24th EDITION

Enhanced DIGITAL VERSION Included

HENRY'S Clinical Diagnosis AND Management BY Laboratory Methods

RICHARD A. McPHERSON
MATTHEW R. PINCUS

ELSEVIER

ASSOCIATE EDITORS

Katalin Banki, MD
Associate Professor
Department of Pathology
SUNY Upstate Medical University
Syracuse, New York

Martin H. Bluth, MD, PhD
Chief, Blood Bank/Transfusion Services
Assistant Director, Clinical Laboratories
Director of Translational Research
Department of Pathology
Maimonides Medical Center
Brooklyn, New York;
Professor of Pathology
Wayne State University School of Medicine
Detroit, Michigan;
Adjunct Professor of Pathology
SUNY Downstate Medical Center
Brooklyn, New York;
Global Medical Director
Kids Kicking Cancer
Founder, Bluth Bio Industries
Southfield, Michigan

Jay L. Bock, MD, PhD
Professor Emeritus
Department of Pathology
Stony Brook Medicine
Stony Brook, New York

Wilbur B. Bowne, MD
Professor of Surgery and Chief of Oncological Surgery
Jefferson Medical Center
Philadelphia, Pennsylvania

Robert E. Hutchison, MD
Professor
Department of Pathology
SUNY Upstate Medical University
Syracuse, New York State University of New York Upstate Medical University
Syrac

Donald S. Karcher, MD
Professor and Immediate Past Chair
Department of Pathology
George Washington University Medical Center
Washington, DC

Mark S. Lifshitz, MD
Clinical Professor
Department of Pathology, Molecular, and Cell-Based Medicine
Icahn School of Medicine at Mount Sinai
New York, New York

H. Davis Massey, DDS, MD, PhD
Chief, Department of Pathology and Laboratory Medicine
McGuire VA Medical Center
Associate Professor
Department of Pathology
Virginia Commonwealth University
Richmond, Virginia

A. Koneti Rao, MBBS, FACP, FAHA
Sol Sherry Professor of Medicine
Professor of Clinical Pathology and Laboratory Medicine
Co-Director, Sol Sherry Thrombosis Research Center
Director, Benign Hematology, Hemostasis and Thrombosis
Lewis Katz School of Medicine at Temple University
Philadelphia, Pennsylvania

Gail L. Woods, MD
Former Professor
University of Arkansas for Medical Sciences
Chief of Pediatric Pathology
Department of Pathology
Arkansas Children's Hospital
Little Rock, Arkansas

سایت کنکور
www.KONKUR.IN
مرجع دانلود رایگان کتب علوم پزشکی و مهندسی
آرشیو کامل و رایگان کنکورهای ارشد، دکتری و آزمونهای مقاطع و گرایشهای مختلف علوم پزشکی

24th EDITION

HENRY'S

Clinical Diagnosis AND Management BY Laboratory Methods

Richard A. McPherson, MD, MSc
Professor Emeritus
Department of Pathology
Virginia Commonwealth University School of Medicine
Richmond, Virginia

Matthew R. Pincus, MD, PhD
Professor
Department of Pathology
SUNY Downstate Medical Center
Brooklyn, New York

ELSEVIER

Elsevier
1600 John F. Kennedy Blvd.
Ste. 1600
Philadelphia, PA 19103-2899

HENRY'S CLINICAL DIAGNOSIS AND MANAGEMENT BY LABORATORY METHODS
TWENTY-FOURTH EDITION

ISBN: 978-0-323-67320-4

Copyright © 2022 by Elsevier Inc.

All rights reserved. No part of this publication may be reproduced or transmitted in any form or by any means, electronic or mechanical, including photocopying, recording, or any information storage and retrieval system, without permission in writing from the publisher. Details on how to seek permission, further information about the Publisher's permissions policies, and our arrangements with organizations such as the Copyright Clearance Center and the Copyright Licensing Agency can be found at our website: www.elsevier.com/permissions. This book and the individual contributions contained in it are protected under copyright by the Publisher (other than as may be noted herein).

Previous editions copyrighted 2017, 2011, 2007, 2001, 1996, 1991, 1984, 1979, 1974, 1969, 1962, 1953, 1948,1943, 1939, 1935, 1931, 1927, 1923, 1918, 1914, 1912, 1908.

Notices

Knowledge and best practice in this field are constantly changing. As new research and experience broaden our understanding, changes in research methods, professional practices, or medical treatment may become necessary. Practitioners and researchers must always rely on their own experience and knowledge in evaluating and using any information, methods, compounds, or experiments described herein. In using such information or methods they should be mindful of their own safety and the safety of others, including parties for whom they have a professional responsibility. With respect to any drug or pharmaceutical products identified, readers are advised to check the most current information provided (i) on procedures featured or (ii) by the manufacturer of each product to be administered, to verify the recommended dose or formula, the method and duration of administration, and contraindications. It is the responsibility of practitioners, relying on their own experience and knowledge of their patients, to make diagnoses, to determine dosages and the best treatment for each individual patient, and to take all appropriate safety precautions. To the fullest extent of the law, neither the Publisher nor the authors, contributors, or editors, assume any liability for any injury and/or damage to persons or property as a matter of products liability, negligence or otherwise, or from any use or operation of any methods, products, instructions, or ideas contained in the material herein.

The Publisher

Library of Congress Control Number: 2020952266

Executive Content Strategist: Michael Houston
Senior Content Development Manager: Katherine DeFrancesco
Publishing Services Manager: Catherine Jackson
Senior Project Manager: John Casey
Senior Designer: Margaret Reid

Printed in Canada

9 8 7 6 5 4 3 2 1

ELSEVIER Book Aid International Working together to grow libraries in developing countries
www.elsevier.com • www.bookaid.org

CONTRIBUTORS

Naif Z. Abraham Jr, MD, PhD
Director, Division of Clinical Pathology
Assistant Professor of Pathology
State University of New York Upstate Medical University
Syracuse, New York

Katsumi Aoyagi, PhD
Head, Research and Development Division
Fujirebio, Inc.
President and CEO
Advanced Life Science Institute, Inc.
Hachioji-shi, Tokyo, Japan

Yoshihiro Ashihara, PhD
President and CEO
Fujirebio Holdings, Inc.
Tokyo, Japan

Jaya Ruth Asirvatham, MBBS
Assistant Professor
Department of Pathology, Immunology, and Laboratory Medicine
University of Florida College of Medicine
Gainesville, Florida

Constantine A. Axiotis, MD
Professor
Department of Pathology
SUNY Downstate Health Sciences University
Brooklyn, New York

Yu Bai, MD, PhD
Professor of Pathology
The University of Texas Health Science Center at Houston
McGovern Medical School
Director, Molecular Pathology at UT Outreach Pathology
Houston, Texas

Ulysses G.J. Balis, MD
Professor
Department of Pathology
University of Michigan
Ann Arbor, Michigan

Katalin Banki, MD
Associate Professor
Department of Pathology
SUNY Upstate Medical University
Syracuse, New York

Katie V. Bean, MD
Nephrology Fellow
Department of Internal Medicine
Virginia Commonwealth University
Richmond, Virginia

Kathleen G. Beavis, MD
Medical Director of Microbiology, Immunology, and
Laboratories' Quality
Professor of Pathology
University of Chicago
Chicago, Illinois

Sylva Bem, MD
Assistant Professor
Department of Pathology
SUNY Upstate Medical University
Syracuse, New York

Jonathan Ben-Ezra, MD
Department of Pathology
Tel Aviv Sourasky Medical Center
Tel Aviv, Israel

Tim B. Bigdeli, PhD
Assistant Professor
Department of Psychiatry
SUNY Downstate Medical Center
Brooklyn, New York

Martin H. Bluth, MD, PhD
Chief, Blood Bank/Transfusion Services
Assistant Director, Clinical Laboratories
Director of Translational Research
Department of Pathology
Maimonides Medical Center
Brooklyn, New York;
Professor of Pathology
Wayne State University School of Medicine
Detroit, Michigan;
Adjunct Professor of Pathology
SUNY Downstate Medical Center
Brooklyn, New York;
Global Medical Director
Kids Kicking Cancer
Founder, Bluth Bio Industries
Southfield, Michigan

Aleh Bobr, MD
Medical Director, Blood Bank and Tissue Services
Associate Medical Director, Apheresis Service
Assistant Professor
Department of Pathology and Microbiology
University of Nebraska Medical Center
Omaha, Nebraska

Jay L. Bock, MD, PhD
Professor Emeritus
Department of Pathology
Stony Brook Medicine
Stony Brook, New York

Michael J. Borowitz, MD, PhD
Professor
Department of Pathology and Oncology
Johns Hopkins Medical Institutions
Baltimore, Maryland

Wilbur B. Bowne, MD
Professor
Director, Division of Oncological Surgery
Department of Surgery
Sidney Kimmel Medical College
Thomas Jefferson University
Philadelphia, Pennsylvania

Paul Brandt-Rauf, MD, PhD, DScD, DrPH
Dean, School of Biomedical Engineering
Drexel University
Philadelphia, Pennsylvania

Robert Bray, PhD
Professor
Department of Pathology
Emory University School of Medicine
Atlanta, Georgia

Cindy L. Bredefeld, DO, FACE
Attending Physician
Division of Endocrinology, Diabetes, and Metabolism
Assistant Professor of Clinical Medicine
Department of Medicine
NYU Long Island School of Medicine
Mineola, New York

Gary Briefel, MD
Clinical Associate Professor
Department of Medicine
SUNY Downstate Medical Center
Brooklyn, New York

M. Jana Broadhurst, MD, PhD, DTM&H
Director, Nebraska Biocontainment Unit Clinical Laboratory
Director, Emerging Pathogens Laboratory
Assistant Professor, Pathology & Microbiology
University of Nebraska Medical Center
Omaha, Nebraska

Robert P. Carty, PhD
Associate Professor
Department of Biochemistry
SUNY Downstate Medical Center
Brooklyn, New York

Angela Ceribelli, MD, PhD
Unit of Rheumatology
Department of Internal Medicine
Humanitas Clinical and Research Center – IRCCS
Rozzano, Milan, Italy

Edward K.L. Chan, PhD
Professor
Department of Oral Biology
University of Florida
Gainesville, Florida

Angella Charnot-Katsikas, MD
Medical Director, MolDx
Chief Medical Officer, Palmetto GBA
Columbia, South Carolina

Sindhu Cherian, MD
Associate Professor
Department of Laboratory Medicine
University of Washington
Seattle, Washington

Spencer Chiang, PhD
Graduate Research Assistant
Weldon School of Biomedical Engineering
Purdue University
West Lafayette, Indiana

William L. Clapp, MD
Professor of Pathology
Director of Renal Pathology
Department of Pathology, Immunology, and Laboratory Medicine
University of Florida College of Medicine
Gainesville, Florida

Laura Lee Cooling, MD, MS
Professor
Department of Pathology
University of Michigan
Ann Arbor, Michigan

Lynsey Daniels, MD
General Surgery Fellow
Department of Surgery
Drexel University College of Medicine
Philadelphia, Pennsylvania

Robertson D. Davenport, MD
Professor
Department of Pathology
University of Michigan
Ann Arbor, Michigan

Robert P. DeCresce, MD, MBA, MPH
Director of Clinical Laboratories
Department of Pathology
Rush University Medical Center
Chicago, Illinois

Julio C. Delgado, MD, MS
Professor
Department of Pathology
University of Utah
Salt Lake City, Utah

Robert A. DeSimone, MD
Assistant Professor
Department of Pathology and Laboratory Medicine
Weill Medical College of Cornell University
New York-Presbyterian Hospital
New York, New York

Margaret A. DiGuardo, MD
Medical Director
Immunohematology Laboratory
Division of Transfusion Medicine
Mayo Clinic
Rochester, Minnesota

Jorge A. Di Paola, MD
Professor of Pediatrics and Molecular Genetics and Genomics
Elizabeth Finney McDonnell Endowed Chair in Pediatric Hematology
Oncology
Division Chief, Pediatric Hematology and Oncology
Washington University School of Medicine in St. Louis
St. Louis, Missouri

Theresa Downs, BS
Laboratory Supervisor
Pathology Blood Bank
University of Michigan
Ann Arbor, Michigan

M. Tarek Elghetany, MD
Professor of Pathology and Immunology and Pediatrics
Department of Pathology
Baylor College of Medicine
Texas Children's Hospital
Houston, Texas

Matthew B. Elkins, MD, PhD
Associate Professor
Department of Pathology
SUNY Upstate Medical University
Syracuse, New York

Ayman Fanous, MD
Professor and Chairman
Department of Psychiatry
SUNY Downstate Medical Center
Brooklyn, New York

Marvin J. Fritzler, PhD, MD
Professor
Department of Medicine
Cumming School of Medicine
University of Calgary
Calgary, Alberta, Canada

Howard M. Gebel, PhD
Professor
Department of Pathology
Emory University Hospital
Atlanta, Georgia

Eve Goldstein, MD
General Surgery Fellow
Department of Surgery
Drexel University College of Medicine
Philadelphia, Pennsylvania

Susan S. Graham, MS
Associate Professor and Chair
Department of Clinical Laboratory Science
SUNY Upstate Medical University
Syracuse, New York

Wayne W. Grody, MD, PhD
Professor
Department of Pathology & Laboratory Medicine, Pediatrics, and Human Genetics
UCLA School of Medicine
Los Angeles, California

Helena A. Guber, MD
Chief, Department of Endocrinology, Metabolism and Diabetes
NY Harbor Healthcare System
Assistant Professor of Medicine
Department of Endocrinology
SUNY Downstate Health Sciences University
Brooklyn, New York

Gaurav Gupta, MD
Associate Professor
Department of Internal Medicine
Virginia Commonwealth University
Richmond, Virginia

Robert G. Hamilton, PhD, D(ABMLI)
Professor
Department of Medicine and Pathology
Johns Hopkins University School of Medicine
Baltimore, Maryland

Amanda Harrington, PhD, D(ABMM)
Associate Professor
Department of Pathology and Laboratory Medicine
Loyola University Chicago
Maywood, Illinois

Neil Selwyn Harris, MBChB, MD
Clinical Professor
Department of Pathology, Immunology, and Laboratory Medicine
University of Florida College of Medicine
Gainesville, Florida

Rong He, MD
Consultant, Department of Laboratory Medicine and Pathology (Hematopathology)
Co-Director, Molecular Hematopathology Laboratory
Mayo Clinic
Rochester, Minnesota

Tim Hilbert, MD, PhD, JD
Medical Director
Blood Bank
NYU Langone Medical Center
New York, New York

Julie Woolworth Hirschhorn, PhD, HCLD
Assistant Professor
Department of Pathology and Laboratory Medicine
Medical University of South Carolina
Charleston, South Carolina

Catherine A. Hogan, MDCM, MSc
Instructor
Department of Pathology
Stanford University
Stanford, California

Joseph Holup, PhD, (D)ABMLI
Assistant Clinical Professor
Department of Pathology
NYU Grossman School of Medicine
New York, New York

Henry A. Homburger, MD
Professor Emeritus
Mayo College of Medicine
Department of Laboratory Medicine and Pathology
Mayo Clinic
Rochester, Minnesota

Yen-Michael S. Hsu, MD, PhD
Director of Immunologic Monitoring and Cellular Products Laboratory
Associate Professor of Medicine
Division of Hematology and Oncology
University of Pittsburgh School of Medicine
UPMC Hillman Cancer Center
Pittsburgh, Pennsylvania

M. Mahmood Hussain, PhD
Director
Diabetes and Obesity Research Center
NYU Langone Hospital–Long Island
Endowed Chair
Department of Foundations of Medicine
NYU Long Island School of Medicine
Mineola, New York;
Distinguished Professor Emeritus
Department of Cell Biology
SUNY Downstate Medical Center
Brooklyn, New York

Robert E. Hutchison, MD
Professor
Department of Pathology
SUNY Upstate Medical University
Syracuse, New York

Peter C. Iwen, PhD, D(ABMM), F(AAM)
Professor
Department of Pathology and Microbiology
University of Nebraska Medical Center
Omaha, Nebraska

Shilpa Jain, MD
Associate Professor
Department of Pathology and Immunology
Director of Gastrointestinal Pathology
Baylor College of Medicine
Houston, Texas

Roohi Jeelani, MD
Director of Research and Education
Reproductive Endocrinology and Infertility
Vios Fertility Institute
Chicago, Illinois

J. Charles Jennette, MD
Professor
Department of Pathology and Laboratory Medicine
University of North Carolina at Chapel Hill
Chapel Hill, North Carolina

Jeffrey S. Jhang, MD, MBA
Professor and Vice Chair
Department of Pathology, Molecular and Cell-Based Medicine
Icahn School of Medicine at Mount Sinai
Medical Director, Center for Clinical Laboratories
Mount Sinai Health System
New York, New York

Donald S. Karcher, MD
Professor and Immediate Past Chair
Department of Pathology
George Washington University Medical Center
Washington, DC

Yasushi Kasahara, PhD, DMSc
Visiting Professor
Department of Clinical Pathology
Showa University School of Medicine
Tokyo, Japan

Samuel W. Kaskovich
MD/MSc Candidate
Medicine & Biomedical Informatics
University of Chicago
Chicago, Illinois

Craig M. Kessler, MD, MACP
Professor of Medicine and Pathology
Director, Division of Coagulation
Georgetown University Medical Center
Washington, DC

Marian Khalili, MD
General Surgery Fellow
Department of Surgery
Drexel University College of Medicine
Philadelphia, Pennsylvania

Jason Kidd, MD
Associate Professor
Department of Internal Medicine, Division of Nephrology
Virginia Commonwealth University Medical Center
Richmond, Virginia

Michael J. Klein, MD
Pathologist-in-Chief and Director Emeritus
Department of Pathology and Laboratory Medicine
Hospital for Special Surgery
Professor of Pathology and Laboratory Medicine
Department of Pathology and Laboratory Medicine
Weill Cornell School of Medicine
New York, New York

Katrin M. Klemm, MD
Medical Director
Aperian Laboratory Solutions
Medical Director
EAMC Hospital Laboratory
Department of Pathology
East Alabama Medical Center
Opelika, Alabama

Stefanie Krick, MD, PhD
Assistant Professor
Department of Medicine
The University of Alabama at Birmingham
Birmingham, Alabama

Scott Krummey, MD, PhD
Assistant Professor
Johns Hopkins School of Medicine
Baltimore, Maryland

Attila Kumánovics, MD
Senior Associate Consultant
Department of Laboratory Medicine and Pathology
Mayo Clinic
Rochester, Minnesota

Anthony Kurec, MS, MASCP, MLT(ASCP)H, DLM
Clinical Associate Professor, Emeritus
Clin Lab Science
SUNY Upstate Medical University
Syracuse, New York

Charles LaDoulis, MD
Chairman Emeritus
Department of Pathology
Maimonides Medical Center
Brooklyn, New York

Raymond G. Lau, MD
Clinical Assistant Professor
Director of Medical Weight Management
Division of Endocrinology, Diabetes, and Metabolism
Division of Bariatric Surgery
Department of Medicine
NYU Long Island School of Medicine
Mineola, New York

Eszter Lázár-Molnár, PhD
Assistant Professor
Department of Pathology
University of Utah
Salt Lake City, Utah

Grace Ming Lee, MD
Assistant Professor
Division of Hematology
Department of Medicine
Duke University
Durham, North Carolina

Peng Lee, MD, PhD
Professor of Pathology and Urology
New York University Langone Medical Center and School of Medicine
Chief, Pathology and Laboratory Medicine Service
VA NY Harbor Healthcare System
New York, New York

Jing Li, PhD
Professor
Department of Oncology
Karmanos Cancer Institute
Wayne State University School of Medicine
Detroit, Michigan

Mark S. Lifshitz, MD
Clinical Professor
Department of Pathology, Molecular, and Cell-Based Medicine
Icahn School of Medicine at Mount Sinai
New York, New York

Bo Lin, MD, PhD
Resident Physician
Department of Pathology
SUNY Downstate Medical Center
Brooklyn, New York

Ronald P. Mageau, MD
KWB Pathology Associates
Tallahassee, Florida

Mariana Markell, MD
Professor
Department of Medicine
SUNY Downstate Health Sciences University
Brooklyn, New York

H. Davis Massey, DDS, MD, PhD
Chief
Department of Pathology and Laboratory Medicine
McGuire VA Medical Center
Associate Professor
Department of Pathology
Virginia Commonwealth University
Richmond, Virginia

Blaine A. Mathison, BS, M(ASCP)
Scientist
Institute for Clinical and Experimental Pathology
ARUP Laboratories
Salt Lake City, Utah

Sharad C. Mathur, MD
Associate Chief of Staff for Education
VA Medical Center
Kansas City, Missouri;
Professor
Department of Pathology and Laboratory Medicine
University of Kansas Medical Center
Kansas City, Kansas

Richard A. McPherson, MD, MSc
Professor Emeritus
Department of Pathology
Virginia Commonwealth University School of Medicine
Richmond, Virginia

Lauren A. McVoy, MD, PhD
Vice Chair of Clinical Integration
Department of Laboratory Medicine
Memorial Sloan Kettering Cancer Center
New York, New York

Kimberly Merkel, MD
Adjunct Assistant Professor
Department of Dermatology
University of Florida College of Medicine
Gainesville, Florida

Jacquelyn L. Meyers, PhD
Assistant Professor
Department of Psychiatry
SUNY Downstate Medical Center
Brooklyn, New York

W. Greg Miller, PhD
Professor
Department of Pathology
Virginia Commonwealth University
Richmond, Virginia

Paul D. Mintz, MD
Chief Medical Officer
Senior Vice President
Verax Biomedical Inc.
Marlborough, Massachusetts

Golam Mohi, PhD
Professor
Department of Biochemistry and Molecular Genetics
University of Virginia School of Medicine
Charlottesville, Virginia

Angela Mojica, MD
Assistant Professor
Department of Pediatrics
SUNY Upstate Medical University
Syracuse, New York

Michel R. Nasr, MD
Interim Chair of Pathology and Laboratory Medicine
Director of Clinical Pathology and Genomics
SUNY Upstate Medical University
Syracuse, New York

Dejan Nikolic, MD, PhD
Director of Microbiology and Immunology
Site Pathology Residency Program Director
Department of Pathology and Laboratory Services
Cooper University Health Care
Assistant Professor of Pathology
Cooper Medical School of Rowan University
Camden, New Jersey

Frederick S. Nolte, PhD
Professor and Vice-Chair for Laboratory Medicine
Department of Pathology and Laboratory Medicine
Medical University of South Carolina
Charleston, South Carolina

Man S. Oh, MD
Professor
Department of Medicine
SUNY Downstate Medical Center
Brooklyn, New York

Juan P. Olano, MD
Professor
Department of Pathology
University of Texas Medical Branch
Galveston, Texas

Mihaela Oprea, MD
Attending Physician
Department of Endocrinology
NY Harbor Healthcare System
Brooklyn, New York

Thomas L. Ortel, MD, PhD
Professor
Departments of Medicine and Pathology
Duke University Medical Center
Durham, North Carolina

Zheng Ouyang, PhD
Professor
Department of Precision Instrument
Tsinghua University
Beijing, China

Mary Ann Perle, PhD
Director of Cytogenetics
Department of Pathology
NYU School of Medicine, Bellevue Hospital Center
New York, New York

Roseann E. Peterson, PhD
Assistant Professor
Virginia Commonwealth University
Virginia Institute for Psychiatric and Behavioral Genetics
Richmond, Virginia

Matthew R. Pincus, MD, PhD
Professor
Department of Pathology
SUNY Downstate Medical Center
Brooklyn, New York

Benjamin A. Pinsky, MD, PhD
Associate Professor
Departments of Pathology and Medicine (Infectious Diseases)
Stanford University School of Medicine
Director, Clinical Virology Laboratory
Stanford Health Care and Stanford Children's Health
Stanford, California

Anna R. Plourde, MD, MPH
Director, Clinical Microbiology Laboratory
Clinical Assistant Professor
Department of Pathology
SUNY Downstate Health Sciences University
Brooklyn, New York

Bobbi S. Pritt, MD, MSc, (D)TMH
Professor
Department of Laboratory Medicine and Pathology
Mayo Clinic
Rochester, Minnesota

Simon Rabinowitz, PhD, MD
Vice Chairman
Department of Pediatrics
SUNY Downstate Children's Hospital
Brooklyn, New York

Nikita Raje, MD, MSc
Section of Allergy/Asthma/Immunology
Department of Pediatrics
Children's Mercy
University of Missouri Kansas City
Kansas City, Missouri

Jacob H. Rand, MD
Professor
Department of Pathology and Laboratory Medicine
Weill Medical College of Cornell University
New York-Presbyterian Hospital
New York, New York

A. Koneti Rao, MBBS, FACP, FAHA
Sol Sherry Professor of Medicine
Professor of Clinical Pathology and Laboratory Medicine
Co-Director, Sol Sherry Thrombosis Research Center
Director, Benign Hematology, Hemostasis and Thrombosis
Lewis Katz School of Medicine at Temple University
Philadelphia, Pennsylvania

Roger S. Riley, MD, PhD
Professor
Department of Pathology
Co-Director, Hematology Laboratory
Director, Hemostasis Laboratory
Program Director, Hematopathology Fellowship
Virginia Commonwealth University School of Medicine
Richmond, Virginia

Rhonda K. Roby, PhD, MPH
Technical Leader/Supervising DNA Criminalist
Crime Laboratory Forensic Biology Unit
Alameda County Sheriff's Office
Oakland, California

Kyle G. Rodino, PhD
Assistant Professor
Department of Pathology and Laboratory Medicine
University of Pennsylvania Perelman School of Medicine
Philadelphia, Pennsylvania

Yan Xue Russell, MD
Fellow
Department of Endocrinology
NY Harbor Healthcare System
Brooklyn, New York

Ravi Sarode, MD
Director, Division of Transfusion and Hemostasis
Professor of Pathology and Internal Medicine (Hematology/Oncology)
UT Southwestern Medical Center
Dallas, Texas

Cynthia A. Schandl, MD, PhD
Professor
Department of Pathology and Laboratory Medicine
Medical University of South Carolina
Charleston, South Carolina

Shabnam Seydhafkan, MD
Resident Physician
Department of Pathology
SUNY Downstate Medical Center
Brooklyn, New York

Haseeb A. Siddiqi, PhD
Professor
Departments of Cell Biology, Pathology, and Medicine
SUNY Downstate Health Sciences University
Brooklyn, New York

Natthapol Songdej, MD, MPH
Assistant Professor of Medicine and Pediatrics
Department of Medicine
Penn State Health Milton S Hershey Medical Center
Hershey, Pennsylvania

Constance H. Stein, PhD
Professor Emeritus
Department of Pathology
SUNY Upstate Medical University
Department of Clinical Pathology
University Hospital
Syracuse, New York

Lisa M. Stempak, MD
System Director of Clinical Pathology
Department of Pathology
University Hospitals Cleveland Medical Center
Clinical Assistant Professor
Case Western Reserve University
Cleveland, Ohio

H. Clifford Sullivan, MD, D(ABHI)
Assistant Professor
Department of Pathology and Laboratory Medicine
Emory University School of Medicine
Atlanta, Georgia

George R. Thompson III, MD, FIDSA
Associate Professor of Medicine
Division of Infectious Diseases
Department of Internal Medicine
University of California–Davis Medical Center
Sacramento, California

Neerja Vajpayee, MD
Laboratory Director
Oneida Health
Oneida, New York

David S. Viswanatha, MD
Consultant, Department of Laboratory Medicine and Pathology (Hematopathology)
Co-Director, Molecular Hematopathology and Clinical Genome Sequencing Laboratories
Mayo Clinic
Rochester, Minnesota

Carlos Alberto von Mühlen, MD, PhD
Chairman of the Board
Department of Immunology
Brazilian Society of Autoimmunity
Porto Alegre, Rio Grande do Sul, Brazil;
Consultant
Immunology and Rheumatology
San Diego, California

David H. Walker, MD
Professor
Department of Pathology
Executive Director
Center for Biodefense and Emerging Infectious Diseases
University of Texas Medical Branch
Galveston, Texas

Hannah Wang, MD
Resident
Department of Pathology
Stanford University
Stanford, California

Victor W. Weedn, MD, JD
Chief Medical Examiner
Office of the Chief Medical Examiner
Maryland Department of Health
Baltimore, Maryland

Eric T. Weimer, PhD, D(ABHI, ABMLI)
Assistant Professor
Department of Pathology and Laboratory Medicine
University of North Carolina
Chapel Hill, North Carolina

Ruth S. Weinstock, MD, PhD
SUNY Distinguished Service Professor
Department of Medicine
SUNY Upstate Medical University
Syracuse, New York

Nancy L. Wengenack, PhD
Professor
Department of Laboratory Medicine and Pathology
Mayo Clinic
Rochester, Minnesota

Nathan P. Wiederhold, PharmD, FCCP, FIDSA, FECMM
Professor
Department of Pathology and Laboratory Medicine
University of Texas Health Science Center
San Antonio, Texas

William E. Winter, MD
Professor
Departments of Pathology, Immunology, and Laboratory Medicine,
Pediatrics, and Molecular Genetics and Microbiology
University of Florida College of Medicine
Gainesville, Florida

Jeffrey L. Winters, MD
Medical Director
Therapeutic Apheresis Treatment Unit
Division of Transfusion Medicine
Mayo Clinic
Rochester, Minnesota

Christina M. Wojewoda, MD
Director, Clinical Microbiology Laboratory
Department of Pathology and Laboratory Medicine
University of Vermont Medical Center
Associate Professor
Department of Pathology and Laboratory Medicine
University of Vermont
Burlington, Vermont

Brent L. Wood, MD, PhD
Professor
Department of Pathology and Laboratory Medicine
Childrens Hospital Los Angeles
University of Southern California
Los Angeles, California

Gail L. Woods, MD
Former Professor
University of Arkansas for Medical Sciences
Chief of Pediatric Pathology
Department of Pathology
Arkansas Children's Hospital
Little Rock, Arkansas

Wenpeng Zhang, PhD
Postdoctoral Research Associate
Department of Chemistry
Purdue University
West Lafayette, Indiana

Yaxia Zhang, MD, PhD
Chief of Clinical Pathology
Head of Pathology Research
Associate Director of Fellowship Program
Department of Pathology and Laboratory Medicine
Hospital for Special Surgery
Associate Professor of Pathology and Laboratory Medicine
Department of Pathology and Laboratory Medicine
Weill-Cornell School of Medicine
New York, New York

PREFACE

Clinical laboratory measurements form the scientific basis upon which medical diagnosis and management of patients is established. These results constitute the largest section of the medical record of patients, and laboratory examinations will only continue to grow in number as new procedures are offered and well-established ones are ordered more frequently in the future. The modern concept of an electronic health record encompasses information from a patient's birth through that individual's entire life, and laboratory testing is a significant component of that record from prenatal and newborn screening through childhood, adulthood, and geriatric years. Traditional areas of testing are well established in clinical chemistry, hematology, coagulation, microbiology, immunology, and transfusion medicine. Genetic testing for disease detection, hereditary disease risk assessment and definitive diagnosis and prognosis is becoming a reality, beginning with individual disease testing that is expected to be followed by whole genome screening for a multitude of conditions. The rapid pace in the introduction of new testing procedures demands that laboratory practitioners be experts in several divergent aspects of this profession. The environment of clinical laboratories is extremely well-suited for translation of research procedures into diagnostic assays because of their traditional involvement in basic analysis, quality control, professional competencies, and cost-effective strategies of operation. All of these applications are made stronger for occurring under regulations of federal and state governments, as well as the standards of accreditation of professional pathology organizations. Clinical laboratories excel in these tasks, and they are now responding to pressures for even greater accomplishments in areas of informatics, advanced analytic methods, interpretation of complex data, and communication of medical information in a meaningful way to physician colleagues and even directly to patients in some health care models. The most successful practitioners of laboratory medicine will incorporate all of these approaches into their daily lives and will be leaders in their institutions for developing initiatives to promote outstanding health care in a fiscally responsible endeavor. This textbook strives to provide the background knowledge by which trainees can be introduced to these practices and to serve as a resource for pathologists and other laboratory personnel to update their knowledge to solve problems that they encounter daily.

This twenty-fourth edition marks more than 100 years since *A Manual of Clinical Diagnosis*, authored by James Campbell Todd, was introduced in 1908. In its current format as *Henry's Clinical Diagnosis and Management by Laboratory Methods*, this textbook remains the authoritative source of information for residents, students, and other trainees in the disciplines of clinical pathology and laboratory medicine, and for physicians and laboratory practitioners. The current edition continues the tradition of partnership between laboratory examinations and the formulation and confirmation of clinical diagnoses followed by monitoring of body functions, therapeutic drug levels, other results of medical treatments, and risk assessment for disease. Beginning with the twenty-first edition, color illustrations have been used throughout the book to accurately and realistically depict clinical laboratory test findings and their analysis. The overriding mission of this book is to incorporate new discoveries and their clinical diagnostic applications alongside the wealth of information that forms the core knowledge base of clinical pathology and laboratory medicine. It is also our objective to call the reader's attention to important unsolved problems in diagnostic medicine and to stimulate the reader to formulate ways to solve these problems. Our contributing authors, who are experts in their specialties, present to the reader the essential basic and new information that is central to clinical laboratory practice.

Part 1, The Clinical Laboratory, covers the organization, purposes, and practices of analysis, interpretation of results, and management of the clinical laboratory from quality control through informatics and finances. The general structure of this section includes general management principles, with emphasis on preanalytic, analytic, and postanalytic components of laboratory analysis as well as oversight functions. Administrative concepts for the laboratory are considered in Chapter 1, with optimization of workflow presented in Chapter 2. Preanalytic factors such as variations arising from specimen collection, transport, and handling and other variables are discussed in Chapter 3. The principles of analysis and instrumentation are presented in Chapter 4. Since the field of mass spectroscopy has begun to play an important role in a wide variety of areas of laboratory medicine, including clinical chemistry and microbiology, we have now introduced a new chapter, Chapter 5, in this new edition that is devoted to the principles and practice of mass spectrometry. Chapter 6 covers laboratory automation. The growing arena of near-patient laboratory services beyond central hospital laboratories in the format of point-of-care testing is presented in Chapter 7 along with presentation on this application in the military. Postanalysis processes of result reporting and medical decision making, are presented in Chapter 8 while a systematic approach that allows the clinician and laboratorian to interpret and assess laboratory results is presented in Chapter 9. This chapter provides the basis for formulation of differential diagnosis from laboratory values, choice of possible reflex testing and the ordering of further testing to confirm diagnoses. A key component to all phases of laboratory processes, interpretation of results, and decision making is statistical analysis, which is presented in Chapter 10. Explicit applications of statistics are in quality control and proficiency testing for oversight of the entire analytic process (Chapter 11). Maintaining order for the complexities of laboratory test result ordering and reporting and the management of clinical information are possible only through sophisticated information systems that are essential to all clinical laboratories (Chapter 12). Management decisions in the clinical laboratory involve the choice of analytic instrumentation, automation to process and deliver specimens to analytic stations, and computer systems to coordinate all of the preanalytic, analytic, and postanalytic processes to meet the mission of the institution. These choices determine the productivity that a laboratory can achieve (especially its ability to respond to increased volumes of testing and complexity of measurements and examinations as the standards of practice advance). Paramount is the manner in which the laboratory can muster its resources in equipment, personnel, reagent supplies, and ingenuity of its leadership to respond to the needs of health care providers and patients in terms of access, timeliness, cost, and quality of test results. New challenges continue to emerge for the laboratory to provide excellent quality services at a fiscally responsible expense; the changing models of reimbursement for medical and laboratory services demand that pathologists and laboratory leaders develop and maintain a strong understanding of the principles of financial management and be well aware of mechanisms that laboratories can utilize for responding to these new approaches to reimbursement (Chapter 13). Chapter 14 on ethics in laboratory medicine provides a framework for appropriate delivery of clinical laboratory testing and human subjects research in accordance with accepted principles of behavior.

Part 2, Clinical Chemistry, is organized to present laboratory examinations according to organ systems and their disorders. Some of the most commonly ordered laboratory tests are directed at the evaluation of renal function, water, electrolytes, metabolic intermediates and nitrogenous wastes, and acid-base balance, all of which are critically important for monitoring acutely ill patients and in the management of patients with kidney and pulmonary disorders (Chapter 15). The important field of bone metabolism and bone diseases, stemming from the enormous public interest in osteoporosis of our aging population, is covered in Chapter 16. The significance of carbohydrate measurements, with particular emphasis on diabetes mellitus, the overall hormonal regulation of glucose metabolism, and disorders of other sugars, is reviewed in Chapter 17. Chapter 18 covers the extremely important topic of lipids and disorders in their metabolism and highlights the critical patterns in lipoprotein profiles that indicate disposition to atherosclerosis and cardiac malfunction, especially myocardial infarction. In Chapter 19, the serodiagnostic markers for cardiac injury evaluation and the related disorders of stroke are elaborated. The clinical significance of specific proteins and their analysis, with emphasis on electrophoresis of blood and body fluids, is covered in Chapter 20. The field of clinical enzymology, with applications to assessment of organ injury,

is covered in Chapter 21. The principles of enzymology (e.g., transition state theory) have been used directly in the design of new effective drugs against specific diseases such as hypertension and AIDS. A new section has been introduced into this chapter concerning the mechanism of infection of cells by the Coronavirus-19, (Covid-19), the cause of the current world pandemic, because, incredibly, this virus binds uniquely to the angiotensin converting enzyme, ACE2, which acts as its receptor on cell surfaces. Laboratory assessment of liver function is presented in Chapter 22 (which includes new treatments for hepatitis C) and that of gastrointestinal and pancreatic disorders in Chapter 23. Toxicological analysis and therapeutic drug monitoring are covered in Chapter 24, with applications of both immunoassays and mass spectroscopy emerging in endocrinology (Chapter 25) and pregnancy and perinatal testing as well (Chapter 26). Nutritional analysis, with examination of vitamins and trace metals, is presented in Chapter 27. Chapter 28 elaborates the chemical principles of analysis, which is crucial to the understanding of virtually all laboratory measurements and the common interferences encountered with blood and biological fluids.

Part 3, Urine and Other Body Fluids, reviews the utility and methods for examining fluids other than blood. Chapter 29 presents the basic examination of urine, with extensive discussions of both chemical testing and microscopic examination of urine sediment. A special area for consideration is body fluid analysis, which has received national attention recently in terms of standardizing the approach to testing of typical fluids and other alternative specimens (Chapter 30). A large range of specimen types is considered in this discussion, with extensive coverage of both microscopic and chemical examinations.

Part 4, Hematology and Transfusion Medicine, introduces techniques for the basic examination of blood and bone marrow (Chapter 31) and provides a wealth of background on the physiological processes involved in hematopoiesis (Chapter 32). Erythrocytic disorders and leukocytic disorders and their diagnosis are covered in Chapters 33 and 34, respectively. Modern techniques for use of flow cytometry for diagnosis of hematopoietic neoplasias are presented in Chapter 35 to round out the approaches to diagnosis in this rapidly changing field. Immunohematology, which is so important for the understanding of erythrocyte, leukocyte, and platelet antibodies and their impact on transfusion, is covered in Chapter 36. Blood component manufacture and utilization are covered in Chapter 37 along with transfusion reactions. Chapters 38 and 39 deal with the rapidly expanding areas of apheresis, with its applications to therapy of multiple blood disorders as well as the collection, processing, and dispensing of hematopoietic progenitor cells (adult stem cells) from bone marrow, peripheral blood, and cord blood for treatment of both malignant and nonmalignant diseases.

Part 5, Hemostasis and Thrombosis, covers the vast increase in our knowledge of the pathways involved in clotting and in fibrinolysis and the panoply of new testing and therapeutic modalities that have evolved as a result. This section continues to reflect the impact of our growing knowledge of coagulation and fibrinolysis (Chapter 40) plus that of platelet function disorders, with emphasis on von Willebrand disease (Chapter 41). Advances in the diagnosis and monitoring of thrombotic disorders are covered extensively in Chapter 42, with particular interest in the prediction of thromboembolic risk. Along with our better understanding of thrombosis have come new drugs for treatment of patients with vascular occlusive disorders, particularly ischemic events in the heart or brain. Principles of antithrombotic therapy and the laboratory's role in its monitoring are covered in Chapter 43. Also discussed in this section is the major advance in pharmacogenomics (fully discussed later in Chapter 75) as it impacts anticoagulant therapies for individual patients.

Part 6, Immunology and Immunopathology, presents a framework both for classifying disorders of the immune system and for the role of laboratory testing in diagnosing those diseases (Chapter 44). Measurements based on immunoassays have long been the essential components of understanding a multitude of disorders; an excellent and comprehensive account of the principles of immunoassay and immunochemistry is included in Chapter 45. Evaluation of the cellular immune system for diagnosing and monitoring immune defects is described in Chapter 46, which is newly updated. Humoral immunity and the examination of immunoglobulins in disease are covered in Chapter 47, with particular emphasis on the evaluation of monoclonal disorders in the blood. Material on complement and its role in inflammation is presented in Chapter 48. Chapter 49 presents cytokines and adhesion molecules that are vital to inflammation and have become targets for therapeutic interventions. Also brought up to date are Chapter 50 on the major histocompatibility complex (MHC), with its significant applications to organ transplantation, and Chapter 51, which looks at MHC and disease associations. The evaluation of immunodeficiency disorders includes many standard examinations for protein and cellular functions plus new genetic tests for specific abnormalities (Chapter 52). The assessment of autoimmune diseases is presented for the systemic rheumatic diseases (Chapter 53), with new chapters covering the vasculitides (Chapter 54) and organ-specific autoimmune diseases (Chapter 55). Allergic diseases, with their ever-increasing laboratory evaluations, are presented in Chapter 56.

Part 7, Medical Microbiology, covers an enormous spectrum of infectious diseases and related topics that include medical bacteriology (Chapter 57); susceptibility testing of antimicrobial agents (Chapter 58); mycobacteria with immense concern for the emergence of resistant strains (Chapter 59); mycotic diseases with a wide array of photographs of cultures and photomicrographs (Chapter 60); spirochete infections (Chapter 61); chlamydial and mycoplasmal infections (Chapter 62); rickettsiae (Chapter 63); viral infections with new material on human coronavirus-19 (Chapter 64); and medical parasitology which has a worldwide significance that is growing as large numbers of people move between countries and continents(Chapter 65). In line with the importance of achieving maximum diagnostic benefit from the laboratory, specimen collection and handling for diagnosis of infectious disease are detailed in Chapter 66. Although classic techniques have consisted of culturing microbiological organisms with identification and antimicrobial susceptibility testing through functional bioassays, modern methods of nucleic acid amplification and detection are now becoming widespread for each type of microbiological organism; these applications are described in each chapter about the various organisms. In addition, the use of mass spectroscopy, that has revolutionized the microbiology laboratory in the identification of pathogens, is likewise discussed in each appropriate chapter.

Part 8, Molecular Pathology, covers some of the most rapidly changing and exciting areas of clinical laboratory testing. Chapter 67 provides an introduction to the role of molecular diagnostics, with an updated discussion of the principles and techniques of the field in Chapter 68. Similar updates are provided for the vital molecular diagnostic techniques of polymerase chain reaction and other amplification methods (Chapter 69) and newer approaches to nucleic acid hybridization (Chapter 70). The application of cytogenetics, with modern methods of karyotyping, including fluorescent in situ hybridization and examination for chromosomal abnormalities, is covered in Chapter 71. Chapter 72 comprehensively presents the application of molecular diagnostics to genetic diseases, for which screening is becoming more widely practiced. In view of the revolutionary development of genome-wide association studies (GWAS), major discoveries of genomic alterations in neuropsychiatric diseases such as Alzheimer's disease, schizophrenia, and post-traumatic stress disorder (PTSD) have been found. Therefore, a new presentation (Chapter 73) on the molecular biology of neuropsychiatric diseases provides understanding for diagnosis and therapy of these disorders. Identity testing as used in modern parentage testing and forensic analysis is presented in Chapter 74. Chapter 75 on pharmacogenomics provides an understanding of how molecular analysis of selected genes crucial for response to therapeutic drugs or for the metabolism of drugs can be used to optimize individualized treatment plans, also known as personalized or precision medicine.

Part 9, Clinical Pathology of Cancer, is a further outgrowth of this section that was introduced in the twenty-first edition. Because of the explosion of new diagnostic information as a result of the successful sequencing of the human genome, genetic profiles of different forms of cancers are now available. Specific forms of cancer are beginning to be diagnosed using microchips containing gene arrays in which patterns of gene expression and mutation are evaluated. In addition, new methods of proteomics (i.e., determination of the patterns of expression of multiple proteins in patients' body fluids and tissues) allow for cancer detection, monitoring, and treatment. Thus there has been a vast increase in information about the principles and applications of laboratory methods for diagnosis and monitoring of malignancies in just the past few years. Chapter 76 deals with the important protein markers for cancer in blood and tissues that are commonly used for the diagnosis and management of malignant diseases. Chapter 77 extends this discussion through exciting new applications of oncoproteins and growth factors and their receptors in the assessment of malignancies and modification of therapies. A broad spectrum of molecular and cytogenetic markers is now commonly used for the initial evaluation of hematopoietic neoplasms (Chapter 78) that could well become a model for assessment of most, if not all, malignancies. Because the methods in molecular pathology used in diagnosing cancer in body fluids are the same as in solid-tissue diagnosis, breaking down the barriers between anatomic and clinical pathology, we include Chapter 79 on the evaluation of solid tumors by these methods.

The prospects for early detection, prognosis, and implementation of treatment regimens for cancer based on specific alterations in the genome have never been more apparent. These chapters on cancer diagnostics emphasize genome-based approaches and other new methods such as proteomics, which has the potential to identify patterns of protein alterations that can be used both for discovery of new targets for examination and for direct detection of clinical abnormalities. Many of these technologies have been developed in the past few years, and many more versions of them are sure to appear as the competitive advantage of rapid and inexpensive genomic analysis emerges. We think it is vital for pathologists to understand the bases of molecular diagnostics, the power of this type of analysis for clinical decision making, and the paths such testing is likely to take in the future. To this end, the final chapter (Chapter 80) presents the diagnostic and prognostic impact of high-throughput genomic and proteomic technologies and the role they can play in the present and future practice of pathology.

The fundamental task for trainees in laboratory medicine is to achieve a sound understanding of analytic principles and the power and limitations of laboratory examinations so that they can interpret whether abnormal results are due to a patient's physical condition or to other potential interferences such as altered physiological state, drug interactions, or abnormalities introduced by specimen mishandling. Based on mastery of these technical aspects of test performance and interpretation, pathologists should be able to recommend strategies to provide the appropriate level of care for multiple purposes: to screen for disease, to confirm a diagnosis, to establish a prognosis, to monitor the effects of treatment, and (more recently) to assess the future risk of disease. National practice recommendations from the American Medical Association and the U.S. Department of Health and Human Services have led to the formulation of standardized panels of multiple individual tests that are targeted to several organ systems, such as the basic metabolic panel and comprehensive metabolic panel (Appendix 7, available online with the other appendices). These panels consist of individual tests that are highly automated and can be conveniently and inexpensively delivered through most hospital laboratories. Such convenience was not always the case when the assays for basic constituents such as potassium, sodium, chloride, bicarbonate, calcium, bilirubin, and all the various metabolites, proteins, and enzyme activities were performed manually, as documented in previous editions of this textbook. Beyond those relatively simple tests, immunoassays have also undergone a similar transformation. A few decades ago, the rapid assay for thyroid-stimulating hormone (TSH) required 2 days, whereas today a third-generation TSH measurement can be completed in 20 minutes or less. Conversion from highly complex and operator-interactive testing to immediately available and inexpensive assays will almost certainly occur with procedures that are now at the cutting edge of technology and require elaborate instrumentation and special expertise to perform. These include tandem mass spectrometry for small molecules such as hormones, vitamins, and drugs; whole genome sequencing for assessing the risk of developing hereditary disorders and diagnosing malignancies; and proteomics for screening a wide array of proteins in blood, body fluids, and tissues for disease detection and evidence of progression. The configuration of these assays will consolidate multiple analyses onto miniature platforms such as chip technologies.

We also note that new methods of microanalysis have now been implemented so as to enable rapid point-of-care testing on critically ill patients on small volumes of whole blood. These include the "stat" analytes (sodium, potassium, chloride, bicarbonate, calcium, BUN, creatinine and glucose and, now, several critical enzymes) in addition to blood gas determinations, all performed on hand-held analyzers and also on blood gas analyzers. In a recent breakthrough in testing, a new mass spectrometer has been devised that is the size of a brief case allowing for point-of-care testing by mass spectroscopy.

Although these new technologies will likely be expensive to implement initially, the hope is that they will reduce costs in other parts of the health care system through initiating prevention or treatment earlier than would be possible without such complex and intimate information about a patient's disease state or propensity to develop a disease.

Within this context, it is clear that the role of the clinical laboratory in the future will involve more than simply providing numeric results for physicians to glance at during rounds or after clinic duty. The complexity and enormity of the test results that will be routinely available will require entirely new approaches to data presentation and interpretation to provide useful information for clinical diagnosis and management. The challenge to laboratories and clinicians alike is to develop "meaningful uses" in which electronic health records can store and present all of this information about a patient—from cradle through an entire life—into which several segments are integrated: genetic background, environmental factors, previous diagnostic and monitoring tests, and contemporaneous monitoring tests. All of these aspects of a patient's history have the potential to be meaningful in the most rigorous sense to provide personalized medical treatments.

This textbook provides grounding in the practice of modern laboratory medicine, and it points the way to new disciplines that will contribute to the evolution of strategies for creating, analyzing, and presenting medical information in the future. We hope that the discussions in this textbook will stimulate our colleagues at all levels to conceive of and/or embrace new diagnostic laboratory technologies (in addition to those that are now standard) and to retain the most valuable from each of these into practices of the future. The legacy of this book over the past century has been to provide a clear and useful account of laboratory tests that generate the solid scientific information upon which medical decisions are based. Building on that foundation, we enthusiastically anticipate new diagnostic capabilities, and we hope that this textbook will be a stimulus to their development.

It is a privilege and an honor to serve as editors for this twenty-fourth edition.

Richard A. McPherson, MD, MSc
Matthew R. Pincus, MD, PhD
April 2021

ACKNOWLEDGMENTS

We gratefully acknowledge the outstanding contributions made by our expert colleagues and collaborators who served as associate editors: Katalin Banki, MD; Martin H. Bluth, MD, PhD; Jay L. Bock, MD, PhD; Wilbur B. Bowne, MD; Robert E. Hutchison, MD; Donald S. Karcher, MD; Mark S. Lifshitz, MD; H. Davis Massey, DDS, MD, PhD; A. Koneti Rao, MBBS; and Gail L. Woods, MD. They all have made extensive contributions to the quality of this book, both through development of textual matter and through the exercise of practiced review of the chapters under their guidance. We deeply appreciate their efforts in this edition. We gratefully acknowledge the participation in previous editions of Elizabeth R. Unger, MD, PhD.

It is with sadness that we note the passing of four authors who made significant contributions to the previous edition of this text. We wish to honor their memories and recognize their professional achievements.

Martin J. Salwen, MD. Dr. Salwen was a Distinguished Service Professor at the State University of New York (SUNY) Downstate Medical Center and former Director of Pathology at both SUNY Downstate University Hospital and the Kings County Hospital. After graduating from SUNY Downstate, he performed his residency in Pathology and Laboratory Medicine at Yale University Medical Center after which he served with distinction in East Asia as a Captain in the medical corps in the United States Air Force. After his military service, he became the Director of Laboratories at Monmouth Medical Center, New Jersey. He then became Director of Pathology at both the Downstate University Hospital and the Kings County Hospital, and Professor of Pathology at SUNY Downstate Medical Center, where he revolutionized the practice of laboratory medicine and trained several generations of pathology residents. Under his leadership the laboratories were equipped with advanced instrumentation using state-of-the art technology, and embarked on the use of efficient laboratory information systems. He revolutionized the clinical pathology services at both medical centers whereby attending physicians and house officers made joint rounds on patients with unusual laboratory findings, greatly increasing the efficacy of both the clinical and anatomic pathology services. His elective course in the interpretation of laboratory data for senior medical students was immensely popular and benefitted them in understanding clinical medicine. In collaboration with Drs. William Sunderman Sr. and Jr., Dr. Salwen helped found and promote the clinical pathology journal, *Annals of Clinical and Laboratory Science* and served on its editorial board for many years. Dr. Salwen made enormous contributions to the clinical pathology literature in many areas including documentation of multisystem failure in gram-negative sepsis, and the graphic presentation of laboratory data that facilitated clinical interpretation and understanding. He received many awards during his tenure at SUNY Downstate Medical Center, including the prestigious Ailanthus Award, the Jean Redmond Oliver Teaching Award, and the Dr. Frank L. Babbott Memorial Award for distinguished service to the medical profession and community. Dr. Salwen's passing is a tremendous loss to SUNY Downstate Medical Center, to the field of clinical pathology, and especially to this book to which he contributed over its many editions.

Geraldine S. Hall, PhD. Dr. Hall was a Clinical Microbiologist at the Cleveland Clinic and served as the Section Head of Microbiology. She was dedicated to education and excelled in the practice of microbiology which she conveyed to numerous trainees. She served in many leadership positions for the American Society of Microbiology both nationally and regionally.

Omar Fagoaga, PhD. Dr. Fagoaga was director of the Histocompatibility Laboratory of the Detroit Medical Center and Wayne State University having immigrated to the United States from El Salvador where he had been the target of terrorists as a youth. Despite that experience, he was known for his warm personality and for being a fast learner of laboratory methodologies. He was at the forefront of DNA typing in histocompatibility testing. Among his greatest accomplishments was the mapping of HLA alleles and antibodies in African American populations.

Nancy S. Jenny, PhD. Dr. Jenny was Associate Professor in the Department of Pathology and Laboratory Medicine at the University of Vermont. Her research in the biochemical mechanisms of diseases of aging including atherosclerosis, dementia, and general frailty led to numerous prestigious publications.

All of our students, residents, and colleagues have for decades contributed enormously to the development of our knowledge of human disease and the use of laboratories for diagnosis and patient management. We are grateful for all of their questions and the stimulus they have provided to our professional growth. We are especially grateful for the mentorship and encouragement provided in our careers by Alfred Zettner, MD; Cecil Hougie, MD; Abraham Braude, MD; Charles Davis, MD; James A. Rose, MD; Robert P. Carty, PhD; Donald West King, MD; George Teebor, MD; Phillip Prose, MD; Fred Davey, MD; and Gerald Gordon, MD. We will always remember them and the standards for excellence they set.

The development of this edition, with its myriad details, would not have been possible without the outstanding professional efforts of our editors at Elsevier: Kathryn DeFrancesco, Michael Houston, and John Casey, each of whom added tremendously to this enterprise. We are sincerely grateful to them and to all the staff of Elsevier. They have made this endeavor a happy one. We also send very special thanks to Anne Erickson, a supreme medical illustrator, who has drawn many of the illustrations in the most recent four editions with a fine eye to beauty in presentation and ease of comprehension.

We are grateful to all of the authors for accepting the challenge to participate in the education of future and present laboratorians and physicians in all fields of medicine by distilling the essential information from each of their fields of expertise and creating a readable and authoritative text for our audience. Special thanks to the authors who have created wholly new chapters on mass spectroscopy, ethics in laboratory medicine, and molecular biology of psycho-neurologic disease for this edition.

We also remember with perpetual gratitude the inspiration provided to us by John Bernard Henry, MD. He provided leadership for seven editions of this book. Moreover, he encouraged us, guided us, and demanded excellence from us in our profession.

Upon the completion of this twenty-fourth edition, we humbly thank all the individuals who have played roles in making it possible. It is not possible to name all of the individuals who have contributed to this textbook. To those mentioned here and to those not explicitly named, we thank you for your prodigious efforts and support. We also gratefully acknowledge the loving support of our wives, Stephanie Sammartino McPherson and Naomi Pincus, in developing this edition and in all our endeavors.

Richard A. McPherson, MD, MSc
Matthew R. Pincus, MD, PhD

CONTENTS

PART 1 The Clinical Laboratory

EDITED BY | Mark S. Lifshitz, Matthew R. Pincus

1 General Concepts and Administrative Issues 2
Tim Hilbert, Anthony Kurec, Mark S. Lifshitz

2 Optimizing Laboratory Workflow and Performance 13
Mark S. Lifshitz

3 Preanalysis 22
Mark S. Lifshitz

4 Analysis: Principles of Instrumentation 35
Matthew R. Pincus, Mark S. Lifshitz, Jay L. Bock

5 Mass Spectrometry and Applications 60
Spencer Chiang, Wenpeng Zhang, Zheng Ouyang

6 Analysis: Clinical Laboratory Automation 74
Robert P. DeCresce, Joseph Holup, Mark S. Lifshitz

7 Point-of-Care Testing and Physician Office Laboratories 81
Lauren A. McVoy, Mark S. Lifshitz

8 Postanalysis: Medical Decision Making 89
Jeffrey S. Jhang, Mark S. Lifshitz

9 Interpreting Laboratory Results 100
Matthew R. Pincus, Naif Z. Abraham Jr., Martin H. Bluth

10 Laboratory Statistics 119
Richard A. McPherson

11 Quality Control 130
W. Greg Miller

12 Clinical Laboratory Informatics 150
Ulysses G.J. Balis

13 Financial Management 162
Mark S. Lifshitz, Robert P. DeCresce

14 Ethics in Laboratory Medicine 174
Richard A. McPherson, Matthew R. Pincus

PART 2 Clinical Chemistry

EDITED BY | Jay L. Bock, Martin H. Bluth, Matthew R. Pincus

15 Evaluation of Renal Function, Water, Electrolytes, and Acid-Base Balance 182
Man S. Oh, Gary Briefel, Matthew R. Pincus

16 Biochemical Markers of Bone Metabolism 208
Katrin M. Klemm, Michael J. Klein, Yaxia Zhang

17 Carbohydrates 225
Angela Mojica, Ruth S. Weinstock

18 Lipids and Dyslipoproteinemia 244
Cindy L. Bredefeld, Raymond Lau, M. Mahmood Hussain

19 Cardiac Injury, Atherosclerosis, and Thrombotic Disease 267
Jay L. Bock

20 Specific Proteins 276
Richard A. McPherson

21 Clinical Enzymology 291
Matthew R. Pincus, Robert P. Carty

22 Evaluation of Liver Function 314
Lynsey Daniels, Marian Khalili, Eve Goldstein, Martin H. Bluth, Wilbur B. Bowne, Matthew R. Pincus

23 Laboratory Diagnosis of Gastrointestinal and Pancreatic Disorders 331
Haseeb A. Siddiqi, Simon Rabinowitz, Constantine A. Axiotis

24 Toxicology and Therapeutic Drug Monitoring 347
Martin H. Bluth, Matthew R. Pincus, Naif Z. Abraham Jr.

25 Evaluation of Endocrine Function 387
Helena A. Guber, Mihaela Oprea, Yan Xue Russell

26 Reproductive Function and Pregnancy 425
Roohi Jeelani, Martin H. Bluth

27 Vitamins and Trace Elements 441
Mariana Markell, Haseeb A. Siddiqi

28 Chemical Basis for Analyte Assays and Common Interferences 453
Matthew R. Pincus, Richard A. McPherson, Jay Bock

PART 3 Urine and Other Body Fluids

EDITED BY | Donald S. Karcher, Richard A. McPherson, Matthew R. Pincus

29 Basic Examination of Urine 468
Roger S. Riley, Richard A. McPherson

30 Cerebrospinal, Synovial, Serous Body Fluids, and Alternative Specimens 510
Donald S. Karcher, Richard A. McPherson

PART 4 Hematology and Transfusion Medicine

EDITED BY | Robert E. Hutchison, Katalin Banki, Richard A. McPherson

31 Basic Examination of Blood and Bone Marrow 540
Neerja Vajpayee, Susan S. Graham, Sylva Bem

32 Hematopoiesis 570
Sharad C. Mathur, Robert E. Hutchison, Golam Mohi

33 Erythrocytic Disorders 588
M. Tarek Elghetany, Katalin Banki

34 Leukocytic Disorders 636
Michel R. Nasr, Robert E. Hutchison

35 The Flow Cytometric Evaluation of Hematopoietic Neoplasia 689
Brent L. Wood, Sindhu Cherian, Michael J. Borowitz

36 Immunohematology 708
Laura Lee Cooling, Theresa Downs

37 Transfusion Medicine 771
Matthew B. Elkins, Robertson D. Davenport, Paul D. Mintz

38 Hemapheresis 788
Margaret A. DiGuardo, Aleh Bobr, Jeffrey L. Winters

39 Tissue Banking and Progenitor Cells 817
Yen-Michael S. Hsu, Matthew B. Elkins

PART 5 Hemostasis and Thrombosis

EDITED BY | A. Koneti Rao, Matthew R. Pincus

40 Coagulation and Fibrinolysis 828
Ravi Sarode, Craig M. Kessler

41 Platelet Disorders and Von Willebrand Disease 847
A. Koneti Rao, Natthapol Songdej, Jorge A. Di Paola

42 Laboratory Approach to Thrombotic Risk 870
Robert A. DeSimone, Jacob H. Rand

43 Antithrombotic Therapy 879
Grace Ming Lee, Thomas L. Ortel

PART 6 Immunology and Immunopathology

EDITED BY | H. Davis Massey, Richard A. McPherson

44 Overview of the Immune System and Immunologic Disorders 894
Richard A. McPherson, H. Davis Massey

45 Immunoassays and Immunochemistry 901
Katsumi Aoyagi, Yoshihiro Ashihara, Yasushi Kasahara

46 Laboratory Evaluation of the Cellular Immune System 929
Roger S. Riley, Ronald Mageau, Jonathan Ben-Ezra

47 Laboratory Evaluation of Immunoglobulin Function and Humoral Immunity 952
Richard A. McPherson, Roger S. Riley, H. Davis Massey

48 Mediators of Inflammation: Complement 969
Katie V. Bean, H. Davis Massey, Gaurav Gupta

49 Mediators of Inflammation: Cytokines and Adhesion Molecules 984
Stefanie Krick

50 Human Leukocyte Antigen: The Major Histocompatibility Complex of Humans 996
Robert Bray, H. Clifford Sullivan, Scott Krummey, Howard M. Gebel

51 The Major Histocompatibility Complex and Disease 1014
Attila Kumánovics, Eszter Lázár-Molnár, Julio C. Delgado

52 Immunodeficiency Disorders 1025
Nikita Raje

53 Clinical and Laboratory Evaluation of Systemic Autoimmune Rheumatic Diseases 1035
Carlos Alberto von Mühlen, Edward K.L. Chan, Angela Ceribelli, Marvin J. Fritzler

54 Vasculitis 1058
Jason Kidd, Eric T. Weimer, J. Charles Jennette

55 Organ-Specific Autoimmune Diseases 1074
William E. Winter, William L. Clapp, Neil Selwyn Harris, Jaya Ruth Asirvatham, Kimberly Merkel

56 Allergic Diseases 1115
Henry A. Homburger, Robert G. Hamilton

PART 7 Medical Microbiology

EDITED BY | Gail L. Woods, Richard A. McPherson

57 Medical Bacteriology 1130
Christina M. Wojewoda, Lisa M. Stempak

58 In Vitro Testing of Antimicrobial Agents 1166
Angella Charnot-Katsikas, Amanda Harrington

59 Mycobacteria 1183
Kyle G. Rodino, Gail L. Woods, Nancy L. Wengenack

60 Mycotic Diseases 1194
Peter C. Iwen, George R. Thompson III, Nathan P. Wiederhold

61 Spirochete Infections 1229
Dejan Nikolic

62 Chlamydial and Mycoplasmal Infections 1246
Dejan Nikolic

63 Rickettsiae and Other Related Intracellular Bacteria 1254
Juan P. Olano, David H. Walker

64 Viral Infections 1266
Catherine A. Hogan, M. Jana Broadhurst, Hannah Wang, Benjamin A. Pinsky

65 Medical Parasitology 1290
Blaine A. Mathison, Bobbi S. Pritt

66 Specimen Collection and Handling for Diagnosis of Infectious Diseases 1352
Anna R. Plourde, Kathleen G. Beavis

PART 8 Molecular Pathology

EDITED BY | Martin H. Bluth, Matthew R. Pincus

67 Introduction to Molecular Pathology 1368
Martin H. Bluth, Matthew R. Pincus

68 Molecular Diagnostics: Basic Principles and Techniques 1373
Martin H. Bluth

69 Polymerase Chain Reaction and Other Nucleic Acid Amplification Technology 1387
Julie Woolworth Hirschhorn, Cynthia A. Schandl, Frederick S. Nolte

70 Hybridization Array Technologies 1401
Martin H. Bluth

71 Applications of Cytogenetics in Modern Pathology 1411
Mary Ann Perle, Constance H. Stein

72 Molecular Diagnosis of Genetic Diseases 1434
Wayne W. Grody

73 Molecular Genetics of Neuropsychiatric Disorders: Current Research and Perspectives 1452
Jacquelyn L. Meyers, Roseann E. Peterson, Tim B. Bigdeli, Ayman Fanous, Bo Lin, Shabnam Seydhafkan, Matthew R. Pincus

74 Identity Testing: Use of DNA Analysis in Parentage, Forensic, and Missing Persons Testing 1468
Rhonda K. Roby, Samuel W. Kaskovich, Victor W. Weedn

75 Pharmacogenomics and Personalized Medicine 1480
Jing Li, Martin H. Bluth

PART 9 Clinical Pathology of Cancer

EDITED BY Matthew R. Pincus, Martin H. Bluth, Wilbur B. Bowne, Richard A. McPherson

76 Diagnosis and Management of Cancer Using Serologic and Other Body Fluid Markers 1508
Peng Lee, Shilpa Jain, Matthew R. Pincus, Marian Khalili, Wilbur B. Bowne, Martin H. Bluth, Richard A. McPherson

77 Oncoproteins and Early Tumor Detection 1525
Matthew R. Pincus, Martin H. Bluth, Paul W. Brandt-Rauf, Wilbur B. Bowne, Charles LaDoulis

78 Molecular Diagnosis of Hematopoietic Neoplasms 1542
Rong He, David S. Viswanatha

79 Molecular Genetic Pathology of Solid Tumors 1579
Yu Bai, Shilpa Jain, Matthew R. Pincus, Peng Lee

80 High-Throughput Genomic and Proteomic Technologies in the Postgenomic Era 1607
Martin H. Bluth

APPENDICES

(AVAILABLE ONLINE AT ELSEVIER EBOOKS FOR PRACTICING CLINICIANS)

1 Physiologic Solutions, Buffers, Acid-Base Indicators, Standard Reference Materials, and Temperature Conversions

2 Desirable Weights, Body Surface Area, and Body Mass Index

3 Approximations of Total Blood Volume

4 Periodic Table of Elements

5 SI Units

6 Common Chimeric Genes Identified in Human Malignancies
Peng Lee, Naif Z. Abraham Jr., Matthew R. Pincus

7 Disease/Organ Panels

PART 1

The Clinical Laboratory

EDITED BY | Mark S. Lifshitz, Matthew R. Pincus

CHAPTER 1

GENERAL CONCEPTS AND ADMINISTRATIVE ISSUES

Tim Hilbert, Anthony Kurec, Mark S. Lifshitz

STRATEGIC PLANNING, 3
QUALITY SYSTEMS MANAGEMENT, 3
HUMAN RESOURCE MANAGEMENT, 5
FINANCIAL MANAGEMENT, 6
LABORATORY DESIGN AND SERVICE MODELS, 6
REGULATION, ACCREDITATION, AND LEGISLATION, 6
SAFETY, 10
Biological Hazards, 10
Chemical Hazards, 11
Ergonomic Hazards, 11
SELECTED REFERENCES, 12

KEY POINTS

- Effective laboratory management requires leaders to provide direction and managers to get things done. Strategic planning, marketing, human resource management, financial management, and quality management are all key elements of a laboratory organization.
- Most laboratory errors occur in the preanalytic and postanalytic stages. Six Sigma and Lean Six Sigma are quality management tools that can be used to reduce laboratory errors and increase productivity.
- Laboratory services are provided in many different ways on a continuum from point-of-care tests producing immediate answers to highly complex laboratory tests that require sophisticated technology and skilled staff.
- Clinical laboratories are highly regulated; many laboratory practices are the direct result of federal or state/local legislation. At the federal level, laboratory activities are regulated through the Clinical Laboratory Improvement Amendments of 1988 (CLIA'88).
- Biological, chemical, and natural disasters, as well as ergonomic and fire hazards, cannot be completely avoided but can be minimized through preplanning and the use of engineering controls, personal protective equipment, and work practice controls.

The laboratory plays a central role in health care. Anecdotal evidence suggests that laboratory results impact up to 70% of medical decisions. While quantitative studies supporting this claim are lacking (Ngo et al., 2017; Amukele & Schroeder, 2017), the clinical laboratory remains a vital tool in the practice of diagnostic medicine. It is of considerable note that although the laboratory is a $100 billion business, annual laboratory costs account for less than 2% of total health care dollars spent, offering high clinical value at relatively low cost (KaufmanHall, 2017; Centers for Medicare and Medicaid Services [CMS], 2018; American Clinical Laboratory Association, 2018). While laboratory testing currently seems to be a relative bargain (0.9% annual growth rate from 2012–2017), an estimated 2.7% annual growth rate is anticipated through the year 2022 (KaufmanHall, 2017). Laboratory test menus have become dynamic, expanding to accommodate the ever-increasing number of new diagnostic tests in response to available advanced technology. In the area of genetic testing, as of August 2017, there were about 75,000 tests available representing approximately 10,000 unique test types. That number is expected to grow about 28% annually through 2020, creating a $7.7 billion worldwide industry (Phillips et al., 2018). Implementing new test modalities and technology will increase expenditures and increase the pressure on laboratory leadership to control costs and guide appropriate test utilization (Bogavac-Stanojevic & Jelic-Ivanovic, 2017).

The purpose of the laboratory is to provide physicians, other health care professionals, and patients with the necessary information to (1) detect a disease or the predisposition to a disease; (2) confirm or reject a diagnosis; (3) establish prognosis; (4) guide patient management; and (5) monitor the efficacy of therapy. The laboratory also plays a leading role in education, research, information technology design and implementation, and quality improvement. To achieve quality goals and ensure a well-functioning laboratory requires skilled personnel who not only understand state-of-the-art technologies but also financial management, business, marketing tactics, and human resource practices. This chapter will discuss key administrative concepts and issues that serve as the basis of sound laboratory practice. Committed leadership with skills to guide staff is crucial to a well-managed laboratory that generates accurate and timely laboratory results. A more detailed discussion of these topics is available elsewhere (Snyder & Wilkinson, 1998; Nigon, 2000; Garcia, 2014).

An organization is only as good as its people, supervised by skilled managers but guided by visionary leaders. While leaders can be managers, not all managers are effective leaders, yet all should aspire to gain such expertise. The terms *leadership* and *management* are often used interchangeably but represent different qualities (Table 1.1). Leadership provides the direction of where a group (or an organization) is going, whereas management provides the "road" to get there. Lewis Carroll pointed out that, "If you don't know where you are going, any road will get you there." This simple concept reminds us that leadership must be visionary and set clear goals with strategic objectives and that leaders ensure that the right things are done. Management is more tactical in practice. Managers implement objectives, control budgets, organize staff, and ensure that things are done right. Good leaders use learned management skills, while great leaders employ both skills and their innate characteristics to effectively grow their organization (Kurec, 2016b). Effective managers use a variety of talents to work with people to get things done. Achieving organizational goals requires an optimal mix of skilled, dedicated, and task-oriented leaders and managers working with committed staff.

Leadership skills manifest as patterns of behavior that engage others to complete tasks in a timely and productive manner. The Situational Leadership model (Hersey et al., 2012) describes four key styles: supporting, directing, delegating, and coaching. A *supportive* leader provides high support but low direction in accomplishing duties. A *directive* leader presents rules, orders, or other defined instructions, but limited support. The former approach offers flexibility and encourages creative problem solving. The latter approach offers concise and detailed instructions from the leader on how to complete a task by independently solving the problems and making all the decisions. A *delegating* leader provides low support and low direction, allowing competent (generally, more experienced) staff to assume accountability and responsibility to complete the goals. The *coaching* leader provides high support and high direction by guiding individuals to make real-time decisions with appropriate support and corrective actions as needed. Most leaders adopt a combination of styles as appropriate to different situations but periodically default to one of the four styles to achieve desired results (Kurec, 2017).

Good managers use a variety of human, financial, physical, and informational resources to meet an organization's strategic goals in the most efficient and effective manner. Some basic managerial responsibilities are listed in Box 1.1. Managers can be stratified as first-line managers (supervisors, team leaders, chief technologists), middle managers (operations managers, division heads), and top managers (laboratory directors, board of directors, and the various C-suite [top-level] executives). Each managerial

TABLE 1.1

Leader Versus Manager Traits

Leader	Manager
Administrator	Implementer
Organizer and developer	Maintains control
Risk taker	Thinks short term
Inspiration	Asks *how* and *when*
Thinks long term	Watches bottom line
Asks *what* and *why*	Accepts status quo
Challenges status quo	Is a good soldier
Does the right thing	Does things right

Modified from Ali M, Brookson S, Bruce A, et al. *Managing for excellence*. London: DK Publishing; 2001, pp 86–149.

level dictates the daily activities and skill sets required for that position. Top-level managers concentrate on strategizing and planning for the next 1 to 5 years, while first-line managers are more concerned about completing the day's work. A top-level manager may or may not possess technical skills that a first-line manager uses every day. Middle managers may straddle both areas to some degree by engaging in a variety of activities that may be strategic as well as tactical.

STRATEGIC PLANNING

Technology has moved the science of laboratory medicine from using numerous manual methods to applying highly automated ones. The introduction of table-top instrumentation, point-of-care technology, and direct-access testing has leveled the playing field of laboratory science to a point at which some testing can be done in the clinic, in the physician's office, at a drugstore, and even in the home by nontraditional laboratorians. In addition, the evolution of telemedicine/telepathology has greatly expanded the laboratory's footprint (Kurec, 2016a). These changes have eliminated some of the market protections that laboratories once enjoyed and made testing a commodity. Labs have been forced to adopt more competitive business practices. To survive and even thrive in a competitive environment, a laboratory must constantly reevaluate its goals and services and adapt to market forces (e.g., fewer qualified laboratory personnel, reduced budgets, stricter regulatory mandates, lower reimbursements, new sophisticated technologies). Leaders must carefully make strategic decisions that can have an impact on the laboratory for years.

The process by which high-level decisions are made is called *strategic planning*, which can be defined as (1) deciding on the objectives of the organization and the need to modify existing objectives if appropriate; (2) allocating resources to attain these objectives; and (3) establishing policies that govern the acquisition, use, and disposition of these resources (Lifshitz & De Cresce, 1996). Strategic planning is usually based on long-term projections and a global view that can have an impact on all levels of a laboratory's operations. It is different from tactical planning, which consists of the detailed day-to-day operations needed to meet the immediate needs of the laboratory and works toward meeting the long-term strategic goals that have been set. For example, a global strategy to develop an outreach business may prompt addressing issues such as bringing more send-out reference work in-house, implementing new technologies, acquiring state-of-the-art instrumentation and/or automation, enhancing information technology tools, and employing adequate and skilled staff to satisfy service expectations. Risk can be involved in initiating a specific strategy. A wrong decision may burden a laboratory with unnecessary costs, unused equipment, and/or overstaffing, making it that much harder to change course in response to future market forces or new organizational strategies. Yet, not taking a risk may result in the loss of opportunities to grow the business and/or improve services.

Successful strategic planning requires appropriate data collection by observing current and projected conditions in the following areas: Social, Technological, Economic, Environmental, and Political (or STEEP) (Kurec, 2014a). Effective data collection is generally not the work of a single individual but rather involves a diverse and dedicated committee. Commitment is an essential factor that each member of the committee must embrace and agree to in the early stages of the strategic planning process. Members must acknowledge that they may have to agree to disagree, setting differences of opinion aside to remain supportive of the overarching goal. Further, committee participation can consume a significant amount of time that is nonproductive if not efficiently organized. A variety of techniques can be used to guide the strategic planning process; these include histograms/graphs/scattergrams, brainstorming, fishbone diagrams, storyboarding, Pareto analyses, Delphi analyses, and SWOT (strengths, weaknesses, opportunities, threats) analyses (Kurec, 2017). Internal environmental factors in a SWOT analysis are generally classified as strengths and weaknesses, while external environmental factors are opportunities and threats. This process is a particularly useful tool for guiding a marketing strategy (Box 1.2) and can be used in developing such a program (Table 1.2). Successful strategic planning requires preplanning, organization, well-defined goals, communication, and a firm belief in what is to be accomplished.

BOX 1.1

Basic Management Responsibilities

Operations Management

Quality assurance
Policies and procedures
Strategic planning
Benchmarking
Productivity assessment
Legislation/regulations/HIPAA compliance
Medicolegal concerns
Continuing education
Staff meetings

Human Resource Management

Job descriptions
Recruitment and staffing
Orientation
Competency assessment
Personnel records
Performance evaluation/appraisals
Discipline and dismissal

Financial Management

Departmental budgets
Billing
CPT coding
ICD-10 coding
Compliance regulations
Test cost analysis
Fee schedule maintenance

Marketing Management

Customer service
Outreach marketing
Advertising
Website development
Client education

CPT, Current Procedural Terminology; *HIPAA,* Health Insurance Portability and Accountability Act; *ICD-10,* International Classification of Diseases, 10th revision.

QUALITY SYSTEMS MANAGEMENT

A key management goal is to ensure that quality laboratory services are provided. To accomplish this, every laboratory should strive to obtain modern equipment, to hire well-trained staff, to ensure a well-designed and safe physical environment, and to create a good management team. A key study from the Institute of Medicine (IOM) is often referred to when quality health care issues and medical error rates are addressed (Wolman, 2000). This study concluded that 44,000 to as many as 98,000 Americans die each year because of medical errors (Kohn& Corrigan, 2000). It has been suggested elsewhere that these numbers may underestimate the problem and that the true figure may top 400,000 deaths per year (Makary & Daniel, 2016). An earlier study that looked at sources of medical error in hospitalized patients reported that the most common causes of "diagnostic errors" were failure to use appropriate tests (50%), failure to act on test findings (32%), and avoidable delays in rendering a diagnosis (55%) (Leape et al., 1991). The frequency of laboratory errors varies across the vast number of laboratory tests performed annually. Error rates for laboratory testing have been estimated to range from 0.1% to 3.0%. The distribution of errors among the testing stages was 46% to 68% occurring in the preanalytic stage, 7% to 13% in the analytic stage, and 18% to 47% in the postanalytic stage (Lippi et al., 2010; Hammerling, 2012). Common preanalytic errors include inaccurate patient identification; ordering the wrong test; and improper specimen collection, transportation, and receipt. Analytic errors

BOX 1.2

SWOT Analysis for a New Hospital Outreach Program

Strengths

1. Use current technology/instrumentation
2. Have excess technical capacity
3. Increased test volume will decrease cost per test
4. Strong leadership support
5. Financial resources available

Weaknesses

1. Staffing shortage
2. Morale issues
3. Inadequate courier system
4. Need to hire additional pathologist
5. Limited experience in providing multihospital/client LIS services
6. Turnaround times are marginal

Opportunities

1. Opening of a new physician health care facility
2. Department of Health mandates lead testing on all children younger than 2 years old
3. Have access to hospital marketing department
4. Hospital X is bankrupt; laboratory will close

Threats

1. Competition from other local hospital laboratories
2. Competition from national reference laboratories
3. Reimbursement decreasing
4. Three local hospitals have consolidated their services, including laboratory
5. Several new patient service centers (phlebotomy stations) already opened

LIS, Laboratory information system; *SWOT,* strengths, weaknesses, opportunities, threats.

occur with inappropriate samples (such as incorrect blood tubes for particular analyses), calibration errors, instrument malfunctions, the presence of interfering substances, and the failure to verify results. Postanalytic errors can include reports being sent to the wrong health care provider, long turnaround times, missing reports, and the improper interpretation of test results by health care providers. Concerted efforts by various governmental regulatory agencies and professional associations have resulted in mandated programs that focus on ways to identify, prevent, and reduce errors.

Total quality management (TQM) and *continuous quality improvement* (CQI) have been standard approaches to quality leadership and management for over 30 years (Deming, 2018; Juran, 1988). TQM is a systems approach that focuses on teams, processes, statistics, and the delivery of services/products that meet or exceed customer expectations (Brue, 2002). CQI is an element of TQM that strives to continually improve practices and not just meet established quality standards. Table 1.3 compares traditional quality thinking versus TQM. TQM thinking strives to continually look for ways to reduce errors ("defect prevention") by empowering employees to assist in problem solving and getting them to understand their integral role within the greater system ("universal responsibility").

Two other tools often used to improve quality throughout the health care industry are Six Sigma (Motorola) and Lean Management (Toyota Production System). While these processes developed independently, the key ideas and techniques are often combined in the methodology frequently referred to as Lean Six Sigma. Six Sigma is a performance improvement program, the goal of which can be summarized by the mantra "improvement by eliminating process variation"—that is, improvements in performance, quality, bottom line, customer satisfaction, and employee satisfaction. Six Sigma is based on statistics and quantitative measurements through which process defects or errors are analyzed, potential causes are identified, and improvements are implemented. A defect is anything that does not meet customer requirements. Some common examples might include a laboratory test result error, a delay in reporting, or a quality control problem. The sigma (σ), or standard deviation, expresses how much variability exists in products or services. By decreasing process variation, thus shrinking the standard deviation or sigma, you can increase the level of sigma (or the number of SD units) that fits between the mean and a predetermined performance limit or between the upper and lower performance limits of a process. Thus, a 6σ process is characterized by creating an environment with less variation than that found in a 4σ or 1σ process. It is more tightly controlled and more likely to produce satisfactory results that fall within established performance limits.

TABLE 1.2

Issues to Consider When Establishing a Marketing Program

Environmental assessment	Remember the four Ps of marketing: • Product • Price • Place • Promotion What are the customer needs? Who is the competition? Do you have the right testing menu, equipment, and facilities? Do you have enough personnel? Do you have adequate financial resources? Do you know what it costs to do a laboratory test (test cost analysis)?
Define your customer segments	Physicians, nurses, dentists, other health care providers Other hospital laboratories, physician office laboratories (POLs) Insurance companies Colleges, universities, and other schools Nursing homes, home health agencies, and clinics Veterinarians and other animal health care facilities Researchers, pharmaceutical companies, clinical trials Identify unique socioeconomic and/or ethnic groups. Look for population shifts and location (urban, rural, suburban).
Process	Develop a sales/marketing plan and team. Set goals. Ensure that infrastructure (courier service, LIS capabilities, customer service personnel, etc.) is adequate. Develop additional test menu items. Educate laboratory personnel in customer service. Support and maintain existing client services. Find advertising/public relations resources.
How to market	Review test menu for comprehensive services (niche testing, esoteric testing, other unique services that could be provided to an eclectic group). Place advertisements. Develop brochures, specimen collection manuals, and other customer-related material. Develop website. Attend/participate in community health forums. Identify specific target customers: • Other hospital laboratories, independent laboratories, reference laboratories • College/school infirmaries, health clinics, county laboratory facilities (preemployment, drug screening) • Nursing homes, extended-care facilities, drug/alcohol rehabilitation centers, correctional facilities • Physician offices, groups, and specialties (pediatrics, dermatology, family medicine, etc.)

LIS, Laboratory information system.

Within Six Sigma, nonconforming products or services are measured and expressed as defects-per-million-opportunities (DPMO). If a laboratory sends out 1000 reports and finds that 10 are reported late, it has a 1% defect rate; this is equivalent to 10,000 DPMO. The observed number of DPMO can be converted to a Sigma level that expresses the control level of an activity. The goal of Six Sigma is to reduce the number of defects to near zero. At only 1σ (adjusted for the 1.5σ shift), there are 691,462.5 DPMO or a success-yield of 30.854% (i.e., percentage of products without defects). To reach the goal of Six Sigma, there can be only 3.4 DPMO in order to obtain a 99.9997% yield (Brue, 2002; Westgard et al., 2018). Most laboratories operate at ±2SD or 45,400 DPMO (less than 4σ or 6210 DPMO) (Kaltra & Kopargonkar, 2016). To put this in perspective per Clinical Laboratory Improvement Amendments (CLIA) guidelines, most proficiency testing (PT) requires an 80% accuracy rate. This translates to 200,000 defects per million tests, or only 2.4σ. Six Sigma practices can be applied to many aspects of patient care and safety, thus providing a tool for meeting process improvement needs (Blick, 2013). Examples based on College

TABLE 1.3

Quality Management: Traditional Versus TQM Thinking

Traditional Thinking	TQM Thinking
Acceptable quality	Error-free quality
Department focused	Organization focused
Quality as expense	Quality as means to lower costs
Defects by workers	Defects by system
Management-controlled worker	Empowered worker
Status quo	Continuous quality improvement
Manage by intuition	Manage by fact
Intangible quality	Quality defined
We versus they relationship	Us relationship
End-process focus	System process focus
Reactive systems	Proactive systems

TQM, Total quality management.

TABLE 1.4

Six Sigma Steps

Six Sigma Step	Example
Define project goal or other deliverable that is critical to quality.	Emergency department results in less than 30 minutes from order
Measure baseline performance and related variables.	Baseline performance: 50% of time results are within 30 minutes, 70% within 1 hour, 80% within 2 hours, etc. Variables: Staffing on each shift, order-to-laboratory receipt time, receipt-to-result time, etc.
Analyze data using statistics and graphs to identify and quantify root cause.	Order-to-receipt time is highly variable because samples are not placed in sample transport system immediately and samples delivered to laboratory are not clearly flagged as emergency.
Improve performance by developing and implementing a solution.	Samples from emergency department are uniquely colored to make them easier to spot among routine samples.
Control factors related to the improvement, verify impact, validate benefits, and monitor over time.	New performance: Results available 90% of time within 30 minutes

of American Pathologists (CAP) Q-Probes and Q-Tracks programs show the outcomes of applying Six Sigma to some common performance quality indicators. In these studies, the median variance (50th percentile) for test order accuracy was 2.3%, or 23,000 DPMO; patient wristband error was 3.13%, or 31,000 DPMO; blood culture contamination was 2.83%, or 28,300 DPMO; and the surgical pathology interpretation discrepancy rate was 5.1%, or 51,000 DPMO (Berte, 2004). By lowering defects (i.e., increasing sigma), quality of care is improved and cost savings are realized by eliminating waste of supplies and materials, staff time, unnecessary testing, and even potential legal actions (Sunyog, 2004). By some estimates, the cost of doing business is reduced by 25% to 40% by moving from 3σ to 6σ. An example of the Six Sigma process is provided in Table 1.4.

Lean management is a system for reducing waste in production or manufacturing processes ("nonvalued activities"). Developed from principles originally instituted by Henry Ford, later adopted by the Toyota Corporation to improve quality and efficiency in automobile production, the Lean system has been applied to production methods in a wide variety of industries, including the clinical laboratory. Lean utilizes a variety of techniques—including 5S (Sort, Set in order, Shine, Standardize, and Sustain), and PDCA (Plan, Do, Check, and Act)—to reduce costs by identifying daily work activities that do not directly add to the delivery of laboratory services in the most efficient or cost-effective ways. A Lean laboratory utilizes fewer resources, reduces costs, enhances productivity, promotes staff morale, and improves the quality of patient care (Naik et al., 2018). Lean directly addresses the age-old concept of "that's the way we always did it" and looks for ways to improve the process. Lean practices can be very broad in nature or unique to a single laboratory work area by focusing on workflow actions in performing specific tasks, procedures, or other activities. Each step in a process must be reviewed to determine where inefficiencies can be eliminated. Some changes require minimal resources and can be accomplished relatively quickly. Examples include relocating analytic equipment to an area where the work is done, resulting in fewer steps and ultimately improving turnaround time; consolidating test menus and associated instrumentation, thus eliminating the expense of maintaining multiple instruments and supplies; placing routinely used supplies (i.e., pipettes, culture plates, gauze pads, etc.) in easy-to-access areas; and reallocating staff to maximize use and minimize wasteful downtime. Many laboratories have found it useful to integrate elements of Six Sigma and Lean into a blend of best practices (Inal et al., 2018). While some Lean and Six Sigma projects can rapidly improve performance, sustained gains generally require modifying the organizational culture, reinforcing systemic changes, and continually monitoring practice (Zarbo, 2012; D'Angelo & Mejabi, 2012).

BOX 1.3

Quality System Essentials

1. Organization
2. Personnel
3. Documents and records
4. Facilities and safety
5. Equipment
6. Purchasing and inventory
7. Information management
8. Occurrence management
9. Assessments—internal/external
10. Process improvement
11. Customer service
12. Process control

Medical laboratories in the United States are required by CLIA to take a focused and stringent approach to quality systems management, similar to the standards set forth by the International Organization for Standardization (ISO), a worldwide federation of accrediting members from over 140 countries. The ISO 15189:2012 has been adopted by the CAP in an effort to improve patient care through quality laboratory practices and complements CAP's CLIA-certified Laboratory Accreditation Program (CAP, 2016). In a similar fashion, the Clinical and Laboratory Standards Institute (CLSI) has created 12 Quality System Essentials (Box 1.3) based on ISO standards. Each of these 12 areas serves as a starting point in establishing a quality system that covers pretesting, testing, and post-testing operations. Quality Systems Management ultimately dispels the concept of "good enough" and promotes one of "it can always be done better" (CLSI, 2014).

HUMAN RESOURCE MANAGEMENT

Recruiting, hiring, training, and retaining qualified personnel have become major challenges for today's manager, and projections indicate that these challenges will continue to grow. Over the past several decades, many accredited Medical Technology programs have closed, resulting in a reduction in the number of graduating students. In recent surveys, the average vacancy rate for all laboratory positions nationally ranged from 6.3% to 9.4%, though rates varied depending upon the position held (Garcia et al., 2018). The employment of medical and clinical laboratory technologists and technicians is projected to increase by 12% to 14% over the next decade (U.S. Bureau of Labor Statistics, 2018). According to American Association of Retired Persons (AARP), 10,000 baby boomers turn 65 each day, with retirement in close view. Of the 322,000 current laboratory professionals, an estimated 6% to 24% will retire over the next few years, adding to the workforce shortage. At the same time, demographic shifts in the general population will increase the need for health care, including laboratory services. Competition with other health care professions has necessitated implementing creative recruitment incentives, such as more competitive salaries, comprehensive benefit packages, and better work environments. Today's job market has become more global; thus, a greater understanding of cultural, ethnic, and gender-related traits and values is necessary to properly evaluate and attract a pool of competent employees who will meet the needs of the laboratory and contribute to accomplishing anticipated goals (Kurec, 2014b).

Labor accounts for 50% to 70% of a laboratory's costs; thus, any new or replacement position must be justified. To ensure that a position is still relevant and cost-effective, the authority level, experience, and education

required, along with specific responsibilities, should be reviewed and compared with any related changes in technology and/or required skills. Ask the question: "If the position remained unfilled or downgraded, how would that impact patient care?" For example, could a position be filled by a less expensive entry-level technologist or a laboratory aide without compromising patient care or creating other staffing hardships? Can the position be eliminated by automating certain tasks? Or, has the test methodology become more sophisticated, requiring a higher-level, specially trained individual?

Once a position has been justified, a criterion-based job description must be developed (Kurec, 2014b). The criterion-based job description should focus on roles and not on specific tasks, because the latter may require frequent changes depending on operational needs. A basic criterion-based job description includes title, grade, and minimum qualifications to fulfill the position (including certification or licensure). It should clearly identify responsibilities, accountability, and internal and external organizational relationships. Any scholarly activities, such as teaching or research, should also be included. This provides clear expectations for both employee and employer, potentially avoiding any future "that's not in my job description" discussion.

The recruiting and hiring process requires an understanding of established strategic goals in order to find qualified individuals who will meet those needs. Managers must be aware of current local and federal hiring guidelines to ensure a fair and legal interview process. An employer must restrict interview questions to what can be legally asked yet still be able to gain insight as to whether the position is the right fit for both parties. Questions must relate to how a candidate is qualified to perform the duties of the job and not contain any personal queries. Discussions that are directed toward gender, generational, political, or racial/cultural differences could be misinterpreted during the interview process and result in legal repercussions (Kurec, 2011).

FINANCIAL MANAGEMENT

The laboratory is a high-value asset in diagnostic medicine. Compared to other clinical specialties, the laboratory generates a high volume of tests requiring expensive equipment and skilled personnel. Laboratory leadership should understand basic financial concepts, such as how services (such as laboratory tests) are reimbursed, why payment may be denied, broad regulations that govern reimbursement as well as basic accounting (e.g., direct and indirect costs, budgets) and financial analyses (e.g., breakeven analyses) (Cleverley & Cleverley, 2018). An understanding of charge masters, Current Procedural Terminology (CPT) codes, and the International Classification of Diseases, 10th revision (ICD-10) is essential to conduct business in a compliant manner and ensure payment for services rendered. A more detailed discussion of financial management is found in Chapter 13.

LABORATORY DESIGN AND SERVICE MODELS

Laboratory services are provided in many different ways and can be thought of as a continuum from point-of-care tests producing immediate answers to highly sophisticated laboratory tests that may take days to complete. Internet access has added a level of transparency to health care and has given the public a better understanding of how care is provided. In particular, websites such as www.webmd.com and www.labtestsonline.org have generated better public understanding of laboratory testing. This has increased awareness among patients of what tests are available and what results mean, offering patients the opportunity to participate in their own health care. This new dynamic has pressured laboratories to achieve greater efficiency, accessibility, safety, and reliability, and to become more transparent and responsive to client needs. Laboratories have changed their internal design from a very compartmentalized environment to a more centralized one, where traditional laboratory sections have been consolidated. Creating a centralized, core laboratory offers a number of efficiencies, such as eliminating the purchase of redundant instrumentation and supplies, better use of technology, sharing of common equipment (centrifuges, incubators, refrigerators, etc.), and access to technical expertise. In some instances, regional laboratories have been developed to perform specialty or complex testing, further capitalizing on existing resources and limiting the need to purchase specialty staffing, equipment, and materials. In many institutions, point-of-care testing (POCT) has been implemented to shorten turnaround time for critical tests and enhance convenience for both patients and caregivers. These internal and external organizational changes have fostered a greater awareness of the importance of laboratory services and how they contribute to the continuum of care.

The *functional design of a laboratory* and its relationship to other testing sites within a facility have evolved from discrete hematology, chemistry, microbiology, and blood bank sections to one where boundaries have been obscured. In an effort to lower costs and respond more rapidly to clinical needs, laboratories have employed both highly automated "core" facilities and distributed testing at peripheral stat laboratories and/or POCT sites. Based on current technology, tests that once were performed in separate laboratory sections are now performed on a single testing platform (single analyzer), on a workcell (two or more linked instruments), or with the use of total laboratory automation (workcell with preanalytic and postanalytic processing). Improvements in preanalytic sample handling (e.g., bar coding, automated centrifuges, decapper) and the use of highly accurate analyzers and timely postanalytic activities (e.g., reporting laboratory results via networked computer systems, the Internet, autofaxing, patient portals) further contribute to enhancing the quality of services provided to health care providers and patients. These configurations are discussed further in Chapters 2 and 6.

Regionalization is a consolidation process on a grand scale. In the "hub and spoke" model, a single core laboratory serves as the hub, providing high-volume routine testing. One or more other laboratories act as the spokes, consolidating certain functions into one highly specialized laboratory. For example, a single laboratory may focus on providing only microbiology, virology, parasitology, mycology, or other related services. In constructing such a specialized site, the redundancy of procuring technical expertise, expensive biohazard hoods, negative-pressure rooms, clinical and molecular testing equipment, and other materials can be minimized. Similar opportunities may exist for other laboratory sections, such as cytogenetics, molecular diagnostics, flow cytometry, mass spectrometry, cytology, histology, or histocompatibility. Establishing regionalized laboratory systems requires significant up-front resources, appropriate space requirements, and commitment from senior personnel from all institutions involved to make this work. In hospital settings, a stat or rapid-response laboratory would be necessary to handle urgent test requests. Challenges to successfully implementing this model include specimen transportation issues or delays, resistance to change, personnel issues, morale issues, "lost identity" of the laboratory, and union problems.

Facility design is important regardless of the type of laboratory and may be accomplished best by implementing Six Sigma/Lean techniques to ensure the highest level of productivity. One must consider the location of the specimen-processing area, patient registration and data entry, specimen testing workflow, short- and long-term storage, and laboratory information system (LIS) connectivity requirements. Determining spatial requirements in relationship to other hospital services (proximity to emergency department, intensive care units, and surgical operating suite) should be viewed as a multidisciplinary process. Robotics, pneumatic tubes, computer information technology, telemedicine, handheld devices, and cell phones are the new tools used in modern laboratories and must be accounted for in the design plans. Electrical power (including emergency power), temperature/humidity controls, access to water (distilled/deionized), drainage sources, and air circulation/ventilation issues must be considered for access, adequate quantity, and safety. Regulatory compliance codes must be reviewed carefully and implemented appropriately to ensure that all needs are met (Box 1.4). Recently, concerns about reducing environmental impact have been expressed (Lopez et al., 2017). Many municipalities and hospitals offer strong incentives, or even mandates, to "go green" by purchasing alternative, nontoxic chemicals, recycling used electronic products, integrating paperless reporting, and generally raising staff awareness of energy-wasting practices. To ensure that one meets local, state, and federal codes, a qualified architect who has had experience in designing clinical laboratories should be consulted at the beginning of relocation or renovation designs. This minimizes costly change orders and maximizes on-time start-up of the new facility.

REGULATION, ACCREDITATION, AND LEGISLATION

Clinical laboratories are among the most highly regulated health care entities (Tables 1.5, 1.6, and 1.7). Understanding the web of laws, regulations, and guidelines that affect laboratory practice is necessary to avoid legal or administrative repercussions that may limit a laboratory's operations or shut it down completely. To operate (and receive reimbursement for services), laboratories must be licensed and often accredited under federal and/or state requirements. (Note that licensure is a mandatory requirement of a governmental agency whereas accreditation is issued by

BOX 1.4

Laboratory Physical Design Considerations

In developing a needs assessment, identify space for offices, personal facilities, storage, conference/library area, and students.

Routinely review all floor plans and elevations for appropriate usage, and ensure that space and function are related; handicapped accessibility may be required.

Develop and use a project scheduler to ensure on-time progress.

Fume hoods and biological safety cabinets must be located away from high-traffic areas and doorways that might cause unwanted air current drafts.

Modular furniture allows for flexibility in moving or reconfiguration of the laboratory according to current and anticipated needs; conventional laboratory fixtures may be considered in building depreciation, whereas modular furniture may not.

Consider HVAC requirements to ensure proper temperature (68° F–76° F), humidity (20%–60%), air flow (12 air exchanges/hour); extremes in any one area can adversely affect patients, staff, and equipment.

Base cabinets (under laboratory counters) provide 20% to 30% more storage space than suspended cabinets.

Noise control in open laboratories may be obtained by installing a drop ceiling. Installation of utilities above a drop ceiling adds to flexibility in their placement.

In general, space requirements are 150 to 200 net square feet (excludes hallways, walls, custodial closets, etc.) per FTE, or 27 to 40 net square feet per hospital bed.

Rooms larger than 100 square feet must have two exits; corridors used for patients must be 8 feet wide, and those not used for patients must be 3 feet 8 inches wide.

An eyewash unit must be within 100 feet of work areas; hands-free units are preferred.

Suggested standard dimensions in planning and designing a laboratory:

- Laboratory counter width: 2 feet 6 inches
- Laboratory counter-to-wall clearance: 4 feet
- Laboratory counter-to-counter clearance: 7 feet
- Desk height: 30 inches
- Keyboard drawer height: 25 to 27 inches
- Human body standing: 4 square feet
- Human body sitting: 6 square feet
- Desk space: 3 square feet

FTE, Full-time equivalent; *HVAC,* heating, ventilating, and air conditioning.
Data from Painter, 1993; Mortland, 1997.

TABLE 1.5

Laboratory Regulations and Their Significance

1983	**Prospective Payment System** for Medicare patients established payment based on diagnosis-related groups (DRGs). Hospitals are paid a fixed amount per DRG, regardless of actual cost, thereby creating an incentive to discharge patients as soon as medically possible. For inpatients, laboratories become cost centers instead of revenue centers (Social Security Amendments P.L. 98-21).
1984	**Deficit Reduction Act** (P.L. 93-369): Established outpatient laboratory fee schedule to control costs; froze Part B fee schedule.
1988	**Clinical Laboratory Improvement Act of 1988 (CLIA '88)** (amended 1990, 1992): Established that all laboratories must be certified by the federal government with mandated quality assurance, personnel, and proficiency testing standards based on test complexity. Until this time, the federal government regulated only the few laboratories conducting interstate commerce or independent or hospital laboratories that wanted Medicare reimbursement. CLIA applies to all sites where testing is done, including physicians' offices and clinics.
1989	**Physician Self-Referral Ban** (Stark I; P.L. 101-239): Prevents physicians from referring Medicare patients to self-owned laboratories.
	Ergonomic Safety and Health Program Management Guidelines: Established OSHA guidelines for employee safety.
1990	**Three-Day Rule** initiated by CMS: Payment for any laboratory testing done 3 calendar days before admission as an inpatient is not reimbursed because testing is considered to be part of the hospital stay (Omnibus Reconciliation Act); directs HHS to develop an outpatient DRG system.
	Occupational Exposure to Hazardous Chemicals in Laboratories: Established OSHA guidelines to limit unnecessary exposure to hazardous chemicals.
1992	**Occupational Exposure to Blood-Borne Pathogens:** Established OSHA guidelines to limit unnecessary exposure to biological hazards.
1996	**Health Insurance Portability and Accountability Act:** Directs how health care information is managed. This law protects patients from inappropriate dispersion (oral, written, or electronic) of personal information and is the basis for many of the privacy standards currently in place.
1997	**OIG Compliance Guidelines** for clinical laboratories: Help laboratories develop programs that promote high ethical and lawful conduct, especially regarding billing practices and fraud and abuse.
2001	**CMS National Coverage Determinations:** Replaced most local medical review policies used to determine whether certain laboratory tests are medically necessary and, therefore, reimbursable. Before this, each Medicare intermediary had its own medical necessity guidelines.
2003	**Hazardous Material Regulations:** Deal with shipment of blood and other potentially biohazardous products (DOT).
2009	**HITECH Act:** Contains incentives related to adoption of health care information technology and the electronic health record (EHR); set goal of "meaningful use" for EHR adoption; improves privacy and security protections available under HIPAA, as well as enforcement and penalties for noncompliance.

CMS, Centers for Medicare and Medicaid Services; *DOT,* U.S. Department of Transportation; *HHS,* U.S. Department of Health and Human Services; *HIPAA*, Health Insurance Portability and Accountability Act; *OIG,* Office of the Inspector General; *OSHA,* Occupational Safety and Health Administration.

a nongovernmental organization and is optional.) Although all pathologists must be state-licensed physicians, 12 states and Puerto Rico currently also require laboratory personnel licensure—a key consideration when attempting to hire technical staff (Box 1.5).

At the federal level, laboratories that test human specimens for diagnosis, prevention, or treatment of disease are regulated under the Clinical Laboratory Improvement Amendments of 1988 (CLIA '88), part of the Public Health Services Act (Public Law 100-578). The U.S. Food and Drug Administration (FDA) and the Centers for Medicare and Medicaid Services (CMS) work in collaboration with the Centers for Disease Control and Prevention (CDC) to oversee the CLIA program. Before CLIA '88, no consistent federal regulatory standards were applied to most laboratories, and there were only sporadic state initiatives that carried various levels of authority and oversight. CLIA '88 was enacted in response to the lack of national laboratory quality standards. Minimum standards are enforced by the federal government or by their designees that have received "deemed status," reflecting standards equivalent to or stricter than those put forth by CLIA. CLIA-certified laboratories are required to meet standards for personnel, operations, safety, and quality based on test complexity (Box 1.6).

TABLE 1.6
Laboratory-Related Governmental Agencies

CDC	**Centers for Disease Control and Prevention** is under the U.S. Department of Health and Human Services (HHS) and provides oversight of public health and safety, including the laboratory (www.cdc.gov).
CMS	**Centers for Medicare and Medicaid Services** (formerly known as the Health Care Finance Administration [HCFA]) oversees the largest health care program in the United States, processing more than 1 billion claims per year. Medicare (see Chapter 12) provides coverage to approximately 40 million Americans over the age of 65 years, some people with disabilities, and patients with end-stage renal disease, with a budget of $309 billion (2004). Medicaid provides coverage to approximately 50 million low-income individuals through a state–federal partnership that costs $277 billion (2004). CMS sets quality standards and reimbursement rates that apply to the laboratory and are often used by other third-party payers (www.cms.hhs.gov).
DHS	**Department of Homeland Security:** Identifies, regulates, and may inspect high-risk chemical facilities and radiation sources (including blood irradiators) that may be risks for terrorism; may require certification for non-U.S. citizens working in the laboratory.
DOT	**U.S. Department of Transportation** has the responsibility of regulating biohazardous materials that include blood and other human products. Laboratory specimens sent to reference laboratories must be packaged per guidelines set by this agency (www.dot.gov).
EPA	**Environmental Protection Agency** sets and enforces standards for disposal of hazardous laboratory materials, such as formalin, xylene, and other potential carcinogens (www.epa.gov).
EEOC	**Equal Employment Opportunity Commission** oversees and enforces Title VIII, which deals with fair employment practices related to the Civil Rights Act of 1964 and the Equal Employment Opportunity Act of 1972. Hiring of laboratory staff falls under the same rules as most businesses (www.eeoc.gov).
FDA	**U.S. Food and Drug Administration** is part of HHS and regulates the manufacture of biologicals (such as blood donor testing and component preparation) and medical devices (such as laboratory analyzers) and test kits through its Office of In-Vitro Diagnostic Device Evaluation and Safety. FDA inspects blood donor and/or component manufacturing facilities irrespective of other regulatory agencies and/or accrediting organizations (www.fda.gov).
HHS	**U.S. Department of Health and Human Services** oversees CMS, OIG, and FDA.
NARA	**National Archives and Records Administration** provides a number of databases, including access to the *Federal Register*, where laboratory and other regulations are published (www.gpoaccess.gov/fr/index.html).
NRC	**Nuclear Regulatory Commission** develops and enforces federal guidelines that ensure the proper use and operation of nonmilitary nuclear facilities. Laboratory tests that use radioactive materials (such as radioimmunoassays) must adhere to guidelines set by this agency (www.nrc.gov).
NIDA	**National Institute on Drug Abuse** regulates standards for performing and maintaining appropriate quality control for drugs of abuse testing (www.nida.nih.gov).
NIOSH	**National Institute of Occupational Safety and Health** is a part of HHS. It provides research, information, education, and training in the field of occupational safety and health. NIOSH makes recommendations regarding safety hazards but has no authority to enforce them (www.cdc.gov/niosh/homepage.html).
NIH	**National Institutes of Health** is an agency of HHS and is a world leader in medical research. It publishes a variety of clinical practice guidelines, some of which are applicable to the laboratory, such as those for diabetes and lipid testing (www.nih.gov).
NIST	**National Institute of Standards and Technology** is a branch of the Commerce Department and has contributed to the development of many health care products. In addition, it has developed standards for calibration, weights and measures, and the International System of Units (www.nist.gov).
OIG	**Office of the Inspector General** is part of HHS. It is responsible for auditing, inspecting, and identifying fraud and abuse in CMS programs, such as laboratory testing. The focus of the OIG is usually noncompliance with reimbursement regulations, such as medical necessity (www.oig.hhs.gov).
OSHA	**Occupational Safety and Health Administration** is part of the U.S. Department of Labor. It develops and enforces workplace standards to protect employees' safety and health. Recommendations from OSHA include guidelines addressing blood-borne pathogens, chemical safety, phlebotomies, latex gloves, ergonomics, and any other potentially hazardous situation that may be found in the workplace (www.osha.gov).
State Departments of Health	**State Departments of Health** vary in the extent to which they regulate laboratories. Some states, such as New York, license all laboratories and oversee mandatory proficiency testing and laboratory inspection programs; others do neither. New York and Washington, D.C., have Clinical Laboratory Improvement Act "deemed status."

Clinical laboratories are big business: in the United States nationwide they are a high-volume health care provider performing over 14 billion tests annually (https://www.cdc.gov/csels/dls/strengthening-clinical-labs.html), employing over 688,000 individuals, and paying $45 billion in wages (https://www.acla.com/economic-impact-of-clinical-labs/). The Laboratory Compliance Program was mandated by Congress (*Federal Register* 63[163], Aug. 24, 1998) in response to concerns from the CMS about fraud and abuse of payments from unnecessary or inappropriate laboratory tests. Over 50% of national health care costs are paid by the federal government through six programs (Medicare, Medicaid, Children's Health Insurance [CHIP], Department of Defense Tricare, Veteran's Health Administration [VHA], and Indian Health Service) (American Hospital Association, 2018). Laboratories that receive payment for services from any federal agency must have policies addressing the medical necessity for tests ordered, ensuring accurate billing for testing, and promoting a standard of conduct to be adopted by laboratory employees. Failure to have an active program could cause a laboratory to be excluded from participating with CMS and could lead to significant financial and legal penalties. Consider, for example, the patient mix that may be encountered over the next decade or so. There are currently 74 million baby boomers rapidly approaching retirement age. It is estimated that those over the age of 55 years consume about 57% of health care spending. As this cohort retires, it will increasingly impact test volume, test mix, and the need to optimize utilization. These forces are already shaping the laboratory business. Ordering the right tests must be justified as medically necessary and must meet evidence-based medicine protocols as emphasized in the "Choosing Wisely" campaign (Sadowski et al., 2017; Wolfson et al., 2014).

The Health Insurance Portability and Accountability Act of 1996 (HIPAA), along with the Privacy Rule of 2000 and the Security Rule of 2003, provide standards that protect the confidentiality, integrity, and availability of an individual's health information while allowing exchange of information in appropriate circumstances with a patient's permission. Various rules have been implemented that have a direct impact on the laboratory and include the use and disclosure of protected health information (PHI). PHI includes any oral, written, electronic, or recorded information such as date of birth, Social Security number, address, phone number, or any other patient identifier. Access to this information among health care professionals is restricted on a "need-to-know" basis with consent from the patient and as described in an employee's job description/title. Failure to adhere to these rules can result in significant fines and, in blatant cases of abuse, prison time. The Health Information Technology for Economic and Clinical Health Act (HITECH, 2009) was enacted under the American Recovery and Reinvestment Act of 2009 to promote and implement better use of health care information. It

TABLE 1.7

Laboratory-Related Nongovernmental Organizations

AABB	Formerly known as **American Association of Blood Banks**, AABB is a peer professional group that offers a blood bank accreditation program that can substitute for (but coordinate with) a CAP inspection. It has CLIA deemed status (www.aabb.org).
ASCP	**American Society for Clinical Pathology** is the largest organization for laboratory professionals and offers certification for various specialties (www.ascp.org).
CAP	**College of American Pathologists** offers the largest proficiency survey program in the United States and has a peer-surveyed laboratory accreditation program that has CLIA deemed status. CAP accreditation is recognized by The Joint Commission as meeting its laboratory standards (www.cap.org).
CLSI	**Clinical and Laboratory Standards Institute** (formerly the National Committee for Clinical Laboratory Standards [NCCLS]) is a peer professional group that develops standardized criteria regarding laboratory practices; accrediting and licensing entities often adopt these as standards (e.g., procedure manual format) (www.clsi.org).
COLA	COLA (originally the **Commission on Office Laboratory Accreditation**) is a nonprofit organization sponsored by the American Academy of Family Physicians, the American College of Physicians, the American Medical Association, the American Osteopathic Association, and CAP. It has CLIA deemed status, and its accreditation is recognized by The Joint Commission. It was originally organized to provide assistance to physician office laboratories (POLs), but it has recently expanded its product line to other services (www.cola.org).
FACT	**Foundation for the Accreditation of Cellular Therapy** is a nonprofit organization that establishes standards for medical and laboratory practice in cellular therapies. FACT provides voluntary inspection and accreditation for a variety of clinical and laboratory services (http://www.factwebsite.org).
TJC	**The Joint Commission** (formerly known as Joint Commission on Accreditation of Healthcare Organizations) is an independent, not-for-profit entity that accredits nearly 17,000 health care organizations and programs in the United States based on a comprehensive set of quality standards. It has CLIA deemed status and may substitute for federal Medicare and Medicaid surveys; it also fulfills licensure requirements in some states and general requirements of many insurers. TJC usually surveys the laboratory as part of an overall health care facility survey (www.jointcommission.org/).

CLIA, Clinical Laboratory Improvement Act.

BOX 1.5

States Requiring Laboratory Personnel Licensure

California
Florida
Georgia
Hawaii
Louisiana
Montana
Nevada
New York
North Dakota
Puerto Rico
Rhode Island
Tennessee
West Virginia

further enhanced some of the privacy and security requirements established in HIPAA as well as penalties for noncompliance. HITECH also included new rules for public notification following PHI data breaches that occur due to the lack of (or ignoring) established policies, possessing unsecured data storage, or from direct malicious ransomware attacks. In October 2014, an additional modification of HIPAA requirements became effective. While in the past, CLIA-regulated labs were not permitted to provide patients direct access to their lab results, HIPAA-covered laboratories are now subject to the same obligations as other health care providers with respect to providing patients access to their health care information, generally within 30 days of the request.

A variety of other government agencies and nongovernmental organizations directly or indirectly influence laboratory operations. Agencies impact the laboratory through regulations addressing business practices, human resource management, transportation of medical specimens, environmental protection issues, and interstate commerce activities (see Tables 1.6 and 1.7). These regulations are designed to protect the public and employees from shoddy laboratory testing practices or unnecessary exposure to biological, chemical, or radioactive hazards. Guidelines from nongovernmental organizations ensure the availability of quality blood products, access to laboratory testing as needed, and a safe work environment for employees. Professional associations (e.g., CAP) play an important part in establishing guidelines and often lobby for their acceptance as standard-of-care practice by governmental agencies. For example, Table 1.8 provides suggested time limits for record and specimen retention based on CAP guidelines.

BOX 1.6

CLIA Categories Included and Excluded

Test categories (based on analyst/operator and complexity to run test)

- Waived (e.g., blood glucose, urine pregnancy)
- Moderate complexity
- High complexity

Not categorized (because they do not produce a result)

- Quality control materials
- Calibrators
- Collection kits (for HIV, drugs of abuse, etc.)

Not currently regulated (by CLIA)

- Noninvasive testing (e.g., bilirubin)
- Breath tests (e.g., alcohol, *Helicobacter pylori*)
- Drugs of abuse testing in the workplace
- Continuous monitoring/infusion devices (e.g., glucose/insulin)

CLIA, Clinical Laboratory Improvement Act; *HIV,* human immunodeficiency virus. Data from Sliva, 2003.

TABLE 1.8

Suggested Guidelines for Record and Specimen Retention*

Record/Specimen Type	Retention
Requisitions	2 years
Accession logs	2 years
Maintenance/instrument logs	2 years
Quality control records	2 years
Blood bank donor/receipt records	10 years
Blood bank deferred donor records	Indefinitely
Blood bank patient records	10 years
Blood bank employee signatures/initials	10 years
Blood bank QC records	5 years
Clinical pathology test records	2 years
Serum/CSF/body fluids	48 hours
Urine	24 hours
Blood/fluid smears	7 days
Microbiology stained slides	7 days
Wet tissue	2 weeks
Surgical pathology (bone marrow) slides	10 years
Paraffin blocks/slides	10 years
Cytology slides	5 years
FNA slides	10 years
Reports (surgical/cytology/nonforensic)	10 years
Cytogenetic slides	3 years
Cytogenetic reports/images	20 years
Flow cytometry plots/histograms	10 years
Retired laboratory procedures	2 years

*College of American Pathologists, Northfield, IL (March 2009) and/or CLIA regulations (42 CFR 293); check with other organizations (such as AABB) or local regulatory agencies for current requirements that may differ from those in this table.
CSF, Cerebral spinal fluid; *FNA,* fine-needle aspiration; *QC,* quality control.

TABLE 1.9
Laboratory Hazard Prevention Strategies

Work practice controls (general procedures/policies that mandate measures to reduce or eliminate exposure to hazard)	Handwashing after each patient contact
	Cleaning surfaces with disinfectants
	Avoiding unnecessary use of needles and sharps and not recapping
	Red bag waste disposal
	Immunization for hepatitis
	Job rotation to minimize repetitive tasks
	Orientation, training, and continuing education
	No eating, drinking, or smoking in laboratory
	Warning signage
Engineering controls (safety features built into the overall design of a product)	Puncture-resistant containers for disposal and transport of needles and sharps
	Safety needles that automatically retract after removal
	Biohazard bags
	Splash guards
	Volatile-liquid carriers
	Centrifuge safety buckets
	Biological safety cabinets and fume hoods
	Mechanical pipetting devices
	Computer wrist/arm pads
	Sensor-controlled sinks or foot/knee/elbow-controlled faucets
Personal protective equipment (PPE; barriers that physically separate the user from a hazard)	Nonlatex gloves
	Isolation gowns
	Masks, including particulate respirators
	Face shields
	Protective eyewear (goggles, safety glasses)
Emergency equipment	Chemical-resistant gloves; subzero (freezer) gloves; thermal gloves
	Hearing protection (earplugs or earmuffs)
	Eyewash station
	Safety shower
	Fire extinguisher
	Laboratory spill kit
	First aid kit

Another area of regulatory interest that has advanced in recent years relates to the regulation of "home brew," in-house, or laboratory-developed tests (LDTs) by entities including the FDA, CLIA, and state governments. While LDTs have always been part of the clinical laboratory, powerful technologies such as next-generation sequencing, deoxyribonucleic acid (DNA) microarrays and matrix-assisted laser desorption ionization time-of-flight (MALDI-TOF) mass spectrometry have recently led to the proliferation of LDTs producing complex data with significant patient impact. As early as 1997, the FDA proclaimed its authority over LDTs by classifying the tests as medical devices and labs employing them as manufacturers. However, until it issued a draft guidance on the issue in 2014, the FDA provided little regulatory framework. The FDA has not finalized the guidance, and it is likely that the government's position on the issue will continue to evolve in response to feedback (Gatter, 2017; Angelo, 2018). In contrast to the FDA, which may regulate LDTs as devices and labs as manufacturers, the CLIA program of the CMS regulates only those laboratories that perform patient testing. CLIA does require validation of a test prior to use but, unlike the FDA, it does not address the clinical validity of a test and does not require submission and approval of the LDT prior to implementation.

SAFETY

Routine clinical laboratory activities can inherently expose staff, and potentially the public, to a variety of hazards, including infectious biologicals, toxic chemicals, and various levels of radioactive materials. All health care facilities must have policies that address routine job-related exposures to these hazards, as well as ergonomic/environmental hazards, fire safety, act-of-God occurrences (tornadoes, hurricanes, floods, etc.), and epidemic, emergency preparedness plans (CDC, 2018a). Laboratories are obligated to identify hazards, implement safety strategies to contain the hazards, and continually audit existing practices to ensure employee compliance. A typical emergency safety plan might include a limited test menu for emergencies, identifying required equipment/reagents/supplies and key staff to perform testing, emergency power and uncontaminated water supply locations, and a procedure to communicate internally and externally. Frequent safety policy reviews, disaster drills, and employee awareness training help maintain safe patient and work environments.

Good safety practices benefit patients and employees as well as a laboratory's bottom line. Injuries and harmful exposures can negatively affect the laboratory financially, by reputation (due to bad press), potential lawsuits, lost workdays and wages, damage to equipment, and poor staff morale (CDC, 2012). An injured person may be absent for an indefinite period and often cannot work at peak efficiency upon return. During this time off, the workload has to be absorbed by existing staff or through expensive additional temporary services. Careful planning and compliance with the laws will minimize undesired outcomes. Although inexperience may be a cause for some accidents, others result from minimizing and ignoring known risks, pressure to do more, carelessness, fatigue, or mental preoccupation (failure to focus attention or to concentrate on what is at hand). A number of strategies may be used to contain hazards, including the use of work practice controls, engineering controls, and personal protective equipment (Table 1.9). The most effective safety programs use all three strategies.

BOX 1.7
Infectious Agents Reported by the Centers for Disease Control and Prevention (CDC)

- COVID-19
- Salmonella
- Listeria
- *Escherichia coli*
- Psittacosis
- Hepatitis
- Ebola
- Measles
- Polio
- Dengue
- Respiratory syncytial virus (RSV)
- Severe acute respiratory syndrome (SARS)
- Nosocomial infections
- Multidrug resistant organisms (MDRO)
- Zoonotic outbreaks to humans
- Bioterrorism (smallpox, anthrax, botulism, plague, tularemia, and viral hemorrhagic fever)

From the CDC's website: https://www.cdc.gov/outbreaks/index.html

BIOLOGICAL HAZARDS

Biological hazards expose an unprotected individual to bacteria, viruses, parasites, or prions that can result in injury. Exposure occurs from ingestion, inoculation, tactile contamination, or inhalation of infectious material from patients or their body fluids/tissues, supplies or materials they have been in contact with or contaminated needles, or by aerosol dispersion. The potential also exists for inadvertent exposure to the public through direct contact with aerosolized infectious materials, improperly processed blood products, and inappropriately disposed of waste products.

Contagious outbreaks (Box 1.7) occur on a worldwide level but quickly can become a local concern. Natural disasters, such as a hurricane or tornado, can often leave an infectious, disease-laden path in its wake. Other outbreaks from bioterrorist activities and even nosocomial infections can activate emergent proceedings (CDC, 2018). Emergency plans to meet personnel and patient safety needs, availability of trained staff, and guidelines to manage the infected patient/community populations are essential.

The spread of COVID-19, hepatitis B virus (HBV), hepatitis C virus (HCV), human immunodeficiency virus (HIV), and tuberculosis (TB) has focused the responsibility on each health care organization to protect its employees, patients, and the general public from infection. The CDC and the Occupational Safety and Health Administration (OSHA) have provided guidelines for safe handling of body fluids and human tissues for all patients, beginning with Universal Precautions in the 1980s (CDC, 1988). OSHA defines *occupational exposure* as "reasonably anticipated skin, eye, mucous membrane, or percutaneous contact with blood or other potentially infectious materials that may result from the performance of an employee's duties" (29 CFR, 1910.1030) (OSHA, 1991). Blood, other body fluids, and any unfixed tissue samples are always assumed to be potentially infectious for various blood-borne pathogens. While working

BOX 1.8

Common Decontamination Agents

Heat (250° C for 15 minutes)
Ethylene oxide (450–500 mg/L at 55° C–60° C)
2% Glutaraldehyde
10% Hydrogen peroxide
10% Formalin
95% Formic acid
5.25% Hypochlorite (10% bleach)*
Formaldehyde
Detergents
Phenols
Ultraviolet radiation
Ionizing radiation
Photo-oxidation

* The only agent effective against prions.

in the laboratory, individuals should avoid mouth pipetting; consumption of food or drinks; smoking; applying cosmetics; potential needlestick situations; and leaving skin, membranes, or open cuts unprotected. Aerosol contamination may be due to inoculating loops (flaming a loop), spills on laboratory counters, expelling a spray from needles, and centrifugation of infected fluids. The CDC has refined its recommendations for Universal Precautions (CDC, 2007) on several occasions, requiring periodic review of any updates on the CDC's website: www.cdc.gov. As experienced in the 1980s with the unexpected emergence of acquired immune deficiency syndrome (AIDS) and the need to develop and implement testing techniques for HIV, clinical laboratories had to respond in a prompt manner. Global outbreaks of Ebola, Zika, influenza, COVID-19, and other contagious diseases require well-developed laboratory safety policies that ensure constant vigilance and the flexibility to adopt evolving recommendations.

Although many laboratories require the wearing of gloves when performing phlebotomies, OSHA strongly recommends that gloves be used routinely as a barrier protection, especially when the health care worker has cuts or other open wounds on the skin, anticipates hand contamination (biological or chemical), performs skin punctures, or is receiving phlebotomy training (OSHA, 1994a) Special precautions must be considered when handling suspected prion-infected blood, tissue, and processing instruments (Pizzella & Kurec, 2018). Employees must wash their hands after removing gloves, after any contact with blood or body fluids, and between patients. Gloves should not be washed and reused because microorganisms that adhere to gloves are difficult to remove (Doebbeling et al., 1988). Masks, protective eyewear, or face shields must be worn to prevent exposure from splashes to the mouth, eyes, or nose. All protective equipment that has the potential for coming into contact with infectious material, including laboratory coats, must be removed before leaving the laboratory area and must never be taken home or outside the laboratory (such as during lunch or personal breaks). Laboratory coats must be cleaned onsite or by a professional. To avoid personal contamination, laboratories should identify what areas (offices, conference rooms, lounges, etc.) and equipment (telephones, keyboards, copy machines, etc.) are designated as clean areas and those that are laboratory work areas. Avoid contamination by not wearing soiled gloves when in these areas or when using nonlaboratory equipment. Box 1.8 outlines some common materials that can be used to decontaminate soiled areas (CLSI, 2014; WHO, 2004). In addition, the number of needlestick and sharps injuries can be reduced by using medical safety devices, practicing proper hygiene procedures, and following standard blood-borne precautions. According to a study, in 2014 approximately 25 sharps injuries per 100 average daily patient census occurred in the United States (Cooke & Stephens, 2017). Injury-related costs—for example, follow-up testing, treatment (if needed), counseling, and other services—have been reported to be up to $5,000 per incident.

CHEMICAL HAZARDS

All clinical laboratories are mandated by OSHA to develop and actively follow plans that protect laboratory workers from potential exposure to hazardous chemicals. To minimize the incidence of chemically related occupational illnesses and injuries in the workplace, OSHA published its *Hazard Communication Standard* (OSHA, 1994b) and *Chemical Hygiene Plan* (OSHA, 1990) requiring the manufacturers of chemicals to evaluate

BOX 1.9

Chemical Hazard Communications Plan

1. Develop written hazard communication program.
2. Maintain inventory of all chemicals with chemical and common names, if appropriate.
3. Manufacturer must assess and supply information about chemical or physical hazards (flammability, explosive, aerosol, flashpoint, etc.).
4. Employers must maintain Safety Data Sheets (SDS) in English for laboratory chemicals.
5. SDS must list all ingredients of a substance greater than 1%, except for known carcinogens if greater than 0.1%.
6. Employers must make SDS available to employees upon request.
7. Employers must ensure that labels are not defaced or removed and must post appropriate warnings.
8. Employers must provide information and training ("right-to-know").
9. Employers must adhere to Occupational Safety and Health Administration permissible exposure limit, threshold limit, or other exposure limit value.
10. Designate responsible person(s) for the program.

the hazards of the chemicals that they produce and to provide written documentation accompanying each product in the form of Safety Data Sheets (SDS; formally Material Safety Data Sheets or MSDS). Employers, then, are responsible for developing hazard communication programs for employees and other users who are exposed to hazardous chemicals (Box 1.9) (OSHA, 2009). OSHA standards are based on the premise that employees have the right to know what chemical hazards they are potentially exposed to and what protective measures the employer and employee need to take to minimize hazardous exposure. Many states have developed individual guidelines and regulations mandating that employers develop and implement safety and toxic chemical information programs for their workers that are reviewed with all employees each year. Labels and SDS are also required to comply with the United Nations Globally Harmonized System of Classification and Labelling of Chemicals (GHS) since its adoption by OSHA in 2012. The GHS was developed with the goal of creating a uniform international standard for the classification and labeling of hazardous chemicals (United Nations, 2011). It should also be noted that specific types of chemicals are required to be stored in safety cabinets or under hoods. Acids and bases are required to be stored in separate chemical safety cabinets.

ERGONOMIC HAZARDS

OSHA presented guidelines (OSHA, 2018) to address ergonomic hazards in the workplace and to assist employers in developing a program to prevent work-related problems that primarily include cumulative trauma disorders or work-related musculoskeletal disorders (WMSDs). This is a collective group of injuries involving the musculoskeletal and/or nervous system in response to long-term repetitive twisting, bending, lifting, or assuming static postures for an extended period of time. These injuries may evolve from constant or excessive repetitive actions, mechanical pressure, vibrations, or compressive forces on the arms, hands, wrists, neck, or back. Human error may also be a causative factor when individuals push themselves beyond their limits or when productivity limits are set too high.

Among laboratory personnel, cumulative trauma disorders are usually related to repetitive pipetting, working at a microscope, using a microtome, keyboard use, or resting their wrists/arms on sharp edges, such as a laboratory counter. These actions can cause carpal tunnel syndrome (compression and entrapment of nerve from wrist to hand), tendonitis (inflammation of tendon), or tenosynovitis (inflammation or injury to synovial sheath) (Scungio & Gile, 2014). Awareness and prevention are essential in managing these disorders by taking personal stock in assuming proper posture when sitting or standing and minimizing eye strain situations, acute twisting or rotating, or gripping. Work practice and engineering controls; various hand, arm, leg, back, and neck exercises; and taking frequent 1- to 2-minute breaks may reduce these problems. The costs of implementing programs to help employees understand and avoid ergonomic hazards can be financially justified. Over a third of WMSDs result in missed workdays at an average of 57 days per incident, with workers' compensation claims amounting to $45 to $54 billion—a total of $120 billion in lost productivity and related costs (Kulakowski, 2018).

SELECTED REFERENCES

Bonini P, Plebani M, Ceriotti F, et al.: Errors in laboratory medicine, *Clin Chem* 48:691–698, 2002.

A review of the literature on laboratory errors, including an analysis of the types and/or volume of preanalytic, analytic, and postanalytic errors, and transfusion errors.

Garcia LS: *Clinical laboratory management*, ed 2, Washington, 2014, ASM Press.

A comprehensive review of laboratory management practices, including financial, operational, human resources, and marketing management.

Lifshitz MS, De Cresce RP: Strategic planning for automation. In Kost GJ, editor: *Clinical automation, robotics, and optimization*, New York, 1996, John Wiley & Sons, pp 471–496.

An overview of the laboratory strategic planning process, with special emphasis on how to assess the environment, define objectives, and audit operations and technology.

Nigon DL: *Clinical laboratory management*, New York, 2000, McGraw-Hill.

Covers fundamental principles of laboratory management and provides many practical examples and case studies that help illustrate concepts.

Snyder J, Wilkinson DS: *Management in laboratory medicine*, ed 3, Philadelphia, 1998, Lippincott.

Comprehensive reference dealing with all aspects of laboratory management, including leadership, human resource management, marketing, safety, and so on.

Access the complete reference list online at Elsevier eBooks for Practicing Clinicians.

REFERENCES

American Clinical Laboratory Association: Value of lab testing. https://www.acla.com/value-of-lab-testing/. (Last accessed December 2018).

American Hospital Association: *Trendwatch Chartbook*, 2018. https://www.aha.org/system/files/2018-07/2018-aha-chartbook.pdf (Last accessed December 2018).

Amukele T, Schroeder L: What is the value of clinical laboratory testing? *J Appl Lab Med* 1(4):339–341, 2017.

Angelo R, Weiss R, Wolfe D, et al.: Facing the inevitable; being prepared for regulatory requirements for laboratory developed tests, *Am J Clin Pathol* 149:484–498, 2018.

Berte LM: Patient safety: getting there from here—quality management is the best patient safety program, *Clin Leadersh Manag Rev* 18(6):311–315, 2004.

Blick KE: Providing critical laboratory results on time, every time to help reduce emergency department length of stay: how our laboratory achieved a six sigma level of performance, *Am J Clin Pathol* 140:193–202, 2013.

Bogavac-Stanojevic N, Jelic-Ivanovic Z: The cost-effective laboratory: implementation of economic evaluation of laboratory testing, *J Med Biochem* 36:238–242, 2017.

Brue G: *Six sigma for managers*, New York, 2002, McGraw-Hill, pp 1–50.

College of American Pathologists (CAP): *Frequently asked questions. ISO15189, Accreditation Program*, https://cap.objects.frb.io/documents/2016-iso-15189-faqs.pdf, June 2016 (Last accessed December 2018).

Centers for Medicare and Medicaid Services. CMS 1990: *Laboratory requirements (clinical laboratory improvement amendments; CLIA'88)*. Title 42, Part 493. 55 FR 9576, https://www.gpo.gov/fdsys/granule/CFR-2011-title42-vol5/CFR-2011-title42-vol5-part493/content-detail.html (Last accessed December 2018).

Centers for Disease Control and Prevention: *CDC emergency preparedness and response*. Updated July 2018a https://emergency.cdc.gov/planning/index.asp (Last accessed December 2018).

Centers for Disease Control and Prevention: CDC 2012: *Morbidity and Mortality Weekly Report (MMWR). Guidelines for safe work practices in human and animal medical diagnostic laboratories*, https://www.cmich.edu/office_provost/ORGS/Lab_Safety/Documents/CDC%20Guidelines%20for%20Safe%20Work%20Practices%20in%20Human%20and%20Animal%20Medical%20Diagnostic%20Laboratories%20010612.pdf (Last accessed December 2018).

Centers for Disease Control and Prevention: CDC 1988: Perspectives in disease prevention and health promotion update: universal precautions for prevention of transmission of human immunodeficiency virus, hepatitis B virus, and other bloodborne pathogens in healthcare settings, *MMWR (Morbidity and Mortality Weekly Report)* 37(24):377–378, 1988.

Centers for Disease Control and Prevention: CDC 2007: *Guideline for isolation precautions: preventing transmission of infectious agents in healthcare settings (2007)*. Updated November 2018, https://www.cdc.gov/infectioncontrol/guidelines/isolation/index.html (Last accessed December 2018).

Centers for Disease Control and Prevention. CDC 2018: *Preparation and planning for bioterrorism emergencies*, https://emergency.cdc.gov/bioterrorism/prep.asp (Last accessed December 2018).

Centers for Medicare and Medicaid Services. CMS 2018: *National health expenditure data*. Updated 4/17/2018, https://www.cms.gov/research-statistics-data-and-systems/statistics-trends-and-reports/nationalhealthexpenddata/nhe-fact-sheet.html (Last accessed December 2018).

Cleverley WO, Cleverley JO: *Essentials of health care finance*, ed 8, Burlington, MA, 2018, Jones & Bartlett Learning.

Clinical and Laboratory Standards Institute: CLSI 2014: *Protection of laboratory workers from occupationally acquired infections; approved guideline*, ed 4, CLSI document M29-A4.2014. www.CLSI.org.

Cooke CE, Stephens JM: Clinical, economic, and humanistic burden of needlestick injuries in healthcare workers, *Med Devices Evid Res* 10:225–235, 2017.

D'Angelo R, Mejabi O: Getting it right for patient safety: specimen collection process improvement from operating room to pathology, *Am J Clin Pathol* 146(1):8–17, 2012.

Deming EW: *Out of Crisis*, Cambridge, 2018, MIT Press.

Doebbeling BN, Pfaller MA, Houston AK, et al: Removal of nosocomial pathogens from the contaminated glove. *Ann Intern Med* 1988; 109:394.

Garcia LS, editor: *Clinical laboratory management*, ed 2, Washington, DC, 2014, American Society for Microbiology.

Garcia E, Kundu I, Ali A, Soles R: The American Society for clinical Pathology's 2016-2017 vacancy survey of medical laboratories in the United States, *Am J Clin Pathol* 149:387–400, 2018.

Gatter K: FDA oversight of laboratory-developed tests: where are we now? *Arch Pathol Lab Med* 141:746–748, 2017.

Hammerling JA: A review of medical errors in laboratory diagnostics and where we are today, *Am J Clin Pathol* 31(2):41–44, 2012.

Health Insurance Portability and Accountability Act. HIPAA. U.S. Dept. of Health & Human Services. https://www.hhs.gov/hipaa/for-professionals/index.html. (Last accessed December 2018).

Health Information Technology for Economic and Clinical Health (HITECH): *Act, Title XIII of Division A and Title IV of Division B of the American Recovery and Reinvestment Act of 2009 (ARRA), P.L. No. 111-5, 123 Stat. 226 (Feb. 17*. codified at 42 U.S.C. §§ 300jj et seq.; §§ 17901 et seq, https://www.healthit.gov/sites/default/files/hitech_act_excerpt_from_arra_with_index.pdf (Last accessed December 2018).

Hersey PH, Blanchard KH, Johnson DE: ed 10, *Management of organizational behavior*, New Jersey, 2012, Pearson-Hall.

Hunt WH: *NACCLS update* 2018, http://www.ascls.org/images/Meetings/CLEC/CLEChandouts/Thursday_230pm_NAACLS-Update_Handout.pdf (Last accessed December 2018).

Inal TC, Ozturk OG, Kibar F, et al.: Lean Six sigma methodologies improve clinical laboratory efficiency and reduce turnaround times, *J Clin Lab Anal* 32:e22180 (1–5), 2018.

Juran J: *Juran on planning for quality*, New York, 1988, The Free Press.

Kaltra J, Kopargonkar A: Quality improvement in clinical laboratories: a six sigma concept, *Pathol Lab Med* 1(1):11–20, 2016.

KaufmanHall M&A Flash Report: Laboratory Services October 2017: https://www.kaufmanhall.com/resources/research/ma-industry-flash-report-laboratory-services-october-2017 (Last accessed December 2018).

Kohn LT, Corrigan JM, Donaldson MS, ed: *Institutes of medicine*, Washington, DC, 2000, National Academies Press.

Kulakowski C: *Laboratory ergonomics. ARUP; March 17, 2018*, (Last accessed December 2018) http://camlt.org/wp-content/uploads/2018/03/Ergonomics-2018-CAMLT-FINAL.pdf, (Last accessed December 2018).

Kurec AS: The new laboratory manager—recruiting & retaining staff, *Clin Leadersh Manage Rev* 25(1):16–21, 2011.

Kurec AS: Employee selection. In Garza LS, editor: *Clinical laboratory management*, Washington, DC, 2014b, American Society for Microbiology Press, pp 295–308.

Kurec AS: Strategic planning without strategic thinking will fail, *Clin Leadersh Manage Rev* 28(1):16–21, 2014a.

Kurec AS: The laboratory of the future moves outside the walls, *Med Lab Observ* 48(5):18–24, 2016a.

Kurec AS: Follow the leader. Developing great leadership skills, *Am Soc Clin Pathol Crit Values* 9(4):24–27, 2016b.

Kurec AS: The skills and characteristics of true leadership, *Med Lab Manage* 6(1):16, 2017.

Leape LL, Brenan TA, Laird N, et al.: The nature of adverse events in hospitalized patients: results of the Harvard medical practice study II, *NEJM* 324(6):377–384, 1991.

Lippi G, Plebani M, Šimundić AM: Quality in laboratory diagnostics: from theory to practice, *Biochem Med* 20:126–130, 2010.

Lopez JB, Jackson D, Gammie A, Badrick T: Reducing the environmental impact of clinical laboratories, *Clin Biochem Rev* 38(1):3–11, 2017.

Makary MA, Daniel M: Medical error—the third leading cause of death in the US, *BMJ* 353:i2139, 2016.

Mortland KK: Facility redesign for your future laboratory requirements, *Clin Lab Manage Rev* 11(3):145–152, 1997.

Naik SR, Khyathi GV, Lokesh AC: Streamlining laboratory work flow using Lean concepts: an exploration study, *Ind J Publ Health Res Develop* 9(6):86–91, 2018.

Ngo A, Gandhi P, Miller G: Frequency that laboratory tests influence medical decisions, *J Appl Lab Med* 1(4):410–414, 2017.

Occupational Safety and Health Administration. OSHA 1991: *29 CFR 1910.1030; 56FR 64004, Dec 6, 1991*, Bloodborne pathogens Updated April 2012, https://www.osha.gov/laws-regs/regulations/standardnumber/1910/1910.1030. (Last accessed December 2018).

Occupational Safety and Health Administration. OSHA 1994a: *The wearing of gloves during routine vena punctures*, vol. 1030. , p 29. 1910, https://www.osha.gov/laws-regs/standardinterpretations/1994-04-01 (Last accessed December 2018).

Occupational Safety and Health Administration. OSHA 1990: *Toxic and hazardous substances. 29 CFR 1910.1450; 55 FR 3327*. Jan 31, 1990, https://www.osha.gov/laws-regs/regulations/standardnumber/1910/1910.1450 (Last accessed December 2018).

Occupational Safety and Health Administration. OSHA 1994b: *Toxic and hazardous substances. 29 CFR 1910.1200, 59 FR 17479, Apr 13, 1994*. Updated 2012, https://www.osha.gov/pls/oshaweb/owadisp.show_document?p_id=10099&p_table=STANDARDS (Last accessed December 2018).

Occupational Safety and Health Administration. OSHA 2009: *Hazard communication standard: safety data sheets*. Updated 2012, https://www.osha.gov/Publications/OSHA3514.html (Last accessed Dec 2018).

Occupational Safety and Health Administration. OSHA Fact Sheet 2018: *Laboratory safety: ergonomics for prevention of musculoskeletal disorders*, . https://www.osha.gov/Publications/laboratory/OSHAfactsheet-laboratory-safety-ergonomics.html (Last accessed December 2018).

Office of Inspector General. Publication of OIG Compliance Program Guidance for Clinical Laboratories. Federal Register 63, no. 163; Aug. 26, 1998. https://oig.hhs.gov/authorities/docs/cpglab.pdf.

Painter P: *Laboratory design workshop*, Clinical Laboratory Management Association annual meeting, 1993.

Peterson-Kaiser Health System Tracker: December 1, 2017 https://www.healthsystemtracker.org/chart-collection/health-expenditures-vary-across-population/#item-people-age-55-account-half-total-health-spending_2015 (Last accessed December 2018).

Phillips KA, Deverka PA, Hooker GW, Douglas MP: Genetic testing and spending: where are we now? Where are we going? *Health Aff* 37(5):710–716, 2018.

Pizzella N, Kurec AS: The proper handling of CJD-infected patient samples in the pathology laboratory, *Med Lab Observ* 50(5):40–42, 2018.

Public Law: Clinical Laboratory Improvements Amendments (CLIA'88). Public Policy 100-578. https://web.archive.org/web/20090118070811/http://www.fda.gov/cdrh/clia/pl100-578.pdf (Last accessed December 2018).

Sadowski BW, Lane AB, Wood SM, et al.: High-value, cost-conscious care: iterative systems-based interventions to reduce unnecessary laboratory testing, *Am J Med* 130(9):1112e1–1112e7, 2017.

Scungio D, Gile TJ: *Complete guide to laboratory safety*, ed 4, HcPro: Marblehead, Mass, 2014.

Sunyog M: Lean management and Six-Sigma yield big gains in hospital's immediate response laboratory, *Clin Leader Manage Rev* 18(5):255–258, 2004.

United Nations: *Globally harmonized system of classification and labelling of chemicals (GHS)*, ed 4, New York and Geneva, 2011.

U.S. Bureau of Labor Statistics: *Occupational outlook handbook: clinical laboratory technologists and technicians* 2018, https://www.bls.gov/ooh/healthcare/medical-and-clinical-laboratory-technologists-and-technicians.htm#tab-6 (Last accessed December 2018).

Westgard S, Bayat H, Westgard J: Analytical sigma metrics: a review of six sigma implementation tools for medical laboratories, *Biochem Med* 28(2):1–12, 2018.

Wolman DM, Kalfoglou AL, LeRoy L, Institute of Medicine (IOM): *Medicare laboratory payment policy, now and in the future*, National Academy of Sciences, 2000, pp 1–57.

Wolfson D, Santa J, Slass L: Engaging physicians and consumers in conversations about treatment overuse and waste: a short history of the Choosing Wisely Campaign, *Acad Med* 89(7):1–6, 2014.

Womack JP, Jones DT, Roos D: *The machine that changed the world*, Free Press, 1990.

World Health Organization (WHO): *Laboratory biosafety manual*, ed 3, Geneva, 2004, WHO. Chapter 14. https://www.who.int/csr/resources/publications/biosafety/Biosafety7.pdf. (Last accessed December 2018).

Zarbo RJ: Creating and sustaining a lean culture of continuous process improvement, *Am J Clin Pathol* 138:321–326, 2012.

CHAPTER 2

OPTIMIZING LABORATORY WORKFLOW AND PERFORMANCE

Mark S. Lifshitz

UNDERSTANDING WORKFLOW, 13
Data Collection Techniques, 13
Workflow Analysis, 16

UNDERSTANDING TECHNOLOGY, 18
The Role of Technology: Principles and Pitfalls, 18

OPTIMIZING PERFORMANCE, 19

SELECTED REFERENCES, 21

KEY POINTS

- An effective testing process requires integration of preanalytic, analytic, and postanalytic steps.
- An understanding of workflow is a fundamental prerequisite to any performance optimization strategy.
- A variety of techniques should be used to collect workflow data. These include sample and test mapping, tube analysis, workstation analysis, staff interviews, and task (process) mapping.
- Though technology is a critical component of every laboratory, it is only a tool to reach a goal. Technology alone does not improve performance and workflow; its success or failure depends on how it is implemented and whether it was truly needed.
- Consolidation, standardization, and integration are key strategies that can optimize workflow. Managing test utilization may also change overall operational needs and workflow patterns.

The clinical laboratory is a complex operation that must smoothly integrate all three phases of the testing process: preanalysis, analysis, and postanalysis. Preanalysis refers to all the activities that take place before testing, such as test ordering and sample collection. The analysis stage consists of the laboratory activities that actually produce a result, such as running a sample on an automated analyzer. Postanalysis comprises patient reporting and result interpretation. Collectively, all of the interrelated laboratory steps in the testing process describe its workflow. This, in turn, occurs within the overall design of a laboratory operation as described in its policies and procedures.

The steps in the testing process can be generally categorized according to testing phase, role (responsibility), or laboratory technology (Fig. 2.1). Note that the testing process and the grouping of steps vary somewhat from one facility to another. Depending on the laboratory service model and technology used, some steps may fall into one category or another. For example, centrifugation may be performed in a physician's office (preanalysis) or in the laboratory as part of a total automation workcell (analysis). Depending on the technology selected, a laboratory may automate some or many of the steps identified in Figure 2.1. Information technology is the essential "glue" that binds these steps. A more detailed discussion of each testing phase is presented in Chapters 3 to 8. This chapter explores the interrelationship of laboratory workflow, technology, and performance.

UNDERSTANDING WORKFLOW

To fully understand a laboratory's workflow, one must audit all phases of the testing process. Only then can one determine how to optimize performance and to what degree technologic or nontechnologic solutions are needed. Table 2.1 provides some of the issues to consider.

Data are of paramount importance in any workflow analysis. Although laboratory data are rather easy to produce because they are readily available from automated analyzers and information systems, they may not be complete, valid, or in the format required. Because laboratory data play a central role in laboratory decision making (e.g., determining which analyzer to acquire), they have to be accurate. Otherwise, one may make wrong downstream decisions that can have a negative impact on operations. One must understand how data are collected by each of these systems and whether they are valid. For instance, do the test statistics pulled from an analyzer provide information on how many patient reportable tests are done, or do they count how many total tests are done (with quality control, repeats, etc.)? Are panel constituents counted individually, is only the panel counted, or are both counted? Are the "collect" times accurate on turnaround time reports that measure "collect to result"? Or are samples indicated as "collected" on a patient floor before they are actually collected, thereby making the turnaround time appear longer than it really is? Ultimately, there is no substitute for carefully reviewing data to determine whether they make sense. Sometimes, this requires manually verifying data collected electronically or directly observing a work area. For example, it may be necessary to observe when samples arrive in the laboratory to determine how long a delay exists before staff assign a receipt time in the computer. By doing so, one can determine the accuracy of the sample receipt time.

DATA COLLECTION TECHNIQUES

Many types of data can be used to assess workflow. Although some of the fundamental data analysis techniques are described in this chapter, they may have to be supplemented with additional data collection to analyze unique characteristics of a laboratory's operation. It is always useful (some would say imperative) to check that the data collected reflect actual laboratory experience rather than anomalies created by unusual workflow patterns or laboratory information system (LIS) programs or definitions.

Sample and Test Mapping

One fundamental data collection technique is to analyze the distribution of samples and tests over time (Fig. 2.2). Depending on what is mapped, the time interval can be a day (e.g., hour increments for frequently ordered tests, such as those in general chemistry) or a week (e.g., daily increments for tests batched several times a week). The goal is to identify overall workload patterns to assess whether resources are appropriately matched to needs and whether turnaround time or other performance indicators can be improved. It is important that the workload measured reflects actual experience. For example, if phlebotomists remotely mark specimens "received" or the laboratory actually orders tests in the LIS, the measured workload distribution may not accurately reflect the underlying processes. As part of the exercise, it is also important to map routine samples versus stat ones and to map locations that may have special needs, such as the emergency department. In addition to sample mapping, one should map key tests and the number or "density" of tests per sample. This is of special interest in the chemistry section. Outpatient samples typically have greater test density than inpatient ones; thus, an equal number of inpatient and outpatient samples may be associated with different inpatient and outpatient workloads. In automated chemistry, sample mapping more closely reflects staffing needs in that much of the labor is associated with handling and processing tubes rather than actually performing the assays. In contrast, test mapping more closely reflects instrument needs (i.e., the test throughput it needs to complete its workload in a timely manner). By mapping samples and tests and relating them to turnaround time and staffing, a laboratory can identify production bottlenecks and alter workflow to achieve better outcomes. Very frequently, laboratories discover that delays are less the result of instrument issues per se and more the result of workflow patterns that are not matched to instrument capabilities.

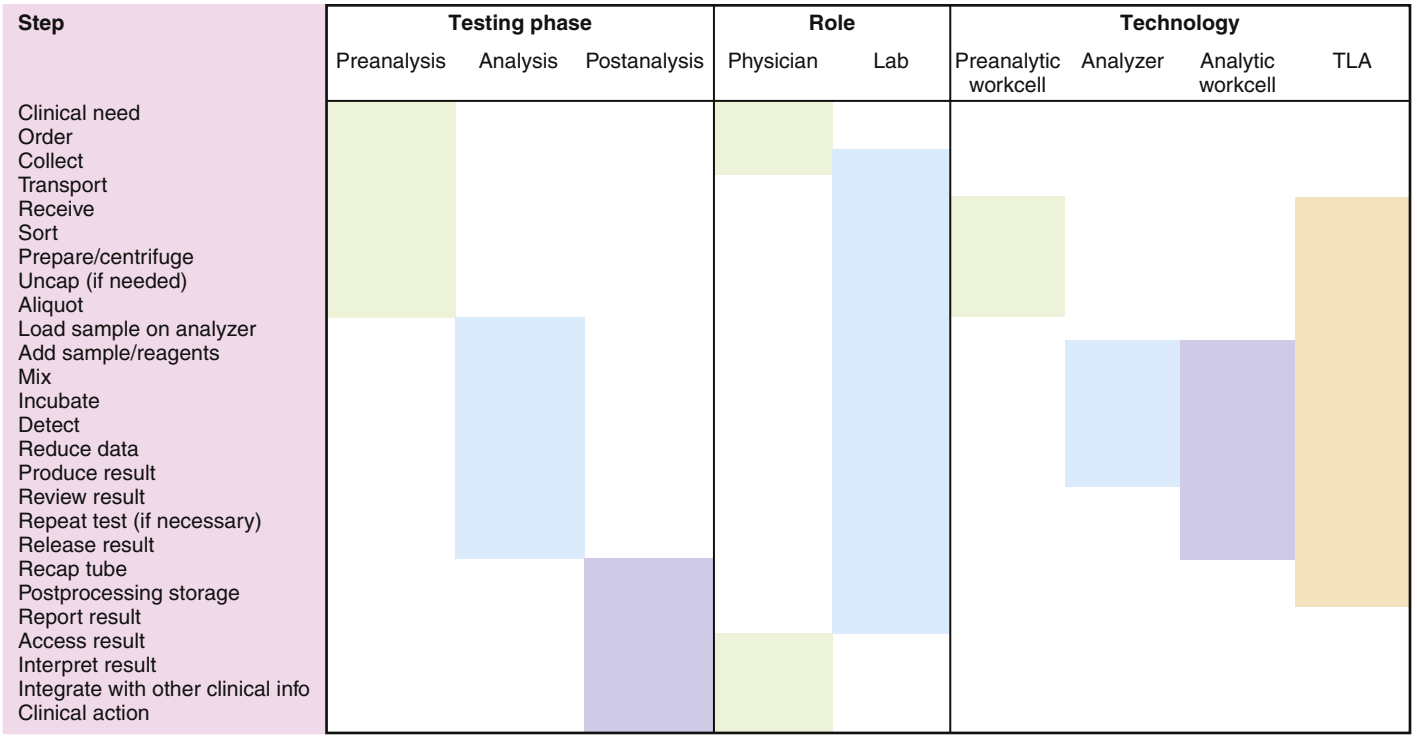

Figure 2.1 Laboratory testing process. Note that the steps can be categorized according to testing phase, role (responsibility), or laboratory technology, as indicated by the shading. *TLA,* Total laboratory automation.

TABLE 2.1

Issues to Consider When Auditing Operations

Test ordering	Where are orders placed—in the laboratory, patient unit, or office? Are inpatient orders handled differently from outpatient ones? Is there a paper or electronic requisition?
Sample collection	Who collects the samples—laboratory or physician? When are they collected—all hours or just in the AM? Are samples bar coded at the site of collection or in the laboratory? How are the labels generated? Is there a positive patient ID system? Does the label contain all the information needed to process the sample?
Transportation	How are samples delivered—by messenger, automatic carrier transport, or a combination? Do all laboratories participate? Are all patient care areas served? How are stats handled? What is their impact? Is there a separate system for emergency department and intensive care units?
Sample receipt	Is there a central receiving area? How are samples distributed to each laboratory? Does physical layout promote efficient sample flow? How are stat samples distinguished from routine ones? How are problem samples handled? Are samples sorted by workstation or department?
Sample processing	Are samples centrifuged centrally or in distributed locations? Are stats handled differently? Are samples aliquoted? If so, where? Is a separate sample drawn for each workstation?
Testing	How many workstations are used? How does capacity relate to need? How are samples stored and retrieved? How long are samples kept? When and why are samples repeated? Are repeat criteria appropriate?
Reporting	How are results reported? Electronically? By remote printer? How are stat and critical values reported, and are criteria appropriate? How many calls for reports does the laboratory receive and why? How are point-of-care tests reported?

Tube Analysis

Part of the laboratory's daily work is related to processing collection tubes or containers. "Tube labor" includes sorting and centrifuging; aliquoting; racking, unracking, loading, and unloading samples on analyzers; retrieving tubes for add-on tests; performing manual dilutions or reruns (depending on instrument); and storing tubes. Although the time needed to perform a tube task may seem insignificant, it has to be repeated many times per day, which can add up to a substantial amount of time. For example, at an average of 10 seconds per tube, it will take a laboratory 3.3 hours to sort 1200 tubes per day. Automation can often reduce this labor, but redesigning the workflow may be a less expensive and more efficient alternative. To the extent that a laboratory reduces the number of tubes and/or the number of tasks associated with each tube, it can reduce tube labor and positively influence workflow and staffing needs. Reducing tube labor is one of the main goals of consolidating chemistry and immunodiagnostic tests into a single analyzer or workcell. Sample mapping provides information about how many containers are received within a specified interval; tube analysis helps to analyze how many additional "tube-related" tasks have to be done. Tube analysis includes the number of containers other than tubes (e.g., fingerstick collections that may require special processing or aliquoting) and the number of reruns (i.e., repeats) needed as the result of instrument flags and/or laboratory policies (Table 2.2).

Workstation Analysis

A typical laboratory is divided into stations for allocating work and scheduling staff. Some workstations consist of a variety of tasks or tests that are grouped together for the purpose of organizing work for one or more staff. For example, all manual or semiautomated chemistry tests may be grouped into a workstation, even though testing might actually be performed at different sites or using different equipment around the laboratory. More typically, a workstation is one physical location (e.g., a fully automated analyzer or group of analyzers, such as hematology cell counters, a chemistry workcell, or an automated track that includes preanalytic processing, analytic modules, and postanalytic storage). Regardless of how a laboratory is organized, it is important to understand where, when, and how the work is performed. This is the goal of a workstation analysis.

Instrument Audit

A key component of any workstation is equipment. By performing an instrument audit (Box 2.1), one can better understand how each analyzer is used, its associated costs, and what potential opportunities might exist to improve performance. The operating characteristics of each instrument should be detailed as part of this process. Examples include the maximum

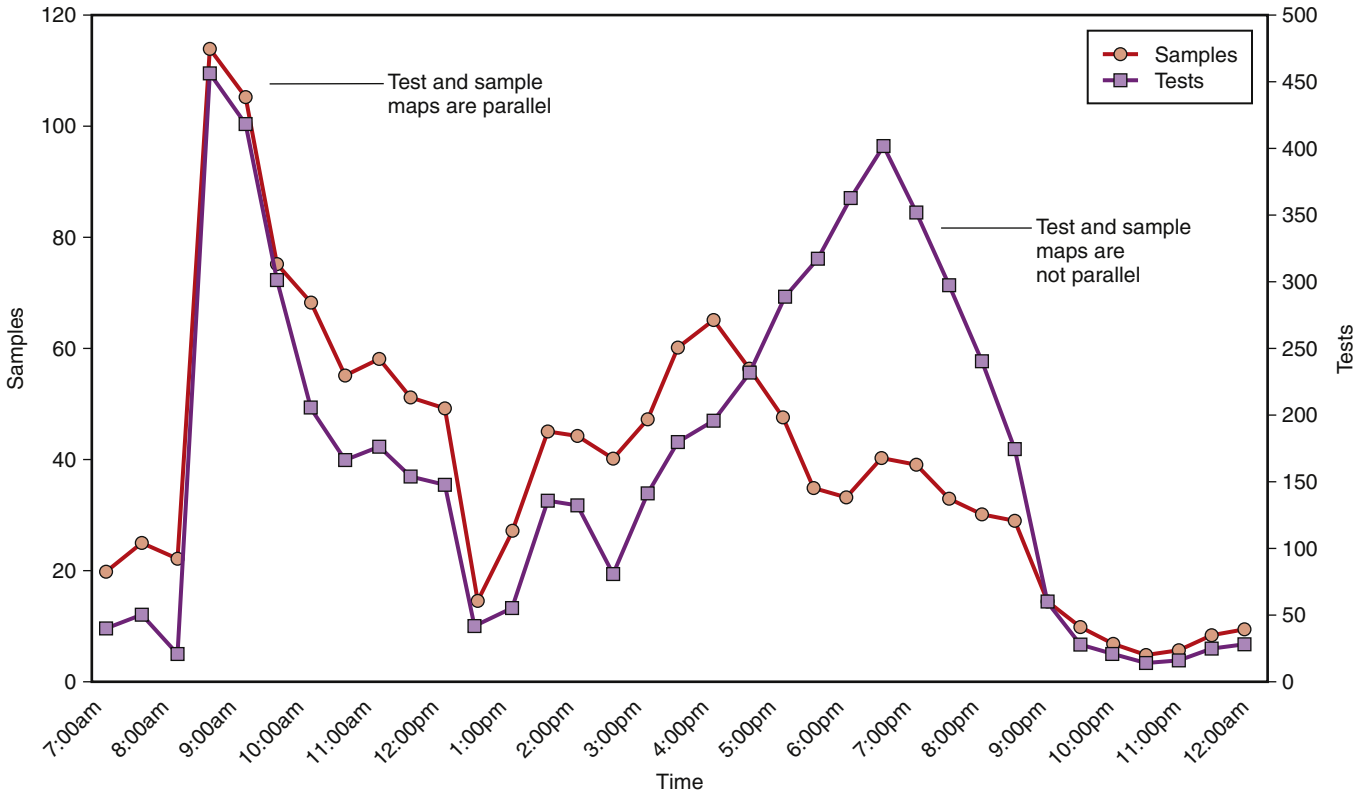

Figure 2.2 Sample and test mapping. Note that the morning volume peak is due to inpatients, and the density is roughly four tests per sample. The evening peak is largely due to outpatients, and density is far greater—about 10 tests per sample. Test density fluctuates during the day; thus, both sample mapping and test mapping are necessary to accurately evaluate workload.

TABLE 2.2

Chemistry Tube Analysis

	Analyzer A	Analyzer B
Total tubes run	500	500
Mechanical error	13	15
Dilution	7	20
Clot/low volume	20	30
Total instrument-related reruns	*40 (32% of total reruns)*	*65 (65% of total reruns)*
Delta check	62	21
Panic value	23	14
Total laboratory criteria–related reruns	*85 (68% of total reruns)*	*35 (35% of total reruns)*
Total reruns	**125**	**100**
% reruns	**25%**	**20%**

Chemistry "reruns" are caused by different factors and can be a source of nonproductive technologist time and/or turnaround time delays. Most Analyzer A reruns are related to overly tight limits for delta checks and panic values that flag too many test results for technologist review and rerun. Most Analyzer B reruns are related to instrument flags caused by a narrow linear range for many methods and a large sample volume requirement per test. A nontechnologic solution (i.e., altering laboratory rerun/review criteria to reduce the number of tubes flagged for rerun) benefits Analyzer A. Only a technologic solution (i.e., a new analyzer) can lower the number of reruns in Analyzer B.

BOX 2.1

Instrument Audit

Instrument model
Vendor
Date acquired
Method of acquisition
Purchased
Leased
Reagent rental
Service cost per year
Supplies cost per year
Reagents
Controls, calibrators
Consumables
Total test volume per year
Patient samples
Controls and calibrators
Test menu
Hours of operation
Days
Shifts
Number of staff trained
Operating mode
Batch versus continuous
Primary system versus backup

number of samples that can be processed per hour, the number of samples that can be loaded at a single time, and the number of reagent containers and assays that can be stored onboard. Instrument throughput (tests/hour) should also be studied by conducting timing studies and reviewing various statistical reports that can be extracted from the instrument and the LIS. Most chemistry analyzers are test-based systems—that is, they perform a specific number of tests per hour irrespective of how many tests are ordered on each sample. On the other hand, some of these systems are affected by test mix (e.g., the relative proportion of electrolytes, general chemistries, and immunoassays). This is the major reason that actual throughput experienced in the laboratory may be lower than what is claimed by the vendor. The latter may assume an ideal test mix that cannot be achieved in a given laboratory. It is important to understand how test mix affects an analyzer's throughput and whether work can be redistributed in a way that enhances throughput. An instrument that was well suited for the laboratory's test mix and volume when initially acquired may no longer provide adequate throughput given a change in test mix. It is important to ensure that a vendor's throughput analysis is based on the laboratory's actual test mix and not on a standard used by the vendor. It may turn out that the number of instruments proposed may not meet the laboratory's needs.

It is equally important to receive a clear and concise definition of uptime from the vendor for the instrument(s). This definition should be simple. If the laboratory cannot report patient results, the instrument is down. Some vendors consider an instrument down only if the vendor is called for

service. This may mean that the percent of up-time by the vendor may be valued higher than the actual up-time experienced by the laboratory. It is important to include this definition in a contract if a laboratory expects a vendor to uphold desired operational performance levels necessary to consistently maintain patient care support.

Last, labor considerations should not be ignored. Must the instrument be attended at all times or does it have walkaway capability? This information can be very useful in identifying processing bottlenecks and redesigning workflow.

Test Menu

A careful review of the laboratory's test offerings should be done during a workstation analysis. Are the tests performed appropriate for the facility given the volume and frequency of test analysis? Just because a laboratory can perform a test does not mean that it should. For example, if a test (e.g., viral load) is performed only once or twice a week and requires dedicated equipment and space, training, and/or labor, it may make more sense to send it to a reference laboratory where it is performed more frequently and, often, at a lower cost. *Sometimes, the best way to improve turnaround time and/or lower the cost of a test is not to perform it*. Unfortunately, this option can be easily overlooked if one focuses only on how to improve the way existing tests are performed instead of analyzing how to best meet clinician needs.

Processing Mode and Load Balancing

These can affect both the cost and the timeliness of testing. Samples can be processed in batches or run continuously as they arrive in the laboratory. When grouped into batches, samples are run at specific intervals (e.g., once a shift, once a day, every other day) or whenever the batch grows to a certain size (e.g., every 20 samples). Batch processing is often less expensive than continuous processing because the setup costs (quality control, labor, etc.) are spread over many specimens (see Table 2.2). However, batch processing produces less timely results. Sometimes, batch processing is a limitation of the instrument that is used. A batch analyzer cannot be interrupted during operation; thus, a newly arrived sample cannot be processed immediately if the instrument is already in use. Most currently available general chemistry and immunoassay analyzers are random-access analyzers that continuously process samples. These analyzers can randomly access samples and reagents and can accommodate an emergency sample at any time. Automation is discussed more fully in Chapter 6. Continuous processing is facilitated by load balancing, a technique that distributes work evenly among analyzers and spreads testing over a longer period to better match instrumentation throughput. For example, outpatient work, which does not require a rapid turnaround time, can be sequenced into the workflow during off hours. This improves testing efficiency, reduces the labor content of individual tests, and reduces throughput requirements (and capital cost) of instruments. In addition, if significant outreach testing (which does not typically require a rapid turnaround) is performed, some or all of this volume can be shifted to times when the laboratory is not as busy. The feasibility of load balancing can be evaluated only if accurate test mapping and tube analysis are performed.

Interviews

Data collection is not complete without interviewing staff. This exercise provides an opportunity for staff to participate in analyzing workflow and improving performance. It also identifies issues that would not be readily apparent from data collection alone. For example, many hospitals require electronic order entry on patient care units. Although this practice may eliminate paper requisitions, laboratory staff members may still be placing orders for "add-on" tests that are called into the laboratory (or added electronically), processing special requests, and troubleshooting incorrect orders, unacceptable samples, or misaligned bar code labels applied by nonlaboratory staff during sample collection. This residual work is likely to be transparent because it probably will not appear on reports, logs, or computer printouts. Thus "computer-generated orders" may still be associated with considerable manual laboratory labor that may be identified only through interviews.

Interviews are particularly valuable in understanding what occurs outside the laboratory. Test ordering patterns or habits can have a significant impact on a laboratory's ability to meet clinician needs. Visits to patient care units and discussions with nursing unit staff can identify preprocessing improvements that cost little to implement but save considerable money downstream.

Early patient discharge can be a challenging task for hospitals trying to shorten length of stay. A full understanding of the discharge process requires interviewing all related staff. One issue that sometimes emerges is the sample collection time for patients awaiting discharge pending a laboratory result. To avoid delays in providing results for discharge patients, some facilities develop elaborate "stat" systems to collect, identify, and process these samples, as well as report results, during the busiest time of the day: the early morning. Sometimes, dedicated (stat instrument) or new technology (point-of-care device) is used for this purpose. However, one can ensure that results are available in the chart during early-morning clinical rounds by simply collecting laboratory samples from patients on the evening before discharge (Sorita et al., 2014). Thus, not all solutions require technology. A careful mix of workflow restructuring and appropriate technology is usually the correct approach and the most cost-effective solution.

Task Mapping

No workflow study is complete without mapping the tasks or processes involved in performing a test (Middleton & Mountain, 1996). A rigorous review will detail every specimen-handling step, each decision point, and redundant activities. Task mapping can be applied to any segment of a laboratory's workflow, whether technical or clerical. A full understanding of the tasks involved usually requires thorough staff interviews, as discussed previously. Task mapping should be an ongoing activity and should also be undertaken whenever one contemplates adding a workstation, test, new technology, or any significant change to a laboratory process. When implementing change, it is important to avoid unnecessary or additional steps that are inadvertently added in the name of "efficiency"; task mapping helps identify these steps. Mapping also helps compare processes before and after change (Fig. 2.3).

WORKFLOW ANALYSIS

Workflow analysis assimilates all of the previously discussed data and transforms them into valuable information. This step can be done manually or, as will be described later, using commercially available software for part of the analysis. A comprehensive workstation analysis should identify bottlenecks and highlight areas where improvements are necessary.

How is this done? The easiest way, and one that does not require computer support, is to follow the path of a specimen or group of specimens through the entire process. This should begin at or near the bedside to see how physicians are ordering tests and should proceed to specimen acquisition and delivery to the laboratory. A flow sheet, which follows the sample from initial order to arrival in the laboratory, should be created. A separate task force is usually assigned to the prelaboratory phase because multiple departments and staff are usually involved. The laboratory often has little or no direct control over this critical portion of workflow, especially when nonlaboratory staff collect samples.

Specimen transit through the laboratory should then be documented, noting areas where batch processing occurs. For example, one should identify minimum and maximum centrifugation times for applicable specimens (such as those that have to be aliquoted). If specimens require 10 minutes for loading and spinning, this should not be assumed to be the average time because a sample queue may form during peak periods. Using the sample arrival mapping done in data collection, an average time can be assigned by time of day. If this is done manually, it is best to select a number of key times and average them, if possible. Similarly, one should note whether loading specimens on the analyzer is delayed. Many other examples of physical bottlenecks need to be identified and quantified. It is not always possible to completely eliminate bottlenecks, but it is possible to mitigate their impact through new technology, alternative processing modes (e.g., random access vs. batch processing), and workflow redesign.

Nonphysical bottlenecks should also be identified and quantified. A classic example is the mode of result verification. Batching results for a technologist to review and accept is every bit as much a bottleneck as is waiting for a centrifuge to process a sample. In contrast, LIS autoverification (where results are automatically released on the basis of preset criteria) can reduce test turnaround time without requiring a major reorganization of the laboratory. However, the degree to which autoverification enhances workflow depends on the manner in which it is implemented and the algorithms defined to qualify a result for this feature. This, in turn, may depend on the LIS used.

Many vendors who want to sell automated equipment systems to the laboratory will provide free workflow analysis. They usually have experienced technical staff who do this, and the information can be very helpful. The laboratory will need to provide the necessary data or access to the laboratory for data collection. Together, the vendor and laboratory leadership need to analyze the workflow to identify opportunities to improve operations, which may well involve the vendor's automated system.

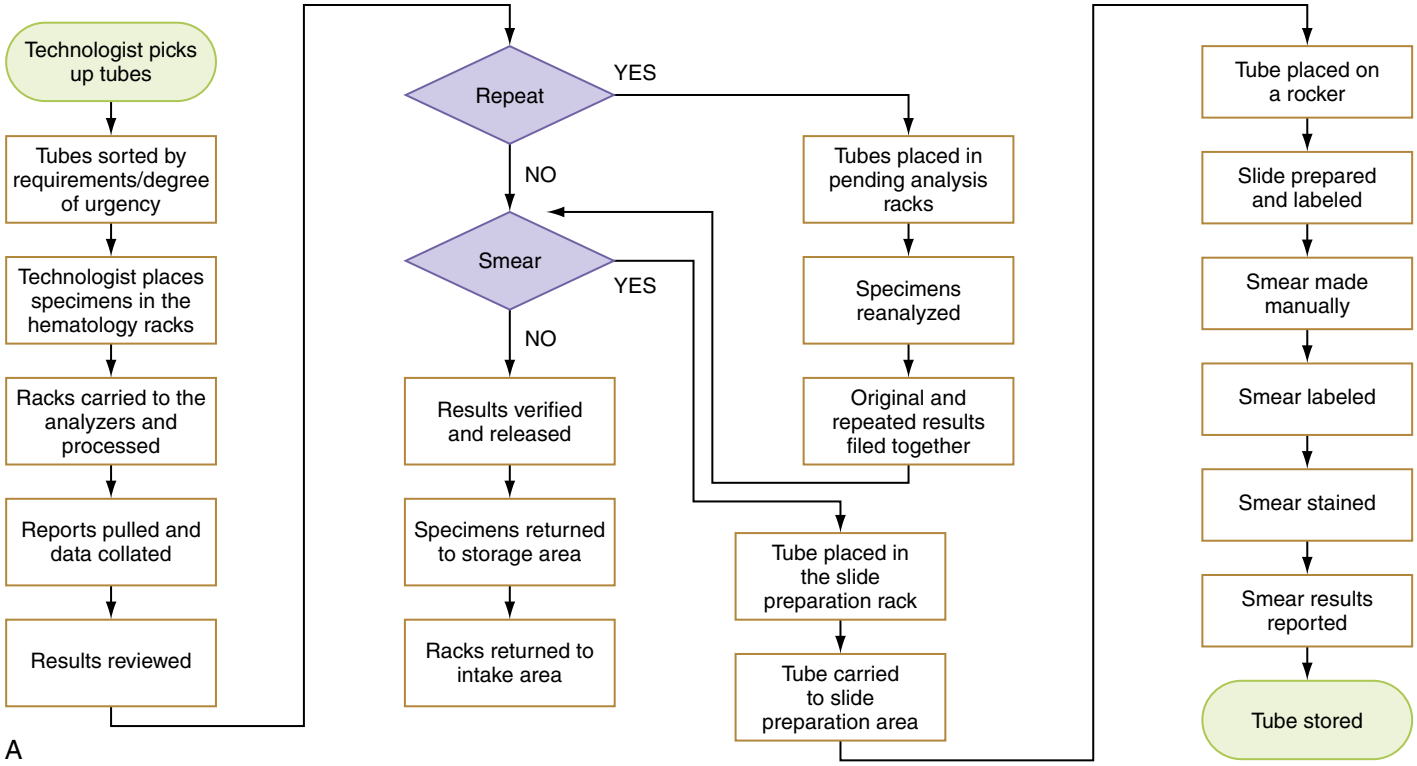

A

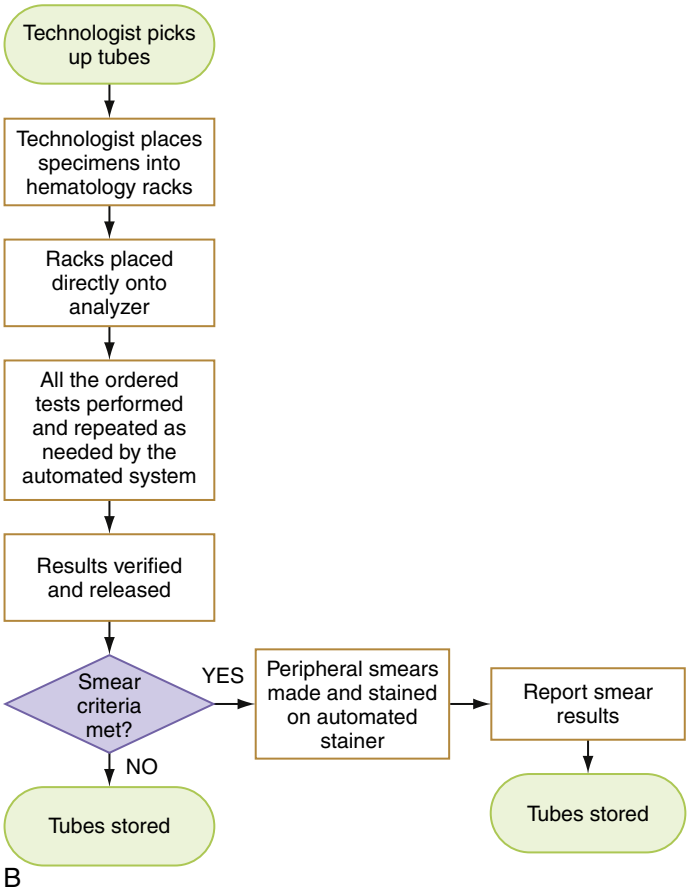

B

Figure 2.3 **A,** Task mapping: Original workflow for hematology cell counting. **B,** Task mapping: Improved workflow for hematology cell counting subsequent to workcell implementation. Note the reduction in steps as compared with part **A.**

Workflow Modeling

Although the analyses discussed earlier are critical to understanding current and proposed workflow designs, they usually provide a somewhat static picture (i.e., each describes a single data element and often how it changes over time). In practice, however, workflow consists of many interrelated variables, and it is difficult to understand (or to evaluate in the laboratory) how a change in one variable affects another. Further, although workflow studies can be very beneficial, they consume resources that may not be available in every laboratory. To address this need, technology vendors have developed workflow simulations. By using sophisticated workflow modeling software, one can analyze these complex interrelationships to better predict the outcome of a given workflow design (Box 2.2). Workflow

BOX 2.2

Interrelated Variables Simulated by Workflow Software Models

Equipment configuration
Facility design
Labor by shift and day
Throughput
Routine maintenance
Downtime
Sample volume (distribution and peak demand)
Sample container type
Review policy and rerun rates
Batch size

modeling can help identify bottlenecks and the impact of staffing changes or different equipment configurations on cost and turnaround time. It can also be used to gain a better understanding of how a given analyzer responds to changes in test volume and test mix. For example, one can simulate the impact of increasing routine test volume on an instrument's turnaround time for stat samples (Mohammad et al., 2004). As with all workflow analyses, however, software modeling must be based on accurate data collection techniques.

Because most simulation programs are proprietary products, they may not allow modeling of all available instruments. Workflow simulation is still a powerful tool, and inferences can be drawn about more efficient processing and testing regardless of the model instrument involved. More important, these programs readily highlight deficiencies in a laboratory's current operations and can point to specific areas where the greatest improvements are achievable.

Pneumatic Tube Transport of Specimens

Many laboratories, especially those in large hospital facilities, use pneumatic tube systems for specimen transport to the laboratory. They can greatly decrease transport time and, thus, total turnaround time for test results. Some of these systems can be extensive, especially the branching systems that can reach most parts of a hospital. Once a laboratory has a tube system, it becomes very dependent on it, requiring a good service and support system to maintain it. Usually, the plant operations or engineering department of the hospital maintains the system on a daily basis. In addition, enough specimen carriers must be available to supply all areas of the hospital in need of specimen transport to the laboratory. It is important to monitor the number of carriers in the system and to order new carriers when existing supplies wear out or "disappear" (it is not uncommon for locations to "stockpile" carriers, at the expense of other locations, to ensure their availability).

UNDERSTANDING TECHNOLOGY

No discussion of workflow is complete without examining the role of technology (De Cresce & Lifshitz, 1988). *Laboratory technology* refers largely to three functional areas: testing equipment (i.e., analyzers), preanalytic processors, and information technology (IT). Although the former two areas are specific to the laboratory, IT is not—its design and role are often determined by factors outside the laboratory. For example, the manner in which a laboratory information system is used for data retrieval and reporting (i.e., whether or not physicians directly access the LIS to view results) depends on whether a clinical information system is available to serve this purpose. In the latter case, laboratory data are accessed and reported through a secondary system. Also, the laboratory system may be part of a broader approach or a single IT vendor solution within the health care center and not a standalone product to be selected by the laboratory. Under these circumstances, the technology selected, although optimal for the general institution, may not be optimal for the laboratory. Changes in hospital-wide systems are rarely made to accommodate efficiencies in ancillary services such as the laboratory. These systems are primarily geared toward easy access to clinical information by caregivers and accurate billing by the hospital finance department.

THE ROLE OF TECHNOLOGY: PRINCIPLES AND PITFALLS

Technology has radically changed the clinical laboratory over the past 30 years and continues to be the driving force behind many new developments. Periodically, a breakthrough technology is introduced that revolutionizes laboratory medicine (Box 2.3). Examples include the random-access

BOX 2.3

Breakthrough Technology

Changes fundamental workflow
Consolidates workstations
Saves labor
Improves service
Sets new performance standard
Leads to premium pricing

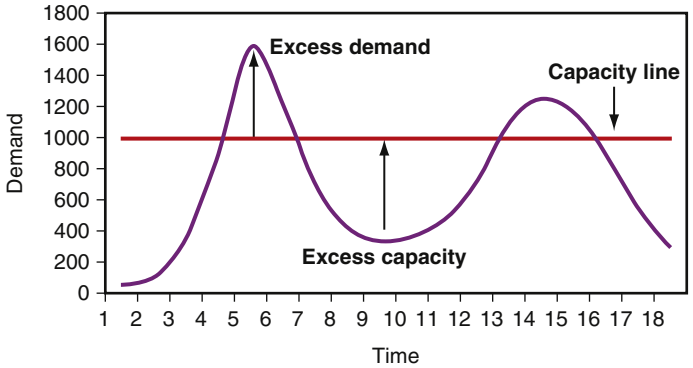

Figure 2.4 Test demand versus instrument capacity. Note that demand exceeds capacity during peak periods, thereby creating backlogs. In many facilities, short backlogs are acceptable. If they are not clinically acceptable, the laboratory should explore ways to more evenly match capacity and demand—for example, by altering blood collection schedules or introducing new work from additional clients. New technology should be the last approach that is considered.

chemistry analyzer, the automated immunodiagnostics system, the chemistry and immunodiagnostics integrated workcell with preanalytic automation, point-of-care testing, and molecular diagnostics. Each change profoundly alters how a laboratory functions and the type of information it provides clinicians. Although breakthrough technologies offer a large potential benefit, they cost more. Over time, a breakthrough technology is adopted by multiple vendors, competition develops, prices fall, and its use becomes widespread among laboratories; in other words, it becomes a current or derivative technology. Early adopters of breakthrough technology often pay more and receive less benefit than those who wait until it becomes a current technology. By thoroughly understanding the role of technology, one can determine how to best use it in the clinical laboratory. The following issues should be considered when evaluating technology.

Is technology needed? Technology is an integral part of a modern laboratory; however, it is not the solution to every problem. Often, a nontechnologic solution provides a faster, better, and less expensive workflow approach than a technologic one. Knowing when to introduce a nontechnologic solution instead of a technologic one can mean the difference between a targeted, cost-effective solution and an expensive one that does not fully address the initial problem, provides unnecessary functionality, or provides necessary functionality but at an unnecessary cost. For example, a laboratory may experience a sharp morning spike in samples, thereby creating workflow backlogs (Fig. 2.4). Instead of purchasing more equipment to provide additional capacity during peak periods, the laboratory should look for ways to distribute work more evenly during the shift. The key is to avoid delivering large sample batches to the laboratory. Outreach samples can be more evenly distributed because the turnaround time is usually not critical. One approach might be to rearrange phlebotomy draw schedules so that blood draws begin earlier and are spread out over a longer period (Sunyog, 2004). Another approach is to have phlebotomists send samples to the laboratory after every few patients instead of waiting to collect a large batch from an entire floor. One consideration is to have the inpatient nursing unit staff perform specimen collection. This may control the number of inappropriate stat orders because nursing units are more familiar than a laboratory phlebotomist with the status of the patient. This requires consistent phlebotomy training for all nursing unit staff that collect specimens to prevent specimen integrity problems. Thus, one should analyze and reengineer processes to the greatest possible degree before embarking on a technology solution; this approach may yield an inexpensive solution that is quicker and easier to implement. Sometimes, nontechnologic solutions, although preferable, are out of the direct control of the laboratory staff and consequently do not receive the attention they deserve. Thus, a technology solution is selected because it can be implemented without the support of other departments.

Technology is a means to an end, not an end. Technology alone does not improve performance and workflow; it is only a tool to reach a goal. Ultimately, new technology succeeds or fails according to how it is implemented. This, in turn, depends on people and their ability to clearly analyze how technology and workflow can be optimally integrated into their setting. What works for one location may not work for another. Sometimes, this means changing long-standing practices or staff schedules. For example, if four chemistry analyzers are consolidated into two, staff need to be reallocated to take into account fewer workstations and/or peak testing needs. Similarly, batching certain tests on a new high-throughput analyzer does not take full advantage of its continuous processing capabilities and in some instances may yield a lower throughput than the analyzer it replaces. Last, manually transcribing physician orders from paper requisitions into an information system provides far less functionality and error reduction capability than is provided by direct electronic order entry by physicians. Because technology has to be "customized" for each site, laboratories implement the same technology in different ways and experience different outcomes. It should never be assumed that improvements and results seen at another facility will automatically occur in one's own facility. The most successful implementations require a total workflow reassessment to evaluate how best to integrate technology. By critically evaluating existing practices, one can avoid perpetuating inefficient processes, even with new equipment.

Overbuying—the cardinal sin. More than anything else, overbuying increases costs that burden an operation over the life of the technology. Although it is tempting to overbuy "just in case" capacity needs grow (such as with new outreach work), these needs may not materialize or may occur slowly over time, allowing for an incremental and more cost-effective approach. A new instrument in the laboratory rarely, if ever, directly translates into new testing volume. The market demand for testing is generally independent of the laboratory's capacity to test, although greater capacity may allow the laboratory to more aggressively market services. Different types of overbuying may occur. For example, one may buy three analyzers instead of two or an analyzer that performs 1000 tests per hour instead of a device that runs 500 tests per hour. Alternatively, a total laboratory automation solution may be implemented instead of one based on several smaller workcells or standalone analyzers. In all instances, overbuying increases costs. All of the previous examples increase depreciation costs, require more service and maintenance, and can lead to ineffective labor utilization and suboptimal workflow. Buying more analyzers than necessary can also increase reagent costs in that each instrument has to be calibrated, controlled, and cross-correlated with other devices running the same test. Reagent waste (due to outdating) may also increase if low-volume tests are set up on all of the analyzers.

Overbuying should not be confused with excess capacity that is sometimes unavoidable when necessary backup systems are implemented. Ultimately, it is the laboratory service model that determines whether backup is needed. For some tests (e.g., cardiac markers), the laboratory may need a backup system; for others (e.g., tumor markers), it may not. Also, a stat laboratory's backup needs will differ from those of a reference laboratory. A well-designed workflow can balance a laboratory's need for some backup without unnecessary overbuying. For a laboratory that needs a 1000 tests/hour capacity, this may mean selecting two 500 tests/hour analyzers instead of two running 1000 tests/hour. Alternatively, it may mean selecting one 1000 tests/hour analyzer and using a laboratory nearby (that is interfaced to the first laboratory's information system) for backup. Last, it may mean selecting two 1000 tests/hour analyzers but running one at a time. This last solution is rarely successful because it duplicates expensive technology and increases maintenance costs. A simple analogy to the family car is often instructive: People rarely buy two automobiles to do what one can do most of the time. Instead, they rely on alternative sources—such as renting, public transportation, or taxis—to fill occasional needs. One must be sure not to underbuy as well. Many times, the number of analyzers is dependent not only on volume throughput but also on stability (uptime). If instrumentation is down a significant amount of time and the effort to bring it back online will take hours or days, a backup instrument is critical for continued testing support. Many large laboratory operations have extensive automation in chemistry and hematology that requires constant availability of service support by the vendor to make sure that the instrumentation is always in working order. In some cases, a vendor will actually have a service engineer routinely present onsite during weekday hours to maintain the automation system and to help train staff to do the same. Because of staffing shortages on a national level, automation has helped laboratories do more with less but only if the automation stays consistently functional. Ultimately, the goal is to "right buy"—that is, to avoid overbuying or underbuying technology.

Do you understand what you are buying? There is a difference between "buying" technology and being "sold" technology by vendors. The former approach requires an analysis by the laboratory to identify what it needs and a thorough understanding of the technology under consideration, whereas the latter relies more heavily on the vendor to provide a solution to the laboratory. The risk of being "sold" a technology is that it might not be the optimal solution. Most instruments work and do what they are advertised to do. Unfortunately, "what they do" may not be "what you need them to do."

The type of technology is also important. Current technology is generally easier to understand and offers a less risky strategy than breakthrough technology, although it might also provide less reward. Breakthrough technology is, by definition, a new technology. It may be difficult to fully understand whether it is appropriate in a given laboratory setting, how best to implement it, or how significant a financial impact it will make.

Other issues to consider relate to the technology itself and whether it currently offers all the features required by a laboratory. A vendor may promote certain enhancements or capabilities scheduled for the future, especially when marketing analyzers. These may include tests in development, instrument or computer hardware improvements, new versions of software, or automatic upgrades to a next-generation system. Although these future enhancements may seem attractive, they may not materialize; thus, they should not be a primary reason for choosing technology. A better approach is to delay purchasing the system until it can offer the laboratory the capabilities it needs. Another potential mistake is overestimating a technology's lifetime or usefulness because this will underestimate its true cost. In the end, the question each laboratorian should ask is not "Does this technology work?" but rather "Does this technology work for me?"

OPTIMIZING PERFORMANCE

Optimizing performance refers to the process by which workflow (including laboratory design) and technology are integrated to yield an operation that best meets the clinical needs and financial goals of the organization: high value. Given that Value = Quality/Cost, enhanced value can be achieved by increasing quality, lowering costs, or a combination of both. In practice, there are times when workflow changes improve service levels and reduce cost. For example, consolidating chemistry systems may lower capital and operating costs and may improve turnaround time. At other times, there is a trade-off between cost and quality. For example, a phlebotomy staff reduction, while lowering costs, may lengthen the time necessary to complete morning blood collection. This, in turn, may delay when test results become available, but this may not be significant if results are not needed until later in the day. On the other hand, if a patient's discharge is contingent on reviewing the result in the morning, a testing delay could increase length of stay. Ultimately, these decisions need to be analyzed within the framework of the overall institution, taking into account the downstream impact of these actions and their effects on other departments.

Optimizing performance is an ongoing process that requires one to constantly assess and reassess workflow and needs. This requires periodic data collection and analysis. Table 2.3 provides examples of workflow metrics that are useful to monitor. Ultimately, the degree to which any of these reports is useful depends on the accuracy of the data. Many different approaches may be taken to optimizing performance; some of the more common ones are discussed here and in Table 2.4.

Consolidation, integration, and standardization are three key interrelated strategies that have assumed increasing importance in recent years as laboratories have become affiliated with one another through large health care networks. These concepts are also relevant to a single facility.

Consolidation. Testing can be consolidated from multiple sites or workstations in a single facility, or selected tests from many facilities can be centralized in one or more locations. Consolidation creates larger sample batches or runs; this improves testing efficiency in that fixed quality control and calibration costs are distributed over more samples. This, in turn, lowers per-unit costs. Consolidation may yield larger reference laboratory test volume. A "make versus buy" analysis can determine whether it is economically feasible to insource tests previously sent to a reference laboratory (Kisner, 2003). Consolidation may also improve turnaround time by making it cost-effective to perform tests more frequently or to use a more automated technology. Some tests may not be appropriate to consolidate. For example, blood gases and other point-of-care tests may have to be performed at multiple sites in a hospital to provide the necessary turnaround time demanded by clinicians. Similarly, little benefit may be derived from performing routine hospital complete blood counts (CBCs) at a central off-site location instead of at the main hospital rapid-response laboratory. In contrast, it may be beneficial to consolidate across facilities those tests

TABLE 2.3
Workflow Metric Examples

Metric	Comments
Turnaround Time (TAT) Studies	
Collection to receipt	Is collection time correct? How long does it take for samples to reach laboratory? Is tube transport system functioning properly? Are messenger pickups reliable?
Receipt to result	How long does testing take once the laboratory receives a sample? Is it held in a central receiving area before it is brought to the technologist? Is the receipt to result time accurate—that is, is there a delay between physical receipt and electronic sample receipt acknowledgment in LIS (Stotler & Kratz, 2012)?
Order (or collection) to result	This is what the physician perceives as total turnaround time. Is it accurate? How long does it take for a released laboratory result to appear in the clinical information system? Do networking issues external to the laboratory delay the appearance of results?
Stat and routine TAT by hour	Is stat TAT longer in the AM when routine samples from morning collection arrive? What is the difference in TAT for routine and stats? Are some tests affected more than others?
Monthly Volume Statistics	
"Billable" tests	How many orderable tests are performed? What is the trend? Has total volume or a specific test's volume changed enough to warrant a reevaluation of workflow or testing capacity? Should any tests be sent to a reference laboratory rather than be performed in-house?
"Exploded" tests	Exploding chemistry panels into individual components provides a more accurate assessment of general testing "load" on analyzers and reagent usage than orderable tests alone. Has volume changed? Is it related to a specific location or a new service?
By location	Has testing volume changed in specific nursing units or outpatient settings? Has the volume of inpatient and outpatient testing changed?
Reference laboratory tests	Are certain tests increasing in volume? If so, why and at what cost? Are total monthly costs changing? (Tests with the highest cost/year are not always the highest volume ones.) Should certain tests be screened for appropriateness? Does it make sense to perform any of these tests in-house ("buy versus make" decision)?
Sample and Test Mapping	
Tubes per hour	Tube handling in chemistry has a direct impact on staff (or automation) and includes centrifugation, aliquoting, and storage.
Tests per hour by department or workstation	This is needed to compare "testing demand" versus "instrument capacity" and can help determine optimal instrument configuration.

that are less time-sensitive (e.g., tumor markers) or that require special skills and/or dedicated equipment at each site (e.g., various microbiology or molecular tests, or electrophoresis). To successfully consolidate tests from multiple facilities, a central site must control new costs (by minimizing additional staff or equipment to perform the tests) and provide better or comparable quality and service to what had been provided (Carter et al., 2004). It must also foster a collaborative approach to ensure that all of the sending facility's needs are met, including common physician concerns, such as longer turnaround time and limited ability to access information or interact with a remote laboratory. A successful consolidation should be transparent to the clinician.

Standardization. Standardized policies, methods, and equipment benefit laboratories in several ways. Direct benefits, such as lower costs, can be realized when the laboratory aggressively negotiates with one vendor to supply all chemistry or hematology equipment and reagents. Indirect benefits are due to the simplified operations that result from standardization and make it easier to cross-train staff or implement policies and procedures. Standardization is a gradual process that can take several years to complete. Rapid transition usually is not possible because of vendor contract lock-ins; a buyout of an existing contract is usually too expensive and can partially or completely offset any intended savings from a new contract. Sometimes, the unique needs of a location may preclude standardization with other laboratories, or a single vendor may not offer a product line that is suitable for each facility. In these instances, it is still possible to significantly lower costs and/or improve performance, albeit using a more varied or limited approach.

Integration. Integration is the process by which services at one location are coordinated, shared, and/or connected to those at another to provide a seamless operation. Although integration is often a by-product of consolidation and standardization, the latter two strategies are not a prerequisite to successful integration. For example, consider a laboratory information system that links several facilities. Although a single seamless operation can be created with a single vendor's system, it is also possible to network systems from different vendors, albeit with greater difficulty and possibly less functionality. Other integration examples include cross-training staff among different laboratory sections or facilities and interfacing point-of-care laboratory data to the main laboratory system.

Six Sigma and Lean. Six Sigma is a management concept that was first introduced by Motorola in 1979 (Gras & Philippe, 2007). The ultimate goal is to reduce defects to fewer than 3.4 per million procedures. Lean is a management concept that reduces waste and streamlines an operation (Sunyog, 2004). It was used to describe the automaker Toyota's business process in the 1980s. (See Chapter 1 for a complete discussion of Six Sigma and Lean.)

Managing utilization. Thus far, strategies to optimize performance have focused on ways to do work better and at lower cost. Although this is important, it does not address the most basic question: Is the work—that is, the test—necessary? After all, the least expensive test is the test that is not done. Lowering test volume may change overall operational needs and workflow patterns. Keep in mind that inpatient laboratory work generally is not reimbursed (see Chapter 13)—each laboratory test is an added cost for the hospital. Thus, lowering inpatient utilization has a direct impact on costs. In contrast, outpatient testing generally is reimbursed by a third-party payer or by the patient. Despite this, the amount reimbursed may not be sufficient to cover the cost of the test. This is especially true for expensive new reference laboratory tests for which the laboratory may receive only 20 to 30 cents for each dollar spent. Therefore selectively controlling outpatient utilization can be financially beneficial. Appropriate utilization of tests does not only mean lowering utilization. In some instances, tests that should be ordered may not be ordered; this could have an impact on patient care and could lengthen stay.

A laboratory may use different strategies to manage utilization. One approach is to decrease tests that are not medically necessary, though defining whether a test is or is not "medically necessary" in a given clinical circumstance may be difficult to establish. Other approaches are more defined and likely to yield greater consensus. For example, one might limit inpatient laboratory testing to only those tests necessary for immediate care or develop an evidence-based laboratory formulary to guide appropriate utilization and to remove obsolete tests. Irrespective of approach, a successful test utilization program requires a broad-based effort. Expert clinicians, pathology leadership, administration, and IT support staff are all critical elements (Kim et al., 2011; Warren, 2013). The American Society for Clinical Pathology (ASCP) has also been instrumental in advancing a dialogue about testing through its Choosing Wisely recommendations (American Board of Internal Medicine, 2018).

Over the years, laboratories have realized large cost savings through productivity improvements. As a result, it is far easier and less costly to run a 10-cent test than to determine whether each one is appropriate. Although this is true for many high-volume tests (such as CBCs and basic metabolic panels), it is not true for many new, complex, and costly reference laboratory tests (such as molecular genetics). Thus, a different strategy is needed to manage utilization of reference laboratory tests that might cost $500 to $1,000 or more than is needed to manage CBCs. One approach is to use a laboratory professional as a gatekeeper to review certain reference laboratory orders and cost with the clinician according to guidelines developed with the clinical services (Greenblatt et al., 2015). This cost avoidance strategy not only ensures that clinical indications are met but it also educates physicians about the cost of a test and challenges each one to evaluate the cost-benefit of ordering it. In contrast, high-volume tests, such as a CBC, require a broader strategy that restricts or guides ordering frequency electronically through various clinical pathways, guideline-based decision support systems (van Wijk et al., 2002) or test frequency filters applied at the point of order (Konger, 2016). For example, a comprehensive or basic metabolic panel might be limited to one order per admission if the patient is stable. Little can be saved by eliminating one low-cost laboratory test from a panel of five other tests. The most significant cost savings is realized when a phlebotomy is eliminated. This usually requires rethinking the frequency of laboratory orders across all clinical services and changing

TABLE 2.4

Strategies to Optimize Performance

Strategy	Example
Consolidate	One facility: Run stat and routine samples together on the same analyzer; run routine and specialty tests on the same platform; collapse number of analyzers and workstations and use workcell, if applicable. Consolidation can reduce "tube labor."
	Multiple facilities: Centralize selected low-volume, high-cost tests/services at a single location (e.g., molecular diagnostics [HIV viral load], blood donor collection).
Standardize	Equipment: All equipment purchased from one vendor yields larger volume discounts and lower costs for reagents and analyzers, especially in chemistry and immunodiagnostics.
	Method: Uniform reference range for all laboratories promotes seamless testing environment for inpatients and outpatients with data comparability and trending results across laboratories. It also provides system backup without excess redundancy.
	Policies: Simplify procedure manuals and compliance documents so they can be shared.
	Staff: Standardized operations make it easier to share staff among facilities.
	LIS: Database management is simplified.
Integrate	Computer: Network LIS with other data systems to promote seamless flow (e.g., sending point-of-care results into the LIS).
Strategic growth	Courier: Use single service to deliver samples among multiple sites.
	Evaluate excess capacity and feasibility of increasing testing workload: Assess outreach infrastructure (couriers, client/sales staff, billing), incremental testing costs, potential revenue, and core mission to determine whether to expand business.
Strategic sourcing	Long-term strategy: Competitively bid equipment, supplies, reference laboratory services, etc., taking into account payment terms, delivery charges, value-added services, and product costs.
Rapid repricing	Short-term strategy: Renegotiate pricing with existing vendors.
"Make versus buy"	Review all send-out tests and low-volume in-house tests to identify which tests to "buy" (i.e., send out or outsource) and which to "make" (i.e., do in-house) based on cost, turnaround time, and/or clinical need. Also, review services, such as couriers.
Review laboratory policies and tasks	Critically review laboratory policies and procedures to determine their relevance and appropriateness: Can delta check limits be narrowed or eliminated to reduce the numbers of test repeats and verifications without compromising quality? Do critical values need to be repeated before they are reported (Lehman et al, 2014)? Are critical call values clinically appropriate or do they generate unnecessary calls to physicians? Can nonurgent expensive tests be batched twice weekly instead of every day? Do clinicians need certain tests daily that are available only several times a week? Are quality control and maintenance procedures excessive?
Make maximum use of simple and/or existing IT solutions	The rule-based autoverification process eliminates the need for the technologist to manually release each result (Crolla & Westgard, 2003); sample racking storage system eliminates most of the time spent looking for samples.
Cross-train staff	Train technologists to perform automated chemistry and hematology tests instead of chemistry or hematology alone.
Adjust skill mix	Adjust skill level (and compensation) of staff to match task performed: Use laboratory helpers instead of technologists to centrifuge samples or load samples on analyzers.
Adjust staff scheduling	Use part-time phlebotomists to supplement peak blood collection periods instead of full-time phlebotomists who are underutilized once morning collection is finished.
Change laboratory layout	Design open laboratory that allows all automated testing to run in the same location and promotes cross-training of staff.
Manage utilization	Require pathologist or director approval to order select costly reference laboratory tests and/or restrict usage of various tests to specialists.

HIV, Human immunodeficiency virus; *IT,* information technology; *LIS,* laboratory information system.

practice patterns to reduce the number of times a patient's blood is collected. Test repetition is a common component of overall test utilization and is costly (van Walraven & Raymond, 2003). It can be reduced using a clinical decision support tool (Procop et al, 2014), using a collaborative approach that includes shared responsibility for establishing clinical guidelines (Rudolf, 2017), using an interactive dashboard to display duplicates per patient or number of tests per patient, establishing minimum retesting intervals, and providing physicians with feedback such as peer comparison statistics on test use (Baird, 2018). Another utilization strategy is charge display, the practice of displaying the charge for a test when it is ordered. Research has shown considerable variation in the ability of this approach to change ordering behavior. In a recent study, it had no significant impact (Schmidt, 2017).

A laboratory-based diagnostic algorithm can assist with medical decision making and reduce test utilization. With this approach, a physician requests the laboratory to perform a diagnostic workup (e.g., thyroid function evaluation) instead of ordering specific tests. Thus, the laboratory determines the appropriate tests to run and in what order (Yang et al., 1996).

SELECTED REFERENCES

American Board of Internal Medicine: *Choosing Wisely recommendations*, Philadelphia, PA, 2018, Initiative of ABIM Foundation.

A useful test utilization strategy guided by experts; it provides a list of commonly performed tests that are potentially unnecessary and should be questioned.

De Cresce RP, Lifshitz MS: Integrating automation into the clinical laboratory. In Lifshitz MS, De Cresce RP, editors: *Perspectives on clinical laboratory automation*, New York, 1988, WB Saunders, pp 759–774.

General overview of how to analyze workflow and evaluate technology, including many practical considerations.

Middleton S, Mountain P: Process control and on-line optimization. In Kost GJ, editor: *Handbook of clinical automation, robotics and optimization*, New York, 1996, John Wiley & Sons, pp 515–540.

Provides an overview of task and process mapping using flow diagrams. Also discusses how to integrate automation, information systems, and staff to optimize performance.

Access the complete reference list online at Elsevier eBooks for Practicing Clinicians.

REFERENCES

Baird GS: What's new in laboratory test utilization management? *Clin Chem* 64(7):1–7, 2018.

Carter E, Stubbs JR, Bennett B: A model for consolidation of clinical microbiology laboratory services within a multihospital health-care system, *Clin Leadersh Manag Rev* 18:211–215, 2004.

Crolla LJ, Westgard JO: Evaluation of rule-based autoverification protocols, *Clin Leadersh Manag Rev* 17:268–272, 2003.

Gras JM, Philippe M: Application of the six sigma concept in clinical laboratories: a review, *Clin Chem Lab Med* 45(6):789–796, 2007.

Greenblatt MB, Nowak JA, Quade CC, et al.: Impact of a prospective review program for reference laboratory testing requests, *Am J Clin Path* 143:627–634, 2015.

Kim JY, Dzik WH, Dighe AS, et al.: Utilization management in a large urban academic medical center. A 10-year experience, *Am J Clin Pathol* 135:108–118, 2011.

Kisner HJ: Make versus buy: a financial perspective, *Clin Leadersh Manag Rev* 17:328–330, 2003.

Konger RL, Ndekwe P, Jones G, et al.: Reduction in unnecessary clinical laboratory testing through utilization management at a US government veteran affairs hospital, *Am J Clin Path* 145:355–364, 2016.

Lehman CM, Howanitz PJ, Souers R, et al.: Utility of repeat testing of critical values. A q-probes analysis of 86 clinical laboratories, *Arch Pathol Lab Med* 138:788–793, 2014.

Mohammad AA, Elefano EC, Leigh D, et al.: Use of computer simulation to study impact of increasing routine test volume on turnaround times of STAT samples on ci8200 integrated chemistry and immunoassay analyzer (abstract), *Clin Chem* 50:1952–1955, 2004.

Procop GW, Yerian LM, Wyllie R, et al.: Duplicate laboratory test reduction using a clinical decision support tool, *Am J Clin Pathol* 141:718–723, 2014.

Rudolf JW, Dighe AS, Coley CM, et al.: Analysis of daily laboratory orders at a large urban academic center, *Am J Clin Path* 148:128–135, 2017.

Schmidt R, Colbert-Getz JM, Milne CK, et al.: Impact of laboratory charge display within the electronic health record across an entire academic medical center, *Am J Clin Path* 148:513–522, 2017.

Sorita A, Patterson A, Landazuri P, et al.: The feasibility and impact of midnight routine blood draws on laboratory orders and processing time, *Am J Clin Pathol* 141:805–810, 2014.

Stotler BA, Kratz A: Determination of turnaround time in the clinical laboratory. "Accessioning-to-result" time does not always accurately reflect laboratory performance, *Am J Clin Pathol* 138:724–729, 2012.

Sunyog M: Lean management and six-sigma yield big gains in hospital's immediate response laboratory, *Clin Leadersh Manag Rev* 18:255–258, 2004.

van Walraven C, Raymond M: Population-based study of repeat laboratory testing, *Clin Chem* 49:1997–2005, 2003.

van Wijk MAM, van der Lei J, Mosseveld M, et al.: Compliance of general practitioners with a guideline-based decision support system for ordering blood tests, *Clin Chem* 48:55–60, 2002.

Warren JS: Laboratory test utilization program. Structure and impact in a large academic medical center, *Am J Clin Pathol* 139:289–297, 2013.

Yang JM, Laposata M, Lewandrowski KB: Algorithmic diagnosis. In Kost GJ, editor: *Handbook of clinical automation, robotics and optimization*, New York, 1996, John Wiley & Sons, pp 911–928.

CHAPTER 3

PREANALYSIS

Mark S. Lifshitz

PRECOLLECTION VARIABLES, 22
Physiologic Factors, 22
Common Interferences, 23
Special Issues That May Impact Analysis, 24
SPECIMEN COLLECTION, 26
The Test Order, 26
Time of Collection, 26
Specimen Acceptability and Identification Issues, 26
BLOOD COLLECTION OVERVIEW, 27
Anticoagulants and Additives, 27
Blood Collection Devices, 29
Blood Storage and Preservation, 29
Importance of Policies and Procedures, 29
BLOOD COLLECTION TECHNIQUES, 29
Arterial Puncture, 29
Finger or Heel Skin Puncture, 30
URINE AND OTHER BODY FLUIDS COLLECTION, 31
Urine, 31
Other Body Fluids, 32
SPECIMEN TRANSPORT, 33
SPECIMEN PROCESSING, 33
Precentrifugation Phase, 33
Centrifugation Phase, 34
Equipment, 34
SELECTED REFERENCES, 34

KEY POINTS

- Errors and variables in the preanalysis stage can affect test results.
- Patient variables include physical activity, diet, age, sex, circadian variations, posture, stress, obesity, smoking, and medication.
- Strict adherence to proper technique and site selection can minimize collection variables such as hemolysis, hemoconcentration, clots, and other causes for sample rejection or erroneous results.
- Blood collection containers are color coded based on additive or preservative, and each is suitable only for specific tests. Failure to use the proper tubes or filling tubes in the wrong sequence can produce erroneous results.
- Blood collection staff must be adequately trained in safety and confidentiality issues.
- Blood, urine, and other body fluid constituents can change during transport and storage. The extent of these changes varies by analyte.
- The most common reasons for specimen rejection are clotted blood for hematology or coagulation tests; insufficient volume in a tube for coagulation tests; and hemolysis, icterus, and lipemia in serum or plasma that can interfere with chemistry testing.

Preanalysis refers to all the complex steps that must take place before a sample can be analyzed. Over the years, a series of studies identified that 32% to 75% of all testing errors occur in the preanalytic phase (Lapworth & Teal, 1994; Stahl et al., 1998; Hofgartner & Tait, 1999; Bonini et al., 2002; Plebani, 2010), and technologic advances and quality assurance procedures have significantly reduced the number of analytic-based errors. This has exposed the preanalysis stage as a major source of residual "error" and/or variables that can affect test results. Preanalytic factors include patient-related variables (diet, age, sex, etc.), specimen collection and labeling techniques, specimen preservatives and anticoagulants, specimen transport, and processing and storage. Potential sources of error or failure in this process include improperly ordered tests, sample misidentification, improper timing, improper fasting, improper anticoagulant/blood ratio, improper mixing, incorrect order of draw, and hemolyzed or lipemic specimens. The most frequent preanalytic errors include improperly filling the sample tube, placing specimens in the wrong containers or preservatives, and selecting the incorrect test (Plebani, 2010). Table 3.1 lists the most common errors associated with specimen collection, including those that occur before specimen collection (e.g., patient ID error), during collection (e.g., incorrect tube or order of draw), and after collection (e.g., improper transport or centrifugation).

Errors in the preanalytic stage create extra work or additional investigation that may cause unnecessary procedures for patients and costs to the health care system (Stankovic & DeLauro, 2010). Preanalytic issues have downstream impact on the use of laboratory resources, hospital costs, and overall quality of care. By some estimates, specimen collection errors cost the average 400-bed hospital about $200,000/year in recollection costs. The estimated average costs of a preanalytical error in North American institutions were estimated at $208, with costs representing between 0.23% and 1.2% of total hospital operating costs (Green, 2013). Proper collection technique is also essential to minimize injury to the phlebotomist and the patient. Treatment for an injury related to a traumatic needlestick can cost $500 to $3000, and poor technique can result in patient injury, such as nerve and arterial damage, subcutaneous hemorrhage, infection, and even death. The Centers for Disease Control and Prevention (CDC) estimates that 385,000 needlestick injuries occur per year (CDC, 2004). Many go unreported. This chapter discusses the preanalytic process, with special emphasis on the clinical impact of variables and sources of failure.

PRECOLLECTION VARIABLES

In preparing a patient for phlebotomy, care should be taken to minimize physiologic factors related to activities that might influence laboratory determinations. These include diurnal variation, exercise, fasting, diet, ethanol consumption, tobacco smoking, drug ingestion, and posture (Haverstick, 2015).

PHYSIOLOGIC FACTORS

Diurnal variation. This may be encountered when testing for hormones, iron, acid phosphatase, and urinary excretion of most electrolytes, such as sodium, potassium, and phosphate (Dufour, 2003). Table 3.2 presents several tests affected by diurnal variations, posture, and stress.

Exercise. Physical activity has transient and long-term effects on laboratory determinations. Transient changes may include an initial decrease followed by an increase in free fatty acids, and lactate may increase by as much as 300%. Exercise may elevate creatine phosphokinase (CK), aspartate aminotransferase (AST), and lactate dehydrogenase (LD) and may activate coagulation, fibrinolysis, and platelets (Garza & Becan-McBride, 2014). These changes are related to increased metabolic activities for energy purposes and usually return to preexercise levels soon after exercise cessation. Long-term effects of exercise may increase CK, aldolase, AST, and LD values. Chronic aerobic exercise is associated with lesser increases in plasma concentration of muscle enzymes such as CK, AST, alanine aminotransferase (ALT), and LD. Decreased levels of serum gonadotropin and sex steroid concentrations are seen in long-distance athletes, while prolactin levels are elevated (Dufour, 2003).

Diet. An individual's diet can greatly affect laboratory test results. The effect is transient and is easily controlled. Glucose and triglycerides, absorbed from food, increase after eating (Dufour, 2003). After 48 hours of fasting, serum bilirubin concentrations may increase. Fasting for 72 hours decreases plasma glucose levels in healthy women to 45 mg/dL (2.5 mmol/L), while men show an increase in plasma triglycerides, glycerol, and free fatty acids, with no significant change in plasma cholesterol. When determining blood constituents such as glucose, triglycerides, cholesterol, and electrolytes, collection should be done in the basal state

TABLE 3.1
Common Preanalytic Errors

Phase	Error
Before Collection	1. Incorrect test ordered 2. Inadequate patient preparation (e.g., not fasting, recent heavy meal—lipemia) or improper timing (e.g., trough drug level drawn too early) 3. Misidentification of patient
During Collection	1. Wrong container/wrong additive 2. Short draws/wrong anticoagulant/blood ratio 3. Hemoconcentration from prolonged tourniquet time 4. Hemolysis due to incorrect technique (e.g., forcing blood through needle, draw via intravenous line)
After Collection	1. Inadequate mixing/clots 2. Mislabeling of specimen 3. Improper transport to lab: Exposure to light/extreme temperatures or delayed delivery 4. Processing errors: Incomplete centrifugation, incorrect log-in, improper storage or aliquoting prior to analysis

(Garza & Becan-McBride, 2014). Eating a meal, depending on fat content, may elevate plasma potassium, triglycerides, alkaline phosphatase, and 5-hydroxyindoleacetic acid (5-HIAA). Stool occult blood tests, which detect heme, are affected by the intake of meat, fish, iron, and horseradish, a source of peroxidase, causing a false-positive occult blood reaction (Dufour, 2003). In addition, consumption of bismuth-containing antacids such as Pepto-Bismol also renders false-positive results. Physiologic changes may include hyperchylomicronemia, thus increasing turbidity of the serum or plasma and potentially interfering with instrument readings.

Certain foods or diet regimens may affect serum or urine constituents. Long-time vegetarian diets are reported to cause decreased concentrations of low-density lipoproteins (LDLs), very-low-density lipoproteins (VLDLs), total lipids, phospholipids, cholesterol, and triglycerides. Vitamin B_{12} deficiency can also occur unless supplements are taken (Young, 2007). A high-meat or other protein-rich diet may increase serum urea, ammonia, and urate levels. High-protein, low-carbohydrate diets, such as the Atkins diet, greatly increase ketones in the urine and increase the serum blood urea nitrogen (BUN). Foods with a high unsaturated-to-saturated fatty acid ratio may show decreased serum cholesterol, while a diet rich in purines will show an increased urate value. Foods such as bananas, pineapples, tomatoes, and avocados are rich in serotonin. When ingested, elevated urine excretion of 5-HIAA may be observed. Beverages rich in caffeine elevate plasma free fatty acids and cause catecholamine release from the adrenal medulla and brain tissue. Ethanol ingestion increases plasma lactate, urate, and triglyceride concentrations. Elevated high-density lipoprotein (HDL) cholesterol, γ-glutamyl transferase (GGT), urate, and mean corpuscular volume (MCV) have been associated with chronic alcohol abuse. Serum concentrations of cholesterol, triglycerides, and apoB lipoproteins are correlated with obesity. Serum LD activity, cortisol production, and glucose increase in obesity. Plasma insulin concentration is also increased, but glucose tolerance is impaired. In obese men, testosterone concentration is reduced (Young, 2007).

Stress. Mental and physical stresses induce the production of adrenocorticotropic hormone (ACTH), cortisol, and catecholamines. Total cholesterol has been reported to increase with mild stress, and HDL cholesterol to decrease by as much as 15% (Dufour, 2003). Hyperventilation affects acid-base balance and elevates leukocyte counts, serum lactate, or free fatty acids.

Posture. Posture of the patient during phlebotomy can have an effect on various laboratory results. An upright position increases hydrostatic pressure, causing a reduction of plasma volume and increased concentration of proteins. Albumin and calcium levels may become elevated as one changes position from supine to upright. Elements that are affected by postural changes are albumin, total protein, enzymes, calcium, bilirubin, cholesterol, triglycerides, and drugs bound to proteins. Incorrect application of the tourniquet and fist exercise can result in erroneous test results. Using a tourniquet to collect blood to determine lactate concentration may result in falsely increased values. Prolonged tourniquet application may also increase serum enzymes, proteins, and protein-bound substances—including cholesterol, calcium, and triglycerides—as the result of hemoconcentration when plasma water leaves the vein because of back pressure. After bed rest in the hospital, a patient's hemoglobin (Hb) can decrease from the original admitting value enough to falsely lead a physician to suspect internal hemorrhage or hemolysis (Dufour, 2003). This effect can be amplified by intravenous fluid administration. Patients should be advised to avoid changes in their diet, consumption of alcohol, and strenuous exercise 24 hours before having their blood drawn for laboratory testing.

TABLE 3.2
Tests Affected by Diurnal Variation, Posture, and Stress

Cortisol	Peaks 4-6 AM; lowest 8 PM–12 AM; 50% lower at 8 PM than at 8 AM; increased with stress
Adrenocorticotropic hormone	Lower at night; increased with stress
Plasma renin activity	Lower at night; higher standing than supine
Aldosterone	Lower at night
Insulin	Lower at night
Growth hormone	Higher in afternoon and evening
Acid phosphatase	Higher in afternoon and evening
Thyroxine	Increases with exercise
Prolactin	Higher with stress; higher levels at 4 and 8 AM and at 8 and 10 PM
Iron	Peaks early to late morning; decreases up to 30% during the day
Calcium	4% decrease supine

Age. Age of the patient has an effect on serum constituents. Young defines four age groups: newborn, childhood to puberty, adult, and elderly adult (Young, 2007). In the newborn, much of the Hb is Hb F, not Hb A, as seen in the adult. Bilirubin concentration rises after birth and peaks at about 5 days. In cases of hemolytic disease of the fetus and newborn (HDFN), bilirubin levels continue to rise. This often causes difficulty in distinguishing between physiologic jaundice and HDFN. Infants have a lower glucose level than adults because of their low glycogen reserve. With skeletal growth and muscle development, serum alkaline phosphatase and creatinine levels, respectively, also increase. The high uric acid level seen in a newborn decreases for the first 10 years of life and then increases, especially in boys, until the age of 16 (Young, 2007). Most serum constituents remain constant during adult life until the onset of menopause in women and middle age in men. Increases of about 2 mg/dL (0.05 mmol/L) per year in total cholesterol and 2 mg/dL (0.02 mmol/L) per year in triglycerides until midlife have been reported. The increase in cholesterol seen in postmenopausal women has been attributed to a decrease in estrogen levels. Uric acid levels peak in men in their 20s but do not peak in women until middle age. The elderly secrete less triiodothyronine, parathyroid hormone, aldosterone, and cortisol. After age 50, men experience a decrease in secretion rate and concentration of testosterone, and women have an increase in pituitary gonadotropins, especially follicle-stimulating hormone (FSH) (Young, 2007).

Sex. After puberty, men generally have higher alkaline phosphatase, aminotransferase, creatine kinase, and aldolase levels than women; this is due to the larger muscle mass of men. Women have lower levels of magnesium, calcium, albumin, Hb, serum iron, and ferritin. Menstrual blood loss contributes to the lower iron values (Young, 2007).

COMMON INTERFERENCES

In Vivo

Tobacco Smoking

Tobacco smokers have high blood carboxyhemoglobin levels, plasma catecholamines, and serum cortisol. Changes in these hormones often result in decreased numbers of eosinophils, while neutrophils, monocytes, and plasma free fatty acids increase. Chronic effects of smoking lead to increased Hb concentration, erythrocyte (red blood cell [RBC]) count, MCV, and leukocyte (white blood cell [WBC]) count. Increased plasma levels of lactate, insulin, epinephrine, and growth hormone and urinary secretion of 5-HIAA are also seen. Vitamin B_{12} levels may be substantially decreased and have been reported to be inversely proportional to serum thiocyanate levels. Smoking also affects the body's immune response. Immunoglobulin A (IgA), IgG, and IgM are lower in smokers, and IgE levels are higher. Decreased sperm counts and motility and increased abnormal morphology have been reported in male smokers when compared with nonsmokers (Young, 2007).

TABLE 3.3

Changes in Serum Concentration (or Activities) of Selected Constituents Due to Lysis of Erythrocytes (RBCs)

Constituent	Ratio of Concentration (or Activity) in RBC to Concentration (or Activity) in Serum	Percent Change of Concentration (or Activity) in Serum after Lysis of 1% RBC, Assuming a Hematocrit of 0.50
Lactate dehydrogenase	16 : 1	+272.0
Aspartate aminotransferase	4 : 1	+220.0
Potassium	23 : 1	+24.4
Alanine aminotransferase	6.7 : 1	+55.0
Glucose	0.82 : 1	–5.0
Inorganic phosphate	0.78 : 1	+9.1
Sodium	0.11 : 1	–1.0
Calcium	0.10 : 1	+2.9

Modified from Caraway WT, Kammeyer CW. Chemical interference by drug and other substances with clinical laboratory test procedures. *Clin Chem Acta* 1972; 41:395; and Laessig RH, Hassermer DJ, Paskay TA, et al. The effects of 0.1 and 1.0 percent erythrocytes and hemolysis on serum chemistry values. *Am J Clin Pathol* 1976; 66:639–644.

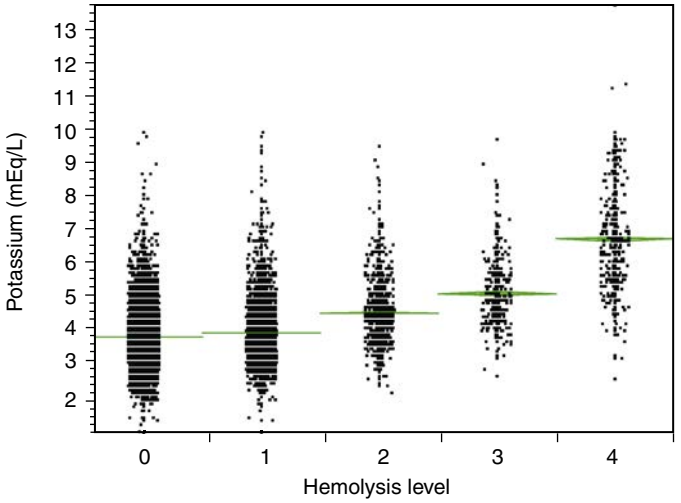

Figure 3.1 Relationship between hemolysis and potassium in 60,989 serum and plasma specimens grouped according to level of hemolysis. The mean values of potassium were 4.12, 4.23, 4.80, 5.36, and 6.93 mEq/L for levels of hemolysis from 0 through 4, respectively.

In Vitro

Collection-Associated Variables

On occasion, when there is a problem finding a vein for phlebotomy, the specimen may be hemolyzed as the result of sheer forces on the RBCs. Hemolysis can also be caused by using a needle that is too small, pulling a syringe plunger back too fast, expelling the blood vigorously into a tube, shaking or mixing the tubes vigorously, or performing blood collection before the alcohol has dried at the collection site. A recent emergency department study concluded that reduced hemolysis is associated with straight stick, antecubital location, shorter tourniquet time (less than 60 seconds) and larger gauge for IV draws (Phelan et al., 2018). Smaller volume and smaller vacuum blood collection tubes can also reduce hemolysis (Phelan et al., 2017). Hemolysis is present when the serum or plasma layer is pink. Hemolysis can falsely increase blood constituents such as potassium, magnesium, iron, LD, phosphorus, ammonium, and total protein (Garza & Becan-McBride, 2014). Table 3.3 shows changes in serum concentrations (or activities) of selected constituents caused by lysis of RBCs.

Because of the extremely important role of potassium in cardiac excitation, elevations due to hemolysis can be problematic, especially for emergency department patients who are at risk of hemolysis during frantic blood collection. The relationship between level of hemolysis and potassium (as determined on a Siemens ADVIA 1650 chemistry analyzer [Siemens Healthcare Diagnostics, Deerfield, IL]) in serum and plasma specimens is shown in Figure 3.1. Even with no hemolysis, the range of potassium concentrations can be broad in a combination of healthy and sick individuals. Low levels of hemolysis cause only minor elevations, but very strong hemolysis can raise the potassium level by 2 to 3 mEq/L into a critical range.

Another special case where pseudohyperkalemia can occur is in patients with extremely high blast counts in acute- or accelerated-phase leukemias. Those blasts can be fragile and may lyse during standard phlebotomy, releasing potassium. In contrast, specimens with very high WBC counts that are collected gently can show pseudohypokalemia when potassium is taken up by highly metabolically active leukemic cells along with glucose. Such specimens can be transported on ice to slow this enzymatically mediated uptake.

Normally, platelets release potassium during clotting; thus serum has a slightly higher value of potassium than plasma from the same individual. This difference is accentuated when the platelet count is extremely elevated.

To avoid problems with hemoconcentration and hemodilution, the patient should be seated in a supine position for 15 to 20 minutes before the blood is drawn (Young, 2007). Extended application of the tourniquet can cause hemoconcentration, which increases the concentrations of analytes and cellular components. When blood collection tubes that contain various anticoagulants/additives are used, it is important to follow the proper order of draw and to thoroughly mix an anticoagulated tube of blood after it has been filled. Failure to mix a tube containing an anticoagulant will result in failure to anticoagulate the entire blood specimen, and small clots may be formed. Erroneous cell counts can result. If a clot is present, it may also occlude or otherwise interfere with an automated analyzer. It is very important that the proper anticoagulant be used for the test ordered. Using the wrong anticoagulant will greatly affect the test results.

Icteric or lipemic serum provides additional challenges in laboratory analysis. When serum bilirubin approaches 430 mmol/L (25 mg/L), interference may be observed in assays for albumin (4-hydroxyazobenzene-2-carboxylic acid [HABA] procedure), cholesterol (using ferric chloride reagents), and total protein (Biuret procedure); the bromcresol green method is less susceptible to bilirubin interference (see Chapter 28). Artifactually induced values in some laboratory determinations result when triglyceride levels are elevated (turbidity) on the basis of absorbance of light of various lipid particles. Lipemia occurs when serum triglyceride levels exceed 4.6 mmol/L (400 mg/dL). Inhibition of assays for amylase, urate, urea, CK, bilirubin, and total protein may be observed (see Chapter 28). To correct for artifactual absorbance readings, "blanking" procedures (the blank contains serum but lacks a crucial element to complete the assay) or dual-wavelength methods may be used. A blanking process may not be effective in some cases of turbidity, and ultracentrifugation may be necessary to clear the serum or plasma of chylomicrons.

SPECIAL ISSUES THAT MAY IMPACT ANALYSIS

In addition to the preanalytic variables discussed earlier, there is a variety of special conditions and interferences that may impact sample analysis.

Immunoassays

Biotin

A variety of substances can interfere with immunoassays; this, in turn, can lead to the misinterpretation of a patient's results. For example, biotin supplements (which have increased in usage in recent years) can create analytic interference in biotin-based immunoassays (Holmes et al., 2017). Dietary supplementation with over-the-counter biotin has recently been recognized to interfere with a multitude of commercial immunoassays, causing either falsely low or falsely high results. The United States Food and Drug Administration (FDA) issued a warning on November 28, 2017, regarding clinically significant errors due to biotin interference. Examples include a falsely low troponin result leading to missed diagnosis of heart attack and hormone errors.

The reason for this interference is assay configuration in which molecular sandwich formation is either blocked or enhanced excessively by high concentrations of biotin. In one such competitive binding assay design, analyte (e.g., thyrotropin, thyroid-stimulating hormone [TSH]) in test blood sample binds to reagent capture antibody, thereby displacing reagent detector analyte (labelled with chemiluminescent molecule). The capture antibody is coupled to biotin (i.e., biotinylated), which, in turn, binds to

streptavidin coated on magnetic beads. After washing off unbound constituents, the amount of analyte from the sample is inversely proportional to the signal from bound detector molecule. If the patient sample has a very high level of free biotin, it will bind to the streptavidin and block binding of the capture antibody to the beads. The resulting signal erroneously looks as if the patient sample had a very high level of the analyte. Other assay configurations can result in erroneously low values.

Daily recommended allowance for biotin is 0.03 mg, but supplements sold for benefit of hair, skin, and nails may have up to 20 mg of biotin. For treatment of multiple sclerosis, up to 300 mg per day may be recommended. These extremely high doses of biotin can lead to concentrations up to 1200 ng/mL in blood, which is very likely to interfere with susceptible immunoassays. A study of various assays from the same manufacturer showed false reductions in high-sensitivity troponin T, TSH, and follicle-stimulating hormone but false elevations in triiodothyronine and vitamin D from biotin, indicating that each assay must be evaluated individually for its particular susceptibility to interference (Li et al., 2018). The prevalence of biotin supplementation was 7.7% in outpatients surveyed by questionnaire; by direct measurement, 7.4% of emergency department patients were found to have concentrations of biotin at or above levels known to interfere with one manufacturer's immunoassays (Katzman et al., 2018). One recommendation for patients taking biotin supplements is to stop taking them for 48 to 72 hours prior to scheduled blood tests to allow the water-soluble biotin to clear from their bodies (Charles et al., 2019). Additional laboratory measures include having backup methods known to be free of biotin interference and to communicate to clinicians through result comments that specific assays are susceptible to biotin interference (Gifford et al., 2019).

Monoclonal Antibodies

Endogenous substances, human antianimal species, or autoantibodies can interfere with the reaction between analyte and reagent antibodies. Manufacturers usually add blocking agents to immunoassay reagents to inhibit or neutralize the interference (Tate & Ward, 2004). Immunoassays use antibodies derived from a variety of species—for example, mouse antibody. Human antimouse antibodies (HAMAs), also referred to as heterophiles, can arise following antigenic stimulation from therapeutic mouse monoclonal antibodies that are administered to alter immune responses (e.g., anti–T cell antibody), to bind and remove toxic levels of drugs (e.g., digoxin), or to attack tumors. Some individuals with HAMAs have no history of therapeutic exposures but could conceivably have had incidental exposure to mouse proteins through contaminated food or other environmental sources. The effect of HAMAs in immunoassays can be to cross-link capture and signal antibodies in a sandwich that mimics true antigen (Klee, 2000). For example, an immunoassay for TSH that has separate antibodies against α and β subunits might yield an astonishingly high false-positive result in a euthyroid person with HAMA. In this case, the other thyroid function tests could be completely normal. The presence of HAMA can be confirmed by direct measurement (usually sent to a reference laboratory) and can also be inferred by adsorption of the HAMA onto special tubes coated with mouse antibodies, followed by repeat measurement of the analyte to look for reduction in signal strength in the treated specimen (Madry et al., 1997). Monoclonal antibodies with specific molecular targets are rapidly moving into clinical practice. One example is emicizumab, which has application as a coagulation factor VIII inhibitor bypass agent as it is a humanized bispecific monoclonal antibody that links activated coagulation factor IX and factor X, which replicates the action of factor VIII (Kitazawa & Shima, 2018). Its initial use is for hemophilia A patients who have developed resistance (i.e., inhibitor) to factor VIII infusion. Future use might extend to all hemophilia patients due to its effectiveness and relative ease of administration by subcutaneous injection. Unfortunately, the binding of emicizumab to factors IX and X also occurs in activated partial thromboplastin time (APTT)–based assays for factor VIII levels and for inhibitor assays even at very low levels of this monoclonal antibody. Because of this interference, the APTT cannot be used to monitor patients receiving emicizumab. One possible solution to this interference is to include in the assay for factor VIII specially prepared anti-idiotype monoclonal antibodies to neutralize any emicizumab present (Nogami et al., 2018).

Another instance of interference from therapeutic monoclonal antibody is daratumumab, which is approved as a treatment for multiple myeloma and is used increasingly for B-cell malignancies (Oostendorp et al., 2015). Although CD38 is present on plasma cells and B-cell proliferations, it is also present on RBCs. Accordingly, daratumumab shows panreactive interference with reagent panel RBCs and acts as an antibody to a high-prevalence antigen in blood bank compatibility procedures (Lancman et al., 2018). This interference can mask the presence of other significant antibodies. Procedures to work around daratumumab interference include use of dithiothreitol to break disulfide bonds in CD38 and inactivate that antigen (but it can also degrade other antigens). Other strategies to neutralize the anti-CD38 activity include use of soluble CD38 fragments and anti-idiotype antibody against the monoclonal antibody of daratumumab.

Specimen Matrix Effects

Common biochemical analytes—such as electrolytes, small molecules, enzymes, and so on—are generally distributed in the water phase of plasma or serum. Consequently, specimens with reduced water phase due to hyperproteinemia (e.g., from very high concentrations of a myeloma protein) or hyperlipidemia (e.g., high chylomicron content) can have reduced content of those solvent analytes even though other properties, such as ionic activities in those specimens, may be within normal physiologic range. This phenomenon is termed the *solvent exclusion effect*, referring to the exclusion of water and small molecules in the aqueous phase when more volume within a specimen is occupied by protein or lipid that excludes water. The content of small molecules per volume is the osmolarity (which is the measurement that can be erroneous), whereas the physiologically important aspect, such as ionic activities, is the osmolality. If excess lipids are the cause, they may be removed by ultracentrifugation. If interference is due to excess protein, an alternative mode of analysis, such as ion-selective electrode in undiluted specimen, can be employed to yield correct electrolyte activity (i.e., equivalent of osmolality).

Matrix effects from very high or very low concentrations of proteins and other constituents may be problematic when dealing with other body fluids, especially when the specimens are highly viscous or otherwise atypical. In those situations, it may be necessary to qualify results in the report to indicate the site of the body fluid and possible limitations in accuracy of measurement.

Molecular Diagnostics

Laboratory manipulations of nucleic acids are susceptible to interferences at various stages, including specimen collection and processing. Introduction of inhibitory substances and contamination with false-positive signals are among the significant interferences. Blood specimens for nucleic acid testing are generally collected into EDTA anticoagulant to inhibit enzymes that might break them down. Heparin is a poor choice for anticoagulant in this application because it can be coextracted with DNA and inhibits DNA polymerase in polymerase chain reactions (PCRs). Hemin from hemolysis in plasma or serum can also inhibit DNA polymerase. RNA is labile in blood or tissues; thus these specimens must be stored appropriately by rapid freezing in liquid nitrogen if the extraction will be delayed.

Extraction of nucleic acids from clinical specimens such as plasma (e.g., for viral load measurement), blood cells (e.g., for genetic testing), or tissues (e.g., for analyzing mutations in tumors) entails lysing cells and separating nucleic acids from proteins and lipids. Reagents for extraction include salts, proteases, and phenol-chloroform to denature the substances complexed with nucleic acids. This process must be optimized for specimen type to recover high-quality nucleic acids with good quantitative yield. Care must be taken to avoid contamination of specimens with target nucleic acids from other specimens or with amplified targets from specimens that have been analyzed previously in that vicinity. Accordingly, laboratories practicing nucleic acid amplification, especially PCR, should have separate preamplification, amplification, and postamplification areas with strict rules about personnel movements between them.

Effects of Drugs

Analytic methods that are based on oxidation–reduction reactions may be influenced positively or negatively by ingested substances such as ascorbic acid (vitamin C). This interference is observed in chemical testing of serum on automated analyzers (Meng et al., 2005) and can also occur in urine testing for glucose (positive interference for reducing substance method; negative interference with enzymatic method). In stool testing for occult blood, peroxidases from meats (myoglobin) or vegetables (horseradish) in the diet can yield a false-positive result with guaiac-based methods, as can topical iodine or chlorine used as a disinfectant.

Drugs can have unanticipated reactions with the reagents intended for specific chemical tests. The list of potential interfering drugs is extremely long, and some methods for a particular analyte may be strongly affected, whereas other methods may not be affected at all. A voluminous compendium of drug interactions has been developed by Dr. Donald S. Young (Young, 2007). In addition to assisting with recognition of potential interferences, this source can be used to evaluate a different method that is unaffected by a particular drug to confirm the accuracy of measurement in cases of suspected interference. These interferences are separated into

those whose effects are manifested directly in the assay in vitro and those that are due to drug actions in vivo, whereby physiologic functions are changed (e.g., prolonged prothrombin time [PT] with Coumadin, lower potassium in blood with some diuretics).

Dyes

Dyes such as methylene blue and pyridium have long been recognized to be cleared into urine and, thus, to have potential for interfering with colorimetric tests. Ascorbic acid has an additional action of reducing intermediates in urine dipstick reactions for constituents such as glucose, thereby causing falsely low values. Conversely, ascorbic acid contributes strongly to tests for reducing substances, which is also used for assessment of urine glucose concentrations as well as other metabolic abnormalities. A systematic review of 1368 FDA-approved single-ingredient drugs found that 134 drugs were known to interfere with at least one clinical laboratory test (Yao, 2017). The most likely drugs to interfere are antibacterial agents, psychotropic drugs, and contrast media; urine was the specimen most likely to be affected. Lists were provided for drugs interfering with urine and blood tests.

Ethanol

Ethanol has been found to cause substantial decreases in measurement of ALT (up to 50%) and LD (up to 70%) in serum pools to which various concentrations of ethanol were added as representative of commonly occurring blood alcohol levels (Gümüş, 2018). Direct bilirubin measurement was also decreased by about 25% and urea decreased by more than 10%. These findings were observed for a single manufacturer but could very well be a general phenomenon that has clinical significance due to the standard use of these laboratory tests in the evaluation of patients presenting for emergency care.

Transgender Reference Ranges and Hormone Therapy

Transgender persons receive hormone therapy with either estrogen or testosterone to affirm gender identity that is incongruent with their birth sex, thus, requiring monitoring for possible organ damage. Interpretation of laboratory testing in these persons does not necessarily follow reference ranges of the reassigned gender. For example, creatinine levels are normally higher in males due to larger muscle mass, which is not altered by estrogen treatment. Thus transgender females (born male) should not be evaluated according to female reference ranges (Roberts et al., 2014). Hematology reference ranges for persons receiving estrogen therapy or testosterone therapy in transgender persons were found clinically the same as for cisgender individuals (Greene et al., 2019). Because the response of other common laboratory tests to hormone therapy has not yet been well established with large numbers of patients, it may be necessary for laboratories to establish these ranges empirically among cohort patients who have achieved stable hormone therapy. Laboratory information systems currently utilize a binary choice for entry of gender: male or female. In order to fully account for hormonal therapy as well as birth sex, this binary choice might be expanded to include male-to-female and female-to-male options as well to apply most accurate reference ranges.

SPECIMEN COLLECTION

THE TEST ORDER

One of the most frequent preanalytic errors involves selecting the wrong laboratory test or panel of tests, leading to inappropriate interpretation of results (Bonini et al., 2002). Laboratory tests are usually ordered electronically (e.g., computer) or in writing (e.g., paper requisition used to transcribe orders into an information system). Online computer input is the most error-free means of requesting laboratory tests. Verbal requests are made in emergency situations and should be documented on a standard form; after the blood is drawn, an official laboratory request or computerized order should be placed. Physician direct order entry and result retrieval provide prompt and accurate patient care. Patient demographics include patient name, sex, age, date of birth (DOB), date of admission (for inpatients), date of test order, location, and physician. Computerized laboratory information systems (LISs), common in today's laboratories, are used to generate requisitions and specimen labels. Some systems also generate requisitions with the number of tubes and types of tubes required for collection.

Most laboratories facilitate test ordering by providing access to an electronic laboratory reference manual that lists available tests, types of specimens required, collection methods, color of blood collection tubes used, amounts of blood/body fluid required, turnaround time, reference intervals, test codes, costs, diagnostic information, and so forth. All specimens must be clearly labeled. Preprinted bar code labels applied after proper patient identification and after the specimen is collected avoid preanalytic transcription errors. Frequently, the laboratory receives a request for an "add-on test." This is an additional test requested on a previously collected sample. Problems are encountered when the specimen is not the proper type for the add-on requested test, the residual volume is not sufficient to perform the test, or storage conditions result in deterioration of the analyte (e.g., bicarbonate). This is usually due to the presence or absence of a particular anticoagulant or additive. All add-on requests must be documented.

Medicolegal concerns include proper identification of the patient, proper labeling of the specimen, patient consent issues, patient privacy issues, and chain of custody. Laboratories should have clearly written policies for these issues. In addition, policies should describe what to do when a patient refuses to have blood drawn, what to do if the patient was unable to be drawn, what to do if a patient is unavailable, and how to deal with a combative patient, as well as emergency measures for patients who become ill or faint during phlebotomy. The Health Insurance Portability and Accountability Act (HIPAA) ensures the security and privacy of health data and protects the confidentiality of all patient record information, including all laboratory data. Employees must be trained to comply with HIPAA.

TIME OF COLLECTION

Sometimes, samples have to be collected at a specific time. Failure to follow the planned time schedule can lead to erroneous results and misinterpretation of a patient's condition. The most common tests in this category are the ASAP and stat collections. *ASAP* means "as soon as possible," and *stat* is an American medical term meaning "immediately" (from the Latin *statim*). The exact definitions of these terms vary from one laboratory to another. Stat specimens are collected and analyzed immediately. They are given the highest priority and are usually ordered from the emergency department and critical care units (Strasinger & DiLorenzo, 2011). Timed specimens are ordered for a variety of reasons, usually to monitor changes in a patient's condition, to determine the level of a medication, or to measure how well a substance is metabolized. For example, a physician may want to monitor a cardiac marker to determine whether it is rising or decreasing. In therapeutic drug monitoring, trough and peak levels of a drug may be ordered. Trough specimens reflect the lowest level in the blood and are generally drawn 30 minutes before the drug is administered. The peak specimen is drawn shortly after the medication is given; the actual collection time varies by medication. Drug manufacturers specify the length of time that must pass between trough and peak collection times.

SPECIMEN ACCEPTABILITY AND IDENTIFICATION ISSUES

All specimens must be collected, labeled, transported, and processed according to established procedures that include sample volume, special handling needs, and container type. Failure to follow specific procedures can result in specimen rejection. Inappropriate specimen type, wrong preservative, hemolysis, lipemia, clots, and so on, are reasons for rejection. Specimen rejection is costly and time-consuming.

An incorrect sample collection may harm the patient, especially when the blood sample in the tube is mislabeled. The first goal of The Joint Commission 2015 Laboratory National Patient Safety Goals is to "identify patients correctly" (http://www.jointcommission.org/standards_information/npsgs.aspx). Patient wristbands that include bar codes or radiofrequency technology promote positive patient identification. A fully integrated, information technology–based preanalytical process has also been described (Barak & Jaschek, 2014). Misidentification of patients during sample collection for transfusion or at the time of transfusion can be a life-threatening medical error. The incidence of patient misidentification at the time of specimen collection has been reported to be approximately 1 in 1000, with 1 in 12,000 patients receiving a unit of blood that was not intended for that individual (Linden et al., 2000; Dzik et al., 2003). Trained phlebotomists appear to have fewer Wrong Blood in Tube (WBIT) errors (1.1 per 1000) than nondedicated staff (2.7 per 1000) (Bolton-Maggs et al., 2015). As a result, the College of American Pathologists requires laboratories to have a plan to reduce the risk of mistransfusion and suggests as options collecting two samples at separate phlebotomy events or utilizing an electronic identification verification system such as an electronic bar code reader for patient identification wristbands (CAP TRM.30575). Therefore it is essential to thoroughly train all medical staff in all aspects of patient identification, specimen collection, transportation, and processing. Box 3.1 lists various reasons for specimen rejection.

BLOOD COLLECTION OVERVIEW

Venipuncture is performed using a needle/adapter assembly attached to an evacuated glass/plastic test tube with a rubber/plastic stopper. Blood may also be collected in a syringe and transferred to the appropriate specimen container (evacuated tube system). A syringe may be helpful when procuring a specimen from the hand or ankle or from small children. In addition, patients with small or poor veins may experience collapse of veins with use of an evacuated tube system. AccuVein (AccuVein LLC, Huntington, N.Y.) is a handheld medical device that helps medical staff visualize veins before phlebotomy. The device emits infrared light and is held about 7 inches over the potential phlebotomy site. Hb in the blood absorbs infrared light and projects an image map of the veins onto the patient's overlying skin. The device is able to distinguish between Hb in the veins and surrounding tissue. This device assists the phlebotomist in determining the best site for needle placement, especially for challenging patients such as the elderly, the obese, burn victims, oncology patients, and patients with other chronic diseases requiring many diagnostic or therapeutic procedures (http://www.accuvein.com).

Blood collection tubes have color-coded stoppers that distinguish the presence of a specific anticoagulant or additive, how the tube is chemically cleaned (e.g., for lead or iron determinations), or if the tube does not contain any additives. Table 3.4 lists the most frequently used anticoagulants/additives based on color-coded tube stoppers. Tubes also come in various sizes for adult and pediatric patient populations. Draw volume is determined by the internal vacuum within the sealed tubes (e.g., 3.5, 4.0, 4.5, or 8.5 mL). By using anticoagulants, plasma (obtained by centrifugation) or whole blood can be analyzed. Plasma contains fibrinogen, which is missing from serum. Many laboratories have converted from glass to plastic collection tubes to minimize exposure to biohazardous material (e.g., blood) and broken glass; to lower biohazard waste disposal costs; and to comply with Occupational Safety and Health Administration (OSHA) guidelines mandating substitution. This change from glass to plastic has required a modification in the order of draw. Glass or plastic tubes with additives, including gel tubes, are drawn after the citrate tube (blue top) to avoid interference with coagulation measurements (Box 3.2). Glass or plastic serum tubes without a clot activator or gel separator may be drawn before the coagulation tubes are drawn, consistent with Clinical and Laboratory Standards Institute (CLSI) guidelines (CLSI GP41, 2017).

BOX 3.1

Reasons for Specimen Rejection

Hemolysis/lipemia
Clots present in an anticoagulated specimen
Nonfasting specimen when test requires fasting
Improper blood collection tube
Short draws, wrong volume
Improper transport conditions (ice for blood gases)
Discrepancies between requisition and specimen label
Unlabeled or mislabeled specimen
Contaminated specimen/leaking container

ANTICOAGULANTS AND ADDITIVES

EDTA is the anticoagulant of choice for hematology cell counts and cell morphology. It is available in lavender-top tubes as a liquid or is spray-dried in the dipotassium or tripotassium salt form (K_2EDTA in plastic, spray-dried and K_3EDTA in liquid form in glass tubes). K_3EDTA is a liquid and will dilute the sample about 1% to 2%. K_2EDTA is spray-dried on the walls of the tube and will not dilute the sample. Pink-top tubes also contain EDTA. The EDTA is spray-dried K_2EDTA. Pink tubes are used in immunohematology for ABO grouping, Rh typing, and antibody screening. These tubes have a special cross-match label for information required by the American Association of Blood Banks (AABB) and are approved by the FDA for blood bank collections. White-top tubes also contain EDTA and gel. They are used most often for molecular diagnostic testing of plasma.

For coagulation testing, a light blue–top tube containing 0.105 M or 0.129 M (3.2% or 3.8%, respectively) sodium citrate is commonly used because it preserves the labile coagulation factors. Coagulation tests require the correct ratio of blood and anticoagulant; thus containers should be adequately filled. An insufficient blood collection volume yields excess citrate in plasma and falsely elevated clotting times. This interference is also important in polycythemia, when the hematocrit is abnormally high and the volume of plasma (where citrate distributes) is

TABLE 3.4

Tube Color and Anticoagulant/Additive

Stopper Color	Anticoagulant/Additive	Specimen Type/Use	Mechanism of Action
Red (glass)	None	Serum/chemistry and serology	N/A
Red (plastic/Hemogard)	Clot activator	Serum/chemistry and serology	Silica clot activator
Lavender (glass)	K_3EDTA in liquid form	Whole blood/hematology	Chelates (binds) calcium
Lavender (plastic)	K_2EDTA/spray-dried	Whole blood/hematology	Chelates (binds) calcium
Pink	Spray-dried K_2EDTA	Whole blood/blood bank and molecular diagnostics	Chelates (binds) calcium
White	EDTA and gel	Plasma/molecular diagnostics	Chelates (binds) calcium
Light blue	Sodium citrate	Plasma/coagulation	Chelates (binds) calcium
Light blue	Thrombin and soybean trypsin inhibitor	Plasma/coagulation	Fibrin degradation products
Black	Sodium citrate	Plasma/sed rates—hematology	Chelates (binds) calcium
Light green/black	Lithium heparin and gel	Plasma/chemistry	Inhibits thrombin formation
Green	Sodium heparin, lithium heparin	Plasma/chemistry	Inhibits thrombin formation
Royal blue	Sodium heparin, K_2EDTA	Plasma/chemistry/toxicology	Heparin inhibits thrombin formation Na_2EDTA binds calcium
Gray	Sodium fluoride/potassium oxalate	Plasma/glucose testing	Inhibits glycolysis
Yellow	Sterile containing sodium polyanetholesulfonate	Serum/microbiology culture	Aids in bacterial recovery by inhibiting complement, phagocytes, and certain antibiotics
Yellow	Acid citrate dextrose	Plasma/blood bank, HLA phenotyping, and paternity testing	WBC preservative
Tan (glass)	Sodium heparin	Plasma/lead testing	Inhibits thrombin formation
Tan (plastic)	K_2EDTA	Plasma/lead testing	Chelates (binds) calcium
Yellow/gray and orange	Thrombin	Serum/chemistry	Clot activator
Red/gray and gold	Clot activator separation gel	Serum/chemistry	Silica clot activator

EDTA, Ethylenediaminetetraacetic acid; *HLA,* human leukocyte antigen; *K_2EDTA,* dipotassium form of EDTA; *K_3EDTA,* tripotassium form of EDTA; *N/A,* not applicable; *Na_2EDTA,* disodium EDTA; *WBC,* white blood cell.

BOX 3.2

Order of Draw: Evacuated Tube and Syringe

1. Blood-culture tubes (yellow)
2. Coagulation sodium citrate tube (blue stopper)
3. Serum tubes with or without clot activator or gel separator
4. Heparin tubes with or without gel (green stopper)
5. Ethylenediaminetetraacetic acid tubes (lavender stopper)
6. Glycolytic inhibitor tubes (gray stopper)

small. Thus, even in an apparently correctly filled tube, polycythemia can lead to falsely prolonged PT and PTT unless the amount of citrate anticoagulant in the tube is reduced proportionally to the decrease in plasma volume. A discard tube (i.e., a partially filled tube that is discarded prior to collecting the one used for testing) is normally needed only when the sample is drawn from a winged set or intravenous catheter. This is because the air space in these collection systems leads to underfilling the first tube (Favaloro et al., 2012). Black-top tubes also contain buffered sodium citrate and are generally used for Westergren sedimentation rates, as are lavender-top tubes. They differ from light blue–top tubes in that the ratio of blood to anticoagulant is 4:1 in the black-top tubes and 9:1 in the light blue–top tubes.

Heparin, a mucoitin polysulfuric acid, is an effective anticoagulant in small quantities without significant effect on many determinations. Heparin was originally isolated from liver cells by scientists looking for an anticoagulant that could work safely in humans. Heparin is available as lithium heparin (LiHep) and sodium heparin (NaHep) in green-top tubes. Heparin accelerates the action of antithrombin III, neutralizing thrombin and preventing the formation of fibrin. Heparin has an advantage over EDTA as an anticoagulant in that it does not affect levels of ions, such as calcium. However, heparin can interfere with some immunoassays. Heparin should not be used for coagulation or hematology testing. Heparinized plasma is preferred for potassium measurements to avoid an elevation due to the release of potassium from platelets as the blood clots (Garza & Becan-McBride, 2014). LiHep may be used for most chemistry tests except for lithium and folate levels; for lithium, a serum specimen can be used instead. NaHep cannot be used for assays measuring sodium levels, but it is recommended for trace elements, leads, and toxicology. NaHep is the injectable form used for anticoagulant therapy.

Gray-top tubes are generally used for glucose measurements because they contain a preservative or antiglycolytic agent, such as sodium fluoride, which prevents glycolysis for 3 days (Strasinger & DiLorenzo, 2011). In bacterial septicemia, fluoride inhibition of glycolysis is neither adequate nor effective in preserving glucose concentration. Red-top tubes have no additive; thus blood collected in these tubes clots.

Red-top tubes can be used for most chemistry, blood bank, and immunology assays. Integrated serum separator tubes are available for isolating serum from whole blood. During centrifugation, blood is forced into a thixotropic gel material located at the base of the tube. The gel undergoes a temporary change in viscosity during centrifugation and lodges between the packed cells and the top serum layer (Strasinger & DiLorenzo, 2011). Pediatric-sized tubes are also available. Advantages of serum separator tubes include (1) ease of use, (2) shorter processing time through clot activation, (3) higher serum yield, (4) minimal liberation of potentially hazardous aerosols, (5) only one centrifugation step, (6) use of single tube (same one as patient specimen), and (7) ease of a single label. A unique advantage is that centrifuged specimens can be transported without disturbing the separation. Some silica gel serum separation tubes may give rise to minute particles that can cause flow problems during analysis. Filtering the serum solves the problem.

A few specialized tubes exist. Red/gray- and gold-top tubes contain a clot activator and a separation gel. These tubes are referred to as *serum separator tubes* (SSTs) and are used most often for chemistry tests. Therapeutic drug monitoring specimens should not be collected in tubes that contain gel separators because some gels absorb certain drugs, causing a falsely lowered result. Significant decreases in phenytoin, phenobarbital, lidocaine, quinidine, and carbamazepine have been reported when stored in Vacutainer SST tubes (Becton, Dickinson and Company [BD], Franklin Lakes, N.J.), while no changes were noted in theophylline and salicylate levels. Storage in standard red-top Vacutainer collection tubes without barrier gels did not affect measured levels of these therapeutic drugs (Dasgupta et al., 1994). Studies indicate that this absorption is time dependent; therefore speed in processing minimizes absorption. Acrylic-based gels do not exhibit the absorption problems associated with silicone and polyester gels (Garza & Becan-McBride, 2014).

TABLE 3.5

Anticoagulant/Additive Effect on Blood Tests

Additive	Test	Effect
EDTA	Alkaline phosphatase	Inhibits
	Creatine kinase	Inhibits
	Leucine aminopeptidase	Inhibits
	Calcium and iron	Decrease
	PT and PTT	Increase
	Sodium and potassium	Increase
	Platelet aggregation	Prevents
Oxalate	Acid phosphatase	Inhibits
	Alkaline phosphatase	Inhibits
	Amylase	Inhibits
	LD	Inhibits
	Calcium	Decreases
	Sodium and potassium	Increase
	Cell morphology	Distorts
Citrate	ALT and AST	Inhibit
	Alkaline phosphatase	Inhibits
	Acid phosphatase	Stimulates
	Amylase	Decreases
	Calcium	Decreases
	Sodium and potassium	Increase
	Labile coagulation factors	Preserve
Heparin	Triiodothyronine	Increases
	Thyroxine	Increases
	PT and PTT	Increase
	Wright's stain	Causes blue background
	Lithium (LiHep tubes only)	Increases
	Sodium (NaHep tubes only)	Increases
Fluorides	Acid phosphatase	Decreases
	Alkaline phosphatase	Decreases
	Amylase	Decreases
	Creatine kinase	Decreases
	ALT and AST	Decrease
	Cell morphology	Distorts

ALT, Alanine aminotransferase; *AST,* aspartate aminotransferase; *EDTA,* ethylenediaminetetraacetic acid; *LD,* lactate dehydrogenase; *LiHep,* lithium heparin; *NaHep,* sodium heparin; *PT,* prothrombin time; *PTT,* partial thromboplastin time.

Tubes containing gels are not used in the blood bank or for immunologic testing because the gel may interfere with the immunologic reactions (Strasinger & DiLorenzo, 2011). Clotting time for tubes using gel separators is approximately 30 minutes. Tubes that have clot activators, such as thrombin, will clot in 5 minutes. Plain red-stoppered tubes with no additives take about 60 minutes to clot completely (Strasinger & DiLorenzo, 2011).

Anticoagulants may affect the transport of water between cell and plasma, thereby altering cell size and constituent plasma concentration. Oxalate anticoagulants may shrink red cells; thus blood anticoagulated with oxalate cannot be used to measure hematocrit. Combined ammonium/potassium oxalate does not have the same effect of shrinking cells.

EDTA, citrate, and oxalate chelate calcium, thereby lowering calcium levels. Fluoride, used for glucose determinations, prevents glycolysis by forming an ionic complex with Mg^{++}, thereby inhibiting the Mg^{++}-dependent enzyme, enolase (Young, 2007). Table 3.5 lists anticoagulants/additives and their effects on various blood tests.

Sample transfer between tubes. A serious error that is sometimes encountered in sample collection occurs when a portion of a sample in the EDTA-containing lavender-top tube for hematologic analysis is poured into a red-top tube for clinical chemistry analysis. EDTA is a potassium salt, artificially increasing the potassium concentration of the sample to values around 25 mEq/L, a value that would be incompatible with life. EDTA itself is an ion exchanger that exchanges potassium for calcium. Therefore calcium levels are greatly reduced in the red-top tube sample to values as low as 0. Very low calcium levels and very high potassium levels in red-top tube samples should be taken as a flag for an error due to EDTA contamination.

BLOOD COLLECTION DEVICES

The most common blood collection system uses a vacuum to pull blood into a container; it consists of a color-coded evacuated collection tube, a double-headed needle, and an adapter/holder. Small tubes are available for pediatric and geriatric collections. The blood collection holder accommodates various sizes (gauge) of blood collection needles. Needles vary from large (16 gauge) to small (23 gauge). Several types of holders have been designed to eject the needle after use. OSHA policies require that the adapters be discarded with the used needle (OSHA, 2002). Pediatric inserts are available for adapters and accommodate the smaller-diameter pediatric blood collection tubes. Also available are a variety of safety needles that cover the needle after use or retract the needle before it is discarded.

Winged infusion sets (butterfly needles) can be used when blood has to be collected from a very small vein. Butterfly needles come in 21, 23, and 25 gauge. These needles have plastic wings attached to the end of the needle that aid in insertion of the needle into the small vein. Tubing is attached to the back end of the needle, which terminates with an adapter for attachment to a syringe or evacuated collection holder. A retractable needle design has significantly reduced needlestick injuries (Hotaling, 2009).

Blood collected in a syringe can be transferred to an evacuated tube. Special syringe safety shield devices are available to avoid unnecessary contact with the blood sample. If blood requires anticoagulation, speed becomes an important factor—the blood must be transferred before clot formation begins. Once the blood has been transferred, the anticoagulated tube must be thoroughly mixed to avoid small clot formation.

Several additional pieces of phlebotomy equipment are necessary. A tourniquet, usually a flat latex strip or piece of tubing, is wrapped around the arm to occlude the vein before blood collection and is discarded after each phlebotomy. OSHA guidelines state that gloves should be worn when performing phlebotomy and should be changed between patients. Gloves are available in various sizes and are made of various materials to avoid latex sensitivity, as experienced by some individuals. Other supplies include gauze pads, alcohol or iodine wipes for disinfection of the puncture site, and a Band-Aid bandage (Johnson & Johnson, New Brunswick, N.J.) to prevent bleeding after completion of the phlebotomy.

BLOOD STORAGE AND PRESERVATION

During storage, the concentration of a blood constituent in the specimen may change as a result of various processes, including adsorption to glass or plastic tubes; protein denaturation; evaporation of volatile compounds, water movement into cells, resulting in hemoconcentration of serum and plasma, and continuing metabolic activities of leukocytes and erythrocytes. These changes occur, although to varying degrees, at ambient temperature and during refrigeration or freezing. Storage requirements vary widely by analyte.

Stability studies have shown that clinically significant analyte changes occur if serum or plasma remains in prolonged contact with blood cells. After separation from blood cells, analytes have the same stability in plasma and serum when stored under the same conditions. Glucose concentration in unseparated serum and plasma decreases rapidly in the first 24 hours and more slowly thereafter. This decrease is more pronounced in plasma. Two approaches have been used to minimize this effect. First, the serum or plasma may be rapidly separated from the red cells, or the specimen may be collected in a fluoride tube to inhibit glycolysis of the red blood cells, thereby stabilizing the glucose level during transport and storage. Fluoride has little effect on reducing glycolysis within the first hour of storage and may not reach complete inhibition until 4 hours of storage. One study has demonstrated a reduction in glucose concentration by 0.39 mmol/L in specimens collected in fluoride that are not immediately separated. The authors suggest that specimens collected in fluoride have a negative bias in blood glucose levels (Shi et al., 2009). Lactate levels increase, and a greater rise is seen in plasma than in serum. Chloride and total carbon dioxide (CO_2) show a steady decrease over 56 hours, with the degree of change more pronounced in plasma. K^+ is reported to be stable for up to 24 hours, after which a rapid increase takes place. The degree of change is slightly more pronounced in plasma. Unseparated serum and plasma yield clinically significant increases in total bilirubin, sodium, urea, nitrogen, albumin, calcium, magnesium, and total protein. These changes are attributed to movement of water into cells after 24 hours, resulting in hemoconcentration (Boyanton & Blick, 2002). Other studies found potassium, phosphorus, and glucose to be the analytes that were least stable in serum not removed from the clot within 30 minutes. Albumin, bicarbonate, chloride, C-peptide, HDL-cholesterol, iron, LDL-cholesterol, and total protein were found to be unstable after 6 hours when the serum was not separated from the clot (Zhang et al., 1998).

When serum and plasma are not removed from the cells, lipids (such as cholesterol) and some enzymes increase over time, with the change more pronounced in plasma than in serum. LD activity continuously increases over 56 hours. AST, ALT, and CK were found to be stable over 56 hours. GGT activity in plasma, with and without prolonged contact with cells, was found to be 27% lower than in serum at 0.5 hours; however, plasma GGT activity steadily increases with prolonged exposure to cells. Creatinine can increase by 110% in plasma and by 60% in serum after 48 to 56 hours (Boyanton & Blick, 2002).

Serum and plasma may yield significantly different results for an analyte. For example, when serum and EDTA plasma results for parathyroid hormone (PTH) are compared from specimens frozen within 30 minutes of collection, EDTA plasma results are significantly higher (>19%) than those obtained from serum (Omar et al., 2001). The effect of freeze–thaw cycles on constituent stability is an important consideration. In plasma or serum specimens, the ice crystals formed cause shear effects that are disruptive to molecular structure(s), particularly to large protein molecules. Slow freezing allows larger crystals to form, causing more serious degradative effects. Thus quick freezing is recommended for optimal stability.

IMPORTANCE OF POLICIES AND PROCEDURES

It is essential to establish institution-specific phlebotomy policies and procedures that include personnel standards with qualifications; dress code and evaluation procedures; safety protocols, including immunization recommendations; universal precautions; needlestick and sharps information; personal protective equipment; test order procedures; patient identification; confidentiality and preparation; documentation of problems encountered during blood collection; needlestick site selection and areas to be avoided (mastectomy side, edematous area, burned/scarred areas, etc.); anticoagulants required and tube color; order of draw; special requirements for patient isolation units; and specimen transport. The laboratory should have available all CDC, College of American Pathologists (CAP), CLSI, OSHA, and The Joint Commission (TJC) guidelines, as well as other government regulations pertaining to laboratory testing. All employees must be trained about safety procedures, and a written blood-borne pathogen exposure control plan must be available. See Chapter 1 for a more complete discussion of safety.

The OSHA Bloodborne Pathogens Standard concluded that the best practice for prevention of needlestick injury following phlebotomy is the use of a sharp with engineered sharps injury protection (SESIP) attached to the blood tube holder and immediate disposal of the entire unit after each patient's blood is drawn (OSHA, 2001). Information on exposure prevention can be found on the Exposure Prevention Information Network (EPINet), a database coordinated by the International Healthcare Worker Safety Center at the University of Virginia (https://internationalsafetycenter.org/). OSHA further mandates that employers make available closable, puncture-resistant, leak-proof sharps containers that are labeled and color-coded. The containers must have an opening that is large enough to accommodate disposal of the entire blood collection assembly (i.e., blood tube, holder, and needle). These containers must be easily accessible to employees in the immediate area of use and, if employees travel from one location to another (one patient room to another), they must be provided with a sharps container that is conveniently placed at each location/facility. Employers must maintain a sharps injury log to record percutaneous injuries from contaminated sharps while at the same time protecting the confidentiality of the injured employee.

BLOOD COLLECTION TECHNIQUES

Box 3.3 summarizes the technique for obtaining blood from a vein (CLSI GP41, 2017).

ARTERIAL PUNCTURE

Arterial punctures are technically more difficult to perform than venous punctures. Increased pressure in the arteries makes it more difficult to stop bleeding, with the undesired development of a hematoma. In order of preference, the radial, brachial, and femoral arteries can be selected.

Before blood is collected from the radial artery in the wrist, one should do a modified Allen test (Box 3.4) to determine whether the ulnar artery can provide collateral circulation to the hand after the radial artery puncture. The femoral artery is relatively large and easy to puncture, but one must be especially careful in older individuals because the femoral artery

BOX 3.3

Venous Puncture Technique

1. Verify that computer-printed labels match requisitions. Check patient identification band against labels and requisition forms. Ask the patient for his or her full name, address, identification number, and/or date of birth.
2. If a fasting specimen or a dietary restriction is required, confirm patient has fasted or eliminated foods from diet as ordered by physician.
3. Position the patient properly. Assemble equipment and supplies.
4. Apply a tourniquet and ask the patient to make a fist without vigorous hand pumping. Select a suitable vein for puncture.
5. Put on gloves with consideration of latex allergy for the patient.
6. Cleanse the venipuncture site with 70% isopropyl alcohol. Allow the area to dry.
7. Anchor the vein firmly but do not touch the alcohol-sterilized area with the gloved finger before inserting the needle.
8. Enter the skin with the needle at approximately a 30-degree angle or less to the arm, with the bevel of the needle up:
   a. Follow the geography of the vein with the needle.
   b. Insert the needle smoothly and fairly rapidly to minimize patient discomfort.
   c. If using a syringe, pull back on the barrel with a slow, even tension as blood flows into the syringe. Do not pull back too quickly to avoid hemolysis or collapsing the vein.
   d. If using an evacuated system, as soon as the needle is in the vein, ease the tube forward in the holder as far as it will go, firmly securing the needle holder in place. When the tube has filled, remove it by grasping the end of the tube and pulling gently to withdraw, and gently invert tubes containing additives.
9. Release the tourniquet when blood begins to flow. Never withdraw the needle without removing the tourniquet.
10. Withdraw the needle, and then apply pressure to the site. Apply adhesive bandage strip over a cotton ball or gauze to adequately stop bleeding and to avoid a hematoma.
11. Mix and invert tubes with anticoagulant; do not shake the tubes. Check condition of the patient. Dispose of contaminated material in designated containers (sharps container) using Universal Precautions.
12. Label the tubes before leaving patient's side with:
    a. patient's first and last name
    b. identification number
    c. date of collection
    d. time of collection
    e. identification of person collecting specimen
13. Deliver tubes of blood for testing to appropriate laboratory section or central receiving and processing area.

can bleed more than the radial or brachial artery. Because the bleeding site is hidden by bedcovers, it may not be noticed until bleeding is massive. The radial artery is more difficult to puncture, but complications occur less frequently. The major complications of arterial puncture include thrombosis, hemorrhage, and possible infection. When performed correctly, no significant complications are reported except for possible hematomas.

Unacceptable sites are those that are irritated, edematous, near a wound, or in an area of an arteriovenous (AV) shunt or fistula (McCall & Tankersley, 1993). Arterial spasm is a reflex constriction that restricts blood flow with possible severe consequences for circulation and tissue perfusion. Radial artery puncture can be painful and is associated with symptoms such as aching, throbbing, tenderness, sharp sensation, and cramping. At times, it may be impractical or impossible to obtain arterial blood from a patient for blood gas analysis. Under these circumstances, another source of blood can be used, with the recognition that arterial blood provides a more accurate result. Although venous blood is more readily obtained, it usually reflects the acid-base status of an extremity—not the body as a whole.

Arterial Puncture Technique

The artery to be punctured is identified by its pulsations, and the overlying skin is cleansed with 70% aqueous isopropanol solution followed by iodine. A nonanesthetized arterial puncture provides an accurate measurement of resting pH and partial pressure of carbon dioxide (pCO_2) in spite of possible theoretical error caused by patient hyperventilation resulting from the pain of the arterial puncture. The use of butterfly infusion sets is not recommended. Using 19-gauge versus 25-gauge needles does not vary the pCO_2 or the partial pressure of oxygen (pO_2) by more than 1 mm Hg. The amount of anticoagulant should be 0.05 mL liquid heparin (1000 IU/mL) for each milliliter of blood. Using too much heparin is probably the most common preanalytic error in blood gas measurement (Garza & Becan-McBride, 2014). Box 3.5 lists the procedure for arterial puncture (CLSI C46-A2, 2009).

BOX 3.4

Modified Allen Test

1. Have the patient make a fist and occlude both the ulnar (opposite the thumb side) and the radial arteries (closest to the thumb) by compressing with two fingers over each artery.
2. Have the patient open his or her fist, and observe whether the patient's palm has become bleached of blood.
3. Release the pressure on the ulnar artery (farthest from the thumb) only, and note whether blood return is present. The palm should become perfused with blood. Adequate perfusion is a positive test indicating that arterial blood may be drawn from the radial artery. Blood should not be taken if the test is negative. Serious consequences may occur if this procedure is not followed, which may result in loss of the hand or its function.

BOX 3.5

Arterial Puncture Procedure

1. Prepare the arterial blood gas syringe according to established procedures. The needle (18-20 gauge for brachial artery) should pierce the skin at an angle of approximately 45 to 60 degrees (90 degrees for femoral artery) in a slow and deliberate manner. Some degree of dorsiflexion of the wrist is necessary with the radial artery, for which a 23- to 25-gauge needle is used. The pulsations of blood into the syringe confirm that it will fill by arterial pressure alone.
2. After the required blood is collected, place dry gauze over the puncture site, and quickly withdraw the needle and the collection device.
3. Compress the puncture site quickly, expel air from the syringe, and activate the needle safety feature; discard into sharps container.
4. Mix specimen thoroughly by gently rotating or inverting the syringe to ensure anticoagulation.
5. Place in ice water (or other coolant that will maintain a temperature of 1°C to 5°C) to minimize leukocyte consumption of oxygen.
6. Continue compression with a sterile gauze pad for a minimum of 3 to 5 minutes (timed). Apply an adhesive bandage.

FINGER OR HEEL SKIN PUNCTURE

For routine assays requiring small amounts of blood, skin puncture is a simple method by which to collect blood samples in pediatric patients. In the neonate, skin puncture of the heel is the preferred site to collect a blood sample; in older children, the finger is the preferred site. The large amount of blood required for repeated venipunctures may cause iatrogenic anemia, especially in premature infants. Venipuncture of deep veins in pediatric patients may rarely cause cardiac arrest, hemorrhage, venous thrombosis, reflex arteriospasm followed by gangrene of an extremity, damage to organs or tissues accidentally punctured, infection, and injury caused by restraining an infant or child during collection. Accessible veins in sick infants must be reserved exclusively for parenteral therapy. Skin puncture is useful in adults with extreme obesity, severe burns, and thrombotic tendencies, with point-of-care testing or with patients performing tests at home (blood glucose). Skin puncture is often preferred in geriatric patients because the skin is thinner and less elastic; thus a hematoma is more likely to occur from a venipuncture.

In newborns, skin puncture of the heel is frequently used to collect a sample for newborn screening tests for inherited metabolic disorders. A deep heel prick is made at the distal edge of the calcaneal protuberance following a 5- to 10-minute exposure period to prewarmed water. The best method for blood gas collection in the newborn remains the indwelling umbilical artery catheter. Box 3.6 lists the steps for a skin puncture (CLSI GP42, 2008).

Central Venous Access Devices

Central venous access devices (CVADs) provide ready access to the patient's circulation, eliminating multiple phlebotomies, and are especially useful in critical care and surgical situations. Indwelling catheters are surgically inserted into the cephalic vein or into the internal jugular, subclavian, or femoral vein and can be used to draw blood, administer drugs or blood products, and provide total parenteral nutrition. Continuous, real-time,

BOX 3.6

Skin Puncture Technique

1. Select an appropriate puncture site.
   a. For infants younger than 12 months old, this is usually the lateral or medial plantar heel surface.
   b. For infants older than 12 months, children, and adults, the palmar surface of the last digit of the second, third, or fourth finger may be used.
   c. The thumb and fifth finger must not be used, and the site of puncture must not be edematous or a previous puncture site because of accumulated tissue fluid.
2. Warm the puncture site with a warm, moist towel no hotter than 42° C; this increases the blood flow through arterioles and capillaries and results in arterial-enriched blood.
3. Cleanse the puncture site with 70% aqueous isopropanol solution. Allow the area to dry. Do not touch the swabbed area with any nonsterile object.
4. Make the puncture with a sterile lancet or other skin-puncturing device, using a single deliberate motion nearly perpendicular to the skin surface. For a heel puncture, hold the heel with the forefinger at the arch and the thumb proximal to the puncture site at the ankle. If using a lancet, the blade should not be longer than 2 mm to avoid injury to the calcaneus (heel bone).
5. Discard the first drop of blood by wiping it away with a sterile pad. Regulate further blood flow by gentle thumb pressure. Do not milk the site, as this may cause hemolysis and introduce excess tissue fluid.
6. Collect the specimen in a suitable container by capillary action. Closed systems are available for collection of nonanticoagulated blood and with additives for whole blood analysis. Open-ended, narrow-bore disposable glass micropipettes are most often used up to volumes of 200 μL. Both heparinized and nonheparinized micropipettes are available. Use the appropriate anticoagulant for the test ordered. Mix the specimen as necessary.
7. Apply pressure and dispose of the puncture device.
8. Label the specimen container with date and time of collection and patient demographics.
9. Indicate in the report that test results are from skin puncture.

intraarterial monitoring of blood gases and acid-base status has been accomplished with fiberoptic channels containing fluorescent and absorbent chemical analytes (Smith et al., 1992).

Central Venous Access Collection Technique

Blood specimens drawn from catheters may be contaminated with whatever was administered or infused via the catheter. The solution (usually heparin) used to maintain patency of the vein must be cleared before blood for analysis is collected. Sufficient blood (minimum of 2–5 mL) must be withdrawn to clear the line so that laboratory data are reliable. Therefore specialized training is necessary before a catheter line is used to collect blood specimens. To obtain a blood specimen from the indwelling catheter, 5 mL of intravenous fluid is first drawn and discarded. In a separate syringe, the amount of blood required for the requested laboratory procedure(s) is then drawn. Strict aseptic technique must be followed to avoid site and/or catheter contamination. Coagulation measurements—such as PT, APTT, and thrombin time (TT)—are extremely sensitive to heparin interference; thus even larger volumes of presample blood must be withdrawn before laboratory results are acceptable for these tests. The appropriate volume to be discarded should be established by each laboratory.

The laboratory is sometimes asked to perform blood culture studies on blood drawn from indwelling catheters. Because the indwelling catheters are in place for a few days, this procedure is not recommended because organisms that grow on the walls of the catheter can contaminate the blood specimen. Lines, such as central venous pressure (CVP) lines, are specifically inserted and used for immediate blood product infusion and are less likely to become contaminated. Determination of catheter contamination requires special handling and careful analysis of multiple samples from the catheter and peripheral blood. Box 3.7 lists the order of draw from catheter lines.

BOX 3.7

Order of Draw from Catheter Lines

1. Draw 3 to 5 mL in a syringe and discard.
2. Blood for blood culture
3. Blood for anticoagulated tubes (lavender, green, light blue, etc.)
4. Blood for clot tubes (red, SST, etc.)

SST, Serum separator tube.

URINE AND OTHER BODY FLUIDS COLLECTION

URINE

Collection and preservation of urine for analytic testing must follow a carefully prescribed procedure to ensure valid results. Laboratory testing of urine generally falls into three categories: chemical, bacteriologic, and microscopic examinations. Several kinds of collection are used for urine specimens: random, clean catch, timed, 24 hour, and catheterized. Random specimens may be collected at any time, but a first-morning-voided aliquot is optimal for constituent concentration, because it is usually the most concentrated and has a lower pH caused by decreased respiration during sleep. Random urine specimens should be collected in a chemically clean receptacle, either glass or plastic. A clean-catch midstream specimen is most desirable for bacteriologic examinations. Proper collection of a clean-catch specimen requires that the patient first clean the external genitalia with an antiseptic wipe; the patient next begins urination, stops midstream, and discards this first portion of urine, then collects the remaining urine in a sterile container. The vessel is tightly sealed, is labeled with the patient's name and date of collection, and is submitted for analysis. A urine transfer straw kit for midstream specimens (BD Vacutainer) can be used to remove an aliquot from the sterile collection container, which then can be transported to the laboratory. The system consists of an adapter that attaches to a yellow evacuated sterile tube. The vacuum draws the urine into the sterile tube. The adapter assembly must be treated like a needle assembly system and be discarded into a biohazard container. A similar product is available for cultures; it uses a sterile gray-top tube containing 6.7 mg/L of boric acid and 3.335 mg/L of sodium formate, along with the adapter device described previously (BD Vacutainer).

Timed specimens are obtained at designated intervals, starting from "time zero." Collection time is noted on each subsequent container. Urine specimens for a 24-hour total volume collection are most difficult to obtain and require patient cooperation. Incomplete collection is the most frequent problem. In some instances, too much sample is collected. In-hospital collection is usually supervised by nurses and generally is more reliable than outpatient collection. Pediatric collections require special attention to avoid stool contamination. One can avoid problems in collecting 24-hour specimens by giving patients complete written and verbal instructions with a warning that the test can be invalidated by incorrect collection technique. The preferred container is unbreakable, measures 4 L (approximately), is plastic, and is chemically clean, with the correct preservative already added. One should remind the patient to discard the first morning specimen, record the time, and collect every subsequent voiding for the next 24 hours. An easy approach is to instruct the patient to start with an empty bladder and to end with an empty bladder. Overcollection occurs if the first morning specimen is included in this routine. The total volume collected is measured and recorded on the request form, the entire 24-hour specimen is thoroughly mixed, and a 40-mL aliquot is submitted for analysis.

It is difficult to determine whether a collection is complete. If results appear clinically invalid, this is cause for suspicion. Because creatinine excretion is based on muscle mass, and because a patient's muscle mass is relatively constant, creatinine excretion is also reasonably constant. Therefore one can measure creatinine on several 24-hour collections to assess the completeness of the specimen and keep this as part of the patient's record. One- and 2-hour timed collection specimens may suffice in some instances, depending on the analyte being measured. Urobilinogen is subject to diurnal variation, with the highest levels reached in the afternoon. Commonly, urine is collected from 2 to 4 PM, when a quantification of urobilinogen is requested.

Special Urine Collection Techniques

Catheterization of the urethra and bladder may cause infection but is necessary in some patients (e.g., for urine collection when patients are unable to void or control micturition). Ureteral catheters can also be inserted via a cystoscope into the ureter. Bladder urine is collected first, followed by a bladder washing. Ureteral urine specimens are useful in differentiating bladder from kidney infection or for differential ureteral analysis, and may be obtained separately from each kidney pelvis (labeled left and right). First morning urine is optimal for cytologic examination.

TABLE 3.6
Changes in Urine with Delayed Testing

Result	Reason
Changes in color	Breakdown or alteration of chromogen or other urine constituent (e.g., hemoglobin, melanin, homogentisic acid, porphyrins)
Changes in odor	Bacterial growth, decomposition
Increased turbidity	Increased bacteria, crystal formation, precipitation of amorphous material
Falsely low pH	Glucose converted to acids and alcohols by bacteria producing ammonia; carbon dioxide (CO_2) lost
Falsely elevated pH	Breakdown of urea by bacteria, forming ammonia
False-negative glucose	Utilization by bacteria (glycolysis)
False-negative ketone	Volatilization of acetone; breakdown of acetoacetate by bacteria
False-negative bilirubin	Destroyed by light; oxidation to biliverdin
False-negative urobilinogen	Destroyed by light
False-positive nitrite	Nitrite produced by bacteria after specimen is voided
False-negative nitrite	Nitrite converts to nitrogen and evaporates.
Increased bacteriuria	Bacteria multiply in specimen before analysis.
Disintegration of cells/casts	Unstable environment, especially in alkaline urine, hypotonic urine, or both

TABLE 3.7
24-Hour Urine Collection Preservatives

Preservative	Tests
None (refrigerate)	Amino acids, amylase, calcium, citrate, chloride, copper, creatinine, delta ALA, glucose, 5-HIAA, heavy metals (arsenic, lead, mercury), histamine, immunoelectrophoresis, lysozyme, magnesium, methylmalonic acid, microalbumin, mucopolysaccharides, phosphorus, porphobilinogen, porphyrins, potassium, protein, protein electrophoresis, sodium, urea, uric acid, xylose tolerance
10 g boric acid	Aldosterone, cortisol
10 mL 6N HCl	Catecholamines, cystine, homovanillic acid, hydroxyproline, metanephrines, oxalate, VMA
0.5 g sodium fluoride	Glucose
If processing delayed longer than 24 hours: equal amounts of 50% alcohol, Saccomanno's fixative, and SurePath or Preserve CT	Cytologic examination

ALA, Alanine aminotransferase; *5-HIAA,* 5-hydroxyindoleacetic acid; *VMA,* vanillylmandelic acid.

Urine Storage and Preservation

Preservation of a urine specimen is essential to maintain its integrity. Unpreserved urine specimens are subject both to microbiologic decomposition and to inherent chemical changes. Table 3.6 lists common changes that occur as urine decomposes. To prevent growth of microbes, the specimen should be refrigerated promptly after collection and, when necessary, should contain the indicated chemical preservative. For some determinations, the addition of a chemical preservative may be best to maintain analytes when performing 24-hour urine collections. If a preservative is added to the empty collection bottle, particularly if acid preservatives are used, a warning label is placed on the bottle. The concentrated acid adds a risk of potential chemical burns; the patient should be warned about this potential danger, and the container labeled accordingly. In this scenario, the clinician must assess the patient's risk of exposure to the preservative. Therefore refrigeration may be more appropriate, and the preservative may be added upon submission to the laboratory. Light-sensitive compounds, such as bilirubin, are protected in amber plastic bottles. Precipitation of calcium and phosphates occurs unless the urine is acidified adequately before analysis.

It is particularly important to use freshly voided and concentrated urine to identify casts and red and white blood cells, as these undergo decomposition upon storage at room temperature or with decreased concentration (<1.015 specific gravity). They disappear rapidly in hypotonic and alkaline urine. Bilirubin and urobilinogen decrease, especially after exposure to light. Glucose and ketones may be consumed, while bacterial contamination and loss of CO_2 lead to increase of pH, formation of turbidity with precipitates, and change in color. Ideally, specimens should be delivered to the laboratory and analyzed within 1 hour of collection.

Urine may be frozen in aliquots to be assayed at a later date for chemical analysis only. When repeat testing is expected, the specimen should be stored in multiple aliquots to circumvent specimen degradation as a result of repeated freeze–thawing of a single specimen. Preservatives may also be added, depending on the substance to be tested. Sodium fluoride can be added to 24-hour urine for glucose determinations to inhibit bacterial growth and cell glycolysis but not growth of yeast. About 0.5 g of sodium fluoride is added to a 3- to 4-L container. Sodium fluoride may inhibit reagent (enzyme-embedded) glucose strip tests. Tablets containing formaldehyde, mercury, and benzoate (95-mg tablet/20 mL urine) have also been used; however, these preservatives elevate specific gravity (0.002/1 tablet/20 mL). Boric acid in a concentration of 1 g/dL preserves urine elements such as estriol and estrogen for up to 7 days. Boric acid maintains the pH at about 6.0 and preserves protein and formed elements well without interfering with routine testing, except for pH. Boric acid is a bacteriostatic preservative, not a bactericidal, and it does not inhibit the growth of yeasts. Boric acid has been reported to interfere with drug and hormone analysis (Strasinger & DiLorenzo, 2001). For catecholamines, vanillylmandelic acid (VMA), or 5-HIAA collections, 10 mL of 6N HCl is added to a 3- to 4-L container. The HCl establishes a pH of approximately less than 3.0, which is good for chemical testing. However, the low pH destroys formed elements and enhances uric acid precipitation. Table 3.7 lists preservatives commonly used for 24-hour urine specimens. The CLSI-approved guidelines for urinalysis and collection, transportation, and preservation of urine specimens provide useful information on various preservatives recommended for 24-hour urine collections (CLSI, 2009).

OTHER BODY FLUIDS

Cerebrospinal Fluid

Lumbar punctures (LPs) are performed to collect cerebrospinal fluid (CSF) for laboratory evaluation to establish a diagnosis of infection (bacterial, fungal, mycobacterial, or amebic meningitis), malignancy, subarachnoid hemorrhage, multiple sclerosis, or demyelinating disorders. The most common site for lumbar puncture is between the third and fourth lumbar vertebrae or between the fourth and fifth lumbar vertebrae. A serious complication of an LP is cerebellar tonsillar herniation in patients with elevated intracranial pressure; LP should be avoided unless CSF findings are expected to improve treatment or outcome. Patients with spinal cord tumors with paresis may progress to paralysis following LP. Patients with sepsis in the lumbar region (skin infection, cellulitis, or epidural abscess) should not have an LP performed to avoid introduction of infection. Other complications of LP include asphyxiation in infants due to hyperextending the head forward, thus occluding the trachea, paresthesia, headache, and, rarely, hematomas. CSF is also collected by cisternal puncture. A needle is inserted into the cisternal subarachnoidea, or small space, that serves as a reservoir for CSF between the atlas and occipital bone in the back of the head or by lateral cervical puncture (Kjeldsberg & Knight, 1993). Specimens can also be collected from ventricular cannulas (shunts) when present.

Before CSF is collected, the pressure should be between 90 and 180 mm Hg; this is measured by allowing fluid to rise in a sterile, graduated manometer. Holding one's breath, abdominal compression, congestive heart failure, inflammation of the meninges, obstruction of intracranial venous sinuses, mass lesions, or cerebral edema may cause the pressure to be elevated (>180 mm Hg). When pressure is normal, 20 mL of specimen may be removed. On closing, the pressure should be between 10 and 30 mm Hg. A marked decrease in pressure following this procedure suggests cerebellar herniation or spinal cord compression; thus no additional CSF should be collected. Patients with partial or complete spinal block may have low pressure (<80 mm Hg), falling to zero after removal of only 1 mL. Again, no additional fluid should be removed. No more than 2 mL can be removed when the pressure is greater than 200 mm Hg. Three aliquots

are generally collected in separate sterile tubes labeled appropriately with name, date, and sequential tube collection number and distributed. Hospital policies differ as to which tube is distributed to which laboratory for analysis. It is generally recommended that Tube #1 goes to chemistry for glucose and protein analysis or to immunology/serology; Tube #2 goes to microbiology for culture and Gram stain; and Tube #3 goes to hematology for cell counts. Tube #3 is the least likely to be contaminated by a bloody tap at collection. Expansion of tests ordered on CSF to include molecular diagnostic procedures has placed even greater demand on proper utilization of the entire volume of CSF collected, with special efforts to conserve specimens in each laboratory section so that additional tests may be performed.

Synovial Fluid

Synovial fluid found in the joint cavities is an ultrafiltrate of plasma that is passed through fenestrations of the subsynovial capillary endothelium into the synovial cavity. Once in the cavity, it is combined with hyaluronic acid, a glycosaminoglycan secreted by the synovial lining cells. Synovial fluid differs from the other serous fluids in that it contains hyaluronic acid (mucin) and may contain crystals. Synovial fluid is collected by arthrocentesis, an aspiration of the joint using a syringe, moistened with an anticoagulant, usually 25 units of sodium heparin per mL of synovial fluid. Oxalate, powdered EDTA, and lithium heparin should not be used because they can produce crystalline structures similar to monosodium urate (MSU) crystals. Once removed, the synovial fluid is usually transferred to three tubes—one sterile, one containing EDTA or heparin, and one red-top tube; 5 to 10 mL of fluid is added to each. The sterile tube is sent to microbiology, the anticoagulated tube is sent to hematology, and the red-top tube, after centrifugation, is used for chemical analysis. Some hospitals transfer synovial fluid to aerobic and anaerobic blood culture bottles for microbiologic culture.

Pleural Fluid, Pericardial Fluid, and Peritoneal Fluid

Pleural fluid is an ultrafiltrate of the blood plasma. It is formed continuously in the pleural cavity. This cavity, normally containing 1 to 10 mL of fluid, is formed by the parietal pleura lining the chest wall and the visceral pleura covering the lung. Each lung is enveloped by this double membrane of contiguous mesothelial layers. Pleural fluid acts as a natural lubricant for contraction and expansion of the lungs during respiration. It is reabsorbed by the lymphatics and the venules in the pleura (Miller, 1999).

Thoracentesis is a surgical procedure to drain fluid (effusions) from the thoracic cavity and is helpful in diagnosing inflammation or neoplastic disease in the lung or pleura. *Pericardiocentesis* and *peritoneocentesis* refer to the collection of fluid from the pericardium (effusion) and the peritoneal cavities (ascites), respectively. These cavities normally contain less than 50 mL of fluid.

The patient, sitting in an upright position with arms and head extended on an overbed table, is prepared with a local anesthetic after appropriate cleansing of the site. A 50-mL syringe is fitted with a stopcock and rubber tubing to assist in the aseptic collection process. Specimens are obtained for chemical, microbiologic, and cytologic examination and are transferred to collection tubes with appropriate additive(s). For most chemical evaluations, no additive is used, and the specimen is allowed to clot. Bacteriologic and cytologic specimens may be collected in EDTA or sterile sodium heparin (without preservatives). Special studies for *Mycobacterium*, anaerobic bacteria, or viruses may require special handling procedures. Special handling procedures must be reviewed before collection is begun.

SPECIMEN TRANSPORT

Transport of blood, urine, body fluids, and tissue specimens from the collection site to the laboratory is an important component of processing. For blood samples, it accounts for approximately one third of the total turnaround time (TAT) (Howanitz et al., 1992). Excessive agitation of blood specimens must be avoided to minimize hemolysis. Specimens should be protected from direct exposure to light, which causes breakdown of certain analytes (e.g., bilirubin). For analysis of unstable constituents such as ammonia, plasma renin activity, and acid phosphatase, specimens must be kept at 4° C immediately after collection and transported on ice. Routine urine is collected in a sterile, disposable, 200-mL plastic container. Pediatric urine collectors are flexible polyethylene bags, which may be sealed for transportation. All laboratory specimens must be transported in a safe and convenient manner to prevent biohazard exposure or contamination of the specimen. Broken or leaking specimens are a biohazard to those who may come in contact with them and require collection of a new specimen. This can delay treatment of the patient and add to the cost.

The stability of the constituents must be determined before specimens are transported. The laboratory usually provides this information along with instructions for specimen preparation and shipping. Polystyrene or other high-impact plastic-type containers are commonly used. Specimens requiring refrigeration must be maintained at between 2° C and 10° C and can be appropriately carried in an insulated container. Large-volume urine specimens should be collected in a leak-proof, 3- to 4-L container. Stool specimens are transported in a cardboard container and placed in a polyethylene bag. To mail a specimen in the frozen state, solid carbon dioxide (dry ice) may be packed in a polystyrene container with the specimen, which can be kept frozen at temperatures as low as –70° C.

The OSHA Bloodborne Pathogens Standard (OSHA: 1910.1030) requires specimens of blood or other potentially infectious materials (OPIM) to be placed in a container that prevents leakage during collection, handling, processing, storage, transport, and/or shipping. This container must be labeled or color-coded according to specific standards (OSHA: 1910.1030[g][1][i]). Furthermore, according to the standard, if contamination of the outside of the primary container occurs or if the specimen could puncture the primary container, the primary container must be placed in a secondary container that is puncture-resistant in addition to having the previous characteristics (OSHA: 1910.1030[d][2][xiii]).

Labeling is required on all containers used to store, transport, ship, or dispose of blood or other potentially infectious materials, except as noted in the OSHA standard. For example, if individual containers of blood or OPIM are placed in a larger container during storage, transport, shipment, or disposal, and that larger container is labeled with the OSHA "BIOHAZARD" label or is color-coded, the individual containers are exempt from the labeling requirement. OSHA accepts the "INFECTIOUS SUBSTANCE" label of the Department of Transportation (DOT) in lieu of the "BIOHAZARD" label on packages where the DOT requires its label on shipped containers but requires the "BIOHAZARD" label where OSHA regulates a material but DOT does not. If the DOT-required label is the only label used on the outside of the transport container, the OSHA-mandated label must be applied to any internal containers containing blood or OPIM. The accepted "BIOHAZARD" label is fluorescent orange.

For local, onsite transport, pneumatic tube systems provide a rapid, efficient, and cost-effective way of transporting laboratory specimens to a specific location. For laboratory use, blood specimens are placed in a carrier with liners to prevent leakage and padding to ensure that specimen containers remain intact. The advantages of a pneumatic tube system are improved TAT; reliability; minimal training; low maintenance; availability 24 hours/day, 7 days/week; and improved staff utilization. Studies have shown that most routine chemical and hematologic evaluations, red cell packs, coagulation tests, and LD values, are not substantially affected by rapid transport (Hardin et al., 1990; Keshgegian & Bull, 1992) and that pneumatic tube system transport does not impact clinical interpretations of blood gases (Carabini et al., 2016).

SPECIMEN PROCESSING

Processing of specimens includes three distinct phases: precentrifugation, centrifugation, and postcentrifugation. Continuing appraisal of all specimen handling activities is an important preanalytic component of total quality control. Appropriate guidelines must be established and adhered to by laboratory personnel in each phase of specimen handling to ensure the generation of reliable and medically meaningful measurement and examination results.

PRECENTRIFUGATION PHASE

Ideally, all measurements should be performed within 45 minutes to 1 hour after collection. If this is not practical, the specimen should be processed to a point at which it can be properly stored to preclude alteration of constituents to be measured. With the exception of blood gases and ammonia determinations, plasma or serum is preferred for most biochemical determinations. In clinical chemistry, serum and plasma are interchangeable except for a few measurements. Serum is required for protein electrophoresis and immunofixation assays, just as plasma is necessary for fibrinogen and other coagulation measurements. Serum is most commonly the specimen of choice, owing to its simplicity in collection and handling. Additionally, interference from anticoagulants is obviated. Plasma may be used in medical emergencies because samples do not have to clot before centrifugation. Usually, a greater volume of plasma than serum is obtained from a given volume of whole blood owing to the clot formation process. Hospitalized patients are likely to be receiving heparin (especially under critical care), which can delay clotting in blood collection tubes even with

activators and lead to fibrin strands that can clog up aspiration probes on instrumentation. Accordingly, it is good practice to collect blood from hospitalized patients into tubes with heparin anticoagulant to obtain plasma for chemical tests.

Blood should be stoppered in the original container until ready for separation. For plasma preparation, centrifuge blood within 1 hour after collection, for 10 minutes at a relative centrifugal force (RCF) of 850 to 1000× gravity (g), keeping the container stoppered to prevent evaporation of plasma or serum water. Adequate time for clotting must be allowed to prevent latent fibrin formation, which may cause undesirable clogging of automated chemistry analyzers. Loosening the clot by "trimming" or "ringing" the tube may cause some hemolysis and should be avoided. When glass tubes are used, they should be centrifuged in an aerosol-contained vessel. Serum or plasma must be stored at 4° C to 6° C if analysis is to be delayed for longer than 4 hours. One study suggests that this may not be necessary (Melanson et al., 2004). Many laboratories store samples for 7 days in case a test is added.

CENTRIFUGATION PHASE

A centrifuge uses centrifugal force to separate phases of suspensions by different densities. It is most frequently used in processing blood to derive plasma or serum fractions. Urine and other body fluids may be centrifuged to concentrate particulate matter as sediment to be examined and to minimize interference with other determinations from the same material. Conditions for centrifugation should specify both the time and the centrifugal force. In selecting a centrifuge, one should look for the highest possible centrifugal force and not the rotational speed. The RCF in g units—that is, multiples of the gravitational force—may be calculated by using the following formula:

$$\mathrm{RCF} = 1.118 \times 10^{-5} \times r \times (\mathrm{rpm})^2$$

where 1.118×10^{-5} is a constant; *r* is the radius, expressed in centimeters, between the axis of rotation and the center of the centrifuge tube; and *rpm* is the speed in revolutions per minute. The RCF can also be obtained from a nomogram that gives the RCF without the need to calculate it from the previous formula.

Several principles must be observed to avoid damage to the centrifuge, or the specimen, and danger to personnel. Tubes, carriers, or shields of equal weight, shape, and size should be placed in opposing positions in the centrifuge head to achieve appropriate balance. Tubes must be balanced across the center of rotation, and each bucket must be balanced with respect to its pivotal axis (Lo, 2015). Specimens must be placed with regard for a geometrically symmetric arrangement, using water-filled tubes to attain balance.

Recentrifugation of gel separator tubes has been associated with pseudohyperkalemia. One study demonstrated that after initial centrifugation, a new serum layer develops under the gel within the cellular layer. During storage, potassium leaks from the cellular layer into the new serum layer, creating hyperkalemia in this layer. When the tube is recentrifuged, the new serum layer will move above the gel layer and cause a pseudohyperkalemia in the serum for analysis. The same authors also demonstrated that a pseudonormokalemia in patients with true hypokalemia may be erroneously reported after recentrifugation (Hira et al., 2001; 2004). Similarly, LD and free hemoglobin can be elevated on recentrifugation due to leakage from the cell layer.

EQUIPMENT

A wide variety of centrifuges and accessories are available to meet specific needs in the clinical laboratory. These include tabletop, general laboratory centrifuges; horizontal head, fixed-angle, or angle-head; high-speed centrifuges; portable floor models, undercounter models; microcentrifuges; refrigerated and unrefrigerated types; and ultracentrifuge models. Ultracentrifuges are high speed and capable of reaching a centrifugal force of 165,000 times gravity. These centrifuges require refrigeration chambers to compensate for the considerable heat produced. Ultracentrifuges are used to clear serum of chylomicrons, which is necessary to avoid interference with clinical testing (Bermes & Young, 2001). An example of a centrifuge designed for fast speed and quick TAT is the StatSpin Express 3 (StatSpin, 2014), a microprocessor-controlled, high-speed, bench-top centrifuge designed to rapidly separate blood in evacuated tubes. This centrifuge accelerates rapidly and brakes very fast, decreasing specimen processing time. The centrifuge operates at a fixed speed of 8500 rpm, produces an RCF of 4440 × (g), and can be operated with a 120- or 180-second spin cycle.

Centrifuge capacities vary with model type and centrifuge head. Specimen volume (per tube), number of tubes to be centrifuged, speed required for adequate separation, and durability of equipment should be considered. For every laboratory procedure requiring centrifuge operation, a written specification identifying centrifuge type, temperature, g forces, and length of centrifugation time is required. Calibration of the centrifuge must be part of the quality assurance process. Speed settings must be calibrated using rpm, and RCFs must be calculated using the earlier formula or a nomogram. Any significant changes will indicate deterioration effects, such as wearing of brushes or bearing problems. Timers must be checked for accuracy.

SELECTED REFERENCES

Boyanton L, Blick K: Stability studies of twenty-four analytes in human plasma and serum, *Clin Chem* 48(12):2242–2247, 2002.

This article studies plasma and serum analyte stability over 56 hours in samples removed from cells and allowed to remain on cells. No significant changes were found in the serum and plasma specimens removed from the cells within 30 minutes of collection. The article provides an excellent historical bibliography of the major studies performed on this topic.

Centers for Disease Control and Prevention: Workbook for designing, implementing, and evaluating a sharps injury prevention program, introduction. Division of Healthcare Quality Promotion—(DHQP Home) privacy policy—Accessibility. Published: June 4, 2004. Reviewed: February 11, 2015. Online. Available at: http://www.cdc.gov/sharpssafety/resources.html. Last accessed 1/25/19.

This excellent Internet publication available as a free download includes an overview of sharps risks and prevention, organizational steps for development of prevention programs, recommendations for selection of sharps injury prevention devices, and education and training materials. The appendices contain useful worksheets for all aspects of sharps injury and prevention documentation.

Garza D, Becan-McBride K: *Phlebotomy handbook: blood specimen collection from basic to advanced*, ed 9, Upper Saddle River, N, 2014, Prentice Hall.

This handbook presents a complete discussion of all aspects related to phlebotomy. Included are safety procedures, equipment, step-by-step procedures, and management and legal issues. It contains an excellent basic discussion of the circulatory system with color diagrams.

Haverstick DM, Groszbach AR: Specimen collection, processing and other preanalytical variables. In Burtis CA, Bruns DE, editors: *Tietz fundamentals of clinical chemistry and molecular diagnostics*, ed 7, St. Louis, 2015, Elsevier Saunders, pp 72–88.

This chapter contains many important preanalysis factors that affect laboratory results.

Strasinger SK, DiLorenzo MS: *The phlebotomy textbook*, ed 3, Philadelphia, 2011, FA Davis.

This text contains a comprehensive presentation of all aspects of phlebotomy. It is an excellent teaching guide and discusses state-of-the-art equipment and techniques. The book is divided into four parts: regulatory, safety, and health care information; techniques for blood collection; medical terminology, anatomy, and physiology; and additional techniques. It also includes a CD with videos demonstrating proper technique. Contained within the various chapters are excellent summary tables and quick reference charts. It also provides an extensive description of the various blood collection tubes and anticoagulants/additives they contain and information on preanalytic factors affecting laboratory results.

Young DS: *Effects of preanalytic variables on clinical laboratory tests*, ed 3, Washington, DC, 2007, AACC Press.

This is the preeminent resource for interference in laboratory tests that covers the effects of drugs as well as other contributing conditions. An online database (www.clinfx.com) is also available.

Access the complete reference list online at Elsevier eBooks for Practicing Clinicians.

REFERENCES

AccuVein website. http://accuvein.com/ Online. Accessed January 25, 2019.

Barak M, Jaschek R: A new and effective way for preventing pre-analytical laboratory errors, *Clin Chem Lab Med* 52(2):e5–e8, 2014.

BD Vacutainer Systems, Franklin Lakes, N.J. Online. Available: http://www.bd.com.

Bermes EW, Young DS: General laboratory techniques, procedures, and safety. In Burtis CA, Ashwood ER, editors: *Tietz fundamentals of clinical chemistry*, ed 5, Philadelphia, 2001, WB Saunders, pp 2–29.

Bolton-Maggs PHB, Wood EM, Wiersum-Osselton JC: Wrong blood in tube—potential for serious outcomes: can it be prevented? *Br J Haematol* 168(1):3–13, 2015.

Bonini P, Plebani M, Ceriotti F, et al.: Errors in laboratory medicine, *Clin Chem* 48:691–698, 2002.

Carabini LM, Nouriel J, Milian RD, et al.: The clinical significance of patient specimen transport modality: pneumatic tube system impact on blood gas analytes, *Respiratory Care* 61:1311–1315, 2016.

Caraway WT, Kammeyer CW: Chemical interference by drug and other substances with clinical laboratory test procedures, *Clin Chem Acta* 41:395, 1972.

Charles S, Agrawal N, Blum M: Erroneous thyroid diagnosis due to over-the-counter biotin, *Nutrition* 57:257–258, 2019.

Clinical and Laboratory Standards Institute (CLSI): *Blood gas and pH analysis and related measurements*, ed 2, Wayne, Pa, 2009, CLSI. Document C46-A2.

Clinical and Laboratory Standards Institute (CLSI): *Collection of diagnostic venous blood specimens*, ed 7, Wayne, Pa, 2017, CLSI. Document GP41.

Clinical and Laboratory Standards Institute (CLSI): *Procedures and devices for the collection of diagnostic capillary blood specimens*, ed 6, Wayne, Pa, 2008, CLSI. Document GP42.

Clinical and Laboratory Standards Institute (CLSI): *Urinalysis: approved guideline*, ed 3, Wayne, Pa, 2009, Document GP16-A3.

Dasgupta A, Dean R, Saldana S, et al.: Absorption of therapeutic drugs by barrier gels in serum separator blood collection tubes. Volume and time dependent reduction in total and free drug concentrations, *Am J Clin Pathol* 101(4):456–461, 1994.

Dufour DR: Sources and control of preanalytical variation. In Kaplan LA, Pesce AJ, Kazmierczak SC, editors: *Clin Chem: Theory, analysis, correlation*, ed 4, St. Louis, 2003, Mosby, pp 64–82.

Dzik WH, Murphy MF, Andreu G, et al.: An international study of the performance of patient sample collection, *Vox Sang* 85:40–47, 2003.

Favaloro EJ, Funk DM, Lippi G: Pre-analytical variables in coagulation testing associated with diagnostic errors in hemostasis, *Lab Med* 43(1–10), 2012.

The FDA warns that biotin may interfere with lab tests: FDA safety communication, *November* 28, 2017, https://www.fda.gov/medicaldevices/safety/alertsandnotices/ucm586505.htm. Accessed November 20, 2019.

Gifford JL, de Koning L, Sadrzadeh SMH: Strategies for mitigating risk posed by biotin interference on clinical immunoassays, *Clin Biochem* 65:61–63, 2019.

Green SF: The cost of poor blood specimen quality and errors in preanalytical processes, *Clin Biochem* 46(13–14):1175–1179, 2013.

Greene DN, McPherson GW, Rongitsch J, et al.: Hematology reference intervals for transgender adults on stable hormone therapy, *Clin Chim Acta* 492:84–90, 2019.

Gümüş S: Evaluation of ethanol interference on routine biochemical tests, *Am J Clin Path* 150:507–511, 2018.

Hardin G, Quick G, Ladd DJ: Emergency transport of AS-1 cell units by pneumatic tube system, *J Trauma* 30:346–348, 1990.

Hira K, Noriaki A, Fukui T: Pseudonormokalaemia caused by recentrifugation of blood samples after storage in gel-separator tubes, *Ann Clin Biochem* 41:82–83, 2004.

Hira K, Ohtani Y, Rahman M, et al.: Pseudohyperkalaemia caused by recentrifugation of blood samples after storage in gel separator tubes, *Ann Clin Biochem* 38:386–390, 2001.

Hofgartner WT, Tait JF: Frequency of problems during clinical molecular-genetic testing, *Am J Clin Pathol* 112:14–21, 1999.

Holmes EW, Samarasinghe S, Emanuele A, et al.: Biotin interference in clinical immunoassays: a cause for concern, (letter to editor), *Arch Pathol Lab Med* 141:1459–1460, 2017.

Hotaling M: A retractable winged Steel (butterfly) needle performance Improvement project, *JCAHO* 35:100–105, 2009.

Howanitz PJ, Steindel SJ, Cembrowski GS, et al.: Emergency department stat test turnaround times. A College of American Pathologists' Q-Probes study for potassium and hemoglobin, *Arch Pathol Lab Med* 116:122–128, 1992.

Katzman BM, Lueke AJ, Donato LJ, Jaffe AS, Baumann NA: Prevalence of biotin supplement usage in outpatients and plasma biotin concentrations in patients presenting to the emergency department, *Clin Biochem* 60:11–l16, 2018.

Keshgegian AA, Bull GE: Evaluation of a soft-handling computerized pneumatic tube specimen delivery system, *Am J Clin Pathol* 97:535–540, 1992.

Kitazawa T, Shima M: Emicizumab, a humanized bispecific antibody to coagulation factors IXa and X with a factor VIIIa-cofactor activity, *Int J Hematol*, 2018, https://doi.org/10.1007/s12185-018-2545-9. Accessed November 20, 2019.

Kjeldsberg CR, Knight AK: *Cerebral spinal fluid in body fluids*, ed 3, Chicago, 1993, American Society of Clinical Pathology, p 65.

Klee GG: Human anti-mouse antibodies, *Arch Pathol Lab Med* 124:921–923, 2000.

Laessig RH, Hassermer DJ, Paskay TA, et al.: The effects of 0.1 and 1.0 percent erythrocytes and hemolysis on serum chemistry values, *Am J Clin Pathol* 66:639–644, 1976.

Lancman G, Arinsburg S, Jhang J, et al.: Blood transfusion management for patients treated with anti-CD38 monoclonal antibodies, *Front Immunol* 9:1–8, 2018.

Lapworth R, Teal TK: Laboratory blunders revisited, *Ann Clin Biochem* 31:78–84, 1994.

Li JL, Wagar E, Meng QH: Comprehensive assessment of biotin interference in immunoassays, *Clin Chim Acta* 487:293–298, 2018.

Linden JV, Wagner K, Voytovich QE, et al.: Transfusion errors in New York State: an analysis of 10 years' experience, *Transfusion* 40:1207, 2000.

Lo SF: Principles of basic techniques and laboratory safety. In Burtis CA, Bruns DE, editors: *Tietz fundamentals of clinical chemistry and molecular diagnostics*, ed 7, St Louis, 2015, Elsevier, pp 108–127.

Madry N, Auerbach B, Schelp C: Measures to overcome HAMA interferences in immunoassays, *Anticancer Res* 17(4B):2883–2886, 1997.

McCall RE, Tankersley CM: *Phlebotomy essentials*, Philadelphia, 1993, JB Lippincott Company, pp 202–206.

Melanson SF, Hsieh B, Flood J, et al.: Evaluation of add-on testing in the clinical chemistry laboratory of a large academic medical center, *Arch Pathol Lab Med* 128:885–889, 2004.

Meng QH, Irwin WC, Fesser J, et al.: Interference of ascorbic acid with chemical analytes, *Ann Clin Biochem* 42:475–477, 2005.

Miller HJ: Pleural effusions. In Davis B, Bishop M, Mass D, editors: *Principles of laboratory utilization and consultation*, Philadelphia, 1999, WB Saunders.

Nogami K, Soeda T, Matsumoto T, et al.: Routine measurements of factor VIII activity and inhibitor titer in the presence of emicizumab utilizing anti-idiotype monoclonal antibodies, *J Thromb Haemost* 16:1383–1390, 2018.

Occupational Safety and Health Administration (OSHA). *Occupational safety bloodborne pathogens standard* 29 CFR 1910.1030. 2001. Online. Available: http://www.osha.gov/SLTC/bloodbornepathogens/index.html.

Occupational Safety and Health Administration (OSHA): Occupational safety Bloodborne needlestick safety prevention act, OSHA, *Revised standards*, 2002.

Omar H, Chamberlin A, Walker V, et al.: Immulite 2000 parathyroid hormone assay: stability of parathyroid hormone in EDTA blood kept at room temperature for 48 hours, *Ann Clin Biochem* 38(Pt 5):561–563, 2001.

Oostendorp M, Lammerts van Bueren JJ, Doshi P, et al.: When blood transfusion medicine becomes complicated due to interference by monoclonal antibody therapy, *Transfusion* 55:1555–1562, 2015.

Phelan MP, Reineks EZ, Berriochoa JP, et al.: Impact of use of smaller volume, smaller vacuum blood collection tubes on hemolysis in emergency department blood samples, *Am J Clin Pathol* 148:330–335, 2017.

Phelan MP, Reineks EZ, Schold JD, et al.: Preanalytic factors associated with hemolysis in emergency department blood samples, *Arch Pathol Lab Med* 142:229–235, 2018.

Plebani M: The detection and prevention of error in laboratory medicine, *Ann Clin Biochem* 47:101–110, 2010.

Roberts TK, Kraft CS, French D, et al.: Interpreting laboratory results in transgender patients on hormone therapy, *Am J Med* 127:159–162, 2014.

Shi RZ, Seeley ES, Bowen R, et al.: Rapid blood separation is superior to fluoride for preventing in vitro reductions in measured blood glucose concentration, *J Clin Pathol* 62:752–753, 2009.

Smith BE, King PH, Schlain L: Clinical evaluation: continuous real-time intra-arterial blood gas monitor during anesthesia and surgery by fibro-optic sensor, *Int J Clin Monit Comput* 9:45–52, 1992.

Stahl M, Lund ED, Bandslund I: Reasons for a laboratory's inability to report results for requested analytical tests, *Clin Chem* 44:2195–2197, 1998.

Stankovic AK, DeLauro E: Quality improvements in the preanalytical phase: Focus on urine specimen workflow, *Med Lab Obs*. 42:20, 22.

StatSpin operator's manual: *StatSpin express 3 centrifuge. Westwood, Mass*, IRIS sample processing, division of IRIS International Inc, 2014. http://www.statspin.com.

Strasinger SK, DiLorenzo MS: *Urinalysis and body fluids*, ed 4, Philadelphia, 2001, FA Davis, pp 23–32.

Tate J, Ward G: Interferences in immunoassay, *Clin Biochem Rev* 25(2):105–120, 2004.

Yao H, Rayburn ER, Shi Q, et al.: FDA-approved drugs that interfere with laboratory tests: a systematic search of US drug labels, *Crit Rev Clin Lab Sci* 54:1–17, 2017.

Zhang DJ, Elswick RK, Miller WG, et al.: Effect of serum-clot contact time on clinical chemistry laboratory results, *Clin Chem* 44:1325–1333, 1998. http://www.jointcommission.org/standards_information/npsgs.aspx. Accessed January 19, 2015.

CHAPTER 4

ANALYSIS: PRINCIPLES OF INSTRUMENTATION

Matthew R. Pincus, Mark S. Lifshitz, Jay L. Bock

PRINCIPLES OF INSTRUMENTATION, 35
Spectrophotometry, 35
Reflectometry, 43
Molecular Luminescence Spectroscopy (Fluorometry), 43
Nephelometry And Turbidimetry, 44
Flow Cytometry, 45
Refractometry, 46
Osmometry, 46
Electrochemistry, 47
Conductance, 48
Impedance, 48
Electrophoresis And Densitometry, 48
Isoelectric Focusing, 48
Chromatography, 49
Mass Spectrometry, 51
Scintillation Counter, 52
Capillary Electrophoresis, 52
Nuclear Magnetic Resonance Spectroscopy, 52
GENERAL ANALYTIC METHODS AND ISSUES, 53
Chemicals, 53
Water, 53
Measurement Of Mass, 54
Laboratory Glassware And Plasticware, 55
Volumetric Laboratoryware, 55
Thermometry, 56
Water Baths, 57
Heating Blocks, Dry-Bath Incubators, And Ovens, 57
Mixing, 57
Aqueous Solution, 57
SELECTED REFERENCES, 59

KEY POINTS

- Many analytic determinations made in clinical laboratories are based on measurements of radiant energy that is absorbed or transmitted. The devices used to measure absorbed or transmitted light energy are photometers and spectrophotometers.
- The basic components of spectrophotometers include a radiant energy source, wavelength selector, cuvette holder, photodetector, signal processors, and readout devices.
- A reflectometer is used to measure analytes by measuring the quantity of light reflected by a liquid sample that has been dispensed onto a grainy or fibrous solid support.
- Nephelometers are used to detect light that is scattered at various angles, whereas turbidimetry measures a reduction in light transmission due to particle formation.
- A flow cytometer measures light patterns produced as particles pass single file through a laser light beam. The flow cytometer is used to count and sort cells. It is also a key component of hematology analyzers and a technology used to differentiate white blood cells.
- Electrochemical principles are used to measure numerous analytes in biologic fluids. Specific electrochemical techniques include potentiometry, amperometry, coulometry, conductivity, and anodic stripping voltammetry.
- Analytes measured by electrochemical techniques include electrolytes, blood gases, pH, metabolites (e.g., glucose, urea nitrogen), ionized calcium, lead, and chloride in sweat.
- Chromatography is a separation technique based on the different interactions of specimen compounds with a mobile phase and a stationary phase, as the compound travels through a support medium.
- Mass spectrometers have become increasingly important clinical instruments, especially in emerging fields such as proteomics. Mass spectrometry is based on fragmentation and ionization of molecules. The relative abundance of each of the ions yields a characteristic mass spectrum of the parent molecule. The basic components of a mass spectrometer include an ion source, a mass analyzer, and an ion detector.

A fundamental understanding of the principles of instrumentation used in clinical laboratories is essential. These instruments must provide the clinician with the best possible data to be of value to the patient. Without a thorough understanding of the necessary principles associated with an analyzer, operators will be ill equipped to perform maintenance procedures and calibrations and to troubleshoot problems that may arise.

The goal of this chapter is to provide the reader with a brief and broad description of the essential principles of analytic instruments in the clinical laboratory. For a more comprehensive review of this topic, the reader is referred to references on clinical instrumentation at the end of this chapter.

PRINCIPLES OF INSTRUMENTATION

SPECTROPHOTOMETRY

Absorption spectroscopy has provided scientists with a means to use both qualitative and quantitative methods of measuring analytes in body fluids. Bouguer initially developed the principles of absorption spectroscopy in the early 1700s. Two other scientists, Lambert and Beer, continued to develop the fundamental principles of absorption spectroscopy, commonly known as Beer's law. Before reviewing the laws of spectroscopy, it is prudent to gain an understanding of light and the effects of its interactions with matter.

Diverse spectrophotometric methods use electromagnetic radiation (EMR), which can take several forms, the most recognizable being light and radiant heat. Other types of EMR include gamma (γ) rays and x-rays, as well as microwaves, radiofrequency radiation, and ultraviolet radiation. The energies involved with specific regions of the electromagnetic spectrum (EMS) and their corresponding wavelengths change dramatically from radio waves to γ radiation. All types of EMR have two component waves that travel at right angles to one another, an electric and a magnetic component, as illustrated in Figure 4.1A.

Some properties of EMR can be described by means of a classical sinusoidal wave model. Parameters associated with this waveform include wavelength, frequency, velocity, and amplitude, as shown in Figure 4.1B. EMR requires no supporting medium for its transmission and passes readily through a vacuum.

The sine wave model does not provide the total picture when discussing the absorption and emission of radiant energy. EMR also exists as a stream of discrete particles, or packets, of energy called *photons*. The energy of the photons is proportional to the frequency of the radiation. This dual nature of EMR is considered complementary and applies to the behavior of streams of electrons, protons, and other elementary particles.

The wave model allows us to represent EMR as both an electrical and a magnetic field that can undergo in-phase, sinusoidal oscillation at right angles both to each other and to the direction of propagation. The electrical and magnetic fields for a monochromatic beam of plane-polarized light (with oscillation of either the electric or magnetic fields within a single plane)* in a specific direction of propagation are shown in Figure 4.1A (Skoog et al., 1998). The electrical vector or component of the waveform is shown in two-dimensional format. Remember that a vector has both

*Unpolarized radiation has waves in many planes.

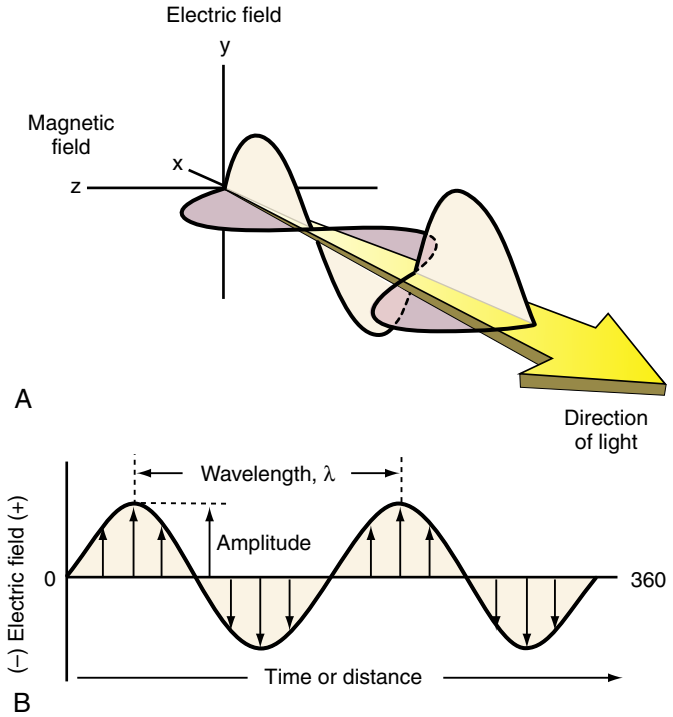

Figure 4.1 Diagram of a beam of monochromatic, plane-polarized light. **A,** Magnetic (*y*-axis) and electrical (*x*-axis) field vectors at right angles to each other. **B,** Two-dimensional view of the electrical vector.

magnitude and direction. The electrical field vector at a certain point in time and space is proportional to its own magnitude.

Time or distance of wave propagation is plotted on the abscissa. Most of the instrument principles widely used in the laboratory involve the electrical component of radiation and will represent the focus of discussion throughout this chapter. An exception will be nuclear magnetic resonance (NMR). With this technique, the magnetic component produces the desired effect.

Several wave parameters will be described. *Amplitude* of the sine wave is shown as the length of the electronic vector at maximum peak height. A *period*, *p*, is defined as the time in seconds required for the passage of successive maxima or minima through a fixed point in space. The number of oscillations of the waveform in a second is called *frequency*, *v*. The unit of frequency is hertz (Hz), which corresponds to one cycle per second. Frequency is also equal to $1/p$. A *wavelength*, λ, is the linear distance between any two equivalent points on a successive wave (Box 4.1). A widely used unit for wavelength in the visible spectrum is the nanometer, nm (10^{-9} m) (Box 4.1). Electromagnetic radiation in the x-rays or gamma region may be expressed in terms of angstrom units, Å (10^{-10} m). Finally, because of its much longer wavelength, EMR in the infrared region may have units corresponding to the micrometer, μm (10^{-6} m).

Velocity of Propagation

Velocity of propagation, v_i in meters per second, is determined by multiplying frequency by wavelength. Thus:

$$\upsilon_i = \upsilon\lambda_i. \qquad \text{(Eq. 4.1)}$$

The frequency of light is determined by the source and does not change, whereas the velocity depends on the composition of the medium through which it passes. Therefore, Equation 4.1 implies that the wavelength of radiation is also dependent on the medium.

The velocity of light traveling through a vacuum is independent of wavelength and is at its maximum. This velocity is represented by the symbol c and is equivalent to 2.99792×10^8 m/s. Equation 4.1 can then be rewritten as follows:

$$c = \lambda\nu = 3X10^8 m/s = 3X10^{10} cm/s. \qquad \text{(Eq. 4.2)}$$

In any medium containing matter, the propagation of radiation is slowed by the interaction between the EMR field of the radiation and the electrons bound in the atoms of that matter. Because the radiant frequency does not vary and is fixed by the source, the wavelength must decrease as radiation passes from air to a slower medium (Box 4.2).

BOX 4.1

Units for Expression of Wavelength

$1\ nm = 10^{-9} m = 10^{-7} cm$;
other units sometimes used include the following:

$$1\ \mu m = 10^{-6}\ m = 10^{-4}\ cm$$
$$1\ Å = 10^{-10}\ m = 10^{-8}\ cm$$

BOX 4.2

Example: Velocity of Propagation

What is the wavelength in nm for EMR having a frequency of 1.58×10^{15} Hz?

Solution

$$\lambda = c/v$$
$$\lambda\,(nm) = \frac{3.00 \times 10^8\ m/s}{1.58 \times 10^{15}\ Hz}$$
$$\lambda\,(nm) = 190$$

BOX 4.3

Example: Energy of EMR

What is the energy in joules and eV of EMR equivalent to (a) 190 nm? (b) 520 nm?

Solution

(a)

$$E = hc/v$$
$$E = \frac{\left(6.626 \times 10^{-34}\ Js\right)\left(3.0 \times 10^8 m/s\right)}{190\ nm\ \left(10^{-9} m/nm\right)}$$
$$E = 1.046 \times 10^{-18}\ J$$

Or, to convert to eV, use the conversion of $1\ J = 6.24 \times 10^{18}$ eV. Therefore, the number of eVs is 6.53.

(b)

$$E = hc/v$$
$$E = \frac{\left(6.626 \times 10^{-34}\ Js\right)\left(3.0 \times 10^8 m/s\right)}{520\ nm\ \left(10^{-9}\ m/nm\right)}$$
$$E = 3.82 \times 10^{-19}\ J \text{ or } 2.38\ eV$$

Energy of EMR

One should note the following safety concern: Optical devices that emit high-frequency EMR generate very high energies and can damage the eyes. Examples include deuterium and xenon lamps.

Wavelength and frequency are related to the energy of a photon, *E*, by Planck's* constant *h*, 6.626×10^{-34} J s, and *c*, the velocity of light in a vacuum (3.00×10^8 ms^{-1}):

$$E = h\upsilon = hc/\lambda, \qquad \text{(Eq. 4.3)}$$

where *E* = energy of a photon in joules or eV, *h* = Planck's constant (6.626×10^{-34} J s), and *v* = frequency in Hz (cycles/s).

Quite often, the energies of photons are stated in terms of an electron volt (eV). An eV is defined as the energy acquired by an electron that has been accelerated through a potential of 1 volt. The conversion factors between joules and eV are as follows:

$$1\ J = 6.24 \times 10^{18}\ eV$$
$$1\ eV = 1.602 \times 10^{-19}\ J$$

To illustrate the difference in energies of photons in the EMS, compare the energy of photons in the ultraviolet (UV) region versus the visible region of the EMS (Box 4.3).

*Also expressed in units 6.626×10^{-27} erg s.

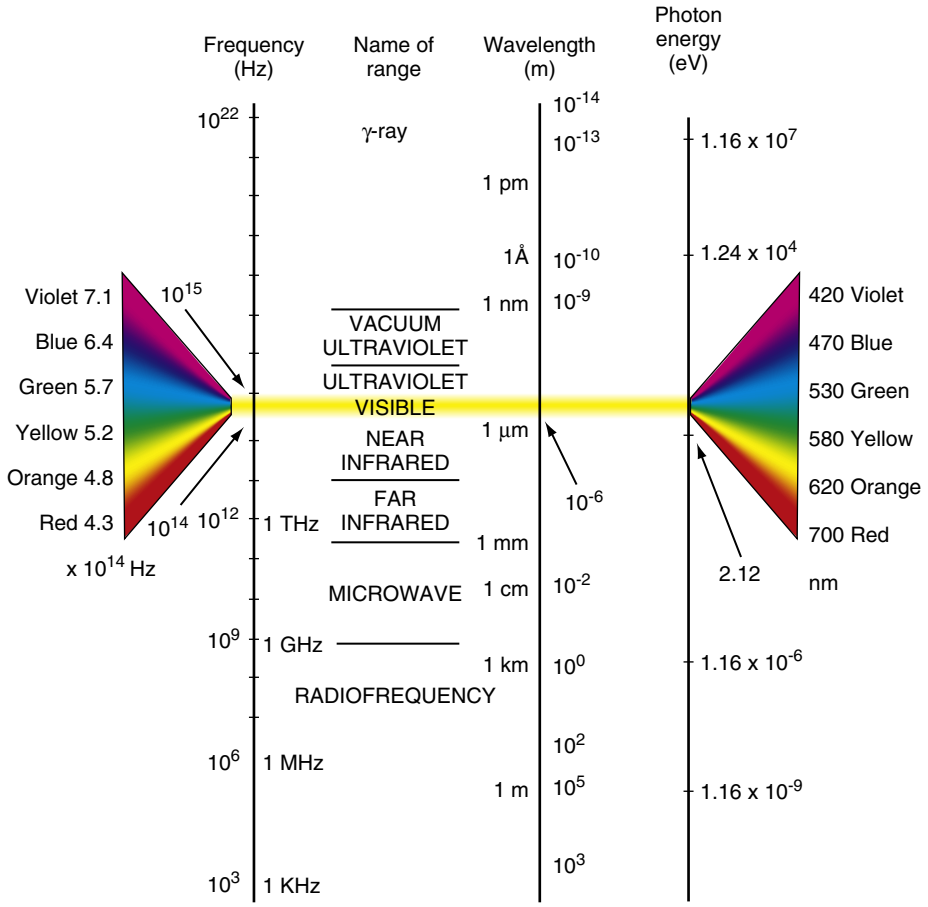

Figure 4.2 A diagram of the names, frequencies, wavelengths, and photon energies of electromagnetic radiation (EMR). Both visible and ultraviolet light are widely used in analytic methods.

The relationship of frequency, wavelength, and photon energy throughout the EMS can be seen in Figure 4.2. This figure illustrates that very-high-energy gamma photons have extremely short wavelengths (top of Fig. 4.2), on the order of 1×10^{-13}m or 1×10^{-4} nm, and very high frequencies, on the order of 1×10^{22} Hz (Rubinson & Rubinson, 2000). The converse is true for television and radio wave parameters shown toward the bottom of Figure 4.2.

Scattering of Radiation

Transmission of radiation in matter can be viewed as a momentary retention of the radiant energy by atoms, ions, or molecules followed by reemission of the radiation in all directions as particles return to their original state. Destructive interference removes most but not all of the reemitted radiation involving atomic or molecular particles that are small relative to the wavelength of the radiation. The exception is radiation that travels in the original direction of the beam; the path of the beam appears to be unaltered because of the interaction. It has been shown that a very small fraction of the radiation is transmitted at all angles from the original path and that the intensity of this scattered radiation increases with particle size.

Rayleigh Scattering

Scattering by molecules or aggregates of molecules with dimensions significantly smaller than the wavelength of the radiation is referred to as *Rayleigh scattering*. The intensity is proportional to the inverse fourth power of the wavelength, the square of the polarizability of the particles, and the dimensions of the scattering particles. In Rayleigh scattering, the wavelengths of absorbed and emitted photons are the same. An example of Rayleigh scattering is the blue color of the sky, which results from increased scattering of the shorter wavelength of the visible spectrum.

Tyndall Effect

The Tyndall effect occurs with particles of colloidal dimensions and can be seen with the naked eye. Measurements of scattered radiation are used to determine the size and shape of polymer molecules and colloidal particles.

Raman Scattering

Raman scatter involves absorption of photons producing vibrational excitation. Emission or scatter occurs at longer wavelengths. Raman scatter always varies from the excitation energy by a constant energy difference.

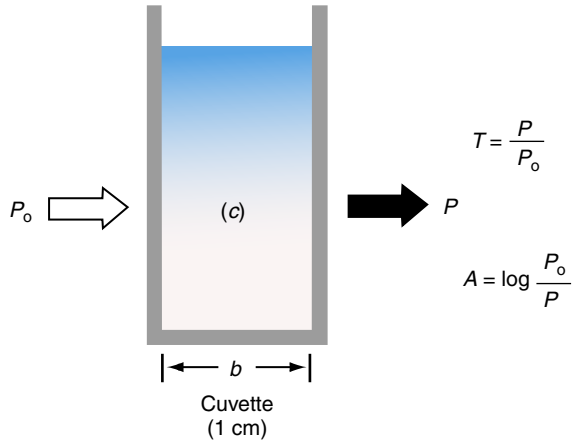

Figure 4.3 Attenuation of monochromatic light by an absorbing solution.

Beer-Lambert Law

Light that has a single wavelength is referred to as monochromatic light. Suppose that monochromatic light, which has an intensity, P_o, is directed toward a cuvette containing a compound that absorbs light at the monochromatic wavelength. Some of the light will be absorbed; the light that is not absorbed will be transmitted through the cuvette. The intensity of this transmitted light is P. We define the transmittance, T, as:

$$T = P/P_o \qquad \text{(Eq. 4.4)}$$

Expressed as a percentage, %T = 100T.

Lambert proved that for monochromatic radiation that passes through an absorber of constant concentration, a logarithmic decrease is seen in the radiant power as the path length increases arithmetically. The absorbance (*A*) of a solution was determined to be equivalent to:

$$A = \log P_o/P. \qquad \text{(Eq. 4.5)}$$

The relationship between transmittance, *T*, or percent transmittance ($P/P_o \times 100$), and absorbance is shown in Figure 4.3. Absorbance

BOX 4.4

Example: Beer-Lambert Law

What is the absorbance of a solution whose transmittance is 10%?

Solution

$$A = 2 - \log \%T$$

$$A = 2 - \log 10\%T = 2 - 1 = 1$$

and percent transmittance (Box 4.4) are inversely related as given by the following:

$$A = 2 - \log\%T. \qquad \text{(Eq. 4.6)}$$

Beer followed with studies on the relationship between radiant power and concentration. His approach was to keep the path length and wavelength constant while determining the relationship of radiant power, *P*, and concentrations of the absorbing species. Based on previous work by Lambert, Beer discovered that for monochromatic radiation, absorbance is directly proportional to the path length, *b*, through the medium and the concentration, *c*, of the absorbing species. The work culminated in the Beer-Lambert law or, simply, Beer's law.

The principles established are represented by the following:

$$A = -\log T = \log P_o/P = abc, \qquad \text{(Eq. 4.7)}$$

where a = absorptivity in L g^{-1} cm^{-1}, b = path length of 1 cm, and c = concentration in units of g/L.

When the concentration in Equation 4.7 is expressed in moles per liter and the path length in centimeters, the term applied is *molar absorptivity*, given the symbol ε, epsilon, and is equivalent to the molar extinction coefficient ("*a*") times gram molecular weight of the absorbing species.

$$A = \varepsilon bc, \qquad \text{(Eq. 4.8)}$$

where units for ε are L mol^{-1} cm^{-1}.

The graph of absorbance versus concentration shows the intercept at zero and a linear plot with a slope equivalent to "*ab*." Absorption spectroscopy is used best for solutions whose absorbance values are less than 2.0. Absorbance values greater than 2.0 may yield erroneous results because of other interactions of light with matter (e.g., variations in the refractive index of a solution). This may cause a deviation from Beer's law, resulting in bending of the linear plot as shown in Figure 4.4.

Deviations from Beer's law may be caused by changes in instrument functions or chemical reactions. Instrument deviation is commonly a result of the finite bandpass of the filter or monochromator. Beer's law assumes monochromatic radiation, but truly monochromatic radiation is best achieved using only unique line emission sources. If absorptivity is constant over the instrument bandpass, then Beer's law is followed within close limits.

Deviations from Beer's law become apparent at higher concentration (i.e., higher absorbance). In Figure 4.4, the curved line bends toward the concentration axis as opacity is approached. This lack of adherence to Beer's law in a negative direction is undesirable because of the somewhat large increase in the relative concentration error.

Deviation from Beer's law can occur with shifts or changes in chemical or physical equilibrium involving the absorbing species. Changes in solution pH, ionic strength, and temperature can result in such deviations.

Components of a Spectrophotometer

A typical photometer or spectrophotometer contains six basic components in a single- or double-beam configuration. These components include a stable source of radiant energy; a filter that isolates a specific region of the EMS; a sample holder (cuvette); a radiation detector, called the photomultiplier; a signal processor; and a readout device. Each component of a typical photometer is shown in Figure 4.5.

The following steps outline the function of each component in any absorption-type photometer as it detects light and provides information to the operator:

1. The light source provides the energy that the sample will modify or attenuate by absorption. The light is polychromatic (i.e., all visible wavelengths are present).
2. A wavelength selector or filter isolates a portion of the spectrum emitted by the source and focuses it on the sample.
3. The sample in a suitable container (e.g., a cuvette) absorbs a fraction of the incident light and transmits the remainder.
4. The light that passes through the cuvette and sample strikes the cathode of a photodetector and generates an electrical signal.

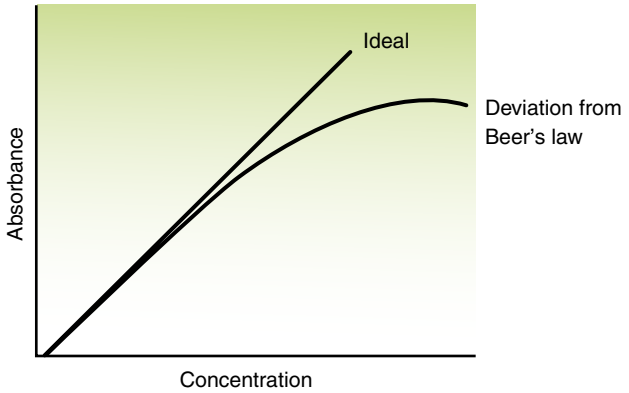

Figure 4.4 A plot of absorbance versus concentration illustrating deviation from Beer's law.

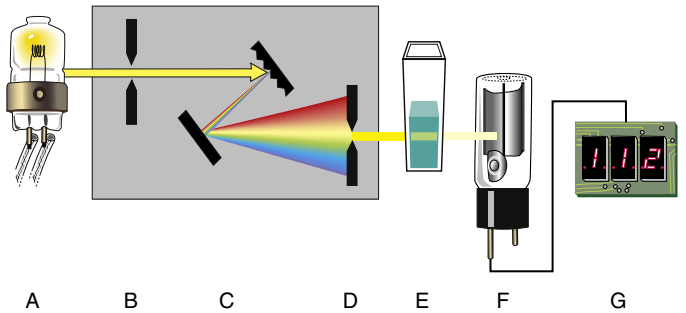

Figure 4.5 Components of a single-beam spectrophotometer. **A,** Exciter lamp. **B,** Entrance slit. **C,** Monochromator. **D,** Exit slit. **E,** Cuvette. **F,** Photodetector. **G,** Light-emitting diode (LED) display.

5. The electrical signal is processed electronically (e.g., amplified, digitized).
6. The processed signal is electronically coupled to the display unit (e.g., light-emitting diode [LED], X-Y strip chart recorder, meter).

Radiant Energy Sources

Radiant energy sources or lamps provide polychromatic light and must generate sufficient radiant energy or power to measure the analyte of interest. A regulated power supply is required to provide a stable and constant source of voltage for the lamp. Radiant energy sources are of two types: *continuum* and *line*. A continuum source emits radiation that changes in intensity very slowly as a function of wavelength. Line sources emit a limited number of discrete lines or bands of radiation, each of which spans a limited range of wavelengths.

Continuum sources find wide applications in the laboratory. Examples of continuum sources include tungsten, deuterium, and xenon. For testing in the visible region of the EMS, tungsten or tungsten-halogen lamps are widely used. The filament in the tungsten-halogen lamp is maintained at a higher temperature than in the normal tungsten lamp. This takes advantage of the Wien and Stefan laws to provide a source with a maximum wavelength near the center of the visible spectrum (whiter), and with a greater energy output (brighter). Introducing a halogen gas into the lamp envelope counteracts the problem of increased atom vaporization from the high-temperature filament.

The deuterium lamp is routinely used to provide UV radiation in analytic spectrometers. The voltage applied is typically about 100 volts, which gives the electrons enough energy to excite the deuterium atoms in a low-pressure gas to emit photons across the full UV range.

The strong atomic interaction in a high-pressure xenon discharge lamp produces a continuous source of radiation, which covers both the UV and the visible range. The discharge light is normally pulsed for short periods with a frequency that determines the average intensity of the light from the source and also its lifetime.

In atomic emission line sources, electrons move between atomic energy levels. If the atom is free of any interaction with other atoms, the amount of energy liberated can be very precise, and all of the photons share a very clearly defined wavelength. This is the characteristic sharp "line" emission from an electronic discharge in a low-pressure gas. Line sources that emit a few discrete lines find wide use in atomic absorption, molecular, and fluorescent spectroscopy. Mercury and sodium vapor lamps provide sharp lines in

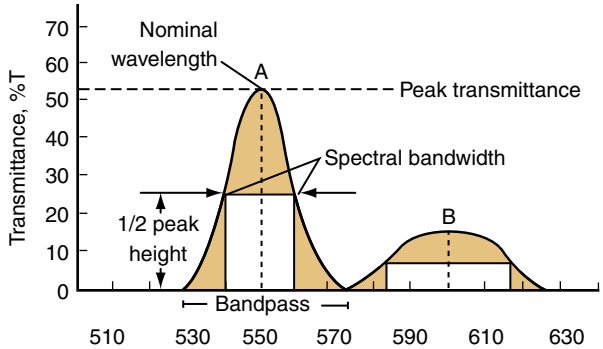

Figure 4.6 Comparison of spectral characteristics of two types of filters. **A,** Interference filter. **B,** Absorption filter. The spectral bandwidth of filter A is much less than filter B and, therefore, allows fewer wavelengths of light through.

the ultraviolet and visible regions and are used in several spectrophotometers. For atomic absorption spectroscopy applications, the hollow cathode lamp provides atomic emission from free metal atoms by using the heat of a gaseous discharge (e.g., in neon) to vaporize metal atoms into the discharge. Typically, each lamp is specific to a particular metal. However, some lamps use two, three, or more metals, although the emission from each of these is reduced.

A laser source is very useful in analytic instrumentation because of its high intensity and narrow bandwidth and the coherent nature of its outputs. Several specific uses of lasers include high-resolution spectroscopy, kinetic studies of processes with lifetimes in the range of 10^{-9} to 10^{-12} s, as light sources for nephelometers, and as ionization inducers in the MALDI and SELDI mass spectrometric techniques (see Chapter 5).

Wavelength Selectors

A critical component of all spectrometers is the device used to select the appropriate wavelength. Several types of wavelength selectors are available, including filters, prisms, grating monochromators, and holographic gratings. The quality of these selectors is described by their nominal wavelengths, spectral bandwidths, and bandpass. *Nominal wavelength* represents the wavelength in nanometers at peak transmittance. Spectral bandwidth is the range of wavelengths above one-half peak transmittance. It is sometimes called the *half power point* or *full width at half peak maximum* (FWHM). The total range of wavelengths transmitted is the *bandpass*. Figure 4.6 summarizes these characteristics of wavelength selectors. This figure also summarizes the difference in wavelength selectivity between interference (Fig. 4.6A, left) and absorbance filters (Fig. 4.6B, right), as we now discuss.

Filters

An important component of the spectrophotometer is the wavelength filter. Its purpose is to isolate monochromatic light, or at least as narrow a range of wavelengths of light as possible, and direct it to the sample or to the photodetector. Remember, the purpose of absorption spectroscopy is to detect how much light is absorbed by the sample. This is a measure of the absorbance of an analyte in a sample that is directly proportional to concentration (see Beer's law discussed earlier). The percent transmittance is the ratio of the amount of light transmitted through the sample to the amount of light transmitted in the absence of the sample (e.g., buffer or solvent without the sample). Theoretically, it should be possible to determine this ratio without any filter at all. However, under these circumstances, most of the light that enters the sample in the cuvette will not be absorbed. Thus, to determine absorbance, it would be necessary to measure a small difference between two large numbers (i.e., the amount of light transmitted in the absence [control] and the presence of the sample). Therefore, to obviate this condition, it becomes necessary to filter out as much "extraneous" light as possible to enable accurate measurements of absorbance.

Two approaches may be taken to filtering light waves. The first is to limit the wavelengths of light that enter the sample with appropriate filters, so-called presample filters. The second is to allow multiwavelength light to pass through the sample and then to break up this light into its component wavelengths using a high-resolution prism and focus each of these component wavelengths on specific detectors, essentially one for each of the component wavelengths. If a sample absorbs light at one wavelength, then the ratio of the light transmittance of this wavelength of the sample to that for the control can be used to compute the percent transmittance and absorbance. This arrangement is termed *postsample filtering*.

Presample Filters (Bender, 1987). Fundamentally, two types of these filters are used: absorption and interference filters. Absorption filters simply absorb regions of the EMS and allow only a limited domain of this spectrum to pass through to the sample cuvette. The simplest sort of absorption filters consists of different forms of glass. One form of glass allows transmission only of wavelengths of light greater than 400 nm, while a second form allows transmission only of wavelengths of light less than 600 nm. If both glasses are arranged serially, they allow for transmission of light of wavelengths of only between 400 and 600 nm, with a peak at 500 nm. As a refinement of this approach, the older spectrophotometers utilize colored glass or transparent plastic materials. These colors are arranged in a circle or wheel so that light of a relatively narrow range of wavelengths is transmitted when each colored sector is in the light path. For example, if light in the green portion of the visible spectrum is desired, the wheel is turned so that the green filter is placed in the light path. The spectral bandwidth of these absorption filters ranges from about 30 to 50 nm (see Fig. 4.6).

This bandwidth is rather large but is adequate for determining the concentration of compounds in solution; absorbance filters are less adequate for scanning the absorption spectra of individual compounds and macromolecules or for accurately determining low concentrations of molecules. To achieve the latter goals, it becomes necessary to use interference filters.

In the simplest interference filter, light on the path to the sample cuvette enters a magnesium fluoride chamber that is coated with micro-mirrors on the interior. As shown in Figure 4.7A, light enters evenly spaced ports or slits on the left. Only light that enters each slit can continue; the rest is absorbed by the chamber. Light entering a slit, at an angle to the horizontal, travels across the chamber and is reflected back to the opposite wall. In Figure 4.7A, if the path length *ab* equals *bc*, and the path length equals the desired wavelength of light, it can be shown from the theory of optics that the light whose wavelength equals that of the path length or integral multiples of this path length will undergo constructive interference (i.e., the waves will add to one another exactly) with incoming light at slits above it. For example, in Figure 4.7A, light of wavelength $L = ab$, reflected from *b* to *c*, will be exactly in phase with light of wavelength L or integral multiples of L, entering the slit at *c*. All other wavelengths will destructively interfere with light entering slit *c*. The light is then reflected again at *c* to *d* and back again to *e* where, again, it will add to (constructively interfere with) only light waves of the same wavelength or integral multiples of it. Eventually, only light at the desired wavelength will be transmitted through the opposite wall at slits *f* and *h*.

It is important to note that because integral multiples of the wavelengths of incident light will constructively interfere with transmitted light in the chamber, more than one wavelength of light can be transmitted from the chamber. The actual quantitative relationship between the wavelengths (L) transmitted by the chamber; the angle of incidence, q, of the light entering a slit; the refractive index, R, of MgF_2 (1.38); and the distance, d, across the chamber is as follows:

$$ML = 2dR\sin(q), \qquad \text{(Eq. 4.9A)}$$

where M is any integer. Note that this equation predicts that for any given distance, d, many wavelengths of integral multiples to the fundamental wavelength where $M = 1$ can be transmitted. In practice, many of these other wavelengths can be excluded by using such techniques as placing appropriate glass filters in series with the interference chamber.

This arrangement successfully transmits (close to) monochromatic light at a particular wavelength. However, it does not allow for scanning of wavelengths to obtain the absorption spectra of different samples. To accomplish this, a similar arrangement is used. In this case, however, advantage is taken of another principle from the theory of optics: the principle of light diffraction. As shown in Figure 4.7B, when monochromatic light is allowed to enter two slits on one surface of a chamber, very much like the one shown in Figure 4.7A except that there is no material (MgF_2) in the chamber, the two light waves interfere with each other such that if a screen is placed on the opposite surface of the chamber, discrete regions of light and dark bands will be seen (Bender, 1987). The light bands are from light waves that have added constructively to one another and are transmitted; the dark bands result from destructive interference of the light waves, and no light waves are transmitted. The position of the bands and the distance between the bands depend on the wavelength of light that enters the two apertures and on the angle of incidence of both beams. Because, for a given angle of incidence, the position of the light bands for transmitted monochromatic light depends exclusively on the wavelength of light, if exit apertures are placed on the opposite surface only where the light bands occur for light of a desired wavelength, only light of that wavelength will be emitted from the chamber. This effect can be enhanced by placing multiple entry apertures next to one another in a sawtooth or grating pattern such that adjacent apertures are at a fixed distance, d, from one another, as shown in Figure 4.7B.

Now, polychromatic light is composed of multiple different monochromatic wavelengths of light. When polychromatic light is allowed to pass through the two apertures, as in Figure 4.7B, each of the wavelengths will

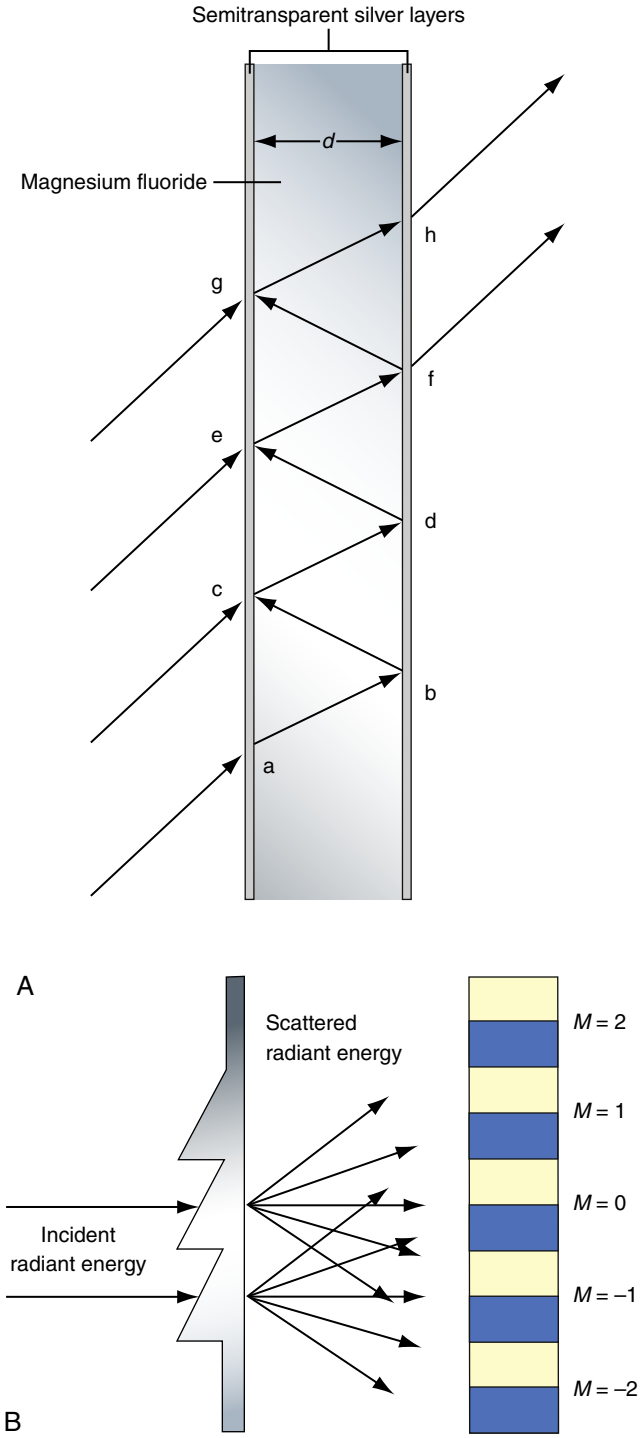

Figure 4.7 **A,** An interference MgF_2 filter. Light enters the filter at regularly spaced apertures at the same angle of incidence at each aperture. Going from the bottom of the figure, the light entering at *a* travels to *b*, where a mirror is reflecting it to *c*. Path lengths *ab* = *bc*. If these, in turn, are equal to the desired wavelength (or integral multiples of it), light of the desired wavelength arriving at *c* will be exactly in phase with light from the light source of that wavelength, which will result in constructive interference. It will be out of phase with all other wavelengths and, therefore, will destructively interact with them. This summation process takes place multiple times until only light of the desired wavelength escapes through exit apertures such as at *f* and *h* (after Bender, 1987). **B,** A diffraction filter. When light enters multiple apertures, as in part A, each of which is equidistant from its two neighbors, light of each of the wavelengths interferes both constructively and destructively with itself, giving rise to light *(yellow)* and dark *(blue)* bands or fringes that can be observed on a screen. The position and spacing of these bands depend only on the wavelength and the angle of incidence. As shown in this figure, if apertures are placed only at the points where light *(yellow)* fringes occur in the figure, only light of a specific wavelength will pass through this exit aperture.

constructively and destructively interfere with itself, as described earlier. Two different wavelengths of light will interfere only destructively with each other unless they are integral multiples of each other, as discussed in the previous case of the MgF_2 chamber. This allows us to "trap" the light of the desired wavelength by placing the exit apertures where the light bands are known to occur on the opposite surface for that monochromatic wavelength. A limiting factor for selecting truly monochromatic light is the size of the aperture that can allow some "stray" light from adjacent light bands for very close wavelengths to exit.

As with the MgF_2 interference chamber described previously, another source of contaminating light can occur from light of wavelengths that are integral multiples of the desired wavelength. The relationship that describes the wavelength as a function of the distance is similar to that for the MgF_2 chamber—that is,

$$ML = d\sin(q). \qquad \text{(Eq. 4.9B)}$$

Here, however, *d* is the distance between two adjacent entry slits on the near surface (toward the light source), *not* the distance across the chamber as with the MgF_2 chamber. Note that for a given distance, *d*, and angle of incidence, *q*, this equation has multiple solutions. For example, if the desired wavelength is 800 nm, $d\sin(q) = 800$. But this is for $M = 1$, $L = 800$ nm. Another solution is $M = 2$, $L = 400$ nm, and another $M = 3$, $L = 266.67$ nm, and so on. As with the MgF_2 chamber, these other wavelengths can be filtered out by the use of appropriate glass or other filters.

Note that the system shown in Figure 4.7B allows for continuous scanning of the absorption spectrum for any analyte. Wavelengths can be continuously changed, most often using electronic devices, by changing the position of the aperture on the exit side of the chamber or by changing the angle of incidence of the entering light by altering the angle of the near surface of the chamber. Filters that have this capacity are called *monochromators*. Both interference systems in Figure 4.7 have spectral bandwidths of approximately 1.5% of the wavelength at peak transmittance, much lower than for the absorption filters illustrated in Figure 4.6.

Postsample Filters. A different approach to obtaining monochromatic light and an accurate determination of absorbance is simply to allow the light to pass through the sample unfiltered. The light is then passed through a prism, where it is broken into its constituent wavelengths. The action of a prism depends on refraction of radiation by the prism material. The dispersive power depends on the variation of the refractive index with wavelength. A ray of radiation that enters a prism at an angle of incidence is bent toward the normal (vertical to the prism face); at the prism–air interface, it is bent away from the vertical. As we describe in the section on photomultipliers that follows, each wavelength is focused onto a photodiode array such that each photodiode responds to only a specific set of wavelengths. The amount of transmitted light in the presence of the sample is compared with that in the absence of the sample. Photodiode arrays are examples of devices that convert photon energy into electrical currents in a system where photons excite the outer electrons in metal to move in the so-called conduction band, generating a current.

Sample Containers (Cuvettes)

Sample containers (i.e., cells or cuvettes) are used to hold samples and must be made of material that is transparent to radiation in the spectral region of interest. In the ultraviolet region of the EMS (below 350 nm), cuvettes are made from fused silica or quartz. Silicate glasses can be used in the region between 350 and 2000 nm. Plastic containers have also found application in the visible region. Generally, the path length of cuvettes is 1 cm, although much smaller path lengths are used in automated systems. However, to increase sensitivity, some cuvettes are designed to have path lengths of 10 cm, increasing the absorbance for a given solution by a factor of 10 (Beer's law; Eq. 4.8).

Many double-beam spectrophotometers are designed with two cuvette holders: one for the sample and the other for the solvent. If two cuvettes are used, they should be optically matched for more accurate results. Matched pairs of cuvettes are obtainable from a manufacturer, but their optical performance should be verified before use by measuring the absorbance of identical solutions and comparing their values. One cell should then be reserved for the sample solution and the other for solvent. Cells should be scrupulously cleaned before and after each use.

Photodetectors

It is necessary to determine how much light passes through the sample in the cuvette. To accomplish this task, advantage is taken of the photoelectric effect that forms the basis of the quantum theory. Photons of specific wavelength excite the outer shell electrons of metals at their resonance frequencies to high-energy states in which they move through the so-called "conduction band" referred to above, where electrons move through the outer shells of the metal, thereby causing a current. This current, the magnitude of which is directly related to the intensity of the incident light, can then be detected and digitized.

Photomultiplier Tubes (PMTs). Perhaps the most common type of photon detector is the photomultiplier. Photomultiplier tubes are

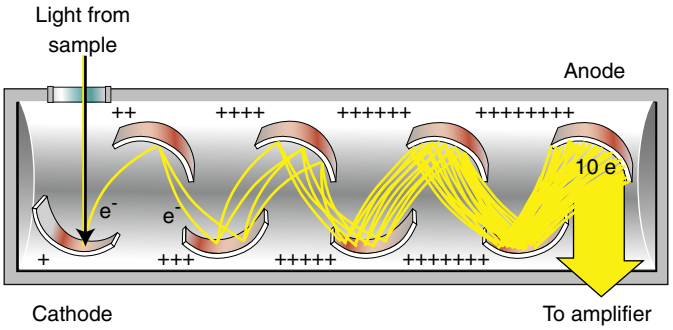

Figure 4.8 Schematic of a photomultiplier tube. In this diagram, a tenfold amplification of the initial signal is produced at the anode. (Redrawn from Simonson MG: In Kaplan LA, Pesce AJ, editors. *Nonisotopic alternatives to radioimmunoassay.* New York, 1981, Marcel Dekker.)

commonly used when radiant power is very low, which is characteristic of very-low-analyte concentrations. The operating principle is similar to the phototube, with one significant difference. Some PMTs are designed to provide an amplified signal nearly 1 million times larger than their phototube counterparts. This is accomplished by using multiple dynodes positioned throughout the PMT. The response of the PMT begins when incoming photons strike a photocathode. Electrons are ejected from the surface of the photocathode. A PMT has several additional electrodes called *dynodes*, each having a potential that is approximately 90 V higher than the previous one. Upon striking a dynode, each photoelectron causes emission of several additional electrons. These, in turn, are accelerated toward a second dynode, which is 90 V more positive than the previous dynode, which further amplifies the incident signal. This process, shown in Figure 4.8, continues within the PMT until all electrons are collected at the anode, where the resulting current is passed to an electronic amplifier.

Photomultiplier tubes are highly sensitive to ultraviolet and visible radiation. They also have very fast response times. These tubes are limited to measuring low-power radiation because intense light causes irreversible damage to the photoelectric surface.

Photovoltaic or Barrier Layer Cell. A variant method of detecting photon-induced current is the photovoltaic cell. This is a basic phototransducer that is used for detecting and measuring radiation in the visible region. This cell typically has a maximum sensitivity at about 550 nm, and the response falls off to about 10% of the maximum at 350 and 750 nm. It consists of a flat copper or iron electrode on which is deposited a layer of semiconductor material, such as selenium. The outer surface of the semiconductor is coated with a thin, transparent metallic film of gold or silver, which serves as the second or collector electrode. When radiation of sufficient energy reaches the semiconductor, covalent bonds are broken, with the result that conduction electrons and holes are formed. The electrons migrate toward the metallic film and the holes toward the base upon which the semiconductor is deposited. The liberated electrons are free to migrate through the external circuit to interact with these holes. The result is an electrical current of a magnitude that is proportional to the number of photons that strike the semiconductor surface and a photocurrent that is directly proportional to the intensity of the radiation that strikes the cells.

These types of photodetectors are rugged and low cost, and they require no external source of electrical energy. Low sensitivity and fatigue are two distinct disadvantages of these cells. For routine analyses at optimum wavelengths, these photocells provide reliable analytic data.

Vacuum Phototubes. A vacuum phototube has a semicylindrical cathode and a wire anode sealed inside an evacuated transparent envelope. The concave surface of the electrode supports a layer of photoemissive material that tends to emit electrons when it is irradiated. When a potential is applied across the electrode, the emitted electrons flow to the wire anode, generating a photocurrent that is generally about one-tenth as great as the photocurrent associated with photovoltaic cells for a given radiant intensity. The number of electrons ejected from a photoemissive surface is directly proportional to the radiant power of the beam that strikes the surface. All of the electrons are collected at the anode. Several types of photoemissive surfaces are used in commercial phototubes. These include highly sensitive bialkali materials made up of potassium, cesium, and antimony; red-sensitive material using multialkalis—for example, Na/K/Cs/Sb; ultraviolet sensitive with UV transparent windows; and flat response-type substances using Ga/As compositions.

Silicon Diode Transducers. Silicon diode transducers are more sensitive than vacuum phototubes but less sensitive than the PMTs described earlier. Photodiodes have spectral ranges from about 190 to 1100 nm. These devices contain positively (P) and negatively (N) charged semiconductive materials

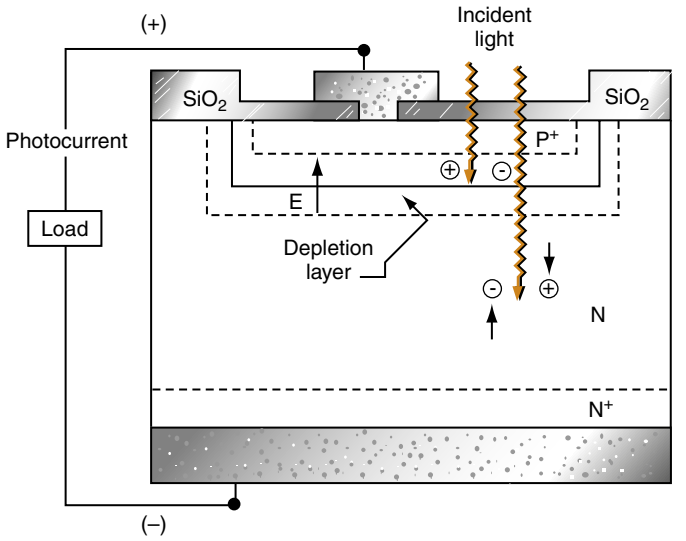

Figure 4.9 Schematic of a semiconductor photodiode used as a detector in many spectrometers.

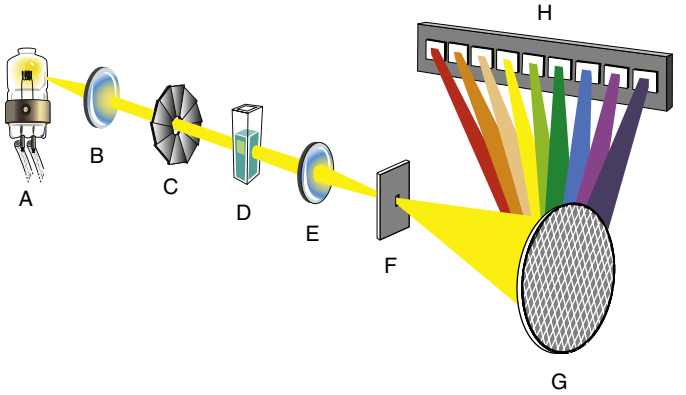

Figure 4.10 Photodiode array. **A,** Lamp. **B,** Lens. **C,** Shutter. **D,** Cell. **E,** Lens. **F,** Slit. **G,** Grating. **H,** Photodiode array.

adjoining one another, embedded on a silicon chip. A power supply is attached to this arrangement so that its positive pole connects to the *N*-type and its negative pole to the *P*-type material. This arrangement results in a depletion layer that reduces the conductance of the junction to nearly zero. If radiation is allowed to impinge on the chip, holes and electrons formed in the depletion layer are swept through the device to produce a current that is proportional to radiant power (Skoog et al., 1998). This process is shown in Figure 4.9.

Multichannel Photon Transducers. In the discussion of postsample filters, it was noted that unfiltered light emerging from the sample could be broken up into its constituent wavelengths using prisms. These different wavelengths are then directed to electronic detectors such that the intensity of light of each of the constituent wavelengths can be quantitated. Here, we describe some of these multiwavelength photodetectors.

A multichannel transducer consists of an array of small photoelectric-sensitive elements arranged linearly or in a two-dimensional pattern on a single semiconductor chip. The chip, which is usually silicon and typically has dimensions of a few millimeters on a side, also contains electronic circuitry that makes it possible to determine the electrical output signal from each of the photosensitive elements sequentially or simultaneously. The alignment of a multichannel transducer is generally in the focal plane of a spectrometer; thus, various elements of the dispersed spectrum can be converted and measured simultaneously. Several types of multichannel transducers currently are used; they may include photodiode arrays (PDAs), charge-injection devices (CIDs), and charge-coupled devices (CCDs).

Photodiode Arrays. By using the modern fabrication techniques of microelectronics, it is now possible to produce a linear (one-dimensional) array of several hundred photodiodes set side-by-side on a single integrated circuit (IC), or "chip" (Fig. 4.10). Each diode is capable of recording the intensity at one point along the line—together, they provide a linear profile of the light variation along the array.

A multiplex method is used to sort all of the signals received from the PDA. It records each signal individually and then feeds the signals sequentially to a single amplifier. The output of the PDA is a histogram profile, along the array, of the charge leaked by each photodiode. This mirrors the variation of light intensity across the array. Thus, the PDA detection occurs in three main stages:

1. Initialization
2. Accumulation of charge at each pixel-integration time
3. Read-out signals

In comparison with the PMT, the PDA has a lower dynamic range and higher noise. It is most useful as a simultaneous multichannel detector (Skoog et al., 1998).

Charge-Transfer Devices

Recent developments in solid-state detection techniques have now produced very effective two-dimensional array detectors that operate on a charge-transfer process as an alternative to photodiodes. A *charge-transfer device* (CTD) is a detection system in which a photon, striking the IC semiconductor material, releases electrons from their bound state into a mobile state. The released charge, consisting of negative electrons and positive holes, then drifts to, and accumulates at, surface electrodes. An array of these surface electrodes divides the detector into separate, light-sensitive "pixels." The charge that accumulates at each electrode is proportional to the integrated light intensity falling on that particular pixel.

Two distinct classes of CTDs are known: charge-injection devices (CIDs) and charge-coupled devices (CCDs). In a CCD, all of the charge packets are moved "in-step" along the array row from one pixel to the next, as in a "bucket chain." At the end of the row, the charge packets are fed sequentially into an *on-chip* low-noise amplifier, which then converts the charge into a voltage signal. The overall signal profile across the two-dimensional array is recorded one row at a time, thus giving a series of voltage signals corresponding to all of the pixels in the detection area.

In a CID, the charge accumulated in each pixel can be measured independently and nondestructively by using a network of "sensing" electrodes, which can monitor the presence of the accumulated charge. This is an important factor that differentiates CID systems from CCD and PDA systems, in which the whole of the detection area is "read" destructively in a single process.

Signal Processors and Readout

The processing of an electrical signal received from a transducer is accomplished by a device that amplifies, rectifies AC to DC (or the reverse), alters the phase of the signal, and filters it to remove unwanted components. In addition, the signal processor may need to perform mathematical operations on the signal such as differential calculations, integration, or conversion to a logarithm. Several readout devices have been used and include digital meters, d'Arsonval meters, recorders, LEDs, cathode-ray tubes (CRTs), and liquid crystal displays (LCDs).

Quality Assurance in Spectrophotometry

Several photometric parameters must be monitored periodically by users. Monitoring these parameters is recommended by most regulatory agencies and accrediting organizations. The parameters routinely monitored include wavelength or photometric accuracy, absorbance check, linearity, and stray light.

Accuracy is the closeness of a measurement to its true value. *Wavelength accuracy* implies that a photometer is measuring at the wavelength that it is set to. *Photometric accuracy* can be assessed easily using special glass-type optical filters. Two examples of commonly used filters include didymium and holmium oxide. Didymium glass has a broad absorption peak around 600 nm, and holmium oxide has multiple absorption peaks with a sharp peak occurring at 360 nm.

An *absorbance check* is performed using glass filters or solutions that have known absorbance values for a specific wavelength. The operator simply measures the absorbance of each solution at a specified wavelength and compares the results with the stated values. Each user should establish a tolerance for the measurements based on accepted criteria.

Linearity is defined as the ability of a photometric system to yield a linear relationship between the radiant power incident on its detector and the concentration (i.e., Beer's law). The linearity of a spectrometer can be determined using optical filters or solutions that have known absorbance values for a given wavelength. Linearity measurements should be evaluated for both slope and intercept.

Stray light is described as any light that impinges on the detector that does not originate from a polychromatic light source. Stray light can have a significant impact on any measurement made. Stray light effect can be evaluated by using special cutoff filters.

Types of Photometric Instruments

Several instrument designs and configurations may be used for absorption photometry. Each has unique terminology associated with its design. The terminology is not universal among users but is presented here as a guide. A *spectroscope* is an optical instrument used for visual identification of atomic emission lines. It has a monochromator, usually a prism or diffraction grating, in which the exit slit is replaced by an eyepiece that can be moved along the focal plane. The wavelength of an emission line can then be determined from the angle between the incident and dispersed beam when the line is centered on the eyepiece.

A *colorimeter* uses the human eye as the detector. The user compares the observed color of the unknown sample against a standard or a series of colored standards of known concentrations. *Photometers* consist of a light source, a filter, and a photoelectric transducer, as well as a signal processor and readout. Some manufacturers use the term *colorimeter* or *photoelectric colorimeter* for a photometer. These photometers use filters for isolation of specific wavelengths, not gratings or prisms.

A *spectrometer* is an instrument that provides information about the intensity of radiation as a function of wavelength or frequency. Spectrophotometers are spectrometers equipped with one or more exit slits and photoelectron transducers that permit determination of the ratio of the power of two beams as a function of wavelength, as in absorption spectroscopy. Most spectrophotometers use a grating monochromator to break up the light into a spectrum, as discussed earlier in the section on presample filters.

Single-beam spectrophotometers are the simplest types of absorption spectrometers. These instruments are designed to make one measurement at a time at one specified wavelength. The absorption maximum of the analyte must be known in advance when a single-beam instrument is used. The wavelength is then set to this value. The reference material (solvent blank) is transferred into a suitable cuvette and is placed in the path of the monochromatic light. The spectrometer is adjusted to read 0%T when a shutter is placed to block all radiation from the detector and is adjusted to read 100%T when the shutter is removed. After these adjustments have been made, the sample is placed in the light path, the absorbance is measured, and the concentration is determined using calculations based on Beer's law or by constructing a calibration curve for the analyte.

A double-beam spectrophotometer splits or chops the monochromatic beam of radiation into two components. One beam passes through the sample and the other passes through a reference solution or blank. In this design, the radiant power in the reference beam varies with the source energy, monochromator transmission, reference material transmission, and detector response, making the difference between the sample and the reference beam largely a function of the sample. The output of the reference beam can be kept constant, and the absorbance of the sample can be recorded directly as the electrical output of the sample beam.

Two fundamental instrument designs are used for double-beam spectrophotometers: double beam in space and double beam in time. A double beam in space design uses two photodetectors: one for the sample beam and the other for the reference beam. The two signals generated are directed to a differential amplifier, which then passes on the difference between the signals to the readout device. A schematic of the double beam in space system is shown in Figure 4.11.

A double beam in time instrument uses one photodetector and alternately passes the monochromatic radiation through the sample cuvette and then to the reference cuvette, using a *chopper*. A chopper is the term used for a device such as a rotating sector mirror that breaks up or rotates radiation beams. Each beam, consisting of a pulse of radiation separated in time by a dark interval, is then directed onto an appropriate detector. A schematic of the double beam in time system is shown in Figure 4.12.

A scanning double-beam system includes a double-beam spectrophotometer and a recorder that can provide an X-Y plot of absorbance versus wavelength for a given test sample. This type of configuration is ideal for determining the wavelength spectrum of an analyte in solution. The spectrophotometer has an automatically driven wavelength cam that can rotate at a predetermined speed. The recorder can be calibrated to the wavelength of the monochromator to facilitate the identification of each peak maximum.

REFLECTOMETRY

Measurement of analytes in biologic fluids using reflectometry has been used for decades. Two clinical applications include urine dipstick analysis and dry slide chemical analysis. The instruments used for these applications include a reflectometer. A reflectometer is a filter photometer that measures the quantity of light reflected by a liquid sample that has been dispensed onto a grainy or fibrous solid support.

The two types of reflectance are specular and diffuse. Specular reflectance occurs on a polished surface where the angle of incidence of the radiant energy is equal to the angle of reflection. Polished surfaces—for example, a mirror—can be used to direct and manage radiant energy but not to determine concentration. Diffuse reflectance occurs on nonpolished surfaces (i.e., a grainy or fibrous surface), as noted earlier. The reflected radiant energy tends to go in many directions. Diffuse reflection occurs within the layers and depends on the properties and characteristics of the layers themselves. A colored substance absorbs the wavelength of its color and reflects all other wavelengths at many different angles. Therefore, the amount of a substance present can be measured as an indirect function of the reflected light.

A typical reflectometer used in a clinical laboratory detects only a constant fraction of the diffuse reflected light. Thus, the reflectance of a sample is represented by the following:

$$R_{(\text{diffuse reflectance})} = \frac{R'_{(\text{fraction of diffuse reflectance of sample})}}{R'_{(\text{fraction of diffuse reflectance of a standard})}}. \qquad \text{(Eq. 4.10A)}$$

The amount of light reflected by a solution dispensed onto a white granular or grainy surface is inversely related to the concentration of the sample, as given by the following:

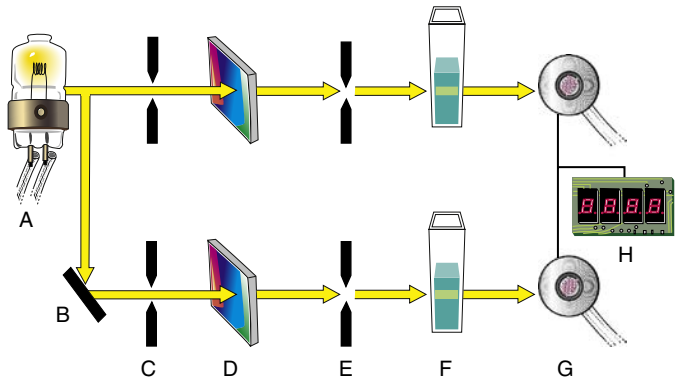

Figure 4.11 Double beam in space design of spectrophotometer. **A,** Exciter lamp. **B,** Mirror. **C,** Entrance slits. **D,** Monochromators. **E,** Exit slits. **F,** Cuvettes. **G,** Photodetectors. **H,** Light-emitting diode (LED).

$$R_{density} = -\log\left(\frac{R_{sample} - R_{black}}{(R_{standard})}\right) \times R_{white}, \qquad \text{(Eq. 4.10B)}$$

where $R_{density}$ = corrected reflectance density of the sample, R_{sample} = measured reflectance of the sample, R_{black} = reflectance of a black reference, R_{white} = reflectance of a white reference, and $R_{standard}$ = reflectance of a standard solution.

The ideal reflectance value of a pure white standard of ceramic material is *one* (i.e., all light is reflected). Conversely, the ideal reflectance value of pure black material is *zero* (i.e., all light is absorbed).

The relationship of percent reflectance and concentration of an analyte is nonlinear. Several algorithms have been developed for linearizing this relationship. The specific algorithm used depends on the reflection characteristics of the composition material of the pad or film, the nature of the illumination, and the geometry of the instrument.

Reflectometers

The components of a reflectometer are very similar to those of a photometer, as shown in Figure 4.13. A tungsten–quartz halide lamp serves as a source of polychromatic radiation. A monochromator (e.g., stationary filter or filter wheel for multiple analytes) is used to isolate the wavelength of interest. Next, the monochromatic light passes through a slit and is directed onto the surface of a urine dipstick pad or dry slide, depending on the instrumentation used. Solid-state photodiodes are typically used to detect reflected radiant energy. Special optical devices—for example, fiber-optics or ellipsoidal mirrors—can be used to direct radiant energy onto the detector. A computer or microprocessor is used to convert nonlinear reflectance signals into direct readout concentration units.

MOLECULAR LUMINESCENCE SPECTROSCOPY (FLUOROMETRY)

Principle

Luminescence is based on an energy exchange process that occurs when certain compounds absorb electromagnetic radiation, become excited, and return to an energy level lower than or equal to their original level. Because some energy is lost before emission from the excited state by collision with the solvent or other molecules, the wavelength of the emitted light is longer than that of the exciting light. Most uncharged molecules contain even numbers of electrons in the ground state. These electrons fill molecular orbits in pairs with their spins in opposite directions. No electron energies can be detected by application of a magnetic field to such spin patterns; this electronic state is called the *singlet state*. Similarly, if an electron becomes excited by electromagnetic radiation and its spin remains paired with the ground state, this creates a singlet excited state. The lifetime of the excited state is the average length of time the molecule remains excited before emission of light. For a singlet excited state, the lifetime of the excited state is on the order of 10^{-9} to 10^{-6} s. The light emission from a singlet excited

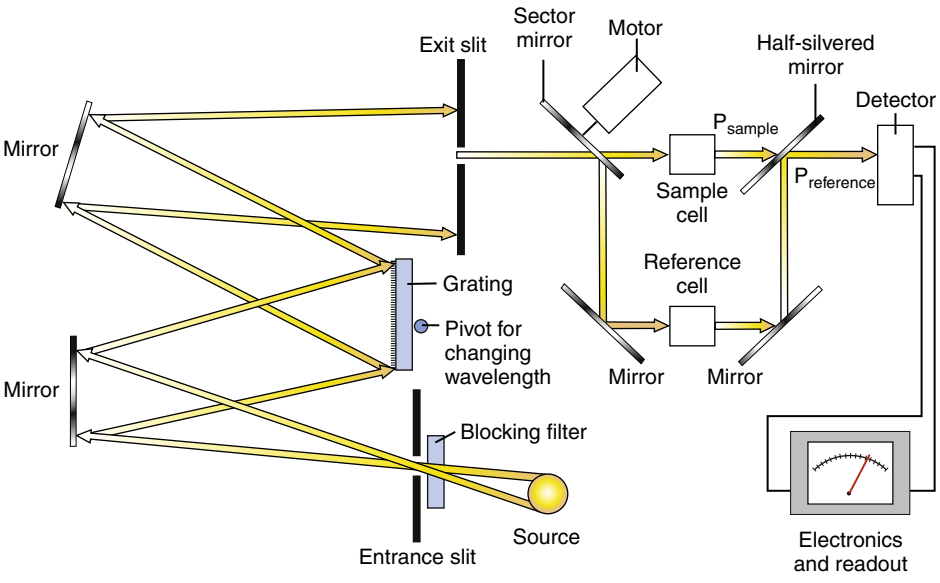

Figure 4.12 Double beam in time design of spectrophotometer.

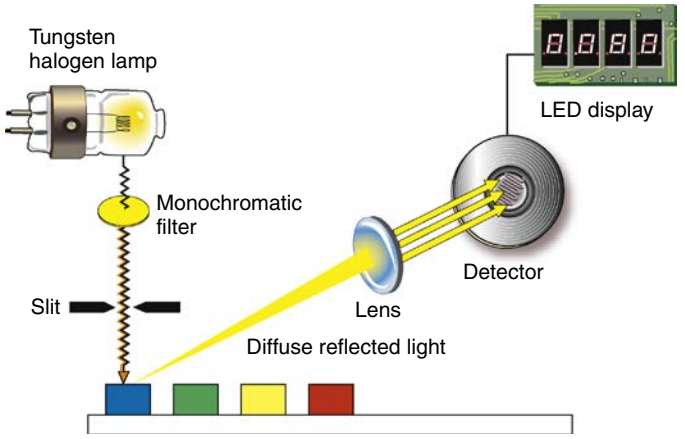

Figure 4.13 Components in a typical reflectometer used to measure analytes on urine dipstick. The different-colored blocks represent different tests performed in urinalysis. *Blue* represents the quantitation of analyte using reflectance (i.e., the reflectance of light focused on the sample and reflected at an angle *[yellow beam]*, where it is detected).

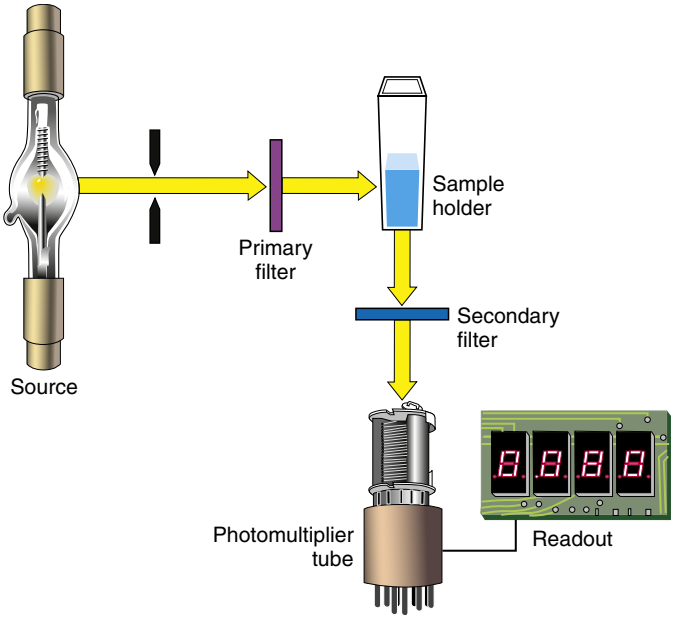

Figure 4.14 Components of a fluorometer. (From Bishop ML, Duben-Engelkirk JL, Fody EP: *Clinical chemistry: Principles, procedures, correlations.* Philadelphia, 1992, JB Lippincott Company; with permission.)

state is called *fluorescence*. When the spins of the electrons in the excited state are unpaired, the electron energy levels will be split if a magnetic field is applied; this electronic state is called a *triplet state*. Triplet state lifetimes range from 10^{-4} to 10 s (Willard et al., 1988). Light emission from an excited triplet state is called *phosphorescence*.

Luminescence is widely used because of its high sensitivity; the signal-to-noise ratio is very high because light is measured against a nearly dark background. High specificity is a function of using two spectra, the excitation and emission spectra, and the possibility of measuring the lifetime of the fluorescent state. Two compounds that are excited at the same wavelength but emit at different wavelengths are readily differentiated with this technique.

Components of Fluorometers and Spectrophotofluorometers

Instruments designed for fluorescence measurement have the following basic components: a light source, an excitation (primary) monochromator, a cuvette, an emission (secondary) monochromator, and a photodetector (Fig. 4.14). The exciter lamp is a high-intensity light source, such as a mercury vapor lamp or a xenon arc lamp. Simple instruments use mercury vapor lamps that do not require any special power supply. Mercury vapor lamps produce discrete and intense resonance lines that are not ideal for compounds with absorption bands at wavelengths not coinciding with these emission bands. For such compounds, xenon arc lamps producing an intense continuous spectrum between 300 and 1300 nm are appropriate. These lamps are used in nearly all commercial spectrophotofluorometers. In fluorescence measurements, the emitted light is detected at a right angle to the incident light to eliminate potential interference by the excitation signal. Phototubes or PMTs are required for fluorescence measurements because the signals are generally of low intensity. Newer fluorometers on the market today use diode array and CTDs, which allow the rapid recording of both excitation and emission spectra and are particularly useful in chromatography and electrophoresis.

Time-resolved fluorescence assays minimize problems inherent in other fluorescent assays, such as overlapping excitation or emission spectra of compounds present in the sample with the fluorophore. The label most commonly used is a chelate of europium (Eu^{3+}). Energy is absorbed by the organic ligand, leading to an excited state as the electrons migrate from the ground state singlet to the excited singlet state. The excitation may lead to any vibrational multiplet of the excited state S_1. The molecule rapidly returns to the lowest energy levels in S_1 by a nonradiative process. The energy is transferred to the metal ion, which becomes excited and subsequently emits characteristic radiation. The radiative transition of excited Eu^{3+} after an energy transfer from triplet state results in an emission wavelength of 613 nm. The fluorescence lifetime of Eu^{3+} chelate is 10 to 1000 μs compared with nanoseconds for the most commonly used fluorophore. Therefore, Eu^{3+} with its longer emission lifetime makes it more attractive to use over a fluorophore-like fluorescein with a lifetime of 4.5 ns. Time-resolved fluorescence instruments are similar to a typical fluorometer except that time-resolved fluorometers use a time-gated measure on only a portion of the total emission spectra.

Chemiluminescence applications have increased dramatically owing to the increased sensitivity over fluorescence. In chemiluminescence, the light signal is measured against a completely dark background because no excitation light is required. The primary application has been in the area of immunoassays where several chemiluminescence compounds have been used as antigen labels. Chemiluminescence differs from fluorescence and phosphorescence in that the emission of light is created from a chemical or electrochemical reaction and not from absorption of electromagnetic energy. The chemical reaction yields an electronically excited compound that emits light as it returns to its ground state or that transfers its energy to another compound, which then produces emission. Chemiluminescence involves the oxidation of an organic compound (e.g., dioxetane, luminol, acridinium ester) by an oxidant (hydrogen peroxide, hypochlorite, or oxygen). These oxidation reactions may occur in the presence of catalysts, such as enzymes that include alkaline phosphatase, horseradish peroxidase, and microperoxidase, metal ions (Cu^{2+} or Fe^{3+} phthalocyanine complex), and hemin. The excited products formed in the oxidation reaction produce chemiluminescence on return to the singlet state. A luminometer is used to detect chemiluminescence; it contains a PMT that provides a very strong electrical output signal. A typical signal from a chemiluminescent compound rises rapidly with time and reaches a maximum when reagent and analyte are completely mixed. An exponential decay of the signal follows until baseline is reached.

NEPHELOMETRY AND TURBIDIMETRY

Nephelometry and turbidimetry are used to measure the concentrations of large particles such as antigen–antibody complexes, prealbumin, and other serum proteins. Nephelometry detects light that is scattered at various angles; scattered light yields a small signal that must be amplified. In contrast, turbidimetry measures a reduction in light transmission due to particle formation; thus, it detects a small decrease in a large signal (Fig. 4.15).

Principle

Nephelometry and turbidimetry are based on the scattering of radiation by particles in suspension. When a collimated light beam strikes a particle in suspension, portions of the light are absorbed, reflected, scattered, and transmitted. Nephelometry is the measurement of the light scattered by a particulate solution. Three types of light scatters occur according to the relative size of the light wavelength (Gauldie, 1981). If the wavelength (λ) of light is much larger than the diameter (d) of the particle ($d < 0.1\lambda$),

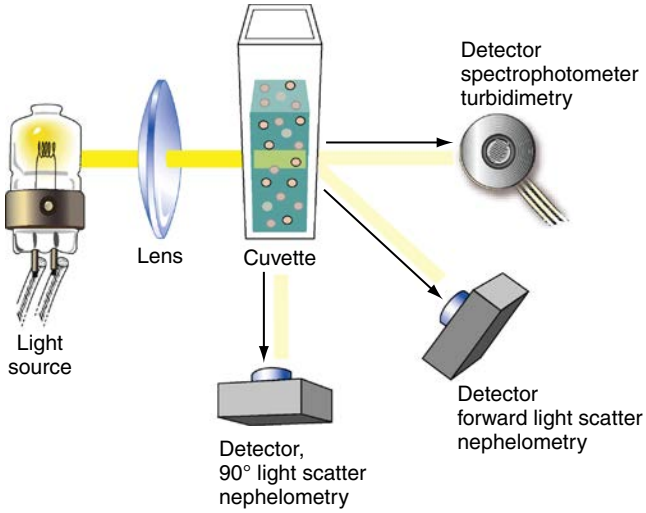

Figure 4.15 Optical arrangements of nephelometry and turbidimetry. Note that nephelometry detects (right-angle or forward) scattered light, and turbidimetry measures a reduction of light transmitted in the forward direction. (Modified from Bishop ML, Duben-Engelkirk JL, Fody EP: *Clinical chemistry: Principles, procedures, correlations.* Philadelphia, 1992, JB Lippincott Company; with permission.)

the light scatter is symmetrical around the particle. Minimum light scatter occurs at 90 degrees to the incident beam and was described by Rayleigh (Rayleigh, 1885). If the wavelength of light is much smaller than the particle diameter ($d < 0.1\lambda$), then the light scatters forward owing to destructive out-of-phase backscatter, as described by the Mie theory. If the wavelength of light is approximately the same as the particle size, more light scatters in the forward direction than in other directions, as defined by the Rayleigh-Debye theory. A common application of nephelometry is the measurement of antigen–antibody reactions. Because most antigen–antibody complexes have a diameter of 250 to 1500 nm and the wavelengths used are 320 to 650 nm, light is scattered forward (Rayleigh-Debye type).

Nephelometer

A typical nephelometer consists of a light source, a collimator, a monochromator, a sample cuvette, a stray light trap, and a photodetector. Light scattered by particles is measured at an angle, typically 15 to 90 degrees to the beam incident on the cuvette (see Fig. 4.15). Light scattering depends on the wavelength of incident light and particle size. For macromolecules with size close to or larger than the light wavelength, measurement of forward light scatter increases the sensitivity of nephelometry. Light sources include a mercury-arc lamp, a tungsten-filament lamp, a light-emitting diode, and a laser.

Lasers produce stable, nearly ideal monochromatic light of narrow bandwidth and emit radiant energy that is coherent, parallel, and polarized. A laser beam can be maintained as a very slim cylinder only a few micrometers in cross-section. A typical helium-neon laser lamp consists of a helium-pumping electrode (cathode) and a hollow glass laser core surrounded by a laser plasma tube (anode). Both the plasma tube and the core are filled with free helium and neon gases. The electrical discharge between the cathode and the anode is confined to the hollow glass core to keep it concentrated for maximum energy transfer. Two mirrors are positioned at the ends of the laser tube. One of them is fully reflective and the other partially transparent. When the electrode is charged, the helium atoms are excited to a higher energy state and then transfer this energy to the neon atoms by collision. In turn, the excited neon atoms emit photons. Photons bounce back and forth between the two end mirrors, stimulating other atoms to emit additional photons, resulting in an amplification process. The amplified light eventually emerges as a laser beam through the partially transparent mirror. With the high-intensity monochromatic beam, a substantial increase in sensitivity has been seen with lasers over conventional light sources. Disadvantages of laser sources include cost, safety and cooling requirements, and limited availability of wavelengths.

Turbidimetry

The measurement of the reduction in light transmission caused by particle formation is termed *turbidimetry*. Light transmitted in the forward direction is detected. The amount of light absorbed by a suspension of particles depends on the specimen concentration and on the particle size. Solutions requiring quantitation by turbidimetry are measured using visible photometers or visible spectrophotometers. Higher sensitivity has been achieved using photodetectors that can detect small changes in photon signals. Sensitivity comparable with nephelometry can be attained using low wavelengths and high-quality spectrophotometers. Many clinical applications exist for turbidimetry. Various microbiology analyzers measure the turbidity of samples to detect bacterial growth in broth cultures. Turbidimetry is routinely used to measure the antibiotic sensitivities from such cultures. In coagulation analyzers, turbidimetric measurements detect clot formation in the sample cuvettes. Turbidimetric assays have long been available in clinical chemistry to quantify protein concentration in biologic fluids, such as urine and cerebrospinal fluid (CSF).

FLOW CYTOMETRY

Scattered light can further be used to determine the size and shape of cells or macromolecules in a suspension using the technique of flow cytometry. The principles of flow cytometry are discussed at length in Chapter 46. Here, we present a brief description of flow cytometry to illustrate how scattered light can be used to image cells.

A flow cytometer measures multiple properties of cells suspended in a moving fluid medium. As each particle passes single file through a laser light source, it produces a characteristic light pattern that is measured by multiple detectors for scattered light (forward and 90 degrees) and fluorescent light (if the cell is stained with a fluorochrome). Flow cytometry is used to count and sort cells as well as viral particles, DNA fragments, bacteria, and latex beads. It is a core component of hematology cell counters and the technology used to differentiate white blood cells.

In flow cytometry, the term *particle* describes any object flowing through the instrument. An *event* is anything that is interpreted by the instrument to be a single particle. An event may be determined correctly or incorrectly by a flow cytometer. Methods have been developed to compensate for measurement of unwanted events. An example is the correction for measuring the simultaneous passing of two particles. Particles must be in suspension as single cells to be analyzed. If not, they can be made suitable for flow cytometry by the use of mechanical disruption or enzymatic digestion. Size restrictions also apply; cells or particles must be from 1 to 30 μm in diameter. Specialized flow cytometers are designed to handle smaller particles such as DNA fragments or bacteria.

Instrument Components

The system shown in Figure 4.16 has all of the design features of a flow cytometer with cell-sorting capabilities. The cell suspension aliquots are introduced into the flow chamber using air pressure. As cells pass through the flow chamber, a low-pressure sheath fluid surrounds them. This outer fluid stream creates a laminar flow that forces the specimen to the center and results in a single-file alignment of the individual cells. This process is called *hydrodynamic focusing*. A laser beam passes through each cell as it flows through the chamber. Forward light scatter is proportional to cell size, and 90-degree or right-angle scatter is related to cell granularity and nuclear irregularity. If the cells are labeled with appropriate fluorochromes, fluorescent signals proportional to the amount of bound label can be measured. Green fluorescence usually means that the dye fluorescein was used as a marker; red fluorescence usually means that a dye such as phycoerythrin was used as the contrasting marker. These dyes are usually attached to antibodies to specifically target selective antigens on cells or particles.

Forward light scatter is directed to the forward scatter photodetector. At right angles to the laser beam are mirrors that divide the right-angle light scatter among the remaining photodetectors (e.g., a right-angle scatter detector and two fluorescence detectors). Across the forward lens is an obscuration bar that blocks the laser beam after it passes through the stream. Only light from the laser that has been refracted or scattered as it strikes a particle in the stream is diverted enough from its original direction to avoid the obscuration bar and strike the forward positioned lens and the photodiode behind it. Granulocytes, monocytes, and lymphocytes are separated on the basis of size and granularity patterns as determined by simultaneously analyzing forward and right-angle light scatter. For example, granulocytes with irregular nuclei scatter more light to the side than do lymphocytes with their spherical nuclei. Cell subpopulations can be identified by using electronic gating and analyzing fluorescence patterns (based on labels used for specific cells).

Fluorescence-activated cell sorter (FACS) describes the ability of a flow cytometer to physically sort cells in a liquid suspension. To do so, the

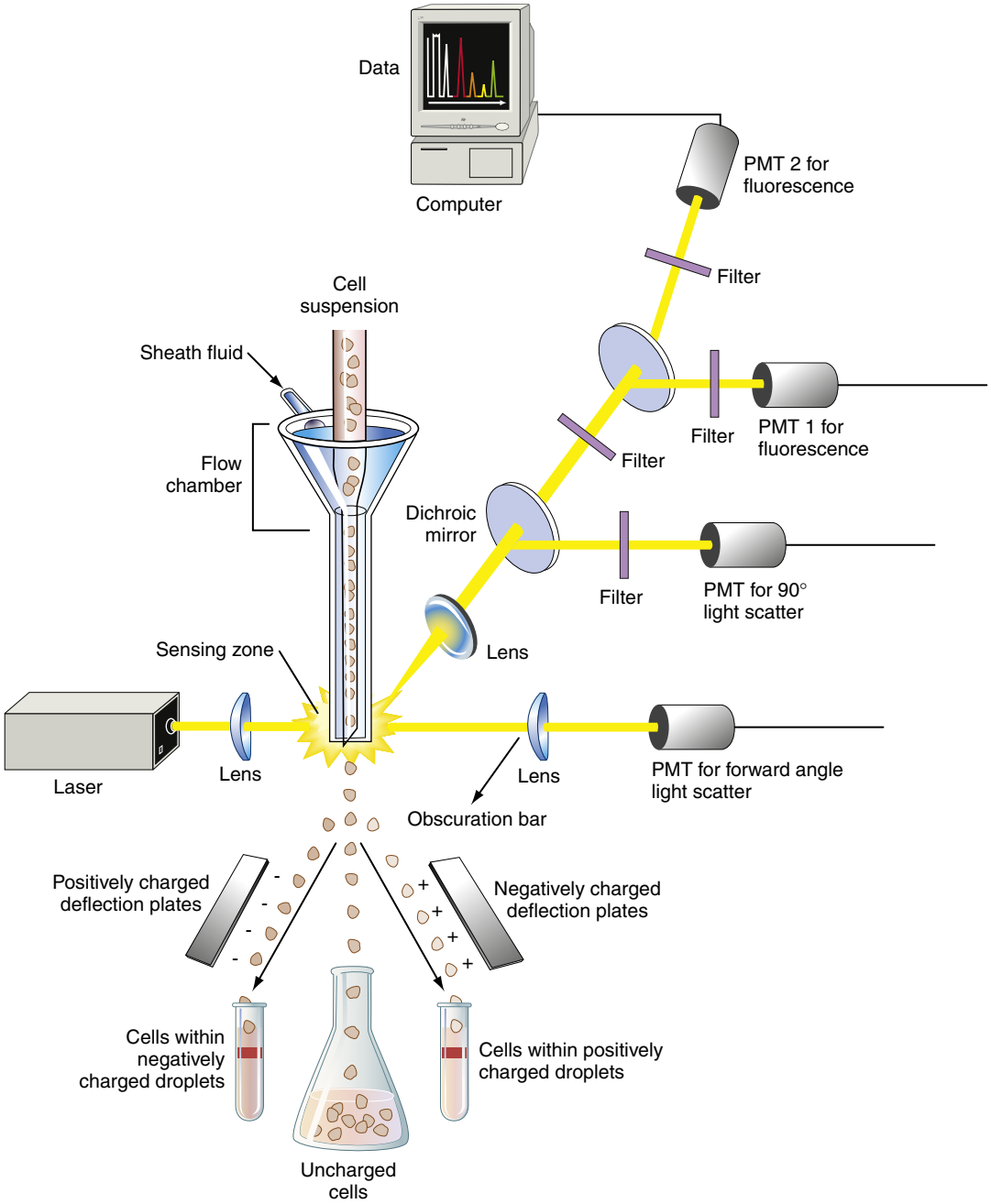

Figure 4.16 Components of a flow cytometer and a cell sorter. (Redrawn from Ward KM, Lehmann CA, Leiken AM: *Clinical laboratory instrumentation and automation: Principles, applications, and selection.* Philadelphia, 1994, WB Saunders; with permission.)

instrument design has to be modified to electrically charge cells of interest. This is done by first vibrating the sheath stream to break it into drops. The stream of drops flows past two charge (high-voltage) plates, where the cells of interest are electrically charged with a voltage pulse. Then the flow stream enters an electrical field, where the charged cells are deflected into suitable collection containers. Unwanted cells are not charged and are not deflected upon passing through the field.

REFRACTOMETRY

Refractometry is based on light refraction. When light passes from one medium into another, the light beam changes its direction at the boundary surface if its speed in the second medium is different from that in the first. The ability of a substance to bend light is called *refractivity*, and it is measured as a difference between the *angle of incidence* and the *angle of refraction*. The refractivity of a liquid depends on the wavelength of the incident light, the temperature, the nature of the liquid medium, and the concentration of the solute dissolved in the medium. If the first three factors are held constant, the refractivity of a solution is an indirect measurement of total solute concentration. Refractometry can be used to measure protein concentration, specific gravity of urine, and concentration of solutes in column effluent of high-performance liquid chromatography analysis.

OSMOMETRY

Osmometry is the measurement of the osmolality of an aqueous solution such as serum, plasma, or urine. As osmotically active particles (e.g., glucose, urea nitrogen, sodium) are added to a solution, causing its osmolality to increase, four other properties of the solution are also affected. These properties are osmotic pressure, boiling point, freezing point, and vapor pressure. They are called *colligative properties* of the solution because they can be related to one another and to the osmolality. As the osmolality of a solution increases, (1) the osmotic pressure increases, (2) the boiling point is elevated, (3) the freezing point is depressed, and (4) the vapor pressure is depressed. Osmometry is based on measuring changes in the colligative properties of solutions that occur owing to variations in particle concentration. Freezing-point depression osmometry is the most commonly used method for measuring the changes in colligative properties of a solution. It is based on the principle that the addition of solute molecules lowers the temperature at which a solution freezes.

Principle of Freezing-Point Osmometry

The freezing point is the temperature at which water and ice are in equilibrium and is related to solute concentration. It is described by the following equation:

$$\Delta T_f = K_f \cdot m, \qquad \text{(Eq. 4.11)}$$

where ΔT_f = change in freezing-point temperature, K_f = freezing-point constant of the solvent, and m = molality.

A 1.0-mOsm/kg solution has a freezing point depression of 0.00186° C when compared with pure solvent (water). Thus, blood plasma, with an osmolality of about 285 mOsm/kg, has a freezing point of about –0.53° C.

Freezing-Point Osmometer

A freezing-point osmometer consists of a sample chamber containing a stirrer and a thermistor (temperature-sensing device) connected to a readout device. The sample is rapidly supercooled to several degrees below its freezing point in a refrigeration chamber containing, for example, ethylene glycol. The sample is then agitated with the stirrer to initiate freezing. As ice crystals form, heat is released from the solution; this raises the temperature of the sample. The rate at which this heat of fusion is released from the ice being rapidly formed reaches equilibrium with the rate of heat removed by the colder temperature of the sample chamber. This equilibrium temperature, known as the freezing point of the solution, stays constant for several minutes once it is reached. This freezing point is detected by the thermistor, and the osmolality of the sample is converted to units of milliosmoles per kilogram of water.

ELECTROCHEMISTRY

Electrochemistry involves measurement of the current or voltage generated by the activity of specific ions. Analytic techniques include potentiometry, coulometry, voltammetry, and amperometry.

Potentiometry

The measurement of potential (voltage) between two electrodes in a solution forms the basis for a variety of procedures for measuring analyte concentration. Electrical potentials are produced at the interface between a metal and ions of that metal in a solution. Such potentials also exist when a membrane semipermeable to that ion separates different concentrations of an ion. To measure the electrode potential, a constant-voltage source is needed as the reference potential. The electrode with a constant voltage is called the *reference electrode*, whereas the measuring electrode is called the *indicator electrode*. Concentration of ions in a solution can be calculated from the measured potential difference between the two electrodes. The measured cell potential is related to the molar concentration by the Nernst equation:

$$E = E^\circ - (RT/nF) \cdot \ln [a_{red}/a_{ox}] = E^\circ - (RT/nF) \cdot (2.303 \log [a_{red}/a_{ox}]), \qquad \text{(Eq. 4.12)}$$

where E = cell potential measured, $E°$ = standard reduction potential, n = number of electrons involved in the reaction, a_{red} = activity of the reduced species, a_{ox} = activity of the oxidized species, F = Faraday (96,485 C/mol), T = absolute temperature, and R = molar gas constant.

Substituting molar concentration, C, for activity (a), common logarithm to the base 10 for natural log and room temperature, approximately 25° C (298° K):

$$E = E^o - (0.0592/n) \log C_{red}/C_{ox}, \qquad \text{(Eq. 4.13)}$$

where C_{red} = concentration of reduced species and C_{ox} = concentration of oxidized species.

The Nernst equation is useful for predicting the electrochemical cell potential given the concentrations of oxidized and reduced species for a given electrode system.

Reference Electrodes

In many electroanalytic applications (e.g., measuring pH), it is desirable that the half-cell potential of one electrode be known, constant, and completely insensitive to the composition of the solution under study. An electrode that fits this description is called a *reference electrode*.

An ideal reference electrode should (1) conform to the Nernst equation, (2) exhibit a potential that is constant with time, (3) return to its original potential after being subjected to small currents, and (4) exhibit little hysteresis (i.e., lags with temperature cycling). The standard hydrogen electrode (SHE) exhibits many of these qualities but is not practical to use in clinical laboratory instrumentation. Thus, the calomel and silver/silver chloride reference electrodes are widely used for clinical measurements.

The calomel electrode (saturated calomel electrode [SCE]) consists of mercury in contact with a solution that is saturated with mercurous (I) chloride (calomel) and that also contains a known concentration of potassium chloride. The silver/silver chloride electrode consists of a silver electrode immersed in a solution of potassium chloride that has been saturated with silver chloride. Silver/silver chloride electrodes can be used at temperatures greater than 60° C, whereas calomel electrodes cannot. Mercuric (II) ions, however, react with fewer sample components than do silver ions (which can react with proteins, for example). Such reactions can lead to plugging of the junction between the electrode and the analyte solution.

Ion-Selective Electrode

An ion-selective electrode (ISE) is an electrochemical transducer capable of responding to one specific ion. An ISE is very sensitive and selective for the ion it measures. It consists of a membrane or other barrier separating a reference solution and a reference electrode from the solution to be analyzed. The complexity of ion-selective electrode design depends on the membrane/barrier composition that determines its ionic selectivity. Many types of ISEs are available, including glass electrodes, liquid membrane electrodes, precipitate-impregnated membrane electrodes, solid-state electrodes, gas electrodes, and enzyme electrodes.

pH Electrode

Glass electrodes were the first and are still the most common electrodes for measuring hydrogen ion activity (pH or negative log of the hydrogen ion concentration). A pH electrode consists of a small bulb made of layers of hydrated and nonhydrated glass, which contains a chloride ion buffer solution. The buffer has a known hydrogen ion concentration. An internal electrode, usually silver/silver chloride, serves as an internal reference electrode. A saturated calomel electrode is used as an external reference electrode. One theory suggests that the sodium ions in the hydrated glass layer drift out. Sodium ions have a large ionic radius. Specimens containing hydrogen ions, which have a smaller ionic radius, replace the sodium ions. The result is a net increase in the external membrane potential. This potential propagates through the thin, dry membrane to the inner hydrated surface of the glass. Chloride ions in the inner buffer solution respond by migrating to the internal glass layer. Potentials generated at the pH electrode are referenced to the external reference electrode (saturated calomel), and the difference or change is displayed as pH units.

pCO_2 Electrode

The pCO_2 electrode is a pH electrode contained within a plastic jacket. This plastic jacket is filled with a sodium bicarbonate buffer and has a gas-permeable membrane (Teflon or silicone) across its opening. When whole blood containing dissolved carbon dioxide (CO_2) contacts the Teflon membrane, CO_2 from the blood passes through and mixes with the buffer. The equilibrium reaction shown in Equation 4.14 shifts, depending on the number of CO_2 molecules in a sample. The hydrogen ion activity is measured by a potentiometric pH indicator system.

$$CO_2 + H_2O \rightleftharpoons HCO_3^- + H^+ \qquad \text{(Eq. 4.14)}$$

Coulometry

Coulometry measures the quantity of electricity (in coulombs) needed to convert an analyte to a different oxidation state. By definition, a coulomb is the quantity of electricity or charge that is transported in 1 second by a constant current of 1 ampere. For a constant current of 1 ampere for t seconds, the number of coulombs (Q) is given by the expression

$$Q = It. \qquad \text{(Eq. 4.15)}$$

A Faraday is the charge in coulombs associated with 1 mole of electrons. The charge of the electron is 1.6018×10^{-19} Q, so 1 Faraday is equal to 96,485 Q/mol.

Coulometry is used to measure chloride ion in serum, plasma, CSF, and sweat samples. In measuring chloride with coulometry, a constant current is applied across the two silver electrodes, which liberate silver ions into the specimen at a constant rate. Chloride ions in the sample combine with released silver ions to produce insoluble silver chloride. A pair of indicator and reference electrodes senses the excess silver ions and stops the titration. The number of silver ions released by ionization, which is exactly equal to that of chloride ions in the sample, can be calculated from Faraday's law:

$$Q = It = znF, \qquad \text{(Eq. 4.16)}$$

where z = number of electrons involved in the reaction, n = number of moles of analyte in the sample, and F = Faraday's constant (96,485 C/mol of electrons).

Amperometry

Amperometry is the measurement of the current flow produced by an oxidation–reduction reaction. Several immobilized enzyme electrodes use this principle, as do pO_2 electrodes (discussed later) and chloride titrators. The measurement of chloride in samples involves the use of two electrochemical methods: coulometry (discussed earlier) and amperometry. In the chloride titrator, a pair of silver electrodes serves as the indicator electrodes. When all of the chloride has been consumed, the silver appears in excess, causing an increase in current. This signals the endpoint of the reaction.

pO_2 Gas-Sensing Electrode

A widely used oxygen-sensing electrode (to determine partial pressure of oxygen in blood) incorporated in blood gas analyzers uses an amperometric or current-sensing electrolytic cell as the indicator electrode.

The pO_2 electrode uses a gas-permeable membrane, usually polypropylene, which allows dissolved oxygen to pass through. This membrane also prevents other blood constituents (that may interfere with the electrode) from passing through. Once the oxygen permeates the membrane, it reacts with a polarized platinum cathode according to the following reaction:

$$O_2 + 4e' \rightarrow 2O^-$$
$$2O^- + 2H_2O \rightarrow 4OH^-. \qquad \text{(Eq. 4.17)}$$

This, in turn, produces a change in the current through the cell, and the change is directly proportional to the partial pressure of oxygen present in the specimen.

Voltammetry

Voltammetry is a method in which a potential is applied to an electrochemical cell and the resulting current is measured. The most important advantages of voltammetry are sensitivity and the capability for multielement measurements. Analytes can be detected in the parts-per-billion range. With careful selection of testing conditions and methods, several analytes can be measured simultaneously in a single voltammetric study. Voltammetry consumes minimal analyte, unlike coulometry, which converts all of the analyte to another state. *Anodic stripping voltammetry* is an electrochemical technique used to measure heavy metals, such as lead. The measurement of lead in blood occurs in basically two steps. First, free lead is electroplated (deposited) onto the platinum cathodes at a characteristic voltage. Second, the lead is stripped off of the platinum cathode, and the current is monitored over time. The current value is proportional to the amount of lead in the blood sample. This technique allows the sample to be preconcentrated at the electrode, which enables the method to detect very low analyte levels.

CONDUCTANCE

The principles of conductance have several applications associated with clinical laboratory procedures. Examples include monitoring water purity, measuring analytes in blood such as urea, and serving as components of detectors used in high-performance liquid chromatography (HPLC), gas chromatography (GC), cell counters, and capillary electrophoresis.

Electrolytic conductivity is a measure of the ability of a solution to carry an electrical current. Solutions of electrolytes conduct an electrical current by migration of ions under the influence of a potential gradient. The ions move at a rate dependent on their charge and size, the microscopic viscosity of the medium, and the magnitude of the potential gradient. Thus, for an applied potential, E, maintained constant but at a value that exceeds the deposition potential of the electrolyte, the current, I, which flows between the electrodes immersed in the electrolyte, varies inversely with the resistance of the electrolytic solution, R. The reciprocal of resistance, $1/R$, is called the *conductance*, G, and is expressed in reciprocal ohms, or mhos.

IMPEDANCE

Electrical impedance measurement is based on the change in electrical resistance across an aperture when a particle in conductive liquid passes through this aperture. As described at length in Chapter 31, electrical impedance is used primarily in the hematology laboratory to enumerate leukocytes, erythrocytes, and platelets. In a cell counter, using impedance in its simplest form, as originally developed by Wallace Coulter, aspirated blood is divided into two separate volumes for measurements. One volume is mixed with diluent and is delivered to the cell bath, where erythrocyte and platelet counts are performed. As a cell passes through the aperture, partially occluding it, the electrical impedance increases, producing a voltage pulse, the size of which is proportional to the cell size. The number of pulses is directly related to the cell count. Particles measuring between 2 and 20 fL are counted as platelets, whereas those measuring greater than 36 fL are counted as erythrocytes. The other blood volume is mixed with diluent and a cytochemical-lytic reagent that lyses only the red blood cells. A leukocyte count is performed as the remaining cells pass through an aperture. Particles greater than 35 fL are recorded as leukocytes.

ELECTROPHORESIS AND DENSITOMETRY

Electrophoresis is the separation of charged compounds based on their electrical charge. This technique is used almost always to separate the proteins in serum, urine, and other body fluids (mainly cerebrospinal fluid) as described in Chapter 20. When a voltage is applied to a salt solution (usually sodium chloride), an electrical current is produced by the flow of ions: cations toward the cathode and anions toward the anode. Conductivity of a solution increases with its total ionic concentration. The greater the net charges of a dissolved compound, the faster it moves through the solution toward the oppositely charged electrode. The net charge of a compound, in turn, depends on the solution pH. However, the mass and shape of a protein molecule also strongly influence its migration rate. The reason is that the larger the protein molecule, the greater is its interaction with the solvent, producing a "solvent drag" effect that retards the migration of the protein. This retardive force is generally proportional to the velocity of the molecule, i.e., aV, where a is the proportionality constant and V is the velocity. For a given electric field, U, and a net charge on the protein of ne, where e is the charge of an electron or a proton and n is the number of net positive or negative charges on the protein, the electric force on the protein is neU. This is counterbalanced by the retardive force, aV, i.e., aV = neU and V = neU/a. Since a increases with increasing mass, the velocity of proteins with higher masses tend to migrate more slowly than proteins with the same net charge but with lower masses (Pincus, 2011).

In the technique of **sodium dodecyl sulfate-polyacrylamide gel electrophoresis (SDS-PAGE)**, advantage is taken of this phenomenon in not only separating proteins using PAGE but also in determining the molecular mass of a protein from its position of migration. A sample of a protein solution is first treated with strong protein denaturing agents, including negatively charged detergents such as SDS. This detergent binds to the denatured proteins making all proteins in the sample highly negatively charged. All of these proteins would migrate to the anode at approximately the same rate except for the difference in their molecular masses; the ones of lowest molecular mass migrate more rapidly while the higher molecular mass proteins migrate more slowly. Thus, the proteins separate solely on the basis of their *molecular masses*. Standard solutions of proteins of different molecular masses serve as controls for this technique so that the molecular mass of a protein of unknown molecular mass can be determined directly from its migration rate (position of migration over a given time).

Electrophoresis separations often require high voltages (50–200 V DC); therefore, the power supply should provide a constant DC voltage at these levels. The buffer solution must have a carefully controlled ionic strength. A dilute buffer causes heat to be generated in the cell, and a high ionic strength does not allow good separation of the fractions. Common support media for electrophoresis in clinical work include cellulose acetate, agarose, and polyacrylamide gels. The total volume of specimen applied depends on the sensitivity of the detection method. For clinical work, 1 μL of serum may be applied. Once the electrophoresis is completed, the support medium is treated with a dye to identify the separated fractions. The most common dyes used for the visualization step include Coomassie blue, Amido Black, Ponceau S, Fat Red 7B, and Sudan Black B. To obtain a quantitative profile of the separated fractions, densitometry is performed on the stained support medium.

A densitometer measures the absorbance of the stain on a support medium. The basic components of a densitometer include a light source, a monochromator and a movable carriage to scan the medium over the entire area, an optical system, and a photodetector. Signals detected by the photodetector are related to the absorbance of the sample stain on the support, which is proportional to the specimen concentration. The support medium is moved through the light beam at a fixed rate; thus, a graph may be constructed that represents multiple density readings taken at different points. Most densitometers have a built-in integrator to find the area under the curve; thus, all sample fractions can be quantified.

ISOELECTRIC FOCUSING

Proteins are polymers of amino acids that can be anions or cations depending on the pH environment. At a specific pH, a protein will have a net charge of zero when the positive charge and the negative charge of its

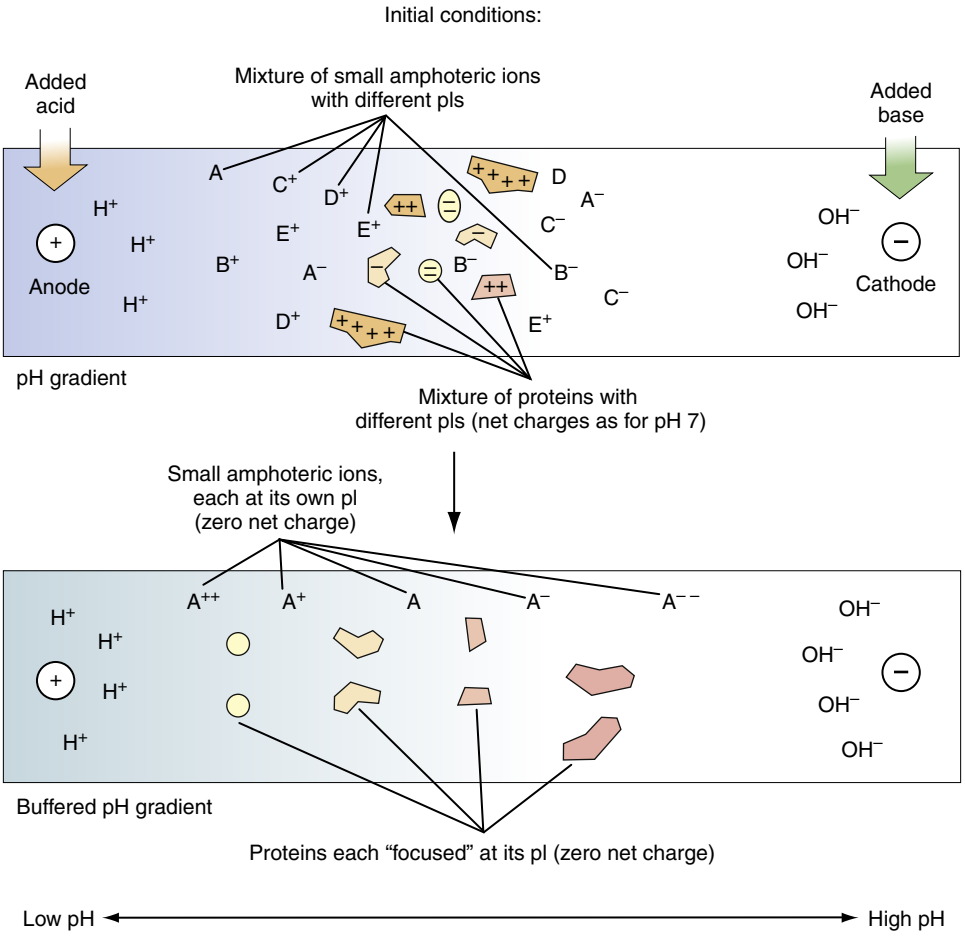

Figure 4.17 Isoelectric focusing (see text). (Redrawn from Schoeff LE, Williams RH: *Principles of laboratory instruments.* St. Louis, 1993, Mosby; with permission.)

amino acids cancel each other out. At this pH value, known as the protein's isoelectric point (pI), the protein is isoelectric. Isoelectric focusing (IEF) techniques are performed similarly to other electrophoresis methods except that the separating molecules migrate through a pH gradient. This pH gradient is created by adding acid to the anodic area of the electrolyte cell and adding base to the cathode area (Fig. 4.17). A solution of ampholytes (mixtures of small amphoteric ions with different pIs) is placed between the two electrodes. These ampholytes have high buffering capacity at their respective isoelectric points. The ampholytes close to the anode carry a net positive charge; those close to the cathode carry a net negative charge. When an electrical voltage is applied, each ampholyte will rapidly migrate to the area where the pH is equal to its isoelectric point. With their high buffering capacity, the ampholytes create stable pH zones for the more slowly migrating proteins. The advantage of isoelectric focusing techniques lies in their ability to resolve mixtures of proteins. Using narrow-range ampholytes, macromolecules differing in isoelectric point by only 0.02 pH units can be identified. Isoelectric focusing has been useful in measuring serum acid phosphatase isoenzymes. Its application has also been extended to detect oligoclonal immunoglobulin bands in CSF and isoenzymes of creatine kinase and alkaline phosphatase in serum.

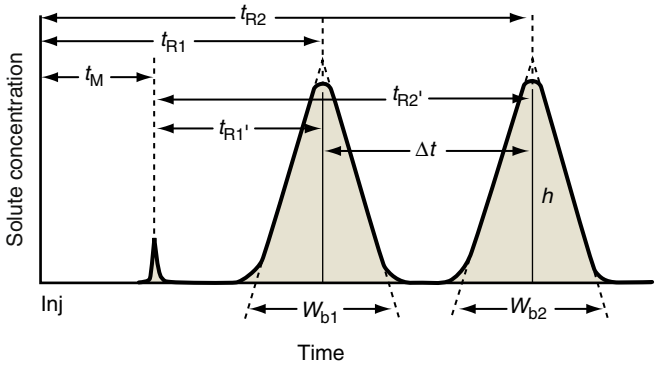

Figure 4.18 Chromatogram for the separation of two compounds. Note that the uncorrected retention time (t_{R1} and t_{R2}) is from injection (Inj) to peak; the corrected time ($t_{R1'}$ and $t_{R2'}$) takes into account the retention time of a nonretained compound (*t*M). (Redrawn from Ravindranath B: *Principles and practice of chromatography.* New York, 1989, John Wiley & Sons; with permission.)

CHROMATOGRAPHY

Chromatography is a separation method based on different interactions of the specimen compounds with the mobile phase and with the stationary phase as the compounds travel through a support medium. Compounds interacting more strongly with the stationary phase are retained longer in the medium than those that favor the mobile phase. Chromatographic techniques may be classified according to their mobile phase: gas chromatography and liquid chromatography. Figure 4.18 shows a typical chromatogram representing the concentration of each detectable compound eluting from the column as a function of time. Retention time (t_R) is the time it takes a compound to elute. This value is characteristic of a compound and is related to the strength of its interaction with the stationary phase and the mobile phase. Therefore, the retention time can be used to determine a compound's identity. In this example, two compounds are separated, and their retention times are represented by t_{R1} and t_{R2}. These are uncorrected retention times and are measured from the injection time, $t = 0$. A column's ability to separate two compounds depends on several factors, which include the difference in retention of the compounds or capacity factor, k'; the selectivity factor, α; and the number of theoretical plates.

The value of k' can be calculated by the following equation:

$$k' = (t_{R1} - t_m)/t_m \text{ or } t_{R1'}/t_m, \qquad \text{(Eq. 4.18)}$$

where t_m = retention time of an unretained compound and $t_{R1'}$ = corrected retention time.

Another measurement derived from the calculated capacity factor is the selectivity factor (α) or relative retention of two solutes. A ratio of both capacity factors is used to calculate the selectivity factor. To measure the width of each peak, draw tangents along the sides of the peak to

the baseline. W_b represents the distance between the two intersected lines. Another useful concept is theoretical plates. This describes the process by which the sample is transported down the column. In each "plate," the sample equilibrates between stationary and mobile phases. The analyte moves down the column as the equilibrated mobile phase transfers sample from one plate to another. To calculate the number of theoretical plates (N), use the following equation:

$$N = 16(t_R/W_b)^2. \quad \text{(Eq. 4.19)}$$

A plate number has no units, and the larger the value of N for a column, the greater is its separation efficiency. The combined effects of solvent efficiency and column efficiency are expressed in the resolution (R_s) of the column:

$$R_s = (t_{R2} - t_{R1})/0.5\,(W_{b1} + W_{b2}). \quad \text{(Eq. 4.20)}$$

The concentration of unknown compound can be derived by integration of peak areas or by using the method of internal standardization.

Gas Chromatography

GC is useful for compounds that are naturally volatile or can be easily converted into a volatile form. GC has been a widely used method for decades owing to its high resolution, low detection limits, accuracy, and short analytic time. Applications involve various organic molecules, including many drugs (see Chapter 24). Retention of a compound in GC is determined by its vapor pressure and volatility, which, in turn, depends on its interaction with the stationary phase. Two types of stationary phases commonly used in GC are solid absorbent (gas–solid chromatography [GSC]) and liquids coated on solid supports (gas–liquid chromatography [GLC]). In GSC, the same material (usually alumina, silica, or activated carbon) acts as both the stationary phase and the support phase. Although this was the first type of stationary phase developed, it is not as widely used as other types, primarily because of the strong retention of polar and low volatile solutes by the column (Ravindranath, 1989). GLC uses liquid phases such as polymers, hydrocarbons, fluorocarbons, liquid crystals, and molten organic salts to coat the solid support material. Calcine diatomaceous earth graded into appropriate-size ranges is often used as a stationary phase because it is a stable inorganic substance. The use of fused silica capillary columns in which the stationary phase is chemically bonded onto the inner surface of the column has become very popular with chromatographers. The advantage of this type of column is that the stationary phase does not leave the solid support and bleed into the detector, and a uniform monomolecular layer of the stationary phase is obtained through the bonding procedure.

Components of a typical GC system are illustrated in Figure 4.19. Its basic design consists of five components: a gas cylinder as a mobile phase source, a sample injector, a column, a detector, and a computer for data acquisition. These systems may be automated to provide the user with a more precise and efficient separation. Carrier gases (mobile phase), which must be chemically inert, include helium, hydrogen, and nitrogen. Other substances used as mobile phases include steam and supercritical fluids. Examples of these are carbon dioxide, nitrous oxide, and ammonia. The carrier gas should be of high purity, and the flow must be tightly controlled to ensure optimum column efficiency and reproducibility of test results. Samples are manually introduced into the GC using a syringe pipet or an automated syringe pipet system. A pipet tip pierces a plastic septum located in the injector port. Each injection port is heated to very high temperatures. Samples are vaporized and swept onto the column. If the molecule of interest is not volatile enough for direct injection, it is necessary to derivatize it into a more volatile form. Most derivatization reactions belong to one of three groups: silylation, alkylation, and acylation. Silylation is the most common technique, which replaces active hydrogens on the compounds with alkylsilyl groups. This substitution results in a more volatile form that is also less polar and more thermally stable.

Retention of compounds in a GC column can also be adjusted by changing the column temperature. The column temperature affects the volatility of the compounds and, thus, the degree of their interaction with the stationary phase. By proper selection of the starting temperature and temperature gradient during the procedure, good resolution of both weakly and strongly retained compounds may be achieved. The GC column, enclosed in a temperature-controlled oven, can be a packed column or a capillary column. Packed columns are usually 1 to 5 m long and 2 to 4 mm in diameter and are filled with a stationary phase. Capillary columns range from 5 to 100 m in length and from 0.1 to 0.8 mm in diameter and have a stationary phase located on their interior surface (Bartle, 1993). Capillary columns generally have higher efficiency and better detection limits. However, packed columns have a larger specimen or sample capacity, making them more useful in purification work. Examples of detectors used in GC include a flame ionization detector, a thermal conductivity detector, a nitrogen-phosphorus detector, an electron capture detector, a flame photometric detector, and a mass spectrometric detector. Flame ionization detectors (FIDs) are commonly used and are capable of detecting a wide variety of organic compounds and many inorganic compounds. This type of detector measures the ions produced by the compounds when burned in a hydrogen-air flame. An electrode collects the ions, and the magnitude of the resulting electrical current is proportional to the amount of substance (Tipler, 1993). FIDs can be modified to make them especially sensitive to molecules, including many drugs that contain either nitrogen or phosphorus (the so-called *nitrogen-phosphorus detector*, or NPD).

Liquid Chromatography

GC as a separation technique has some restrictions that make liquid chromatography a suitable alternative. Many organic compounds are too unstable or are insufficiently volatile to be assayed by GC without prior chemical derivatization. Liquid chromatography techniques use lower temperatures for separation, thereby achieving better separation of thermolabile compounds. These two factors allow liquid chromatography to separate compounds that cannot be separated by GC. Finally, it is easier to recover a sample in liquid chromatography than in gas chromatography. The mobile phase can be removed, and the sample can be processed further or reanalyzed under different conditions.

Many forms of liquid chromatography are available; the selection of an appropriate form depends on a variety of factors. These factors include analysis time, type of compound, and detection limits. Paper, thin-layer (discussed in Chapter 24), ion-exchange, and exclusion liquid chromatography often result in poor efficiency and a very long analysis time owing to low mobile phase flow rates. HPLC, also discussed in Chapter 24, emerged in the late 1960s as a viable form of liquid chromatography that provided advantages over other forms of liquid chromatography and GC. HPLC uses small, rigid supports and special mechanical pumps, producing high pressure to pass the mobile phase through the column. HPLC columns can

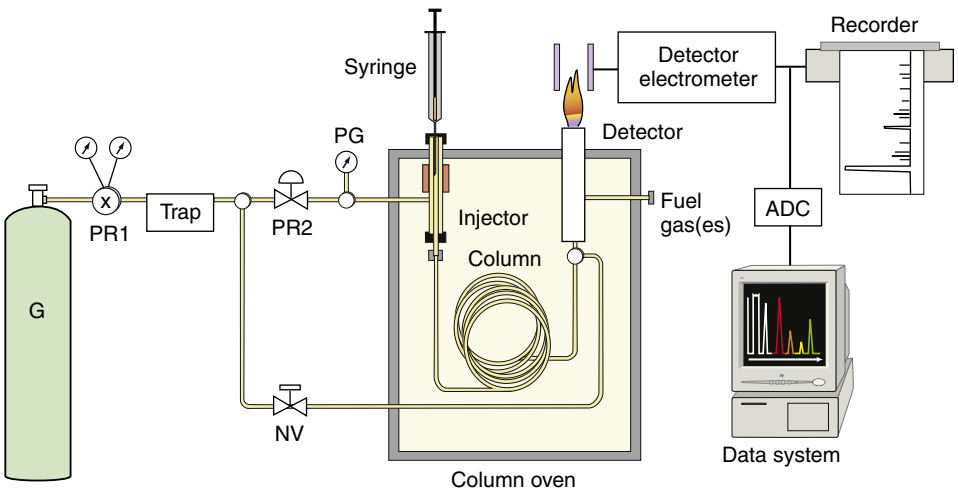

Figure 4.19 Components of a gas chromatographic system. *G,* Gas cylinder. *NV,* Valve for adjusting the gas flow rate. *PG,* Pressure gauge. *PR1* and *PR2,* Regulators. (*Redrawn from Ravindranath B: Principles and practice of chromatography.* New York, 1989, John Wiley & Sons; with permission.)

be used many times without regeneration. The resolution achieved with HPLC columns is superior to that of other forms of liquid chromatography, analysis times are usually much shorter, and reproducibility is greatly improved. All of these attributes of HPLC render it a better method of separation over other forms of liquid chromatography.

Five separation techniques are commonly used in liquid chromatography. They include adsorption, partition, ion-exchange, affinity, and size exclusion. Each is characterized by a unique combination of stationary phase and mobile phase. In *adsorption (liquid–solid) chromatography*, the compounds are adsorbed to a solid support, such as silica or alumina. Although this was the first type of column liquid chromatography developed, it is not widely used owing to the strong retention of many compounds by the supports, making them difficult to elute from the column. *Partition (liquid–liquid) chromatography* separates compounds based on their partition between a liquid mobile phase and a liquid stationary phase coated on a solid support. Partition chromatography includes normal-phase liquid chromatography, which uses a polar liquid stationary phase, and reverse-phase liquid chromatography, which uses a nonpolar stationary phase, such as C18. *Ion-exchange chromatography* uses column packing material that has charge-bearing functional groups attached to a polymer matrix. The mechanism in this type of chromatography is the exchange of sample ions and mobile-phase ions with the charged group of the stationary phase. *Affinity chromatography* uses immobilized biochemical ligands as the stationary phase to separate a few solutes from other unretained solutes. This type of separation uses the so-called *lock-and-key binding* that is widely present in biologic systems. *Size-exclusion* chromatography separates molecules according to differences in their size. The support material has a certain range of pore sizes. As solutes travel through, the small molecules can enter the pores, whereas the larger ones cannot and will elute first from the column.

Liquid chromatography is similar in many aspects to GC; therefore, the instrumentation is similar. A typical liquid chromatography system consists of a liquid mobile phase, a sample injector (manual or automatic), a mechanical pump, a column, a detector, and a data recorder (Fig. 4.20). The liquid mobile phase is pumped from a solvent reservoir through the column. A mechanical pump must provide precise and accurate flow, often working at high pressures (typically up to 6000 PSI). The pump must have low internal volume and be constructed of material that does not react with the solvent. Sample injection is achieved using a syringe and depositing the sample into a loop. The injection may be performed manually or automatically using a microprocessor control autosampler. Most analytic separations are performed using packed columns. Many types of packing materials are available. Selection of the appropriate packing material is largely dependent on the type of compound(s) to be separated. In liquid chromatography, the physical properties of the sample and the mobile phase are often very similar. Two basic types of detectors have been developed. One is based on the differential measurement of a physical property common to both the sample and the mobile phase; examples include refractive index, conductivity, and electrochemical detectors. The other is based on the measurement of a physical property that is specific to the sample, either with or without the mobile phase; examples include absorbance and fluorescent detectors.

A widely used clinical application of HPLC is the separation and quantitation of various hemoglobins associated with specific diseases (e.g., thalassemia). Whole blood measurement of glycosylated hemoglobin (HbA_{1c}) can be accomplished using HPLC with complete analysis within 5 minutes. As discussed in Chapter 24, HPLC is also employed to determine serum levels of therapeutic drugs, such as the tricyclic antidepressants.

MASS SPECTROMETRY

Because of its versatility, mass spectrometry (MS) has become a widely used technique in the clinical laboratory for such diverse purposes as determination of the concentrations of therapeutic drugs or drugs of abuse in patients' sera or urine, amino acid sequencing of proteins, and proteomic analysis of proteins in sera and other body fluids to diagnose specific diseases. Incredibly, it is now a primary method for identification of bacteria and other organisms in the microbiology laboratory. Because of its ever-expanding applications to diverse areas of the clinical laboratory, its uniqueness and the special technical requirements of this method, we devote Chapter 5 to describing this unique technology. Here, we give a preliminary description of this technique since it is used to identify specific clinically important molecules and can itself be used as a means for separating different molecules from one another using the so-called *mass spectroscopy-mass spectroscopy* (MS-MS) methodology.

MS is based on the process of subjecting molecules separated from one another—usually in the gas phase, as in gas-liquid chromatography—to electron beams that induce their loss of electrons, resulting in the generation of molecule ions, almost always cations, whose molecular masses are the masses of the original molecules. Most of these have single positive charges; thus, the mass-to-charge (M/z) ratio is 1. These so-called "parent" molecule ions then undergo fragmentation to lower molecular mass forms, which also have mostly single positive charges and, again, have characteristic M/z ratios. All of these molecule ions are moved via an inert transporting gas through a tube containing a segment that is in an alternating electric field (often a quadrupole or octupole field). The higher M/z fragments migrate onto the tube at positions that are closer to the electron beam while the smaller cationic fragments move farther away from the beam, i.e., the smaller cationic fragments move farther along the tube than do the larger cationic fragments. At each position where a fragment "hits" the tube, a change in voltage occurs that represents a particular M/z ratio. The size of the voltage change gives the abundance of the particular fragment. A plot of the voltage changes versus the M/z ratios yields the mass spectrum. For given electron beam strengths, temperature, and field strengths, these fragments and their relative abundances characterize the parent molecule, allowing identification of the original molecule present in a patient sample. As emphasized in Chapters 5 and 24, each compound or macromolecule has a unique mass spectrum—a "fingerprint" of the molecule. Mass spectra are shown and discussed in the succeeding Chapter 5.

Modern mass spectrometers are extremely powerful and versatile instruments that themselves can be interfaced to liquid chromatographs (LC; eliminating the need to make volatile derivatives) and can perform separations in tandem (i.e., a gentle ionization step allows separation of parent

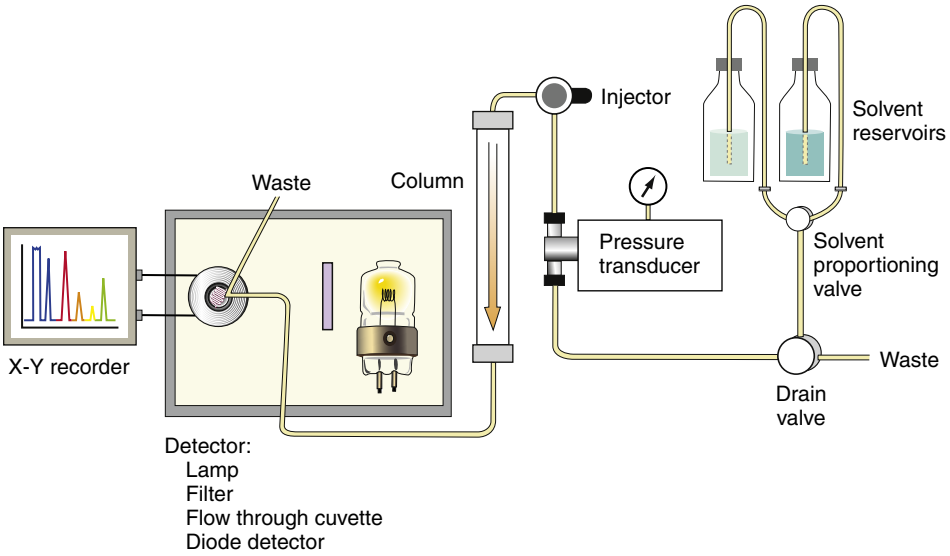

Figure 4.20 Components of a high-performance liquid chromatograph.

ions, which can then be identified by their individual fragmentation patterns on a second MS) (Karasek & Clement, 1988). Such MS-MS and LC/MS/MS techniques are finding increased application in clinical laboratories.

SCINTILLATION COUNTER

This technique is used to quantitate the level of radioactive emissions from radiolabeled compounds. Because the use of radioactivity has been largely replaced by more sensitive techniques, such as fluorescence and chemiluminescence (discussed previously), and because radioactivity and radioactive waste disposal have become major health hazards, this technique has been largely abandoned. Some radioassays are still performed in such areas as endocrinology. Therefore, we will discuss the basis for radioassays, namely, scintillation counting.

Scintillations are flashes of light that occur when gamma rays or charged particles interact with matter. Chemicals used to convert their energy into light energy are called scintillators. If gamma rays or ionizing particles are absorbed in a scintillator, some energy absorbed by the scintillator is emitted as a pulse of visible light or near-UV radiation. A photomultiplier tube detects light directly or through an internally reflecting optic fiber. A scintillation counter is an instrument that detects scintillations using a photomultiplier tube and counts the electrical impulses produced by the scintillations. An application for scintillation counting is the radioimmunoassay (RIA). Two types of scintillation methods exist: crystal scintillation and liquid scintillation.

Crystal scintillation generally is used to detect gamma radiation. When a gamma ray penetrates the sodium iodide (NaI) crystal, which contains 1% thallium, it excites the electrons of iodide atoms and raises them to higher-energy states. When the electrons return to ground state, energy is emitted as UV radiation. The UV radiation is promptly absorbed by the thallium atoms and emitted as photons in the visible or near-UV range. The photons pass through the crystal and are detected by a photomultiplier tube. A pulse-height analyzer sorts out the pulse signals from the photomultiplier tube according to their pulse height and allows only those within a restricted range to reach the rate meter for counting.

Liquid scintillation is primarily used to count radionuclides that emit beta particles. A sample is suspended in a solution (or "cocktail") consisting of a solvent such as toluene, a primary scintillator such as 2,5-diphenyloxazole (PPO), and a secondary scintillator such as 2,2′-p-phenylenebis (5-phenyloxazole [POPOP]). Beta particles from the radioactive sample ionize the primary scintillator of the solvent. A secondary scintillator absorbs the photons emitted by the primary scintillator and reemits them at a longer wavelength. The secondary scintillator facilitates more effective energy transmission from the beta particles, especially when a large amount of quenching is present. Quenching is a process that results in a reduction of the photon output from the sample. This phenomenon may be due to chemical quenching, in which impurities in the sample compete with the scintillators for energy transfer, or color quenching, in which colored substances such as hemoglobin absorb the light photons produced by scintillation. The light photons produced in the sample are detected and amplified by the photomultiplier tubes in the same manner as for the crystal scintillation counter.

CAPILLARY ELECTROPHORESIS

Capillary electrophoresis (CE) represents another alternative in separation techniques. A typical CE system, as shown in Figure 4.21, consists of a fused silica capillary, two electrolyte buffer reservoirs, a high-voltage power supply, and a detector linked to a data acquisition unit. The sample is introduced into the capillary inlet. When high voltage is applied across the capillary ends, the sample molecules are separated by electro-osmotic flow, a bulk flow resulting from excess positive ions at the inner capillary surface moving toward the cathode. The positive ions in the specimen emerge early at the capillary outlet because the electro-osmotic flow and the ion movement are in the same direction. Negative ions in the specimen also move toward the capillary outlet but at a slower rate. As the sample ions migrate toward the capillary outlet, different types of detectors—including optical, conductivity, electrochemical, MS, or radioactivity detectors—are used to detect and measure them. Advantages of CE over conventional electrophoresis and HPLC are its short analytic time, improved resolving power, and microsample volumes (Love & Ward, 1994). Using nanoliter quantities of specimen, complex mixtures of molecules can be separated with a theoretical plate number approaching 1 million. Separations may be completed in less than 10 minutes by applying very high voltage. The application of high voltage is made possible by the capillary's high surface/volume ratio, which allows for efficient heat transfer through the capillary wall. Applications of capillary electrophoresis include separation of serum proteins and hemoglobin variants.

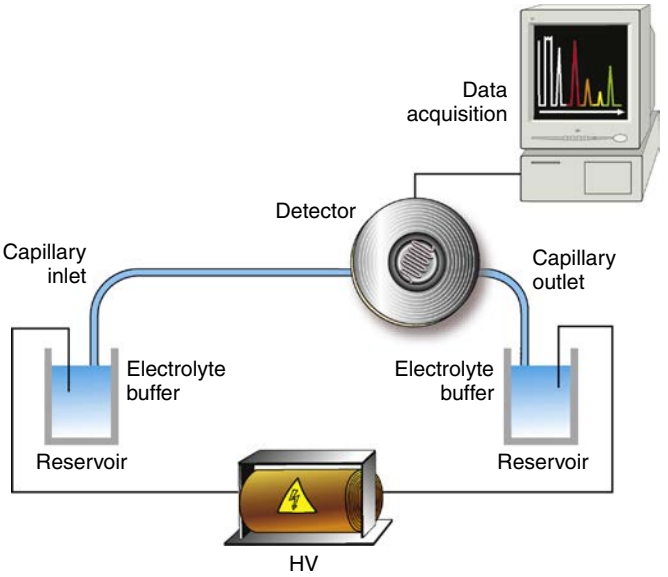

Figure 4.21 Capillary electrophoresis system. *HV,* High-voltage source. (Redrawn from Ward KM, Lehmann CA, Leiken AM: *Clinical laboratory instrumentation and automation: Principles, applications, and selection.* Philadelphia, 1994, WB Saunders; with permission.)

NUCLEAR MAGNETIC RESONANCE SPECTROSCOPY

NMR spectroscopy is a technique for determining the structure of organic compounds. Unlike MS, NMR spectroscopy is nondestructive, although it does require a larger sample volume than MS. Although NMR spectroscopy is widely used as a diagnostic imaging technique, it has been adapted for only a limited number of clinical laboratory analyses, the most popular being lipoprotein particle measurements (see Chapter 18). It also has the unique capability of performing chemical analysis in vivo.

NMR is a phenomenon that occurs when the nuclei of certain atoms are immersed in a static magnetic field and are exposed to a second oscillating magnetic field (i.e., the magnetic component of EMR). Some nuclei experience this phenomenon and others do not depending on whether they possess a property called *spin*. A single proton, or hydrogen nucleus, possesses spin; because hydrogen atoms occur very frequently, they are useful in determining structure.

When EMR is used to bombard molecules, the hydrogen atoms present will absorb photons of different energies depending on the atoms to which they are attached and to their local environments. The energy absorbed by the spinning nuclei can be plotted versus the frequency of the applied EMR to obtain an NMR spectrum of the molecule.

In lipoprotein subclass measurements, the NMR signal originates in the protons of the terminal methyl groups of the lipid carried in the particles (primarily the cholesterol ester and triglycerides of the particle core, and the phospholipids of the particle shell). Signals from these different lipids combine to produce one signal with a characteristic frequency and shape related to particle size (i.e., the diameter of the phospholipid shell), excluding the influence of the apolipoprotein attached to the particle.

Basic components of an automated NMR spectrometer designed to provide fast, simultaneous subclass quantitative analysis of very-low-density lipoprotein (VLDL), low-density lipoprotein (LDL), and high-density lipoprotein (HDL) are presented in Figure 4.22. The automated sampler provides a microsample probe that aspirates an aliquot of serum or plasma from a tray and transfers it to the NMR probe in a flow injection mode. Each sample passes through the 400-MHz magnet. The magnetic property of lipoproteins that gives them a characteristic resonance is a difference in their magnetic behavior induced by the degree of orientation of phospholipids in the shell surrounding the neutral lipid core. The equation describing this effect reveals that all lipoprotein particles of different diameters should have a different lipid NMR signature. This is displayed on the NMR processor.

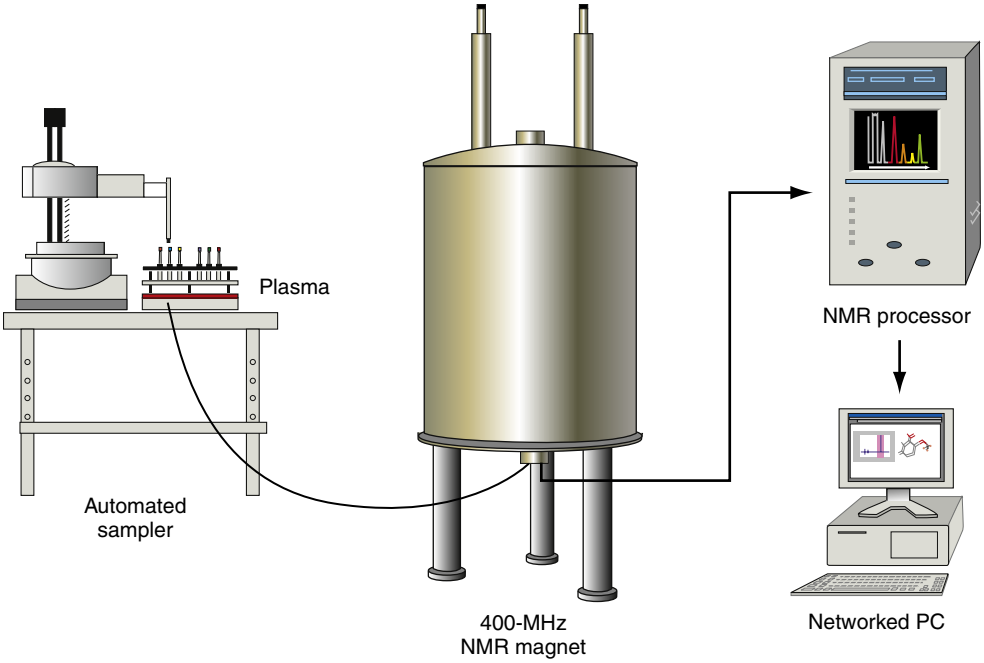

Figure 4.22 Schematic of an automated nuclear magnetic resonance (NMR) system using an automated flow-injector sampler.

The signature patterns are relayed to a networked PC, which provides access to high-quality spectral data from isolated subclasses of lipoproteins incorporated into proprietary analysis software. The information is contained in a reference library that is accessible with permission from the vendor.

GENERAL ANALYTIC METHODS AND ISSUES

Perhaps the most fundamental aspect of the analytic process is the preparation of high-quality reagents that will be used in the analytic procedure. In this process, the quality of water, the purity of the chemical, the selection of correct glassware or plasticware, and the correct preparations of reagents are all important for the proper operation of laboratory equipment and the performance of testing procedures. In this section, several topics will be presented that relate to analytic process and will ultimately have an impact on the results of a test performed on a patient's specimen.

CHEMICALS

Use of chemicals for preparation of reagents, solvents, dyes, and so on has been steeply declining over the past decade in view of the extensive automation of the clinical laboratory. Almost all solutions or reaction slides used for testing are now being prepared by manufacturers who either are the companies providing the individual tests being performed on their autoanalyzers or who provide them to the manufacturer that provides these analyzers to the clinical laboratories. Most chemical preparations that require manual manipulations involve mixing preprepared reagents to one another. For the few chemicals used to prepare reagents for chemical testing, proper selection of chemicals is important so that the desired results may be attained. Chemicals acquired for reagent preparation are characterized by a grading system. The grading of any chemical is greatly influenced by its purity. The types and quantities of impurities are usually stated on the label affixed to the chemical container. Less pure grades of chemicals include practical grade, technical grade, and commercial grade. These grades of chemicals are unsuitable for use in most quantitative assays performed in a clinical laboratory.

Most qualitative and quantitative procedures performed in the clinical laboratory require the use of chemicals that meet the specifications of the American Chemical Society (ACS). These chemicals are classified as analytic grade or reagent grade. Examples of other designations of chemicals that meet high standards of purity include spectrograde, nanograde, and HPLC grade. These are often referred to as ultrapure chemicals.

Pharmaceutical chemicals are produced to meet the specifications defined in *The United States Pharmacopeia* (USP), *The National Formulary*, and *The Food Chemical Index*. These specifications define impurity tolerances that are not injurious to health.

The International Union for Pure and Applied Chemistry (IUPAC) has developed standards and purity levels for certain chemicals. These include atomic weight standard (grade A), ultimate standard (grade B), primary standard (grade C), working standard (grade D), and secondary substances (grade E).

A very good source of highly purified chemicals, especially reference materials, is the National Institute of Standards and Testing (NIST; Gaithersburg, MD). The NIST defines its chemical and physical properties for each compound and provides a certificate documenting their measurements. The NIST also provides Standard Reference Materials (SRMs) in solid, liquid, or gaseous form. The solids may be crystalline, powder, or lyophilized.

Two professional organizations can provide laboratory staff with guidelines for proper chemical selection and reagent preparation. They are the College of American Pathologists (CAP; Northfield, IL) and the Clinical and Laboratory Standards Institute (CLSI), formerly the National Committee for Clinical Laboratory Standards (NCCLS; Wayne, PA).

WATER

Water has numerous uses in the clinical laboratory. Water is used to prepare reagents, as diluent for controls and calibrators, to flush and clean internal components of analyzers, to serve as a heating bath for cuvettes, and to wash and rinse laboratory glassware. For most of these uses, the water must be of the highest purity, whereas the water required for rinsing glassware may be of a lesser purity.

Types of Water Purity

The CLSI and CAP have defined three grades of water purity: types I, II, and III. The criteria for each type are outlined in the CLSI guidelines (CLSI, 2006). When selecting a water purification system, the purchaser must pay strict attention to these criteria so that all of the appropriate filters and components necessary to produce type I water (purest water) are included. Also, special attention must be given to the "feed-water," which is usually the laboratory tap water. The feed-water may contain unique contaminants or may have a high mineral content (hardness), which will often require the inclusion of additional components in the water processing system.

Purification

Many laboratories produce or purify their own water. Several means are available by which to produce reagent-grade water. Most water filtration systems use a prefilter to begin the process. This prefilter has feed-water running through it to trap any particulates before sending it on to the next component. At this point in the water filtration process, water may be distilled or passed through a reverse osmosis filter. Distillation is the process by which a liquid is vaporized and condensed and is used to purify or concentrate a substance or separate a volatile substance from a less volatile substance. Water that has been distilled does not meet the specific resistivity requirements of CAP type I water. Reverse osmosis (RO) is a process

by which water is forced through a semipermeable membrane that acts as a molecular filter. The RO filter removes 95% to 99% of organic compounds, bacteria, and other particulate matter, and about 95% of all ionized and dissolved minerals, but not as many gaseous impurities. RO alone does not produce type I water, but, like distillation, if additional filters such as ion-exchange and carbon particulate filters are added to the system, type I water may be produced.

Ion-exchange filters remove ions to produce mineral-free deionized water. Deionization is accomplished by passing water through insoluble resin polymers that contain anion- or cation-exchange resins. These exchange resins replace H^+ and OH^- ions for impurities present in ionized form in the water. Another type of material used is a mixed bed resin that contains both anion and cation-exchange materials. Deionizers are capable of producing water that has specific resistance exceeding 1 to 10 megaohms·cm (Mohm·cm or MΩ·cm).

Carbon filters containing activated charcoal may be added to the water purification system to help remove several types of organic compounds that may still be in the water. When these filters are used, the CLSI/CAP considers the end product to contain minimal organic material.

A particulate filter may be added to the end of the system. This filter, with a mean pore size down to about 0.22 μm, will serve to trap any remaining particulates as large as or larger than the pore size.

Monitoring Water Purity

Because water is such an integral part of laboratory analysis, its purity must be monitored on a consistent basis. The frequency of water testing is dependent on many factors, including the composition of the feed-water, the availability of staff to perform water testing, and the amount of water the laboratory uses during a given period of time. At the very least, resistivity and bacterial content of the water should be monitored on a regular basis. In addition, pH, silica content, and organic contaminants may be determined. Depending on the laboratory's resources, some or all of these parameters should be checked on a periodic basis.

Most water filtration systems will have an in-line resistivity meter available. Resistivity measurements are used to assess the ionic content of purified water. The higher the ion concentration in water, the lower the resistivity value will be. the CLSI/CAP requires that type I water have a resistivity greater than 10 MΩ·cm.

Bacterial contamination can be monitored easily. The water should be allowed to run for at least 1 minute to flush the system. Next, an aliquot of water is taken, depending on the procedure used, and is plated on appropriate media. After an appropriate incubation time, the number of colony-forming units on the agar plate is determined. The most commonly found organisms in water after the purification process is complete are Gram-negative rods.

Once Your System Has Been Installed

Most water purification systems are designed for easy access to end-product type I water. Therefore, it is advisable to use only type I water for most applications in the laboratory. Type II or III water could be used for rinsing glassware and cleaning exterior surfaces. If a procedure—for example, heavy metal testing or HPLC—requires the use of specially prepared water, then type I water should not be used. Ultra-pure water can be purchased from NERL Diagnostics Corporation (East Providence, RI).

MEASUREMENT OF MASS

Mass is the quantity of matter contained within an object. The weight of a body is the gravitational acceleration exerted on it; unlike mass, it varies with altitude. The weight is equal to mass times gravity. In the laboratory, we are measuring the mass of an object.

Types of Balances

Several different types of balances are available, depending on what needs to be weighed. For example, to weigh a fecal fat specimen, an appropriate balance to use would be a top-loading precision balance capable of accurately weighing kilogram amounts. Preparation of standards for toxicology assays requires microgram quantities; thus, a single-pan microbalance would be appropriate.

Unequal-Arm Substitution Balances

Unequal-arm substitution balances are typically single-pan types and are commonly used in laboratories, although almost all of these balances are being replaced by electronic-type balances. The single-pan, mechanical, unequal-arm balance operates on the principle of removing weights rather than adding them. A fixed mass counterweight is used to balance the combined mass of the pan and the removable weights across two arms of unequal weight. When a sample is placed on the weighing pan, internal weights in 1-g or 10-g increments are moved one at a time by the operator turning a set of knobs. This is continued until the system returns to equilibrium, at which time the sum of the weights removed is equal to the weight of the object.

Magnetic Force Restoration Balance

Another widely used balance is the single-pan balance that relies on magnetic force restoration. The restoring force is the force required to put the balance back into equilibrium. The unknown mass is placed on the pan, and this system goes out of equilibrium. The operator who adjusts the internal weights restores partial equilibrium. The null detector optics circuit senses when equilibrium is near and provides a signal to the sensor motor to generate a restoring current until equilibrium is reached. At this time, the unknown mass is equal to the mass of the weights removed plus the force due to the restoring current.

Top-Loading Balances

Single-pan top-loading balances operate on the same principle as single-pan analytic balances (i.e., weighing by substitution). Damping is accomplished by magnetic rather than an air-release mechanism. These balances are especially suitable for rapidly weighing larger masses (up to 10,000 g) that do not require as much analytic precision, such as large-volume reagent preparation.

Electronic Balances

Several electronic balance designs are available. One design uses a strain gauge load cell. This is a small, thin device that changes electrical resistance when it is stretched or compressed. Typically, several strain gauges are used in a Wheatstone bridge arrangement, and they are glued onto the load cell in a protected location. A load cell is usually in the shape of a beam or plate. When the beam or plate is displaced, it bends a tiny amount, and this tiny bending is detected by the strain gauges. The amount of bending might be only a thousandth of an inch, but that is enough for a strain gauge to measure.

Another electronic balance design operates on the principle of electromagnetic force (EMF) compensation. A coil, placed between the poles of a cylindrical electromagnet, is mechanically connected to a weighing pan. Mass placed on the pan produces a force that displaces the coil within the magnetic field. A regulator generates a compensation current just sufficient to return the coil to its original position. The more mass that is placed on the pan, the larger the deflecting force and the stronger the current required to correct the deflection of the coil. The measuring principle is based on a strict linear relationship between compensation current and force produced by the load placed on the pan.

Several additional features may be available on some models of electronic balances. For example, some electronic balances include an electronic vibration damper. Any excess vibration can be detected when variation of the pointer or oscillation of the number in the last decimal place of the digital display is observed. Another feature available in some models is built-in taring. This allows the weight of the weighing container to be "zeroed." Also, electronic balances can be interfaced with computers to provide calculations such as weight averaging and statistical analysis of multiple weighing. The fundamental design of electronic balances allows for faster weighing, which is advantageous when doing multiple readings (e.g., pipet calibrations).

Calibration

Laboratory balances require calibration at regular intervals. The NIST states that there is no fixed calibration interval for scientific applications. Calibration intervals should coincide with the requirements of the laboratory's licensing and accrediting organizations.

The mass standard and test weight accuracy classes for weights used in calibrating balances have been updated and replace the older requirements specified by National Bureau of Standards (NBS) class S and class S1 weights. The new mass standards and test weight accuracy classes appropriate for laboratory balances include the American Society for Testing and Materials (ASTM; West Conshohocken, PA) classes 1 and 2. Reference should also be made to ASTM E617-13 for specific information regarding range, readability, and best uncertainty applicable to these classes.

NIST class 1 weights (extra-fine accuracy) are available up to 250 mg and may be used for high-precision (e.g., single-pan and electronic) balances that are precise to four decimal places. The range of weight for class 2 balances may be in excess of 1000 g.

Handling Weights Used for Testing Accuracy

Meticulous care must be used when handling class 1 or 2 weights. The operator must avoid direct contact with the weights by using clean gloves

or special lifting tools (e.g., forceps). Hand contact with the weights can cause corrosion. The weights should not be dragged across any surface, including the stainless steel weighing pan. Usually, the weights are sent in a covered box and should always be stored in that box.

Environmental Concerns for Best Weighing Accuracy

Several aspects of the environment may have an impact on the performance of a laboratory balance. They include temperature, air drafts, floor vibrations, table instability, and static electricity. The effects of the environment on your weighing procedures can often be minimized easily. For example, if air drafts are present in the room, a shroud or enclosure can be placed around the balance. A marble table can be used to reduce table vibrations or instability.

Balance Specifications

An operator should be knowledgeable about several important specifications related to balances. They include the following:

- Capacity—which represents the maximum load one can weigh
- Accuracy—which is dependent on the smallest mass one will be weighing
- Linearity—the ability of a balance to provide accurate output over its full range
- Resolution (readability)—the smallest increment of weight that may be discernible

Laboratory accrediting agencies require verification of accuracy of balances at various time intervals. Several sources are available to guide the laboratory through this requirement.

LABORATORY GLASSWARE AND PLASTICWARE

Because of the extensive automation of laboratories, the need for glass- and plasticware and manually operated pipettes has diminished to the point where many clinical laboratories have ceased using these implements. Nonetheless, some laboratories continue to use some or all of these, including specialty laboratories that employ nonautomated methods. We discuss these in the next several sections.

Types of Glassware

The most common type of glassware encountered in volume measurements is borosilicate glass. This glass is characterized by a high degree of thermal resistance, has low alkali content, and is free from the magnesium-lime-zinc group of elements, heavy metals, arsenic, and antimony. Commercial brands are known as Pyrex (Corning, Corning, NY) and Kimax (Kimble, Vineland, NJ). The caustic conditions involved in storing concentrated alkaline solutions in borosilicate glass will etch or dissolve the glass and destroy the calibration. Borosilicate glassware with heavy walls—such as bottles, jars, and even larger beakers—should not be heated with a direct flame or hotplate. Glass should not be heated above its strain point (for Pyrex, 515°C) because rapid cooling strains and cracks glass easily when it is heated again. In the case of volumetric glassware, heating can destroy the calibration.

Corex (Corning, NY) brand glassware is a special alumina-silicate glass strengthened chemically rather than thermally. Corex is six times stronger than borosilicate glass (e.g., Corex pipets have a typical strength of 30,000 psi, compared with 2000 to 5000 psi for borosilicate pipets) and will outlast conventional glassware by tenfold. Corex also resists clouding and scratching better.

Low-actinic glassware is a glass of high thermal resistance with an amber or red color added as an integral part of the glass. The density of the red color is adjusted to permit adequate visibility of the contents, yet give maximum protection to light-sensitive materials, such as bilirubin standards. Low-actinic glass is commonly used in containers used to store control material and reagents.

Types of Plasticware

Several types of plasticware are used in clinical laboratories—for example, pipet tips, beakers, flasks, cylinders, and cuvettes. Polypropylene, polyethylene, Teflon, polycarbonate, and polystyrene are all examples of types of plastics used for laboratory plasticware.

Plastic pipet tips are made primarily of polypropylene. This type of plastic may be flexible or rigid, is chemically resistant, and can be autoclaved. These pipet tips are translucent and come in a variety of sizes. Polypropylene is also used in several tube designs, including specimen tubes and test tubes. Specially formulated polypropylene is used for cryogenic procedures and can withstand temperatures down to –190°C.

Polyethylene is widely used in plasticware, too, including test tubes, bottles, graduated tubes, stoppers, disposable transfer pipets, volumetric pipets, and test tube racks. Polyethylene may bind or absorb proteins, dyes, stains, and picric acid.

Polycarbonate is used in tubes for centrifugation, graduated cylinders, and flasks. The usable temperature range is broad: –100°C to +160°C. It is a very strong plastic but is not suitable for use with strong acids, bases, and oxidizing agents. Polycarbonate may be autoclaved but with limitations (refer to furnished instructions).

Polystyrene is a rigid, clear type of plastic that should not be autoclaved. It is used in an assortment of tubes, including capped graduated tubes and test tubes. Polystyrene tubes will crack and splinter when crushed. This type of plastic is not resistant to most hydrocarbons, ketones, and alcohols.

Teflon is widely used for manufacturing stirring bars, tubing, cryogenic vials, and bottle cap liners. Teflon is almost chemically inert and is suitable for use at temperatures ranging from –100° to +400°F (–73°C to 204°C). This type of plastic is resistant to a wide range of chemical classes, including acids, bases, alcohol, and hydrocarbons.

VOLUMETRIC LABORATORYWARE

Class A Designation

Volumetric glassware designated as Class A has been manufactured to Class A tolerances as established by the American Society for Testing and Materials (ASTM) E694 for volumetric apparatus. Other standards include ASTME 542 for calibration of volumetric apparatus and ASTME 288 for volumetric flasks.

Pipets

Many kinds of pipets are available for use in a clinical laboratory, each intended to serve a specific function. They are used for reconstituting controls and calibrators, preparing serum or plasma dilutions, and aliquoting specimens. Thus, a high degree of accuracy and precision is required. Manual pipets fall into two general categories: transfer (volumetric) and measuring. Three subclassifications include to contain (TC), to deliver (TD), and to deliver/blow-out (TD/blow-out).

Types of Pipets

Pipets designed to contain (TC) are often referred to as *rinse-out pipets* because they must be refilled or rinsed out with the appropriate solvent after the initial liquid has been drained from the pipet. TC pipets contain an exact amount of liquid that must be completely transferred for accurate measurement. Examples of TC pipets are Sahli hemoglobin and Long-Levy pipets. These pipets do not meet Class A certification criteria.

TD pipets are designed to drain by gravity. TD pipets must be held vertically and the tip placed against the side of the container and must not touch the liquid in it. The stated volume is obtained when draining stops. This type of pipet should not be blown out. Examples of TD pipets include Mohr, serologic, and volumetric transfer pipets. These pipets are designed to meet the requirements of Class A–type pipets.

Volumetric TD pipets have an open-ended bulb that holds the bulk of the liquid. On one side of the pipet is a long glass tube with a line indicating the extent to which the pipet is to be filled. The other end is tapered for smooth delivery of liquid. These pipets should be allowed to drain freely and not be shaken or hit against the container. Any disruption of the free-flowing liquid may result in an inaccurate delivery of the liquid.

Some TD pipets are designed so that most of the contents are allowed to drain freely, after which the remaining fluid in the tip is blown out. These pipets are not rinsed out. Examples of pipets designed to be blow-out–type pipets include Ostwald-Folin and serologic pipets. TD/blow-out pipets are identified by the presence of one or two frosted bands near the mouthpiece of the pipet. It is vital to remember that one should never pipet or blow out solutions by mouth. It is always necessary to use an appropriate pipetting aid—for example, a bulb.

Serologic glass or plastic pipets are long tubes with uniform diameters. They have volume graduations extending to the delivery tip of the pipet. The last volume of liquid blown out is included in the delivery volume. The design of the Mohr TD pipet is different from that of the serologic pipet. Mohr pipets are not graduated to the tip. The accuracy of the Mohr pipets is valid only when the pipet is filled. If smaller volumes are dispensed, the accuracy decreases proportionally.

Micropipets

The two most widely used types of micropipets are the air displacement and positive displacement. These pipets are capable of delivering liquid volumes from 1 to 1000 μL. Some micropipets are designed to deliver a fixed volume, while others can deliver variable amounts of sample.

Air-displacement pipets are piston-operated devices. A disposable, one-time use polypropylene tip is attached to the pipet barrel. The pipet tip is placed into the liquid to be aspirated and drawn into and dispensed from this tip.

Positive-displacement pipets use a capillary tip that may be siliconized glass, glass, or plastic. This type of pipet is useful if a reagent reacts to plastics. Positive-displacement pipets use a Teflon-tipped plunger that fits tightly inside the capillary. These capillary tips are reusable and carryover is negligible if the pipet is properly maintained. Some procedures require a washing or flushing step in between samples.

Pipet Calibration

Monitoring the performance of pipetting devices is not only mandatory in most states that issue licenses to laboratories that perform diagnostic testing, but it is also very wise. Micropipets should be verified for accuracy and precision before they are put into use and monitored during the course of the year. The frequency of verification depends in part on the amount of use and requirements by the licensing and/or accrediting agency. Proper maintenance of air-displacement pipets is very important. This type of pipet has a fixed stroke length that must be maintained. These pipets also have seals to prevent air from leaking into the pipet when the piston is moved. These seals require periodic greasing to maintain their integrity.

Positive-displacement micropipets need to have their spring checked and the Teflon tip replaced periodically. A slide wire is used to quickly check the plunger setting. This check does not replace the scheduled precision and accuracy checks.

There are several procedures used by laboratories to verify precision and accuracy of micropipets. Most of these procedures are time-consuming, especially the procedures that require the weighing of water. At any rate, this verification procedure must be done to ensure proper performance of the laboratory micropipets.

The CLSI has provided an acceptable procedure for determining pipet accuracy and precision (I8-P, NCCLS; CLSI, 1984). This gravimetric procedure is labor intensive but does provide a low-cost means of complying with the regulations set forth by the various accrediting agencies.

More expensive procedures for calibrating micropipets include the following:

- Commercial photometric pipet calibration products
- Calibration services providers
- Pipet Tracker (Labtronics Inc., Canada)

One of the major concerns when considering the cost attributed to pipet calibration procedures is technologist time. The technologist time required for the photometric procedures is often 50% to 60% less than the inexpensive manual weighing techniques.

Volumetric Flasks

Volumetric flasks represent a special type of glassware in the laboratory. These flasks are often used to prepare standards for quantitative procedures. Therefore, the accuracy must be optimal. Volumetric flasks used for the preparation of standards and other solutions requiring optimal accuracy must meet Class A specifications as defined by NIST. These specifications are imprinted on the flasks. Volumetric flasks are used to contain (TC) an exact volume when the flask is filled to the mark. A Teflon or ground-glass stopper should be used to seal the flask. Volumetric flasks should not be used for reagent storage.

Calibration of Volumetric Glassware

According to the strictest of standards, every piece of volumetric glassware in the clinical laboratory should be coded and a record kept of its calibration. Any piece of glassware that does not meet Class A tolerance should be rejected. To prepare a piece of glassware for calibration, thoroughly wash and dry it using appropriate cleaning procedures. The CLSI can provide the laboratory with an appropriate procedure to calibrate volumetric flasks.

THERMOMETRY

Thermometers and other types of temperature-sensing devices are used in the laboratory to monitor the temperatures in refrigerators, freezers, water baths, heating blocks, and incubators. Special applications of thermometry include osmometry, refrigerated centrifuges, refrigerated reagent compartments of automated analyzers, warming compartments of automated analyzers, and circulating water baths for cuvette compartments in automated analyzers. All of these temperature-monitoring applications have the same requirements, which are accurate measurements and a constant temperature.

Appropriate quality control procedures must be carried out and documented routinely for all of these temperature-monitoring devices. Any temperature-sensitive device that fails to perform within established tolerances must be replaced. Because many assays performed in the laboratory are enzymatic in nature, even the slightest deviation from the optimal temperature required to perform the assay may yield an erroneous result.

Types of Thermometers

The two types of liquid-in-glass thermometers most widely used are total immersion and partial immersion. A total immersion thermometer requires that the bulb and entire column of liquid be immersed into the medium measured. These thermometers are used to monitor freezers and refrigerators. Partial immersion thermometers must have the bulb and stem immersed to the immersion line or defined depth on the thermometer. This type of thermometer is often used for water baths and heating blocks.

Special Applications of Temperature-Sensing Devices

Thermistors are used in several types of instruments found in the laboratory, including freezing-point depression osmometers. A thermistor is a transducer that converts changes in temperature (heat) to resistance. It consists of a small bead constructed of a fused mixture of metal oxides, attached to two leads and encapsulated in glass. The metal oxide mixture has a large negative temperature coefficient of resistance. Thus, a small decrease in temperature causes a relatively large increase in the resistance of the thermistor.

A thermocouple is a sensor that consists of two dissimilar metals joined together at one end. When the junction of the two metals is heated or cooled, a voltage is produced that can be correlated back to the temperature. Thermocouples come in several designs, including beaded wire, probes, and surface probes. An important feature of most thermocouples used in laboratory analyzers is their fast response times. The response time of a thermocouple is defined as the time required by a sensor to reach 63.2% of a step change in temperature under a specified set of conditions. Five time constants are required for the sensor to approach 100% of the step change value.

Laboratory applications for thermocouple use include gas and liquid chromatography, surface temperature measurements in heating compartments in automated analyzers, thermo-cuvettes, and circulating water baths in chemistry analyzers.

Mercury-Free Laboratories

There are initiatives nationwide to make laboratories mercury-free. For example, in June 1998, a landmark agreement was put together between the American Hospital Association (AHA) and the U.S. Environmental Protection Agency (EPA) (JCAHO, 2002). A memo of understanding was signed between the two organizations in an effort to decrease and eventually eliminate hospital pollution practices over a 5- to 10-year period. One of the goals is to eliminate mercury waste.

Mercury is contained in numerous chemical reagents used by the laboratory and, of course, in mercury thermometers. The cost associated with proper disposal of mercury and the impact of mercury in the environment make replacing mercury thermometers a sound idea. Several alternatives exist for replacement thermometers that provide the necessary accuracy for laboratories procedures, including the following:

- Thermometers containing an organic red-spirit and pressurized with nitrogen gas
- Thermometers containing blue biodegradable liquid (isoamyl benzoate and dye)
- A red liquid thermometer filled with kerosene
- Bimetal digital thermometers
- Digital thermometers with stainless-steel stems

Thermometer Calibration

Monitoring the temperature accuracy of thermometers is necessary to ensure the reliability of procedures requiring temperature regulation. Thermometers may be purchased with a certificate to indicate traceability to standards provided by the NIST. Also, many commercially available thermometers meet or exceed NIST and American National Standards Institute (United States)/Scientific Apparatus Makers Association (United Kingdom) (ANSI/SAMA) tolerance for accuracy.

Noncertified thermometers can be calibrated by using a NIST SRM 934 thermometer or a NIST SRM 1968 gallium melting point cell. The SRM 934 clinical laboratory thermometer is calibrated per specifications

by the International Temperature Scale 1990 (ITS-90) at 0°C, 25°C, 30°C, and 37°C. A gallium melting point cell consists of about 25 g of very pure (99.99999%) gallium metal that has a single fixed melting point at 29.7646°C (as defined by ITS-90). The gallium is sealed in an inert plastic crucible and surrounded in a stainless-steel envelope (Strouse et al., 1997).

Temperature monitoring devices should be verified for accuracy at 6- or 12-month intervals. Guidelines and procedures for proper monitoring and tolerances are available (NCCLS-approved standard I2-A2, 1990).

WATER BATHS

For general clinical laboratory use, constant temperature water baths must offer variable temperature control from +5°C above ambient temperature to 100°C, with accurate control to ±0.2°C. Water baths can be circulating or noncirculating. The circulating water baths provide the best temperature control. Another important consideration in the selection of a constant temperature bath is that the model be large enough to accommodate the desired working volume.

Maintenance

Maintenance of a constant temperature water bath is improved by filling it with type II (or type I) water. This prevents the accumulation of mineral deposits from regular tap water, which can affect the temperature-sensing elements and generally lead to poor heat transfer. However, if an accumulation of these minerals does occur, a weak hydrochloric acid solution will dissolve the deposits. Frequent cleaning and fresh water will prevent overgrowth of bacteria and algae. Also, a 1:1000 dilution of thimerosal (Merthiolate) can be added to help prevent bacterial growth. Overheating and subsequent damage can occur if the bath goes dry. At higher temperatures, the bath should be covered, both to maintain proper temperature control and to prevent rapid evaporation to dryness.

Quality Control

A thermometer calibrated against another certified by the NIST must be a component of any water bath. The temperature should be noted and recorded for each assay. This function by the operator ensures that, indeed, the temperature of the bath is the same as the reading of the thermometer.

HEATING BLOCKS, DRY-BATH INCUBATORS, AND OVENS

Heating blocks and dry-bath incubators are commonly used for incubating liquids at higher temperatures. Most incubators are constructed of an aluminum alloy that is capable of distributing the heat in a uniform manner. Their heating efficiency is less than a circulating water bath but will maintain a constant temperature within ±0.5°C. A certified thermometer or NIST-calibrated thermometer must be present in the heating block to monitor the temperature.

Heating ovens are used in chromatography procedures, to dry chemicals, to assist in extraction, and to dry membrane or gels in electrophoresis. Several different designs are available, depending on the desired temperature and purpose. Oven designs include programmable, vacuum, or standard laboratory types. Temperature control is usually within ±1°C. The oven must have a certified thermometer or NIST-calibrated thermometer available to monitor the interior temperature.

MIXING

Mixing is an operation intended to form a homogeneous mass or create a uniform heterogeneous system. Mixing is used to bring solids into solution; to bring phases into intimate contact, for instance, in extraction procedures; to wash suspended solids; to homogenize liquid phases; and to perform many other operations. A serious consequence of inadequate mixing can be failure to completely resuspend protein that settles out under long-term frozen storage of serum controls, resulting in invalid data. In some instances, excessive mixing may cause denaturation of protein or hemolysis. A phase separation occurs when serum (or plasma) specimens stand for a period of time and must be thoroughly mixed before analysis. The concentration of even small molecules in such a system will be heterogeneous as proteins settle and become more concentrated; thus, effective water concentration decreases in this layer. This produces a water concentration gradient throughout the system and, consequently, a concentration gradient of all components.

BOX 4.5

Example: Molarity

How many grams of NaCl are required to prepare 1 L of a 0.5 M solution? The gram molecular weight (GMW) of NaCl is 58.5.

Solution

$$\text{GMW} \times \text{M} = \text{g/L}$$

$$58.5 \times 0.5 = 29.25 \text{ g/L}$$

Single-Tube Mixers

A vortex mixer is capable of a variable-speed oscillation that results in a swirling motion to liquid contents of a test tube or other container. The angle of contact and degree of pressure can be regulated for optimal mixing action. A very effective mixing action is created by a multiple-touch sequence (i.e., touching and withdrawing the tube from the neoprene oscillating cup of the mixer). The operator must be careful not to fill the container too full or to mix the liquid contents too fast because spillage can occur.

Multiple-Tube Mixers

Various mixers are available that handle a number of tubes and tube sizes and have different types of mixing motions. A Thermolyne Maxi-Mix (Sybron Corporation, Dubuque, IA) can conveniently be used for vortex mixing one tube or several tubes at one time. Changing the pressure of the container against the replaceable foam rubber top varies mixing action. Circular motion on a tilted disk provides continuous inversion of contents in tubes, which are clip-mounted at the circumference of the rotating disk. Rotational speed can be varied to provide gentle or more vigorous mixing. Control sera are conveniently reconstituted on this type of mixer. Tube shakers that operate by tilting back and forth at variable speeds provide thorough mixing of whole blood samples.

AQUEOUS SOLUTION

The concentration of a solution may be expressed as molarity (M), normality (N), and, less frequently, molality (m). Accurate preparation of reagents requires fundamental knowledge of solution chemistry, basic mathematics, and techniques.

Molarity

Molarity (M) is equal to the number of moles of solute per liter of solution. A *mole* of a substance is the number of grams equal to the atomic or molecular weight of the substance. The atomic or molecular weight of a substance is the actual mass of the chemical particle (atom or molecule) relative to the mass of the carbon atom. One mole of any substance will contain approximately 6.02×10^{23} particles (Avogadro's number). Thus, a 1 molar solution contains 1 mole of solute per liter of solution (Box 4.5). Therefore, the procedure is to weigh out 29.25 g of NaCl, transfer it to a 1-L volumetric flask, and then add water to the 1-L mark on the flask.

Millimoles

When small concentrations are used, they are frequently expressed in millimoles per liter (1000 mmol = 1 mol). For example, to prepare 10 mL of a 10-mmol (0.01 moles) NaOH solution, 4 mg NaOH is diluted to 10 mL.

Normality

Normality (N) is equal to the number of gram equivalents of solute per liter of solution and is dependent on the type of reaction involved (e.g., acid-base, oxidation). One-gram equivalent weight of an element or compound equals the gram molecular weight divided by the number of replaceable hydrogens or hydroxyls (also valence; Boxes 4.6 through 4.8):

$$\text{Gram Equivalent Weight} = \text{GMW/Number of replaceable hydrogens, hydroxyls or valence}$$

$$1\text{N} = \text{Number of gram equivalents of solute/L of solution}$$

Molal

In the laboratory, the physical properties of solutions are sometimes measured—for example, when the osmolality of serum or urine is measured. The molality of the solution is determined instead of the molarity. A molal

BOX 4.6

Example 1: Normality

What is the gram equivalent weight of $Ca(OH)_2$ (GMW = 74)?

Solution

Gram equivalent weight = 74/2 = 37

1 mole = 2 equivalents

BOX 4.7

Example 2: Normality

What is the gram equivalent weight of H_2SO_4 (GMW = 98)?

Solution

Gram equivalent weight = 98/2 = 49

1 mole = 2 equivalents

BOX 4.8

Example 3: Normality

How many milliliters of concentrated H_2SO_4 (specific gravity, 1.84; percent purity, 96.2%) are required to prepare 1 L of a 1 normal solution?

Solution

Step 1: A 1 N solution of H_2SO_4 is a 0.5 M solution of H_2SO_4.

Step 2: The molecular mass of H_2SO_4 is 98 g. Thus, a 1 N solution of H_2SO_4 = 0.5 M = 98/2 g = 49 g/L.

Step 3: Therefore, we need 49 g of H_2SO_4 in 1 L. We need to know what volume of H_2SO_4 will give us 49 g. We will then dilute this volume to 1 L with water. Our solution of H_2SO_4 has a density or specific gravity of 1.84 g/mL, but not all of the 1 g is H_2SO_4; only 96.2%, or 0.962 of the 1 g is actually H_2SO_4. Thus, in 1 mL of this acid, only 0.962 × 1.84 g = 1.77 g is H_2SO_4.

Step 4: Now, to determine how many mL of the acid solution we need in order to get 49 g, since we have 1.77 g of the acid/mL, we ask how many 1.77 g there are in 49 g. Since each 1.77 g is in a volume of 1 mL, then the total number of mL of acid is 49 g/1.77 g = 27.68 mL. This will be diluted with water either by transferring the 27.68 mL of acid solution to one 1-L volumetric flask and adding water to the 1 L mark or by transferring the 27.68 mL of acid solution to a beaker and adding 973.32 L of water to the acid solution.

solution is 1 mole of solute in 1 kilogram of solvent. Molal solutions are based on weight, not volume. Because the density of water at room temperature is approximately 1 gram per milliliter, 1000 grams of water occupies about 1 liter. Therefore, a 1-molal aqueous solution is approximately the same as a 1-molar solution (Box 4.9).

Dilutions

Dilution procedures are not performed as frequently as in the past owing to improvements in computers and instruments whereby the system performs the dilution automatically. But, on occasion, a dilution has to be prepared. A brief review follows.

A laboratory procedure may involve the addition of one substance to another to reduce the concentration of one of the substances. This mixture is called a *dilution*. Laboratory staff often confuse the terminology associated with dilutions and ratios. The term *ratio* is more general and refers to an amount of one thing relative to an amount of something else with no other implications. *Dilution*, as the term is used in laboratories, is more specific. It refers to the number of parts of a substance in the total number of parts of mixture containing the substance. The implication is how the mixture was made or how it is going to be made. The following are examples of ratios followed by dilutions (Box 4.10):

Ratios

1. The serum/saline ratio is 1 : 9.
2. The saline/serum ratio is 9 : 1.
3. The serum/total volume ratio is 1 : 10.

BOX 4.9

Example: Molal Solutions

How many grams of NaOH are needed to make a 2.00 molal solution?

Solution

Step 1: Determine the GMW of NaOH = 40 g.

Step 2: Compute the number of grams of NaOH required to prepare the solution by using the following formula:

$$\text{Molality} = \frac{\text{Grams of solute/GMW of solute}}{\text{1.0 kg of solvent}}$$

$$\text{2 Molal} = \frac{\text{X g of NaOH/40.00 g}}{\text{1.0 kg of solvent}}$$

$$X = 80 \text{ g of NaOH}$$

BOX 4.10

Example: Dilutions

Prepare a 1 mL/10 mL dilution of a serum sample.

Solution

Pipet 1.0 mL of serum and add 9.0 mL of saline for a total volume of 10 mL.

Note that a colon is used as the ratio symbol.

Dilutions

1. Make a 1 : 10 dilution of serum in saline.
2. Make a 1 : 10 dilution of serum with saline.

A clinical application may involve the dilution of a patient serum sample because the bilirubin result exceeds the upper limit of linearity. The technologist decides to make a 1 : 2 dilution of the sample and assay the diluted sample. To prepare the dilution, the technologist pipets 100 μL of patient serum and adds 100 μL of water, for a total volume of 200 μL. The sample is assayed for bilirubin, and the analyzer prints out a value of 12 mg/dL. Before reporting the patient's bilirubin result, the technologist must multiply the analyzer value times 2 (the dilution factor) and then report the value of 24 mg/dL.

Acids, Alkalis, and pH

An acid molecule yields hydrogen ions (protons) in aqueous solutions; an alkali accepts these. At room temperature in pure water:

$$[H^+] = [OH^-] = 1 \times 10^{-7} \text{ molar}$$

In all aqueous solutions, both acid and alkaline:

$$Kw = [H^+] \times [OH^-] = 10^{-14}$$

In an acid solution, $[H^+]$ is greater than 1×10^{-7} mol. In an alkaline solution, $[H^+]$ is less than 1×10^{-7} mol. pH is the minus the logarithm of the hydrogen ion concentration, $[H^+]$, exponent, that is,

$$pH = -\log [H^+].$$

When pH is	1	H^+ is	10^{-1}	and OH^- is	10^{-13}
	2		10^{-2}		10^{-12}
	4		10^{-4}		10^{-10}
	6		10^{-6}		10^{-8}
	10		10^{-10}		10^{-4}
	13		10^{-13}		10^{-1}

A change of one pH unit indicates a tenfold change in H^+ concentration.

Buffer Solution. The theory of buffers and their preparation can be found in Appendix 1. For most commonly used buffers, the quantities of salts of the acids and bases have been predetermined and may be found in reference books (e.g., Bates, 1973, which contains a very good discussion of the theoretical aspects of buffers and extensive information on how to prepare several buffer solutions).

SELECTED REFERENCES

ASTM: E288-10 Standard specification for laboratory glass volumetric flasks, *ASTM International*. Online. Available at http://www.astm.org.

ASTM: E542-01 (Reapproved 2012). Standard practice for calibration of laboratory volumetric apparatus, *ASTM International*. Online. Available at http://www.astm.org.

ASTM: E694-99 (Reapproved 2010). Standard specification for laboratory glass volumetric apparatus, *ASTM International*. Online. Available at http://www.astm.org.

For referenced ASTM standards, visit the ASTM website, or contact ASTM Customer Service at service@astm.org. For annual book of ASTM standards volume information, refer to the standard's document summary page on the ASTM website.

Clinical and Laboratory Standards Institute (CLSI): Formerly the National Committee for Clinical Laboratory Standards (NCCLS) (Wayne, PA).

Provides comprehensive guidelines and procedures for basic laboratory methods.

Skoog DA, Holler FJ, Nieman TA: *Principles of instrumental analysis*, vol. 5. Philadelphia, 1998, Harcourt Brace.

Provides a comprehensive explanation of instrument principles for nearly all clinical laboratory equipment.

Access the complete reference list online at Elsevier eBooks for Practicing Clinicians.

REFERENCES

ASTM. E617-13: Standard specification for laboratory weights and precision mass standards. *ASTM International.* Online. http://www.astm.org.

Bartle KD: Introduction to the theory of chromatographic separations with reference to gas chromatography. In Baugh PJ, editor: *Gas chromatography: A practical approach*, ed 1. New York, 1993, Oxford University Press, pp 9–10.

Bates RG: *Determination of pH—theory and practice*, ed 2. New York, 1973, John Wiley and Sons.

Bender GT: *Principles of chemical instrumentation*, Philadelphia, 1987, WB Saunders.

CLSI: *Determining performance of volumetric equipment*, *Proposed Standard I8-P*, Wayne, Pa., 1984, CLSI.

CLSI: Preparation and testing of reagent water in the clinical laboratory. In *Approved Guideline GP40-A4-AMD*, ed 4. Wayne, Pa, 2006, CLSI.

Gauldie J: Principles and clinical applications of nephelometry. In Kaplan LA, Pesce AJ, editors: *Nonisotopic alternatives to radioimmunoassays*, New York, 1981, Marcel Dekker Inc, pp 289–291.

Joint Commission on Accreditation of Health Care Organizations (JCAHO): Eliminating mercury in hospitals, *Environmental best practices for health care facilities, US Environmental Protection Agency*, 2002.

Karasek FW, Clement RE: *Basic gas chromatography—mass spectrometry: principles and techniques*, Amsterdam, 1988, Elsevier.

Love JE, Ward KM: Electrophoretic instrumentation systems. In Ward KM, Lehmann CA, Leiken AM, editors: *Clinical laboratory instrumentation and automation: principles, applications, and selection*, Philadelphia, 1994, WB Saunders, pp 173–174.

Pincus MR: The Physiological structure and function of proteins. In Sperelakis N, editor: *Principles of cell Physiology (chapter 2)*, Fourth Ed., Philadelphia, 2011, Elsevier, pp 19–47.

Ravindranath B: *Principles and practice of chromatography*, Chichester, England, 1989, Ellis Horwood, pp 89–127.

Rayleigh LB: On waves propagated along the plane surface of an elastic solid, *Proc London Math Soc xviv* 4–11, 1885.

Rubinson KA, Rubinson JF: *Contemporary instrumental analysis*, Upper Saddle River, N.J., 2000, Prentice Hall.

Schoeff LE, Williams RH: *Principles of laboratory instruments*, St. Louis, 1993, Mosby.

Strouse GF, Furukawa GT, Mangum BW, et al.: *NIST standard reference materials for use as thermometric fixed points*, Gaithersburg, Md, 1997, NIST.

Tipler A: Gas chromatography instrumentation, operation, and experimental considerations. In Baugh PJ, editor: *Gas chromatography: A practical approach*, ed 1. New York, 1993, Oxford University Press, pp 63–67.

Willard HH, Merritt LL, Dean JA, et al.: *Instrumental methods of analysis*, Belmont, Calif., 1988, Wadsworth.

CHAPTER 5

MASS SPECTROMETRY AND APPLICATIONS

Spencer Chiang, Wenpeng Zhang, Zheng Ouyang

OVERVIEW, 60

DEFINITIONS AND TERMINOLOGY, 60
Molecular Weight, 60
Mass-to-Charge Ratio, 60
Internal Standard, 61
Sample Matrix, 61
Matrix Effect, 61
Reference Laboratories, 61
Clinical Laboratories, 61
Point-of-Care Settings, 61
False Positives/Negatives, 61
Resolution, 62
Reproducibility, 62
Relative Standard Deviation, 62
Limits of Quantitation/Limit of Detection, 62

PRINCIPLES OF MASS SPECTROMETRY, 62
Primary Components of Mass Spectrometry Systems, 62
Separation and Extraction, 62
Ionization, 62
Mass Analyzer, 62
Ion Detector, 64

ANALYTIC METHODS, 64
Tandem Mass Spectrometry, 64
Quantitative Analysis, 65
Chemical Profiling, 65

MASS SPECTROMETRY IN A CLINICAL ENVIRONMENT, 65
Targeted Analytic Mass Spectrometry Systems, 66
Gas Chromatography–Mass Spectrometry, 66
Liquid Chromatography–Mass Spectrometry, 66
Mass Spectrometry Imaging, 66

MS-BASED OMICS, 67
Proteomics, 67
Metabolomics, 68
Biomolecule Database Building, 68

CHALLENGES IN IMPLEMENTING MASS SPECTROMETRY INTO CLINICAL LABORATORIES, 68
Ambient Mass Spectrometry, 68
Direct Sampling Ionization, 69
Point-of-Care Mass Spectrometry Devices, 71

FUTURE PERSPECTIVES ON CLINICAL MASS SPECTROMETRY, 73

SELECTED REFERENCES, 73

KEY POINTS

- Mass spectrometry can identify and quantify analytes in human fluids and tissues.
- Mass spectrometry is based on volatilizing samples and ionizing the analytes of interest, which can then be identified from their times of flight (TOF) or in electric fields based on their molecular masses and the relative masses of their molecular ion fragments.
- New special techniques are now able to analyze patient samples by immediate direct sampling.
- These techniques include matrix-assisted laser-desorption ionization (MALDI), paper spray ionization (PSI), desorption electrospray ionization (DESI), direct analysis in real time (DART), and coated-blade spray techniques.
- As a result of these techniques and new, ultra-high-resolution mass spectrometers, mass spectrometry is able to analyze the presence and concentrations of many critical proteins, lipids, and small-molecule metabolites in patient samples.
- Consequently, mass spectrometry is now being used to perform proteomic analysis of cells in different disease states and is able to identify proteins in disease-causing microorganisms—for example, bacteria—allowing for rapid identification of these organisms.
- Mass spectrometry is now able to distinguish between normal and malignant tissue.
- Recent innovations in mass spectrometry allow the size of the mass spectrometer to be greatly reduced so that it can be used to perform point-of-care tests, including a mass spectrometer that can be placed in operating rooms, allowing surgeons to sample tissue to determine if tissue margins contain malignant cells.

OVERVIEW

Clinical methods employing mass spectrometric techniques, termed *clinical mass spectrometry*, is a well established but relatively unknown field that encompasses a wide range of current medical diagnostics. Mass spectrometry provides undeniable merits in comparison with other analytic methods, such as structure identification, and qualitative and quantitative analysis in complicated samples. Many recent applications are focusing on biomedical research, such as proteomics, metabolomics, and drug development. In recent years, several significant advancements in mass spectrometry have allowed for the translation of these methods into clinical applications. Development of new instrumentation and novel methodologies have pushed the limits of mass spectrometry and increasingly expanded its applications in a clinical environment over a relatively short period of time, as summarized in Figure 5.1. Currently, mass spectrometry is playing a progressively important role in medical diagnostics, especially for biomarker research, toxicology, and newborn metabolite screening. This chapter will go over the principles of mass spectrometry and emphasize its application as a comprehensive system for clinical and biological analyses.

DEFINITIONS AND TERMINOLOGY

A summary of necessary terminology for the principles of mass spectrometry, criteria, and field of clinical analysis is provided in this section to assist in understanding clinical mass spectrometry.

MOLECULAR WEIGHT

Mass spectrometry focuses on the molecular weight of each specific component within a sample. Molecules are expressed in terms of atomic mass units (amu) or Daltons (Da). Both terms are interchangeable and are scaled by 1/12th to the reference carbon isotope, ${}^{12}_{6}C$, defined at exactly 12 amu. The following equalities summarize the relation of amu, Da, and kg:

$$1\ mol\ of\ {}^{12}_{6}C = 12\ g$$

$$1\ Da\ (Dalton) = 1\ amu\ (atomic\ mass\ unit) = 1.66054 \times 10^{-27} \frac{kg}{atom\ {}^{12}_{6}C}.$$

MASS-TO-CHARGE RATIO

Mass-to-charge ratio (m/z) comes from dividing the relative mass (m) in terms of amu or Da to the number of charges (z). The charge number is an integer value indicated in multiples of the elementary charge. Most

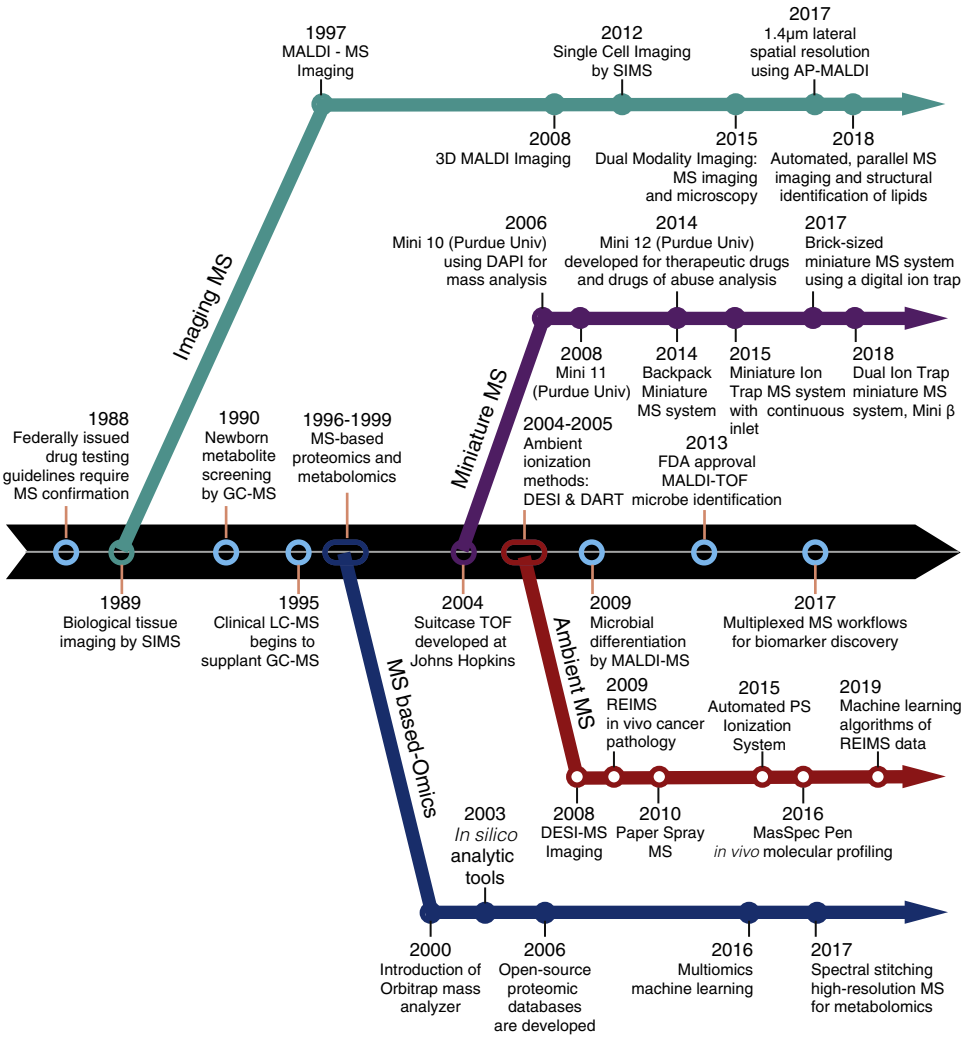

Figure 5.1 Approximate timeline of major developments in mass spectrometry technologies in the last few decades. *AP,* Atmospheric pressure; *3D,* three-dimensional; *DAPI,* discontinuous atmospheric pressure interface; *DART,* direct analysis in real time; *DESI,* desorption electrospray ionization; *FDA,* U.S. Food and Drug Administration; *GC,* gas chromatography; *LC,* liquid chromatography; *MALDI,* matrix-assisted laser desorption ionization; *MS,* mass spectrometry; *PS,* paper spray; *REIMS,* rapid evaporative ionization mass spectrometry; *SIMS,* secondary ion mass spectrometry; *TOF,* time of flight; *Univ,* university.

positive ions or negative ions correspond to the loss or addition of a single electron, respectively. In most cases, these ions directly reflect the relative mass. However, large molecules, such as proteins, have multiple sites that can hold a charge, forming multiply charged ions. It should be noted that multiply charged molecules have apparent m/z values that represent only a fraction of its actual mass. A mass spectrometer separates the ions by m/z, which is plotted in the x-axis of a mass spectrum against their relative abundance (y-axis).

INTERNAL STANDARD

Absolute quantitation by mass spectrometry requires an internal standard (IS) to correlate signal intensity to concentration. The IS is usually a compound that is similar but not the same as the species of interest in the sample. In most cases, this entails a deuterated form where several hydrogens have been replaced with deuterium. The similarity to the species of interest minimizes significant differences in ionization to the target species. Further detail on absolute quantitation is provided in the following section.

SAMPLE MATRIX

The sample matrix refers to all other components besides the species of interest. In the case of biological samples—such as blood, urine, or saliva—this encompasses a wide range of proteins, lipids, and other molecules that can easily confound mass analysis.

MATRIX EFFECT

Matrix effect is the effect of other components in a sample excluding the analyte of interest. In most cases, this is associated with a lowered specificity and sensitivity due to an excess of nonrelevant compounds in the mass spectrometer.

REFERENCE LABORATORIES

Reference laboratories are laboratory sites that perform analysis that is not commonly done in the hospital or other local laboratories. In most cases, these sites are far away from hospitals or other health care buildings and require long-term biosafe transport to analyze patient samples. These laboratories do not have to use high-throughput methods and analyze patient samples as needed.

CLINICAL LABORATORIES

Clinical laboratories are sites that are located within or nearby hospitals. Clinical laboratories can vary greatly depending on location, such as acute-care hospitals or medical centers. These laboratories maintain mostly automated instrumentation to run all routine clinical exams at a high volume. For low-volume tests or confirmations, samples are referred to reference laboratories.

POINT-OF-CARE SETTINGS

Point-of-care settings are environments in which health care is administered. This can include hospitals, intensive care centers, and surgery rooms. Rapid, simple tests are conventionally administered here to obtain preliminary information on whether more in-depth analysis is needed for diagnostics. In most cases, examinations at this setting are to make the initial diagnosis and collect patient samples for analysis in clinical or reference laboratories.

FALSE POSITIVES/NEGATIVES

Clinical tests are evaluated based the level of false positives or false negatives that occur in a controlled patient sample set. False positives refer to samples that are returned as positive by the clinical test but are negative. False negatives are samples that are returned as negative but are positive. In terms of clinical test efficacy, false positives prove the least amount of

risk and can be mitigated with consecutive tests. However, false negatives are extremely problematic, especially in diseases that require early intervention.

RESOLUTION

Resolution refers to the ability of a mass analyzer to separate two nearby peaks. In mass spectrometry, this is defined through the following equation:

$$R = \frac{M}{\Delta M},$$

where R refers to resolution, M is the mass of the peak, and ΔM is resolving power. In mass spectrometry, resolving power is defined through several methods. The peak width definition calculates the resolving power to be equal to the width of the peak measured at a fraction of the peak height. In most cases, this is defined to be at 50%, otherwise called *full-width at half maximum (FWHM)*. The valley definition is defined as the minimum distance between two overlapping peaks that form a valley (lowest value of signal) at a specified fraction of peak height. In most cases, this refers to either 10% or 50% loss of peak height.

REPRODUCIBILITY

Reproducibility is the ability for the same sample to be analyzed with the same or statistically similar outcomes. This is measured using criteria such as relative signal deviation and evaluated through large-volume clinical samples.

RELATIVE STANDARD DEVIATION

A measure of variability during repeats of the same sample. Relative standard deviation (RSD) values are calculated using the standard deviation and weighted to the average sample mean. These values are provided in percentages.

LIMITS OF QUANTITATION/LIMIT OF DETECTION

The lower bounds of an analyte that can be quantified or detected by mass spectrometry.

PRINCIPLES OF MASS SPECTROMETRY

Mass spectrometry is an analytic technique that outlines the composition of a sample. This is shown by a mass spectrum, where the x-axis represents the m/z and the y-axis is its relative abundance within the sample. Mass spectrometry systems comprise several major components: (1) an ion source, (2) mass analyzer, and (3) detector. In the last several decades, each of these components has undergone advancements that either improved on existing instruments or realized novel hybrid systems that enable unique mass spectrometric analyses. Current research using mass spectrometry has slowly begun to transition from instrumentation into biological applications, translating research-based analytic techniques for high-throughput clinical use.

PRIMARY COMPONENTS OF MASS SPECTROMETRY SYSTEMS

Before mass analysis, sample extraction and separation are critical steps for highly sensitive and specific analysis. Especially with clinical samples such as blood, urine, or even biopsy tissues, these matrices are immensely complex, containing numerous proteins, lipids, and salts. This step is commonly done to remove unwanted matrices and provide a preliminary separation, preventing detector overloads. However, solid samples such as biopsy tissue sections do not require extraction or separation and rely solely on the mass spectrometer for specificity. Afterwards, the three basic components of a mass spectrometer work sequentially to ionize, identify, and detect ions: the ion source, mass analyzer, and ion detector. Depending on the product from sample extraction—whether it is solid, liquid, or gas—the sample inlet must be adjusted accordingly to promote effective and comprehensive sample ionization.

SEPARATION AND EXTRACTION

External to the mass spectrometer, sample separation is predominantly based on gas or liquid chromatography. A typical system includes a sample injector, column, and detector (covered by mass spectrometry), illustrated in Figure 5.2. Current systems are automated to eliminate human errors and rely on chemical interactions between the mobile and stationary phase for separation. The column holds the stationary phase, which is composed of differing materials based on targeted chemical interaction (see Chapter 24). In gas chromatography (GC), compounds are converted into the gas phase to interact with a heated column comprising solid absorbent material (usually, alumina, silica, or activated carbon) or liquid-coated solid supports (e.g., polymers, hydrocarbons, fluorocarbons coating a solid material). Gaseous samples are introduced into a chemically inert carrier gas (mobile phase) and propelled through the column, separating based on vapor pressure and volatility. This requires compounds that are naturally or easily made volatile. This encompasses various organic molecules and most drugs that are ideal for toxicology and pharmacokinetic analysis. GC has been used for decades, providing high resolution, specificity, and relatively short analysis time.

Liquid chromatography provides a suitable alternative for compounds that are insufficiently volatile or unstable in the gas phase. Without the dependency on volatility, separation of thermally labile compounds can be achieved. Both factors encompass the remaining class of compounds that cannot be analyzed through GC. In most cases, liquid chromatography paired with mass spectrometry involves high-performance liquid chromatography (HPLC), which greatly improves the mobile phase flow rates, separation efficiency, and reproducibility. As the name suggests, the mobile phase of HPLC includes the use of liquid solvents to carry the sample through the column. Automated sample injectors and specialized mechanical pumps provide and maintain a high-pressure environment (up to 6000 PSI). Five different separation techniques are most commonly used: adsorption, partition, ion exchange, affinity, and size exclusion. The versatility of HPLC for different types of molecules enables a wide range of clinical applications, from separating small drugs to proteins for mass spectrometric analysis.

IONIZATION

The ion source is responsible for ionizing molecules from samples that are provided in either gas, liquid, or solid forms. Acting as an intermediary for the transition of samples from their native phase into the gas phase, ionization occurs in various modalities. By providing adequate conditions—such as high temperatures, voltage potentials, gas flow, or a vacuumed environment—sample molecules are easily ionized. Some ionization modalities are highly energetic and cause extensive fragmentation before entering the mass spectrometer. Others are soft ionization methods, which only produce molecular ions. Most ion sources produce ions mainly by attaching charges in the gas phase through electron ejection, electron capture, protonation, deprotonation, adduct formation, or transfer of charged species.

For gas-phase molecules, *electron ionization* and *chemical ionization* are commonly used ionization methods. *Electron ionization* or *electron-impact ionization* bombards a sample with a beam of electrons formed from a heated filament. *Chemical ionization* uses a reagent gas that is ionized by the electron beam and is then exposed to the sample. Both methods are limited to volatile and thermally stable samples, resulting in its main use being paired to gas chromatography–mass spectrometry (GC-MS). Molecules that fall outside of these categories must be directly converted from the condensed phase to the gas phase. Liquid-phase ion sources depend on a nebulizer to initiate or assist droplet formation. *Electrospray ionization* (ESI) applies high voltage to the solvent/sample capillary to form a charged Taylor cone at the tip, in which an external nebulizing gas is often applied to assist with charged droplet formation and desolvation. Other processes include *atmospheric pressure chemical ionization* and *atmospheric pressure photoionization*, in which a nebulizing gas is applied to form small droplets from the sample and ionized by a corona discharge electrode or UV lamp, respectively. Both gas- and liquid-phase samples are commonly coupled to extraction or separation instrumentation. However, solid-phase samples cannot and do not use GC or HPLC without any previous homogenization or dissolving. These solid-phase ion sources require an external matrix that coats the sample surface. This external matrix is usually a solid or viscous liquid that produces ions when irradiated by photons or charged particles. *Matrix-assisted laser desorption ionization* uses a laser beam to irradiate the matrix and sample collectively to form ions. Similarly, *fast atom bombardment* employs a liquid matrix layered over the solid sample and bombarded with protons or other charged particles. Both ionization techniques require extensive optics and 3D stands to finely manipulate the intensity and location of the laser beam.

MASS ANALYZER

Following the formation of negative or positive gaseous ions, a strong voltage gradient and countercurrent curtain gas focus and accelerate the sample

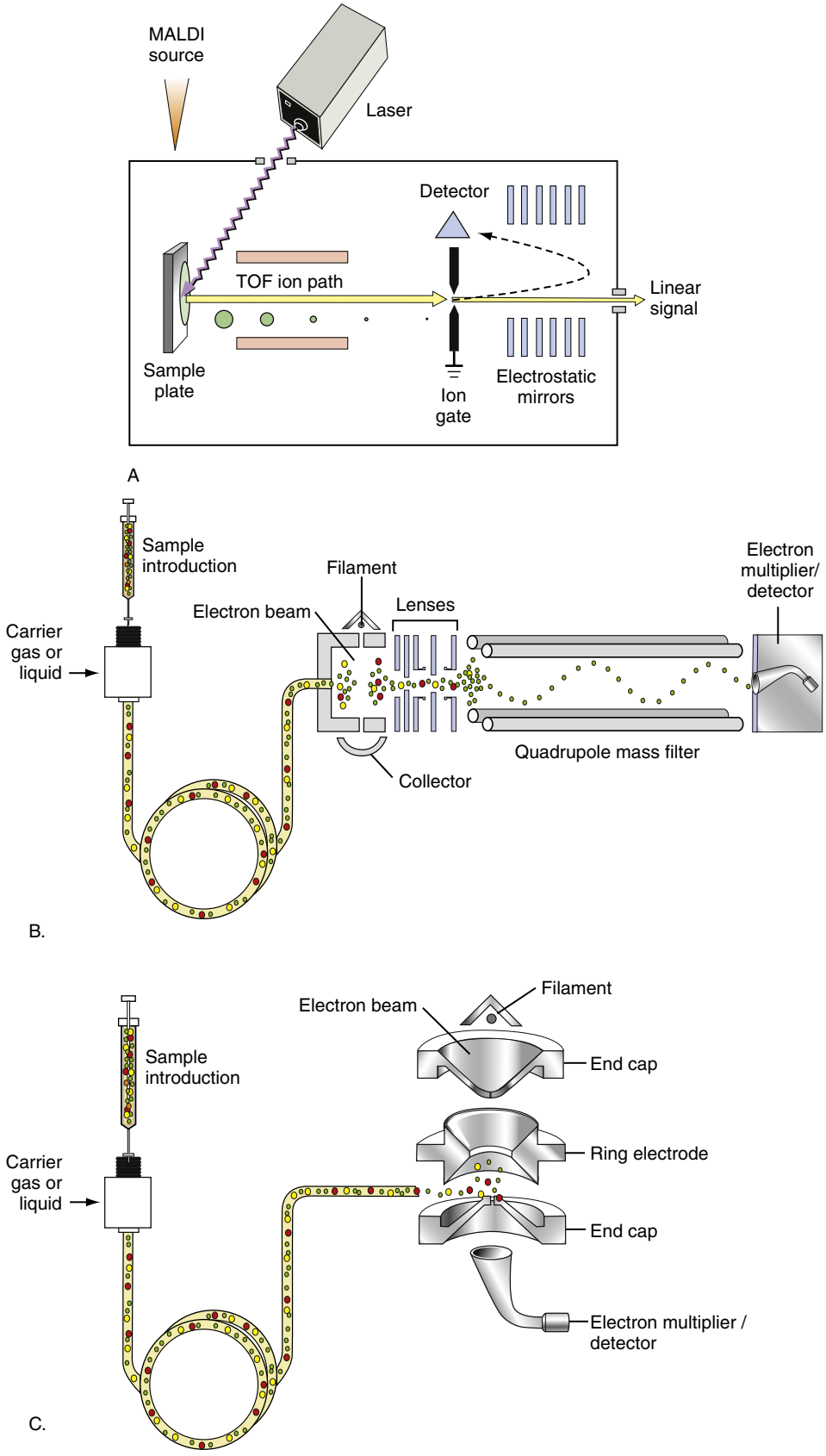

Figures 5.2 Mass spectrometry analytic systems. **A,** Sample processing. In this example, the sample is present on a matrix that is exposed to intense laser light. In this process of matrix-assisted laser desorption ionization (MALDI), ions from the sample are created and moved by a carrier gas (often, N_2) into the mass spectrometer analyzer or detector. When passing through the mass spectrometer, these ions enter a quadrupole field and eventually hit the detector, where they give rise to a change in voltage recorded as a peak. Low-molecular-mass ions travel farther than higher-molecular-mass ions. Therefore, low-molecular-mass ions travel for greater times, and higher-molecular-mass ions travel for lesser times, known as *times of flight* (TOFs), as in the figure. **B,** The mass spectrometer detector. The sample initially processed in **A** is carried by the carrier gas into the mass spectrometer, where it enters a chamber called the *collection* or *collision chamber*, which produces high-energy electrons that collide with the sample molecules, resulting in ion fragments. These ion fragments are focused into the quadrupole field wherein they accelerate at rates that are directly related to their molecular masses. Detection is by voltage change, as mentioned earlier. **C,** Ion trap. This is a special adaptation of the collection chamber wherein ions are collected in a so-called ion trap and accelerated through the quadrupole field.

ions into the mass analyzer. Similar to the numerous ionization modalities present, varying mass analyzers have been developed using a combination of electric and magnetic fields to separate molecules by m/z. Separation can be achieved by manipulating various properties. *Time-of-flight* (TOF) analyzers separate based on ion velocity, using an electric field to accelerate and transfer identical amounts of kinetic energy to each ion. A metal flight tube and reflectron comprise a sufficiently long flight path to separate ions. With the same kinetic energy, low-m/z ions will travel faster than high-m/z ions. Precisely measuring the amount of time to travel the ion path results in an accurate measurement of m/z. *Quadrupole mass analyzers* utilize two pairs of metallic rods, each of which have both a direct electrical current and radiofrequency voltages applied at selected magnitudes. These two pairs of rods, termed *quadrupole*, act as a mass filter. Only a specified m/z can pass through the quadrupole undeflected and strike the detector.

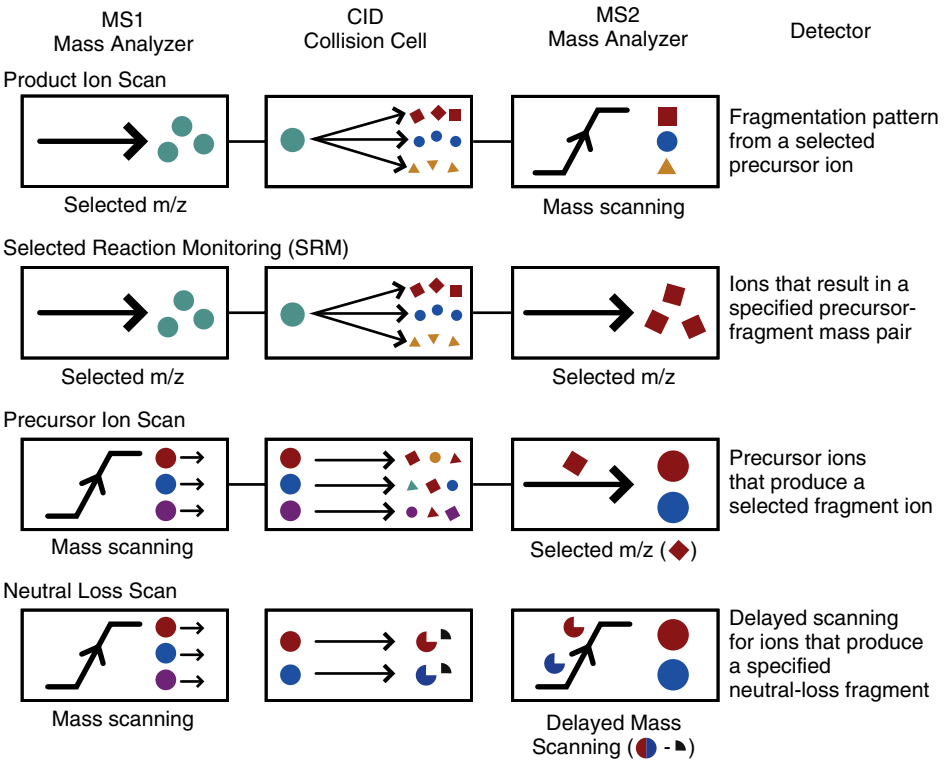

Figure 5.3 Tandem mass spectroscopic (MS) scan modes. These are for two MS units in tandem with one another. *Top line:* Product ion scan. A particular parent ion from MS1 (mass spectrometer 1), represented by the *green circles*, is transported to MS2. Just prior to its entering MS2, it enters a collision cell where the parent ion collides with electrons to produce lower-molecular-mass ion fragments represented by *red squares*, *blue circles*, and *gold triangles*. These fragments are then scanned in the quadrupole tubes in MS2. The horizontally upward tilted arrow in MS2 on the upward slanted line symbolizes the scanning of these ion fragments. *Second line:* Selected reaction monitoring. This is similar to the product ion scanning above, but the presence of only one ion, represented by the *red squares*, is monitored. *Third line:* Precursor ion scan. In this instance, the ionization of all molecules of interest is achieved on MS1. These precursor ions are then fragmented in the collision cell. *Red circle* and *blue circle* ion fragments both give rise to the *red diamond* subfragment. This is the ion species that is monitored on MS2. *Fourth line:* Neutral loss scan. This is similar to the precursor ion scan above except, in this case, *red* and *blue circle* ion fragments lose a neutral (uncharged) fragment (*black sector*) in the collision cell, resulting in lower-molecular-mass *red* and *blue partial circle* fragments, both of which are monitored in MS2. *CID,* Collision-induced dissociation; *m/z,* mass-to-charge ratio.

By ramping either the electrical current or radiofrequency magnitudes, a range of m/z can be detected sequentially. Both TOF and quadrupole mass spectrometers control the path of the ion beam for analysis. *Ion trap mass analyzers*, however, capture the ions in an electromagnetic field with several direct current end caps and can analyze only in select pulses. Various ion trap types have been proposed, such as ring and linear ion traps. Ions orbit within the analyzer and can be selectively ejected from the trap by scanning radiofrequency magnitudes that correspond to specific m/z resonant frequencies. These analyzers can detect much lower sample concentrations and scan across a wide m/z range. The *orbitrap mass analyzer* is a relatively recent innovation in comparison with other analyzers, developed in 2005. This analyzer is similar to ion traps by capturing the ions but measures the ion orbit frequencies rather than scanning resonant frequencies. A polished metal spindle is held within a hollow barrel for the ions to orbit at its natural frequency under an electromagnetic field. Fourier transforms are used to obtain mass spectra and show impressive performances at high masses and high resolution, making them the gold standard for large biomolecules such as proteins.

ION DETECTOR

The ion detector is placed in the direct path of the ion beam or ion ejection in the case of TOF/quadrupoles or ion traps, respectively. Most mass spectrometers utilize an electron multiplier that exponentially magnifies the ion charge as it strikes the first dynode. After the ion collides into the first dynode, a release of secondary electrons and, in turn, tertiary electrons, travels through the tube and amplifies the signal into a detectable charge. Other detectors, such as *ion-photon conversion detectors*, operate in similar parameters but utilize photons instead of electrons. Although these detectors are effective in amplifying charge, they have a lifetime of only 1 to 2 years owing to sample contamination or poor vacuum conditions, which can affect electron transfer. However, orbitrap analyzers utilize a nondestructive method to detect ions. Several electrodes on the opposing side of the analyzer are used to detect image current formed by orbiting ions. This provides the raw data needed for a Fourier transform, eliminating issues with contamination and gaussian noise from each dynode.

ANALYTIC METHODS

TANDEM MASS SPECTROMETRY

Tandem mass spectrometry (MS/MS or MS^2) performs mass analysis at least twice while performing a dissociation process or chemical reaction to change the mass or charge of an ion. MS/MS improves specificity beyond separation by molecular weight and provides insight into structure elucidation and identifying elementary composition. The most common dissociation method is collision-induced dissociation (CID), in which the first analyzer is used to isolate a specified target ion (precursor ion) and, subsequently, undergoes a fragmentation process to yield neutral fragments and fragment ions (product ions). The second analyzer analyzes these product ions and forms a unique pattern based on the precursor ion structure and components. Other dissociation processes exist and form varying fragmentation patterns, such as ultraviolet photodissociation or electron-transfer dissociation (ETD), which are used for specific applications such as proteomics. Chemical reactions, such as charge-exchange or partial charge transfers, can also be done to further study ion-molecule reactions. Furthermore, multiple MS/MS steps can be performed by sequentially selecting the precursor ion, then a single fragment ion, and so on. Depending on the number of steps, this is called MS^n, where *n* defines the generation of ion being analyzed. This technique can be done either in space or in time. In-space mass analyzers, such as TOF and quadrupoles, conduct MS/MS analysis by using several distinct mass analyzers (i.e., triple quadrupole MS). A dedicated quadrupole acts as the reaction region, containing inert gas to fragment the precursor ions. The final analyzer scans all fragment ions. To obtain higher MS^n spectra, additional analyzers and collision cells must be added to the mass spectrometer at prohibitive costs and complexity. However, mass spectrometers with ion trap mass analyzers conduct in-time MS/MS or MS^n using a single analyzer. A single ion is isolated and fragmented sequentially and can perform up to MS^7 or MS^8. Minimal ion losses occur at each step of the process; however, practical limitations, such as minute mass fragments and multiple fragments, limit the number of steps that can be performed.

Various MS/MS scan modes have been developed for different applications and can significantly improve sensitivity and specificity (Fig. 5.3). Here, we define the four main scan modes that are commonly used in clinical analysis, focusing on CID as the major dissociation method.

Product Ion Scan

A precursor ion of a targeted m/z is first selected and then fragmented by a collision cell or in an ion trap mass analyzer. All product ions are analyzed and observed in the resulting mass spectra.

Precursor Ion Scan

Instead of scanning for the product ions, this scan mode scans all precursor ions that produce a specified product ion. The second mass analyzer is focused on a single product ion formed from CID, while the first analyzer scans all precursor ions. This cannot be performed by in-time analyzers, such as ion traps.

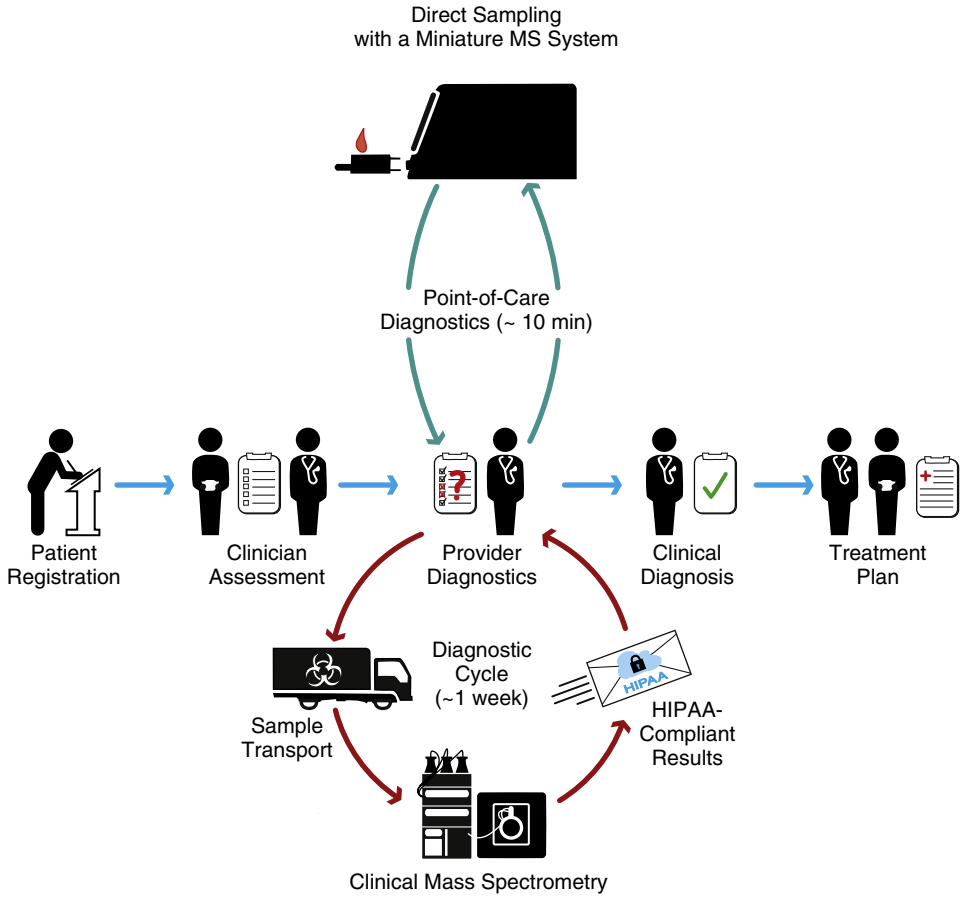

Figure 5.4 Overall workflow of clinical diagnostics involving clinical mass spectrometry (MS) assays.

Neutral Loss Scan

This scan mode detects all fragmentations that lead to the formation of a specific neutral fragment. Both the first and second mass analyzers are scanned at the same time but with a constant mass offset correlated to the selected neutral fragment. For example, a neutral loss scan of x Da would require an ion mass of m in the first analyzer and a fragment ion (m-x Da) for detection. Similar to precursor ion scans, this mode is not available to in-time analyzers.

Selected Reaction Monitoring

Selected reaction monitoring selects a single precursor-product reaction by focusing the first and second analyzer to a single mass. No scanning is needed, and detection occurs only if ions selected by the first mass analyzer produce the preset fragment ion. Multiple reactions can be monitored at the same time, which is called *multiple reaction monitoring* (*MRM*).

QUANTITATIVE ANALYSIS

In a clinical environment, quantitative analysis plays a key role. For applications such as toxicology and drug abuse detection, deriving the absolute concentration of certain molecules in patient samples helps establish legal limits or monitor the appropriate drug concentrations within a patient. Absolute quantification of drugs by mass spectrometry requires the addition of an IS. Without an IS, ion signal intensity provides only a relative quantification in comparison to the rest of the sample. This signal intensity can differ greatly among instrumentation, succumbing to randomness in ion formation, sample parameters, and detector amplification. The IS serves as a calibrant to correct for the loss of analyte during analysis. A calibration curve is drawn from standards of varying concentrations and a single concentration of IS. Placing a set concentration of IS into a patient sample enables the user to correlate the resulting signal intensity to concentration. By doing so, the concentration of other ions can be deduced without being affected by sample or instrument noise.

CHEMICAL PROFILING

Chemical profiling encompasses the remaining mass spectrometric analysis that seeks to identify or compare a wide range of chemical components within a patient sample. Some applications profile patient samples to identify the presence of disease-specific biomarkers. The presence of one or several molecules is enough for diagnosis without calculating the absolute concentration. Unlike quantitative analysis, an IS is not needed. The use of high-resolution mass spectrometers maintains molecular specificity while providing enough sensitivity to detect low concentration molecules. Other profiling methods include monitoring ion ratios, which change in correlation to disease progression.

MASS SPECTROMETRY IN A CLINICAL ENVIRONMENT

Mass spectrometry systems have had various clinical applications since the end of the 20th century. Initially designed as a specialized tool for reference-level analyses, mass spectrometry has rapidly transitioned into clinical laboratories through its main features of merit: structure identification and quantitative analysis in mixtures. In the current clinical landscape, mass spectrometry plays a role as the secondary follow-up test after initial in-field or preliminary screening. Several reasons contribute to the existence of this role: (1) the lack of appropriate sensitivity and specificity of preliminary screening tests and (2) the inability for mass spectrometry to be implemented as a routine screening tool due mainly to cost and the need for technical expertise in the operation and maintenance of the mass spectrometers and in the interpretation of results. However, in recent developments, new much smaller mass spectrometers have been developed that have the potential to perform in-house laboratory testing and point-of-care tests, as illustrated in Figure 5.4 (Li et al., 2014).

Currently, preliminary screens such as immunoassays can be administered at the point of care and provide near instantaneous results, ideal for in-field analysis and areas with limited resources. However, erroneous results can occur, forming false positives or false negatives. In most cases, these preliminary screens err toward false positives and, thus, must rely on secondary exams to rule out the initial diagnosis. Upon the physician's request for further diagnostic exams, patient samples are carefully packaged and sent to specialized clinical laboratories that perform mass spectrometry analysis. Results are returned, following health care guidelines such as the Health Insurance Portability and Accountability Act (HIPAA),

and can take up to a week. With the involvement of point-of-care diagnostics, this workflow can be significantly simplified, eliminating the need for biosafe sample transport as well as complications owing to HIPAA compliant results.

Starting from the inception of GC-MS for clinical use, quantitative analysis of drugs and organic compounds was achieved and established in specialized clinical laboratories. These laboratories have been dedicated to toxicology, metabolite screening, or volatile compound analysis, but have expanded into other nonvolatile or thermally labile species with the introduction of liquid chromatography-mass spectrometry (LC-MS). More recently, these systems have seen an uptick in solving biochemical problems, identifying the underlying phenomena that exist within the human biome. Proteomics, metabolomics, and high-throughput drug discovery are just several high-profile topics that have been guided through mass spectrometry systems. With such an expansive field, mass spectrometry systems have established themselves as the gold standard for analytic techniques for two different method classes: targeted analytes and global chemical profiling.

TARGETED ANALYTIC MASS SPECTROMETRY SYSTEMS

Targeted clinical analytic methods focus on identifying a subset of *known* diagnostic molecules within patient samples. These methods are used for applications such as toxicology (see Chapter 24), metabolite screening, and therapeutic drug monitoring in which specified ions can be separated and analyzed. In most cases, quantitative analysis is necessary to be effective along with constant addition of ISs. Tandem mass spectrometry is also used to increase the method's specificity toward all analytes of interest. For the analysis of clinical samples, sample preparation and extraction are key steps owing to the complex nature of biological matrices. The different limitations in sample type, gas/liquid chromatography, and ion source need to be accounted for to ensure compatibility and analytic efficiency.

GAS CHROMATOGRAPHY–MASS SPECTROMETRY

GC-MS was one of the first official clinical-use mass spectrometers. Owing to the gaseous sample introduction from GC to the mass spectrometer, minimal compatibility and combinatory issues arose from preliminary ion sources, such as electron impact and chemical ionization. A major push for the use of mass spectrometers (and, in relation, GC-MS) came about during an accident aboard the aircraft carrier USS Nimitz. In 1981, a plane crashed trying to land aboard the Nimitz. During the investigation, it was found that several seamen were under the influence of drugs such as marijuana and cocaine, prompting further drug evaluations for the rest of the military (Jannetto and Fitzgerald, 2016). Immunoassays were used to identify major marijuana metabolites but had numerous false positives. Thus, a new rule-out test was needed to confirm whether these metabolites were present. GC-MS along with mass spectrometry slowly was implemented into toxicology laboratories and was advocated for further development and expansion into other fields, such as newborn metabolite screening.

Newborn Screening

Newborn metabolite screening is a rapid examination to test for any inborn errors that could have lasting effects or elevated mortality rates. Many of these disorders—such as phenylketonuria, cystic fibrosis, or other hematologic disorders—result from enzyme defects within metabolism, leading to unnatural accumulation of intermediate metabolites that can be toxic. These disorders can be screened using two groups of analytes: amino acids and acylcarnitines. Amino acids are easily analyzed by GC-MS in biofluids after derivatization. However, acylcarnitines were better analyzed using other methods, such as fast-atom bombardment. The use of tandem MS/MS systems enables GC-MS analysis for several amino acids derived from dried blood spots (DBSs). Samples are collected from the heel of a newborn and sent to clinical labs to run. Several minutes are required for each run, quantifying both phenylalanine and tyrosine ratios for routine screening of phenylketonuria with low detection limits of 1.2 μM and 1.6 μM, respectively (Deng et al., 2002). However, GC-MS has obvious limitations. It relies on volatile and thermally stable samples to be analyzed by using gas-phase ionization methods such as electron impact and chemical ionization. For samples that do not have these characteristics, extensive derivation is needed for the analytes to be sufficiently volatile. GC-MS is not suitable for the analysis of most biological molecules, especially proteins.

LIQUID CHROMATOGRAPHY–MASS SPECTROMETRY

Limitations in GC-MS propelled research and development using liquid chromatography. Without the need for volatile compounds, liquid chromatography enables differing separation based on chemical properties for an extensive analyte list. However, converting the sample from liquid-phase to gas-phase in the ion source proved to be difficult. The introduction of electrospray ionization (ESI), atmospheric pressure photoionization (APPI), and atmospheric pressure chemical ionization (APCI) were instrumental in developing the first liquid chromatography–mass spectrometry (LC-MS) system. Through nebulization and its subsequent ionization, a successful pairing of LC-MS brought forth MS as a viable instrument for routine clinical use.

LC-MS has grown into a method that has supplanted some more time-consuming applications that were previously established by GC-MS. Several clinical tests include hormone and steroid testing. Endocrine testing for normal circulating levels of aldosterone in blood is critical in diagnosing hyperaldosteronism, which has a direct correlation to secondary arterial hypertension. GC-MS was an accurate and specific method to quantify circulating aldosterone but required extensive sample preparations unfit for routine clinical laboratory use. Instead, in-lab developed immunoassays were used to directly measure or analyze after a simple preextraction and, therefore, lacked standardization. LC-MS supplanted this by enabling semiautomated analysis with a limit of quantitation of 69.4 pmol/L (Taylor et al., 2009). Another hormone test is cortisol measurements in Cushing syndrome, in which elevated serum levels of cortisol occur. Three tests are required to quantify cortisone levels in the body, starting from urinary free cortisol measurement, midnight plasma cortisol, and low-dose dexamethasone suppression test due to interference from endogenous metabolites. LC-MS/MS assays improved the limit of detection (LOD) from 30 nmol/L to 6 nmol/L, while holding an interassay imprecision of less than 10% (Grebe and Singh, 2011).

LC-MS is also commonly applied to therapeutic drug monitoring for various drugs, such as immunosuppressants. Immunosuppressants are a class of drugs that suppress the immune system to regulate autoimmune conditions in cases such as organ transplantation or arthritis. These drugs have very narrow therapeutic ranges, such as tacrolimus (5–20 ng/mL) and sirolimus (5–15 ng/mL), and life-threatening side effects owing to a weakened immune system. LC-MS provides a method for the simultaneous measurements of four different immunosuppressants in blood with an analytic run time of 9.5 minutes (Christians et al., 2000). Other types of drugs that are monitored include anticonvulsants and antibiotics.

MASS SPECTROMETRY IMAGING

Mass spectrometry imaging adds a new dimension to the information provided by traditional clinical mass spectrometry. Spatial resolution and distribution of certain analytes can be generated to form heatmaps. This is usually applied for differentiation between healthy and diseased tissue biopsies or observing drug distributions within an organ. One notable application of mass spectrometry imaging is the transference of therapeutic drugs across the blood-brain barrier, providing valuable biological insight into therapeutic drug response for brain diseases (Liu et al., 2013). Much of mass spectrometry imaging is focused on monitoring multiple biomolecules, such as lipids and peptides, rather than quantifying the absolute concentration. Chemical profiling is more commonly used to establish healthy ratios of biomolecules and record disease-affected biomolecule ratios. Labs rarely use tandem MS, instead opting for higher-resolution mass spectrometers to maintain high levels of sensitivity. These methods usually undergo minimal to no sample preparation by only selectively eliminating matrices. Locations and relative concentrations of various compounds are overlaid over optical images to verify and locate areas of disease.

Matrix-Assisted Laser Desorption Ionization

Matrix-assisted laser desorption ionization (MALDI)–mass spectrometry is a powerful analytic counterpart that utilizes high-resolution mass spectrometry through its TOF analyzer. Samples are coated in a chemical matrix and ionized by a laser to produce intact gas-phase ions. This is highly advantageous for several reasons. Large, thermally labile and nonvolatile compounds, including proteins and oligopolymers, can be ionized with minimal decreases in sensitivity due to matrix effects. Furthermore, the laser desorbs and ionizes samples at a single spot, enabling spatial analysis of samples. Several applications of MALDI-MS include targeted analyte detection of large biomolecules. An example of this is the direct analysis of hemoglobin glycation, used to monitor diabetes progression.

With further selectivity in chemical matrices, a wide array of molecules can be analyzed, including peptides, lipids, drugs, and nucleotides. Furthermore, direct single-spot sampling by MALDI has been standardized and implemented largely for characterization of bacterial and fungal growths (Freiwald and Sauer, 2009).

The other main application of MALDI is its imaging capabilities through sequential irradiation throughout a tissue section without radiolabeling. Computer postprocessing enables the generation of numerous heatmaps on specific analytes or groups of analytes to highlight areas of disease. Although largely performed in research labs, MALDI imaging has greatly advanced in the last decade. Sequential analysis of tissue sections has enabled three-dimensional (3D) reconstruction of cancer tissue biopsies, such as malignant pleural mesotheliomas (Giordano et al., 2016). Spatial drug distributions across the tumor can be visualized three-dimensionally, elucidating a very limited drug penetration in subvolumes. MALDI also has a unique advantage in generating molecular snapshots of protein expression within tissues. Localization of biomarkers such as β-amyloid peptides in Alzheimer rats has been reported, providing highly useful data for disease classifications (Schuerenberg et al., 2007). Recently, 3D molecular imaging by MALDI has reached the subcellular level, mapping the spatial distribution of lipids in a single cell. Zebrafish embryos were used to visualize local changes in lipid concentrations during various stages of cell development (Dueñas et al., 2017). This provides a powerful set of information, assisting studies in lipid metabolism and dynamics during embryonic development. In concurrence with novel applications, MALDI has undergone technological advancements that improve spatial resolution and throughput. Imaging of lipid profiles and spatial locations in rat cerebellar tissue paired with automated structural assignments show rapid validation of over 100 molecular lipids in each pixel without increasing acquisition times (Ellis et al., 2018).

Several derivatives of MALDI have been introduced to overcome MALDI limitations. Whole tissue samples and specimens that are unanalyzable under vacuum conditions can be analyzed by atmospheric pressure (AP)-MALDI, although in such conditions, spatial resolutions are generally diminished due to stochastic ion paths when ionized. However, advancements to AP-MALDI include lateral spatial resolutions at 1.4 μm in various tissues and cells and improvements continue (Kompauer et al., 2017). Another aspect of MALDI is matrix-free laser desorption ionization (LDI), in which different fixed substrates are utilized instead of chemical matrices. The removal of matrices eliminates any confounding matrix peaks that dominate the low mass spectra. This can greatly improve the throughput of mass spectrometry imaging, eliminating any sample preparation procedures.

Secondary Ion Mass Spectrometry

Secondary ion mass spectrometry (SIMS) pushes the boundaries on mass spectrometry imaging with high spatial resolution. An ion beam (usually Ar, Ga, or Cs) is used to bombard the surface with keV energy and high precision to form secondary ions measured by mass spectrometry. Although this method has reported much lowered sensitivities and mass ranges, its spatial resolution is unparalleled, providing images at submicron levels. This is highly applicable for subcellular level analysis, such as stem cell division and metabolism. Molecular snapshots of these systems help elucidate metabolic pathways without radiolabeling or external components that may affect cellular activity. SIMS has also been used for high-resolution detection and visualization of protein expression in human breast tumors (Angelo et al., 2014). Antibodies tagged with isotopic elemental metals bind to their targeted surface protein receptors. During ion bombardment, elemental metals are released as the secondary ions and analyzed through mass spectrometry. Localization of protein receptors provides unique insights and potential targets for cancer drugs and other novel disease therapies.

MS-BASED OMICS

In recent years, *omics* research has expanded greatly following the success of genome research. Whereas the genome describes what can potentially happen, proteomics and metabolomics study the definite initiators and products, respectively. Proteins initiate and regulate biological pathways and change in response to diseases. Metabolites comprise the signaling intermediates and products that result from metabolic pathways. Thus, proteins are generally affected in disease states, while metabolomics is highly dynamic, responding to second-to-second changes within the body. Both research fields hold valuable data regarding cellular biology and are highly relevant to disease diagnostics. Recently, high-resolution mass spectrometry has undergone the most significant level of technical evolution for mass spectrometry. Mass analyzers, such as orbitraps and TOF, can resolve analytes to the nearest 0.001 amu, providing enough selectivity for the user to observe minute changes in the structure and wide mass ranges. These high-resolution mass spectrometers are highly suitable for biomolecule profiling and are commonly tied to liquid chromatography for improved sensitivity. As such, proteomics, metabolomics, and other omics research are largely driven through high-resolution mass spectrometry. These mass spectrometers are maintained in reference laboratories due to its cost and high clinical research value, especially in biomarker discovery and other basic translational research. Further validation studies for biomarkers and disease metabolic profiling can easily be translated for routine clinical screening. As such, omics research is critical as a clinical mass spectrometric method despite its standing in a reference laboratory.

PROTEOMICS

Much of the omics research is dedicated to identifying novel, significant high-impact biomolecules that potentially revolutionize disease diagnostics. One major category is proteomics, or the study of proteins (Aebersold and Mann, 2003; Domon and Aebersold, 2006). This class encompasses everything about proteins—their identification, structure, complex formation, posttranslational modification, and quantitation under different disease states. Proteomic research is separated into two categories: bottom-up and top-down protein research. Both methods generally require extensive sample preparation procedures to isolate individual proteins. Two-dimensional electrophoresis (as further described in Chapter 76) is performed in agar to select a single protein, which is cut and dissolved into a solution. LC-MS/MS is performed, and protein fragments are subsequently observed and connected to an appropriate database of protein for identification. High-resolution mass spectrometers are often used to improve the specificity of highly charged peptides and proteins, and can separate isotopic peptides that differ in their composition (e.g., lysine vs. glutamine, differing by 0.0364 Da) without using tandem MS (Mann and Kelleher, 2008) (see also Chapters 76 and 79).

Bottom-up proteomics is highly amenable to the LC-MS/MS workflow by first enzymatically digesting a protein and separating its peptides by LC. All peptides are eluted from the column, and amino acid sequencing is done by tandem MS. Subsequent algorithms combine and compare the precursor ion mass to a database for protein identification. This method is simple and reliable for amino acid sequencing and can also be used to identify certain posttranslational modifications. Another method, called *shotgun proteomics*, can be performed by enzymatically digesting protein extract or raw biofluids, such as serum. Commonly, abundant proteins are first removed by protein depletion to focus on lower-concentration peptides with biological significance. After chromatographic separation, enzymatically cleaved peptides are identified and sequenced by tandem MS. Peptide spectral libraries are used to assemble the numerous identified fragments into protein identification. This has been applied to various microorganisms, as discussed in Chapter 57, posttranslational modification, discovery of biological pathways and various other clinical applications to study biological mechanisms and highlight significant drug targets or biomarkers. However, there are specific limitations to this method, including limited protein sequence coverage, limited labile posttranslational modification analysis, and ambiguity of redundant peptide sequences from isoform proteins.

In contrast, top-down proteomics ionizes whole, intact proteins and fragments them within the mass analyzer using various methods such as CID and ETD. The limitations of bottom-up proteomics can be overcome through whole protein analysis. Using this method, information regarding proteins can be identified, such as degradation products, sequence variants, isoforms, and, most commonly, posttranslational modifications. Posttranslational modifications are analyzed based on characteristic additional masses to unmodified amino acid residues. This method is also amenable to low-mass protein detection, in which enzyme digests may not result in sufficient peptide fragments for analysis.

A significant part of proteomics research is dedicated to biomarker discovery. Initial characterization studies identify thousands of potential protein candidates that are narrowed down with increased sample tests (Drabovich et al., 2015; Rifai et al., 2006). Bottom-up proteomics is used for both untargeted and targeted analysis. There are three phases to the biomarker pathway: discovery, verification, and validation, as discussed in Chapter 76. In the discovery phase, untargeted analysis is used to identify any significant differences between patients with differing disease states. Samples are depleted for all known, insignificant proteins and digested into peptide fragments. Labelling of each fragment and combining the samples allows for a relative quantitative comparison between samples. LC-MS/MS using a high-resolution mass spectrometer provides high-quality mass spectra, in which data analysis

and statistical tests are performed. Potential biomarker candidates that correlate with the labelled disease states are highlighted and identified for the next stage. Verification uses a targeted proteomic methodology, in which initial sample preparations are focused on extracting these biomarker candidates. In many cases, immunoenrichment is used owing to its specificity toward these biomarkers, including methods such as stable isotope standards and capture by antipeptide antibodies (SISCAPA) (Anderson et al., 2004) Afterwards, absolute quantitation is done with the addition of ISs and further statistical analysis to eliminate nonsignificant candidates. The final step is validation, which utilizes a high-throughput methodology—commonly, immunoassays—for large-scale cohort studies and to quantify the efficacy of the biomarker candidates.

METABOLOMICS

Metabolomics, in comparison with proteomics, is even more encompassing and expansive. Biological pathways—such as epigenetic mechanism, pluripotency, bloodstream transport, and cellular responses—all rely on metabolites in some form. To understand and clarify the human biome and its extensive pathways, metabolomics seeks to find differences within biological samples (Fernie et al., 2004). This can be from disease-related disruptions in the biological pathways, validation of potential biomarkers, excluding proteins, or even drug disruptions at the cellular levels. In many cases, this includes an extensive and expansive list of small molecules under 1 kDa in size. This encompasses molecules such as amino acids, nucleotides, antioxidants, and vitamins. Major metabolomic pathways, such as fatty acid synthesis and the glyoxylate cycle, are largely interconnected, resulting in elevated or diminished levels of specific fatty acids, lipids, carbohydrates, and organic acids. Tracking and identifying these metabolites is an arduous task and requires an extensive library for global profiling. Several applications for mass spectrometry–based metabolomics is metabolic fingerprinting and metabolic profiling (Griffin and Shockcor, 2004). These differ in fundamental purpose—fingerprinting focuses on analyzing all analytes within a sample at a specified disease state. No prior knowledge is needed and, in most cases, multivariate statistical analysis is needed to elucidate less obvious trends and outliers as well as to gauge data quality. Afterwards, connections to expansive metabolite databases are needed for identification. Metabolic profiling identifies a significant subset of metabolites that can differentiate disease states. This more targeted analytic method relies heavily on the specificity of MS to isolate and analyze metabolites. Standards are obtained and analyzed through tandem MS for confirmation of actual identity. This helps validate any statistically significant molecules emerging from untargeted analytic methods and provides more specific information regarding their identity.

BIOMOLECULE DATABASE BUILDING

A key area emerging from high-resolution mass spectrometry is the development of biomolecule databases. Due to extensive clinical samples being run and monitoring of hundreds of biomolecules, it is a physically enormous task to identify and validate each statistically significant peak. Unknown compounds with biological significance can remain unknown. With the increasing development of machine learning and deep learning, use of in silico prediction tools have become critical for metabolite identification. Fragment predictions are highly useful in targeted metabolomics, which can supplant standard analysis for compound identification. Other in silico prediction tools can automate identification and peak recognition with improved analytic comparison versus by hand. Metabolite databases such as METLIN, HHMBD, and MassBank compile a wealth of information, such as m/z and retention time. Over 2500 metabolites, 1200 drugs, and 3500 food components found within the human biome have been catalogued and reported in the literature. Current workflows are highly dependent on accurate mass-to-charge ratios and tandem MS for proper identification and subsequent validation. Other resources, such as MetaboAnalyst, have provided a comprehensive platform for metabolomic data. Statistical analyses and computer-generated metabolic pathway analysis using these resources greatly increase the throughput of identifying patterns and elucidation of biological mechanisms.

CHALLENGES IN IMPLEMENTING MASS SPECTROMETRY INTO CLINICAL LABORATORIES

Mass spectrometry faces its own set of challenges that need to be considered when being implemented into a clinical setting. Even being the gold standard for analytic techniques, with unparalleled specificity and sensitivity, mass spectrometry faces significant laboratory-to-laboratory variability. This highlights several critical issues that need to be addressed for mass spectrometry to be further established in the clinical lab (Clarke, 2017; Clarke et al., 2013).

Standardization of operations is key to minimize the variability that exists through mass spectrometry–based methods. In the current landscape, many general clinical labs utilize their own proprietary laboratory-developed tests. This is common practice owing to the wide range of commercial mass spectrometers available, all with differing sensitivities and capabilities. Performance elements—such as accuracy, precision, analytic sensitivity, specificity, and reportable ranges—are key in validating and characterizing lab-specific methods. However, mass spectrometers vary widely in parameters and variables that affect assay performance. Current assay guidelines have been established by the U.S. Food and Drug Administration (FDA) and the Clinical Laboratory Improvement Amendments (CLIA) to guide assays for toxicology, biochemical genetics, steroid analysis, and many others (Lynch, 2016). This includes several FDA-cleared, MS-based assays for immunosuppressant monitoring and newborn screening. However, mass spectrometry has a much wider reach beyond these applications, most notably excluding imaging mass spectrometry and omics research. Currently, there have been little to no applications of mass spectrometry for protein and peptide measurement, largely owing to the wide variability in operations (Lathrop et al., 2016). Numerous workflows, starting from chromatographic separation to mass analysis, have been reported but lack a unifying effort for large-scale studies using one standard method. This has largely been reflected in low numbers of validated MS proteomic methods and related device performances.

Another key challenge is standardizing diagnostic values correlated to disease detection. As mentioned earlier, mass spectrometry has been widely used for chemical profiling, imaging, and quantitation. However, numerous applications have outlined the potential or established proof-of-concept studies. This is especially apparent in chemical profiling of omics research and MS imaging. Statistical differences between healthy and normal samples have been widely observed, but these standards have not been established based on these observed differences. Although several studies have been done to validate potential biomarkers discovered by MS-based methods, many of these studies are unable to maintain the same pace as the development of new MS technologies. This issue is further compounded with variability introduced in the first challenge, in which numerous commercial mass spectrometers and potential workflows are available. Quantitative efforts in tandem with extensive long-term evaluation of a standardized method through cohort studies will greatly further the extensive use of mass spectrometry in clinical environments.

The last challenge is the relatively low sample throughput of current clinical mass spectrometry. Current methods require a skilled workforce with a considerable amount of experience and training to develop and subsequently validate these laboratory-developed tests. Many of these steps require sample preparation procedures, chromatographic separation, data analysis, and safety guidelines to ensure proper data distribution and transport. Thus, a limited number of samples can be analyzed during a workday, which hinders effective treatment response to those in urgent need. Automation should play a large role in increasing the throughput of mass spectrometric analysis but will still be limited owing to collection and transportation times to maximize efficiency rather than speed. The next section addresses this challenge and is highly significant to the future of mass spectrometry. Many of these methodologies are relatively novel up-and-coming methods that provide end users with instant diagnostic results by translating mass spectrometry into a point-of-care environment.

AMBIENT MASS SPECTROMETRY

Current clinical mass spectrometry is still heavily reliant on instruments in reference laboratories to run low-volume patient samples or research for method development. With the advancements in the early 2000s, mass spectrometry instrumentation took an immense leap, introducing technologies such as the orbitrap (see earlier discussion) and significantly improving existing analyzers. The combination of liquid chromatography with mass spectrometry widened the application of mass spectrometry to almost all possible analytes, while MALDI-MS brought about bacterial, fungal, and tissue diagnostics of bacteria with imaging capabilities. In addition, a new class of mass spectrometry, ambient mass spectrometry, seeks to move it to solely clinical laboratories or, further downstream, at the point of care.

Unlike conventional clinical mass spectrometry, the main goal of ambient mass spectrometry is to bring it to the point of care. To do so, there are several

obstacles that must be overcome to translate MS systems. One such obstacle is the reliance on chromatography for sample preparation and separation. Although chromatography provides excellent separation and remains the gold standard for some biomedical applications, it requires extensive sample preparation, purification, and long-time separations, which largely delay the overall clinical testing and make it difficult to realize high-throughput analysis. Based on direct sampling ionization methods and cartridge technologies, ambient mass spectrometry has achieved several significant advancements for its eventual translation to the clinical analysis, such as fast analysis of therapeutic drugs and biomarkers, MS imaging and in vivo chemical profiling.

DIRECT SAMPLING IONIZATION

Direct sampling ionization has closely followed the development of commercial clinical MS systems, developing applications for quantitative and profiling analysis. These methods, also termed *ambient ionization*, are an emerging class of ion sources that combine separative methods with ionization to reduce the pretreatment requirement of biological sample analysis. Samples can be directly injected into the mass spectrometer without chromatographic separation, which is typically labor-intensive and time-consuming. At the point of care, quantitative analysis plays a highly impactful role for clinical diagnostics. In most cases, species of interest are known and require quantitative knowledge for disease diagnostics and routine screening. As mentioned in the previous section, consistent incorporation of IS will greatly improve stability and reproducibility needed for quantitation. In order to assess the quantitative power of direct sampling ionization methods, several bioanalytic method validation criteria are used: lower limit of quantitation (LOQ), relative standard deviation (RSD), and matrix-matched calibration curve linearity (r-squared value). Selectivity, stability, and reproducibility are other indicators used to validate bioanalytic methods (Pu et al., 2019b). For qualitative applications, analyte ratios based on relative signal intensity with appropriate statistical tests are satisfactory for point-of-care clinical analysis. Within the last decade, numerous direct sampling methods have been presented. Several major direct sampling methods are highlighted in this section: paper spray ionization (PSI), desorption electrospray ionization (DESI), and other emerging noteworthy techniques.

Paper Spray Ionization

This technique is illustrated in Figure 5.5A. It was first introduced in 2010; various types of derivatives have been reported since. PSI is an extremely simplistic and robust method for directly analyzing biofluid samples, such as blood. Typically, chromatography paper is used as the substrate. The paper is cut into an isosceles triangle to form a relatively sharp tip, and a drop of blood (≈0.4 μL) is placed in the center. The substrate provides an extensive fiber network in which salts, cell debris, and other macromolecules within the sample matrix can be captured and bound. After letting the blood spot dry for several minutes, a small amount of solvent (5–30 μL), typically, a methanol and water solution, is applied to the dried sample spot. Subsequently, analytes are eluted into the solvent. Around 3 kV is applied to the wetted paper to form an electrospray at the tip of the paper that generates ions analyzed by mass spectrometry. PSI can also be applied to solid samples, such as powdered drugs and tissues (Wang et al., 2011).

However, PSI's simplicity in analysis has resulted in calls for mandatory improvements in reproducibility and minimization of background noise from its nonselective extraction. Advancements such as standardized incorporation of IS have greatly improved reproducibility. Several methods have been presented, such as spiking the sample or even preprinting the IS into the substrate. Taking advantage of the fibrous network in paper, certain compounds can be preloaded and eluted during the presence of a solvent. Several studies have reported a marked increase in reproducibility in similar methods (RSDs of <8%) for therapeutic drug analysis (Liu et al., 2013). Tandem MS analysis is also typically used to overcome the diminished sensitivity from background noise. Relying on the resolving power of the mass analyzer, PSI has reported numerous quantitative applications such as drugs of abuse and therapeutic drug analysis (Table 5.1).

PSI for drugs of abuse analysis promotes a simple and versatile applicability needed for in-field analysis. Numerous studies have been published on various drugs of abuse—such as cocaine, heroin, and methamphetamine—using PSI and dried blood spots. ISs are premixed into samples and analyzed across wide linear dynamics ranges with LOQ under screening cut-off levels. Other studies have developed preliminary methods to quantify multiple drugs simultaneously using PSI, mimicking conventional clinical diagnostic methods. Other sample types and forms can be analyzed by PSI, limited only by imagination. One study analyzed fingerprints for drug residue collected on prepared IS-spiked paper. After analyzing 239 fingerprint samples from habitual drug users and control groups, PSI-MS identified a 99% true-positive rate and a 2.5% false-positive rate for the detection of cocaine (Costa et al., 2017).

Similarly, PSI for therapeutic drug analysis in blood has been extensively analyzed, including anticancer drugs and immunosuppressants. Comprehensive characterization of imatinib, an anticancer drug, resulted in linear

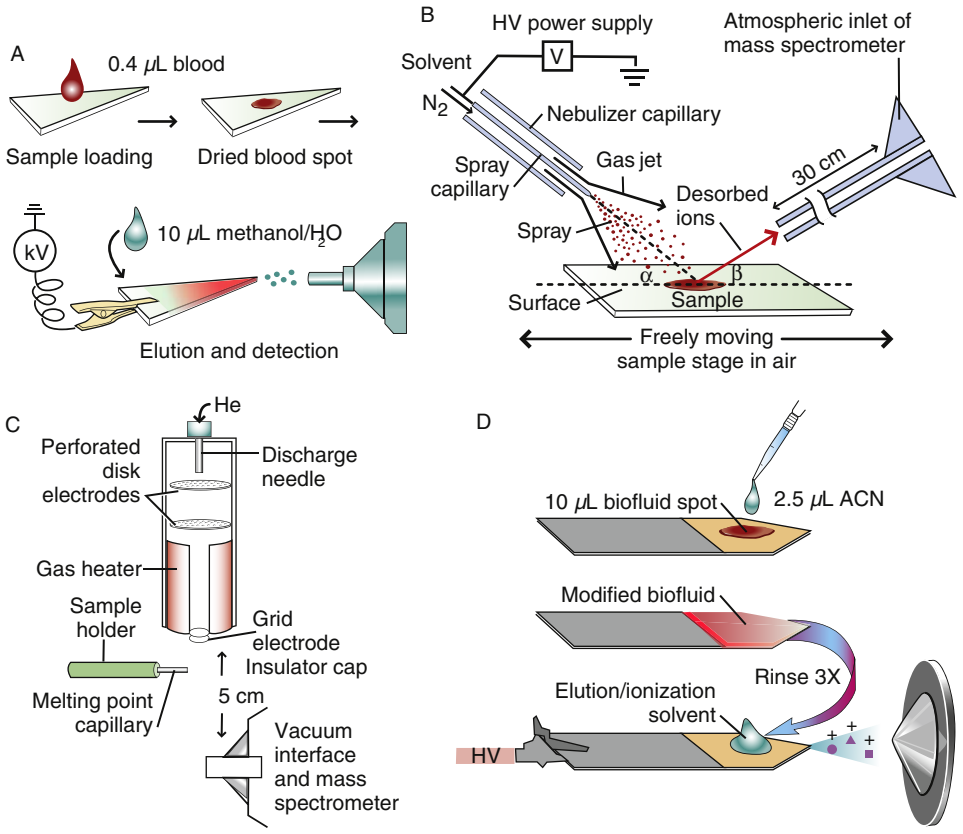

Figures 5.5 Major direct sampling methods for clinical use. **A,** Paper spray ionization (PSI). **B,** Desorption electrospray ionization (DESI). **C,** Direct analysis in real time (DART). **D,** Coated blade spray. See text for explanation of each method. ACN, acetonitrile; HV, high voltage.

dynamic ranges from 62.5 ppb (ng/mL) to 4 ppm (μg/mL) (Wang et al., 2010). Other drugs, such as sitamaquine and amitriptyline, were observed to have limits of quantitation lower than 10 ppb (ng/mL) (Manicke et al., 2011). Calibration and standards and quality control samples were developed to further characterize reproducibility of each method. With the IS loaded onto the substrate, RSD increased to 10%, with an imprecision of 22%. ISs spiked into wet patient samples showed RSD of less than 5% and imprecision of 2% across all samples. All analyzed samples identified linear dynamic ranges encompassing therapeutic ranges, displaying satisfactory sensitivity and rapid analytic times to attain on-demand pharmacokinetic curves.

Furthering the applicability of PSI, clinical validation by real clinical samples has begun to be explored. An automated PSI source and cartridge was developed by Purdue University and commercialized by Prosolia for therapeutic drug monitoring use. Tacrolimus, an immunosuppressant drug that has high clinical value, was evaluated by cross-validating a PSI method with FDA-approved immunoassays and LC-MS/MS methods. PSI showed a significant correlation and adequate capabilities (Shi et al., 2015). Further simultaneous evaluation of commonly paired immunosuppressants, sirolimus and cyclosporine, was completed to establish PSI as a novel and simple direct sampling method for therapeutic drug monitoring of immunosuppressants.

Multiple derivates of PSI have been reported to improve the sensitivity, separative capabilities and ionization efficiencies. Coating materials such as graphene, zirconia, and metal-organic frameworks onto the paper substrate have reported significant improvements to these figures of merit. The use of silica as a coating reported increases in LOQ of up to 50-fold for lidocaine, citalopram, verapamil, and sunitinib compared with traditional chromatography paper (Zhang et al., 2012). Coatings such as silane-treated hydrophobic paper enable a highly selective online extraction to occur on the substrate surface (Damon et al., 2016a). Organic solvents can penetrate the substrate, while aqueous samples remained as a blood spheroid. Interaction between solvent and sample results in an online liquid-liquid extraction without matrix interference. Another type of paper-based modification under investigation is paper-based microfluidics through wax-printing. Formation of microchannels by wax printing provides a more stable electrospray and minimizes solvent evaporation to improve ionization efficiency (Damon et al., 2016b). The development of these smarter yet simplistic devices on paper is slowly transforming traditional paper spray and opening doors for other novel applications of PSI that have not been explored yet.

Desorption Electrospray Ionization

DESI is one of the pioneering ambient mass spectrometry methods that has been applied to various clinical and biomedical applications. The methodology behind DESI is very similar to MALDI but uses a charged solvent stream instead of a laser (Figure 5.5B). The charged droplets are angled toward the sample surface to impact and form charged sample ions that are analyzed by mass spectrometry. MALDI matrices are not needed for this method, which does not require any prior sample preparation. DESI can rapidly analyze dried blood spots. Several therapeutic drugs have been analyzed using DESI and dried blood spots, including aspirin, sitamaquine, and terfenadine, by using verapamil as the IS. The highest LOD observed for all drugs analyzed is 8 ppb (ng/mL) with an LOQ at 10 ppb (ng/mL) (Wiseman et al., 2010). Linear dynamic ranges were generated from 10 ppb (ng/mL) to 10 ppm (μg/mL), with RSDs below 14% in all samples. Other biofluid sample analyses, such as urine, were also performed in tandem with solid-phase microextraction reporting LODs less than 50 ppb

TABLE 5.1

Illicit and Therapeutic Drugs Analyzed by Paper Spray Ionization Mass Spectrometry

Analyte Name	Analyte Use	Molecular Weight (Da)	Reported LOD/LOQ (ppb)
Acetaminophen	Therapeutic	151.16	250
Amitriptyline	Therapeutic	277.41	1
Amphetamine	Abused substance	135.21	1
Atenolol	Therapeutic	266.34	50
Benzethonium	Therapeutic	412.637	0.02
Benzoylecgonine	Metabolite	289.33	1
Buprenorphine	Abused Substance	467.64	1.6
Citalopram	Therapeutic	324.39	0.1
Cocaine	Abused substance	303.12	0.05
Cotinine	Metabolite	176.219	3, 2, 5
Cyclophosphamide	Therapeutic	261	11
Cyclosporine	Therapeutic	1202.63	5
Dextromethorphan	Therapeutic	271.4	0.6
Docetaxel	Therapeutic	807.88	13
Heroin	Abused substance	369.41	125
Hydralazine	Therapeutic	160.176	16
Ibuprofen	Therapeutic	206.28	500
Imatinib	Therapeutic	493.6	9
Lidocaine	Therapeutic	234.34	4
MDMA	Abused Substance	193.24	0.04
Methamphetamine	Abused Substance	149.23	0.3
Morphine	Therapeutic and Abused	285.34	12
Oxycodone	Abused Substance	315.36	16
Paclitaxel	Therapeutic	853.9	12, 15
Pazopanib	Therapeutic	437.52	0.5
Proguanil	Therapeutic	253.73	0.08
Simvastatin	Therapeutic	418.57	50
Sirolimus	Therapeutic	914.19	0.5
Sitamaquine	Therapeutic	343.51	5
Sunitinib	Therapeutic	398.47	0.1
Tacrolimus	Therapeutic	804.01	0.2
Tamoxifen	Therapeutic	371.51	8
Verapamil	Therapeutic	454.6	3, 0.75, 0.1

LOD, Limit of detection; *LOQ,* limit of quantitation; *MDMA,* 3,4-methylenedioxymethamphetamine.
Data from Chiang S, Zhang W, Ouyang Z: Paper spray ionization mass spectrometry: recent advances and clinical applications. *Expert Rev Proteomics* 2018;15:781–789.

(ng/mL). Although the LODs observed for therapeutic drugs are relatively higher than PSI, DESI has a higher throughput by eliminating any need for cutting or punch-out methods in dried blood spot analysis.

DESI provides a great advantage in biomolecule profiling and imaging capabilities under ambient environments. Molecular-specific images can be generated from tissue samples placed on the sample stage and manipulated in the X, Y and Z directions. The highest spatial resolution for clinical applications is 40 μm, with most applications using 200 μm for routine imaging (Kertesz and Van Berkel, 2008). Applications such as rapid, on-site discrimination of healthy and cancerous tissues in surgical suites using DESI were proposed. Several studies on lipid and metabolite profiling by DESI-based mass spectrometry imaging were performed and could discriminate gray matter, white matter, and different tumor tissues in brain tumor tissue samples (Jarmusch et al., 2016). DESI was also used to monitor the oncometabolite 2-hydroxyglutarate, a brain cancer biomarker that identifies a mutation in isocitrate dehydrogenase I and II (Pirro et al., 2017). After normalization of 2-hydroxyglutarate signal intensity to total ion counts, heat maps of 2-hydroxyglutarate concentrations can be overlaid for determination of tumor presence. In another study, DESI profiling of glucose to citrate ion ratios was also used for prostate cancer prediction (Banerjee et al., 2017). Statistical analysis of significant metabolites resulted in a differentiation of healthy and cancerous prostate tissue sections with a nearly 90% accuracy. Tumor margins in brain, kidney, and liver cancers have all been reported to be analyzed through monitoring altered lipid profiles correlated to changes in diseased cellular membranes.

Nano-DESI improves upon DESI by improving spatial resolution capabilities while maintaining ambient ionization conditions. The electrospray used by DESI forms a wide, charged plume that is focused by the nebulizing gas. However, this charged solvent beam cannot be accurately focused, resulting in relatively low resolution. Nano-DESI separates the desorption and ionization steps, forming a liquid droplet between the sample and electrospray capillary (Figure 5.5B). The liquid droplet is subsequently ionized by electrospray, away from the sample and in front of the mass spectrometer inlet. Using this method, tissue imaging at a resolution of 12 μm was achieved (Laskin et al., 2012). Quantitative tissue imaging was also realized by adding the IS into the nano-DESI solvent. Absolute concentrations of nicotine, endogenous phosphatidylcholines, and small-molecule neurotransmitters were quantified and mapped in rat brain tissue sections (Bergman et al., 2016; Lanekoff et al., 2014, 2013). Nano-DESI has also been utilized to profile endogenous molecules in single cells and to perform 3D tissue imaging of lipids and metabolites (Lanekoff et al., 2015). Several diseases, such as papillary renal cell carcinomas in human tissue samples and MYC-induced lymphomas in mice samples, have also been analyzed.

Other Direct Sampling Methods

Several other notable direct sampling methods include direct analysis in real time, coated blade spray, slug-flow microextraction, and laser absorption electrospray ionization. These methods provide unique advantages in specific clinical applications or are precursors to potentially impactful direct sampling methods.

Direct analysis in real time (DART) is illustrated in Figure 5.5C. It uses a more similar ionization method to electron impact as it bombards samples with charged ions. A corona discharge is used to charge incoming gases such as helium or nitrogen and is focused into a sharp ion beam. This beam is then exposed to a sample held on a probe, forming analyte ions to be analyzed by the mass spectrometer. Applications of DART are relatively limited in clinical use and instead mainly are used for food safety, forensics, and explosives. Similar to electron impact, this ionization method generates many ion fragments before mass analysis. As a result, larger biomolecule analysis cannot be done using DART. However, there are a few reports on drugs of abuse and therapeutic drug analysis. Blood samples spiked with therapeutic drugs such as verapamil and loperamide were found to have LODs below 5 ppb (ng/mL) and linear ranges from 0.5 ppb (ng/mL) to 2 ppm (μg/mL) (Zhao et al., 2008). DART was also applied to analyze dried blood spots to quantify endogenous cholesterol in human serum and quantified by spotting IS onto the paper (Hsieh et al., 2017). Sixty-three serum samples from 21 ultramarathon runners at several time points were analyzed and validated by fluorometric-enzymatic assay tests.

Coated blade spray, illustrated in Figure 5.5D, is a notable derivative of PSI (see Figure 5.5A) using a coated stainless steel sheet cut into a small sampling strip with a triangular tip. Various coatings, such as C_{18}-polyacrylonitrile (orange area in Figure 5.5D), are bound to the stainless steel surface to selectively capture analytes in a similar methodology to solid-phase microextraction. A typical procedure for coated blade spray takes around 3 minutes, starting from preconditioning by methanol: water. The coated blade is submerged in sample solution and agitated for approximately 1 minute and quickly rinsed with water. Afterwards, a high voltage is applied (≈3.5 kV) along with 20 μL of solvent for desorption and ionization. The stainless steel substrate eliminates background noise associated with the accidental elution of matrix bound to the porous substrate, while a washing step can remove loosely bound substances to minimize matrix effects. A robotic sampling preparation system was also developed to automate preconditioning, extraction, and washing. Quantitation of various drugs of abuse and therapeutic drugs were performed with limits of quantitation under 10 ppb (ng/mL) (Gómez-Ríos et al., 2018; Tascon et al., 2017). Immunosuppressive drugs were also analyzed in whole blood samples. However, it must be noted that relatively large sample amounts are needed for analysis (>100 μL).

Along the lines of improving the specificity and extraction capabilities of other direct sampling methods, slug-flow microextraction simplifies the liquid-liquid extraction method into a small-volume interaction. Two plugs of blood and solvent, each 5 μL, are placed next to each other within a glass capillary. Back and forth movement of these plugs introduce an internal turbulence that transfers analytes from the sample into the solvent. Due to the constantly refreshed interface between the two plugs, equilibrium is achieved after 5 cycles of slug-flow movement. Quantitative studies investigating methamphetamine and its related IS identified a linear dynamic range from 1 to 100 ppb (ng/mL) with an RSD of 10% in concentrations above 10 ppb (ng/mL) (Deng et al., 2016).

Laser ablation electrospray ionization (LAESI) is a hybrid direct sampling method, combining MALDI with ESI without the use of a matrix. A mid-infrared (mid-IR) laser is used to generate neutral species from the surface of a sample and exposed to charged droplets formed by ESI. Introduced in 2005, LAESI is one of the first laser-based methods to introduce direct sampling profiling and imaging. This method is amenable to water-rich samples, such as biological tissues, due to the strong absorption of mid-IR energy by water molecules. Tissue analysis of small metabolites and lipids in rat brain tissue, along with top-down MSI of intact proteins in mouse lung tissue sections, were performed from a commercial LAESI source (Kiss et al., 2014; Shrestha et al., 2010). LAESI has also been largely applied to imaging of biological tissues and biofilms, monitoring proteins, and lipid distributions. Other applications, such as bacterial identification and single-cell analysis, have been reported.

POINT-OF-CARE MASS SPECTROMETRY DEVICES

To fully appreciate the point-of-care capabilities of direct sampling ionization, device development and validation is critical in ensuring reliability and robustness. The potential and efficacy of direct sampling methods have been well documented; however, there remain variations in experimental results. This was observed in PSI due to the variety of experimental conditions that can affect analysis: substrate type, tip quality, distance to MS inlet, and more. When factoring in human operators and routine sampling in a point-of-care setting, these variations may be more serious. Developing devices that are easy to use, cost-effective, high-throughput, and reliable is vital for the implementation of ambient mass spectrometry to point-of-care testing.

Cartridge Development

Cartridges for mass spectrometry were introduced shortly after the development of paper spray. The simplicity of paper spray held immense potential for the development of a device to automate and increase the throughput for point-of-care analysis. Initial designs of a moving platform holding 14 paper spray tips on a moving stage were developed (Shen et al., 2013). Preliminary disposable PSI cartridges were fabricated using stereolithography to form a holder, lid, and electrode (Yang et al., 2012). These cartridges fit all the needs of transitioning to point-of-care applications by providing users with one-step operation, cheap materials, and prevention of cross-contamination. An automated source, as mentioned in the PSI section earlier, was commercialized by Prosolia and used to characterize the reproducibility and efficacy of PSI for clinical sample analysis. Various other designs have been presented, implementing other functions such as solid-phase extraction. A recently designed top with a solid-phase extraction (SPE) precolumn (which helps separate analytes of interest from contaminating material) enables a fast, selective enriching of target analytes while removing any matrix effects (Zhang and Manicke, 2015). Thus, significant improvement (≈14- to 70-fold) in drug analysis was observed compared with direct PSI. Similarly, antibody columns were attached to paper spray for highly selective extraction and ionization of apolipoprotein, hemoglobin species, and transthyretin mutants in human plasma samples

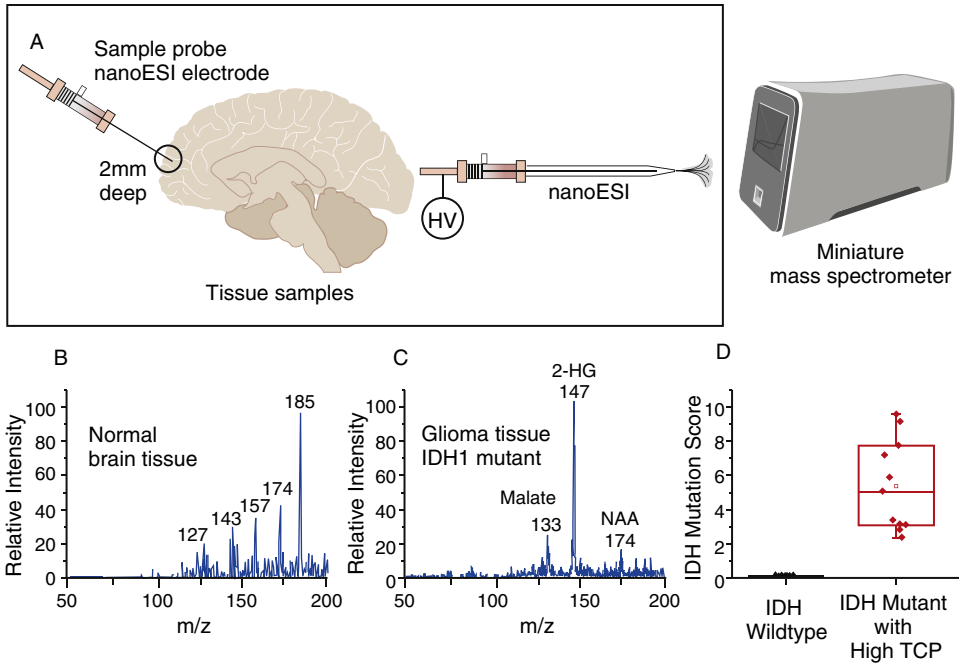

Figures 5.6 Glioma tissue analysis (**A**) by a miniature mass spectrometer. Comparative spectra of healthy (**B**) and glioma (**C**) tissue samples obtained using the miniature mass spectrometer. Statistical analysis of isocitrate dehydrogenase (IDH) mutation score (**D**) between healthy (IDH wildtype) and high-grade glioma tissues (IDH mutant with high tumor cell percentage [TCP]). *ESI,* Electrospray ionization; *HV,* high voltage; *m/z,* mass-to-charge ratio.

(Zhang et al., 2017). A carbon nanotube coated porous polyethylene tip is used to prevent protein-substrate binding and facilitate formation of electrospray. Cartridges with continuous solvent supply features have also been developed, enabling a continuous spray of up to 10 minutes. 3D printing was recently implemented in PSI cartridge designs, implementing sheath gas inlets for improved desolvation or ion optics, such as electrostatic lenses to focus the electrospray (Salentijn et al., 2017, 2014).

In Vivo Clinical Analysis

In vivo devices are mainly focused for surgical suite applications, where samples can be analyzed on demand and guide surgeons during surgery. In a time-sensitive environment such as surgical suites, samples need to be analyzed quickly and accurately, presenting results that can be easily interpreted. A current emerging in vivo device called MasSpec Pen was introduced in 2017 (Zhang et al., 2017). This biocompatible device utilizes a direct sampling method similar to nano-DESI. An automated sampling probe generates a water droplet to contact the tissue for several seconds and transports it to a mass spectrometer for analysis. During the quick liquid-solid interaction, significant biomolecules are eluted into the solvent from the tissue and monitored within the mass spectrometer. From previous ex vivo analysis of tissue samples, statistical analysis is applied to build a prediction model for cancer tissue. Proof-of-concept analysis was done for in vivo cancer diagnostics during surgery on a mouse model, which identified an 87.5% sensitivity and 100% specificity for cancer, and 95.6% accuracy for breast cancer detection. Utilization of machine learning and previously published molecular information were applied to improve the statistical algorithms and published sensitivity, specificity, and accuracies for breast cancer at 96.4%, 96.2%, and 96.3%, respectively. Other cancers have been discriminated using this method, including ovarian cancer, thyroid cancer, and lung cancer. Tumor margins have also been identified in high-grade serous ovarian cancer next to normal ovarian stroma tissue (Sans et al., 2019).

Rapid evaporative ionization mass spectrometry (REIMS), another direct sampling method, has been developed into an in vivo device called the iKnife. As an attachment to current electrosurgical tools, the iKnife transports the aerosol by-product when cutting to a nearby mass spectrometer. As electrosurgical tools cut or coagulate tissue, heat is generated within the tissue and ionizes the tissue contents. The overall device provides tissue analysis in 1.8 seconds after the initial cut. Mass spectra profiles in the phospholipid range (600–850 Da) of ex vivo healthy and cancerous tissues were generated and studied through computational algorithms (i.e., machine learning) for predictive use. The resulting ex vivo prediction model derived from 359 individual specimens (253 normal, 106 tumor) resulted in an overall accuracy of 94.4%, with sensitivity and specificity at 93.4% and 94.9% (Balog et al., 2013). Several statistically significant phospholipid species were reported to be elevated compared with normal tissues. Proof-of-principle intraoperative methods were also performed in six case studies, which reported that the REIMS system provides a significant advantage with little to no disruption to the current oncologic workflow. Other cancers, such as breast and gastrointestinal, have also been differentiated by REIMS (Balog et al., 2015; St John et al., 2017). For example, real-time identification of tumor margins during mastectomies for breast cancer has been achieved. In addition, REIMS has been found to be able to identify normal gastrointestinal tissue, tissue from adenomatous polyps, and tissue from gastrointestinal cancers. In general, these in vivo devices show immense potential for the transition of mass spectrometry into surgical suites pending biocompatibility tests and further clinical evaluation (Schäfer et al., 2009).

Miniature Mass Spectrometry Systems for Clinical Use

Miniature mass spectrometers are also key in translating MS methods for point-of-care applications (Fig. 5.6). Major considerations before introducing commercial mass spectrometers in clinical laboratories prevent the implementation of mass spectrometry at point-of-care settings. In accordance with other criteria set for point-of-care devices, miniature mass spectrometry systems must achieve low power consumption, portability on par with its environment, robust analysis, and adequate analytic performance for its targeted applications. Several trade-offs exist in the miniaturization of mass spectrometry. Flow rates of gas systems, limited pumping speeds, ion trap operating pressure, and power consumption are all variables that need balancing to develop a miniature mass spectrometer. One major obstacle is in the miniaturization of the extensive pumping systems in commercial instruments to maintain the appropriate low-pressure environment for mass analysis. Limited pumping capacities significantly hinder mass analysis by restricting the intake of analytes, affecting instrument sensitivities.

One solution was to introduce a miniature differential pumping system with two chambers in a small form-factor. Using direct sampling ionization sources, ions enter the first chamber maintained at a pressure of 1 to 10 Torr by a diaphragm pump. The second chamber is maintained at 10^{-3} to 10^{-4} Torr, where the ion trap resides along with the detector. Between the two chambers is a 5.0- to 0.3-mm funnel-shaped pinhole where ions can be transferred between chambers (Zhai et al., 2015). Characterization of the miniature mass spectrometer using reserpine, cytochrome C and protein Gly-Pro-Arg-Pro (GPRP) showed that unit resolution could be achieved with scan times under 3000 Da/s. Spectra with mass ranges from 200 to 1000 Da per charge could be obtained. Lowering the AC ejection frequency can increase the mass range to 2500 Da, ideal for larger macromolecules. With the availability of a 1 Torr pressure chamber, several other modifications have been integrated, such as in-vacuum plasma ionization, ion funnels, and laser spray ionization (Zhai et al., 2017, 2016).

Another solution is the introduction of a discontinuous atmospheric pressure interface (DAPI). Instead of a continuously open ion inlet, a pinch value with an electrically conductive membrane is used to close the vacuum system. The inlet opens only briefly during ion introduction. This discontinuous method allows the vacuum chamber to maintain 10^{-5} Torr using small pumps. Furthermore, ion manipulations such as tandem MS and transfers

can be done at optimal pressure in accordance with the generated characteristic pressure curves. A series of these miniature mass spectrometers have been developed at Purdue University, such as the Mini 12, backpack Mini, and the Mini β. The Mini 12 was designed with a smaller rectilinear ion trap, as with previous generations. Characterization of the Mini 12 using clenbuterol, tacrolimus, imatinib, and amitriptyline reported a resolution of 500 using a scan rate of 3000 Da per second (Li et al., 2014). Mass ranges to a maximum of 850 Da were obtained, and tandem MS performed up to MS^5. Several direct sampling methods have been used in tandem with the Mini 12, such as paper spray. Amitriptyline spiked in whole blood using paper spray and the Mini 12 reported LODs of 7.5 ppb (ng/mL). Synthetic cannabinoids in biofluids reported LOQs under 20 ppb (ng/mL) (Ma et al., 2015). Digital microfluidic systems were also performed in conjunction with the Mini 12, where extraction of cocaine from dried urine spots was completed before mass analysis (Kirby et al., 2014). Further exploration for the use of the Mini 12 for pharmacokinetics and therapeutic drug monitoring was performed in conjunction with an automated blood sampler (Pu et al., 2017). Blood samples were automatically drawn from freely moving rats dosed with therapeutic drugs. Slug-flow microextraction direct sampling was used to extract the therapeutic drugs from whole blood and analyzed using the Mini 12. High levels of accuracy and precisions were obtained, along with therapeutic drug monitoring curves that met FDA-recommended criteria. A new model of miniature mass spectrometer has been introduced recently, with dual ion traps to realize the scanning modes only available to triple quadrupoles. Precursor ion scans and multiple reaction monitoring scanning modes were performed using dual linear ion traps. Other applications, such as beam-type CID and improved ion transfer efficiency for MS^n, were also reported, identifying a significant advancement in miniature mass spectrometry systems (Liu et al., 2019). Tissue analysis of glioma samples was also performed using a miniature mass spectrometer, identifying 2-hydroxylglutarate (2-HG) as a main metabolite biomarker (see Figure 5.6). 2-HG accumulation within gliomas stems from a genetic mutation in isocitrate dehydrogenase (IDH) I and II. This has been confirmed through comprehensive metabolomic analysis of glioma samples (Dang et al., 2009). Using extraction nanospray as the direct sampling ionization method, a clinical miniature mass spectrometer determined IDH mutation status by monitoring 2-HG in 44 biopsies from 15 subjects (Pu et al., 2019a).

FUTURE PERSPECTIVES ON CLINICAL MASS SPECTROMETRY

As the field of mass spectrometry matures, it becomes reasonable to imagine the prevalence of mass spectrometric methods in the clinical field. In the last decade or so, there has been a noticeable shift from instrumentation development toward applications in imaging, omics research and point-of-care diagnostics, all of which contribute to advancing health care. Imaging applications in both clinical and reference laboratories provide spatial information of drug or biomolecule distributions in tissues, while omics research continually delves into the human biome to understand biological pathways and discover new biomarkers. Most importantly, ambient MS is beginning to move toward entering point-of-care settings, where techniques such as REIMS and MasSpec Pen are currently being applied for intrasurgical applications. Emerging new miniature mass spectrometers are beginning to undergo commercialization paired with further validation of direct sampling applications for point-of-care diagnostics.

However, a significant limitation to clinical mass spectrometry systems is the lack of standardization, even with commercial instruments in clinical labs. Many current clinical laboratory assays based on LC-MS or GC-MS are developed in-house, called *laboratory-developed tests*. Based on individual needs and priorities, differences in balancing MS assay elements in the interactive triangle of *sensitivity–specificity–throughput* could result in interassay inconsistencies. Regulatory guidelines and bodies such as the Clinical Laboratory Improvement Act and the Food and Drug Administration can help guide and regulate assays to maintain a standard performance level, which helps improve standardization. The importance of standardization and validation is further compounded for the field of ambient MS. Numerous direct sampling methods have been reported, along with their potential for point-of-care testing, but methods that have reported comprehensive validation and comparison to conventional assays are severely lacking. Even within the same direct sampling method, such as paper spray, experimental conditions such as IS addition methodology or biofluid type differ greatly. This confounds the ability to accurately characterize the capabilities of direct sampling methods for implementation. The lack of standardization remains one of the biggest concerns regarding translating ambient MS to the clinical field. Future emphasis on direct sampling implementation rather than innovation would significantly propel ambient MS into a point-of-care environment.

Further improvements that are envisioned for clinical mass spectrometry is its eventual automation and ease of use. Current mass spectrometers enable users to modify numerous parameters to achieve optimal signal-to-noise ratios but, again, are limited in standardization. Training and employing a skilled workforce to continually operate clinical mass spectrometers is unfeasible in a point-of-care environment, whereas automation and/or simplification for use can greatly improve adoption of mass spectrometry. Miniature mass spectrometry systems are expected to improve significantly. Several miniature mass spectrometers have been introduced as capable for targeted quantitative applications, such as therapeutic drug monitoring and drugs of abuse analysis. Development of integrated miniature MS systems for point-of-care quantitative use with even smaller sizes and improved performance can be expected in the future, along with eventual implementation in a point-of-care setting.

SELECTED REFERENCES

Aksenov AA, Da Silva R, Knight R, Lopes NP, Dorrestein PC: Global chemical analysis of biology by mass spectrometry, *Nat Rev Chem* 1:1–20, 2017.
Comprehensive review on utilizing mass spectrometry to investigate the diverse chemistry within biological systems.

Cooks RG, Ouyang Z, Takats Z, Wiseman JM: Ambient mass spectrometry, *Science* 311:1566–1570, 2006.
Review on the innovations in ambient ionization and its implications for clinical analysis and miniature mass spectrometers.

Jannetto PJ, Fitzgerald RL: Effective Use of mass spectrometry in the clinical laboratory, *Clin Chem* 62:92–98, 2016.
Guidelines on the effective implementation and application of mass spectrometry in the clinical laboratory.

Lathrop JT, Jeffery DA, Shea YR, Scholl PF, Chan MM: US Food and Drug Administration Perspectives on clinical mass spectrometry, *Clin Chem* 62:41–47, 2016.
Perspectives from the US-FDA on introducing mass spectrometry into clinical laboratories and its implementation for clinical use in the future.

Pirro V, Alfaro CM, Jarmusch AK, Hattab EM, Cohen-Gadol AA, Cooks RG: Intraoperative assessment of tumor margins during glioma resection by desorption electrospray ionization-mass spectrometry, *Proc Natl Acad Sci U S A* 114:6700–6705, 2017.
Clinical application of ambient mass spectrometry for assessing glioma tumor margins during surgery by providing on-demand molecular measurements.

Snyder DT, Pulliam CJ, Ouyang Z, Cooks RG: Miniature and Fieldable mass spectrometers: Recent Advances, *Anal Chem* 88:2–29, 2016.
Review on the current state of miniature mass spectrometry systems and future directions.

Access the complete reference list online at Elsevier eBooks for Practicing Clinicians.

REFERENCES

Anderson NL, Anderson NG, Haines LR, et al.: *Mass spectrometric quantitation of peptides and proteins using stable isotope standards and capture by Anti-peptide antibodies*, SIS-CAPA), 2004, https://doi.org/10.1021/PR034086H.

Aebersold R, Mann M: Mass spectrometry-based proteomics, *Nature* 422:198–207, 2003, https://doi.org/10.1038/nature01511.

Angelo M, Bendall SC, Finck R, Hale MB, Hitzman C, Borowsky AD, et al.: Multiplexed ion beam imaging of human breast tumors, *Nat Med* 20:436–442, 2014, https://doi.org/10.1038/nm.3488.

Balog J, Kumar S, Alexander J, Golf O, Huang J, Wiggins T, et al.: In vivo endoscopic tissue identification by rapid evaporative ionization mass spectrometry (REIMS), *Angew Chemie Int Ed* 54:11059–11062, 2015, https://doi.org/10.1002/anie.201502770.

Balog J, Sasi-Szabó L, Kinross J, Lewis MR, Muirhead LJ, Veselkov K, et al.: Intraoperative tissue identification using rapid evaporative ionization mass spectrometry, *Sci Transl Med* 5:194ra93, 2013, https://doi.org/10.1126/scitranslmed.3005623.

Banerjee S, Zare RN, Tibshirani RJ, Kunder CA, Nolley R, Fan R, et al.: Diagnosis of prostate cancer by desorption electrospray ionization mass spectrometric imaging of small metabolites and lipids, *Proc Natl Acad Sci U S A* 114, 2017https://doi.org/10.1073/pnas.1700677114. 3334–9.

Bergman H-M, Lundin E, Andersson M, Lanekoff I: Quantitative mass spectrometry imaging of small-molecule neurotransmitters in rat brain tissue sections using nanospray desorption electrospray ionization, *Analyst* 141:3686–3695, 2016, https://doi.org/10.1039/C5AN02620B.

Chiang S, Zhang W, Ouyang Z: Paper spray ionization mass spectrometry: recent advances and clinical applications, *Expert Rev Proteomics* 15, 2018, https://doi.org/10.1080/14789450.2018.1525295. 781–9.

Christians U, Jacobsen W, Serkova N, Benet LZ, Vidal C, Sewing K-F, et al.: Automated, fast and sensitive quantification of drugs in blood by liquid chromatography–mass spectrometry with on-line extraction: immunosuppressants, *J Chromatogr B Biomed Sci Appl* 748:41–53, 2000, https://doi.org/10.1016/S0378-4347(00)00380-7.

Clarke W: Mass spectrometry in the clinical laboratory: determining the need and avoiding pitfalls, *Mass Spectrom Clin Lab*1–15, 2017, https://doi.org/10.1016/B978-0-12-800871-3.00001-8.

Clarke W, Rhea JM, Molinaro R: Challenges in implementing clinical liquid chromatography-tandem mass spectrometry methods - Seeing the light at the end of the tunnel, *J Mass Spectrom* 48:755–767, 2013, https://doi.org/10.1002/jms.3214.

Costa C, Webb R, Palitsin V, Ismail M, De Puit M, Atkinson S, et al.: Rapid, secure drug testing using fingerprint development and paper spray mass spectrometry, *Clin Chem* 63:1745–1752, 2017, https://doi.org/10.1373/clinchem.2017.275578.

Damon DE, Davis KM, Moreira CR, Capone P, Cruttenden R, Badu-Tawiah AK: Direct biofluid analysis using hydrophobic paper spray mass spectrometry, *Anal Chem* 88, 2016a, https://doi.org/10.1021/acs.analchem.5b04278. 1878–84.

Damon DE, Maher YS, Yin M, Jjunju FPM, Young IS, Taylor S, et al.: 2D wax-printed paper substrates with extended solvent supply capabilities allow enhanced ion signal in paper spray ionization, *Analyst* 141:3866–3873, 2016b, https://doi.org/10.1039/C6AN00168H.

Dang L, White DW, Gross S, Bennett BD, Bittinger MA, Driggers EM, et al.: Cancer-associated IDH1 mutations produce 2-hydroxyglutarate, *Nature* 462:739–744, 2009, https://doi.org/10.1038/nature08617.

Deng C, Deng Y, Wang B, Yang X: Gas chromatography–mass spectrometry method for determination of phenylalanine and tyrosine in neonatal blood spots, *J Chromatogr B* 780:407–413, 2002, https://doi.org/10.1016/S1570-0232(02)00632-3.

Deng J, Wang W, Yang Y, Wang X, Chen B, Yao Z-P, et al.: Slug-flow microextraction coupled with paper spray mass spectrometry for rapid analysis of complex samples, *Anal Chim Acta* 940, 2016, https://doi.org/10.1016/j.aca.2016.08.037. 143–9.

Domon B, Aebersold R: Mass spectrometry and protein analysis, *Science* 312:212–217, 2006, https://doi.org/10.1126/science.1124619.

Drabovich AP, Martínez-Morillo E, Diamandis EP: Toward an integrated pipeline for protein biomarker development, *Biochim Biophys Acta - Proteins Proteomics* 1854:677–686, 2015, https://doi.org/10.1016/j.bbapap.2014.09.006.

Dueñas ME, Essner JJ, Lee YJ: 3d MALDI mass spectrometry imaging of a single cell: spatial mapping of lipids in the embryonic development of zebrafish, *Sci Rep* 7:14946, 2017, https://doi.org/10.1038/s41598-017-14949-x.

Ellis SR, Paine MRL, Eijkel GB, Pauling JK, Husen P, Jervelund MW, et al.: Automated, parallel mass spectrometry imaging and structural identification of lipids, *Nat Methods* 15, 2018, https://doi.org/10.1038/s41592-018-0010-6. 515–8.

Fernie AR, Trethewey RN, Krotzky AJ, Willmitzer L: Metabolite profiling: from diagnostics to systems biology, *Nat Rev Mol Cell Biol* 5, 2004, https://doi.org/10.1038/nrm1451. 763–9.

Freiwald A, Sauer S: Phylogenetic classification and identification of bacteria by mass spectrometry, *Nat Protoc* 4:732–742, 2009, https://doi.org/10.1038/nprot.2009.37.

Giordano S, Morosi L, Veglianese P, Licandro SA, Frapolli R, Zucchetti M, et al.: 3d mass spectrometry imaging reveals a very heterogeneous drug distribution in tumors, *Sci Rep* 6:37027, 2016, https://doi.org/10.1038/srep37027.

Gómez-Ríos GA, Tascon M, Reyes-Garcés N, Boyacı E, Poole JJ, Pawliszyn J: Rapid determination of immunosuppressive drug concentrations in whole blood by coated blade spray-tandem mass spectrometry (CBS-MS/MS), *Anal Chim Acta* 999:69–75, 2018, https://doi.org/10.1016/J.ACA.2017.10.016.

Grebe SK, Singh RJ: LC-MS/MS in the clinical laboratory - where to from here? *Clin Biochem Rev* 32(5–31), 2011.

Griffin JL, Shockcor JP: Metabolic profiles of cancer cells, *Nat Rev Cancer* 4:551–561, 2004, https://doi.org/10.1038/nrc1390.

Hsieh H-Y, Li L-H, Hsu R-Y, Kao W-F, Huang Y-C, Hsu C-C: Quantification of endogenous cholesterol in human serum on paper using direct analysis in real time mass spectrometry, *Anal Chem* 89, 2017, https://doi.org/10.1021/acs.analchem.7b00943. 6146–52.

Jannetto PJ, Fitzgerald RL: Effective use of mass spectrometry in the clinical laboratory, *Clin Chem* 62, 2016, https://doi.org/10.1373/clinchem.2015.248146. 92–8.

Jarmusch AK, Pirro V, Baird Z, Hattab EM, Cohen-Gadol AA, Cooks RG: Lipid and metabolite profiles of human brain tumors by desorption electrospray ionization-MS, *Proc Natl Acad Sci U S A* 113, 2016, https://doi.org/10.1073/pnas.1523306113. 1486–91.

Kertesz V, Van Berkel GJ: Improved desorption electrospray ionization mass spectrometry performance using edge sampling and a rotational sample stage, *Rapid Commun Mass Spectrom* 22, 2008, https://doi.org/10.1002/rcm.3812. 3846–50.

Kirby AE, Lafrenière NM, Seale B, Hendricks PI, Cooks RG, Wheeler AR: Analysis on the go: quantitation of drugs of abuse in dried urine with Digital microfluidics and miniature mass spectrometry, *Anal Chem* 86, 2014, https://doi.org/10.1021/ac5012969. 6121–9.

Kiss A, Smith DF, Reschke BR, Powell MJ, Heeren RMA: Top-down mass spectrometry imaging of intact proteins by laser ablation ESI FT-ICR MS, *Proteomics* 14:1283–1289, 2014, https://doi.org/10.1002/pmic.201300306.

Kompauer M, Heiles S, Spengler B: Atmospheric pressure MALDI mass spectrometry imaging of tissues and cells at 1.4-μm lateral resolution, *Nat Methods* 14, 2017, https://doi.org/10.1038/nmeth.4071. 90–6.

Lanekoff I, Burnum-Johnson K, Thomas M, Cha J, Dey SK, Yang P, et al.: Three-dimensional imaging of lipids and metabolites in tissues by nanospray desorption electrospray ionization mass spectrometry, *Anal Bioanal Chem* 407, 2015, https://doi.org/10.1007/s00216-014-8174-0. 2063–71.

Lanekoff I, Thomas M, Carson JP, Smith JN, Timchalk C, Laskin J: Imaging nicotine in rat brain tissue by Use of nanospray desorption electrospray ionization mass spectrometry, *Anal Chem* 85, 2013, https://doi.org/10.1021/ac302308p. 882–9.

Lanekoff I, Thomas M, Laskin J: Shotgun Approach for quantitative imaging of phospholipids using nanospray desorption electrospray ionization mass spectrometry, *Anal Chem* 86, 2014, https://doi.org/10.1021/ac403931r. 1872–80.

Laskin J, Heath BS, Roach PJ, Cazares L, Semmes OJ: Tissue imaging using nanospray desorption electrospray ionization mass spectrometry, *Anal Chem* 84, 2012, https://doi.org/10.1021/ac2021322. 141–8.

Lathrop JT, Jeffery DA, Shea YR, Scholl PF, Chan MM: US Food and Drug Administration Perspectives on clinical mass spectrometry, *Clin Chem* 62, 2016, https://doi.org/10.1373/clinchem.2015.244731. 41–7.

Li L, Chen T-C, Ren Y, Hendricks PI, Cooks RG, Ouyang Z: Mini 12, miniature mass spectrometer for clinical and other applications—introduction and characterization, *Anal Chem* 86, 2014, https://doi.org/10.1021/ac403766c. 2909–16.

Liu J, Cooks RG, Ouyang Z: Enabling quantitative analysis in ambient ionization mass spectrometry: internal standard coated capillary samplers, *Anal Chem* 85, 2013, https://doi.org/10.1021/ac401056q. 5632–6.

Liu X, Ide JL, Norton I, Marchionni MA, Ebling MC, Wang LY, et al.: Molecular imaging of drug transit through the blood-brain barrier with MALDI mass spectrometry imaging, *Sci Rep* 3:2859, 2013, https://doi.org/10.1038/srep02859.

Liu X, Wang X, Bu J, Zhou X, Ouyang Z: Tandem analysis by a dual-trap miniature mass spectrometer, *Anal Chem* 91, 2019, https://doi.org/10.1021/acs.analchem.8b03958. 1391–8.

Lynch KL: Clsi C62-A: a new standard for clinical mass spectrometry, *Clin Chem* 62, 2016, https://doi.org/10.1373/CLINCHEM.2015.238626. 24–9.

Ma Q, Bai H, Li W, Wang C, Cooks RG, Ouyang Z: Rapid analysis of synthetic cannabinoids using a miniature mass spectrometer with ambient ionization capability, *Talanta* 142, 2015, https://doi.org/10.1016/j.talanta.2015.04.044. 190–6.

Manicke NE, Abu-Rabie P, Spooner N, Ouyang Z, Cooks RG: Quantitative analysis of therapeutic drugs in dried blood spot samples by paper spray mass spectrometry: an avenue to therapeutic drug monitoring, *J Am Soc Mass Spectrom* 22, 2011, https://doi.org/10.1007/s13361-011-0177-x. 1501–7.

Mann M, Kelleher NL: Precision proteomics: the case for high resolution and high mass accuracy, *Proc Natl Acad Sci U S A* 105, 2008, https://doi.org/10.1073/pnas.0800788105. 18132–8.

Pirro V, Alfaro CM, Jarmusch AK, Hattab EM, Cohen-Gadol AA, Cooks RG: Intraoperative assessment of tumor margins during glioma resection by desorption electrospray ionization-mass spectrometry, *Proc Natl Acad Sci U S A* 114, 2017, https://doi.org/10.1073/pnas.1706459114. 6700–5.

Pu F, Alfaro CM, Pirro V, Xie Z, Ouyang Z, Cooks RG: Rapid determination of isocitrate dehydrogenase mutation status of human gliomas by extraction nanoelectrospray using a miniature mass spectrometer, *Anal Bioanal Chem* 411, 2019a, https://doi.org/10.1007/s00216-019-01632-5. 1503–8.

Pu F, Chiang S, Zhang W, Ouyang Z: Direct sampling mass spectrometry for clinical analysis, *Analyst* 144:1034–1051, 2019b, https://doi.org/10.1039/C8AN01722K.

Pu F, Zhang W, Bateman KP, Liu Y, Helmy R, Ouyang Z: Using miniature MS system with automatic blood sampler for preclinical pharmacokinetics study, *Bioanalysis* 9:1633–1641, 2017, https://doi.org/10.4155/bio-2017-0160.

Rifai N, Gillette MA, Carr SA: Protein biomarker discovery and validation: the long and uncertain path to clinical utility, *Nat Biotechnol* 24:971–983, 2006, https://doi.org/10.1038/nbt1235.

Salentijn GI, Oleschuk RD, Verpoorte E: 3d-printed paper spray ionization cartridge with integrated desolvation feature and ion optics, *Anal Chem* 89, 2017, https://doi.org/10.1021/acs.analchem.7b02490. 11419–26.

Salentijn GI, Permentier HP, Verpoorte E: 3d-printed paper spray ionization cartridge with fast wetting and continuous solvent supply features, *Anal Chem* 86:11657–11665, 2014, https://doi.org/10.1021/ac502785j.

Sans M, Zhang J, Lin JQ, Feider CL, Giese N, Breen MT, et al.: Performance of the MasSpec pen for rapid diagnosis of ovarian cancer, *Clin Chem* 65:674–683, 2019, https://doi.org/10.1373/clinchem.2018.299289.

Schäfer K-C, Dénes J, Albrecht K, Szaniszló T, Balog J, Skoumal R, et al.: In vivo, in situ tissue analysis using rapid evaporative ionization mass spectrometry, *Angew Chemie Int Ed* 48, 2009, https://doi.org/10.1002/anie.200902546. 8240–2.

Schuerenberg M, Luebbert C, Deininger S-O, Ketterlinus R, Suckau D: MALDI tissue imaging: mass spectrometric localization of biomarkers in tissue slices, *Nat Methods* 4, 2007, https://doi.org/10.1038/nmeth1039. 462–462.

Shen L, Zhang J, Yang Q, Manicke NE, Ouyang Z: High throughput paper spray mass spectrometry analysis, *Clin Chim Acta* 420:28–33, 2013, https://doi.org/10.1016/j.cca.2012.10.025.

Shi R-Z, El Gierari ETM, Manicke NE, Faix JD: Rapid measurement of tacrolimus in whole blood by paper spray-tandem mass spectrometry (PS-MS/MS), *Clin Chim Acta* 441:99–104, 2015, https://doi.org/10.1016/j.cca.2014.12.022.

Shrestha B, Nemes P, Nazarian J, Hathout Y, Hoffman EP, Vertes A: Direct analysis of lipids and small metabolites in mouse brain tissue by AP IR-MALDI and reactive LAESI mass spectrometry, *Analyst* 135:751, 2010, https://doi.org/10.1039/b922854c.

St John ER, Balog J, McKenzie JS, Rossi M, Covington A, Muirhead L, et al.: Rapid evaporative ionisation mass spectrometry of electrosurgical vapours for the identification of breast pathology: towards an intelligent knife for breast cancer surgery, *Breast Cancer Res* 19:59, 2017, https://doi.org/10.1186/s13058-017-0845-2.

Tascon M, Gómez-Ríos GA, Reyes-Garcés N, Poole J, Boyacı E, Pawliszyn J: High-Throughput screening and quantitation of target compounds in biofluids by coated blade spray-mass spectrometry, *Anal Chem* 89, 2017, https://doi.org/10.1021/acs.analchem.7b01877. 8421–8.

Taylor PJ, Cooper DP, Gordon RD, Stowasser M: Measurement of aldosterone in human plasma by semiautomated HPLC-tandem mass spectrometry, *Clin Chem* 55:1155–1162, 2009, https://doi.org/10.1373/clinchem.2008.116004.

Wang H, Liu J, Cooks RG, Ouyang Z: Paper spray for direct analysis of complex mixtures using mass spectrometry, *Angew Chemie* 122:889–892, 2010, https://doi.org/10.1002/ange.200906314.

Wang H, Manicke NE, Yang Q, Zheng L, Shi R, Cooks RG, et al.: Direct analysis of biological tissue by paper spray mass spectrometry, *Anal Chem* 83:1197–1201, 2011, https://doi.org/10.1021/ac103150a.

Wiseman JM, Evans CA, Bowen CL, Kennedy JH: Direct analysis of dried blood spots utilizing desorption electrospray ionization (DESI) mass spectrometry, *Analyst* 135:720, 2010, https://doi.org/10.1039/b922329k.

Yang Q, Wang H, Maas JD, Chappell WJ, Manicke NE, Cooks RG, et al.: Paper spray ionization devices for direct, biomedical analysis using mass spectrometry, *Int J Mass Spectrom* 312, 2012, https://doi.org/10.1016/j.ijms.2011.05.013. 201–7.

Zhai Y, Feng Y, Wei Y, Wang Y, Xu W: Development of a miniature mass spectrometer with continuous atmospheric pressure interface, *Analyst* 140:3406–3414, 2015, https://doi.org/10.1039/C5AN00462D.

Zhai Y, Jiang T, Huang G, Wei Y, Xu W: An aerodynamic assisted miniature mass spectrometer for enhanced volatile sample analysis, *Analyst* 141:5404–5411, 2016, https://doi.org/10.1039/C6AN00956E.

Zhai Y, Zhang X, Xu H, Zheng Y, Yuan T, Xu W: Mini mass spectrometer integrated with a miniature ion funnel, *Anal Chem* 89, 2017, https://doi.org/10.1021/acs.analchem.7b00195. 4177–83.

Zhang C, Glaros T, Manicke NE: Targeted protein detection using an all-in-one mass spectrometry cartridge, *J Am Chem Soc* 139, 2017, https://doi.org/10.1021/jacs.7b05571. 10996–9.

Zhang C, Manicke NE: Development of a paper spray mass spectrometry cartridge with integrated solid phase extraction for bioanalysis, *Anal Chem* 87, 2015https://doi.org/10.1021/acs.analchem.5b00884. 6212–9.

Zhang J, Katta N, Suliburk J, Rector J, Garza KY, Sans M, et al.: Nondestructive tissue analysis for ex vivo and in vivo cancer diagnosis using a handheld mass spectrometry system, *Sci Transl Med* 9, 2017, https://doi.org/10.1126/scitranslmed.aan3968. eaan3968.

Zhang Z, Xu W, Manicke NE, Cooks RG, Ouyang Z: Silica coated paper substrate for paper-spray analysis of therapeutic drugs in dried blood spots, *Anal Chem* 84, 2012, https://doi.org/10.1021/ac202058w. 931–8.

Zhao Y, Lam M, Wu D, Mak R: Quantification of small molecules in plasma with direct analysis in real time tandem mass spectrometry, without sample preparation and liquid chromatographic separation, *Rapid Commun Mass Spectrom* 22, 2008, https://doi.org/10.1002/rcm.3726. 3217–24.

CHAPTER 6

ANALYSIS: CLINICAL LABORATORY AUTOMATION

Robert P. DeCresce, Joseph Holup, Mark S. Lifshitz

EVOLUTION OF AUTOMATION, 74
PREANALYTIC AND POSTANALYTIC AUTOMATION, 75
Automated Delivery, 75
Automated Specimen Processing, 75
Postanalytic Processing, 75
THE AUTOMATED CHEMISTRY ANALYZER: CORE COMPONENTS, 76
Sampling, 76
Reagent Handling, 76
Mixing And Incubation, 76
Detection, 76
Data Processing And Real-Time Monitoring, 76
THE CONTINUUM OF CHEMISTRY AUTOMATION, 77
Workstation, 77
Workcell, 77
Total Laboratory Automation, 77
AUTOMATION IN OTHER SECTIONS OF THE LABORATORY, 77
Hematology, 77
Microbiology, 79
PLANNING FOR LABORATORY AUTOMATION, 79
SELECTED REFERENCES, 80

KEY POINTS

- Laboratory testing has undergone revolutionary changes over the past decade. Typically, all routine chemistry and hematology testing is completely automated.
- Automated solutions are available for preanalytic, analytic, and postanalytic stages of laboratory testing. The degree of automation implemented in a laboratory should match its needs and can vary from a freestanding analyzer to a workcell or totally automated solution.
- Preanalytic automation is heavily dependent on uniquely identifying (often with a bar code) the primary collection container. Analyzers automatically perform many tasks and when integrated with other automated modules can significantly reduce hands-on time, thereby enabling staff to concentrate on exception processing, problem solving, and quality oversight.
- A continuum of automation strategies has been developed to meet scalable needs and to offset staff shortages. Other key benefits are shorter turnaround time, fewer errors, safer staff working environment, and focus on value-based testing.

What is automation? In the context of the clinical laboratory, it can be described as the process by which an instrument automatically performs tasks that would otherwise have to be performed manually by laboratory staff. In recent years, *laboratory automation* has also been used to describe a broader process wherein multiple devices, often linked together, are capable of automating preanalytic, analytic, and postanalytic stages of testing (see Chapter 2). Thus, in addition to performing tests, automation now includes solutions for specimen sorting, processing, transport, sample introduction, and storage. At the core of these configurations is a sophisticated information system that monitors and controls these tasks, optimizes performance, self-monitors analytic performance, and interfaces with the laboratory information system (LIS). This chapter discusses the fundamental concepts of automation as it relates to both of the preceding definitions, with specific emphasis on clinical chemistry.

EVOLUTION OF AUTOMATION

Prior to the introduction of automation in the 1950s, laboratory testing was a completely manual process that required technologists to hand-pipette specimen and reagent into glass test tubes, incubate, read reaction changes in a spectrophotometer, and extrapolate values from a calibration curve that was plotted on paper. These tasks are still performed today—only on automated platforms that eliminate manual intervention, significantly improving the reproducibility, accuracy, flexibility, and turnaround time of testing while lowering costs, eliminating errors, and enhancing patient safety through robust sample identification and test reporting technologies (Battisto, 2004; Shim, et al., 2011).

The first automated analyzers were based on continuous-flow technology (i.e., reagents would continuously flow through the channels); they sequentially analyzed each sample in a single or multiple parallel channel configuration. The same group of tests was performed on each sample irrespective of which tests were ordered; in other words, there was no test selectivity. These devices were followed by variable profile analyzers that could perform a subset of tests from the master profile or suppress those that were not ordered. The one characteristic shared by these analyzers was that their operating cycles were sample-based—that is, they processed a set number of samples per hour irrespective of the number of tests ordered per sample. Another approach to testing was the batch analyzer (e.g., centrifugal analyzer), which could perform a single test on a large number of samples. These devices were "run-based" systems; once the batch testing began, it could not be interrupted to add a new sample. By the early 1980s, the inflexibility of these designs started to be addressed with the introduction of a totally new concept: the random access analyzer.

Unlike its predecessors, the random access analyzer selects sample and reagent randomly without regard to placement on the analyzer. This type of operation implies several unique characteristics that differentiate it from other instruments:

1. It has a single analytic pathway for all testing instead of dedicated channels for each test.
2. Tests are initiated sequentially based on what is ordered—that is, tests are not batched.
3. It has a flexible configuration to process each test's unique parameters (e.g., wavelength, number of readings, reagent additions).
4. It performs tests discretely, each in its own cuvette.
5. Throughput is based on the number of tests run per hour, not the number of samples per hour.

Virtually all of today's automated chemistry systems are based on random access design. This flexible design has allowed many tests that previously were performed on a variety of platforms to be consolidated into one.

Although the random access analyzer was originally introduced for general chemistry and homogeneous immunoassay testing, many of its operating characteristics were adapted in the 1990s to heterogeneous immunoassay testing. These tests typically require more flexible assay parameters, such as variable incubation times, reagent additions and wash steps, and unique detection systems (e.g., luminometer) that require testing to be performed in a specially designed unit. Because of these testing requirements, immunoassay throughput is significantly lower than that of a general chemistry analyzer. Although immunoassay analyzers were originally introduced as standalone units, they are also typically available as an integrated subsystem within a single chemistry/immunoassay platform.

After great strides were made in automating sample analysis, more attention was focused on the preanalytic processes that increasingly accounted for errors and workflow delays. These included sample labeling

BOX 6.1

Factors That Drive Laboratory Automation

Turnaround time (TAT) demands
Specimen integrity issues
Staff shortages
Economic factors
Need to lower maintenance
Need to reduce calibration
Need to reduce downtime
Faster start-up times
24/7 uptime
Throughput
Computer and software technology
Primary tube sampling
Increasing the number of different analytes on one system
Increasing the number of different methods on one system
Reducing laboratory errors
Number of specimens
Types of fluids
Safety
Environmental concerns (i.e., biohazard risks)

(or relabeling with bar codes), loading and unloading centrifuges, manual aliquoting (e.g., splitting samples to be used at several workstations or transferring samples into another container to be sent out for testing or used by in-house instruments), and sorting samples for different workstations. Each step could potentially lead to an error, such as a misidentified sample resulting in an incorrect report. Finally, the uncapping and capping of samples posed biohazard risks due to aerosol exposure and contact with blood and body fluids. In response to these issues, preanalytic automation was introduced in the form of standalone units or preanalytic processing modules integrated into an automated laboratory configuration.

In addition to refining the capabilities of automated analyzers, in the past 10 to 15 years, laboratories have primarily focused on automating the entire testing process from collection to reporting, with a major emphasis on integrating these activities and optimizing preanalytic tasks and sample storage. Total laboratory automation (TLA) is the culmination of this design strategy (Sarkozi et al., 2003), one that uses intralaboratory sample transportation systems such as conveyors or tracks to move samples between analyzers and into and out of processing stations that centrifuge, decap/cap, and store sample containers. TLA is discussed in greater detail later.

As we enter a new era in health care, with enhanced emphasis on value-based management, the diversity of laboratory automation solutions is well positioned to meet the needs of small-, medium-, and high-volume clinical laboratories (Burtis & Bruns, 2014). Some of the factors that will continue to drive automation are presented in Box 6.1.

PREANALYTIC AND POSTANALYTIC AUTOMATION

AUTOMATED DELIVERY

The preanalytic stage focuses on sample collection and processing (see Chapter 3). The first processing step begins with the delivery of samples from the collection location. For decades, specimens drawn within a facility were transported to the laboratory by phlebotomists or other staff. If the specimens were obtained from outside the facility, a courier service was often used. Both of these batch processes were usually based on scheduled pick-ups. One of the earliest automated transport systems to be introduced—and still the most popular one today—is the pneumatic tube (e.g., TransLogic Pneumatic Tube System, Swisslog Healthcare, Denver, CO; Pevco, Baltimore, MD). Typically, these systems rapidly transport 4- or 6-inch-diameter high-impact polycarbonate carriers from one point (or carrier station) in a facility to another. Each station is uniquely identified, and carriers are programmed to travel to a specific station. Thus, the sender can load blood collection tubes into a carrier and program it to go to the laboratory, and blood units from transfusion services or medications from pharmacies can be delivered to patient care units. Pneumatic tube carriers are lined with foam to cushion contents and reduce the potential for breakage. These systems are also designed to prevent hemolysis by avoiding significant elevation of *g* forces during acceleration and deceleration.

Other automated delivery systems have also been developed for use predominantly in the laboratory and, in some instances, outside it.

BOX 6.2

Automation: Preanalytic and Postanalytic Steps

Primary tube identification/labeling (if not done remotely)
Laboratory information system receiving
Sorting (and prioritizing stats)
Centrifuging
Decapping
Secondary tube labeling
Volume checks/clot detection
Aliquoting
Destination sorting into analyzer racks
Recapping
Sample storage and retrieval

Electrical track vehicles can transport a larger number of specimens than pneumatic tubes; they require a station for loading and unloading specimens, which may pose a problem in facilities with limited space. They can also transport ice or refrigerated packs with samples because of their larger carrying capacity. Mobile robots offer another transportation option: They can deliver samples directly to the workstation. These devices either follow a line in the floor or use a more sophisticated, flexible, and expensive guidance system. Mobile robots are batch delivery systems, requiring staff to load and unload samples at each stop. Conveyors or track systems are used in some laboratory facilities, especially if the laboratory receives a very large number of samples. Conveyor or track systems are designed to transport specimens horizontally (i.e., across the floor) and vertically (i.e., to a different floor).

AUTOMATED SPECIMEN PROCESSING

Automated specimen processing minimizes non-value-added steps in the laboratory testing process (e.g., aliquoting, sorting tubes) and improves quality by reducing manual handling errors; it also addresses reproducibility and throughput issues. Automation enhances worker safety: It reduces operator exposure to potentially hazardous biological material and eliminates repetitive stress injuries. Box 6.2 lists common specimen handling steps; some or all of these tasks have been included in front-end automation systems. Standalone units (with or without centrifugation) selectively target a group of preanalytic or postanalytic steps. For example, a unit may include sample sorting, sample uncapping, and aliquoting. After processing, samples are manually transported to a workstation. In contrast to this *targeted automation* approach, these tasks can also be integrated into a larger, fully automated modular design that is connected to an analytic and storage (postanalytic) component and eliminates any handling after initial loading. One example of a standalone automated unit is the Automate 800 (Beckman Coulter Inc., Brea, CA). It can perform sample receipt, sorting, centrifugation, decapping, sample volume detection, and aliquoting functions. In addition, this system stores all analyzed samples and places them in refrigerated storage so that any sample can be easily identified should a sample require further analysis. The fully automated Beckman system—in which all clinical chemistry, immunochemistry, hematology, and coagulation samples are identified, preanalytically processed (including centrifugation where necessary), and sent to the appropriate workstation for analysis and then stored—is on display at the Beckman Vision Center (Jersey City, NJ).

Automated specimen inspection can potentially address two of the most significant preanalytic concerns: identifying sample identification errors and sample integrity issues. Ideally, an automated device could sort a random collection of different-sized containers with different additives and assess each one for proper labeling, adequate volume, and interference from icterus, lipemia, or hemolysis. This recently described invention uses optical character recognition to identify potentially mislabeled samples (Hawker et al., 2014).

POSTANALYTIC PROCESSING

Standalone systems are also available to archive and retrieve bar-coded specimens; samples are scanned and placed in numbered positions in numbered racks. Specimens are retrieved by entering the patient's sample accession number or a medical record number into the archival system's database. The rack number and sample position are displayed for the user. Some systems include a refrigerator for sample storage and automatic disposal of samples at predetermined times. The Cobas p 701 (Roche Diagnostics, Indianapolis, IN) and the Beckman Automate 800 are examples

of postanalytic units that can be used as freestanding devices or can be connected to a preanalytic system. The Cobas p 701 can store up to 27,000 tubes in a walk-in refrigerator; samples are automatically disposed based on user-defined short- and long-term storage time frames.

THE AUTOMATED CHEMISTRY ANALYZER: CORE COMPONENTS

The automated analyzer is central to the operation of the clinical laboratory. Chapter 4 discusses many of the testing principles used by these devices. This section discusses various physical operating characteristics and design features that enable these devices to function in an automated manner (Box 6.3).

BOX 6.3

Automation: Analytic Steps

Sample introduction and transport to cuvette or dilution cup
Addition of reagent
Mixing of sample and reagent
Incubation
Detection
Calculations
Readout and result reporting

SAMPLING

All fully automated general chemistry analyzers are capable of sampling directly from the collection tube. Direct tube sampling along with bar code reading has eliminated the need to transfer samples into another container, reduced errors, and minimized technologist exposure to potentially biohazardous materials. Tubes are typically decapped before sampling; however, cap-piercing technology is available on all high-throughput hematology analyzers.

Automatic sampling may be accomplished in different ways. The peristaltic pump is an example of an older technology that is still used in some instrument designs (e.g., electrolyte measurements). More commonly, positive liquid displacement pipettes are used to transfer sample from cups or tubes to the analytic module. These pipettes dispense sample into the reaction container, or they flush out sample together with diluent. Computer-controlled stepper motors can precisely control the amount of liquid that is aspirated and dispensed. A similar configuration is used for reagent dispensing.

In most analyzers, samples are aspirated and dispensed using a thin, stainless-steel probe. In some analyzers, the probe pierces a rubber stopper; in others, it passes directly into a test tube or a cup. A potential problem is the formation of a sample clot that adheres to the probe. The clot may plug the probe, preventing further use; occupy sample volume, thereby leading to a "short sample" measurement error; or adhere to the sample probe, thereby leading to an instrument malfunction and/or sample probe misalignment. Most sample probe designs can detect clots and reject the sample. Liquid level sensors detect the presence of an inadequate or short sample; they typically travel a specified distance into the sample container to determine whether liquid is present.

Reusable pipette probes are subject to carryover—that is, contamination of one sample by the previous sample. This can create spurious results. Several instrument modifications have been used to reduce carryover. One approach is to aspirate a wash solution between pipetting cycles. Another technique is to back-flush the probe using a wash solution. The wash solution flows through the probe into a waste container in a direction opposite to that of the aspiration. This technique minimizes the risk of pulling a small clot deeper into the system. To completely eliminate carryover, some devices use disposable plastic pipette tips to transfer each sample, although this slightly increases consumable costs.

REAGENT HANDLING

Automated analyzers need to address how reagents are stored, handled, prepared, proportioned, and dispensed. Most laboratories use bulk reagents that are ready to use with little or no preparation. If the reagent is lyophilized, most analyzers will automatically reconstitute the contents with diluent. Some analyzers use unit test reagents (i.e., reagent is present for the performance of a single test). In dry technology, reagents are impregnated on a solid phase strip or slide. Another type of unit test reagent is a container or test tube with premeasured liquid or powdered material to which water, buffer, or sample is added.

Reagents are stored in environmentally controlled compartments, and inventory is monitored in real time. Most of the methods used in the laboratory require only a single reagent, but some require two or more. When a reagent becomes depleted, the computer alerts the operator to replace the empty container with a new one. Onboard reagent storage compartments are refrigerated to maintain reagent stability.

Bar code labels uniquely identify each reagent container so that multiple containers of a high-volume reagent can be loaded and the analyzer will sequentially use the contents of each. The bar code label may contain additional information such as expiration dates, lot numbers, and volume of reagent (or number of tests) in the container. Some analyzers may couple a liquid level sensor onto the reagent probe, which confirms reagent aspiration and also measures remaining test inventory in the container.

For all tests, the bar-coded reagent label stores calibration information, such as concentration, expected detector responses, calibration curve algorithms, and tolerances for acceptability of calibration. This information is often referred to as *master lot* or *master calibration*.

Automated analyzers are categorized as *open* or *closed* reagent systems, a distinction that may influence purchasing decisions. An open reagent system can accommodate reagents from third-party (i.e., non-instrument manufacturer) vendors and allows the operator to modify test parameters to implement these tests. *Open* reagent systems provide users with greater flexibility and adapt easily to new methods and analytes. As a note of caution, many of the instruments do not allow full access to all of the functions and calculations that the manufacturer uses, and third-party methods often cannot be optimized. A *closed* reagent system can use only the instrument manufacturer's reagents and therefore may not offer a new or proprietary test that is available only from an external vendor. Although reagents may cost more in a closed system, reagent handling and identification are usually more tightly integrated with the analyzer operation, thereby leading to hidden benefits. Most laboratories predominantly use reagents from their instrument vendor. Even "closed" systems sometimes have some limited ability to accommodate third-party reagents.

MIXING AND INCUBATION

Many unique approaches are used to mix sample and reagent in automated systems. They include magnetic stirring, rotating paddles, forceful dispensing, the use of ultrasonic energy, and vigorous lateral displacement. Dry slide analyzers, originally developed by Eastman Kodak (Rochester, NY) and now manufactured by Ortho Diagnostics (Raritan, NJ) do not require sample and reagent mixing because samples need only flow through the reagent layers to accomplish this task.

An incubator must provide a constant and accurate temperature for the reaction; this is achieved by using circulating air or water baths or heated metal blocks. Electronic thermocouples and thermistors monitor and maintain required temperatures.

DETECTION

An automated analyzer may typically include several detection systems depending on the test menu offered. For example, general chemistry assays may be measured by absorption or reflectance spectroscopy; electrolytes may be measured by ion-selective electrodes; and some immunoassays may be based on chemiluminescence and thus require a luminometer. These technologies are discussed in Chapters 4 and 28. Most of the chemistry analyzers marketed today incorporate several measuring subsystems. Typically, they are dedicated chemistry, dedicated immunoassay, or chemistry/immunoassay integrated platforms.

DATA PROCESSING AND REAL-TIME MONITORING

The instrument computer controls signal processing, data handling, and process control. Signal processing converts an analog signal from the detector to a digital signal that is usable by all communication devices. Data processing can transform nonlinear input signals into linear calibration plots, thereby enabling nonlinear assays (e.g., those based on reflectance spectrophotometry) to be automated. Within the analyzer, the computer controls electromechanical processes so that they are uniform, repeatable, and in the correct sequence. These operations include activating pipetting devices, moving cuvettes from one point to another, moving sample tubes, and dispensing reagents. User-friendly software can display Levey-Jennings quality control charts and calibration curves, and online

troubleshooting can be accessed along with "how to" videos that help guide users through instrument training and maintenance. Real-time monitoring (using Internet connectivity) has allowed vendors to continuously analyze instrument subsystems and identify components that could potentially fail before they actually do. Based on these data, vendors can schedule service and avoid potential unscheduled downtime during off-hours.

THE CONTINUUM OF CHEMISTRY AUTOMATION

Laboratory vendors offer a variety of automation solutions designed to meet the needs of laboratories of all sizes. Often, these solutions are scalable, allowing the same technology to be used across a network of laboratories, albeit implemented in different configurations. What follows is a brief description of these configurations. Automation is a constantly evolving technology, with new solutions often introduced by vendors. Thus, it is important to review the latest offerings and competitive differences when new automation is considered. Currently, the major vendors in core chemistry and immunodiagnostics are Abbott Diagnostics, Lake Forest, IL; Beckman Coulter Inc., Brea, CA; Ortho Clinical Diagnostics, Raritan, NJ; Roche Diagnostics U.S. Headquarters, Indianapolis, IN; and Siemens Healthcare Diagnostics, Inc., Tarrytown, NY.

WORKSTATION

The most basic unit of automation is the workstation, which is typically an automated clinical analyzer (described earlier). The analyzer may be dedicated to general chemistry testing, immunoassay testing, or a single platform that integrates both technologies. Although samples have to be manually loaded and unloaded, this standalone device automates the entire testing process. The instrument operator usually initiates calibration, quality control, and daily maintenance activities and replenishes reagents. Typically, bar-coded samples and bidirectional LIS interfaces allow analyzers to automatically determine which tests to run on each sample and automatically upload (and autoverify) results. Provided the analyzer can accommodate a sufficient number of samples and reagents, the operator can walk away for a period of time. However, all instrument alerts appear on the local device and need to be reviewed. Another drawback of this approach is that the operator must manually gauge how to load balance the daily routine work and stat requests to achieve optimal throughput and performance across several freestanding workstations.

WORKCELL

To further enhance productivity, vendors have developed integrated groups of analyzers that can function as a single unit and can be monitored by a single technologist. A "virtual" workcell is a cluster of such devices—for example, chemistry analyzers, hematology cell counters, or coagulation instruments—that is not physically connected by a track, but in which the devices are interfaced to one another through common software known as *middleware*. A physical workcell is a similar cluster of devices that is connected by a track and thus has a single sample loading and unloading station. The middleware is a central hub that can consolidate most of the user interaction emanating from all the devices and present it to the technologist on a single display. For example, it can display the status of all the samples processed on each system, the pending list of stat samples, the error messages from different systems, and the samples that require reruns (and that may have to be manually reloaded). It can also autoverify samples that meet the preset criteria. Also, it can load balance by either indicating to the technologist where to load a sample on the virtual workcell or by automatically doing so on the physical one.

TOTAL LABORATORY AUTOMATION

The idea of totally automating a clinical laboratory has its roots in Japan, and the concept was first introduced in the early 1980s. Early designs used one-arm robots, conveyor belts, and modifications to existing chemistry analyzers to perform as many preanalytic and analytic tasks as possible with no human intervention (Olsen, 2012). Each laboratory workstation was coupled to the conveyor belts so that the samples could be moved from one workstation to another. Continued research and modifications to these earlier systems led to the development of commercial TLA systems designed for hospital-based laboratories.

In a TLA design, multiple analyzers are coupled to a specimen management and transportation system; process control software (middleware) coordinates the activities of the various automation modules (Box 6.4) and is interfaced to the LIS. These systems are typically designed for laboratories that process 1000 to 10,000 or more samples per day—for example, a core laboratory within a health system's network of laboratories. TLA can include a wide variety of modules, including analytic units to perform chemistry, hematology, coagulation, and immunochemistry tests, as well as preanalytic/postanalytic units such as centrifuges, specimen sorting modules, specimen decappers and recappers, specimen aliquot modules, and refrigerated storage units (Fig. 6.1).

BOX 6.4

Process Control Software Functions

1. Calculate number of aliquots and volume needed for each workstation
2. Route samples to analyzers in most optimal way
3. Recap sample
4. Autoretrieval of samples for reflex or repeat testing
5. Autoverification of results

TLA benefits include a decrease in labeling and other preanalytic errors, shorter turnaround times, and a reduction in full-time equivalents (FTEs) necessary to process a given test volume—that is, increased productivity. The latter is of special interest given the current shortage of laboratory technologists. Laboratories using a high degree of automation thus have the ability to introduce new assays and/or process additional testing volume without adding staff. Staff savings from automated testing can be reassigned to other areas or projects, such as increasing the frequency of testing for tests currently run on a limited schedule or implementing new tests in-house that were previously sent to a reference laboratory.

The major limitations of TLA include the need for substantial financial investment and increased floor space. Initial investment may reach millions of dollars, and floor space requirements may exceed 4000 square feet. Another factor that requires the attention of planners because of the complex nature of TLA is the need for highly technical personnel to operate and troubleshoot the system. Other challenges to TLA include infrastructure remodeling, personnel team building, and software interfacing. In addition, some systems may not be able to easily interrupt workflow to analyze emergency (stat) samples (Lippi, 2019).

Most TLA vendors assist (when requested) in the planning, budgeting, implementation, and optimization of their system. For example, the vendor will often perform a Six Sigma/Lean analysis of the laboratory (see Chapter 2) to develop a proposed layout and determine the optimal configuration of preanalytic, analytic, and storage units. After implementation, vendors typically review performance to assess and suggest minor modifications.

AUTOMATION IN OTHER SECTIONS OF THE LABORATORY

In addition to the major advances in chemistry automation discussed earlier, transformational changes have also occurred and continue to evolve in other laboratory sections. What follows is a brief overview of some of these changes, the technology of which is discussed in greater detail in other chapters.

HEMATOLOGY

Hematology analyzers use a variety of technologies (e.g., electrical impedance, flow cytometry, light scatter, and absorbance) to count and classify red cells, white cells, and platelets and to identify morphologic abnormalities. (These principles are discussed in Chapter 31.) Recent trends in hematology have focused on automating all aspects of cell counting, including manual review of the white blood cell (WBC) differential and automating unrelated tests that typically could be run on the same ethylenediaminetetraacetic acid (EDTA) collection container (e.g., hemoglobin A1C).

Hematology automation is available as a standalone workcell or as a component of a larger track system that includes chemistry and preanalytic modules. For most users, a compact workcell provides most of the functionality that can be realized from hematology automation. In either configuration, the system is typically comprised, at a minimum, of multiple cell counters, a slidemaker stainer, and a tube sorter; these devices are usually physically connected by a track. Devices can also be virtually connected; this requires samples to be loaded and unloaded from each module. As with chemistry systems, middleware connects the modules, balances testing load

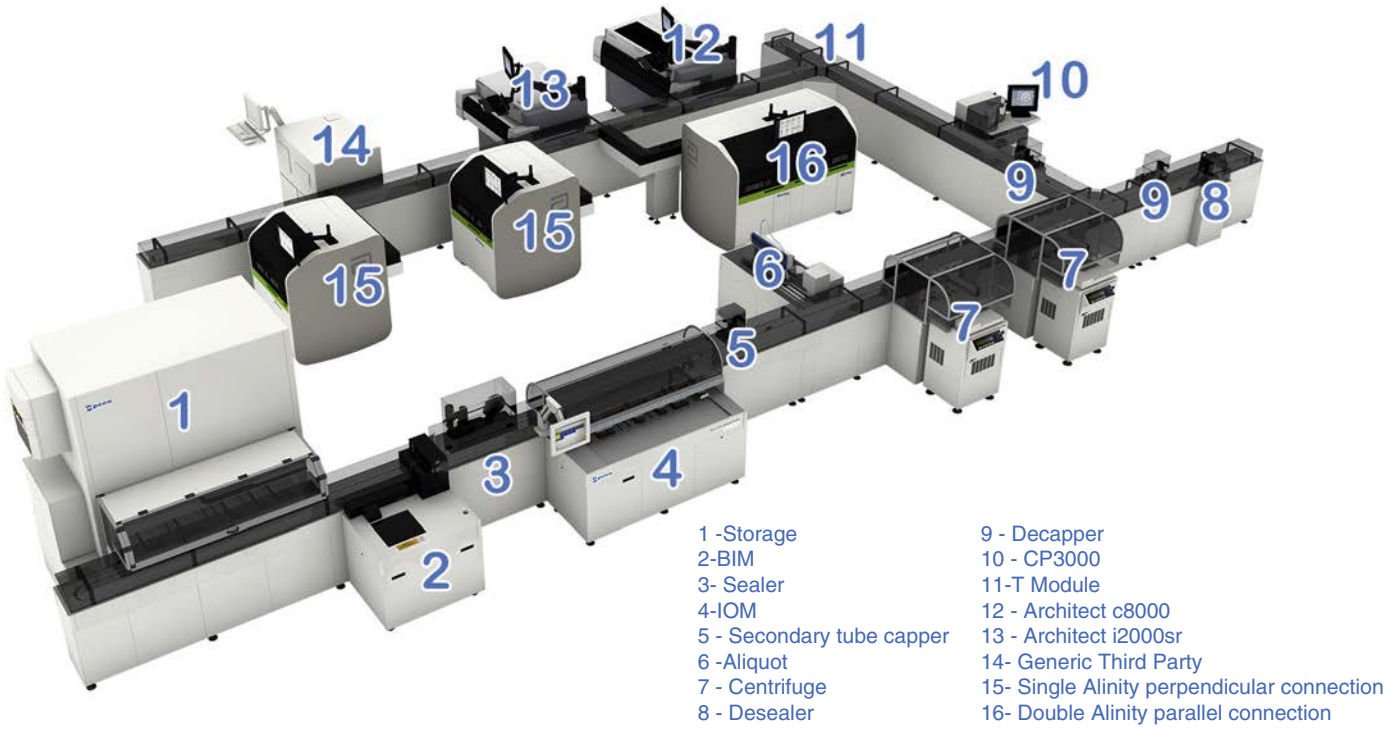

Figure 6.1 Abbott Diagnostics (Lake Forest, IL) total laboratory automation (TLA). This example of a chemistry TLA configuration includes preanalytic, analytic, and postanalytic modules that can be expanded to meet a laboratory's specific needs. Refer to component numbers in figure. Note that sample is introduced via the bulk input module (BIM) that can accommodate different tube types and sizes (2) or the input/output module (IOM) that contains configurable lanes for sample tubes, for example, separate lanes for spun and unspun tubes (4). Tubes are centrifuged (7), desealed (8), or decapped (9), and a secondary aliquot tube can be prepared (6). Samples are then transported to testing modules, for example, CP3000 coagulation (10), Architect c8000 chemistry (12), Architect i2000sr immunoassay (13), single (15) and double (16) Alinity chemistry and/or immunoassay modules, and generic third-party system (14). Alinity (ALingnment, INnovation, unITY) stations are standalone workstations that can perform multiple types of tests, for example, chemistry assays and immunoassays, at the same station. After testing, samples are sealed (3) and secondary tubes are capped (5) and transported to the temperature-controlled storage and retrieval module (1). The T module (11) is an extension of the track module. (*From Abbott Diagnostics, Lake Forest, IL, with permission.*)

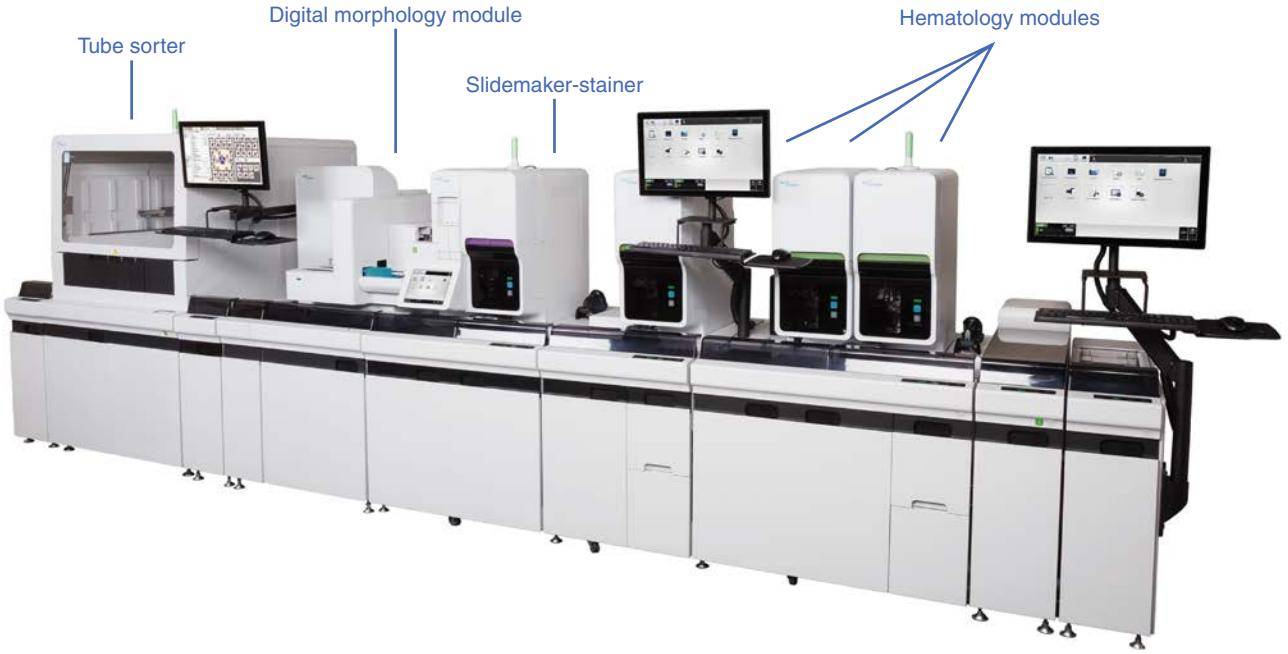

Figure 6.2 Sysmex XN-9100 (Sysmex Corporation). The Sysmex XN-9100 can be configured with automated modules that perform cell counting, slidemaking/staining, tube sorting, and digital automated microscopy. An optional HbA1c testing module can also be added. *(From Sysmex Corporation, with permission.)*

among analyzers, and determines which samples require staining or other follow-up. More sophisticated versions may also include a module for automated slide microscopy (e.g., CellaVision Inc., Durham, NC) and/or A1C testing (by high-performance liquid chromatography method). Thus, all tasks historically performed on an EDTA tube can be automated with minimal operator intervention. Compact analytic units and concentrated reagents that are automatically reconstituted onboard have significantly downsized the footprint of these systems and have decreased the space needed to store offline reagents. User interaction and manual slide reviews are kept to a minimum. One example of scalable hematology automation is the Sysmex XN-9100 (Sysmex America Inc., Lincolnshire, IL; Fig. 6.2). It can include up to nine analytic modules, along with the capability to connect slide preparation units, tube sorters, HbA1c testing, and automated microscopy. The system is driven by Sysmex's proprietary WAM middleware, which enables multisite connectivity and systemwide rules that can yield autovalidation rates greater than 88%.

MICROBIOLOGY

Although continuous-monitoring blood culture systems and automated microbial identification and antimicrobial susceptibility testing systems have been widely implemented for many years, microbiology sample processing and workup have largely been manual, time-consuming tasks. Samples need to be plated on culture media, incubated, and then monitored at periodic intervals. This entails much hands-on time, and plates are constantly shuffled between workstations and incubators. Until recently, microbiology lagged behind chemistry and hematology in its ability to automate manual tasks. However, with the introduction of new approaches to address these long-standing issues, the microbiology laboratory is in the midst of a transformational change. These core changes are driven by sophisticated specimen-processing devices that can address the unique intricacies of this discipline and laboratory automation solutions that can integrate the various workstations (including plating, incubation, identification, and susceptibility testing) into a single unit. Systems such as Vitek (Biomerieux, Durham, NC), Kiestra TLA (Becton-Dickinson, Sparks, MD) and WASP (Copan Diagnostics Inc., Murrieta, CA) provide automated solutions for a variety of microbiology tasks. For example, blood cultures can be automatically screened every 20 minutes for growth and positive cultures can be moved to automated workstations for plating and incubation.

Innovative technology continues to improve test turnaround time and promote rapid diagnosis. For example, as described in Chapters 5 and 57, matrix-assisted laser desorption ionization time of flight (MALDI-TOF) mass spectroscopy can identify pure bacterial colonies (from plate culture) in hours instead of days. MALDI-TOF spectroscopy can identify species and genus with 90% and 98% specificity, respectively. Rapid PCR methods, such as the GenXpert system (Cepheid, Sunnyvale, CA), Biofire FilmArray (Biofire Diagnostics LLC, Salt Lake City, UT) and the BD MAX system (Becton-Dickinson, Franklin Lakes, NJ) are user-friendly systems that provide results in 1 to 2 hours or less. Depending on method, a system can perform individual tests, for example, methicillin-resistant *Staphylococcus aureus* (MRSA), or a panel of tests, for example, for respiratory or gastrointestinal pathogens. As the microbiology laboratory continues to introduce non-growth-dependent techniques (e.g., molecular diagnostics) coupled with sophisticated automation, it is likely that the boundaries between this discipline and others will continue to erode (Bourbeau & Ledeboer, 2013).

PLANNING FOR LABORATORY AUTOMATION

An understanding of laboratory workflow and the role of technology is a key prerequisite to developing a performance optimization strategy. This is more fully discussed in Chapter 2. The application of these concepts is particularly important in TLA, in which project costs are measured in millions of dollars. Objectives need to be clearly defined and decisions must be based on accurate data. For example, one must fully understand the capabilities of the LIS and its limitations; the current result turnaround time; the laboratory layout to determine whether automation will fit (and whether there is sufficient space to support existing operations during construction); specimen and test mapping; and the current cost and test volume to share with vendors in the request for proposal (RFP). Ultimately, vendors will propose solutions based on these data. To adequately evaluate and compare bids, one must understand what they are based on.

The RFP outlines the laboratory's strategies, service needs, and goals (Melanson et al., 2007). It also provides a standardized framework and a deadline for vendors to respond. Table 6.1 provides examples of the type of information requested in an RFP.

After the RFP has been distributed, vendors can be invited to present their analysis of the laboratory's current and future needs/goals, along with a proposed solution and project timeline. Vendors also provide useful information about the competitive advantages of their system and the drawbacks of others; this may highlight issues that may not otherwise be apparent. Subsequent to these presentations, it is useful to conduct customer phone interviews to clarify potential concerns about a specific issue that may have surfaced during the vendor presentation or to validate that performance expectations are met. Box 6.5 provides examples of questions that can be used to probe customer experience.

TABLE 6.1

Laboratory Automation RFP: Examples of Needs, Goals, and Terms to Consider

Laboratory turnaround time	90th percentile for test completion: general chemistry (30 minutes), immunoassay (45 minutes), CBC (20 minutes), basic coagulation (30 minutes)
	Ability to prioritize stats
Throughput	During peak periods, throughput adequate to meet TAT and grow business by 20% with existing configuration
Method	Proposed test menu and (current) volume with ability to add open (user-defined) channels
Specimen management	Operator alerts for sample integrity issues (such as hemolysis, icterus), insufficient sample, label error
	System should be able to store, locate, and retrieve sample for add-on or repeat tests
LIS needs	Seamless and bidirectional interface
	Can operate independent of TLA
Financial impact and contract terms	Budget neutral; with reallocation of staff
	Contract length; fixed reagent and consumable pricing over contract period versus annual adjustment
	Service included for life of contract versus initial 2 years
Environment and safety	Will not generate excessive heat or noise
	System will minimize workplace exposure to hazards
Downtime and service	Dedicated service engineer for first 2 months
	24/7 on-call service thereafter with 2-hour response time
	Minimal downtime
References	Contact information for at least two current customers using the proposed or a similar configuration

CBC, Complete blood count; *LIS,* laboratory information system; *RFP,* request for proposal; *TAT,* turnaround time; *TLA,* total laboratory automation

BOX 6.5

Strategic Planning for Automation: Site Visit and Customer Questions

Why did you choose to automate?
Why did you pick your current manufacturer?
How did your lab function before automation?
Do you ever have downtime?
How is the service response?
Are there any recurrent problems?
How did the staff react to the new automation?
What LIS do you have?
What kind of remodeling did your lab perform?
Are there any expectations that were never met?
What were your ultimate goals after the automation?
Did you realize all your goals?
Would you buy this product again?
What is the one idea or "words of wisdom" that you would give us?

In the last phase of the process, the vendor selection team identifies two or three final candidates based on RFP responses, vendor presentations, and customer feedback. This is an optimal time to visit customer sites and see the proposed system in operation. Typically, these vendors are also invited back to present their final financial proposal and system configuration. After selecting a vendor, the final contractual terms are negotiated by the legal and purchasing experts, and an implementation plan is developed. It is a good idea to assess the expected results of the implemented automation about 6 months after the installation.

SELECTED REFERENCES

Burtis CA, Bruns DE, Tietz: *Fundamentals of clinical chemistry and molecular diagnostics*, vol. 7. St. Louis, 2014, Elsevier.

Provides substantial detailed information on all aspects of the preanalytic, analytic, and postanalytic stages in automation and clinical testing.

Melanson SEF, Lindeman NI, Jarolim P: Selecting automation for the clinical chemistry laboratory, *Arch Pathology Lab Med* 131:1063, 2007.

Lists the topics and tasks needed to prepare for automation.

Sarkozi L, Simson E, Ramanathan L: The effects of total laboratory automation on the management of a clinical chemistry laboratory: Retrospective analysis of 36 years, *Clin Chim Acta* 329(1–2):89–94, 2003.

Shows the results of a consolidation project serving a multihospital system.

Access the complete reference list online at Elsevier eBooks for Practicing Clinicians.

REFERENCES

Bourbeau PP, Ledeboer NA: Automation in clinical microbiology, *J Clin Micro* 51(6):1658–1665, 2013.

Hawker CD, McCarthy W, Cleveland D, et al.: Invention and validation of an automated camera system that uses optical character recognition to identify patient name mislabeled samples, *Clin Chem* 60:463–467, 2014.

Lippi G, Da Rin G: Advantages and limitations of total laboratory automation: a personal overview, *Clin Chem Lab Med* 57(6):802–811, 2019.

Olsen K: The first 110 years of laboratory automation: technologies, applications, and the creative scientist, *J Lab Autom* 17:469, 2012.

Shim H, Uh Y, Lee SH, et al.: A new specimen management system using RFID technology, *J Med Syst* 35:1403–1412, 2011.

CHAPTER 7

POINT-OF-CARE TESTING AND PHYSICIAN OFFICE LABORATORIES

Lauren A. McVoy, Mark S. Lifshitz

INTRODUCTION: DEFINITION OF POINT-OF-CARE TESTING, 81
REGULATORY REQUIREMENTS, 81
LABORATORY DIRECTORSHIP, 82
COMPLIANCE, 83
TYPES OF POINT-OF-CARE TESTING, 83
Hematology, 83
Chemistry, 83
Microbiology, 84
ADVANTAGES AND DISADVANTAGES OF POINT-OF-CARE TESTING, 85
CONNECTIVITY AND DATA MANAGEMENT, 85
IMPLEMENTATION OF A POINT-OF-CARE TESTING PROGRAM, 85
Physician Offices, 85
Hospitals And Medical Centers, 86
Policies And Procedures, 87
MAINTENANCE OF A POINT-OF-CARE TESTING PROGRAM, 87
Quality Assurance Program, 87
CONCLUSIONS, 87
SELECTED REFERENCES, 88

KEY POINTS

- Point-of-care testing refers to the scope of laboratory tests that are performed where patient care is delivered. This includes physician office testing as well as various hospital locations outside the laboratory, such as the emergency department, operating room, and intensive care unit.
- When performed in a physician office, simple tests (such as urine dipstick and whole blood glucose meters) are exempt from most regulations involving personnel, proficiency testing, and rigorous quality assurance requirements. These are referred to as waived tests under the Clinical Laboratory Improvement Amendments. In hospitals, these tests fall under the laboratory certificate of the parent hospital or health care facility and generally are subject to stricter requirements.
- Special personnel requirements are necessary (including those for laboratory director) if a physician office laboratory performs moderate-complexity testing.
- Key components of a hospital point-of-care testing program include method validation, training of nonlaboratory staff, and clear policies and procedures to establish who is responsible for each part of the program. Laboratory oversight is mandatory.
- Current technology of select tests in hematology, chemistry, and microbiology is reviewed, and limitations are discussed.

INTRODUCTION: DEFINITION OF POINT-OF-CARE TESTING

Point-of-care testing (POCT) is laboratory testing that is performed outside the central or core laboratory and generally at the site of clinical care or close to the patient. In most settings, POCT is performed by clinical staff rather than laboratorians. Some POCT is also performed by the patient at home. This is the case for home glucose monitoring for diabetics and home coagulation testing for patients on warfarin.

Because POCT is mainly performed by nonlaboratorians, there are many challenges to ensuring that testing is performed in an appropriate and accurate manner. Regulatory requirements are available to help guide outpatient locations in the implementation and maintenance of important components of POCT, such as training, creating procedure manuals, performance of quality control, test validation, and documentation of results. Because testing is generally performed by people who are not trained in laboratory sciences and do not have a background in quality assurance and error reduction in laboratory testing, device manufacturers have built-in features to reduce the possibility of errors. These features include passwords for individual users with lock-out if training is not up-to-date, requirements for external and internal quality control prior to patient testing, and electronic transmission of results.

Some of the clinical settings in which POCT is performed include emergency departments (EDs) or urgent care settings, where quick decisions often need to be made; inpatient settings to maintain tight glucose control; physicians' offices; health fairs; cancer centers that perform infusions; radiology sites prior to contrast administration; presurgical testing; nursing homes; and blood drives. This variety of settings involves a diverse group of health care workers who perform different types of tests. Depending on the type of testing, the clinical setting, and the test categorization (mandated by the Clinical Laboratory Improvement Amendments [CLIA]), testing may be performed by nurses, medical assistants, physicians, or office assistants. This diversity of clinical roles and levels of education means that training and testing responsibilities must be tailored to the individuals' backgrounds as appropriate. For instance, a medical assistant may be trained to perform urine dipsticks in an outpatient setting, but a nurse may be responsible for reviewing daily quality control. Similarly, a physician or medical director on the CLIA certificate may be responsible for writing the procedure manual and oversight of training.

Oversight of POCT programs can be very complex and challenging owing to the mix of tests and devices, the number of people performing the tests, and the focus on clinical care over laboratory testing. Testing in a clinical laboratory is generally performed by a relatively small number of people trained in laboratory sciences whose primary focus is lab testing. Testing is also generally performed on only a few laboratory analyzers. This is in contrast to POCT, which is performed in a clinical site by health care providers who have other responsibilities besides POCT. They are generally trained in patient care, not clinical laboratory sciences. Also, POCT is frequently distributed over a larger number of devices, with each performing a relatively low volume of testing, requiring more validation, calibration, quality control, and so on.

REGULATORY REQUIREMENTS

The Clinical Laboratory Improvement Amendments of 1988 (CLIA 88) set basic standards for laboratories to follow to ensure the accuracy of patient test results regardless of the setting in which they are performed (Code of Federal Regulations, Part 493). These standards apply to central or core laboratories performing testing on samples received from inpatient and outpatient locations; they also apply to any other site performing testing, including POCT and provider-performed microscopy procedures (PPMPs). CLIA defines four different categories of tests based on the following factors: level of training and education required to perform the test, reliability and stability of the reagents, complexity of operational steps, availability and stability of quality control and proficiency of testing materials, requirements for maintenance of the test system, and the level of judgment and interpretation required to perform the test and compile the results. The levels of complexity are waived testing, provider-performed microscopy, moderate-complexity, and high-complexity testing. The United States Food and Drug Association (FDA) determines the level of

BOX 7.1

Types of CLIA Certificates

Certificate of Waiver

- Certificate issued to a laboratory to perform only waived tests
- Certificate for provider-performed microscopy procedures
- Certificate issued to a laboratory in which a physician, midlevel practitioner, or dentist performs no tests other than the microscopy procedures; permits the laboratory to also perform waived tests

Certificate of Registration

- Certificate issued to a laboratory that enables the entity to conduct moderate- or high-complexity laboratory testing, or both, until the entity is determined by survey to be in compliance with CLIA regulations

Certificate of Compliance

- Certificate issued to a laboratory after an inspection that finds the laboratory to be in compliance with all applicable CLIA requirements

Certificate of Accreditation

- Certificate issued to a laboratory on the basis of the laboratory's accreditation by an accreditation organization approved by the Health Care Finance Administration

Data from Centers for Medicare and Medicaid Services. *CLIA: How to obtain a CLIA certificate of waiver.* Obtained at http://www.cms.gov/CLIA/downloads/HowObtainCertificateofWaiver.pdf. Accessed February 24, 2015.

complexity based on the preceding criteria (http://www.fda.gov/MedicalDevices/DeviceRegulationandGuidance/IVDRegulatoryAssistance/ucm393229.htm). Waived testing requires minimal training and education to perform and/or would theoretically cause minimal harm if the results were not accurate (Box 7.1). Many point-of-care tests are waived, including any tests approved for home use. Testing such as urine dipsticks, qualitative human chorionic gonadotropin (hCG), and glucose are generally waived. Some point-of-care international normalized ratio (INR) devices are waived, and the U.S. Food and Drug Administration (FDA) has recently granted CLIA waivers to a few nucleic acid–based influenza diagnostic tests. PPMPs are a discrete set of tests in which specimens that are time-dependent are examined under a microscope at the point of care (Table 7.1). PPMP can be performed only by licensed professionals such as physicians and dentists, as well as nurse practitioners and physician assistants under the direction of a physician, depending on the state in which they practice. Moderate- and high-complexity testing is usually performed in larger and more advanced laboratory settings, including hospital and reference laboratories.

A CLIA certificate must be issued for a site to perform laboratory testing. Five different types of certificates are issued: Certificate of Waiver, Certificate for Provider-Performed Microscopy Procedures, Certificate of Registration, Certificate of Compliance, and Certificate of Accreditation (Box 7.2). Some examples of accreditation organizations are The Joint Commission and the College of American Pathologists (CAP). When a hospital laboratory is issued a certificate, all testing that is performed in that building or any contiguous buildings falls under the laboratory's certificate. Any testing that is performed at a separate location, even if it is overseen by the hospital laboratory and has the same laboratory director, must have its own certificate.

CLIA 88 established the laboratory requirements for testing personnel, supervisory personnel, laboratory directors, testing facilities, test validation, procedure manuals, personnel training and competency, quality control, proficiency testing, and reporting results. Some states, including New York, California, and Florida, have more stringent laboratory regulations than those mandated by CLIA. Also, laboratories that choose to be accredited by CAP face some stricter requirements.

LABORATORY DIRECTORSHIP

Laboratories that operate under a Certificate of Waiver or with a certificate for PPMP can perform waived testing without the overhead of having personnel who meet established qualifications in training, experience, job performance, and competency. However, if any moderate-complexity tests or measurements are performed, CLIA requires that the laboratory be directed by a laboratory director and/or a laboratory consultant with appropriate credentials. This director is responsible for determining the qualifications of individuals performing and reporting test results, as well as ensuring compliance with all applicable regulations. The director is also responsible for the analytic performance of all assays and must monitor ongoing proficiency testing, accuracy, and precision. If more than one individual in the practice qualifies as a laboratory director, the laboratory is required to designate one as being responsible. It must be demonstrated that the laboratory director is providing effective direction for the operation of the laboratory. If one does not provide onsite direction, one must provide phone consultation or delegate to qualified personnel with specific responsibility as required by regulation.

For POCT, a separate certification is usually not necessary when it is performed under the supervision of the laboratory director responsible for laboratory services in a health care facility. POCT that occurs within a health care facility at sites that are located in contiguous buildings on the same campus and under common direction can be performed under the certificate of the parent organization. When assays and procedures are performed in a situation such as this, the terms *waived* and *complexity* no longer apply. The test menu is no longer restricted to waived testing—more frequent inspections and higher scrutiny are received in return. Because the parent organization typically has a certificate that allows testing at all levels of complexity, it is the responsibility of the laboratory director to ensure that the test method used at the POCT site is appropriate for the skills

TABLE 7.1

Waived Tests

Chemistry	Albumin, amylase, ALT, AST, GGT, alkaline phosphatase, total protein, bilirubin (total), carbon dioxide, glucose, sodium, potassium, calcium (ionized), calcium (total), phosphorus, urea (BUN), creatinine, uric acid, brain natriuretic peptide (BNP), glycated hemoglobin (HbA1c), fructosamine, cholesterol, LDL, HDL, triglyceride, creatine kinase (CK), lactic acid, ketones, lead, collagen type 1 N-telopeptides
Endocrinology	TSH, FSH, LH, ovulation tests (LH) by visual color comparison, estrone 3-glucuronide
Drugs	Alcohol (saliva), barbiturates, benzodiazepines, buprenorphine, cannabinoids (THC), cocaine metabolites, methadone, methamphetamines/amphetamines, MDMA, morphine, oxycodone, nicotine, opiates, PCP, propoxyphene, tricyclic antidepressants, lithium
Hematology	Hemoglobin, hematocrit, ESR (nonautomated), platelet aggregation (VerifyNow), prothrombin time (PT)
Microbiology	*H. pylori* antibodies, HIV-1 and -2 antigens/antibodies, adenovirus antigens, RSV, *Treponema pallidum* antibodies, influenza A and B, group A streptococcus, trichomonas antigen, Lyme antibodies, vaginal aerobes/anaerobes, hepatitis C virus antibody, infectious mononucleosis antibodies
Urine	pH, glucose, ketone, protein, nitrite, urobilinogen, bilirubin, leukocyte esterase, catalase, hCG, albumin, microalbumin, specific gravity, leukocytes, ascorbic acid
Miscellaneous	Vaginal pH, matrix metalloproteinase-9 (MMP-9), glucose (fluid), gastric pH, semen, osmolality (tears), fecal occult blood, gastric occult blood, bladder tumor–associated antigen

Data from U.S. Food and Drug Administration. Obtained at http://www.accessdata.fda.gov/scripts/cdrh/cfdocs/cfClia/analyteswaived.cfm. Accessed February 24, 2015.

BOX 7.2

Provider-Performed Microscopy Procedures

- Wet mounts, including preparations of vaginal, cervical, or skin specimens
- Potassium hydroxide (KOH) preparations
- Pinworm examinations
- Fern test
- Postcoital direct, qualitative examinations of vaginal or cervical mucus
- Urinalysis with microscopy
- Fecal leukocyte examination
- Semen analysis; presence and/or motility of sperm
- Nasal smears for eosinophils

Data from Centers for Disease Control and Prevention. Obtained at http://wwwn.cdc.gov/CLIA/Resources/TestComplexities.aspx. Accessed February 24, 2015.

and training of those performing the test. What inspectors do not tolerate could be called "rogue testing." This occurs when a clinic or service sets up a test without the knowledge and supervision of the laboratory director. With the tracer method used by accrediting agencies such as The Joint Commission, if an inspector finds a lab result and traces it back to a laboratory that is not adequately supervised by the laboratory director, a citation may be issued to the health care facility.

COMPLIANCE

In addition to CLIA, all laboratories must adhere to regulatory procedures, particularly in the outpatient setting. First, all testing for which Medicare is billed must be medically necessary. Screening tests and other measures of wellness generally are not covered. Medical necessity determination is implemented by Medicare, Medicaid, and other insurance carriers through Current Procedural Terminology (CPT) codes used in conjunction with International Classification of Disease (ICD) codes. When the ICD-10 code does not warrant the CPT-4 code, payment is rejected. Even worse, if it is determined that a laboratory deliberately added codes to obtain a higher payment than it deserves or payment for work that it has not done, it can be charged with fraud, which is a felony, and the laboratory will be subjected to fines. Errors are assumed to be deliberate unless a compliance program is in place that actively seeks to uncover billing errors.

Another potential pitfall is Stark regulations. The Stark laws, which are named after their original sponsor, Representative Fortney Pete Stark (D-Calif.), were intended to prevent unnecessary self-referrals intended to boost revenue. Under Stark, physicians are prohibited from referring Medicare patients to laboratories in which the physician (or a close family member) has a financial interest. Because this prohibition would be detrimental to most physician office laboratories (POLs), it is important to understand the "safe harbors" that allow legitimate self-referral.

CLIA 88 created standards for POLs and POCT in the United States that predated similar measures on the international scene. However, an international working group has proposed and adopted ISO 22870-2006 as an international standard for POCT. These standards are more extensive than current CLIA requirements; however, CLIA is a minimum federal requirement, and states and other accrediting agencies can impose standards that are more rigorous. Thomas (2008) has published a summary of these international standards with cross-referencing to current CAP accreditation standards.

TYPES OF POINT-OF-CARE TESTING

Many different analytes can be used for point-of-care tests. Some of these tests are single-use cartridges, such as rapid HIV tests and urine pregnancy tests, and manual tests that require testing personnel to record a result, such as a urine dipstick or fecal occult blood testing. Other tests are performed on portable multiuse devices that may require a blood draw or fingerstick. These include many glucometers, coagulation monitoring devices, blood gas analyzers, and point-of-care chemistry analyzers (Table 7.2).

HEMATOLOGY

POCT in hematology has generally been limited to hemoglobin and hematocrit on a blood gas or chemistry device. In 2017, the FDA cleared the first waived device for performing a complete blood cell count (CBC), including a white cell count and platelet count (US Food and Drug Administration, 2017). This access to point-of-care CBC testing should facilitate rapid diagnosis and care in emergency settings as well as cancer centers. In an ED or urgent care center, a rapid CBC may help the clinician determine whether a patient has an infection and whether the patient needs admission and antibiotics. In a cancer center, some treatment decisions are based on the white blood cell count. If the CBC had to be sent to the central laboratory for testing, the delay could hold up the patient's treatment and lead to inefficiencies in productivity for the cancer center.

POC coagulation testing mainly consists of prothrombin time (PT) and INR for monitoring patients on warfarin and the activated clotting time (ACT) for monitoring patients on heparin during cardiac bypass surgery. Point-of-care coagulation monitoring for patients on warfarin is well established. This testing may be performed in an anticoagulation clinic, a cardiology practice, a primary care setting, or at home by the patient. Many of these devices are waived, but some are of moderate complexity, which would necessitate meeting all the requirements of a moderate-complexity laboratory. POC PT/INR testing can significantly improve monitoring for patients on warfarin. Their dose can be adjusted during their office visit based on results from POCT performed in the clinical setting. This alleviates the burden on office staff of contacting patients once their laboratory results are complete. Patients may also self-monitor with a home use device, alleviating the need for regular office visits. POC PT/INR testing generally correlates well with testing performed in clinical laboratory settings in patients with INRs below 5. Many manufacturers recommend confirming elevated results with a sample sent to the lab. Because of the risk of improperly adjusting or failing to adjust a patient's dose of warfarin, this testing should be performed only in a setting where strict attention is given to performing the testing properly, appropriately documenting results, and questioning unexpected results. The same is applicable for patients who will perform their own monitoring at home; they should clearly understand the risks of an erroneous result and be capable of following the manufacturer's instructions.

TABLE 7.2
Examples of Common Point-of-Care Tests

Test	Clinical Setting
Glucose	Home monitoring for diabetics, inpatient monitoring for glycemic control
Blood gases	Critical care units, operating rooms
Cardiac markers	Emergency departments
Urinalysis	Physicians' offices
Creatinine	Radiology suites prior to contrast administration
PT/INR	Coagulation clinics, cardiology practices, home monitoring
Infectious diseases (HIV, RSV, influenza, etc.)	Outpatient and emergency settings for treatment decisions and cohorting or isolation
Drug screening	Emergency departments, outpatient treatment programs, workplace testing

In a CAP Q Probes survey of quality control performance for POCT on PT/INR and ACT at 87 institutions, 95.6% of expected quality control was performed. However, only 79.5% of out-of-range quality control was associated with corrective action, and 9.6% of the time, patient testing was performed even though no corrective action was taken. Additionally, for the sites performing routine INR comparisons with the central laboratory, 10% of the time there was a difference of greater than 0.5 units (Meier & Jones, 1999). This study highlights some of the common quality issues facing POCT programs, such as failure to perform quality control, lack of follow-up on missing or inaccurate quality control, and potential discrepancies among testing methods. These are issues that every POCT program should strive to avoid and/or improve through proper laboratory oversight, user training, and well-defined procedures.

A more specialized type of coagulation assessment that can be performed as a point-of-care test is viscoelastography (thromboelastogram [TEG] or rotational thromboelastogram [ROTEM]). This testing is of moderate complexity and is generally performed in a bleeding patient to predict the need for blood product administration to correct the coagulopathy. A curve is generated based on the oscillations of a pin in a cup (or vice versa) as the patient's blood clots. Depending on the shape of the curve, the provider can predict whether the patient needs fresh frozen plasma, cryoprecipitate, or platelets to maintain hemostasis. This testing is often used in liver transplantation, cardiac surgery, trauma, and obstetric hemorrhage (Sharp & Young, 2018).

The added challenge with this type of testing is the need for providers at the bedside or in the operating room to be able to view the curve in real time. If the testing is not done close to the patient, local information technology resources are needed to provide remote viewing capabilities, set up user accounts, and maintain the privacy and security of the data. Additionally, providers must be trained in interpretation. This testing is also more costly and labor-intensive than traditional coagulation testing. Thus, consideration must be given to cost versus the potential clinical advantages at any given institution. There are many studies demonstrating reduction in blood product use with potential cost savings and benefit to patients with TEG or ROTEM testing (Wikkelso et al., 2017).

CHEMISTRY

By far, the most ubiquitous POCT performed is glucose testing. Point-of-care glucose testing is performed at home by diabetic patients, in physician offices and nursing homes, and in inpatient settings. Glucose testing devices were originally designed for home monitoring in diabetic patients to maintain glycemic control. Many studies have demonstrated

the patient benefits of this approach, including reduction in morbidity and mortality and decreases in retinopathy, nephropathy, neuropathy, and cardiovascular disease. To achieve tight glycemic control (TGC), these home use devices were later adopted in inpatient settings, such as critical care and postoperative units, as well as general inpatient units. However, these devices were never intended for use in these patient populations, nor were they validated in them. In 2014, the FDA published guidance documents proposing that these devices should be redefined as moderate complexity owing to the use in critically ill patients. This had the potential to significantly increase the regulatory burden on hospitals as POC glucose testing performed in an inpatient setting would have been considered "off label" use, placing the burden on the manufacturers or the hospital to validate the devices in the appropriate patient populations. Fortunately, some manufacturers of POC glucometers quickly recognized the need to perform their own validations on different patient populations in order to meet the FDA's new requirements. This issue demonstrates the potential need to define appropriate use for these devices in different patient populations and settings.

POC measurement of hemoglobin A1c (HbA1c) is increasingly being performed in outpatient settings to monitor glucose control in diabetics. This allows a physician to determine how well a patient's glucose has been controlled over the past few months and whether any changes in medications or lifestyle need to be made. Thus, the patient does not have to return for a follow-up visit or wait for a phone call from the doctor's office. Also, if any new prescriptions need to be issued, this can be done at the time of the office visit. Thus, while POC HbA1c testing does not necessarily provide critical clinical information, it does help improve patient care because important clinical decisions can be made during the visit without waiting a day or more for the lab results to be available. This decreases the burden on the physician's staff and potentially improves adherence to treatment changes as well as patient satisfaction. Thus, the cost, labor, and expertise involved in implementing POCT for HbA1c must be weighed against the benefits to the patient and the provider.

Some other examples of chemistry testing that are commonly performed at the point of care are creatinine, β-hCG, and cardiac markers. Creatinine measurements and pregnancy tests are used to determine whether patients can be appropriately referred for radiologic procedures. Creatinine is also commonly used to assess renal function prior to infusion of certain chemotherapeutic agents. Nichols and colleagues (2007) questioned the accuracy of two POCT creatinine assays. The authors concluded that when a creatinine result is close to a decision point, the sample can be sent to the central laboratory for confirmation while the clinically acceptable values on the remaining and majority of patients promote more rapid care. A more recent study of POC creatinine compared performance characteristics of three POC devices with a laboratory analyzer. The authors concluded that one of the devices demonstrated acceptable performance with a whole blood sample while the other two did not compare favorably enough. They also concluded that fingerstick samples were not ideal for testing (van der Heijden et al., 2019).

POC pregnancy testing is generally a qualitative urine β-hCG with analytic sensitivity of 25 mIU/mL for a positive result and 5 to 25 mIU/mL for an equivocal result. A recent study of qualitative urine β-hCG at a major medical center in Boston showed a false-negative rate of 11 out of over 9000 tests (Herskovitz et al., 2019). While this study was performed in the clinical laboratory, it demonstrates how accurate these tests can be. In a POCT setting, operator variability will lead to more testing issues; however, the benefit of knowing a patient's pregnancy status prior to performing a procedure or starting a medication that may be harmful to a fetus is critical.

In a review of POCT cardiac markers, Storrow and colleagues (2009) found general agreement that POCT led to significantly decreased turnaround time for results reporting to the ordering physician. In addition, improvements in other ED efficiency measures (e.g., time to therapy and total ED length of stay) were seen. However, investigators could find no evidence that POCT for cardiac biomarkers had any effect on clinical outcomes of patients evaluated for acute coronary syndrome. In a multicenter, randomized controlled study comparing laboratory and POC cardiac marker testing strategies, Ryan and colleagues (2009) found similar reductions in turnaround time, but effects on ED length of stay varied among institutions. Across all sites, POCT did not decrease time to disposition for admitted or discharged patients (Ryan et al., 2009). A more recent study compared a high-sensitivity troponin assay to two POC tests performed in the ED of a hospital in Frankfurt, Germany. Testing was performed on all three platforms in patients suspected of having acute coronary syndrome (ACS). All three tests demonstrated similar performance characteristics for predicting ACS (Wilke et al., 2017).

MICROBIOLOGY

Over the past decade or so, POC testing for infectious diseases has become more and more common. Given the long turnaround times with culture-based microbiology testing—or even traditional laboratory molecular testing, in which tests may be batched—the availability of effective POCT can radically change practice in infectious disease diagnosis and treatment. This is evident with the emergence of effective POCT for human immunodeficiency virus (HIV). Performance characteristics of the first- and second-generation POC HIV assays have been reviewed and were found to have comparable sensitivity and specificity to conventional enzyme immunoassays (Campbell & Fedoriw, 2009). In early infection, however, these assays are less sensitive than nucleic acid amplification testing. Appiah and colleagues (2009) compared POC HIV testing in a voluntary counseling and testing (VCT) clinic and in a tuberculosis (TB) clinic in Ghana and found that in both clinics, 100% of patients offered POCT accepted it, but only 93% of VCT clients and 40% of TB patients had accepted a standard HIV test offered 6 months earlier. Moreover, all patients attending the VCT or TB clinics who tested positive for HIV with the POC test returned to the HIV clinic for care, but only 64% and 95%, respectively, of patients who tested positive in the previous cohort had returned for follow-up, indicating a change in patient behavior when access to POCT with immediate results is provided (Appiah et al., 2009).

More recently, several manufacturers have developed POC HIV-1 ribonucleic acid (RNA) tests, both qualitative and quantitative. These are particularly helpful in resource-limited settings where a clinical laboratory may not be readily accessible for testing. In a systematic review by Agatu et al. (2019), 32 studies were considered, 30 of which compared the POC diagnostics with clinical laboratory testing. Their conclusions were that accuracy was acceptable for these POC tests when plasma was the specimen type and that whole-blood or dried-blood spot testing was not as accurate. An important conclusion from this review of testing in resource-limited settings is the need for trained phlebotomists, centrifuges, refrigeration, and systems for documentation of results. One other observation is that the POC viral load tests were not as accurate at the cutoff of 1000 copies/mL and tended to overestimate the viral load. This could potentially lead to changing antiretroviral therapy before necessary.

Several lateral flow assays are available for diagnosis of pathogens as diverse as malaria, *Cryptococcus*, and *Legionella*. These are immunoassays that detect antigens for these organisms present in a patient's blood, cerebrospinal fluid (CSF), or urine. They are simple, single-use devices with relatively good performance characteristics. While these are often moderate-complexity tests, they are relatively simple to use and perform well in resource-limited settings where a larger central laboratory may not be readily available.

In 2015, Roche released the LIAT, the first CLIA-waived molecular test for influenza A and B. This device also performs rapid Group A *Streptococcus* and respiratory syncytial virus (RSV) testing. Since then, four other manufacturers have received FDA approval for POC molecular influenza tests. As waived tests, these rapid diagnostics can be performed in a provider's office by a nurse, medical assistant, physician, or other staff member. Given the high sensitivity and specificity of molecular testing, the potential for an accurate, rapid diagnosis in the office is much greater than with older immunoassays, which lacked sensitivity. However, considering the small amount of nucleic acid necessary for a positive result, there is concern among laboratorians about the risk of false-positive results due to contamination by amplicons in the environment. There is also the theoretical risk of a false-negative result due to operator error in the hands of medical staff who are not trained in laboratory sciences (Babady et al., 2019). For rapid molecular testing of Group A *Streptococcus*, the sensitivity is high enough that there is no longer any need to perform culture on all negative samples as with older, less sensitive immunoassays. Thus, the provider can be confident of the negative result and the laboratory can be spared the extra work of performing the culture. In a study by Donato et al. (2019), the performance of the LIAT Group A Strep testing in a POCT setting was compared with Group A Strep polymerase chain reaction (PCR) testing in the clinical laboratory. The authors found a 97.2% concordance rate and a 6.6% failure rate in this study, indicating that the concern for false-positive results due to amplicon contamination may not be an issue.

There are also now many multiplexed molecular microbiology tests that are moderate complexity but are potentially simple enough to be performed as a POC test. These multiplexed molecular tests often cost more than $100 per test, which is significantly more costly than the few dollars a culture costs or even the cost of some other rapid immunoassays

BOX 7.3

Advantages and Disadvantages of Point-of-Care Testing

Advantages

- Decreased turnaround time
- Decreased time to treatment
- Decreased length of stay
- Fewer follow-up visits or calls
- Improved patient and provider satisfaction
- Less traumatic sample collection
- Collaboration between laboratory and clinical staff

Disadvantages

- Increased cost, direct and indirect
- Increased regulatory burden
- Increased work for clinical staff
- Increased oversight for laboratory
- Greater potential for error
- Results may not correlate with central laboratory

TABLE 7.3

Point-of-Care Testing Device Software Features

Feature	Details
System lockouts	Quality control out of range or not performed, no patient ID, no operator training
Calibration	
Security access	Different levels for users and managers
Reference ranges	May transmit to LIS
Quality control ranges	
Bar code scanner	For patient identification, reagent and quality control identification
Data management	Patient results, quality control records, maintenance and calibration documentation
Connectivity	Data manager or middleware, LIS

used for microbiological diagnosis. In an outpatient setting, the cost to the patient can be significant. This brings about a debate over utilization versus benefit to the patient and health care organization. There has been much discussion and confusion regarding how to code these tests and what the reimbursement rates will be. This is still an area in flux as the Centers for Medicare and Medicaid Services (CMS) continues to refine how these tests are reimbursed. There is, as discussed earlier, the concern regarding false-positive results due to either manufacturing issues or amplicon contamination from the testing environment. This is potentially more likely in a busy patient care setting where unexpected results may not be noted and questioned as readily as in a clinical microbiology laboratory.

ADVANTAGES AND DISADVANTAGES OF POINT-OF-CARE TESTING

POCT has many advantages, including improved turnaround time, convenience, shorter length of stay, and improved patient satisfaction (Box 7.3). However, whether these benefits are realized can be challenging to quantify. Crocker and colleagues (2014) showed some benefits to implementing POCT in an outpatient setting, including fewer follow-up tests, fewer phone calls and repeat visits, and reduced cost of care. However, these advantages have to be weighed against the disadvantages, including the higher cost of testing, regulatory requirements, consequences of erroneous results, and differences in technology compared with the central laboratory.

The pros and cons of implementing POCT vary depending on the clinical setting and need. For instance, in an inpatient setting, point-of-care glucose testing is practically a necessity. The volume of glucose tests regularly performed in an inpatient setting would rapidly overwhelm the central laboratory and slow down everything from accessioning to processing. Also, it would add to the workload of the nursing staff responsible for drawing the specimens and sending them to the laboratory. Finally, the patient would require more blood draws and could even develop iatrogenic anemia. In an emergency department, time is of the essence. Rapid turnaround times guide decisions for treatment, further testing, and admission or discharge. For a patient presenting with symptoms of ACS without classic electrocardiogram (ECG) changes, the cardiac markers help the clinicians decide whether the patient needs an intervention such as cardiac catheterization or thrombolysis. Many studies have shown that the time to intervention is critical to salvaging precious cardiac muscle (Ryan et al., 2009). In an outpatient, POCT may be considered when treatment decisions can be guided by the test results at the visit. This is the case for INR monitoring for patients on warfarin. However, erroneous results can lead to improper dosage adjustments, and any questionable results should be confirmed by the laboratory. Testing for HbA1c is a good example of a noncritical test that may improve patient care in an outpatient visit. Having the test results at the office visit allows the clinician to adjust treatment and counsel the patient appropriately to improve glycemic control in the future. Finally, home monitoring is appropriate for insulin-dependent diabetics to properly adjust their dose. Home INR monitoring frees a patient from coming to the physician's office for a fingerstick or blood draw on a regular basis. However, patients still need to consult with their clinicians when adjustments are appropriate.

CONNECTIVITY AND DATA MANAGEMENT

Data management in POCT can be quite extensive. Test results must be recorded in the patient's chart, whether electronic or on paper, and appropriate units of measure and reference ranges must be included with the report. Other data that must be maintained by the site are records of validation of devices; validation and tracking of new lots of reagent; quality control data, including proficiency testing results that must be performed; all testing personnel; and operator training and competency. To meet regulatory requirements, it must be possible to link each patient result to a specific operator, device, and lot of reagent and quality control. For an outpatient practice, this documentation may not be too cumbersome. For a hospital or health care system with many types of devices, tests, and operators, however, this documentation can quickly become overwhelming.

To make maintenance of this data easier, many device vendors have implemented certain features for result reporting and data management (see Table 7.3). In addition to device-specific information processing features, middleware systems can electronically connect with multiple types of devices to manage patient and QA/QC data. Thus, in a complex health care system using multiple POCT devices, there can be one central repository for the data. Interfaces with the laboratory information system (LIS) and the electronic medical record (EMR) further improve functionality, reduce errors, and transmit patient data very rapidly. Many devices now have wireless transmission of data; thus, the device does not even need to be docked to send the patient's results across an interface to an LIS or EMR.

The Clinical and Laboratory Standards Institute (CLSI) has developed standards for transmitting POCT data based on the specifications of the Connectivity Industry Consortium (CIC) (Dunka et al., 2014). The CIC is a group of 49 health care institutions, POC diagnostic vendors, diagnostic test system vendors, and system integrators. This document describes two types of interfaces: the device interface and the observation reporting interface (Fig. 7.1). It sets standards for the POCT industry to maintain some level of uniformity among vendors and promotes cost-effective and easy-to-implement data management.

IMPLEMENTATION OF A POINT-OF-CARE TESTING PROGRAM

PHYSICIAN OFFICES

POCT programs differ significantly, depending on the scope of testing and the setting where they will be performed. In an outpatient physician office setting where only waived testing will be performed, establishing a program may be relatively simple. A physician or the medical director for the practice will generally serve as the director on the Certificate of Waiver. It will be their responsibility to develop policies and procedures and lead the practice in deciding what testing to perform and what methods to use. However, the director should solicit feedback from other practitioners, nurses, and clinical staff who will play a role in the testing. After clinical need and performance criteria, the most important factors in test selection are usually ease of use and cost per test. A system for initial training and subsequent competency will need to be established. The practice should follow the manufacturer's recommendations for quality control

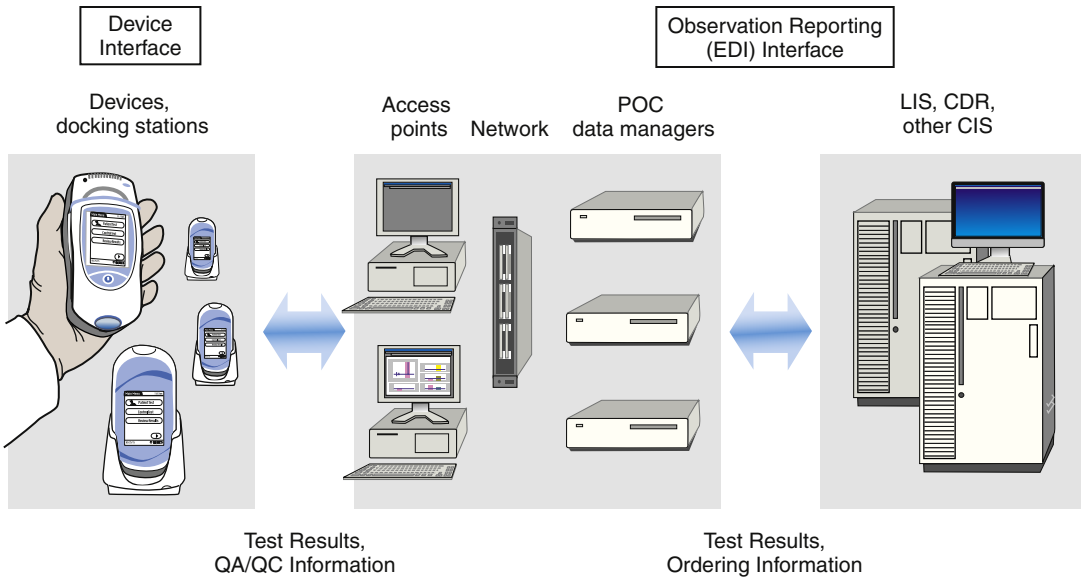

Figure 7.1 Point-of-care testing interfaces. (From CLSI: Point-of-care connectivity; approved standard, ed 2, CLSI document POCT01-A2. Wayne, PA, 2006, Clinical and Laboratory Standards Institute; 2006. Redrawn with permission.)

procedures, specimen collection, and testing procedures. Appropriate logs with patient information and lots of reagent and quality control material should be maintained if electronic reporting is not performed.

HOSPITALS AND MEDICAL CENTERS

Point-of-Care Committee and Management Team

A first step in implementing a POCT program at a hospital or medical center is to establish a Point-of-Care Committee. This committee should consist of representatives from the clinical laboratory, particularly the medical director responsible for POCT, the POC manager and/or administrator from the clinical laboratory, nursing (particularly nursing educators), information technology (IT), regulatory, and medical staff from departments who frequently use POCT. These could include the emergency department, the intensive care units, outpatient clinics, and so on. Nurses should play a vital role in the committee because they will be overseeing training, verifying correct use of tests, and ensuring proper storage of reagents, kits, and quality control materials. They may also be performing the tests, depending on the institution. Members of hospital administration should have a role on the committee because they can provide information about future growth and addition of new sites and technologies that will help guide the committee. A member from the hospital regulatory team might also be involved to ensure regulatory compliance and keep the committee apprised of impending inspections, new regulations, or deficiencies noted in mock inspections. Finally, representation of the information technology department is critical because more and more devices have the capability to report electronically. Many devices can now report results wirelessly, an important consideration in a fast-paced setting where a device may not be docked between patients.

In addition to a Point-of-Care Committee, it may be necessary to have a point-of-care team as part of the clinical laboratory staff. This depends on the number of sites that are performing testing and the diversity of devices and tests in use. In a smaller community hospital where only point-of-care glucose testing is done, it may be adequate to have one laboratory technologist run the program. However, in a large medical center where many inpatient and outpatient locations perform POCT (e.g., rehabilitation, cancer centers, same-day surgery, cardiac catheterization suites, radiology, and endoscopy), it is important to have a laboratory team that can meet the many needs of these different locations. A clinical staff member at the site should oversee the POCT program in conjunction with the clinical laboratory POCT team. This person would ensure that quality control was being performed and was acceptable, that new employees received training, and that procedures were being followed. The laboratory POCT team member might visit once a month to make sure that documentation was in order; devices were in good working order; reagents, kits, and quality control materials were labeled and stored correctly; and that any necessary calibrations and instrument comparisons were performed. This lab representative should also make sure that proficiency testing (PT) materials were being handled and tested appropriately, although the PT must be performed at the site by the staff normally performing patient testing. The number of people on the point-of-care laboratory team will depend on the number of sites and the complexity of testing. These should be technologists who are organized, competent to perform validations on new instruments and analyze the data, and can help troubleshoot problems with instruments. Also, the ability to communicate clearly with clinical staff at different locations is an important attribute.

Selection of Appropriate Tests

After instituting the Point-of-Care Committee, it is important to survey the institution to determine what testing is currently performed. This will involve talking to clinicians and nurses, as well as actually visiting testing locations to observe what is being done. Reagents and other testing materials may be discovered by laboratory representatives by visiting inpatient floors and outpatient testing locations. Some locations may not report all the testing they are doing. For instance, on labor and delivery, physicians may not realize that the microscopy they do for fern testing is a PPMP that requires an appropriate CLIA certificate. Other locations may be performing fecal occult blood testing and not realize that it is a laboratory test requiring appropriate procedures, training, and documentation of results. Once the survey is complete, it is important to assess the needs of each location performing the testing. Some locations may not need all of the testing they are performing or may be able to scale back on the number of devices and/or tests. Other locations may have a valid clinical need to add more testing.

When a location wants to add a new POC test, some basic information should be collected for review by the Point-of-Care Committee. This information includes testing to be added, anticipated volume of testing, reason for performing the testing on-site rather than sending it to the clinical laboratory, number of personnel who will be performing testing and their qualifications, person who will be the site manager and that person's qualifications, and person who will be the medical director and that person's qualifications. Perhaps the most important consideration is the reason for the testing to be performed as a POC test. Some important factors are impact on the number of patient visits, length of stay, treatment initiation, morbidity and mortality, patient/clinician satisfaction, and compliance with therapy (CLSI POCT09-A). A standard form could be used for this purpose, followed by a visit from a laboratory representative, either the medical director for POCT or the administrator/laboratory manager, depending on the request. Once this information has been collected, it should be presented to the Point-of-Care Committee for review. Criteria for accepting the request might include clinical need, cost considerations, complexity of testing (waived or moderate), and the location's track record with other POCT.

Selection of Appropriate Testing Devices and Methods

During the initial survey to determine what POCT is being performed, it is important to start moving toward standardization of equipment as well as manual tests such as urine dipsticks and urine pregnancy. This approach

has several advantages. One is that policies and procedures can be uniform for all locations. Sometimes, inpatient policies may differ slightly from outpatient policies if, for instance, an outpatient will be sent to the emergency department for a critical result. Training and competency can also be the same for all locations, for the most part. Reagents, quality control, and any other material can be bought in larger quantities by the central lab and distributed appropriately. This way, the laboratory can be sure that the correct materials are being used. It also ensures appropriate storage of reagents requiring specific storage conditions. It may also help to keep costs down and can be a tremendous help with lot-to-lot changes in reagents and quality control because these comparisons can be performed centrally, if required. Any other documentation can be consolidated, such as logs for quality control and temperature and humidity logs.

Selection of which manufacturer's tests and devices to use is an important function of the Point-of-Care Committee. Vendors may be invited to give a presentation to the Committee and provide a demonstration. Other clinical sites that are using the test under consideration can be contacted for input and feedback on their experiences. Considerations such as ease of use, frequency of quality control, electronic quality control, lockouts for unacceptable quality control results, lockouts for users whose training has expired, electronic data transmission to a middleware product or LIS, wireless downloads, and robust construction of the device are all important. Other important considerations include complexity of testing, cost of device, cost and stability of reagent/cartridges/kits, and validation procedures. From an analytic perspective, the accuracy and precision, analytic sensitivity and specificity, reportable range, and comparison to laboratory methods in use at the institution are important considerations (Zucker et al., 2014). Ultimately, input from the laboratory professionals on the committee is important because they will be responsible for overseeing the testing and ensuring the quality of the results. Also, laboratory professionals are familiar with the process of assessing new equipment and determining which equipment best suits the testing needs for the situation. However, it is also important that the end users are comfortable with device selection and that the testing, quality control, calibration, and other aspects of maintenance are relatively easy to perform.

POLICIES AND PROCEDURES

Test procedures should adhere to CLSI guidelines and follow the manufacturer's instructions. The procedure should act as a reference for the person performing testing and contain institution- or practice-specific information, such as critical values, reference ranges, and acceptable specimen types. Procedures should be reviewed annually and signed by the director on the CLIA certificate or by the director's designee. Procedures should be uniform for all locations using the same device or manual test. The procedure is generally written by the laboratory POC team in a hospital or medical center. However, input from nursing or other clinical users may be appropriate to be sure that the procedure actually fits the testing workflow. Also, because nurses frequently bear much of the responsibility for training, they should be familiar with the procedures and comfortable with training on them.

Method Validations

Prior to implementation, POC tests must be validated and approved by the director. Validation may be a simple procedure for a manual test, such as a urine dipstick, where results can be compared to those run on a laboratory analyzer. Ten to 20 specimens are usually adequate as long as all components have normal and abnormal results. Additionally, some simple precision studies using normal and abnormal quality control material should be performed. More complex validations are required for POC devices reporting analytes such as blood gases, chemistries, and cardiac markers. CLSI guidelines should be followed for these validations with method comparison to the main laboratory analyzer(s). Precision studies and reference range verifications may be warranted. When multiple devices are being validated at once, it is acceptable to compare one device to the laboratory method and then compare other devices to that one. This can streamline the process and decrease the burden on the central laboratory when implementing new POCT throughout a large institution.

Oversight of Training and Competency

Regulatory requirements must be considered when developing training and competency programs and documents for new POCT. Generally, oversight of training and competency is a shared responsibility between nursing and the POC team in the clinical laboratory. The POC team may set up logins and passwords for devices and coordinate with vendors for training large groups of employees. Many devices require a login that can automatically lock an employee out when training is not up-to-date. Nursing keeps records of who has been trained and is due for competency and makes sure that new employees receive the appropriate training.

MAINTENANCE OF A POINT-OF-CARE TESTING PROGRAM

QUALITY ASSURANCE PROGRAM

Once the POCT program has been established, including the Point-of-Care Committee, POC management team, and standardization and implementation of appropriate tests, ongoing work is necessary to maintain the program. Each inpatient and outpatient location should have a clinical staff member who is responsible for the daily operations. This includes maintaining appropriate inventory, reviewing quality control, and ensuring that staff are trained and following procedures. Devices also need to be checked regularly for damage that may affect function, and reagents should be properly labeled in a temperature-controlled environment. This also may include retraining when necessary and following up on critical and erroneous results. The laboratory POC team member should visit each location on a routine basis to ensure compliance with policies and procedures, spot check the site for any problems, and discuss issues with the clinical staff.

Hospital-based programs in which POCT falls under the laboratory's certificate are obliged to perform regular proficiency testing. While the proficiency testing may be overseen by the laboratory, the testing itself must be performed by the staff that regularly perform patient testing. An attempt should be made to rotate proficiency testing throughout the staff. This can also be used as evidence of competency because it demonstrates the ability to produce accurate test results. The laboratory POC team will generally review the results and perform root cause analysis for any unacceptable results. Ultimately, this will be reviewed and signed off by the laboratory director.

Inventory management can be challenging in a complex organization with many POCT sites. Inventory may be maintained by the central laboratory and distributed as needed. Alternatively, a lot mortgage may be sequestered by the vendor or distributor to maintain uniformity across all testing sites of an organization. In this situation, individual locations are responsible for ordering their own supplies but may order only what has been approved by the laboratory. The advantage of keeping the entire hospital or medical center on the same lot of reagent is that the lab POC team can perform lot-to-lot studies where appropriate and does not have to worry about remote locations complying with this requirement. This control over inventory also prevents ordering the wrong reagent, strip, or quality control materials.

Maintenance of devices, periodic calibration, and instrument comparisons also must be performed. These tasks are generally performed or at least coordinated by the laboratory POC team because they may require a more in-depth understanding of laboratory processes and coordination with the central laboratory. Once the data for the method comparisons are compiled, the director must review and approve them. The POC team may also maintain a few backup devices that will be available in the event that devices are damaged or require maintenance.

Finally, the POC team and the information technology department are responsible for the appropriate results reporting, implementing and maintaining any middleware products or data repositories, and installing any software upgrades or other technology changes. The POC manager or administrator should make sure that any data in the middleware are reviewed for errors or problems, such as critical high or low values or out-of-range values. If the procedure states that a sample should be sent to the laboratory under these circumstances, the POC manager can verify that this was done. Noncompliant users can be retrained and, if the issue persists, testing privileges revoked. Middleware databases also may track proper patient identification in the case where a wristband is scanned or patient number is entered. Improper use of generic numbers that do not link to a patient can be tracked down and prevented in the future.

CONCLUSIONS

POCT is a rapidly expanding and evolving area of laboratory medicine. With new technologies and tests becoming available on a regular basis, as well as expansion of routine POCT to more locations, it is a constant challenge to maintain a program that delivers accurate results and maintains regulatory compliance. Wireless connectivity and middleware products facilitate order and result transmission, as well as documentation of quality control, testing personnel, and problematic results. Data management is

a constant challenge for POCT programs, including training and competency, quality control, calibrations, and validations. Electronic options for maintaining this information have become a critical component of a POCT program for a large hospital or medical center. Perhaps the most important consideration when implementing a new POC test should be whether the benefit to the patient and/or provider outweighs the cost, including the added expenses related to maintaining testing (personnel, quality control, proficiency testing, etc.). As our health care system focuses more on resource management and test utilization, it will be interesting to see how this impacts POCT.

SELECTED REFERENCES

Appiah LT, Havers F, Gibson J, et al.: Efficacy and acceptability of rapid, point-of-care HIV testing in two clinical settings in Ghana, *AIDS Patient Care STDS* 23:365–369, 2009.
Demonstrates improved patient behavior with immediacy of POCT.

Campbell S, Fedoriw Y: Point-of-care human immunodeficiency virus testing, *Point Care* 8:32–35, 2009.
Reviews sensitivities of POCT HIV assays.

Crocker JB, Lee-Lewandrowski E, Lewandrowski N, et al.: Implementation of point-of-care testing in an ambulatory practice in an academic medical center, *Am J Clin Pathol* 142:64–646, 2014.
Benefits of implementation of POCT in an outpatient setting.

Meier FA, Jones BA: *Q-Probes: point-of-care coagulation testing (99-04)*, College of American Pathologists, 1999, pp 1–15.
Survey of coagulation POCT at 87 sites.

Ryan RJ, Lindsell CJ, Hollander JE, et al.: A multicenter randomized controlled trial comparing central laboratory and point-of-care cardiac marker testing strategies: the disposition impacted by serial point-of-care markers in acute coronary syndromes (DISPO-ACS) trial, *Ann Emerg Med* 53:321–328, 2009.
Analyzes outcomes when POCT is available.

Storrow AB, Lyon JA, Porter MW, et al.: A systematic review of emergency department point-of-care cardiac markers and efficiency measures, *Point Care* 8:121–125, 2009.

Thomas MA: Quality assurance and accreditation in point-of-care testing, *Point Care* 7:227–232, 2008.
Compares CLIA and international standards.

U.S. Food and Drug Administration: *FDA grants first CLIA waiver for nucleic acid–based flu diagnostic test*. http://www.fda.gov/NewsEvents/Newsroom/PressAnnouncements/ucm429127.htm, 2015.
Guidelines for standardization of POCT connectivity and data management.

Zucker ML, Anderson R, POCT09-A, et al.: *Selection criteria for point-of-care testing devices; Approved guideline*, Clinical and Laboratory Standards Institute, 2014.
Guidelines for selecting POCT devices.

Access the complete reference list online at Elsevier eBooks for Practicing Clinicians.

REFERENCES

Agatu CA, Ngetsa CJ, Proce MA, Rinke de Wit TF, Omosa-Manyoni G, Sanders EJ, Graham SM: *PLOS ONE;June* 27, 2019.

Babady NE, Dunn JJ, Madej R: CLIA-waived molecular influenza testing in the emergency department and outpatient settings, *J Clin Virol* 116:44–48, 2019.

Code of Federal Regulation: Title 42: *Part 493—laboratory requirements*, vol. 5. 2011, pp 516–536.

Donato LJ, Myhre NK, Murray MA, et al.: Assessment of test performance and potential for environmental contamination associated with a point-of-care molecular assay for group A *Streptococcus* in an end user setting, *J Clin Microbiol* 57(Issue 2), February 2019.

Dunka L, Allen B, et al.: *POCT01-A2. Point of care connectivity*, vol. 2. Clinical and Laboratory Standards Institute, 2014.

Herskovitz AZ, Chen Y, Latifi N, Ta RM, Kriegel G: False-negative urine human chorionic gonadotropin testing in the clinical laboratory, *Lab Med* XX:1–8, 2019.

Nichols JH, Bartholomew C, Bonzagi A, et al.: Evaluation of the IRMA TRUpoint and i-STAT creatinine assays, *Clin Chim Acta* 377:201–205, 2007.

Sharp G, Young C: Point-of-care viscoelastic assay devices (rotational thromboelastometry and thromboelastography): a primer for surgeons, *ANZ J Surg* 89(4):291–295, 2019.

Wikkelso A, Wetterslez J, Moller AM, Afshari A: Thromboelastography (TEG) or rotational thromboelastogrametry (ROTEM) to monitor haemostatic treatment in bleeding patients: a systematic review with meta-analysis and trial sequential analysis, *Anaesthesia* 72:519–531, 2017.

Wilke P, Masuch A, Fahron O, Zylla S, Leipold T, Petersmann A: Diagnostic performance of point-of-care and central laboratory cardiac troponin assays in an emergency department, *PloS One* 12(11), 2017. November 28.

US Food and Drug Administration: *FDA clears common blood cell count test that offers faster results for patients and providers*, https://www.fda.gov/NewsEvents/Newsroom/PressAnnouncements/ucm583997.htm, 2017.

CHAPTER 8

POSTANALYSIS: MEDICAL DECISION MAKING

Jeffrey S. Jhang, Mark S. Lifshitz

ASSESSMENT OF ANALYTIC CORRECTNESS OF RESULTS, 89
Alarms and Flags, 89
Delta Checks, 90
ASSESSMENT OF CLINICAL SIGNIFICANCE OF RESULTS, 90
Critical Values, 90
Reference Ranges, 90
GENERAL PRINCIPLES FOR THE INTERPRETATION OF LABORATORY RESULTS, 92
Diagnostic Accuracy, 92
Bayes Theorem, 94
Likelihood Ratio, 94
Receiver Operator Characteristic Curves, 95
Positivity Criterion, 96
EVIDENCE-BASED MEDICINE, 97
SYSTEMATIC REVIEWS OF CLINICAL EFFECTIVENESS RESEARCH AND CLINICAL PRACTICE GUIDELINES, 98
Systematic Reviews, 98
Clinical Practice Guidelines, 98
SELECTED REFERENCES, 99

KEY POINTS

- Laboratory results must undergo a two-step postanalytic review for analytic correctness (using delta checks, linearity ranges, etc.) and for clinical significance for the patient (applying critical values, reference ranges, pretest and posttest probability, etc.).
- Reference intervals are most commonly defined as the range of values into which 95% of nondiseased individuals will fall. This definition implies that 5% of nondiseased individuals can have laboratory results outside the reference range.
- The ability of a test to discriminate disease from no disease is described by the sensitivity and specificity of the test. Sensitivity is the probability of a positive result in a person with the disease (true-positive rate). Specificity is the probability of a negative result in a person without disease (true-negative rate).
- Screening tests require high sensitivity so that no case is missed. Confirmatory tests require high specificity to be certain of the diagnosis.
- Altering a test cutoff has a reciprocal effect on sensitivity and specificity. A cutoff can be lowered to include all patients with disease (100% sensitivity), but this reduces the specificity (i.e., increases false-positives).
- Receiver operator characteristic (ROC) curves plot the true-positive rate (sensitivity) versus the false-positive rate (1-specificity) and graphically present the range of sensitivities and specificities at all test cutoffs. If two tests are compared, the more accurate test is closer to the upper-left-hand corner of the ROC curve.
- The likelihood ratio of a test refers to the ratio of the probability of a given test result in the disease state over the probability of the same result in the nondisease state. The likelihood ratio of a test changes as the cutoff value defining disease and nondisease is varied.
- Predictive value describes the probability of disease or no disease for a positive or negative result, respectively. The predictive value of a positive test increases with disease prevalence.
- The Bayes theorem uses information about test characteristics (sensitivity and specificity) and disease prevalence (pretest probability) to obtain the posttest probability of disease given a positive test. Similarly, it can be used to determine the posttest probability of no disease given a negative test.
- Evidence-based medicine is a process by which medical decisions can be made using as many objective tools as possible; it integrates the most current and the best medical evidence with clinical expertise and patient preferences.
- Clinical practice guidelines (CPGs) can be used to decrease practice variability, establish monitoring parameters, improve health, increase safety, and decrease cost.
- Systematic reviews of clinical effectiveness are transparent, scientifically rigorous, and reliable syntheses of literature that evaluate specific medical interventions and are often used to inform groups developing CPGs.

Every time a clinical laboratory produces a test result, the value must undergo a two-step postanalytic evaluation process. The result needs to be assessed for analytic correctness and for clinical significance. It is often assumed that these two tasks can be easily divided between the performing laboratory, which is responsible for determining analytic correctness, and the clinical team, which is responsible for evaluating the clinical meaning of the results. However, significant overlap is seen in the responsibilities for these tasks. Although the laboratory performs most of the review of laboratory results for analytic reliability by using techniques such as delta checks, flagging of questionable results, moving averages, and linear ranges, it is incumbent on the clinician to review every laboratory result with regard to the patient's clinical situation and to question the analytic reliability of implausible results. When evaluating the clinical significance of a laboratory result, one of the most important factors to consider is the reference range. In most settings, the laboratory determines reference ranges, with varying degrees of input from the clinical staff. Postanalytic decision making is therefore a shared responsibility of the laboratory and the clinical staff; it behooves both groups to maintain close communication to optimize every part of the process. The purpose of this chapter is to discuss postanalytic review of laboratory data and its use in medical decision making and to provide tools that can be used to objectively interpret results.

ASSESSMENT OF ANALYTIC CORRECTNESS OF RESULTS

ALARMS AND FLAGS

Modern diagnostic laboratories often analyze large numbers of samples using highly automated instruments. Many results are released into patients' electronic medical records without prior review by a laboratory employee (e.g., autoverification). To prevent the release of erroneous results, most laboratories utilize a variety of "flags" or alarms. Automated analyzers can flag specimens that require additional or repeat testing before results are released (i.e., reported) by specialized middleware (see Chapter 6) or by the laboratory information system. Flags can indicate a problem with the specimen (e.g., the presence of an interfering substance) or an issue with the result (e.g., a numeric value outside the analytic range of the method, or the need for confirmation by an additional assay).

Flags for Problem Specimens

Many automated instruments can measure the amount of sample present in a collection tube and flag samples that contain amounts that are inadequate for a reliable analysis. The laboratory will have to identify another tube containing an adequate sample volume or will request the collection of a new sample. Another frequent cause of inadequate samples is the presence of high concentrations of interfering substances in the specimen, most commonly lipids (lipemia), hemoglobin (Hb; hemolysis), paraproteins (gammopathies), or bilirubin (icterus). The mechanism for this interference is dependent on the substance and the analytic method. For example, in spectrophotometric assays, lipids interfere mainly by increasing light

scatter (turbidity); in assays using ion-specific electrodes for measurement, lipids will affect results by solvent exclusion. A more detailed discussion of interference mechanisms is provided in Chapters 3 and 28. Most commercial assays will list concentrations of interfering substances above which assay results are no longer valid. Visual inspection is often an adequate means of assessing the presence of unacceptable concentrations of interfering substances. A technologist may immediately flag samples that are grossly hemolyzed or icteric as inappropriate for analysis. However, automated analyzers are also able to detect troublesome levels of interfering substances even when they are not apparent to the laboratorian at the macroscopic level. Automated systems can measure the concentrations of bilirubin, lipid, and hemoglobin in samples and can report the degree of interference as an index (Kroll & Elin, 1994; Vermeer et al., 2005). If the index exceeds a given threshold, then the sample is flagged as problematic and should be rejected or rerun after sample treatment to remove the interfering substance. Serum bilirubin and Hb levels have been shown to correlate very closely with interference indices, but because of the chemical heterogeneity of serum lipids, lipemia indices do not correlate as well (Fossati & Prencipe, 1982).

Flags for Specimens That Require Additional Analysis With Another Method

Some laboratory technologies are screening methods used to analyze large numbers of samples, rapidly report results on most samples, and identify potentially abnormal samples that require retesting with a more labor-intensive method. Automated cell counters are the paradigm of such instruments. These instruments can often analyze more than 100 samples per hour in a highly automated fashion; samples that are normal or that show only quantitative abnormalities (e.g., increased or decreased percentage of lymphocytes, low platelet counts, low red cell counts) can be reported immediately, and samples that could potentially contain qualitative abnormalities (e.g., atypical lymphocytes, platelet clumps, red cell fragments) are flagged for preparation of a blood smear and further evaluation. The flags are generally based on forward- and side-scatter and impedance measurements that provide information about size and nuclear complexity/granularity of the cells, and on special stains that help identify the potential presence of immature cells (Fujimoto, 1999). The sensitivities and specificities of these flags show poor discriminatory power; clinical judgment is needed if suspicion of an underlying hematologic abnormality is high (Thalhammer-Scherrer et al., 1997; Kweon et al., 2018).

Flags for Problematic Results

An analyte concentration outside the validated linear range is another common problem affecting samples. Generally, package inserts of commercial assays will provide end users with an estimated range within which an increase in signal is linearly related to an increase in the analyte concentration. The laboratory may validate this range or may establish its own acceptable linear range when the assay is introduced. Analyzers, middleware, or the laboratory information system will identify and flag samples in which the measured analyte values fall outside the linear range. If the analyte falls above the linear range, many instruments can automatically dilute and reanalyze the sample. In some cases, a manual dilution may be necessary, or the information that the result is higher than a certain value may be sufficient for the requesting clinician. For example, patients in diabetic ketoacidosis will have glucose measurements over 1000 mg/dL, far exceeding the linearity of most analyzers. These samples will be flagged, diluted by a predetermined factor, and then rerun before reporting. If an analyte concentration falls below the linear range, the sample is usually reported as "less than the limit of detection."

DELTA CHECKS

Advances in computer technology have facilitated the storage of data from large numbers of patients and increasingly complex calculations in laboratory information systems. This has made it possible to use patient data for quality control purposes in real time. For example, most laboratories routinely submit the results of certain laboratory assays to "delta checks" before releasing them into the patient record. Delta checks are defined as comparing a current laboratory result with results obtained on a previous specimen from the same patient. Parameters chosen for delta checks should not be subject to large intraindividual variations; for example, many laboratories have delta checks in place for the mean corpuscular volume of red cells. Suggested assays, thresholds, and time intervals between measurements can be found in the literature (Ladenson, 1975). Some studies have suggested the comparison of multiple test parameters to decrease the false-positive rate of the delta check; however, few laboratories have implemented such delta checks. Delta checks can detect preanalytic (e.g., mislabeling of specimens) and analytic issues (e.g., aspiration of insufficient sample volume by the instrument sample probe), though the latter are much less common (Schifman, 2017). Laboratories should define procedures for samples that have been flagged by delta checks; protocols usually incorporate repeating the assay, reviewing the specimen identification, and notifying the clinical staff of the possibility of a mislabeled specimen. Refer to Chapter 11 for a more comprehensive discussion of this topic.

ASSESSMENT OF CLINICAL SIGNIFICANCE OF RESULTS

CRITICAL VALUES

A critical value (also known as a *panic value*) is a laboratory result that may represent a life-threatening situation that may not otherwise be readily detectable. It must be reported immediately to a health care provider who can provide necessary medical interventions. Federal law, regulatory agencies, and The Joint Commission require rapid communication of such results; it is one of the most common, recurring Joint Commission Laboratory National Patient Safety Goals (The Joint Commission, 2019). To be sure that results are correctly communicated, regulations require the health care provider to read back the critical value and the patient name. The laboratory then has to document the event, including the name and title of the caregiver who is notified, the time and date of notification, and the read-back by the care provider.

No universally accepted guidelines indicate which assays should have critical values, what the thresholds should be, whether critical values should be repeated before reporting, and what is an acceptable time from result availability to caregiver notification. Although it is generally established that critical values must be called in to a caregiver who has the ability to act on the information, there is no universal agreement regarding the types of caregivers (e.g., physician assistant, registered nurse) who fulfill this definition. This has caused significant variation in procedures related to critical values at different institutions. It is ultimately the responsibility of the medical director of the laboratory to work with clinical colleagues to develop a critical values policy that meets the needs of patients and staff served by the laboratory.

REFERENCE RANGES

Definition of Reference Intervals

Comparison of a laboratory result versus a reference or "normal" range is often one of the most important aspects of medical decision making. Reference intervals are usually defined as the range of values into which 95% of nondiseased ("normal") individuals will fall; the corollary of this definition is that 2.5% of nondiseased individuals will have laboratory results below the reference range, and 2.5% of nondiseased individuals will have laboratory results above the reference range (CLSI, 2008). For some analytes, the reference range is defined as "less than" or "greater than" a certain value. For example, a prostate-specific antigen (PSA) level of 4 ng/mL is often used to distinguish patients who require no further follow-up ("normal") from those who require a prostate biopsy ("abnormal"). Some reference ranges have been defined by professional organizations without adherence to the 95% rule. A paradigm of this is the recommendation of American and European cardiology associations: "An increased cardiac troponin concentration is defined as a value exceeding the 99th percentile of a normal reference population" (upper reference limit [URL]) (Jaffe, 2013). For other analytes (e.g., cholesterol/lipids), laboratories frequently provide therapeutic target ranges that represent recommendations based on clinical trials and/or epidemiologic studies (Grundy et al., 2004). Finally, it is common practice to provide therapeutic and/or toxic ranges for drug measurements.

In the future, the efforts to standardize methods should minimize the effects of site-to-site differences in the implementation of methods. With such standardization, each laboratory would not need to establish its own reference intervals unless its patient population was clearly distinct and exhibited a unique range of values—for example, the protein differences seen in various Asian populations (Myron et al., 2004). The Joint Committee for Traceability in Laboratory Medicine has established a process for standardization by identifying, reviewing against agreed criteria, and publishing list(s) of Higher Order Certified Reference Materials and Reference Measurement Procedures. One effort made by all U.S. manufacturers of in vitro diagnostics is to reduce interlaboratory variability by calibrating and using materials traceable to the isotope dilution mass spectrometry (IDMS) reference measurement procedure (Myers et al., 2006). This allows for comparability of estimated glomerular filtration (eGFR) and calculated creatinine clearance rates across laboratories (Levey et al., 1999).

Factors That Influence Reference Ranges

A variety of factors can influence reference ranges. Different laboratory methods often yield significantly different results and therefore require different reference ranges. This phenomenon is best documented and understood for methods in which measurement of the analyte is based on one or more antibody–antigen interactions, but it can affect all analytic methods. Because of differences in age, genetic background, or exposure to environmental factors, different populations may need different reference ranges for certain laboratory analytes. Many other factors can affect reference ranges, including sample collection container (e.g., glass vs. plastic tubes), sample transport (e.g., by messenger or pneumatic tube), the time between specimen collection and analysis, and sample storage before analysis (Bowen et al., 2005; Victor et al., 2011; Zhao & Lv, 2013).

Determination of Reference Ranges

Because many factors can affect reference ranges, laboratories are strongly encouraged to perform their own studies to establish reference ranges for all analytes they report, usually by testing at least 120 samples from nondiseased individuals in each "partition" (e.g., gender, age group). If this is not possible, the laboratory can verify a reference interval that it has previously established for a different method by transference (i.e., demonstrating that the new method yields identical results to the previous method). The laboratory can verify another laboratory's or the manufacturer's reference interval if the analyte was not previously tested for in the laboratory (CLSI, 2008).

Variability of Laboratory Results

Interindividual variation of laboratory results often occurs because of factors specific to individual patients. For example, creatine kinase (CK) levels are proportional to muscle mass. Thus, a population of normal subjects will express a range of CK values according to each individual's muscle mass, but an individual patient will have a unique set value that is "normal" for that individual. In clinical practice, this unique value, if known, is the best reference value for a particular individual. Comparison of test results from a patient versus such an individualized reference value has to take into account random variability. Random variability is the sum of analytic and intraindividual variability. Analytic variability is the result of assay imprecision. It is usually determined during validation studies for a new method by running the same sample multiple times and is expressed quantitatively as the coefficient of variation (CV), as discussed in Chapter 11. Intraindividual variability is due to biologic changes that cause analyte levels to fluctuate over time. Well-known examples of this phenomenon include diurnal variations in cortisol levels, estrogen levels that vary with the menstrual cycle, and seasonal variations of vitamin D. Many other analytes show some biologic variability, including changes related to exercise or food intake. Table 8.1 provides

TABLE 8.1

Interindividual and Intraindividual Biologic Variability for Common Analytes

Analyte Individual	Interindividual CV, %	Intraindividual CV, %	Index of CV, %	Method
Alanine aminotransferase	50.2	23.7	0.47	3.2
Albumin	8.9	2.8	0.31	3.4
Alkaline phosphatase	33.4	4.4	0.13	6.5
Apolipoprotein A	17.8	7.0	0.39	4.8
Apolipoprotein B	27.6	9.5	0.34	2.7
Aspartate aminotransferase	29.1	15.1	0.52	3.4
β-Carotene	67.4	24.2	0.36	7.4
Bicarbonate	13.3	11.0	0.83	2.4
Bilirubin, total	43.9	24.6	0.56	3.0
C-peptide	65.7	28.4	0.43	7.2
Calcium, ionized	3.6	2.4	0.67	1.4
Calcium, total	4.7	3.3	0.70	2.2
Chloride	3.1	1.9	0.61	1.0
Cholesterol, total	22.3	8.2	0.37	2.3
Creatinine	18.7	6.8	0.36	1.0
Creatinine, urine	61.3	43.0	0.70	2.2
Fibrinogen, plasma	25.6	16.2	0.63	3.9
Folate	64.3	22.6	0.35	3.6
γ-Glutamyl transferase	59.8	16.2	0.27	1.7
Glucose, plasma	12.5	8.3	0.66	1.7
Glycohemoglobin, blood	9.6	1.5	0.16	3.1
HDL cholesterol	28.3	12.4	0.44	2.5
Homocysteine	36.6	18.0	0.49	6.0
Insulin, plasma	55.9	25.2	0.45	13.0
Iron	41.6	29.0	0.70	3.2
Iron binding capacity, total	15.5	6.9	0.45	3.3
Lactate dehydrogenase	21.6	7.9	0.37	6.0
Phosphorus	15.8	9.2	0.58	2.0
Potassium	7.7	5.4	0.70	0.5
Protein, total	6.2	3.5	0.56	0.9
Selenium	13.2	5.1	0.39	4.8
Sodium	1.6	1.3	0.81	0.7
Triglycerides	56.8	28.8	0.51	4.7
Urea nitrogen	32.1	18.0	0.56	3.7
Uric acid	27.1	9.0	0.33	0.7
Varicella antibody	43.2	13.7	0.32	6.7
Vitamin A	30.7	9.5	0.31	2.5
Vitamin B_{12}	41.6	13.4	0.32	6.2
Vitamin E	35.1	11.3	0.32	2.9

Data from Lacher DA, Hughes JP, Carroll MD: Estimate of biologic variation of laboratory analytes based on the Third National Health and Nutrition Examination Survey, *Clin Chem* 51(2):450–452, 2005.
CV, Coefficient of variation; *HDL,* high-density lipoprotein.

TABLE 8.2
Clinically Significant Difference Between Two Consecutive Patient Results

Analyte	Change
Total T_4	2.2 μg/dL
Free T_4	0.5 ng/dL
Total T_3	35 ng/dL
Free T_3	0.1 ng/dL
TSH	0.75 mIU/L
Thyroglobulin	1.5 ng/mL

Data from Baloch Z, Carayon P, Conte-Devolx B, et al.: Laboratory medicine practice guidelines: laboratory support for the diagnosis and monitoring of thyroid disease, *Thyroid* 13(1):3–126, 2003.
T_3, Triiodothyronine; *T_4,* thyroxine; *TSH,* thyroid-stimulating hormone.

estimates of interindividual and intraindividual biologic variation for common analytes. As expected, intraindividual variation is generally less than interindividual variation. The index of individuality is the ratio of intraindividual CV to interindividual CV. A low index (<0.6) means that results from a given individual fluctuate within a narrow range of the reference interval. In such instances, serial changes in an individual's analyte may be more useful in detecting disease than in comparing each of the measurements to the reference interval (Lacher et al., 2005). Table 8.1 also shows that the method CV or degree of analytic variability is usually much lower than the biologic variability and thus is much less of a factor in affecting the overall random variability of measurements. For some analytes, guidelines have been published as to what constitutes a clinically significant difference between two consecutive patient sample results. As an example, Table 8.2 provides this information for various thyroid function tests (Baloch et al., 2003).

GENERAL PRINCIPLES FOR THE INTERPRETATION OF LABORATORY RESULTS

DIAGNOSTIC ACCURACY

Truth Table

Clinicians often find it helpful and intuitive to dichotomize a continuous test result into a binary one by applying a threshold value for the analyte. Although the reference range can be used to separate normal from abnormal values, clinically validated thresholds are also commonly used for disease classification. For example, the reference range for hemoglobin A1c (HbA1c) in a laboratory may be 4.0% to 6.0%, but the clinically established threshold to classify a patient as diabetic is 6.5%. This means that a patient's result can be outside the reference range without meeting the threshold for diabetes.

A test with perfect diagnostic accuracy could determine the presence or absence of disease with certainty, and the established cutoff point would perfectly separate diseased from nondiseased populations (Galen & Gambino, 1975) (Fig. 8.1). However, nearly all laboratory tests are imperfect, and overlap is seen between populations at both low and high cutoffs (Fig. 8.2). In both figures, there are two cutoffs: the leftmost is for low values of a marker analyte that signify disease (e.g., low albumin in the diagnosis of liver failure) and the rightmost cutoff is for elevated values of a marker analyte that signify disease (e.g., elevated troponin in the diagnosis of myocardial infarction).

The diagnostic accuracy of a test is determined by comparing its ability to discern true disease from nondisease as determined by a diagnostic gold standard (i.e., truth). Based on results from the test and the gold standard, patients can be classified into four groups in a 2 × 2 table (see Fig. 8.2 and Table 8.3). Patients correctly classified as abnormal are called true-positives (TPs) and those correctly classified as normal are called true-negatives (TNs). These true results are the nonoverlapping areas of the two patient distributions. False results occur because the two populations overlap (i.e., because a test cannot completely discriminate all abnormal patients from normal ones). Patients incorrectly classified as normal are false-negatives (FNs), and those incorrectly classified as abnormal are false-positives (FPs). As seen in Figure 8.3—where, for ease of illustration, a single cutoff is used to discriminate disease from normal populations—varying the cutoff changes the numbers of true and false results in a given population. False results can also be produced when an analyte has two relevant cutoffs (e.g., thyroid-stimulating hormone), with overlapping populations at both the low end and the high end.

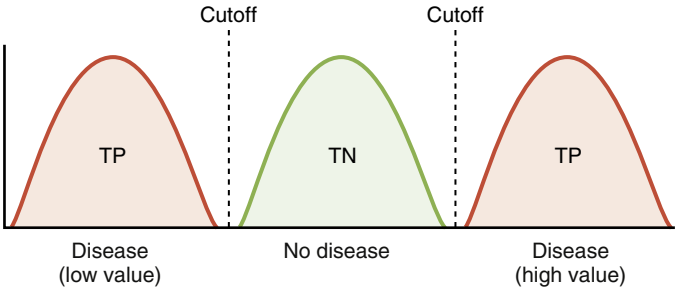

Figure 8.1 Distribution of test results from nonoverlapping populations of patients with and without disease (see Table 8.3). *TN,* True-negative; *TP,* true-positive.

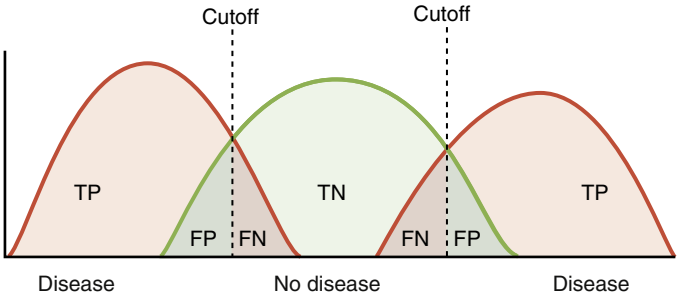

Figure 8.2 Distribution of test results from overlapping populations of patients with and without disease (see Table 8.3). *FN,* False-negative; *FP,* false-positive; *TN,* true-negative; *TP,* true-positive.

TABLE 8.3
Truth (2 × 2) Table: Classifying Patients

Result	Disease	No Disease	Total
Positive	TP	FP	TP + FP
Negative	FN	TN	FN + TN
Total	TP + FN	FP + TN	TP + FP + FN + TN

$$\text{Sensitivity \%} = 100 \times \left(\frac{TP}{TP + FN}\right)$$

$$\text{Specificity (\%)} = 100 \times \left(\frac{TN}{TN + FP}\right)$$

$$\text{Positive predictive value (\%)} = 100 \times \left(\frac{TP}{TP + FP}\right)$$

$$\text{Negative predictive value (\%)} = 100 \times \left(\frac{TN}{TN + FN}\right)$$

FN, False-negative; *FP,* false-positive; *TN,* true-negative; *TP,* true-positive.

Sensitivity and Specificity

Sensitivity and specificity are measures of the diagnostic accuracy of a test; they are indicators of a test's ability to distinguish between disease and absence of disease at a chosen cutoff. Sensitivity and specificity therefore are not fixed characteristics of a test and must be calculated from a different 2 × 2 table for each cutoff chosen.

Sensitivity is the ability of a test to detect disease and is expressed as the proportion of persons with disease in whom the test is positive (see Tables 8.3 and 8.4). It may also be thought of as the probability of a positive test given a true disease state as defined by the gold standard. A test that is 90% sensitive will give positive results in 90% of diseased patients (TP) and negative results in 10% of diseased patients (FN). Specificity is the ability to detect the absence of disease and is expressed as the proportion of persons without disease in whom the test is negative (see Tables 8.3 and 8.4). It may be thought of as the probability of a negative test, given no disease as defined by the gold standard. Thus, a test that is 90% specific will give negative results in 90% of patients without disease (TN) and positive results in 10% of patients without disease (FP). A test with a higher sensitivity identifies a greater proportion of persons with disease, and a test with a higher specificity excludes a greater proportion of persons without disease.

Sensitivity is also the TP rate, and the inverse (1 – sensitivity) is the FN rate. If the sensitivity is 95%, 5 of 100 individuals with the disease will test

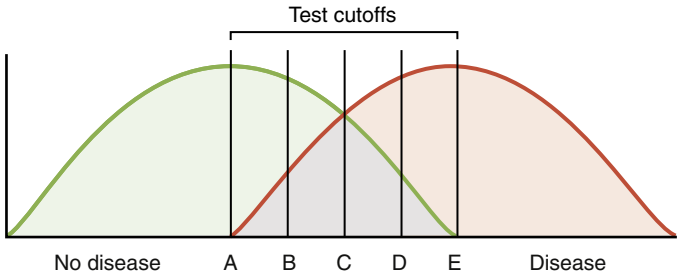

Figure 8.3 Effects of varying the test cutoff on overlapping populations of patients with and without disease.

TABLE 8.4

Example Truth (2 × 2) Table

Result	Disease	No Disease	Total
Positive	196	20	216
Negative	4	180	184
Total	200	200	400

$$\text{Sensitivity \%} = 100 \times \left(\frac{196}{196+4}\right) = 98\%$$

$$\text{Specificity (\%)} = 100 \times \left(\frac{180}{180+20}\right) = 90\%$$

$$\text{Positive predictive value (\%)} = 100 \times \left(\frac{196}{196+20}\right) = 91\%$$

$$\text{Negative predictive value (\%)} = 100 \times \left(\frac{180}{180+4}\right) = 98\%$$

In this evaluation study of a hypothetical cardiac marker, 200 patients with acute myocardial infarction (AMI) and 200 healthy subjects are recruited for a study designed to mimic a prevalence of 50%. The assay is performed and is compared with a gold standard test for AMI, and the 2 × 2 truth table shown here is generated. Measures of diagnostic accuracy are determined according to the formulas outlined in Table 8.3.

negative. Specificity is the TN rate, and the inverse (1 – specificity) is the FP rate. If the specificity is 95%, 5 of 100 individuals without disease will test positive.

Effect of Altering the Test Cutoff

When a test cutoff is altered, an inverse relationship between sensitivity and specificity is noted, and a trade-off between the numbers of FP and FN results can be seen. Altering a cutoff changes a test's sensitivity and specificity because it relates to overlapping normal and abnormal patient distributions along the test value continuum (see Fig. 8.3). For tests in which high values indicate disease, lowering the cutoff (i.e., moving the cutoff line to the left) will lead to more diseased patients being classified as abnormal. Thus, in Figure 8.3, changing the cutoff from C to B increases sensitivity. If the cutoff is moved to A, then all diseased persons will have a positive test, and the sensitivity will be 100%. However, increased sensitivity is associated with decreased specificity, and the number of nondiseased persons with a positive test (FPs) increases as the cutoff is moved from C to B to A. If the cutoff is raised (i.e., the cutoff line is moved to the right), more nondiseased patients are classified correctly, and specificity increases. If the cutoff is moved to E, then all nondiseased persons will have a negative test, and the specificity will be 100%. However, this will be accompanied by concomitant decreased sensitivity and additional FN results.

The Need for High Sensitivity Versus High Specificity

FP and FN results can lead to misdiagnosis and inappropriate clinical management with adverse clinical and financial consequences. For example, an FP result may cause the unnecessary admission of a patient, needless additional testing, and invasive procedures. Similarly, an FN result may lead to a patient's release from the emergency department despite a life-threatening disorder. Enhanced assays that provide improved sensitivity and specificity—thereby allowing better discrimination between diseased and nondiseased populations—continue to be developed. However, it is nearly impossible to eliminate false results entirely because some overlap between diseased and nondiseased persons is always evident. In most situations, the cost of an FP or an FN result supersedes the other, and the cutoff that delineates normal from abnormal can be shifted to reduce the more significant of the two consequences.

In general, the sensitivity of a test used to screen a population for a serious disease should be high to capture the majority of cases for confirmation by a gold standard. When PSA is used to screen for prostate cancer, a low threshold is used to capture all potential cases. Many men without a malignancy (e.g., prostatitis, nodular hyperplasia) will also have a positive result and need to undergo an invasive procedure for a definitive diagnosis. These "unnecessary" prostate biopsies, which are performed to confirm the true cases of prostate cancer, are the FP cost of this sensitive, but not specific, screening test. In contrast, high specificity is required when the definitive diagnosis of a serious condition will be based on a positive result; initiation of toxic or costly therapy can be based only on a test with the ability to "rule in" the disease with high confidence. A highly specific test excludes persons without disease (eliminates FPs). In a test for which higher values indicate disease, specificity can be increased by increasing the cutoff, thereby excluding all persons without the disease. However, this will also exclude some persons with the disease (see Fig. 8.3).

Less expensive and less labor-intensive screening procedures with high sensitivity are often used in combination with more complex, highly specific tests for confirmation. For example, an immunoassay is used as an initial test to screen for drugs of abuse and may cross-react with substances other than the analyte of interest, thereby producing an FP result. These FP individuals can be identified with a highly specific, albeit expensive, follow-up test, such as gas chromatography/mass spectrometry (GC/MS). In many combinations of screening and confirmatory tests, the confirmatory test is both highly specific and highly sensitive, but it is inappropriate to use as a screening test because of cost or test complexity.

Predictive Value and Prevalence of Disease

The predictive value of a positive test (sometimes referred to as positive predictive value) may be understood as the probability that a positive test indicates disease. It is the proportion of persons with a positive test who truly have the disease (see Tables 8.3 and 8.4). The predictive value of a negative test (sometimes referred to as negative predictive value) is the probability that a negative test indicates absence of disease. It is the proportion of persons with a negative test who are truly without disease (see Tables 8.3 and 8.4).

The diagnostic accuracy of a test tends to diminish as the test becomes more widely used in a population. Initial validation studies are often performed on a small group of individuals in whom disease is clearly absent or present. Those who lack the disease are often selected from a population of subjects in overall good health. In practice, however, patients exhibit a spectrum of illness, including early or mild disease, which overlaps with nondiseased individuals, including those with other diseases, some cases of which might cause an abnormal test result. Thus, the proportion of false test results is often higher in clinical practice than is claimed by the manufacturer from more limited studies in healthy individuals.

The predictive value of a positive test is highly dependent on the prevalence of the disease being tested. The higher the prevalence, or pretest probability, the higher the posttest probability, or predictive value of a positive test. Consider a test with a sensitivity of 90% and a specificity of 90% for a disease with a prevalence of 0.1%. Based on the formula, the predictive value of a positive result (PV+) would be 0.9%. If the prevalence increases to 5.0%, the PV+ increases to 32%. Thus, the predictive value of a positive test increases as the prevalence increases. This effect of prevalence on predictive value is shown in Tables 8.5 and 8.6.

The impact of prevalence on predictive value theory has a practical application in that it enables one to derive a higher predictive value from results of a test performed in a high-prevalence setting as compared with a low-prevalence setting (see Table 8.6). For example, consider the serum antiheparin/platelet factor (PF4) immunoassay for suspected heparin-induced thrombocytopenia (HIT). The positive predictive value of antiheparin/PF4 antibodies in a patient suspected of HIT is 40%, and the negative predictive value is 100% (Bakchoul et al., 2009). However, if a clinical scoring system were used to stratify patients based on several clinical criteria (e.g., thrombocytopenia, time course of thrombocytopenia, thrombosis), then the positive predictive value would be higher if testing were performed only on patients with a high probability of HIT using the clinical scoring system. We can also examine this situation from a pretest probability point of view. The clinical suspicion of HIT, or the pretest probability, is significantly higher when the clinical score is high. Because pretest probability determines posttest probability, the stronger pretest suspicion translates into stronger prediction of disease (see the Bayes theorem discussed later).

TABLE 8.5

Positive Predictive Value Decreases With Decreasing Disease Prevalence

Result	Disease	No Disease	Total
Positive	49	95	144
Negative	1	855	856
Total	50	950	1000

$$\text{Positive predictive value (\%)} = 100 \times \left(\frac{49}{49+95}\right) = 34\%$$

$$\text{Negative predictive value (\%)} = 100 \times \left(\frac{855}{855+1}\right) = 100\%$$

In this study, a population of 1000 hospitalized patients is studied. Of the patients, 50 are determined to have an acute myocardial infarction (AMI) and 950 patients do not have an AMI according to a gold standard (prevalence = 5%). If the cardiac marker described in Table 8.4 is performed on this population, we would expect a TP rate of 49 (50 AMI patients × sensitivity = 50 × 0.98) and an FN rate of 1 (FN = total AMI – TP = 49 – 1); a TN rate of 855 (950 non-AMI × specificity = 950 × 0.90) and an FP rate of 95 (total non-AMI – TN = 950 – 855). The positive predictive value of the test decreases with a lower prevalence.
FN, False-negative; *FP,* false-positive; *TN,* true-negative, *TP,* true-positive.

TABLE 8.6

Predictive Value of a Positive Test: Effect of Prevalence and Accuracy

	PREDICTIVE VALUE OF A POSITIVE TEST	
Prevalence, %	**Sensitivity, 90% Specificity, 90%**	**Sensitivity, 99% Specificity, 99%**
0.01	0.09	0.9
0.1	0.9	9
5	32.1	83.9
50	90.0	99

For a disease with low prevalence, even a test with high sensitivity and specificity will yield a low predictive value because most positive test results will be FPs. For example, consider a disease with a prevalence of 1 in 10,000 and a test that is 99% sensitive and 99% specific. The PV+ will be only about 1% because 99 of every 100 who test positive have a FP result. One can see that the accuracy of tests for rare conditions must be very high to reliably predict disease. Thus, besides requiring near perfect sensitivity, tests that are used to screen for rare diseases have greater utility in selected populations that offer a higher pretest probability.

On the other hand, the predictive value of a negative test decreases as the prevalence of disease increases. However, the effect is small, especially when sensitivity and specificity are high. Prevalence influences the predictive value of a negative test to a noticeable extent only when the starting prevalence is high.

Predictive Value and Accuracy

Improved accuracy (i.e., sensitivity and specificity) enhances the predictive value of a test. The formula for predictive value (see Table 8.3) from the Bayes theorem shows that sensitivity and specificity influence the predictive value. Further, Table 8.6 shows that the predictive value of a positive test increases with increasing prevalence and improved accuracy. Specificity has the biggest impact on the predictive value of a positive test, whereas sensitivity determines the predictive value of a negative test. This is also appreciated from Table 8.5, in which the number of FPs directly influences the predictive value of a positive test, whereas the number of FNs has the same effect on a negative test.

When a test cutoff changes, its accuracy (sensitivity/specificity) and predictive value also change. As an example, D-dimer testing is used to exclude deep vein thrombosis in patients who present to the emergency department. In the reference population, a value greater than 400 U/mL is considered abnormal and indicative of thrombosis. For a patient in the emergency department with symptoms suggestive of thrombosis, an even lower D-dimer value will predict thrombosis to the same extent as the greater than 400 U/mL value in the general population. (Recall that posttest probability is dependent on pretest probability.) Because a cutoff of 400 U/mL is not 100% sensitive, it excludes some patients with thrombosis, thereby yielding FNs. Because one cannot risk neglecting a possible case of thrombosis, a lower value of 200 U/mL could be selected to improve sensitivity, decrease the proportion of FNs, and greatly improve the predictive value of a negative test. A negative test could then be used to exclude thrombosis and obviate the need for additional costly diagnostic studies, such as radiologic scans or lower extremity Doppler.

BAYES THEOREM

Clinical assessment and diagnostic tests are inherently flawed; these uncertainties must be considered when medical decisions are made. Sensitivity and specificity represent a summary of the diagnostic accuracy of a test, but they do not indicate the probability that an individual patient has a disease after the test result is obtained. It would be useful to know how the test result changes the probability of disease (i.e., posttest probability), given certain assay characteristics and disease prevalence (i.e., pretest probability). Alternatively, it is useful to know that a condition can be ruled out given a negative test if the probability of disease after a negative test is very low. To determine this information, one must consider predictive value theory, also known as the Bayes theorem. The Bayes theorem describes the relationship between posttest and pretest probability of disease or no disease based on the sensitivity and specificity of the test. $P(D)$ is the probability of disease before the test result is obtained; this is also known as clinical suspicion, prevalence, or pretest probability. $P(D|T)$ is the probability of the disease after the test result is known; this is the posttest probability. $P(D|T)$ is the probability that the test is positive when the disease is present, or the TP rate. $P(\overline{D})$ is the probability of not having the disease. $P(T|\overline{D})$ is the FP rate. The probability (posttest) of disease or no disease is calculated; examples are shown in Table 8.7.

$$P(D|T) = \frac{P(T|D) \times P(D)}{P(T|D) \times P(D) + P(T|\overline{D}) \times P(\overline{D})}$$

$$\text{Posttest probability} = \frac{\text{sensitivity} \times \text{pretest probability}}{(\text{sensitivity} \times \text{pretest probability}) + (\text{FP} \times [1 - \text{pretest probability}])}$$

The theorem applies population data and test characteristics directly to an individual subject and calculates the probability of the presence of a disease for a particular patient after a positive test result is obtained and, alternatively, the probability of the absence of disease given a negative test. Although sensitivity and specificity describe a test at a particular cutoff value (e.g., what percent of diseased patients have abnormal results?), the predictive value describes the state of the patient (e.g., how likely is it that a given patient's positive result indicates disease?). The predictive value depends on sensitivity, specificity, and prevalence of the disease being tested. Table 8.6 illustrates how disease prevalence, test accuracy, and predictive value of a test are interrelated (Bayes theorem).

This approach requires information about the individual patient and clinical suspicion of disease, which includes prevalence of the disease in different populations, to establish the pretest probability of a patient having a disease. For example, if nothing is known about a patient other than the test result, then the pretest probability of disease would be the prevalence of the disease in the population. Clinical suspicion may raise this pretest probability to 50% based on a thorough clinical history and physical examination, the clinician's personal experience, and knowledge of relevant literature. Pretest probability, or a priori probability, is the prevalence of disease in the patient's clinical setting. For example, the prevalence of myocardial damage among subjects with chest pain is higher in the cardiac care unit than it is in the emergency department.

The pretest probability is used in conjunction with the characteristics of diagnostic accuracy as summarized in the sensitivity and specificity of the test. Posttest probability, or a posteriori probability, is the probability of disease in the posttest situation and is commonly referred to as the predictive value of the test. As described earlier, pretest probability and posttest probability are related through the Bayes theorem (see Table 8.7). Additionally, posttest probability = posttest odds/(posttest odds + 1). The value of posttest odds is equal to the pretest probability × the likelihood ratio (LR). The LR is used to change the probability based on test characteristics, as described in the next section.

LIKELIHOOD RATIO

The LR is a convenient measure that combines sensitivity and specificity into a single number (Table 8.8). Similar to these other measures of test accuracy (sensitivity and specificity), the LR is an assessment of test performance, and not of disease status, in the patient being tested. The

TABLE 8.7

Posttest Probability (Predictive Value) from Bayes Theorem

Posttest probability of disease (predictive value) depends on diagnostic accuracy and disease prevalence. A test for rheumatoid factor is positive in 95 of 100 patients with rheumatoid arthritis (RA; sensitivity of 95%), but it is also positive in 10 of 100 non-RA patients (specificity of 90%). The RA pretest probability (prevalence) is 5% in a rheumatology practice.

$$\text{Posttest probability} = \frac{\text{sensitivity} \times \text{pretest probability}}{(\text{sensitivity} \times \text{pretest probability}) + ([1 - \text{specificity}] \times [1 - \text{pretest probability}])}$$

$$\text{Posttest probability} = \frac{0.95 \times 0.05}{(0.95 \times 0.05) + (0.1 \times 0.95)} = 33\%$$

Posttest probability of no disease for the same test characteristics

$$\text{Posttest probability} = \frac{(1 - \text{pretest probability}) \times \text{specificity}}{([1 - \text{pretest probability}] \times \text{specificity}) + ([1 - \text{sensitivity}] \times [1 - \text{pretest probability}])}$$

$$\text{Posttest probability} = \frac{0.95 \times 0.9}{(0.95 \times 0.9) + (0.05 \times 0.05)} = 99.7\%$$

TABLE 8.8

Likelihood Ratio

Definition

$$\text{LR} = \frac{\text{probability of test result in persons with disease}}{\text{probability of same result in persons with no disease}}$$

Example

$$\text{LR}+ = \frac{\text{sensitivity}}{1 - \text{specificity}}$$

From Table 8.7, using the test for rheumatoid factor (RF) that is positive in 95 of 100 rheumatoid arthritis (RA) patients (sensitivity of 95%) but also positive in 10 of 100 non-RA patients (specificity of 90%)

$$\text{LR}+ = \frac{\frac{95}{100}}{\frac{10}{100}} = 9.5$$

$$\text{LR}- = \frac{1 - \text{sensitivity}}{\text{specificity}}$$

The same test for RF is negative in 90 of 100 non-RA patients but is also negative in 5 of 100 RA patients.

$$\text{LR}- = \frac{\left(\frac{5}{100}\right)}{\left(\frac{90}{100}\right)} = 0.06$$

TABLE 8.9

Likelihood Ratio and Probability of Disease

The likelihood ratio (LR) and pretest probability (prevalence) can be used to calculate posttest probability (predictive value). This is best understood by expressing probability in terms of odds.

Definitions

$$\text{Pretest odds} = \frac{\text{pretest probability}}{1 - \text{pretest probability}}$$

Step 1. Pretest probability is converted to pretest odds to calculate posttest odds of disease or no disease (see examples).

$$\text{Posttest odds} = \text{pretest odds} \times \text{LR}$$

Step 2. Posttest odds are calculated. Note: As the LR of a positive or negative result increases, so do the odds that the result will predict disease or no disease, respectively.

$$\text{Posttest probability} = \frac{\text{posttest odds}}{(1 + \text{posttest odds})}$$

Step 3. Odds are converted back into probability to calculate the posttest probability (predictive value) of a positive or negative test.

Example 1

From Table 8.7, the rheumatoid arthritis pretest probability (prevalence) is 5% in a rheumatology practice. From Table 8.8, the LR of a positive rheumatoid factor test is 9.5. Note that the probability of disease increases from 5% (pretest) to 33% (posttest) because of the positive test result.

$$\text{Pretest odds} = \frac{\text{pretest probability}}{1 - \text{pretest probability}} = \frac{0.05}{1 - 0.05} = 0.053$$

$$\text{Posttest odds} = \text{pretest odds} \times \text{LR}+ = 0.053 \times 9.5 = 0.5$$

$$\text{Posttest probability} = \frac{\text{posttest odds}}{(1 + \text{posttest odds})} = \frac{0.5}{(1 + 0.5)} = 0.33 \text{ or } 33\%$$

Example 2

From Table 8.8, the LR of a negative rheumatoid factor test is 0.06. Although the probability of disease increases from 5% (pretest) to 33% (posttest) because of the positive test result (Example 1), the probability of disease decreases from 5% (pretest) to 0.3% (posttest) because of the negative test result.

$$\text{Pretest odds} = \frac{\text{pretest probability}}{1 - \text{pretest probability}} = \frac{0.05}{1 - 0.05} = 0.053$$

$$\text{Posttest odds} = \text{pretest odds} \times \text{LR}+ = 0.053 \times 0.06 = 0.003$$

$$\text{Posttest probability} = \frac{\text{posttest odds}}{(1 + \text{posttest odds})} = \frac{0.003}{1 + 0.003} = 0.3\%$$

LR of a positive test (LR+) is the ratio of two probabilities: the probability of a positive test result when disease is present (TP) divided by the probability of the same test result when disease is absent (FP). In other words, the calculation gives the likelihood that a test result will occur in a diseased patient as opposed to a healthy one. For example, serum lipase is used to detect acute pancreatitis; it may be elevated (higher than the cutoff of 200 U/L) in 90 of 100 individuals with acute pancreatitis, but it may be similarly elevated in 10 of 100 individuals with other causes of abdominal pain. The LR+ at the 200 U/L cutoff is 9, which means that an abnormal lipase is nine times more likely in individuals with pancreatitis than in those without, or nine times as many patients with pancreatitis than with other abdominal diseases will have an elevated lipase. The LR refers to the likelihood of the test result, given the disease. This is not the same as the likelihood of pancreatitis being nine times greater, given an abnormal lipase. The latter would be the predictive value of a positive lipase. Alternatively, the LR of a negative test (LR–) is the probability that an individual with the disease will have a negative test divided by the probability that an individual without the disease will have a negative test. Additional advantages of the LR are that it is not influenced by disease prevalence, and the LR can be calculated for multiple test cutoffs. Thus, a result's degree of abnormality can be taken into account, and medical decisions can be made at a point where fewer FN and FP results are seen.

The LR may also be used, along with pretest probability (prevalence), to calculate posttest probability (predictive value). Although the concept is similar to the Bayes theorem, the LR is used to calculate posterior probabilities in terms of odds and not direct probabilities, making it less intuitive than the Bayes method. This is illustrated in the examples in Table 8.9. For a positive test, an LR+ higher than 1 will increase the posttest probability. The larger the LR, the greater the difference between pretest and posttest probabilities. Regardless of prevalence, a high LR increases the probability that a positive test result predicts disease. The converse applies for a negative test result, for which any LR– less than 1 will decrease the posttest probability. Thus, tests likely to be useful in clinical practice are those for which a positive result has a high LR and a negative result has a low LR.

RECEIVER OPERATOR CHARACTERISTIC CURVES

Because diagnostic tests are not perfect, there is always a trade-off between sensitivity and specificity, making it difficult to determine an optimal cutoff. The receiver operator characteristic (ROC) curve is a useful tool for identifying the optimal cutoff for a diagnostic test by calculating the sensitivity and specificity combinations across the entire range of cutoff values. In addition, the ROC curves of two or more tests can be compared to identify the one with the greatest discriminating ability (Zweig & Campbell, 1993).

An ROC curve is constructed by calculating sensitivity and specificity across the entire range of cutoffs for the diagnostic test being evaluated. Sensitivity is plotted on the *y*-axis, and 1– specificity (or the FP rate) is plotted on the *x*-axis; construction of the curve shows the trade-off between sensitivity and specificity at each cutoff. The ROC curve for a test with no ability to predict disease (i.e., random chance) is a 45-degree line drawn

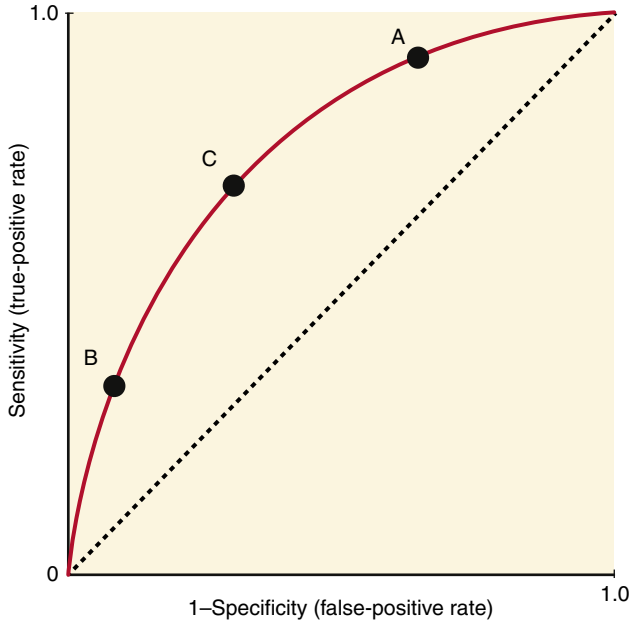

Figure 8.4 Receiver operator characteristic curve: effect of varying the cutoff value for separating disease from no disease (also see Fig. 8.3).

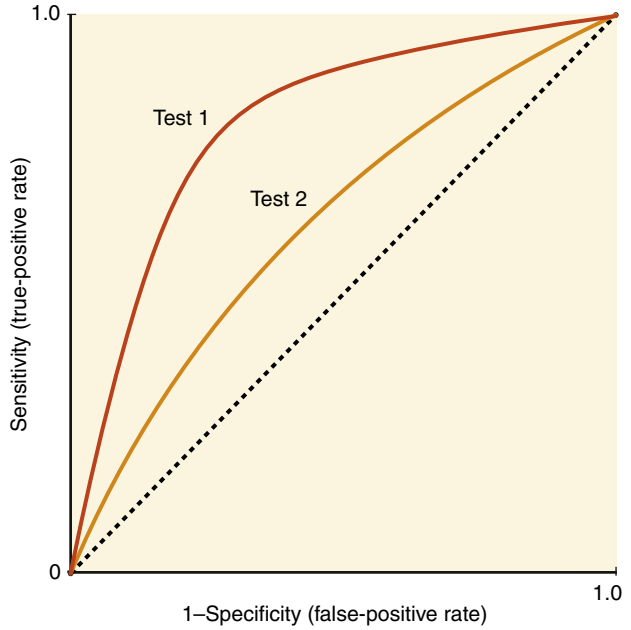

Figure 8.5 Receiver operator characteristic curves for two tests. Note that Test 1 is always superior to Test 2 because it has higher sensitivity than Test 2 (i.e., it is always above and to the left of Test 2).

through the origin. As the discriminatory ability of a test increases, the curve progresses outward toward the upper-left-hand corner. The area under the ROC curve (AUC) is a single measure of the overall discriminating ability of a test. The minimum AUC is 0.5, which is the area under the 45-degree line, and the maximum AUC is 1.0 for a perfect diagnostic test. Because diagnostic tests are not absolutely perfect, the AUC will range from 0.5 to 1.0; the higher the AUC, the greater the overall discriminating ability of the test. In general, an AUC that is greater than 0.8 suggests that the diagnostic test has good discriminatory power.

Point A on the ROC curve in Figure 8.4 has the highest sensitivity but has low specificity. Increasing the specificity to point B trades the higher specificity for lower sensitivity. The optimal cutoff is identified by the coordinate that maximizes discriminatory power, which, in this example, is point C. Point C is also the location on the ROC curve with the farthest distance perpendicular from the 45-degree line. The second useful application for the ROC curve is to compare two or more diagnostic methods by calculating the AUC. If the AUC is similar, then no difference is observed between the two tests. However, if one ROC curve has a greater AUC than a comparison test, it has better sensitivity and specificity at all cutoffs. For example, in Figure 8.5, Test 1 is better than Test 2 at all cutoffs and therefore would be the better test. However, curves may cross, indicating that performance depends on the desired use of the test (i.e., whether a higher sensitivity or specificity is required for clinical use). In the example in Figure 8.6, Test B has a lower FP rate than Test A at high sensitivity, which makes it a better screening test; Test A would be the better confirmatory test because it has greater sensitivity at high specificities.

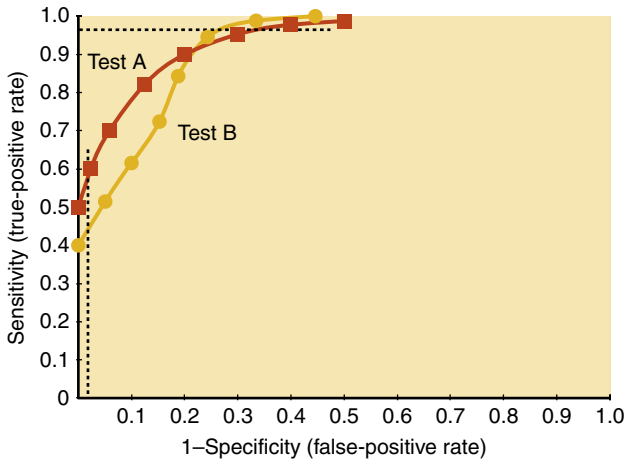

Figure 8.6 Receiver operator characteristic curves for two tests. Note that the curves cross. See text for interpretation.

POSITIVITY CRITERION

The LR may be used to select the optimal cutoff for an assay that best separates disease from nondisease. As was previously discussed, the LR, like sensitivity and specificity, varies with the cutoff. To select the optimal discriminatory cutoff, one might simply pick the cutoff resulting in the greatest LR for a positive test. However, this approach does not take into account the clinical impact of the test result. The clinical consequences of an FP test (e.g., unnecessary surgery) or an FN test (e.g., a missed chance to treat) need to be weighed when the optimal cutoff is determined. The *positivity criterion* is a method that allows one to assess the optimal cutoff with numeric estimates for clinical impact, or consequences, of test results.

In determining which cutoff will serve as the positivity criterion, a finite list of possible cutoffs is generated, and an LR for a positive test is calculated for each cutoff value. Next, the consequences of each of the four possible testing outcomes (TP, TN, FP, and FN) are assigned numeric estimates with respect to some outcome (e.g., morbidity, mortality, cost). For example, the clinical consequence of missing propionic acidemia on newborn screening by tandem mass spectroscopy is an increased risk of metabolic decompensation before diagnosis, with resultant developmental delay and long-term disability. One might estimate the consequence of this FN as 0.1; quality of life (QOL) lived in this state of misdiagnosis has 10% of the QOL lived without disease. It is important to note that the consequence of TP may not always be 100% or equivalent to healthy life. Indeed, for propionic acidemia, even neonatal diagnosis may not completely alleviate the burden of disease. A possible estimate of the consequence of a TP on morbidity would be 80%. Similar estimates are determined for the remaining two outcomes. Values for the estimated consequences, as well as prevalence estimates of the disease, are then used in the equation that follows, where cTN, cFP, cTP, and cFN are the estimated consequences of each diagnostic category, and $P(D)$ is disease prevalence and $P(\overline{D})$ is 1 – prevalence. The $LR_{threshold}$ is the optimal assay cutoff.

$$LR_{threshold} = \frac{P(\overline{D})}{P(D)} \times \frac{cTN - cFP}{cTP - cFN}$$

From the list of possible analyte concentrations, one can now select the cutoff that most closely approximates the $LR_{threshold}$. In this way, one may select a test cutoff that not only optimizes the discriminatory power of the assay but also fits the clinical need that the test is meant to address.

Consider a theoretical test for a disease shown in Table 8.10 with a prevalence (pretest probability) of 10%. R1 to R5 represent possible assay cutoffs, where R1 represents a barely positive result and R5 a strong positive test result. Table 8.10 shows the percentage of diseased patients (defined

TABLE 8.10
Positivity Criterion

Cutoff	% Disease With This Value or Greater on Assay	% Without Disease With This Value or Greater on Assay	LR-Positive Test
R1—barely positive	5	30	0.17
R2—weakly positive	20	40	0.5
R3—intermediate positive	20	15	1.33
R4—strongly positive	25	10	2.50
R5—very strongly positive	30	5	6.00

The characteristics of a theoretical test for a disease with a prevalence of 10% are shown. Possible cutoff values for this assay ranging from a barely positive reading to a very strongly positive reading are denoted as R1 to R5, respectively. The percentage of patients with and without disease at or above each cutoff is also provided. The likelihood ratio (LR) for a positive test for R1–R5 is calculated from the information in the table (see explanation in text).

by a gold standard) with a test result greater than the cutoffs defined as R1 to R5. In addition, the percentage of patients without disease at each cutoff is shown. As the value for the cutoff increases from R1 to R5, the percentage of patients with disease increases. Using this information, an LR for a positive test can be calculated for each cutoff level.

Next, we consider the consequences of an FN/FP and TP/TN result on the assay in terms of QOL. It is important to note that consequences can be estimated in terms of a variety of outcomes, including cost, excess mortality, or even cost-benefit, and each of these will result in a different positivity criterion. Assume that a missed diagnosis (FN) results in a QOL that is 70% that of a healthy person. Furthermore, assume that an FP result will lead to an unnecessary workup and anxiety, with a QOL that is 93% that of a healthy person. Finally, QOL for a TP living with a correctly diagnosed disease may be considered as 80% the QOL of a healthy person. Finally, a TN person experiences 95% the QOL as a fully healthy, untested person. Values for consequences are generally estimated from the literature or from expert opinion. By plugging the values for consequences into the formula presented earlier for $LR_{threshold}$, we obtain a value of 1.8. In other words, the assay is most efficient, in terms of maximized QOL, at an LR+ of 1.8. From Table 8.10, the positivity criterion for this assay should be between R3 and R4, and closer to R3.

EVIDENCE-BASED MEDICINE

Historically, medical decisions have relied heavily on clinical experience, expert opinions, and other subjective or uncontrolled sources of information. This has also been true in laboratory medicine, in which often an inadequate foundation of evidence is found to support existing practices (Price, 2000; 2003). There may be no clear understanding of why a test is ordered or what clinical question it is trying to answer. Alternatively, there may be no information on whether or how a test affects morbidity, mortality, cost, patient satisfaction, risk, and QOL (Bruns, 2001). For example, it is not clear whether point-of-care testing improves patient diagnosis and discharge in the emergency department (Kendall et al., 1998; Bruns, 2001; Asha et al., 2014). Studies of clinical effectiveness in the clinical laboratory are hard to find because they are expensive and difficult to design (Price, 2000; McQueen, 2001). In addition, laboratory consultation is often based on the tradition of clinical and laboratory experience and less on a systematic approach to determining the current best evidence. In contrast to traditional approaches, evidence-based medicine (EBM) is a process by which medical decisions can be made by using as many objective tools as possible. This, in turn, can help reduce the uncertainty of medical decision making. EBM is a systematic practice that integrates the most current and best evidence with clinical expertise and patient preferences when making medical decisions (Sackett et al., 2000). EBM places emphasis on critically analyzing information from the literature and developing knowledge for medical practice (Sackett, 1983; Sackett et al., 1991; Elstein, 2004; Ludmerer, 2004). EBM encourages the cultivation of continuous learning and

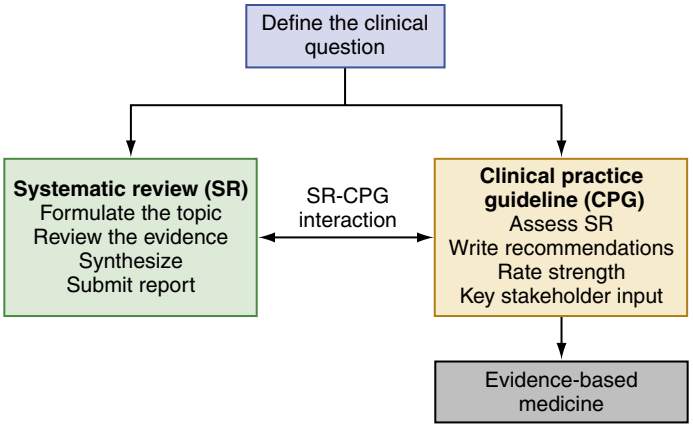

Figure 8.7 Flowchart showing the process of evidence-based medicine. The development of systematic reviews (SRs) informs the group developing the clinical practice guidelines (CPGs). The SRs may be developed independently or specifically to inform the CPG group.

sharing of medical knowledge at all levels of training, from medical student to attending physician (Ludmerer, 2004). Since the time of its introduction, EBM has grown to become a key tool for all health care providers.

Practicing EBM consists of five steps (Price, 2000, 2003; Fig. 8.7): ask a clinical question based on a patient encounter; acquire information by searching resources; analyze and critically evaluate the information and reach a conclusion that answers the clinical question; apply the information to individual patients; and audit effectiveness and monitor the literature.

A clinical encounter of a patient with a health care provider generally results in a clinical question that necessitates one or more laboratory tests—whether for screening, diagnosis, prognosis, or monitoring of treatment. The question that is developed should be specific to a decision that must be made for that patient. The question compares an intervention such as ordering a diagnostic test versus accepted practice. The clinical question can be described in four parts and summarized with the acronym PICO (Sackett, 2000; Elstein, 2004):

- Problem (P): What is the problem of interest for the specific patient?
- Intervention (I): What intervention is being considered?
- Comparison (C): To what alternatives can the intervention be compared?
- Outcome (O): Is there a quantifiable clinical outcome that can be measured?

For example, a laboratory director is asked to provide instrumentation for diabetes screening at an employee health fair. The clinical question can be summarized as follows:

- Problem: Is a portable glucometer and fingerstick blood sample appropriate for population screening for diabetes? (Sturgeon & Diamandis, 2010)
- Intervention/Test: Portable fingerstick glucose
- Comparison: Glucose measurement on venous plasma in an accredited laboratory
- Outcome: Predictive value of fingerstick glucose in screening for diabetes

A second example might be the following: A 58-year-old man with hepatocellular carcinoma (HCC) undergoes liver resection.

- Problem: Should serum alpha-fetoprotein (AFP) be routinely monitored after liver resection for HCC recurrence? (National Academy of Clinical Biochemistry, 2011)
- Intervention: Serum AFP measured after liver resection
- Comparison: Serum AFP not measured after liver resection
- Outcome: Predictive value of serum AFP to detect HCC recurrence and survival rates

The strategy for answering these questions must be determined before searching the resources to prevent the introduction of selection bias. Information sources include textbooks, journals, electronic textbooks, and summary journals. Journal articles provide more up-to-date information than textbooks, but they can also be outdated by the time the articles have been written, accepted, and published. Journal articles reporting the results of randomized controlled trials (RCTs) that are double-blinded are the most valuable because they are the least biased. However, RCTs are still highly dependent on the methods employed in the blinding and treatment of subjects (Lijmer et al., 1999).

SYSTEMATIC REVIEWS OF CLINICAL EFFECTIVENESS RESEARCH AND CLINICAL PRACTICE GUIDELINES

Patients assume that their physician bases diagnostic testing and treatment recommendations on EBM. However, practitioners cannot stay abreast of the rapidly expanding literature, which can be of variable quality, and the labor-intensive steps required answering each clinical question using EBM. Therefore, practitioners are increasingly turning to systematic reviews (SRs) for a summary of the current best evidence and to clinical practice guidelines (CPGs) for diagnostic testing and treatment recommendations. However, how does a clinician determine which SRs and CPGs are trustworthy? The quality of SRs can be variable due to developer bias, lack of scientific rigor, and subsequent incorrect conclusions. CPGs can be affected by the quality of the SRs used to inform the CPGs, particularly with respect to strength of the evidence and recommendation appraisals; unmanaged conflicts of interest (COI); and overall failure to use rigorous methodologies in CPG development. The Institute of Medicine (IOM) created a common set of standards addressing the group structure, transparent process, scientific rigor, and reporting of SRs and CPGs (AHRQ, 2012).

SYSTEMATIC REVIEWS

SRs identify, select, assess, and synthesize the findings of the relevant literature and clarify what is known and not known about the potential benefits and harms of medical interventions. They are increasingly being used to guide clinicians who want to practice EBM. Professional medical societies and other organizations that develop CPGs rely on SRs to inform their recommendations. An SR of comparative effectiveness research (CER) is a specific type of SR that analyzes two or more medical interventions (e.g., fingerstick vs. plasma glucose) for the same disease. For example, an SR of CER in transfusion medicine may compare plasma versus four-factor prothrombin complex concentrates for the treatment of intracranial bleeding in a patient requiring warfarin reversal.

The IOM standards for producing an SR (AHRQ, 2012) are shown in Box 8.1. After formulating the question of the SR, a multidisciplinary team consisting of the relevant experts and key stakeholders (e.g., professional organizations) is assembled. Management of conflicts of interest must begin at the start of the process with full transparency. After having defined searching methods, the studies are analyzed and synthesized using a qualitative, or preferably a quantitative, method such as meta-analysis (a statistical technique to integrate results from multiple studies). The group publishes the SR for peer review and then may publish it as a standalone document, or it can be used to specifically inform a group developing a CPG. The Centre for Evidence-Based Medicine (http://www.cebm.net), the Cochrane Collaboration/Cochrane Library (http://www.cochrane.org), and Up-to-Date (http://www.uptodate.com/) are sources that present summarized information. The Evidence-Based Medicine (ebm.bmjjournals.com) series of journals are also an excellent resource for up-to-date SRs.

CLINICAL PRACTICE GUIDELINES

CPGs are statements, usually by a governmental agency or professional organization, that include recommendations intended to optimize patient care, make clinical practice more uniform, establish performance measures, improve patient outcomes, improve patient safety, and reduce medical costs (Box 8.2). They are usually informed by one or more SRs. The process of developing a CPG starts with selecting a group of experts and key stakeholders who will develop the CPG. It is important to manage conflicts of interest within the CPG group and the SR group if one is specifically selected to inform the CPG. It is indisputable that a trustworthy CPG should be based on high-quality SRs. The summary of the CPG should include the scope of the CPG (e.g., objective, interventions considered, major outcomes considered), methodology (e.g., ratings for strength of evidence, ratings for strength of recommendations), major recommendations, and the risks and benefits of implementing the recommendations. For example, the *Guidelines on the Use of Therapeutic Apheresis in Clinical Practice* provides the details of the systematic approach for the SR and CPG, uniform criteria to assign a category for the indications for therapeutic apheresis (i.e., Categories I through IV), and an assignment of the strength of the recommendation (i.e., 1A-C or 2A-C) (Padmanabhan et al., 2019). In the use of tumor markers in liver, bladder, cervical, and gastric cancers, the strength of the evidence and the strength of the recommendations are well described (Sturgeon & Diamandis, 2010) (Box 8.3). Finally, there should be a comment period, which should be published—ideally, with free access.

BOX 8.1

Institute of Medicine Standards for Systematic Reviews

- Establish a team with appropriate expertise and experience.
- Ensure end user and stakeholder input.
- Manage bias and conflict of interest.
- Formulate the topic.
- Develop a systematic review protocol.
- Conduct a comprehensive systematic search for evidence.
- Screen and select studies; critically appraise.
- Use a prespecified method to evaluate the body of evidence.
- Conduct a qualitative and/or quantitative analysis (e.g., meta-analysis).
- Prepare a draft, obtain peer reviews, and publish with free public access.

(AHRQ, 2012).

BOX 8.2

Standards for Clinical Practice Guidelines (CPGs)

- Establish transparency of how the CPG is going to be developed and funded.
- Manage conflicts of interest.
- CPG development group should be composed of a variety of methodological experts, clinicians, and patients served.
- Use systematic reviews that meet the Institute of Medicine standards for systematic reviews.
- Establish the foundations for and rating strength of recommendations.
- Provide recommendations in a standardized form; clinical flexibility should be built in.
- Prepare a draft, obtain peer reviews, and publish with free public access.
- Regularly update as new literature is published.

(AHRQ, 2012).

BOX 8.3

Rating Schemes for Systematic Reviews and Clinical Practice Guidelines

Example of Rating Scheme for Level of Evidence

I. Evidence from a single high-powered, prospective-controlled study that is specifically designed to test marker data or evidence from a meta-analysis, pooled analysis, or overview of level II or III studies
II. Evidence from a study in which marker data are determined in relation to prospective therapeutic trials that are performed to test therapeutic hypotheses but not specifically designed to test marker utility
III. Evidence from large prospective studies
IV. Evidence from small retrospective studies
V. Evidence from small pilot studies

Example of Rating Scheme for Strength of Recommendation

A. High: Further research is very unlikely to change the panel's confidence in the estimate of effect.
B. Moderate: Further research is likely to have an important impact on the panel's confidence in the estimate of effect and is likely to change the estimate.
C. Low: Further research is very likely to have an important effect on the panel's confidence in the estimate of effect and is likely to change the estimate.
D. Very Low: Any estimate of effect is very uncertain.

Level of evidence from Sturgeon & Diamandis (2010); strength of recommendation from National Academy of Clinical Biochemistry (2011).

SELECTED REFERENCES

Clinical and Laboratory Standards Institute (CLSI): *Defining, establishing, and verifying reference intervals in the clinical laboratory—Approved guideline*, 3rd ed., 950 West Valley Road, Suite 2500, Wayne, PA 19088-1898, 2010, CLSI document EP28-A3c. Clinical and Laboratory Standards Institute.

A reference procedure for determining the reference range for a clinical laboratory test.

Galen RS, Gambino SR: *Beyond normality: the predictive value and efficiency of medical diagnoses*, New York, 1975, John Wiley & Sons.

This book serves as an introduction to understanding the interpretation of a laboratory test. The basics of diagnostic test accuracy and the predictive value of tests are well outlined.

Institute of Medicine of the National Academies: *Clinical practice guidelines we can trust. Standards for developing trustworthy clinical practice guidelines (CPGs)*, 2011.

The published standards by the Institute of Medicine for the Systematic Review of Clinical Effectiveness Research and Clinical Practice Guidelines. These standards are important for determining whether an SR or a CPG is trustworthy.

The Joint Commission: *Laboratory National patient safety Goals*. Retrieved from https://www.jointcommission.org/lab_2017_npsgs/, 2019.

The Joint Commission requires that laboratories and hospitals address the National Patient Safety Goals, which are revised every year.

McQueen MJ: Overview of evidence-based medicine: Challenges for evidence-based laboratory medicine, *Clin Chem* 47(8):1536–1546, 2001.

General overview of the practice of EBM as it relates to the laboratory, including examples and useful resources.

Myron JA, Hyloft PP, Whicher JT, et al.: On behalf of the International Federation of clinical Chemistry and laboratory medicine committee on plasma proteins: reference intervals for serum proteins: Similarities and differences between adult Caucasian and Asian Indian males in Yorkshire, UK, *Clin Chem Lab Med* 42:792–799, 2004.

An example of different reference ranges between two reference populations.

National Academy of Clinical Biochemistry (NACB): *Guidelines and recommendation for laboratory analysis in the diagnosis and management of diabetes mellitus*, Washington, D.C., 2011, National Academy of Clinical Biochemistry (NACB), p 104.

Example of the development of a clinical practice guideline according to IOM standards for the laboratory aspects of testing for types I and II diabetes.

Padmanabhan A, Connelly-Smith L, Aqui N, et al.: Guidelines on the use of therapeutic apheresis in clinical practice—evidence-based approach from the Writing Committee of the American Society of Apheresis: the eighth special issue, *J Clin Apher* 24:171–254, 2019.

Example of the development of a clinical practice guideline according to IOM standards for the treatment of diseases with apheresis.

Sackett DL, Straus SE, Richardson WS, et al.: *Evidence-based medicine: how to practice and teach EBM*, ed 2, London, 2000, Churchill Livingstone.

Comprehensive, easy-to-read primer on all facets of EBM that includes many examples.

Sturgeon CM, Diamandis E, editors: *Use of tumor markers in liver, bladder, cervical and gastric cancers*, Washington, D.C., 2010, National Academy of Clinical Biochemistry (NACB), p 57.

Example of the development of a clinical practice guideline according to IOM standards for the laboratory aspects of tumor marker testing.

Zweig MH, Campbell G: Receiver-operating characteristic (ROC) plots: a fundamental evaluation tool in clinical medicine, *Clin Chem* 39(4):561–577, 1993.

An in-depth article on the concept, use, and application of ROC curves in clinical testing. A comparison with other measures of test accuracy is part of the discussion.

Access the complete reference list online at Elsevier eBooks for Practicing Clinicians.

REFERENCES

AHRQ: *Clinical practice guidelines Archive*, . https://www.ahrq.gov/prevention/guidelines/archive.html. [Accessed 16 September 2019], September, 2012.

Asha SE, Chan AC, Walter E, et al.: Impact of point-of-care devices on emergency department patient processing times compared with central laboratory testing of blood samples: a randomized controlled trial and cost-effectiveness analysis, *Emerg Med* 31:714–719, 2014.

Bakchoul T, Giptner A, Najaoui A, et al.: Prospective evaluation of PF4/heparin immunoassays for the diagnosis of heparin-induced thrombocytopenia, *J Thromb Haemost* 7:1260–1265, 2009.

Baloch Z, Carayon P, Conte-Devolx B, et al.: Laboratory medicine practice guidelines. Laboratory support for the diagnosis and monitoring of thyroid disease, *Thyroid* 13(1):3–126, 2003.

Bowen R, Chan Y, Coehn HA, et al.: Effect of blood collection tubes on total triiodothyronine and other laboratory assays, *Clin Chem* 51(2):424–433, 2005.

Bruns DE: Laboratory-related outcomes in healthcare, *Clin Chem* 47(8):1547–1552, 2001.

Clinical and Laboratory Standards Institute (CLSI): *Defining, establishing, and verifying reference intervals in the clinical laboratory: Approved guideline*, ed 3, Wayne, PA, 2008, Clinical and Laboratory Standards Institute, p 59.

Elstein AS: On the origins and development of evidence-based medicine and medical decision making, *Inflamm Res* 53(Suppl 2):S184–S189, 2004.

Fossati P, Prencipe L: Serum triglycerides determined colorimetrically with an enzyme that produces hydrogen peroxide, *Clin Chem* 28(10):2077–2080, 1982.

Fujimoto K: Principles of measurement in hematology analyzers manufactured by Sysmex Corporation, *Sysmex Journal International* 9:31–40, 1999.

Grundy SM, Cleeman JI, Merz CN, et al.: Implications of recent clinical trials for the national cholesterol education Program adult treatment panel III guidelines, *Circulation* 110(2):227–239, 2004.

Jaffe AS: Third universal definition of myocardial infarction, *Clin Biochem* 46(1–2):1–4, 2013.

Kendall J, Reeves B, Clancy M: Point of care testing: Randomised controlled trial of clinical outcome, *BMJ* 316(7137):1052–1057, 1998.

Kroll MH, Elin RJ: Interference with clinical laboratory analyses, *Clin Chem* 40(11 Pt 1):1996–2005, 1994.

Kweon OJ, Lee M-K, Kim HR: Evaluation of the flagging performance of the hematology analyzer Sysmex XN series on the basis of "Q values", *Arch Pathol Lab Med* 142:83–88, 2018.

Lacher DA, Hughes JP, Carroll MD: Estimate of biologic variation of laboratory analytes based on the third national health and nutrition examination survey, *Clin Chem* 51(2):450–452, 2005.

Ladenson JH: Patients as their own controls: use of the computer to identify "laboratory error", *Clin Chem* 21(11):1648–1653, 1975.

Levey AS, Bosch JP, Lewis JB, et al.: A more accurate method to estimate glomerular filtration rate from serum creatinine: a new prediction equation. Modification of Diet in Renal Disease Study group, *Ann Intern Med* 130(6):461–470, 1999.

Lijmer JG, Mol BW, Heisterkamp S, et al.: Empirical evidence of design-related bias in studies of diagnostic tests, *J Am Med Assoc* 282(11):1061–1066, 1999.

Ludmerer KM: Learner-centered medical education, *N Engl J Med* 351(12):1163–1164, 2004.

Myers GL, Miller WG, Coresh J, et al.: Recommendations for improving serum creatinine measurement: a report from the laboratory working group of the National Kidney Disease Education Program, *Clin Chem* 52(1):5–18, 2006.

National Academy of Clinical Biochemistry (NACB): *Guidelines and recommendation for laboratory analysis in the diagnosis and management of diabetes mellitus*, Washington, D.C., 2011, National Academy of Clinical Biochemistry (NACB), p 104.

Price CP: Evidence-based laboratory medicine: Supporting decision making, *Clin Chem* 46(8 Pt 1):1041–1050, 2000.

Price CP: Application of the principles of evidence-based medicine to laboratory medicine, *Clin Chim Acta* 333(2):147–154, 2003.

Sackett DL: Interpretation of diagnostic data: 1. How to do it with pictures, *Can Med Assoc J* 129(5):429–432, 1983.

Sackett DL, Haynes RB, Tugwell P, et al.: *Clinical epidemiology: a basic science for clinical medicine*, ed 2, Boston/Toronto/London. Little and Brown, 1991.

Schifman RB, Talbert M, Souers RJ: Delta check practices and outcomes. A Q-probes study involving 49 health care facilities and 6541 delta check alerts, *Arch Pathol Lab* Med141:813–823, 2017.

Padmanabhan A, Connelly-Smith L, Aqui N, et al.: Guidelines on the use of therapeutic apheresis in clinical practice—evidence-based approach from the writing committee of the American Society of Apheresis: the eighth special issue, *J Clin Apher* 24:171–254, 2019.

Sturgeon CM, Diamandis E, editors: *Use of tumor markers in liver, bladder, cervical and gastric cancers*, Washington, D.C., 2010, National Academy of Clinical Biochemistry (NACB), p 57.

Thalhammer-Scherrer R, Knobl P, Korninger L, et al.: Automated five-part white blood cell differential counts: Efficiency of software-generated white blood cell suspect flags of the hematology analyzers Sysmex SE-9000, Sysmex NE-8000, and Coulter STKS, *Arch Pathol Lab Med* 121(6):573–577, 1997.

The Joint Commission: 2019 laboratory national patient safety Goals. Retrieved from https://www.jointcommission.org/lab_2017_npsgs/. [Accessed 16 September 2019].

Vermeer HJ, Thomassen E, de Jonge N: Automated processing of serum indices used for interference detection by the laboratory information system, *Clin Chem* 51(1):244–247, 2005.

Victor JV, Patole S, Joseph HJH, et al.: Agreement between paired blood gas values in samples transported either by a pneumatic tube system or by human courier, *Clin Chem Lab Med* 49(8):1303–1309, 2011.

Zhao Y, Lv G: Influence of temperature and storage duration on measurement of activated partial thromboplastin time, D-dimers, fibrinogen, prothrombin time, and thrombin time in citrate-anticoagulated whole blood specimens, *Int J Lab Hematol* 35(5):566–570, 2013.

CHAPTER 9

INTERPRETING LABORATORY RESULTS

Matthew R. Pincus, Naif Z. Abraham Jr., Martin H. Bluth

INTERPRETING AND CORRELATING ABNORMAL LABORATORY VALUES, 100
General Considerations, 100
Fundamental Principles in Interpretation of Values, 101
ABNORMALITIES IN THE HEMATOLOGY PROFILE, 101
Anemias, 101
Quantitative White Blood Cell Abnormalities, 104
Coagulation Disorders, 105
ABNORMALITIES IN CLINICAL CHEMISTRY: CHEMICAL PATHOLOGY, 106
Electrolyte Abnormalities, 106
Renal Disease, 108
Blood Gas Abnormalities, 110
Glucose Abnormalities, 111
Other Abnormal Laboratory Findings in Diabetes Mellitus, 112
Liver Function Tests, 112
Cardiac Function Tests, 113
Skeletal Muscle Function, 114
Pancreatic Function Tests, 114
Markers for Inflammatory Conditions, 114
Endocrine Function Testing, 114
Adrenal Function, 115
EXAMPLES OF CLINICAL CASES WITH CLINICOPATHOLOGIC CORRELATIONS, 116
Case A: Electrolyte Disorder, 116
Case B: Complex Electrolyte Disorder, 117
Case C: Disorders Related To Liver Failure, 117
Case D: Severe Rhabdomyolysis, 117
SELECTED REFERENCES, 118

KEY POINTS

- Accurate differential diagnoses can be made from a systematic study of the laboratory profiles of patients in a large majority of cases.
- There are basically four types of anemia: iron deficiency, anemia of chronic disease, hemolytic anemia, and macrocytic/nutritionally deficient anemia. These can be readily distinguished from one another both by the hematologic profile and simple laboratory testing.
- By examining the urinary sodium, potassium, and osmolarity, the causes of hyponatremia and hypernatremia can be readily determined.
- Liver function tests can distinguish among six different diseases of the liver: hepatitis, cirrhosis, biliary disease, space-occupying lesions of the liver, passive congestion, and fulminant hepatic failure.
- Renal failure can be readily diagnosed by observing elevated blood urea nitrogen and creatinine; it is possible to pinpoint the site of renal failure—that is, glomerular or tubular—from the ratio of serum to urine osmolality.
- Blood gas results allow determination of the causes of metabolic versus respiratory acidosis or alkalosis; there is a critical relationship between the partial pressure of oxygen and carbon dioxide such that, in respiratory diseases, high levels of carbon dioxide block oxygenation of venous blood, leading to respiratory crisis.
- Elevation of cardiac troponin in serum, in the proper clinical context, is diagnostic of myocardial infarction.
- Elevations of serum C-reactive protein indicate inflammatory disease.
- Elevations of serum amylase and lipase point to acute pancreatitis.
- Two types of endocrine disease are discussed: thyroid and adrenal. Serum levels of T_4 (or, better, free T_4) and thyroid-stimulating hormone (TSH) can be used to diagnose primary or secondary hypothyroidism or hyperthyroidism; serum levels of cortisol and adrenocorticotropic hormone (ACTH) can be used to diagnose primary or secondary hypoadrenalism or hyperadrenalism.

INTERPRETING AND CORRELATING ABNORMAL LABORATORY VALUES

GENERAL CONSIDERATIONS

The major purpose of performing analyte determinations in the clinical laboratory is to aid in the diagnosis and management of disease and in health assessment. In this regard, the clinical pathologist is often called on as a consultant to explain abnormal laboratory values, especially those that do not seem to correlate with one another, and to recommend or even to order laboratory tests that may lead to the correct diagnosis in the workup of patients for particular medical problems. In addition, evaluation of laboratory test results on individual patients by the clinical pathologist can not only reveal the (infrequent) occurrence of laboratory errors but can help in the selection of appropriate, cost-effective tests from a wide variety of increasingly complex test choices (Witte et al., 1997; Dighe et al., 2001; Bonini et al., 2002).

For evaluation of test results, the laboratory computer is an invaluable aid. Virtually all such systems perform daily checks for patient values that lie significantly outside of their established reference intervals or that have undergone large changes over a 24-hour period. These are often reported as "failed delta checks." Thus, patients with significant laboratory findings can be identified.

This chapter presents an approach to the interpretation of laboratory values that will enable laboratorians to aid in the establishment of clinical diagnoses and to assist in clinical management. This discussion is by no means comprehensive and cannot possibly cover every conceivable illness afflicting patients. Rather, this presentation is concerned with general approaches to interpreting abnormal values and discussion of the most common causes of such findings so that the reader has a framework for interpreting abnormal values.

The reader may prefer to complete the Clinical Chemistry (Part 2) and Hematology and Transfusion Medicine (Part 4) sections of this book before reading this chapter, which gives an overview of both of these vital diagnostic areas. Alternatively, the reader may decide to read this chapter before the several chapters on chemistry and hematology to benefit from the overview presented here.

FUNDAMENTAL PRINCIPLES IN INTERPRETATION OF VALUES

Before embarking on a discussion of specific conditions giving rise to abnormal values, certain precepts should always be followed:

1. Never rely on a single out-of-reference range value to make a diagnosis. It is vital to establish a trend in values. A single sodium value of, for example, 130 mEq/L does not necessarily indicate hyponatremia. This single abnormal value may be spurious and may reflect such factors as improper phlebotomy technique, laboratory variability, and so on. Rather, a series of low sodium values in successive serum samples from

a given patient does indicate this condition. Thus, it is vital to follow trends in particular values.

2. Osler's rule. Especially if the patient is under the age of 60 years, try to attribute all abnormal laboratory findings to a single cause. Only if there is no possible way to correlate all abnormal findings should the possibility of multiple diagnoses be entertained.

ABNORMALITIES IN THE HEMATOLOGY PROFILE

Often, in laboratory reports, the first section contains the hematology profile, including the complete blood count (CBC). Comprehensive discussions of clinical hematopathology are given in Part 4. Here, we discuss very basic patterns of abnormalities to provide an overall reference frame for interpreting values and for the ordering of further examinations. Though this part of the book is concerned with clinical chemistry or chemical pathology, we discuss the hematology profile because the interpretation of hematopathologic results often depends on the results of quantitative determinations performed in clinical chemistry.

ANEMIAS

Anemia, a common hematologic disorder, is defined pathophysiologically as a decrease in the oxygen-carrying capacity of the blood. All oxygen-carrying capacity of the blood is due to the binding of oxygen to hemoglobin contained uniquely in red blood cells. Because anemia can cause tissue hypoxia, it often produces such symptoms as fainting, fatigue, pallor, and difficulty in breathing.

Practically, the best indicator for this condition is a low red blood cell count or number of red blood cells per volume of whole blood. Although the reference range for the red cell count varies with age, sex, and population, it encompasses values from around 4 to 6 × 10^6 red blood cells per cubic millimeter (cu mm) or microliter. This range may change somewhat depending on population. Red blood cell counts below the lower limit of the reference range suggest the presence of anemia. In addition, red blood cells occupy a well-defined range in terms of the percent of the volume that they occupy of whole blood or the hematocrit. Generally, normal adult hematocrit values range from about 36% to 45% (normal values for females are generally slightly lower than those for males). In addition, the concentration of hemoglobin in whole blood is about 12 to 15 g/dL or approximately 33 to 36 g/dL in red blood cells—that is, the mean corpuscular hemoglobin concentration. Normal values are also dependent on patient age and altitude of residence. Normally, the hematocrit is about three times the value of the hemoglobin concentration, which, in turn, is about three times the value of the red blood cell count.

If anemia has been diagnosed, it is then mandatory to determine the cause of the anemia. An excellent history and physical examination are required for appropriate test selection, diagnosis, and the best possible patient care and treatment. In addition, a review of the peripheral blood film with respect to red and white cell morphology is often helpful.

To narrow further the differential diagnosis and to facilitate appropriate test selection, a number of classification schemes for anemia have been developed, with no single ideal scheme available. A particularly useful approach utilizes the common red cell indices of mean corpuscular volume (MCV), measured in femtoliters (fL), or 1 × 10^{-15} L, in conjunction with the red cell distribution width (RDW) and the reticulocyte count (percent reticulocytosis) or reticulocyte production index (RPI). A further aid in diagnosis is the chromicity of the red cells—that is, the intensity of the red color of the cells due to intracellular hemoglobin. The chromicity is measured quantitatively by the mean corpuscular hemoglobin concentration (MCHC). Taken together, these indices help to form a working hypothesis for the underlying cause of the anemia.

Electronic determination of MCV directly from red cell distribution data allows for classification on the basis of red blood cell size as macrocytic (MCV generally >100 fL), microcytic (MCV generally <80 fL), or normocytic (MCV generally between 80 and 100 fL). The sizes (volumes) of red cells vary within a certain range in which the number of cells of particular volumes form a bell-shaped or Gaussian distribution (see Chapter 10). The standard deviation of the cell volumes divided by the mean cell volume gives what is called the red cell distribution width, or RDW, measured as a percent. As it happens, the RDW is a parameter that helps to further classify an anemia because it reflects the variation of red blood cell size. The RDW generally varies between about 12 and 17 and is dependent on the patient's age, sex, and ethnic subgroup. It can be helpful in differentiating causes of microcytosis, because moderate to severe iron deficiency anemia is associated with an increased RDW, whereas thalassemia and anemia of chronic disease (ACD) are associated with a normal RDW.

Peripheral blood reticulocytosis is a measure of bone marrow response in the face of anemia. A similar measure, the reticulocyte proliferation index (RPI) corrects the reticulocyte count with respect to the proportion of reticulocytes present in a patient without anemia and the premature release of reticulocytes into the peripheral circulation. Bone marrow response to anemia may be appropriate (hyperproliferative), with an RPI over 3 generally indicating marrow red cell hyperproliferation. However, the anemia may be due to defective red blood cell production or marrow failure (hypoproliferative), which is generally indicated by an RPI less than 2. Thus, although these red cell indices are not pathognomonic of the cause of a particular type of anemia, the combination of MCV, RDW, and RPI examined together will often significantly narrow the differential diagnosis and facilitate further test selection. Table 9.1 illustrates common examples of anemia and their diagnostic workup using these red cell indices as well as other helpful analytic abnormalities.

TABLE 9.1
Common Types of Anemias and Their Diagnostic Workups[a]

Anemia	Cause	Common Analyte Abnormality
1. Hypoproliferative, microcytic	Iron deficiency	Low ferritin Increased IBC Decreased serum iron Reduced Fe/TIBC ratio Generally increased RDW
2. Hypoproliferative, microcytic	Anemia of chronic disease	Generally high ferritin Normal IBC Decreased serum iron Normal Fe/TIBC ratio Generally normal RDW
3. Hyperproliferative, normocytic	Hemolytic anemia	Schistocytosis Increased reticulocytes Low haptoglobin Elevated carboxyhemoglobin Elevated LD and potassium Elevated indirect bilirubin Generally increased RDW
4. Hypoproliferative, normocytic	Aplastic anemia	Leukopenia Thrombocytopenia Hypocellular bone marrow Generally normal RDW
5. Hypoproliferative, normocytic	Renal failure	Elevated BUN and creatinine Low erythropoietin Burr cells may be present Generally normal RDW
6. Hypoproliferative, macrocytic		
A. Megaloblastic	Vitamin B_{12} and/or folate deficiency	Low vitamin B_{12} and/or folate Hyperlobulated polymorphonuclear leukocytes Macro-ovalocytes Increased RDW
B. Nonmegaloblastic	Hypothyroidism	Elevated TSH Normal RDW

[a]Low is equivalent to depressed, and high is equivalent to elevated. Ferritin, haptoglobin, LD, bilirubin, BUN, creatinine, erythropoietin, TSH, and T_4 are all expressed as concentrations. All of these analytes are measured in serum.
BUN, Blood urea nitrogen; *Fe,* iron; *IBC,* iron-binding capacity; *LD,* lactate dehydrogenase; *RDW,* red cell distribution width; *TIBC,* total iron-binding capacity; *TSH,* thyroid-stimulating hormone.

Microcytic Anemia

Common microcytic anemias include iron deficiency anemia (IDA) and the thalassemias. Some hemoglobinopathies and ACD may also be microcytic.

In our discussion, we focus on IDA and ACD, a common differential diagnosis for patients with microcytic anemia. Both anemias appear to be disorders involving iron metabolism.

In IDA, there is a primary deficiency of iron available to the red cell (usually due to blood loss, but other causes include dietary deficiency, malabsorption, and pregnancy); chronic blood loss should always lead to further investigation because it is commonly associated with malignancy. ACD, however, appears to be due to defective iron utilization/metabolism and is associated with chronic nonhematologic disorders such as chronic infections, connective tissue disorders, malignancy, and renal, thyroid, and pituitary disorders. Because iron levels in red cells are low, hemoglobin levels are also low in both of these conditions. Thus, the MCHC mentioned earlier tends to be low, giving rise to what is termed a *hypochromic* (low red color in red cells or low MCHC), *microcytic* (low MCV) anemia.

To distinguish between IDA and ACD, a number of different laboratory measurements are very useful in addition to the RDW. The diagnosis is typically made using additional serum or whole blood laboratory tests. However, because IDA is always accompanied by loss of iron that is stored bound to the protein ferritin in bone marrow macrophages, the diagnosis can always in principle be made with a bone marrow biopsy with an iron stain—that is, nitroprusside—that shows the absence of marrow iron. This procedure is, of course, invasive and should be performed only as a last resort.

Serum Ferritin Levels

Normally, there is an equilibrium between intracellular and extracellular ferritin. The lower the stored iron becomes, the lower the intracellular ferritin is, and, consequently, the lower the extracellular ferritin becomes. The level of extracellular ferritin can be directly measured by determining the serum ferritin level, which is readily and accurately performed on serum aliquots, using enzyme-linked immunosorbent assay (ELISA) techniques, described in Chapter 45. Overall, therefore, serum ferritin levels give an excellent measure of available iron stores noninvasively. Because, in ACD, iron stores are abundant, serum ferritin levels are characteristically normal to elevated. In contrast, in IDA, in which iron stores become depleted, serum ferritin levels are characteristically decreased. Thus, serum ferritin level is one assay that can be used in differentiating IDA from ACD.

One caveat in using serum ferritin values to provide this distinction is the fact that ferritin also happens to be an acute-phase reactant. Acute-phase reactants are proteins (discussed in Chapter 20) that rise in response to an acute process, usually an acute inflammatory condition. Thus, if a patient has an acute infection, the serum ferritin level may be spuriously elevated. The net effect may be a ferritin in the reference interval. Usually, in IDA, accompanied by an acute process, this level is in the low reference range.

Use of Serum Iron and Iron-Binding Capacity

In addition to ferritin levels, serum iron and serum iron-binding capacity (IBC) can be measured as discussed in Chapters 24 and 28). On average, serum iron is, of course, reduced in IDA and normal or sometimes low in ACD. The IBC is a direct measure of the protein transferrin, which transports iron from the gut to iron storage sites in bone marrow. In IDA, the serum iron is reduced, and the IBC increases.

However, both serum iron and transferrin are subject to wide fluctuations because of such factors as diet, and they do not always reliably reflect iron stores. Also, transferrin is a beta-protein—that is, it migrates in the beta-region in serum protein electrophoresis (discussed in Chapter 20)—and is an acute-phase reactant—that is, its serum levels change (usually decrease, as a so-called "negative acute-phase reactant") in inflammatory conditions. There is considerable overlap between serum levels of iron and IBC in IDA and ACD. A somewhat more reliable discriminating measure of IDA is the ratio of serum iron to the IBC, known as the *transferrin saturation* (*TS*). This ratio is around 1 : 3 for normal individuals, while in IDA it is significantly reduced to values of around 1 : 5 or lower. Again, there is considerable overlap even in this ratio for patients with IDA and ACD; thus, the values should always be interpreted with care.

Use of Red Blood Cell Distribution Width

Finally, use of automated procedures for determination of cell counts and indices enables us to obtain average erythrocyte sizes and size distributions. In IDA, there is a marked dispersion in cell volumes (sizes) so that the RDW increases, whereas it generally remains within normal limits in ACD. Normal RDWs occur in the range of 12% to 17%. Unfortunately, the standard deviations for normal subjects and for patients with IDA or ACD can overlap significantly, tending to limit the validity of using the RDW exclusively for distinguishing between these conditions.

The major laboratory findings that distinguish IDA from ACD are summarized as entries 1 and 2 in Table 9.1. Note that most of the major tests used to distinguish these two conditions are performed in the clinical chemistry laboratory. This emphasizes the strong interdependence of both of these services in obtaining definitive diagnoses through laboratory measurements.

Normocytic Anemia

In these anemias, the red cells show normal MCVs and MCHCs—that is, they are normocytic and normochromic. Common causes of normocytic anemia include acute hemorrhage, hemolytic anemia, marrow hypoplasia, renal disease, and ACD. It may seem paradoxical that acute hemorrhage presents as normocytic anemia because it involves major blood loss that is associated with loss of iron stores. However, iron depletion requires time to develop; acutely, major blood loss presents as normocytic anemia.

A very useful measurement in determining the cause of normocytic anemia is the reticulocyte count. Reticulocytes are newly formed red blood cells that have recently lost their nuclei but retain high levels of cytosolic mRNA dedicated to the synthesis of hemoglobin. This RNA reacts with the dye, methylene blue, to give a bright-green color, making it possible to perform reticulocyte counts. In addition, reticulocytes and other red blood cell precursors react with the Wright stain to give dark-staining cytoplasm, in contrast to the cytoplasm of mature red blood cells. This darker staining of the cytoplasm of precursors is termed *polychromasia*. In cases, prominently in hemolytic anemia, where there is a loss of red blood cells due to peripheral destruction of these cells, there is an increased synthesis in bone marrow of red blood cells and an early release of red blood cell precursors, especially reticulocytes.

Hyperproliferative Normocytic Anemias

Hyperproliferative normocytic anemias, associated with an increased reticulocyte count, include both hemolytic anemia and the anemia associated with acute blood loss, while hypoproliferative anemias, associated with a decreased reticulocyte count, include such causes as renal disease, ACD, and, variably, bone marrow aplasia/hypoplasia. Renal disease can affect juxtaglomerular cells that are involved in the synthesis of erythropoietin, the growth factor that induces differentiation of bone marrow hematopoietic stem cells into the red cell line. Bone marrow aplasia/hypoplasia can give rise to low reticulocyte counts if caused by agents, such as chemotherapeutic agents, that kill bone marrow hematopoietic stem cells. In such conditions as myelofibrosis, clonal expansion of cancer cells such as occurs in leukemia, lymphoma, myeloma, and metastatic cancer, there may be a release of early red and white blood cell precursors from bone marrow (the leukoerythroblastic picture discussed later), leading to increased nucleated red blood cell and reticulocyte counts.

As mentioned earlier, a history and a complete physical, as well as an examination of the patient's peripheral blood film, are helpful in establishing a differential diagnosis. In this section, we focus on the most common causes of normocytic anemia: hemolytic anemia, aplastic anemia, and the anemia associated with renal disease.

Hemolytic Anemia

Hemolysis is defined as the destruction of the red cell membrane, causing hemoglobin release. This may occur slowly as a normal physiologic process or may be accelerated in pathologic states. Many different underlying causes exist for the decrease in survival/increase in destruction of red blood cells. These include membrane defects (e.g., hereditary spherocytosis), enzyme defects (e.g., glucose-6-phosphate dehydrogenase [G6PD] deficiency), hemoglobinopathies (e.g., sickle cell disease or beta-thalassemia), immune destruction (e.g., autoimmune hemolytic anemia or hemolytic transfusion reaction), and nonimmune destruction. Immune and nonimmune destruction include destruction due to infectious agents, toxic agents/drugs, physical agents, hypersplenism, and microangiopathic hemolytic anemias. Microangiopathic hemolytic anemias are caused by the mechanical destruction of red blood cells, mainly in bone marrow where they are synthesized, from such factors as fibrin deposition in the blood vessels of the bone marrow microvasculature, fibrosis, or malignancies such as leukemia, lymphoma, and metastatic cancer. In addition, mechanical destruction can result from extramedullary causes such as prosthetic heart valves.

Hemolytic anemia can be recognized from hemoglobin in plasma/serum and breakdown products of heme. Specific laboratory measurements that readily confirm the diagnosis of hemolytic anemia are based on the natural events that occur subsequent to hemolysis. After erythrocyte membrane

breakdown, hemoglobin is extruded. Thus, plasma and urine may contain free hemoglobin or its degradation products. Free hemoglobin may be present acutely in the plasma (hemoglobinemia) or urine (hemoglobinuria), while hemosiderin may be present in the urine (hemosiderinuria) in more chronic episodes of hemolysis. Extruded hemoglobin becomes bound to the alpha-2 fraction protein, haptoglobin. The hemoglobin–haptoglobin complex becomes catabolized by macrophages that engulf these complexes by receptor-mediated endocytosis. Thus, an excellent indicator for hemolytic anemia is a *low haptoglobin value*. Extremely sensitive and rapid ELISA tests for haptoglobin are available for this purpose.

Because the red cell contents are extruded into the plasma, besides hemoglobin, there are other indicators of red cell damage: high serum potassium because intracellular potassium concentration is much higher in red cells than in the extracellular fluid and serum elevations of the enzyme lactate dehydrogenase (LD). As discussed in Chapters 19 and 21, this enzyme has five major isozymes, labeled LD1 through LD5. Peculiarly, the predominant isozyme of LD in red cells is LD-1, which occurs predominantly in cardiac tissue.

Carbon monoxide (CO) and unconjugated bilirubin become elevated in blood in hemolytic anemia. When hemoglobin is extruded, large amounts of it become oxidized to methemoglobin. The heme portion dissociates and then becomes oxidized ultimately to bilirubin. The first step in this process is the oxidative opening of the porphyrin ring of heme with the attendant liberation of CO. CO may be measured easily by gas chromatographic techniques, or even more conveniently by co-oximetry, based on spectrophotometry (see Chapter 4), as carboxyhemoglobin (see Chapter 31). Elevated CO levels in normochromic, normocytic anemias are an excellent indicator of hemolytic anemia.

Because there is an increased production of bilirubin, which is unconjugated (see Chapter 22), there will be at least a transient elevation of serum indirect bilirubin. This elevation, in the presence of normal liver function, will be modest, usually in the range of about 2 to 2.5 mg/dL. (The upper limit of normal is around 1.2 mg/dL.)

Hemolytic anemia is almost always accompanied by an increased reticulocyte count and by evidence of red cell damage. As mentioned earlier, the reticulocyte count will be elevated (increase in polychromasia on the blood film), with erythroid hyperplasia present in the bone marrow, indicative of increased red cell production. In addition, the peripheral blood film may show evidence of the particular type of red cell damage associated with the particular type of hemolytic anemia (e.g., sickle cells in sickle cell disease or schistocytes/helmet cells in microangiopathic hemolytic anemia). There is also a noticeable difference in red cell size (anisocytosis) and shape (poikilocytosis) due to the presence of damaged and/or young cells. Because of the often marked changes in size and/or shape, the RDW is usually elevated. A number of nucleated red blood cells may also be identified.

Other findings in hemolytic anemia can identify the cause. A direct antiglobulin test (DAT)/direct Coombs test can be used to detect immunoglobulin attached to the red cell surface that identifies immune hemolytic anemia as the cause of red cell destruction. In this case, red cells are incubated with antihuman immunoglobulin. If the red cells are coated with antibody, they will agglutinate in the presence of the antihuman immunoglobulin, but if not coated with antibody, they will not agglutinate. A positive test suggests that an autoantibody or alloantibody may be responsible for the anemia. A positive screening test for G6PD deficiency will identify this enzyme deficiency as the cause of the hemolytic anemia. The selection of these tests will be dependent on the clinical evaluation as well as the preliminary laboratory data.

Laboratory findings that are diagnostic of hemolytic anemia are summarized in entry 3 in Table 9.1. Note that virtually all of the quantitative diagnostic testing for hemolytic anemia—that is, serum and urine hemoglobin, haptoglobin, carboxyhemoglobin, indirect bilirubin, and LD—are performed in the clinical chemistry laboratory, again emphasizing the strong interdependence of the clinical chemistry and hematology laboratories.

Microangiopathic Hemolytic Anemia

As previously mentioned, red cell fragments (schistocytes) may be present on peripheral blood films due to mechanical (e.g., prosthetic heart valve) or thermal (severe burns) destruction. Mechanical rupture of red cells within the microvasculature may also occur by physical damage to red cells in the microvasculature of bone marrow. This may be due to space-occupying lesions, such as metastatic tumors or leukemia or lymphoma, to myelofibrosis, or to the intravascular deposition of fibrin strands on endothelial cell surfaces. Because red blood cells are damaged and destroyed, this process leads to so-called microangiopathic (i.e., lesions in the microvasculature) hemolytic anemia (MHA).

Besides space-occupying lesions, other causes of this type of anemia include disease states in which fibrin is deposited on endothelial surfaces, also resulting in the shearing and fragmentation of newly synthesized red blood cells, as in disseminated intravascular coagulopathy (DIC). In this condition, there is an abnormal activation of the coagulation process in which fibrin-platelet clots form intravascularly and embolize to virtually any tissue. These clots block the microvasculature of tissues, including that of bone marrow, resulting in the destruction of newly synthesized red cells. In addition, other disease states may give rise to MHA, in which there may be an immunologic component—that is, antibodies to determinants on endothelial cells or on other structures in the microvasculature, resulting in immune complex deposits with or without fibrin deposits.

In thrombotic thrombocytopenic purpura (TTP), the microvascular disease is caused by platelet thrombi. A prominent cause of this condition is dysfunction due to the absence of a critical chymotrypsin-like protease known as ADAMTS13 (A Disintegrin And Metalloproteinase with a Thrombospondin type 1 motif, member 13) that hydrolyzes large multimer forms of von Willebrand factor (vWF) into lower molecular mass forms; the high molecular mass forms promote platelet aggregation, leading to this condition. However, this condition can also arise, rarely, in patients with no known abnormality of ADAMTS13 in cases of acquired TTP. Because the microvasculature is blocked in this condition, there is multiple system pathology—prominently renal failure—evidenced by high serum levels of creatinine and BUN (blood urea nitrogen), as described in the Abnormalities in Clinical Chemistry section, neural signs and symptoms due to cerebral infarctions and thrombocytopenia, and widespread purpura from local hemorrhaging.

In the closely related condition called the hemolytic anemic/uremic syndrome (HUS), which occurs mainly in children, bacterial infection by certain toxin-producing strains of organisms such as *E. coli*, *S. pneumoniae*, *Mycoplasma*, and *Shigella* induce platelet aggregation. This is believed to arise in part from toxin-induced inhibition of ADAMST13, although the full pathophysiology of this condition still remains unexplained. Here, as in TTP, there is renal failure anemia, and, though less prominent than in TTP, neural symptoms.

MHA may also occur with other immune-mediated disorders—for example, connective tissue disorders such as disseminated lupus erythematosus, where endothelial damage from the attachment of immune complexes and complement produces fibrin deposition on endothelial surfaces. More important, because MHA results from traumatic destruction of newly formed red blood cells in the microvasculature where both red and white blood cell precursors are being formed, often both red and white blood cell precursors are released into the circulation. Thus, all of the findings of hemolytic anemia are present, in addition to which a significant number of precursor cells are seen in the peripheral blood, such as nucleated red blood cells, myelocytes, and metamyelocytes, a pattern termed the *leukoerythroblastic picture*.

As discussed later, in DIC and occasionally in TTP, laboratory findings include thrombocytopenia and increased prothrombin time, activated partial thromboplastin time, thrombin time, fibrin degradation products, and D-dimer levels (described later); fibrinogen levels, however, are low. As discussed earlier, BUN and creatinine are also elevated.

Hypoproliferative Normocytic Anemias

Bone Marrow Hypoplasia/Aplastic Anemia

This is a hypoproliferative anemia, with MCV and RDW usually within normal limits, that typically affects all peripheral blood elements (red cells, white cells, and platelets; see later discussion). Immature white cells and red cells are not usually present on peripheral blood films. Bone marrow biopsy is commonly performed to obtain the diagnosis and typically shows severely hypoplastic/aplastic marrow with severe depletion of all hematopoietic marrow precursors. Aplastic anemia may be primary/inherited or secondary/acquired, with the latter due to chemotherapy, chemical toxins, infection, radiation, or immune dysfunction. Serum iron may be elevated due to lack of erythropoiesis. The typical hematologic findings in this condition are summarized in entry 4 in Table 9.1. More important, *none of the quantitative serum diagnostic tests for hemolytic anemia, such as haptoglobin, carboxyhemoglobin, and indirect bilirubin elevation, are positive in this condition.*

Myelodysplastic Syndrome

Another less common condition, but nonetheless an important cause of hypoproliferative normocytic anemia, is myelodysplastic syndrome (MDS). This syndrome, which often presents as a normocytic anemia, although it can also on occasion present as a mildly macrocytic or microcytic anemia, is refractory to treatment such as transfusions of packed red blood cells. It may present simply as a refractory anemia in its early stages and is thought to progress to

refractory anemia with ringed sideroblasts and eventually to so-called preleukemic stages, in particular refractory anemia with an excess of blasts in bone marrow (generally in the myeloid or lymphoid lines) and an excess of blasts in transformation. The condition may also present initially as a refractory cytopenia that involves all three (erythroid, granulocytic, megakaryocytic) hematopoietic cell lines. As might be surmised from this latter observation, MDS appears to be a clonal stem cell disorder that is characterized by ineffective hematopoiesis. Further discussion of this fascinating disease can be found in Chapter 33.

Anemia of Renal Failure

Another normocytic, hypoproliferative anemia is the anemia of chronic renal failure. Loss of the kidneys' excretory function produces an increase in BUN and creatinine (discussed later) as well as a buildup of metabolic byproducts. The resulting uremia appears to be responsible for changes in red cell shape, with burr cells (echinocytes) and ellipsoidal cells commonly present on peripheral blood films. Identification of burr cells on peripheral blood films during the course of illness may signal the development of renal dysfunction. In addition to a decreased excretory function, there is a decrease in the kidneys' ability to produce erythropoietin, resulting in impaired erythropoiesis, such that the marrow's response to hypoxia becomes inadequate. Distinguishing this condition from aplastic anemia (entry 4 in Table 9.1), white cell and platelet counts usually remain within normal limits. The typical findings in this condition are summarized in entry 5 in Table 9.1. Again, as in bone marrow hypoplasia/aplastic anemia (entry 4, Table 9.1), none of the quantitative serum diagnostic tests for hemolytic anemia (e.g., haptoglobin, carboxyhemoglobin, indirect bilirubin elevation), are positive in this condition.

Macrocytic Anemia

Macrocytic anemia can be diagnosed from the hemogram from a low red blood cell count and a high MCV, often exceeding 100 fL. By far the most common cause of macrocytic anemia is nutritional deficiency, such as vitamin B_{12} and/or folate deficiency. Lack of either factor is thought to disrupt DNA synthesis but not RNA synthesis, such that the nucleus and cytoplasm of the cell no longer mature in synchrony. Morphologically, the cell cytoplasm matures, while the nucleus remains immature, and the cell appears megaloblastic. This lack of synchrony produces hypersegmented neutrophils (five-lobed nuclei in more than 5% of the neutrophils or any neutrophil with six or more lobes) and large, oval-shaped red cells termed *macroovalocytes*, both of which are present on blood films of patients with megaloblastic anemia. In addition, the RDW is typically increased, and the reticulocyte count is decreased.

If macrocytic anemia is diagnosed, the first serum analytes whose concentrations should be determined are B_{12} and folate, for which rapid and accurate ELISA tests are performed. If these analytes are both found to be within the reference range, assays for thyroid function should be performed because hypothyroidism is a cause of macrocytosis. As discussed later in the Endocrine Function Testing section, elevated thyroid-stimulating hormone (TSH) with low or normal thyroxine (T_4) serum levels confirm the diagnosis of primary hypothyroidism. Because certain therapeutic drugs—particularly azidothymidine (AZT), used in the treatment of retroviral disease—are known also to induce macrocytic anemia, it is important to ascertain whether a patient is being treated with such drugs.

In this era of the automated CBC, it is possible also that red cell precursor forms, such as nucleated red blood cells, may be counted as mature erythrocytes. Therefore, in a patient with a "macrocytic" anemia with normal B_{12}, folate, and thyroid hormone levels, it is important to check the reticulocyte and nucleated red blood cell count to determine whether these are significantly elevated. If so, the possibility of a hemolytic anemia should be considered. Thus, the diagnostic workup for hemolytic anemia described in the preceding section should be instituted.

Other possible causes of macrocytic anemia include posthemorrhagic states (differentiated by an elevation of the reticulocyte count and polychromasia), alcoholism (associated with folate deficiency), liver disease, and myelodysplasia. Note again that the definitive tests for determining the cause of macrocytic anemia—that is, B_{12}, folate, and thyroid function tests—are often performed in the clinical chemistry section.

Major clinical laboratory findings for macrocytic anemia are summarized as entries 6A and B in Table 9.1. Note that macrocytic anemias are divided into megaloblastic (entry 6A), typical of B_{12} and folate deficiency, and nonmegaloblastic (entry 6B), typical of hypothyroidism. Whether the macrocytic anemia is megaloblastic can be determined only by bone marrow biopsy. This procedure is not necessary in most cases because the cause of the macrocytosis can be determined by the assays described earlier.

Table 9.1 summarizes some of the pertinent findings and specific determinations used to distinguish and diagnose common anemias previously discussed. Note that this table is a guide as to what specific tests should be ordered and, by implication, what tests need not be ordered. For example, a microcytic anemia should be worked up with orders for ferritin levels, IBC, and Fe/IBC ratios, but generally there is no need to order B_{12} and folate levels. Conversely, there is no need to order ferritin, IBC, and so on for a macrocytic anemia, for which B_{12} and folate levels should be ordered.

QUANTITATIVE WHITE BLOOD CELL ABNORMALITIES

The white blood cell (WBC) count encompasses several types of commonly circulating nucleated cells: granulocytes (principally, mature neutrophils, basophils, and eosinophils), lymphocytes, and monocytes. It should be noted that absolute concentrations (and not percentages) of these cells are significant in interpreting the WBC count. An increase above the normal physiologic level in the WBC count, termed *leukocytosis*, may primarily involve any of these white cells, depending on which cell type is chiefly elevated (i.e., neutrophilia, basophilia, eosinophilia, monocytosis, and lymphocytosis). Occasionally, plasma cells may be found in the peripheral blood. Likewise, a decrease in the WBC count, termed *leukopenia*, may also center on a single cell series (i.e., neutropenia, monocytopenia, and lymphocytopenia). Absolute decreases in the eosinophils and basophils are difficult to identify because of the low numbers present normally. Certain differential diagnoses are commonly associated with certain WBC changes (e.g., infection and/or inflammation with neutrophilia; allergic reactions and parasitic infections with eosinophilia). In addition, elevations may be due to a benign process (e.g., infection) or a malignant process (e.g., leukemia). Here, we note several quantitative patterns and their associations that correlate with abnormal chemical findings.

Again, clinical history and physical findings are important in diagnosis and management of the patient. In addition, the CBC and white cell differential are important laboratory findings used, in conjunction with the clinical impression, to formulate the differential diagnosis. In adults, the reference range for the WBC count is approximately 4000 to 7000 white cells/μL; approximately two thirds of the white cells are neutrophils, and slightly less than one third are lymphocytes.

Infection

Infection is the most common cause of an elevated WBC count. An elevated WBC count of between about 10,000 and 20,000/μL commonly points to an infectious/reactive process. In general, neutrophilia is associated with infection (bacterial, fungal, viral), inflammatory states (trauma, surgery), certain drugs (e.g., corticosteroids), and myeloproliferative conditions. Exceptions to the neutrophilia seen in bacterial infections are tuberculosis; brucellosis; pertussis, in which the predominant cells are lymphocytes; and infections, mainly in newborns, with *Listeria monocytogenes*, for which a monocytic response is predominant.

Eosinophilia is commonly associated with allergic reactions, parasitic infections, and hematologic malignancies (Boyer, 2016; Brito-Babapulle, 2003; Fischbach et al., 2008; Brigden & Graydon, 1997; Rothenberg, 1998). Basophilia is also commonly associated with hematologic malignancies (e.g., chronic myelogenous leukemia [CML]), but it may be seen in some inflammatory states and allergic reactions. Lymphocytosis is commonly associated with acute viral infections, such as infectious mononucleosis (Epstein-Barr virus infection); chronic infections, such as tuberculosis, brucellosis, and pertussis; and hematologic disease and immune stimulation. Monocytosis is commonly associated with hematologic disease, such as acute monocytic leukemia (M5 by the French-American-British, or FAB, classification system), acute myelomonocytic leukemia (M4, in the FAB system), or chronic myelomonocytic leukemia, as well as with some infectious processes, such as tuberculosis, rickettsia, and listeria.

Elevated White Blood Cell Count Due to Leukemoid Reaction

In patients who do not have leukemia, very high white blood cell counts (generally $>50 \times 10^3/\mu L$) may produce a peripheral blood film appearance similar to leukemia. This is termed a *leukemoid reaction*. The more common type of leukemoid reaction is granulocytic, although lymphocytic reactions may also occur. The granulocytic type usually reveals reactive neutrophils present in the peripheral blood film, with a left shift in the neutrophil series (i.e., immature forms such as bands, metamyelocytes, and myelocytes). Changes in the cells' cytoplasmic appearance, such as toxic granulation and Döhle body production (see Chapter 33), are also commonly present. Causes of the granulocytic type of reaction include bacterial infection (e.g., diphtheria), malignancy (Hodgkin disease), and reactive conditions such as rebound granulocytosis. Although these changes are helpful, C-reactive protein (CRP), an acute-phase plasma protein, rapidly rises and falls with the onset and resolution of inflammation. CRP appears to be an earlier

and more sensitive indicator of acute inflammation and infection (Sproston & Ashworth, 2018; Dantzer et al., 2008; Seebach et al., 1997) and can now be quickly measured using present-day analyzers. Leukemoid reaction must be distinguished from CML and other myeloproliferative conditions. More important, the enzyme *neutrophil alkaline phosphatase* will be normal or elevated in a granulocytic leukemoid reaction but is decreased in CML.

Elevated White Blood Cell Count Due to Chronic Myelogenous Leukemia

At present, definitive diagnosis of CML rests on the demonstration of the Philadelphia chromosome (i.e., the BCR/c-abl translocation between chromosomes #9 and #22) by either cytogenetics or molecular techniques (e.g., see Jabbor & Kantarijan, 2018; George & Arber, 2003; Hughes & Branford, 2003; Sattler & Griffin, 2003; Silver, 2003; Ross & Hughes, 2008; also, see Chapters 34, 70, and 77). Detection of molecular or cytogenetic abnormalities is also of diagnostic (and can be of prognostic) significance in other hematologic diseases, including acute myeloid leukemia, acute lymphoblastic leukemia, T cell leukemia/lymphoma, and myelodysplasia (Swerdlow et al., 2008). Molecular techniques are also currently utilized to detect very early stages of disease as well as to detect minimal residual disease—that is, disease that may only be apparent at the molecular level. For example, quantitative polymerase chain reaction can be used to monitor BCR/c-abl translocation levels in CML patients being treated with the kinase inhibitor imatinib (Gleevec) (Ross & Hughes, 2008). An important clue for diagnosing CML is an increase, in peripheral blood, of the basophil count often also accompanied by an increased eosinophil count (El-Ghammaza, 2015). Basophilia is an independent adverse prognostic factor in patients with CML.

Elevated White Blood Cell Count Due to Chronic Lymphocytic Leukemia

When the lymphocytes appear normal but are significantly increased in number in an older individual, the possibility of chronic lymphocytic leukemia (CLL) must be considered. Again, molecular techniques, such as flow cytometric, immunophenotypic, and cytogenetic/fluorescence in situ hybridization analysis (Hallek, 2018; Oscier et al., 2004; Shanafelt & Call, 2004) can help establish the diagnosis. In CLL, the neoplastic B lymphocytes will be found to express an unusual (but characteristic) human leukocyte differentiation antigen designated CD5, which is typical for this disease. Other CD antigens can also be detected by flow cytometry and have become useful in resolving other hematologic diagnostic problems.

Leukocytosis Due to Acute Leukemias

Both acute myeloid and lymphoid leukemias present often as markedly elevated white cell counts. In lymphoblastic leukemia, numerous lymphoblasts are seen on the peripheral smear. The myeloid leukemias can present in a myriad of forms, including myeloblastic, promyelocytic, monoblastic/monocytic, myelomonocytic, erythroblastic, and megakaryoblastic. Again, flow cytometric, immunophenotypic, and karyotypic/molecular analysis can help establish the diagnosis as well as define prognosis (Winton & Langston, 2004, Jabbour, 2018). These are discussed fully in Chapters 34 and 77. Here, we point out that blast forms of any kind on a peripheral blood smear raise the strong diagnostic possibility of an acute leukemia.

Low White Blood Cell Counts

Aplastic Anemia

Low WBC counts, if accompanied by marrow hypoplasia and two out of three of anemia (with corrected reticulocyte count <1%), neutropenia (neutrophil count <500/μL), and thrombocytopenia (platelet count <20,000/μL) may be part of generalized pancytopenia secondary to marrow failure (DeZern & Brodsky, 2011; Marsh, 2005; Marsh et al., 2003; Guinan, 1997). Also known as aplastic anemia, this condition may be primary/inherited or acquired/secondary. Known causes of the acquired type include chemotherapy, drugs/toxins, infections (including hepatitis), radiation, and immune dysfunction (Gordon-Smith et al., 2002). Cytogenetic study may be utilized to rule out myelodysplasia; if unsuccessful, molecular techniques such as fluorescent in situ hybridization (FISH) may be necessary for chromosome analysis (Guinan, 1997). The primary/inherited types may not always be present at birth (i.e., congenital), and diagnosis of this type of marrow failure relies heavily on clinical assessment in conjunction with appropriate laboratory evaluation (Alter, 1999; 2002).

Gram-Negative Sepsis as a Cause of Leukopenia

Leukopenia may also be seen in other conditions, including gram-negative sepsis. Interestingly, gram-negative sepsis with a low WBC count is often accompanied by a cholestatic pattern in the liver (i.e., a mild rise in bilirubin and alkaline phosphatase), discussed later and in Chapter 22.

COAGULATION DISORDERS

This vast and complex topic is discussed in Part 5. For our review, we focus on four hematologic parameters that may be important in correlation with test results in chemistry determinations: the platelet count; the bleeding time; the activated partial thromboplastin time (APTT), reflecting the function of the intrinsic coagulation system; and the prothrombin time (PT), reflecting the function of the extrinsic coagulation system. Diminished values of the platelet count and/or abnormalities in platelet aggregation can lead to abnormal bleeding times. Elevated PTs and/or APTTs are not generally associated with abnormal bleeding times except mainly in factor VIII deficiency with concomitant deficiency of vWF. This latter factor is needed for platelet aggregation.

Bleeding Time Measures Platelet Function. Historically, the bleeding time (BT) was utilized as a screening test for platelet function. It should be noted that the BT is not felt to correlate accurately with or to predict bleeding (DeCaterina et al., 1994; Gerwirtz et al., 1996) and is now uncommonly used to screen for platelet function abnormalities (Kottke-Marchant & Corcoran, 2002; Posan et al., 2003).

Major Causes of Increased PT or APTT. The anticoagulant heparin, which accelerates the inactivation of thrombin and other coagulation factors (such as factor Xa), preferentially blocks the intrinsic system of coagulation, leading to prolonged APTTs but not significant elevations in PTs. On the other hand, the vitamin K antagonist Coumadin preferentially blocks factor VII in the extrinsic system, leading to prolonged PTs but not APTTs.

International Normalized Ratios for Patients Being Treated with Coumadin. The PTs of patients who are being anticoagulated on Coumadin must be followed carefully to ensure that the therapeutic effect is occurring but that the effective levels of Coumadin are not sufficiently elevated as to initiate hemorrhage. Thus, it is important to establish a therapeutic range for PTs for patients on Coumadin. Because different methods for determining PTs exist, somewhat different reference ranges for PTs among different laboratories have resulted, making it difficult on occasion to compare PT results from different laboratories for a given patient. To attempt to correct for these differences, the PT values are used in a formula that standardizes these "raw" values. This formula takes the ratio of the observed PT to the mean value for the PT reference range of the particular laboratory and then raises the resulting ratio to the power of what is termed the *international standardized index* (ISI). This index is determined from the slope of a correlation plot of the logarithm of a laboratory's PTs for blood samples that contain different Coumadin concentrations against the logarithm of the PTs determined by a reference (gold standard) method. Thus, the international normalized ratio (INR) is $(\text{PTpat}/\text{PTmean})^{\text{isi}}$, where PTpat is the measured PT for the patient and PTmean is the mean value for the laboratory's reference range (Kamath & Kim, 2009). In most circumstances, INR values of 2 to 3 are considered to be therapeutic for patients who have atrial fibrillation and 3 to 4 for patients with prosthetic heart valves, while values over 4 are considered to require lowering of the Coumadin dose or temporary cessation of treatment. Note that INRs are appropriate principally for patients who are being treated with Coumadin.

The Other Cause of Isolated PT or APTT Elevation Is Coagulation Factor Deficiency. If the PT or APTT becomes elevated, in the absence of treatment with heparin or Coumadin, and the platelet count is normal, it is important to perform mixing studies of the patient's plasma with normal plasma to determine whether the coagulation time normalizes—that is, whether there is a factor deficiency. A not infrequent cause of factor deficiency is liver failure, discussed subsequently and in Chapter 22. Thus, liver function measurements should also be checked in these instances. If mixing studies do not completely correct the prolonged coagulation times, the presence of coagulation inhibitors, such as *circulating lupus anticoagulant* or *antifactor antibodies*, should be suspected.

The Major Cause of Elevated PT and APTT Is DIC. If the platelet count diminishes and the APTT and PT both rise, the diagnosis of DIC should be entertained. This diagnosis is confirmed by the finding of elevated D-dimer, discussed in Chapter 40, the D–D fragment of fibrin that results from the proteolytic action of plasmin upon the fibrin clot that forms during intravascular coagulation. D-dimer is detected in an assay utilizing a very specific monoclonal antibody to this cross-linked fibrin degradation product. This method has largely replaced the less specific assay for fibrin split products (FSPs), which are likewise elevated in this condition. DIC is an extremely dangerous condition and must be diagnosed rapidly, as indicated earlier.

In this condition, there is an abnormal activation of both coagulation cascades and a consumption of platelets. This activation may be caused by gram-negative sepsis (activation of the cascades may be from bacterial endotoxins), cancer, chronic inflammatory states such as in collagen vascular diseases, leukemia (especially acute promyelocytic leukemia), complications of pregnancy, blood transfusion complications, liver failure, and physical trauma such as burns, drowning, and central nervous system (CNS) injuries. DIC causes the formation of microemboli that can result in widespread tissue infarction or ischemia with attendant abnormal chemical values—for example, elevated liver function enzymes; elevated BUN and creatinine, suggestive of renal failure; and even elevation of cardiac troponin, indicating myocardial damage. Thus, low platelet counts and elevated APTT and PT, together with chemical abnormalities suggestive of multisystem dysfunction, strongly suggest DIC. Anticoagulant therapy must be instituted rapidly to block further embolization and tissue destruction.

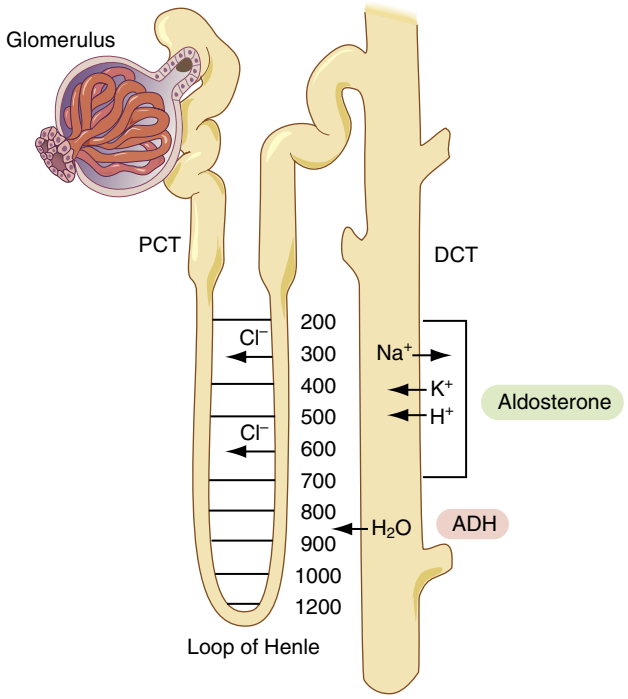

Figure 9.1 A schematic representation of a nephron showing the fundamental mechanism of water and salt conservation by the kidneys. Filtration occurs at the glomerulus (*upper left,* showing capillaries in *red*), and the filtrate passes through the proximal convoluted tubule (PCT), where about 70% of the total filtered sodium is reabsorbed. In the loop of Henle, the countercurrent multiplier mechanism is operative. Chloride ion (Cl^-) is extruded from the ascending limb into the interstitial space *(upper middle part of figure)*. Sodium ion passively follows. The cells of the ascending limb of the loop of Henle are impermeable to water, and the cells of the descending limb are impermeable to chloride ions. The result of this system is that high concentrations of NaCl are built up at the tip of the loop of Henle. The numbers beside the loop of Henle are osmolalities at different levels along the loop that, in humans, reach a maximum of 1200 mOsm/kg, as shown in the figure. At the top of the loop, the filtrate becomes isotonic (where the 300 mOsm/kg mark occurs) and then hypotonic due to the continuous extrusion of chloride ion. The hypertonic interstitium allows water to diffuse in from the collecting ducts provided that antidiuretic hormone *(ADH, labeled and highlighted in color)* is secreted. More sodium ion can be conserved in the distal convoluted tubule (DCT), provided aldosterone *(labeled and highlighted in color)* is secreted, resulting in the one-to-one exchange of Na^+ for K^+ and H^+.

ABNORMALITIES IN CLINICAL CHEMISTRY: CHEMICAL PATHOLOGY

ELECTROLYTE ABNORMALITIES

This topic is treated at length in Chapter 15 and in Oh (2003). Here, we present an overview of the regulation of the serum levels of critical electrolytes to enable accurate formulation of the possible causes of abnormalities in their serum levels. Figure 9.1 summarizes the basic mechanisms by which the kidneys control electrolyte and water balance. Functionally, keep in mind that the purpose of the kidneys is to conserve fluids or, tantamount to this, to concentrate the urine. The mechanism by which this conservation of fluids is effected is by the building up of high–sodium chloride gradients in the interstitial space between the descending and ascending limbs of the loop of Henle, using the countercurrent multiplier mechanism. In this mechanism, sodium chloride is extruded into the interstitial space such that NaCl concentrations become greater toward the tip of the loop of Henle. The ascending limb of the loop of Henle is impermeable to water, as are the distal convoluted tubules and collecting ducts. However, under the effect of antidiuretic hormone (ADH), the collecting ducts are made permeable to water, allowing it to flow into the interstitial space and to penetrate the vasa recta. The entire driving force for this process is the high concentrations of NaCl in the interstitium. Any interference with the countercurrent multiplier will block reabsorption of water because the ion gradients are eliminated.

As also shown in Figure 9.1, sodium ion, 70% of which is reabsorbed in the proximal convoluted tubule, can be further reabsorbed in the distal convoluted tubules and collecting ducts under the effect of aldosterone from the zona glomerulosa of the adrenal cortex. This hormone promotes the 1 : 1 exchange of sodium for potassium or hydrogen ion. Sodium levels in serum depend almost completely on the interplay between aldosterone and ADH. With these simple considerations in mind, the most common causes of hyponatremia and hypernatremia are now summarized with an explanation of how to identify them. It should be kept in mind that normal renal function is assumed. If renal failure occurs, the kidneys ultimately fail to be able to concentrate the urine so that hyponatremia will result, as is discussed in the Renal Disease section to come.

Hyponatremia

The four most common causes of hyponatremia are given in Table 9.2, together with a fifth, rare, cause: Bartter syndrome. A sixth, metabolic cause, diabetes mellitus, is also presented in this table. In all forms of hyponatremia, the chloride ion concentration is also generally low because chloride is the chief counterion for sodium.

Basic Principle. All confirmed serum sodium abnormalities must be followed up with urinalysis on the patient who must be fluid restricted. This urinalysis should include the urine sodium and urine osmolality. For conditions 1 and 2 in Table 9.2, the serum sodium tends to correct over a 24-hour period when the patient is fluid restricted.

Overhydration. In this condition, the most common cause of which is the consumption of large amounts of water or hypotonic fluids due to such causes as psychogenic polydipsia, serum sodium is reduced below 135 mEq/L. Because the consumed water is excreted by the kidneys, the urine is also dilute in this ion. In fact, the osmolality of urine will be low—that is, less than 300 mOsm/kg. Often accompanying hyponatremia in overhydration are low values of the hematocrit and low values of BUN, discussed

TABLE 9.2
Common Causes of Hyponatremia and Electrolyte Patterns in Serum and Urine with Normal Renal Function[a]

Cause	Serum Na	Urine Na (UNa)	Urine Osmolality	Serum K	24-Hour UNa
1. Overhydration	Low	Low	Low	Normal or low	Low
2. Diuretics	Low	Low	Low	Low	High
3. SIADH[b]	Low	High	High	Normal or low	High
4. Adrenal failure	Low	Mildly elevated	Normal	High	High
5. Bartter syndrome	Low	Low	Low	Low	High
6. Diabetic hyperosmolarity[c]	Low	Normal	Normal	High	Normal

[a]All Na and K values are concentrations, except for 24-hour UNa, which is the total number of milliequivalents of Na excreted in 24 hours in the urine.
[b]Syndrome of inappropriate antidiuretic hormone secretion.
[c]In this condition, serum glucose is markedly elevated.

subsequently. This triad of findings strongly suggests overhydration as the cause. Urinalysis in the fluid-restricted patient will reveal urinary sodium of less than 25 mEq/L and low osmolalities. The potassium may also be low, although it often remains within the reference range. Because mainly water is excreted in urine in this condition, the total 24-hour sodium excretion will be low (cause number 1 in Table 9.2).

Use and/or Abuse of Diuretics. Loop diuretics block the chloride pump in the loop of Henle, thereby blocking the formation of the ion gradients via the countercurrent multiplier, necessary for water conservation. Thus, water is lost. Also, because sodium is no longer retained because it follows chloride in the loop, it also is depleted from serum. Thus, unlike in overhydration, the total 24-hour sodium excretion is high (compare 24-hour urinary sodium [UNa] for entries 1 and 2 in Table 9.2). Except for this difference, the pattern for diuretics resembles overhydration (dilute serum and urine), except that loop diuretics cause severe potassium depletion unless the diuretic is combined with a potassium-sparing diuretic such as triamterene. Combined hyponatremia and hypokalemia with a high urinary sodium and potassium 24-hour excretion point to diuretic use. Of course, a history will generally also reveal use of diuretics.

Syndrome of Inappropriate Antidiuretic Hormone (SIADH) Secretion (entry 3, Table 9.2). In this condition, secondary to head trauma, seizures, other CNS diseases, and neoplastic conditions, especially lung, breast, and ovarian cancers that secrete ADH-like hormones, the serum sodium is depressed due to the excess retention of water in the collecting ducts. This results in depletion of water in the renal tubules, thereby concentrating the urine. Therefore, while the serum is dilute in sodium (hypotonic), the urine is concentrated to levels of over 40 mEq/L and the urine osmolality exceeds 300 mOsm/kg, while the serum osmolality is less than 280 mOsm/kg. This pattern clearly is diagnostic of SIADH.

Aldosterone Deficit (entry 4, Table 9.2). This condition is secondary to Addison disease and AIDS-related hypoadrenalism. Without aldosterone, the Na^+–K^+ and Na^+–H^+ exchange in the distal convoluted tubules and collecting ducts does not occur. Therefore, serum sodium concentration is reduced, while serum potassium concentration increases, and there is a mild metabolic acidosis. Urinary sodium increases but not to the high levels seen in SIADH, and the osmolality of urine is also not so elevated as in SIADH.

Bartter Syndrome (entry 5, Table 9.2). This rare condition resembles diuretic use except that the hyponatremia is not corrected with fluid restriction. This syndrome is actually a complex of diseases, each of which is caused by mutations of genes that encode ion transporter proteins in the thick portion of the ascending loop of Henle. There are two forms of neonatal Bartter syndrome, caused by absence or mutations of the Na-K-2Cl symporter protein (*SLC12A2* or *NKCC2* gene) or the ROMK/KCNJ1-encoded potassium channel protein. In so-called classic Bartter syndrome, the *CLCNKB* gene–encoded chloride channel protein is defective. In a form of Bartter syndrome that is associated with hearing loss (sensorimotor loss–associated Bartter syndrome), the *BSND* gene–encoded accessory chloride channel protein is dysfunctional. In another Bartter variant, the *CASR* (calcium-sensing receptor) gene–encoded calcium transporter protein is defective, leading to Bartter syndrome with superimposed hypocalcemia. In Gitelman syndrome, which parallels Bartter syndrome but is a milder form of disease, mutations in the *NCC* gene–encoded sodium-chloride symporter protein, also termed the *thiazide-sensitive Na^+-Cl^- cotransporter protein* (Pedersen et al., 2010), cause malfunction of reabsorption of sodium and chloride ions from the tubular fluid into the cells of the distal convoluted tubule. In all forms of this disease, as in diuretic use, there is a high 24-hour sodium and potassium excretion.

Diabetic Hyperosmolar State (entry 6, Table 9.2). In patients with diabetes mellitus, if they are in a hyperosmolar state—that is, in which the serum glucose is markedly elevated (say, around 700 mg/dL)—the hyperosmolarity of serum causes efflux of cellular water, with a consequent osmotic dilution of serum sodium. Roughly, for each 100 mg/dL increase in serum glucose, there is a 1.6 mEq/L decrease in the serum Na^+ concentration. Because transport of glucose into cells is accompanied by concurrent transport of potassium into cells, low insulin levels also cause high serum potassium. Thus, the net effect of diabetic hyperosmolar states is a low serum sodium and a high serum potassium. This resembles hypoaldosteronism (entry 4 in Table 9.1), but the presence of abnormally high glucose levels signals the possibility of diabetes mellitus as the cause.

Pseudohyponatremia

This condition is usually caused by the presence of excess lipids in serum. No sodium ions are dissolved in lipids, which can take up a considerable volume of serum. If the absolute amount of sodium in a given volume of serum is determined, as is performed when using such methods of sodium determination as flame photometry, this value is divided by the sample volume to get the concentration. However, part of this volume is lipid that has no sodium; thus, a falsely low value of sodium can be obtained. This artifact is eliminated by the use of ion-selective electrodes that directly determine the concentration of sodium and do not depend on knowledge of the volume of serum. Note that although most modern, high-throughput chemistry analyzers measure serum sodium using ion-selective electrodes, they perform a predilution (dilution prior to analysis) of the specimen (so-called *indirect* potentiometry); thus, the measurement is relative to volume and *is* susceptible to pseudohyponatremia. This phenomenon is discussed further in Chapter 28.

Hypernatremia

Table 9.3 summarizes the three basic causes of hypernatremia. Note that each cause is the counterpart of a cause for hyponatremia. These causes are summarized as follows.

Dehydration (entry 1, Table 9.3). This can be caused by excess renal loss with high positive free water clearance (i.e., loss of water in excess of NaCl), excess sweating, and low water intake. The serum sodium is elevated, as is the hematocrit (possibly masking a true anemia), and the urine sodium is also high due to increased renal excretion of NaCl.

Diabetes Insipidus (DI; entry 2, Table 9.3). DI may be central (neurogenic; i.e., due to decreased vasopressin secretion) or nephrogenic (i.e., due to decreased renal response). Functionally, this condition is the reverse of SIADH—that is, water retention in the tubules is not adequate. Although this condition is not completely understood and may be multifactorial, current research suggests that either mutation and/or changes in protein expression of "water channel molecules" (renal aquaporins) and/or the vasopressin V2 renal collecting tubule cell receptor may play a role in both pathologic water loss, such as in nephrogenic DI, and pathologic water retention, such as in SIADH (Nielsen et al., 2002; Brown, 2003; Oh, 2003; Schrier & Cadnapaphornchai, 2003; Nguyen et al., 2003). The pattern is elevated serum sodium but dilute urinary sodium due to the functionally inadequate levels of ADH.

Hyperaldosteronism (entry 3, Table 9.3). This condition may result from adrenal hyperplasia, Cushing syndrome, Cushing disease (see endocrine section to come) and Conn syndrome, in which there is hypersecretion of aldosterone from the zona glomerulosa. The levels of circulating aldosterone are inappropriately high, causing excessive reabsorption of Na^+ and excretion of K^+ and H^+ ions. The patient will be hypernatremic and hypokalemic and exhibit a mild metabolic alkalosis.

Hypokalemia

Many of the causes of hypokalemia overlap with those of hyponatremia, including overhydration; use of loop diuretics; SIADH; and Bartter syndrome, as discussed earlier. In addition to these causes overlapping with those of hyponatremia, the following states lead uniquely to hypokalemia:

1. Infusion of insulin to diabetics. This results in rather large influxes of potassium into cells, lowering its concentration in serum.
2. Alkalosis. Red blood cells are themselves excellent buffers. They are capable of exchanging potassium for hydrogen ions. Thus, in acidosis, H^+ ions enter red cells in exchange for K^+ ions. Conversely, in alkalosis, H^+ ions leave red cells (to neutralize excess base), while K^+ ions enter the red cells.

TABLE 9.3

Common Causes of Hypernatremia and Electrolyte Patterns in Serum and Urine with Normal Renal Function[a]

Cause	Serum Na	Urine Na (UNa)	Urine Osmolality	Serum K	24-Hour UNa
1. Dehydration	High	High	High	Normal	Varies
2. Diabetes insipidus	High	Low	Low	Normal	Low
3. Cushing disease or syndrome	High	Low	Normal	Low	Low

[a]All Na and K values are concentrations, except for 24-hour UNa, which is the total number of milliequivalents of Na excreted in 24 hours in the urine.

3. Vomiting. The major loss is both H^+ and K^+ from the stomach. Loss of K^+ in gastric fluid may be less important than the overall fluid loss, which causes activation of aldosterone and renal wasting of K^+.

Hyperkalemia

Among the major causes are those that also cause hypernatremia—for example, dehydration and DI—acidosis and diabetes mellitus (as discussed earlier), and hemolysis. Hypoadrenalism resulting in low levels of aldosterone also causes hyperkalemia. Any kind of cell damage, such as rhabdomyolysis, and especially hemolysis of erythrocytes, can cause hyperkalemia. In hemolysis, all of the intracellular K^+ is extruded into plasma. Another analyte that is concentrated in red cells that rises with K^+ in hemolysis is LD. Concomitant elevations of potassium and LD in serum should be taken as indications of hemolysis either artifactually after a blood sample has been taken from the patient or, less commonly, hemolysis from an underlying hemolytic condition.

Anion Gap

All sodium ions must be neutralized by counterions, most of which, in blood, are constituted by chloride and bicarbonate ions, and, to a lesser degree, by phosphate, sulfate, and protein carboxylate groups. Normal serum sodium is about 140 mEq/L, chloride is usually around 100 mEq/L, and bicarbonate is around 24 mEq/L. The anion gap is defined as $Na^+ - (Cl^- + HCO_3^-)$, which, for normal individuals, is around 16. This 16 mEq/L really comprises the other counterions that neutralize sodium but are not measured in serum.

If an individual has a metabolic acidosis in which the rise in H^+ ion concentration is accompanied by a corresponding rise in Cl^- ions, the acid will be buffered by bicarbonate (converted to H_2CO_3). The bicarbonate value will therefore decrease, but there will be a 1:1 increase in chloride ion. Thus, there will be no change in the anion gap. If the metabolic acidosis is due to the presence of an acid whose counterion is not Cl^-, such as acetoacetic acid (in diabetic acidosis) or lactic acid as in sepsis or hypoperfusion, then bicarbonate is reduced, as discussed earlier, but there is no corresponding increase in Cl^-. Therefore, there is an increase in the anion gap that can reach values of 25 to 30 mEq/L. The presence of a widened anion gap signifies the presence of a metabolic acidosis due to a non-chloride-containing acid.

Low Anion Gaps. Consistently low anion gaps, typically in the range of 1 to 3 mEq/L, signify the presence of high levels of basic protein, often a monoclonal paraprotein as occurs in plasma cell dyscrasias. Basic protein contains ammonium ions, the counterions for which are chloride and bicarbonate. Now the "invisible" ion is ammonium, while there is a measurable increase in chloride and bicarbonate ions. This tends to decrease the anion gap. Persistently low anion gaps are a serious sign of possible malignancy—for example, multiple myeloma.

RENAL DISEASE

The four analytes that aid in the diagnosis of this condition are BUN, creatinine, calcium, and phosphate. It is amazing that neither BUN or creatinine is produced in the kidneys, yet both are excellent indicators of renal conditions (Schnermann & Sayegh, 1998; Oh, 2003).

BUN and Creatinine

BUN is blood urea nitrogen. Urea nitrogen is generally measured in plasma or serum, but it has historically been referred to as BUN. The formula for urea is $H_2N—CO—NH_2$. There are two moles of nitrogen per mole of urea. This is the end product of NH_3 metabolism in the liver, as discussed in Chapter 22. Urea is excreted by the renal tubules at a rate that is roughly proportional to the glomerular filtration rate (GFR). Note, therefore, that the retained urea—that is, plasma or serum urea or BUN—is approximately inversely proportional to the GFR—that is,

$$\text{BUN} \propto 1/\text{GFR}. \qquad \text{(Eq. 9.1)}$$

Creatinine is secreted but is also reabsorbed to an approximately equal extent over a rather wide range for the GFR so that the net effect is that the amount filtered is the amount excreted. The total amount of creatinine filtered then is its urinary concentration, Ucr × the volume of urine, V, over a given time. The total plasma volume that delivered this quantity of creatinine to the glomerulus in a given time period is the GFR and is the total amount of creatinine filtered divided by the plasma concentration, Pcr. This quantity is also the creatinine clearance, Ccr. Thus, the GFR is:

$$\text{GFR} = \text{Ccr} = \text{Ucr} \times \text{V} / \text{Pcr} \qquad \text{(Eq. 9.2)}$$

Prerenal Disease. Suppose the BUN is abnormally high (reference range = 10–20 mg/mL). There are two possible reasons for this. The first is prerenal, where renal plasma flow is reduced from such lesions as renal artery stenosis, renal vein thrombosis, and the like. This causes a reduction in the GFR. From Equation 9.1, the BUN will then rise. However, the serum creatinine levels (Pcr in Eq. 9.2), reference range about 0.5 to 1.0 mg/dL, will generally remain within normal limits or may be mildly elevated because, from Equation 9.2, a low GFR will result in lower urine flow (V in Eq. 9.2). The Pcr and Ucr will remain generally within normal limits. Thus, there will be a disproportionate rise in BUN over creatinine. The normal BUN/creatinine ratio is 10:1 to 20:1; in prerenal disease, it rises to well above 20:1.

Renal and Postrenal Disease. The second cause of elevated BUN is true renal disease. Here again, there will be a rise in BUN due to low GFR. Now, however, creatinine filtration will be compromised so that its serum level will rise correspondingly. Thus, in true renal disease, both BUN and creatinine rise together, maintaining the BUN/creatinine at 10:1 to 20:1 (Oh, 2003). This pattern also occurs in so-called postrenal disease, that is, obstructive uropathy due to renal or ureteral stones (nephro- or urolithiasis), prostatic enlargement from benign prostatic hypertrophy or prostatic carcinoma, urinary tract infection, bladder stasis, and urothelial carcinomas.

Pinpointing the Lesion. Suppose a patient is found to have a BUN of 60 mg/dL and a creatinine of 3.5 mg/dL. True renal failure can therefore be diagnosed. Now, consider the kidney to be two compartments, one a filtration compartment (glomerulus) and the other a concentration compartment (renal tubules). If renal failure is present, where is the lesion—in the filtration or concentration compartment? As discussed previously, the function of the kidneys is to conserve fluids or to concentrate the urine. Therefore, if a patient is on a fluid-restricted diet, the osmolality of urine (Uosm) should be significantly higher than the osmolality of plasma (Posm). In fact, Uosm/Posm is higher than 1.2 for normal individuals. If a 24-hour urine specimen collection from this patient on a fluid-restricted diet is measured for Uosm, we can determine where the lesion has occurred. If Uosm/Posm is less than 1.2, then the urine is not being concentrated; thus, there must be a tubular lesion. On the other hand, if there is a normal ratio, then the lesion must be glomerular. Confirmation of glomerular lesions can be performed by urinalysis, as described in Chapter 29. The presence of albumin and/or globulins in urine suggests compromise of the filtration function of the glomerulus. Causes of glomerular lesions are many: glomerulonephritis, pyelonephritis, lupus nephritis, crescentic disease such as Goodpasture syndrome, immune complex disease, pauci-immune crescentic disease, diabetes, and infarction number among these; tubular lesions also have many causes, including pyelonephritis, diabetes, papillary necrosis, acute tubular necrosis (ATN), infarction, shock, and ischemia, among others. It is remarkable that from a blood specimen of only 100 μL and several urine aliquots, not only can we determine the presence of renal failure, but we can localize the lesion, and all of this virtually noninvasively.

Nephrotic Versus Nephritic Disease

In glomerular disease, filtration mechanisms become nonfunctional such that proteins are filtered and consequently are present in urine. Therefore, urinalysis should reveal elevated protein concentrations. Assay of urine for albumin should likewise be performed. If the albumin level is approximately the same as the total protein, then only albumin was filtered in the glomerulus. This condition is termed *nephrosis* or the *nephrotic pattern* and has sometimes been termed *lipoid nephrosis* because β-lipoprotein is often concurrently elevated in serum. This condition is also termed *minimal change disease* because there is little morphologic change in the glomerulus histopathologically. If the albumin level is elevated but is significantly less than that for total protein in urine, then many proteins, besides albumin, pass through the glomerulus, which, in contrast to the glomerulus in minimal change disease, is morphologically damaged. The presence of multiple proteins in urine is called the *nephritic pattern*. These two patterns can also be diagnosed by observing the patterns of urine protein electrophoresis, as discussed in Chapter 20. If only albumin is present, the pattern is nephrotic; if multiple protein bands, that is, albumin and α, and/or β, and/or γ are present, the pattern is nephritic.

Types of glomerular disease can now be diagnosed by ELISA on sera (Mastroianni-Kirsztajn et al., 2015; Caliskan & Kiryluk, 2014). Glomerular diseases often have immunological causes that are of two types: immune complex disease, in which immune complexes are present as subendothelial or subepithelial deposits in the glomerulus; and autoimmune disease, in which specific antibodies to components of the glomerulus, such as the glomerular basement membrane, are present. In some cases, both types may be present. Both patterns can be identified in immunohistochemical studies on renal biopsies. Fortunately, the same antibodies in the immune complexes and in glomerular tissue are frequently present in the circulation where they can be identified in ELISA in serum. These assays are explained in Chapter 45. In fact, due to improved ELISA techniques, there is currently a major trend for relying on these assays on patients' sera to

determine the cause of glomerulopathies. This approach has the advantage that it allows avoidance of performing renal biopsies, which are invasive procedures. In addition, there are studies suggesting that assays for specific proteins in urine samples of patients with glomerular and tubular diseases may result in direct diagnosis of these diseases (Akankwasa et al., 2018) and can be used to monitor progress in disease treatment such as for diabetes mellitus (Zylka et al., 2018). Here, we focus on serologic markers for specific proteins that have been validated as markers for specific glomerular diseases. While there are numerous conditions for which these assays are now available, we list the most prominent among them.

A common cause of primary glomerulonephritis has been found to be deposition of polymeric IgA1 in the mesangium of the glomerulus. This immunoglobulin is discussed in Chapter 47. The cause of this condition appears to be antibodies to this immunoglobulin. An important component of this condition is a defect in the posttranslational modification of IgA1 in that there is the absence of O-glycosylation by galactose of the hinge region of this antibody, resulting in galactose-deficient IgA1 (Gd-IgA1). This results in an unexpected antigenic determinant that provokes an immune response. However, other antibodies against IgA1 are also required for full expression of this disease. Expression in serum of both antiglycan antibodies and of Gd-IgA1 in the presence of proteinuria appear to identify glomerulonephritis at an early stage.

It has further recently been found that high proportions of patients presenting with membranous glomerular nephropathies have high serum titers of circulating antibodies to a membrane receptor for phospholipase A2 on podocytes (glomerular visceral epithelial cells), the so-called PLA-2 antigen. In membranoproliferative glomerulonephritis, a major finding is subendothelial deposition of immune complexes, containing high levels of C3 from the primary complement cascade that may result from concurrent infectious or other diseases provoking an immune response. A diagnostic serologic finding is depletion of circulating levels of C3.

Interestingly, minimal change disease and focal segmental glomerulosclerosis do not seem to have an immunologic component. Rather, in both of these conditions, it has been found that there are elevated serum levels of a soluble (non-membrane-bound) form of the urokinase receptor, called *suPAR*, suggesting that both conditions are manifestations of the same underlying disease, although this view is not universally accepted. A current hypothesis is that binding of suPAR to integrin 3 on the membrane surface of podocytes seems to induce changes in overall cell-cell orientation, resulting in abnormal spacing between cells.

Often, cytotoxic antibodies to glomerular cells result from autoimmune systemic diseases that are not confined to the kidneys. Prominent among these is systemic lupus erythematosus, in which antinuclear antibodies (ANAs) circulate and cause polysystemic disease, including renal nephropathy. It appears that two prominent antibodies that cause direct glomerular damage are ANAs and antinucleosome antibodies. Circulating antibodies against neutrophil cytoplasmic antigen (ANCA) that occur in Wegener granulomatosis affecting both lung and kidney, with a specificity for myeloperoxidase (ANCA-MPO), are serodiagnostic for this condition. These antibodies have been identified as occurring in so-called pauci-immune complex disease identified in the immunohistochemistry on renal biopsies on patients with this disease. Anti-glomerular basement membrane (anti-GBM) antibody has been identified as a prominent causative factor of Goodpasture syndrome that, like Wegener granulomatosis, is a systemic disease affecting both kidney and lung. Interestingly, about 20% of patients with Goodpasture syndrome who have high titers of anti-GBM antibodies also have high titers of ANCA-MPO.

Thus, serodiagnostic markers for renal disease can not only indicate the presence of renal disease but can further identify the location of the disease in the kidneys and further identify the cause of the disease in a virtually noninvasive manner.

Calcium and Phosphate

The kidneys play an important role in the regulation of calcium levels. In renal failure, calcium levels tend to fall, while phosphate levels correspondingly tend to rise. The topic of calcium and phosphorus metabolism is discussed in detail in the context of bone metabolism (see Chapter 16) and the endocrine system (see Chapter 25). Here, we discuss these two analytes for diagnostic purposes.

Remember that calcium is the most abundant cation in the body, most of it stored in bone as a calcium hydroxyphosphate in hydroxyapatite crystal. Calcium complexes with phosphate in several different forms, depending on the ionization state of phosphate—that is,

$$H_3PO_4 \leftrightarrow H_2PO_4^- + H^+ \quad \text{(Eq. 9.3)}$$

$$H_2PO_4^- \leftrightarrow HPO_4^{2-} + H^+ \quad \text{(Eq. 9.4)}$$

$$HPO_4^{2-} \leftrightarrow PO_4^{3-} + H^+ \quad \text{(Eq. 9.5)}$$

The most insoluble calcium phosphate forms are those with the most basic phosphates (i.e., those in Eq. 9.5). Thus, alkaline conditions promote calcium deposition in bone, while acidic conditions promote leaching of calcium from bone. Therefore, alkalosis promotes hypocalcemia, while acidosis promotes hypercalcemia.

Note also that there is an equilibrium between soluble calcium phosphate and insoluble calcium phosphate in bone. We represent this equilibrium as:

$$\text{Ca} + \text{P} \leftrightarrow (\text{CaP})\ \text{insoluble}, \quad \text{(Eq. 9.6)}$$

where P represents all ionic phosphate forms and where the left side is all soluble calcium phosphate salts and the right side is the insoluble salt forms. The equilibrium constant, Ksp, for this equilibrium is:

$$\text{Ksp} = (\text{Ca}) \times (\text{P}) / (\text{CaP})\ \text{insoluble}. \quad \text{(Eq. 9.7)}$$

Because (CaP) insoluble is constant in concentration, the product of soluble Ca × soluble P is a constant, called the solubility constant or Ksp. Thus, there is an inverse relationship between Ca and P. Hypocalcemic states are almost always accompanied by hyperphosphatemic states and vice versa. Of the soluble calcium, in the numerator of Equation 9.7, there are two forms, calcium bound to albumin and globulin, and small molecules in chelate form, and so-called ionized or nonchelated calcium. Biologically active calcium is in the ionized form. Therefore, serum levels of ionized calcium are considered to be the best measure of hypocalcemia, normocalcemia, or hypercalcemia.

Causes of Hypocalcemia. The kidneys are vital in calcium metabolism and regulate calcium levels in two ways. First, parathyroid hormone (PTH) stimulates the renal tubules to excrete phosphate. By Equation 9.7, the serum calcium level must then rise. Also, the kidneys are vital to the formation of active vitamin D in the synthesis of 1,25-dihydroxycholecalciferol, which is necessary for the absorption of calcium in the gut. In renal disease, where there is tubular failure, phosphate excretion is inhibited due to the nonresponsiveness of the tubules to PTH. Therefore, phosphate levels rise, while calcium levels fall. In addition, active vitamin D production is reduced, lowering absorbed calcium. Hypocalcemia and hyperphosphatemia in the face of elevated BUN and creatinine, indicative of renal disease, strongly suggest tubular failure.

Other Causes of Hypocalcemia. Besides alkalosis and renal failure, hypocalcemia may be caused by hypoparathyroidism, also leading to hyperphosphatemia. Rarely, such as in medullary thyroid carcinomas and other amine precursor uptake and decarboxylase (APUD) activity cell tumors, the elaboration of calcitonin, a well-known calcium-lowering hormone, may lead to decreased serum calcium levels. In addition, vitamin D levels may be low, resulting in diminished reabsorption of calcium for the gut. These causes may be encapsulated in the acronym CHARD (Calcitonin, Hypoparathyroidism, Alkalosis, Renal failure, and vitamin D deficit).

Causes of Hypercalcemia. Besides acidosis, the possible causes of this condition may be summarized by Bakerman's CHIMPS mnemonic (Bakerman & Strausbauch, 1994), or Cancer, Hyperthyroidism, Iatrogenic causes, Multiple myeloma, Hyperparathyroidism, and Sarcoidosis.

Calcium and Albumin

About half of calcium circulating in blood is bound to serum protein, mainly albumin; the remainder is either chelated in tight complexes with ions such as citrate and oxalate or is in ionic complexes with counterions such as chloride, so-called "free" calcium. As is true for most hormones in the body, serum levels of PTH are determined by the levels of the free target of the hormone, in this case, free calcium. Also, virtually all of the effects of calcium in the body are induced by free calcium. Free or ionized calcium can be measured directly by an ion selective electrode method described in Chapter 28. However, most laboratories measure total serum calcium using appropriate chelating dye methods; the concentrations of the calcium-dye complexes can be measured spectrophotometrically. Several formulas, none too reliable, have been developed to compute serum free-calcium concentration from the total calcium ion concentration and serum albumin concentration (Larsson & Magnusson, 2003). More relevant is the computation of the "corrected" calcium concentration, most usually in hypocalcemia (Labriola et al., 2009). Generally, even if serum albumin concentrations fluctuate substantially, resulting in changes in total calcium levels, the ionized calcium levels in serum may remain relatively stable. If a patient has a total serum calcium that is lower than the lowest value for the reference range, and if the serum albumin level is concurrently low, a correction formula is used in which the total calcium is computed as the observed total calcium in mg/dL plus a correction factor. There are several different correction factors, perhaps the most commonly used of which is 0.8 × (4 g/dL—serum albumin concentration in g/dL). This correction is based on the ratio of bound calcium to albumin and the mean "normal"

TABLE 9.4
Patterns of pH, PCO_2, and Bicarbonate in Different Conditions

Condition	pH	Bicarbonate	PCO_2	Typical Causes
1. Metabolic acidosis	<7.40	Low	Low	Diabetic keto-acidosis; lactic acidosis
2. Metabolic alkalosis	>7.40	High	High	Vomiting
3. Respiratory acidosis	<7.40	High	High	COPD; paralysis of respiratory muscles
4. Respiratory alkalosis	>7.40	Low	Low	Anxiety; acute pain

COPD, Chronic obstructive pulmonary disease.

albumin value of 4 g/dL. If the corrected value results in total calcium in the reference range, then it is assumed that the free calcium is in the normal range. In other words, the "lost" calcium was all bound to albumin; thus, no free calcium was lost. Conversely, dehydration or hemoconcentration may elevate serum albumin, resulting in a falsely elevated total serum calcium. In this case, the correction will be a negative one because the albumin levels are elevated above 4 g/dL.

BLOOD GAS ABNORMALITIES

We have discussed the effects of acidosis and alkalosis on serum calcium levels. The actual diagnosis of acidosis or alkalosis, however, depends on measurement of the pH of arterial blood. This topic is discussed in depth in Chapter 15. Here, we focus on how to interpret abnormal results and to correlate them with other laboratory findings.

Blood gas determinations refer to the quantitative measurement of the pH of arterial blood, the partial pressure of carbon dioxide (PCO_2), the bicarbonate, the partial pressure of oxygen (PO_2), oxygen saturation, and base excess. Three of these quantities are interdependent—the PCO_2, the bicarbonate, and the pH—by the Henderson-Hasselbalch equation—that is,

$$pH = 6.1 + \log[(HCO_3^-)/(H_2CO_3)]. \qquad \text{(Eq. 9.8)}$$

Because the H_2CO_3 concentration in blood is directly proportional to the PCO_2—that is, at room temperature, $H_2CO_3 = 0.03 \times PCO_2$—Equation 9.8 can be written as:

$$pH = 6.1 + \log[(HCO_3^-)/(0.03 \times PCO_2)] \qquad \text{(Eq. 9.9)}$$

Note that if bicarbonate, in the numerator of Equation 9.9, decreases due to HCO_3^- consumption, as occurs in metabolic acidosis, the respiratory rate will increase, thereby decreasing the PCO_2, causing the denominator of this equation to fall, resulting in compensation. If the PCO_2 increases as in respiratory acidosis, the kidneys retain bicarbonate so that both numerator and denominator increase so as to maintain the ratio relatively constant.

In interpreting blood gas results, the first number to note is the pH. Regardless of the values of the bicarbonate and PCO_2, if the pH is less than 7.4, the patient is acidotic; that is, the hydrogen ion concentration in the blood is elevated, which must reflect acidosis—excessive production or retention of acid. If the pH is greater than 7.4, the patient is alkalemic—that is, there is an abnormally low H^+ ion concentration in the blood. If the pH is close or equal to 7.4, the patient is neither acidemic nor alkalemic but could still have compensating processes of acidosis and alkalosis. Once the diagnosis of acidosis or alkalosis is made, then the bicarbonate and the PCO_2 can be used to decide whether it is of metabolic or respiratory origin.

Table 9.4 summarizes the four basic abnormal states: metabolic and respiratory acidosis and metabolic and respiratory alkalosis. In **metabolic acidosis**, the primary problem is production of acid as in diabetic keto-acidosis, lactic acidosis (e.g., from gram-negative sepsis), renal failure, and diarrhea. The latter condition results from excretion of bicarbonate in the gastrointestinal tract. This acid is buffered by bicarbonate, which is therefore consumed. To compensate for the bicarbonate loss, the breathing rate increases to lower the PCO_2. Thus, a low pH combined with a low bicarbonate and a low PCO_2 point to metabolic acidosis, as shown in condition 1 in Table 9.4.

As shown in condition 2 in Table 9.4, the opposite condition, **metabolic alkalosis**, results in reversal of the levels shown in condition 1. The most common cause of metabolic alkalosis is vomiting, with a loss of HCl from the stomach and an attendant rise in bicarbonate.

Respiratory Acidosis

When CO_2 is abnormally retained by the lungs, as in chronic obstructive pulmonary disease (COPD), the denominator of Equation 9.9 increases, causing the pH of blood to fall. To compensate, the kidneys retain bicarbonate, thus increasing the numerator of this equation. If the blood pH is below 7.4 and the CO_2 and bicarbonate are both increased (condition 3 in Table 9.4), the acidosis is of respiratory origin. Note the mirror image condition (opposite levels) for respiratory alkalosis in condition 4 of this table. Besides COPD, major causes of respiratory acidosis include diseases such as myasthenia gravis, in which there is partial paralysis of the accessory muscles of breathing; pneumonia; and CNS diseases affecting the brainstem in areas involved in respiratory control. **Respiratory alkalosis** is due mainly to hyperventilation, often of psychogenic origin, but can also result from such states as pain from trauma or underlying disease, especially inflammation. Here, the PCO_2 is reduced because of the rapidity of breathing.

The pH of blood can affect the levels of electrolytes in serum. In acidosis, besides bicarbonate buffering, red cells also buffer the excess H^+ ions by exchanging these for intracellular K^+ ions, the net effect being a mild hyperkalemia. An attendant hypokalemia occurs in alkalosis. Remember also that acidosis can cause a mild hypercalcemia; alkalosis can cause a mild hypocalcemia.

Combined Acid-Base Conditions

Combined conditions result from two general circumstances: situations in which there appears to be overcompensation of an acidosis or an alkalosis and apparent absence of compensation of these two conditions. Here, we present three examples that are the most commonly encountered combined conditions.

1. **"Overcompensation" of metabolic acidosis in salicylic acid overdose.** This condition is seen mainly in the pediatric population when a child swallows multiple aspirin tablets. Since aspirin is salicylic acid, the first manifestation of this condition is metabolic acidosis with a partially compensated reduced PCO_2 and an increased anion gap. However, salicylate anion induces increased respiratory rates, causing lowering of the PCO_2 to levels significantly lower than those in the normal compensatory process, resulting in a respiratory alkalosis that masks the fundamental metabolic acidosis. This "overcompensation" results from the independent action of salicylate anion on respiratory centers in the CNS.
2. **Underlying stimulus for rapid breathing from inflammatory conditions in metabolic acidosis.** In uncontrolled diabetics who develop ketoacidosis with increased anion gaps, inflammatory conditions such as gastritis, pancreatitis, and arthritis, which themselves promote hyperglycemia and further ketoacidosis, respiratory rates can increase secondary to the pain from acute exacerbations of these inflammatory states. This results in increasing breathing rates beyond the levels that occur in compensation of the ketoacidosis resulting in an overall respiratory alkalosis. The giveaway finding is the increased anion gap and generally marked elevations in serum glucose (levels >300 mg/dL).
3. **Combined metabolic acidosis and respiratory acidosis.** In the next section, we discuss how oxygen levels in the circulation can be affected by high levels of PCO_2. In severe COPD, such as in advanced emphysema, accumulation of CO_2 occurs in alveoli, blocking entrance of O_2 molecules into the alveoli. This results in a steep drop in the PO_2 of arterial blood, resulting in tissue hypoxia, resulting in decreased Krebs cycle activity and increased glycolysis, producing increased lactic acid. This event then results in metabolic acidosis. Because of the buildup of CO_2 in the alveoli, there is no ability for the lungs to clear the excess CO_2 due to the primary condition of COPD and consequent respiratory acidosis. As discussed in the next section, the most effective maneuver to reverse this trend is to ventilate the patient to remove the excess alveolar CO_2, enabling more O_2 to enter the alveoli and the arterial blood.

Oxygenation

Blood gases also give an excellent measurement of tissue perfusion through measurement of the PO_2 and the oxygen saturation of hemoglobin. Normal PO_2 values should be 90 to 100 mmHg, while O_2 saturation should be 100%. Low values of either or both of these numbers flag underlying pathology. The major causes of low values for these measurements are myocardial infarction, pulmonary embolus, severe pulmonary interstitial disease (e.g., interstitial pneumonia), and tissue anoxic states secondary to

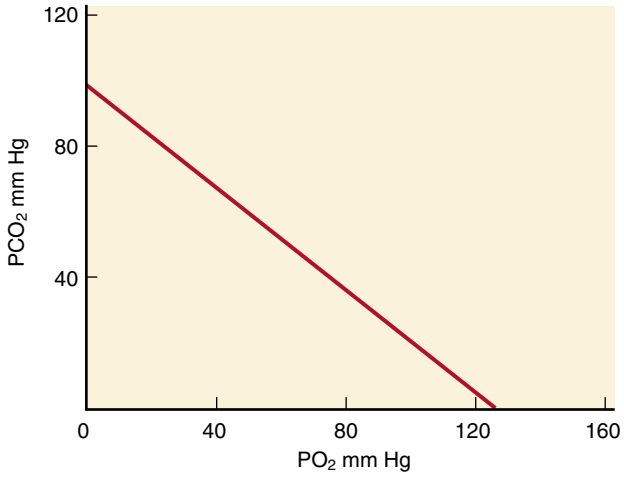

Figure 9.2 The effect of increased PCO_2 on the PO_2 in the alveolus and in arterial blood. This figure demonstrates that as the PCO_2 increases, there is greater than a one-to-one decrease of PO_2.

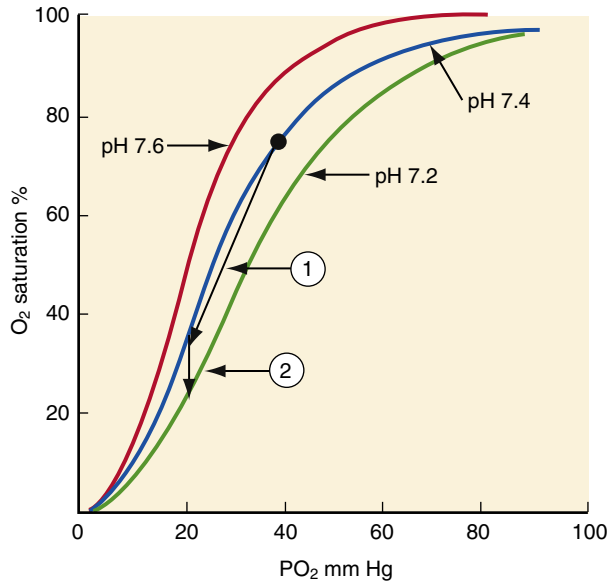

Figure 9.3 The effects of decreasing PO_2 in the allosteric zone of the oxygen–hemoglobin dissociation curve. On the pH 7.4 *(middle, blue)* curve, if the PO_2 drops from 80 to 60 mmHg, there is little effect on the oxygen saturation. However, a drop from 40 to 20 mmHg results in a large drop in oxygen saturation from about 80% to 30% *(arrow 1)*. With this low oxygen saturation, there is a marked tissue lactic acidosis from anaerobic metabolism. The increased acidosis results in a drop in blood pH to 7.2, shifting the oxygen–hemoglobin dissociation to the right (pH 7.2, *green curve*). Now, for a PO_2 of 20 mmHg, the oxygen saturation drops even further *(arrow 2)* to about 20%, setting a vicious cycle in motion.

hypoperfusion, as in septicemia and severe congestive heart failure. In pulmonary embolus, there is blockage of the pulmonary circulation by the embolus, despite adequate ventilation, giving rise to ventilation/perfusion inequalities. The hallmark of pulmonary embolus is a marked drop in the PO_2.

Hypercarbia as a Cause of Hypoxia. Another major cause of hypoxic states in arterial blood is CO_2 retentive states, as in severe COPD. This occurs because as CO_2 builds up in alveoli, it reduces the volume of O_2 in the air space. At PCO_2 values of over 50 mmHg, the effect on alveolar PO_2, represented as PAO_2, becomes important, as illustrated in Figure 9.2. Oxygen, unlike CO_2, is not soluble in water or membranes; thus, there is a difference of about 10 to 15 mmHg pressure between alveolar and arterial O_2 (represented as PaO_2), called the A–a gradient. Thus, the PaO_2 is even lower than the decreased PAO_2. It is important to remember that the total oxygen breathed in, called the PIO_2, is partitioned, therefore, between the alveolar sac and the arterial blood. This relationship may be written as:

$$PIO_2 = PAO_2 + PaO_2 . \qquad \text{(Eq. 9.10)}$$

For each mole of O_2 consumed, approximately 0.8 mole of CO_2 is produced. The ratio of CO_2 produced to O_2 consumed is called the *respiratory quotient* (RQ). The PaO_2 may therefore be written as $PaCO_2/RQ$. Overall, Equation 9.10 can be rewritten as:

$$PAO_2 = PIO_2 - PaCO_2 / RQ . \qquad \text{(Eq. 9.11)}$$

For an RQ of 0.8:

$$PAO_2 = PIO_2 - 1.25 \times PaCO_2. \qquad \text{(Eq. 9.12)}$$

This equation states that, for each increment in the $PaCO_2$, there will be a more than one-to-one decrease in the PAO_2. This will result in severe oxygen deficits.

Figure 9.3 is the oxygen–hemoglobin dissociation curve. Note that the curve is sigmoidal due to the allosteric nature of the binding of oxygen to hemoglobin. For PO_2 values between 70 and 100 mmHg, the saturation of hemoglobin is close to 100%. But at PO_2 values of less than 70 mmHg, there is a steep drop in the saturation fraction so that small drops in PO_2 lead to large decreases in percent saturation. Compounding this effect is the disproportionate decrease in PO_2 whenever PCO_2 increases, as described previously. While these detrimental events transpire, tissue perfusion severely diminishes because of the diminished oxygen saturation of arterial blood. The result is tissue acidosis (mainly from lactic acid as a result of anaerobic metabolism). Acidosis shifts the oxygen–hemoglobin dissociation to the right, as in Figure 9.3, causing even lower saturation for a given PO_2, causing further diminished tissue perfusion and more tissue acidosis. This vicious circle can be corrected by placing the patient on a respirator to cause increased expiration of CO_2.

The pattern of arterial blood gas determinations for this type of patient will be low arterial blood pH, low PO_2, low oxygen saturation, high PCO_2, and low bicarbonate. This pattern is not typical of the four basic patterns given in Table 9.4 because, on top of a fundamental respiratory acidosis (high PCO_2), there is a superimposed tissue metabolic lactic acidosis, causing low bicarbonate. These findings, together with the low PO_2, indicate the immediate need for ventilation of the patient on a respirator.

Unlike the two conditions—myocardial infarction and pulmonary embolus—the treatment of the acute hypercarbic state is not to administer oxygen unless the patient is being adequately ventilated. Hypercarbia causes a CO_2-induced inhibition of the respiratory centers in the pons and the medulla oblongata in the brainstem. In fact, the only impetus to breathe is the hypercarbia-induced hypoxia, causing chemoreceptors in the aortic arch to send signals to the respiratory center in the brain to continue breathing. Administration of oxygen to patients with this condition without ventilation can cause cessation of respiration and the acute demise of the patient.

GLUCOSE ABNORMALITIES

Reference Range for Serum Glucose. The reference range for fasting serum glucose is between 70 and 100 mg/dL. As described in Chapter 17, the two basic abnormalities that occur with serum glucose levels are hyperglycemia, almost always associated with diabetes mellitus, and hypoglycemia due to iatrogenic (overdose with insulin in the diabetic patient) or other underlying causes (such as reactive hypoglycemia due to "hypersensitivity" to insulin, insulinoma, etc.). Hypoglycemia should be considered if the fasting serum glucose is <50 mg/dL.

Besides single serum glucose levels, two other diagnostic tests for diabetes mellitus are used: hemoglobin A1C and the oral glucose tolerance test (OGTT).

Hemoglobin A1C. Glucose reacts covalently with the α-amino group of the beta chain of hemoglobin to form a Schiff base that is then reduced. This covalent reaction product is called *hemoglobin A1c* or *glycosylated hemoglobin*. Levels of glycosylated hemoglobin change slowly over time and therefore constitute a stable and reliable indicator of serum glucose levels over the past 2 to 3 months. Glycosylated hemoglobin levels are measured as a percentage of total hemoglobin; percentage levels that are greater than 6.5% are considered to be indicative of diabetes mellitus (Nathan, 2009; American Diabetes Association, 2018), and efficacy of treatment is gauged by whether this serum level is reduced to less than 6.5%. Of all of the methods for diagnosing and especially for monitoring treatment of diabetes mellitus, measurement of glycosylated hemoglobin levels is perhaps the most accurate and should be measured in conjunction with blood glucose determinations (Blincko & Edwards, 2001; Krishnamurti & Steffes, 2001; Kilpatrick, 2004; Nathan, 2009; American Diabetes Association, 2018).

Oral Glucose Tolerance Test. In the glucose tolerance test (see Chapter 17), after giving the patient, who has not eaten for 12 hours overnight, a well-defined amount of glucose orally, the blood and urine glucose levels are followed. Normally, serum glucose levels rise and then

TABLE 9.5
Six Fundamental Patterns of Liver Function Tests

Condition	AST	ALT	LD	AP	TP	Albumin	Bilirubin	Ammonia
1. Hepatitis	H	H	H	H	N	N	H	N
2. Cirrhosis	N	N	N	N–sl H	L	L	H	H
3. Biliary obstruction	N	N	N	H	N	N	H	N
4. Space-occupying lesion	N or H	N or H	H	H	N	N	N–H	N
5. Passive congestion	sl H	sl H	sl H	N–sl H	N	N	N–sl H	N
6. Fulminant failure	Very H	H	H	H	L	L	H	H

ALT, Alanine aminotransferase; *AP,* alkaline phosphatase; *AST,* aspartate aminotransferase; *H,* high; *L,* low; *LD,* lactate dehydrogenase; *N,* normal; *sl,* slightly; *TP,* total protein.

fall within about a 2-hour period. If the glucose levels remain elevated, however, the diagnosis of diabetes mellitus may again be made. Also, if glucose is detected in the urine at any point, evidence for this condition is also obtained, although absence of urinary glucose does not rule out diabetes mellitus.

Criteria for Diagnosing Diabetes Mellitus

The criteria for diagnosing diabetes mellitus in a patient are as follows:

1. Two random fasting serum glucose levels greater than or equal to 126 mg/dL, or
2. One random fasting serum glucose level greater than or equal to 200 mg/dL, or
3. A 2-hour postload plasma glucose concentration greater than or equal to 200 mg/dL during an oral glucose tolerance test (Nathan, 2009; American Diabetes Association, 2018).
4. Hemoglobin A1C levels > 6.5%.

If serum glucose levels are found to be in the range of 100 to 125 mg/dL and/or the hemoglobin A1C is found to be in the range of 5.7% to 6.5%, the diagnosis of prediabetes or hyperglycemia can be made.

OTHER ABNORMAL LABORATORY FINDINGS IN DIABETES MELLITUS

As discussed in the electrolyte section earlier, under the influence of insulin, whenever glucose is transported into the cell, it is accompanied by potassium. In diabetes, in the absence of insulin, blood glucose is elevated, as is potassium. Due to increased metabolism of fats, there is a buildup of acetoacetic acid, leading to metabolic acidosis. In diabetes in which the blood glucose becomes exceptionally elevated—for example, over 300 mg/dL—serum osmolality becomes dangerously high and can cause nonketotic, hyperosmolar coma. In this condition, red (and white) cell water flows from the cells into the vascular volume, tending to dilute analytes such as sodium. Thus, the nonketotic, hyperosmolar coma patient may have a hyperosmolar serum, hyperglycemia, hyperkalemia, and hyponatremia. In ketotic states, the patient will also have a metabolic acidosis and a large anion gap.

Serum glucose levels of lower than 60 mg/dL on a series of random fasting serum specimens strongly suggest hypoglycemia. The low glucose values should be associated with adrenergic and/or neuroglycopenic symptoms, which are relieved upon administration of glucose (the Whipple triad). Glucose tolerance tests show that after an initial sharp rise of serum glucose levels, there is an abnormally rapid drop to levels substantially below 60 mg/dL. If hypoglycemia is suspected, it is advisable to give the patient a 5-hour glucose tolerance test because the hypoglycemic "dip" often is not seen until after 3 hours. Glucose tolerance tests on patients with suspected hypoglycemia should be performed with great caution because the procedure can induce severe reactive hypoglycemia, causing loss of consciousness and even shock.

LIVER FUNCTION TESTS

Liver function is discussed in depth in Chapter 22. Here, we summarize a set of principles that will enable the reader to formulate differential diagnoses of liver disease from the pattern of the so-called liver function tests. The liver may be considered as three systems:

1. A chemical metabolic system
2. A reticuloendothelial system based on Kupffer cells (macrophages) that line the sinusoids in the vascular system of the liver that are concerned with metabolism of hemoglobin released from red blood cells
3. A metabolic system for the secretion of bilirubin, a hemoglobin metabolite, into the biliary tract

The functioning of the first system can be tested by measuring the serum levels of two critical aminotransferases or transaminases: aspartate aminotransferase (AST) and alanine aminotransferase (ALT). High serum levels of these enzymes occur most commonly in acute hepatitis and/or mechanical damage to the liver. The liver is the site of extensive metabolic processes, including the Krebs cycle and glycolysis that occur in hepatocytes, and a prominent metabolic enzyme is LD. In hepatitis or in other conditions resulting in hepatocytic injury, including mass lesions of the liver, LD levels increase.

Because the liver is the site for the synthesis of over 90% of the proteins in the body, including all of the albumin, levels of total protein and albumin also reflect liver function. Unlike with the two aminotransferases, however, liver pathology is recognized by *decreases* in the serum levels of total protein and albumin. These decreases do not occur unless 80% or more of liver tissue is destroyed, as in cirrhosis and fulminant hepatic failure.

The liver is the only tissue in the body that can metabolize ammonia, the end product of amino and nucleic acid metabolism via the Krebs-Hennseleit cycle, in which ammonia is converted to urea. When more than 80% of liver tissue is destroyed, as in the conditions mentioned earlier, serum ammonia rises to toxic levels.

The functioning of the second system is concerned with circulating hemoglobin from lysed red blood cells. In Kupffer cells, the iron of heme is oxidized to the ferric state, and the heme is released from its complex with globin. The porphyrin ring of heme is opened into a straight chain compound with release of CO called *biliverdin* that is then further oxidized to bilirubin.

In the third system, bilirubin enters the hepatocyte, where it undergoes conjugation to glucuronic acid and is then transported to the interface between the hepatocyte and the epithelial cell of the bile canaliculus, where it is secreted into the canaliculus and then into the bile ductules. Two enzymes are strongly associated with the canalicular system in the liver: on the hepatic surface is γ-glutamyltransferase (GGT) and on the canalicular surface is the enzyme alkaline phosphatase (AP). Also useful in diagnosis is the enzyme 5′-nucleotidase (5′-N). In cases in which there is obstruction of the flow of conjugated bilirubin into the canaliculus, there is an increase in serum bilirubin, most of it conjugated or direct bilirubin, and a rise generally in both AP and γ-glutamyltransferase. Six patterns of liver function tests are useful in diagnosing the major diseases affecting liver tissue (Table 9.5).

Hepatitis and acute injuries and/or necrotic lesions in the liver cause primarily a marked rise in the levels of AST and ALT. Cell injury and necrosis also cause the rise of other enzymes, such as LD. These include acute hepatitis (e.g., infectious and chemically induced), infarction, and trauma. The biliary tract is always affected so that direct bilirubin rises from interference with bile flow. Because of biliary tract injury, the enzyme AP rises along with GGT and 5′-N. Hepatocyte injury causes loss of conjugation of transported bilirubin so that indirect (unconjugated) bilirubin also rises.

Because in hepatitis much less than 80% of the liver generally is destroyed, total regeneration will occur, and enough tissue is present to enable adequate levels of protein synthesis and ammonia fixation as urea. Therefore, the total protein and albumin and ammonia levels remain normal. These typical results are summarized in condition 1 in Table 9.5.

Cirrhosis of the liver is characterized by two cardinal features: fibrosis, preventing regeneration of liver tissue wherever this has occurred, and nodules of regenerating liver tissue, which are the only source of any kind of hepatocytic function. Thus, in cirrhosis, as shown in condition 2 in Table 9.5, almost the reverse pattern occurs from the one seen in condition 1 in Table 9.5 for hepatitis. Because in panhepatic cirrhosis there is destruction of more than 80% of liver tissue, with no regeneration of damaged liver tissue, the AST, ALT, and LD levels (all from the regenerating nodules)

tend to be normal or low, or occasionally mildly elevated. However, the total protein and albumin are both abnormally low. Because the liver is the sole site of ammonia detoxification via the urea cycle and because, in this condition, there is loss of hepatocytic function, serum ammonia levels are elevated. Because there is insufficient viable liver tissue remaining, and because fibrosis destroys the cholangioles, both unconjugated (indirect) and conjugated (direct) bilirubin tend to be elevated.

Acute biliary obstruction caused by stones in the biliary tree or by neoplasms that block bile excretion results in elevations in direct bilirubin and biliary tract AP, along with the enzymes GGT and 5′-N (see earlier discussion). All other liver function test results are normal. For simple biliary obstruction, therefore, the pattern is as shown in condition 3 in Table 9.5.

Space-occupying lesions of the liver are characterized, for reasons that are not well understood, by isolated elevations of the enzymes ALP and LD. This pattern is shown in condition 4 in Table 9.5. The most common causes of this condition are metastatic carcinoma to the liver and hepatocellular carcinoma.

Passive congestion of the liver is characterized by a mild elevation of aminotransferases (AST/ALT) and LD and, in more severe cases, elevations of total bilirubin and AP. This pattern is also seen in infectious mononucleosis, in which the rise in bilirubin may be marked. The general passive congestion pattern is shown in condition 5 in Table 9.5.

Acute fulminant hepatic failure from a variety of causes, which include Reye syndrome, hepatitis C (Gill & Sterling, 2001; Schiodt & Lee, 2003), panhepatitic hepatitis (mainly from hepatitis B-delta), severe hypoperfusion states, cirrhosis, and multiple abdominal surgeries, is discussed in Chapter 22. This condition is total liver failure. The overall pattern (Sunheimer et al., 1994) is shown in condition 6 in Table 9.5. It appears as a combination of hepatitis and cirrhosis. Here, AST and ALT reach exceptionally high values, often in excess of 10,000 IU/L. At the same time, total protein and albumin are markedly reduced, and the ammonia levels are abnormally elevated, causing hepatic encephalopathy. LD, AP, and bilirubin are also elevated. Besides the marked rise in AST and ALT, combined with hyperammonemia, there is a characteristic disproportional rise of AST over ALT, further confirming the diagnosis. It is vital to recognize this pattern because the underlying condition is a medical emergency that must be treated promptly. The treatment is liver transplantation.

Correlations of Liver Function Test Results with Other Laboratory Findings

In severe liver failure, secondary to cirrhosis or to fulminant hepatic failure, it is not uncommon to find electrolyte abnormalities and abnormalities in renal function tests and in the coagulation profile. Patients with either condition 2 or 6 in Table 9.5 often have ascites, with marked third-space fluid loss. This results in increased levels of both ADH and aldosterone to retain intravascular water. Depending on which levels "win out," the patient may become hyponatremic or hypernatremic.

Severe liver failure can also cause hepatorenal syndrome—that is, renal dysfunction secondary to hepatic failure. This disease is characterized by the typical patterns shown in conditions 2 and 6 in Table 9.5. As discussed earlier in the renal section, renal failure results in elevations in BUN and creatinine with a 10:1 to 20:1 ratio, indicative of renal failure. The Uosm/Posm ratio is less than 1.2:1, indicating tubular dysfunction.

Severe coagulopathies with elevated APTTs and PTs may be seen due to the absence of production of coagulation factors. Not infrequently, DIC will accompany liver failure. This condition must be distinguished from low coagulation factor production combined with hepatosplenomegaly due to portal hypertension, as in cirrhosis. The splenomegaly may result in sequestration of platelets; thus, the overall pattern may resemble DIC but may not be true DIC. To clinch the diagnosis of DIC, there should be elevations of D-dimer levels. Because in DIC emboli occur in the microvasculature of different tissues, including bone marrow, bone marrow–induced hemolytic anemia may develop in which schistocytes, burr cells, and fragmented forms appear in the peripheral blood smear. In addition, nucleated red cells and myeloid precursor cells, such as myelocytes and metamyelocytes, may also be seen in the blood smear—the so-called *leukoerythroblastic picture* referred to in the earlier coagulation section. Also, in severe liver failure, abnormal red cell forms, called *target cells*, may be seen in the peripheral blood smear.

Patients with cirrhosis and acute fulminant hepatic failure tend to be immunocompromised. Many of these patients have defective T cell function but produce an excess of (ineffective) immunoglobulin. Thus, these patients tend to have low serum albumin levels from diminished albumin synthesis but elevated serum immunoglobulins.

CARDIAC FUNCTION TESTS

Diagnosis of Myocardial Infarction and Acute Coronary Syndrome

Myocardial infarction (MI) and acute coronary syndrome are discussed at length in Chapter 19. Because acute MI (AMI) requires rapid and accurate diagnosis, especially now that new treatment options with thrombolytic agents are available, the clinical laboratory has been called upon to provide serum diagnostic tests that can make this diagnosis at an early stage. Until recently, laboratory diagnosis was based on serial determinations of the MB fraction of creatine phosphokinase (CK-MB). Confirmation of the diagnosis was provided by the so-called "flipped ratio" of the isozymes of LD 24 to 36 hours after the initial acute event and/or by observation of the characteristic time courses for elevations of the three enzymes: CK, AST, and LD. These tests have all been confirmatory, not diagnostic, because of the long times necessary to establish a definitive diagnosis

These approaches have been replaced mainly by two other analytes—cardiac troponin (cTn) (Aviles et al., 2002) and myoglobin (MY)—that provide more rapid and specific diagnostic capabilities (Morrow et al., 2007). MY is an oxygen-binding/transport protein found in both cardiac and skeletal muscle. Its relatively small size and function allow for early release from irreversibly damaged cells. However, current methods of measurement cannot distinguish MY's tissue of origin. Therefore, its use is confined to screening patients for possible AMI; positive results suggest further workup for AMI. A negative result indicates the strong likelihood that MI did *not* occur, that is, MY testing has a high negative predictive value (see Chapter 8 for definition).

Troponin is a regulatory protein complex in muscle tissue; it comprises three subunits designated troponin I (TnI), troponin T (TnT), and troponin C (TnC). Different genes encode TnI in skeletal and cardiac muscle, giving rise to isoforms that differ significantly in sequence. In addition, cardiac TnI or cTnI, contains an additional 31 amino acid residues on its N-terminal. Rapid, sensitive, and accurate immunoassays for cardiac TnT and cardiac TnI have been developed (Thygesen et al., 2012). The most useful assays appear to be for TnI because they are specific for the cardiac form, and TnT may be elevated in patients with renal failure without MI (Diris et al., 2004). In AMI, cardiac TnI becomes elevated 4 to 8 hours after onset of chest pain, reaches a peak at about 12 to 16 hours, and remains elevated for 5 to 9 days. Values at or above 1.5 ng/mL are considered to be suggestive of AMI. However, because different assays (all immunoassays) measure different domains of TnI, reference ranges differ depending on the antibodies used in the assays. Because cTn levels rise relatively rapidly and remain elevated for prolonged times, troponin determinations have replaced the so-called "flipped ratio" of the two isozymes of LD, LD1, and LD2 (LD1:LD2 ratio rises to >0.75 and often exceeds 1.0), which occurs only about 36 to 48 hours after the onset of symptoms.

CK-MB is another biomarker that can be used in diagnosing AMI. This is an isozyme of CK that has three isozymes composed of two chains (called the M and B chains): MM, MB, and BB. The MB fraction is predominantly found in cardiac muscle (Roberts, 1997). To diagnose AMI from CK-MB serum levels, it is important to show both a rise in the concentration of CK-MB and in the ratio of CK-MB to total CK (also called the *cardiac index*) (Thompson et al., 1988; Woo et al., 1992). An increase in the sensitivity of the CK-MB assay has been developed by quantitation of two CK-MB isoforms, CK-MB-2 and its posttranslationally modified CK-MB1, that results from proteolytic cleavage of the carboxyl terminal lysine residue from CK-MB-2 (Bock et al., 1999). Because there is a small amount of CK-MB in skeletal muscle, diseases of skeletal muscle that cause the level of CK-MM to rise to high values will also cause the levels of CK-MB to rise to high absolute concentrations in serum, which can cause false-positive values for CK-MB although most of these can be identified by the low cardiac indices. In addition, to increase both the sensitivity and specificity of CK-MB in the diagnosis of acute AMI, it has been found necessary to perform serial determinations of MB fraction (at 3- to 4-hour intervals over a 12- to 16-hour period) that show a progressive rise that reaches a peak, followed by a fall to low levels. This pattern is virtually 100% diagnostic of MI (Lott, 1984; Wu et al., 1999). More important, CK-MB generally rises 4 to 6 hours, and sometimes only 2 hours, after the onset of chest pain, peaking within 12 hours. Therefore, MY and CK-MB were recommended (Wu et al., 1999; Alpert et al., 2000; Fromm & Roberts, 2001; Lewandrowski et al., 2002) for use as early markers of AMI. However, elevated TnT and TnI levels are more specific for cardiac injury than are elevated CK-MB levels. Like CK-MB, they rise within 4 to 6 hours, and sometimes within 2 hours, after the onset of chest pain. More recent studies suggest that use of cTnI alone has the same diagnostic accuracy as use of both cTnI and CK-MB and that it may be more cost-effective

to employ cTnI alone (Ducatman, 2017) although this conclusion is controversial (Hueb et al., 2016).

Current protocols for the laboratory diagnosis of AMI vary and are evolving as assays for cTnI improve (see Chapter 19). In some medical centers TnI or TnT is used exclusively, while in other centers, troponin and CK-MB are used together.

Diagnosis of Congestive Heart Failure

Until recently, this condition was diagnosed strictly on the basis of symptomatology and/or as a result of procedures such as echocardiography. More recently, a biomarker for this condition is the brain form or B-type natriuretic peptide (BNP), which has been approved as a definitive test for this condition and appears to be an excellent marker for early heart failure. This test may also be both diagnostically and prognostically significant in patients presenting with acute dyspnea and chest pain. The differential diagnosis in these patients includes dyspnea caused by chronic heart failure (signs and symptoms of which are typically nonspecific) versus other causes of acute dyspnea (e.g., pneumonia, carcinoma, effusion, asthma). Normal levels (i.e., a high negative predictive value for this test) appear useful in excluding a cardiac etiology in these patients. Levels of BNP may also be an independent predictor of arrhythmia, stroke, and death (Clerico & Emdin, 2004; Clerico et al., 2012; Ishii et al., 2003; Mueller et al., 2004; Prahash & Lynch, 2004; Wang et al., 2004; Winter & Elin, 2004; Novo et al., 2009). Studies suggest that serum BNP levels are useful in evaluating the efficacy of treatment of congestive heart failure (Novo et al., 2009).

SKELETAL MUSCLE FUNCTION

As noted in the earlier Cardiac Function Tests section, an elevated serum CK-MB is a useful marker for myocardial disease. The MB fraction is one of three possible isozyme dimer states of the M and B chains. The MM fraction is by far the most prominent of the three isozymes; this isozyme of CK is found in skeletal muscle. Thus, diseases affecting skeletal muscle are often accompanied by substantial serum elevations of this CK isozyme. The most common cause of skeletal muscle disease is myositis, a general inflammation of skeletal muscle fibers affecting the sarcolemma. This condition has many causes, including viral causes, especially coxsackie B viral infections that predominantly affect skeletal muscle, autoimmune conditions, and drugs. One of the most common causes of drug-induced myositis is the statin class of cholesterol-lowering drugs such as lovastatin. Another closely related condition is rhabdomyolysis, which is the breakdown of skeletal muscle due to such causes as trauma, drug abuse (especially intravenous drug abuse from needle damage to skeletal muscle), severe, generalized myositis due to viral infections, and third-degree burns. Thus, serum CK levels should always be obtained in patients complaining of generalized muscle pain. If these levels are elevated, efficacy of treatment may be followed by serial levels of total CK.

As noted in the Cardiac Function Tests section, both cardiac and skeletal muscle contain the oxygen transport protein myoglobin. In conditions of acute myositis of skeletal muscle, myoglobin is released from damaged muscle cells, giving elevated levels of this protein in serum. Because this protein has a relatively low molecular mass, it is filtered in the kidneys and excreted in the urine, causing myoglobinuria. Because myoglobin is toxic to renal tubules, high serum concentrations of myoglobin can cause renal failure, a potentially serious complication of myositis and especially of rhabdomyolysis (Melli et al., 2005; Ouyang et al., 2009).

PANCREATIC FUNCTION TESTS

Elevations in serum pancreatic amylase and lipase are definitive markers for pancreatic disease. The most common cause for such increases in the serum levels of these enzymes is pancreatitis. In acute pancreatitis, both enzymes are elevated. Because amylase can also be produced by the salivary glands, amylase is less specific than lipase as a marker for pancreatitis. Elevations in the latter enzyme are definitive for pancreatic disease.

MARKERS FOR INFLAMMATORY CONDITIONS

As discussed previously in the hematology section, increases in the WBC count, especially with a predominance of neutrophils, indicate acute infection. In most acute inflammatory conditions, as noted previously, acute-phase reactant proteins are also found to be increased. These proteins occur in the alpha (including alpha-1-antitrypsin, alpha-2-macroglobulin) and beta (including ferritin and CRP) regions of the serum protein electrophoretogram, as discussed in Chapter 20 on serum protein electrophoresis. In this regard, quantitative determinations for serum CRP are very helpful in recognizing acute inflammatory states (Sproston & Ashworth, 2018). Recently, specific antibodies to CRP have allowed for highly sensitive measurement of CRP (termed *high-sensitivity CRP* [*hs-CRP*]) at lower concentrations than were previously measurable (Roberts et al., 2000). Currently, elevated levels of hs-CRP appear to serve as an early marker of inflammation and may have utility in assessing cardiovascular risk for stroke and MI (Abrams, 2003; Ridker, 2003; Libby & Ridker, 2004).

Fibrinogen, also an acute phase reactant, may increase as well. Often, the platelet count tends to rise, and platelets themselves have been considered as "acute-phase reactants." In addition, in both acute and chronic inflammatory conditions, erythrocytes exhibit increased mobilities. Thus, there is an increase in the erythrocyte sedimentation rate (ESR). Recent studies suggest that the best marker for inflammation, especially as a guide to therapeutic efficacy, is CRP (Crowson et al., 2009).

Finally, one common cause of acute inflammation is gout—that is, hyperuricemia, or elevations of uric acid in serum. Uric acid crystals cause a severe, acute arthritic condition (gout). Serum levels of uric acid over 7.5 mg/dL are indicative of this condition. Less constant findings are the presence of uric acid crystals in the urinary sediment (see Chapter 28) or in joint fluid (see Chapter 29).

ENDOCRINE FUNCTION TESTING

We noted that abnormal functioning of the thyroid and adrenal cortex can give rise to important abnormal laboratory findings. Hypothyroidism, for example, can give rise to macrocytic anemia, while hypoadrenalism gives rise to electrolyte abnormalities—that is, hyponatremia and hyperkalemia and an acidosis. Hyperadrenalism produces the opposite effect—that is, hypernatremia, hypokalemia, and an alkalosis. It is therefore important to confirm that these endocrine glands are malfunctioning. The important topic of endocrine function testing is discussed in Chapter 25. Here, we present simple principles for the laboratory diagnosis and identification of the site of origin of thyroid, adrenal, and parathyroid conditions.

Principle

All endocrine systems involve a stimulating hormone that is synthesized and secreted into the blood from one tissue, such as the pituitary, parathyroid glands, and so on. These hormones are delivered to their targets, which may be the thyroid gland, adrenal glands, or a nonendocrine target, such as the renal tubules in the case of the parathyroid glands. In all cases, for normally functioning endocrine systems, *elevations of the hormones or, in the case of the parathyroid glands, elevations in serum ionized calcium levels, will result in decreased levels of the stimulating hormones. Conversely, decreased levels of the target, such as thyroxine (T_4) or ionized calcium, will result in increased levels of the stimulating hormones.* For example, high levels of circulating T_4 will result in low levels of TSH, a condition called *primary hyperthyroidism*, and, conversely, low levels of T_4 will result in high levels of TSH, a condition called *primary hypothyroidism*. In contrast, if the pituitary gland secretes an excess of TSH due to an adenoma or other pathologic condition, this increase in TSH will result in elevated T_4. This condition is also referred to as *secondary hyperthyroidism*. Thus, if both T_4 and TSH levels are elevated, a diagnosis of pituitary disease—that is, pituitary adenoma in which there is hypersecretion of TSH—can be made. Conversely, decreases of both TSH and T_4 point to pituitary hyposecretive states, also referred to as *secondary hypothyroidism*. These considerations may be summed up as the following principle: C*hanges in opposite directions of the stimulating and target hormones (e.g., T_4) or effectors (e.g., ionized calcium) point to endocrine target (e.g., thyroid gland) disease, while changes of the two hormones in the same direction point to stimulating hormone gland (e.g., pituitary) disease.*

Thyroid Function

Thyroid function tests are the most commonly ordered tests for endocrine function. It is important to note that in a hospital population (as opposed to an ambulatory population), thyroid screening tests may be diagnostically misleading. This is due to endocrine stress responses (as well as medications) that may affect hormone levels (Van den Berghe, 2003). As discussed in Chapter 25, the thyroid gland synthesizes thyroid hormone, tetraiodothyronine, or T_4, with four iodines, which requires iodine uptake by the gland. This activity is strongly stimulated by the peptide hormone TSH from the pituitary. In the periphery, T_4 is converted to T_3 (three iodines). Over 99% of T_4 is bound to serum proteins—that is, thyroid-binding globulin (TBG) and albumin. However, it is the free T_4 (<1% of total T_4) that exerts all biological effects. Accurate methods exist that directly measure serum free T_4. While, most commonly, both total and free T_4 rise and fall together in serum, there are circumstances in which total T_4 may be elevated but T_4-binding proteins may also be elevated so that free T_4

TABLE 9.6

Patterns of Serum Levels of TSH and T_4 in Different Thyroid Gland Conditions

Condition	T4 (Most Accurate, Free T4)	TSH	Site of Disease
Euthyroid	Normal	Normal	None
Primary hypothyroidism	Low	High	Thyroid gland
Secondary hypothyroidism	Low	Low to normal	Pituitary
Primary hyperthyroidism	High	Low	Thyroid
Secondary hyperthyroidism	High	High	Pituitary

TSH, Thyroid-stimulating hormone.

levels are normal. This results in a euthyroid state in which TSH levels are also normal. Of prime importance, high T_4 (more correctly, high free T_4) causes inhibition of TSH secretion, while low T_4 (more correctly, low free T_4) causes elevation of TSH. In primary hypothyroidism (primary thyroid gland disease), T_4 is present at low serum levels, while TSH becomes elevated. More important, often, in subclinical hypothyroidism, T_4 can be within the reference range, but TSH is elevated. In ambulatory patients, elevated TSH in the presence of low levels of T_4 is diagnostic of primary hypothyroidism. In secondary hypothyroidism, TSH is low due to pituitary failure, resulting in low T_4.

In primary hyperthyroidism (primary thyroid gland disease), excess T_4 is secreted by the thyroid gland, which is the source of the problem. As a result, TSH is decreased, and T_4 is elevated. If, however, there is a primary lesion in the pituitary gland—for example, hyperplasia or adenoma—then TSH is oversecreted. Because TSH is elevated, T_4 secretion is elevated. This is secondary hyperthyroidism (secondary to pituitary disease). These conditions and the patterns of T_4 and TSH levels that occur in them are summarized in Table 9.6.

ADRENAL FUNCTION

As discussed in depth in Chapter 25, the adrenal gland is divided anatomically into two endocrine glands: the adrenal cortex and the adrenal medulla. Adrenal cortical hormones are steroid hormones of three basic types: mineralocorticoids, such as aldosterone, that regulate sodium and potassium ions in the distal convoluted tubule, as discussed earlier; the glucocorticoids, such as cortisol, that are gluconeogenic; and the sex hormones—that is, the estrogens and the androgens. The adrenal medulla is a neuroendocrine gland that secretes epinephrine and norepinephrine that act on the sympathetic nervous system. By far the most commonly ordered serum analyte used to measure adrenal cortical function is cortisol. Cortisol secretion by the adrenal cortex is stimulated by the pituitary hormone adrenocorticotropic hormone (ACTH). ACTH secretion, in turn, is stimulated by the hypothalamic hormone corticotropin-releasing hormone (CRH). Its serum levels are under diurnal control such that serum ACTH levels peak at about 200 pg/mL in the morning hours (about 7:00 AM), while they decline to their lowest values of around 100 pg/mL at midnight. Cortisol secretion follows ACTH secretion such that its serum levels are highest at around 8:00 to 9:00 AM. Cortisol inhibits ACTH secretion by the pituitary gland both by directly blocking pituitary ACTH secretion and by inhibiting CRH secretion by the hypothalamus.

Therefore, if the adrenal cortex hypersecretes cortisol secondary to such conditions as adrenal hyperplasia, adenoma, or carcinoma, serum cortisol levels increase and block ACTH secretion. This condition is called primary hyperadrenalism. Serum cortisol levels are elevated (Cushing syndrome), but ACTH levels decrease.

On the other hand, as with thyroid hormone secretion, if ACTH levels are elevated by an ACTH pituitary tumor (Cushing disease) or as ectopic ACTH secretion—for example, by a nonpituitary tumor—cortisol levels will also rise, producing secondary hyperadrenalism. Both cortisol and ACTH are elevated in this condition. Here, notice that both cortisol and ACTH change in the same direction (both are elevated), pointing to pituitary, not adrenal, disease. In cases of Cushing disease or syndrome, the diurnal variation of serum ACTH is absent.

In addition to measurements of serum cortisol, it is often desirable to measure urinary free cortisol in cases of hypercortisolemia. Normally, almost all cortisol is bound to serum protein, mainly transcortin; in hypercortisol states, cortisol exceeds the capacity of transcortin to bind to it and is consequently filtered by the kidneys. The reference range for morning serum cortisol is approximately 10 to 25 μg/dL, and for urinary free cortisol, it is approximately 24 to 108 μg/24 h for healthy males.

In cases of hypercortisolism, especially in which ACTH levels may remain in the reference range or have "borderline" high or low values, it is often desirable to perform the dexamethasone suppression test. Dexamethasone is a potent glucocorticoid that strongly suppresses normal pituitary ACTH secretion. This can be accomplished with low-dose dexamethasone. If low-dose dexamethasone results in diminished serum cortisol levels and low values for urinary free cortisol, pituitary function is most likely normal while the adrenals are hypersecreting cortisol—that is, primary hyperadrenalism. This test may further be used to distinguish the possible source of primary hyperadrenalism—that is, hyperplasia versus adenoma or carcinoma. High-dose dexamethasone will generally lower serum cortisol levels in adrenal hyperplasia, while it will have no effect in adrenal adenoma or carcinoma.

Conversely, in pituitary failure, serum ACTH levels decrease, as do serum cortisol levels, because ACTH stimulation of the adrenal gland decreases. This condition is referred to as *secondary hypoadrenalism*. If the adrenal gland function is compromised (primary adrenal insufficiency), serum cortisol levels decrease, resulting in less inhibition of pituitary secretion of ACTH and, consequently, in elevated serum levels of ACTH. This condition is referred to as *primary hypoadrenalism* or *Addison disease*. These conditions and the patterns of serum cortisol and ACTH levels in these conditions, including dexamethasone suppression test results, where relevant, are summarized in Table 9.7.

Parathyroid Hormone and Vitamin D

In the renal section, it was noted that PTH induces elevated serum calcium levels by causing increased secretion of phosphate in the renal tubules and by promoting increased calcium ion absorption in the gut. Hypocalcemia with elevated PTH points to causes having to do with calcium metabolism—for example, alkalotic states, decreased albumin, low dietary calcium and/or lack of absorption of calcium from the gut, and low vitamin D levels. Hypocalcemia with low serum PTH levels points to parathyroid gland dysfunction. In rare instances, hypocalcemia that is not responsive to calcium infusions and vitamin D supplements can be caused by secretion of high levels of calcitonin, a serum calcium–lowering peptide that blocks osteoclastic resorption of bone, thereby blocking release of calcium in the circulation. Calcitonin is synthesized and secreted from the medullary cells of the thyroid. In medullary thyroid carcinoma, high levels of calcitonin are sometimes secreted. At high levels of calcitonin, hypocalcemia will result.

Hypercalcemia with low PTH again points to primary calcium metabolic causes, as in the CHIMPS mnemonic mentioned in the renal section and acidotic states, while hypercalcemia with elevated PTH indicates parathyroid diseases such as adenoma (most commonly) or carcinoma (uncommonly). These conditions and the patterns of serum calcium and PTH levels in serum in these conditions are summarized in Table 9.8.

Vitamin D

Vitamin D induces absorption of calcium from the gut by acting on vitamin D receptors in the cells lining the gut. It is produced from 7-dehydrocholesterol in skin by ultraviolet (UV) light that induces the synthesis of cholecalciferol. In the liver, cholecalciferol is converted to 25-hydroxycholecalciferol, which has a half-life of several weeks. This form is further hydroxylated in the kidneys to 1,25-dihydroxycholecalciferol, the active form of vitamin D. The half-life of active vitamin D is on the order of hours. Thus, in serum assays for vitamin D, the analyte whose serum level best reflects vitamin D levels is the precursor, 25-hydroxycholecalciferol (Zerwekh, 2008). This may give falsely elevated levels of vitamin D in cases of renal failure in which conversion of the precursor to active vitamin D is impaired. However, 25-hydroxycholecalciferol itself has some effects on calcium reabsorption, although its affinity for the vitamin D receptor is only about one-one thousandth of that for the fully active form. The reference range for serum 25-hydroxycholecalciferol, also called *25-hydroxy vitamin D*, is 30 to 100 ng/mL, although this is method-dependent (Yates et al., 2008).

Over the past few years, there has been a large increase in requests for serum vitamin D levels, especially in the pediatric and geriatric populations. This is due at least in part to the availability of reliable chromatographic, mass spectroscopic, and immunochemical methods that quantitate serum vitamin D levels. In the pediatric population, vitamin D levels are determined and followed for the diagnosis and treatment of vitamin D–dependent rickets. In the elderly, vitamin D levels are determined in the

TABLE 9.7
Patterns of Serum Levels of ACTH and Cortisol in Different Adrenal Gland Conditions

Condition	Cortisol	ACTH	Dexamethasone Suppression, Low Dose	Dexamethasone Suppression, High Dose	Site of Disease
Normal adrenal	Normal	Normal	N/A	N/A	None
Primary hypoadrenalism	Low	High	N/A	N/A	Adrenal gland
Secondary hypoadrenalism	Low	Low	N/A	N/A	Pituitary
Primary hyperadrenalism—high cortisol, low ACTH	High	Low	N/A	N/A	Adrenal
Primary hyperadrenalism—high cortisol, borderline low ACTH	High	Borderline low	Positive	N/A	Adrenal
Primary hyperadrenalism due to adrenal hyperplasia—high cortisol, borderline low ACTH	High	Borderline low	Negative	Positive	Adrenal
Primary hyperadrenalism due to adrenal adenoma/carcinoma—high cortisol, borderline low ACTH	High	Borderline low	Negative	Negative	Adrenal
Secondary hyperadrenalism	High	High	N/A	N/A	Pituitary

ACTH, Adrenocorticotropic hormone.

TABLE 9.8
Patterns of Serum Levels of Calcium and PTH in Different Conditions

Condition[a]	Ionized Calcium	PTH	Cause of Disease
Normocalcemia	Normal	Normal	None
"Primary" hypocalcemia	Low	High	CHARD[b]
"Secondary" hypocalcemia	Low	Low	Parathyroid glands
"Primary" hypercalcemia	High	Low	CHIMPS[c]
"Secondary" hypercalcemia	High	High	Parathyroid glands (e.g., adenoma, carcinoma)

[a]The terms *primary* and *secondary* are not usually employed for hypocalcemia and hypercalcemia. They are used here to emphasize the site of the disease to keep consistent with the conditions described in Tables 9.6 and 9.7.
[b]Mnemonic for **C**alcitonin, **H**ypoparathyroidism, **A**lkalosis, **R**enal failure, and vitamin **D** deficit.
[c]Mnemonic for **C**ancer, **H**yperthyroidism, **I**atrogenic causes, **M**ultiple myeloma, hyper**P**arathyroidism, and **S**arcoidosis.

treatment of such diseases as osteoporosis and osteomalacia, because vitamin D supplements have been found to diminish the extent and severity of these diseases.

The discovery that many cells, besides epithelial cells of the gut—the principal site of vitamin D activity—have abundant receptors for vitamin D suggests that this vitamin has effects that go beyond regulation of calcium homeostasis (Autier, 2017; Bilke, 2009). Indeed, studies suggest that vitamin D can induce apoptosis in breast cancer and other malignant cells (Sergeev, 2014; Feldman, 2014; Mathiasen, 1999) and can be used to treat such diseases as multiple sclerosis (Thomas & Ellen, 2018), heart failure (Moretti, 2017), psoriasis (Barrea, 2017), asthma (Ali, 2017), Crohn disease and inflammatory bowel disease (Del Pinto et al., 2017), and a number of other conditions. Thus, there has been an increased demand for vitamin D levels for patients with a variety of conditions.

EXAMPLES OF CLINICAL CASES WITH CLINICOPATHOLOGIC CORRELATIONS

Given the overview of many salient features of the causes of the more common abnormal laboratory findings, the laboratory results from a number of different patients are now presented to illustrate how analyte levels change in different disease states and how these analyte concentrations are used to diagnose these conditions.

CASE A: ELECTROLYTE DISORDER

A 64-year-old white male was found unconscious in his home after suffering a cerebrovascular accident (CVA) and brought to the emergency department. His hematocrit was 44%, but his red blood cell count was 4.3 million/μL (lower limit of normal, 4.6 million/μL), with an MCV of 104 fL; a series of serum sodium values ranged from 164 to 175 mEq/L; admission BUN was 33 mg/dL; and creatinine was 1.5 mg/dL. The total serum osmolality was 357 mOsm/kg (upper limit of normal, 290 mOsm/kg), while the urine osmolality was 1008 mOsm/kg (upper limit of normal, 1000 mOsm/kg); the random urine sodium was 228 mEq/L.

A liver panel showed a marginally elevated AST at 41 IU/L (upper limit of normal, 39 IU/L), elevated but continually decreasing LD (admission value of 426 IU/L; upper limit of normal, 200 IU/L), GGT of 72 U/L (upper limit of normal, 43 IU/L), total protein of 7.8 g/dL (normal), and a low albumin of 2.8 g/dL (normal 3.5–5.0 g/dL). Lipase was mildly elevated at 127 IU/L (upper limit of normal, 60 IU/L). Occult blood was found in his stool, which was found positive for *Clostridium difficile*. Urine was nitrite positive (indicative of bacteriuria) and was markedly positive for hemoglobin, red cells, and white cells. After infusion of half-normal saline, the hematocrit was reduced to 34% but then rose to 38% with a persistently elevated MCV. The sodium and the BUN were reduced to within the reference range.

Evaluation

The basic diagnosis of this patient's condition is hypernatremia. This patient was dehydrated, as shown by the markedly elevated serum sodium (average value of 169 mEq/L), high normal hematocrit, and elevated BUN. Note that the diagnosis of dehydration was confirmed by the finding of a high serum and urinary (228 mEq/L) sodium and a high urinary osmolality of 1008 mOsm/kg (see Table 9.3). The red blood cell count was low, which seems to contradict the high normal hematocrit. This apparent discrepancy may be explained by the macrocytosis, causing each erythrocyte to occupy a greater than normal volume. Yet, the total number of cells was reduced. The low red cell count indicates a true anemia. The macrocytosis was caused by a nutritional (vitamin B_{12}) deficiency. All of these findings may be attributed to malnutrition and insufficient fluid consumption, a not uncommon finding in the elderly, especially in this stroke victim.

Note that the BUN and creatinine were mildly elevated in a pattern with a ratio of over 20 : 1, suggesting a prerenal (low perfusion) etiology. The renal tubules were evidently functioning well, as evidenced by the high urine-to-serum osmolality ratio (1008/357 = 2.8, which is greater than 1.2 : 1). Hypoperfusion may have also caused the mild abnormalities found in some of the liver function tests and the elevated pancreatic lipase.

Note also that the total protein was normal even though the albumin, the most abundant serum protein, was low. Because of possibly two infectious diseases identified in urine and stool examinations, the patient may have produced elevated levels of immunoglobulins. Accompanying the CVA was a peptic ulcer, the so-called *Cushing ulcer*, known to be associated with this condition—hence, the occult blood in this patient's stool. *C. difficile* is known to infect patients with chronic debilitating disease. The urinary tract infection was responsible for the high red cell count and hemoglobin in this patient's urine.

CASE B: COMPLEX ELECTROLYTE DISORDER

A 31-year-old white male patient with known type 1 diabetes mellitus, end-stage renal disease secondary to diabetic nephropathy, and a history of alcoholism was admitted with acute abdominal pain in the midepigastrium, with a serum glucose of 736 mg/dL that rose as high as 933 mg/dL at one point. Serum sodium was 134 mEq/L, which decreased to as low as 124 mEq/L. Potassium was 7.1 mEq/L, BUN was 64 mg/dL, and creatinine was 18 mg/dL. These values were confirmed and found to follow a consistent trend. Serum osmolality was 316 mOsm/kg. Blood gas values on admission were pH of 7.58, PO_2 of 121 mmHg, O_2 saturation of 99%, PCO_2 of 20 mmHg, and bicarbonate of 20 mEq/L. The anion gap rose in one day from 13 (high end of normal) to 20. Serum lipase was elevated at 469 IU/L (upper limit of normal is 60 IU/L). There was no urine output, and the patient was subjected to peritoneal dialysis.

Evaluation

This diabetic patient was evidently in a hyperosmolar state due to abnormally elevated glucose levels. The low serum sodium and high serum potassium might appear to be due to low circulating aldosterone or renal tubular failure. However, there was no urine output; thus, no filtration could occur. The end-stage renal disease is reflected in the BUN and especially in the creatinine value (18 mg/dL). The BUN/creatinine ratio of about 4 confirms the diagnosis of true renal failure.

As noted in earlier discussions on sodium and glucose, in diabetes mellitus with high serum glucose levels, there is an efflux of cell water that causes dilution of serum analytes such as sodium. Whenever glucose is transported into cells under the influence of insulin, it is accompanied by potassium. Low insulin levels can therefore result in hyperkalemia. This mechanism was operative in this patient. Though the anion gap increased after admission, it was normal on admission. Thus, this patient was in a nonketotic, hyperosmolar state but subsequently became ketotic. The admission blood gas picture suggests a respiratory alkalosis because the arterial blood pH was 7.57 (alkalosis), but the PCO_2 was low at 20 mmHg, and the bicarbonate was low at 20 mEq/L (condition 4 in Table 9.4). This is an unusual finding in a patient with diabetes mellitus, in whom a finding of metabolic acidosis is more frequently encountered.

An explanation for this finding may be found in the serum lipase, which was markedly elevated, denoting pancreatitis, a common finding in patients with a history of alcoholism. The sharp epigastric pain caused increased respiration (respiratory rate on admission was 25/min) precipitating a lowering of the PCO_2, which was partially compensated by a lowering of the bicarbonate. This condition, acute pain inducing respiratory alkalosis and an underlying diabetes-induced metabolic ketoacidosis, gives the combined blood gas pattern of "overcompensated" metabolic acidosis discussed in the earlier section on blood gas.

Treatment of this patient with dialysis, hydration, and insulin corrected the abnormal laboratory findings, and the patient was discharged on chronic dialysis.

CASE C: DISORDERS RELATED TO LIVER FAILURE

A 39-year-old white female with a past medical history of multiple abdominal surgical procedures over a 7-year period, sporadic alcohol abuse, pancreatitis, and a 30 pack-year history of smoking was brought to the emergency department in shock and acute abdominal distress. Significant laboratory values included white blood cell count of $12.1 \times 10^3/\mu L$, red cell count of $3.0 \times 10^6/\mu L$, hematocrit of 34.6%, and red cell indices that showed macrocytosis and hypochromia (low mean corpuscular hemoglobin concentration). Vitamin B_{12} and folate levels were normal. The peripheral blood smear showed a leukoerythroblastic pattern. Serum glucose was low at 38 mg/dL; total protein was 4.3 g/dL and albumin was 1.5 g/dL. Lactate levels were elevated. The AP was elevated at 241 IU/L (upper limit of normal, 129 IU/L), and the bilirubin was mildly elevated at 1.6 mg/dL (upper limit of normal, 1.2 mg/dL). Serum ammonia was found to be elevated at 146 μmol/L (upper limit of normal, 30 μM). Screens for hepatitis A, B, and C were all negative. The patient was placed on broad-spectrum antibiotics. Multiple blood, urine, and throat cultures were negative. Exploratory laparotomy revealed abdominal adhesions and cholestasis. Postoperatively, the patient became encephalopathic; her liver function deteriorated, as evidenced by dramatic elevations of AST and ALT from normal levels to 1660 and 545 IU/L, respectively; of LD to 2190 IU/L; bilirubin to 14.5 mg/dL; and ammonia to 177 μM, despite lactulose administration. A liver-spleen scan performed on the fifth hospital day showed no dye uptake in the liver, consistent with functional liver failure. The serum sodium, normal on admission, increased within 5 days to 166 mEq/L, together with chloride levels that rose to 123 mEq/L, a pattern that persisted throughout the hospital course despite aggressive intravenous infusion of half-normal saline. Serum potassium was consistently less than 3.5 mEq/L. The BUN and creatinine both rose to abnormally high levels, with a ratio of over 20:1, suggesting renal failure. Plasma aldosterone was elevated at 13.2 ng/dL (upper limit of normal, 8.5 ng/dL). The platelet count dropped rapidly, while the APTT and PT rose to values at least twice those of the corresponding normal controls; her level of FSPs (this evaluation occurred prior to the standard use of D-dimer) became abnormally elevated. Her condition worsened, and the patient expired on the eighth hospital day.

Evaluation

Although a complex patient presentation, the fundamental problem with this patient lay in the dramatically abnormal liver function test profile. Note how there was an acute elevation in the aminotransferases (transaminases), with the AST/ALT ratios significantly greater than 1. There were concurrent rapid elevations in the bilirubin and the LD. At the same time, the total protein and albumin were abnormally low. The ammonia levels rose rapidly (despite high doses of lactulose). The pattern is that of fulminant hepatic failure shown in condition 6 in Table 9.5. This condition is a medical emergency and is associated with fatal encephalopathy and severe DIC, as evidenced by the low platelet counts, elevated PT and APTT, and FSP levels. This condition can cause multiple system infarcts, resulting in multiple-organ failure.

The patient's peripheral blood picture showed a macrocytosis but, concurrently, a leukoerythroblastic picture. This pattern suggests that the macrocytosis was caused by an increased number of erythrocyte precursor forms. This condition was most likely caused by DIC that causes microangiopathic hemolytic anemia with a leukoerythroblastic picture. It is also possible that with the persistently elevated WBC count and the elevated lactate levels, gram-negative sepsis affecting bone marrow may have contributed to the leukoerythroblastic picture. Though cultures were consistently negative, the patient was being treated with broad-spectrum antibiotics, the effects of which may have blocked growth of the organism(s) in culture. As noted previously, patients with liver failure from either cirrhosis or acute fulminant hepatic failure are generally immunocompromised. In both panhepatic cirrhosis and fulminant hepatic failure, there is severe third-space fluid loss associated with ascites that invariably develops. We noted previously that to retain vascular volume, both aldosterone and ADH rise. It appears that aldosterone became elevated to markedly high values, causing abnormal sodium retention and potassium loss in this patient. Almost always accompanying both cirrhosis and acute fulminant hepatic failure is renal failure, generally manifested by the hepatorenal syndrome. In fulminant hepatic failure, an additional possible cause is ATN (Sunheimer et al., 1994). Also associated with this condition is hypoglycemia (serum glucose was 38 mg/dL), thought to be due to the absence of glycogen stores in the liver caused by the massive necrosis of hepatocytes and the resultant absence of enzymes involved in gluconeogenesis.

CASE D: SEVERE RHABDOMYOLYSIS

A 25-year-old previously healthy African American male in the U.S. Navy collapsed while performing running exercises as part of his military training. He reported that he had developed severe bilateral calf and thigh pain prior to this episode. His medical history was significant for sickle trait, and the only medication he had been taking was an over-the-counter "performance-enhancing" dietary supplement, ephedra. In the emergency department, the patient became hypotensive and showed signs of respiratory distress. He reported increasing bilateral lower extremity pain. A provisional diagnosis of anterior compartment syndrome—that is, muscle tissue necrosis on the anterior aspect of the lower extremities—was made. An electrocardiogram showed sinus tachycardia, inferolateral ischemia, and left ventricular hypertrophy. Arterial blood gas revealed a blood pH of 7.16, a PCO_2 of 33.5 mmHg (lower limit, 35.0 mmHg), a PO_2 of 245 mmHg while the patient was receiving 40% O_2, and a low serum bicarbonate (6.0 mEq/L; lower limit, 24 mEq/L).These findings suggested metabolic acidosis (low blood pH, low bicarbonate, and a modestly decreased PCO_2). Further significant findings were elevated creatine kinase (total CK) of 269 IU/L (upper limit, 174 IU/L), elevated creatinine (2.1 mg/dL; upper limit, 1.2 mg/dL), elevated AST (73 IU/L; upper limit, 42 IU/L) and ALT (84 IU/L; upper limit, 40 IU/L), and a high anion gap of 33 mOsm (upper limit, 11 mOsm). Blood lactate was elevated at 11.7 mM (upper limit, 1.5 mM) and reached its highest level of 21 mM on the 26th hospital day. Serum glucose was found to be elevated at 233 mg/dL (upper limit, 115 g/dL). CBC showed elevated WBC count ($16.6 \times 10^3/\mu L$; upper limit, $11 \times 10^3/\mu L$) and red cell count of 4.4×10^6 (lower limit, 4.5×10^6),

hematocrit 37.3 (lower limit, 40), and normal MCV and MCHC. Troponin I was found to be elevated at 4.72 ng/mL (positive >0.78 ng/mL), which is strongly suggestive of AMI. Over several hours, the AST was found to increase to 2035 IU/L, the ALT to 728 IU/L, and the CK to 95,775 IU/L. The serum total protein (lower limit, 6.4 mg/dL) and albumin (lower limit, 3.8 mg/dL) were low, reaching levels as low as 3.8 and 1.9 mg/dL, respectively. The serum sodium concentration was 133 mEq/L (lower limit, 135 mEq/L), and the potassium increased to 7.5 mEq/L. Urinalysis showed severe myoglobinuria, proteinuria, glucosuria, bacteriuria, and elevated WBC count. The patient was transferred to the medical intensive care unit (MICU), where it was further found that the platelet count dropped to $97 \times 10^3/\mu L$ (lower limit, $150 \times 10^3/\mu L$). The PT and APTT were both found to be elevated at 21.3 sec (upper limit, 13.8 sec) and 59.1 sec (upper limit, 38.4 sec), respectively. The D-dimer level was found to be elevated at greater than 5000 ng/mL (upper limit, 230 ng/mL). On the second hospital day, in the MICU, the red cell count dropped to $2.1 \times 10^6/\mu L$, with normal MCV and MCHC values. The patient was intubated and placed on mechanical ventilation, with aggressive hydration therapy. In addition, he was treated with anticoagulant therapy and transfusions of packed red blood cells and fresh frozen plasma. In view of the elevated WBC count and a persistent fever, the patient was placed on a broad-spectrum antibiotic regimen. On the twelfth hospital day, cultures of the patient's femoral catheter tip and a urethral swab showed *Pseudomonas aeruginosa* and *Enterococcus faecium*. By the seventeenth hospital day, chest x-ray showed cardiomegaly and BNP values that increased from 86 ng/mL (upper limit, 100 ng/mL) 1 week after admission to 422 ng/mL on hospital day 23 and 6300 ng/mL on day 25. The AST and ALT levels increased to as high as 11,443 and 5949 IU/L, respectively, accompanied by large rises in bilirubin, alkaline phosphatase, and LD; the CK level was as high as 98,000 IU/L. BUN and creatinine increased to as high as 108 and 5.7 mg/dL, respectively, indicative of severe renal failure. After persistent treatment and a bilateral lower extremity fasciotomy to relieve compartment syndrome, the patient improved symptomatically, but after about 1 week, he relapsed, became septic from *Acinetobacter baumannii*, and expired on the twenty-fifth hospital day.

Evaluation

Based on this patient's history—compartment syndrome/rhabdomyolysis—the laboratory results in this complex case are diagnostic of this condition. As with Case C, there is a key abnormality that can explain the other findings: the initial elevated CK followed by a massive increase of this enzyme level over a short time period. The initial value of CK in the emergency department might have been attributed to AMI, as confirmed by troponin and ECG, but the subsequent values could not have been attributed to this condition alone. Values of CK in the thousands and tens of thousands are clearly indicative of severe muscle tissue breakdown, as occurs in rhabdomyolysis and polymyositis. In this condition, as discussed in the section on CK, damaged myocytes release myoglobin into the circulation. This small protein is filtered by the glomerulus and enters the tubules, where it induces tubular damage and tubular necrosis. This results in (often severe) renal disease, thus the rise in BUN and creatinine, as was observed in this case. Another major consequence of massive muscle tissue necrosis is the release of potassium, the chief intracellular cation, into the circulation, causing severe hyperkalemia, which is cardiotoxic and was life-threatening to this patient because he already appears to have suffered an MI and had an arrhythmia. The patient was therefore treated with insulin, which induces glucose and potassium transport across the cell membranes of viable cells. In this patient, not only did this lower the serum potassium but the serum glucose as well, a beneficial effect because the serum glucose was abnormally elevated, possibly a result of the adrenergic ephedra and/or underlying diabetes).

Massive tissue necrosis also releases tissue fragments that activate the coagulation cascades. As a result, coagulation factors are consumed, as are platelets in the formation of microemboli that often block the microvasculature, causing further tissue necrosis. This condition of DIC can cause microangiopathic hemolytic anemia, which could explain the normochromic, normocytic anemia. As discussed in the section on elevated PT and APTT, in this condition, the PT and APTT are elevated, as is D-dimer, and the platelet count is low, as occurred in this case. Because oxygenation of tissues is compromised by the microemboli, metabolism in these tissues becomes anaerobic, leading to a buildup of lactic acid. This is compounded by rhabdomyolysis that releases large quantities of lactic acid from stressed muscle tissue. This condition gives rise to severe lactic acidosis. In this patient, lactate levels reached as high as 21 mM.

Accompanying the rise in CK early in this patient's hospital stay was a dramatic rise in the AST and ALT levels to the point that the AST levels were much higher than the corresponding ALT levels. In addition, there were concomitant increases in bilirubin, LD, and alkaline phosphatase and major decreases in total protein and albumin. From entry 5 in Table 9.6 and Case C, this pattern of liver function tests suggests acute hepatic failure. Liver failure in this case may have been caused by the drop in systemic blood pressure experienced by this patient, leading to severe liver hypoperfusion (so-called "shock liver"), a known cause of this condition and/or the DIC, causing microemboli in the microcapillaries of the liver.

This patient's condition involved three unusual complications: AMI documented by significantly elevated serum levels of troponin and positive ECG findings (i.e., elevated ST wave elevations), severe congestive heart failure documented by severely elevated serum levels of BNP and positive chest x-ray findings, and recurrent bacterial infection and septicemia. The first two findings are rare complications of acute rhabdomyolysis. They suggest that the patient's sickle trait may have contributed to the overall pathophysiology of this disease. The extreme level of military exercise, exacerbated by the use of the drug ephedra, which is now prohibited given its severe adrenogenic effects, may have precipitated a sickle crisis due to the severe oxygen demand, simulating the events that might transpire in sickle trait patients at high altitudes where oxygen pressures are low. Sickling may have further added to blockade of the microvasculature, including the coronary circulation.

With respect to bacterial infections, a total of three different gram-negative organisms were cultured from this patient, two—*P. aeruginosa* and *E. faecium*—from a catheter tip and a urethral swab and one—*Acinetobacter baumannii*—from blood cultures. Recurrent infections over a short time span suggest the possibility of an immunosuppressive state, due likely to massive tissue necrosis and protein loss, and fulminant hepatic failure as in Case C, although the patient was able to mount a strong white cell response, as indicated by the elevated WBC count. An unusual accompaniment of gram-negative sepsis is the Waterhouse-Friderichsen syndrome in which there are petechial hemorrhages on body surfaces and in the adrenal glands, leading to adrenal failure. A sign of this condition is hyponatremia (sodium of 133 mEq and lower values during the course of hospitalization) and hyperkalemia due to low production of aldosterone. Because the patient was found to have both hyponatremia and hyperkalemia, though most of the elevated potassium was most likely due to rhabdomyolysis, the possibility of gram-negative sepsis–induced adrenal failure must be considered. gram-negative sepsis from *A. baumannii* is thought to be acquired in immunosuppressed patients in intensive care units.

SELECTED REFERENCES

Bakerman S, Strausbauch P: In Myrtle Beach SC, editor: *ABC's of interpretive laboratory data*, ed 2, Interpretive Laboratory Data, 1994.

This is an excellent review of not only the use of laboratory testing but also of the underlying methodology.

Bonini P, Plebani M, Ceriotti F, et al.: Errors in laboratory medicine, *Clin Chem* 48:691–698, 2002.

This is an important review of laboratory errors and how to recognize them.

Caliskan Y, Kiryluk K: Novel biomarkers in glomerular disease, *Adv Chron Kid Dis* 21:205–216, 2014.

This is a concise summary of urine and serum diagnostic markers for glomerular disease.

Mastroianni-Kirsztajn G, Hornig N, Schlumberger W: Autoantibodies in renal diseases-clinical significance and recent developments in serological detection, *Front Immunol* 6:1–18, 2015.

This is an outstanding review of the major glomerulopathies and their diagnostic serological markers.

Nathan D: (corresponding author for the international Expert Committee, American Diabetes Association): international Expert Committee report on the role of the A1C assay in the diagnosis of diabetes, *Diabetes Care* 32:1327–1334, 2009.

This summarizes the current standards for diagnosis of diabetes mellitus.

Oh M: *Acid-base, electrolytes, old Westbury*, NY, 2003, OHCO, LLC.

This is an excellent, concise discussion of renal physiology, electrolyte regulation, and acid-base balance.

Sunheimer R, Capaldo G, Kashanian F, et al.: Serum analyte pattern characteristic of fulminant hepatic failure, *Ann Clin Lab Sci* 24:101–109, 1994.

This paper summarizes serum liver function analyte patterns that have been found to occur in this uncommon but fatal disease. It correlates analyte patterns with tissue pathological findings.

Access the complete reference list online at Elsevier eBooks for Practicing Clinicians.

REFERENCES

Abrams J: C-reactive protein, inflammation, and coronary risk: an update, *Cardiol Clin* 21:327–331, 2003.

Ali NS, Nanji K: A review on the role of vitamin D in asthma, *Cureus* 9(5):e1288, 2017, https://doi.org/10.7759/cureus.1288.

Alpert JS, Thygesen K, Antman E, et al.: Myocardial infarction redefined—a consensus document of the joint European Society of Cardiology/American College of Cardiology Committee for the Redefinition of myocardial infarction, *J Am Coll Cardiol* 36:959–969, 2000.

Alter BP: Bone marrow failure syndromes, *Clin Lab Med* 19:113–133, 1999.

Alter BP: Bone marrow failure syndromes in children, *Pediatr Clin North Am* 49:973–988, 2002.

American Diabetes Association: Classification and diagnosis of diabetes: standards of medical care in diabetes-2018, *Diabetes Care* 41:S13–S27, 2018.

Akankwasa G, Jianhua L, Guixue C, Changjuan A, Xiaosong Q: Urine markers of podocyte dysfunction: a review of podocalyxin and nephrin in selected glomerular diseases, *Bio Med* 12, 2018, https://doi.org/10.2217/bmm-2019-0152. Published Online: 6 Jul 2018.

Autier P, Mullie P, Macacu A, et al: Effect of vitamin D supplementation on non-skeletal disorders: a systematic review of meta-analyses and randomised trials, Lancet Diabetes & Endocrinology 5(12): 986 -1004, 2017.

Aviles RJ, Askari AT, Lindahl B, et al.: Troponin T levels in patients with acute coronary syndromes, with or without renal dysfunction, *N Engl J Med* 346:2047–2052, 2002.

Barrea L, Savanelli C, Di Somma C, Napolitano M, Megna M, Colao A, Savastano S: Vitamin D and its role in psoriasis: an overview, *Rev Endocr Metab Disord* 18:195–205, 2017.

Bilke D: Nonclassic actions of vitamin D, *J Clin Endocrinol Metab* 1:26–34, 2009.

Blincko S, Edwards R: Current issues in glycated haemoglobin measurement, *Clin Lab* 47:377–385, 2001.

Bock JL, Brogan Jr GX, McCuskey CF, Thode Jr HC, Hollander JE, Gunther T: Evaluation of CK-MB isoform analysis for early diagnosis of myocardial infarction, *J Emerg Med* 17:75–79, 1999.

Boyer DF: Blood and bone marrow evaluation for eosinophilia, *Archives Pathol Lab Med* 140:1060–1067, 2016.

Brigden M, Graydon C: Eosinophilia detected by automated blood cell counting in ambulatory North American outpatients: Incidence and clinical significance, *Arch Pathol Lab Med* 121:963–967, 1997.

Brito-Babapulle F: The eosinophilias, including the idiopathic hypereosinophilic syndrome, *Br J Haematol* 121:203–223, 2003.

Brown D: The ins and outs of aquaporin-2 trafficking, *Am J Physiol Renal Physiol* 284:F893–F901, 2003.

Caliskan Y, Kiryluk K: Novel biomarkers in glomerular disease, *Adv Chron Kid Dis* 21:205–216, 2014.

Clerico A, Emdin M: Diagnostic accuracy and prognostic relevance of the measurement of cardiac natriuretic peptides: a review, *Clin Chem* 50:33–50, 2004.

Clerico A, Zaninotto M, Prontera C, et al.: State of the art of BNP and NT-proBNP immunoassays: the CardioOrmoCheck study, *Clin Chim Acta* 414:112–119, 2012.

Crowson CS, Rahman MU, Matteson EL: Which measure of inflammation to use? A comparison of erythrocyte sedimentation rate and C-reactive protein measurements from randomized clinical trials of golimumab in rheumatoid arthritis, *J Rheum* 36:1606–1610, 2009.

Dantzer R, Capuron L, Irwin MR, et al.: Identification and treatment of symptoms associated with inflammation in medically ill patients, *Psychoneuroendocrinology* 33:18–29, 2008.

DeCaterina R, Lanza M, Manca G, et al.: Bleeding time and bleeding: an analysis of the relationship of the bleeding time test with parameters of surgical bleeding, *Blood* 84:3363–3370, 1994.

Del Pinto R, Ferri C, Cominelli F: Vitamin D axis in inflammatory bowel diseases: role, current uses, and future perspectives, Int J Molec Sci 18:2360, 2017.

DeZern AE, Brodsky RA: Clinical management of aplastic anemia, *Expert Rev Hematol* 4:221–230, 2011.

Dighe AS, Soderberg BL, Laposata M: Narrative interpretations for the clinical laboratory evaluations: an overview, *Am J Clin Pathol* 116(Suppl 1):S123–S128, 2001.

Diris JH, Hackeng CM, Kooman JP, et al.: Impaired renal clearance explains elevated troponin T fragments in hemodialysis patients, *Circulation* 109:23–25, 2004.

Ducatman AM, Tacker DH, Ducatman BS, Long D, Perotta PL, Lawther H, et al.: Quality improvement intervention for reduction of redundant testing, *Acad Path* 4:1–10, 2017.

El-Ghammaza AM, Hamedb GM, Fattahb MFA, Attiaa MH: Basophil progenitor marker histamine and its relation to the treatment response in Egyptian chronic myeloid leukemia patients, Egyptian Society of Haematology 40:30-36, 2015.

Feldman D, Krishnan AV, Swami S, et al: The role of vitamin D in reducing cancer risk and progression, Nature Reviews: Cancer 14:342-357, 2014.

Fischbach F, et al.: *A manual of laboratory and diagnostic tests*, Philadelphia, Pa, 2008, Lippincott Williams & Wilkins.

Fromm Jr RE, Roberts R: Sensitivity and specificity of new serum markers for mild cardionecrosis, *Curr Probl Cardiol* 26:246–284, 2001.

George TI, Arber DA: Pathology of the myeloproliferative diseases, *Hematol Oncol Clin North Am* 17:1101–1127, 2003.

Gerwirtz AS, Miller ML, Keys TF: The clinical usefulness of the preoperative bleeding time, *Arch Pathol Lab Med* 120:353–356, 1996.

Gill RQ, Sterling RK: Acute liver failure, *J Clin Gastroenterol* 33:191–198, 2001.

Gordon-Smith EC, Marsh JC, Gibson FM: Views on the pathophysiology of aplastic anemia, *Int J Hematol* 76(Suppl 2):163–166, 2002.

Guinan EC: Clinical aspects of aplastic anemia, *Hematol Oncol Clin North Am* 11:1025–1044, 1997.

Hallek M, Cheson BD, Catovsky D, et al.: Guidelines for diagnosis, indications for treatment, response assessment and supportive management of chronic lymphocytic leukemia, *Blood* 2745–2760, 2018.

Hueb W, Gersh BJ, da Costa LMA, Oikawa FTC, de Melo RMV, Rezende PC, et al.: Accuracy of myocardial biomarkers in the diagnosis of myocardial infarction after revascularization as assessed by cardiac resonance: the Medicine, Angioplasty, Surgery Study V (MASS-V) Trial, *Ann Thorac Surg* 101:2202–2208, 2016.

Hughes T, Branford S: Molecular monitoring of chronic myeloid leukemia, *Semin Hematol* 40(Suppl 2):62–68, 2003.

Ishii J, Cui W, Kitagawa F, et al.: Prognostic value of combination of cardiac troponin T and B-type natriuretic peptide after initiation of treatment in patients with chronic heart failure, *Clin Chem* 49:2020–2026, 2003.

Jabbour E, Kantarijan H: Chronic myeloid leukemia: 2018 update on diagnosis, therapy and monitoring, *Am J Hematol* 93:442–459, 2018.

Kamath PS, Kim WR: *The International Normalized Ratio of prothrombin time in the model for end-stage liver disease score: a reliable measure in clinics in liver disease*, Philadelphia, 2009, WB Saunders, pp 63–68.

Kilpatrick ES: HbA1c measurement, *J Clin Pathol* 57:344–345, 2004.

Kottke-Marchant K, Corcoran G: The laboratory diagnosis of platelet disorders: an algorithmic approach, *Arch Pathol Lab Med* 126:133–146, 2002.

Krishnamurti U, Steffes MW: Glycohemoglobin: a primary predictor of the development or reversal of complications of diabetes mellitus, *Clin Chem* 47:1157–1165, 2001.

Labriola L, Wallemacq P, Gulbis B, et al.: The impact of the assay for measuring albumin on corrected ("adjusted") calcium concentrations, *Nephrol Dial Transplant* 24:1834–1838, 2009.

Larsson L, Magnusson P: Ionized calcium or corrected total calcium? *J Bone Miner Res* 18:1554–1555, 2003.

Lewandrowski K, Chen A, Januzzi J: Cardiac markers for myocardial infarction, *Am J Clin Pathol* 118(Suppl 1):S93–S99, 2002.

Libby P, Ridker PM: Inflammation and atherosclerosis: role of C-reactive protein in risk assessment, *Am J Med* 116(Suppl 6A):9S–16S, 2004.

Lott JA: Serum enzyme determinations in the diagnosis of acute myocardial infarction: an update, *Hum Pathol* 15:706–716, 1984.

Marsh JC: Bone marrow failure syndromes, *Clin Med* 5:332–336, 2005.

Marsh JC, Ball SE, Darbyshire P, et al.: Guidelines for the diagnosis and management of acquired aplastic anemia, *Br J Haematol* 123:782–801, 2003.

Mastroianni-Kirsztajn G, Hornig N, Schlumberger W: Autoantibodies in renal diseases-clinical significance and recent developments in serological detection, *Front Immunol* 6:1–18, 2015.

Melli G, Chaudhry V, Cornblath DR: Rhabdomyolysis: an evaluation of 475 hospitalized patients, *Medicine (Baltimore)* 84:377–385, 2005.

Moretti H, Colucci VJ, Berry BD: Vitamin D3 repletion versus placebo as adjunctive treatment of heart failure patient quality of life and hormonal indices: a randomized, double-blind, placebo controlled trial, *BMC Cardiovasc Disord* 17:274–286, 2017.

Morrow DA, Cannon CP, Jesse RL, et al.: National Academy of Clinical Biochemistry Laboratory Medicine Practice guidelines: clinical characteristics and utilization of biochemical markers in acute coronary syndromes, *Circulation* 115:e356–e375, 2007.

Mueller C, Scholer A, Laule-Kilian K, et al.: Use of B-type natriuretic peptide in the evaluation and management of acute dyspnea, *N Engl J Med* 350:647–654, 2004.

Nguyen MK, Nielsen S, Kurtz I: Molecular pathogenesis of nephrogenic diabetes insipidus, *Clin Exp Nephrol* 7:9–17, 2003.

Nielsen S, Froklar J, Marples D, et al.: Aquaporins in the kidney: from molecules to medicine, *Physiol Rev* 82:205–244, 2002.

Novo G, Amoroso GR, Fazio G, et al.: Biomarkers in heart failure, *Front Biosci* 14:2484–2493, 2009.

Oscier D, Fegan C, Hillmen P, et al.: Guidelines on the diagnosis and management of chronic lymphocytic leukemia, *Br J Haematol* 125:294–317, 2004.

Ouyang J, Dalal Dalal S, Blumenthal D, et al.: Unusual complications of exertional rhabdomyolysis in a patient with sickle-cell trait, *Fed Pract*14–26, 2009.

Pedersen NB, Hofmeister MV, Rosenbaek LL, et al.: Vasopressin induces phosphorylation of the thiazide-sensitive sodium chloride cotransporter in the distal convoluted tubule, *Kidney Int* 78:160–169, 2010.

Posan E, McBane RD, Grill DE, et al.: Comparison of PFA-100 testing and the bleeding time for detecting platelet hypofunction and von Willebrand disease in clinical practice, *Thromb Haemost* 90:483–490, 2003.

Prahash A, Lynch T: B-type natriuretic peptide: a diagnostic, prognostic, and therapeutic tool in heart failure, *Am J Crit Care* 13:46–53, 2004.

Ridker PM: High-sensitivity C-reactive protein and cardiovascular risk: Rationale for screening and primary prevention, *Am J Cardiol* 92(Suppl):17K–22K, 2003.

Roberts R: Rapid MB CK subform assay and the early diagnosis of myocardial infarction, *Clin Lab Med* 17:669–683, 1997.

Roberts WL, Sedrick R, Moulton L, et al.: Evaluation of four automated high-sensitivity C-reactive protein methods: Implications for clinical and epidemiological applications, *Clin Chem* 46:461–468, 2000.

Ross DM, Hughes TP: Current and emerging tests for the laboratory monitoring of chronic myeloid leukaemia and related disorders, *Pathology* 40:231–246, 2008.

Rothenberg ME: Eosinophilia, *N Engl J Med* 338:1592–1600, 1998.

Sattler M, Griffin JD: Molecular mechanisms of transformation by the BCR-ABL oncogene, *Semin Hematol* 40(Suppl 2):4–10, 2003.

Schiodt FV, Lee WM: Fulminant liver disease, *Clin Liver Dis* 7:331–349, 2003.

Schnermann JB, Sayegh SI: *Kidney physiology*, New York, 1998, Lippincott-Raven.

Schrier RW, Cadnapaphornchai MA: Renal aquaporin water channels: from molecules to human disease, *Prog Biophys Mol Biol* 81:117–131, 2003.

Seebach JD, Morant R, Ruegg R, et al.: The diagnostic value of the neutrophil left shift in predicting inflammation and infectious disease, *Am J Clin Pathol* 107:582–591, 1997.

Sergeev IN: Vitamin D-mediated apoptosis in cancer and obesity, Horm Mol Biol Clin Invest 20: 43-49, 2014.

Shanafelt TD, Call TG: Current approach to diagnosis and management of chronic lymphocytic leukemia, *Mayo Clin Proc* 79:388–398, 2004.

Silver RT: Chronic myeloid leukemia, *Hematol Oncol Clin North Am* 17:1159–1173, 2003.

Sproston NR, Ashworth JJ: Role of C-reactive protein at sites of inflammation and infection, *Front Immunol* 9:1–11, 2018.

Mathiasen IS, Lademann U, Jaattela M: Apoptosis induced by vitamin D compounds in breast cancer cells is inhibited by Bcl-2 but does not involve known caspases or p53, *Cancer Res* 59:4849–4856, 1999.

Swerdlow SH, Campo E, Harris NL, et al.: *WHO classification of tumours of hematopoietic and lymphoid tissues*, Lyon, 2008, International Agency for Research on Cancer.

Thomas JS, Ellen MM: A review of vitamin D supplementation as disease-modifying therapy, Multiple Sclerosis J 24: 6-11, 2018.

Thompson WG, Mahr RG, Yohannan W, et al.: Use of creatine kinase MB isoenzyme for diagnosing myocardial infarction when total creatine kinase activity is high, *Clin Chem* 34:2208–2210, 1988.

Thygesen K, Mair J, Giannitsis E, et al.: How to use high-sensitivity cardiac troponins in acute cardiac care, *Eur Heart J* 33:2252–2257, 2012.

Van den Berghe G: Endocrine evaluation of patients with critical illness, *Endocrinol Metab Clin North Am* 32:385–410, 2003.

Wang TJ, Larson MG, Levy D, et al.: Plasma natriuretic peptide levels and the risk of cardiovascular events and death, *N Engl J Med* 350:655–663, 2004.

Winter WE, Elin RJ: The role and assessment of ventricular peptides in heart failure, *Clin Lab Med* 24:235–274, 2004.

Winton EF, Langston AA: Update in acute leukemia 2003: a risk adapted approach to acute myeloblastic leukemia in adults, *Semin Oncol* 31(Suppl 4):80–86, 2004.

Witte DL, VanNess SA, Angstadt DS, et al.: Errors, mistakes, blunders, outliers, or unacceptable results: how many? *Clin Chem* 43:1352–1356, 1997.

Woo J, Zaman S, Patel L: The diagnostic value of specific CK-MB assay in acute myocardial infarction. In Miyai K, Kanno T, Ishikawa E, editors: *Progress in clinical biochemistry*, London, 1992, Elsevier, pp 243–246.

Wu AH, Apple FS, Gibler WB, et al.: National Academy of Clinical Biochemistry standards of laboratory practice: Recommendations for the use of cardiac markers in coronary artery diseases, *Clin Chem* 45:1104–1121, 1999.

Yates AM, Bowron A, Calton L, et al.: Interlaboratory variation in 25-hydroxyvitamin D2 and 25-hydroxyvitamin D3 is significantly improved if common calibration material is used, *Clin Chem* 54:2082–2084, 2008.

Zerwekh J: Blood biomarkers of vitamin D status, *Am J Clin Nutr* 87:1087S–1091S, 2008.

Zylka A, Dumnicka P, Kusnierz-Cabala B, et al.: *Markers of glomerular and tubulardamage in the early stage of kidney disease in type 2 diabetic patients*, Med Inflammat Hind, 2018, https://doi.org/10.1155/2018/7659243: 1-12. Article ID 7659243 2018.

CHAPTER 10

LABORATORY STATISTICS

Richard A. McPherson

DEFINITIONS, 119
VARIABLES, 120
PREPARING TO ANALYZE DATA, 120
DESCRIPTIVE STATISTICS, 120
Central Tendency, 120
Gaussian (Normal) Distribution, 121
Dispersion, 121
Nonparametric Measures, 122
COMPARATIVE STATISTICS, 122
Student *T*-Test, 122
Nonparametric Tests, 124
ANALYZING DISCRETE DATA: TESTING PROPORTIONS, 124
Chi-Square Test, 124
TREND EVALUATION AND CORRELATIVE STATISTICS, 125
Linear Regression, 125
Method Comparisons, 125
Analysis of Variance, 126
Analysis Involving Multiple Variables, 126
METHOD VALIDATION AND PROCESS CONTROL, 127
Reference Ranges, 127
Accuracy, 127
Precision, 127
Analytic Sensitivity, 127
Analytic Specificity, 128
Acceptability of a Method, 128
Misuse of Statistics, 128
Risk of False-Positive Results, 128
RESOURCES FOR STATISTICAL ANALYSIS, 128
SELECTED REFERENCES, 129

KEY POINTS

- For statistical analyses, nominal variables can take on only a limited number of values (or categories), whereas continuous variables are used to report quantitative data.
- Independent variables are considered input (cause), and dependent variables are considered output (effect).
- Distributions of continuous data are described by a measure of central tendency (e.g., mean or median) and dispersion (standard deviation). Gaussian distributions derive from a mathematical formula and thus are parametric. A common application of descriptive statistics is to establish reference ranges.
- Statistical tests, such as comparisons of different groups of data points, may be parametric (i.e., assume Gaussian distributions; an example is the Student *t*-test) or nonparametric (i.e., make no assumption of distributions; an example is a test based on rank order).
- Confidence intervals are preferable over point estimates to express level of certainty in the calculation of any statistical parameter.
- Nominal data are conveniently analyzed with proportions using the chi-square test.
- The effects of multiple factors in a model system can be assessed through analysis of variance.
- Regression analysis between two continuous variables is usually done by least squares fit to a straight line. Applications of regression analysis are common when different analytic methods for validation are compared in clinical laboratories.
- Investigators should take measures to avoid bias in their experimental design and planning of statistical analysis to avoid misuse and be aware of high potential for false-positive results, especially when the power is low and other personal and professional factors are at stake.

The quantification of information in meaningful summaries and comparisons is the domain of statistical analysis. The first task in analysis is to provide a description of the magnitude of the observations and how close the different measurements are to one another. Descriptive statistics provide a consistent framework for calculating or estimating the central tendency of continuous data in the familiar forms of mean, median, and mode. The variation in data is generally described by the mathematical calculations of variances and standard deviations or by the simple allocation of data points into a range of percentiles (e.g., interquartile range). These approaches are everyday phenomena in clinical laboratories for the monitoring of all quantitative assays. Reference ranges are initially set up with these techniques. Methods of quality control for precision and proficiency testing for accuracy also are based on these principles. For data that are not continuous but take on only two or a few discrete values (e.g., positive or negative), the analysis might consist of counting the number in each category and looking at the proportions of all values by category.

Comparison of data typically asks the question whether one group is different from another group. These comparisons are usually done by *t*-test or by analysis of variance depending on whether two or more groups of continuous data are compared. If the data are discrete, comparison is done by chi-square analysis. When data can take on a range of different values, it is convenient to do a correlation between two different data sets with a straight line fit. The newcomer to statistical analysis frequently poses the question "Which statistical test is best?" The question of which test to use depends largely on whether the data are continuous or discrete and whether continuous data follow particular distributions. However, statistics is based on convention; thus, the investigator should try diligently to understand the importance of differences between tests and whether possible findings and conclusions are likely to reflect accurately the nature and significance of the question being asked. In contrast to the investigator who is interested in finding the right test for data already collected, the statistician is more interested in helping the investigator plan the experiment and collect data so that statistical tests are most valid. This chapter relies heavily on common clinical laboratory examples for which specific statistical tests are applied to demonstrate some useful choices.

DEFINITIONS

- *Variables:* The things that we measure, count, or otherwise delineate are termed *variables* because the values they can assume vary. Variables are usually considered to fall into one of the following scales.
- *Nominal scale* is where a variable can take on only a limited number of values, usually called *categories* (or *characters*). Examples of nominal variables are gender (male or female) and risk factors (e.g., smoker or nonsmoker).
- *Ordinal scale* is where the variable takes on specific values that have some inherent order, such as magnitude but without equivalent distances between categories (e.g., trace amount, 1+, 2+, etc., of protein in urine).
- *Interval scale* is where a variable takes on values in a quantitative range with defined differences between points. It is conventional to treat most numeric laboratory measurements as continuous variables, even though they may be reported as discrete values (e.g., glucose values of 123 or 124 mg/dL, but not 123.857… mg/dL).
- *Coefficient of variation (CV)* is the standard deviation of a set of data points divided by the mean result expressed as a percentage or as a decimal fraction.
- *Confidence interval (CI)* is the interval that is computed to include a parameter such as the mean with a stated probability (e.g., commonly 90%, 95%, 99%) that the true value falls into that interval.

- *Degrees of freedom (df)* is a parameter related to the sample size (n). df indicates the number of quantities free to vary and is usually n – 1 for applications such as the *t*-test. For the chi-square test, it is the number of rows minus one times the number of columns minus one. df is employed in calculating the *p* value for a statistical test.
- *Gaussian (normal) distribution* is a spread of data in which elements are distributed symmetrically around the mean, with most values close to the center. It is explicitly described by a mathematical equation, as is a parametric distribution. Random scatter or random selection of a population often results in a Gaussian normal distribution. This type of distribution is often a criterion for completely valid application of many parametric tests.
- *Linear regression* is the mathematical process for calculating the best straight line to fit the relationship observed between two variables measured on the same items. *Simple* or *least squares linear regression* yields the best fit for x and y data sets by minimizing the sum of the squared *y*-axis (vertical distance) differences between each data point *(x, y)* and the line. This approach assumes the *x*-axis data to be nearly perfect or without error. Uneven distribution of data points across the entire range may significantly alter the reliability of linear regression. *Deming linear regression* does not assume the *x*-axis data to be free of error, but instead uses the weighted sum of squared *y*-axis and *x*-axis differences between the data points and the line. The *correlation coefficient (r)* describes how well the line fits the data (*r* ranges from –1 to 1).
- *Mean* is the sum of all results divided by the number of results. Also related are the *median*, which is the middle value that divides the distribution of data points into upper and lower halves (also called the 50th percentile), and the *mode*, which is the most common value. The mean, median, and mode are all measures of central tendency. The *geometric mean* is calculated as the *n*th root of the product of a distribution of *n* numbers; its use for estimating central tendency minimizes the effects from extreme values such as are found in a log-normal distribution.
- *Parametric statistics* are statistical measures that are calculated based on the assumption that the data points follow a Gaussian distribution and include parameters such as mean, variance, and standard deviation. *Nonparametric statistics* are based on rank or order of data.
- *Null hypothesis (H_0)* is the proposal that there is no difference in a comparison. The alternative hypothesis is that there is a difference. When the critical value of a statistic is exceeded, rejection of the null hypothesis occurs, thereby favoring the acceptability of the alternative hypothesis.
- *Significance level (p or α)* is the probability that a difference between groups occurred by chance alone, by convention set at less than 0.05.
- *Statistical power (1 – β)* is the probability that a difference between groups will be detected by the study, generally set to at least 80%.
- *Standard deviation (SD)* is the square root of the sum of the squared differences of each data point from the mean divided by *n – 1* for samples (divided by *n* for populations). The SD is a predictable measure of dispersion from the mean in a Gaussian normal distribution.
- *Standard deviation index (SDI)* is the difference between the value of a data point and the mean value divided by the group's SD. The *z-transformation* is the expression of a result from the mean in SD units. The *Z*-value is the probability of a result being *z* SDs from the mean value. The SDI is commonly used in reporting performance in proficiency testing for an individual laboratory compared with peers.
- *Student* t-*test* is a statistical test for comparing means between two sample groups. The test can be paired (e.g., two separate measurements on the same individuals before and after some intervention) or unpaired. Values of *t* and *df* yield a level of statistical significance (*p* value).
- *Type I error (alpha error, α)* is incorrectly rejecting the null hypothesis and stating that two groups are statistically different when they really are not.
- *Type II error (beta error, β)* is incorrectly failing to reject the null hypothesis and stating that two groups are not statistically different when they really are.

VARIABLES

Statistical questions are often posed in terms of input versus output, cause and effect, or correlation between two or more variables. The input or cause is considered an *independent variable* because it is already determined and therefore is not influenced by other factors. Examples of independent variables are age, gender, temperature, and time. In contrast, *dependent variables* are those things that might change in response to the independent variable. Examples of dependent variables are blood glucose concentration, enzyme activities, and the presence or absence of malignancy. Of course, we can change our thinking and switch which is the independent and which is the dependent variable if the experimental question changes. For graphical display, the independent variable is plotted along the horizontal *(x)* axis or abscissa, while dependent variables are plotted along the vertical *(y)* axis or ordinate. With a single independent variable (e.g., time) on the *x*-axis, more than one dependent variable can be plotted on the *y*-axis to demonstrate different relationships simultaneously. The relationship observed between an independent variable and dependent variables is used to predict future outcomes of the dependent ones based on what values the independent variable assumes.

PREPARING TO ANALYZE DATA

Most statistical calculations today are done automatically by computer with software programs that present multiple sophisticated options for analysis and even graphical displays of the data. To prepare data for these automated analyses, it is always necessary to enter them into readable format for the program. This process can entail automated transfer from one electronic data set to the statistical program or manual entry from printed sheets of data. Manual entry is obviously fraught with opportunity for typographic errors, but even automated transfer of data can result in erroneous entries, especially when translating older data sets that have been stored on media that might have been corrupted (e.g., magnetic tapes reexamined decades later). Even converting data strings to columns and rows of data points can leave some values in the wrong places. Consequently, it is always good practice to examine the data set for accuracy before performing the statistical analysis. This examination could be done by proofreading every entry or by double entry of each value and automatic comparison for discrepancies, although both of these approaches may be impractical when the data sets contain hundreds, thousands, or more values. At the very least, visual examination of the plotted values provides a quick idea of whether some serious data entry errors have occurred. For example, an incorrectly entered value of 50.0 for potassium (instead of 5.0) can be immediately identified by scanning all values on a graphic plot. The person preparing to perform statistical analyses should do this visual test to identify and correct the most obvious errors and to search for any systematic errors that might have arisen in data transfer and entry.

DESCRIPTIVE STATISTICS

When multiple data points are collected, it is useful to provide a summary of those results that makes them easier to understand rather than simply listing all values. The methods used to summarize data are termed *descriptive statistics* because they describe what the magnitude of results is and how the data points differ from one another. In the case of categorical variables, this description can be a simple count of discrete values (e.g., how many men and how many women had blood drawn in a clinic). For continuous variables, it is conventional to use some measure of *central tendency* about which the data points cluster and a measure of how far apart they are *dispersed* from one another (e.g., the ages of the patients who had blood drawn).

CENTRAL TENDENCY

The most widely recognized measure of central tendency is probably the mean or average value (also referred to as the *arithmetic mean*), which is calculated by adding the values of all the individual data points and dividing that sum by the total number of data points, expressed mathematically as follows:

$$\text{Mean} = \bar{x} = (x_1 + x_2 + \cdots x_n) \div n = \frac{1}{n}\sum_{i=1}^{n} x_i \qquad \text{(Eq. 10.1)}$$

Because this technique derives the mean value from a defined formula, it is termed a *parametric method*. An alternative measure of central tendency is the *median*, which divides all data points exactly in half, with one half being higher and one half lower. The median is also called the 50th percentile. It is not calculated from a formula because it is taken from a straight count of the data points; thus, it is termed a *nonparametric method*. The third commonly used measure of central tendency is the *mode*, which is the most common value (i.e., the value of the variable that has the greatest number of data points). The mode is not a very useful measure for describing or comparing data sets, but it does have a role in understanding when a data set consists of two or more different populations that result in more than one mode. If two separate subpopulations are present, it is called a *bimodal population*.

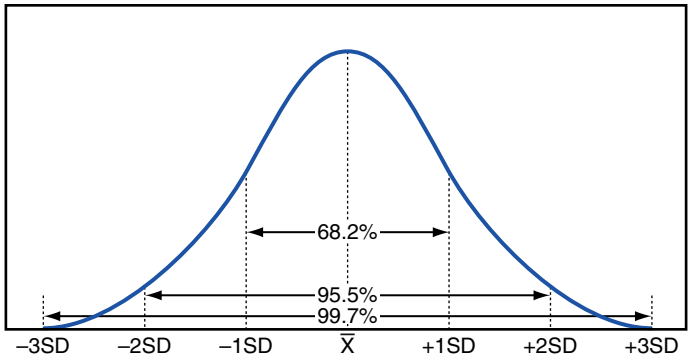

Figure 10.1 Idealized Gaussian (normal) distribution showing areas under the curve corresponding to mean ±1, 2, and 3 standard deviations (SD).

Another measure of central tendency is the *geometric mean*, which has the feature of minimizing the influence from extreme values in a distribution. The geometric mean is calculated as the *n*th root of the product of all *n* values from a population, or:

$$\text{Geometric mean} = \sqrt[n]{x_1 \times x_2 \times \cdots x_n}. \qquad \text{(Eq. 10.2A)}$$

The following transformation is more convenient for calculating the geometric mean:

$$\log \text{Geometric mean} = \sum_{i=1}^{n} \frac{\log x_i}{n} \qquad \text{(Eq. 10.2B)}$$

Thus, the log of the geometric mean equals the mean of the logarithm of all observations, and taking the antilog of this summation yields the value of the geometric mean.

Consider the following distribution of values, which is heavily weighted toward the lower end but with some high values:

$$3, 3, 4, 4, 4, 5, 5, 5, 6, 6, 8, 9, 10, 15, 21$$

The arithmetic mean for these values is 7.2, whereas the geometric mean is 6.09, which better reflects the preponderance of values at the lower end than does the arithmetic mean.

In general, parametric methods allow numerous additional calculations for application of many different statistical tests that are based on specific formulas. The advantage of nonparametric methods is that they do not assume or require that the data points must follow any particular distribution for them to be applicable. Parametric methods can be applied to data sets that deviate from preferred distributions, but those calculations and conclusions may not be fully warranted if the deviations are extreme.

GAUSSIAN (NORMAL) DISTRIBUTION

The Gaussian (also called *normal*) distribution is a symmetric, bell-shaped curve centered about the mean value (Fig. 10.1). It is described by the following mathematical formula:

$$P(x) = \frac{1}{\sigma\sqrt{\pi}} e^{-\left(\frac{(x-\bar{x})^2}{2\sigma^2}\right)}, \qquad \text{(Eq. 10.3)}$$

where σ is the standard deviation of the ideal Gaussian population (Dawson-Saunders & Trapp, 1994). It corresponds to the distance from the mean to the *x* value at which the curve has an inflection point.

The area under this curve within ±1 σ from the mean is approximately 68.2% of the total area, meaning that 68.2% of data points from a Gaussian distribution should fall within ±1 σ of the mean. Similarly, 95.5% of the data points will be within ±2 σ of the mean, and 99.7% will be within ±3 σ of the mean.

DISPERSION

A common parametric measure (based on the Gaussian distribution) of the dispersion of data points about the mean value of a population under examination is the standard deviation, mathematically calculated as:

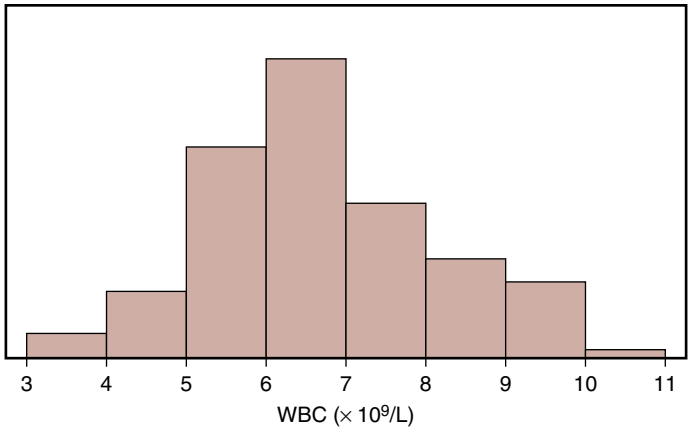

Figure 10.2 Distribution of white blood cells (WBCs) in the blood of 85 healthy individuals.

$$SD = \sqrt{\frac{\sum_{i=1}^{n}(x_i - \bar{x})^2}{n-1}} \qquad \text{(Eq. 10.4)}$$

The quantity under the square root sign is termed the *variance*. Use of the SD assumes that the data follow a bell-shaped curve that can be described mathematically by the formula for a normal or Gaussian distribution. To the extent that the data are normally distributed, the SD is a good estimate of the dispersion.

Two additional terms derive from the SD. One is the *coefficient of variation (CV)*, which is calculated as the SD divided by the mean. The CV is often expressed as a percentage, although it can also be expressed as a decimal fraction less than 1. For a situation in which the mean = 25 and the SD = 5, the CV = 20%, or 0.20. The other term is the *standard deviation index (SDI)*, which is the distance that an individual data point is away from the mean value divided by the SD. The main use for the SDI is in such applications as proficiency testing, where performance of any one laboratory is standardized according to the dispersion of data in the performance by all laboratories.

A common clinical laboratory application of the normal distribution is to calculate the central 95% of values obtained from a healthy population when trying to establish the reference range for an analyte. This range, of course, is easily calculated as mean ±2 SD for a truly Gaussian normal population. An example of this application is calculation of the central 95% of values of the white blood cell (WBC) count in a group of 85 healthy medical students (Fig. 10.2). The bar graph plot is roughly bell-shaped and symmetric, although there is a slight asymmetry that can probably be ignored. The mean value is 6.60×10^9 cells/L, with an SD of 1.457×10^9 cells/L, and the calculated central 95% range is from 3.69 to 9.52×10^9 cells/L. This is a small group of individuals compared with what might be used for actual reference range calculations, but it does show a few persons with WBCs higher than this range and some lower. Thus, this estimate of central 95% appears appropriate.

Another way of thinking about these calculations is that the persons tested represent only a sample of all persons to whom we are interested in generalizing these findings (Daniel, 1999). The mean value actually observed would probably be somewhat different if another group of 85 healthy people were tested. Based on the values observed and their spread, a confidence interval can be placed around the mean such that we can be certain by a desired percent that the true mean of WBCs from all healthy persons falls in that range. The confidence limit is calculated as follows:

$$\text{Confidence interval} = \bar{x} \pm z\frac{SD}{\sqrt{n}}, \qquad \text{(Eq. 10.5)}$$

where the critical factor *z* derives from transformation of the problem to a standard normal distribution. The quantity $\frac{SD}{\sqrt{n}}$ is termed the *standard error of the mean*. In this example, let the confidence interval be 95%, for which *z* = 1.96. The 95% confidence interval around the mean value is:

$$6.60 \pm 1.96 \times \frac{1.457}{\sqrt{85}} \text{ or } 6.295 - 6.914 \times 10^9 \text{cells/L}.$$

Note that this range is the 95% confidence interval on the mean value alone, whereas the earlier calculations yielded the central 95% of all data

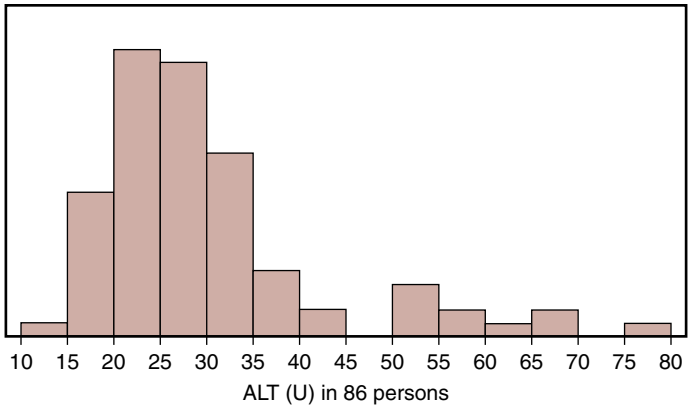

Figure 10.3 Distribution of alanine aminotransferase (ALT) in the serum of 86 healthy individuals.

points. Confidence intervals are used to give an idea of the broadness of the estimate of something. This can be made more certain by using 99% confidence intervals (i.e., 99% confident that the true mean falls in the interval), in which case $z = 2.575$ for the calculation, and the 99% confidence interval is broader at:

$$6.60 \pm 2.575 \times \frac{1.457}{\sqrt{85}} \quad \text{or} \quad 6.193 - 7.007 \times 10^9 \text{cells/L}.$$

NONPARAMETRIC MEASURES

The median value of WBCs for this group of healthy persons is 6.4×10^9 cells/L, which is roughly the same as the mean value. For a perfectly Gaussian normal distribution, values of the mean, median, and mode are exactly the same. Delineation of the range from the 2.5-percentile to the 97.5-percentile also gives an estimate of the central 95% range (for the example of WBCs, it is 3.94 to 9.89×10^9 cells/L, which is really the exact range for this specific population). This is a nonparametric estimate of the range because it does not use a calculation but rather divides the data points only according to their order. Many applications of median use the central 50% of data points from the 25th percentile to the 75th percentile (also called interquartile range) to describe central tendency by the nonparametric method.

Sometimes, the parametric method of mean ±2 SD produces an erroneous estimate of the central 95% range. An example of this situation arises with the distribution of alanine aminotransferase (ALT) activities in the serum of apparently healthy individuals (Fig. 10.3). In this population, the mean value is 30.1 U, the SD is 12.69 U, and the calculated reference range (mean ±2 SD) is 4.73 to 55.48 U. This range is not appropriate because the actual lowest value observed in the group was much higher (12 U). This estimate of the lower end of the range (4.73 U) is far too low. Similarly, the estimate of the upper end (55.48 U) is too low and excludes about 10% of the data points instead of only 2.5%. Another clue that the parametric method may not work here is that the median value is 27.0 U, which is somewhat different from the mean. The reason for this discrepancy is apparent upon looking at the distribution, which is skewed to the right with many values tailing off at the upper end. In this case, a much more useful estimate of the central 95% can be obtained simply from the 2.5-percentile to the 97.5-percentile range. It is 15.2 to 68.0 U. The form of this distribution for ALT is sometimes termed *log-normal*, because it can be converted to a normal distribution by using the values of log ALT instead.

Many laboratory measurements show distinctly non-Gaussian normal distributions. Values of 25-OH vitamin D in 12,434 serum specimens from 2000 through 2008 showed a skewed distribution, with lowest value 0.5 ng/mL and highest value 260.0 ng/mL (Fig. 10.4A). The arithmetic mean of these values is 25.55 ng/mL, and the median is 20.90 ng/mL, reflecting the nonnormal distribution. Plotting log 25-OH vitamin D shows a nearly normal distribution with mean value 1.3130 (Fig. 10.4B). Then, the geometric mean is $10^{1.3130} = 20.56$ ng/mL, which appears to be a better measure of central tendency for 25-OH vitamin D than the arithmetic mean.

COMPARATIVE STATISTICS

One of the questions frequently asked by statistical means is whether one group is different from another group in some characteristic. The question boils down to a comparison of the central tendency of one group versus that of the other and the scatter that each group exhibits about the central values. If the scatter of data is extreme, then calculated differences between mean values of two groups might not be important but rather the result of adding in the extreme values. Another way to think about these comparisons is that of signal/noise ratio. If there is little noise (scatter of data), then the difference in the signal from each group is more believable.

STUDENT *T*-TEST

The most common method for comparison of a continuous variable between groups is probably the Student *t*-test (Dawson-Saunders & Trapp, 1994). The pseudonym *Student* was used by William Gosset, a statistician working for the Guinness brewery, who wanted to keep his work for optimizing productivity unrecognized by competing companies. The *t*-test is based on a parametric calculation of the *t* statistic as follows:

$$t = \frac{\bar{x}_1 - \bar{x}_2}{SD_{12}\sqrt{\frac{1}{n_1} + \frac{1}{n_2}}} \qquad \text{(Eq. 10.6)}$$

where
$\bar{x}_1$ = mean value in group 1
n_1 = number of values in group 1
$\bar{x}_2$ = mean value in group 2
n_2 = number of values in group 2
SD_{12} = standard deviation of groups 1 and 2 combined

Fortunately, the calculation of *t* statistics is conveniently performed by computers in modern times; thus, the analyst now has the responsibility of vouching for the accuracy of data input and the correct choice of statistical tests and their validity for the situation.

Some specific assumptions about the data sets are also necessary for applicability. For example, it is necessary to have sufficient numbers of data points in each group to make a valid comparison with approximately equal numbers in each. The spread of the data points should be equivalent (usually assessed by whether the variances of the groups are equivalent). The selection of data points should be independent of one another; for example, it would be inappropriate to include the same patient twice in one group. The issue of independence is usually handled experimentally by a random selection of subjects or patients. Randomization of treatments is an exacting process for important research such as clinical trials. For laboratory use, it is more likely that data come from patients who present themselves to the hospital or clinic for testing rather than being a random sample of all people in a city or from a country. The more random the selection process, the more likely it is that results can be generalized to a much larger target population for which inference is desired.

The statistical question for consideration is reduced to two mutually exclusive hypotheses that include all the possible situations. The null hypothesis (H_0) states that there is no difference between groups. The alternative hypothesis (H_{alt}) is that the difference between mean values is significant. If the *t* statistic has a sufficiently high value, we can reject the null hypothesis and consequently must accept the alternative hypothesis that there is a significant difference. If the *t* value is on the low side, we cannot reject the null hypothesis, but neither can we accept it. This decision is somewhat like that of the verdict from a trial in which the possible outcomes are "guilty" and "not guilty." The innocence of the defendant is never established; similarly, the null hypothesis is never proven. We could end up thinking that the null hypothesis is correct (particularly because the alternative hypothesis now seems unlikely), but the test we performed did not strictly lead to that conclusion.

Consider the distribution of hemoglobin (Hb) values in the whole blood of 36 healthy males and 49 healthy females (Fig. 10.5). Visual inspection of the bar graphs for Hb shows that the females generally have lower values (mean 13.2 g/dL, SD 0.80 g/dL) than the males (mean 15.1 g/dL, SD 0.96 g/dL). Only a portion of the males and females overlap one another in Hb values. In this example, the value of $t = 9.898$. One other factor must be taken into account—the degrees of freedom, which is obtained from the total number of data points minus 2 or $df = n_1 + n_2 - 2 = 36 + 49 - 2 = 83$.

Significance

The value of the *t* statistic is assessed for significance according to the degrees of freedom. One way to approach the assessment is to look up the value of *t* for which the degrees of freedom yield a probability (*p*) value that is to be applied for significance using a table of values. More often, the software does this calculation automatically. Generally, *p* values of 0.05 or less are required to claim statistical significance. A *p* value of 0.05 (also called *alpha*) means that the difference observed between the two groups could have occurred one time in 20 with the particular spread of data actually observed. The value of alpha is also thought of as the risk that we

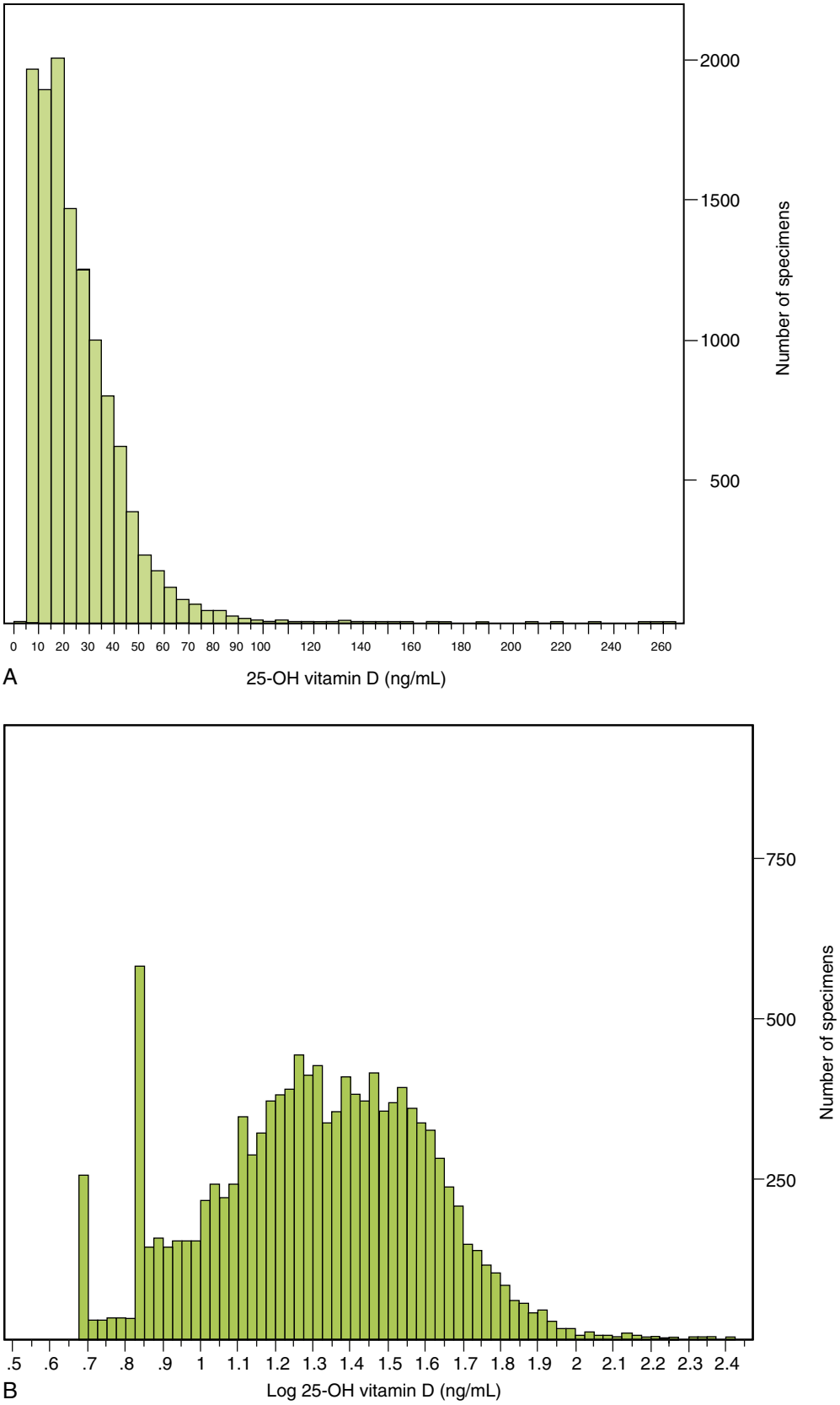

Figure 10.4 **A,** Distribution of 25-OH vitamin D in 12,434 serum specimens showing skewness to the right at higher values. **B,** Plotting log of 25-OH vitamin D shows normal distribution following logarithmic transformation.

are willing to take to conclude falsely that there is a significant difference when, in fact, none exists (type I error). The use of alpha = 0.05 is merely an arbitrary convention, but it is ingrained in the minds of reviewers and protocols for evaluating studies. Of course, if the p value is much smaller, such as 0.01 or 0.001, then the statistical significance of a difference between group means is that much more credible.

Even though an observed difference between groups might have an extraordinarily impressive p value (p = 0.001 means that the result should happen by chance only 1 in 1000 times), it is incumbent upon the investigator to conclude whether the observation is clinically significant. The statistical significance of any difference can always be amplified, no matter how insignificant it is for decision making, simply by increasing the number of data points (see the formula for calculating t, Eq. 10.6).

A potential problem arises when a large number of comparisons are done in studies in which no clear hypothesis is stated, but instead the data are mined for whatever might fall out upon examination. In this case, the minimal level of significance should be adjusted to reflect the large number of tests that could conceivably discover "significant results" by chance alone.

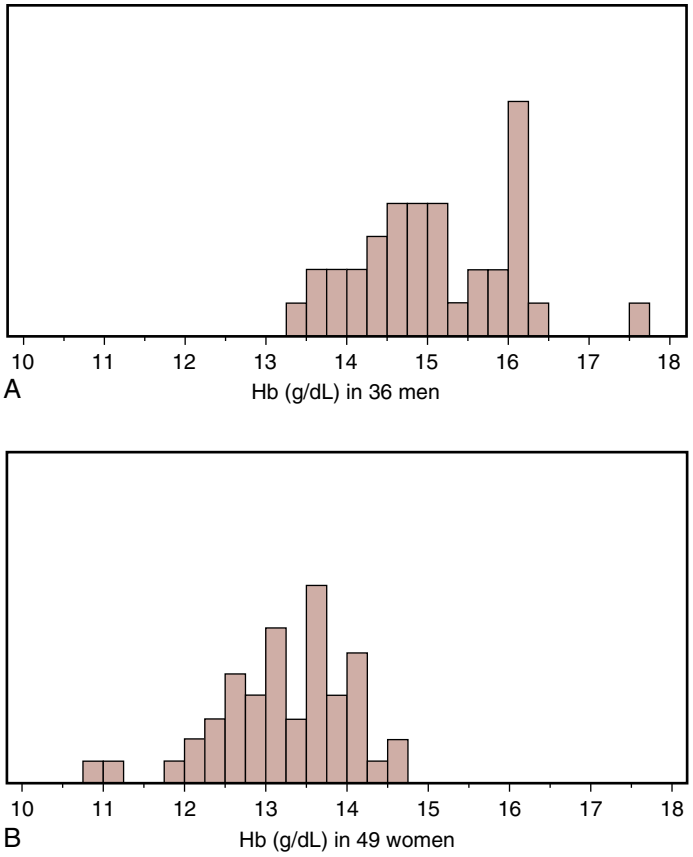

Figure 10.5 Distribution of hemoglobin (Hb) in the blood of healthy men (**A**) and healthy women (**B**).

After all, if a p value of 0.05 is used, then by doing 20 different comparisons, one should find on average some comparison with a statistically significant difference regularly. The Bonferroni correction is done to lower the risk of such false discovery. It consists of dividing the usually accepted p value by the number of comparisons. Thus, for five different comparisons, the correction is p value = 0.05/5 = 0.01 as the acceptable threshold value for significance.

For this particular example, comparing Hb values between males and females, the p value is less than 0.0001. Thus, we can reject the null hypothesis and can conclude that there is a significant difference between groups. Most statisticians would not report this level but would be satisfied with saying that the p value was less than 0.001. Another condition to denote is whether this test is two-sided or one-sided, meaning that the question being asked is whether one group is simply different from the other (two-sided) as opposed to the question of whether one group is only higher than the other group (one-sided). Most journals require the use of two-sided t-tests because they are more demanding.

Sample Size

Suppose that the two groups being compared showed a difference that was not quite statistically significant, with a p value of 0.06. One way to achieve statistical significance is to increase the number of subjects studied. This will be the case if the difference remains the same, because the t-value will be increased by a greater n. A pilot study can be done in a clinical trial to establish roughly the difference between groups and the scatter of the data. These pieces of information are then used in a formula to calculate the sample size necessary to bring the results to statistical significance. Calculation of sample size also takes into account another factor, called *beta*, which is the risk one has of missing a true effect by chance (type II error). The power of the study is 1 – beta. When beta is set to 0.20, the power of the study is 0.80, which says that the number of subjects calculated for use will yield a statistically significant result 80% of the time with the specified difference between groups and scatter of data.

The t-test used for this example was unpaired because the comparison was between different individuals. If the experimental design included a comparison of values on the same individuals before and after treatment, then it is appropriate to use a paired t-test. A paired test is potentially a more powerful mathematical tool because it looks only at the change between the values within each person and is not influenced by variation in background values between individuals.

TABLE 10.1
Observed Values of Contamination in Blood Cultures

Result	Baseline Period	Post-Training
Number of cultures contaminated	53	32
Number of cultures not contaminated	978	891

NONPARAMETRIC TESTS

If the assumption about normality of the data is not valid, other nonparametric tests can be used to compare distributions between groups. The *Wilcoxon signed-ranks test* is such a technique. By this method, all values for both groups are given a numeric rank according to their magnitude. In the case of ties for the same value, both are assigned the intermediate rank (e.g., if 4th and 5th places are tied, then both are given the rank 4.5). All ranks are summed in each group and divided by the number of data points in each group. The difference between the rank scores is then given a probability. This technique is easily done by computer software and may be quite useful when assumptions required for a parametric method are not met by a data set.

ANALYZING DISCRETE DATA: TESTING PROPORTIONS

Analysis of discrete data takes on a different form from that of continuous variables that can be expressed as distributions. With discrete data, answers are typically dichotomous: Something is present or absent, patient gender is male or female, the patient lived or died. Consider the fictitious example of an intervention to lower contamination rates in blood culture collection. (This is a universal problem in all laboratories, but these data are only hypothetical.) Before the intervention, baseline information over a 2-month period showed that 53 cultures were considered contaminated and 978 were not. After training and implementation of the new collection process, a second 2-month period showed 32 contaminated cultures and 891 that were not. These nominal data are conveniently expressed in a 2 × 2 display termed a *contingency table of observed values* (Table 10.1). These data consist of simple counts in one category or another. The question to be asked is whether the proportion of contaminated cultures was significantly different in the two time periods.

CHI-SQUARE TEST

The statistical test to be used is the chi-square test. It is calculated as:

$$\chi^2 = \sum \frac{(\text{observed} - \text{expected})^2}{\text{expected}}, \qquad \text{(Eq. 10.7A)}$$

where the observed values are as listed earlier and the expected values are calculated from the overall assortment of counts (Dawson-Saunders & Trapp, 1994). In this example, the expected number of contaminated cultures in the baseline period is the total number of cultures done in that period (53 + 978 = 1031) times the proportion of contaminated cultures in both time periods together (proportion calculated as [53 + 32]/[53 + 978 + 32 + 891] = 0.0435), or 1031 × 0.0435 = 44.8. Calculation of the other expected values follows similarly, resulting in a contingency table of expected values (Table 10.2). Then, calculation of the χ^2 value is done by summing the squares of the differences (this converts all differences to positive values) between expected and observed values and dividing by the expected value in each cell of the table. In this example,

$$\chi^2 = \frac{(53-44.8)^2}{44.8} + \frac{(978-986.2)^2}{986.2} + \frac{(32-40.2)^2}{40.2} + \frac{(891-882.8)^2}{882.8} = 3.3 \qquad \text{(Eq. 10.7B)}$$

With one degree of freedom ([number of rows – 1][number of columns – 1]), the p value is 0.07, which does not meet the universal threshold of at least 0.05 for statistical significance. It is fair to say that a trend toward less contamination was observed after the intervention but that it was not quite statistically significant. It is important to keep in mind that for χ^2 testing to

TABLE 10.2

Expected Values of Contamination in Blood Cultures

Result	Baseline Period	Post-Training
Number of cultures contaminated	44.8	40.2
Number of cultures not contaminated	986.2	882.8

be valid, each cell must have a minimum value of five observations. When the cell sizes are expected to be small (less than 5), *Fischer's exact test* can be used for looking at the relationship between two categorical variables.

TREND EVALUATION AND CORRELATIVE STATISTICS

The relationship between an independent variable and a dependent variable is demonstrated by plotting them on a scattergram or a plot with the independent (input) variable on the *x*-axis or abscissa and the dependent (output) variable on the *y*-axis or ordinate. If there is no relationship between the two variables, the data scatter randomly over the graph. If there is a relationship, it can be described mathematically by finding a line that is the best fit through all the data points. This line can be calculated by the least squares approach, in which the vertical distances from each point to the calculated line are minimized for the entire population of values. This statistical method is referred to as *linear regression* (National Committee for Clinical Laboratory Standards, 2003).

LINEAR REGRESSION

The general form for the equation of a straight line is:

$$y = a + bx \qquad \text{(Eq. 10.8)}$$

in which the slope (*b*) indicates how the value of *y* changes when *x* changes. When $b = 1$, the relationship of change between *x* and *y* is one-to-one. The intercept (*a*) indicates how the relationship between *x* and *y* is offset or biased by a constant factor. The calculation is easily done by any of several statistical programs that also provide information about the goodness of fit of the line. This approach is commonly used when comparing an existing method (A) with a new method (B) for the same analyte (Fig. 10.6A). This example shows a strong correlation between method A and method B because the data points fall very close to the line, which is described by the following equation: *Method B* = 0.62 + 0.99 × *Method A*. The slope of 0.99 is almost perfect, and the intercept of 0.62 is quite small on the scale of possible values. In fact, the 95% confidence limits on *b* are –0.47 to 1.72, which includes the value 0, indicating that the intercept is not significantly different from 0.

The vertical (*y*-axis) distances from each data point to the best-fit line are termed the *residuals*. The most valid line fits are associated with relatively constant values of the residuals over the entire range of values. If the residuals grow larger at one end of the graph, then the line fit is less certain in that portion of the range. The *standard error of regression* (also called *standard error of the estimate*), denoted $S_{y.x}$, is used to estimate the variation that could be expected from doing the regression again with another sample of data points. The $S_{y.x}$ is calculated as the square root of the sum of residuals squared, divided by n – 2. It is important that data points from patient specimens be spread over the entire analytic range to yield the most valid comparison of methods unbiased by overrepresentation or underrepresentation of data in any region (National Committee for Clinical Laboratory Standards, 2002).

In laboratory practice, regression or correlation analysis is frequently used to compare the performance of a new method versus an old method. In this situation, the old method could have worse precision than the new one; thus, it would not be appropriate to base a judgment just on how the new method compares with the old one as a gold standard. A common approach to this issue is Deming regression analysis, named for W. Edwards Deming (1900–1993), a mathematician influential in principles of quality improvement. In Deming regression, the best line is obtained by minimizing the sum of squares of both *x* and *y* distances from the data points to the line (Cornbleet & Gochman, 1979). In addition, Deming regression applies a weighting factor (λ) that incorporates the relative variances of both *x* and *y* data. The result is more heavily weighted in favor of the data set with better precision.

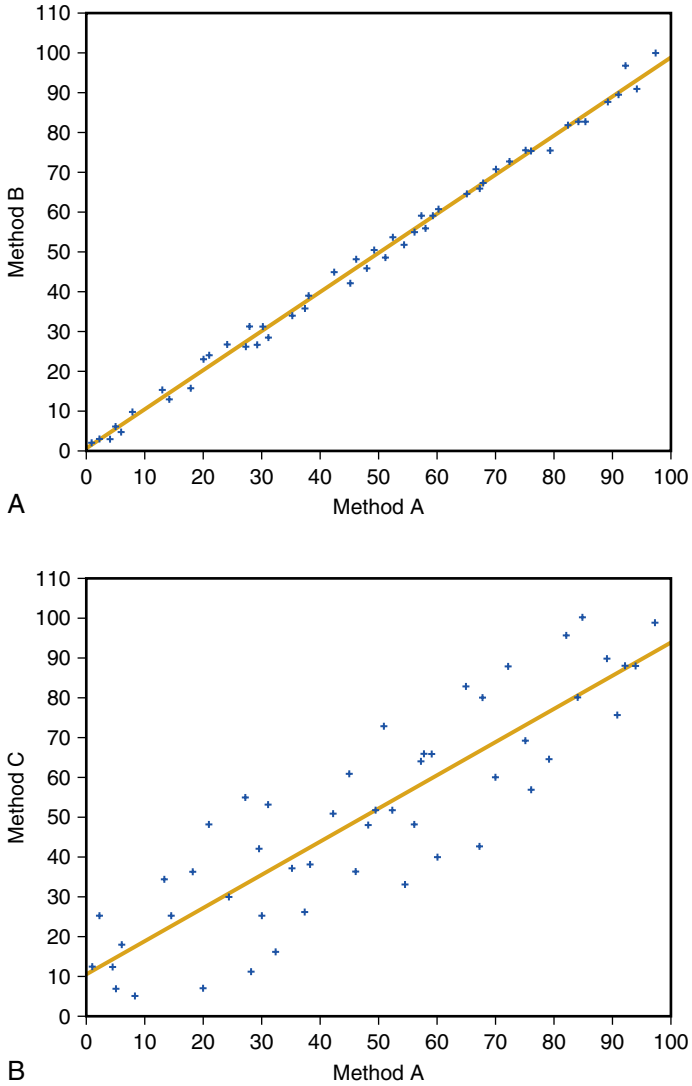

Figure 10.6 **A,** Regression analysis between method A and method B; strong correlation. **B,** Regression analysis between method A and method C; weaker correlation.

The relationship between method A and method B is further described by the *correlation coefficient (r)*, which can range in value from –1 to +1. A value of 0 indicates no relationship, and a value of 1 indicates a perfect relationship (–1 is also a perfect but inverse relationship). Other values between –1 and +1 indicate intermediate relationships. The square of the correlation coefficient is termed the *coefficient of determination* (r^2), which describes the amount of variation observed in the dependent variable that is due to the relationship between the two variables. In this example, $r = 0.9976$ and $r^2 = 0.9952$, both of which are very high values that show an extremely strong relationship between method A and method B that accounts for 99.52% of the variation. The *p* value on this correlation is less than 0.0001.

In contrast with the very good correlation between method A and method B, the performance of method C versus method A (Fig. 10.6B) is not nearly as good. By simple visual examination, the data points are scattered farther from the line and the line is shifted upward. The value of $r = 0.8757$ is somewhat less than between method A and method B, but it still shows a strong correlation, with *p* value less than 0.0001. The value of $r^2 = 0.7668$; thus, 76.68% of the variation can be accounted for by the relationship between method C and method A. The equation for this line is *Method C* = 10.2 + 0.84 × *Method A*; thus, the change in values using method C compared with method A is slightly less (slope of 0.84). A significant upward bias is seen by method C (intercept of 10.2 with 95% confidence limits of 2.8 to 17.6). A special example of regression analysis termed *logistic regression* is employed when the outcome is a dichotomous or binary variable for continuous independent (predictor) variables.

METHOD COMPARISONS

These two examples show somewhat different relationships, although both are statistically significant. It is up to the person assessing the performance

to determine which is sufficient for the application. The comparison of method A with method B is extraordinarily strong both by visual review and by statistical analysis; thus, it can comfortably be said that these methods are equivalent for the purposes of replacing one with the other in clinical practice. On the other hand, the comparison of method A with method C is messier because of the larger amount of data scatter. The smaller slope suggests that the two methods do not react equivalently with the analyte; furthermore, there is a positive bias by method C. With expectations for excellent precision and accuracy on modern instrumentation, method C would probably be rejected if method B were a viable alternative. Yet, the level of correlation observed between method A and method C might be very welcome to researchers trying to ask a different question related to cause and effect between biological processes that have inherently high levels of variation.

In clinical laboratory applications for method evaluation, the question to be asked is not how certain we are that two things are different but rather how certain we are that a new method yields results comparable to those from an existing method. The Clinical and Laboratory Standards Institute provides the software titled StatisPro, which does such analysis for method comparability with input from the user about tolerances for differences between methods at low and high values and correlation, bias, and scatter of the data that are acceptable for a particular analyte. StatisPro incorporates standard measures of quality control and also regulatory requirements for documenting assay performance in formats that are readily accepted for laboratory inspections. Instead of analyzing for differences between methods, this approach is for their trueness to one another (Fig. 10.7).

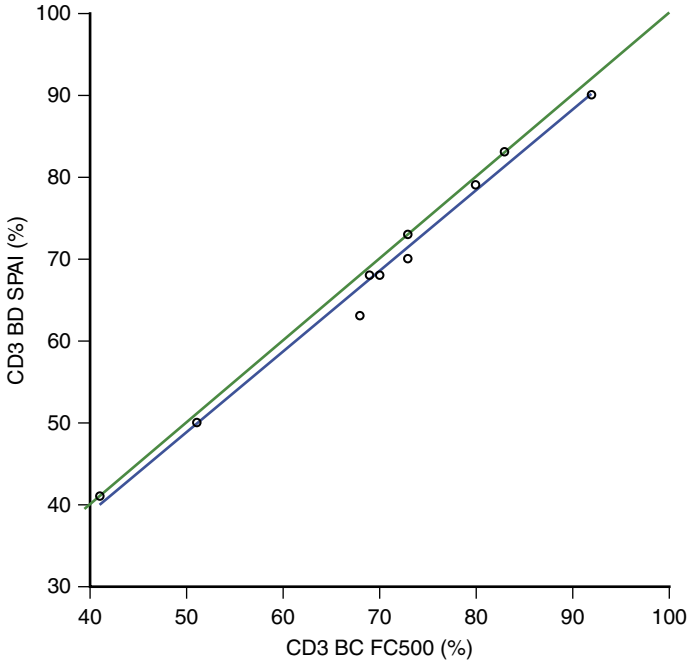

Figure 10.7 StatisPro analysis of two flow cytometric methods for percent CD3 cells in whole blood. The correlation coefficient is excellent (r = 0.994; 95% confidence interval = 0.897–1.069), with an acceptable slightly downward plot *(blue line)* compared with the line of identity *(green line)* that has the small value for intercept of 0.33% (95% confidence interval = –6.46% to 5.80%).

ANALYSIS OF VARIANCE

When the mean values of more than two different groups are to be compared, the process is termed *analysis of variance* (*ANOVA*) (Dawson-Saunders & Trapp, 1994). This analysis can be thought of as extending the t-test beyond two independent samples to three or more. The null hypothesis in this situation is that the mean values of all groups are the same. The alternative hypothesis is that not all the means are equal (some could be the same, but others different). The test statistic is the F-ratio of the mean squares among all groups (MS_A) to the error mean square (MS_E):

$$\text{F} - \text{ratio} = \frac{\text{MS}_\text{A}}{\text{MS}_\text{E}}. \qquad \text{(Eq. 10.9)}$$

It compares the variance of the group means with the mean of all the data (numerator) and the variance of individual data points within each group (denominator). If the group means differ from one another (signal) more than the variation within groups (noise), then the F-ratio will exceed a critical value for significance.

An example of ANOVA is the comparison of serum albumin values from patients at two inpatient sites, an outpatient (OP) clinic and a student health (SH) clinic (Fig. 10.8). One hundred consecutive specimens from each site were recorded. The horizontal line shows the grand mean of all 400 values of 3.17 g/dL. Within each group, the diamonds indicate group means (midline) and 95% confidence intervals on those means (upper and lower vertices). The F-ratio is 279, for which the p value is less than 0.0001. Thus, the null hypothesis can be rejected with the conclusion that at least some of the means are different. This approach is more conservative and realistic than comparing each group with every other group using a series of different t-tests (with four groups, six comparisons could be made). The problem with too many comparisons is the possibility of "accidentally finding significance" that is not true. To extend ANOVA, comparisons of group means by such procedures as Tukey's honestly significant difference (HSD) can be done. In the example in Figure 10.8, Tukey's HSD indicates that IP1 and IP2 (inpatient wards 1 and 2) are not different from each other but that OP and SH are both different from all other groups. At this stage, the investigator is free to elaborate on potential reasons for these observed differences without putting further statistical significance on the individual differences.

Some conditions should be met for parametric ANOVA to be completely valid mathematically:

- The data were collected using random sampling in which all observations are independent of one another.
- The data in each group are normally distributed.
- Each group has an equal number of data points.
- Each group has equal variances.

If this set of ideal criteria is not met, other methods are available for comparisons. The Mann-Whitney test can be used to compare medians. The Wilcoxon and Kruskal-Wallis tests for rank sums are nonparametric alternatives. This example of serum albumin shows greater variances for the inpatient groups than for the outpatients; thus, nonparametric analysis could be more appropriate. (The Wilcoxon test also showed significant differences among the groups of this example.) This case dealt with one variable; thus, it was one-way ANOVA. To deal with two variables, the procedure can be extended to two-way ANOVA.

Linear regression might be used in error to analyze continuous outcome data when the independent variable has the appearance of being continuous but is actually categorical. Such a situation is seen with tumor grade (1 through 4) as an independent variable. Tumor grade is not continuous but rather consists of discrete categories that are not necessarily evenly spaced along a dimension. Although statistical programs would permit calculation of a regression on tumor grade, the proper approach would be one-way ANOVA to look for differences in the dependent variable (e.g., survival time) among groups (e.g., tumor grade).

ANALYSIS INVOLVING MULTIPLE VARIABLES

Two-way analysis of variance (*two-way ANOVA*) is used when the experimental design has two categorical independent variables (input) and a continuous dependent variable (output). An example is the effects of both gender and different (fixed) drug levels on a physiologic measurement such as blood pressure. In addition to the one-way effects of gender on blood pressure and of drug level on blood pressure, it is necessary to investigate a possible interaction of gender and drug level in two-way ANOVA. If such an interaction is significant, then response to drug level might be different in men versus women. These interactions are conveniently displayed graphically (e.g., a plot of response to drug in men and one for women; noninteraction results in parallel lines; intersection of the lines indicates an interaction).

Multivariate analysis of variance (*MANOVA*) applies to a model with multiple categorical independent variables and two or more continuous dependent variables. Sometimes, the way a comparison is set up by selection of subjects into different groups can lead to a confounding effect from another variable besides the variable of primary interest. In this case, it is revealing to perform *analysis of covariance* (*ANCOVA*) to account for potential influence from the covariable. The intention of ANCOVA is to use statistical methods to eliminate effects arising from confounding variables that were not accounted for by random assignment in the original selection of subjects. Typically, these effects might be due to an imbalance of subjects with certain characteristics in the experimental group compared with the control group (e.g., the treatment group might have 75% smokers and the control group only 25%; without adjusting for this potential

confounding factor, one could not be certain that results from treatment were not, in fact, merely due to different proportions of smokers in each group).

As a laboratory example of ANCOVA, consider the comparison of serum calcium measurements in 61 male and 41 female healthy adults to establish whether different reference ranges of calcium would be necessary for males and females. Simple one-way ANOVA similar to that in Figure 10.8 yielded a statistically significant ($p = 0.0045$) difference between the group means of calcium (males 9.3 mg/dL, females 9.1 mg/dL). (Performing ANOVA with only two groups is equivalent to an unpaired *t*-test.) This finding was consistent with those of previous studies; thus, it probably is appropriate to have gender-specific reference ranges for serum calcium. However, does this make sense from a physiologic view? It is also well recognized that serum albumin influences total calcium levels by binding some of the calcium. A linear regression for these subjects confirmed this relationship. The effects of gender and of the covariable albumin on calcium are sorted out by ANCOVA. In this example, the effect on calcium from gender was completely accounted for by the effect of albumin on calcium and the different distribution of albumin in males versus females. ANCOVA can be enlightening to discover and eliminate by statistical analysis those covariables that might not be known and planned for in the design of an experiment. Further discussion of ANCOVA can be found in more advanced texts on statistics (Matthews & Farewell, 1988).

When multiple continuous independent variables (x_1, x_2, x_3, etc.) are tested to predict a continuous dependent variable (y) as outcome, *multiple regression analysis* is used to calculate the weighting factors (b_i) for a linear combination as follows:

$$y = a + b_1x_1 + b_2x_2 + b_3x_3 + \cdots \qquad \text{(Eq. 10.10)}$$

This analysis also allows use of nominal independent variables with so-called "dummy variables" that are arbitrarily given values of 1 or 0 (e.g., 1 for female and 0 for male). Thus, if x_1 is gender, the coefficient b_1 is multiplied by 1 for females in calculating the values of y; however, for males, b_1 is multiplied by 0. This dummy coding permits convenient use of nominal variables in regression analysis.

Structural equation modeling (*SEM*) is a method for evaluating linear relationships among multiple variables, with the added value of taking measurement error into account simultaneously instead of linearly. SEM has been used extensively for multivariate analysis in psychological research because it allows for the introduction of latent variables that are not directly observed, although they might have causal relationships with observed outcomes. SEM has the potential to analyze complex relationships among variables and estimate the strength of their correlations. Applications in medicine include epidemiology and genetics (Beran & Violato, 2010; Valente et al., 2013). A common platform for SEM analysis is the LISREL (Linear Structural Relationships) software.

METHOD VALIDATION AND PROCESS CONTROL

Statistical analysis is integral to the validation of new laboratory methods and to the monitoring of analytic and workflow processes in clinical laboratories (Lott, 1998).

REFERENCE RANGES

The examples depicted in Figures 10.2 through 10.5 demonstrate some of the issues encountered when reference ranges are established through application of descriptive statistics. The basic aim is to establish a range of values within which the majority of healthy people will fall, while excluding individuals with disease. The simplest approach is to use the central 95% of data points from healthy individuals by calculating mean ±2 SD whenever the distribution is normal or bell-shaped, as for WBCs in Figure 10.2. This parametric approach fails to provide a complete reference range when the data are skewed, as for ALT in Figure 10.3. In this case, the central 95% can be determined nonparametrically by using the range 2.5-percentile to 97.5-percentile, which excludes 2.5% at both the upper and lower ends. The distribution of ALT actually appears to have two subpopulations in these healthy people. Consequently, basing reference ranges solely on observed ranges in apparently healthy persons might not be the best approach. In fact, some new recommendations for ALT set the upper range much lower than wide-based population studies would suggest. The new guidelines try to eliminate persons who might have mild, asymptomatic liver changes, such as steatosis (Prati et al., 2002). This approach is

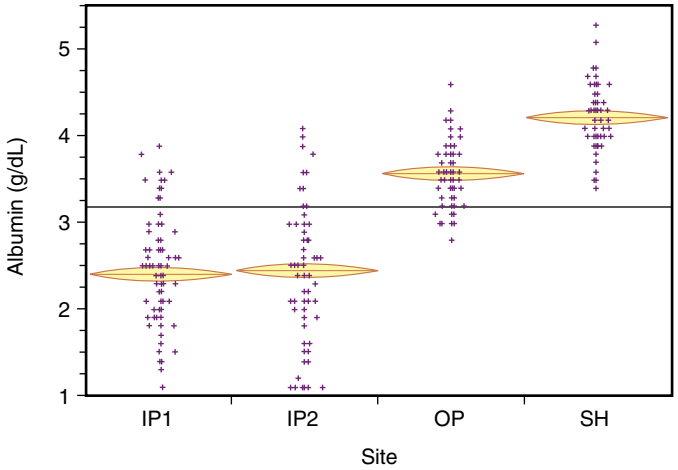

Figure 10.8 Analysis of variance. Serum albumin at different patient sites. *IP1, IP2,* Inpatient wards 1 and 2; *OP,* outpatient; *SH,* student health.

similar to the strategy used for setting desirable or healthy levels of cholesterol and lipid fractions (National Cholesterol Education Program, 2002) and of glucose (Report of the Expert Committee on the Diagnosis and Classification of Diabetes Mellitus, 2003). In the future, recommendations from other consensus groups or professional organizations will probably be even more useful in setting desirable ranges for other analytes in place of population-based reference ranges.

Finally, healthy subgroups of people should be recognized by separate reference ranges whenever major differences occur according to factors such as age or gender (see Fig. 10.5).

ACCURACY

The performance of a new method can be assessed for accuracy (e.g., the ability to correctly detect and quantify an analyte) by assaying patient specimens or interlaboratory survey materials with known values. The example of a strong correlation between methods in Figure 10.6A indicates that the analyte reacts in a nearly one-to-one manner by each method (slope ≈ 1) with essentially no bias (intercept ≈ 0). In contrast, the correlation depicted in Figure 10.6B, has a slope different from 1, indicating that the analyte reacts differently with the two methods. One explanation for this type of discrepancy is found when tumor markers are measured by two immunoassays that employ different antibodies that potentially recognize different epitopes. A bias such as that shown by method C versus method A in Figure 10.6B also suggests a basic methodologic difference that has an impact on accuracy, albeit in a predictable way that could be compensated for with calibration adjustment.

The accuracy of any assay depends heavily on the calibrators—that is, how they are originally constituted, how they remain stable over time, and how they compare with calibrators from other vendors (see Chapter 11). The best situation is to have an assay calibrated against internationally distributed standards, such as from the World Health Organization or other professional group. By using calibrators with such traceability and standardized units of measurement, it is feasible to use values from different assays interchangeably for the same patient or to compare outcomes in different groups of patients being monitored with different methods.

After implementation of a method, periodic proficiency survey testing of unknown specimens is usually reported in terms of SDIs away from the mean of all laboratories. For example, if the mean of creatinine measurements is 11 mg/dL for all participants with SD of 2 mg/dL, then a laboratory reporting a value of 8 mg/dL would have SDI = (8 – 11)/2 = –1.5.

PRECISION

The reproducibility of an assay is conveniently expressed with the CV that allows the observed SD to be normalized by the magnitude of the signal being measured. It should be kept in mind that assays typically have different CVs for different ranges of analyte values. Therefore, it is good practice to establish CVs for an assay at high-, low-, and midrange values.

ANALYTIC SENSITIVITY

The lowest value that an assay can reliably detect is termed the *analytic sensitivity*. A common approach to making this judgment is to measure a zero

standard multiple times (e.g., 10 times) and calculate the SD of the signal detected, which is noise. Then, set the lowest reliable detection threshold at three or four times the value of the SD. This approach is often individualized within laboratories. This characteristic is also termed the *detection limit*. Another use of the term *analytic sensitivity* refers to the change in response of an assay for a given change in the amount or concentration of the analyte (Giacomo, 1984). In this respect, a highly sensitive assay has the characteristic of readily detecting small changes in analyte at concentrations in the midrange of measurement.

ANALYTIC SPECIFICITY

The major interferents in laboratory measurements are hemolysis, icterus, and lipemia, due either to interference with optical absorbances (or light scattering) or to actual chemical interactions (e.g., peroxidase activity of Hb in many immunoassays that use horseradish peroxidase as an indicator). Beyond these endogenous interferents, drugs can also interact with various chemical or immunologic assays. The magnitude of these interactions (or lack thereof) is typically documented by the addition of known, large amounts of the substances to serum samples that are tested for recovery of the analyte in the serum.

ACCEPTABILITY OF A METHOD

The final decision of whether to accept a method as valid depends on a combination of factors. Do the statistical tests show a new method to perform analytically as it should with good accuracy and precision? Does the new method provide useful medical information that is not otherwise available? Is the method feasible to do (easy to perform, low cost, rapid)? Does the maximum error fall within medically acceptable limits? The final decision is a professional judgment based on all of these items.

MISUSE OF STATISTICS

Mark Twain wrote in his 1906 *Chapters from My Autobiography*, "There are three kinds of lies: lies, damned lies, and statistics" (also attributed to various British politicians). The point is supposed to be that numerical data can be used nefariously to support otherwise dubious positions. This statement should be strong incentive to any investigator contemplating statistical analysis so as to establish an experimental design that minimizes or eliminates any possible bias, thereby avoiding false-positive findings that are inaccurate despite apparent statistical significance.

Consultation with a biostatistician should be considered prior to setting experimental design. This review by a neutral party who has no preconception (and presumably no *a priori* bias) about experimental outcome will lead to a more powerful design and also facilitate proper collection of data to allow best choice of statistical test for analysis. In short, it is preferable to design an experiment knowing which statistical tests will be used for analysis before collecting data rather than to have already collected data before deciding which statistical tests would be appropriate.

RISK OF FALSE-POSITIVE RESULTS

The power for use of a statistical test is directly related to the number of observations (e.g., patients in a clinical trial) and to the strength of the effect being measured (e.g., the difference in outcome between the experimental group and the control group). Many studies can be underpowered due to inadequate number of subjects or due to an overestimation of what the true effect is. Such studies are somewhat futile because they do not have a good chance of finding any effect. The result can be either missing a true effect because of underpowered design or accidentally finding an apparent effect that is bogus.

An important publication on this subject by Ioannidis (2005a) elucidated the reasons why published research findings are often false. In addition to inadequate study power, another important factor is bias that can occur in the experimental study design itself or in the selection/exclusion of data for use in the statistical analysis. Furthermore, when the study includes many relationships, each of which will be tested, the chances of finding a false-positive result (e.g., statistically significant) also increases. When the investigators have a financial interest or some other important reward, such as academic advancement and tenure based on the outcome of studies, false-positive results are more likely. When multiple research teams are exploring the same experimental question, the risk increases for at least one group to report false-positive results simply because of the way that statistical significance allows for such false outcomes on occasion. For example, if 20 different groups perform the same investigation with a threshold p value of 0.05 for statistical significance, then on average one group can be expected to make statistically significant observations even when there is no true difference to be found (i.e., false-positive result).

The remedy for this latter problem is to include results from all studies exploring the same question to avoid excluding negative results that might otherwise go unreported. This approach would rely on some type of registry so that all such similar studies can be included in the final analysis. Another aspect of small versus large studies is that relatively infrequent but medically important side-effects of treatments can be missed in early-phase clinical trials involving only tens or hundreds of patients, but they can be recognized when the treatment moves to large phase IV randomized clinical trials and even later in the postmarketing phase when it is administered to an entire population, which is then monitored for side-effects (see Chapter 14).

Ioannidis (2005b) extended the discussion of reasons why most published research findings are false with an investigation of follow-up studies to highly cited clinical research. This examination looked at all original clinical research studies published in three major journals from 1990 to 2003 that were later cited more than 1000 times. Of the 49 studies so identified, 45 claimed clinical effectiveness. Of those 45, subsequent studies contradicted 7 cases, showed weaker effects than initially reported in 7 other cases, and replicated findings in 20 cases; 11 studies were unchallenged by later studies. Contradiction of findings and initially stronger effects that were not borne out were associated with nonrandomized design and especially with smaller sample size. The publication of only positive studies with statistically significant findings can introduce bias by excluding negative studies that could be more representative of the phenomenon under investigation; without balance from perhaps more numerous negative studies, a single positive one might erroneously be considered to represent truth when it actually does not (publication bias). With so much of academic and institutional success as well as commercial viability depending on effectiveness of new treatments, positive results from initial studies naturally have a great deal of appeal. Statistical tests may give an air of authenticity to early positive results, but exercising caution is prudent while searching for sources of bias that could lead to false-positive initial studies.

A counter-example often cited to the approach of using large numbers of patients in clinical trials is how penicillin was introduced to standard medical practice (Rothman, 2016). The first few patients treated with penicillin did not survive due to limited supply of the antibiotic. Mass production of penicillin led to several more patients being treated successfully for life-threatening infections, with one woman in the United States recovering from septicemia after receiving half the national supply in 1942. Once manufacture of large stores of penicillin was accomplished, it would have been impractical and probably even unethical to delay treatment until the antibiotic's effectiveness could be proven in a large randomized clinical trial in which untreated controls would have had an extremely high mortality rate.

Consequently, there is a balance in clinical trials between sufficiently large numbers of patients to provide solid statistical significance and numbers that are practical both from a financial standpoint (recruiting subjects and putting each person through months of a trial) and for the desire to make available truly effective treatments on a timely basis without undue delay.

RESOURCES FOR STATISTICAL ANALYSIS

Calculation of descriptive statistics and performance of statistical tests are now widely done using statistical software on computers. In the scientific realm, a few software packages are particularly popular, although applications from other vendors are also available. One of the most popular in the biomedical sciences is from the SAS (originally Statistical Analysis System) Institute, Inc., in Cary, North Carolina. SAS also provides JMP Software that has graphics linked to the statistics for ready visualization of results. Another well-established statistical software product is the Statistical Package for the Social Sciences (SPSS), which is now a part of IBM (SPSS Inc., Chicago, IL). SPSS is still recognized for its prominence in the social sciences. Microsoft Excel also can provide statistical analyses along with expanded graphical capabilities.

An alternative software package for scientific data analysis is the free open-source program named R for the first names of its creators Ross Ihaka and Robert Gentleman from the University of Auckland in New Zealand. While R requires programming abilities, it has the advantage of transparency in its written code, for which many users have posted applications on the Internet for others to use at no cost. Statistical analysis

using R programs has gained considerable popularity with graduate students as well as with users of standard procedures in pathology (Cuff & Higgins, 2012).

Resources for performing statistical calculations directly online are available with simple searching. One such site is Martindale's Calculators On-Line Center at http://www.martindalecenter.com/Calculators.html. A listing of similar sites is available on "Web Pages that Perform Statistical Calculations!" at https://statpages.info/.

When planning statistical analysis of data—in fact, even before planning the experimental design of a project—it is appropriate to consult with a biostatistician to ensure the most efficient design and one that is most likely to provide statistically sound results. A simple review of which statistical tests to employ for different combinations of categorical and continuous variables as independent (input) and dependent (output) variables can be found at The Decision Tree for Statistics at http://www.microsiris.com/Statistical%20Decision%20Tree/.

SELECTED REFERENCES

Daniel WW: In *Biostatistics: a foundation for analysis in the health sciences*, ed 7, New York, 1999, John Wiley & Sons.

This book is a more rigorous text on the use of statistical analysis in medicine and life sciences.

Dawson-Saunders B, Trapp RG: In Norwalk CT, editor: *Basic & clinical biostatistics*, ed 2, Appleton & Lange, 1994.

This very readable book provides excellent descriptions of statistical procedures applied to multiple examples in the life sciences and medicine.

Ioannidis JPA: Why most published research findings are false, *PLoS Med* 2:696–701, 2005a.

This article provides a mathematical explanation of why many published studies showing statistical significance probably are based on false-positive results due to inadequate factors such as small sample size and other aspects of power.

Lott JA: Process control and method evaluation. In Snyder JR, Wilkinson DS, editors: *Management in laboratory medicine*, ed 3, Philadelphia, 1998, Lippincott, pp 293–325.

This book is a comprehensive source for all aspects of management in the clinical laboratory.

Momeni, A, Pincus MR, Libien J: In introduction to statistics for pathologists, New York, 2017, Springer.

This text provides examples of statistical analysis commonly encountered in the practice of pathology.

National Committee for Clinical Laboratory Standards: *Evaluation of the linearity of quantitative measurement procedures: a statistical approach—approved guideline. Document EP6-A*, Wayne, PA, 2003, NCCLS.

This and all of the NCCLS guidelines have been developed through a consensus process involving international representatives from industry, government, and user laboratories to yield recommendations that can be applied worldwide. In January 2005, the NCCLS changed its name to the Clinical and Laboratory Standards Institute (CLSI).

Access the complete reference list online at Elsevier eBooks for Practicing Clinicians.

REFERENCES

Beran TN, Violato C: Structural equation modeling in medical research: a primer, *BMC Res Note* 3:267–276, 2010.

Cornbleet PJ, Gochman N: Incorrect least-squares regression coefficients in method-comparison analysis, *Clin Chem* 25:432–438, 1979.

Cuff J, Higgins JPT: Statistical analysis of surgical pathology data using the R program, *Adv Anat Pathol* 19:131–139, 2012.

Giacomo P: *International vocabulary of basic and general terms in metrology*, *Geneva*, Switzerland, 1984, International Organization for Standardization, pp 4–40.

Ioannidis JPA: Contradicted and initially stronger effects in highly cited clinical research, *J Am Med Assoc* 294:218–228, 2005b.

Matthews DE, Farewell VT: In *Using and understanding medical statistics*, ed 2, *Basel*, Switzerland, 1988, Karger.

National Cholesterol Education Program: *Detection*, *evaluation*, *and treatment of high blood cholesterol in adults (Adult Treatment Panel III)*, *final report. National Heart*, *Lung*, *and Blood Institute*, Bethesda, Md, 2002, National Institutes of Health.

National Committee for Clinical Laboratory Standards: *Method comparison and bias estimation using patient samples; approved guideline. Document EP9-A2*, Wayne, Pa., 2002, NCCLS. ISBN 1-56238-472-4.

Prati D, Taioli E, Zanella A, et al.: Updated definitions of healthy ranges for serum alanine aminotransferase levels, *Ann Inern Med* 137:1–10, 2002.

Expert Committee on the Diagnosis and Classification of Diabetes Mellitus: *Report of the expert committee on the diagnosis and classification of diabetes mellitus*, *Diabetes Care* 26(Suppl 1):S5–S20, 2003.

Rothman L: This is what happened to the first American treated with penicillin, *Time*, http://time.com/4250235/penicillin-1942-history/, 2016.

Valente BD, Rosa GJM, Gianola D, et al.: Is structural equation modeling advantageous for the genetic improvement of multiple traits? *Genetics* 194:561–572, 2013.

CHAPTER 11

QUALITY CONTROL

W. Greg Miller

ANALYTIC BIAS AND IMPRECISION, 130

CALIBRATION CONSIDERATIONS IN QUALITY CONTROL, 131

Calibration Traceability to a Reference System and Commutability Considerations, 131

OVERVIEW OF QUALITY CONTROL PROCEDURES, 132

IMPLEMENTING QUALITY CONTROL PROCEDURES, 133

Selecting Quality Control Materials, 133

Establishing Quality Control Target Value and Standard Deviation that Represent a Stable Measurement Operating Condition, 134

Performance of a Measurement Procedure for Its Intended Medical Use, 136

Establishing Rules to Evaluate Quality Control Results, 137

Frequency to Measure Quality Control Samples, 139

Corrective Action when a Quality Control Result Indicates a Measurement Problem, 140

Reviewing Quality Control Data, 140

VERIFYING QUALITY CONTROL EVALUATION PARAMETERS FOLLOWING A REAGENT LOT CHANGE, 141

VERIFYING METHOD PERFORMANCE FOLLOWING USE OF A NEW LOT OF CALIBRATOR, 143

USING PATIENT DATA IN QUALITY CONTROL PROCEDURES, 143

Delta Check with a Previous Result for a Patient, 143

Verifying Consistency of Results Between More Than One Instrument or Method, 143

Using Patient Data for Statistical Quality Control, 144

PROFICIENCY TESTING, 144

Noncommutability of Proficiency Testing Materials and Peer Group Grading, 145

Reporting Proficiency Testing Results when One Measurement Procedure Is Adjusted to Agree with Another Measurement Procedure, 145

Interpreting Proficiency Testing Results, 145

Accuracy-Based Proficiency Testing Programs with Commutable Samples, 147

QUALITY MANAGEMENT, 147

SELECTED REFERENCES, 149

KEY POINTS

- Quality control samples are assayed on a schedule to verify that a laboratory procedure is performing correctly.
- Interpretation of quality control results is based on acceptance criteria that will identify bias, trend in bias, or imprecision that exceeds expected method performance characteristics.
- In the event of an unacceptable quality control result, corrective action is taken to fix the method problem, and all patient results since the time of the previous acceptable quality control result are repeated to determine whether a result correction is needed.
- Because of commutability limitations, quality control samples cannot be used to verify that two different methods, or two different lots of reagents, produce the same results for patient samples.
- Proficiency testing provides external evaluation that a laboratory is using a method correctly and in conformance with the manufacturer's specifications.

The purpose of a clinical laboratory test is to evaluate the pathophysiologic condition of an individual patient to assist with diagnosis, to guide or monitor therapy, or to assess risk for a disease or for progression of a disease. To have value for clinical decision making, an individual laboratory test result must have total error small enough to reflect the biological condition being evaluated. The total error of a measured result is influenced by the following:

- Preanalytic variability in sample collection, transportation, processing, and storage
- Analytic variability in test performance
- Interfering substances such as drugs or metabolic components in the clinical sample

Quality control (QC) is also called *internal quality control* (meaning internal to the laboratory testing process and distinct from built-in QC, to be discussed later) or *statistical process control*. QC is a process to periodically examine a measurement procedure to verify that it is performing according to preestablished specifications. This chapter addresses QC of an analytic measurement procedure using QC sample materials intended to simulate clinical samples. Such QC sample materials are called surrogate samples. The QC samples are measured periodically in the same manner as clinical samples, and their results are examined to determine that the measurement procedure meets performance requirements appropriate for patient care. Techniques for using results from patient samples in the QC program are also included. This chapter is organized as follows:

- Analytic bias and imprecision
- Calibration considerations in quality control
- Overview of quality control procedures
- Implementing quality control procedures
- Reagent and calibrator lot changes
- Using patient data in quality control procedures
- Proficiency testing
- Quality management

ANALYTIC BIAS AND IMPRECISION

Figures 11.1 and 11.2 illustrate the meaning of bias and imprecision for a measurement. In Figure 11.1, the horizontal axis represents the measured numeric value for an individual result, and the vertical axis represents the number of repeated measurements with the same value made on different samples of a QC material. The red line shows the distribution of different results for repeated measurements of the same QC material, which is the random imprecision of the measurement. If we assume that repeated measurements of a QC sample follow a Gaussian (normal) distribution, as discussed in Chapter 10, the standard deviation (SD) is a measure of the expected imprecision or variability in a measurement procedure when it is performing correctly. Note that results near the mean (average value) occur more frequently than results farther away from the mean. An interval of ±1 SD includes 68% of the measured values, and an interval of ±2 SD includes 95% of the values. A result that is more than 2 SD from the mean is expected to occur 5% of the time (100%–95%) in a positive (2.5% of the time) or a negative (2.5% of the time) direction from the mean value. The mean of repeated measurements of a QC sample when the measurement procedure is performing within specifications becomes the expected, or target, value for that QC sample.

Figure 11.2 illustrates that if the calibration changes for any reason, a systematic bias is introduced into the results. The systematic bias is the difference between the observed mean and the original target value for a QC material. Note that the imprecision of an incorrectly calibrated method is the same as when correctly calibrated. All measurement procedures have an inherent imprecision. The purpose of measuring QC samples is to statistically evaluate the measurement process to verify that the measurement procedure continues to perform within the specifications consistent

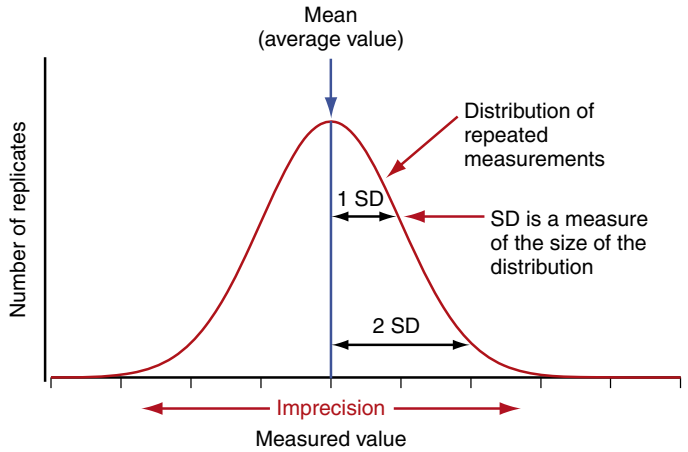

Figure 11.1 Illustration of results distribution showing the mean value and imprecision for repeated measurements of a quality control sample assuming a Gaussian (normal) distribution. *SD,* Standard deviation.

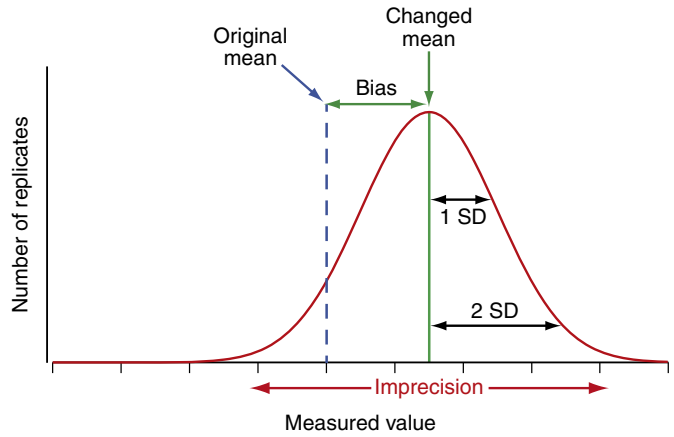

Figure 11.2 Illustration of systematic bias when a change in calibration has occurred. *SD,* Standard deviation.

with acceptable systematic bias and imprecision, and to identify whether a change in performance occurred that needs to be corrected. QC result acceptance criteria, discussed in a later section, are based on the probability for an individual QC result to be different from the variability in results expected when the measurement procedure is performing correctly. The imprecision observed in QC results provides a measure of the variability expected for individual patient results caused by the inherent variability of the measurement procedure.

CALIBRATION CONSIDERATIONS IN QUALITY CONTROL

Calibration of the analytic measurement procedure is a key component in achieving quality results. Figure 11.3 shows calibration of a measurement procedure that establishes the relationship between the signal measured and the quantitative value of analyte in the calibrator materials. This relationship is used to convert the measurement signal from a patient sample into a reportable concentration for the analyte. Specific techniques for calibration are unique to individual methods and will not be covered here. However, some general principles for implementing calibration procedures can contribute to the stability and clinical reliability of laboratory results.

Measurement procedure calibration is most often performed by the laboratory using end-user calibrator materials provided by the method or instrument manufacturer. In some cases (e.g., point-of-care devices), methods are calibrated during the manufacturing process and the laboratory performs a verification of that calibration. In either situation, traceability of result accuracy to the highest-order reference system is provided by the method manufacturer. The measurement procedure manufacturer's calibrator material(s) and assigned value(s) are designed to produce accurate results with clinical patient samples measured using that particular manufacturer's routine measurement procedure. One manufacturer's end-user

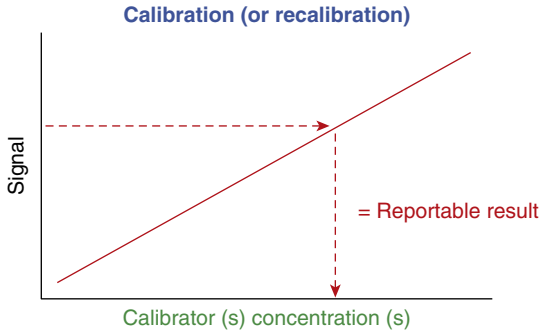

Figure 11.3 Calibration using measurement procedure–specific calibrators establishes the relationship between measurement signal (e.g., absorbance, voltage, impedance, etc.) and concentration in the sample measured.

calibrator is not intended for use with other measurement procedures; laboratories should not use calibrator materials intended for one measurement procedure with any other measurement procedure. Use of a calibrator with a measurement procedure for which it was not specifically intended can produce miscalibration and erroneous patient results (see next section).

One of the common causes of drift in QC results is inadequate frequency of calibration of measurement procedures. Measurement procedure manufacturers provide instructions on calibration frequency. Instructions to recalibrate when QC indicates a problem are not usually effective and lead to excessive result variability that is easily prevented by calibrating at a suitable interval. This condition is identified by a drift in QC results on a Levey-Jennings chart that returns to the target value when a recalibration is performed and typically looks like a sawtooth pattern. QC rules (see later section) are designed to identify that a measurement procedure does not meet its performance expectations and results for patient samples should not be reported. While it is possible that recalibration is necessary to correct the erroneous measurement condition, QC rules are not designed to identify when recalibration is needed during normal operation of a measurement procedure.

CALIBRATION TRACEABILITY TO A REFERENCE SYSTEM AND COMMUTABILITY CONSIDERATIONS

Whenever possible, calibration of routine measurement procedures should be traceable to a higher-order reference measurement procedure or international certified reference material (ISO, 2020; Vesper & Thienpont, 2009; Miller et al., 2014). For commercially available measurement procedures cleared by the U.S. Food and Drug Administration (FDA), the in vitro diagnostics (IVD) manufacturer offers end-user calibrators that provide calibration traceable to the applicable reference system for an analyte (called a *measurand* when fully specified to include the sample type and the molecular substance measured).

Commutability is a property of a reference material, such as a higher-order certified reference material, a QC material, or a proficiency testing (PT) material. As shown in Figure 11.4A, a commutable reference material has a numeric relationship between two or more measurement procedures that closely agrees with the relationship observed for a panel of clinical patient samples (Miller & Myers, 2013; Miller et al., 2018). Consequently, a commutable reference material (or calibrator) reacts in a measurement procedure to give a numeric result that would be in close agreement to that observed for a patient sample with the same amount of analyte. A noncommutable material (Figure 11.4B) has some other relationship between measurement procedures than that observed for clinical samples. Differences in commutability are caused by matrix-related bias between a reference material and clinical patient samples. Note that noncommutability is also an important limitation of QC and PT materials discussed in later sections.

A reference material's certificate of analysis should be reviewed for commutability documentation. If a reference material is commutable with patient samples for a given measurement procedure, it can be used for calibration or verification of calibration traceability to the reference system. Use of a noncommutable reference material for calibration will cause the clinical laboratory measurement procedure to be miscalibrated and produce erroneous patient results (Franzini & Ceriotti, 1998; Vesper et al., 2007; Miller & Myers, 2013; Miller et al., 2014). Similarly, use of a noncommutable reference material to verify calibration will give incorrect information regarding the calibration status of a method. Many higher-order certified reference materials have not been evaluated for commutability with patient

samples measured using clinical laboratory measurement procedures. If a reference material's commutability status is unknown, it must be assumed not to be commutable with patient samples.

It is important to recognize that IVD manufacturer–provided calibrators typically have matrix characteristics and assigned values that are intended only for use with that specific measurement procedure and cannot be used with any other manufacturer's measurement procedures. An IVD manufacturer can assign a value to a measurement procedure–specific calibrator that corrects for any matrix-related bias that may be present so that results for clinical samples are correctly traceable to the reference system for an analyte. However, if such a measurement procedure–specific calibrator is used with a different measurement procedure, it will cause miscalibration, because it does not compensate for a different matrix-related bias with that different measurement procedure.

A clinical laboratory may wish to verify that a measurement procedure's calibration conforms to a manufacturer's claim for traceability to the reference system used for a given analyte. Some manufacturers provide calibration verification materials specifically intended for this purpose. Such materials may be provided as measurement procedure–specific QC materials. Such measurement procedure manufacturer–provided QC materials typically have matrix characteristics and target values that are intended only for use with the specific measurement procedures claimed in the instructions for use and cannot be used with any other manufacturers' measurement procedure. Such measurement procedure–specific calibration verification materials may have assigned values that are specific for stated reagent lots or may have values certified by the manufacturer to be suitable for all reagent lots.

National and international certified reference materials are available for some analytes. In many cases, these reference materials are intended for use with higher-order reference measurement procedures and may not be suitable for use with clinical laboratory measurement procedures. Laboratories should not use national or international certified reference materials to calibrate, or to verify calibration, of a routine measurement procedure unless the reference material's commutability with patient samples has been verified for the specific measurement procedure used by a clinical laboratory.

Third-party QC materials (i.e., those provided by a manufacturer other than the clinical laboratory measurement procedure's manufacturer) are not suitable to verify calibration traceability. These materials are not validated for commutability with clinical samples for different clinical laboratory measurement procedures, and they do not have assigned values that are traceable to higher-order reference measurement procedures. Such third-party QC materials are designed to be used as QC samples for statistical process control, with target values and SD values assigned as described later in the Implementing Quality Control Procedures section. When third-party QC materials are used in an interlaboratory method comparison program with method-specific peer group mean values, these values can be used to confirm that a laboratory is using a specific method in conformance with other users of the same method (see Proficiency Testing section).

OVERVIEW OF QUALITY CONTROL PROCEDURES

Statistical QC is a component of a quality management system as shown in Figure 11.5. Figure 11.6A illustrates that a QC sample is periodically measured along with clinical samples. If the QC result is within acceptable limits of its target value, the measurement procedure is performing as expected, and results for patient samples can be reported with good probability that they are suitable for clinical use. If a QC result is not within

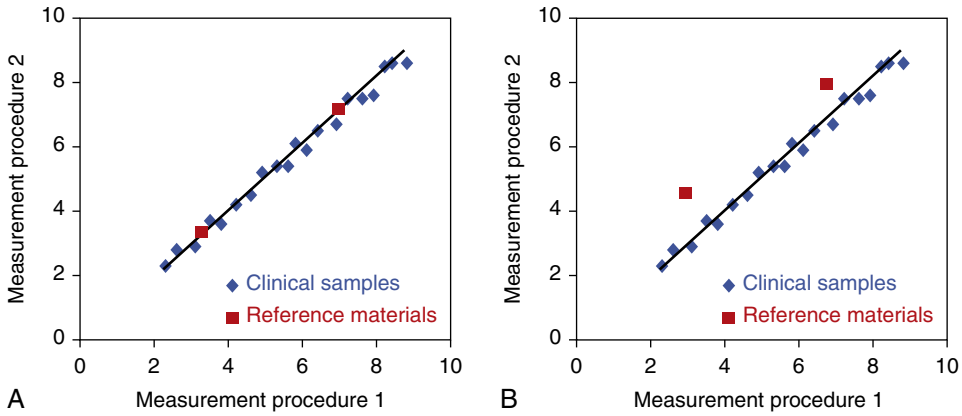

Figure 11.4 Panel A shows that commutable reference materials have the same numeric relationship between two (or more) measurement procedures as observed for clinical samples from patients. Panel B shows that noncommutable reference materials have a relationship that is different than that observed for clinical samples.

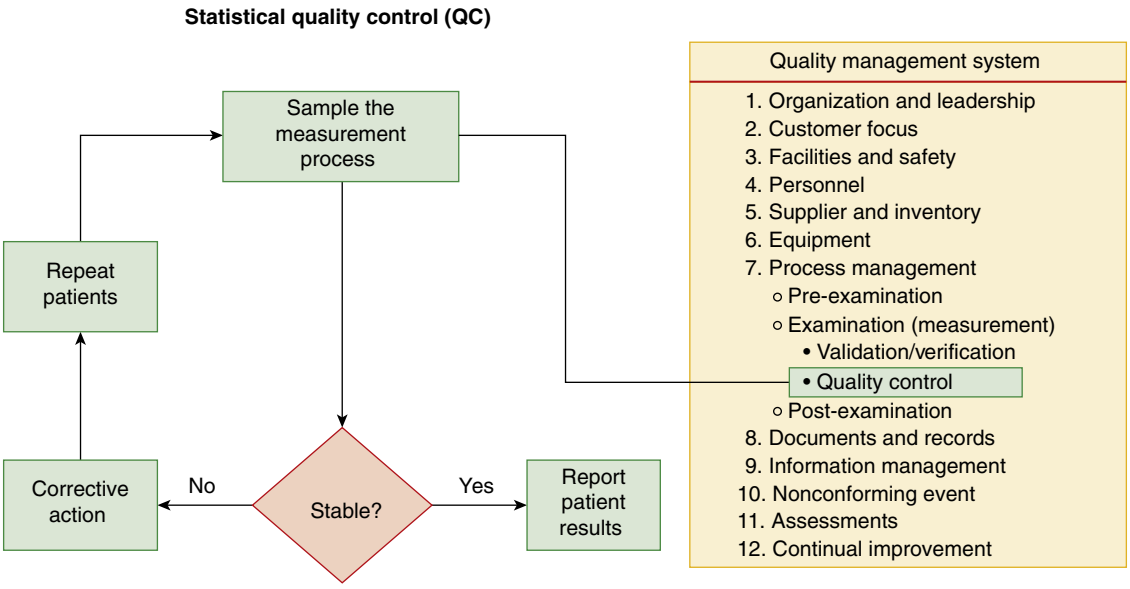

Figure 11.5 Overview of statistical quality control and its integration into a quality management system. The quality management system essentials are summarized from CLSI QMS-01 *A Quality Management System Model for Laboratory Services*, 5th edition (CLSI 2019).

acceptable limits (Figure 11.6B), the measurement procedure is not performing correctly, results for patient samples are not reported, and corrective action is necessary. Following corrective action, patient sample measurements that have already been reported since the time of the last acceptable QC result are repeated. Good laboratory practice requires verification that a measurement procedure is performing correctly at the time patient results are measured.

Statistical QC is part of the process management component of the quality system that integrates good laboratory practices to ensure correct patient results. Written standard operating procedures (SOPs) are required for all aspects of laboratory operation, including statistical quality control. The SOP for QC should include all aspects of the program, including the selection of QC materials, how to determine statistical parameters to describe method performance, criteria for acceptability of QC results, how frequently to measure the QC materials, corrective action when problems are identified, and documentation and review processes. The SOP should include who is authorized to establish acceptable control limits and interpretive rules for release of results; who should review performance parameters, including statistical QC results; and who can authorize exceptions to or modify an established QC policy or procedure.

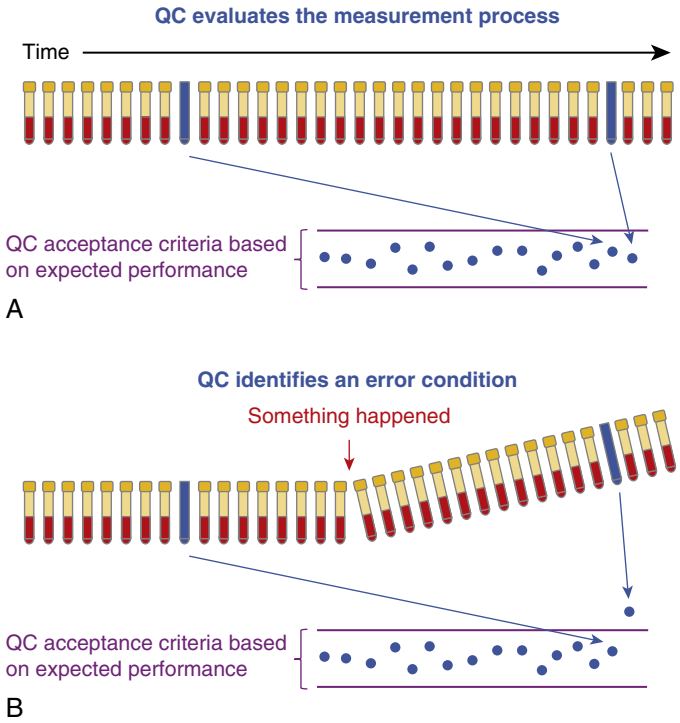

Figure 11.6 Panel A shows that quality control (QC) samples *(blue)* are periodically measured in place of patient samples *(yellow/red)* to determine whether the results for QC samples are within expected performance limits for a measurement procedure. Panel B shows that a QC result can identify that a measurement error condition occurred at some time since the last acceptable QC result was measured.

Figure 11.7 shows a Levey-Jennings (Levey & Jennings, 1950), also called Shewhart (Shewhart, 1931), plot, which is the most common presentation for evaluating QC results. This format shows each QC result sequentially over time and allows a quick visual assessment of measurement procedure performance, including trend detection. Assuming that the measurement procedure is performing in a stable condition consistent with its specifications, the mean value represents the target (or expected) value for the result, and the SD lines represent the expected imprecision for the measurements. Assuming a Gaussian (normal) distribution of imprecision, the results are distributed uniformly around the mean, with results observed more frequently closer to the mean than near the extremes of the distribution. Note that seven results are greater than 2 SD, four results are on the 2 SD lines, and two results slightly exceed 3 SD, which are expected on the basis of a Gaussian distribution of imprecision. For a large number of repeated measurements, the number of results expected within the SD intervals is as follows:

- ±1 SD = 68.3% of observations
- ±2 SD = 95.4% of observations
- ±3 SD = 99.7% of observations

Interpretation of an individual QC result is based on its probability to be part of the expected distribution of results when the measurement procedure is performing correctly. A later section provides details regarding interpretive rules for evaluation of QC results. Note that evaluation of individual QC results may be performed by computer algorithms. However, the underlying logic of such algorithms is illustrated by the Levey-Jennings chart example.

IMPLEMENTING QUALITY CONTROL PROCEDURES

SELECTING QUALITY CONTROL MATERIALS

Generally, two different concentrations are necessary for adequate statistical QC. For quantitative methods, QC materials should be selected to provide analyte concentrations that monitor the analytic measurement range of the method. In practice, laboratories are frequently limited by concentrations available in commercial QC products. When possible, it is important to confirm that method performance is stable near the limits of its analytic measurement range, because defects may affect these concentrations before others. Many quantitative measurement procedures have a linear response over the analytic measurement range—it is reasonable to assume that their performance over the range is acceptable if the results near the assay limits are acceptable. In the case of nonlinear response, it is necessary to use additional controls at intermediate concentrations. Critical concentrations for clinical decisions (e.g., glucose, therapeutic drugs, thyroid-stimulating hormone, prostate-specific antigen, troponin) may also warrant QC monitoring. In the case of analytes that have poor precision at low concentrations, such as troponin or bilirubin, the concentration should be chosen to provide an adequate SD for practical evaluation. For procedures with extraction or other pretreatment, controls must be used in the extraction or pretreatment step.

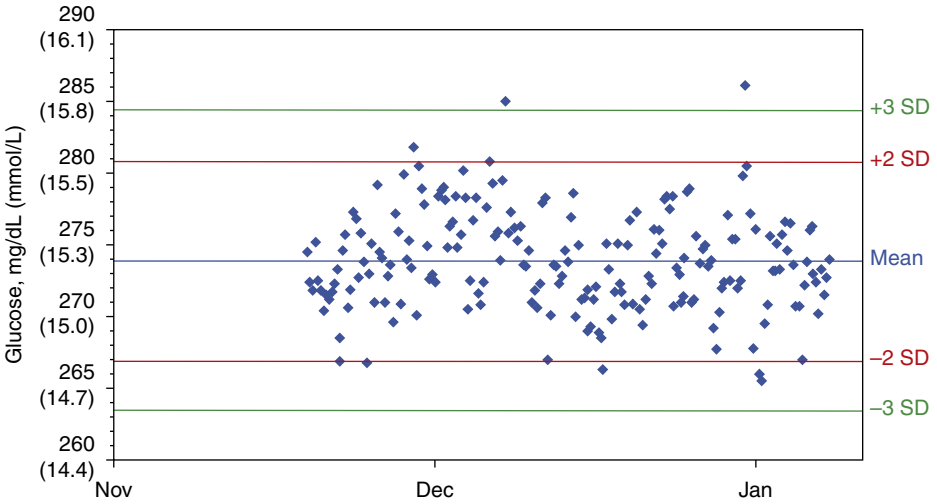

Figure 11.7 Levey-Jennings plot of quality control (QC) results (N = 199) for a single lot of QC material used for a 49-day interval. *SD,* Standard deviation.

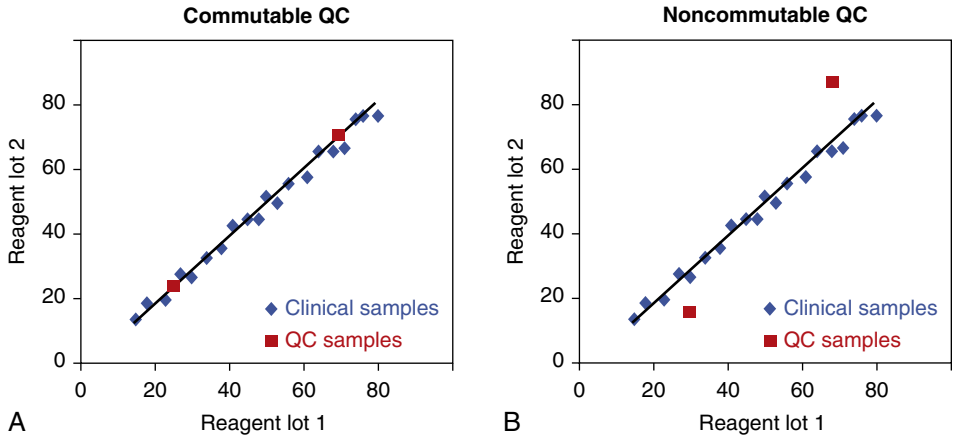

Figure 11.8 Panel A shows that commutable QC materials have the same numeric relationship between two reagent lots used for a measurement procedure as observed for clinical samples from patients. Panel B shows that noncommutable QC materials have a relationship that is different than that observed for clinical samples.

This chapter is primarily focused on QC procedures for quantitative methods. However, the principles can be adapted to most qualitative procedures. For tests based on qualitative interpretation of quantitative measurements (e.g., drugs of abuse), the same principles of QC assessment can be applied to the numeric results, and the negative and positive controls should be selected to have concentrations relatively near the decision threshold to adequately control for discrimination between negative and positive. For qualitative procedures with graded responses (e.g., dipstick urinalysis), negative, positive, and graded response controls are required. For qualitative tests based on other properties (e.g., electrophoretic procedures, stain adequacy, immunofluorescence, organism identification), it is necessary to ensure that the QC procedure will appropriately discriminate normal from pathologic conditions.

The QC samples selected must be manufactured to provide a stable material that can be used for an extended time period, preferably 1 or more years for stable analytes. Use of a single lot for an extended period allows reliable interpretive criteria to be established that will permit efficient identification of a measurement procedure problem, avoid false alerts due to poorly defined expected ranges for the QC results, and minimize limitations in interpreting values following reagent and calibrator lot changes.

Limitations of Quality Control Materials

Limitations are inherent in commercially available QC materials. One limitation is that a QC material is frequently noncommutable with clinical patient samples. A commutable QC material is one that reacts in a measurement system to give a result that would closely agree with that expected for a clinical sample with the same amount of analyte. The property of commutability is shown in Figure 11.8, in which measurement responses for a QC material and patient samples are compared. In panel A, the QC samples are commutable with clinical samples because they have the same relationship as observed for results for the clinical samples when two different reagent lots are used. In panel B, the QC samples are noncommutable with clinical samples because they have a different relationship than observed for the results for the clinical samples. In the case of panel B, the results for clinical samples correctly show that equivalent results are obtained with either reagent lot, while the results for the QC samples do not mimic those for patients and incorrectly suggest that a bias exists for results with the two different reagent lots.

QC (and PT) materials are frequently noncommutable with clinical samples because the serum or other biological fluid matrix is usually altered from that of a clinical sample (Franzini & Ceriotti, 1998; Miller, 2003; Thienpont et al., 2003; Miller et al., 2005; Miller et al., 2008; Miller et al., 2011a; Miller et al., 2018). The matrix alteration is due to processing of the biological fluid during product manufacturing, use of partially purified human and nonhuman analyte additives to achieve desired concentrations, and various stabilization processes that alter proteins, cells, and other components. The impact of the matrix alteration on the recovery of an analyte in a measurement procedure is not predictable and is frequently different for different lots of QC material, for different lots of reagent within a given measurement procedure, and for different measurement procedures (Miller et al., 2011b). Because of the noncommutability limitation, special procedures are required (discussed in later sections) when changing lots of reagent or comparing QC (or PT) results among two or more measurement procedures.

A second limitation of QC materials is deterioration of the analyte during storage. Analyte stability during unopened storage is generally excellent, but slow deterioration eventually limits the shelf life of a product and can introduce a gradual drift into QC data. Analyte stability after reconstitution, thawing, or vial opening can be an important source of variability in QC results and can vary substantially among analytes in the same vial. User variables to be controlled are the time spent at room temperature and the time spent uncapped with the potential for evaporation. An expiration time after opening is provided by the QC material manufacturer but may need to be established by a laboratory for each QC material under the conditions of use in that laboratory and may be different for different analytes in the same QC product. For QC materials reconstituted by adding a diluent, vial-to-vial variability can be minimized by standardizing the pipetting procedure (e.g., using the same pipet or filling device—preferably an automated device—and having the same person prepare the controls) whenever practical.

Another limitation of QC materials is that analyte concentrations in multi-constituent materials may not be at levels optimal for the different measurement procedures. This limitation may be caused by solubility considerations or potential interactions between different constituents, particularly at higher concentrations. It may be necessary to use supplementary QC materials to adequately monitor the analytic measurement range and clinically important decision concentrations.

ESTABLISHING QUALITY CONTROL TARGET VALUE AND STANDARD DEVIATION THAT REPRESENT A STABLE MEASUREMENT OPERATING CONDITION

QC target values and acceptable performance limits are established to optimize the probability to detect a measurement defect that is large enough to have an impact on clinical care decisions while minimizing the frequency of "false alerts" due to statistical limitations of the criteria used to evaluate QC results. The measuring system must be correctly calibrated and operating within acceptable performance specifications before the statistical parameters to establish QC interpretive rules can be established. Some sources of measurement variability that are expected to occur during typical operation of a measurement procedure are listed in Table 11.1.

A QC material must have a reliable target value that represents the condition when systematic bias is as small as possible. This condition requires the method to be calibrated correctly. For practical reasons, the typical sources of measurement variability in Table 11.1 are rarely all represented in the time available to establish a target value; consequently, the target value has some uncertainty and needs to be refined over time to reflect the expected fluctuations in measurement conditions that occur when the measuring system remains within its performance specifications. The generally accepted protocol for target value assignment is to use the mean value from measuring a QC material a minimum of 10 times on 10 different days (CLSI, 2015a). If a 10-day protocol is not possible—for example, if an emergency replacement lot of QC material is necessary—a provisional target value can be established with fewer data but should be updated as additional results are available. When applicable, more than one calibration should be represented in the 10-day period to include this source of variability in the target value. If a QC material will be used for longer than 1 day, a single vial should be stored correctly and measured on as many days as the material is planned to be used to allow any variability caused by deterioration of the analyte to be averaged into the target value.

TABLE 11.1

Common Sources of Measurement Variability

Source	Time Interval for Fluctuation	Likely Statistical Distribution
Pipette volume	Short	Gaussian
Pipette seal deterioration	Long	Drift
Instrument temperature control	Short or long	Gaussian or other
Electronic noise in the measuring system	Short	Gaussian
Calibration cycles	Short to long	Gaussian or periodic drift/shift
Reagent deterioration in storage	Long	Drift
Reagent deterioration after opening	Intermediate	Cyclic, periodic drift/shift
Calibrator deterioration in storage	Long	Drift
Calibrator deterioration after opening	Intermediate	Cyclic, periodic drift/shift
Control material deterioration in storage	Long	Drift
Control material deterioration after opening	Intermediate	Cyclic, periodic drift/shift
Environmental temperature and humidity	Variable	Variable
Reagent lot changes	Long	Periodic shift
Calibrator lot changes	Long	Periodic shift
Instrument maintenance	Variable	Cyclic or periodic shift
Deterioration of instrument components	Variable	Drift, cyclic, or periodic shift

Some QC materials are provided by the measurement procedure manufacturer with preassigned target values and ranges intended to confirm that the measurement procedure meets the manufacturer's specifications. Such assigned values may be used initially by the laboratory. It is recommended that both the target value and the SD be reevaluated and adjusted by the laboratory after adequate replicate results have been obtained because the QC interpretive rules used in a single laboratory should reflect performance for the measurement procedure in that laboratory. The acceptability limits (product insert ranges) suggested by a measurement procedure manufacturer typically are based on data collected from several laboratories. These acceptability limits will inevitably be greater than the variability expected for a measurement procedure used in an individual laboratory. Use of product insert ranges that are too large will reduce a laboratory's ability to detect an erroneous measurement condition.

QC materials with assigned target values are also available from third-party manufacturers (i.e., manufacturers not affiliated with the measurement procedure manufacturer). Caution should be used with target values assigned by third-party QC material providers because the target values may have been assigned using reagent and calibrator lots that are no longer available (see the section on Verifying Quality Control Evaluation Parameters Following a Reagent Lot Change). A laboratory should establish a target value that reflects the measurement conditions for a particular measurement procedure used in a specific laboratory. Some QC material providers offer an interlaboratory data aggregation service and report peer group target values for large numbers of laboratories using the same measurement procedure. Such interlaboratory QC data aggregation target values can be useful to determine that a laboratory is obtaining results similar to other users of the same measuring system in conformance to the manufacturer's specifications. However, such target values should not be used within a laboratory because those values will be influenced by reagent lot–specific noncommutability biases and other differences between measurement procedures in different laboratories that will make the target value less reliable for use in QC rules to identify errors in a laboratory's measurement procedure.

In addition to a target value, an SD is estimated for a QC material that represents the expected imprecision of the measurement procedure when it is performing according to its design specifications. As shown in Table 11.1, measurement variability includes sources with short time interval

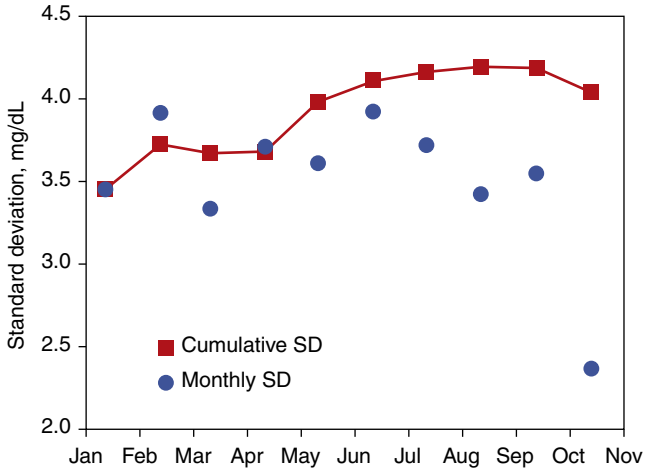

Figure 11.9 Cumulative standard deviation (SD) versus single monthly values calculated from the data in Figure 11.12.

frequencies, many of which can be described by Gaussian error distributions. Measurement variability also includes influences from intermittent and longer time interval sources that are not described by Gaussian error distributions. Such longer-term variability can cause cyclic fluctuations over several days or weeks, small drift over weeks or months, and more abrupt small shifts in results when a measurement procedure is performing within its specifications. QC interpretive rules are based on an assumption of Gaussian distribution of imprecision. However, the actual QC results are frequently non-Gaussian and it is very important to base the estimate of SD on a long enough time interval that all or most sources of variability that are consistent with the measurement procedure performing to specifications are reflected in the SD.

A minimum of 20 observations is recommended for an initial estimate of SD (CLSI, 2015a). It is desirable to have as many of the events that contribute to measurement variability, in particular calibration and maintenance, included during the time interval over which the SD is estimated. The initial estimate of SD will not include contributions from all expected sources of variability in Table 11.1 and will need to be updated when additional data are available. CLSI document EP05 provides guidance on establishing the SD for a measurement procedure under carefully defined conditions that do not include longer-term components of variability (CLSI, 2014). Consequently, an SD determined by this protocol is inevitably an underestimate of the SD needed for use in QC interpretive rules.

The SD for stable measurement performance should be estimated from the cumulative SD over a 6- to 12-month period for a single lot of QC material. The cumulative SD is likely to include most expected sources of variation in Table 11.1 and thus provide a realistic SD for use in QC interpretive rules. See an important limitation when determining a cumulative SD, described later in the section Verifying Quality Control Evaluation Parameters Following a Reagent Lot Change. Figure 11.9 illustrates (with data for a glucose method) the fluctuation in SD that occurs when calculated for monthly intervals compared with the relatively stable value observed for the cumulative SD after a period of 6 months. Note that the cumulative SD is not the average of the monthly values but is the SD determined from all individual results obtained over a time interval since the lot of QC material was first used. Different sources of long-term variability occur at different times during the use of a measurement procedure. The monthly SD does not adequately reflect the longer-term components of variability. Consequently, the cumulative SD will typically be larger than the monthly values and will better represent the actual variability of the method when it is operating to its specifications.

If the SD expected during stable operation is underestimated, the acceptable range for QC results will be too small, and the false alert rate will be unacceptably high. If the SD for the stable operating condition is overestimated, such as when using the SD from an interlaboratory comparison program, the acceptable range will be too large, and a significant measurement error could go undetected. Some QC material providers offer an interlaboratory data aggregation service that reports peer group SDs for laboratories using the same measurement procedure. Such SDs should not be used within a laboratory because those values will be influenced by reagent lot–specific noncommutability biases and other differences between measurement procedures in different laboratories that do not apply in a particular laboratory and will make the SD inappropriate for use in QC rules to identify errors in a laboratory's measurement procedure.

The statistical QC packages in instrument and laboratory computer systems are designed with the assumption that the SD for a Gaussian (normal) distribution is used for the QC rules criteria even though non-Gaussian components of variability influence the QC results. Because there are non-Gaussian components to measurement variability over time, it is very important that they be represented in the data used to estimate an SD. We use an estimate of SD to make conclusions regarding the acceptability of an individual QC value; thus, the SD must be as realistic as possible to represent the variability expected for a measurement procedure when its performance meets its specifications.

It is important to include all valid QC results in the calculation of SD to ensure that the SD correctly represents expected measurement procedure variability. A valid QC result is one that was, or would have been in the case of preliminary value assignment, used to verify acceptable performance and reporting of patient results. Only QC results that were, or would have been, responsible for not releasing patient results should be excluded from summary calculations. If inappropriate editing of QC results occurs, the method SD may be inappropriately small, which will produce inappropriately small evaluation limits and an increase in false QC alerts, with concomitant reduction in the effectiveness of statistical QC evaluation.

When a method has been established in a laboratory and a new lot of QC material is being introduced, the target value for the new lot of QC material is used along with the well-established SD from the previous lot (CLSI 2015a). This practice is appropriate because measurement imprecision is a property of the measurement procedure and equipment used and is unlikely to change with a different lot of QC material. If target values for the old and new lots of QC materials are substantially different, a different SD may occur and adjustment to the SD may be necessary as additional experience with the new lot is accumulated.

If a new measurement procedure is introduced for which no historical performance information is available, the SD and target value assignment of the QC materials must be established using data available from the measurement procedure validation. In this case, the initial SD will underestimate the long-term SD, and evaluation criteria will need to be monitored closely and adjustments made as additional experience allows measurement imprecision from all sources to be reflected in the cumulative SD.

PERFORMANCE OF A MEASUREMENT PROCEDURE FOR ITS INTENDED MEDICAL USE

It is important to understand how a test's performance impacts clinical decision making in order to determine the criteria used to evaluate acceptability and the optimal QC frequency. The sigma metric is commonly used to assess how well a measurement procedure performs relative to the medical requirement. Sigma is the Greek letter used to denote standard deviation. The sigma scale compares the variability of a measurement process in standard deviations to the variability that is medically acceptable because it has a low probability to cause an error in diagnosis or treatment of a patient.

For laboratory measurements, the sigma metric is calculated as:

$$(TE_a - |\text{bias}|)/SD,$$

where TE_a is the total error allowed based on medical interpretation requirements, and the absolute value of bias and the SD refer to performance characteristics of the laboratory measurement procedure. The SD is estimated from the long-term QC data as previously described. It is critically important that the SD uses QC data that represents all or most components of variability that occur over an extended time period. It is difficult for a laboratory to estimate true bias because it requires comparison with a reference method, which is not usually a feasible approach. In practice, QC results are used to determine whether a change in bias has occurred compared with the condition established by calibration of a measurement procedure. Consequently, the bias is usually assumed to be zero when calculating sigma for the purpose of establishing suitable QC rules. In a situation in which different measurement procedures are used in different laboratories in the same health care system and there is a known bias between the measurement procedures, a bias value can be used to reflect the overall sigma performance for clinical sample results that might be measured in different laboratory locations. However, this overall sigma value may not be suitable for establishing QC parameters for a single measurement procedure in one laboratory location.

TE_a can be estimated in several ways. The preferred way to set the TE_a is from laboratory practice guidelines. For example, the National Cholesterol Education Program recommends that total cholesterol be measured with a TE_a of 9% or less (National Institutes of Health, 1990), and the National Kidney Disease Education Program recommends that creatinine be measured with a TE_a of less than approximately 0.10 mg/dL in the concentration range 1 to 1.5 mg/dL, which is 7% to 10% (Myers et al., 2006). When practice guidelines are not available, the recommended way to estimate the TE_a is to consult clinicians to determine the magnitude of change in a laboratory result that will prompt a patient care decision.

Another approach is to base the TE_a on a fraction of the within- and between-individual biological variations for an analyte (Fraser, 2001; Lund et al., 2015; Panteghini & Sandberg, 2015). Tables of optimal, desirable, and minimal TE_a based on biological variation are available (Perich et al., 2015). However, biological variation–based estimates of TE_a should be used with caution because the estimates of biological variation in many cases are based on minimal data, and the experimental designs of the estimates and the process to select the listed estimates have been challenged (Oosterhuis, 2011; Roraas et al., 2012; Aarsand et al., 2015). For example, reports of biological variation for AST, alanine aminotransferase (ALT), and γ-glutamyl transferase (GGT) varied between 11% and 58%, 3% and 32%, and 4% and 14%, respectively, among different studies (Carobene et al., 2013). In addition, the biological variability has typically been derived from data for nondiseased individuals and may be different for pathologic conditions. The European Federation of Clinical Chemistry and Laboratory Medicine is addressing some of the limitations of biological variability data, has published a checklist for quality of data (Aarsand et al., 2018), and is updating the older published values (EFLM, 2019).

Because sigma assumes a Gaussian or normal distribution for repeated measurements, the probability of a defect—that is, an erroneous laboratory result—can be predicted as shown in Table 11.2. The sigma metric represents the probability that a given number of erroneous results—which could cause risk of harm to a patient—are expected to occur when the test method is performing to its specifications. The phrase "six sigma" refers to a condition when the variability in the measurement process is sufficiently smaller than the medical requirement that erroneous results are very uncommon (see Chapter 2). A "four sigma" method would be less robust and have a higher probability that erroneous results could be produced but still at a fairly low frequency. A "two sigma" method would produce enough erroneous results even though it met its performance specifications that it would be less suitable for patient care.

Figure 11.10 shows how the sigma metric describes the performance of a laboratory test. Panel A shows the performance of a "six sigma" test that has the TE_a limits six SD away from the center point of the expected distribution of variability in measurements when the test procedure is performing to its analytic specifications. In the "six sigma" situation, some bias or increased imprecision will have little influence on the number of erroneous results produced, and less stringent QC will be appropriate because the risk of producing an erroneous result is very low even with some loss of performance. Panel B shows the performance of a "three sigma" test that has the TE_a limits three SD away from the center point of the expected distribution of variability in measurements when the test procedure is performing to its analytic specifications. In the "three sigma" situation, a small amount of bias or increased imprecision will cause the number of erroneous results to increase substantially, and more stringent QC is needed to identify when such an error condition occurs. Note that no amount of QC will improve the performance of a marginal measurement procedure. However, more frequent QC and more stringent acceptance criteria will allow the laboratory to identify when small changes in performance occur so that they can be corrected to minimize the risk of harm to a patient from erroneous results being acted on to make clinical care decisions.

TABLE 11.2

Probability of Acceptable or Erroneous Results Based on the Sigma Scale[a]

Sigma Value	Percent of Results within Specification	Percent of Results With an Error (Defect)	Errors (Defects) Per Million Opportunities
1	68	32	317,311
2	95.5	4.5	45,500
3	99.7	0.3	2,700
4	99.994	0.006	63
5	99.99994	0.00006	0.6
6	99.9999998	0.0000002	0.002

[a]The values in this table are based on a Gaussian statistical distribution and do not include the "1.5 sigma shift" frequently introduced to recognize that many manufacturing processes have been observed to have a long-term drift approximately ±1.5 SD when operating in a stable condition. The 1.5 sigma shift is not used for QC rules design.

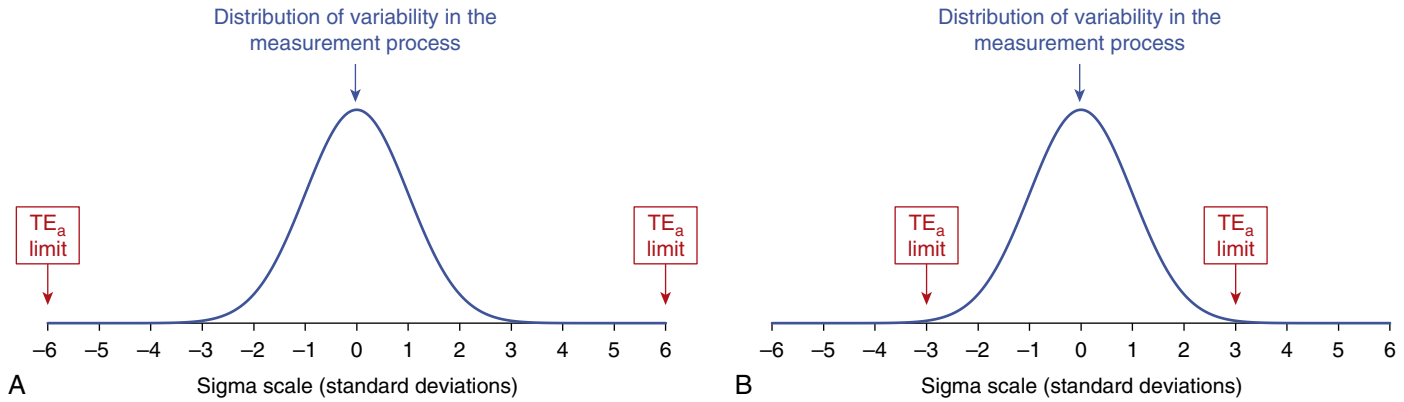

Figure 11.10 Test performance relative to the sigma scale to describe how well performance meets medical requirements. Part A shows a "six sigma" method, and part B shows a "three sigma" method. Note that the measurement SD is the same in both cases, but the fraction of the TE_a consumed by the SD is different. *SD,* Standard deviation; *TE_a*, allowable total error.

TABLE 11.3

Abbreviation Nomenclature for Quality Control Evaluation Rules

Rule	Meaning	Detects
1_{2S}	One observation exceeds 2 SD from the target value. The 1_{2S} rule is not recommended because it has a large false alert rate.	Not recommended except for "low sigma" measurement procedures
1_{3S}	One observation exceeds 3 SD from the target value.	Imprecision or bias
2_{2S} ($2_{2.5S}$)	Two sequential observations, or observations for two QC samples in the same run, exceed 2 SD (or 2.5 SD) from the target value in the same direction.	Bias
R_{4S}	Range between observations for two QC samples in the same run, or for two sequential observations of the same QC sample, exceeds 4 SD.	Imprecision
10_x or 10_m	Ten sequential observations for the same QC sample are on the same side of the target value (x or mean). The 10_x rule is not recommended because it has a large false alert rate.	Not recommended
8_{1S} ($8_{1.5S}$)	Eight sequential observations for the same QC sample exceed 1 SD (or 1.5 SD) in the same direction from the target value.	Bias trend
CUSUM	Cumulative sum of SDI for a specified number of previous results.	Bias trend
EWMA	Exponentially weighted moving average with newer results having more influence (weight).	Bias trend

CUSUM, Cumulative sum; *EWMA*, exponentially weighted moving average; *QC*, quality control; *SD*, standard deviation; *SDI*, standard deviation interval.

ESTABLISHING RULES TO EVALUATE QUALITY CONTROL RESULTS

The acceptable range and rules for interpreting QC results are based on the probability of detecting a significant analytic error condition with an acceptably small false alert rate. The measurement procedure performance characteristics—that is, the SD—and the acceptable TE_a must be established for each analyte before the appropriate QC rules can be selected.

The conventional way to express QC interpretive rules is with an abbreviation nomenclature popularized among clinical laboratories by Westgard and colleagues (1981) and summarized in Table 11.3. Note that fractional SD intervals are permissible, as in the $2_{2.5S}$ example. Statistical procedures such as cumulative sum (CUSUM), moving average (MA) or exponentially weighted moving average (EWMA) are preferred to monitor for bias trends (Ryan, 1989). One of these more advanced trend detection procedures is recommended if supported by an available computer system because they are more powerful than the 8_{1S}, or similar approaches based on sequential observations exceeding a specified SD from the target value. EWMA and CUSUM must be implemented carefully to avoid being too sensitive to small changes that may cause an excessive frequency of false alerts.

Power function graphs have been used to express the probability that a QC interpretive rule will detect an analytic error of a given magnitude (Westgard & Groth, 1979). Westgard's statistical model assumed Gaussian (normal) error distributions and, despite the fact that non-Gaussian error distributions exist in measurement procedures, has provided useful guidance for selecting rules to interpret QC results. Other literature reports have addressed rule selection criteria using other statistical models and assumptions regarding distribution of errors (Linnet, 1989; Parvin, 1997; Parvin & Gronowski, 1997).

Figure 11.11 shows a power function graph that plots the probability to detect a measurement error (*y*-axis), which is the probability that a result will exceed a particular interpretive rule, versus a systematic bias of known magnitude in a result (*x*-axis) with a fixed random imprecision of ±1 SD when there are two QC samples being measured along with the group of patient samples. The three lines in Figure 11.11 represent the probabilities of different interpretive rules to detect systematic biases of various magnitudes. For example, for the 1_{2S} rule, a result with a systematic bias of 1 SD (*x*-axis) has a 0.35 (35%) probability (*y*-axis) of violating the rule (i.e., of having a result more than 2 SD from the target value). Note that this figure shows only systematic bias as SD on the *x*-axis, and a result with 1 SD systematic bias will also have an imprecision component that may cause the 1_{2S} rule to be exceeded. Thus, a 1_{2S} interpretive rule has a 35% probability to detect a systematic error that is 1 SD in magnitude. Similar graphs can be created for other interpretive rules for both systematic bias and imprecision error conditions.

Note in Figure 11.11 that none of these interpretive rules has a 100% probability to detect a systematic bias until the error becomes relatively large. The 1_{2S} rule has a good probability of detecting errors (e.g., almost 90% probability of detecting a 2.5 SD bias) but has a high false alert rate, as indicated by the *y*-intercept (because of imprecision, the probability of indicating an error condition for zero bias is approximately 10%). Because of this high false alert rate, a 1_{2S} rule is generally not recommended unless the measurement procedure is a "low sigma" method and the laboratory desires to identify small biases that could cause inappropriate risk for a patient care decision. The 1_{3S} rule has a low false alert rate but a lower probability to detect an error (e.g., a 50% probability to detect a 2.5 SD bias). The efficiency of QC interpretive rules is improved by combining two or more rules and applying them simultaneously as multirule criteria. For example, the $1_{3S}/2_{2S}$ multirule identifies an error condition if one control exceeds ±3 SD from the target value or if two controls exceed ±2 SD in the same direction from the target value. The $1_{3S}/2_{2S}$ multirule has a low false alert rate similar to the 1_{3S} rule but improved probability to detect an error (e.g., a 65% probability to detect a 2.5 SD bias and a 90% probability to detect a 3.2 SD bias). In this multirule example, the 1_{3S} component is sensitive to imprecision or large systematic bias, while the 2_{2S} component is sensitive to systematic bias.

A challenge in selecting interpretive rules for evaluating QC results is that the different sources of variation listed in Table 11.1 occur in most contemporary automated measurement procedures but at various frequencies that cause longer-term cyclic and step fluctuations in performance to occur at different times in the course of using a measurement procedure. These longer-term types of variability are not adequately described by Gaussian models for rules selection. At certain periods of time, the short-term SD will be noticeably smaller than the long-term cumulative SD. One must avoid concluding that the SD used for evaluation is too large because over time the cumulative value will be more consistent with measurement procedure performance as periodic sources of variability are encountered.

Figure 11.12 shows how non-Gaussian error sources influenced results for a single lot of QC material used over a 10-month period for an automated glucose method. The glucose method stability and performance over the 10 months were considered acceptable for clinical use. Data for the first 49 days are the same as in Figure 11.7 and represent the initial experience with this lot of QC material. Examination of these data shows several fluctuations that cannot be described by a Gaussian statistical model. The first reagent lot change caused a step shift to higher values that was too small to initiate a change in target value (see later section on Verifying Quality Control Evaluation Parameters Following a Reagent Lot Change). The second reagent lot change had no effect on QC results. Between March and April, a transition to lower values occurred that did not correspond to any maintenance, reagent lot change, or calibration events. Throughout the 10-month period, intervals of several weeks' duration occurred when the imprecision was better or worse than at other time periods (also see Fig. 11.9 calculated from the same data).

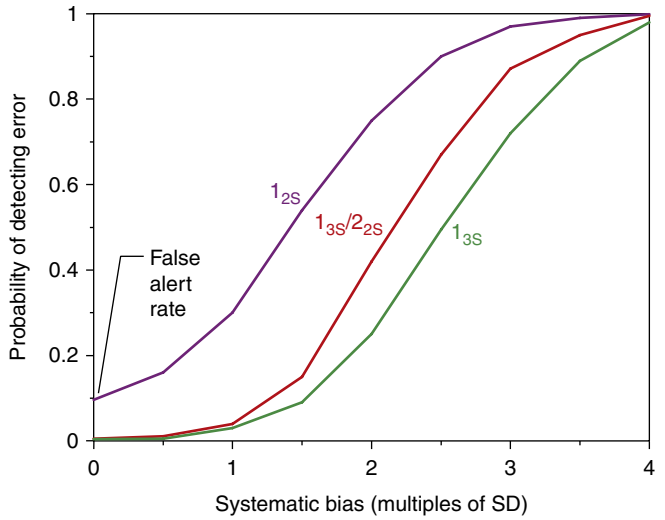

Figure 11.11 Power function graphs for the ability of different quality control interpretive rules to detect systematic error using two controls. Systematic error is expressed as number of standard deviations (SDs) from the target value. (Modified from Westgard JO, Groth T: Power functions for statistical control rules, *Clin Chem*, 25:863–9, 1979; used with permission.)

In practice, empirical judgment is frequently used to establish acceptance criteria (rules) to evaluate QC results based on data acquired over a long enough time to adequately quantify the expected variability when a method is working correctly. QC rules should not be selected based only on Gaussian models of imprecision because the rules will not correctly accommodate all types of variability observed for measurement procedures when they are operating within specifications.

Table 11.4 gives an example of an empirically developed multirule based on the data in Figure 11.12. This multirule had 0.6% false alerts when applied to the data in Figure 11.12, using the mean from the November to January period (see Fig. 11.7) as the target value and the SD for the 10-month period to represent overall imprecision. If a 2_{2S} rule was used instead of a $2_{2.5S}$ rule, the false alert rate would increase to 1.2%, but the rule would detect slightly smaller biases. An $8_{1.5S}$ rule was used to provide detection of bias trends because it had a 0% false alert rate (compared with 0.5% for an 8_{1S} rule) and was adequate to detect a developing trend before it became clinically important because the SD was small, 4.0 mg/dL, at a concentration of 274 mg/dL. If a 10% TE_a is considered acceptable for glucose at this concentration, then the sigma is 6.8, suggesting a very low error rate, and these QC rules with a low false alert rate will be suitable to alert the laboratory to an error condition that is large enough to affect patient care decisions. At other clinical concentration ranges, or for other analytes, a 2_{2S}, 8_{1S}, or $6_{1.5S}$ rule may be more appropriate. A 10_x rule was not used because it would have increased the false alert rate to 11%. A 10_x rule is generally not recommended because this condition does not infer a problem with clinical interpretation of patient results when the magnitude of the difference from the target value is small.

Whatever statistical approach is used, the balance between false alerts and the probability of detecting an error is improved when multiple rules are used in combination. When establishing rules to interpret QC results, it is important to remember that statistical process control can only verify at a point in time that a measuring system is producing results that conform to the expected variability when the system is performing in a stable operating condition. Periodic measurement of QC samples does not identify random events (e.g., a temporary clot in a sample pipette, a random reagent pipette error) that do not persist until the next QC sample is measured. QC rules are chosen to detect changes in bias and changes in imprecision that are significant enough to require correction before patient results are reported.

In the process of reviewing statistical parameters for QC data, a laboratory may determine that a measurement procedure's performance is marginal or inadequate to meet medical requirements. Determining the sigma

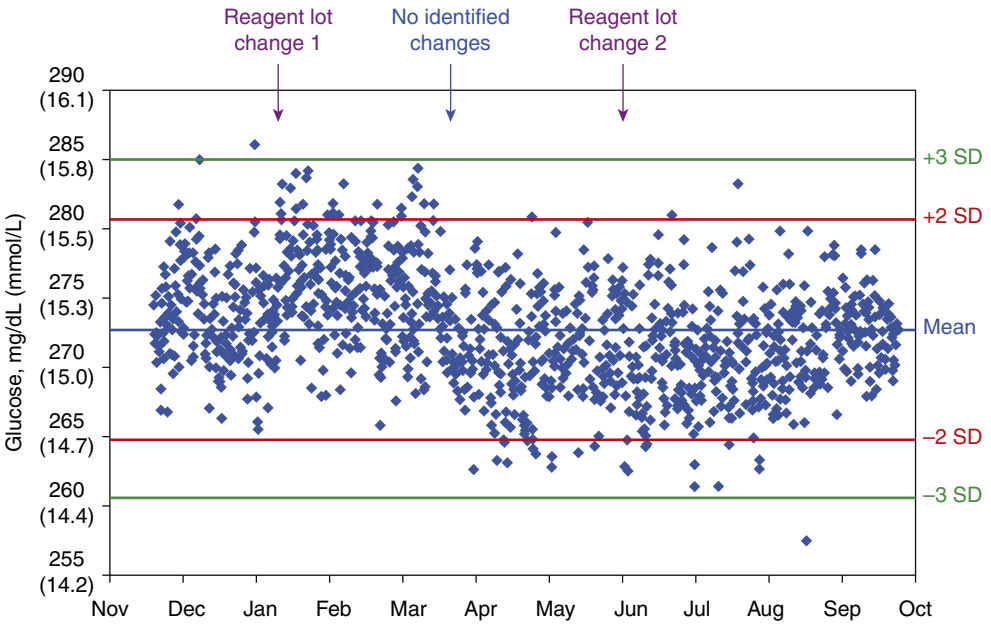

Figure 11.12 Levey-Jennings plot of quality control (QC) results (N = 1232) for a single lot of QC material used over a 10-month interval. *SD,* Standard deviation. (Modified with permission from Miller WG, Nichols JH: Quality control. In Clarke WA, editor: Contemporary practice in clinical chemistry, ed 2, Washington DC, 2010, AACC Press.)

TABLE 11.4

Empirical Multirule for the Quality Control Data in Figure 11.12

Multirule Components	Type of Variability Detected
1_{3S}	Imprecision or bias
$2_{2.5S}$	Bias
R_{4S}	Imprecision
$8_{1.5S}$	Bias trend

metric is helpful to make this assessment because the sigma value gives a prediction of the number of erroneous results expected. If the measurement procedure's performance cannot be improved and a better measurement procedure is not available, the laboratory can either discontinue the test if the performance is inadequate or apply more stringent QC practices to identify small changes in performance. In addition, the measurement procedure limitations should be communicated to patient care providers.

More stringent QC practices include selecting rules that will give an alert at smaller error conditions, using additional rules in a multirule set, assaying QC more frequently, using more than two QC samples, and not releasing patient results until QC assessment is complete for the time interval during which patient samples were measured. For lower sigma methods, the more stringent QC rules will cause more QC alerts, some of which will be false alerts, in order to detect error conditions that could affect interpretation of a patient's result. It is important to recognize that more stringent QC will not improve measurement procedure performance but is intended to identify smaller changes in performance that could produce results that affect patient care decisions.

A plan for statistical QC using surrogate QC samples specifies the number of controls, the concentration levels of the controls, the acceptance rules, and the frequency to measure the QC samples. The choice of the parameters will depend on the performance characteristics of the measurement procedure, the number of potentially erroneous patient results that could occur before the next QC event, and the risk of harm to a patient if potentially erroneous results were used in clinical care decisions. The relationship between these components of a QC strategy has been reviewed by Yundt-Pacheco and Parvin (2013).

FREQUENCY TO MEASURE QUALITY CONTROL SAMPLES

The frequency to assay QC samples is a function of several parameters:

- Analytic stability of the measurement procedure
- Risk of harm to a patient from clinical action being taken before a significant error is detected
- Number of patient results produced in a period of time when an error condition existed but was not yet detected
- Scheduled events such as recalibration or maintenance that may alter the current performance condition of the measuring system
- Training and competency of the test operator, particularly for manual or semiautomated methods
- Risk of failure of the measuring device

Analytic Stability of the Measurement Procedure

The stability of the measurement procedure is a fundamental determinant of how frequently a QC sample needs to be assayed. The more stable the system, the less frequently a statistical QC evaluation needs to be performed. The minimum requirement, consistent with Clinical Laboratory Improvement Amendments (CLIA) regulations, section 493.1256 (Department of Health and Human Services, 2003), is to assay controls at least once per 24 hours or more frequently if specified by the method manufacturer or if the laboratory determines that more frequent QC assays are necessary for the performance characteristics of a measurement procedure. Some types of tests have more stringent requirements. For example, CLIA section 493.1267 requires that at least one QC be measured every 8 hours (including both high and low concentrations over a period of 24 hours) for blood gas measurements; in addition, a QC must be run with each patient sample unless the instrument automatically calibrates at least every 30 minutes.

Risk of Harm to a Patient and Number of Patients Who May Be at Risk

The risk of clinical action being taken before a significant measurement error is detected is an important consideration for more frequent QC measurements than one based strictly on measurement procedure stability characteristics or on regulatory minimum requirements. More frequent QC measurements are appropriate to avoid the situation of discovering a methodologic problem many hours after a physician has performed a clinical intervention based on an erroneous result. For example, QC sampling performed on a 24-hour cycle might be performed at 9 AM. If QC results indicate a measurement procedure problem, the erroneous condition could have started at any time during the previous 24 hours. If the problem had occurred at 3 PM the previous day, potentially erroneous results would have been reported for 18 hours, likely putting a large number of patients at risk of an inappropriate medical decision. Parvin (2008, 2018) reported an assessment of the frequency of QC testing and the number of potentially incorrect patient results that could be reported before errors of different magnitudes were detected.

The medical risk of harm to a patient from erroneous results must be considered and the frequency of QC testing established to minimize risk. From a practical perspective, the cost of a medical error, or simply the cost of repeating questionable patient samples since the last acceptable QC results, could be more expensive than a more frequent QC measurement schedule that would detect an error condition in a more timely manner.

CLSI has published guideline EP23 addressing risk-based QC procedures (CLSI, 2011). The document provides guidance to clinical laboratories on how to develop a QC plan based on evaluation of risk of harm to a patient and assessment of the effectiveness of risk mitigation procedures using information from the manufacturer and from other literature sources, combined with the clinical requirements of the local health care setting and measurement procedure performance in the laboratory.

In general terms, the laboratory director is responsible for ensuring that a result has a high probability to be correct at the time it is reported for clinical use. To make this judgment, the laboratory director needs to understand the risks that can cause a measurement technology to perform incorrectly, needs to evaluate the effectiveness of built-in control processes to mitigate those risks, and needs to ensure that adequate control procedures are in place to confirm that a result is correct at the time it is reported. A combination of built-in and QC sample-based monitoring procedures can be utilized to ensure that all risks have been appropriately mitigated and/or monitored at a frequency commensurate with the risk of malfunction and the risk of harm to a patient if an incorrect result was reported.

Individualized Quality Control Plan

The Centers for Medicare and Medicaid Services (CMS) introduced an Individualized Quality Control Plan (IQCP) in 2013 (Department of Health and Human Services, 2013). The IQCP is an alternate QC option allowed by the CLIA 88 QC policy in 42CFR493.1250. After January 1, 2016, the QC requirements as written in the 2003 CLIA quality control requirements (Department of Health and Human Services, 2003) or the IQCP option are allowed in U.S. laboratories. Note that either QC practice is acceptable and it is voluntary if a laboratory implements an IQCP.

The IQCP option was derived from the CLSI guideline EP23 that introduced a risk-based process for developing a QC plan in 2011 (CLSI, 2011). The IQCP option is applicable to any measurement procedure but is primarily intended for measurement procedures that have been designed with sophisticated built-in control procedures to mitigate the risk that an erroneous result could be produced. Built-in control procedures may include QC materials integrated with reagent packaging and sensors that monitor electronic components and the measurement process with algorithms that prevent a result from being produced if any monitored conditions fail to meet criteria. Some of these measuring systems may be sufficiently stable and self-monitored to justify reduced frequency of traditional surrogate QC sample testing. The approach to risk assessment is qualitative in the CMS IQCP and in the CLSI EP23 guideline. This chapter includes risk assessment in developing a QC plan, particularly for the frequency to perform QC and the criteria to accept a QC value to confirm acceptable method performance. However, this chapter does not specifically address all components of the IQCP or EP23 recommendations.

Scheduled Event-Based Measurement of Quality Control Samples

Laboratory operations typically implement two types of testing schedules. Batch processes measure a group of clinical samples as a batch and testing for all samples is completed before reporting the results. For batch processes, QC samples can be measured at the beginning and end of the batch to ensure that all results have high probability to be correct before reporting. Continuous measurement processes are common in higher-volume settings—for example, automated chemistry or hematology—when clinical samples are measured and results reported continuously as they are

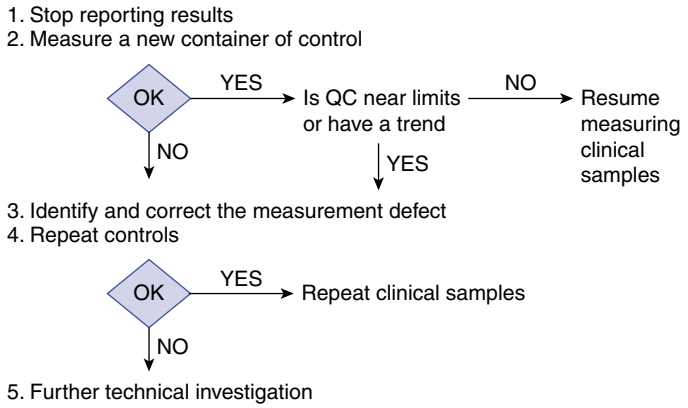

Figure 11.13 Generalized troubleshooting sequence following an unacceptable quality control (QC) result.

received in the laboratory with QC sample measurements made periodically during the course of the process.

For continuous measurement processes, QC samples must be measured before scheduled events such as recalibration or maintenance that could alter the current performance condition. Each of these operations is intended to restore the measurement conditions to optimal specifications and to correct for any calibration drift or component deterioration that may have occurred. It is necessary to measure QC samples before these operations to verify that no significant errors in results have occurred since the last time QC samples were measured because recalibration or maintenance alters the condition of the measurement procedure. Otherwise, it is not possible to know whether erroneous results could have been reported since the time of the last acceptable QC assessment. It is also necessary to measure QC samples after these scheduled events to verify correct measurement procedure performance before restarting measurement of patient samples.

If a malfunction occurs during a continuous measurement process such that the measuring system becomes nonoperable, that condition must be treated as a QC failure with follow-up to repeat and confirm the acceptability of reported clinical sample results. This follow-up action is required because the malfunction prevents measuring QC samples to determine whether erroneous results could have been reported since the time of the last acceptable QC assessment.

CORRECTIVE ACTION WHEN A QUALITY CONTROL RESULT INDICATES A MEASUREMENT PROBLEM

A QC alert occurs when a QC result fails an evaluation rule, which indicates that an analytic problem may exist. A QC alert means there is a high probability that the measurement procedure is producing results unreliable for patient care. When this condition occurs, it is necessary to take corrective action to investigate the cause of the QC alert. Figure 11.13 presents a generalized troubleshooting sequence. The first action is to stop making measurements and reporting results for clinical samples. The next step is to repeat the QC measurement . If the value on the repeat measurement is acceptable, testing of patient samples can resume; if the result is still unacceptable, the possibility that the QC material has deteriorated should be investigated. QC materials can deteriorate after opening caused by improper handling and storage or because of unstable analytes. Thus, repeating the measurement on a new vial or container of the QC material is recommended to determine whether the alert was caused by deteriorated QC material rather than by a measurement procedure problem. In this situation, if the result for the new QC sample is acceptable, testing of patient samples can resume. However, if the repeat QC result is acceptable but near the acceptability limits, it is important to consider that the repeat and original results may be essentially of the same magnitude and the probability is fairly high that a measurement problem exists that should be investigated. In addition, current and preceding QC results should be examined for a trend in bias that indicates a measurement issue needing to be corrected. These precautions in evaluating repeat results for a new QC sample can be challenging or impossible for automated evaluation by computer systems, thus requiring the laboratory technologist to be vigilant in reviewing results.

When repeat testing of a new QC sample does not resolve the alert situation, the instrument and reagents should be inspected for component deterioration, empty reagent containers, mechanical problems, and so on.

TABLE 11.5

Example for Selected Chemistry Analytes of Empirical Criteria for Patient Test Result Agreement between Repeated Measurements and for Agreement Among Results for a Single Patient Sample Measured on Multiple Instruments

Analyte	Acceptance Criteria (Difference between Results)
Albumin	0.4 g/dL
ALP	10 U/L or 10%*
ALT	10 U/L or 10%*
Amylase	15 U/L or 10%*
AST	10 U/L or 10%*
Bilirubin, total	0.3 or 10%*
Calcium, total	0.5 mg/dL
Chloride	4 mmol/L
Cholesterol	5%
CK	10 U/L or 10%*
CO_2	4 mmol/L
Creatinine	0.2 mg/dL or 10%*
GGT	10 U/L or 10%*
Glucose	6 mg/dL or 5%*
Iron	10 μg/dL or 10%*
Lactate	0.32 mmol/L
LD	10 U/L or 10%*
Lipase	10 U/L or 10%*
Magnesium	0.3 mg/dL
Phosphorus	0.4 mg/dL
Potassium	0.3 mmol/L
Protein, total	0.4 g/dL
Sodium	4 mmol/L
Triglycerides	10%
Urea nitrogen (BUN)	3 mg/dL or 10%*
Uric acid	0.4 mg/dL

ALP, Alkaline phosphatase; *ALT*, alanine aminotransferase; *AST*, aspartate aminotransferase; *BUN*, blood urea nitrogen; *CK*, creatine kinase; *CO_2*, carbon dioxide; *GGT*, γ-glutamyltransferase; *LD*, lactate dehydrogenase.
*Whichever is greater.

In many cases, it will be necessary to recalibrate. When the problem is identified and corrected, QC samples should be measured to verify the correction and all patient samples since the time of the last acceptable QC results should be remeasured. The laboratory director must establish acceptable criteria to determine whether the repeat results agree adequately to permit reporting of original results without issuing a corrected report. Otherwise, corrected results must be reported. As an example, Table 11.5 lists empirical criteria used in the author's laboratory for this purpose. The criteria for acceptability of repeated tests are based on measurement procedure performance characteristics and clinical requirements of the medical services.

In some cases, sample volume may not be adequate (quantity not sufficient [QNS]) for repeat testing. In these situations, no results can be reported unless it is documented that the impact of the measurement procedure defect on the original results was small enough to have minimal effect on clinical interpretation. A protocol to evaluate the clinical impact of the methodological problem is to repeat those samples that have adequate volume. The repeated samples must represent the concentration range of the QNS samples, must represent the time span since the previous acceptable QC results, and should include a substantial proportion of the total samples originally measured while the measurement procedure was in the unacceptable condition. If the repeat results are within established criteria for repeat testing of patient samples, the original results for the QNS samples can be reported. Otherwise, the original results for the QNS samples are considered erroneous; no results can be reported and the original results already reported need to be corrected to a "no reportable result" condition with a comment that the original result was incorrect.

REVIEWING QUALITY CONTROL DATA

The immediate use of QC data is to determine whether patient results can be reported and used for clinical decision making. In addition, QC data

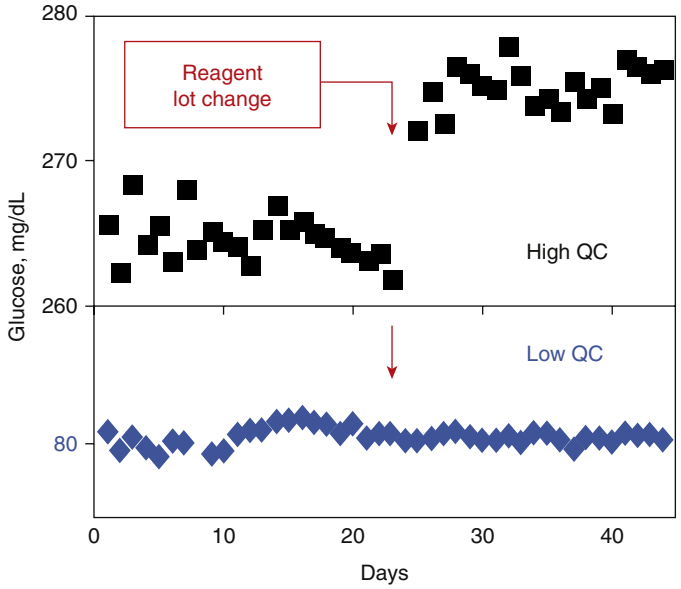

Figure 11.14 Levey-Jennings plot showing impact of a reagent lot change on matrix bias with quality control (QC) samples. (Modified with permission from Miller WG, Nichols JH: Quality control. In Clarke WA, editor: Contemporary practice in clinical chemistry, ed 2, Washington DC, 2010, AACC Press.)

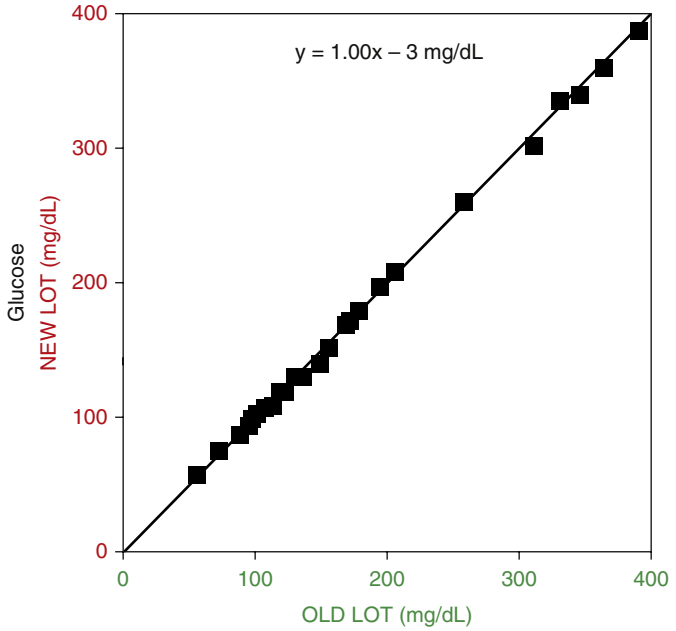

Figure 11.15 Deming regression analysis of results from a comparison of a patient's sample results between the same old and new lots of reagent shown in Figure 11.14 for quality control samples.

must be reviewed by laboratory management on a regular schedule. Typical review schedules are weekly or twice weekly by senior medical technologists and/or supervisors and at least monthly by the laboratory director. The weekly review process should determine that correct follow-up of any QC alerts was conducted, that all patient samples that may have had erroneous results were repeated, and that the process was properly documented in QC records. The monthly review should include any issues identified by the weekly review process as well as examination of the Levey-Jennings chart or other tool to identify trends or changes in assay performance that may need to be addressed. The monthly review should also include consistency of reagent lot changes, calibrator lot changes, and any patient data–based QC procedures described in the following sections.

Note that automated systems to assist in the review of QC data are acceptable, and individual Levey-Jennings charts do not need to be examined every month. A report that compares the mean and SD for QC results over a defined time interval, such as 1 month, with the expected values consistent with stable assay performance can be useful to focus the review on assays that may need attention. For example, the report might identify QC statistical values that deviate more than a specified amount, such as a mean over 1 SD from the target value or an SD that exceeds its expected value. QC values that are identified as needing further examination can then be followed up with review of a Levey-Jennings chart or other records of measurement procedure conditions such as maintenance, calibration, and reagent change.

The QC review process serves two major functions: It verifies that test procedures are stable and meet performance specifications, and it identifies test procedures that may need intervention to address trends in performance deterioration. In addition, other adjustments can be made, such as QC frequency, QC acceptance criteria, calibration and maintenance frequency, and so on based on a measurement procedure's performance characteristics. Quality indicators from the quality management program—such as number of QC failures, number of result corrections, or number of patient samples that are repeated due to QC issues—can be helpful in determining whether changes may be needed to the QC plan. The QC review is an opportunity to examine any aspect of performance that is relevant for a given measurement procedure to provide results that meet the requirements for clinical care decisions.

VERIFYING QUALITY CONTROL EVALUATION PARAMETERS FOLLOWING A REAGENT LOT CHANGE

Changing reagent lots can have an unexpected impact on QC results. Careful reagent lot crossover evaluation of QC target values is necessary. Because the matrix-related interaction between a QC material and a reagent can change with a different reagent lot, QC results are usually not a reliable indicator of a measurement procedure's performance for patient samples following a reagent lot change. In a large study of 661 reagent lot changes for 8 QC materials for 82 analytes using 7 different instrument platforms, 41% of 1483 QC material–reagent lot combinations had significant differences in QC values between the reagent lots that were not observed for patient samples (Miller et al., 2011b). In the example in Figure 11.14, QC values for the high concentration control shifted following the change to a new lot of reagents, but there was no change in results for the low control. A comparison of results for a panel of patient samples measured using the new and old reagent lots, shown in Figure 11.15, verified that patient results were the same when either lot of reagents was used. Patient results spanned the analytic measurement range and had nearly identical values, as indicated by the slope of 1.00 and the small intercept of –3 mg/dL. Consequently, the change in QC values for the high concentration material was due to a difference in matrix-related bias between the QC material and each of the reagent lots.

It is necessary to use patient samples to verify the consistency of results between old and new lots of reagents because of the unpredictability of a matrix-related bias being present for QC materials. Figure 11.16 presents a procedure to verify or adjust QC sample target values following a reagent lot change. A group of patient samples and the QC samples are measured using both the current (old) and new reagent lots. The first step is to verify that results for a group of patient samples with the new reagent lot are consistent with results from the current (old) lot. The patient sample results, not the QC results, provide the basis for verifying that the new reagent lot is acceptable for use. If a problem is identified, the calibration of the new reagent lot must be investigated and corrected or the new reagent lot may be defective and should not be used. When evaluating the patient results, keep in mind that the calibration of the old reagent lot may have drifted and should be verified before concluding that the new reagent lot is not giving acceptable results for the patient samples.

The number of patient samples to use for verifying the performance of a new reagent lot will depend on the analytic measurement range, the imprecision of the measurement procedure, and the concentrations at which key clinical decisions are made. CLSI document EP26 (CLSI, 2013) recommends a minimum of 3 patient samples, possibly more, depending on the number of key clinical decision concentrations and the imprecision of a measurement procedure. This CLSI guideline includes a statistical analysis to determine whether a difference in patient results is less than a critical difference that would represent risk for an inappropriate patient care decision based on a particular laboratory test result. An alternate approach is to select 10 or more patient samples that span the analytic measurement range and use Deming regression analysis (Cornbleet & Gochman, 1979; Linnet, 1993; Martin, 2000), which allows assessment of average performance over the range of concentrations represented by the patient samples. (See Chapter 10 for Deming analysis).

There are no well-established clinical acceptance criteria for agreement between results. Consequently, the laboratory must establish acceptance

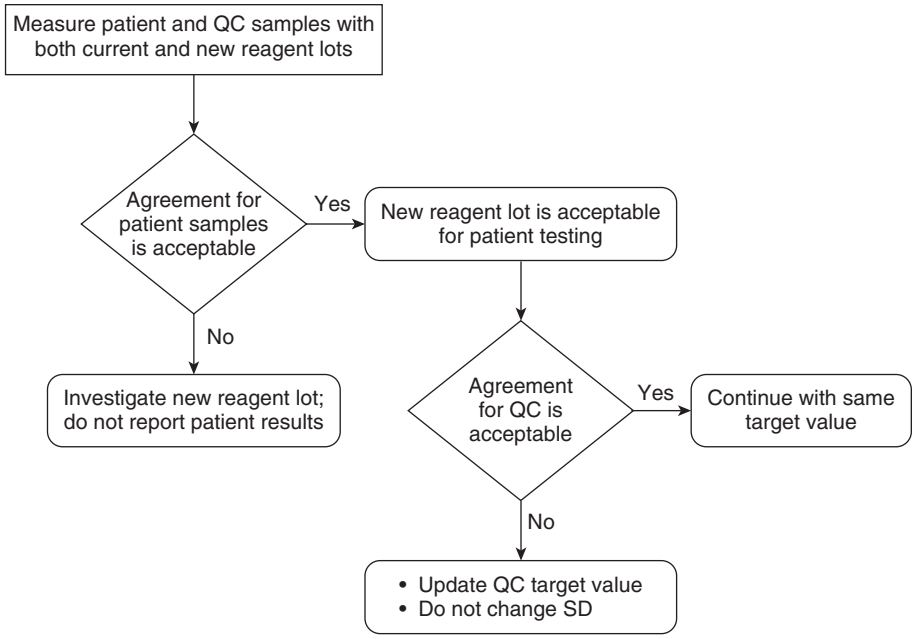

Figure 11.16 Process for assessment of potential matrix impact on quality control (QC) target values following a reagent lot change. *SD,* Standard deviation.

criteria consistent with the relatively small number of samples used, the analytic capability of a measurement procedure, and the clinical requirements for interpreting results. As an example, empirical acceptance criteria used in the author's laboratory for assessment of individual results are provided in Table 11.5.

Once the results for patients are determined to be acceptable, the second step in Figure 11.16 evaluates results for each QC material to determine whether its target value is correct for use with the new lot of reagent(s). If the target value has changed, it must be adjusted to correct for the change in matrix-related bias between the QC material and the old and new lots of reagent(s). This adjustment keeps the expected variability centered around the QC target value so that QC interpretive rules will remain valid. Failure to make a target value adjustment will introduce an artifactual (and incorrect) bias in subsequent QC results, causing both an increased false alert rate and a decreased ability to detect some error conditions. These effects are illustrated in Figure 11.17, where the shift in target value would cause some of the results shown by red symbols to exceed the old upper 1–3S threshold, when in reality there is no defect in patient results because the QC results are artifactually increased due to the matrix-related bias with the new reagent lot. Similarly, the increased magnitude of the gap to the old lower 1–3S limit will permit a low-bias condition, as shown by the last two red points, to be undetected until the low bias becomes larger than the QC rule is intended to detect. A reagent lot verification is typically performed on a single day and will likely provide only a few QC results from which to evaluate if the target value has changed. Consequently, when the QC target value is adjusted for a new reagent lot, it is necessary to carefully monitor QC results as more data are acquired using the new reagent lot and, if needed, to further refine the new target value.

The SD used to evaluate QC results will not typically change when a new lot of reagent(s) is put into service. The SD represents expected variability when the method is stable and is performing according to specifications. In most cases, the variability of a method will be approximately the same with different lots of reagent(s). However, occasional exceptions may occur—for example, if the new reagent lot is a reformulation, it may be necessary to adjust the SD after additional numbers of QC results are accumulated with the new reagent lot.

Note that a reagent lot–induced matrix-related change in the numeric values for the QC results will cause an artifactual increase in the cumulative SD such that the cumulative SD may be larger than the inherent measurement variability and not be suitable for use in QC rules. For this reason, the cumulative SD from a single QC and reagent lot pairing or from reagent lots that did not have a matrix-related change in QC target value should be used when determining the long-term cumulative SD to use for interpreting QC rules. However, such single QC and reagent lot pairing intervals may not adequately include all sources of long-term variability. To ensure that long-term sources of variability are included, the SD can be determined as a pooled value from several intervals of single

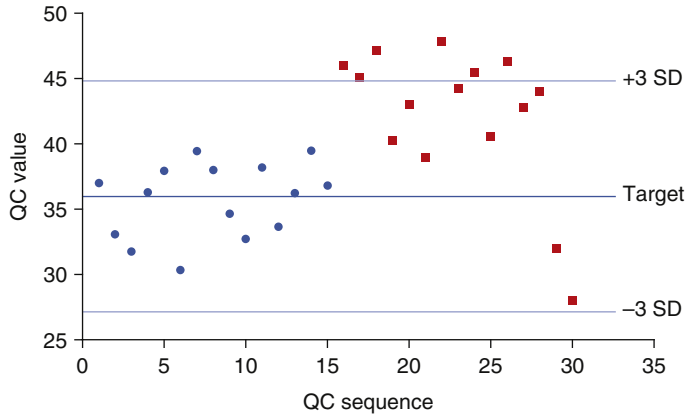

Figure 11.17 Influence on the failure rate for a quality control (QC) rule when failing to adjust the target value for a matrix-related shift. A new reagent lot was introduced at sequence number 16. *SD,* Standard deviation. *Blue symbols,* values with old reagent lot; *red symbols,* values with new reagent lot.

QC and reagent lot pairings. Pooling SD is a well-established statistical approach to obtain a SD value that represents the accumulated influences represented in different partitions or intervals of single QC and reagent lot pairings. The formula for pooling SD is

$$SD_{pooled} = \sqrt{\frac{(n_1 - 1) \text{ x } SD_1^2 + (n_2 - 1) \text{ x } SD_2^2 + \ldots + (n_i - 1) \text{ x } SD_i^2}{n_1 + n_2 + \ldots + n_i - i}}, \quad \text{(Eq. 11.1)}$$

where n is the number of QC results in a partition from 1 to i.

Experience in clinical laboratories has shown that there are changes, other than reagent lot changes, in measurement procedures that can also affect the QC values but not the results for patient samples. Such changes could be caused by maintenance, component replacement, or other causes. In theory, there should be an assignable cause for such effects, but such a cause is not always identifiable. In practice, any condition that affects QC results but does not affect patient results is treated in the same manner as described for reagent lot changes. The important QC principle is that if the results for patient samples are consistent between the two conditions, then the target value for the QC sample should be adjusted, if necessary, to reflect its value under the new condition. Failure to adjust the QC target value will cause inappropriate acceptability criteria to be used for evaluating the QC results.

VERIFYING METHOD PERFORMANCE FOLLOWING USE OF A NEW LOT OF CALIBRATOR

When a new lot of calibrator is used with no change in reagents, there is no change in matrix interaction between the QC material and the reagents. In this situation, QC results provide a reliable indication of calibration status with the new lot of calibrator. If the QC results indicate a bias following use of a new lot of calibrator, the calibration has changed and needs to be corrected to ensure consistent results for patient samples.

Some measurement procedures are packaged as kits that include reagents, calibrators, and QC materials. In this case, QC results could fail to identify a calibration shift when a new kit lot is used. It is then necessary to measure patient samples with the old and new kit lots to verify consistency of patient results. When possible, it is recommended to use QC materials that are independent of the kit lot and to avoid changing lots of QC material at the same time as changing lots of reagent or calibrators. Assaying patient samples always provides a reliable approach to verifying the consistency of results following changes in lots of reagents or calibrators.

USING PATIENT DATA IN QUALITY CONTROL PROCEDURES

Results from patient samples are used in four principal ways to support the QC processes in a laboratory:

- To verify consistency of patient results when changing lots of reagent or calibrators (discussed in the previous section)
- To identify inconsistent results using a delta check with a previous result for a patient
- To verify consistency of patient results when an analyte is measured using more than one instrument or method in a health care system
- To verify measurement procedure performance using results from patient samples in a statistical QC scheme

DELTA CHECK WITH A PREVIOUS RESULT FOR A PATIENT

Some types of laboratory errors can be identified by comparing a patient's current test result to a previous result for the same analyte. This comparison is called a *delta check*. The previous result is taken from a specified time interval in the past during which the result is not likely to have changed physiologically. This limitation restricts the analytes that can be effectively monitored with a delta check. Delta checks are most useful to detect mislabeled samples and samples altered by dilution with intravenous fluid during collection from a patient. Consequently, an effective delta check process for panels of tests from a sample can be established using a limited number of analytes. The difference between results that cause a delta check alert must be sufficiently large to avoid excessive numbers of false alerts and adequate to allow identification of samples that may be compromised and require follow-up investigation. Table 11.6 shows, as an example, the delta check parameters for automated chemistry used in the author's laboratory designed to identify compromised patient samples.

Delta checks can detect analytic errors; however, the threshold values necessary to identify analytic errors will be fairly small compared with physiologic changes and may cause a large number of false alerts that reduce the efficiency of laboratory workflow. A well-designed statistical QC plan will be more effective in detecting analytic errors. However, delta checks might be useful to identify an interfering substance—for example, from a new drug—that may appear in a patient's sample. Kazmierczak (2003) has reviewed and presented recommendations for using delta checks and other patient data–based QC procedures. The CLSI has published guideline EP33 for using delta checks in the clinical laboratory (CLSI, 2015b).

VERIFYING CONSISTENCY OF RESULTS BETWEEN MORE THAN ONE INSTRUMENT OR METHOD

Another common use of patient results in a QC process is to verify consistency of patient results when an analyte is measured using more than one instrument or method technology within the same health delivery system. Good laboratory medicine requires that multiple instruments or different measurement procedures for the same analyte be calibrated to produce the same results for patient samples whenever possible. It may be necessary to modify the calibration settings of one measurement procedure to match another measurement procedure's results. This strategy allows a common reference interval to be used, provides continuity in results between different laboratory testing locations, and avoids clinical confusion regarding interpretation of laboratory results.

As illustrated in Figure 11.18, equivalence of patient results is verified by measuring aliquots of patient samples using each of two or more measurement procedures (or analyzers) to evaluate and adjust the calibration as needed to achieve agreement in results for patient samples. Such an analysis design is called a *round robin*. One measurement procedure/analyzer may be chosen to represent the primary measurement procedure to which others will be adjusted to achieve equivalent results. The primary measurement procedure should be chosen based on quality and reliability of results with consideration of its calibration traceability to national or international standards, its performance stability, its analytic specificity for the analyte, and its susceptibility to interfering substances. An alternate approach is to evaluate each measurement procedure for agreement with the mean of all measurement procedures and to adjust the calibration of any measurement procedures/analyzers as necessary to produce equivalent results among the group. When like analyzers in a group are compared, if results for one analyzer are different from results for the others, that analyzer's calibration is adjusted to conform to that of the group.

There are no well-established guidelines regarding the number of samples to use for a round robin exchange. The laboratory needs to establish the frequency of evaluation and the number of samples based on the stability of the measurement procedures, the frequency of reagent and calibrator lot changes, and the clinical requirements of the health delivery

TABLE 11.6

Example Delta Check Criteria Intended to Identify Samples That Are Potentially Mislabeled or Contaminated With Intravenous Fluids Due to Incorrect Collection

Test	Delta Criteria
Sodium	5% change within previous 48 hours
Urea nitrogen	60% change within previous 48 hours
Creatinine	50% change within previous 48 hours
Calcium	25% change within previous 48 hours
Osmolality	5% change within previous 48 hours

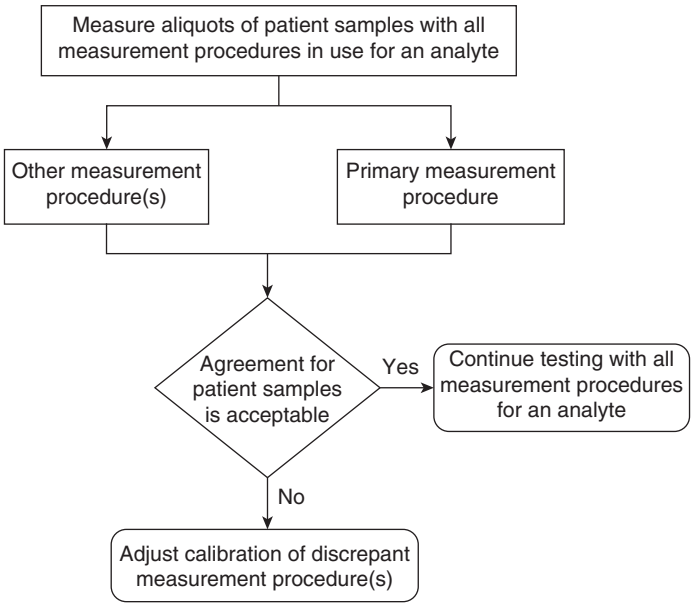

Figure 11.18 Process used to evaluate agreement between measurement procedures and to adjust calibration, if necessary, to achieve equivalent results from different measurement procedures.

system. Common practices include a round robin exchange of one or more individual patient samples or a pool prepared from several samples on a weekly basis for high-volume analytes; on a monthly or quarterly basis for lower-volume or very stable methods; or the regulatory minimum of every 6 months. CLIA regulations, section 493.1281, require that the relationship between test results from different measurement procedures/analyzers or from multiple locations should be evaluated at least twice a year (Department of Health and Human Services, 2003). For frequent comparisons with one or two samples, concentrations should be chosen to evaluate the analytic measurement range over a period of several examinations. For less frequent comparisons, a larger number of samples is recommended to cover the analytic measurement range. When establishing interpretation criteria, the laboratory needs to consider the limited statistical power for the number of results available. CLSI document EP31, *Verification of Comparability of Patient Results within One Healthcare System*, provides a statistical approach suitable for using one to five samples in a comparison (CLSI, 2012).

Table 11.5 provides, as an example, empirical criteria used in the author's laboratory for evaluation of agreement among results for a single patient sample assayed weekly among multiple analyzers. These criteria were established based on the expected imprecision of the measurement procedures used and the clinical impact of discrepant results. To allow for the limitations of a single measurement of a single sample in a comparison, a result outside a criterion is typically not acted on unless the magnitude of a difference is somewhat larger than the criterion or the situation persists for 2 or more weeks.

Patient samples are recommended to verify agreement between multiple measurement procedures or analyzers. Results for QC materials should not be used for the purpose of verifying equivalence of results for patient samples measured using different measurement procedures or analyzers. As discussed earlier, QC materials are not validated to be commutable with patient samples between different measurement procedures. Even when more than one measurement procedure/analyzer from the same manufacturer is used, differences may be seen in the measured value for QC materials between different reagent lots. In theory, if more than one of the same model analyzer with the same reagent lots are used, all should have the same results for the same lot of QC material. In practice, differences in measurement details among different analyzers cause small differences in QC results. The acceptance criteria can be set to allow for such differences. However, more reliable conclusions will be drawn when patient samples are used to evaluate agreement among different analyzers.

USING PATIENT DATA FOR STATISTICAL QUALITY CONTROL

Patient results can be used in a statistical QC process to monitor method performance. For a sufficiently large number of results, the mean (or preferably median) value may be sufficiently stable to be used as an indicator of measurement procedure consistency over time. This approach can be used on a periodic basis by extracting data for a specified time interval (e.g., 1 month), calculating the mean and SD for the distribution of results, and comparing one time interval to another to determine whether any changes have occurred. This type of periodic evaluation can identify changes in calibration stability or in overall imprecision for a method. The mean and SD can also be compared for consistency among multiple measurement procedures/analyzers for the same analyte.

An important limitation for using patient data to evaluate consistency within a single measurement procedure or between different measurement procedures for the same analyte is the physiologic homogeneity of results. Important considerations include parameters likely to influence the reference interval, such as disease status, pediatric versus adult, gender, and ethnic differences. Figure 11.19 shows an example of the potential impact of a nonhomogeneous sample of patients on distribution of albumin results for hospital general medicine inpatients compared with a student health outpatient clinic. The histograms are very different because the two patient groups differ in severity of disease and in recumbent versus supine position for blood collection, which influences vascular water volume and the concentration of albumin.

Automated approaches to determine the mean (or median) for groups of sequential patient results used as a continuous process control parameter have been described. These methods have been called *average of normals* (*AON*) or *moving average* techniques and are suitable for use in higher-volume measurements in chemistry and hematology (Cembrowski et al., 1984; Smith & Kroft, 1996; Westgard et al., 1996; Ye et al., 2000; Kazmierczak, 2003; Ng et al., 2016; Badrick et al., 2019). In general, these approaches evaluate sequential patient results over time intervals from minutes to hours or days. The time interval that can be confidently

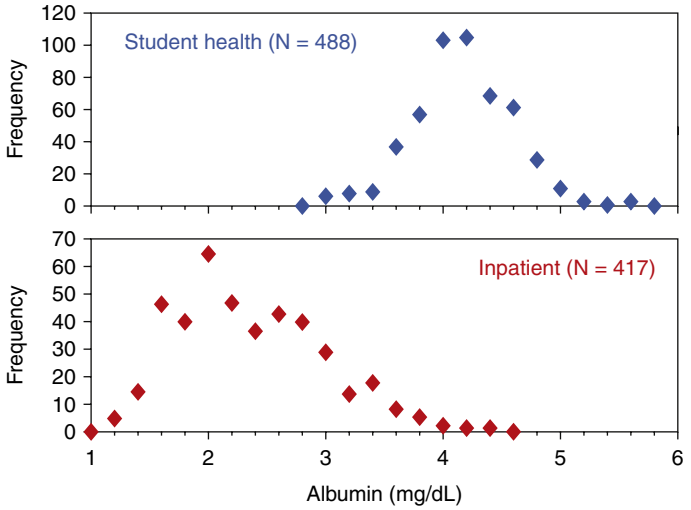

Figure 11.19 Histograms for distribution of sequential patient results for albumin from a student health outpatient clinic and a hospital general medicine inpatient unit.

examined depends on the number of results in the time interval and the relative homogeneity of the clinical conditions represented in the patients. For some analytes, patients may need to be partitioned to obtain subgroups whose results are expected to be homogeneous. Consideration of influences for partitioning include age, gender, ethnicity, and disease conditions. Some approaches have arbitrarily trimmed abnormal results in an attempt to restrict results to more normal health conditions. Trimming approaches must be used with caution because excessive trimming will create an artificial subset of results that may not reflect a method's calibration condition. The median is not influenced by extreme values and is recommended as the most robust estimate for tracking method stability over time based on patient results.

The median, mean, or other statistical parameter for a group of results is tracked over sequential time intervals to monitor measurement procedure performance. Statistical procedures, such as cumulative sum or exponentially weighted or unweighted moving average, are used to monitor trends in measurement procedure calibration status. These approaches can be useful for supplementing traditional surrogate sample–based statistical QC techniques to monitor a measurement procedure's stability and to monitor calibration uniformity between multiple measurement procedures/analyzers in higher-volume settings. However, patient-based monitoring procedures have not been widely adopted because of lack of consensus guidelines for their use and lack of computer support from measurement procedure and laboratory information system suppliers. When computer support is available, patient data–based statistical monitoring is a useful addition to conventional QC measurements, especially for analytes such as sodium and others with low sigma metric performance capability. Moving averages are frequently applied in hematology complete blood count measurement procedures based originally on the Bull's Algorithm approach (Lunetsky et al, 1987).

PROFICIENCY TESTING

Proficiency testing (PT) (also called *external quality assessment*) is a program to evaluate measurement procedure performance by comparison of results versus those of other laboratories for the same set of samples (Miller et al., 2011a). PT providers circulate a set of samples among a group of laboratories. Each laboratory measures the PT samples as if they were patient samples and reports the results for the PT samples to the PT provider for evaluation. The PT provider assigns a target value to the PT samples and determines whether the results for an individual laboratory are in close enough agreement with the target value to be consistent with acceptable measurement procedure performance. PT allows a laboratory to verify that its results are consistent with those of other laboratories and to verify that it is using a measurement procedure in conformance with the manufacturer's specifications.

PT is not available for some analytes because a particular test may be new to the clinical laboratory, is not commonly performed, or because analyte stability makes it difficult to include in a PT material. In these situations, the laboratory is required to use an alternate approach to periodically verify acceptable performance of the measurement procedure. CLSI guideline QMS24 provides information on PT and approaches for verifying measurement procedure performance when formal PT is not available (CLSI, 2016).

NONCOMMUTABILITY OF PROFICIENCY TESTING MATERIALS AND PEER GROUP GRADING

The materials commonly used for PT samples are derived from blood or urine but are altered in the process to manufacture PT samples such that the matrix is modified and the samples do not have the same measurement characteristics as observed for unaltered clinical patient samples (Miller et al., 1993; Ross et al., 1998; Miller, 2003; Miller et al., 2005; Miller et al., 2008; Miller et al., 2011a). In addition, some PT samples—for example, cerebrospinal fluid or blood gas—are prepared as synthetic materials that are not derived from patient fluids. Consequently, many PT samples, as for QC samples, are noncommutable with authentic patient samples. As shown in Figure 11.4, for any type of reference materials, including PT or QC materials, a commutable PT sample will have a relationship between results for the PT sample measured by different measurement procedures that is in close agreement to the relationship observed for results from patient samples. The results for a noncommutable PT sample will have a different relationship in their numeric values among different measurement procedures than would be observed for patient samples.

PT providers organize results into "peer groups" of measurement procedures that represent similar technology expected to have the same result for a noncommutable PT sample. The mean value of the peer group results is used as the target value. Because the peer group mean value may be influenced by a matrix-related bias, that value can be used only to evaluate labs using the same measurement procedure(s) and cannot be used to evaluate laboratories using other measurement procedures or to evaluate whether different measurement procedures agree with one another. Figure 11.20 illustrates the effects of noncommutable PT materials on interpretation of results and demonstrates why "peer group" evaluation is used. In this older but still valid example, pooled patient sera and PT samples were assayed by the duPont Dimension Analyzer and by the Abell-Kendall reference measurement procedure for cholesterol (Naito et al., 1993). The Abell-Kendall method was shown to be unaffected by matrix-induced changes in PT samples (Ellerbe et al., 1990). The patient samples showed excellent agreement between the two measurement procedures (average bias = 0.2%). However, the PT samples had a large negative bias (–9.5%) between the two measurement procedures, caused by a matrix-related bias with the duPont measurement procedure that was not present with the reference measurement procedure (Kroll & Chesler, 1990).

In this example, the duPont measurement procedure was correctly calibrated and produced results for patient samples that were equivalent to and thus traceable to the reference measurement procedure. However, PT results gave an incorrect conclusion regarding the duPont measurement procedure's calibration relationship to the reference measurement procedure. If the duPont measurement procedure's calibration had been erroneously adjusted on the basis of PT results, the results for patient samples would then be incorrect. PT results from the noncommutable materials were useful for evaluating the performance of all laboratories using the duPont measurement procedure because the matrix-related bias was uniform within this peer group. In general, if an individual laboratory's results agree with those of the peer group, the individual laboratory can conclude that its measurement procedure is performing in conformance with the manufacturer's specifications. An individual laboratory depends on the manufacturer to correctly calibrate a clinical laboratory measurement procedure to be traceable to the reference system for an analyte but calibration traceability cannot be evaluated from results for noncommutable PT samples.

REPORTING PROFICIENCY TESTING RESULTS WHEN ONE MEASUREMENT PROCEDURE IS ADJUSTED TO AGREE WITH ANOTHER MEASUREMENT PROCEDURE

It is good laboratory practice (and consistent with CLIA regulations section 493.1281) to adjust the calibration of different measurement procedures for the same analyte used within a health care system so that the results for patient samples are consistent irrespective of which measurement procedure is used. Such harmonization of results is important for uniform use of reference intervals and decision thresholds within a health care system. In this situation, it is important to report PT results such that they can be properly evaluated against the peer group target value. The peer group target value will reflect the measurement procedure calibration established by the measurement procedure manufacturer. For an individual laboratory's PT result to be evaluated against the peer group mean, that individual result must be reported to the PT provider after removing any laboratory applied calibration adjustments so that the reported result is consistent with the manufacturer's nonadjusted calibration.

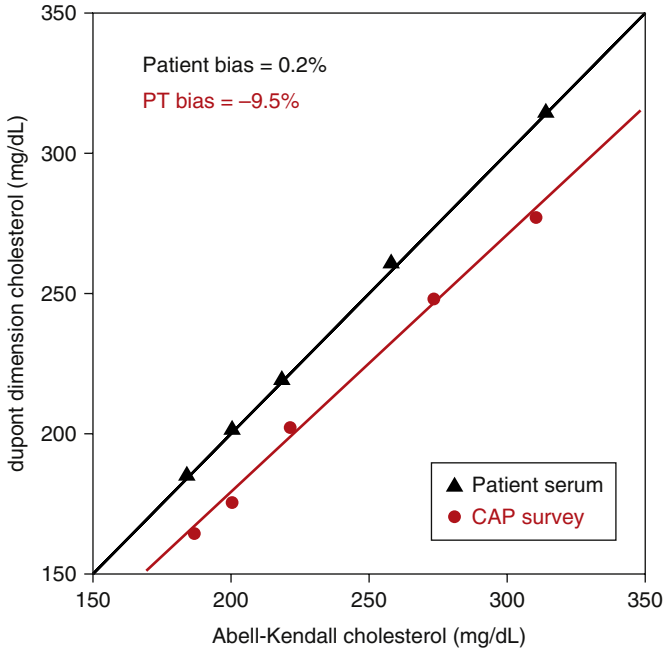

Figure 11.20 Example of noncommutable results between proficiency testing materials and pooled patient samples for two measurement procedures. *CAP,* College of American Pathologists; *PT,* proficiency testing. (Modified from Naito HK, Kwak YS, Hartfiel JL, et al.: Matrix effects on proficiency testing materials: Impact on accuracy of cholesterol measurement in laboratories in the nation's largest hospital system, *Arch Pathol Lab Med*, 117:345–351, 1993; used with permission.)

The most convenient way to remove a calibration adjustment is to first measure PT samples with the laboratory-applied measurement procedure calibration adjustment as would be the usual measurement process for patient samples. After the measurement, mathematically remove the calibration adjustment factor and report the results with any laboratory-applied adjustment factors removed. One should not recalibrate the instrument for the purpose of measuring PT samples because this practice would violate regulations requiring the PT material to be measured in the same manner as patient samples.

For example, a laboratory has performed a patient sample comparison between measurement procedure A used in the main laboratory and measurement procedure B used in a satellite laboratory location. Measurement procedure B consistently gave 10% higher results for patient samples. Measurement procedure B was adjusted to agree with measurement procedure A by applying the adjustment factor 0.9091 (calculated as 1/1.10) to automatically multiply each measurement procedure B result by 0.9091 to lower the reported result by 10%. When PT results from measurement procedure B are reported, it is necessary to remove the 0.9091 factor to allow the reported result to reflect the original manufacturer's calibration and thus to be compared with the peer group mean of results from all laboratories using measurement procedure B. Removing the 0.9091 factor is accomplished by multiplying the reported PT result from measurement procedure B by the factor 1.100 (calculated as 1/0.9091) to increase its numeric value by 10% to the nonadjusted value that was actually measured by the instrument according to the manufacturer's defined calibration procedure. This process allows the PT result measured by measurement procedure B to be appropriately evaluated in comparison with its peer group mean, which will reflect the manufacturer's established calibration. This process permits the PT sample to be measured in the same manner as patient samples and the numeric result reported to the PT provider to reflect the actual measured result using the manufacturer's recommended calibration settings.

INTERPRETING PROFICIENCY TESTING RESULTS

Many countries have regulations (e.g., CLIA in the United States) requiring PT and specifying the evaluation criteria for acceptable performance. When criteria are not set by regulations, the PT provider sets evaluation criteria on the basis of clinically acceptable performance and/or the analytic capability of the measurement procedures in use. PT evaluation criteria are designed to evaluate the total error of a single measurement.

Proficiency testing participant evaluation report
Shipment date: 10/13/2019
Evaluation date: 11/21/2019

Test units peer group	Specimen	Reported result	Mean	SD	N labs	SDI	Limits of acceptability Lower	Upper
Calcium	1	9.6	9.92	0.23	587	–1.4	8.9	11.0
mg/dL	2	8.8	8.86	0.26	592	–0.2	7.8	9.9
Arsenazo	3	7.5	7.65	0.23	587	–0.7	6.6	8.7
dye	4	8.2	8.43	0.23	590	–1.0	7.4	9.5
Analyzer B3	5	10.8	10.87	0.25	589	–0.3	9.8	11.9
Iron	1	190	192.5	7.0	397	–0.4	154	232
µg/dL	2	65	65.0	3.4	394	0.0	51	78
Pyridyl azo	3	74	69.2	3.2	395	+1.5	55	83
dye	4	124	107.9	4.6	395	+3.5	86	130
Analyzer B3	5	277	260.9	8.8	396	+1.8	208	314

Figure 11.21 Example of an external proficiency testing evaluation report sent to a participating laboratory. *N,* Number of laboratories; *SD,* standard deviation; *SDI,* standard deviation interval.

The acceptability limits for PT include bias and imprecision components considered clinically acceptable for an analyte plus other error components that are unique to PT samples, such as between-laboratories variation in calibration; homogeneity of the PT material vials; stability variability in the PT material both in storage/shipping and after reconstitution or opening in the laboratory; and variable matrix–related bias with different lots of reagent within a peer group. Consequently, the acceptability limits for PT samples are frequently larger than what might be expected for clinically acceptable total error for patient samples.

Figure 11.21 is an example of a typical evaluation report sent to a participating laboratory. Each reported result is compared with the mean result for the peer group using the same measurement procedure. The report also includes the SD for the distribution of results in the peer group, the number of laboratories in the peer group, and the SDI (also called a *z-score*), which expresses the reported result as the number of SDs it is from the mean value [SDI = (result – mean) / SD]. The limits of acceptability are shown. Acceptability criteria may be a number of standard deviations from the mean value, a fixed percent from the mean value, or a fixed concentration from the mean value. In Figure 11.21, calcium acceptability criteria are ±1 mg/dL from the mean value, and iron criteria are ±20% from the mean value.

Peer group evaluation allows a laboratory to verify that it is using a measurement procedure according to the manufacturer's specifications and is producing patient results that are consistent with those of other laboratories using the same measurement procedure (Miller et al., 2011a). In Figure 11.21, the calcium results are in close agreement with the peer group mean (SDI ranges from –0.2 to –1.4). However, the iron results show greater variability, with one result +3.5 SDI. Although that iron result is within the acceptability criteria, it is good laboratory practice to investigate the measurement procedure, as discussed next.

If an unacceptable PT result is identified, the method must be investigated for possible causes and any necessary corrective action taken. Even when a PT result is within acceptability criteria, it is good laboratory practice to investigate PT results that are more than approximately 2.5 SDI from the peer group mean. When the SDI is 2.5, there is only a 0.6% probability that the result will be within the expected distribution for the peer group; consequently, there is a reasonable probability that a measurement procedure problem may exist. In addition, PT results that have been near the failure limits for more than one PT event, even if the results have passed the PT acceptance criteria, should initiate a review of systematic problems with the measurement procedure. These practices support identification of potential problems before they progress to more serious situations. When results are investigated, a limitation of SD-based grading criteria should be considered. Very precise methods may have a very small SD, and a result may be outside an SD limit when the magnitude in reporting units is small and may be of no concern regarding using results for clinical care decisions.

Common causes for PT failure are listed in Box 11.1. Incorrect handling and reporting are usually unique to PT events and may not reflect the same process used in the laboratory for patient samples. Nonetheless, these situations reflect attention to detail, which is a necessary attribute for quality laboratory testing. Occasionally, the PT material may have a defect that causes it to perform inappropriately for all or a subgroup of measurement procedures. In this case, the PT provider should identify the situation and not grade participants for that sample.

PT evaluations are usually received several weeks after the date of testing. Consequently, investigation of unacceptable results requiring review of quality control, reagent, calibration, and maintenance records for the date of the test and the preceding several weeks or months is necessary. It is common practice to save any remaining PT samples to investigate an unacceptable result. Care must be taken to store the residual PT samples to preserve the stability of the analytes. In some cases, the analyte will not be stable for storage. In addition, when remeasuring stored samples, degradation may have occurred during storage or possibly before storage while still being used in the laboratory for the PT event, which may affect any remeasured value. If review of these records suggests a stable operating condition and review of the PT material handling and documentation does not identify a cause for the erroneous PT result, it may be concluded that the PT failure was a random event. Investigative steps, data reviewed, and conclusions from the review of the unacceptable PT result must be documented in a written report and reviewed by the laboratory director.

Limitations in Interpreting Proficiency Testing Results

PT providers also prepare a summary report, which includes the mean and SD for all peer groups represented by the participants' results. Similar reports are available from interlaboratory QC programs. Summary reports are very useful but must be interpreted with consideration of the limitations of noncommutable samples. The peer group mean and SD are useful for evaluating the uniformity of results between laboratories using the same measurement procedure, to confirm that an individual laboratory is using the measurement procedure correctly as designed by the manufacturer, and to evaluate the consistency of an individual laboratory's measurement procedure performance relative to the peer group over time intervals from one PT event to the next (trend monitoring). Summary information also allows evaluation of the imprecision of various measurement procedure groups, and the number of users in each peer group reveals which measurement procedures are commonly used.

The frequent occurrence of noncommutability of PT materials makes it incorrect to use PT summary reports to compare an individual laboratory's result with the peer group mean for another measurement procedure group, to compare measurement procedure peer group mean values to each other, or to compare an individual measurement procedure peer group value to a value from a reference measurement procedure. The noncommutability limitation prevents PT (or QC) results from being used to infer agreement, or lack of agreement, for patient results among different measurement procedures for the same analyte.

QC material manufacturers may provide a data analysis service that compares results from different laboratories using the same QC material by calculating group statistics for performance evaluation. As with PT evaluation, this type of interlaboratory QC data analysis allows a laboratory to verify that it is producing QC results that are consistent with those of other laboratories using the same measurement procedure. This information

BOX 11.1

Classification of Potential Problems Identified When Investigating Unacceptable PT/EQA Results[a]

1. Clerical errors:
   - Incorrectly transcribed PT result from the instrument readout to the report form
   - The PT sample was mislabeled in the laboratory
   - Incorrect instrument or method was reported on the results submission form
   - Incorrect units were reported
   - Decimal point was misplaced
2. Methodological problems:
   - Inadequate standard operating procedure
   - Problem with manufacture or preparation of reagents or calibrators (e.g., unstable)
   - Lot-to-lot variation in reagents or calibrators
   - Incorrect value assignment of calibrators
   - Method lacks adequate specificity for the measurand
   - Method lacks adequate sensitivity to measure the concentration
   - Carryover from a previous sample
   - Inadequate QC procedures used
3. Equipment problems:
   - Obstruction of instrument tubing/orifice by clot
   - Misalignment of instrument probes
   - Incorrect instrument data processing functions
   - Incorrect instrument setting
   - Automatic pipettor not calibrated to acceptable precision and accuracy
   - Equipment component malfunction (e.g., light source, membrane, fluidics, detector)
   - Incorrect instrument conditions (e.g., water quality, surrounding temperature)
   - Instrument maintenance not performed appropriately
4. Technical problems caused by personnel errors:
   - Did not operate equipment correctly or did not conform to method standard operating procedure
   - Incorrect storage, preparation, or handling of reagents or calibrators
   - Delay causing evaporation or deterioration of the PT sample
   - Failure to follow recommended instrument function checks or maintenance
   - Pipetting or dilution error
   - Calculation error
   - Misinterpretation of test result
5. A problem with the PT material, such as:
   - Incorrect storage, preparation, or handling of PT materials
   - Differences between PT samples and patient samples (e.g., matrix, additives, stabilizers)
   - Sample deteriorated in transit or during laboratory storage
   - Sample had weak or borderline reaction
   - Sample contained interfering factors (that may be method-specific)
   - Sample was not homogeneous among vials

[a]This classification scheme assists in developing an appropriate corrective action plan. Reprinted with permission from Miller WG, Jones GRD, Horowitz GL, et al.: Proficiency testing/external quality assessment: Current challenges and future directions, *Clin Chem,* 57:1670–80, 2011.

EQA, External quality assurance; *PT,* proficiency testing.

can be helpful for troubleshooting measurement procedure issues and for assessing performance of a new measurement procedure being introduced to a laboratory.

ACCURACY-BASED PROFICIENCY TESTING PROGRAMS WITH COMMUTABLE SAMPLES

The preferred sample for PT is one that is commutable with patient samples for use with all of the measurement procedures in a PT event (Miller et al., 2011a). Commutable samples are typically prepared by pooling clinical patient samples with minimal processing or additives to avoid any alteration of the sample matrix. To achieve samples with abnormal values for analytes, donors are identified with known pathologic conditions or blood and serum units from a general donor population can be prescreened for selected analytes. Supplementing patient samples or pools with purified analytes may be acceptable in some cases but requires assessment of commutability of the final material (Cobbaert et al., 2012; Shinohara et al., 2016). Commutable PT samples are more difficult to prepare and are more expensive than the more commonly used noncommutable samples. When commutable PT samples can be prepared, the results reflect what would be expected if patient samples were sent to each of the different laboratories. Thus, agreement among different laboratories and different measurement procedures (called *harmonization*) can be evaluated. The agreement between an individual laboratory result and a reference measurement result (accuracy) and the agreement between a measurement procedure group mean value and the reference measurement result (called *trueness*) can be evaluated when a reference measurement procedure is available for an analyte.

For example, the College of American Pathologists glycohemoglobin survey for many years has used pooled, freshly collected whole blood from both normal and diabetic donors. The target values for the pooled blood are assigned by reference measurement procedures for hemoglobin A_{1c}. In this survey, the accuracy of individual laboratory results and the trueness of measurement procedure group means versus the reference measurement procedure values can be evaluated because the PT samples are commutable with patient samples. Measurement procedure trueness can be used by the respective measurement procedure manufacturers to monitor the effectiveness of their calibration processes.

Preparing commutable materials for use in large PT programs has been challenging. However, use of commutable materials adds substantial value to the information obtained from the results (Miller et al., 2011a). Procedures have been developed to validate the commutability of QC, PT, and reference materials (Miller et al., 2018; Nilsson et al., 2018; Budd et al., 2018).

QUALITY MANAGEMENT

Quality management (QM) refers to the overall process used to ensure that laboratory results meet the requirements for health care services to patients. The components of a QM system shown in Figure 11.5 were derived from the CLSI document QMS01, *A Quality Management System Model for Laboratory Services* (CLSI, 2019) and are consistent with the International Organization for Standardization (ISO) document 15189:2012, *Medical Laboratories—Requirements for Quality and Competence* (ISO, 2012). Laboratories are required to develop procedures to monitor and ensure quality in all aspects of laboratory services. A QM program is an accreditation requirement, and good documentation of the quality indicators (also called *metrics*), the review process, and the improvements made are necessary.

Statistical QC and PT, covered in detail earlier in this chapter, are two important components of a QM program that address measurement procedures. Quality indicators related to QC activities may be evaluated as part of monitoring the performance of a measurement procedure. The following may be useful indicators of measurement procedure performance:

- Frequency of QC alerts
- Frequency of recalibration based on QC alerts
- Number of reagent changes due to QC alerts
- Number of times controls were repeated because of QC alerts
- Frequency of unscheduled maintenance due to QC alerts
- Number of patient samples repeated based on QC alerts
- Frequency that patient samples are repeated based on QC alerts
- Number of patient results corrected

Directly related to the quality of test results are preanalytic components such as patient preparation; sample collection, transportation, storage, and preparation for testing; and postanalytic components such as result reporting, critical value notification, and provision of interpretive information. All of the quality system essentials listed in Figure 11.5 are important to ensure that quality laboratory results are available for patient care. In some cases, the quality requirements extend outside the laboratory and require cooperation with health care partners who order laboratory tests and act on the results.

A QM program defines data-based quality indicators or metrics that are monitored at regular recurring intervals to provide information on the adequacy of important influences on laboratory quality. The CLSI document QMS01 includes an appendix with examples of quality indicators for all of the quality system essentials. An International Federation of Clinical Chemistry (IFCC) working group has also recommended a number of specific quality indicators for laboratory testing (Sciacovelli, 2017).

A laboratory QM committee oversees the development of quality indicators and their regular review and initiates quality improvement actions in response to quality indicators that indicate a need for improved performance in a particular aspect of laboratory service. A QM committee is typically chaired by a laboratory director or section director and includes senior-level representation from all service areas, including the laboratory information system. Monthly meetings to review data collected from the previous month are typical. However, automation of data management can make some quality indicators available close to real time for more immediate monitoring and intervention. For example, turnaround time from specimen receipt to result reporting can be monitored continuously with a scrolling computer display report to assist medical technologists in tracking stat requests.

Table 11.7 provides a list of some typical quality indicator metrics that could be included in a QM program. In addition to the metrics, thresholds for acceptable values are defined for most metrics. Thresholds are established on the basis of what is considered good laboratory practice and may be different in different situations. Quality indicators that meet thresholds confirm that the laboratory is meeting its quality goals for those service requirements. Quality indicators that exceed thresholds require analysis and a plan for corrective and preventive action. The example thresholds in Table 11.7 are illustrative and should not be taken as recommendations. It is not possible to have zero mistakes in laboratory service; consequently, thresholds need to be realistic and can be changed as quality improvement programs are applied to reduce and prevent errors of various types. The total number of observations examined by a metric should be recorded along with the data for a given reporting interval.

The metrics should be reported in a manner that allows trends to be identified—for example, by showing data for 6 or more months on a page. Graphic presentation is very effective to monitor trends and can easily include 1 or more years on a single graph. Many quality indicators are useful to track indefinitely to document that laboratory service continues to meet performance expectations and to have an alert mechanism if a change in the environment has adversely affected laboratory service. Data cannot be collected for all possible quality indicators; the QM committee needs to determine which aspects of laboratory performance are most critical or in need of improvement and should develop suitable metrics to drive a quality improvement process. Specific interventions should be documented with a written report that describes the quality issue, the data used to understand the issue, the improvements made, and the data that document the effectiveness of the improvement.

TABLE 11.7

Examples of Quality Indicators (Metrics)

Quality Indicator (Metric)	Threshold	Total Number Reviewed	Example Data	Analysis and Action Plan
Result Reporting				
Gram stain correlation with culture (% disagreement)	≤1%	1513	0%	
Blood culture contamination	≤3%	2468	2.7%	
Percent bone marrow cases reviewed in consensus conference	≥10%	146	28.8%	
Number of bone marrow cases with disagreements	2	146	0	
PT reports; number flagged unacceptable (list by laboratory section)	0			
POCT: Glucose meters, QC failures	≤3%	9058	2.3%	
POCT: Glucose meter, critical value not confirmed by repeating on meter	≤5%	439	2.5%	
Turnaround times in minutes for 90% completed (shown as in-laboratory/total); examples follow, recommend for all applicable work shifts; threshold is for in-laboratory turnaround time				
Potassium, stat, day shift	45 min	1477	47/91	Reviewed, no action indicated
Troponin I, ED, stat, day shift	60 min	476	58/121	
Hb, stat, day shift	45 min	520	40/81	
PT, stat, day shift	60 min	528	41/94	
Urinalysis pH, stat, day shift	60 min	240	56/106	
Bacterial vaginosis, ED, Gram stains	60 min	231	40/91	
Critical value callback delay; minutes for 90% completed; examples shown				
Critical value delay, hemoglobin, inpatient	30 min	215	14	
Critical values not called Hematology	0	2474	4	SOP reviewed with medical technologist
Result corrections (list by laboratory sections)				
Specimens rejected/corrected at log-in (list by receiving location and type of problem; examples shown)				
Lost/not received	<5	109,851	5	
Incomplete label or form	<20	109,851	25	
Hemolyzed	<50	109,851	19	
Clotted	<100	109,851	289	
QNS	<100	109,851	204	
Exceeds time limit	<20	109,851	8	
Improper collection, container, specimen	<20	109,851	32	
Improperly ordered	<20	109,851	16	
Interfering substance		109,851	25	
Mislabeled specimens (identified by delta check or by notification from clinical staff; list by receiving location)	<20	109,851	83	
Blood bank: Emergency units not accounted for in ED and OR	0	35	0	
Sweat chloride QNS specimens, %	≤5%	18	0%	

Continued

TABLE 11.7 —cont'd

Quality Indicator (Metric)	Threshold	Total Number Reviewed	Example Data	Analysis and Action Plan
Customer Satisfaction				
Client services: % calls lost	≤5%	5932	7%	See below
Client services: Calls answered within 60 seconds	≥90%	5932	87%	Consider if additional staff needed
Patient safety incident reports from clinical units (number received/number for which the laboratory was responsible)	0		10/7	See attached report (each incident has an individual review)
Personnel				
Safety (number of incidents)				
Infectious agent exposure	0		1	See attached report
Chemical exposure	0		0	
Job-related injury/illness	0		2	See attached report
On-call utilization (number of instances a person was called in; list by laboratory section)				
Overtime utilization (hours paid; list by laboratory section)				
Vacancies and proportion of staff in training status (graph by laboratory section)				
Continuing education (total hours CE received/number staff receiving CE/total number staff); list by laboratory section)				

CE, Continuing education; *ED*, emergency department; *Hb*, hemoglobin; *OR*, operating room; *POCT*, point-of-care testing; PT, prothrombin time; *QC*, quality control; *QNS*, quantity not sufficient; *SOP*, standard operating procedure.

SELECTED REFERENCES

Badrick T, Bietenbeck A, Cervinski MA, et al.: Patient-based real-time quality control: review and recommendations, *Clin Chem* 65:962–971, 2019.

Review of the strengths and limitations of patient sample–based statistical control procedures.

CLSI: *Laboratory quality control based on risk management; approved guideline EP23-A*, Wayne, PA, 2011, Clinical and Laboratory Standards Institute.

Guidance on developing a quality control plan based on assessment and management of risk of harm to a patient if an erroneous result was reported.

CLSI: *Statistical quality control for quantitative measurements: principles and definitions; approved guideline C24-A4*, Wayne, PA, 2015a, Clinical and Laboratory Standards Institute.

Consensus document describing the principles and implementation guidelines for a statistical quality control system.

Department of Health and Human Services: 42: CFR Part 493, Medicare, Medicaid, and CLIA programs: laboratory requirements relating to quality systems and certain personnel qualifications; final rule, *Fed Regist* 68:3639–3714, 2003.

Clinical Laboratory Improvement Act of 1988; final rule containing the regulatory requirements for quality practices in laboratories in the United States.

Lunetzky ES, George MS, Cembrowsky GS: Performance characteristics of Bull's multirule algorithm for the quality control of multichannel hematology analyzers Am J Clin Path 88:634-638, 1987.

Miller WG, Jones GRD, Horowitz GL, et al.: Proficiency testing/external quality assessment: current challenges and future directions, *Clin Chem* 57:1670–1680, 2011a.

Review of proficiency testing, including the value of commutable PT materials and the limitations when using noncommutable PT materials.

Miller WG, Myers GL: Commutability still matters, *Clin Chem* 59:1291–1293, 2013.

Editorial describing the importance of commutable reference materials and the errors that can occur when commutability is ignored.

Miller WG, Tate JR, Barth JH, et al.: Harmonization: the sample, the measurement, and the report, *Ann Lab Med* 34:187–197, 2014.

Review of calibration traceability, including commutability of reference materials and pre- and postmeasurement considerations.

Miller WG, Schimmel H, Rej R, et al.: IFCC working group recommendations for assessing commutability Part 1: general experimental design, *Clin Chem* 64:447–454, 2018.

Recommendations for experimental design for assessing commutability of reference materials, PT materials and QC materials.

Yundt-Pacheco J, Parvin CA: Validating the performance of QC procedures, *Clin Lab Med* 33:75–88, 2013.

Review of the QC process, including guidance on acceptance criteria and frequency to assay QC materials with consideration of risk of harm to a patient if an erroneous result was reported.

Access the complete reference list online at Elsevier eBooks for Practicing Clinicians.

REFERENCES

Aarsand AK, Rorass T, Sandberg S: Biological variation—reliable data is essential, *Clin Chem Lab Med* 53:153–4, 2015.

Aarsand AK, Rorass T, Fernandez-Calle P, et al.: The biological variation data critical Appraisal checklist: a standard for evaluating studies on biological variation, *Clin Chem* 64:501–514, 2018.

Budd JR, Weykamp C, Rej R, et al.: IFCC working group recommendations for assessing commutability Part 3: using the calibration effectiveness of a reference Material, *Clin Chem* 64:465–474, 2018.

Carobene A, Braga F, Roraas T, et al.: A systematic review of data on biological variation for alanine aminotransferase, aspartate aminotransferase and g-glutamyltransferase, *Clin Chem Lab Med* 51:1997–2007, 2013.

Cembrowski GS, Chandler EP, Westgard JO: Assessment of "average of normals" quality control procedures and guidelines for implementation, *Am J Clin Pathol* 81:492–499, 1984.

CLSI: *Verification of Comparability of patient results within one Healthcare system; approved guideline EP31-A-IR*, Wayne, PA, 2012, Clinical and Laboratory Standards Institute.

CLSI: *User evaluation of between-reagent lot variation; approved guideline EP26-A*, Wayne, PA, 2013, Clinical and Laboratory Standards Institute.

CLSI: *Evaluation of precision of quantitative measurement procedures; approved guideline EP05-A3*, Wayne, PA, 2014, Clinical and Laboratory Standards Institute.

CLSI: *Delta checks; approved guideline EP33-A*, Wayne, PA, 2015b, Clinical and Laboratory Standards Institute.

CLSI: *Using proficiency testing and alternative assessment to improve medical laboratory quality*, 3rd Ed, QMS24, Wayne, PA, 2016, Clinical and Laboratory Standards Institute.

CLSI: *A quality management system model for laboratory services*, 5th ed, CLSI guideline QMS01, Wayne, PA, 2019, Clinical and Laboratory Standards Institute.

Cobbaert C, et al.: Systematic monitoring of standardization and harmonization status with commutable EQA-samples-five year experience from The Netherlands, *Clin Chim Acta* 414:234–240, 2012.

Cornbleet PJ, Gochman N: Incorrect least-squares regression coefficients in method comparison analysis, *Clin Chem* 25:432–438, 1979.

Department of Health and Human Services: *Centers for Medicare & Medicaid services, IQCP announcement letter for CLIA CoC and PPM laboratories*, September 30 2013, http://www.cms.gov/Regulations-and-Guidance/Legislation/CLIA/Individualized_Quality_Control_Plan_IQCP.html. Accessed August 17, 2019.

EFLM, European Federation of Clinical Chemistry and Laboratory Medicine, Biological Variation Database, https://biologicalvariation.eu/, Accessed August 17, 2019.

Ellerbe P, Myers GL, Cooper GR, et al.: Comparison of results for cholesterol in human serum obtained by the reference method and by the definitive method of the National Reference System for cholesterol, *Clin Chem* 36:370–375, 1990.

Franzini C, Ceriotti F: Impact of reference materials on accuracy in clinical chemistry, *Clin Biochem* 31:449–457, 1998.

Fraser CG: Biological variation: from principles to practice, *American Association for Clinical Chemistry*, 2001, AACC Press, ISBN 1-890883-49-2.

ISO 15189:2012: medical laboratories—requirements for quality and competence, Geneva, Switzerland, 2012, ISO.

ISO 17511:2020: in vitro diagnostic medical devices—requirements for establishing metrological traceability of values assigned to calibrators, control materials and human samples, Geneva, Switzerland, 2020, ISO.

Kazmierczak SC: Laboratory quality control: using patient data to assess analytical performance, *Clin Chem Lab Med* 41:617–627, 2003.

Kroll MH, Chesler R: Effect of serum lyophilization on the rate constants of enzymatic methods for measuring cholesterol, *Clin Chem* 36:534–537, 1990.

Levey S, Jennings ER: The use of control charts in the clinical laboratory, *Am J Clin Pathol* 20:1059–1066, 1950.

Linnet K: Choosing quality-control systems to detect maximum clinically allowable errors, *Clin Chem* 35:284–288, 1989.

Linnet K: Evaluation of regression procedures for methods comparison studies, *Clin Chem* 39:424–432, 1993.

Lund F, Peterson PH, Fraser CG, et al.: Calculation of limits for significant bidirectional changes in two or more serial results of a biomarker based on a computer simulation model, *Ann Clin Biochem* 52:434–440, 2015.

Martin RF: General Deming regression for estimating systematic bias and its confidence interval in method-comparison studies, *Clin Chem* 46:100–104, 2000.

Miller WG: Specimen materials, target values and commutability for external quality assessment (proficiency testing) schemes, *Clin Chim Acta* 327:25–37, 2003.

Miller WG, Erek A, Cunningham TD, et al.: Commutability limitations influence quality control results with different reagent lots, *Clin Chem* 57:76–83, 2011b.

Miller WG, Kaufman H, McLendon WW: College of American Pathologists Conference XXIII: matrix effects and accuracy assessment in clinical chemistry, *Arch Pathol Lab Med* 117:343–436, 1993.

Miller WG, Myers GL, Ashwood ER, et al.: Creatinine measurement: State of the art in accuracy and inter-laboratory harmonization, *Arch Pathol Lab Med* 129:297–304, 2005.

Miller WG, Myers GL, Ashwood ER, et al.: State of the art in trueness and interlaboratory harmonization for 10 analytes in general clinical chemistry, *Arch Pathol Lab Med* 132:838–846, 2008.

Myers GL, Miller WG, Coresh J, et al.: Recommendations for improving serum creatinine measurement: a report from the laboratory working group of the national kidney disease education program, *Clin Chem* 52:5–18, 2006.

Naito HK, Kwak YS, Hartfiel JL, et al.: Matrix effects on proficiency testing materials: impact on accuracy of cholesterol measurement in laboratories in the nation's largest hospital system, *Arch Pathol Lab Med* 117:345–351, 1993.

National Institutes of health: recommendations for improving cholesterol measurement: a report from the Laboratory Standardization Panel of the National Cholesterol Education Program, Bethesda, MD, 1990, *National Institutes of Health*. NIH publication no, pp 90–2964.

Ng D, Poliyo FA, Cervinski MA: Optimization of a moving averages program using a simulated Annealing algorithm: the goal is to monitor the process not the patients, *Clin Chem* 62:1361–1371, 2016.

Nilsson G, Budd JR, Greenberg N, et al.: IFCC working group recommendations for assessing commutability Part 2: using the difference in bias between a reference material and clinical samples, *Clin Chem* 64:455–464, 2018.

Oosterhuis WP: Gross overestimation of total allowable error based on biological variation, *Clin Chem* 57:1334–1336, 2011.

Panteghini M, Sandberg S: Defining analytical performance specifications 15 years after the Stockholm conference, *Clin Chem Lab Med* 53:829–832, 2015.

Parvin CA: Quality-control (QC) performance measures and the QC planning process, *Clin Chem* 43:602–607, 1997.

Parvin CA: Assessing the impact of the frequency of quality control testing on the quality of reported patient results, *Clin Chem* 54:2049–2054, 2008.

Parvin CA: Planning statistical quality control to minimize patient risk: it's about time, *Clin Chem* 64:249–250, 2018.

Parvin CA, Gronowski AM: Effect of analytical run length on quality-control (QC) performance and the QC planning process, *Clin Chem* 43:2149–2154, 1997.

Perich C, Minchinela J, Ricos C, et al.: Biological variation database: Structure and criteria used for generation and update, *Clin Chem Lab Med* 53:399–405, 2015.

Roraas T, Petersen PH, Sandberg S: Confidence intervals and power calculations for within-person biological variation: effect of analytical imprecision, number of replicates, number of samples, and number of individuals, *Clin Chem* 58:1306–1313, 2012.

Ross JW, Miller WG, Myers GL, et al.: The accuracy of laboratory measurements in clinical chemistry—a study of 11 routine chemistry analytes in the College of American Pathologists chemistry survey with fresh frozen serum, definitive methods, and reference methods, *Arch Pathol Lab Med* 122:587–608, 1998.

Ryan TP: *Statistical methods for quality control*, New York, 1989, John Wiley & Sons.

Shewhart WA: *Economic control of quality of manufactured product*, New York, 1931, Van Nostrand.

Sciacovelli L, Panteghini M, Lippi G, et al.: Defining a roadmap for harmonizing quality indicators in Laboratory Medicine: a consensus statement on behalf of the IFCC working group "laboratory error and patient Safety" and EFLM Task and nish group "performance specifications for the extra-analytical phases, *Clin Chem Lab Med* 55:1478–1488, 2017.

Shinohara K, Hamasaki N, Takagi Y, et al.: Multianalyte Conventional Reference Material (MacRM): a useful tool for nationwide standardization of laboratory measurements for medical care—a model study in Japan, *Clin Chem* 62:392–406, 2016.

Smith FA, Kroft SH: Exponentially adjusted moving mean procedure for quality control—an optimized patient sample control procedure, *Am J Clin Pathol* 105:44–51, 1996.

Thienpont LM, Stockl D, Friedecky B, et al.: Trueness verification in European external quality assessment schemes: time to care about the quality of the samples, *Scand J Clin Lab Invest* 63:195–201, 2003.

Vesper HW, Miller WG, Myers GL: Reference materials and commutability, *Clin Biochem Rev* 28:139–147, 2007.

Vesper HW, Thienpont LM: Traceability in laboratory medicine, *Clin Chem* 55:1067–1075, 2009.

Westgard JO, Barry PL, Hunt MR: A multi-rule Shewhart chart for quality control in clinical chemistry, *Clin Chem* 27:493–501, 1981.

Westgard JO, Groth T: Power functions for statistical control rules, *Clin Chem* 25:863–869, 1979.

Westgard JO, Smith FA, Mountain PJ, et al.: Design and assessment of average of normals (AON) patient data algorithms to maximize run lengths for automatic process control, *Clin Chem* 42:1683–1688, 1996.

Ye JJ, Ingels SC, Parvin CA: Performance evaluation and planning for patient-based quality control procedures, *Am J Clin Pathol* 113:240–248, 2000.

CHAPTER 12

CLINICAL LABORATORY INFORMATICS

Ulysses G.J. Balis

FUNDAMENTALS OF CLINICAL INFORMATICS, 150
Definition, 151
Brief History, 151
DATABASE FUNDAMENTALS: DESIGN, IMPLEMENTATION, AND MAINTENANCE, 151
Key Database Concepts, 151
Key Database Structures, 152
Data Normalization and Single Source of Truth, 153
Common Database Operations, 153
Transformational Operations, 153
Database Insertions, 153
Database Updates, 153
Database Deletions, 154
POSITIVE PATIENT AND SPECIMEN IDENTIFICATION AND BARCODING, 154
LABORATORY INFORMATION SYSTEMS, 155
LIS System Selection, 155
Specialized Lab Information System Modules, 156
ARTIFICIAL INTELLIGENCE AND MACHINE LEARNING, 157
GLOSSARY, 159
SELECTED REFERENCES, 161

KEY POINTS

- The practice of Pathology Informatics/Clinical Laboratory Informatics is central to all aspects of data stewardship in the clinical laboratory.
- Fundamental knowledge of database technology and database principles is critical to understanding key aspects of laboratory information system (LIS) operation.
- The LIS is an integral element of the larger enterprise-wide portfolio of information technology solutions that may be rendered as either a stand-alone vendor solution or as an integral module of the larger integrated electronic health record (EHR).
- The LIS supports laboratory workflow and automation in all phases of the generation of clinical results (preanalytical, analytical and postanalytical).
- Data interoperability is an increasingly important aspect of data stewardship and is supported by a growing ecosystem of standards.
- Informatics will increasingly play an important role in data analysis and stewardship as machine learning techniques and solutions are incrementally applied to primary laboratory results, creating derivatized versions of base knowledge, representing incremental and medically actionable knowledge.

Clinical laboratory informatics is a subdiscipline of clinical informatics, which encompasses all of the subject matter of informatics in the general discipline of clinical informatics, and a potpourri of unique topics distinct to the fields of clinical laboratory medicine. This growing assemblage of core material and specialized niche topics poses a challenge for the generalist pathologist or laboratorian to effectively master and utilize in daily practice. Owing to this reality, it is increasingly likely to find pathology groups, both in academia and community practice, making use of specifically trained pathology informaticists who may devote a fraction or even the entirety of their time to this pursuit.

Clinical laboratory informatics encompasses many areas of expertise, with not all of them being within information technology fields per se. The most important aspects of informatics are in many cases nontechnical, with examples being the application of effective interpersonal communications, sound management strategies, robust project management skills, and user experience-centered design. When adding these to the litany of technical subspecialties within pathology informatics, it can be easily seen that the breadth and depth of possible expertise in this area is astonishing, making the case for a multidisciplinary team approach in even midsized projects (noting that it is becoming increasingly unreasonable to expect that any one individual would possess all of the skills and domain expertise typically required for the successful execution of a typical contemporary solution).

Given the significant range of pathology informatics topics and the larger range of clinical informatics topics, this chapter will make selective use of the general framework provided by the American Medical Informatics Association's "Clinical informatics subspecialty delineation of practice" document (Silverman et al., 2019), The material contained within this chapter constitutes a reasonable contemporary survey of the areas of expertise and topics that pathology informaticists might typically encounter during their daily activities. In topic areas in which substantial additional domain knowledge is available but exceeds the level of coverage provided by this chapter, appropriate references are provided, along with mention of the significantly expanded knowledge base that can be perused and assimilated as required.

FUNDAMENTALS OF CLINICAL INFORMATICS

While it is true that clinical informatics—and, specifically, the collective areas of pathology informatics—makes extensive use of information technology, it should be emphasized that these clinical fields are distinct and separate from computer science. They should be viewed from the more holistic perspective of supporting the underlying collective needs of health care in general and the clinical laboratory specifically to generate, analyze, disseminate, and curate primary data. In so doing, raw information is transformed into medically actionable knowledge and wisdom. As such, the practice of clinical informatics and pathology informatics exists at the crossroads of many knowledge domains, including information technology, project management, data sciences and analytics, data curation, change management, and, of course, laboratory medicine. In recognition of this broad scope and vast sets of requisite skills required to practice pathology informatics effectively, it should be immediately seen that to be maximally effective, a team-based, multidisciplinary approach is highly desirable, if not absolutely required. Whereas many, if not most, medical specialties define the value proposition they provide to the overall health care system in terms of direct clinical interaction with patients and procedurally based activities (often carried out in direct contact with the patient), the practice of laboratory medicine fundamentally differs in that the value-added contribution is information itself (and, increasingly, knowledge), in the form of data products that are shared with clinician colleagues and, by proxy, their patients as well. As the information that the clinical laboratory generates is increasingly, if not universally, now in the form of multiple forms of digital communication channels to various downstream information repositories, not the least of which is a health enterprise's central electronic health record (EHR), it is incumbent on practitioners of laboratory medicine to have definitive command of the constitutive technologies and methodologies that enable effective data curation, transformation, interrogation, and dissemination. This expectation and its associated requirements will only grow in importance as the data that contemporary clinical laboratories now generate increases in both scale and complexity. Most of the core concepts of clinical laboratory informatics covered in this chapter are covered in much greater detail in the Pantanowitz text (Pantanowitz et al., 2012). Note that anatomic pathology informatics topics as covered in that text are generally beyond the scope of this chapter.

DEFINITION

As stated by the Association for Pathology Informatics (https://www.pathologyinformatics.org/about_api.php),

"Pathology Informatics involves collecting, examining, reporting, and storing large complex sets of data derived from tests performed in clinical laboratories, anatomic pathology laboratories, or research laboratories to improve patient care and enhance our understanding of disease-related processes. Pathology Informaticians seek to continuously improve existing laboratory information technology and enhance the value of existing laboratory test data, and develop computational algorithms and models aimed at deriving clinical value from new data sources."

This definition is significant in that it underscores the major role of pathology informatics in transforming raw, laboratory-derived primary data into medically actionable knowledge and, in so doing, creating additional clinical utility. As has been borne out in recent years by the explosive growth of machine learning and general artificial intelligence techniques as applied to laboratory medicine data, it is now well recognized that the primary data generated by the various clinical laboratory sections contains extensive incremental data in encoded form that can be accessed only by advanced analytical and data sciences methodologies. The application of such approaches to primary data as generated by the clinical laboratory is fully within the purview of pathology informatics and its practitioners.

BRIEF HISTORY

With the advent of commercially available computers, as early as the 1950s, pioneers such as Homer Warner (Seising et al., 2013) and Octo Barnett (Celebrating G. Octo Barnett, 2020) systematically explored the utility of applying computational and analytical methodologies on health care data sets and workflow models. Up to that point, analysis of such data had been entirely dependent on manual approaches and clerically dependent data entry methods. Besides the obvious benefit of reduction in transcription-based error rates (which can be uniformly seen to be typically between 1.5% and 3%, at minimum), there emerged an expansive range of possibilities for value-added use of primary data once it was properly registered and/or logged in electronic form. In time, this recording process of primary data came to be known as database technology. With its emergence came an expansive portfolio of derivative uses and technologies that continue to expand into the present era.

Commensurate with these early works were attempts to develop both so-called "expert systems" (which were programs that could assist in the rendering of diagnoses and treatment plans, given input data) and EHRs. In their earliest forms, these efforts were only partial successes in terms of both functionality and adoption, underscoring the actual level of complexity inherent in appropriately capturing and curating health information data in surgical/anatomic pathology and laboratory medicine data specifically. Creating applications mirroring actual laboratory workflow has been the critically needed elixir that enabled the development of solutions that truly support productivity and safety. This goal remains one of the singular challenges in the continuous development of new generations of software solutions that support the ever-increasing complexity of the contemporary testing laboratory environment.

DATABASE FUNDAMENTALS: DESIGN, IMPLEMENTATION, AND MAINTENANCE

No informatics chapter would be complete without at least a cursory introduction and coverage of this important topic, as database technology is a central enabling component of any contemporary laboratory information system. At its simplest possible definition, a database is a program (or assembly of programs, recognizing modern distributed software architecture) that allows for the aggregation, storage, curation, retrieval, transformation, and dissemination of primary data, as well as derivatized and extracted forms of this data. A database serves the very important purpose of adding a critical layer of *provenance* to every accumulated data element that is housed within it such that both its source and level of confidence concerning its veracity (e.g., patient identity, documentation of results validation prior to release, and history of addended or amended information and/or reports, etc.) can be examined and confirmed upon demand. Such capabilities are central to all of clinical informatics and not just pathology informatics, as information throughout the clinical chart is always subject to change through the accumulation of incremental knowledge as well as by point-wise amendments and corrections to existing records. Just as fundamental as correct initial information and correctly updated records is the need to ensure that all records are updated for correct patient identity, necessitating that positive patient identification be extended to all aspects of laboratory workflow. Ultimately, this has led to the creation of an entire workflow and computational "fabric" of an overall laboratory results verification process so that the correct results are always attributed to the correct patient. Some of the most injurious patient care events have resulted from identification errors (e.g., "wrong blood in tube," leading to major hemolytic transfusion reactions). This underscores the need for constant vigilance and error proofing in workflow to maintain best practices for validating the identity of all information flowing in or out of the database underlying the laboratory information system.

TABLE 12.1
Key Database Operations: Create, Read, Update and Delete (CRUD)

Function	Definition	Typical SQL Example
Create	Insert a new table into a database schema or a new data row into an existing table. (Example: inserting a new patient record into the Patient Identity Table)	INSERT INTO Patient_Identity_Table (Last_Name, First_Name, MI, DOB, Gender, MRN) VALUES ('Doe', 'John', 'M', '1987-05-21', 'M', '00001234567');
Read	Extract one or more records from a database. (Example: extracting patient name and DOB when providing a name and medical record number)	SELECT Last_Name, First_Name, DOB FROM Patient_Identity_Table PIT Where PIT.Last_Name='Doe' and First_Name='John' and MRN='00001234567';
Update	Replace a data element of an existing table row with a new one. (Example: changing the data of birth for a specific patient, using multiple identifiers)	UPDATE Patient_Identity_Table SET DOB = '1987-05-23' WHERE Last_Name='Doe' and First_Name='John' and MRN='00001234567';
Delete	Remove one or more rows from a table. (Example: remove a patient record row from the Patient Identity Table, using the MRN as the deletion key)	DELETE FROM Patient_Identity_Table WHERE MRN='00001234567';

KEY DATABASE CONCEPTS

Recognizing that modern databases (of which the laboratory information is unquestionably a member of this class of information technology solution) are fundamentally transactional systems, it is important to recognize the primary transaction classes that databases facilitate. Known informally as CRUD, short for Create, Read, Update and Delete (Table 12.1), these four basic functions allow for essentially all required information stewardship operations. Some additional commentary on the deletion operation is warranted as, in most cases, actual data deletion is contraindicated for both auditing and patient safety purposes. The highly effective and almost universally implemented alternative approach to data deletion is the use of "inactivation flags," whereby the database can selectively deprecate data elements and concepts that are no longer in active use, while at the same time keeping them available for any necessary historical look back or auditing activity. Use of this approach is how the important data curation concept of *data provenance* is maintained. Specific examples of where data deprecation takes place in the laboratory information system include patient name

TABLE 12.2
ACID Properties of Databases

Property	Definition
Atomicity	Database updates must be all-or-none operations. If a multipart transformation is requested, it must complete in toto or not at all. Thus, the database is left unchanged.
Consistency	Change requests to any database table row data must result in the database being left in a form in which all fields are left with valid data.
Isolation	Isolation enforces concurrent execution of transactions to operate in the same manner that would have been obtained if the same transactions were executed sequentially.
Durability	Engineered software and operating system robustness such that, once a transaction has been committed, it will remain committed even in the setting of system failure (e.g., system crashes, power failures).

changes and reference interval updates, both of which represent relatively common events. In the case of the latter, for example, a revised reference interval update in the LIS database schema would affect only the reporting of new results. All prior reported results would remain associated with the reference interval with which they were originally associated.

In the language of most database programming (Structured Query Language [SQL]), the four common operations on tables—adding, reading, updating, and deleting (in select circumstances) data—are carried out via four general classes of SQL commands: *insert*, *select*, *update*, and *delete*. The vast majority of database operations, as carried out on the contemporary lab information system database schema, could be contained within variations of these four general command classes alone. Consequently, having even cursory familiarity with this aspect of the SQL programming language can confer on the laboratorian greatly enhanced ability to converse with vendor database architects, thereby allowing for active participation in any requests for LIS architectural modifications or enhancements. Similarly, for the pathology informaticist, possession of a broader knowledge base for SQL databases and actual SQL programming can be of great utility in efficiently generating custom reports not already provided by the LIS vendor. Such reports can support laboratory operations without the need for additional vendor support, which can be time-consuming and expensive. The availability of such skill sets within the clinical laboratory can be of significant strategic value, recognizing that the generation of specific data extractions for time-sensitive needs (periodic laboratory inspections, state and federal reporting of infectious disease and pandemic data, etc.) is not an infrequent occurrence.

Another key concept integral to database technology and stewardship of any compendium of systematized information is the list of ACID properties: atomicity, consistency, isolation, and durability (Table 12.2). Of these four fundamental concepts, atomicity is perhaps the most important in that it ensures that any intended transaction is either fully executed or not executed at all. To understand the importance of this concept, consider the routine task of updating a patient's demographics, including name, date of birth, and current address. Typically, such updates are carried out on the core database as a monolithic transaction such that all fields associated with the record in question are updated at the same time. Without the database possessing atomicity as a core property, it would be possible, under certain circumstances, for an update to successfully carry out modification of some fields in a patient's demographic record, but not all fields. Such a partially completed update would create an errant record, which not only would incorrectly represent the patient, but also could, by coincidence, correctly match a different patient. Such referential integrity problems were manifested in the earliest days of clinical database implementations, and subsequently became far less likely in the setting of adoption of ACID principles by contemporary database solutions.

KEY DATABASE STRUCTURES

Tables

Fundamentally, most contemporary databases are rendered as relational databases, implying that tabular information is stored in separate and distinct tables, which have both rows and columns. By convention, any given database table's structure defines the columns to represent the distinct classes of information held by a given table and defines rows to represent individual entries housed in a given table, which specify all of the required (or optional) data elements (e.g., the columns) needed to comprise a complete record (Fig. 12.1) for that given table. In addition to externally added content, most database tables will contain one or more keys, which are simply unique identifiers

PATH-MSSQL-A...comprehensive

Column Name	Data Type	Allow Nulls
person_id	bigint	☐
empi_id	bigint	☑
source_id	bigint	☑
creation_datetime	datetime	☑
active	varchar(1)	☑
inactivation_datetime	datetime	☑
alias_id	bigint	☑
ext_pat_mrn	varchar(50)	☑
external_check_digit	varchar(50)	☑
ext_check_digit_scheme	bigint	☑
ext_assign_fac_id	bigint	☑
ext_id_type	bigint	☑
int_pat_mrn	varchar(50)	☑
lastname	varchar(100)	☐
firstname	varchar(100)	☑
middlename	varchar(100)	☑
date_of_birth	datetime	☑
middle_initial	varchar(25)	☑
prefix	varchar(50)	☑
suffix	varchar(50)	☑
gender	varchar(1)	☑
address_1	varchar(500)	☑
address_2	varchar(500)	☑
address_3	varchar(500)	☑
mailstop	varchar(500)	☑
city	varchar(500)	☑
state	varchar(500)	☑
country	varchar(500)	☑
postal_code_1	varchar(500)	☑
postal_code_2	varchar(500)	☑
home_tel	varchar(25)	☑
office_tel	varchar(25)	☑
email	varchar(100)	☑
		☐

Figure 12.1 Typical table definition matrix. In this example, a patient demographics table configuration definition matrix is depicted. Primary row element attributes include the data type and whether the data element can be left blank (Allow Nulls). The primary table key is the first element (depicted by gold key at left).

generated by the database itself (typically, sequential numbers or alphanumeric sequences) that serve to uniquely identify each individual row in a table, thereby distinguishing it from all other rows. Keys are also of fundamental importance, as will be subsequently described, in that they form the underlying construct by which a relational database can be realized.

Tables are constructed such that each column can house a particular class of data (e.g., simple text, dates, numbers, etc.) with the option at design time to instruct the database as to whether that class of data will be enforced for that column. With enforcement in place, all attempts to place a nonconforming data element in a constrained column will result in an error. When enforcement is suspended, data classes other than the originally specified type can be included. This type of data storage is defined as a *data type overload*. There are reasons that a database architect might choose one or more columns to have enforcement of a data class suspended, including the provisioning for general-purpose containers that might need to hold various classes of data concurrently. However, for the vast majority of data representation needs, designing table columns with

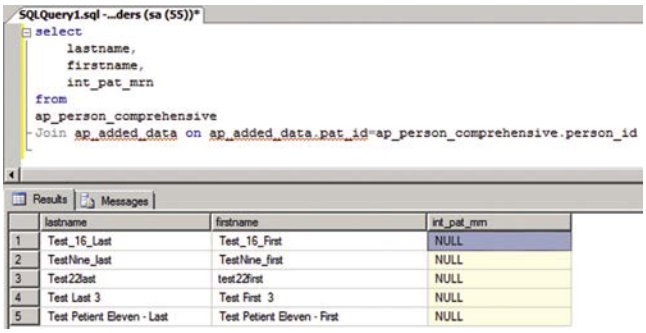

Figure 12.2 Typical select statement. The SQL language join operator is used to link subordinate tables to the primary table being queried by matching all foreign key rows in the subordinate table to the primary key of the primary table.

data enforcement in place is a sound practice, as it ensures that columns with specific intended meaning and function are always populated with appropriate data types and, therefore, correct information.

DATA NORMALIZATION AND SINGLE SOURCE OF TRUTH

With the availability of individual tables comes the added potential to link them in meaningful ways such that specific information can be easily recovered while at the same time eliminating (or at least minimizing) the need to reduplicate atomic data elements in multiple tables. As a brief digression, the issue of data reduplication in contemporary database design is a central topic, as any instance in which a unique data element is repeated more than once in the overall database represents an opportunity for the incursion of errors over time. This is especially true as a database grows and evolves. As a simple example, in a hypothetical LIS database in which the system architect chose to include patient demographics in both the orders and results tables, a patient name change requested by the laboratory's host health organization (a relatively common event) would necessarily require an update in the demographics fields of both tables. As database table count and table complexity would grow, there would be increasing instances in which single data elements are multiply reproduced throughout the overall database. Such growth could represent an exponential (and, thus, unsupportable) increase in complexity, with the associated need to identify and then update all instances of the repeated data element. In the setting of a data element update request, if not all copies of the affected data element are correctly changed to their new correct value, a very real possibility exists for the database to be placed into a condition known as *referential integrity failure*. For example, a patient's name would not be represented consistently throughout the multiple tables where it resides, leading to having multiple concurrent names for the same individual in different parts of the overall database schema. Clearly, this is an undesirable outcome.

To address this vulnerability, contemporary relational databases have espoused the notion of data normalization, in which important data elements, such as patient name and medical record number, are contained in only one table of an overall database schema, with all references to such data elements, as may be present in other tables, carried out by use of a pointer to this single referential source data element. This construct, commonly referred to as *single source of truth*, ensures that when an update takes place to a particular data element, that update is guaranteed to cascade throughout the entire database schema with no possibility that prior values of that data element will remain active.

In specialized settings, in which there is the need for extremely high database performance, it is permissible to reduplicate data elements so that they are immediately available for retrieval without interrogating multiple tables concurrently. Repeating such data elements for performance purposes is known as *data denormalization*. While very useful in select circumstances, it should be recognized that this process should be carried out with great care to avoid the possibility of referential integrity failure.

COMMON DATABASE OPERATIONS

By virtue of data normalization, most database queries typically require access to more than one table and, in some cases, many tables. This is both expected and routine. To accomplish a typical query, the most encountered operation in the SQL language is the *select* statement. Figure 12.2 highlights a typical *select* statement involving multiple tables and is representative of the usual fashion in which data elements that span different areas of a relational database schema can be brought into a single construct of extracted tabular information. Fundamental to the *select* statement is the use of table keys—specifically, master keys and subordinate keys.

Master Keys

A table that contains master keys for its various rows of tabular data necessarily implies that each row contains elements of unique identity data, with each row distinguished from all other rows in that same table by a key variable, which is defined to be unique. A table key can be all-numeric or alphanumeric but must follow the single overriding rule that no two keys can be identical. In most cases, the underlying database engine and software environment will enforce referential integrity, thus making it an impossibility for either the user or the software itself to insert additional rows in a master-key-enabled table, where keys are identical. Rather, the database engine would generate a referential integrity error, which typically would then require inspection of the underlying programming code and correction by the vendor, as such errors are considered as "never events" for production-grade code.

Subordinate Keys

Conversely, a table that contains subordinate keys necessarily implies that generation of a more complete view of any single table row entry is predicated on using the subordinate key to identify the row in the linked table where the master key of that row matches the subordinate key. There is no limit to the number of rows within external tables to which any given table row can point, necessarily implying that any table may contain any number of subordinate keys in its respective rows. Similarly, a table with a unique master key may itself be subordinate to other tables for additional classes of information, thus generating a construct in which a table may contain a master key and any number of subordinate (or so-called *foreign*) keys. Collectively, the assemblage of tables and their respective key-based interconnections is known as the *database schema* or, simply, *schema* for short. In making queries against any relational database, having access to the database schema, including table column definitions and key linkages, is essential for assembling complete and correct data extractions. For this reason, it is highly desirable for the clinical laboratory, when selecting and installing any new laboratory information system, to secure the contractual assurance from the LIS vendor that the associated database's schema will be shared with the laboratory. Absent such documentation, the laboratory could run the risk of not being able to generate any required operational or regulatory reports and/or data extractions without the continued assistance and support of the LIS vendor. While LIS vendors do play a substantial role in providing ongoing support and data product solutions to laboratories, there is significant utility, as already discussed, in a laboratory's ability to carry out such data product generation independently. Toward this goal, knowledge of the schema is a key enabling step.

TRANSFORMATIONAL OPERATIONS

So far, in describing the *select* statement, and the role that master and subordinate keys play in joining multiple tables into a single unified query, the resultant database operations have been nonmodifying (also known as *read-only*). In addition to read-only operations, there are several routine operations carried out on databases that result in modification to table/row contents. These are the insertion, update, and deletion operations.

DATABASE INSERTIONS

With database insertions, the intent is to add one or more rows of data to existing tables while at the same time ensuring that the overall database schema's referential integrity is not compromised. In many cases, the database engine's integral business logic will assist with the insertion process by automatically generating a unique key value for the inserted row's or rows' key identifier column. Similarly, most database engines will facilitate validation of the existence of a corresponding master key in a linked table when a new entry is placed in any table that has one or more subordinate keys linking that row to table/row locations elsewhere in the overall database. This validation step is essential in preventing so-called "orphan rows" that, by definition, do not point to a valid row in external tables.

DATABASE UPDATES

With the database update operation, one or more data elements in one or more rows of a given table are replaced by new information. In some cases, behind the scenes, the database engine will keep a transactional record of the update so that if an audit is requested in the future, the prior stored information can be retrieved along with additional transactional information about the update (such as the process or user identity that requested the update, as well as the time and date of the update). This feature is routinely employed in laboratory information systems, with an example being

amended laboratory results. Although new results are both stored locally and forwarded to downstream clinical information systems, the auditing feature intrinsic to most LIS database engines' update logic ensures that all aspects of the update process itself are documented, including the initial information that was updated and who carried out the update.

DATABASE DELETIONS

With the database deletion operation, one or more data elements from one or more rows in a given table are requested for deletion. Similarly, as in the case of database updates, the underlying database engine routinely carries out associated auditing operations so that the contents of the deleted records are maintained in an external set of auditing tables. The availability of such information allows for both after-the-fact interrogation of prior deletion operations and for the more sophisticated operation of "rolling back" a database to a prior state at an earlier point in time. Such rollback operations might be useful, for example, in the setting in which a known series of transactional operations was deemed after the fact to be incorrect, such as an incorrectly applied patient identity merge operation. With the availability of the rollback operation, the database can be selectively restored to a prior known correct configuration, thus alleviating the manual work that would otherwise be required to manually reconstruct the configuration of the affected table rows prior to the errant update.

In practice, however, actual database deletions are quite uncommon in contemporary systems, as the relational nature of interconnected tables in a relational database often generates dependencies in which the presence of any row of data in a given table is required to satisfy the referential integrity of the overall database. This reality is necessitated by virtue of other tables that may make use of a specific row in the table in question. By way of example, consider the scenario in which a laboratory analyte reference interval is being updated, with this being a common recurring activity. The solution to effectively carrying out a reference interval update is not as simple as merely changing the values for the reference interval in the existing reference interval table row. Although such an operation would address the data representation needs for new tests being performed, which presumably would operate under the operating conditions of the new reference interval, all prior reported tests would similarly then point to the same updated row and, therefore, would contain incorrect information as to the actual reference interval that was prevailing at the time of the original testing. Thus, it becomes necessary to resolve this conflict by both preserving the original reference interval information while, at the same time, allowing newly reported tests to benefit from an updated reference interval. The solution to this conundrum is not a database deletion but, rather, a status transformation. This is typically accomplished by signifying that the existing reference interval row data for prior reported results is now for historical use only, and not currently active. The most typical way to accomplish this task is including a column in each table depicting active status, commonly known as a *status flag*. When a particular record is inactivated, the active status flag can be switched to false, with the row being left otherwise unchanged and still very much present in the overall schema. In this manner, historically reported results can continue to benefit from possessing the correct reference interval, while at the same time allowing new results to be associated with the new reference interval, which is now manifested in the reference interval table as a new row with its active flag set to true. Thus, in the typical deployment of relational database technology, with respect to modern laboratory information systems, data are not typically deleted; they are merely inactivated. This is a fundamental best practice of data stewardship in contemporary LIS architecture, allowing for the most transparent representation and auditing of the data transformation steps that take place in the course of routine information flow and database stewardship.

POSITIVE PATIENT AND SPECIMEN IDENTIFICATION AND BARCODING

An expected consequence of the significant automation and ability to operate at large production scale, as witnessed in the contemporary clinical laboratory, has been the need to deploy solutions and technologies that can assist with both positive patient identification and positive specimen identification along every step associated with the preanalytical, analytical, and postanalytical journeys that specimens and primary data take in the hopeful generation of an accurate result. In the late 1970s, as high throughput clinical analyzers became more widespread in use, it was immediately noted that the contemporary practices of that era concerning worklist generation, which were based on manual clerical steps for data entry, were not able to maintain satisfactorily low error rates (recognizing that Six Sigma performance requires maintaining less than 3.4 errors per million events). Attention then necessarily turned to the exploration of workflows, forcing functions, and technology solutions that could reliably drive patient and specimen identification error rates toward zero.

As a first step, laboratory-generated labels that also included the accession number and barcode format proved to be a useful innovation. In the initial period of barcode deployment within the clinical lab, multiple barcode symbologies were employed. This created what might be considered to be one of the first interoperability challenges in that there was no guarantee that a barcode label specimen generated at one laboratory could be utilized by the barcode reader technology and established barcode/accession number format at a remote reference laboratory. In the absence of this standardization, clinical laboratory specimens that are transported between laboratories usually required the receiving reference laboratory to relabel all incoming specimens with a locally generated label that itself contained the locally agreed upon barcode symbology and accession number format. This relabeling practice is problematic in that it exhibits an error rate for the relabeling of specimens that is extremely difficult to reduce below a baseline (nonzero) value. This risk remains unacceptably high (similar to the previously described setting of clerical entry of accession numbers into worklists).

A further technical limitation of the currently ubiquitous linear (one-dimensional) barcode symbologies in use is their variability for providing for reliable error detection, which could easily occur when a label is partially obscured or defaced during the routine course of transport throughout the laboratory. Even with error detection, studies such as those exploring advanced barcoding solutions (Snyder et al., 2010; Hawker, 2010) have conclusively demonstrated that error detection, in even ostensibly robust one-dimensional symbologies such as Code 128 (linear barcode symbology that incorporates all 128 alphanumeric ASCII [American Standard Code for Information Interchange] characters), are not as reliable as previously thought. The limitations of one-dimensional barcodes had already been identified in many other industries, including settings in which extremely high production volumes necessitated the lowest possible identification error rates. The resulting evolved barcode technologies brought forth by these limitations as seen in the first-generation 1-D barcodes manifested in the invention of the two-dimensional (2D) barcode: a technology that allows for both substantially higher data density per aerial surface and, concomitantly, robust error *correction* instead of having only error detection.

The error correction aspect of 2D barcode symbologies merits expanded discussion as this feature is now the center point of major efforts in the laboratory standards space to create an extremely reliable and interoperable universal specimen label format. Specifically, error-correcting formats within 2D symbologies allow for highly degraded and even defaced barcoded labels to still be able to be read completely and accurately, including the retrieval of all elements of the original encoded message sequence. This is made possible by the redundant placements of multiple error correction data elements throughout the surface area of the barcode, creating substantial resilience from multiple individual point-wise spatial defects in the barcode. An important secondary benefit of the use of such error correcting algorithms in 2D barcodes is the observation that, in the setting of defacement, the highly undesirable misread event is now reduced to an exceptionally small statistical likelihood owing to the redundancy of the newer error detection methods. Therefore, anticipated use of 2D error-correcting barcode symbologies has, as an added benefit, the near-total extinction of misread events (with misread events now being further diminished to less than 1 in 10.5 million). Nonread events are the only remaining failure mode (in addition to the ubiquitous wrong specimen in tube eventuality), which is a manageable exception condition that can be readily rectified by the usual manual corrective actions by laboratory personnel.

In the past decade, the Clinical Laboratories Standards Institute (CLSI) has extensively explored the need for standardization of specimen barcoded labels, initially offering a one-dimensional barcode specimen label standard (Auto-12). More recently, it has been expending much effort on a slightly revised label format that supports 2D barcodes, with all the benefits that they offer (Auto-14). The Auto-14 standard is in final preparation as of this writing. It is expected to not only solve the current misidentification shortcomings of one-dimensional barcodes but also to solve the patient safety issues created by the ubiquitous practice of relabeling of specimens upon transfer from one laboratory to another. In short, the need to relabel will be eliminated by the establishment of a unique laboratory identifier (ULI) number for every clinical laboratory globally, with this number serving as a prefix to the local specimen accession number. In this manner, by virtue of the unique prefix, every specimen label generated throughout the world in each local laboratory will be both unique in its alphanumeric sequence and identical in its overall barcode content format. If adopted as hoped, the

Figure 12.3 Contemporary 1D and prototype 2D barcoded specimen label. The use of a 2D error-correcting barcode format in the Auto-14 candidate label (lower label), such as DataMatrix or QR-Code, promises to reduce identification errors and the need for specimen relabeling. 2D barcodes are placed multiple times on the Auto-14 candidate format layout to maximize readability under extended radial viewing angle conditions, as might be typically encountered on a lab automation line.

need for specimen relabeling in the clinical lab will become a thing of the past. Figure 12.3 depicts a contemporary specimen label juxtaposed to the near-final Auto-14 2D label format. Additionally, of note is the reduplication of the 2D barcode, a minimum of three times, at different vertical positions in the label. This redundant placement is intended to assist automation lines in effectively reading barcodes on specimen tubes, recognizing that tube placement, rotationally in an automation rack, may not be perfectly aligned in every instance.

LABORATORY INFORMATION SYSTEMS

Stewardship of the LIS is one of the core activities of central interest to pathology informatics. All aspects of the LIS application lifecycle—including selection, deployment, and continued operation—are under the aegis of informatics support, and merit discussion.

LIS SYSTEM SELECTION

This is an area that is not without some measure of contemporary controversy given the constricting universe of typically deployed solutions in the setting of a very small number of leading EHR solution providers that are also offering an integrated LIS as an integral module to the overall EHR solution. Indeed, in the past decade, companies such as Epic and Cerner have witnessed substantial growth of their respective LIS market share, essentially at the expense of all other remaining stand-alone LIS vendors. The resultant controversy arises not from the question of whether such monolithic solutions provide adequate capabilities. Rather, the concern is that the rapidly constricting market share available to all remaining best-of-breed LIS vendors threatens their very existence and, with that, the potential capacity for the pathology informatics field to maintain a critical mass of diversity in its vendor field of solution providers and, thus, continued innovative capacity. While it is true that for the duration of the 50 or so years that the field of Pathology Informatics has existed as a domain and has enjoyed a diverse offering of commercial LIS solutions, this era may regrettably be coming to an end. While the competition in the LIS vendor sector to gain visibility and market share historically has been a driving force for both innovation and partnership with clinical laboratories themselves, who often contribute in substantive ways to the continued evolution of LIS capabilities, the current predominance of a very small number of "big box" integrated EHR solution providers offering their own integrated LIS solutions is effectively squeezing the best-of-breed LIS vendors out of the market despite the latter having arguably superior solutions. This constriction potentially jeopardizes the model of partnered innovation between the LIS vendor and the clinical lab, replacing it with a rapidly evolving monoculture of a very short list of enterprise-wide solution providers who potentially view the LIS as a subordinate information system to the larger overall EHR and not as a distinct repository requiring careful domain-specific data modeling and curation. Only time will tell whether the current ecosystem of independent LIS vendors will continue to survive or whether they will fade away and be replaced by EHR lab solutions that espouse ancillary modules supporting the laboratory.

As a counterpoint, the argument can be made that there are distinct advantages of a primary vendor solution in that, ostensibly, total cost of ownership for the enterprise is lowered. In tandem, a number of additional benefits are claimed, including: (1) simplified implementation of a monolithic EHR/LIS solution, (2) better integration of data flow from the LIS module to other EHR modules and departments across the health enterprise, and (3) reduction in the total computing complexity that an enterprise would need to curate. These assertions require some clarification and rebuttal. First and foremost, implementing an LIS, even if it is an integral component of a larger "wall-to-wall" EHR enterprise solution that is ostensibly already included in the overall application expense, is not free. Most EHR vendors charge a substantial implementation fee or require the use of duly licensed channel partners to assist with implementation (e.g., Deloitte). These expenses quickly mount and are often comparable to, if not more than, the total costs that would have been otherwise incurred in the implementation of a traditional stand-alone/best-of-breed LIS solution. Pertaining to the other common assertions, the level of difficulty for implementing lab modules of monolithic LIS solutions has recently proven to be comparable or even more complex than traditional stand-alone LISs, recognizing that the former, in order to gain the needed interconnectivity with lab instrumentation and other devices, make use of third-party "middleware" solutions (e.g., Epic Beaker's reliance on Data Innovations' portfolio of middleware solutions). This adds an entirely new layer of complexity to configuration, staff training, and long-term application stewardship. With respect to the enhanced LIS data integration across all EHR modules assertion that often accompanies primary vendor EHR claims, a careful architectural analysis will often reveal an entirely different reality. In truth, the core LIS software in use was separately developed under its own software development stack and, for the purposes of computational workflow, the LIS module can be seen to actually operate as a stand-alone software package with its integration architecture with the larger EHR being no different than what is seen with traditional settings in which specific interfaces needed to be developed to link the lab and EHR schemas. In this scenario, the only primary difference is that the interface logic is under the stewardship of one vendor and not shared between two, potentially making corrective efforts easier for the client when data does not flow as expected (as it is no longer possible to encounter a scenario in which two separate vendors are blaming each other for the untoward interface operation). Thus, while some advantages of interface defect resolution can be realized with a primary vendor solution, it should be similarly noted that this approach, in and of itself, is no guarantee that the internal LIS-EHR module integration or data flow will be superior to that of a conventional best-of-breed LIS implementation. Finally, with respect to the assertion that a primary vendor EHR system will lead to a reduction in the total computing complexity needed to provide comprehensive LIS support, this too is illusory. In practice, the incremental information technology (IT) footprint of technology layers such as compulsory middleware and workstation virtualization hardware and software (e.g., Citrix) matches and even exceeds the IT requirements of most typical stand-alone LIS solutions. This reality is further compounded when factoring in the additional laboratory sections that must be provisioned with their own stand-alone "mini-LIS solutions" in the settings in which the primary vendor solutions do not provide such a module (e.g., human leukocyte antigen testing, blood bank, cytogenetics, flow cytometry, molecular pathology/next-generation sequencing pipeline scheduling, just to name a few). Interestingly, these missing modules in the primary vendor EHR solution are usually readily available in stand-alone/best-of-breed LIS solutions, which should be seen as a further differentiating factor as to why primary vendor solutions with an integrated LIS are not entirely the panacea that they are cast as being. In summary, primary vendor solutions that include the LIS are certainly trending, but by no means have they completely obsolesced the rationale or need for considering the deployment of stand-alone LIS solutions in select circumstances.

With the earlier cautionary notes of comparison as a preface, it is still very germane to cover the important topic of LIS selection, as that avenue of deployment remains a possibility for at least a subset of clinical labs in operation. Over the past decade, it is interesting to note that the selection of LIS solutions, which traditionally was based on use of a request for proposal (RFP) process, has necessarily evolved to becoming simpler and perhaps more streamlined, with a considerably accelerated timeline. One of the well-established critiques of the use of the RFP has been the long overall timeline and considerable spacing between critical-path milestones leading up to the final selection event. For example, with the scheduling of vendor demonstrations historically being spaced quite far apart from each other, to minimize impact on local laboratory staff schedules, it became difficult for individuals to effectively compare the merits of the different systems being considered (with first impressions fading substantially over time). This led to the realization that vendor demonstrations should be held sequentially and as temporally close as possible to each other to afford laboratory staff the best possible chance of comparing and contrasting the various solutions, while they are still fresh in memory. However, scheduling multiple system demonstrations in a rapid-fire manner could be quite taxing on the available time of laboratory staff unless there is a concurrent effort to shorten and constrain the sessions to being highly scripted, targeted, and moderated, in which vendors are provided with a structured and exact sequence of activities to demonstrate. This approach has come to be known as the "mini-RFP" process, often leading to an improved ability of laboratories to make the best-possible informed decision concerning LIS selections.

With respect to the RFP (or mini-RFP) process, it is important to recognize the general stages leading up to the determination that an RFP is even required and the subsequent steps needed, including RFP development, RFP dissemination, vendor invitation for demonstration, vendor selection, contract negotiations, implementation schedule development, implementation, go-live, post-live stabilization, post-live optimization, and continued stewardship. Fundamental to this entire approach is the analytical process by which a laboratory determines whether the current LIS solution is salvageable by conventional software enhancement means. In settings in which corrective action is deemed to be monumental in scope, the RFP process can represent both a liberating direction and an expanding set of possibilities for leveraging the existing vendor to provide critically needed functionality (via the forcing-function intrinsic in responding to an RFP) or seeking new and alternative vendors who might offer a solution that is better matched to the acute needs of the contemporary and evolving laboratory circumstances. However, given the substantial effort and resources associated with executing the complete RFP process, such an exercise should not be initiated without fully understanding the commitment necessary to fully execute a logical and successful conclusion.

As "common things are common," organizations such as the Association for Pathology Informatics have recognized the universal need for tools to assist in the RFP construction process and, concurrently, the inherent difficulty of executing the RFP process itself. This recognition has brought about the creation of a freely available LIS Functionality Assessment Toolkit (LIS–FAT) aimed at simplifying the LIS selection process. This same document also provides comprehensive attributes organized by laboratory section that should be included in the RFP document as vendor-directed questions. This document is well informed of the instrumentation and workflow diversity that accompanies the modern clinical laboratory. As a consequence, it provides targeted evaluative criteria across the multiple areas of LIS stewardship, including general laboratory, microbiology, blood bank, specimen procurement, quality control, molecular pathology and genetics, anatomic pathology, interfaces, and information security. The following resources contain a synopsis of the general high-level categories contained in the LIS–FAT: https://www.pathologyinformatics.org/toolkit.php and https://www.pathologyinformatics.org/docs/1._Use_of_the_LIS_Toolkit_-_White_Paper_-_V_1.0.pdf.

The toolkit provides as a preface a white paper describing the rationale, background, and intended uses of the various modules contained within. The toolkit proper is composed of three appendices: LIS functionality statements, LIS scenarios, and total cost of ownership elements. These three assemblages, when used together, allow for the construction of a highly precise and complete RFP, and provide the associated criteria by which vendor responses can be quantitatively scored and compared in support of a final vendor/LIS solution selection.

SPECIALIZED LAB INFORMATION SYSTEM MODULES

Although the core LIS provides adequate support for the core clinical laboratory sections—including clinical chemistry, hematology, and microbiology—there are additional subspecialties and associated lab sections that manifest either different or more complex lab workflow, including all aspects of results preparation (preanalytical, analytical, and postanalytical). This recognition has fostered the emergence and exuberant growth of a niche industry comprising best-of-breed ancillary lab section solutions, notable examples being histocompatibility, flow cytometry, molecular diagnostics, and cytogenetics. The incremental presence of one or more of these ancillary LIS solutions imparts a necessary increase in complexity for the stewardship of the overall LIS. Consequently, the pathology informatics team in these settings is tasked with the added challenge of integrating such ancillary systems and then maintaining them with the same level of acuity and precision as the core system. This added burden represents one of the ongoing existential challenges for contemporary pathology informatics in that it is often seen that available resources are not commensurate with the incremental complexity of shouldering multiple systems concurrently. Thus, sometimes difficult decisions are required concerning reduction of features or diminution of total system integration. This, of course, is problematic as any ancillary LIS that remains computationally disparate from the primary system in terms of orders and results will likely become a source for substantial incremental manual workflow as well as an ongoing source of clerical transcription errors.

Histocompatibility

The modern histocompatibility laboratory exhibits complex workflow that differs in its level of internal documentation and process steps. For this reason, a number of stand-alone HLA lab solutions have been developed that are commonly deployed in tandem with a core LIS solution. The existence of an added HLA-specific module necessitates the creation of specific orders and results interfaces and, in tandem, additional data center hardware to run the specialized program. Stewardship of this module is further compounded by the fact that HLA laboratories are accredited by organizations in addition to the typical CLIA required status annual inspections (e.g., CAP), such as by the American Society for Histocompatibility and Immunogenetics (ASHI), thus requiring an added body of evidentiary documentation as to software system implementation and maintenance.

Flow Cytometry

The flow cytometry laboratory section is another area of complex and intense workflow, in which specialized data capture and analysis capabilities are required. In the past several decades, there has been an increasing trend of the larger, unified LIS vendors offering specific flow cytometry modules, with it being observed that these sometimes meet the mark for the minimum set of functional requirements. It can also be seen, however, that in the case of the more complex flow cytometry labs, which also maintain substantially higher case volume, big-box LIS vendor solutions can prove inadequate, leading to opportunities for niche vendors and local software development units within laboratories themselves to supplant functional deficits by offering their own custom-developed applications. In this latter case, it is incumbent upon the flow cytometry laboratory—in tandem with local pathology informatics expertise (if present)—to fully integrate, validate, and *document* any resultant stand-alone solutions and workflow into the larger resident LIS solution in hopes of realizing an intact electronic orders-to-results reconciliation process. Without this last attribute, any large-volume flow cytometry lab would be hard-pressed to justify the substantial expenditure of effort needed in building a custom module, if only to realize a workflow that is electronically isolated from the greater LIS solution. This follows for the obvious reasons of both patient safety and required efficiencies when operating at high production volumes.

At the actual technical and workflow level, the flow cytometry laboratory represents complexity in the size of the primary data captured from contemporary flow cytometry instrumentation in tandem with the complex and often multilayered analytical process required to transform raw information into actionable medical knowledge (vis-à-vis rendered final flow cytometry reports). Most flow cytometry laboratories, for example, make use of so-called list-mode data, which is a rendering of the full transcript of cellular detection events from the flow cytometer's detection apparatus (typically enumerating the optical and fluorescent properties of each detected cell, with high-precision floating point numbers). Given that most contemporary flow cytometers possess many channels, the data set associated with each individual cell can include forward-scatter, side-scatter, and multichannel fluorescent magnitude variables that collectively need to be stored, gated, and then classified within the larger context of the tens of thousands of similar events that constitute even a single analytical run of a sample. While some of this workflow is often carried out by the integrated application software that accompanies the instrument, there is still a substantial plurality of analytical and postanalytical data processing required

to fully interpret the primary data in support of rendering a final medical report. It is this latter postanalytical data processing step that often falls short in the offerings provided by big-box LIS vendors. This, in turn, creates the opportunity for niche best-of-breed flow cytometry software solution providers and locally developed intramural solutions.

The flow cytometry lab also represents something of a challenge in terms of data stewardship. The larger list-mode data files, stored in a standardized format known as FSC, require substantial on-premises data storage and, therefore, expertise to maintain such repositories. While some of this functionality can be seen to be intrinsic to the flow cytometer's vendor-provided application suite platform, there is often the incremental need for additional storage to address clinical archival of primary data sets, which are not sent to the local EHR and would be otherwise lost forever if not specifically curated locally under laboratory stewardship.

Molecular Diagnostics

Without question, the molecular diagnostics laboratory is one of the "heavy hitters" in terms of requiring significant pathology informatics expertise and operational support. The intrinsic workflow of this lab section is complex, involving many steps, very large data sets, and utilizing extraordinarily sophisticated algorithms for data analysis. All of these attributes are in need of initial validation, ongoing maintenance, version curation, and exceptionally nimble modular design to facilitate feature-swapping and innovation. In addition to these requirements, the molecular diagnostics lab workflow is further compounded by the concurrent need for tracking of not only specimens but also component reagents along every step of the data generation process. This added documentation is necessary to address quality issues that may arise in the setting of postanalytical notification by a reagent vendor—for example, that a specific lot of supplies was somehow defective. This could indicate the need for repeat testing. In such settings, the availability of an extremely granular database of reagent lot documentation, as associated with each production run and patient sample, could allow the laboratory to carry out a strategy of precise repeat testing of only the samples and analytical stages affected by the defective reagents. Conversely, without such granularity of documentation as to the disposition of how reagents were previously applied toward specimens, it would be necessary to carry out complete retesting of patient samples, including all preanalytical, analytical, and postanalytical steps (potentially representing great incremental expense and effort).

Given the rapid pace of innovation seen in the molecular diagnostics laboratory, it is often the case that the larger integrated LIS vendors substantially lag behind "the art of the possible" and the state of the art. This vacuum is filled by locally developed solutions and the ever-present growing field of specialized software application vendors who specifically cater to the molecular diagnostics field. As a high-level observation, the very large size of the primary data generated by next-generation sequencing (NGS) instrumentation necessitates the availability of tools and methodologies that operate at an enhanced level of performance as compared with the more traditional approaches used by other laboratory sections to address tabular data (e.g., conventional spreadsheet software). Electronic workflow, as seen in the modern clinical NGS laboratory, generates data in multiple steps, with several initial classes of data representing the largest-sized file class of data constructs in laboratory medicine. These activities are in need of the highest-performance class computational tools in order to carry out the typical tasks of fragment alignment and subsequent variant calling. Specifically, FASTQ files, which are the largest, primarily differ from BAM files in that the former contain read fragments that are completely unaligned. In contrast, the latter have been exhaustively parsed toward the goal of aligning all individually generated DNA fragments into a single and globally optimized exome or whole-genome sequence, where every base pair can be adjudicated to its position in the genome/exome and, therefore, confirmed against however many reading frames provided in the level of coverage associated with a particular NGS protocol.

It is not difficult to understand why specialized software is required to carry out the initial alignment task. Historically, before the widespread availability of clinical NGS testing platforms, many genetic-based tests were based on Sanger-sequencing, yielding primary data sets that were still within the capabilities of contemporary software spreadsheets (~100,000 rows). Indeed, for many years, use of spreadsheet software (specifically, Microsoft Excel), with integrated macro commands and cell operations, was the gold standard and workhorse of molecular diagnostics laboratories, representing a manual and generally unavoidable intermediary step in the overall process by which final molecular reports would be generated. With the advent of the larger data sets made possible by NGS technology, primary data set size rapidly overtook the capabilities of spreadsheet technology, necessitating the creation of specialized software specifically designed to handle the larger size and complexity of the fragment alignment process. Overall, the process by which unaligned FASTQ files are transformed to aligned files—initially (BAM files) and then subsequently to called variants (VCF files)—is known as the NGS pipeline or simply the pipeline for short. Every molecular diagnostics laboratory that offers NGS-based testing maintains an internal pipeline or makes use of one or more cloud-based services that supplant missing or inadequate segments of their partially rendered internal pipeline. A typical hybrid workflow model employed by many molecular diagnostic laboratories includes initial local bench testing on locally placed NGS sequencing instruments followed by alignment of the resultant FASTQ files into aligned BAM files via an external cloud-based computational pipeline that is vendor-hosted. Following repatriation of the postanalytical data back in the local laboratory, final variant calling and adjudication of the clinical significance of the variants is determined and a final clinical report is issued. This hybrid model is attractive in that it allows smaller laboratories to benefit from sophisticated and actively curated analytical pipelines maintained by a larger central team, leveraging the economies of scale that come with greater testing volume. This provides a greater support model than would be possible if the lab were to attempt such activities with intramural resources alone. In essence, the emergence of web-based computational services has greatly democratized clinical NGS-based testing in that smaller laboratories can now effectively generate high-quality reports by leveraging the computational scale offered by external services while at the same time preserving the all-important personal relationships that local laboratories maintain with their clinician and patient clientele.

Cytogenetics

The cytogenetics laboratory, by virtue of the image-intensive subject matter that it generates and then analyzes, requires specialized software for image management and analysis as well as for assistance in assembly of the specialized descriptive language used to communicate genetic alterations in a systematized and consistent manner. The unique aspects of information technology in use by this laboratory section span the full range of preanalytical, analytical and postanalytical workflow settings, and should be reviewed individually.

Preanalytically, the cytogenetics laboratory shoulders a significant burden for maintaining an active cell-culture facility, with the requirement of knowing the location and status of a myriad number of live patient cell samples undergoing expansion in preparation for cytologic and cytogenetic analyses. This workflow is not unlike the microbiology laboratory that similarly needs to maintain inventory tracking for the many bacterial cultures incubating and awaiting detection of growth. Consequently, the preanalytical aspects of the cytogenetics laboratory from an informatics perspective can be viewed as an inventory and scheduling system, satisfying the need for flagging cultures that are sufficiently mature for further cytogenetic preparation and subsequent image capture/analysis.

With respect to the analytical phase, the cytogenetics laboratory is a sophisticated consumer of advanced image capture and analysis technology, with functional requirements that often fall outside the scope of intrinsic features offered by core LIS solutions. These unique requirements have fostered the creation and continued existence of a distinct ecosystem of best-of-breed solution providers, which often offer carefully paired image acquisition hardware and the required image analysis packages to realize a complete overall solution. In selecting such independent packages, the local pathology informatics team is left with the more manageable task of simply integrating the required electronic orders and results interfaces to the host LIS system, while leaving the complex intralaboratory workflow challenges to the purview of the third-party solution. While such incremental modules add complexity to the stewardship of the overall software portfolio that a larger collective clinical lab might need to maintain, the reduction in complex image analysis-based workflow usually more than justifies their inclusion. To be clear, an increasing number of integrated LIS solution providers are now beginning to offer their own cytogenetics module as part of their larger application suite portfolio. However, such big-box solutions are often devoid of the necessary incremental image acquisition hardware, making them at least partially incomplete. Consequently, it is expected that niche clinical LIS solution providers, such as those who provide integrated cytogenetics solutions, will continue to exist for the foreseeable future.

ARTIFICIAL INTELLIGENCE AND MACHINE LEARNING

The past decade has witnessed substantial accelerated adoption of various machine learning techniques in both commerce and science, with

laboratory medicine similarly identifying an increasing number of opportunities in which these technologies can be successfully applied for value-added operational, safety, and discovery activities. The term *artificial intelligence* is generally discouraged from use in the data sciences fields, with *machine learning* being the far-preferred term. This stems from the simple observation that the vast majority of algorithms and approaches currently in use represent an attempt to extract additional information from primary data that would otherwise be unavailable by human cognitive interrogation alone.

To understand the utility of machine learning techniques, consider the use case of a clinician interpreting two common laboratory panels in tandem: a complete blood count and comprehensive chemistry. Taken together, typically these panels represent between 28 and 30 individual scaler variables, with each result value having its own reference interval (which itself could be age- or gender-based, adding further interpretive variability). From a human cognitive standpoint, these 30 variables represent individual results that can be considered in isolation (a relatively straightforward cognitive task) and, at the same time, groupings of two or more results that necessarily should be considered collectively. Simple probability theory (e.g., "N Choose N" methodologies using the factorial function) necessarily dictates that the number of potential grouping—and, therefore, associated deviations from homeostasis—can grow geometrically in complexity and beyond the capacity of human cognitive interpretation alone. In essence, the example of two commonly ordered panels represents a 30-dimensional space computationally, which absolutely requires application of one or more multidimensional analytical methodologies to exhaustively identify and classify perturbations from the expected homeostatic setpoints of laboratory indices (both individually and in groups of varying size). Figure 12.4 underscores the geometrical challenge of increasing numbers of data elements from the perspective of human cognitive interpretation. Of primary note is the sobering observation that any collection of data elements exceeding between 7 and 11 individual classes of information already is at the level of complexity that requires computational assistance to fully extract all reproducible data present, with potentially many clusters in this high-dimensional space representing medically actionable information. A parallel can be drawn to a human's ability to effectively visualize dimensional spaces of increasing order. Fully comprehending event associations in two- and three-dimensional spaces (e.g., concurrent assessment of three variables at the same time) is cognitively feasible, but even four dimensions can represent something of an interpretive challenge to some individuals. As the dimensional order continues to increase, this cognitive challenge can be seen to exponentially compound—for example, a six-dimensional space perhaps being visualizable as a three-dimensional continuum of discrete three-dimensional spaces. Not every individual can effectively carry out such a mental exercise, nor would an individual be expected to have such ability. As the order of dimension grows further, it should be immediately evident that human cognitive insight alone is simply inadequate for seeing causal linkages and clusters in any larger N-dimensional space.

Conversely, there should be no doubt in any laboratorian's mind that, no matter the complexity of the dimensional order, there exist reproducible clusters and linkages of lab analyte results that manifest in

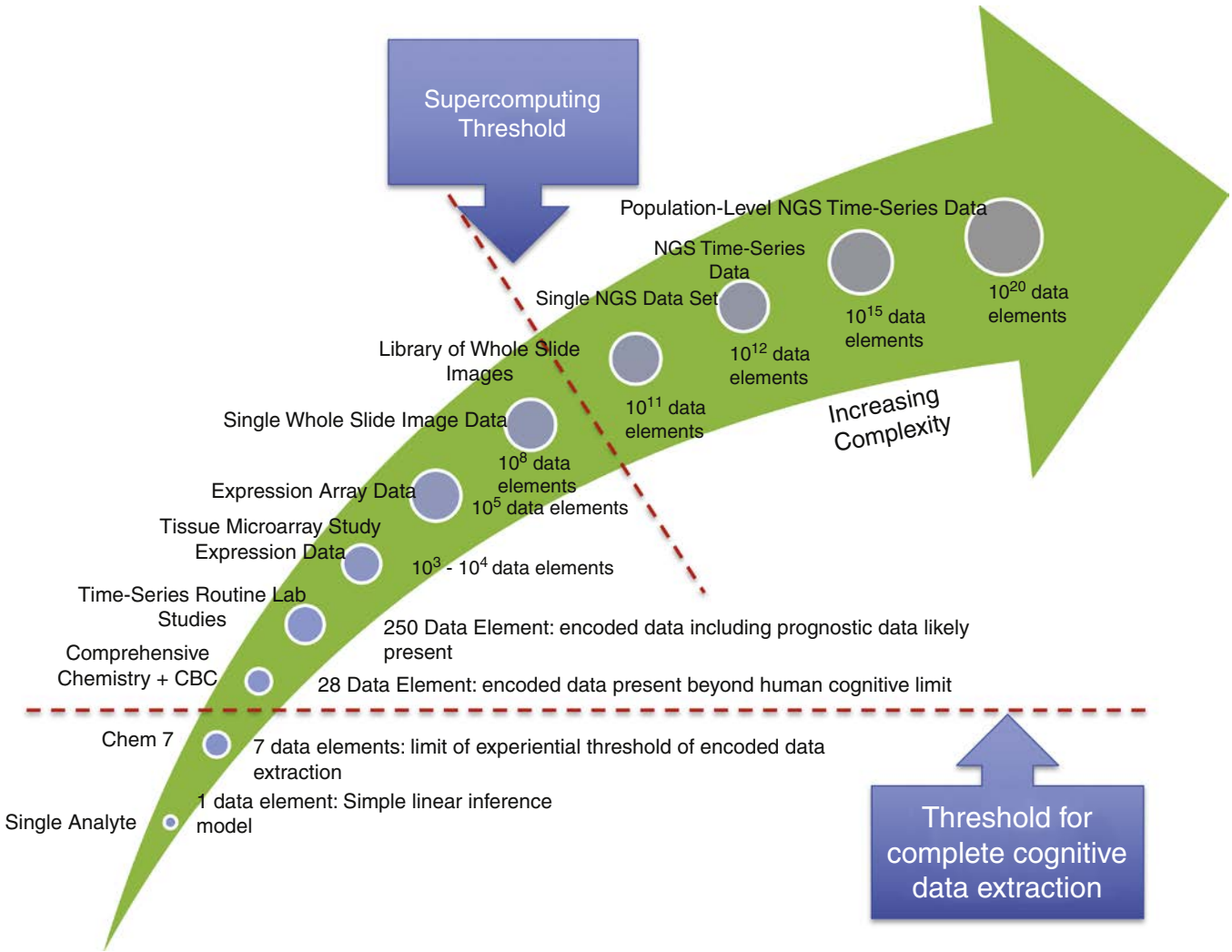

Figure 12.4 The cognitive challenge associated with increasing dimensional complexity. As the number of variables in tandem increases in the pursuit of fully evaluating clinical laboratory results, it should be noted that the threshold in terms of number of data elements, in which computational assistance is necessary to fully extract high-dimensional patterns, is quite modest (somewhere between 7 and 11). This implies that computational and machine learning approaches are requisite for even small panels of results. More importantly, without such computational support, biologically relevant and reproducibly present patterns of disease as manifest in these higher-dimensional spaces will absolutely be missed by dependence on human cognition alone. Another reality borne out by the increasingly large data sets that are being generated by the clinical lab is that laboratory medicine is becoming a supercomputing-dependent specialty for at least some of its core workflow. This makes a compelling case for the augmentation of data sciences and machine learning content in contemporary clinical pathology residency and medical technologist curricula, as without these added skills, the specialty will soon be unable to effectively analyze the very data that it generates.

high-dimensional space. These clusters and systematic shifts represent distinct and reproducible patterns, many of which correlate to a physiologic process or disease entity. Fundamentally, one of the hallmarks of machine learning techniques is the identification and classification of these clusters and cluster shifts in high-dimensional space and their associated correlation with both disease status and outcomes prediction. This observation also underscores the sobering reality that for essentially the entire modern period of laboratory medicine leading to the present, our field has been reporting only a fraction of the total data present in the primary data that has been generated from routine testing.

When extending this observation to the growing availability of high-throughput technologies for clinical testing (NGS, transcriptomics, and metabolomics, to name a few), it should be immediately evident that the actual dimensionality of the spaces now available for interrogation are in the hundreds or thousands, creating immense possibilities for new diagnostic and predictive assays that are specifically tailored to identify and classify clusters of events (which may be diagnoses) that reproducibly exist in high-order dimensions.

GLOSSARY

- **BYOD (bring your own device):** A central IT strategy for cost savings by which employees are encouraged to purchase their own IT devices (PCs, laptops, and smartphones) and bring them to work for routine work-related activities. This approach has the significant advantage of substantially decreasing central IT expenses that would otherwise be needed to cover the high cost of episodically replacing fleets of devices when they reach their expected end-of-life interval (typically every five to seven years). Conversely, this approach also exhibits the significant disadvantage of potentially introducing substantial device configurational and performance variability at both the hardware and software levels, leading to inconsistent or even absent antivirus/antimalware protection and varying capabilities for effectively running enterprise-standard software. With the emerging trend of health care enterprises leveraging thin client software in support of its core business solutions, these concerns can be partially mitigated with the use of browser-only-based devices that are otherwise locked down configurationally (e.g., Google Chromebook) and, therefore, much more resilient to malware intrusion (i.e., designed to cause damage to a computer or system) and less subject to variable performance across brands and models.
- **Client-Server Model:** In computing and business applications, the client-server model remains one of the dominant contemporary approaches for deploying solutions. In this model, computational burden of implementing business rules and carrying out transactions is carried out by a bifurcated transactional model in which tasks are divided between the central server and the plurality of attached nodes or devices that share in the computational burden. In the typical division of effort, the central server is usually tasked with the roles of validating access credentials upon users logging into the system and providing raw tabular data in support of transactions, with the remainder of the application of business rules assigned to the client, toward the goal of completing transactions. By dividing computational effort more or less equally between the central server and a multitude of attached client sessions, overall application throughput can be increased, making it possible to render an overall computing solution that can operate at greater scale (in terms of both number of users and number of transactions) for any given server configuration. The net benefit of utilizing the client-server model is decreased total cost of ownership (TCO) for the rendered database solution as a consequence of being able to reduce required hardware resources to a near-theoretical minimum.
- **Data Security Strategy:** Recognizing that health institutions are under increasing scrutiny to implement and maintain best practice for ensuring data security of all classes of protected health information, the implementation of a data security strategy has become an essential element of most IT organizations' overall data stewardship strategy. At minimum, policies are set in place to define minimum password length and any additional requirements for embedding of special characters (toward the goal of making brute-force password guessing attempts more difficult) as well as password expiration and replacement policies. Many institutions have also implemented *two-factor authentication*, in which a system user must enter another credentialing data element in addition to a fixed password to gain access to said secure systems. Typically, such systems are based on downloadable applications that can run on smartphones or self-contained key fobs. Both serve the purpose of dynamically generating a second credentialing data element that must be presented to the secure system in tandem with the password for authorization to be granted.
- **DHCP (Dynamic Host Configuration Protocol):** As a response to the configurational burden of adding new devices to any given network, in which IP numbers would need to be manually assigned and entered into the network configuration settings of that device prior to it being able to correctly operate, network engineers developed a "zero knowledge" protocol whereby an uninitiated device, upon its connection to a new network to which it had not previously connected, could utilize an interactive protocol to receive a centrally assigned IP number along with a stipulated lease time, whereupon another (and possibly different) IP number would be assigned. This protocol is fully autonomous, providing all information needed for a device to successfully interoperate on any given network (including the three essential elements of an IP address: the address itself, the subnet mask, the gateway address and, finally, the one or more needed DNS addresses). Use of the DHCP protocol has both simplified and compounded the installation and stewardship of instrumentation in the clinical laboratory. On-boarding of devices is now a trivial task, but the fact that IP addresses can change over time as leases expire, causing DHCP servers to possibly assign a different IP address, creates a challenge for laboratory information systems to always know the network address of instruments for which a constant connection is required for transport of orders and results. The general solution to this conundrum has been the parallel implementation of a DHCP Reservation process along with use of DHCP IP assignment.
- **DHCP Reservation:** An extension of the DHCP, whereby any device attaching to a network, upon presenting its six-byte *MAC Address*, will be assigned the same IP number by the DHCP server if it is the case that the MAC ID in question is already registered in that DHCP server's assignment table as having a permanently reserved IP number. This has the effect of ensuring that any network device that is preregistered with the DHCP server will always receive the same IP number upon reconnecting. Devices that have completed the DHCP reservation process always are assigned the same IP number, with such numbers not having an expiration time interval (as typically encountered with routine DHCP IP assignment). This permanence creates the necessary circumstances whereby network devices that require address permanence, such as clinical instruments and automation lines, are always in a stationary network address, where the central lab information system can find them.
- **Domain Name System (DNS):** As an integral element of the Internet, the DNS layer was developed to allow for a simplified way of assigning human-readable and easily remembered/recognized textual names to each of the IP numbers that constitute unique devices/nodes on the Internet. The DNS paradigm is divided into a number of top-level domains (e.g., .com, .org, .net, .edu), upon which subdomains can be appended to formulate a fully qualified domain name (FQDN). To facilitate converting domain names to their assigned IP number, the Internet itself (as well as most enterprises) makes use of the domain name server, whose role it is to provide the IP address of FQDNs upon being interrogated. For example, a user querying the CNN website in a browser (by entering CNN.com) is ultimately routed to CNN's website, which is actually located at IP #151.101.001.067, by a DNS server that looks up the textual name in a locally held table and provides the registered IP number in return. The DNS system is globally linked to a number of top-level DNS servers, which periodically cascade their master tables, thus allowing for synchronization of the global Internet to a matching set of FQDN-to-resolved-IP# tables.
- **Firewall:** An integral hardware component of any private network that serves as a physical and topological demarcation between internal intranet traffic and all external Internet traffic. Firewalls typically operate by a set of rules that are applied on a specific IP address basis, against a range of IP addresses, whereby specific data packet classes (identified by port number and transmission class) are allowed or disallowed from originating or destinating. In this manner, the firewall can (1) exclude unwanted types of data and data classes from exiting an enterprise's secure intranet network segment and (2) exclude unwanted packets from the Internet-large from entering a secure intranet. Often, specific rules of a firewall will be accompanied by general class rules that are intended to protect the enterprise-large (e.g., if the port number of an incoming packet is not identified in the acceptable port type list, then disallow it).
- **List-Mode Data (Flow Cytometry):** Flow cytometry data is high-dimensional data by virtue of the multichannel nature of the quantitative indices captured for each individual cell interrogated in a flow cell by the light of a columnated laser beam. This complexity creates the need for several approaches to data stewardship depending on the intended analysis methodology and long-term requirements for curation of the resultant primary data. In the simpler form of data archi-

val, numeric gating "windows" allow for the capture of cell-population histogram and bitmap data, which essentially is a running tally of the number of events in the forward scatter, side scatter, and multiple fluorescent channels. For applications in which there is no intent of re-windowing primary data, this capture format suffices in appropriately documenting the expression characteristics of the multiple cell populations typically present in a clinical sample. However, in settings for which there is the need and/or expectation that re-gating of individual cell data will be required for current and future diagnostic and/or investigative evaluations, especially in settings of multichannel gating, it is desirable to capture individual cell signal intensities, including forward scatter, side scatter, and all individual fluorescent channels, with high-precision numeric values. Such fully documented data sets of flow cytometry runs are termed *List-Mode Data*, stored in a particular file format (Flow Cytometry Standard [FCS], a standard maintained by the International Society for Advancement of Cytometry [ISAC]), facilitating both ease of use and interoperability. The latest version, which was introduced in 2010, is FCS 3.1. The FCS format makes use of an array configuration, with individual cell measurements forming the rows and the various scatter and fluorescent channels forming the columns. FCS files can be quite large owing to the requirement of capturing every data channel for every cell. Consequently, clinical and scientific judgment should be exercised in deciding which flow cytometry assays and protocols merit the substantial increase in storage required to support FCS-based documentation.

- **Internet/Intranet:** In any institution's network topology, there is an almost always present demarcation between the internal network (the intranet), where secure business information (and protected health information [PHI], in the case of health care–related institutions, including clinical laboratories) can be exchanged internally, and the remainder of the world (the Internet). These two domains are typically separated by an institutional firewall, which operates under a set of information exchange rules to determine which packets of internal data are allowed to leave the intranet for the Internet and, conversely, which external classes of data from the outside are allowed to enter an enterprise's intranet. This demarcation is important; most examples of data compromise involve some type of exploitation that allows external threat actors to penetrate the security layers imparted by an institution's firewall, thus creating an unauthorized channel (or "tunnel") between the Internet proper and an organization's intranet.
- **IP Address:** This is one of the two device address classes (the other being the Media Access Control Address) that any device on a network will possess and with which it will identify itself when interrogated. An IP (Internet Protocol) number can be assigned by the network itself on a device being activated on the network (Dynamic Host Configuration Protocol [DHCP]) or it can be preprogrammed with a fixed number that will always be used to identify itself when a device is connected. IP addresses are available in two forms: IPv4 (IP version four) and IPv6 (IP version six). The latter format was developed to address the address exhaustion of top-level IPv4 pools that took place in 2011, with the newer IPv6 format allowing for an inconceivably large number of network addresses (3.4×10^{38}), making it unlikely that another device numbering schema will be required in the foreseeable future. At present, most contemporary router and switch devices in most intranets (and the Internet at large) make it possible for IPv4- and IPv6-based traffic to interoperate seamlessly across the same network.
- **Media Access Control Address (MAC Address):** The MAC address is a unique, six-byte identifier assigned by the device manufacturer to the network interface controller (NIC) of any network-capable device, allowing for physical identification of a specific device by network devices such as routers and switches. As this number is typically permanently assigned to the physical network port of a device, it represents a convenient stationary fiduciary anchoring point by which network hardware can positively identify an instrument and assign it a reserved IP number (e.g., the DHCP reserved IP number protocol). MAC addresses are also sometimes used as part of a network's intrinsic security model in a protocol known as Network Admission Control (NAC). With NAC implemented in an intranet, only devices with known MAC addresses are allowed to join the internal network, with all other devices being ignored. This approach prevents personally owned machines that have not had their MAC addresses registered with the enterprise from being able to make use of an enterprise's network infrastructure.
- **MODEM (MOulator/DEModulator**): In telecommunications, the modem is a fundamental hardware device that allows for a serial digital data stream to be converted to the audio format of common carrier telephony networks (telephone lines). In the earlier days of computing, prior to the availability of high-speed Internet access, modems were an essential solution in allowing remote sites to access a data center through telephone line access. Modems are still utilized to provide instrument and printer connectivity where the cost of a fixed high-speed Internet connection cannot be justified for low transactional settings and locations, where operating expenses of a phone line are far below that required for higher bandwidth connectivity, which is not required anyway. Typically employed with conventional copper telephone line service, the overall approach is commonly referred to as a Modem/POTS (modem–plain old telephone service) connection.
- **Network:** This is a general term that refers to the collective assembly of data channel interconnections within an enterprise (which can be extended as a concept to the whole of the Internet), by which devices (e.g., nodes) on the network communicate with all other devices on that same network. Complex networks are typically managed, implying the utilization of one or more central switches/routers to manage data traffic, both internally within a secure intranet zone and externally to the public Internet at large. For most institutions, an important demarcation is the crossover point at which internal and external data traffic overlaps, which typically is managed by a top-level router. Traffic that stays within an enterprise is said to be intranet traffic. Intranet traffic that crosses the router to reach the greater Internet is said to be external or Internet-bound traffic. An important aspect of network topology is ensuring that appropriate security measures and safeguards are always in place between internal intranet traffic and the outside world of the Internet.
- **Relational Database:** In the general field of database technology, relational databases are application environments that provide database functionality in the form of normalized information, where atomically distinct data elements are typically not reduplicated within a plurality of tables. In a typical transactional system, such as any contemporary LIS, common categorical classes of information (e.g., tables) typically include orders, patients, and tests. In the relational database model, the need to reduplicate information in any one table to other tables is usually avoided. For example, an orders table, with distinct laboratory test orders in each of its rows of data, would not also directly include patient data in that row. Rather, each order row would simply contain a "pointer" to the correct row of the Patient Demographics table, where such patient data would be maintained. In such a manner, changing the information for a given patient in the Patient Demographics table would ensure that all Order Table rows pointing to this Patient Demographics table row would also benefit from the fully updated and correct information when the Patient Demographics table is updated. Prior to the development of relational databases, a common problem with so-called flat-database models, in which information was repeated many times in many separate places of the overall database, was referential integrity failure, in which updates in one piece of information were not uniformly applied in all sections of the database, where that piece of data was reduplicated. By removing duplicate information, this problem was seen to essentially disappear and was one of the original driving motivations for transitioning to near-universal use of relational database technology.
- **Router:** In data network architecture, the router is a fundamental building block of both intranets and the Internet proper. In intranet settings, an enterprise will employ one or more routers to manage IP traffic between nodes within the enterprise as well as traffic between nodes of the enterprise and the outside world. Given that each IP-based packet is labeled with both a unique socket number (indicating the class of information being transported) and a datagram class (e.g., TCP or UDP, indicating stateful or stateless channel transmission), routers make use of this packet prefix information to decide if and where to route it. IP packets with socket numbers or destination address that fall outside of known destination targets are excluded by the router from being relayed, whereas IP packets with sanctioned prefix information are allowed to pass through to their intended destination. Given that routers are responsible for managing all incoming and outgoing data of any given enterprise, these devices at the hardware abstraction level tend to be constructed as high-performance/high-reliability devices capable of handling enormous transactional volume. Indeed, as they have often been identified as being single points of failure, many enterprises employ two or more routers in a typical N+1 configuration to allow for fault tolerance and uninterrupted operation in the setting of point failure.
- **TCP/UDP Packet Type:** IP packets are generally exchanged as both stateful (TCP, Transmission Control Protocol) and stateless (UDP,

User Datagram Protocol); the former mode provides a managed channel, which can be opened, monitored, and subsequently closed. The stateless channel alternative, as provided by the UDP datagram model, allows for simplified provision of communication between source and destination network nodes, where traffic management is handled by the application layer and not the Internet itself. Use of TCP and UDP datagram models have respective advantages and disadvantages, which must be considered when developing an interconnection protocol.

- **Thick Client:** In the client-server model, when the software running on a client is a conventional application specifically designed for the operating system and hardware of the client hardware, the client is said to be a *thick client.* Such programs are typically designed to run on specific hardware and operating system versions and, therefore, are not "portable" across differing operating system environments. A thick client version of a LIS solution designed for the MS Windows 10 environment, for example, would not be expected to be able to be run from an Apple-based (Mac OS) hardware platform.
- **Thin Client:** With the advent of the so-called Web 2.0 and HTML-5 markup language, it has become possible to develop client applications that can run entirely within a web browser while still providing a similar level of computational throughput and functional capability as provided by the more traditional thick client application model, where programs run directly within a specific operating system. So-called thin client applications, which can run entirely within a browser environment, are significantly more portable and, therefore, can be executed from a variety of device platforms, including all brands of personal computers, browser-only workstations (e.g., Google Chromebooks), tablets, and even smartphones. The only requirement for such portability is that the host device is capable of running a contemporary browser that supports the current HTML-5 markup language extensions. Utilizing a thin client app in client-server-based solutions is attractive in that end users may make use of the application from a diverse range of hardware appliances. This extends the reach of the software to more work and applications settings than would otherwise be possible with the use of a dedicated workstation hardware version alone.
- **Transmission Lines:** The physical means by which electronic data are exchanged, both internally within an institution and externally from an institution to the Internet proper, as well as to other external destination networks. This term can apply equally to two separate conceptual constructs: the physical abstraction layer and the interconnection topology layer. In the physical abstraction layer, transmission lines refer to the actual methodology used to connect workstations and instruments to the local area network and to other devices and resources on this network. Typical examples of physical transmission lines include Category 5e and Category 6 twisted pair cable, and fiber optical cable. In terms of the topological definition of transmission lines, the same physical cable may be capable of carrying multiple signal formats. For example, a 1 Gigabit Cat-6 cable can effectively relay 1-Gbit, 100-Mbit and 10-Mbit signal formats, depending on the configuration of the attached network switch.
- **VPN Tunnel:** Recognizing the increasing frequency with which enterprises are being asked to extend their intranet to geographically diverse locales that are physically separated from their primary campus, IT departments and their network engineering groups have effectively made use of VPN (virtual private network) tunnel technology. In constructing a VPN tunnel, it is possible to extend an institution's private intranet through the public Internet proper into a distant locale where devices on that separately instantiated intranet are viewed as being also within the intranet of the enterprise's main campus. Packet traffic between the geographically diverse and separate two intranet locations is made to "tunnel" through the Internet proper in a manner in which the utilized encryption prevents third parties along the public Internet route in use from being able to decode and read the information being transmitted. Such tunnels have become essential in extending LIS workflow to outreach locations (supporting blood draw sites and outpatient reporting) in a manner that does not require dedicated and expensive point-to-point high-speed network connectivity. Rather, with VPN tunnels, it is possible to extend an enterprise's intranet to as many external locations as needed, while being dependent only on a distant site's ability to offer general access to the Internet itself. Implementation of VPN tunnel technology, however, is not without its challenges, as the burden of appropriately configuring the VPN tunnel itself and the associated network firewalls on each end of the tunnel can be substantial both in terms of initial setup and ongoing stewardship.

SELECTED REFERENCES

Pantanowitz L, Tuthill JM, Balis UGJ: *Pathology informatics: theory and practice*, Chicago, 2012, ASCP Press.
A comprehensive review of informatics.

Sinard JH: *Practical pathology informatics: Demystifying informatics for the practicing anatomic pathologist*, London, 2006, Springer-Verlag, p 380.
A useful general reference anatomic pathology informatics text.

REFERENCES

Aller RD: Connectivity from source to action, *Clin Chemistry* 47(8):1521–1525, 2001.

Baron JM, Mermel CH, Lewandrowski KB, et al.: Detection of preanalytic laboratory testing errors using a statistically guided protocol, *Am J Clin Pathol* 138(3):406–413, 2012.

Celebrating G. Octo Barnett, MD, *J Am Med Inform Assoc*. 27(8):1187–1189, 2020.

Hawker CD: Bar codes may have poorer error rates than commonly believed, *Clin Chem* 56(10):1513–1514, 2010 Oct, https://doi.org/10.1373/clinchem.2010.153288. Epub 2010 Aug.25. PMID: 20739634.

Lippi G, Blanckaert N, Bonini P, Green S, Kitchen S, Palicka V, Vassault AJ, Mattiuzzi C, Plebani M: Causes, consequences, detection, and prevention of identification errors in laboratory diagnostics, *Clin Chem Lab Med* 47(2):143–153, 2009, https://doi.org/10.1515/CCLM.2009.045. PMID: 19099525.

Louis DN, Gerber GK, Baron JM, et al.: Computational pathology: an emerging definition, *Arch Pathol Lab Med* 138(9):1133–1138, 2014.

Murphy MF, Kay JD: Barcode identification for transfusion safety, *Curr Opin Hematol* 11(5):334–338, 2004 Sep, https://doi.org/10.1097/01.moh.0000142801.38087.e5. PMID: 15666657.

O'Moore RR: Decision support based on laboratory data, *Methods Inf Med* 27(4):187–190, 1988 Oct. PMID: 3067058.

Pringle M: Using computers to take patient histories, *BMJ* 297(6650):697–698, 1988 Sep 17, https://doi.org/10.1136/bmj.297.6650.697. PMID: 3147730; PMCID: PMC1834108.

Piemme TE: Computer-assisted learning and evaluation in medicine, *J Am Med Assoc* 260(3):367–372, 1988 Jul 15. PMID: 3288776.

Patel AA, Gilbertson JR, Showe LC, et al.: A novel cross-disciplinary multi-institute approach to translational cancer research: Lessons learned from Pennsylvania Cancer Alliance Bioinformatics Consortium (PCABC), *Cancer Inform* 3:255–274, 2007.

Sarkar IN, Butte AJ, Lussier YA, et al.: Translational bioinformatics: linking knowledge across biological and clinical realms, *J Am Med Inform Assoc* 18:354–357, 2011.

Seising R, Homer Richards Warner, 1922-2012. *Artif Intell Med*. 58(3):133–138, 2013.

Silverman HD, Steen EB, Carpenito JC et al.: Domains, tasks, and knowledge for clinical informatics subspecialty practice: results of a practice analysis. *J Am Med Inform Assoc* 2019.

Snyder ML, Carter A, Jenkins K, Fantz CR: Patient misidentifications caused by errors in standard bar code technology, *Clin Chem* 56(10):1554–1560, 2010 Oct, https://doi.org/10.1373/clinchem.2010.150094. Epub 2010 Aug 11. PMID: 20702784.

Staes CJ, Evans RS, Rocha BH, et al.: Computerized alerts improve outpatient laboratory monitoring of transplant patients, *J Am Med Inform Assoc* 15(3):324–332, 2008.

Tate A: Middleware: Don't rule it out, *MLO Med Lab Obs* 44(10):20, 2012.

Van Cott EM: Laboratory test interpretations and algorithms in utilization management, *Clin Chim Acta* 427:188–192, 2014.

Westbrook JI, Georgiou A, Dimos A, et al.: Computerised pathology test order entry reduces laboratory turnaround times and influences tests ordered by hospital clinicians: a controlled before and after study, *J Clin Pathol* 59(5):533–536, 2006. [Epub 2006 Feb 3].

Westra BL: Radio frequency identification, *Am J Nurs* 109:34–36, 2009.

Weilert M, Tilzer LL: Putting bar codes to work for improved patient care, *Clin Lab Med* 11(1):227–238, 1991 Mar. PMID: 2040145.

CHAPTER 13

FINANCIAL MANAGEMENT

Mark S. Lifshitz, Robert P. DeCresce

INDUSTRY OVERVIEW, 162
DEFINING AND IDENTIFYING COSTS, 162
REVENUE, 164
PAYERS AND REIMBURSEMENT, 164
Private Insurance, 164
Government Payers, 164
REIMBURSEMENT CODING SYSTEMS, 166
Why Accurate Coding Is Important, 166
Medicare Reimbursement, 167
FINANCIAL PERFORMANCE AND MONITORING, 169
Budgeting, 169
Variance Analysis, 169
Financial Reporting and Statements, 170
Benchmarking and Productivity Measures, 171
EVALUATING A CAPITAL PROJECT, 171
Payback Period, 171
Breakeven Point, 171
Return on Investment, 171
Net Present Value, 171
Internal Rate of Return, 171
Interpretation of Financial Calculations, 171
CAPITAL ACQUISITION METHODS, 172
SELECTED REFERENCES, 173

KEY POINTS

- Costs can be described in different ways depending on how they relate to laboratory operations (direct/indirect), change with test volume (variable/fixed), pertain to staffing (salary/nonsalary), or are associated with the useful life of supplies or equipment (operating/capital). Cost per reportable result is a key indicator.
- Reimbursement for laboratory services comes mostly from third-party payers, such as Medicare (government) and insurance companies (nongovernment/private insurance), and payments are almost always less than charges.
- Inpatient laboratory testing charges are usually not reimbursed directly; they are considered part of a per diem rate (i.e., general hospital daily room reimbursement rate) or a case rate, such as diagnosis-related group rate (i.e., set rate for the entire hospital stay, regardless of actual length of stay). Thus inpatient laboratory testing is usually considered a "cost center." In contrast, outpatient laboratory charges are reimbursed directly; therefore, outpatient testing is usually considered a "revenue center."
- For reimbursement purposes, Current Procedural Terminology codes describe tests, and *International Classification of Diseases, Tenth Revision (ICD-10)* codes describe the diagnosis. Medical necessity requirements may limit reimbursement to those tests associated with specific predefined diagnoses.
- Budgeting is the process of planning, forecasting, controlling, and monitoring the financial resources of an organization.
- A variety of financial tools are used to evaluate a capital project, such as purchasing a chemistry analyzer. These measure how long it takes to recoup an investment (payback) and how much it generates in today's dollars (net present value) and its rate of return (internal rate of return).
- Laboratory equipment can be acquired in different ways, including purchase, lease, and per-test payment. Each has pros and cons.

Every organization, no matter the products or services it provides, must be concerned with the management, oversight, and accounting of its monetary resources. To sustain a viable, competitive entity, an organization not only must recoup the cost of operations but must have a positive net income to reinvest in itself. The laboratory is no exception. To be successful in the financial management of the laboratory, the director/manager must be able to identify and categorize costs, understand the relationships between revenue and reimbursement, become familiar with the budget process, and use financial ratios and information to make sound decisions. Credibility with administrators and colleagues demands that the director/manager be comfortable and confident when explaining financial issues and when justifying the need for additional resources.

INDUSTRY OVERVIEW

Most industries in the United States are subject to traditional free-market competition. However, this principle does not fully apply to health care because relatively few people who use health care pay directly for it. Most people are beneficiaries of some form of health insurance. This, in combination with the number of uninsured and underinsured, has led to a system that provides services even when no one pays adequately for them. Most medical claims are paid by a third party, such as the government (Medicare, Medicaid) or a private insurance company. Thus someone other than the patient usually pays the provider of health care.

The health care industry is one of the largest industries in the United States and continues to be a growing sector of the gross domestic product, having increased from 5.1% ($27 billion) in 1960 to 17.9% ($3.5 trillion or $10,739 per person) in 2017 (Centers for Medicare & Medicaid Services [CMS], 2018b). Hospitals continue to be a driving force behind escalating health care costs. Most U.S. hospitals are tax exempt, not-for-profit entities. Though "not-for-profit" suggests that no profit is made, it actually means that profits are not distributed to owners or shareholders; instead, profits are reinvested in the organization. Historically, not-for-profit status led hospital administrators to be less profit conscious than counterparts in other businesses. However, today's hospitals are having a difficult time just covering operating costs given dwindling reimbursement and increasing supply and labor costs. With scarce money left for capital reinvestment in equipment, buildings, facilities, and technology, hospitals are aggressively seeking new ways to produce a profit to invest for the future.

DEFINING AND IDENTIFYING COSTS

A cost (expense) is the supply, labor, and overhead money spent on a product or service (Travers, 1997). It is important to understand costs to accurately price tests and other services, to determine when and how to offer new tests, and to determine whether to acquire new outreach client business or a managed care contract. Costs can be classified in different ways (Table 13.1).

Direct costs are expenses that can easily be traced directly to an end product. In the laboratory setting, the end product is a billable test. Examples are reagents, consumables, and hands-on technologist time. In contrast, *indirect costs* are not directly related to a billable test but are necessary for its production. Indirect costs are often referred to as overhead. Examples are proficiency testing and utility expenses.

Variable costs change proportionately with the volume of tests. As test volume grows, so do reagent costs. If the reagent cost per test is $1.00, when 1000 tests are performed, the reagent cost is $1000; when 20,000 tests are performed, the reagent cost is $20,000. *Fixed costs* do not change with the volume of tests performed. If a laboratory pays $5000 per month to rent its space, this expense remains the same if the laboratory produces 1000 or 20,000 tests per month (Fig. 13.1).

TABLE 13.1
Cost Classification

	Direct	Indirect	Variable	Fixed	Salary	Nonsalary	Operating	Capital
Reagents	■		■			■	■	
Proficiency testing		■		■		■	■	
Analyzer service	■			■		■	■	
Analyzer	■			■		■		■
Testing staff	■			■	■		■	
Management staff		■		■	■		■	
Rent		■		■		■	■	

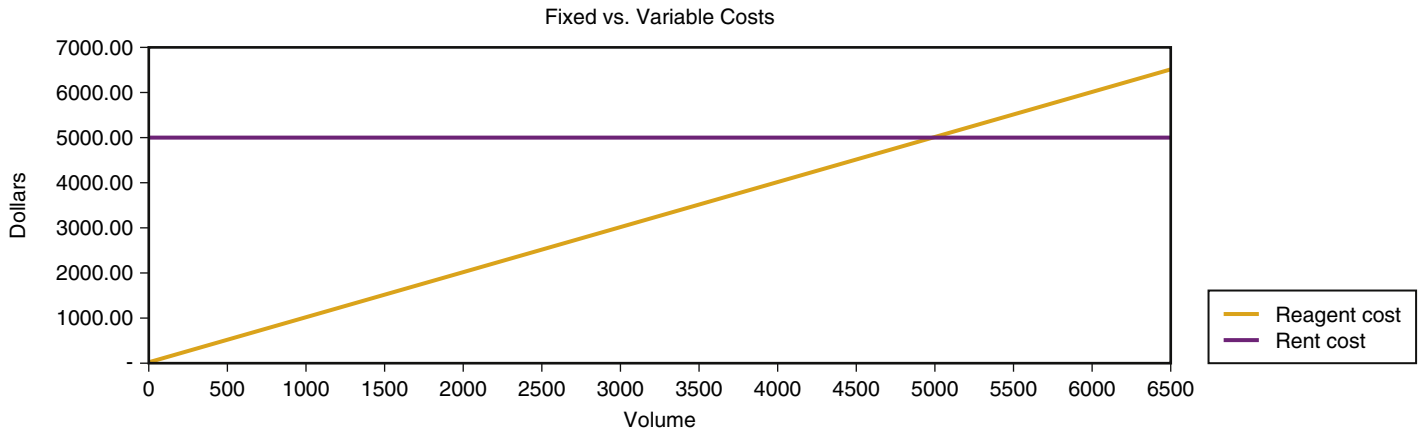

Figure 13.1 Fixed costs, such as rent, remain constant. Variable costs, such as reagents, are directly proportional to test volume.

Because fixed costs do not vary with activity, the goal is to produce as much as possible from fixed costs to achieve economies of scale. The more that is produced, the lower the *fixed cost per activity*. In the preceding scenario, if the laboratory produced 1000 tests, the fixed cost per test is $5.00; with 20,000 tests, the fixed cost per test falls to $0.25. Note that even some fixed costs have a variable component. For example, if an instrument's capacity is 20,000 tests per month and the volume increases beyond that, another instrument will have to be purchased, increasing the fixed costs per test. Fixed costs that change with increments of volume are called *step costs*.

Salary costs need to be looked at differently from *nonsalary costs* because salary costs have fringe benefits associated with them. Salary expenses account for approximately 50% to 70% of the laboratory budget. Because salary expenses are generally fixed, it is important to strive for economies of scale. The hourly pay or salaried wage of an employee is not the entire cost of employment. Fringe benefits such as Social Security, health insurance, tuition reimbursement, pension plans, and life insurance can represent an additional 16% to 28% expense above the base salary. Costs are also associated with the recruitment, interview, and selection process. Once an employee is hired, orientation, training, and ongoing growth and development costs are incurred.

Operating costs are the expenses incurred to produce a product or service. Many items have only a one-time use and, once used, the item has no further value. Examples of one-time operating costs include reagents, electricity, disposable pipettes, and the salary expense in the production of a test. Other items, such as analytic equipment, computers, and the physical plant, have a useful life greater than one production cycle. These items are capital items. To qualify as a *capital* item, it must meet three criteria: time, price, and purpose. To meet the time criterion, the item must have a useful life of longer than 1 year. The institution must designate a minimum dollar amount, usually $1000 to $5000, that qualifies an item as capital. The purpose of acquiring capital items is usually to replace older equipment with safer and more efficient models or to add new equipment to support new products or services. With time, capital equipment loses its value. The annual loss of a capital item's value is called *depreciation* and is an annual expense that is deducted from the revenue of a business. Depreciation is not a cash expense (i.e., you do not "pay it" each year), but it is a real expense in that it recognizes the "wearing out" of an asset that was acquired with cash and eventually will have to be replaced. If an analyzer has not yet been fully depreciated, it still has "book value." Note that operating and capital costs are budgeted separately (see later discussion).

The cost of producing a test can be derived in different ways. *Microcosting* determines the total direct labor and supply costs of producing a test, and it is the starting point for determining the fully loaded cost and ultimately the price for a test. Most testing in the clinical laboratory is performed in batches or continuous "runs" of many samples during one or more shifts. A run can be a group of tests that are performed once or many times during a shift or an entire 24-hour period. A run includes all quality control and calibration costs needed to produce patient results. When microcosting a test, it is important to consider how a test is performed because labor and supply costs vary according to workflow and laboratory policy for quality control and repeats. The *cost per reportable result* (CPRR) distributes the total direct costs of a run over the patient "reportable" results for that run. Testing efficiency is defined as the total reportable patient results/total test results. Thus the more repeats and controls performed, the lower the efficiency and the higher the CPRR. As testing efficiency increases, the CPRR decreases. The *incremental cost* is the cost of producing one additional test that, typically, does not require additional salary or capital. For example, the incremental cost of running a chemistry test is usually the cost of dispensing reagent for one additional test assuming that there are no sample collection costs. Other associated costs, such as technologist time, equipment, or quality control, are fixed costs that are incurred irrespective of the additional test. The incremental cost is usually the lowest possible cost incurred to produce a result. It is best used to assess how much it costs to produce small increments in test volume. As volume grows, a laboratory may need additional staff and equipment; these costs would have to be included in the incremental costing analysis. Incremental costing is especially useful when one is trying to determine whether additional outreach work is profitable or not. The *fully loaded cost* for a test is the sum of direct and indirect costs. The allocation of indirect costs is usually done using a formula. The goal of allocating indirect costs is to apply the costs based on the strongest correlation between the indirect cost and to what it is being applied. For example, utilities could be based on

departmental square footage, while human resources costs could be based on the number of employees in the department. *Make-versus-buy* decisions should be based on the fully loaded cost to produce the test compared with the price offered by a commercial or reference laboratory. If it costs more to produce a test than to buy it from another supplier, the test should be considered for outsourcing. However, when make-versus-buy decisions are made, cost is only one factor to consider. Medically necessary turnaround time, methods, and reliability of the potential alternative supplier should also be considered. The price charged for a test needs to be marked up (increased) from the fully loaded cost to realize a profit. However, a profit may also be realized on additional business priced lower than the fully loaded cost, as long as the incremental revenue from the work exceeds the incremental cost of doing the work. One must also take into consideration the expected collection rate, relative to charge. The *contribution margin* is the balance remaining after the fully loaded costs are deducted from the price charged for a test. Table 13.2 demonstrates various ways to determine the cost of a test and how to establish its charge.

The *total cost of ownership* (TCO) for a laboratory is the life cycle cost of its capital assets. It focuses attention on the sum of all costs of owning and maintaining all assets for a specific service or product as opposed to the initial capital or operating costs. In the laboratory, TCO includes acquisition, setup (construction, training), support (ordering supplies, dealing with backorders), ongoing maintenance (scheduled and unscheduled downtime), service, and operating expenses (reagents, controls, repeat testing, inventory control, proficiency testing, testing personnel, supervisory personnel) of a specific workbench and its associated testing instrumentation. TCO is useful in considering make-versus-buy decisions, but determining an accurate TCO can be very difficult.

REVENUE

Revenue is the total price of services rendered or products sold (Harmening, 2012). It is the money a business is entitled to receive for the services and products it produces. In health care, revenue should not be confused with reimbursement or cash collected. *Gross patient revenue* consists of the total charges at a facility's full-established rates (list price) for provision of inpatient and outpatient care before deductions from revenue are applied. *Net patient revenue* is the gross inpatient and outpatient revenue minus all related deductions. *Deductions* from revenue include contractual adjustments, provision for bad debts, charity care, and other adjustments and allowances that reduce gross patient revenue. *Contractual adjustments* account for the difference between billings at full-established rates and amounts received or receivable from third-party payers under formal contract agreements. For example, if the list price of a test is $10 but the contracted payment from the insurance company is $6, the adjustment is $4. If all deductions and contractual allowances are correct, net patient revenue should equal cash collected, or $6 in this example.

In health care, it is important to distinguish between inpatient and outpatient care because they are reimbursed differently. Inpatient laboratory testing charges usually are not reimbursed separately; they are considered to be part of a per diem rate (i.e., general hospital daily room reimbursement rate) or diagnosis-related group (DRG) rate (i.e., set rate for the entire hospital stay, regardless of actual length of stay). Thus inpatient laboratory testing is considered a "cost center." The hospital is paid the same rate regardless of how many tests are provided. In contrast, outpatient laboratory testing has historically been a revenue center because each test is separately reimbursed, usually by a third party (Table 13.3). Thus there has been a financial disincentive to perform inpatient tests and an incentive to perform outpatient tests. However, because new reimbursement models focus on accountable care, shared risk, and bundled payments, incentives to perform outpatient testing are likely to change.

PAYERS AND REIMBURSEMENT

Hospitals in early America served a different purpose from those of today. A visiting physician usually provided health care in the patient's home, and care was administered by family members, midwives, and servants. Early hospitals were founded to shelter older adults, the dying, orphans, those with mental illness, and vagrants, and to protect the citizens of a community from contagious diseases and the dangerously insane. Many of today's county, municipal, or religious order hospitals were originally a combination of these almshouses and isolation hospitals (Young, 2017).

The transformation of hospitals from charitable institutions to complex technical organizations came about with the passage of the Hill-Burton Hospital Construction Act of 1946 and the growth of private hospital insurance. The Hill-Burton Act provided federal money to the states to plan and construct new facilities. The first private health insurance policy was formed by a group of teachers and Baylor Hospital in Dallas to provide coverage for certain hospital expenses. This arrangement created the model for the development of what was to become Blue Cross Insurance. The development of health insurance to provide reimbursement for routine medical care carried gigantic implications. The original concept of any insurance was to guard against the low risk of a rare occurrence such as premature death or accident. Today's health insurance provides for coverage of routine, predictable services and unforeseen illnesses and injuries (Young, 2017).

PRIVATE INSURANCE

Private health insurance falls into two main categories: indemnity and managed care. Indemnity plans, also known as fee-for-service, are traditional insurance plans that give patients absolute freedom to choose their physicians and medical facilities. Insurance companies usually require the beneficiaries to fulfill a yearly deductible, which can often exceed $1,000 per person per year. After the deductible is fulfilled, the insurance company pays a certain coinsurance rate of the usual and customary charge (UCC). The UCC (or fee schedule) is set by the payer and is usually less than the actual billed charge, in which case the patient may be responsible for the balance. Generally, the coinsurance is split 70%/30% or 80%/20%, where the insurance company pays the higher percentage and the insured the lower. Indemnity plans were the mainstay of the health insurance world before the 1980s. Today, managed care is the norm. Some employers still offer indemnity plans despite their high premium payments to allow their employees the freedom to choose medical services.

As an alternative to indemnity health insurance, managed care was introduced in 1973 with the passage of the Health Maintenance Organization Act. This act encouraged and funded the development of health maintenance organizations (HMOs) as a strategy to contain the rising cost of health care (Young, 2017). HMOs utilized managed care features that coupled health care reimbursement with delivery of service and allowed payers significant economic control over how, where, and what services were delivered. In managed care, specific physicians and hospitals are selected to care for members; referrals from a case manager are usually necessary for specialty or inpatient services; and providers share in the financial risk through capitation agreements and per diem rates.

Capitation agreements pay the service provider (e.g., physician) a fixed dollar amount per member per month (PMPM). From this amount, the provider agrees to cover all care for plan members. For example, if a laboratory signs a capitation agreement to accept $1.50 PMPM for the outpatient testing needs of 2000 HMO members, the laboratory receives $3000 per month and $36,000 per year. If it costs the laboratory more than $36,000/year to provide the services, it realizes a financial loss; if it costs less than $36,000, it realizes a profit. In a capitation testing agreement, a laboratory assumes the risk of spending more than it is paid. One key to managing this risk is gaining access to test utilization of plan members and accurately assessing laboratory costs.

Per diem rates are negotiated with hospitals to provide all necessary care and services for managed members requiring inpatient care. Reimbursement for any laboratory testing during the inpatient stay is included in the per diem amount. As with capitation, if it costs more to provide inpatient services than the per diem rate, the hospital is at financial risk.

Sometimes, a service is separately negotiated (i.e., it is not included as part of the capitation or per diem rate). This is called a "carve out." Expensive esoteric tests (e.g., certain molecular and genetic tests) should be carved out of the outpatient laboratory capitation agreement. A negotiated fee-for-service price for these tests is appropriate. By excluding these tests from capitation, one can avoid huge financial losses due to unexpectedly high utilization of these costly services.

GOVERNMENT PAYERS

Medicare is federal health insurance for individuals age 65 and older, individuals who are permanently disabled, and those with end-stage renal disease who have met the specified waiting period. Medicare was established in 1965 by Title XVIII of the Social Security Act. It is administered by the Centers for Medicare and Medicaid Services (CMS), a division of the U.S. Department of Health and Human Services (HHS). Coverage is provided under Parts A, B, C, and D. Claims are processed by CMS-approved contractors. These contractors are usually private companies that serve as fiscal intermediaries (generally processing Part A claims) and carriers (generally processing Part B claims). However, CMS is moving to a new model, whereby the Medicare Administrative Contractor (MAC) will administer

TABLE 13.2

Test Cost Analysis*

Test: Prostate-Specific Antigen

A. Microcosting: Instrument Run of One Reportable Test

Direct Labor

Determine the total "hands-on" time in minutes required to perform an instrument "run" of one patient test. Assume labor cost is $20 per hour.

	Minutes	Expense
Prepare specimen	5	
Prepare reagents	10	
Prepare instrument	10	
Computer and/or worksheet setup	5	
Documentation of results/quality control/maintenance	10	
Cleanup	10	
Total direct labor	50	$16.67

Direct Supplies

List all consumables needed to perform the test. Note that four tests (one sample and three controls) are needed to produce one patient reportable result. Calibration costs should be added if they are required with each run.

	Unit cost	Units	Expense
Reagent ($700 kit/100 tests)	$7	4	$28.00
Disposable pipettes ($10/100 pipettes)	$0.10	4	$0.40
Disposable reagent cups ($10/200 cups)	$0.05	4	$0.20
Low-, medium-, and high-control material (0.05 mL/test @ $20/mL)	$1	3	$3.00
Total direct supplies			$31.60
Total direct costs			$48.27
Cost per reportable (total direct cost/reportable results)	$48.27/1		$48.27
Testing efficiency (reportable patient results/tests)	1 result/4 tests		25%

B. Microcosting: Instrument Run of 15 Reportable Tests

Direct Labor

For a group of tests run on automated analyzers, use direct labor expense from microcosting. For manual batch testing, direct labor costs may apply to each batch; additional labor time studies may be necessary to derive accurate data.

	Minutes	Expense
Total direct labor per batch (same as microcosting in this example)	50	$16.67

Direct Supplies

Note: 18 tests (15 samples and 3 controls) are needed to produce 15 reportable results. Fixed costs (controls) are spread over more than 1 sample, in contrast to first example.

	Unit cost	Units	Expense
Reagent ($700 kit/100 tests)	$7	18	$126.00
Disposable pipettes ($10/100 pipettes)	$0.10	18	$1.80
Disposable reagent cups ($10/200 cups)	$0.05	18	$0.90
Low-, medium-, and high-control material (0.05 mL/test @ $20/mL)	$1	3	$3.00
Total direct supplies			$131.70
Total direct costs			$148.37
Cost per reportable (total direct cost/reportable results)	$148.37/15		$9.89
Testing efficiency (reportable patient results/tests)	15 results/18 tests	83%	

C. Incremental Cost: Cost for One More Test

	Units	Expense
Reagent ($700 kit/100 tests)	1	$7
Disposable pipettes ($10/100 pipettes)	1	$0.10
Disposable reagent cups ($10/200 cups)	1	$0.05
Total		$7.15

	Unit cost	Units	Expense
D. Fully Loaded Cost			
Direct cost (cost per reportable result for typical size run) from Example B	$9.89		
Indirect cost (estimated by typical hospital as 2.5 × direct costs)	$24.73		
Fully loaded cost			$34.62
E. Contribution Margin			
Example of Charging a 20% Markup for Laboratory Tests			
Fully loaded cost plus 20% mark-up (test charge at list price)	$34.62 × 1.2		$41.54
Fully loaded cost from Example D			($34.62)
Contribution margin			$6.92

*This analysis is for illustration purposes only; real-life costs may be different.

TABLE 13.3
Reimbursement Comparison for PSA* by Payer Type

	List Price	Reimbursement Terms	Amount Paid	Contractual Allowance
Inpatient				
Managed care (HMO)	$41.54	No separate reimbursement for laboratory tests because they are included in the contracted per diem rate	0	N/A
Medicare	$41.54	No separate reimbursement for laboratory tests because they are included in the DRG rate	0	N/A
Outpatient				
Indemnity insurance	$41.54	Usual and customary charge (UCC) is $38; insurance pays 80% of UCC.	$30.40	$11.14
Managed care (PPO)	$41.54	Contract pays 110% of Medicare fee schedule ($25.70 for PSA).	$28.27	$13.27
Managed care (HMO)	$41.54	No separate reimbursement for laboratory tests because of capitation arrangement: Laboratory receives per member per month payment irrespective of usage	N/A	N/A
Medicare	$41.54	Medicare fee schedule	$25.09	$16.45

DRG, Diagnosis-related group; *HMO,* health maintenance organization; *N/A,* not applicable; *PPO,* preferred provider organization; *PSA,* prostate-specific antigen.
*Reimbursement amounts are for illustrative purposes only and may not accurately reflect current Medicare reimbursement.

both Part A and Part B claims via 12 MAC jurisdictions (as of 2018). For a clinical laboratory to qualify for Medicare/Medicaid reimbursement, the laboratory must maintain Clinical Laboratory Improvement Act of 1988 certification (CMS, 2017e).

Medicare Part A covers inpatient hospitalization, hospice care, skilled nursing care, and home health care. Coverage is automatic for those who are eligible. Before the Tax Equity and Fiscal Responsibility Act of 1982 (TEFRA), inpatient hospitalization was reimbursed on a retrospective cost-based system. This system paid hospitals for all costs incurred during an inpatient stay. After TEFRA, the system switched to a prospective payment system (PPS), which reimbursed hospitals on the basis of preset payments for services provided to patients with similar diagnoses. With this DRG payment system, hospitals are reimbursed the same amount for a specific DRG no matter how many discrete units of services are provided. Thus hospitals can earn a profit or realize a loss on each inpatient stay, depending on whether their costs are lower or higher than the DRG payment. The aim of the PPS, with its fixed DRG reimbursements, was to force hospitals to contain costs by reducing the length of stay and eliminating unnecessary and/or overutilized services (Young, 2017).

Medicare Part B covers outpatient laboratory tests, physician professional services, and other medical services and devices. Coverage is not automatic. Eligible beneficiaries must enroll for Part B coverage and pay premiums. Beneficiaries must pay an annual deductible and a 20% copayment for all Part B services, except for clinical laboratory testing, which is covered in full, provided certain conditions are met (see later discussion).

The Part B fee schedule plays an important role in reimbursement because it is a baseline that nongovernment payers use to establish their own rates. For example, a private insurance company may set its fee schedule at 110% of the Part B fee schedule.

Medicare Part C (also known as Medicare Advantage) is an alternative to the traditional Part B fee-for-service program. It is designed to reduce patient "out-of-pocket" costs by providing services through health maintenance organizations and other managed care service models. *Medicare Part D* provides prescription drug coverage.

Medicaid is a federal program that offers health care coverage for select low-income families. It was authorized in 1965 as a federal/state-sponsored program designed to pay medical costs for certain families with low income or inadequate resources. Eligibility extends to people who are aged, blind, or disabled, and those in families with dependent children. Although Medicaid is a federal program, it is under the jurisdiction of each individual state. This means that each state determines who is eligible, the range of health services offered, and how they are reimbursed. It is a common misconception that Medicaid covers health care costs for all low-income persons. Medicaid does not provide paid medical assistance to every single poor person. To receive medical assistance, a person must meet eligibility requirements.

REIMBURSEMENT CODING SYSTEMS

To be paid, a medical claim must document the patient's medical condition (or diagnosis) and must list the services (or tests) provided. This information is conveyed via a standardized coding system, recognized by all government and private payers: Healthcare Common Procedure Coding System (HCPCS) codes describe the test or service (AMA, 2017b), and *International Classification of Diseases, Tenth Revision, Clinical Modification* (*ICD-10-CM*) codes describe the patient's condition or diagnosis (AMA, 2019). These coding standards allow data to be accurately communicated among physicians, patients, and third-party payers.

The HCPCS was developed in 1983 and consists of two levels of codes. Level I is the Current Procedural Terminology (CPT) coding system, used to identify nearly all clinical laboratory tests and most medical services (AMA, 2017a). CPT codes are assigned by the American Medical Association (AMA) and are reviewed and updated annually to keep current with changes in technology and medical practice. Each CPT code consists of five digits and a description of the test or service. For example, the CPT code for a total prostate-specific antigen (PSA) test is 84153.

Level II HCPCS codes are assigned by the CMS. CPT does not contain all the codes needed to report services or to describe special circumstances that may apply to Medicare. The CMS developed this second level of codes to fill the gap. HCPCS Level II codes begin with a single letter (A through V), followed by four digits. These codes are updated annually by the CMS. An example of Level II coding is PSA for cancer screening, G0103. Note that the CMS treats this test differently than the PSA CPT code described earlier, even though the tests are identical to those of the laboratory. This allows the CMS to assign different criteria for reimbursement based on why a test is ordered.

The ICD was originally developed by the World Health Organization (WHO) as a classification system for reporting of mortality and morbidity statistics by physicians throughout the world. The *ICD-10-CM* is a U.S. clinically modified revision of the WHO *ICD-10*. This modification is maintained and updated by the National Center for Health Statistics. These modifications assist health care providers to index patient records, retrieve case data for clinical studies, and submit claims for health care services. In contrast to *ICD-9*, *ICD-10* (implemented in 2015) provides much greater detail, precisely defines location (including laterality), and provides changes in terminology and expanded concepts for injuries and other related factors. As a result, *ICD-10* is composed of about 68,000 codes (three to seven characters long), in contrast to *ICD-9*'s approximately 13,000 codes (three to five characters long) (AMA, 2012).

WHY ACCURATE CODING IS IMPORTANT

Correct coding is important for three reasons. First, one should be paid for services rendered. Insufficient or incorrect coding may yield lower reimbursement than is rightfully due. Second, one must not receive more reimbursement than is rightfully due. Coding for services not provided or assigning a code that recoups more reimbursement (this practice is known as "up-coding") is illegal and constitutes fraud. Third, one must comply with *medical necessity* requirements established by the CMS for Medicare patients. These policies define under what conditions a test is considered "medically necessary" and thus reimbursable. Certain tests are considered "medically necessary" only if they are associated with specific diagnoses. Thus reimbursement depends on whether the diagnosis or medical condition code (*ICD-10* code) supports the test code (HCPCS code). For example, "malignant neoplasm of the prostate" supports the medical necessity of doing a PSA test, so Medicare would pay for the test. In contrast, "congestive heart failure" is not considered a medically necessary reason for a PSA

TABLE 13.4
National Coverage Determinations for Laboratory Testing

General Testing Category	CPT Codes Included
Alpha-fetoprotein	82105
Blood counts	85004, 85007, 85008, 85013, 85014, 85018, 85025, 85027, 85032, 85048, 85049
Blood glucose testing	82947, 82948, 82962
Carcinoembryonic antigen	82378
Collagen crosslinks, any method	82523
Digoxin therapeutic drug assay	80162
Fecal occult blood test	82272
Gamma-glutamyl transferase	82977
Glycated hemoglobin/glycated protein	82985, 83036
Hepatitis panel/acute hepatitis panel	80074
Human chorionic gonadotropin	84702
Human immunodeficiency virus (HIV) testing (diagnosis)	86689, 86701, 86702, 86703, 87390, 87391, 87534, 87535, 87637, 87538
HIV testing (prognosis, including monitoring)	87536, 87539
Lipids	80061, 82465, 83700, 83701, 83704, 83718, 83721, 84478
Partial thromboplastin time	85730
Prostate-specific antigen	84153
Prothrombin time	85610
Serum iron studies	82728, 83540, 83550, 84466
Thyroid testing	84436, 84439, 84443, 84479
Tumor antigen by immunoassay CA 125	86304
Tumor antigen by immunoassay CA 15-3 (CA 27.29)	86300
Tumor antigen by immunoassay CA 19-9	86301
Urine culture, bacterial	87086, 87088

From CMS (2018a).

test; in that case, the test would not be reimbursed. Note that a physician (or other provider) can order any test on a patient, even if it is not "medically necessary," but it will not be reimbursed.

Most laboratory fee schedules are set by the local Medicare contractor (fiscal intermediary or carrier). Historically, each contractor established separate guidelines for determining which tests were subject to medically necessary diagnosis codes. *Local medical review policies* and local coverage decisions differ from one carrier to another, making it very difficult to submit and process claims. In some instances, a diagnosis code that is valid for a test from one carrier may not be considered medically necessary by another carrier. In an effort to standardize all carrier reimbursement guidelines for specific outpatient laboratory tests, 23 tests have been assigned *national coverage determinations* (*NCDs*); these medical necessity guidelines apply to all carriers in the country. Table 13.4 lists the NCD tests (CMS, 2018a).

Coding at any level should be as specific as possible. Medicare contractors employ the national Correct Coding Initiative to ensure correct coding practices based on the codes defined in the AMA's CPT code set (CMS, 2018f). These software edits flag inappropriate code combinations that should not be billed together for the same patient on the same day of service. Medicare has also added a system of medically unlikely edits (MUEs) that limit the units of service payable for a particular CPT code per patient, per provider, per day of service. Claims that exceed the MUE are rejected. Most analytes or tests have a specific CPT, similar to that of PSA. However, sometimes a new test does not have its own code. When that happens, the test must be identified by the method used to perform the analysis (e.g., 83520—Immunoassay, quantitative, not otherwise specified). A method code is usually reimbursed at a lower rate than a CPT code for a specific analyte.

Certain tests that are performed together (i.e., as a panel) must be coded correctly. Eleven panels have been approved by the AMA (though only eight are considered covered services by Medicare, the exceptions being the General Health and Obstetrics panels; Table 13.5). When these 11 panels are performed, they must be coded with the unique panel code and not by each individual test's CPT code. Reimbursement is much lower for a panel than it is for the sum total reimbursement of each test. Coding for each individual test component as opposed to one panel code is considered "unbundling," which is a fraudulent billing practice.

Professional pathology physician services (e.g., test interpretation, slide review) are not included in the laboratory fee schedule. They are paid by the Medicare physician fee schedule, which uses a resource-based relative value scale to determine the payment based on a service's relative value unit. Relative value units are determined by the Specialty Society Relative Value Update Committee of the American Medical Association and consist of three parts: physician work, practice expense, and malpractice expense. The sum is then multiplied by a geographic factor to account for differences in wages and overhead costs in different regions of the country and then multiplied by a conversion factor by Medicare to obtain the final payment. These amounts are adjusted to reflect local economic factors. Unlike the laboratory fee schedule, these professional services are subject to the annual deductible and the 20% copayment.

MEDICARE REIMBURSEMENT

Medicare is the largest insurance program in the country. In many hospitals, it accounts for 25% to 40% of all revenue. Outpatient services are reimbursed differently from inpatient ones.

Medicare Inpatients

DRGs make up a patient classification system that is used to reimburse inpatient (Part A) hospital costs for Medicare patients. Although the costs associated with inpatient clinical laboratory tests are included in the DRG, it does not cover physician services (Part B). After a Medicare patient has been discharged from the hospital, the patient's medical record is reviewed by health information management coders and is assigned appropriate *ICD-10-CM* and HCPCS codes for one or more diagnoses and procedures for the inpatient stay. These codes, along with the patient's demographic information, are grouped by decision trees (this process is computerized) into a specific DRG. Currently, more than 500 DRGs are used. The CMS assigns a weight to each DRG based on the severity of the diagnoses, the types of procedures performed, the number of laboratory tests, the volume and type of drugs administered, and the presence of complications or comorbid conditions. The CMS assigns each hospital a specific rate that is calculated on the basis of the type of facility (community hospital vs. teaching hospital), the setting (urban vs. rural), and the location (West Coast vs. Midwest). The CMS-assigned rate for the DRG is multiplied by the hospital's assigned rate to determine reimbursement for the hospital stay. This amount is payment-in-full for the inpatient hospitalization. If it costs the hospital more than the reimbursed amount to treat the patient, the hospital must absorb the cost. The patient cannot be billed for any nonreimbursed Part A services (Young, 2017).

Medicare Outpatients

For many years after the enactment of DRGs, each outpatient service continued to be reimbursed individually (Harmening, 2012). However, the reimbursement system changed when the CMS started to implement an outpatient prospective payment system with the introduction of the Ambulatory Payment Classification (APC) system in 2000. Under this system, virtually all hospital-based outpatient services (e.g., emergency department and clinic visits, oncology treatment, and surgery) provided to Medicare patients are reimbursed on a prospective basis according to a preset rate, similar to DRGs. Clinical diagnostic laboratory tests are not currently included in the APC and are still reimbursed individually on the basis of the CMS fee schedule, with some exceptions.

Under certain conditions, Medicare does not pay for laboratory tests (Table 13.6). If a laboratory expects Medicare to deny payment because a test does not meet medical necessity requirements, it must inform the patient before the service is provided. An *advanced beneficiary notice (ABN)* is used to document that the beneficiary was told the test might not be covered by Medicare, the reason(s) for the possible denial, and the decision by the patient to pay for the test if Medicare does not reimburse or to refuse the test entirely (CMS, 2017d).

An important consideration for hospitals that have laboratories that perform outpatient testing on Medicare patients is the *72-hour rule* (CMS, 2018c). This rule states that a hospital cannot bill an outpatient claim for laboratory tests performed within 72 hours of an inpatient admission. Outpatient testing that is performed 72 hours before the admission must be included with the inpatient claim and is reimbursed according to the assigned DRG for that stay. Hospital laboratories must identify outpatient Medicare services that are affected by this rule and must make sure they are not billed separately. A nonhospital independent laboratory is not subject to the 72-hour rule. Thus preadmission tests performed 3 days before

TABLE 13.5

AMA Organ or Disease-Oriented Panels

CPT	Panel	Required Components	
80047	Basic metabolic panel (calcium, ionized)	Calcium, ionized	(82330)
		Carbon dioxide	(82374)
		Chloride	(82435)
		Creatinine	(82565)
		Glucose	(82947)
		Potassium	(84132)
		Sodium	(84295)
		Urea nitrogen, blood (BUN)	(84520)
80048	Basic metabolic panel (calcium, total)	Calcium, total	(82310)
		Carbon dioxide	(82374)
		Chloride	(82435)
		Creatinine	(82565)
		Glucose	(82947)
		Potassium	(84132)
		Sodium	(84295)
		BUN	(84520)
80050	General health panel	Comprehensive metabolic panel	(80053)
		Blood count, complete (CBC)	(85025) or (85027) and (85004)
		or	
		CBC	(85027) and (85007) or (85009)
		Thyroid-stimulating hormone	(84443)
80051	Electrolyte panel	Carbon dioxide	(82374)
		Chloride	(82435)
		Potassium	(84132)
		Sodium	(84295)
80053	Comprehensive metabolic panel	Albumin	(82040)
		Bilirubin, total	(82247)
		Calcium	(82310)
		Carbon dioxide	(82374)
		Chloride	(82435)
		Creatinine	(82565)
		Glucose	(82947)
		Phosphatase, alkaline	(84075)
		Potassium	(84132)
		Protein, total	(84155)
		Sodium	(84295)
		Transferase, alanine amino	(84460)
		Transferase, aspartate amino	(84450)
		BUN	(84520)
80055	Obstetric panel	CBC	(85025) or (85027) and (85004)
		or	
		CBC	(85027) and (85007) or (85009)
		Hepatitis B surface antigen	(87340)
		Antibody, rubella	(86762)
		Syphilis test, qualitative	(86592)
		Antibody screen, RBC	(86850)
		Blood typing, ABO	(86900)
		Blood typing, Rh	(86901)
80081	Obstetric Panel (includes HIV)	HIV-1 antigen with HIV-1 and HIV-2 antibodies (single result) plus all tests in Obstetric Panel 80055	(87389) plus codes above
80061	Lipid panel	Cholesterol, total	(85465)
		HDL cholesterol	(83718)
		Triglycerides	(84478)
80069	Renal function panel	Albumin	(82040)
		Calcium	(82310)
		Carbon dioxide	(82374)
		Chloride	(82435)
		Creatinine	(82565)
		Glucose	(82947)
		Phosphorus, inorganic	(84100)
		Potassium	(84132)
		Sodium	(84295)
		BUN	(84520)

Continued

TABLE 13.5 —cont'd

National Coverage Determinations for Laboratory Testing

CPT	Panel	Required Components	
80074	Acute hepatitis panel	Hepatitis A antibody, IgM	(86709)
		Hepatitis B core antibody, IgM	(86705)
		Hepatitis B surface antigen	(87340)
		Hepatitis C antibody	(86803)
80076	Hepatic function panel	Albumin	(82040)
		Bilirubin, total	(82247)
		Bilirubin, direct	(82248)
		Phosphatase, alkaline	(84075)
		Protein, total	(84155)
		Transferase, alanine amino	(84460)
		Transferase, aspartate amino	(84450)

ABO, Blood group; *HDL,* high-density lipoprotein; *IgM,* immunoglobulin M; *RBC,* red blood cell.
From AMA (2017a).

TABLE 13.6

National Coverage Determinations (NCDs) for Laboratory Testing

Category	Medicare Coverage	ABN Necessary?
LMRP or NCD tests	Provider paid according to outpatient fee schedule if medical necessity met	No, unless test is not "medically necessary"
FDA cleared or "homebrew" tests not included above	Provider paid according to outpatient fee schedule if medical necessity met	No, unless test is not "medically necessary"
Investigational use only or research tests (i.e., not FDA cleared)	Not covered, no payment	Yes
Health and wellness screening	Not covered, with few exceptions: PAP smears covered every 2 years for all women and every year for those with high cancer risk or abnormal smear; PSA covered every year for men older than 50	Yes, unless it is one of the allowable exceptions

ABN, Advanced beneficiary notice; *FDA,* U.S. Food and Drug Administration; *LMRP,* local medical review policies; *NCD,* national coverage determinations; *PAP,* Papanicolaou smear; *PSA,* prostate-specific antigen.
From CMS (2018a).

hospitalization are not reimbursed if performed in the admitting hospital's laboratory but are reimbursed if done in an independent laboratory. Post-discharge testing may also be bundled into the DRG if the test/service is ordered by the patient's physician less than 14 days following the date of the patient's discharge from the hospital (42 CFR § 414.510).

FINANCIAL PERFORMANCE AND MONITORING

BUDGETING

Budgeting is the process of planning, forecasting, controlling, and monitoring the financial resources of an organization (Garcia, 2013). The *operational budget* provides a target of day-to-day revenues and expenditures that are to be achieved in the forthcoming year.

Different budget-planning strategies are used based on the type and seasonality of the business. However, all use a method to forecast and project what will occur in the next budget cycle. Projections are made for the expected increases and decreases in revenues and expenses based on historical information and adjustments for inflation, loss of business, new business, and new product lines. The laboratory typically uses a *pro forma* budget. It provides in a pro forma or "predetermined set form" the expected annual revenue and expense based on various projections and assumptions, including test volume. It uses actual costs, ratios, and percent calculations to extrapolate from historical data what the new budget will be. Table 13.7 presents an example of a pro forma budget.

In contrast to the pro forma budget, which uses baseline data from 1 year to develop data for the next, a *zero-based budget* has no baseline. A zero-based budget requires management to annually evaluate all services and products to determine which should be funded or eliminated. Each department manager must justify its budget as if all of its activities are new. It assumes that no existing program is entitled to automatic budget approval but rather must prove its financial merit when compared with the organization's other programs. Programs are ranked and funded by merit priority to the level of the organization's available funds. Laboratories use a zero-based approach to propose a new service (e.g., blood donor program, outpatient blood collection center) or laboratory section (e.g., mycology) or test (polymerase chain reaction assay) (Travers, 1997).

The *capital budget* is used to fund large capital projects such as acquiring an instrument or information system or remodeling the laboratory (Garcia, 2013). These projects may cost thousands or millions of dollars and require several years to plan or implement. The laboratory's proposed projects must compete with those of other hospital departments for limited capital dollars. Each project is evaluated (see later discussion) and ranked on the basis of a variety of financial and clinical factors. The operational budget must be linked to the capital budget, because it is the revenues generated by operations that are used to fund needed capital items and projects. Operational budgets must generate surplus revenue to fund capital projects; a business must reinvest in itself to remain competitive.

VARIANCE ANALYSIS

The operational budget should be reviewed periodically, usually monthly, to determine how closely the projected budget matches actual revenues and expenses (Garcia, 2013). A variance is the difference between the projected budget and the actual revenue and expenses (Budget – Actual = Variance). Both favorable variances (more than expected revenue or less than expected expenses) and unfavorable variances (less than expected revenue or more than expected expenses) need to be analyzed. By analyzing a variance, one can identify whether or not it can be controlled. Once the cause is determined, one can take necessary action to improve performance and more accurately prepare future budgets.

If revenues (and expected test volume) are within budget but laboratory supplies show an unfavorable variance, one must investigate the reason for the discrepancy. For example, technologists may be repeating tests too frequently, running too many controls, or scheduling work inefficiently, in many small batches. This is an example of a variance that can be controlled by the laboratory if it changes its practices. Actions to consider include increasing the frequency of instrument maintenance to reduce problems that require repeats and controls, providing staff education to reinforce policies on when repeats and controls are needed, and rescheduling work into more efficient batch sizes.

TABLE 13.7
Pro Forma Laboratory Budget

Category	Current Year	Assumptions	Change	Projection for New Year
Revenue	$3,000,000	4% growth	$120,000	$3,120,000
Total tests	370,000	4% growth	14,800	384,800
Revenue/test	$8.11			$8.11
Expenses				
Salaries	$950,000	3% cost of living increase	$28,500	$978,500
Laboratory supplies	$421,000	4% growth (no price increase)	$16,840	$437,840
Reference lab fees	$250,000	4% growth	$10,000	$260,600
		1% price increase (on projected $260,000)	$2600	
Phlebotomy supplies	$35,500	4% growth	$1420	$36,920
Maintenance contracts	$40,000	No change		$40,000
Total expense	$1,696,500		$59,360	$1,755,860
Cost per test	$4.59			$4.56

TABLE 13.8
Cost Center: Microbiology

		CURRENT MONTH			YEAR TO DATE		
		REVENUE					
Account number	**Account name**	**Actual**	**Budget**	**Variance**	**Actual**	**Budget**	**Variance**
20100	Inpatient revenue	$1,414,245	$1,403,172	$11,073	$2,892,427	$2,764,597	$127,830
20200	Outpatient revenue	$906,343	$894,405	$11,938	$1,699,418	$1,748,169	$(48,751)
Total revenue		$2,320,588	$2,297,577	$23,011	$4,591,845	$4,512,766	$79,079
		EXPENSES					
40100	Salary, management	$22,045	$21,811	$234	$43,310	$43,622	$(312)
40200	Salary, technical	$85,161	$105,410	$(20,249)	$170,437	$210,820	$(40,383)
40201	Overtime	$3385	$3907	$(522)	$6713	$7814	$(1101)
Total salary expense		$110,591	$131,128	$(20,537)	$220,460	$262,256	$(41,796)
41580	Laboratory supplies	$109,961	$96,114	$13,847	$193,102	$188,461	$4641
41590	Medical-surgical supplies	$1682	$1715	$(33)	$3964	$3362	$602
41890	Service contracts	$75	$355	$(280)	$150	$710	$(560)
42010	Minor equipment	$1112	$1083	$29	$2568	$2166	$402
45300	Sendout test expense	$14,973	$13,750	$1223	$28,812	$27,500	$1312
46300	Accreditation expense	$—	$100	$(100)	$—	$200	$(200)
Total nonsalary expense		$127,803	$113,117	$14,686	$228,596	$222,399	$6197
Total expense		$238,394	$244,245	$(5851)	$449,056	$484,655	$(35,599)

An example of an uncontrollable variance occurs if a hospital decides to eliminate the cardiac disease prevention service. In this scenario, a favorable reagent expense variance (i.e., less money spent on reagents than expected) would be related to doing fewer cardiac disease–related tests. A laboratory manager can do nothing to correct this variance. However, this does not absolve the manager from a duty to review it. One must verify the amount of the variance and must determine whether it is appropriate for the amount of lost business. When forecasting for the next budget cycle, one should decrease projected revenues and expenses attributed to the loss of cardiac services.

FINANCIAL REPORTING AND STATEMENTS

Managerial accounting is used to prepare and monitor budgets. Revenue and expenses are organized into logical groupings known as cost centers that represent a laboratory section (such as microbiology, core lab, blood bank) or function (phlebotomy). Each cost center is subdivided into a variety of expense and revenue categories. Salary and nonsalary expense categories are grouped separately. Periodic review, at least monthly, of the cost center's accounts is needed to monitor the variances and put corrective action in place to keep the organization on its expected financial plan. Table 13.8 provides an example of a laboratory cost center's accounts.

Financial accounting is a system used to report business information to external entities, such as the Internal Revenue Service or stockholders. Generally accepted accounting principles are used to standardize this information. Balance sheets, income statements, and statements of cash flows are the financial statements most commonly used to assess an organization's financial position. Banks and investors rely heavily on these statements to determine whether to lend money to a business or to purchase shares of stock.

The *balance sheet* is the statement of an organization's financial position at a specific point in time. This statement is usually generated at the end of an organization's fiscal year or at the end of the calendar year. It records the organization's assets (what it owns), its liabilities (what it owes), and its equity or net worth (what is left after subtracting what it owes from what it owns). From this statement is derived the fundamental accounting equation: Assets = Liabilities + Equity (net worth). This statement is used to assess an organization's level of indebtedness to what it owns.

The *income statement*, also known as the *statement of profit and loss*, summarizes the organization's revenues and expenses over an accounting period, usually quarterly or annually. The income statement records all of a laboratory's gross patient revenue, less allowances for a given period, and deducts the expenses for that same period to arrive at net income before taxes. Taxes are paid only if the organization is for-profit. Net income is realized when net revenues exceed expenses. A net loss is realized when expenses exceed net revenues. Note that revenue does not necessarily equate to cash generated. Many times a test is performed and recorded as income, although the payment (cash) may not be received for several months. The income statement records the organization's ability to make a profit; it does not reflect its cash position.

The *statement of cash flows* shows the amount of cash generated by an organization over a period of time, usually a calendar or fiscal year. Cash

TABLE 13.9

Common Productivity Measures for Clinical Laboratories

Productivity Measure	Target*	Quarter 1	Quarter 2
Billable tests/paid FTE	>3680	3798	3500
Billable tests/worked FTE	>4000	4128	4080
Worked FTE/paid FTE	>92%	95.2%	90%
Labor cost/billable test	<$5.00	$4.68	$5.01
Supply cost/billable test	<$1.00	$0.99	$1.01
Overtime/worked straight time	<3%	2.7%	3.5%

FTE, Full-time equivalent or 2080 paid hours in a year; *paid FTE,* all salaries paid (benefit time plus worked time).
*Target is for illustration purposes only. It should not be considered a laboratory standard.

outflows (cash paid out) are subtracted from cash inflows (cash received) to calculate the net change in cash for the period. Excess cash in a given period can be reinvested in the organization, used to make additional debt payments, or placed in easily liquidated securities for emergency use. If the net cash position for a period is negative, the organization must meet its cash obligations by using cash reserves from previous periods. If this trend is not reversed, the organization eventually will run out of cash.

BENCHMARKING AND PRODUCTIVITY MEASURES

Benchmarking and productivity measures go hand in hand. It does no good to collect productivity data if they are not compared with a standard or evaluated for trends over time. Benchmarking is the measurement of an organization's products or services against specific standards for comparison and improvement. Benchmarking can be internal or external.

Internal benchmarking trends an organization's productivity over time. Productivity is the relationship between input (labor and supplies) and output (product or service) (Travers, 1997). It is usually expressed as a ratio of the product or service to the various inputs used for the production of the product or service. Table 13.9 provides the common productivity ratios used in the laboratory. The purpose of trending internal productivity is to determine whether internal standards are being met, exceeded, or not met. If adjustments to workflow or personnel are made, the next period's benchmarking data can be used to determine whether the adjustments were the probable cause for improvements or for decreased productivity.

External benchmarking compares a laboratory's productivity with that of other laboratories. Its purpose is to identify top performers in a particular field. Top performers can be contacted to find out what processes or resources have been used to achieve high productivity. This information may guide a laboratory to make similar changes that could result in higher productivity. Professional organizations such as the College of American Pathologists or Vizient offer external laboratory-specific benchmarking programs. Caution should always be used when interpreting external benchmarking information. Although clinical laboratories are similar, no two are exactly alike. Despite best efforts, sometimes data are collected and reported differently. A laboratory may never be able to achieve productivity as high as its peers because of factors beyond the laboratory's control. Labor availability, the disease and acuity mix of patients, and access to technology and automation will each have an effect on how productive a laboratory is and how much more productive it can become.

EVALUATING A CAPITAL PROJECT

A hospital has limited capital; it cannot fund all requested projects, so it must prioritize them according to a variety of factors, including clinical need, patient or employee safety, and financial impact. Irrespective of whether money is borrowed to finance these projects, it may be necessary for the project or investment to pay for itself and even generate excess cash to fund other projects. The following section discusses different ways to evaluate a capital project to answer the question "Is it a good investment?" Table 13.10 compares these methods.

PAYBACK PERIOD

The payback period is commonly used to evaluate a capital project. The payback is the length of time required for an investment's net revenue to cover the cost of the initial investment (Brigham & Houston, 2015). Because laboratory equipment or technology can become obsolete in a very short period of time, it is important to recover the investment cost as soon as possible. Many institutions want to see a payback in 3 years or less. Once the initial investment is recovered, net revenue (Revenue – Expense) from this investment represents a profit to the organization. The sooner a capital project's payback period is reached, the sooner an organization can realize a profit from the investment.

BREAKEVEN POINT

The breakeven point of a capital project is reached when the volume of sales is such that total revenue equals total costs (fixed and variable) and, therefore, profit is zero. Before the breakeven point is reached, the project is operating at a loss; after it is reached, the project is realizing a profit (Brigham & Houston, 2015). As with the payback period, the sooner the breakeven point is reached, the better it is for the organization.

RETURN ON INVESTMENT

The rate of return on investment (ROI) for a capital project is the ratio of net income it generates to the total investment of the project (Travers, 1997). ROI is a standard for evaluating how wisely management uses its capital dollars, whether from its own cash reserves or from borrowing activities. The higher the rate of return is, the better the capital dollars are used. ROI is the formal means of expressing the phrase "better bang for your buck." Some institutions have automated the ROI process. Most information can be pulled from the financial data banks of the hospital computer system after a limited amount of information is provided by the laboratory. An ROI is pretty much a standard requirement of most facilities for any capital project.

NET PRESENT VALUE

Money loses its value over time; $10,000 today is more valuable than $10,000 3 years from now. This concept is known as the time value of money. The payback period and ROI calculations do not consider the time value of money. They assume that the value of future cash flows remains constant. To address this shortcoming, the *net present value (NPV)* calculation is used to determine whether a project's cash flows (i.e., cash it generates in the future) are sufficient to repay the original investment taking into account that money loses value over time. Thus cash received in the future has to be *discounted* (i.e., the value has to be reduced) to determine how much it is worth in today's dollars. The discount rate is usually the inflation rate (if no money was borrowed to finance the project) or the interest rate on a loan used to fund the project. NPV is defined as the present value of future cash flows, which have been discounted at the interest rate used to fund the capital project (Brigham & Houston, 2015).

When the NPV is a positive number, the project will generate enough cash to pay for the original investment. When the NPV is a negative number, the project cost is not recouped and/or the future cash flows are not sufficient to cover the interest costs for borrowing the money.

INTERNAL RATE OF RETURN

The internal rate of return (IRR) also discounts cash flow into today's value. It determines the actual rate of return that the investment earns. The IRR is the discount rate at which the present value of a capital project's expected cash inflows equals the present value of its costs or, in other words, when the NPV equals zero.

Identifying a project's IRR is necessary to ensure that its rate is higher than the cost of the capital borrowed for the project. The higher the IRR, the faster the project pays for itself. Hospitals and corporations use the IRR as one way to rank projects.

INTERPRETATION OF FINANCIAL CALCULATIONS

Although the preceding calculations are important tools, an organization should not make its capital decisions based strictly on the outcome of the equations. As with all budgeting activities, there is an element of the unknown in assumptions. Predicting future cash flows for replacement instrumentation is usually more reliable than predicting it for new product lines or technology. Assigning an expected life to a piece of capital equipment is also an educated estimate. Having a good sense of how reliable predictions are will determine how much credence should be given to the calculations.

If only the payback period, breakeven analysis, and ROI were considered when evaluating the example in Table 13.10, the project would look

TABLE 13.10
Financial Evaluation of a New Automated Analyzer

Given		
Investment (cost of analyzer)		$200,000
Discount rate (rate of inflation or interest rate of borrowed money)		10.00%
Useful life of analyzer	5 years	
Annual depreciation expense	$200,000/5 years	$40,000
Annual revenue	100,000 tests at $5.00/test	$500,000
Annual labor expense	100,000 tests at $2.50/test	$250,000
Annual supply expense	100,000 tests at $2.00/test	$200,000
Annual net revenue (Annual revenue – Annual expense)	$500,000 – ($250,000 + $200,000)	$50,000
Net revenue per test (Test revenue – Test expense)	$5.00 – ($2.50 + $2.00)	$0.50
Calculations		
PAYBACK PERIOD = Investment/Annual net revenue	$200,000/$50,000	4 years
BREAKEVEN per year = Depreciation/Net revenue per test	$40,000/$0.50	80,000 tests
Life of analyzer = Investment/Net revenue per test	$200,000/$0.50	400,000 tests
RETURN ON INVESTMENT (ROI) = Annual net revenue/Investment	$50,000/$200,000	25% per year
NET PRESENT VALUE (NPV) = Present value of the sum of future net revenue (cash flows) minus investment. *Note:* Present value interest factor (PVIF) for each year based on 10% discount rate is multiplied by net revenue to determine present value. PVIF is available from any financial data resource. NPV can also be calculated with financial calculator.		
Today's investment	($200,000)	
Year 1 Net revenue × PVIF	$50,000 × 0.9091 = $45,455	
Year 2 Net revenue × PVIF	$50,000 × 0.8264 = $41,320	
Year 3 Net revenue × PVIF	$50,000 × 0.7513 = $37,565	
Year 4 Net revenue × PVIF	$50,000 × 0.6830 = $34,150	
Year 5 Net revenue × PVIF	$50,000 × 0.6209 = $31,045	
Present value of sum of future NPV net revenue	$189,535	$(10,465)
INTERNAL RATE OF RETURN (IRR) = Discounted interest rate at which NPV = 0. *Note:* Financial calculator is used to determine IRR by entering cash flow and discount rate.		
Today's investment	($200,000)	
Year 1 Net revenue × PVIF	$50,000 × 0.9265 = $46,326	
Year 2 Net revenue × PVIF	$50,000 × 0.8585 = $42,923	
Year 3 Net revenue × PVIF	$50,000 × 0.7954 = $39,769	
Year 4 Net revenue × PVIF	$50,000 × 0.7369 = $36,847	
Year 5 Net revenue × PVIF	$50,000 × 0.6828 = $34,140	
Present value of sum of future net revenue	$200,000	
NPV		$0
IRR		8%

TABLE 13.11
Capital Acquisition Options

	Advantages	Disadvantages
Purchase	Ownership	Risk of obsolescence; opportunity cost
Operating (true) lease	Hedging obsolescence; flexibility in financing; cancelable	Nonownership; interest/financing cost
Financial lease	Ownership; flexibility in financing	Noncancelable; interest/financing cost
Rental	Hedging obsolescence; flexibility in length of use	High cost; nonownership

acceptable. However, when the NPV and IRR are also considered, it does not look as good. The NPV is unfavorable, and the IRR is much less than the ROI because the cost of capital is high (10%). Does this mean the project should not go forward? Not necessarily. Depending on other issues, it may be determined that this new chemistry analyzer is absolutely essential to support the mission of the organization.

These calculations have other inherent drawbacks. As mentioned earlier, some of the calculations take into account the time value of money and others do not. The time value of money is a very important consideration when the cost of capital is high (as in the example in Table 13.10) or during periods of high inflation. The rate of return calculations yield a percentage, but the actual dollars they represent are not immediately apparent. A capital project that yields an ROI of 15% might look better initially than one that yields 10%. However, the size of the projects may differ considerably. For example, in the former, an initial investment of $10,000 could produce $1500 in net revenue, but in the latter project, an initial investment of $200,000 produces $20,000 in net revenue. None of these financial calculations should be considered in isolation, but they should be used in aggregate to assist in the analysis of capital projects.

CAPITAL ACQUISITION METHODS

When a capital project is evaluated, the method for acquiring the equipment is also an important consideration. Table 13.11 summarizes the advantages and disadvantages of acquisition methods: purchase, leasing, and renting. Just as there is not a single best financial calculation when evaluating a project, there is not a single best acquisition method. The method selected depends on individual needs, characteristics and financial philosophy of the organization, and availability of capital dollars.

The concept of purchasing needed equipment is easy to understand, but is it the wisest use of an organization's money? If the capital (money) needed to fund the project is currently invested in a security that is earning a higher interest rate than the rate needed to borrow money, it makes financial sense to borrow the needed capital. Conversely, if capital earns

a lower interest rate than the borrowing rate, it makes sense to use the organization's capital.

Once the equipment is purchased, it is an asset of the organization and is depreciated by a method appropriate for such a piece of equipment. Most laboratory equipment is depreciated over a 5-year period using the straight line depreciation method. The depreciation expense is noted in the income statement but probably will not be included in the monthly operational budget documents. It will depend on each organization as to whether depreciation is listed on the monthly budget reports. The operational expense for the equipment will consist of the supplies, maintenance, and labor needed to support it.

Many different variations and contract terms may be associated with a leasing agreement. Being certain to "read the fine print" never rings truer than when an equipment leasing arrangement is considered. Nonetheless, no matter how complicated the terms of a leasing contract are, there are only two types of leases.

An *operating lease* (also known as a "true" lease) allows an organization (lessee) full use of the equipment for a predetermined time. The time period is usually 1 to 3 years, but it is always less than the useful life of the equipment. A termination clause could be included in the agreement. Equipment maintenance is included in an operating lease. The lessee has no right to ownership during or after the lease period. No equity is established during the term. The owner (lessor) retains full ownership of the equipment and full responsibility for it. The leasing agreement may or may not contain an option to allow the lessee to purchase the equipment at the end of the term. This is only an option, however, and should not be misinterpreted as established equity over the course of the agreement. If a purchase option is provided, it is usually for the equipment's fair market value at the end of the lease period. If the original lessee decides not to purchase the equipment at the end of the lease term, the lessor could release it to the original lessee or to another organization, because the equipment still has useful life (Brigham & Houston, 2015).

The other lease type is a financial lease. With a *financial lease* (also known as a capital lease or lease-purchase), the lessee eventually gains ownership of the equipment. The lease period corresponds to the economic life of the equipment. Through lease payments, the lessor recovers the cost of the equipment plus an interest factor to ensure a return on its investment. A financial lease is not cancelable, and equipment maintenance is not included (Brigham & Houston, 2015).

Renting equipment is not the same as leasing it. The major differentiators are that renting does not carry an option for later purchase, renting has no predetermined specified length of time, renting can be terminated at any time, and maintenance and repairs are the responsibilities of the owner, not the renter (Travers, 1997). A reagent rental agreement is a misnomer; it is not a rental but a lease. These agreements require the lessee to purchase reagents that are specific for a particular piece of equipment. The price of the reagents is marked up by a certain amount to cover the "rent" of the equipment. The markup is a lease payment to cover the cost of the capital. Whether the equipment will be owned at the end of the reagent rental agreement will determine if the agreement was a financial lease. Federal legislation requires vendors to clearly state the proportion of annual payments that are allocated to the capital portion of the lease. This simplifies the analysis of competing lease agreements.

Regardless of which method of capital acquisition is utilized, you should always have the vendor or lessor break out the agreement into cost of equipment, cost of service agreement, and costs of reagents and supplies. This way, you can see and negotiate the cost of each. It is prudent to include someone from the institution's purchasing department to help with negotiations.

SELECTED REFERENCES

Brigham EF, Houston JF: In Mason OH, editor: *Fundamentals of financial management*, ed 14, Cengage Learning, 2015.

An introduction to finance textbook written for the undergraduate business student.

CMS (Centers for Medicare & Medicaid Services): Clinical Labs Center. http://www.cms.gov/Center/Provider-Type/Clinical-Labs-Center.html. Accessed December 16, 2018a.

This website contains the most comprehensive collection of lab-related information, including fee schedules, coverage explanations, legislation, policies, and coding.

Garcia LS, editor: *Clinical laboratory management*, ed 2, Washington, DC, 2013, ASM Press.

A multiauthored textbook with comprehensive coverage of all aspects of laboratory management.

Harmening DM: *Laboratory management: principles and processes*, ed 3, St. Petersburg, FL, 2012, D.H. Publishing & Consulting.

A textbook designed to balance theory and practical applications of laboratory management.

Young KM, Kroth PJ: *Sultz & Young's Health care USA: Understanding its organization and delivery*, ed 9, Sudbury, MA, 2017, Jones & Bartlett.

A text describing the changing roles of the components of the health care system, in addition to the technical, economic, political, and social forces responsible for these changes.

Access the complete reference list online at Elsevier eBooks for Practicing Clinicians.

REFERENCES

American Medical Association: *Cpt 2018*, professional edition, Chicago, 2017a, American Medical Association.

American Medical Association: *HCPCS 2018 level II*, professional edition, Chicago, 2017b, American Medical Association.

American Medical Association: *International Classification of diseases, Tenth revision, clinical modification (ICD-10-CM)*, Chicago, 2019, American Medical Association.

American Medical Association: Fact sheet 2. Preparing for the ICD-10 code set. www.ama-assn.org/go/ICD-10, September 25, 2012.

CMS (Centers for Medicare & Medicaid Services): *National health expenditure data*. U.S. Department of Health & Human Services. Available at: http://www.cms.hhs.gov/nationalhealthexpenddata. Accessed December 16, 2018b.

CMS (Centers for Medicare & Medicaid Services): Medicare claims processing manual: Chapter 3 Inpatient hospital billing. U.S. Department of Health & Human Services (Revised 2018). Available at: http://www.cms.gov/Regulations-and-Guidance/Guidance/Manuals/downloads/clm104c03.pdf. Accessed December 18, 2018c.

CMS (Centers for Medicare & Medicaid Services): Advanced beneficiary notice of noncoverage (ABN), September 2017d, http://www.cms.gov/Outreach-and-Education/Medicare-Learning-Network-MLN/MLNProducts/downloads/abn_booklet_icn006266.pdf. Accessed December 18, 2018.

CMS (Centers for Medicare & Medicaid Services): Clinical laboratory improvement Amendments (CLIA), August 2017e, http://www.cms.gov/Outreach-and-Education/Medicare-Learning-Network-MLN/MLNProducts/Downloads/CLIABrochure.pdf. Accessed December 18, 2018.

CMS (Centers for Medicare & Medicaid Services): National correct coding initiative edits for 2019, Revised December 12, 2018f, http://www.cms.gov/Medicare/Coding/NationalCorrectCodInitEd/index.html. Accessed December 18, 2018.

Travers EM: *Clinical laboratory management*, Baltimore, MD, 1997, Williams & Wilkins.

CHAPTER 14

ETHICS IN LABORATORY MEDICINE

Richard A. McPherson, Matthew R. Pincus

HIPPOCRATIC OATH TODAY, 174
REGULATIONS, 174
Conflict Of Interest, 175
Privacy, 175
HUMAN SUBJECT RESEARCH, 175
DEVELOPMENT OF FEDERAL REGULATIONS FOR HUMAN SUBJECTS RESEARCH, 176
CASE REPORTS, 176
CATEGORIES OF HUMAN SUBJECTS RESEARCH, 176
Exempt Review Category, 176
Expedited Review, 177
Full Institutional Review Board Panel Review, 177
METHOD VALIDATION OR NEWLY DEVELOPED ASSAYS—TRIALS FOR U.S. FOOD AND DRUG ADMINISTRATION SUBMISSION, 177
CLOSE OUT OF A RESEARCH STUDY, 177
RESEARCH IN THE CLINICAL LABORATORY, 177
CONFIDENTIALITY OF GENETIC INFORMATION, 178
CLINICAL TRIAL PHASES, 178
AUTHORSHIP, 179
DISHONEST BEHAVIOR, 179
KICKBACKS/BRIBERY, 179
OWNERSHIP OF SPECIMENS, 179
SUMMARY, 180
SELECTED REFERENCES, 180

KEY POINTS

- Ethical behavior in professional affairs is essential to maintain trust of patients and physicians.
- Conflicts of interest can arise when transparency of motives and rewards is not practiced.
- Privacy of protected health information is mandated by the U.S. federal government under the Health Insurance Portability and Accountability Act.
- Following atrocities and war crimes of unethical research on human subjects during World War II, the Helsinki Declaration (1964) and the Belmont Report (1978) established ethical principles for human subjects research.
- Federal regulations under the Common Rule for human subjects research incorporate respect for persons, beneficence, and justice.
- Institutional review boards (IRBs) are responsible for approving human subjects research in the categories of exempt, expedited, or full panel review.
- While standard clinical laboratory procedures of method validation, quality control, quality assurance, and more do not fall under the purview of an IRB (because they are not research activities), new method development does; therefore, adequate provisions should be made for commercial or other support of the research.
- Clinical trials of new therapeutics can involve both conventional and experimental laboratory tests that laboratory personnel should be aware of.
- Dishonest behavior, kickbacks, and fraud in laboratory medicine can be crimes and may rely on whistleblowers to report them.
- Ownership of diagnostic specimens and genetic information has led to court cases in which patients have generally not been able to maintain ownership. However, they should be made aware of any possible future uses of those specimens.

Why is ethical behavior desirable and applicable to today's practices in medicine? News media recount daily examples of unethical performance in business, government, finance, entertainment, professional sports, interpersonal/marital relationships, international/diplomatic affairs, and more. In essence, bad behavior seems to abound in modern society although it is not new but probably simply more revealed in recent years.

Unethical behavior has often become expected or even normal, with rewards of monetary gain, personal advancement, and individual power. Yet, the scorn heaped on those who are revealed to break ethical norms speaks to the expectations that most people have for good behavior from persons in positions of responsibility. The field of medicine has special respect from patients who expect that physicians will treat them with competence and will hold their information in strictest confidence. They expect physicians to be their dedicated and unbending advocates for pursuing the correct diagnosis and treatment. The respect that people have for medical practitioners might be unique among all professions. Nevertheless, ethical behavior is not simply a consequence of a medical diploma but rather develops from years of experience, beginning with family values and maturing under the influence of educational oversight, with special significance from the examples of attending physicians during medical school, residency, and fellowships. By the time that medical professionals begin practice, they clearly have an ethical framework upon which to rely for making many decisions. However, the study of medicine does not provide an exhaustive review of ethics nor is that education in ethics necessarily equivalent between specialties or institutions. Consequently, ethical guidelines have become more prevalent in recent years to provide a path to best (and expected) behaviors in areas that are crucial for maintaining the trust that patients and society as a whole have for medical practice.

HIPPOCRATIC OATH TODAY

The earliest codification of medical ethics in Western culture dates to the Hippocratic oath for physicians that originated in Greece in the fifth to third century BCE. The basic tenets of that oath are to treat patients appropriately and as best as can be done without harming them, to maintain patient confidentiality, and to teach the practice of medicine to ensuing generations of student physicians (North, 2002; Shiel, 2018). The original oath has been modernized, and some form of it is generally used in most medical schools. Schools of osteopathy have a similar osteopathic oath (American Osteopathic Association, 2019). These oaths are highly relevant to ethics applied to the practice of laboratory medicine.

REGULATIONS

Most individuals have an inherent sense of what constitutes ethical behavior, but to ensure that we operate at the appropriate and expected levels, the U.S. government has issued rules of such conduct. This discussion covers different regulations that are currently in effect for medical practice and human subjects research, with emphasis on issues that frequently arise in laboratory medicine.

Because these regulations are relatively new, having been produced in recent decades, they should be expected to evolve further, especially with regard to new therapies and their accompanying diagnostic procedures based on discoveries of molecular biology. Accordingly, medical practitioners should become familiar with current regulations and should be prepared to learn and follow new ones as they are enacted.

CONFLICT OF INTEREST

Many situations prone to possible unethical behavior have at their core a *conflict of interest* in which a medical professional has interests beyond those of treating patients in an open and unbiased manner (Muth, 2017). Such conflicts may arise if the medical professional has potential financial gain from particular diagnostic or therapeutic procedures and thus preferentially recommends or orders those procedures over other competitive ones that might be equivalent or superior in effectiveness or might cost substantially less. Full disclosure to patients should include any potential financial interests of physicians in such procedures to promote true and complete informed consent about treatment course. Most, if not all, institutions now require faculty and employees to make conflict of interest disclosures (COIDs) for their own investments (and those of family members) and other interests related to medical practice. These disclosures include consulting agreements and honoraria for presentations at meetings. Complete disclosure of financial relationships is essential to truly transparent operations. Special note should be made of strict regulations pertaining to federal employees, such as those at military and Veterans Affairs hospitals or agencies of the National Institutes of Health and of the Centers for Disease Control and Prevention. U.S. government employees are not permitted to participate in consulting relationships and may not receive honoraria for speeches or writing.

PRIVACY

Ethical guidelines for handling patient information have been established as law by the U.S. government under the Health Insurance Portability and Accountability Act (HIPAA) of 1996 and subsequently amended, including the HIPAA Omnibus Rule effective March 26, 2013 (see Chapter 1). The Privacy Rule of HIPAA protects the confidentiality of medical information having to do with a patient's past, current, and future medical encounters. This Protected Health Information (PHI) is covered for 50 years after the patient's time of death. HIPAA deals with covered entities (the hospital, medical group, insurance company, and other organizations that might be involved in providing medical care and storing PHI for clinical purposes or for transmitting it to substantiate insurance claims). HIPAA defines protected data, with emphasis on identifiers that might break the confidentiality of PHI if revealed—such as patient names, dates (of birth, admission, discharge, death), telephone numbers, social security numbers, email addresses, geographic subdivision, photographic images, or biometric markers. Patients are provided with a HIPAA form at the time of medical care that discloses the health care provider's privacy practice. HIPAA also guarantees patients' rights to access their own PHI, to copy it, and to correct it if necessary.

Through these provisions, HIPAA defines the basics of how patient information should be respected and kept confidential. One might say it is self-evident that these regulations are good behavior that should always be in place. Yet, by codifying these privacy measures as federal law, anyone on the verge of revealing PHI either through casual conversation or in an orchestrated effort to breach confidentiality will know that it is wrong and that serious consequences can result. Thus HIPAA sets what might be termed the base of ethical behavior for handling PHI. Because clinical laboratories generate an immense amount of PHI through test results, HIPAA is extremely important—from test order entry through test performance, result reporting, and storing in systems (usually electronic) that can retrieve results for purposes such as future medical care, billing, compliance with other regulations, and other informatics applications. To facilitate care of patients, personnel at medical centers—such as physicians, nurses, and technologists—usually have ready electronic access to medical records of a wide range of patients, including family members, friends, neighbors, celebrities, and others. However, unless those personnel are part of a care team and have a professional reason to do so, they should not read medical records of persons who are not their patients. Along with ease of electronic access to medical records comes complete documentation of who entered medical records, which can support disciplinary actions regarding their inappropriate use.

HUMAN SUBJECT RESEARCH

Modern ethics of research performed on human subjects came into being partly as a response to atrocities forced on prisoners by the Nazi regime of World War II. Revelations of these inhumane experiments occurred during the Nuremburg trials for war crimes.

The Helsinki Declaration adopted in 1964 by the World Medical Association and subsequently revised was an international effort to establish ethical principles for physicians performing medical research with human subjects or identifiable human material/data.

BOX 14.1

Belmont Report: Principles of Human Subjects Research

1. *Respect for the individual.* Human subjects should have the research fully explained to them, including possible risks and benefits. Their participation is strictly voluntary, without coercion or undue incentives. Informed consent should be done in writing by each subject. Special protections are provided for vulnerable populations: prisoners, children, pregnant women/fetuses, mentally impaired persons.
2. *Beneficence.* Experimental procedures should have the possibility of benefit, such as a successful new treatment for a disease. For treatments that can have adverse effects, such as chemotherapy, benefits should be balanced against risk of harm.
3. *Justice.* Research subjects should reflect the population for whom an experimental treatment is likely to be made available in the future.

A comprehensive study by the National Commission for the Protection of Human Subjects of Biomedical and Behavioral Research resulted in the Belmont Report (1978) that set the guidelines for ethical behavior in research. Three principles are elaborated in the Belmont Report (Box 14.1):

1. **Respect for persons.** The principle of respect is embodied in obtaining informed consent from prospective subjects before they enter an experimental study. The informed consent document should be written in language appropriate for age and educational level. It should describe why the subject is being asked to participate in the research (e.g., if the subject has a particular disease which is being studied or if a subject is being recruited as a healthy control who does not have the disease) and what to expect in terms of experimental manipulations or treatments, known side effects of those actions, and what the subjects will be expected to do (e.g., time and effort to attend medical clinics for research purposes). It should be clear in the consent process that subjects are free to refuse participating and can leave the study at any time. Special provisions must be made for consent from children (including parental consent) and other vulnerable populations (e.g., pregnant women and their fetuses, mentally impaired persons, prisoners, or otherwise incapacitated individuals). Sometimes, an experimental design includes deception to study its effects. However, truthfulness is paramount to the informed consent process; thus, deception would be extremely unlikely to gain approval from a research review panel. Although written informed consent is the expected practice, oral consent with documentation can be used if keeping a record of the subject's name could lead to embarrassment or other adverse consequences. Some research consists of potentially life-saving actions, such as at the onset of a heart attack, seizure, or trauma, in which a delay in treatment to fully explain the research to the subject (who might be unconscious) or relatives is not feasible because of the emergent medical condition. This type of research may be conducted as an Exempt From Informed Consent (EFIC) study without the usual written consent before initiating the experimental treatment, although written consent must be obtained subsequently from the subject or relative. EFIC studies should be extensively advertised and explained to the community where they will be conducted in advance of their approval.
2. **Beneficence.** Any experimentation performed on humans should carry the prospect of being good for the subjects. This principle excludes research that has the possibility of harm with no likelihood of good. Direct physical harm merely to study the result of that harm would be forbidden. Some research could potentially do harm to subjects, such as a trial of a new and unproven chemotherapy agent that has known toxicities but might have desirable antitumor effects based on preliminary research using animals or tissue culture models of the disease. Psychosocial research must build in safeguards when subjects could be frightened or alarmed by the research process, especially when deception might be part of the experimental design. Likewise, biomedical research should foresee probable or possible discomforts to subjects and take measures to minimize such effects.
3. **Justice.** This principle states that the subjects who are being experimented on should represent the population that is expected to benefit from products or treatments that might be developed based on experimental findings. Thus, it would be unethical to recruit subjects solely from low socioeconomic levels if the intended new treatment could be afforded only by wealthy people.

The Belmont Report and its principles form the basis for modern human subjects research, although it is not the actual law.

DEVELOPMENT OF FEDERAL REGULATIONS FOR HUMAN SUBJECTS RESEARCH

The U.S. Public Health Service (USPHS) conducted observational experimentation on African-American males diagnosed with syphilis from 1932 to 1972. Termed the Tuskegee Health Survey, this study consisted of monitoring these men with regular physical examinations plus laboratory evaluation of blood and cerebrospinal fluid specimens to document the natural progression of syphilis, which was untreated in the study. This experimental design violated all three principles of the Belmont Report:

1. Whatever informed consent used was inadequate, as participants were deceived into thinking that their visits and the collection of specimens was therapeutic.
2. There was no beneficence, as the disease was not treated.
3. Surely, there was no justice in the study, as subjects with clearly diagnosed disease were denied standard-of-care treatment that would have cured them simply to study the progression of untreated syphilis.

When the nature of the Tuskegee study was made known publicly, the USPHS was in an indefensible position, which led to a complete overhaul of human subjects research and the development of a code of ethical behavior that is now in effect for approval and conduct of the research. These regulations are published in the code of federal regulations 45 CFR 46 and are referred to as the Common Rule, which is mandatory for human subjects research supported by the U.S. Department of Health and Human Services and has been adopted by other research entities as well.

This presentation will focus on guidelines for human subjects research in which laboratory professionals are likely to be engaged. The federal guidelines deal with some additional categories of research, such as taste testing and opinion surveys, that will not be considered here.

The definition of human subjects research is crucial to decisions about what studies require review and approval by a panel such as an institutional review board (IRB). All human subjects research receiving federal funding either directly or indirectly must have institutional review. IRBs at individual institutions are regulated, in turn, by the Office for Human Research Protection (OHRP) of the Department of Health and Human Services under Title 45 Code of Federal Regulations Part 46 (45 CFR 46).

Research consists of (1) a systematic investigation with (2) the intent of contributing to generalizable knowledge (45 CFR 46.102). Human subjects research meeting these two criteria requires IRB review of a study proposal before it is initiated. By federal code, each IRB has at least five members, with at least one member who works in scientific areas, at least one member whose primary concerns are in nonscientific areas, and at least one member not otherwise affiliated with the institution. Efforts should be made to avoid an IRB that is all men or all women. No IRB member may be part of the review of a project for which that member has a conflict of interest. IRB members must maintain current knowledge and certification with continuing education in human subjects research regulations.

Routine and usual laboratory practices—such as method validation for establishing standard procedures (e.g., when changing instrumentation to upgraded equipment), quality assurance (QA), and quality improvement (QI) studies—are not considered research (they are not intended to contribute new generalizable knowledge). Thus, they do not fall under IRB review. It is important to note here that the intent to publish, as stated in OHRP policy, is "an insufficient criterion for determining whether a project involves research." Therefore, since QA and QI studies are not considered research, the results may be published without the need for IRB approval provided that all patient identifiers are removed so that results cannot be traced to any particular patients (see later discussion). Included in these QA studies would be results concerning mass analysis of patient values, such as running averages for specific analytes, in which there is no patient identification.

Waived and Expedited IRB Reviews: Discarded Specimens. There are situations in which it is desired to perform research studies on patient samples that would normally be discarded after a fixed period (usually 1 week for serum samples). These are so-called "discarded samples." These studies must be submitted to an IRB. However, if the studies involve deidentification of all patient samples and fulfill other requirements of the IRB, special (or short) forms are given to the investigators to complete. The Chief Officer of the IRB and other senior IRB officials then evaluate the investigators' filled out special forms. If these officials conclude that the forms are acceptable, one of two actions can then be taken. A waiver can be issued by the IRB exempting the study from any further IRB review or an expedited review can be performed. In case of the latter, approval is issued for 1 year for the study. For continuance of the study, the investigators must submit an annual review of their study and, if desired, request renewed IRB approval for another year.

BOX 14.2

Common Rule: Institutional Review Board Oversight of Human Subjects Research

1. *Exempt from IRB oversight.* Minimal risk typically for retrospective research using data already collected for other purposes and, thus, informed consent is impractical to obtain; main risk is to patient confidentiality, thus, data should be deidentified after collection. No annual review is required. The IRB should determine that research is exempt, not the investigators.
2. *Expedited.* Minimal risk for prospective data collection; can usually expect to obtain informed consent unless a waiver is granted (rare event).
3. *Full Panel.* More than minimal risk; must have annual review of research progress, occurrence of adverse events, and likelihood of completing the study.

CASE REPORTS

In the normal course of usual clinical practice, unexpected observation of an interesting patient finding (e.g., serum protein disorder, autoantibody, histopathologic abnormality, variation in therapeutic drug clearance, etc.) could lead to the publication of that unique *case report*. Because that unanticipated action was not a systematic investigation, it does not meet the criteria for human subjects research. Thus, it should not require IRB review to proceed with publication. However, if a second or more cases of the same unusual finding appear, then collection of data from the multiple cases is a systematic investigation. This constitutes research that requires IRB review, which should be completed prior to collection of data from patient records. One might think that collection of patient data and even analysis could be done before IRB approval. However, proceeding with these actions prior to review is a breach of confidentiality of the patient medical record, thus should not be done prematurely.

CATEGORIES OF HUMAN SUBJECTS RESEARCH

The general categories of research are defined according to whether the project is retrospective or prospective and according to level of risk to subjects (Box 14.2). Individual IRBs have the authority to apply more stringent criteria for approval of human subjects research according to local sensibilities and practices.

EXEMPT REVIEW CATEGORY

If a study is performed retrospectively on information already in existence (i.e., in medical records not collected for research purposes), then it might qualify as being exempt from review. Studies in the exempt category should be designated as such by an IRB, not by the investigators themselves, to avoid potential conflict of interest. Inherent in approval for exempt status is to strip patient identifiers from research data after collection from the medical record to preserve patient confidentiality. Typically, patients for retrospective study can be identified by a search through computer or paper medical records according to the clinical parameters of interest to qualify as subjects for the study. A list of subjects can be kept in an electronic spreadsheet from which each subject name and identifiers can be purged upon completion of data collection. It is appropriate to establish and submit to the IRB for approval an information collection sheet (electronic or paper) that lists all the data elements that will be extracted from the medical record. This approach has the advantage of not requiring informed consent from subjects who might not be accessible retrospectively, but it limits the investigator to collecting only the information stated in the research proposal. Patient confidentiality is maintained by stripping identifiers from data prior to analysis. These data are said to be deidentified (as opposed to anonymous data, which would have been collected without identifiers). This category of exempt research does not allow for collecting additional relevant information (such as medication) that might not have been originally proposed. To do so would require an additional

IRB review of an amended protocol in which data collection should be done completely anew, as already collected research data should have been deidentified. An exempt protocol does not require annual review. When the study is complete, it should be closed out with the institution's IRB.

EXPEDITED REVIEW

The category of expedited review (45 CFR 46.110) can be applied to research in which minimal to no harm is expected to occur to subjects or for minor changes to previously approved research. This category includes prospective research with collection of data not yet in existence. In this case, subjects are available for informed consent; thus, research data need not be deidentified. Expedited protocols do not include clinical trials of medications that might cause harm. They do allow for collection of data and of clinical specimens, such as age- and health status–defined volumes of blood or body fluids not requiring invasive collection, such as urine. The main risk to subjects in this category is breach of confidentiality, which must be adequately explained in the informed consent form. Both exempt and expedited protocols may be reviewed by a single member of an IRB (e.g., IRB chairperson or designee from IRB members), as the risk is considered to be no more than minimal.

FULL INSTITUTIONAL REVIEW BOARD PANEL REVIEW

Review by a full IRB panel is necessary whenever a protocol has a potential risk that is greater than minimal. For example, the use of a new chemotherapy agent with known or suspected side effects would require extensive explanation to potential subjects in the informed consent process and form. Laboratory personnel generally would not initiate such studies, but they could easily be co-investigators with specific tasks of examining specimens collected for the research before, during, and after experimental treatment. Accordingly, they should be aware of the impact of the research manipulations on subjects.

METHOD VALIDATION OR NEWLY DEVELOPED ASSAYS—TRIALS FOR U.S. FOOD AND DRUG ADMINISTRATION SUBMISSION

The use of a clinical laboratory to analyze research specimens is outside the usual authority of individual laboratory directors to approve if the facility is a public lab or a private lab not owned by the director, who is merely its steward. The director's role is to ensure timely and accurate testing at reasonable operating expenses, all of which require quality control and proficiency testing in a fiscally responsible operation. Introduction of new tests or equipment entails method validation using excess specimens submitted for routine clinical analysis. All of these activities are standard for laboratory management. Manufacturers of reagents for new tests generally do not have immediate access to the hundreds of specimens covering all expected normal and abnormal test results. Thus, they must contract with clinical laboratories to provide such clinical specimens in order to document fitness of the new procedure. Remuneration for collection of those specimens or their analysis by a new test should be structured to include relevant costs of the institution, including labor of the technical staff. It is not appropriate for the company purchasing those services simply to write a check to the laboratory director for the director's personal use unless that person has ownership of the laboratory and is authorized to commit use of the entity's resources. Certainly, hospital-based laboratories are not owned by their directors, but they do have governing bodies that review and approve research (i.e., IRBs) as well as those empowered to authorize grants and contracts. Accordingly, the steps to negotiating a contract for evaluating a new commercial assay should include:

1. Approval of the research with specific provisions to protect patient confidentiality, as medical records could well be utilized to provide information such as diagnosis, current treatments, therapeutic responses, and other test results
2. Approval of a budget to adequately reimburse the institution for the time and efforts of its employees, including that of the laboratory director, and, typically, additional funds to further research activities. Such payments from companies to institutions are fair and expected for the privilege of access to patient specimens in sufficient numbers and variety to provide supporting evidence for clearance of a new assay by the U.S. Food and Drug Administration (FDA).

Because most institutions do not have previously banked specimens with a full range of results and with patient diagnoses to evaluate effectiveness of a new assay, research projects for new method evaluation must use newly acquired specimens. Thus, they are prospective studies. Such prospective studies would not fall under exempt review because patients are actually available for obtaining their informed consent. However, to do so might be extremely unwieldy. For example, particular specimens with a full range of test results might be recognized as appropriate for a study only after being analyzed, at which time the patient could have gone home and not be immediately available for consent. One way to handle this situation is to have a member of the technical staff select and set aside specimens for research based on review of results to ensure that the full spectrum of appropriate results are included. That staff member should not be a member of the research team (thus should not be a coauthor on any resulting manuscript). That person would be responsible for deidentifying specimens so that the research team members do not know from which patients they were extracted. The staff member could review medical records to ascertain relevant aspects of the patients, such as diagnosis, treatments, and medical outcomes, assuming that the protocol to collect such information along with specimens is approved by the IRB with jurisdiction.

After initial approval by an IRB of expedited and full panel–reviewed protocols, annual continuing review is required of those protocols that remain active. Continuing reviews report progress in the research, including number of subjects recruited and their current status (e.g., actively participating, participation concluded, dropped out of study before completion, etc.). This information will allow the IRB to conclude whether a protocol has a good chance of successfully achieving its recruitment goal in the projected research period or whether it might be futile to continue. Exempt protocols need only initial IRB approval; thus, they do not require continuing annual review unless the risk profile to subjects has substantially increased since study onset. New changes to the Common Rule effective January 21, 2019, allow expedited protocols to proceed without annual review subsequent to their initial approval.

CLOSE OUT OF A RESEARCH STUDY

Once a research study has been completed, the principle investigator (PI) should file with the IRB to close out that protocol. Records of a closed study should be kept by the PI for at least 3 years if PHI is not included (OHRP regulation) or for a minimum of 6 years after each subject signed authorization for records with PHI (HIPAA requirement). The FDA requires records of research on drugs, devices, or biologics for testing in humans to be retained for 2 years beyond the date a marketing application is approved. These guidelines for record retention can be extended by individual institutions or sponsors. It should be noted that research records are owned by the university where the work is conducted and not by the investigators themselves.

At the conclusion of a mandated storage period, and when approval to destroy research data has been obtained, it should be disposed of in an irreversible manner to prevent the information from being recreated. Modern data storage can include both paper and magnetic/electronic files, such as disc and individual or central computer systems. Data disposal methods for all of these modes should be approved by the university and might entail physical destruction of storage media by special procedure and not merely by dumping in the trash, where it might be discovered by an unauthorized individual who could gain inappropriate access to confidential information.

RESEARCH IN THE CLINICAL LABORATORY

Types of human subjects research performed in clinical laboratories include the following general areas:

1 *Method comparison.* New methods for conventionally measured analytes are routinely compared on the same specimens with the existing methods prior to introduction of new reagents and/or instrumentation (Clinical Laboratory Improvement Amendments [CLIA] regulation). Examples are clinical chemistry and hematology procedures widely used for patient diagnosis and monitoring. This practice is standard and is required for laboratories to conduct when introducing a new method into routine use. Such method comparison for establishing validity of a new technique or instrumentation for clinical use is not research; thus, it requires no IRB approval. However, prior to FDA clearance of new methods, manufacturers generally enlist the participation of clinical laboratories for the necessary numbers and types of specimens for comparison with existing methods. This activity contributes new knowledge; therefore, it is research that entails IRB approval. These data would typically be used by the manufacturer in an FDA submission.

2 *Wholly new method.* This category refers to new laboratory procedures for which no analysis currently exists. Examples could be newly discovered autoantibodies, peptide markers of inflammation, or DNA sequences and mutations. For these new methods, the evaluation compares test results with clinical findings such as presence of disease or syndrome, response to therapy, and clinical outcome, all of which information must be extracted from the medical record. These data would also typically be used by the manufacturer for FDA submission.

3 *Support of clinical trial.* Performance of a clinical trial, such as when evaluating a new chemotherapy drug, usually requires measurement of a spectrum of analytes, some standard and others that could be research entities themselves. Thus, the laboratory should be prepared to participate in treatment protocols to assist in diagnosis (or specific study entry criteria), monitoring progress and guiding therapy, and, finally, for clinical outcome. Large multi-institution protocols can have funding for performance of novel methods or to collect, store, and transport specimens to a central laboratory that has established that testing. Routine testing of patients in many cancer protocols can be billed to insurance companies as standard of practice. The laboratory should maintain procedures for proper handling, reporting, and billing of specimens as well as their local testing or transport to a centralized institution.

Laboratory tests that are part of a research protocol (e.g., DNA sequencing, measurement of low-level protein concentrations, etc.) but that are not standard of practice would not be billed to insurance or to the patient. In that case, research funding should be established to support the portion of testing that is not standard of care and to collect, process, store, transport, and, finally, to perform the testing.

If specimens are labile and not viable after transport, they could be tested at the medical site where the patient is located. In that case, funding should be procured to support all aspects of specimen handling and analysis, including time and effort of technical staff as well as of a laboratory director and others who oversee the validation, performance, and any interpretation of the testing.

The informed consent form that a research subject signs and the oral explanation of the research should include a specific list of all tests that will be performed as research, how much blood or other body fluid or specimens will be collected and how often; any pain or discomfort subjects might experience related to specimen collection; how the information obtained from testing will be used and its confidentiality maintained; whether the subject could benefit from the testing and knowing the results; how specimens will be stored long-term and whether other tests might be performed on them in the future; and how subjects can opt out of future specimens testing or storage if they change their minds about participating.

CONFIDENTIALITY OF GENETIC INFORMATION

For many decades, clinical laboratories have been performing procedures that reveal selected genetic abnormalities about patients. This information has largely been in the form of single pieces of information, such as presence of metabolic abnormality detected by neonatal heel stick blood testing for serious disorders that can result in neurologic impairment if not properly treated (often simply through dietary exclusions). Other examples are screening for hemoglobinopathies or testing for hemophilia in children with a hemorrhagic diathesis. Screening for carrier status is also carried out for Tay-Sachs disease in high-risk populations (e.g., Ashkenazi Jews) with arranged courtships and marriages to avoid conception of an afflicted homozygous child (who would be severely mentally impaired and who would live only a few years at best). This match-making pairs only noncarriers with carriers; children of such a marriage would be nonaffected carriers or noncarriers (Merz, 1987).

In contrast to that historic line of single disorder or restricted panel testing, modern nucleic acid sequencing has the capacity to examine the entire human exome and even the entire genome. Thus, a patient might have revealed any of a multitude of genetic disorders that could be less severe than ones that are lethal in children but could have the effect of altered longevity, susceptibility to disease, mental and physical fitness, neuropsychiatric disease, etc. Once such extended genetic testing becomes a standard of practice, patients should be made aware of the possibility that these types of sensitive findings might be inadvertently revealed. Furthermore, knowledge of an individual's genetic background could also lead to suspicion that family members could have the same risk for disease even though they had not requested or consented to that testing. Examination of an individual's genetics thus has an impact on genetic knowledge of family members as well.

Another example of unintended effects of genetic testing on others has been the recent use of genetic markers shared by family members to find perpetrators of heinous crimes, such as rape or murder, through comparison of crime scene specimens of DNA with existing data bases of DNA sequences collected voluntarily from family members for the express purpose of studying ancestry. Although this practice has been done in selected legal cases, it has the potential for application to myriad types of identity testing; thus, it should be explained to persons prior to testing them. Admittedly, many future applications might not be recognized at present, but the risk of impinging on the confidentiality of genetic information should be understood by participants. Certainly, the legal treatment of genetic information will have precedent set in the near future.

Commercial DNA testing companies that actively market their services to the public act through anonymous consent on the Internet using unique identification coding to permit customers to look up their own results. Because these commercial endeavors derive support directly from customers and not from the federal government, they are not constrained to follow the same regulations for informed consent as in federally funded research at universities and institutions. Consequently, the explanation about genetic results is not always thorough and may lead to more questions from customers who need to evaluate their own potential for hereditary diseases and their progression. While some genetic counseling might be available from these companies, there remains the need for more genetic counselors to meet the increasing workload nationwide.

CLINICAL TRIAL PHASES

The design for a clinical trial involves a regular sequence of phases that evaluate both the side effects and the therapeutic action of a new drug or other treatment. Before administration to human subjects, animal trials as well as biochemical and tissue culture experiments with a new drug should provide some evidence for therapeutic success and low or acceptable toxicity. The ethical principle of *equipoise* (or *clinical equipoise*) indicates uncertainty that a new experimental treatment will be beneficial (i.e., it could be better than existing therapies or it could be ineffective or even harmful). This uncertainty can be answered by a clinical trial with treatment arms designed to show effectiveness if it is true.

Phase 0 trials constitute the first administration of an experimental drug to humans, largely to ascertain how it is metabolized and cleared from the body and what toxicities it might have. Only a few persons (10 to 15) are included in a phase 0 trial.

Phase I trials determine the best dose for which fewest side effects occur. Using 15 to 30 patients, initial participants receive very low doses while later patients receive escalating doses until side effects become severe or projected effects on the disease are attained. Phase I is often called a safety trial. Phase I participation may be offered to patients with the disease intended to be treated with the new drug who have exhausted other standard therapies.

Phase II trials can proceed after an initial safety profile has been established in phase I. Phase II uses more patients with a specific disease; treatment is often with combinations of drugs. Phase II looks at safety in the larger group of patients as well as whether the drug works.

If toxicities are acceptable and the drug shows some efficacy, it may proceed to *phase III trials* with 100 or more patients. At this stage, patients are randomized to different treatments or control (typically standard of care for the disease). Neither the patient nor local medical personnel choose the specific treatment received. This masking (also called blinding) to treatment group is intended to eliminate bias from participants who otherwise might feel they are getting a new drug that is effective and so report major improvement or might think they are receiving an ineffective control and expect it to fail. Once the trial is over, patients may be told which group they were in. The informed consent form for participation in the study should include this information that patients and doctors will not know group assignment during the study. Based on success in phase III, the FDA can approve use of a new treatment for the general public.

Phase IV trials are for drugs already approved by the FDA and are tested in up to thousands of patients. This larger number of carefully monitored patients facilitates detection of rare side effects and gives a better understanding of drug efficacy in different contexts of care.

Although these phases of 0 to IV are generally recognized as the basic steps for evaluating a new drug, additional postmarketing surveillance for side effects is done in very large numbers of patients. This monitoring can lead to recognition of infrequent adverse events that are serious for some patients.

AUTHORSHIP

Participation in research projects is rewarded in part by sharing authorship in scientific publications generated from that research. Coauthorship on publications is crucial for academic advancement and for establishing the reputation of researchers. Accordingly, it is appropriate that the authors on scientific manuscripts should have provided substantial effort that was essential for the project. Efforts generally expected for being included as an author include planning the project (including both experimental and statistical design), participation in data collection and data interpretation and managing the work, data analysis, and writing the manuscript. If the study concerns a new test or a new drug, the inventor(s) may also be included as authors of the final manuscript. If someone has not done one of these activities or others critical to the completion of the study, then that person probably should not be listed as an author but could be acknowledged in the manuscript.

DISHONEST BEHAVIOR

Professional interactions in medicine require open and honest communication between parties, including patients' primary care physicians and consulting physicians. To this end, the huge majority of laboratory tests are automated with computer interfaces that transmit test results directly into patient medical records with a strong audit trail, thereby avoiding possible fraudulent changes by laboratory personnel. However, some manual procedures or those using complex equipment or even interpretations of results might not be directly connected to laboratory computers, which could require data input by hand for reporting purposes. This situation is susceptible to falsification of results by unscrupulous persons or just by simple human error. To guard against false reporting by this means, a regular review of instrument printouts should be reconciled against actually reported values. While such fraudulent result reporting could appear highly unlikely to occur, in fact, a notorious case of massive numbers of false cytologic reports from examinations that were not actually performed (sometimes referred to as "dry lab" results) was a major factor leading to adoption of the Clinical Laboratory Improvement Amendments of 1988 (CLIA 88) by the U.S. federal government (see Chapter 1). It behooves laboratory directors to have policies and procedures in place for preventing and detecting any fraudulent results that could be considered criminal activity.

Human resources departments certainly should have policies to manage employees found performing fraudulent actions. Typically, a series of actions could be taken, including immediate suspension or termination if an employee has committed a serious infraction, such as falsification of results that could lead to patient harm or death due to incorrect diagnosis and inappropriate treatment. If an employee is retained after documented fraud, the trust that laboratory directors and other personnel have for the person might never be restored, leading to a contentious and untrusting workplace. The maxim that someone who is found to be lying under oath can never be completely believed in other testimony has its counterpart in the laboratory workplace.

It may be difficult to understand the reasons for prevarication, especially in the setting of the clinical laboratory where testing is an objective process. Perhaps the perception of personal gain is an inducement, or professional advancement, or even simple curiosity or retribution against an acquaintance under medical care. Regaining trust in someone who falsified findings can be a difficult process and should include that person admitting responsibility for one's actions and being committed to making positive efforts to avoid similar actions in the future. If the person is a student in training, supervisory personnel should be obliged to develop a personalized plan of corrective action with frequent monitoring. An analogous program of rehabilitation has been adopted for medical personnel who are addicted to drugs or alcohol.

Honor codes require anyone who witnesses fraud or cheating to report those violations even if the observer is not a participant in the illicit activity. Doing so might carry significant personal loss if an organization or persons in powerful positions choose to cover up wrongdoing and take aggressive steps against a legitimate whistleblower. Such countersteps against a whistleblower might include loss of income, position, or employment and even punishment such as lawsuits and attacks on the individual's reputation. Countersuits on behalf of a whistleblower can lead to reinstatement and payment of damages, although it may take years to settle. Most persons would probably not be willing to pursue such a course owing to the toll on living conditions; yet, that might be the only way to bring fraud to light. A recent case of whistleblowers bringing a fraudulent laboratory enterprise to public attention is documented in investigative articles published in the *Wall Street Journal* and in the book *Bad Blood* by John Carreyrou about the Silicon Valley company Theranos and its supposed multipurpose instrument called Edison. The promise of that system to perform a spectrum of chemical analyses inexpensively on a drop of blood was very attractive. However, the concept was not realized, leading to extensive coverups and false claims that were eventually exposed through whistleblowers who were threatened with legal action for telling the truth. Because clinical laboratory practices are so well regulated both by laboratory professionals and by outside accrediting and licensing entities, it is highly unlikely that laboratory fraud could go on indefinitely; rather, it will be discovered and reported.

KICKBACKS/BRIBERY

In order to obtain preferred services or to influence decisions about contractual arrangements when multiple bidders are making formal proposals, some companies may resort to illicit payments to secure a large volume of business. Such circumstances include decisions to purchase or lease equipment for a clinical laboratory with long-term purchase of special reagents for that instrumentation. Payments to influence decision makers can also include free travel, meals, gifts, cash, or honoraria far out of line for actual value of presentation on a company's products—all of which should be avoided. Major institutions now require employees to disclose any and all such payments on a regular basis, even from national organizations that merely reimburse expenses incurred by speakers at national conferences. Revealing all personal gifts and obtaining permission for reimbursed expenses are appropriate means to avoid bribery and other illicit pressures in financial practice.

In daily practice, contracts and payments should be constructed so that actual effort is reimbursed. Thus, laboratory directors should receive compensation in their negotiated salary for administrative efforts and not simply be expected to direct a laboratory in return for the privilege of billing patients and insurance for interpretive work. Physicians should also not expect kickback payments from hospitals or laboratories for referring patients or specimens to those organizations.

Laboratory personnel should have an understanding of the nature of fraudulent and other unethical behaviors, such as kickbacks, so that they can be prepared to reject them and avoid conflicts of interest that could compromise their professional standards.

OWNERSHIP OF SPECIMENS

In the normal course of doing business, clinical laboratories store patient specimens for a brief period of hours to days after analysis in order to repeat testing if initial testing was questioned, to perform additional testing that might be requested, or to evaluate the authenticity of specimens if they are questioned. Then, typical specimens—such as blood, urine, and other body fluids—are disposed of by incineration or other biohazard-free means generally within at least a week after collection and completion of testing. During the period of testing and storage, routinely requested specimens are generally considered to be under the protection of the clinical laboratory; thus, they would not be owned by the patient. In fact, it has been successfully argued that patients who consent to have diagnostic specimens collected have also abandoned those specimens and no longer have ownership rights over them (Allen et al., 2010).

The same general principle has been applied to specimens collected for research studies as long as subjects have been appropriately informed about what will be done with the specimens, about the nature and extent of subject involvement, and about what might be expected from findings of the study (e.g., papers could be published with academic advancement of the investigators, patents could be filed, and the researcher and institution might receive subsequent royalties from any discoveries). A celebrated case in which such transparency was not practiced began in 1976 when the patient John Moore had his spleen removed at the University of California Los Angeles Medical Center for standard treatment of hairy cell leukemia. UCLA researchers created a cell line that was later patented using the biological material removed from Moore without his knowledge or consent. He was asked to return to UCLA from his home in Seattle multiple times at his own expense and inconvenience to collect further blood specimens from 1976 to 1983, although those specimens were not strictly necessary for his therapy. After discovering that the cell line had been commercialized and that UCLA was collecting royalties for

its use (on more than three billion dollars of products based on the cell line between 1984 and 1990), Moore sued UCLA for ownership of the cell line (Gitter, 2004). The California Supreme Court verdict dismissed his claim to ownership and to a share of the royalties in part because the cell line was different from the tissues taken from Moore (even though they had his genetic material). To rule in Moore's favor might also have resulted in suppression of biomedical research of a similar nature. The court did allow that Moore could proceed with claims that his doctors at UCLA had breached their fiduciary responsibility to obtain his informed consent and had not disclosed their research interest and possible monetary rewards. This decision and others subsequently have reinforced the need for researchers to be fully transparent with subjects about the issues of informed consent and who might benefit from scientific discoveries (generally not the subjects) (Petrini, 2012).

Future legal cases on ownership of biological materials will certainly arise in the absence of clear legislation on the matter and likely will further define rights of patients and family members, especially when considering genetic information that is unique to individuals and their kindreds.

SUMMARY

Ethical behavior is a cornerstone of medical practice and is essential to the trust between patients and their physicians. Prospective transparency in motivation and potential financial gain allows physicians to manage potential conflicts of interest when they arise. Basic regulations for privacy of PHI is mandated in HIPAA. Separate regulations apply to human subjects research as elucidated in the Common Rule (in the U.S. Code of Federal Regulations) with protections for persons, beneficence, and justice (also principles of the Belmont Report). IRBs are responsible for approving human subjects research. Many laboratory activities, such as quality control, quality assurance, and method validation, do not require IRB review. IRB approval is necessary for new method development and evaluation when using human specimens and information from medical records for those tasks. Clinical trials frequently require laboratory support. Fraudulent activities can be criminal and may come to light through whistleblowers. Ownership of patient specimens for clinical or research use can be assumed to be the right of a laboratory and not the subject, although that relationship should be explained in advance to subjects before entry into a research protocol.

SELECTED REFERENCES

Allen MJ, Powers MLE, Gronowski KS, Gronowski AM: Human tissue ownership and use in research: what laboratorians and researchers should know, *Clin Chem* 56:1675–1682, 2010.

This article reviews cases and issues that have emerged concerning ownership of human specimens collected for research purposes.

Declaration of Helsinki, https://www.who.int/bulletin/archives/79%284%29373.pdf.

Historical declaration of the rights of human research subjects first adopted in 1964.

National Commission for the Protection of Human Subjects of Biomedical and Behavioral Research: *The Belmont report: ethical principles and guidelines for the protection of human subjects of research*, Bethesda, MD, 1978, U.S. Government Printing Office.

The Belmont Report puts forth the central principles for ethical behavior in human subjects research.

National Comprehensive Cancer Network: Phases of clinical trials, https://www.nccn.org/patients/resources/clinical_trials/phases.aspx.

This website provides a brief outline of the goals and structure of clinical trials.

The Common Rule, 45 CFR 46. https://www.hhs.gov/ohrp/regulations-and-policy/regulations/45-cfr-46/index.html.

These regulations are established by the U.S. federal government to provide strict guidelines for conducting human subjects research.

Access the complete reference list online at Elsevier eBooks for Practicing Clinicians.

REFERENCES

American Osteopathic Association: *Osteopathic oath*, https://osteopathic.org/about/leadership/aoa-governance-documents/osteopathic-oath/, 2019.

Carreyrou J: *Bad blood: Secrets and Lies in a Silicon Valley Startup*, New York, 2019, Alfred A. Knopf.

Gitter DM: *Ownership of human tissue: a proposal for federal recognition of human research participants' property rights in their biological material*, vol. 61. Wash & Lee Rev, 2004.

Expedited review, https://www.hhs.gov/ohrp/regulations-and-policy/guidance/categories-of-research-expedited-review-procedure-1998/index.html.

Muth CC: *JAMA* patient page: conflict of interest in medicine, *J Am Med Assoc* 317:1812, 2017.

Merz B: Matchmaking scheme solves Tay-Sachs problem, *J Am Med Assoc* 258:2636, 1987.

North M: *Greek medicine: the Hippocratic oath*, https://www.nlm.nih.gov/hmd/greek/greek_oath.html, 2002.

Petrini C: Ethical and legal considerations regarding the ownership and commercial use of human biological materials and their derivatives, *J Blood Medicine* 3:87–96, 2012.

Shiel WC: *Medical definition of Hippocratic oath*, https://www.medicinenet.com/script/main/art.asp?articlekey=20909, 2018.

PART 2

Clinical Chemistry

EDITED BY | Jay L. Bock, Martin H. Bluth, Matthew R. Pincus

CHAPTER 15

EVALUATION OF RENAL FUNCTION, WATER, ELECTROLYTES, AND ACID-BASE BALANCE

Man S. Oh , Gary Briefel , Matthew R Pincus

INTRODUCTION, 182

VOLUMES AND OSMOLALITY OF BODY FLUID, 183
Measurement Of Body Fluid Volumes, 183
Body Fluid Volumes, 183
Composition Of The Body Fluid, 184
Measurement Of Plasma Osmolality, 185

REGULATION OF EXTRACELLULAR VOLUME, 186
Nonrenal Control Of Water And Electrolyte Balance, 187

MEASUREMENT OF RENAL FUNCTION, 187
Concept Of Clearance, 187
Measurement Of Glomerular Filtration Rate, 188
Urea Clearance And Urea/Creatinine Ratio In Serum, 191
Glomerular Filtration Rate, Renal Plasma Flow (RPF), And Filtration Fraction (FF), 191
Fractional Excretion (FE), 192
Renal Failure Index (RFI), 192
Fractional Reabsorption (FR), 192

BIOMARKERS OF ACUTE KIDNEY INJURY (AKI), 192
Kidney Injury Molecule-1 (KIM-1), 193
Neutrophil Gelatinase-Associated Lipocalin (NGAL), 193
Interleukin-18 (IL-18), 193
Fatty Acid-Binding Protein (FABP), 193

DISORDERS OF POTASSIUM, 193
Control Of Transcellular Flux Of Potassium, 193
Control Of Renal Excretion Of Potassium, 194
Plasma Renin Activity (PRA), Plasma Aldosterone (PA) Concentration And Abnormalities In Potassium Metabolism, 194
Aldosterone Paradox And Role Of Sodium Chloride Reabsorption In The Distal Convoluted Tubule, 194
Causes And Pathogenesis Of Hypokalemia, 195
Differential Diagnosis Of Hypokalemia, 196
Causes And Pathogenesis Of Hyperkalemia, 196
Differential Diagnosis Of Hyperkalemia, 197

DISORDERS OF WATER, SODIUM, AND ANTIDIURETIC HORMONE (ADH) METABOLISM, 197
Regulation Of Thirst And ADH Release, 197
Urine Concentration And Dilution, 198
Polyuria, 199
Causes And Pathogenesis Of Hyponatremia, 199
Causes And Pathogenesis Of Hypernatremia, 200

ACID-BASE DISORDERS, 201
Bicarbonate And Co_2 Buffer System, 201
Definitions Of Acid And Base, 201
Whole Body Acid-Base Balance, 201
Metabolic Acidosis, 202
Metabolic Alkalosis, 205
Respiratory Acidosis, 206
Respiratory Alkalosis, 206
Mixed Acid-Base Disorders, 207

SELECTED REFERENCES, 207

INTRODUCTION

Laboratory tests for evaluation of disorders of renal, water, electrolyte, and acid-base status are the most common procedures performed in clinical chemistry laboratories. Screening tests in most laboratories are often grouped together in a basic metabolic panel because acid-base and electrolyte disorders are seen in a high percentage of hospitalized individuals, and electrolyte disorders are frequent complications of treatment for a variety of common conditions. Furthermore, renal disease is one of the major sequelae of common disorders such as diabetes and hypertension. Hence, proper interpretation of laboratory tests of renal, electrolyte, and acid-base disorders requires an understanding of pathophysiology of these systems. Most central to the understanding of these disorders is knowledge of renal function and how the kidneys regulate extracellular volume and tonicity.

VOLUMES AND OSMOLALITY OF BODY FLUID

The body fluid is an aqueous solution containing electrolytes and nonelectrolytes, consisting of intracellular and extracellular compartments. The intracellular compartment is not a single compartment; rather, each cell has its own separate environment, communicating with other cells only through interstitial fluid and plasma. Consequently, differences exist among cells in various tissues in their solute composition and concentrations. However, because cell membranes are permeable to water through the ubiquitous presence of aquaporins (water channels), osmotic equilibrium is maintained so that the osmolality of all cells is the same as that of extracellular fluid (Carroll & Oh, 1989a).

Before the discovery of aquaporins, it was believed, erroneously, that all cell membranes are readily permeable to water. We now know that cell membranes are virtually impermeable to all substances, large and small. Even a molecule as small as water, with the molecular mass of a mere 18 Da, needs aquaporins in order to cross the cell membrane. Even after the discovery of aquaporins, it was widely believed that small gaseous substances such as carbon dioxide (CO_2) can readily diffuse across cell membranes. It has been shown subsequently that CO_2 cannot diffuse across cell membranes easily in some cells in the absence of aquaporins. For example, the apical membrane of the gastric mucosa is impermeable to CO_2 because of the absence of aquaporins, whereas the basolateral membrane of the same cell allows ready diffusion of CO_2 owing to the presence of aquaporin (Cooper et al., 2002). The same appears true of the colonic mucosa (Maiuolo et al., 2015; Endeward & Gros, 2005).

Operation of normal metabolic functions of the body requires maintenance of an optimal ionic strength of its environment, primarily the intracellular fluid, where most metabolic activities occur. The main functions of homeostatic mechanisms of the body are to provide such an environment. Because the extracellular fluid is not the site of major metabolic activity, substantial alteration in its ionic strength may occur without adverse effects on body function. The main function of the extracellular fluid is to serve as a conduit among cells and among organs. The plasma is a route of rapid transit, and the interstitial fluid serves as a slow supply zone. The ability of extracellular fluid to function efficiently as a conduit requires maintenance of optimal volume, particularly of vascular volume. An additional important function of the extracellular fluid is regulation of the intracellular volume and its ionic strength. Because osmotic equilibrium exists between cells and the extracellular fluid, any alteration in extracellular osmolality is followed by an identical change in intracellular osmolality, which is accompanied by a reciprocal change in cell volume through transcellular water movement (Carroll & Oh, 1989b).

Although cells and organs can be supplied with substrate and relieved of metabolic products with a much slower rate of circulation, normal cardiac output is required to supply sufficient amounts of oxygen for the body's metabolic needs. Normal plasma volume is a prerequisite for maintenance of normal circulation. Because plasma is in equilibrium with the interstitial fluid, the maintenance of normal vascular volume requires normal extracellular volume. Low extracellular volume results in impaired organ perfusion, which manifests most promptly as insufficient oxygen delivery. Excessive extracellular volume leads to increased blood volume, eventually leading to pulmonary edema.

Transfer of fluid between the vascular space and the interstitial space is regulated by the Starling forces. The ultimate purpose of maintaining adequate intravascular volume is to maintain adequate hydrostatic pressure, which is necessary for diffusion of fluid from the vascular space into the interstitial space. Movement of fluid, nutrients, and electrolytes occurs in systemic capillaries through the vascular endothelial fenestrae. On the other hand, movement of solutes and water across the capillaries of the brain is entirely transcellular through endothelial cells because the intercellular gap (endothelial fenestrae) of the brain capillary endothelium is tightly closed. This is termed the *blood-brain barrier* (Spector, 2010). In order to supply nutrients and oxygen to the brain, perfusion is what matters, not perfusion pressure. The position of the brain in relation to the heart is such that when blood pressure is too low, perfusion of the brain will cease before that of other organs (Spector, 2010).

MEASUREMENT OF BODY FLUID VOLUMES

Total body water can be determined by dilution of various substances, including deuterium, tritium, and antipyrine. The gold standard of the measurement is using either tritiated water or deuterium oxide. The former is a radioactive isotope, and the latter requires a complicated method for its measurement. Both are very expensive. Furthermore, deuterium hydrogen is also known to equilibrate with H atoms besides those found in water molecules; as a result, total body water obtained with D_2O was shown to be slightly higher (Brans et al., 1990; Forro et al., 2017). Another nonradioisotope used for the measurement of total body water is H_2O with ^{18}O isotope, which, unlike D_2O, does not equilibrate with O atoms outside of H_2O. Consequently, total body water measured with D_2O is about 3% larger than that measured with $H_2{}^{18}O$. As a cheap alternative, antipyrine has been introduced, which was used extensively in the 1940s and 1950s (Brans et al., 1990). However, subsequent studies indicated that antipyrine is not a very reliable dilution marker. It is metabolized in the liver; therefore, the equilibrium concentration at time zero must be obtained by interpolating the results (Brans et al., 1990).

More recently, the measurement of body fluid volumes by bioelectrical impedance analysis has become very popular. However, the results are not as accurate as the dilution methods and the technology is still evolving. The main advantages of this method are easy applicability, noninvasiveness, and portability of measurements. The portability allows measurements of body fluid volumes in outpatient clinics and at the bedside. The method is based on the principle that the body is an electrical conductor with a certain amount of resistance to flow (impedance), and resistance (R) is proportional to its length (L) and inversely proportional to the cross-sectional area (A). Hence, R (resistance) = $\rho L/A$, where ρ is the resistivity of the conducting material, that is, the body. Since $V = AL$, $V = \rho L2/R$. The body fluid offers two types of resistance to an electrical flow: resistive resistance and capacitative resistance. The former is simply called *resistance*, whereas the latter is called *reactance*. Impedance of the body to an electrical flow is the combination of these two types of resistance. The cell membrane, which is made of lipid, acts like capacitance, and is the cause of capacitative resistance. At zero or low frequency, electrical current does not penetrate the cell membrane and, therefore, flows only through the extracellular fluid. At a very high frequency, electrical current flows through both extracellular and intracellular fluid compartments (Lemos & Gallagher, 2017; Peyton & Chong, 2010).

The term *bioelectrical impedance analysis* is used when single or multiple frequencies of up to 8 frequencies are used, whereas the term *bioelectrical spectroscopy* is used when 256 or more multiple frequencies are used. Bioelectrical impedance analysis has been used to measure fat-free mass, extracellular fluid volume and intracellular fluid volume, and total body water. In bioelectrical spectroscopy, mathematical modeling and mixture equations are used to generate the relationship between R and body fluid volumes.

A mathematical model widely used is called the *Xitron equation*, which has been further modified. Another model, called the *body composition spectroscopy equation*, using different assumptions, has been developed subsequently. Comparison of the two methods in dialysis patients whose change in total body water can be determined from the ultrafiltration volume during dialysis, indicated that the latter method was more accurate (Forro et al., 2017).

BODY FLUID VOLUMES

Total body water measured with antipyrine in hospitalized adults without fluid and electrolyte disorders is about 54% of body weight. The fractional water content is higher in infants and children and decreases progressively with aging. The water content also depends on the body content of fat; women and obese persons, because of their higher fat content, have less water for a given weight. A useful shortcut for the calculation of total body water, using the fact that 54% of body weight in kg is body water and 1 kg is 2.2 lb, is:

$$\text{TOTAL BODY WATER (L)} = \text{BODY WEIGHT (LBS)}/4 \quad \text{(Eq. 15.1)}$$

For an obese subject, subtract 10% from the calculated body water; for a lean person, add 10%. For a very obese person, subtract 20%. Women have about 10% less body water than men for the same body weight (Carroll & Oh, 1989c).

Extracellular volume is measured directly; intracellular volume is estimated as the difference between total body water and extracellular volume. The measurement of total body water is reliable, but the measurement of extracellular volume is not. Although many different markers have been used to measure extracellular volume, no ideal marker has been found. Markers that have been used to measure extracellular volume include sodium, chloride, bromide, mannitol, inulin, sucrose, sulfate, thiosulfate, and thiocyanate. Markers such as sodium, chloride, and bromide are not located exclusively in the extracellular compartment; rather, they penetrate the cells to varying extents. Other markers, such as mannitol, inulin, sucrose, sulfate, thiosulfate, and thiocyanate, do not penetrate certain parts of the extracellular fluid. Extracellular volume has also been estimated indirectly by the degree of dilution of serum Na following administration of mannitol on the principal that mannitol in the extracellular fluid would cause osmotic withdrawal of water from the cell. Thus, depending on the type of marker used, extracellular fluid volume could vary from 27% to 53% of total body water. Extracellular volume has also been estimated by a formula using body weight and height (Carroll & Oh, 1989c).

Extracellular volume measured with chloride and expressed as percent of total body water varies from 42% to 53%, greater in older subjects and women. Extracellular volume measured with inulin or sulfate is smaller, about 30% to 33% of total body water. For discussion in this chapter, a value of 40% of total body water will be considered to represent extracellular volume. Extracellular volume is further divided into 3 fractions: interstitial (space between cells) volume (28% of total body water), plasma volume (8%), and transcellular water volume (4%; Box 15.1). Transcellular water includes luminal fluid of the gastrointestinal tract, the fluids of the central nervous system, and fluid in the eye as well as the lubricating fluids at the serous surface.

COMPOSITION OF THE BODY FLUID

Extracellular Composition

The concentrations of electrolytes in plasma are easily measured and their values well known. These concentrations increase by about 7% when expressed in plasma water, because about 7% of plasma is solids. Thus, plasma sodium is 140 mEq/L but the concentration in plasma water is about 150 mEq/L. The concentrations of electrolytes in interstitial fluid are different from those in plasma because of the difference in protein concentrations between plasma and interstitial fluid. The differences in electrolyte concentrations between plasma and interstitial fluid can be predicted by the Donnan equilibrium (Table 15.1). With normal plasma protein concentrations, the concentrations of diffusible cations are higher in plasma water than in interstitial water by about 4%, while the concentrations of diffusible anions are lower in plasma than in interstitial fluid by about 4%. The concentrations of calcium and magnesium in the interstitial fluid are lower than the values predicted by the Donnan equilibrium, because they are substantially protein bound (Elkin et al., 2010).

The extracellular fluid space is not merely the site of passive passageway for the movement of nutrients and metabolites between plasma and cells and the exchange of oxygen and CO_2. The extracellular space also contains extracellular matrix, which provides structural integrity and support for the surrounding cells but also participates in signaling transduction to the cells. The main molecules contained in the extracellular space are many different types of fibrous proteins, such as collagen, elastin, laminin, and fibronectin, and glycoproteins and hyaluronic acid (Burg, 1995). Glycoproteins consist of sulfated glycosaminoglycan attached covalently to protein; examples include heparan sulfate, dermatan sulfate, and chondroitin sulfate. Hyaluronic acid is one form of glycosaminoglycan, which is neither sulfated nor attached to protein, and is the most abundant glycosaminoglycan in the extracellular space. Both hyaluronic acid and sulfated glycoproteins are highly anionic and surrounded by many water molecules in a gel-like state. This space excludes distribution of proteins. In the other part, proteins diffuse freely and communicate with lymphatics. Interspersed within the interstitial space is elastin, which provides the elastic property of the interstitial tissue. This property is necessary for generation of a normal negative pressure of the interstitial space and a positive pressure with the development of edema (Burg, 1995; Aukland and Reed, 2017; Aukland and Reed, 1993).

BOX 15.1

Volumes of Body Fluid Compartments*

INTRACELLULAR VOLUME: 24 L (60%)
EXTRACELLULAR VOLUME: 16 L (40%)
- Interstitial Volume: 11.2 L (28%)
- Plasma Volume: 3.2 L (8%)
- Transcellular Volume: 1.6 L (4%)

*A normal man weighing 73 kg (160 lbs) with 40 L of total body water is used as a model.

The fact that extracellular matrix proteins participate in cellular signaling is shown by the findings that many extracellular matrix proteins—such as collagen, laminin, fibronectin, and vitronectin—are ligands for the transmembrane receptor proteins, such as integrin. In fact, as another name for integrin is *vitronectin receptor*, many important physiologic effects of vitronectin are mediated through integrin (Moreno-layseca et al., 2019).

Intracellular Composition

While sodium, chloride, and bicarbonate are the main solutes in extracellular fluid, potassium, magnesium, phosphate, and proteins are the main solutes in the cell. The intracellular concentrations of sodium and chloride cannot be measured accurately and are estimated by subtracting the amount that is extracellular from the total tissue value. Since concentrations of electrolytes in the extracellular fluid are high, a small error in extracellular water volume measurement will cause a large error in the measurement of intracellular concentration of these ions. The concentration of bicarbonate is calculated from cell pH, and the bicarbonate concentration shown in Table 15.1 is based on the assumption that average cell pH is 7.0. It should be noted further that the intracellular fluid consists of many different subcompartments, such as mitochondria. In many cells, such as skeletal muscle and the liver, mitochondria represent a large fraction of the cell mass and the electrolyte composition of the mitochondria is often quite different from the cell cytoplasm. For example, the pH of mitochondrial matrix is about 7.8, which is 0.7 pH units higher than the pH of the cytoplasm. Since transport of phosphate through the inner mitochondrial membrane occurs as neutral phosphoric acid, the eventual total concentration of phosphate in the mitochondria is expected to be about 5 times higher than that in the cytoplasm (Burg, 1995).

The electrolyte composition of intracellular fluid is not identical throughout the tissues. For example, the concentration of chloride in muscle is very low, about 3 to 4 mEq/L, but it is about 75 mEq/L in erythrocytes. A very low chloride concentration in skeletal muscle is attributed to the strongly negative resting membrane potential, about −90 mV. In contrast, the electrical potential of red blood cells is about −10 mV. Distribution of chloride across muscle estimated from the Nernst equation would predict the concentration of 3.5 mEq/L when the electrical potential is −90 mV in the muscle cell and 72 mEq/L when the potential is −10 mV in the red blood cell. Slightly higher values can be explained by secondarily active transporters, such as sodium-potassium-chloride transporters (NKCC). The concentration of potassium in the muscle cell is about 140 mEq/L, but in the platelets only about 118 mEq/L, and the lower potassium concentration is also explained by lower membrane potential, about −70 mV.

The concentration of sodium in the cell cannot be predicted by the membrane potential since the values are far from the equilibrium predicted by the Nernst equation. If it were the electrochemical equilibrium, the intracellular concentration of sodium would be much greater than that of the extracellular fluid. The much lower concentration of sodium in the cell of the latter than predicted from the equation can be explained by Na^+-K^+-ATPase that pumps sodium out of the cell constantly. The

TABLE 15.1

Electrolyte Concentrations in Extracellular and Intracellular Fluids

	PLASMA		INTERSTITIAL FLUID		PLASMA WATER		CELL WATER (MUSCLE)	
	(mEq/L)	(mmol/L)	(mEq/L)	(mmol/L)	(mEq/L)	(mmol/L)	(mEq/L)	(mmol/L)
Na^+	140	140	145.3	145.3	149.8	149.8	13	13
K^+	4.5	4.5	4.7	4.7	4.8	4.8	140	140
Ca^{++}	5.0	2.5	2.8	1.4	5.3	5.3	10^{-7}	0.5×10^{-7}
Mg^{++}	1.7	0.85	1.0	0.5	1.8	0.9	7.0	3.5
Cl^-	104	104	114.7	114.7	111.4	111.4	3	3
HCO_3^-	24	24	26.5	26.5	25.7	25.7	10	10
$SO_4^=$	1.0	0.5	1.2	0.6	1.1	0.55	–	–
P	2.1	1.2[+]	2.1[++]	1.2[+]	2.2	1.25[+]	107	57[+++]
Protein	15	1	8	0.5	16	1	40	2.5*
Organic anion	5	5	5.6	5.6	5.3	5.3	–	–

[+]The calculation is based on the assumption that the pH of the extracellular fluid is 7.4 and the pK of inorganic $H_2PO_4^-$ is 6.8.
[++]The concentration of P in the interstitial fluid is higher than that of plasma by the Donnan effect but lower by lower protein-bound phosphate. These two opposing effects keep interstitial phosphate concentration about equal to that of plasma.
[+++]The intracellular molal concentration of phosphate is calculated with the assumption that the pK of organic phosphates in the cell is 6.1 and the intracellular pH 7.0.
*The calculation is based on the assumption that each mmol of intracellular protein has, on average, 15 mEq.

concentration of sodium in the muscle and red blood cell is about 13 mEq/L, but in the leukocytes about 34 mEq/L. The main phosphate in the red blood cell is 2,3 DPG, but in the muscle ATP and creatinine phosphate are the main phosphates. Because the muscle represents the bulk of the body cell mass, it is customary to use the electrolyte concentration of the muscle cells as representative of the intracellular electrolyte concentration. A substantial part of the anions inside the cell are polyvalent ions, such as phosphate and protein; consequently, the total ionic concentration in the cell in mEq/L is higher than that of the extracellular fluid in order to maintain osmotic equilibrium with the extracellular fluid (Oh, 2003).

Even then, the total solute concentration of electrolytes in the cell is less than the total solute concentration of electrolytes in the extracellular fluid. The difference is explained by the accumulation of organic solutes in the cell at concentrations that are much higher than those in the extracellular fluids. These organic solutes include sorbitol, myoinositol, taurine, betaine, and glycerophosphocholine. These solutes are not only the constituents of normal solutes in the cell but also participants in the regulation of cell volumes in the presence of changes in extracellular tonicity. For example, in the presence of hypertonicity, the intracellular concentrations of these solutes increase either by increased synthesis or by increased cellular uptake. The concentration of sorbitol in the cell with hypertonicity increases by the increased production by activating the enzyme aldose reductase while reducing its metabolism to fructose. Similarly, the concentration of glycerophosphocholine increases by the increased activity of the main synthetic enzyme, NTE (neuropathy target esterase). On the other hand, the increased cellular concentration of betaine, myoinositol, and taurine are achieved by the increased number of transporters—namely, BGT1 (betaine-GABA transporter), SMIT (sodium myoinositol transporter), and TauT (taurine transporter). Regulation of production of these various chemicals is orchestrated by the TonEBP transcription factor described earlier (Lee et al., 2011).

MEASUREMENT OF PLASMA OSMOLALITY

Osmolarity refers to the number of moles of solute in a liter of solution, whereas osmolality refers to the number of moles of solute in a kilogram of water (solvent). *Osmolality* is the preferred term, since measurements of both osmolarity and osmolality are based on colligative properties, which are based on the number of particles dissolved in a given number of water molecules. Examples of colligative properties, which depend on the number of solute particles, include freezing point depression, boiling point elevation, and vapor pressure lowering. The molecular mass of water represents the number of water molecules more accurately than the volume, because water volume changes with temperature and the molecular mass does not. One should note, however, that 1 kg of water occupies exactly 1 L at 4° C. However, the terms *osmolality* and *osmolarity* are often used interchangeably because changes in volume of liquid water with temperature are negligible (Oh, 2003).

One mole of NaCl in solution contains 2 osmoles because NaCl is dissociated to Na^+ and Cl^-. One mole of D-glucose in solution contains 1 osmole since glucose does not dissociate. One mole of Na_3PO_4 in solution contains 4 osmoles, since it will dissociate into 3 Na^+ ions and one $PO_4^{\equiv}$ ion. To calculate the osmolality of a solution whose solute dissociates into more than one particle, the following equation is used:

$$M \times a = \text{Osm/L}, \qquad \text{(Eq. 15.2)}$$

where M is molarity and a is the number of particles into which a molecule of the substance dissociates.

When the osmolal concentration of the extracellular fluid increases by accumulation of solutes that are restricted to the extracellular fluid (effective osmols)—for example, glucose, mannitol, and sodium—osmotic equilibrium is reestablished as water shifts from the cell to the extracellular fluid (ECF), increasing intracellular osmolality to the same level as the extracellular osmolality. When the extracellular osmolality increases by accumulation of solutes that can enter the cell freely (ineffective osmols)—for example, urea and alcohol—the osmotic equilibrium is achieved by entry of those solutes into the cell. Since most of the solutes normally present in the extracellular fluid are effective osmols, loss of extracellular water (e.g., insensible losses) will increase effective osmolality and, hence, cause shift of water from the cells. Reduction in extracellular osmolality either by loss of normal extracellular solutes or by retention of water reduces effective osmolality for the same reasons, causing a shift of water into the cells.

Osmolality of serum or plasma can be measured directly with an osmometer as described in Chapter 4 on the principles of instrumentation or estimated as the sum of the concentration of all the solutes in the plasma. Because an osmometer does not distinguish between effective and ineffective osmols, effective osmolality can only be estimated. As it happens, urea is the only ineffective osmol that is present in substantial concentrations in the normal plasma, 5 mOsm/L. In the normal plasma, therefore, total osmolality is nearly equal to effective osmolality. Plasma osmolality is estimated as follows:

$$\text{Serum osmolality} = \{\text{serum } Na^+ \text{ (mEq/L)} \times 2\} + \{\text{glucose (mg/dL)}/18\} + \{\text{urea (mg/dL)}/2.8\} \qquad \text{(Eq. 15.3)}$$

In the use of this formula, osmolality of sodium and accompanying anions are overestimated by not considering the osmotic coefficient and assuming that all serum anions are univalent. On the other hand, osmolality is underestimated by ignoring nonsodium cations and their accompanying anions. At normal serum glucose and urea concentrations, osmolality almost equals serum $Na^+ \times 2$ because the opposing errors cancel each other. It should be noted that for the contribution of urea and glucose for serum osmolality, their values in mg/dL is divided by one-tenth of each (2.8 and 18) of their molecular weights (28 and 180) because osmolality is expressed as mOsm/L, not mOsm/dL (Oh, 2003).

Many of the solutes that may accumulate in the body in certain abnormal states are anions of an acid, for example, salicylate, glycolate, formate, lactate, and beta-hydroxybutyrate. These substances should not be added in estimating plasma osmolality since they are largely balanced by sodium and, therefore, already accounted for when plasma sodium is multiplied by 2. Nonelectrolyte solutes that accumulate abnormally in the serum—for example, ethanol, ethylene glycol, methanol, and mannitol—will cause the measured osmolality to exceed the calculated osmolality, producing an osmolal gap. This osmolal gap is a useful clinical clue to the presence of the toxic substances listed earlier. Accumulation of neutral and cationic amino acids also causes a serum osmolal gap (Oh & Carroll, 1995).

Effect of Hyperglycemia on Serum Na^+

The permeability of a membrane for a given solute varies with the cell type. For example, glucose does not accumulate in muscle. It does not enter the muscle cell freely and, after entering the cell with the help of insulin, it is quickly metabolized. Thus, glucose is an effective osmol for the muscle cell—for example, hyperglycemia will cause a shift of water from the muscle cell. On the other hand, glucose is an ineffective osmol for red blood cells, liver, kidney cells, and most brain cells because it enters these cells freely. Glucose is generally categorized as an effective osmol mainly because muscle cells represent the largest body cell mass, as noted previously in this chapter. Accumulation of glucose or mannitol in the extracellular fluid is a well-known cause of hyponatremia because, as discussed in Chapter 9, glucose is osmotically active and induces diffusion of water from the cells to the extracellular fluid, diluting its electrolytes. The fluid shift affects concentrations of all extracellular electrolytes, but its absolute effect is greatest on serum sodium because of its highest concentration. The relationship between change in serum sodium and change in glucose concentration in a normal adult is about 1.6 mEq/L of Na^+ for 100 mg/dL of glucose. However, the correction factor is not linear. When hyperglycemia is more severe, the change in serum sodium for a given change in glucose tends to be less, approaching 1.4 at serum glucose concentration of 1000 mg/dL. In sharp contrast, Hillier et al. (1999), on the basis of experiments on normal subjects, concluded that the correction factor was much larger, a 2.4 mEq/L change in serum sodium for every 100 mg/dL change in glucose. A problem with this experiment and the conclusion was that the authors disregarded the effect of water contained in intravenous glucose and urine output on serum sodium (Hillier et al. (1999)). Furthermore, infusion of somatostatin during induction of hyperglycemia would have increased serum potassium, and infusion of insulin during treatment of hyperglycemia would have had an opposite effect on serum potassium concentration. Changes in serum potassium have the opposite effects on serum sodium concentration (Oh & Carroll, 1995; Oh, 2003).

These figures suggested by various formulas are valid, however, only when the volume of distribution of glucose is between 40% and 50% of total body water. Volume of distribution of glucose refers to a theoretical volume into which glucose would be evenly distributed when none of the administered glucose is excreted and none metabolized. For example, if 10 g (10,000 mg) of glucose is given to a person, and the serum concentration were to increase by 1000 mg/L (100 mg/dL, with the assumption that none was metabolized and none excreted), the volume of distribution would be 10 L. Normally, the volume of distribution of glucose is slightly greater than the extracellular volume because some cells allow free diffusion

of glucose. As the volume of distribution of glucose in relation to total body water is increased, the effect of glucose on serum sodium decreases. Decreased volume of distribution of glucose has an opposite effect. The change in serum Na caused by hyperglycemia can be estimated with the following formula:

$$\Delta Na^{+} \text{ (mEq/L)} = (5.6 - 5.6a)/2, \qquad \text{(Eq. 15.4)}$$

where ΔNa is a reduction in serum Na^+ in mEq/L for each 100 mg/dL increase in glucose, and a the fraction of the volume of glucose distribution over total body water (Oh, 2003).

In conditions with marked expansion of extracellular volume—for example, congestive heart failure and other edema-forming states—the volume of distribution of glucose represents a much greater fraction of total body water and, hence, a fall in serum sodium caused by hyperglycemia would be much less than usual. For example, when the volume of distribution of glucose is 80% of total body water (0.8), the decrease in serum Na^+ for 100 mg/dL rise in glucose would be only 0.56 mEq/L; $(5.6 - 5.6 \times 0.8)/2 = 0.56$. When the volume of distribution of glucose is 20% of total body water, ΔNa^+ would be 2.2 mEq/L for a 100 mg/dL increase in glucose (Oh & Carroll, 1995).

Tonicity

The concept of tonicity of a solution is based on the effect of a particular solution on the volume of cells. A hypertonic solution is one that shrinks the cells, while a hypotonic solution is one that causes swelling of the cells. An isotonic solution is one that does not induce any volume change in the cells. A solution of 0.9% saline (154 mM solution of sodium chloride) is isotonic in relation to the normal body fluid. When the term *tonicity* is applied to a fluid in vitro, as in the urine, it is used almost interchangeably with total osmolality since voided urine is no longer in contact with cells. Thus, urine with a high concentration of urea is called hypertonic (Oh, 2003; Mallie, 1998).

Osmolality and Specific Gravity

The specific gravity of a solution is the mass of the solution divided by the volume of the solution. Whereas osmolality of fluid depends on the osmolal concentration of its solute, specific gravity is determined by the weight of the solute relative to the volume that it displaces in solution. Plasma protein contributes little to osmolality because of its low molal concentration despite its great weight but is the major factor determining specific gravity of plasma. Urinary specific gravity and osmolality usually change in parallel, but discrepancy occurs between the two with heavy proteinuria and severe glycosuria. Sometimes, specific gravity is confused with the molecular mass, and specific gravity is thought to correlate with the molecular mass. This may lead to the erroneous conclusion that the larger the molecular mass, the greater the specific gravity. Such correlations do not exist. Glucose, for example, has a molecular mass of 180 Da, but has a greater effect on urine specific gravity than albumin, which has nearly 40 times the molecular mass of glucose. Triglyceride has a molecular mass of about 850 Da, but urine specific gravity is less than 1 (Oh, 2003; Oppliger et al., 2005; Trudnowski & Rico, 1974).

The main determinant of specific gravity of plasma is protein, much more than NaCl and glucose, not because it has a greater effect than the latter but because the normal protein concentration at 70 g/L dominates over all other solutes. The normal plasma concentration of NaCl is merely 9 g/L and that of glucose only 1 g/L. Consequently, iso-osmotic plasma has a specific gravity of 1.020 to 1.030, whereas iso-osmotic urine has a specific gravity of about 1.010.

REGULATION OF EXTRACELLULAR VOLUME

As discussed later, extracellular volume depends primarily on its sodium concentration, which is closely regulated by two hormones: antidiuretic hormone (ADH), which promotes water retention, and aldosterone, which promotes sodium retention, which, in turn, causes water to be retained with it, as discussed in Chapter 9. Because the extracellular sodium concentration is maintained within a narrow range through the regulation of ADH release, the extracellular volume depends primarily on its sodium content. In most clinical situations, extracellular volume correlates well with vascular volume, which, in turn, usually correlates positively with the effective vascular volume. Effective vascular volume is an imaginary volume that reflects cardiac output in relation to the tissue's demand for oxygen. Sometimes, effective vascular volume does not correlate well with vascular volume or extracellular volume (Oh & Carroll, 1995; Oh, 2003).

Effective vascular volume, rather than extracellular volume or vascular volume, is the chief determinant of how much extracellular fluid is retained. The location and type of sensors that perceive changes in effective vascular volume is not well known. Most physiologists consider the baroreceptors—located in the carotid sinus, the atria of the heart, and the aortic arch—likely candidates that send neural signals to the central nervous system, resulting in increases or decreases of ADH and altered sympathetic tone. However, the preponderance of evidence argues against effectiveness of such receptors in chronic states of altered effective vascular volume. For example, in a hypertensive patient with congestive heart failure, both atrial low pressure and arterial high pressure baroreceptors would sense a higher than normal pressure. Yet, the neurohumoral responses (e.g., high ADH, high catecholamines, and high renin and angiotensin concentrations) in such states suggest that the body somehow senses low effective vascular volume. In such conditions, the kidney responds appropriately by reducing urinary excretion of sodium and chloride. These physiologic responses to low effective vascular volume sometimes lead to a pathologic retention of salt. For example, salt is retained in congestive heart failure despite markedly expanded extracellular volume and vascular volume because effective vascular volume is decreased (Oh & Carroll, 1995).

Theoretically, there are two ways to alter the salt content of the body: to alter the intake of salt or to alter renal salt output. There is no well-developed mechanism that influences salt intake in response to changes in effective vascular volume. Thus, alterations in salt content of the body are achieved primarily through changes in renal salt output. Changes in renal salt output can be achieved through physical and humoral factors. The physical factors for renal salt regulation work through changes in the glomerular filtration rate (GFR) and in peritubular capillary oncotic and hydrostatic pressures. When other factors that influence renal salt output are kept unchanged, the greater the GFR, the greater the amount of sodium filtered and the greater the amount of sodium excreted. In general, however, tubular reabsorption rather than glomerular filtration plays the major role in the regulation of renal excretion of sodium. In advanced renal failure, the GFR may be 10% of normal, but patients with renal failure excrete the usual amount of sodium intake as people with normal renal function (Carvounis et al., 2002).

Tubular reabsorption of sodium is regulated by humoral factors and physical factors. The latter's influence on sodium reabsorption is limited mainly to the proximal tubule, where much of sodium reabsorption occurs passively through the paracellular (between cells) pathway. Increased hydrostatic pressure on the peritubular capillary retards passive fluid reabsorption through the paracellular pathway while it promotes passive back diffusion of fluid into the tubular lumen. Increased oncotic pressure has the opposite effects. For example, in congestive heart failure, peritubular hydrostatic pressure is reduced because of the increased renal vascular resistance caused by constriction of both afferent and efferent arterioles. Constriction of afferent arterioles would also tend to reduce glomerular capillary hydrostatic pressure. However, the glomerular pressure does not decrease much because the constriction of efferent arterioles is even greater than that of afferent arterioles. The maintenance of glomerular filtration pressure helps to minimize a fall in GFR in volume depletion states. The result is an increase in filtration fraction (the ratio of GFR to renal plasma flow), which increases the concentration of plasma protein in the blood, leaving the glomerular capillary through the efferent arterioles to a greater extent than usual. Because the blood in the efferent arterioles flows into the peritubular capillaries, the oncotic pressure of the peritubular capillary would be higher than usual. A lower than usual hydrostatic pressure and a higher than usual oncotic pressure of peritubular capillary blood in volume depletion states tend to favor reabsorption of salt and water through the paracellular pathway of the proximal tubule, the tubular segment in which passive reabsorption of salt through the paracellular pathway plays a big role in overall renal tubular salt transport. Normally, the oncotic pressure of peritubular capillary plasma in the proximal tubule is about 25% higher than the peripheral blood plasma because the filtration fraction is 0.2. In states of volume depletion with a filtration fraction of 25%, the value would be 33% higher than that of the peripheral plasma. This anomalous behavior of changes in plasma protein concentration following glomerular filtration of plasma can be explained by the fact that the filtered volume of plasma must be expressed as a fraction of the remaining plasma volume. For example, when 120 mL of plasma is filtered with renal plasma flow of 600 mL, the filtered volume (120 mL) now represents 25% of the remaining plasma volume (480 mL). The protein concentration of the remaining plasma will increase accordingly (Oh & Carroll, 2008; Oh, 2003b).

Humoral factors that influence tubular reabsorption of sodium include angiotensin II, aldosterone, atrial natriuretic peptide family of

hormones, and catecholamines. Angiotensin II directly increases proximal tubular sodium reabsorption through its effect on the sodium-hydrogen exchanger-3 (NHE-3), and also indirectly by increasing aldosterone secretion, which in turn increases sodium reabsorption in the cortical collecting duct. Catecholamines influence sodium reabsorption mainly through their effects on renal blood flow, but may have some direct tubular effect in the proximal nephron.

Different types of atrial natriuretic peptide hormones exist. The most widely known are ANP, BNP, CNP, and urodilatin. ANP is produced mainly by the atrium of the heart; BNP, despite its original name, brain natriuretic peptide, is produced mainly by ventricles. Although BNP is now used widely as a marker of heart failure as its levels increase with dilatation of the ventricles (see Chapter 20), its physiologic relevance as the regulator of renal sodium excretion is doubtful. Despite a marked increase in ANP and BNP in congestive heart failure, there is markedly increased sodium reabsorption by the kidney in patients with congestive heart failure. The most important natriuretic peptide hormone for the renal excretion of sodium appears to be urodilatin. (Nishikimi et al., 2011; Kerkelä et al., 2015; Carstens et al., 2007).

The role of ADH in the regulation of extracellular volume is modest because of the overwhelming importance of osmolality as the main regulator of ADH secretion. For this reason, *salt content of the body is the main determinant of the extracellular volume*. When sodium is retained, a proportionate amount of water is retained in order to maintain normal serum osmolality. ADH secretion will occur despite hyponatremia only when the effective vascular volume depletion is very great (Oh & Carroll, 1995).

In the presence of primary water retention, as in the syndrome of inappropriate ADH secretion, extracellular volume could theoretically increase in the absence of sodium retention. However, massive water retention without sodium retention will cause only a modest increase in extracellular volume. For example, if a person with 40 L of total body water gains 10 L of water without a change in sodium content, serum sodium would decrease from 140 mEq/L to 112 mEq/L (140 × 40/50 = 112), a value that would cause severe morbidity or even death. This would increase the extracellular volume by only 4 L since the bulk (60%) of retained water would enter the cell. On the other hand, the same fluid volume retained with salt would remain almost exclusively in the extracellular space. In other words, the amount of water that can be retained without salt is limited by severe and fatal hyponatremia. This is the reason why a massive increase in extracellular volume, as in severe congestive heart failure, is possible only with massive sodium retention (Oh & Carroll, 1995).

The ultimate source of energy for reabsorption of sodium at various nephron segments is Na^+-K^+-ATPase located on the basolateral membrane, which transports 3 Na^+ out of the cell in exchange for 2 K^+ transported into the cell. The resulting reduction in intracellular sodium concentration and the negative cellular electrical potential allow passive diffusion of Na^+ into the cell through the luminal membrane. Four major sites of sodium reabsorption in the nephron utilize 4 different mechanisms of luminal sodium entry (Fig. 15.1). Among humoral factors that have been proven or suggested as participating in the regulation of renal salt output, those with well-proven physiologic effects are aldosterone, catecholamines, angiotensin II, and perhaps ADH and prostaglandins (Oh & Carroll, 1995).

Some of the humoral substances that influence renal sodium excretion have an indirect effect on renal sodium output. For example, adenosine is currently the best candidate for the regulation of GFR through the tubuloglomerular feedback mechanism. Increased production of adenosine in response to a high NaCl concentration at the macula densa results in constriction of afferent arterioles, resulting in reduced GFR. The ultimate effect is reduced excretion of sodium. Likewise, constriction of efferent arterioles by angiotensin II can secondarily increase tubular reabsorption of NaCl, as the increased filtration fraction results in a higher peritubular oncotic pressure and a lower hydrostatic pressure.

NONRENAL CONTROL OF WATER AND ELECTROLYTE BALANCE

Insensible Loss of Water from the Skin

Water is lost from the skin primarily as a means of eliminating heat. Water loss from the skin without sweat is called *insensible perspiration*. Sweat contains about 50 mEq/L of sodium and 5 mEq/L of potassium. The maintenance of low NaCl concentration in the sweat requires the normal functioning of CFCR (chloride channel implicated in cystic fibrosis), and hence the loss of NaCl in sweat is greater in those with cystic fibrosis. Because the main purpose of water loss from the skin is elimination of heat, water loss from the skin depends mainly on the amount of heat generated in the body (Oh & Carroll, 1995):

$$\text{Water loss from the skin} = 30 \text{ mL per 100 calories.} \quad \text{(Eq. 15.5)}$$

Caloric expenditure depends on the basal metabolic rate and the rate of skin water loss may be sharply reduced in a cachectic malnourished person, especially an anuric person with impaired mental state.

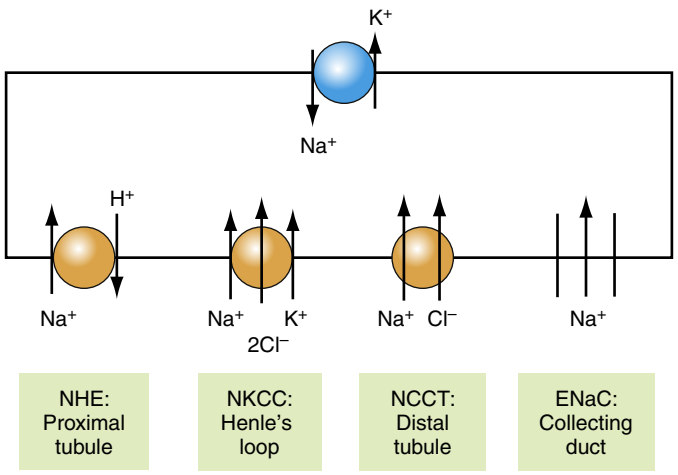

Figure 15.1 Mechanisms of sodium reabsorption at different nephron segments. The main source of energy for sodium reabsorption at all nephron segments is the basolateral Na^+-K^+-ATPase, which transports $3Na^+$ out of the cell in exchange for $2K^+$ into the cell. This pump creates a low intracellular sodium concentration and negative cellular potential, which allow passive diffusion of Na^+ into the cell through the luminal membrane. In the proximal tubule, Na^+ entry is accompanied by exit of H^+ through sodium-hydrogen exchanger type 3 (NHE-3). In the thick ascending limb of Henle, Na^+ enters along with K^+ and $2Cl^-$ through the sodium-potassium-chloride cotransporter (NKCC). In the distal convoluted tubule, sodium enters with chloride through the sodium chloride cotransporter (NCCT) and, in the cortical collecting duct, sodium enters through the epithelial sodium channel (ENaC).

Loss of Respiratory Water

The water content of inspired air is less than that of the expired air; hence, water is lost during normal ventilation. Because the ventilatory volume is determined by the amount of CO_2 production, which is, in turn, determined by the caloric expenditure, ventilatory water loss in normal environmental conditions depends also on caloric expenditure:

$$\text{Respiratory water loss} = 13 \text{ mL per 100 calories at normal } pCO_2. \quad \text{(Eq. 15.6)}$$

By coincidence, the quantity of water lost during normal respiration is about equal to the metabolic water production. Hence, in calculating water balance, respiratory water loss may be ignored in the measurement of insensible water loss provided that metabolic water gain is also ignored. Respiratory water loss increases with hyperventilation or fever disproportionately to metabolic water production (Oh, 2003).

Loss of Water in the Gastrointestinal Tract

The net activity of the gastrointestinal tract to the level of the jejunum is secretion of water and electrolytes. The net activity from jejunum to colon is reabsorption. Most of the fluid entering the small intestine is absorbed in the small intestine and the remainder is absorbed in the colon, leaving only about 100 mL of water to be excreted daily in the feces. The contents of the gastrointestinal tract are isotonic or slightly hypotonic to plasma, and any fluid that enters the gastrointestinal tract becomes isotonic. Thus, the loss of fluid from the gastrointestinal tract never causes hyponatremia but may cause hypernatremia in the absence of water ingestion (Oh, 2003).

MEASUREMENT OF RENAL FUNCTION

CONCEPT OF CLEARANCE

Renal clearance relates to the rate of urinary clearance of a substance in relation to the plasma concentration of the substance. It is defined as the

theoretical volume of plasma that contains the substance excreted in the urine in a given period. In order to calculate the clearance, one must know the amount of the substance excreted in a given time period, which is calculated from volume and concentration. The next step is to know the plasma concentration of the substance (P_x) in order to determine the volume of plasma needed to account for the material excreted. For example, a person excreting 1500 mg of creatinine in a day would need 150 L of plasma to account for that 1500 mg of creatinine if the plasma concentration were 10 mg/L (1 mg/dL); creatinine clearance (C_{creat}), then, would be 150 L/day. At a plasma concentration of 100 mg/L (10 mg/dL), as in patients with renal diseases, only 15 L of plasma would be needed to account for the same 1500 mg of creatinine; C_{creat} in this case would be 15 L/day. Customarily, clearance is expressed in m/min, but any volume and time units can be used. Thus, a clearance of 150 L/day is equal to 6.25 L/hour and 104 mL/min (Oh, 2003). The formal equation for clearance is:

$$C_x = (U_x V)/P. \qquad \text{(Eq. 15.7)}$$

C_x is clearance of a substance x, U_x and P_x are concentrations of the substance in urine and plasma, respectively, and V the volume of urine per unit time.

In estimating clearance, concentration and volume units must be consistent. For example, if urine creatinine concentration is 70 mg/dL and volume is 2000 mL/day, urine creatinine must also be expressed in mg/mL, not mg/dL. Thus, the total amount excreted is 0.7 mg/mL × 2000 mL/day = 1400 mg/day.

A clearance in mL/24 hours can be converted to a clearance in mL/min by the dividing the value by 1440, since 24 hours equals 1440 minutes.

Quick Formulas for the Calculation of Clearance

When calculating a 24-hour clearance in mL/min, urine creatinine excretion may be expressed in g/24 hours instead of mg/24 hours while expressing the plasma creatinine as mg/dL instead of mg/mL as long as the incorrect use of these units is corrected by multiplying the final result by 1000 (for using g instead of mg) and then by 100 (for using mg/dL instead of mg/mL). A further correction requires dividing the value by 1440 in order to convert a 24-hour clearance value to a value in mL/min as follows (Oh, 2003):

$$C_x = U_x V \ (\text{g/24 hours})/P_x\,(\text{mg/dL}) \times 100{,}000 \times 1/1440. \qquad \text{(Eq. 15.8)}$$

$$\text{Since } 100{,}000/1440 = 70,$$

$$C_x\ (\text{mL/min}) = 70 \times \{U_x\,(\text{g/day})/P_x\,(\text{mg/dL})\}. \qquad \text{(Eq. 15.9)}$$

Conversion of Clearance in L/Week to mL/min (Oh, 2003)

The conventional unit for clearance is mL/min; however, in certain situations, different units are more useful. For example, when one compares clearances of peritoneal dialysis in a patient on a CAPD (continuous ambulatory peritoneal dialysis) program with clearance in hemodialysis, the clearance unit often used is L/week. A patient on CAPD treatment typically has 2 L of dialysate exchanged every 6 hours. Since the volume drained is usually about 2.5 L (a slightly higher volume because of transudation of fluid from the blood to peritoneal cavity), creatinine clearance is about 10 L per day, or 70 L per week. As comparison, hemodialysis provides about 48 L of creatinine clearance with each treatment, or 144 L of clearance per week since usually 3 treatments are given each week. If weekly clearance in L/week is to be converted to mL/min, the following shortcut may be useful.

$$\text{L/week} = 1000\ \text{mL/week} = 1000\ \text{mL}/(7 \times 24 \times 60)\ \text{minutes}$$
$$= 1000/10{,}080 = 0.1\ \text{mL/min. In other words,}$$
$$(\text{weekly clearance in L/week})/10 = \text{minute clearance in mL/min.} \qquad \text{(Eq. 15.10)}$$

For example, 70 L/week of clearance is equal to 7 mL/min of clearance.

MEASUREMENT OF GLOMERULAR FILTRATION RATE

GFR is generally considered the best overall indicator of the level of kidney function. Two different approaches have been utilized for the measurement of GFR. One approach has been to use an endogenous substance and the other to use an exogenous substance. It is important that whatever molecular marker is used to determine GFR, the substance is minimally reabsorbed and minimally secreted by the renal tubules.

Measurement of Glomerular Filtration Rate With Exogenous Substances

Inulin clearance is widely regarded as the gold standard for measuring GFR. Inulin clearance in healthy young adults has a mean value of 127 mL/min/1.73 m^2 in men and 118 mL/min/1.73 m^2 in women. GFR declines with age. After age 20 to 30 years, GFR decreases by approximately 1.0 mL/min/1.73 m^2 per year. The classic method of inulin clearance requires an intravenous infusion and timed urine collections over many hours. Inulin is expensive and the procedure is very time consuming and so is generally not performed clinically.

Consequently, a number of alternative measures for estimating GFR have been introduced. The urinary clearance of exogenous radioactive markers such as ^{125}I-iothalamate and ^{99m}Tc-DTPA (metastable technetium^{99} labeled diethylene triamine pentaacetic acid) provides good measures of GFR. Plasma disappearance of exogenous substances such as iohexol and ^{51}Cr-EDTA has also been used to estimate GFR; an advantage of this method is that it does not require urine collection. However, plasma clearance methods are not as accurate as those that require urine collection. GFR has also been measured with nonradiolabeled iothalamate in blood and urine. An obvious advantage of this method is avoidance of radioactive materials (Agarwal, 2003; Stevens & Levey, 2009; Shemesh et al., 1985).

Measurement of Glomerular Filtration Rate With Endogenous Substances

Endogenous substances that are widely used to determine GFR include urea, creatinine, cystatin C, beta trace protein, beta-2 microglobulin, and tryptophan glycoconjugate. The first two are widely used in clinical practice mainly because of their ready availability, but cystatin C is gaining popularity.

Creatinine as Measure of Renal Function

Creatinine is an endogenous substance with a molecular weight of 113 Da. It is produced by the muscle from creatine and creatine phosphate by a nonenzymatic dehydration process. The rate of production of creatinine is proportionate to the creatine-creatine phosphate pool, which, in turn, is proportionate to the muscle mass. An additional source of creatinine is creatine contained in ingested meat. The rate of in vitro conversion of creatine to creatinine in meat is dependent on temperature and acidity; high temperature and low pH increase conversion. Creatinine is the most widely used marker of GFR for several reasons. First, it is an endogenous substance with a fairly constant rate of production. Second, creatinine is not bound to plasma proteins; therefore, it is filtered freely by the glomerulus. It is not reabsorbed by the renal tubules, and only a small amount is secreted by the tubules (Kar & Islam, 2018; Price & Finney, 2000).

In the use of creatinine clearance, the inconvenience of urine collection and uncertainty of its completeness can be avoided by estimating the excretion rate. When renal function is normal and stable, creatinine excretion is almost equal to its production, which depends primarily on muscle mass. Muscle mass varies with sex, age, and body weight (Chen, 2013). The creatinine production rate is estimated as age (A):

$$\text{Creatinine production (mg/kg/day)}: 28 - 0.2A \ \text{(men)} \qquad \text{(Eq. 15.11A)}$$

$$\text{Creatinine production (mg/kg/day)}: 23.8 - 0.17A \ \text{(women)} \qquad \text{(Eq. 15.11B)}$$

In both obese and wasted patients, this formula will overestimate creatinine production. Normally, creatinine excretion in urine is slightly less than its production because some creatinine is broken down by the colonic bacteria. The discrepancy increases progressively with decreasing renal function, because of the increasing fraction of nonrenal clearance of creatinine, which is about 0.04 L/kg/day. However, the metabolism of creatinine by the colonic bacteria is inducible and is increased more in chronic renal failure than in acute renal failure. Normally, a 70-kg man would have an extrarenal creatinine clearance of 2.8 L/day or 2 mL/min, less than 2% of the normal renal clearance. However, at a renal clearance of 4 mL/min, 2 mL/min of extrarenal clearance would represent one-third of the total plasma clearance of creatinine.

However, there are several drawbacks to the use of creatinine as a measure of GFR. First, although the rate of production in a given individual remains constant, it has substantial inter-individual variation, depending mainly on the muscle mass. In the presence of severe muscle wasting, production of creatinine could be reduced to less than 25% of the amount predicted from the body weight. Second, creatinine is also derived from dietary meat, and the quantity of meat ingestion can substantially influence the total daily production. Third, creatinine measurement is still frequently made by the alkaline picrate method (see later, more detailed, discussion), and a

number of chromogens, both endogenous and exogenous, interfere with its measurement by this technique. Finally, creatinine is partially secreted by the proximal tubules via the organic cation transport pathway and tubular secretion is blocked by various drugs, including cimetidine, trimethoprim, pyrimethamine, and salicylate. The extent of tubular secretion varies with individuals and variation is much greater in the presence of renal dysfunction; tubular secretion could be as much as 50% of the amount excreted in the urine in advanced renal failure. In order to obviate the errors due to tubular secretion, creatinine clearance has been obtained with the simultaneous administration of cimetidine, which inhibits tubular secretion of creatinine. However, suppression of creatinine secretion by cimetidine is not complete and also has wide individual variations (Schwartz & Work, 2009).

Creatinine Measurement

Historically, the most widely used method of creatinine measurement has been the reaction of creatinine with picrate (2,4,6-trinitrophenol) at alkaline pH, described by Jaffe more than 100 years ago. More recently, enzymatic methods have been developed using creatinine amidohydrolase or creatinine iminohydrolase (Fossati et al., 1994). Creatinine is hydrolyzed by creatinine iminohydrolase to ammonia and N-methylhydantoin. The ammonia then combines with 2-oxoglutarate and NADH in the presence of glutamate dehydrogenase to produce glutamate and NAD+. The consumption of NADH, measured as a decrease in absorbance at 340 nm, is used to measure the concentration of creatinine. Creatinine can also be measured by converting creatinine to creatine by creatinine amidohydrolase. Creatine is then hydrolyzed by iminohydrolase and sarcosine oxidase to produce hydrogen peroxide. In the presence of horseradish peroxidase, 2,4-dichlorophenolsulfonate is converted to a colorless polymer by hydrogen peroxide. The concentration of the polymer is then measured at 510 nm.

Several substances—such as ketones, glucose, fructose, protein, urea, and ascorbic acid—also react with picrate and falsely increase creatinine concentration by Jaffe methods. Interference by glucose on creatinine measurement becomes significant when glucose concentration is very high, as in diabetic ketoacidosis or hyperglycemic coma. Glucose concentration is extremely high in dialysate fluid used in peritoneal dialysis; a correction for the high glucose is needed when creatinine concentration is measured in the effluent of peritoneal dialysate. The magnitude of glucose interference of creatinine measurement has been shown not only on glucose concentration but also on creatinine concentration. The interference by glucose in creatinine measurement does not occur in the enzymatic methods. Bilirubin and hemoglobin also interfere with the alkaline picrate method, resulting in falsely low values. Cephalosporin antibiotics also positively interfere with the alkaline picrate method, resulting in falsely elevated values (Lipman et al., 2003; Nah et al., 2016; Soldin et al., 1978; Petrykiv et al., 2017; Hoste et al., 2015).

Without removing noncreatinine chromogens, the upper limit of normal measured by the Jaffe reaction is 1.6 to 1.9 mg/dL for adults. The upper limit of normal for serum creatinine measured after removing the chromogens is 1.2 to 1.4 mg/dL. Values for women are 0.1 to 0.2 mg/dL lower. When serum creatinine is very high, noncreatinine chromogens contribute proportionally less to the total reaction. With normal renal function, noncreatinine chromogens make up 14% (range 4.5%–22.3%) of the total; however, in advanced renal dysfunction, it contributes only about 5% (Oh, 2003).

Use of Mass Spectroscopy in Creatinine Level Determination

Because of the possible interference of noncreatinine chromogens to the absorbance measurements for creatinine using the Jaffe method and because accurate creatinine measurements are required for computing the GFR as described elsewhere in this chapter, it has been recommended that all creatinine assays should be standardized by a validation procedure in which creatinine assay results on samples are correlated with the values obtained on the same samples using a gold standard method, which is mass spectroscopy based (see Chapter 5), called *isotope dilution mass spectroscopy* (*IDMS*) (Myers et al., 2006). Results using this method are usually not affected by extraneous chromogens. In this method, in its simplest form, serum samples are extracted so as to separate creatinine from other serum components. A known amount of a C^{13} isotope-enriched creatinine is then added to the sample. The mass spectrum of this sample is taken. The height (relative abundance) of the parent creatinine C^{13} isotope peak represents the known concentration of the C^{13} creatinine. This concentration is corrected for losses that may have been incurred in the extraction procedure using an internal standard. The corrected peak height (minus the corrected known height of unlabeled creatinine in the isotopically labeled creatinine) is then compared with the height of the corresponding parent peak of the sample creatinine, and the ratio of the two peaks is computed. Since the concentration of the C^{13}-labeled creatinine is known, the concentration of the sample creatinine can be directly calculated. This procedure has the disadvantage of the extracted sample possibly containing compounds that may have a molecular mass that occurs at the unlabeled creatinine parent peak, which can result in overestimation of creatinine concentration. Currently, standardization of creatinine determinations has not been adopted universally, in part because the values obtained using IDMS are significantly lower than those obtained in patients who are being followed over prolonged times, making interpretation of results more difficult.

Cimetidine-Enhanced Creatinine Clearance

Tubular secretion of creatinine results in falsely elevated values in creatinine clearance, especially in renal insufficiency. Measurement of creatinine clearance with inhibition of tubular secretion with cimetidine substantially improves the creatinine clearance estimate of GFR in patients with mild to moderate renal impairment. However, tubular secretion of creatinine is not completely blocked by cimetidine; hence, the method still overestimates GFR (Shemesh et al., 1985; Hoste et al., 2015).

In addition to cimetidine, a number of other drugs also interfere with tubular secretion of creatinine by inhibiting organic cation transporters. These include trimethoprim, pentamidine, and amiloride (Hoste et al., 2015).

Formulas to Estimate Creatinine Clearance as an Estimate of Glomerular Filtration Rate

With the realization that accurate urine collection is a major limitation in creatinine clearance as a measure of GFR, attempts have been made to mathematically transform serum creatinine to estimate GFR. In part because of the convenience, these methods are widely used in clinical practice. The two most widely used formulas are the Cockcroft and Gault formula and the MDRD formula (Cockcroft and Gault, 1976):

$$((140 - \text{Age}) \cdot (\text{IBW}))/(72 \times \text{SCr}), \text{ multiply by 0.85 if female,}$$

where *IBW* is ideal body weight and *SCr* is serum creatinine concentration. IBW is calculated by the following formula:

$$\text{Males: IBW} = 50 \text{ kg} + 2.3 \text{ kg for each inch over 5 feet.} \quad \text{(Eq. 15.12A)}$$

$$\text{Females: IBW} = 45.5 \text{ kg} + 2.3 \text{ kg for each inch over 5 feet.} \quad \text{(Eq. 15.12B)}$$

The Cockcroft and Gault formula reduces the variability of serum creatinine estimates of GFR caused by a difference in creatinine production due to differences in muscle mass based on sex and age. However, because the formula does not take into account differences in creatinine production due to variation in muscle mass caused by disease states, it systematically overestimates GFR in individuals who have relatively low muscle mass in relation to their body weight, such as obese, edematous, or chronically debilitated subjects. Moreover, it does not take into account variations caused by extrarenal elimination and tubular secretion (Oh, 2003).

In the Modification of Diet in Renal Disease (MDRD) study, Levey and coworkers measured GFR by I^{125}-iodothalamate to derive a formula for estimating GFR using six variables: age, sex, race, serum urea nitrogen, serum creatinine, and serum albumin concentration (Levey et al., 1999). In 2000, the same investigators produced a simplified MDRD formula based on 4 variables, serum creatinine, age, race, and sex. Few diabetic individuals were included in the original studies and these formulas tested in diabetic patients were found to be inaccurate (Levey et al., 2000). Furthermore, the use of exponents in the formula has prevented routine use in clinical practice (Levey et al., 1999). GFR calculators based on the equations below are now available online, facilitating these calculations.

MDRD formula (mL/min/1.73 m^3):

$$\text{GFR} = 170 \cdot \text{Cr}^{-0.999} \cdot \text{Age}^{-0.176} (0.762 \text{ if female}) \cdot (1.180 \text{ if black}) \cdot \text{BUN}^{-0.170} \cdot \text{Alb}^{0.318} \quad \text{(Eq. 15.13A)}$$

The simplified MDRD formula (mL/min/1.73 m^3) based on 4 variables (serum creatinine, age, race, and sex) (44):

$$\text{GFR} = 186.3 \cdot \text{Cr}^{-1.154} \cdot \text{Age}^{-0.203} \times 1.212 \text{ (for black)} \times 0.742 \text{ (for women),} \quad \text{(Eq. 15.13B)}$$

where *Cr* = serum creatinine (mg/dL), *Wt* = body weight (kg), *BUN* = blood urea nitrogen (mg/dL), and *Alb* = serum albumin (g/dL). More recently, a modified GFR equation proposed by the CKD Epidemiology Collaboration, known as the CKD-EPI formula, has been added to the consortium of formulas to calculate estimated GFR (eGFR) (Levey et al., 1999). Despite the claim that this formula more accurately predicts eGFR than the original MDRD equation, errors caused by variability in serum creatinine concentration due to individual variations in creatinine production remain unresolved.

Whereas the Cockcroft and Gault formula includes the body weight, the MDRD formula does not include the body weight, because the result of the latter is expressed in mL/min/1.73 m^3 rather than an absolute value. The same errors resulting from variations in creatinine production rate caused by disease states are not eliminated in the Cockcroft and Gault formula as well as the MDRD formula. Both the Cockcroft-Gault and MDRD formulas estimate GFR in adults and are not applicable to measurement of GFR in children, obese, bedridden patients, or amputees. Following are the formulas used most often for estimating creatinine clearance for children:

Schwartz formula:

$$\text{GFR} = 0.55 \times \text{height (cm)/serum creatinine (mg/dL)} \quad \text{(Eq. 15.14A)}$$

$$\text{GFR} = 43 \times \text{height (cm)/serum creatinine (}\mu\text{mol/L)} \quad \text{(Eq. 15.14B)}$$

Counahan Barrett formula:

$$\text{GFR} = 40 \times \text{height (cm)/serum creatinine (}\mu\text{mol/L)} \quad \text{(Eq. 15.15)}$$

In 2009, Schwartz et al. further modified their formula to estimate GFR more accurately in children. The new formula is very similar to the MDRD equation in that it uses multiple exponential functions; the use of the formula requires knowing values of serum creatinine, height, BUN, and serum cystatin C. Like the MDRD formula, a computer program is usually needed to use the formula (Filler & Lepage, 2003; Pierrat et al., 2003).

Modified Schwartz formula:

$$\text{GFR}\ (\text{mL/min per 1.73 m}^2) = 39.1\,[\text{height (m)/Scr (mg/dL)}]^{0.516} \times [1.8/\text{cystatin C (mg/L)}]^{0.294}[30/\text{BUN (mg/dL)}]^{0.169}[1.099]^{\text{male}}\,[\text{height (m)}/1.4]^{0.188}. \quad \text{(Eq. 15.16)}$$

In addition, the Chronic Kidney Disease Epidemiology Collaboration (CDK-EPI) group has an alternate equation that can be used to compute GFR values for GFRs > 60 mL/min per 1.73 m^2 (Levey, 2009).

It has been shown that GFR estimated from these various formulas is not very accurate. However, creatinine clearance values estimated from the formulas are still more accurate than those from direct measurements mainly because of the inaccurate urine collections and variations in plasma creatinine concentration in the latter. Consequently, K/DOQI (Kidney Disease Outcomes Quality Initiative) guidelines have recommended the use of these formulas in calculating creatinine clearance instead of direct measurements (Schwartz & Work, 2009).

All of these formulas are useful in the estimation of GFR in chronic states when creatinine production is assumed to be equal to the amount excreted in the urine. In acute renal failure when serum creatinine rises rapidly during the development of renal failure and falls rapidly during the recovery phase, such an assumption is invalid. Hence, the estimation of GFR by either method is invalid. Measurement of creatinine in the urine with timed urine collection is more useful in determining creatinine clearance in acute renal failure.

Urea as Measure of Renal Function

Urea is the main waste product of nitrogen-containing chemicals in the body. It has a molecular weight of 60 Da. However, by custom, the concentration of urea is expressed only by the nitrogen content of urea. For this reason, the term *serum or urine urea nitrogen* is widely used in place of *serum or urine urea*. Because a molecule of urea contains 2 nitrogen atoms, the molecular weight of urea nitrogen is 28 Da (Oh, 2003).

Serum urea is widely used as a measure of renal dysfunction, but its value as a measure of GFR is not very good for several reasons. First, urea concentration in the serum depends not only on the renal function but also on the rate of urea production, which depends largely on protein intake. The rate of protein intake varies widely from individual to individual.

Urea is freely filtered at the glomerulus but is reabsorbed substantially in the proximal convoluted tubule and the inner medullary collecting duct. Reabsorption of urea in the proximal tubule occurs passively through the lipid membrane without the help of urea transporters, whereas in the inner medullary collecting duct, urea reabsorption is mediated by urea transporters. Some of the urea reabsorbed from the inner medullary collecting duct then reenters the tubule in the thin descending limb of the cortical nephrons, which also express urea transporters. The amount of urea reabsorbed in the proximal tubule varies greatly depending on the status of effective vascular volume; reabsorption is markedly increased in states of volume depletion because the luminal concentration of urea is high owing to the increased fractional reabsorption of salt and water. The amount reabsorbed in the inner medullary collecting duct is increased when urine osmolality is high because of the high urea concentration. For these reasons, urea clearance does not reflect GFR accurately, but serum urea nitrogen is still widely used as a measure of renal dysfunction. In the presence of normal renal function without volume depletion, urea clearance is about 50% of creatinine clearance, but in the presence of severe volume depletion, its clearance could be as little as 10% of creatinine clearance. In advanced renal failure, urea clearance approaches unity with GFR and is better than creatinine clearance as a measure of GFR (Cowley et al., 2013; Price & Finney, 2000).

Measurement of Urea

Essentially, there are 3 methods for the measurement of urea. The gold standard, which is used only as a reference method because of its high cost, is isotope dilution mass spectrometry. In clinical laboratories, urea is measured either by the colorimetric method based on a reaction of urea with diacetyl monoxime or by enzymatic methods. In the former, urea reacts directly with diacetyl monoxime under strong acidic conditions to produce a yellow condensation product. The reaction is intensified by the presence of ferric ions and thiosemicarbizide. The intense red color formed is measured at 540 nm (Rahmatullah & Boyde, 1980; Barbour & Welch, 1992).

The initial reaction in all enzymatic methods is hydrolysis of urea by urease, which produces ammonia and CO_2. Ammonia and CO_2 produced are measured by various methods to calculate the concentration of urea in the original sample. Measurement of ammonia is most often used. In one of these methods, ammonia produced by urease converts glutamate and ATP to glutamine and ADP. The ADP so produced is consumed in reactions catalyzed sequentially by pyruvate kinase and pyruvate oxidase to generate hydrogen peroxide. The hydrogen peroxide is then measured as an indirect estimate of urea concentration. In another enzymatic method, as in the one used for creatinine described in the preceding section, ammonia produced from urea hydrolysis reacts with alpha-keto-glutarate and NADH to produce glutamic acid and NAD^+ by glutamate dehydrogenase. The amount of NADH consumed is measured photometrically to determine the urea concentration. Another urease method involves the indophenol method, in which ammonium produced by urease reacts with hypochlorite to form monochloramine. In the presence of phenol and an excess of hypochlorite, the monochloramine forms a blue-colored compound, indophenol, the concentration of which is determined spectrophotometrically at 630 nm. In yet another enzymatic method, CO_2 produced by urease is measured by thermal conductivity gas chromatography.

Other Measures of Glomerular Filtration Rate

Cystatin C

Cystatin C is a 122 amino acid protein with a molecular weight of 13,000 Da, and is an inhibitor of cysteine proteinase. The substance is produced by all nucleated cells. Its production rate is relatively constant from age 4 months to 70 years and is proportionate to GFR. The rate of production is not affected by muscle mass, sex, and race. Because of its small size (small for a protein) and a positive net charge, it is freely filtered at the glomerulus at the same concentration as in the plasma. It is completely reabsorbed by the proximal tubule, and in the absence of proximal tubular defect, none is excreted in the urine. Hence, appearance of cystatin C signifies proximal tubular damage.

A common assumption in the use of cystatin C as a marker of GFR is that the production rate of cystatin C is constant. However, this is probably not true. It is now known that cystatin C production is regulated by interleukin 10 (IL-10), and the high IL-10 inhibits its production. There is evidence that glucocorticoids reduce production of cystatin C; this might result in overestimation of renal function in renal transplantation patients, who are regularly given a glucocorticoid. Nevertheless, a number of studies made comparison of serum creatinine and serum cystatin C as an indicator of renal function; the general consensus is that cystatin C is better than creatinine. However, cystatin C is not widely used clinically because measurements are difficult and expensive. It must be noted that cystatin C renal clearance cannot be measured because normally it is completely reabsorbed and none excreted in the urine. For this reason, changes in serum concentration of cystatin C are used as indirect estimates of GFR. A complex equation to estimate GFR using the exponential functions and plasma cystatin C concentrations has been developed. The results were found to be better than those obtained by the MDRD equation and the Schwartz formula for estimation of GFR (Price & Finney, 2000).

Modified Cystatin C equation:

$$\text{GFR}\left[\text{mL}\cdot\text{min}^{-1}\cdot\left(1.73\ \text{m}^2\right)^{-1}\right] = 84.69 \times \text{cystatin C (mg/L)}^{-1.680} \times 1.384 \ \text{(if a child <14 years)} \quad \text{(Eq. 15.17)}$$

Beta-2 microglobulin

Beta-2 microglobulin, a polypeptide with molecular weight of 11.6 kDa with a length of 99 amino acids, is a component of major histocompatibility complex (MHC) class I molecule. It is present in all nucleated cells. Its production is increased in multiple myeloma and lymphoma. Because of the low molecular weight, beta-2 microglobulin is freely filtered at the glomerulus and then reabsorbed and metabolized completely by the proximal tubule. Like cystatin C and beta trace protein, the plasma level increases in renal failure. The protein appears in the urine when reabsorption is incomplete because of the proximal tubular damage as in acute kidney injury. The protein has the tendency to fold into a beta-sheet configuration, resulting in amyloid formation; it is a common cause of dialysis-associated amyloidosis, which occurs less often because of the widespread use of high flux hemodialysis (Bianchi et al., 2001).

Beta Trace Protein

Beta trace protein (BTP) is a low-molecular-weight glycoprotein with 168 amino acids. The molecular weight varies between 23,000 and 29,000 Da depending on the degree of glycosylation. BTP belongs to the lipocalin protein family and functions as prostaglandin D synthase. Because prostaglandin D is the major prostaglandin in the brain, BTP is isolated primarily from cerebrospinal fluid. Plasma BTP originates from the brain and is freely filtered at the glomerulus, then reabsorbed completely by the proximal tubule and catabolized there. The plasma level is increased in patients with renal diseases because of the reduced filtration in the presence of constant production. White et al. and Poge et al. developed formulas to estimate GFR on the basis of plasma concentration of BTP and urea or creatinine. They claimed that the results were better than those obtained by the MDRD equation and serum cystatin C measurements. However, others showed that BTP was less sensitive than cystatin C (Inker et al., 2016).

White formula using beta trace protein:

$$\text{GFR1} = 112.1 \times \text{BTP}^{-0.662} \times \text{urea}^{-0.280} \times (0.880 \text{ if female}) \quad \text{(Eq. 15.18A)}$$

$$\text{GFR2} = 167.8 \times \text{BTP}^{-0.758} \times \text{creatinine}^{-0.204} \times (0.871 \text{ if female}) \quad \text{(Eq. 15.18B)}$$

Poge formula using BTP:

$$\text{GFR1} = 89.85 \times \text{BTP}^{-0.5541} \times \text{urea}^{0.3018} \quad \text{(Eq. 15.19A)}$$

$$\text{GFR2} = 974.31 \times \text{BTP}^{-0.2594} \times \text{creatinine}^{-0.647} \quad \text{(Eq. 15.19B)}$$

GFR in mL/min/1.73 m^2; BTP in mg/dL; urea in mmol/L; creatinine in μmol/L.

Tryptophan Glycoconjugate

MPT (mannopyranosyl-L-tryptophan) is a substance normally produced in the body by glycoconjugation of tryptophan. It is filtered at the glomerulus freely but not reabsorbed. There is a strong linear correlation between clearances of MPT and inulin clearance in rats (r = 0.97) and humans (r = 0.87), indicating that renal handling of MPT is similar to that of inulin. The current limitation for the use of MPT for renal function estimation is that it can be measured only by the high-performance liquid chromatography method, which is time-consuming and expensive. Serum level of MPT increases progressively with declining renal function; however, unlike creatinine, serum MPT concentrations are not affected by muscle mass. It is not known whether dietary intake of tryptophan affects the serum concentration (Takahira et al., 2001).

UREA CLEARANCE AND UREA/CREATININE RATIO IN SERUM

In the absence of renal dysfunction and severe dehydration, urea clearance is about 50% of creatinine clearance and, hence, about 50% of GFR, because about 50% of the filtered urea is reabsorbed. The bulk of urea reabsorption occurs in the proximal tubule, about 40% of the filtered load. Among the distal nephron sites, the inner medullary collecting duct reabsorbs urea extensively along a concentration gradient when urine is being concentrated. Some of the urea reabsorbed from the inner medulla reenters the tubule at the descending thin limb; this reentry represents intrarenal recycling of urea. Urea reentry occurs mainly in the short loop of Henle of the cortical nephron. Some of the urea reabsorbed from the inner medullary collecting duct is carried away from the medulla by the ascending vasa recta. This amount represents about 10% of the filtered load with normal urine flow; however, with marked urine concentration, the amount can increase greatly.

A marked reduction in urea clearance occurs when the proximal reabsorption of urea is greatly increased by a reduction in effective vascular volume. Reabsorption of urea in the proximal tubule is passive and depends on a favorable urea concentration gradient. This gradient is created by reabsorption of water in the proximal tubule. Normally, about 83% of the filtered water is reabsorbed in the proximal tubule as a result of reabsorption of salt (mainly sodium chloride). Loss of 83% of the water in the tubule increases urea concentration in the tubule sixfold, creating a favorable gradient for urea diffusion out of the tubule. When the water reabsorption is 90% to 95% of the filtered load, the urea concentration would increase to 10 to 20 times the plasma concentration. Volume depletion and decreased renal plasma flow without volume depletion, for example, renal artery stenosis, also reduces GFR, thereby reducing clearance of both creatinine and urea. Volume depletion decreases creatinine clearance only by reduced filtration, and urea clearance by both reduced filtration and increased reabsorption. Hence, in volume depletion, urea clearance decreases more than creatinine clearance does. Normally, the ratio of plasma urea nitrogen to plasma creatinine is about 10 to 1; in volume depletion, the ratio may be greater than 20 to 1 (Oh, 2003b).

The prediction of volume status by the urea/creatinine ratio is based on the assumption of constancy of urea and creatinine production, which is often not the case. Glucocorticoids and a high-protein diet increase urea production, whereas chronic protein malnutrition decreases it. Creatinine production also varies considerably; marked muscle wasting can reduce its production to less than one-fifth of a usual value. Currently, the main cause of a high BUN/creatinine ratio in the hospital is not dehydration but rather adequate protein intake (often by a tube feeding) in a patient with severe muscle wasting. Thus, fractional excretion of urea (see later discussion) would be a more reliable index of volume status than plasma urea/creatinine ratio. The mechanisms by which low effective vascular volume increases the proximal reabsorption of salt and water were explained earlier in the section on the control of extracellular volume.

As stated previously, because about 50% of filtered urea is reabsorbed, urea clearance normally underestimates GFR greatly, whereas creatinine clearance slightly overestimates GFR. As renal function declines, the fraction of urea reabsorbed declines progressively, whereas the tubular secretion of creatinine increases progressively. As a result, urea clearance is a better predictor of GFR than creatinine clearance in the presence of advanced renal dysfunction.

GLOMERULAR FILTRATION RATE, RENAL PLASMA FLOW (RPF), AND FILTRATION FRACTION (FF)

As discussed in the preceding section, because inulin is filtered freely at the glomerulus but is neither reabsorbed nor secreted by the tubules, its clearance equals GFR, which is the rate (mL/min) of plasma filtered by the glomerulus from the blood into the tubular system. The clearance of para-aminohippurate (PAH) measures another aspect of renal function. As it happens, whatever PAH is not filtered at the glomerulus is almost all secreted into the proximal tubule, thereby allowing PAH clearance to be a measure of renal plasma flow, which is the total quantity of plasma perfusing the glomerular capillary. The quantity of plasma filtered as a fraction of the total quantity perfusing the glomerular capillary is the filtration fraction. Because inulin clearance represents GFR and PAH clearance the quantity of plasma perfusing the glomerulus,

$$\text{Filtration Fraction (FF)} = C_{IN}/C_{PAH}, \quad \text{(Eq. 15.20)}$$

where C_{IN} is inulin clearance and C_{PAH} is PAH clearance.

Filtration fraction in man is normally about 0.2. As discussed earlier, low effective vascular volume, as in heart failure, decreases renal perfusion, but GFR decreases to a lesser degree because glomerular capillary pressure is maintained by increased efferent arteriolar tone. The result is an increase in filtration fraction. An increase in glomerular filtration for a given plasma flow, that is, increased filtration fraction, increases the concentrations of plasma proteins by concentrating the nonfilterable plasma constituents. This increases the oncotic pressure of peritubular capillary blood, resulting in increased fluid movement from the tubular interstitium to the capillary. This, in turn, helps to increase fluid reabsorption from the proximal tubule into the interstitial space. Similarly, increased tone of efferent arterioles in an attempt to maintain a high glomerular capillary pressure tends to reduce the peritubular capillary hydrostatic pressure. This also contributes to increased salt reabsorption by the proximal tubule (Oh, 2003).

The expanded effective vascular volume decreases filtration fraction because the increase in renal plasma flow is greater than the increase in GFR. Changes in oncotic pressure and hydrostatic pressure in the peritubular capillary blood and their effects on proximal salt and water reabsorption are the opposite of those encountered in conditions of reduced effective vascular volume.

FRACTIONAL EXCRETION (FE)

Fractional excretion is the quantity of a substance excreted in the urine expressed as a fraction of the filtered load of the same substance.

$F_x = P_x * GFR$ (16), where F_x is the amount of a substance x filtered.

$$F_x = P_x * C_{creat} \ (GFR = C_{creat}) = P_x * (U_{creat} V / P_{creat})$$

$E_x = V * U_x$, where E_x is the amount excreted in the urine and U_x the urine concentration of substance x.

$$\text{Hence, } FE = [(V * U_x)] / [P_x * (V * U_{creat}/P_{creat})] \qquad \text{(Eq. 15.21)}$$

When V is cancelled on both sides, the equation is simplified as:

$$FE = (U_x/P_x) / (U_{creat}/P_{creat}) \ (20) \text{ or}$$

$$FE = (U_x/P_x) * (P_{creat}/U_{creat}) \qquad \text{(Eq. 15.22)}$$

Thus, the measurement of fractional excretion can be obtained in a spot urine sample. When the substance excreted in the urine has a clearance that is less than creatinine clearance, fractional excretion is less than 1. When FE is multiplied by 100, the result is %FE. FE of sodium is often used to distinguish between acute tubular necrosis (acute kidney injury) and prerenal azotemia. A value of FE of sodium of less than 0.01 (less than 1%) suggests prerenal azotemia, while a value greater than 0.01 suggests acute tubular necrosis (acute kidney injury) (Oh, 2003b).

RENAL FAILURE INDEX (RFI)

The renal failure index is another formula used for differential diagnosis of acute renal failure. It is expressed as $U_{Na^+}/(U_{creat}/P_{creat})$. The renal failure index is different from fractional excretion of sodium by the exclusion of plasma Na^+ concentration in the formula. Hence, the value of the renal failure index will be 140 times the value of fractional excretion of Na^+ when the serum Na^+ concentration is 140 mEq/L. When fractional excretion of Na^+ is expressed as a % value:

$$\%FE_{Na^+} \times 1.4 = \text{Renal failure index} \qquad \text{(Eq. 15.23)}$$

A word of caution: Both FE of Na^+ and the renal failure index are used only in the differential diagnosis of acute renal failure (acute kidney injury) in the presence of oliguria. It must be realized that the usual fractional excretion of Na^+ on regular salt intake in a normal person is less than 0.01. Thus, low FE of Na in a normal person without oliguria does not indicate the presence of prerenal azotemia (Oh, 2003).

FRACTIONAL REABSORPTION (FR)

Fractional reabsorption is the quantity of a substance reabsorbed expressed as a fraction of the filtered load. It is estimated from fractional excretion as:

$$FR = 1 - FE. \qquad \text{(Eq. 15.24)}$$

BIOMARKERS OF ACUTE KIDNEY INJURY (AKI)

Acute kidney injury (AKI) is defined as a decrease in kidney function, usually reflected as an increase in serum creatinine or decrease in urine output within hours to days. There are several consensus definitions that are all based on changes in serum creatinine and/or urine output. Initially, AKI was classified into 5 categories (Table 15.2). Subsequently, it was simplified into 3 categories (Table 15.3). Persistent renal damage consequent to AKI is termed *acute kidney disease* (*AKD*) and is a risk factor for chronic kidney disease (CKD). Identifying AKI does not distinguish among the various causes that encompass prerenal azotemia, acute tubular necrosis (ATN), acute interstitial nephritis (AIN), acute glomerulonephritis/vasculitis and obstructive uropathy. These distinctions today are made based on history, physical exam, renal ultrasound, urinalysis/urine chemistries, and various currently available blood tests.

TABLE 15.2
RIFLE Criteria For Acute Kidney Injury

	GFR and Serum Creatinine Changes	Urine Volume Changes
R (Risk)	Increase in S_{creat} >1.5× Decrease in GFR >25%	Urine volume <0.5 mL/kg/h >6 h
I (Injury)	Increase in S_{creat} >2× Decrease in GFR >50%	Urine volume <0.5 mL/kg/h >12 h
F (Failure)	Increase in S_{creat} >3× Decrease in GFR >75% S_{creat} >4 mg/dL	Urine volume <0.3 mL/kg/h >24 h Anuria >12 h
L (Loss)	Complete loss of kidney function > 4 weeks	
E (ESRD)	End Stage Kidney Disease > 3 months	

TABLE 15.3
New Classification For Acute Kidney Injury Criteria

Stage	Serum Creatinine	Urine Output
1	> 0.3 mg/dL (26.4 μmol/L) or >150%–200%	<0.5 mL/kg for >6 h
2	>200%–300%	<0.5 mL/kg for >12 h
3	> 300%, 4 mg/dL (354 μmol/L) or acute increase of > 0.5 mg/dL	<0.3 mL/kg for >24 h or anuria >12 h

There are a number of limitations to the current diagnostic tests. The current tests are not able to detect AKI in its earliest stages when interventions would be more likely to be successful. They do not reliably distinguish between the various etiologies of AKI and they do not provide prognostic information, such as which patients would likely need renal replacement therapy (RRT). New biomarkers are being developed that could help resolve these problems (McCullough, 2017; Alge & Arthur, 2015; Kashani et al., 2013).

It is known that changes in serum creatinine are insensitive markers for detecting early AKI, particularly in small individuals or those receiving large amounts of fluids (dilutional). Earlier detection of renal injury can prepare for the better care of patients in anticipation of clinically overt AKI or perhaps allow physicians to intervene by employing specific therapeutic measures and thereby prevent progression to overt AKI (Deng et al., 2017). According to the evaluation of clinically available renal biomarkers in critically ill adults, the prospective multicenter observational study showed that the urine has yielded the most promising markers for the early detection of AKI (Zhou et al., 2008). These urinary markers are either produced by the kidney due to kidney injury or filtered by the glomerulus but not well reabsorbed by the tubules because of injury to the tubules. Increased renal excretion occurs in part because some of these chemicals are produced in increasing amounts owing to renal injury or conditions associated with renal injury. The advantage of these biomarkers over the conventional markers of AKI, such as serum creatinine and serum urea nitrogen, is that the levels often increase long before any changes occur in serum creatinine or urea nitrogen or a change in urine output (Dennen & Park, 2007)

Thus, biomarkers of AKI help diagnose AKI before changes in serum creatinine. The biomarkers also help to identify the primary location of injury, that is, proximal tubule, distal tubule, interstitium, or vasculature, to distinguish among different subtypes of AKI, for example, prerenal, intrinsic renal, or postrenal, and delineate etiologies of AKI, for example, ischemia, toxins, sepsis, or a combination (Devarajan, 2008). Urine is likely to contain biomarkers of renal origin; therefore, urinary biomarkers are most widely used. On the other hand, urine samples are more prone to protein degradation, and their concentrations may be affected by urine flow rate. Serum samples are readily available and serum biomarkers more stable, but serum biomarkers may reflect the systemic response to a disease process rather than specific organ involvement.

Conventional urinary biomarkers such as casts and fractional excretion of sodium are shown to be insensitive and nonspecific for the early

recognition of AKI. Other traditional urinary biomarkers such as filtered high-molecular-mass proteins and tubular proteins or enzymes suffer from the lack of specificity. The application of innovative technologies has uncovered several new candidates that are promising biomarkers of AKI. Several of these candidates have now progressed through the first three stages of the biomarker development process and have entered phase IV of drug trials. There are more than 20 biomarkers of AKI that have been extensively studied.

KIDNEY INJURY MOLECULE-1 (KIM-1)

Kidney injury molecule-1 (KIM-1) is a type I cell membrane glycoprotein containing an immunoglobulin-like domain and a mucin domain in its extracellular region. KIM-1 mRNA levels increase more than any other known gene after kidney injury. The ectodomain of KIM-1 is shed into the urine after proximal tubular injury. In preclinical and clinical studies using several different models of kidney injury, urinary KIM-1 serves as an earlier diagnostic indicator of kidney injury when compared with any of the conventional biomarkers, for example, plasma creatinine and BUN (Charlton et al., 2014; Vanmassenhove et al., 2013).

NGAL (to be discussed in the next section) appears to be the most sensitive at the earliest time points, but KIM-1 potentially adds specificity at later time points because expression of KIM-1 is limited to the kidney and no systemic source of KIM-1 has been detected. KIM-1 is induced in the kidney and upregulated in the urine by a large number of nephrotoxins, including cyclosporin, cisplatin, cadmium, gentamicin, mercury, and chromium.

NEUTROPHIL GELATINASE-ASSOCIATED LIPOCALIN (NGAL)

Human neutrophil gelatinase-associated lipocalin (NGAL) is a 25-kDa protein initially identified bound to gelatinase in granules of the neutrophil. Other names for NGAL are lipocalin 2 (LCN2) and human neutrophil lipocalin (HNL).

NGAL is synthesized during a narrow window of granulocyte maturation in the bone marrow but also may be induced in epithelial cells in the setting of inflammation or malignancy. NGAL is upregulated and can be detected in the kidney and urine of mice 3 hours after cisplatin administration (Mishra, 2004; Mishra, 2005; Mishra, 2006) and has been proposed as an early biomarker for diagnosing AKI. A prospective study of pediatric and adult patients undergoing cardiopulmonary bypass for cardiac corrective surgery found urinary NGAL to be a powerful early marker of AKI, showing increased concentrations within 2 to 6 hours of the insult, preceding any increases in serum creatinine by 1 to 3 days (Bennet, 2008; Dent, 2007; Mishra, 2006; Devarajan, 2008). However, serum NGAL levels are known to increase in the setting of a number of inflammatory and infective conditions; more studies are needed to determine specificity of urinary NGAL for AKI in the setting of sepsis. NGAL has also been evaluated as a biomarker of AKI after contrast-induced nephropathy (Hirsch, 2007).

INTERLEUKIN-18 (IL-18)

Interleukin-18 (IL-18) is a cytokine, which is an interferon γ (IFN-γ)-inducing factor. IL-18 activity has been described in a number of inflammatory diseases across a broad range of tissues. Renal IL-18 mRNA levels have been shown to be significantly upregulated in the proximal tubule following ischemia-reperfusion injury, inflammatory/autoimmune nephritis, and cisplatin-induced nephrotoxicity. Urinary IL-18 levels are elevated in patients with AKI and delayed graft function compared with normal subjects and patients with prerenal azotemia, urinary tract infection, chronic renal insufficiency, and nephrotic syndrome. Increased urinary IL-18 was found to be an early marker of AKI, preceding changes in serum creatinine by 1 to 2 days, and was an independent predictor of death (Arthur et al., 2014; Schrezenmeier et al., 2017).

FATTY ACID-BINDING PROTEIN (FABP)

Fatty acid-binding proteins (FABPs) are 14- to 15-kDa cytoplasmic proteins abundantly expressed in all tissues, particularly in the proximal convoluted and straight tubule of the kidney. Urinary L-FABP has been identified in preclinical and clinical models of AKI and has been found to be a potential biomarker in a number of pathologic conditions, including CKD, diabetic nephropathy, IgA nephropathy, and contrast nephropathy. In a model of cisplatin-induced AKI, there was increased shedding of urinary L-FABP within the first 24 hours, whereas a rise in serum creatinine was not detectable until after 72 hours of cisplatin treatment. Urinary L-FABP levels were significantly increased before the increase in serum creatinine only in those patients who developed AKI post contrast dye. In a recent study involving 12 living related kidney transplant patients, a significant direct correlation was found between urinary L-FABP level and both peritubular capillary blood flow and the ischemic time of the transplanted kidney. In AKI following cardiac surgery, increases in serum creatinine occurred 2 to 3 days postsurgery, whereas urine L-FABP levels increased at 4 hours after surgery (Schrezenmeier et al., 2017).

The U.S. Food and Drug Administration has approved NephroCheck, which is a point-of-care assay for urinary biomarkers predicting the risk of AKI. The biomarkers used in this assay are insulin-like growth factor binding protein 7 (IGFBP7) and tissue inhibitor of metalloproteinases (TIMP-2) (Ronco et al., 2017; Gunnerson et al., 2016). These biomarkers were selected from among 340 putative biomarkers in a study of patients with AKI and were validated in two subsequent studies. TIMP-2 and IGFBP7 are expressed in renal tubular cells and act to induce a state of G1 cell cycle arrest, which is thought to be a response to cell injury that is important for cell repair. In the most recent validation study performed in 420 critically ill patients, in whom 17% reached the clinical end point of moderate to severe AKI within 12 hours, the test ([TIMP-2] x [IGFBP7]) was 92% sensitive using a cutoff of 0.3 $(ng/mL)^2/1000$ and identified a group that was 7 times more likely to develop AKI than using clinical indicators alone (Kashani et al., 2017). In a study of patients undergoing cardiac surgery, using these biomarkers to identify patients at high risk for developing postoperative AKI, it was shown that interventions aimed at reducing the risk of AKI were effective in the study group (Beker et al., 2018; Schrezenmeier et al., 2017). More studies need to be done in different settings before these biomarkers can be used widely.

DISORDERS OF POTASSIUM

Total body K^+ in hospitalized adults is about 43 mEq/kg of body weight, only about 2% of which is found in the extracellular fluid. When potassium concentrations across the cell membrane are in electrochemical equilibrium, the transcellular gradient of K^+ is the main determinant of, and can be also predicted by, the membrane potential (Em) according to the Nernst equation:

$$\text{Em (mV)} = -61 \log\left(\text{intracellular } K^+/\text{extracellular } K^+\right) \qquad \text{(Eq. 15.25)}$$

The normal ratio of (intracellular K^+/extracellular K^+) for the skeletal muscle is about 35, and normal Em is about −90 mV. Hence, most cells are slightly less negatively charged than the concentration ratio would predict. As a result, the increased permeability of the cell membrane to potassium tends to cause hyperpolarization as potassium diffuses out of the cell. Conversely, inhibition of the K permeability causes depolarization. The membrane potential tends to increase with hypokalemia and to decrease with hyperkalemia. In hypokalemia, both intra- and extracellular K^+ tend to decrease, but the extracellular concentration tends to decrease proportionately more than the intracellular concentration. Hence, the ratio of (intracellular K^+/extracellular K^+) tends to increase. In hyperkalemia, the membrane potential tends to decrease because an increase in the extracellular K^+ is proportionately greater than that in the intracellular K^+. However, in dogs with severe chronic hypokalemia, resting membrane potential of the skeletal muscle is shown to be reduced rather than increased, indicating that the permeability of the membrane to potassium may change with severe hypokalemia (Oh, 2003; Bilbrey et al., 1973).

CONTROL OF TRANSCELLULAR FLUX OF POTASSIUM

Transmembrane electrical gradients cause diffusion of cellular K^+ out of cells and Na^+ into cells. Because the Na^+-K^+ pump, which reverses this process, is stimulated by insulin and catecholamines (through beta-2-adrenergic receptors), alterations in levels of these hormones can affect K^+ transport and its serum levels (Meister & Aperia, 1993; Bilbrey et al., 1973).

Cells can act as buffers to prevent marked changes in extracellular K^+ concentrations. In acidosis, cells can take up H^+ ions in exchange for K^+ ions, and, in alkalosis, cells extrude H^+ ions in exchange for K^+ ions. These effects are summarized in Figure 15.2. Although there is no direct exchange of K^+ for H^+, a change in the extracellular pH can influence K^+ movement across the cell membrane through the Na^+-H^+ exchanger. When H^+ concentration in the ECF falls (alkaline pH), exchange of Na^+ for H^+ will result in a higher Na^+ concentration in the cell, which secondarily stimulates Na^+-K^+-ATPase,

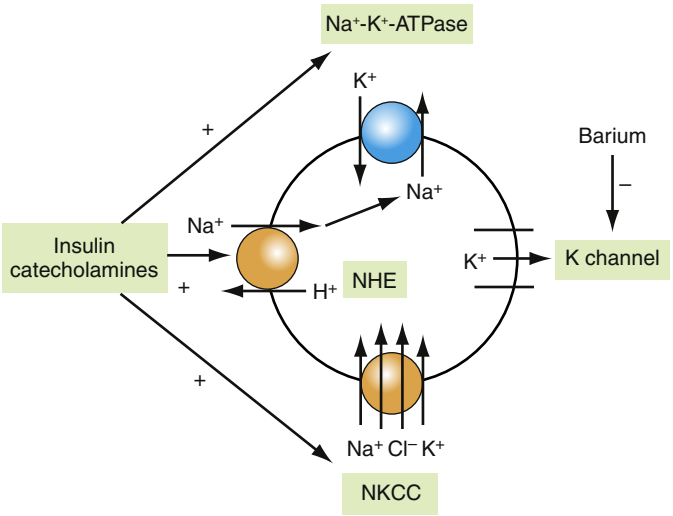

Figure 15.2 Control of transcellular movement of potassium. Potassium enters the cell through Na^+-K^+-ATPase (stimulated by beta-adrenergic agents or insulin) or through the sodium-potassium-chloride cotransporter (NKCC; stimulated by insulin and catecholamines). Stimulation of the Na-H exchanger (NHE) by a high extracellular pH, catecholamines, or insulin increases intracellular sodium concentration, which stimulates Na^+-K^+-ATPase and thereby increases intracellular movement of potassium.

causing an intracellular shift of K^+. The effect of acidosis and alkalosis on transcellular K^+ flux depends not only on the pH but also on the type of anion that accumulates. In general, metabolic acidosis causes greater K^+ efflux than respiratory acidosis. Metabolic acidosis due to inorganic acids, for example, sulfuric acid and hydrochloric acid, causes greater K^+ efflux than that due to organic acids, for example, lactic acid and keto acids. The reason is that organic anions accumulate substantially in the cell as well as in the ECF, whereas inorganic anions, such as chloride and sulfate, accumulate mainly in the ECF. Acidosis causes efflux of K^+ from the cell because of the shift of H^+ into the cell in exchange for K^+. A modifying factor appears to be anion accumulation in the cells. In organic acidosis, much of the H^+ entering the cell is balanced by organic anions; therefore, efflux of K^+ is prevented. In respiratory acidosis, the anion that accumulates in the cell to balance the incoming H^+ is bicarbonate. This explains why there is little K^+ efflux from the cell in respiratory acidosis. Alkalosis tends to lower serum K^+, because, as noted earlier, H^+ leaves cells in exchange for K^+, which enters the cells. As with acidosis, K^+ influx varies with the type of alkalosis. In respiratory alkalosis, with its lower pCO_2 and attendant lower intracellular bicarbonate by cellular buffering, K^+ influx is not as much as in metabolic alkalosis. When pH is kept normal with proportionately increased concentration of bicarbonate and pCO_2, K^+ tends to move into the cells; accumulation of bicarbonate in the cell must be accompanied by Na^+ and K^+. Similarly, when pH is kept normal with proportionately low bicarbonate and low pCO_2, K^+ tends to move out of the cells (Halperin & Kamel, 1998b; Oh, 2003).

Inhibition of K^+ diffusion across the cell would cause decreased plasma K^+ concentration. Barium, chloroquine, and hydroxychloroquine are examples of K^+ channel inhibitors (Clemessy et al., 1995).

CONTROL OF RENAL EXCRETION OF POTASSIUM

When Na^+ is accompanied by anions that are less permeable than $C1^-$, luminal negativity is increased, resulting in enhanced K^+ secretion. Examples of such anions include sulfate, bicarbonate, and anionic antibiotics such as penicillin and carbenicillin (Halperin & Kamel, 1998c). Bicarbonate in the tubular fluid enhances K^+ secretion not only through its effect as a poorly reabsorbable anion but also by enhancing renal outer medullary potassium (ROMK) activity. An increase in renal K^+ excretion in patients who vomit and develop metabolic alkalosis may be explained by this mechanism. ADH also increases the luminal K^+ channel activity. K^+ secretion is increased by rapid urine flow by maintaining a low luminal K^+ concentration. Renal K^+ wasting during osmotic diuresis could be explained by this mechanism. The more Na^+ presented to the distal nephron, the more that can be absorbed and more K^+ can be secreted "in exchange." The increased Na^+ delivery to the collecting duct also increases renal K^+ excretion by its effect on urine flow (Fig. 15.3). A higher urine flow allows greater secretion of potassium into the luminal fluid while reducing back diffusion of potassium into the tubular cells because the luminal concentration would be lower for a given amount of potassium secretion (Halperin et al., 2006; Halperin & Kamel, 1998a).

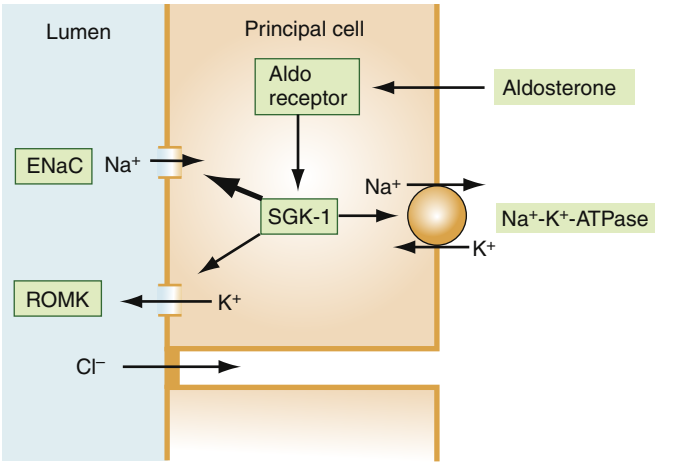

Figure 15.3 Control of potassium secretion at the cortical collecting duct. Sodium enters from the luminal fluid into the cell through the epithelial sodium channel (ENaC) and is transported out of the cell through Na^+-K^+-ATPase on the basolateral membrane. These processes create the luminal electrical potential that is more negative than the electrical potential of the peritubular fluid. The electrical charge imbalance created by sodium reabsorption causes paracellular reabsorption of chloride and allows entry of potassium into the lumen through the renal outer medullary potassium (ROMK) channel. Binding of aldosterone to its receptor results in upregulation of SGK1 (serum and glucocorticoid regulated kinase 1), which results in the increased expression of ENaC on the luminal membrane. Upregulation of SGK1 also stimulates ROMK and Na-K-ATPase. All three effects help to increase potassium secretion.

PLASMA RENIN ACTIVITY (PRA), PLASMA ALDOSTERONE (PA) CONCENTRATION AND ABNORMALITIES IN POTASSIUM METABOLISM

Because abnormalities in PRA and PA are frequently either responsible for or caused by abnormalities in K^+ metabolism, it is important to understand their relationships. The general principles are as follows. (1) Expansion of effective arterial volume caused by primary increase in aldosterone (primary aldosteronism) or by other mineralocorticoids will cause suppression of PRA. When mineralocorticoids other than aldosterone are present in excess, they induce retention of salt and water; the resulting volume expansion leads to suppression of both PRA and PA. (2) A primary increase in PRA will always lead to an increase in PA (secondary aldosteronism). On the other hand, a primary defect in aldosterone secretion will cause volume depletion and secondarily increase PRA. PRA may be high because of:

a. Volume depletion secondary to renal or extrarenal salt loss
b. Abnormality in renin secretion, for example, reninoma (hemangiopericytoma of afferent arteriole), malignant hypertension, renal artery stenosis
c. Increased renin substrate production, for example, oral contraceptives

Elevation in serum K^+ can directly stimulate the adrenal cortex to release aldosterone. When renin is deficient primarily, aldosterone is always low, for example, hyporeninemic hypoaldosteronism.

ALDOSTERONE PARADOX AND ROLE OF SODIUM CHLORIDE REABSORPTION IN THE DISTAL CONVOLUTED TUBULE

It is well known that aldosterone secretion is stimulated by two different mechanisms: high angiotensin II and high plasma potassium. The high angiotensin II is usually due to high renin concentration, which is usually due to low effective vascular volume. The kidney's responses to these two situations are quite different. When aldosterone secretion is stimulated by low effective vascular volume leading to high renin, high angiotensin II, and eventually high aldosterone, there is little increase in urinary potassium excretion, but the kidney conserves sodium avidly. On the other hand, when aldosterone secretion is stimulated by hyperkalemia, renal sodium reabsorption is not increased, but urinary potassium excretion is greatly increased (Palmer, 2015). In fact, a high-potassium diet tends to cause renal sodium wasting and reduced blood pressure. The contradictory response is called the aldosterone paradox (Box 15.2). We now understand the mechanism of the aldosterone paradox, which is due to differing effects of hyperkalemia and angiotensin II on the sodium reabsorption in the distal convoluted tubule. Hyperkalemia inhibits sodium reabsorption, whereas high angiotensin II stimulates sodium reabsorption in the distal convoluted tubule. These effects are mediated through their effects on WNK4 and WNK1, both of which

BOX 15.2

Aldosterone Paradox

Volume Depletion → Angiotensin II → Aldosterone

Angiotensin II → K channel (KCNJ10) stimulation of DCT → membrane hyperpolarization → low DCT Cl → activation of WNK 4 & 1 → activation of NCCT → NaCl reabsorption in DCT with reduced Na delivery to CCD → Na retention without renal K wasting

Hyperkalemia → Aldosterone

Hyperkalemia → membrane depolarization of DCT → high DCT Cl → inhibition of WNK 4 &1 → inhibition of NCCT → increased Na delivery to CCT → hypersecretion of K with Na wasting.

stimulate NCCT (sodium chloride cotransporter). In short, the activation of WNK4 and WNK1 requires low intracellular chloride concentration, which in turn depends on the transmembrane potential (Kamel 2018). Hyperkalemia increases intracellular chloride by reducing the transmembrane potential whereas angiotensin II reduces intracellular chloride by increasing the transmembrane potential. Thus, hyperkalemia inhibits NaCl reabsorption in the distal convoluted tubule, whereas angiotensin II stimulates it.

The reduced NaCl reabsorption in the distal convoluted tubule in hyperkalemia results in increased delivery of NaC1, which increases secretion of potassium. Angiotensin II increases NaCl reabsorption in the distal convoluted tubule, resulting in reduced delivery of NaC1 to the cortical collecting duct, and thus decreases secretion of potassium. As stated earlier, the amount of Na delivery to the cortical collecting duct is of paramount importance in determining the amount of potassium secreted by the cortical collecting duct (Kamel et al., 2018).

CAUSES AND PATHOGENESIS OF HYPOKALEMIA

Hypokalemia occurs by one of three main mechanisms: intracellular shift, reduced intake, and increased loss (Box 15.3). Because the intracellular K^+ concentration greatly exceeds the extracellular concentration, K^+ shift into the cell can cause severe hypokalemia with little change in its intracellular concentration. Alkalosis, insulin, and beta-2-agonists can cause hypokalemia by stimulating Na^+-K^+-ATPase activity. Defective activity of dihydropyridine-responsive Ca^{++} channels and potassium channels has been documented in some patients with hypokalemic periodic paralysis. A defect in sodium channel is also known to cause hypokalemic periodic paralysis, but a defect in sodium channel sometimes causes hyperkalemic or normokalemic paralysis (Lin & Halperin, 2007). In barium poisoning, K^+ accumulates in the cell and hypokalemia develops because of the inhibition of the K^+ channel by barium, resulting in inhibition of K^+ efflux from the cell in the face of continuous cellular uptake of K^+ through the action of Na^+-K^+-ATPase (Bradberry & Vale, 1995). Poisoning with chloroquine or hydroxychloroquine produces hypokalemia by the same mechanism as barium (Jordan et al., 1999). Both drugs are cationic, like barium, and can inhibit the K^+ channel. K^+ accumulates in the cell along with anions as the cell mass increases during nutritional recovery because K^+ is the main intracellular cation.

Poor intake of K^+ is rarely a cause of hypokalemia by itself; it is usually accompanied by poor caloric intake, which causes catabolism and release of K^+ from the tissues. Vomiting and diarrhea are common causes of hypokalemia. Diarrhea causes direct K^+ loss in the stool; however, in vomiting, hypokalemia is mainly the result of K^+ loss in the urine rather than in the vomitus since vomiting causes metabolic alkalosis and the subsequent renal excretion of bicarbonate leads to renal K^+ wasting (Halperin & Kamel, 1998c).

Renal loss of K^+ is by far the most common cause of hypokalemia. With rare exceptions, hypokalemia due to increased renal wasting of potassium can be attributed to an increased activity of aldosterone or other mineralocorticoids. Increased aldosterone could be a primary disorder, as in primary hyperaldosteronism, or due to increased renin secretion, as in secondary hyperaldosteronism. Even with increased aldosterone, renal K^+ wasting occurs only if it is accompanied by adequate distal delivery of Na^+. In primary aldosteronism, distal delivery of Na^+ is increased because increased NaCl reabsorption in the cortical collecting duct by the action of aldosterone inhibits salt reabsorption in the proximal tubule because of volume expansion. In secondary aldosteronism, hypokalemia occurs only in conditions that are accompanied by increased distal Na^+ delivery. Examples of secondary hyperaldosteronism that result in hypokalemia include renal artery stenosis, diuretic therapy, and malignant hypertension, and congenital defects in renal salt transport such as Bartter syndrome and Gitelman syndrome. It must be noted that, in the absence of extrarenal salt loss, renal salt excretion ultimately equals salt intake even in conditions of increased

BOX 15.3

Causes of Hypokalemia

Intracellular Shift
- Alkalosis
- Hypokalemic periodic paralysis
- Beta-2-adrenergic agonists
- Barium poisoning
- Chloroquine and hydroxychloroquine poisoning
- Insulin
- Administration of carbohydrates
- Nutritional recovery state

Poor Intake

Gastrointestinal Loss
- Vomiting
- Diarrhea
- Intestinal drainage
- Laxative abuse

Excessive Renal Loss
- Primary aldosteronism (adrenal adenoma or hyperplasia); PRA is suppressed
- Secondary aldosteronism (increase in aldosterone is secondary to increase in renin)
- Malignant hypertension
- Renal artery stenosis
- Reninoma
- Diuretics
- Bartter syndrome
- Gitelman syndrome
- Excess mineralocorticoids other than aldosterone, e.g., Cushing syndrome, ACTH-producing tumor, licorice
- Chronic metabolic acidosis
- Delivery of poorly reabsorbed anions to the distal tubule, e.g., bicarbonate, ketone anions, carbenicillin
- Miscellaneous causes: magnesium deficiency, acute leukemia, Liddle syndrome.

aldosterone or aldosterone deficiency since prolonged imbalance between intake and output is impossible. Without eventual balance, an individual could not survive volume excess or volume depletion. However, when salt reabsorption is increased at the mineralocorticoid active site (i.e., cortical collecting duct), the amount of salt delivered to this site must be increased when the final salt output eventually equals the intake. When balance is achieved, an increased amount is delivered to the site and the increased amount is reabsorbed so that the normal amount equaling the intake is excreted. Ultimate balance is possible only when the amount entering the body equals the amount leaving the body. This is the mechanism by which salt delivery to the aldosterone site remains increased in primary hyperaldosteronism as well as all cases of secondary hyperaldosteronism that are associated with hypokalemia (Lin & Halperin, 2007; Oh, 2003).

Bartter syndrome is caused by defective NaCl reabsorption in the thick ascending limb of Henle, whereas in Gitelman syndrome the defect in NaCl reabsorption is in the distal convoluted tubule. Reabsorption of NaCl in the thick ascending limb is mediated by an NKCC, which reabsorbs one Na^+ and one K^+ accompanied by 2 Cl^-. The continuous reabsorption of these electrolytes requires constant leak back of K^+ into the lumen through ROMK channels, while Na^+ entering the cell is transported out the cell by Na^+-K^+-ATPase, and Cl^- entering the cell diffuses out of the cell through the chloride channel, CLCKB. The process stops when any one of these steps is impaired; thus, Bartter syndrome may be due to a defect in NKCC, ROMK, or CLCKB. Finally, the fourth type of Bartter syndrome is due to a defective barttin, the molecule necessary for the normal function of CLCKB (Koulouridis & Koulouridis, 2015).

Defective Na^+ reabsorption proximal to the aldosterone effective site in these conditions results in increased delivery of Na^+ to the cortical collecting duct and hence in hypokalemia. Heart failure does not lead to hypokalemia despite secondary hyperaldosteronism unless distal delivery of Na^+ is increased by diuretic therapy.

Substances that are not aldosterone but have mineralocorticoid activity include corticosterone, deoxycorticosterone (DOC), and synthetic mineralocorticoid, such as 9-α-fludrocortisone (Florinef). Licorice, a chemical present in licorice-containing candies, increases the mineralocorticoid activity of cortisol by inhibiting the catabolism of cortisol in the principal cells of the cortical collecting duct. Cortisol is normally a

potent mineralocorticoid but has a negligible concentration in the cortical collecting duct cells owing to the rapid breakdown by the enzyme 11-beta-hydroxy steroid dehydrogenase type 2, which converts cortisol to cortisone (Krozowski et al., 1999).

Rare causes of renal potassium wasting that are not accompanied by increased mineralocorticoid activity is Liddle syndrome. Liddle syndrome is a congenital disorder that is characterized by increased ENaC activity in the collecting duct in the absence of increased aldosterone, resulting in increased sodium reabsorption and enhanced potassium secretion. Aldosterone secretion is reduced because salt retention due to the increased ENaC activity leads to physiologic suppression of renin secretion. In chronic metabolic acidosis, hypokalemia develops probably because reduced proximal reabsorption of NaCl allows increased delivery of NaCl to the distal nephron. Direct stimulation of aldosterone secretion by metabolic acidosis appears to be an additional mechanism that contributes to hypokalemia (Lin et al., 2017).

Stimulation of aldosterone secretion by acidic pH is through the pH-sensitive K^+ channel, which is inhibited by the low intracellular pH. Inhibition of K^+ channel causes membrane depolarization, which, in turn, activates voltage-dependent Ca^{++} channels. Activation of Ca^{++} channels is ultimately responsible for increased aldosterone secretion (Holtzclaw et al., 2011)

During pregnancy, plasma concentration of progesterone I is greatly increased, but renal K wasting of patients with aldosterone-producing adenoma may be greatly reduced, and the patient may not require any treatment because of the antialdosterone effect of progesterone (Kamel et al., 2002).

A rare cause of hypokalemia is a genetic mutation of the aldosterone receptor that recognizes progesterone as a mineralocorticoid, resulting in renal potassium wasting and hypokalemia. These patients do not respond to allopurinol—rather, the drug worsens hypokalemia because the same abnormal receptor recognizes allopurinol as a receptor agonist.

One of the most exciting new developments in the area of aldosterone pathophysiology is the mechanism of aldosterone-producing adenoma (Choi et al., 2011). Following the initial report of 8 patients among 24 cases of unselected patients with aldosterone-producing adenoma, additional cases of aldosterone-producing adenoma due to the same mutation are being reported all over the world. Clearly, this mechanism is a major cause of aldosterone-producing adenoma. The mechanism of stimulation of aldosterone secretion and subsequent hyperplasia of the affected cell, turning into an adenoma, is mutation of a G-protein coupled receptor–associated potassium channel, known as KCNJ5 (Choi et al., 2011). The mutation is a loss of function mutation, and the defect in K^+ channel results in the membrane depolarization and the subsequent activation of the voltage-dependent Ca^{++} channel, which is ultimately responsible for the stimulation of aldosterone secretion. Angiotensin II normally stimulates aldosterone secretion by binding to the same receptor, which results in inhibition of the K^+ channel. Subsequently, many reports of other mutations that cause aldosterone-producing adenoma are appearing; the final pathway appears to be membrane depolarization resulting in activation of Ca^{++} channels.

Recently, it has been shown that the mutant KCNJ5 channel is selectively blocked by macrolide antibiotics. This mechanism may be used for diagnosis and treatment of adenoma caused by the same mutation (Scholl et al., 2017).

DIFFERENTIAL DIAGNOSIS OF HYPOKALEMIA

The first step in the differential diagnosis is to measure urinary excretion of K^+. If urinary K^+ excretion is low (<20 mEq/day or <0.01 mEq/mg of creatinine), the cause is low intake, extrarenal loss of K^+, or intracellular shift. Superacute development of hypokalemia usually suggests intracellular shift as the mechanism. The most common cause of extrarenal loss is diarrhea, which can be suspected by history and a low or negative urine anion gap (urine $Na^+ + K^+ -$ urine Cl^-); the normal urine anion gap is about 40 mmol/24 hours. Intracellular shift is suggested by the history and clinical findings. If urinary excretion is normal or increased (urine K^+> 30 mEq/day or 0.02 mEq/mg of creatinine), the cause is renal loss. Once a real cause is suspected, the next step should be the measurement of PRA and plasma aldosterone (Oh, 2003; Halperin & Kamel, 1998c).

High PRA and high aldosterone suggest secondary hyperaldosteronism, the causes of which include diuretic therapy, renal artery stenosis, malignant hypertension, renin-producing tumors, and hereditary defects in renal salt transport (Bartter syndrome and Gitelman syndrome). Blood pressure would be normal in subjects with Bartter syndrome or Gitelman syndrome and a normotensive person on diuretic therapy. Blood pressure would be high in all other conditions and in a hypertensive subject on diuretic therapy. Low PRA and high plasma aldosterone suggest primary hyperaldosteronism, which is caused by adrenal adenoma or bilateral hyperplasia. If PRA and plasma aldosterone are low, the likely conditions include Liddle syndrome, apparent mineralocorticoid excess states (both hereditary and drug-induced), 11-hydroxylase deficiency, and 17-hydroxylase deficiency. Reduction in renal K^+ excretion will be achieved with spironolactone in all of these conditions except for Liddle syndrome, which will respond to ENaC blockers such as triamterene and amiloride and aldosterone-receptor mutation (Loffing and Korbmacher, 2009; Halperin et al., 2006).

BOX 15.4

Causes of Hyperkalemia

PSEUDOHYPERKALEMIA

Thrombocytosis, severe leukocytosis, use of tourniquet with fist exercise, in vitro hemolysis

TRUE HYPERKALEMIA

Due to Extracellular Shift

- Acute acidosis (more with inorganic acidosis)
- Catabolic states
- Periodic paralysis
- Succinylcholine (esp. in those with muscular dystrophy)
- Cationic amino acids (epsilon aminocaproicacid)
- Vigorous exercise
- Digitalis intoxication, digitalis-like chemicals (herb chansu, bufotoxins)
- Fluoride poisoning

Due to Excessive Ingestion: Rare If Renal Excretion of K^+ Is Normal

Decreased Renal Excretion

- Hypoaldosteronism: Addison disease; selective hypoaldosteronism (hyporeninemic hypoaldosteronism, heparin, congenital adrenal enzyme deficiencies, angiotensin converting enzyme inhibitors)
- Tubular unresponsiveness to aldosterone (pseudohypoaldosteronism types I and II): congenital, salt-losing nephropathy (acquired)
- Potassium-sparing diuretics: spironolactone, amiloride, triamterene, drospirenone birth control pill
- Antibiotics with epithelial sodium channel (ENaC)-blocking effects: pentamidine, trimethoprim
- Antirejection medications: cyclosporine, tacrolimus
- Severe dehydration

CAUSES AND PATHOGENESIS OF HYPERKALEMIA

Hyperkalemia may be caused by one of three mechanisms: (1) a shift of potassium from the cells to the extracellular fluid, (2) increased potassium intake, and (3) reduced renal potassium excretion (Box 15.4). Hyperkalemic familial periodic paralysis, administration of succinylcholine in paralyzed patients, administration of cationic amino acids such as arginine and lysine, epsilon-aminocaproic acid (this chemical is neutral in its charge, but becomes a cationic amino acid in the cell after addition of an amine group) (Perazella & Biswas, 1999) rhabdomyolysis or hemolysis, and acute acidosis all cause hyperkalemia by extracellular potassium shift. Rhabdomyolysis and hemolysis cause hyperkalemia only when they are accompanied by renal failure. Although hyperkalemia is not as predictable with organic acidosis as with inorganic acidosis in experimental situations, hyperkalemia is common in diabetic ketoacidosis and phenformin-induced lactic acidosis. The more frequent occurrence of hyperkalemia in clinical organic acidosis may be explained by the longer duration of acidosis and the presence of other factors such as dehydration and renal failure and insulin deficiency in diabetic ketoacidosis (Halperin & Kamel, 1998a; Chothia et al., 2014; Kamel et al., 1994).

Hyperkalemia occurs quite regularly during vigorous muscular exercise. The likely mechanism is extracellular shift of potassium due to depolarization of the cell membrane. A transient rise in intracellular pH at the start of exercise as conversion of creatine phosphate to creatine and phosphate has been suggested as the mechanism of hyperkalemia. However, this is an unlikely mechanism since conversion of creatine phosphate to creatine is triggered by a falling pH, not a rise in pH (Sahlin et al., 1975).

Hyperkalemia can also occur in severe digitalis intoxication by extracellular shift of potassium as digitalis inhibits the Na^+-K^+-ATPase pump. A number of drugs have digitalis-like activity. Intoxication with these drugs, such as bufogenins, bufadienolides, or bufotoxins, are contained in toad skin bufo marinus. The same chemical is contained in Chinese medicine as chansu, and hyperkalemia due to chansu has been reported (Halperin &

Kamel, 1998c; Fazekas et al., 1993; Kamel et al., 1994; Rajapakse, 2009; Kanji & MacLean, 2012).

Fluoride poisoning is mainly known as a cause of severe hypocalcemia, but it can also cause hyperkalemia by the extracellular shift of potassium caused by activation of K^+ channels. As fluoride causes an intracellular shift of Ca^{++} in the cell, leading to hypocalcemia, the high intracellular Ca^{++} stimulates Ca^{++}-activated K^+ channels (McIvor et al., 1985), resulting in hyperkalemia (Bradberry & Vale, 1995).

The kidney's ability to excrete potassium is so great that hyperkalemia rarely occurs solely on the basis of increased intake of potassium. Thus, hyperkalemia is almost always due to impaired renal excretion. There are three major mechanisms of diminished renal potassium excretion: reduced aldosterone or aldosterone responsiveness, renal failure, and reduced distal delivery of sodium. Aldosterone deficiency may be part of a generalized deficiency of adrenal hormones (e.g., Addison disease) or it may represent a selective process (e.g., hyporeninemic hypoaldosteronism). Hyporeninemic hypoaldosteronism is the most common cause of all aldosterone deficiency states and by far the commonest cause of chronic hyperkalemia among nondialysis patients (Oh et al., 1974; Phelps et al., 1980). Selective hypoaldosteronism can also occur with heparin therapy, which inhibits steroid production in the zona glomerulosa (Phelps et al., 1980) In patients with reduced aldosterone secretion, any agent that limits the supply of renin or angiotensin II may provoke hyperkalemia, for example, ACE (angiotensin-converting enzyme) inhibitors, nonsteroidal antiinflammatory agents, and beta-blockers. The latter compound interferes with potassium transport into cells. Renal tubular unresponsiveness to aldosterone (pseudohypoaldosteronism) may be congenital, but it is more often an acquired defect. This defect may involve only potassium secretion (pseudohypoaldosteronism type II) or sodium reabsorption as well as potassium secretion (pseudohypoaldosteronism type I). Most cases of so-called "salt-losing nephritis" represent the latter defect. Severe volume depletion may cause hyperkalemia despite secondary hyperaldosteronism because volume depletion causes a marked reduction in delivery of sodium to the cortical collecting duct (Uribarri et al., 1983).

Pseudohyperkalemia is defined as an increase in potassium concentration only in the local blood vessel or in vitro and has no physiologic consequences. Prolonged use of a tourniquet with fist exercises can increase the serum potassium level by as much as 1 mEq/L. Thrombocytosis and severe leukocytosis cause pseudohyperkalemia through potassium release from the platelets and white blood cells, respectively, during blood clotting (see Box 15.4) (Kim et al., 1990; Colussi & Cipriani, 1995).

In vitro hemolysis is by far the most common cause of pseudohyperkalemia; the destruction of red blood cells occurs when blood is injected into a vacuum tube through a narrow needle. When hemolysis occurs, the common practice is to repeat the measurement, hoping that hemolysis would not recur. An easier way is to measure free hemoglobin concentration in the serum if the sample is saved and to calculate the likely addition of potassium to serum by red blood cell lysis on the basis that the ratio of released K^+ is proportionate to released hemoglobin. It has been shown, however, that there are wide individual variations in the ratio between released K^+ and hemoglobin, ranging from 2.1 mEq/g of hemoglobin to 5 mEq/g. The difference exists probably because the quantities of K^+ and hemoglobin released from partially lysed red blood cells differ (Oh, 2003; Oh, 2003a).

DIFFERENTIAL DIAGNOSIS OF HYPERKALEMIA

The first step in the differential diagnosis of hyperkalemia should be to rule out pseudohyperkalemia. Electrocardiogram (ECG) abnormalities of hyperkalemia are absent in pseudohyperkalemia, but the absence of ECG changes does not rule out true hyperkalemia because ECG changes are often absent with severe hyperkalemia when the condition is chronic. Pseudohyperkalemia should be suspected when conditions known to cause pseudohyperkalemia, such as thrombocytosis or in vitro hemolysis (pink serum) exist. In pseudohyperkalemia due to thrombocytosis, both serum and plasma K^+ should be obtained simultaneously. The higher serum K^+, which is always the case, is due to release of K^+ from platelets during clotting. Once pseudohyperkalemia is ruled out, the next step is to differentiate among the 3 major causes of hyperkalemia: increased K^+ intake, shift of K^+ from the cell, and impaired renal excretion. Measurement of a 24-hour urine K^+ will distinguish increased intake from the other two causes. Although hyperkalemia due to a shift of K^+ from the cell would result in an increased urinary excretion of K^+, renal excretion of K^+ is often not increased because conditions that impair renal excretion of K^+ often coexist. A careful dietary history will be necessary to rule out hyperkalemia due to increased intake unless the patient is deliberately trying to deceive the physician.

An important principle is that extracellular shift is never a cause of chronic hyperkalemia since the amount of potassium that can be released from the cell is always very limited. Once net movement of potassium from the cell stops, the plasma K^+ concentration will depend on the factors that affect renal K^+ excretion. This explains why in types I and II renal tubular acidosis (RTA), hypokalemia is a common finding despite systemic acidemia (Oh, 2003).

Chronic hyperkalemia is almost always due to impaired renal excretion; a 24-hour urine K^+ measurement is rarely needed to prove impaired renal excretion of K^+ as the cause of hyperkalemia. Among the renal causes of hyperkalemia, acute renal failure is the most common cause of acute hyperkalemia, which will be obvious from serum creatinine and blood urea nitrogen (BUN). For differential diagnosis of chronic hyperkalemia of renal causes, the first step is to measure plasma renin activity, plasma aldosterone, and urinary excretion of Na^+ and K^+. A very low urinary Na^+ and a low K^+ in the absence of polyuria suggest that the aldosterone effect is normal. In this setting, K^+ excretion is impaired because of the reduced availability of Na^+ and a marked reduction in collecting duct urine flow. Markedly increased proximal reabsorption of Na^+ due to low effective vascular volume, such as severe congestive heart failure, can cause hyperkalemia by such a mechanism. If urinary Na^+ is adequate (>20 mEq/L), plasma renin activity and aldosterone should be measured.

Low PRA and low aldosterone suggest hyporeninemic hypoaldosteronism, whereas high PRA and low aldosterone suggest a primary defect in aldosterone secretion, such as Addison disease, heparin therapy, and aldosterone biosynthetic defect. When PRA and aldosterone are both increased, likely culprits are pseudohypoaldosteronism and very low Na^+ delivery to the cortical collecting duct, drugs that impair the ENaC function, or aldosterone action, such as potassium-sparing diuretics (e.g., amiloride, triamterene, spironolactone) and certain antibiotics (e.g., trimethoprim, pentamidine). The presence of low PRA and high aldosterone in the setting of hyperkalemia is not a very likely combination but has been observed occasionally in a patient with a genetic defect of an enzyme WNK kinase, called pseudohypoalteronism type II (also known as Gordon syndrome). The defect in WNK kinase causes increased NaCl transport in the distal convoluted tubule, resulting in hypertension and a defect in potassium secretion. The condition is a mirror image of Gitelman syndrome and is characterized by low PRA (due to volume expansion caused by hyperabsorption of NaCl) and low aldosterone, resulting in hyperkalemia. A variant of the condition is characterized by a separate severe defect in K^+ secretion, resulting in hyperkalemia despite normal or sometimes high aldosterone. In such a patient, a high plasma aldosterone occurs in response to hyperkalemia, but renin is low because of volume expansion. By far, the commonest cause of chronic hyperkalemia due to impaired renal excretion of potassium is hyporeninemic hypoaldosteronism, which is caused by chronic renal insufficiency of primarily tubulointerstitial diseases. The suggested mechanism is primary renal salt retention caused by the renal disease, which leads to physiologic suppression of renin secretion and hence of aldosterone, ultimately resulting in hyperkalemia, often accompanied by hypertension (Oh, 2003).

DISORDERS OF WATER, SODIUM, AND ANTIDIURETIC HORMONE (ADH) METABOLISM

REGULATION OF THIRST AND ADH RELEASE

A rise in effective osmolality shrinks the hypothalamic osmoreceptor cells, which then stimulate the thirst center in the cerebral cortex and stimulate ADH production in the supraoptic and paraventricular nuclei. Conversely, a decline in effective osmolality causes swelling of the osmoreceptor cells, resulting in inhibition of ADH production. ADH produced in the hypothalamus is carried through long axons and is secreted from the posterior pituitary gland. Stimulation and inhibition of osmoreceptor cells affect both production by the hypothalamus and secretion by the pituitary of ADH (Bourque & Oliet, 2002; Oldfield & McKinley, 2014).

Regulation of ADH secretion by a change in effective osmolality is extremely sensitive. ADH secretion in response to a change in effective osmolality was so sensitive that a change of only 2% to 3% stimulates ADH secretion sufficiently to result in a maximally concentrated urine and decline in plasma osmolality of only 2% to 3% produces maximally dilute urine (<100 mOsm/L). However, a more recent study has shown that changes in serum sodium concentration by 2% to 3% in venous blood is accompanied by a much greater change in arterial serum sodium concentrations when oral intake of water is rapid. For example, drinking 20 m/kg

of water in 15 minutes reduced arterial serum sodium by about 8 mmol/L and resulted in rapid water diuresis, but the same amount given by slow sipping did not produce water diuresis. With rapid intake of water, venous sodium concentration was about 4 mmol/L higher than that of venous blood. The osmoreceptors, of course, would respond to the arterial, rather than venous, sodium concentration (Oh, 2003).

ADH release is also regulated by nonosmotic factors. Low effective vascular volume provokes thirst and ADH release, and high effective vascular volume has the reverse effects. These effects are mediated through baroreceptors as well as some humoral factors. Alpha catecholamines suppress and beta catecholamines enhance ADH output. Prostaglandins inhibit the effect of ADH on the kidney. Angiotensin II stimulates thirst and ADH release. Lack of glucocorticoid enhances ADH action on the kidney and increases ADH release. ADH in the pituitary gland acts like corticotropin-releasing hormone and stimulates production of ACTH. Cortisol, in turn, inhibits the release of ADH. Physical and emotional stress, for example, major surgery, increases ADH output, possibly in part through emetic stimuli, which are common complications of major surgery and are attributed to the effects of anesthesia and surgical trauma. Many drugs affect ADH release or its action; ethanol inhibits the output of ADH. Lithium and demeclocycline inhibit the antidiuretic effect of ADH on the kidney (Kortenoeven et al., 2012). Chlorpropamide increases the action of ADH on the kidney. Some drugs may operate through the emetic stimulus, which is one of the most potent physiologic stimuli to ADH release (Oh, 2002). The urine may become osmotically concentrated in the absence of ADH if effective vascular volume is very low. The combination of reduced GFR and enhanced proximal reabsorption of filtrate reduces urine flow to the collecting duct so greatly that even the limited permeability of the membrane permits withdrawal of a sufficient amount of water to concentrate urine (Moritz, 2019; Halperin & Bohn, 2002).

There are 3 classes of ADH receptors: V1 receptors cause a rise in vasomotor tone and have certain metabolic effects, V2 receptors are associated with antidiuresis, and V3 receptors cause stimulation of ACTH secretion in the anterior pituitary. The antidiuretic effect of ADH is mediated by promoting the expression of aquaporin 2 on the luminal membrane of the collecting duct to make the tubule permeable to water and by stimulating reabsorption of salt on the outer medullary thick ascending limb of Henle's loop. Vasopressinase, which normally breaks down ADH, may be increased in pregnancy and may cause polyuria. DDAVP, a synthetic analogue of arginine vasopressin, which resists vasopressinase, is useful in polyuria of pregnancy (Marques et al., 2015).

URINE CONCENTRATION AND DILUTION

About 180 L of water are filtered daily in humans; 150 L are reabsorbed in the proximal tubule and about 5 L in the descending limb of Henle of cortical nephrons. About 25 L of dilute urine are delivered to the ascending limb of Henle. Since the tubules from this point to the beginning of the cortical collecting duct are water impermeable, the volume remains unchanged at 25 L, but the osmolality decreases progressively to about 60 to 80 mOsm/L. Because of the conditional expression of aquaporin 2 on the luminal membrane of collecting ducts, which depends on the action of ADH, no water reabsorption occurs in the cortical and outer medullary collecting ducts when ADH is absent (Fig. 15.4). However, a small amount of water (about 3–5 L during water diuresis) is reabsorbed in the terminal portion of the inner medullary collecting duct even when ADH is absent. Aquaporins may be present constitutively in this part of the nephron or some other chemical may cause expression of aquaporins in the inner medullary collecting duct. During the maximal water diuresis, the combined effect of further salt reabsorption in the collecting duct and small additional reabsorption of water in the inner medullary collecting duct allow final excretion of about 20 L of dilute urine at an osmolality of about 40 mOsm/L. It must be noted that the maximal urine output during water diuresis depends greatly on salt intake, because the maximal urine output can never exceed the amount delivered into the ascending limb of Henle. Even with a mild salt restriction, for example, 2 g per day, the resulting mild volume depletion increases reabsorption of salt and water in the proximal tubule sufficiently to reduce the volume delivery to the ascending limb of Henle's loop to 12 to 15 L per day and the final maximal urine output to 10 to 12 L per day (Oh, 2003).

In the presence of maximal ADH, urine can be concentrated to as high as 1200 mOsm/L as water is reabsorbed in the cortical and medullary collecting duct, with urine volume as low as 0.5 L per day (see Fig. 15.4). The osmolality of urine as it enters the ADH effective site, that is, the cortical collecting duct, is the same during water diuresis and antidiuresis, and the value is quite low, about 60 mOsm/L. Urine osmolality is

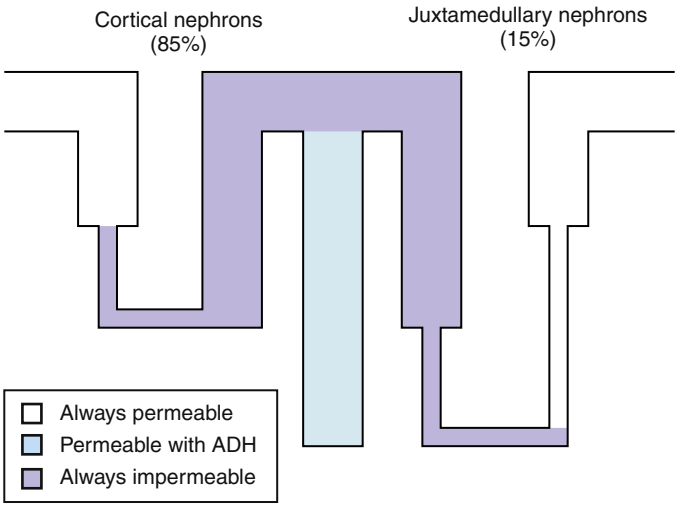

Figure 15.4 Transport of water at various nephron sites. The proximal tubules are always water permeable because aquaporins are constitutively expressed at these sites. The descending thin limbs of juxtamedullary nephrons (15% of all nephrons) also have expression of aquaporins and are therefore water permeable, but descending thin limbs of cortical nephrons (85%) lack aquaporins and are water impermeable. This view is not widely accepted; the majority view is that the entire thin descending limb of Henle of both cortical and juxtamedullary nephrons is water permeable. The ascending thin limb and ascending thick limb of Henle, the distal convoluted tubule, and the connecting tubule do not express aquaporins, and are always water impermeable. The collecting duct is water permeable when ADH action allows expression of aquaporins. *ADH,* antidiuretic hormone.

reduced by continuous salt reabsorption without water reabsorption in the ascending thin and thick limbs of Henle and the distal convoluted tubule and connecting table. The concentration of urine is achieved by reabsorption of water in the collecting duct through transcellular reabsorption of water through the cells of the collecting duct; water first enters the cell through the luminal membrane and then leaves the cell through the basolateral membranes. Diffusion of water through each membrane requires expression of aquaporins. Aquaporin 3 is constitutively expressed in the basolateral membrane of the cortical collecting duct and aquaporin 4 in the basolateral membrane of the medullary collecting duct. Entry of water in the collecting duct, both cortical and medullary, from the lumen into the cell requires the expression of aquaporin 2 on the luminal membrane, which is an ADH-mediated process.

Increase in urine osmolality from a very low value at the beginning of the cortical collecting duct to an isotonic value at the corticomedullary junction requires the presence of ADH and the tubular responsiveness to ADH since the interstitium of the cortex is always isotonic. However, the reabsorption of water in the medullary collecting duct requires not only the ADH action but also the hypertonicity of the medullary interstitium. Maintenance of medullary hypertonicity is achieved by the countercurrent multiplication mechanism. In short, the medullary interstitial fluid becomes progressively hypertonic starting at the isotonic level at the corticomedullary junction, increasing to a level of about 1200 mOsm/L at the tip of the papilla. Medullary hypertonicity in the outer medullary area is achieved by the active reabsorption of salt in the thick ascending limb of Henle that is not accompanied by water reabsorption. In the inner medulla, salt reabsorption in the thin ascending limb of Henle (the inner medulla lacks the thick ascending limb of Henle) is passive, occurring with the help of urea that diffuses from the inner medullary collecting duct. The mechanism by which urea contributes to the concentration of urine is still hotly debated and is beyond the scope of this discussion. The achievement of medullary hypertonicity is attributed to the countercurrent mechanism, which had been traditionally explained in the following manner: (1) selective reabsorption of salt from the ascending limbs of Henle without water reabsorption, (2) selective reabsorption of water from the descending limb of Henle, and (3) the countercurrent arrangement of the descending and ascending limbs of Henle by bending of the tubule at the tip of Henle's loop (Oh, 2003; Kamel & Halperin, 2016).

It is now clear, however, that this sequence of events to achieve the progressive hypertonicity of the fluid in the descending thin limb of Henle is applicable only to a small fraction of the nephrons, the juxtamedullary nephrons, which represent only 15% of the total nephron population. The cortical nephrons, representing 85% of the nephron populations in humans, do not express aquaporins on the thin descending limb of Henle; therefore, those tubular segments are water impermeable. The progressive

urine concentration that occurs along the descending limb of Henle occurs instead by sodium and chloride entry. This would create a wasted effort in that sodium entering the descending limb will have to be reabsorbed again in the ascending limb, but the absence of water permeability of the descending limb of Henle allows relatively constant urine flow rates entering the distal convoluted tubule during water diuresis and antidiuresis (Kamel & Halperin, 2016).

POLYURIA

Polyuria is arbitrarily defined as urine volume in excess of 2.5 L a day. There are two types of polyuria: osmotic diuresis and water diuresis.

Osmotic Diuresis

Osmotic diuresis is defined as increased urine output due to an excessive rate of solute excretion; the commonly accepted level of solute excretion for osmotic diuresis is a rate in excess of 60 mOsm/hour or 1440 mOsm/day in the adult. Urine osmolality is usually greater than that of plasma, but it may be lower than plasma osmolality when it coexists with water diuresis. Solutes commonly responsible for osmotic diuresis are glucose, urea, mannitol, radiopaque media, and NaCl. Marked increase in urine output following the administration of a diuretic, such as intravenous furosemide, is a form of osmotic diuresis; the increased urine output is in response to increased excretion of a solute in the form of NaCl (Kamel & Halperin, 2016).

Water Diuresis

Water diuresis is characterized by excretion of a large volume of dilute urine. The polyuria is caused by reduced reabsorption of water in the collecting duct. Reasons for reduced water reabsorption in the collecting duct are lack of ADH or unresponsiveness to ADH (nephrogenic diabetes insipidus). Nephrogenic diabetes insipidus (DI) can be either congenital or acquired. Congenital nephrogenic DI is due to either a defective ADH receptor or an aquaporin defect (Kamel & Halperin, 2016; Oh, 2003).

The lack of ADH, which could be congenital or acquired, is either due to primary deficiency (central DI) or physiologic suppression by low serum osmolality (primary polydipsia, dipsogenic DI). The deficiency of ADH could be mild, moderate, or severe. When ADH deficiency is partial, urine osmolality may be fairly close to normal. In rare instances, ADH is made but cannot be released in response to a rise in body fluid osmolality because of a defect involving the osmoreceptor cells, for example, hypothalamic lesions. In such instances, ADH may be released in response to hypovolemia or to drugs. During pregnancy, ADH deficiency may be caused by excessive production of vasopressinase (gestational DI). Causes of polyuria, including central and nephrogenic DI, are listed in Box 15.5.

Primary polydipsia is defined as increased water drinking that is not caused by physiologically stimulated thirst, that is, hyperosmolality or volume depletion. Primary polydipsia is usually psychogenic in origin, hence the term *psychogenic polydipsia*. In contrast, polydipsia in patients with DI or diabetic patients with severe glycosuria is secondary polydipsia, which is due to thirst stimulation in response to hyperosmolality. In primary polydipsia, increased urine output is due to physiologic suppression of ADH secretion; hence, serum Na^+ is usually at the low range of normal. In contrast, in secondary polydipsia, as in central or nephrogenic DI, serum sodium is in the high normal range. Serum sodium is frankly low in severe primary polydipsia, indicating that the capacity of the GI tract to absorb water exceeds the capacity of the kidney to excrete water (Halperin et al., 2010)

BOX 15.5

Causes of Polyuria Due to Water Diuresis

Lack of ADH
- Central DI: congenital or acquired (idiopathic cell degeneration, tumors and granulomas, surgery, trauma, infarction, and infection of the pituitary or hypothalamus)
- Dipsogenic: psychogenic, organic brain disease, iatrogenic
- Gestational DI: excess vasopressinase

Failure of the Kidney to Respond to ADH (Nephrogenic DI)
- Congenital nephrogenic DI: defect in ADH receptor, defect in aquaporin expression
- Chronic renal failure
- Acquired nephrogenic DI: lithium toxicity, demeclocycline toxicity, methoxyflurane toxicity, amyloidosis, light chain nephropathy, hypercalcemia, hypokalemia, obstructive uropathy

ADH, Antidiuretic hormone; *DI,* diabetes insipidus

CAUSES AND PATHOGENESIS OF HYPONATREMIA (BOX 15.6)

Hyponatremia, the most common electrolyte disorder, is defined as a reduced plasma sodium concentration to a value less than 135 mEq/L. Generally, clinical concern arises when the concentration is less than 130 mEq/L.

The term *pseudohyponatremia*, as discussed in Chapter 9, is applied to a spurious reduction in serum sodium concentration due to an error in the measurement. The commonest, yet not widely appreciated, cause of pseudohyponatremia is in vitro hemolysis, a well-known cause of pseudohyperkalemia. Since cell lysis does not change osmolality of the plasma, any rise in serum potassium must be met by a reciprocal decrease in serum sodium. However, the reduction in serum Na^+ from hemolysis is somewhat greater than the increase in serum K^+ by a factor of 1.3, because hemoglobin released from the red cells causes additional reduction in serum Na^+, as in hyperproteinemia. This error occurs because hemoglobin has the same effect as hyperproteinemia in displacing plasma water. This additional error by the effect of released hemoglobin occurs only when samples are diluted before the measurement of serum sodium.

Other causes of pseudohyponatremia include hyperlipidemia, hyperproteinemia, and increased viscosity of the plasma. The error in measurement in pseudohyponatremia due to hyperproteinemia and hyperlipidemia results from the dilution of the sample. The same error occurs even when Na is measured with an ion-specific electrode when samples are diluted before the measurements. In hypergammaglobulinemia, as in multiple myeloma, low serum Na is partly false due to high protein volume and partly true as cationic charges of the protein replace Na to balance Cl (Kamel & Halperin, 2016).

Pseudohyponatremia due to high protein is most often observed in patients with multiple myeloma, and pseudohyponatremia due to hyperlipidemia is due either to high triglyceride or high cholesterol concentrations. In the latter, the cause of high cholesterol is almost always due to primary or secondary biliary cirrhosis. When high cholesterol causes hyperlipidemia-induced hyponatremia, the solid that displaces plasma water is mainly phospholipid, which is the major component of lipoprotein X (Hussain et al., 2015).

Hyponatremia induced by acute hyperglycemia is not pseudohyponatremia, since sodium concentration in the extracellular fluid is truly low; this occurs as a result of water shift from the cell caused by hyperglycemia.

BOX 15.6

Classification of Hyponatremia by Pathogenesis

Due to Renal Na^+ Loss
- Thiazide diuretics in the presence of ADH
- Saline infusion in the presence of ADH

Due to Water Retention
- Excessive water intake: primary polydipsia
- Advanced renal failure with water intake
- Appropriate ADH secretion: Edema-forming states (CHF, nephritic syndrome, ascites), salt depletion states (GI loss, diuretic therapy, aldosterone deficiency, hypothyroidism)
- Inappropriate ADH secretion
  - Tumors: Cancers of the lung, pancreas, duodenum, ureter, bladder, prostate, lymphoma, thymoma, mesothelioma, Ewing sarcoma
  - Intrathoracic causes: Bacterial and viral pneumonia, tuberculosis, lung abscess, aspergillosis, asthma, positive pressure breathing, pneumothorax, cystic fibrosis
  - CNS abnormalities: encephalitis, meningitis, brain tumors and abscess, head trauma, subdural hematoma, cerebrovascular accidents, Guillain-Barré syndrome, acute intermittent porphyria, brain atrophy, schizophrenia, hydrocephalus, acute psychosis, multiple sclerosis, cavernous vein thrombosis, lupus cerebritis, Shy-Drager syndrome, Rocky Mountain Spotted Fever, delirium tremens, seizure disorder
  - Drugs: arginine vasopressin and its analogs, sulfonylureas, tricyclic antidepressants, clofibrate, carbamazepine, vinca alkaloids, cyclophosphamide, selective serotonin reuptake inhibitors, opiates, phenothiazines, haloperidol
  - Surgical and emotional stress
  - Emesis
  - Endocrine causes: glucocorticoid deficiency and myxedema

ADH, Antidiuretic hormone; *CHF,* congestive heart failure; *CNS,* central nervous system; *GI,* gastrointestinal.

Serum sodium decreases by 1.6 mEq/L for every 100 mg/dL rise in serum glucose, as discussed earlier (Katz, 1973).

The immediate mechanisms responsible for a reduction in extracellular sodium concentration are (1) shift of water from the cell caused by accumulation of extracellular solutes, such as glucose, other than sodium salts; (2) retention of excess water in the body; (3) loss of sodium; and (4) shift of sodium into the cells. The appropriate physiologic response to hypotonicity is suppression of ADH release, which leads to rapid excretion of excess water and correction of hyponatremia. Persistence of hyponatremia therefore indicates the failure of this compensatory mechanism. In most instances, hyponatremia is maintained because the kidney fails to produce water diuresis. However, ingestion of water in excess of the limits of normal renal excretion is sometimes responsible. The reasons for inability of the kidney to excrete water include (1) renal failure, (2) reduced delivery of glomerular filtrate to the distal nephron, and (3) the inappropriate presence of ADH (Kamel & Halperin, 2016).

The mechanism for impaired water excretion in renal failure is obvious and needs no further explanation. Reduced distal delivery of filtrate results from low glomerular filtration rate and enhanced proximal tubular reabsorption of salt and water when effective vascular volume is reduced (Oh, 2003).

In most cases of hyponatremia, the main reason for the fall of serum sodium is abnormal retention of water, which is either ingested as such or administered as hypotonic fluids. However, in certain clinical settings, reduction in serum sodium can occur without the administration of hypotonic fluid. The latter phenomenon occurs when urine is excreted containing sodium and potassium at concentrations that exceed the sum of serum concentrations of the two ions. For example, if urine contains sodium at 140 mEq/L and potassium at 100 mEq/L, the combined concentration of 240 mEq/L is far greater than the sum of serum sodium and potassium. The physiologic requirement for the excretion of hypertonic urine is an increased amount of ADH in the presence of sodium diuresis. Clinical examples include (1) a patient who receives a large amount of isotonic fluid in the immediate postoperative period, (2) a patient with secretion of inappropriate antidiuretic hormone who is treated with isotonic fluid, and (3) a patient who receives a thiazide diuretic. It must be noted that development of hyponatremia with excretion of hypertonic urine occurs only when hypertonicity of urine is caused by increased excretion of sodium or potassium. Hypertonic urine by increased excretion of urea would not produce hyponatremia for obvious reasons. Loss of potassium has a very similar effect on serum sodium as loss of sodium, because loss of potassium from the cell is accompanied either by entry of sodium into the cell or exit of water from the cell in order to maintain osmotic balance and electrical neutrality.

The normal dilution of urine requires delivery of adequate amounts of fluid to the diluting segment and the reabsorption of solute without water at that segment. An increased body fluid tonicity causes release of ADH, which allows reabsorption of water in the collecting duct, helping to restore the body fluid tonicity. The response is considered appropriate when ADH is released in response to hypertonicity of the body fluid. However, release of ADH in the presence of hyponatremia is also considered appropriate if the effective vascular volume is reduced. The term, *syndrome of inappropriate ADH secretion* (*SIADH*) is therefore reserved for ADH secretion that occurs despite hyponatremia and a normal or increased effective vascular volume (Kamel & Halperin, 2016; Oh, 2003).

Causes of SIADH include tumors, pulmonary diseases such as tuberculosis and pneumonia, central nervous system diseases, and drugs (Hill et al., 1990). Hyponatremia in clinical states associated with reduced effective vascular volume, such as congestive heart failure and cirrhosis of the liver, is caused by a combination of reduced delivery of fluid to the distal nephron and increased secretion of ADH. Salt restriction and diuretics increase severity of hyponatremia. ADH secretion may be increased in the presence of hyponatremia in myxedema and glucocorticoid deficiency states. ADH secretion in these conditions, however, may be considered appropriate, since both conditions have some clinical evidence of volume depletion. Finally, mild hyponatremia may be caused by "resetting of the osmostat" at an osmolality lower than the usual level. In such cases, urine dilution occurs normally when the plasma osmolality is reduced below the reset level. Resetting of the osmostat is a form of SIADH, since ADH secretion occurs inappropriately at hyponatremic levels in the absence of reduced effective vascular volume. Patients with chronic debilitating diseases such as pulmonary tuberculosis often manifest this phenomenon (Robertson, 2006).

Some authorities believe in the existence of a cerebral salt wasting syndrome, which is defined as renal loss of salt caused by humoral substances released in response to cerebral disorders such as acute subarachnoid hemorrhage. These patients are thought to manifest volume depletion that results in hyponatremia. However, a careful analysis of the existing data does not support the existence of such an entity, and those cases labeled as cerebral salt wasting syndrome are probably cases of inappropriate ADH secretion. The one common finding of acute vascular volume depletion in the absence of bleeding is a sharp rise in hematocrit, but there is not a single case of "cerebral salt wasting syndrome" in which an acute increase in hematocrit has been well documented (Oh & Carroll, 1999; Sterns & Silver, 2008).

BOX 15.7

Causes of Hypernatremia

Reduced Water Intake
- Defective thirst due to altered mental state or thirst center defect
- Inability to drink water
- Lack of access to water

Increased Water Loss (Water Intake Must Be Impaired)
- Gastrointestinal loss: vomiting, osmotic diarrhea
- Cutaneous loss: sweating and fever
- Respiratory loss: hyperventilation and fever
- Renal loss: diabetes insipidus, osmotic diuresis

Increased Sodium Content of the Body (Water Intake Must Be Impaired)
- Increased oral or intravenous intake of sodium chloride
- Hypertonic saline or sodium bicarbonate infusion
- Ingestion of sea water
- Renal salt retention, usually in response to primary water deficit

CAUSES AND PATHOGENESIS OF HYPERNATREMIA

Hypernatremia is defined as an increased sodium concentration in plasma water and is generally diagnosed at serum sodium levels >145 mEq/L. Whereas hyponatremia may not be accompanied by hypoosmolality, hypernatremia is always associated with an increased effective plasma osmolality and hence with a reduced cell volume. However, the extracellular volume in hypernatremia may be normal, decreased, or increased.

Hypernatremia is caused by loss of water, gain of sodium, or both (Box 15.7). Loss of water could be due to increased loss or reduced intake, and gain of sodium is due either to increased intake or to reduced renal excretion. Increased loss of water can occur through the kidney (e.g., in DI or osmotic diuresis), the gastrointestinal tract (e.g., gastric suction or osmotic diarrhea), or the skin. Reduced water intake occurs most commonly in comatose patients or in those with a defective thirst mechanism. Less frequent causes of reduced water intake include continuous vomiting, lack of access to water, and mechanical obstruction to the esophagus, e.g., esophageal tumor or stricture. Gain of sodium in a conscious person does not result in hypernatremia because a proportional amount of water is retained to maintain normal body fluid osmolality as long as the person has a normal perception of thirst, is able to drink water, and has access to water. Whereas the main physiologic defense against hyponatremia is increased renal water excretion, the most effective physiologic defense against hypernatremia is increased water drinking in response to thirst. Because thirst is such an effective and sensitive defense mechanism against hypernatremia, it is virtually impossible to increase serum sodium by more than a few mEq/L if the water drinking mechanism is intact. Therefore, in a patient with hypernatremia, there will always be reasons for reduced water intake. These reasons include defective thirst mechanism, inability to drink water, and unavailability of water. The excess gain of sodium leading to hypernatremia is usually iatrogenic, for example, from hypertonic saline infusion, accidental entry into maternal circulation during abortion with hypertonic saline, or administration of hypertonic sodium bicarbonate during cardiopulmonary resuscitation or treatment of lactic acidosis. Reduced renal sodium excretion leading to sodium gain and hypernatremia is usually in response to volume depletion caused by primary water deficit. Water depletion due to DI, osmotic diuresis, or insufficient water intake leads to secondary sodium retention through volume-mediated activation of sodium-retaining mechanisms. Consequently, in chronic hypernatremia, sodium retention plays a more important role than water loss. Of course, net sodium retention is possible only if sodium is ingested or administered (Oh, 2003; Kamel & Halperin, 2016).

Whether hypernatremia is due to sodium retention or water loss can be determined by examination of the patient's volume status. For example, if a patient with a serum sodium concentration of 170 mEq/L had no obvious evidence of dehydration, one must conclude that hypernatremia is caused by water loss as well as salt retention. Increasing the serum sodium to 170 mEq/L by water deficit alone would require loss of more than 20% of total body water.

ACID-BASE DISORDERS

BICARBONATE AND CO_2 BUFFER SYSTEM

All body buffers are in equilibrium with protons (H^+) and therefore with pH, as shown in the following equation (Siggaard-Andersen, 2006; Shafiee, Kamel & Halperin, 2002):

$$pH = pK + \log A^- / HA, \text{ where } A^- \text{ is a conjugate base of an acid HA.} \quad \text{(Eq. 15.26)}$$

Because HCO_3^- and CO_2 are the major buffers of the body, pH is typically expressed as a function of their ratio and shown in the Henderson-Hasselbalch equation:

$$pH = 6.1 + \log HCO_3^- / pCO_2 \times 0.03, \quad \text{(Eq. 15.27)}$$

where 6.1 is the pK of the HCO_3^- and CO_2 buffer system and 0.03 is the solubility coefficient of CO_2 at the normal body temperature.

The equation can be further simplified by combining the 2 constants, pK and solubility coefficient of CO_2:

$$pH = 6.1 + \log HCO_3^- / pCO_2 \times 0.03 = 6.1 + \log 1/0.03 + \log HCO_3^- / pCO_2 = 7.62 + \log HCO_3^- / pCO_2 \text{ (Carroll, 1989).}$$

Hence,

$$pH = 7.62 - \log pCO_2/HCO_3^- = 7.62 + \log HCO_3^- - \log pCO_2. \quad \text{(Eq. 15.28)}$$

When H^+ is expressed in nM instead of a negative log value (pH), pCO_2 can be related to HCO_3^- in the following equation:

$$H^+ \text{ (nM)} = 24 \times pCO_2 \text{ (mmHg)} / HCO_3^- \text{ (mM)} \quad \text{(Eq. 15.29)}$$

The Henderson-Hasselbalch equation indicates that pH depends on the ratio of HCO_3^-/pCO_2. pH increases when the ratio increases (alkalosis), and pH decreases when the ratio decreases (acidosis). The ratio may be increased by an increase in HCO_3^- (metabolic alkalosis) or by a decrease in pCO_2 (respiratory alkalosis). The ratio may be decreased by a decrease in HCO_3^- (metabolic acidosis) or by an increase in pCO_2 (respiratory acidosis).

DEFINITIONS OF ACID AND BASE

Arrhenius's definition: an acid is a substance that increases the concentration of hydrogen ion (H^+) when dissolved in water and a base is a substance that increases the concentration of hydroxyl ion (OH^-) when dissolved in water (Kamel et al., 2012). Bronsted and Lowry's definition: an acid is a substance that donates a proton in a chemical reaction, while a base is a substance that accepts a proton in a chemical reaction. Lewis's definition: an acid is a molecule or ion that accepts a pair of electrons to form a covalent bond, and a base is a molecule that donates a pair of electrons for a covalent bond. The definition of Bronsted-Lowry is the most widely accepted and most relevant clinically.

WHOLE BODY ACID-BASE BALANCE

Metabolic acidosis occurs either because net acid production is increased or net acid excretion is reduced. Because a typical modern diet results in net acid production, the normal function of the kidney is to excrete acid in order to remain in acid-base balance. For these reasons, proper understanding of disorders of acid-base balance requires the knowledge of the sources of acid production as well as the mechanisms by which acids are disposed of.

Net Acid Production

On a typical American diet, the daily production of nonvolatile acid is about 90 mEq/day. The main acids are sulfuric acid (about 40 mEq/day), which originates from metabolism of sulfur-containing amino acids such as methionine and cysteine and incompletely metabolized organic acids (about 50 mEq/day). The source of sulfuric acid is protein, but the sulfate content varies greatly with the types of protein that are ingested. In general, proteins of animal sources (meat, fish, milk, and egg) have higher amounts of sulfur-containing amino acids for a given amount of protein than proteins of plant origin (cereal, beans, and nuts). The sulfur content is much greater in fruits, vegetables, and potatoes, but these food groups are not important sources of protein in the amounts usually eaten. The total amount of acid/alkali content depends not only on the sulfur content but also on the alkali content of food, which is present mainly as salts of organic acids. When both factors are considered, milk has a net alkali value, whereas meat and fish have a net acid value. As a whole, fruits and vegetables contain a large amount of net alkali because they contain large amounts of organic anions. The total amount of organic acids produced normally is much more than 50 mEq/day, but the bulk of organic acids produced in the body is metabolized; only a small amount is lost in the urine as organic anions that escape metabolism (e.g., citrate) or as a metabolic end product (e.g., urate). On typical American diets, the amount of alkali absorbed from the GI tract is about 30 mEq/day (Oh, 1989; Uribarri et al., 1995). Thus, the net amount of acid produced daily can be estimated as

$$\text{Net acid production} = (\text{urine sulfate} + \text{urine organic anions}) - \text{net alkali absorbed from GI tract} \quad \text{(Eq. 15.30)}$$

An assumption in the use of Equation 15.30 has been that urinary sulfate originates entirely from the metabolism of sulfur-containing amino acids via sulfuric acid. This assumption is not entirely accurate in view of the fact that the modern diet contains a fair amount of oxidized sulfur in the form of sulfate additives, such as in wine (Florin, 1991). Thus, measurement of net acid excretion by Equation 15.30 would slightly overestimate net acid production.

Determination of the net alkali (or acid) content of diet is based on the metabolic fates of the chemicals in the diet after absorption into the body rather than its in vitro states. For example, citric acid in food is considered neutral, because it would be metabolized to CO_2 and water in the body, whereas K^+ citrate is an alkali because it would be converted to K^+ bicarbonate after metabolism. Similarly, arginine Cl^- is an acid, because metabolism of arginine in the body would result in the formation of HCl (Lemann, 1959). Thus, net alkali value of the diet is best determined by the total amount of noncombustible cations (Na^+, K^+, Ca^{++}, and Mg^{++}) in comparison with the total amount of noncombustible anions (Cl^- and P):

$$\text{Net alkali content} = (Na^+ + K^+ + Ca^{++} + Mg^{++}) - (Cl^- + 1.8\,P). \quad \text{(Eq. 15.31)}$$

All units are expressed as mEq/day except for P, which is expressed as mmol/day multiplied by 1.8, because phosphate valence depends on pH, and at pH 7.4 the average valence of phosphate is 1.8. Only the above 6 ions are considered in the equation because other noncombustible ions are present in negligible amounts in normal food. Sulfate is not included here because sulfate is derived almost entirely from the metabolism of sulfur-containing amino acids and not ingested as such. The amount of alkali absorbed from food is not equal to the amount present in food, because the absorption of divalent noncombustible ions, Ca^{++}, Mg^{++}, and P, is incomplete. Hence, traditionally, the measurement of the net GI alkali absorption required analysis of food as well as stool, which necessitated prolonged collection of stool (Goodman et al., 1965; Oh, 1989). Thus, the net GI alkali absorption is expressed as

$$\text{Net GI alkali absorbed} = \text{net alkali of food} - \text{net alkali of stool.} \quad \text{(Eq. 15.32)}$$

The analysis of food for the measurement of net alkali content is cumbersome and analysis of stool is even more cumbersome. Such analyses typically require admitting patients to a special metabolic unit. An alternative method has been developed to measure net GI alkali absorption. In this method, urine electrolytes are measured instead of diet and stool electrolytes. The method is based on the principle that noncombustible ions absorbed from the GI tract would eventually be excreted in the urine and therefore that the individual amounts of these electrolytes excreted in the urine would equal those absorbed from the GI tract. Hence,

$$\text{Net GI alkali absorption} = \text{urine } (Na^+ + K^+ + Ca^{++} + Mg^{++}) - \text{urine } (Cl^- + 1.8\,P). \quad \text{(Eq. 15.33)}$$

Twenty four hour urine can be collected in outpatient settings while the subjects are eating their usual diets. The amount of net alkali absorbed on a typical American diet stated earlier, 30 mEq/day, was measured by the analysis of urine electrolytes using the Equation 15.33. An assumption in this equation as well as the diet and stool analysis of net alkali content has

BOX 15.8

Causes of Metabolic Acidosis According to Net Acid Excretion

Renal Acidosis: Absolute or Relative Reduction in Net Acid Excretion
- Uremic acidosis
- Renal tubular acidosis
- Distal renal tubular acidosis (type I)
- Proximal renal tubular acidosis (type II)
- Aldosterone deficiency or unresponsiveness (type IV)

Extrarenal Acidosis: Increase in Net Acid Excretion
- Gastrointestinal loss of bicarbonate
- Ingestion of acids or acid precursors: ammonium chloride, inorganic sulfur or sulfur-containing compounds
- Acid precursors or toxins: salicylate, ethylene glycol, methanol, toluene, acetaminophen, paraldehyde
- Organic acidosis
- L-lactic acidosis
- D-lactic acidosis
- Ketoacidosis
- Pyroglutamic acidosis

been that only 6 electrolytes are nonmetabolizable electrolytes contained in the normal diet, and the presence of sulfate in the diet would therefore result in overestimation of net alkali content of the diet. However, the overestimation of net acid production by ignoring dietary sulfate would be exactly equal to the overestimation of net alkali content of the diet by ignoring dietary sulfate content. The overall whole body acid-base balance would not be affected by the presence of dietary sulfate.

Net Acid Excretion

The most important function of the kidney in acid-base homeostasis is excretion of acid, which is tantamount to generation of alkali. Acid is excreted in the form of NH_4^+ and titratable acid. Another important function of the kidney is excretion of HCO_3^-. Usually, the main function of renal excretion of HCO_3^- is prevention of metabolic alkalosis, but a small amount of bicarbonate is normally excreted in the urine (about 10 mEq/day). Thus, net acid excretion, which is tantamount to net renal production of alkali, can be determined by subtracting HCO_3^- excretion from acid excretion (Uribarri et al., 1995; Relman, 1959).

$$\text{Net acid excretion} = NH_4^+ + \text{titratable acid} - HCO_3^-. \quad \text{(Eq. 15.34)}$$

Normally, about two-thirds of acid excretion occurs in the form of NH_4^+, but in severe acidosis NH_4^+excretion may increase as much as 10-fold. Excretion of titratable acid is usually modest because of the limited amount of buffer that produces titratable acid, that is, phosphate, creatinine, and urate, but may be increased markedly in disease states, for example, beta-hydroxybutyrate in diabetic ketoacidosis. Maintenance of acid-base balance requires that net acid production equals net acid excretion. Metabolic acidosis develops when net acid production exceeds net acid excretion, and metabolic alkalosis develops when net acid excretion exceeds net acid production.

METABOLIC ACIDOSIS

Classification

All metabolic acidoses result from reduction in bicarbonate content of the body with two minor exceptions: acidosis resulting from dilution of the body fluid by administration of a large amount of saline solution that does not contain alkali (dilution acidosis) and acidosis that results from the shift of H^+ from the cell. Reduction in bicarbonate content may be due to a primary increase in acid production (extrarenal acidosis) or due to a primary reduction in net acid excretion (renal acidosis; Box 15.8). In this classification, nonrenal loss of bicarbonate or an alkali precursor is considered as part of increased acid production. In extrarenal acidosis, net acid excretion is increased as the kidney compensates to correct the acidic pH. On the other hand, net acid excretion may be restored to normal in chronic renal acidosis as acidosis stimulates renal H^+ excretion. Normal net acid excretion in the presence of acidic pH suggests a defect in renal acid excretion and therefore renal acidosis. If the renal acid excretion capacity is normal, net acid excretion would be increased in the presence of extrarenal acidosis (Oh, 2003).

Renal Acidosis

Renal acidosis is further classified into 2 types: uremic acidosis and RTA. In uremic acidosis, reduced net acid excretion results from reduced nephron mass or generalized renal dysfunction, that is, chronic or acute renal failure. In RTA, reduction in net acid excretion results from a specific tubular dysfunction in acid excretory function. Because development of renal acidosis depends on the rate of net acid excretion as well as the rate of net acid production, and the latter varies greatly according to the diet of individuals, the level of renal failure at which uremic acidosis develops depends on the dietary intake of acid. On a usual diet, uremic acidosis typically develops when GFR falls below 20% of normal.

There are 3 types of RTA. Type I RTA, also called *classical RTA* or *distal RTA*, is characterized by inability to reduce urine pH below 5.5. Since acidification of urine to a very low urine pH occurs at the collecting duct, the site of defect is the collecting duct, which is a part of the distal nephron, hence the term *distal RTA*. Because H^+ secretion in the collecting duct is also impaired in type IV RTA, some authors consider both type I and type IV RTA a form of distal RTA. More often, the terms *type I RTA* and *distal RTA* are used synonymously. Type I RTA can develop as a primary disorder or secondary to drug toxicity, tubulointerstitial renal diseases, or other renal diseases (Shafiee et al., 2002).

Type II RTA, also called *proximal RTA*, has defective proximal bicarbonate reabsorption characterized by reduced renal bicarbonate threshold. Urine can be made free of bicarbonate and acidified normally when serum bicarbonate decreases to a sufficiently low level. Most patients with proximal RTA have evidence of generalized proximal tubular dysfunction, that is, Fanconi syndrome, which is manifested by bicarbonaturia, aminoaciduria, glycosuria, phosphaturia, and uricosuria. Of these, renal glycosuria (glycosuria in the presence of normal blood glucose) is most useful in diagnosing Fanconi syndrome. Type II RTA may be a primary disorder or secondary to genetic or acquired renal dysfunction. A common cause of type II RTA at present is toxicity from antiretroviral drugs. Hypokalemia is a characteristic finding of both type I and type II RTA but tends to be more severe in type I. The mechanism of hypokalemia in chronic metabolic acidosis was discussed earlier in potassium disorders. *Type III RTA*, a term describing a hybrid form of types I and II RTA, is no longer in use.

Type IV RTA is caused by aldosterone deficiency or tubular unresponsiveness to aldosterone, resulting in impaired renal tubular potassium secretion and hence hyperkalemia. Although reduced H^+ secretion in the collecting duct plays some role, the major mechanism of acidosis in type IV RTA is hyperkalemia-induced suppression of ammonia production in the proximal tubule. Type IV RTA is far more common than either type I or type II RTA, and the most common cause of type IV RTA is hyporeninemic hypoaldosteronism. Diabetic nephropathy is the most common cause of hyporeninemic hypoaldosteronism leading to type IV RTA (Phelps et al., 1980).

Organic Acidosis

Among external causes of acidosis, overproduction of endogenous acids, especially lactic acid and ketoacids, is the most important mechanism. Only a marked overproduction, well in excess of 1000 mEq/day of lactic acid, leads to acidosis because of the enormous capacity to metabolize organic acids. When organic acids react with bicarbonate, organic anions and CO_2 are formed. Retention of organic anions results in increased anion gap. The retained organic anions are potential bicarbonate; when they are metabolized, bicarbonate is regenerated. However, renal excretion of organic anions results in hyperchloremic acidosis with a normal anion gap. Thus, loss of organic anions in the urine is tantamount to loss of bicarbonate. If an organic anion produced from organic acid is entirely retained, subsequent metabolism of the entire amount will result in the complete recovery of the lost alkali. Characteristically, organic acidosis is rapid in onset and in recovery (Halperin, 1977).

Lactic Acidosis. Lactic acid is produced from pyruvic acid by the action of the enzyme LDH and the cofactor NADH. Metabolism of lactic acid requires its conversion back to pyruvic acid using the same enzyme and NAD^+ as a cofactor. For this reason, both production and metabolism of lactic acid depends on the same enzyme but different cofactors, NADH for the former and NAD for the latter. Increased concentration of pyruvic acid and increased ratio of NADH/NAD^+ increase lactic acid production and reduce its metabolism. Consequently, in most cases of lactic acidosis, lactic acid production is increased while its metabolism is reduced. By far the most common cause of lactic acidosis is tissue hypoxia, which results from circulatory shock, severe anemia, severe heart failure, acute pulmonary edema, cardiac arrest, carbon monoxide poisoning, seizures, vigorous muscular exercise, and more. Lactic acidosis in the absence of tissue hypoxia is called *type B lactic acidosis*, whereas that associated with tissue hypoxia is called *type A lactic acidosis*. Currently, two most common causes of type B lactic acidosis are antiretroviral drugs and metformin. Impaired metabolism of lactic acid is the cause of lactic acidosis in acute alcoholism and severe liver disease (Box 15.9) (Halperin & Kamel, 1996).

BOX 15.9

Causes of L-Lactic Acidosis

Type A Lactic Acidosis: Due to Tissue Hypoxia
- Circulatory shock
- Severe hypoxemia
- Heart failure
- Severe anemia
- Grand mal seizure

Type B Lactic Acidosis: No Tissue Hypoxia
- Acute alcoholism
- Drugs and toxins, e.g., metformin, antiretroviral drugs, salicylate intoxication
- Diabetes mellitus
- Leukemia
- Deficiency of thiamin or riboflavin
- Idiopathic

BOX 15.10

Classification of Metabolic Acidosis by Anion Gap

Metabolic Acidosis with Increased Anion Gap (Normochloremic Acidosis)
- Ketoacidosis
- L-Lactic acidosis
- D-Lactic acidosis
- Beta-hydroxybutyric acidosis
- Uremic acidosis
- Ingestion of toxins: salicylate, methanol, ethylene glycol, acetaminophen

Metabolic Acidosis with Normal Anion Gap (Hyperchloremic Acidosis)
- Renal tubular acidosis
- Uremic acidosis (early)
- Acidosis following respiratory alkalosis
- Intestinal loss of bicarbonate
- Administration of chloride-containing acid: HCl, NH_4Cl
- Ketoacidosis during recovery phase
- Toluene intoxication (occasionally, it causes high anion gap acidosis)

D-Lactic Acidosis. Lactic acidosis, unless specified, refers to acidosis caused by L-lactic acid, which is the isomer produced in the human body because the enzyme LDH is L-isomer specific. The accumulation of D-lactic acid causes D-lactic acidosis. The condition is characterized by severe acidosis accompanied by neurologic manifestations such as mental confusion and staggering gait, mimicking ethanol intoxication without elevated plasma levels of ethanol. The mechanism of D-lactic acidosis is the colonic overproduction of D-lactic acid by bacteria. Necessary requirements for overproduction of D-lactic acid in the colon are delivery of a large amount of carbohydrate to the colon, that is malabsorption syndrome, and proliferation of D-LDH-forming bacteria in the colon. Treatment of D-lactic acidosis includes oral administration of poorly absorbable antibiotics such as neomycin and measures to alter the colonic bacterial flora.

Other causes of D-lactic acidosis include propylene glycol poisoning and diabetic ketoacidosis. In the former, propylene glycol is converted to methylglyoxal, which is further converted to D-lactic acid. The mechanism of D-lactic acid production in diabetic ketoacidosis is not entirely clear (Oh et al., 1979; Uribarri et al, 1998; Halperin & Kamel, 1996).

Ketoacidosis. Keto acids, acetoacetic acid, and beta-hydroxybutyric acid are produced in the liver from free fatty acids (FFAs) and metabolized by the extrahepatic tissues, especially by the brain. Increased production of keto acids is the main mechanism for keto acid accumulation, although decreased utilization of keto acids by the brain with the patient in a coma may accelerate keto acid accumulation. Increased production requires a high concentration of FFA and its conversion to keto acids in the liver. Insulin deficiency is responsible for increased mobilization of FFA from the adipose tissue, and glucagon excess and insulin deficiency stimulate conversion of FFA to keto acids in the liver. The initial step in keto acid production from FFA is the entry of FFA into the mitochondria, which requires acyl-carnitine transferase. This step is stimulated by glucagon excess. The next step is metabolism of FFA to acetyl coenzyme A (acetyl-CoA), and finally to keto acids. Diversion of acetyl-CoA to fatty acid resynthesis requires the enzyme acetyl-CoA carboxylase. Inhibition of this enzyme by insulin deficiency, glucagon excess, and excess of stress-induced hormones such as catecholamines further contributes to increased keto acid synthesis. Consumption of medium-chain fatty acids, for example, goat milk, results in ketoacidosis even in the presence of insulin, because entry of medium-chain fatty acids into the mitochondria does not require carnitine (Davids et al., 2004).

The clinical diagnosis of ketoacidosis is usually made with Acetest, which detects acetoacetate (AA) but not beta-hydroxybutyrate (BB). Although BB is the predominant acid in typical ketoacidosis (the usual ratio of BB/AA is about 2.5–3.0), the reaction to Acetest represents a fair estimate of the total concentration of ketoacids as long as the ratio remains within a usual range. When the ratio of BB/AA is greatly increased, Acetest may be negative or only slightly positive despite retention of a large amount of total ketones in the form of BB. This condition is called *beta-hydroxybutyric acidosis*, which is commonly seen in alcoholic ketoacidosis (Halperin et al., 1983).

Differential Diagnosis

One approach to the differential diagnosis of metabolic acidosis is to calculate the serum anion gap. The increased anion gap suggests organic acidosis, uremic acidosis, and acidosis due to various toxic alcohols (Box 15.10). The normal anion gap suggests RTA and acidosis due to diarrheal loss of bicarbonate. Most cases of uremic acidosis are accompanied by a normal anion gap; only in advanced chronic and acute renal failure is the anion gap increased. Furthermore, the vast majority of patients with ketoacidosis pass through a phase of hyperchloremic acidosis (normal anion gap) during the recovery phase (Oh et al., 1978).

Another approach to the differential diagnosis of metabolic acidosis is to classify it into renal and extrarenal acidosis. Three major causes of extrarenal acidosis are organic acidosis, diarrheal loss of bicarbonate, and acidosis due to exogenous toxins. The presence of organic acidosis is usually obvious from clinical findings, for example, evidence of tissue hypoxia in lactic acidosis, or hyperglycemia, ketonuria, and ketonemia in ketoacidosis. History of drug ingestion and acute onset suggests acidosis due to exogenous toxins (Oh, 2003).

Diarrhea as the cause of metabolic acidosis is first suspected from history, but history is often misleading because the severity of diarrhea cannot be easily determined. The measurement of urine anion gap is useful in determining the severity of diarrhea. The urine anion gap, which is measured as urine ($Na^+ + K^+$) – urine Cl^-, is reduced or negative when diarrhea is severe. The low urine anion gap in diarrhea is explained by the preferential loss of $Na^+ + K^+$ in excess of Cl^- because diarrheal fluid contains more $Na^+ + K^+$ than Cl^-, as some of these cations are balanced by bicarbonate and organic anions. In other types of metabolic acidosis, the urine anion gap is not altered as long as there is no extrarenal loss of electrolytes that are components of the urine anion gap (Oh & Carroll, 2002).

Once extrarenal acidosis is excluded, renal acidosis is the only alternative diagnosis. Of the two types of renal acidosis, uremic acidosis can be readily ruled out by normal values of serum creatinine and BUN. If renal acidosis is confirmed but uremic acidosis is ruled out, the diagnosis must be RTA. Among the 3 types of RTA, type IV RTA is suspected by the presence of hyperkalemia. Hypokalemia suggests either type I or type II RTA. If spontaneous urine pH is below 5.5, type I RTA is ruled out. If urine pH is higher than 5.5, urine pH should be measured after oral administration of 40 mg of furosemide or 10 mg of torsemide. The latter drug has higher sensitivity and specificity. If the urine pH remains above 5.5, the likely diagnosis is type I RTA. The evidence of Fanconi syndrome (the best evidence is renal glycosuria) suggests type II RTA (Fogh-Andersen et al., 1995).

Serum Anion Gap (AG)

Serum anion gap is estimated as $Na^+ - (Cl^- + HCO_3^-)$ or $(Na^+ + K^+) - (Cl^- + HCO_3^-)$. Since normal serum potassium concentration is quantitatively a minor component of serum electrolytes, the fluctuation in its concentration has a minor effect on the overall result. Hence, the first of the two equations is more commonly used to estimate the anion gap. The normal value is about 12 mEq/L (8–16 mEq/L). Although the term *anion gap* implies that there is a gap between cation and anion concentrations, the total concentration of all cations in the serum is exactly equal to the total concentration of all anions. The anion gap, $Na^+ - (Cl^- + HCO_3^-)$, is 12 mEq/L because the total concentration of unmeasured anions (i.e., all anions other than chloride and bicarbonate) is about 23 mEq/L, and the total concentration of unmeasured cations (i.e., all cations other than sodium) is about 11 mEq/L (Kraut & Madias, 2007; Oh & Carroll, 1977).

Let us assume that total serum cations = Na^+ + unmeasured cations (UCs), and that total serum anions = $Cl^- + HCO_3^-$ + unmeasured anions (UAs). Since total serum cations = total serum anions, Na^+ + UC = $(Cl^- + HCO_3^-)$ + UA. Hence, Na+ – $(Cl^- + HCO_3^-)$ = UA – UC. Since the anion gap = $Na^+ - (Cl^- + HCO_3^-)$, the anion gap = UA – UC (Fig. 15.5).

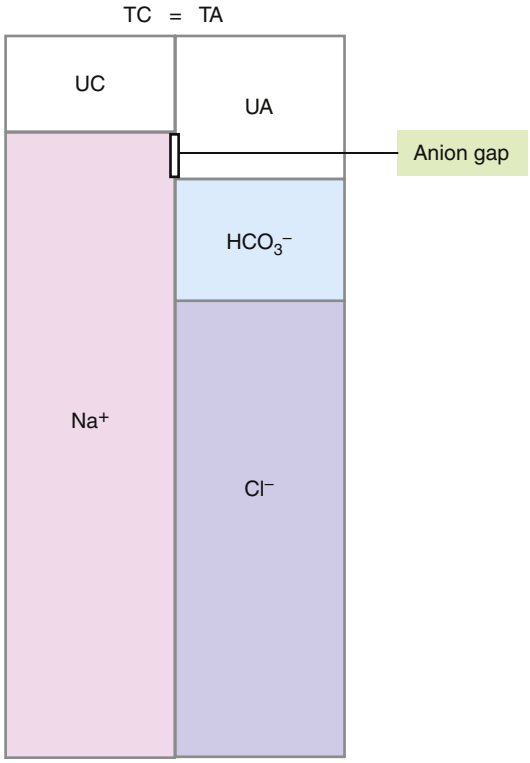

Figure 15.5 The anatomy of the anion gap. When an unmeasured cation (UC) is defined as all serum cations other than Na, and unmeasured anion (UA) as all serum anions other than Cl or bicarbonate, the serum anion gap can be stated as UA minus UC.

It is apparent that a change in the anion gap must involve changes in unmeasured anions or unmeasured cations unless there is a laboratory error involving the measurement of Na^+, Cl^-, or HCO_3^-. The anion gap can be increased by increased UA or decreased UC or by a laboratory error resulting in a false increase in serum Na^+ or a false decrease in serum Cl^- or HCO_3^-. AG can be decreased by decreased UA or increased UC or by a laboratory error resulting in a false decrease in serum Na^+ or a false increase in serum Cl^- or HCO_3^-. The equation also predicts that a change in UA may not change AG if UC is also changed by the same extent in the same direction (Halperin et al., 1988; Oh & Carroll, 2002).

A decreased AG is most commonly due to reduction in serum albumin concentration, while an increased AG is most often due to accumulation of anions of acids, such as sulfate, lactate, and ketone anions. Although bromide is an unmeasured anion, bromide intoxication is accompanied by a low serum anion gap because bromide causes a false increase in serum Cl^-. A change in serum Na^+ usually does not cause a change in AG because serum Cl^- usually changes in the same direction. For the same reason, HCO_3^- concentrations cannot be used to predict a change in AG. For example, when the serum HCO_3^- concentration increases in metabolic alkalosis, Cl^- concentration usually decreases reciprocally in order to maintain electrical neutrality so that the anion gap is unchanged. When the HCO_3^- concentration decreases, the Cl^- concentration may remain unchanged or be increased. If bicarbonate is replaced by another anion, the Cl^- concentration remains unchanged, resulting in normochloremic acidosis with an increased anion gap. Examples are organic acidosis, uremic acidosis, and acidosis due to toxic alcohols. When bicarbonate concentration decreases without another anion replacing it, electrical neutrality is maintained by a higher Cl^- concentration, resulting in hyperchloremic acidosis with a normal anion gap. Proper interpretation of the serum anion gap requires the knowledge of existence of conditions that influence the anion gap even though they may have no direct effect on metabolic acidosis. For example, if a person with hypoalbuminemia develops lactic acidosis, the anion gap could be normal because the low albumin and the lactate accumulation have opposite effects on the anion gap. Similarly, hypermagnesemia (increased unmeasured cation) does not decrease the anion gap if it is accompanied by increased sulfate (unmeasured anion), as in magnesium sulfate intoxication. Sometimes, the anion gap is increased with magnesium sulfate intoxication because the increase in sulfate exceeds the increase in magnesium. The likely explanation is that sulfate, being mainly an extracellular electrolyte, has a smaller volume of distribution than magnesium, which has a higher concentration in the cell than in the ECF.

It has been suggested that in pure high anion gap metabolic acidosis, the decrease in serum bicarbonate is about equal to the increase in serum anion gap. A concentration of serum bicarbonate higher than expected has been taken as evidence for the presence of complicating metabolic alkalosis. However, this rule often does not apply in individual cases (Oh, 2003).

Arguments Against Strong Ion Difference and Buffer Base

The term *strong ion difference* was first introduced by Peter Stewart in 1978 (Stewart, 1978). However, essentially the same concept was introduced in 1948 by Singer and Hastings with a different nomenclature: *buffer base* (Singer & Hastings, 1948). According to Singer and Hastings, base is any cation and hence buffer bases are cations balanced by buffering anions, which have the same meaning as weak anions of Stewart, which participate in buffering of acids. Stewart as well as Singer and Hastings assumed that normal plasma contained only strong cations and no weak cations. In contrast, anions in plasma exist either as strong anions or weak anions (buffering anions). Hence, strong ion difference, which is defined as strong cations minus strong anions, is, in fact, mathematically identical to buffer base, which has the same meaning as weak anions of Stewart. Since all cations are either strong cations or weak cations, and all anions are either strong anions or weak anions, strong ion difference must equal weak ion difference. In the absence of strong cations, strong ion difference then equals weak anions, which is identical to the buffer base of Singer and Hastings (Singer & Hastings, 1948).

Perhaps because of this confusing definition of the term *base*, the concept of buffer base is rarely used in modern discussions of clinical acid-base disorders. In contrast, the concept of *strong ion difference*, perhaps because it is a catchy term, has received a renewed interest recently after a period of dormancy. The concept is particularly popular among those who specialize in critical care medicine, anesthesia, surgery, and emergency medicine. In the past several years, while some articles were critical of its merits (Adrogué et al., 2009; Siggaard-Andersen & Fogh-Andersen, 1995), many more articles have appeared in respectable journals praising its value (Kellum, 2007; Seifter, 2014; Berend et al., 2014; Morgan, 2011).

Our overall assessment of strong ion difference is strongly negative. We believe that it has a few limited values but has many more flaws. The use of the concept in understanding and diagnosis of acid-base disorders is accompanied by unnecessary complexities with limited usefulness. The purpose of this review is to list major flaws of the concept, with the ultimate aim of persuading the medical community to stop using the concept. The same basic flaws are applicable to the concept of buffer base, but since the latter is hardly used in discussions of acid-base disorders at present, we shall limit our discussion to strong ion difference.

According to Stewart and his followers, all electrolytes in plasma are either strong or weak electrolytes. Strong electrolytes remain fully, or almost fully, dissociated within usual ranges of physiologic pH and do not participate in acid-base buffering. Hence, their concentrations are not affected by addition of acid or alkali. In contrast, weak electrolytes are not fully dissociated and their concentrations vary with changes in blood pH. In order to maintain electrical neutrality, total cations of plasma must equal total anions of plasma. Since all cations of plasma exist either as a strong cation or a weak cation, while all anions of plasma must be either a strong anion or weak anion, total strong cations + total weak cations = total strong anions + total weak anions.

According to Stewart, strong cations of plasma are Na, K, Ca, and Mg, whereas strong anions of plasma are Cl, sulfate, and organic anions, most notably lactate. Stewart believes that plasma contains no weak cations but contains 3 weak anions—bicarbonate, plasma proteins (mainly albumin), and phosphate. Thus, strong ion difference is expressed as (Na + K + Ca + Mg) – (Cl + lactate + sulfate). Since strong ion difference must equal weak ion difference, and weak ion difference equals plasma weak anions, as no weak cations exist. Hence, strong ion difference = (Na + K + Ca + Mg) – (Cl + lactate + sulfate) = (HCO_3^- + plasma proteins + phosphate). This assumes that the sum of Ca and Mg is about equal to the sum of all normal organic anions plus sulfate. Strong ion difference (SID) is then further simplified as

$$\text{SID} = \text{Na} + \text{K} - \text{Cl} = \text{proteins} + \text{bicarbonate} + \text{phosphate}.$$

The following is the list of objections for the definition, characterization, and classification of strong ion difference.

1. Many so-called strong cations of plasma are actually weak cations.
   a. In normal plasma, about 50% of Ca is complexed to protein and other anions. In the duodenum, where pH is as high as 8.0, much of calcium is complexed to carbonate. Thus, characterization of Ca as a strong ion is in error.

b. Similarly, about one third of plasma Mg is bound to plasma proteins, and in the small intestine, the concentration of carbonate is sufficiently high to form $MgCO_3$ as insoluble complexes. Hence, Mg is not a true strong cation.

2. Plasma protein has about 15 mEq/L of net negative charges, which is almost entirely due to greater amounts of anionic amino acids (glutamate and aspartate) than the amounts of cationic amino acids (lysine and arginine). The buffering capacity of plasma proteins is not due to these anionic amino acids but rather due mainly to histidine. Histidine exists either as a cation or a neutral substance. The buffering effect of plasma proteins comes from neutral histidine, not from anionic charges of amino acids. Hence, plasma proteins are not weak anions but rather strong anions, and contain some weak cations in the form of cationic histidine. It is an unfortunate accident of nature that the approximate net charge difference of plasma proteins was approximately equal to the buffering capacity of plasma proteins. This coincidence allowed designation of plasma proteins as weak organic acids.
3. All organic anions are considered strong anions according to Stewart, but only plasma lactate is included in the calculation of strong ion difference despite the fact that the sum of all other organic anions is far greater than lactate.
4. The existence of hypoalbuminemic alkalosis (Morgan, 2011) and hyperalbuminemic acidosis has not been proven to exist, and their existence is theoretically untenable. Those who advocate the use of a separate category of hypoalbuminemic alkalosis assumed that unchanged strong difference must be accompanied by unchanged weak ion difference. It is further reasoned that if the total weak anion remains the same, a lower albumin anion concentration must be accompanied by a higher bicarbonate concentration, hence hypoalbuminemic metabolic alkalosis. That is not what actually happens in reality. Since protein's charge difference is made mainly by the difference between cationic amino acids (lysine and arginine, total 83) and anionic amino acids (glutamate and aspartate, total 98), one may predict that the metabolism of albumin would result in net production of alkali. However, the magnitude of rise in bicarbonate would be quite meager because the entire plasma contains a mere 30 mmol of net charge difference in favor of anionic amino acids in 5 L of blood. Actually, the catabolism of albumin will result in a net gain of acid because each albumin molecule contains 41 molecules of cysteine plus methionine, which will collectively produce 82 mEq of sulfuric acid. Hence, albumin loss by catabolism will result in a net gain of a huge amount of acids, producing metabolic acidosis. Likewise, with renal loss of albumin as in nephrotic syndrome, there will be little increase in bicarbonate concentration, as the reduced negative charges due to albumin loss would be compensated mostly by the increased chloride concentration.
5. The use of a complex exponential formula to estimate changes in negative charges of plasma proteins and phosphate caused by abnormal pH is based on the assumption that changes in strong ion difference and in anion gap are due entirely to buffering of proteins and phosphate charges in response to abnormal pH. In reality, those changes are more due to changes in concentrations of organic acids. For example, in a dog experiment by Adrogué et al., in metabolic acidosis with serum bicarbonate of 10 mEq/L, the anion gap decreased by 5 mEq/L; in metabolic alkalosis with serum bicarbonate of 40 mEq/L, the anion gap increased by 8 mEq/L. Protein charge variation explained less than 20% of changes in total charge variations.
6. When total inorganic phosphate in plasma is kept constant, a charge difference due to changes in pH is quite negligible—far less than the usual ranges of error in serum Na measurements. Since errors in Na measurement are about 1% and errors in Cl measurement are around 1.5%, variations in concentrations of Na and Cl would be several mEq/L. In contrast, at a plasma phosphate concentration of 1.2 mmol/L, concentrations in mEq/L would be 2.16 mEq/L at pH 7.4 and 2 mEq/L at pH 7.1, a difference of a mere 0.16 mEq/L.
7. When protein buffers participate in buffering acids, net positive charges change (strong ion difference decrease), not because net negative charges of proteins decrease, but because net positive charges of proteins increase. Of course, effects on the strong ion difference calculation would be identical, but the statements and assumptions are factually wrong.

Compensation

Compensation of metabolic acidosis is achieved by hyperventilation, which results in decreased pCO_2. Compensation is moderately effective in restoring normal pH; maximal compensation is completed within 12 to 24 hours.

BOX 15.11

Mechanisms and Causes to Increase Extracellular Bicarbonate Concentration

- Loss of HCl from the stomach, e.g., gastric suction, vomiting
- Administration of bicarbonate or bicarbonate precursors, e.g., sodium lactate, sodium acetate, sodium citrate
- Shift of H^+ into the cell, e.g., K^+ depletion refeeding alkalosis
- Rapid contraction of extracellular volume without loss of bicarbonate, e.g., contraction alkalosis by the use of loop diuretics
- Increased renal excretion of acid, e.g., diuretic therapy, high aldosterone state, potassium depletion, high pCO_2, secondary hypoparathyroidism

The formula that predicts the expected decrease in pCO_2 (ΔpCO_2) is as follows (Oh, 2003):

$$\Delta pCO_2 = \Delta HCO_3^- \times 1.2 \pm 2$$

(ΔHCO_3^- a given decrease in a serum HCO_3^- concentration).

(Eq. 15.35)

METABOLIC ALKALOSIS

Causes and Pathogenesis

At normal serum bicarbonate concentrations, bicarbonate filtered at the glomerulus is almost completely reabsorbed. As serum bicarbonate concentrations rise above the normal level, bicarbonate reabsorption is incomplete and bicarbonaturia begins. A slight increase in serum bicarbonate above 24 mEq/L causes marked bicarbonaturia. Hence, when renal tubular bicarbonate handling and GFR are normal, maintenance of a high plasma bicarbonate concentration is extremely difficult unless an enormous amount of bicarbonate is administered. Therefore, maintenance of metabolic alkalosis requires two conditions: a mechanism to increase plasma bicarbonate and a mechanism to maintain an increased concentration. A bicarbonate concentration may be increased by net gain of alkali by one of the following mechanisms: administration of alkali, gastric loss of HCl through vomiting or nasogastric suction, or by renal generation of bicarbonate (Box 15.11). Maintenance of high plasma bicarbonate concentration occurs in advanced renal failure or when renal threshold for bicarbonate is increased. The two most common causes for increased renal bicarbonate threshold are volume depletion and K^+ depletion. Potassium deficiency reduces the intracellular pH of the proximal tubules, which stimulates bicarbonate reabsorption. Increased reabsorption of potassium in exchange for protons by K^+-H^+-ATPase in the collecting duct also contributes to metabolic alkalosis in potassium deficiency states. Metabolic alkalosis corrected by administration of chloride-containing fluid, for example, NaCl or KCl solution, is called *chloride-responsive metabolic alkalosis*, for example, vomiting-induced alkalosis. Patients with chloride-responsive metabolic alkalosis are typically volume depleted. However, in edema-forming conditions, administration of Cl^- may not improve metabolic alkalosis even though the mechanism of high renal bicarbonate threshold is volume depletion, because administered chloride is retained mostly in the edema fluid with little increase in effective vascular volume. Parathyroid hormone (PTH) normally interferes with bicarbonate reabsorption in the proximal tubule, and the renal tubular bicarbonate threshold tends to be increased in a low PTH state, such as primary and secondary hypoparathyroidism (Oh, 2003).

Compensation

Compensation of metabolic alkalosis is achieved by hypoventilation that results in increased pCO_2. Partly because hypoxemia is inevitable with hypoventilation in the absence of oxygen supplement, compensation is least effective in metabolic alkalosis among the four types of acid-base disorders. The formula that predicts the expected increase in pCO_2 (ΔpCO_2) is as follows:

$$\Delta pCO_2 = \Delta HCO_3^- \times 0.7 \pm 5$$

(ΔHCO_3^- a given decrease in a serum HCO_3^- concentration)

(Eq. 15.36)

The maximal compensation is completed within 12 to 24 hours. Observations have shown that no matter how severe the metabolic alkalosis, pCO_2 rarely exceeds 60 mm Hg unless a complicating independent respiratory disorder that compromises ventilation coexists (Oh, 2003).

BOX 15.12

Causes of Respiratory Acidosis

- Lung diseases: chronic obstructive lung disease, advanced interstitial lung disease, acute asthma
- Thoracic deformity or airway obstruction
- Diseases of respiratory muscle and nerve: myasthenia gravis, hypokalemia paralysis, botulism, amyotrophic lateral sclerosis, Guillain-Barré syndrome
- Depression of the respiratory center: barbiturate intoxication, stroke, myxedema.

BOX 15.13

Causes of Respiratory Alkalosis

- Diseases of the lung: any intrapulmonary pathology such as pneumonia, pulmonary fibrosis, pulmonary congestion, pulmonary embolism
- Hypoxemia
- Central nervous system lesions
- Gram-negative sepsis
- Liver disease
- Drugs: salicylate, progesterone

RESPIRATORY ACIDOSIS

Causes and Pathogenesis

The causes of respiratory acidosis are usually quite apparent. They include diseases of the lung (by far the most common causes), respiratory muscle, respiratory nerve, thoracic cage, and airways, and suppression of the respiratory center by stroke, drugs such as phenobarbital, or severe hypothyroidism (Box 15.12).

Compensation

The normal compensatory response to respiratory acidosis is to increase HCO_3^- concentration in an attempt to minimize the reduction in pH. This occurs in two distinct stages: first, by tissue buffering of CO_2 and second, by increased renal excretion of acid.

Tissue Buffering

This phase of compensation is extremely fast, and occurs within a second. The chemical reaction is as follows:

$$CO_2 + H_2O \rightarrow H_2CO_3 \qquad \text{(Eq. 15.37)}$$

$$H_2CO_3 + KBuff \rightarrow HBuff + KHCO_3 \qquad \text{(Eq. 15.38)}$$

KBuff is a non-HCO_3^- buffer, and the reaction proceeds to the right because of the rising pCO_2. Because extracellular fluid contains little non-HCO_3^- buffers, most of this buffering occurs in the cell. The increased concentration of cellular HCO_3^- in red blood cells causes an extracellular shift of HCO_3^- in exchange for Cl^- through the ubiquitous anion exchanger, also known as *band 3 protein*, on the red blood cell membrane. The relationship between an increase in pCO_2 (ΔpCO_2) and the increase in serum levels of HCO_3^- (ΔHCO_3^-) in acute respiratory acidosis is shown in the equation

$$\Delta HCO_3^- \text{ (mEq/L)} = \Delta pCO_2 \text{ (mmHg)} \times 0.07 \pm 1.5. \qquad \text{(Eq. 15.39)}$$

Renal Compensation

Renal compensation for respiratory acidosis is delayed, but it increases the HCO_3^- concentration to a much higher level. The increased concentration of HCO_3^- is achieved by increased net acid excretion, primarily in the form of NH_4^+. Maximal compensation requires 5 days but is 90% complete in 3 days. Increased excretion of NH_4^+ is accompanied by Cl^-. As new HCO_3^- is retained, Cl^- is lost. It follows therefore when respiratory acidosis is corrected, excretion of HCO_3^- must be accompanied by retention of Cl^-, which is possible only if Cl^- is taken in. Restriction of NaCl intake during the recovery phase of chronic respiratory acidosis would prevent the compensation, resulting in persistent metabolic alkalosis. Such a condition is called post-hypercapnic metabolic alkalosis.

The relationship between the increase in pCO_2 (ΔpCO_2) and the increase in HCO_3^- (ΔHCO_3^-) in chronic fully compensated respiratory acidosis is shown in the following equation (Carroll et al., 1989c):

$$\Delta HCO_3^- \text{ (mEq/L)} = \Delta pCO_2 \text{ (mmHg)} \times 0.4 \pm 3. \qquad \text{(Eq. 15.40)}$$

RESPIRATORY ALKALOSIS

Causes and Pathogenesis

With the exception of respirator-induced alkalosis and voluntary hyperventilation, respiratory alkalosis is the result of stimulation of the respiratory center. The two most common causes of respiratory alkalosis are hypoxic stimulation of the peripheral respiratory center (carotid body and aortic arch chemoreceptors) and stimulation of the pulmonary receptors caused by various disorders of the lung, such as pneumonia, pulmonary congestion, and pulmonary embolism.

Certain drugs, for example, salicylate and progesterone, stimulate the respiratory center directly. High progesterone levels are responsible for chronic respiratory alkalosis of pregnancy (Wise, 2006). Respiratory alkalosis is also common in gram-negative sepsis and liver disease through unknown mechanisms. Blood pH tends to be extremely high when respiratory alkalosis is caused by psychogenic stimulation of the respiratory center because the condition is usually very acute and therefore there is no time for compensation. Causes of respiratory alkalosis are listed in Box 15.13.

Compensation

Two types of compensation lower plasma HCO_3^- and minimize the increase in blood pH in respiratory alkalosis: tissue buffering and renal compensation.

Tissue Buffering

Compensation by buffering of HCO_3^- is completed within a second with the reactions:

$$HBuff + HCO_3^- \rightarrow H_2CO_3 + Buff \qquad \text{(Eq. 15.41)}$$

$$H_2CO_3 \rightarrow CO_2 + H_2O \qquad \text{(Eq. 15.42)}$$

The reactions proceed to the right because CO_2 is lost by hyperventilation. The magnitude of reduction in HCO_3^- content depends on the amount of cellular acid buffers (HBuff) that react with HCO_3^-. As cellular HCO_3^- is consumed in the buffer reaction, extracellular HCO_3^- enters the cell in exchange for cellular Cl^- that enters the extracellular fluid. An additional mechanism of tissue buffering is increased production of lactic acid and other organic acids (Hood, 1998). Increased lactic acid production is explained in part by the stimulatory effect of alkaline pH on phosphofructokinase, a rate-limiting enzyme for glycolysis. The magnitude of reduction in plasma HCO_3^- concentration by acute compensation is predicted from the following equation:

$$\Delta HCO_3^- \text{ (mEq/L)} = \Delta pCO_2 \text{ (mmHg)} \times 0.2 \pm 2.5 \qquad \text{(Eq. 15.43)}$$

ΔHCO_3^- (mEq/L) is the expected decrease in plasma HCO_3^- for a given decrease in pCO_2 (ΔpCO_2 in mmHg) (Carroll et al., 1989c).

Renal Compensation

Renal compensation of respiratory alkalosis is achieved by reduction in net acid excretion. This is achieved initially by increased excretion of HCO_3^- but later by reduced excretion of NH_4^+ and titratable acid. The magnitude of reduction in plasma HCO_3^- concentration due to renal compensation can be predicted from the following equation:

$$\Delta HCO_3^- \text{ (mEq/L)} = \Delta pCO_2 \text{ (mmHg)} \times 0.2 \pm 2.5 \qquad \text{(Eq. 15.44)}$$

ΔHCO_3^- (mEq/L) is the expected decrease in plasma HCO_3^- for a given decrease in pCO_2 (ΔpCO_2 in mmHg) (Carroll et al., 1989c).

Among the four types of acid-base disorders, compensation is most effective in respiratory alkalosis; pH after compensation sometimes returns to normal levels. Compensation is completed within 2 to 3 days. When complete compensation does occur, one should look for evidence of complicating metabolic acidosis.

BOX 15.14

Formulas For Predicting Normal Acid-Base Compensation

- Metabolic acidosis: $\Delta pCO_2 = \Delta HCO_3^- \times 1.2 \pm 2$
- Metabolic alkalosis*: $\Delta PCO_2 = \Delta HCO_3^- \times 0.7 \pm 5$
- Acute respiratory acidosis: $\Delta HCO_3^- = \Delta pCO_2 \times 0.07 \pm 1.5$
- Chronic respiratory acidosis: $\Delta HCO_3^- = \Delta pCO_2 \times 0.4 \pm 3$
- Acute respiratory alkalosis: $\Delta HCO_3^- = \Delta pCO_2 \times 0.2 \pm 2.5$
- Chronic respiratory alkalosis: $\Delta HCO_3^- = \Delta pCO_2 \times 0.5 \pm 2.5$

ΔHCO_3^- and ΔpCO_2 represent the difference between normal and actual values in bicarbonate and pCO_2, respectively.

* No matter how high the serum HCO_3^- rises, pCO_2 rarely rises above 60 mm Hg in metabolic alkalosis.

MIXED ACID-BASE DISORDERS

The term *mixed acid-base disorder* refers to a clinical condition in which two or more primary acid-base disorders coexist. They generally present with one obvious disturbance with what appears to be an inappropriate (excessive or inadequate) compensation. The "inappropriateness" of the compensatory process is probably the result of a separate primary disorder. The appropriate degrees of compensation for primary acid-base disorders have been determined by analysis of data from a large number of patients and are expressed in the form of equations in Box 15.14. When two disorders influence the blood pH in opposite directions, the blood pH will be determined by the dominant disorder. If disorders cancel out each other's effects, blood pH can be normal. When there is any degree of compensation for acid-base disorders, both pCO_2 and HCO_3^- change in the same direction, that is, both are high or both are low. If pCO_2 and HCO_3^- have changed in opposite directions, for example, pCO_2 is high and HCO_3^- is low or pCO_2 is low and HCO_3^- is high, the presence of a mixed acid-base disorder is certain. Appropriateness of compensation can be determined by consulting Box 15.14. Compensation could be excessive, insufficient, or appropriate. One can also have an approximate idea about the appropriateness of compensation from the degree of pH deviation without consulting the formula for normal compensation.

In general, compensation is most effective in respiratory alkalosis (pH is often normalized), the next best is respiratory acidosis (pH may become normal), and the third best is metabolic acidosis. Compensation is least effective in metabolic alkalosis, probably because hypoxemia, an inevitable consequence of hypoventilation, stimulates ventilation. If a patient has low pCO_2 and low HCO_3^- with normal pH, the likely diagnosis is compensated respiratory alkalosis rather than compensated metabolic acidosis (Oh, 2003).

SELECTED REFERENCES

Aukland K, Reed RK: Interstitial lymphatic mechanisms in the control of extra cellular fluid volume, *Physiol Rev* 73:1–78, 1993.

Carroll HJ, Oh MS: *Water, electrolyte, and acid-base metabolism*, Philadelphia, 1989, J. B. Lippincott.

Frantz C, Stewart KM, Weaver BM: The extracellular matrix at a glance, *J Cell Sci* 123:4195–4200, 2010.

Gennari FJ: Current concepts. Serum osmolality. Uses and limitations, *N Engl J Med* 310:102–105, 1984.

Gietz R, Mohammadi M: Exploring the mechanisms of FGF signaling through the lens of structural biology, *Nature Rev Mol Cell Biol* 14:166–180, 2013.

Giebisch GH: A trail of research on potassium, *Kidney Int* 62:1498–1512, 1984.

Halperin ML, Kamel KS, Oh MS: Mechanisms to concentrate the urine: an opinion, *Curr Opin Nephrol Hypertens* 17:416–422, 1984.

Kraut JA, Madias NE: Serum anion gap: its uses and limitations in clinical medicine, *Clin J Am Soc Nephrol* 2:162–74, 2007.

Kyle UG, Bosaeusb I, De Lorenzoc AD, et al.: Bioelectrical impedance analysis—part I: review of principles and methods, *Clinical Nutrition* 23:1226–1243, 2004.

Mehta R, Kellum JA, Shah S, et al.: Acute kidney injury Network: report of an initiative to improve outcomes in acute kidney injury, *Crit Care* 11:R31, 2007.

Moore F: *The body cell mass and its supporting environment*, Philadelphia, 1963, WB Saunders Co.

Oh MS, Carroll HJ: The anion gap, *N Engl J Med* 297:814–817, 1977.

Oh MS: Does serum creatinine rise faster in rhabdomyolysis? *Nephron* 63:255–257, 1993.

Oh MS, Carroll HJ: Regulation of intracellular and extracellular volume. In Arieff AI, DePronzo RA, editors: *Fluid, Electrolyte, and Acid-Base Disorders*, ed 2, New York, 1995, Churchill Livingstone.

Oh MS: *Acid-base electrolytes*, New York, 2003, OHCO, LLC.

Relman AS, Lennon EJ, Lemann Jr J: Endogenous production of fixed acid and the measurement of the net balance of acid in normal subjects, *J Clin Invest* 40:1621–1630, 1961.

Rose BD: New approach to disturbances in the plasma sodium concentration, *Am J Med* 81(6):1033, 1986.

Smith HW: *The kidney: Structure and function in Health and disease*, New York, 1951, Oxford University Press, pp 231–238.

Access the complete reference list online at Elsevier eBooks for Practicing Clinicians.

REFERENCES

Adrogué HJ, et al.: *Assessing acid-base disorders*, *Kidney Int* 76(12):1239–1247, 2009, https://doi.org/10.1038/ki.2009.359.

Agarwal R: Ambulatory GFR measurement with cold iothalamate in adults with chronic kidney disease, *Am J Kidney Dis*, 2003, https://doi.org/10.1016/S0272-6386(03)00022-2.

Alge JL, Arthur JM: Biomarkers of AKI: a review of mechanistic relevance and potential therapeutic implications, *Clin J Am Soc Nephrol*, 2015, https://doi.org/10.2215/CJN.12191213.

Arthur JM, et al.: Evaluation of 32 urine biomarkers to predict the progression of acute kidney injury after cardiac surgery, *Kidney Int*, 2014, https://doi.org/10.1038/ki.2013.333.

Aukland K, Reed RK: Interstitial-lymphatic mechanisms in the control of extracellular fluid volume, *Physiol Rev*, 1993, https://doi.org/10.1152/physrev.1993.73.1.1.

Aukland K, Reed RK: Interstitial-lymphatic mechanisms in the control of extracellular fluid volume, *Physiol Rev*, 2017, https://doi.org/10.1152/physrev.1993.73.1.1.

Barbour HM, Welch C: Development and evaluation of a kinetic diacetyl monoxime method for urine urea, *Ann Clin Biochem*, 1992, https://doi.org/10.1177/000456329202900116.

Beker BM, et al.: Novel acute kidney injury biomarkers: their characteristics, utility and concerns, *Int Urol Nephrol*, 2018, https://doi.org/10.1007/s11255-017-1781-x.

Berend K, de Vries APJ, Gans ROB: Physiological approach to assessment of acid–base disturbances, *N Engl J Med*, 2014, https://doi.org/10.1056/NEJMra1003327.

Bianchi C, et al.: Reappraisal of serum β2-microglobulin as marker of GFR. In *Ren fail*, 2001, https://doi.org/10.1081/JDI-100104725.

Bilbrey GL, et al.: Skeletal muscle resting membrane potential in potassium deficiency, *J Clin Invest*, 1973, https://doi.org/10.1172/JCI107499.

Bourque WC, Oliet SHR: Osmoreceptors in the central nervous system, *Ann Rev Physiol*, 2002, https://doi.org/10.1146/annurev.physiol.59.1.601.

Bradberry SMB, Vale A: Disturbances of potassium homeostasis in poisoning, *Clin Toxicol*, 1995, https://doi.org/10.3109/15563659509028915.

Brans YW, et al.: Simultaneous estimation of Neonatal total body water by antipyrine and H218O dilution, *Neonatology*, 1990, https://doi.org/10.1159/000243253.

Burg MB: Molecular basis of osmotic regulation, *Am J Physiol*, 1995, https://doi.org/10.1152/ajprenal.1995.268.6.F983.

Carroll H, Oh M: Aquaporin water channels. In *Biosci Rep*, 1989a, https://doi.org/10.1007/s10540-005-2577-2.

Carroll H, Oh M: Toxic alcohol ingestions: clinical features, Diagnosis, and management, *Clin J Am Soc Nephrol*, 1989b, https://doi.org/10.2215/CJN.03220807.

Carroll H, Oh M: *Water*, *electrolytes*, *and acid-base metabolism*, 2nd ed., Philadelphia, 1989c, Lippincott.

Carstens J, et al.: Effects of urodilatin on natriuresis in cirrhosis patients with sodium retention, *BMC Gastroenterol*, 2007, https://doi.org/10.1186/1471-230X-7-1.

Carvounis CP, Nisar S, Guro-Razuman S: Significance of the fractional excretion of urea in the differential diagnosis of acute renal failure, *Kidney Int*, 2002, https://doi.org/10.1046/j.1523-1755.2002.00683.x.

Charlton JR, Portilla D, Okusa MD: A basic science view of acute kidney injury biomarkers, *Nephrol Dial Transplant*, 2014, https://doi.org/10.1093/ndt/gft510.

Chen S: Retooling the creatinine clearance equation to estimate kinetic GFR when the plasma creatinine is changing acutely, *J Am Soc Nephrol*, 2013, https://doi.org/10.1681/ASN.2012070653.

Choi M, et al.: K+channel mutations in adrenal aldosterone-producing adenomas and hereditary hypertension, *Science*, 2011, https://doi.org/10.1126/science.1198785.

Chothia MY, et al.: Bolus administration of intravenous glucose in the treatment of hyperkalemia: a randomized controlled trial, *Nephron Physiol*, 2014, https://doi.org/10.1159/000358836.

Clemessy JL, et al.: Hypokalaemia related to acute chloroquine ingestion, *Lancet*, 1995, https://doi.org/10.1016/S0140-6736(95)92711-5.

Cockcroft DW, Gault MH: Prediction of creatinine clearance from serum creatinine, *Nephron*, 1976, https://doi.org/10.1159/000180580.

Colussi G, Cipriani D: Pseudohyperkalemia in extreme leukocytosis, *Am J Nephrol*, 1995, https://doi.org/10.1159/000168883.

Cooper GJ, et al.: Transport of volatile solutes through AQP1, *J Physiol*, 2002, https://doi.org/10.1113/jphysiol.2002.023218.

Cowley AW, et al.: Progression of glomerular filtration rate reduction determined in conscious Dahl salt-sensitive hypertensive rats, *Hypertension*, 2013, https://doi.org/10.1161/HYPERTENSIONAHA.113.01194.

Davids MR, et al.: An unusual cause for ketoacidosis, *QJM - Monthly Journal of the Association of Physicians*, 2004, https://doi.org/10.1093/qjmed/hch064.

Deng Y, et al.: Evaluation of clinically available renal biomarkers in critically ill adults: a prospective multicenter observational study, *Crit Care*, 2017, https://doi.org/10.1186/s13054-017-1626-0.

Dennen P, Parkh CP: Biomarkers of acute kidney injury: can we replace serum creatinine?, 2007, *Clin Nephrol*, 2007.

Elkin BS, Shaik MA, Morrison B: Fixed negative charge and the Donnan effect: a description of the driving forces associated with brain tissue swelling and oedema, 2010, *Philos Trans A Math Phys Eng Sci* 368:585–603, 1912, https://doi.org/10.1098/rsta.2009.0223.

Endeward V, Gros G: Low carbon dioxide permeability of the apical epithelial membrane of guinea-pig colon, *J Physiol*, 2005, https://doi.org/10.1113/jphysiol.2005.085761.

Fazekas S, et al.: Magnesium and the Hem: Antiarrhythmic therapy with magnesium, *Clin Cardiol* 16:768–774, 1993.

Filler G, Lepage N: Should the Schwartz formula for estimation of GFR be replaced by cystatin C formula? *Pediatric Nephrol*, 2003, https://doi.org/10.1007/s00467-003-1271-5.

Fogh-Andersen N, et al.: Composition of interstitial fluid, *Clin Chem*, 1995.

Forro M, et al.: Total body water and ECFV measured using bioelectrical impedance analysis and indicator dilution in horses, *J Appl Physiol*, 2017, https://doi.org/10.1152/jappl.2000.89.2.663.

Fossati P, et al.: A step forward in enzymatic measurement of creatinine, *Clin Chem*, 1994.

Goodman AD, et al.: Production, excretion, and net balance of fixed acid in patients with, *J Clin Invest*, 1965, https://doi.org/10.1172/JCI105163.

Gunnerson KJ, et al.: TIMP2•IGFBP7 biomarker panel accurately predicts acute kidney injury in high-risk surgical patients, *J Trauma Acute Care Surg*, 2016, https://doi.org/10.1097/TA.0000000000000912.

Halperin ML: *Lactic acidosis and ketoacidosis: biochemical and clinical implications*, CMAJ, 1977.

Halperin ML, et al.: Metabolic acidosis in the alcoholic: a pathophysiologic approach, *Metabolism*, 1983, https://doi.org/10.1016/0026-0495(83)90197-X.

Halperin ML, et al.: The urine osmolal gap: a clue to estimate urine ammonium in "hybrid" types of metabolic acidosis, *Clin Invest Med*, 1988.

Halperin ML, et al.: Control of potassium excretion: a Paleolithic perspective, *Curr Opin Nephrol Hypertens*, 2006, https://doi.org/10.1097/01.mnh.0000232884.73518.9c.

Halperin ML, Bohn D: Clinical approach to disorders of salt and water balance: emphasis on integrative physiology, *Crit Care Clin*, 2002, https://doi.org/10.1016/S0749-0704(01)00008-2.

Halperin ML, Kamel KS: D-lactic acidosis: turning sugar into acids in the gastrointestinal tract, *Kidney Int*, 1996, https://doi.org/10.1038/ki.1996.1.

Halperin ML, Kamel KS: Electrolyte quintet: potassium, *Lancet*, 1998a, https://doi.org/10.1016/S0140-6736(98)85044-7.

Halperin ML, Kamel KS: Electrolyte quintet: sodium, *Lancet*, 1998b, https://doi.org/10.1016/S0140-6736(98)85044-7.

Halperin ML, Kamel KS: *Potassium*, *Lancet*, 1998c, https://doi.org/10.1016/S0140-6736(98)85044-7.

Halperin ML, Kamel KS, Goldstein MB: Fluid, electrolyte, and acid-base physiology: a problem-based approach. In *Fluid*, *electrolyte and acid-base physiology: a problem-based approach*, *fourth edition*, fourth edition, 2010, https://doi.org/10.1016/B978-1-4160-2442-2.00043-5.

Hill AR, et al.: Altered water metabolism in tuberculosis: role of vasopressin, *Am J Med*, 1990, https://doi.org/10.1016/0002-9343(90)90489-Z.

Hillier TA, Abbott RD, Barrett EJ. Hyponatremia: evaluating correction factor for hyperglycemia. Am J Med. 1999; 106:399-403

Holtzclaw JD, Grimm R, Sansom SC: *Role of BK channels in hypertension and potassium secretion*, 2011, https://doi.org/10.1097/MNH.0b013e3283488889.

Hoste L, et al.: Routine serum creatinine measurements: how well do we perform? *BMC Nephrol* 16(1):1–9, 2015, https://doi.org/10.1186/s12882-015-0012-x.

Hussain I, Ahmad Z, Garg A: Extreme hypercholesterolemia presenting with pseudohyponatremia - a case report and review of the literature, *J Clin Lipidol*, 2015, https://doi.org/10.1016/j.jacl.2014.11.007.

Inker LA, et al.: GFR estimation using β-trace protein and β2-microglobulin in CKD, *Am J Kidney Dis*, 2016, https://doi.org/10.1053/j.ajkd.2015.07.025.

Jordan P, et al.: Hydroxychloroquine overdose: Toxicokinetics and management, *J Toxicol Clin Toxicol*, 1999, https://doi.org/10.1081/CLT-100102466.

Kamel KS, et al.: Disorders of potassium homeostasis: an approach based on pathophysiology, *Am J Kidney Dis*, 1994, https://doi.org/10.1016/S0272-6386(12)80220-4.

Kamel KS, et al.: Interpretation of electrolyte and acid-base parameters in blood and urine. In *Brenner and Rector's*, *kidney*, 2012, https://doi.org/10.1016/b978-1-4160-6193-9.10026-0.

Kamel KS, Halperin ML: Sodium and water physiology. In *Fluid*, *electrolyte acid-base Physiol*, 2016, https://doi.org/10.1016/b978-0-323-35515-5.00009-9.

Kamel KS, Oh MS, Halperin ML: Bartter's, Gitelman's, and Gordon's syndromes: from physiology to molecular biology and back, yet still some unanswered questions. In *Nephron*, 2002, https://doi.org/10.1159/000065373.

Kamel KS, Schreiber M, Halperin ML: Renal potassium physiology: integration of the renal response to dietary potassium depletion, *Kidney Int*, 2018, https://doi.org/10.1016/j.kint.2017.08.018.

Kanji S, MacLean RD: Cardiac Glycoside toxicity. More than 200 Years and counting, *Crit Care Clin*, 2012, https://doi.org/10.1016/j.ccc.2012.07.005.

Kar S, Paglialunga S, Islam R: Cystatin C is a more reliable biomarker for determining eGFR to support drug development studies, *J Clin Pharmacol*, 2018, https://doi.org/10.1002/jcph.1132.

Kashani K, et al.: Discovery and validation of cell cycle arrest biomarkers in human acute kidney injury, *Crit Care*, 2013, https://doi.org/10.1186/cc12503.

Kashani K, Cheungpasitporn W, Ronco C: Biomarkers of acute kidney injury: the pathway from discovery to clinical adoption, *Clin Chem Laborat Med*, 2017, https://doi.org/10.1515/cclm-2016-0973.

Katz MA: Hyperglycemia-induced hyponatremia — calculation of expected serum sodium Depression, *Engl J Med*, 1973, https://doi.org/10.1056/NEJM197310182891607.

Kellum JA: Acid-base disorders and strong ion gap, *Contribut Nephrol* 156:pp158–p166, 2007, https://doi.org/10.1159/000102079.

Kerkelä R, Ulvila J, Magga J: Natriuretic peptides in the regulation of cardiovascular physiology and metabolic events, *J Am Heart Associat*, 2015, https://doi.org/10.1161/JAHA.115.002423.

Kim HJ, et al.: *Determinants of magnitude of pseudohyperkalemia in thrombocytosis*, Korean JIntMed, 1990.

Kortenoeven MLA, et al.: Lithium reduces aquaporin-2 transcription independent of prostaglandins, *Am J Physiol Cell Physiol*, 2012, https://doi.org/10.1152/ajpcell.00197.2011.

Koulouridis E, Koulouridis I: Molecular pathophysiology of Bartter's and Gitelman's syndromes, *World J Pediatr*, 2015, https://doi.org/10.1007/s12519-015-0016-4.

Kraut JA, Madiast NE: Serum anion gap: its uses and limitations in clinical medicine, *Clin J Am Soc Nephrol*, 2007, https://doi.org/10.2215/CJN.03020906.

Krozowski Z, et al.: The type I and type II 11β-hydroxysteroid dehydrogenase enzymes. In *J steroid Biochem mole Biol*, 1999, https://doi.org/10.1016/S0960-0760(99)00074-6.

do Lee S, et al.: TonEBP stimulates multiple cellular pathways for adaptation to hypertonic stress: organic osmolyte-dependent and -independent pathways, *Am J Physiol Renal Physiol*, 2011, https://doi.org/10.1152/ajprenal.00227.2010.

Lemann J, Relman AS: The relation of sulfur metabolism to acid-base balance and electrolyte excretion: the effects of DL-methionine in normal man, *J Clin Invest*, 1959, https://doi.org/10.1172/JCI104001.

Lemos T, Gallagher D: Current body composition measurement techniques, *Curr Opin Endocrinol, Diabet Obesity*, 2017, https://doi.org/10.1097/MED.0000000000000360.

Levey AS et al: A simplified equation to predict glomerular filtration rate from serum creatinine. J Am Soc Nephrol. 2000; 11:155A.

Levey AS, et al.: A more accurate method to estimate glomerular filtration rate from serum creatinine: a new prediction equation, *Modification of Diet in Renal Disease Study Group, AnnIntern Med*, 1999.

Levey AS, Stevens LA, et al.: A new equation to estimate glomerular filtration rate, *Ann Intern Med* 150:604–612, 2009.

Lin SH, et al.: Control of excretion of potassium: lessons from studies during prolonged total fasting in human subjects, *AmJ Physiol-Renal Physiol*, 2017, https://doi.org/10.1152/ajprenal.1997.273.5.f796.

Lin SH, Halperin M, Hypokalemia: A practical approach to diagnosis and its genetic basis, *Curr Med Chem*, 2007, https://doi.org/10.2174/092986707780831050.

Lipman J, Wallis SC, Boots RJ: Cefepime versus cefpirome: the importance of creatinine clearance, *Anesth Analg*, 2003, https://doi.org/10.1213/01.ANE.0000077077.54084B0.

Loffing J, Korbmacher C: Regulated sodium transport in the renal connecting tubule (CNT) via the epithelial sodium channel (ENaC), *Pflugers Arch Europ JPhysiol*, 2009, https://doi.org/10.1007/s00424-009-0656-0.

Maiuolo J, et al.: Regulation of uric acid metabolism and excretion, *Int J Cardiol* 213:8–14, 2015, https://doi.org/10.1016/j.ijcard.2015.08.109.

Mallie JP, Haperin ML: *Tonicity balance: a tool to explain the basis for the dysnatremias*, Nephrologie, 1998.

Marques P, Gunawardana K, Grossman A: *Transient diabetes insipidus in pregnancy*, 2015, https://doi.org/10.1530/EDM-15-0078.

McCullough PA: Contrast-induced acute kidney injury. In *Critical Care Nephrology*, ed 3. 2017, https://doi.org/10.1016/B978-0-323-44942-7.00048-0.

McIvor ME, et al.: The manipulation of potassium efflux during fluoride intoxication: implications for therapy, *Toxicology*, 1985, https://doi.org/10.1016/0300-483X(85)90086-1.

MeisterB AA: Molecular mechanisms involved in catecholamine regulation of sodium transport. In *Semin Nephrol*, 1993.

Myers GL, Miller WK, Coresh J, Fleming J, Greenberg N, et al.: Recommendations for improving serum creatinine measurement: a report from the laboratory working group of the National kidney disease Education program, *Clin Chem* 52:5–18, 2006.

Moreno-layseca P, et al.: Review article | Focus integrin trafficking in cells and tissues, *Nature Cell Biol*, 2019, https://doi.org/10.1038/s41556-018-0223-z.

Morgan TJ: Partitioning standard base excess: a new approach, *J Clin Monitor Comput*, 2011, https://doi.org/10.1007/s10877-011-9324-y.

Moritz ML: Syndrome of inappropriate antidiuresis, *Pediat Clin North Am*, 2019, https://doi.org/10.1016/j.pcl.2018.09.005.

Nah H, et al.: Evaluation of bilirubin interference and accuracy of six creatinine assays compared with isotope dilution-liquid chromatography mass spectrometry, *Clin Biochem*, 2016, https://doi.org/10.1016/j.clinbiochem.2015.10.015.

Nishikimi T, Kuwahara K, Nakao K: Current biochemistry, molecular biology, and clinical relevance of natriuretic peptides, *J Cardiol*, 2011, https://doi.org/10.1016/j.jjcc.2011.01.002.

Oh MS, Carroll HJ: In ArieffAI DFR, editor: *Regulation of extra- and intracellular fluid composition and content*, New York, NY, 1995, Churchill Livingstone, pp 1–38.

Oh M: Determinants of magnitude of pseudohyperkalemia in thrombocytosis, *Korean JInt med*, 2003a.

Oh M: Prediction of creatinine clearance from serum creatinine, *Nephron*, 2003b, https://doi.org/10.1159/000180580.

Oh MS, et al.: D-lactic acidosis in a man with the short-Bowel syndrome, *N Engl J Med*, 1979, https://doi.org/10.1056/NEJM197908023010505.

Oh MS, et al.: A mechanism for hyporeninemic hypoaldosteronism in chronic renal disease, *Metabolism*, 1974, https://doi.org/10.1016/0026-0495(74)90032-8.

Oh MS, et al.: Hyperchloremic acidosis during the recovery phase of diabetic ketosis, *Ann Int Med*, 1978, https://doi.org/10.7326/0003-4819-89-6-925.

Oh MS: A new method for estimating G-I absorption of alkali, *Kidney Int*, 1989, https://doi.org/10.1038/ki.1989.280.

Oh MS: Pathogenesis and diagnosis of hyponatremia, *InNephron*, 2002, https://doi.org/10.1159/000065370.

Oh MS: *Acid-base, electrolytes*, 1st edn, New York, NY, 2003, OHCO, LLC.

Oh MS, Carroll HJ: The anion gap, *N Engl J Med*, 1977, https://doi.org/10.1056/NEJM197710132971507.

Oh MS: Carroll HJCerebral salt-wasting syndrome: we need better proof of its existence, *Nephron*, 1999, https://doi.org/10.1159/000045385.

Oh MS, Carroll HJ: Value and determinants of urine anion gap, *Nephron*, 2002, https://doi.org/10.1159/000049059.

Oh MS, Carroll HJ: External balance of electrolytes and acids and alkali. In *Seldin and Giebisch's, kidney*, 2008, https://doi.org/10.1016/B978-012088488-9.50013-9.

Oldfield BJ, McKinley MJ: Circumventricular organs. In *The rat nervous system*, Fourth Edition, 2014, https://doi.org/10.1016/B978-0-12-374245-2.00015-2.

Oppliger RA, et al.: Accuracy of urine specific gravity and osmolality as indicators of hydration status, *Int J Sport Nutr Exerc Metab*, 2005, https://doi.org/10.1123/ijsnem.15.3.236.

Palmer BF. Regulation of potassium homeostasis. Clin J Am Soc Nephrol 2015; 10: 1050-1060.

Perazella MA, Biswas P: Acute hyperkalemia associated with intravenous Epsilon-aminocaproic acid therapy, *Am J Kidney Dis*, 1999, https://doi.org/10.1016/S0272-6386(99)70234-9.

Petrykiv S, et al.: Differential effects of dapagliflozin on cardiovascular risk factors at varying degrees of renal function, *Clin J Am Soc Nephrol*, 2017, https://doi.org/10.2215/CJN.10180916.

Peyton PJ, Chong SW: Minimally Invasive measurement of cardiac output during surgery and critical care A Meta-analysis of accuracy and Precision, *Anesthesiology* 113:1220–35, 2010.

Phelps KR, et al.: Pathophysiology of the syndrome of hyporeninemic hypoaldosteronism, *Metabolism*, 1980, https://doi.org/10.1016/0026-0495(80)90145-6.

Phelps KR, Oh MS, Carroll HJ: *Heparin-induced hyperkalemia: report of a case, nephron*, 1980.

Pierrat A, et al.: Predicting GFR in children and adults: a comparison of the Cockcroft-Gault, Schwartz, and Modification of diet in renal disease formulas, *Kidney Int*, 2003, https://doi.org/10.1046/j.1523-1755.2003.00208.x.

Price CP, Finney H: Developments in the assessment of glomerular filtration rate, *Clin Chim Acta*, 2000, https://doi.org/10.1016/S0009-8981(00)00233-3.

Rahmatullah M, Boyde TRC: Improvements in the determination of urea using diacetyl monoxime; methods with and without deproteinisation, *Clin Chim Acta*, 1980, https://doi.org/10.1016/0009-8981(80)90407-6.

Rajapakse S: Management of yellow oleander poisoning, *Clin Toxicol*, 2009, https://doi.org/10.1080/15563650902824001.

Robertson GL: Regulation of arginine vasopressin in the syndrome of inappropriate antidiuresis, *Am J Med*, 2006, https://doi.org/10.1016/j.amjmed.2006.05.006.

Ronco C, Rizo-Topete LM, Soto MS: Acute kidney injury: from clinical to molecular diagnosis. From clinical to molecular diagnosis. In *Critical care Nephrol*, Third Edition, 2017, https://doi.org/10.1016/B978-0-323-44942-7.00011-X.

Sahlin K, Harris RC, Hultman E: Creatine kinase equilibrium and lactate content compared with muscle pH in tissue samples obtained after Isometric exercise, *Biochem J* 152:173–180, 1975.

Scholl UI, et al.: Macrolides selectively inhibit mutant KCNJ5 potassium channels that cause aldosterone-producing adenoma, *J Clin Invest*, 2017, https://doi.org/10.1172/JCI91733.

Schrezenmeier EV, et al.: Biomarkers in acute kidney injury – pathophysiological basis and clinical performance, *Acta Physiol*, 2017, https://doi.org/10.1111/apha.12764.

Schwartz GJ, Work DF: Measurement and estimation of GFR in children and adolescents, *Clin J Am Soc Nephrol*, 2009, https://doi.org/10.2215/CJN.01640309.

Seifter JL: Integration of acid–base and electrolyte disorders, *N Engl J Med*, 2014, https://doi.org/10.1056/NEJMra1215672.

Shafiee MA, Kamel KS, Halperin ML: A conceptual approach to the patient with metabolic acidosis: application to a patient with diabetic ketoacidosis, *Nephron*, 2002, https://doi.org/10.1159/000065377.

Shemesh O, et al.: Limitations of creatinine as a filtration marker in glomerulopathic patients, *Kidney Int*, 1985, https://doi.org/10.1038/ki.1985.205.

Siggaard-Andersen O: Acid-base balance, *EncyclopRespirat Med*, 2006, https://doi.org/10.1016/B0-12-370879-6/00003-X.

Siggaard-Andersen O, Fogh-Andersen N: Base excess or buffer base (strong ion difference) as measure of a non-respiratory acid-base disturbance, *Acta Anaesth Scand* 39(106):123–128, 1995.

Singer RB, Hastings AB: An improved clinical method for the estimation of disturbances of the acid-base balance of human blood, *Medicine (Baltim)* 27:223–242, 1948.

Soldin SJ, Henderson L, Gilbert Hill J: The effect of bilirubin and ketones on reaction rate methods for the measurement of creatinine, *Clin Biochem*, 1978, https://doi.org/10.1016/S0009-9120(78)90028-0.

Spector R: Nature and consequences of mammalian brain and CSF efflux transporters: four decades of progress, *J Neurochem*, 2010, https://doi.org/10.1111/j.1471-4159.2009.06451.x.

Sterns RH, Silver SM: Cerebral salt wasting versus SIADH: what difference? *J Am Soc Nephrol*, 2008, https://doi.org/10.1681/ASN.2007101118.

Stevens LA, Levey AS: Measured GFR as a confirmatory test for estimated GFR, *J Am Soc Nephrol*, 2009, https://doi.org/10.1681/ASN.2009020171.

Stewart PA: Independent and dependent variables of acid-base control, *Respir Physiol*, 1978, https://doi.org/10.1016/0034-5687(78)90079-8.

Takahira R, et al.: Tryptophan glycoconjugate as a novel marker of renal function, *Am J Med* 110(3):192–197, 2001, https://doi.org/10.1016/S0002-9343(00)00693-8.

Trudnowski RJ, Rico RC: Specific gravity of blood and plasma at 4 and 37 °C, *Clin Chem*, 1974.

Uribarri J, Douyon H, Oh MS: A re-evaluation of the urinary parameters of acid population and excretion in patients with chronic renal acidosis, *Kidney Int*, 1995, https://doi.org/10.1038/ki.1995.79.

Uribarri J, Oh MS, Carroll HJ: Salt-losing nephropathy: clinical presentation and mechanisms, *Am J Nephrol*, 1983, https://doi.org/10.1159/000166709.

UribarriJ, Oh MS, Carroll HJ: D-lactic acidosis: a review of clinical presentation, biochemical features, and pathophysiologic mechanisms, *Medicine*, 1998, https://doi.org/10.1097/00005792-199803000-00001.

Vanmassenhove J, et al.: Urinary and serum biomarkers for the diagnosis of acute kidney injury: an in-depth review of the literature, *Nephrol Dial Transplant*, 2013, https://doi.org/10.1093/ndt/gfs380.

Zhou Y, et al.: Comparison of kidney injury molecule-1 and other nephrotoxicity biomarkers in urine and kidney following acute exposure to gentamicin, mercury, and chromium, *Toxicol Sci*, 2008, https://doi.org/10.1093/toxsci/kfm260.

CHAPTER 16

BIOCHEMICAL MARKERS OF BONE METABOLISM

Katrin M. Klemm, Michael J. Klein, Yaxia Zhang

MINERAL AND BONE METABOLISM, 208
Calcium, 208
Phosphorus, 210
Magnesium, 211
Hormones Regulating Mineral Metabolism, 212
DISORDERS OF MINERAL METABOLISM, 215
Hypercalcemia, 215
Hypocalcemia, 217
Hyperphosphatemia, 218
Hypophosphatemia, 219
Hypermagnesemia, 219
Hypomagnesemia, 219
BIOCHEMICAL MARKERS OF BONE REMODELING, 219
Bone Resorption Markers, 220
Bone Formation Markers, 220
METABOLIC BONE DISEASE, 221
Osteoporosis, 221
Osteomalacia And Rickets, 222
Renal Osteodystrophy, 222
Paget Disease, 223
SELECTED REFERENCES, 224

KEY POINTS

- The plasma concentration of calcium, phosphate, and magnesium is dependent on the net balance of bone mineral deposition and resorption, intestinal absorption, and renal excretion. The principal hormones regulating these processes are parathyroid hormone (PTH), calcitonin, 1,25-dihydroxyvitamin D, and fibroblast growth factor-23 (FGF-23).
- The most common causes of hypercalcemia are primary hyperparathyroidism (elevated PTH) and malignant neoplasms (decreased PTH and usually elevated PTH-related peptide). They account for 80% to 90% of all patients with hypercalcemia.
- The most common causes of hypocalcemia are chronic renal failure, hypomagnesemia, hypoparathyroidism, pseudohypoparathyroidism, vitamin D deficiency, and acute pancreatitis.
- Biointact PTH measures biologically active PTH; it is useful in patients with impaired renal function when various metabolites accumulate and interfere with traditional PTH assays.
- In patients undergoing surgery for primary hyperparathyroidism, intraoperative PTH measurements are useful in identifying whether the abnormal tissue is completely removed.
- Osteoporosis is the most common metabolic disease of bone and is characterized by decreased organic bone matrix. Serial bone resorption marker measurements can predict early response to therapy.
- Osteomalacia is failure to mineralize newly formed organic matrix (osteoid) in the mature skeleton.
- Phosphatonins comprise a newly described cascade of hormones, enzymes, and proteins related to phosphate metabolism.

MINERAL AND BONE METABOLISM

The skeleton is a metabolically active organ that undergoes continuous remodeling throughout life. This remodeling is necessary both to maintain the structural integrity of the skeleton and to fulfill its metabolic functions as a storehouse of calcium and phosphorus. Skeletal remodeling can be triggered by changes in mechanical forces or microdamage and by hormonal response to changes in circulating calcium and phosphorus levels. The skeleton also serves as the second line of defense against acidosis, and it is able to liberate buffers in the form of inorganic phosphates (Raisz, 1999).

Bone can be classified into two types: cortical or compact bone, and cancellous or trabecular bone (Fig. 16.1). Cortical bone plays an important role in the supportive, protective, and mechanical functions of the skeleton; it comprises the shafts of long bones and the outer envelope of all bones. It constitutes approximately 80% of skeletal mass, and it is 90% bone and 10% space (vascular canals, osteocyte lacunae, and canaliculi) by volume. Cancellous bone, which constitutes the remaining 20% of skeletal mass, is 25% bone and 75% space by volume. It is present at the ends of long and short tubular bones, within carpal and tarsal bones, and in the medullary cavities of vertebral bodies and flat bones. It is arranged in highly perforated vertical plates interconnected by horizontal struts and has a honeycombed appearance. It serves as a repository for hematopoietic cells and provides a large surface area for short-term mineral exchange (Watts, 1999). Even though cancellous bone represents only 20% of the total skeletal mass, it provides such a large surface area—one that equals that of cortical bone because of its honeycombed structure—that it accounts for 50% of active bone turnover at any given time (Erikson et al., 1994). Both compact and cancellous bones are composed primarily of inorganic minerals (calcium and phosphorus) and an organic matrix. Approximately 90% to 95% of this organic matrix is type I collagen. The remaining 5% to 10% consists of noncollagenous proteins, including osteocalcin, osteopontin, osteonectin, thrombospondin, sialoproteins, and other less well characterized proteins. Osteoclasts actively resorb bone by producing hydrogen ions to mobilize the minerals and proteolytic enzymes to hydrolyze the organic matrix. Osteoblasts synthesize the organic matrix and control the mineralization of the newly synthesized matrix (Endres & Rude, 1999).

The plasma concentration of calcium, phosphate, and magnesium is dependent on the net balance of bone mineral deposition and resorption, intestinal absorption, and renal excretion. The principal hormones regulating these processes are PTH, calcitonin, and 1,25-dihydroxyvitamin D. Much of bone metabolism reflects the body's effort to maintain serum calcium and phosphorus levels.

CALCIUM

Physiology

Distribution

Calcium is the fifth most common element and is the most prevalent cation in the human body. A healthy adult contains approximately 1 to 1.3 kg of calcium, 99% of which is in the form of hydroxyapatite in the skeleton. The remaining 1% is contained in the extracellular fluid (ECF) and soft tissues. Additionally, less than 1% of the skeletal content of calcium is in bone fluid and exchanges freely with the ECF (Mundy & Guise, 1999).

Serum (plasma) calcium exists in three distinct forms: free or ionized calcium, which is the physiologically active form, accounting for approximately 50% of the total serum calcium; complexed calcium, which is bound tightly to a variety of anions, including bicarbonate, lactate, phosphate, and citrate, accounting for approximately 10%; and plasma protein-bound calcium, accounting for approximately 40%. Both ionized calcium and the calcium complexes are freely dialyzable. Approximately 80% of the protein-bound calcium fraction is associated with albumin.

Because ionized calcium binds to negatively charged sites on the protein molecules, there is competition with hydrogen ions for binding sites on albumin and other calcium-binding proteins, and its binding is pH dependent. Although total serum calcium levels may remain unchanged, the relative

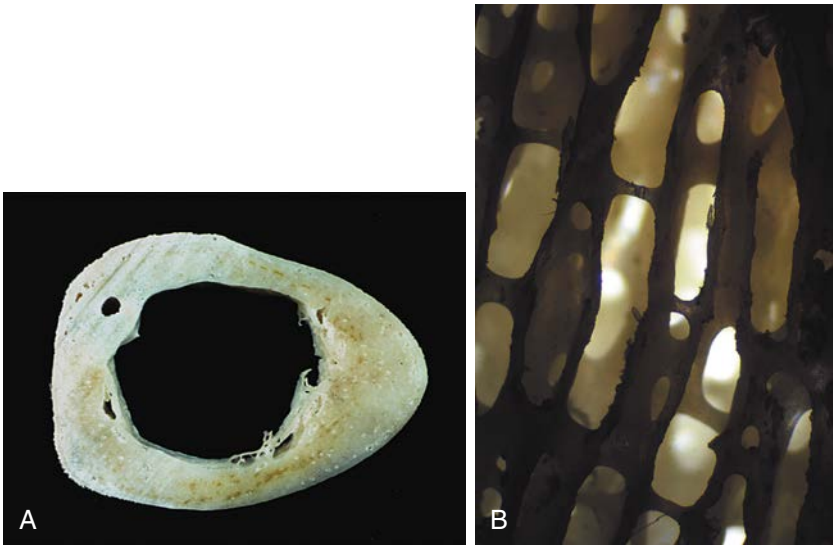

Figure 16.1 **A,** Compact bone, long bone, cross-section. The compact bone of the cortex of the femur in this 30-year-old male is continuous and solid, and the vascular spaces are not grossly visible. The hollow medullary cavity is filled with fatty marrow in vivo. **B,** Cancellous bone, longitudinal section. The cancellous bone is arranged in highly perforated vertical plates interconnected by delicate horizontal struts (braces). Most of its volume appears to be empty space once the marrow has been removed.

distribution of the three forms is altered as a result of pH changes in ECF. Alkalosis promotes increased protein binding, with a subsequent decrease in free calcium, whereas acidosis decreases protein binding, causing an increase in free calcium levels. Because calcium is bound to proteins, total calcium levels are also altered by plasma protein concentration.

Function

In addition to its obvious importance in skeletal mineralization, calcium plays a vital role in such basic physiologic processes as blood coagulation, neural transmission, plasma buffering capacity and enzyme activity, and in the maintenance of normal muscle tone and excitability of skeletal and cardiac muscle. It is an activator of intracellular signal transduction processes and is essential for DNA and RNA biosynthesis. Calcium is also involved in glandular synthesis and in regulation of exocrine and endocrine glands, as well as in the preservation of cell membrane integrity and permeability, particularly in terms of sodium and potassium exchange.

The average dietary intake of calcium for most adults in the United States is approximately 15 to 20 mmol/day (600 to 800 mg/day), most of which is derived from milk or other dairy products. The National Osteoporosis Foundation recommends that all adults have a daily intake of at least 1200 mg of elemental calcium with diet plus supplements. Lactating females and postmenopausal females not given exogenous estrogen therapy should probably have at least 1500 mg/day (Lewiecki, 2004).

Calcium is absorbed in the duodenum and upper jejunum via an active transport process. Less than half of dietary calcium is absorbed in adults. However, calcium absorption increases during periods of rapid growth in children, in pregnancy, and during lactation. It decreases with advancing age. Absorption also decreases at doses greater than 500 mg, suggesting that split doses may be more effective if supplemental calcium is consumed. The major stimulus to calcium absorption is vitamin D (see later discussion). Calcium absorption is also enhanced by growth hormone, an acid medium in the intestines, and by increased dietary protein. The ratio of calcium to phosphorus in the intestinal contents is also important, because a ratio greater than 2:1 results in the formation of insoluble calcium phosphates and tends to inhibit calcium absorption. Phytic acid, derived from various cereal grains, can also form insoluble calcium compounds, as can dietary oxalate and fatty acids. Cortisol and excessive alkalinity of the intestinal contents are both inhibitory to calcium absorption.

Estimates of daily calcium excretion in sweat vary widely—from 15 mg to more than 100 mg. The loss can greatly exceed this range during extreme environmental conditions. The major net loss of calcium occurs via urinary excretion and varies between 2.5 and 10 mmol/day (100 and 200 mg/day). In normal individuals, wide variations in dietary calcium intake have little effect on urinary calcium. Urinary calcium excretion is enhanced by hypercalcemia, phosphate deprivation, acidosis, and glucocorticoids. Parathyroid hormone (PTH), certain diuretics, and probably vitamin D diminish urinary calcium excretion. The physiology of calcium, its regulating hormones, and alterations of calcium homeostasis in disease have been extensively reviewed (Boden & Kaplan, 1990; Bazydlo, 2014).

Calcium Homeostasis

Ionized calcium concentration of the ECF is kept constant within a narrow range of approximately 1.25 mmol/L (Fig. 16.2). It is the ionized calcium concentration of the ECF that is the primary determinant of the hormonal

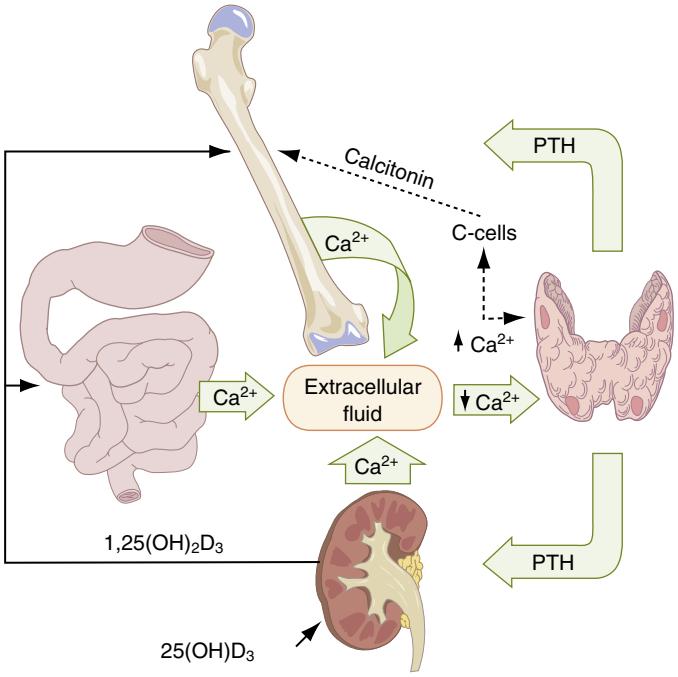

Figure 16.2 Calcium homeostasis. *Solid arrows* and *block arrows* indicate effects that increase serum calcium levels; *dashed arrows* indicate negative effects that decrease serum calcium.

influences that exert effects on ECF calcium levels. These effects are sometimes achieved at the expense of bone integrity. Adjustment of the ionized calcium concentration of the ECF is achieved mainly by the actions of PTH and active 1,25-dihydroxyvitamin D_3 ($1,25[OH]_2D_3$); calcitonin plays a smaller, yet significant, role. The principal target organs of these hormones are bone, kidneys, and intestines. When plasma-ionized calcium concentration decreases, the parathyroid glands sense the change via a membrane-bound calcium sensor receptor (CaSR) and secrete PTH immediately. Although PTH has no direct effect on osteoclasts, it stimulates osteoblasts and their precursors to produce RANKL (the receptor activator of nuclear factor κB ligand). This substance, a member of the tumor necrosis factor superfamily, activates its receptor, RANK, which is expressed on osteoclasts and their precursors. This, in turn, promotes osteoclast formation and activity and prolongs osteoclast survival by suppressing apoptosis (Hsu et al., 1999). This explains why bone formation and bone resorption are coupled in normal bone physiology. The resorption of bone matrix releases calcium and phosphate into the ECF. At the same time, PTH also acts on the kidney to stimulate increased urine phosphate excretion and some calcium reabsorption in the distal nephron, returning the ionized calcium concentration to normal. It has been suggested that sufficient action of $1,25(OH)_2D_3$ is mandatory for these steps to work appropriately. The kidney is almost exclusively responsible for this vitamin D activation (Kurokawa & Fukagawa, 1999). Calcitonin may play a role in the regulating process, although its significance

in humans is controversial. Other hormones that affect calcium metabolism but whose secretions are not primarily affected by changes in plasma calcium and phosphate include thyroid hormone, growth hormone, adrenal glucocorticoids, and gonadal steroids.

Analytic Techniques

Total calcium measurements include protein-bound calcium and ionized calcium; alternatively, ionized calcium alone can be measured. The total calcium measurement is easier to perform in the laboratory, but this result must be interpreted in clinical context. For example, patients with malignancies often exhibit hypoalbuminemia, a condition that may result in misleadingly low total calcium levels. When this occurs, the total calcium level (expressed in mg/dL) can be corrected with the following equation:

$$\text{Total calcium (mg/dL) corrected for hypoalbuminemia} = \text{measured total calcium} + [(\text{normal albumin-patient's albumin}) \times 0.8] \quad \text{(Eq. 16.1)}$$

An albumin of about 4.4 is typically used as the normal value in the previous formula. This corrected value is a more accurate assessment of the patient's calcium status. Because albumin is the primary protein that binds calcium, variations in this protein are clinically significant. Only a small percentage of calcium binds to other proteins, such as γ-globulins. Therefore, clinical states such as hypogammaglobulinemia are unlikely to drastically alter total calcium levels.

Total and Ionized Calcium

Although many total calcium procedures have been reported, only three methods are commonly used: colorimetric analysis with metallochromic indicators, atomic absorption spectrometry (AAS), and indirect potentiometry. Total calcium is most widely measured by spectrophotometric determination of the colored complex when various metallochromic indicators or dyes bind calcium. Orthocresolphthalein complexone (O-CPC) and arsenazo III are the most widely used indicators. The structures of both of these dyes are shown in Chapter 28. O-CPC reacts with calcium to form a red color in alkaline solution, which is measured at near 580 nm. Interference by magnesium ions is reduced by the addition of 8-hydroxyquinoline. Arsenazo III reacts with calcium to form a calcium-indicator complex, usually measured at near 650 nm. The stable reagent exhibits high specificity for calcium at slightly acidic pH. These reactions are also discussed in Chapter 28.

AAS is the reference method for determining calcium in serum. Despite its greater accuracy and precision compared with other methods, very few laboratories continue to use AAS for routine determination of total calcium. This may be because laboratories performing large numbers of sample determinations rely on automated methods that are not widely available for this technique. In addition, the level of equipment maintenance required in this technique is difficult for high-volume laboratories.

In indirect potentiometry, an electrode selective for calcium measures a sample that is also measured against a sodium-selective electrode, and calcium concentrations are proportional to the difference in potential between the electrodes.

Instruments with calcium-selective electrodes (see Chapter 28) provide accurate, precise, and automatic determinations of free (ionized) calcium. Calcium ion-selective electrodes (ISEs) consist of a calcium-selective membrane enclosing an inner reference solution of $CaCl_2$, AgCl, and other ions, as well as a reference electrode. ISEs are discussed in Chapters 4 and 28. In Chapter 28, use of ISEs to measure total calcium is also discussed.

Reference Interval

The reference interval for total calcium in normal adults ranges between 8.8 and 10.3 mg/dL (2.20 and 2.58 mmol/L). Serum is the preferred specimen for total calcium determination, although heparinized plasma is also acceptable. Citrate, oxalate, and ethylenediaminetetraacetic acid (EDTA) interfere with commonly used methods. Other factors that have been reported to interfere with the colorimetric methods include hemolysis, icterus, lipemia, paraproteins, and magnesium.

The reference interval for *ionized (free) calcium* in normal adults is 4.6 to 5.3 mg/dL (1.16–1.32 mmol/L). Whole blood, heparinized plasma, or serum may be used. Specimens should be collected anaerobically, transported on ice, and stored at 4°C to prevent loss of carbon dioxide (CO_2) and glycolysis and to stabilize pH (because pH changes alter the ionized calcium fraction). Proper collection technique is important to ensure accurate ionized calcium results; a tourniquet left on too long can lower pH at the site of collection and falsely elevate levels.

The reference interval for *urinary calcium* varies with diet. Individuals on an average diet excrete up to 300 mg/day (7.49 mmol/day). Urine specimens should be collected with appropriate acidification to prevent calcium salt precipitation.

PHOSPHORUS

Physiology

Distribution

The total body phosphorus content in normal adults is around 700 to 800 g. Approximately 80% to 85% is present in the skeleton; the remaining 15% is present in the ECF in the form of inorganic phosphate and intracellularly in the soft tissues as organic phosphates such as phospholipids, nucleic acids, and adenosine triphosphate (ATP). The skeleton contains primarily inorganic phosphate, predominantly as hydroxyapatite and calcium phosphate.

In blood, organic phosphate is located primarily in erythrocytes, with the plasma containing mostly inorganic phosphate. Approximately two-thirds of blood phosphorus is organic, while only about 3 to 4 mg/dL of the total of 12 mg/dL represents the inorganic form. Inorganic phosphate in serum exists as both divalent (HPO_4^{2-}) and monovalent ($H_2PO_4^-$) phosphate anions, both of which represent important buffers. The ratio of $H_2PO_4^-$:HPO_4^{2-} is pH dependent and varies between 1:1 in acidosis, 1:4 at pH of 7.4, and 1:9 in alkalosis. Approximately 10% of the serum phosphorus is bound to proteins; 35% is complexed with sodium, calcium, and magnesium; and the remaining 55% is free. Only inorganic phosphorus is measured in routine clinical settings.

Function

In addition to its role in the skeleton, phosphate has important intracellular and extracellular functions. Phosphate is an important constituent of nucleic acids in that both ribonucleic acid (RNA) and deoxyribonucleic acid (DNA) represent complex phosphodiesters. In addition, phosphorus is contained in phospholipids and phosphoproteins. It forms high-energy compounds (ATP) and cofactors (nicotinamide adenine dinucleotide phosphate [NADPH]) and is involved in intermediary metabolism and various enzyme systems (adenylate cyclase). Phosphorus is essential for normal muscle contractility, neurologic function, electrolyte transport, and oxygen carrying by hemoglobin (2,3-diphosphoglycerate).

Phosphorus Homeostasis

Most blood phosphate is derived from diet, but some is derived from bone metabolism. Phosphorus is present in virtually all foods. The average dietary intake for adults is about 800 to 1400 mg, most of which is derived from dairy products, cereals, eggs, and meat. About 60% to 80% of ingested phosphate is absorbed in the gut, mainly by passive transport. However, there is also an active energy-dependent process, which is stimulated by $1,25(OH)_2D_3$. Serum calcium and phosphorus generally maintain a reciprocal relationship. Phosphorus is freely filtered in the glomerulus. More than 80% of the filtered phosphorus is reabsorbed in the proximal tubule, and a small amount is reabsorbed in the distal tubule. Proximal reabsorption occurs by passive transport coupled to sodium (Na–P cotransport). Phosphorus intake and PTH mainly regulate this cotransport. Phosphorus restriction increases reabsorption, and intake decreases it. PTH induces phosphaturia by inhibition of Na–P cotransport. The effect is exerted mainly in the proximal tubule. The hormone binds to specific receptors in the basolateral membrane, resulting in the activation of two pathways—the adenylate cyclase/cyclic adenosine monophosphate/protein kinase A and the phospholipase C/calcium/protein kinase C systems—both of which are involved in inhibition of Na–P cotransport (Bellorin-Font et al., 1990).

Although PTH lowers serum phosphate, serum levels of phosphate are increased by administration of vitamin D and growth hormone. Vitamin D increases intestinal absorption and renal reabsorption of phosphorus. Growth hormone is a main regulator of skeletal growth. Its presence in the bloodstream reduces renal excretion of phosphates, thereby increasing serum levels.

Recently, a regulation cascade comprising a hormone, fibroblast growth factor-23 (FGF-23), an enzyme termed PHEX (phosphate-regulating gene with homologies to endopeptidases) thought to be involved in the metabolism of FGF-23, and a protein (matrix extracellular glycoprotein [MEPE]) has been elucidated (Quarles, 2003). This cascade is involved in phosphate homeostasis. FGF-23 is normally produced by osteocytes and osteoblasts as well as in marrow pericytes, thymus, and lymph nodes. However, current data support that most of FGF-23 is derived from bone in response to phosphate levels (Lu & Quarles, 2007) and provide the first evidence of an independent hormonal regulation of phosphate levels. FGF-23 is also involved in the regulation of the amount of vitamin D and dietary phosphate absorbed by the intestines (Bazydlo, 2014). Elevated levels of FGF-23 result in hyperphosphaturia,

primarily by inhibiting sodium-dependent phosphate resorption channels. FGF-23 also inhibits intestinal phosphorus absorption by inhibiting 25OH-vitamin D 1-α-hydroxylase in the renal proximal tubules (Lu & Quarles, 2007). Mutations involving FGF-23, PHEX, and MEPE have been implicated in phosphate wasting by the kidneys and have been associated with various mineralization abnormalities, including hereditary hypophosphatemic rickets, hyperphosphatemic familial tumoral calcinosis, and kidney stones (Quarles, 2003, 2012).

Analytic Techniques

Most commonly used methods for determination of inorganic phosphate are based on the reaction of phosphate with ammonium molybdate to form phosphomolybdate complex (see Chapter 45). Direct ultraviolet (UV) measurement of the colorless unreduced complex by absorption at 340 nm, as originally described by Daly and Ertinghausen in 1972, has been adapted for use on most of the automated analyzers. Alternatively, the phosphomolybdate complex can be reduced by a wide variety of agents (e.g., aminonaphtholsulfonic acid, ascorbic acid, methyl-*p*-aminophenol sulfate, ferrous sulfate) to produce molybdenum blue, which can be measured at 600 to 700 nm. The formation of phosphomolybdate complex is pH dependent, and the rate of its formation is influenced by protein concentration. Measurements of unreduced complexes have the advantages of being simple, fast, and stable. An enzymatic method has also been described whereby phosphorus undergoes successive enzymatic reactions catalyzed by glycogen phosphorylase, phosphoglucomutase, and glucose-6-phosphate dehydrogenase. The NADPH produced can be quantitated fluorometrically or spectrophotometrically. The reaction takes place at neutral pH, thus permitting the measurement of inorganic phosphorus in the presence of unstable organic phosphate.

Serum is preferred because most anticoagulants, except heparin, interfere with results and yield falsely low values. Phosphorus levels are increased by prolonged storage with cells at room temperature. Hemolyzed specimens are unacceptable because erythrocytes contain high levels of organic esters that are hydrolyzed to inorganic phosphate during storage and thus yield elevated levels. Additional interferences are created by icterus and lipemia. False elevations in phosphorus levels can also occur in the setting of dysproteinemia associated with monoclonal gammopathy of uncertain significance, multiple myeloma, or Waldenstrom's macroglobulinemia (Bazydlo, 2014).

Reference Interval

In normal adults, serum phosphorus varies between 2.8 and 4.5 mg/dL (0.89 and 1.44 mmol/L). Higher phosphorus levels occur in growing children (between 4.0 and 7.0 mg/dL, or 1.29 and 2.26 mmol/L). Serum phosphate is best measured in fasting morning specimens because of diurnal variation, with higher levels in the afternoon and evening as well as a reduction in serum phosphate after meals. Levels are influenced by dietary intake, meals, and exercise.

MAGNESIUM

Physiology

Distribution

Magnesium is the fourth most abundant cation in the body after calcium, sodium, and potassium; it is the second most prevalent intracellular cation. The normal body magnesium content in an adult is approximately 1000 mmol, or 22.66 g, of which 50% to 60% is in bone; the remaining 40% to 50% is in the soft tissues. One-third of skeletal magnesium is exchangeable and probably serves as a reservoir for maintaining a normal extracellular magnesium concentration.

Only 1% of total body magnesium (TBMg) is in extracellular fluid. In serum, about 55% of magnesium is ionized or free magnesium (Mg^{++}), 30% is associated with proteins (primarily albumin), and 15% is complexed with phosphate, citrate, and other anions. The interstitial fluid concentration is approximately 0.5 mmol/L. In cerebrospinal fluid (CSF), 55% of the magnesium is free or ionized, and the remaining 45% is complexed with other compounds (Elin, 1988).

Approximately 99% of TBMg is in bone matrix or is intracellular. About 60% of this total is within bone matrix; the other 40% is within skeletal muscle, within blood cells, or in the cells of other tissues. Intracellular magnesium concentration is approximately 1 to 3 mmol/L (2.4–7.3 mg/dL). Within the cell, magnesium is compartmentalized, and most of it is bound to proteins and negatively charged molecules; approximately 80% of cytosolic magnesium is bound to ATP. Significant amounts of magnesium are found in the nucleus, mitochondria, and endoplasmic reticulum. Free magnesium accounts for 0.5% to 5.0% of the total cellular magnesium; it is the fraction that is probably important as a cofactor supporting enzyme activity.

Function

Magnesium is essential for the function of more than 300 cellular enzymes, including those related to the transfer of phosphate groups, all reactions that require ATP, and every step related to the replication and transcription of DNA and the translation of messenger RNA. This cation is also required for cellular energy metabolism and has an important role in membrane stabilization, nerve conduction, ion transport, and calcium channel activity. In addition, magnesium plays a critical role in the maintenance of intracellular potassium concentration by regulating potassium movement through the membranes of the myocardial cells. Thus, magnesium deficiency can result in a variety of metabolic abnormalities and clinical consequences, including refractory plasma electrolyte abnormalities (especially depressed potassium) and cardiac arrhythmias, most often observed after stress such as cardiac surgery (Weisinger & Bellorin-Font, 1998).

Magnesium Homeostasis

TBMg depends mainly on gastrointestinal (GI) absorption and renal excretion. The average dietary intake of magnesium fluctuates between 300 and 350 mg/day, and intestinal absorption is inversely proportional to the ingested amount. The factors controlling the intestinal absorption of magnesium remain poorly understood.

The kidney is the principal organ involved in magnesium regulation. Renal excretion is about 120 to 140 mg/24 hours for a person on a normal diet. Approximately 70% to 80% of plasma magnesium is filtered through the glomerular membrane. Tubular reabsorption of Mg^{++} is different from that for other ions because the proximal tubule has a limited role and 60% to 70% of the reabsorption of Mg^{++} takes place within the thick ascending loop of Henle (Quamme, 1989). Even though the distal tubules reabsorb only 10% of the filtered Mg^{++}, they are the major sites of magnesium regulation. Many factors, both hormonal and nonhormonal (e.g., parathyroid hormone, calcitonin, glucagon, vasopressin, magnesium restriction, acid-base changes, potassium depletion), influence both Henle's loop and distal tubule reabsorption. However, the major regulator of reabsorption is the plasma concentration of Mg^{++} itself. Increased Mg^{++} concentration inhibits loop transport, whereas decreased concentration stimulates transport, regardless of whether or not there is magnesium depletion. The mechanisms appear to be regulated by the Ca^{++}/Mg^{++}-sensing receptor, located on the capillary side of the thick-ascending-limb cells, which senses the changes in Mg^{++} (Quamme, 1997). Other factors that may play a role in magnesium regulation include calcium concentration and rate of sodium chloride reabsorption.

In magnesium deficiency, serum levels decrease, which leads to reduced urinary excretion. Later, bone stores of magnesium are affected as the process of equilibration with bone stores takes place over several weeks.

Because serum contains only about 1% of TBMg, it may not accurately reflect total stores. In general, a low serum level indicates deficiency and a high level indicates adequate stores. However, the most common result—a normal level—should be interpreted with caution because it does not exclude an underlying deficiency. The most accurate assessment of magnesium status is generally considered to be the loading test, wherein magnesium is given intravenously. Magnesium-deficient individuals retain a greater proportion of the load and excrete less in the urine than normal individuals (Papazachariou et al., 2000). However, the test is not commonly used because it is difficult to administer.

Analytic Techniques

Total Magnesium

Serum is preferred over plasma for magnesium determination because anticoagulant interferes with most procedures. Serum magnesium is usually measured by photometry. The reference method for total magnesium is AAS. Most clinical laboratories use a photometric method on an automated analyzer. These methods use metallochromic indicators or dyes that change color upon selectively binding magnesium from the sample. Some of the chromophores used include calmagite, methylthymol blue, formazan dye, and magon (see Chapter 28). In the calmagite photometric method, which is the one most commonly used, calmagite, whose structure is shown in Chapter 28 (see Fig. 28.2), forms a colored complex with magnesium in alkaline solution. This complex is stable for over 30 minutes, and its absorbance at 530 to 550 nm (depending on the indicator) is directly proportional to the magnesium concentration in the specimen aliquot. Some of these measurements are affected by increased serum bilirubin levels, which can result in a significant underestimation of Mg in the sample.

Ionized (Free) Magnesium

Ionized magnesium can be measured with magnesium ISEs that have been incorporated into several commercial clinical analyzers (Huijgen et al., 1999).

These ISEs employ neutral carrier ionophores that are selective for Mg^{++}. However, in addition to Mg^{++}, these ISEs measure Ca^{++}, thus requiring a chemometric correction to calculate the true free magnesium levels in the sample. Studies have shown significant differences in the measured ionized magnesium on different analyzers that were attributed to interference from free calcium in the sample as well as to insufficient specificity and lack of standardization of the calibrators (Hristova et al., 1995; Cecco et al., 1997). Further improvements in the method for ISEs for ionized magnesium will improve the performance and increase the availability of Mg^{++} determination in the clinical laboratory.

As with ionized calcium determinations, ionized magnesium measurements are affected by pH. The rate of change of ionized magnesium measurements is not as significant as that seen in ionized calcium determinations. Changes in magnesium in relation to alterations of pH are similar to those in ionized calcium, although less well characterized. With an increase in pH, ionized magnesium is decreased; with a decrease in pH, it is increased (Wang et al., 2002). There is a potential for discrepancies between free and total magnesium levels in the setting of alcoholism, diabetes mellitus, cardiovascular disease, and even pregnancy (Bazydlo, 2014).

Reference Interval

The reference interval for serum total magnesium in normal adults ranges between 0.75 and 0.95 mmol/L (1.7 and 2.2 mg/dL, or 1.5 and 1.9 mEq/L). There appear to be no significant sex or age differences. Erythrocyte magnesium is about three times that of serum. The magnesium concentration in CSF is 2.0 to 2.7 mg/dL (1.0–1.4 mmol/L). The reference interval for ionized magnesium depends on the analyzer used for its measurement and varies from 0.44 to 0.60 mmol/L (Hristova et al., 1995).

HORMONES REGULATING MINERAL METABOLISM

The three principal hormones regulating mineral and bone metabolism are PTH, $1,25(OH)_2D_3$, and calcitonin. PTH and $1,25(OH)_2D_3$ are the primary hormones that exert an effect; calcitonin is less prominent in the cycle that maintains mineral metabolism. In addition, the metabolic effects of calcitonin are less well understood.

Parathyroid Hormone

Physiology

Synthesis. PTH is synthesized and secreted by the chief cells of the parathyroid gland. Intact PTH is a single-chain polypeptide consisting of 84 amino acids with a molecular mass of 9500 Da. It is derived from a larger precursor, pre-pro-PTH, of 115 amino acids, which undergoes two successive cleavages, both at the amino-terminal sequences. This gives rise to an intermediate precursor, pro-PTH, and then to the hormone itself. Any pro-PTH that reaches the circulation is immediately converted to PTH and other products.

Secretion. Multiple factors control the release of PTH from the parathyroid glands, but only a small number are known to be physiologically important. PTH secretion is regulated on a time scale of seconds by extracellular ionized calcium and represents a simple negative-feedback loop. Extracellular signals are detected by a calcium-sensing receptor, located on the plasma membrane of the parathyroid chief cell. Stimulation of this receptor leads to suppression of the rate of PTH secretion via intracellular signals (inositol triphosphate and diacylglycerol) generated by the active receptor. The receptor is present in parathyroid glands, the calcitonin-secreting cells of the thyroid, brain, and kidney. This G-protein–linked receptor is mutated in the disorders of familial hypocalciuric hypercalcemia, neonatal severe hyperparathyroidism, and autosomal-dominant hypocalcemia (Mundy & Guise, 1999).

Ionized magnesium has also been shown to influence the secretion of PTH. Hypocalcemic patients with low serum magnesium concentration often require administration of magnesium to increase serum PTH levels before the serum calcium concentration can be restored to the desired interval. Chronic severe hypomagnesemia such as that seen in alcoholism has been associated with impaired PTH secretion, whereas an acute decrease in serum magnesium concentration can lead to increased PTH levels.

Other levels of PTH control include regulation of PTH gene transcription and parathyroid chief cell mass by vitamin D and extracellular calcium. $1,25(OH)_2D_3$ chronically suppresses the synthesis of PTH by interacting with vitamin D receptors in the parathyroid gland.

Function. The primary physiologic function of PTH is to maintain the concentration of ionized calcium in the ECF, which is achieved by the following mechanisms: (1) stimulation of osteoclastic bone resorption and release of calcium and phosphate from bone; (2) stimulation of calcium reabsorption and inhibition of phosphate reabsorption from the renal tubules; and (3) stimulation of renal production of $1,25(OH)_2D_3$, which increases intestinal absorption of calcium and phosphate. The amino-terminal end of the PTH molecule binds to the PTH receptor, which modulates adenylate cyclase and phospholipase C. Activating mutations in this receptor may cause the hypercalcemia and epiphyseal disorganization seen in Jansen's chondrodysplasia (Bastepe et al., 2004).

The net effects of PTH actions on bone, the kidney, and indirectly on the intestine include increased serum total and ionized calcium concentrations and decreased serum phosphate. Its immediate effects on the kidney are to increase renal plasma flow and cause diuresis. At the level of the distal convoluted tubule, it causes increased reabsorption of calcium and chloride with the exchange of phosphate into the urine. These effects are mediated through its activation of renal adenyl cyclase. As a result, urinary cyclic adenosine monophosphate (cAMP) and urinary phosphate are increased with a mild secondary hyperchloremic acidosis. In the absence of disease, the increase in serum calcium reduces PTH secretion through a negative-feedback loop, thus maintaining calcium homeostasis. If this negative-feedback loop is sufficiently interrupted by an autonomously functioning parathyroid gland to increase resting calcium to abnormally high levels, the capacity of the distal tubules to reabsorb calcium is exceeded, and hypercalciuria results.

Heterogeneity. PTH metabolism is complex and produces several fragments of varying biologic and immunologic reactivity. The intact PTH is the biologically active form and has a half-life in the circulation of less than 4 minutes. The kidney and liver clear intact PTH rapidly. In the liver, intact PTH is cleaved into discrete fragments and smaller peptides that are released into the circulation. The released inactive carboxy-terminal fragments circulate considerably longer than the intact hormone, mainly because they are cleared exclusively by glomerular filtration (Mundy & Guise, 1999).

Analytic Techniques

Historically, PTH immunoassays were developed to measure mid-region, N-terminal, and C-terminal regions. However, these assays cross-reacted with amino acid sequences present in both mid-region and carboxyl fragments of the intact hormone and measured mostly inactive fragments because they are present in greater concentration than the intact molecule. Because the kidney clears inactive PTH fragments, results from these assays were difficult to interpret, especially in patients with impaired renal function. PTH intact is measured by noncompetitive immunometric (sandwich) assays (see Chapter 45), which, depending on the type of detection system used, are divided into immunoradiometric assay (IRMA), when radiolabeled, and immunochemiluminometric assay, when labeled with a chemiluminescent compound. Most automated systems use immunochemiluminometric assays. These immunometric assays have several advantages over earlier assays: increased sensitivity and specificity through the use of sequence-specific and affinity-purified antibodies, extended assay concentration range, and decreased incubation time. Also, they do not utilize radioactive compounds.

Reference Interval

The reference interval for intact PTH in normal adults is 10 to 65 pg/mL (ng/L) when a two-site immunometric method is used. Studies have demonstrated that intact PTH is secreted in episodic or pulsatile fashion, with an overall circadian rhythm characterized by a nocturnal rise in intact PTH. Serum is the preferred specimen for measurement of PTH. Prolonged storage of the specimen aliquot causes falsely decreased levels.

Biointact PTH

Physiology

Traditional tests for intact PTH detect and measure both the biologically intact 84 amino acid PTH molecule (1-84) and its minimally active to inactive metabolites. Recall that the intact, biologically active molecule is cleaved within minutes to the many metabolites that have a longer half-life and of which there is a much higher concentration in the circulation at any given time. One of these cleavage products, the 7-84 PTH breakdown fragment, is a weak antagonist to PTH activity and may actually lower patient serum calcium levels. It is therefore important to distinguish between intact PTH and breakdown products in the setting of patients with chronic renal failure (Brossard et al., 2000). In uremic patients, the metabolites, including the 7-84 breakdown fragment, accumulate as the result of decreased renal clearance and can therefore give the impression of an elevated PTH (Quarles et al., 1992).

Intact PTH testing has been utilized to bypass inaccuracies of testing created by chronic renal disease, where inactive metabolites of PTH may accumulate. This third-generation test eliminates interference by the metabolites and is of great clinical utility in patients with impaired renal function. The biointact PTH test specifically measures the (1-84) molecule via a two-site

chemiluminescent assay. This assay yields a higher specificity than second-generation tests for the biologically active intact PTH, but cost and availability considerations make this a second-line test that is used primarily in following metabolic bone status in patients with renal insufficiency.

Normal ranges for this test show seasonal variation, in part because of lower serum 25(OH)D during winter in the healthy population. Normal values for this test range from 8 to 50 pg/mL (Nichols Advantage, 2004).

Intraoperative PTH

Historically, parathyroid surgery has consisted of bilateral neck exploration in an attempt to identify enlarged parathyroid glands. In recent years, clinical practice has moved away from this costly and invasive procedure, which often requires an overnight hospital stay, to minimally invasive parathyroidectomy with or without the use of a handheld gamma probe. This procedure consists of preoperative administration of technetium-99m sestamibi 2 hours preoperatively followed by performance of a parathyroid scan. The parathyroid adenoma, with its increased numbers of cytoplasmic mitochondria, selectively absorbs large amounts of this radioactive substance, which then allows identification of the adenoma(s) with a handheld gamma probe. This method of identifying the enlarged gland allows for removal of only the hyperfunctional parathyroid gland in cases of parathyroid adenoma. Cases of parathyroid hyperplasia still require bilateral neck exploration. Depending on the size of these enlarged glands, they may or may not be identified on the preoperative parathyroid scan (Sofferman et al., 1998; Goldstein et al., 2000; Sokoll et al., 2000).

Once the hyperfunctioning parathyroid gland is identified via sestamibi scan and only a single parathyroid gland has been shown to be involved, patients are taken to surgery for minimally invasive parathyroidectomy. This approach has reduced surgical and hospital costs, as well as admission time (Goldstein et al., 1991).

Prior to surgery, a baseline PTH value is obtained. Following incision, dissection to the radioactive parathyroid gland is guided by the use of a gamma probe. Once identified, the parathyroid gland is removed. After removal, the surgeon waits about 10 to 20 minutes and then obtains a postremoval PTH value. This postremoval PTH value should decrease to at least 50% to 75% below the preoperative level or should have a "significant" trend toward normal in patients with markedly elevated preoperative PTH levels. The decrease in PTH levels reassures the surgeon that the adenomatous gland has been removed. If no or minimal decrease is noted in the intraoperative PTH level, the surgeon is obligated to resume neck exploration for additional abnormal glands, and multiple adenomas or hyperplasia is suggested as the underlying process. Intraoperative PTH testing is recommended for patients undergoing surgery for primary hyperparathyroidism, reoperative hyperparathyroidism, and venous/tumor localization presurgery in the angiography suite (Sokoll et al., 2004).

Analytic Techniques

The intraoperative technique for intact PTH customarily requires blood collected in an EDTA tube (plasma) or a red-top tube (serum). The sample is maintained at a cold temperature to minimize breakdown, and it is then submitted for rapid PTH testing. These immunochemiluminometric assays provide rapid results by modifying certain test parameters on the standard assay. Specifically, increased incubation temperature, continuous shaking of the reaction contents, and alterations in sample and reagent volumes are used to expedite antibody–antigen reactions. The end result is a more rapid assay, albeit one that is more costly, less sensitive, and more imprecise than the standard assay. These assays correlate well with standard assays and are totally acceptable for measuring large drops in PTH concentration during surgery.

Parathyroid Hormone–Related Peptide

Physiology

Parathyroid hormone–related peptide (PTH-rP) was first discovered in tumors derived from head and neck, lung, breast, kidney, and other solid tissues. It has since been described as a hormone with paracrine and autocrine functions. PTH-rP is composed of 141 amino acids and shows significant homology with PTH in the first 13 amino acids. It is the product of a large gene on chromosome 12 that is syngeneic to the PTH gene on chromosome 11. This peptide shares the same receptor as PTH. While PTH production is limited to the parathyroid glands, PTH-rP can be produced by virtually all tissues and exhibits a wide range of physiologic functions. Its actions include binding to and activating the PTH receptor, thus simulating the PTH biological effects on bone, kidney, and intestine. Similar to PTH, PTH-rP increases bone resorption by stimulating osteoclasts and promotes renal tubular reabsorption of calcium. The net effect is elevated serum calcium concentration. It is now known that PTH-rP is produced by approximately 50% of primary breast cancers, and its production may be enhanced by bone-derived factors such as transforming growth factor-β (Yin et al., 1999; see Chapter 76 for a description of this growth factor). Other malignant tumors also elaborate this peptide. PTH-rP has been implicated as the agent responsible for humoral hypercalcemia in patients with malignancy.

Elevation of PTH-rP has been observed in approximately 50% to 90% of patients with malignancy-associated hypercalcemia. Increased PTH-rP is seen in squamous cell carcinomas of the lung, esophagus, cervix, and skin, as well as in other malignancies (e.g., islet cell carcinomas, T-cell and B-cell lymphomas, multiple myeloma). PTH-rP levels are normal in patients with primary hyperparathyroidism, hypoparathyroidism, chronic renal failure, and other conditions with hypercalcemia.

Some benign hyperplasias, including massive mammary hypertrophy, vasoactive intestinal peptide-secreting tumors, pheochromocytomas, and lactational changes of the breast, may elaborate this peptide (Strewler, 1997).

A more recent study demonstrated that PTH-rP has therapeutic potential in the treatment of postmenopausal osteoporosis; PTH-rP increased bone mineral density by nearly 5%—a rate that exceeds those of current therapeutic approaches (Horwitz et al., 2003). Currently, PTH 1-34 (teriparatide) represents the only PTH analog approved in the United States for anabolic bone treatment purposes. Synthetic PTH-rp (1-36) and a PTH-rP analog (1-34) known as BA058 have shown therapeutic effects as well (Augustine, 2013).

Analytic Technique and Reference Interval

PTH-rP is measured by immunometric assay. The limit of detection of these assays is between 0.1 and 1.0 pmol/L (Endres et al., 1999). The reference interval for PTH-rP is method dependent. In normal individuals, PTH-rP levels range from undetectable to around 2 pmol/L, whereas the mean concentration of PTH-rP in patients with humoral hypercalcemia of malignancy has been reported to be 22.2 pmol/L. Recent studies have shown that most patients (95%) with a PTH level over 26 ng/mL had no increased PTH-rP, a number that increased to 100% when only patients with hypercalcemia were evaluated. This study suggests that testing for PTH-rP in patients with low or low normal PTH may not be of clinical utility (Fritchie et al., 2009).

Calcitonin

Physiology

Synthesis and Metabolism. Calcitonin is synthesized and secreted by specialized C cells (parafollicular cells) of the thyroid gland and acts on the bones, kidneys, and GI tract. Circulating immunoreactive calcitonin is derived from a larger precursor, and the monomeric form is the only biologically active entity. Calcitonin monomer is a 32 amino acid peptide with a molecular mass of 3500 Da. The ionized calcium concentration is the most important regulator of calcitonin secretion. Increases in ionized calcium lead to an increase in calcitonin secretion. Other potent calcitonin secretagogues include the GI peptide hormones and gastrin in particular (Care et al., 1971). The latter could explain the presence of a mild postprandial increase in calcitonin concentration.

The calcitonin receptor is structurally similar to PTH/PTH-rP and secretin receptors. It exists in several isoforms, and its expression seems to be influenced by ambient concentrations of calcitonin itself (Mundy & Guise, 1999). Calcitonin is metabolized within minutes of secretion, primarily by the kidney.

Physiologic Role and Clinical Use. Although calcitonin has been viewed as a major calcium-regulating factor because of its calcium-lowering and phosphorus-lowering properties, its precise physiologic role is still unclear. Calcitonin directly inhibits osteoclastic bone resorption by directly binding to osteoclasts. The effect of this binding action is observed within minutes after calcitonin administration. This inhibition is transient and likely has little role in overall calcium homeostasis, although it may be important in the short-term control of calcium loads. Calcitonin also inhibits the action of PTH and vitamin D. Although some clinical studies suggest that serum calcium does not appear to be affected in patients with total thyroidectomy, other studies suggest that medullary thyroid carcinoma and an excess of calcitonin can give rise to marked hypocalcemia. In the kidney, calcitonin causes increased clearance of calcium and phosphate. The mechanisms of its action on the GI tract have not been elucidated entirely.

In addition to evaluation of calcitonin in the setting of bony abnormalities, testing for calcitonin is an important adjunct in the evaluation of the patient with nodular thyroid disease and is often performed in the hope of

identifying the patient with early medullary thyroid carcinoma, which may be seen in the setting of multiple endocrine neoplasia type 2 (MEN 2), as described in Chapter 25. Therapeutic success in medullary thyroid carcinoma hinges on its early identification; slight elevations of calcitonin with subsequent surgical exploration of the thyroid may identify this lesion in its early, nonpalpable stage of development. It is well known that the therapeutic efficacy is poor in cases that are identified as well-developed palpable tumors because many such patients already have metastatic disease (Rieu et al., 1995; Horvit & Gagel, 1997). Until recently, routine testing for calcitonin in patients with nodular thyroid disease was not considered cost-effective in the United States. Studies in Europe, however, have shown this to be cost-effective. A recent cost-effectiveness analysis performed in the United States concluded that routine calcitonin testing in patients with nodular thyroid disease is, in fact, of comparable cost-effectiveness as other screening tests, such as those for thyroid-stimulating hormone, breast cancer (mammography), and colon cancer (colonoscopy) (Cheung et al., 2008). Diagnostic sensitivity for medullary thyroid carcinoma is increased by pentagastrin stimulation before calcitonin level testing. A high index of suspicion for this aggressive neoplasm should exist in patients with plasma or serum calcitonin levels over 100 pg/nL (Vierhapper et al., 1997).

Therapeutic applications of calcitonin have been explored and include its use in the treatment of osteoporosis and in the treatment of Paget disease, the early stages of which are characterized by increased bone resorption.

Analytic Technique and Reference Interval

In the past, serum calcitonin was measured primarily by radioimmunoassay (RIA). However, differences in assay specificity and sensitivity, matrix and nonspecific serum effects, and heterogeneity of the circulating calcitonin have contributed to contradicting results and discrepancies in reference values for the hormone. At present, a number of highly sensitive (limit of detection as low as 2 pg/mL), two-site immunometric methods (electroimmunoassays and IRMAs) for serum calcitonin are available. These tests are now regarded as the most reliable methods of testing for serum calcitonin.

The reference interval for serum calcitonin in normal adults is less than 25 pg/mL for males and less than 20 pg/mL for females. Gender, age, growth, pregnancy, lactation, and ingestion of food have been reported to affect the levels of calcitonin.

Vitamin D and Metabolites

Physiology

Synthesis and Metabolism. (See also Chapters 9 and 27.)

The steroid hormone $1,25(OH)_2D_3$ is the major biologically active metabolite of the vitamin D sterol family. The vitamin D precursor (cholecalciferol or vitamin D_3) may be ingested in the diet or synthesized in the skin from 7-dehydrocholesterol (provitamin D_3) through exposure to sunlight. The plant-derived form of vitamin D is called vitamin D_2 or ergosterol. Neither form of vitamin D has any significant biological activity; both must be metabolized to hormonally active forms. This activation occurs in two steps, the first of which takes place in the liver and the second of which takes place in the kidney. Cholecalciferol is transported to the liver bound to a specific α_1-globulin. In the liver, vitamin D undergoes hydroxylation to produce 25-hydroxyvitamin D (calcidiol), a metabolite with limited biological activity. Because the liver only loosely regulates this step, circulating levels of 25-hydroxyvitamin D mirror the amounts of vitamin D that may be ingested or synthesized by the skin. The 25-hydroxyvitamin D is then bound by the vitamin D–binding protein and is transported to the kidney, where it undergoes further hydroxylation by 1-α-hydroxylase in the proximal tubular mitochondria to form the more potent metabolite $1,25(OH)_2D_3$ (calcitriol). Renal hydroxylation of 25-hydroxyvitamin D is the major controlling point in vitamin D metabolism—a step that is regulated by serum phosphate, calcium, and circulating PTH concentrations. PTH and phosphate depletion act independently to increase $1,25(OH)_2D_3$ production by inducing 1-α-hydroxylase activity, with PTH being the more potent stimulus. Decreased blood calcium stimulates the parathyroid glands to secrete PTH, which, in turn, increases production of $1,25(OH)_2D_3$ in the renal proximal tubules. Conversely, a rise in blood calcium suppresses PTH secretion, which lowers the production of $1,25(OH)_2D_3$. The only other known important extrarenal sites of $1,25(OH)_2D_3$ production are the placenta and the granulomatous tissue. In humans, the half-life of $1,25(OH)_2D_3$ in the circulation is approximately 5 hours. It is excreted as urinary and fecal metabolites (Mundy & Guise, 1999). Several other vitamin D metabolites are produced in the kidney; most of these have been shown to be biologically inert. The most notable of these is 24,25-dihydroxyvitamin D_3, produced by the action of 24-α-hydroxylase in the kidney. It is activated when PTH levels are low or when inorganic phosphate levels are elevated (Fig. 16.3).

Physiologic Role. $1,25(OH)_2D_3$ bound to a vitamin D–binding protein is delivered to the intestine, where the free form is taken up by the cells and transported to a specific nuclear receptor protein. Although the receptor binds several forms of vitamin D, its affinity for 1,25-dihydroxyvitamin D_3 is about 1000 times that of 25-hydroxyvitamin D_3, accounting for why the former is so much more biologically active than the latter. As a result of this interaction in the intestine, calcium-binding protein is synthesized. In bone, osteocalcin, osteopontin, and alkaline phosphatase are produced. In the intestine, the net effect of $1,25(OH)_2D_3$ is to transport calcium and phosphate from the lumen of the small intestine into the circulation by stimulating the expression of calcium-carrying proteins, increasing plasma calcium and phosphate concentrations. It also increases bone resorption and enhances the effects of PTH in the nephron to promote renal tubular calcium reabsorption. $1,25(OH)_2D_3$ is a powerful differentiating agent for committed osteoclast precursors, causing their maturation to form multinucleated cells that are capable of resorbing bone. These pathways enable $1,25(OH)_2D_3$ to provide a supply of calcium and phosphate available at bone surfaces for the formation of normal mineralized bone (Mundy & Guise, 1999).

The demonstration that the sites of action of $1,25(OH)_2D_3$ are not limited to its target tissues—namely, the intestine, bone, and kidney—has expanded the therapeutic function of vitamin D. Administration of vitamin D hormone has been shown to be effective in the therapeutic management and prevention of postmenopausal and age-related osteoporosis. A recent study showed that higher-than-recommended (700–800 vs. the recommended 600 IU) doses of vitamin D in nursing home residents reduced the number of patients with falls and the total number of falls in nursing home residents (Kerry et al., 2007). Another study showed that a similar dose acts to prevent fracture in a comparable population (Bischoff-Ferrari et al., 2005). Evidence suggests that, besides exhibiting calciotropic properties, vitamin D may be a developmental hormone. As discussed in Chapters 9 and 27, vitamin D has been found to exhibit antitumor growth activity.

Analytic Techniques

Of the more than 35 metabolites of vitamin D_2 and vitamin D_3, only 25(OH)D and $1,25(OH)_2D$ measurements are clinically important. 25(OH)D is a better marker than vitamin D for evaluation of vitamin D status because of its longer half-life (2–3 weeks vs. 5–8 hours) (Papapoulos et al., 1982), more limited fluctuation with exposure to sunlight and dietary intake, larger concentration, and ease of measurement. Measurement of $1,25(OH)_2D_3$ is useful in detecting certain states of inadequate or excessive hormone production in the evaluation of hypercalcemia, hypercalciuria,

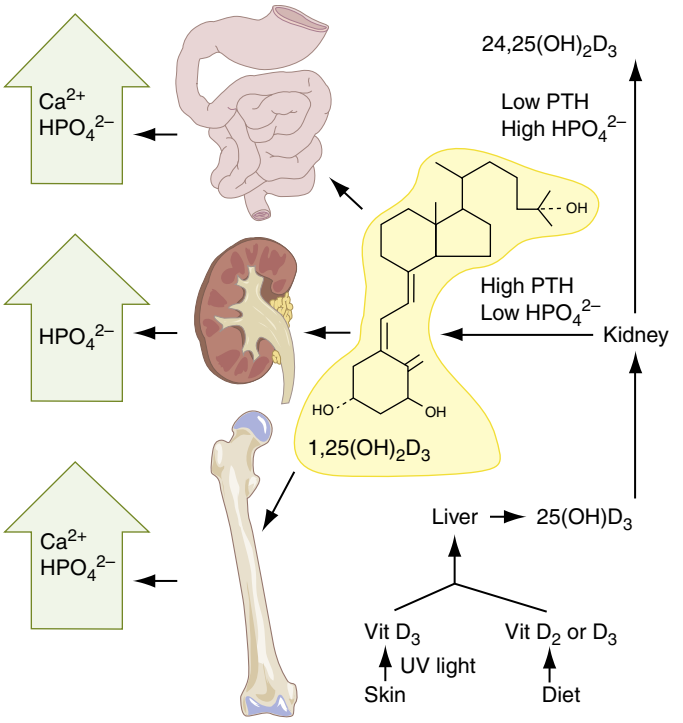

Figure 16.3 Pathways of vitamin D synthesis and their end-organ effects. The *large green arrows* indicate increases in calcium and phosphate induced by vitamin D (dihydroxycholecalciferol).

and hypocalcemia, as well as in bone and mineral disorders. Because both vitamin D_2 and vitamin D_3 are metabolized to compounds of similar if not equal biological activity, for clinical purposes the assays should measure $25(OH)D_2$ and $25(OH)D_3$ or $1,25(OH)_2D_2$ and $1,25(OH)_2D_3$, respectively. At present, the reference method for the assay of $25(OH)D_2$ and $25(OH)D_3$ is dual mass spectrometry. Most other assays for vitamin D metabolites are measured by RIA or chemiluminescent immunoassay.

Reference Interval

The reference interval for 25(OH)D in serum is approximately 10 to 50 ng/mL (25–125 nmol/L), and for $1,25(OH)_2D$ is 15 to 60 pg/mL (36–144 pmol/L) (Endres & Rude, 1999). Levels for 25(OH)D are influenced by sunlight exposure, latitude, skin pigmentation, sunscreen use, and hepatic function. 25(OH)D levels also exhibit seasonal variation. Winter values may be 40% to 50% lower than summer values because of reduced UV radiation exposure. Concentrations of vitamin D metabolites vary with age and are increased in pregnancy.

Phosphatonins

Phosphatonins represent a new group of phosphate-regulating factors that remain incompletely understood yet have thus far shed much light on the many disorders of phosphate and calcium metabolism. These factors include FGF-23, MEPE, and secreted frizzled-related protein 4 (sFRP4). These substances act to reduce renal inorganic phosphate reabsorption both directly by their action on the renal tubules and indirectly through the inhibition of 25-hydroxyvitamin D_1 α-hydroxylase, causing a reduction in $1\alpha25(OH)_2D$ formation that results in decreased inorganic phosphate absorption and reduced calcium absorption. Both mechanisms produce decreased serum inorganic phosphate levels, resulting in rickets in children and osteomalacia in adults. Increased levels of these factors, as well as the previously discussed PHEX, have been causally implicated in tumor-induced osteomalacia, X-linked hypophosphatemic rickets, and autosomal-dominant hypophosphatemic rickets (ADHR). X-linked hypophosphatemic rickets is associated with varied mutations of the *PHEX* gene, and ADHR is due to activating mutations of FGF-23 (Schiavi & Kumar, 2004; Roetzer et al., 2007; Ichikawa et al., 2008; Pettifor, 2008; Gaucher et al., 2009). All of these entities are clinically characterized by reduced serum phosphate, increased urinary phosphate levels, and aberrant bone mineralization. In addition, these entities are customarily seen in the setting of normal serum calcium.

Although the previous entities result largely from increased FGF-23, mutations in FGF-23 resulting in a net reduced level of effective FGF-23 have also been described at multiple loci. They produce disease through a common mechanism of reduced phosphaturic activity, creating the clinical picture of hyperphosphatemic tumoral calcinosis (Araya et al., 2005; Larsson et al., 2005; Masi et al., 2009). Another factor implicated in the hyperphosphatemic form of this disease is UDP-*N*-acetyl-α-D galactosamine/polypeptide *N*-acetylgalactosaminyltransferase 3. Inactivating mutations of this gene result in accelerated degradation of FGF-23 into inactive metabolites (Jueppner, 2007). FGF-23 is of interest to nephrologists and endocrinologists alike for its predictive abilities for adverse events in chronic renal disease and as a measurable substance useful in identifying tumors associated with oncogenic osteomalacia.

Klotho is a cofactor that serves to provide tissue specificity for FGF-23. It is a single-pass transmembrane protein that is expressed in the renal distal tubule, pituitary gland, parathyroid gland, and the sinoatrial node of the heart. Defective or decreased Klotho results in aging-like changes in mice, including osteomalacia; those mice with overexpression show aging suppressor–like changes, including increased bone density (Cavalli, 2012).

Analytic Techniques

These growth factors have been evaluated experimentally via polymerase chain reaction (PCR) and more recently by enzyme-linked immunosorbent assay for intact FGF-23 and the processed fragments (18 and 12 kDa). In addition, reverse transcriptase-PCR (RT-PCR) for FGF-23 has been performed on formalin-fixed, paraffin-embedded tissue in the setting of phosphaturic mesenchymal tumors of the mixed connective tissue type with high sensitivity and specificity (Bahrami et al., 2009). More recently, an immunometric sandwich enzyme assay was developed that is now being utilized for testing commercially. The results of these tests for FGF-23 must be interpreted in the context of serum calcium, phosphate, magnesium, PTH, $1,25(OH)_2D$, and 25(OH)D (Fukumoto, 2014). Tumor-induced osteomalacia may be suspected in patients with normal serum calcium, magnesium, and PTH; with low to very low serum phosphorus; and increased urine phosphorus and magnesium. $1,25(OH)_2D$ will be low to low normal in these patients, while 25(OH)D is usually normal to low normal. In this clinical setting, serum FGF-23 measurements are indicated and may be of assistance in identifying oncogenic osteomalacia (Fukumoto & Yamashita, 2003). This test may also assist in follow-up for patients who have had tumors removed. The half-life of FGF-23 is very short, requiring rapid turnaround. This feature may also be of assistance in identifying small or occult tumors via systemic venous sampling, whereby the location of a tumor is established by venous sampling from different areas of the body and comparing the levels of FGF-23.

Reference Interval

FGF-23 values can be markedly increased (>900 RU/mL) in infants less than 3 months of age. Thereafter, the values are reduced to 230 RU/mL or less in patients 3 months to 17 years of age and 180 RU/mL or less in those 18 years of age and older. While values in patients with oncogenic osteomalacia are often at least twice the normal upper limit of the reference interval, making this a useful test in that setting, there is some concern about the use of FGF-23 testing in patients with chronic kidney disease, where it is utilized to predict the development of secondary hyperparathyroidism and adverse outcomes, because there is some variation as to test analytes and lack of reproducible cutoff points (Wesseling-Perry, 2011).

DISORDERS OF MINERAL METABOLISM

HYPERCALCEMIA

Increased serum calcium is associated with anorexia, nausea, vomiting, constipation, hypotonia, depression, high-voltage T waves on electrocardiography, and occasionally lethargy and coma. Persistent hypercalcemia or persistently elevated calcium–phosphorus ionic activity product may cause ectopic depositions of calcium in tissues throughout the body. This may take the form of ectopically calcified blood vessel walls associated with necrotic skin lesions in calciphylaxis. It may also lead to calcifications in viable tissues (metastatic calcification/tumoral calcinosis), particularly those developing pH gradients with localized relative alkalosis (e.g., pulmonary alveolar walls, renal medullary pyramids, deep gastric mucosa). The most common causes of hypercalcemia are primary hyperparathyroidism and malignant neoplasms, which account for 80% to 90% of all patients with hypercalcemia. Less frequent causes include renal failure, diuretics, vitamins A and D intoxication, lithium therapy, milk–alkali syndrome, immobilization, hyperthyroidism and other nonparathyroid endocrinopathies, and familial hypercalciuric hypercalcemia (Box 16.1). Recently, mutations in *FGF-23* and in another gene encoding the so-called N-terminal sterile α motif protein (*SAMD9* gene) have also been implicated in tumoral calcinosis. Mutations in *FGF-23* characteristically cause hyperphosphatemic tumoral calcinosis, while mutations in *SAMD9* cause normophosphatemic tumoral calcinosis. The tumoral calcinosis caused by both is familial (Araya et al., 2005; Larsson et al., 2005; Chefetz et al., 2005, 2008; Topaz et al., 2006; Masi et al., 2009). Disease due to *SAMD9* mutations appears to affect Yemenite Jews predominantly. *Primary hyperparathyroidism* (PHPT) is characterized by excessive secretion of PTH in the absence of an appropriate physiologic stimulus and with no response to the physiologic negative-feedback loop of hypercalcemia. This results in a generalized disorder of calcium, phosphate, and bone metabolism. Approximately 100,000 cases of

BOX 16.1

Causes of Hypercalcemia

Parathyroid Hormone (PTH)-Mediated

Primary hyperparathyroidism (most common)
Sporadic
Multiple endocrine neoplasia (types 1 and 2)
Familial hypocalciuric hypercalcemia
Ectopic secretion of PTH by neoplasms (rare)?

Non–PTH-Mediated

Malignancy associated (most common)
Vitamin D mediated
Vitamin D intoxication
Increased generation of $1,25(OH)_2D$
Other endocrinopathies
Thyrotoxicosis
Hypoadrenalism
Immobilization with increased bone turnover
Milk–alkali syndrome
Sarcoidosis
Multiple myeloma

Figure 16.4 Hyperparathyroid bone disease (osteitis fibrosa cystica). **A,** The hand radiograph demonstrates scalloped cortical resorption on the radial *(left)* side of the phalanges and radiolucency of the terminal phalangeal tufts. **B,** Biopsy of compact bone with advanced hyperparathyroid disease demonstrates conversion of compact to cancellous bone with internal resorption of Haversian systems by osteoclastic cutting cones (CC) and paratrabecular fibrosis (100 ×).

PHPT occur each year in the United States, and the incidence increases with age. The disease affects women twice as frequently as it affects men. Most cases are caused by solitary parathyroid adenomas. Other causes include multiple parathyroid adenomas, hyperplasia, and, rarely, parathyroid carcinoma. Hypercalcemia in PHPT is characteristically associated with decreased serum phosphate due to PTH-induced phosphate diuresis and is frequently accompanied by mild acidosis from decreased renal reabsorption of bicarbonate. The hypercalcemia is attributed to the direct action of PTH on bone, causing increased resorption; PTH-activated renal tubular reabsorption; and PTH-stimulated increased renal biosynthesis of $1,25(OH)_2D_3$, which increases intestinal absorption of calcium (Boden & Kaplan, 1990). Half or more of patients with PHPT are asymptomatic. Symptomatic patients usually present with recurrent nephrolithiasis, chronic constipation, mental depression, neuromuscular dysfunction, recurrent chronic pancreatitis, or peptic ulcer, and less frequently with unexplained or premature osteopenia (Deftos et al., 1993).

The unique bone manifestation of PHPT is osteitis fibrosa cystica generalizata. This is characterized by diffuse skeletal radiolucency with focal cystic bone lesions, subperiosteal bone resorption most pronounced in the digits, and osseous deformities on routine radiographs. Histologically, paratrabecular fibrosis and marrow hypervascularity are accompanied by increased numbers of osteoclasts, causing trabecular scalloping (Howship lacunae) as a result of accelerated bone resorption (Fig. 16.4). As the disease progresses, the marrow cavity is gradually replaced by fibrous tissue. The process is even more pronounced in compact bone, where large aggregates of osteoclasts demonstrate wedge-shaped "tunneling" resorption that enlarges Haversian canals (cutting cones). Tunneling resorption is also seen in cancellous bone, and its presence is almost always indicative of hyperparathyroidism. When these changes are widespread and chronic, they result in radiographic alterations, including the so-called "salt and pepper" appearance of the skull and subperiosteal resorption pattern of the fingers. Fractures that develop through this altered bone tend to heal poorly and result in space-occupying lesions filled with fibrous tissue, multinucleated giant cells, hemorrhage, and hemosiderin; these are sometimes referred to as "brown tumors" even though they are not neoplastic. Generalized osteitis fibrosa cystica is now very uncommon because serum calcium and phosphate screening usually reveal early parathyroid hyperfunction long before signs or symptoms develop. However, even in advanced cases, bony changes are often reversible with successful removal of the tumor.

PHPT may be inherited as an autosomal dominant trait and may present as a part of MEN. MEN 1 consists of hyperparathyroidism and tumors of the pituitary gland and pancreas. It is often associated with Zollinger-Ellison syndrome, characterized by islet cell tumors with gastrin hypersecretion and peptic ulcer disease. MEN 2A consists of hyperparathyroidism, pheochromocytoma, and medullary carcinoma of the thyroid. Studies have identified the molecular defects in hyperparathyroidism. A gene locus on chromosome 11 has been associated with MEN 1. The same locus appears to be lost in approximately 25% of solitary parathyroid adenomas, implying that the defect responsible for MEN 1 can also cause the sporadic disease.

Secondary hyperparathyroidism is present when there is resistance to the metabolic actions of PTH, as occurs in patients with renal failure, vitamin D deficiency (osteomalacia), and pseudohypoparathyroidism. This leads to parathyroid gland hyperplasia and excessive production of PTH. The pathogenesis varies somewhat, depending on the nature and severity of renal disease. However, decreased renal excretion of phosphate as a consequence of impaired glomerular filtration is paramount. In such patients, there is an initial tendency toward hypocalcemia owing to the fact that as phosphate levels rise, calcium levels decrease because their ionic activity product constant makes their serum concentrations inversely related (see Chapter 9 for a discussion of the solubility product constant). In addition, chronic renal failure includes reduced production of $1,25(OH)_2D$ by the kidney. Decreased $1,25(OH)_2D$ causes a reduced response of the skeleton to PTH and decreased calcium absorption from the intestine, contributing to hypocalcemia. Because of the decreased serum ionic calcium, there is positive feedback to increase parathyroid hormone secretion; this causes parathyroid gland hyperplasia. Initial clinical manifestations include low to normal serum calcium and hyperphosphatemia. Later, in cases with severe secondary hyperparathyroidism, both hypercalcemia and hyperphosphatemia develop. In addition, bone pain, ectopic calcifications, and pruritus may be seen. The complex bone disease occurring in secondary hyperparathyroidism and renal failure is usually termed *renal osteodystrophy* (Fig. 16.5) and is discussed in greater detail later. Autonomous hyperparathyroidism may sometimes supervene in the setting of chronic parathyroid stimulation. Typical patients are those with chronic renal failure or with some other disease that chronically lowers serum ionized calcium levels and stimulates long-term parathyroid hormone secretion. This chronic parathyroid stimulation results in increased parathyroid mass and diffuse parathyroid hyperplasia. If increased levels of parathyroid hormone are not diminished by hypercalcemia, whether it occurs in the setting of continued calcium wasting or if the calcium level is corrected (e.g., after renal transplantation), the clinical syndrome is sometimes referred to as *tertiary hyperparathyroidism*. Patients with this syndrome may have parathyroid adenomas, parathyroid hyperplasia, and even parathyroid carcinomas. There is also a tendency for these patients to develop metastatic calcifications in soft tissues, blood vessels, and organs because their transiently increased calcium and phosphate levels may exceed the ionic activity product for these ions and cause precipitation of the excess.

Malignant tumors are the most frequent cause of hypercalcemia in the hospital inpatient population. *Malignancy-associated hypercalcemia* can be divided into cases with or without bony metastases. Radiolucent bone lesions indicative of metastatic disease are frequently seen in patients with hematologic malignancies (multiple myeloma, lymphomas, and leukemias), lung carcinoma, renal cell carcinoma, and thyroid carcinoma. Several possible mechanisms have been implicated in the development of malignancy-associated hypercalcemia, including direct tumor lysis, secretion of osteoclast-activating factor by tumor cells, and secretion of lymphokines with osteoclast potentiating activity, such as interleukin-1 and tumor necrosis factor. Conventional bone radiographs and bone scanning can detect most bony metastases. Hypercalcemia without bony metastases is also known as *humoral hypercalcemia of malignancy* (HHM). Diagnosis in these cases, in general, is more difficult because the primary tumor may be occult. A variety of tumor types have been associated with this syndrome, including renal carcinoma, hepatocellular carcinoma, carcinomas of the head and neck, lung carcinomas, and islet cell tumors of the pancreas. The most common cause of HHM is secretion of PTH-rP by the tumor. The diagnosis is highly suggestive when urinary cAMP excretion (typically seen in hyperparathyroidism) is increased in the setting of reduced or normal PTH.

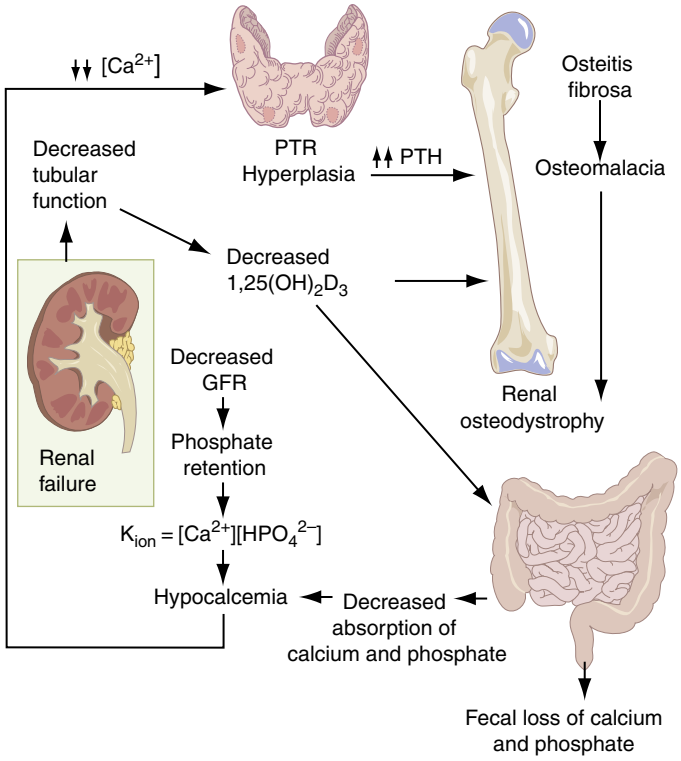

Figure 16.5 Relationships leading to renal osteodystrophy in chronic renal failure.

Vitamin D intoxication is another cause of hypercalcemia and is usually the result of excessive intake of vitamin supplements over a prolonged period of time. Excess vitamin D causes increased calcium absorption by the intestines, enhanced bone resorption, and hypercalciuria. PTH is suppressed, but the frequent development of renal failure may make it difficult to exclude hyperparathyroidism; 25(OH)D has been implicated as the major metabolite responsible for the syndrome. The diagnosis is supported by careful history taking, measurements of 25(OH)D, and a prompt response following steroid administration. Clinically, vitamin D intoxication is manifest by weakness, irritability, nausea, vomiting, and diarrhea. Soft-tissue calcification is a common feature because serum phosphorus tends to be elevated. Intoxication may persist for months because of storage of vitamin D in adipose tissue.

Hypercalcemia associated with *granulomatous disorders* is seen commonly in patients with sarcoidosis and less frequently in patients with tuberculosis, silicone-induced granulomas, and fungal diseases such as coccidioidomycosis and candidiasis. Renal failure, soft-tissue calcification, nephrolithiasis, and severe hypercalcemia are potential manifestations. Different mechanisms in the development of hypercalcemia have been implicated, including enhanced sensitivity to vitamin D, increased concentration of vitamin D metabolites, and unregulated generation of $1,25(OH)_2D$ by macrophages in granulomatous tissue.

Milk–alkali syndrome was first reported in patients with peptic ulcer disease taking large amounts of milk and absorbable alkali (e.g., calcium carbonate). Recently, a rise in the incidence of the syndrome has been reported; this may be due to the widespread use of calcium carbonate preparations in the treatment and prophylaxis of osteoporosis. The syndrome is manifest by hypercalcemia, hypocalciuria, alkalosis, azotemia, and soft-tissue calcifications.

Laboratory testing in the differential diagnosis of hypercalcemia includes measurements of serum total and ionized calcium, urine calcium, serum and urine phosphorus, alkaline phosphatase, albumin, intact PTH, PTH-rP, and urine cAMP. Determination of various other analytes (e.g., growth hormone, cortisol, cortisone suppression test, selective venous catheterization with measurement of local PTH concentration, measurements of vitamin D metabolites) can provide valuable information in selected cases. Meaningful interpretation of relevant laboratory data often requires various special studies in addition to a complete history and physical examination. Renal function tests and studies of acid-base balance may be indicated. Histopathologic examination of bone biopsy specimens from appropriate sites can be of unique value in selected cases.

BOX 16.2

Causes of Hypocalcemia

Parathyroid Hormone (PTH)-Mediated

PTH deficiency
Permanent
Acquired
Postsurgical
Hereditary
Idiopathic hypoparathyroidism
DiGeorge syndrome (branchial dysgenesis)
Polyglandular autoimmune syndromes
Reversible
Severe hypomagnesemia
Long-standing hypercalcemia
PTH resistance
Pseudohypoparathyroidism

Vitamin D–Mediated

Vitamin D deficiency
25(OH)D deficiency
$1,25(OH)_2$ deficiency
Reversible inhibition of 1-hydroxylase
Intrinsic renal defects (chronic renal failure, tubulopathies, Fanconi syndrome)
Defective response to $1,25(OH)_2D$
Mutations of vitamin D receptor

HYPOCALCEMIA

Chronic hypocalcemia presents with neuromuscular and neurologic manifestations, including muscle spasms, carpopedal spasm, peripheral and perioral paresthesias, cardiac arrhythmias, lengthening of the QT interval and low-voltage T waves on the electrocardiogram, and, in severe cases, laryngeal spasm and convulsions. Respiratory arrest may occur. Severe hypocalcemia will eventually result in tetany. Hypocalcemia has many causes, which can be divided into several major categories: deficiencies in PTH production or secretion, resistance to PTH action, deficiency of vitamin D or vitamin D metabolites, and deficiencies in bone mineralization with normal metabolism of PTH and vitamin D (Box 16.2). The most common causes of hypocalcemia are chronic renal failure, hypomagnesemia, hypoparathyroidism, pseudohypoparathyroidism, vitamin D deficiency, and acute pancreatitis. Less frequently, low plasma calcium may be seen in critically ill patients with sepsis, burns, and acute renal failure. Transient hypocalcemia can be observed after administration of a number of drugs, including heparin, glucagon, and protamine, as well as after massive transfusions of citrated blood products.

Hypoparathyroidism, hereditary or acquired, is characterized by diminished or absent PTH production by the parathyroid glands, which leads to a fall in plasma calcium and corresponding hyperphosphatemia. In addition, these patients have absent or low levels of $1,25(OH)_2D$. In the past, acquired hypoparathyroidism secondary to neck surgeries and thyroidectomies, in particular, was more common than hereditary hypoparathyroidism. With improvement in surgical techniques, however, its incidence has diminished dramatically. Hereditary hypoparathyroidism can occur as an isolated entity with a variable pattern of inheritance (idiopathic hypoparathyroidism), in association with defective development of both the thymus and the parathyroid glands (DiGeorge syndrome or branchial dysgenesis), or as part of a complex hereditary autoimmune syndrome involving failure of the adrenals, ovaries, and parathyroids, usually referred to as *autoimmune polyglandular deficiency*. Hereditary hypoparathyroidism is often manifested within the first decade of life. In addition to low or absent PTH and hypocalcemia, certain skin manifestations, such as alopecia and candidiasis, occur frequently.

Pseudohypoparathyroidism (PHP), also known as *Albright hereditary osteodystrophy*, is a rare genetic disorder characterized by ineffective PTH action rather than failure of parathyroid gland hormone production. Clinically, PHP presents with some of the features of hypoparathyroidism, such as extraosseous calcifications, extrapyramidal symptoms and signs such as choreoathetotic movements and dystonia, chronic changes in fingernails and hair, lenticular cataracts, and increased intracranial pressure with papilledema. Serum calcium is depressed despite an increased concentration of PTH, suggesting resistance to PTH. Moreover, whereas infusion of PTH in patients with hypoparathyroidism generally results in a marked increase in both urinary cAMP and phosphaturia, patients with PHP usually respond with subnormal urinary phosphate excretion and cAMP

production. This is due to a defect in the stimulatory G-protein of adenylate cyclase that is necessary for the action of PTH.

Hypocalcemia associated with hypomagnesemia may be the result of deficient PTH release from the parathyroid glands or impaired responsiveness to the hormone. Hypocalcemia associated with hypovitaminosis D may occur as a result of inadequate production of vitamin D_3 in the skin, insufficient dietary supplementation, inability of the small intestine to absorb adequate amounts of the vitamin from the diet, and resistance to the effects of vitamin D. The latter may be due to deficient or defective receptors for $1,25(OH)_2D$ or to the use of drugs that antagonize vitamin D action. Hypovitaminosis D is associated with disturbances in mineral metabolism and secretion of PTH and mineralization defects in the skeleton, such as rickets in children and osteomalacia in adults (see later discussion). Decreased levels of vitamin D lead to insufficient intestinal absorption of calcium and hypocalcemia, followed by increased secretion of PTH (secondary hyperparathyroidism). Increased PTH stimulates calcium release from bone and decreases calcium clearance by the kidney, increasing calcium levels in the circulation. If hypovitaminosis D persists, severe hypocalcemia may occur.

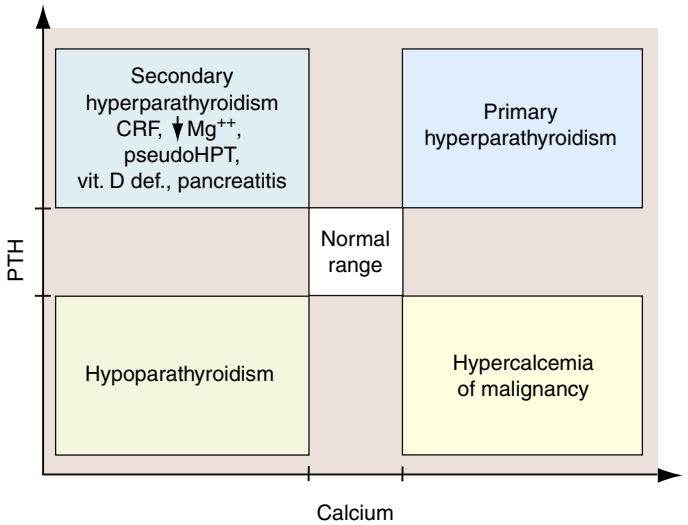

Figure 16.6 Graph correlating alterations in serum calcium levels and parathyroid hormone levels with the diseases most frequently causing these alterations.

An inherited disorder, characterized by defective production of $1,25(OH)_2D$ in the kidney, has been described. In this syndrome, known as *pseudovitamin D–deficient rickets* or *vitamin D–dependent rickets type I*, there is a deficiency in renal 25(OH)D-1α-hydroxylase activity, which results in low production of $1,25(OH)_2D$ and decreased levels in the circulation, but with a normal response to physiologic doses of calcitriol. In vitamin D–dependent rickets type II, mutations impair the function of the $1,25(OH)_2D$ receptor by altering the binding of the hormone to the receptor, causing elevated levels of circulating $1,25(OH)_2D$. Although administration of high doses of calcitriol produces further increases in the levels of $1,25(OH)_2D$, no physiologic response occurs. Another inherited disease associated with impaired vitamin D metabolism is X-linked hypophosphatemic rickets. This condition is characterized by a functional defect in 25(OH)D-1α-hydroxylase, hypophosphatemia, and normal or low serum levels of $1,25(OH)_2D$. Figure 16.6 summarizes the more common causes of abnormal calcium levels, along with their differential diagnoses. Tables 16.1 and 16.2 summarize serum calcium, phosphate, vitamin D levels, and other laboratory values in altered metabolic states.

HYPERPHOSPHATEMIA

Hyperphosphatemia is usually caused by decreased renal excretion in acute and chronic renal failure; increased intake with excessive oral, rectal, or intravenous administration; or an increased extracellular load due to a transcellular shift in acidosis. Less common causes include increased tubular reabsorption in hypoparathyroidism; pseudohypoparathyroidism; and increased extracellular load due to cell lysis in rhabdomyolysis, intravascular hemolysis, leukemia, lymphoma, and cytotoxic therapy. In addition,

TABLE 16.1
Serum Calcium, Phosphate, and Vitamin D Levels in Various Disorders

Disorder	Calcium	25(OH)D	1,25(OH)D	Phosphate
25(OH)D intoxication	High	High	Low, normal	Normal, high
Primary hyperparathyroidism	High	Normal	Normal, high	Low
Secondary hyperparathyroidism	Low	Low, normal, high	Low, normal, high	Low, normal, high
Tertiary hyperparathyroidism	Normal, high*	Low, normal, high	Low, normal, high	Low, normal, high
Malignancy	High	Normal	Low, normal	Low
Vitamin D deficiency	Low	Low	Low, normal, high	Low
Renal failure	Low	Normal	Low	High
Hyperphosphatemia	Low	Normal	Low	High
Vitamin D rickets types I, II	Low	Normal, high	Low, normal, high	Low
Granulomatous diseases (sarcoid/TB)	High	Low, normal, high	High	Normal, high
Postmenopausal osteoporosis	Normal	Normal	Normal	Normal
Senile osteoporosis	Normal	Normal	Normal	Normal
Osteomalacia	Low, normal	Low, normal	Low	Low, normal, high

*Calcium may be normal in the setting of concurrent $1,25(OH)_2D_3$ deficiency.

TABLE 16.2
Laboratory Values in Various Altered States of Calcium Metabolism

	Primary Hyperparathyroidism	Humoral Hypercalcemia of Malignancy	Secondary Hyperparathyroidism	Tertiary Hyperparathyroidism	Familial Hypocalciuric Hypercalcemia
Urine calcium	High	High	Normal, high	Normal, high	Low
Serum phosphate	Low	Low	Low, normal, high	Low, normal, high	Low
Urine phosphate	High	High	High	High	High
1,25(OH)D	Normal, high	Low, normal	Low, normal, high	Low, normal, high	Normal, high
PTH intact	High	Low	High	High	High
PTH-r protein	Normal	High	Normal	Normal	Normal

PTH, Parathyroid hormone; *PTH-r,* parathyroid hormone related.

hyperphosphatemia may be seen secondary to overmedication with vitamin D and production of vitamin D by granulomatous diseases such as sarcoidosis and tuberculosis.

No direct symptoms result from hyperphosphatemia. When high levels are maintained for long periods, however, mineralization is enhanced, and calcium phosphate may be deposited in abnormal sites. Ectopic calcification is a frequent complication in patients with chronic renal failure receiving supplements of vitamin D when correction of hyperphosphatemia is inadequate (Weisinger & Bellorin-Font, 1998).

HYPOPHOSPHATEMIA

Hypophosphatemia is observed in 0.25% to 2.15% of general hospital admissions. Alcohol abuse is the most common cause of severe hypophosphatemia, probably as a result of poor food intake, vomiting, antacid use, and marked phosphaturia. It is also caused by ingestion of large amounts of nonabsorbable antacids that bind phosphate. Hypophosphatemia is induced by several mechanisms, including internal redistribution, increased urinary excretion, decreased intestinal absorption, or a combination of these abnormalities. The most common cause is a shift of phosphorus from extracellular fluid into cells, which can be observed in acute respiratory alkalosis associated with sepsis, salicylate poisoning, alcohol withdrawal, heatstroke, hepatic coma, increased insulin during glucose administration, recovery from diabetic ketoacidosis, and refeeding of malnourished patients. Increased urinary excretion is usually secondary to hyperparathyroidism; renal tubular defects, as in Fanconi syndrome and familial hypophosphatemia; X-linked vitamin D–resistant rickets; aldosteronism; glucocorticoid and mineralocorticoid administration; and diuretic therapy. Hypophosphatemia due to urinary losses is observed in osmotic diuresis, acute volume expansion, and up to 30% of patients with malignant neoplasms such as certain leukemias and lymphomas. In oncogenic hypophosphatemia with osteomalacia, also referred to as tumor-induced osteomalacia, mesenchymal tumors, which are more often benign than malignant, produce hyperphosphaturia by a mechanism in which overproduction of FGF-23 has been implicated (Nelson et al., 2003; Folpe et al., 2004; Florenzano, 2017). Increased intestinal loss is due to vomiting, diarrhea, and use of phosphate-binding antacids. Decreased intestinal absorption is observed in malabsorption, vitamin D deficiency, and steatorrhea (Box 16.3).

Symptomatic hypophosphatemia is usually observed when plasma phosphorus falls below 0.32 mmol/L. Clinical manifestations include proximal weakness, anorexia, dizziness, myopathy, dysphagia, ileus, respiratory failure due to weakness of the respiratory muscles, impairment of cardiac contractility due to depletion of ATP in myocardial cells, and metabolic encephalopathy.

HYPERMAGNESEMIA

Hypermagnesemia (i.e., plasma Mg^{++} concentration >0.9 mmol/L) is rare and usually iatrogenic. Those most at risk are the elderly and patients with bowel disorders or renal insufficiency. Clinical manifestations of hypermagnesemia include hypotension, bradycardia, respiratory depression, depressed mental status, and electrocardiographic abnormalities (Weisinger & Bellorin-Font, 1998).

BOX 16.3

Causes of Abnormal Phosphate Levels

Elevated

Hypoparathyroidism and pseudohypoparathyroidism
Renal failure
Hypervitaminosis D
Cytolysis
Pyloric obstruction

Decreased

Alcohol abuse
Primary hyperparathyroidism
Acute respiratory alkalosis
Myxedema
Exogenous/endogenous steroids
Diuretic therapy
Renal tubular defects
Oncogenic phosphaturia
Diabetic coma

HYPOMAGNESEMIA

Magnesium deficiency is found in approximately 11% of hospitalized patients. The usual reason is loss of magnesium from the GI tract or the kidney. Depletion by GI tract occurs during acute and chronic diarrhea, malabsorption, and steatorrhea after extensive bowel resection, and in patients with the rare inborn error of metabolism, primary intestinal hypomagnesemia. Na^{+} resorption may serve as the basis for magnesium depletion in the kidney because of a sodium-dependent magnesium efflux pathway in the same tubular segment (Ikari et al., 2003) or because of a primary defect in renal tubular reabsorption of Mg^{++}. Factors that can cause Mg^{++} losses from the urine include thiazide and loop diuretics, increased sodium excretion and volume expansion (parenteral fluid therapy), hypercalcemia and hypercalciuria (hyperthyroidism or malignancy), and nephrotoxic drugs (aminoglycoside antibiotics, cisplatin, amphotericin B, cyclosporine). Diabetes mellitus is a common cause of hypomagnesemia, probably secondary to glycosuria and osmotic diuresis. Another important and very common cause of magnesium deficiency is alcohol; this is found in approximately 30% of alcoholic patients admitted to the hospital. Sustained and extensive stress, including that seen with varied surgical procedures and acute illnesses, may be associated with depressed serum magnesium levels (Box 16.4).

Signs and symptoms of magnesium depletion do not usually appear until extracellular levels have fallen to 0.5 mmol/L or less. Manifestations of significant magnesium depletion are largely due to the associated hypocalcemia and include neuromuscular hyperexcitability characterized by carpopedal spasm, seizures, muscular weakness, depression, and psychosis; metabolic abnormalities (carbohydrate intolerance, hyperinsulinism); and cardiac arrhythmias.

BIOCHEMICAL MARKERS OF BONE REMODELING

The skeleton constantly undergoes a process of remodeling that is essential for bone health. Bone remodeling is a coupled process that begins with resorption of old bone by osteoclasts, a process that takes approximately 50 days, followed by formation of new bone by osteoblasts, which takes

BOX 16.4

Causes of Hypomagnesemia

Decreased Intake/Absorption

Protein-calorie malnutrition
Starvation
Alcoholism
Prolonged intravenous therapy
Inadequate parenteral supplementation
Malabsorption (e.g., celiac sprue)
Neonatal gut immaturity
Excessive gastrointestinal losses
Prolonged gastric suction
Laxatives
Intestinal or biliary fistula
Severe diarrhea

Excessive Renal Losses

Diuretics
Acute tubular necrosis—diuretic phase
Acute renal failure—diuresis
Primary aldosteronism
Hypercalcemia
Renal tubular acidosis
Idiopathic renal wasting
Chronic renal failure with wasting

Miscellaneous

Idiopathic
Acute pancreatitis
Porphyria with syndrome of inappropriate antidiuretic hormone (SIADH)
Multiple transfusions with citrated blood
Endocrine
Hyperthyroidism
Hyperparathyroidism
Diabetes mellitus with diabetic ketoacidosis
Hyperaldosteronism
Medications (e.g., cisplatin, cyclosporine, gentamicin, ticarcillin)

another 150 days, for a total turnover cycle lasting approximately 200 days (Erikson et al., 1994). Beginning at middle age or earlier, net bone loss occurs because resorption exceeds formation, a fact that was identified more than 60 years ago by Fuller Albright, the father of metabolic bone disease. He noted that postmenopausal women had elevated urinary calcium levels and deduced that this reflects a negative calcium balance that can result in osteoporotic fractures. Estrogen deficiency and many other diseases and conditions accentuate bone resorption (Watts, 1999).

Three major diagnostic procedures are available to monitor bone turnover and evaluate metabolic bone disease: bone imaging techniques, bone biopsy, and biochemical markers of bone turnover. Although bone density measurement is an important diagnostic tool in osteoporosis, it is difficult for the test to detect increased bone turnover in its early stages or to monitor acute changes. Also, bone densitometry gives a summated measure of mineralized bone matrix; it does not define abnormal distribution of bone loss. Bone biopsy can define the distribution of bone mass and can answer questions about bone mineralization that cannot be answered with bone densitometry. However, bone biopsy is invasive, and, in the absence of mineralization defects, it provides a relatively static glimpse into long and slowly developing processes. Thus, it is not useful in routine clinical management of osteoporosis. In osteoporosis, net bone loss is caused by only a slight imbalance of bone resorption over formation; thus, conventional markers such as calcium and PTH are usually normal. In contrast, bone turnover markers are more sensitive to subtle change and can be used to noninvasively detect and monitor the progression of metabolic bone disease. Laboratory assessment of these markers has been the focus of much attention in recent years (Ju et al., 1997; Souberbielle et al., 1999; Eastell, 2017; Greenblatt, 2017).

BONE RESORPTION MARKERS

Bone tissue has three components: an organic matrix (called *osteoid*), bone mineral, and bone cells. Bone resorption markers have included constituents of bone matrix such as calcium and collagen degradation products such as hydroxyproline, pyridinium cross-links, and telopeptides, as well as cellular products involved with degradation of the mineralized matrix, such as tartrate-resistant acid phosphatase (TRAP). Urinary calcium is affected by diet and renal function; thus, it is not sensitive or specific for assessment of bone remodeling (Watts, 1999). TRAP, a lysosomal enzyme found in osteoclasts, is not considered a useful test. Measurement of the amino acids hydroxyproline and glycosylated (galactosyl and glucosyl-galactosyl) hydroxylysine is not specific for skeletal collagen and has been found to correlate poorly with bone resorption as determined by bone histomorphometry and calcium kinetics. The most useful tests measure pyridinium cross-links and cross-linked telopeptides. Bone resorption markers have a diurnal rhythm, making the timing of sample collection critical. Serial samples that are to be utilized for monitoring response to antiresorptive medications should be collected at the same time of day. Values are highest in the mornings; thus, collection of the sample during this time is indicated.

Recently, serum cathepsin K, the primary enzyme involved in proteolysis of bone type I collagen by osteoclasts, has been implicated as a possible valuable marker of bone resorption. However, the data are incomplete with respect to its efficacy as a useful clinical marker. Several other bone metabolism regulators, such as RANK, RANKL, and even osteoprotegerin, a decoy receptor of nuclear factor κ, may be of interest. None of these have been evaluated to the extent at which they have proven efficacy in following bone metabolism clinically. In fact, conflicting reports have described the utility of determining an osteoprotegerin/RANKL ratio, with some suggesting that this ratio in patients beginning therapy for rheumatoid arthritis was the single most important predictor of joint erosion measured 11 years later (van Tuyl et al., 2010). Another study with shorter follow-up did not show that this ratio predicted disease progression.

Pyridinium Cross-Links (Pyridinoline and Deoxypyridinoline)

Collagen fibrils consist of many cross-linked amino acids that effectively stabilize the mature collagen molecule. These include pyridinoline (Pyr), a cross-linked polymer formed from three hydroxylysine residues, and deoxypyridinoline (DPyr), which is formed from two hydroxylysine residues and one lysine residue. These cross-links are found in collagen types I, II, and III. Although these cross-links are not unique to bone, they are found in a unique ratio in the bone, a fact that makes these substances ideal candidates as markers for bone breakdown. In the collagen of most other tissues, the ratio of Pyr/DPyr is 10:1, while in bone it is 3-3.5:1. This difference means that DPyr is more pronounced in bone and metabolic bone disease. DPyr is essentially specific for bone, in that it is found in relatively significant amounts in bone and has been shown to correlate well with bone turnover (Robins, 1995). An additional characteristic that makes evaluation of pyridinium cross-links ideal is that they are neither metabolized upon their release nor absorbed from the diet. They are excreted in urine in free form (40%) and in peptide-bound form (60%). Because cross-link molecules are found only in mature collagen, their excretion in the urine reflects breakdown of mature collagen and is not an expression of newly synthesized bone collagen (Watts, 1999). Thus, their presence in urine suggests active bone resorption. Excretion of Pyr and DPyr is increased after menopause and can be utilized to study the effects of hormone replacement therapy on bone turnover (Fledelius et al., 1994). The clinical applications of measuring these substances include identification of individuals at risk for bone loss and fracture, assessment of metabolic bone disease, prediction of bone metastases, subsequent skeletal complications, and even outcome in cancer patients afflicted by solid tumors (prostate, breast, and lung most commonly) and primary bone tumors, as well as management of antiresorptive therapy. Pyr and DPyr are measured in urine by high-performance liquid chromatography (HPLC; see Chapter 24) or immunoassays. Care must be taken to account for the marked diurnal variation that is seen with urinary pyridinolines, with a peak late at night and early in the morning. Although a 24-hour urine collection avoids this issue and does not require correction for the creatinine concentration, an early-morning fasting sample corrected for creatinine concentration is a more sensitive marker of bone turnover (Bettica et al., 1992).

Cross-Linked Telopeptides

During bone resorption, only 40% of cross-links are released as free pyridinium cross-links; the remaining 60% are peptide-attached cross-links (Risteli & Risteli, 1993). Type I collagen has two sites with attached cross-links. These are called telopeptides, which occur in the amino-terminal and carboxy-terminal regions of the collagen molecule. These telopeptides are released into the circulation as collagen is degraded; they are then excreted into the urine. Amino-telopeptides (NTx) and carboxy-telopeptides (CTx) are excreted in the urine and can be measured by immunoassay. Testing for these cross-links is widely available.

Cross-linked telopeptides have been utilized in estimating relative risks of hip fracture in postmenopausal women and show promise in predicting such complications of osteoporosis (Chapurlat et al., 2000; Swaminathan, 2001).

Although baseline levels of cross-linked telopeptides do not necessarily correlate with baseline bone mineral density, their serial measurement has shown the capacity to predict early response to therapy (Fink et al., 2000). Studies have shown reductions of urinary CTx and NTx in the range of 50% to 60% with 3 to 6 months of antiresorptive therapy (Eastell et al., 2003) and correlation of these reductions with the prediction of long-term bone mass response (Ravn et al., 2003).

BONE FORMATION MARKERS

Bone formation markers include alkaline phosphatase and three byproducts of bone matrix synthesis, including osteocalcin and amino- and carboxy-terminal procollagen I extension peptides.

Alkaline Phosphatase

(See Chapter 21.)

Bone alkaline phosphatase (ALP-B), an osteoblast membrane-bound enzyme, is released into the circulation by phosphatidylinositol glycanase activity and formation of membrane vesicles. Studies have shown that the amount of ALP-B activity in osteoblasts and in bone is proportional to collagen formation; thus, it can provide an index of the rate of bone formation. Human serum contains a variable mixture of ALP isoenzymes from the liver, intestine, kidney, and bone. During pregnancy, ALP may be derived from the placenta (Farley et al., 1994). Certain malignant tumors may also produce a heat-stable ALP isoenzyme. The function of ALP is unknown; however, it has been postulated that ALP probably has a role in the mineralization of newly formed bone. Measurements of total serum ALP are useful to follow disease activity when the amount of bone isoenzyme is exceptionally high, as in Paget disease or osteosarcoma.

The two major circulating ALP isoenzymes, bone and liver, are difficult to distinguish because they are the products of a single gene and differ only by posttranslational glycosylation. Separation of skeletal ALP can be achieved by heat inactivation, wheat germ agglutinin precipitation, electrophoresis, isoelectric focusing, and two-site immunoradiometric assays. At present, immunoassay is the method of choice because of high specificity and satisfactory precision.

Osteocalcin

Osteocalcin is the major noncollagenous protein of the bone matrix and is produced by osteoblasts, odontoblasts, and even chondrocytes. It is a 49 amino acid polypeptide that is rich in glutamic acid. Its function is incompletely understood, but it may serve as a site of deposition for hydroxyapatite crystals. In addition, recent studies suggest that osteocalcin has effects on energy metabolism by affecting the production and even the action of insulin (Lee et al., 2007). During bone matrix synthesis, some osteocalcin is released into the circulation and is rapidly cleared by the kidneys. Osteocalcin can be measured by immunoassay in plasma or serum. However, assays for osteocalcin are not yet standardized because different antibodies recognize different fragments. Antibodies that recognize both the intact molecule and the large amino-terminal mid-molecule fragment appear to provide the best clinical information (Watts, 1999). Recent studies have shown that although vitamin K does not affect the amount of osteocalcin concentration, it does affect the amount of carboxylation. Undercarboxylated osteocalcin has been suggested to be a better predictor of certain outcomes, such as fracture (Vergnaud et al., 1997). Osteocalcin is metabolized mainly in the kidneys and, to a lesser extent, in the liver; the half-life in the circulation is about 5 minutes. Osteocalcin is increased when there is high bone turnover, as occurs in hyperparathyroidism, acromegaly, and Paget disease. It is decreased in hypoparathyroidism and hypothyroidism and in patients on glucocorticoid therapy. Osteocalcin reference intervals are approximately 1.1 to 11 ng/mL (adult male) and 0.7 to 6.5 ng/mL (adult female), and testing is not routinely available.

Procollagen Type I N-Terminal and C-Terminal Peptides

Procollagen type I N-terminal peptide and procollagen type I C-terminal peptide are the precursor peptides that are removed from procollagen type I to produce type I collagen. Upon cleavage, these peptides are released into the circulation, where they can be measured, serving as markers of collagen type I synthesis. Of the two markers, procollagen type I N-terminus is more stable and thus is a more reliable marker. Incidentally, the procollagen type I C-terminal peptide has also been implicated as a potentially useful marker in predicting the extent and severity of disease in systemic sclerosis (Kikuchi et al., 1994).

METABOLIC BONE DISEASE

Metabolic bone diseases encompass a heterogeneous group of entities that diffusely affect the mass and microstructure of bones. They may be caused by nutritional deficiencies, acquired metabolic disorders, or even by genetic disorders. Because the disease is generalized, by definition every bone is involved. Consequently, a biopsy of any bone in the body should reflect these metabolic alterations to some extent. However, the disease manifestations may vary in different areas of the skeleton, and the laboratory findings are also somewhat variable (Chang, 2016). Although a very few metabolic disorders (e.g., fluorosis, vitamin A toxicity) may increase bone density, the vast majority of metabolic bone diseases result in decreased bone density. Decreased bone density may be a consequence of decreased organic matrix with normal mineralization (e.g., osteoporosis), decreased mineral content without a significant change in organic matrix (e.g., osteomalacia), or bones with both altered organic matrix and decreased mineral content (e.g., renal osteodystrophy). The purpose of this section is to review the underlying pathophysiologic mechanisms as well as the histopathologic findings of the common metabolic bone diseases, including osteoporosis, osteomalacia and rickets, and renal osteodystrophy. Because of its similarity to a metabolic bone disease histologically, Paget disease of bone is also included.

OSTEOPOROSIS

Osteoporosis, the most common metabolic bone disease (Box 16.5), is a systemic skeletal disorder characterized by decreased organic bone matrix and microarchitectural deterioration of bone tissue, with a subsequent increase in bone fragility and susceptibility to fracture (Ferrari et al., 1999). The abnormality is a result of imbalance between bone formation and bone resorption, with resorption exceeding bone formation.

Bone mass and strength are related to volumetric density, bone size, microarchitecture, and intrinsic tissue quality. These factors are likely to change during bone growth and bone loss, with selective modifications according to the skeletal site. Postmenopausal white and Asian women who are thin or small and have a positive family history are at greatest risk. Other risk factors include cigarette smoking, alcohol abuse, a sedentary lifestyle, and consumption of too little calcium. Strong evidence indicates that genetic and lifestyle factors are important determinants of peak bone mass.

BOX 16.5

Deficiencies in Organic Bone Matrix

Primary Osteoporosis

Idiopathic (children and young adults)
Postmenopausal
Senile

Secondary Osteoporosis

Hyperparathyroidism
Hyperadrenocorticism
Hypogonadism
Thyrotoxicosis
Immobilization
Calcium deficiency
Prolonged heparin administration
Miscellaneous (alcoholism, malnutrition, liver disease, rheumatoid arthritis, malabsorption)

Disorders of Connective Tissue

Osteogenesis imperfecta
Ehlers-Danlos syndrome
Marfan syndrome

As the density of bone decreases, it becomes more radiolucent; this appearance may be due to decreased collagen and/or decreased mineral. Collectively, this state is called *osteopenia*, a radiographic term that does not discriminate between the various sorts of metabolic bone disease. The term *osteopenia* should not be confused with its use in bone densitometric studies, wherein osteopenia refers to a significant loss of bone density that is about one standard deviation less than the definition of osteoporosis. Radiologic loss of bone mass is due to loss of compact and cancellous bone, but the most common skeletal problems associated with osteoporosis arise from the loss of cancellous bone. This is as much due to the arrangement of each bone type as it is to actual decreased bone mass.

As long as the bony cortex forms a continuous ring, the strength of the shaft of a long bone is proportional to the distance from the center of the medullary cavity to the outside of the cortex raised to the third power. Its stiffness is proportional to the same distance raised to the fourth power. Because resorption of compact bone is primarily an endosteal event caused by osteoclasts, this means that as compact bones become more osteoporotic, their shafts become hollower. Hollowing of the shafts is somewhat compensated for by intramembranous ossification by osteoblasts on the cortical surface. Consequently, when the medullary cavity enlarges by endosteal osteoclasis, the diameter of the cortex also enlarges. This enlargement means that the radius from medullary midpoint to outer cortex increases. Because the strength of the intact bone is proportional to this distance raised to the third power, a small increase in appositional bone can biomechanically compensate for a relatively large loss of endosteal bone (Fig. 16.7).

Cancellous (trabecular) bone, on the other hand, is affected earlier by osteoporosis not only because it has less mass but because of its architecture. Cancellous bone is arranged in thin, highly perforated, vertically oriented parallel plates braced laterally by even thinner horizontal struts. Only 25% of the cancellous bone compartment is bone by volume; the remainder consists of intertrabecular spaces filled with fat, bone marrow, and blood vessels. (see Fig. 16.1B). Compared with the cortex, the surface/volume ratio in the cancellous bone is very high, giving all bone cells free access to the delicate surfaces of the trabeculae. As a result, cancellous bone is resorbed more rapidly than cortical bone. Furthermore, if osteoclastic resorption progresses at an equal rate in all parts of the cancellous bone, the horizontal struts that serve to brace and reinforce the vertical plates are lost earlier because they began with significantly less bone mass than the vertical plates. Resorption of these horizontal braces contributes proportionately more to the morbidity of osteoporosis than the diffuse loss of bone mass because of the altered distribution of forces that results. As these struts disappear, the vertical trabeculae form increasingly longer vertical line segments that are subject to progressively increased bending forces (Fig. 16.8). Increasing the length of each of these vertical trabecular line segments increases their susceptibility to fatigue fracture by a factor of the incremental length squared. If the unprotected length of a vertical plate is doubled, it is four times more likely to fracture. For example, the vertebral bodies are composed of 5% cortical bone and 95% trabecular bone. A 50%

loss of horizontal trabecular bone can result in a 75% loss of load-bearing capacity. It is not surprising that pain, skeletal deformities, and fractures are common sequelae.

Osteoporosis may be divided etiologically into primary and secondary types. In primary osteoporosis, there are typical complex associations and patient ages, but the exact cause of bone loss is not known. The most common type of primary osteoporosis is postmenopausal osteoporosis, which occurs in the setting of hormonal decrease, has its maximal loss of bone mass in the first menopausal decade, and seems to be associated with increased osteoclastic activity. It is manifest primarily as a loss of cancellous bone (Black, 2016). So-called senile osteoporosis manifests a decade or more later than the postmenopausal variety and is associated with a decline in osteoblast number proportionate to the demand for their activity; it affects mainly compact bone (Manolagas & Jilka, 1995). Idiopathic juvenile osteoporosis occurs in the peripubertal period and is associated with increased osteoclastic activity. Unlike the postmenopausal and senile varieties, it is usually self-limited, and the skeleton may regain much of its bone mass.

In secondary osteoporosis, there is a known reason for the loss of bone mass, which may sometimes be preventable or even reversed. Etiologies include hyperparathyroidism and other endocrinopathies, space-occupying marrow lesions causing increased pressure in the marrow cavity, calcium deficiency, malabsorption, administration of steroids or heparin, and immobilization. Certain connective tissue disorders, such as osteogenesis imperfecta, Marfan syndrome, and Ehlers-Danlos syndrome, also result in structural or functional osteoporosis.

Clinically, patients with osteoporosis often have pain and fractures due to increased bone fragility. One-third of women and one-fifth of men older than 50 years will eventually develop osteoporotic fractures. The wrist, the hip, and the spine are the three most common fracture locations. According to the World Health Organization (WHO), osteoporosis is defined as "a bone mineral density that is 2.5 or more standard deviations (SD) less than that of a young healthy adult as measured with dual-energy x-ray absorptiometry (DEXA) (T-Score of –2.5 or less)." However, this definition can be confusing. An individual may still develop osteoporotic fractures when the bone mineral density decreases significantly comparing to that prior to the bone loss and yet the T-Score may still not be in the osteoporotic range.

Current treatment efforts are aimed at preventing resorption or stimulating new bone production. Current antiresorptive treatments include estrogens, selective estrogen receptor modulators (SERMs), vitamin D, calcitonin, and bisphosphonates, and even anti-RANK monoclonal antibodies (denosumab). The only anabolic agent currently approved for use is PTH. However, antiremodeling drugs decrease bone formation as well as bone resorption and PTH analogues increase bone formation but also may activate bone resorption. Treatment is generally recommended in postmenopausal women who have a bone mineral density T score of –2.5 or less, a history of spine or hip fracture, or a Fracture Risk Assessment Tool (FRAX) score indicating increased fracture risk. Bisphosphonates are commonly used as first-line treatment in women who do not have contraindications (Eriksen, 2014). Bisphosphonates and denosumab reduce the risk of hip, nonvertebral, and vertebral fractures; teriparatide (a form of PTH) reduces the risk of nonvertebral and vertebral fractures. Romosozumab, a specific inhibitor of sclerostin that activates bone formation while reducing bone resorption, may in the future be an exciting potential therapy for osteoporosis (clinical trials and safety evaluation are still ongoing). More rapid therapeutic effects are measurable with antiresorptive agents; anabolic medications require a longer time to produce measurable effects.

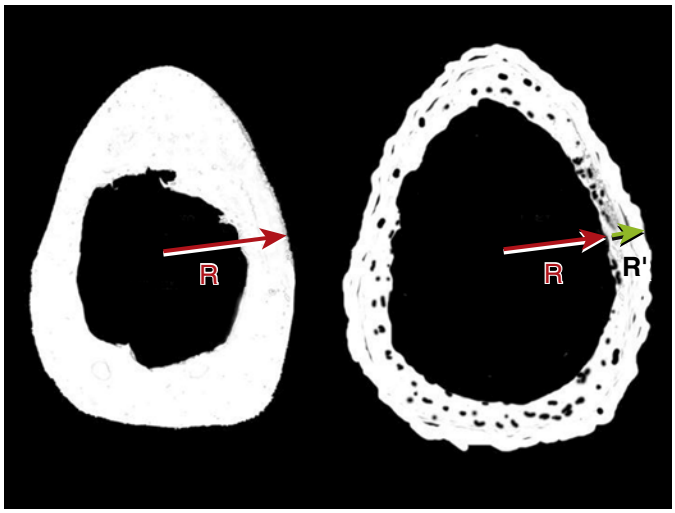

Strength ≈ R^3 Strength ≈ $(R + R')^3$

Figure 16.7 Schematic comparison of femoral cortex in a 30-year-old male *(left)* and a 75-year-old male *(right)*. Note that the proportionate strength of the bone shaft on the right is greater than that on the left.

OSTEOMALACIA AND RICKETS

Osteomalacia and rickets are disorders of inadequate bone mineralization. Osteomalacia is a failure to mineralize newly formed organic matrix (osteoid) in the mature skeleton. Osteoid formation continues, but the bones gradually become softer as the ratio of osteoid to mineralized bone increases over time. Rickets, a disease of children, is the designation for osteomalacia that occurs before cessation of growth—that is, before closure of the epiphyseal plates of long bones.

Optimal mineralization requires (1) an adequate supply of calcium and phosphate ions from the extracellular fluid, (2) an appropriate pH (around 7.6), (3) bone matrix of normal chemical composition and rate of synthesis, and (4) control of inhibitors of mineralization. The major categories of disease that produce osteomalacia or rickets are vitamin D deficiency states, phosphate depletion, systemic acidosis, and inhibitors of mineralization. Vitamin D deficiency is particularly important in childhood and may be caused by inadequate dietary intake, intestinal malabsorption, diminished synthesis of active metabolites, increased catabolism, or peripheral resistance to vitamin D action (Fukumoto, 2015). Dietary deficiency is very uncommon in the United States because of the widespread use of fortified milk and bread and vitamin supplements. When vitamin D deficiency occurs in adults, it is usually a consequence of malabsorption. Because vitamin D is a fat-soluble vitamin, its absorption is impaired in celiac disease, biliary and pancreatic disease, or steatorrhea from other causes. Systemic resistance to vitamin D can be of major importance in the osteomalacia that accompanies chronic renal disease. On the other hand, hereditary resistance to $1,25(OH)_2D_3$, often called *vitamin D-dependent rickets type II*, is a rare disorder caused by a variety of defects in the vitamin D receptor. Osteomalacia can also be caused by the overproduction of FGF-23. Tumor-induced osteomalacia (TIO) is a rare paraneoplastic disorder caused by the overproduction of FGF-23 by small mesenchymal tumors.

Clinically, weakness, skeletal pain and deformities, and fractures can occur as the disease progresses. Roentgenographic examination reveals a generalized decrease in skeletal radiodensity. Although the skeleton becomes less radiodense, this does not discriminate between absolute loss of mineralization and loss of mineralized organic matrix (osteoporosis). Looser zones are another distinct radiographic feature in late-stage osteomalacia. These are the deposition of unmineralized osteoid at sites of stress or along nutrient vessels. They are often bilateral and symmetric, and appear as transverse lucent bands (pseudofractures). The skeletal deformities in rickets are accentuated as a consequence of compensatory overgrowth of epiphyseal cartilage, wide bands of which remain unmineralized and unresorbed. In severe cases of rickets, decreased growth can be associated with such evident deformities as swelling of the costochondral junctions of the ribs (rachitic rosary), a protuberant sternum, costodiaphragmatic depression (Harrison sulcus), delayed closure of the anterior fontanelle with frontal bossing, and radiographically widened metaphyses of the long bones.

Laboratory tests for detecting osteomalacia include a routine serum chemistry panel (calcium, phosphorus, and ALP), vitamin D screening, and PTH. Serum FGF-23 is often elevated in patients with tumor-induced osteomalacia. The definitive diagnosis of osteomalacia is based on microscopic examination of undecalcified bone biopsy, which is characterized by an increase in the amount of unmineralized osteoid. Tetracycline uptake studies often show irregular, patchy, blurred uptake. The choice of therapy depends on the underlying etiology of the disease. Complete tumor resection is curative for TIO.

RENAL OSTEODYSTROPHY

Renal osteodystrophy (ROD) refers to the spectrum of bone abnormalities that occur in patients with end-stage renal disease (ESRD). ROD affects both bone quality and quantity through metabolic (low calcium, high phosphorus) and hormonal disturbances (secondary hyperparathyroidism) (Moe, 2017; Ott, 2017). Patients with ESRD have an increased risk for fracture, predominantly osteitis fibrosa cystica, osteomalacia, or a

combination of the two (see Fig. 16.5). Osteitis fibrosa cystica is characterized by increased bone turnover due to secondary hyperparathyroidism, a consequence of decreased levels of $1,25(OH)_2D_3$ and ionized calcium. (In general, bone dissolution is accelerated and bone formation decreased.) Osteomalacia is characterized by poor mineralization of bone, resulting in the accumulation of surface osteoid (unmineralized bone). Osteoclasts cannot penetrate (resorb) these osteoid surfaces because they are attracted only to mineralized surfaces. Thus, osteoclasts dig cutting cones through the few remaining mineralized surfaces into the mineralized cores of old trabeculae. This phenomenon is histologically referred to as *tunneling resorption* because of the manner in which osteoclasts gain access to mineralized bone (Fig. 16.9).

Figure 16.8 Osteoporosis of lumbar vertebra. There is generalized loss of bone. The vertical plates have become more perforated and the number of horizontal cross-braces is decreased markedly in proportion to the vertical plates (compare to Fig. 16.1B).

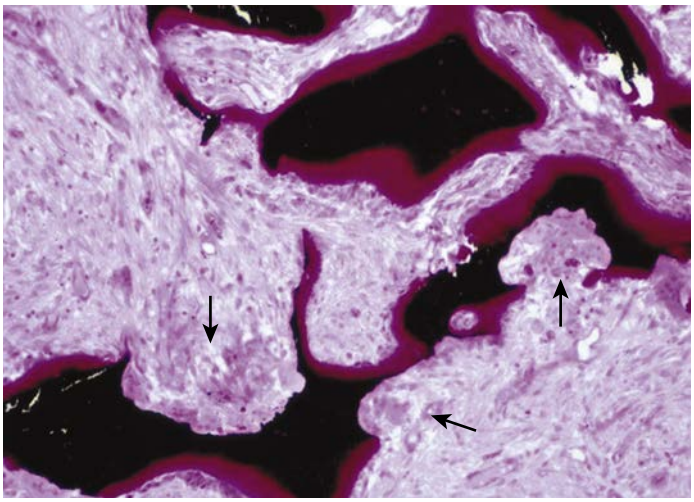

Figure 16.9 Renal osteodystrophy with hyperparathyroidism and osteomalacia. This undecalcified section is stained by the Von Kossa method, which stains mineralized bone black and osteoid with Alizarin red. The *thick red areas* represent seams of newly formed osteoid resulting from renal failure (see Fig. 16.10A). The *solid black arrows* point to the cutting cones of osteoclasts tunneling into the mineralized substance of the bone trabeculae. Note that these scalloped resorption surfaces occur only in the black areas. The red areas are devoid of osteoclasts and are smooth (250 ×).

The defective mineralization process in osteomalacia of ESRD patients can be attributed to low serum calcium levels, the accumulation of aluminum in bone, or other as yet unexplained factors. Renal failure patients who are treated orally with aluminum-containing phosphate binders to control hyperphosphatemia, or who undergo hemodialysis using aluminum-containing dialysates, can experience osteomalacia because aluminum ion can interfere with normal hydroxyapatite lattice formation. Undecalcified bone biopsies stained for aluminum can distinguish between this and the more usual types of osteomalacia (Fig. 16.10).

Radiographs in patients with ROD may show diffuse osteosclerosis, more common in the axial skeleton. Brown tumors are observed as radiolucent lesions. The gold standard for the diagnosis and classification of ROD is tetracycline double-labelled transiliac bone biopsy along with microscopic and histomorphometric evaluation (Aguiar, 2018; Evenepoel, 2017). Histologic abnormalities are heterogeneous; standardized biopsy reports should include the "TMV" classification system, in which "T" represents bone turnover, "M" represents mineralization and "V" stands for volume. There is little evidence to guide proper treatment and drugs have not been developed specifically for ROD. Renal transplantation can arrest disease progression.

PAGET DISEASE

Paget disease of bone (osteitis deformans; PDB) is a chronic disorder of bone that may be unifocal or multifocal. Although it resembles a metabolic disease because involved bones are structurally and functionally abnormal, it is not a true metabolic disease because uninvolved bones are normal. The cause of PDB is currently unknown; however, it has been suspected to be of viral origin because paramyxovirus-like particles have been identified in the nuclei of osteoclasts from affected bone. A familial occurrence of the disease has been recognized and mutations in the *SQSTM1* gene, which encodes the sequestosome protein that targets specific proteins for autophagy, have been discovered in about 30% of familial cases. The decline in prevalence and severity of Paget disease, even in those with a genetic predisposition over the years, argues that exposure to some predisposing environmental agents has lessened (Cundy, 2018).

In a high proportion of patients, PDB is discovered incidentally. Pain, worse at rest and relieved by exercise, is the most common symptom. Radiographs often show a mixed lucent and sclerotic picture. Bone scintigraphy is the best method to evaluate the extent of the disease (Winn, 2017). Any bone in the skeleton can be involved, with pelvis, spine, and sacrum being more common.

PDB is characterized by the uncoupling of osteoclast and osteoblast function, with osteoclastic activity predominating early in the disease and osteoblastic activity predominating late in the disease. The osteoclasts are often large and bizarre, with 50 or more nuclei; trabecular scalloping with multiple Howship lacunae, paratrabecular fibrosis, and marrow hypervascularity may occur. The early histologic picture resembles osteitis fibrosa of hyperparathyroidism. As osteoblastic new bone production takes place, the Howship lacunae are filled in by irregular patches

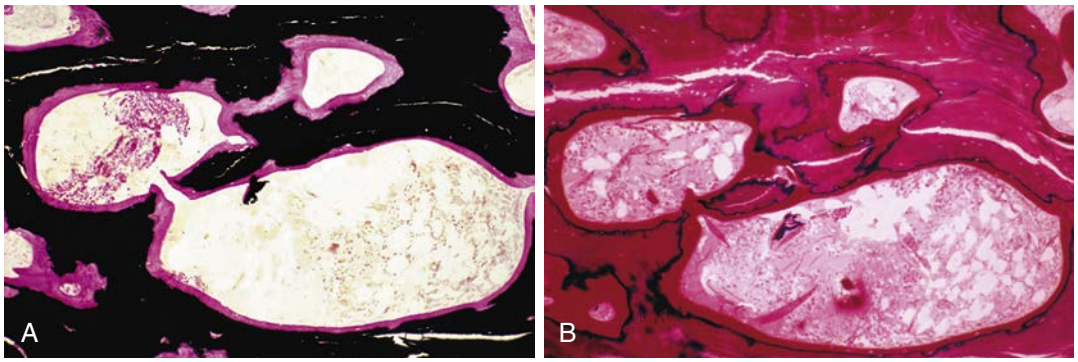

Figure 16.10 Osteomalacia in renal osteodystrophy. **A,** Von Kossa stain shows previously formed bone in black; newly synthesized, unmineralized osteoid stains magenta. Note that all surfaces are covered with thick magenta osteoid seams (125 ×). **B,** The same field of the same biopsy stained with solochrome azurine to detect aluminum. Note that the lines corresponding to the demarcation between black and magenta in the Von Kossa section are stained with a dark-blue line. This corresponds to aluminum derived from dietary phosphate binders that has been incorporated into the hydroxyapatite matrix of the bone and interferes with further mineralization (125 ×).

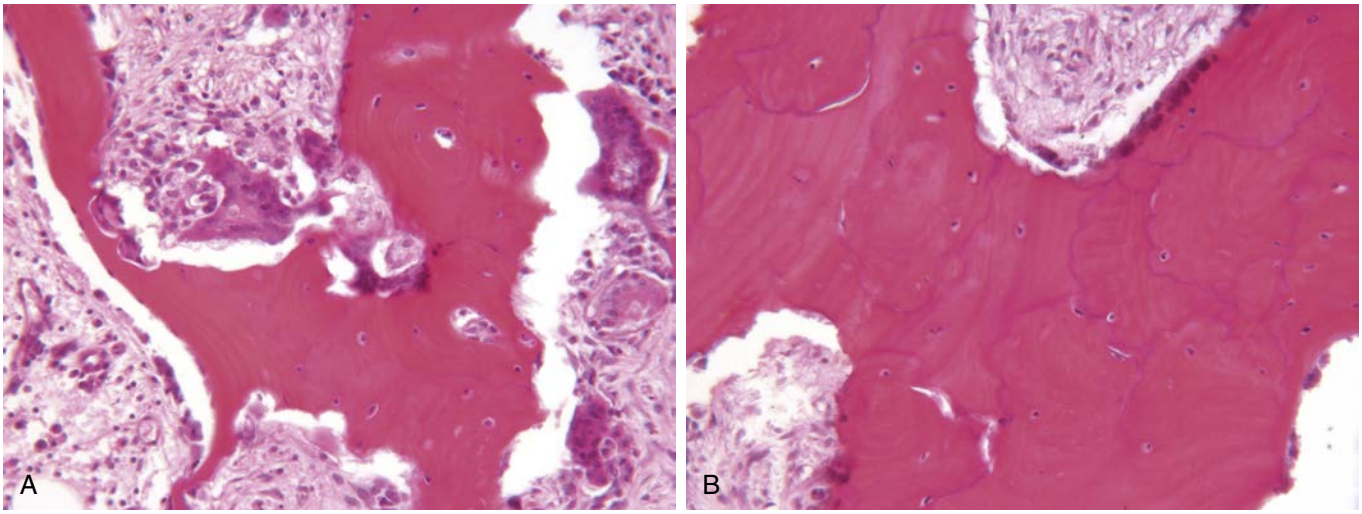

Figure 16.11 Paget disease of bone. **A,** Early phase of Paget disease is dominated by large and bizarre osteoclasts causing secondary scalloping of the bone trabeculae. The marrow is fibrotic and the marrow vasculature is preserved. **B,** In the later phase of Paget disease, the fibrotic marrow is retained. The trabeculae are thick and retain some surface scalloping, and irregular reversal lines separate areas of synthesized new bone to form a mosaic pattern.

of mature and immature bone. The outlines of the original delimitations of osteoclast resorption are preserved as irregularly disposed reversal cement lines, and the resulting bone comes to resemble a tile mosaic (Singer, 2016) (Fig. 16.11). This results in structurally weak bone that is prone to both deformities and fractures (Kravets, 2018; Ralston, 2013). Patients with extensive bone lesions who have underlying heart disease may develop high-output cardiac failure as a complication. Approximately 1% of patients eventually develop bone sarcomas, usually with osteosarcomatous differentiation. Laboratory findings are of some interest. Although serum calcium and inorganic phosphorus concentrations are typically normal, they may occasionally become elevated. Serum calcium levels may, in fact, become very elevated if an extensive area of Paget disease is immobilized. Once osteoblast activity begins, serum ALP increases and may be used to follow the activity of the bone-synthesizing phase of the disease. ALP levels rise further if a patient with Paget disease develops osteosarcoma. Urinary excretion of calcium and phosphorus is normal or increased, whereas excretion of hydroxyproline is usually significantly increased. Paget disease frequently responds both clinically and pathologically to therapeutic administration of calcitonin. The effects of calcitonin, introduced as a therapeutic modality in 1968, are incomplete and short-lived; thus, calcitonin was rapidly replaced by bisphosphonates. Zoledronate is the most potent bisphosphonate—a single intravenous infusion may be adequate for lifelong treatment for the majority of PDB patients, suggested by a recent study (Muschitz, 2017).

SELECTED REFERENCES

Mundy GR, Guise TA: Hormonal control of calcium homeostasis, *Clin Chem* 45:1347–1352, 1999.

Overview of calcium physiology and pathophysiology, including the roles of PTH, vitamin D, PTH-related peptide, and calcitonin. Also presents physiologic defenses against hypercalcemia and hypocalcemia.

Sokoll L, Remaley A, Sena S, et al.: National Academy of Clinical Biochemistry Laboratory Medicine practice guidelines: evidence-based practice for POCT, *Intraoperative PTH, Draft* 2, 2004. October 15.

This comprehensive evidence-based review proposes practice guidelines for all intraoperative PTH-related issues, including clinical indications, timing of draws, method, locations of testing, and financial impact. Guidelines are organized in clear question-and-answer format.

Watts NB: Clinical utility of biochemical markers of bone remodeling, *Clin Chem* 45:1359–1368, 1999.

This is a thorough overview of bone resorption and formation markers, including biological and assay variability issues and clinical uses. The latter are presented in a useful clinical question-and-answer format, such as "Is the patient responding to treatment?".

Access the complete reference list online at Elsevier eBooks for Practicing Clinicians.

REFERENCES

Aguiar F, Meng C, Pereira L, Brito I, Frazao JM: Bone biopsy: an ally in the management of fragility fractures in chronic kidney disease, *Acta reumatologica portuguesa* 43(3):201–209, 2018.

Araya K, Fukumoto S, Backenroth R, et al.: A novel mutation in fibroblast growth factor 23 gene as a cause of tumoral calcinosis, *J Clin Endocrinol Metab* 90:5523–5527, 2005.

Augustine M, Horowitz M: Parathyroid hormone and parathyroid hormone-related protein analogs as therapies for Osteoporosis, *Curr Osteoporos Rep* 11(4):400–406, 2013.

Bahrami A, Weiss S, Montgomery E, et al.: RT-PCR Analysis for FGF32 using paraffin sections in the diagnosis of phosphaturic mesenchymal tumors with and without known tumor induced osteomalacial, *Am J Surg Pathol* 33:1348–1354, 2009.

Bastepe M, Raas-Rothschild A, Silver J, et al.: A form of Jansen's metaphyseal chondrodysplasia with limited metabolic and skeletal abnormalities is caused by a novel activating parathyroid hormone (PTH)/PTH-related peptide receptor mutation, *J Clin Endocrinol Metab* 89(7):3595–3600, 2004.

Bazydlo L, Needham M, Harris N: Calcium, magnesium, and phosphate, *Lab Medicine* 45(1):e44–e50, 2014.

Bellorin-Font E, Starosta R, Milanes CL, et al.: Effect of acidosis on PTH-dependent renal adenylate cyclase in phosphorus deprivation: role of G proteins, *Am J Physiol* 258:F1640–F1649, 1990.

Bettica P, Moro L, Robins SP, et al.: Bone-resorption markers galactosyl hydroxylysine, pyridinium cross-links, and hydroxyproline compared, *Clin Chem* 38:2313–2318, 1992.

Bischoff-Ferrari HA, Willett WC, Wong JB, et al.: Fracture prevention with vitamin D supplementation: a metaanalysis of randomized controlled trials, *J Am Med Assoc* 293:2257–2264, 2005.

Black DM, Rosen CJ: Clinical practice. Postmenopausal osteoporosis, *N Engl J Med* 374(3):254–262, 2016.

Boden SD, Kaplan FS: Calcium homeostasis, *Orthop Clin North Am* 21(1):31–42, 1990.

Brossard JH, Lepage R, Cardinal H, et al.: Influence of glomerular filtration on non-(1–84) parathyroid hormone (PTH) detected by intact PTH assays, *Clin Chem* 46:697–703, 2000.

Care AD, Bruce JB, Boelkins LJ, et al.: Role of pancreozymin-cholecystokinin and structurally related compounds as calcitonin secretagogues, *Endocrinology* 89(1):262–271, 1971.

Cavalli L, Mazzotta C, Brandi M: Phosphatonins: physiological role and pathological changes, *Clin Cases Mineral Bone Metabol* 9(1):9–12, 2012.

Cecco SA, Hristova EN, Rehak NN, et al.: Clinically important intermethod differences for physiologically abnormal ionized magnesium results, *Am J Clin Pathol* 108:564–569, 1997.

Chapurlat RD, Garnero P, Brart G, et al.: Serum type I collagen breakdown product (SerumCTX) predicts hip fracture risk in elderly women: the EPIDOS study, *Bone* 27:283–286, 2000.

Chang CY, Rosenthal DI, Mitchell DM, Handa A, Kattapuram SV, Huang AJ: Imaging findings of metabolic bone disease, *Radiographics : A Review Publication of the Radiological Society of North America, Inc* 36(6):1871–1887, 2016.

Chefetz I, Amitai DB, Browning S, et al.: Normophosphatemic familial tumoral calcinosis is caused by deleterious mutations in SAMD9, encoding a TNF-α responsive protein, *J Invest Dermatol* 128:1423–1429, 2008.

Chefetz I, Heller R, Galli-Tsinopoulou A, et al.: A novel homozygous missense mutation in FGF23 causes familial tumoral calcinosis associated with disseminated visceral calcification, *Hum Genet* 118(2):261–266, 2005.

Cheung K, Roman SA, Wang TS, et al.: Calcitonin measurement in the evaluation of thyroid nodules in the US: a cost-effectiveness and decision analysis, *J Clin Endocrinol Metab* 93(6):2173–2180, 2008.

Cundy T: Paget's disease of bone, *Metabolism, Clin Exp* 80:5–14, 2018.

Deftos LJ, Parethemore JG, Stabile BE: Management of primary hyperparathyroidism, *Annu Rev Med* 44:19–26, 1993.

Eastell R, Barton I, Hannon RA, et al.: Relationship of early changes in bone resorption to the reduction in fracture risk with risedronate, *J Bone Miner Res* 18(6):1051–1056, 2003.

Eastell R, Szulc P: Use of bone turnover markers in postmenopausal osteoporosis, *Lancet Diabet Endocrinol* 5(11):908–923, 2017.

Elin RJ: Magnesium metabolism in health and disease, *Dis Mon* 34:161–218, 1988.

Endres DB, Rude RK: Mineral and bone metabolism. In Burtis CA, Ashwood ER, editors: *Tietz textbook of clinical chemistry*, vol. 3. Philadelphia, 1999, WB Saunders, pp 1395–1457.

Erikson EF, Axelrod DW, Melsen F: *Bone histomorphometry*, New York, 1994, Raven Press.

Eriksen EF, Diez-Perez A, Boonen S: Update on long-term treatment with bisphosphonates for postmenopausal osteoporosis: a systematic review, *Bone* 58:126–135, 2014.

Evenepoel P, Behets GJS, Laurent MR, D'Haese PC: Update on the role of bone biopsy in the management of patients with CKD-MBD, *J Nephrol* 30(5):645–652, 2017.

Farley JR, Hall SL, Ilacas D, et al.: Quantification of skeletal alkaline phosphatase in osteoporotic serum by wheat germ agglutinin precipitation, heat inactivation, and two-site immunoradiometric assay, *Clin Chem* 40:1749–1756, 1994.

Ferrari S, Rizzoli R, Bonjour JP: Genetic aspects of osteoporosis, *Curr Opin Rheumatol* 11:294–300, 1999.

Fink E, Cormier C, Steinmetz P, et al.: Differences in the capacity of several biochemical markers to assess high bone turnover in early menopause and response to alendronate therapy, *Osteoporos Int* 11(4):295–303, 2000.

Fledelius C, Riis BJ, Overgaard K, et al.: The diagnostic validity of urinary free pyridinolines to identify women at risk of osteoporosis, *Calcif Tissue Int* 54:381–384, 1994.

Florenzano P, Gafni RI, Collins MT: Tumor-induced osteomalacia, *Bone Reports* 7:90–97, 2017.

Folpe AL, Fanburg-Smith JC, Billings SD, et al.: Most osteomalacia-associated mesenchymal tumors are a single histopathologic entity: an analysis of 32 cases and a comprehensive review of the literature, *Am J Surg Pathol* 28(1):1–30, 2004.

Fritchie K, Zadek D, Grenache D: The clinical utility of parathyroid hormone related peptide in the assessment of hypercalcemia, *Clin Chim Acta* 402(1–2):146–149, 2009.

Fukumoto S: Diagnostic modalities for FGF23 producing tumors in patients with tumor induced osteomalacia, *Endocrinol Metab (Seoul)* 29(2):136–143, 2014.

Fukumoto S, Ozono K, Michigami T, Minagawa M, Okazaki R, Sugimoto T, et al.: Pathogenesis and diagnostic criteria for rickets and osteomalacia - proposal by an expert panel supported by Ministry of health, Labour and Welfare, Japan, the Japanese Society for bone and mineral Research and the Japan endocrine Society, *Endoc J* 62(8):665–671, 2015.

Fukumoto S, Yamashita T, in letter to the editor in response to, Jonsson KB, Zahradnik R, Larsson T: Fibroblast Growth Factor 23 in oncogenic osteomalacia and X-linked hyperphospatemia, *N Engl J Med* 349:505–506, 2003.

Gaucher C, Walrant-Debray O, Nguyen TM, et al.: PHEX analysis in 118 pedigrees reveals new genetic clues in hypophosphatemic rickets, *Hum Genet* 125(4):401–411, 2009.

Goldstein RE, Blevins L, Delbeke D, et al.: Efficacy of minimally invasive radioguided parathyroidectomy on efficacy, length of stay, and costs in the management of primary hyperparathyroidism, *Ann Surg* 15:716–723, 1991.

Goldstein RE, Blevins L, Delbeke D, et al.: Effect of minimally invasive radioguided parathyroidectomy on efficacy, length of stay, and costs in the management of primary hyperparathyroidism, *Ann Surg* 231(5):732–742, 2000.

Greenblatt MB, Tsai JN, Wein MN: Bone turnover markers in the diagnosis and monitoring of metabolic bone disease, *Clin Chem* 2017. 63(2):464–474, 2017.

Horvit PK, Gagel RF: The goitrous patient with an elevated serum calcitonin—what to do? *J Clin Endocrinol Metab* 82(2):335–337, 1997.

Horwitz MJ, Tedesco MB, Gundberg C, et al.: Short-term high-dose parathyroid hormone-related protein as a skeletal anabolic agent for the treatment of postmenopausal osteoporosis, *J Clin Endocrinol Metab* 88(2):569–575, 2003.

Hristova EN, Cecco S, Niemela JE, et al.: Analyzer-dependent differences in results for ionized calcium, ionized magnesium, sodium, and pH, *Clin Chem* 41:1649–1653, 1995.

Hsu H, Lacey DL, Dunstan CR, et al.: Tumor necrosis factor receptor family member RANK mediates osteoclast differentiation and activation induced by osteoprotegerin ligand, *Proc Natl Acad Sci U S A* 96(7):3540–3545, 1999.

Huijgen HJ, Sanders R, Cecco SA, et al.: Serum ionized magnesium: comparison of results obtained with three ion-selective analyzers, *Clin Chem Lab Med* 37:465–470, 1999.

Ichikawa S, Traxler EA, Estwck SA, et al.: Mutational survey of the PHEX gene in patients with X-linked hypophosphatemic rickets, *Bone* 43(4):663–666, 2008.

Ikari A, Nakajima K, Suketa Y, et al.: Arachidonic acid-activated Na+-dependent Mg2+ efflux in rat renal epithelial cell, *Biochim Biophys Acta* 1618(1):1–7, 2003.

Ju HSJ, Leung S, Brown B, et al.: Comparison of analytical performance and biological variability of three bone resorption assays, *Clin Chem* 43:1570–1576, 1997.

Jueppner H: Novel regulators of phosphate homeostasis and bone metabolism, *Ther Apher Dial* 11(Suppl 1):S3–S22, 2007.

Kerry E, Broe M, Tai C, et al.: A higher dose of vitamin D reduces the risk of falls in nursing home residents: a randomized, multiple dose study, *J Am Geriatr Soc* 55(2):234–239, 2007.

Kikuchi K, Ihn H, Sato S, et al.: Serum concentration of procollagen type I carboxyterminal propeptide in systemic sclerosis, *Arch Dermatol Res* 286(2):77–80, 1994.

Kravets I: Paget's disease of bone: diagnosis and treatment, *Am J Med* 131(11):1298–1303, 2018.

Kurokawa K, Fukagawa M: Introduction to renal osteodystrophy: calcium metabolism in health and uremia, *Am J Med Sci* 317:355–356, 1999.

Larsson T, Yu X, Davis SI, et al.: A novel recessive mutation in fibroblast growth factor-23 causes familial tumoral calcinosis, *J Clin Endocrinol Metab* 90:2424–2427, 2005.

Lee NK, Sowa H, Hinoi E, et al.: Endocrine regulation of energy metabolism by the skeleton, *Cell* 130:456–469, 2007.

Lewiecki EM: Management of osteoporosis, *Clin Mol Allergy* 2(9), 2004.

Lu S, Quarles D: How fibroblast growth factor 23 works, *J Am Soc Nephrol* 18:1637–1647, 2007.

Manolagas SC, Jilka RL: Mechanisms of disease: bone marrow, cytokines, and bone remodeling—Emerging insights into the pathophysiology of osteoporosis, *N Engl J Med* 332:305–311, 1995.

Masi L, Gozzini A, Franchi A, et al.: A novel recessive mutation of fibroblast growth factor-23 in tumoral calcinosis, *J Bone Joint Surg Am* 91:1190–1198, 2009.

Moe SM: Renal osteodystrophy or kidney-induced osteoporosis? *Curr Osteopor Rep* 15(3):194–197, 2017.

Muschitz C, Feichtinger X, Haschka J, Kocijan R: Diagnosis and treatment of Paget's disease of bone : a clinical practice guideline, *Wiener medizinische Wochenschrift* 1946. 167(1–2):18–24, 2017.

Nelson AE, Bligh RC, Mirams M, et al.: Clinical case seminar. Fibroblast growth factor 23: a new clinical marker for oncogenic osteomalacia, *J Clin Endocrinol Metab* 88(9):4088–4094, 2003.

Nichols Advantage: *BIO-INTACT PTH assay directional insert*, *ADS document*, vol. 7040. 2004.

Ott SM: Renal osteodystrophy-time for common Nomenclature, *Curr Osteopor Rep* 15(3):187–193, 2017.

Papapoulos SE, Clemens TL, Sandler LM, et al.: The effect of renal function on changes in circulating concentrations of 1,25 dihydroxycholecalciferol after an oral dose, *Clin Sci* 62(4):427–429, 1982.

Papazachariou IM, Martinez-Isla A, Efthimiou E, et al.: Magnesium deficiency in patients with chronic pancreatitis identified by an intravenous loading test, *Clin Chim Acta* 302(1–2):145–154, 2000.

Pettifor JM: What's new in hypophospataemic rickets? *Eur J Pediatr* 167:493–499, 2008.

Quamme GA: Control of magnesium transport in the thick ascending limb, *Am J Physiol* 256:F197–F210, 1989.

Quamme GA: Renal magnesium handling: new insights in understanding old problems, *Kidney Int* 52:1180–1195, 1997.

Quarles LD: FGF23, PHEX, and MEPE regulation of phosphate homeostasis and skeletal mineralization, *Am J Physiol Endocrinol Metab* 285(1):E1–E9, 2003.
Quarles LD, Lobaugh B, Murphy G: Intact parathyroid hormone overestimates the presence and severity of parathyroid mediated osseous abnormalities in uremia, *J Clin Endocrinol Metab* 75:145–150, 1992.
Quarles LD: Role of FGF23 in vitamin D and phosphate metabolism: Implications in chronic kidney disease, *Exp Cell Res* 318(9):1040–1048, 2012.
Raisz LG: Physiology and pathophysiology of bone remodeling, *Clin Chem* 45:1353–1358, 1999.
Ralston SH: Clinical practice. Paget's disease of bone, *N Engl J Med* 368(7):644–650, 2013.
Ravn P, Thompson DE, Ross PD, et al.: Biochemical markers for prediction of 4-year response in bone mass during bisphosphonate treatment for prevention of postmenopausal osteoporosis, *Bone* 33(1):150–158, 2003.
Rieu M, Lame MC, Richard A, et al.: Prevalence of sporadic medullary thyroid carcinoma: the importance of routine measurement of serum calcitonin in the diagnostic evaluation of thyroid nodules, *Clin Endocrinol* 42:453–460, 1995.
Risteli L, Risteli J: Biochemical markers of bone metabolism, *Ann Med* 25:385–393, 1993.
Robins SP: Collagen cross-links in metabolic bone disease, *Acta Orthop Scand* 66(Suppl 266):171–175, 1995.
Roetzer KM, Varga F, Zwettier E: Novel PHEX mutation associated with hypophosphatemic rickets, *Nephron Physiol* 106(1):8–12, 2007.
Schiavi SC, Kumar R: The phosphatonin pathway: new insights in phosphate homeostasis, *Kidney Int* 65(1–14), 2004.
Singer FR: Bone quality in Paget's disease of bone, *Curr Osteopor Rep* 14(2):39–42, 2016.
Sofferman RA, Standage J, Tang ME: Minimal-access parathyroid surgery using intraoperative parathyroid hormone assay, *Laryngoscope* 108:1497–1503, 1998.
Sokoll LJ, Drew H, Udelsman R: Intraoperative parathyroid hormone analysis: a study of 200 consecutive cases, *Clin Chem* 46:1662–1668, 2000.
Souberbielle JC, Cormier C, Kindermans C: Bone markers in clinical practice, *Curr Opin Rheumatol* 11:312–319, 1999.
Strewler GJ: Hypercalcemia of malignancy and parathyroid hormone-related protein. In Clark OH, Duh Q-Y, editors: *Textbook of endocrine surgery*, Philadelphia, 1997, WB Saunders, pp 426–431.
Swaminathan R: Biochemical markers of bone turnover, *Clin Chim Acta* 313:95–105, 2001.
Topaz O, Indelman M, Chefetz I, et al.: A deleterious mutation in SAMD9 causes normophosphatemic familial tumoral calcinosis, *Am J Hum Genet* 79(4):759–764, 2006.
van Tuyl LH, Voskuyl AE, Boers M, et al.: Baseline RANKL/OPG-ratio and markers of bone and cartilage degradation predict annual radiological progression over 11 years in rheumatoid arthritis, *Ann Rheum Dis* 69(9):1623–1628, 2010.
Vergnaud P, Garnero P, Meunier PJ, et al.: Undercarboxylated osteocalcin measured with a specific immunoassay predicts hip fracture in elderly women: the EPIDOS study, *J Clin Endocrinol Metab* 82:719–724, 1997.
Vierhapper H, Raber W, Bieglmayer C, et al.: Routine measurement for plasma calcitonin in nodular thyroid diseases, *J Clin Endocrinol Metab* 82:1589–1593, 1997.
Wang S, McDonnell EH, Sedor FA, et al.: pH effects on measurements of ionized calcium and ionized magnesium in blood, *Arch Pathol Lab Med* 126(8):947–950, 2002.
Weisinger JR, Bellorin-Font E: Magnesium and phosphorus, *Lancet* 352:391–396, 1998.
Wesseling-Perry K: FGF23: is it ready for prime time? *Clin Chem* 57(11):1476–1477, 2011.
Winn N, Lalam R, Cassar-Pullicino V: Imaging of Paget's disease of bone, *Wien Med Wochenschr* 167(1–2):9–17, 1946. 2017.
Yin JJ, Chirgwin JM, Dallas M, et al.: Blockage of TGF-β signaling inhibits PTH-rP secretion by breast cancer cells and the development of bone metastasis, *J Clin Invest* 103:197–206, 1999.

CHAPTER 17

CARBOHYDRATES

Angela Mojica, Ruth S. Weinstock

FUNCTION OF THE ENDOCRINE PANCREAS, 226
Insulin and Amylin, 226
Glucagon, 227
Somatostatin, 227
Ghrelin and Pancreatic Polypeptide, 228
Incretins, 4

GLUCOSE MEASUREMENTS, 228
Glucose Measurement Methods, 228
Specimen Considerations, 228
Whole Blood Glucose, 228
Interstitial Glucose, 229

DIABETES MELLITUS, 229
Type 1 Diabetes, 230
Type 2 Diabetes, 232
Measures of Glycemic Control, 232
Ketone Testing, 234

HYPOGLYCEMIA, 234
Drug-Induced Hypoglycemia, 234
Severe Medical Illnesses, 235
Hormone Deficiencies, 235
Non–Beta Cell Tumors, 235
Endogenous Hyperinsulinism, 236
Alimentary Hypoglycemia, 236
Autoimmune-Related Hypoglycemia, 236
Hypoglycemia in Infancy and Childhood, 236

INBORN ERRORS OF CARBOHYDRATE METABOLISM, 238
Glycogen Storage Diseases, 238
Disorders of Gluconeogenesis, 238
Defects in Galactose Metabolism, 242
Defects in Fructose Metabolism, 242
Lactic Acidosis, 242

SELECTED REFERENCES, 243

KEY POINTS

- Normal fasting plasma glucose is less than 100 mg/dL (5.6 mmol/L), and normal glucose levels 2 hours after a 75-g glucose load are less than 140 mg/dL (7.8 mmol/L). Impaired fasting glucose (100–125 mg/dL; 5.6–6.9 mmol/L), impaired glucose tolerance (a 2-hour plasma glucose value of 140–199 mg/dL [7.8–11.0 mmol/L] after a 75-g glucose load), or "prediabetes" (a glycated hemoglobin (HbA_{1c}) of 5.7%–6.4%) indicates increased risk for developing diabetes.
- The diagnosis of diabetes requires 2 abnormal test results: a fasting plasma glucose of ≥126 mg/dL (7.0 mmol/L), a random plasma glucose level ≥200 mg/dL (11.1 mmol/L) with hyperglycemic symptoms, a plasma glucose level 2 hours after a 75-g glucose load of ≥200 mg/dL (11.1 mmol/L), and/or HbA_{1c} of ≥6.5% using a method that is National Glycohemoglobin Standardization Program certified and standardized to the Diabetes Control and Complications Trial (DCCT) assay. Results can be from samples obtained on the same day or on 2 different days. Oral glucose tolerance tests should be used to diagnose cystic fibrosis–related diabetes. Oral glucose tolerance tests, with pregnancy-specific cutoff levels, should be performed to diagnose gestational diabetes.
- Whole blood capillary glucose values obtained with point-of-care devices and interstitial fluid glucose readings measured with continuous glucose monitoring devices are useful for the detection of hyperglycemia and hypoglycemia and help to monitor and direct therapy in individuals with diabetes. They should not be used to diagnose diabetes or hypoglycemic disorders. To establish these diagnoses, confirmation with laboratory measures of plasma glucose is recommended because of their greater accuracy.
- HbA_{1c} levels should be performed every 3 to 6 months in individuals with diabetes to monitor glycemic control using a certified method traceable to the DCCT reference method. Reliability and accuracy are diminished in the presence of shortened red blood cell survival, lower mean blood cell age as seen with certain hemoglobinopathies and hemolytic conditions, or need for blood transfusions as well as with uremia.
- Direct methods for measuring β-hydroxybutyrate in blood are available in point-of-care devices as well as in the laboratory. These tests are preferable to use of sodium nitroprusside strips and tablets for urine ketone testing, which do not detect β-hydroxybutyrate. Because β-hydroxybutyrate levels are high in diabetic ketoacidosis (DKA) and fall with treatment, whereas acetoacetic acid and acetone levels rise with treatment, urine ketone testing is not useful for monitoring therapy. Calculation of the anion gap is also commonly used to monitor recovery from DKA.
- Circulating pancreatic autoantibodies may be present before and after the onset of autoimmune type 1 diabetes. These include antibodies to glutamic acid decarboxylase (GAD65), insulinoma-associated protein 2 (IA-2A), the zinc transporter ZnT8A, insulin (IAA) and islet cell antibodies (ICA). These tests should not be used for routine screening of asymptomatic nondiabetic individuals except in a research setting. When performed, assays should be used that have been shown by the Islet Autoantibody Standardization Program to have the best performance.
- Hypoglycemic symptoms with a plasma glucose level of ≤55 mg/dL (3.1 mmol/L) in an individual who is not receiving medications for diabetes warrant further evaluation. A careful drug and medical history and measurements of insulin, C-peptide, proinsulin, insulin autoantibodies, β-hydroxybutyrate, and drug levels (sulfonylureas, repaglinide, nateglinide) during the hypoglycemic episode are recommended to determine the diagnosis.
- Hypoglycemia in neonates, infants, and children is usually a problem of fasting adaptation. Infants and young children have higher glucose turnover than adults, which makes them more susceptible to developing hypoglycemia during times of illness when feeding patterns are disturbed. Hypoglycemia can harm the developing brain; therefore, it is a medical emergency that demands immediate investigation and treatment.
- Inborn errors of carbohydrate metabolism constitute a group of inherited disorders caused by abnormalities of the enzymes that regulate glycogen metabolism (glycogen storage diseases) and gluconeogenesis. These disorders cause persistent hypoglycemia in young infants and children and can potentially affect childhood development and growth. Some of these disorders can lead to life-threatening metabolic emergencies if not diagnosed in a timely manner.

Carbohydrates are major constituents of physiologic systems. They are organic compounds composed of carbon, hydrogen, and oxygen [$C_x(H_2O)_y$], which, along with lipids and proteins, provide energy and contribute to the structure of organisms. Complex carbohydrates are digested into simple sugars, principally glucose, which are used primarily as energy sources or are stored as glycogen. The most important dietary hexoses (six carbon-containing carbohydrates) are D-glucose, D-galactose, and D-fructose, but the principal sugar circulating in the bloodstream is glucose. Lactose (glucose and galactose) and sucrose (glucose and fructose) are important disaccharides. Carbohydrates are needed for specific cellular functions (such as ribose in nucleic acids) and can modify proteins and their

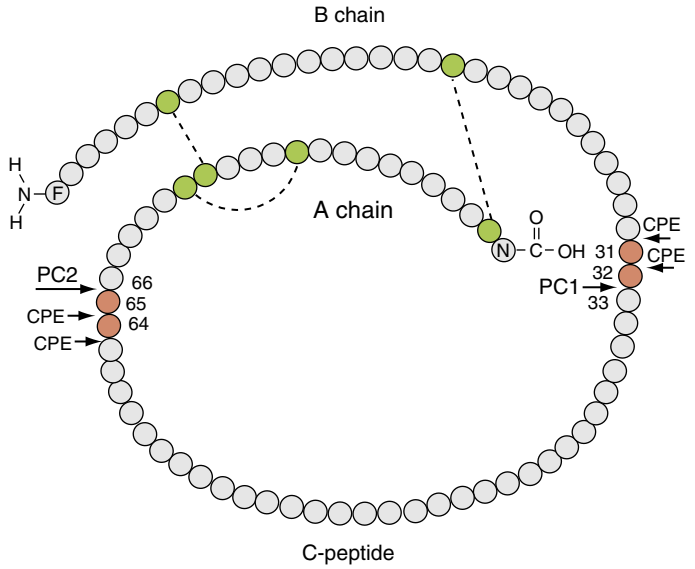

Figure 17.1 Human proinsulin, with cleavage sites for the proprotein convertases PC1 and PC2 and for carboxypeptidase H (CPE). *Orange circles* represent the two pairs of basic amino acids used for proteolytic processing, and *green circles* represent cysteine residues that participate in disulfide bonding. F, phenylalanine; N, asparagine. (Diagnosis and classification of diabetes mellitus. Copyright © 2004 American Diabetes Association. From Mackin RB. Proinsulin: Recent observations and controversies. *Cell Mol Life Sci* 54:696–702, 1998, with permission.)

function by glycosylation. Carbohydrates are measured in whole blood, serum, or plasma. In addition, measurements of glucose in urine, cerebrospinal fluid, interstitial fluid, and other body fluids are important clinically.

The concentration of glucose in blood is normally controlled within narrow limits by many hormones, the most significant of which, insulin, is produced by the endocrine pancreas. Diabetes mellitus is the most common disease of carbohydrate metabolism. Most individuals with diabetes have either type 1 (autoimmune beta cell destruction with absolute insulin deficiency) or type 2 (insulin resistance and defective insulin secretion). Measurements of glycemic control are increasingly important in diabetes, because the development and progression of microvascular and macrovascular complications are associated with hyperglycemia. This chapter reviews the aspects of carbohydrate metabolism most critical to the practice of medicine.

FUNCTION OF THE ENDOCRINE PANCREAS

The pancreas functions as both an endocrine and an exocrine organ in the control of carbohydrate metabolism. As an exocrine gland, it produces and secretes amylase responsible for the breakdown of ingested complex carbohydrates. Further digestion leads to the production of monosaccharides. Once absorbed, the monosaccharides signal the endocrine pancreas, which regulates hormones involved in energy homeostasis. Enteroendocrine cells in the gastrointestinal tract are also stimulated by nutrients to secrete incretins, peptide hormones that affect pancreatic function, gastric emptying, appetite, and intestinal motility.

The endocrine pancreas secretes several hormones from different cells residing in the islets of Langerhans. Insulin and amylin (islet amyloid polypeptide [IAPP]) are produced by the beta cells (55%–70% of islet cells), glucagon by the alpha cells (20% of islet cells), somatostatin by the delta cells (5%–10% of islet cells), ghrelin by the epsilon cells (<1%–3% of islet cells), and pancreatic polypeptide (PP) by the PP (gamma or F) cells (≤5% of islet cells). Alpha cells can also produce glucagon-like peptide 1 (GLP-1) after there has been injury to beta cells.

INSULIN AND AMYLIN

Insulin is an anabolic hormone. In insulin-sensitive tissues such as skeletal muscle, fat, and liver, insulin stimulates glucose uptake and the formation of glycogen, inhibits glucose production, and increases protein and triglyceride synthesis. It is a peptide hormone with a mass of approximately 5800 daltons (Da), with a 21 amino acid A chain and a 30 amino acid B chain that are linked by two disulfide bonds. Insulin is synthesized initially as a longer single-chain peptide precursor hormone, preproinsulin (11,500 Da). Proinsulin (≈9000 Da), the immediate precursor of insulin, is processed into insulin in the secretory granules of the beta cells by enzymatic

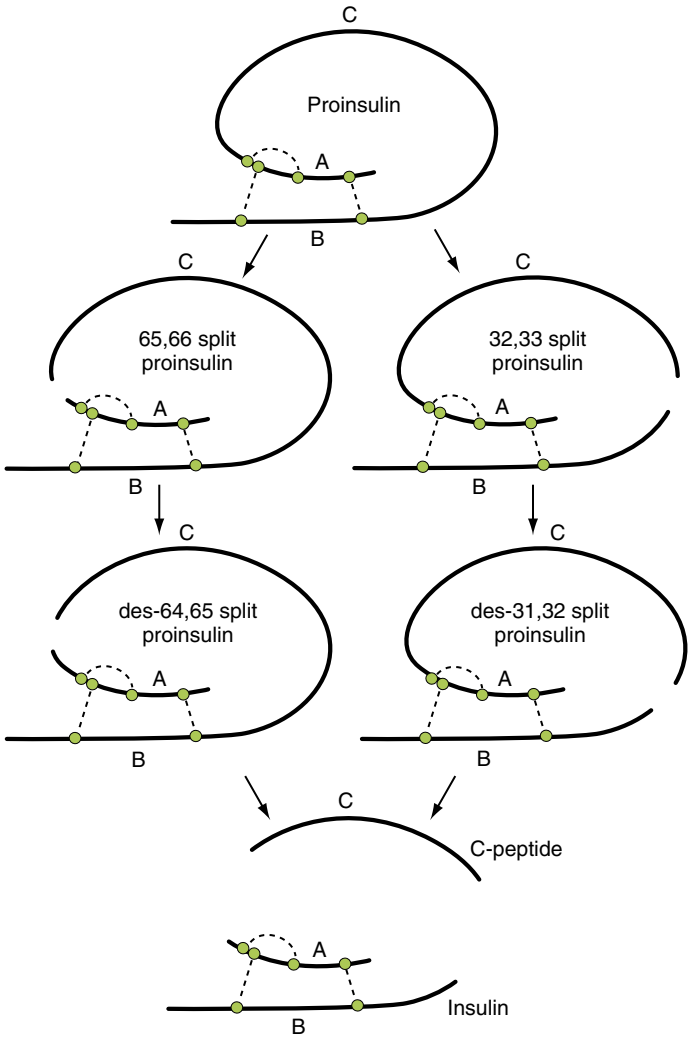

Figure 17.2 Processing of proinsulin to insulin. *Green circles* represent cysteine residues that participate in disulfide bonding. (Copyright John Wiley and Sons Ltd; reproduced with permission from Temple R, Clark PM, Hales CN. Measurement of insulin secretion in type 2 diabetes: Problems and pitfalls. *Diabetic Med* 9:503–512, 1992.)

removal of the 31 amino acid peptide segment that connects the A and B chains, known as C-peptide (Figs. 17.1 and 17.2). This proteolytic processing is catalyzed by proprotein convertases PC2 and PC1/PC3, which first convert proinsulin into the intermediate metabolites 32,33 split proinsulin and 65,66 split proinsulin, and then, after cleavage by carboxypeptidase H, to des-31,32 split proinsulin and des-64,65 split proinsulin. In adults, small amounts of intact proinsulin and these metabolically active conversion intermediates, especially des-31,32 split proinsulin, are cosecreted with insulin. Healthy infants and preterm neonates have higher proinsulin and 32,33 split proinsulin levels than adults. Proinsulin and its metabolites may cross-react with insulin in some insulin immunoassays. This can be significant, especially because the half-life of proinsulin is at least three times as long as that of insulin. In vivo studies of proinsulin have shown that it has 10% to 15% of the biological activity of insulin.

Elevated proinsulin levels (intact and partially processed proinsulin) and high proinsulin : insulin ratios have been found in type 2 diabetes. This is associated with reduced PC1/PC3 activity and decreased ability of the beta cells to secrete insulin (Roder et al., 1998; Ozawa et al., 2014). An increase in proinsulin : insulin levels has also been observed in recent-onset type 1 diabetes and after partial pancreatectomy (Seaquist et al., 1996), where there are reductions in beta cell function and increases in secretory demand. Less common conditions associated with high proinsulin levels include insulinomas. Familial hyperproinsulinemia is a rare condition caused by mutations in the proinsulin gene. In affected families, these genetic abnormalities can be associated with impaired glucose tolerance or type 2 diabetes (Nishi & Nanjo, 2011). C-peptide and insulin are secreted in equimolar amounts into the portal vein, but the ratio in serum is about 5:1 (fasting) to 15 : 1. The molar concentration of C-peptide in blood is higher than that of insulin, primarily because of the hepatic clearance of

insulin. Approximately 50% of insulin is rapidly removed by its initial passage through the liver, but hepatic extraction of C-peptide is negligible. In cirrhosis, hyperinsulinemia is observed as the result of decreased hepatic insulin clearance. In healthy individuals, the half-life of both C-peptide and proinsulin is approximately 30 minutes, whereas it is only 4 to 9 minutes for insulin. There is some evidence that C-peptide has biological activity, but its potential therapeutic role is unclear (Pinger et al., 2017).

Disease states occur when insulin concentrations are inappropriate for given blood glucose levels. Insulin deficiency, either absolute or relative, leads to diabetes mellitus. Serum insulin levels should be measured with a concomitant glucose level because insulin secretion is regulated primarily by glucose. Whereas a high insulin level in the presence of a low glucose level suggests inappropriate secretion or administration of insulin, high insulin levels can be observed in insulin-resistant individuals who need to secrete extra insulin to keep blood glucose levels normal.

Unregulated excess insulin secretion causes hypoglycemia. This is seen in insulin-secreting tumors, especially insulinomas, in which patients have low serum glucose levels (<50 mg/dL; <2.8 mmol/L), and elevated insulin and proinsulin levels with hypoglycemic symptoms (e.g., shakiness, palpitations, diaphoresis, confusion). There are also congenital genetic defects, usually diagnosed in childhood, known as congenital hyperinsulinism, which cause dysregulation in insulin secretion and hypoglycemia. C-peptide levels are measured in hypoglycemic states to help identify the cause of the hypoglycemia. Sera from insulinoma patients or patients with congenital hyperinsulinism have high insulin and C-peptide levels, whereas hypoglycemia from injected or exogenous insulin is characterized by high insulin levels and low C-peptide levels. Commercially available insulin preparations are free of C-peptide and proinsulin. Because C-peptide is less stable than insulin, serum samples should be separated quickly and frozen.

In people with diabetes mellitus, C-peptide and glucose can be measured after an overnight 8-hour fast and after stimulation by an oral mixed meal or after glucagon stimulation to provide information concerning beta cell secretory capacity. Urine C-peptide:creatinine has also been used to assess beta cell function (Besser et al., 2011). Low C-peptide levels are characteristic of the absolute insulin deficiency of type 1 diabetes. C-peptide measurements during the mixed meal tolerance test are commonly used in clinical trials of type 1 diabetes for the evaluation of preservation of beta cell function (Greenbaum et al., 2008). C-peptide measurement can also be useful in follow-up evaluations after pancreatectomy and postpancreatic transplantation. Unlike insulin, both C-peptide and proinsulin are primarily degraded in the kidneys; thus, levels are elevated in renal failure.

Many commercial immunoassays for insulin, C-peptide, and proinsulin are available. Progress has been made concerning the standardization of these assays, and ultrasensitive immunoassays are available (Miller et al., 2009; Wang et al., 2012; Little et al., 2017). It is recommended that all assays be standardized to one reference method. Manufacturers are encouraged to publish data concerning the performance of their assays, including accuracy, recovery, precision, specificity, linearity, and lowest measurable concentration statistically different from zero/limits of quantitation. Laboratory certification is also encouraged. In the United States, an external quality assessment program for insulin and C-peptide measurements is available through the College of American Pathologists (Northfield, IL).

Serum insulin measurements may be falsely low in the presence of hemolysis. An insulin-degrading enzyme found in red blood cells, as well as in other tissues, is responsible for this problem. C-peptide and proinsulin measurements appear to be less affected by hemolysis. Insulin antibodies will also interfere with insulin immunoassays, with both falsely elevated and suppressed levels reported.

In addition to the hormones mentioned earlier, the pancreatic beta cell secretes a 37 amino acid protein called *islet amyloid polypeptide* (IAPP), or amylin. First discovered in 1986, amylin is colocalized and cosecreted with insulin in response to stimulation by nutrients. Amylin slows gastric emptying and inhibits postprandial glucagon secretion. The overall result is a lowering of postprandial hyperglycemia. It can also reduce food intake and can be associated with weight loss. Oligomeric forms are associated with an increase in beta cell apoptosis. Amylin is first synthesized as a larger 89 amino acid precursor peptide that is processed within the beta cell. This processing is abnormal in type 2 diabetes. High levels of amylin have been observed in hyperinsulinemic, insulin-resistant states, such as impaired glucose tolerance and early type 2 diabetes, and low levels are seen in type 1 diabetes and insulin-requiring type 2 diabetes. Amyloid deposits, fibroid material derived from IAPP, are observed in islets in type 2 diabetes. Amylin levels can also be elevated in pancreatic cancer. Amylin assays are not used in clinical practice, but amylin analogs may be helpful in diabetes management by limiting postprandial glucose excursions and promoting satiety. A synthetic analog of amylin, pramlintide acetate, is available for use by injection before major meals for patients with insulin-requiring diabetes.

GLUCAGON

Proglucagon is synthesized in the pancreatic alpha cells and the L cells of the distal small bowel. Through differential processing, the glucagon family of gene products is formed. This includes the production of glucagon in the pancreatic alpha cells and the incretin glucagon-like peptide 1 (GLP-1) in the L cells of the intestines. In diabetes, the processing of proglucagon in alpha cells can be altered, producing GLP-1.

Fasting plasma glucagon concentrations are normally 25 to 50 pg/mL. Pancreatic glucagon stimulates glucose production. It is an important regulator of hepatic glycogenolysis, gluconeogenesis, ketogenesis, and hepatic amino acid turnover. In type 1 diabetes, over time, progressive glucagon deficiency develops. This deficiency of glucagon results in increased glycemic fluctuations and difficulty recovering from hypoglycemia. In type 2 diabetes, inappropriately elevated postprandial levels of glucagon are observed.

The ratio of insulin to glucagon is important in the regulation of carbohydrate metabolism. Anabolism is favored when there is a relative increase in the insulin-to-glucagon ratio, as in the postprandial state; catabolism is favored with a relative decrease in this ratio, as in the fasting state. The ratio of insulin to glucagon is influenced by somatostatin, neural input, intestinal peptides, and the concentrations of glucose and other metabolites. The ratio of insulin to glucagon is tightly regulated to keep blood glucose concentrations within the normal range.

Serum glucagon concentrations are rarely measured in clinical practice. Glucagonomas are rare islet cell tumors that produce excessive glucagon. Clinically, glucagonomas present with a characteristic necrotizing migratory erythematous rash, stomatitis, glossitis, weight loss, anemia, and mild diabetes mellitus. These tumors are usually associated with fasting glucagon levels >120 pg/mL, but levels can range from 900 to 7800 pg/mL. The processing of proglucagon is impaired, and large molecular weight forms can be seen. Milder elevations in blood glucagon levels are observed in patients with multifunctional neuroendocrine tumors, cirrhosis, nonalcoholic fatty liver disease, renal insufficiency, Cushing syndrome, pancreatitis, acromegaly, and after gastric bypass surgery. In these circumstances, more accurate measurements of glucagon are obtained using glucagon sandwich enzyme-linked immunosorbent assay (ELISA) assays (Albrechtsen et al., 2014). In familial hyperglucagonemia, an autosomal-dominant disorder, glucagon levels are high in the absence of tumor. Family history is helpful in making this diagnosis.

SOMATOSTATIN

Somatostatin, a tetradecapeptide with a disulfide bond, was originally discovered as a hypothalamic hormone that inhibited growth hormone secretion, but the discovery of somatostatin in the islets of Langerhans prompted further investigation of its function in the endocrine pancreas. Subsequently, somatostatin was found in the gastrointestinal tract and nervous system. It inhibits the secretion of pituitary (growth hormone and thyrotropin) and pancreatic (insulin, glucagon, PP) hormones, as well as gastric inhibitory polypeptide (GIP), gastrin, secretin, vasoactive intestinal peptide, cholecystokinin, motilin, arginine vasopressin, acetylcholine, epidermal growth hormone, neurotensin, and serotonin. Nonendocrine functions include inhibition of gastric acid secretion; gastrointestinal motility, including gastric emptying time; gallbladder contractions; and pancreatic enzyme release. The first isolated somatostatin peptide had 14 amino acids and is called *somatostatin-14*. Subsequently, somatostatin-28, which contains an N-terminal extension, was isolated and is a more potent inhibitor of insulin secretion.

Somatostatin is produced in the delta cells of the islets and in extra-islet neuroendocrine cells. Rare islet cell tumors, somatostatinomas, secrete high levels of somatostatin, causing diabetes mellitus, diarrhea, and gallstones. Elevated somatostatin levels can also be seen in small cell lung cancer, medullary thyroid cancer, and pheochromocytoma. Somatostatin has a very short half-life and is rarely measured in clinical practice. Long-acting somatostatin analogs, octreotide and lanreotide, which bind primarily to the somatostatin receptor subtype 2 (SSTR2), are used to treat pituitary tumors (acromegaly, adrenocorticotropic hormone [ACTH]– and thyroid-stimulating hormone [TSH]–producing tumors), as well as carcinoid syndrome, VIPomas, glucagonomas, insulinomas, pancreatic fistulas, Zollinger-Ellison syndrome, human immunodeficiency virus (HIV)–associated diarrhea, and other disorders of the gastrointestinal tract (the only labeled indications are for acromegaly, VIPomas, and metastatic carcinoid

tumors). Octreotide scintigraphy has also been used for the diagnosis, localization, and detection of metastatic disease, and for prediction for success of treatment with somatostatin analogs for gastroenteropancreatic neuroendocrine tumors.

GHRELIN AND PANCREATIC POLYPEPTIDE

Ghrelin is a 28 amino acid peptide that is primarily synthesized in the stomach but also is made in islets, the heart, lungs, kidney, immune system, and hypothalamus and pituitary glands. It stimulates appetite primarily by actions in the hypothalamus and is associated with weight gain and adiposity. In the pancreas, there is evidence that ghrelin inhibits glucose-stimulated insulin secretion and stimulates glucagon secretion. Ghrelin also increases growth hormone secretion, gastric emptying, and acid secretion. Ghrelin is not routinely measured in clinical practice.

Nutrient ingestion, through vagal-cholinergic stimulation, increases the secretion of PP, a 36 amino acid peptide. The PP family also includes peptide YY and neuropeptide Y, which are found in the gastrointestinal tract and nervous system, and affect gastrointestinal function, food intake, and satiety. PP increases satiety, delays gastric emptying, and inhibits gall bladder motility and exocrine pancreas secretion. Excessive PP is released by tumors of PP cells and some insulinomas, gastrinomas, glucagonomas, and VIP-secreting tumors. In these rare reported cases of islet cell tumors overproducing PP, or in PP hyperplasia, some patients are asymptomatic, whereas other cases are associated with a watery diarrhea syndrome (Tomita et al., 1980; Bellows et al., 1998; Pasieka & Hershfield, 1999).

INCRETINS

Oral nutrients stimulate the release of incretins from the intestines. The incretin effect refers to the greater and earlier insulin response to the oral administration of glucose compared with intravenous glucose. The most important incretins in the regulation of insulin secretion are GLP-1 and glucose-dependent insulinotropic peptide (gastric inhibitory polypeptide [GIP]), both of which are members of the glucagon superfamily (Drucker et al., 2017). GLP-1 (7-37), the most common active form, has a half-life of only 2 to 3 minutes. It is rapidly cleaved by circulating aminopeptidases to the inactive GLP-1 (9-37). This inactive form represents 80% of the circulating GLP-1. Both forms of GLP-1 are short-lived and cleared by the kidneys. Dipeptidyl peptidase-4 (DPP-4), a serine peptidase present on the surface of endothelial cells, inactivates GLP-1 by removing two N-terminal amino acids.

GLP-1 rapidly stimulates insulin and somatostatin secretion, suppresses glucagon secretion, and slows gastric emptying in response to a meal. GLP-1 may also reduce appetite and promote weight loss. In vitro and animal studies indicate that GLP-1 can inhibit beta cell apoptosis, stimulate beta cell proliferation and neogenesis from precursor duct cells, and decrease alpha cell mass (Drucker et al., 2017). Beneficial actions of GLP-1 on the kidney and cardiovascular system have also been described (Drucker et al., 2017). C-cell hyperplasia and medullary cancer of the thyroid have been observed in rodents after prolonged administration of GLP-1 receptor agonists, but increased tumor formation has not been reported in humans.

Plasma meal-stimulated GLP-1 levels are decreased in type 2 diabetes mellitus (Toft-Nielsen et al., 2001). Injectable long-acting GLP-1 receptor agonists are effective in improving glycemic control in patients with type 2 diabetes. Oral inhibitors of DPP-4 are also used for the treatment of type 2 diabetes.

GLUCOSE MEASUREMENTS

GLUCOSE MEASUREMENT METHODS

Measurements of glucose are critical for the diagnosis and management of diseases affecting carbohydrate metabolism. Glucose is measured in whole blood, plasma, serum, cerebrospinal fluid, pleural fluid, and urine for a variety of diagnostic and management purposes. In addition, devices can measure glucose from interstitial fluid for continuous monitoring of glucose levels in people with diabetes. The standard clinical laboratory analysis of glucose is performed on plasma or serum derived from a phlebotomy specimen. For the diagnosis of diabetes, laboratory plasma glucose measurements with an analytic imprecision ≤2.9%, a bias ≤2.2% and a total error ≤6.9% are recommended (Sacks et al., 2011). Most measurements of glucose employ enzymatic methods (see Chapter 28). These methods provide specificity and can be packaged to furnish point-of-care determinations. Enzyme systems that have been commonly used to measure glucose are glucose oxidase and hexokinase; rarely, glucose dehydrogenase methods are employed. How and when specimens are collected and handled and the sites of collection affect the clinical interpretation of the analytic result.

SPECIMEN CONSIDERATIONS

Glycolysis causes plasma glucose to decline over time while the plasma is in contact with cells. The decline can be 10 mg/dL/0.56 mmol/L (average 5%–7%) per hour, depending on leukocyte counts, temperature, and other factors (Sacks et al., 2011). A specimen is appropriate for glucose analysis if serum or plasma is separated from the cells within 30 minutes (Weissman & Klein, 1958; Chan et al., 1989; Sacks et al., 2011). Until separation has been performed, it is recommended that specimens be kept on ice. Sodium fluoride, long used to prevent in vitro glycolysis, is now recognized to be ineffective (Gambino, 2013). Several studies have reported differences in glucose stability in collection tubes containing a variety of glycolysis inhibitors. Less glycolysis was found in tubes containing citrate buffer and in tubes in which serum was rapidly separated by a gel barrier (Winter et al., 2018).

WHOLE BLOOD GLUCOSE

Whole blood glucose specimens, analyzed with point-of-care monitoring devices, are used in the home, in the physician's office, or at the bedside in the hospital to monitor for hypoglycemia and hyperglycemia. Most of these devices have been calibrated to give results similar to plasma levels and can report plasma or whole blood readings. Whole blood tends to give approximately 10% to 15% lower glucose readings than plasma, but the percentage varies on the basis of hematocrit, analysis technique, and sample timing (fasting vs. post-glucose load). Capillary blood is the source for most of these whole blood glucose measuring devices. Capillary blood glucose is similar to arterial glucose but can vary markedly from venous samples depending on timing relative to food ingestion. For example, a postprandial specimen is higher in the capillary sample than in the venous sample. In general, capillary glucose tests performed with point-of-care devices should not be used to diagnose diabetes or hypoglycemic disorders. To establish these diagnoses, confirmation with laboratory measurements of plasma glucose is recommended because of their greater accuracy.

Home blood glucose monitoring devices help people with diabetes to better self-manage their disease. A wide variety of devices are available for home measurements. Proper training of patients in the use of individual meters is critical in avoiding operator errors. Errors that may contribute to inaccurate readings in certain devices include the application of an insufficient volume of blood, milking the finger to acquire sufficient blood, use of outdated test strips, use of alternative sites, environmental factors (humidity, heat, altitude), use of a malfunctioning meter, use of a dirty meter, hypertriglyceridemia, hypotension, measurements outside of the hematocrit or temperature range, and other factors (Schmid et al., 2013; Erbach et al., 2016). Some blood glucose monitoring devices are influenced by high levels of salicylate, acetaminophen, levodopa, vitamin C, uric acid, bilirubin, lipids, or low oxygen levels; others are altered by touching the reaction area. Results can be misleading when samples are obtained from critically ill patients with poor perfusion and edema. Oxygen pressure can also affect accuracy in systems that use glucose oxidase.

The accuracy of point-of-care home blood glucose monitoring devices varies, especially at very high and low glucose concentrations (Ekhlaspour et al., 2017; King et al., 2018). Accuracy is critical, because patients, caregivers, and providers use results to direct therapy and avoid serious hypoglycemia and hyperglycemia. The International Organization for Standardization (ISO) 1197 accuracy standards changed in 2013. The 2013 standards require that 95% or more of glucose levels be ±15 mg/dL when reference glucose is less than 100 mg/dL, within 15% for glucose of 100 mg/dL or higher, and 99% within zone A or B (little or no effect on clinical outcome) of Parkes Consensus Error Grid for type 1 diabetes. Testing on three lots of strips is now required. Compliance with these standards is not mandatory, and many devices do not meet these standards (Freckmann et al., 2012). On November 29, 2018, the U.S. Food and Drug Administration (FDA) issued new draft accuracy recommendations for glucose monitoring devices used in health care and home settings (https://www.fda.gov/news-events/fda-brief/fda-brief-fda-takes-steps-advance-safety-and-accuracy-blood-glucose-monitors-empower-patients). In these documents, they recommend the following: for health care settings, 95% of all glucose readings should be within ±12% and 98% within ±15% of results from the comparator method. For home use, 95% of all glucose readings should be within ±15% and 99% within ±20% of comparator results. The FDA, however, does not monitor the performance

of these devices after they are approved and become commercially available. Because some of the devices on the market have been found to be unreliable, the Diabetes Technology Society developed a post-market surveillance program to assess the performance of home glucose monitoring devices in the United States (Klonoff et al., 2016).

Desirable features of home blood glucose monitoring devices, aside from performance characteristics (precision and accuracy), include ease of use, requirement of a small volume of blood, low maintenance, large print readout, rapid testing, appropriate alarms, minimal interfering substances, and memory storage and download capabilities. Some meters permit alternative site testing (such as forearm, upper arm, thigh), but results from alternative sites may be less accurate when rapid changes in glucose levels occur. Others incorporate insulin dose calculators and electronic logbooks for recording events, insulin doses, and carbohydrate intake. This information can be downloaded to a computer or smartphone in displays such as logbooks, graphs, charts, and summary statistics. There is also wireless communication between certain home blood glucose monitoring devices and insulin pumps.

INTERSTITIAL GLUCOSE

Interstitial glucose measuring devices have been developed for the continuous monitoring of glucose levels. Continuous glucose monitoring (CGM) helps individuals with diabetes better self-manage their disease, reducing hypoglycemia, glucose variability, and HbA_{1c} levels (Rodbard, 2017). Most CGM devices measure glucose levels using electrochemical methods; one of the devices uses a fluorescence-based sensor. These devices measure glucose levels in the interstitial fluid using a subcutaneous tissue sensor that is changed every 7, 10, 14, or 90 days. Newer devices are factory calibrated; older devices require calibrations using capillary glucose. A transmitter is placed on the skin directly over the sensor. For the "real-time" CGM devices, glucose readings are automatically transmitted to a smartphone, insulin pump, smartwatch, or device-specific receiver every 5 minutes. "Flash" (intermittently scanned) CGM devices measure glucose every minute, record readings every 15 minutes, and require the user to intermittently scan a reader over the transmitter to view results. The person with diabetes views glucose readings along with trend arrows that indicate the direction and rate of change of glucose. Tracings display glucose readings over time, providing information about glucose patterns over hours or days. This glucose "trend analysis" can reveal unsuspected nocturnal hypoglycemia or postprandial hyperglycemia and is used for modifying treatment. Some CGM devices have "share" features so that family members, friends, or caretakers can also view the glucose readings. Accuracy has improved such that the FDA has approved some devices to be used for treatment decisions (e.g., insulin dosing) without verification by capillary glucose testing. The mean absolute relative difference (MARD) is frequently used to assess CGM accuracy. The MARD for most devices is <10% (Edelman et al., 2018). With the real-time CGM devices, alarms/alerts can be set for current or approaching hypoglycemia and hyperglycemia. Alarms/alerts are available with newer flash CGM devices.

Integrated CGM (iCGM) devices can transmit glucose readings to different digitally connected devices such as insulin pumps or can be used alone. When communicating with an insulin pump, CGM devices can help direct insulin delivery. In some systems, the insulin pump will stop delivering insulin if a hypoglycemic threshold has been reached or is predicted to occur. In the "hybrid" artificial pancreas systems, basal insulin is delivered automatically based on CGM readings. Clinical trials are in progress testing fully automated systems ("artificial pancreas"). Early studies of a bionic pancreas (an automated wearable insulin and glucagon subcutaneous infusion system that communicates with a continuous glucose monitor and uses an automated adaptive algorithm) are promising (Russell et al., 2014).

Interstitial glucose is in slow (5–30 min) equilibrium with capillary blood glucose and therefore is not equal to blood glucose, except in stable systems (Zierler, 1999; Cheyne et al., 2002). Particularly during times when glucose levels are rapidly changing, such as after meal ingestion or recovery from hypoglycemia or with exercise, interstitial fluid readings will lag behind blood glucose levels. Capillary glucose measurements need to be used if hypoglycemia is suspected but not observed by CGM.

DIABETES MELLITUS

Diabetes mellitus is a group of diseases in which blood glucose levels are elevated. Diabetes is the most common set of disorders of carbohydrate metabolism, affecting approximately 30.3 million Americans in 2015, 9.4% of the total population, 12.2% of U.S. adults and 25.2% of those 65 years of age and older (CDC, 2017). This chronic disease is responsible for significant morbidity, mortality, and cost. Diabetes is the leading cause of treated end-stage renal disease, the most common cause of nontraumatic amputations, and the foremost cause of new blindness in adults ages 20 to 74 years. Nerve damage, known as diabetic neuropathy, occurs in 60% to 70% of people with diabetes. Most diabetes-related deaths, however, are related to the increased risk of developing atherosclerotic disease. People with diabetes are at least two to four times more likely to have heart disease and cerebrovascular disease than those without diabetes. In 2017, it was estimated that diabetes in the United States cost approximately $360.54 billion: $327.2 billion for diagnosed diabetes, $31.7 billion for undiagnosed diabetes and nearly $1.6 billion for gestational diabetes (Dall et al., 2019). Fortunately, in recent years—associated with better glycemic and blood pressure control, use of angiotensin-converting enzyme inhibitors or angiotensin receptor blockers for renoprotection, use of statin drugs to lower LDL cholesterol, and better foot care—complication rates have been falling (Gregg et al., 2014).

The Expert Committee on the Diagnosis and Classification of Diabetes Mellitus revised the criteria for the diagnosis of diabetes in 1997, with later modifications by the American Diabetes Association (ADA, 2019). As shown in Table 17.1, to diagnose diabetes, two abnormal results from one or more of the following tests are required: (1) fasting plasma glucose level of 126 mg/dL (7.0 mmol/L) or higher (the glucose level should be obtained after an 8-hour fast), (2) a plasma glucose level ≥200 mg/dL (11.1 mmol/L) 2 hours after a glucose load (75-g oral glucose tolerance test [OGTT]), (3) a random glucose ≥200 mg/dL (11.1 mmol/L) with symptoms of hyperglycemia, and/or (4) hemoglobin A_{1c} (HbA_{1c}) of ≥6.5%. Tests can be performed on two different days or 2 different tests can be performed on the same day. If the patient has discordant results from two different tests, then the test for which the result is above the diagnostic cut point should be repeated.

Prediabetes designates conditions in which glucose homeostasis is abnormal, but serum glucose levels are not high enough to be classified as diabetes. This group includes individuals with impaired fasting glucose and impaired glucose tolerance (see Table 17.1). They are also at increased risk for cardiovascular and cerebrovascular diseases. In 2015, 33.9% of U.S. adults (84.1 million) and 48.3% (23.1 million) of adults ≥65 years of age had prediabetes (CDC, 2017). In 2017, this cost was estimated to be $43.4 billion (Dall et al., 2019).

Formal OGTTs are not generally recommended for routine clinical use in the diagnosis of diabetes. If used, the procedure described by the World Health Organization (1985) utilizing a 75-g glucose load should be followed. For children, 1.75 g glucose/kg up to 75 g is recommended. There are 2 exceptions. The first is the diagnosis of cystic fibrosis–related diabetes. Annual screening with a 2-hour 75-g (1.75 g/kg) OGTT is recommended beginning at least by age 10 years. HbA_{1c} testing for screening for cystic fibrosis–related diabetes is not recommended (Moran et al., 2018). The other exception is for the diagnosis of diabetes during pregnancy. Pregnant women with risk factors for type 2 diabetes should be screened using an OGTT test at their initial prenatal visit. If testing results are abnormal during the first trimester using standard criteria, the woman is considered to have had undiagnosed diabetes prior to pregnancy. All other women should be screened between 24 and 28 weeks' gestation.

There is ongoing debate concerning the optimal screening method for diagnosing gestational diabetes (ADA, 2019). The "one-step" method,

TABLE 17.1
Diagnosis of Prediabetes and Diabetes Mellitus

	FASTING PLASMA GLUCOSE		2-HOUR PLASMA GLUCOSE LEVEL (AFTER 75 G GLUCOSE LOAD)		HBA_{1C}
	mg/dL	**mmol/L**	**mg/dL**	**mmol/L**	**%**
Normal	<100	<5.6	<140	<7.8	
Prediabetes					5.7–6.4
Impaired fasting glucose	100–125	5.6–6.9			
Impaired glucose tolerance			140–199	7.8–11.0	
Diabetes mellitus	≥126	≥7.0	≥200	≥11.1	≥6.5

From American Diabetes Association (2019).
HbA_{1c}, Hemoglobin A_{1c}.

TABLE 17.2
Diagnosis of Gestational Diabetes Mellitus

One-Step (IADPSG Consensus)

Perform a 75-g OGTT, with plasma glucose measurement fasting and at 1 and 2 h, at 24–28 weeks of gestation in women not previously diagnosed with overt diabetes.

The OGTT should be performed in the morning after an overnight fast of at least 8 h.

The diagnosis of GDM is made when any of the following plasma glucose values are exceeded:

- Fasting: ≥92 mg/dL (5.1 mmol/L)
- 1 h: ≥180 mg/dL (10.0 mmol/L)
- 2 h: ≥153 mg/dL (8.5 mmol/L)

Two-Step (NIH Consensus)

Perform a 50-g GLT (nonfasting), with plasma glucose measurement at 1 h (Step 1), at 24–28 weeks of gestation in women not previously diagnosed with overt diabetes.

If the plasma glucose level measured 1 h after the load is ≥130 mg/dL (7.2 mmol/L), 135 mg/dL (7.5 mmol/L), or 140 mg/dL (7.8 mmol/L), proceed to 100-g OGTT (Step 2). The 100-g OGTT should be performed when the patient is fasting.

The diagnosis of GDM is made when at least two of the following four plasma glucose levels (measured fasting, 1 h, 2 h, 3 h after the OGTT) are met or exceeded*:

	Carpenter/Coustan	**NDDG**
Fasting	95 mg/dL (5.3 mmol/L)	105 mg/dL (5.8 mmol/L)
1 h	180 mg/dL (10.0 mmol/L)	190 mg/dL (10.6 mmol/L)
2 h	155 mg/dL (8.6 mmol/L)	165 mg/dL (9.2 mmol/L)
3 h	140 mg/dL (7.8 mmol/L)	145 mg/dL (8.0 mmol/L)

GDM, Gestational diabetes mellitus; *NDDG,* National Diabetes Data Group; *NIH,* National Institutes of Health; *OGTT,* oral glucose tolerance test
*The American College of Obstetricians and Gynecologists (ACOG) comments that one abnormal elevated value (instead of two) may be used to diagnose gestational diabetes.
From American Diabetes Association. Standards of medical care in diabetes—2019. *Diabetes Care* 2019 Jan; 42(Suppl 1): S13–S28.

based on the International Association of Diabetes and Pregnancy Study Groups [IADPSG] consensus meeting, uses a 75-g OGTT, measuring glucose levels after fasting and at 1 and 2 hours (Table 17.2). Cutoff glucose concentrations are based on those values associated with a 1.75-fold increase in the risk of neonatal complications in the Hyperglycaemia and Adverse Pregnancy Outcomes (HAPO) study. The other method (National Institutes of Health consensus) uses the two-step protocol shown in Table 17.2. The use of this protocol avoids a large increase in the prevalence of gestational diabetes that is without clear benefit.

Before an OGTT is performed, individuals should ingest at least 150 g/day of carbohydrates for the 3 days preceding the test without limitation in physical activity, and the test should be performed after an overnight 8- to 14-hour fast. The individual should not eat food; drink tea, coffee, or alcohol; or smoke cigarettes during the test, and the individual should be seated.

The classification of diabetes is shown in Box 17.1 (ADA, 2019). The most common forms of diabetes are type 1 and type 2 (Table 17.3). Type 1 diabetes, characterized by absolute insulin deficiency and beta cell destruction, used to be called *juvenile-onset diabetes* or *insulin-dependent diabetes*. Although this disease is most commonly diagnosed in young people, its onset can occur at any age. Because people with other forms of diabetes also use insulin therapy, the term *insulin-dependent* is confusing and should not be used. Type 2 diabetes, characterized by insulin resistance and insulin secretory defects, has been referred to in the past as *adult-onset* or *non-insulin-dependent diabetes*. These terms also should no longer be used. Although the onset of type 2 diabetes is most common in older adults, it can occur at any age, including childhood. Many patients with type 2 diabetes use insulin therapy, so it should not be referred to as *non-insulin-dependent diabetes*. Other types of diabetes include gestational diabetes, diabetes secondary to pancreatic diseases, such as cystic fibrosis–related diabetes or pancreatitis, monogenic diabetes, drug or chemical-induced diabetes, including post-transplantation diabetes, and diabetes associated with endocrinopathies such as Cushing syndrome, acromegaly, and pheochromocytoma (see Box 17.1).

TYPE 1 DIABETES

Type 1 diabetes mellitus represents approximately 5% to 10% of all cases of diabetes. There usually is autoimmune destruction of insulin-producing beta cells in the islets of the pancreas, causing an absolute deficiency in insulin production. The genetic susceptibility to develop type 1 diabetes is related, at least in part, to the inheritance of specific immune response genes associated with HLA-DR/DQ on chromosome 6, as well as other genes and genetic markers. It is hypothesized that a precipitating event occurs, such as a viral infection, toxin exposure, or other environmental influence, which triggers the autoimmune destruction of the beta cells. The prediabetes period of gradual and progressive beta cell destruction can last for months, years, or decades. During this period, the acute insulin response to intravenous glucose, called the *first-phase insulin release*, becomes depressed or absent. The absence of first-phase insulin response is also found in other forms of diabetes. Eventually, in most people with type 1 diabetes, most or all of the beta cells are destroyed, resulting in inadequate or absent insulin secretion and hyperglycemia. Therefore, C-peptide levels and endogenous insulin levels are very low or undetectable. People with untreated type 1 diabetes develop diabetic ketoacidosis (DKA). Insulin therapy is required for all people with type 1 diabetes.

Antibody markers of beta cell destruction are commonly present before and at the time of onset of type 1 diabetes. Measurements of pancreatic autoantibodies can be useful for prediction and diagnosis of type 1 diabetes, for research on the treatment and prevention of type 1 diabetes, and for screening nondiabetic family members who are considering becoming a pancreatic transplant donor. Autoantibody assays are available for the 65 kDa isoform of glutamic acid decarboxylase (GAD65), insulin (IAA), insulinoma-associated protein 2 (IA-2, a tyrosine phosphatase–related protein), and zinc transporter 8 (ZnT8A). ZnT8 and IA-2 are found on the surface membrane of pancreatic islet beta cell secretory granules. Older assays measured islet cell antigen 512 autoantibodies (ICA512), which were autoantibodies to parts of the IA-2 antigen (IA-2A). Although the presence of antibodies may help in the differentiation of type 1 diabetes from other types of diabetes early in the course of the disease, the absence of antibodies does not exclude this diagnosis.

Those individuals at greatest risk of developing type 1 diabetes have high titers of multiple autoantibodies. In family as well as in population studies, the detection of at least two autoantibodies is associated with increased risk of developing type 1 diabetes. Composite levels from assays for autoantibodies to GAD65, IA-2, insulin, and ZnT8 increase prediction (Sosenko et al., 2013). GAD65 has the highest sensitivity (91%) as a single screening marker for detecting multiple antibody-positive individuals (Krischer et al., 2003). IAAs are more common in young children who develop type 1 diabetes, whereas GAD65 is more common in adults. Prediction for the development of type 1 diabetes is enhanced by use of the Diabetes Prevention Trial-Type 1 risk score that includes parameters related to glycemia, age, body mass index (BMI) and C-peptide levels (Sosenko et al., 2014).

The Islet Autoantibody Standardization Program (IASP), previously called the Diabetes Antibody Standardization Program, began as a collaboration between the Immunology of Diabetes Society and the Centers for Disease Control and Prevention (CDC), and established a Proficiency Testing Service. This program has the following goals: evaluation and improvement of assays for type 1 diabetes–associated autoantibodies, provision of standard reference samples, and validation of novel candidate

BOX 17.1

Classification of Diabetes Mellitus

I. Type 1 diabetes (beta cell destruction, usually leading to absolute insulin deficiency)
   A. Immune mediated
   B. Idiopathic
II. Type 2 diabetes (may range from predominantly insulin resistance with relative insulin deficiency to a predominantly secretory defect with insulin resistance)
III. Gestational diabetes mellitus
IV. Other specific types
   A. Maturity onset diabetes of the young (MODY): gene (locus)
      1. MODY1: HNF4A (20q12)
      2. MODY2: GCK (7p13)
      3. MODY3: HNF1A (12q24.2)
      4. MODY4: PDX1(13q12.1)
      5. MODY5: HNF1B (17q21)
      6. MODY6: NEUROD1 (2q31.3)
      7. MODY7: KLF11 (2p25)
      8. MODY8: CEL (9p34)
      9. MODY9: PAX4 (7q32)
      10. MODY10: INS (11pl5.5)
      11. MODY11: BLK (8p23)
      12. MODY12: ABCC8 (11pl5.1)
      13. MODY13: KCNJ11 (11p15.13)
      14. MODY14: APPL1 (3pl4.3)
   B. Other genetic defects: gene (locus)
      1. Neonatal diabetes: >20 genetic defects identified
      2. Diabetes and deafness: Mitochondrial tRNA
      3. Type A insulin resistance: INSR (19p13)
      4. Wolfram syndrome 1: WFS1 (4p16)
      5. Wolfram syndrome 2: CISD2 (4q24)
      6. Thiamine-responsive megaloblastic anemia syndrome: SLC19A2 (1q23)
      7. Mitchell-Riley syndrome: RFX6 (6q22)
      8. Alstrom syndrome: ALMS1 (2p13)
      9. Bardet-Biedl syndrome: BBS1-BBS21
      10. Donohue syndrome (Leprechaunism): INSR Rabson-Mendenhall syndrome: INSR
      11. Some forms of lipodystrophic diabetes
      12. Others
   C. Diseases of the exocrine pancreas
      1. Pancreatitis
      2. Trauma/pancreatectomy
      3. Neoplasia
      4. Cystic fibrosis
      5. Hemochromatosis
      6. Fibrocalculous pancreatopathy
      7. Others
   D. Endocrinopathies
      1. Acromegaly
      2. Cushing syndrome
      3. Glucagonoma
      4. Pheochromocytoma
      5. Hyperthyroidism
      6. Somatostatinoma
      7. Aldosteronoma
      8. Others
   E. Drug or chemical induced
      1. Vacor
      2. Pentamidine
      3. Nicotinic acid
      4. Glucocorticoids
      5. Antiretroviral protease inhibitors
      6. Nucleoside reverse-transcription inhibitors
      7. Atypical antipsychotic drugs
      8. Thyroid hormone
      9. Diazoxide
      10. β-Adrenergic agonists
      11. Thiazides
      12. Dilantin
      13. γ-Interferon
      14. Others
   F. Infections
      1. Congenital rubella
      2. Cytomegalovirus
      3. Coxsackievirus
      4. Others
   G. Uncommon forms of immune-mediated diabetes
      1. "Stiff-man" syndrome
      2. Anti-insulin receptor antibodies
      3. Others
   H. Other genetic syndromes sometimes associated with diabetes
      1. Down syndrome
      2. Klinefelter syndrome
      3. Turner syndrome
      4. Friedreich ataxia
      5. Huntington chorea
      6. Laurence-Moon-Biedl syndrome
      7. Myotonic dystrophy
      8. Porphyria
      9. Prader-Willi syndrome
      10. Others

Adapted from American Diabetes Association. Diagnosis and classification of diabetes mellitus. *Diabetes Care* 37:(Suppl 1):S81–S90, 2014; Sanyoura M, Philipson LH, Naylor R. *Curr Diab Rep* 18:58, 2018.

TABLE 17.3

Characteristics of Type 1 and Type 2 Diabetes Mellitus

	Type 1 Diabetes	Type 2 Diabetes
Frequency	5%–10%	90%–95%
Age of onset	Any, but most common in children and young adults	More common with advancing age, but can occur in children and adolescents
Risk factors	Genetic, autoimmune, environmental	Genetic, obesity, sedentary lifestyle, race/ethnicity, hypertension, dyslipidemia, polycystic ovarian syndrome
Pathogenesis	Destruction of pancreatic beta cells, usually autoimmune	No autoimmunity Insulin resistance and progressive insulin deficiency
C-peptide levels	Very low or undetectable	Detectable
Prediabetes	Pancreatic autoantibodies (GAD65, IA-2, IAA, ZnT8) may be present	Pancreatic autoantibodies absent
Medication therapy	Insulin absolutely necessary; multiple daily injections or insulin pump	Oral agents and/or noninsulin injectable hypoglycemic drugs Insulin commonly needed
Therapy to prevent or delay onset of diabetes	None known Clinical trials in progress	Lifestyle (weight loss if overweight or obese and increased physical activity) Oral medications (metformin, acarbose) may be helpful

autoantibody antigens. The IASP is now at the TrialNet Islet Cell Autoantibody Core Laboratory at the University of Florida. Proficiency evaluations have been reported for different assays of GAD65, IA-2, IAA, and ZnT8 autoantibodies (Bingley et al., 2003; Torn et al., 2008; Schlosser et al., 2010; Lampasona et al., 2011).

TYPE 2 DIABETES

Type 2 diabetes is the most common type of diabetes, affecting approximately 90% of Americans with diabetes. This disease is familial, but the underlying genetic defects for most of those affected have yet to be determined. Risk factors in adults include overweight or obesity (BMI ≥25 kg/m^2 or ≥23 kg/m^2 in Asian Americans), sedentary lifestyle, first-degree relative with diabetes, advanced age (≥45 years), high-risk ethnicity (African Americans, Latinos, Native Americans, Asian Americans, and Pacific Islanders), polycystic ovary disease, as well as history of gestational diabetes or delivery before diabetes of a baby weighing >9 pounds, hypertension, vascular disease or dyslipidemia (HDL cholesterol ≤35 mg/dL [0.90 mmol/L] and/or triglyceride level ≥250 mg/dL [2.82 mmol/L]), HbA_{1c} ≥5.7%, impaired fasting glucose, impaired glucose tolerance, and other conditions associated with insulin resistance (i.e., acanthosis nigricans). Unlike type 1 diabetes, this is not an autoimmune disease; thus, pancreatic autoantibodies are absent. C-peptide levels are measurable in type 2 diabetes, but there is usually a reduction in beta cell mass over time. Unlike undiagnosed type 1 diabetes, in which patients are usually symptomatic, people with new-onset type 2 diabetes can be free of symptoms. It is not unusual to diagnose type 2 diabetes after the onset of complications. Therefore, routine screening for high-risk individuals is recommended.

The American Diabetes Association (ADA, 2019) recommends screening for type 2 diabetes in any overweight or obese adult if one or more risk factors are present. In general, it is recommended that adults ages ≥45 years be screened for diabetes every 3 years, but screening should be performed earlier and more frequently if the individual is at high risk. The preferred test is a fasting plasma glucose or HbA_{1c} level. If a random plasma glucose level is 160 mg/dL (8.9 mmol/L) or higher, a fasting plasma glucose, HbA_{1c}, or 2-hour 75-g OGTT should be performed (see Table 17.1). Home blood glucose monitoring devices should not be used to diagnose diabetes. If, however, an individual does have a capillary glucose test on one of these instruments that reads ≥140 mg/dL (7.8 mmol/L), the individual should be rescreened with a fasting plasma glucose, HbA_{1c}, or OGTT, using venous samples (see Table 17.1). In general, point-of-care HbA_{1c} assays are not recommended for diagnosis.

In recent years, type 2 diabetes has been diagnosed in younger individuals, including children. The American Diabetes Association (ADA, 2019) recommends screening children and adolescents, beginning at age 10 years or at onset of puberty, who are overweight (BMI ≥85th percentile) or obese (≥ 95th percentile) with one or more of the following risk factors: family history (type 2 diabetes in first- and second-degree relatives), high-risk race/ethnicity (Native Americans, African Americans, Hispanic Americans, Asians/South Pacific Islanders), signs of insulin resistance (acanthosis nigricans, hypertension, dyslipidemia, polycystic ovary syndrome), small for gestational age birth weight, or maternal history of diabetes or gestational diabetes during the child's gestation.

Most people with type 2 diabetes are insulin resistant, overweight or obese, and have a relative or absolute deficiency in insulin secretion. Inappropriately high hepatic glucose production occurs, along with impaired glucose utilization peripherally. Decreased glucose transport can be demonstrated in muscle and adipose tissue. Hyperglycemia is toxic to beta cell function and further impairs insulin secretion. Over time, beta cell failure is usually progressive, and the beta cells produce lesser amounts of insulin, contributing to increasing insulin deficiency. Inappropriately high postprandial glucagon and low postprandial GLP-1 levels have been observed. Although many people with type 2 diabetes can be effectively treated with diet and exercise, oral glycemic control agents and/or noninsulin injectable medications, others require insulin therapy.

MEASURES OF GLYCEMIC CONTROL

It has been established that good glycemic control is associated with preventing or delaying the progression of microvascular complications in diabetes. The Diabetes Control and Complications Trial (DCCT) demonstrated that lowering glucose levels in patients with type 1 diabetes slows or prevents the development of retinopathy, neuropathy, and nephropathy (DCCT Research Group, 1993). A 50% to 75% decrease in complications was observed in the intensively treated group, in which an HbA_{1c} of 7.2% was achieved (compared with 9.0% in the conventionally treated group). In the DCCT follow-up Epidemiology of Diabetes Interventions and Complications (EDIC) study, reduction in cardiovascular disease was also found in the groups that had been intensively treated (DCCT/EDIC Study Research Group, 2016). Reduction in microvascular complications in type 2 diabetes was reported in the United Kingdom Prospective Diabetes Study (UKPDS) as well as in a smaller Japanese study (Ohkubo et al., 1995; United Kingdom Prospective Diabetes Study Group, 1998a, 1998b). In the UKPDS, microvascular complications were decreased by 25% in intensively treated patients by lowering the HbA_{1c} from 7.9% to 7.0%. In the UKPDS follow-up study, macrovascular disease was reduced as well. The standard of care is to measure HbA_{1c} levels every 3 to 6 months to monitor glycemic control (ADA, 2019). Glycemic goals are shown in Table 17.4.

Glycosylated hemoglobin (HbA_{1c}) is formed nonenzymatically by the two-step reaction shown in Figure 17.3. The first reaction is rapid, reversible, dependent on the ambient glucose concentration, and produces a labile aldimine or Schiff base. Over time, the aldimine slowly undergoes Amadori rearrangement and is converted to a stable ketoamine, glycosylated hemoglobin. Most HbA_{1c} assays measure this stable ketoamine, not the labile product, which is more prone to be influenced by recent dietary intake.

HbA_{1c} is defined by the International Federation of Clinical Chemistry Working Group on HbA_{1c} as the hemoglobin A that is irreversibly glycosylated at one or both N-terminal valines of the β-chains of the tetrameric hemoglobin molecule, including hemoglobin that may also (but not solely) be glycosylated on lysine residues. HbA_{1c} testing provides an index of average blood glucose levels over the past 2 to 4 months. Although the

TABLE 17.4

Glycemic Goals in Adults[a]

		PREPRANDIAL GLUCOSE		POSTPRANDIAL GLUCOSE[b]	
	Hemoglobin A_{1c} (%)	**mg/dL**	**mmol/L**	**mg/dL**	**mmol/L**
ADA[c]: Adults	<7.0[d]	80–130	4.4–7.2	<180	<10.0
Pregnant adults[c]	<6.0	<95	<5.3	<140 (1 h) <120 (2 h)	<7.8 (1 h) <6.7 (2 h)
Older adults[c]:					
Healthy	<7.5	80–130	4.4–7.2	90–180	5.0–10.0
Intermediate	<8.0	90–150	5.0–8.3	100–180	5.6–10.0
Poor health	<8.5[e]	100–180	5.6–10.0	110–200	6.1–11.1
AACE[f,g]	≤6.5	≤110	≤6.1	≤140	<7.8

[a]Youth <18 years of age: goal hemoglobin A_{1c}<7.5%.
[b]1 to 2 hours after beginning a meal for adults, except bedtime for older adults.
[c]American Diabetes Association (2019)
[d]Lower goals may be appropriate for selected individuals if this can be accomplished safely (without significant hypoglycemia). Higher goals may be appropriate in some individuals (e.g., with a history of severe hypoglycemia, limited life expectancy, advanced complications, extensive comorbid conditions, or long-standing diabetes in whom the goal is difficult to achieve with appropriate education, monitoring, and therapies, including insulin).
[e]Avoid reliance on HbA_{1c} ; avoid hypoglycemia and symptomatic hyperglycemia (American Diabetes Association revised 2021: https://care.diabetesjournals.org/content/44/Supplement_1/S168.figures-only).
[f]AACE, American Association of Clinical Endocrinologists https://www.aace.com/pdfs/diabetes/AACE_2019_Diabetes_Algorithm_FINAL_ES.pdf accessed July 15, 2019.
[g]For patients without concurrent serious illness and at low hypoglycemia risk.

life span of red blood cells is approximately 90 to 120 days, HbA_{1c} levels represent a "weighted" average of glucose levels, with the youngest erythrocytes contributing to a greater extent than older ones. Approximately 50% of the HbA_{1c} level is determined by plasma glucose levels over the previous month. To avoid confusion for the general public, the American Diabetes Association, American College of Endocrinology, and National Diabetes Education Program recommend using the term A1c testing when referring to HbA_{1c} results. In 2007, a consensus statement on the international standardization of HbA_{1c} assays was issued by the American Diabetes Association, the European Association for the Study of Diabetes, the International Federation of Clinical Chemistry and Laboratory Medicine (IFCC), and the International Diabetes Federation (Consensus Committee, 2007). HbA_{1c} assays should be calibrated using the reference measurement system developed by the IFCC that measures only HbA_{1c} (not non-A_{1c} components). The Consensus Committee also recommended that results be reported in a standardized manner (A_{1c} [%]; A_{1c} [mmol/mol], and estimated average glucose [eAG]). The United States reports National Glycohemoglobin Standardization Program (NGSP) numbers (% HbA_{1c} and eAG) but not IFCC numbers (mmol/mol). IFCC units can be converted to NGSP units as follows: NGSP = (0.915 × IFCC) + 2.15 (Hoelzel et al., 2004).

The NGSP began in 1996, with the goal of standardizing glycosylated hemoglobin tests to the high-performance liquid chromatography (HPLC) method reported as HbA_{1c} or HbA_{1c} equivalent, as used in the DCCT. Several types of certified methods are available for measuring hemoglobin A_{1c}: immunoassay, ion-exchange HPLC, electrophoresis, boronate affinity HPLC, and enzyme methods. Reliable benchtop point-of-care analyzers, such as the one that uses a cassette-based immunoassay method, also are available. These devices permit results to be accessible at the time of the patient visit so that they can be discussed with the patient and immediate action taken when needed. The performance of 13 point-of-care devices has been examined and found to vary in bias and diagnostic accuracy (Hirst et al., 2017). In the United States, one point-of-care device (Afinion), which has superior accuracy and precision, has been approved by the FDA for use in the diagnosis of diabetes.

Most U.S. laboratories use a certified method and participate in the College of American Pathologists' proficiency testing program. To obtain and retain a Certificate of Traceability to the DCCT Reference Method in the NGSP, the laboratory must annually satisfy certification criteria.

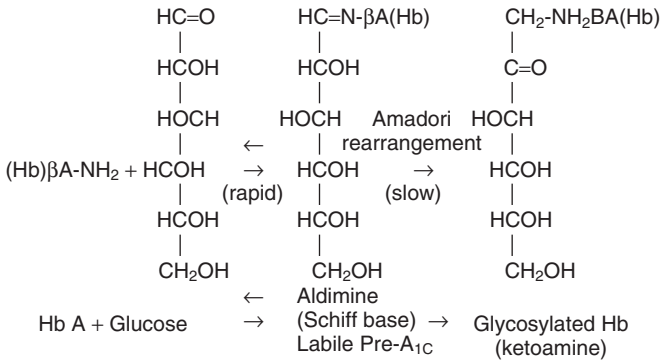

Figure 17.3 Formation of glycosylated hemoglobin (GHb).

TABLE 17.5
Correlation Between Hemoglobin A_{1c} and Plasma Glucose Levels

Hemoglobin A_{1c} (%)	APPROXIMATE MEAN PLASMA GLUCOSE	
	mg/dL	mmol/L
5	97 (76–120)	5.4 (4.2–6.7)
6	126 (100–152)	7.0 (5.5–8.5)
7	154 (123–185)	8.6 (6.8–10.3)
8	183 (147–217)	10.2 (8.1–12.1)
9	212 (170–249)	11.8 (9.4–13.9)
10	240 (193–282)	13.4 (10.7–15.7)
11	269 (217–314)	14.9 (12.0–17.5)
12	298 (240–347)	16.5 (13.3–19.3)

From Nathan et a0.l (2008).
See http://professional.diabetes.org/eAG for a calculator to convert hemoglobin A1c (%) to estimated mean glucose level.

The process compares 40 whole blood patient samples with a Secondary Reference Laboratory (SRL). Beginning in 2019, for manufacturer method certification and Level II Laboratory certification, criteria are 36/40 results within ±5%, and for Level 1 Laboratory certification 37/40 results within ±5%. The NGSP website contains certification criteria, procedures to obtain certification, and information on assay interferences (http://www.ngsp.org/index.asp).

All HbA_{1c} assays are affected by blood loss, blood transfusions, and conditions that affect the age or survival of red blood cells, such as hemolysis, pregnancy, and the use of drugs that stimulate erythropoiesis (Little et al., 2019). Shortened red blood cell survival or lower mean age will lower HbA_{1c} levels as a result of reduced exposure to plasma glucose. HbA_{1c} assays vary in reliability in the presence of a variety of other factors. Interference by carbamylated hemoglobin can occur with uremia in some older methods, and salicylates can cause interference by acetylated species. Hemoglobinopathies (HbSS, HbSC, HbCC, HbD trait, HbE trait, elevated fetal hemoglobin HbF) can adversely affect accuracy in certain assays (for an updated list, see http://www.ngsp.org/interf.asp), as can iron deficiency and hemodialysis (Tarim et al., 1999; Little et al., 2019). Vitamins C and E can falsely lower levels by inhibiting glycosylation, but vitamin C can also increase levels in some assays. Sample storage effects may occur. Hyperglycemia has been associated with a decrease in erythrocyte survival, suggesting that HbA_{1c} levels in poorly controlled patients may underestimate their mean plasma glucose concentration (Virtue et al., 2004).

The correlation between HbA_{1c} and estimated average plasma glucose levels is shown in Table 17.5 (Nathan et al., 2008). This is based on data from the International A1c Derived Average Glucose trial. There is evidence that the relationship between HbA_{1c} and mean blood glucose may vary in different racial and ethnic groups owing to differences in hemoglobin glycation, genetics, and/or other factors that are not well understood (Herman & Cohen, 2012). Whereas, on average, black compared to white individuals had somewhat higher HbA_{1c} levels at the same mean glucose levels (measured using CGM), HbA_{1c} levels at the same mean glucose level vary considerably between individuals regardless of race, with greater differences within races than between races (Bergenstal et al., 2017). For example, an HbA_{1c} of 7.0% was associated with a mean CGM glucose (95% CI) of 128 to 190 mg/dL (7.1–10.6 mmol/L) and an HbA_{1c} of 8.0% was associated with a mean glucose of 155 to 218 mg/dL (8.6–12.1 mmol/L) (Beck et al., 2017).

For patients in whom HbA_{1c}/eAG and measured blood glucose appears to be discordant, clinicians should consider the possibility of interfering factors discussed earlier. In the presence of abnormal red cell turnover, such as with pregnancy, recent blood loss, or transfusions, only blood glucose criteria should be used to diagnose diabetes. For patients with an abnormal hemoglobin but normal red cell turnover, such as sickle cell trait, an HbA_{1c} assay without interference from the abnormal hemoglobin should be used.

Since the estimated HbA_{1c} (eA_{1c}) in some individuals based on CGM readings may be lower or higher than the laboratory measured HbA_{1c}, using the HbA_{1c} alone to assess glycemic control can be misleading (Beck et al., 2017). To address this dilemma, a new term, *glucose management indicator* (GMI), has been introduced (Bergenstal et al., 2018). The GMI estimates HbA_{1c} from mean CGM data (GMI% = 3.31 + 0.02392 × mean glucose [mg/dL]; https://www.jaeb.org/gmi). The GMI can be useful when setting glycemic goals for specific individuals to help avoid overtreatment and hypoglycemia.

The turnover time of serum proteins, primarily albumin (14–20 days), is much shorter than that of erythrocytes; thus, their glycosylation reflects glycemic control over narrower periods of time (2–3 weeks). The nonenzymatic glycation of these serum proteins occurs similarly to that of hemoglobin, with the formation of ketoamine-linked glucose protein. Fructosamine and glycated albumin assays may be useful in patients for whom HbA_{1c} assays are inaccurate, such as those with hemoglobinopathies, advanced chronic kidney disease, and hemolytic anemias. However, unlike HbA_{1c} levels, their clinical utility has not been firmly established. Fructosamine assays primarily measure glycosylated albumin; additional glycosylated proteins, such as globulins and lipoproteins, are measured as well. These measurements can be affected by alterations in serum protein levels that are present during acute illnesses, nephrotic syndrome, thyroid disease, and liver disease.

Fructosamine assays use serum samples and automated equipment; thus, they are simple to perform and low cost. However, they are not well standardized and are sensitive to variations in temperature (Danese et al., 2015). Fructosamine values are not commonly corrected for serum protein or albumin concentrations; thus, the assay should not be performed if the serum albumin level is ≤3.0 g/dL (0.45 mmol/L). **Glycated albumin**

assays are better standardized, more precise, and inexpensive (Danese et al., 2015). Several methods are available for measuring glycated albumin, including boronate affinity chromatography, ion-exchange chromatography, HPLC, immunoassays, and enzymatic methods. Glycated albumin results can be reported as a percent of total albumin and are not affected by elevated serum bilirubin levels. Although the results of fructosamine and glycated albumin assays are well correlated, glycated albumin assays overall have better specificity and accuracy and are less expensive.

Neither HbA_{1c} nor fructosamine values capture the magnitude of glycemic excursions. There is evidence that wide glycemic fluctuations contribute to vascular damage independent of mean glucose concentrations. Tests providing information about glycemic excursions may be useful for risk stratification. One such test is **1,5-anhydroglucitol (1,5-AG)**, the results of which reflect postprandial glycemia and short-term (1- to 2-week) hyperglycemia. 1,5-AG, a dietary monosaccharide, is filtered in the glomerulus and competes with glucose for reabsorption in the renal tubules. Hyperglycemia decreases 1,5-AG blood concentrations. Abnormal renal function will interfere with the accuracy of this test (Lawler & Mora, 2014). Several studies have suggested an association between 1,5-AG and microvascular and macrovascular complications. In the Atherosclerosis Risk in Communities (ARIC) study, adults with diabetes and low 1.5-AG levels developed more coronary heart disease, heart failure, stroke, and death over 20 years of follow-up (Selvin et al., 2016). More recently, with the increased availability and use of continuous glucose monitoring, glucose metrics, particularly standard deviation and coefficient of variation, are being used to assess glycemic variability.

KETONE TESTING

The ketone bodies β-hydroxybutyric acid, acetoacetic acid, and acetone are products of fatty acid degradation. β-Hydroxybutyric acid and acetoacetic acid are normally present in a 1:1 ratio at concentrations of 0.5 to 1.0 mmol/L each. Ketone testing, using urine or blood, is particularly important for individuals with type 1 diabetes to detect ketosis. DKA is a serious and potentially fatal hyperglycemic condition requiring urgent treatment. It is frequently associated with nausea, vomiting, abdominal pain, electrolyte disturbances, and severe dehydration. Type 2 diabetes patients who are poorly controlled, particularly in the presence of extreme stress or severe acute illness, can also develop DKA. Ketone testing may be useful in pregnancy and in determining the cause of hypoglycemic disorders.

The ratio of β-hydroxybutyric acid to acetoacetic acid is greatly increased in DKA as a result of the altered redox state and elevated levels of NADH in the hepatic mitochondria. The most commonly used strips and tablets use sodium nitroprusside (sodium nitroferricyanide) and turn purple in the presence of elevated levels of acetoacetic acid. Acetone is detected in the presence of glycine. False-negative results can occur with old strips and with strips that have had excessive contact with air and after ingestion of large amounts of vitamin C (very acidic urine). False-positive results have been observed with the use of sulfhydryl-containing medications such as captopril (but not other angiotensin-converting enzyme inhibitors not containing the sulfhydryl group) and in the presence of highly colored urine (Sacks et al., 2011). β-Hydroxybutyric acid is not detected by these methods. Because β-hydroxybutyric acid levels fall and acetoacetic acid and acetone levels rise during the treatment of DKA, these tests are not useful for the monitoring of therapy. Given these shortcomings and the availability of direct measurement of β-hydroxybutyrate in serum (by laboratories and by ambulatory patients and caregivers using point-of-care devices), direct measurement of β-hydroxybutyrate is preferred over older nitroprusside-based tests. The use of these point-of-care devices in ambulatory settings (as an alternative to urine ketone tests) is limited by their higher cost. Compared with laboratory measurements, point-of-care devices have poor accuracy at very high ketone concentrations (>5 mmol/L) (Yu et al., 2011).

β-Hydroxybutyric acid can be measured in serum by enzymatic, electrochemical, chromatographic, electrophoretic, and colorimetric methods. Reference ranges of β-hydroxybutyrate vary among assay methods, but concentrations in healthy individuals who have fasted overnight are generally less than 0.5 mmol/L. Patients who meet biochemical criteria for diagnosis of DKA (i.e., HCO_3 <17 mmol/L, arterial pH <7.3, plasma glucose >250 mg/dL [14.9 mmol/L]) generally have β-hydroxybutyrate concentrations >2.0 mmol/L (Sacks et al., 2011).

For the monitoring of recovery from DKA in the hospital setting, serial measurements of serum electrolytes, including bicarbonate with calculation of the anion gap, are often used. Serial measurement of β-hydroxybutyric acid provides an additional tool to monitor resolution of DKA. This can be especially useful in patients with DKA in the presence of a concomitant additional acid-base abnormality interfering with proper interpretation of bicarbonate concentrations and the anion gap, such as seen in renal failure.

HYPOGLYCEMIA

Hypoglycemia results from an imbalance between glucose utilization (by brain, erythrocytes, muscle, and kidneys) and production (endogenous glucose production by liver and kidneys and from ingestion of carbohydrates) in such a manner that the rate of glucose utilization exceeds the rate at which glucose is being produced (Guettier & Gordon, 2006). The symptoms of hypoglycemia can be divided into two categories: neurogenic and neuroglycopenic. Neurogenic symptoms are triggered by the autonomic nervous system. Tremulousness, palpitations, and anxiety are catecholamine mediated; diaphoresis, hunger, and paresthesias are related to acetylcholine release. The neuroglycopenic symptoms are due to diminished glucose supply to the central nervous system and include dizziness, tingling, difficulty concentrating, blurred vision, confusion, behavioral changes, seizure, and coma (Schwartz et al., 1987; Mitrakou et al., 1991; Towler et al., 1993). Severe hypoglycemia, if not corrected in a timely fashion, can be fatal (Cryer, 2007).

Treatment of diabetes mellitus with insulin or agents that increase insulin secretion (insulin secretagogue drugs), such as sulfonylureas, is the major cause of hypoglycemia. A number of other drugs and medical conditions can also cause hypoglycemia (Box 17.2). Pancreatic hyperinsulinemic hypoglycemia can be diagnosed by demonstrating that insulin secretion is not suppressed normally when the individual develops hypoglycemia. Measurements of insulin, C-peptide, proinsulin, insulin and insulin receptor autoantibodies, β-hydroxybutyrate, and drugs (i.e., sulfonylurea and meglitinide levels) are recommended to determine the correct diagnosis. Insulin and proinsulin autoantibodies may interfere with the immunoassays for insulin, proinsulin, and C-peptide.

Whipple's triad, initially proposed by Whipple for the diagnosis of hypoglycemic disorders, continues to be an important tool in assessing patients with episodes suggestive of low plasma glucose levels. *Whipple's triad* refers to symptoms consistent with hypoglycemia associated with a documented low plasma glucose level and relief of symptoms with correction of hypoglycemia (Whipple, 1938). Further evaluation is indicated if a person who is in good health presents with symptoms of hypoglycemia and a laboratory plasma glucose level ≤55 mg/dL (3.1 mmol/L) in the absence of treatment of diabetes mellitus (Cryer et al., 2009; Haymond, 1989; Sperling & Menon, 2004).

DRUG-INDUCED HYPOGLYCEMIA

Most cases of drug-induced hypoglycemia have been described in patients with diabetes mellitus who are on glucose-lowering medications such as insulin and insulin secretagogue drugs (sulfonylureas, repaglinide, and nateglinide). Elevated insulin with low C-peptide values are observed when exogenous insulin has been administered. High insulin and C-peptide levels with a positive drug screen for an insulin secretagogue would be expected when these oral agents have been used surreptitiously. It is important that these blood tests be drawn during the hypoglycemic episode. The assays for sulfonylureas and meglitinides should be sent to a laboratory that has the capability to measure very low levels of these drugs, because assays using higher detection limits can lead to an inaccurate diagnosis (Manning et al., 2003).

Many other drugs have been reported to cause hypoglycemia, including quinolones, pentamidine, quinine, and beta blockers. Pentamidine directly damages pancreatic beta cells. Hypoglycemia can occur within a few hours to days of administration of pentamidine. Plasma insulin levels are high despite low glucose concentrations, indicating excessive insulin leakage (Bouchard et al., 1982; Assan et al., 1995). Sulfonamide-induced hypoglycemia is also associated with increased insulin and C-peptide levels in susceptible individuals (Hekimsoy et al., 1997). Salicylate-induced hypoglycemia may be due to increased peripheral glucose utilization secondary to uncoupling of oxidative phosphorylation, decreased hepatic glyconeogenesis, and increased insulin release (Marks & Teale, 1999). Beta blockers such as propranolol can cause hypoglycemia by antagonizing catecholamine-mediated glycogenolysis (Chavez et al., 1999).

Adenosine triphosphate (ATP)–sensitive potassium (K_{ATP}) channels play a major role in the regulation of insulin secretion from pancreatic beta cells. Blockage of these channels causes depolarization of the beta cell membrane, opening of voltage-dependent calcium channels, and increased influx of calcium that causes release of insulin from the beta cell and lowering of blood glucose. The K_{ATP} channel consists of eight subunits (four

BOX 17.2

Clinical Classification of Hypoglycemia

Drugs
Insulin
Sulfonylureas
Repaglinide
Nateglinide
Alcohol
Pentamidine
Quinolones
Beta blockers
Quinine
Salicylates
Sulfonamides
Haloperidol
Propoxyphene
Paraaminobenzoic acid
Cibenzoline
Indomethacin
Lithium
Glucagon
Artesunate
Artemisin
Artemether
Chloroquineoxaline sulfonamide
Insulin-like growth factor-1

Critical Illnesses
Hepatic failure
Renal failure
Cardiac failure
Sepsis
Malnutrition

Hormonal Deficiencies
Glucagon
Epinephrine
Cortisol
Growth hormone

Endogenous Hyperinsulinism
Pancreatic beta cell disorders
Tumor (insulinoma)
Nontumor (nesidioblastosis or diffuse hyperplasia of the islets)

Autoimmune Hypoglycemia
Insulin antibodies
Insulin receptor antibodies

Non–Beta Cell Tumors
Mesenchymal: Fibrosarcoma, mesothelioma, rhabdomyosarcoma, leiomyosarcoma, liposarcoma, lymphosarcoma, hemangiopericytoma
Carcinomas: Hepatomas, adrenocortical tumors, hypernephroma, Wilms tumor
Neurologic and neuroendocrine tumors: Pheochromocytoma, carcinoid tumor, neurofibroma
Hematologic: Leukemias, lymphoma, myeloma

Hypoglycemia of Infancy and Childhood
Hyperinsulinism: Genetic defects in pancreas beta cells
Transient hyperinsulinism: Infant of mother with diabetes, Beckwith-Wiedemann syndrome, prolonged neonatal hyperinsulinism (perinatal stress, intrauterine growth restriction, maternal toxemia), erythroblastosis fetalis
Idiopathic ketotic hypoglycemia
Glycogen storage diseases
Hereditary fructose intolerance
Galactosemia
Defects in gluconeogenesis
Glucose transporter defects
Fatty acid oxidation disorders
Ketogenesis disorders
Disorders of protein metabolism
Defects in mitochondrial function
Miscellaneous: Reye syndrome, gastroenteritis, malaria, drugs, malnutrition

Alimentary Hypoglycemia
Postgastric bypass surgery
Post-Nissen fundoplication with gastrostomy (children)
Idiopathic (functional) postprandial hypoglycemia

Adapted from Lteif & Schwenk (1999); Cryer et al. (2009); Murad et al. (2009); Ghosh et al. (2016).

Kir6.0 and four SUR). Saraya and colleagues (2004) showed that the Kir6.2 subunit of the pancreatic beta cell is blocked by fluoroquinolone, gatifloxacin, and to a lesser extent by levofloxacin and temafloxacin (Park-Wyllie et al., 2006). Gatifloxacin has been withdrawn.

Alcohol consumption can inhibit hepatic gluconeogenesis and increase glycogen phosphorylase activity, depleting hepatic glycogen stores and resulting in hypoglycemia. Alcohol-induced hypoglycemia is usually seen in the setting of a history of alcohol intake of 50 to 300 g without food intake for the preceding 6 to greater than 36 hours. Alcohol can be detected in the blood or breath. Plasma β-hydroxybutyrate levels are elevated, and plasma insulin and C-peptide levels are low during the hypoglycemic episode (Arky, 1989; Marks & Teale, 1999).

SEVERE MEDICAL ILLNESSES

Widespread hepatic disease and severe cardiac failure can result in hypoglycemia. Pathogenic mechanisms can include impaired gluconeogenesis, hepatic congestion with decreased oxygen delivery to hepatocytes, impaired insulin degradation, and shunting of portal blood into the systemic circulation (Khoury et al., 1998). A decrease in glycogen reserves coupled with failure of gluconeogenesis and enhanced glucose utilization may be the cause of hypoglycemia in patients with severe sepsis (Miller et al., 1980). In addition, patients with very low muscle mass, such as those with spinal muscular atrophy and congenital myopathy, are at risk for hypoglycemia during prolonged fasting (23 hours), presumably related to poor availability of the gluconeogenic substrate alanine. Low plasma insulin and high plasma glucagon levels are observed during the hypoglycemia (Orngreen et al., 2003).

Hypoglycemia in end-stage renal disease (ESRD) can be related to defective gluconeogenesis, as well as impaired hepatic glycogenolysis due to poor nutritional status (Arem, 1989). ESRD is also associated with reduced insulin clearance. Alcohol ingestion, use of insulin or sulfonylurea drugs, sepsis, malnutrition, liver disease, and cardiac failure can increase the likelihood of hypoglycemic events in a patient with renal failure (Haviv et al., 2000). Gabapentin has been associated with hypoglycemia in a patient with ESRD on peritoneal dialysis. Plasma insulin and C-peptide levels were elevated during the hypoglycemic episode (Penumalee et al., 2003).

HORMONE DEFICIENCIES

Glucose counterregulation, mediated by glucagon, catecholamines, cortisol, and growth hormone, is important in preventing hypoglycemia. Glucagon initially stimulates glycogenolysis and later gluconeogenesis to increase plasma glucose levels. Catecholamines increase glycogenolysis, gluconeogenesis, and lipolysis; decrease insulin-mediated glucose uptake; and inhibit insulin release. Both growth hormone and cortisol decrease insulin-mediated tissue glucose uptake and increase release of glucose into the circulation. Growth hormone and cortisol mediate glycogenolysis and gluconeogenesis. A deficiency in the secretion of these counterregulatory hormones can contribute to low blood glucose levels. Hypoglycemia in adults is rarely attributable to deficiencies of glucagon or catecholamines, but poor glucagon and epinephrine responses to hypoglycemia are common in patients with long-standing diabetes mellitus and are associated with prolonged hypoglycemic episodes. Infants and children with a deficiency of cortisol and growth hormone are prone to develop hypoglycemia, especially during fasting and acute illness. Adults with glucocorticoid or growth hormone deficiency can also develop hypoglycemia, usually after a prolonged fast (Smallridge et al., 1980; Zuker et al., 1995; Bunch et al., 2002).

NON–BETA CELL TUMORS

Non–islet cell tumor hypoglycemia (NICTH) originates from non–beta cell tumors, which cause hypoglycemia without producing insulin. Tumors of mesenchymal origin (mesothelioma, hemangiopericytoma, solitary fibrous tumors) and epithelial origin (hepatocellular, gastrointestinal stromal tumor) are commonly associated with NICTH. The tumor is usually detected on physical examination and is confirmed by radiologic diagnostic studies. These tumors are associated with increased paraneoplastic production of insulin-like growth factor-II (IGF-II). Normally, IGF-II is produced

by the liver and is relatively independent of growth hormone (GH) action. The primary transcription product is pre-proIGF-II. Posttranslational processing of pre-proIGF-II leads to the formation of proIGF-II that is cleaved to form IGF-II. The intermediate product proIGF-II may be secreted. Non–islet cell tumor hypoglycemia is associated with aberrant paraneoplastic production of proIGF-II, also known as "big" IGF-II (Fukuda et al., 2006; de Groot et al., 2007). It is believed that elevated levels of IGF-II increase glucose utilization and suppress endogenous glucose production (Chung & Henry, 1996; Daughaday, 1989). The diagnosis of NICTH can usually be made by the presence of fasting hypoglycemia, low insulin, proinsulin, and C-peptide levels; an elevated IGF-II–to–IGF-I ratio; and low growth hormone and β-hydroxybutyrate levels. The glucagon level is usually within the normal range despite hypoglycemia because of the suppressive effect of "big" IGF-II on glucagon secretion. Hypokalemia is frequently associated with hypoglycemia due to insulin-like activity of big IGF-II. Levels of big IGF-II and IGF binding protein 2 (IGF-BP 2) can be determined by immunometric assays and are usually elevated (van Doorn et al., 2002). Size-exclusion acid chromatography is considered the gold standard method for detecting big IGF-II in NICTH. However, this is a time-consuming procedure. A rapid, reproducible, and sensitive method for the determination of big IGF-II by immunoblot analysis after separating IGF-II peptides using 16.5% tricine sodium dodecyl sulfate-polyacrylamide gels has been described (Miraki-Moud et al., 2005). There are also rare reports of ectopic insulin secretion by tumors.

ENDOGENOUS HYPERINSULINISM

Hypoglycemia from endogenous insulin secretion can be due to (1) insulin-secreting beta cell tumors (insulinomas), (2) congenital hyperinsulinism, and (3) autoantibodies to insulin in patients who have never been treated with insulin (Hirata & Uchigata, 1994). A supervised 72-hour fast is recommended for the diagnosis of insulinoma with frequent clinical and biochemical monitoring for signs of hypoglycemia. During the hypoglycemic episode, blood is drawn for glucose, insulin, proinsulin, C-peptide, and β-hydroxybutyrate levels. Blood or urine screening tests for sulfonylurea/meglitinide drugs are also performed.

Insulinomas are the most common tumors of islet cells. The diagnostic criteria for an insulinoma are the presence of signs and symptoms of hypoglycemia, with a plasma glucose level of ≤55 mg/dL (3.1 mmol/L); insulin level ≥3 μU/mL (18 pmol/L) by immunochemiluminometric assay; C-peptide concentration of ≥0.6 ng/mL (0.2 nmol/L); proinsulin concentration of ≥5.0 pmol/L; β-hydroxybutyrate of ≤2.7 mmol/L; an increase in the plasma glucose concentration of ≥25 mg/dL (1.4 mmol/L) in response to a 1-mg glucagon injection given intravenously; and a negative sulfonylurea/meglitinide blood/urine screen (Cryer et al., 2009). An abnormally high amended fasting insulin-glucose ratio (ratio >53.6 pmol/L/mmol/L using an amended glucose value [1.7 mmol/L; 30 mg/dL] subtracted from the measured glucose concentration) has also been reported to have high specificity and positive predictive value in the diagnosis of insulinoma (Nauck & Meier, 2012). Those patients who are found to have endogenous hyperinsulinemic hypoglycemia with negative screening for oral antihyperglycemic agents and no evidence of insulin antibodies need further diagnostic tests to localize the insulinoma. These tests may include computed tomography (CT), magnetic resonance imaging (MRI), transabdominal and endoscopic ultrasonography (USG), and positron emission tomography (PET) imaging with or without tracers (i.e., F-FDOPA and GLP-1 receptor analogs). Selective pancreatic arterial calcium injections with measurement of hepatic venous insulin levels can be used when conventional noninvasive means (CT, MRI, USG) have failed to localize the insulin-producing islet cell tumors (Guettier et al., 2009).

ALIMENTARY HYPOGLYCEMIA

Alimentary ("reactive") hypoglycemia occurs usually within 4 hours after eating a meal. The OGTT is unreliable in diagnosing this condition. Individuals who have had gastric surgery are at risk. The dumping syndrome is characterized by vasomotor symptoms, such as sweating, dizziness, and weakness, which usually occur less than an hour after ingestion of a meal. Hypoglycemia is not a characteristic of early dumping syndrome.

Hypoglycemia has been described in patients who have undergone bariatric surgery for obesity, particularly after Roux-en-Y gastric bypass (Service et al., 2005). The onset is usually >1 year after surgery. There is rapid gastric emptying associated with an early, rapid, exaggerated transient peak in blood glucose concentrations. Increased insulin and GLP-1 levels, as well as alterations in glucagon secretion, have been reported (Salehi et al., 2018). These patients usually have a history of "spells" of postprandial hypoglycemia that fulfill Whipple's triad. Typically, the pattern is postprandial hypoglycemia in the absence of fasting hypoglycemia. OGTTs are poorly tolerated and not recommended.

Some individuals without gastrointestinal pathology report spontaneous symptoms suggestive of hypoglycemia 1 to 4 hours after intake of carbohydrate-rich meals but have a normal laboratory evaluation. These patients are believed to have idiopathic reactive hypoglycemia. The oral glucose tolerance test is also not useful for the diagnosis of this condition (Lefebvre et al., 1988). Increased insulin sensitivity has been seen in some patients exhibiting features of postprandial hypoglycemia (Tamburrano et al., 1989). Contributing factors may also include delayed release of insulin in response to a meal and concomitant alcohol ingestion (Flanagan et al., 1998).

Up to 33% of children with a Nissen fundoplication and gastrostomy tube are at risk for late dumping syndrome and hypoglycemia. In these patients, a rapid rise in glucose triggers a rapid rise in insulin. Glucose is absorbed quickly, resulting in high circulating insulin levels that cause hypoglycemia 1 to 2 hours later. These children do not have the gastrointestinal symptoms typically seen with the dumping syndrome. Laboratory results from samples at the time of hypoglycemia may suggest hyperinsulinism. These patients have normal glucose readings for fasting and do not develop hypoglycemia if there is slow weaning of their continuous feedings. Acarbose, a glucosidase inhibitor that slows carbohydrate digestion and attenuates both postprandial glucose hyperglycemia and reactive postprandial hypoglycemia, in combination with a complex carbohydrate formula, have been used successfully in infants as young as 6 months old (De León et al., 2001; DeCunto et al., 2011).

AUTOIMMUNE-RELATED HYPOGLYCEMIA

Hypoglycemia can be due to antibodies directed against endogenous insulin or the insulin receptor. Hypoglycemia associated with autoantibodies to insulin in patients who have not received insulin injections is a rare condition called the *autoimmune insulin syndrome* (*AIS*). Individuals with autoimmune diseases or recent ingestion of sulfhydryl-containing medications (i.e., methimazole, penicillamine, captopril, imipenem, hydralazine, procainamide, isoniazid, penicillin G) are at increased risk for AIS. These patients commonly experience episodes of postprandial hypoglycemia. In some patients, fasting hypoglycemia, as well as hypoglycemia precipitated by increased physical activity, have been reported. Excessive amounts of insulin secreted after a meal are bound to antibodies; as a result, insulin becomes unavailable to target tissues. Hours later, insulin dissociates from the antibodies, resulting in hyperinsulinemia and hypoglycemia. Insulin levels are extremely elevated and distinctly higher than in insulinoma. C-peptide levels are incompletely suppressed, and a high insulin–to–C--peptide molar ratio is present. Serum insulin antibodies are elevated (Hirata & Uchigata, 1994; Dozio et al., 1998; Lidar et al., 1999; Cavaco et al., 2001; Vogeser et al., 2001; Yaturu et al., 2004; Lupsa et al., 2009).

Antibodies directed against the insulin receptor can cause hypoglycemia or hyperglycemia with extreme insulin resistance (type B insulin resistance). Type B insulin resistance is a rare condition typically diagnosed in the third to fifth decades of life. It is more common in women and in persons of African heritage. Hyperglycemia may be the initial metabolic derangement in 80% of these patients; however, 20% may present with hypoglycemia. Hypoglycemia may develop some time later in 14% of patients who initially present with hyperglycemia (Fareau et al., 2007). Other autoimmune diseases, such as systemic lupus erythematosus and Hashimoto thyroiditis, may also be present in these patients (Bao et al., 2007; Kato et al., 2008; Qing et al., 2009). In this condition, insulin receptor antibodies block insulin from attaching to the insulin receptor. In some patients, hyperglycemia is due to receptor degradation or downregulation, leading to insulin resistance. Hyperglycemia and hypoglycemia sometimes can be seen in the same patient. Plasma glucose, β-hydroxybutyrate, and proinsulin levels are low, and insulin and the insulin–to–C-peptide ratio are inappropriately high. Insulin receptor antibodies can be detected by immunoprecipitation assays (Taylor et al., 1989; Redmon & Nuttall, 1999). Mutations in the insulin receptor gene are another rare cause of hypoglycemia.

HYPOGLYCEMIA IN INFANCY AND CHILDHOOD

Hypoglycemia in neonates, infants, and children is usually a problem of fasting adaptation. Postprandial hypoglycemia is rare and limited to special situations, such as those with Nissen fundoplication (discussed earlier) or hereditary fructose intolerance (described later). Glucose utilization rates are significantly higher in infants compared with adults because of their

larger brain weight to body weight ratio. Normal infants and children develop hyperketonemia and hypoglycemia after 24 to 36 hours of fasting compared with 48 to 72 hours in normal adults. This results in normal infants and children being more susceptible to fasting hypoglycemia during illnesses that impair feeding. Hypoglycemia during the first 2 years of life may cause significant and permanent neurologic damage since this is a crucial period for brain growth and development.

Endocrine adaptive responses at birth help mobilize endogenous glucose, preventing hypoglycemia when the maternal transfer of glucose to the fetus is acutely interrupted at delivery. These include a decrease in insulin levels, an increase in glucagon and catecholamine concentrations, and elevated growth hormone levels. These hormonal changes at birth help mobilize glucose through glycogenolysis and gluconeogenesis, activate lipolysis, and promote ketogenesis. Blood glucose concentrations are usually lower in neonates, especially in the first day of life, compared with those observed in older infants and children. However, because of increased production and use of alternative fuels such as free fatty acids and ketones, glucose is spared for brain use and this "transitional hypoglycemia" is not associated with adverse effects. Whereas it has been traditional to accept lower glucose values in newborns as normal, pediatric endocrinologists recommend using the same definition of hypoglycemia in neonates as in older children (De León et al., 2008; Gandhi, 2017).

Transient neonatal hypoglycemia can occur in normal-term infants and is associated with immature hepatic gluconeogenesis and ketogenesis. The normal newborn is highly dependent on hepatic glycogen stores to maintain normoglycemia during the first day of life and acquires mature fasting systems after the first 24 hours of life. Plasma glucose concentrations fall below 50 mg/dL (2.8 mmol/L) during the first 6 hours of life in one-third of infants after delivery. By the second day of life, the frequency of glucose levels below 50 mg/dL (2.8 mmol/L) is less than 0.5% (De León et al., 2008; Farrag & Cowett, 2009).The risk of fasting hypoglycemia in the immediate postnatal period is considerably higher in the preterm infants compared with full-term neonates. This may be explained by lower glycogen reserves in preterm infants and more limited hormonal responses. (Thornton et al., 2015; Gandhi, 2017).

Neonatal hyperinsulinism due to maternal factors can also cause transient neonatal hypoglycemia. This is seen in infants of women with poorly controlled diabetes mellitus. Babies are usually large and plethoric. Hypoglycemia in these infants is mainly due to hyperinsulinemia; diminished glucagon secretion may also be contributory. Transient hyperinsulinism in an infant of a mother with diabetes usually resolves in 1 or 2 days. If hypoglycemia persists, there should be further evaluation. A blunted glucagon surge (possibly mediated by intravenous glucose or formula feeds) or insufficient catecholamine release (due to maternal β-blocker medication use) can also lead to transient neonatal hypoglycemia and require treatment.

Neonates exposed to perinatal stress—such as birth asphyxia, maternal toxemia, prematurity, intrauterine growth restriction, or other perinatal stress—are at high risk for prolonged hypoglycemia due to **prolonged neonatal hyperinsulinism**. These neonates have high glucose utilization and require high glucose infusion rates to maintain normal blood glucose concentrations. At the time of hypoglycemia, they have inappropriately normal or high levels of insulin, low β-hydroxybutyrate, and low free fatty acids. The hypoglycemia is responsive to administration of glucagon (glucose level rise of ≈30 mg/dL [1.7 mmol/L]). Unlike the hyperinsulinism seen in infants of mothers with poorly controlled diabetes, perinatal stress–induced hyperinsulinism persists for several weeks. Median age of resolution is 6 months. These infants respond to medical therapy with diazoxide (De León et al., 2008; Farrag & Cowett, 2009; Thornton et al., 2015).

Persistent hypoglycemia in infants and children is due to deficiencies of counterregulatory hormones (growth hormone deficiency and glucocorticoid deficiency), congenital hyperinsulinism, ketotic hypoglycemia and inborn errors of metabolism (see earlier section **Hormone Deficiencies**). Older infants and children with hypoglycemia due to hypopituitarism present with ketotic hypoglycemia. However, in the newborn period, they do not have elevated β-hydroxybutyrate levels at the time of hypoglycemia. The incidence of hypoglycemia in infants and children with hypopituitarism and a combination of growth hormone and/or ACTH deficiency is 20%. Hypoglycemia can be the presenting clinical feature in infants with hypopituitarism. These infants can also have midline anatomic abnormalities and microphallus, a sign of coexistent gonadotropin deficiency. Liver disease similar to cholestatic liver disease is another clinical feature in infants with hypopituitarism. (Thornton et al., 2015; Gandhi, 2017).

Congenital Hyperinsulinism

In congenital hyperinsulinism (CHI) there is inappropriate secretion of insulin by pancreatic beta cells that leads to hyperinsulinemic hypoglycemia (HH). The estimated incidence of CHI is 1/50,000 live births (up to 1/2500 in Saudi Arabia because of a high rate of consanguinity). Infants have large-for-gestational-age birth weight and severe, persistent hypoglycemia requiring high glucose infusion rates (>10 mg/kg/min) to treat the hypoglycemia. Compensatory ketogenesis is prevented by elevated insulin levels, causing a lack of alternate sources of fuel to protect the brain from hypoglycemia (Arnoux et al., 2011). The diagnosis of CHI in children relies heavily on markers of excessive insulin action at the time of hypoglycemia (suppressed ketogenesis and lipolysis). The plasma insulin concentration is rarely dramatically elevated. Biochemical criteria that support the diagnosis of hyperinsulinism at the time of plasma glucose <50 mg/dL (<2.8 mmol/L) include (1) detectable insulin, (2) hypoketonemia (β-hydroxybutyrate <2.0 mmol/L), (3) inhibition of lipolysis (free fatty acids <1.5 mmol/L), and (4) inappropriate glycemic response to glucagon 1 mg IV/IM (change in glucose >30 mg/dL [1.7 mmol/L]) (Lord & De León, 2013; Thornton et al., 2015).

Figure 17.4 displays genetic defects in the pancreatic beta cell that cause hyperinsulinism. Glucose-induced insulin secretion requires glucose uptake

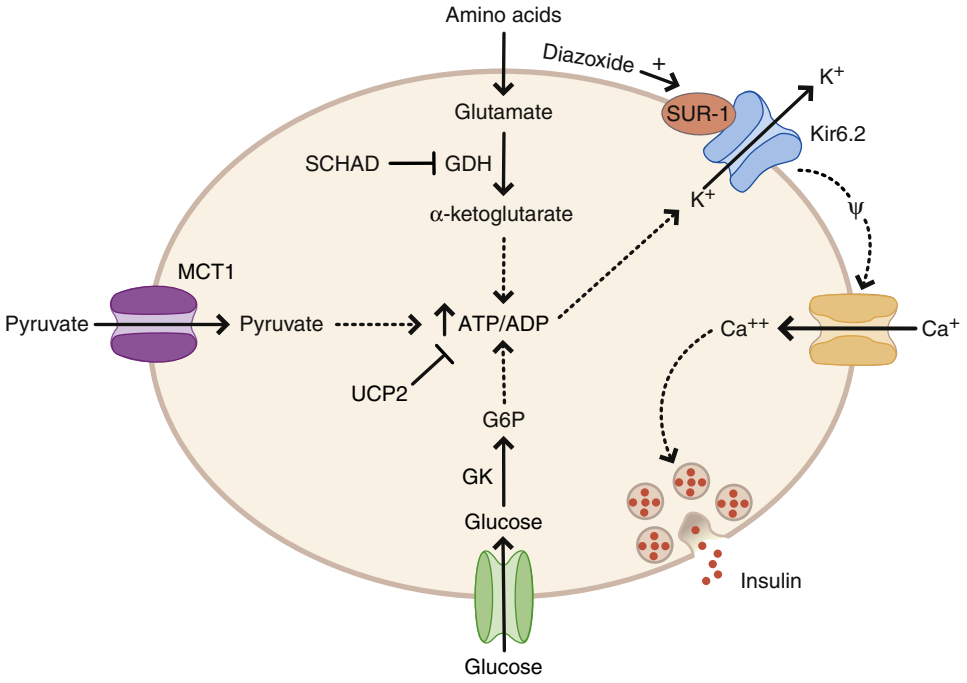

Figure 17.4 Genetic defects in the pancreatic beta cell leading to hyperinsulinism. The plus sign (+) above the arrow from "Diazoxide" indicates that this agent induces channel opening with inhibition of insulin release. (Reproduced with permission from Lord K and De León D. Monogenic hyperinsulinemic hypoglycemia: Current insights into the pathogenesis and management. Int J Pediatr Endocrinol 2013:3, 2013.)

by the GLUT 2 glucose transporter, where it is metabolized by glucokinase (GCK). Increases in the ATP/ADP ratio lead to closure of plasma membrane ATP-dependent potassium channel (K_{ATP}), depolarization of cellular membrane, influx of calcium, and release of insulin from storage granules. The beta cell K_{ATP} channel has 2 subunits: Kir6.2 and a regulatory subunit SUR1 (sulfonylurea receptor). Mutations in the genes that encode these 2 subunits are the main causes of the most severe cases of CHI. Both recessive and dominantly expressed genetic forms of CHI have been described. Inactivating K_{ATP} channel mutations, that is, mutations that result in closing of the potassium channel, cause the most common and severe type of CHI, which occur in both a focal and a diffuse form. These mutations, which are usually autosomal recessive, include loss of function of SUR1 (encoded by ABCC8) or Kir6.2 (encoded by KCNJ11). Loss of function of either of these two channel regulatory proteins results in closure of the potassium channel and continuous membrane depolarization with resulting increased release of insulin. The drug diazoxide, which opens ATP-dependent potassium channels, has been used to treat this condition (Fig. 17.4). The effects of these mutations on channel expression and function determines the clinical phenotype, including the response to diazoxide. Unfortunately, these patients usually do not respond to diazoxide because there are no functional K_{ATP} channels (recessive defects) or their function is severely impaired (dominant defects). Therefore, most of these patients require pancreatectomy to control hypoglycemia (Stanley, 2016; Lord & De León, 2013).

Mutations in glucokinase (GCK) or glutamate dehydrogenase (GDH) are additional causes of CHI. These are usually gain of function mutations and are dominantly expressed. Activating mutations of GDH result in the hyperinsulinism/hyperammonemia syndrome (HI/HA). This is the second most common cause of CHI. In the beta cell, GDH is involved in amino acid–stimulated insulin secretion. Individuals with HI/HA have fasting and protein-induced hypoglycemia, which can be treated with diazoxide. Ammonia levels are typically elevated to 3–5 times above normal, but these individuals do not exhibit the classical symptoms associated with hyperammonemia (Stanley, 2016; Lord & De León, 2013; Gandhi, 2017).

Activating mutations of GCK, the "glucose sensor" of the beta cell, lowers the glucose threshold for insulin release. These individuals have fasting hypoglycemia with variable degrees of severity. Less than one-third of the patients are diazoxide responsive. More recently identified genetic causes of CHI include mutations in the genes encoding short-chain 3-hydroxyacyl-CoA (SCHAD), uncoupling protein 2 (UCP2), hepatocyte nuclear factor 4-alpha (HNF-4α), hepatocyte nuclear factor 1-alpha (HNF-1α), and the monocarboxylate transporter 1 (MCT-1), which results in a very rare form of CHI triggered by exercise (Stanley, 2016; Lord & De León, 2013; Gandhi, 2017). In addition, mutations in enzymes involved in mitochondrial fatty acid oxidation can cause HH (Molven et al., 2004).

The noninsulinoma pancreatogenous hypoglycemia syndrome reported in adults is rare and related to islet hyperplasia. These patients usually present with postprandial hypoglycemia. Serum insulin and C-peptide levels are elevated, and the drug screen for sulfonylureas and meglitinides is negative (Service et al., 1999).

Beckwith Wiedemann syndrome (BWS) is a fetal overgrowth syndrome caused by genetic defects affecting an imprinted region on 11p15.4 that is close to the two K_{ATP} channel genes. This BWS locus contains the paternally expressed growth promoting gene IGF2 and maternally expressed growth suppressor genes and voltage-gated potassium channel gene (H19 and CDKN1C; KCNQ1). Hyperinsulinism occurs in about half of BWS neonates. Hyperinsulinism is usually transient but may be persistent and nonresponsive to pharmacologic therapy (diazoxide). CHI in these patients is associated with a large area of islet adenomatosis and is usually accompanied by additional manifestations in other organs (e.g., hemihypertrophy, macroglossia).

The **Kabuki syndrome** is linked to monoallelic de novo mutations of lysine-specific methyltransferase 2D (MLL2, encoded by KMT2D), and lysine-specific demethylase 6A (KDM6A on Xp11.3), two closely related genes that affect histone methylation in promoter and transcription initiation sites of target genes. Hyperinsulinism presents in a significant proportion of patients and is usually responsive to pharmacologic therapy (diazoxide). CHI has also been reported to occur with increased frequency in infants with **Turner syndrome**. The mechanism is unknown. Some cases have responded to diazoxide therapy and others required surgical therapy (pancreatectomy). Three genetic defects that disrupt protein glycosylation have been associated with CHI: CDG1a (phosphomannomutase 2 deficiency), CDG1b (mannosephosphate isomerase deficiency), and CDG1t (phosphoglucomutase 1 deficiency). Other genetic syndromes associated with CHI include Sotos, Simpson-Golabi-Behmel, and Costello syndromes, and trisomy 13 (Stanley, 2016).

Ketogenic hypoglycemia is the most common noniatrogenic cause of hypoglycemia in children between 18 months and 5 years of age. Hypoglycemia remits spontaneously by 8 or 9 years of age. These patients have recurrent morning hypoglycemia. Usually, an episode of illness or prolonged fasting is associated with the hypoglycemia. The mechanism of the hypoglycemia is not well understood but several studies have shown that these children have limited glucose stores. There are no clear defects in gluconeogenesis. The majority of children with ketotic hypoglycemia are small and have reduced muscle mass with low levels of the gluconeogenic substrate alanine. The reduced muscle mass may limit the availability of alanine at the time when glucose demands are high and there is a reduced epinephrine response to hypoglycemia (Langdon et al., 2008; Wolfsdorf & Weinstein, 2009). At the time of hypoglycemia, these patients have high blood and urine ketones and low plasma insulin levels. Ketosis in these patients is adaptive, producing an alternative energy source for the brain. Ketotic hypoglycemia is a diagnosis of exclusion, as episodic hypoglycemia with ketosis also occurs in other conditions, such as with deficiencies of counter regulatory hormones and defects of gluconeogenesis or glycogen metabolism (Ghosh et al., 2016).

INBORN ERRORS OF CARBOHYDRATE METABOLISM

Normal plasma glucose levels are maintained by absorption of glucose from the diet, synthesis of glucose during gluconeogenesis, and the release of glucose from glycogen, the principal storage form of glucose. There are many inherited conditions that adversely affect the function of enzymes that regulate glycogen metabolism (glycogen storage diseases) and gluconeogenesis that result in hypoglycemia.

GLYCOGEN STORAGE DISEASES

These inherited diseases, which present in late infancy or childhood, are caused by defects in the enzymes that regulate glycogen synthesis or glycogenolysis, resulting in abnormal quality or quantity of glycogen. Liver and muscle, the main storage sites for glycogen, are most commonly affected by defects in glycogen metabolism. Glycogen storage diseases (GSDs) that primarily affect the liver (hepatic glycogenoses) usually are associated with hypoglycemia and hepatomegaly. Muscle cramps, exercise intolerance, fatigue, and weakness are common complaints in GSDs affecting muscles (muscle glycogenoses). Cardiac involvement is variable, with cardiomyopathy and conduction defects observed. Some forms of these disorders have both liver and muscle abnormalities, with or without neurologic involvement and hemolysis. Affected children present with failure to thrive or hepatomegaly, and display a significant tolerance to chronic hypoglycemia. Blood glucose levels of 20 to 50 mg/dL (1.1–2.8 mmol/L) are not often associated with symptoms, possibly because ketones and lactic acid serve as alternate sources of energy for the central nervous system. Fifteen GSD types have been identified, including glycogen storage disease types I (glucose-6-phosphatase deficiency), III (debrancher deficiency), VI (liver phosphorylase deficiency), IX (phosphorylase kinase deficiency), and 0 (glycogen synthase deficiency). GSD type Ia is the only GSD to involve glycogenolysis and gluconeogenesis. Diagnostic testing can include examination of liver and/or muscle biopsies and genetic testing. DNA mutation analysis can be used for prenatal diagnosis. Table 17.6 shows clinical and biochemical characteristics of hepatic glycogenoses (Langdon et al., 2008; Weinstein et al., 2009; Froissart et al., 2011, Chen & Weinstein, 2016). Muscle glycogenoses or GSDs affecting the muscles (Table 17.7) include type V (muscle phosphorylase deficiency), type VII (muscle phosphofructokinase deficiency), and GSDs secondary to defects in phosphoglycerate kinase, phosphoglycerate mutase, lactate dehydrogenase, fructose 1,6-biphosphate aldolase A, pyruvate kinase, muscle phosphorylase kinase, lysosomal acid alpha-glucosidase (type II, Pompe disease), and cardiac-specific phosphorylase kinase (Tsujino et al., 2000; Weinstein et al., 2009; Chen & Weinstein, 2016).

DISORDERS OF GLUCONEOGENESIS

The major enzymatic defects in gluconeogenesis that cause hypoglycemia are deficiencies in fructose 1-phosphate aldolase (hereditary fructose intolerance), fructose-1,6-diphosphatase, phosphoenol pyruvate carboxykinase (PEPCK) and pyruvate carboxylase (Langdon et al., 2008; Sansaricq & Balwani, 2009). Hypoglycemia usually occurs during periods of metabolic decompensation, which can be spontaneous or triggered by illnesses or prolonged fasting. Vomiting and tachypnea are the most prominent

TABLE 17.6

Hepatic Glycogenoses

Type (GSD)	Defect	Clinical Features	Laboratory Findings/Diagnosis	Treatment
Ia/von Gierke disease	Glucose-6-phosphatase. Glycogenolysis and gluconeogenesis affected. Autosomal recessive.	• Thin extremities, failure to thrive, short stature, round "doll" face, skin xanthomas, retinal changes, severe hepatomegaly, hypoglycemic seizures, pancreatitis, progressive renal failure • Long-term complications: Growth failure, anemia, renal disease (renal tubular dysfunction), osteoporosis, pancreatitis due to hyperlipidemia, hepatic adenomas that can give rise to hepatocellular carcinoma (Franco et al., 2005)	• Hypoglycemia, lactic acidosis, hyperuricemia, very high triglycerides, low ketones • No glycemic response to glucagon • Diagnosis: Targeted gene mutation analysis: noninvasive method of diagnosis for most patients • Liver biopsy to demonstrate glucose-6-phosphatase activity in both intact and fully disrupted microsomes	• High complex carbohydrate feeds during the day, total parenteral nutrition, nocturnal nasogastric or gastrostomy tube infusion of glucose at night, uncooked starch from age 6 to 12 months • Restrict fructose, lactose, and galactose • Treatment of other manifestations when indicated (e.g., gout, dyslipidemia). • ACE inhibitors can slow the progression of renal disease • Liver transplantation may be considered in patients who do not respond to dietary therapy or in those who develop hepatic adenomas (Faivre et al., 1999).
Ib	Glucose-6-phosphatase transporter. Autosomal recessive.	• Same as for GSD Ia, plus consequences of neutrophil abnormalities: recurrent bacterial infections, brain abscess and inflammatory bowel disease, GSD enterocolitis • Inflammatory bowel disease is the major cause of morbidity	• Same as for GSD Ia, plus neutropenia	• Same as for GSD Ia, plus granulocyte and granulocyte/macrophage colony-stimulating factor for neutropenia
IIIa (also called "Cori" or Forbes disease)	Glycogen debranching enzyme (in both liver and muscle). Less severe hypoglycemia because gluconeogenesis is intact.	• Childhood: Hepatomegaly, fasting hypoglycemia, growth retardation • Adult: Proximal myopathy, cardiomyopathy • Long-term complications: Cardiomyopathy, hepatic fibrosis and cirrhosis, hepatic adenomas (25% adults)	• Childhood: Dyslipidemia (high triglycerides), ketotic hypoglycemia, markedly elevated transaminases, increased creatine kinase; normal lactate and uric acid • Adult: EMG shows myopathy • Diagnosis: Demonstration of abnormal glycogen and abnormal enzyme activity on liver and muscle biopsy • Gene-based mutation analysis is a noninvasive method of diagnosis	Childhood: Frequent small amounts of uncooked cornstarch. Large quantities of cornstarch may worsen myopathy. High protein diet improves myopathy and growth failure. No dietary restriction of fructose and galactose. • Adult: No effective treatment of myopathy
IIIb	Glycogen debranching enzyme in liver (normal muscle debranching enzyme)	• Same as in GSD IIIa, with no muscle symptoms	• Same as in GSD IIIa, with no muscle findings	• Same as in GSD IIIa
VI (also called Hers disease)	Glycogen phosphorylase (in liver). Autosomal recessive.	• Typically mild and may be confused with "ketotic hypoglycemia" • Hepatomegaly, growth retardation in early childhood • Hepatomegaly improves with age • In older children and adults, tendency to develop hypoglycemia abates and can tolerate 18- to 24-hour fasting	• Mild hypoglycemia, dyslipidemia and transaminitis, ketosis • Normal uric acid and lactic acid • Diagnosis: Abnormal enzyme activity in biopsy of affected tissues • Molecular genetic testing: PYGL is the only gene associated with GSD VI and can be detected by sequence analysis	• Diet with high content of protein and complex carbohydrates • Cornstarch at bedtime to prevent ketosis • Intravenous glucose may be required during periods of illness or fasting
IX	Phosphorylase kinase (in liver and muscle). Autosomal recessive and X-linked.	• Hepatomegaly, growth retardation, delay in motor development	• Mild dyslipidemia, mildly elevated liver transaminases, fasting ketosis, mild hypoglycemia • Diagnosis: Abnormal enzyme activity in biopsy of affected tissues	• High-carbohydrate diet, frequent feeds • Course usually benign
0	Glycogen synthase Autosomal recessive.	• Severe fasting hypoglycemia and with illness • No hepatomegaly • Mild growth delay (in few cases) • Tolerance to fasting improves with age (by age 7) • 22% of the patients with developmental delay	• Fasting hypoglycemia, hyperketonemia • Hyperglycemia and elevated lactate level after meals • Glycemic response to glucagon after meals but not usually after 12-hour fast • Diagnosis: Mutation analysis of the hepatic glycogen synthase gene	• Frequent feedings during day with high protein content to provide substrate for gluconeogenesis • Low glycemic index complex carbohydrates to minimize postprandial hyperglycemia and hyperlactatemia • Uncooked starch feeding during night
XI (also called Fanconi-Bickel syndrome	GLUT 2	• Protuberant abdomen due to hepatomegaly and renomegaly, rickets, failure to thrive	• Glucosuria, phosphaturia, aminoaciduria, bicarbonate wasting, hypophosphatemia, elevated alkaline phosphatase level, mild fasting hypoglycemia and dyslipidemia, postprandial hyperglycemia • Rickets on radiologic studies	• No specific therapy • Symptomatic replacement of water, electrolytes, vitamin D • Restriction of galactose • Frequent small meals with corn starch supplement

Adapted from Langdon et al., 2008; Weinstein et al., 2009; Froissart et al., 2011, Chen & Weinstein, 2016.
ACE, Angiotensin-converting enzyme; *EMG,* electromyography; *GSD,* glycogen storage disease.

TABLE 17.7

Muscle Glycogenoses

Type (GSD)	Defect	Clinical Features	Laboratory Findings/Diagnosis	Treatment
II/Pompe disease	Lysosomal acid alpha glucosidase (GAA; acid maltase)	• Infant: Muscle weakness, feeding problems, macroglossia, hepatomegaly, cardiomyopathy • Late childhood: Proximal muscle weakness, swallowing difficulties, respiratory muscle weakness • Adult: Proximal muscle weakness with pelvic girdle, paraspinal and diaphragm muscles affected seriously	• ↑ Creatine kinase, ↑ aspartate transaminase, LD • Diagnosis: decreased or absent acid alpha-glucosidase (GAA) activity in muscle or cultured skin fibroblasts • Molecular genetic testing: GAA is the only gene associated with GSD11 and can be detected by sequence analysis or deletion/duplication analysis (Montalvo et al., 2006; Pittis et al., 2008).	• Infant: Enzyme replacement therapy with myozyme (alglucosidase alfa) by slow intravenous infusion every 2 weeks should be initiated as soon as the diagnosis is established (Kishnani et al., 2007). • Late childhood and adult: High-protein diet • Ventilatory support
IV (also called Anderson disease)	Glycogen branching enzyme. Autosomal recessive.	• Variable phenotype • Hepatosplenomegaly, failure to thrive, liver cirrhosis, portal hypertension, ascites, esophageal varices, and fatal by 5 years of age. Hypoglycemia rare but may occur in liver cirrhosis. • Perinatal: Fetal akinesia deformation sequence, hydrops, death in perinatal period. • Congenital: Hypotonia, muscle atrophy, cardiomyopathy, neural abnormalities in respiratory centers, early infant demise. • Childhood: Myopathy or cardiomyopathy • Adulthood: Diffuse central and peripheral nervous system dysfunction (adult polyglucosan body disease)	• Variable transaminitis and elevations of creatine kinase • Normal serum amino acids and urine organic acids • Muscle biopsy: Tissue deposition of amylopectin-like material • Deficiency of branching enzyme in liver • Adult polyglucosan body disease: Deficient branching enzyme in leukocytes or nerve biopsy	• No specific treatment • Maintenance of normoglycemia • Liver transplantation in selected cases
V (McArdle disease)	Muscle phosphorylase. Autosomal recessive.	• Exercise intolerance, muscle cramps • Dark red urine after intense exercise • Usually presents in 2nd or 3rd decade	• Myoglobinuria, ↑ creatine kinase at rest and increases after exercise • Diagnosis: enzymatic evaluation of muscle or mutation analysis	• Avoidance of rhabdomyolysis from strenuous exercise • Low-dose creatine supplementation • Ingestion of sucrose, glucose, or fructose immediately prior to exercise (Quinlivan et al., 2008)
VII (Tarui disease)	Phosphofructokinase	• Same as in type V plus: Severe exercise intolerance or myopathy in childhood	• ↑ Creatine kinase • Increased muscle isoforms of lactate dehydrogenase and aspartate transaminase • Hemolysis with sustained exercise: Reticulocytosis and hyperbilirubinemia • Hyperuricemia • Diagnosis: Biochemical or histochemical demonstration of enzyme defect	• Avoid strenuous exercise for prevention of muscle cramps and myoglobinuria.
Phosphoglycerate kinase deficiency	Phosphoglycerate kinase	• Same as in type V plus hemolytic anemia, CNS dysfunction, and/or myopathy	• ↑ Creatine kinase (not always) • Abnormal enzyme assays in muscles/RBCs	• Same as in type VII • Bone marrow transplantation
GSD IXd (Muscle phosphorylase kinase deficiency)	Muscle phosphorylase kinase (muscle specific)	• Same as type V plus muscle weakness and atrophy	• ↑ Creatine kinase (not always)	Same as type VII
GSD X (Phosphoglycerate mutase deficiency)	Phosphoglycerate mutase M subunit	• Same as in type V	• ↑ Serum creatine kinase level • Diagnosis: Muscle biopsy and enzyme assay; DNA testing	Same as type VII
GSD XI (Lactate dehydrogenase deficiency)	Lactic acid dehydrogenase M subunit	Same as in type V plus erythematous rash, difficulties in childbirth (uterine stiffness)	• ↑ Creatine kinase level (not always) • Diagnosis: Muscle or RBC enzyme assay; DNA testing	Same as type VII
GSD XII (Fructose-1,6-bisphosphate aldolase A deficiency)	Fructose-1,6-bisphosphate aldolase A	Same as type V plus muscle weakness, hemolytic anemia	• ↑ Creatine kinase (not always) • Diagnosis: Muscle or RBC enzyme assay; DNA testing	Same as type VII
GSD XIII	Beta enolase deficiency	Muscle cramps, exercise intolerance	• ↑ Creatine kinase and rhabdomyolysis. • Diagnosis: Muscle biopsy, enzyme assay; DNA testing	Same as type VII

TABLE 17.7

Muscle Glycogenoses—cont'd

Type (GSD)	Defect	Clinical Features	Laboratory Findings/Diagnosis	Treatment
GSD XIV	Phosphoglucomutase 1 deficiency in muscle	Exercise intolerance, rhabdomyolysis	• Myoglobinuria, increased CPK • Diagnosis: Muscle biopsy, enzyme assay, DNA testing	No specific treatment
GSD XV	Glycogenin 1 deficiency in muscle	Muscle weakness, arrhythmias	Muscle biopsy (glycogen depletion), DNA testing	No specific treatment

ACE, Angiotensin converting enzyme; DNA, deoxyribonucleic acid; *GSD,* glycogen storage disease; LD, lactate dehydrogenase; RBCs, red blood cells.
Adapted from Tsujino et al., 2000; Weinstein et al., 2009; Chen & Weinstein, 2016.

symptoms. Growth retardation or impaired neuromuscular development are seen even when severe episodes are infrequent.

Fructose-1,6-bisphosphatase deficiency is an autosomal-recessive disorder resulting in failure of hepatic glucose generation by gluconeogenic precursors such as lactate, glycerol, and alanine. Fructose 1,6 bisphosphatase also plays an important role in the utilization of ingested fructose. Maintenance of euglycemia is dependent on intake of exogenous glucose or galactose and glycogenolysis. This disorder commonly presents during the first week of life but up to 50% of patients are diagnosed later. Most infants present during the first week of life with a severe, life-threatening metabolic acidosis and hypoglycemia. Affected newborns, who fast and/or have decreased intake, rapidly deplete their glycogen stores and develop hypoglycemia, hyperventilation (from ketoacidosis and lactic acidosis), irritability, lethargy, seizures, and respiratory or cardiac arrest. In some patients, symptoms may not develop for years and, when they do, are triggered by stress (prolonged fasting and intercurrent illnesses) or ingestion of fructose. Children develop anorexia, vomiting, hypoglycemia, and metabolic acidosis. Between crisis, patients are metabolically stable with mild, intermittent or chronic metabolic acidosis. Development is usually normal unless there has been prolonged untreated hypoglycemia. Additional laboratory findings are elevated levels of lactate, pyruvate, alanine, glycerol, uric acid, free fatty acids and an increased ratio of lactate:pyruvate (ratio up to 30). Ketone levels may be elevated; in some patients, however, the elevation is modest or absent. Liver function and renal tubular function are normal. Fructose-induced hypoglycemia cannot be reversed by glucagon administration, but there is a hyperglycemic response to glucagon in the fed state. The diagnosis is established by demonstrating enzyme deficiency in a liver, kidney cortex, or jejunum biopsy specimen. Correction of hypoglycemia and acidosis with intravenous fluids is the treatment of choice during acute attacks. Fructose, sucrose, and sorbitol should be limited in the diet, especially during childhood. A diet excessively high in protein or fat can also provoke hypoglycemia and metabolic acidosis (Langdon et al., 2008; Sansaricq & Balwani, 2009).

Hereditary fructose intolerance occurs when there is a defect of fructose-1,6-bisphosphate aldolase B activity in the liver, kidney, and intestine, resulting in failure of conversion of fructose-1-phosphate and fructose-1,6-bisphosphate into dihydroxyacetone phosphate, glyceraldehyde-3-phosphate, and glyceraldehyde. Accumulated fructose-1-phosphate impairs gluconeogenesis and glycogenolysis, resulting in hypoglycemia and acidosis. This is an autosomal recessive disorder. Clinical manifestations are variable and depend on age, level of enzyme activity and amount/duration of fructose intake. Exclusively breastfed infants remain asymptomatic. Symptoms appear with the introduction of sucrose in formula, fruits, and/or fruit juices. After fructose intake, there is acute onset of abdominal pain, vomiting, diarrhea that may progress to hypoglycemia, shock, apneic spells, seizures, and liver failure. The greater the amount of fructose ingested, the worse the symptoms. Chronic low-level exposure to fructose causes anorexia, failure to thrive, renal tubular acidosis, and liver and kidney failure. Infants who survive the first episode develop aversion to fructose products. Laboratory evaluation shows abnormal liver function and elevated tyrosine and methionine. Hypoglycemia may be missed because the low blood glucose concentration may be transient. Aminoaciduria, proximal tubular acidosis, and hypophosphatemia may be present due to development of Fanconi tubulopathy. Hyperuricemia, anemia, and thrombocytopenia are also seen. Fructosuria is present and can be detected by analyzing the urine for reducing substances. Oral or intravenous fructose tolerance testing is contraindicated as it can be potentially life-threatening. A definitive diagnosis can be made by assay of aldolase B activity in a liver biopsy specimen. DNA sequencing of the aldolase B gene can also be performed. However, a negative DNA test does not rule out the diagnosis because the patient may have a previously unreported mutation. Acute treatment of hypoglycemia includes intravenous glucose administration and discontinuation of fructose intake. Chronic treatment includes elimination of fructose-, sucrose-, and sorbitol-containing foods in the diet, and avoidance of infant formulas or medications that contain fructose. Laboratory parameters normalize after a fructose-restricted diet is instituted (Langdon et al., 2008; Sansaricq & Balwani, 2009).

GLUT 2 is a monosaccharide transporter primarily present in the plasma membranes of pancreatic beta cells, renal tubule cells, and hepatocytes. It has also been found in the hypothalamus and intestines. The **Fanconi-Bickel syndrome (GLUT2 deficiency)** is associated with impairment of gluconeogenesis, which causes fasting hypoglycemia and leads to glycogen accumulation and enlargement of the liver and kidney. These patients also have postprandial hyperglycemia due to reduced glucose sensing by pancreatic beta cells. Renal tubular function is impaired and leads to a Fanconi-like tubulopathy. Renal tubular defects cause glucosuria, aminoaciduria, metabolic acidosis, phosphaturia, and hypophosphatemic rickets. Severe growth failure can be seen. Treatment is symptomatic, with replacement of water, electrolytes, and vitamin D (Langdon et al., 2008; Weinstein et al., 2009).

Pyruvate carboxylase is a mitochondrial enzyme that catalyzes the conversion of pyruvate to oxaloacetate, a key substrate in gluconeogenesis. In **pyruvate carboxylase deficiency**, the cells that are most affected are in the tissues that depend heavily on energy from glucose oxidation, such as the central and peripheral nervous systems. The developing brain and basal ganglia are particularly susceptible. There is wide heterogeneity in the clinical presentation and severity of disease. Measurements of the enzyme activity or the nature of the causative mutations do not correlate with the clinical presentation. Clinical manifestations fall into 2 categories: metabolic and neurologic. Metabolic consequences can include fatal severe lactic acidosis and hypoglycemia in the newborn or infant associated with elevated pyruvate and alanine levels. A subgroup of patients develop hyperammonemia. Neurologic manifestations—such as developmental delay, hypotonia, seizures, ataxia, and peripheral neuropathy—occur in the absence of primary myopathy or cardiomyopathy. This condition is diagnosed by measuring the enzyme activity in fibroblasts, blood lymphocytes or muscle. Treatment is symptomatic, with correction of metabolic acidosis. Long-term therapy options are limited. A ketogenic diet has been used in an attempt to provide alternative energy sources to the nervous system (β-hydroxybutyrate and acetone) and skeletal muscle and heart (fatty acids). The ketogenic diet has been used effectively in infants but is difficult to maintain in older children. Supplementation with L-carnitine may be beneficial for those following the ketogenic diet to prevent secondary carnitine deficiency. Replacement of Krebs cycle intermediates (citrate, aspartate) as well as thiamine have been used (De León et al., 2008; Kerr & Zinn, 2009).

Phosphoenolpyruvate carboxykinase (PEPCK) catalyzes the decarboxylation of oxaloacetate to phosphoenolpyruvate (PEP), which, in turn, can be converted to glucose, glycerol, or pyruvate. **PEPCK deficiency** is uncommon and not well characterized. Since very few cases have been reported, the degree of variability in the clinical presentation

is unclear. There is impaired gluconeogenesis and accumulation of lactate and pyruvate. The diagnosis can be made by measuring PEPCK activity in fibroblasts or a liver biopsy. Clinical manifestations of PEPCK deficiency in the few reported cases in infants included hepatomegaly, hypoglycemia, and hyperlactatemia. These patients did not have hyperammonemia. Death occurred in early infancy or childhood. The same approach that is used for treating patients with pyruvate carboxylase deficiency has been suggested, but successful treatment of PEPCK deficiency has not been reported (De León et al., 2008; Kerr & Zinn, 2009).

DEFECTS IN GALACTOSE METABOLISM

Galactose is the monosaccharide, together with glucose, that constitutes the disaccharide lactose. Milk and milk products are the main sources of galactose. Although galactose can contribute to formation of glycogen, its main role is the formation of complex glucolipids and glycoproteins. These complex molecules are vital components of cell surface receptors as well as myelin in the central nervous system. The metabolism of galactose to glucose occurs in a series of three reactions known as the Leloir pathway. Enzymatic defects in the three main enzymes in this pathway—galactokinase (GALK), galactose-1-phosphate uridyl transferase (GALT), and uridine diphosphate (UDP) galactose 4′-epimerase (GALE)—result in the accumulation of galactose and its metabolites (Roth & Sansaricq, 2009; Welling et al., 2017). Greater oxidative stress is associated with low GALT or GALE activity.

GALT deficiency (classic galactosemia) has an autosomal-recessive mode of inheritance. The most common mutation of the GALT gene is the Q188R mutation for the protein encoded by the gene on chromosome 9. When the GALT enzyme is missing or altered, there is accumulation of galactose, galactose-1-phosphate (Gal-1-P), galactiol, and galactonate. There is also a lack of production of UDP galactose, which is a precursor for glycoprotein and glycolipid formation in various tissues, including the brain. If GALE enzyme function is intact, UDP galactose can be derived from UDP glucose and the disease can be treated with galactose-free formula. Untreated patients develop diffuse fibrotic changes in the liver that mimic alcoholic cirrhosis. Changes in the central nervous system have been linked to membrane damage due to insufficient antioxidant protection, possibly related to elevated concentrations of Gal-1-P. In females, streak ovaries have been found, which may be due to defective migration of embryonic germ cells to the developing gonads as well as alterations in FSH activity due to defects in glycosylation. There are abnormalities in leukocyte function during the neonatal period, increasing susceptibility to developing gram-negative sepsis (*Escherichia coli*). Symptoms start as soon as the baby starts ingesting milk (breast milk or formula) and have been seen as early as the second day of life. Clinical findings include feeding intolerance (vomiting, diarrhea, bloating), irritability, and failure to thrive. As liver dysfunction develops, these infants have jaundice, hepatomegaly, and easy bruisability due to coagulopathy. Early changes in the lens have been described as "oil drop changes" and cataract formation occurs. Hypoglycemia is not a common feature in the absence of liver failure. These patients are at risk of developing cerebral edema. They can also have hyperchloremic metabolic acidosis, albuminuria and aciduria (renal Fanconi syndrome), galactosuria, glycosuria, and vitreous hemorrhage. Patients become hypoalbuminemic and develop ascites and anasarca. Long-term complications in GALT deficiency include impaired cognition, ovarian failure in females, impaired growth, and ataxic neurologic disease. Testicular function does not appear to be affected. Bone mineral density is diminished and may contribute to poor growth. A milder form of galactosemia known as the "Duarte variant" is also caused by a mutation within the *GALT* gene and is characterized by decreased red cell enzyme activity, which generally is of no clinical significance (Roth & Sansaricq, 2009; Welling et al., 2017).

The diagnosis of galactosemia should be confirmed by measuring GALT enzyme activity in red blood cells (absent or significantly decreased) and/or performing GALT gene analysis. The measurement of reducing urine substances should only be used as a screening test. This test is helpful for the diagnosis of classic galactosemia, but interpretation of results is complicated by the following: (1) reducing substances (i.e., glucose) other than galactose may give a false-positive result, (2) galactosuria may be found in patients with liver disease, and (3) intravenous fluids given to neonates in crisis can dilute the galactose in the urine. Microbiological and fluorometric assays are used in newborn screening (NBS) to detect galactosemia (GALT activity). Many NBS laboratories also quantify "total galactose" (galactose + galactose-1-P), which can be elevated in affected infants, especially if they have consumed milk. An abnormal screening test result should be followed by biochemical or molecular confirmation of the diagnosis. Quantitative assays can produce false-negative results after blood transfusion. If classical galactosemia is suspected in an infant, treatment with galactose-free formula should be started immediately without waiting for confirmatory test results. In the first year of life, clinicians should measure red blood cell Gal-1-P levels at diagnosis, and after 3 and 9 months of dietary galactose restriction. After 1 year of age, Gal-1-P levels should be monitored annually (Roth & Sansaricq, 2009, Welling et al., 2017).

Treatment of GALT deficiency consists of restriction of galactose in the diet (e.g., soy-based, casein hydrolysate, or elemental formula). Galactose from nonmilk products may be allowed as their contribution to dietary galactose is minimal. Intake of calcium and vitamin D should be evaluated annually as well as levels of 25(OH) vitamin D. If necessary, calcium and vitamin D supplements should be given following age-specific recommendations.

In **GALK deficiency**, galactose cannot be converted into Gal-1-P. Patients accumulate galactose, which is converted to galactiol and galactonate, leading to cataract formation. Cataracts may be the only major clinical manifestation in older children with GALK deficiency. Conversion of galactose to galactiol is mediated by aldose reductase, which is downregulated in the kidney. This may explain why these patients do not have renal impairment. Pseudotumor cerebri is a rare, transitory complication, possibly related to galactiol accumulation. The diagnosis is made by demonstrating an elevated blood galactose level with normal uridyl transferase activity and absence of galactokinase activity in erythrocytes. A galactose-free diet can reverse cataracts if started in early infancy (Bosch et al., 2002; Roth & Sansaricq, 2009).

The benign form of uridine diphosphate GALE deficiency is associated with enzyme deficiency limited to erythrocytes and leukocytes. These affected individuals are usually asymptomatic and do not require treatment. In the severe form, clinical findings are similar to those seen in GALT deficiency, with additional findings of hypotonia and sensorineural deafness. Treatment consists of dietary restriction of galactose (Holton et al., 2001; Roth & Sansaricq, 2009).

DEFECTS IN FRUCTOSE METABOLISM

Fructose is an important source of carbohydrate. It is a component of table sugar, honey, fruits and various vegetables. Fructose, sucrose, and sorbitol (metabolized mainly via conversion to fructose) are frequent food additives. Oral fructose is absorbed in the small intestine and primarily metabolized in the liver. Significant fructose metabolism also takes place in the kidney and small intestine. Essential fructosuria, hereditary fructose intolerance, and fructose-1,6-diphosphatase deficiency are the clinical conditions resulting from defects in fructose metabolism.

Essential fructosuria is an autosomal-recessive disorder resulting from fructokinase deficiency. Fructokinase catalyzes the conversion of fructose to fructose-1-phosphate. The condition is asymptomatic and usually is diagnosed incidentally by the detection of fructose in urine as a reducing substance. No treatment is necessary. **Hereditary fructose intolerance** and **fructose-1,6-bisphosphatase deficiency** were discussed earlier (see Disorders of Gluconeogenesis).

LACTIC ACIDOSIS

Lactic acid is a product of pyruvic acid metabolism. Approximately 1400 to 1500 mmol of lactic acid is produced daily in healthy individuals, most of which is derived from glucose via the glycolytic pathway and deamination of alanine (Kreisberg, 1980; Marko et al., 2004). This enormous amount of lactic acid is eliminated by several mechanisms, including buffering by extracellular buffers and removal primarily by the liver and kidneys. Under normal circumstances, the rates of lactate entry and exit from the blood are in equilibrium, and net lactate accumulation is zero. Excessive accumulation of L-lactic acid is caused by overproduction and/or underutilization of L-lactate.

Lactic acidosis is classified as either Type A, which includes etiologies related to the presence of tissue hypoxia, or Type B, which is not associated with tissue hypoxia (Seheult et al., 2017). Selected causes of lactic acidosis are shown in Box 17.3. Lactic acid production increases during ischemia, seizures, vigorous exercise, and some leukemic conditions. High levels of lactic acid produced during strenuous exercise are rapidly cleared by both renal and hepatic mechanisms as well as by aerobic metabolism in muscle (half-life approximately 60 minutes).

BOX 17.3

Selected Causes of L-Lactic Acidosis

Tissue Hypoxia

Septic shock
Cardiogenic shock
Hemorrhagic shock
Acute hypoxemia
Carbon monoxide poisoning
Splanchnic ischemia
Aortic thromboembolism

Metabolic/Medical Conditions

Uncontrolled diabetes mellitus (diabetic ketoacidosis)
Hepatic insufficiency
Renal insufficiency
Thiamine deficiency

Tumors

Leukemia
Lymphoma
Pheochromocytoma
Solid tumors (especially with liver metastases)

Drugs/Toxic Substances

Nucleoside reverse transcriptase inhibitors
Metformin
Ethanol
Salicylates
Isoniazid
Cyanide
Methanol
Ethylene glycol
Acetaminophen
Propofol
Beta agonists (cocaine, epinephrine, inhaled salbutamol and terbutaline)

Inborn Errors of Metabolism

Type 1a glycogen storage disease (von Gierke disease)
Fructose-1,6-bisphosphatase deficiency
Pyruvate dehydrogenase deficiency
Organic acidurias: Propionic acidemia, methylmalonic acidemia

Mitochondrial Diseases

KSS (Kearns-Sayre syndrome)
PEO (progressive external ophthalmoplegia)
PS (Pearson syndrome)
MERRF (myoclonic epilepsy with ragged-red fibers)
MELAS (mitochondrial encephalopathy, lactic acidosis, and stroke-like episodes)
MILS (maternally inherited Leigh syndrome)

A decrease in lactic acid utilization can also lead to accumulation of lactic acid. This is generally seen in diseases of the liver and kidneys. Defects in the removal of lactic acid have been associated with hepatic insufficiency, specific enzymatic defects, and severe acidosis. Metformin, which is widely prescribed for the treatment of type 2 diabetes, rarely causes lactic acidosis. Risk factors for metformin-related lactic acidosis include congestive heart failure, tissue hypoxia, renal insufficiency, and sepsis (Salpeter et al., 2003; Misbin, 2004). Nucleoside reverse transcriptase inhibitors used in the treatment of human immunodeficiency virus infection can also induce lactic acidosis (John & Mallal, 2002; Ogedegbe et al., 2003).

D-Lactic acidosis results from excessive accumulation of D-lactic acid (the dextrorotary form of lactic acid). It has been described in patients with jejunoileal bypass or small bowel disease or resection. In these conditions, glucose and other carbohydrates are converted into D-lactic acid in the colon by bacteria. Elevated D-lactate levels have also been found in severe diabetic ketoacidosis (Seheult et al., 2017). The D-lactic acid is absorbed into the systemic circulation and is slowly metabolized. Affected patients present with episodes of metabolic acidosis and encephalopathy.

Hyperlactatemia is defined as blood lactate concentration of ≥2 mmol/L. Severe hyperlactatemia ("lactic acidosis") is diagnosed by the presence of high blood lactate levels (>45 mg/dL or >5.0 mmol/L), an elevated anion gap, and a low blood pH (<7.35). For accurate measurements of lactate, tourniquet use should be minimal and the patient should not clench the fist at the time of blood draw. Specimens should be processed promptly to avoid glycolysis. Lactate (L-lactate) is measured using a variety of methods and instruments. In addition to the traditional laboratory measurements of lactate, point-of-care testing has become widely available in acute care settings. This provides rapid results, facilitating prompt treatment and leading to better outcomes. There is a lack of standardization and reference standards, which is recognized as a concern that should be addressed. In the case of ethylene glycol poisoning, falsely elevated lactate concentrations have been reported when using blood gas analyzers that detect the presence of ethylene glycol metabolites that are structurally similar to L-lactate (Seheult et al., 2017). D-Lactate levels can be measured using specific D-lactate enzymatic assays (Luft & Schwenk, 2001; Zhang et al., 2003).

Treatment of lactic acidosis consists of correction of underlying conditions that initiated the disruption in normal lactate metabolism. Tissue oxygenation, improved fluid status, amplification of cardiac status, and treatment of sepsis play important roles in the treatment of lactic acidosis. Dialysis is sometimes necessary for removal of lactate.

SELECTED REFERENCES

American Diabetes Association: Standards of medical care in patients with diabetes—2019, *Diabetes Care* 42(Suppl 1):S1–S181, 2019.

Summarizes the criteria for the classification and diagnosis of diabetes, and provides recommendations for assessment of glycemic control, management goals, and strategies to prevent complications.

Bergenstal RM, Beck RW, Close KL, et al.: Glucose Management Indicator (GMI): a new term for estimating A1c from continuous glucose monitoring, *Diabetes Care*, 41:2275–2280, 2018; and Edelman SV, Argenta NB, Pettus J, Hirsch IB: Clinical implications of real-time and intermittently scanned continuous glucose monitoring. *Diabetes Care*, 41:2265-2274, 2018.

These articles review current issues related to continuous glucose monitoring, and describe the derivation and use of the Glucose Management Indicator (GMI).

Bingley PJ, Bonifacio E, Mueller PW, And participating laboratories: diabetes antibody standardization program: first assay proficiency evaluation, *diabetes*, 52:1128–1136, 2003; and Lampasona V, Schlosser M, Mueller PW, et al.: Diabetes Antibody Standardization Program: First proficiency evaluation of assays for autoantibodies to zinc transporter 8. First assay proficiency evaluation, *Clin Chem*, 57:1693–1702, 2011.

The first article is a report of the first proficiency evaluation of the Diabetes Antibody Standardization Program, which includes information concerning the performance of different assays for GAD, IA-2, and insulin autoantibodies. The second article is a report of the first proficiency evaluation of ZnT8 antibodies.

Chen M, Weinstein DA: Glycogen storage diseases: diagnosis, treatment and outcomes, *Translat Sci Rare Dis* 1:45–72, 2016.

Reviews in detail the major glycogen storage diseases.

Cryer PE, Axelrod L, Grossman AB, et al.: Evaluation and management of adult hypoglycemic disorders: an Endocrine Society clinical practice guideline, *J Clin Endocrinol Metab* 94:709–728, 2009.

Reviews hypoglycemic disorders, with detailed clinical classification and a description of diagnostic testing, including a protocol for performing the 72-hour fast, mixed-meal diagnostic tests, and management strategies.

Lord K, De León D: Monogenic hyperinsulinemic hypoglycemia: current insights into the pathogenesis and management, *Int J Pediatr Endocrinol* 2013:3, 2013.

Reviews congenital hyperinsulinism disorders in detail, including the pathogenesis, genetics, classification, and management.

Little RR, Rohlfing C, Sacks DB: The National Glycohemoglobin Standardization Program: over 20 years of improving hemoglobin A_{1c} measurement, *Clin Chem* 65:839–848, 2019.

Summarizes the National Glycohemoglobin Standardization Program and progress in standardization nationally and internationally.

Sacks DB, Arnold M, Bakris GL, et al.: Guidelines and recommendations for laboratory analysis in the diagnosis and management of diabetes mellitus, *Clin Chem* 57:e1–e47, 2011.

Provides recommendations for laboratory testing in diabetes.

Sarafoglou K, Hoffmann G, Roth K, editors: *Pediatric endocrinology and inborn errors of metabolism*, New York, 2009, McGraw-Hill, pp 71–82 and 127–140.

Reviews in detail the major glycogen storage diseases, gluconeogenesis disorders, galactosemia, and disorders of fructose metabolism.

Sosenko JM, Skyler JS, Mahon J, et al.: Use of the diabetes prevention Trial—type 1 risk score (DPTRS) for improving the accuracy of the risk classification of type 1 diabetes, *Diabetes Care* 37(4):979–984, 2014; and Sosenko JM, Skyler JS, Palmer JP, et al.: The prediction of type 1 diabetes by multiple autoantibody levels and their incorporation into an autoantibody risk score in relatives of type 1 diabetic patients, *Diabetes Care* 36(9):2615–2620, 2013.

These articles review the use of pancreatic autoantibodies and other factors in the prediction of type 1 diabetes.

Thornton P, Stanley C, De Leon D, et al.: Recommendations from the Pediatric Endocrine Society for Evaluation and Management of Persistent Hypoglycemia in Neonates, Infants, and Children, *J Pediatr* 167(2):238–245, 2015.

Reviews evaluation and management of hypoglycemia in newborns and persistent hypoglycemia in infants and children without diabetes.

Access the complete reference list online at Elsevier eBooks for Practicing Clinicians.

REFERENCES

Albrechtsen NJW, Hartmann B, Veedfald S, et al.: Hyperglucagonaemia analysed by glucagon sandwich ELISA: nonspecific interference or truly elevated levels? *Diabetologia* 57:1919–1996, 2014.

American Diabetes Association: Standards of medical care in patients with diabetes 2019, *Diabetes Care* 42(Suppl 1):S1–S181, 2019.

Arem R: Hypoglycemia associated with renal failure, *Endocrinol Metab*, *Clin N Amer* 18(1):103–121, 1989.

Arky RA: Hypoglycemia associated with liver disease and ethanol, *Endocrinol Metab Clin N Amer* 18(1):75–90, 1989.

Arnoux JP, Verkarre V, Saint-Martin C, et al.: Congenital hyperinsulinism: current trends in diagnosis and therapy, *Orphanet J Rare Dis* 6:63, 2011.

Assan R, Perronne C, Assan D, et al.: Pentamidine-induced derangements of glucose homeostasis. Determinant roles of renal failure and drug accumulation: a study of 128 patients, *Diabetes Care* 18(1):47–55, 1995.

Bao S, Root C, Jagasia S: Type B insulin resistance syndrome associated with systemic lupus erythematosus, *Endocr Pract* 13(1):51–55, 2007.

Bellows C, Haque S, Jaffe B: Pancreatic polypeptide islet cell tumor: case report and review of the literature, *J Gastrointest Surg* 2(6):526–532, 1998.

Beck RW, Connor CG, Mullen DM, et al.: The fallacy of average: how using HbA_{1c} alone to assess glycemic control can be misleading, *Diabetes Care* 40:994–999, 2017.

Bergenstal RM, Beck RW, Close KL, et al.: Glucose Management Indicator (GMI): a new term for estimating A_{1c} from continuous glucose monitoring, *Diabetes Care* 41:2275–2280, 2018.

Bergenstal RM, Gal RL, Connor CG, et al.: Racial differences in the relationship of glucose concentrations and hemoglobin A_{1c} levels, *Ann Intern Med* 167:95–102, 2017.

Besser RE, Ludvigsson J, Jones AG, et al.: Urine C-peptide creatinine ratio is a noninvasive alternative to the mixed-meal tolerance test in children and adults with type 1 diabetes, *Diabetes Care* 34(3):607–609, 2011.

Bingley PJ, Bonifacio E, Mueller PW: And participating laboratories: diabetes Antibody Standardization Program: first assay proficiency evaluation, *Diabetes* 52:1128–1136, 2003.

Bosch AM, Bakker HD, van Gennip AH, et al.: Clinical features of galactokinase deficiency: a review of the literature, *J Inherit Metab Dis* 25(8):629–634, 2002.

Bouchard P, Sai P, Reach G, et al.: Diabetes mellitus following pentamidine-induced hypoglycemia in humans, *Diabetes* 31(1):40–45, 1982.

Bunch TJ, Dunn WF, Basu A, et al.: Hyponatremia and hypoglycemia in acute Sheehan's syndrome, *Gynecol Endocrinol* 16(5):419–423, 2002.

Cavaco B, Uchigata Y, Porto T, et al.: Hypoglycaemia due to insulin autoimmune syndrome: report of two cases with characterization of HLA alleles and insulin autoantibodies, *Eur J Endocrinol* 145(3):311–316, 2001.

Centers for Disease Control and Prevention: National Diabetes Statistics Report. Available at: http://www.cdc.gov/diabetes/pdfs/data/statistics/national-diabetes-statisticsreport.pdf, 2017. Accessed July 15, 2019.

Chan AY, Swaminathan R, Cockram CS: Effectiveness of sodium fluoride as a preservation of glucose in blood, *Clin Chem* 35:315–317, 1989.

Chavez H, Ozolins D, Losek JD: Hypoglycemia and propranolol in pediatric behavioral disorders, *Pediatrics* 103(6):1290–1292, 1999.

Chen M, Weinstein DA: Glycogen storage diseases: diagnosis, treatment and outcomes, *Translat Sci Rare Dis* 1:45–72, 2016.

Cheyne EH, Cavan DA, Kerr D: Performance of a continuous glucose monitoring system during controlled hypoglycaemia in healthy volunteers, *Diabetes Technolo Ther* 4(5):607–613, 2002.

Chung J, Henry RR: Mechanisms of tumor-induced hypoglycemia with intraabdominal hemangiopericytoma, *J Clin Endocrinol Metab* 81(3):919–925, 1996.

Consensus Committee: Consensus statement on the worldwide standardization of the HbA_{1c} measurement, *Diabetes Care* 30:2399–2400, 2007.

Cryer PE: Hypoglycemia, functional brain failure, and brain death, *J Clin Invest* 117:868–870, 2007.

Cryer PE, Axelrod L, Grossman AB, et al.: Evaluation and management of adult hypoglycemic disorders: an endocrine Society clinical practice guideline, *J Clin Endocrinol Metab* 94:709–728, 2009.

Dall TM, Yang W, Gillespie K, et al.: The economic burden of elevated blood glucose levels in 2017: diagnosed and undiagnosed diabetes, gestational diabetes, and prediabetes, *Diabetes Care*, 2019. pii: dc181226. doi: 10.2337/dc18-1226. [Epub ahead of print].

Danese E, Montagnana M, Nouvenne A, Lippi G: Advantages and pitfalls of fructosamine and glycated albumin in the diagnosis and treatment of diabetes, *J Diabetes Sci Technol* 9:169–176, 2015.

Daughaday WH: Hypoglycemia in patients with non-islet cell tumors, *Endocrinol Metab Clin N Amer* 18(1):91–101, 1989.

de Groot JW, Rikhof B, van Doorn J, et al.: Non-islet cell tumour-induced hypoglycaemia: a review of the literature including two new cases, *Endocr Relat Cancer* 14(4):979–993, 2007.

DeCunto A, Barbi E, Minen F, et al.: Safety and efficacy of high-dose acarbose treatment for dumping syndrome, *J Pediatr GastroenterolNut* 53:113–114, 2011.

De León D, Ferry L, Kelly A, et al.: Acarbose treatment of postprandial hypoglycemia in children after Nissen fundoplication, *J Pediatr* 139:877–879, 2001.

De León D, Stanley C, Sperling M: Hypoglycemia in neonates and infants. In ed 3, Sperling MA, editor: *Pediatric Endocrinology*Philadelphia, 2008, Elsevier, pp 165–197.

Diabetes ControlComplications Trial Research Group: The effect of intensive treatment of diabetes on the development and progression of long-term complications in insulin-dependent diabetes mellitus, *N Engl J Med* 329:977–986, 1993.

Diabetes control and complications trial (DCCT)/Epidemiology of diabetes Interventions and complications (EDIC) study research group: intensive diabetes treatment and cardiovascular outcomes in type 1 diabetes: the DCCT/EDIC study 30 – year follow-up, *Diabetes Care* 39:686–693, 2016.

Dozio N, Scavini M, Beretta A, et al.: Imaging of the buffering effect of insulin antibodies in the autoimmune hypoglycemic syndrome, *J Clin Endocrinol Metab* 83(2):643–648, 1998.

Drucker DJ, Habener JF, Holst JJ: Discovery, characterization, and clinical development of the glucagon-like peptides, *J Clin Invest* 127:4217–4227, 2017.

Edelman SV, Argenta NB, Pettus J, Hirsch IB: Clinical implications of real-time and intermittently scanned continuous glucose monitoring, *Diabetes Care* 41:2265–2274, 2018.

Ekhlaspiur L, Mondesir D, Lautsch N, et al.: Comparative accuracy of 17 point-of-care glucose meters, *J Diabetes Sci Technol* 11:558–566, 2017.

Erbach M, Freckmann G, Hinzmann R, et al.: Interferences and limitations in blood glucose self-testing: an overview of the current knowledge, *J Diabetes Sci Technol* 10:1161–1168, 2016.

Faivre L, Houssin D, Valayer J, et al.: Long-term outcome of liver transplantation in patients with glycogen storage disease type Ia, *J Inherit Metab Dis* 22:723–732, 1999.

Fareau GG, Maldonado M, Oral E, et al.: Regression of acanthosis nigricans correlates with disappearance of anti-insulin receptor autoantibodies and achievement of euglycemia in type B insulin resistance syndrome, *Metabolism* 56(5):670–675, 2007.

Farrag H, Cowett R: Hypoglycemia in the newborn. In ed 5, Lifshitz F, et al.: *Pediatric Endocrinology*, New York, 2009, Informa, pp 329–358.

Flanagan D, Wood P, Sherwin R, et al.: Gin and tonic and reactive hypoglycemia: what is important—the gin, the tonic, or both? *J Clin Endocrinol Metab* 83(3):796–800, 1998.

Franco LM, Krishnamurthy V, Bali D, et al.: Hepatocellular carcinoma in glycogen storage disease type Ia: a case series, *J Inherit Metab Dis* 28:153–162, 2005.

Freckmann G, Schmid C, Baumstark A, et al.: System accuracy evaluation of 43 blood glucose monitoring systems for self-monitoring of blood glucose according to DIN EN ISO 15197, *J Diabetes Sci Technol* 6:1060–1075, 2012.

Froissart R, Piraud M, Boudjemline AM, et al.: Glucose 6 phosphatase deficienc, *Orphanet J Rare Dis* 6:27, 2011.

Fukuda I, Hizuka N, Ishikawa Y, et al.: Clinical features of insulin-like growth factor-II producing non-islet-cell tumor hypoglycemia, *Growth Horm IGF Res* 16:211–216, 2006.

Gambino R: Sodium fluoride: an ineffective inhibitor of glycolysis, *Ann Clin Biochem* 50:3–5, 2013.

Gandhi K: Approach to hypoglycemia in infants and children, *Transl Pediatr* 6(4):408–420, 2017.

Ghosh A, Banerjee I, Morris A: Recognition, assessment and management of hypoglycaemia in childhood, *Arch Dis Child* 101:575–580, 2016.

Greenbaum CJ, Mandrup-Poulsen T, McGee PF, et al.: Mixed-meal tolerance test versus glucagon stimulation test for the assessment of beta-cell function in therapeutic trials in type 1 diabetes, *Diabetes Care* 31(10):1966–1971, 2008.

Gregg EW, Li Y, Wang J, et al.: Changes in diabetes related complications in the United States, 1990-2010, *N Engl J Med* 370:1514–1523, 2014.

Guettier JM, Gordon P: Hypoglycemia, *Endocrinol Metab Clin N Amer* 35(4):753–766, 2006.

Guettier JM, Kam A, Chang R, et al.: Localization of insulinomas to regions of the pancreas by intra-arterial calcium stimulation: the NIH experience, *J Clin Endocrinol Metab* 94(4):1074–1080, 2009.

Haviv YS, Sharkia M, Safadi R: Hypoglycemia in patients with renal failure, *Ren Fail* 22(2):219–223, 2000.

Haymond MW: Hypoglycemia in infants and children, *Endocrinol Metab Clin N Amer* 18(1):211–252, 1989.

Hekimsoy Z, Biberoglu S, Comlekci A, et al.: Trimethoprim/sulfamethoxazole-induced hypoglycemia in a malnourished patient with severe infection, *Eur J Endocrinol* 136(3):304–306, 1997.

Herman WH, Cohen RM: Racial and ethnic differences in the relationship between HbA_{1c} and blood glucose: implications for the diagnosis of diabetes, *J Clin Endocrinol Metab* 97(4):1067–1072, 2012.

Hirata Y, Uchigata Y: Insulin autoimmune syndrome in Japan, *Diabetes Res Clin Pract* 24(Suppl):S153–S157, 1994.

Hirst JA, McLellan JH, Price CP, et al.: Performance of point-of-care HbA1c test devices: implications for use in clinical practice a systematic review and meta-analysis, *Clin Chem Lab Med* 55:167–180, 2017.

Hoelzel W, Weykamp C, Jeppsson JO, et al.: IFCC reference system for measurement of hemoglobin A1c in human blood and the national standardization schemes in the United States, Japan, and Sweden: a method comparison study, *Clin Chem* 50:166–174, 2004.

Holton JB, Walter JH, Tyfield LA: Galactosemia. In ed 8, Scriver CR, Beaudet al, Sly WS, et al.: *The metabolic and molecular bases of inherited disease*New York, 2001, McGraw-Hill, pp 1553–1587.

John M, Mallal S: Hyperlactatemia syndromes in people with HIV infection, *Curr Opin Infect Dis* 15(1):23–29, 2002.

Kato Y, Ichiki Y, Kitajima Y: A case of systemic lupus erythematosus presenting as hypoglycemia due to anti-insulin receptor antibodies, *Rheumatol Int* 29(1):103–105, 2008.

Kerr D, Zinn A: Disorders of pyruvate metabolism. In ed 1, Sarafoglou K, Hoffmann G, Roth K, editors: *Pediatric Endocrinology and Inborn Errors of Metabolism*, McGraw-Hill, 2009, pp 231–244.

Khoury H, Daugherty T, Ehsanipoor K: Spontaneous hypoglycemia associated with congestive heart failure attributable to hyperinsulinism, *Endocr Pract* 4(2):94–95, 1998.

King F, Ahn D, Hsiao V, et al.: A review of blood glucose monitor accuracy, *Diabetes Technol Ther* 20:843–856, 2018.

Kishnani PS, Corzo D, Nicolino M, et al.: Recombinant human acid α-glucosidase: major clinical benefits in infantile-onset Pompe disease, *Neurology* 68:99–109, 2007.

Klonoff DC, Lias C, Beck S, et al.: Development of the Diabetes Technology Society blood glucose monitor system surveillance protocol, *J Diabetes Sci Technol* 10:697–707, 2016.

Kreisberg RA: Lactate homeostasis and lactic acidosis, *Ann Intern Med* 92:227–237, 1980.

Krischer JP, Cuthbertson DD, Yu L, et al.: Screening strategies for the identification of multiple antibody-positive relatives of individuals with type 1 diabetes, *J Clin Endocrinol Metab* 88(1):103–108, 2003.

Lampasona V, Schlosser M, Mueller PW, et al.: Diabetes Antibody Standardization Program: first proficiency evaluation of assays for autoantibodies to zinc transporter 8. First assay proficiency evaluation, *Clin Chem* 57:1693–1702, 2011.

Langdon D, Stanley C, Sperling M: Hypoglycemia in the infant and child. In ed 3, Sperling MA, editor: *Pediatric Endocrinology*Philadelphia, 2008, Elsevier, pp 422–443.

Lawler P, Mora S: Moving beyond mean glycemia: 1,5-Anhydroglucitol and microvascular complications of diabetes, *Clin Chem* 60:11-1359–61, 2014.

Lefebvre PJ, Andreani D, Marks V, et al.: Statement on postprandial hypoglycemia, *Diabetes Care* 11(5):439–440, 1988.

Lidar M, Rachmani R, Half E, et al.: Insulin autoimmune syndrome after therapy with imipenem, *Diabetes Care* 22(3):524–525, 1999.

Little RR, Rohlfing C, Sacks DB: The national Glycohemoglobin standardization program: over 20 years of improving hemoglobin A_{1c} measurement, *Clin Chem* 65:839–848, 2019.

Little RR, Wielgosz RI, Josephs R, et al.: Implementing a reference measurement system for c-peptide: successes and lessons learned, *Clin Chem* 63:1447–1456, 2017.

Lord K, De León D: Monogenic hyperinsulinemic hypoglycemia: current insights into the pathogenesis and management, *Int J Pediatr Endocrinol* 2013:3, 2013.

Lteif AN, Schwenk WF: Hypoglycemia in infants and children, *Endocrinol Metab Clin N Amer* 28(3):619–646, 1999.

Luft AN, Schwenk WF: Lactic acidosis update for critical care clinicians, *J Am Soc Nephrol* 12(Suppl 17):S15–S19, 2001.

Lupsa BC, Chong AY, Cochran EK, et al.: Autoimmune forms of hypoglycemia, *Medicine* 88(3):141–153, 2009.

Manning PJ, Espiner EA, Yoon K, et al.: An unusual cause of hyperinsulinaemic hypoglycaemia syndrome, *Diabet Med* 20(9):772–776, 2003.

Marko P, Gabrielli A, Caruso LJ: Too much lactate or too little liver? *J Clin Anesth* 16(5):389–395, 2004.

Marks V, Teale JD: Drug-induced hypoglycemia, *Endocrinol Metab Clin N Amer* 28(3):555–577, 1999.

Miller WG, Thienpont LM, Van Uytfanghe K, et al.: The insulin standardization Work group: toward standardization of insulin immunoassays, *Clin Chem* 55:1011–1018, 2009.

Miller SI, Wallace Jr RJ, Musher DM, et al.: Hypoglycemia as a manifestation of sepsis, *Am J Med* 68(5):649–654, 1980.

Miraki-Moud F, Grossman AB, Besser M, et al.: A rapid method for analyzing serum pro-insulin-like growth factor-II in patients with non-islet cell tumor hypoglycemia, *J Clin Endocrinol Metab* 90(7):3819–3823, 2005.

Misbin RI: The phantom of lactic acidosis due to metformin in patients with diabetes, *Diabetes Care* 27(7):1791–1793, 2004.

Mitrakou A, Ryan C, Veneman T, et al.: Hierarchy of glycemic thresholds for counterregulatory hormone secretion, symptoms, and cerebral dysfunction, *Am J Physiol* 260(1 Pt 1):E67–E74, 1991.

Molven A, Matre GE, Duran M, et al.: Familial hyperinsulinemic hypoglycemia caused by a defect in the SCHAD enzyme of mitochondrial fatty acid oxidation, *Diabetes* 53:221–227, 2004.

Montalvo AL, Bembi B, Donnarumma M, et al.: Mutation profile of the GAA gene in 40 Italian patients with late onset glycogen storage disease type II, *Hum Mutat* 27:999–1006, 2006.

Moran A, Pillay K, Becker D, Granados A, Hameed S, Acerini CL: ISPAD Clinical Practice Consensus Guidelines 2018:management of cystic-fibrosis-related diabetes in children and adolescents, *Pediatr Diabetes* 19(Suppl 27):64–74, 2018.

Murad HA, Coto-Yglesias F, Wang AT, et al.: Drug-induced hypoglycemia: a systematic review, *J Clin Endocrinol Metab* 94(3):741–745, 2009.

Nathan DM, Kuenen J, Borg R, et al.: Translating the A1C assay into estimated average glucose values, *Diabetes Care* 31(1–6), 2008.

Nauck MA, Meier JJ: Diagnostic Accuracy of an "amended" insulin-glucose ratio for the biochemical diagnosis of insulinoma, *Ann Intern Med* 157:767–775, 2012.

Nishi H, Nanjo K: Insulin gene mutations and diabetes, *J Diabetes Investig* 2:92–100, 2011.

Ogedegbe AE, Thomas DL, Diehl AM: Hyperlactataemia syndromes associated with HIV therapy, *Lancet Infect Dis* 3(6):329–337, 2003.

Ohkubo Y, Kishikawa H, Araki E, et al.: Intensive insulin therapy prevents the progression of diabetic microvascular complications in Japanese patients with non-insulin-dependent diabetes mellitus: a randomized prospective 6-year study, *Diabetes Res Clin Pract* 28:103–117, 1995.

Orngreen MC, Zacho M, Hebert A, et al.: Patients with severe muscle wasting are prone to develop hypoglycemia during fasting, *Neurology* 61:997–1000, 2003.

Ozawa S, Katsuta H, Suzuki K, et al.: Estimated proinsulin processing activity of prohormone convertase (PC) 1/3 rather than PC2 is decreased in pancreatic β-cells of type 2 diabetic patients, *Endocrine J* 61:607–614, 2014.

Park-Wyllie LY, Juurlink DN, Kopp A, et al.: Outpatient gatifloxacin therapy and dysglycemia in older adults, *N Engl J Med* 354(13):1352–1361, 2006.

Pasieka JL, Hershfield N: Pancreatic polypeptide hyperplasia causing watery diarrhea syndrome: a case report, *Can J Surg* 42(1):55–58, 1999.

Penumalee S, Kissner PZ, Migdal SD: Gabapentin-induced hypoglycemia in a long-term peritoneal dialysis patient, *Am J Kidney Dis* 42(6):E3–E5, 2003.

Pinger CW, Entwistle K, Bell TM, et al.: C-peptide replacement therapy in type 1 diabetes: are we in the trough of disillusionment? *Mol Biosyst* 13:1432–1437, 2017.

Pittis MG, Donnarumma M, Montalvo AL, et al.: Molecular and functional characterization of eight novel GAA mutations in Italian infants with Pompe disease, *Hum Mutat* 29:E27–E36, 2008.

Qing Y, Zhou J-G, Yuan G: Systemic lupus erythematosus presenting as hypoglycaemia with insulin receptor antibodies and insulin autoantibodies, *Lupus* 18(5):457–459, 2009.

Quinlivan R, Beynon RJ, Martinuzzi A: Pharmacological and nutritional treatment for McArdle disease (Glycogen Storage Disease type V), *Cochrane Database Syst Rev*, CD003458, 2008.

Redmon JB, Nuttall FQ: Autoimmune hypoglycemia, *Endocrinol Metab Clin N Amer* 28(3):603–618, 1999.

Roder ME, Porte Jr D, Schwartz RS, et al.: Disproportionately elevated proinsulin levels reflect the degree of impaired B cell secretory capacity in patients with noninsulin-dependent diabetes mellitus, *J Clin Endocrinol Metab* 83(2):604–608, 1998.

Rodbard D: Continuous glucose monitoring: a review of recent studies demonstrating improved glycemic outcomes, *Diabetes Technol Ther* 19(Suppl 3):S25–S37, 2017.

Roth K, Sansaricq C: The galactosemias. In ed 1, Sarafoglou K, Hoffmann G, Roth K, editors: *Pediatric Endocrinology and Inborn Errors of Metabolism*, McGraw-Hill, 2009, pp 127–134.

Russell SJ, El-Khatib FH, Sinha M, et al.: Outpatient glycemic control with a bionic pancreas in type 1 diabetes, *N Engl J Med* 371:313–325, 2014.

Sacks DB, Arnold M, Bakris GL, et al.: Guidelines and recommendations for laboratory analysis in the diagnosis and management of diabetes mellitus, *Clin Chem* 57:e1–e47, 2011.

Salehi M, Vella A, McLaughlin T, Patti M-E: Hypoglycemia after gastric bypass surgery: concepts and controversies, *J Clin Endocrinol Metab* 103:2815–2826, 2018.

Salpeter SR, Greyber E, Pasternak GA, et al.: Risk of fatal and nonfatal lactic acidosis with metformin use in type 2 diabetes mellitus: systematic review and meta-analysis, *Arch Intern Med* 163(21):2594–2602, 2003.

Sansaricq C, Balwani M: Disorders of fructose metabolism. In ed 1, Sarafoglou K, Hoffmann G, Roth K, editors: *Pediatric Endocrinology and Inborn Errors of Metabolism*, McGraw-Hill, 2009, pp 135–140.

Saraya A, Yokokura M, Gonoi T, et al.: Effects of fluoroquinolones on insulin secretion and beta-cell ATP-sensitive K+ channels, *Eur J Pharmacol* 497:111–117, 2004.

Schlosser M, Mueller PW, Törn C, Bonifacio E, Bingley PJ: Participating laboratories. Diabetes antibody standardization program: evaluation of assays for insulin autoantibodies, *Diabetologia* 53:2611–2620, 2010.

Seheult J, Fitzpatrick G, Boran G: Lactic acidosis: an update, *Clin Chem Lab Med* 55:322–333, 2017.

Schmid C, Haug C, Heinemann L, et al.: System accuracy of blood glucose monitoring systems: Impact of use by patients and ambient conditions, *Diabetes Technol Ther* 15(10):889–896, 2013.

Schwartz NS, Clutter WE, Shah SD, et al.: Glycemic thresholds for activation of glucose counterregulatory systems are higher than the threshold for symptoms, *J Clin Invest* 79(3):777–781, 1987.

Seaquist ER, Kahn SE, Clark PM, et al.: Hyperproinsulinemia is associated with increased beta cell demand after hemipancreatectomy, *J Clin Invest* 97(2):455–460, 1996.

Selvin E, Rawlings A, Lutsey P, et al.: Association of 1,5-anhydroglucitol with cardiovascular disease and mortality, *Diabetes* 65:201–208, 2016.

Service FJ, Natt N, Thompson GB, et al.: Noninsulinoma pancreatogenous hypoglycemia: a novel syndrome of hyperinsulinemic hypoglycemia in adults independent of mutations in Kir6.2 and SUR1 genes, *J Clin Endocrinol Metab* 84(5):1582–1589, 1999.

Service GJ, Thompson GB, Service FJ, et al.: Hyperinsulinemic hypoglycemia with nesidioblastosis after gastric-bypass surgery, *N Engl J Med* 353:249–254, 2005.

Smallridge RC, Corrigan DF, Thomason AM, et al.: Hypoglycemia in pregnancy. Occurrence due to adrenocorticotropic hormone and growth hormone deficiency, *Arch Intern Med* 140(4):564–565, 1980.

Sosenko JM, Skyler JS, Mahon J, et al.: Use of the diabetes prevention Trial—type 1 risk score (DPTRS) for improving the accuracy of the risk classification of type 1 diabetes, *Diabetes Care* 37(4):979–984, 2014.

Sosenko JM, Skyler JS, Palmer JP, et al.: The prediction of type 1 diabetes by multiple autoantibody levels and their incorporation into an autoantibody risk score in relatives of type 1 diabetic patients, *Diabetes Care* 36(9):2615–2620, 2013.

Sperling MA, Menon RK: Differential diagnosis and management of neonatal hypoglycemia, *Pediatr Clin N Amer* 51(3):703–723, 2004.

Stanley C: Perspective on the genetics and diagnosis of congenital hyperinsulinism disorders, *J Clin Endocrinol Metab* 101(3):815–826, 2016.

Tamburrano G, Leonetti F, Sbraccia P, et al.: Increased insulin sensitivity in patients with idiopathic reactive hypoglycemia, *J Clin Endocrinol Metab* 69(4):885–890, 1989.

Tarim O, Kucukerdogan A, Gunay U, et al.: Effects of iron deficiency anemia on hemoglobin A1c in type 1 diabetes mellitus, *Pediatr Int* 41:357–362, 1999.

Taylor SI, Barbetti F, Accili D, et al.: Syndromes of autoimmunity and hypoglycemia. Autoantibodies directed against insulin and its receptor, *Endocrinol Metab Clin N Amer* 18(1):123–143, 1989.

Thornton P, Stanley C, De Leon D, et al.: Recommendations from the Pediatric Endocrine Society for Evaluation and Management of Persistent Hypoglycemia in Neonates, Infants, and Children, *J Pediatr* 167 (2):238–245, 2015.

Toft-Nielsen MB, Damholt MB, Madsbad S, et al.: Determinants of the impaired secretion of glucagon-like peptide-1 in type 2 diabetic patients, *J Clin Endocrinol Metab* 86:3717–3723, 2001.

Tomita T, Kimmel JR, Friesen SR, et al.: Pancreatic polypeptide cell hyperplasia with and without watery diarrhea syndrome, *J Surg Oncol* 14(1):11–20, 1980.

Torn C, Mueller PW, Schlosser M, et al.: Diabetes Antibody Standardization Program: evaluation of assays for autoantibodies to glutamic acid decarboxylase and islet antigen-2, *Diabetologia* 51:846–852, 2008.

Towler DA, Havlin CE, Craft S, et al.: Mechanism of awareness of hypoglycemia. Perception of neurogenic (predominantly cholinergic) rather than neuroglycopenic symptoms, *Diabetes* 42(12):1791–1798, 1993.

Tsujino S, Nonaka I, DiMauro S: Glycogen storage myopathies, *Neurol Clin* 18(1):125–150, 2000.

United Kingdom Prospective Diabetes Study Group: Effect of intensive blood glucose control with metformin on complications in overweight patients with type 2 diabetes (UKPDS 34), *Lancet* 352(9131):854–865, 1998a.

United Kingdom Prospective Diabetes Study Group: Intensive blood-glucose control with sulphonylureas or insulin compared with conventional treatment and risk of complications in patients with type 2 diabetes (UKPDS 33), *Lancet* 352(9131):837–853, 1998b.

van Doorn J, Hoogerbrugge CM, Koster JG, et al.: Antibodies directed against the E region of pro-insulin-like growth factor-II used to evaluate non-islet cell tumor-induced hypoglycemia, *Clin Chem* 48:1739–1750, 2002.

Virtue MA, Furne JK, Nuttall FQ, et al.: Relationship between GHb concentration and erythrocyte survival determined from breath carbon monoxide concentration, *Diabetes Care* 27:931–935, 2004.

Vogeser M, Parhofer KG, Furst H, et al.: Autoimmune hypoglycemia presenting as seizure one week after surgery, *Clin Chem* 47(4):795–796, 2001.

Wang L, Lovejoy NF, Faustman DL: Persistence of prolonged c-peptide production in type 1 diabetes as measured by an ultrasensitive c-peptide assay, *Diabetes Care* 35:465–470, 2012.

Weinstein D, Roth K, Wolfsdorf JI: Glycogen storage diseases. In ed 1, Sarafoglou K, Hoffmann G, Roth K, editors: *Pediatric Endocrinology an Inborn errors of Metabolism*McGraw-Hill, 2009, pp 71–82.

Weissman M, Klein B: Evaluation of glucose determinations in untreated serum samples, *Clin Chem* 4:420, 1958.

Welling L, Bernstein L, Berry G, et al.: International clinical guideline for the management of classical galactosemia: diagnosis, treatment, and follow-up, *J Inherit Metab Dis* 40:171–176, 2017.

Whipple AE: The surgical therapy of hyperinsulinism, *J Int Chir* 3:237–276, 1938.

Winter T, Hannemann A, Suchsland J, et al.: Long-term stability of glucose: glycolysis inhibitor vs gel barrier tubes, *Clin Chem Lab Med* 56:1251–1258, 2018.

Wolfsdorf JI, Weinstein D: Hypoglycemia in children. In ed 5, Lifshitz F, et al.: *Pediatric Endocrinology*, New York, 2009, Informa, pp 291–328.

World Health Organization: *Diabetes mellitus: Report of a WHO study group. (Technical report series, No. 727)*, Geneva, Switzerland, 1985, WHO.

Yaturu S, DePrisco C, Lurie A: Severe autoimmune hypoglycemia with insulin antibodies necessitating plasmapheresis, *Endocr Pract* 10(1):49–54, 2004.

Yu HE, Agus M, Kellogg MD: Clinical utility of Abbott Precision Xceed Pro® ketone meter in diabetic patients, *Pediatr Diabetes* 12:649–655, 2011.

Zhang DL, Jiang ZW, Jiang J, et al.: D-lactic acidosis secondary to short bowel syndrome, *Postgrad Med J* 79(928):110–112, 2003.

Zierler K: Whole body glucose metabolism, *Am J Physiol* 276(3 Pt 1):E409–E426, 1999.

Zuker N, Bissessor M, Korber M, et al.: Acute hypoglycaemic coma—a rare, potentially lethal form of early onset Sheehan syndrome, *Aust N Z J Obstet Gynaecol* 35(3):318–320, 1995.

CHAPTER 18

LIPIDS AND DYSLIPOPROTEINEMIA

Cindy L. Bredefeld, Raymond Lau, M. Mahmood Hussain

OVERVIEW, 244

LIPOPROTEINS, APOLIPOPROTEINS, AND RELATED PROTEINS, 246
Major Lipoproteins, 246
Minor and Abnormal Lipoproteins, 248
Important Proteins in Lipoprotein Metabolism, 248

LIPID TRANSPORT AND LIPOPROTEIN METABOLISM, 248

LIPID AND LIPOPROTEIN MEASUREMENT, 251
Blood Sampling and Storage, 252
Estimation of Plasma Lipids, 253
Estimation of Lipoproteins and Lipoprotein Cholesterol, 254
Ultracentrifugation Methods, 255
Electrophoretic Methods, 255
Polyanion Precipitation Methods, 255
Determining HDL-C Values, 255
LDL-C Measurement, 255
Friedewald and Martin-Hopkins Calculation, 255
Selective Chemical Precipitation, 256
Direct LDL-C Measurement, 256

ADDITIONAL METHODS IN THE STUDY OF DYSLIPIDEMIA, 256
Measurement of Lipoprotein Particle Number, 256
Measurement of Lipoprotein Subclasses, 256
Standing Plasma Test, 257
Detection of β-VLDL and Lp(a), 257
VLDL-C/Plasma Triglyceride Ratio, 257
Reliability of Measurements, 257
Hypertriglyceridemia, 258

GUIDELINES FOR CHOLESTEROL TESTING AND MANAGEMENT, 258
Estimating Risk Factors, 258
High Cholesterol in Children, 260

LIPIDS, LIPOPROTEINS, AND DISEASE, 260
High Cholesterol with High LDL-C, 260
Polygenic (Nonfamilial) Hypercholesterolemia, 260
Familial Hypercholesterolemia, 261
Familial Defective ApoB, 263
Sitosterolemia, 263
Autosomal-Dominant Hypercholesterolemia, 263
Autosomal-Recessive Hypercholesterolemia, 263
High Triglycerides with Normal Cholesterol, 264
Familial Hypertriglyceridemia, 264
Lipoprotein Lipase Deficiency (Hyperlipoproteinemia Type 1 or Hyperchylomicronemia), 264
ApoC-II Deficiency, 264
High Cholesterol with High Triglycerides, 264

HIGH TRIGLYCERIDE AND LOW HDL CHOLESTEROL, 265
Lipids, Obesity and Metabolic Syndrome, 265
Low Total Cholesterol and Triglyceride, 265
Isolated Low HDL-C, 265
Isolated High HDL-C, 266

SELECTED REFERENCES, 266

KEY POINTS

- Although ultracentrifugation and electrophoretic techniques are of historical significance, most useful lipid and lipoprotein testing methods are now enzymatic.
- Low-density lipoprotein (LDL) cholesterol is considered the primary target in assessing cardiac risk and directing therapy.
- LDL cholesterol can be measured directly but is usually calculated using the Friedewald equation and more recently using the Martin-Hopkins formula. The Martin-Hopkins formula has demonstrated improved accuracy at lower LDL levels and in the setting of hypertriglyceridemia.
- Given the cumulative impact of hyperlipidemia over a lifespan, identifying and treating hyperlipidemia early reduces an individual's lifetime risk for cardiovascular disease.
- New guidelines emphasize a personalized approach to the management of hyperlipidemia, incorporating more detailed risk assessments and new cholesterol-lowering drug options.

OVERVIEW

Disorders of lipid metabolism play a major role in atherosclerosis and coronary heart disease (CHD). A clear-cut relationship is evident between elevated serum cholesterol and myocardial infarction. At the tissue level, cholesterol deposits occur in areas of endothelial cell damage and are a prominent part of atherosclerotic lesions. Although cholesterol may be considered "bad" because of its association with myocardial infarction, it is actually a vital structural component of cell membranes and a precursor of steroid hormones and bile acids. Another lipid, triglyceride, is a major source of energy for cells. Cholesterol and triglycerides are the most important lipids in the study and management of CHD risk.

Lipids are soluble in nonpolar organic solvents such as chloroform and ether but relatively insoluble in polar solvents such as water. Thus, cholesterol and triglycerides travel in plasma not as free-floating molecules but rather as part of water-soluble complexes called *lipoproteins*. These particles contain cholesterol in two forms: free cholesterol, a polar nonesterified alcohol (about 30%), and cholesteryl ester, a hydrophobic form wherein cholesterol is linked to a fatty acid (about 70%). The lipoprotein is arranged like a micelle (Fig. 18.1). The most hydrophobic lipids, such as cholesteryl esters and triglycerides, are located in the core of the particle. Lipids with some hydrophilicity, such as free cholesterol and phospholipids, are arranged on the surface with polar groups pointing outward. *Apolipoproteins* (apo), the protein moiety of lipoproteins, are arrayed on the surface. They show amphiphilic characteristics; hydrophobic residues interact with the hydrophobic core, whereas hydrophilic residues interact outside the aqueous environment.

Four major lipoprotein classes are chylomicrons (CMs), very-low-density lipoprotein (VLDL), low-density lipoprotein (LDL), and high-density lipoprotein (HDL). The classification is based on the buoyant density of the particles (see later discussion). Several minor lipoproteins have also been identified, including intermediate-density lipoprotein (IDL) and lipoprotein(a) (Lp[a]) (Tables 18.1 and 18.2). Lipoproteins can be differentiated by density, particle size, chemical composition, and

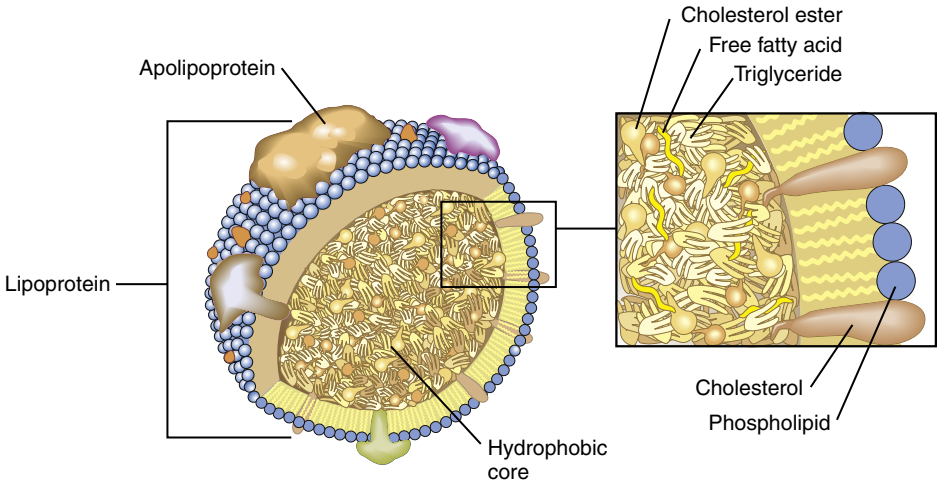

Figure 18.1 Lipoprotein structure. Lipoproteins are spherical particles with a hydrophobic core and an amphiphilic surface. The surface consists of a single layer of phospholipids. This surface layer also contains proteins and free cholesterol. The hydrophobic core mainly contains triglycerides and cholesteryl esters.

TABLE 18.1
Major Classes of Human Plasma Lipoproteins: Physicochemical Characteristics

Particle	Electrophoretic Mobility*	Major Apolipoproteins	Diameter (Å)	Density (kg/L)	Sf†
Chylomicrons	Origin	ApoA-I, A-IV, B-48, C-I, C-II, C-III, E	750–12,000	<0.95	>400
VLDL	Pre-β	ApoB-100, C-I, C-II, C-III, E	300–700	0.95–1.006	20–400
IDL	β or pre-β	ApoB-100, E1.006–1.019	12–20		
LDL	β	ApoB-100	180–300	1.019–1.063	0–12
HDL_2	α	ApoA-I, A-II, E	50–120	1.063–1.125	
HDL_3	α	ApoA-II, A-I, E	50–120	1.125–1.210	
Lp(a)	Pre-β	ApoB-100, Apo(a)		1.045–1.080	

HDL_2, Ultracentrifugation subclass of high-density lipoprotein; *HDL_3,* ultracentrifugation subclass of high-density lipoprotein; *IDL,* intermediate-density lipoprotein; *LDL,* low-density lipoprotein; *Lp(a),* lipoprotein A; *VLDL,* very-low-density lipoprotein.
*Agarose gel electrophoresis.
†Svedberg flotation rate.

TABLE 18.2
Chemical Composition of Major Classes of Plasma Lipoproteins

	Protein (%)*	Free Cholesterol (%)	Cholesteryl Esters (%)	Triglyceride (%)	Phospholipid (%)
Chylomicrons	1–2	1–3	2–4	80–95	3–6
VLDL	6–10	4–8	16–22	45–65	15–20
IDL	Intermediate between VLDL and LDL				
LDL	18–22	6–8	45–50	4–8	18–24
HDL	45–55	3–5	15–20	2–7	26–32

*Percentage of dry weight.
HDL, High-density lipoprotein; *IDL,* intermediate-density lipoprotein; *LDL,* low-density lipoprotein; *VLDL,* very-low-density lipoprotein.
Data from Albers (1974), Gaubatz et al. (1983), Fless et al. (1984), Gotto et al. (1986), Gries et al. (1988), and Hegele (2009).

electrophoretic mobility. These physical properties are due to differences in protein, triglyceride, and cholesterol content and reflect the role of each lipoprotein in lipid metabolism (see later discussion). Each lipoprotein is associated with specific apos that play important roles in lipid transport, such as activating or inhibiting the enzymes involved in lipid metabolism and binding lipoproteins to cell surface receptors. The apo composition of the lipoprotein classes is summarized in Table 18.1.

Lipoproteins are commonly differentiated from one another based on their buoyant density and electrophoretic mobility (Fig. 18.2). Ultracentrifugation separates lipoproteins by buoyant density. Lipids and proteins have average densities of 1.0 and 1.4 g/mL, respectively. If centrifuged in solutions of different densities, these particles band at characteristic densities. The density of a lipoprotein particle is determined mostly by its protein and triglyceride content. As illustrated in Figure 18.2, the higher the lipid content the less dense the lipoprotein particle, therefore, the closer they migrate to the top of the tube. Lipoproteins with high triglyceride and low protein content (CM and VLDL) are less dense than those with high protein and low triglyceride content (HDL). LDL and IDL are more dense than VLDL but less dense than HDL. When plasma lipoproteins are separated by agarose gel electrophoresis, CM remains at the origin and HDL migrates fastest in the α-region, followed by VLDL in the "pre-β" region and IDL and LDL in the β region.

Based on the presence and absence of apoB, lipoproteins can be classified as apoB-containing (CM, VLDL, IDL, LDL) and non–apoB-containing (HDL) lipoproteins. This classification is important because apoB is a nonexchangeable apolipoprotein, and only one molecule of apoB is present per lipoprotein. ApoB-containing lipoproteins (B-Lps) may or may not contain additional apolipoproteins such as apoA1, apoC, and apoE. ApoB serves as a structural protein for these lipoproteins and is always associated with these particles. B-Lps are synthesized mainly by hepatocytes and enterocytes.

B-Lps are mainly involved in delivering lipids to tissues for storage or use in energy production. CM (formed in the intestine from dietary fat) and VLDL (formed in the liver) are triglyceride-rich particles that are metabolized after entering the circulation. Through the action of lipoprotein lipase (LPL), found predominantly in microvasculature, they deliver fatty acids to tissues. The remnant CM and VLDL particle that have shed triglycerides and cholesterol esters are now transformed into denser

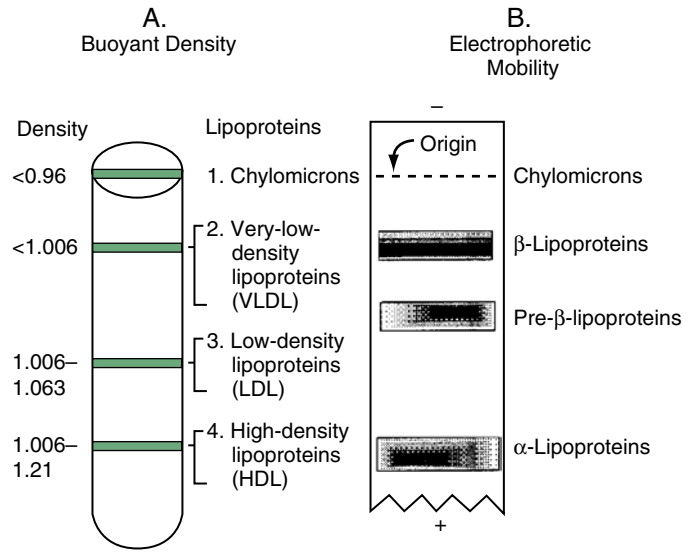

Figure 18.2 Lipoprotein classification. Lipoproteins are classified on the basis of buoyant density (A) or electrophoretic mobility (B). Separation of lipoproteins based on buoyant density depends on the ratio between lipids and proteins present in them. Lipoproteins that contain higher amounts of lipids have lower buoyant density and are collected on top of the centrifuge tube. Separations based on electrophoretic mobility are based on the number of charges present on lipoproteins and are independent of their size and buoyant density.

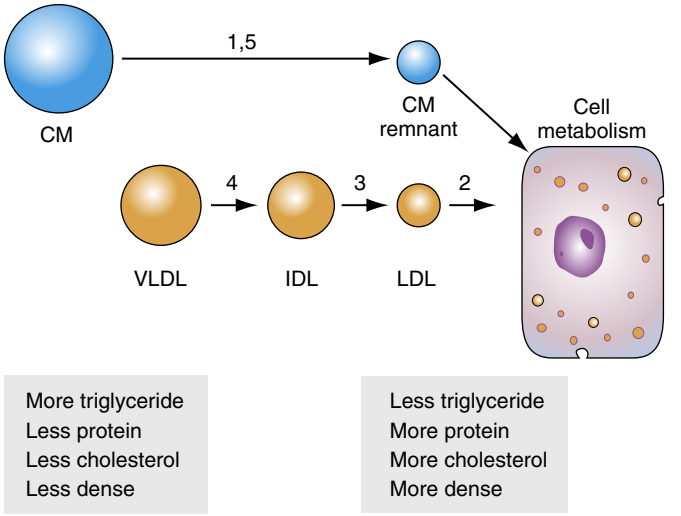

Figure 18.3 Metabolism of lipoprotein particles. The figure depicts successive shrinkage in the size of lipoproteins as a consequence of the lipolysis of triglycerides present in the particles. The number over each step in the pathway represents the functional hyperlipoproteinemia caused by a block between two intermediates (see Table 18.3). *CM,* Chylomicron; *IDL,* intermediate-density lipoprotein; *LDL,* low-density lipoprotein; *VLDL,* very-low-density lipoprotein.

lipoproteins with a higher percentage of cholesterol. The well-known LDL is the densest of these B-Lps, and elevated serum LDL-cholesterol (LDL-C) is a primary cardiac risk factor. Treatment of CHD-causing dyslipidemia is generally aimed at lowering LDL.

One way to understand heterogeneity in B-Lps is to view them as metabolic products in which CM and VLDL are acted upon by LPL, resulting in the release of free fatty acids to tissues with progressive decreases in their sizes. Because of this interaction with LPL, CM and VLDL become triglyceride depleted, denser, and relatively protein and cholesterol rich, giving rise to CM remnants and LDL. These particles are internalized and metabolized by cells—CM remnants by the liver and bone marrow cells and LDL by liver cells and by other cells throughout the body. LDL serves as the major source of cholesterol for tissues. This metabolic progression is presented in Figure 18.3.

A block in any step of the pathway leads to the accumulation of one or more lipoproteins. In Figure 18.3, the number over each step in the pathway represents the functional hyperlipoproteinemia (originally described by Fredrickson [1967]) caused by a block between two intermediates. For example, a block in the progression from CM to CM remnants results in the accumulation of CM—Type 1 or 5 disease—and presents with high triglycerides and normal cholesterol. A block in the conversion of VLDL to IDL and LDL results in Type 4 disease (i.e., VLDL accumulation with elevated triglycerides and frequently elevated cholesterol). Often, the cause of Types 1, 5, and 4 disease is LPL deficiency and the resulting inability to break down triglycerides. Type 2 disease results from a block in LDL metabolism and may have a genetic basis. Four possible known defects include a defective apoB protein that does not bind to the LDL receptor (LDLR), a mutant LDLR that does not recognize apoB, a gain in function mutation in proprotein convertase subtilisin/kexin type 9 (PCSK9), or a defective LDL adaptor protein. Type 2 is further subcategorized based on triglyceride levels. Note that other studies (see later discussion) may be necessary to distinguish Type 2B and Type 3 because both present with elevated cholesterol and triglycerides. This functional classification is presented in Table 18.3. No ideal system is known for classifying lipid disorders. They can be categorized in many different ways: primary versus secondary, hereditary versus acquired, and by lipoprotein fraction phenotypes. In general, each category is heterogeneous with respect to genetic, clinical, and pathologic factors. These are discussed in greater detail at the end of the chapter.

The major protein present in non–apoB-containing HDL is apoA-I, which makes up about 70% of the HDL protein. HDL is formed in the liver and small intestine. HDL plays a key role in reverse cholesterol transport, the process by which excess cholesterol is returned from tissues to the liver, where it is reused or excreted in bile. Besides apoA-I, HDL contains several apos. In addition to reverse cholesterol transport, other functions of HDL based on in vitro assays include anti-inflammatory, antioxidant, antithrombotic, and nitric oxide–inducing activities. Although the role of reverse cholesterol transport is suggested as a protective mechanism against atherosclerosis, these other properties of HDL might also contribute to the "protective" effect. Consequently, such protection may stem from HDL function rather than from increased plasma levels of HDL. In fact, interventions increasing HDL-C levels in plasma have not consistently shown clinical benefit (Tall & Rader, 2018).

LIPOPROTEINS, APOLIPOPROTEINS, AND RELATED PROTEINS

Lipoprotein particles are dynamic entities that acquire and shed protein and lipid components as they circulate in the body. As mentioned earlier, CM and VLDL particles lose triglycerides and become smaller as they are catabolized. Thus, young VLDL and CM particles are larger and less dense than their more mature counterparts. For this reason, it is best to view each of the lipoprotein classes not as a collection of identical particles but as a heterogeneous group. In fact, distinct lipoprotein subfractions or subclasses have been well described.

MAJOR LIPOPROTEINS

Chylomicrons

CMs are large particles produced by the intestine that transport lipids of dietary origin to the tissues of the body. They are very rich in triglycerides but relatively poor in free cholesterol, phospholipids, and protein. These particles are secreted into mesenteric lymphatics and reach circulation at the thoracic duct. These lipoproteins acquire apoC-II, a cofactor for LPL, from plasma. The interaction of CMs with LPL at the luminal surface of capillary endothelium results in the depletion of triglycerides and surface elements. The resulting smaller particles, called CM remnants, are removed from circulation by the liver (Hussain et al., 1996), primarily through the interaction of apoE with receptors such as proteoglycans, the LDLR, and the LDLR-related protein (LRP). The half-life of the CM in human circulation is short—only minutes. Because of the very high lipid/protein ratio, CMs are considerably less dense than water and float without centrifugation. When present at high levels, CMs result in "milky" plasma and accumulate as a floating creamy layer when left undisturbed for several hours. The apolipoproteins in CMs include apoB-48, apoA-I, apoA-IV, apoC-I, apoC-II, apoC-III, and apoE. In metabolism of CMs, apoC-II serves as an activator of LPL.

Very-Low-Density Lipoproteins

VLDL particles are produced by the liver and supply the tissues of the body with triglycerides of endogenous, primarily hepatic origin, and cholesterol. As compared with CMs, VLDL particles are smaller and produce turbid plasma when present in excessive amounts. They are rich in triglycerides,

TABLE 18.3

Classic Hyperlipidemia Phenotypes

WHO ICD and OMIM Numbers	Type	Particle	Triglycerides	Cholesterol	Comments
E78.3 238600	1 (familial chylomicronemia or LPL deficiency)	CM	High	Normal	Low cardiac risk; hereditary, found mostly in pediatric patients and young adults; autosomal-recessive mutation in *LPL* or *APOC2*; *APOA5*, *LMF-1*, and *GPIHBP1* mutations are linked to this phenotype.
E78.0 143890	2A (heterozygous and homozygous familial hypercholesterolemia)	LDL	Normal	High	High cardiac risk; mostly polygenic disease; about 10% are monogenic; heterozygous form is due to mutations in *LDLR*, *APOB*, or *PCSK9*; homozygous form is due to mutations in *LDLR* or *LDLRAP1* (ARH).
E78.4 144250	2B (combined hyperlipoproteinemia)	VLDL, LDL	High	High	High cardiac risk; polygenic disease; links to mutations in *USF1*, *APOB*, and *LPL*.
E78.2 107741	3 (dysbetalipoproteinemia)	IDL	High	High	High cardiac risk; mutations in *APOE* gene or homozygous for E2 allele of *APOE*.
E78.1 144600, 145750	4 (primary hypertriglyceridemia)	VLDL	High	Normal	Lower cardiac risk than type 2 or 3; polygenic disease
E78.3 144650	5 (mixed hyperlipidemia)	VLDL, CM	High	High	Low cardiac risk; polygenic disease; 10% of patients have mutations in *LPL*, *APOC2*, and *APOA5*; mutations in *APOE*, *TRIB1*, *CHREBP*, *GALNT2*, *GCKR*, and *ANGPTL3* are thought to contribute to this disease.

ANGPTL3, Angiopoietin-like 3; *APOA5,* apolipoprotein A-V; *APOB,* apolipoprotein B; *APOC2,* apolipoprotein C-II; *APOE,* apolipoprotein E; *CHREBP,* carbohydrate response element binding protein (or *MLXIPL*); *CM,* chylomicron; *GALNT2,* UDP-N′-acetyl-alpha-D-galactosamine-polypeptide *N*-acetylgalactosaminyltransferase 2; *GCKR,* glucokinase regulator; *ICD,* International Classification of Diseases; *IDL,* intermediate-density lipoprotein; *LDL,* low-density lipoprotein; *LDLRAP1,* LDLR adaptor protein 1 (also known as ARH); *OMIM,* Online Mendelian Inheritance in Man; *TRIB1,* tribbles homologue 1; *USF1,* upstream transcription factor 1; *VLDL,* very-low-density lipoprotein; *WHO,* World Health Organization.

although to a lesser extent than CMs, and have a higher buoyant density because of their lower lipid/protein ratio. By mass, VLDL particles contain approximately 50% triglyceride, 40% cholesterol and phospholipid, and 10% protein, mostly apoB-100 and apoC-I, apoC-II, and apoC-III, but also apoE. VLDL particles vary widely in size and chemical composition. Larger particles are rich in triglycerides and apoC. Smaller particles have less of these two components. LPL hydrolyzes VLDL, and this produces highly atherogenic, smaller triglyceride and surface material–depleted particles called VLDL remnants and IDL. LDLRs on hepatocytes recognize apoE in CM remnants and VLDL remnants and remove them from plasma.

Low-Density Lipoproteins

LDL is produced through the metabolism of VLDL/IDL in circulation and constitutes about 50% of the total lipoprotein mass in human plasma. The particles are much smaller than the triglyceride-rich lipoproteins (VLDL and CM) and do not scatter light or alter the clarity of plasma even at greatly increased concentrations. LDL consists of approximately 50% cholesterol, mostly esterified; 25% protein, mostly apoB-100 with traces of apoC; 20% phospholipid; and some triglycerides. Although each VLDL and LDL particle is thought to contain only one apoB-100 molecule, the extraordinary size of this protein allows it to be the largest protein component of these particles. The liver takes up most of the LDL in circulation (≈75%), with apoB-100 serving as a ligand for the hepatic LDLRs. The remaining LDL is delivered to other tissues. Some LDL is modified and is removed from the circulation by scavenger cells such as those found in atheromatous plaque. Small, dense LDL contains less cholesteryl ester, has a lower cholesterol/apoB ratio, and is believed to be atherogenic. Increased amounts of the small particles have been found in patients with several common forms of dyslipoproteinemia that are associated with CHD. People with high levels of small, dense LDL are at high risk of a CHD event, which is independent of total LDL concentration.

High-Density Lipoprotein

HDL is a small particle, consisting mostly of protein, cholesterol, and phospholipids, with only traces of triglycerides. ApoA-I is the major apolipoprotein for HDL, which is synthesized in the liver and small intestine. Different from B-Lps, most of HDL particles have more than one apoA-I molecule. Produced by the liver and intestine, HDL is involved in reverse cholesterol transport. In vitro studies suggest that HDL is involved in anti-inflammatory, antioxidant, antithrombotic, and nitric oxide–inducing mechanisms. The major site for the clearance of HDL cholesterol is the liver, and the best-understood mechanism is the selective uptake of cholesteryl esters from HDL by the SR-B1 receptor expressed in the liver. In the selective uptake process, SR-B1 promotes cholesteryl ester uptake without apoA-I degradation. Cholesteryl esters are removed from the internalized HDL particles, and cholesterol-depleted HDLs are resecreted. Mouse models that lack SR-B1 exhibit increased plasma HDL, slower HDL uptake by the liver, and increased atherosclerosis. Reverse cholesterol transport is reduced. In contrast, mouse models overexpressing SR-B1 in the liver show increased reverse cholesterol transport with reduced HDL plasma levels; however, these same mice also exhibit reduced atherosclerosis. In studies done on humans who maintain normal lipid profiles, the contribution of SR-B1 to HDL uptake is minimal. The cholesteryl ester transfer protein (CETP) pathway is considered an alternative pathway for HDL metabolism. CETP transfers triglycerides from B-Lps in exchange for cholesteryl esters in HDL. The result is an HDL particle depleted of cholesteryl esters but enriched with triglycerides. Cholesterol transferred to B-Lps is then cleared by LDLRs.

HDLs are also heterogeneous particles. Discrete HDL particle subpopulations have been identified on the basis of differences in size or charge, including two major ultracentrifugation subclasses, HDL_2 and HDL_3 (MacKenzie et al., 1973; Sundaram et al., 1974; Blanche et al., 1981). HDL_3 is smaller than HDL_2.The distinction is significant because HDL_2 is thought to be more cardioprotective than HDL_3, and people with low levels of HDL_2 are thought to be at increased risk for premature CHD. By surface charge, HDL is divided into three different subpopulations, from small to large: pre-β, pre-α, and α. Pre-βHDL is also called *lipid-poor apoA-I*. Each pre-βHDL contains one apoA-I molecule, three to four phospholipid molecules, and one to two cholesterol molecules. Additionally, HDL has been subfractionated into particles that contain apoA-I but not apoA-II, and those that contain both apoA-I and apoA-II (Fruchart & Ailhaud, 1992). ApoA-I is present on virtually all HDL particles and makes up 70% of the protein content. ApoA-II makes up about 20% of the HDL lipoprotein and is present on about two-thirds of all HDL particles in humans. The physiologic function of apoA-II is not fully understood. In a study with 306 individuals from 25 families with CHD family history, the apoA-II plasma level is significantly correlated with the serum free fatty acid level. In a mouse model, human apoA-II inhibits hepatic lipase activity on hydrolysis of HDL triglyceride (Warden et al., 1993). ApoA-II plays an important role in maintaining HDL particle size and levels of HDL in plasma. It is known that apoA-II is associated with insulin resistance and increased body fat (Corella et al., 2011). ApoE also associates with HDL particles. Laboratory measurement of particles with different apolipoprotein composition may eventually prove to be clinically useful (Shao & Heinecke, 2018).

TABLE 18.4
Significant Human Apolipoproteins

Apolipoprotein	Major Lipoproteins	Mr* (kDa)	Amino Acids	Chromosome	PLASMA CONCENTRATION mmol/L	PLASMA CONCENTRATION mg/dL
A-I	HDL	29	243–245	11	32–46	90–130
A-II	HDL	17.4	154	1	18–29	30–50
A-IV	HDL, LDL	44.5	396	11		
(a)	Lp(a)	350–700	Variable	6		
B-100	VLDL, IDL, LDL	512.7	4536	2	1.5–1.8	80–100
B-48	CM	240.8	2152	2	<0.2	<5
C-I	CM, LDL	6.6	57	19	6.1–10.8	4–7
C-II	CM, LDL	8.9	78 or 79	19	3.4–9.1	3–8
C-III	CM	8.8	79	11	9.1–17.1	8–15
D	HDL	19	169	3		
E	CM, LDL, IDL	34.1	299	19	0.8–1.6	3–6
F	HDL, LDL, VLDL	29	162	12		8.35
H	VLDL	50	326	17		20
J	HDL	80	449	8		
L	HDL	39–42	383	22	Absent in plasma	
M	HDL, LDL, VLDL, CM	26	188	6		2–15
O	HDL, LDL, VLDL	22.3	198	X		

CM, Chylomicron; *HDL,* high-density lipoprotein; *IDL,* intermediate-density lipoprotein; *LDL,* low-density lipoprotein; *Lp(a),* lipoprotein A; *VLDL,* very-low-density lipoprotein.
*Relative molecular mass.

MINOR AND ABNORMAL LIPOPROTEINS

Intermediate-Density Lipoproteins

Formed through the metabolism of VLDL in circulation, IDL can be removed from circulation quickly through interaction with the LDLR or it can be further metabolized to LDL. As expected, the lipid content, size, and density of IDL are intermediate between VLDL and LDL. Concentrations of IDL also contribute to the development of CHD, together with VLDL and LDL in humans.

Lipoprotein(a)

Lp(a) is similar to LDL in terms of density and overall composition. It can be thought of as an LDL particle to which a large glycoprotein, apo(a), has been linked to apoB-100 via a disulfide bond (Gaubatz et al., 1983; Fless et al., 1984, 1985). The electrophoretic mobility of Lp(a) is usually pre-β but can vary between that of LDL (β) and albumin (pre-α). Lp(a) is generally present in much lower concentrations than LDL. However, in normal subjects, values can range from less than 20 to 1500 mg/L or more. Increased levels are primarily genetically determined and its distribution varies between racial groups. Lp(a) levels show an autosomal-dominant pattern of inheritance and have been associated with an increased risk of CHD, cerebrovascular disease, and stroke (Thanassoulis, 2019). When concentrations in the plasma are increased to above 200 to 300 mg/L, Lp(a) appears electrophoretically as a lipid-staining pre-β band in the plasma fraction containing lipoproteins of density greater than 1.006 g/mL.

Lp(a) is synthesized in the liver. It binds to the LDLR by virtue of its apoB-100 component, albeit with lower affinity than LDL (Floren et al., 1981). Several mechanisms exist for the association of Lp(a) with cardiovascular disease (CVD). The removal of apo(a) from Lp(a) increases the affinity of the residual apoB-containing particle for the LDLR (Armstrong et al., 1985), and it has been suggested that apo(a) may interfere with the uptake of apoB-100–containing particles (Scanu, 1988). Additionally, the VLDL receptor on macrophages in atherosclerotic lesions can bind and mediate the catabolism of Lp(a), leading to accumulation of lipids within macrophages. Supporting this hypothesis is the observation that Lp(a) is ubiquitous in human coronary atheroma (Dangas et al., 1998). It has been speculated that Lp(a) and apo(a) might interfere with normal thrombolysis by virtue of their similarity to plasminogen. In vitro, it competes with plasminogen and tissue-type plasminogen activator for fibrin binding (Loscalzo et al., 1990). Human apo(a) transgenic mice are resistant to tissue plasminogen activator–mediated thrombolysis.

Screening for Lp(a) is considered when either familial or personal history of premature atherosclerotic cardiovascular disease (ASCVD) is not explained by major risk factors (Tsimikas, 2017). Niacin, estrogen, and Lp(a) apheresis have been shown to lower Lp(a). However, apart from the newer PCSK9 inhibitors, traditional LDL-lowering therapies are not effective in this regard. Antisense gene therapy to lower Lp(a) is an area of active research. At present, no clinical trials have demonstrated that lowering Lp(a) influences clinical outcomes.

LpX Lipoprotein

LpX is an abnormal lipoprotein found in patients with obstructive biliary disease and in patients with familial lecithin/cholesterol acyltransferase (LCAT) deficiency. Lipids account for more than 90% of its weight (mostly phospholipids: phosphatidylcholine, unesterified cholesterol, and very little esterified cholesterol). Proteins, primarily apoC and smaller amounts of albumin, constitute less than 10% of LpX by weight. A study has shown that LpX formation associates with a high level of hepatic cholesterol synthesis, but it is independent of LCAT activity, as well as ABCA1 and SR-BI expression (Bravo et al., 2007).

β-VLDL ("Floating *β*" Lipoprotein)

β-VLDL (floating β lipoprotein) is an abnormal lipoprotein that accumulates in type 3 hyperlipoproteinemia. It is richer in cholesterol than VLDL and apparently results from the defective catabolism of VLDL. The particle is found in the VLDL density range but migrates electrophoretically with or near LDL. β-VLDL is enriched in apoE. Cholesterol-fed animals accumulate β-VLDL in plasma. Uptake of cholesteryl ester-rich β-VLDL by macrophages induces foam cell formation.

IMPORTANT PROTEINS IN LIPOPROTEIN METABOLISM

Apolipoproteins

As mentioned previously, apos constitute the major protein component of lipoproteins. They are commonly referred to using the nomenclature introduced by Alaupovic (1971). Some significant properties of the apos are in Tables 18.4 and 18.5.

Lipolytic Enzymes and Other Proteins

The major enzymatic systems that are known to participate in plasma lipoprotein metabolism are the LCAT and lipolytic enzymes, LPL, hepatic triglyceride lipase (HL), and endothelial lipase (EL). Many other proteins are also involved in lipoprotein metabolism. Some significant attributes of these proteins are in Table 18.6.

LIPID TRANSPORT AND LIPOPROTEIN METABOLISM

Triglycerides and cholesterol enter circulation as part of triglyceride-rich lipoprotein particles, CMs produced in the intestine, and VLDLs produced

TABLE 18.5
Apolipoprotein Functions and Significant Characteristics

Apolipoprotein	Main Distribution	Function (If Known)	Comments
A-I	HDL	Activates LCAT that esterifies cholesterol in plasma. Ligand for *ABCA1*.	Synthesized in liver and intestine; HDL biosynthesis.
A-II	HDL		May inhibit lipoprotein and hepatic lipases and increases plasma triglyceride.
A-IV	HDL, CM, and free in plasma		May be a cofactor for LCAT; increased during fat absorption; HDL biosynthesis.
B-100	VLDL and LDL	Synthesis of VLDL; carboxy-terminal recognition signal targets LDL to the LDL (apoB, E) receptor.	Very large structural protein, synthesized in liver with lipids of endogenous origin (i.e., not chylomicrons).
B-48	CM	Synthesis of CM; not recognized by LDLR.	Synthesized in intestine, encoded by same gene and same amino terminus as apoB-100. Differential production of the two proteins involves RNA editing.
C-I	CM and VLDL		May inhibit hepatic uptake of VLDL and cholesteryl ester transfer protein.
C-II	CM and VLDL	Activates lipoprotein lipase.	Deficiency causes reduced clearance of triglyceride-rich lipoproteins.
C-III	VLDL, HDL	Inhibits lipolysis of triglyceride-rich lipoproteins; decreases clearance rate of remnant particles.	Deficiency causes reduced clearance of triglyceride-rich lipoproteins.
D	HDL	Activates LCAT.	
E	CM, VLDL, IDL, remnants and HDL	Recognition factor that targets CM and VLDL remnants to hepatic receptor; also binds to cell surface LDL receptors and proteoglycans.	E-2, E-3, and E-4 isoforms; E-4 is associated with high LDL-C, higher risk of CHD and Alzheimer's disease; E-2 associated with type 3 hyperlipoproteinemia.
F	HDL, LDL, VLDL	Regulates CETP function.	
H	VLDL	Related to activation of LPL; triglyceride metabolism.	Antibodies against apoH or β_2-glycoprotein-I are a subset of antiphospholipid antibodies, and may be associated with hyperthrombosis and stroke.
J		Cell-aggregating factor in Sertoli cells; inhibitor of the C5b*7 complement complex; beta-amyloid clearance in glial cells; cholesterol trafficking in brain.	Involved in apoptosis; linked to neurologic diseases like Pick and Alzheimer; also known as clusterin.
L	HDL		May be linked to reverse cholesterol transport
M	HDL, CM, LDL, VLDL		May be linked to HDL remodeling.
Apo(a)	Lp(a)		Homologous to plasminogen, may be prothrombotic; bound to apoB-100 by disulfide linkage.

ABCA1, ATP-binding cassette transporter; *CETP,* cholesteryl ester transfer protein pathway; *CHD,* congenital heart disease; *CM,* chylomicron; *HDL,* high-density lipoprotein; *IDL,* intermediate-density lipoprotein; *LCAT,* lecithin/cholesterol acyltransferase; *LDL,* low-density lipoprotein; *LDL-C,* low-density lipoprotein cholesterol; *Lp(a),* lipoprotein A; *LPL,* lipoprotein lipase; *VLDL,* very-low-density lipoprotein.

primarily by the liver. Their synthesis requires an intracellular chaperone microsomal triglyceride transfer protein (MTP) that transfers different lipids in in vitro systems (Hussain et al., 2003, 2012). In addition, MTP physically interacts with apoB. These two properties of MTP play a critical role in the biosynthesis of B-Lps. It is believed that MTP physically associates with nascent apoB in endoplasmic reticulum and lipidates it, forming a lipoprotein particle that is further matured and secreted (Walsh & Hussain, 2017; Sirwi & Hussain, 2018). Enterocytes synthesize CMs under postprandial conditions. In fasting conditions, they synthesize VLDL and smaller lipoproteins (Hussain et al., 1996). These lipoproteins are concentrated into mesenteric lymphatics and are delivered to blood at the thoracic duct. Hepatocytes synthesize VLDL and directly secrete into the circulation. Their synthesis is also dependent on MTP activity. The main function of B-Lps is to deliver cholesterol and triglyceride to different tissues. CMs are primarily involved in the absorption and delivery of dietary fat and fat-soluble vitamins, whereas VLDLs deliver endogenous lipids to other tissues.

Only one *APOB* gene is present in the human genome. Nevertheless, enterocytes and hepatocytes make two different forms of apoB protein to synthesize CMs and VLDL, respectively. In both tissues, the human *APOB* gene is transcribed into messenger ribonucleic acid (mRNA) that is 15 kilobases long. This transcript is translated into a single polypeptide in the liver, called apoB-100. In the intestine, however, *APOB* mRNA undergoes a posttranscriptional change. One cytosine residue (at position 6666) is deaminated to a uracil. This changes a glutamine codon into a stop codon. Translation of the edited mRNA gives rise to a polypeptide of 2152 amino acids that is 48% of the apoB-100 (synthesized by the liver). This editing enzyme is not expressed in the human liver; therefore, the liver synthesizes only full-length apoB-100.

These lipoprotein particles begin to undergo intravascular change almost immediately after entry into the circulation through the action of LPL. This enzyme hydrolyzes triglycerides and diglycerides, releasing fatty acids and monoglycerides, which are taken up by cells and used as a source of energy. ApoC-II stimulates the hydrolysis of triglycerides. In addition to losing triglycerides by LPL-mediated hydrolysis, the CM loses surface lipids and apos by transfer of these components to HDL. Overall, CMs lose significant mass in the form of triglyceride and the A and C apolipoproteins. The depleted CM remnant particle contains apoB-48 and apoE as its major apolipoproteins. These particles are rapidly removed from plasma and are sequestered in the space of Disse by binding to proteoglycans or taken by hepatocyte after binding to the LDLRs. The sequestered particles can undergo further hydrolysis by hepatic lipase and are enriched with apoE. Eventually, they are internalized and degraded by means of a rapid and specific receptor-mediated endocytic process involving LDLRs, LRP, and proteoglycans. C apos inhibit the uptake of CM remnants, allowing them to remain in the circulation long enough to complete the hydrolysis of triglycerides. In the fasting state, the intestine continues to make apoB and secretes "intestinal VLDL" (small CMs). These particles may constitute up to 10% or 20% of the circulating "VLDL," but they are probably metabolized as CMs (Byers & Friedman, 1960; Cenedella & Crouthamel, 1974; Risser et al., 1978; Green & Glickman, 1981).

VLDL is synthesized in the liver. Similar to CM, VLDL is catabolized upon entry into the circulation, in part by LPL, and is converted to

TABLE 18.6

Enzymes and Other Proteins Important for Lipoprotein Metabolism

Enzyme	Gene Location	Function	Deficiency	Tissue Expression
ABCG5	2p21	Forms heterodimers with ABCG8 to pump out plant sterols back into the intestinal lumen.	Increased plant sterol levels in plasma that can disrupt cell membranes and cause sitosterolemia; influences cholesterol levels in plasma.	Tissue expression in liver, colon, and intestines
ABCG8	2p21	Forms heterodimers with ABCG5 to pump out plant sterols back into intestinal lumen; also associated with cholesterol and sterol excretion in bile.	Increased plant sterol levels in plasma that can disrupt cell membranes and cause sitosterolemia; influences cholesterol levels in plasma.	Tissue expression in the liver, intestines, and gallbladder
ABCA1	9q22-31	Efflux of cholesterol from peripheral cells into HDL.	Tangier disease, with very low HDL and accumulation of lipids in peripheral cells.	Many cell types, prominently in the liver, testis, and adrenal
CETP	16q21	Transfers CE, PL, and TG among lipoproteins, especially the transfer of CE from HDL to apoB-100–containing lipoproteins in exchange for TG.	Deficiency results in large cholesterol-laden HDL.	Produced in liver and circulates with HDL.
EL	18q21.1	Hydrolysis of PL and TG in lipoproteins, especially PL in HDL. Homologous to LPL and EL and pancreatic lipase.	Increased levels of HDL_2, and large buoyant LDL. Overexpression in mice, decreased TC, PL, and HDL-C.	Expressed in many tissues, including liver. Synthesized by endothelium.
HL	15q22-23	Hydrolysis of TG and PL, especially from HDL_2, and may be necessary for HDL metabolism. Also active on lipids in VLDL remnants and IDL. Not very active on newly released VLDL or CM.	Increased TC, TG, and HDL-C in deficiency.	Associates with nonparenchymal liver cells.
LCAT	16q22.1	Catalyzes the esterification of cholesterol, especially in HDL, by promoting transfer of fatty acids from lecithin to cholesterol. Enables HDL to accumulate cholesterol as CE. Activated by apoA-I.	Deficiency results in decreased HDL.	Produced in liver and circulates with HDL.
LPL	8q22	Hydrolysis of TG in lipoproteins (especially VLDL and CM), releasing free fatty acids and glycerol to tissues. ApoC-II are essential cofactors.	Large CM and VLDL with very high TG levels.	Present on surface of capillary endothelial cells in adipose tissue and skeletal and heart muscle, but not produced by endothelial cells.
LDLR	19p13.2	Binds apoE and apoB-100 and mediates endocytosis of lipoproteins, mostly LDL, but also VLDL, IDL, and CM remnants.	Familial hypercholesterolemia results primarily in elevated LDL.	Expressed on most cell types, but hepatic receptors clear 70% of LDL.
MTP	4q24	Lipidates and regulates secretion of ApoB particles from the liver and intestines.	Deficiency of MTP function leads to abetalipoproteinemia, in which ApoB lipoproteins are virtually undetectable in plasma.	Expression is seen in liver, intestines, heart, kidney, and eye.
PLTP	20q12	Transfer of PL to and from HDL. Important for HDL growth and remodeling.	Deficiency in mice results in low HDL.	Expressed on many cell types.
PCSK9	1p32.3	Influences the number of LDLRs expressed on cell surface.	Depending on mutation—either gain of function or loss of function—the presence of PCSK9 affects availability of LDLR on cell surface and, consequently, the levels of LDL in plasma; gain of function leads to more LDL in plasma; loss of function associates with increased LDLR expression and thus less LDL in plasma.	Secreted protein by the liver cells; expressed in pancreatic islet beta cells and neuronal cells.
SR-B1	12q24.31	Binds HDL on cell surface. Plays a role in selective uptake of CE from HDL in liver and steroidogenic tissues. May also enable macrophages to bind oxidized LDL.	Accumulation of large CE-rich HDL, and accelerated atherosclerosis in mice.	Macrophage, adrenal, liver and testis

ABCA1, ATP-binding cassette protein A1; *Apo,* apolipoprotein; *CE,* capillary electrophoresis; *CETP,* cholesteryl ester transfer protein; *CM,* chylomicron; *EL,* endothelial lipase; *HDL,* high-density lipoprotein; HDL_2, ultracentrifugation subclass of HDL; *HDL-C,* high-density lipoprotein cholesterol; *HL,* hepatic lipase; *IDL,* intermediate-density lipoprotein; *LCAT,* lecithin/cholesterol acyltransferase; *LDL,* low-density lipoprotein; *LDLR,* LDL receptor; *LPL,* lipoprotein lipase; *MTP,* microsomal triglyceride transfer protein; *PL,* phospholipid; *PLTP,* phospholipid transfer protein; *SR-B1,* scavenger receptor class B, member 1; *TC,* total cholesterol; *TG,* triglycerides; *VLDL,* very-low-density lipoprotein.

cholesterol-enriched VLDL remnants, IDL. Some of these remnants are removed from circulation by the liver via receptor-mediated endocytosis; others are further catabolized to LDL (Bachorik & Kwiterovich, 1988). LDL carries most of the circulating cholesterol and transports cholesterol to hepatic and extrahepatic tissues, where it is taken up by LDLR-mediated endocytosis (Brown et al., 1981). LDL binds to the LDLR via apoB-100 and is subsequently internalized and directed to the lysosome, where apoB-100 is degraded and cholesteryl ester and other lipids are hydrolyzed. LDLRs are recycled back to the cell membrane (Fig. 18.4).

The unesterified cholesterol produced via lysosomal hydrolysis becomes available for membrane, hormone, and bile acid synthesis. Excess cholesterol is reesterified by the microsomal enzyme acyl:cholesterol acyl

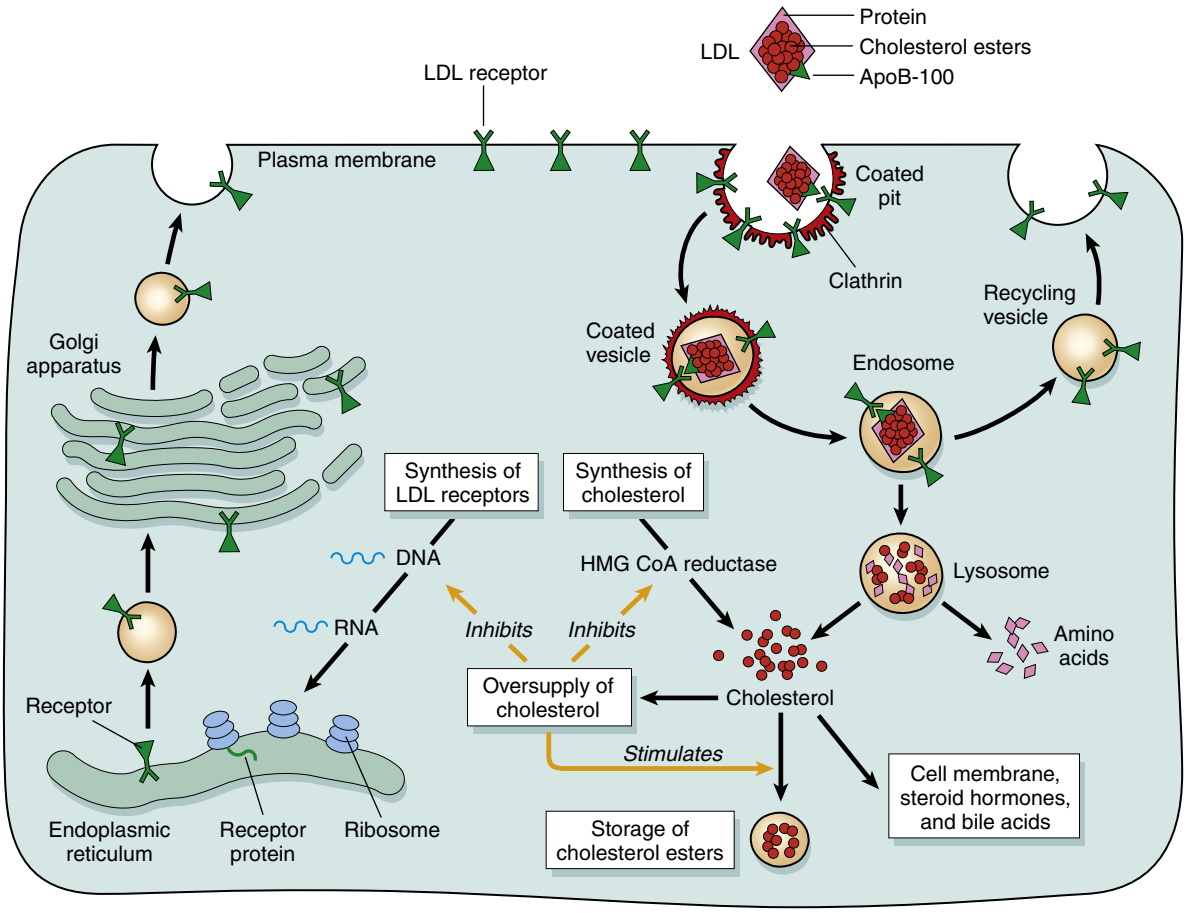

Figure 18.4 The low-density lipoprotein (LDL) receptor pathway and regulation of cholesterol metabolism.

transferase (ACAT) and is stored until it is needed. High cellular free cholesterol downregulates the expression of LDLR on the cell surface, leading to reductions in LDL uptake. About two-thirds of LDL is removed from plasma via hepatic LDLRs. Although most tissues use cholesterol only for membrane synthesis or store it as cholesteryl ester, the liver can utilize cholesterol to make bile acids and excrete it into the bile both as unesterified cholesterol and after conversion to bile acids. The liver also reuses cholesterol for lipoprotein synthesis and secretes it with VLDL into the circulation. Steroid-secreting tissues use cholesterol as a precursor for the synthesis of steroid hormones.

LDL and CM remnants deliver lipids to the tissues. In contrast, HDL is thought to be the vehicle for reverse cholesterol transport, the process by which excess cholesterol is removed from peripheral tissues and transported back to the liver. HDL is secreted from both the liver and the intestine as nascent, disk-shaped particles that contain apos, cholesterol, and phospholipid (Havel, 1980; Scanu et al., 1982; Oram, 1986; Oppenheimer et al., 1987). The formation of nascent HDL particles is almost exclusively dependent on the synthesis and release of apoA-I. HDL also arises de novo in circulation from excess surface material (e.g., free cholesterol, apoA-I, apoA-II, apoC, phospholipid) removed from the triglyceride-rich lipoproteins as they are catabolized. In peripheral tissues, excess cholesterol is exported from cells (including macrophages), in part through the action of the protein ATP-binding cassette transporter 1 (ABCA1) to apoA-I or HDL. The free cholesterol in nascent HDL particles is esterified by LCAT into cholesteryl esters. As cholesteryl esters move into the hydrophobic core, the particle becomes spherical and larger, developing eventually into HDL_3 and then HDL_2. Two plasma proteins are involved in the remodeling of HDL: phospholipid transfer protein (PLTP) and CETP. CETP catalyzes the transfer of cholesteryl esters to apoB-100–containing particles in exchange for triglycerides (Tall, 1990). PLTP facilitates the transfer of phospholipids from other lipoproteins to HDL, allowing the particle to grow by acquiring surface phospholipid as it accumulates esterified cholesterol and triglyceride in its core. Once formed, HDL delivers excess lipids, especially cholesterol, to the liver and other tissues (Glass et al., 1983; Stein et al., 1984; Bachorik et al., 1987). This may occur directly when HDL gives cholesterol to the hepatocytes, mainly via Scavenger receptor class B member 1 (SR-B1). Lipids may also return to the liver indirectly or be directed to peripheral tissues via B-Lps to which they are transferred from HDL by CETP.

Although HDL particles may return to the liver soon after formation, the bulk of HDL seems to remain in circulation for several days, continuously exchanging lipids and apos with other lipoprotein particles, retrieving additional cholesterol from peripheral tissues, and delivering those lipids to the liver and steroid-producing tissues. This is supported by the fact that apoA-I has a half-life of several days in circulation. Eventually, mature HDL is internalized by the liver SR-B1 or small lipid-depleted HDL may be catabolized in the kidney following filtration and cubulin-mediated reuptake in the proximal tubule. Lipid-poor apoA-I is eliminated from the body mainly by the kidney through the renal glomerulus. Patients with kidney disease exhibit impaired cholesterol efflux capacity and are at high risk of cardiovascular disease (Moore & Fisher, 2013).

LIPID AND LIPOPROTEIN MEASUREMENT

Lipoprotein concentrations have been measured and described in several ways. Some of these measurements, including particle mass and mass concentration (the mass of each lipoprotein particle as solute per liter of solution), are not easily applied for screening or routine clinical purposes. Fortunately, other methods may be used to describe the lipoprotein content of blood. Because the cholesterol composition of each lipoprotein class is similar from individual to individual, lipoprotein cholesterol is commonly used to evaluate lipoprotein concentration. For example, it is easier to determine the amount of LDL-C in a specimen than it is to determine the mass of LDL (cholesterol + triglyceride + protein) in solution, yet both measurements provide similar information about the LDL content of plasma. Lipoprotein-cholesterol concentrations correlate well with analytic ultracentrifugation values. Also, because these values have been used in most population studies of cardiovascular risk, they have documented predictive value.

When various methods of lipid analysis are considered, several issues should be kept in mind. First, the more complicated the analytic procedures, the greater the variability of the analyses (Bookstein et al., 1990; Brown et al., 1990). For example, the measurement of plasma lipoproteins usually requires two steps: separating lipoprotein classes and measuring the class of interest. Both steps contribute to the error in the measurements.

Consistent with this, lipoprotein cholesterol analyses are generally more variable than total cholesterol (TC) analyses because of the additional manipulations required in preparing the lipoprotein-containing fractions. Second, in addition to analytic sources of error, significant preanalytic variables may affect measured lipid and lipoprotein levels. In fact, plasma lipoprotein concentrations can change dramatically as a result of normal physiologic variation. In this section, issues of sampling and storage are considered, along with methods for measuring lipids and lipoproteins.

BLOOD SAMPLING AND STORAGE

Variation and error may occur before or during venipuncture or when the samples are handled and stored before analysis. Therefore, it is important to standardize conditions under which blood specimens are drawn and prepared for analysis.

Biological Variation

Physiologic variations in cholesterol, triglyceride, and lipoproteins have been examined in a number of studies (Warnick et al., 1979; Demacker et al., 1982; Bookstein et al., 1990; Brown et al., 1990; Kafonek, 1992). For cholesterol, the coefficient of physiologic variation within an individual averages about 6.5%, but it can be higher in certain individuals (Tables 18.7 and 18.8). When measured in serial samples from the same person, cholesterol levels in 95% of the samples will vary by about 13% above or below that person's mean level. As a result, physiologic variation can be several times greater than analytic error; thus, measurements must be made in several blood samples taken at least a week apart to establish the individual's usual lipoprotein concentration. Determinations of these levels is important for consideration of appropriate therapy for documented hypercholesterolemia, such as use of statins shown in Table 18.9. Table 18.10 summarizes levels of serum total cholesterol and their significance. Table 18.11 summarizes some of the clinical presentations of hypercholesterolemias and/or hypertriglyceridemias.

A variety of biological factors can affect lipid and lipoprotein levels. Cholesterol levels rise with age, starting in early adulthood, in both sexes. Women have lower cholesterol levels than men, except in childhood and after the early fifties. Age-related variation forms the basis for the National Cholesterol Education Program (NCEP) recommendation that cholesterol screening should be repeated every 5 years. Seasonal variation also occurs, such that cholesterol levels are slightly higher in the winter (Robinson et al., 1992). In addition, dietary intake of saturated fat and cholesterol significantly influences plasma lipid levels. The effects of dietary modification take several weeks to become apparent; thus before individuals' cholesterol levels are ascertained, it is important that they be on their usual diet for 2 weeks and are neither gaining nor losing weight. Several common medications, including oral contraceptives, postmenopausal estrogens, and some antihypertensive drugs, significantly alter lipid levels. Medical disorders that lead to secondary dyslipoproteinemia include thyroid, hepatic, and kidney disease (see Table 18.12). In such cases, management of hyperlipidemia is predominantly a function of treating the underlying disorder. Lifestyle and biological factors that produce short-term deviations from baseline lipid values include alcohol consumption, fasting, posture, venous occlusion, anticoagulants, recent myocardial infarction, stroke, cardiac catheterization, trauma, acute infection, and pregnancy. It is recommended that lipoprotein measurements be made no sooner than 8 weeks after any form of trauma or acute bacterial or viral infection and 3 to 4 months after childbirth.

Fasting

Patients should fast for 12 hours before venipuncture. CMs are usually present in postprandial plasma and, depending on the type and amount of food ingested, can markedly increase the plasma triglyceride (TG) concentration. Concentrations of LDL- and HDL-cholesterol (LDL-C and HDL-C) also decline transiently after eating, in part as a consequence of CETP-mediated compositional changes that occur during the catabolism of CMs (Cohn et al., 1988). CMs are almost completely cleared within 6 to 9 hours; their presence after a 12-hour fast is considered abnormal. Generally, TC and HDL-C levels can be measured in nonfasting individuals, greatly facilitating screening and monitoring. Fasting has little effect on plasma TC levels; although nonfasting HDL-C levels can be a few mg/dL lower than fasting levels, this should not lead to misclassification of patients with low HDL levels. When TG and LDL-C are being measured, fasting becomes a requirement.

Posture

When a standing patient reclines, extravascular water transfers to the vascular system and dilutes nondiffusible plasma constituents. Decreases of as much as 10% in the concentrations of TC, LDL-C, HDL-C, apoA-I, and apoB have been observed after a 20-minute period of recumbence (Miller et al., 1992). The decrease in TG is about 50% greater, suggesting that factors other than simple hemodilution may also be involved. These effects are about half as great in a standing subject who sits (Miller et al., 1992). Postural changes are reversible when the patient resumes the standing position. Current NCEP guidelines recommend that patients be seated for 5 minutes before sampling to prevent hemoconcentration. If it is necessary to use the recumbent position, it should be used each time the patient is sampled to minimize postural change. Prolonged venous occlusion can lead to hemoconcentration and cholesterol increases of 10% to 15%. Tourniquets should not be applied for longer than a minute or two, if possible.

TABLE 18.7
Physiologic Variation of Plasma Lipids, Lipoproteins, and Apolipoproteins

Component	CVP (%)*	CVP (%)†
Total cholesterol	5.0	6.4
Triglycerides	17.8	23.7
LDL-cholesterol	7.8	8.2
HDL-cholesterol	7.1	7.5
ApoA-I	7.1	—
ApoB	6.4	—

CVP, Coefficient of physiologic variation; *HDL,* high-density lipoprotein; *LDL,* low-density lipoprotein.
*Data from patients of a lipid clinic (Kafonek et al., 1992).
†Data from the National Cholesterol Education Program 1995 Working Group on Lipoprotein Measurement.

Venous Versus Capillary Samples

Although it is generally assumed that venous and capillary samples are equivalent, the available information at present is limited and somewhat contradictory. Some investigators have found that cholesterol measurements in the two kinds of samples agreed in about 4% (Koch et al., 1987) or less (Lunz et al., 1987; Law et al., 1997), but others have reported differences of 8% to 12% (Bachorik et al., 1990). In general, measurements in capillary blood samples seem to be a little lower than in venous samples. Additionally, measurements in fingerstick samples tend to be more variable than in venous samples obtained at the same time, probably as the result of preanalytic sources of error. Estimates for the biological component of within-subject variations have been made for lipid and lipoprotein in venous and fingerstick samples and are similar in both kinds of samples for cholesterol, TG, HDL, and LDL (Kafonek et al., 1996). Although the use of capillary samples may be unavoidable under some conditions, it is good to keep in mind, first, that the epidemiologic data from which risk levels for lipids and lipoproteins are derived are based on measurements in venous samples and, second, that for various physiologic and methodologic reasons, the measurements in the two kinds of samples may differ.

Plasma Versus Serum

Plasma or serum can be used when only cholesterol, TG, and HDL-C are measured, and LDL-C is calculated from these three measurements (see later discussion). However, plasma is preferred when the lipoproteins are measured by ultracentrifugal or electrophoretic methods because the samples can be cooled to 4° C immediately to retard changes that can occur in the lipoproteins at room temperature. When plasma is to be used, blood is cooled in an ice bath as soon as it is drawn, and the cells are removed as soon as possible, generally within 3 hours. The plasma is then stored at 4° C until it is analyzed. Plasma should not remain in contact with the cells overnight. Even in the presence of the anticoagulant, protein aggregation can occur in plasma that is stored in the refrigerator for a few days or frozen for longer periods. This can make it difficult to obtain a homogeneous aliquot for analysis and can interfere with the flow of sample in automated analyzers, resulting in inaccurate or variable results. Protein aggregation occurs less frequently in serum.

The choice of anticoagulant is also important. Some anticoagulants, such as citrate, exert rather large osmotic effects that result in falsely low plasma lipid and lipoprotein concentrations. Heparin, because of its relatively high molecular weight, has little effect on plasma volume but can alter the electrophoretic mobilities of the lipoproteins. Ethylenediaminetetraacetic acid (EDTA) is the preferred anticoagulant even though

cholesterol and triglyceride concentrations in EDTA plasma are about 3% lower than in serum (Laboratory Methods Committee of the Lipid Research Clinics Program, 1977). This anticoagulant retards certain kinds of oxidative and enzymatic alterations that occur in the lipoproteins during storage.

Storage

Generally, TC, triglycerides, and HDL-C can be satisfactorily analyzed in frozen samples, and LDL-C concentrations can be estimated. Apolipoproteins can also be measured in frozen samples (see later discussion). Frozen samples are not appropriate for ultracentrifugal analysis because the triglyceride-rich lipoproteins do not withstand freezing. HDL free cholesterol and VLDL free fatty acid decrease by about 35%, and LDL cholesteryl ester increases by 35% upon single freeze and thaw (Zivkovic et al., 2009). When serum or plasma must be stored for long periods, it should be maintained at temperatures of –70° C or lower. For short-term storage (up to 1 or 2 months), the samples can be kept at –20° C, but they should not be stored in a self-defrosting freezer. The temperature in a self-defrosting freezer actually cycles between about –20° C and 2° C during the defrost cycle and effectively subjects the samples to daily freeze–thaw cycles, which can hasten their deterioration and cause the lipid and lipoprotein measurements to become variable (i.e., less reproducible). Quantification of lipid and apos are not affected within three freeze-and-thaw cycles. In most lipid classes, the effect of storage temperature over 1 week is minimal between 4° C, –20° C, and –80° C (Zivkovic et al., 2009).

ESTIMATION OF PLASMA LIPIDS

Cholesterol and triglycerides are the plasma lipids of greatest interest in the diagnosis and management of lipoprotein disorders. Phospholipid analyses generally provide little additional information and are seldom required. Occasionally, they may be requested in cases of obstructive liver disease or disorders associated with abnormally low lipoprotein levels.

Cholesterol

Cholesterol accounts for almost all of the sterol in plasma. It exists as a mixture of unesterified (30%–40%) and esterified (60%–70%) forms; the proportion of the two forms is fairly constant among normal individuals. TC and lipoprotein-cholesterol concentrations are usually expressed in terms of the sterol nucleus without distinguishing the esterified and unesterified fractions. In general, it is not necessary to distinguish the two forms, except in cases in which the contribution of the fatty acid moiety to cholesteryl ester mass must be accounted for or when the cholesterol/cholesteryl ester mass ratio is of interest.

This discussion considers primarily the enzymatic methods of cholesterol quantification, which have virtually replaced the chemical methods that were used for most clinical and research purposes (Bachorik et al., 1976; Wood et al., 1980; Lipid Research Clinics Program, 1982). However, one chemical method, a modification of the Abell-Kendall method (Abell et al., 1952), continues as the reference method for cholesterol used by the Centers for Disease Control and Prevention (CDC) and a network of secondary reference laboratories (Myers et al., 1989). In the Abell-Kendall method, cholesteryl esters are hydrolyzed with alcoholic potassium hydroxide (KOH), and the unesterified cholesterol is extracted with petroleum ether and measured with the Liebermann-Burchard reagent using purified cholesterol standards. This method can be accurate within about 0.5% of true value.

Enzymatic Methods

These methods measure TC directly in plasma or serum through a series of reactions in which cholesteryl esters are hydrolyzed. The 3-OH group of cholesterol is oxidized, and hydrogen peroxide, one of the reaction products, is quantified enzymatically:

$$\text{Cholesterylester} + H_2O \xrightarrow[\text{esterase}]{\text{Cholesterol}} \text{Cholesterol} + \text{Free fatty acid} \quad \text{(Eq. 18.1)}$$

$$\text{Cholesterol} + O_2 \xrightarrow[\text{oxidase}]{\text{Cholesterol}} \text{Cholest-4-en-3-one} + H_2O_2 \quad \text{(Eq. 18.2)}$$

$$2H_2O_2 + \text{Phenol} + 4\text{-aminoantipyrine} \xrightarrow{\text{Peroxidase}} \text{Quinoneimine dye} + 4H_2O \quad \text{(Eq. 18.3)}$$

To complete the enzymatic measurement of TC, there must be a way to quantify the by-products of the reaction. Currently, the most common method of quantifying the cholesterol oxidase reaction is to measure the amount of hydrogen peroxide produced (Eq. 18.3). The hydrogen peroxide produced in the cholesterol oxidase reaction can be oxidatively coupled to two chromogenic substrates by catalysis with a peroxidase, most commonly horseradish peroxidase (HRP). The chromogens used are usually phenol and 4-aminoantipyrine. When coupled with hydrogen peroxide, they produce a quinoneimine dye that can be read photometrically at 500 nm. The catalytic properties of HRP are very nonspecific; therefore, this step is most subject to interference from other components of serum/plasma.

Interfering Substances

Enzymatic methods are less subject to interference by nonsterol substances that react in the chemical methods; however, they are not absolutely specific for cholesterol. Cholesterol oxidase (Eq. 18.2) can react with sterols other than cholesterol that are present in plasma such as plant sterols, which are present in appreciable concentrations in the circulation of patients with β-sitosterolemia. These sterols also contribute to the cholesterol values measured via most chemical methods. Another type of interfering agent is ascorbic acid, a reducing agent, which competes with the chromogenic substrates of Equation 18.3 for hydrogen peroxide. Therefore, plasma/serum samples with elevated levels of ascorbic acid can result in lower measured levels of TC. It is currently accepted that ascorbic acid levels over 30 mg/dL should be accounted for in TC measurements, although levels that high are infrequent (Rifai et al., 2000). Another interfering agent that acts in a similar manner is bilirubin. Bilirubin can interfere with TC measurements because of its own spectral properties; bilirubin absorbs light at 500 nm (Rifai et al., 2000). This tends to increase measured cholesterol values. However, bilirubin is also oxidized by H_2O_2; as a result, it loses its absorbance at 500 nm. This complicates the application of a serum blank to correct for bilirubin absorbance. Overall, interference by bilirubin seems to be significant only at concentrations exceeding 5 mg/dL, at which level it has been reported to decrease apparent cholesterol values by 5% to 15% (Pesce & Bodourian, 1977; Deacon & Dawson, 1979; Naito & David, 1984). Sample turbidity because of hypertriglyceridemia can also interfere with enzymatic methods (Pesce & Bodourian, 1977). Hemoglobin is another possible interfering agent in the measurement of TC. It has a pseudo-peroxidase activity that can consume the hydrogen peroxide produced in Equation 18.2. More important, however, is that hemoglobin has an inherent color that can falsely elevate TC levels. Just as hemoglobin is a product of red blood cell hemolysis, other products of hemolysis, such as catalase, can compete with the peroxidase for hydrogen peroxide. However, hemolyzed products do not significantly affect cholesterol measurements even at abnormally high plasma concentrations (Pesce & Bodourian, 1977; Deacon & Dawson, 1979).

In addition to their relative resistance to interference, enzymatic methods have other significant benefits. They consume only microliter quantities of sample and do not require a preliminary extraction step. They are rapid, and if the cholesteryl ester hydrolase step is omitted, they can be used to measure unesterified cholesterol. Finally, enzymatic methods are precise, with coefficients of variation generally in the range of 1% to 2%. For the most part, they use stabilized pure cholesterol standards or serum calibration standards for which the stated values are traceable to the CDC reference method for cholesterol (Pesce & Bodourian, 1977). Enzymatic values generally agree with reference values within 1% to 2% when measured in a laboratory setting with modern equipment. Serum-based calibrators are inherently preferable to pure cholesterol because they are subject to all analytic reactions undergone by patient samples.

Triglycerides

A wide variety of methods have been used to measure plasma triglycerides, but the methods most commonly used for clinical or epidemiologic purposes are based on the hydrolysis of triglycerides and the measurement of glycerol that is released in the reaction:

$$\text{Triglyceride} + 3H_2O \xrightarrow{\text{Lipase}} \text{Glycerol} + \text{Fatty acids} \quad \text{(Eq. 18.4)}$$

Because each glycerol molecule is calculated to represent a triglyceride molecule, TG concentrations are often overestimated if endogenous unesterified glycerol is not subtracted. Even after correction for glycerol, TG levels are overestimated because of the presence of monoglyceride and diglyceride molecules. Despite this knowledge and the availability of reagents and methods to correct for endogenous glycerol, only about 5% of American clinical laboratories actually correct for endogenous glycerol. The reason for this is that in most normal individuals, endogenous glycerol levels are negligible.

Enzymatic methods (Bucolo & David, 1973) are now universally used for TG analysis in the clinical laboratory. They are relatively specific, rapid, and easy to use. The analyses are performed directly in plasma or serum and are not subject to interference by phospholipids or glucose.

Common to most enzymatic methods is the hydrolysis of triglycerides to free fatty acids and glycerol, followed by the phosphorylation of glycerol to glycerophosphate.

$$\text{Triglycerides} \xrightarrow{\text{Lipase}} \text{Glycerol} + \text{Fatty acids} \quad \text{(Eq. 18.5)}$$

$$\text{Glycerol} + \text{ATP} \xrightarrow{\text{Glycerokinase}} \text{Glycerophosphate} + \text{ADP} \quad \text{(Eq. 18.6)}$$

However, several methods may be used to quantify the amount of glycerolphosphate formed and thus the amount of triglyceride in plasma. In one approach, glycerophosphate reacts as follows:

$$\text{Glycerophosphate} + \text{NAD} \xrightarrow[\text{dehydrogenase}]{\text{Glycerophosphate}} \text{Dihydroxyacetone phosphate} + \text{NADH} + \text{H}^+ \quad \text{(Eq. 18.7)}$$

$$\text{NADH} + \text{Tetrazolium dye} \xrightarrow[\text{oxidase}]{\text{Diaphorase}} \text{Formazan} + \text{NAD}^+ \quad \text{(Eq. 18.8)}$$

NADH formation can be measured spectrophotometrically at 340 nm. In other methods, Equation 18.8 has been added so that absorbance readings can be made in the 500- to 600-nm region of the spectrum, using instruments that are more commonly available in the clinical laboratory.

In a common variation, the glycerophosphate formed in Equation 18.6 is oxidized by the action of glycerophosphate oxidase:

$$\text{Glycerophosphate} + \text{O}_2 \xrightarrow[\text{oxidase}]{\text{Glycerophosphate}} \text{Dihydroxyacetone} + \text{H}_2\text{O}_2 \quad \text{(Eq. 18.9)}$$

The resulting H_2O_2 is measured as described previously for cholesterol methods (Eq. 18.3).

In a third approach, adenosine diphosphate (ADP) rather than glycerophosphate is formed in Equation 18.6, and is quantified:

$$\text{ADP} + \text{Phosphoenolpyruvate} \xrightarrow{\text{Pyruvate}} \text{ATP} + \text{Pyruvate} \quad \text{(Eq. 18.10)}$$

$$\text{Pyruvate} + \text{NADH} + \text{H}^+ \xrightarrow[\text{dehydrogenase}]{\text{Lactate}} \text{Lactate} + \text{NAD}^+ \quad \text{(Eq. 18.11)}$$

In this method, the disappearance of NADH is measured at 340 nm.

Enzymatic TG methods generally perform well. The reagents are available commercially as lyophilized preparations that need only to be reconstituted before use. Based on recent College of American Pathologists (CAP) surveys, the interlaboratory coefficients of variation (CVs) for TG measurement using a variety of enzymatic methods were about 5% to 6%. It is prudent before selecting an enzymatic method to evaluate its accuracy and precision over the range of triglyceride concentrations likely to be encountered most frequently (1.299–12.987 mmol/L; 50–500 mg/dL).

Triglyceride Blanks

Enzymatic measurements of triglyceride involve the generation and measurement of glycerol. Although phospholipids and glucose do not interfere with enzymatic methods, free glycerol does. Glycerol is normally present in plasma in concentrations below 0.163 mmol/L (1.5 mg/dL) equivalent to a triglyceride concentration of about 14 mg/dL. However, concentrations can be higher in the following circumstances: after extremely vigorous exercise; in patients with uncontrolled diabetes; after chance contamination with the glycerol lubricant used on the stoppers of some blood collection tubes; after recent ingestion of glycerol-containing medications; or in a relatively rare disorder, hyperglycerolemia, which arises secondary to a mutation in the glycerol kinase gene on chromosome Xp21.3. A blank assay, without the addition of lipase, provides a measure of preexisting glycerol. Increased readings in the blank indicate the presence of glycerol; measured TG values can be corrected accordingly. In an alternative procedure, free glycerol is consumed in a preliminary reaction before triglyceride hydrolysis is initiated. In this case, the measured value is the equivalent of a blanked triglyceride.

The blanking procedures described earlier are satisfactory for correcting spurious measurements that arise from many glycerol sources but not for those that result from partial glycerides (diglycerides and monoglycerides). Partial glycerides are generally present at very low concentrations in fresh plasma or serum but can form through the slow hydrolysis of triglycerides when samples are stored. It is not clear whether partial glycerides in fresh plasma should be subtracted, but those that form during storage probably should not be subtracted because they arise from triglycerides that were originally present in the sample.

Fortunately, as complex as the blanking problem is, it is usually of little practical importance. Blanks are not determined routinely in many laboratories, and their use continues to be a matter of uncertainty. When measured, the magnitude of the blanks encountered in most fresh samples is on the order of 0.056 to 0.112 mmol/L (5–10 mg/dL), expressed as triglyceride, although they can be higher in samples with high triglyceride concentrations. However, blanks can assume importance in the standardization and quality control of triglyceride measurements because they can be about 0.226 to 0.339 mmol/L (20–30 mg/dL) or greater in serum pools used for these purposes. This is probably a result of the partial hydrolysis of triglycerides during preparation of the pools.

Interfering Substances

As with cholesterol measurement interference, TG measurement is subjected to similar interference by the same substances. Plasma ascorbic acid is an antioxidant that can interfere with the oxidation/reduction reactions involved in the measurement of TG. Bilirubin can also cause interference, both spectrally and chemically. Significant plasma hemolysis can spectrally interfere with TG measurements and may cause the dilution of lipid constituents.

Phospholipids

Most of the phospholipid in human plasma is phosphatidylcholine (70%–75%) or sphingomyelin (18%–20%). Remaining phospholipids include phosphatidylserine, phosphatidylethanolamine (3%–6%), and lysophosphatidylcholine (4%–9%). Phospholipid measurement is not routinely performed in the clinical laboratory. The reason for this is that phospholipid analysis usually provides little additional information in cases of dyslipoproteinemia. Another reason is that the phospholipid concentration in plasma is not altered as markedly as that of cholesterol and TG in various pathologic conditions. However, estimation of lipoprotein phospholipids provides information that at times can be more important than cholesterol or TG concentrations. For example, only 10% to 20% of the total weight of HDL is cholesterol, but almost 25% to 30% of it is phospholipids, making it a far more accurate reflection of HDL content (Rifai et al., 2000). Furthermore, the phospholipid content of HDL is more important than cholesterol or even apolipoprotein A-I in reverse cholesterol transport; abnormalities in HDL phospholipid composition have been noted to have a greater effect on HDL function than cholesterol concentration. Phospholipids are also important substrates for a number of lipoprotein metabolizing enzymes (e.g., LCAT, LPL, HL); therefore, changes in the composition could adversely affect the function of these enzymes. Most important, the dietary status of essential fatty acids is more accurately assessed by the fatty acid composition of phospholipids rather than total lipids. It has also been noted that the saturated fatty acid content of plasma phospholipids is reported to be an independent risk factor for atherosclerosis.

The only unique structural feature common to all phospholipids is the presence of lipid-bound phosphate. Therefore, most of the methods originally designed to determine plasma phospholipids depend on the estimation of lipid phosphorus. Lipids are extracted from the sample and are oxidized completely to convert phospholipid phosphorus to inorganic phosphate, which is then determined colorimetrically. These procedures are reproducible and sensitive and can be adapted to measure total phospholipid phosphorus in 100 μL or less of plasma or serum. Each mole of phosphorus contributes about 4% to the total phospholipid mass; thus, phospholipid mass can be determined by multiplying the phospholipid phosphorus concentration (expressed in mg/dL) by 25.

Serum or plasma phospholipids can also be measured enzymatically using commercially available methods. In the method available from WAKO Pure Chemical Industries, Ltd. (Osaka, Japan), lecithin (phosphatidylcholine), sphingomyelin, and lysolecithin are hydrolyzed using phospholipase D, and the choline liberated is oxidized.

$$\text{Phospholipid} \xrightarrow{\text{Phospholipase D}} \text{Choline} \quad \text{(Eq. 18.12)}$$

$$\text{Choline} \xrightarrow[\text{oxidase}]{\text{Choline}} \text{Betaine} + \text{H}_2\text{O}_2 \quad \text{(Eq. 18.13)}$$

The resulting H_2O_2 produced is measured in a manner similar to that shown in Equation 18.3. Analysis of individual phospholipid classes is seldom required for evaluation of dyslipoproteinemia and is not discussed in this chapter.

ESTIMATION OF LIPOPROTEINS AND LIPOPROTEIN CHOLESTEROL

Because lipoproteins share common lipid and apolipoprotein components, the central problem in lipoprotein analysis is the separation of different lipoprotein classes from one another. Many methods have been applied to lipoprotein separation, including ultracentrifugation, adsorption, gel filtration, affinity chromatography, electrophoresis in various media, polyanion and alcohol precipitation, immunochemical procedures, and various combinations of methods. Some of these methods require special skills and

equipment and are not easily adapted for clinical or epidemiologic purposes. This discussion is limited to several procedures that have been used by clinical laboratories.

ULTRACENTRIFUGATION METHODS

These take advantage of two properties of lipoproteins. First, by virtue of their lipid content, lipoproteins have lower densities than other plasma macromolecules. Second, each class of lipoproteins has a different density. Thus, lipoproteins can be readily separated on the basis of their densities by using ultracentrifugation techniques. The proportion of lipids, in particular TG, associated with appropriate proteins determines the density of a particular lipoprotein class. VLDL and CMs are the most lipid-rich lipoprotein classes in human blood. This fact leaves them as the most buoyant in plasma. These lipoproteins have a density of less than 1.006 kg/L (density measurement). LDL particles are smaller in size and in lipid content, causing their density to range from 1.006 to 1.063 kg/L. HDL, the densest lipoprotein, ranges from 1.063 to 1.210 kg/L (Rifai et al., 2000). Ultracentrifugation methods are considered the best means to compare lipoprotein classes. However, the technique is difficult, time-consuming, and expensive, leaving it for research settings rather than clinical measurement.

ELECTROPHORETIC METHODS

In the past, electrophoresis was widely used in the clinical laboratory to separate and measure lipoproteins. However, because the method has significant limitations (described later), it generally is not required for the diagnosis of dyslipoproteinemia and its use in routine clinical practice has diminished in recent years. In general, the cost of the procedure, in terms of both time and money, is rarely justified by the information provided.

The most commonly used support medium for lipoprotein electrophoresis is agarose gel because of its speed, sensitivity, and ability to resolve the lipoprotein classes. CMs, if present, remain at the origin. Of the remaining major lipoproteins, HDL migrates the fastest, LDL the slowest, and VLDL at a rate intermediate between HDL and LDL. The electrophoretically separated lipoproteins have been named according to their mobilities: HDL (α-lipoprotein) moves with the α_1-globulins; LDL (β-lipoprotein) migrates with the β-globulins, and VLDL (pre-β lipoprotein) migrates with the β_2-globulins. Different properties of lipoproteins form the basis for electrophoretic and ultracentrifugal separation; analogous fractions separated by the two techniques may not be identical. For example, β-VLDL (found in type 3 hyperlipidemia; see later discussion) is isolated with VLDL by ultracentrifugation but moves electrophoretically with LDL. In the absence of additional information, a sample containing β-VLDL would appear to have an elevated VLDL concentration by ultracentrifugation and an increased LDL concentration by electrophoresis. Another example is that Lp(a) is isolated in the LDL–HDL density range by ultracentrifugation, but it has an electrophoretic mobility similar to that of VLDL. This dichotomy is responsible for naming Lp(a) "sinking pre-β-lipoprotein."

Electrophoresis can be performed using unfractionated plasma or in plasma fractions that contain other serum proteins. Lipoprotein electrophoretograms are usually visualized with a lipid-staining dye such as Oil Red O, Fat Red 7B, or Sudan Black B. These lipid stains react primarily with the ester bonds in triglycerides and cholesteryl esters. Lipoproteins rich in free cholesterol and phospholipids (such as LpX) stain very poorly and thus are grossly underestimated by electrophoretic techniques.

POLYANION PRECIPITATION METHODS

Some lipoproteins are precipitated with polyanions such as heparin sulfate, dextran sulfate, phosphotungstate, and others in the presence of divalent cations such as Ca^{++}, Mg^{++}, and Mn^{++}. Conditions have been established in which the major classes of lipoproteins can be precipitated in stepwise fashion beginning with the lower-density, lipid-rich lipoproteins (Burstein & Legmann, 1982). The more dissimilar the lipoproteins are from one another, the better the separation. Thus, it is easier to separate B-Lps from HDL than it is to separate VLDL from LDL or HDL_2 from HDL_3. Historically, polyanion precipitation was most commonly used to remove B-Lps before analysis of HDL-C. This requires a sample pretreatment that is not fully automated. Most clinical laboratories have replaced precipitation techniques with automated homogeneous assays for HDL-C and LDL-C.

DETERMINING HDL-C VALUES

Epidemiologic studies have shown and current guidelines recognize HDL-C as an independent risk factor for CHD and recommend its measurement in conjunction with TC measurements. Historically, HDL-C has been measured in the supernatant of samples following the precipitation of B-Lps by polyanion-divalent cations. Several combinations of polyanion-divalent cations have been used, and not all of them give precisely the same results. HDL-C values determined with heparan sulfate–Mn^{++} procedures agree closely with those obtained using analytic or preparative ultracentrifugation (Bachorik et al., 1976; Warnick et al., 1979). This method was widely used in epidemiologic studies. Dextran sulfate (relative molecular mass 50,000 Da)–Mg^{++} and sodium phosphotungstate–Mg^{++} methods gained popularity because they do not interfere with enzymatic cholesterol studies. However, they give results about 5% lower than ultracentrifugation. Heparin-Ca^{++} appears to give results that are about 10% higher. Moreover, the use of different concentrations of cation may give different estimates of HDL-C. These differences arise, in part, from the underprecipitation of B-Lps, which leads to overestimation of HDL-C, or the overprecipitation of HDL, which can lead to underestimation of HDL-C. Increased triglycerides interfere with precipitation methods and overestimate HDL-C. Attempts were made to simplify precipitation methods by using dextran sulfate–coated magnetic beads to achieve selective separation of HDL from the B-Lps (Naito & Kwak, 1995).

Currently, homogeneous assays are the most popular method for measuring HDL-C. Unlike precipitation methods, these fully automated two-reagent procedures do not require offline pretreatment and separation (hence the term *homogeneous*) and can be adapted to most chemistry analyzers. Thus, they reduce hands-on time and overall assay costs. Test kits distributed in the United States are based on a variety of methods. Usually, the first reagent forms a stable complex with non-HDL lipoproteins, preventing them from participating in the reaction, and the second reagent releases HDL-C that is then measured enzymatically. According to CAP 2005 surveys, the most common method uses a synthetic polymer together with a polyanion to block non-HDL lipoproteins, followed by a selective detergent to release HDL-C (Genzyme Diagnostics, Cambridge, MA; Beckman Coulter, Inc., Brea, CA). Other methods use polyethylene glycol–modified enzyme (Roche Diagnostics, Indianapolis) or immunoinhibition (Wako Chemicals USA, Inc., Richmond, VA) to block non-HDL lipoproteins. A fourth method (Polymedco Inc., Cortlandt Manor, NY) uses a special reagent to selectively eliminate cholesterol in non-HDL lipoproteins, followed by a second reagent that releases cholesterol from HDL (Denka Seiken Co., Niigata, Japan). These methods generally are not affected by high triglycerides, bilirubin, and globulins. See Chapter 28 for further discussion of methods that distinguish HDL and LDL cholesterol.

In a comprehensive review (Warnick et al., 2001), multiple HDL-C homogeneous assays were compared with traditional precipitation and ultracentrifugation procedures. The authors concluded that the new procedures simplify the determination of HDL-C and are accurate, precise, and meet NCEP criteria for total error. However, atypical lipoproteins evaluated by homogeneous assay may show discrepant results when compared with the established precipitation method. These differences are seen in patients with hyperlipidemia or liver or kidney disease when abnormal lipoprotein forms occur. Laboratories that encounter a high proportion of atypical lipoproteins (e.g., lipid clinics or research settings) should thoroughly validate a homogeneous assay for use with their patient population.

LDL-C MEASUREMENT

LDL cholesterol plays a causal role in the development of atherosclerosis. Several methods have been used to measure LDL-C. The first, a reference laboratory procedure, involves ultracentrifugation to separate LDL from other lipoproteins, followed by analysis as described previously to measure cholesterol. This method is not extensively discussed here. A much more common method uses the Friedewald formula to calculate LDL-C. The Martin-Hopkins formula for the estimation of LDL-C has also been implemented with improved accuracy over the Friedewald calculation in certain clinical circumstances and will be discussed later. Finally, homogeneous methods for measuring LDL-C are also available, as discussed in Chapter 28.

FRIEDEWALD AND MARTIN-HOPKINS CALCULATION

LDL-C can be determined by using the Friedewald formula, originally described by Friedewald, Levy, and Fredrickson (Friedewald et al., 1972). Generally, in fasting plasma samples, LDL contains the cholesterol that is not present in HDL or VLDL. Thus, LDL-C can be determined by the following equation in which concentrations are expressed in mmol/L, and the term *[Plasma TG]/2.175* is used to represent VLDL-C:

$$[\text{LDL} - \text{cholesterol}] = [\text{Total cholesterol}] - [\text{HDL} - \text{cholesterol}] - [\text{Plasma TG}]/2.175.$$

The term *[Plasma TG]/5* is used when concentrations are expressed in mg/dL. In this method, the plasma TC, TG, and HDL-C concentrations are determined as described. Because VLDL carries most plasma triglyceride, VLDL-C concentration is estimated from the ratio of triglyceride to cholesterol in VLDL:

$$\text{VLDL} - \text{C} = \text{Plasma TG}/2.175.$$

The Friedewald formula has significant limitations (Sniderman et al., 2003). These limitations arise largely from two assumptions on which the method is based. First, the calculation assumes that essentially all plasma triglycerides are carried in VLDL. Second, the method assumes that the triglyceride/cholesterol ratio of VLDL is invariant. Neither assumption is entirely true; as a result, this method is unsuitable for nonfasting samples that contain CMs or samples that contain β-VLDL. As compared with VLDL, the ratio of triglycerides to cholesterol in CMs is much higher. Thus, when CM is present, the use of the factor TG/2.175 to account for non-HDL cholesterol can overestimate the amount of cholesterol in VLDL, leading to underestimation of LDL-C. Similarly, the ratio of triglyceride to cholesterol in β-VLDL is much lower than in VLDL; use of the factor TG/2.175 in the presence of β-VLDL can underestimate VLDL-C and thus overestimate LDL-C. A patient with type 3 hyperlipoproteinemia can be misclassified as having an elevated LDL-C. It is important to distinguish the two conditions because their treatments differ.

Even in CM-free samples, the ratio of VLDL-C to triglyceride changes as triglyceride levels increase, which can lead to errors in estimates of VLDL-C. Because VLDL generally carries only about 25% of the TC in plasma, resulting errors in LDL-C are usually less than 5 to 10 mg/dL (0.130–0.260 mmol/L). However, the calculation is not suitable for samples with high triglyceride concentrations. Errors in LDL-C become noticeable at triglyceride levels over 2.26 mmol/L (200 mg/dL) and become unacceptably large at triglyceride levels over 4.52 mmol/L (400 mg/dL). The accuracy of LDL-C calculation also suffers at low LDL-C levels, indicating that calculated LDL-C values may not provide the best assessment of cardiac risk in patients who already are receiving cholesterol-lowering therapy (Sniderman et al., 2003). If its limitations are appreciated, the Friedewald equation has broad utility, both as a screening tool and for following patients.

Given these limitations, Martin and colleagues have derived and validated a novel method to estimate LDL-C. Rather than assuming a fixed factor of 2.175, this method applies an adjustable factor for the TG:VLDL-C ratio based on triglyceride and non-HDL-C concentrations. This approach led to improved accuracy in LDL-C determinations as compared with Friedewald estimates. The overall accuracy of the Martin-Hopkins equation compared with direct ultracentrifugation was 92% as opposed to 85% for the Friedewald estimation. Improved accuracy is preserved across all ranges of LDL-C. A significant clinical advantage of this equation is in classification of LDL-C concentrations less than 70 mg/dL, particularly in individuals with hypertriglyceridemia (Martin et al. 2013). The Martin-Hopkins calculation has received external validation in several studies (Chung, 2019).

Another issue to consider is non-LDL lipoproteins. Generally, LDL contributes most of the cholesterol to the measurement, and IDL and Lp(a) contribute only a few mg/dL each. However, these lipoproteins can contribute significantly to cholesterol measurements in some hyperlipidemia patients. Because Lp(a) levels are not lowered by a number of treatments that effectively lower LDL levels, Lp(a) measurements can, in some circumstances, reveal why a patient does not respond well to LDL-lowering therapy.

SELECTIVE CHEMICAL PRECIPITATION

LDL-C is calculated as the difference between TC and the amount remaining after precipitation of LDL-C. Such methods are reasonably accurate if TG concentrations are low enough. However, this method allows only for the separation of B-Lps, separating HDL from non-HDL particles.

DIRECT LDL-C MEASUREMENT

Largely, the ability to calculate LDL-C has eliminated the need for direct measurements. However, homogeneous direct LDL-C methods are useful when triglycerides are elevated because they are not subject to interference by triglycerides even at relatively high concentrations (600 mg/dL) (Bachorik, 2000). Direct assays have been adapted for use on a variety of analyzers and have been reviewed (Nauck et al., 2002; Miller et al., 2002). Although these methods differ significantly, in general, they use a combination of two reagents. The first reagent usually selectively removes non-LDL lipoproteins (and/or stabilizes or inhibits LDL from reacting with enzymes). The second reagent releases cholesterol from LDL so that it can be measured enzymatically.

In one method (Equal Diagnostics, Exton, PA; Genzyme Diagnostics), the first reagent uses a detergent polymer mixture to disrupt non-LDL lipoproteins, releasing their cholesterol. The cholesterol is then deesterified and reacts with cholesterol oxidase to generate hydrogen peroxide, which reacts to form a colorless compound. The second reagent contains a detergent that releases cholesterol from LDL. After deesterification, the LDL-C proceeds through a similar set of reactions, except that the final step generates a colored compound. The intensity of the color is proportional to the concentration of LDL-C. Another method (Roche Diagnostics) is based on selective micellary solubilization of LDL by a nonionic detergent as well as the interaction of a sugar compound with HDL, VLDL, and CMs to inhibit participation in the measurement assay (Sugiuchi et al., 1998). A third method exploits the fact that reactivity of cholesterol in the different lipoproteins is affected by the hydrophile:lipophile balance (HLB) of solubilizing detergents. In this method, as discussed in Chapter 28, non–LDL-C is reacted with cholesteryl esterase and cholesterol oxidase in conditions in which LDL-C is inhibited, and the resulting peroxide is eliminated by catalase. A second reagent then alters the HLB of the detergent, creating conditions in which LDL-C reacts. This reagent also contains an azide that inhibits catalase and allows the colorimetric detection of peroxide (see Eq. 18.3) (Polymedco Inc.; Reference Diagnostics, Bedford, MA). In a fourth method, the first reagent contains amphoteric surfactants that protect LDL, allowing the elimination of non–LDL-C and resulting peroxide as described earlier. The second reagent contains nonionic surfactants that displace the protecting surfactants and allow measurement of LDL-C (Sigma Diagnostics, St. Louis, MO).

Although these methods are precise, they produce discrepancies in comparison with the reference ultracentrifugation procedures in a number of circumstances, including the presence of abnormal lipoproteins. When the triglyceride level is less than 400 mg/dL, homogeneous methods perform no better than the Friedewald calculation for classifying patients into treatment groups (Miller et al., 2002). However, unlike the Friedewald calculation, homogeneous assays can provide clinically useful results when triglycerides are over 400 mg/dL. Alternatively, as mentioned before, the Martin-Hopkins estimation of LDL-C can be applied with accuracy in this scenario.

ADDITIONAL METHODS IN THE STUDY OF DYSLIPIDEMIA

MEASUREMENT OF LIPOPROTEIN PARTICLE NUMBER

Each apoB-containing lipoprotein has one apoB molecule; therefore, serum concentration of apoB reflects the LDL particle number closer than LDL-C level. It has been claimed that serum apoB concentration is a stronger indicator for CHD prediction. In contrast, serum apoA-I concentration does not reflect the HDL particle number (HDL-P). HDL-P shows stronger association with CVD risk compared with apoA-I levels. The most popular method in measuring LDL- and HDL-P is nuclear magnetic resonance (NMR) spectroscopy (see Chapter 4).

MEASUREMENT OF LIPOPROTEIN SUBCLASSES

Subpopulations or subclasses have been identified in VLDL, LDL, and HDL by techniques such as analytic ultracentrifugation, gradient gel electrophoresis, and NMR spectroscopy (Krauss, 1987; Krauss & Blanche, 1992; Otvos et al., 1992). Some subclass distinctions are of clinical significance, yet the number of subclasses identified varies among methods of separation, and the nomenclature for subclasses is less than uniform. For example, when NMR technology is used to identify lipoprotein subclasses, particle subclass numbers tend to increase with increasing particle size; thus, LDL particles of the L2 subclass are larger than L1 particles. When electrophoresis or ultracentrifugation is used, the opposite is true, and particles tend to decrease in size with higher numbers. Thus, in segmented gradient gel electrophoresis, LDL subclass IV (or LDL4) particles are smaller than subclass II (LDL2) particles; in gradient ultracentrifugation, subclass LDL4 particles are smaller than LDL3 particles.

Interest has focused on the role of subclasses in the development of atherosclerosis, specifically the smallest and least dense LDL particles. This fraction is thought to be more atherogenic than large LDL. Small

HDL and large VLDL subclasses have also been associated with an increased incidence of atherosclerosis. The NMR Lipoprofile (LipoScience, Raleigh, NC) allows the quantification of lipoprotein particles by subclass based on their unique NMR-spectral characteristics. This profile provides information about CHD risk by quantifying the subclass distribution of lipoprotein particles (Otvos, 2002). At least partially, the appeal of this technique arises from the idea that the migration of LDL particles into the artery wall is gradient driven based on the LDL particle number. When large numbers of small LDL particles are present, LDL-C measurements tend to underestimate the number of LDL particles and thus the atherosclerotic effects of LDL. Triglyceride levels over 100 mg/dL and HDL-C less than 60 mg/dL are associated with high levels of small LDL particles; when these conditions are present, NMR profiling may be a useful technique for assessing CHD risk. Sensitive electrophoretic methods should provide similar results. These methods are not currently viewed as screening tools. They are more appropriate for refining risk assessment and treatment in patients with previously identified CHD risk: those under treatment and patients who have LDL-C values at or close to treatment goals. This is consistent with most accepted guidelines that stress the importance of LDL-C as the primary goal of therapy in most types of dyslipidemia.

HDL is also highly heterogeneous. HDL_2 and HDL_3 are defined according to density and particle size by sequential ultracentrifugation. NMR divides them into large, intermediate, and small HDL. In two-dimensional electrophoresis, HDL is separated into several subpopulations, such as α1, α2, α3, α4, pre-β1, pre-β2, and pre-β3. Different subpopulations of HDL exhibit different functionalities. For example, small, dense HDL is potent in cholesterol efflux via ABCA1, and large HDL is potent in cholesterol efflux via ABCG1 and SR-B1. Small, dense HDL plays a major role in antioxidative activity (Kontush & Chapman, 2006).

STANDING PLASMA TEST

CMs, if present in appreciable quantities, are detected using the "standing plasma" test. An aliquot of plasma (2 mL) in a 10 × 75 mm test tube is allowed to stand in the refrigerator at 4° C undisturbed overnight. CMs accumulate as a floating "cream" layer and can be detected visually. The presence of CMs in fasting plasma is considered to be abnormal. A plasma sample that remains turbid after standing overnight contains excessive amounts of VLDL; if a floating "cream" layer also forms, CMs are present as well.

DETECTION OF β-VLDL AND LP(A)

As mentioned earlier, the abnormal lipoprotein β-VLDL has the density of VLDL but migrates electrophoretically with LDL in the β-region. It can be detected when the ultracentrifugal fraction of d < 1.006 kg/L is examined electrophoretically. In practice, unfractionated plasma and both ultracentrifugal fractions (< and >1.006 kg/L) are examined at the same time. Each sample thus serves as its own control to establish the relative migration of the lipoprotein bands. In normal plasma, the β (LDL and IDL), pre-β (VLDL), and α (HDL) lipoprotein bands are visible in unfractionated plasma; only the pre-β band is present in the d < 1.006 kg/L fraction, and the β- and α-lipoprotein bands are seen in the d > 1.006 kg/L fraction. When present, β-VLDL is observed as a band with β-mobility in the d < 1.006 kg/L fraction. Its presence is abnormal and is usually associated with dysbetalipoproteinemia (type 3 hyperlipoproteinemia), although occasionally it is seen in other disorders. CMs, which often are seen in type 3 patients, remain at the origin on agarose gel.

Lp(a) has a density similar to LDL, but it migrates similarly to VLDL on electrophoresis. Thus, it can be detected when the d > 1.006 g/mL protein is examined electrophoretically. When Lp(a) is present in concentrations exceeding 20 to 30 mg/dL (i.e., when it contributes to more than 10 mg/dL to the LDL-C measurement), an additional band with pre-β mobility is observed in the d > 1.006 kg/L fraction (hence the name "sinking pre-β-lipoprotein"). Under these conditions, the physician may wish to request a quantitative Lp(a) measurement. Lp(a) can now be measured using immunoturbidimetric methods. When the Lp(a) level is very high, it may be necessary to correct LDL-C for the contribution of Lp(a)-cholesterol. The following relationship has been used to estimate the contribution of Lp(a)-cholesterol to the measured LDL-C value, where the values are given in mg/dL:

$$\text{Lp(a)-cholesterol} = 0.3 \times [\text{Lp(a) mass}]$$

$$\text{LDL C} = \text{TC} - [\text{HDL-cholesterol}] - [\text{Plasma TG}]/5 - (0.3\,[\text{Lp(a) mass}]).$$

VLDL-C/PLASMA TRIGLYCERIDE RATIO

The ratio of VLDL-C to plasma triglycerides may be useful in the evaluation of type 3 hyperlipoproteinemia. This ratio, expressed in mol/mol or (mass/mass), is generally in the range of 0.230 to 0.575 (0.10–0.25) in samples without β-VLDL, depending on the relative amounts of VLDL, LDL, and HDL present, and on the errors inherent in the VLDL-C and plasma triglyceride measurements. Type 3 subjects have ratios greater than 0.689 (0.3), usually in the range of 0.689 to 0.919 (0.3–0.4), and higher ratios can be observed. Again, because of errors in the measurements, the observation of a ratio of 0.689 (0.3) on a single occasion may or may not be significant. Overt type 3 patients manifest both β-VLDL and a VLDL-C/plasma triglyceride ratio of 0.689 (0.3) or greater. Occasionally, a lipid disorder treatment clinic may request the assessment of apoE phenotype to supplement the diagnosis of type 3 hyperlipoproteinemia (see later discussion), because homozygosity for apoE-2 is associated with this disorder. However, not all homozygous patients have type 3 hyperlipoproteinemia, and ultracentrifugation is still required for assessing the presence of β-VLDL.

Apolipoprotein Analysis

Studies have indicated that apoA-I and apoB may be better discriminators of atherosclerotic disease than lipid or lipoprotein determinations. Because apoA-I is present primarily in HDL while apoB (in fasting samples) is present in VLDL, IDL, and LDL, it stands to reason that low apoB and high apoA-I levels, as well as a low apoB–to–apoA-I ratio, would be a good thing. In general, the evidence for this has been more consistent for apoB than for apoA-I, but the reason for this is not clear. A large-scale, placebo-controlled intervention trial, AFCAPS (Gotto et al., 2000), found that apoB was the best single lipid, lipoprotein, or apolipoprotein measurement to predict both baseline and on-treatment coronary artery disease risk, followed by apoA-I. ApoB–to–A-I ratios may also be useful in assessing risk.

Apolipoproteins are usually measured by immunoassay, such as immunonephelometry. These techniques rely on measurement of the turbidity caused by apolipoprotein–antibody complexes (Lopes-Virella et al., 1980). A potential limitation of this method stems from the inherent turbidity of lipemic samples or even nonlipemic samples after repeated freezing and thawing. To some extent, automated systems can correct for such turbidity. Now, enzyme-linked immunosorbent assay (ELISA)–based assays are becoming available that are better in laboratory settings.

Modified Lipoprotein

Researchers first noted the enrichment of oxidized lipoproteins in atherosclerosis lesions from both human and animal models decades ago. Native LDL does not accumulate in macrophages. Also, when the intracellular cholesterol level is high, LDLR and the key enzyme in cholesterol biosynthesis, HMG-CoA reductase, will be downregulated as a negative feedback regulation to keep the intracellular cholesterol level under control. It is believed that oxidized LDL (oxLDL) is taken up by scavenger receptors in macrophages, which causes lipid accumulation, as the early stage of foam cell formation. Reactive oxygen species (ROS)–induced lipid peroxidation and lipoxygenase expressed in cells might be the main source of oxLDL. It is well accepted that the plasma level of oxLDL is a marker for CHD risk. A sensitive ELISA with monoclonal antibodies specific to oxLDL has been developed to quantify its concentration in plasma. In chow diet–fed apoE knockout mice, the plasma level of oxLDL showed a transient peak before the onset of atherosclerosis (Kato et al., 2009). Oxidized HDL is commonly considered as dysfunctional because native HDL is protective to atherosclerosis. HDL isolated from human atherosclerotic lesions is rich in nitrotyrosine- and chlorotyrosine-containing apoA-I (Bergt et al., 2004; Zheng et al., 2004). Both of these modifications of tyrosine in apoA-I are produced by a heme-containing enzyme myeloperoxidase (MPO), which is present in inflammatory conditions (Mohiuddin et al., 2006). Modified HDL shows reduced ABCA1-mediated cholesterol efflux capacity from macrophages. One population study shows that fasting plasma glucose significantly and positively associates with the oxHDL level in plasma (Kotani et al., 2012). Therefore, the measurement of oxidized lipoproteins might be a useful marker of CHD.

RELIABILITY OF MEASUREMENTS

Previous NCEP guidelines shifted the focus from recognizing abnormal and normal cholesterol values to assessing overall cardiovascular risk based on cutoffs for cholesterol, triglycerides, HDL-C, and LDL-C. The adoption of a single set of cutoffs imposes a mandate on clinical laboratories to measure lipids and lipoproteins accurately and precisely. The

Laboratory Standardization Panel of NCEP (NCEP, 1995) guidelines are presented in Table 18.8. Note that each test has a single maximum acceptable value for total error that includes assay bias (i.e., a measure of accuracy) and CV (i.e., a measure of imprecision). Total error is calculated as follows:

$$\%\ \text{total error} = \%\ \text{bias} + 1.96\,(\%\text{CV}).$$

For each test, Table 18.8 provides an example of a target bias and CV that, when considered together, would yield the maximum acceptable total error. Note that by using total error, a laboratory can slightly exceed the limit for bias provided that the CV is sufficiently small to maintain the total error within the guideline (the opposite is also true). For example, cholesterol has a target bias of 3% and a target CV of 3%. A laboratory with a bias of 3.5% and a CV of 2% exceeds the target for bias, even though it still meets the target for CV. However, the total error of 7.5% (i.e., 3.5% + 1.96 × 2%) is acceptable because it is less than the 9% target.

HYPERTRIGLYCERIDEMIA

Triglyceride levels are classified as normal (<150 mg/dL), borderline high (150–199 mg/dL), high (200–499 mg/dL), or very high (≥500 mg/dL) based on measurement after a 12-hour fast. The 2011 AHA scientific statement on triglycerides and CVD reaffirms that triglyceride is an important biomarker of CVD risk rather than a directly atherogenic factor (Miller et al., 2011). Causes of very high triglycerides that may be associated with pancreatitis include genetic disorders (LPL deficiency, apolipoprotein C-II deficiency, apolipoprotein A-V deficiency, GPIHBP1 deficiency, Marinesco-Sjögren syndrome, familial hypertriglyceridemia); acquired disorders of the metabolism (hypothyroidism, pregnancy, poorly controlled insulinopenic diabetes); drugs (α-interferon, atypical antipsychotics, β-blockers such as atenolol, bile acid resins, L-asparaginase, estrogens [oral, not transcutaneous]); protease inhibitors; raloxifene; retinoic acid drugs; sirolimus; steroids; tamoxifen; thiazides; diet (alcohol excess, especially with a high–saturated fat diet); and other diseases (autoimmune chylomicronemia [e.g., antibodies to LPL, SLE], chronic idiopathic urticaria, renal disease). Measurement of non–HDL-C, apoB, or both are especially useful in those with obviously abnormal triglyceride/HDL because LDL-C measurements may underestimate atherosclerotic vascular risk. Use of triglyceride-lowering drugs to treat individuals with triglyceride levels of 500 mg/dL or higher is justified to prevent pancreatitis in conjunction with therapeutic lifestyle change. As monotherapy, fibrates can reduce triglyceride levels by 30% to 50%, immediate-release niacin by 20% to 50%, omega-3 methyl esters by 20% to 50%, extended-release niacin by 10% to 30%, statins by 10% to 30%, and ezetimibe by 5% to 10%.

TABLE 18.8

NCEP Guidelines for Acceptable Measurement Error

Analyte	Total Error	Bias	CV*
Cholesterol	≤9%	≤3%	≤3%
Triglyceride	≤15%	≤5%	≤5%
HDL-cholesterol	≤13%	≤5%	≤4%†
LDL-cholesterol	≤12%	≤4%	≤4%

HDL, High-density lipoprotein; *LDL,* low-density lipoprotein; *NCEP,* National Cholesterol Education Program.
*Coefficient of variation defined as standard deviation/mean × 100.
†Precision criteria applied to HDL-cholesterol levels of 42 mg/dL (1.09 mmol/L) and higher. At lower levels, CV is not used; rather, standard deviation should not exceed 1.7 mg/dL (0.044 mmol/L).

GUIDELINES FOR CHOLESTEROL TESTING AND MANAGEMENT

ESTIMATING RISK FACTORS

The 2013 American College of Cardiology/American Heart Association (ACC/AHA) guidelines developed new equations to estimate the 10-year risk of developing a first ASCVD event (CHD death, nonfatal myocardial infarction, and fatal or nonfatal stroke), using the best available data from community-based cohorts of adults. The 2018 ACC/AHA Task Force on Clinical Practice Guidelines used state-of-the-art statistical methods to derive and internally validate the Pooled Cohort Equations, which provide sex- and race-specific estimates of the 10-year risk of ASCVD for African American and white men and women aged from 40 to 79. The variables included in the equations are age, TC, HDL-C, systolic BP (including treated or untreated), diabetes, and current smoking status. If a risk-based treatment decision is uncertain by the equations, assessment of one or more of the following ASCVD risk enhancers (Box 18.1) as proposed in the 2018 AHA/ACA guidelines is recommended. Further risk refinement can also be applied using coronary artery calcium (CAC) scoring. Coronary artery scoring can reclassify risk upward, particularly when the score is greater than 100 or downward if the score is zero. Most individuals with CAC scores >100 Agatston units will have a 10-year ASCVD risk of >7.5%, a threshold for statin initiation. Statin therapy is also suggested for borderline-risk patients >55 years old with a 10-year ASCVD risk of 5% to <7.5% and a CAC of 1 to 99 Agatston units. Alternatively, an individual with borderline risk and a CAC score of zero suggests low risk for the subsequent 10 years and possibly statin deferment (Greenland et al., 2018).

The 2018 evidence-based guidelines for cholesterol testing and management provide detailed information on other topics, including CHD risk assessment, lifestyle intervention, drug treatment, and treatment adherence issues (Grundy et al., 2019). Previously, in 2013, the ACC/AHA issued guidelines focusing predominantly on evidence from high-quality randomized clinical trials. At that time, there was limited data to support specific LDL-C goals and for the routine use of non-statin therapies. The authors created an algorithm of four groups who were most likely to benefit from either moderate- or high-intensity statin (Andrus & Lacaille, 2014) (Table 18.9 and Box 18.1). The guideline classifies statin therapy as high-intensity (lowers LDL-C by an average of ≥50%), moderate-intensity (lowers LDL-C by an average of 30%–50%), and low-intensity (lowers LDL-C by an average of <30%). Strong evidence indicates that the following four groups of individuals should receive moderate- or high-intensity statin therapy to reduce ASCVD risk:

1. Clinical ASCVD
2. Primary elevations of LDL-C of 190 mg/dL or higher
3. Individuals 40 to 75 years of age with diabetes, LDL-C 70 to 189 mg/dL without clinical ASCVD
4. Individuals without clinical ASCVD or diabetes, age 40 to 75 years, LDL-C 70 to 189 mg/dL, and an estimated 10-year ASCVD risk of 7.5% or greater

The 2018 ACC/AHA guidelines maintained these four treatment groups but also incorporated data from nonstatin-LDL lowering therapies, including PCSK9 inhibitors and ezetimibe. Additionally, specific LDL-C thresholds were implemented based on proven ASCVD outcome data. The recommendation for the use of ezetimibe over PCSK9 inhibitors was based

BOX 18.1

2018 AHA/ACC/ACCVPR/AAPA/ABC/ACPM/ADA/AGS/APhA/ASPC/NLA/PCNA Guideline on the Management of Blood Cholesterol in Adults

A. Heart-healthy lifestyle habits should be encouraged for all individuals across the lifespan.
B. Evaluate for secondary causes of hyperlipidemia if indicated.
C. The appropriate intensity of statin therapy should be initiated or continued with consideration for additional LDL-C–lowering therapies depending on the clinical scenario.
D. Assess adherence, response to therapy, and adverse effects within 4 to 12 weeks following statin initiation or change in therapy and every 3 to 12 months once adherence is established.
E. In individuals intolerant of the recommended intensity of statin therapy, use the maximally tolerated intensity of statin. In individuals with statin-associated symptoms, an assessment of symptoms and evaluation for nonstatin causes and predisposing factors is recommended.
F. Statin therapy is not routinely recommended for individuals with NYHA class II to IV heart failure or who require hemodialysis. However, in patients with heart failure and reduced ejection fraction secondary to ischemic heart disease with a life expectancy of >3 years, consider initiation of moderate intensity statin.

Continued

BOX 18.1

2018 AHA/ACC/ACCVPR/AAPA/ABC/ACPM/ADA/AGS/APhA/ASPC/NLA/PCNA Guideline on the Management of Blood Cholesterol in Adults—Cont'd

Clinical ASCVD*

Treatment Category	Recommended Treatment	Additional Remarks
Age 75 years or less and not meeting criteria for very high risk**	High-intensity statin with aim to reduce LDL-C by 50%	If high-intensity statin not tolerated, use moderate-intensity statin with aim to reduce LDL-C by 30%–49%. If on maximally tolerated statin therapy and LDL-C ≥70 mg/dL, consider adding ezetimibe.
Individuals considered very high risk**	High-intensity statin or maximally tolerated statin	If on maximally tolerated statin and LDL-C is ≥70 mg/dL, consider adding ezetimibe. If on maximally tolerated LDL-C–lowering therapy and LDL-C is ≥70 mg/dL or non–HDL-C is ≥100 mg/dL, adding PCSK9-I is reasonable.
Age >75 years	Initiate moderate- or high-intensity statin following assessment of clinical benefit and risk as well as patient preference.	If already on high-intensity statin, continuation is reasonable.

Primary Prevention (Including Individuals With Severe Hypercholesterolemia and Diabetes Mellitus)

Treatment Category	Recommended Treatment	Additional Remarks
40–75 years of age, LDL-C 70–189 mg/dL (≥1.8–<4.9 mmol/L)	Estimate 10-year ASCVD risk using the Risk Calculator based on the Pooled Cohort Equations (PCE)+ in those not receiving statin; estimate every 4–6 years <5%, low risk: Emphasis on healthful lifestyle to reduce risk factors 5% to <7.5%, borderline risk: Assess for risk enhancers++and consider moderate-intensity statin. >7.5% to <20% intermediate risk: Initiate moderate-intensity statin to reduce LDL-C by 30%–49%. >20%, high risk: Initiate statin to reduce LDL-C ≥50%.	Engage in a clinician-patient discussion of the potential for ASCVD risk reduction, adverse effects, drug-drug interactions and patient preferences. If risk decision is uncertain, consider measuring coronary artery calcium (CAC). CAC = 0: Consider no statin unless family history of premature CHD or cigarette smoking are present). CAC = 1–99: Favors statin (especially after age 55 years) CAC = 100+ and/or 75th percentile: Initiate statin therapy.
20–39 years of age	Consider statin if family history of premature ASCVD and LDL-C ≥160 mg/dL (≥4.1 mmol/L).	Estimate lifetime risk using PCE to encourage lifestyle to reduce ASCVD risk.
0–19 years of age	Lifestyle changes to prevent or reduce ASCVD risk Assess for familial hypercholesterolemia (FH)	Statins may be considered for ages ≥10 years who have FH and have not responded to 3–6 months of lifestyle therapy. Age 8 years in the presence of concerning family history, extremely elevated LDL-C or Lp(a).
Severe Hypercholesterolemia LDL-C >190 mg/dL (4.9 mmol/L)	Begin high-intensity statin without calculating 10-year ASCVD risk.	In patients 21 years or older who achieve <50% reduction in LDL-C while receiving maximally tolerated statin and have LDL-C ≥100 mg/dL (≥2.6 mmol/L), consider adding ezetimibe. In patients who achieve <50% reduction in LDL-C and have fasting triglycerides <300 mg/dL (<3.4 mmol/L) on maximally tolerated statin and ezetimibe therapy, consider the addition of a bile acid sequestrant. In patients with a baseline LDL-C >220 mg/dL (>5.7 mmol/L) or higher and achieve on-treatment (maximally tolerated statin and ezetimibe therapy) LDL-C of >130 mg/dL (>3.4 mmol/L) or higher, consider a PCSK9-I.
Individuals with diabetes 40–75 years of age and LDL-C 70–189 mg/dL (≥1.8–<4.9 mmol/L)	Initiate moderate-intensity statin regardless of estimated 10-year ASCVD risk.	Consider high-intensity statin with aim to reduce LDL-C by 50% when 10-year ASCVD risk using the PCE is ≥7.5% in individuals with multiple risk factors or those 50–75 years of age. In adults with diabetes and a 10-year ASCVD risk of 20% or higher, consider the addition of ezetimibe to maximally tolerated statin to reduce LDL-C by 50% or more.
Individuals with diabetes older than 75 years	Following clinical discussion of potential risks and benefits, consider statin therapy.	In those individuals already on statin therapy, it is reasonable to continue treatment.
Individuals with diabetes 20–39 years of age	Consider statin therapy in individuals with the following qualifiers.+++	

* Clinical ASCVD includes acute coronary syndrome, history of MI, stable or unstable angina, coronary or other arterial revascularization, stroke, transient ischemic attack (TIA), or peripheral arterial disease presumed to be of atherosclerotic origin.

** Clinical ASCVD with very high risk includes those with a history of multiple major ASCVD events or 1 major ASCVD event and multiple high-risk conditions. Major ASCVD event includes recent ACS (within the past 12 months), history of MI (other than recent ACS listed previously), history of ischemic stroke, symptomatic peripheral arterial disease (history of claudication with ankle brachial index (ABI) <0.85, or previous revascularization or amputation). High-risk conditions include: Age ≥65 years, heterozygous familial hypercholesterolemia, history of prior coronary artery bypass surgery or percutaneous coronary intervention outside of the major ASCVD event(s), diabetes mellitus, hypertension, chronic kidney disease (CKD; eGFR 15–59 mL/min/1.73 m^2), current smoking, persistently elevated LDL-C (≥100 mg/dL [≥2.6 mmol/L]) despite maximally tolerated statin therapy and ezetimibe, history of congestive heart failure.

+ PCE can be calculated using this link: http://tools.acc.org/ASCVD-Risk-Estimator-Plus/#!/calculate/estimate/

See text under Estimating Risk Factors

++ ASCVD Risk Enhancers: Family history of premature ASCVD, persistently elevated LDL-C ≥160 mg/dL (≥4.1 mmol/L), chronic kidney disease, metabolic syndrome, conditions specific to women (e.g., preeclampsia, premature menopause), inflammatory diseases (especially rheumatoid arthritis, psoriasis, HIV), ethnicity (e.g., South Asian ancestry), persistently elevated triglycerides ≥175 mg/dL (≥2.0 mmol/L), hs-CRP ≥2.0 mg/L, Lp(a) levels >50 mg/dL or >125 nmol/L, apoB ≥130 mg/dL, ankle-brachial index (ABI) <0.5.

+++ Long duration (≥10 years for type 2 diabetes mellitus or ≥20 years for type 1 diabetes mellitus, albuminuria ≥30 μg of albumin/mg creatinine, eGFR <60 mL/min/1.73 m^2, retinopathy, neuropathy, ABI <0.9.

From Grundy et al., 2019.

AAPA, American Academy of Physician Assistants; *AACVPR,* American Association of Cardiovascular and Pulmonary Rehabilitation; *ABC,* Association of Black Cardiologists; *ACC,* American College of Cardiology; *ACPM,* American College of Preventive Medicine; *ADA,* American Diabetes Association; *AGS,* American Geriatrics Society; *AHA,* American Heart Association; *APhA,* American Pharmacists Association; *ASCVD,* atherosclerotic cardiovascular disease; *ASPC,* American Society for Preventive Cardiology; *NLA,* National Lipid Association; *NYHA,* New York Heart Association; PCE, pooled cohort equation; *PCNA,* Preventive Cardiovascular Nurses Association.

TABLE 18.9
High-, Moderate-, and Low-Intensity Statin Therapy

Statin Therapy	High-Intensity (Daily Dose Lowers LDL-C Levels by an Average of ≥50%)	Moderate-Intensity (Daily Dose Lowers LDL-C Levels by an Average of 30% to <50%)	Low-Intensity (Daily Dose Lowers LDL-C Levels by an Average of <30%)
Atorvastatin	40–80 mg	10 (20) mg	—
Rosuvastatin	20 (40) mg	(5) 10 mg	—
Simvastatin	—	20–40 mg	10 mg
Pravastatin	—	40 (80) mg	10-20 mg
Lovastatin	—	40 mg	20 mg
Fluvastatin	—	80 mg (Fluvastatin XL) 40 mg twice daily	—
Pitavastatin	—	2–4 mg	1 mg

TABLE 18.10
Normal and Abnormal Lipid Values in Childhood

Category	Total Cholesterol (mg/dL)	LDL-Cholesterol (mg/dL)
Acceptable	<170	<110
Borderline	170–199	110–129
Abnormal	≥200	≥130

From Grundy et al., 2019
CHD, Coronary heart disease; *LDL,* low-density lipoprotein.

on cost considerations at the time of publication. The 2018 ACC/AHA guidelines emphasized shared decision making when deciding on treatment and provided additional elements to consider, called *risk-enhancing factors*, favoring the use of statins when there is uncertainty. Finally, a focus on population subgroups was expanded. A detailed algorithm is provided (Box 18.1).

The 2018 ACC/AHA treatment guidelines recommend an LDL-C of <70 mg/dL for very high-risk individuals. Nevertheless, increasing evidence for the safety and efficacy of even lower targets exist for such patients, including those post-ASCVD. Randomized clinical trials have demonstrated that the use of nonstatin LDL-C-lowering therapies (i.e., ezetimibe/PCSK9 inhibitors) in addition to statins in this population can safely lower LDL-C to less than 50 mg/dL and further reduce major adverse cardiovascular events (Cannon et al., 2015; Sabatine et al., 2017; Schwartz et al., 2018). As such, clinician-patient risk discussion is encouraged to optimize an individual's treatment plan.

In regards to the management of mild to moderate hypertriglyceridemia, cardiovascular outcomes trials (Ginsberg et al., 2010; Investigators et al., 2011; Group et al., 2014) while not designed to test the effect of lowering TG levels in patients with TG <500 mg/dL after statin therapy, failed to demonstrate cardiovascular benefit of adding either a fibrate or formulations of niacin. However, 2 trials investigating the use of omega 3 fatty acids, specifically eicosapentaenoic acid (EPA) and at 3 g daily, in a population on background statin with well controlled LDL-C (mean LDL-C 75 mg/dL) have demonstrated reduction in major adverse cardiovascular events (Yokoyama et al., 2007; Bhatt et al., 2019).

HIGH CHOLESTEROL IN CHILDREN

Current evidence indicates that atherosclerotic lesions can begin in childhood; children with high blood cholesterol levels typically maintain high blood cholesterol through adulthood. In an effort to intervene early in children with an atherosclerotic predisposition, guidelines for assessing CHD risk in children and adolescents have been promulgated by organizations such as the NCEP (NCEP Expert Panel on Children and Adolescents) (NCEP, 1992) and the AHA (Grundy et al., 2019). Current recommendations support selective screening (starting at 2 years of age) of children and adolescents with a family history of premature CVD or those with at least one parent with high blood cholesterol. Table 18.10 classifies these children by total and LDL-C levels. In children and adolescents without cardiovascular risk factors or family history of early CVD, it may be reasonable to measure a fasting lipid panel or nonfasting non-HDL-C once between 9 and 11 years of age and again between 18 and 21 years to detect moderate to severe lipid abnormalities (Grundy et al., 2019). Intervention aimed at reducing risk is outlined in Table 18.10. As in adults, intervention focuses on a search for medical causes of lipid abnormalities and pharmacologic intervention when necessary.

LIPIDS, LIPOPROTEINS, AND DISEASE

Lipoprotein and lipid levels are used to predict CHD and form the basis of the NCEP guidelines discussed earlier. However, for many years, the Fredrickson Classification (alluded to in Table 18.3) was used to characterize lipid disorders (Hansen, 1998). The Fredrickson Classification used electrophoresis and a standing plasma test for CMs to correlate clinical disease syndromes with laboratory phenotypes (Fredrickson et al., 1967). Note that each phenotype is not a specific disease but rather a variety of disorders that affect the same lipoproteins and therefore express the same lipid pattern. Thus, treatment is usually the same for all disorders falling within the same phenotype. One limitation of this system is that it does not consider low HDL as a risk factor for CHD. In recent years, the Fredrickson Classification has proved less useful given modern analytic techniques and an evolving understanding of the genetics of these disorders. Nevertheless, the nomenclature for a few pathognomonic syndromes (e.g., Type 1 and Type 3 hyperlipidemias) has remained in use. Some pertinent details of the Fredrickson Classification are presented in Table 18.11.

As our understanding of lipids, lipoprotein metabolism, and genetics has evolved, far more complex systems for describing clinical lipid disorders have been conceived. Presently, no ideal scheme to categorize these disorders is available. They can arise from lifestyle or secondary causes as well as from mutations in genes encoding apolipoproteins, apolipoprotein receptors, or enzymes of lipoprotein metabolism. Some genes (e.g., apoA-I, apoC-III, apoA-IV) are in close proximity and share similar response elements, allowing a single mutation to alter multiple aspects of lipoprotein metabolism. The following disorders of lipoprotein metabolism are categorized on the basis of laboratory findings. Lifestyle factors affecting lipid profiles and causes of secondary hyperlipidemia are listed in Table 18.12 in association with their most common laboratory presentation. As with the genetic dyslipidemias, these factors can produce overlapping and somewhat variable lipoprotein profiles. In Figures 18.5 and 18.6, some of the disorders described later are incorporated into the schemes of forward and reverse cholesterol transport so that their cause and pathogenesis may be more readily understood.

HIGH CHOLESTEROL WITH HIGH LDL-C

These disorders share one feature, hyperbetalipoproteinemia (Fredrickson Type 2A), which is characterized by elevated LDL-C and normal triglycerides. It is associated with a high cardiac risk that is not surprising given the elevations in LDL, a highly atherogenic particle. This is a commonly encountered laboratory presentation.

POLYGENIC (NONFAMILIAL) HYPERCHOLESTEROLEMIA

Polygenic (nonfamilial) hypercholesterolemia is a general term used to describe individuals for whom the cause of hypercholesterolemia is likely multifactorial (Soutar, 1998). Although some of the causative factors in this disease are thought to be genetic, before a patient's hypercholesterolemia is labeled "polygenic," secondary and familial hypercholesterolemia (autosomal dominant) must be ruled out. Approximately 85% of the hypercholesterolemia in the population may fall into this category. Some clinicians use

TABLE 18.11
Pertinent Details of the Fredrickson Classification

Type	Refrigerator Test	Gel Electrophoresis	Clinical Presentation
1	Positive; clear plasma	Normal	Eruptive xanthoma; acute, recurrent pancreatitis in early childhood; lipids improve on low-fat diet
2a	Negative; clear plasma	Increased β band	Xanthelasma, tendon xanthoma; premature coronary disease; autosomal-dominant familial inheritance; commonly known as familial hypercholesterolemia
2b	Negative; cloudy plasma; increased β and pre-β band		Isolated xanthelasma may be present; premature coronary disease; autosomal-dominant pattern; affected family members must have varied patterns (e.g., isolated hypertriglyceridemia, isolated hypercholesterolemia, combined hyperlipidemia) to meet diagnostic criteria for familial combined hyperlipidemia
3	Occasional cloudy plasma	Increased pre-β band	Eruptive xanthoma and palmar xanthoma; premature coronary disease; autosomal-recessive pattern; a secondary cause of dyslipidemia, such as hypothyroidism, can unmask type 3, and treatment of the secondary condition can return lipids to normal
4	Negative; cloudy plasma	Increased α_2 band	May or may not be associated with premature coronary disease
5	Positive; cloudy plasma	Increased α_2 band	Eruptive xanthoma; may be associated with pancreatitis; may be associated with premature coronary disease

TABLE 18.12
Lifestyle Factors and Causes of Secondary Dyslipidemia

Lipoprotein Profile	Secondary Causes	Lifestyle Factors
High cholesterol and high LDL-C with or without low HDL-C	Hypothyroidism and nephrotic syndrome Medications such as thiazide diuretics and steroids Chronic obstructive liver disease Cholestatic liver disease (primary biliary cirrhosis and related diseases) ApoE-4 may increase susceptibility	Obesity Excess dietary cholesterol and/or saturated fat
High triglycerides with normal total and LDL-C with or without low HDL-C	Medications such as thiazide diuretics, estrogens, corticosteroids, retinoids, cyclosporine, and beta blockers (without intrinsic sympathomimetic) Insulin resistance/diabetes Chronic renal failure and nephrotic syndrome Antipsychotic drugs (clozapine/olanzapine)	Obesity Physical inactivity Cigarette smoking Excess alcohol intake High-carbohydrate diets
High cholesterol and high triglycerides with or without low HDL-C	Medications—notably, high-dose steroids or cyclosporine Severe hypothyroidism, diabetes/insulin resistance, and nephrotic syndrome	Obesity HIV antiretroviral drugs
Isolated low HDL-C	Medications such as isotretinoin, probucol, anabolic steroids, beta blockers, and certain progestogens	Physical inactivity Increased body weight High-carbohydrate, low-fat diets
Isolated high HDL-C	Medications such as phenytoin, phenobarbital, rifampicin, griseofulvin, and estrogens	Alcohol intake

HDL-C, High-density lipoprotein cholesterol; *HIV,* human immunodeficiency virus; *LDL-C,* low-density lipoprotein cholesterol.

this term to describe patients who develop age-related increases in cholesterol that do not respond to lifestyle modification.

FAMILIAL HYPERCHOLESTEROLEMIA

Familial hypercholesterolemia (FH), with severely elevated serum cholesterol levels, is caused by a group of inherited genetic defects. LDLR gene mutations (deletion, missense, nonsense, and insertion) are the most common cause of FH, resulting in loss of LDLR activity in the clearance of LDL-C from circulation. Patients can be LDLR negative (little to no LDLR activity) or receptor defective (LDLR isotypes with reduced affinity for LDL on the hepatocyte surface). These are the five major classes of LDLR defects:

Class I: LDLR is not synthesized at all.

Class II: LDLR is not properly transported from the endoplasmic reticulum to the Golgi apparatus for expression on the cell surface.

Class III: LDLR does not properly bind LDL on the cell surface because of a defect in either apoB-100 (R3500Q) or in the LDLR.

Class IV: LDLR bound to LDL does not properly cluster in clathrin-coated pits for receptor-mediated endocytosis.

Class V: LDLR is not recycled back to the cell surface.

FH is an autosomal-dominant disorder caused by one of several mutations in the LDLR gene on chromosome 19. The resulting defective receptors cannot bind or clear LDL from the circulation (Hobbs et al., 1992). Several hundred mutations have been identified in the LDLR gene, which affect most aspects of receptor synthesis, transport, and function (Fig. 18.7). This genetic heterogeneity has led to variability in presentation and responsiveness to therapy (Varret et al., 2008). Heterozygous FH occurs in 1 in 200 to 500 individuals and is associated with premature atherosclerotic disease. Affected heterozygous men usually present in their fourth decade and women 10 to 15 years later. Untreated LDL-C levels are typically over 220 mg/dL. Further, FH heterozygotes exhibit LDL-C levels that vary with environmental factors and genetics. Homozygous FH presents in childhood with LDL levels over 400 mg/dL. Vascular deposition of lipid results in premature symptomatic CHD. In addition, homozygotes are less affected by environmental factors in terms of LDL-C levels. Large valvular and supravalvular cholesterol deposits can produce symptomatic aortic stenosis. Other stigmata of the disease include corneal arcus, tendinous xanthomata, and xanthelasma. These stigmata generally develop in early childhood in homozygotes and by adulthood in heterozygotes. Statins, which inhibit 3-hydroxy-3-methylglutar yl-coenzyme A (HMG-CoA) reductase, may be effective. However, because these drugs may act indirectly by increasing LDLR activity, not all heterozygous patients will normalize their LDL-C despite receiving maximum doses of statins. PCSK9 inhibitors are indicated in FH when the LDL-C threshold is not achieved. These medications have demonstrated both significant LDL-C–lowering efficacy as well as improved ASCVD outcomes in this very-high-risk population (Raal et al., 2012; Karatasakis et al., 2017).

Homozygous patients have two abnormal LDLR genes, making statin drugs ineffective unless combined with apheresis (Ose, 1999). Patients with homozygous FH are classified into two groups based on tests for LDLR activity in skin fibroblasts: patients with less than 2% of normal LDLR activity are receptor negative; patients with 2% to 25% of normal LDLR activity are receptor defective. Receptor-negative patients rarely live past the second decade; receptor-defective patients often develop significant atherosclerotic disease by the age of 30 years.

FH should be suspected when adults (≥20 years) have LDL-C of 190 mg/dL or greater or non–HDL-C of 220 mg/dL or greater (Goldberg et al., 2011). In children, adolescents, and young adults (<20 years), LDL-C of 160 mg/dL or greater or non–HDL-C of 190 mg/dL or greater indicates FH. As previously mentioned, signs of the disease include corneal arcus, tendinous xanthomata, and xanthelasma. Adult FH patients should receive initial treatment with higher-potency statins titrated to achieve an LDL-C reduction of 50% or more from baseline. Heterozygous FH patients with

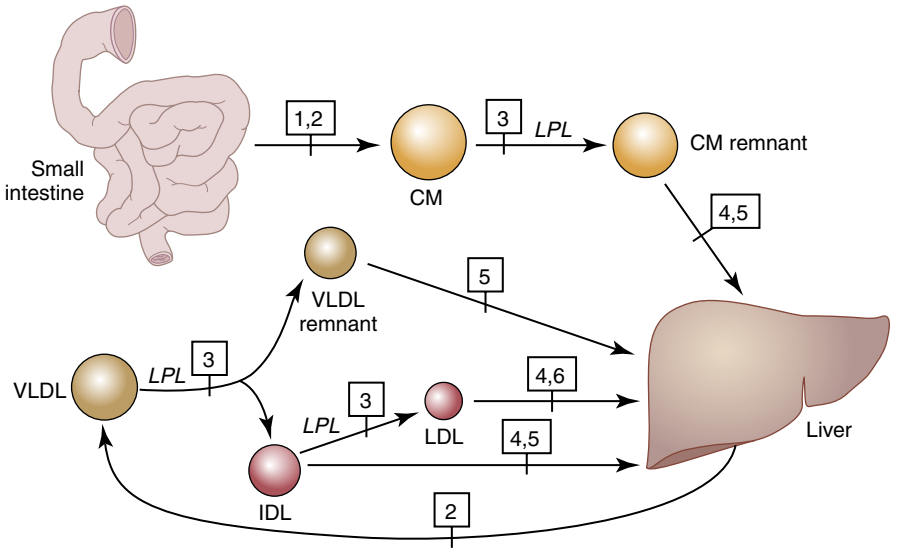

1 - Chylomicron retention (Apo B-48 defect)
2 - Hypobetalipoproteinemia/Abetalipoproteinemia
3 - LPL deficiency/Apo C II deficiency
4 - Familial hypercholesterolemia
5 - Dysbetalipoproteinemia (Type III hyperlipoproteinemia, associated with Apo-E-2)
6 - Familial defective Apo B

Figure 18.5 Disorders associated with the transport of lipids. *Apo,* Apolipoprotein; *CM,* chylomicron; *IDL,* intermediate-density lipoprotein; *LPL,* lipoprotein lipase; *VLDL,* very-low-density lipoprotein.

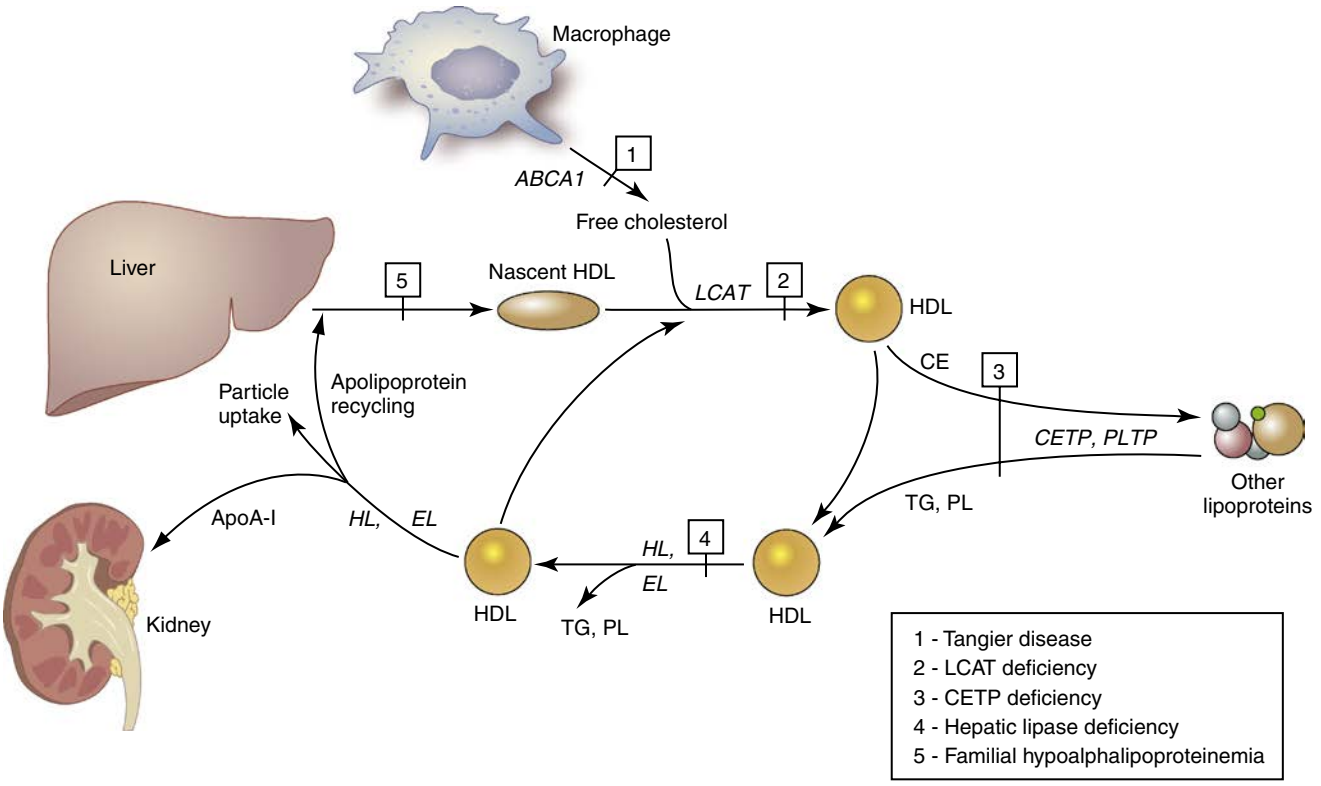

1 - Tangier disease
2 - LCAT deficiency
3 - CETP deficiency
4 - Hepatic lipase deficiency
5 - Familial hypoalphalipoproteinemia

Figure 18.6 Disorders associated with the reverse cholesterol transport. *ABCA1,* Adenosine triphosphate (ATP)–binding cassette protein A-1; *Apo,* apolipoprotein; *CE,* cholesteryl ester; *CETP,* cholesteryl ester transfer protein; *EL,* endothelial lipase; *HDL,* high-density lipoprotein; *HL,* hepatic lipase; *LCAT,* lecithin/cholesterol acyltransferase; *PL,* phospholipids; *PLTP,* phospholipid transfer protein; *TG,* triglycerides.

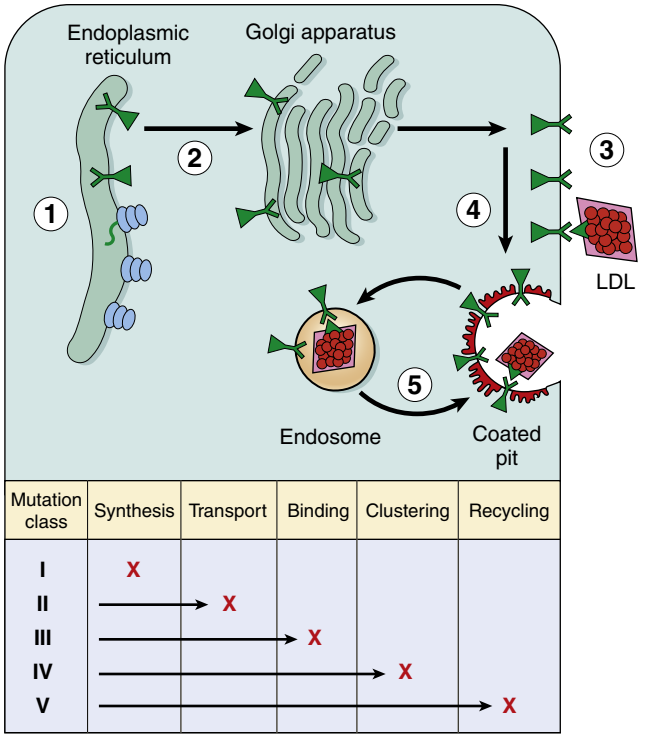

Figure 18.7 Classification of low-density lipoprotein (LDL) receptor mutations based on abnormal function of the mutant protein. These mutations disrupt the receptor's synthesis in the endoplasmic reticulum, transport to the Golgi complex, binding of apoprotein ligands, clustering in coated pits, and recycling in endosomes. Each class is heterogeneous at the DNA level (Modified with permission from Hobbs HH, Russell DW, Brown MS, Goldstein JL: The LDL receptor locus in familial hypercholesterolemia: Mutational analysis of a membrane protein. *Annu Rev Genet* 24:133–170, 1990.)

50% functional LDLRs respond well to statin therapy. Generally, homozygous FH patients with LDLR-defective mutations cannot achieve the LDL-C goal by statins. However, some FH homozygotes having sufficient LDLR activity respond to statin therapy well. If an individual with FH cannot achieve the LDL-C goal with the maximum and tolerable dose of statin, other LDL-C–lowering therapies—such as PCSK9 inhibitors, ezetimibe, niacin, or bile acid sequestrants—should be combined with the statins. If maximum drug therapy after 6 months is inadequate for LDL-C reduction, not tolerated, or contraindicated, LDL apheresis may be considered for the following individuals: functional heterozygous FH patients with LDL-C of 300 mg/dL or greater (or non–HDL-C ≥330 mg/dL) and no or only one risk factor; functional heterozygous FH patients with LDL-C of 200 mg/dL or greater (or non–HDL-C ≥230 mg/dL) and high-risk characteristics such as two or more risk factors or high Lp(a) of 50 mg/dL or greater; and functional heterozygotes with LDL-C of 160 mg/dL or greater (or non–HDL-C ≥190 mg/dL) and very-high-risk characteristics (established CHD, other cardiovascular disease, or diabetes). With the introduction of PCSK9 inhibitors to the treatment armamentarium, the need for LDL apheresis has decreased for some individuals (Moriarty et al., 2016).

Given the limited treatment options and the severe morbidity and mortality of homozygous familial hypercholesterolemia (HoFH), two new drugs have been approved by the U.S. Food and Drug Administration (FDA): lomitapide and mipomersen. Lomitapide inhibits MTP and thus decreases LDL production. Lomitapide was initially targeted for hypercholesterolemic patients, but because of substantial side effects such as frequent elevations of liver enzymes and liver steatosis, the FDA approved it to treat only patients with HoFH. Mipomersen is an antisense oligonucleotide that inhibits production of apoB-100. It is administered as a subcutaneous injection once a week. Mipomersen also was initially developed for patients with lipid disorders but was ultimately targeted to HoFH patients because of adverse effects and safety concerns, such as hepatic steatosis, interactions with CYP3A4 inhibitory drugs, and inflammatory injection site reactions.

FAMILIAL DEFECTIVE APOB

Familial defective ApoB is an autosomal-dominant disorder of the apoB gene on chromosome 2 that interferes with the recognition of apoB-100 by the LDLR (Hansen, 1998). The disease results from a missense mutation (*Arg3500Gln*) in the LDLR-binding domain of ApoB-100, although other mutations that occur less frequently can cause this disease. Estimated frequency in the population is 1 in 750. Patients with familial defective apoB have similar physical stigmata to those of FH: tendinous xanthomata, xanthelasma, and premature coronary disease. Untreated LDL-C levels can overlap those seen in FH but tend to be slightly lower. Further, patients with familial defective ApoB have levels of plasma LDL-C comparable with those in FH heterozygotes. Statin drugs are effective.

SITOSTEROLEMIA

Sitosterolemia is an extremely rare autosomal-recessive disorder in which phytosterols (plant sterols) are absorbed and accumulate in plasma and peripheral tissues. This disease results from mutations in the *ABCG8* or *ABCG5* gene, both of which are located at chromosome 2p21. Mutations in these genes disrupt the ABCG5 or ABCG8 proteins from forming the proper channel to pump back absorbed plant sterols into the intestinal lumen as well as the ability of liver to secrete absorbed phytosterols into bile. Most patients identified with sitosterolemia have had high plasma LDL-C levels during childhood. Tendon xanthomas or tuberous xanthomas can occur in childhood at heels, knees, elbows, and buttocks (Niu et al., 2010). Premature atherosclerosis is present and can lead to angina, aortic valve involvement, myocardial infarction, and sudden death. Hemolytic anemia, abnormally shaped erythrocytes (stomatocytes), and large platelets (macrothrombocytopenia) can be the initial presentation or the only clinical feature of the disorder (Wang et al., 2011). Cholesterol levels may be normal or elevated. A distinctive clinical presentation of sitosterolemia is the occurrence of low-level hemolysis. Red blood cells may be incorporating the plant sterols into their membranes. Diagnosis of sitosterolemia should be considered if the patient presents with xanthomatosis and hypercholesterolemia yet has parents who have normal levels of cholesterol. In untreated individuals with sitosterolemia, the sitosterol concentration can be increased 30- to 100-fold—that is, as high as 10 to 65 mg/dL (Kidambi & Patel, 2008). Plasma concentrations of sitosterol greater than 1 mg/dL are diagnosed as sitosterolemia (except in infants, in whom further testing may be necessary). Treatment goals are to reduce plasma concentration of plant sterols (ideally <1 mg/dL), to control plasma concentration of cholesterol, and to prevent xanthoma formation and/or to reduce the size and number of xanthomas. Main therapy is a diet low in sterols and use of ezetimibe, a sterol absorption inhibitor (Tsubakio-Yamamoto et al., 2010). If patients do not respond to ezetimibe, the use of cholestyramine and/or partial ileal bypass surgery is recommended.

AUTOSOMAL-DOMINANT HYPERCHOLESTEROLEMIA

Autosomal-dominant hypercholesterolemia (ADH) is an autosomal-dominant disorder of the *PCSK9* gene on chromosome 1 that is involved in cholesterol homeostasis in the liver (Abifadel et al., 2003). Mutations in this gene may lead to a gain of function. Individuals with gain-of-function mutations present clinically with increased plasma levels of LDL-C and exhibit a higher risk of CHD. Relatively little is known about the frequency of ADH since the discovery of the mutation in three families in 2003. However, more gain-of-function *PCSK9* patients have been reported (*D374Y*). PCSK9 is a member of the proprotein convertase family of proteins. It is secreted into plasma and binds to LDLR on the cell surface. This leads to endocytosis and intracellular degradation of the LDLR. Consequently, gain of function of *PCSK9* decreases levels of LDLR protein. In addition to the gain-of-function mutations, loss-of-function mutations have been found. These missense (*R46L*) and nonsense (*Y142X* and *C697X*) mutations have led to hypocholesterolemia in patients. Based on these findings, monoclonal antibodies that inhibit the function of PCSK9 have been developed for clinical practice. Alirocumab and evolocumab are currently available for the treatment of hyperlipidemia in individuals on maximally tolerated statin with established ASCVD and in FH. By preventing LDLR destruction, these agents lower LDL-C levels by 50% to 60% and have been shown to reduce major adverse cardiovascular events above that achieved by statin therapy alone (Sabatine et al. 2017; Schwartz et al., 2018).

AUTOSOMAL-RECESSIVE HYPERCHOLESTEROLEMIA

Autosomal-recessive hypercholesterolemia (ARH) involves the ARH gene found on chromosome 1. ARH is also known as *LDLRAP1*. In these patients, LDLR expression is normal, but LDL clearance rates are low and comparable with those of patients with homozygous FH. ARH is thought to express

a protein that is involved in internalization of the LDLR–LDL complex. Plasma levels of LDL-C in ARH patients tend to be between FH heterozygotes and FH homozygotes. The onset of atherosclerotic disease presents later than in homozygous FH patients. ARH patients can present with large, bulky xanthomas. Patients with ARH respond to lipid-lowering medications. However, most ARH patients are maintained on LDL apheresis as part of their treatment.

HIGH TRIGLYCERIDES WITH NORMAL CHOLESTEROL

These disorders are related to elevations of triglyceride-rich particles—namely, CMs or VLDL (Fredrickson Types 1 and 4). This commonly encountered laboratory presentation is usually due to hyperprebetalipoproteinemia (VLDL) and may be due to secondary causes such as excess alcohol or a high-carbohydrate diet. LDL and LDL-C are typically normal.

FAMILIAL HYPERTRIGLYCERIDEMIA

Familial hypertriglyceridemia occurs along with other lipoprotein abnormalities as part of a number of familial hyperlipidemia syndromes. Isolated hypertriglyceridemia (or Type 4 hyperlipidemia) is a relatively common autosomal-dominant disorder, having a population prevalence of 5% to 10%, and is defined by the familial occurrence of isolated high VLDL levels with triglyceride values most commonly in the 200- to 500-mg/dL range. The pathophysiology remains elusive, but VLDL triglyceride production is increased in the setting of normal apoB production, resulting in the formation of "fluffy," triglyceride-rich VLDL particles. Some kindreds have premature CHD, but it is unclear whether the CHD results from hypertriglyceridemia or from the frequently coexisting exacerbating factors: obesity and insulin resistance (Brunzell, 1983). The increased prevalence of the metabolic syndrome alone could account for the elevated CVD risk associated with familial hypertriglyceridemia. Thus, the growing prevalence of both obesity and metabolic syndrome appears to increase the frequency, onset of expression, and severity of genetic triglyceride syndromes (Hopkins et al., 2003).

LIPOPROTEIN LIPASE DEFICIENCY (HYPERLIPOPROTEINEMIA TYPE 1 OR HYPERCHYLOMICRONEMIA)

LPL deficiency is a rare, autosomal-recessive disorder that presents in childhood with abdominal pain and pancreatitis. Defective or absent LPL creates an inability to clear CMs, creating the classic "type 1" chylomicronemia syndrome (see Tables 18.3 and 18.11). Fasting triglyceride levels may be over 100 mg/dL and may rise to over 10,000 mg/dL postprandially. Treatment with a low-fat diet to reduce CM input is effective, fat-soluble vitamins should be supplemented, and drug therapy can be considered to lower endogenous VLDL production (Brunzell, 1995). Heterozygotes have half-normal LPL activity and occur in the general population at a frequency of 1 in 500. It has been speculated that heterozygous individuals with the defective *LPL* gene constitute a subset of families with familial combined hyperlipidemia (Babirak et al., 1989).

APOC-II DEFICIENCY

ApoC-II is an activating cofactor for LPL. Thus, the absence of apoC-II creates a functional LPL deficiency, which presents similarly to LPL deficiency as a rare autosomal-recessive form of familial hyperchylomicronemia. The disorder presents in children and young adults as recurrent bouts of abdominal pain and pancreatitis. Several defects in the apoC-II gene have been described (Fojo & Brewer, 1992). Patients can be treated with plasma transfusions during severe hypertriglyceridemia providing apoC-II, which will activate endogenous LPL.

ApoC-III Excess

ApoC-III excess interferes with the activity of LPL and binds to the carboxy-terminal portion of apolipoprotein B, preventing the binding of lipoproteins to the LDLR. Excess apoC-III, especially within the B-Lps LDL and VLDL, may be an independent risk factor for CHD (Ooi et al., 2008). ApoC-III levels can be increased in patients with diabetes type 2, hyperbilirubinemia, kidney deficiency, and thyroid dysfunction; further, genetic mutations in the apoC-III gene are known. In addition to genetic factors, serum apoC-III is affected by age and alcohol consumption in men and women; oral contraceptive use in women has also been associated with high levels of apoC-III. Several genetic polymorphisms of the apoC-III gene are known (Li et al., 1995). They include point mutations at –641T/C, –482C/T, –455T/C, 1100C/T, 3175C/G, and 3026T/G of the start site of the apoC-III gene. The mutations at –455T/C and 1100C/T are more common in white adult males and boys. It is thought that the point mutation at –455T/C affects a transcription factor–binding site associated with insulin response. Consequently, lack of response to insulin at the apoC-III promoter, which downregulates apoC-III transcription, is thought to contribute to high levels of triglycerides in plasma. Meta-analysis showed that ApoC-III Sst I and T-455C polymorphisms, other than C-482T and C1100T, might be associated with CHD risk (Lin et al., 2014). Genetic mutations at other genes such as *APOA4* or carrying APOE E4 alleles have been suggested to influence serum apoC-III levels as well.

ApoA-V

ApoA-V is a highly hydrophobic protein that has a preference for binding to lipids and HDL particles. The function of ApoA-V has been hypothesized as being involved in VLDL assembly; in addition, it has been postulated that ApoA-V may be involved in activation of LPL-mediated triglyceride hydrolysis. Consequently, low levels of ApoA-V may promote hypertriglyceridemia, whereas high levels of ApoA-V would have the opposite effect. One variant of ApoA-V has been found in humans that has a strong correlation with hypertriglyceridemic patients. The actual function of ApoA-V and its role in triglyceride metabolism require further investigation.

HIGH CHOLESTEROL WITH HIGH TRIGLYCERIDES

These disorders are related to elevations of LDL and triglycerides (Fredrickson Types 2B and 3). Familial combined hyperlipidemia (2B) is the most common primary hyperlipoproteinemia and presents with a variety of lipoprotein phenotypes within a family. The relatively rare dysbetalipoproteinemia (Type 3) is characterized by an abnormal LDL (IDL) that appears as a broad beta electrophoretic band and distinguishes it from familial combined hyperlipidemia. These disorders are associated with increased cardiac risk because of the elevated LDL.

Familial Combined Hyperlipidemia (Type 2B)

Familial combined hyperlipidemia (type 2B) is a relatively common disorder in which affected individuals may have simple hypercholesterolemia, simple hypertriglyceridemia, or a mixed defect. Because of the disorder's phenotypic heterogeneity and the lack of a definitive biochemical marker for the disorder, considerable overlap and confusion with other forms of hyperlipidemia have occurred. Estimated frequency in the population is 1 in 100. Affected families must have more than one pattern of lipid disorder to meet diagnostic criteria for familial combined hyperlipidemia.

Acquired Combined Hyperlipidemia

Acquired combined hyperlipidemia is common in patients who have metabolic syndrome. As the name suggests, the disease stems from a syndrome of conditions that include type 2 diabetes mellitus, hypertension, central obesity, and CHD. It is thought that the liver increases the production of VLDL through high levels of free fatty acids in plasma. As a result, the increased VLDL levels mature to LDL until this process is saturated. When LDL levels get high enough, VLDL levels follow, causing both hypercholesterolemia and hypertriglyceridemia.

Dysbetalipoproteinemia (Type 3)

ApoE is present on chylomicrons, VLDL, IDL, and CM remnants. By binding to the LDLR, and probably other receptors, apoE helps to clear these lipoproteins from circulation. Three common electrophoretic isoforms of apoE are known, each form attributable to several different genetic mutations. The most common isoform is E-3, followed by E-4 and E-2. ApoE-2 has lower affinity for the LDLR (less than 2% of binding ability of E-3); thus, lipoprotein particles accumulate in the blood of patients who are homozygous for E-2. However, although individuals with this genotype are relatively common in the white population (1 in 100), expression of an overt Type 3 phenotype occurs in 1 to 5 per 5000 individuals. Thus, the manifestation of the Type 3 hyperlipidemia phenotype is thought to contribute to the disease. Secondary factors implicated in the manifestation of disease include obesity, diabetes mellitus, hypothyroidism, and medications such as protease inhibitors.

Type 3 hyperlipidemia primarily affects adults and is more common in men than in women (Mahley & Rall, 1995). Symptomatic individuals typically have roughly equal elevations of cholesterol and triglycerides; presence of β-VLDL or cholesterol-enriched remnants of intestinal CMs and hepatic VLDL; xanthomas; and premature vascular disease, such as CHD and peripheral artery disease. Type 3 has a pathognomonic feature: a broad

abnormal band between VLDL and LDL known as "abnormally migrating beta lipoprotein," or β-VLDL. The cholesterol content in VLDL is also increased, and measurement of the VLDL-C:triglyceride ratio is a useful screen. Normally, the VLDL-C/triglyceride ratio is 0.2; typical Type 3 patients have a ratio over 0.3. Day-to-day variation in lipid levels is more pronounced than usual. Other clinical stigmata include palmar xanthoma and tuberoeruptive xanthoma on the elbows, knees, and buttocks. Premature atherosclerosis is highly prevalent and, unlike FH, more often involves abdominal and femoral arteries. The atherosclerosis appears reversible with treatment of the lipid disorder (Kuo et al., 1988). Patients are responsive to low-fat diets, weight loss, and most classes of lipid-lowering drugs.

Hepatic Lipase Deficiency

Generally resulting from mutations of the HL gene, this rare familial disorder is associated with combined hyperlipidemia characterized by TC levels of 250 to 1500 mg/dL and TG levels of 400 to 8000 mg/dL. Levels of HDL-C are normal or increased. Physical stigmata include palmar and tuberoeruptive xanthoma; the risk of atherosclerosis is thought to be increased. In contrast to Type 3 hyperlipidemia, although β-VLDL is increased, the TC/TG ratio is not increased. The triglyceride content of all lipoproteins is increased three- to fivefold. Families with compound heterozygous mutations have been described (Connelly & Hegele, 1998). Patients with hepatic lipase deficiency are able to convert large VLDL to smaller VLDL particles; however, they are unable to convert VLDL to IDL and also LDL from IDL. HDL and LDL particles from hepatic lipase deficiency patients are large and enriched with triglycerides.

Cholesterol 7-Alpha-Hydroxylase Deficiency

Cholesterol 7-alpha-hydroxylase deficiency is a recessive disorder of the *CYP7A1* gene that encodes cholesterol 7-alpha-hydroxylase protein. *CYP7A1* encodes an enzyme that is involved in the first step of the classical pathway for bile acid biosynthesis. The few patients who present with this rare disease exhibit not only high cholesterol but also high triglycerides in plasma. Very little is known about the disease. However, it has been reported that the few patients diagnosed with this disease are resistant to statin therapy, although the same patients managed to lower their plasma cholesterol with atorvastatin and niacin therapy. Lack of cholesterol 7-alpha-hydroxylase is thought to reduce hepatic LDLR activity. However, because so few patients have been identified with this condition, more information and patients will be necessary to confirm the relationship between the deficiency and its clinical presentation.

HIGH TRIGLYCERIDE AND LOW HDL CHOLESTEROL

LIPIDS, OBESITY AND METABOLIC SYNDROME

Dyslipidemias are one of the most common comorbidities associated with substantial increases in body weight (Frayn et al., 2003). In particular, visceral adipose tissue is associated with greater lipolytic activity, insulin resistance and atherogenic dyslipidemia (Bamba & Rader, 2007; Hwang et al., 2016). Atherogenic dyslipidemia is a phenotype characterized by elevated fasting and postprandial triglyceride, low HDL, and increased levels of small, dense LDL particles. The changes in lipid metabolism seen with visceral adiposity are frequently associated with the term *metabolic syndrome*. The metabolic syndrome is a constellation of metabolic derangements that confer significant risk for CHD exceeding its individual components (McNeill et al., 2005). According to a joint international statement (Samson & Garber, 2014), patients with metabolic syndrome meet three or more of the following:

1. Obesity: Waist circumference ≥102 cm (40.2 in) in men and ≥88 cm (34.6 in) in women (based on NCEP/ATPIII 2004 criteria). These numbers may vary with region and ethnicity.
2. HDL-C <40 mg/dL (men) and <50 mg/dL (women)
3. Triglycerides ≥150 mg/dL (or drug therapy for hypertriglyceridemia)
4. Hyperglycemia: Fasting plasma glucose ≥100 mg/dL (or drug therapy for hyperglycemia)
5. Hypertension: Systolic: ≥130 mmHg; Diastolic: ≥85 mmHg (or antihypertensive drug therapy/history of hypertension)

LOW TOTAL CHOLESTEROL AND TRIGLYCERIDE

These uncommon disorders are associated with defective apoB synthesis, metabolism, leading to low or nonexistent levels of apo-B lipoproteins such as CM, VLDL, and LDL. Triglycerides and cholesterol are low. Fat-soluble vitamin deficiencies are common.

Abetalipoproteinemia

Abetalipoproteinemia (also known as *Bassen-Kornzweig syndrome*) is a rare, autosomal-recessive disorder involving mutations in the *MTTP* gene located on chromosome 4. *MTTP* encodes an 894 amino acid protein called *microsomal triglyceride transfer protein* (MTP). MTP forms a heterodimer with a chaperone protein called protein disulfide isomerase (PDI) in the endoplasmic reticulum. Mutations in *MTTP* affect its binding to PDI and its ability to transfer lipids. Clinically, abetalipoproteinemia patients present with undetectable plasma apoB-containing lipoproteins. During apoB translation, MTP incorporates lipids onto the nascent apoB protein and prevents it from proteasomal degradation. Consequently, the lack of functional MTP still allows for apoB protein production. However, the protein ends up misfolded and destroyed by endoplasmic reticulum (ER)-associated degradation mechanisms. Neither apoB-48 nor apoB-100 is present in plasma. Patients present in childhood or early adolescence with fat malabsorption, hypolipidemia, retinitis pigmentosa, cerebellar ataxia, and acanthocytosis. Laboratory testing usually shows decreased apoB, triglycerides, and TC (typically <50 mg/dL). Patients develop fat-soluble vitamin deficiencies caused by malabsorption of vitamins A, K, and E. Vitamin D does not require CMs for absorption and therefore is typically not deficient. Because both vitamins A and K have transport systems independent of lipoproteins, clinical deficiency is not as severe as that seen with vitamin E, which not only depends on CMs for absorption but relies on VLDL and LDL for delivery to tissues. Children with this disorder respond to a low-fat diet rich in medium-chain fatty acids and supplemented with high-dose fat-soluble vitamins, especially vitamin E. Replacing vitamin E stores improves the retinal and peripheral neuropathic symptoms. Heterozygotes have no symptoms and no evidence of abnormal plasma lipid levels.

Hypobetalipoproteinemia

Hypobetalipoproteinemia is an autosomal-dominant disorder explained by nonsense or missense mutations in the *apoB* gene, leading to synthesis of various truncated forms of apoB. Severity of disease depends on the type of apoB synthesized. Generally, patients have very low LDL-C levels (Wu et al., 1999). The familial form is associated with a decreased risk for cardiovascular disease. Homozygous individuals have TC levels less than 50 mg/dL and present at an early age with fat malabsorption and low plasma cholesterol levels. Heterozygous individuals are usually asymptomatic and have low plasma LDL concentrations. They develop progressive neurologic degenerative disease, retinitis pigmentosa, and acanthocytosis, similar to patients with abetalipoproteinemia. Complications from vitamin E deficiency can be prevented by treatment with very high doses of vitamin E (100–300 IU/kg/day). Heterozygous individuals have LDL-C levels approximately half that of age- and sex-matched controls but are otherwise asymptomatic.

Chylomicron Retention Disease

Chylomicron retention disease (Anderson disease) presents in childhood with fat malabsorption and low levels of plasma lipids. This syndrome is distinct from abetalipoproteinemia because only apoB-48 appears to be affected. Further, the disease is characterized by hypocholesterolemia, chronic diarrhea, failure to thrive, and deficiency of fat-soluble vitamins (vitamin E in particular); the latter can lead to neurologic deficits. The genetic abnormality associated with this disorder is linked to the *SARA2* gene on chromosome 5q3 that encodes the Sar1 GTPase protein. This protein belongs to a family of GTPases that govern the intracellular trafficking of proteins in protein-coated vesicles (Jones et al., 2003). Sar1 GTPase most likely plays a role in the steps involving intracellular trafficking of newly synthesized apoB-48–containing lipoproteins in the enterocytes. After proper folding and lipidation in the ER by the MTP, apoB-48 lipoproteins leave the ER through prechylomicron transfer vesicles (PCTVs). These vesicles fuse with a recipient Golgi membrane and are ultimately secreted. The precise role of Sar1 GTPase in intracellular trafficking has not been elucidated.

ISOLATED LOW HDL-C

Low HDL levels are associated with CHD, presumably because insufficient HDL is available to participate in reverse cholesterol transport, the process by which cholesterol is eliminated from peripheral tissues.

Familial Hypoalphalipoproteinemia

Familial hypoalphalipoproteinemia is a common autosomal-dominant disorder that occurs in 1 in 400 people. Affected men have HDL-C levels less than 30 mg/dL, and women have HDL-C levels less than 40 mg/dL. The criteria for familial hypoalphalipoproteinemia include (1) low HDL cholesterol in the presence of normal VLDL cholesterol and LDL cholesterol

levels; (2) absence of diseases or factors that lead to secondary effects of hypoalphalipoproteinemia; and (3) the presence of a similar lipoprotein pattern in a first-degree relative. Half of affected families appear to have hepatic lipase or apoA-I/C-III/A-IV gene defects (Breslow, 1995). Mutations in the *ABCA1* gene, the same gene that is mutated in Tangier disease, have been associated with some cases of hypoalphalipoproteinemia. Premature CHD is typically present.

ApoA-I Deficiency and ApoC-III Deficiency

ApoA-I deficiency with ApoC-III deficiency is a rare autosomal-recessive condition characterized by a reduction in the formation of HDL. It has been linked to point mutations in the *apoA-I* gene and to deletions/gene rearrangements at the *apoA-I/C-III/A-IV* gene locus on the long arm of chromosome 11 (Assman et al., 1995). HDL-C levels are less than 5 mg/dL; both corneal opacification and premature coronary disease are seen in some patients.

ApoA-I Variants

ApoA-I variants due to specific amino acid substitutions in the *apoA-I* gene are rare. They have been shown to increase catabolism of HDL and apoA-I (Breslow, 1995). Homozygous patients generally present with autosomal-recessive inheritance of low HDL-C levels (≈10 mg/dL), corneal opacifications, xanthomata, and premature coronary disease. Heterozygous individuals may present with low HDL-C. One mutation, *apoA-I-Milano*, shows autosomal-dominant inheritance and is associated with low HDL-C levels but is not associated with premature coronary disease (Calabresi & Franceschini, 1997).

Tangier Disease

Tangier disease is a rare autosomal-recessive disorder characterized by very low HDL levels due to a mutation in the *ABCA1* gene on chromosome 9. The mutation leads to an inability to effectively transfer cholesterol and phospholipids from within the cell onto nascent apoA1 proteins in plasma. The resulting buildup of cholesterol within the cell becomes toxic. LDL cholesterol is reduced. In the homozygous state, patients present with low or undetectable HDL in plasma, hepatosplenomegaly, peripheral neuropathy, orange tonsils, and premature coronary disease (Rust et al., 1999). In normal cells, the ABCA1 protein enables cholesterol to exit the cell, upon which it combines with apoA-I to form the HDL. The small amount of HDL that is present in patients with this disorder differs qualitatively from normal HDL.

Lecithin/Cholesterol Acyltransferase Deficiency

LCAT deficiency is characterized by corneal opacities, normochromic anemia, and renal failure in young adults. It is a very rare autosomal-recessive disorder. The disease occurs in two forms: a classic (or complete) familial LCAT deficiency and a milder partial deficiency phenotype known as *fish-eye disease* (Peelman et al., 1999). In complete deficiency, HDL-C levels are typically less than 10 mg/dL, but total cholesterol levels are normal or high. Without LCAT, most cholesterol remains unesterified, and HDL synthesis is impeded. Patients with complete LCAT deficiency have anemia, increased proteinuria, and renal failure. Diagnosis is made by LCAT quantification and cholesterol esterification activity in the plasma. Partial LCAT deficiency exhibits progressive corneal opacification, low plasma HDL levels (<10 mg/dL), and variable hypertriglyceridemia (also seen in complete LCAT deficiency). Premature CHD has been reported even in cases of partial LCAT deficiency (Kuivenhoven et al., 1997). No treatment can be given to raise LCAT levels; however, therapies for this condition involve dietary restriction of fat and management of complications from this disease.

ISOLATED HIGH HDL-C

Cholesteryl Ester Transfer Protein Gene Defects

HDL is involved in the reverse transport of cholesterol from peripheral tissues to the liver. An important step in this process involves CETP, the plasma protein that facilitates the transfer of cholesteryl esters from HDL to apoB-100–rich proteins (VLDL and LDL) in exchange for triglycerides. CETP deficiency is an autosomal-recessive disorder in which the transfer of cholesteryl esters is inhibited. As a result, HDL particles are large and laden with cholesteryl ester, and apoA-I is increased, as is HDL-C (typically >100 mg/dL). The association of higher HDL-C plasma levels with risk of CHD is still unclear based on genetic studies of humans with *CETP* mutations. Heterozygotes have moderately increased HDL-C levels.

SELECTED REFERENCES

Grundy SMNJ, Stone AL, Bailey C, et al.: 2018 AHA/ACC/AACVPR/AAPA/ABC/ACPM/ADA/AGS/APhA/ASPC/NLA/PCNA guideline on the management of blood cholesterol: a report of the American College of Cardiology/American Heart Association Task Force on clinical practice guidelines, *Circulation* 139(25):e1082–e1143, 2019.

A comprehensive review of present treatment modalities for hypercholesterolemia and risk factors for use of these modalities. These are correlated with ranges for LDL and HDL cholesterol.

National Cholesterol Education Program Expert Panel: Third report of the National Cholesterol Education Program (NCEP) Expert panel on detection, evaluation, and treatment of high blood cholesterol in adults (adult treatment panel III): final report, *Circulation* 106:3143–3421, 2002.

A comprehensive monograph that includes the latest recommendations for screening, evaluating, and treating hyperlipidemia.

Nauck M, Warnick GR, Rifai N: Methods for measurement of LDL-cholesterol: a critical assessment of direct measurement by homogenous assays versus calculation, *Clin Chem* 48(2):236–254, 2002.

bib53A comprehensive review of current LDL-C methods, including the advantages and disadvantages of each, performance characteristics, and an explanation of the chemistry and technology upon which the assay is based.

Warnick GR, Nauck M, Rifai N: Evolution of methods for measurement of HDL-cholesterol: from ultracentrifugation to homogeneous assays, *Clin Chem* 47:1579–1596, 2001.

A comprehensive review of all methods used to measure HDL-C, with particular emphasis on the new homogeneous assays. It discusses the pros and cons of each assay and its accuracy, precision, and clinical usefulness, as well as the chemistry or technology upon which each is based.

Access the complete reference list online at Elsevier eBooks for Practicing Clinicians.

REFERENCES

Abell LL, Levy BB, Brodie BB, et al.: A simplified method for the estimation of total cholesterol in serum and demonstration of its specificity, *J Biol Chem* 195:357–366, 1952.

Abifadel M, Varret M, Rabes JP, et al.: Mutations in PCSK9 cause autosomal dominant hypercholesterolemia, *Nat Genet* 34:154–156, 2003.

AIM-HIGH Investigators, Boden WE, Probstfield JL, et al.: Niacin in patients with low HDL cholesterol levels receiving intensive statin therapy, *N Engl J Med* 365(24):2255–2267, 2011.

Alaupovic P: Apolipoproteins and lipoproteins, *Atherosclerosis* 13:141–146, 1971.

Albers JJ, Hazzard WR: Immunochemical quantification of human plasma Lp(a) lipoprotein, *Lipids* 9:15–26, 1974.

Andrus B, Lacaille D: 2013 ACC/AHA guideline on the assessment of cardiovascular risk, *J Am Coll Cardiol* 63(25 Pt A):2886, 2014.

Armstrong VW, Walli AK, Seidel D: Isolation, characterization, and uptake in human fibroblasts of an apo(a)-free lipoprotein obtained on reduction of lipoprotein (a)1, *J Lipid Res* 26:1314–1323, 1985.

Assman G, von Eckardstein A, Brewer HB: Familial high-density lipoprotein deficiency: Tangier's disease. In Scriver CR, Beaudet al, Sly SW, editors: *The metabolic basis of inherited disease*, ed 7, New York, 1995, McGraw-Hill, pp 2053–2072.

Babirak SP, Iverius PH, Fujimoto WY, et al.: Detection and characterization of the heterozygote state for lipoprotein lipase deficiency, *Arteriosclerosis* 9:326–334, 1989.

Bachorik PS, Kwiterovich Jr PO: Apolipoprotein measurements in clinical biochemistry and their utility vis-a-vis conventional assays, *Clin Chim Acta* 178:1–34, 1988.

Bachorik PS, Rock R, Cloey T, et al.: Cholesterol screening: Comparative evaluation of on-site and laboratory-based measurements, *Clin Chem* 36:255–260, 1990.

Bachorik PS, Virgil DG, Kwiterovich PO: Effect of apolipoprotein E-free high-density lipoproteins on cholesterol metabolism in cultured pig hepatocytes, *J Biol Chem* 262:13636–13645, 1987.

Bachorik PS, Wood PDS, Albers JJ, et al.: Plasma high-density lipoprotein cholesterol concentrations determined after removal of other lipoproteins by heparin/manganese precipitation or by ultracentrifugation, *Clin Chem* 22:1828–1834, 1976.

Bachorik PS: Measurement of low density lipoprotein cholesterol. In Rifai N, Warnick GR, Dominiczak MH, editors: *Handbook of lipoprotein testing*, Washington, DC, 2000, AACC Press.

Bamba V, Rader DJ: Obesity and atherogenic dyslipidemia, *Gastroenterology* 132(6):2181–2190, 2007.

Bergt C, Pennathur S, Fu X, et al.: The myeloperoxidase product hypochlorous acid oxidizes HDL in the human artery wall and impairs ABCA1-dependent cholesterol transport, *Proc Natl Acad Sci U S A* 101(35):13032–13037, 2004.

Bhatt DL, Steg PG, Miller M, et al.: Cardiovascular risk reduction with Icosapent Ethyl for hypertriglyceridemia, *N Engl J Med* 380(1):11–22, 2019.

Blanche PJ, Gong EL, Forte TM, et al.: Characterization of human high-density lipoproteins by gradient gel electrophoresis, *Biochim Biophys Acta* 665:408–419, 1981.

Bookstein L, Gidding SS, Donovan M, et al.: Day-to-day variability of serum cholesterol, triglyceride and high-density lipoprotein cholesterol levels, *Arch Intern Med* 150:1653–1657, 1990.

Bravo I, Amigo L, Cohen DE, et al.: Role of plasma and liver cholesterol- and lipoprotein-metabolism determinants in LpX formation in the mouse, *Biochim Biophys Acta* 1770(6):979–988, 2007.

Breslow JL: Familial disorders of high-density lipoprotein metabolism. In Scriver CR, Beaudet al., Sly WS, et al.: editors: *The metabolic basis of inherited disease*, 7th ed, New York, 1995, McGraw-Hill, pp 2031–2052.

Brown MS, Kovanen PT, Goldstein JL: Regulation of plasma cholesterol by lipoprotein receptors, *Science* 212:628–635, 1981.

Brown SA, Boerwinkle E, Kashanian FK, et al.: Variation in concentrations of lipids, lipoprotein lipids, and apolipoproteins A-I and B in plasma from healthy women, *Clin Chem* 36:207–210, 1990.

Brunzell JD, Albers JJ, Chait AI, et al.: Plasma lipoprotein in familial combined hyperlipidaemia and monogenic familial hypertriglyceridaemia, *J Lipid Res* 24:147–155, 1983.

Brunzell JD: Familial lipoprotein lipase deficiency and other causes of the chylomicronemia syndrome. In Scriver CR, Beaudet al., Sly WS, et al.: editors: *The metabolic basis of inherited disease*, ed 7, New York, 1995, McGraw-Hill, pp 1913–1932.

Bucolo G, David H: Quantitative determination of serum triglycerides by the use of enzymes, *Clin Chem* 19:476–482, 1973.

Burstein M, Legmann P: Lipoprotein precipitation. In Clarkson TB, Kritchevsky D, Pollak OJ, editors: *Monographs on atherosclerosis (vol II)*, Basel S, 1982, Karger AG.

Byers SO, Friedman M: Site of origin of plasma triglyceride, *Am J Physiol* 198:629–631, 1960.

Calabresi L, Franceschini G: High-density lipoprotein and coronary heart disease: Insights from mutations leading to low high-density lipoprotein, *Curr Opin Lipidol* 8:219–224, 1997.

Cannon CP, Blazing MA, Giugliano RP, et al.: Ezetimibe added to statin therapy after acute coronary syndromes, *N Engl J Med* 372(25):2387–2397, 2015.

Cenedella RJ, Crouthamel WG: Intestinal versus hepatic contribution to circulating triglyceride levels, *Lipids* 9:35–42, 1974.

Chung S: Update on low-density lipoprotein cholesterol quantification, *Curr Opin Lipidol* 30(4):273–283, 2019.

Cohn JS, McNamara JR, Schaefer EJ: Lipoprotein cholesterol concentrations in plasma of human subjects as measured in the fed and fasted states, *Clin Chem* 34:2456–2459, 1988.

Connelly PW, Hegele RA: Hepatic lipase deficiency, *Crit Rev Clin Lab Sci* 35:547–572, 1998.

Corella D, Tai ES, Sorli JV, et al.: Association between the APOA2 promoter polymorphism and body weight in Mediterranean and Asian populations: Replication of a gene-saturated fat interaction, *Int J Obes (Lond)* 35(5):666–675, 2011.

Dangas GR, Mehran PC, Harpel SK, et al.: Lipoprotein(a) and inflammation in human coronary atheroma: association with the severity of clinical presentation, *J Am Coll Cardiol* 32(7):2035–2042, 1998.

Deacon AC, Dawson PJG: Enzymic assay of total cholesterol involving chemical or enzymic hydrolysis—a comparison of methods, *Clin Chem* 25:976–984, 1979.

Demacker PNM, Schade RWB, Jansen RTP, et al.: Intra-individual variation of serum cholesterol, triglycerides, and high-density lipoprotein cholesterol in normal humans, *Artherosclerosis* 45:259–266, 1982.

Fless GM, Rolih CQ, Scanu AM: Heterogeneity of human plasma lipoprotein(a). Isolation and characterization of the lipoprotein subspecies and their apoproteins, *J Biol Chem* 259:11470–11478, 1984.

Fless GM, ZumMallen ME, Scanu AM: Isolation of apolipoprotein(a) from lipoprotein(a), *J Lipid Res* 26:1224–1229, 1985.

Floren C-H, Albers JJ, Bierman EL: Uptake of Lp(a) lipoprotein by cultured fibroblasts, *Biochem Biophys Res Commun* 102:636, 1981.

Fojo SS, Brewer HB: Hypertriglyceridaemia due to genetic defects in lipoprotein lipase and apolipoprotein C-II, *J Intern Med* 231:669–677, 1992.

Frayn KN, Karpe F, Fielding BA, et al.: Integrative physiology of human adipose tissue, *Int J Obes Relat Metab Disord* 27(8):875–888, 2003.

Fredrickson DS, Levy RI, Lees RS: Fat transport in lipoproteins—an integrated approach to mechanisms and disorders, *N Engl J Med* 276(34–42):94–103, 1967. 148–156, 215–225, 273–281.

Friedewald WT, Levy RI, Fredrickson DS: Estimation of the concentration of low-density lipoprotein cholesterol in plasma without use of the preparative ultracentrifuge, *Clin Chem* 18:499–502, 1972.

Fruchart JC, Ailhaud G: Apolipoprotein A-containing particles: Physiological role, quantification and clinical significance, *Clin Chem* 38:793–797, 1992.

Gaubatz JW, Heideman C, Gotto Jr AM, et al.: Human plasma lipoprotein(a). Structural properties, *J Biol Chem* 258:4582–4589, 1983.

Ginsberg HN, Elam MB, Lovato LC, et al.: Effects of combination lipid therapy in type 2 diabetes mellitus, *N Engl J Med* 362(17):1563–1574, 2010.

Glass C, Pittman RC, Weinstein DB, et al.: Dissociation of tissue uptake of cholesterol ester from that of apoprotein A-I of rat plasma high-density lipoprotein: selective delivery of cholesterol ester to liver, adrenal and gonad, *Proc Natl Acad Sci U S A* 80:5435–5439, 1983.

Goldberg AC, Hopkins PN, Toth PP, et al.: Familial hypercholesterolemia: screening, diagnosis and management of pediatric and adult patients: clinical guidance from the National Lipid Association Expert Panel on familial hypercholesterolemia, *J Clin Lipidol* 5(3):133–140, 2011.

Gotto Jr AM, Pownall HJ, Havel RJ: Introduction to the plasma lipoproteins, *Meth Enzymol* 128(3–41), 1986.

Gotto AM, Whitney E, Stein EA, et al.: The relation between baseline and on-treatment lipid parameters and first acute major coronary events in the Air Force/Texas Coronary Artery Prevention Study (AFCAPS/TEXCAPS), *Circulation* 101:477–484, 2000.

Green PHR, Glickman RM: Intestinal lipoprotein metabolism, *J Lipid Res* 22:1153–1173, 1981.

Greenland P, Blaha MJ, Budoff MJ, Erbel R, Watson KE: Coronary calcium score and cardiovascular risk, *J Am Coll Cardiol* 72(4):434–447, 2018.

Gries A, Fievet C, Marcovina S, et al.: Interaction of LDL, Lp(a), and reduced Lp(a) with monoclonal antibodies against apoB, *J Lipid Res* 29(1–8), 1988.

Grundy SM, Stone NJ, Bailey AL, et al.: 2018 AHA/ACC/AACVPR/AAPA/ABC/ACPM/ADA/AGS/APhA/ASPC/NLA/PCNA guideline on the management of blood cholesterol: a report of the American College of Cardiology/American Heart Association Task Force on clinical practice guidelines, *Circulation* 139(25):e1082–e1143, 2019.

Hansen PS: Familial defective apolipoprotein B-100, *Danish Med Bull* 45:370–382, 1998.

Havel RJ: Lipoprotein biosynthesis and metabolism, *Ann N Y Acad Sci* 348:16–29, 1980.

Hegele RA: Plasma lipoproteins: genetic influences and clinical implications, *Nat Rev Genet* 10:109–121, 2009.

Hobbs HH, Brown MS, Goldstein JL: Molecular genetics of the LDL-receptor gene in familial hypercholesterolemia, *Hum Mutation I*445–466, 1992.

Hopkins PN, Heiss G, Ellison RC, et al.: Coronary artery disease risk in familial combined hyperlipidemia and familial hypertriglyceridemia: a case-control comparison from the National Heart, Lung, and Blood Institute Family Heart Study, *Circulation* 108:519–523, 2003.

HPS2-THRIVE Collaborative Group, Landray MJ, Haynes R, et al.: Effects of extended-release niacin with laropiprant in high-risk patients, *N Engl J Med* 371(3):203–212, 2014.

Hussain MM, Kancha RK, Zhou Z, et al.: Chylomicron assembly and catabolism: role of apolipoproteins and receptors, *Biochim Biophys Acta* 1300:151–170, 1996.

Hussain MM, Rava P, Walsh M, et al.: Multiple functions of microsomal triglyceride transfer protein, *Nutr Metab* 9(14), 2012.

Hussain MM, Shi J, Dreizen P: Microsomal triglyceride transfer protein and its role in apoB-lipoprotein assembly, *J Lipid Res* 44(22–32), 2003.

Hwang YC, Fujimoto WY, Hayashi T, Kahn SE, Leonetti DL, Boyko EJ: Increased visceral adipose tissue is an independent predictor for Future development of atherogenic dyslipidemia, *J Clin Endocrinol Metab* 101(2):678–685, 2016.

Jones B, Jones EL, Bonney SA, et al.: Mutations in a Sar1 GTPase of COPII vesicles are associated with lipid absorption disorders, *Nat Genet* 34:29–31, 2003.

Kafonek SD, Derby CA, Bachorik PS: Biological variability of lipoproteins and apolipoproteins in patients referred to a lipid clinic, *Clin Chem* 38:864–872, 1992.

Kafonek SD, Donovan L, Lovejoy KL, et al.: Biological variation of lipids and lipoproteins in fingerstick blood, *Clin Chem* 42:2002–2007, 1996.

Karatasakis A, Danek BA, Karacsonyi J, et al.: Effect of PCSK9 inhibitors on clinical outcomes in patients with hypercholesterolemia: a Meta-analysis of 35 randomized controlled trials, *J Am Heart Assoc* 6(12), 2017.

Kato R, Mori C, Kitazato K, et al.: Transient increase in plasma oxidized LDL during the progression of atherosclerosis in apolipoprotein E knockout mice, *Arterioscler Thromb Vasc Biol* 29(1):33–39, 2009.

Kidambi S, Patel SB: Sitosterolaemia: pathophysiology, clinical presentation and laboratory diagnosis, *J Clin Pathol* 61:588–594, 2008.

Koch TR, Mehta U, Lee H, et al.: Bias and precision of cholesterol analysis of physician's office analyzers, *Clin Chem* 33:2262–2267, 1987.

Kontush A, Chapman MJ: Antiatherogenic small, dense HDL—Guardian angel of the arterial wall? *Nat Clin Pract Cardiovasc Med* 3(3):144–153, 2006.

Kotani K, Sakane N, Ueda M, et al.: Oxidized high-density lipoprotein is associated with increased plasma glucose in non-diabetic dyslipidemic subjects, *Clin Chim Acta* 414:125–129, 2012.

Krauss RM, Blanche PJ: Detection and quantitation of LDL subfractions, *Curr Opin Lipidol* 3:377–383, 1992.

Krauss RM: Relationship of intermediate and low-density lipoprotein subspecies to risk of coronary heart disease, *Am Heart J* 113:578–582, 1987.

Kuivenhoven JA, Pritchard H, Hill J, et al.: The molecular pathology of lecithin:cholesterol acyltransferase (LCAT) deficiency syndromes, *J Lipid Res* 38:191–205, 1997.

Kuo PT, Wilson AC, Kostis JB: Treatment of type III hyperlipoproteinemia with gemfibrozil to retard progression of coronary artery disease, *Am Heart J* 116:85–90, 1988.

Laboratory Methods Committee of the Lipid Research Clinics Program: Cholesterol and triglyceride concentrations in serum/plasma pairs, *Clin Chem* 23:60, 1977.

Law WT, Doshi S, McGeehan J, et al.: Whole-blood testing for total cholesterol by a self-metering, self-timing disposable device with built in quality control, *Clin Chem* 43:384–389, 1997.

Li WW, Dammerman MM, Smith JD, et al.: Common genetic variation in the promoter of the human apo CIII gene abolishes regulation by insulin and may contribute to hypertriglyceridemia, *J Clin Invest* 96:2601–2605, 1995.

Lin B, Huang Y, Zhang M, et al.: Association between apolipoprotein C3 Sst I, T-455C, C-482T and C1100T polymorphisms and risk of coronary heart disease, *BMJ Open* 4(1):e004156, 2014.

Lipid Research Clinics Program: *Manual of laboratory operations. Lipid and lipoprotein analysis.U.S. Department of Health and Human Services*, *Publication No.(NIH)* 75, 1982. Revised September.

Lopes-Virella MFL, Virella G, Evangs G, et al.: Immunocephelometric assay of human apoliprotein A, *J Clin Chem* 26:1205–1208, 1980.

Loscalzo J, Weinfeld M, Fless GM, et al.: Lipoprotein(a), fibrin binding, and plasminogen activation, *Arteriosclerosis* 10(2):240–245, 1990.

Lunz ME, Castleberry BM, James K, et al.: The impact of the quality of laboratory staff on the accuracy of laboratory results, *J Am Med Assoc* 258:361–363, 1987.

MacKenzie SL, Sundaram GS, Sodhi HS: Heterogeneity of human high-density lipoprotein (HDL2), *Clin Chim Acta* 43:223–229, 1973.

Mahley RW, Rall SC: Type III hyperlipoproteinaemia (dysbetalipoproteinemia): the role of apolipoprotein E in normal and abnormal lipoprotein metabolism. In Scriver CR, Beaudet al, Sly WS, et al.: *The metabolic basis of inherited disease*, ed 7, New York, 1995, McGraw-Hill, pp 1953–1986.

Martin SS, Blaha MJ, Elshazly MB, et al.: Comparison of a novel method vs the Friedewald equation for estimating low-density lipoprotein cholesterol levels from the standard lipid profile, *J Am Med Assoc* 310(19):2061–2068, 2013.

McNeill AM, Rosamond WD, Girman CJ, et al.: The metabolic syndrome and 11-year risk of incident cardiovascular disease in the atherosclerosis risk in communities study, *Diabetes Care* 28(2):385–390, 2005.

Miller M, Bachorik PS, Cloey TA: Normal variation of plasma lipoproteins: postural effects on plasma concentrations of lipids, lipoproteins and apolipoproteins, *Clin Chem* 38:569–574, 1992.

Miller M, Stone NJ, Ballantyne C, et al.: Triglycerides and cardiovascular disease: a scientific statement from the American Heart Association, *Circulation* 123:2292–2333, 2011.

Miller WG, Waymack PP, Anderson FP, et al.: Performance of four homogenous direct methods for LDL-cholesterol, *Clin Chem* 48(3):489–498, 2002.

Mohiuddin I, Chai H, Lin PH, et al.: Nitrotyrosine and chlorotyrosine: clinical significance and biological functions in the vascular system, *J Surg Res* 133(2):143–149, 2006.

Moore KJ, Fisher EA: Dysfunctional HDL takes its toll in chronic kidney disease, *Immunity* 38(4):628–630, 2013.

Moriarty PM, Parhofer KG, Babirak SP, et al.: Alirocumab in patients with heterozygous familial hypercholesterolaemia undergoing lipoprotein apheresis: the ODYSSEY ESCAPE trial, *Eur Heart J* 37(48):3588–3595, 2016.

Myers GL, Cooper GR, Winn CL, et al.: The Centers for Disease Control–National Heart, Lung and Blood Institute lipid standardization Program. An approach to accurate and precise lipid measurements, *Clin Lab Med* 9:105–135, 1989.

Naito HK, David JA: Laboratory considerations: determination of cholesterol, triglyceride, phospholipid, and other lipids in blood and tissues. In Story JA, editor: *Lipid research methodology*, New York, 1984, Alan R Liss.

Naito HK, Kwak YS: The evaluation of a new high-density lipoprotein cholesterol (HDL-C) technology; selective separation of lipoproteins by magnetic separation, *Clin Chem* 41:S135, 1995.

National Cholesterol Education Program Working Group on Lipoprotein Measurement: *Recommendations on lipoprotein measurement*, *Bethesda*, *Md*, 1995. NIH. Publication No. 95-3044.

National Cholesterol Education Program: Highlights of the report of the Expert panel on blood cholesterol levels in children and adolescents, *Pediatrics* 89:495–501, 1992.

Niu DM, Chong KW, Hsu JH, et al.: Clinical observations, molecular genetic analysis, and treatment of sitosterolemia in infants and children, *J Inherit Metab Dis* 33:437–443, 2010.

Ooi EM, Barrett PH, Chan DC, Apolipoprotein III C-, et al.: Understanding an emerging cardiovascular risk factor, *Clin Sci (Lond)* 114:611–624, 2008.

Oppenheimer MJ, Oram JF, Bierman EL: Downregulation of high-density lipoprotein receptor activity of cultured fibroblasts by platelet-derived growth factor, *Arteriosclerosis* 7:325–332, 1987.

Oram JF: Receptor-mediated transport of cholesterol between cultured cells and high-density lipoproteins, *Meth Enzymol* 129:645–659, 1986.

Ose L: An update on familial hypercholesterolaemia, *Ann Med* 31(Suppl 1):13–18, 1999.

Otvos J, Jeyarajah E, Bennett DW, et al.: Development of a proton nuclear magnetic resonance spectroscopic method for determining plasma lipoprotein concentrations and subspecies distributions from a single, rapid measurement, *Clin Chem* 39:1632–1638, 1992.

Otvos JD: Measurement of lipoprotein subclass profiles by nuclear magnetic resonance spectroscopy, *Clin Lab* 48(3–4):171–180, 2002.

Peelman F, Verschelde JL, Vanloo B, et al.: Effects of natural mutations in lecithin:cholesterol acyltransferase on the enzyme structure and activity, *J Lipid Res* 40:59–69, 1999.

Pesce MA, Bodourian SH: Interference with the enzymatic measurement of cholesterol in serum by use of five reagent kits, *Clin Chem* 23:757–760, 1977.

Raal F, Scott R, Somaratne R, et al.: Low-density lipoprotein cholesterol-lowering effects of AMG 145, a monoclonal antibody to proprotein convertase subtilisin/kexin type 9 serine protease in patients with heterozygous familial hypercholesterolemia: the Reduction of LDL-C with PCSK9 Inhibition in Heterozygous Familial Hypercholesterolemia Disorder (RUTHERFORD) randomized trial, *Circulation* 126(20):2408–2417, 2012.

Rifai N, Warnick GR, Dominiczak MH: Handbook of lipoprotein testing, *Am Assoc Clin Chem*, 2000.

Risser TR, Reaven GM, Reaven EP: Intestinal contribution to secretion of very-low-density lipoproteins into plasma, *Am J Physiol* 234:E277–E281, 1978.

Robinson D, Bevan EA, Hinohara S, et al.: Seasonal variation in serum cholesterol levels—evidence from the UK and Japan, *Atherosclerosis* 95:15–24, 1992.

Rust S, Rosier M, Funke H, et al.: Tangier disease is caused by mutations in the gene encoding ATP-binding cassette transporter 1, *Nat Genet* 22:352–355, 1999.

Sabatine MS, Giugliano RP, Keech AC, et al.: Evolocumab and clinical outcomes in patients with cardiovascular disease, *N Engl J Med* 376(18):1713–1722, 2017.

Samson SL, Garber AJ: Metabolic syndrome, *Endocrinol Metab Clin North Am* 43(1):1–23, 2014.

Scanu AM, Byrne RE, Mihovilovic M: Functional roles of plasma high-density lipoproteins, *CRC Crit Rev Biochem* 13:109–140, 1982.

Scanu AM: Lipoprotein(a). A potential bridge between the fields of atherosclerosis and thrombosis, *Arch Pathol Lab Med* 112:1045–1047, 1988.

Schwartz GG, Steg PG, Szarek M, et al.: Alirocumab and cardiovascular outcomes after acute coronary syndrome, *N Engl J Med* 379(22):2097–2107, 2018.

Shao B, Heinecke JW: Quantifying HDL proteins by mass spectrometry: how many proteins are there and what are their functions? *Expert Rev Proteomics* 15(1):31–40, 2018.

Sirwi A, Hussain MM: Lipid transfer proteins in the assembly of apoB-containing lipoproteins, *J Lipid Res* 59(7):1094–1102, 2018.

Sniderman AD, Blank D, Zakarian R, et al.: Triglycerides and small dense LDL: the twin Achilles heels of the Friedewald formula, *Clin Biochem* 36:499–504, 2003.

Soutar AK: Update on low-density lipoprotein receptor mutations, *Curr Opin Lipidol* 9:141–147, 1998.

Stein O, Stein Y, Coetzee GA, et al.: Metabolic fate of low-density lipoprotein and high-density lipoprotein labeled with an ether analogue of cholesteryl ester, *Klin Wochenschr* 62:1151–1156, 1984.

Sugiuchi H, Irie T, Uji Y, et al.: Homogenous assay for measuring low-density lipoprotein cholesterol in serum with triblock co-polymer and alpha-cyclodextrin sulfate, *Clin Chem* 44:522–531, 1998.

Sundaram GS, MacKenzie SL, Sodhi HS: Preparative isoelectric focusing of human serum high-density lipoprotein (HPL3), *Biochem Biophys Acta* 337:196–203, 1974.

Tall AR: Plasma high-density lipoproteins: metabolism and relationship to atherogenesis, *J Clin Invest* 86:379–384, 1990.

Tall AR, Rader DJ: Trials and Tribulations of CETP inhibitors, *Circ Res* 122(1):106–112, 2018.

Thanassoulis G: Using genetics to plan Future randomized trials of lipoprotein(a) lowering-how much reduction, for how long, and in whom? *JAMA Cardiol* 4(6):513–514, 2019.

Tsimikas S: A test in Context: lipoprotein(a): diagnosis, Prognosis, Controversies, and emerging therapies, *J Am Coll Cardiol* 69(6):692–711, 2017.

Tsubakio-Yamamoto K, Nishida M, Nakagawa-Toyama Y, et al.: Current therapy for patients with sitosterolemia—effect of ezetimibe on plant sterol metabolism, *J Atheroscler Thromb* 17:891–900, 2010.

Varret M, Abifadel M, Rabes JP, et al.: Genetic heterogeneity of autosomal dominant hypercholesterolemia, *Clin Genet* 73(1–13), 2008.

Walsh MT, Hussain MM: Targeting microsomal triglyceride transfer protein and lipoprotein assembly to treat homozygous familial hypercholesterolemia, *Crit Rev Clin Lab Sci* 54(1):26–48, 2017.

Wang G, Wang Z, Liang J, et al.: A phytosterolemia patient presenting exclusively with macrothrombocytopenia and stomatocytic hemolysis, *Acta Haematol* 126:95–98, 2011.

Warden CH, Daluiski A, Bu X, et al.: Evidence for linkage of the apolipoprotein A-II locus to plasma apolipoprotein A-II and free fatty acid levels in mice and humans, *Proc Natl Acad Sci U S A* 90(22):10886–10890, 1993.

Warnick GR, Cheung MC, Albers JJ: Comparison of current methods for high-density lipoprotein cholesterol quantitation, *Clin Chem* 25:596–604, 1979.

Wood PD, Bachorik PS, Albers JJ, et al.: An investigation of the effects of sample aging on total cholesterol values determined by the automated ferric chloride-sulfuric acid and Liebermann–Burchard procedures, *Clin Chem* 26:592–597, 1980.

Wu J, Kim J, Li Q, et al.: Known mutations of apoB account for only a small minority of hypobetalipoproteinemia, *J Lipid Res* 40:955–959, 1999.

Yokoyama M, Origasa H, Matsuzaki M, et al.: Effects of eicosapentaenoic acid on major coronary events in hypercholesterolaemic patients (JELIS): a randomised open-label, blinded endpoint analysis, *Lancet* 369(9567):1090–1098, 2007.

Zheng L, Nukuna B, Brennan ML, et al.: Apolipoprotein A-I is a selective target for myeloperoxidase-catalyzed oxidation and functional impairment in subjects with cardiovascular disease, *J Clin Invest* 114(4):529–541, 2004.

Zivkovic AM, Wiest MM, Nguyen UT, et al.: Effects of sample handling and storage on quantitative lipid analysis in human serum, *Metabolomics* 5(4):507–516, 2009.

CHAPTER 19

CARDIAC INJURY, ATHEROSCLEROSIS, AND THROMBOTIC DISEASE

Jay L. Bock

OVERVIEW, 267
BACKGROUND, 267
MARKERS OF MYOCARDIAL DAMAGE, 269
Historical Development, 269
Cardiac Troponin, 269
Other Markers—Copeptin, 270
Assay Procedures, 270
Clinical Protocols, 270
MARKERS OF CORONARY RISK, 272
C-Reactive Protein, 272
Homocysteine, 272
MARKERS OF CONGESTIVE HEART FAILURE, 273
Cardiac Natriuretic Peptides, 273
Other Heart Failure Biomarkers, 275
OTHER CONDITIONS ASSOCIATED WITH ATHEROSCLEROSIS OR THROMBOSIS, 275
SELECTED REFERENCES, 275

KEY POINTS

- The most important disease affecting the heart is atherosclerotic cardiovascular disease (ASCVD), caused by plaque in the coronary arteries. ASCVD can lead to thrombotic occlusion of coronary blood flow, causing an acute coronary syndrome (ACS). ACS with frank necrosis of any amount of myocardium is known as myocardial infarction (MI).
- The primary tests for diagnosing and evaluating ACS are electrocardiography (ECG) and laboratory measurement of cardiac troponin (cTn).
- Troponin is a complex of three proteins, part of the contractile apparatus of all muscle cells but with two isoforms that are specific to myocardium: cTnI and cTnT. These two proteins have different properties, but their clinical applications are similar. Clinically, MI is now essentially defined as an ACS that causes release of cTn.
- The latest generation of cTn tests, referred to as high-sensitivity cTn (hs-cTn), can measure levels of the protein down to the normal range. With hs-cTn, elevated levels can typically be detected within an hour after the onset of MI. Plasma cTn then peaks in about 24 hours and declines to baseline over the next several days.
- Patients presenting to an emergency department with symptoms suggesting ACS must be processed rapidly and precisely to provide lifesaving interventions as needed yet avoid the cost and morbidity of unnecessary procedures. Rapid measurement of cTn, and possibly secondary markers such as copeptin, plays a critical role.
- The clinical laboratory also measures risk factors associated with the development and progression of ASCVD. Significant laboratory markers of risk include lipids (cholesterol, triglycerides, and specific lipoprotein fractions—see Chapter 18), homocysteine (Hcy), and C-reactive protein (CRP). Hcy is an amino acid that exacerbates thrombosis. CRP is an inflammatory marker that appears to reflect the severity of ASCVD and may contribute to its pathogenesis.
- ASCVD and other heart diseases can impair the heart's ability to pump blood, causing the clinical syndrome of heart failure (HF). B-type natriuretic peptide (BNP), a 32 amino acid peptide secreted by the cardiac ventricles in response to wall-stretch stimuli, is a marker of the presence and severity of HF. BNP testing is particularly useful for aiding the differential diagnosis of patients who present to an emergency department with shortness of breath.
- Atherosclerosis affecting the carotid arteries or brain vasculature can lead to ischemic or hemorrhagic stroke. Some biomarkers show promise for the diagnosis or evaluation of stroke, but none are sufficiently discriminatory for routine use at present.
- Measurement of D-dimer, a degradation product of fibrin, has excellent sensitivity but poor specificity for the diagnosis of pulmonary embolism and venous thrombotic disease in general.
- Advances in methodology, standardization, and decision-point assignment for hs-cTn, BNP, D-dimer, and other cardiac-related tests are ongoing and essential for optimizing clinical outcomes.

OVERVIEW

Heart disease is an affliction intimately tied to high technology. Technology has had a causal role, in part by allowing people to live longer and in part by enabling a sedentary and overly consumptive lifestyle. During the twentieth century, heart disease rose from obscurity to become the leading cause of morbidity and mortality in developed nations (Box 19.1). Diagnosis and treatment of heart disease also depend heavily on advanced technology, including electrophysiologic, imaging, catheterization, surgical, and clinical laboratory modalities. The following major laboratory applications will be the subject of this chapter.

1. Measurement of proteins present in cardiac myocytes indicates recent damage to cardiac muscle. These tests are used mainly for the diagnosis and management of ischemic events (acute coronary syndromes [ACSs]). Although many different markers of ischemic damage have been used in the past, at present the most important marker by far is *cardiac troponin* (cTn).
2. Measurement of substances that are damaging to the coronary arteries, or at least have proven association with atherosclerotic cardiovascular disease (ASCVD), is used to assess risk and select appropriate preventive measures. The most important laboratory risk factors are lipids, which are discussed in Chapter 18. Two others will be discussed in this chapter: homocysteine (Hcy) and C-reactive protein (CRP).
3. Measurement of natriuretic peptides released from myocardium, particularly *B-type natriuretic peptide* (BNP) and the related inactive fragment, *N-BNP* or *NT-pro-BNP*, reflects the presence and severity of heart failure.
4. Laboratory testing has been less applicable to cerebrovascular disease, but some new biomarkers show promise. Measurement of D-dimer is useful in ruling out pulmonary embolus.

BACKGROUND

It is ironic that for the heart, an organ that pumps several liters of blood each minute, the most important disease process is ischemia—the lack of an adequate blood supply. This is so because heart muscle depends on constant nutrition through a system of coronary arteries, which are highly vulnerable to the process of atherosclerosis. Atherosclerosis is a chronic process involving damage to endothelium and the buildup of vessel-occluding lesions called *plaque*. In the early stages of atherosclerosis, as coronary blood flow is gradually reduced, there are typically no symptoms or laboratory evidence of cardiac injury. Once the diameter of a coronary artery is reduced to less than 10% to 20% of its original size, chest pain (angina pectoris) often develops when demand for oxygen increases, particularly during exercise (exertional angina). More rapid reduction in blood flow can occur when plaque stimulates formation of a thrombus in a coronary artery, leading to an ACS. When a thrombus completely cuts off blood flow, the supplied muscle will develop irreversible ischemic damage, and the syndrome is a myocardial infarction (MI). When the blockage is not complete, irreversible muscle damage may be avoided, but the patient

BOX 19.1

Heart Disease Statistics for the United States

- An estimated 48% of the adult population (≥20 years of age), has some form of cardiovascular disease (including ASCVD, HF, stroke, and hypertension). Excluding hypertension, that reduces to 9.0% of the population, or about 24.3 million adults.
- 805,000 new or recurrent MIs occur each year, and 18.2 million Americans have experienced an MI or have other history of ASCVD.
- 795,000 new or recurrent strokes occur each year, and 7.0 million Americans have experienced a stroke.
- 6.2 million Americans have HF.
- The economic cost of cardiovascular disease, including indirect costs such as loss of work productivity, etc., is estimated at about $555 billion for 2015, and to increase substantially in subsequent years, particularly for the elderly.
- Favorable trends in ASCVD include less cigarette smoking and effective pharmacotherapy for hypertension and hyperlipidemia. However, the epidemic is now growing due to an alarming increase in the prevalence of obesity and type 2 diabetes.

From Benjamin EJ, Muntner P, Alonso A, et al.: Heart disease and stroke statistics—2019 update: a report from the American Heart Association. *Circulation* 139:e56–e528, 2019. *ASCVD,* atherosclerotic cardiovascular disease; *CVD,* cardiovascular disease; *HF,* heart failure; *MI,* myocardial infarction.

will experience severe angina, even at rest, and this syndrome is known as unstable angina (UA). The broad spectrum of heart disease resulting from impaired coronary blood flow has been referred to by many names and acronyms over the years: for example, atherosclerotic heart disease (ASHD), coronary heart disease (CHD), ischemic heart disease (IHD), etc. Organizations that publish consensus guidelines, such as the American Heart Association, have recently adopted the term *atherosclerotic cardiovascular disease* (ASCVD), which we will employ henceforth. Common acronyms used to describe heart disease are listed in Table 19.1.

MIs can be categorized by whether they are accompanied by characteristic changes on the electrocardiogram (ECG), a recording of electrical activity in the heart. Only requiring simple voltage recordings between electrodes attached to the skin surface, the ECG was introduced in the late nineteenth century and has played a central role in cardiac diagnosis ever since. Portions of the waveform associated with each heartbeat are assigned the letters P through U. Severe MIs, generally involving transmural damage to the myocardium, disrupt electrical flow and typically cause the rapid appearance of readily identified changes known as ST-segment elevations and the later appearance of Q-waves. These are categorized as ST-elevation MIs (STEMIs). Lesser amounts of damage may cause ECG alterations that are not sufficiently specific for diagnosis or may cause no ECG change whatsoever. These smaller MIs are known as non-ST elevation MIs (NSTEMIs). Even with only a small amount of damage to myocardium, any ACS event carries risk for possibly lethal arrhythmias and for future events. Damage to a sizable quantity of cardiac muscle carries the additional risk of compromising the heart's ability to pump blood, leading to the clinical syndrome of heart failure (HF), which is discussed later.

Cardiac muscle is relatively resistant to ischemia compared with other cells, such as neurons and renal tubular epithelial cells, in which even short duration of ischemia can lead to cell death. In experimental animals, complete blockage of blood flow to an area of the heart does not cause cell death (MI) until after at least 20 to 30 minutes of ischemia; if blood flow had been previously restricted, cell death often is delayed for up to an hour. With complete coronary artery occlusion, there is typically a gradient of ischemia, with oxygen deprivation worst in areas receiving blood flow last (the subendocardial portions of the ventricular wall). Cells near the border between ischemic myocardium and normally perfused myocardium may receive some oxygen supply and thus may remain viable for several hours. The longer the duration of ischemia, the higher is the percentage of cells at risk that will die; 3 hours of ischemia increases cell death to 80% of cells at risk, and 6 hours of ischemia causes the death of almost 100% of cells at risk. For this reason, early recognition of persistent ischemia and intervention to restore blood flow are needed to minimize cell death. Blood flow is most commonly restored by manipulating the plaque (usually by inflating a balloon) via a catheter inserted into a peripheral vein and then threaded into the coronary circulation (percutaneous coronary intervention [PCI]). A mesh tube, or stent, may be inserted at the same time to maintain the patency of the coronary artery. When flow is blocked at multiple sites, it may be necessary to perform a coronary artery bypass graft (CABG).

TABLE 19.1

Clinical Abbreviations

ACS	Acute coronary syndrome
ASCVD	Atherosclerotic cardiovascular disease (also referred to as coronary heart disease [CHD], ischemic heart disease [IHD], and others)
CVD	Cardiovascular disease (comprising ASCVD, HF, stroke, and hypertension)
HF	(Congestive) heart failure
MI	(Acute) myocardial infarction
NSTEMI	Non–ST-elevation myocardial infarction
STEMI	ST-elevation myocardial infarction
UA	Unstable angina

Despite the central role of atherosclerosis and thrombosis in ACS, infarction can be the result of other processes causing an imbalance between oxygen supply and demand in the myocardium. The classical "heart attack" caused by coronary artery occlusion is now referred to as a *type 1 MI*. A type 2 MI is a similar clinical syndrome, not involving thrombotic occlusion of a coronary artery but rather caused by vasospasm, anemia, or other situations, often related to severe systemic illness, leading to insufficient oxygen delivery to myocardium. Extending this classification system, a type 3 MI occurs by definition when there is strong clinical evidence for MI but the patient succumbs before it can be confirmed by ECG and biochemical evidence. Types 4a, 4b, 4c, and 5 MI are related to cardiac interventional procedures (Thygesen et al., 2018).

The pathobiology of atherosclerosis and ACS remains incompletely understood (Usman et al., 2015; Wu et al., 2017). Formation of obstructive plaques probably begins with nonobstructive lesions known as fatty streaks, which have been observed in the coronary arteries of young individuals dying in combat or in accidents. The lesions are likely triggered by uptake of oxidized low-density lipoprotein (LDL) particles by macrophages, which then invade the coronary endothelium. Inflammatory cells and mediators play a role in the evolution of the lesion, which eventually becomes a structure containing a lipid core (mainly cholesterol esters) surrounded by numerous macrophages and other inflammatory cells and covered with a cap of endothelialized connective tissue. Advanced lesions also contain new blood vessels and calcium deposits. Plaques in coronary arteries were formerly regarded as passive, physiologically irreversible barriers to blood flow. In recent years, their more dynamic role in ACS has been appreciated. A balance of inflammatory mediators, shear forces, and other factors can cause the fibrous cap of the plaque to strengthen or weaken. Erosion of the cap can expose thrombogenic material, leading to deposition of platelets and eventually enlargement of the lesion. More ominous is actual rupture of the plaque, causing thrombosis with enough occlusion to result in ACS (Bentzon et al., 2014; Cornelissen et al., 2019). A major contributor to this concept of plaque vulnerability has been the finding that cholesterol-lowering statin drugs can diminish the risk of ACS substantially without causing appreciable diminution of the degree of stenosis caused by atherosclerotic lesions (see Chapter 18). The severity of coronary atherosclerotic disease has traditionally been evaluated by coronary angiography, which uses a radiopaque "dye" to image blood flow through the coronary arteries. Besides being invasive, this test has the limitation that it can identify restrictions only to coronary blood flow; it says nothing about the biology of the plaque lesions. Computed tomography can noninvasively image the accumulation of calcium in atherosclerotic lesions (the "calcium score"), but ability to predict the future behavior of lesions is still limited (Neves et al., 2017). Blood tests that directly reflect plaque vulnerability and the extent of atherosclerosis may be available in the future, but at present a patient's propensity to an ASCVD event is assessed indirectly through the measurement of risk factors, each of which appears to play a contributory but not necessarily definitive role. Several clinical parameters, summarized in Table 19.2, have been established as important risk factors. Additionally, hundreds of laboratory tests have been studied in relation to ASCVD risk. Of these, several lipid tests, as discussed in Chapter 18, have the best-established role in risk assessment. Two newer markers, Hcy and CRP, are discussed later.

Next to ASCVD, and often as a direct consequence of it, the most important heart disease is HF. HF is a clinical syndrome with prominent symptoms—including fatigue, shortness of breath, and pulmonary edema—resulting from impairment in the heart's pumping ability. It is most commonly caused by damage to the myocardium, as results from ASCVD. Because of the high incidence of ASCVD and the improving survival of people who suffer from it, HF is a rapidly increasing problem, especially in the elderly. HF can also be caused by mechanical problems,

TABLE 19.2

Nonlaboratory Risk Factors Used in Assessment of ASCVD Risk

Risk Factor	Recommendations
Age	In earlier guidelines, arbitrary age cutoffs, e.g., male >45 years, female >55 years, were used as indicators of ASCVD risk. Current guidelines recommend a continuous risk calculation based on the "pooled cohort equations" that incorporates age, gender, and race along with clinical and laboratory data. Risk assessment at regular healthcare visits is recommended for adults age 40–75 years who do not have a history of ASCVD.
Smoking	All adults should be assessed at every healthcare visit for tobacco use; those who use tobacco should be assisted and strongly advised to quit.
Poor diet	Diet should emphasize intake of vegetables, fruits, nuts, whole grains, lean vegetable or animal protein, and fish and minimize the intake of trans fats, processed meats, refined carbohydrates, and sweetened beverages.
Obesity	For adults with overweight and obesity, counseling and caloric restriction are recommended for achieving and maintaining weight loss.
Sedentary Lifestyle	Adults should engage in at least 150 minutes per week of accumulated moderate-intensity physical activity or 75 minutes per week of vigorous-intensity physical activity.
Hypertension	Nonpharmacologic interventions are recommended for all adults with elevated blood pressure or hypertension. For those requiring pharmacologic therapy, the target blood pressure should generally be <130/80 mm Hg.
Diabetes	For adults with type 2 diabetes mellitus, lifestyle changes, such as improving dietary habits and achieving exercise recommendations, are crucial. If medication is indicated, metformin is first-line therapy, followed by consideration of a sodium-glucose cotransporter 2 inhibitor or a glucagon-like peptide-1 receptor agonist.
Family history	Premature ASCVD in primary relatives (males, age <55 years; females, age <65 years) is a risk-enhancing factor for patient-clinician discussion.
Other	Chronic inflammatory disease, chronic kidney diseases, and some other conditions are risk-enhancing factors for patient-clinician discussion.
	Aspirin has little or no net benefit for primary prevention.

Recommendations are from a joint task force of the American College of Cardiology and American Heart Association.
Data from Arnett DK, Blumenthal RS, Albert MA, et al.: 2019 ACC/AHA Guideline on the Primary Prevention of Cardiovascular Disease. *Circulation* 140:e596-e646 2019.
ASCVD, Atherosclerotic cardiovascular disease.

such as valvular disease, which interfere with the pump function of the heart. When the problem is related to filling of the left ventricle during diastole, it is often referred to as diastolic HF.

Diagnosing HF and monitoring its progression can be difficult. A defining parameter for systolic HF is the left ventricular ejection fraction (LVEF), which is the fraction of the left ventricle's blood volume that is ejected during systole. It can be measured by echocardiography or by radionuclide ventriculography. Symptomatic HF is usually associated with LVEF <40%, but correlation between LVEF and subjective symptoms is poor. Laboratory testing can contribute to the evaluation and management of HF via measurement of natriuretic peptides and other biomarkers, as discussed later.

Of the myriad other diseases that can affect the heart, brief mention should be made of genetic diseases that, although relatively uncommon, have disproportionate importance because of their potentially life-threatening consequences. The advent of molecular diagnostics—sometimes referred to as "personalized cardiology" in this context—has created a major role for the clinical laboratory in diagnosis and management of these disorders. The syndrome of hypertrophic cardiomyopathy, described more than a century ago, occurs in 1 in 500 individuals and is the most common cause of sudden death in the young. At this date, thousands of variants in at least 15 genes have been related to this disorder; they affect various proteins of the contractile apparatus, including the troponins, actin, and myosin, and generally are inherited in autosomal-dominant fashion (Burns et al., 2017). The long-QT syndrome, an abnormality in ventricular repolarization that can cause sudden death, occurs in about 1 in 2000 individuals. It has several distinct variants caused by both autosomal-dominant and -recessive mutations in ion channels and other proteins (Tester & Ackerman, 2014). Identifying the affected gene can guide therapy in some cases as well as provide diagnostic confirmation (Pasipoularides, 2017).

MARKERS OF MYOCARDIAL DAMAGE

HISTORICAL DEVELOPMENT

Biochemical markers of myocardial damage were essentially a serendipitous discovery in the early 1950s, when Ladue and coworkers were investigating the enzymes now known as aspartate and alanine transaminase (Ladue et al., 1954). Surveying patients on the hospital wards, which at that time had many patients with suspected or confirmed MI, these investigators noted that serum transaminase levels rose sharply after an MI. They also put forward a rapid and practical spectrophotometric assay for serum transaminase (Karmen, 1955) and thus was born the era of "cardiac enzymes." The simple underlying principle, as with other organ markers, is that cell death will cause release of cellular proteins into the circulation. (A more difficult question, still not fully resolved, is the extent to which *reversible* cell damage can cause protein leakage (Mair et al., 2018; Wu, 2017).

It was immediately recognized that transaminases were abundant in liver muscle, skeletal muscle, and other tissues and therefore offered poor sensitivity and specificity for cardiac diagnosis. Superior enzymic markers were sought. Over the next few decades, testing for CK-MB (the MB isoenzyme of creatine kinase, also known as CK2) and, to a lesser extent, the LD1 isoenzyme of lactate dehydrogenase became popular. However, these required cumbersome isoenzyme separations and still offered limited cardiac specificity. It was only with the introduction of monoclonal antibody technology that a systematic search could be made for proteins specific to myocardium; that search led to the discovery of cardiac troponins (Bodor et al., 1992). For further discussion of transaminases and the classical "cardiac enzymes," see Chapter 21.

CARDIAC TROPONIN

Troponin (Tn) is a regulatory complex of three proteins that resides at regular intervals in the thin filament of striated muscle (Katrukha, 2013; Park et al., 2017). The three individual proteins are tropomyosin-binding subunit (TnT, 36 kDa), inhibitory subunit (TnI, 24 kDa), and calcium-binding subunit (TnC, 18 kDa). The Ca^{++} trigger for muscle contraction is transmitted via the Tn complex, which causes a conformational change in another thin-filament component, tropomyosin, allowing interaction between actin and myosin to proceed. In contrast to nearly all other muscle proteins, TnT and TnI both have distinct forms, coded by different genes, in cardiac muscle (myocardium), as well as in type 1, or "slow-twitch" and type 2, or "fast twitch," skeletal muscle fibers. Note that in a clinical context, "troponin" nearly always refers to cardiac-specific troponin because measurement of the noncardiac form has no clinical application. Here, we will employ the terms *cTnI* and *cTnT* for the respective cardiac proteins.

cTnI is always produced in the heart but never (or extraordinarily rarely) at any other site. Hence, cTnI is a tissue marker with extremely high sensitivity and specificity. With cTnT, the situation is a little more complicated because it has been detected in fetal skeletal muscle and diseased skeletal muscle. Posttranslational modifications may cause detectable differences between cTnT produced in myocardium and cTnT produced in diseased skeletal muscle that can improve their distinction by immunoassay (Apple, 1999). However, in rare cases. patients may have neuromuscular disease, without cardiac involvement, associated with increases in cTnT but not cTnI (Rittoo et al., 2014; Schmid et al., 2018).

The cTnT and cTnI within cardiac myocytes are predominantly bound to the muscle fibers and released slowly over the course of 1 to 2 weeks following myocardial injury. Thus, although cTnI and cTnT are relatively small proteins that are rapidly cleared, their plasma levels fall slowly after MI. A small fraction of cTn in the myocardial cell is free within the cytoplasm (or more loosely bound): 6% to 8% for cTnT and slightly less (2%–4%) for cTnI (Park et al., 2017). This fraction is released rapidly from injured cardiac myocytes. An increase in cTn is generally detectable using the most sensitive assays within 1 hour of an MI. cTn then reaches a peak at about 24 hours postevent, which may be thousands-fold greater than the baseline level (Fig. 19.1). Due to brisk renal clearance, a rapid decline in serum cTn follows, but because of the slow release of fiber-bound cTn, the rate of decline slows and there may even be a small secondary increase. It is important that such an increase *not* be interpreted as evidence of reinfarction. Circulating cTn declines to baseline levels in about 5 to 10 days, depending on infarct size.

cTnT and cTnI are present at very low concentrations in normal serum. Assays introduced in the 1990s, which we may refer to as "traditional"

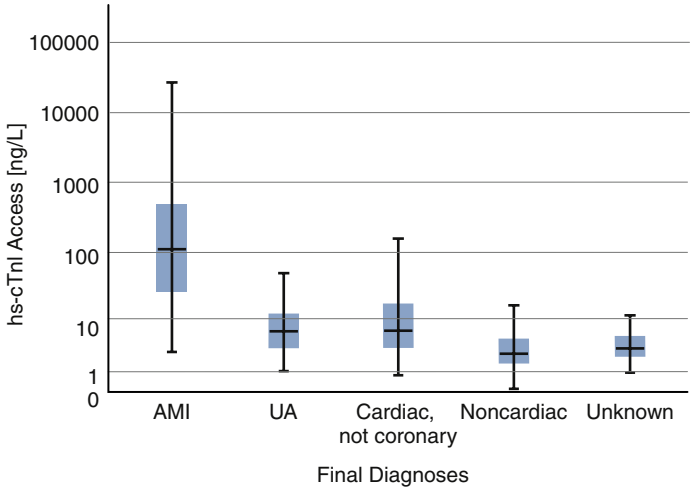

Figure 19.1 Box plots showing plasma cardiac troponin I levels in patients presenting to an emergency department with symptoms suspicious of an acute coronary syndrome (ACS) as a function of their final adjudicated diagnosis. Cardiac troponin I was measured using the Access high-sensitivity assay as part of a multi-institutional study of rapid myocardial infarction diagnosis. Boxes represent medians and intraquartile ranges, and whiskers display the smallest and the largest nonoutliers. *AMI*, acute myocardial infarction; UA, unstable angina. (Modified with permission from Boeddinghaus J, Nestelberger T, Twerenbold R, et al.: High-sensitivity cardiac troponin I assay for early diagnosis of acute myocardial infarction. *Clin Chem* 65:893–904, 2019.)

assays, had detection limits around 10 to 50 ng/L and could not reliably measure cTn in healthy individuals. More modern high-sensitivity (hs) assays have detection thresholds around 1 to 2 ng/L and an upper 99th percentile, commonly used as the reference range limit, of around 10 to 30 ng/L depending on patient characteristics (age, gender) and the particular assay. Levels above this threshold indicate myocardial damage, but it is important to recognize that slight elevations can reflect a very small amount of myocyte damage having questionable clinical significance. Even substantial elevations have many causes unrelated to MI or ASCVD. cTn elevations have been observed in pericarditis, myocarditis, pulmonary embolism, renal failure, sepsis, other critical illness, and even after intense exercise (Baker et al., 2019; Kelley et al., 2009). Pediatric data are limited, but it is clear that both cTnI and cTnT are increased in the neonatal period (Caselli et al., 2016; Jehlicka et al., 2018). The range of cTnI concentrations measured in patients presenting to an emergency department (ED) with suspicion of ACS is illustrated in Figure 19.1.

OTHER MARKERS—COPEPTIN

As discussed earlier, the history of cardiac markers dates to the 1950s, and many possible markers of cardiac injury have been considered over this long period. These include CK-MB and the other classical cardiac enzymes, myoglobin, glycogen phosphorylase BB isoenzyme, heart fatty-acid binding protein, myosin, and others (Mair, 1997). All of these are diagnostically inferior to cTn and do not usefully complement cTn testing, except perhaps in some very unusual circumstances; thus, they are not further discussed here. However, especially before the recent advent of hs-cTn, there has been some consideration that a nonspecific, rapidly secreted marker of stress might usefully complement cTn for early evaluation of ACS. The molecule copeptin has shown greatest promise in this regard. Copeptin is a 39-amino-acid peptide, molecular weight 5 kDa, that is produced in the hypothalamus as the C-terminus of pro-arginine-vasopressin, precursor of the water-conserving hormone arginine vasopressin (AVP) or antidiuretic hormone (ADH; see Chapters 9 and 15). Under conditions of acute stress, AVP and copeptin are secreted in stoichiometrically equivalent amounts, but copeptin is more suitable for laboratory analysis because of its greater stability. Following demonstration that copeptin is elevated following MI (Khan et al., 2007), studies suggested that copeptin measurement could improve early rule-out of NSTEMI compared with cTn alone (Reichlin et al., 2009; Ricci et al., 2016). Even with the newest hs-cTn assays, it may offer benefit (Roffi et al., 2016; Wildi et al., 2015).

ISCHEMIA-MODIFIED ALBUMIN AND GLYCOGEN PHOSPHORYLASE BB

Several other serodiagnostic protein markers have been proposed for the diagnosis of unstable angina and ACS, including ischemia-modified albumin (IMA) and the BB isozyme of glycogen phosphorylase (GPBB). IMA results from free radical-induced oxidation of a histidine residue of the amino terminal domain of albumin causing a conformational change blocking its binding to heavy metals such as cobalt. Assays for IMA are available that determine extent of binding of cobalt to albumin in sera. There are fundamentally three different isoenzymes of glycogen phosphorylase (GP): GPMM (present mainly in skeletal muscle), GPLL (mainly in liver), and GPBB (brain and myocardium). Immunoassays for GPBB are available to detect serum elevations of this GP isozyme. Although studies indicate that these two analytes can aid in the diagnosis of unstable angina and ACS, they are not currently in general use.

ASSAY PROCEDURES

cTn and other protein or peptide markers are universally measured by sensitive immunometric assays employing monoclonal antibodies, as described in Chapter 45. Measurement by mass spectrometry is possible and useful for standardization but not currently practical for direct clinical application (Schneck et al., 2018). Immunoassays can be adapted for either automated high-volume testing or manual point-of-care methodology. Recent improvements in sensitivity and specificity of the assays have resulted from adjustments of the methodology rather than major innovations. Performance characteristics of available methods have been summarized by the International Federation of Clinical Chemistry and Laboratory Medicine (IFCC) on their website (http://www.ifcc.org/ifcc-education-division/emd-committees/committee-on-clinical-applications-of-cardiac-bio-markers-c-cb/).

Despite the high performance of modern immunometric assays, they have intrinsic limitations that affect the clinical application of cTn. All proteins are heterogeneous analytes, making standardization difficult. cTn is especially heterogeneous, because it originates in a protein complex that degrades as it is released into the circulation. Circulating forms that have been identified include a ternary cTnT-I-C complex, binary cTnI-C, free cTnT (but not free cTnI), oxidized forms (cTnI but not cTnT contains cysteine residues that can be oxidized to form an intramolecular disulfide bond), phosphorylated forms, and degraded forms (Vylegzhanina et al., 2019). Immunoassays may react differently with these various forms depending on which epitopes the monoclonal antibodies are directed against. Tenfold or greater differences have been observed among commercial assays for cTnI (Tate et al., 2015), whereas cTnT assays at this time are marketed by only one manufacturer. International efforts at harmonization have resulted in preparation of certified reference material; its widespread adaptation will reduce systemic interassay bias, but individual specimens may still behave differently with assays that recognize different epitopes.

Immunoassays are also subject to interference. Because the normal level of plasma cTn is very low, even a minuscule degree of assay interference can elevate a result to the abnormal range. The most recent cTn assays seem much less prone to positive interferences than earlier generations, but heterophilic antibodies may still occasionally cause positive (Lippi et al., 2013) or negative interference (Eriksson et al., 2005). Another possible cause of negative interference is biotin (Schrapp et al., 2018), a vitamin normally present in plasma at minute concentrations but which can reach high concentrations if the patient is taking high-dose biotin supplements. Interference occurs when the assay uses biotin labeling of antibodies to allow capture by avidin-coated particles, in which case the capture is disrupted by exogenous biotin.

CLINICAL PROTOCOLS

Diagnosis of acute coronary syndrome

MI used to be loosely defined clinically based on the triad of clinical history, ECG, and cardiac "enzymes"—the diagnostic power of any one arm of this triad being quite limited. The exquisite tissue specificity of cTn has forced a rethinking since detecting its elevation in plasma suffices (with rare exceptions) to prove myocardial damage. Redefinitions of MI and related syndromes have therefore placed cTn testing in a central role; the current consensus approach is summarized in Table 19.3 (Thygesen et al., 2018). The dilemma remains that myocardial damage has diverse causes; thus, clinical judgment and other diagnostic modalities are still essential.

More than 8 million ED visits in the United States each year are related to chest pain or other symptoms, including shortness of breath, dizziness, or loss of consciousness, which may suggest ACS (Rui et al., 2016). Although diagnosis is often straightforward, the challenge is to achieve a very high level of accuracy. Missed diagnosis of ACS, which may occur in about 2% of cases, carries an increased risk of mortality and has been the leading cause of malpractice payout for emergency physicians (Karcz et al., 1996; Pope et al., 2000). On the other hand, the conservative practice of

TABLE 19.3

Guidelines Relating Cardiac Troponin Testing to Clinical Diagnoses in the Fourth Universal Definition of Myocardial Infarction

Diagnosis	Criteria
Myocardial injury	• Any elevated result for cTn, defined as a result above the 99th percentile of a reference population
Acute myocardial injury	• At least one elevated result for cTn • Evidence of a rise and/or fall in cTn
Acute myocardial infarction (MI), Type 1, 2, or 3 (not related to a cardiac interventional procedure)	• Acute myocardial injury, as defined above • Clinical, ECG, or imaging evidence of myocardial ischemia
Acute myocardial infarction, Type 4a (following percutaneous coronary intervention)	• Within 48 hours of the procedure, cTn is >5 times the 99th percentile • If the preprocedure value was already elevated, there is an increase of at least 20% • Evidence to support ischemic etiology
Acute myocardial infarction, Type 5 (following coronary artery bypass grafting)	• Within 48 hours of the procedure, cTn is >10 times the 99th percentile • If the preprocedure value was already elevated, there is an increase of >20% • Evidence to support ischemic etiology
Reinfarction (defined as an acute MI occurring within 28 days of incident or recurrent MI)	• If the cTn concentration had been elevated but stable or decreasing at the time of suspected reinfarction, there is a >20% increase in cTn over a 3–6 h time span (or less with a high-sensitivity assay) • If the first specimen had a normal cTn result, the criteria for new acute MI apply

Data from Thygesen K, Alpert JS, Jaffe AS, et al.: Fourth universal definition of myocardial infarction (2018). *Circulation* 138:e618–e651, 2018.

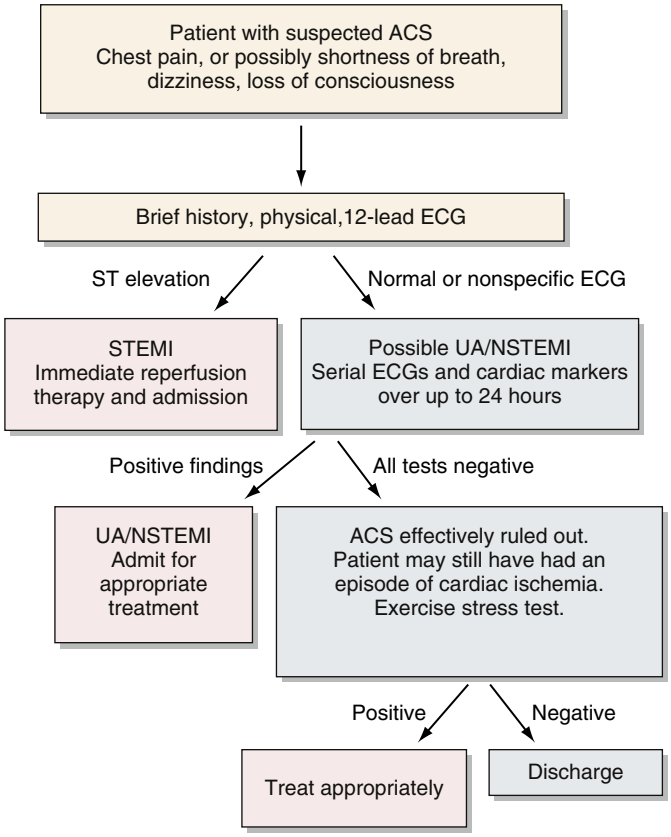

Figure 19.2 Outline of a clinical algorithm for treating patients presenting to an emergency department with symptoms suggesting acute coronary syndrome (ACS). The protocol is general and has to be customized to particular institutions and used with proper clinical judgment. *ECG,* Electrocardiogram, *NSTEMI,* non-ST elevation myocardial infarction; *STEMI,* ST-elevation myocardial infarction; *UA,* unstable angina.

hospital admission and/or elaborate workup for most patients with suspected ACS spends billions of dollars unnecessarily, because two-thirds or more of these patients turn out not to have ACS (Amsterdam et al., 2010).

Biochemical markers play a secondary role in the initial management of patients with suspected ACS. The earliest decision-making, which ideally should take place within 10 minutes of the patient's arrival in the ED (or possibly in the ambulance en route to the hospital), is based on history, physical examination, and 12-lead ECG (Amsterdam et al., 2014; Roffi et al., 2016) (Fig. 19.2). The ECG may establish the diagnosis of STEMI, at which point the patient is a candidate for immediate intervention to restore coronary blood flow (Ibanez et al., 2018). Biochemical marker results are not necessary before these interventions are provided and may even be misleadingly negative at this early time.

If the initial ECG is negative for STEMI, biochemical markers assume greater importance. As detailed in the Fourth Universal Definition of MI (Thygesen et al., 2018), it is now agreed that cTn is the preferred marker, with little to choose between I and T. Because it takes time for markers to be released into the circulation, serial testing has long been a staple of diagnosis. However, with the advent of hs-cTn, the time frame of serial testing can be shortened. Even a single hs-cTn measurement at the time of presentation is very informative, because if it is not only normal but well below the 99th percentile, a diagnosis of MI is very unlikely (Vasile & Jaffe, 2017), whereas a value well above the 99th percentile makes the diagnosis highly likely (Arslan et al., 2019). A second specimen 1 to 3 hours later allows another comparison to the 99th percentile and also a determination of the rate of change (or "delta"). The delta is important because a large number of chronic conditions can cause a persistent, relatively stable elevation in cTn. If cTn is increasing, it implies a recent acute event; if decreasing, it implies an acute event further back in time. Optimal time points and decision thresholds have not been established. However, it appears that rapid and accurate patient triage can be accomplished with hs-cTn measurements in the first hour of patient presentation, possibly supplemented by copeptin measurement (Body et al., 2019; Boeddinghaus et al., 2019; Chapman et al., 2017; Fabbri et al., 2019; Mueller-Hennessen et al., 2019; Neumann et al., 2019). For example, in a multicenter study enrolling 1282 patients, a 1-hour rapid protocol classified 14.4% as "rule-in" MI. Of these, 77.2% had a final adjudicated diagnosis of MI; 63.4% of patients were classified as "rule-out," of whom 0.9% had a final diagnosis of MI; and 22.2% were placed in an "observe" category, of whom 22.5% had a final diagnosis of MI (Mueller et al., 2016). The promise of such an approach, as well as caveats and limitations, have been discussed (Crea et al., 2016). It should be emphasized that assessing diagnostic strategies is made challenging by patient heterogeneity. Even in large multicenter trials, the number of MI cases is likely to be small once they are stratified based on age group, gender, prior history of ASCVD, nature of symptoms, time after symptom onset, comorbidities, and/or other factors.

NSTEMI is confirmed by positive cTn results with appropriate changes over time (see Table 19.3). Negative cTn results with ischemic ECG changes (ST depression or T-wave inversions) or other evidence may establish the diagnosis of UA. The increased sensitivity of cTn assays has led many cases that may have been diagnosed as UA in the past to be considered NSTEMI instead. However, it appears that ACS without elevation of cTn is still an important clinical entity and that diagnosis of UA will not become extinct (Braunwald & Morrow, 2013; Eggers et al., 2017). In any case, UA and NSTEMI are managed similarly, frequently with invasive artery-opening therapy (Amsterdam et al., 2014).

If the patient's presenting symptoms have resolved after several hours and ECG and cTn have been consistently negative, then an ACS has been effectively ruled out. For increased safety, before such a patient is discharged, additional testing for ASCVD is commonly performed, such as a simple exercise ECG, or various imaging modalities. These tests must be rapidly and continuously available if the ED is to achieve the desired rapid discharge of low-risk patients. They have the drawbacks of expense and significant numbers of false-positive and false-negative results, depending on the test modality chosen. Carefully evaluated algorithms may allow safe avoidance of this additional testing in many instances (Mahler et al., 2018).

Because both clinical care and patient flow through the ED require rapid risk assessment, cardiac marker test results must be available quickly. It has been advocated that point-of-care testing be considered when the central laboratory cannot reliably provide results within about 1 hour. That time frame can be challenging for a central laboratory, given pre- and post-analytic delays and the need for relatively long incubation times in a high-sensitivity immunoassay. Both qualitative and quantitative tests for cardiac markers that are suitable for point-of-care testing are now available and have demonstrated effectiveness, but central laboratory methods may be superior in accuracy and cost. Point-of-care methodology has until recently

not been suitable for rapid protocols based on hs-cTn (Januzzi et al., 2019), but that may be changing as technology advances (Pickering et al., 2018).

Other Applications

Besides ruling in or ruling out the diagnosis of MI, cTn testing can be useful in determining prognosis and adjusting treatment. Higher cTn levels indicate a larger volume of infarcted muscle and a worse prognosis (Bohmer et al., 2009; Kurz et al., 2009; Reinstadler et al., 2016). Although more experience has been acquired in testing for reinfarction using CK-MB, which declines more rapidly after an uncomplicated MI than cTn, it appears that the latter can be equally effective in diagnosing reinfarction (Apple & Murakami, 2005). Criteria for diagnosing reinfarction as well as MIs related to invasive cardiac procedures are summarized in Table 19.3.

MARKERS OF CORONARY RISK

Since ASCVD can cause events with irreversible consequences, preventing its onset or progression is paramount. As summarized earlier in the Background section, our understanding of the causation of ASCVD is still incomplete; therefore, definitive preventive measures are not foreseeable at this time. However, many lines of evidence, the most important being large epidemiology studies, have identified several risk factors associated with ASCVD. Most of these risk factors pertain not just to the heart but also to the general processes of atherosclerosis and/or thrombosis. Hence, they have important implications for stroke and peripheral vascular disease as well.

Once an individual has been diagnosed with ASCVD, there is a markedly increased risk of future ASCVD-related events. Efforts to prevent these are known as *secondary prevention*, whereas preventing initial ASCVD events constitutes *primary prevention*. The risk factors in either case are similar, but secondary prevention demands more stringent interventions. Some risk factors for ASCVD that are not related to laboratory tests are listed in Table 19.2, along with a summary of guidance from a recent report of an American College of Cardiology/American Heart Association task force (Arnett et al., 2019). Of risk factors that can be identified by the clinical laboratory, the earliest identified, and still one of the most important, is serum cholesterol. It is actually the LDL fraction of cholesterol, which generally contains about 70% of the total circulating cholesterol, that is directly associated with risk; the HDL fraction is a negative risk factor. The other major lipid class commonly measured in plasma, triglyceride, has been an issue of controversy but now is generally accepted as a significant risk factor and is very useful in the computation of LDL cholesterol levels (see Chapter 18). Lipid testing and its relationship to ASCVD risk assessment are discussed in Chapter 18.

Aside from the lipids, a wide array of plasma constituents has been related to ASCVD risk. These include various nutrients, hormones, clotting factors, drugs, toxins, oxidants, antioxidants, and markers of inflammation or infection. In this chapter, two markers that have been extensively studied will be discussed: CRP and Hcy.

C-REACTIVE PROTEIN

First isolated in 1930 from the plasma of patients with pneumococcal pneumonia (Tillett & Francis, 1930), CRP was so named because it binds to the C-polysaccharide of the pneumococcus. It was later found that the protein appeared in plasma during many infectious or inflammatory conditions, and CRP was the original acute-phase reactant. CRP has now been characterized as a member of the pentraxin family of proteins. It comprises five protomers, each of 206 amino acids and molecular weight 23 kDa, arranged in cyclic symmetry. With the participation of Ca^{++} ions, it binds various proteins and phospholipids, particularly phosphocholine. It opsonizes particles and activates complement via the classical pathway, but its actual biological function is unknown (Boncler et al., 2019).

In plasma from normal individuals, the median CRP concentration is about 1 mg/L, and the 99th percentile is about 10 mg/L. In individuals with acute illness, cytokines, chiefly interleukin-6, stimulate hepatic production of CRP, and plasma levels may increase to 300 mg/L or more. Plasma CRP is increased in a variety of disorders, including most bacterial (but usually not viral) infections. MI is among the acute illnesses associated with elevation of plasma CRP (de Beer, 1982).

Epidemiologic studies have established that individuals with higher baseline levels of plasma CRP are at increased risk for ASCVD and stroke. In the relatively early Physicians Health Study, which enrolled 22,000 male U.S. physicians to examine the cardioprotective effects of aspirin and beta-carotene, plasma CRP averaged 1.51 mg/L in participants who developed MI, 1.38 mg/L in those who developed stroke, and 1.13 mg/L in controls who did not suffer vascular events (Ridker et al., 1997). In the subsequent Reykjavik study, the average baseline CRP was 1.75 mg/L in participants who developed MI versus 1.25 in those without vascular events (Danesh et al., 2004). A report on the Women's Health Study suggested that CRP was actually more predictive than LDL cholesterol (Ridker et al., 2002), whereas the Reykjavik study found CRP less predictive than total cholesterol, cigarette smoking, or systolic blood pressure. Meta-analyses published in 2009 (Buckley et al., 2009) and 2012 (Kaptoge et al., 2012) supported at least modest independent predictive power of CRP measurement. The 2012 analysis, examining 52 prospective studies with a total of 246,669 participants, concluded that adding CRP testing to traditional risk assessment could prevent one ASCVD event over 10 years for every 440 individuals screened.

The elevations of plasma CRP just described that confer excess coronary risk are minute compared to the hundred- to thousand-fold increases that occur with overt inflammatory or infectious diseases. For this reason, testing of CRP related to cardiac risk has been given the somewhat misleading name of *high-sensitivity CRP* (*hs-CRP*). Even at concentrations around 1 mg/L or less, CRP is a relatively abundant plasma protein (10^6-fold more abundant than cTn!), not requiring the most sensitive technology for accurate measurement. Methods such as nephelometry, which had been established for measuring CRP as an inflammatory marker, have been readily adapted to hs-CRP assays; the main differences involve degree of dilution and calibration. Commercial hs-CRP assays have adequate precision, and the long-term stability of hs-CRP in individual patients appears to be comparable with that of other risk factors, such as blood pressure and cholesterol (Danesh et al., 2004).

Although diverse evidence points to a role of inflammation in ASCVD (Packard & Libby, 2008; Pant et al., 2014), a precise mechanism for the relationship of plasma CRP to ASCVD risk is lacking. A key question still unresolved is whether the elevation in CRP is a cause or a consequence of the disease (or possibly both) (Hingorani et al., 2009). The inflammatory response associated with atheromatous lesions may trigger enough cytokine production to be associated with a measurable rise in plasma CRP. CRP may, in turn, through its proinflammatory effects, increase plaque vulnerability or have other effects that worsen the severity of ASCVD. The presence of CRP in human atheromatous lesions has been demonstrated (Reynolds & Vance, 1987), and in rats it has been shown that injection of human CRP after ligation of the coronary artery enhances infarct size (Griselli et al., 1999). Another intriguing possibility is that the risk associated with CRP relates to cytokine production by adipocytes and that CRP is essentially a biochemical marker of the metabolic syndrome (Reddy et al., 2019).

Given the variations in quantitative risk estimates, the unclear pathogenic role of CRP, and the lack of specific treatment for high CRP, the clinical usefulness of the hs-CRP test has been controversial. A joint committee of the Centers for Disease Control and Prevention and the American Heart Association issued recommendations in 2003, some of which are listed in Box 19.2. The 2019 ACC/AHA guideline on primary prevention (Arnett et al., 2019) does not endorse widespread hs-CRP screening but

BOX 19.2

Recommendations of a Joint Committee of the American Heart Association and the Centers for Disease Control and Prevention on CRP Testing to Assess CHD Risk

- If inflammatory markers are to be used in assessment of CHD risk, hs-CRP is the current analyte of choice.
- Optimally, hs-CRP results should be averaged from two specimens drawn about 2 weeks apart. If a level >10 mg/L is identified, there should be a search for an obvious cause of infection or inflammation. This result should then be discarded and another test done 2 weeks later.
- Decision intervals are as follows: <1 mg/L, low risk; 1–3 mg/L, intermediate risk; >3 mg/L, high risk (approximately corresponding to tertiles in the adult population).
- Patients most likely to benefit from an hs-CRP test would be those in whom the risk estimate from established factors is moderate (i.e., ≈10%–20% risk of CHD in the next 10 years); the physician needs additional information to guide preventive therapy.
- The role of hs-CRP in secondary prevention (i.e., prevention of disease progression in patients with established CHD) is limited because it is not likely to alter management (which needs to be aggressive regardless of additional information provided by CRP or other markers).
- Universal hs-CRP screening of the adult population is *not* warranted.

Modified from Pearson TA, Mensah GA, Alexander RW, et al.: Markers of inflammation and cardiovascular disease: Application to clinical and public health practice. A statement for healthcare professionals from the Centers for Disease Control and Prevention and the American Heart Association. *Circulation* 107:499–511, 2003. *CHD,* Coronary heart disease; *CRP,* C-reactive protein; *hs-CRP,* high-sensitivity C-reactive protein.

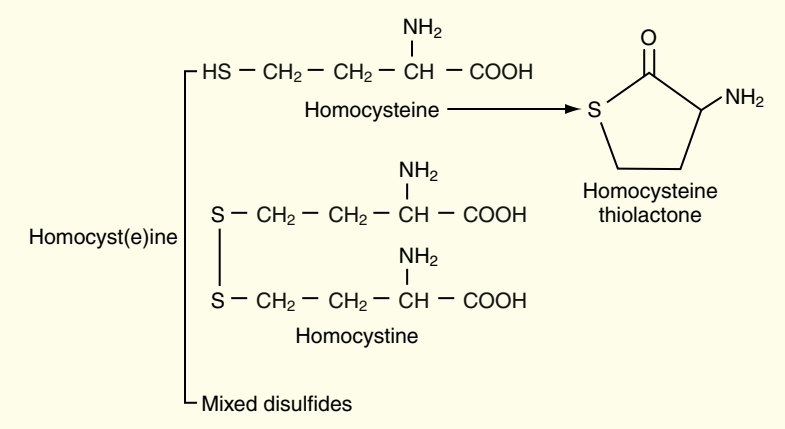

Figure 19.3 Chemical structure of homocysteine and related compounds.

does advise that CRP ≥ 2.0 mg/L is an "ASCVD risk enhancer" that may influence therapeutic decisions when it is measured.

HOMOCYSTEINE

Hcy (Fig. 19.3) is a sulfur-containing amino acid that is not incorporated into protein but is a metabolic intermediate. It can be methylated to form methionine or it can be converted through the transsulfuration pathway to cystathionine and then to cysteine. Hcy can exist in plasma as the species with a free sulfhydryl group, as a disulfide (homocystine), or as a mixed disulfide, linked to a plasma protein via one of its cysteine residues. It is the sum of these, which may be referred to as "total homocysteine," "homocyst(e)ine," or simply "homocysteine" that is generally measured.

Excessive levels of circulating Hcy generally reflect a diminished activity of one of the enzymes involved in its metabolism. The classical syndrome of homocystinuria, first described in 1962 (Carson & Neill, 1962; Gerritsen et al., 1962), is due to a homozygous defect in the enzyme cystathionine-β-synthase (CBS). It results in severely elevated circulating levels of the various forms of Hcy and methionine. Elevated Hcy levels have been classified as mild (16–30 μmol/L), moderate (30–100 μmol/L), and severe (>100 μmol/L) (Djuric et al., 2018; Hankey&Eikelboom, 1999). Clinical manifestations include dislocation of the optical lens, osteoporosis with associated skeletal abnormalities, intellectual impairment, psychiatric disturbance, and thromboembolic disease (Sacharow et al., 2017).

The basis of the damaging effects of Hcy is uncertain. At a biochemical level, oxidant stress and inhibition of transmethylation reactions are likely possibilities. Cellular effects that have been documented in experimental systems include endothelial injury, alteration of nitric oxide metabolism, platelet activation, smooth muscle proliferation, and activation of Toll-like receptors (Djuric et al., 2018; Thambyrajah & Townend, 2000). Some of the toxicity of Hcy may derive from its enzymatic conversion to Hcy thiolactone (see Fig. 19.3), which can modify LDL and enhance its uptake by macrophages (McCully, 1993; Vignini et al., 2004). Hcy is likely pro-inflammatory and has been linked to production of CRP, the risk factor discussed in the previous section (Pang et al., 2014).

The development of Hcy as an ASCVD risk marker in some ways parallels that of cholesterol: the regular occurrence of atherosclerosis in persons with massive elevation, due to an inborn error of metabolism, led to the hypothesis of increased risk in individuals with more moderate elevations. Experimentally induced hyperhomocysteinemia in animals lent support to the hypothesis (McCully, 1993). In humans, mild to moderate elevations in Hcy can have many causes. Genetic causes include a heterozygous defect in CBS, a defect in methionine synthase (rare), or a defect in 5,10-methylenetetrahydrofolate reductase (generally rare, except for a temperature-sensitive form that is relatively common). Nutritional causes include a deficiency of any of the vitamin cofactors involved in metabolism of Hcy: folate, B_{12}, or pyridoxine (B_6).

Many of the earlier epidemiology studies seemed to confirm a correlation between moderate Hcy levels and ASCVD. For example, in the Physicians Health Study, it was initially reported that having a Hcy level in the upper 5% of the population conferred a 3- to 4-fold higher risk (Stampfer et al., 1992). However, other studies, including a longer-term follow-up in the Physicians Health Study (Chasan-Taber et al., 1996) and many of the larger and more recent studies, have shown little or no association between moderate elevations of Hcy and ASCVD risk. A recent meta-analysis could support no benefit of Hcy-lowering vitamin therapy in a general population for MI or any-cause death, but there was a small benefit for stroke (Marti-Carvajal et al., 2017). Also, widespread folate supplementation of food has probably tended to diminish average circulating Hcy in the U.S. population. For these reasons, general screening for Hcy is not advised, but testing is warranted in individuals who develop ASCVD despite being at relatively low risk according to traditional risk factors.

Hcy was originally measured by chromatographic techniques, and there was variability in results due to the heterogeneous nature of the substance. More recently, mass spectrometric methods were introduced, standard reference material was developed, and automated methods using either enzymic assay or immunoassay have become available (Ghassabian et al., 2014; La'ulu et al., 2008; Satterfield et al., 2006). Attention must be paid to proper sample collection and storage to prevent an artifactual increase in measured Hcy (Willems et al., 2004).

MARKERS OF CONGESTIVE HEART FAILURE

CARDIAC NATRIURETIC PEPTIDES

The heretical concept that the heart could be an endocrine organ was enforced by two reports in 1956: (1) that inflating a balloon inside the left atrium of a dog caused an increase in urine flow (Henry & Pearce, 1956) and (2) that structures resembling secretory granules were visible on electron micrographs of guinea pig atrial cells (Kisch, 1956). In 1981, extracts of rat heart atria (but not ventricles) were found to have a natriuretic effect (de Bold et al., 1981). In 1984, a peptide named *atrial natriuretic peptide* (*ANP*) was isolated from human heart (Kangawa & Matsuo, 1984). A short time later, a similar peptide named *brain natriuretic peptide* (*BNP*) was isolated from porcine brain (Sudoh et al., 1988). It turns out that in humans, BNP is produced mainly in the cardiac ventricle (Mukoyama et al., 1991)thus, the hormone now is commonly referred to as B-type natriuretic peptide.

Members of the natriuretic peptide family are illustrated in Figure 19.4. Their notable common feature is a 17 amino acid ring structure, closed by a cystine bridge, with substantial homology among the family members. C-type natriuretic peptide (CNP), described in 1990, is produced not in the heart but rather in endothelial cells (Sudoh et al., 1990). D-type natriuretic peptide (DNP) was isolated in 1992 from the green mamba snake, *Dendroaspis angusticeps* (Schweitz et al., 1992). DNP immunoreactivity was later reported in human plasma (Schirger et al., 1999), but this peptide has not been definitively demonstrated in humans. Finally, urodilatin is a form of ANP with four additional amino acids at the N-terminus. It is likely produced in the kidney by alternative splicing of the same gene product (Schulz-Knappe et al., 1988).

These peptides act via two distinct G-protein–coupled receptors (NPR-A and NPR-B). They downregulate the renin-angiotensin-aldosterone system, decrease sympathetic nerve activity in the heart and kidney, increase renal blood flow, and increase sodium excretion via a direct effect on the renal collecting duct (Potter et al., 2009; Spevack & Schwartzbard, 2004).

Another peptide with natriuretic properties is adrenomedullin (ADM), originally isolated from a pheochromocytoma (Kitamura et al., 1993) but now known to be produced in heart and other tissues. Though also containing an intrapeptide disulfide bond, it is in a distinct structural family from the traditional "natriuretic peptides" and acts via different receptor pathways. ANP, ADM, and BNP all have elevated plasma levels in HF patients, and their use in diagnosis and management have been extensively explored. Application of ANP and ADM has been hampered by their instability in plasma. The midregions of the peptide prohormones (MRproANP and MRproAM) are more stable in plasma and reflect the rate of hormone production. Commercial assays of these have been developed and shown to be informative in

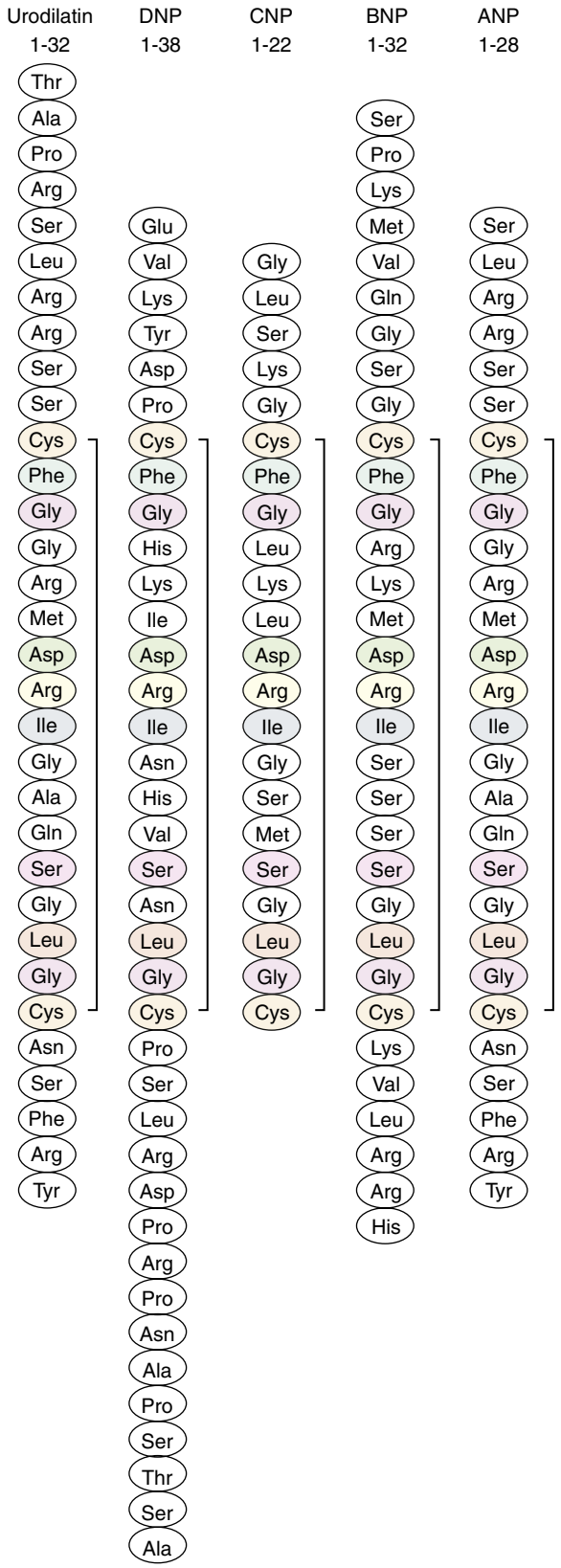

Figure 19.4 Amino acid sequences of the natriuretic peptides. Amino acids preserved through the family are indicated in color. *ANP,* Atrial natriuretic peptide; *BNP,* B-type natriuretic peptide; *CNP,* C-type natriuretic peptide; *DNP,* D-type natriuretic peptide.

HF (Maisel et al., 2002; Nishikimi & Nakagawa, 2018; Roberts et al., 2015). However, only BNP-related assays are widely applied at the present time; thus, the following discussion will be limited to the BNP system.

BNP derives from a 134 amino acid precursor, preproBNP, which is rapidly cleaved to the 108 amino acid proBNP, and then by the endoproteases furin and corin to a 32 amino acid C-terminal fragment, the active BNP, and

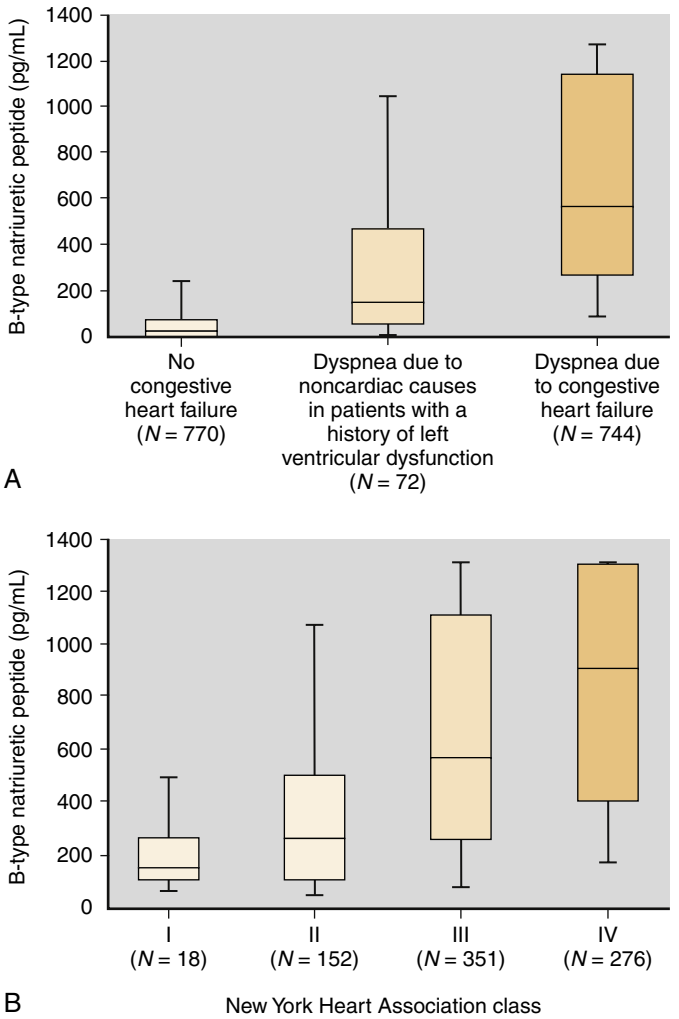

Figure 19.5 Box plots showing median levels of B-type natriuretic peptide in patients presenting to an emergency department with dyspnea in the Breathing Not Properly study. **A,** Patients in different diagnostic categories. **B,** Patients with heart failure, classified according to the New York Heart Association criteria. A higher class indicates more severe disease, as evidenced by a lesser amount of activity needed to provoke symptoms. Boxes show interquartile ranges, and I bars represent highest and lowest values. (With permission from Maisel AS, Krishnaswamy P, Nowak RM, et al. Rapid measurement of B-type natriuretic peptide in the emergency diagnosis of heart failure. *N Engl J Med* 347:161–167, 2002.)

an inactive 76 amino acid N-terminal fragment, N-BNP or NT-proBNP (Chow et al., 2017). Secretion of both fragments is enhanced by ventricular wall stretch and volume overload, as occur in HF (Tabbibizar & Maisel, 2002). BNP is eliminated by binding to a clearance receptor (NPR-C) and also through the action of endopeptidases in serum; its circulating half-life is approximately 22 minutes. The circulating half-life of N-BNP is considerably longer (60–120 minutes), and its mechanism of clearance seems to be mainly renal. Complicating measurement, a variety of truncated and glycosylated forms of BNP, N-BNP, and the precursor preproBNP are known to circulate and cross-react in various immunoassays (Halfinger et al., 2017).

Plasma levels of BNP are less than 100 pg/mL in most healthy individuals; reference ranges may vary with age, gender, and body weight. N-BNP levels are roughly comparable in healthy individuals but show greater increases in HF. The best-established application of BNP or N-BNP measurement is for diagnosing acutely ill patients presenting to emergency service with shortness of breath (Ponikowski et al., 2016; Yancy et al., 2017). Distinguishing HF from lung disease, such as emphysema, in these patients can be difficult. The multinational Breathing Not Properly study enrolled patients who presented to emergency centers with dyspnea and used a point-of-care method for measurement of BNP. At a decision point of 100 pg/mL, the BNP test had the following characteristics for diagnosis of HF: sensitivity 90%, specificity 76%, positive predictive value 79%, and negative predictive value 89% (Maisel et al., 2002). Among patients with a history of ventricular dysfunction, BNP was higher in those whose current symptoms were thought to be caused by HF; it was also higher in patients with more severe failure (Fig. 19.5). With N-BNP, levels below 300 pg/mL make a diagnosis of acute HF unlikely (Januzzi et al., 2006; Ponikowski et al., 2016).

BNP testing has poor clinical specificity for HF. ACS, valve disease, and other cardiac diseases increase BNP, as do many noncardiac conditions, including advancing age, anemia, renal failure, pulmonary disease, sleep apnea, critical illness, sepsis, and severe burns (Roberts et al., 2015; Yancy et al., 2017; Yancy et al., 2013). Obesity tends to decrease levels, and patients with symptomatic HF, especially when it is chronic and stable, can have normal levels (Tang et al., 2003). Intraindividual variability is relatively high; in a group of patients with stable, chronic HF, week-to-week variability for BNP and N-BNP was 30% to 40% (Bruins et al., 2004).

As might be expected, BNP and N-BNP levels decrease with effective treatment of HF, and serial testing, possibly combined with other markers such as cTn, may be used to assess treatment response and prognosis. This role is still evolving, and there is limited evidence at present to support improved patient outcomes based on serial BNP testing (Brunner-La Rocca & Sanders-van Wijk, 2019; Khan et al., 2018; McQuade et al., 2017; Zhang et al., 2018). Testing may also be useful for screening patients before any overt symptoms of HF are present, particularly in the context of predisposing factors such as hypertension and diabetes (Chow et al., 2017).

Besides being a biomarker for HF, BNP has natriuretic, vasodilatory, and other effects that are ameliorative for the syndrome. In the past, BNP has been administered as a drug, known as nesiritide (Natrecor). However, more recently, better results have been achieved with drugs that inhibit neprilysin, a peptidase that breaks down BNP. When such pharmacotherapy is employed, BNP—but not N-BNP—levels are directly affected, and the latter is the preferred monitor of clinical response. Otherwise, BNP and N-BNP testing appear to have equal clinical efficacy provided that appropriate reference ranges are employed (Ponikowski et al., 2016).

As with cTn, BNP and N-BNP are measured clinically by immunoassay. Unfortunately, standardization of these assays has lagged due to the varying cross-reactivities with different peptides and lack of agreed-upon reference material. Results from different assays cannot be reliably compared (Halfinger et al., 2017; Semenov & Feygina, 2018). Powerful mass spectrometry methods have been applied in the research setting. These may aid in standardizing immunoassays in the near term and become suitable for clinical application over the longer term (Xiao et al., 2019). Performance characteristics of commercial immunoassays for BNP, N-BNP, and MR-proANP have been summarized by the IFCC at their website (http://www.ifcc.org/ifcc-education-division/emd-committees/committee-on-clinical-applications-of-cardiac-bio-markers-c-cb/).

OTHER HEART FAILURE BIOMARKERS

Given the limited diagnostic power of BNP testing, there has been interest in developing additional markers and possibly pursuing a multimarker strategy for diagnosis and management of HF (Ibrahim & Januzzi, 2017; Ky et al., 2012). Two markers of current interest are Gal-3 (galectin-3) and ST-2 (suppressor of tumorigenicity 2) (Karayannis et al., 2013). Gal-3, first named "Mac-2" when it was discovered in mice (Ho & Springer, 1982), was later characterized as one of a family of lectins with an affinity for β-galactosides. Having a role in cell adhesion and other cellular processes, it is present in diverse tissues and elevated in many diseases (Sciacchitano et al., 2018). Studies in model systems have suggested that it may contribute to progression of HF, particularly in the formation of fibrosis. ST-2, a member of the Toll-like/interleukin-1 receptor superfamily, has both a soluble and transmembrane form. It is involved in allergic and inflammatory responses. Like Gal-3, soluble ST-2 is elevated in HF but also in many other diseases and may contribute to disease progression (Aleksova et al., 2019). These markers are diagnostically inferior to BNP and do not have a well-defined clinical role at present. However, elevated levels appear to independently imply poorer prognosis and may thus aid in selecting patients for more aggressive interventions.

OTHER CONDITIONS ASSOCIATED WITH ATHEROSCLEROSIS OR THROMBOSIS

A cerebrovascular accident, or stroke, is another dreaded complication of atherosclerotic disease. About 795,000 Americans suffer a stroke per year, about the same number as those who suffer an MI (see Box 19.1). Many strokes are presumably caused by a mechanism similar to ACS, where atherosclerotic plaque eventually becomes unstable and ruptures, resulting in thrombotic occlusion. However, additional mechanisms can cause ischemic stroke, and 20% of strokes result from hemorrhage rather than from vascular occlusion. Considerable effort has been directed at finding biomarkers for stroke that might rival the utility of cTn and other markers for cardiac disease. Candidate markers have included neurotransmitters; proteins produced in neurons or glia such as tau, S100b, and neuron-specific enolase; inflammatory mediators such as CRP, interleukins, and matrix metalloproteinases; natriuretic peptides; and others. At the time of this writing, none has been shown to have sufficient sensitivity and specificity for incorporation into routine practice (Montaner et al., 2019; Ng et al., 2017; Whiteley et al., 2012). Possibly a multiple-marker approach will eventually be successful; however, at present, the diagnosis and management of stroke rests on clinical findings and imaging studies.

Thrombosis in peripheral veins can result in dislodging of part of the thrombus—embolization—which, after passing through the right side of the heart, will lodge in the lung, causing the syndrome of a pulmonary embolus (PE). Depending on the size of the PE, consequences can range from minimal to sudden death. PE can cause chest pain, ECG abnormalities, and increased cTn levels and thus may be confused with an ACS. Measurement of D-dimer, a specific degradation product of fibrin (see Chapter 40), has become a useful laboratory test for ruling out PE and venous thrombotic disease in general. Almost any activation of the coagulation cascade, anywhere in the body, leads to production of D-dimer; hence elevated levels are widespread, especially in hospitalized patients, and have little meaning. When pretest probability of thrombotic disease is low, however, low levels of D-dimer have high negative predictive value in excluding the diagnosis of PE (as well as any venous thrombosis) (Linkins & Takach Lapner, 2017). (See Chapter 8 for discussion of pre- and posttest probabilities.) Hence, if a patient's pretest probability of PE is significant but low, a D-dimer test should be performed; if it is negative, further testing can be omitted. If the pretest probability is moderate or high, further testing (imaging) should be performed in any case, and a D-dimer test is not useful.

Determining that a D-dimer result is "negative" or "positive" depends on the choice of cutoff. The cutoff is not really related to the "reference range" for D-dimer, which would be its concentration range in a healthy population, but rather has to be chosen to optimize clinical outcomes in the context of diagnosing PE. D-Dimer is measured by commercial immunoassays; the cutoff for ruling out thrombosis is generally specified by the manufacturer, typically at 500 μg/L fibrinogen equivalent units (FEUs). However, a conservative (low) cutoff may lead to an undesirable number of false positives; therefore, adjusting the cutoff for certain variables may be considered. For example, ambient D-dimer levels increase with age; thus, it has been proposed that the cutoff be adjusted for patient age, possibly using 500 in patients younger than 50 years but ten times age in older patients (Douma et al., 2010; Nybo & Hvas, 2017; Righini et al., 2014). Alternatively, clinical criteria may be used to select patients with very low pretest probability in whom the cutoff might be, for example, increased to 1000 (Takach Lapner et al., 2017). Clearly, as with all of the other tests discussed in this chapter and this textbook, close collaboration between the laboratory and clinical departments is essential so that tests are properly interpreted and optimally applied to patient care.

SELECTED REFERENCES

Arnett DK, Blumenthal RS, Albert MA, et al.: 2019 ACC/AHA guideline on the primary prevention of cardiovascular disease: a report of the American College of Cardiology/American Heart Association task force on clinical practice guidelines, *Circulation*, 2019. CIR0000000000000678. Available at the websites of the American College of Cardiology (www.acc.org) and the American Heart Association (professional.heart.org/).

A comprehensive discussion of risk factors related to ASCVD, with consensus guidelines.

Thygesen K, Alpert JS, Jaffe AS, et al.: Fourth universal definition of myocardial infarction, 2018, *Circulation* 138:e618–e651, 2018.

Discusses diagnosis of myocardial infarction, emphasizing the role of cardiac troponin.

Djuric D, Jakovljevic V, Zivkovic V, Srejovic I: Homocysteine and homocysteine-related compounds: an overview of the roles in the pathology of the cardiovascular and nervous systems, *Can J Physiol Pharmacol* 96:991–1003, 2018.

Reviews the role of homocysteine in ASCVD.

Boncler M, Wu Y, Watala C: The multiple faces of C-reactive protein-physiological and pathophysiological implications in cardiovascular disease, *Molecules* 24:E2062, 2019.

Reviews the role of CRP in ASCVD.

Januzzi JL Jr, Mahler SA, Christenson RH, et al.: Recommendations for institutions transitioning to high-sensitivity troponin testing: JACC Scientific Expert Panel, *J Am Coll Cardiol* 73:1059–1077, 2019.

Practical guidance on cardiac troponin testing, particularly with regard to high-sensitivity troponin.

Access the complete reference list online at Elsevier eBooks for Practicing Clinicians.

REFERENCES

Aleksova A, Paldino A, Beltrami AP, et al.: Cardiac biomarkers in the emergency department: the role of soluble ST2 (sST2) in acute heart failure and acute coronary syndrome-there is meat on the bone, *J Clin Med* 8:270, 2019.

Amsterdam EA, Kirk JD, Bluemke DA, et al.: Testing of low-risk patients presenting to the emergency department with chest pain: a scientific statement from the American Heart Association, *Circulation* 122:1756–1776, 2010.

Amsterdam EA, Wenger NK, Brindis RG, et al.: AHA/ACC guideline for the management of patients with non-ST-elevation acute coronary syndromes: a report of the American College of Cardiology/American Heart Association Task Force on Practice Guidelines, 2014, *J Am Coll Cardiol* 64:e139–e228, 2014.

Apple FS: Tissue specificity of cardiac troponin I, cardiac troponin T and creatine kinase-MB, *Clin Chim Acta* 284:151–159, 1999.

Apple FS, Murakami MM: Cardiac troponin and creatine kinase MB monitoring during in-hospital myocardial reinfarction, *Clin Chem* 51:460–463, 2005.

Arnett DK, Blumenthal RS, Albert MA, et al.: ACC/AHA guideline on the primary prevention of cardiovascular disease, *Circulation*, 2019. CIR0000000000000678, 2019.

Arslan M, Dedic A, Boersma E, Dubois EA: Serial high-sensitivity cardiac troponin T measurements to rule out acute myocardial infarction and a single high baseline measurement for swift rule-in: a systematic review and meta-analysis, *Eur Heart J Acute Cardiovasc Care 2048872618819421*, 2019.

Baker P, Leckie T, Harrington D, Richardson A: Exercise-induced cardiac troponin elevation: an update on the evidence, mechanism and implications, *Int J Cardiol Heart Vasc* 22:181–186, 2019.

Bentzon JF, Otsuka F, Virmani R, Falk E: Mechanisms of plaque formation and rupture, *Circ Res* 114:1852–1866, 2014.

Bodor GS, Porter S, Landt Y, Ladenson JH: Development of monoclonal antibodies for an assay of cardiac troponin-I and preliminary results in suspected cases of myocardial infarction, *Clin Chem* 38:2203–2214, 1992.

Body R, Twerenbold R, Austin C, et al.: Diagnostic accuracy of a high-sensitivity cardiac troponin assay with a single serum test in the emergency department, *Clin Chem* 65:1006–1014, 2019.

Boeddinghaus J, Nestelberger T, Twerenbold R, et al.: High-sensitivity cardiac troponin I assay for early diagnosis of acute myocardial infarction, *Clin Chem* 65:893–904, 2019.

Bohmer E, Hoffmann P, Abdelnoor M, et al.: Troponin T concentration 3 days after acute ST-elevation myocardial infarction predicts infarct size and cardiac function at 3 months, *Cardiology* 113:207–212, 2009.

Boncler M, Wu Y, Watala C: The multiple faces of C-reactive protein-physiological and pathophysiological implications in cardiovascular disease, *Molecules* 24:E2062, 2019.

Braunwald E, Morrow DA: Unstable angina: is it time for a requiem? *Circulation* 127:2452–2457, 2013.

Bruins S, Fokkema MR, Romer JW, et al.: High intraindividual variation of B-type natriuretic peptide (BNP) and amino-terminal proBNP in patients with stable chronic heart failure, *Clin Chem* 50:2052–2058, 2004.

Brunner-La Rocca HP, Sanders-van Wijk S: Natriuretic peptides in chronic heart failure, *Card Fail Rev* 5:44–49, 2019.

Buckley DI, Fu R, Freeman M, et al.: C-reactive protein as a risk factor for coronary heart disease: a systematic review and meta-analyses for the U.S. Preventive Services Task Force, *Ann Intern Med* 151:483–495, 2009.

Burns C, Bagnall RD, Lam L, et al.: Multiple gene variants in hypertrophic cardiomyopathy in the era of next-generation sequencing, *Circ Cardiovasc Genet* 10:e001666, 2017.

Carson NA, Neill DW: Metabolic abnormalities detected in a survey of mentally backward individuals in Northern Ireland, *Arch Dis Child* 37:505–513, 1962.

Caselli C, Cangemi G, Masotti S, et al.: Plasma cardiac troponin I concentrations in healthy neonates, children and adolescents measured with a high sensitive immunoassay method: high sensitive troponin I in pediatric age, *Clin Chim Acta* 458:68–71, 2016.

Chapman AR, Lee KK, McAllister DA, et al.: Association of high-sensitivity cardiac troponin I concentration with cardiac outcomes in patients with suspected acute coronary syndrome, *J Am Med Assoc* 318:1913–1924, 2017.

Chasan-Taber L, Selhub J, Rosenberg IH, et al.: A prospective study of folate and vitamin B6 and risk of myocardial infarction in US physicians, *J Am Coll Nutr* 15:136–143, 1996.

Chow SL, Maisel AS, Anand I, et al.: Role of biomarkers for the prevention, assessment, and management of heart failure: a scientific statement from the American Heart Association, *Circulation* 135:e1054–e1091, 2017.

Cornelissen A, Jinnouchi H, Sakamoto A, et al.: Evaluation and management of the vulnerable plaque, *Curr Cardiovasc Risk Rep* 13(14), 2019.

Crea F, Jaffe AS, Collinson PO, et al.: Should the 1h algorithm for rule in and rule out of acute myocardial infarction be used universally? *Eur Heart J* 37:3316–3323, 2016.

Danesh J, Wheeler JG, Hirschfield GM, et al.: C-reactive protein and other circulating markers of inflammation in the prediction of coronary heart disease, *N Engl J Med* 350:1387–1397, 2004.

de Bold AJ, Borenstein HB, Veress AT, Sonnenberg H: A rapid and potent natriuretic response to intravenous injection of atrial myocardial extract in rats, *Life Sci* 28:89–94, 1981.

Djuric D, Jakovljevic V, Zivkovic V, Srejovic I: Homocysteine and homocysteine-related compounds: an overview of the roles in the pathology of the cardiovascular and nervous systems, *Can J Physiol Pharmacol* 96:991–1003, 2018.

Douma RA, le Gal G, Sohne M, et al.: Potential of an age adjusted D-dimer cut-off value to improve the exclusion of pulmonary embolism in older patients: a retrospective analysis of three large cohorts, *BMJ* 340:c1475, 2010.

Eggers KM, Jernberg T, Lindahl B: Unstable angina in the era of cardiac troponin assays with improved sensitivity-a clinical dilemma, *Am J Med* 130:1423–1430, e1425, 2017.

Eriksson S, Halenius H, Pulkki K, et al.: Negative interference in cardiac troponin I immunoassays by circulating troponin autoantibodies, *Clin Chem* 51:839–847, 2005.

Fabbri A, Bachetti C, Ottani F, et al.: Rapid rule-out of suspected acute coronary syndrome in the emergency department by high-sensitivity cardiac troponin T levels at presentation, *Intern Emerg Med* 14:403–410, 2019.

Gerritsen T, Vaughn JG, Waisman HA: The identification of homocystine in the urine, *Biochem Biophys Res Commun* 9:493–496, 1962.

Ghassabian S, Rethwan NS, Griffiths L, Smith MT: Fully validated LC-MS/MS method for quantification of homocysteine concentrations in samples of human serum: a new approach, *J Chromatogr B Analyt Technol Biomed Life Sci* 972:14–21, 2014.

Griselli M, Herbert J, Hutchinson WL, et al.: C-reactive protein and complement are important mediators of tissue damage in acute myocardial infarction, *J Exp Med* 190:1733–1740, 1999.

Halfinger B, Hammerer-Lercher A, Amplatz B, et al.: Unraveling the molecular complexity of O-glycosylated endogenous (N-terminal) pro-B-type natriuretic peptide forms in blood plasma of patients with severe heart failure, *Clin Chem* 63:359–368, 2017.

Hankey GJ, Eikelboom JW: Homocysteine and vascular disease, *Lancet* 354:407–413, 1999.

Henry JP, Pearce JW: The possible role of cardiac atrial stretch receptors in the induction of changes in urine flow, *J Physiol* 131:572–585, 1956.

Hingorani AD, Shah T, Casas JP, et al.: C-reactive protein and coronary heart disease: predictive test or therapeutic target? *Clin Chem* 55:239–255, 2009.

Ho MK, Springer TA: Mac-2, a novel 32,000 Mr mouse macrophage subpopulation-specific antigen defined by monoclonal antibodies, *J Immunol* 128:1221–1228, 1982.

Ibanez B, James S, Agewall S, et al.: 2017 ESC guidelines for the management of acute myocardial infarction in patients presenting with ST-segment elevation: the task force for the management of acute myocardial infarction in patients presenting with ST-segment elevation of the European Society of Cardiology (ESC), *Eur Heart J* 39:119–177, 2018.

Ibrahim NE, Januzzi Jr JL: Beyond natriuretic peptides for diagnosis and management of heart failure, *Clin Chem* 63:211–222, 2017.

Januzzi Jr JL, Mahler SA, Christenson RH, et al.: Recommendations for institutions transitioning to high-sensitivity troponin testing: JACC Scientific Expert Panel, *J Am Coll Cardiol* 73:1059–1077, 2019.

Januzzi JL, van Kimmenade R, Lainchbury J, et al.: NT-proBNP testing for diagnosis and short-term prognosis in acute destabilized heart failure: an international pooled analysis of 1256 patients: the International Collaborative of NT-proBNP Study, *Eur Heart J* 27:330–337, 2006.

Jehlicka P, Huml M, Rajdl D, et al.: How to interpret elevated plasmatic level of high-sensitive troponin T in newborns and infants? *Physiol Res* 67:191–195, 2018.

Kangawa K, Matsuo H: Purification and complete amino acid sequence of alpha-human atrial natriuretic polypeptide (alpha-hANP), *Biochem Biophys Res Commun* 118:131–139, 1984.

Kaptoge S, Di Angelantonio E, Pennells L, et al.: C-reactive protein, fibrinogen, and cardiovascular disease prediction, *N Engl J Med* 367:1310–1320, 2012.

Karayannis G, Triposkiadis F, Skoularigis J, et al.: The emerging role of Galectin-3 and ST2 in heart failure: practical considerations and pitfalls using novel biomarkers, *Curr Heart Fail Rep* 10:441–449, 2013.

Karcz A, Korn R, Burke MC, et al.: Malpractice claims against emergency physicians in Massachusetts: 1975-1993, *Am J Emerg Med* 14:341–345, 1996.

Karmen A: A note on the spectrometric assay of glutamic-oxalacetic transaminase in human blood serum, *J Clin Invest* 34:131–133, 1955.

Katrukha IA: Human cardiac troponin complex, structure and functions, *Biochemistry (Mosc)* 78:1447–1465, 2013.

Kelley WE, Januzzi JL, Christenson RH: Increases of cardiac troponin in conditions other than acute coronary syndrome and heart failure, *Clin Chem* 55:2098–2112, 2009.

Khan MS, Siddiqi TJ, Usman MS, et al.: Does natriuretic peptide monitoring improve outcomes in heart failure patients? A systematic review and meta-analysis, *Int J Cardiol* 263:80–87, 2018.

Khan SQ, Dhillon OS, O'Brien RJ, et al.: C-terminal provasopressin (copeptin) as a novel and prognostic marker in acute myocardial infarction: Leicester Acute Myocardial Infarction Peptide (LAMP) study, *Circulation* 115:2103–2110, 2007.

Kisch B: Electron microscopy of the atrium of the heart. I. Guinea pig, *Exp Med Surg* 14:99–112, 1956.

Kitamura K, Kangawa K, Kawamoto M, et al.: Adrenomedullin: a novel hypotensive peptide isolated from human pheochromocytoma, *Biochem Biophys Res Commun* 192:553–560, 1993.

Kurz K, Schild C, Isfort P, et al.: Serial and single time-point measurements of cardiac troponin T for prediction of clinical outcomes in patients with acute ST-segment elevation myocardial infarction, *Clin Res Cardiol* 98:94–100, 2009.

Ky B, French B, Levy WC, et al.: Multiple biomarkers for risk prediction in chronic heart failure, *Circ Heart Fail* 5:183–190, 2012.

La'ulu SL, Rawlins ML, Pfeiffer CM, et al.: Performance characteristics of six homocysteine assays, *Am J Clin Pathol* 130:969–975, 2008.

Ladue JS, Wroblewski F, Karmen A: Serum glutamic oxaloacetic transaminase activity in human acute transmural myocardial infarction, *Science* 120:497–499, 1954.

Linkins LA, Takach Lapner S: Review of D-dimer testing: Good, Bad, and Ugly, *Int J Lab Hematol* 39(Suppl 1):98–103, 2017.

Lippi G, Aloe R, Meschi T, et al.: Interference from heterophilic antibodies in troponin testing. Case report and systematic review of the literature, *Clin Chim Acta* 426:79–84, 2013.

Mahler SA, Lenoir KM, Wells BJ, et al.: Safely identifying emergency department patients with acute chest pain for early discharge, *Circulation* 138:2456–2468, 2018.

Mair J: Progress in myocardial damage detection: new biochemical markers for clinicians, *Crit Rev Clin Lab Sci* 34:1–66, 1997.

Mair J, Lindahl B, Hammarsten O, et al.: How is cardiac troponin released from injured myocardium? *Eur Heart J Acute Cardiovasc Care* 7:553–560, 2018.

Maisel AS, Krishnaswamy P, Nowak RM, et al.: Rapid measurement of B-type natriuretic peptide in the emergency diagnosis of heart failure, *N Engl J Med* 347:161–167, 2002.

Marti-Carvajal AJ, Sola I, Lathyris D, Dayer M: Homocysteine-lowering interventions for preventing cardiovascular events, *Cochrane Database Syst Rev* 8, 2017. Cd006612.

McCully KS: Chemical pathology of homocysteine. I. Atherogenesis, *Ann Clin Lab Sci* 23:477–493, 1993.

McQuade CN, Mizus M, Wald JW, et al.: Brain-Type natriuretic peptide and amino-terminal pro-brain-type natriuretic peptide discharge thresholds for acute decompensated heart failure: a systematic review, *Ann Intern Med* 166:180–190, 2017.

Montaner J, Ramiro L, Simats A, et al.: Matrix metalloproteinases and ADAMs in stroke, *Cell Mol Life Sci* 76:3117–3140, 2019.

Mueller-Hennessen M, Lindahl B, Giannitsis E, et al.: Combined testing of copeptin and high-sensitivity cardiac troponin T at presentation in comparison to other algorithms for rapid rule-out of acute myocardial infarction, *Int J Cardiol* 276:261–267, 2019.

Mueller C, Giannitsis E, Christ M, et al.: Multicenter evaluation of a 0-Hour/1-Hour algorithm in the diagnosis of myocardial infarction with high-sensitivity cardiac troponin T, *Ann Emerg Med* 68:76–87, e74, 2016.

Mukoyama M, Nakao K, Hosoda K, et al.: Brain natriuretic peptide as a novel cardiac hormone in humans. Evidence for an exquisite dual natriuretic peptide system, atrial natriuretic peptide and brain natriuretic peptide, *J Clin Invest* 87:1402–1412, 1991.

Neumann JT, Twerenbold R, Ojeda F, et al.: Application of high-sensitivity troponin in suspected myocardial infarction, *N Engl J Med* 380:2529–2540, 2019.

Neves PO, Andrade J, Moncao H: Coronary artery calcium score: current status, *Radiol Bras* 50:182–189, 2017.

Ng GJL, Quek AML, Cheung C, et al.: Stroke biomarkers in clinical practice: a critical appraisal, *Neurochem Int* 107:11–22, 2017.

Nishikimi T, Nakagawa Y: Adrenomedullin as a biomarker of heart failure, *Heart Fail Clin* 14:49–55, 2018.

Nybo M, Hvas AM: Age-adjusted D-dimer cut-off in the diagnostic strategy for deep vein thrombosis: a systematic review, *Scand J Clin Lab Invest* 77:568–573, 2017.

Packard RR, Libby P: Inflammation in atherosclerosis: from vascular biology to biomarker discovery and risk prediction, *Clin Chem* 54:24–38, 2008.

Pang X, Liu J, Zhao J, et al.: Homocysteine induces the expression of C-reactive protein via NMDAr-ROS-MAPK-NF-kappaB signal pathway in rat vascular smooth muscle cells, *Atherosclerosis* 236:73–81, 2014.

Pant S, Deshmukh A, Gurumurthy GS, et al.: Inflammation and atherosclerosis--revisited, *J Cardiovasc Pharmacol Ther* 19:170–178, 2014.

Park KC, Gaze DC, Collinson PO, Marber MS: Cardiac troponins: from myocardial infarction to chronic disease, *Cardiovasc Res* 113:1708–1718, 2017.

Pasipoularides A: Genomic translational research: Paving the way to individualized cardiac functional analyses and personalized cardiology, *Int J Cardiol* 230:384–401, 2017.

Pearson TA, Mensah GA, Alexander RW, et al.: Markers of inflammation and cardiovascular disease: application to clinical and public health practice: a statement for healthcare professionals from the Centers for Disease Control and Prevention and the American Heart Association, *Circulation* 107:499–511, 2003.

Pickering JW, Young JM, George PM, et al.: Validity of a novel point-of-care troponin assay for single-test rule-out of acute myocardial infarction, *JAMA Cardiol* 3:1108–1112, 2018.

Ponikowski P, Voors AA, Anker SD, et al.: ESC guidelines for the diagnosis and treatment of acute and chronic heart failure: the task force for the diagnosis and treatment of acute and chronic heart failure of the European Society of Cardiology (ESC), Developed with the special contribution of the heart failure association (HFA) of the ESC, *Eur J Heart Fail* 18:891–975, 2016. 2016.

Pope JH, Aufderheide TP, Ruthazer R, et al.: Missed diagnoses of acute cardiac ischemia in the emergency department, *N Engl J Med* 342:1163–1170, 2000.

Potter LR, Yoder AR, Flora DR, et al.: Natriuretic peptides: their structures, receptors, physiologic functions and therapeutic applications, *Handb Exp Pharmacol* 341–366, 2009.

Reddy P, Lent-Schochet D, Ramakrishnan N, et al.: Metabolic syndrome is an inflammatory disorder: a conspiracy between adipose tissue and phagocytes, *Clin Chim Acta* 496:35–44, 2019.

Reichlin T, Hochholzer W, Stelzig C, et al.: Incremental value of copeptin for rapid rule out of acute myocardial infarction, *J Am Coll Cardiol* 54:60–68, 2009.

Reinstadler SJ, Feistritzer HJ, Klug G, et al.: High-sensitivity troponin T for prediction of left ventricular function and infarct size one year following ST-elevation myocardial infarction, *Int J Cardiol* 202:188–193, 2016.

Reynolds GD, Vance RP: C-reactive protein immunohistochemical localization in normal and atherosclerotic human aortas, *Arch Pathol Lab Med* 111:265–269, 1987.

Ricci F, Di Scala R, Massacesi C, et al.: Ultra-sensitive copeptin and cardiac troponin in diagnosing non-ST-segment elevation acute coronary syndromes--the COPACS study, *Am J Med* 129:105–114, 2016.

Ridker PM, Cushman M, Stampfer MJ, et al.: Inflammation, aspirin, and the risk of cardiovascular disease in apparently healthy men, *N Engl J Med* 336:973–979, 1997.

Ridker PM, Rifai N, Rose L, et al.: Comparison of C-reactive protein and low-density lipoprotein cholesterol levels in the prediction of first cardiovascular events, *N Engl J Med* 347:1557–1565, 2002.

Righini M, Van Es J, Den Exter PL, et al.: Age-adjusted D-dimer cutoff levels to rule out pulmonary embolism: the ADJUST-PE study, *J Am Med Assoc* 311:1117–1124, 2014.

Rittoo D, Jones A, Lecky B, Neithercut D: Elevation of cardiac troponin T, but not cardiac troponin I, in patients with neuromuscular diseases: implications for the diagnosis of myocardial infarction, 2014, *J Am Coll Cardiol* 63:2411–2420, 2014.

Roberts E, Ludman AJ, Dworzynski K, et al.: The diagnostic accuracy of the natriuretic peptides in heart failure: systematic review and diagnostic meta-analysis in the acute care setting, *BMJ* 350:h910, 2015.

Roffi M, Patrono C, Collet JP, et al.: 2015 ESC guidelines for the management of acute coronary syndromes in patients presenting without persistent ST-segment elevation: task force for the management of acute coronary syndromes in patients presenting without persistent ST-segment elevation of the European Society of Cardiology (ESC), *Eur Heart J* 37:267–315, 2016.

Rui P, Kang K, Ashman JJ: *National hospital Ambulatory Medical care Survey: 2016 emergency department summary tables*. Available from https://www.cdc.gov/nchs/data/ahcd/nhamcs_emergency/2016_ed_web_tables.pdf, 2016.

Sacharow SJ, Picker JD, Levy HL: Homocystinuria caused by cystathionine beta-synthase deficiency 2004 Jan 15. In Adam MP, Ardinger HH, Pagon RA, Wallace SE, Bean LJH, Stephens K, Amemiya A, editors: *GeneReviews®[Internet]*, Seattle, Seattle (WA), 2017 May 18, University of Washington.

Satterfield MB, Sniegoski LT, Sharpless KE, et al.: Development of a new standard reference material: SRM 1955 (homocysteine and folate in human serum), *Anal Bioanal Chem* 385:612–622, 2006.

Schirger JA, Heublein DM, Chen HH, et al.: Presence of Dendroaspis natriuretic peptide-like immunoreactivity in human plasma and its increase during human heart failure, *Mayo Clin Proc* 74:126–130, 1999.

Schmid J, Liesinger L, Birner-Gruenberger R, et al.: Elevated cardiac troponin T in patients with skeletal myopathies, *J Am Coll Cardiol* 71:1540–1549, 2018.

Schneck NA, Phinney KW, Lee SB, Lowenthal MS: Quantification of cardiac troponin I in human plasma by immunoaffinity enrichment and targeted mass spectrometry, *Anal Bioanal Chem* 410:2805–2813, 2018.

Schrapp A, Fraissinet F, Hervouet C, et al.: Biotin and high-sensitivity cardiac troponin T assay, *Biochem Med* 28:030901, 2018.

Schulz-Knappe P, Forssmann K, Herbst F, et al.: Isolation and structural analysis of "urodilatin", a new peptide of the cardiodilatin-(ANP)-family, extracted from human urine, 2018, *Klin Wochenschr* 66:752–759, 1988.

Schweitz H, Vigne P, Moinier D, et al.: A new member of the natriuretic peptide family is present in the venom of the green mamba (Dendroaspis angusticeps), *J Biol Chem* 267:13928–13932, 1992.

Sciacchitano S, Lavra L, Morgante A, et al.: Galectin-3: one molecule for an alphabet of diseases, from A to Z, *Int J Mol Sci* 19, 2018.

Semenov AG, Feygina EE: Standardization of BNP and NT-proBNP immunoassays in light of the diverse and complex nature of circulating BNP-related peptides, *Adv Clin Chem* 85:1–30, 2018.

Spevack DM, Schwartzbard A: B-type natriuretic peptide measurement in heart failure, *Clin Cardiol* 27:489–494, 2004.

Stampfer MJ, Malinow MR, Willett WC, et al.: A prospective study of plasma homocyst(e)ine and risk of myocardial infarction in US physicians, *J Am Med Assoc* 268:877–881, 1992.

Sudoh T, Kangawa K, Minamino N, Matsuo H: A new natriuretic peptide in porcine brain, *Nature* 332:78–81, 1988.

Sudoh T, Minamino N, Kangawa K, Matsuo H: C-type natriuretic peptide (CNP): a new member of natriuretic peptide family identified in porcine brain, *Biochem Biophys Res Commun* 168:863–870, 1990.

Tabbibizar R, Maisel A: The impact of B-type natriuretic peptide levels on the diagnoses and management of congestive heart failure, *Curr Opin Cardiol* 17:340–345, 2002.

Takach Lapner S, Julian JA, Linkins LA, et al.: Comparison of clinical probability-adjusted D-dimer and age-adjusted D-dimer interpretation to exclude venous thromboembolism, *Thromb Haemost* 117:1937–1943, 2017.

Tang WH, Girod JP, Lee MJ, et al.: Plasma B-type natriuretic peptide levels in ambulatory patients with established chronic symptomatic systolic heart failure, *Circulation* 108:2964–2966, 2003.

Tate JR, Bunk DM, Christenson RH, et al.: Evaluation of standardization capability of current cardiac troponin I assays by a correlation study: results of an IFCC pilot project, *Clin Chem Lab Med* 53:677–690, 2015.

Tester DJ, Ackerman MJ: Genetics of long QT syndrome, *Methodist Debakey Cardiovasc J* 10:29–33, 2014.

Thambyrajah J, Townend JN: Homocysteine and atherothrombosis--mechanisms for injury, *Eur Heart J* 21:967–974, 2000.

Thygesen K, Alpert JS, Jaffe AS, et al.: Fourth universal definition of myocardial infarction (2018), *Circulation* 138:e618–e651, 2018.

Tillett WS, Francis T: Serological reactions in pneumonia with a non-protein somatic fraction of pneumococcus, *J Exp Med* 52:561–571, 1930.

Usman A, Ribatti D, Sadat U, Gillard JH: From lipid retention to immune-mediate inflammation and associated angiogenesis in the pathogenesis of atherosclerosis, *J Atheroscler Thromb* 22:739–749, 2015.

Vasile VC, Jaffe AS: High-sensitivity cardiac troponin for the diagnosis of patients with acute coronary syndromes, *Curr Cardiol Rep* 19:92, 2017.

Vignini A, Nanetti L, Bacchetti T, et al.: Modification induced by homocysteine and low-density lipoprotein on human aortic endothelial cells: an in vitro study, *J Clin Endocrinol Metab* 89:4558–4561, 2004.

Vylegzhanina AV, Kogan AE, Katrukha IA, et al.: Full-size and partially truncated cardiac troponin complexes in the blood of patients with acute myocardial infarction, *Clin Chem* 65:882–892, 2019.

Whiteley W, Tian Y, Jickling GC: Blood biomarkers in stroke: research and clinical practice, *Int J Stroke* 7:435–439, 2012.

Wildi K, Zellweger C, Twerenbold R, et al.: Incremental value of copeptin to highly sensitive cardiac troponin I for rapid rule-out of myocardial infarction, *Int J Cardiol* 190:170–176, 2015.

Willems HP, den Heijer M, Lindemans J, et al.: Measurement of total homocysteine concentrations in acidic citrate- and EDTA-containing tubes by different methods, *Clin Chem* 50:1881–1883, 2004.

Wu AHB: Release of cardiac troponin from healthy and damaged myocardium, *Frontiers in Laboratory Medicine* 1:144–150, 2017.

Wu MY, Li CJ, Hou MF, Chu PY: New insights into the role of inflammation in the pathogenesis of atherosclerosis, *Int J Mol Sci* 18:E2034, 2017.

Xiao P, Li H, Li X, Song D: Analytical barriers in clinical B-type natriuretic peptide measurement and the promising analytical methods based on mass spectrometry technology, *Clin Chem Lab Med* 57:954–966, 2019.

Yancy CW, Jessup M, Bozkurt B, et al.: ACCF/AHA guideline for the management of heart failure: a report of the American College of Cardiology Foundation/American Heart Association task force on practice guidelines, 2013, *J Am Coll Cardiol* 62:e147–239, 2013.

Yancy CW, Jessup M, Bozkurt B, et al.: ACC/AHA/HFSA focused update of the 2013 ACCF/AHA guideline for the management of heart failure: a report of the American College of Cardiology/American Heart Association task force on clinical practice guidelines and the heart failure Society of America, 2017, *J Am Coll Cardiol* 70:776–803, 2017.

Zhang ZL, Li R, Yang FY, Xi L: Natriuretic peptide family as diagnostic/prognostic biomarker and treatment modality in management of adult and geriatric patients with heart failure: remaining issues and challenges, *J Geriatr Cardiol* 15:540–546, 2018.

CHAPTER 20

SPECIFIC PROTEINS

Richard A. McPherson

PROTEIN STRUCTURE, 276
TECHNIQUES OF PROTEIN SEPARATION, 277
Electrophoresis, 277
Precipitation, 279
Column Separations, 279
PROTEIN DETECTION AND QUANTITATION, 279
SPECIFIC PLASMA PROTEINS, 280
Major Components, 280
Minor Components, 285
Protease Inhibitors, 287
Acute-Phase Reactants, 287
PATTERNS OF PROTEIN ABNORMALITIES, 288
SELECTED REFERENCES, 289

KEY POINTS

- The primary structure of a protein is its linear sequence of amino acids with different side groups, which determine how the protein folds on itself (secondary and tertiary structures) and how it reacts with other molecules and cells (i.e., its molecular identity).
- Methods to quantitate and fractionate proteins are based on turbidimetry, colorimetry, absorption spectrophotometry, dye binding, column chromatography, electrophoresis, and immunoassays.
- Protein electrophoresis separates proteins according to their electrical charges (usually at pH 8.6).
- The major proteins in plasma that contribute to the electrophoretic pattern are albumin, α_1-antitrypsin, α_2-macroglobulin, haptoglobin, β-lipoprotein, transferrin, complement C3, fibrinogen, and immunoglobulins.
- Several minor components of plasma proteins—such as ceruloplasmin, C-reactive protein, prealbumin, and protease inhibitors—have clinical utility in diagnosing and monitoring diseases and are quantitated by immunoassays.
- Patterns of protein electrophoresis in serum and urine are characteristic of specific diseases primarily involving changes in synthetic rates (liver), loss (renal), or inflammatory states.
- Hereditary deficiency of some plasma proteins leads to significant diseases (e.g., α_1-antitrypsin).
- Proteins in plasma play several roles, including maintaining oncotic pressure, transporting small molecules, and promoting or inhibiting inflammatory reactions.
- The major clinical use of serum and urine protein electrophoresis is to screen for monoclonal gammopathies.

Examination of the proteins in plasma can provide information reflecting disease states in many different organ systems. The most frequently performed measurement—that for total protein—is usually performed on serum, which has no fibrinogen and no anticoagulant that may slightly dilute proteins in plasma. Although total protein determination gives the physician some information as to a patient's general status regarding nutrition or severe organ disease (as in protein-losing states), further fractionations yield far more clinically useful information.

Additional quantitation of albumin, for example, is more informative regarding nutritional status, liver synthetic capacity, and protein-losing nephropathy or enteropathy. It allows the clinician to interpret high or low calcium and magnesium levels, because albumin binds about one-half of each of those ions on a molar basis. Calculated differences between total protein and albumin represent the value of all globulins, a composite of the other fractions that individually may rise several-fold in severe disorders.

Protein electrophoresis separates the globulins from albumin and resolves the major proteins of serum into patterns that may be highly specific for some diseases. High-resolution techniques can provide a display of all components in concentrations down to about 1 g/L (0.1 g/dL in traditional units). However, at that level, quantitation by scanning of stained proteins is not highly reliable, and alternative methods should be employed. Such techniques, involving immunologic detection of individual proteins, have the dual advantages of specificity and sensitivity over electrophoresis (see Chapter 45).

Yet, there is much to be appreciated from visual inspection of an electrophoretogram of proteins because the human eye is highly efficient at detecting subtle variations in individual proteins as well as alterations in protein patterns. Identification of these patterns is a useful screening method to be followed by more specific confirmatory procedures to identify and quantitate aberrant protein bands. Protein electrophoresis also can be a useful tool for monitoring patients over long periods of time when marked alterations are noted in levels of particular proteins, such as in myeloma, nephrotic syndrome, cirrhosis, or extensive body burn.

This chapter reviews protein structure, methods of measurement and separation, the major plasma proteins (except coagulation factors, immunoglobulins, and the complement system, which are covered in Chapters 40, 47, and 48), and some of the patterns encountered in particular disease states.

PROTEIN STRUCTURE

The backbone of all protein molecules is a continuous chain of carbon and nitrogen atoms joined through peptide bonds between adjacent amino acids. At one end (the amino-terminus) is a free amino group; at the other end (the carboxy-terminus) is a free carboxyl group. Whereas the peptide backbone is qualitatively invariant between different proteins (its total length is equivalent to the total number of amino acids in a particular protein), proteins have structural identity by virtue of the side groups or residues of the constituent amino acids. The average molecular weight of an amino acid is 120 Da. Serum proteins range in size from roughly 66 kDa to over 700 kDa. These amino acid side chains are conventionally grouped according to chemical nature: hydrogen (glycine), aliphatic (alanine, valine, leucine, and isoleucine), hydroxymethylamino (serine and threonine), aromatic (tyrosine, phenylalanine, and tryptophan), imino (proline and hydroxyproline), acidic (aspartate and glutamate), basic (arginine, histidine, and lysine), amides (asparagine and glutamine), and sulfur-containing (cysteine and methionine). These different side chains may be charged, polar, or hydrophobic, resulting in the tendency for them to be relatively soluble or insoluble in water, respectively. Writing complete amino acid sequences of peptides or proteins becomes very complicated using their common three letter abbreviations; thus, single-letter abbreviations have become standard practice for writing such primary sequences (Table 20.1).

The linear sequence of amino acids in a protein is called its *primary structure*; this sequence of amino acids determines the identity of a protein, what its molecular structure is, what functions it can perform, how it can bind to other molecules, and how it can participate in the processes of recognition between molecules and cells. These biological interactions are guided by reactivities between charged groups on one molecule and those on another, and similarly by hydrophobic interactions between molecules. Analytic processes such as chromatography, electrophoresis, dye binding, light absorbance, and others also depend on the primary amino acid sequence.

The *secondary structure* refers to specific regular three-dimensional conformations into which portions of the polypeptide chain fold. Three such structures have been identified (Branden & Tooze, 1991). First is the α-helix,

in which the chain forms a regular helix such that the backbone C=O of the *i*th peptide group participates in a hydrogen bond with the N–H of the (*i*+4) th peptide unit. The second is β-pleated sheets in fully extended structures, in which the chain forms a flat structure such that the side chains of adjacent amino acids point in opposite directions. In this conformation, two or more extended chains can associate so that the maximum number of C=O ●●●H–N bonds form between them. β-Pleated sheets can have their individual β-strands in parallel or antiparallel orientations. Finally, a third grouping of structures is the bend conformation, in which the direction of the polypeptide chain reverses itself, thereby allowing long primary structures to bend back on themselves and assume compact conformations.

The core of a protein molecule typically consists of combinations of α-helices and β-strands linked by loops of various lengths and shape. This inner core generally contains hydrophobic amino acids, whereas the loops and other surface portions of the protein molecule are richer in polar and charged amino acids that are hydrophilic. Upon degradation, some proteins (e.g., serum amyloid–associated protein, immunoglobulin light chains, prealbumin) release fragments rich in β-regions. These fragments are capable of coming together spontaneously in vivo to form deposits of β-sheets in fibrils that constitute amyloid. Recent work has shown an association between the genotype of apolipoprotein E (especially the allele apoE-4) and the progression of late-onset Alzheimer disease, in which cerebral plaques of amyloid form within the brain. These genetic findings suggest that Alzheimer disease may be understood and treated as a disease that has a biochemical basis in β-pleated sheet generation (Roses, 1994; Hayashi et al., 2004).

Molecular regions with clusters of hydrophobic side groups tend to remain on the interior of a protein that is soluble in water, whereas those regions with clusters of charges or other hydrophilic moieties tend to appear on the protein's surface. Conversely, proteins that are membrane bound usually have a distinct hydrophobic segment that protrudes to anchor the protein molecule in the lipid phase of the membrane. The actual three-dimensional structure or folding pattern of the protein, uniquely determined by its amino acid sequence, is termed its *tertiary structure*. Individual proteins or monomeric subunits may form more stable complexes, such as dimers, trimers, and tetramers; this is termed *quaternary structure*.

TABLE 20.1

Amino Acids by Chemical Nature of Side Chains and Their Commonly Used Abbreviations

Aliphatic		
Glycine	gly	G
Alanine	ala	A
Valine	val	V
Leucine	leu	L
Isoleucine	ile	I
Hydroxymethylamino		
Serine	ser	S
Threonine	thr	T
Aromatic		
Tyrosine	tyr	Y
Phenylalanine	phe	F
Tryptophan	try	W
Imino		
Proline	pro	P
Hydroxyproline*		
Acidic		
Aspartate	asp	D
Glutamate	glu	E
Basic		
Arginine	arg	R
Histidine	his	H
Lysine	lys	K
Amidic		
Asparagine	asn	N
Glutamine	gln	Q
Sulfur-containing		
Cysteine	cys	C
Methionine	met	M

*Hydroxyproline derives from posttranslational modification of proline.

The sulfhydryl group on a cysteine residue can form a disulfide (covalent) bond with another cysteine within the same protein to hold different segments tightly together. This action helps stabilize the whole structure from disruption by mechanical, thermal, or other forces. These intramolecular disulfide bonds most likely form after spontaneous protein folding along the linear amino acid sequence into most thermodynamically stable conformations. Disulfide bonds can also form between cysteine residues on different molecules, thereby stabilizing multimeric molecular structures (e.g., haptoglobin, von Willebrand antigen).

The acidic and basic amino acids determine the net charge on a protein and thus its electrophoretic mobility. The charge on carboxyl and amino groups is a function of pH (i.e., whether a hydrogen ion is bound to or dissociated from the group). Combining all the different side groups and their different degrees of dissociation, the pH at which a particular protein has net charge equal to zero is called its *isoelectric point* (pI). Proteins with pI less than 7 are acidic and tend to have carboxyl side groups exposed, whereas those with pI greater than 7 are basic (e.g., histones that, in turn, bind to the external helical structure of DNA that is negatively charged with phosphate groups).

Proteins are synthesized from the amino end to the carboxyl end by ribosomes translating from the information encoded in messenger RNA. The initial translation product of some proteins is acted on before secretion by proteolytic enzymes that convert a preform to the mature protein by removal of a signal peptide (generally hydrophobic) that otherwise holds the new protein molecule to the endoplasmic reticulum. Release of a preprotein from the endoplasmic reticulum entails passage through a membrane pore with the participation of various translocation factors (Brodsky, 1998). The correct assembly of a protein may critically depend on the function of so-called molecular chaperones, which are other proteins that guide the folding of nascent proteins in concert with proteases that remove selective segments to achieve functional conformations (Wickner et al., 1999). Many genetic diseases are due to harmful mutations in DNA, leading to alterations in the amino acid sequence of a protein that may block this complex assembly process or that may render any assembled protein molecules nonfunctional (Kuznetsov & Nigam, 1998).

Additional modifications to protein structures occur posttranslationally (i.e., after joining of the amino acids is complete) (Harding, 1985). Phosphorylation consists of the enzymatically regulated attachment of phosphate groups to serine and threonine groups as well as tyrosine (e.g., by tyrosine kinases) in the peptide backbone, thereby forming phosphoproteins with a more negative charge that can alter protein functions and state of activation. Glycosylation may occur spontaneously, in the presence of sugar molecules, or in a directed manner under enzymatic control, in which oligosaccharides, frequently terminating with sialic acid (which carries a negative charge), are attached to the protein (Van den Steen et al., 1998). These species of molecules are termed *glycoproteins*. Linkages are generally to asparagine residues through *N*-acetylglucosamine or to serine and threonine residues through *N*-acetylgalactosamine. Proteolysis results in the cleavage or removal of short segments of the peptide backbone that can open up catalytic sites of a zymogen (e.g., plasminogen to plasmin) or facilitate recognition by a receptor molecule (e.g., proinsulin to insulin). Many of these posttranslational steps are unique to eukaryotic cells and do not occur in prokaryotic cells. This point is very important to the biotechnology industry, which uses cloned genes to produce human proteins in bacteria, yeast, or other artificial cell types and thus must take additional steps to synthesize accurate molecules (Jenkins et al., 1996). Posttranslational changes in the structure of proteins influence their antigenicity, specific chemical or catalytic activities, abilities to bind to receptors, and electrophoretic mobilities.

Proteins that normally remain intracellular ultimately undergo degradation and clearance by the proteasome enzyme complex. This normal breakdown is essential to prevent accumulation of aging of otherwise faulty protein molecules and to allow newly synthesized fully functional proteins to take their place. Prior to degradation, protein molecules are tagged by conjugation with ubiquitin (ubiquitinylation), a small (8.5 kDa) protein that is found in all eukaryotic cells. Attachment of ubiquitin also directs proteins to other parts of the cell and modifies their molecular interactions. Conjugation with a single ubiquitin molecule is followed by attachment of further ubiquitin molecules, leading to a polyubiquitin chain that binds to the proteasome, which then degrades the protein into peptides and amino acids to be used to synthesize new proteins. This crucial proteasome action is the target of the inhibitor bortezomib, which has had clinical application for treatment of multiple myeloma and mantle cell lymphoma (Merin & Kelly, 2015).

TECHNIQUES OF PROTEIN SEPARATION

ELECTROPHORESIS

Modern understanding of the protein composition of serum and plasma derives from the electrophoretic techniques introduced by Tiselius. He

separated proteins dissolved in an electrolyte solution by application of an electric current through a U-shaped quartz tube that held the protein solution. At pH 7.6, four serum protein fractions, designated albumin, α, β, and γ, were identified and quantified optically by change in refractive index at the boundaries among these bands. Because separation was achieved in a homogeneous solution without solid support medium, convective forces prevented resolution into distinct zones. Hence, this technique has been termed *moving boundary* or *frontal electrophoresis*. Introduction of filter paper as an anticonvection support medium permitted separation of the protein fractions into discrete bands or zones in a process termed *zonal electrophoresis*. On solid support medium and at pH 8.6, the α fraction further splits into two groups of proteins: α_1 and α_2. Other support media, such as cellulose acetate membrane, agarose gel, starch gel, and polyacrylamide gel, have been used. Cellulose acetate and agarose have predominated in the clinical laboratory because of ease of use, low cost, and commercial availability (Jeppsson et al., 1979).

Application of samples can be done in wells that are cut into the gel, but this process typically leaves an artifact that can interfere with the scan. A method to get around this problem involves soaking the sample into the gel by means of an overlying template. Each end of the gel is then immersed into separate buffer chambers in which electrodes are mounted. A voltage is applied between the electrodes, generating a current that passes through the gel, usually for a period of about 30 minutes, to achieve the desired resolution. The ionic strength of the buffer determines the amount of current and the movement of the proteins for a fixed voltage. If ionic strength is low, relatively more current is carried by the charged proteins. If ionic strength is high, less current is carried by the proteins, which move a shorter distance. If the electrodes are not properly aligned, the current may be denser on one side of the gel than on the other; proteins will migrate farther on the side with more current. If electrophoresis proceeds too long, the proteins may migrate off the gel into the buffer. If there is a break in the electrical circuit and no current passes, the proteins will not move from the point of application. Frequently, gels show the "smile artifact," in which samples at the center of the gel migrate farther than those at the edges.

After electrophoresis, the gel is treated with a mild fixative, such as acetic acid, that precipitates the proteins at the positions to which they have migrated. They are then stained, and the gel is dried and cleared of excess stain. Protein patterns can be inspected visually for qualitative identification of abnormal proteins. Densitometric scanners are used to generate tracings and to quantitate the relative percentages of protein in each fraction. Those percentages are then multiplied by the total protein (separately measured) in the sample to yield the concentration of protein in each fraction.

When an electrophoretic support medium has a negative charge, the electromotive force to which it is subjected tends to move it toward the anode (positive pole; Fig. 20.1). However, the solid support medium is fixed; thus, it cannot move. The complementary positively charged ions in the surrounding buffer are free to move under the electromotive force; they carry with them molecules of the solvent water, which are clustered around their charges. The net result is flow of buffer toward the cathode. This buffer flow is termed *electro-osmosis* or *endosmosis*, which also carries the proteins with it to some extent by mechanical flow, not by charge. The actual distance traveled by a particular protein migrating in an electrical field is determined by the combined magnitudes of the electromotive force (a feature of the protein itself and the pH) and the electro-osmotic force (a function primarily of the support medium). When the electro-osmotic force is greater than the electrophoretic force acting on weakly anionic proteins (e.g., γ-globulins), those proteins move from the application point toward the cathode even though their charge is slightly negative.

Through critical manipulations of buffer salt composition, endosmotic properties of the medium, and means of sample application, commercially available electrophoretic agarose plates now achieve consistently high-resolution quality that allows routine separation of all major serum protein species (Fig. 20.2). Because of variability in the chemical formulations of gels, it should not necessarily be expected that each manufacturer's electrophoretic system will yield identical protein separation patterns. Furthermore, optimal separation of isoenzymes generally requires different buffer and gel composition compared with the conditions for best resolution of serum proteins versus lipoproteins versus hemoglobins. A significant variation in conditions for protein electrophoresis is that for optimizing the separation of the γ-region to resolve and detect oligoclonal bands of immunoglobulin in cerebrospinal fluid (CSF). In this case, the endosmosis is set high to maximize the cathodal movement of immunoglobulins from the point of application over a span of the gel that is convenient for visual inspection.

Polyacrylamide is an inert support medium whose porosity is easily adjusted by changing the composition of acrylamide before polymerization. Although polyacrylamide gel electrophoresis (PAGE) is applicable to standard separation of native proteins, it can also be used for separating proteins according to molecular weight when they are denatured in the presence of sodium dodecyl sulfate (SDS). SDS-PAGE is at present the most widely used protein electrophoretic technique for research in molecular biology. However, its very power for resolving proteins and separating them into multitudinous subunits has virtually excluded it from routine use in the clinical laboratory. Nevertheless, there is promise for clinical application of two-dimensional electrophoresis (2-DE), which uses standard separation in one direction followed by SDS-PAGE in the perpendicular direction. 2-DE results in perhaps hundreds of identifiable protein peaks, from which it may be possible to obtain important diagnostic information by sophisticated pattern analysis.

Isoelectric focusing affords superior resolution of closely migrating proteins or various forms of a single protein that differ in charge owing

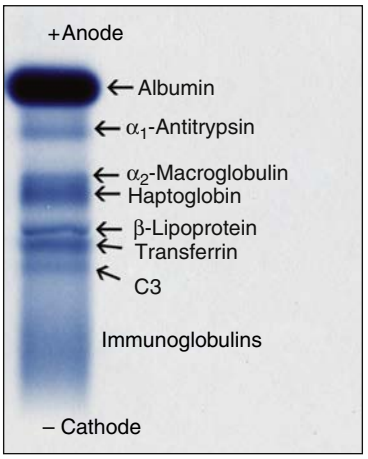

Figure 20.1 Positions of major serum proteins in a normal person using electrophoresis in agarose. Individual proteins separate according to their electrical charge between the anode (positive pole) and the cathode (negative pole).

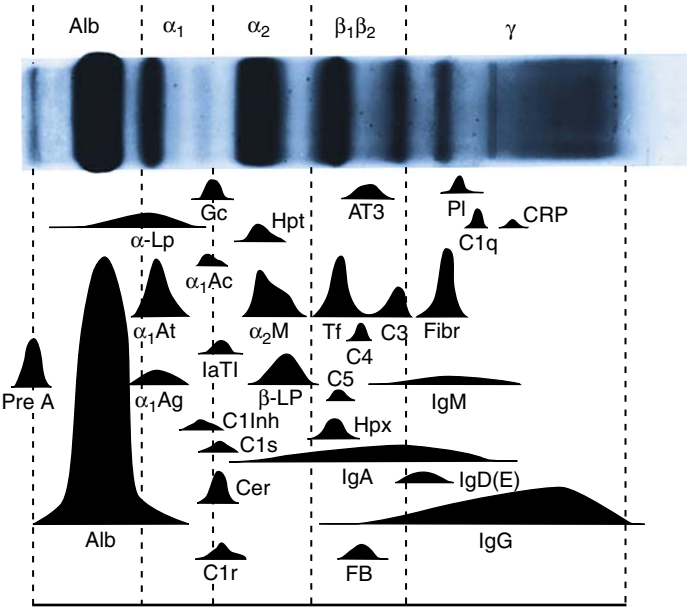

Figure 20.2 Plasma protein electrophoresis pattern in agarose gel is composed of five fractions, each composed of many individual species. Some of the major proteins are shown here in an artist's rendition for clarity. *α_1Ac,* α_1-Antichymotrypsin; *α_1Ag,* α_1-acid glycoprotein; *α_1At,* α_1-antitrypsin; *α_2-M,* α_2-macroglobulin; *α-Lp,* α-lipoprotein; *Alb,* albumin; *AT3,* antithrombin III; *β-Lp,* β-lipoprotein; complement components *C1q, C1r, C1s, C3, C4, C5,* as designated; *C1Inh,* C1 esterase inhibitor; *Cer,* ceruloplasmin; *CRP,* C-reactive protein; *FB,* factor B; *Fibr,* fibrinogen; *Gc,* Gc-globulin (vitamin D–binding protein); *Hpt,* haptoglobin; *Hpx,* hemopexin; immunoglobulins *IgA, IgD, IgE, IgG, IgM,* as designated; *IαTI,* inter-α-trypsin inhibitor; *Pl,* plasminogen; *Pre A,* prealbumin; *Tf,* transferrin. *(Modified from Laurell CB: Electrophoresis, specific protein assays, or both in measurement of plasma proteins?* Clin Chem *19:99, 1973, with permission.)*

to minor modification (e.g., posttranslational; see Chapter 4). By this technique, proteins migrate through a gel containing a gradient of pH established with a mixture of ampholytes. As each protein reaches the gel location where the pH is equal to its pI, the net charge on it becomes zero. It no longer has electromotive force acting on it, and it comes to rest. Thus, the final pattern is strictly according to pI.

PRECIPITATION

Chemical precipitations of serum proteins have been devised to resolve albumin and the globulins into two or more fractions that can then be measured for protein content. With the addition of sodium sulfate, sodium sulfite, ammonium sulfate, or methanol, the globulins tend to precipitate, leaving albumin in solution. By measuring total protein in the original serum and protein in the precipitate or the supernatant, values for albumin and globulin can be derived. Additionally, total protein concentration may be determined spectrophotometrically using an appropriate dye such as Coomassie blue or the biuret reagent, and the albumin concentration can likewise be determined spectrophotometrically using a dye that binds to it specifically, that is, bromocresol green or bromocresol purple. The globulin concentration can then be computed as total protein-albumin, and then the albumin to globulin (A/G) ratio can be determined. The ratio of these values (A/G ratio) has been used extensively because it accentuates abnormalities in serum protein composition, which in disease generally involves depression of albumin and elevation of one or more globulin fractions. Albumin may be depressed owing to decreased synthesis (malnutrition, malabsorption, liver failure, diversion to synthesis of other proteins) or increased loss (proteinuria, accumulation of ascites fluid, enteropathy). Globulins may be elevated owing to increased synthesis of many different proteins as part of acute or chronic reactions to disease. Lowering of albumin and elevation of globulins tend to occur simultaneously in disease, thus leading to exaggerated changes in the A/G ratio as the numerator and denominator move in opposite directions. Precipitation methods are not as accurate as zonal electrophoresis because some α-globulins may fail to precipitate, thus leading to an overestimate of the albumin fraction.

Preparative procedures for the isolation of a single minor protein constituent usually begin with a precipitation step to remove the bulk of other undesired serum proteins. The next step in protein isolation typically involves a column that separates on the basis of molecular size (gel filtration) or charge (ion exchange).

COLUMN SEPARATIONS

Gel filtration media such as Sephadex or agarose beads are rated according to pore size, which, in turn, determines what size molecules can pass through the interior of each bead or particle of the column. After application of a sample composed of various-sized proteins in aqueous solvent containing buffer and salt, more of the buffer is applied to drive the sample through the column. Very large molecules tend to flow through interstices of the column without entering the beads and emerge first from the bottom of the column in the void volume. Slightly smaller molecules enter the largest pores before being washed through; thus, they are slightly retarded in passing through the column. Small protein molecules pass into still smaller pores and are retained still longer. Finally, particles the size of dissolved salt penetrate farthest into the interior of gel filtration beads and come out after all of the proteins have emerged in an amount of applied buffer called the *salt volume*. Thus, in gel filtration, the order of protein elution is by molecular weight or size, from largest first to smallest last. Because all protein species continuously move through a gel filtration column all at the same time but at different rates, it is necessary to apply the sample in a small and uniform volume to optimize separation between peaks. Gel filtration requires that the medium be inert and not interact chemically or by charge with the proteins. It is not a method to be employed for high-resolution separation.

Ion-exchange chromatography, on the other hand, takes advantage of the charge on proteins to bind them to beads of a support medium with positively charged components such as diethylaminoethyl or quaternary aminoethyl. In anion-exchange chromatography, proteins are usually applied at a basic pH such as 8.6, at which they may be negatively charged (albumin and α_1-, α_2-, and β-globulins are anions) or may have no net charge (γ-globulins). The neutral proteins pass immediately through an anion-exchange column, whereas the anionic ones stick to the positively charged column matrix. If a buffer with a higher salt concentration is washed through, anions of the salt displace the anionic proteins and exchange for them by binding to the support medium. The proteins then elute from the column. By using a steadily increasing gradient of salt concentration in the eluting buffer, the proteins can be resolved according to charge. The ones with a small amount of charge will elute first, whereas those with the greatest charge (e.g., albumin) elute only when displaced by higher salt levels.

Alternatively, if pH is lowered while salt concentration is held low, anionic proteins acquire a net neutral or slightly positive charge and pass through the column. A gradient of falling pH can be used to resolve anionic proteins, with the order of elution being roughly β-, α_2-, and α_1-globulins, and albumin. Note that this order of elution is the reverse order of electrophoretic migration at pH 8.6, because in anion-exchange chromatography, mobility is retarded according to net negative charge, whereas in electrophoresis, mobility is enhanced by that charge.

Cation-exchange chromatography begins at an acid pH, with the proteins having positive charge (cations) and adhering to a negatively charged column matrix such as carboxymethylcellulose. They can be displaced by the cations of high salt in an eluting buffer or by increasing the pH, which will reverse the charge on the proteins to negative. By cation exchange, albumin should elute first, followed by α_1-, α_2-, β-, and γ-globulins.

Another separation modality by column is hydrophobic chromatography, in which samples are applied at high salt and are eluted with low salt. The support medium interacts with proteins with a hydrophobic nature; this is a good complementary technique to follow ion-exchange chromatography, in which the sample was eluted with high salt.

Affinity chromatography is based on specific binding between a protein of interest and another protein that has been covalently linked to the solid support medium of a column. For example, coagulation factor VIII complexed with von Willebrand factor (vWF) can be selectively removed from the other plasma proteins by passing plasma through a column that contains monoclonal anti-vWF antibody linked to the solid-phase matrix. The factor VIII-vWF complex selectively binds to the column as other plasma proteins wash through. The factor VIII is then dissociated from the vWF, thereby allowing it to elute in a purified fraction suitable for transfusion therapy. Such antigen–antibody interactions may be disrupted by high salt concentration, change in pH, or a chemical denaturant, such as urea, in different applications. Other affinity chromatography gels use a binding phenomenon that mimics naturally occurring molecular interactions. Thus, some dyes coupled to agarose are able to bind albumin, thereby removing it selectively from serum. Therapeutic antibodies or their Fab portions are concentrated with affinity columns containing their intended target antigens (e.g., Digibind for digoxin, CroFab for crotalid snake venom). Immunoglobulins can also be absorbed from a sample by staphylococcal protein A coupled to the gel matrix. Many other separation schemes can effect a high degree of purification in a single step with affinity chromatography medium coupled to dyes, drugs, nucleotide cofactors, and sugars. A clinical test using affinity chromatography is quantitation of glycosylated hemoglobin using a dihydroxyboronate affinity matrix that selectively binds molecular species of hemoglobin to which glucose has been covalently attached while allowing the nonglycosylated forms to pass through the column. The glycosylated hemoglobin is then separately eluted and quantitated.

Capillary electrophoresis is a separation method based on flow through a capillary tube that can be tailored to resolution of different molecules based on size, hydrophobicity, or stereospecificity. It is applicable to large molecules such as DNA or proteins, as well as to small ones such as hormones or therapeutic drugs. Physically, the method is similar to high-performance liquid chromatography (HPLC), in which solvent is pumped through a column that retains or passes solutes according to chemical interactions. Capillary electrophoresis for serum proteins employs a column with properties similar to agarose; thus, the separation of proteins is comparable with that from electrophoresis. This analysis can be automated with a detector at the effluent end that detects and quantitates protein bands without the need for staining and separate scanning. Although equipment costs are relatively high for capillary electrophoresis, reagent and labor costs are low, and the procedure is fast and very quantitative, leading to the promise of more widespread clinical applications in the future (Chen, 1991; Brinkman et al., 2004). When a monoclonal immunoglobulin band is suspected by capillary electrophoresis, further treatment of the specimen with anti-IgG, anti-IgA, anti-IgM, anti-κ, and anti-λ antisera is done in separate aliquots prior to performing the electrophoresis again; the monoclonal protein type is identified as the band that disappears with that antiserum. This approach is satisfactory for relatively high concentrations of monoclonal proteins, but it does not have good detection and quantitation power at lower concentrations of those proteins (Huang et al., 2014).

PROTEIN DETECTION AND QUANTITATION

The ultimate reference method for determining concentration of protein is the analysis for nitrogen content. Nitrogen is present uniformly along

the peptide bonds throughout the length of a protein and more irregularly in the side groups, wherever tryptophan, arginine, lysine, histidine, asparagine, or glutamine is present. The Kjeldahl technique consists of acid digestion to release ammonium ions from nitrogen-containing compounds. The ammonium can then be quantitated by conversion to ammonia gas and titration as a base, or by nesslerization, in which double iodides (potassium and mercuric) form a colored complex with ammonia in alkali. Although determination of nitrogen content can be extremely precise, its use for calculation of protein concentration depends on the exact protein composition of a sample because each protein has a somewhat different nitrogen content according to amino acid composition. However, for a sample of a purified protein, nitrogen content is highly accurate for estimating protein concentration when the nitrogen content on a molar basis is already known for that purified protein. Knowledge of a protein's exact amino acid sequence allows an accurate calculation of what the nitrogen content should be. Because clinical samples consist of unpredictable mixtures of different proteins and measurement of nitrogen content is not a simple procedure, it is not commonly used in clinical laboratories.

The refractive index can be accurate for measuring serum protein concentration as dissolved solute for levels above 2.5 g/dL. Hemolysis, lipemia, icterus, and azotemia produce erroneously high results. The refractive index cannot be used for urine protein measurements because of excess amounts of solutes in relation to the protein.

Specific gravity (and thus, by inference, protein content) can be estimated by pipetting drops of serum or blood into a graded series of copper sulfate solutions. A protein–copper shell forms about the drop to prevent dissolution for a short interval, during which time the drop falls to the bottom, remains stationary, or rises to the top. The protein concentration of a sample is estimated from the specific gravity of the copper sulfate solution in which the drop remains stationary. This technique is simple and has been used widely as a screening test for hemoglobin concentration in whole blood.

Proteins in solution absorb ultraviolet light at 280 nm (A_{280}), owing mostly to tryptophan but also to tyrosine and phenylalanine (Layne, 1957). For accurate conversion of A_{280} readings to protein concentration, the molar absorptivity must be used because each protein contains a different amount of these three amino acids. However, the A_{280} of a mixture of proteins is not a perfect measure of protein content because molar absorptivities vary greatly among different proteins. Because nucleic acids (which absorb strongly at 260 nm and also somewhat at 280 nm) may be present in protein preparations, a better estimate of protein concentration in the presence of nucleic acids is given by the following formula:

$$\text{Protein concentration (mg/mL)} = 1.55 \times A_{280} - 0.76 \times A_{260}.$$

Direct measurements of absorbance can be used for quantitating proteins in the range of 0.05 to 1.5 mg/mL.

Turbidimetric methods are often used for a similar concentration range in CSF or urine. Protein forms precipitate on the addition of trichloroacetic acid, sulfosalicylic acid, or other acid reagent. The resulting turbidity can be used for protein quantitation by increment in optical density in comparison with similarly treated standards. However, these techniques are not specific to proteins, because other acid-insoluble substances, such as nucleic acids, can also precipitate.

A colorimetric technique highly specific for proteins and peptides is the biuret method, by which copper salts in alkaline solution form a purple complex with substances containing two or more peptide bonds. Interferences are minimal, although ammonium ion may acidify the reaction, while hemoglobin and bilirubin absorb in the same region as the biuret complex (540–560 nm). The biuret method is extensively used in clinical laboratories, particularly in automated analyzers in which protein concentration can be measured down to 10 or 15 mg/dL.

Greater sensitivity can be obtained using the Folin-Ciocalteu reagent (or phenol reagent, phosphotungstomolybdic acid), which oxidizes phenolic compounds such as tyrosine and, in addition, tryptophan and histidine to give a deep-blue color.

Lowry and colleagues (1951) used the biuret method followed by the phenol reagent, which greatly enhanced color formation, because the phenol reagent can react with biuret complexes involving all peptide bonds. The Lowry assay has been extensively used for consistently accurate determinations of protein concentration. Further sensitivity for detection down to 1 μg of protein can be obtained using Coomassie brilliant blue dye, which is free of interferences from a very wide range of substances.

Comparable sensitivity is obtained with ninhydrin, which develops a violet color by reacting with primary amines. This reagent is widely used for detection of peptides and amino acids after paper chromatography and amino acid analyses from ion-exchange columns as well as for detection of drugs on toxicology screens using thin-layer chromatography (see Chapter 24).

Quantitation of albumin in the presence of other proteins is possible by virtue of the specific binding of albumin to certain dyes such as bromophenol blue, methyl orange, hydroxybenzeneazobenzoic acid, bromocresol purple, and bromocresol green (BCG). BCG is used extensively in automatic analyzers for determining serum albumin in parallel with biuret reagent for total protein. Dyes bound to albumin absorb maximally at slightly different wavelengths, thus allowing direct spectrophotometric quantitation of the albumin.

The standard dyes used for staining electrophoresis are Coomassie brilliant blue, Ponceau S, and amido black. For detection of minor components in high-resolution gels, silver staining is very sensitive down to nanogram quantities (Merril et al., 1981). In addition, special dyes, such as Oil Red O and Sudan Black, stain lipoproteins, and periodic acid–Schiff stains glycoproteins separated in special electrophoretic applications.

Because electrophoresis followed by staining does not afford explicit identification of serum proteins, immunologic measurements have been instituted for quantitation of individual proteins (Laurell, 1966). Nephelometry detects the turbidity produced usually within minutes or less by the precipitation of a reagent antibody with its target protein in a serum sample (Maachi et al., 2004). The major serum proteins are now widely measured by this method on automated immunochemistry analyzers that have supplanted former measurements by radial immunodiffusion. Owing to the specificity of the antibody reagent, nephelometry has great specificity for quantitating individual proteins, even in the presence of others. Proteins present in lower concentrations may be quantitated by specific immunoassays (Chapter 45).

SPECIFIC PLASMA PROTEINS

MAJOR COMPONENTS

The major serum proteins are those components that are readily resolved and detected on electrophoretic gels stained by conventional clinical laboratory techniques (Table 20.2, and see Fig. 20.1).

Prealbumin

Prealbumin is defined electrophoretically as the fraction that migrates in a position faster than albumin toward the anode. Prealbumin has a tetrameric structure with a total molecular weight of 62,000 Da, making it one of the smaller serum proteins. Each monomer can bind a molecule of thyroxine. As such, it is also called *thyroxine-binding prealbumin* (*TBPA*) or *transthyretin* (*TTR*), although only a small fraction of thyroxine is actually bound to TBPA in normal individuals because thyroxine-binding globulin has a 100-fold greater affinity for thyroxine (Oppenheimer, 1968). However, at least one molecular variant of prealbumin, inherited in a familial pattern, has a greatly increased affinity for thyroxine, resulting in elevated serum thyroxine content, although those individuals have normal free thyroxine concentrations and thus are euthyroid (Moses et al., 1982).

TTR is produced mostly in the liver (about 90%) with smaller amounts being made in epithelium of the choroid plexus from whence it enters CSF. Some TTR is also synthesized in retinal pigment epithelium and pancreatic islet of Langerhans cells as well as trace amounts in various organs (Vieira & Saraiva, 2014). Prealbumin plays a significant role in the metabolism of vitamin A by complexing with retinol-binding protein (RBP), which, in turn, complexes with vitamin A to transport it through the body (Peterson, 1971). RBP is a small protein of only 182 amino acids; thus, it would be rapidly removed from the circulation by filtration through the kidney if it were not held in the plasma by the larger protein prealbumin, which is not cleared into the glomerular filtrate. The complex of retinol, RBP, and TTR appears to be assembled in the endoplasmic reticulum of hepatocytes (Gaetani et al., 2002).

Prealbumin is rich in tryptophan (sometimes called *tryptophan-rich prealbumin*) and has considerable β-pleated sheet conformation. A portion of prealbumin is the source of the β-fibrillar amyloid component in type I familial amyloidotic polyneuropathy (Glenner, 1980). This hereditary amyloidosis derives from a mutation in the prealbumin gene that produces a protein (e.g., TTR Met 30 variant or FAP V30M) susceptible to proteolytic cleavage to create the β-structured fragments that are the building blocks of amyloid in nerve fibers (Saraiva et al., 1989; Ii et al., 1991). More than 80 different mutations in transthyretin have been recognized, mostly affecting nerve or heart with amyloid. These pathogenetic variants of prealbumin cannot be distinguished from normal by standard protein electrophoresis. Current diagnosis is based on analysis at the DNA level. A different variant of prealbumin (TTR T60A leading to FAP T60A) presents with a slightly

TABLE 20.2

Characteristics of Major Plasma Proteins

Protein	Concentration Range (g/L)	Molecular Weight	Actions
Prealbumin	0.15–0.36	62,000	Binds thyroxine; transports vitamin A
Albumin	39–51	66,000	Oncotic pressure; amino acid reservoir; carries small molecules
α_1-Antitrypsin	2.0–4.0	54,000	Protease inhibitor
α_2-Macroglobulin	1.5–3.5	725,000	Protease inhibitor
Haptoglobulin	0.4–2.9	100,000 (Type 1-1)	Binds hemoglobin
β-Lipoprotein	2.7–7.4	380,000	Lipid transport
Transferrin	2.0–4.0	80,000	Transports iron
C3	0.6–1.4	185,000	Component of complement system
Fibrinogen	1.0–4.0	340,000	Clot formation
Immunoglobulin A	0.4–3.5	160,000	Surface immunity
Immunoglobulin D	0.1–0.4	180,000	
Immunoglobulin E	50–600 (μg/L)	180,000	Binds to mast cells; hypersensitivity reactions
Immunoglobulin G	7–15	150,000	Humoral immunity
Immunoglobulin M	0.25–2.0	850,000	Humoral immunity primary response

different clinical picture in which disease appears later in life and in which cardiac amyloidosis is more frequent than in FAP V30M. Liver transplantation alone to remove the source of variant prealbumin did not reverse the cardiac amyloid, partly because these patients have significant involvement of multiple organs; consequently, a more favorable outcome might occur with the use of inhibitors of amyloid formation (Sattianayagam et al., 2012). Recently, novel new drugs have been introduced for treatment of hereditary transthyretin amyloidosis that act by suppressing both mutant and wild-type TTR protein production (Mickle et al., 2019). These medications are patisiran, which is a small interfering RNA molecule inside a lipid nanoparticle for transporting the oligonucleotide into hepatic cells (Rizk & Tüzman, 2019); and inotersen, which is also a modified antisense oligonucleotide (Benson et al., 2018). These gene-silencing drugs have the capacity to stabilize the disease (Plante-Bordeneuve, 2018).

Prealbumin has a relatively short half-life in the circulation (roughly 2 days) compared with other major serum proteins. Its synthetic rate is also exquisitely sensitive to intake of adequate nutrition and to alterations in hepatic function where it is produced. Therefore, prealbumin concentrations in serum fluctuate more rapidly in response to alterations in synthetic rate than do those of other proteins, such as albumin. For this reason, quantitation of serum prealbumin has major clinical utility as a marker for nutritional status (Gofferje, 1978; Keller, 2019; Loftus, 2019). Because of the rapid dynamics of its synthesis and clearance, prealbumin is considered to be a better early indicator of change in nutritional status than other commonly used markers, such as albumin and transferrin, which are more abundant but whose levels respond to other factors as well and at slower time scales. In a study of 7815 hemodialysis patients, low levels of prealbumin were associated with greater risks of mortality and hospitalization for infection that were independent of other risk factors, including serum albumin (Chertow et al., 2005). Thus, prealbumin measurements can be very important for planning patient management.

Concentrating CSF before electrophoresis allows visualization of a distinct prealbumin band in CSF. CSF normally contains a major peak of albumin plus prealbumin and a small amount of transferrin. Electrophoresis of CSF is usually requested for detection of oligoclonal bands of immunoglobulin, and the presence of a distinct band of prealbumin is used only as a landmark to confirm that the specimen was likely CSF. True prealbumin is generally below the level of detection by serum electrophoresis; instead, it is best quantified by immunologic measurements such as nephelometry. A protein band frequently appears in the prealbumin position of serum from patients who have had heparin therapy. In the circulation, heparin activates and releases lipoprotein lipase activity, which attacks triglycerides in lipoprotein fractions, thereby greatly enhancing their electrophoretic migration anodally. Protein stain reveals apolipoproteins in the prealbumin position but no β-lipoprotein fraction. This is an in vivo effect that does not occur if heparin is added to samples already collected.

Albumin

The single most abundant protein in normal plasma is albumin, usually constituting up to two-thirds of total plasma protein (Peters, 1975). For this reason, depressions in albumin level due to impaired synthesis (e.g., malnutrition, malabsorption, hepatic dysfunction) (Rothschild et al., 1972) or due to losses (e.g., ascites, protein-losing nephropathy or enteropathy) result in serious imbalance of intravascular oncotic pressure. This loss is manifested clinically by the development of peripheral edema (Slater et al., 1975). However, the congenital absence of albumin (analbuminemia) generally does not lead to such problems, presumably because of lifelong compensatory mechanisms that control hydrostatic pressures (Waldman et al., 1964). Albumin also serves as a mobile repository of amino acids for incorporation into other proteins. A third function ascribed to albumin is that of a general transport or carrier protein. Many organic and inorganic ligands (e.g., thyroxine, bilirubin, penicillin, cortisol, estrogen, free fatty acids, warfarin [Coumadin], calcium, magnesium, heme) are complexed with different regions of the albumin molecule in covalent (e.g., δ-bilirubin) (Lauff et al., 1982) or dissociable binding (Koch-Weser et al., 1976). These binding interactions with very different ligands are possible because of a wide variety of binding sites on the albumin molecule, which consists of 585 amino acids arranged in nine loops held together by the disulfide bonds between cysteine residues (Meloun et al., 1975). The primary sequence of albumin contains three major regions with three peptide loops each, suggesting that it arose from gene duplication of some ancestral gene in a tandem rearrangement process (Peters, 1977; Sevall, 1986). It is also interesting to note that α-fetoprotein has regions of homology with serum albumin, which may indicate a common ancestral gene origin for these two proteins.

In addition to the genetic abnormality of analbuminemia, many hereditary variants of albumin differ from the most common allotype, albumin A, by single amino acid substitutions. These variants can be rapid or slow migrating compared with albumin A, leading to two distinct albumin peaks (bisalbuminemia) in the heterozygous state (Fig. 20.3). None of the variant albumins appears to affect health, but one variant does have greatly enhanced affinity for thyroxine, which leads to elevated thyroxine content in the serum of such persons, who nevertheless remain euthyroid (Ruiz et al., 1982). At least 77 different mutations in albumin are recognized, 65 of which lead to bisalbuminemia; 12 cause analbuminemia, and 3 have strong binding of thyroid hormones, whereas others show variations due to frameshifts, with modifications near the carboxy-terminus of the albumin molecule (Minchiotti, 2008).

Up to 8% of albumin circulating in normal persons becomes glycosylated nonenzymatically, whereas up to 25% becomes glycosylated during hyperglycemia in analogy with glycosylated hemoglobin (Guthrow et al., 1979). The half-life of circulating albumin is about 17 days; thus, measurements of the glycosylated form may be useful in monitoring diabetic control during an interval of a few weeks. Measurement of glycosylated albumin can be very useful for assessing diabetic control in patients with hemolytic anemias (e.g., sickle cell disease, thalassemia, autoimmune hemolysis), whose red cell survival is greatly shortened and in whom measurement of glycosylated hemoglobin is unreliable. A similar measurement is termed fructosamine, which is total glycosylated (or glycated) proteins, the large majority of which is glycated albumin (see Chapter 17). Glycosylated albumin measurements may not be reliable for assessing diabetic control in patients with protein-losing nephropathy, in which albumin clearance

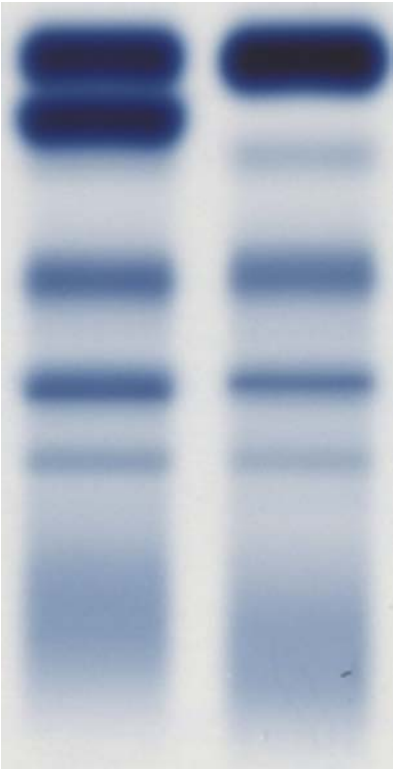

Figure 20.3 Bisalbuminemia. Serum protein electrophoresis with normal pattern in right lane and bisalbuminemia consisting of two equal intensity bands of albumin in left lane. The additional band of albumin in this patient migrated more slowly than normal albumin into the α_1-region.

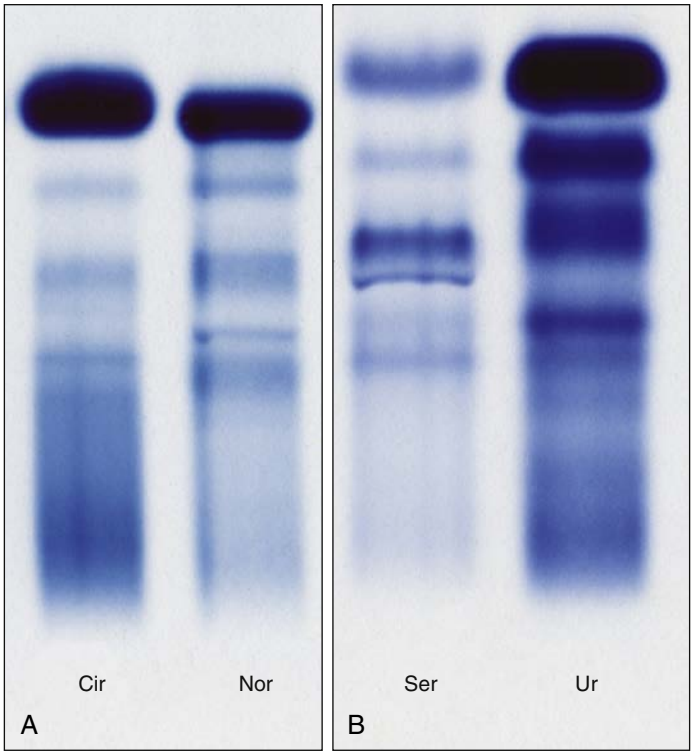

Figure 20.4 A, Serum protein electrophoresis in cirrhosis (Cir) shows more rapidly migrating albumin compared with normal serum (Nor) because of the additional negative charge from covalently linked conjugated bilirubin (i.e., δ-bilirubin). The γ-globulins are broadly increased in the polyclonal elevation characteristic of cirrhosis of the liver. B, Protein electrophoretic patterns of serum (Ser) and concentrated urine (Ur) in a patient with nephrotic syndrome. Smaller molecular-sized proteins such as albumin are preferentially lost from blood into urine. Larger proteins such as α_2-macroglobulin and β-lipoprotein are retained in the blood and constitute major bands in the serum pattern.

is accelerated. Diabetic patients on hemodialysis can be monitored with glycosylated hemoglobin or glycosylated albumin (Ghacha et al., 2001).

Analysis of newly synthesized albumin from intracellular sites has revealed the existence of a precursor proalbumin, which has an additional hexapeptide at its amino-terminal end. The primary structure of albumin consists of 35 cysteine residues, of which 34 form intramolecular disulfide bonds and one remains free. On storage for many days, albumin forms covalently linked dimers through the free cysteines, resulting occasionally in an extra band of albumin on electrophoresis.

Clinical measurements of albumin are very frequent, with determinations of total protein and albumin often included in chemistry panel profiles. Organ- or disease-oriented panels of chemistry tests in current use include the following measurements: comprehensive metabolic panel has albumin and total protein; renal function panel has albumin; and hepatic function panel has albumin and total protein.

Elevations of serum albumin concentration are infrequent, although they do occur in dehydration as the plasma water phase shrinks. Following rehydration, the albumin level should fall to within the normal reference range. Elevation of serum albumin may also occur artefactually as the result of prolonged application of a tourniquet for venipuncture. In this instance, increased hydrodynamic pressure from venous backup forces water and small solutes out of the intravascular space, thereby concentrating cellular elements, micellar forms of lipoproteins, and proteins such as albumin.

Depression of albumin concentrations is frequent in sick individuals; a review of hospitalized patients reveals that a substantial proportion of albumin measurements are below healthy reference ranges (see Fig. 20.7). Although some of these decreases are likely dilutional, owing to the administration of intravenous fluids, others are caused by loss of albumin into urine, ascitic fluid, or the gastrointestinal tract in enteropathies, or by decreased synthesis in the liver caused by hepatic disease such as cirrhosis or by secondary effects on synthesis resulting from compromised nutrition or diversion of synthetic capacity to other proteins. This sensitive but nonspecific reduction of albumin in so many different conditions has led to referring to it as a "negative acute-phase reactant" (Post et al., 1991). Measurements of albumin concentrations are vital to the understanding and interpretation of calcium and magnesium levels because these ions are bound to albumin; thus, decreases in albumin are directly responsible for depression of their concentrations as well. In some disease states, decreases in albumin are at least partially compensated for by increases in other serum proteins, thereby stabilizing oncotic pressures intravascularly. In particular, cirrhosis shows a major polyclonal increase of immunoglobulins in the γ-fraction (Fig. 20.4A) and nephrotic syndrome shows high levels of α_2-macroglobulin (Fig. 20.4B). In acute heart failure of elderly patients, increased albumin has been shown to be associated with decreased 180-day mortality in patients over 80 years old (Metra et al., 2014).

Body fluids that form normally, such as CSF, or pathologically, such as filtrates of plasma (e.g., ascites), contain albumin as the major component, with very little contribution from other plasma proteins. The presence of albumin in the urine is generally considered abnormal even in trace amounts above 30 μg/g creatinine, although some healthy individuals exhibit albuminuria following intense exercise. Progression of diabetic nephropathy can be assessed by the quantitative measurement of albuminuria, as it tends to appear ahead of the other serum proteins in urine during the course of renal glomerular damage. Immunologic measurement of microalbumin in urine is now considered a standard of care for management of diabetes mellitus and the early detection of diabetic complications. The nephrotic syndrome, which is marked by extensive hypoalbuminemia, is often due to diabetic nephropathy or one of several other primary glomerular diseases (Orth & Ritz, 1998).

α_1-Antitrypsin

The major component of the α_1-globulins is the protease inhibitor α_1-antitrypsin (AAT), which has the capacity to combine with and inactivate trypsin (Eriksson, 1965; Berninger, 1985a). The first clue to this function came with the discovery that the serum of some young adults with pulmonary emphysema was deficient in α_1-globulin. Further investigation revealed a similar deficiency of AAT in children with cirrhosis (Sveger, 1976). Usually, no appreciable circulating levels of trypsin are found in blood, but other related proteases, such as elastase, are released from leukocytes responding to irritants or inflammation. AAT is able to neutralize the activity of these proteases as well; thus, it is an intrinsic factor in the homeostatic mechanism modulating endogenous proteolysis within the body and preventing inappropriately severe biochemical response to inflammation (Cox, 1986).

AAT is coded for by the gene *SERPINA1* on chromosome 14. A majority of people are homozygous for the normal fully active *M* allele of AAT, or phenotype MM (Lieberman et al., 1972). About 10% of whites (and

lower percentages of other races) are heterozygous for *M* and some other allele of the protease inhibitor (or Pi) system. More than 2% carry the *PiZ* allele and exhibit the phenotype MZ. Although these individuals have somewhat reduced levels of trypsin-inhibitory capacity in serum, they are generally asymptomatic. However, their homozygous ZZ offspring (who have very low levels of AAT) are susceptible to pulmonary or hepatic disease. The ZZ phenotype occurs in about 1 in 4000 individuals. Another common variant is the *PiS* allele, which shows moderate reduction in synthesis. Although the MS phenotype does not show related disease, both SS and SZ phenotypes are suspected to have increased risk of lung or liver disease. Another allele that may need special attention to detect is the null variant that produces no AAT protein.

Although AAT deficiency can be recognized on serum protein electrophoresis, an efficient diagnostic algorithm employs measurement of AAT concentration followed by phenotyping with isoelectric focusing electrophoresis and genotyping with molecular assays designed to detect specific mutations (Snyder et al., 2006; Bornhorst et al., 2007). Definitive typing may require analysis of the DNA sequence for the *AAT* gene. At least 75 different alleles exist for *AAT*. About 17 alleles have sufficiently low protein production to lead to pulmonary disease, and only a few are responsible for liver disease (Cox, 1986).

Therapy for pulmonary emphysema secondary to AAT deficiency has been greatly advanced by intravenous replacement of AAT, using concentrates or recombinant protein to bring circulating levels into ranges sufficient for antielastase protection to the lungs (Snider, 1989). Augmentation therapy using plasma-derived AAT administered intravenously allows protective concentrations to accumulate in alveolar epithelial lining fluid (Strange, 2018). Gene therapy for AAT deficiency using recombinant adeno-associated virus AAT vector administered by single intramuscular injection has resulted in sustained low-level expression (2.0%–2.5% of target level) of AAT in serum over 1 to 5 years. This treatment also led to partial correction of neutrophil defects (Mueller et al., 2017).

Further replacement has also been successful with AAT inhalation for patients in whom pulmonary disease has not yet become extensive (Hubbard et al., 1989). Avoidance of cigarette smoking by homozygous individuals is essential because cigarette smoke is a major source of irritants that trigger leukocytes in the lung to release proteases (Gelb et al., 1977). Cirrhosis in young children is treated by hepatic transplantation, because the liver is the site of AAT synthesis. An interesting aspect of cirrhosis and the ZZ phenotype is the presence of unsialylated mutant-type AAT granules in the hepatocytes, implying a defect of secretion in those alleles. Cirrhosis secondary to AAT abnormality has not been improved by replacement therapy. Children with this disorder can develop progressive, severe cholestasis, prompting liver transplantation. Following transplant, the recipient takes the AAT phenotype of the donor. One approach suggested for treatment of AAT ZZ phenotype is to enhance the secretion of that abnormal molecule with a chemical chaperone and thus reverse or prevent the intracellular deposits of AAT that cause damage to hepatocytes (Chanprasert & Scaglia, 2015).

AAT is one of the serum glycoproteins that rise in response to acute inflammation, but such elevations lack clinical specificity. The α_1-fraction never appears completely empty in AAT deficiency because other proteins (e.g., α-lipoprotein, α_1-acid glycoprotein) migrate there but do not resolve into distinct bands. Genetic screening for AAT deficiency may be useful in targeted populations, resulting in early diagnosis, improved outcomes, and guidance for affected kindreds (Aboussouan & Stoller, 2009).

α_2-Macroglobulin

α_2-Macroglobulin (AMG) is the largest major nonimmunoglobulin protein in plasma, with a molecular weight of 725,000 Da (Roberts, 1985). The serum concentration in normal individuals is comparable with that of the other major protease inhibitor, AAT, although women have higher levels than men in response to estrogen (Horne et al., 1970). The concentration of AMG rises 10-fold or more in the nephrotic syndrome when other lower-molecular-weight proteins are lost (Beetham & Cattell, 1993). The loss of AMG into urine is prevented by its large size. The net result is that AMG reaches serum levels equal to or greater than those of albumin (≈2–3 g/dL) in the nephrotic syndrome, which has the effect of maintaining oncotic pressure (see Fig. 20.4B). Synthesis of AMG in nephrotic syndrome may also be enhanced, which accounts for its absolute increase in concentration. AMG inactivates proteases by complexing with them and forming covalent bonds to them. Its own conformation is thereby altered, which enhances clearance by the reticuloendothelial system. At least four molecular forms of AMG differ in sialic acid, mannose, and galactose content and can be separated by isoelectric focusing. Other molecular variations probably are the result of proteases linked to AMG before removal from the circulation. The spectrum of inhibition by AMG is very wide, including virtually all types of serine, carboxyl, thiol, and metal proteases. AMG complexes with prostate-specific antigen (PSA) in a form that is not detected by immunoassay for PSA (see Chapter 76). Although AMG function is certainly important for maintaining balance in the ebb and flow of proteolysis, no specific deficiency with associated disease has been recognized and no disease state is generally attributed to low concentrations of AMG. Mild but distinct elevations of AMG can be observed on serum protein electrophoresis early in the course of diabetic nephropathy.

AMG inactivates proteases through a molecular trap mechanism using a bait region to bind proteases that then are bound to AMG and cleared by macrophage receptors (Armstrong, 2006). AMG also has separate binding sites for β-amyloid peptide, transforming growth factor-β, nerve growth factor-β, and platelet-derived growth factor-BB. Polymorphisms of AMG may be important in the modulation and clearance of these substances, leading to varying risk for disorders such as Alzheimer disease (Mettenburg & Gonias, 2005).

Haptoglobin

The other major protein migrating in the α_2-region is haptoglobin, which has the function of combining with hemoglobin released by lysis of red cells to preserve body iron and protein stores. The circulating half-life of haptoglobin, free of hemoglobin, is roughly 4 days. Hemoglobin–haptoglobin complexes are removed from the circulation within minutes by the reticuloendothelial system, where the hemoglobin is broken down into globin and heme, which further degrades to iron and bilirubin. Haptoglobin–hemoglobin complexes bind to the CD163 monocyte/macrophage scavenger receptor for removal from the circulation by endocytosis (Buehler et al., 2009). When the hemoglobin-binding capacity of haptoglobin is exceeded, free hemoglobin enters the glomerular filtrate as α-chain–β-chain dimers that are subsequently reabsorbed in the proximal renal tubules and converted to hemosiderin.

Haptoglobin has two heavy chains and two light chains linked by disulfide bonds in analogy to the basic structure of immunoglobulins. Some persons have a light-chain gene that is duplicated in a head-to-tail arrangement (Type 2). Normal haptoglobin (Type 1-1) gives rise to a single molecular species of molecular weight 100,000. Heterozygous individuals (1-2) have, in addition to Type 1-1 haptoglobin, a series of multimers (e.g., dimers, trimers) by virtue of intermolecular disulfide linkages through the duplicated light chain. Type 2-2 haptoglobin consists of a different series of multimers, because the Type 2 light chain has a different molecular weight from the Type 1 light chain (Konigsberg, 1974). These different forms of haptoglobin can be distinguished by high-resolution electrophoresis (Fig. 20.5).

Haptoglobin can be quantitated in terms of its hemoglobin-binding capacity or by immunologic means, especially nephelometry. Owing to steric hindrance between molecular sites on the multimers, the different phenotypes of haptoglobin yield measurements of antigen- or hemoglobin-binding capacity that may be discrepant with the absolute amount of haptoglobin protein present in a sample. Accordingly, the reference range for haptoglobin is broader for an entire population of different phenotypes than within individual phenotypes. For this reason, interpretation of haptoglobin concentrations is soundest for serial measurements in the same individual. However, very high levels can readily be distinguished from very low ones, which can be important in the first-time evaluation of a patient for hemolysis. Congenital deficiency of haptoglobin appears not to have clinical consequences (Manoharan, 1997).

In diabetes mellitus, patients with Type 2-2 haptoglobin have shown higher risk for vascular complications, perhaps owing to different ability to clear hemoglobin, thus leading to altered iron handling and heightened oxidative load (Van Vlierberghe et al., 2004; Levy et al., 2010).

Serum haptoglobin rises in response to stress, infection, acute inflammation, or tissue necrosis, probably by stimulation of synthesis (see later discussion under Acute-Phase Reactants). After a hemolytic episode, haptoglobin concentrations fall as the complexes with hemoglobin are cleared from the circulation. This effect is dramatic following massive hemolysis in situations of hemolytic transfusion reaction, thermal burns, or autoimmune hemolytic anemia. It is also a useful measurement for serially monitoring patients who have a slow but steady rate of red cell breakdown, such as by mechanical heart valves, hemoglobinopathies, or exercise-associated trauma. Low haptoglobin concentrations may accompany liver disease when hepatic synthetic capacity is impaired. There are also individuals with congenital deficiency of haptoglobin who apparently use other mechanisms to conserve body iron stores. Serum samples from blood hemolyzed in vitro during phlebotomy or processing show a displaced band of haptoglobin–hemoglobin complex on protein electrophoresis.

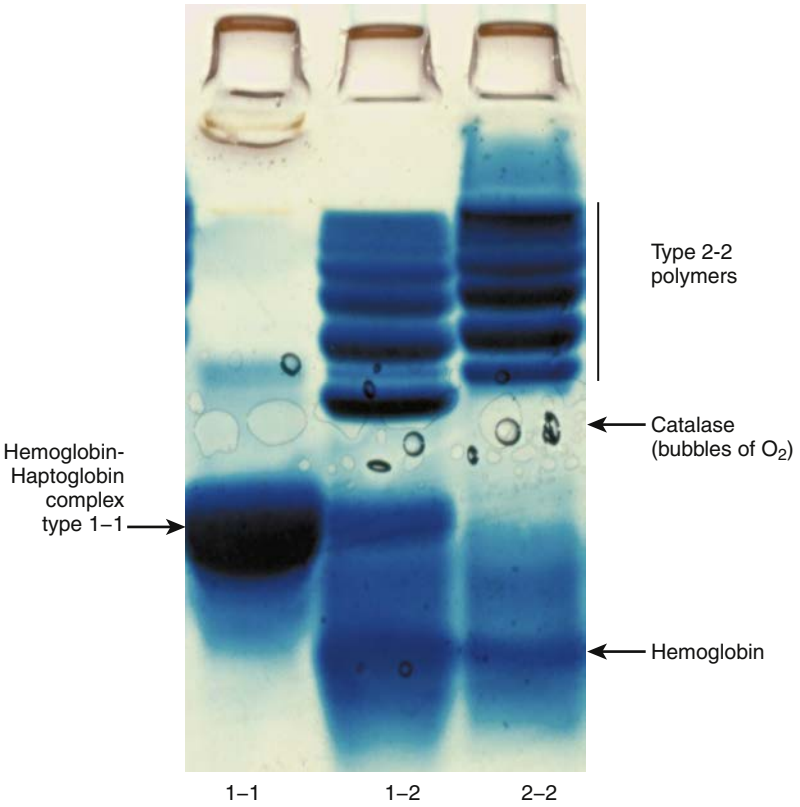

Figure 20.5 Phenotyping of haptoglobin. Patient serum specimens were mixed with free hemoglobin from erythrocytes lysed in vitro and electrophoresed in a polyacrylamide gel with high resolution of different molecular weight proteins. After electrophoresis, the gel was developed in a solution of substrate 3,3′,5,5′-tetramethylbenzidine and hydrogen peroxide. Hemoglobin exhibits pseudoperoxidase activity that converts substrate to a blue product wherever it has migrated, including complexes with haptoglobin. Bubbles of oxygen formed in the gel at the location of catalase, which is also present in the lysate. Type 1-1 haptoglobin *(arrow in left lane)* migrated deeply into the gel *(from top to bottom)*, although unbound hemoglobin migrated even farther. Type 2-2 haptoglobin showed no band in the 1-1 position but migrated as a series of high-molecular-weight polymers, each binding hemoglobin *(bar next to right lane)*. Type 1-2 haptoglobin *(middle lane)* showed a minor band of 1-1 plus a series of high-molecular-weight polymers different from the bands observed with 2-2.

It should be noted that myoglobin does not bind to haptoglobin; therefore, release of large amounts of myoglobin by rhabdomyolysis does not diminish haptoglobin levels in serum. This difference can be useful in the workup of a positive dipstick test for blood (actually a test for pseudoperoxidase activity of heme in hemoglobin or myoglobin) in urine with no coexisting red cells. In this case, low serum haptoglobin suggests hemoglobinuria (hemolysis), whereas high serum haptoglobin suggests myoglobinuria. Lactate dehydrogenase (LD) isoenzyme 1 in serum is also associated with hemolysis, whereas LD5 and creatine kinase are released in rhabdomyolysis.

β-Lipoprotein

β-Lipoprotein (low-density lipoprotein [LDL]) migrates with a characteristic sharp leading cathodal edge and feathery trailing region more anodally. Although it is better quantitated by stains for lipid, apoprotein content is sufficient to be a distinct band on staining for protein. The exact position of the β-lipoprotein band is sensitive to recent ingestion of fatty foods; thus, samples from fasting versus postprandial collections will show the β-lipoprotein in slightly different positions. The other lipoproteins (very-low-density lipoprotein, high-density lipoprotein, and chylomicrons) are relatively small in intensity, and they occur in overlapping electrophoretic positions with other serum proteins; thus, these fractions generally are not appreciated on protein stain. Administration of heparin activates postheparin lipoprotein lipase, which degrades triglycerides in the circulating lipoprotein fractions. Consequently, heparinized patients transiently demonstrate an anomalous band of β-lipoprotein that can migrate very rapidly and unevenly across the electrophoretic path, even into the prealbumin region. Elevations of LDL, with greater staining intensity to the β-lipoprotein band, occur in hypercholesterolemia. Lipoproteins are discussed more thoroughly in Chapter 18.

Transferrin

The major β-globulin is transferrin (siderophilin), which transports ferric ions from the iron stores of intracellular or mucosal ferritin to bone marrow, where erythrocyte precursors and lymphocytes have transferrin receptors on their surfaces (Irie & Tavassoli, 1987).

Transferrin consists of 687 amino acids with a calculated molecular weight of 79,550 Da (MacGillivray et al., 1982). Analysis of the amino acid sequence shows that transferrin has two homologous domains that may have arisen by contiguous duplication of an ancestral transferrin gene. Each domain has a binding site with very high affinity for iron. Transcription of mRNA for transferrin synthesis in the liver is regulated by the concentration of iron in the circulation and surrounding the hepatocytes.

In normal serum, transferrin ranges in concentration from 200 to 400 mg/dL, which is conveniently measured as iron-binding capacity (IBC) (Tsung et al., 1975). In response to short-term iron deficiency, transferrin levels rise markedly to twice normal levels or higher. Because transferrin is a single molecular species with a tight electrophoretic mobility, an elevated level can have the appearance of a paraprotein (pseudoparaproteinemia) in cases of severe iron deficiency (Zawadzki, 1970). At least some iron deficiency and elevation of transferrin should be expected with pregnancy (Mendenhall, 1970). Administration of iron to deficient patients increases saturation; this is followed by return of transferrin to normal.

Chronic saturation of transferrin occurs in idiopathic hemochromatosis and transfusional hemosiderosis. Because almost no unsaturated IBC is found in those syndromes, iron cannot be mobilized normally for excretion, resulting in excess deposition in tissues that is toxic. Current strategies to screen for hemochromatosis include measurement of serum iron and serum transferrin (usually by nephelometric immunoassay), with the calculation of percent saturation as the best index for identifying previously unrecognized cases. Hemochromatosis is a hereditary disorder that results in cirrhosis, diabetes, cardiomyopathy, arthritis, and other endocrine disorders owing to the toxic effects of excess free iron. Screening for hemochromatosis is desirable because disease progression can be halted by lowering the body burden of iron by such means as phlebotomy or chelation therapy.

Transferrin may also demonstrate an antibacterial effect by complexing iron and removing it from bacteria that require iron for growth (Reddy et al., 1970; Weinberg, 1978). Congenital deficiency of transferrin (atransferrinemia) is a rare disorder characterized by microcytic anemia and iron overload (Aslan et al., 2007). In protein-losing nephropathy of sufficient severity, transferrin is lost from the circulation into the urine, carrying iron with it. This loss may contribute to the development of hypochromic anemia.

Electrophoretic variants of transferrin occur occasionally in serum owing to allotypic variation in the amino acid sequence and thus have a different charge on the molecule. In this case, the heterozygous state shows a doublet in place of a single electrophoretic band for transferrin (Kamboh & Ferrell, 1987).

Transferrin is a glycoprotein in which various sugar molecules are added to newly synthesized protein molecules in the liver. Persons who engage in heavy alcohol consumption demonstrate abnormal carbohydrate-deficient

transferrin (CDT) in their serum (Stibler, 1991). CDT refers to a group of human transferrin (hTf) molecules lacking carbohydrate chains that normally attach to two sites on hTf. These aberrant molecules of disialo- and asialotransferrin, as opposed to normally glycosylated tetrasialotransferrin, may be due to failure of glycosyltransferases in hepatocytes, to increased sialidase activity in serum, or to a combination of the two (Xin et al., 1995).Considerable microheterogeneity occurs with up to eight sialic acid (SA) residues on hTf. These negatively charged SA residues are probably involved in the binding and transport of positively charged iron ions. Alcohol intake causes a reduction in the hepatic enzymes responsible for attaching SA, thus leading to release of asialo-hTf (Paterlini et al., 2019).

CDT can be detected by anion-exchange chromatography or isoelectric focusing of isoforms in serum followed by immunoblotting. Other methods include HPLC, capillary zone electrophoresis, mass spectrometry, and turbidimetric immunoassay (Bean et al., 2001). Although CDT is generally considered to be a highly specific marker for chronic alcohol abuse (Arndt, 2001), false negatives can occur in women, in nonsmokers, and in persons who have a high body mass index (both overweight and obese) (Whitfield et al., 2008).

A variant of transferrin has been recognized in CSF (Zaret et al., 1992), aqueous and vitreous humor of the eye (Tripathi et al., 1990), and perilymph of the ear (Thalmann et al., 1994). Chemically, it lacks sialic acid in glycosylation compared with the transferrin found in plasma (Hoffmann et al., 1995); it is called *asialotransferrin*, *τ protein*, or β_2-transferrin, which has slightly different electrophoretic migration (toward the cathode), because it carries less negative charge than plasma transferrin (Blennow & Fredman, 1995). CSF contains both forms of plasma transferrin and asialotransferrin, whereas plasma contains only one form. Consequently, detection of asialotransferrin in fluid from a fistula or drainage is presumptive evidence for the presence of CSF in cases of skull fracture or other head trauma with nasal drainage (Solomon et al., 1999) or for the presence of perilymph in fistula fluid from otologic procedures such as cochlear implants (Delaroche et al., 1996). Asialotransferrin reacts immunologically as transferrin; thus, it can be readily detected by immunoblotting following electrophoresis (Roelandse et al., 1998). This procedure is easily done by adapting commercially available agarose gel electrophoresis systems already used in many laboratories for direct immunofixation of immunoglobulins (Normansell et al., 1994); using an antitransferrin antibody demonstrates a single band of transferrin in serum samples but two bands if the specimen contains CSF (Fig. 20.6). It is necessary to include serum in addition to test fluid from the patient to rule out allelic variants of transferrin that could cause false positives if not recognized (Sloman & Kelly, 1993). The presence of CSF in drainage fluid may require surgical repair or antibiotic therapy; thus, detection of asialotransferrin as a marker for CSF can have a substantial clinical impact.

Complement

A separate fraction of β-globulin consists of the C3 component of complement. Although this protein can be resolved easily with a fresh serum sample, in stored specimens and commercial control serum that has been lyophilized, C3 is cleaved to form C3c, which migrates anodally to native C3 as a band nondistinct from other β-globulins. Depression of C3 occurs in autoimmune disorders when the complement system is activated and C3 becomes bound to immune complexes deposited in tissues, thereby removing them from plasma. Thus, C3 (and also C4) concentration is a convenient marker for assessing disease activity in rheumatic disorders such as lupus erythematosus and rheumatoid arthritis. C4 is not appreciated on serum protein electrophoresis because its concentration is normally only about one-fifth that of C3. Both C3 and C4 are now easily quantitated by nephelometry for monitoring rheumatic disease activity. No particular diagnostic significance is ascribed to higher than normal levels of C3 or C4, except as mild indicators of an acute-phase response. The complement system and its inhibitors are discussed further in Chapter 48.

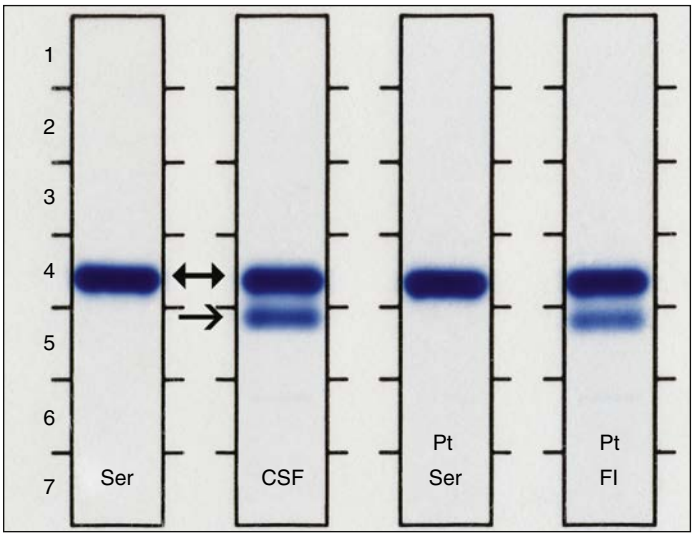

Figure 20.6 Immunofixation with transferrin antibody to test for presence of cerebrospinal fluid (CSF). *Ser,* Normal serum showing position of transferrin (Tf; *double-headed arrow*); *CSF,* normal position of Tf and asialotransferrin (aTf, *single-headed arrow*); *Pt Ser,* patient serum included to rule out electrophoretic variant of Tf; *Pt Fl,* unknown fluid from patient demonstrating bands of both Tf and aTf that confirm the presence of CSF in that fluid.

Fibrinogen

Plasma contains 100 to 400 mg/dL of fibrinogen, which is the most abundant of the coagulation factors and which forms the fibrin clot. With an overall molecular weight of 340,000 Da, fibrinogen is a dimer consisting of three pairs of peptide chains (A-α, B-β, and γ) linked with multiple disulfide bonds near their amino-terminal ends (Doolittle, 1975; Doolittle et al., 2001). This region of the molecule is termed the *E domain* or *disulfide knot*. The chains extend outward into two other identical domains (D) at their carboxyl ends, where all three chains are intertwined. Thrombin cleaves fibrinopeptides A and B from the amino ends of the A-α and B-β chains, thereby resulting in a fibrin monomer that polymerizes into fibrils that macroscopically form a fibrin clot. Factor XIII then produces covalent bonds between lysine and glutamine residues on adjacent γ-chains of different fibrin molecules, making the fibrin clot essentially a single molecule. A cross-linked clot is refractory to dissolution by chemical denaturants and is mechanically very stable.

Numerous hereditary variants of fibrinogen (dysfibrinogenemias) have been identified, in which a functionally abnormal fibrinogen molecule is synthesized with altered amino acid sequence owing to genetic mutation. Some dysfibrinogenemias exhibit impairment of clotting and a hemorrhagic diathesis, whereas others show increased tendency to thrombosis (Menache, 1973). Congenital afibrinogenemia, in which essentially no fibrinogen is synthesized, results in a hemorrhagic disorder that paradoxically is not as severe as the hemophilias in terms of joint abnormalities secondary to hemorrhage (hemarthroses).

Fibrinogen levels become elevated with the other acute-phase reactants, occasionally to over 1.0 g/L. In such instances, the erythrocyte sedimentation rate (ESR) is also markedly elevated owing to fibrinogen content directly. Fibrinogen levels also rise with pregnancy and use of contraceptive medications. Low levels generally indicate extensive activation of coagulation with consumption of fibrinogen. During this process, plasminogen is also activated into plasmin, which degrades fibrin and fibrinogen into split products that are measured for the assessment of intravascular coagulation. Normally, clots that form are removed by the action of plasmin, which, in turn, is inactivated by antiplasmin and the other protease inhibitors.

Fibrinogen is absent from normal serum but should appear in plasma electrophoresis as a distinct band between the β- and γ-globulins (Fig. 20.7). Not infrequently, blood drawn from heparinized patients does not fully clot; thus, a fibrinogen band is present on electrophoresis. It can be distinguished by examining the specimen for a fine clot and by repeat electrophoresis of a thoroughly clotted sample. This maneuver is important to distinguish a residual fibrinogen band from a monoclonal spike of immunoglobulin that can migrate in the same electrophoretic position.

MINOR COMPONENTS

The next group of individual proteins consists of those that are not usually detected by standard protein electrophoresis owing to low levels in serum. Their quantitation is typically performed by immunologic methods.

Ceruloplasmin

Migrating with the α_2-globulins is a copper-binding protein, ceruloplasmin, which contains most of the copper in plasma and exhibits ferroxidase activity that is important in iron metabolism (Hellman & Gitlin, 2002). Synthesized in the liver, it has a molecular weight of 132,000 Da and consists of a single polypeptide chain. Although lower at birth (Al-Rashid & Spangler, 1971), serum levels are 20 to 40 mg/dL in normal adults, with twofold elevations found in oral contraceptive therapy and pregnancy (Burrows & Pekala, 1971) or as an acute-phase reactant. Each molecule of ceruloplasmin can bind six atoms of copper, which imparts a blue color to the protein. The combination of this blue with the yellow from other

chromogens of plasma imparts a greenish color to plasma with elevated ceruloplasmin concentrations (Schenker et al., 1971); this green appearance is frequently noted in bags of plasma donated for transfusions. Iron is oxidized from ferrous to ferric ions by ceruloplasmin, which may be a means of releasing iron from ferritin for binding to transferrin (Roeser et al., 1970).

Wilson disease (hepatolenticular degeneration) results from disordered copper metabolism, in which hepatic excretion of copper into the bile is impaired, leading to toxic deposition of copper in tissues. Normally, the copper-transporting protein ATP7B mediates incorporation of copper into ceruloplasmin, which is then secreted into the plasma. In Wilson disease, this process is impaired, and copper that has been absorbed by the body and transported to the liver fails to reenter the circulation as part of ceruloplasmin. Normal excretion of copper through the bile is diminished, with an overall increase in body copper deposits that are toxic to liver, brain, cornea, kidneys, bones, and parathyroids. Diagnosis is usually made in childhood or adolescence, when damage to the liver is first noticed. Other affected persons may present later in life when neurologic changes also occur. Treatment is long-term chelation with penicillamine or, in severe cases, liver transplantation, which may be curative.

Diagnosis of Wilson disease is based on physical findings (liver disease, neurologic signs, Kayser-Fleischer ring in the cornea), measurement of low serum ceruloplasmin level by such methods as immunoassay (Guttman, 2018), and increased copper concentrations in urine and on liver biopsy. The oxidase activity of ceruloplasmin can be used in a colorimetric assay, with *p*-phenylenediamine as substrate, for quantitation. Additionally, immunochemical methods are used, because the band is too faint to be used reliably on protein electrophoresis. If the combination of clinical findings and classical laboratory tests are insufficient to make or exclude the diagnosis of Wilson disease, RT-PCR methods (see Chapter 69) for detection of mutations in the *ATP7B* gene can be employed (Ferenci, 2004, Guttman, 2018). There are over 650 mutations that are known to be associated with dysfunctional ceruloplasmin (Guttman, 2018). Mutations in the ceruloplasmin gene leading to aceruloplasminemia result in iron overload affecting the pancreas, liver, and brain with a spectrum of neurologic disease (McNeill et al., 2008).

Gc-Globulin

Vitamin D binds to the group-specific component (Gc)-globulin (vitamin D–binding protein [DBP]) (Daiger et al., 1975; Bikle et al., 1986), which migrates as an α_1-globulin and has a molecular weight of about 51,000 Da. Normal serum concentration is 20 to 55 mg/dL. It may be decreased in severe liver disease. Gc-globulin has two autosomal-codominant alleles expressed as three phenotypes: 1-1, 2-2, and 1-2 (Giblett, 1969). Congenital absence of this protein may be a lethal mutation, owing to impairment of vitamin D transport, because vitamin D has low solubility in aqueous media. Gc-globulin binds vitamin D and its metabolites on a mole-per-mole basis; however, in plasma, it probably is not fully saturated. Nephrotic syndrome results in urinary loss of DBP, some of which is complexed with vitamin D. This loss of vitamin D may contribute to subsequent problems of calcium metabolism encountered in nephrotic syndrome (Goldstein et al., 1981). As a minor component of plasma proteins, Gc-globulin can be quantitated by radioimmunoassay, radioimmunodiffusion, or rocket immunoelectrophoresis (Walsh & Haddad, 1982; Westwood & Werrett, 1986). More recent studies with immunonephelometry have shown lower levels of Gc-globulin in trauma patients who develop organ dysfunction and sepsis (Dahl et al., 2003). Plasma concentrations of 25-hydroxyvitamin D are affected by polymorphisms of the vitamin D–binding protein (Sinotte et al., 2009) presumably caused by varying levels of this protein associated with the different phenotypes (Lauridsen et al., 2001).

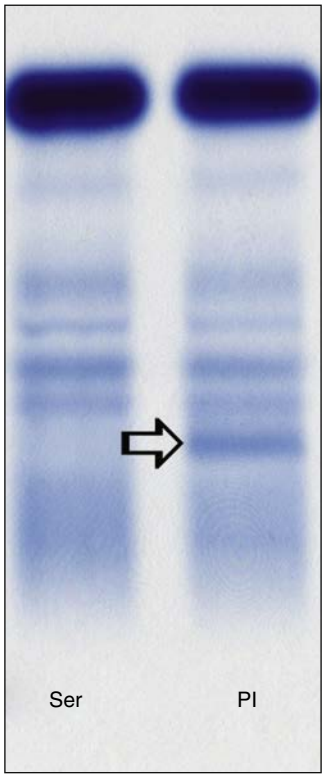

Figure 20.7 Comparison of serum (Ser) and citrated plasma (Pl) from the same individual demonstrates the position of fibrinogen *(arrow)* in plasma that should not be confused with a monoclonal immunoglobulin.

Hemopexin

The β-migrating globulin hemopexin binds heme released by degradation of hemoglobin (Muller-Eberhard, 1970). By this means, this small porphyrin molecule with its iron atom is protected from excretion, thereby contributing to the preservation of body iron stores. Among plasma proteins, hemopexin has the strongest binding affinity for heme, which probably helps to limit the toxicity of free heme (Tolosano & Altruda, 2002). Normal serum concentration is 50 to 120 mg/dL; thus, it must be quantitated by immunologic means. It has a molecular weight of 70,000 Da, of which 20% is carbohydrate and consists of a single polypeptide chain. Although low levels of hemopexin can occur with nonspecific urinary loss or as the result of decreased synthesis in liver failure, the most profound decreases occur following intravascular hemolysis, when the amount of free hemoglobin exceeds the binding capacity of haptoglobin. The circulating plasma hemoglobin can then degrade to release heme, which is bound molecule per molecule by hemopexin. Heme–hemopexin complexes are cleared from the circulation by hepatocytes, which markedly lower hemopexin concentration in serum. Excess heme then binds to albumin as methemalbumin. As more hemopexin is made available by new synthesis, heme passes from methemalbumin to hemopexin, which continues to depress the hemopexin level. As such, this can be an additional aid for diagnosing hemolysis at an earlier time, after haptoglobin levels have returned to normal but before full clearance of the heme (Wochner et al., 1974). Hemopexin can also be decreased in porphyrias and in rhabdomyolysis and chronic neuromuscular disease (Delanghe & Langlois, 2001).

α_1-Acid Glycoprotein

This protein, also known as *orosomucoid*, has a very high carbohydrate content, which minimizes its visualization by standard protein stains (Alvan, 1986). With a molecular weight of roughly 44,000 Da, it passes into the glomerular filtrate to a large extent, resulting in a half-life of only about 5 days in the circulation. Serum levels are normally 40 to 105 mg/dL, with elevations during pregnancy (Schmid, 1975). It is an acute-phase reactant, but its biological function is not known. As a binder of progesterone, it may be important in the transport or metabolism of that steroid hormone. It also binds some drugs (e.g., lidocaine) and keeps them in an inactive circulating pool. Measurements of this protein have clinical utility in interpreting levels of drugs, such as lidocaine, that may achieve high serum concentrations without expected therapeutic effect owing to being complexed in inactive form to higher than normal amounts of α_1-acid glycoprotein. Some genetic polymorphisms of this protein may be additionally complicated by isomorphic forms from specific tissue sources, although the primary site of its synthesis appears to be the liver. Although measurements of this protein have not been widely employed, its ability to bind various drugs such as the tyrosine kinase inhibitor STI571 (Gleevec, used in chronic myeloid leukemia) has led to concerns over possible drug-refractory states through binding and drug inactivation (Jorgensen et al., 2002; Le Coutre et al., 2002).

C-Reactive Protein

This serum constituent was discovered by mixing the serum of patients who had recovered from pneumococcal infections with C-polysaccharide of that bacterium. Visible flocculates formed, which allowed extensive study and purification of the C-reactive protein (CRP) from serum in the 1940s. It was found that CRP is present in the serum of patients with disorders other than pneumococcal infection but that it rises strikingly whenever there is tissue necrosis. Many other substances react with

CRP, such as DNA, nucleotides, various lipids, and other polysaccharides (Hokama, 1982). Thus, it appears to serve as a general scavenger molecule. Its molecular weight is between 118,000 and 144,000 Da, with substantial carbohydrate content. In its native molecular form, CRP exists as a pentameric conformation (pCRP). At inflammatory sites, pCRP dissociates into monomeric form (mCRP) which has strong proinflammatory properties that affect endothelial cells, neutrophils, macrophages, and platelets (Wu et al., 2015).

Normal serum concentrations are about 100 ng/mL at birth, 170 ng/mL in children, and 470 to 1340 ng/mL in adults. Despite these low concentrations, CRP has major significance as a highly sensitive acute-phase reactant (Deodhar, 1989). It is generally measured by immunoassay. By electrophoresis, CRP is a γ-migrating protein that may form a minor but distinct monoclonal-appearing band in patients having a severe inflammatory response. CRP levels are sometimes used as a rapid test for presumptive diagnosis of bacterial infection (high CRP) versus viral infection (low CRP) (Clyne & Olshaker, 1999). CRP is often used by rheumatologists to monitor the progression or remission of autoimmune disease. The gene for CRP has been localized to human chromosome 1 (Whitehead et al., 1983). Recent epidemiologic studies have shown that a high-sensitivity assay for CRP can add to the predictive value of serum lipids for identifying individuals at risk of cardiovascular events, presumably owing to the role that inflammation plays in atherogenesis (Ridker et al., 2000). Persons with high normal CRP concentrations are at greater risk for stroke or myocardial infarction than those with low normal values (discussed in greater detail in Chapter 19).

Serial measurements of CRP over a 14-month period in a test subject undergoing personal omics profiling showed marked elevations of CRP corresponding to periods of infection with two different viruses: human rhinovirus and respiratory syncytial virus. This intense profiling demonstrated the continuing utility of CRP for assessing inflammatory responses (Chen et al., 2012).

PROTEASE INHIBITORS

In addition to α_1-antitrypsin and α_2-macroglobulin, which have already been considered, other distinct inhibitors of different proteases are present in plasma. They include α_1-antichymotrypsin (AAC) (Berninger, 1985b), inter-α-trypsin inhibitor (IATI) (Daniels, 1975), antithrombin III (AT3), antiplasmin, C1 esterase inhibitor (Prograis et al., 1985), protein C (Stenflo, 1984), and plasminogen activator inhibitor-1 (PAI-1) (Nilsson & Tengborn, 1984). None of these proteins attains plasma concentrations appreciable on stained protein electrophoresis. Whereas the other inhibitors show inhibition over a rather wide range of proteases, AAC is highly specific for neutralizing chymotrypsin, which cleaves peptide bonds at the carboxyl side of tyrosine and phenylalanine residues. AAC has a molecular weight of 68,000 Da, with about 25% carbohydrate content. Normal serum concentration is 40 to 60 mg/dL, but AAC can rise rapidly to five times normal as an acute-phase reactant that remains elevated throughout a period of inflammation (Kosaka & Tazawa, 1976). AAC complexes with PSA, measured as the bound form of PSA by immunoassay (see Chapter 76. It can be lost along with other low-molecular-weight serum proteins in the proteinuria of nephrotic syndrome.

IATI is a glycoprotein of molecular weight 160,000 Da. Its concentration normally is about 50 mg/dL. IATI does not rise appreciably as an acute-phase reactant. Its role in disease states is probably similar to that of the major protease inhibitors in preventing autodigestion of tissues by endogenous cellular enzymes (Daniels, 1975).

AT3 is of special clinical interest because of the role it plays in neutralizing thrombin, which normally becomes activated intravascularly from prothrombin during clot formation. This 62,000-Da protein forms a covalently bonded complex with thrombin over a period of several minutes when mixed in solution. On addition of heparin, the complex formation occurs almost instantaneously (Rosenberg, 1975; Rosenberg et al., 1985; Rosenberg & Bauer, 1987). Although AT3 is probably essential for successful therapeutic administration of heparin, only those rare individuals with marked deficiencies seem to have thrombotic disorders (Carvalho & Ellman, 1976). The action of AT3 extends to other coagulation factors (IX, X, XI, XII, and kallikrein). Serum levels of AT3 may be depressed in severe liver disease or in protein-losing disorders when the similar-sized molecule albumin is lost and also in disseminated intravascular coagulopathy (DIC). A new experimental protocol for treating DIC involves replacing AT3 by infusion of concentrates when the patient's AT3 level falls to very low concentrations as part of the consumptive coagulopathy. Presumably, return to normal levels of AT3 has the effect of blocking further thrombosis systemically. AT3 levels are lower in heparin therapy and slightly elevated in oral anticoagulant therapy owing to increased and reduced turnover, respectively.

Although AAT, AMG, and AT3 provide the bulk of plasmin-neutralizing activity in serum (Harpel & Rosenberg, 1976), a distinct antiplasmin migrates as an α_2-globulin (Lijnen & Collen, 1985). This cross-reactivity of serum protease inhibitors for plasmin illustrates the difficulty in sorting out the precise physiologic function of each molecular species because each one appears capable of substituting for another in different instances. However, antiplasmin binds quantitatively to the majority of plasmin that is generated from plasminogen in human plasma that undergoes clotting. Antiplasmin thus serves as one of the critical checks within the joint coagulation–fibrinolytic system, which maintains hemostasis by balancing clot formation against dissolution. By this mechanism, clot formation and breakdown are generally contained within local regions of the vasculature without extending to the entire circulation. Hereditary deficiency of antiplasmin results in a bleeding disorder due to relatively unlimited fibrinolysis.

PAI-1 acts to prevent activation of plasminogen, thereby blocking fibrinolysis at an early step. Deficiency of PAI-1 results in less inhibition, leading to greater fibrinolysis and potentially a bleeding disorder. Elevated levels of PAI-1 prevent fibrinolysis, leading to thrombotic disorders and to the progression of atherosclerosis. Protein C (with its cofactor protein S) inactivates activated coagulation factors V and VIII. Deficiency of protein C or S (Griffin et al., 1987) allows prolonged activity in vivo of procoagulant factors, leading to thrombotic disorders.

The C1 esterase inhibitor is capable of inhibiting activated complement components C1r and C1s plus some other coagulation and fibrinolytic factors. It rises as an acute-phase reactant. Hereditary deficiency of C1 esterase inhibitor allows activation of complement to proceed relatively unabated, a disorder termed *hereditary angioedema*. The complement system and its inhibitors are described in depth in Chapter 48.

ACUTE-PHASE REACTANTS

The acute-phase reactant proteins share the property of showing elevations in concentrations in response to stressful or inflammatory states that occur with infection, injury, surgery, trauma, or other tissue necrosis (Daniels et al., 1974; Laurell & Jeppsson, 1975; Dowton & Colten, 1988). They include AAT, α_1-acid glycoprotein, haptoglobin, ceruloplasmin, fibrinogen, serum amyloid A protein, and CRP. Others are factor VIII, ferritin, lipoproteins, complement proteins, and immunoglobulins. It is easy to see how such a response of the plasma proteins would be advantageous to the body: Inflammation causes release from leukocytes of proteolytic enzymes in tissue that must be neutralized by enzyme inhibitors to limit their extent of destruction; scavenger proteins (haptoglobin, CRP) help collect and transport cellular debris and breakdown products to phagocytic cells (reticuloendothelial system) to process them and conserve vital substances (e.g., iron); and healing of wounds requires a large amount of fibrin, which arrives via the circulation as fibrinogen. Thus, the humoral response of the acute-phase reactants can be viewed as a phenomenon that is geared to handle extensive insult each time it is triggered, even though not all components will be needed on every occasion. The elevation of acute-phase reactants is likely a response to the cytokines, including interleukin-1, tumor necrosis factor, interferon-γ, and interleukin-6. The total physiologic response includes induction of fever, recruitment of leukocytes, catabolism of muscle, and a shift in protein synthesis patterns with reduction in albumin production.

For clinical use in diagnosis, other parameters in fact may be as sensitive as these and far easier to measure (e.g., fever, leukocytosis, ESR). However, these proteins provide another dimension of quantitation that can be useful for monitoring the course of a patient by serial determinations (Van Oss et al., 1975). Of course, those patients with congenital deficiencies (Gitlin & Gitlin, 1975), those with other impairment of synthesis due to drugs or organ disease, and newborns who normally have lower levels of many constituents (Gitlin & Biasucci, 1969) may not show the dramatic increases expected. However, a generally useful acute-phase reactant for monitoring response is CRP, which is the fastest-rising acute-phase reactant and one that returns to normal quickly following successful therapies (Fischer et al., 1976). CRP is frequently applied to the detection and preliminary classification of occult infections, because bacterial infections can stimulate much higher levels of CRP than viral ones. It is also widely used for assessing disease activity in autoimmune disorders because it is rarely elevated persistently without continued inflammatory response. Elevations of CRP can be up to 1000 times normal levels, which greatly assists in detecting abnormal states compared with the other acute-phase reactants, which may

rise at most only several-fold in such responses, although ferritin levels may occasionally rise to values greater than 20,000 ng/mL.

PATTERNS OF PROTEIN ABNORMALITIES

Some of the most frequently encountered patterns of protein abnormalities in electrophoresis are shown as densitometric scans in Figure 20.8. Scanning allows quantitation of each fraction, but visual inspection of the electrophoretic strip provides more detailed information about individual proteins separated in high-resolution systems (Ritzman & Daniels, 1975). Interpretation of electrophoretic results depends on visual inspection to identify abnormal patterns or aberrant bands and on quantitation by scan to gauge the relative quantities of individual fractions.

Patterns of hypoproteinemia due to malnutrition or gross loss of protein show decreases in all fractions, but the most dramatic reduction is often seen in albumin compared with its normally high value as the most abundant serum protein (Fig. 20.9, lane 3). Severe starvation, malabsorption, or inanition associated with severe chronic disease will show marked reduction in albumin to levels below 20 g/L. The other serum proteins, including AAT, AMG, haptoglobin, transferrin, and C3, appear even fainter on electrophoresis. Reduction in staining intensity for the β-lipoprotein parallels a marked decrease in serum cholesterol concentration. The immune system is strongly affected by severe starvation, with decreased synthesis of immunoglobulins resulting in hypogammaglobulinemia and impaired resistance to bacterial and other infections. Protein-losing enteropathy (Fig. 20.8H) shows a variation in the hypoproteinemia pattern, in which most fractions are diminished owing to the combination of decreased synthesis and increased loss, although α_2 may be relatively higher owing to a coexisting acute-phase response (haptoglobin) or to preferential retention of larger molecules (α_2-macroglobulin).

Specific loss of proteins into the urine as in nephrotic syndrome occurs on a molecular weight basis, with smaller proteins being lost more rapidly than larger ones. Accordingly, albumin appears early in the course of protein-losing nephropathies, followed by smaller quantities of AAT, transferrin, and, ultimately, immunoglobulins (Fig. 20.10, lanes 1 and 2). The very large molecule AMG is retained, as are the large micelles of β-lipoprotein. The result is complementary patterns of proteins in the

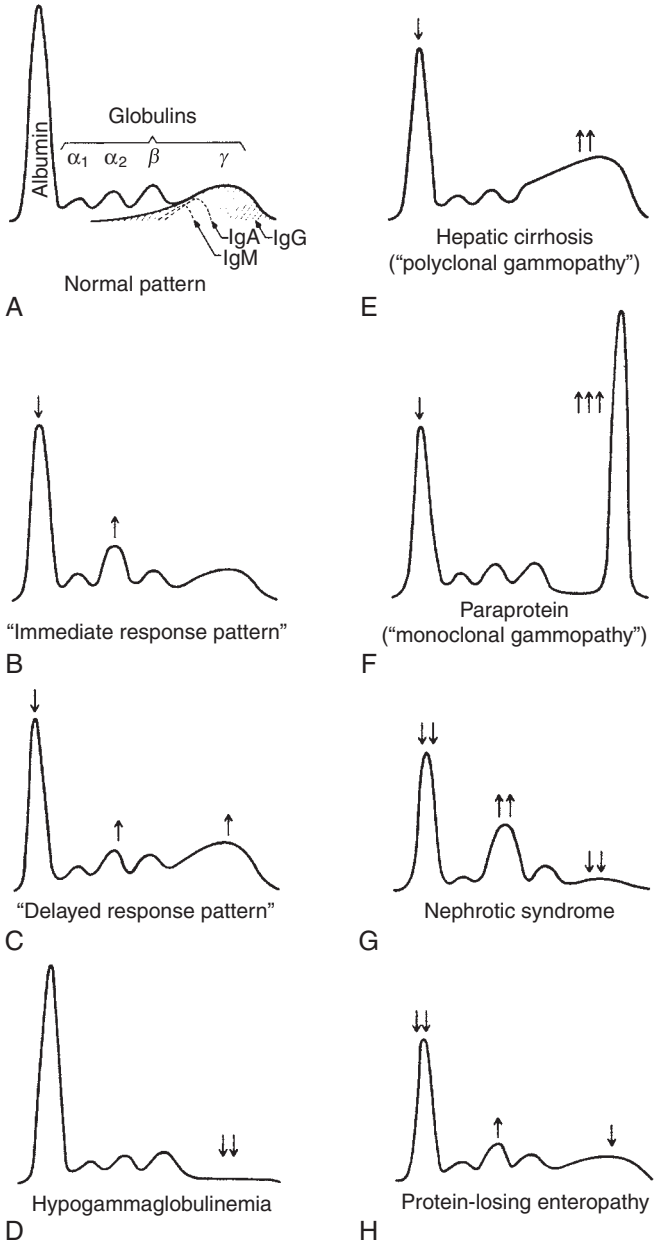

Figure 20.8 Serum protein electrophoresis: clinicopathologic correlations. *(Courtesy of Dr. A. E. Krieg.)*

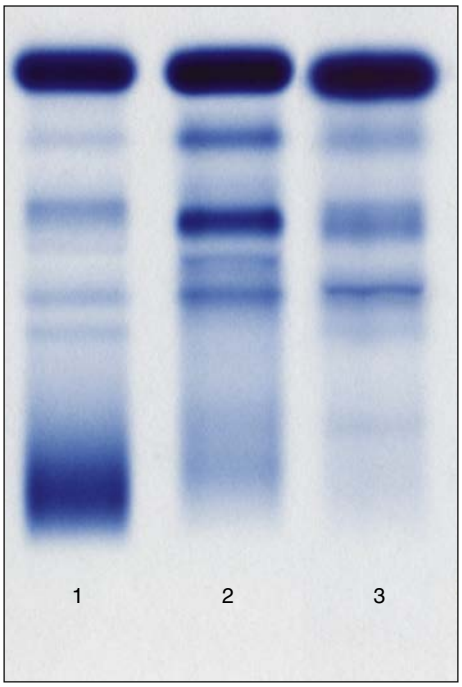

Figure 20.9 Serum protein patterns in (1) chronic inflammation with decreased albumin and increased γ-globulins; (2) acute inflammation with increased α_2-fraction (haptoglobin) and decreased C3 due to activation and consumption of complement; and (3) inanition post–spinal cord injury with hypoproteinemia of several fractions.

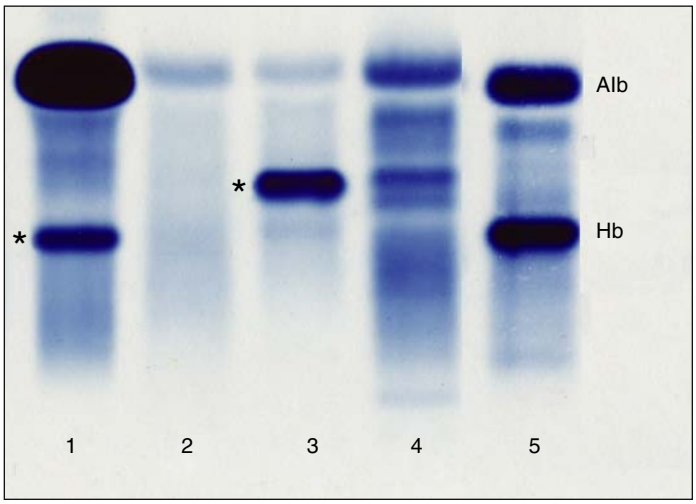

Figure 20.10 Patterns of urine protein electrophoresis in different disorders. (1) Severe glomerular proteinuria with a major band of albumin plus a secondary one of transferrin (*). (2) Trace proteinuria with a faint band of albumin and other diffuse proteins. (3) Immunoglobulin light chains in a case of multiple myeloma (*). (4) Tubular proteinuria with multiple bands that do not correspond to major serum proteins. (5) Hematuria with a major band of hemoglobin (not to be confused with monoclonal gammopathy), in addition to albumin.

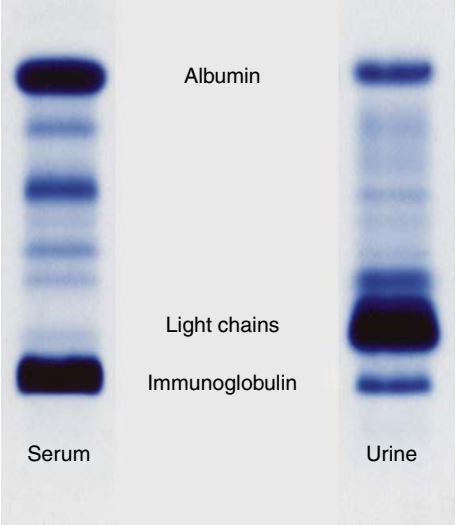

Figure 20.11 Serum and urine protein electrophoretic patterns in a patient with multiple myeloma. Serum demonstrates a predominance of the larger complete immunoglobulin; the urine has a large amount of the smaller-sized light chains, with only a small amount of the whole immunoglobulin.

serum (decreases in albumin and α_1-, β-, and γ-globulins; increased α_2-macroglobulin and elevated β-lipoprotein) versus those in urine (see Fig. 20.4B; glomerular proteinuria with albumin, α_1-, β-, and γ-fractions present but without α_2-macroglobulin in the urine sample). Tubular proteinuria that is due to impaired renal tubular reabsorption of small proteins shows a pattern of α, β, and γ in the urine with only minimal albumin loss into the urine (Killingsworth, 1982) (see Fig. 20.10, lane 4). In addition to glomerular and tubular patterns of proteinuria (Maachi et al., 2004), it is essential to recognize the important pattern of a monoclonal gammopathy in urine (see Fig. 20.10, lane 3, and Fig. 20.11). A similar pattern of a single large band occurs in hemoglobinuria (see Fig. 20.10, lane 5), which must be distinguished from a monoclonal immunoglobulin or free light chains.

Acute-phase or immediate response patterns have the greatest effect on serum protein electrophoresis by increasing the amount of haptoglobin while slightly decreasing the concentration of albumin. Increases in haptoglobin usually indicate some form of response, whether acute or chronic, to stressful stimuli (see Fig. 20.9). Other proteins, such as AAT, can contribute to this response; minor components such as CRP do not contribute significantly to this protein stain pattern, although immunologic measurement of CRP may show up to 1000-fold elevations. If the haptoglobin has been depleted in a patient as a result of active hemolysis, an independent band of hemoglobin may be migrating in the β- or α_2-region. Hemolysis of a sample in vitro may show a red band (on the unstained gel) of the haptoglobin–hemoglobin complex that migrates differently from hemoglobin alone. The pattern of delayed response or chronic pattern is an extension of the acute-phase response (high haptoglobin, slight reduction in albumin) with greater decrease in albumin and polyclonal increase in immunoglobulins broadening the γ-region.

A striking elevation of transferrin in the β-region sometimes occurs in patients suffering from iron deficiency anemia. The increase in transferrin corresponds to increased IBC, and the percent saturation is low (Koerper & Dallman, 1977). This variation may be confused with a myeloma protein because the transferrin band forms a narrow, clonal-appearing band.

Cirrhosis of the liver creates a protein pattern that is recognizable (see Fig. 20.4A). Hepatocellular damage from cirrhosis results in diminished capacity to synthesize albumin. Furthermore, the imbalance of hemodynamic pressures in portal hypertension secondary to cirrhosis leads to the formation of ascitic fluid, which contains almost exclusively albumin. This decreased synthesis, coupled with increased loss, greatly reduces serum albumin concentrations. The loss of albumin is balanced to some extent by marked polyclonal increase in immunoglobulins with a γ-fraction that may contribute significantly to oncotic pressures. The increase in γ-globulin involves all immunoglobulins; the increase in immunoglobulin A (IgA) in the slow β-region shows a continuum with the γ (also termed *β–γ bridging*).

In contrast to polyclonal increases, oligoclonal bands consist of only a few clones of distinct immunoglobulins that migrate in defined positions. This pattern is seen in serum in cases in which an immunologic disorder is present or in some patients treated with chronic immunosuppression for organ transplantation (Myara et al., 1991). Oligoclonal bands in the CSF are used to indicate immunologic activity in the central nervous system and occur in infectious diseases or autoimmune or demyelinating disorders (see Chapter 46).

Hypogammaglobulinemia is manifested as a nearly to completely absent γ-fraction. It occurs normally in neonates before maturation of the immune system. It also occurs in some congenital immunodeficiency states, such as Bruton agammaglobulinemia and other states involving B cell function. Perhaps more commonly, this pattern is seen in adults with lymphoreticular disorders in whom normal plasma cells have been displaced by lymphocytic proliferations, and to some extent after chemotherapy for eradication of malignancies, as well as in hypoproteinemic states (see Fig. 20.9, lane 3).

The single most important and widespread clinical application of serum protein electrophoresis is used for the detection of monoclonal gammopathies. This very explicit pattern comes from a paraprotein (immunoglobulin) secreted by a monoclonal proliferation of plasma cells and is generally found without normal amounts of polyclonal γ as normal plasma cells are replaced by the malignant clone (see Fig. 20.11). The presence of a paraprotein with normal polyclonal γ suggests a possible plasmacytoma that has not yet spread throughout the bone marrow. Laboratory evaluation of myeloma should include serum and urine protein electrophoreses to detect aberrant clonal bands, immunoelectrophoresis or immunofixation to type the heavy and light chains of the paraprotein, and quantitation of immunoglobulins to provide a baseline for monitoring the patient's response to therapy or disease progression. Other proteins that may sometimes be mistaken for monoclonal bands of immunoglobulin on serum protein electrophoresis include haptoglobin–hemoglobin complexes, C3 and its variants, β-lipoprotein, transferrin, fibrinogen, immune complexes, CRP, and, occasionally, α_2-macroglobulin. Immunoglobulins, disorders of the immune system, and abnormalities of complement are discussed further in Chapters 47, 48, and 52.

SELECTED REFERENCES

Bean P, Harasymiw J, Peterson CM, et al.: Innovative technologies for the diagnosis of alcohol abuse and monitoring abstinence, *Alcohol Clin Exp Res* 25:309–316, 2001.
Comprehensive review of assays for carbohydrate-deficient transferrin and strategies for their use.

Bornhorst JA, Procter M, Meadows C, et al.: Evaluation of an integrative diagnostic algorithm for the identification of people at risk for α_1-antitrypsin deficiency, *Am J Clin Pathol* 128:482–490, 2007.
This article describes the modern approach to diagnosis of AAT deficiency using the combined modalities of immunoassay, phenotyping by isoelectric focusing, and genotyping.

Delanghe JR, Langlois MR: Hemopexin: a review of biological aspects and the role in laboratory medicine, *Clin Chim Acta* 312:12–23, 2001.
This review article provides a comprehensive description of the biochemistry of hemopexin and how it fluctuates in different disease states.

Ferenci P: Review article: diagnosis and current therapy of Wilson's disease, *Aliment Pharmacol Ther* 19:157–165, 2004.
Up-to-date account of the role of laboratory testing in diagnosing Wilson disease.

Hellman NE, Gitlin JD: Ceruloplasmin metabolism and function, *Annu Rev Nutr* 22:439–458, 2002.
This article is an excellent summary of ceruloplasmin chemistry and its clinical importance.

Lauff JJ, Kasper ME, Wu TW, et al.: Isolation and preliminary characterization of a fraction of bilirubin in serum that is firmly bound to protein, *Clin Chem* 28:629–637, 1982.
Early account of δ-bilirubin and its relationship to albumin.

Layne E: Spectrophotometric and turbidimetric methods for measuring proteins, *Meth Enzymol* 3:447–455, 1957.
Classical paper on protein measurements.

Maachi M, Felahi S, Regeniter A, et al.: Patterns of proteinuria: urinary sodium dodecyl sulfate electrophoresis versus immunonephelometric protein marker measurement followed by interpretation with the knowledge-based system MDI-LabLink, *Clin Chem* 50:1834–1837, 2004.
This paper presents patterns of proteinuria and new methods for their discrimination.

Minchiotti L, Galliano M, Kragh-Hansen U, et al.: Mutations and polymorphisms of the gene of the major human blood protein serum albumin, *Hum Mutat* 29:1007–1016, 2008.
This article provides a comprehensive listing of known genetic mutations in the human albumin gene.

Paterlini V, Porpiglia NM, De Palo EF, Tagliaro F: Asialo-transferrin: biochemical aspects and association with alcohol abuse investigation, *Alcohol* 78:43–50, 2019.
This review covers the molecular structures of transferrin variants and how they reflect disease.

Peters T: Serum albumin: recent progress in the understanding of its structure and biosynthesis, *Clin Chem* 23:5–12, 1977.
Comprehensive review of clinically important structure–function relationships of albumin.

Tolosano E, Altruda F: Hemopexin: structure, function, and regulation, *DNA Cell Biol* 21:297–306, 2002.
Comprehensive discussion of the chemistry and roles of hemopexin.

Vieira M, Saraiva MJ: Transthyretin: a multifaceted protein, *Biomol Concepts* 5:45–54, 2014.
Up-to-date review of variations in the structure of the transferrin molecule and their role in disease.
Wu Y, Potempa LA, Kebir DE, Filep JG: C-reactive protein and inflammation: conformational changes affect function, *Biol Chem* 96:1181–1197, 2015.
Excellent review of variations in the molecular structure of C-reactive protein and their functions.
Zaret DL, Morrison N, Gulbranson R, et al.: Immunofixation to quantify beta 2-transferrin in cerebrospinal fluid to detect leakage of cerebrospinal fluid from skull injury, *Clin Chem* 38:1908–1912, 1992.
Description of assay for a specific marker for CSF in unknown fluid.
Access the complete reference list online at Elsevier eBooks for Practicing Clinicians.

REFERENCES

Aboussouan LS, Stoller JK: Detection of alpha-1 antitrypsin deficiency: a review, *Respir Med* 103:335–341, 2009.

Al-Rashid RA, Spangler J: Neonatal copper deficiency, *N Engl J Med* 285:841–843, 1971.

Alvan G: Ethnic differences in reactions to drugs and xenobiotics. Other protein variants with pharmacogenetic consequences: albumin and orosomucoid, *Prog Clin Biol Res* 214:345–355, 1986.

Armstrong PB: Proteases and protease inhibitors: a balance of activities in host-pathogen interaction, *Immunobiology* 211:263–281, 2006.

Arndt T: Carbohydrate-deficient transferrin as a marker of chronic alcohol abuse: a critical review of preanalysis, analysis, and interpretation, *Clin Chem* 47:13–27, 2001.

Aslan D, Crain K, Beutler E: A new case of human atransferrinemia with a previously undescribed mutation in the transferrin gene, *Acta Haematol* 118:244–247, 2007.

Beetham R, Cattell WR: Proteinuria: Pathophysiology, significance and recommendations for measurement in clinical practice, *Ann Clin Biochem* 30:425–434, 1993.

Benson MD, Waddington-Cruz M, Berk JL, et al.: Inotersen treatment for patients with hereditary transthyretin amyloidosis, *N Engl J Med* 379:22–31, 2018.

Berninger RW: Protease inhibitors of human plasma. Alpha 1-antichymotrypsin, *J Med* 16:101–128, 1985a.

Berninger RW: Protease inhibitors of human plasma. Alpha 1-antitrypsin, *J Med* 16:23–99, 1985b.

Bikle DD, Halloran BP, Gee E, et al.: Free 25-hydroxyvitamin D levels are normal in subjects with liver disease and reduced total 25-hydroxyvitamin D levels, *J Clin Invest* 78:748–752, 1986.

Blennow K, Fredman P: Detection of cerebrospinal fluid leakage by isoelectric focusing on polyacrylamide gels with silver staining using the PhastSystem, *Acta Neurochir* 136:135–139, 1995.

Branden C, Tooze J: *Introduction to protein structure*, New York, 1991, Garland Publishing.

Brinkman JW, Bakker SJ, Gansevoort RT, et al.: Which method for quantifying urinary albumin excretion gives what outcome? A comparison of immunonephelometry with HPLC, *Kidney Int Suppl* 92:569–575, 2004.

Brodsky JL: Translocation of proteins across the endoplasmic reticulum membrane, *Int Rev Cytol* 178:277–328, 1998.

Buehler PW, Abraham B, Vallelian F, et al.: Haptoglobin preserves the CD163 hemoglobin scavenger pathway by shielding hemoglobin from peroxidative modification, *Blood* 113:2578–2586, 2009.

Burrows S, Pekala B: Serum copper and ceruloplasmin in pregnancy, *Am J Obstet Gynecol* 109:907–909, 1971.

Carvalho A, Ellman L: Hereditary antithrombin III deficiency. Effect of antithrombin on platelet function, *Am J Med* 61:179–183, 1976.

Chanprasert S, Scaglia F: Adult liver disorders caused by inborn errors of metabolism: review and update, *Mol Genet Metab* 114:1–10, 2015.

Chen FA: Rapid protein analysis by capillary electrophoresis, *J Chromatogr* 559:445–543, 1991.

Chen R, Mias GI, Li-Pook-Than J, et al.: Personal omics profiling reveals dynamic molecular and medical phenotypes, *Cell* 148:1293–1307, 2012.

Chertow GM, Goldstein-Fuchs DJ, Lazarus JM, et al.: Prealbumin, mortality, and cause-specific hospitalization in hemodialysis patients, *Kidney Int* 68:2794–2800, 2005.

Clyne B, Olshaker JS: The C-reactive protein, *J Emerg Med* 17:1019–1025, 1999.

Cox DW: Clinical and molecular studies of alpha 1-antitrypsin deficiency, *Prog Clin Biol Res* 214:373–384, 1986.

Dahl B, Schiodt FV, Ott P, et al.: Plasma concentration of Gc-globulin is associated with organ dysfunction and sepsis after injury, *Crit Care Med* 31:152–156, 2003.

Daiger SP, Schanfield MS, Cavalli-Sforza LL: Group-specific component (Gc) proteins bind vitamin D and 25-hydroxy-vitamin D, *Proc Natl Acad Sci U S A* 72:2076–2080, 1975.

Daniels JC: Abnormalities of protease inhibitors. In Ritzmann SE, Daniels JC, editors: *Serum protein abnormalities, diagnostic and clinical aspects*, Boston, 1975, Little, Brown & Co.

Daniels JC, Larson DL, Abston S, et al.: Serum protein profiles in thermal burns. II. Protease inhibitors, complement factors and C-reactive proteins, *J Trauma* 14:153–162, 1974.

Delaroche O, Bordure P, Lippert E, et al.: Perilymph detection by beta 2-transferrin immunoblotting assay. Application to the diagnosis of perilymphatic fistulae, *Clin Chim Acta* 245:93–104, 1996.

Deodhar SD: C-reactive protein: the best laboratory indicator available for monitoring disease activity, *Cleveland Clin J Med* 56:126–130, 1989.

Doolittle RF: Fibrinogen and fibrin. In Putnam FW, editor: *The plasma proteins. Vol II*, vol. 2. New York, 1975, Academic Press, p 110.

Doolittle RF, Yang Z, Mochalkin I: Crystal structure studies on fibrinogen and fibrin, *Fibrinogen*, *Ann N Y Acad Sci* 936:31–43, 2001.

Dowton SB, Colten HR: Acute phase reactants in inflammation and infection, *Semin Hematol* 25:84–90, 1988.

Eriksson S: Studies in alpha 1-antitrypsin deficiency, *Acta Med Scand* 177(Suppl):1–85, 1965.

Fischer CL, Gill C, Forrester MG, et al.: Quantitation of "acute phase proteins" postoperatively. Value in detection and monitoring of complications, *Am J Clin Pathol* 66:840–846, 1976.

Gaetani S, Bellovino D, Apreda M, et al.: Hepatic synthesis, maturation and complex formation between retinol-binding protein and transthyretin, *Clin Chem Lab Med* 40:1211–1220, 2002.

Gelb AF, Klein E, Lieberman J: Pulmonary function in nonsmoking subjects with alpha-1-antitrypsin deficiency (MZ phenotype), *Am J Med* 62:93–98, 1977.

Ghacha R, Sinha AK, Karkar AM: HbA1c and serum fructosamine as markers of the chronic glycemic state in type 2 diabetic hemodialysis patients, *Dial Transplant* 30:214–217, 2001.

Giblett ER, editor: *Genetic markers in human blood*, Oxford, 1969, Blackwell Scientific.

Gitlin D, Biasucci A: Development of gamma G, gamma A, gamma M, C′1 esterase inhibitor, ceruloplasmin, transferrin, hemopexin, haptoglobin, fibrinogen, plasminogen, alpha 1-antitrypsin, orosomucoid, beta-lipoprotein, alpha 2-macroglobulin, and prealbumin in the human conceptus, *J Clin Invest* 48:1433–1446, 1969.

Gitlin D, Gitlin JD: Genetic alterations in the plasma proteins of man. In Putnam FW, editor: *The plasma proteins*, vol. II. New York, 1975, Academic Press, p 321.

Glenner GG: Amyloid deposits and amyloidosis. The beta-fibrilloses, *N Engl J Med* 302:1283–1292, 1980.

Gofferje H: Prealbumin and retinol binding protein, highly sensitive parameters for the nutritional state in respect to protein, *Med Lab* 5:38–44, 1978.

Goldstein DA, Haldimann B, Sherman D, et al.: Vitamin D metabolites and calcium metabolism in patients with nephrotic syndrome and normal renal function, *J Clin Endocrinol Metab* 52:116–121, 1981.

Griffin JH, Heeb MJ, Schwarz HP: Plasma protein S deficiency and thromboembolic disease, *Prog Hematol* 15:39–49, 1987.

Guttman S, Bernick F, Naorniakowska M, Michgehl U, Groba SR, et al.: Functional characterization of novel ATP7B variants for diagnosis of Wilson disease, *Frontiers in Pediatrics* 6:1–8, 2018, https://doi.org/10.3389/fped.2018.00106.

Guthrow CE, Morris MA, Day JF, et al.: Enhanced nonenzymatic glucosylation of human serum albumin in diabetes mellitus, *Proc Natl Acad Sci U S A* 76:4258–4261, 1979.

Harding JJ: Nonenzymatic covalent posttranslational modification of proteins in vivo, *Adv Protein Chem* 37:247–334, 1985.

Harpel PC, Rosenberg RD: Alpha-2-macroglobulin and antithrombin–heparin cofactor: Modulators of hemostatic and inflammatory reactions, *Prog Hemost Thromb* 3:145–189, 1976.

Hayashi H, Kimura N, Yamaguchi H, et al.: A seed for Alzheimer amyloid in the brain, *J Neurosci* 24:4894–4902, 2004.

Hoffmann A, Nimtz M, Getzlaff R, et al.: "Brain-type" N-glycosylation of asialotransferrin from human cerebrospinal fluid, *FEBS Lett* 359:164–168, 1995.

Hokama Y: Methods of assay and role of acute phase C-reactive protein in human diseases. In Nakamura RM, Dito WR, Tucker ES, editors: *Immunologic analysis. recent progress in diagnostic laboratory immunology*, New York, 1982, Masson Publishing, p 239.

Horne CHW, Weir RJ, Howie PW, et al.: Effect of combined oestrogen–progesterone oral contraceptives on serum levels of alpha-2-macroglobuin, transferrin, albumin, and IgG, *Lancet* 1:49–50, 1970.

Huang RS, Dasgupta A, Nguyen AN, et al.: Inability to measure M-protein with capillary electrophoresis (CAPPILLARYS2) in tracings with nondiscernable peaks, *J Clin Lab Anal*, 2014. https://doi.org/10.1002/jcla.21776. [Epub ahead of print].

Hubbard RC, Brantly ML, Sellers S, et al.: Anti-neutrophil-elastase defenses of the lower respiratory tract in alpha 1-antitrypsin deficiency directly augmented with an aerosol of alpha 1-antitrypsin, *Ann Intern Med* 111:206–212, 1989.

Ii S, Minnerath S, Ii K, et al.: Two-tiered DNA-based diagnosis of transthyretin amyloidosis reveals two novel point mutations, *Neurology* 41:893–898, 1991.

Irie S, Tavassoli M: Transferrin-mediated cellular iron uptake, *J Med Sci* 293:103–111, 1987.

Jenkins N, Parekh RB, James DC: Getting the glycosylation right: implications for the biotechnology industry, *Nat Biotechnol* 14:975–981, 1996.

Jeppsson J-O, Laurell CB, Franzén B: Agarose gel electrophoresis, *Clin Chem* 25:629–638, 1979.

Jorgensen HG, Elliott MA, Allan EK, et al.: α_1-Acid glycoprotein expressed in the plasma of chronic myeloid leukemia patients does not mediate significant in vitro resistance to STI571, *Blood* 99:713–715, 2002.

Kamboh MI, Ferrell RE: Human transferrin polymorphism, *Hum Hered* 37:65–81, 1987.

Keller U: Nutritional laboratory markers in malnutrition, *J Clin Med* 8:775, 2019.

Killingsworth LM: Clinical applications of protein determinations in biological fluids other than blood, *Clin Chem* 28:1093–1102, 1982.

Koch-Weser J, Sellers EM: Drug therapy. Binding of drugs to serum albumin, *N Engl J Med* 294:311–316, 1976.

Koerper MA, Dallman PR: Serum iron concentration and transferrin saturation in the diagnosis of iron deficiency in children: normal developmental changes, *J Pediatr* 91:870–874, 1977.

Konigsberg W: Molecular diseases. In Bondy PK, Rosenberg LE, editors: *Duncan's diseases of metabolism*, vol. 7. Philadelphia, 1974, WB Saunders, p 86.

Kosaka S, Tazawa M: Alpha-1-antichymotrypsin in rheumatoid arthritis, *Tohoku J Exp Med* 119:369–375, 1976.

Kuznetsov G, Nigam SK: Folding of secretory and membrane proteins, *N Engl J Med* 339:1688–1695, 1998.

Laurell CB: Quantitative estimation of proteins by electrophoresis in agarose gel containing antibodies, *Anal Biochem* 15:45–52, 1966.

Laurell CB: Electrophoresis, specific protein assays, or both in measurement of plasma proteins? *Clin Chem* 19:99–102, 1973.

Laurell CB, Jeppsson J-O: Protease inhibitors in plasma. In Putnam FW, editor: *The plasma proteins*, vol. 2. New York, 1975, Academic Press, p 299. (vol. I.

Lauridsen AL, Vestergaard P, Nexo E: Mean serum concentration of vitamin D-binding protein (Gc globulin) is related to the Gc phenotype in women, *Clin Chem* 47:753–756, 2001.

Le Coutre P, Kreuzer K-A, Na I-K, et al.: Determination of α-1 acid glycoprotein in patients with Ph+ chronic myeloid leukemia during the first 13 weeks of therapy with STI571, *Blood Cells Mol Dis* 28:75–85, 2002.

Levy AP, Asleh R, Blum S, et al.: Haptoglobin: basic and clinical aspects, *Antioxid Redox Signal* 12:293–304, 2010.

Lieberman J, Gaidulis L, Garoutte B, et al.: Identification and characteristics of the common alpha-1-antitrypsin phenotypes, *Chest* 62:557–564, 1972.

Lijnen HR, Collen D: Protease inhibitors of human plasma. Alpha 2-antiplasmin, *J Med* 16:225–284, 1985.

Loftus TJ, Brown MP, Slish JH, Rosenthal MD: Serum levels of prealbumin and albumin for preoperative risk stratification, *Nutr Clin Pract* 34:340–348, 2019.

Lowry OH, Rosebrough NJ, Farr L, et al.: Protein measurement with Folin phenol reagent, *J Biol Chem* 193:265–275, 1951.

MacGillivray RTA, Mendez E, Sinha S, et al.: The complete amino acid sequence of human serum transferrin, *Proc Natl Acad Sci U S A* 79:2504–2508, 1982.

Manoharan A: Congenital haptoglobin deficiency, letter, *Blood* 90:1709, 1997.

McNeill A, Pandolfo M, Kuhn J, et al.: The neurological presentation of ceruloplasmin gene mutations, *Eur Neurol* 60:200–205, 2008.

Meloun B, Moravek L, Kostka V: Complete amino acid sequence of human serum albumin, *FEBS Lett* 58:134–137, 1975.

Menache D: Abnormal fibrinogens: a review, *Thromb Diath Haemorrh* 29:525–535, 1973.

Mendenhall HW: Serum protein concentrations in pregnancy. I. Concentrations in maternal serum, *Am J Obstet Gynecol* 106:388–399, 1970.

Merin NM, Kelly KR: Clinical use of proteasome inhibitors in the treatment of multiple myeloma, *Pharmaceuticals* 8:1–20, 2015.

Merril CR, Goldman D, Sedman SA, et al.: Ultrasensitive stain for proteins in polyacrylamide gels shows regional variation in cerebrospinal fluid proteins, *Science* 211:1437–1438, 1981.

Metra M, Mentz RJ, Chiswell K, et al.: Acute heart failure in elderly patients: Worse outcomes and differential utility of standard prognostic variables. Insights from the PROTECT trial, *Eur J Heart Fail*, 2014. https://doi.org/10.1002/ejhf.207.

Mettenburg JM, Gonias SL: Beta-amyloid peptide binds equivalently to binary and ternary alpha2-macroglobulin-protease complexes, *Protein J* 24:89–93, 2005.

Mickle K, Lasser KE, Hoch JS, et al.: The effectiveness and value of patisiran and inotersen for hereditary transthyretin amyloidosis, *J Manag Care Spec Pharm* 25:10–14, 2019.

Moses AC, Lawlor J, Haddow J, et al.: Familial euthyroid hyperthyroxinemia resulting from increased thyroxine binding to thyroxine-binding prealbumin, *N Engl J Med* 306:966–969, 1982.

Mueller C, Gernoux G, Gruntman AM, et al.: 5 year expression and neutrophil defect repair after gene therapy in alpha-1 antitrypsin deficiency, *Mol Ther* 25:1387–1394, 2017.

Muller-Eberhard U: *Hemopexin*, *N Engl J Med* 283:1090–1094, 1970.

Myara I, Quenum G, Storogenko M, et al.: Monoclonal and oligoclonal gammopathies in heart transplant recipients, *Clin Chem* 37:1334–1337, 1991.

Nilsson IM, Tengborn LA: A family with thrombosis associated with high level of tissue plasminogen activator, *Haemostasis* 14(24), 1984.

Normansell DE, Stacy EK, Booker CF, et al.: Detection of beta-2 transferrin in otorrhea and rhinorrhea in a routine clinical laboratory setting, *Clin Diagn Lab Immunol* 1:68–70, 1994.

Oppenheimer JH: Role of plasma proteins in the binding, distribution and metabolism of the thyroid hormones, *N Engl J Med* 278:1153–1162, 1968.

Orth SR, Ritz E: The nephrotic syndrome, *N Engl J Med* 338:1202–1211, 1998.

Peters TJr: Serum albumin. In Putnam FW, editor: *The plasma proteins*, vol. 2. New York, 1975, Academic Press, p 133.

Peterson PA: Studies on interaction between pre-albumin, retinol-binding protein and vitamin A, *J Biol Chem* 246:44–49, 1971.

Plante-Bordeneuve V: Transthyretin familial amyloid polyneuropathy: an update, *J Neurol* 265:976–983, 2018.

Post DJ, Carter KC, Papaconstantinou J: The effect of aging on constitutive mRNA levels and lipopolysaccharide inducibility of acute phase genes, *Ann N Y Acad Sci* 621:66–77, 1991.

Prograis LJ, Brickman CM, Frank MM: Protease inhibitors of human plasma. C1-inhibitor (C1-Inh), *J Med* 16:303–350, 1985.

Reddy S, Adcock KJ, Adeshina H, et al.: Immunity, transferrin, and survival in kwashiorkor, *BMJ* 4:268–270, 1970.

Ridker PM, Hennekens CH, Buring JE, et al.: C-reactive protein and other markers of inflammation in the prediction of cardiovascular disease in women, *N Engl J Med* 342:836–843, 2000.

Ritzmann SE, Daniels JC, editors: *Serum protein abnormalities. Diagnostic and clinical aspects*, Boston, 1975, Little, Brown & Co.

Rizk M, Tzmen S: Patisiran for the treatment of patients with familial amyloid polyneuropathy, *Drugs Today* 55:315–327, 2019.

Roberts RC: Protease inhibitors of human plasma. Alpha 2-macroglobulin, *J Med* 16:129–224, 1985.

Roelandse FW, van der Zwart N, Didden JH, et al.: Detection of CSF leakage by isoelectric focusing on polyacrylamide gel, direct immunofixation of transferrins, and silver staining, *Clin Chem* 44:351–353, 1998.

Roeser HP, Lee GR, Nacht S, et al.: The role of ceruloplasmin in iron metabolism, *J Clin Intest* 49:2408–2417, 1970.

Rosenberg RD: Actions and interactions of antithrombin and heparin, *N Engl J Med* 292:146–151, 1975.

Rosenberg RD, Bauer KA: Thrombosis in inherited deficiencies of antithrombin, protein C, and protein S, *Hum Pathol* 18:253–262, 1987.

Rosenberg RD, Bauer KA, Marcum JA: Protease inhibitors of human plasma. Antithrombin-III: the heparin–antithrombin system, *J Med* 16:351–416, 1985.

Roses AD: Apolipoprotein E is a genetic locus that affects the rate of Alzheimer disease expression, *Neuropsychopharmacology* 10:55, 1994.

Rothschild MA, Oratz M, Schreiber SS: Albumin synthesis, *N Engl J Med* 286(748):816–821, 1972.

Ruiz M, Rajatanavin R, Young RA, et al.: Familial dysalbuminemic hyperthyroxinemia. A syndrome that can be confused with thyrotoxicosis, *N Engl J Med* 306:635–639, 1982.

Sattianayagam PT, Hahn AF, Whelan CJ, et al.: Cardiac phenotype and clinical outcome of familial amyloid polyneuropathy associated with transthyretin alanine 60 variant, *Eur Heart J* 33:1120–1127, 2012.

Saraiva M, Alves IL, Costa PP: Simplified method for screening populations at risk for transthyretin met 30 associated familial amyloidotic polyneuropathy, *Clin Chem* 35:1033–1035, 1989.

Schenker JG, Jungreis E, Polishuk WZ: Oral contraceptives and serum copper concentrations, *Obstet Gynecol* 37:233–237, 1971.

Schmid K: Alpha-1-acid glycoprotein. In Putnam FW, editor: *The plasma proteins*, vol. 2. New York, 1975, Academic Press. (vol. I.

Sevall JS: The albumin gene: DNA–protein interaction, *Fed Proc* 45:2412–2415, 1986.

Sinotte M, Diorio C, Berube S, et al.: Genetic polymorphisms of the vitamin D binding protein and plasma concentrations of 25-hydroxyvitamin D in premenopausal women, *Am J Clin Nutr* 89:634–640, 2009.

Slater L, Carter PM, Hobbs JR: Measurement of albumin in the sera of patients, *Ann Clin Biochem* 12:33–40, 1975.

Sloman AJ, Kelly RH: Transferrin allelic variants may cause false positives in the detection of cerebrospinal fluid fistulae, *Clin Chem* 39:1444–1445, 1993.

Snider GL: Pulmonary disease in alpha1-antitrypsin deficiency, *Ann Intern Med* 111:957–959, 1989.

Snyder MR, Katzmann JA, Butz ML, et al.: Diagnosis of α-1-antitrypsin deficiency: an algorithm of quantification, genotyping, and phenotyping, *Clin Chem* 52:2236–2242, 2006.

Solomon P, Chen J, D'Costa M, et al.: Extracranial drainage of cerebrospinal fluid: a study of beta-transferrins in nasal and lymphatic tissues, *Laryngoscope* 109:1313–1315, 1999.

Stenflo J: Structure and function of protein C, *Semin Thromb Hemost* 10:109–121, 1984.

Stibler H: Carbohydrate-deficient transferrin in serum: a new marker of potentially harmful alcohol consumption reviewed, *Clin Chem* 37:2029–2037, 1991.

Strange C: Anti-proteases and alpha-1 antitrypsin augmentation therapy, *Respir Care* 63:690–698, 2018.

Sveger T: Liver disease in alpha 1-antitrypsin deficiency detected by screening of 200,000 infants, *N Engl J Med* 294:1316–1321, 1976.

Thalmann I, Kohut RI, Ryu J, et al.: Protein profile of human perilymph: in search of markers for the diagnosis of perilymph fistula and other inner ear disease, *Otolaryngol Head Neck Surg* 111:273–280, 1994.

Tripathi RC, Millard CB, Tripathi BJ, et al.: Tau fraction of transferrin is present in human aqueous humor and is not unique to cerebrospinal fluid, *Exp Eye Res* 50:541–547, 1990.

Tsung SH, Rosenthal WA, Milewski KA: Immunological measurement of transferrin compared with chemical measurement of total iron-binding capacity, *Clin Chem* 21:1063–1066, 1975.

Van den Steen P, Rudd PM, Dwek RA, et al.: Concepts and principles of O-linked glycosylation, *Crit Rev Biochem Mol Biol* 33:151–208, 1998.

Van Oss CJ, Bronson PM, Border JR: Changes in the serum alpha glycoprotein distribution in trauma patients, *J Trauma* 15:451–455, 1975.

Van Vlierberghe H, Langlois M, Delanghe J: Haptoglobin polymorphisms and iron homeostasis in health and in disease, *Clin Chim Acta* 345:35–42, 2004.

Waldman TA, Gordon RS, Rosse W: Studies on the metabolism of the serum proteins and lipids in patients with analbuminemia, *Am J Med* 37:960–968, 1964.

Walsh PG, Haddad JG: "Rocket" immunoelectrophoresis assay of vitamin D-binding protein (Gc globulin) in human serum, *Clin Chem* 28:1781–1783, 1982.

Weinberg ED: Iron and infection, *Microbiol Rev* 42:45–66, 1978.

Westwood SA, Werrett DJ: Group-specific component: a review of the isoelectric focusing methods and auxilliary methods available for the separation of its phenotypes, *Forensic Sci Int* 32:135–150, 1986.

Whitehead AS, Bruns GAP, Markham AF, et al.: Isolation of human C-reactive protein complementary DNA and localization of the gene to chromosome 1, *Science* 221:69–71, 1983.

Whitfield JB, Dy V, Madden PAF, et al.: Measuring carbohydrate-deficient transferrin by direct immunoassay: factors affecting diagnostic sensitivity for excessive alcohol intake, *Clin Chem* 54:1158–1165, 2008.

Wickner S, Maurizi MR, Gottesman S: Posttranslational quality control: folding, refolding, and degrading proteins, *Science* 286:1888–1893, 1999.

Wochner RD, Spilberg I, Iio A, et al.: Hemopexin metabolism in sickle cell disease, porphyrias and control subjects: effect of heme injection, *N Engl J Med* 290:822–826, 1974.

Xin Y, Lasker JM, Lieber CS: Serum carbohydrate-deficient transferrin: mechanism of increase after chronic alcohol intake, *Hepatology* 22:1462–1468, 1995.

Zawadzki Z, Edwards G: Pseudoparaproteinemia due to hypertransferrinemia, *Am J Clin Pathol* 54:802–809, 1970.

CHAPTER 21

CLINICAL ENZYMOLOGY

Matthew R. Pincus, Robert P. Carty

GENERAL PROPERTIES OF ENZYMES, 291
Catalysis, 291
Enzyme Specificity, 291
Enzyme Concentration and Activity, 292
Molecular Basis for Enzyme Catalysis, 292
Nomenclature of Enzymes, 293
Isozymes, 293
Enzyme Cofactors, 293
Factors Affecting Plasma Enzyme Activities, 294
Factors Affecting the Lifetime of Enzymes In Blood, 294

ENZYME KINETICS: DETERMINATION OF TOTAL ENZYME CONCENTRATIONS IN SERUM AND OTHER BODY FLUIDS, 295
Determination of Total Enzyme Concentration In Serum and Other Body Fluids by Michaelis-Menten Equation, 295
Other Factors Affecting Enzyme Activity, 298
Caveats in Enzyme Assays, 299
Antibody-Based Techniques for Measuring Enzymes, 300

INHIBITION OF ENZYMES, 300
Competitive Inhibition, 300
How Competitive Inhibitors Affect the Michaelis-Menten Equation, 300
Uncompetitive Inhibition, 301
Effect of Uncompetitive Inhibitors on the Michaelis-Menten Equation, 301
Simple and Mixed Noncompetitive Inhibition, 301
Effects of Noncompetitive Inhibitors on the Michaelis-Menten Equation, 302

CATALYTIC EFFICIENCY: TRANSITION STATE THEORY AND DRUG DESIGN, 302
Enzymes Achieve High Rates of Reaction That Greatly Exceed Those for Uncatalyzed Reactions, 302
Enzymes Achieve High Rate Enhancements by Binding to the Transition State on the Reaction Pathway, 303
Transition State Theory in Drug Design, 303

SPECIFIC ENZYMES, 305
Acid Phosphatase (Ec 3.1.3.2), 305
Alkaline Phosphatase (Ec 3.1.3.1), 306
Angiotensin-Converting Enzyme (Ec 3.4.15.1), 308
Acetylcholinesterase (Ec 3.1.1.7) and Butyrylcholinesterase (Ec 3.1.1.8), 310
Lactate Dehydrogenase (Ec 1.1.1.27), 311
5′-Nucleotidase (Ec 3.1.3.5) (5′-NT), 312
Skeletal Muscle Injury: Creatine Phosphokinase, 313

SELECTED REFERENCES, 313

KEY POINTS

- Enzymes are protein catalysts utilized by essentially all mammalian cells in specific biochemical reactions in different organs of the body, which may also be physically located in different organelles and structures within a cell.
- Enzymes lower the activation energies of the chemical reactions that they catalyze so as to cause greatly enhanced rates of reaction. They do not become modified in these reactions and do not affect the equilibrium between reactants and products in the reaction.
- Most enzymes have a practical or trivial name as well as a name based on standardized nomenclature of the International Union of Biochemistry; the latter is based on the type of reaction catalyzed by the enzyme.
- Along with certain narrow ranges of pH, temperature, and protein and salt concentrations, most enzymes require additional organic molecules and/or inorganic ions for optimal enzyme function.
- An understanding of enzyme kinetics allows for laboratory measurement of serum and other body fluid enzyme levels, as well as determination of possible enzyme inhibition.
- Transition state theory of enzyme action has resulted in major breakthroughs in drug design.
- Damaged or dying cells within organs can release enzymes into the circulation. These plasma enzyme levels can be used clinically to develop a differential diagnosis of a patient with respect to specific organ disease and dysfunction.
- In addition, many enzymes have isozymes (i.e., polypeptide chains that differ in sequence but have similar enzymatic activity). Some enzymes are composed of two or more different polypeptide chains, such as the M and B chains of creatine phosphokinase, giving rise to isozymes that differ in chain composition (e.g., the MM, MB, and BB forms of creatine phosphokinase). In a number of diseases, specific isozymes become elevated in serum, facilitating diagnosis.

GENERAL PROPERTIES OF ENZYMES

All enzymes are proteins and function as catalysts. This means that they accelerate the rates of chemical reactions in the body but do not become chemically altered themselves in these reactions. Virtually every reaction that occurs in the body, both intracellularly and extracellularly, is catalyzed by an enzyme. The molecule for which a particular enzyme catalyzes a reaction is called the *substrate*. As explained later, enzymes interact very specifically with their substrates and, with the possible exceptions of closely related molecules, do not interact with any molecules other than their substrates. The concentrations and/or activities of different enzymes in blood give vital information about the functioning of specific tissues. Furthermore, many enzymes exist predominantly in specific tissues and not in other tissues. Thus, certain enzymes can serve as biomarkers for diseases in specific tissues. Therefore, a vital focus of the medical laboratory is determination of the concentrations and/or activities of specific enzymes in blood and other body fluids. The fact that an enzyme interacts selectively with only specific substrates facilitates determination of enzyme concentrations. The concentration of an enzyme can be determined simply by adding a specific substrate to serum or other body fluid and observing the rate at which the substrate disappears or the product of the reaction forms. This chapter is concerned with the principles of how enzyme concentrations are determined.

CATALYSIS

A catalyst accelerates the rate of a chemical reaction. The acceleration may occur in solution, and the process is called *homogeneous catalysis*. Catalysis on an insoluble surface is termed *heterogeneous catalysis*. Biological catalysts are called *enzymes* and for the most part are proteins that exhibit homogeneous catalysis. However, some enzymes are embedded in membrane structures and should be considered insoluble, heterogeneous catalysts.

ENZYME SPECIFICITY

Enzyme specificity defines the capacity of protein catalysts to recognize and bind only one or a few molecules, the substrate(s), excluding all others,

a process referred to as *binding specificity*. An enzyme catalyzes a unique chemical process (i.e., a solitary type of covalent bond is broken or formed). This is called *reaction specificity*. Most enzymes exhibit absolute reaction specificity, that is, no minor by-products are formed. Binding specificity permits many biochemical reactions to occur simultaneously within the same biological space. Absolute reaction specificity saves energy because it reduces the pool of unwanted metabolites.

Enzymes are stereoselective because of the asymmetry of their active sites. They recognize only one enantiomeric form (i.e., one of a pair of compounds having a mirror image relationship) of a chiral substrate. Hence, proteases exclusively bind polypeptides made up of L-amino acids (and not D-amino acids) and catalyze their hydrolysis. Enzymes exhibit geometric specificity exemplified by the fumarase reaction, in which the Krebs cycle intermediate, fumarate (the *trans* isomer), but not maleate (the *cis* isomer), undergoes hydration.

ENZYME CONCENTRATION AND ACTIVITY

The concentration of enzyme molecules within a given intracellular or extracellular space depends on their rate of synthesis and degradation. Control of enzyme synthesis occurs at both transcriptional and translational levels. In eukaryotes, cells of different organs express different isoforms, called *isozymes* (discussed later), of the same enzyme, which alters rates and specificity suitable for selective cellular homeostasis. The presence of substrate, or other inducing molecules, can cause a sudden increase in enzyme levels.

Enzymatic activity is also subject to control through the binding of small molecules that produce conformational changes in the structure of the enzyme. This binding can alter substrate affinity for the enzyme or change the enzyme's catalytic activity, or both. Generally, enzymes that catalyze rate-determining steps in metabolic pathways are subject to this type of regulation.

Enzymes do not affect the value of the equilibrium constant between reactants and products. In a reversible reaction, they accelerate forward and reverse reactions by the same relative amount. The equilibrium distribution of reactants and products is unchanged whether the equilibrium state has been achieved in the presence or absence of an enzyme.

As noted previously, almost all known enzymes are proteins or conjugated proteins. A few enzymes are nucleoproteins, which are ribonucleic acid (RNA) molecules complexed to proteins. Enzymes contain a surface region referred to as the *active site*, where binding and catalysis occur. It is a cleft or crevice in which are embedded specific groups, suitably oriented, which carry out the roles of binding and bond-making, or bond cleavage. The three-dimensional shape of the active site is a vital determinant in the recognition and specificity process. The enzyme-substrate complex is the adduct formed by the physical adsorption of the substrate to the active site. Enzyme-substrate complex formation requires specific alignment of atoms in the active site with atoms in the substrate molecule. This complementary arrangement is referred to as the *lock-and-key fit* of the substrate in the active site and is illustrated in Figure 21.1. Sometimes, the shape of the substrate molecule does not exactly match the contour of the active site. Yet, the substrate binds tightly because of its capacity to reshape the active site to a conformation that binds the substrate with high affinity. This type of substrate adsorption is described as *induced fit*. It is illustrated in Figure 21.2. Active sites of induced-fit enzymes become complementary only after the substrate is bound. Some of the favorable binding energy is used in reorganizing the shape of the active site.

MOLECULAR BASIS FOR ENZYME CATALYSIS

The free energy of activation is the energy absorbed by reactant molecules before they have a chance to convert to products. The free energy of activation is a barrier to chemical reactivity. When this barrier is large, the rate of a chemical reaction is very slow. The lower the barrier, the faster is the reaction rate. The barrier exists for almost all chemical reactions because, for bonds to be broken, they must be stretched and sometimes bent away from their equilibrium positions. These deformations require energy. Enzymes lower the free energy of activation. Most metabolic reactions have very high activation barriers and, in the absence of enzymes, reaction rates are imperceptibly slow. Cells can selectively reduce metabolic reaction rates to near zero by abolishing enzyme activity. This feature of metabolism allows cells to "turn on" and "turn off" metabolic pathways during different stages of the cell cycle. Enzymes lower the free energy of activation in various ways. Binding and appropriate orientation of the substrate in the active site increase its proximity to the catalytic groups. Various types of catalysis are used by enzymes. The major types of catalysis are acid-base, electrophilic, nucleophilic, elimination reactions, decarboxylation reactions, and metal ion and electrostatic catalysis. Reductions in the free energy of activation occur through preferential binding of the transition state (or intermediate enzyme-substrate complex) to active site groups. The side chains of different amino acids participate in catalysis. The side chain of histidine is an effective acid-base catalyst, and the side chains of serine, cysteine, lysine, histidine, and aspartic acid participate in covalent catalysis. The side chains of lysine and arginine, as well as metal ions, can act as electrostatic catalysts by stabilizing negative charges that develop during catalysis. Conversely, the side chains of aspartate and glutamate residues can stabilize the positive charges that develop during catalysis.

The rate of the reaction is proportional to the concentration of molecules that have attained energy equal to the free energy of activation, $\Delta G\ddagger$. This energy is higher for the uncatalyzed reaction. The idea that enzymes accelerate chemical reactions by lowering $\Delta G\ddagger$ is illustrated in Figure 21.3, where the free energy needed for a productive reaction is compared for an uncatalyzed and an enzyme-catalyzed reaction. As shown in this figure, enzymes lower the activation energy. As explained later, an enzyme binds to its substrate to form an enzyme-substrate complex in an initial recognition step. In the subsequent step, the substrate is converted to product. The enzyme-substrate complex is more stable than the two separated species (i.e., has a lower free energy). However, this energy cannot be too low, as in the case of the dotted lines in Figure 21.3, because, in this case, the activation energy would be raised and the reaction rate would be slower. As explained later, an enzyme binds to what is called the *transition state* on the reaction pathway. This is the reactive form of the substrate that is of relatively high free energy compared with the free energy of the ground state of the substrate. Thus, although the energy of the substrate is raised in the

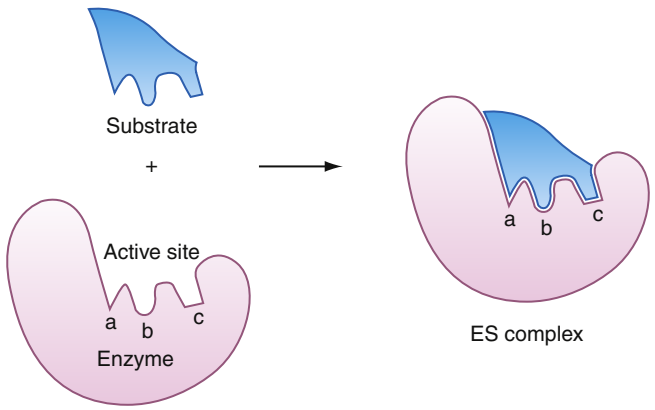

Figure 21.1 The lock-and-key model of substrate binding to the enzyme active site. The enzyme exhibits preformed steric and electronic complementarity to the shape and charge distribution of the substrate. No shape changes or electronic redistributions in the enzyme or the substrate are necessary for optimal binding. (By permission of W. H. Freeman and Company, San Francisco; Stryer L: Biochemistry, ed 2. Stanford, CA, 1981, Stanford University.)

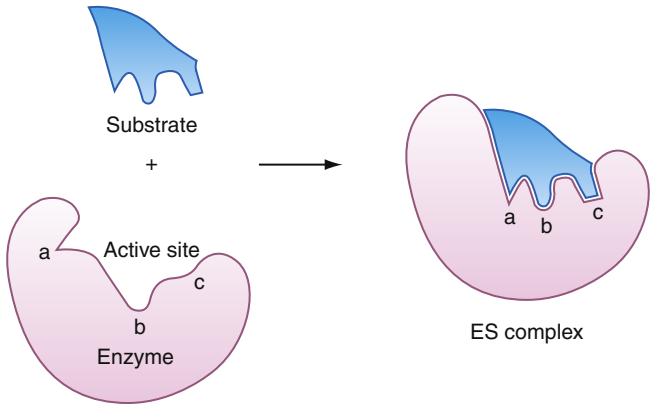

Figure 21.2 The induced-fit model of substrate binding to the enzyme active site. The induced-fit model postulates an initial weak, flexible interaction of the substrate with groups in the enzyme's substrate (ES) binding site. This is sufficient to trigger a conformational rearrangement of the enzyme's surface that exposes additional ligand binding groups that enhance the binding affinity of the substrate for the enzyme. (By permission of W. H. Freeman and Company, San Francisco; Stryer L: Biochemistry, ed 2. Stanford, A, 1981, Stanford University.)

transition state complex, the enzyme provides stabilizing interactions with the transition state that result in overall stabilization of the complex and in an enhanced rate of reaction.

Enzymes have developed as extremely efficient catalysts because their active sites have evolved to bind transition states very tightly. It is this tight binding that stabilizes the transition state and lowers the free energy of activation. Enzymes do not alter the ground state energies of reactants and products of a chemical reaction. The equilibrium state is characterized as a state of lowest energy; the composition of the reactant and product mixture at equilibrium is a reflection of these ground state energies. Enzymes emerge from the catalytic process unaltered, although some undergo transient chemical modification during the reaction.

NOMENCLATURE OF ENZYMES

The nomenclature of commonly measured enzymes was standardized by the Enzyme Commission (EC) of the International Union of Biochemistry (1979, 1992). Each enzyme has two names: a practical or trivial name and a systematic name. The latter consists of a unique numeric code designation and the nature of the catalytic reaction, as follows: Enzymes are named by citing the name of the substrate molecule and by following that with the suffix, -ase; sometimes the name also includes a designation of the type of reaction catalyzed. Examples are as follows.

1. RNA is hydrolyzed by an enzyme called *ribonuclease*.
2. Lactic acid is oxidized to pyruvic acid by an enzyme called *lactic acid dehydrogenase*.

Older trivial names persist in the literature. Examples are trypsin, a protein-hydrolyzing enzyme secreted into the gut, and papain, a plant enzyme that also hydrolyzes proteins. A more systematic classification of enzymes has been implemented in the biochemical literature (International Union of Biochemistry, 1979, 1992). Enzymes have been organized by reaction type into six major classes, as shown in Table 21.1.

ISOZYMES

Many enzymes have isoenzymes, called isozymes, of different forms that catalyze the same reaction. These different forms occur because of differences in the amino acid sequences of enzymes. Despite these differences in sequence, the enzymes fold to the same three-dimensional structures and frequently exhibit similar affinities for and catalytic rates with substrates. Often, isozymes occur as the result of differences in the chain composition of enzymes, as discussed later. Most commonly, different isoenzymes are found in specific organs or tissues; determination of the type of isoenzyme present can then be of use in identifying the damaged tissue and releasing the enzyme. The standard nomenclature of isoenzymes is based on their electrophoretic migration, with the isoenzyme migrating farthest toward the anode designated **isoenzyme 1**. The most widely recognized isoenzymes are those that are composed of varying combinations of subunits; common examples are creatine kinase (CK), a dimer of muscle (M) and brain (B) subunits, and lactate dehydrogenase (LD), a tetramer of heart (H) and M subunits. In other cases, isoenzymes may have the same protein component but may differ based on modifications made by the cell of origin. For example, the bone, renal, and liver isoenzymes of alkaline phosphatase (ALP) have identical amino acid sequences but differ in carbohydrate composition.

In some cases, isoenzymes may have completely different protein structures. Distinct cytoplasmic and mitochondrial isoenzymes of both CK and aspartate aminotransferase (AST) have markedly differing structures. Placental and intestinal ALP isoenzymes have a different protein structure compared with that of the tissue-nonspecific forms found in liver, bone, and other organs.

Finally, enzymes can be modified by proteases present in serum to produce forms that differ slightly from each other; these are termed *isoforms*. As an example, CK-M subunits are partially metabolized by carboxypeptidase N, removing a lysine residue from the carboxy-terminal end of the molecule and converting the tissue isoform to a differently charged plasma isoform. The relative amounts of the tissue and plasma isoforms can be used as a marker of duration of injury to CK-containing cells. The official names and EC numbers of the commonly measured, clinically useful enzymes are given in Table 21.2 (Zollner, 1989).

ENZYME COFACTORS

Two-thirds of all enzymes contain cofactors that are a group of heat-stable substances required for catalysis. They are low-molecular-weight organic molecules and inorganic ions. The combination of cofactor plus the protein portion, the apoenzyme, forms the complete catalytic entity and is known as the *holoenzyme*. Organic cofactors are bound covalently or noncovalently to the apoenzyme. Covalently bound cofactors are sometimes referred to as *prosthetic groups*. Cofactors are observed in oxidation-reduction, group transfer, and isomerization reactions, and in reactions that form covalent bonds. Hydrolytic reactions generally do not require cofactors. Organic cofactors are listed in Table 21.3. Inorganic cofactors that include mainly metal ions are listed in Box 20.1. A cosubstrate is an organic cofactor that behaves as a second substrate in an enzyme-catalyzed

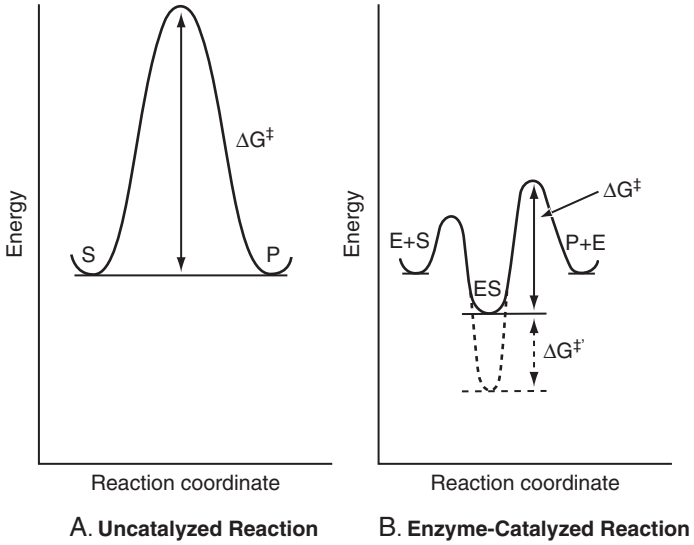

Figure 21.3 The free energy path of a reactant molecule through its transition state on its way to becoming a product molecule. The energy trajectory followed by a molecule undergoing a chemical reaction is the minimum free energy pathway known as the *reaction coordinate*. The transition state, the state of highest free energy, is the point where there is an equal probability that a reaction will take place, or that the activated complex will decompose back to the reactant. The free energy change, ΔG‡, is the energy that the substrate molecule must acquire to reach the activated complex, also called the *activation energy barrier.* **A,** The uncatalyzed reaction. The reactant, called *S*, must acquire the necessary energy, ΔG‡, to become converted into the product, P. This energy is the difference between the energy of the transition state and the ground-state energy of S. **B,** The enzyme-catalyzed reaction. In this case, the enzyme binds noncovalently to the substrate, resulting in a stable enzyme–substrate (ES) complex. In most textbooks, the ES complex is shown as having slightly higher energy than that for free E and S. This is because the energy of the substrate increases when it binds to the enzyme because the enzyme recognizes the transition state of the substrate (discussed later), which is a higher energy form for the substrate. However, overall, the energy of the ES complex is lower than that for the free enzyme and free substrate, as reflected in the favorable affinity constant (usually measured as $1/K_M$, explained later) for the binding of S to E. This is why the energy of ES is shown as lower than for the two isolated species. However, although this complex has a lower free energy than that for the two separated species (S and E), it should not be too much lower, as discussed later. The energy of activation, ΔG‡, now becomes the difference in energy between that of the transition state in the ES complex, and not for S alone, and that of the ground-state ES complex. This energy is less than that for the uncatalyzed reaction. A major reason why ΔG‡ for the enzyme-catalyzed reaction is less than for the uncatalyzed reaction in **A** is that the enzyme has a high affinity for the transition state, lowering its energy relative to that for the ground-state ES complex. Note in **B** what would happen if the enzyme had a very high affinity for ground-state ES *(broken line).* If the same transition state is assumed, the energy barrier to reach this transition state, instead of just being ΔG‡, will now be ΔG‡ + ΔG‡′, resulting in a slower rate of reaction.

TABLE 21.1
Enzyme Classification

Class	Type of Reaction Catalyzed
1. Oxidoreductases	Oxidation-reduction reactions
2. Transferases	Transfer of functional groups
3. Hydrolases	Hydrolysis reactions
4. Lyases	Group elimination to form double bonds
5. Isomerases	Isomerizations
6. Ligases	Bond formation coupled with ATP hydrolysis

ATP, Adenosine triphosphate.

TABLE 21.2
Names, Enzyme Numbers, Substrates for Enzymes

Enzyme (IUB Group, EC Number)	Substrate	Comments
AChE (hydrolase, EC 3.1.1.7)	Acetylcholine, acetyl thiocholine; hydrolyzes acetyl-β-methylcholine	Choline is $HO\text{-}CH_2\text{-}CH_2\text{-}N^+\text{-}(CH_3)_3$, a quaternary amine; many esters with the OH group are substrates. Critical in regulating acetylcholine neurotransmission.
PChE (hydrolase, EC 3.1.1.8)	Many aliphatic esters of choline; unlike AChE, does not hydrolyze acetyl-β-methylcholine but, also unlike AChE, does hydrolyze butyryl- and benzoylcholine.	Largely unknown function; it is critical in hydrolyzing the muscle relaxant succinylcholine.
ACP (hydrolase, EC 3.1.3.2)	G6P, phenyl-P, 3-glycerophosphate, phenolphthalein-P, thymolphthalein-P, naphthol-P	Cleaves phosphate esters like ALP (see next entry) but at pH values around 5.0.
ALP (hydrolase, EC 3.1.3.1)	See ACP	ALP has unusual pH optimum of about 9. Optimum pH varies with substrate and buffer.
ACE (bradykinin, hydrolase, EC 3.4.15.1)	Splits C-terminal His-Leu dipeptide of angiotensin 1 to yield angiotensin 2; also splits hippuryl-His-Leu to hippurate + His-Leu.	Considered a nonspecific hydrolase; acts on Met- and Leu-enkephalin.
LD (oxido reductase, 1.1.1.27)	Pyruvate and other keto acids + NADH Also lactate and other 2-hydroxy acids + NAD^+	Moderately specific
5′-Nucleotidase (hydrolase, EC 3.1.3.5)	5′-Monoribonucleotides	Wide specificity for 5′-monoribonucleotides

ACE, Angiotensin-converting enzyme; *AChE,* acetylcholinesterase; *ACP,* acid phosphatase; *ADP,* adenosine diphosphate; *ALP,* alkaline phosphatase; *ATP,* adenosine triphosphate; *EC,* Enzyme Commission; *G6P,* glucose-6-phosphate; *IUB,* International Union of Biochemistry; *LD,* lactate dehydrogenase; *NAD^+,* nicotinamide-adenine dinucleotide; *NADH,* the reduced form of NAD^+; *P,* phosphate; *PChE,* pseudocholinesterase; *pNPP, p*-nitrophenylphosphate.

reaction. Cofactors such as nicotinamide adenine dinucleotide (NAD^+) can serve as cosubstrates for many oxidoreductases. A single molecule of NAD^+ may act as a cosubstrate many thousands of times. The product, NADH (reducing agent derived from NAD^+), must first be oxidized back to NAD^+ before it can participate again as an electron and H atom acceptor. The recycling of the NAD-NADH oxidation-reduction couple depends on the ready availability of a chemical system capable of regenerating NAD^+ from NADH. A substrate molecule is usually irreversibly changed in a reaction. In contrast, cosubstrate molecules are recycled.

TABLE 21.3
Enzyme Cofactors

Coenzyme(s)	Reaction Type	Deficiency
Coenzyme A	Acyl transfer	
Thiamine pyrophosphate	Aldehyde transfer	Beriberi
Folic acid coenzymes	One-carbon transfer	Megaloblastic anemia
Cobamide (B_{12}) coenzymes	Alkylation	Pernicious anemia
Nicotinamide coenzymes	Oxidation-reduction	Pellagra
Flavin coenzymes	Oxidation-reduction	
Biotin	Carboxylation	
Lipoic acid	Acyl transfer	
Pyridoxal phosphate	Amino group transfer	
Coenzyme Q	Electron transfer	

FACTORS AFFECTING PLASMA ENZYME ACTIVITIES

Plasma levels of enzymes may be increased by several mechanisms. Because enzymes are high-molecular-weight compounds, the most common cause for increased plasma enzymes is death of enzyme-containing cells. As cells die, activation of phospholipases leads to development of holes in the plasma membrane, allowing leakage of cytoplasmic macromolecules, such as proteins. Enzymes are also released in the process of normal cell turnover; this is thought to be the source of normal plasma levels of various enzymes. Increased synthesis of enzymes by cells also leads to increased plasma enzyme levels. With increased activity of osteoblasts, plasma levels of the bone isoenzyme of ALP increase. This may be responsible for the increase in muscle-related enzymes seen with increased exercise (Dickerman et al., 1999). Many drugs that stimulate microsomal enzymes, including ethanol and antiepileptic agents, lead to increased plasma γ-glutamyl transferase (GGT). In some cases, release of enzyme from cells occurs without cell death or increased synthesis.

As discussed in Chapter 22 on liver function, acute liver injury from trauma, hepatitis, or toxic compounds such as ethanol causes release into blood of the aminotransferases, AST and ALT, and LD from damaged and necrotic hepatocytes. For ethanol, which also induces not only cellular damage but also mitochondrial damage to hepatocytes, there is likewise consequent release of the mitochondrial isoenzyme of AST, MT-AST, into blood. Where there is a blockade of bile flow, as occurs from stones in the common bile duct, retrograde buildup of bile salts induces membrane damage to hepatocytes and bile ductule epithelial cells at the cell-cell junction. This results in the release into blood of a number of liver enzymes, such as ALP, leucine aminopeptidase (LAP), and 5′-nucleotidase (5′-NT), which are bound to the canalicular membrane, and GGT, which is bound to the hepatocyte membrane at this junction.

Ischemia of myocardial cells leads to loss of troponin, CK, including the MB isozyme of CK, and glycogen phosphorylase into plasma. Ingestion of food leads to release of intestinal ALP into lymphatic fluid and may transiently increase plasma levels of ALP. Increased concentrations of bile salts with canalicular obstruction may release fragments of membrane with enzyme attached into the circulation or may solubilize the membrane-binding domain (Van Hoof et al., 1997). Finally, increased plasma enzyme levels may be due to decreased clearance of enzymes from the circulation. Some smaller enzymes, such as amylase and lipase, are partially cleared by glomerular filtration; renal failure increases their plasma levels. For many enzymes, autoantibodies against one or more isoenzymes may cause the development of enzyme–antibody complexes (often termed *macroenzymes*), which result in enzyme half-lives similar to the 3-week half-life of immunoglobulin G (Remaley & Wilding, 1989). Most commonly, no specific clinical feature is associated with such macroenzymes. However, it is common to see antibodies against the intestinal isoenzyme of ALP in persons with bacterial infection (Mader et al., 1994). A similar phenomenon can occur when enzymes are bound to antibodies directed against other antigens, such as LD complexes with antibodies to streptokinase (Podlasek et al., 1989).

FACTORS AFFECTING THE LIFETIME OF ENZYMES IN BLOOD

The time course of appearance and disappearance of enzymes with cell injury is dependent on a number of factors. With cell death, defects in cellular membranes enlarge gradually over time; thus, smaller cytoplasmic enzymes will leak from damaged cells sooner than larger ones. For example, with myocardial injury, CK and AST are smaller than LD and appear in plasma sooner. Some enzymes are not cytoplasmic but may be within mitochondria (isoenzymes of CK and AST) or bound to plasma membranes (such as ALP and GGT); cell death typically does not lead to release of such enzymes. If cell death is due to infarction caused by interruption of blood flow to a portion of an organ, enzymes released from damaged cells must diffuse away from the nonperfused region before appearing in the circulation. For example, in myocardial infarction, CK peaks later in persons whose coronary arteries are not successfully reperfused by the use

of thrombolytic agents. The degree of elevation of an enzyme is related to the number of cells injured, the gradient in concentration between cell and plasma, and the rates of enzyme entry into and clearance from plasma. In myocardial infarction, the amount of CK released is strongly correlated to size of infarction; thus, enzyme levels with one-time injury are related to the amount of cell injury occurring. If injury is ongoing, plasma enzyme levels will continue to be elevated for a longer time period. For example, in acute hepatic injury, the time course of enzyme changes can be used to differentiate viral hepatitis, in which immunologic damage causes ongoing cell death and prolonged enzyme elevation, from ischemic and toxic injury, in which damage is immediate but short-lived and enzyme elevations rapidly return to normal.

Other important determinants of the time course of enzyme changes include the relative gradient in enzyme levels between cells and serum and the rate of clearance of enzyme from plasma. For any given amount of cell damage, the enzyme with the higher gradient between cells and serum will show greater elevation of plasma levels. For example, with hepatocyte injury, AST levels in hepatocytes are higher than those of alanine aminotransferase (ALT), and both are many times higher than levels of LD. Immediately after injury, therefore, AST will show a greater degree of elevation than will ALT, and LD will show the least degree of increase. In cardiac tissue, the gradient of CK between myocardial cells and plasma is several times higher than that for LD, leading to higher peak CK than LD levels. Once an enzyme reaches plasma, the rate of clearance also becomes important. For example, the half-life of AST is much shorter than that of ALT, and the half-life of CK is shorter than that of the cardiac isoenzymes of LD. With hepatic injury, therefore, plasma ALT often becomes higher than AST within a short time after injury. Following myocardial infarction, CK returns to normal several days earlier than does LD.

ENZYME KINETICS: DETERMINATION OF TOTAL ENZYME CONCENTRATIONS IN SERUM AND OTHER BODY FLUIDS

The basic objective of clinical enzymology is the determination of the total concentrations of specific enzymes in serum and other body fluids. Qualitatively, detecting the presence of enzymes in body fluids is fortunately quite simple because each enzyme has almost total specificity for one or at most a few substrate(s). By adding the substrate, say, to serum, and observing either its disappearance or the appearance of the product, the presence of the enzyme can be ascertained. As is now explained, the rate at which substrate disappears or product appears can be directly used to determine the concentration of enzyme present (Cleland, 1970, 1990; Dixon & Webb, 1979; Cornish-Bowden, 1995; Fersht, 1999; Segel, 2009).

DETERMINATION OF TOTAL ENZYME CONCENTRATION IN SERUM AND OTHER BODY FLUIDS BY MICHAELIS-MENTEN EQUATION

Enzymes exhibit saturation, which occurs when the rate becomes unresponsive to further increases in substrate concentration. Ordinary chemical reactions occur with rates proportional to the entire range of reactant concentrations. In an enzyme-catalyzed reaction, at low substrate concentrations, rates are proportional to substrate concentration. At higher concentrations, the rate does not increase in direct proportion. At still higher substrate concentrations, the rate becomes constant and unresponsive to any further change in substrate concentration. This led to the proposal that enzyme catalysis is a two-step process that consists of an initial adsorption whereby the substrate combines with the enzyme to form a noncovalent enzyme–substrate (ES) complex, followed by a second step in which the ES complex decomposes into product (P) and free enzyme (E) as follows:

$$E + S \underset{k_{-1}}{\overset{k_1}{\rightleftharpoons}} ES \xrightarrow{k_2} P + E \qquad \text{(Eq. 21.1)}$$

The formation of enzyme–substrate may be regarded as the step in which the enzyme recognizes the substrate. This process involves the formation of specific *noncovalent* interactions between enzyme and substrate. These interactions include ionic interactions, hydrophobic interactions, hydrogen bonding, and van der Waals interactions.

The physical explanation for saturation is that binding reduces the number of active sites available to form the enzyme-substrate complex. When all sites are filled, no further binding can occur until an active site discharges its contents. The step that determines the overall rate is the k_2 step. Adding additional substrate molecules under saturating conditions does not change the rate because all unbound substrate molecules must wait until an active site becomes vacant. This kinetic model is now used to derive the Michaelis-Menten equation that enables direct determination of total enzyme concentration or activity.

Derivation of the Michaelis-Menten Equation

The velocity, v, the rate at which product forms, of an enzyme-catalyzed reaction is defined as:

$$v = v_0 = d[p]/dt = k_2[ES] \qquad \text{(Eq. 21.2)}$$

where *t* is time. Note that *v* is the *initial* velocity of the reaction, referred to as v_0, where we know the concentration of the substrate. It is important to measure initial velocities to ensure the absence of product inhibition (when time [t] = 0, [P] = 0) and the loss of enzyme due to proteolysis, denaturation, or time-dependent adsorption onto glass or plastic surfaces.

The differential rate law, which gives the rate of change of [ES] with time, is the difference between the rate of the k_1 step leading to formation of the complex and the rates of the steps leading to the disappearance of [ES] and k_1 and k_2 steps:

$$d[ES]/dt = k_1[E][S] - k_{-1}[ES] - k_2[ES] \qquad \text{(Eq. 21.3)}$$

For a wide variety of enzyme-catalyzed reactions, it has been found that, over long periods of time, after an initial transient phase lasting a few milliseconds, the concentration of the ES complex remains constant (i.e., does not change in time), especially when S >> E. This is the steady-state assumption. Therefore,

$$d(ES)/dt = 0 = k_1[E][S] - k_{-1}[ES] - k_2[ES] = k_1[E][S] - (k_{-1} + k_2)[ES] \qquad \text{(Eq 21.4)}$$

and

$$[ES] = k_1[E][S]/(k_{-1} + k_2) = [E][S]/K_M \qquad \text{(Eq. 21.5)}$$

where the ratio of the rate constants $k_1/(k_{-1} + k_2)$ is defined as $1/K_M$. K_M is termed the *Michaelis constant*, whose significance is discussed later.

If E_T is the total concentration of enzyme, it is equal to free enzyme plus enzyme bound to substrate, that is,

$$[E_T] = [E] + [ES] \qquad \text{(Eq. 21.6)}$$

Then, using Equation 21.5,

$$[E_T] = [E] + [E][S]/K_M \qquad \text{(Eq. 21.7)}$$

and

$$[E] = [E_T]/(1 + [S]/K_M) \qquad \text{(Eq. 21.8)}$$

and substituting for [E] in Equation 21.5,

$$\begin{aligned}[ES] &= [E][S]/K_M \\ &= [ET]/(1 + [S]/K_M) \times [S]/K_M \\ &= [ET][S]/(K_M + [S])\end{aligned} \qquad \text{(Eq. 21.9)}$$

$$\begin{aligned}[ES] &= [E][S]/K_M \\ &= [E_T]/[(1 + [S]/K_m)[S]/K_M].\end{aligned}$$

Combining Equation 21.9 with Equation 21.2, we have

$$\frac{d[P]}{dt} = V_0 = k_2[ES] = \frac{k_2[E_T][S]}{(K_M + S)}. \qquad \text{(Eq. 21.10)}$$

Equation 21.10, termed the **Michaelis-Menten equation,** accurately describes virtually all single-substrate enzyme-catalyzed reactions and many bisubstrate reactions in which the concentration of one substrate is constant throughout the course of the reaction.

BOX 21.1

Inorganic Cofactors for Enzymes

Mg^{++}	Ca^{++}
Fe^{++}/Fe^{+++}	Mn^{++}
Zn^{++}	Co^{++}
Cu^{+}/Cu^{++}	

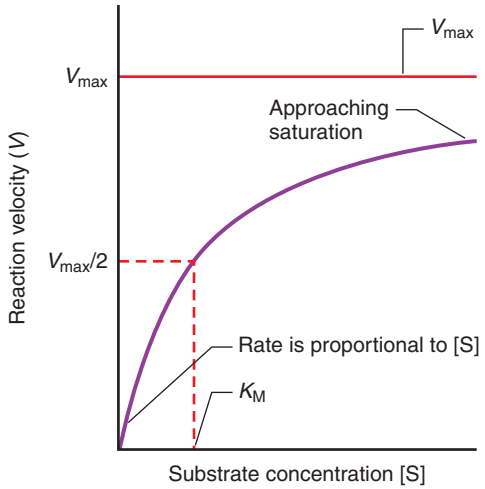

Figure 21.4 The effect of substrate concentration [S] on the velocity (V) of an enzyme-catalyzed reaction. The plot is for an enzyme that obeys Michaelis-Menten kinetics, where the maximal velocity is V_{max} and [S] equals K_M where (v) equals $V_{max}/2$.

Total Enzyme Concentration Can Be Determined from the Initial Rate at Saturation

A typical plot of v_0 versus initial substrate concentration is shown in Figure 21.4. The curve is a rectangular hyperbola, and the initial rate increases up to a particular substrate concentration beyond which the rate remains constant. This occurs on the curve where $[S] >> K_M$. This is referred to as *saturation*, in which all of the enzyme molecules are bound to the substrate, making it impossible to increase the rate any further by increasing [S]. Note that S is *free* S, unbound to the enzyme. The only manner in which S can be greater than K_M is if the total concentration of S is greater than the total enzyme concentration.

Note that, where saturation occurs, that is, where $[S] >> K_M$, Equation 21.10 reduces to

$$d[P]/dt = V_0 = k_2[E_T] \qquad \text{(Eq. 21.11)}$$

Because the rate is constant at saturation, the rate is zero order with respect to substrate; the rate does not depend on the concentration of reactants. There is a dependence on E_T, which, however, is not consumed in the reaction. At saturation, the initial velocity of the reaction is referred to as the *maximal velocity*, or $V_{max} = k_2E_T$. Under this saturating condition, the initial rate of the reaction is directly proportional to the total enzyme concentration. If k_2 is known, then E_T can be directly computed as the observed initial rate divided by k_2. This equation solves the problem of determining the total enzyme concentration from measurements of the rate of the enzyme-catalyzed reaction where $[S] >> K_M$.

Knowledge of k_2 and K_M Allows Determination of [S] Values That Will Saturate the Enzyme

To fulfill the conditions of Equation 21.11, it is necessary to know both K_M and k_2. These can be estimated from plots similar to the one shown in Figure 21.4. To generate these plots, the purified enzyme is dissolved in aqueous solution in a series of tubes at the same concentration. A different concentration of substrate is added to each of these tubes, and the initial rate of reaction for each tube is determined

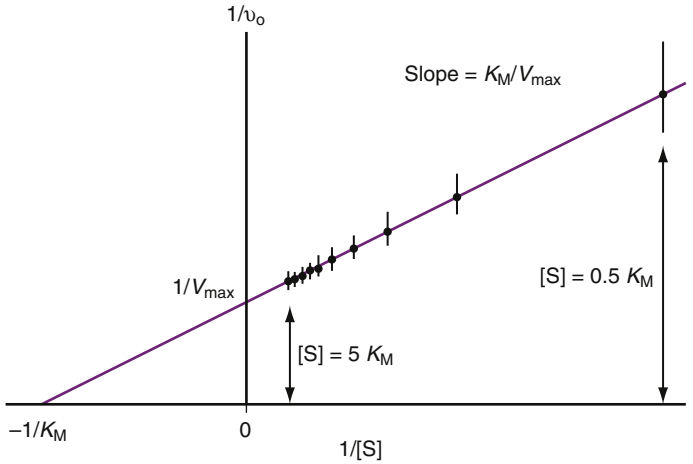

Figure 21.5 A typical Lineweaver-Burk ($1/v_o$ vs. 1/[S]) plot, from Equation 21.12, for an enzyme-catalyzed reaction. v_0 is the initial velocity of the reaction at time t = 0, where the substrate concentration, [S], is known. The figure shows that [S] must cover a range from where it is significantly less than K_M (0.5 K_M) to where it is significantly greater than K_M (5 K_M) to obtain reliable values for K_M and V_{max}. The Y-intercept is $1/V_{max}$, and the X-intercept is $-1/K_M$. The slope is K_M/V_{max}.

using a suitable (mostly spectrophotometric) technique. The value of v_0 versus initial substrate concentration [S] can be plotted; the value of S at which the rate levels off (i.e., becomes constant) can be estimated from the plot.

The Lineweaver-Burk Plot Gives k_2 and K_M

The problem with this approach is that, in the v_0 versus [S] plot, the rate approaches V_{max} asymptotically. Therefore, V_{max} can only be estimated, often inaccurately, from such a plot. A more accurate method by which to accomplish this goal is to linearize the Michaelis-Menten equation (Eq. 21.10) by taking the reciprocal of both sides of the equation and rearranging the terms, that is,

$$\frac{1}{V_0} = \frac{K_M}{V_{MAX}} \cdot \frac{1}{[S]} + \frac{1}{V_{MAX}} \qquad \text{(Eq. 21.12)}$$

As can be seen from Equation 21.12, a plot of $1/v_0$ versus 1/[S], called the *double reciprocal plot*, also called the *Lineweaver-Burk plot*, should be linear; the Y-intercept should be $1/V_{max}$, and the slope should be K_M/V_{max}. Because $1/V_{max}$ is the Y-intercept, K_M can be computed as the slope/Y-intercept. Because from Equation 21.12 the X-intercept is $-1/K_M$, K_M can also be computed directly from this relationship. K_M can be computed directly from the Michaelis-Menten equation (Eq. 21.10) from V_{max}. When [S] = K_M, from Equation 21.10, $v_0 = V_{max}/2$. Thus, the K_M is the substrate concentration necessary to reach $V_{max}/2$. A typical Lineweaver-Burk plot is shown in Figure 21.5.

Practically, after the points are obtained from the double reciprocal plot, the least squares best line is drawn through the points from which the slope and X- and Y-intercepts are directly determined. The correlation coefficient, which is a measure of the closeness of fit of the experimental points to the best line, is also calculated and should be greater than 0.9, that is, a high correlation.

Note in the above procedure and as is illustrated in Figure 21.5 that substrate concentrations must span a range that brackets K_M. Measurements of v_0 at low [S] have relatively large errors, as illustrated in the upper-right portion of the line in Figure 21.5, yet it is these estimates that are critical in determining accurate values of K_M and V_{max}. Modern computer programs provide reasonably accurate values for K_M and V_{max} based on weighted values of the initial velocities. Weights are assigned based on the magnitude of v_0. In addition, other computer programs use nonlinear regression analysis to fit the weighted data to a hyperbolic v_0 versus [S] curve, as in Equation 21.10, and a Lineweaver-Burk plot is used only for visual display of the kinetic data.

Once K_M is known, saturating concentrations of substrate can be used such that $[S] >> K_M$. Thus, for example, if $K_M = 1 \times 10^{-5}$ M for a certain enzyme for which an assay is desired, we can use a substrate concentration of 1×10^{-3} M (1 mM) and be assured that $[S] >> K_M$, here by a factor of 100, so that Equation 21.11 applies. The substrate at this concentration is added to a patient sample (most often, serum), and the rate is observed and then divided by k_2 to obtain the total concentration of enzyme. As

discussed later, because many enzymes exist as different isozymes with different k_2 and K_M values, division by k_2 is not performed and the results are reported directly as k_2E_T, referred to as *total activity units*.

A Word About K_M

Equation 21.1 shows that the ES complex is in equilibrium with free E and free S. We can write an equilibrium constant for this process as a dissociation constant, K_s, as k_{-1}/k_1, which is equal to [E][S]/[ES]. The reciprocal of this constant, or the association constant, K_A, is k_1/k_{-1} = [ES]/[E][S]. From Equation 21.5, K_M is defined as $(k_{-1} + k_2)/k_1$. Note that when $k_{-1} >> k_2$, K_M is the same as K_S. This condition actually pertains to most enzyme-catalyzed reactions; k_{-1} is the rate of dissociation for the enzyme-substrate complex that almost always involves the breaking of noncovalent bonds, and k_2 is the rate for the breaking and/or making of covalent bonds. Usually, the energy necessary for the former process is much less than for the latter; therefore, the rate of dissociation, k_{-1}, of the noncovalent ES complex is higher than the rate, k_2, for the covalent catalysis step. Thus, K_M is the dissociation constant for the ES complex. The reciprocal of this is K_A, the association constant, and it is the affinity of the substrate for the enzyme.

However, in some cases, the rate for the covalent catalytic step is greatly enhanced. Examples include carbonic anhydrase ($k_2 = 10^6$ sec^{-1}; carbon dioxide is the substrate) and catalase ($k_2 = 10^7$ sec^{-1}; hydrogen peroxide is the substrate). For these enzymes, because k_2 is large, K_M is not a dissociation constant but rather a steady-state constant, equal to k_2/k_1.

Enzyme Activity

As noted previously, computation of total enzyme concentration using Equation 21.11 is often not performed because many enzymes have multiple isozymes. For example, at least five isozymes of LD are known, each having a different set of values for K_M and k_2. In this case, the total enzyme activity of LD is given, that is, $k_2 \times [E_T]$. In these cases, enzyme activities are all reported in units called *international units*, defined originally in 1964 by the International Commission on Enzymes. One international unit (IU) is the amount of enzyme that catalyzes the formation of one micromole of product (or the disappearance of 1 micromole of substrate) in 1 minute. It applies only under specified conditions of pH, temperature, and ionic strength, all factors that influence enzyme activity, as discussed later.

With development of the Système International d'Unités system and the use of moles and seconds as base units, a second definition for the unit of enzyme activity was developed, the katal: 1 katal is defined as the amount of enzyme that catalyzes the conversion of 1 mol of substrate to product in 1 second under the conditions used in the assay. One IU is equal to 16.7 nanokatal (nkat), and 1 katal is equal to 6×10^7 IU. Both definitions unfortunately omit volume. Generally, 1 IU is reported per liter (L); the right side of Equation 21.11 has the units of concentration per time so that IU/L conforms to these units. It is vital that, if total enzyme activity is reported, the substrate used in the assay for the enzyme also be reported because the k_2 value differs for different substrates.

As discussed later, many factors affect enzymatic activity, including pH, temperature, ionic strength, concentration of cofactors of an enzyme, presence of inhibitors, use of other enzyme reactions as indicators, and whether the forward or backward reaction is used to measure the enzyme concentration. For example, LD measured using the forward reaction has approximately one-third the activity of LD measured using the reverse reaction, and lipase measured with colipase present has 5 to 10 times the activity of lipase measured without its cofactor.

Therefore, even if the same substrate is used by different laboratories, the reference ranges of enzymes may differ dramatically among these laboratories. Furthermore, differences in reference ranges between two different laboratories can still exist even if the above factors are the same for both, because of different assay conditions.

To attempt to standardize enzyme activities, one approach is to have each laboratory set the upper boundary of the reference range to 100 (Langdon, 1994). Then all other values are expressed as percentages or ratios. A result indicating that an enzyme level was 10 times normal is useful to a physician. If the result is 10X U/L, then the physician must hunt the value of X and calculate the ratio. As long as the assays are performed with internal consistency in a highly reproducible manner, quantitative results are comparable between one laboratory and another if relative activities are reported. More commonly, the results of enzyme assays are now expressed in IU along with the reference ranges for each enzyme, allowing for evaluation of the patient's condition, progression of disease, or efficacy of therapy.

Measuring Enzyme Activity

In principle, in the measurement of enzyme activity, either the rate of disappearance of substrate or the rate of appearance of product can be measured. In general, it is easier to measure small increases in product than to measure small decreases in a relatively high concentration of substrate often needed to achieve saturation. As discussed previously, to measure enzyme activity in a sample, it is most common to use substrates at saturating concentrations where zero-order kinetics with respect to [S] occur. Under these conditions, the reaction rate is directly proportional to the total amount of enzyme present.

Equation 21.11 states that, at saturation, the rate of product formation with time is constant. This implies that the concentration of product increases linearly with time. Experimentally, P is determined at different time points, and a least-squares best-fit line through the points is determined. If the correlation coefficient is high, [P] increases linearly with t, confirming saturation of the enzyme by substrate. The slope of this line is V_{max}, which may be reported directly as activity or divided by k_2 to give enzyme concentration.

The most common cause of a *nonlinear* relationship between P and t is the presence of an inhibitor that will be discussed later. In cases such as these, dilution of the serum or other body fluid sample is warranted because this will dilute the concentration of the inhibitor, although it will also dilute the total enzyme concentration. However, as long as [S] is present at saturating conditions and [P] can be measured, valid total enzyme concentrations or activities can be measured.

Typically, in enzyme assays, a lag phase follows mixture of the specimen and reagents when preliminary reactions and mixing of sample occur. The initial absorbance of the sample is based on the absorbance due to the reagents and the sample and is considered to be zero in terms of making an interpretation of enzyme activity. Once the reaction begins, the graph will follow a straight line for a period of time. At this point, the reaction is zero-order and enzyme activity can be determined. If the reaction is allowed to proceed, substrate is consumed and [S] falls toward K_M. If [S] falls substantially below K_M, the reaction will then be first-order, and v_0 will be affected both by the amount of substrate (which is not a constant) and by the enzyme activity.

Spectrophotometric Assays

In most cases, enzyme activity is measured spectrophotometrically. In addition, other detection methods are used as appropriate, depending on the product being measured. For example, lipase acts on emulsions of lipid; these are often turbid so that measurement of the rate of clearance of turbidity could be used to determine lipase activity. Glucose oxidase, widely used to measure glucose concentration, is a flavoprotein that uses oxygen as an electron acceptor. The change in potential due to alteration in charge on the acceptor can be measured to determine the reaction rate. Urease is widely used to measure urea concentration; urease splits urea into bicarbonate and ammonium ions. The change in conductance of the specimen due to the appearance of the ions in the sample can be used to determine the rate of reaction.

Because assay methods based on spectrophotometry are the most common, we will focus on these in describing how enzyme assays are performed. In the simplest case, the substrate does not absorb light at a particular wavelength at which the product absorbs strongly. An excellent example of this is LD, which catalyzes reversibly the oxidation of lactate to pyruvate. Because lactate is a unique substrate for LD, it is preferred. Pyruvate can be used as the substrate, except that it is also the substrate for several other enzymes such as pyruvate dehydrogenase and ALT, among others.

When lactate is oxidized to pyruvate, the cofactor, NAD^+, becomes reduced to NADH. For each mole of lactate oxidized to pyruvate, 1 mole of NADH forms. NADH absorbs strongly at 340 nm; NAD^+ does not absorb light at this wavelength. Therefore, the addition of saturating concentrations of both lactate and NAD^+ to a patient's serum will result in a linear increase in absorbance at 340 nm over a given period, from which total enzyme activity is directly determined as described earlier. In this case, the increase in concentration of NADH, ΔP, over the time period, Δt, is proportional to the increase in absorbance, ΔA, at 340 nm, by Beer's law, as described in Chapter 4, that is,

$$\Delta P/\Delta t = \varepsilon \times (\Delta A/\Delta t) \times L \qquad \text{(Eq. 21.13)}$$

L in Equation 21.13 is the path length of the reaction vessel or cuvette, almost always equal to 1 cm. ε is a proportionality constant (most often, the molar extinction coefficient) in Beer's law, which is 6.22×10^3 L mol^{-1} cm^{-1}

for NADH at 340 nm. On most current chemistry analyzers, a volume of a patient's serum sample is added to the reaction cuvette containing the reaction components (lactate and NAD^+), and ΔA is observed. This results in dilution of the volume (Vp) of the patient's serum to the total volume of the reaction mixture (Vo), so that

$$\text{Enzyme activity} = \Delta P/\Delta t = \varepsilon \cdot (\Delta A/\Delta t) \cdot L \cdot (V_0/V_P) \qquad \text{(Eq. 21.14)}$$

One caveat in the previous assay is that LD also catalyzes the reverse reaction (i.e., pyruvate to lactate). Therefore, as pyruvate forms, it can serve as an end-product competitive inhibitor (see the Inhibition of Enzymes section later in the chapter) and can drive the reaction back to lactate. Therefore, it is important to be able to take the measurements in Equation 21.14 over a short time before pyruvate builds up to significant levels.

Coupled Enzymatic Reactions

In many instances, however, neither the product nor the substrate of a chemical reaction can be measured conveniently. In such instances, the enzymatic reaction can be "coupled" to another reaction that uses the product of the enzyme-catalyzed reaction to produce an indicator substance. An example of a typical coupled enzymatic reaction is the Oliver-Rosalki method for measurement of CK activity, illustrated in Equations 21.15 through 21.17, later. The reverse reaction of CK is used, producing adenosine triphosphate (ATP), which is used in a second reaction to produce glucose-6-phosphate (G6P) from glucose + ATP. The third reaction in the sequence results in the reduction of nicotinamide adenine dinucleotide phosphate, or $NADP^+$, to NADPH, the indicator of the reaction. In these coupled reactions, it is critical that the rate-limiting step in the overall reaction is the CK-mediated step that generates ATP. This can be achieved by using high concentrations of the indicator enzymes to ensure rapid conversion of the substrates of the subsequent reactions.

One potential problem with CK measurements when this reaction scheme is used is the presence of other enzymes that can generate ATP. Adenylate kinase, an enzyme found in red blood cells and liver, converts adenosine diphosphate (ADP) to ATP (see Eq. 21.34); specimens with high adenylate kinase activity will have falsely elevated values for CK activity.

Creatine phosphate + ADP → Creatine + ATP (catalyzed by CK) (Eq. 21.15)

Glucose + ATP → G6P + ADP (catalyzed by hexokinase) (Eq. 21.16)

G6P + $NADP^+$ → 6 - Phosphogluconate + NADPH (catalyzed by glucose -6-phosphate dehydrogenase, or G6PD) (Eq. 21.17)

Complication:

2 ADP → ATP + AMP (catalyzed by adenylate kinase) (Eq. 21.18)

The absorbance increase at 340 nm due to NADPH is proportional to the [ATP] generated as the end-product of the CK reaction, as expressed in Equation 21.15.

In assays of enzyme activity, some methods use **endpoint** measurements, discussed in Chapter 28, determining the concentration of substrate or product at a specific time after addition of the sample. Endpoint methods are typically used in simple methods, such as bedside glucose testing or dipstick reactions, as for glucose or leukocyte esterase in urine. Endpoint methods may give erroneously low results in situations in which enzyme activity is very high. Most enzymatic assays use **kinetic** methods of measurement (as discussed earlier), whereby the rate of change in concentration of substrate or product is determined. (For the sake of simplicity, throughout the rest of this section, only measurement systems that detect appearance of product will be described. The same principles, however, would apply to situations in which rate of disappearance of substrate is being monitored.) Kinetic methods are more accurate and make it easier to detect changes in reaction conditions and samples requiring dilution. In a time-course study, the rate of reaction can be expressed as ΔP/Δt, the change in amount of product per unit time. Because the IU and the katal represent the amount of enzyme producing a specific amount of product in a given time period, this approach allows direct reporting of enzyme activity in either IU or katal, as desired.

Enzyme Assays Under Nonsaturating Conditions: First-Order Rate Processes

As discussed later, there are circumstances under which it may not be possible to perform an enzyme assay under saturating conditions in which Equation 21.11 applies. In these circumstances, assay conditions may be used in which $S < K_M$. The Michaelis-Menten equation (21.10) then becomes

$$V_0 = d[p]/dt = k_2 E_T \cdot [S]/K_M \qquad \text{(Eq. 21.19)}$$

Because E_T is constant, the initial rate of the reaction depends only on the concentration of S. When S decreases, ES and P increase so that $-d[S]/dt = d[ES]/dt + d[P]/dt$. But, under the reaction condition that $[S] >> [E]$, the steady-state assumption, $d[ES]/dt = 0$, is valid. Therefore, the rate of product formation equals the rate of substrate depletion, that is,

$$V_0 = d[p]/dt = -[S]d/dt = k_2 E_T \cdot [S]/K_M \qquad \text{(Eq. 21.20)}$$

This is the equation for a first-order process, that is, the rate depends only on the concentration of a single species, in this case the substrate. Because the rate also formally depends on E_T, it is properly called a second-order reaction. However, in this case, E_T is constant and does not change during the reaction. It is therefore referred to as a *pseudo–first-order* reaction. E_T can be determined from determination of the initial rate of the reaction in which the initial substrate concentration, S_0, is known. Because K_M and k_2 are known,

$$E_T = (V_0/[S_0]) \times (K_M/k_2) \qquad \text{(Eq. 21.21)}$$

If only total enzyme activity is to be reported, then v_0/S_0, which is equal to $(k_2/K_M)[E_T]$, is reported because this quantity is directly proportional to E_T. Note, though, that these are not the same activity units as are used under saturating conditions because the total enzyme concentration in that case is multiplied only by k_2 and, in the current circumstance, it is multiplied by k_2/K_M because of the fact that saturation has not occurred.

Another approach to determination of E_T under nonsaturating conditions is to integrate Equation 21.20 for S in terms of t. This results in the following relationship:

$$\ln([S]/[S_0]) = 2.303\log([S]/[S_0]) = -(K_2 K_T/K_M) \cdot t \qquad \text{(Eq. 21.22)}$$

where ln is the natural logarithm to the base e and $[S_0]$ is the initial substrate concentration. If the substrate concentration is determined at specific times, a plot of the log (S/S_0) versus time should give a straight line whose slope is $-(k_2E_T/K_M)/2.303$. Because both k_2 and K_M are known, E_T can be directly evaluated. This method eliminates the need to measure initial velocities involving small changes in [S]. This method is advantageous when the substrate solubility does not permit saturating substrate concentrations to be reached.

The above first-order rate equation is the general equation for all first-order rate processes that abound in biology. Many reactions in the body occur either by first-order processes or by pseudo–first-order processes in which the rate depends only on the concentration of one species. As discussed in Chapter 24, when drugs are administered to the body, they decay very often by a first-order process, where the rate of disappearance of the drug depends only on the concentration of the drug. One important feature of this process is the so-called *half-time*. Note, from Equation 21.22, that the half-time, $t_{1/2}$, or the time required for half of S_0 to be consumed, that is, when $[S] = [S_0]/2$, is a constant that depends only on the rate constant in the equation. The nondependence of $t_{1/2}$ on concentration is a cardinal feature of first-order rate processes.

Because log (2) = 0.3, the above equation reduces to

$$t_{1/2} = 0.69/k \qquad \text{(Eq. 21.23)}$$

where, in this case, $k = K_M/k_2E_T$ and $t_{1/2}$ is the half-time, that is, the time required for half of the substrate to be consumed. Thus, if the half-time for substrate consumption is known, E_T can also be directly computed from Equation 21.23 provided that K_M and k_2 are known.

OTHER FACTORS AFFECTING ENZYME ACTIVITY

Temperature

Enzyme-catalyzed reaction rates are extremely sensitive to temperature changes; to ensure accuracy, the temperature of the reaction mixture must not deviate by more than ±0.1° C from the assigned temperature. In general, every 10° C increase in temperature leads to an approximate doubling of

enzyme activity, although this varies slightly from one enzyme to another. The use of higher temperatures gives faster reaction rates and improves sensitivity—an advantage when enzyme activities are low. Lower temperatures increase the linear limit of an assay, requiring fewer dilutions. The choice of temperature with most modern instruments is governed by the capabilities of the instrument. There is a limit to the amount of temperature increase that can be used; most enzymes start to denature and become inactive as the temperature is increased. For example, CK starts to denature at 37° C, and amylase begins to denature at 45° C. On the other hand, some enzymes remain stable at extremely high temperatures. As an extreme case, the Taq polymerase used in the polymerase chain reaction is stable at 95° C. Taq polymerase and the polymerase chain reaction are discussed in Chapter 69.

Another issue concerning thermal stabilities of clinically significant enzymes is the effect of low temperatures on their stabilities, that is, when samples are stored prior to reassay or to initial assay. In the former case, it is sometimes necessary to perform a reassay for an enzyme if the first result was questionable clinically. Normally, patient samples that have been assayed are stored at 4° C (refrigeration temperature) for about 1 week, after which time they are discarded. The question is whether the reassay result is reproducible in this 1-week time period. Some earlier studies suggested that ALP, ALT, AST, CK, but not LDH are stable in this time period (Heins, 1995) while other studies found that ALP was not stable, especially in the presence of magnesium ions. On the other hand, recent studies suggest that the stabilities of ALP, ALT, AST, CK, and LDH are all reproducible (statistically identical) over this time period (Chua, 2017). In the latter case, in which samples are stored frozen either at –20° C or –80° C (dry ice temperature) prior to assay, there is a recent study on the activities of salivary ALP, ALT, AST, and LDH that suggests that the activities of all of these enzyme decrease in a statistically significant manner over a 2-week period when stored at –20° C but not when stored at –80° C (Dos Santos, 2018). In contrast, the activities of the same enzymes and CK in serum were found to be statistically reproducible over a 1-month period except for ALT when stored at –20° C (Chua, 2018). These results suggest that the medium (salivary fluid vs. serum) may be an important determinant of reproducibility and that storage of serum samples over 1 month at –20° C will yield reproducible results for these enzymes, except for ALT.

pH

Enzymes have a pH optimum for maximal activity; usually, the pH of the reaction conditions is chosen to be that at which the enzyme exhibits the greatest activity. Selection of pH is not always critical; some enzymes have a very broad pH maximum so that small changes in pH do not appreciably change activity. For example, ALP has maximum activity at pH values between 9 and 10. In some cases, particularly for enzymes with multiple isoenzymes, selection of pH represents a compromise, as different isoenzymes may have maximum activity at differing pH values. In this situation, the pH for the reaction is selected to allow measurement of the activities of all isozymes.

Salt and Protein Concentrations

The ionic strength of solutions affects enzyme activity; if ionic strength is too high, enzyme activity drops. The activity of many enzymes is also affected by protein concentration. When enzyme activity is over the linear limits of the assay, dilution of plasma typically requires use of **enzyme diluents** containing plasma proteins. Human plasma contains about 70 g protein/L, but normal urine has almost no protein; use of proteins such as albumin increases the activity of urinary amylase and standardizes its measurement. In protein-free solutions, enzymes lose activity rapidly either by denaturation or by adsorption to the walls of the container.

Inhibitors and Interferences

Typically, enzymes are measured in serum samples. Heparinized plasma is generally considered an equivalent sample to serum for most routine analytes; however, this may not be the case for enzymes. Heparin may inhibit the activity of some enzymes—notably, amylase and AST (using some, but not all, methods). Citrate, used in evacuated collection tubes for coagulation testing and as a preservative in blood products, complexes divalent cations, among which calcium ion is most prominent. Citrate-containing specimens may cause falsely low results for enzymes such as CK and ALP. Ethylenediaminetetraacetic acid (EDTA) and fluoride inhibit the activity of many enzymes and should almost never be used for specimens for enzyme analysis. An exception is in measurement of renin, in which EDTA inhibits the action of enzymes that convert prorenin to the active enzyme renin and prevents artifactual increase in renin activity.

CAVEATS IN ENZYME ASSAYS

Some of the causes of errors in enzyme assays, such as the presence of inhibitors, have been mentioned previously. Here, we summarize the most common problems that can be encountered.

K_M-Type Mutations

In certain deficiency states, the conditions of the in vitro assay may not mirror the in vivo conditions that give rise to the deficiency state. In cases in which a genetic defect does not alter normal protein levels of enzyme and the k_{cat} value is unchanged, by applying the principle that the assay should be carried out at saturating substrate concentration, it is possible that a K_M-type mutation may go undetected. This is due to the fact that the enzyme, inactive at low substrate levels, exhibits full or nearly full activity at the higher [S] used in the assay. For example, a variant erythrocyte hypoxanthine-guanine-phosphoribosyltransferase is inactive in assays at low [S], but full activity is restored by increasing the substrate concentration. To guard against such a false positive, a clinical evaluation should include a determination of the K_M for the mutant enzyme.

One technique that can be employed to detect enzyme mutations that affect activity is the use of monoclonal antibodies directed against the enzyme of interest. Immunoassays for enzymes are discussed later. Correspondence between measurement of enzyme activity and the protein (enzyme) concentration from immunoassays will pertain as long as the enzyme antigen is fully active. Such is not always the case when inherited deficiencies associated with point mutations are involved. In these instances, estimates of enzyme concentration based on immunoassays can exceed those based on measurements of enzyme activity, indicating a defect in the enzyme. If the underlying basis of disease is genetic, it is best to estimate enzyme activity from kinetic measurements and compare these with normal values. Some mutations destabilize protein structure, leading to rapid intracellular proteolysis of the enzyme. In this instance, the results derived from immunologic methods and enzyme activity measurements can concur. The presence of inhibitors in the source biological fluid may lead to underestimation of the amount of enzyme present based on activity but not immunologic measurements. Usually, reversible enzyme inhibitors will not interfere with immunologic estimates of enzyme concentration.

Cyclic Enzyme Instability

In some cases, an enzyme defect may go undetected because the clinical evaluation occurs at an inappropriate time. Administration of the antimalarial primaquine to a glucose-6-phosphate dehydrogenase (G6PD)-deficient individual carrying the common type **A–** variant (G6PD **A–**) causes transient hemolytic anemia. Patients can recover completely from the anemia despite continued drug treatment. The type **A–** variant has normal kinetic parameters but reduced thermal stability. The initial episode clears older erythrocytes that have reduced G6PD activity. The older cells are replaced by new cells that have higher amounts of enzyme. The quantity of G6PD molecules in erythrocytes is a function of erythrocyte age, and the rate of loss of enzyme molecules in type **A–** variant cells exceeds that in normal cells by a significant margin. Levels of G6PD activity following recovery from anemia will be substantially higher than if assays are performed before or during the hemolytic episode, because hemolysis selectively destroys older cells containing smaller amounts of enzyme. Recovery results in the replacement of these older cells with new cells with higher levels of G6PD **A–** molecules. During and following recovery, the younger set of cells is able to cope with the primaquine treatment because of the presence of higher levels of enzyme activity.

Presence of Enzyme Inhibitors

As discussed later, enzyme inhibitors present in biological fluids may permit underestimation of the amount of enzyme present. It is important to note that if the presence of an inhibitor is suspected, the most effective procedure is to dilute the sample so that the effect of the inhibitor will be minimal. In case of the possibility of end-product inhibition, initial velocity determinations eliminate this effect because, initially, at $t = 0$, $[P] = 0$, where there will be no inhibitory effect. In rare cases, in enzyme-catalyzed reactions in which the product binds to the enzyme with a much higher affinity than the substrate, $\Delta P/\Delta t$ or $-\Delta S/\Delta t$ may be curvilinear, and estimates of the initial velocity are best made from tangents drawn to the substrate or product time-course curves at $t = 0$. These tangents are best determined from continuous traces of substrate disappearance or product formation.

Protease Degradation of Unstable Enzymes

Proteases in plasma may attack the enzyme while the velocity estimate is being made. This is especially true for enzymes that may have reduced thermal stability, as discussed earlier. If the enzymes become unfolded, they are subject to attack by serum proteases, including trypsin and chymotrypsin and a number of other proteases. Enzyme damage through proteolysis and substrate decomposition may be corrected by the use of suitable blanks and preincubation studies.

Presence of Inhibitory Compounds in Blood Collection Tubes

As discussed previously, in many cases, serum or plasma and not whole blood must be used for the determination of enzyme activity in whole blood samples collected in anticoagulant-containing tubes. Polyanionic anticoagulants, such as citrate, heparin, and EDTA, inactivate metal-containing enzymes. For example, EDTA inactivates the zinc-containing enzyme ALP, an enzyme that is commonly assayed.

Competing Reactions in an Enzyme Assay

As noted in the preceding section, substrates used to assay specific enzymes may be subject to attack by other enzymes normally present in biological fluids. Assays for LD using pyruvate as the substrate can be complicated by the presence of other enzymes, such as pyruvate dehydrogenase and ALT, that react with this substrate. The coupled assay system for CK activity can be complicated by the presence in serum of the enzyme adenylate kinase, which can consume the substrate ADP (see Eq. 21.18.) This problem cannot be corrected by using saturating concentrations of ADP because the product of the adenylate kinase reaction is also ATP, and the ATP produced in the CK reaction has to be used to determine the amount of G6P produced to accurately determine the CK level.

Time-Dependent Inactivation of Certain Enzymes

Sample age may be important in determining enzyme activity. Enzymes whose activity depends on active-site sulfhydryl groups may suffer slow inactivation through oxidation and/or disulfide exchange reactions. In many instances, these processes are irreversible and lead to underestimation of the enzyme concentration by activity measurements.

ANTIBODY-BASED TECHNIQUES FOR MEASURING ENZYMES

As mentioned earlier, immunoassays can be used to measure the mass of enzyme protein. These assays are described at length in Chapter 24 and in Part 6. Immunoassays are the method of choice when it is desired to quantitate one or more isoenzymes of an enzyme in a sample because specific antibodies raised against each individual isoenzyme will identify and quantitate each of the variants present in the sample.

Immunoassays are, in general, less affected by factors that affect enzyme activity and are often more precise. As with enzyme activity, however, the determination of enzyme mass may vary depending on the reagents used; calibrators often lead to different results for mass activity between different methods. Examples include the MB isoenzyme of CK, the pancreatic isoenzymes of amylase, the prostatic and bone isoenzymes of acid phosphatase (ACP), and the bone isoenzyme of ALP. Antibodies can also be used to selectively inhibit or bind particular enzyme subunits. This approach allows the total and isoenzyme measurements to be expressed in the same units. For example, antibodies to CK-M subunits inhibit half of CK-MB isoenzyme and all of CK-MM isoenzyme. Measurement of CK activity of a sample after incubation with an anti-M antibody can be used to determine the activity of non-M subunits of CK.

Antibodies can also be used as **capture** antibodies to separate a particular isoenzyme from other forms of the same enzyme, followed by measurement of enzymatic activity. Examples of such capture assays include tests for the bone isoenzyme of ALP and the bone and prostate isoenzymes of ACP. Some enzymes circulate bound to antiproteases, such as prostate-specific antigen (PSA; see Chapter 76) and α-1-antichymotrypsin or trypsin and α-1-antitrypsin. Antibodies may differ in their ability to measure free and bound forms. Some enzymes are also bound to β-2-macroglobulin, such as PSA (Otto et al., 1998) and ACP (Brehme et al., 1999); enzyme bound to this antiprotease usually is not enzymatically active and cannot be measured by most immunoassays because the binding site is hidden from antibody recognition. Finally, in common with other immunoassays, measurement of enzymes by immunoassay can show interferences from substances that bind to reagent antibodies, such as heterophile antibodies (Sosolik et al., 1997) and rheumatoid factor (Dasgupta et al., 1999).

INHIBITION OF ENZYMES

The inhibition of enzymes may be reversible or irreversible. In irreversible inhibition, a covalent bond is formed between the inhibitor and the enzyme, and enzyme activity cannot be restored by dissociation of the inhibitor. Examples include the inhibition of acetylcholinesterase (AChE) and pseudocholinesterase (PChE) by chemical warfare agents such as sarin and tabun that irreversibly phosphorylate the side chain **OH** group of the active-site serine residue. The first fluorinated anesthetic, fluroxene (**$CF_3CH_2OCH{=}CH_2$**) proved to be too toxic for use as a general anesthetic because it irreversibly alkylated a heme ring N atom in the cytochrome P450 monooxygenase responsible for its detoxification. This alkylation led to complete loss of enzyme activity.

Reversible inhibition is one of three types: competitive, uncompetitive, and noncompetitive. As noted earlier, if the presence of an inhibitor is suspected in an enzyme assay of a patient's sample, such as by observation of a nonlinear [P] versus time curve, an effective strategy is to dilute the sample so that the effect of the inhibitor is reduced. Even if this procedure concurrently dilutes the enzyme, the enzyme assay can still be effectively performed, especially if the substrate is present at saturating conditions.

COMPETITIVE INHIBITION

Competitive inhibition occurs when the inhibitor binds at the same site as the substrate. The molecular basis for the binding of competitive inhibitors at the active site is that the substrate and the inhibitor are structurally similar, with the result that the enzyme is "deceived" into recognizing and binding the inhibitor. Examples of competitive inhibition include the inhibition of trypsin by α-1-antitrypsin, chymotrypsin by α-1-antichymotrypsin, dihydrofolate reductase by the chemotherapeutic agent methotrexate, and the Krebs cycle enzyme succinic dehydrogenase by malonate. In serum assays, urea inhibits LD, and inorganic phosphate inhibits alkaline phosphatase. Fluoride ion competitively inhibits the glycolytic enzyme enolase. In some reactions, the product of the reaction, which may be structurally similar to the substrate, may competitively inhibit the reaction, a phenomenon known as **end-product inhibition.** A variation of this phenomenon can occur occasionally in which the buildup of the end-product can reverse the forward reaction, regenerating the substrate. Not infrequently, drugs are used as competitive inhibitors of targeted enzymes. For example, as discussed later, a major target of antihypertensive drugs is angiotensin-converting enzyme (ACE).

HOW COMPETITIVE INHIBITORS AFFECT THE MICHAELIS-MENTEN EQUATION

The kinetic mechanism for **competitive inhibition** is shown in Figure 21.6B. The inhibitor is assumed to be in rapid equilibrium with free **E** and the **EI** complex. Kinetically, the inhibitor reduces the concentration of free **E** available to combine with **S**. The equation of conservation of enzyme now reads

$$[E_T] = [E] + [EI] + [ES]. \qquad \text{(Eq. 21.24)}$$

[EI] is defined in terms of the equilibrium constant, $\mathbf{K_I}$, for the dissociation of the inhibitor from the **EI** complex, and

$$[EI] = [E]\,[I]/K_I \qquad \text{(Eq. 21.25)}$$

Because the steady-state equation for ES (Eqs. 21.3, 21.4, and 21.5) remains the same, Equation 21.24 becomes

$$E_T = E + [E]\,[S]/K_M + [E]\,[I]/K_I \qquad \text{(Eq. 21.26)}$$

$$[E] = \frac{[E_T]}{\left(1 + \frac{[S]}{K_M} + \frac{[I]}{K_I}\right)} \qquad \text{(Eq. 21.27)}$$

Because, as in Equation 21.2,

$$d[P]/dt = k_2[ES] = [E]\,[S]/K_M \qquad \text{(Eq. 21.28)}$$

$$\frac{dP}{dt} = \frac{k_2[S]}{K_M} \cdot \frac{[E_T]}{\left(1 + \frac{[S]}{K_M} + \frac{[I]}{K_I}\right)} \qquad \text{(Eq. 21.29)}$$

and

$$\frac{d[P]}{dt} = k_2[ES] = \frac{k_2[E_T]\,[S]}{K_M\left(1 + \frac{[I]}{K_I}\right) + [S]} \qquad \text{(Eq. 21.30)}$$

Note from this equation that the factor $(1 + [I]/K_I)$ multiplies K_M in the denominator. This means that K_M is multiplied by a number ≥1. Thus, if a competitive inhibitor is present at an appreciable concentration so that this factor > > 1, concentrations of S that would have saturated the enzyme will now no longer be able to do so. If a competitive inhibitor is present, its effect can be eliminated by increasing the substrate concentration such that $S >> K_M(1+[I]/K_I)$.

Reactions Schemes for the Three Types of Inhibitior of Enzyme-Catalyzed Reactions

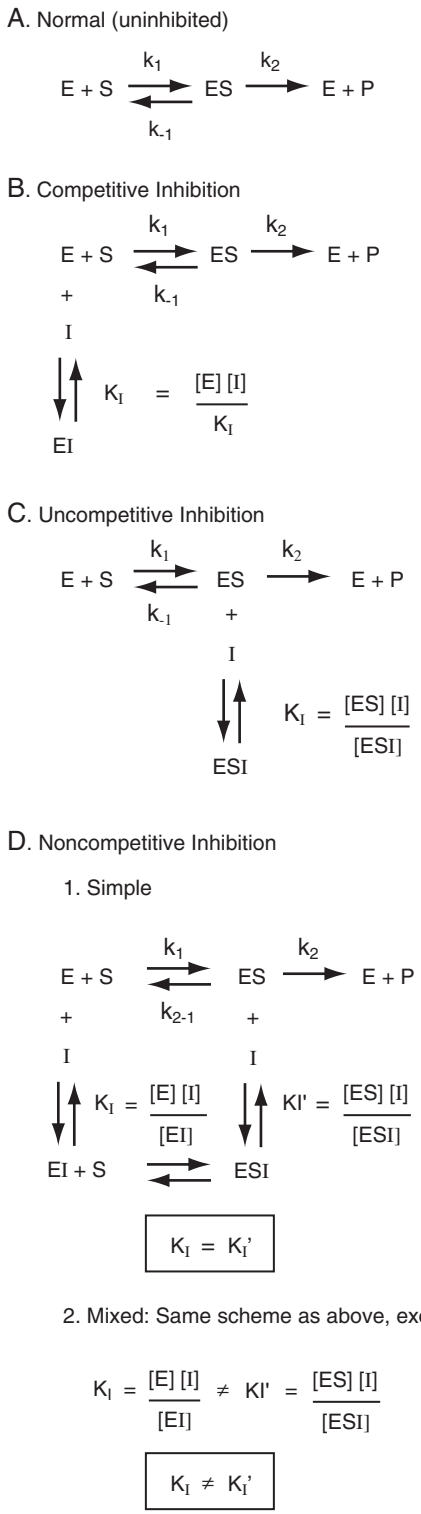

Figure 21.6 Schemes for all types of inhibition of enzyme activity. **A,** The scheme for an uninhibited reaction. **B,** The scheme for competitive inhibition, showing that the inhibitor binds competitively to free enzyme, decreasing the binding of the substrate to the free enzyme. This results in a lower apparent affinity of the substrate for the enzyme, making the apparent K_M higher than the true K_M. However, this inhibition does not affect the catalytic rate, V_{max}. K_I is the dissociation constant for the enzyme–inhibitor complex ([EI]). **C,** The scheme for uncompetitive inhibition, showing that the inhibitor binds only to the enzyme–substrate complex such that it blocks catalysis but not the binding of the substrate to the enzyme and therefore affects V_{max} but not K_M. K_I in this case is the dissociation constant for the enzyme–substrate–inhibitor ternary complex ([ESI]). **D,** The scheme for noncompetitive inhibition, which is of two types: (1) simple and (2) mixed. In both cases, the inhibitor binds both to the free enzyme *and* to the enzyme-substrate complex, affecting both V_{max} and K_M. In simple noncompetitive inhibition (1), the affinity of the inhibitor both for the free enzyme and for the enzyme–substrate complex is the same, making the two respective dissociation constants, K_I and K_I', equal. In mixed noncompetitive inhibition (2), K_I and K_I' are not equal.

Inversion of Equation 21.30 gives the Lineweaver-Burk linear transform as follows:

$$\frac{1}{V_0} = \frac{K_M\left(1 + \frac{[I]}{K_I}\right)}{V_{MAX}} \cdot \frac{1}{[S]} + \frac{1}{V_{MAX}} \qquad \text{(Eq. 21.31)}$$

Plots of $1/v_o$ versus $1/[S]$ at different inhibitor concentrations give linear traces in which the slope, but not the intercept, is altered in the presence of a competitive inhibitor. V_{max} is unchanged, and only K_M is altered. K_M is modified by the coefficient $(1 + [I]/K_I)$. The X-intercept of this equation (where $1/v_o$ is 0) is $-1/[(1 + I/K_I)K_M]$. The effect of competitive inhibitors on enzyme-catalyzed reactions is summarized in Figure 21.7.

UNCOMPETITIVE INHIBITION

As shown in Figure 21.6C, **uncompetitive** inhibition occurs when the inhibitor binds only to the ES complex and not to free E. Therefore, no EI complex forms. Binding of the substrate causes a conformational change, creating a site for binding of the inhibitor. An example of uncompetitive inhibition is the inhibition of tertiary amines, like choline, on acetylcholinesterase.

EFFECT OF UNCOMPETITIVE INHIBITORS ON THE MICHAELIS-MENTEN EQUATION

In keeping with a similar procedure that was used for deriving Equation 21.30, we obtain the following expression:

$$V_0 = \frac{V_{MAX}[S]}{K_M + [S]\left(1 + \frac{[I]}{K_I}\right)} \qquad \text{(Eq. 21.32)}$$

Note here that the same factor, $(1 + [I]/K_I)$, now multiplies S, rather than K_M, in the denominator of the Michaelis-Menten equation, as in the case of competitive inhibition discussed previously. This has the paradoxical effect of causing saturation to be reached at *lower* values of S than for the normal, uninhibited case (see Fig. 21.6) because S is multiplied by a factor that is >1. However, the *rate* of the uncompetitively inhibited enzyme-catalyzed reaction at saturation is *lower* than it normally should be; the maximal rate at saturation is $V_{max}/(1 + I/K_I)$. No matter how high the substrate concentration is in this case, the normal rate at saturation, that is, V_{max}, cannot be reached, unlike in the case of competitive inhibition discussed in the preceding section.

At low **[S]** values, v_o approaches $V_{max}/K_M[S]$, as for the uninhibited case, and the uncompetitive inhibitor is without effect. This suggests that dilution of the specimen will remove the effect of the inhibitor and will enable the uninhibited rate of the reaction to be determined. Under these conditions, E_T or activity can be directly computed from the first-order kinetic analysis (Eq. 21.19) at low substrate concentration.

The double reciprocal form of Equation 21.32 is as follows:

$$\frac{1}{V_0} = \frac{K_M}{V_{MAX}} \cdot \frac{1}{[S]} + \left(1 + \frac{[I]}{K_I}\right) \cdot \frac{1}{V_{MAX}} \qquad \text{(Eq. 21.33)}$$

The Lineweaver-Burk plot of this equation has a slope that is the same as for the uninhibited (normal) reaction, but the intercept, $(1/V_{max})(1 + [I]/K_I)$, will be higher for uncompetitive inhibition than for the normal case, that is, $1/V_{max}$, as shown in Figure 21.6C. The X-intercept (where $1/v_o = 0$) is $-(1 + [I]/K_I)/K_M$. If [I] is known, either intercept can be used to compute K_I. The effect of uncompetitive inhibitors on enzyme-catalyzed reactions is summarized in Figure 21.7.

SIMPLE AND MIXED NONCOMPETITIVE INHIBITION

Noncompetitive inhibition occurs when the inhibitor, similar to the uncompetitive inhibitor, binds at a site distinct from the substrate-binding site. Both the inhibitor and the substrate are capable of binding the enzyme simultaneously. Binding of the inhibitor to this second site may completely abolish enzyme activity or may only partially reduce it. Hence, noncompetitive inhibition may be **full** or **partial**. An example is the noncompetitive inhibition of pyruvate kinase by alanine. Unlike

uncompetitive inhibitors, noncompetitive inhibitors bind both to free E and to ES. If the binding of the inhibitor and of the substrate occurs independently of each other, **simple noncompetitive inhibition** exists. If bound substrate alters the affinity of the enzyme for the inhibitor, a condition of **mixed competitive inhibition** exists. Binding of the noncompetitive inhibitor alters the conformation of the substrate-binding site. The substrate can still bind; however, the binding affinity and/or the catalytic activity are reduced.

EFFECTS OF NONCOMPETITIVE INHIBITORS ON THE MICHAELIS-MENTEN EQUATION

The kinetic scheme for this type of inhibition is shown in Figure 21.6D. Here, the inhibitor can bind *both* to the free enzyme *and* to the enzyme-substrate complex. If the affinity or dissociation constants for each of these processes are the same, as shown in Figure 21.6, then the pattern appears to be a combination of competitive and uncompetitive inhibition and is termed *simple noncompetitive inhibition*. Thus, in this case, the term $(1 + [I]/K_I)$ multiplies both terms in the denominator of the Michaelis-Menten equation (see Eq. 21.10), or

$$V_0 = \frac{V_{MAX} \cdot [S]}{\left(1 + \frac{[I]}{K_I}\right) \cdot K_M + \left(1 + \frac{[I]}{K_I}\right) \cdot [S]} \qquad \text{(Eq. 21.34)}$$

If the two K_I constants differ, the inhibition is termed mixed *noncompetitive inhibition*. For this latter case, if K_I is the dissociation constant for the inhibitor when it binds to free enzyme, and if K_I' is the dissociation constant for the inhibitor when it binds to the enzyme-substrate complex, then the Michaelis-Menten rate law for noncompetitive inhibition is

$$V_0 = V_{MAX}[S] / \left[(1 + I/K_I)\, K_M + \left(1 + I/K_I'\right)[S]\right] \qquad \text{(Eq. 21.35)}$$

The Lineweaver-Burk equation for simple noncompetitive inhibition is

$$\frac{1}{V_0} = \frac{K_M}{V_{MAX}} \cdot \left(1 + \frac{[I]}{K_I}\right) \cdot \frac{1}{[S]} + \frac{1}{V_{MAX}} \cdot \left(1 + \frac{[I]}{K_I}\right) \qquad \text{(Eq. 21.36)}$$

And, for mixed inhibition,

$$\frac{1}{V_0} = \frac{K_M}{V_{MAX}} \cdot \left(1 + \frac{[I]}{K_I}\right) \cdot \frac{1}{[S]} + \frac{1}{V_{MAX}} + \left(1 + \frac{[I]}{K_I'}\right) \qquad \text{(Eq. 21.37)}$$

As can be seen from Equation 21.35, for simple noncompetitive inhibition, in the presence of inhibitor, both the slope and the intercept increase in value by the factor $(1 + [I]/K_I)$. This result is based on the assumption that the substrate does not modify the affinity of the enzyme for the inhibitor, and vice versa. Note that, because the inhibitor binds to the enzyme-substrate complex, thereby inactivating it, the maximal velocity is lowered, as was the case for uncompetitive inhibition, as discussed earlier. Therefore, the intercept for this condition is $1/V_{max}$ $(1 + [I]/K_I)$, that is, instead of $1/V_{max}$ as in the normal case. Likewise, K_M is increased by the same factor. However, as discussed previously, K_M is computed as the **ratio** of the slope of the Lineweaver-Burk plot to the intercept. Because both of these terms contain the factor $(1 + [I]/K_I)$, this factor cancels, and the computation yields the value of the actual K_M. This, of course, does not happen in mixed noncompetitive inhibition, in which the two constants for inhibitor binding differ from one another. In this case, K_M^{app} is $K_M \bullet (1 + [I]/K_I)/(1 + [I]/K_I')$. The X-intercept for simple noncompetitive inhibition from Equation 21.36 is $-1/K_M$; for mixed noncompetitive inhibition, it is $-(1 + [I]/K_I')/(1 + [I]/K_I)K_M$. The effect of simple noncompetitive inhibitors (that have the same K_I value for free enzyme and enzyme-substrate complex) on enzyme-catalyzed reactions is summarized in Figure 21.7.

Table 21.4 summarizes changes in the apparent values of V_{max} and K_M derived from the intercepts and slopes of double reciprocal Lineweaver-Burk plots for competitive, uncompetitive, and simple noncompetitive inhibition. Figure 21.7 summarizes the Lineweaver-Burk plots for a normal enzyme-catalyzed reaction and for the three types of inhibition of enzyme-catalyzed reactions and the values of the Y- and X-intercepts in each condition.

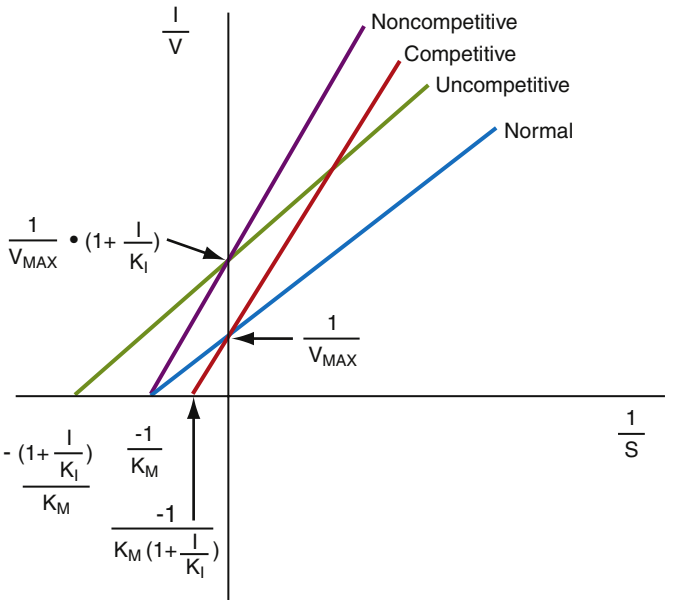

Figure 21.7 Lineweaver-Burk plots for each type of inhibition shown in Figure 21.6, showing Y- and X-intercepts. To avoid cluttering, the slopes are not shown. The slopes of the lines for uninhibited reaction *(blue)* and uncompetitive inhibition *(green)* are K_M/V_{max}. The slopes of the lines for competitive *(red)* and noncompetitive *(purple)* inhibitions are K_M $(1 + I/K_I)$.

CATALYTIC EFFICIENCY: TRANSITION STATE THEORY AND DRUG DESIGN

Equation 21.19 applies to circumstances in which the substrate concentration is present at concentrations below the value of K_M for an enzyme. The rate constant for this reaction is k_2/K_M, which is formally a second-order rate constant because this reaction depends on the concentrations of both the substrate and the enzyme. (As noted previously, the reaction is actually pseudo–first-order in that the total enzyme concentration, E_T, is constant and only the substrate concentration, [S], changes.) Catalytic efficiency is assessed in terms of the rate constants of the catalyzed reaction. The constant k_2/K_M, often written as k_{cat}/K_M, is a reflection of the frequency of productive encounters of enzyme and substrate molecules in solution.

ENZYMES ACHIEVE HIGH RATES OF REACTION THAT GREATLY EXCEED THOSE FOR UNCATALYZED REACTIONS

An upper boundary to the frequency of encounters is determined by the temperature and the diffusion coefficients of the substrate and enzyme. This limiting value is on the order of 10^8 to 10^9 $M^{-1}sec^{-1}$, called the *diffusion-controlled limit*. If the value of k_{cat}/K_M is at the diffusion-controlled limit, every encounter of the enzyme and substrate leads to product formation and the enzyme has achieved what may be termed *catalytic perfection*. Some enzymes have actually approached this state. These include superoxide dismutase ($k_{cat}/K_M = 2.8 \times 10^9$ $M^{-1}sec^{-1}$), AChE ($k_{cat}/K_M = 1.5 \times 10^8$ $M^{-1}sec^{-1}$), and catalase ($k_{cat}/K_M = 4.0 \times 10^8$ $M^{-1}sec^{-1}$). Most other enzymes do not have constants of this magnitude but have values that vastly exceed those for the corresponding uncatalyzed reactions, the second-order rate constants that are termed k_{uncat} (*uncatalyzed*).

The ratio k_{cat}/k_{uncat} gives the rate enhancement, which is often difficult to obtain because most cellular reactions occur very slowly in the absence of enzymes. For enzymes, rates are in the range of 10^8 to 10^{12}, but some are even higher. For example, the rate acceleration for adenosine deaminase, which catalyzes the deamination of adenosine to inosine, is 10^{14}, and the rate acceleration of ALP is 10^{17}. Both adenosine deaminase and ALP have modest k_{cat} values, 10^2 sec^{-1}. Their unusually large rate accelerations stem from the stability of their substrates at pH 7.0 and 25° C. For example, the half-time for the deamination of adenosine to inosine at 20° C and pH 7.0 is approximately 20,000 years, and k_{uncat} is 10^{-12} sec^{-1}! The nonenzymatic rate constant for the hydrolysis of phosphate esters under neutral, room temperature conditions is estimated to be on the order of 10^{-15} sec^{-1}. The question arises as to how enzymes can induce such large rate enhancements and, in some instances, attain rates that are the highest that can physically be achieved.

TABLE 21.4

Slopes and Intercepts from Double Reciprocal Plots and Computed Values of V_{max} and K_M from These Plots for Various Types of Reversible Inhibitors

Type of Inhibition	Slope	Y-Intercept	X-Intercept	V_{max} (apparent)*	K_M (Apparent)*
None	K_M/V_{max}	$1/V_{max}$	$-1/K_M$	V_{max}	K_M
Competitive	$(K_M/V_M)(1 + I/K_I)$	$1/V_{max}$	$-1/[K_M(1 + I/K_I)]$	V_{max}	$K_M(1 + I/K_I)$
Uncompetitive	K_M/V_{max}	$(1/V_{max}) \bullet (1 + I/K_I)$	$-(1 + I/K_I)/K_M$	$V_{max}/(1 + I/K_I)$	K_M
Noncompetitive (simple)	$K_M/V_{max} \bullet (1 + I/K_I)$	$(1/V_{max}) \bullet (1 + I/K_I)$	$-1/K_M$	$V_{max}/(1 + I/K_I)$	K_M

*The observed value that equals the derived expression from the double reciprocal plots shown for each condition.

ENZYMES ACHIEVE HIGH RATE ENHANCEMENTS BY BINDING TO THE TRANSITION STATE ON THE REACTION PATHWAY

From Figure 21.3, it can be seen that when the enzyme binds noncovalently to the substrate, if the energy of the resulting enzyme-substrate complex is lowered significantly relative to the energies of the separated species, this would lead to an increased activation energy. However, if the enzyme stabilizes the transition state leading to the formation of products, then the activation energy would be greatly lowered, as indicated in Figure 21.3. Considerable accumulating evidence suggests that enzymes have high affinities for **transition states.** Because, in the transition state, the substrate is somewhat distorted from its ground state structure by the incipient breaking and making of covalent bonds, the resulting increase in energy of the substrate is greater than that compensated by favorable interactions of the distorted substrate with the enzyme. It should be realized that transition states in reactions are not stable structures but rather are inferred from knowledge of the reaction path. However, substrate molecules have been designed that have critical features of inferred transition states; these modified substrates have been found to bind to the enzymes with enhanced affinities (Fersht, 1999).

These considerations have direct clinical applicability in two areas: drug design and the advent of so-called *catalytic antibodies*, that is, antibodies that have been designed to have strong and specific enzyme activity. We give one example of each of these applications to illustrate the importance of transition state theory to practical clinical problems.

TRANSITION STATE THEORY IN DRUG DESIGN

HIV Protease Inhibitors in Treating HIV-AIDS

A host of new drugs have been developed as protease inhibitors that block the protease enzymes of the human immunodeficiency virus (HIV) involved in viral replication of the acquired immunodeficiency syndrome (AIDS) virus (Vance et al., 1997). Proteases catalyze hydrolytic reactions in which peptide or amide bonds are cleaved by water into a carboxylic acid and a primary (or, in the case of proline, secondary) amine. HIV proteases are vital for cleaving large protein precursors into gag and pol proteins that enable viral replication. Absence of this protease activity results in inability of the virus to replicate. Thus, this protease has become the target for the design of inhibitory compounds (Vance et al., 1997).

HIV protease functions as a homodimer, that is, two subunits having the exact same sequence. It catalyzes the hydrolysis of X-Pro (proline) peptide bonds where X is an aromatic amino acid, such as phenylalanine (Phe) or tyrosine (Swain et al., 1990; Vance et al., 1997). Two critical aspartic acid residues (25 and 125) are known to be the actual catalytic residues effecting peptide bond cleavage (Swain et al., 1990). Thus, HIV protease, similar to a number of other proteases such as ACE, discussed in the next section, is an aspartic acid peptidase. It has been known for many years that the hydrolysis of peptide (and ester) bonds involves the formation of a so-called *tetrahedral intermediate*, as illustrated for a peptide bond in Figure 21.8. This intermediate results from the addition of water to the unsaturated carbonyl carbon on the reaction pathway. The carbonyl carbon and the three atoms to which it is attached all lie in the same plane, the so-called *planar configuration.* Attack by the oxygen atom of water on the carbonyl carbon results in the addition of a fourth atom attached to the carbonyl carbon, causing replacement of the planar arrangement of the atoms by a tetrahedral arrangement of these atoms. Note that the transition state leading to this intermediate is inferred also to have tetrahedral features and a partially negatively charged oxygen. Thus, substrates have been designed that have, in place of the normally occurring amide bond, a tetrahedral structure with an oxyanion or a hydroxyl group at this position that resembles the transition state.

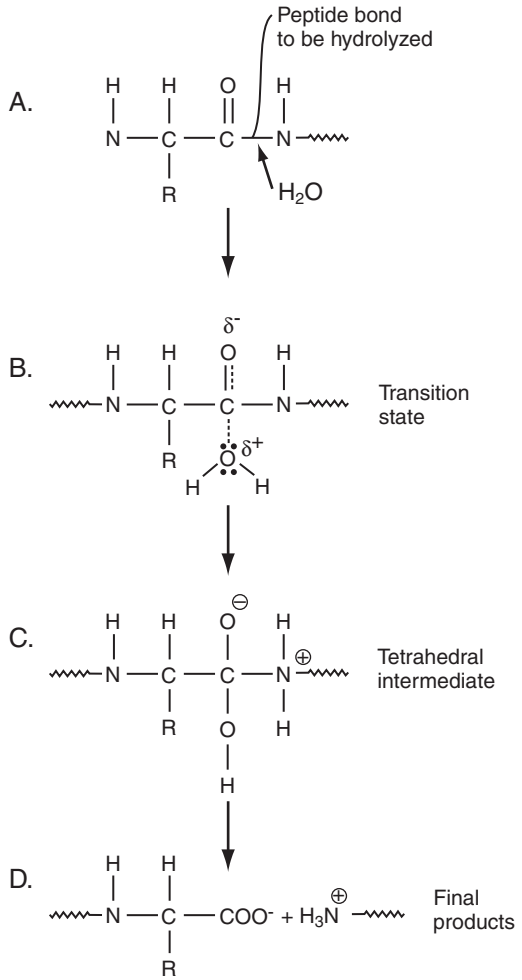

Figure 21.8 Steps in the hydrolysis of a peptide bond. **A,** A typical peptide bond for two amino acids in a peptide bond link. R is the side chain of the first amino acid. This bond will be cleaved by addition of water to the carbonyl group, as shown by the arrow. **B,** The transition state on the way to the addition of water to the carbonyl group. The carbonyl oxygen takes on a partial negative charge (δ^-). **C,** The tetrahedral intermediate that results from the addition of water. Note that an oxyanion forms on the former carbonyl oxygen. The attacking water molecule has given up a proton that can add to the amino nitrogen of the leaving group, that is, the amino acid on the right of the peptide bond, or to the oxyanion of the former carbonyl group. **D,** The final products, that is, a carboxylate from the left amino acid and an amine (ammonium ion) from the right amino acid.

An example of an inhibitory transition state analog of HIV protease is shown in Figure 21.9. For comparison, a typical substrate of HIV protease is also shown (Matayoshi et al., 1990). As can be seen in Figure 21.9, in the Phe residue in the transition state analog, the normally occurring planar C–O group in the peptide backbone is replaced with a tetrahedral C(H)–OH group, giving rise to the so-called *Phe-Psi residue*. This occurs at the normal peptide cleavage site. This analog binds to HIV protease with a K_I (dissociation constant) of 0.24 nM (Swain et al., 1990). The substrate has a K_M on the order of 103 μM (Matayoshi, 1990). This K_M is a true dissociation constant in that the k_2 is much lower than the noncovalent dissociation constant. Therefore, the ratio of the affinity constant (reciprocal of the

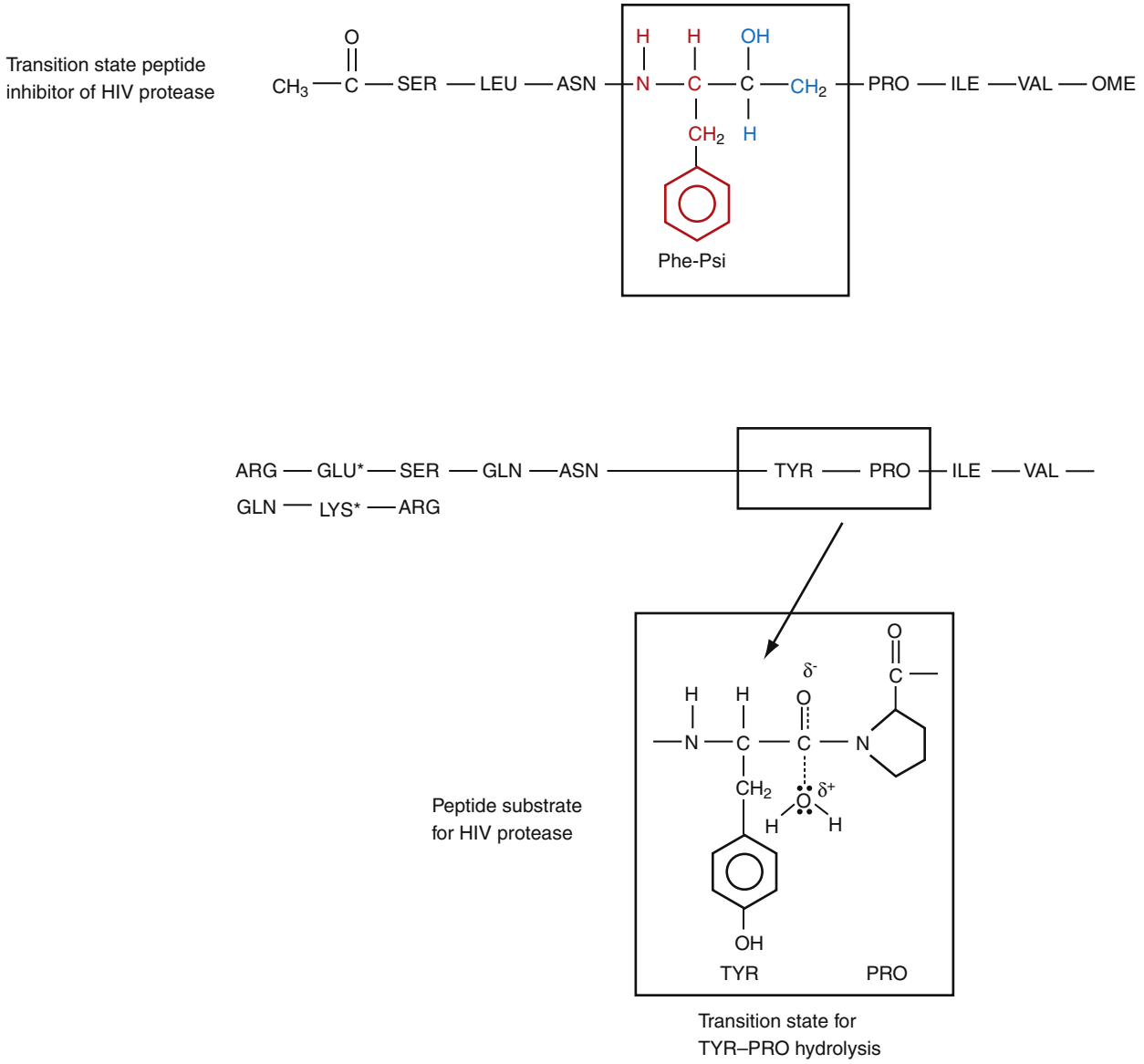

Figure 21.9 Human immunodeficiency virus (HIV) protease transition state analog peptide inhibitor. HIV protease cleaves at X-Pro bonds, where X is an aromatic amino acid such as Tyr and Phe. In this case, X is a modified Phe residue, labeled Phe-Psi, most of whose atoms are colored red such that, in place of the normally occurring C=O (carbonyl) group, a tetrahedral carbon is present attached to an OH group. The tetrahedral atoms are shown in blue. This mimics the transition state shown for a substrate of HIV protease whose amino acid sequence is shown below that for the transition state analog. This sequence contains the bond cleavage site, TYR-PRO, as shown in the small box. The tetrahedral transition state for this cleavage is shown in the larger box. The asterisks on the two substrate residues denote that these residues can be attached to fluorescent probes in an enzyme assay for this protease using this substrate. Because the transition state analog resembles the transition state in the hydrolysis of the Tyr-Pro peptide bond, it is a strong and specific inhibitor of the protease.

dissociation constant) for the transition state analog to that of the substrate is on the order of 400,000! Thus, the application of transition state theory has resulted in the design of a very potent HIV protease inhibitor. Newer HIV protease transition state inhibitors, such as the modified peptide KNI-272, that have substantially lower K_I values have been designed (Adachia et al., 2009). The x-ray crystal structures of the transition state analogs bound to HIV protease have been determined (Swain et al., 1990; Adachia et al., 2009). The two critical Asp residues interact strongly with the tetrahedral atoms of the modified Phe residue and are clearly involved in stabilization of the tetrahedral transition state (Swain et al., 1990; Adachia et al., 2009).

One drawback to the HIV protease inhibitors currently being used clinically in the treatment of AIDS is that viral mutations result in HIV proteases that have lower affinities for these inhibitors. More recently, therefore, new transition state analogs have been designed such that they interact with amino acid residues that surround the active site and actually bind to critical backbone atoms of sections of the polypeptide chain that have well-defined secondary structures (such as α-helices and β-sheets), greatly increasing their affinities (K_I's in the picomolar range) (Ghosh et al., 2008). In this case, because mutations of constant structural residues would be expected to decrease the stability of the protease greatly, it is hoped that viral mutations will have much less effect on their efficacies.

Design of New Catalytic Antibodies with Predetermined Enzyme Activity

Antibodies generally bind to antigens with high affinities. If antibodies can be raised to transition state analogs of compounds that undergo specific chemical reactions, by stabilizing the transition state for these specific chemical reactions they might themselves serve as enzymes that catalyze these reactions. Although still in its infancy, this area of enzymology has achieved some notable success, providing, in turn, further support for the transition state theory of enzyme action. As an example, a clinically important finding using this approach is seen in the design of antibodies that induce hydrolysis of cocaine. Hydrolysis of the benzoate and acetyl esters results in effective inactivation of this drug of abuse, as discussed in Chapter 24. The structure of cocaine and a tetrahedral transition state analog are shown in Figure 21.10 (Cashman et al., 2000). This analog has a tetrahedral structure for the benzoyl moiety in which a nonhydrolyzable phenyl phosphonate ester replaces the normally occurring carbonyl group. Antibodies have been raised to a thiol derivative of cocaine and then assayed for their abilities to bind to the transition state analog. Several antibodies have been isolated that bind strongly to the transition state analog and also catalyze, with large rate enhancements over the uncatalyzed reaction, the hydrolysis of the benzoyl ester of cocaine, resulting in a cocaine derivative of much lower potency. It is of considerable interest that, using another

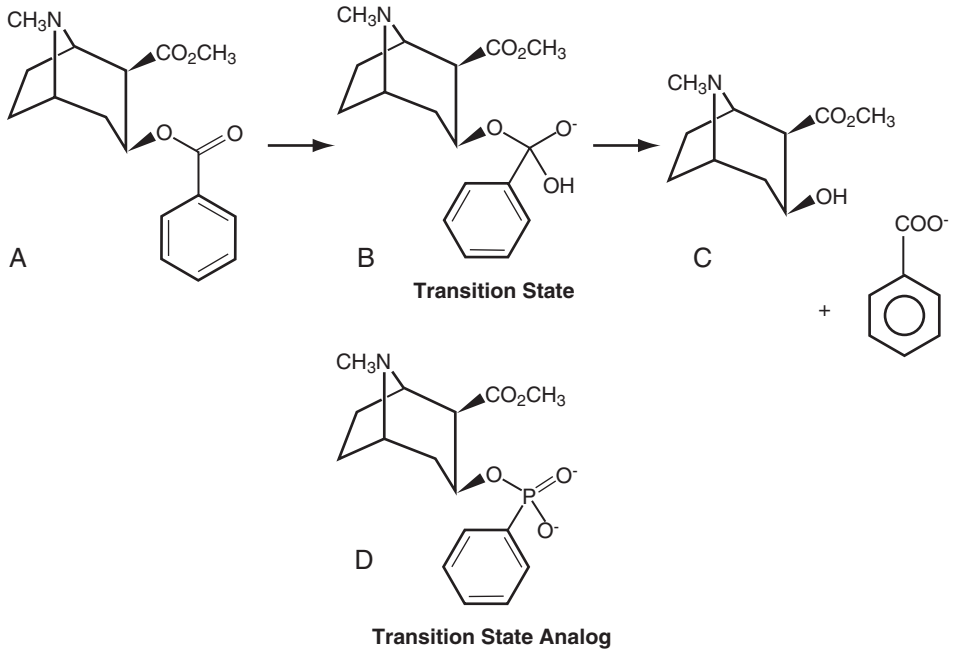

Figure 21.10 Hydrolysis of the benzoate ester moiety of cocaine (**A**) an ecgonine derivative, occurs via a tetrahedral intermediate (**B**) containing an oxyanion, and, presumably, a tetrahedral transition state resulting in the free –OH group of an ecgonine derivative shown in **C** and benzoic acid. This results in a cocaine derivative that is much less active. **D,** A nonhydrolyzable benzyl phosphonate ester transition state analog that has a tetrahedral structure that likewise contains an oxyanion. An antibody that binds with high affinity to this analog has been found to catalyze the hydrolysis of cocaine with a greatly enhanced rate over that for the noncatalyzed reaction.

approach, the serum enzyme butyrylcholinesterase, discussed in the next section, has been modified based on the x-ray crystal structure of this enzyme bound to inhibitors using site-specific mutagenesis techniques so that it is active in the debenzoylation of cocaine, leading to its inactivation. The rates of catalysis of the catalytic antibodies and the engineered butyrylcholinesterase are similar to one another. Both approaches may provide rational treatment modalities for detoxification of harmful substances, in this case, drugs of abuse.

SPECIFIC ENZYMES

Numerous enzymes are clinically useful in recognition and monitoring of particular disease processes. In all but a few circumstances, abnormal conditions in specific tissues are recognized by *elevations* of one or more enzymatic activities or enzyme concentrations. For example, elevations of the activity of serum CK suggest the presence of muscle disease. The reason for elevation of specific enzymes in blood and other body fluids as the result of disease processes in specific tissues is not completely understood. One explanation for this occurrence is that disease processes that cause cell injury or death result in damage to the cell membrane, leading to the release of specific intracellular enzymes into tissue spaces and the microvasculature, causing increased enzymatic activity in serum or other body fluids. On occasion, mutant forms of enzymes occur, resulting in *lowering* of their activities although, generally, not of their concentrations. One prominent example of this phenomenon is butyrylcholinesterase (discussed earlier and later).

Several enzymes are distributed predominantly in a single tissue so that damage to this tissue results in elevations of the enzyme in serum. For example, as discussed in Chapter 22 on liver function, elevation of the level of the enzyme ALT, which is distributed predominantly in the liver, indicates acute hepatic injury, often as a result of hepatitis. Although measured by immunoassay, PSA is a form of chymotrypsin and occurs almost exclusively in the prostate gland. Serum elevations of PSA, therefore, suggest prostate pathology, often prostate cancer. Other enzymes do not have selective tissue distributions but have isozymes that do have selective distributions, making elevations of these isozymes valuable in diagnosing specific tissue pathology. For example, as discussed in Chapter 19, elevation of serum levels of CK-MB (also, see previous discussion) points to myocardial disease, most often infarction. As discussed later, elevations of specific isozymes of ALP point to specific tissue disease. The biliary tract form is elevated in biliary disease and the bone form is elevated in diseases of bone.

For enzymes with no tissue-specific isozymes, the relative amounts of different enzymes in plasma provide a clue as to the type of organ injured. For example, LD, AST, and ALT are found in many organs, but the relative amounts in each differ (Table 21.5). If LD is markedly elevated while AST and ALT are only slightly elevated, this would suggest damage to an organ or tissue (such as red blood cells, white blood cells, or tumors) with a high LD/AST ratio. On the other hand, if AST and ALT are elevated but LD is only slightly elevated, this suggests damage to liver, which has a low LD/AST ratio.

TABLE 21.5

Relative Amounts of Enzymes in Various Organs (Relative to Serum)*

Tissue	AST†	ALT	LD	CK
Liver	7000	3000	7000	
Kidney	4500	1200	500	10
Brain				1700
Spleen	700	150		
Heart	8000	500	600	5000–8000
Skeletal muscle	5000	300	700	20,000–30,000
Smooth muscle				300–600
Red blood cells	15	7	500	0

ALT, Alanine aminotransferase; *AST,* aspartate transaminase; *CK,* creatine kinase; *IU,* international unit; *LD,* lactate dehydrogenase.
*Relative amount is calculated by dividing the activity of enzyme in tissue (in IU/kg of tissue) by the upper reference limit of plasma activity of the enzyme (in IU/L), assuming that 1 L of plasma = 1 kg. Because the data are derived from multiple publications, the relative amounts among enzymes may be approximate, but the relative amount of a single enzyme in each tissue is accurate.
†Total amount in cells; varying amounts represent mitochondrial isoenzyme, which reaches serum in only small amounts.

Many other enzymes, elevations of which denote damage to specific tissues, are discussed in other chapters of this book. Discussion of enzymes and enzyme inhibitors in serum and urine for recognition of renal disease is found in Chapter 15; enzymes of bone metabolism are presented in Chapter 16; enzymes and other proteins utilized for the diagnosis of myocardial infarction are discussed in Chapter 19; enzymes useful in recognition of liver and biliary tract disease are discussed in Chapter 22; pancreatic enzymes are covered in Chapter 23; and enzyme deficiencies that produce hemolytic anemia are discussed in Part 4. Commonly used assays for these enzymes are discussed in Chapter 28.

The remainder of this chapter is concerned with a discussion of enzymes, each of whose isozymes is specific for a different tissue (e.g., acid and alkaline phosphatases, 5′-NT, LD), and two enzymes that are not tissue specific but whose activities have major systemic effects: ACE, vital for control of blood pressure, and AChE, which is critical in neuromuscular and sympathetic nervous system transmission.

ACID PHOSPHATASE (EC 3.1.3.2)

Biochemistry and Physiology

ACPs belong to the hydrolase class of enzymes (see Table 21.1) and occur as several isoenzymes with a common enzymatic function (the hydrolytic breakdown of phosphate monoesters). They all show optimal enzyme activity below a pH of 7.0. They possess some tissue specificity (greatest

concentrations occur in prostate, liver, spleen, erythrocytes, and bone). The major forms are coded for by different genes and possess different molecular weights and structures, as well as differences in sensitivity to tartrate inhibition. Lysosomal, prostatic, erythrocyte, macrophage, and osteoclastic ACPs are five important types found in humans. Normally, concentrations in serum are low (Moss & Henderson, 1999; Bull et al., 2002). The activity of erythrocyte ACP can be distinguished from that of the other ACP isoenzymes in that it is inhibited by 2% formaldehyde solution and 1-mM cupric sulfate solution. This is in contrast to the other isoenzymes, which are not inhibited by these agents. In addition, erythrocyte ACP is not inhibited by 20-mM tartrate solution, which does inhibit the other isoenzymes. It is important to note that tartrate-resistant acid phosphatase (TRAP) is present in certain chronic leukemias and some lymphomas, most notably in hairy cell leukemia, as described in Chapter 34. In addition, a particular isoform of TRAP, called *TRAP-5b*, occurs predominantly in osteoclasts in bone marrow and is used as a marker for bone remodeling (Lu et al., 2006). It has also been proposed as a marker for metastatic cancer (e.g., breast cancer) in bone marrow (Chao et al., 2005).

Reference Ranges and Preanalytic Variation

Reference values depend on age, gender, and hormonal status (in women). Total and tartrate-resistant ACP values are high in children, rising through the first decade to peak at three to four times adult levels in adolescence, paralleling changes in ALP (Chen et al., 1979). In the late teen years, levels decline to adult values that are constant to approximately 80 years of age in both genders. Normal men and women up to about 55 years of age have the same reference ranges for ACP. In women, total and tartrate-resistant ACPs increase after menopause (Schiele et al., 1988) and increase with the use of depot medroxyprogesterone acetate in premenopausal women (Mukherjea et al., 1981).

The enzymatic activity of ACP is unstable at normal plasma pH; specimens must be acidified to prevent loss of ACP activity (Theodorsen, 1985). The effect of specimen pH is not as consistently seen with immunoassays for prostatic ACP; some studies have recommended routine use of acidification for all ACP specimens, but it is not clear that this is essential (Panteghini et al., 1992).

The half-life of prostatic ACP is about 1 to 3 hours (Wadstrom et al., 1985). Day-to-day variation in ACP is relatively high; average variation of the prostatic isoenzyme is 30% (Maatman, 1993), although it may be as high as 100% in patients with prostatic carcinoma (Brenckman et al., 1981), and bone isoenzyme variation averages about 35% (Panteghini & Pagani, 1995).

Measurement

Assays for all phosphatases utilize the strategy that phosphate esters, which have no visible light absorbance, are hydrolyzed to inorganic phosphate and a strongly visible light-absorbing alcohol or alcohol anion. Total ACP is typically measured by its ability to cleave phosphate groups at an acid pH. Usually, the test is utilized for the measurement of prostatic serum ACP in the diagnosis or monitoring of prostatic adenocarcinoma. A variety of substrates and conditions have been used to measure enzymatic activity with increased specificity; these include thymolphthalein monophosphate and α-naphthyl phosphate, both of which give rise to strongly absorbing products, α-naphthol and thymolphthalein. *High bilirubin causes falsely low values for TRAP activity* but not for total ACP (Alvarez et al., 1999).

Isozymes of ACP can be separated by electrophoresis (Moss, 1986); however, there is usually little interest in isoenzymes other than prostate and bone. Immunoassays (Bull et al., 2002) for both prostatic and bone isoenzymes of ACP have been developed; the former are widely available. The reference range for serum ACP is ≤ 2 ng/mL.

Causes of Abnormal Results

The main cause of increased ACP is prostate disease; with development of PSA as the major serum test for prostate (see Chapter 76), ACP has become less popular for use in prostate cancer although, with the availability of newer immunochemical methods, its use in the diagnosis of prostate cancer has been maintained (Pontes, 2006). In early prostate cancer, the sensitivity of ACP is inferior to that of PSA (Burnett et al., 1992) although ACP, similar to PSA, is elevated in a significant percentage of patients with benign prostatic hyperplasia (Salo et al., 1990) or prostatic infarction, making ACP of little use for prostate cancer screening (Kaplan et al., 1985). Almost all patients with prostate cancer and elevated ACP have extracapsular extension or metastases (Salo et al., 1990; Burnett et al., 1992); thus, an elevated ACP may provide useful information in staging of patients. Occasionally, elevated prostatic ACP may be due to other causes. Urinary tract obstruction and acute urinary retention may cause elevated ACP (Collier & Pain, 1986). Extensive prostatic massage, prostatic inflammation, infarction/ischemia, and prostatic manipulations such as needle biopsy and cystoscopy may also cause a transient increase in serum ACP; testing should be done before any procedures are performed.

After surgical treatment of prostate cancer, ACP falls faster than PSA (Price et al., 1991), and levels should become undetectable after complete tumor resection. Because PSA is an androgen-dependent protein, androgen deprivation therapy decreases PSA production but has no effect on ACP (Price et al., 1991; Narayan et al., 1995), suggesting that ACP may be of use in monitoring patients treated in this fashion.

Another important use of ACP is in the differential diagnosis of acute lymphoblastic leukemia (ALL). ALL of T-cell origin is ACP positive while ALL of B-cell origin is ACP negative (Catovsky, 1978).

ACP has been used for many years in cases of suspected rape. Fluid collected from the vagina on a cotton swab will give a positive test for ACP if semen is present, provided that a stabilizing fluid with an acidic pH is used (Ricci & Hoffman, 1982). Peak values are generally present in the first 12 hours, and values remain elevated for up to 4 days.

There has been a recent interest in the use of TRAP as a tumor marker for following specific tumors. In one study, it was found that expression of this enzyme in gastric carcinoma cells is associated with an increased probability of peritoneal involvement (Kawamura et al., 2014). On the other hand, another study found that expression of TRAP by specific subclasses of macrophages in patients with colon cancer was associated with a 22% increase in 5-year survival and a 47% risk reduction in death due to this disease (How et al., 2014).

ALKALINE PHOSPHATASE (EC 3.1.3.1)

Biochemistry and Physiology (Sharma, 2014)

Similar to ACP, ALPs are a type of hydrolase (see Table 21.1). Discussion of ALP in the canalicular (biliary) system can be found in Chapter 22 on liver function. ALPs represent a family of enzymes coded for by different genes. Their physiologic role is not completely understood. The most abundant plasma ALP isoforms are coded for by a single gene on chromosome 1, producing the tissue-nonspecific isozyme found in the kidney, liver, and bone. However, in different tissues, this **parent** isozyme is subjected to different posttranslational modifications, resulting in differences in their carbohydrate side chains. Two other genes on chromosome 2 code for ALP of placental and intestinal origin; another gene on chromosome 2 codes for the so-called *germ cell* or placental-like isoenzyme, which has some antigenic and physical similarities to the placental isozyme (Sharma, 2014).

In cells, ALP is primarily bound to cell membranes, where it appears to be involved in cleavage of phosphate-containing compounds and may facilitate movement of substances across cell membranes. Hepatocytes produce ALP in the liver, where it is found attached to the canalicular surface of the cells (see Chapter 22). Osteoblasts produce bone ALP, which appears to be involved in cleavage of pyrophosphate, an inhibitor of bone mineralization. Intestinal epithelial cells produce intestinal ALP, which is released into the intestine following ingestion of fatty foods.

There appear to be different mechanisms for release of ALP from cells, leading to varying forms of ALP in plasma. With liver injury, ALP synthesis increases, but bile acids dissolve fragments of canalicular cell membranes with attached enzymes (including ALP, GGT, leucine aminopeptidase, and 5′-NT [Moss, 1997]). In normal serum, a single form (of liver or bone origin) of ALP is typically seen. However, with hepatobiliary disease, both the normal product and the membrane-attachment form (high molecular weight) bound to lipoproteins can be found (Wolf, 1994). The intestinal isoenzyme of ALP is released in large amounts into duodenal fluid (Deng et al., 1992), and large amounts enter lymphatic fluid, draining the intestinal tract following a meal (Reynoso & Elias, 1971). However, much of the isoenzyme apparently becomes bound to red blood cell (RBC) ABO antigens (Bayer et al., 1980), so that only small amounts reach the plasma except in individuals who possess both the secretor gene and a large amount of H substance (group O or B), where ALP may increase by up to 30 IU/L following a meal (Domar et al., 1993). ALP is also higher in individuals of blood group O or B than in A and AB individuals (Agbedana & Yeldu, 1996) because of differences in intestinal ALP levels (Domar et al., 1993). It is curious that placental ALP is also lower in pregnant women of groups A and AB (Ind et al., 1994).

The half-lives of isoenzymes of ALP differ significantly. Thus, it is necessary to know the isoenzyme that is elevated before rate of clearance can be evaluated: intestine, minutes; bone, 1 day; liver, 3 days; and placenta, 7 days. Day-to-day variation in total ALP is 5% to 10%, although the bone isozyme shows 20% day-to-day variability.

TABLE 21.6

Relative Levels of Enzymes by Gender, Relative to Young Adult Males (1.0)*

		AGE, YEARS							
Enzyme	**Gender**	**8**	**12**	**16**	**22**	**30**	**40**	**50**	**60**
Aspartate aminotransferase	Male	0.75	0.86	0.82	1.00	1.16	1.26	1.21	1.11
	Female	0.73	0.80	0.69	0.89	0.89	1.01	0.77	0.96
Alanine aminotransferase	Male	1.14	1.09	0.89	1.00	1.03	1.11	1.06	0.83
	Female	0.11	0.89	0.83	0.75	0.75	0.75	0.72	0.83
Alkaline phosphatase	Male	3.61	4.76	4.48	1.52	1.00	1.00	0.95	0.95
	Female	3.14	4.10	2.52	0.81	0.86	0.76	1.00	1.38
γ-glutamyl transferase	Male	0.25	0.29	0.37	0.62	1.00	1.07	1.16	0.99
	Female	0.24	0.28	0.33	0.38	0.52	0.58	0.9	1.09

Data from Siest G, Henry J, Schiele F, Young DS. *Interpretation of clinical laboratory tests: reference values and their biological variation*. Foster City, CA: Biomedical Publications; 1985.

*Results expressed as upper reference limits as a fraction of the upper reference limits for healthy young males.

Reference Ranges and Preanalytic Variation

Reference ranges for ALP are highly dependent on age and gender (Table 21.6). During childhood, levels gradually rise throughout the first decade, reaching peak values three to four times normal adult levels, and are higher in boys than in girls. The higher values in children are due to the bone isoenzyme. After a peak in the early teens, values gradually decrease to adult levels by the early 20s and are similar in men and women until 50 years of age. After menopause, the bone isoenzyme increases slightly in women, causing a rise in reference limits after 50 years of age. Reference limits are 15% higher in African American men and 10% higher in African American women (Manolio et al., 1992). Pregnancy causes a two- to threefold increase in ALP, mainly due to the placental isoenzyme, but also because of an increase in bone isoenzyme (Valenzuela et al., 1987).

A number of other factors affect ALP levels as well. High body mass index is associated with a 10% average increase in ALP (Salvaggio et al., 1991). Oral contraceptives decrease ALP by an average of 20% (Schiele et al., 1988; Dufour, 1998); fibric acid derivatives decrease total ALP by 25% and the liver isoenzyme by 40% (Day et al., 1993). Antiepileptic agents commonly cause increased total ALP, mainly because of increases in the liver isoenzyme. However, in some cases, the bone isozyme may also be elevated (Nijhawan et al., 1990). Smoking causes an average 10% increase in total ALP as the result of pulmonary production of placental-like ALP (Kallioniemi et al., 1987). Blood transfusion and cardiopulmonary bypass decrease alkaline phosphatase, often causing low levels (Kyd et al., 1998); this may be due to chelation of necessary cations by citrate.

Measurement

Although numerous methods are known, ALP activity is usually measured using *p*-nitrophenyl phosphate as the substrate at alkaline pH. Hydrolysis of this phosphate ester yields inorganic phosphate plus the highly colored (and, therefore, easily measured) *para*-nitrophenoxide anion. A variety of buffers are used to bind phosphate groups; this increases activity, because inorganic phosphate (as well as some other anions) inhibits ALP (competitive end-product inhibition). Zinc is a component of the enzyme; magnesium and other cations activate the enzyme. Chelators present in collection tubes (such as EDTA, citrate, and oxalate) falsely lower ALP activity; in the case of EDTA, activity is often too low to measure. The activity of the enzyme increases slowly on storage because of loss of inhibitors, but specimens are stable at 4° C for at least 6 days (Chua, 2017).

Isoforms

High-performance liquid chromatography (see Chapter 24) using weak anion-exchange columns has been able to separate at least six different isoforms of ALP in the sera of healthy individuals (Haarhaus et al., 2009). These are bone/intestinal (B/I), two bone isoforms, called B1 and B2, and three liver isoforms termed *L1*, *L2*, and *L3*. Recently, another bone isoform was isolated, termed *B1x*, that appears in the serum of dialysis patients (Swolin-Eide et al., 2006). These bone isoforms have been used to study low bone mineral disease (BMD) in patients with chronic kidney disease and have been found to rise in BMD of the hip, which is predominantly made up of trabecular bone. It is interesting to note that acid phosphatase TRAP-5b, discussed in the preceding section, was also found to be a marker for this condition (Haarhaus et al., 2009).

In addition, several other methods have been used to separate ALP isoenzymes. Inhibition by phenylalanine reduces reactivity of intestinal and placental isoenzymes, and levamisole inhibits bone and liver isoenzymes. Inhibition assays are poorly reproducible and are seldom used. Heat fractionation has been used for many years to determine the source of an elevated total ALP. The most heat-stable isoenzyme is placental (and germ cell) ALP; the liver isoenzyme is moderately stable, and the bone isoenzyme is the most heat labile. To achieve reliable results, use of standards of known composition and careful control of both temperature and time are essential. For these reasons, electrophoretic separation has been used for a number of years. Standard cellulose acetate and agarose gel electrophoresis cannot completely resolve bone and liver isoenzymes, making them unsuitable for other than qualitative studies. Because the difference between these isoenzymes is seen in their carbohydrate side chains, use of neuraminidase (to remove sialic acid) and wheat germ lectin (to bind to other isoenzymes) improves separation of bone and liver forms, allowing their quantitation. High-resolution electrophoresis using polyacrylamide gel and isoelectric focusing is capable of resolving multiple bands of ALP. Immunoassays for bone and placental isoenzymes of ALP are available commercially. Bone isoenzyme assays typically show some degree of cross-reactivity with the liver isoenzyme, and placental isoenzyme assays have varying cross-reactivity with the germ cell isoenzyme.

Causes of Abnormal Results

The most common causes of increased ALP are liver and bone disease. Hepatic causes of elevated ALP are discussed in greater detail in Chapter 22; disorders causing cholestasis more frequently cause elevation of ALP than do hepatocellular disorders. Increased osteoblastic activity in Paget disease, osteosarcoma, tumor metastatic to bone, and metabolic bone disease are the most common causes of elevated bone isoenzyme. It appears that acid phosphatase TRAP-5b is associated with bone resorption conditions and that the three major isoforms of bone ALP (B/I, B1, and B2) are associated with conditions involving bone deposition. Occasionally, patients will have elevations of both bone and liver isoenzymes, especially in metastatic carcinoma. Rarely, marked transient elevations of ALP occur, usually in children and often following trivial illness. These may reach several thousand IU/L and may persist for weeks to months before resolving (Steinherz & Steinherz, 1984).

Increases in intestinal ALP may occur in patients with intestinal infarction, inflammation, and ulceration. Increases in placenta-like isoenzymes, such as Regan and Nagao, are commonly found in patients with malignancies (ovary, cervix, lung, breast, colon, pancreas) and are due to ectopic production by the neoplasm.

As mentioned earlier, low ALP may occur transiently after blood transfusion or cardiopulmonary bypass. Prolonged, severely low ALP levels occur in hypophosphatasia, a rare inherited disorder of bone metabolism (Whyte et al., 1996), as the result of missense mutations of tissue-nonspecific ALP (Haarhaus et al., 2009). Decreased ALP can also occur in zinc deficiency because zinc is a necessary cofactor for ALP activity as well as other conditions.

Placental alkaline phosphatase (PLAP) is a useful tumor marker in serum and cerebrospinal fluid (CSF) for most germ cell tumors. In the latter case, CSF levels of PLAP are of diagnostic value in discerning whether a tumor in the pineal body is a pinealoma or a germ cell tumor. Because most germ cell tumors are radiosensitive, elevated CSF levels of PLAP suggest radiation treatment for this condition, allowing circumvention of surgical removal.

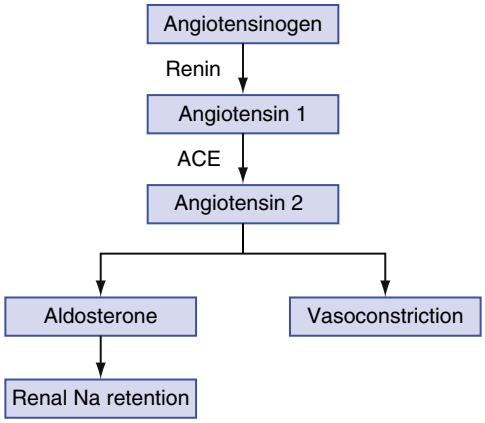

Figure 21.11 The renin-angiotensin system.

Elevated levels of alkaline phosphatase and phosphate have been found in patients with coronary artery disease but not in patients with stroke. However, levels of this enzyme appear to be an independent prognostic factor for long-term functional outcome post–cerebral infarction (Kim et al., 2013).

ANGIOTENSIN-CONVERTING ENZYME (EC 3.4.15.1)

Biochemistry and Physiology

ACE, also known as *kininase II* and *peptidyl-dipeptidase A*, belongs to the hydrolase class of enzymes (see Table 21.1) and is usually involved in the hydrolysis of peptide bonds at a free C-terminus, releasing the dipeptide His-Leu in the reaction. However, it may also act as an endopeptidase or an aminopeptidase. Its chief function is to cleave the His-Leu sequence from a decapeptide called *angiotensin 1*, whose sequence is Asp-Arg-Val-Tyr-Ile-His-Pro-Phe-His-Leu. This peptide, in turn, is cleaved by the enzyme renin from an α-2-macroglobulin called *angiotensinogen*, produced predominantly in the liver. Angiotensin 1 travels to the lungs, where ACE cleaves its carboxyl-terminal His-Leu peptide to produce angiotensin 2. The latter peptide has two major activities: it is a potent vasoconstrictor in arterioles and it induces the secretion of aldosterone from the zona glomerulosa of the adrenals. As discussed in both Chapters 9 and 25, aldosterone induces sodium retention in the collecting ducts in the kidneys, resulting in conservation of water. This action results in an increase in vascular volume. Therefore, by increasing arteriolar resistance via vasoconstriction and by increasing vascular volume, thereby increasing flow, angiotensin 2 induces higher arteriolar pressures. The renin-angiotensin system is summarized in Figure 21.11.

It is interesting to note that ACE also inactivates bradykinin (in the kallikrein-kinin system) by cleaving a dipeptide from its carboxyl terminus. Although the catalytic action of ACE is somewhat nonspecific in vitro, only angiotensin 1, bradykinin, and the hemoregulatory peptide Ac-DSKP are definite in vivo substrates (Macours et al., 2004). Because angiotensin 2 induces increased blood pressure, and because it is produced uniquely by the activity of ACE, the latter enzyme is a major target of competitively inhibiting drugs in the treatment of hypertension.

ACE consists of a single polypeptide chain, with two homologous, zinc-binding catalytic sites (ACE is a zinc-metalloprotease). Enzyme activity is lost if zinc is bound to a chelating agent, such as EDTA, or is replaced by a different cation. It is important to note that ACE, similar to HIV protease, as discussed earlier, is an aspartic acid protease; that is, two Asp residues are involved in catalysis at each active site. In cells, ACE is a transmembrane protein with a large amino-terminal extracellular domain, a very short hydrophobic transmembrane domain, and a small intracellular carboxyl-terminal domain. The cell-bound molecule is referred to as tissue ACE. The two catalytic sites are present in the extracellular domain: one near the amino-terminus and one nearer the carboxyl-terminus. The carboxyl-terminal active site is thought to harbor the predominant angiotensin 1 hydrolytic activity, and the amino-terminal active site has activity against bradykinin. Proteolytic cleavage releases the functional enzyme from the cell membrane into the extracellular environment, producing circulating ACE.

The majority of ACE is tissue bound (>90%), with much lower levels circulating in plasma. ACE is found predominantly in endothelial cell membranes throughout the body. The lungs and the testes are particularly rich in ACE. Information on the molecular biology and structure of ACE is available (Dzau et al., 2002; Macours et al., 2004). There appear to be two distinct forms of ACE: a somatic form (sACE) and a smaller isoform found in testes (tACE). A single gene encodes both forms by utilizing alternative promoters. sACE is found in many tissues and contains two active sites (as described previously); tACE contains only the C-terminal active site and is exclusively found in testes. Although both active sites of sACE require zinc ion, their biochemical properties are not identical (Dzau et al., 2002; Macours et al., 2004).

The Design of ACE Inhibitors

As mentioned earlier, ACE is a critical target for inhibitory drugs designed to lower blood pressure. Because ACE and HIV protease are Asp proteases, many of the considerations used for the design of these inhibitors were subsequently used in the design of HIV protease inhibitors, as discussed earlier. It was known that the nonapeptide teprotide, from the snake *Bothrops jararaca*, whose sequence is Glu-Trp-Pro-Arg-Pro-Gln-Ile-Pro-Pro, was a potent antihypertensive that acted by competitively inhibiting ACE (Crantz et al., 1980). This was the first effective therapeutic ACE inhibitor, but it could not be given orally because of its hydrolysis in the stomach and the gut. Because it was known that there was a critical positively charged Arg residue in the active site, in addition to the positively charged Zn ion, and that the enzyme had a high affinity for Phe and Pro residues, the inhibitor succinyl proline was developed. The affinity of this inhibitor was greatly enhanced if the carboxylate of the succinic acid moiety was replaced with a thiol that had a high affinity for the bound Zn ions. This resulted in the synthesis of 3-mercapto-2-methylpropanoyl-L-proline, also called *captopril*, a highly effective agent that had several undesirable side effects, however, such as skin rash and loss of taste (Cushman & Ondetti, 1991). In addition, Phe-containing tripeptides that contained carboxylate groups were synthesized, allowing for tight binding to the active site and to Zn concurrently (i.e., enalapril and lisinopril—both effective agents). In addition, transition state analog inhibitors, such as the ones discussed for HIV protease, have been developed (Dive, 2004; Gerogiadis et al., 2004; Redelinghuys et al., 2006). Several contain modified Phe as seen in the HIV protease inhibitors, except that they also contain nonhydrolyzable tetrahedral phosphinic acid in place of the normally occurring backbone carbonyl group. Several of these inhibitors inhibit the carboxyl-terminal active site preferentially, making them good antihypertensive agents because it is this active site that predominantly hydrolyzes angiotensin 1. At the same time, considerable bradykinin hydrolytic activity still occurs in the amino-terminal active site. This is considered desirable in that bradykinin itself induces vasodilatation and angioedema and can compound the lowering of blood pressure. This can result in some cases in induction of hypotension, an undesirable side effect. More recently, peptides, in particular, derivatives of pyroglutamyl (Pyr)-apelin 13 and apelin 17, have been found to block ACE activity, resulting in vasodilatation (Wang, 2016).

Reference Ranges and Preanalytic Variation

ACE activity is higher in children than in adults; during adolescence, values are higher in boys than in girls (Beneteau-Burnat et al., 1990), gradually falling to adult levels by 18 years of age. Men and women have the same values, although not all studies show this pattern. ACE appears to be cleared by the liver; the half-life in plasma is roughly 48 hours. Average day-to-day variation is less than 10%, with no diurnal variation (Thompson et al., 1986).

A number of other factors affect ACE levels. Smokers have ACE activities about 30% lower than in nonsmokers or former smokers who have stopped smoking for at least 10 years (Ninomiya et al., 1987). Thyroid hormone stimulates ACE synthesis. Postmenopausal estrogen replacement causes a 20% fall in ACE activity in serum (Proudler et al., 1995). Rare families lack an endogenous inhibitor of ACE activity and, consequently, have markedly elevated serum ACE levels (Luisetti et al., 1990).

Measurement

ACE is typically measured by its ability to cleave synthetic peptides, releasing hippuric acid (Hip) or other indicator molecules, as in the following reaction:

$$\text{Hip-L-His-L-Leu} + H_2O \rightarrow \text{Hip} + \text{L-His-L-Leu} \qquad \text{(Eq. 21.38)}$$

Hip is then extracted, and its absorption is measured at 228 nm. A modification of the assay is required in CSF samples because of their much lower ACE activity (Oksanen et al., 1985).

Causes of Abnormal Results

The most common reason for ordering ACE levels involves the diagnosis and monitoring of sarcoidosis. In general, ACE levels are directly related to the number of organs affected (Muthuswamy et al., 1987) and the activity of granulomas;

mature granulomas tend to produce less ACE than developing ones (Mimori, 1998). In sarcoidosis, a general correlation has been noted between disease activity and ACE levels (Gupta et al., 1992); as disease progresses to fibrosis, ACE levels decline. ACE is more likely to be elevated with pulmonary involvement than with purely hilar adenopathy. ACE is also increased in many other granulomatous diseases, although not as frequently as in sarcoidosis. Although most individuals with sarcoidosis have elevated ACE, the frequency of elevation of ACE in other granulomatous disorders is 10% (Studdy et al., 1978). For this reason, ACE is not usually considered a diagnostic test, although it may be helpful in patients with primarily ocular involvement, in whom biopsy cannot be readily performed (Power et al., 1995).

ACE is frequently elevated in a number of other disorders, including multiple sclerosis (Constantinescu et al., 1997), Addison disease (Falezza et al., 1985), hyperthyroidism (Reiners et al., 1988), diabetes mellitus (Schernthaner et al., 1984), alcoholic hepatitis (Borowsky et al., 1982), peptic ulcer (D'Onofrio et al., 1984), and nephrotic syndrome (Huskic et al., 1996), and at various stages in patients with bacterial (Kerttula & Weber, 1986) or *Pneumocystis* pneumonitis (Singer et al., 1989). Other pulmonary disorders with a significantly increased ACE are emphysema, asthma, small cell carcinoma, and squamous cell carcinoma (Ucar et al., 1997). In chronic renal failure, it is increased only in those on hemodialysis and rises during the course of a dialysis procedure (Docci et al., 1988); it is decreased in those with chronic renal failure who are not on dialysis (Le Treut et al., 1983). In HIV infection, the frequency and degree of elevation correlate with stage of disease (Ouellette et al., 1992). Decreased ACE levels are seen in various malignancies (Romer & Emmertsen, 1980; Schweisfurth et al., 1985), in chronic liver disease (Sakata et al., 1991), in anorexia nervosa (Matsubayashi et al., 1988), and in hypothyroidism (Reiners et al., 1988).

Use of CSF ACE levels for diagnosis and monitoring of neurosarcoidosis has been criticized (Dale & O'Brien, 1999). A number of other diseases cause elevated CSF ACE, among them viral encephalitis, multiple sclerosis, and central nervous system (CNS) syphilis (Schweisfurth et al., 1987).

In all cases of assays for ACE, attention should be paid to the possible use of ACE inhibitors in hypertensive patients. Because virtually all ACE inhibitors are competitive inhibitors, if competitive inhibition is suspected, use of higher concentrations of Hip-His-Leu substrate in the ACE assay can be used to overcome the inhibition. Alternatively, the sample can be diluted to remove the effect of the inhibitor. Assays for the levels of ACE inhibitors such as captopril have been developed (Prior et al., 2007).

Angiotensin Converting Enzyme 2 (ACE 2)

Surprisingly, ACE2, which has 805 amino acid residues, which is closely related to ACE1 and tACE and is also intercalated in cell membranes mainly in pneumocytes and the gastrointestinal tract, is the *receptor for coronaviruses* including the COVID SARS virus and the COVID-19 virus that is the cause of the current worldwide pandemic. This protein has strong sequence homology to the carboxy-terminal domain of ACE1 discussed earlier. In fact residues 19 to 805 of ACE2 have strong homology to residues 614 to 1196 of ACE1 (Towler et al., 2004). In contrast to ACE1, ACE2 contains only one catalytic site. Also, unlike ACE1, ACE2 is not a dipeptidyl peptidase because it cleaves only a single carboxy-terminal residue from peptides (see later discussion). Importantly, ACE2 cleaves angiotensin 2 to a heptapeptide and the carboxy-terminal phenylalanine residue, inactivating it. However, ACE2 does not apparently affect blood pressure. It seems mainly to be involved in regulation of cardiac function (Crackower et al., 2002). Since it cleaves only one amino acid residue at a time from the carboxy-terminal end—unlike ACE1, which cleaves two amino acid residues from the carboxy-terminal end of a peptide sequence, like angiotensin 1—it is classified as a carboxypeptidase rather than a dipeptidyl peptidase. Membrane-bound ACE2 is cleaved in a domain between residues 716 and 741, where the transmembrane domain begins, by disintegrin and metalloprotease 17 (ADAM17) (Jia et al., 2009). Soluble ACE2, or sACE2, circulates in serum at a mean concentration of about 500 ng/dL. Its half-life in serum is on the order of 10 hours (Haschke et al., 2013).

ACE2–COVID-19 Interactions. The three-dimensional structure of ACE2 has been determined both as the free enzyme (residues 19–615) (Towler et al., 2004) and as the enzyme bound to the COVID-19 spike protein receptor binding domain (RBD; residues 336–615) (Lan et al., 2020; Shang et al., 2020). The structure of ACE2 bound to the COVID-19 RBD is shown in Figure 21.12. ACE2 is represented as the green-colored structure and can be seen to be an almost all α-helical protein. In this figure, the first α-helix, called α1, involving residues 19 to 55, is colored blue. It is this helical segment that serves predominantly as the site to which the coronavirus binds, although a number of residues from the α10 domain and a few other residues in other domains make contacts with the viral RBD of the receptor binding protein. The coronavirus has a set of surface,

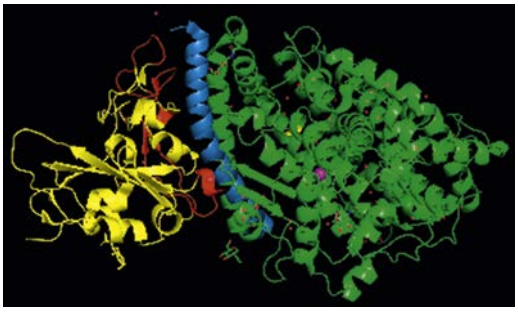

Figure 21.12 Ribbon representation of the x-ray crystal structure of residues 19 to 615 of ACE2 *(green structure)* bound to residues 336 to 516 of the COVID-19 spike (S) protein. The latter is shown in two colors: red and yellow. The red section is the receptor binding motif (RBM), residues 438 to 506, of the COVID-19 spike protein that interacts with the ACE2 protein receptor. The yellow-colored section shows the structure of the remainder of the S protein. The large arrows denote regions of beta-pleated sheets in the structure of the complex. Alpha helices are shown by the coiled ribbon structures. The blue-colored domain of ACE2 is the α1 domain, residues 19 to 55. The purple or magenta ball in the middle of the ACE2 structure is the location of the zinc ion. This structure is shown in a rotated view of the x-ray crystal structure deposited in the Protein Data Bank, 6VW1 (With permission from Shang J, Ye G, Shi K, et al.: Structural basis of receptor recognition by SARS-CoV-2, *Nature* 581:221–224, 2020.)

crown-shaped proteins called spike proteins (S proteins) (Lan et al., 2020). These are homotrimers consisting of proteins S1 and S2. S1 contains a series of domains that include the RBD, that is, residues 336 to 516, and the receptor binding motif (RBM), involving residues 438 to 506 that contain the residues that interact with ACE2. (These are mainly residues in the subsequence 449–505). The structure of the RBM of the virus is also shown in Figure 21.12 in yellow and the segment involved in interacting with residues of ACE2 is shown in red. Many of the interactions between the viral S protein and the α1 helix of ACE2 are polar (salt bridges and hydrogen binding interactions) at the interface. Two important ACE2 residues involved in multiple contacts with the viral S protein are Gln 24 and Gln 42 (Lan et al., 2020). Cryoelectron microscopy has suggested that, subsequent to binding of the virus to the ACE2 receptor, the S1 subunit dissociates from the receptor, inducing activation of the S2 protein that facilitates the fusion of the viral membrane to the cell membrane, allowing for viral transport into the cell (Lan et al., 2020).

Figure 21.12 shows a magenta ball in the middle of ACE2. This is the location of the zinc ion in the active site. As can be seen in this figure, the active site of the enzyme is removed by a long distance from the α1 helix, the major site of binding of the viral S protein. Thus, catalysis and/or inhibition of catalysis may be expected to have little effect on the viral binding process and vice versa.

The Active Site of ACE2 and Its Specificity (Towler et al., 2004**).** The active site of ACE2 is similar to that of tACE, which also has only one active site for peptide cleavage. Like ACE1 and tACE, ACE2 utilizes zinc to aid in the splitting of peptide bonds. In ACE2, the Zn is stabilized by two His residues, His 374 and His 378. Unlike tACE, however, the active site cannot accommodate more than two residues between which the peptide bond is cleaved. A peptide can be represented, proceeding from amino- to carboxy-terminal end, as P2-P1-P1′-P2′, each P representing a single amino acid residue. ACE1, but not ACE2, could cleave this peptide at the P1-P1′ bond. ACE 2 cannot effect this cleavage but can cleave a peptide that is P2-P1-P1′ into P2-P1 + P1′. The reason for this specificity is the absence of a P2′ binding site in ACE2 due to the presence in the binding site for P1′ that has Arg 273 with a large side chain that interacts with the COO– group of the carboxy-terminal amino acid P1′ and blocks any potential P2′ binding site. tACE has a glutamine in the corresponding position that is more permissive because it has a smaller side chain. In addition, the P1 site is "covered" by the side chain of Tyr 510. This results in a restricted P1 binding site, that is, amino acids with small, but not large, side chains can be accommodated in this site in ACE2. Thus, the peptide sequence Ala-Trp or Ala-Lys or Pro-Trp or Pro-Lys would be cleaved by ACE2 either as dipeptides or the dipeptides occurring at the carboxy-terminal end of a peptide sequence. ACE2 would not cleave the reverse sequences. The reaction mechanism for peptide bond cleavage has not been fully elucidated but is known to involve His 345, His 505, Tyr 515, Glu 402, and Glu 375 (Towler et al., 2005).

Assays for ACE2. There appears to be little clinical use at present for serum or other body fluid assay for ACE2. Most assays performed for this enzyme relate to extent of inhibition of this enzyme by specific inhibitors. Fundamentally, assays for ACE2 are of two types: enzyme-linked

immunosorbent assays (ELISAs) and activity assays. ELISAs use monoclonal antibodies to determine ACE2 mass concentration. Activity assays are based on use of a fluorogenic substrate such as MCA-Ala-Pro-Lys-DNP, where DNP is a dinitrophenyl group attached to the side chain amino group of Lys. MCA is the methoxycoumadinyl group in amide bond with Ala. MCA is fluorescent, but this fluorescence is quenched by the DNP moiety. ACE2 induces hydrolysis of the Pro-Lys amide bond, removing the DNP group from the peptide, allowing for the MCA moiety to fluoresce unquenched. The fluorescence intensity is directly related to the activity of ACE2.

ACETYLCHOLINESTERASE (EC 3.1.1.7) AND BUTYRYLCHOLINESTERASE (EC 3.1.1.8)

Biochemistry and Physiology

AChE (true cholinesterase or choline esterase I) and PChE (or choline esterase II) are carboxylic ester hydrolases (class 3; see Table 21.1) that have different specificities (Abdallah & Udomtecha, 2007). AChE catalyzes the following reaction:

$$\text{Acetylcholine} + H_2O \rightarrow \text{Choline} + \text{Acetate} \qquad \text{(Eq. 21.39)}$$

PChE catalyzes this reaction:

$$\text{Acylcholine} + H_2O \rightarrow \text{Choline} + \text{Carboxylate} \qquad \text{(Eq. 21.40)}$$

AChE and PChE are two different enzymes produced by different tissues that are able to cleave acetylcholine, one of the body's major neurotransmitters. True cholinesterase has acetylcholine (ACh) as its primary natural substrate and is also inhibited by it at approximately 10^{-2} mol/L or 10 mM. It is found in high activity in the CNS, RBCs, lung, and spleen. ACh is a primary neurotransmitter at various sites in the CNS, and AChE rapidly hydrolyzes ACh, producing rapid termination of neurotransmission. AChE is not normally found in amniotic fluid.

The normal function of the enzyme found in serum, PChE (also called *acetylcholine acylhydrolase*), is not known but it is important in the cleavage of acetylcholine antagonists such as succinylcholine and mivacurium, a neuromuscular blocking agent, and muscle relaxants used during surgery. Serum PChE is not subject to substrate inhibition by high levels of ACh. PChE production occurs primarily in the liver, although other tissues, such as myocardium and pancreas, can also produce it. Although both enzymes hydrolyze ACh, AChE, but not PChE, hydrolyzes acetyl-β-methylcholine. Conversely, PChE, but not AChE, hydrolyzes butyryl- and benzoylcholine.

A number of genetic variants of PChE have reduced affinity (higher K_M) for acetylcholine as well as for competitive inhibitors such as dibucaine and fluoride when compared with the common U (usual) form. These are termed *A* (for atypical), *F* (for fluoride resistant), and *S* (for silent). The S variant actually represents a number of mutations that may cause absence of enzymatic activity or absence of PChE synthesis. Heterozygous deficiency is found in about 4% of the population, and homozygous deficiency affects 0.3% to 0.5% of individuals. These variants cause decreased (or, in the case of the S variant, absent) PChE activity when present in homozygous or mixed heterozygous forms (AA, AF, AS, FF, FS, SS). Because of the broad range of normal values, reduced PChE activity is not usually found in U-form heterozygotes.

Another way to detect such variants is to measure the percent of enzyme activity remaining after in vitro incubation of serum enzyme with dibucaine or fluoride (termed *dibucaine number*, or *DN*, and *fluoride number*, respectively) (Soliday, 2010). As mentioned previously, increased K_M of variants produces less effective catalysis than normal; decreased affinity thus exists for dibucaine and fluoride, making these variants more resistant to inhibition than normal. In general, dibucaine inhibits U plasma cholinesterase activity by approximately 70% to 90%. Variant cholinesterase activity is more resistant to inhibition, such that heterozygote activity is inhibited by approximately 50% to 70%, and homozygous variant activity is inhibited by approximately 10% to 30%. The DN will then reflect percentage inhibition of enzyme activity and will give a rough measure of the enzyme's activity. This, in turn, will indicate the presence or the absence of a variant form of the enzyme. The DN is calculated using the formula in Equation 21.41. For example, the UU form may show 85% inhibition, or 15% remaining activity, and may yield a DN of 85.

$$\text{Dibucaine (fluoride) number} = 100 \times (1 - \text{Enzyme activity with inhibitor}/\text{Enzyme activity without inhibitor}) \qquad \text{(Eq. 21.41)}$$

Newer molecular biology techniques, such as the use of polymerase chain amplification with separation of the reaction products by gel electrophoresis (Cerf et al., 2002), allow much more accurate identification of variants as compared with traditional biochemical analysis.

Pseudocholinesterase as an Antixenobiotic Enzyme

In addition to its involvement in the metabolism of anticholinergic drugs, PChE has been found to catalyze the debenzoylation of cocaine (Duysen et al., 2008; Yang et al., 2009) and the hydrolysis of procaine (Duysen et al., 2008). Although catalysis by PChE of debenzoylation of cocaine is inefficient, absence of this enzyme or mutations that reduce its activity, discussed in the preceding section, can prolong and exacerbate the negative effects of cocaine, such as its cardiotoxicity (Duysen et al., 2008). It is interesting to note that recently, based on transition state theory analysis and molecular modeling of this enzyme bound to cocaine, site-specific mutagenesis of the gene encoding this enzyme has resulted in forms of rodent PChE that can debenzoylate cocaine with increasing catalytic efficiency, thereby totally inactivating it (Yang et al., 2009; Gao, 2009; Chen, 2015). Humanized forms of this engineered enzyme may soon prove to have significant therapeutic value.

Reference Ranges and Preanalytic Variation

PChE values are low in infants and gradually rise to adult levels by 4 months of age (Karlsen et al., 1981). Values in men do not change after this point until 45 years of age; in women, they fall by about 10% at menarche and increase by 15% after menopause. A study by Abou-Hatab et al. (2001) found no significant correlation between older patient age and changes in plasma enzyme activities of AChE and PChE; healthy young and older individuals (study age range, 18–85 years) showed similar enzyme activities. Values in men are about 15% to 20% higher than in women until 45 years of age, when values in women become equal. Oral contraceptives cause a decrease of about 15% in PChE activity (Lepage et al., 1985) suggesting possible enzyme inhibition. About a fourfold range of values is seen in normal individuals. Increased body mass index is associated with an increase in PChE, and low protein intake leads to decreased PChE.

The half-life of PChE has been estimated at between 2 and 10 days. Average day-to-day variation is about 7% (Moses et al., 1986)—much smaller than that for most other enzymes.

Measurement

Enzyme activity is typically measured using an acylthiocholine ester as a substrate. Released thiocholine reacts with Ellman's reagent (dithiobisnitrobenzoic acid), releasing 5-mercapto-2-nitrobenzoic acid, which is measured spectrophotometrically at 412 nm. Pseudocholinesterase activity is measured in serum, and AChE activity is measured in a hemolysate of washed RBCs. AChE may also be determined in amniotic fluid by gel electrophoresis. To measure dibucaine or fluoride numbers, serum is incubated with dibucaine (30 μmol/L) or fluoride (4 mmol/L) in the assay reaction mixture.

Causes of Abnormal Results

The main reasons for measuring PChE are (1) to monitor exposure to cholinesterase inhibitors, (2) for use as a liver function test, or (3) for diagnosis of genetic variants. Organophosphate insecticides and nerve poisons such as sarin (methyl isopropyl fluorophosphate) form covalent complexes with the OH group of the catalytic serine residue of both AChE and PChE, inactivating both forms of this enzyme, although typically PChE plasma activity falls before AChE activity in RBCs with poisoning (Areekul et al., 1981). As discussed in Chapter 24, this inactivation can be acutely overcome by treating the patient with pralidoxime, a hydroxylamine derivative of N-methylpyridine that forms a phosphate ester with the phosphate group attached to the critical serine residue, allowing regeneration of the free hydroxyl group of this serine. Because of small individual variation and large interindividual variation in PChE values, it is advisable to obtain baseline values for PChE before individuals are exposed to organophosphates (Trundle & Marcial, 1988). A decrease of 40% from baseline is needed before symptoms develop, and severe symptoms typically occur with falls in values greater than 80%. Thus, symptoms often occur with PChE values within the reference range. If no baseline values are present, serial determinations are helpful. In one study, 90% of symptomatic organophosphate poisonings were associated with PChE values within the reference range, and postexposure levels showed a rise, confirming toxicity (Coye et al., 1987). Although PChE reflects acute toxicity, AChE (RBCs) better reflects chronic exposure.

In contrast to other hepatocyte enzymes, PChE production by the liver appears to reflect synthetic function rather than hepatocyte injury. Levels of PChE are decreased in acute hepatitis, cirrhosis, and carcinoma

metastatic to liver. PChE is decreased in malnutrition but is normal or increased in nephrotic syndrome. As is the case when monitoring organophosphate exposure, changes in values compared with baseline are more useful than single values, limiting the diagnostic usefulness of PChE as a nutritional or liver injury monitor.

The other common use of PChE measurements is in recognizing the presence of genetic variants. Most commonly, such testing involves family members of individuals who have prolonged apnea after use of succinylcholine or mivacurium (neuromuscular blocking agents/muscle relaxants) during anesthesia. Testing typically involves both total PChE and determination of fluoride and dibucaine numbers to recognize homozygous or compound heterozygous variants that put an individual at risk from exposure to cholinesterase inhibitors. Patients at risk (with variant cholinesterase forms) may more slowly hydrolyze the neuromuscular blocking agent, unexpectedly increasing the duration of respiratory muscle relaxation and prolonging apnea. This is in contrast to the usual rapid drug hydrolysis seen with the U forms, leading to rapid recovery of the patient.

As mentioned previously, measurement of RBC AChE is useful in organophosphate exposure and poisoning. In addition, qualitative analysis of AChE in amniotic fluid may be useful in the diagnosis of neural tube defects, especially in high-risk groups (Muller, 2003). AChE can be identified in amniotic fluid from pregnancies with neural tube defects as well as some other types of birth defects. AChE is absent in amniotic fluid from normal pregnancies. More recently, PChE (butyrylcholinesterase) has been found to have a strong inverse relationship to long-term survival in patients diagnosed with coronary artery disease (CAD) (Goliasch et al., 2012).

LACTATE DEHYDROGENASE (EC 1.1.1.27)

Biochemistry and Physiology

Lactate dehydrogenase (LD) is a class 1 enzyme (oxidoreductase; see Table 21.1) that acts on a CH–OH group of donors with NAD^+ as acceptor and catalyzes the transfer of hydrogen in the form of a hydride ion:

$$\text{(L)-Lactate} + NAD^+ \leftrightarrow \text{Pyruvate} + NADH + H^+ \quad \text{(Eq. 21.42)}$$

The enzyme is also capable of oxidizing other (L)-2-hydroxymonocarboxylic acids.

LD is a zinc-containing enzyme that is part of the glycolytic pathway; it is found in the cytoplasm of all cells and tissues in the body. LD is a tetramer of two active subunits: H and M with a molecular weight of 134 kDa. Combinations of subunits produce five isoenzymes ranging from LD_1 (HHHH) to LD_5 (MMMM); the intermediate isoenzymes contain differing combinations of H and M subunits (LD_2, HHHM; LD_3, HHMM; LD_4, HMMM). Inherited forms of deficiency of H (Joukyuu et al., 1989) and M (Kanno et al., 1980), subunits of LD, are associated with low LD levels in plasma and only one isoenzyme on electrophoresis. Another form of LD composed of four C subunits is found in spermatozoa and in semen but has never been detected in serum, even in individuals with seminoma (Vogelzang et al., 1982). Rarely, another band detected in electrophoresis and termed **LD_6** can be seen. This probably represents alcohol dehydrogenase, which can also metabolize lactate (Podlasek et al., 1984; Kato et al., 1984).

The tissue distribution of LD varies primarily in its isoenzyme composition, not in its content of LD (see Table 21.5). It is important to note that LD_1 and LD_2 are expressed at high levels in myocardial tissue and in erythrocytes and at much lower levels in tissues such as liver and muscle; the reverse is true for LD_4 and LD_5. In myocardial damage, the predominant isozymes that become elevated in serum are LD_1 and LD_2; in liver or skeletal muscle disease, the LD_4 and LD_5 isozymes become elevated predominantly in serum. In contrast to enzymes such as AST, ALT, and CK, which show marked variation in enzyme activity between tissues, the range in values for LD is only about 1.5-fold between those with the highest amounts (such as liver) and those with lower amounts (such as kidney). Most tissues have LD activities that are 500 to 1000 times greater in tissue than those found in normal serum (see Table 21.5). Thus, significant elevation of plasma levels occurs with a small amount of tissue damage/breakdown. The tissue distribution of LD isoenzymes is shown in Table 21.7. The specific composition of elevated isoenzyme levels found in plasma will reflect tissue origin. In plasma, the majority of LD comes from breakdown of erythrocytes and platelets, with varying contributions from other organs. LD is apparently eliminated in bile, as injection of radiolabeled LD results in radioactivity in the gallbladder and small intestine (Smith et al., 1988).

Reference Ranges and Preanalytic Variation

LD values are highest in newborns and infants; values do not change with age in adults, and there is no gender difference. Persons older than 65 years of age tend to have slightly higher values. Exercise causes, at most, slight increases in total LD; even strenuous exercise causes only a 25% rise in average values (Tanada et al., 1993). Even trace to slight hemolysis invalidates LD and LD isoenzyme analyses. Contact with the clot increases LD, and physical agitation of specimens, as occurs in most pneumatic tube systems, tends to cause some hemolysis and increased LD. Hemolysis affects both total LD and the LD_1/LD_2 ratio. Exercise has little effect on LD or its isoenzymes. Extreme exercise can cause LD_1 to become greater than LD_2. Total LD increases transiently after blood transfusion but returns to baseline within 24 hours (Wiesen et al., 1998). Delayed separation of RBCs from serum does not affect LD values for 1 to 2 days. Few drugs directly affect LD activity, but granulocyte-macrophage colony-stimulating factor appears to increase LD in parallel to the increase in white blood cell (WBC) count (Sarris et al., 1995).

The half-life of LD isoenzymes varies greatly, from approximately 4 to 4.5 days for LD_1 to 4 to 6 hours for LD_5. Day-to-day variation of LD is only 5% to 10%.

TABLE 21.7
Relative Percentage of LD Isoenzymes in Various Tissues

Tissue	LD_1	LD_2	LD_3	LD_4	LD_5
Serum	25	35	20	15	5
Heart	45	40	10	5	0
Red blood cells	40	35	15	10	0
Renal cortex	35	30	25	10	0
Lung	10	15	40	30	5
Skeletal muscle	0	0	10	30	60
Liver	0	5	10	15	70

LD, Lactate dehydrogenase.

Measurement

LD activity can be measured using either the forward (lactate-to-pyruvate) or the reverse (pyruvate-to-lactate) direction of the reaction. A vast majority of laboratories use the forward reaction. The reverse reaction, predominantly used in the dry-slide method for LD, produces activities that have good correlation with the forward reaction but at measured activities approximately threefold higher. This underscores the point made earlier—if total activity units are reported, it is vital to list the substrate and to provide the reference range for that substrate.

The reverse (pyruvate-to-lactate) reaction is used in a few laboratories currently because of faster reaction kinetics, the less costly cofactor (NADH) needed, and the smaller specimen volume requirement. Disadvantages of the pyruvate-to-lactate reaction include early loss of linearity of reaction kinetics, the effect of potent LD inhibitors in some NADH preparations, and use of suboptimal concentrations of pyruvate because of substrate inhibition. Also, lactate is a more specific substrate for this enzyme; pyruvate is less specific and serves as a substrate for such enzymes as pyruvate dehydrogenase.

Assay for LD Isozymes. Electrophoretic separation of LD isoenzymes is typically used when quantitation of different isoenzymes is required; agarose gel is most commonly used. Quantitation usually uses the forward reaction, allowing detection of fluorescent NADH or a reduced formazan dye in a colorimetric development step, a reaction sequence that is described in Chapter 28. The electrophoretic support and developing agent affect the results, and the reference ranges for the different methods are not the same.

Assays for LD_1. As discussed later, LD_1 elevation, which occurs 36 to 72 hours subsequent to initial symptoms of myocardial infarction (MI), was used to confirm this diagnosis. Using the electrophoretic methods described earlier, the ratio of LD_1/LD_2 was determined. Normally, the ratio of LD_1/LD_2 is approximately 0.75 to 0.80. This ratio is reversed after an MI to >1, the so-called "flipped ratio." Replacing this assay, methods for direct determination of LD_1 have been developed, including use of inhibitors that selectively block LD_1 activity. Results are often expressed as the ratio of LD_1 to total LD. Since LD_1 uniquely catalyzes the oxidation of β-hydroxybutyrate to β-ketobutyrate, this substrate has been used to determine LD_1 activity. (Until the early 1970s, measurement of **hydroxybutyrate dehydrogenase** was used as a diagnostic test for MI.) Currently, the most widely used method is direct immunoassay for LD_1. Serum LD is, on average, 30 IU/L higher than plasma LD owing to release of LD from platelets. With prolonged incubation of plasma-containing platelets (separated at <1200 *g* centrifugation), LD can leak from damaged platelets,

increasing plasma LD as well (Hollaar & Van der Laarse, 1979). As discussed earlier (Chua, 2017), LD activity is stable for at least 6 days on storage at 4° C. The LD activity of serum samples frozen at –20° C has been found to be stable for 1 month (Chua, 2018).

Causes of Abnormal Results

LD is a highly nonspecific test; an abnormal value is not specific for damage to any particular organ. Relative amounts of LD, AST, and ALT (along with CK) may provide clues to the source of LD elevation. If LD is markedly elevated, but AST, ALT, and CK are normal or minimally increased, this suggests damage to cells such as RBCs, WBCs, kidney, lung, lymph nodes, or tumors. Increases in both CK and LD, with greater increases in AST than ALT, occur with cardiac or skeletal muscle injury. Increases in LD occur in liver disease and LD can be elevated in hepatitis, although these increases by themselves are not specific to liver injury (Cassidy & Reynolds, 1994). Recently, it was found that in fulminant hepatic failure (see Chapters 9 and 22), the serum levels of ALT and LD both increase such that LD increases more rapidly initially. An ALT-LD index has been computed in these patients and was found to be a reliable predictor of survival in patients with this condition (Kotoh et al., 2008). As discussed in Chapters 9 and 22, serum elevations of LD and ALP frequently occur in space-occupying lesions of the liver; most cases are identified as metastatic carcinoma or primary hepatocellular carcinoma.

In many conditions, such as shock and metastatic carcinoma, LD is increased because of damage to multiple organs so that mixed patterns can be seen. Marked elevations of LD (>5–10 times normal) are seen in megaloblastic anemia, hemolytic anemias, advanced malignancies (particularly lymphoma and leukemia), sepsis or other causes of shock, and cardiopulmonary arrest. LD is often moderately elevated in *Pneumocystis carinii* pneumonia (Smith et al., 1988) but is often normal in most other forms of pneumonia (Rotenberg et al., 1988). Although LD is highly sensitive (so that normal values make the diagnosis unlikely) (Quist & Hill, 1995), the positive predictive value of LD is not adequate to establish a diagnosis in an HIV patient (Grover et al., 1992). In patients with biliary pancreatitis (inflammation due to gallstones impacted in the bile duct), the LD/AST ratio is elevated, which appears to indicate the presence of pancreatic necrosis (Isogai et al., 1998). Note that 10% to 20% of patients with biliary pancreatitis may present with normal liver function tests (Dholakia et al., 2004).

In cases in which the cause of elevated LD cannot be determined by other means, LD isoenzymes may be useful in determining the source of injury. In normal serum, the LD isoenzymes, in decreasing order of activity, are 2 > 1 > 3 > 4 > 5. In germ cell tumors (particularly seminoma and dysgerminoma), LD_1 is increased and can serve as a tumor marker (von Eyben et al., 2000; von Eyben, 2001).

As noted earlier, LD increases in serum over about a 36- to 48-hour period, during which time the LD_1/LD_2 ratio, which is normally less than 1, increases to values of 1 or above, the flipped ratio. This confirmed the diagnosis of MI but could not be used to make acute diagnoses of MI because of the prolonged time (36 hours) required for the flipped ratio to develop. As discussed in Chapter 19, better biomarkers, specifically troponin (TnT) and its inhibitory subunit TnI, are available for the acute diagnosis of MI and for confirmation of the diagnosis (serum troponin levels remain elevated for longer than 1 week after the acute event). Also, hemolytic anemia (RBCs have elevated LD_1 levels), megaloblastic anemia, and renal cortical diseases such as renal infarcts and renal cell carcinoma cause increases in LD_1 and, often, a flipped LD_1/LD_2 ratio. In tumors of WBCs (leukemia, lymphoma, multiple myeloma), LD_3 and often LD_4 are typically increased, whereas the relative amounts of LD_1 and LD_2 are decreased (Ricerca et al., 1988; Copur et al., 1989; Pandit et al., 1990). Pulmonary disease can produce a similar pattern. Increases in LD_5 and sometimes LD_4 are typically seen with skeletal muscle injury or with ischemic or toxic hepatic injury. The presence of LD_6 is associated with a poor prognosis (Ketchum et al., 1984). An isomorphic pattern, in which total LD is increased but isoenzymes are present in normal proportions, and a **tombstone** pattern, seen when the relative amount of each isoenzyme is roughly the same, are typically noted in persons with diffuse tissue damage, often accompanied by shock or hypoxemia.

More recently, serum LDH levels have been used in cancers as an important prognostic factor, as with prediction of response to therapy in multiple myeloma (Moreau et al., 2014) (high levels indicating lower likelihood of response to specific therapy) and overall survival in metastatic melanoma (Kelderman, 2014), with high levels indicating a worse prognosis. Interestingly, LDH levels have been useful in evaluating pulmonary damage induced by silicate exposure in agate workers wherein the ratio of serum to RBC LD was much higher for exposed workers than for a nonexposed control group (Aggarwal, 2014). In patients who have undergone radiotherapy for prostate cancer, elevated LD_5 levels have been found to be strongly indicative of high tumor proliferation rates and relapse following radiotherapy (Koukourakis et al., 2014).

5′-NUCLEOTIDASE (EC 3.1.3.5) (5′-NT)

Biochemistry and Physiology

5′-NT is a phosphoric monoester hydrolase (class 3 enzyme; see Table 21.1), also known as *5′-ribonucleotide phosphohydrolase*, which catalyzes the following reaction:

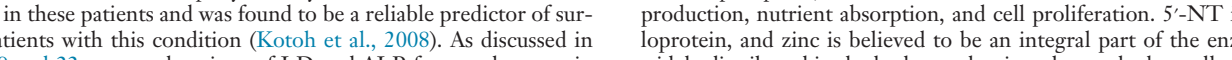

5’-Ribonucleotide + H2O → Ribonucleoside + Phosphate (Eq. 21.43)

It is a cytoplasmic membrane–bound phosphatase with a wide specificity for 5′-ribonucleotides and a molecular weight of about 70 kDa. It acts only on nucleotides (such as adenosine 5′-monophosphate and guanosine 5′-monophosphate) and is believed to function in extracellular adenosine production, nutrient absorption, and cell proliferation. 5′-NT is a metalloprotein, and zinc is believed to be an integral part of the enzyme. It is widely distributed in the body, predominantly attached to cell membranes (similar to ALP and GGT). Plasma 5′-NT is derived predominantly from the liver. A detailed review of 5′-NT is available (Sunderman, 1990).

Reference Ranges and Preanalytic Variation

5′-NT is normally present at low activities in children, rises in adolescence, and plateaus until 40 years of age, when levels increase significantly (Moses et al., 1986). Reference values are independent of gender and race. A slight increase in 5′-NT is seen during the second and third trimesters of pregnancy (Bacq et al., 1996). Similar to ALP and GGT, antiepileptic drugs can increase 5′-NT activity. However, values are usually less than twice the reference limits, and less than 25% of those taking such agents show elevated 5′-NT activity (Fortman & Witte, 1985). For adults, the reference range is 2 to 15 IU/L although other ranges have been determined, such as 0 to 10 IU/L.

Measurement

Measurement of 5′-NT is difficult because other phosphatases, notably ALP, are capable of cleaving the substrate used to measure the lower activity of 5′-NT present in the sample. Approaches usually utilize large quantities of other nonnucleoside substrates to “competitively inhibit” ALP (although they are actually undergoing reactions catalyzed by ALP, they prevent ALP from acting on nucleotide phosphates). Although it would be simplest to measure generated phosphate, this cannot be done because cleavage of other phosphates by ALP would produce incorrect results. Therefore, measurement of the nucleoside released by the action of 5′-NT is required. The most common method is to use adenosine-5′-monophosphate as the substrate, which is converted to adenosine by 5′-NT. This product is then converted to inosine + ammonia in the presence of adenosine deaminase. The ammonia is then reacted with α-ketoglutarate to form glutamate in a reductive amination reaction catalyzed by glutamate dehydrogenase (see Chapter 28), a reaction in which NADH is converted to NAD, resulting in a decrease in absorbance at 340 nm. Most chelating agents such as EDTA inhibit enzyme activity, presumably by making zinc unavailable.

Causes of Abnormal Results

Similar to GGT, 5′-NT is most commonly used to determine whether the source of an elevated ALP is liver or bone. Although 5′-NT is more commonly elevated in cholestatic disorders, acute hepatitis causes an increase in 5′-NT synthesis by the liver and a slight elevation in 5′-NT in plasma (Fukano et al., 1990). 5′-NT is increased in ovarian carcinoma (Chatterjee et al., 1981) and in rheumatoid arthritis, where levels correlate with extent of inflammation as reflected by erythrocyte sedimentation rate (Johnson et al., 1999). Sapey and colleagues (2000) prospectively studied ALP, GGT, and 5′-NT in 80 cholestatic patients, correlating intrahepatic (i.e., secondary to intrahepatic parenchymal disease) and extrahepatic (i.e., secondary to biliary tree obstruction) causes with enzyme changes. They found markedly increased levels with extrahepatic causes (compared with intrahepatic disease) and noted that elevations in GGT and 5’-NT levels were independently linked to cause. The GGT/5′-NT ratio differed significantly between the two groups, with a ratio <1.9 highly suggestive of (but insensitive to) intrahepatic disease (Sapey et al., 2000). More recently, a study suggests that 5′-NT is elevated in viral hepatitis and alcoholic liver disease (including alcoholic hepatitis) and, surprisingly, in cirrhosis (Hyder, 2016).

SKELETAL MUSCLE INJURY: CREATINE PHOSPHOKINASE

The basic assay for this enzyme was discussed earlier (see Eqs. 20.15 to 20.17) and is further discussed in Chapter 28. The cytosolic form of this enzyme has two major isoenzymes, M and B, each of which has the same activity. CK is composed of three types of dimers: MM (mainly in skeletal muscle), MB (found mainly in cardiac tissue), and BB (found predominantly in brain and intestine). There are also two other forms of CK, the intramitochondrial forms, termed *MtCK*, *nonmuscle* or *ubiquitous MtCK*, and *sarcomeric muscle CK.* MtCK is a supplier of phosphocreatine that shuttles to the cytosol where it is used to drive various cellular processes by inducing synthesis of ATP that is used as an energy source serving as a substrate for cytosolic ATPases (Wallimann et al., 1992).

As discussed at length in Chapter 19, because CK-MB is found mainly in myocardial tissue, CK-MB is used as a serodiagnostic test for MI. In this section, CK is discussed as a biomarker for skeletal muscle injury.

Skeletal muscle injury can occur from a variety of sources. Direct trauma, as occurs with physical injury (including contact sports), surgery, strenuous exercise, and intramuscular injection, are common causes of mild elevations of CK (up to about five to six times reference limits). In these situations, CK typically increases rapidly and then falls quickly, returning to baseline with a half-life of approximately 24 hours. An important clinical disorder associated with acute muscle injury is neuroleptic malignant syndrome, a rare complication of treatment with phenothiazines or other psychotropic agents. Typically, affected individuals present with muscle rigidity, fever, and elevated WBC counts; CK is considered a diagnostic test for this disorder. Prompt recognition and treatment are necessary to prevent death from this syndrome; discontinuation of medications and use of the muscle-stabilizing agent dantrolene are the cornerstones of treatment (Pelonero et al., 1998).

Chronic damage to muscle causes more persistent elevation of CK, which may be mild or more extensive. The broad range of normal values and the preanalytic variation seen in total CK values can hamper recognition of mild, ongoing muscle injury. Generally, persistent elevation above the reference limits for an appropriate comparison group despite cessation of any other factors known to affect CK is needed to diagnose muscle injury in asymptomatic individuals (Moghadam-Kia, 2016). Common causes of chronic muscle injury include IV drug abuse (injecting heroin induces muscle damage), medications (particularly the statins, used to lower LDL cholesterol, that are 3-hydroxy-3-methylglutaryl-coenzyme A reductase inhibitors and glucocorticoids), congenital myopathies (such as Duchenne muscular dystrophy), inflammatory disorders (such as polymyositis and dermatomyositis), hypothyroidism, and alcohol abuse. In chronic myopathies, CK-MB is often increased, reflecting its production by regenerating muscle.

With severe acute damage to muscle, a clinical picture termed *rhabdomyolysis* may develop. In such situations, CK-MB/total CK may be elevated above normal in the absence of myocardial infarction (cardiac troponin levels are normal); this is commonly seen in patients with inflammatory muscle disease (Kiely et al., 2000). In addition to normal cardiac troponin levels with elevated CK levels, two distinct isoforms (representing fast or slow skeletal fiber types) of serum skeletal troponin I may be identified (Simpson et al., 2002).

No specific criteria are known for differentiating rhabdomyolysis from lesser degrees of muscle injury. Among the more important features are the higher total CK (one suggested diagnostic level is CK >20 times upper reference limits), the rapid rise and fall of CK, and the appearance of myoglobinuria. Many assays for myoglobin (found in skeletal, smooth, and cardiac muscle) are relatively insensitive, and myoglobin has a short half-life; thus, CK is a more reliable test for establishing the diagnosis. As a form of **cell lysis syndrome**, rhabdomyolysis is associated with the release of other cell contents, such as potassium, phosphate, and nucleotides that can be converted to uric acid. Qualitative testing for myoglobin in the urine is important because myoglobin is potentially toxic to the kidneys; thus, the patient is at risk for acute renal failure. Myoglobinuria may lead to the development of acute tubular necrosis, with the appearance of pigmented casts in the urine sediment. If renal failure develops, hyperkalemia, hyperphosphatemia, and hyperuricemia typically also will be present, as described in the fourth clinical case presentation in Chapter 9. No direct relationship has been discerned between the degree of elevation of CK and the likelihood of development of renal failure (Gabow et al., 1982; Ward, 1988). Common causes of rhabdomyolysis include drugs (particularly ethanol and cocaine), viral infection, extreme exertion, hyperthermia, trauma including crush injuries, ischemia of the lower extremities, and inflammatory myopathy. In addition, strenuous exercise in individuals with sickle trait can result in massive rhabdomyolysis, leading to myoglobin-induced renal failure and the other sequelae discussed previously (see Chapter 9 and Mitchell, 2007; Ouyang et al., 2008).

In a recent study (Enooku et al., 2014), elevation of serum MtCK in patients with cirrhosis or hepatitis C was found to be a reliable independent predictor of development of hepatocellular carcinoma. The cutoff value was 9 IU/L. There also appeared to be a correlation between serum MtCK levels and degree of liver fibrosis and hepatocellular damage.

SELECTED REFERENCES

Bull H, Murray PG, Thomas D, et al.: Acid phosphatases, *J Clin Pathol Mol Pathol* 55:65–72, 2002.
Recent review of acid phosphatases, with emphasis on tartrate-resistant acid phosphatase and its function and clinical usefulness in processes involving bone resorption.

Dzau VJ, Bernstein K, Celermajer D, et al.: Pathophysiologic and therapeutic importance of tissue ACE: a consensus report, *Cardiovasc Drugs Ther* 16:149–160, 2002.
Report from a recent consensus conference examining the actions of angiotensin-converting enzymes (ACEs) in the pathology of cardiovascular disease and the use of tissue ACE inhibitors as antihypertensive agents in these patients.

Macours N, Poels J, Hens K, et al.: Structure, evolutionary conservation, and functions of angiotensin- and endothelin-converting enzymes, *Int Rev Cytol* 239:47–97, 2004.
Overview of both angiotensin-converting enzymes and endothelin-converting enzymes examining the structure and biological roles of these molecules.

von Eyben FE: A systematic review of lactate dehydrogenase isoenzyme 1 and germ cell tumors, *Clin Biochem* 34:441–454, 2001.
Review of lactate dehydrogenase isoenzyme 1 as a possible serum marker in patients with germ cell tumors.

Access the complete reference list online at Elsevier eBooks for Practicing Clinicians.

REFERENCES

General

Brehme CS, Roman S, Shaffer J, et al.: Tartrate-resistant acid phosphatase forms complexes with alpha 2-macroglobulin in serum, *J Bone Miner Res* 14:311–318, 1999.

Chua C, Tifigiu E, Momeni A, Laskar D, Shaffique K, Zuretti A, et al.: Stability of values for the activities of critical enzymes assayed in serum, *Clin Diagn Pathology*, 2017, https://doi.org/10.15761/CDP.1000115.

Chua C, Tifigiu E, Boroujeni AM, Lin B, Laskar D, Shafique K, et al.: Stability of values for the activities of critical enzymes assayed in serum frozen for prolonged time periods, *Ann Clin Lab Sci* 48:55–63, 2018.

Crackower MA, Sarao R, Oudit GY, Yagil C, Kozieradzki I, Scanga S, Oliveira-dos-Santos AJ, da Costa J, Zhang L, Pei Y, Scholey J, Ferrario CM, Manoukian AS, Chappell MC, Backx PH, Yagil Y, Penninger JM: Angiotensin-converting enzyme 2 is an essential regulator of heart function, *Nature* 417:822–828, 2002.

Dasgupta A, Banerjee SK, Datta P: False-positive troponin I in the MEIA due to the presence of rheumatoid factors in serum: elimination of this interference by using a polyclonal antisera against rheumatoid factors, *Am J Clin Pathol* 112:753–756, 1999.

Dickerman RD, Pertusi R, Zachariah NY, et al.: Anabolic steroid induced hepatotoxicity: is it overstated? *Clin J Sports Med* 9:34–39, 1999.

Dos Santos DR, Souza RO, Dias LB, Ribas TB, de Oliveira LCF, Sumida DH, et al.: The effects of storage time and temperature on the stability of salivary phosphatases, transaminases and dehydrogenase, *Arch Oral Biol* 85:160–165, 2018.

Haschke M, Schuster M, Poglitsch M, Loibner H, Salzberg M, Bruggisser M, Penninger J, Krähenbühl S: Pharmacokinetics and pharmacodynamics of recombinant human angiotensin-converting enzyme 2 in healthy human subjects, *Clin Pharmacokinet* 52:783–792, 2013.

Heins M, Heil W, Withold W: Storage of serum or whole blood samples? Effects of time and temperature on 22 serum analytes, *Eur J Clin Chem Clin Biochem* 33:231–238, 1995.

International Union of Biochemistry: Enzyme nomenclature, 1978. In *Recommendations of the nomenclature Committee of the international union of Biochemistry of the nomenclature and classification of enzymes*, San Diego, 1979, Academic Press.

International Union of Biochemistry and Molecular Biology: *Nomenclature Committee: enzyme nomenclature: recommendations 1992*, San Diego, 1992, Academic Press.

Jia HP, Look DC, Tan P, Shi L, Hickey M, Gakhar L, Chappell MC, Wohlford-Lenane C, McCray Jr PB: Ectodomain shedding of angiotensin converting enzyme 2 in human airway epithelia, *Am J Physiol Lung Cell Mol Physiol* 297, 2009. L84–L96.

Lan J, Ge J, Yu J, Shan S, Zhou H, Fan S, Zhang Q, Shi X, Wang Q, Zhang l, Wang X: Structure of the SARS-CoV-2 spike receptor-binding domain bound to the ACE2 receptor, *Nature* 581:215–219, 2020.

Langdon DE: Enzyme neurosis—a clinician's plan for standardization, *Ann Intern Med* 121:234–235, 1994.

Mader M, Kolbus N, Meihorst D, et al.: Human intestinal alkaline phosphatase-binding IgG in patients with severe bacterial infections, *Clin Exp Immunol* 95:98–102, 1994.

Moss DW, Henderson AR: Clinical enzymology. In Burtis CA, Ashwood ER, editors: *Tietz textbook of clinical chemistry*, ed 3, Philadelphia, 1999, WB Saunders, pp 617–721.

Otto A, Bar J, Birkenmeier G: Prostate-specific antigen forms complexes with human alpha 2-macroglobulin and binds to the alpha 2-macroglobulin receptor/LDL receptor-related protein, *J Urol* 159:297–303, 1998.

Podlasek SJ, Dufour DR, McPherson RA: Alterations in lactate dehydrogenase isoenzyme pattern after streptokinase administration or streptococcal infection, *Clin Chem* 35:1763–1766, 1989.

Remaley AT, Wilding P: Macroenzymes: biochemical characterization, clinical significance, and laboratory detection, *Clin Chem* 35:2261–2270, 1989.

Shang J, Ye G, Shi K, Wan Y, Luo C, Aihara H, Geng Q, Auerbach A, Li F: Structural basis of receptor recognition by SARS-CoV-2, *Nature* 581:221–224, 2020.

Sosolik RC, Hitchcock CL, Becker WJ: Heterophilic antibodies produce spuriously elevated concentrations of the MB isoenzyme of creatine kinase in a selected patient population, *Am J Clin Pathol* 107:506–510, 1997.

Towler P, Staker B, Prasad SG, Menon S, Tang J, Parsons T Ryan D, Fisher M, Williams D, Dales NA, Patane MA, Pantoliano MW: ACE2 x-ray structures reveal a large hinge-bending motion important for inhibitor binding and catalysis, *J Biol Chem* 279:17996–18007, 2004.

Van Hoof VO, Deng DT, De Broe ME: How do plasma membranes reach the circulation? *Clin Chim Acta* 266(23–31), 1997.

Zollner H: *Handbook of enzyme inhibitors*, New York, 1989, VCH Publishers.

Enzyme Kinetics

Cleland WW: Steady state kinetics. In ed 3, Boyer PD, editor: *The enzymes*, vol. 2. San Diego, 1970, Academic Press, pp 1–65.

Cleland WW: Steady-state kinetics. In ed 3, Sigman DS, Boyer PD, editors: *The enzymes*, vol. 19. San Diego, 1990, Academic Press, pp 99–158.

Cornish-Bowden A: *Fundamentals of enzyme kinetics*, revised edition, London, 1995, Portland Press.

Dixon M, Webb EC: *Enzymes*, ed 3, San Diego, 1979, Academic Press. Chapter IV.

Fersht A: *Structure and mechanism in protein science*, New York, 1999, Freeman. Chapters 3–7.

Segel I: *Enzyme kinetics: behavior and analysis of rapid equilibrium and steady-state enzyme systems*, New York, 2009, Wiley Classics Library.

Catalytic Efficiency

Adachia M, Ohharaa T, Kuriharaa K, et al.: Structure of HIV-1 protease in complex with potent inhibitor KNI-272 determined by high-resolution x-ray and neutron crystallography, *Proc Natl Acad Sci U S A* 106:4641–4646, 2009.

Cashman JR, Berkman C, Underiner GE: Catalytic antibodies that hydrolyze (-)-cocaine obtained by a high throughput procedure, *J Pharmacol Exp Ther* 293:952–961, 2000.

Ghosh AK, Chapsal BD, Weber IT, et al.: Design of HIV protease inhibitors targeting protein backbone: an effective strategy for combating drug resistance, *Acc Chem Res* 41:78–86, 2008.

Matayoshi ED, Wang GT, Krafft GA, et al.: Novel fluorogenic substrates for assaying retroviral proteases by resonance energy transfer, *Science* 247:954–958, 1990.

Swain A, Miller MM, Green J, et al.: X-ray crystallographic structure of a complex between a synthetic protease of human immunodeficiency virus 1 and a substrate-based hydroxyethylamine inhibitor, *Proc Natl Acad Sci U S A* 87:8805–8809, 1990.

Vance JE, LeBlanc DA, Wingfield P, et al.: Conformational selectivity of HIV-1 protease cleavage of X-Pro peptide bonds and its implications, *J Biol Chem* 272:15603–15606, 1997.

Specific Enzymes

Abdallah C, Udomtecha D: Pseudocholinesterase activity: determination and interpretation in pediatric anesthesia, *Middle East, J Anesthesiol* 19:423–428, 2007.

Abou-Hatab K, O'Mahony MS, Patel S, et al.: Relationship between age and plasma esterases, *Age Ageing* 30:41–45, 2001.

Aggarwal BD: Lactate dehydrogenase as a biomarker for silica exposure-induced toxicity in agate workers, *Occup Environ Med* 71:578–582, 2014.

Agbedana EO, Yeldu MH: Serum total, heat and urea stable alkaline phosphatase activities in relation to ABO blood groups and secretor phenotypes, *Afr J Med Med Sci* 25:327–329, 1996.

Alvarez L, Peris P, Bedini JL, et al.: High bilirubin levels interfere with serum tartrate-resistant acid phosphatase determination: relevance as a marker of bone resorption in jaundiced patients, *Calcif Tissue Int* 64:301–303, 1999.

Areekul S, Srichairat S, Kirdudom P: Serum and red cell cholinesterase activity in people exposed to organophosphate insecticides, *Southeast Asian J Trop Med Public Health* 12:94–98, 1981.

Bacq Y, Zarka O, Brechot JF, et al.: Liver function tests in normal pregnancy: a prospective study of 103 pregnant women and 103 matched controls, *Hepatology* 23:1030–1034, 1996.

Bayer PM, Hotschek H, Knoth E: Intestinal alkaline phosphatase and the ABO blood group system: a new aspect, *Clin Chim Acta* 108:81–87, 1980.

Beneteau-Burnat B, Baudin B, Morgant G, et al.: Serum angiotensin-converting enzyme in healthy and sarcoidotic children: comparison with the reference interval for adults, *Clin Chem* 36:344–346, 1990.

Borowsky SA, Lieberman J, Strome S: Elevation of serum angiotensin-converting enzyme level: occurrence in alcoholic liver disease, *Arch Intern Med* 142:893–895, 1982.

Brenckman Jr WD, Lastinger LB, Sedor F: Unpredictable fluctuations in serum acid phosphatase activity in prostatic cancer, *J Am Med Assoc* 245:2501–2504, 1981.

Burnett AL, Chan DW, Brendler CB, et al.: The value of serum enzymatic acid phosphatase in the staging of localized prostate cancer, *J Urol* 148:1832–1834, 1992.

Cassidy WM, Reynolds TB: Serum lactic dehydrogenase in the differential diagnosis of acute hepatocellular injury, *J Clin Gastroenterol* 19:118–121, 1994.

Catovsky D, Cherchi M, Greaves MF, Janossy G: Phosphatase reaction in acute lymphoblastic leukemia, *Lancet* 8067:749–751, 1978.

Cerf C, Mesguish M, Gabriel I, et al.: Screening patients with prolonged neuromuscular blockade after succinylcholine and mivacurium, *Anesth Analg* 94:461–466, 2002.

Chao TY, Yu JC, Ku CK, et al.: Tartrate-resistant acid phosphatase 5b is a useful serum marker for extensive bone metastasis in breast cancer patients, *Clin Cancer Res* 11:544–550, 2005.

Chatterjee SK, Bhattacharya M, Barlow JJ: Evaluation of 5′-nucleotidase as an enzyme marker in ovarian carcinoma, *Cancer* 47:2648–2653, 1981.

Chen J, Yam LT, Janckila AJ, et al.: Significance of "high" acid phosphatase activity in the serum of normal children, *Clin Chem* 25:719–722, 1979.

Chen X, Huang X, Geng L, Xue L, Hou S, Zheng X, et al.: Kinetic characterization of a cocaine hydrolase engineered from mouse butyrylcholinesterase, *Biochem J* 466:243–251, 2015.

Collier DS, Pain JA: Acute and chronic retention of urine: relevance of raised serum prostatic acid phosphatase levels. A prospective study, *Urology* 27(34–37), 1986.

Constantinescu CS, Goodman DB, Grossman RI, et al.: Serum angiotensin-converting enzyme in multiple sclerosis, *Arch Neurol* 54:1012–1015, 1997.

Copur S, Kus S, Kars A, et al.: Lactate dehydrogenase and its isoenzymes in serum from patients with multiple myeloma, *Clin Chem* 35:1968–1970, 1989.

Coye MJ, Barnett PG, Midtling JE, et al.: Clinical confirmation of organophosphate poisoning by serial cholinesterase analyses, *Arch Intern Med* 147:438–442, 1987.

Crantz FR, Swartz SL, Hollenberg NK, et al.: Differences in response to the dipeptidyldipeptide hydrolase inhibitors SQ 20,881 and SQ 14,225 in normal-renin essential hypertension, *J Am Heart Assoc* 2:604–609, 1980.

Cushman DW, Ondetti MA: History of the design of captopril and related inhibitors of angiotensin converting enzyme, *J Am Heart Assoc* 17:589–592, 1991.

Dale JC, O'Brien JF: Determination of angiotensin-converting enzyme levels in cerebrospinal fluid is not a useful test for the diagnosis of neurosarcoidosis, *Mayo Clin Proc* 74:535, 1999.

Day AP, Feher MD, Chopra R, et al.: The effect of benzafibrate on serum alkaline phosphatase isoenzyme activities, *Metabolism* 42:839–842, 1993.

Deng JT, Hoylaerts MF, Van Hoof VO, et al.: Differential release of human intestinal alkaline phosphatase in duodenal fluid and serum, *Clin Chem* 38:2532–2538, 1992.

Dholakia K, Pitchumoni CS, Agarwal N: How often are liver function tests normal in acute biliary pancreatitis? *J Clin Gastroenterol* 38:81–83, 2004.

Dive V: Review: phosphinic peptides as zinc metalloproteinase inhibitors, *Cell Mol Life Sci* 61:2010–2019, 2004.

Docci D, Delvecchio C, Turci F, et al.: Effect of different dialyzer membranes on serum angiotensin-converting enzyme during hemodialysis, *Int J Artif Organs* 11:28–32, 1988.

Domar U, Karpe F, Hamsten A, et al.: Human intestinal alkaline phosphatase: release to the blood is linked to lipid absorption, but removal from the blood is not linked to lipoprotein clearance, *Eur J Clin Invest* 23:753–760, 1993.

D'Onofrio GM, Levitt S, Ilett KF: Serum angiotensin converting enzyme in Crohn's disease, ulcerative colitis and peptic ulceration, *Aust N Z J Med* 14:27–30, 1984.

Dufour DR: Effects of oral contraceptives on routine laboratory tests, *Clin Chem* 44:A137, 1998.

Duysen EG, Li B, Carlson M, et al.: Increased hepatotoxicity and cardiac fibrosis in cocaine-treated butyrylcholinesterase knockout mice, *Basic Clin Pharmacol Toxicol* 103:514–521, 2008.

Enooku K1, Nakagawa H, Soroida Y, et al.: Increased serum mitochondrial creatine kinase activity as a risk for hepatocarcinogenesis in chronic hepatitis C patients, *Int J Cancer* 135:871–879, 2014.

Falezza G, Lechi Santonastaso C, Parisi T, et al.: High serum levels of angiotensin-converting enzyme in untreated Addison's disease, *J Clin Endocrinol Metab* 61:496–498, 1985.

Fortman CS, Witte DL: Serum 5′-nucleotidase in patients receiving anti-epileptic drugs, *Am J Clin Pathol* 84:197–201, 1985.

Fukano M, Amano S, Hazama F, et al.: 5′-Nucleotidase activities in sera and liver tissues of viral hepatitis patients, *Gastroenterol Jpn* 25:199–205, 1990.

Gabow PA, Kaehny WD, Kelleher SP: The spectrum of rhabdomyolysis, *Medicine (Baltim)* 61:141–152, 1982.

Gao Y, Brimijoin S: Lasting reduction of cocaine action in neostriatum—a hydrolase gene therapy approach, *J Pharm Exptl Therap* 330:449–457, 2009.

Gerogiadis D, Guniasse P, Cotton J, et al.: Structural determinants of RXPA 380, a potent and highly selective inhibitor of the angiotensin-converting enzyme C-domain, *Biochemistry* 43:8048–8054, 2004.

Goliasch G, Haschemi A, Marculescu R, et al.: Butyrylcholinesterase activity predicts long-term survival in patients with coronary artery disease, *Clin Chem* 58:1055–1058, 2012.

Grover SA, Coupal L, Suissa S, et al.: The clinical utility of serum lactate dehydrogenase in diagnosing *Pneumocystis carinii* pneumonia among hospitalized AIDS patients, *Clin Invest Med* 15:309–317, 1992.

Gupta SK, Chakraborty M, Mitra K: Serum angiotensin converting enzyme in respiratory diseases, *Indian J Chest Dis Allied Sci* 34:19–24, 1992.

Haarhaus M, Fernstrom A, Magnusson M, et al.: Clinical significance of bone alkaline phosphatase isoforms, including the novel B1x isoform, in mild to moderate chronic kidney disease, *Nephrol Dial Transplant* 24:3382–3389, 2009.

Hollaar L, Van der Laarse A: Interference of the measurement of lactate dehydrogenase (LDH) activity in human serum and plasma by LDH from blood cells, *Clin Chim Acta* 99:135–142, 1979.

How J, Brown JR, Saylor S, et al.: Macrophage expression of tartrate-resistant acid phosphatase as a prognostic indicator in colon cancer, *Histochem Cell Biol* 142:195–204, 2014.

Huskic J, Kulenovic H, Culo F: Serum angiotensin-converting enzyme activity in patients with endemic nephropathy, *Nephron* 74:120–124, 1996.

Hyder MA, Hasan M, Mohieldein A: Comparative study of 5'-nucleotidase test in various liver diseases, *J Clin Diagn Res* 10, 2016. BCO1-BC03.

Ind TE, Iles RK, Carter PG, et al.: Serum placental-type alkaline phosphatase activity in women with squamous and glandular malignancies of the reproductive tract, *J Clin Pathol* 47:1035–1037, 1994.

Hyder MA, Hasan M, Mohieldein A: Comparative study of 5'-nucleotidase test in various liver diseases, *J Clin Diagn Res* 10, 2016. BCO1–BC03.

Isogai M, Yamaguchi A, Hori A, et al.: LDH to AST ratio in biliary pancreatitis—a possible indicator of pancreatic necrosis: preliminary results, *Am J Gastroenterol* 93:363–367, 1998.

Johnson SM, Patel S, Bruckner FE, et al.: 5′-Nucleotidase as a marker of both general and local inflammation in rheumatoid arthritis patients, *Rheumatology* 38:391–396, 1999.

Joukyuu R, Mizuno S, Amakawa T, et al.: Hereditary complete deficiency of lactate dehydrogenase H-subunit, *Clin Chem* 35:687–690, 1989.

Kallioniemi OP, Nieminen MM, Lehtinen J, et al.: Increased serum placental-like alkaline phosphatase activity in smokers originates from the lungs, *Eur J Respir Dis* 71:170–176, 1987.

Kanno T, Sudo K, Takeuchi I, et al.: Hereditary deficiency of lactate dehydrogenase M-subunit, *Clin Chim Acta* 108:267–276, 1980.

Kaplan LA, Chen IW, Sperling M, et al.: Clinical utility of serum prostatic acid phosphatase measurements for detection (screening), diagnosis, and therapeutic monitoring of prostatic carcinoma: assessment of monoclonal and polyclonal enzymes and radioimmunoassays, *Am J Clin Pathol* 84:334–339, 1985.

Karlsen RL, Sterri S, Lyngaas S, et al.: Reference values for erythrocyte acetylcholinesterase and plasma cholinesterase activities in children: implications for organophosphate intoxication, *Scand J Clin Lab Invest* 41:301–302, 1981.

Kato S, Zishii H, Kano S, et al.: Evidence that "lactate dehydrogenase isoenzyme 6" is in fact alcohol dehydrogenase, *Clin Chem* 30:1585–1586, 1984.

Kawamura M, Tanaka K, Toiyama Y, et al.: Clinical significance of tartrate-resistant acid phosphatase type-5 expression in human gastric cancer, *Anticancer Res* 34:3425–3429, 2014.

Kelderman S, Heemskerk B, van Tinteren H, et al.: Lactate dehydrogenase as a selection criterion for ipilimumab treatment in metastatic melanoma, *Cancer Immunol Immunother* 63(5):449–458, 2014.

Kerttula Y, Weber TH: Serum angiotensin converting enzyme in pneumonias, *J Clin Pathol* 39:1250–1253, 1986.

Ketchum CH, Robinson CA, Hall LM, et al.: Clinical significance and partial biochemical characterization of lactate dehydrogenase isoenzyme 6, *Clin Chem* 30:46–49, 1984.

Kiely PDW, Bruckner FE, Nisbet JA, et al.: Serum skeletal troponin I in inflammatory muscle disease: relation to creatine kinase, CKMB and cardiac troponin I, *Ann Rheum Dis* 59:750–751, 2000.

Kim J, Song TJ, Song D, et al.: Serum alkaline phosphatase and phosphate in cerebral atherosclerosis and functional outcomes after cerebral infarction, *Stroke* 44:3547–3549, 2013.

Kotoh K, Enjoji M, Kato M, et al.: A new parameter using serum lactate dehydrogenase and alanine aminotransferase level is useful for predicting the prognosis of patients at an early stage of acute liver injury: a retrospective study, *Comp Hepatol* 7(1–8), 2008. [open access].

Koukourakis MI, Giatromanolaki A, Panteliadou M, et al.: Lactate dehydrogenase 5 isoenzyme overexpression defines resistance of prostate cancer to radiotherapy, *Br J Cancer* 11:2217–2223, 2014.

Kyd PA, Vooght KD, Kerkhoff F, et al.: Clinical usefulness of bone alkaline phosphatase in osteoporosis, *Ann Clin Biochem* 35:717–725, 1998.

Lepage L, Schiele F, Gueguen R, et al.: Total cholinesterase in plasma: biological variations and reference limits, *Clin Chem* 31:546–550, 1985.

Le Treut A, Chevet D, Guenet L, et al.: Serum angiotensin-converting enzyme levels in patients with chronic renal failure, *Pathol Biol* 31:182–185, 1983.

Lu K-C, Tseng C-F, Wu C-C, et al.: Effects of calcitriol on type 5b tartrate-resistant acid phosphatase and interleukin-6 in secondary hypoparathyroidism, *Blood Purif* 254:423–430, 2006.

Luisetti M, Martinetti M, Cuccia M, et al.: Familial elevation of serum angiotensin converting enzyme activity, *Eur Respir J* 3:441–446, 1990.

Maatman TJ: Comparative analysis of fluctuation of serum tumor markers in advanced cancer of prostate, *Urology* 42:672–676, 1993.

Manolio TA, Burke GL, Savage PJ, et al.: Sex- and race-related differences in liver-associated serum chemistry tests in young adults in the CARDIA study, *Clin Chem* 38:1853–1859, 1992.

Matsubayashi S, Tamai H, Kobayashi N, et al.: Angiotensin-converting enzyme and anorexia nervosa, *Horm Metab Res* 20:761–764, 1988.

Mimori Y: Sarcoidosis: correlation of HRCT findings with results of pulmonary function tests and serum angiotensin-converting enzyme assay, *Kurume Med J* 45:247–256, 1998.

Mitchell BL: Sickle trait and sudden death—bringing it home, *J Natl Med Assoc* 99:300–305, 2007.

Moghadam-Kia S, Oddis CV, Aggarwal R: Approach to asymptomatic creatine kinase elevation, *Cleveland Clin J Med* 83:37–42, 2016, https://doi.org/10.3949/ccjm.83a.14120. PMC 4871266. PMID 26760521.

Moreau P, Cavo M, Sonneveld P, et al.: Combination of international scoring system 3, high lactate dehydrogenase, and t(4;14) and/or del(17p) identifies patients with multiple myeloma (MM) treated with front-line autologous stem-cell transplantation at high risk of early MM progression-related death, *J Clin Oncol* 32:2173–2180, 2014.

Moses GC, Tuckerman JF, Henderson AR: Biological variance of cholinesterase and 5′-nucleotidase in serum of healthy persons, *Clin Chem* 32:175–177, 1986.

Moss DW: Electrophoresis of human alkaline and acid phosphatases, *Clin Lab Med* 6:507–523, 1986.

Moss DW: Physicochemical and pathophysiological factors in the release of membrane-bound alkaline phosphatase from cells, *Clin Chim Acta* 257:133–140, 1997.

Mukherjea M, Mukherjee P, Biswas R, et al.: Effect of medroxyprogesterone acetate contraception on human serum enzymes, *Int J Fertil* 26:35–39, 1981.

Muller F: Prenatal biochemical screening for neural tube defects, *Childs Nerv Syst* 19:433–435, 2003.

Muthuswamy PP, Lopez-Majano V, Ranginwala M, et al.: Serum angiotensin-converting enzyme (SACE) activity as an indicator of total body granuloma load and prognosis in sarcoidosis, *Sarcoidosis* 4:142–148, 1987.

Narayan P, Tewari A, Jacob G, et al.: Differential suppression of serum prostatic acid phosphatase and prostate-specific antigen by 5-alpha-reductase inhibitor, *Br J Urol* 75:642–646, 1995.

Nijhawan R, Wierzbicki AS, Tozer R, et al.: Antiepileptic drugs, hepatic enzyme induction and raised serum alkaline phosphatase isoenzymes, *Int J Clin Pharmacol Res* 10:319–323, 1990.

Ninomiya Y, Kioi S, Arakawa M: Serum angiotensin converting enzyme activity in ex-smokers, *Clin Chim Acta* 164:223–226, 1987.

Oksanen V, Fyhrquist F, Somer H, et al.: Angiotensin converting enzyme in cerebrospinal fluid: a new assay, *Neurology* 35:1220–1223, 1985.

Ouellette DR, Kelly JW, Anders GT: Serum angiotensin-converting enzyme level is elevated in patients with human immunodeficiency virus infection, *Arch Intern Med* 152:321–324, 1992.

Ouyang J, Dalal S, Blumenthal D, et al.: Myocardial infarction, congestive heart failure and septicemia: rare complications of exertional rhabdomyolysis in a patient with sickle cell trait, *Fed Pract* 26:25–26, 2008. 14–16, 19–20.

Pandit MK, Joshi BH, Patel PS, et al.: Efficacy of serum lactate dehydrogenase and its isozymes in monitoring the therapy in patients with acute leukemia, *Indian J Pathol Microbiol* 33:41–47, 1990.

Panteghini M, Pagani F: Biological variation in bone-derived biochemical markers in serum, *Scand J Clin Lab Invest* 55:609–616, 1995.

Panteghini M, Pagani F, Bonora R: Preanalytical and biological variability of prostatic acid phosphatase and prostate-specific antigen in serum from patients with prostatic pathology, *Eur J Clin Chem Clin Biochem* 30:135–139, 1992.

Pelonero AL, Levenson JL, Panduranji AK: Neuroleptic malignant syndrome: a review, *Psychiatr Serv* 49:1163–1172, 1998.

Podlasek SJ, McPherson RA, Threatte GA: Characterization of apparent lactate dehydrogenase isoenzyme 6: a lactate independent dehydrogenase, Clin Chem 30:266-270, 1984.

Pontes JE: Clinical significance of serum and bone marrow acid phosphatase, *Prostate* 1:465–470, 2006.

Power WJ, Neves RA, Rodriguez A, et al.: The value of combined serum angiotensin-converting enzyme and gallium scan in diagnosing ocular sarcoidosis, *Ophthalmology* 102:2007–2011, 1995.

Price A, Attwood SE, Grant JB, et al.: Measurement of prostate-specific antigen and prostatic acid phosphatase concentrations in serum before and 1-42 days after transurethral resection of the prostate and orchidectomy, *Clin Chem* 37:859–863, 1991.

Prior JA, Santos JL, Lima JL: Exploiting kinetic spectrophotometric determination of captopril, an angiotensin-converting enzyme inhibitor, in a multi-pumping flow system, *Anal Chim Acta* 600:183–187, 2007.

Proudler AJ, Ahmed AI, Crook D, et al.: Hormone replacement therapy and serum angiotensin-converting-enzyme activity in postmenopausal women, *Lancet* 346:89–90, 1995.

Quist J, Hill AR: Serum lactate dehydrogenase (LDH) in *Pneumocystis carinii* pneumonia, tuberculosis, and bacterial pneumonia, *Chest* 108:415–418, 1995.

Redelinghuys P, Nchinda AT, Chibale K, et al.: Novel ketomethylene inhibitors of angiotensin 1-converting enzyme (ACE): inhibition and molecular modeling, *Biol Chem* 387:461–466, 2006.

Reiners C, Gramer-Kurz E, Pickert E, et al.: Changes of serum angiotensin-I-converting enzyme in patients with thyroid disorders, *Clin Physiol Biochem* 6:44–49, 1988.

Reynoso G, Elias EG, Mittelman A: The contribution of the intestinal mucosa to the total serum alkaline phosphatase activity, *Am J Clin Pathol* 56:707–712, 1971.

Ricci LR, Hoffman SA: Prostatic acid phosphatase and sperm in the post-coital vagina, *Ann Emerg Med* 11:530–534, 1982.

Ricerca BM, Storti S, Campisi S, et al.: Serum lactate dehydrogenase isoenzyme pattern in non-Hodgkin's lymphomas, *Int J Biol Markers* 3:237–242, 1988.

Romer FK, Emmertsen K: Serum angiotensin-converting enzyme in malignant lymphomas: leukaemia and multiple myeloma, *Br J Cancer* 42:314–318, 1980.

Rotenberg Z, Weinberger I, Davidson E, et al.: Significance of isolated increases in total lactate dehydrogenase and its isoenzymes in serum of patients with bacterial pneumonia, *Clin Chem* 34:1503–1505, 1988.

Sakata T, Takenaga N, Endoh T, et al.: Diagnostic significance of serum angiotensin-converting enzyme activity in biochemical tests with special reference of chronic liver diseases, *Jpn J Med* 30:402–407, 1991.

Salo JO, Rannikko S, Haapiainen R: Serum acid phosphatase in patients with localised prostatic cancer, benign prostatic hyperplasia or normal prostates, *Br J Urol* 66:188–192, 1990.

Salvaggio A, Periti M, Miano L, et al.: Body mass index and liver enzyme activity in serum, *Clin Chem* 37:720–723, 1991.

Sapey T, Mendler M-H, Guyader D: Respective value of alkaline phosphatase, gamma-glutamyl transpeptidase and 5′ nucleotidase serum activity in the diagnosis of cholestasis, *J Clin Gastroenterol* 30:259–263, 2000.

Sarris AH, Majlis A, Dimopoulos MA, et al.: Rising serum lactate dehydrogenase often caused by granulocyte- or granulocyte-macrophage colony stimulating factor and not tumor progression in patients with lymphoma or myeloma, *Leuk Lymphoma* 17:473–477, 1995.

Schernthaner G, Schwarzer C, Kuzmits R, et al.: Increased angiotensin-converting enzyme activities in diabetes mellitus: analysis of diabetes type, state of metabolic control and occurrence of diabetic vascular disease, *J Clin Pathol* 37:307–312, 1984.

Schiele F, Artur Y, Floc'h AY, et al.: Total, tartrate-resistant, and tartrate-inhibited acid phosphatases in serum: biological variations and reference limits, *Clin Chem* 34:685–690, 1988.

Schweisfurth H, Schioberg-Schiegnitz S, Kuhn W, et al.: Angiotensin I converting enzyme in cerebrospinal fluid of patients with neurological diseases, *Klin Wochenschr* 65:955–958, 1987.

Schweisfurth H, Schmidt M, Brugger E, et al.: Alterations of serum carboxypeptidases N and angiotensin-I-converting enzyme in malignant diseases, *Clin Biochem* 18:242–246, 1985.

Simpson JA, Labugger R, Hesketh GG, et al.: Different detection of skeletal troponin I isoforms in serum of a patient with rhabdomyolysis: markers of muscle injury, *Clin Chem* 48:1112–1114, 2002.

Sharma U, Pal D, Prasad R: Alkaline phosphatase: an Overview, *Ind J Clin Biochem* 29:269–278, 2014.

Singer F, Talavera W, Zumoff B: Elevated levels of angiotensin-converting enzyme in *Pneumocystis carinii* pneumonia, *Chest* 95:803–806, 1989.

Smith RL, Ripps CS, Lewis ML: Elevated lactate dehydrogenase values in patients with *Pneumocystis carinii* pneumonia, *Chest* 93:987–992, 1988.

Soliday F, Conley YP, Henker R: Pseudocholinesterase deficiency: a comprehensive review of genetic, acquired, and drug influences, *AANA J (Am Assoc Nurse Anesth)* 38:313–320, 2010.

Steinherz PG, Steinherz LJ, Nisselbaum JS, et al.: Transient, marked, unexplained elevation of serum alkaline phosphatase, *J Am Med Assoc* 252:3289–3292, 1984.

Studdy P, Bird R, James DG: Serum angiotensin-converting enzyme (SACE) in sarcoidosis and other granulomatous disorders, *Lancet* 2:1331–1334, 1978.

Sunderman Jr FW: The clinical biochemistry of 5′-nucleotidase, *Ann Clin Lab Sci* 20:123–139, 1990.

Swolin-Eide D, Hansson S, Larsson L, et al.: The novel bone alkaline phosphatase B1x isoform in children with kidney disease, *Pediatr Nephrol* 21:1723–1729, 2006.

Tanada S, Higuchi T, Nakamura T, et al.: Evaluation of exercise intensity indicated by serum lactate dehydrogenase activity in healthy adults, *Acta Biol Hung* 44:153–160, 1993.

Theodorsen L: Collection and storage of samples for the determination of prostatic acid phosphatase in serum, *Scand J Clin Lab Invest Suppl* 179:57–65, 1985.

Thompson PJ, Kemp MW, McAllister WA, et al.: Angiotensin-converting enzyme: investigation of diurnal variation, the effect of a large dose of prednisolone, and prednisolone pharmacokinetics in patients with sarcoidosis, *Am Rev Respir Dis* 134:1075–1077, 1986.

Trundle D, Marcial G: Detection of cholinesterase inhibition: the significance of cholinesterase measurements, *Ann Clin Lab Sci* 18:345–352, 1988.

Ucar G, Yildirim Z, Ataol E, et al.: Serum angiotensin converting enzyme activity in pulmonary diseases: correlation with lung function parameters, *Life Sci* 61:1075–1082, 1997.

Valenzuela GJ, Munson LA, Tarbaux NM, et al.: Time-dependent changes in bone, placental, intestinal, and hepatic alkaline phosphatase activities in serum during human pregnancy, *Clin Chem* 33:1801–1806, 1987.

Vogelzang NJ, Lange PH, Goldberg E: Absence of sperm-specific lactate dehydrogenase-x in patients with testis cancer, *Oncodev Biol Med* 3:269–272, 1982.

von Eyben FE, Liu FJ, Amato RJ, et al.: Lactate dehydrogenase isoenzyme 1 is the most important LD isoenzyme in patients with testicular germ cell tumor, *Acta Oncol* 39:509–517, 2000.

Wadstrom J, Wenk M, Huber P: Serum half life of prostatic acid phosphatase, *Urol Res* 13:131–132, 1985.

Wallimann T, Wyss M, Brdiczka D, et al.: Intracellular compartmentation, structure and function of creatine kinase isoenzymes in tissues with high and fluctuating energy demands: the "phosphocreatine circuit" for cellular energy homeostasis, *Biochem J* 281(Pt 1):21–40, 1992.

Wang W, McKinnie SMK, Farhan M, Paul M, McDonald T, McLean B, et al.: Angiotensin-converting enzyme 2 metabolizes and partially inactivates pyr-apelin-13 and apelin-17 physiological effects in the cardiovascular system, *Hypertension* 68:365–377, 2016.

Ward MM: Factors predictive of acute renal failure in rhabdomyolysis, *Arch Intern Med* 148:1553–1557, 1988.

Whyte MP, Walkenhorst DA, Fedde KN, et al.: Hypophosphatasia: levels of bone alkaline phosphatase immunoreactivity in serum reflect disease severity, *J Clin Endocrinol Metab* 81:2142–2148, 1996.

Wiesen AR, Byrd JC, Hospenthal DR, et al.: Transient abnormalities in serum bilirubin and lactate dehydrogenase levels following red blood cell transfusions in adults, *Am J Med* 104:144–147, 1998.

Wolf PL: Clinical significance of serum high-molecular-mass alkaline phosphatase, alkaline phosphatase-lipoprotein-X complex, and intestinal variant alkaline phosphatase, *J Clin Lab Anal* 8:172–176, 1994.

Yang W, Pan Y, Zheng F, et al.: Free-energy perturbation simulation on transition states and redesign of butyrylcholinesterase, *Biophys J* 96:1931–1938, 2009.

CHAPTER 22

EVALUATION OF LIVER FUNCTION

Lynsey Daniels, Marian Khalili, Eve Goldstein, Martin H. Bluth, Wilbur B. Bowne, Matthew R. Pincus

NORMAL LIVER FUNCTION, 314
Metabolic Functions, 314
Synthetic Functions, 318
TESTS OF LIVER INJURY, 320
Plasma Enzyme Levels, 320
α-Fetoprotein, 322
Autoimmune Markers, 322
Testing For Viral-Induced Hepatitis, 323
DIAGNOSIS OF LIVER DISEASES, 327
Hepatitis, 327
Chronic Passive Congestion, 327
Cirrhosis, 327
Posthepatic Biliary Obstruction, 329
Space-Occupying Lesions, 329
Fulminant Hepatic Failure, 330
SELECTED REFERENCES, 330

KEY POINTS

- The liver is composed of three systems: the hepatocyte, concerned with metabolic reactions, macromolecular (especially protein) synthesis, and degradation and metabolism of xenobiotics (e.g., drugs); the biliary system, involved with the metabolism of bilirubin and bile salts; and the reticuloendothelial system, concerned with the immune system and the production of heme and globin metabolites (e.g., bilirubin).
- The function of each of these systems can be measured conveniently and virtually noninvasively by determining the serum levels of specific analytes, in the so-called liver function test profile.
- One of the most common causes of acute liver injury is viral hepatitis, mainly hepatitis A, B, and C, all of which induce acute elevations of serum alanine and aspartate aminotransferase.
- Diagnosis of viral hepatitis can be made by screening for viral antigens, especially in hepatitis B, and for immunoglobulin M and G directed against specific viral antigens. Confirmation of the diagnosis of a particular form of viral hepatitis is carried out using suitable molecular diagnostic techniques such as real-time polymerase chain reaction using primers encoding specific viral gene sequences.
- Treatment of hepatitis C has changed dramatically recently. The standard treatment of pegylated interferon and ribavirin has now been replaced with specific viral protease (e.g., NS3 protein) inhibitors such as telaprevir, simeprevir, and boceprevir.
- The diagnosis of specific liver diseases, including hepatitis, cirrhosis, chronic passive congestion, acute biliary obstruction, space-occupying lesions, autoimmune diseases, and fulminant hepatic failure, can be made from specific patterns of serum liver function tests and from the presence of specific antibodies in serum.

NORMAL LIVER FUNCTION

The liver is the largest and most complex organ of the gastrointestinal tract. Overall, it comprises three systems: first, the biochemical hepatocytic system, which is responsible for the vast majority of all metabolic activities in the body, including protein synthesis; aerobic and anaerobic metabolism of glucose and other sugars; glycogen synthesis and breakdown; amino acid and nucleic acid metabolism; amino acid and dicarboxylic acid interconversions via transaminases (aminotransferases); lipoprotein synthesis and metabolism; xenobiotic metabolism (e.g., drug metabolism), usually involving the cytochrome P450 oxidation system; storage of iron and vitamins such as A, D, and B_{12}; and synthesis of hormones such as angiotensinogen, insulin-like growth factor I, and triiodothyronine. It is also the site of clearance of many other hormones such as insulin, parathyroid hormone, estrogens, and cortisol. Uniquely, the liver is the site of metabolism of ammonia to urea.

Albumin in the body is synthesized in the liver, as are all coagulation factor proteins with the exception of von Willebrand factor, which is synthesized in endothelial cells and megakaryocytes. Patients with liver disease may have signs or symptoms related to disturbance of any of the functions outlined earlier.

The second major hepatic system is the hepatobiliary system, which is concerned with the metabolism of bilirubin, a process that involves transport of bilirubin into the hepatocyte and its conjugation to glucuronic acid and its secretion into bile canaliculi and the enterohepatic system. Last is the reticuloendothelial system—that is, Kupffer cells. These are a form of macrophage involved (a) with the immune system, including being a major site of defense against intestinal bacteria and the primary location for removal of antigen–antibody complexes from the circulation, and (b) with the breakdown of hemoglobin from dead erythrocytes, giving rise to bilirubin, which, together with bilirubin from the spleen, enters the hepatocyte.

Because clinical symptoms in liver disease often lag behind the progression of disease, it is important to detect the presence and even the onset of these conditions. Fortunately, evaluation of liver function can often be achieved by determination of serum analytes in a test profile known as *liver function tests*, many of whose components are not unique to the liver but, when evaluated together, allow for accurate diagnosis of abnormalities of liver function. An outline of liver function tests and their interpretation has been presented in Chapter 9.

This chapter reviews the most common laboratory tests for evaluation of liver function and injury, methods used for their measurement, testing for causes of liver injury, and patterns of laboratory abnormalities seen in specific liver diseases.

METABOLIC FUNCTIONS

Bilirubin

Normal Bilirubin Metabolism

Bilirubin is the major metabolite of heme, the iron-binding tetrapyrrole ring found in hemoglobin, myoglobin, and cytochromes. Approximately 250 to 350 mg of bilirubin is produced daily in healthy adults, about 85% of which is derived from turnover of senescent red blood cells (Berlin & Berk, 1981; Chowdhury et al., 1988; Berk & Noyer, 1994a). In macrophages mainly in the spleen, methemoglobin from red cells is split to give free globin chains and heme. The porphyrin ring of heme is oxidized by microsomal heme oxygenase, producing the straight-chain compound biliverdin and releasing iron. In this ring-opening reaction, 1 mole of carbon monoxide is released, which is transported ultimately as carboxyhemoglobin, whose serum levels can be useful in the diagnosis of hemolytic anemia, as discussed in Chapter 9. Biliverdin is then reduced to bilirubin (Fig. 22.1;

Crawford, 1998b) by the nicotinamide adenine dinucleotide phosphate (NADPH)-dependent enzyme, biliverdin reductase. Bilirubin, bound mainly to albumin, is then transported mainly in the portal system to the liver, where it enters the hepatocyte through its membrane surface in contact with the sinusoids, as shown in Figure 22.2. Specific transporters on the sinusoidal (basolateral) plasma membrane of hepatocytes help mediate the transport and uptake of bile acids and non-bile acid organic anions such as bilirubin, sulfobromophthalein (BSP), various drugs, and hormones. The fenestrated sinusoidal endothelium of the liver permits these compounds to have access to hepatocytes. These transporters include organic anion transport proteins (oatps), a family of 12 transmembrane domain glycoproteins and Na+/taurocholate transporting protein (ntcp), a seven transmembrane domain glycoprotein (Wolkoff, 2014; Russell, 2007).

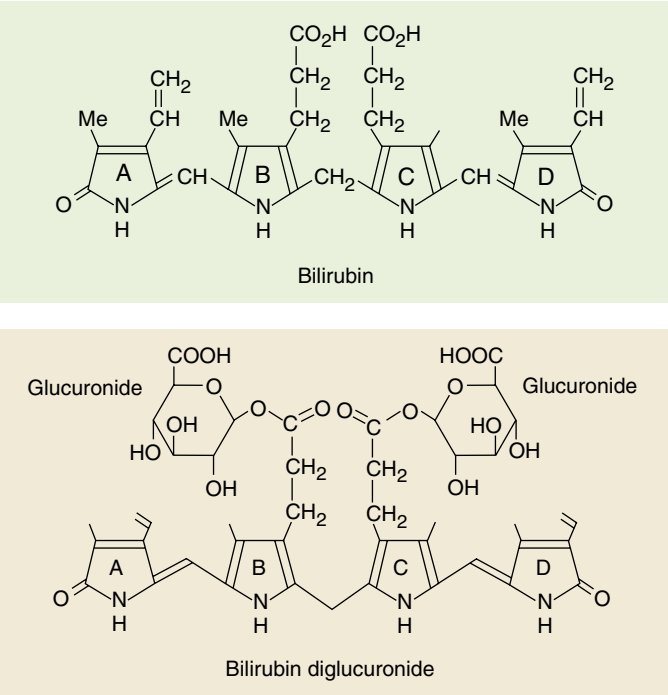

Figure 22.1 Structures of critical molecules in the metabolism of bilirubin to its diglucuronide. Bilirubin is transported into the hepatocyte, where it is converted into the diglucuronide form and secreted into canaliculi. (From Crawford JM, Hauser SC, Gollan JL: Formation, hepatic metabolism, and transport of bile pigments: A status report. *Semin Liver Dis* 8:105–18, 1988b.)

As free bilirubin enters hepatocytes, additional bilirubin dissociates from albumin. This process is highly efficient; clearance of unconjugated bilirubin at normal values is about 5 mg/kg/day or, for a 75-kg individual, about 400 mg/day (Berk & Noyer, 1994b). The half-life of unconjugated bilirubin is short; 60% of labeled bilirubin appears within hepatocytes within 5 minutes of injection (Bloomer et al., 1973). The clearance rate increases with an increasing concentration of unconjugated bilirubin up to at least 4 mg/dL (Berk & Noyer, 1994b).

In its most common isomeric (*trans*-) form, bilirubin is highly insoluble in water, and most of it is transported bound to albumin, with only a small fraction of free bilirubin. Light can cause photoisomerization of bilirubin, from a *trans*- form to a more compact *cis*- form, making it much more water soluble and allowing it to be excreted in urine (Onishi et al., 1986). This forms the basis for phototherapy in the treatment of neonatal (unconjugated) hyperbilirubinemia. The pathway for clearance of bilirubin by the liver is illustrated in Figure 22.2. Note that unconjugated bilirubin enters the hepatocyte at the membrane surface adjacent to the sinusoids, opposite the face that is in contact with bile canaliculi.

Bilirubin enters hepatocytes by two mechanisms: passive diffusion and receptor-mediated endocytosis. As summarized in Figure 22.2, once in the hepatocyte, bilirubin is "handed-off" from one protein complex to another in a chain. First, it complexes with the so-called Y and Z proteins; then, it binds sequentially to a protein complex called *ligandin*. From this complex, it is transported to the smooth endoplasmic reticulum (SER). In the SER, bilirubin becomes the substrate of the enzyme glucuronyl transferase, encoded by the *UGT1A1* gene, which catalyzes the esterification of the propionic acid side chains of bilirubin with glucuronic acid (present as uridine diphosphoglucuronic acid) to form mainly the diglucuronide conjugate shown in Figure 22.1 (bottom) (Chowdhury et al., 1988). Some monoglucuronide and a small amount of triglucuronide also form. The ratio of monoconjugated to diconjugated pigment in bile is 1:4, whereas the ratio is nearly 1:1 in plasma, suggesting that monoconjugates reflux into plasma more readily.

Both monoconjugated and diconjugated pigments undergo ATP-dependent transport via an ABC cassette that is mediated by multidrug resistance protein (MRP1). Additionally, there is a distinct canalicular isoform (MRP2). Both

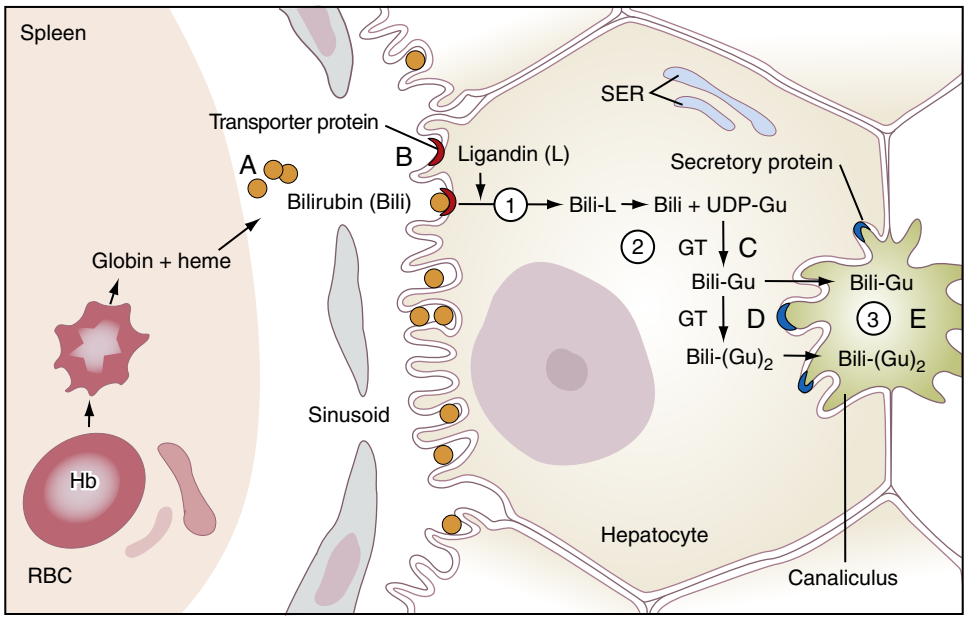

Figure 22.2 Schematic summary of the pathway of bilirubin *(Bili, in brown circles)* transport and metabolism. Bilirubin is produced from metabolism of heme, primarily in the spleen, and is transported to the liver bound to albumin. It enters the hepatocyte by binding to a transporter protein *(red crescents)* and crosses the cell membrane *(circled 1)*, thus entering the cell. It binds to Y and Z proteins *(not shown)* and then to ligandin for transport to the smooth endoplasmic reticulum (SER). In the SER, bilirubin is conjugated to glucuronic acid by UDP-glucuronyl transferase 1 *(circled 2 and labeled GT)*, producing monoglucuronides and diglucuronides of bilirubin: Bili-Gu and Bili-$(Gu)_2$. Conjugated bilirubin is then secreted into the canaliculi *(circled 3)* by the adenosine triphosphate–binding cassette transporter protein MRP2/cMOAT/ABCC2 *(shown as blue crescents)*. In overproduction disease *(A)*, such as hemolytic anemia, unconjugated bilirubin is produced at rates that exceed the ability of the liver to clear it, leading to a usually transient increase in unconjugated bilirubin in serum. In both Gilbert and Crigler-Najjar syndromes, mutations in the gene encoding UDP glucuronyl transferase *(UDPGT1A1)*, shown at C in the figure, result in buildup of unconjugated bilirubin in hepatocytes and ultimately in serum. In Gilbert syndrome, there may also be a defect in the bilirubin transporter protein, shown at *B* in the figure. Mutations in the *MRP2/cMOAT/ABCC2* gene result in defective secretory proteins, causing buildup of conjugated bilirubin in hepatocytes and, ultimately, in serum, resulting in the Dubin-Johnson syndrome *(D)*, an autosomal-recessive disease. Conjugated hyperbilirubinemia is also found in Rotor syndrome, possibly virus induced. In adults, blockade of any of the major bile ducts, especially the common bile duct, by stones or space-occupying lesions such as tumors *(E)*, is the most common cause of conjugated hyperbilirubinemia. *Hb,* Hemoglobin; *RBC,* red blood cell.

MRP1 and MRP2 are ATP-dependent export pumps. This transporter function is deficient in Dubin-Johnson syndrome (Jedlitschky, 1997), discussed later.

As shown in Figure 22.2, an energy-dependent mechanism transports the conjugated bilirubin to the canalicular face of the hepatocyte, at which it is directly secreted into the canaliculi. Only conjugated bilirubin can be directly excreted into the canaliculi; unconjugated bilirubin cannot traverse this membrane.

Once bilirubin is excreted into the canaliculi and ultimately into the intestinal tract, it is further metabolized by intestinal bacteria, which effect its deconjugation and oxidation or reduction with the formation of compounds collectively called *urobilinogen* and *urobilin*, which can then be reabsorbed from the gut. Most urobilinogen absorbed is reexcreted by the liver. A minor fraction may be excreted in the urine. Larger quantities are found in the urine in conditions leading to hyperbilirubinemia or in conditions in which the liver cannot readily secrete urobilinogen absorbed from the gut. Ultimately, intestinal urobilinogen is converted to stool pigments such as stercobilin. Their absence leads to clay-colored stools, often an early sign of impaired bilirubin metabolism.

When conjugated bilirubin is present in serum, it can become covalently bound to albumin, producing biliprotein or delta-bilirubin (Lauff et al., 1982; McDonagh, 1984). Although conjugated bilirubin has a half-life of less than 24 hours, delta-bilirubin has a half-life similar to that for albumin at 17 days (Fevery & Blanckaert, 1986), causing prolonged jaundice during recovery from hepatocellular injury (Van Hootegem et al., 1985) or biliary obstruction (Kozaki et al., 1998). Conjugated bilirubin, being water soluble, can be filtered by the glomerulus and can appear in urine, where it may be detected by dipstick examination. Urobilinogen measurement, however, adds little to standard tests of liver function or injury (Binder & Kupka, 1989). Urinary bilirubin is elevated in most patients with increased serum conjugated bilirubin (Binder & Kupka, 1989).

Derangements of Bilirubin Metabolism

As shown in Figure 22.2, in each step in the processing of bilirubin, a possible lesion leads to elevated serum levels of unconjugated or conjugated bilirubin. Each of these is discussed in turn.

Causes of Elevated Serum Levels of Unconjugated Bilirubin. Hemolysis. As discussed in Chapter 9, in hemolytic anemias, unconjugated bilirubin rises as a result of abnormally high levels of hemoglobin released from erythrocytes. If the rate of bilirubin formation exceeds the rate of liver clearance (i.e., a state of overproduction of bilirubin), there will be a rise in the bilirubin level in serum. Virtually all of this bilirubin will be unconjugated bilirubin. This is particularly likely to occur in neonates, whose glucuronyl transferase activity is low. Thus, one manner of confirming a diagnosis of hemolytic anemia is the finding, in adults, of elevated indirect bilirubin levels in serum. Usually, these levels are not dramatically elevated and are generally in the 1.5 to 3.0 mg/dL range.

Gilbert syndrome and Crigler-Najjar syndrome are caused by gene mutations and deletions. In Gilbert syndrome, characterized by a mild unconjugated hyperbilirubinemia, the most common genetic lesion appears to be the insertion of two bases into the promoter region of the *UGT1A1* gene that encodes glucuronyl transferase, resulting in lower transcriptional rates (Kraemer & Scheurlen, 2002; Maruo et al., 2004) and overall lower enzymatic activity (reduced to about 30% of normal). In the more serious Crigler-Najjar syndrome, frequently characterized by high serum levels of unconjugated bilirubin, multiple mutations are found to occur in this gene, including shifts in the reading frames, stop codons, and critical amino acid substitutions, all of which give rise to a spectrum of dysfunctional proteins, from mildly dysfunctional to completely nonfunctional (Kraemer & Scheurlen, 2002).

In Gilbert syndrome, which occurs in a significant fraction (3%–5%) of the population, the genetic defect may be necessary but not sufficient because, in an earlier study (Persico et al., 1999), a significant percentage of males with this defect were found to have hyperbilirubinemia, but no females with this enzyme deficit were found to have elevated serum bilirubin levels (Bosma et al., 1995). In some patients with Gilbert syndrome, the rate of organic anion uptake has been found to correlate negatively with serum bilirubin (Persico et al., 1999), suggesting that an additional defect may be present to cause hyperbilirubinemia that may be related to a transport deficit in the sinusoidal membrane of the hepatocyte. In this condition, total bilirubin, virtually all of which is unconjugated, is typically elevated to 2 to 3 mg/dL; levels can increase further with fasting but seldom exceed 5 mg/dL. Because passive diffusion of bilirubin into hepatocytes occurs, this condition is rarely serious and may result in mild elevations of bilirubin such as those seen in hemolytic anemia, as described previously.

Gilbert syndrome has perhaps been overdiagnosed; it is most frequently diagnosed in young adults ranging in age from 20 to 30 years. However, normal bilirubin ranges are age dependent and actually reach their highest levels in adolescents and young adults (Rosenthal et al., 1984), as discussed further later. Diagnosis of UGT1A1 mutations have an important practical value, not just for the accurate diagnosis of Gilbert syndrome, but also because carriers of various genotypes of UGT1A1 differ in their metabolism of a number of common medications. This may assist in adjusting the dosage of these medications when considering a patient's individual genetics. Recent studies show that DNA melting curve analysis is an effective method for rapidly diagnosing Gilbert syndrome (Hsieh et al., 2014).

In the more serious or type I form of the Crigler-Najjar syndrome (i.e., homozygously nonfunctioning proteins), the unconjugated hyperbilirubinemia becomes marked, almost always exceeding 5 mg/dL and causing jaundice and sometimes exceeding 20 mg/dL. Affected infants develop severe unconjugated hyperbilirubinemia, which typically leads to kernicterus, deposition of bilirubin in the brain, particularly affecting the basal ganglia, mainly the lenticular nucleus, causing severe motor dysfunction and retardation. In the less severe type II form, enzyme activity is approximately 10% of normal, and survival to adulthood is possible (Berk & Noyer, 1994c). The danger of kernicterus is a certainty at levels exceeding 20 mg/dL. It is vital to treat these infants with phototherapy, as discussed earlier, to cause excretion of the unconjugated bilirubin.

Causes of Elevated Serum Levels of Conjugated Bilirubin. Excretion deficits: Dubin-Johnson syndrome. In another inborn error of metabolism, called *Dubin-Johnson syndrome*, there is a blockade of the excretion of bilirubin into the canaliculi, caused by defects in the adenosine triphosphate (ATP)-binding cassette (ABC) canalicular multispecific organic anion transporter, MRP2/cMOAT/ABCC2 (Paulusma et al., 1997; Tsujii et al., 1999; Gottesman & Ambudkar, 2001). This protein is a member of a family of approximately 100 different transporter proteins that share homology within the ABC region and contain transmembrane domains involved in recognition of substrates, which are transported across, into, and out of cell membranes and include proteins involved in multiple-drug resistance to chemotherapeutic agents in cancer treatment. Some protein members utilize ABCs to regulate ion channels. Several genetic diseases result from transporter mutations, including Dubin-Johnson syndrome, cystic fibrosis, age-related macular degeneration, Tangier disease, and progressive familial intrahepatic cholestasis (Gottesman & Ambudkar, 2001).

Dubin-Johnson syndrome is associated with increased plasma conjugated bilirubin, typically with mild jaundice (total bilirubin, 2–5 mg/dL), and intense dark pigmentation of the liver due to accumulation of lipofuscin pigment, brown granules from liposomal degradation of lipids. Thus, conjugated bilirubin accumulates within the hepatocyte and eventually backdiffuses into the circulation, where it is detected in serum. This inborn error can sometimes be confused with Rotor syndrome, possibly of viral origin, where there is also a block in the excretion of conjugated bilirubin but without liver pigmentation (Berk & Noyer, 1994d). In these cases, liver biopsy often will reveal cytosolic inclusion bodies within hepatocytes.

Biliary obstruction. In adults, cholelithiasis is the most common cause of hyperbilirubinemia. This condition results from the presence of bile stones (composed of bilirubin or cholesterol), most commonly in the common bile duct (choledocholithiasis). Most frequently, patients presenting with this condition are parous white females in early middle age (giving rise to the alliterative, semi-mnemonic, "fair, fecund, fortyish female"). Biliary obstruction due to cholelithiasis results in elevation of total bilirubin, with over 90% being direct bilirubin. In more than 90% of such patients, a concomitant rise in alkaline phosphatase (ALP) occurs. The levels of this enzyme are variable but are frequently above 300 international units (IU)/L.

Inflammatory conditions of the biliary tract, such as ascending cholangitis, also give rise to elevated serum levels of direct bilirubin and ALP, as discussed later in this chapter. The rise in direct bilirubin often exceeds 5 mg/dL. In gram-negative sepsis, there can be what appears to be a mild inflammation of the biliary tract, resulting in mild elevation of direct bilirubin to levels of 2 to 3 mg/dL. A concomitant elevation of ALP to levels of 200 to 300 IU/L is also observed.

In hepatitis, in which toxic destruction of hepatocytes is due to viral, chemical, or traumatic causes, focal necrosis and/or cellular injury results both in blocking conjugation of bilirubin and in excretion of conjugated bilirubin. Thus, elevation of both direct and indirect bilirubin occurs. Serum levels of bilirubin are variable, depending on the severity of infection and the extent of disease. In viral hepatitis, such as hepatitis B, as discussed subsequently, serum bilirubin levels often reach levels of 5 to 10 mg/dL or greater.

Aside from liver disease, elevations of conjugated bilirubin may occur with a few other disorders. Septicemia (as noted previously), total parenteral nutrition, and certain drugs such as androgens commonly cause increased conjugated bilirubin, but the mechanism is not understood (Zimmerman, 1979; Jenniskens, 2016). Fasting causes increases in unconjugated bilirubin in normal individuals but to a lesser degree than is seen in Gilbert syndrome.

Laboratory Tests for Bilirubin

Bilirubin is typically measured using diazotized sulfanilic acid, which forms a conjugated azo compound with the porphyrin rings of bilirubin, resulting

in reaction products that absorb strongly at 540 nm (see Chapter 28). Because unconjugated bilirubin reacts slowly, accelerants such as caffeine or methanol are used to measure total bilirubin. Deletion of these accelerants allows determination of direct-reacting, or direct, bilirubin.

Until the early 1980s, it was accepted that direct bilirubin was equal to conjugated bilirubin. The introduction of dry-slide technology, using differential spectrophotometry to measure conjugated and unconjugated bilirubin separately, led to the observation that the sum of these two entities did not equal total bilirubin and to the characterization of delta-bilirubin. Approximately 70% to 80% of conjugated bilirubin and delta-bilirubin and a small percentage of unconjugated bilirubin are measured in the direct bilirubin assay (Lo & Wu, 1983; Doumas & Wu, 1991). Although good data support the measurement of conjugated bilirubin instead of estimating it from direct bilirubin (Arvan & Shirey, 1985; Doumas et al., 1987), the direct bilirubin assay is still widely used. The accuracy of direct bilirubin assays is dependent on sample handling and reagent composition. Prolonged exposure to light causes photoisomerization, increasing direct-reacting bilirubin (Ihara et al., 1997; McDonagh, 2008). Use of wetting agents or incorrect pH buffers increases the amount of unconjugated bilirubin measured as direct bilirubin (Doumas & Wu, 1991). Typically, direct bilirubin should measure 0 to 0.1 mg/dL in normal individuals, with rare values of 0.2 mg/dL in the absence of liver or biliary tract disease.

Reference values for total bilirubin are both age and gender dependent. Bilirubin levels typically reach peak values at around ages 14 to 18 years, falling to stable adult levels by age 25 years (Rosenthal, 1984; Notter, 1985; Zucker, 2004). Values are higher in males than in females at all ages (Rosenthal, 1984; Carmel et al., 1985; Notter et al., 1985; Dufour, 1998a; Zucker et al., 2004). Strenuous exercise causes a significant increase in bilirubin values compared with those seen in sedentary individuals or those engaging in chronic exercise (Dufour, 1998b; Fragala et al., 2017; Witek et al., 2016; Swift et al., 2012). African Americans have bilirubin levels significantly lower than those of other ethnic groups.

Other Metabolic Tests

Ammonia

This critical and toxic compound is metabolized exclusively in the liver. Ammonia is derived mainly from amino acid and nucleic acid metabolism. Some ammonia is also produced from metabolic reactions such as the action of the enzyme glutaminase on glutamine, resulting in the production of glutamic acid and ammonia. As it happens, ammonia can be metabolized only in the liver because the liver uniquely contains the critical enzymes for the Krebs-Henseleit or urea cycle, in which ammonia, a toxic substance, is ultimately converted into urea, a nontoxic compound that is readily excreted. In this cycle, ammonia, with the enzyme carbamoyl phosphate synthetase, is condensed with carbon dioxide (CO_2) and ATP to form carbamoyl phosphate that then, in the rate-determining step, carboxamidates the delta-amino group of ornithine to form citrulline using the enzyme ornithine carbamoyltransferase (OCT), an enzyme that is unique to the liver. Congenital deficiency of this or other urea cycle enzymes leads to increased levels of ammonia in serum and in cerebrospinal fluid (Batshaw, 1994).

A unique feature of liver tissue is its ability to regenerate. To abolish liver tissue function, more than 80% of the liver must be destroyed. If most of the liver is destroyed by such conditions as cirrhosis (Stahl, 1963) or, less commonly, acute fulminant hepatic failure, including Reye syndrome (Heubi et al., 1984; Sunheimer et al., 1994), urea cycle enzymes are no longer present. This leads to a toxic buildup of ammonia and some of the amino acid intermediates in the urea cycle, such as arginine, which has known neurotoxic effects. The result is an increase in ammonia and these amino acid intermediates in the circulation and in the central nervous system (CNS), giving rise to hepatic encephalopathy. In addition, in most cirrhotics, intrahepatic portal-systemic shunting occurs, causing ammonia to bypass the liver and resulting in elevated serum ammonia concentrations. Elevated serum levels of ammonia therefore often indicate some form of liver failure, although other conditions can also induce increases in serum ammonia levels.

In patients with cirrhosis or fulminant hepatic failure, there has been some dispute as to whether ammonia itself is the cause of the observed metabolic encephalopathy; possibly other toxins that accumulate as a result of absent hepatic detoxification are the cause. One of the arguments often used is that there is no clear correlation between the severity of the encephalopathy and serum ammonia concentrations (Lewis & Howdle, 2003). Countering this argument is the finding that, although venous ammonia levels do not correlate with the degree of encephalopathy (Stahl, 1963), arterial levels of ammonia do generally correlate with the degree of encephalopathy. Furthermore, in patients with cirrhosis or fulminant hepatic failure, lowering serum ammonia invariably diminishes the severity of the encephalopathy (Pincus et al., 1991). Furthermore, idiopathic hyperammonemia, not related to liver disease, also induces lethal encephalopathy (Shepard et al., 1987; Davies et al., 1996). An important mechanism by which ammonia can cause toxicity to the CNS is its ability to lower the concentration of γ-aminobutyric acid (GABA), a critically important neurotransmitter in the CNS, by reacting with glutamic acid to form glutamine via reversal of the glutaminase-catalyzed reaction (Butterworth et al., 1987). This depletes glutamic acid in the CNS. However, GABA is formed directly from the decarboxylation of glutamic acid; thus, GABA levels consequently decrease, with potentially serious effects on neurotransmission (see Chapter 24). Because ammonia causes accumulation of glutamine in the CNS, there is the suggestion that, at least in valproic acid–induced hyperammonemia, cerebrospinal fluid levels of glutamine can be used in the diagnosis and management of hepatic encephalopathy (Vossler et al., 2002). More recently, besides evidence that ammonia in the CNS is directly toxic to astrocytes, there is growing recognition that there is a complex and synergistic relationship between ammonia, inflammation, and oxidative stress in the pathogenesis of hepatic encephalopathy. Neutrophil dysfunction results in the generation of reactive oxygen species contributing to oxidative stress and inflammation, with lowered ability of the CNS to block infectious agents. In accordance with these findings, strategies targeting systemic inflammation, such as rifaximin-α and other anti-inflammatory agents being studied, are quickly becoming the new mainstay in the treatment of hepatic encephalopathy (Shawcross et al., 2010; Aldridge et al., 2014). One major new finding put forth by these studies is that treatment of hepatic encephalopathy with suitable anti-inflammatory agents may be effective.

At present, most commonly, elevated serum ammonia concentrations in hepatic encephalopathy are reduced by the agent lactulose, which is metabolized by a wide range of gut bacteria to lactic acid (Mao et al., 2014). The acid so produced in the intestinal lumen traps ammonia as ammonium ion, which can no longer diffuse across the intestinal membrane and is thus excreted. Ammonia-producing bacteria in the intestine are removed by treatment with antibiotics such as neomycin.

Assays for Ammonia. Ammonia is typically measured by enzymatic assays using glutamate dehydrogenase, which catalyzes the reaction of α-ketoglutarate and ammonia to form glutamate, with oxidation of NADPH to NADP as the indicator (decrease in absorbance at 340 nm, as described in Chapter 21). Ammonia is also measured via a dry-slide method (e.g., on the Ortho Diagnostics Vitros systems) using alkaline pH buffers to convert all ammonium ions to ammonia gas, with bromophenol blue as the indicator (Huizenga et al., 1994). Because ammonia is a product of cellular metabolism, methods used in specimen collection and transportation are critical in preventing artifactually increased levels. Arterial blood is the preferred specimen for measurement of ammonia. Although venous blood is not recommended, if used, tourniquets should be used minimally, and fist clenching and relaxing should be avoided during collection. Specimens should be kept in ice water until separation of cells from plasma occurs (Howanitz et al., 1984; da Fonseca-Wollheim, 1990).

Lipids

Cholesterol and Other Lipids (see Chapter 18). Because the liver is vital in lipoprotein synthesis and interconversions, hepatic disorders often cause derangements in lipoprotein metabolism. Although none of these abnormalities is used to diagnose liver pathology, it is important to recognize that they may result from liver disease. In severe liver injury, including cirrhosis, these abnormalities include a decrease in high-density lipoprotein (HDL), particularly the HDL_3 (but often not the HDL_2) subfraction, and in other altered lipoprotein distributions, caused in part by deficiencies of lecithin/cholesterol acyltransferase (LCAT, the enzyme that esterifies cholesterol) and of lipoprotein lipases, resulting in elevated levels of unesterified cholesterol and hypertriglyceridemia (triglyceride levels ranging from 250 to 500 mg/dL), respectively. In addition, there are increased levels of phospholipids, including lecithins, in blood and in the very-low-density lipoprotein (VLDL) fraction. Overall, the resulting lipoprotein pattern is that of the so-called abnormally migrating β-lipoprotein, typical of type III hyperlipoproteinemia (see Chapter 18). However, in cirrhotics with poor nutrition, despite critical enzyme deficiencies, low levels of cholesterol (<100 mg/dL) may be found.

In contrast, in alcohol-induced liver injury, alcohol induces increased expression of apolipoprotein (apo) A-I protein. Thus, HDL—especially HDL_3—may be elevated if alcohol ingestion continues. Because apoA-I protein decreases in cirrhosis, serum levels of this protein have been used to diagnose this disease using the so-called PGA index (Teare et al., 1993), discussed later in this chapter, a combination of prothrombin time (PT),

which increases, with γ-glutamyl transferase activity (discussed later), which also increases, and apoA-I protein. This index differs for alcoholic hepatitis, enabling the distinction to be made between these two conditions without the necessity of liver biopsy (Mun et al., 2003).

In cholestasis, regurgitation of biliary contents into the bloodstream results in the buildup of lipoprotein X (LpX; discussed in Chapter 18) and elevation of biliary lipids. Because LpX carries high levels of unesterified cholesterol, cholesterol levels in serum can become markedly elevated (Turchin et al., 2005).

Bile Salts. Bile salts, which are products of cholesterol metabolism, facilitate absorption of fat from the intestine. They are stored in the gallbladder and released to the intestine after meals through gallbladder contraction mediated by cholecystokinin. They are not usually used in the diagnosis of abnormal liver function but are important in that they constitute a substantial amount of bile in bilirubin excretion and can therefore be of use in diagnosing cholestasis. Also, in severe biliary obstruction, the buildup of bile salts in serum causes symptomatic illness in the form of intractable itching, although this has been disputed (Jones & Bergasa, 1999). The primary bile salts, cholate and chenodeoxycholate, are produced in the liver and excreted into the biliary and enterohepatic systems. In the intestinal lumen, bacteria utilize 7-α-dehydroxylation to produce secondary bile salts (i.e., lithocholate, deoxycholate, and ursodeoxycholate) (Carey & Cahalane, 1988). Ursodeoxycholate, an end-product of bile salt metabolism in humans, is produced by isomerization of secondary bile salts and has been found to be therapeutic in cholestatic diseases (Rost et al., 2004). These bile salts are conjugated, in the microsomal system discussed later, to glycine and taurine and are also sulfated and glucuronidated. Conjugation of bile salts to taurine and sulfates increases with the severity of cholestasis in conditions causing obstruction to bile outflow. Recirculation of bile salts to the liver occurs by reabsorption from the terminal ileum, where deoxycholate is almost completely reabsorbed, and chenodeoxycholate is about 75% reabsorbed. In cirrhosis, a disproportionate decrease in cholic acid is seen, along with a reduced ratio of primary to secondary bile salts. With cholestasis, secondary bile salts are not formed; thus, the ratio of primary to secondary bile salts is markedly increased.

Renal clearance of bile salts is negligible in normal patients, but in cholestasis, renal excretion of bile salts, mainly in the form of sulfates and glucuronides, is enhanced. Fasting bile salts, when normal, can exclude the presence of parenchymal liver disease in patients with Gilbert syndrome (Vierling et al., 1982), as discussed previously. It should also be recognized that defective production of bile salts, which helps solubilize the contents of bile, in the liver may predispose to the formation of bilirubinate or cholesterol stones and posthepatic biliary obstruction.

Analysis of bile salts must be performed on serum taken from patients who are in the fasting state or on serum taken at a specified time after meals, because food ingestion causes a significant increase in bile acid levels. Bile salts can be measured by many techniques, but chromatographic methods, particularly high-performance liquid chromatography, as discussed in Chapter 24, are most widely used and allow separation of different bile salts.

Drug Metabolism

Many xenobiotics, such as drugs, are metabolized in the liver, mainly in the microsomes of hepatocytes. Complex series of reactions occur, many of which are dependent on cytochrome P450, which is involved in the oxidation of these compounds. Whether specific exogenous compounds are converted to metabolites depends on the isoforms of cytochrome P450, such as CYP1A and CYP2B (cytochrome P450 1A and 2B, respectively). Often, the conversion of xenobiotics into metabolites using this system involves two phases: Phase I reactions involve oxidations/hydroxylations, and phase II reactions conjugate the metabolite (or parent compound) to polar compounds, such as glucuronic acid, glycine, taurine, and sulfate. In more severe liver disease, which involves microsomal damage, this ability to metabolize xenobiotics is compromised. Thus, the ability of hepatocytes to metabolize drugs can be used to measure liver damage.

This is generally accomplished by administering a known dose of isotopically labeled (usually ^{13}C-labeled) drug and measuring the $^{13}CO_2$ exhaled over time in a patient's breath. Two categories of breath tests have been developed based on the rate-limiting step in metabolism. The first group includes drugs such as aminopyrine, caffeine, and diazepam, which are metabolized at rates that are independent of hepatic blood flow to the liver and depend only on the enzymatic activity of different cytochromes P450 (e.g., CYP1A). The second group is composed of drugs such as methacetin, phenacetin, and erythromycin, whose rates of metabolism depend on the rate of blood flow (i.e., their rates of metabolism are fast compared with their rates of delivery to the liver). These types of dynamic tests appear not to be so useful in the initial diagnosis of hepatic disease; rather, they are more useful in estimating the extent of liver damage in known liver disease (Nista et al., 2004).

Some interferences that complicate interpretation of the results of these tests include dependence of the demethylation of aminopyrine (the methyl group is oxidized to CO_2) on vitamin B_{12}. In cases of vitamin B_{12} deficiency, less than normal amounts of $^{13}CO_2$ will be exhaled because of low B_{12} levels, not necessarily because of liver damage. Rates of caffeine metabolism generally decrease with increasing age but are increased by smoking; these findings can complicate interpretation of test results.

SYNTHETIC FUNCTIONS

Protein Synthesis

The liver is the site of synthesis for most plasma proteins. Major exceptions include immunoglobulin (Ig) and von Willebrand factor. Synthesis of more than 90% of all protein and 100% of albumin occurs in the liver. Thus, extensive destruction of liver tissue will result in low serum levels of total protein and albumin. In cirrhosis, besides hepatocyte destruction, another cause of diminished protein production is portal hypertension, which decreases delivery of amino acids to the liver. Two vital measurements of liver function, therefore, are total protein and albumin levels in serum. However, it should always be kept in mind that other major causes of low serum total protein and albumin have been identified. These include renal disease, malnutrition, protein-losing enteropathy, and, less commonly, chronic inflammatory disease. These alternative causes must always be considered when liver function status is evaluated.

In liver disease with widespread injury or necrosis, such as fulminant hepatic failure and cirrhosis, plasma levels of liver-synthesized proteins fall such that proteins with longer half-lives tend to decrease more slowly. Albumin has a half-life of about 20 days; thus, decreases in its serum levels occur more slowly than those of proteins with shorter half-lives. Among the liver-produced proteins with shorter half-lives are factor VII (4–6 hours), transthyretin (1–2 days), and transferrin (6 days).

Determination of Serum Protein Levels

This is based usually on the biuret method as described in Chapter 28. This method reflects the ability of the peptide backbone C=O groups of proteins to form color complexes with copper that absorb strongly at 540 nm. Some methods utilize a dye-binding method in which the proteins form a complex with the dye Coomassie blue. Albumin forms a unique color complex with the dyes bromocresol green and bromocresol purple, such that they absorb maximally at slightly different wavelengths, thus allowing direct spectrophotometric quantitation (Ihara et al., 1991; Duly et al., 2003; Bertholf, 2014; Moreira et al., 2018). Bromocresol purple tends to react more exclusively with albumin than does bromocresol green (which reacts to a minor extent with some globulins); thus, serum albumin levels may be slightly lower when determined with bromocresol purple. The reference range for total serum protein levels is generally in the 6.0 to 7.8 g/dL range. At least 60% of this should be albumin, the normal range for which is about 3.5 to 5.0 g/dL.

Serum protein electrophoresis and quantitative Ig may reveal characteristic changes in liver disease, as discussed in Chapter 20. Typically, in cirrhosis, albumin is significantly decreased, as are the α-1, α-2, and β (principally transferrin) bands. However, a polyclonal increase in Ig, which is seen frequently, produces the characteristic β-γ bridging pattern, as discussed in Chapter 20. In autoimmune hepatitis, albumin is typically decreased; this is accompanied by a marked polyclonal increase in IgG. Primary biliary cirrhosis, an autoimmune disease, is accompanied by a polyclonal increase in IgM. However, as noted later, this polyclonal IgM does not react with the mitochondrial antigens against which the autoimmune antibodies in this disease do react (Reshetnyak, 2015).

Albumin

Albumin is the major protein produced by the liver. Its synthesis is increased by low plasma oncotic pressure and is decreased by cytokines, particularly interleukin-6. Although normal albumin synthesis occurs at about 120 mg/kg/day, the rate of synthesis can approximately double with low oncotic pressure. A decrease in albumin is one of the major prognostic features in patients with cirrhosis. Albumin measurements were discussed previously in Chapter 20 and are further discussed in Chapter 28.

Albumin is a transport protein for many substances, both endogenous (e.g., bilirubin, thyroid hormone) and exogenous (e.g., drugs). Low serum albumin levels due to liver disease are almost always caused by massive destruction of liver tissue and are seen primarily in cirrhosis, most often secondary to alcoholism. The diminution in albumin is paralleled by a fall

in total serum protein. Because albumin is the osmotically active intravascular colloid, hypoalbuminemia often results in edema. In cirrhosis, in which increased resistance to blood flow in the sinusoids causes portal hypertension, the combined effect of elevated hydrostatic pressure in the portal system and low colloid osmotic pressure results in ascites, a frequent finding in cirrhosis. These same changes may also be seen acutely in fulminant hepatic failure (Sunheimer et al., 1994; Garcovich et al., 2009).

Other Serum Proteins

Although most of the proteins discussed in Chapter 20 are produced by the liver, two bear special importance in the detection of congenital liver disorders.

α_1-Antitrypsin. α_1-antitrypsin (AAT), the most abundant α_1-globulin, is the most important protease inhibitor in plasma. Although its name indicates that it inhibits trypsin, it also is an inhibitor of other serine proteases, such as elastin. AAT is coded for by the *Pi* gene on chromosome 14; several genetic variants are due to point mutations, leading to single amino acid substitutions (Chappell et al., 2004). The most common variant, M, is associated with normal serum AAT levels. The mutations present in the S and Z variants prevent normal protein glycation, leading to accumulation of AAT within hepatocytes and reduced plasma AAT levels (Propst et al., 1994; Bartels et al., 2009; Bengtson et al., 2016; Hidvegi et al., 2005; Kelly et al., 2010). In the United States, the overwhelming genotype is PiMM, where Pi is the protease inhibitor. The other genotypes—PiZZ, PiSS, PiSZ, PiMZ, and PiMS—all contain measurable activity of antiprotease, except a rare null genotype, Pi^{-}. If the antiprotease activity of the MM phenotype is used as the reference, then the activity in phenotype ZZ is 15%, SS is 60%, MZ is 57.5%, and MS is 80%. Adults with PiZZ are most prone to develop emphysema relatively early in life as a result of uninhibited trypsin activity on alveolar wall elastin. Patients with PiZZ tend to accumulate the Z protein in periportal hepatocytes, where it forms discrete cytoplasmic bodies and may also develop neonatal hepatitis. Curiously, although infants may die of hepatic injury, it resolves in most infants and progresses to cirrhosis in only about 3% (Sveger, 1988). In adults, the likelihood of liver injury is increased in patients heterozygous or homozygous for the Z variant of AAT. This may be due to accumulation of AAT in the endoplasmic reticulum that induces autophagy and apoptosis of hepatocytes (Teckman et al., 2004). AAT phenotyping can be performed using isoelectric focusing (Propst et al., 1994; Greene et al., 2017). Because AAT is an acute-phase reactant, its serum levels can be normal in MZ heterozygotes.

Ceruloplasmin. The major copper-containing protein in serum, ceruloplasmin, is also the enzyme present in highest circulating concentration. Ceruloplasmin is a ferroxidase, which is essential for converting iron to the ferric state to allow binding to transferrin. Low levels of ceruloplasmin are found in Wilson disease, a rare congenital disorder (1 in 30,000 individuals) associated with one of many mutations in the gene on chromosome 13 coding for a cellular adenosine triphosphatase (ATPase), ATP7B, a member of the cation-transporting p-type ATPase family (Bull et al., 1993; Gitlin, 2003; Medici, 2007). This protein is principally expressed in the liver and promotes copper secretion into plasma, coupled with ceruloplasmin synthesis, and into the biliary tract. More than 500 mutations of this Wilson disease gene have been detected, with over 300 causing disease, resulting in impairment of ATP7B function and intracellular copper accumulation (Langner & Denk, 2004; Kenny & Cox, 2007; Roberts & Schilsky, 2008). Excess intracellular copper is deposited in lysosomes in hepatocytes; it induces free-radical reactions such as lipid peroxidation and membrane instability. Resultant liver damage can lead to chronic active hepatitis, cirrhosis, or, uncommonly, fulminant hepatic failure. In addition, steatosis and inflammation can result in this condition. Copper becomes deposited in the CNS, especially in the lenticular nucleus of the basal ganglia, causing neuropsychiatric disease. It can also be deposited at the edge of the iris, forming the observed Keyser-Fleischer rings.

The diagnosis of Wilson disease is made on the basis of typical clinical and laboratory findings, including low serum ceruloplasmin, which can be measured by immunoassay or by enzymatic assay, increased urinary copper excretion, and increased hepatic copper content. Although ceruloplasmin is characteristically low in Wilson disease, factors that increase ceruloplasmin synthesis (e.g., cytokines, pregnancy, estrogens) may cause normal ceruloplasmin levels in up to 15% of patients overall and in as many as 35% with hepatic manifestations of Wilson disease (Dufour & Kaplan, 1997), particularly acute Wilsonian hepatitis (Berman et al., 1991; Eisenbach et al., 2007). Genetic testing is the most reliable means to establish the diagnosis, but it is difficult because more than 300 mutations have been shown to cause disease.

Clotting Factors

As mentioned earlier, except for von Willebrand factor, which is made by endothelial cells and megakaryocytes, coagulation proteins are synthesized in the liver. In addition, inhibitors of coagulation, such as antithrombin III, α_2-macroglobulin, α_1-antitrypsin, C1 esterase inhibitor, and protein C, are synthesized in the liver. In addition, fibrin degradation products are catabolized in the liver. Low levels of antithrombin III in patients with cirrhosis and hepatitis may be caused by decreased synthesis, increased consumption, or alteration in the transcapillary flux ratio (Kelly, 1987). The most common coagulopathy seen in liver failure (i.e., cirrhosis and acute fulminant hepatic failure) is disseminated intravascular coagulopathy (DIC), as discussed in Chapter 9 and extensively throughout Part 5 of this book. This condition is characterized by increased consumption of clotting factors and platelets, causing thrombocytopenia and elevations of both PT and partial thromboplastin time (PTT). The mechanism has been postulated to be decreased synthesis of clotting inhibitory factors, decreased clearance of activated clotting factors, or release of tissue thromboplastin from hepatocytes (Kelly & Tuddenham, 1986). D-Dimer and, in the past, fibrin split products, detected in DIC, have been found in up to 80% of patients with liver disease without evidence of fibrinolysis (Van de Water et al., 1986). It is important that the diagnosis of DIC be made certain by determination of elevated blood D-dimer levels, as described in Part 5 on hemostasis and thrombosis. In some cases of liver failure, platelet counts are decreased because of sequestration in an enlarged spleen due to hepatosplenomegaly. This condition, combined with elevated levels of PT and PTT caused by low levels of synthesis of coagulation factors, can masquerade as DIC. In these cases, D-dimer levels are not elevated, excluding this diagnosis.

Perhaps the most frequently ordered laboratory test for detecting liver-associated coagulation abnormalities is PT and its associated measurement, the international sensitivity ratio, as described in Part 5. The PT measures the efficacy of the extrinsic clotting system in which factor VII is activated by tissue factor, as discussed in Part 5. Because factor VII is uniquely synthesized in the liver, its measurement can be used to evaluate liver function status. Often, PT is computed as the international normalized ratio (INR), which attempts to standardize all PT measurements relative to a gold standard PT-measuring method, using the international sensitivity index (ISI), as described in Part 5.

Some Caveats in Using PT and INR to Evaluate Liver Function. Because PT and PTT measure the status of the coagulation cascades (extrinsic and intrinsic, respectively), any coagulation disorder will give rise to abnormal PT and/or PTT, independent of liver function. In addition, in patients with cholestasis (i.e., disease of the biliary tract) with no hepatocytic dysfunction (e.g., cirrhosis, fulminant hepatic failure), absorption of fat-soluble vitamin K from the gut may be impaired because of low levels of bile salts that allow membrane transport of this vitamin. Because factors II, VII, IX, and X depend on vitamin K for biosynthesis via carboxylation, coagulation abnormalities often result. Therefore, in patients with cholestasis, normal serum levels of inactive precursor forms of these four coagulation factors can be detected, as discussed later. Correction of PT by the administration of vitamin K is usually possible when factor V is normal in patients with cholestatic liver disease.

Also, use of the INR in evaluating liver function can provide misleading results. As discussed in Part 5, the INR is based on PT values for patients treated with Coumadin (warfarin, which blocks mainly the extrinsic system). Thus, its appropriateness for evaluating non–Coumadin-induced coagulopathies has been questioned, especially in view of the finding that PT increases much less with lower ISI in patients with liver disease than in patients being treated with Coumadin (Kovacs et al., 1994; Ts'ao et al., 1994; Johnston et al., 1996; Robert & Chazouilleres, 1996).

Prothrombin Times Are Used to Compute the MELD Score. PT is an integral part of the model for end-stage liver disease (MELD) score in evaluating priority for liver transplantation in liver disease (Trotter et al., 2004). This score is a computed number based on the values of bilirubin, creatinine, and INR and is applied in categories of 10 (i.e., scores of 40 or higher predict 100% mortality [30–39, 83%; 20–29, 76%; 10–19, 27%; <10, 4%]). Although this score appears to predict accurately the 3-month mortality for cirrhotic patients awaiting liver transplantation (Farnsworth et al., 2004), it must be used with caution both because reference ranges of these analytes differ among different laboratories, making standardization difficult, and because caveats are associated with using INR values, as described earlier.

Des-γ-Carboxy Prothrombin

The vitamin K–dependent coagulation factors (II, VII, IX, X) are synthesized in the liver and require a vitamin K–mediated posttranslational modification (γ-carboxylation of a number of terminal glutamic acid residues to

γ-carboxyglutamic acid) to occur before secretion into the blood, which is necessary for functional activity of these factors in the coagulation cascade. The unmodified precursor of prothrombin, des-γ-carboxy prothrombin (DCP), has been found to be elevated in the sera of patients with hepatocellular carcinoma. DCP is measured using two monoclonal antibodies, 19B7 and MU-3. A rapid immunoassay for DCP is available (Yamaguchi et al., 2008). Increases of DCP in patients with hepatocellular carcinoma predict decreased survival times (Nagaoka et al., 2003). The overall sensitivity and specificity of elevated serum DCP levels in diagnosing hepatocellular carcinoma is 67% and 92%, respectively (Gao et al., 2012). However, assays for DCP do not have the same general use as α-fetoprotein (AFP), discussed later, for diagnosing and following this disease. However, a study has found that use of both DCP and AFP together reliably predicts survival rates of patients with recurrent hepatocellular carcinoma (Okamura et al., 2014).

TESTS OF LIVER INJURY

PLASMA ENZYME LEVELS

As metabolically complex cells, hepatocytes contain high levels of a number of enzymes. With liver injury, these enzymes may leak into plasma and can be useful for diagnosis and monitoring of liver injury. Although enzymes are discussed in Chapter 21, knowledge of the cellular locations of enzymes and patterns of enzyme change is critical in understanding the findings in various types of liver disease.

Cellular Locations of Enzymes

Within the hepatocyte, the commonly measured enzymes are found in specific locations; the type of liver injury will determine the pattern of enzyme change. Figure 22.3 illustrates the locations of the most important hepatocytic enzymes. Cytoplasmic enzymes include lactate dehydrogenase (LD), aspartate aminotransferase (AST), and alanine aminotransferase (ALT). Mitochondrial enzymes, such as the mitochondrial isoenzyme of AST, are released with mitochondrial damage. Canalicular enzymes, such as ALP and γ-glutamyl transferase (GGT), are increased by obstructive processes.

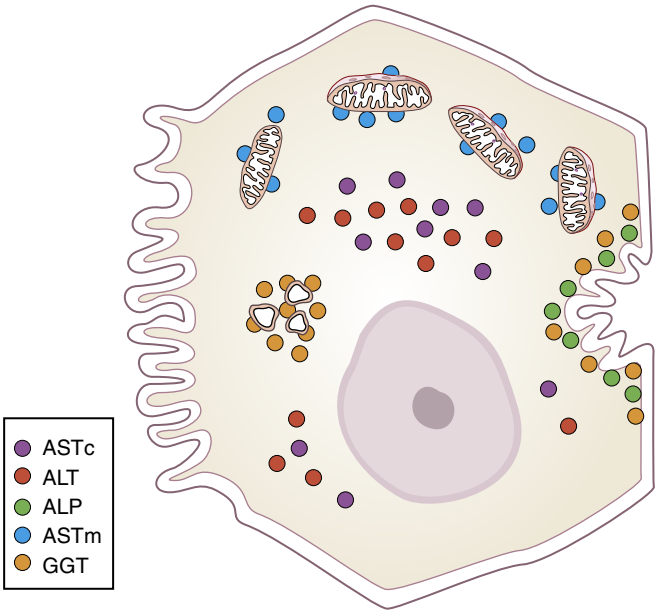

Figure 22.3 Location of hepatocellular enzymes. The major diagnostic hepatocellular enzymes are located at various sites in the hepatocyte, giving rise to different patterns of enzyme release with different causes of injury. Alanine aminotransferase (ALT) and the cytoplasmic isoenzyme of aspartate aminotransferase (ASTc) are found primarily in the cytosol. With membrane injury, as in viral or chemically induced hepatitis, these enzymes are released and enter the sinusoids, raising plasma AST and ALT activities. Mitochondrial aspartate aminotransferase (ASTm) is released primarily with mitochondrial injury caused by ethanol, as in alcoholic hepatitis. Alkaline phosphatase (ALP) and γ-glutamyl transferase (GGT) are found primarily on the canalicular surface of the hepatocyte. Bile acids accumulate in cholestasis and dissolve membrane fragments, releasing bound enzymes into plasma. GGT is also found in the microsomes, represented as pink rings in the figure; microsomal enzyme-inducing drugs, such as phenobarbital and Dilantin (phenytoin), can also increase GGT synthesis and raise plasma GGT activity.

Mechanisms of Enzyme Release

Enzymes are released from hepatocytes as a result of injury to the cell membrane that directly causes extrusion of the cytosolic contents. In addition, agents such as ethanol cause release of mitochondrial AST from hepatocytes and its expression on cell surfaces (Zhou et al., 1998a). Accumulation of bile salts with canalicular obstruction causes release of membrane fragments with attached canalicular enzymes (Schlaeger et al., 1982; Moss, 1997). Increased synthesis of GGT, and to a lesser extent ALP, can occur with medications that induce microsomal enzyme synthesis, notably ethanol, phenytoin, and carbamazepine (Aldenhovel, 1988).

Aminotransferases (Transaminases)

Two diagnostically very useful enzymes in this category are AST, also known as *serum glutamate oxaloacetate transaminase* (*SGOT*), and ALT, formerly called *serum glutamate pyruvate transaminase* (*SGPT*). These enzymes catalyze reversibly the transfer of an amino group of AST or ALT to α-ketoglutarate to yield glutamate plus the corresponding ketoacid of the starting amino acid (i.e., oxaloacetate or pyruvate, respectively). Both enzymes require pyridoxal phosphate (vitamin B_6) as a cofactor. Using ALT as an example, alanine reacts with pyridoxal phosphate to yield pyruvate plus pyridoxine. Pyridoxine then reacts with α-ketoglutarate to yield glutamate plus regenerated pyridoxal phosphate.

In many of the serum assays for ALT and AST, it is assumed that the patient's serum provides a sufficient complement of pyridoxal phosphate, a circumstance that does not always apply. In a most poignant case illustrating this point, a patient, a known alcoholic, was admitted to a hospital with a presumptive diagnosis of alcoholic hepatitis, a condition described at length later. His admission clinical chemistry profile showed normal to low serum levels of ALT and AST. This finding is unusual in alcoholic hepatitis because, as we discuss later, both enzymes become significantly elevated such that AST levels, that source both from the cytosol *and* mitochondria, are higher than those for ALT. During the course of the next 24 hours, he was treated for his condition, with apparent clinical improvement. However, a repeat liver function profile on the original blood sample showed marked elevations of both enzymes to levels greater than 200 IU/L. This presented a diagnostic dilemma, which was resolved when it was realized that, as part of the protocol for treatment of alcoholic hepatitis, the patient had received vitamin supplements, including vitamins B_6 and B_{12}. Because the serum assays for both ALT and AST required vitamin B_6 supplied by the patient's serum, and the patient, an alcoholic, was vitamin B_6 deficient (common in alcoholics), the assays for both enzymes showed normal to low levels caused by the absence of vitamin B_6. Upon therapeutic intervention, when vitamins were administered, sufficient serum levels of vitamin B_6 were present to allow full enzyme activities. This clinical history illustrates the central role of pyridoxal phosphate in enzyme catalysis by AST and ALT and the importance of understanding the chemical basis for enzyme assays.

AST and ALT have blood half-lives of 17 and 47 hours, respectively, and have upper reference range limits of around 40 IU/L. (See Chapter 21 for the definition of international units [IU]) AST is both intramitochondrial and extramitochondrial, but ALT is completely extramitochondrial. Mitochondrial AST isoenzyme has a half-life of 87 hours (Panteghini, 1990). AST is ubiquitously distributed in the body tissues, including the heart and muscle, whereas ALT is found primarily in the liver, although significant amounts are also present in the kidney.

Total cytoplasmic AST is present in highest activity in hepatocytes, with a cell AST level approximately 7000 times that in plasma. ALT is also present in highest activity in hepatocytes, with a cell ALT level approximately 3000 times that in plasma. With pyridoxine deficiency, hepatic synthesis of ALT is impaired; a similar phenomenon occurs in hepatic fibrosis and cirrhosis. The enzyme changes seen in hepatic injury can be readily explained by differing hepatic activity levels and half-lives of enzymes. With most forms of acute hepatocellular injury, such as hepatitis, AST will be higher than ALT initially because of the higher activity of AST in hepatocytes. Within 24 to 48 hours, particularly if ongoing damage occurs, ALT will become higher than AST, based on its longer half-life.

An exception to these observations is seen in acute alcohol-induced hepatocyte injury, as in alcoholic hepatitis. Studies suggest that alcohol induces mitochondrial damage, resulting in the release of mitochondrial AST, which, besides being the predominant form of AST in hepatocytes, has a significantly longer half-life than do extramitochondrial AST and ALT. This frequently results in the disproportionate elevation of AST over ALT, yielding an AST/ALT quotient, also called the DeRitis ratio, of 3 to 4:1 in alcohol-induced liver disease. Whether cessation of alcohol consumption reduces this ratio is a topic of disagreement. In one early study, serum mitochondrial AST was measured in cirrhotic and noncirrhotic

patients who abused alcohol (Nalpas et al., 1986). Patients with chronic alcohol abuse, regardless of the extent of their underlying liver disease, had more consistent mitochondrial AST elevations than other patients; values dropped by more than 50% with abstinence for longer than 1 week. On the other hand, in more recent studies involving more than 300 patients, it was found that high AST/ALT ratios suggest advanced alcoholic liver disease (Nyblom et al., 2004). It should also be noted that many alcoholics are vitamin B_6 deficient, causing lower rates of synthesis of ALT and suppression of existing ALT activity.

In chronic hepatocyte injury, mainly in cirrhosis, ALT is more commonly elevated than AST; however, as fibrosis progresses, ALT activities typically decline and the ratio of AST to ALT gradually increases. Thus, by the time cirrhosis is present, AST is often higher than ALT (Williams & Hoofnagle, 1988; Sheth et al., 1998). However, in end-stage cirrhosis, the levels of both enzymes generally are not elevated and may be low as the result of massive tissue destruction. In acute fulminant hepatic failure, as discussed later and in Chapter 9, the serum levels of both aminotransferases are markedly increased and are such that the AST/ALT ratio is often significantly greater than 1 (Sunheimer et al., 1994).

Overall, ALT activity is more specific for detecting liver disease in nonalcoholic, asymptomatic patients. Mild elevations are often seen in hepatitis C infection. AST is used for monitoring therapy with potentially hepatotoxic drugs; a result more than three times the upper border of normal should signal stopping of therapy. Chronic elevation of aminotransferase activities in asymptomatic patients may have several causes, including alcohol or medication use, chronic viral hepatitis, or nonalcoholic fatty liver disease. Weight reduction may lower ALT in overweight patients whose ALT is elevated (Palmer & Schaffner, 1990). Ursodeoxycholic acid lowers ALT as well as GGT (see later discussion) when these are found to be elevated in blood donors (Bellentani et al., 1989).

Assays for AST and ALT

The chemical basis for these assays is described in Chapter 28. Several variants of assays can be used with these enzymes. In one, alanine for ALT or aspartate for AST is added to force the reaction to the right, yielding glutamate. Production of the latter is then coupled to the enzyme glutamate dehydrogenase in the so-called indicator reaction, yielding α-ketoglutarate. In this reaction, nicotinamide adenine dinucleotide (NAD) is converted to NADH (reducing agent derived from NAD), which can be measured as an increase in absorbance at 340 nm. These reactions must be evaluated over short periods because one of the substrates for these enzymes, α-ketoglutarate, is regenerated by the indicator reaction. Another variant for AST involves coupling the oxaloacetate (OAA) that is formed from aspartate in the reaction to malate dehydrogenase, which converts OAA to malate, and in which NADH is converted to NAD that is measured by a decrease in absorbance at 340 nm. For ALT, conversion of alanine to pyruvate allows coupling to the pyruvate dehydrogenase complex in which pyruvate is converted to acetyl coenzyme A, and in which NAD is converted to NADH that can be directly measured by an increase in absorbance at 340 nm. As noted earlier, it is vital that pyridoxal phosphate be present in sufficient quantity to allow these reactions to proceed.

Lactate Dehydrogenase

As described in Chapter 21, this cytosolic glycolytic enzyme catalyzes the reversible oxidation of lactate to pyruvate. As discussed in Chapter 18, five major LD isozymes exist, consisting of tetramers of two forms, H and M, the former having high affinity for lactate, the latter for pyruvate. Progressing from HHHH to MMMM, the five possible isozymes are labeled LD_1 to LD_5. LD_1 and LD_2 predominate in cardiac muscle, kidney, and erythrocytes. LD_4 and LD_5 are the major isoenzymes in liver and skeletal muscle. The upper reference range limit for total LD activity in serum is around 150 IU/L (see Chapter 21 for the definition of international units, or IU). Serum LD levels become elevated in hepatitis; often, these increases are transient and return to normal by the time of clinical presentation (Dufour & Teot, 1988; Singer et al., 1995; Fuchs et al., 1998) because LD isozymes originating in liver (LD_4 and LD_5) have relatively low activity in hepatocytes relative to plasma (about 500 times) and a half-life of approximately 4 to 6 hours.

More important is the large increase in total LD to levels of 500 IU/L or more combined with a significant increase in ALP, discussed later and in Chapter 21, to levels of greater than 250 IU/L, in the absence of other dramatic abnormalities in liver function enzyme levels, especially AST and ALT. These selective increases often accompany space-occupying lesions of the liver, such as metastatic carcinoma and primary hepatocellular carcinoma or, rarely, benign lesions, such as hemangiomata and adenomas. The source of the LD, most often the LD_5 isozyme, is not clear because it can originate from hepatocytes, the tumor, or both. The rise in ALP is due to blockage of local canaliculi and ductules by the masses in the liver, as discussed later. Assays for LD are described in Chapters 21 and 28.

Enzymes Primarily Reflecting Canalicular Injury

As shown in Figure 22.3, these enzymes are located predominantly on the canalicular membrane of the hepatocyte and include ALP, γ-glutamyl transferase, and 5′-nucleotidase. In contrast to cytoplasmic enzyme activities, canalicular enzyme activities within hepatocytes are typically quite low; focal hepatocyte injury seldom causes significant increases in canalicular enzyme levels.

Alkaline Phosphatase

As discussed at length in Chapter 21, ALP is present in a number of tissues, including liver, bone, kidney, intestine, and placenta, each of which contains distinct isozymes that can be separated from one another by electrophoresis. Total ALP in serum is mainly present in the unbound form and, to a lesser extent, is complexed with lipoproteins or, rarely, with Ig.

ALP in the liver, which has a half-life of about 3 days, is a hepatocytic enzyme that is found on the canalicular surface and is therefore a marker for biliary dysfunction. The bone isozyme is particularly heat labile, allowing it to be distinguished from the other major forms. In addition, small intestinal and placental ALP is antigenically distinct from liver, bone, and kidney ALP. The bulk of ALP in the serum of normal patients is made up of liver and bone ALP.

In obstruction of the biliary tract by stones in the ducts or ductules, or by infectious processes resulting in ascending cholangitis, or by space-occupying lesions, biliary tract ALP rises rapidly to values sometimes in excess of 10 times the upper limit of normal. The reasons for this increase probably include a combination of increased synthesis and decreased excretion of ALP. In obstructive cholestasis, ALP most commonly rises to twice the upper limit of normal or greater, roughly paralleling the rate of rise in serum bilirubin. If obstruction is partial, ALP usually increases as much as with complete obstruction, often out of proportion to the increase in conjugated bilirubin (dissociated jaundice). Passive congestion of the liver can occasionally result in moderate ALP elevations, more so than abnormal bilirubin levels. ALP is also moderately elevated in most instances of jaundice resulting from hepatic injury. When the resulting cholestasis is relieved, serum ALP levels fall to normal more slowly than bilirubin.

A high-molecular-weight ALP appears in serum in cholestasis. This ALP is attached to fragments of canalicular membrane. Bile salts solubilize the enzymes from the sinusoidal and canalicular membranes. In serum, the membrane-bound enzymes aggregate with lipids and lipoproteins. This may explain the relationship that has been observed, for instance, with LpX (see Chapter 18). Another form of high-molecular-weight ALP, which migrates differently on electrophoresis from the isozyme just described, has been found in malignant disease involving the liver (Viot et al., 1983).

Intestinal ALP is increased in a variety of disorders of the intestinal tract and in cirrhosis. Serum intestinal ALP is detected in more than 80% of cirrhotic patients as compared with 10% of normal controls. Measurement of this enzyme activity was suggested as one method of discriminating intrahepatic from extrahepatic jaundice because intestinal ALP may be absent in extrahepatic obstruction, but it lacks adequate sensitivity and specificity (Collins et al., 1987). Assays for ALP are described in Chapters 21 and 28.

γ-Glutamyl Transferase

This enzyme regulates the transport of amino acids across cell membranes by catalyzing the transfer of a glutamyl group from glutathione to a free amino acid. Its major use is to discriminate the source of elevated ALP (i.e., if ALP is elevated and GGT is correspondingly elevated, then the source of the elevated ALP is most likely the biliary tract). The highest values, often greater than 10 times the upper limit of normal, may be found in chronic cholestasis due to primary biliary cirrhosis or sclerosing cholangitis. This enzyme is also elevated in about 60% to 70% of those who chronically abuse alcohol, with a rough correlation between the amount of alcohol intake and GGT activity (Whitehead & Clark, 1978). Levels often decline slowly with abstention from alcohol and remain elevated for at least 1 month after abstinence begins (Belfrage et al., 1977; Moussavian et al., 1985). GGT has a half-life of 10 days; however, in recovery from alcohol abuse, the half-life may be as long as 28 days. It tends to be higher in obstructive disorders and with space-occupying lesions in the liver than with hepatocyte injury (Kim et al., 1977).

The gene for human GGT has been cloned, and the nucleotide sequence has been identified (Rajpert-De Meyts et al., 1988). GGT can be detected in three major forms in serum (Wenham et al., 1985), but such

determinations are not readily available. A high-molecular-mass form is present in normal serum, as well as in biliary obstruction, and more frequently in malignant infiltration of the liver. An intermediate-molecular-mass form consists of two fractions—the major one detected in liver disease and the other one found in biliary obstruction. Determination of these fractions lacks sufficient sensitivity and specificity to be worthwhile (Collins et al., 1987). The third form is a low molecular mass compound of uncertain importance.

Serum levels of GGT differ from those of ALP during pregnancy, in which GGT remains normal even during cholestasis in pregnancy. GGT is often increased in alcoholics even without liver disease; in some obese people; and in the presence of high concentrations of therapeutic drugs, such as acetaminophen and phenytoin and carbamazepine (increased up to five times the reference limits), even in the absence of any apparent liver injury. Similarly, elevated GGT and albuminuria have been found to predict the development of hypertension (Li & McDermott, 2014). These increases in GGT may occur in order to restore glutathione used in the metabolism of these drugs. Glutathione is conjugated to these drugs via the glutathione S-transferase system, and the complex is then excreted.

As described in Chapter 28, most assays for GGT utilize the substrate γ-glutamyl–*p*-nitroanilide. In the reaction catalyzed by GGT, *p*-nitroaniline is liberated and is chromogenic, enabling this colored product to be measured spectrophotometrically.

Other Enzymes

5′-Nucleotidase activity is increased in cholestatic disorders with virtually no increase in activity in patients with bone disease. This enzyme is discussed further in Chapter 21. Measurement of 5′-nucleotidase can corroborate the elevation of ALP from a hepatic source. Other enzymes, such as leucine aminopeptidase (LAP), can be used for the same purpose but virtually never are. Isocitrate dehydrogenase and ornithine carbamoyltransferase (the latter unique to the liver) activities are elevated in hepatocellular injury and parallel ALT and AST. Again, as with LAP, they are virtually never used in routine laboratory assays.

α-FETOPROTEIN

α-Fetoprotein (AFP) is synthesized by embryonic hepatocytes and fetal yolk sac cells and peaks in the second trimester of pregnancy, reaching levels that constitute up to one-third of fetal serum protein. The function of AFP is not known. It may be immunosuppressive, preventing fetal destruction by circulating maternal antibodies.

As discussed in Chapter 26, AFP becomes elevated to abnormal levels in fetal neural tube deficits. The reasons for this correlation are unclear. It is important to note that normal AFP levels vary considerably with gestational age. Therefore, the decision that the serum level of this protein is abnormally high will depend on the reference interval for the gestational age of the patient. Shortly after birth, AFP levels fall, reaching the adult normal range at around 1 year of age. There is evidence that early screening for neural tube deficits can begin at 11 to 13 weeks of gestation (Bredaki et al., 2012). After acute hepatic injury, a rise in AFP (typically 100–200 ng/dL) from regenerating hepatocytes usually occurs. Often, however, these typical elevations after acute hepatic insults do not occur after surgical resection of the liver. Regeneration is therefore not a sufficient impetus for the occurrence of elevated AFP levels.

As discussed in Chapter 75, AFP has been found to be an important marker for hepatocellular carcinoma (HCC) (Zhou et al., 2006). Elevated levels occur in more than 90% of patients with this disease. As noted previously, elevated levels can also occur after acute liver disease and fibrosis, making this marker somewhat nonspecific. However, at levels greater than 400 ng/dL, there is a high probability of HCC, but at these levels of AFP, the tumor is widespread. Therefore, its use as an early detector of HCC is limited. In screening patients with cirrhosis, a cutoff value of 20 ng/mL can be used with a sensitivity of 52.9%, specificity of 93.3%, PPV of 69.8%, and NPV of 87.0% (Chang et al., 2015). Recent studies have shown that serial measurements of AFP in those with HCC receiving chemotherapy may serve as a good prognostic tool (Chan et al., 2009). Serum levels of AFP in HCC are also dependent on the extent and degree of differentiation of the tumor and the age of the patient. As noted earlier, AFP and DCP have been found to predict survival rates in patients with recurrent hepatocellular carcinoma (Okamura et al., 2014).

The value of serum levels of AFP in diagnosing HCC may be increased by looking at additional laboratory values, such as circulating cell-free DNA (cfDNA), which is a potential biomarker for tumor diagnosis. Recent studies have shown that cfDNA in combination with AFP had a higher diagnostic power than AFP alone (Yan et al., 2018).

In addition, AFP has been used as a marker for rare germ cell tumors, especially yolk sac (endodermal sinus) tumors of infants, and other even rarer tumors such as Sertoli-Leydig cell tumors (Watanabe et al., 2008).

AUTOIMMUNE MARKERS

Antimitochondrial Antibody Is a Marker for Primary Biliary Cirrhosis

Occasionally, autoimmune disease may be the primary cause of liver injury. The most common autoimmune liver disease is primary biliary cirrhosis (PBC), which occurs primarily in women, usually in the fifth decade, often accompanied by other autoimmune diseases (especially Sjögren syndrome). There is a strong association of occurrence of this disease among siblings. This condition, which is discussed at length in Chapter 55, causes fibrosis of the bile canaliculi in the portal triads. Bile eventually seeps into hepatocytes, causing necrosis. Granulation tissue replaces hepatocytes; thus, fibrosis eventually spreads into the liver parenchyma, giving rise to the pattern of fibrosis and regenerating nodules. A similar course occurs in secondary biliary cirrhosis as a result of other underlying conditions, such as choledocholithiasis, carcinoma of the head of the pancreas, and, occasionally, hepatitis and sepsis.

A vital difference between primary and secondary biliary cirrhosis is that the former uniquely appears to be part of a generalized autoimmune condition. More than 90% of patients with primary biliary cirrhosis are found by immunofluorescence to have serum antibodies that react with liver, kidney, stomach, and thyroid tissue. These circulating antibodies, which can be detected in serum using an enzyme-linked immunosorbent assay, are directed against mitochondrial antigens (anti–mitochondrial antigen [AMA]) from the inner mitochondrial membrane, called M2, which has been found to be dihydrolipoamide acetyltransferase, a component of the pyruvate dehydrogenase multienzyme complex (Kaplan et al., 1984; Dähnrich et al., 2009; Coppel et al., 1988; Krams et al., 1989). Antimitochondrial antibodies have been found in a variety of disease states, but two anti-M2 antibodies in primary biliary cirrhosis uniquely react either with a protein of molecular mass 62 kilodalton (kDa)—the E2 subunit of pyruvate dehydrogenase (Manns et al., 1987; Fussey et al., 1988), the predominant autoantibody—or with a 48-kDa E2 subunit of branched-chain oxo-keto-acid dehydrogenase. In other disorders, AMA against M1 antigen has been found in syphilis, anti-M5 in collagen vascular disease, anti-M6 in iproniazid-induced hepatitis, and anti-M7 in cardiomyopathy (Berg et al., 1986). AMA with anti-M2 specificity is 100% specific for primary biliary cirrhosis.

In a human genome–wide study (see Chapters 73, 79, and 80), DNA samples from more than 500 patients with this condition and a control group were genotyped for more than 300,000 single-nucleotide polymorphisms (SNPs). This analysis revealed that PBC has a strong association with two SNPs in the HLA-2 region, particularly in the gene-encoding interleukin (IL)-12, and a more modest but significant association with SNPs at the signal transducer and activator of transcription 4 (STAT4) locus and the CTLA4 locus, encoding cytotoxic T lymphocyte–associated protein 4. These results now implicate IL-12 signaling and CD4-positive helper T cells in the pathogenesis of this condition (Hirschfield et al., 2009). Recent genome-wide association studies have mapped autoimmunity association signals to 17q12-21 for a number of autoimmune diseases, including PBC (Ustiugova et al., 2019). However, the association between specific SNPs and IL-12 coding and PBC is still unclear and requires further investigation. Also, how these findings relate to the production of anti-M2 and anti-M1 auto-antibodies that actually cause this disease remains unsolved. Because there is considerable overlap of symptoms between PBC, sclerosing cholangitis, and autoimmune hepatitis (the latter two conditions are discussed in the following two sections), there is a strong likelihood that these conditions may share a similar pathogenesis (Webb & Hirschfield, 2014).

ANCA Is a Marker for Primary Sclerosing Cholangitis

Primary sclerosing cholangitis (PSC) is an autoimmune disease associated with destruction of extrahepatic and intrahepatic bile ducts. More than 80% (26%–94%) of patients with this disease have circulating perinuclear antineutrophil cytoplasmic antibodies (p-ANCAs) (Chapman, 2005; Hov et al., 2008; Hov et al., 2017) with specificities against antigens such as bactericidal/permeability-increasing protein, cathepsin G, elastase, and/or lactoferrin (Mulder et al., 1993; Roozendaal et al., 1998; Hov et al., 2008; Kyriakidi et al., 2016). Up to 75% also have other autoantibodies, such as antinuclear antibodies (ANAs) or anti–smooth muscle antibodies (ASMAs) (Chapman et al., 1986; Björnsson et al., 2002; Hov et al., 2008). There is some question as to whether pANCA, which is a reliable indicator of large cholangiole disease, can likewise serve as a reliable biomarker for PSC involving small cholangioles (Tervaert et al., 2009). Recent studies suggest that the strongest

genetic risk factors for PSC are encoded in the HLA complex. However, the clinical significance of the presence of pANCA is still under investigation (Hov et al., 2017). Unlike primary biliary cirrhosis, PSC occurs primarily in young to middle-aged men and is often associated with inflammatory bowel disease (IBD), particularly ulcerative colitis, although it was found that PSC is also associated with Crohn disease (Stinton et al., 2014). PSC patients with positive pANCA have been shown to be diagnosed earlier and have a lower frequency of cholangiocarcinoma. Although PSC is often associated with IBD, there does not appear to be a correlation between positive pANCA and IBD status or IBD subtype (Hov et al., 2017). Recently, a new sensitive chemiluminescent immunoassay (CIA) has been developed that detects neutrophil cytosolic serine protease 3, called PR3-ANCA. This antigen appears to be more specific for PSC (Stinton et al., 2014). Strength of positivity of the assay correlates with the extent of elevation of liver function enzyme levels and may be specific for more advanced stages of this condition.

Serum Markers for Autoimmune Hepatitis

Autoimmune hepatitis is responsible for as much as 3% to 5% of chronic hepatitis and occasionally may present as acute hepatitis. Several variants of autoimmune hepatitis are associated with various markers (Czaja, 1995; Czaja et al., 1995; Zachou et al., 2004; Zeman and Hirschfield, 2010; Czaja, 2016). In the United States, the most common variant, type 1, is associated with ANAs most commonly as well as with antibodies to actin (often detected as ASMAs). Titers of ANAs and/or ASMAs greater than 1:80 support the diagnosis in patients with hepatitis (Johnson et al., 1993; Moy & Levine, 2014). Type 2 autoimmune hepatitis typically affects children and is much more common in Europe than in the United States, where it is rarely encountered. ANAs and ASMAs are often negative in type 2, and antibodies to liver–kidney microsomal antigens are positive in most cases (Moy & Levine, 2014). Lower-level titers of ANAs or ASMAs are commonly seen in other forms of liver disease, particularly hepatitis C, in which they may be found in up to 40% of cases (Czaja, 1995; Czaja et al., 1995). Both types of autoimmune hepatitis affect females predominantly.

As with primary biliary cirrhosis, gene clusters have been identified as conferring susceptibility to this disease. Most of these occur in the HLA-DRB1 that affect antigen presentation (Moy & Levine, 2014).

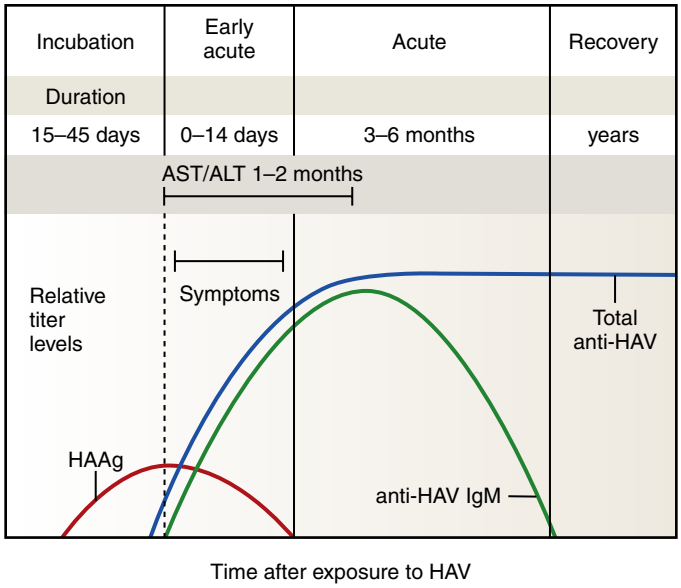

Figure 22.4 Typical time course for appearance of viral antigens and antiviral antibodies in hepatitis A viral (HAV) infection. The appearance of the hepatitis A antigen, HAAg, occurs early on; it is no longer present during the acute phase, during which time jaundice may develop. During the incubation period (which averages 2–3 weeks), HAV RNA is replicating, and viral particles can be detected in stool by immune electron microscopy. Viral RNA is also detectable during this time by real-time polymerase chain reaction (PCR). The most effective diagnostic determination of hepatitis A acute infection is the detection of anti-HAV immunoglobulin (Ig) M. Also shown in this figure is the rise of the aminotransferases, aspartate aminotransferase (AST) and alanine aminotransferase (ALT), which occurs at the beginning of the early acute phase and lasts for several weeks to 1 to 2 months. The patient ceases to be infectious after anti-HAV IgM falls to undetectable levels in 3 to 6 months post early phase. Permanent anti-HAV IgG rises over several months and lasts for many years, conferring immunity on the exposed or infected individual. (Adapted from Abbott Laboratories Diagnostic Educational Services. *Hepatitis A diagnostic profile.* North Chicago, IL: Abbott Labs; 1994, with permission.)

TESTING FOR VIRAL-INDUCED HEPATITIS

Numerous viruses cause liver damage. Some, such as hepatitis A, B, and C viruses and the arboviruses, are hepatotoxic, but others, such as Epstein-Barr virus, cytomegalovirus, varicella zoster virus, herpes simplex virus, human herpesvirus 6, human immunodeficiency virus (HIV), adenovirus, and echovirus, induce transient to moderately aggressive hepatitis. Even newly identified hepatitis G causes only a self-limited form of hepatitis. In actuality, viruses are the cause of 80% to 90% of acute and chronic hepatitis. Although a variety of such viruses can affect the liver, most viral-induced liver pathology is caused by five viruses that are known to cause hepatocyte injury and are termed *hepatitis viruses*—namely, hepatitis A, B, C, D, and E.

Hepatitis A

Hepatitis A virus (HAV) is a member of the picornavirus family of RNA viruses. It is transmitted by the fecal–oral route and typically has an incubation period of 15 to 50 days, with a mean time of about 1 month, depending on the inoculum (Brown & Stapleton, 2003). Epidemics or clusters of HAV infection often occur with conditions of poor sanitation, in daycare centers, with military actions, and from contaminated food. Epidemics of HAV occur generally in crowded urban areas, especially where there is a preponderance of uncooked food. Infection with HAV is almost always self-limiting, although in 5% to 10% of cases, a secondary rise in enzymes occurs. The time course of markers of HAV infection is shown in Figure 22.4.

During the incubation period, HAV RNA is present in stool and in plasma and remains detectable for an average of 18 days after clinical onset of hepatitis (Fujiwara et al., 1997). The initial immune response to the virus is IgM anti-HAV, which typically develops about 2 to 3 weeks after infection; increasing AST and ALT develop after antibody development. IgM antibodies typically persist for 3 to 6 months after infection. The presence of elevated titers of IgM anti-HAV is considered to be diagnostic of acute infection, although some apparently false-positive results have been found (Funk, 2005), resulting in the recommendation that only symptomatic individuals be screened for acute infection using IgM titers. IgG antibodies develop within 1 to 2 weeks of IgM antibodies and typically remain positive for life (Skinhoj et al., 1977).

"Total" anti-HAV assays detect both IgM and IgG antibodies. The prevalence of total anti-HAV varies, ranging from 5% to 10% in children younger than 5 years to 75% in those older than 50 years of age (Koff, 1995). Following HAV immunization, using attenuated HAV, detectable antibody develops in 2 to 4 weeks and persists to 5 years in 99% of responders (Totos et al., 1997). Vaccination against hepatitis A appears to be effective in preventing disease in children traveling to endemic areas (Martinez et al., 2014). Similar protection from the use of Ig in passive immunization seems to occur, although this conclusion is tentative (Liu et al., 2009). If necessary for epidemiologic purposes, polymerase chain reaction (PCR) assays are available to identify HAV RNA in plasma and stool. However, there is no need to incorporate the use of PCR for routine diagnostic purposes.

Hepatitis B

Hepatitis B virus (HBV) is a member of the hepadnavirus (i.e., hepato-DNA virus) family, a group of related DNA viruses that cause hepatitis in various animal species. This virus causes infection of the liver with clinical features that are extremely variable, ranging from absent or mild disease to severe liver failure (Horvat et al., 2003). Viral particles attach to host cells by an unknown receptor, where they enter the cell by receptor-mediated endocytosis and are transferred to the nucleus by so-called chaperone proteins.

Once in the nucleus, HBV replicates by an unusual mechanism (Beck & Nassal, 2007; Kay & Zoulim, 2007). The viral DNA is partially duplex and consists of a shorter plus strand and a longer minus strand. It consists of four known genes: C, which encodes the core protein; X, whose protein product is unknown; P, which encodes DNA polymerase; and S, which encodes the surface protein, also called the surface antigen. The latter consists of three open reading frames, giving rise to three types of surface proteins—large, middle, and small. During viral replication, the two unequal strands elongate and become circular. Several messenger RNAs (mRNAs) are transcribed, and the longest is longer than the original coding DNA. This mRNA is secreted into the cytosol, where it is involved in the replication of more virions, requiring the use of reverse transcriptase, as in retroviruses. Thus, HBV replication requires reverse transcriptase, making it susceptible to reverse transcriptase inhibitors. Four serotypes of HBV (adr, adw, ayr, ayw) and eight genotypes, some of which occur in geographically different regions, have different virulences and may respond differently to different treatment modalities (Kramvis et al., 2007).

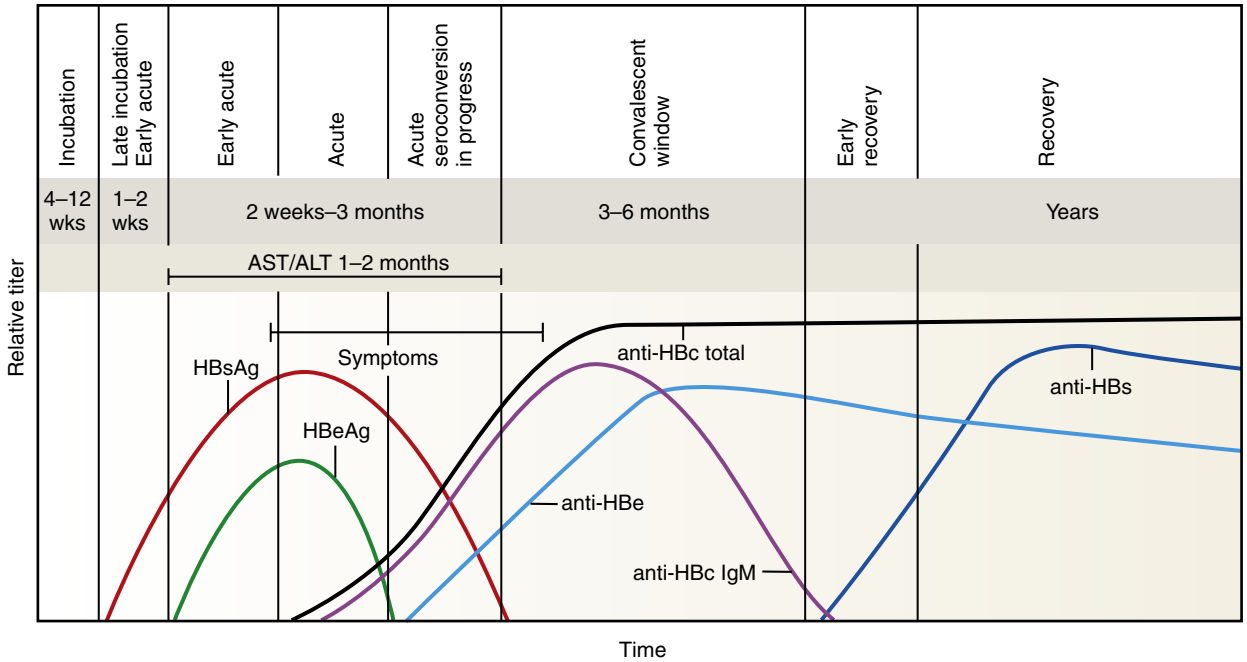

Figure 22.5 Typical time course for appearance of viral antigens and antiviral antibodies in hepatitis B viral (HBV) infection. In the early acute phase, the HBV surface antigen (HBsAg) *(red curve)* appears and lasts for several months. Detection of this antigen signifies acute HBV infection. Between the time the titer of HBsAg falls and the titer of anti-HBV immunoglobulin (Ig) G *(dark-blue curve),* which confers immunity, rises, there is a gap of about 6 months. In this time period, the titers of anti-HBV core antigen (anti-HBc) IgM *(purple curve)* and IgG *(black curve)* rise, indicating acute HBV infection. This is the so-called core window. IgG anti-HBV e antigen (anti-HBe) *(cyan or light-blue curve)* also rises during this core window period. Permanent immunity is conferred by anti-HBsAg IgG (anti-HBs) *(dark-blue curve).* It is difficult to determine the time at which the patient is no longer infectious. Generally, an individual is considered noninfectious when no HBsAg or HBeAg, and no anti-HBcAg IgM, can be detected, and the anti-HBsAg IgG has plateaued. Also shown in this figure is the pattern of aspartate aminotransferase (AST) and alanine aminotransferase (ALT) elevations. These occur in the early acute phase, slightly after HBsAg rises. AST and ALT levels may remain elevated for several weeks to several months, after which time they decline. In HBV chronic active hepatitis, HBsAg is present continuously. AST and ALT generally remain elevated, although they can oscillate throughout the course of the disease. (Adapted from Abbott Laboratories Diagnostic Educational Services. *Hepatitis B diagnostic profile.* North Chicago, IL: Abbott Labs; 1994, with permission.)

Hepatitis B is transmitted primarily by body fluids, especially serum. It is spread effectively by sex and can be transmitted from mother to baby. In Southeast Asian and African countries, horizontal transmission between children under age 4 years has also been observed (Prince et al., 1981; Hurie, 1992). Hepatitis B produces several protein antigens that can be detected in serum: a core antigen (HBcAg), a surface antigen (HBsAg or HBs), and an e antigen (HBeAg), related to the core antigen; commercial assays are available for HBsAg and HBeAg. Antibodies to each of these antigens can also be measured, and commercial assays for each are available. The time course of self-limited infection with HBV is illustrated in Figure 22.5. Different groups of tests are recommended for three different clinical situations as follows:

1. Acute HBV hepatitis: HBsAg, IgM anti-HBc
2. Chronic HBV hepatitis: HBsAg, IgG anti-HBc, IgG anti-HBs
3. Monitoring chronic HBV infection: HBsAg, HBeAg, IgG anti-HBs, IgG anti-HBe, and ultrasensitive quantitative PCR

The initial serologic marker of acute infection is HBsAg, which typically becomes detectable 2 to 3 months after infection. After another 4 to 6 weeks, IgM anti-HBc appears, accompanied by increases in AST and ALT. When symptoms of hepatitis appear, most patients still have detectable HBsAg, although a few patients have neither detectable HBsAg nor anti-HBs, leaving anti-HBc the only marker of infection (core window). IgM anti-HBc typically persists for 4 to 6 months; however, it may be intermittently present in patients with chronic HBV infection (Czaja et al., 1988; Liang, 2009; Puri, 2013).

In most individuals, HBV hepatitis is self-limited and the patient recovers. About 1% to 2% of normal adolescents and adults have persistent viral replication, which causes chronic hepatitis. The frequency of chronic HBV infection is 5% to 10% in immunocompromised patients and 80% in neonates, with the likelihood of chronic infection declining gradually during the first decade of life. With recovery from acute infection, HBsAg and HBcAg disappear, and IgG anti-HBs and IgG anti-HBe appear; development of anti-HBs is typically the last marker in recovery and is thought to indicate clearance of virus. Anti-HBs and anti-HBc are believed to persist for life, although in about 5% to 10% of cases, anti-HBs ultimately disappears (Seeff et al., 1987). Isolated anti-HBc can also occur during periods of viral clearance in acute and chronic hepatitis and as a false-positive result. The titer of anti-HBc is important in determining its significance; low titers are typically false-positive results, and high titers almost always (50%–80% of cases) indicate immunity to HBV infection, as demonstrated by an anamnestic response to hepatitis B vaccine (Aoki et al., 1993).

The newest assay to assess HBV infection is the ultrasensitive quantitative real-time PCR technology, which is discussed extensively in Part 8. This quantitative HBV DNA PCR detects a highly conserved region of the surface gene at a level as low as 200 copies of viral genome per mL (0.001 pg/mL) with a range up to 2×10^8 copies/mL. Its primary use is to monitor therapeutic responsiveness in clinically infected patients.

Also available is the quantitative digene hybrid capture assay, which employs a signal amplification antibody capture microplate test that utilizes chemiluminescent detection. However, this quantitative HBV PCR technique utilizes an RNA probe and has detection limits of 5000 copies/mL (0.02 pg/mL), making it less sensitive than ultraquantitative assays (Qiu et al., 2014), although branched-DNA assays, discussed in Chapter 68, are also used, with detection limits of 2000 copies/mL. Patients who have clinically recovered from HBV infection and are anti–HBs positive have no detectable HBV DNA using most assays.

Using sensitive PCR assays, circulating HBV DNA can be found in a high percentage of anti–HBs-positive patients who have clinically recovered from HBV infection (Cabrerizo et al., 1997; Yotsuyanagi, 1998) as well as in patients with hepatitis C and isolated anti-HBc (Cacciola et al., 1999). The significance of finding low levels of HBV DNA is not known, although in patients with concurrent hepatitis C viral infection, this finding may be associated with more severe liver damage. The e antigen has historically been used to detect the presence of circulating viral particles; a good correlation has been noted between levels of HBeAg and the amount of HBV DNA (Hayashi et al., 1996). In chronic HBV infection, approximately 1% to 1.5% of patients will spontaneously clear HBeAg each year. Some will recover, but others enter a nonreplicative phase in which HBV DNA integrates into the cell genome. This transition phase is often associated with a rise in AST and ALT and, occasionally, jaundice. Rarely, HBeAg may again be detectable in plasma in such patients. Patterns of HBV markers and their interpretation are shown in Table 22.1.

At present, approved antiviral therapies reducing morbidity and mortality related to HBV include interferon and nucleos(t)ide analogs (Lin, 2016). Complete cure cannot be obtained in the treatment of chronic hepatitis B (CHB) owing to persistence of covalently closed circular DNA (ccDNA) in the nucleus of hepatocytes, posing a lifelong risk for reactivation of infection. However, immunologic cure, defined by HBsAg loss and

sustained HBV DNA suppression, can be attained. HBsAg loss, though infrequently achieved, is the best predictor of sustained remission (Terrault, 2015).

Hepatitis C

Hepatitis C (HCV) is an RNA virus of the flavivirus group consisting of an icosahedral viral protein coat, embedded in cellular lipid and surrounding RNA. The viral RNA encodes a single protein with more than 3000 amino acids that is then processed into individual proteins using viral and host cellular proteases. These include two core proteins, E1 and E2, and a series of proteins labeled as NS1 to NS5. NS2 is a transmembrane protein, NS3 contains protease and RNA helicase activities, and NS4A and B proteins are known cofactors; NS5A is an interferon-resisting protein, and NS5B is RNA polymerase. The virus has a tropism for hepatocytes that it enters via specific receptors, including CD 81 protein. Once inside the hepatocyte, HCV initiates the lytic cycle utilizing the intracellular translational machinery required for its replication (Lindenbach & Rice, 2005). Replication using NS5B RNA polymerase produces a negative-strand RNA intermediate, which then serves as a template for the production of new positive-strand viral genomes. Because viral replication does not involve proofreading, the mutation rate for HCV is high. On the basis of sequencing studies, six genotypes, labeled 1 to 6, that have been further divided into subgroups (e.g., 1a, 1b, 2a, 2b) have been recognized. Genotype 1a predominates in North America, and 1b predominates in Europe. Genotypes 4 and 5 are unique to Africa. It is important to note that genotypes 1 and 4 are more resistant to interferon therapy than are the other genotypes, resulting in longer treatment times (48 vs. 24 weeks). Thus, genotyping has therapeutic implications.

Treatment of HCV has dramatically improved in recent years. Peginterferon (PEG-IFN) and ribavirin (RBV), long-time mainstays of treatment, have side effects that include severe flu-like symptoms (fever, headache, myalgias, arthralgias, fatigue), nausea, diarrhea, depression, pruritus, alopecia, anemia, neutropenia, and thrombocytopenia. Ribavirin has a black box warning for hemolytic anemia, can worsen cardiac disease, and has significant teratogenic effects. Interferon can cause life-threatening neuropsychiatric, autoimmune, ischemic, and infectious disorders. This leads to a cessation of therapy and thus a resurgence of the viral load in these patients.

Following the advances of HIV therapy, developers created direct-acting antivirals (DAAs), NS3/4A protease inhibitors, NS5A inhibitors, and NS5B polymerase inhibitors. One of these NS3/4A protease inhibitors, boceprevir, in combination with PEG-IFN and RBV, reduced HCV RNA load to half the level of the group treated with PEG-IFN/RBV alone (Poordad et al., 2011). New DAAs (consisting of NS3/4A protease inhibitors and nucleotide inhibitors) include ledipasvir, boceprevir, telaprevir, simeprevir/sofosbuvir, glecaprevir, pibrentasvir, velpatasvir, and voxilaprevir (Kim et al., 2014; Ferraro et al., 2019). These drugs have excellent cure rates, lower side effect profiles, and increased ease of use (Gane et al., 2013; Poordad et al., 2013; Kowdley et al., 2014; Ferraro et al., 2019).

In patients undergoing treatment for HCV infection, successful therapy with direct-acting antivirals is measured by sustained virologic response (SVR). This is demonstrated with continuingly decreasing viral loads in patients. Many patients who are treated with direct-acting antivirals show decreases in their viral load in the first 4 to 8 weeks of treatment. An undetectable HCV RNA level indicates SVR and requires sensitive and precise methods to detect such low copy numbers of HCV viral load. Both lavender top tubes (LTTs) for specimens and plasma preparation tubes (PPTs) are approved for molecular diagnosis assays, with the only difference between the two tubes being a plasma separator insert gel on the bottom of the PPTs. Recent studies have shown that viral loads in LTTs are significantly higher than in PPTs. This suggests a need for further research and the standardization of collection tubes for measuring HCV viral response to DAAs (Wang et al., 2018).

With the use of novel DAAs, recent studies, including a prospective study published in *Gastroenterology*, have demonstrated 5-year survival of 88.6%, with 50.5% of patients receiving SVR. Achieving SVR results in decreased mortality (hazard ratio [HR] = 0.27), decreased hepatic decompensation (HR= 0.26), and lowered rates of HCC (HR= 0.29) (Nahon et al; 2017, Ferraro et al; 2019).

HCV, formerly known as non-A, non-B hepatitis, is the primary etiologic agent, transmitted via blood transfusions and transplantation before 1990. At present, 60% of all new cases occur in injection drug users, but other serum modes of transmission are also seen, such as accidental needle punctures in health care workers, dialysis procedures in patients, and, rarely, transmission from mother to infant. Although sexual transmission is thought to be an inefficient means of transmitting infection, it nevertheless accounts for at least 10% of new cases. Monogamous sexual partners of HCV-infected patients rarely become infected, although a history of multiple sexual partners has been recognized as a risk factor. In contrast to HAV and HBV, chronic infection with HCV occurs in about 75% to 85% of infected individuals, with an estimated 4 million individuals chronically infected in the United States alone (Alter et al., 1999; Liang et al., 2000; Zaltron et al., 2012; Hofmeister et al., 2019). About half of HCV chronically infected individuals with persistent viremia will have elevated ALT levels. Physical symptoms are absent for the first 2 decades after infection. As the disease progresses, inflammation and liver cell death can lead to fibrosis, and in about 20% of patients, fibrosis will advance to cirrhosis. The risk for HCC in a patient with chronic HCV is about 1% to 5% after 20 years. HCC is seen only in patients with cirrhosis (Shuhart & Gretch, 2003). Laboratory tests for HCV infection and their common uses are summarized in Table 22.2.

HCV has not been grown in culture; however, HCV genomes can be amplified by recombinant technology. A number of structural and nonstructural antigens have been identified. An immunoassay for the core antigen of HCV has been developed (Aoyagi et al., 2001) but has been found to be less sensitive than HCV RNA assays (Krajden et al., 2004). The major diagnostic test for HCV infection has been the second-generation anti-HCV assay, which detects the presence of antibody to one of four different viral antigens at an average of 10 to 12 weeks after infection (Alter, 1992). A third-generation anti-HCV assay detects antibody at an average of 7 to 9 weeks after infection (Barrera et al., 1995). IgM anti-HCV is present in both acute and chronic HCV infection and is therefore not helpful diagnostically (Brillanti et al., 1993; Quinti et al., 1995; Nikolaeva et al., 2002). Total anti-HCV typically persists for life, although it may disappear with recovery from HCV infection (Seeff & NHLBI Study Group, 1994; Beld et al., 1999).

TABLE 22.1
Interpretations of Patterns of HBV Markers

Interpretation	IgM Anti-HBc	Total Anti-HBc	HBsAg	Anti-HBs	HBeAg	Anti-HBe
Incubation period of HBV infection	–	–	+	–	–	–
Acute HBV infection	+	+	+	–	+	–
Recent, resolving HBV infection	+	+	–	++		
Acute HBV infection in core window	+	+	–	–	–	–
Active chronic HBV infection	–	+	+	–	+	–
Chronic HBV carrier state	–	+	+	–	–	+
Resolved HBV infection	–	+	–	+	–	+
HBV immunity after vaccination	–	–	–	+	–	–

HBV, Hepatitis B virus; *HBc,* hepatitis B core; *HBeAg,* hepatitis B e antigen; *HBsAg,* hepatitis B surface antigen; *IgM,* immunoglobulin M.

TABLE 22.2
Interpretation of Patterns of HCV Markers

Interpretation	Anti-HCV	HCV RNA
Acute HCV infection	–	+
Active HCV infection	+	+
Possible HCV clearance	+	–
False-positive HCV test	+	–
Requires further study	+	–

HCV, Hepatitis C; RNA, ribonucleic acid.

The best screening test for hepatitis C is anti-hepatitis C antibody (95% sensitivity, 99% specificity). The antibody can be detected 4 to 10 weeks after exposure; in >97% of cases, the antibody is detected by 10 weeks after exposure. If the result of the antibody test is positive, confirmatory testing is then performed by determining hepatitis C RNA viral load by PCR and genotyping. HCV RNA can be detected 2 to 3 weeks after exposure. If results of hepatitis C viral load are negative in a patient with suspected high risk of exposure in the past 6 months, HCV RNA should be ordered every 4 to 8 weeks or repeat antibody testing can be performed at 12 weeks. If hepatitis C antibody is positive but the hepatitis C RNA viral load is negative, the patient is diagnosed with acute infection, for which treatment is not recommended. Hepatitis C RNA viral load should be monitored for 6 months to evaluate spontaneous clearance (Ferraro, 2019).

In high-risk populations, the predictive value of anti-HCV for HCV infection is over 99%; thus, further testing is not typically needed to prove viral exposure (Pawlotsky et al., 1998). In low-risk populations, such as blood donors, the predictive value of positive anti-HCV is only 25%. In low-risk patients, or when needed to confirm HCV exposure, supplemental tests for anti-HCV should be used. The original test for this purpose, the HCV Recombinant Immuno-Blot Assay (RIBA), has been discussed in detail in the previous edition of this text but is no longer widely available. Briefly, the RIBA uses recombinant HCV proteins isolated in a dot or strip blot assay; this is analogous to Western blot tests used to confirm positivity in other types of infectious disease. In the latest (third-generation) RIBA, three antigens—core and NS3 and NS5 proteins—are immobilized on a membrane; positive enzyme-linked immunosorbent assay (ELISA) reactions to two or more antigens is considered to be positive, while reaction with only one antigen is considered to be equivocal or indeterminate (Kamili et al., 2012). Isolated antibody to the NS5 antigen is virtually never associated with HCV viremia, suggesting that it may indicate a false-positive result (Vernelen et al., 1994; LaPerche et al., 1999).

The primary test for confirming persistence of HCV infection is HCV RNA, detected by a variety of amplification techniques. Quantitative assays can typically detect as few as 1000 copies/mL; however, results from different assays are not interchangeable, and detection limits vary among methods (Ravaggi et al., 1997; Lunel et al., 1999). Qualitative HCV RNA assays generally have lower limits of detection compared with quantitative methods using the same amplification technique, are less expensive, and are more useful for detecting the presence or absence of infection.

A World Health Organization standard has been developed to improve comparability between methods (Saldanha et al., 1999) and is based on an international unit or IU/mL of serum or plasma and on recently developed real-time PCR techniques, which have a detection range of 5 to 200 million IU/mL, thereby eliminating the need to obtain qualitative and quantitative levels. A 2003 study (Shiffman et al., 2003) found, using the international standard, that approximately 90% of serum values for HCV RNA were within 1 log unit irrespective of which virologic assay was used. However, significant differences in results have been found, a few samples giving a maximum of 2 log unit differences (factor of 100). Such discrepant results may have an impact on the management of patients receiving interferon therapy. These findings suggest that it is important to obtain more than one HCV RNA determination before making treatment decisions (Shiffman et al., 2003).

With acute infection, HCV RNA is typically present within 2 weeks of infection but falls with development of antibody; as many as 15% of those with acute HCV infection have negative HCV RNA (Alter et al., 1992; Villano et al., 1999). Viral RNA may be intermittently present for the first year of infection but then becomes persistently present (Villano et al., 1999). In later stages of infection, HCV RNA levels generally fluctuate by no more than 0.5 to 1.0 log around mean values (Nguyen et al., 1996). HCV has a high rate of mutation, similar to that of other reverse transcriptase viruses, such as HIV. This produces a number of "quasispecies" of HCV that may emerge, often associated with fluctuating ALT levels (Yuki et al., 1997). Unique species of HCV are termed *genotypes*. In the United States, the most common is genotype 1, divided into subtypes 1a and 1b. These together cause about 65% of HCV infections in whites but 90% to 95% of infections in African Americans (McHutchison et al., 1999; Reddy et al., 1999). Genotypes 2 and 3 are generally more responsive to treatment (McHutchison et al., 1998; Poynard et al., 1998); other strains are responsible for 1% to 2% of infections. Detection of the unique nucleic acid sequences of each strain by one of several nucleic acid methods (Lau et al., 1995), discussed at length in Part 8, is the most reliable means to identify the responsible genotype in an individual.

Hepatitis C–Induced Hepatocellular Carcinoma

Approximately 20% of patients who have hepatitis C develop cirrhosis of the liver (discussed later), which has been attributed to chronic inflammation due to chronic hepatitis C infection (Selimovic et al., 2012; Bandiera et al., 2016; Irshad et al., 2017; Axley et al., 2018). Of these 20%, approximately 20% develop HCC. The issue thus arises as to whether HCV may be a causative factor for HCC. It has been found that expression of individual hepatitis C proteins in normal hepatocytes can lead to their malignant transformation. Interestingly, expression of HCV protein by hepatocytes in a transgenic mouse model was sufficient to induce HCC in these mice and the immortalization of primary human hepatocytes. Core protein has also been found to activate telomerase in immortalized hepatocytes and to induce the expression of interleukin (IL)-6, gp130, leptin receptor, and signal transducer and activator of transcription 3. Upregulation of these proteins is thought to upregulate c-myc and cyclin D1, both promitotic proteins (see Chapters 76 and 77), which may further promote cell transformation.

More important, it has been found that transfection of HCV NS3-encoding genomic DNA into quiescent NIH 3T3 cells (mouse fibroblasts) induces cell transformation. Overexpression of NS3 protein in human hepatocytes likewise was found to induce cell transformation. NS3 protein has also been found to form inactivating complexes with the antioncogene protein p53 and the proapoptotic protein waf-p21.

HCV NS5A protein has been found to cause dysregulation of the cell cycle and to induce aberrant mitosis. The NS5B protein induces downregulation of the antioncogene protein Rb and promotes elongation factor-2 (E2F)–induced transcription. These studies suggest that drugs that can block the interactions of these viral proteins with the critical proteins in hepatocytes may reduce the occurrence of HCC in these patients. Studies further suggest that interferon may reduce the occurrence of HCC in these patients (Selimovic et al., 2012; Morgan et al., 2013; Webster et al., 2015; Yamada et al., 2019).

Hepatitis D

Hepatitis D (delta-agent; HDV) is an RNA virus that can replicate only in the presence of HBsAg; circulating viral particles have viral RNA inside a shell of HBsAg. Although HDV is rare in the United States, occurring primarily in injecting drug users and hemophiliacs via multiple transfusions, it is endemic in some parts of the world (London & Evans, 1996). Overall, about 20 million individuals may be infected with HDV (Taylor, 2006). In patients with HBV infection, HDV may occur in two forms. If infection with both viruses occurs at about the same time (coinfection), the course of infection is more severe, often follows an atypical course, is a cause of acute fulminant hepatic failure (Sunheimer et al., 1994), and has a higher fatality rate than HBV infection alone. If HDV infection occurs in the presence of persistent HBV infection (superinfection), progression of disease may be faster. The major diagnostic test is the presence of anti-HDV; both total and IgM antibody tests are available. Both antibodies may eventually disappear following convalescence. The simultaneous assessment of anti-HBc IgM will help differentiate coinfections (present) from superinfections (absent).

Hepatitis E

Hepatitis E (HEV), an RNA virus, now classified as a herpesvirus, with a clinical course similar to that of HAV infection, is common in parts of Asia, Africa, and Mexico. It is rarely seen in the United States, except in individuals who have traveled to endemic areas (Erker et al., 1999). Similar to HAV, it is spread by the fecal–oral route. Person-to-person transmission of HEV appears to be uncommon. For travelers to endemic areas, the usual food and water hygiene precautions are recommended. Evidence suggests that humans can contract this virus from animal reservoirs (e.g., from uncooked boar and deer meat), but this route of transmission has not been fully verified (Kuniholm & Nelson, 2008). When infection occurs in pregnancy, there is an increased fatality rate of about 20%, although in general the fatality rate is between 0.5% and 4%. HEV infections range from inapparent illness to severe acute hepatitis, sometimes leading to fulminant hepatitis and death. The signs and symptoms cannot be distinguished from those associated with cases of acute hepatitis caused by other hepatotropic viruses (Schlauder et al., 2003).

The viral genome encodes at least six proteins, including a capsid protein, whose x-ray structure has been determined (Guu et al., 2009). There are presumed to be five genotypes: 1 and 2 are from humans, 3 and 4 are from humans and swine, and a fifth genotype is an avian HEV found in chickens that represents a branch distinct from human and swine HEVs. Genotypes 1 and 2 occur in younger populations, whereas genotypes 3 and 4 occur in older age groups that may be immunocompromised. Antibody tests for HEV are available but appear to have frequent false-positive

results depending on the antigens used to detect reactivity (Mast et al., 1998). Two serologic tests are available: anti-HEV IgM, which detects recent or current infection, and anti-HEV IgG, which detects current or past infection. Because of the current questionable specificity of serologic assays, a confirmatory test is required. A PCR amplification of an HEV RNA-specific product using serum, plasma, bile, or feces becomes the definitive indicator of acute infection. However, the PCR test window of detection is from 2 to 7 weeks after infection. Recently, a new ELISA assay for hepatitis E antigen has been developed that appears to detect the presence of this virus in known cases at significantly higher rates than either anti–hepatitis E IgM or viral RNA. Using this antigen test, it was found that, in primates, the viral antigen is present for 3 weeks longer than previously thought and for most of the acute phase (Wen et al., 2014).

Hepatitis G

Two other viruses have been suspected, but not proven, to cause posttransfusion hepatitis: hepatitis G virus (HGV, sometimes called G-B) (Laskus et al., 1997) and transfusion-transmitted virus (Matsumoto et al., 1999). Although both viruses can be isolated from a high percentage of persons with posttransfusion hepatitis and viremia is found in at least 1% of blood donors, they do not seem to cause liver disease in these cases. To date, no serologic or PCR assays that can detect these agents are commercially available. Although acute and chronic HGV can be detected at some research centers with a qualitative PCR assay for HGV RNA, no routine testing is recommended because the clinical significance of HGV remains unknown (Shuhart et al., 2003). Several other viruses, including herpes viruses, can cause hepatitis, but they typically affect other organs as well.

DIAGNOSIS OF LIVER DISEASES

In Chapter 9, the fundamental patterns of laboratory findings in liver function abnormalities are summarized and are encapsulated in Table 9.5. In this section, the major hepatic disorders are discussed, with emphasis on laboratory evaluations that enable diagnoses to be made, often without the need to perform invasive procedures such as liver biopsies.

It is important to remember that in acute hepatitis, the principal changes include significant elevations of aminotransferases. In cirrhosis, these tend to remain normal or become slightly elevated, while total protein and albumin are depressed and ammonia concentrations in serum are elevated. In posthepatic biliary obstruction, bilirubin and ALP become elevated; in space-occupying diseases of the liver, ALP and LD are elevated. In fulminant hepatic failure, the aminotransferases and ammonia are elevated, but total protein and albumin are depressed.

HEPATITIS

Hepatitis usually first manifests clinically with the symptoms of fatigue and anorexia. Microscopically, cell injury and generally minimal necrosis are caused both by direct virus (or toxic agent)–induced cell damage and by the immune response to the virus. Jaundice may be present. By far, the most common cause (>90% of cases) of hepatitis is viral, with about 50% of cases due to hepatitis B, 25% to hepatitis A, and 20% to hepatitis C. Jaundice is often initially seen as scleral icterus when the patient has total serum bilirubin concentrations above 2 mg/dL. The cause of acute hepatitis is likewise almost always (>90% of cases) viral, although chemical exposure—such as to carbon tetrachloride or chloroform or to drugs such as acetaminophen, especially in children—should be considered. A special category of toxin-induced hepatitis is that induced by alcohol, discussed later.

The cardinal finding in hepatitis is a rise in the aminotransferases to values greater than 200 IU/L and often to 500 or even 1000 IU/L. An exception to this finding is seen in hepatitis C, in which only modest elevations of ALT (but not AST) can occur. The AST/ALT ratio generally favors ALT. The bilirubin is frequently elevated and is composed of both direct and indirect types. Frank jaundice occurs in about 70% of cases of acute hepatitis A (Lednar et al., 1985), 33% of cases of hepatitis B (McMahon et al., 1985), and about 20% of acute hepatitis C cases (Hoofnagle, 1997). Elevations of indirect bilirubin are due to the inability of injured hepatocytes to conjugate bilirubin, and the rise in direct bilirubin is due to the blockage of compromised canaliculi secondary to the inflammatory process that occurs in the acute phase. Because of hepatocyte damage, LD levels are mildly elevated to values typically around 300 to 500 IU/L. Because of inflammation and/or necrosis or apoptosis of canalicular and ductular lining cells, the ALP may also be elevated, typically to values of 200 to 350 IU/L. Unless the hepatitis is severe and involves the whole liver, progressing to fulminant hepatic failure, total protein and albumin are within their normal ranges. The γ-globulin fractions may be elevated as a result of infection (Lotfy et al., 2006).

Given the pattern of the analytes suggestive of hepatitis as previously discussed, screens for specific causes should be made (i.e., determination of serologic markers for hepatitis A, B, and C). Screening for anti–hepatitis A IgM and for HBsAg can be performed within 1 day. If either of these is positive, the diagnosis is established. If negative, further screening for hepatitis B should be undertaken (i.e., determination of serum titers of anti-HBcAg IgM and IgG [core window] and anti-HBsAg IgG, as already described). If only the latter is positive, it may be difficult to establish whether hepatitis B is the cause of the infection or whether the patient has had past exposure to the virus. Unless the patient has chronic active or persistent hepatitis, in which case HBsAG is continuously present, elevated titers of anti-HBsAg IgG occur long after the aminotransferases return to normal levels. Screens for hepatitis C should also be performed. If these are negative, other viral causes should be sought (e.g., cytomegalovirus, Epstein-Barr virus). Especially in the event that a viral hepatitis screen is negative, nonviral causes, such as chemical toxins, should be considered. In addition, less common causes of hepatitis, such as Wilson disease (discussed earlier), in which decreased serum ceruloplasmin and increased urinary copper are found, and autoimmune hepatitis should be considered. Both conditions can present as acute or chronic disease; in chronic forms, both can give rise to chronic active hepatitis and, less commonly, cirrhosis. In the chronic form of autoimmune hepatitis (often accompanied by elevations in ANA titers), polyclonal increases in the γ-globulins can usually be detected.

Alcoholic Hepatitis

In alcoholic hepatitis, the previously described pattern of abnormal analyte concentrations holds except that AST, much of it mitochondrial AST, often becomes disproportionately elevated over ALT. In addition, marked elevations of the enzyme GGT are often out of proportion to elevations in alkaline phosphatase. Unless malnutrition or compromised renal function exists in the alcoholic patient, total protein and albumin are found to be within their reference ranges.

Chronic Hepatitis

In chronic hepatitis, hepatocyte damage is ongoing and chronic inflammation is seen in hepatocytes on biopsy. This condition is caused mainly by chronic hepatitis B or C infection, detected by persisting HBsAg or real-time PCR for hepatitis C sequences, respectively, and is a major predisposing factor for cirrhosis and hepatocellular carcinoma, the two leading causes of death from liver disease. Chronic hepatitis may be asymptomatic or mildly symptomatic. A mild elevation of AST and ALT is seen, and, more commonly in hepatitis C, a mild elevation of only ALT may be noted.

CHRONIC PASSIVE CONGESTION

In chronic passive congestion of the liver, most often secondary to congestive heart failure, back pressure from the right heart is transmitted to the hepatic sinusoids from the inferior vena cava and the hepatic veins. Increased pressure causes sinusoidal dilation, which may cause physical damage to hepatocytes. The result is a mild increase in aminotransferases and occasionally mild hyperbilirubinemia. Other analytes that measure liver function are usually within their reference ranges.

CIRRHOSIS

Cirrhosis of the liver is a condition that results in parenchymal fibrosis and hepatocytic nodular regeneration and can be caused by alcoholism (macronodular or Laennec's cirrhosis), panhepatic hepatitis, chronic active hepatitis, toxins and drugs, and diseases of the biliary tract, such as primary and secondary biliary cirrhosis, as discussed previously.

In addition, systemic disease can predispose to cirrhosis. In hemochromatosis, for example, excess iron becomes deposited in a variety of tissues, including liver, and becomes toxic to hepatocytes, predisposing to cirrhosis. As discussed in Chapter 24, this disease is associated with single amino acid substitutions, most commonly tyrosine for cysteine 282 (C282Y), in the protein product of the *HFE* gene on chromosome 6 (Feder et al., 1996; Crawford et al., 1998a). This protein is thought to be involved in the interaction of transferrin with the transferrin receptor (Zhou et al., 1998b) and in amino acid substitutions such as C282Y, which induce protein malfunction, resulting in abnormal iron deposition in tissues, including liver. More recent work suggests that the HFE protein can regulate intracellular iron storage independently of its interaction with transferrin receptor-1 (Carlson et al., 2005).

However, homozygosity for the C282Y HFE protein appears to be a necessary but not a sufficient condition for causing this disease because known homozygous individuals with this mutant protein do not have the disease. This finding suggests that one or more other factors are involved in causing this disease. In a recent large-scale. genome-wide association study on 474 unrelated homozygous individuals, associations were examined for quantitative iron burden indices and patient follow-up with 534,213 SNPs (de Tayrac et al., 2014). The only gene found to have an association with aberrant iron metabolism was the transferrin (TF) gene. The implication of this finding is that hemochromatosis may be a "two-hit" disease—that is, one that requires two mutant proteins to have full expression of the clinical features of this disease.

Testing for this condition involves determination of the serum iron-binding saturation, discussed in Chapter 24, which is greater than or equal to 45%. This test has high sensitivity but low specificity, diminishing its screening value. Other tests for this condition include determination of iron content of liver biopsy samples and genetic analysis as just described.

As discussed previously, in Wilson disease, copper deposits in liver are also toxic and can likewise lead to a form of chronic active hepatitis and cirrhosis. In α_1-antitrypsin deficiency, because of continuing proteolysis in hepatocytes, patients have a significantly increased propensity to develop cirrhosis. Chronic hepatitis due to persistent circulating hepatitis B or C virus and autoimmune disease with elevated ANA or ASMA also predispose to cirrhosis.

In general, irrespective of the cause, cirrhosis is a chronic but gradually worsening condition that can occasionally progress to fulminant hepatic failure, as discussed later (Sunheimer et al., 1994). At its inception, it is often focal and may not be evident clinically.

Diagnosing and Following Cirrhosis, Fibrosis, and Necroinflammation of the Liver Noninvasively Using Serum Analytes

The definitive diagnosis of fibrosis and/or necrosis and inflammation of the liver is attained by liver biopsy. Because this invasive procedure carries with it morbidity such as bleeding and pneumothorax and because the liver biopsy itself has the confounding problem of sampling errors, a search is underway to devise methods to diagnose and follow these disease processes noninvasively using the levels of serum analytes that measure liver function. The first of these was the PGA index (Poynard et al., 1991), computed from the PT and serum levels of GGT and apolipoprotein A-I. Ranges of values for each of these analytes are divided into five categories, numbered 0 to 4, in increasing order of severity. For example, GGT values between 20 and 49 are scored as 1, values between 50 and 99 are scored 2, and so on. For apoA-I, increasing severity of disease correlates with decreasing concentration of this protein in serum. The prothrombin time increases with severity of disease because the liver is the sole site for synthesis of coagulation factors. These scores are then summed to give the PGA index. Higher PGA scores have been found to correlate with the degree of hepatic fibrosis and with the severity of cirrhosis as judged both by clinical grading and from liver biopsies (Teare et al., 1993). This index also has a good correlation with the level of procollagen type III propeptide in serum, also used to follow active cirrhosis.

More recently, other indices have been developed that appear to be more effective. These include the FibroTest (FT) and the ActiTest index (Poynard et al., 2004), which utilize the measurement of six analyte levels (i.e., apolipoprotein A1, GGT [these two analytes also being in the PGA index], haptoglobin, total bilirubin, α_2-macroglobulin, and ALT) and also include the patient's age and gender. Also commercially available is the Enhanced Liver Fibrosis (ELF) test, which combines 3 direct serum markers of extracellular matrix remodeling and fibrogenesis. These included hyaluronic acid, tissue inhibitor of metalloproteinase-1 and the N-terminal propeptide for collagen type III. The ELF score has shown good performance for prediction of histologic stage of fibrosis (Moreno, 2019).

Correlations with liver biopsy results are then performed based on an artificial intelligence algorithm, resulting in an equation that computes the score on a scale of 0 to 1.0. These scores correspond to the scores of one or more histopathologic staging systems, the most commonly used one of which is called METAVIR (METAVIR Cooperative Group & Bedossa, 1994; Bedossa & Poynard, 1996), as follows: F0, no fibrosis; F1, portal fibrosis; F2, bridging fibrosis with few septa; F3, bridging fibrosis with many septa; and F4, frank cirrhosis. ActiTest scores are computed likewise on a scale of 0 to 1.0, using the same parameters except that they are correlated with necroinflammatory activity using a METAVIR grading system (Bedossa & Poynard, 1996) as follows: A0, no activity; A1, minimal activity; A2, moderate activity; and A3, severe activity. One important aspect of the METAVIR score is that the interobserver agreement of the METAVIR score depends on the experience of the histopathologist. The utility of this score can be improved by more experienced pathologists or consensus reading (Rousselet, 2005).

Some disagreement has been seen as to the efficacy of these indices in diagnosing and following liver fibrosis and necrosis/inflammatory activity. For example, in one study (Rossi et al., 2003) on 125 patients with hepatitis C, serum samples were obtained and assayed for the six analytes in the FibroTest and ActiTest. Using cutoffs of less than 0.1 to signify minimal fibrosis and greater than 0.6 to indicate severe fibrosis, of 33 patients with a score less than 0.1, 6 (18%) were found to have significant fibrosis. Of 24 patients with scores greater than 0.6, 5 (21%) were found to have mild fibrosis on biopsy. On the other hand, in another similar study of more than 300 patients with hepatitis C for whom analyses were performed before and after a treatment regimen using antiviral agents, high values (almost 0.8) for the areas under the receiver-operator curves (see Chapter 8) were found at pretreatment and posttreatment. The overall sensitivity (see Chapter 8) of the method was 90%, and the positive predictive value was 88%. These values indicate that the index is of value in detecting fibrosis. Recently, FibroTest was validated as a prognostic marker for liver-related mortality in patients with chronic hepatitis C (Poynard et al., 2014).

It has been pointed out that false-positive results may occur as the result of treatment for hepatitis C with ribavirin because this drug can induce hemolysis, thereby reducing haptoglobin and increasing unconjugated bilirubin, both of which will change the index in a manner unrelated to increasing liver fibrosis (Halfon et al., 2008). This interference is less likely to occur now that new direct acting anti-hepatitis C agents are replacing ribavirin for treatment of this disease. Other conditions that are unrelated to liver fibrosis and that can change the index are acute hepatitides, extrahepatic cholestasis (as from choledocholithiasis), Gilbert disease, acute inflammatory conditions, and severe hemolysis (Halfon et al., 2008), as mentioned previously. With these caveats, Poynard has estimated that 18% of discordances between liver biopsy and FibroTest and ActiTest results are due to sampling errors on liver biopsy, a known problem with this procedure, especially for small biopsy sample sizes of less than 15 mm, and that 2% were due to the test (Poynard et al., 2004). For biopsy sizes of greater than 15 mm, correlation of FibroTest scores with biopsies resulted in an area of 0.88 under the receiver-operator curve (see Chapter 8). Other investigators have concluded from studies that there is a need for standardization of methods so that all testing laboratories obtain similar values for individual test results (Rosenthal-Allieri et al., 2005), as well as a need for large prospective studies (Afdhal & Nunes, 2004). It has been found that, overall, FibroTest, which is commercially available from the Laboratory Corporation of America (LabCorp, Philadelphia) under the name FibroSure, has a similar prognostic value to that obtained from liver biopsy and appears to be the most accurate of the noninvasive biomarker indices (Naveau et al., 2009).

These other indices (reviewed and evaluated in Parkes et al., 2006) include the FIBROSpect II index based on tissue inhibitors of metalloproteinases, α_2-macroglobulin, as in the ELF test, and hyaluronic acid, the latter appearing to give better correlations with liver fibrosis than procollagen type III peptide, as mentioned earlier; the INR; platelet count; ratio of AST to ALT; AST/platelet ratio index; and the Forns index, which correlates age, platelet count, GGT, and cholesterol with extent of liver fibrosis (Forns et al., 2002). These appear to have similar, although somewhat lower, sensitivities and/or specificities than those for the FibroTest and the ActiTest (Thabut et al., 2003; Naveau et al., 2009).

Computed Indices Used to Predict Survival of Patients with Extensive Liver Disease

Combinations of serum analytes, as described in the preceding section, are being employed to predict the survival of patients with severe disease. There are two major indices that are employed: MELD and the Child-Turcotte-Pugh (CTP) indices. Both utilize total serum bilirubin, serum creatinine, and the INR. The CTP system also uses serum levels of albumin and the extent of ascites and encephalopathy. One of the major purposes of these indices is to predict which patients are the "sickest" and who would require a liver transplant in a short time period.

MELD System

The MELD score was mentioned in the prior section on the INR (Bambha & Kamath, 2014; Reverter et al., 2014). The purpose is to compute the probability of survival for patients with liver disease. The score uses serum bilirubin, the INR, and serum creatinine to compute a score based on these values. The interpretation of the scores varies with the particular condition.

Patients with liver failure who require liver transplantation and who have high MELD scores are predicted to have lower predicted survival times; therefore, they must be given high priority. Originally, the MELD system was employed to predict the probability of a 3-month survival of patients with liver disease who had undergone a transjugular intrahepatic portosystemic shunt (TIPS). Predicted survival and actual survival in a number of different studies correlated well. The prediction scheme was then extended to prediction of the 3-month survival of any patients with extensive liver disease as described earlier. The following equation is used to compute the MELD score:

$$\text{MELD score} = 3.8 \times \ln[\text{serum bilirubin (mg/dL)}] + 11.2 \times \ln[\text{INR}] + 9.6 \times \ln[\text{serum creatinine (mg/dL)}] + 6.4$$

As an illustration of the use of this formula in guiding treatment, for patients who are considered to be candidates for TIPS placement, it has been found that the best outcomes for this procedure are for patients with MELD scores under 14. TIPS is not recommended for patients with MELD scores of over 24. For scores between 14 and 24, clinical evaluation of the risks and benefits is required.

Child-Turcotte-Pugh Score

This system categorizes patients with liver disease into three stages labeled A, B, and C based on the number of points that are assigned to specific results, the higher number of points increasing with severity of disease (Cholongitas et al., 2005; Bambha & Kamath, 2014). The condition severity is graded as follows: If a patient has a serum bilirubin of less than 2 mg/dL, albumin of greater than 3.5 g/dL, INR of less than 1.7, and no ascites or hepatic encephalopathy, the total number of points is 5 (1 for each of the three values and the two clinical conditions). The patient's condition would then be classified as category A. This category is for 5 to 6 points; if the score is 7 to 9 points, the patient's condition is ranked as category B, and 10 to 15 points places the condition in category C. The projected 2-year survival for category A is 85%; for category B, 57%; and for category C, 35%.

Biochemical and Clinical Correlations of Cirrhosis

As cirrhosis progresses to involve most (>80%) of the liver parenchyma, liver function becomes compromised. Total protein synthesis drops to low levels, as does synthesis of albumin. Portal hypertension, together with the drop in colloid osmotic pressure, results in ascites and even anasarca. Compression of the intrahepatic bile ductules and cholangioles results in diminished excretion of bilirubin and bile salts, causing hyperbilirubinemia and a rise in ALP, GGT, and 5′-nucleotidase. The serum concentrations of hepatocyte enzymes such as AST, ALT, and LD may be normal or diminished. If injury to viable hepatocytes is ongoing, the levels of these enzymes in serum may become mildly elevated. In more advanced stages of cirrhosis, serum ammonia levels become significantly elevated and correlate roughly with the degree of encephalopathy.

Four clinically graded levels of hepatic encephalopathy have been identified: motor tremors detected as asterixis, in which, when pressed back and then released, the patient's hands move back and forth in a flapping motion; a lethargic, stuporous state; severe obtundation; and frank coma. Lowering ammonia levels reduces the degree of encephalopathy. More recently, earlier signs of encephalopathy have been observed, including sleep disturbance and abnormal results on neuropsychiatric tests.

Because the liver is the site of synthesis of all of the coagulation factors except von Willebrand factor, and because synthesis of these factors is markedly diminished in cirrhosis, coagulation disorders may result, as discussed previously. Accelerated partial thromboplastin and prothrombin times become prolonged, often accompanied by diminished platelet counts. The latter may be caused by splenic sequestration due to splenomegaly caused by portal hypertension. However, disseminated intravascular coagulopathy may occur in cirrhosis, as evidenced by high levels of D-dimer and fibrin split products in serum, and may be the cause of the diminished platelet count. Because of derangements in lipid metabolism in the liver, fats enter the circulation and become deposited in erythrocyte membranes, causing these cells to appear as target cells.

Loss of vascular volume from ascites and anasarca can cause low tissue perfusion and lactic acidosis. Volume receptors, sensitive to volume loss, stimulate the secretion of antidiuretic hormone. The retained water causes serodilution, leading to hyponatremia.

Cirrhosis of the liver is often associated with renal failure as a result of the hepatorenal syndrome. In this condition, which is not well understood, renal tubular function is compromised. Serum blood urea nitrogen and creatinine rise to markedly elevated levels, indicating renal failure. Low tissue perfusion may also cause acute tubular necrosis. In hepatorenal syndrome, restoration of liver function generally reverses the renal failure.

Primary and secondary types of biliary cirrhosis have been discussed previously in this chapter. The diagnosis of these conditions is made difficult by the changing pattern of serum analyte concentrations used to evaluate liver status. Usually beginning as an obstructive pattern, in which alkaline phosphatase and sometimes bilirubin are elevated, the pattern progresses to one that resembles hepatitis because of the toxic effects of bile salts on hepatocytic function. With time, this pattern gives way to a cirrhotic pattern in which the aminotransferases decrease, total protein and albumin decrease, and ammonia rises. In patients with a persistent obstructive pattern indicated by laboratory results, with no evidence of mass lesions or stones causing blockage of bile flow, the presence of anti-M2 antimitochondrial antibody should be ascertained. Increased titers of this antibody are virtually 100% diagnostic of primary biliary cirrhosis. In addition, assays for serum p-ANCA antibodies should be performed to detect secondary biliary cirrhosis, which can also produce a cholestatic pattern.

Survival for patients with primary biliary cirrhosis can be computed from the MELD score (Bambha & Kamath, 2014) or computed using an empirical formula analogous to the MELD score that utilizes the age of the patient, the serum albumin and bilirubin, the prothrombin time, and the extent of edema (Dickson et al., 1989). This formula gives an estimate of the time within which the patient may undergo liver transplantation.

POSTHEPATIC BILIARY OBSTRUCTION

Posthepatic biliary obstruction refers to blockage of the intrahepatic and extrahepatic ducts and/or to blockage of bilirubin excretion from the hepatocyte into the canaliculi, leading to backflow of bile into the hepatocyte and ultimately into the circulation. The most common cause of this condition is cholelithiasis. Other causes include primary biliary cirrhosis and primary sclerosing cholangitis, as discussed earlier, and inflammation of the biliary tract, as occurs in ascending cholangitis and in gram-negative sepsis. Drugs such as the neuroleptics, like chlorpromazine, can cause cholestatic jaundice. Mass lesions, such as carcinoma of the head of the pancreas or lymphoma, can also cause posthepatic biliary obstruction by blocking the common bile duct at the porta hepatis. These conditions cause elevated bilirubin (most of it direct), ALP, and GGT. Often, however, especially in inflammatory conditions in the biliary tract, obstruction to bile flow is incomplete, resulting in partial flow of bile. Under these conditions, bilirubin remains normal or is only mildly increased. However, ALP, GGT, and 5′-nucleotidase become significantly elevated.

Occasionally, hyperbilirubinemia may be observed in patients who are otherwise normal. The bilirubin is of the indirect type and most often results from hemolysis, usually in hemolytic anemia. Hemolytic anemias may be triggered by hepatic disease. For example, viral hepatitis may precipitate hemolysis in patients with glucose-6-phosphate dehydrogenase deficiency. In Zieve syndrome, hemolysis occurs in conjunction with alcoholic hepatitis and hyperlipidemia. Wilson disease is sometimes associated with acute hemolysis. Patients with chronic hepatitis secondary to autoimmune disease may develop severe hemolytic disease, sometimes requiring splenectomy.

SPACE-OCCUPYING LESIONS

In space-occupying lesions of the liver, a high percentage of which are due to metastatic cancer; a smaller percentage to lymphoma, primary HCC, and angiosarcoma of the liver; and a small percentage to benign lesions such as hemangioma of the liver, the cardinal finding is isolated increases in the two enzymes LD and ALP. Increases in the latter are caused by encroachments of the mass(es) on canaliculi and cholangioles and even on the main bile ducts. The reasons for increases in LD are not clear. Most commonly, it is the LD_5 fraction that is responsible for the increase. This fraction may be produced by the liver but also may be produced by tumors, especially if LD is greater than 500 to 1000 IU/L and alkaline phosphatase is greater than 500 IU/L. If a malignant tumor spreads widely through the liver, mild elevation in the aminotransferases may be seen, along with hyperbilirubinemia due to bile duct obstruction, and low protein and albumin. The latter findings may not be caused as much by liver dysfunction as by generalized cachexia associated with tumor spread. A number of cancers that originate in the liver can be identified using serodiagnostic tests. For example, as discussed earlier in this chapter, serum levels of AFP are elevated in HCC. As discussed in Part 9 of this book, angiosarcomas can be diagnosed using specific antibodies to mutated ras-p21 protein.

FULMINANT HEPATIC FAILURE

In acute fulminant hepatic failure, an uncommon but highly fatal condition, massive destruction of liver tissue results in complete liver failure. Depending on the nature and extent of the destruction, ultimate liver regeneration frequently does not occur, although if cell death is limited and if hepatocytes can recover from the acute injury, normal liver function may return. The causes of this condition are largely unknown. Reye syndrome is an example of this condition, in which a child has an acute viral infection with fever and is treated with aspirin. Within 1 to 2 weeks after the infection and fever have dissipated, the child suddenly becomes encephalopathic secondary to hyperammonemia caused by acute hepatic failure. An adult form of Reye syndrome has also been described. Other possible causes of fulminant hepatic failure include acute hepatitis B with hepatitis D superinfection, Budd-Chiari syndrome and other hepatic vein thrombotic conditions, vascular hypoperfusion of the liver, ileojejunal bypass for obesity, acetaminophen intoxication, alcoholism, and cirrhosis. Another significant predisposing condition is the fatty liver of pregnancy (Sunheimer et al., 1994; Gotthardt, et al., 2007).

Two histopathologic forms of fulminant hepatic failure are known: panhepatic necrosis, in which all hepatocytes have become necrotic, and microvesicular steatosis, in which sinusoidal enlargement and cholestasis are present. The latter is most commonly observed in Reye syndrome and the fatty liver of pregnancy. It is important to note that, because the microvesicular steatosis pattern often shows only minimal changes histologically, liver biopsy is unrevealing. It is necessary to rely on laboratory analysis of liver function for a definitive diagnosis, as described later.

Many of the pathophysiologic sequelae of cirrhosis also occur in fulminant hepatic failure (Sunheimer et al., 1994). Patients develop ascites and become encephalopathic as the result of hyperammonemia. Total serum protein and serum albumin are depressed. Virtually all patients with fulminant hepatic failure exhibit severe coagulopathy, particularly disseminated intravascular coagulopathy, and virtually all are anemic. All develop renal failure as a result of the hepatorenal syndrome and acute tubular necrosis.

In addition, many patients become hypoglycemic, possibly because of the absence of enzymes involved in glycogenolysis. Lactic acidosis also develops as the result of poor tissue perfusion. It is interesting to note that, unlike in cirrhosis, in which patients become hyponatremic, patients with fulminant hepatic failure may become hypernatremic and hypokalemic. This observation may be explained by the finding that circulating levels of aldosterone in the serum of some of these patients are quite high (Sunheimer et al., 1994). Perhaps failure of the liver to clear aldosterone from the circulation results in the observed high levels of this hormone.

Diagnostic laboratory findings for fulminant hepatic failure include rapid increases in serum levels of the aminotransferases to markedly elevated levels, such that AST, which can reach levels greater than 20,000 IU/L, may be at least 1.5 times greater in value than ALT because of acute release of mitochondrial AST, as discussed previously. Although these enzymes rise in value, the total protein and albumin become markedly depressed. Overall, this pattern resembles hepatitis and end-stage cirrhosis combined, except that usually in acute hepatitis, save alcoholic hepatitis, AST and ALT rise in a ratio of about 1:1 or in a ratio that favors ALT. Shortly after these patterns occur, serum ammonia increases rapidly, leading to encephalopathy. LD, ALP, and bilirubin all increase markedly. All of the changes described previously occur over a period of about 1 week. After another week, the serum AST and ALT return to low, sometimes undetectable, levels. This finding signifies complete destruction of all viable liver tissue (Sunheimer et al., 1994).

Patients whose AST and ALT undergo the stereotypic changes described should be observed closely for fulminant hepatic failure, especially if there is any indication of encephalopathy. Although supportive therapy can sometimes result in restoration of normal liver function, for most patients in fulminant hepatic failure, the only ultimate cure is liver transplantation. The MELD score has been shown to have prognostic value in patients with hepatic failure, in particular those with alcoholic hepatitis, and serves as a predictor of patient survival among liver transplant candidates (Dunn et al., 2005; Srikureja et al., 2005).

SELECTED REFERENCES

Farnsworth N, Fagan SP, Berger DH, et al.: Child-Turcotte-Pugh versus MELD score as a predictor of outcome after elective and emergent surgery in cirrhotic patients, *Am J Surg* 188:580–583, 2004.

This is an excellent survey of the efficacy of different predictive methods for patients with cirrhosis.

Gottesman MM, Ambudkar SV: Overview: ABC transporters and human disease, *J Bioenerg Biomembr* 33:453–458, 2001.

This is a succinct discussion of the family of transporter proteins that share homology within the ATP-binding cassette (ABC) region and contain transmembrane domains involved in recognition of substrates, which are transported across, into, and out of cell membranes, including the bilirubin glucuronides that are secreted by an ABC protein in the canaliculi.

Kim DY, Ahn SH, Han K-H: Emerging therapies for hepatitis C, *Gut and Liver* 8(5):471–479, 2014.

This is an important summary of the issues concerning standardized international units for assays for hepatitis C.

Shiffman ML, Ferreira-Gonzalez A, Reddy KR, et al.: Comparison of three commercially available assays for HCV RNA using the international unit standard: implications for management of patients with chronic hepatitis C virus infection in clinical practice, *Am J Gastroenterol* 98:1159–1166, 2003.

This is an important review of the treatment therapies for hepatitis C.

Sunheimer R, Capaldo G, Kashanian F, et al.: Serum analyte pattern characteristic of fulminant hepatic failure, *Ann Clin Lab Sci* 24(–109):101, 1994.

This describes the major pathophysiologic aspects of fulminant hepatic failure and gives a summary of liver function profiles in different liver disease states.

Access the complete reference list online at Elsevier eBooks for Practicing Clinicians.

REFERENCES

Afdhal NH, Nunes D: Evaluation of liver fibrosis: a concise review, *Am J Gastroenterol* 99:1160–1174, 2004.

Aldenhovel HG: The influence of long-term anticonvulsant therapy with diphenylhydantoin and carbamazepine on serum gamma-glutamyltransferase, aspartate aminotransferase, alanine aminotransferase and alkaline phosphatase, *Eur Arch Psychiatry Neurol Sci* 237:312–316, 1988.

Aldridge DR, Tranah EJ, Shawcross DL: Pathogenesis of hepatic encephalopathy: role of ammonia and systemic inflammation, *J Clin Exp Hepatol* 5:S7–S20, 2014.

Alter HJ: New kit on the block: evaluation of second-generation assays for detection of antibody to the hepatitis C virus, *Hepatology* 15:350–353, 1992.

Alter MJ, Kruszon-Moran D, Nainan OV, et al.: The prevalence of hepatitis C virus infection in the United States, 1988 through 1994, *N Engl J Med* 341:556–562, 1999.

Alter MJ, Margolis HS, Krawczynski K, et al.: The natural history of community acquired hepatitis C in the United States. The Sentinel Counties Chronic non-A, non-B Hepatitis Study Team, *N Engl J Med* 327:1899–1905, 1992.

Aoki SK, Finegold D, Kuramoto IK, et al.: Significance of antibody to hepatitis B core antigen in blood donors as determined by their serologic response to hepatitis B vaccine, *Transfusion* 33:362–367, 1993.

Aoyagi K, Iida K, Matsunaga Y, et al.: Performance of a conventional enzyme immunoassay for hepatitis C virus core antigen in the early phases of hepatitis C infection, *Clin Lab* 47:119–127, 2001.

Arvan D, Shirey TL: Conjugated bilirubin: a better indicator of impaired hepatobiliary excretion than direct bilirubin, *Ann Clin Lab Sci* 15:252–259, 1985.

Axley P, Ahmed Z, Ravi S, et al.: Hepatitis C virus and hepatocellular carcinoma: a narrative review, *J Clin Transl Hepatol* 6:79–84, 2018.

Bambha K: *Kamath PS model for end-stage liver disease (MELD). UpToDate on-line publication. Literature review through November*, 2014.

Bandiera S, Billie Bian C, Hoshida Y, et al.: Chronic hepatitis C virus infection and pathogenesis of hepatocellular carcinoma, *Curr Opin Virol* 20:99–105, 2016.

Barrera JM, Francis B, Ercilla G, et al.: Improved detection of anti-HCV in post-transfusion hepatitis by a third-generation ELISA, *Vox Sang* 68:15–18, 1995.

Bartels CL, Marchetti AL, Highsmith EW, et al.: Real time PCR detection of the PI*Z and PI*S mutations associated with alpha-1 antitrypsin deficiency, *Am J Transl Res* 1:406–411, 2009.

Batshaw ML: Inborn errors of urea synthesis, *Ann Neurol* 35:133–141, 1994.

Beck J, Nassal M: Hepatitis B virus replication, *World J Gastroenterol* 13:48–64, 2007.

Bedossa P, Poynard T: The METAVIR Cooperative Study Group: an algorithm for the grading of activity in chronic hepatitis C, *Hepatology* 24:289–293, 1996.

Beld M, Penning M, van Putten M, et al.: Quantitative antibody responses to structural (core) and nonstructural (NS3, NS4, and NS5) hepatitis C virus proteins among seroconverting injecting drug users: impact of epitope variation and relationship to detection of HCV RNA in blood, *Hepatology* 29:1288–1298, 1999.

Belfrage P, Berg B, Hagerstrand I, et al.: Alterations of lipid metabolism in healthy volunteers during long-term ethanol intake, *Eur J Clin Invest* 7:127–131, 1977.

Bellentani S, Tabarroni G, Barchi T, et al.: Effect of ursodeoxycholic acid treatment on alanine aminotransferase and gamma-glutamyltranspeptidase serum levels in patients with hypertransaminasemia: results from a double-blind controlled trial, *J Hepatol* 8(7–12), 1989.

Bengtson P, Valtonen-André C, Jonsson M: Phenotyping of α-1-Antitrypsin by liquid chromatography–high resolution mass spectrometry, *Clin Mass Spectrometry* 2:34–40, 2016.

Berg PA, Klein R, Lindenborn-Fotinos JL: Antimitochondrial antibodies in primary biliary cirrhosis, *J Hepatol* 2:123–131, 1986.

Berk PD, Noyer C: Clinical chemistry and physiology of bilirubin, *Semin Liver Dis* 14:346–351, 1994a.

Berk PD, Noyer C: Structure, formation, and sources of bilirubin and its transport in plasma, *Semin Liver Dis* 14:325–330, 1994b.

Berk PD, Noyer C: The familial unconjugated hyperbilirubinemias, *Semin Liver Dis* 14:356–385, 1994c.

Berk PD, Noyer C: The familial conjugated hyperbilirubinemias, *Semin Liver Dis* 14:386–394, 1994d.

Berlin NI, Berk PD: Quantitative aspects of bilirubin metabolism for hematologists, *Blood* 57:983–999, 1981.

Berman DH, Leventhal RI, Gavaler JS, et al.: Clinical differentiation of fulminant Wilsonian hepatitis from other causes of hepatic failure, *Gastroenterology* 100:1129–1134, 1991.

Bertholf RL: *Proteins and Albumin*, *Laboratory Medicine* 45, 2014. e25–e41.

Binder LD, Kupka T: Failure of prediction of liver function test abnormalities with the urine urobilinogen and urine bilirubin assays, *Arch Pathol Lab Med* 113:73–76, 1989.

Björnsson E, Boberg KM, Cullen S, et al.: Patients with small duct primary sclerosing cholangitis have a favourable long term prognosis, *Gut* 51:731–735, 2002.

Bloomer JR, Berk PD, Vergalla J, et al.: Influence of albumin on the extravascular distribution of unconjugated bilirubin, *Clin Sci Mol Med* 45:517–526, 1973.

Bosma PJ, Chowdhury JR, Bakker C, et al.: The genetic basis of the reduced expression of bilirubin UDP-glucuronosyltransferase 1 in Gilbert's syndrome, *N Engl J Med* 333:1171–1175, 1995.

Bredaki FE, Poon LC, Birdir C, et al.: First-trimester screening for neural tube defects using alpha-fetoprotein, *Fetal Diagn Ther* 31:109–114, 2012.

Brillanti S, Masci C, Miglioli M, et al.: Serum IgM antibodies to hepatitis C virus in acute and chronic hepatitis C, *Arch Virol Suppl* (8)213–218, 1993.

Brown EA, Stapleton JT: Hepatitis A virus. In Murray PR, editor: *Manual of clinical microbiology*, ed 8, Washington, DC, 2003, ASM Press, pp 1452–1463.

Bull PC, Thomas GR, Rommens JM, et al.: The Wilson disease gene is a putative copper transporting P-type ATP-ase similar to the Menkes gene, *Nat Genet* 5:327–337, 1993.

Butterworth RF, Giguere JF, Michaud J, et al.: Ammonia: Key factor in the pathogenesis of hepatic encephalopathy, *Neurochem Pathol* 6(1–12), 1987.

Cabrerizo M, Bartolome J, De Sequera P, et al.: Hepatitis B virus DNA in serum and blood cells of hepatitis B surface antigen-negative hemodialysis patients and staff, *J Am Soc Nephrol* 8:1443–1447, 1997.

Cacciola I, Pollicino T, Squadrito G, et al.: Occult hepatitis B virus infection in patients with chronic hepatitis C liver disease, *N Engl J Med* 341(22–26), 1999.

Carey MC, Cahalane MJ, et al.: Enterohepatic circulation. In Arias IM, Jakoby WB, Popper H, editors: *The liver: Biology and pathobiology*, 2nd ed, New York, 1988, Raven Press, pp 573–616.

Carlson H, Zhang AS, Fleming WH, et al.: The hereditary hemochromatosis protein, HFE, lowers intracellular iron levels independently of transferrin receptor 1 in TRVb cells, *Blood* 105:2564–2570, 2005.

Carmel R, Wong ET, Weiner JM, et al.: Racial differences in serum total bilirubin levels in health and in disease (pernicious anemia), *J Am Med Assoc* 253:3416–3418, 1985.

Chan SL, Mo FK, Johnson PJ, et al.: New utility of an old marker: serial alpha-fetoprotein measurement in predicting radiologic response and survival of patients with hepatocellular carcinoma undergoing systemic chemotherapy, *J Clin Oncol* 27:446–452, 2009.

Chang TS, Wu YC, Tung SY, et al.: Alpha-fetoprotein measurement benefits hepatocellular carcinoma surveillance in patients with cirrhosis, *Am J Gastroenterol* 110:836–845, 2015.

Chapman RW: The enigma of anti-neutrophil antibodies in ulcerative colitis primary sclerosing cholangitis: important genetic marker or epiphenomenon, *Hepatology* 21:1473–1474, 2005.

Chapman RW, Cottone M, Selby WS, et al.: Serum autoantibodies, ulcerative colitis and primary sclerosing cholangitis, *Gut* 27:86–91, 1986.

Chappell S, Guetta-Baranes T, Batowski K, et al.: Haplotypes of the alpha-1 antitrypsin gene in healthy controls and Z deficiency patients, *Hum Mutat* 24:535–536, 2004.

Cholongitas E, Papatheodoridis GV, Vangeli M, et al.: Systematic review: the model for end-stage liver disease—should it replace Child-Pugh's classification for assessing prognosis in cirrhosis? *Alimentary Pharm Ther* 22:1079–1089, 2005.

Chowdhury JR, Wolkoff AW, Arias IM: Heme and bile pigment metabolism. In Arias IM, Jakoby WB, Popper H, et al.: *The liver: Biology and pathobiology*, ed 2, New York, 1988, Raven Press, pp 419–449.

Collins D, Goold MF, Rosalki SB, et al.: Plasma intestinal alkaline phosphatase and intermediate molecular mass gamma glutamyltransferase activities in the differential diagnosis of jaundice, *J Clin Pathol* 40:1252–1255, 1987.

Coppel RL, McNeilage LJ, Surh CD, et al.: Primary structure of the human M2 mitochondrial autoantigen of primary biliary cirrhosis: dihydrolipoamide acetyl transferase, *Proc Natl Acad Sci U S A* 85:7317–7321, 1988.

Crawford JM, Hauser SC, Gollan JL: Formation, hepatic metabolism, and transport of bile pigments: a status report, *Semin Liver Dis* 8:105–118, 1988a.

Crawford DH, Jazwinska EC, Cullen LM, et al.: Expression of HLA-linked hemochromatosis in subjects homozygous or heterozygous for the C282Y mutation, *Gastroenterology* 114:1003–1008, 1988b.

Czaja AJ: Autoimmune hepatitis: Evolving concepts and treatment strategies, *Dig Dis Sci* 40:435–456, 1995.

Czaja AJ: Diagnosis and management of autoimmune hepatitis: current status and Future Directions, *Gut and Liver* 10:177–203, 2016.

Czaja AJ, Ming C, Shirai M, et al.: Frequency and significance of antibodies to histones in autoimmune hepatitis, *J Hepatol* 23:32–38, 1995.

Czaja AJ, Shiels MT, Taswell HF, et al.: Frequency and significance of immunoglobulin M antibody to hepatitis B core antigen in corticosteroid-treated severe chronic active hepatitis B, *Mayo Clin Proc* 63:119–125, 1988.

da Fonseca-Wollheim F: Preanalytical increase of ammonia in blood specimens from healthy subjects, *Clin Chem* 36:1483–1487, 1990.

Dähnrich C, Pares A, Caballeria L, et al.: New ELISA for detecting primary biliary cirrhosis-specific antimitochondrial antibodies, *Clin Chem* 55:978–985, 2009.

Davies SM, Szabo E, Wagner JE, et al.: Idiopathic hyperammonemia: a frequently lethal complication of bone marrow transplantation, *Bone Marrow Transplant* 17:1119–1125, 1996.

de Tayrac M, Roth M, Jouanolle A, et al.: Genome-wide association study identifies TF as a significant modifier gene of iron metabolism in HFE hemochromatosis, *J Hepatol*, 2014, https://doi.org/10.1016/j.jhep.2014.10.017. Oct 18. pii: S0168-8278(14)00778-8, [Epub ahead of print].

Dickson ER, Grambsch PM, Fleming TR, et al.: Prognosis in primary biliary cirrhosis: model for decision making, *Hepatology* 10(1–7), 1989.

Doumas BT, Wu TW: The measurement of bilirubin fractions in serum, *Crit Rev Clin Lab Sci* 28:415–445, 1991.

Doumas BT, Wu TW, Jendrzejczak B: Delta bilirubin: absorption spectra, molar absorptivity, and reactivity in the diazo reaction, *Clin Chem* 33:769–774, 1987.

Dufour DR: Effects of habitual exercise on routine laboratory tests, *Clin Chem* 44:A136, 1998a.

Dufour DR: Gender-related differences in liver function and integrity tests, *Clin Chem* 44:A137, 1998b.

Dufour JF, Kaplan MM: Muddying the water: Wilson's disease challenges will not soon disappear, *Gastroenterology* 113:348–350, 1997.

Dufour DR, Teot L: Laboratory identification of ischemic hepatitis (shock liver), *Clin Chem* 34:A1287, 1988.

Duly EB, Grimason S, Grimason P, et al.: Measurement of serum albumin by capillary zone electrophoresis, bromocresol green, bromocresol purple, and immunoassay methods, *Journal of clinical pathology* 56:780–781, 2003.

Dunn W, Jamil SH, Brown LS, et al.: MELD accurately predicts mortality in patients with alcoholic hepatitis, *Hepatology* 42:353–358, 2005.

Eisenbach C, Sieg O, Stremmel W, et al.: Diagnostic criteria for acute liver failure due to Wilson disease, *World J Gastroenterol* 13:1711–1714, 2007.

Erker JC, Desai SM, Schlauder GG, et al.: A hepatitis E virus variant from the United States: molecular characterization and transmission in *Cynomolgus macaques*, *J Gen Virol* 80:681–690, 1999.

Feder JN, Gnirke A, Thomas W, et al.: A novel MHC class I-like gene is mutated in patients with hereditary haemochromatosis, *Nat Genet* 13:399–408, 1996.

Ferraro M, Painter MS: Hepatitis C–screening, diagnosis, management & treatment, *Osteopathic Family Physician* 11:12–19, 2019.

Fevery J, Blanckaert N: What can we learn from analysis of serum bilirubin? *J Hepatol* 2:113–121, 1986.

Forns X, Ampurdance S, Llovet JM, et al.: Identification of chronic hepatitis C patients without hepatic fibrosis by a simple predictive model, *Hepatology* 36:986–992, 2002.

Fragala MS, Bi C, Chaump M, et al.: Associations of aerobic and strength exercise with clinical laboratory test values, *PloS One* 12:e0180840, 2017.

Fuchs S, Bogomolski-Yahalom V, Paltiel O, et al.: Ischemic hepatitis: clinical and laboratory observations of 34 patients, *J Clin Gastroenterol* 26:183–186, 1998.

Fujiwara K, Yokosuka O, Ehata T, et al.: Frequent detection of hepatitis A viral RNA in serum during the early convalescent phase of acute hepatitis A, *Hepatology* 26:1634–1639, 1997.

Funk B: Reactive hepatitis A virus IgM antibody tests do not always indicate acute disease: a review of 10 case reports, *State of Alaska Epidemiology Bulletin* 3(1), 2005.

Fussey SP, Guest JR, James OFW, et al.: Identification and analysis of the major M2 autoantigens in primary biliary cirrhosis, *Proc Natl Acad Sci U S A* 85:8654–8658, 1988.

Gane EJ, Stedman CA, Hyland RH, et al.: Nucleotide polymerase inhibitor sofosbuvir plus ribavirin for hepatitis C, *N Engl J Med* 368(1):34–44, 2013, https://doi.org/10.1056/NEJMoa1208953.

Gao P, Lim M, Tian QB, et al.: Diagnostic performance of des-γ-carboxy prothrombin (DCP) for hepatocellular carcinoma: a bivariate meta-analysis, *Neoplasma* 201:150–159, 2012.

Garcovich M, Zocco MA, Gasbarrini A: Clinical use of albumin in hepatology, *Blood transfusion* 7:268–277, 2009.

Gitlin JD: Wilson disease, *Gastroenterology* 125:1868–1877, 2003.

Gotthardt D, Riediger C, Weiss KH, et al.: Fulminant hepatic failure: etiology and indications for liver transplantation, *Nephrol Dial Trans* 22(suppl_8):viii5–viii8, 2007.

Greene DN, Elliott-Jelf MC, Grenache DG: AAT phenotype identification by isoelectric focusing, *Methods Mol Biol* 1639:33–44, 2017.

Guu TS, Liu Z, Ye Q, et al.: Structure of the hepatitis E virus-like particle suggests mechanisms for virus assembly and receptor binding, *Proc Natl Acad Sci U S A* 106:12992–12997, 2009.

Halfon P, Munteanu M, Poynard T: FibroTest-ActiTest as a non-invasive marker of liver fibrosis, *Gastroenterol Clin Biol* 32(22–39), 2008.

Hayashi PH, Beames MP, Kuhns MC, et al.: Use of quantitative assays for hepatitis B e antigen and IgM antibody to hepatitis B core antigen to monitor therapy in chronic hepatitis B, *Am J Gastroenterol* 91:2323–2328, 1996.

Heubi JE, Daugherty CC, Partin JC, et al.: Grade 1 Reye's syndrome—outcome and predictors of progression to deeper coma grades, *N Engl J Med* 311:1539–1542, 1984.

Hidvegi T, Schmidt BZ, Hale P, et al.: Accumulation of mutant α1-antitrypsin Z in the endoplasmic reticulum activates caspases-4 and -12, NFκB, and BAP31 but not the unfolded protein response, *J Biol Chem* 280:39002–39015, 2005.

Hirschfield GM, Liu X, Xu C, et al.: Primary biliary cirrhosis associated with HLA, IL12A and IL12B variants, *N Engl J Med* 360:2544–2555, 2009.

Hofmeister MG, Rosenthal EM, Barker LK, et al.: *Estimating prevalence of hepatitis C virus infection in the United States*, 2013-2016, Hepatology, 2019.

Hoofnagle JH, Hepatitis C: The clinical spectrum of disease, *Hepatology* 26(3 Suppl 1) :15S-20S, 1997.

Horvat RT, Tegtmeier GE: Hepatitis B and D viruses. In Murray PR, editor: *Manual of clinical microbiology*, ed 8, Washington, DC, 2003, ASM Press, pp 1480–1494.

Hov JR, Boberg KM, Karlsen TH: Autoantibodies in primary sclerosing cholangitis, *World J Gastroenterol* 14:3781–3791, 2008.

Hov JR, Boberg KM, Taraldsrud E, et al.: Antineutrophil antibodies define clinical and genetic subgroups in primary sclerosing cholangitis, *Liver Int* 37:458–465, 2017.

Howanitz JH, Howanitz PJ, Skrodzki CA, et al.: Influences of specimen processing and storage conditions on results for plasma ammonia, *Clin Chem* 30:906–908, 1984.

Hsieh TY, Shiu TY, Chu NF, et al.: Rapid molecular diagnosis of the Gilbert's syndrome-associated Exon 1 mutation within the UGT1A1 gene, *Genet Mol Res* 13:670–679, 2014.

Huizenga JR, Tangerman A, Gips CH: Determination of ammonia in biological fluids, *Ann Clin Biochem* 31:529–543, 1994.

Hurie MB, Mast EE, Davis JP: Horizontal transmission of hepatitis B virus infection to United States-born children of Hmong refugees, *Pediatrics*, 1992. From: http://www-ncbi-nlm-nih-gov.ezproxy2.library.drexel.edu/pubmed/1734395. [Accessed 16 November 2014]. Retrieved.

Ihara H, Nakamura H, Aoki Y, et al.: Effects of serum-isolated vs. synthetic bilirubin-albumin complexes on dye-binding methods for estimating serum albumin, *Clin Chem* 31:1269–1272, 1991.

Ihara H, Shino Y, Hashizume N, et al.: Effect of light on total and direct bilirubin by an enzymatic bilirubin oxidase method, *J Anal Biol Sci* 20:349–354, 1997.

Irshad M, Gupta P, Irshad K: Molecular basis of hepatocellular carcinoma induced by hepatitis C virus infection, *World J Hepatol* 9:1305–1314, 2017.

Jedlitschky G, Leier I, Buchholz U, et al.: ATP-dependent transport of bilirubin glucuronides by the multidrug resistance protein MRP1 and its hepatocyte canalicular isoform MRP2, *Biochem J* 327(Pt 1):305–310, 1997.

Jenniskens M, Langouche L, Vanwyngaerden YM, et al.: Cholestatic liver (dys)function during sepsis and other critical illnesses, *Intensive Care Med* 42:16–27, 2016.

Johnson PJ, McFarlane IG, Alvarez F, et al.: Meeting report: international autoimmune hepatitis group, *Hepatology* 18:998–1005, 1993.

Johnston M, Harrison L, Moffatt K, et al.: Reliability of the international normalized ratio for monitoring the induction phase of warfarin: Comparison with the prothrombin time ratio, *J Lab Clin Med* 128:214–217, 1996.

Jones EA, Bergasa NV: The pruritus of cholestasis, *Hepatology* 29:1003–1006, 1999.

Kamili S, Drobeniuc J, Araujo AC, Hayden TM: Laboratory diagnostics for hepatitis C virus infection, *Clin Infect Dis* 55(Suppl 1):S43–S48, 2012, https://doi.org/10.1093/cid/cis368.

Kaplan MM, Gandolfo JV, Quaroni EG: An enzyme-linked immunosorbent assay (ELISA) for detecting antimitochondrial antibody, *Hepatology* 4:727–730, 1984.

Kay A, Zoulim F: Hepatitis B virus genetic variability and evolution, *Virus Res* 127:164–176, 2007.

Kelly DA, Summerfield JA: Hemostasis in liver disease, *Semin Liver Dis* 7:182–191, 1987.

Kelly DA, Tuddenham EGD: Hemostatic problems in liver disease, *Gut* 27:339–349, 1986.

Kelly E, Greene CM, Carroll TP, et al.: Alpha-1 antitrypsin deficiency, *Respir Med* 104:763–772, 2010.

Kenney SM, Cox DW: Sequence variation database for the Wilson disease copper transporter, ATP7B, *Hum Mutat* 28:1171–1177, 2007.

Kim NK, Yasmineh WG, Freier EF, et al.: Value of alkaline phosphatase, 5′nucleotidase, gamma-glutamyltransferase, and glutamate dehydrogenase activity measurements (single and combined) in serum in diagnosis of metastasis to the liver, *Clin Chem* 23:2034–2038, 1977.

Koff RS: Seroepidemiology of hepatitis A in the United States, *J Infect Dis* 171(Suppl 1):S19–S23, 1995.

Kovacs MJ, Wong A, MacKinnon K, et al.: Assessment of the validity of the INR system for patients with liver impairment, *Thromb Haemost* 71:727–730, 1994.

Kowdley KV, Lawitz E, Poordad F, et al.: Phase 2b trial of interferon-free therapy for hepatitis C virus genotype 1, *N Engl J Med* 370(3):222–232, 2014, https://doi.org/10.1056/NEJMoa1306227.

Kozaki N, Shimizu S, Higashijima H, et al.: Significance of serum delta-bilirubin in patients with obstructive jaundice, *J Surg Res* 79:61–65, 1998.

Kraemer D, Scheurlen M: Gilbert disease and Type I and II Crigler-Najjar syndrome due to mutations in the same UGT1A1 gene locus, *Med Klin* 15:528–532, 2002.

Krajden M, Shivji R, Gunadasa K, et al.: Evaluation of the core antigen assay as a second-line supplemental test for diagnosis of active hepatitis C virus infection, *J Clin Microbiol* 42:4054–4059, 2004.

Krams SM, Surh CD, Coppel RL, et al.: Immunization of experimental animals with dihydrolipoamide acetyltransferase, as a purified recombinant polypeptide, generates mitochondrial antibodies but not primary biliary cirrhosis, *Hepatology* 9:411–416, 1989.

Kramvis A, Kew M, François G: Hepatitis B virus genotypes, *Vaccine* 23:2409–2423, 2007.

Kuniholm MH, Nelson KE: Of organ meats and hepatitis E virus: one part of a larger puzzle is solved, *J Infect Dis* 198:1727–1728, 2008.

Kyriakidi KS, Tsianos VE, Karvounis E, et al.: Neutrophil anti-neutrophil cytoplasmic autoantibody proteins: bactericidal increasing protein, lactoferrin, cathepsin, and elastase as serological markers of inflammatory bowel and other diseases, *Ann Gastroenterol* 29:258–267, 2016.

Langner C, Denk H: *Wilson disease*, *Virchows Arch* 445:111–118, 2004.

LaPerche S, Courouce AM, Lemaire JM, Coste J, Defer C, Cantaloube JF: GB virus type C/hepatitis G virus infection in French blood donors with anti-NS5 isolated reactivities by recombinant immunoblot assay for hepatitis C virus, *Transfusion* 39(7):790–791, 1999, https://doi.org/10.1046/j.1537-2995.1999.3907790.x.

Laskus T, Radkowski M, Wang LF, et al.: Lack of evidence for hepatitis G virus replication in the livers of patients coinfected with hepatitis C and G viruses, *J Virol* 71:7804–7806, 1997.

Lau JY, Mizokami M, Kolberg JA, et al.: Application of six hepatitis C virus genotyping systems to sera from chronic hepatitis C patients in the United States, *J Infect Dis* 171:281–289, 1995.

Lauff JJ, Kasper ME, Wu TW, et al.: Isolation and preliminary characterization of a fraction of bilirubin that is firmly bound to protein, *Clin Chem* 28:629–637, 1982.

Lednar WM, Lemon SM, Kirkpatrick JW, et al.: Frequency of illness associated with epidemic hepatitis A virus infections in adults, *Am J Epidemiol* 122:226–233, 1985.

Lewis M: Howdle PD: the neurology of liver failure, *Q J Med* 96:623–633, 2003.

Li M, McDermott R: *Obesity, albuminuria, and gamma-glutamyl transferase predict incidence of hypertension in indigenous Australians in rural and remote communities in northern Australia*, J Hypertens, 2014. [Epub ahead of print].

Lindenbach B, Rice C: Unravelling hepatitis C virus replication from genome to function, *Nature* 436:933–938, 2005.

Liang TJ, Rehermann B, Seeff LB, et al.: Pathogenesis, natural history, treatment, and prevention of hepatitis C, *Ann Intern Med* 132:296–305, 2000.

Liang TJ: Hepatitis B: the virus and disease, *Hepatology 49 (Baltimore, Md*(5 Suppl)49, 2009.

Lin CL, Kao JH: Review article: novel therapies for hepatitis B virus- advances and perspectives, *Aliment Pharmacol Therapeut* 44:213–222, 2016.

Liu JP, Nikolova D, Fei Y: Immunoglobulins for preventing hepatitis A, *Cochrane Database Syst Rev*(2)CD004181, 2009.

Lo DH, Wu TW: Assessment of the fundamental accuracy of the Jendrassik-Grof total and direct bilirubin assays, *Clin Chem* 29:31–36, 1983.

London WT, Evans AA: The epidemiology of hepatitis viruses B, C, and D, *Clin Lab Med* 16:251–271, 1996.

Lotfy M, El-Kady IM, Nasif WA, et al.: Distinct serum immunoglob ulins pattern in Egyptian patients with chronic HCV infection analyzed by nephelometry, *J Immunoassay Immunochem* 27:103–114, 2006.

Lunel F, Cresta P, Vitour D, et al.: Comparative evaluation of hepatitis C virus RNA quantitation by branched DNA, NASBA, and monitor assays, *Hepatology* 29:528–535, 1999.

Manns M, Gerken G, Kyriatsoulis A, et al.: Two different subtypes of antimitochondrial antibodies are associated with primary biliary cirrhosis: identification and characterization by radioimmunoassay and immunoblotting, *Hepatology* 7:893–899, 1987.

Mao B, Li D, Zhao J, Liu X, Gu Z, Chen YQ, Zhang H, Chen W: In vitro fermentation of lactulose by human gut bacteria, *Agric Food Chem* 62:10970–10977, 2014, https://doi.org/10.1021/jf503484d. Epub 2014 Nov 3.

Martínez A, Broner S, Sala MR, et al.: Changes in the epidemiology of hepatitis A outbreaks 13 years after the introduction of a mass vaccination program, *Hum Vaccin Immunother* e35861, 2014. [Epub ahead of print].

Maruo Y, Addario C, Mori A, et al.: Two linked polymorphic mutations [A(TA) 7TAA and T3279G] of UGT1A1 as the principal cause of Gilbert syndrome, *Hum Genet* 115:525–526, 2004.

Mast EE, Alter MJ, Holland PV, et al.: Evaluation of assays for antibody to hepatitis E virus by a serum panel, *Hepatitis E Virus Antibody Serum Panel Evaluation Group*, *Hepatology* 27:857–861, 1998.

Matsumoto A, Yeo AE, Shih JW, et al.: Transfusion-associated TT virus infection and its relationship to liver disease, *Hepatology* 30:283–288, 1999.

McDonagh AF: Photolysis and photoisomerization of bilirubin in serum specimens exposed to room lighting, *Clin Chim Acta* 393:130, 2008.

McDonagh AF, Palma LA, Lauff JJ, et al.: Origin of mammalian biliprotein and rearrangement of bilirubin glucuronides in vivo in the rat, *J Clin Invest* 74:763–770, 1984.

McHutchison JG, Gordon SC, Schiff ER, et al.: Interferon alfa-2b or in combination with ribavirin as initial treatment for chronic hepatitis C. Hepatitis Interventional Therapy Group, *N Engl J Med* 339:1485–1492, 1998.

McHutchison JG, Poynard T, Gordon SC, et al.: The impact of race on response to anti-viral therapy in patients with chronic hepatitis C, *Hepatology* 30:A302, 1999.

McMahon BJ, Alward WL, Hall DB, et al.: Acute hepatitis B virus infection: Relation of age to the clinical expression of disease and subsequent development of the carrier state, *J Infect Dis* 151:599–603, 1985.

Medici V, Rossaro L, Sturniolo GC: Wilson disease–a practical approach to diagnosis, treatment and follow-up, *Dig Liver Dis* 39:601–609, 2007.

METAVIR Cooperative Group, Bedossa P: Intraobserver and interobserver variations in liver biopsy interpretation in patients with chronic hepatitis C (French), *Hepatology* 20:15–20, 1994.

Moreira VG, Vaktangova NB, Gago NDM, et al.: Overestimation of albumin measured by bromocresol green vs bromocresol purple method: influence of acute-phase globulins, *Lab Med* 49:355–361, 2018.

Moreno C, Mueller S, Szabo G: Non-invasive diagnosis and biomarkers in alcohol-related liver disease, *J Hepatol* 70:273–283, 2019.

Morgan RL, Baack B, Smith BD, et al.: Eradication of hepatitis C virus infection and the development of hepatocellular carcinoma: a meta-analysis of observational studies, *Ann Intern Med* 158:329–337, 2013.

Moss DW: Physicochemical and pathophysiological factors in the release of membrane-bound alkaline phosphatase from cells, *Clin Chim Acta* 257:133–140, 1997.

Moussavian SN, Becker RC, Piepmeyer JL, et al.: Serum gamma-glutamyl transpeptidase and chronic alcoholism: influence of alcohol ingestion and liver disease, *Dig Dis Sci* 30:211–214, 1985.

Moy L, Levine J: Autoimmune hepatitis: a classic autoimmune liver disease, *Curr Probl Pediatr Adolesc Health Care* 44:341–346, 2014.

Mulder AH, Horst G, Haagsma EB, et al.: Prevalence and characterization of neutrophil cytoplasmic antibodies in autoimmune liver diseases, *Hepatology* 17:411–417, 1993.

Mun BS, Ahn HS, Ahn DS, et al.: The correlation of Child-Pugh score, PGA index and MELD score in the patient with liver cirrhosis and hepatocellular carcinoma according to the cause of alcohol and hepatitis B virus, *Korean J Hepatol* 9:107–115, 2003.

Nagaoka S, Yatsuhashi H, Hamada H, et al.: The des-gamma-carboxy prothrombin index is a new prognostic indicator for hepatocellular carcinoma, *Cancer* 98:2671–2677, 2003.

Nahon P, Bourcier V, Layese R, et al.: Eradication of hepatitis C virus infection in patients with cirrhosis reduces risk of liver and non-liver complications, *Gastroenterology* 152:142–156, 2017.

Nalpas B, Vassault A, Charpin S, et al.: Serum mitochondrial aspartate aminotransferase as a marker of chronic alcoholism: diagnostic value and interpretation in a liver unit, *Hepatology* 6:608–614, 1986.

Naveau S, Gaude G, Asnacios A, et al.: Diagnostic and prognostic values of non-invasive biomarkers of fibrosis in patients with alcoholic liver disease, *Hepatology* 49:97–100, 2009.

Nguyen TT, Sedghi-Vaziri A, Wilkes LB, et al.: Fluctuations in viral load (HCV RNA) are relatively insignificant in untreated patients with chronic HCV infection, *J Viral Hepat* 3:75–78, 1996.

Nikolaeva LI, Blokhina NP, Tsurikova NN, et al.: Virus–specific antibody titres in different phases of hepatitis C virus infection, *J Viral Hepat* 9:429–437, 2002.

Nista EC, Fini L, Armuzzi A, et al.: 13C-breath tests in the study of microsomal liver function, *Eur Rev Med Pharmacol Sci* 8:33–46, 2004.

Notter D, et al.: Bilirubin. In Siest G, Schiele F, Henny J, editors: *Interpretation of clinical laboratory tests*, *Foster city*, *Calif.*, Biomedical Publications, 1985.

Nyblom H, Berggren U, Balldin J, et al.: High AST/ALT ratio may indicate advanced alcoholic liver disease rather than heavy drinking, *Alcohol* 39:336–339, 2004.

Okamura Y, Ashida R, Ito T, et al.: The tumor marker score is an independent predictor of survival in patients with recurrent hepatocellular carcinoma, *Surg Today*, 2014. [Epub ahead of print].

Onishi S, Isobe K, Itoh S, et al.: Metabolism of bilirubin and its photoisomers in newborn infants during phototherapy, *J Biochem (Tokyo)* 100:789–795, 1986.

Palmer M, Schaffner F: Effect of weight reduction on hepatic abnormalities in overweight patients, *Gastroenterology* 99:1408–1413, 1990.

Panteghini M: Aspartate aminotransferase isoenzymes, *Clin Biochem* 23:311–319, 1990.

Parkes J, Guha IN, Roderick P, et al.: Performance of serum marker panels for liver fibrosis in chronic hepatitis C, *J Hepatol* 44:462–474, 2006.

Paulusma CC, Kool M, Bosma PJ, et al.: A mutation in the human canalicular multispecific organic anion transporter gene causes the Dubin-Johnson syndrome, *Hepatology* 25:1539–1542, 1997.

Pawlotsky JM, Lonjon I, Hezode C, et al.: What strategy should be used for diagnosis of hepatitis C virus infection in clinical laboratories? *Hepatology* 27:1700–1702, 1998.

Persico P, Persico E, Bakker C, et al.: Hyperbilirubinemia in subjects with Gilbert syndrome (GS) mutations is determined by the rate of hepatic uptake of organic anions, *Hepatology* 30:A501, 1999.

Pincus JH, Cohan JL, Glaser GH: Neurologic complications of internal disease. In Baker AB, Baker LH, editors: *Clinical neurology*, New York, 1991, Harper and Row, pp 10–13.

Poordad F, Lawitz E, Kowdley KV, et al.: Exploratory study of oral combination antiviral therapy for hepatitis C, *N Engl J Med* 368(1):45–53, 2013, https://doi.org/10.1056/NEJMoa1208809.

Poordad F, McCone J, Bacon BR, et al.: Boceprevir for untreated chronic HCV genotype 1 infection, *N Engl J Med* 364(13):1195–1206, 2011, https://doi.org/10.1056/NEJMoa1010494.

Poynard T, Aubert A, Bedossa P, et al.: A simple biological index for detection of alcoholic liver disease in drinkers, *Gastroenterology* 100:1397–1402, 1991.

Poynard T, Marcellin P, Lee SS, et al.: Randomised trial of interferon alpha2b plus ribavirin for 48 weeks or for 24 weeks versus interferon alpha2b plus placebo for 48 weeks for treatment of chronic infection with hepatitis C virus, *International Hepatitis Interventional Therapy Group (IHIT)*, *Lancet* 352:1426–1432, 1998.

Poynard T, Munteanu M, Imbert-Bismut F, et al.: Prospective analysis of discordant results between biochemical markers and biopsy in patients with chronic hepatitis C, *Clin Chem* 50:1344–1355, 2004.

Poynard T, Vergniol J, Ngo Y, et al.: Staging chronic hepatitis C in seven categories using fibrosis biomarker (FibroTest™) and transient elastography (FibroScan®), *J Hepatol* 60:706–714, 2014. [Editor: Year mismatch].

Prince AM, White T, Pollock N, et al.: Epidemiology of hepatitis B infection in Liberian infants, *Infect Immun* 32(2):675–680, 1981.

Propst T, Propst A, Dietze O, et al.: Alpha-1-antitrypsin deficiency and liver disease, *Dig Dis* 12:139–149, 1994.

Puri P: Acute exacerbation of chronic hepatitis B: the dilemma of differentiation from acute viral hepatitis B, *Journal of Clinical and Experimental Hepatology* 3:301–312, 2013.

Qiu N, Li R, Yu JG, et al.: Comparison of Abbott and Da-an real-time PCR for quantitating serum HBV DNA, *World J Gastroenterol* 20:11762–11769, 2014.

Quinti I, Hassan N, Salman D, et al.: Hepatitis C virus-specific B cell activation: IgG and IgM detection in acute and chronic hepatitis C, *J Hepatol* 23:640–647, 1995.

Rajpert-De Meyts E, Heisterkamp N, Groffen J: Cloning and nucleotide sequence of human gamma-glutamyl transpeptidase, *Proc Natl Acad Sci U S A* 85:8840–8844, 1988.

Ravaggi A, Biasin MR, Infantolino D, et al.: Comparison of competitive and non-competitive reverse transcription-polymerase chain reaction (RT-PCR) for the quantification of hepatitis C virus (HCV) RNA, *J Virol Methods* 65:123–129, 1997.

Reddy KR, Hoofnagle JH, Tong MJ, et al.: Racial differences in response to therapy with interferon in chronic hepatitis C. Consensus Interferon Study Group, *Hepatology* 30:787–793, 1999.

Reshatnyak VI: Primary biliary cirrhosis: clinical and laboratory criteria for its diagnosis, World *J Gastroenterol* 7:7683–7708, 2015.

Reverter E, Tandon P, Augustin S, et al.: A MELD-based model to determine risk of mortality among patients with acute variceal bleeding, *Gastroenterology* 146:412–419, 2014.

Robert A, Chazouilleres O: Prothrombin time in liver failure: time, ratio, activity percentage, or international normalized ratio? *Hepatology* 24:1392–1394, 1996.

Roozendaal C, Van Milligen de Wit AW, Haagsma EB, et al.: Antineutrophil cytoplasmic antibodies in primary sclerosing cholangitis: defined specificities may be associated with distinct clinical features, *Am J Med* 105:393–399, 1998.

Rosenthal-Allieri MA, Peritore ML, Tran A, et al.: Analytical variability of the Fibrotest proteins, *Clin Biochem* 38:473–478, 2005.

Rosenthal P, Pincus MR, Fink D: Sex and age-related differences of bilirubin in serum, *Clin Chem* 30:1380–1382, 1984.

Rossi E, Adams L, Prins A, et al.: Validation of the FibroTest biochemical markers score in assessing liver fibrosis in hepatitis C patients, *Clin Chem* 49:450–454, 2003.

Rost D, Rudolph G, Kloeters-Plachky P, et al.: Effect of high-dose ursodeoxycholic acid on its biliary enrichment in primary sclerosing cholangitis, *Hepatology* 40:693–698, 2004.

Roberts EA, Schilsky ML: Diagnosis and treatment of Wilson disease: an update, *Hepatology* 47:2089–2111, 2008.

Rousselet MC, Michalak S, Dupre F, et al.: Sources of variability in histological scoring of chronic viral hepatitis, *Hepatology* 41:257–264, 2005.

Russell DW: The enzymes, regulation, and genetics of bile acid synthesis, *Annu Rev Biochem* 72:137–174, 2003.

Saldanha J, Lelie N, Heath A: Establishment of the first international standard for nucleic acid amplification technology (NAT) assays for HCV RNA. WHO Collaborative Study Group, *Vox Sang* 76:149–158, 1999.

Schlaeger R, Haux P, Kattermann R: Studies on the mechanism of the increase in serum alkaline phosphatase activity in cholestasis: significance of the hepatic bile acid concentration for the leakage of alkaline phosphatase from rat liver, *Enzyme* 28(3–13), 1982.

Schlauder GC, Dawson GJ: Hepatitis E virus. In Murray PR, editor: *Manual of clinical microbiology*, ed 8, Washington, DC, 2003, ASM Press, pp 1495–1511.

Seeff LB, Beebe GW, Hoofnagle JH, et al.: A serologic follow-up of the 1942 epidemic of post-vaccination hepatitis in the United States Army, *N Engl J Med* 316:965–970, 1987.

Seeff LB, the NHLBI Study Group: Mortality and morbidity of transfusion-associated non-A, non-B hepatitis and type C hepatitis: an NHLBI multi-center study, *Hepatology* 20:A204, 1994.

Selimovic D, El-Khattouti Haikel Y, Abdelkader O, et al.: Hepatitis C virus-related hepatocellular carcinoma: an insight into molecular mechanisms and therapeutic strategies, *World J Hepatol* 4:342–355, 2012.

Shawcross DL, Shabir SS, Taylor NJ, et al.: Ammonia and the neutrophil in the pathogenesis of hepatic encephalopathy in cirrhosis, *Hepatology* 51:1–8, 2010.

Shepard RL, Kraus SE, Babayan RK, Sirosky MB: The role of ammonia toxicity in the post transurethral prostatectomy syndrome, *Br J Urol* 60:349–351, 1987.

Sheth SG, Flamm SL, Gordon FD, et al.: AST/ALT ratio predicts cirrhosis in patients with chronic hepatitis C virus infection, *Am J Gastroenterol* 93:44–48, 1998.

Shuhart MC, Gretch DR: Hepatitis C and G viruses. In Murray PR, editor: *Manual of clinical microbiology*, ed 8, Washington, DC, 2003, ASM Press, pp 1480–1494.

Singer AJ, Carracio TR, Mofenson HC: The temporal profile of increased transaminase levels in patients with acetaminophen-induced liver dysfunction, *Ann Emerg Med* 26(49–53), 1995.

Skinhoj P, Mikkelsen F, Hollinger FB: Hepatitis A in Greenland: importance of specific antibody testing in epidemiologic surveillance, *Am J Epidemiol* 105:140–147, 1977.

Srikureja W, Kyulo NL, Runyon BA, et al.: MELD score is a better prognostic model than Child-Turcotte-Pugh score or discriminant function score in patients with alcoholic hepatitis, *J Hepatol* 42:700–706, 2005.

Stahl J: Studies of the blood ammonia in liver disease: its diagnostic, prognostic, and therapeutic significance, *Ann Intern Med* 58(1–24), 1963.

Stinton LM, Bentow C, Mahler M, et al.: PR3-ANCA: a promising biomarker in primary sclerosing cholangitis (PSC), *PloS One* 9(1–8), 2014.

Sveger T: The natural history of liver disease in alpha-1-antitrypsin deficient children, *Acta Paediatr Scand* 77:847–851, 1988.

Swift DL, Johannsen NM, Earnest CP, et al.: Effect of different doses of aerobic exercise training on total bilirubin levels, *Med Sci Sports Exerc* 44:569–574, 2012.

Taylor JM: Hepatitis delta virus, *Virology* 344:71–76, 2006.

Teare JP, Sherman D, Greenfield SM, et al.: Comparison of serum procollagen III peptide concentrations and PGA index for assessment of hepatic fibrosis, *Lancet* 342:895–898, 1993.

Teckman JH, An JK, Blomenkamp K, et al.: Mitochondrial autophagy and injury in the liver in alpha 1-antitrypsin deficiency, *Am J Physiol Gastrointest Liver Physiol* 286:G851–G862, 2004.

Terrault NA, Bzowej NH, Chang KM, et al.: AASLD guidelines for treatment of chronic hepatitis B, *Hepatology* 63:261–283, 2015.

Tervaert JWC, van Hoek B, Koek G: Antineutrophil cytoplasmic antibodies in small-duct primary sclerosing cholangitis, *Gastroenterology* 136:364, 2009.

Thabut D, Simon M, Myers RP, et al.: Noninvasive prediction of fibrosis in patients with chronic hepatitis C, *Hepatology* 37:1220–1221, 2003.

Totos G, Gizaris V, Papaevangelou G: Hepatitis A vaccine: persistence of antibodies 5 years after the first vaccination, *Vaccine* 15:1252–1253, 1997.

Trotter JF, Brimhall B, Arjal R, et al.: Specific laboratory methodologies achieve higher model for endstage liver disease (MELD) scores for patients listed for liver transplantation, *Liver Transpl* 10:995–1000, 2004.

Ts'ao C, Swedlund J, Neofotistos D: Implications of use of low international sensitivity index thromboplastins in prothrombin time testing, *Arch Pathol Lab Med* 118:1183–1187, 1994.

Tsujii H, Konig J, Rost D, et al.: Exon-intron organization of the human multidrug-resistance protein 2 (MRP2) gene mutated in Dubin–Johnson syndrome, *Gastroenterology* 117:653–660, 1999.

Turchin A, Wiebe DA, Seely EW, et al.: Severe hypercholesterolemia mediated by lipoprotein X in patients with chronic graft-versus-host disease of the liver, *Bone Marrow Transplant* 35:85–89, 2005.

Ustiugova AS, Korneev KV, Kuprash DV, et al.: Functional SNPs in the human autoimmunity-associated locus 17a12-21, *Genes* 10:77, 2019.

Van de Water L, Carr JM, Aronson D, et al.: Analysis of elevated fibrinogen degradation product levels in patients with liver disease, *Blood* 67:1468–1473, 1986.

Van Hootegem P, Fevery J, Blanckaert N: Serum bilirubins in hepatobiliary disease: Comparison with other liver function tests and changes in the post-obstructive period, *Hepatology* 5:112–117, 1985.

Vernelen K, Claeys H, Verhaert H, Volckaerts A, Vermylen C: Significance of NS3 and NS5 antigens in screening for HCV antibody, *Lancet* 343(8901):853, 1994, https://doi.org/10.1016/s0140-6736(94)92054-0.

Vierling JM, Berk PD, Hoffman AF, et al.: Normal fasting-state levels of serum cholyl-conjugated bile acids in Gilbert's syndrome: an aid to the diagnosis, *Hepatology* 2:340–343, 1982.

Villano SA, Vlahov D, Nelson KE, et al.: Persistence of viremia and the importance of long-term follow-up after acute hepatitis C infection, *Hepatology* 29:908–914, 1999.

Viot M, Thyss A, Schneider M, et al.: Alpha 1 isoenzyme of alkaline phosphatases: clinical importance and value for the detection of liver metastases, *Cancer* 52:140–145, 1983.

Vossler DG, Wilensky AJ, Cawthon DF, et al.: Serum and CSF glutamine levels in valproate-related hyperammonemic encephalopathy, *Epilepsia* 43:54–59, 2002.

Wang XH, Momenti A, Eid I, et al.: Major Discrepancies of HCV viral loads determined by real time polymerase chain reaction caused by Use of collection tubes that differ only with the presence or absence of serum separator, *ACLS (Ann Clin Lab Sci)* 48:286–295, 2018.

Watanabe T, Yamada H, Morimura Y, et al.: Ovarian Sertoli-Leydig cell tumor with heterologous gastrointestinal epithelium as a source of alpha-fetoprotein: a case report, *J Obstet Gynaecol Res* 34:418–421, 2008.

Webb GJ, Hirschfield GM: Genetics of autoimmune liver disease: a brief summary for clinicians, *Dig Dis* 32(5):e1–e6, 2014, https://doi.org/10.1159/000366174. Epub 2014 Aug 22.

Webster DP, Klenerman P, Dusheiko GM: *Hepatitis C*, *Lancet* 385:1124–1135, 2015.

Wen G, Tang Z, Yang F, et al.: A valuable antigen detection method for the diagnosis of acute hepatitis E, *J Clin Microbiol*, 2014. pii: JCM.01853-14. [Epub ahead of print].

Wenham PR, Horn DB, Smith AF: Multiple forms of gamma-glutamyl-transferase: a clinical study, *Clin Chem* 31:569–573, 1985.

Whitehead TP, Clarke CA, Whitfield AG: Biochemical and haematological markers of alcohol intake, *Lancet* 1:978–981, 1978.

Williams AL, Hoofnagle JH: Ratio of serum aspartate to alanine aminotransferase in chronic hepatitis: relationship to cirrhosis, *Gastroenterology* 95:734–739, 1988.

Witek K, Ścisłowska J, Turowski D, et al.: Total bilirubin in athletes, determination of reference range, *Biol Sport* 34:45–48, 2016.

Wolkoff AW: Organic anion uptake by hepatocytes, *Comprehensive Physiology* 4:1715–1735, 2014.

Yamada R, Hiramatsu N, Oze T, et al.: Incidence and risk factors of hepatocellular carcinoma change over time in HCV patients who achieved sustained virologic response, *Hepatol Res*, 2019.

Yamaguchi I, Nakamura K, Kitano H, et al.: Development of des-gamma-carboxy prothrombin (DCP) measuring reagent using the LiBASys clinical analyzer, *Clin Chem Lab Med* 46:411–416, 2008.

Yan L, Chen Y, Zhou J, et al.: Diagnostic value of circulating cell-free DNA levels for hepatocellular carcinoma, *Int J Infect Dis* 67:92–97, 2018.

Yotsuyanagi H, Yasuda K, Iino S, et al.: Persistent viremia after recovery from self-limited acute hepatitis B, *Hepatology* 27:1377–1382, 1998.

Yuki N, Hayashi N, Moribe T, et al.: Relation of disease activity during chronic hepatitis C infection to complexity of hypervariable region 1 quasispecies, *Hepatology* 25:439–444, 1997.

Zachou K, Rigopoulou E, Dalekos GN: Autoantibodies and autoantigens in autoimmune hepatitis: important tools in clinical practice and to study pathogenesis of the disease, *J Autoimmune Dis* 1(1–17), 2004.

Zaltron S, Spinetti A, Biasi L, et al.: Chronic HCV infection: epidemiological and clinical relevance, *BMC Infect Dis* 12(Suppl 2):S2, 2012. Suppl 2.

Zeman MV, Hirschfield GM: Autoantibodies and liver disease: uses and abuses, *Can J Gastroenterol* 24:225–231, 2010.

Zhou SL, Gordon RE, Bradbury M, et al.: Ethanol up-regulates fatty acid uptake and plasma membrane expression and export of mitochondrial aspartate aminotransferase in Hep G2 cells, *Hepatology* 27:1064–1074, 1998a.

Zhou L, Liu J, Luo F: Serum tumor markers for detection of hepatocellular carcinoma, *World J Gastroenterol* 12:1175–1181, 2006.

Zhou XY, Tomatsu S, Fleming RE, et al.: HFE gene knockout produces mouse model of hereditary hemochromatosis, *Proc Natl Acad Sci U S A* 95:2492–2497, 1998b.

Zimmerman HJ: Intrahepatic cholestasis, *Arch Intern Med* 139:1038–1045, 1979.

Zucker SD, Horn PS, Sherman KE: Serum bilirubin levels in the U.S. population: gender effect and inverse correlation with colorectal cancer, *Hepatology* 40:827–835, 2004.

CHAPTER 23

LABORATORY DIAGNOSIS OF GASTROINTESTINAL AND PANCREATIC DISORDERS

Haseeb A. Siddiqi, Simon Rabinowitz, Constantine A. Axiotis

PANCREATIC DISORDERS, 331
Pancreas in Systemic Disease, 331
Cystic Fibrosis (CF), 331
Hemochromatosis, 332
Inflammatory Diseases of the Pancreas, 332
Acute Pancreatitis, 332
Chronic Pancreatitis, 334
GASTROENTEROLOGIC DISORDERS, 335
Peptic Ulceration, 335
Zollinger-Ellison Syndrome, 335
Pepsin and Pepsinogen, 336
Diarrhea and Malabsorption, 336
Diarrhea, 336
Malabsorption Syndromes, 340
Gastrointestinal Bleeding, 343
Fecal Occult Blood Testing, 343
Blood in Newborn's Feces (Apt Test for Swallowed Blood), 343
Gastrointestinal and Pancreatic Neuroendocrine Neoplasms, 343
Pancreatic Adenocarcinoma, 343
Neuroendocrine Neoplasms, 344
Laboratory Diagnosis, 345
STOOL COLLECTION AND EXAMINATION, 345
Collection, 345
Macroscopic Examination, 345
Microscopic Examination, 345
SELECTED REFERENCES, 346

KEY POINTS

- Almost all patients with duodenal ulcers and most with chronic gastritis have demonstrable *Helicobacter pylori* infection. *H. pylori* stool antigen assays and urea breath tests are useful in diagnosis and in monitoring for eradication after treatment.
- Acute pancreatitis presents with abdominal pain and elevated levels of serum amylase or lipase. Reversible etiologies, including drug exposure, must be excluded in patients with recurrent episodes of acute pancreatitis. Routine laboratory testing is of limited value in diagnosing chronic pancreatitis.
- Sweat chloride determination is the necessary initial test in the workup for cystic fibrosis (CF). Malnutrition and other conditions can yield a false-negative result. Genetic testing can then be used to identify the mutations associated with CF.
- Patients with chronic diarrhea should be evaluated for fecal blood, fat, leukocytes, reducing substances, pH, and stool pathogens (bacterial culture on routine media, ova, and parasite examination). Fecal calprotectin should be measured to rule out colonic inflammation.
- *Clostridium difficile* should be considered a cause of diarrhea in patients on antibiotic therapy or hospitalized for >3 days. Community-acquired infection is being recognized with increasing frequency. Prompt recognition and treatment is crucial as many isolates have increased virulence, especially in patients >65 years old.
- Diagnostic evaluation of a patient suspected of celiac disease should be initiated with anti–tissue transglutaminase immunoglobulin (Ig) A, and total serum IgA before placing the patient on a gluten-free diet.
- Acquired lactose intolerance related to decreased expression of lactase gene is common in adults. Secondary lactose intolerance may occur in infection, in inflammatory bowel disease, and in other conditions causing small-bowel mucosal damage.
- Positivity of perinuclear antineutrophil cytoplasmic antibody (p-ANCA) is most often associated with ulcerative colitis and that of anti-*Saccharomyces cerevisiae* antibody (ASCA) with Crohn disease.
- Endoscopy with biopsy has replaced gastric acid aspiration for diagnosis of upper gastrointestinal tract disorders. Gastric acid output testing is useful when acid levels are very high or very low.
- Gastrin, the most powerful gastric acid stimulator, varies inversely with gastric acid secretion. Serum gastrin levels are elevated in gastric atrophy and in the presence of *H. pylori* infection while the gastric acid levels are reduced.
- Secretin stimulates gastrin production in patients with a gastrinoma but not in patients with other causes of hypergastrinemia.
- Intraoperative gastrin measurements are useful in identifying whether the abnormal tissue is completely removed in patients undergoing surgery for gastrinomas.
- An immunochemical fecal occult blood test is used to screen for colon cancer.

Diagnosis of gastrointestinal (GI) disease is guided by the patient's history and the significant signs and symptoms. Findings with strong negative predictive values exclude some possible etiologies and focus the differential diagnosis. Initially, noninvasive procedures are preferentially performed. Patient preparation is as important as the correct selection of the diagnostic tests or procedures indicated. Endoscopy, when warranted, can provide direct visualization of the entire upper gastrointestinal mucosa and permits biopsy. Colonoscopy permits detailed examination of the entire colon and terminal ileum. More comprehensive and accurate radiographic investigations, such as magnetic resonance enterography and video capsule endoscopy, have largely replaced the traditional upper GI series. Imaging-assisted invasive techniques may be required in the critically ill with GI bleeding or obstruction. To ensure interpretable endoscopic results and to avoid false-positive and false-negative results, stringent patient preparation is required. Similarly, testing requires appropriately collected specimens. Emphasis is given in this chapter to frequently used diagnostic tests.

PANCREATIC DISORDERS

PANCREAS IN SYSTEMIC DISEASE

Cystic Fibrosis (CF)

CF is the most common genetic disorder in white North Americans and is often fatal in childhood. Some Native American tribes (Pueblo) have a similar incidence. It is also frequent in Hispanics but uncommon in Asians and African Americans. More than 25,000 Americans have CF at this writing, with almost 1000 new cases expected to be diagnosed every year. The incidence is 1 in 1600 white births and 1 in 17,000 African American births in the United States. With the advent of more widespread prenatal screening, the incidence is declining. While much less frequent, CF still is the most common cause of steatorrhea in African American children.

CF of the pancreas is an autosomal-recessive disease of chloride ion transport. It is caused by mutations in the CF transmembrane conductance regulator (CFTR) gene on chromosome 7, which encodes for an epithelial chloride channel protein. More than 2000 CFTR gene mutations with different associations with the disease have been identified; 15% of these are not associated with CF. The available genetic testing can identify 70 mutations that account for >90% of the CF cases. When genetic screening fails to identify a mutation in affected patients, whole exome sequencing can be performed (Elborn, 2016).

Newborn screening for CF is now routinely performed in many states. The initial test, which has high sensitivity and poor specificity, determines immunoreactive trypsinogen; gene sequencing is then performed for confirmation.

CF is characterized by abnormally viscous mucous secretions from the various exocrine glands of the body, including the pancreas and the salivary, peritracheal, peribronchial, and sweat glands. Involvement of the intestinal glands may result in the presence of meconium ileus at birth. Two-thirds are diagnosed before 1 year of age. Chronic lung disease and malabsorption resulting from pancreatic insufficiency are the major clinical problems of those who survive beyond infancy, but intelligence and cognitive functions are unaffected and are normal (Cheng et al., 1990; Elborn, 2016).

The degree of the defect depends on the nature of the mutation, and well-defined genotype-phenotype associations are now known. There are several characterized mutations that lead to a milder form of the disease. The classic ΔF508 (or Phe508del) mutation leads to cystic fibrosis when two copies of the gene are inherited. Persons heterozygous for the R117H (or Arg117His) mutation may develop pancreatic insufficiency due to plugging of ducts, causing idiopathic chronic pancreatitis (Elborn, 2016; Dechecchi et al., 2018).

Heterozygotes have no recognizable clinical symptoms. Most homozygotes fully express the syndrome of recurrent pulmonary infections, pancreatic insufficiency, steatorrhea, and malnutrition. These manifestations are caused by abnormally dehydrated tenacious secretions of all exocrine glands. The viscid inspissated mucus plugs ducts and causes chronic inflammation with atrophy of acini, fibrosis, dilatation, and cystic duct changes.

Pancreatic abnormalities occur in >80%. Islets of Langerhans are initially spared, but diabetes often develops during adolescence. The pancreatic lipase deficiency causes maldigestion of fat and steatorrhea. Thick intestinal mucus may cause intestinal obstruction in the neonate due to meconium ileus. Most men with CF are infertile, with azoospermia due to duct obstruction. Pulmonary changes are the most serious in CF. No cure is available. Median survival has increased in the past 25 years from 18 to 36 years of age due to advances in treatment. A total of 90% die from pulmonary complications.

In a child with suspected CF, the demonstration of increased chloride in the sweat is a useful initial test in the workup. More than 99% of children with CF have concentrations of sweat chloride greater than 60 mmol/L. The sweat chloride may not be as dramatically increased in adolescent or adult patients. The test needs be performed with care (LeGrys et al., 2007).

Pilocarpine is introduced into the skin by iontophoresis to stimulate locally increased sweat gland secretion. The resulting sweat is absorbed by filter paper or gauze, weighed, diluted with water, and analyzed for sodium and chloride concentrations. High rates of incorrect results have been attributed to problems associated with sweat specimen sample collection and test analysis (NCCLS, 2000; LeGrys et al., 2007). In children, chloride concentrations of over 60 mmol/L in sweat on at least two occasions are diagnostic, with a sensitivity of 90% to 99%. Levels of between 50 and 60 mmol/L are suggestive of CF in the absence of adrenal insufficiency.

Patients with indeterminate sweat chloride results in whom CF is suspected may undergo confirmatory testing following administration of a mineralocorticoid such as fludrocortisone. In those patients with CF, the electrolyte values would remain unchanged, whereas normal controls would show a decrease in sweat electrolytes. Sodium concentrations in sweat tend to be slightly lower than those of chloride in patients with CF, but the reverse is true in normal subjects. Alternatively, genetic mutation analysis of the CFTR gene can be performed.

False-positive elevations of sweat chloride concentrations of >60 mmol/L may be seen in malnutrition, hyperhidrotic ectodermal dysplasia, nephrogenic diabetes insipidus, renal insufficiency, glucose-6-phosphatase deficiency, hypothyroidism, mucopolysaccharidosis, and fucosidosis. These disorders are usually easily differentiated from CF by their clinical symptoms. False-negative sweat test results have been seen in patients with CF in the presence of hypoproteinemic edema.

Sweat electrolytes in about half of a group of premenopausal adult women were shown to undergo cyclic fluctuation, reaching a peak chloride concentration most commonly 5 to 10 days prior to the onset of menses. Peak values were slightly under 65 mmol/L. Men showed random fluctuations up to 70 mEq/L. For this reason, interpretation of sweat electrolyte values in adults must be approached with caution (Rosenstein & Cutting, 1998; NCCLS, 2000).

Hemochromatosis

Excessive body iron accumulation from any source is directly toxic to cells and causes fibrosis. The symptoms include the triad of bronze coloration of the skin, cirrhosis, and diabetes, among others. Humans have no major iron excretory pathway. The screening test consists of transferrin saturation (TS) = serum iron/total iron binding capacity × 100. Interpretation: Abnormal, >60% in women and >50% in men. Confirm with fasting TS and ferritin levels. Genetic testing and liver biopsy with assay for iron is used to confirm and assess extent of tissue iron load (Powell, 2002; Adams & Barton, 2007). Recently, MRI has been utilized to quantify liver iron overload and to monitor response to chelation therapy (Hernando et al., 2014).

Primary or hereditary hemochromatosis (HH) is a human leukocyte antigen (HLA)-linked autosomal recessive defect in duodenal iron absorption regulation. Mutations (C282Y, H63D) in the *HFE* gene, on the short arm of chromosome 6, are responsible for >80% of HH cases (see Chapters 22 and 72). The disease is most common in white males; the homozygosity frequency is 1 in 220. When HH is diagnosed, other family members should be screened; one quarter of siblings will be positive (Bulaj et al., 2000; Powell et al., 2016).

Secondary hemochromatosis is typically seen in congenital or hemolytic anemias that require multiple blood transfusions, or when oral iron intake is increased, resulting in excess iron storage.

Early diagnosis and chelation therapy and/or phlebotomies are effective in preventing tissue damage. In disease, the pancreas is slightly enlarged and deep brown due to accumulated hemosiderin, the iron containing pigment. When untreated, progressive fibrosis of the pancreas with atrophy occurs. The iron is deposited in the acinar and duct cells and in the β-cells of the islets. Other cells of the islets appear spared. Similar pigments are in the skin. The β-cell loss results in bronze diabetes. Hypogonadism with pituitary dysfunction is present in half of cases and cardiomegaly and osteoarthritis is present in most cases. Cirrhosis is seen in 70% of the cases. Hepatocellular carcinoma occurs in 30% of cases; this tumor has become a chief cause of death in HH (Bacon et al., 2011; Powell et al., 2016).

The American Association for the Study of Liver Diseases has recommended liver biopsy and a quantitative serum iron assay for (1) all homozygotes with clinical evidence of liver disease; (2) all homozygotes with serum ferritin greater than 1000 ng/ml; (3) all homozygotes older than 40 years with other risk factors for liver disease; and (4) compound or C282Y heterozygotes with elevated transferrin saturation, particularly those who have had abnormal liver enzyme levels or clinical evidence of liver disease (Bacon et al., 2011).

INFLAMMATORY DISEASES OF THE PANCREAS

Pancreatitis is an inflammation of the pancreas caused by injury to acinar cells due to activation of digestive enzymes within the pancreatic parenchyma and is characterized by significant morbidity and mortality. Clinical manifestations of pancreatitis are very variable.

Acute Pancreatitis

Acute reversible inflammation is due to necrosis of the pancreatic tissue by proteolytic digestive enzymes that are inappropriately activated. It can occur at any age, most commonly between 30 to 70 years, but is also noted in children. Its diagnosis is based on compatible clinical features, including abdominal pain, nausea, and vomiting. The clinical suspicion is supported by finding elevations of the serum amylase and/or lipase (Table 23.1). The pancreas contributes 40% of total serum amylase; the rest is mostly from the salivary glands (Halangk & Lerch, 2005).

In 30% of patients, the diagnosis of acute pancreatitis was not suspected and was only made at autopsy (Wilson et al., 1985). There are many causes. Gallstones continue to be the leading cause (30%–60%). Alcohol is the second most common cause, responsible for 15% to 30%. Other causes include duct obstruction due to tumors, duct anomalies such as pancreas divisum, infections (mumps, coxsackievirus A, parasites), blunt trauma or post–endoscopic retrograde cholangiopancreatography (ERCP), many drugs (diuretics, sulfonamides), organophosphates, methyl alcohol, nitrosamines, hypertriglyceridemia, and hypercalcemia (Lankisch et al., 2015; Forsmark et al., 2016).

Hemorrhagic pancreatitis, a severe form of acute pancreatitis, results from necrosis within and around the pancreas with hemorrhage, which may cause shock and death. Initially, necrosis is coagulative, but the necrotic cells rapidly undergo liquefaction. Biliary tract disease with gallstones or inflammation of the gallbladder or bile ducts, or alcoholism, are present in about 80% of the patients. The male:female ratio is 1:3 in acute pancreatitis associated with biliary tract disease and 6:1 in alcoholism. Pancreatic microlithiasis may be responsible for many of the other cases.

The sequence of changes following release of activated intrapancreatic enzymes in acute pancreatitis are microvascular leakage causing edema, necrosis of fats, and acute inflammatory reaction. Proteolytic destruction of pancreatic tissue and blood vessels causes edema and focal dilatation of acini with variable amounts of hemorrhage. In fat necrosis, neutral fats are broken down, glycerol is reabsorbed, and the fatty acids combine with calcium salts to form soaps (saponification) with a zone of acute inflammation around the foci of necrosis. After a few days, secondary infection with suppuration and abscesses may occur.

In 15% to 30% of those with pancreatic necrosis, poorly defined areas of acute fluid collection occur, with fibrosis. The liquefied areas are walled off and pseudocysts form. A pseudocyst contains pancreatic fluid enclosed in fibrous tissue with no epithelial lining; they often communicate with a pancreatic duct and continue to increase in mass.

Computed tomography (CT) is the most useful test to establish diagnosis, with characteristic radiologic findings of enlarged edematous and inflamed pancreas with or without surrounding fluid collection, with or without necrosis. An ultrasonogram may be useful in showing a diffusely enlarged, hypoechoic pancreas, and may show presence of gallstones in the gallbladder, indicating a possible etiology. A CT severity score (the Balthazar score) is based on the degree of necrosis, inflammation, and the fluid collections. There is a 23% mortality rate associated with any degree of pancreatic necrosis plus a strong association between necrosis and morbidity and mortality. After initial assessment, a CT scan need not be repeated unless one suspects development of a complication such as pancreatic necrosis. Magnetic resonance imaging (MRI) is being increasingly used to detect pancreatitis and to characterize the "pancreatic necrosis" seen on CT into peripancreatic necrotic fluid collection, necrotic pancreatic parenchyma, and hemorrhagic foci. MRI can also detect pancreatic duct disruption, seen early in the course of acute pancreatitis. Endoscopic ultrasound is now recognized as an invaluable tool to diagnose and drain pseudocysts.

Predictors of severe acute pancreatitis are a hematocrit >44% with a failure to decrease at 24 hours, which is indicative of pancreatic necrosis and organ failure, and a C-reactive protein (CRP) >150 mg/L. Serum creatinine >2.0 mg/dL or marked hyperglycemia >150 mg/dL are predictive of mortality (Lankisch et al., 2001). There is a strong association between the extent of urea nitrogen increase and mortality at 24 hours. Each increase in urea nitrogen of 5 mg/dL was associated with a corresponding increase in mortality, and a decrease was associated with significantly improved survival (Wu et al., 2009; Forsmark et al., 2016) (Table 23.2).

Amylase

Amylase in serum and urine is stable for 1 week at ambient temperature and for at least 6 months under refrigeration in well-sealed containers. Plasma specimens that have been anticoagulated with citrate or oxalate should be avoided for amylase determination because amylase is a calcium-containing enzyme. Heparinized plasma specimens do not interfere with the amylase assay.

Diagnosis is confirmed by detection of elevated serum amylase threefold above normal. It peaks in 20 to 30 hours, often at 10 to 20 times the upper reference limit (Papachristou & Whitcomb, 2005). Amylase returns to normal in 48 to 72 hours. Elevated values persisting longer suggest continuing necrosis or possible pseudocyst formation. Serum amylase has poor sensitivity (72%) for pancreatitis; it is not increased in about 20% of patients with pancreatitis. Serum amylase has 99% specificity for pancreatitis (Treacy et al., 2001). Serum amylase increases nonspecifically in many acute abdominal conditions. In hyperlipemic patients with pancreatitis, normal serum and urine amylase levels are frequently encountered. The spuriously normal levels are believed to be the result of suppression of amylase activity by triglyceride or by a circulating inhibitor in serum. Serum amylase levels do not correlate with etiology or severity of pancreatitis. Amylase is also produced by the salivary glands.

While there are a variety of reliable amylase methods available, care is required in specimen handling. Caution must be exercised to avoid contamination of specimens with saliva because its amylase content is approximately 700 times that of serum. Red cells contain no amylase; thus, hemolysis does not affect most methods except those coupled-enzyme methods in which the released peroxide is determined by a coupled-peroxidase reaction.

The urine amylase activity rises promptly, often within several hours of the rise in serum activity, and may remain elevated after the serum level has returned to the normal range. Values of over 1000 Somogyi units/hour are seen almost exclusively in patients with acute pancreatitis. (A Somogyi unit is 1 mg of glucose hydrolyzed in 30 minutes from a standard starch solution in a volume of 100 mL.) In a majority of patients with acute pancreatitis, serum amylase activity is elevated and there is a concomitant increase in urine amylase activity.

Increased renal clearance of amylase can be used in the diagnosis of acute and relapsing pancreatitis. However, the ratio of amylase clearance to creatinine clearance expressed as a percentage adds little to the diagnosis since elevated ratios may be found in unrelated conditions.

Lower than normal serum amylase activity may be found in patients with chronic pancreatitis and has also been seen in such diverse conditions as congestive heart failure, pregnancy (during the second and third trimesters), gastrointestinal cancer, bone fractures, and pleurisy.

Serum amylase may be elevated in patients with pancreatic carcinoma but often too late to be diagnostically useful. Serum amylase activity may also be elevated in patients with cholecystitis, peptic ulcer, postgastrectomy, renal transplant, viral hepatitis, or ruptured ectopic pregnancy.

Serum and urine amylase elevations occur in many conditions other than pancreatitis, such as renal failure, parotitis, and diabetic ketoacidosis. Patients with acidemia may have spurious elevations of serum amylase. This explains why patients with diabetic ketoacidosis may have marked elevations of serum amylase without any other evidence of acute pancreatitis.

Increased ascites fluid amylase levels have been seen in patients with pancreatitis, a leaking pancreatic pseudocyst, pancreatic duct rupture, pancreatic cancer, abdominal tumors that secrete amylase, and perforation of a hollow viscus.

Fractionation of amylase in serum, urine, or other body fluids can be done by physical means, such as electrophoresis, chromatography, or isoelectric focusing. Each isoenzyme is then quantitated by direct densitometry.

TABLE 23.2
Laboratory Findings in Acute Pancreatitis

At Presentation		At 48 Hours	
Age	>55 years	Hematocrit	Fall by ≥10%
Leukocyte count	>16,000/mm^3	Urea nitrogen	Increase by ≥5 mg/dL despite fluids
Blood glucose	>200 mg/dL	Serum calcium	<8 mg/dL
LD	350 U/L	pO_2	<60 mmHg
AST	>250 U/L	Base deficit	>4 mEq/L
		Fluid sequestration	>6000 mL

AST, aspartate aminotransferase; *LD,* lactate dehydrogenase; *pO_2,* partial pressure of oxygen.

TABLE 23.1
Laboratory Tests in Acute Pancreatitis

Laboratory Test	Purpose	Usage and Limitations
Amylase	Diagnosis	Accurate over 3× the upper normal limit; decreased specificity in renal failure; elevated in macroamylasemia; hypertriglyceridemia interferes; elevated from other sources, such as salivary glands and/or intra-abdominal inflammation (not above 3×); can be normal in alcohol-induced pancreatitis.
Lipase	Diagnosis	Decreased specificity in renal failure; immune complexes create false positives; elevated from salivary glands and intra-abdominal inflammation.
Trypsinogen 2	Diagnosis	Limited use; unclear if superior to amylase/lipase.
AST/ALT	Etiology	If greater than 3× upper normal limit, gallstones present as etiology in 95% of cases. Low sensitivity.
Lipase/amylase ratio	Etiology	>5 is diagnostic for alcohol-induced pancreatitis. Low sensitivity.
CDT	Etiology	Useful in patients who deny alcohol; remains elevated for weeks after binge drinking; not widely available.
Hematocrit	Severity	>44% on admission, or rising over initial 24 hours; associated with pancreatic necrosis.
C-reactive protein	Severity	>150 mg/L associated with pancreatic inflammation. Useful after first 36–48 hours.

ALT, Alanine aminotransferase; *AST,* aspartate aminotransferase; *CDT,* carbohydrate-deficient transferrin.

Macroamylasemia

Macroamylasemia is not a disease but rather an acquired benign condition, more frequent in men and usually discovered incidentally in the fifth through seventh decades (Remaley & Wilding, 1989). There is a persistent increase in the serum amylase without clinical symptoms. Urine amylase is normal or low. Macroamylases are heterogeneous complexes of normal amylase (usually salivary isoenzyme) with immunoglobulin G (IgG), IgA, or polysaccharide (Van Deun et al., 1989). Because of their large size, macroamylases cannot be filtered through the glomerulus. They are retained in the plasma and are not present in urine. The plasma amylase activity is often increased two- to eightfold. Serum lipase is normal. Macroamylasemia is found in about 1% of randomly selected patients. Renal function is normal and the amylase/creatinine clearance ratio is low (Table 23.3) (Kleinman & O'Brien, 1986).

Lipase

The pancreas is the major and primary source of serum lipase. Human pancreatic lipase is a glycoprotein with a molecular weight of 45,000 Da. Lipase is not present in the salivary glands. Lipases are defined as enzymes that hydrolyze preferentially glycerol esters of long-chain fatty acids at the carbon 1 and 3 ester bonds, producing 2 moles of fatty acid and 1 mole of β-monoglyceride per mole of triglyceride. After isomerization, the third fatty acid can be split off at a slower rate. Lipolysis increases in proportion to the surface area of the lipid droplets; the absence of bile salts in duodenal fluid with a resultant lack of emulsification renders lipase ineffective.

Serum lipase is more specific for the diagnosis of acute pancreatitis. Serum lipase increases in 4 to 8 hours and remains elevated for 8 to 14 days. Increased lipase activity rarely lasts longer than 14 days; prolonged increases suggest a poor prognosis or the presence of a pancreatic cyst. Hyperglycemia and elevated bilirubin concentrations may be present. Leukocytosis is frequently present.

Pancreatic lipase must be differentiated from lipoprotein lipase, aliesterase, and arylester hydrolase, which are related but different enzymes. These enzymes' activities may be included in the measurement of lipase activity unless suitable assay conditions for pancreatic lipase are adapted. Lipase is also present in the liver, stomach, intestine, white blood cells, fat cells, and milk.

Calcium is necessary for maximal lipase activity, but at higher concentrations it has an inhibitory effect. It is speculated that the inhibitory effect is due to its interference with the action of bile salts at the water-substrate interface. Like serum albumin, bile salts prevent the denaturation of lipase at the interface. Heavy metals and quinine inhibit lipase activity.

Lipase is filtered by the glomeruli owing to its low molecular weight; it is normally completely reabsorbed by the proximal tubules and is absent from normal urine. In patients with failure of renal tubular reabsorption caused by renal disorders, lipase is found in the urine. Urine lipase activity in the absence of pancreatic disease is inversely related to creatinine clearance.

Serum lipase is stable up to 1 week at room temperature and may be kept stable longer if it is refrigerated or frozen. The optimal reaction temperature is about 40° C. The optimal pH is 8.8, but other values ranging from 7.0 to 9.0 have been reported. This difference probably is due to the effect of the difference in types of substrate, buffer, incubation temperature, and concentrations of reagents used. Serum is the specimen of choice for blood lipase assays. Icterus, lipemia, and hemolysis do not interfere with turbidimetric lipase assays.

TABLE 23.3

Differential Diagnosis of Hyperamylasemia and Macroamylasemia

Condition	Serum Amylase	Serum Lipase	Urinary Amylase	C_{am}:C_{cr}	Serum Macroamylase
Pancreatic hyperamylasemia	High	High	High	High	Absent
Salivary hyperamylasemia	High	Normal	Low or normal	Low or normal	Absent
Macroamylasemia	High	Normal	Low	Low	High

C_{am}:C_{cr}, Amylase clearance: creatinine clearance ratio = (urinary amylase/serum amylase) × (serum creatinine/urinary creatinine)
Adapted from Kleinman DS, O'Brien JF: Macroamylase, *Mayo Clin Proc* 61:66–-670, 1986.

Both serum lipase and amylase are useful in ruling out acute pancreatitis. Although determination of serum lipase has diagnostic advantages over serum amylase for acute pancreatitis, it is not specific for acute pancreatitis. Serum lipase may also be elevated in patients with chronic pancreatitis, obstruction of the pancreatic duct, and nonpancreatic conditions, including renal diseases, acute cholecystitis, intestinal obstruction or infarction, duodenal ulcer, and liver disease, as well as alcoholism and diabetic ketoacidosis, and in patients who have undergone ERCP. Patients with trauma to the abdomen uniformly have increases in both serum amylase and lipase. Elevation of serum lipase activity in patients with mumps strongly suggests significant pancreatic involvement by the disease.

There are no data that measuring both amylase and lipase adds significant diagnostic accuracy. Once the diagnosis is established, daily determination of either amylase or lipase has little value in gauging the clinical course or the prognosis.

Trypsinogen

Trypsin is produced in the exocrine pancreas as two proenzymes, known as trypsinogen 1 and trypsinogen 2. The proenzymes are activated in the duodenum by an enterokinase that yields trypsin 1 and trypsin 2, respectively, and can also be autoactivated by trypsin itself. Trypsin present within the peripheral circulation is inactivated by complexing with either α_2-macroglobulin or α_1-antitrypsin. Trypsin, unlike amylase, is solely produced by the pancreatic acinar cells and is therefore a specific indicator of pancreatic damage. Premature activation of the proenzyme to active trypsin within the pancreatic parenchyma is thought to be a key mechanism in the development of acute pancreatitis (Andersen et al., 2001). Irrespective of the cause, all etiologies allow the activation of the inactive proenzyme trypsinogen to trypsin, which then activates most of the other digestive enzymes and produces tissue damage and necrosis of the pancreas, the surrounding fat, and adjacent structures. Elevated serum concentrations of immunoreactive trypsin, measured by quantitative radioimmunoassay (RIA), may prove useful in diagnosing acute pancreatitis.

Other enzymes that have been proposed as diagnostic tools include pancreatic isoamylase, phospholipase A, elastase 1, and trypsinogen-2 (Forsmark & Baillie, 2007). Other tests—aspartate aminotransferase (AST), alanine aminotransferase (ALT), CRP, hematocrit, carbohydrate-deficient transferrin (CDT), and trypsinogen activation peptide (TAP)—have shown low sensitivity for diagnosing acute pancreatitis. CDT is a marker for chronic alcoholism. Markers of inflammatory response (e.g., CRP) peak following interleukin-1 (IL-1) and IL-6 increase on day 3 after onset of abdominal pain, which is useful in predicting severity of pancreatitis (Smotkin & Tenner, 2002).

Complications of Acute Pancreatitis

Hypocalcemia related to saponification of calcium by the liberated fats and mild to significant jaundice may appear after 24 hours because of biliary obstruction. A sepsis-like syndrome due to the digestive enzymes in the systemic circulation may cause the release of inflammatory cytokines, a systemic immune response syndrome, with severe systemic complications. About 75% of patients with acute pancreatitis have a benign course and recover rapidly. No treatment has proven to interrupt the inflammatory process effectively.

Idiopathic acute pancreatitis occurs in about 10% to 20% of patients with pancreatitis. It is believed that many are germline mutations of either cationic trypsinogen (PRSS1) or serine protease inhibitor, kazal type 1 (SPINK1). There is high risk for development of endocrine or exocrine insufficiency and pancreatic adenocarcinoma. These mutations can cause an autosomal recessive hereditary acute or chronic pancreatitis with onset in childhood or early adulthood. PRSS1 abrogates the inactivation of trypsinogen for cleavage of trypsin. SPINK1 mutation inactivates pancreatic secretory trypsin inhibitor (Howes et al., 2005; Schneider, 2005).

Patients with these disorders typically have recurrent acute pancreatitis sometime between infancy and the fourth decade. Chronic pancreatitis and pancreatic cancer develop at a relatively young age. No specific treatment exists for the prevention or treatment of hereditary pancreatitis. Clinical testing is available for the disorders described (Etemad & Whitcomb, 2001).

Chronic Pancreatitis

It is the irreversible damage, and often progressive inflammation with irregular fibrosis, duct dilatation and loss of pancreatic parenchyma, that characterize chronic pancreatitis. It occurs after repeated bouts of acute pancreatitis, obstruction of the pancreatic duct by mechanical blockage or congenital defect, by neoplasm, gallstone duct obstruction, or alcoholism. Early in the course, the pancreas is enlarged. Subsequently, due to scarring,

the gland usually shrinks, with loss of acini and still later a loss of ductules. Preserved or even increased islets are seen in the fibrous scar. Patients seek medical attention because of abdominal pain or maldigestion.

Maldigestion/malabsorption and steatorrhea are due to pancreatic insufficiency with loss of enzymes, glucose intolerance or diabetes, and islet damage. Low fecal elastase levels correlate well with disease. Clinically, there is recurrent or chronic pain. Since only a small number of patients with acute pancreatitis go on to develop chronic pancreatitis, the incidence of the latter is lower than that of acute pancreatitis but is increasing. Incidence is greater in males than in females, and the average age of onset is 40 years. It is more prevalent in tropical countries; the main form is chronic calcifying pancreatitis with duct calcifications, which can often be seen on plain films of the abdomen. In temperate areas, chronic alcoholism is found in more than half of the cases. Etiology is not apparent in 40% of the cases.

The central enzyme involved in activation of all the digestive proenzymes is trypsin. Trypsin is synthesized and maintained as inactive trypsinogen in secretory granules in the pancreatic acinar cell. After release through the pancreatic duct into the intestinal lumen, trypsinogen is cleaved by enterokinase on the brush border of the duodenum to yield active trypsin. Trypsin is stabilized in the pancreatic acini by a serine protease inhibitor, SPINK1. Mutations in SPINK1 increase the risk of chronic pancreatitis almost 12-fold by impairing the ability of acinar cells to counteract and inhibit the damaging effects of intracellular trypsin (Schneider et al., 2004; DiMagno & DiMagno, 2005). Cationic trypsinogen (PRSS1) mutations involving codon 29 and 122 cause autosomal-dominant forms of hereditary pancreatitis (Whitcomb, 2000; Cohn et al., 2005).

GASTROENTEROLOGIC DISORDERS

PEPTIC ULCERATION

Helicobacter pylori causes the most frequent and persistent bacterial infection worldwide. It has been recognized as the principal cause of duodenitis and duodenal ulcers and is strongly associated with chronic antral gastritis, gastric ulcers, nonulcer dyspepsia, gastric carcinoma, and mucosa-associated lymphoid tissue (MALT) lymphomas (MALTomas) (Peterson, 1991; Thiede et al., 1997; Wotherspoon, 1998). The use of nonsteroidal anti-inflammatory drugs (NSAIDs) causes or aggravates peptic and gastric inflammation and ulceration. Gastric hypersecretory states are a much rarer cause of peptic ulcer disease. Data gathered by history and physical examination may initially suggest peptic ulcer disease. While radiologic and endoscopic examinations may be useful, definitive diagnosis requires laboratory analysis.

Since *H. pylori* is the most important cause of peptic ulcer disease and is significantly associated with multiple other types of upper GI pathology, there has been a great deal of research on its detection and treatment and confirmation of its eradication following treatment. A cogent argument has been made that all patients found to harbor this organism should be treated (Graham, 1997). Numerous commercial products are available for the laboratory diagnosis of this infection. These tests support both specific diagnosis and determination of eradication in population groups with different infection and antibiotic-resistance prevalence. Each of these tests has advantages, disadvantages, and limitations (Garza-González et al., 2014). Thus, appropriate test selection and result interpretation are imperative.

Test selection depends on the test objective (initial diagnosis or determination of eradication) and whether endoscopy with tissue sampling is indicated. The biopsied tissue can be subjected to direct urease test, nucleic acid amplification tests (NAATs), cultured, or histologically examined following conventional or immunochemical staining. The noninvasive tests include urea breath tests that detect exhaled $^{13}CO_2$ or $^{14}CO_2$ following orally administered labeled urea, antibody detection in serum or saliva, and stool antigen assays using antibodies against *H. pylori*. NAATs are not widely available or routinely used.

The rapid urease test and breath test are most often used for diagnosis and determination of eradication, respectively. Both utilize the organism's ability to produce urease, which hydrolyzes urea into ammonia and CO_2; the latter is absorbed into blood and then exhaled. Breath tests using nonradioactive ($^{13}CO_2$) and radioactive ($^{14}CO_2$) carbon isotopes require different systems for detection of labeled CO_2. The sensitivity and specificity of breath tests generally exceed 90% in determining eradication. The tests are useful for both initial diagnosis and monitoring efficacy of eradication therapy. The breath tests may yield false-negative results if performed too soon after treatment, before the bacterial load is insufficient for detection (Atherton & Spiller, 1994), and in patients with corpus-predominant gastritis (Capurso et al., 2006; Garza-González et al., 2014).

Urease-based chemical tests are routinely used to detect *H. pylori* in biopsy specimens obtained via endoscopy. Fresh biopsy specimens are placed into gels containing urea. The bacterial urease splits the urea, producing ammonia that changes pH and affects a color indicator, thus providing the basis for the detection. Bacterial load determines the amount of urease present and thus the rapidity of reaction; tissue samples with low bacterial loads may yield false-negative results (Xia et al., 1994). If endoscopy must be performed for other reasons, a rapid direct urease test is the least expensive means of documenting the presence of *H. pylori* in antral biopsies (Suerbaum & Michetti, 2002).

Tests dependent on detection of urease activity may yield false-negative results from the incidental use of proton pump inhibitors (PPIs), antibiotics, or bismuth-containing antacids (Lewis et al., 1997). Treatment of *H. pylori* may not lead to complete eradication of the organisms, particularly in the face of clarithromycin and metronidazole resistance.

In addition to serving as an adjunct in diagnosis of *H. pylori* infection, histologic examination is invaluable in assessing disease severity and the inflammatory changes in gastric mucosa. Multiple biopsies collected from antrum and corpus are usually stained with any two of the conventional stains; Warthin-Starry and Giemsa stains are most frequently employed to demonstrate *H. pylori*, and hematoxylin and eosin (H&E) staining is used to evaluate gastric mucosa. The organism can also be demonstrated immunochemically. In H&E-stained sections, absence of antral inflammation has been found to exclude infection (Cutler et al., 1995; Smith et al., 2012). Other studies have reported H&E stain adequate in detecting organisms, essentially obviating the need for routine immunohistochemistry (Wang et al., 2010).

Culture of the organism is not routinely performed for diagnosis. However, with the increasing rates of antibiotic resistance, it yields much needed antimicrobial susceptibility data in patients with more than one treatment failure (Garza-González et al., 2014). Meticulously collected, transported, and cultured gastric biopsies are more likely to grow the fastidious microaerophilic organism, when present, than attempts at isolation from gastric fluid, stool, or vomitus (Han et al., 1995; Ndip et al., 2003).

Stool antigen tests are reliable alternatives to urea breath tests for both initial diagnosis and determination of eradication. A variety of commercial immunochromatographic and enzyme immunoassays (EIAs) are available that use monoclonal or polyclonal antibodies against *H. pylori* (Garza-González et al., 2014). EIAs employing monoclonal antibodies have generally superior sensitivity, specificity, and positive and negative predictive values than other assays (Gisbert et al., 2006; Choi et al., 2011; Korkmaz et al., 2013).

Serologic tests are inexpensive, widely available, and reliable in documenting exposure to or colonization with *H. pylori* (Feldman & Evans, 1995; Feldman et al., 1995; van de Wouw et al., 1996). These tests are of limited utility in both initial diagnosis and monitoring eradication, and are subject to misinterpretation (Suerbaum & Michetti, 2002; Garza-González et al., 2014). However, these tests are of negative predictive value, and may be useful in patients with recent use of antibiotics or PPIs, and those with bleeding ulcers or gastric atrophy. Office-based serologic tests on blood, urine, or saliva yield inconsistent results and are not recommended for diagnosis of *H. pylori* infection (Malfertheiner et al., 2007; Garza-González et al., 2014).

Hypersecretory states are suggested by extensive peptic ulcer disease, especially in the absence of *H. pylori* and NSAIDs. Failure to respond to the usual doses of histamine-2 (H_2)-receptor blocking agents and PPIs also suggests oversecretion of hydrochloric acid. Although gastric analysis remains the gold standard for measurement of gastric acid, it is used infrequently. Care must be taken to avoid the use of antisecretory medications for the appropriate time intervals before testing. H_2-receptor blockers should be held for 48 hours and PPIs should be avoided for 7 days. Antisecretory agents are available without prescription; thus, patient education is important. Physicians must remember to review all of the medications that their patients are taking.

ZOLLINGER-ELLISON SYNDROME

The syndrome is defined by the triad of peptic ulceration, hyperchlorhydria, non-β islet cell tumors (gastrinomas). Duodenal ulcers do not occur in achlorhydric individuals but are present in those with extreme hyperchlorhydria. Gastrinomas may occur in the body or tail of the pancreas or in the upper duodenum; they may be multiple and malignant. About 25% of patients with Zollinger-Ellison (ZE) syndrome have multiple endocrine neoplasia type 1 (MEN-1) with hyperparathyroidism (Hung et al., 2003).

Gastrin levels, with and without secretin stimulation, can be used to diagnose ZE syndrome. Serum gastrin levels greater than 150 ng/L (reference: <100 ng/L), especially with simultaneous gastric pH values of <3, are highly suggestive of a gastrinoma. For equivocal results, secretin (2 U/kg in 10 mL 0.9% sodium chloride) can be given intravenously in 30 seconds and serial gastrin levels can be drawn at 0, 2, 5, 10, 15, 20, and 30 minutes.

An increase in gastrin of >200 ng/L within 15 minutes of the injection is considered a positive test. Octreotide, a synthetic form of somatostatin, has been used for localization of the tumor(s). Radiolabeled octreotide binds to somatostatin receptors and can be subsequently localized by scintigraphy (Zimmer et al., 1995). If such tumors are surgically removed, gastrin levels can be used to assess potential success or future recurrence (see Gastrinoma in "Functional Neuroendocrine Tumors").

Gastrin is a primary GI hormone, produced mainly by the antral G cells, that regulates gastric acid secretion and stimulates growth of the gastric mucosa, among other functions. To a lesser extent, gastrin is produced by the G cells of the proximal small intestine and delta cells of the pancreas. Gastrin acts on the parietal cells located in the fundus of the stomach, stimulating the secretion of gastric acid. Gastrin also increases blood flow to the stomach and is responsible for increased gastric and intestinal motility. Other functions include stimulation of gastric pepsinogens and intrinsic factor secretion, release of secretin from the small intestine, and secretion of pancreatic enzymes as well as bicarbonate (Hill, 2006). This hormone is secreted from antral distention mainly after the detection of digested protein products. Maximal stimulation of gastrin secretion occurs within a pH range of 5 to 7. An acid environment serves as a negative-feedback mechanism for the release of gastrin, with 80% reduction in secretion at a pH of 2.5 (Hill, 2006). This serves to protect the stomach from overacidification from excess stimulation of gastrin. For this reason, individuals on acid suppression therapy for peptic ulcer disease may have elevated gastrin levels. Homeostatic mechanisms to minimize excessive gastrin secretion include the apocrine effect of antral somatostatin, which inhibits gastrin release by neighboring G cells.

Three main forms of gastrin exist in human blood and tissues: G34, G17, and G14, known as *big gastrin*, *little gastrin*, and *mini-gastrin*, respectively. There are different assay sensitivities to these forms. All gastrins originate from a single precursor, preprogastrin, which is cleaved by the action of trypsin. Interestingly, in pathologic cases of increased gastrin production, as with achlorhydric gastritis or gastrinomas, larger molecular forms of gastrin and incompletely processed precursors are present and are beyond the scope of detection by conventional assays. In such cases, only little gastrin would be detectable in serum (Goetze & Rehfeld, 2003).

Laboratory determination of gastrin levels with RIA or EIA is indicated for the confirmation of suspected gastrin-secreting tumors, namely, gastrinomas or ZE syndrome. The antibodies present in these assays are specific for the biologically active C-terminal of the gastrin molecule and have minimal cross-reactivity with CCK peptides. Prior to determination of gastrin levels, a patient must be fasting for 12 hours because the concentration of G34 doubles and the concentration of G17 quadruples following a meal, altering the results of the assay. Specimens must be frozen immediately because gastrin is unstable in serum. Due to the action of proteolytic enzymes, 50% of the specimen's immunoreactivity may be lost within 48 hours at a temperature of 4° C. It is recommended that specimens should be kept in a freezer at a temperature of –70° C without a self-defrosting cycle if long-term storage is required. Specimens must be analyzed immediately after thawing, avoiding refreezing and thawing.

Fasting serum gastrin levels are increased with increasing age, especially in patients older than 60 years, in part due to gastric mucosal atrophy. Approximately 15% of individuals older than 60 years may have gastrin levels between 100 and 800 ng/L (Hill, 2006). Reference intervals for infants and children differ from those for adults; interpretation should use age-specific reference ranges. Gastrin concentration greater than 1000 ng/L with gastric acid hypersecretion (basal acid secretion >15 mmol/hour) is diagnostic of gastrinomas. The secretin stimulation test is a provocative biochemical test that can help confirm the diagnosis of ZE syndrome in questionable cases. Infused secretin should cause a drop in gastrin levels in normal individuals. However, in patients with ZE syndrome, there is a dramatic increase in gastrin level following secretin infusion. The mechanism by which secretin stimulates an increase in gastrin levels in these patients is poorly understood; however, it is thought to be due to a direct local effect on the blood flow to the tumor (Ashley et al., 1999). Limitations include altered results from conditions that may lead to elevated gastrin levels, such as gastric ulcer disease, chronic renal failure, hyperparathyroidism, pyloric obstruction, vagotomy, retained gastric antrum, short bowel syndrome, and pernicious anemia. Certain medication can also increase gastrin measurements, such as antacids, H_2-blocking agents, and PPIs, all commonly used in the treatment of patients with peptic ulcer disease. However, these elevations are moderate and certainly not as high as in a patient with a gastrin-secreting tumor.

Intraoperative testing for gastrin is of potential use because gastrinomas can be multiple and are often difficult to locate as they can be distributed widely in the stomach, pancreas, and duodenum or periaortic lymph nodes. Gastrin has a short half-life of approximately 10 minutes, and the catabolic breakdown of most peptide hormones follows first-order exponential decay (see Chapters 21 and 24). Therefore, if the entire hormone-secreting tissue is surgically resected, only approximately 12.5% of the baseline concentration would be present in serum after three half-lives. When patients with ZE syndrome or gastrinomas were evaluated with intraoperative gastrin assays, a drop of gastrin levels to within reference values within 20 minutes of resection was indicative of cure (Sokoll et al., 2004).

Pepsin and Pepsinogen

Pepsinogens are the biologically inactive proenzymes of pepsins that are produced by the chief cells and other cells in the gastric mucosa. They are found in two distinct types, pepsinogen I (PGI), also known as *pepsinogen A*, and pepsinogen II (PGII), also known as *pepsinogen C*. Pepsinogen secretion is stimulated by the vagus nerve, gastrin, secretin, and CCK. It is inhibited by gastric inhibitory peptide (GIP), anticholinergics, H_2-receptor antagonists, and vagotomy (Hill, 2006). PGI is produced in the chief cells and mucous cells of oxyntic glands; PGII is produced in mucous cells in oxyntic and pyloric regions and the duodenum. The ratio of concentration of PGI to PGII in serum or plasma of healthy individuals is approximately 4:1 (Samloff, 1982). Pepsinogen is converted to the active form, pepsin, by gastric acid that can activate additional pepsinogen autocatalytically. Both groups of pepsinogen are activated at an acid pH below 5 and destroyed by alkaline pH. Both types can be detected in blood. Only type I pepsinogens are present in the urine. Pepsins are responsible for the hydrolysis of proteins to polypeptides. The pepsinogen released from the gastric mucosa constitutes a major component of gastric fluid. Only approximately 1% gets into the peripheral blood. Active pepsin is rapidly inactivated in the bloodstream, whereas pepsinogen is stable in the blood. Pepsinogen is then filtered by the kidneys and is excreted in the urine, where the slightly acidic pH converts the pepsinogen, now called *uropepsinogen to uropepsin* (Hill, 2006). Immunoassay is the method used to detect serum pepsinogen. However, the PGI isoform is commonly analyzed in the clinical laboratory since it is the isoform commonly associated with disease.

Serum levels of PGI are an accurate estimate of parietal cell mass and correlate with acid-secretory capacity of the stomach. Increased pepsinogen levels and associated activity is observed in patients with disease states that lead to increased gastric output or with increased parietal cell mass, namely, gastrinomas, ZE syndrome, duodenal ulcer disease, and acute and chronic gastritis. Decreased levels of pepsinogen are associated with decreased parietal cell mass, atrophic gastritis and gastric carcinoma, as well as in patients with myxedema, Addison disease and hypopituitarism (Hill, 2006). The PGI/PGII ratio decreases linearly with worsening atrophic gastritis. Absence of pepsinogen is noted in patients with achlorhydria. PGI levels measured by immunoassay usually range from 20 to 107 μg/L and PGII levels usually range from 3 to 19 μg/L.

Pepsinogen assays are being explored for their utility in the noninvasive identification of patients with chronic atrophic gastritis and to provide an estimate of the extent of atrophic gastritis, a known precursor of gastric carcinoma. Severe atrophic body gastritis causes a four- to fivefold increase in the risk of gastric carcinoma compared with healthy individuals (Miki et al., 2003). This will hopefully identify a subgroup of individuals with chronic atrophic gastritis that would benefit from endoscopic evaluations for detection of early-stage gastric tumors. These assays are currently utilized in Japan, an area marked by high prevalence of gastric cancer, as a potential method for widespread screening of high-risk individuals (Miki et al., 2003). Study authors recommended that criteria for diagnosing chronic atrophic gastritis be persons with PGI <70 μg/L and PGI/PGII ratio <3.0. In Japan, the pepsinogen serum screening test has been demonstrated to detect a higher percentage of early cancers compared with conventional methods; a considerable number of patients have subsequently been candidates for treatments with endoscopic surgery (Miki et al., 2003). The most sensitive test for fundic atrophic gastritis is considered to be the PGI/II serum ratio, with 99% sensitivity and 94% specificity (Hill, 2006). Furthermore, PGII levels may be a useful marker of prognosis, serving as an independent predictor of tumor biology and survival in patients with gastric carcinoma. The absence of PGII production has been associated with aggressive tumor behavior and shorter overall survival in gastric cancer patients (Fernandez et al., 2000). Pepsinogen assays may therefore prove to be a useful serum screening method for detection of gastric carcinoma among high-risk individuals.

DIARRHEA AND MALABSORPTION

Diarrhea

About 8 to 10 L of fluid enters the duodenum every 24 hours. Much of this fluid is absorbed in the small intestine and about 1.5 L enters the large intestine. However only 100 to 150 mL is voided in stools. Increased fluid secretion or decreased fluid absorption in either the small or large intestine, or increased intestinal motility, results in diarrhea. One of the most

important parameters defining diarrhea in an individual patient is a change in the usual bowel habit to more frequent looser stools. Diarrhea is the passage of three or more loose or liquid stools per day or more frequently than is normal for the individual (WHO, 2009). Decrease in fecal consistency (i.e., increased fluidity) is difficult to measure; thus, increased stool weight, frequency, and duration are used in defining diarrhea.

The diagnosis of diarrhea starts with a thorough history to characterize the condition. Is the diarrhea bland or bloody (dysentery)? Are there constitutional symptoms? What is the duration of the illness? Important issues to determine are travel history, the use of antibiotics and other medications, ingestion of uncooked fish or meats, exposure to animals, and previous history of diarrhea and family history of gastrointestinal illness. Self-limited, acute diarrhea (<2 weeks in duration) without bleeding or constitutional symptoms rarely requires diagnostic testing. Chronic diarrhea, the passage of blood, and constitutional symptoms all suggest the need for a specific diagnosis. History is the key to developing the differential diagnosis and guiding the laboratory evaluation (Table 23.4). The physical examination, although usually less helpful than the history, must still be comprehensive.

TABLE 23.4

Laboratory Tests in the Differential Diagnosis of Diarrhea

Test	Method	Use
Initial Screening Tests		
Fecal leukocytes	Wright's or methylene blue stain	Identify inflammatory diarrhea
Fecal occult blood test	Immunochemical	Detect blood
Fecal osmotic gap	290 – 2 × (fecal N^+ + fecal K^+)	Distinguish secretory vs. osmotic diarrhea
Stool pH	pH determination; fecal phenolphthalein test	Lactose intolerance; laxative abuse; malabsorption of any carbohydrate
Infectious Causes		
Stool bacterial culture/special culture*	Culture and sensitivity, serotyping; NAAT	Identify bacterial pathogens
Stool mycobacteria	Acid-fast stain, culture and sensitivity, NAAT	Detect mycobacteria, antibiotic selection
HIV serology	EIA, Western blot	HIV enteritis
Viral gastroenteritis	EIA, NAAT	Rotavirus, norovirus, adenovirus, astrovirus
Stool ova and parasites	Concentration, stain, microscopy	Enteric parasitic infection
Intestinal protozoa	Acid-fast stain, EIA, NAAT	See below
Endocrine Causes		
Urine 5-HIAA or blood serotonin	HPLC	Carcinoid syndrome, rarely pheochromocytoma
Serum VIP	RIA, immunoassay	VIPoma
Serum TSH, free T4	Immunoassay	Hyperthyroidism
Serum gastrin	RIA	Zollinger-Ellison syndrome
Serum calcitonin	RIA, immunoassay	Hypocalcemia-related diarrhea
Serum somatostatin	RIA, immunoassay	Somatostatinoma
Malabsorption		
Lactose tolerance test	See text	Lactase deficiency
Stool reducing sugars	Clinitest reaction	Carbohydrate intolerance
Sweat chloride	See text	Cystic fibrosis
D-xylose absorption test	See text	Evaluate small-bowel absorption
Fecal fat stain	Fat stain	Lipid malabsorption
Serum carotene	Spectrophotometry	Lipid malabsorption
Serum IgA	Nephelometry	Rule out IgA deficiency
Anti-tissue transglutaminase antibody	EIA	Celiac disease; see Table 23.6
Hydrogen breath test	Gas chromatography	Carbohydrate malabsorption
Bacterial colony count	Small-bowel aspirate and quantitative culture	Bacterial overgrowth
Other		
Fecal calprotectin	EIA	Screen for IBD
Serum ionized calcium	Ion-selective electrode	Hypocalcemia-related diarrhea
Serum protein and albumin	Nephelometry	IBD, protein-losing enteropathy
Stool α_1-antitrypsin	Nephelometry	IBD, protein-losing enteropathy from multiple causes
Quantitative immunoglobulins	Nephelometry	Agammaglobulinemia
Fecal elastase	EIA	Pancreatic exocrine insufficiency
Intestinal biopsy	Endoscopic or open biopsy	Whipple disease, MAI, abetalipoproteinemia, neoplasia, lymphoma, amyloidosis, eosinophilic gastroenteritis, agammaglobulinemia, intestinal lymphangiectasia, Crohn disease, tuberculosis, graft-versus-host disease, *Giardia,* other parasitic infections, collagenous colitis, microscopic colitis
Extraintestinal causes	See text	Hyperthyroidism, diabetes, hypoparathyroidism, adrenal cortical insufficiency, hormone-secreting tumors

5-HIAA, 5-Hydroxyindole acetic acid; *Ag,* antigen; *Ab,* antibody, *EIA,* enzyme immunoassay, *HIV,* human immunodeficiency virus; *HPLC,* high-performance liquid chromatography; *IBD,* inflammatory bowel disease; *MAI, Mycobacterium avium-intracellulare*; *NAAT,* nucleic acid amplification test; *RIA,* radioimmunoassay; *TSH,* thyroid-stimulating hormone; *VIP,* vasoactive intestinal peptide.

*May involve routine culture and sensitivity, and culture on special media and serotyping for *Salmonella* spp., *Shigella* spp., *Campylobacter* spp., *Escherichia coli* O157:H7, *Yersinia* spp., and stool toxin immunoassays or NAAT for Shiga toxin-producing *E. coli*, *Clostridium perfringens*, and food toxin detection for *Bacillus cereus* and *Staphylococcus aureus, Entamoeba histolytica*, *Giardia* sp., *Cryptosporidium* spp., *Cyclospora cayetanensis*, *Cystoisospora belli*, modified trichrome stain for microsporidia.

Adapted from Khare R, et al.: Comparative evaluation of two commercial multiplex panels for detection of gastrointestinal pathogens by use of clinical stool samples, *J Clin Microbiol* 52:3667-3673, 2014; Shane AL, et al.: 2017 Infectious Diseases Society of America clinical practice guidelines for the diagnosis and management of infectious diarrhea, *Clin Infect Dis* 65:1963–1973, 2017; Paulos S, et al.: Comparative performance evaluation of four commercial multiplex real-time PCR assays for the detection of the diarrhea-causing protozoa *Cryptosporidium hominis/parvum*, *Giardia duodenalis* and *Entamoeba histolytica*, *PloS One* 14:e0215068, 2019.

Acute diarrheas, defined as <4 weeks' duration, generally have an infectious etiology. Those with a course of >4 weeks are considered to be chronic diarrheas (Fine & Schiller, 1999) and are categorized as osmotic, secretory, or inflammatory. Hypermotility or shortened gut may reduce the transit time and absorptive surface, resulting in diarrhea and/or some degree of malabsorption.

Osmotic diarrhea results from unabsorbable or poorly absorbed solutes. These include polyethylene glycol in colon-cleansing solutions, magnesium salts (magnesium citrate in cathartics, magnesium hydroxide in some antacids), sorbitol in chewing gum, lactulose in the treatment of hepatic encephalopathy, and lactose in lactase-deficient individuals. These osmotically active substances in the lumen alter the osmotic gradient that normally favors Na+ absorption, drawing fluid into the lumen.

Fasting or cessation of consumption of the suspected solute for 24 hours stops osmotic diarrhea. Microbial fermentation of malabsorbed carbohydrates yields short-chain fatty acids. The increased osmolarity draws additional water into the colon and lowers the stool pH to values of <5.6 (Fine & Schiller, 1999). Sodium and potassium concentrations in stool water are measured to calculate the fecal osmotic gap, which estimates the contribution of electrolytes and nonelectrolytes to water retention in the gut lumen. The osmotic gap is useful in differentiating osmotic from secretory diarrhea; it is best calculated as: $290 - 2 \times (\text{fecal } Na^+ + \text{fecal } K^+)$, where 290 represents the stool osmolality that approximates plasma osmolality, and a factor of 2 is used to account for associated anions. Osmotic gaps of >125 mOsm/kg characterize osmotic diarrhea and those of <50 mOsm/kg are seen in secretory diarrhea (Fine & Schiller, 1999).

Stool osmolality must be measured on a freshly collected specimen. Because of continued degradation of stool carbohydrates, osmolality of the specimen increases over hours. Continued diarrhea during a 48-hour fast is suggestive of a secretory process, although fecal weight may decrease because of increasing dehydration (Fordtran, 1967; Fine & Schiller, 1999).

Disaccharidase Deficiency

Many of the previously listed conditions causing malabsorption may also be associated with intolerance to disaccharides. Disaccharide absorption is diminished either from primary disaccharidase deficiencies, such as sucrase-isomaltase deficiency, lactase deficiency, primary alactasia, primary trehalase deficiency, or secondary disaccharidase deficiencies due to celiac disease, tropical sprue, acute viral gastroenteritis, or drugs such as orally administered neomycin, kanamycin, and methotrexate. These secondary disaccharidase deficiencies involve injury to the villi, are usually transient, and implicate more than one enzyme. Lactase is located at the tips of villi; any injury will impair lactose digestion. More extensive enteropathy results in deficits in sucrose and maltose hydrolysis. Although the incidence of lactose intolerance due to congenital lactase deficiency is low, the prevalence of lactose intolerance in adults is quite high. About 10% of whites, 70% to 80% of African Americans, and an even greater percentage of Asians manifest some degree of lactose intolerance even though they were able to digest lactose well as infants. In these disorders, intestinal bacteria ferment unhydrolyzed and unabsorbed carbohydrates, producing hydrogen gas, small (3- or 4-carbon) fatty acids, and draw water into the lumen. Normally, absorption of digested carbohydrates is rapid and fairly complete in the proximal small intestine. Unhydrolyzed disaccharides or monosaccharides unabsorbed because of deficiencies in transport are osmotically active and hence cause secretion of water and electrolytes into the small and large intestines. This can result in protracted diarrhea as well as complaints of bloating and flatulence.

Screening tests for disaccharidase deficiencies include oral challenge of suspected disaccharides to reproduce the abdominal symptomatology, followed by stool analysis. The stools are usually watery, acidic, explosive, and fermentative. Stool pH of less than 5.5 is suggestive, but the measurement of pH is not valid if the patient is taking oral antibiotics. High pH does not exclude the diagnosis. Normal infants between 3 to 7 days of age commonly have high stool pH. Stools can be analyzed for sugars by chromatography or by one of the semiquantitative nonspecific tests for urinary sugar adapted for stool analysis. The Clinitest tablet (Bayer Diagnostics, Australia) is suitable for this purpose. The presence of 0.25 g/dL reducing substances is considered normal; from 0.25 to 0.5 g/dL is regarded as suspicious; more than 0.5 g/dL is considered abnormal. In patients with intolerance to sugar, the amount of total reducing substances in the stool usually exceeds 0.25 g/dL feces.

An oral tolerance test using a specific sugar such as lactose or sucrose can be used to establish a specific carbohydrate intolerance. Although the oral tolerance test is fairly specific and sensitive, in some instances, 23% to 30% false-positive results were noted following administration of lactose—that is, a flat tolerance curve and less than a 20 mg/dL (1.1 mmol/L) increase in blood sugar (Krasilnikoff et al., 1975). Delayed gastric emptying appears to be the cause of the false-positive result, because duodenal instillation of lactose eliminates the flat tolerance curve.

Definitive diagnosis of disaccharidase deficiencies depends on the demonstration of low specific enzyme activity in the mucosa of small intestinal biopsy material. An assay for disaccharidase has been published (Dahlqvist, 1968).

Lactose Tolerance Test

A lactose tolerance test provides presumptive diagnosis of lactase deficiency. In patients with alactasia or hypolactasia, whether primary or secondary to mucosal disease, oral lactose results in an insignificant rise in blood glucose. Following an overnight fast, a blood sample is drawn and 50 g of lactose dissolved in 400 mL of water is orally administered. A 100-g lactose dose has been reported to yield more definitive results. Blood samples are collected at 30, 60, and 120 minutes after lactose ingestion. An optional 5-hour stool specimen can be collected, and its appearance, consistency, and pH noted.

Patients with lactase deficiency exhibit a peak rise of <20 mg/dL of reducing substances, expressed as glucose. In individuals with flat tolerance curves, the test should be repeated in 2 days and the less abnormal of the two curves used for interpretation. In patients with lactase deficiency, the nonabsorbed lactose, upon reaching the colon, is degraded to gas and lactic acid, which inhibits salt and water absorption, resulting in abdominal discomfort and diarrhea. In children, the oral dose of lactose or other sugars is 2 g/kg body weight. Lactase can also be detected in a mucosal biopsy specimen.

Secretory diarrhea is evoked by a variety of exogenous and endogenous secretagogues. The hypersecretion of isotonic fluid exceeds the absorptive capacity of the colon. Cholera toxin activates mucosal cyclic adenosine monophosphate (cAMP), which results in outpouring of vast quantities of salt and water in the jejunum with normal structure. In Verner-Morrison syndrome (pancreatic cholera), vasoactive intestinal peptide also activates cAMP. Thus, secretory diarrhea remains unrelieved despite fasting.

Diarrhea also occurs in hypergastrinemic states (e.g., ZE syndrome). Sustained hypersecretion of acid lowers intestinal pH, providing a suboptimal pKa for the pancreatic enzymes (causing steatorrhea), and precipitates bile salts (causing bile salt malabsorption). The latter irritates the colonic mucosa, inducing excess water secretion. In patients with mastocytosis, excessive histamine release stimulates acid hypersecretion but their plasma gastrin concentrations remain low or normal. Gastrointestinal dysfunction caused by release of mast cell mediators can be observed in both cutaneous and systemic mastocytosis (Liu et al., 2010). Signs and symptoms include abdominal pain, diarrhea, nausea, vomiting, peptic ulcer disease, and gastrointestinal bleeding. Diarrhea can result from increased motility induced by prostaglandin D_2 (PGD2) secretion or from decreased rectal compliance and overactive rectal contractility (Jensen, 2000).

Drug-Induced Diarrhea

Prokinetic agents (metoclopramide, domperidone, cisapride), PPIs, and antibiotics (erythromycin and other macrolides) produce loose stools or diarrhea. Erythromycin binds motilin receptors on the GI smooth muscle membranes (motilin agonist). When used as a prokinetic agent, intravenous administration is more effective than oral dosage, and long-term use downregulates motilin receptors.

Other Causes of Diarrhea

Diarrhea may occur in patients with a variety of GI illnesses, including inflammatory bowel disease and celiac disease, hypo- and hyperthyroidism, diabetes and adrenal insufficiency, tumors (villous adenoma, small-bowel carcinoid), and infiltrative disorders (scleroderma, reactive amyloidosis, gut lymphoma). Ethanol abuse, ischemic bowel disease, and radiation enteritis also produce diarrhea. Heat-labile enterotoxin of *Escherichia coli*, toxins of *Staphylococcus aureus* and *Clostridium perfringens* activate biochemical events that induce a secretory response.

Gut Peptides in Diarrhea

In acute infectious diarrheas, the plasma concentrations of glucagon, PYY, and motilin may be increased, contributing most likely to the altered gut motility and promoting mucosal repair. Patients with Crohn disease have an elevated pancreatic polypeptide, GIP, motilin, and glucagon, while in ulcerative colitis there is a modest elevation in PP, GIP, motilin, and gastrin, the last in response to the associated hypochlorhydria. No demonstrable abnormalities in gut peptides account for disordered motility in irritable bowel syndrome.

Vasoactive Intestinal Peptide

VIPomas are rare neuroendocrine neoplasms that secrete vasoactive intestinal polypeptide (VIP). This peptide hormone activates adenyl cyclase in epithelial cells and suppresses gastric acid secretion, resulting in secretory diarrhea with hypokalemia. Stool volume exceeds 700 mL/day in all patients (even during fasting) and 3 L/day in approximately 70%. The stools are tea-colored, odorless, with features of a secretory diarrhea, such as persistence with fasting, high sodium concentration, and a low stool osmotic gap. Often referred to as Verner-Morrison syndrome, it is characterized by watery diarrhea, hypokalemia, and achlorhydria (WDHA) (Verner & Morrison, 1958). The diagnosis of VIPoma is established by the presence of an otherwise unexplained high-volume secretory diarrhea in the presence of an elevated VIP concentration and tumor localization by somatostatin receptor scintigraphy. It is important to replace fluid losses in these patients and long-acting somatostatin analogs (octreotide) control symptoms in >90% (Kapoor et al., 2009).

Patients usually present between 30 and 50 years of age; 90% of these tumors are primary pancreatic tumors—most commonly arising in the body or tail. Metastatic spread occurs in 60% to 70% of the patients prior to presentation. These VIP-secreting tumors account for 10% of neuroendocrine neoplasms of the GI tract. Approximately 60% of VIPomas are malignant and 6% are associated with MEN-1.

VIP, released in response to gut distention, is a potent vasodilator and is responsible for the relaxation of vascular and nonvascular smooth muscle of the intestinal tract. It is also a potent stimulator of water and electrolyte secretion, activating adenylate cyclase through stimulation of cAMP. Similar to glucagons, VIP stimulates breakdown of glycogen and lipid stores and inhibits histamine-stimulated acid secretion in the stomach, resulting in hypochlorhydria or achlorhydria.

VIPomas produce a severe, secretory diarrhea that has been termed *pancreatic cholera*. Diarrhea may be present for several years prior to the diagnosis of VIPoma. Patients typically produce more than 3 L of watery stools per day, though volume can be as high as 30 L/day. Diarrhea is not controlled with fasting and an average secretion of 300 mmol of potassium per 24 hours occurs. Patients with stool volume of <700 mL/day are unlikely to have VIPoma. If the diagnosis is missed or delayed, as is often the case, the chronic diarrhea results in severe fluid and electrolyte imbalances that produce a myriad of clinical symptoms, the most severe of which is sudden death from cardiac arrhythmias resulting from electrolyte disturbances with potassium depletion and acidosis.

Laboratory evaluations for determination of VIP levels are clinically relevant for diagnosis of VIPomas. RIAs or EIAs for VIP are sensitive and specific. The normal value for circulating VIP levels is <75 pg/mL. However, in patients with functional VIPomas, VIP concentrations may range from 675 to 965 pg/mL (Thomas et al., 2003). Appropriate handling of the blood sample is critical to the accuracy of the VIP assay because VIP has a half-life of 1 minute. A fasting blood specimen should be collected in tubes containing ethylenediaminetetraacetic acid, mixed gently, spun immediately, and plasma frozen at –20° C until assayed. False-positive elevations of VIP can be observed in patients with small-bowel ischemia or severe low-flow states resulting from diarrhea and subsequent dehydration not associated with VIP-producing lesions. In addition, the plasma level of pancreatic polypeptide should be determined at the time of the VIP assay. This value will be elevated if the VIPoma is located within the pancreas.

Clostridium difficile Infection

Clostridium difficile, a gram-positive, spore-forming anaerobic bacillus, is the principal cause of nosocomial diarrhea in adults, with greater than 300,000 cases per year in the United States. It is thought to be associated with approximately 25% of all antibiotic-associated cases of diarrhea and 50% to 75% of cases involving antibiotic-associated colitis (Malnick & Zimhony, 2000). *C. difficile* infections in persons without prior antibiotic use or exposure to hospital or health care environment have been reported since the early to mid-2000s (Kelly & LaMont, 2008; Svensson & LaSala, 2012). It may present clinically, from a mild watery diarrhea to life-threatening pseudomembranous colitis and toxic megacolon. This can lead to colonic perforation and peritonitis, with a mortality rate as high as 38% (Poutanen & Simor, 2004). Patients can present with watery diarrhea, lower abdominal pain/cramping, systemic symptoms such as fever and malaise, or can have occult GI bleeding. The pathogenesis of this disease entity usually involves disruption of the normal colonic flora, typically following a course of antibiotic therapy in hospitalized patients, and exposure to a toxigenic strain of *C. difficile*. Broad-spectrum antibiotics such as quinolones, clindamycin, and cephalosporins have been particularly implicated. However, any antibiotic can lead to development of *C. difficile* colitis. Clinical suspicion of the disease is confirmed with detection of *C. difficile* toxin A or B virulence factors in stool samples. Both toxins A and B lead to increased vascular permeability and have potential to cause hemorrhage. They induce the production of tumor necrosis factor α and inflammatory interleukins that are responsible for the inflammatory response and pseudomembrane formation (Poutanen & Simor, 2004).

Endoscopic visualization of the colonic mucosa is required for diagnosis of pseudomembranous colitis associated with *C. difficile*. However, endoscopy should be avoided in cases of suspected fulminant colitis because of the risk of perforation. Laboratory methods are available for confirmation of *C. difficile* infection. Tissue culture cytotoxicity assays, which take at least 48 hours to complete, for detecting *C. difficile* cytotoxin B in stool specimens are considered the gold standard, with a sensitivity ranging between 80% and 90% and specificity of approximately 99%. This tissue culture assay can detect as little as 10 pg of toxin in stool specimens. Rapid EIAs, which can be completed within several hours, have been developed for the detection of toxin A or B in stool specimens. However, the sensitivity and specificity of these immunoassays are 65% to 85% and 95% to 100%, respectively, compared with cytotoxic assays. The EIA can detect 100 to 1000 pg of toxin in stool specimens. In hospitalized patients with greater than six stools per day, EIA is the optimal diagnostic test (Malnick & Zimhony, 2000). Stool cultures can also be performed but require up to 96 hours for completion. NAATs for toxigenic *C. difficile* have sensitivity and specificity profiles similar to cytotoxic assays (Poutanen & Simor, 2004). These assays, however, are unable to distinguish between asymptomatic carriage and symptomatic infection. It is currently recommended that these tests be performed on diarrheal stools; in most cases, one stool sample is sufficient for diagnosis of *C. difficile* infection (Poutanen & Simor, 2004; Surawicz et al., 2013). Diarrheic stools can also be screened by an immunoassay for glutamate dehydrogenase, a *C. difficile*–specific antigen, and those positive should be tested for toxins A and B by EIA. NAATs should be performed on specimens yielding discordant antigen and toxin screening results (LaSala et al., 2012; Baron et al., 2013; Surawicz et al., 2013). Refer to Table 23.5 for laboratory tests available for the diagnosis of *C. difficile*–associated diarrhea (Fenner et al., 2008).

TABLE 23.5

Laboratory Tests for the Diagnosis of *Clostridium difficile*–Associated Diarrhea

Test	Advantages	Disadvantages
Clostridium difficile cytotoxin assay	Excellent specificity (99%–100%).	Decreased diagnostic sensitivity (80%–90%); results not available until after 48 hours; requires tissue culture facility; detects toxin B only.
Immunoassay for glutamate dehydrogenase antigen (GDA) of *C. difficile*	High negative predictive value without additional tests.	Toxin assay required because GDA assay does not distinguish toxigenic and nontoxigenic strains.
Immunoassay for *C. difficile* toxin A or toxins A and B	Good specificity (95%–100%); results available within 4 hours; technically simple.	Decreased sensitivity (65%–85%) as compared with cytotoxin assay.
Stool culture for *C. difficile* with cytotoxin assay of isolate	Excellent sensitivity (<90%) and specificity (<98%); enables strain typing for outbreak investigation.	Results not available for at least 72–96 hours; labor intensive; requires tissue culture facility.
Nucleic acid amplification assay for *C. difficile* toxin genes	Excellent sensitivity (93%–100%); useful in confirmation of results of GDA or toxin immunoassays.	Useful only in acute disease; false positives of concern.

Adapted from Poutanen SM, Simor AE: *Clostridium difficile*–associated diarrhea in adults, *Can Med Assoc J* 171:51–58, 2004; Fenner L, et al.: Rapid and reliable diagnostic algorithm for detection of *Clostridium difficile*, *J Clin Microbiol* 46:328–330, 2008; Surawicz CM, et al.: Guidelines for diagnosis, treatment, and prevention of *Clostridium difficile* infections. *Am J Gastroenterol* 108:478-498, 2013.

Human Immunodeficiency Virus–Related Diarrhea

Diarrheal disease in human immunodeficiency virus (HIV)–infected individuals is frequently caused by infectious agents but may also be due to infiltrative diseases, such as lymphoma or Kaposi sarcoma. Common enteric pathogens with sufficient virulence that cause disease in healthy hosts can also cause diarrheal disease in HIV-infected individuals with intact or compromised immunologic function. Less virulent pathogens, such as *Cryptosporidium parvum*, which appear to require some immunocompromise to establish disease, are more common in patients with more advanced HIV infection or acquired immune deficiency syndrome (AIDS).

Mycobacterium avium-intracellulare complex (MAC) is predominantly associated with lung infections in immunocompetent patients. MAC may also produce disseminated disease with bowel infiltration and malabsorption in patients with severe immunocompromise and should be considered in the differential diagnosis. In these patients, blood should also be obtained in fungal isolator tubes for culture.

In patients with HIV, it is important to ascertain the nature and chronicity of symptoms and the CD4 cell count. Patients with CD4 cell counts <100 cells/μL are at risk for opportunistic infections that are typically chronic, such as *C. parvum*, MAC, cytomegalovirus, *Isospora belli*, or microsporidia.

An epidemiologic history with focus on travel history (*Entamoeba histolytica*, *Giardia lamblia*), sexual exposure (history of unprotected anal intercourse suggesting transmission of herpes simplex virus, *Neisseria gonorrhoeae*, *Chlamydia trachomatis*, or occasionally *E. histolytica*), and food associations (lactose intolerance) should be sought. In patients who are taking highly active antiretroviral therapy (HAART), medication-induced diarrhea (nelfinavir, ritonavir) should be considered, particularly when diarrhea is the sole presenting symptom. *C. difficile* should be considered since the majority of patients with HIV are given antibiotics for treatment of various infections (Sanchez et al., 2005).

Malabsorption Syndromes

Malabsorption is the pathologic state of impaired nutrient absorption in the GI tract. Normal nutrient absorption occurs in three steps: luminal and brush border processing, absorption into the intestinal mucosa, and transport into the circulation. Disruption in any one or a combination of these steps can result in inadequate mucosal absorption of carbohydrates, proteins, fats, vitamins, or minerals. Malabsorption can also result from the presence of substances in the bowel that cannot be absorbed, e.g., lactulose and sorbitol. Maldigestion results from an intraluminal defect that leads to the incomplete breakdown of nutrients into their absorbable substrates. This can occur with pancreatic insufficiency and loss of exocrine function, resulting in increased osmotic load of the colon and diarrhea. In addition, patients can have selective malabsorption/maldigestion of specific nutrients, resulting in associated clinical sequelae. Irrespective of the cause, diarrhea, including steatorrhea, is the most common feature of malabsorption.

Hepatic maldigestion results from interference or obstruction of bile flow. Loss of bile salts compromises formation of mixed micelles and thus interferes with fat emulsification, diminishing the surface area available for lipolytic action. In addition, bile salt activation of lipase activity is lost. Patients are usually jaundiced, pass dark urine, and have other signs of cholestatic liver disease. Hepatic steatorrhea may coexist with pancreatic steatorrhea, as in patients with a neoplasm obstructing the ampulla of Vater. The inability to assimilate fats and proteins due to maldigestion also occurs in patients with vasculitis, diabetes mellitus, carcinoid syndrome, hypogammaglobulinemia, and relative vitamin B_6 or B_{12} deficiency.

Enteric malabsorption comprises a variety of conditions that have in common normal digestion but inadequate net assimilation of nutrients. This may result from competition by bacteria or altered bacterial flora, as in the blind loop syndrome, bacterial overgrowth, diverticulosis of the small bowel, and from obstruction to the flow of lymph. It may also result from diseases affecting the small-bowel mucosa, such as amyloidosis, inflammation following irradiation (radiation enteritis), diminished mucosal surface area as in gastroileostomy (gastric bypass), or small-bowel resection. Depending on the location within the intestinal tract of such pathology, preferential loss of specific substrates may occur. One of the most common clinical scenarios encountered is regional enteritis localized to the distal ileum, the site of vitamin B_{12} and bile salt absorption, which will result in vitamin B_{12} deficiency as well as a decreased pool of circulating bile salts for metabolism.

Steatorrhea is a hallmark finding in patients with malabsorption, resulting in fluid, semifluid, or soft and pasty, pale, bulky, and foul-smelling stools. These stools may be foamy due to the high fat content and may float on water. However, the latter may occur with stools from healthy individuals and is therefore a nonspecific sign of malabsorption.

In patients with steatorrhea, unabsorbed fecal dietary fat is passed in stools above and beyond the normal 1% to 9%, along with as much as 40% of the ingested fat. The quantity of fecal fat depends on the dietary fat intake. Thus, dietary fat intake must be known to properly interpret fecal fat, which is expressed as percentage of dietary fat, allowing assessment of variation in an individual patient. Normally, >93% of dietary fat is absorbed but diarrhea of any cause may lead to a slight increase in fecal fat content.

Another clinical presentation of fat malabsorption is the development of fat-soluble vitamin (A, D, E, and K) deficiencies. Primary and secondary alterations of the bowel mucosa may also result in deficiencies of water-soluble vitamins. Other evidence of nutritional deficiencies, such as hypoprothrombinemia, glossitis, anemia, edema, ascites, and osteomalacia may be evident in these individuals. These patients may experience significant weight loss due to diarrhea leading to cachexia in severe cases.

Quantitative fecal fat measurement has many limitations and should be abandoned (Holmes & Hill, 1988; Hill, 2001). Sample collection is known to be incomplete (Ditchburn et al., 1971; West et al., 1981). Also, there is poor precision in analytic performance, making interpretation uncertain (Duncan & Hill, 1998). Newer tests provide improved sensitivity and specificity for the diagnosis of malabsorption (Hill, 2001): the ^{14}C-glycerol trioleate breath test (Turner et al., 1987) and mixed-chain triglyceride breath test are widely available (Ventrappen et al., 1989; Amarri et al., 1997). However, these tests have limited reliability in diabetes, obesity, hyperthyroidism and hypothyroidism, and chronic respiratory insufficiency, and should not be performed in pregnancy.

The test is based on the measurement of $^{14}CO_2$ in expired air following the ingestion of various ^{14}C-labeled triglycerides (triolein, tripalmitin, and trioctanoin). Steatorrhea from pancreatic insufficiency or other causes results in a decreased absorption of triglycerides. This, in turn, results in a decrease in expired CO_2 derived from metabolism of triglyceride fatty acids.

After an overnight fast, the patient consumes ^{14}C-labeled triglyceride. Periodically, breath CO_2 is collected in a trapping solution containing an indicator that changes color when a predetermined amount of CO_2 is in solution. The radioactivity of the $^{14}CO_2$ is then measured in a liquid scintillation counter and the results are reported as a percentage of the dose of $^{14}CO_2$ excreted per hour.

To distinguish pancreatic insufficiency from other causes of steatorrhea, some investigators have developed a two-stage breath test (Goff, 1982). In the first stage of the test, the patient consumes a ^{14}C-labeled triglyceride and the $^{14}CO_2$ is measured as previously described. The second stage of the test is performed 5 to 7 days later and is the same as the first stage except that the patient is given an oral dose of pancreatic enzymes along with the dose of ^{14}C-labeled triglyceride. In patients with steatorrhea due to pancreatic insufficiency, the amount of $^{14}CO_2$ expired should increase relative to the amount of $^{14}CO_2$ expired in the first stage of the test. Patients with steatorrhea from other causes should show no significant change in the amount of $^{14}CO_2$ expired following the oral administration of pancreatic enzymes.

Agammaglobulinemia

X-linked agammaglobulinemia is a primary humoral immunodeficiency characterized by recurrent bacterial infections of the respiratory tract and increased susceptibility to enteroviral infections. Absence of humoral immunity makes the patient susceptible to bacterial gastroenteritis.

Abetalipoproteinemia

Abetalipoproteinemia is a rare autosomal-recessive disorder that is characterized by defective assembly and secretion of apolipoprotein B (apo B) and apo B–containing lipoproteins resulting from mutations in the gene encoding the microsomal triglyceride transfer protein; the serum β-lipoprotein is absent. It causes defective absorption of lipids. The patients may have neurologic manifestations, acanthocytes, fat malabsorption, steatorrhea, and associated fat-soluble vitamin deficiencies (Gregg & Wetterau, 1994).

Tests for Steatorrhea

Screening tests for detection of steatorrhea include microscopic examination of feces for fat globules and determination of serum carotenoid. Carotenoids are a group of compounds that are the major precursors of vitamin A in humans. Absorption of carotenoids in the intestines depends on the presence of dietary fat. Because carotenoids are not stored in the body to any appreciable degree, lack of carotenoids in the diet or disturbances in absorption of lipids from the intestine can

result in decreasing levels of serum carotenoid. This is a simple and useful screening test for steatorrhea. In addition to steatorrhea and poor dietary intake, liver disease and high fever may also cause a low level of serum carotenoid. Elevated serum carotenoid levels are seen in patients with hypothyroidism, diabetes, hyperlipidemia, and excessive intake of carotene.

Tests for Malabsorption

When a diagnosis of malabsorption is being entertained, it is important to distinguish pancreatic maldigestion from enteric malabsorption. Pancreatic malabsorption is often associated with an increased appetite while enteropathy is usually accompanied by compromised intake. In children, the main cause of pancreatic malabsorption is CF, and the sweat chloride determination should be used when clinical evidence warrants it. Screening tests based on absent stool trypsin have also been used. One of the most valuable differential diagnostic tests, especially in adults, is the D-xylose absorption test.

The cellobiose-mannitol sugar permeability test and lactulose-mannitol test have been used in the diagnosis of celiac disease. The modern evaluation of this disorder has been described earlier. Isotopic techniques and the starch tolerance test have been used as alternatives to the D-xylose test. Quantitative specific fecal trypsin and chymotrypsin assays may be helpful, as may be the Schilling test for vitamin B_{12} absorption, which tends to be abnormal in patients with enteric steatorrhea and in which the abnormality is not correctable with intrinsic factor. Endoscopy, radiologic studies, and biopsy have replaced these methods in many cases.

Fecal Elastase. Elastase-1 is a proteolytic enzyme produced by the pancreas. Pancreatic elastase survives intestinal transit intact and is five- to sixfold concentrated in the feces (Lankisch, 2004). Reduced pancreatic elastase-1 in feces indicates pancreatic insufficiency in infants over 2 weeks of age with CF and in older children with the disorder (Phillips et al., 1999; Cade et al., 2000; Leus et al., 2000).

This EIA is unaffected by pancreatic enzyme replacement therapy. Although sensitive for detection of severe pancreatic insufficiency, it lacks sensitivity for detection of milder forms. Fecal elastase is better than fecal chymotrypsin, para-aminobenzoic acid, bentiromide, and pancreolauryl tests (Lankisch, 2004). A single analysis of a 100-mg stool sample is adequate for determination of fecal elastase levels. If borderline values are detected, a repeat sample may be useful. This test should only be performed on formed stool. With a cutoff of 200 μg/g stool, the positive predictive value of fecal elastase determination is estimated to be approximately 50% (Lüth, 2001).

Xylose Absorption Test. The D-xylose absorption test is a valuable test for the differential diagnosis of malabsorption. In this procedure, a 25-g dose of the pentose sugar (which is not normally found in the body or diet) in water is administered orally and the amount excreted in urine over a 5-hour period is determined. If the amount excreted is less than 3 g, the diagnosis is mostly likely enterogenous malabsorption because pancreatic enzymes are not required for absorption of D-xylose. D-Xylose is passively absorbed in the small intestine and is not metabolized by the liver, although a portion of an orally or intravenously administered dose is destroyed. The accuracy of the method depends not only on the rate of absorption of D-xylose but also on the rate of renal excretion. Therefore, in patients with renal disease, xylose should be quantified in blood 2 hours after its oral administration because urine values are difficult to interpret in the absence of reference values.

Isotopic techniques and the starch tolerance test have been used as alternatives to the D-xylose test. Quantitative specific fecal trypsin and chymotrypsin assays may be helpful, as may be the Schilling test, which is used to assess the function of the terminal ileum. An oral dose of radioactive vitamin B_{12} is followed by an intramuscular large dose of nonradioactive vitamin B_{12}, and radioactivity in urine is measured. Urinary radioactivity reflects the absorbed amount of vitamin B_{12}. A repeat test to diagnose pernicious anemia or gastric pathology in a patient with steatorrhea involves coadministration of intrinsic factor and vitamin B_{12}. An abnormal result indicates ileal disease.

Laxative Abuse

Surreptitious laxative abuse is a frequently overlooked cause of chronic diarrhea and is the final diagnosis for chronic diarrhea in 15% to 26% of patients at referral centers (Bytzer et al., 1989; Duncan et al., 1992). In Munchausen syndrome by proxy, adults administered laxatives surreptitiously to young children (Duncan, 2000). The main prerequisite for making the diagnosis of surreptitious laxative abuse is clinical suspicion. Analysis of urine and fecal samples taken during diarrhea is necessary. Phenolphthalein is less frequently found since over-the-counter sales were banned. Senna, aloin, and cascara are colonic stimulants that are abused and can be detected by thin-layer chromatography.

Celiac Disease

Celiac disease (CD), or gluten-sensitive enteropathy, is an immune-mediated disorder that is precipitated by the ingestion of gluten in genetically predisposed individuals. CD is characterized by intestinal malabsorption of nutrients due to villous damage secondary to sensitivity to the alcohol-soluble portion of gluten, known as *gliadin*. Gluten is the major storage protein in wheat, rye, and barley. It can induce mucosal damage in the gut, causing nonspecific villous atrophy of the small intestinal mucosa. CD does not develop unless a person has HLA-DQ2 or HLA-DQ8 haplotypes. When expressed on the surface of antigen-presenting cells, these proteins bind deaminated (activated) gluten peptides, leading to an aberrant immune response. CD has most often been diagnosed in whites of Northern European descent in developed countries and is now being recognized with increasing frequency in developing countries. The worldwide prevalence is estimated to be as high as 1%; women are 2 to 3 times more frequently affected than men (Green & Cellier, 2007; Sabatino & Corazza, 2009; Fasano & Catassi, 2012).

CD has most often been recognized in children but it can manifest at any age; some individuals remain asymptomatic into their 50s. Astute clinicians may suspect this disorder when patients present with thin stature, iron deficiency anemia, weight loss, chronic bloating, and/or diarrhea. In severe cases, one may see malabsorption, steatorrhea, and wasting. There are associations between CD and type 1 diabetes mellitus, Down syndrome, dermatitis herpetiformis, IgA deficiency, autoimmune thyroid disease, and others (Barr & Grehan, 1998; Fasano & Catassi, 2012). Due to the enteropathy associated with the disorder, multiple hematologic and biochemical abnormalities may be found in persons with untreated CD, including deficiencies of iron, folate, or vitamin D.

Patients with the clinical diagnosis of CD and their first-degree relatives are screened by serologic tests. Positive findings from serologic testing require confirmation of diagnosis by histologic examination of multiple biopsies of the affected small-bowel mucosa for villous atrophy and crypt hyperplasia. Despite its shortcomings because of patchy mucosal lesions and sampling errors, histologic examination of small-bowel mucosa has remained the gold standard for diagnosis of CD. However, endoscopy and biopsy are most often reserved for patients with HLA-DQ2 or HLA-DQ8 in whom the diagnosis is suspected based on signs or symptoms of the disease and with supporting serologic findings (see later discussion). Patients with confirmed diagnosis of CD must be maintained on a gluten-free diet for the rest of their lives to control symptoms and mitigate cancer risk (Green & Cellier, 2007; Ensari, 2010).

Serologic tests have variable performance characteristics depending on the antigen and test method employed. Sensitivities and specificities of these tests, now available for different age and population groups, should guide test selection. Some tests are more useful in CD diagnosis and others more useful in monitoring compliance with gluten-free diet. Features of the most commonly performed laboratory studies are provided here. Detailed guidelines on diagnosis and management of CD are available elsewhere (Rubio-Tapia et al., 2013).

Biomarkers used in the diagnosis of CD or monitoring compliance to a gluten-free diet are summarized in Table 23.6 (Caio, 2019; Husby et al., 2019). The serologic studies include testing for antibodies to gliadin (AGA-IgA and AGA-IgG), deamidated gliadin (IgA and IgG), endomysium (EMA-IgA and IgG), and tissue transglutaminase (tTG-IgA and tTG-IgG). AGA-IgA and AGA-IgG have low sensitivity and specificity, and have been replaced by antideaminated gliadin antibodies (IgG and IgA) and EMA-IgA and IgG (see Chapter 55). Antireticulin antibodies, which have long been used in diagnosing CD, are no longer recommended for routine diagnostic use because of their suboptimal sensitivity and specificity (Nandiwada & Tebo, 2013). Specific IgA tests have better sensitivity and specificity than the IgG tests. Results of serologic testing for CD must be analyzed with caution since this disease is associated with selective IgA deficiency that will produce false-negative serum IgA antibody tests (Thomas et al., 2003). Transient IgA deficiency may be seen in patients on phenytoin, penicillamine, and sulfasalazine. Therefore, total IgA levels should be measured and specific IgG serology used in IgA-deficient patients with suspected CD. Endomysial antibodies (EMAs) have high sensitivity and specificity; these are detected by indirect immunofluorescence of sections of monkey esophagus or human umbilical cord, but are costly, cumbersome, and subject to interobserver interpretive variability.

Wheat storage protein, gliadin, is used as an antigen in EIAs for AGA-IgA and AGA-IgG. Titers of these tests are frequently elevated in untreated CD; however, these tests are of only moderate sensitivity and

TABLE 23.6
Biomarkers in the Diagnosis of Celiac Disease (CD) and Monitoring Compliance to Gluten-free Diet

Biomarker	Method	Comments
Anti-reticulin antibodies—IgG/IgA	IFA (rat kidney)	Lack optimal sensitivity and specificity for routine diagnostic use.
Total IgA	Quantitative nephelometry	Useful in ruling out IgA deficiency; specific IgG antibodies need to be tested in IgA-deficient individuals.
Anti-gliadin antibodies—IgG/IgA	Quantitative EIA	Low sensitivity and specificity; limited use in monitoring dietary compliance.
Antideaminated gliadin antibodies—IgG/IgA	Quantitative EIA	Inferior performance relative to other diagnostic assays.
Antiendomysial antibodies—IgG/IgA	IFA (rhesus monkey esophagus; human umbilical cord)	High sensitivity and specificity in CD; observer bias limits usefulness.
Antitissue transglutaminase antibodies—IgG/IgA	Quantitative EIA	Assays using purified human or recombinant human tTG are more sensitive than those using guinea pig tTG; useful in both diagnosis and monitoring dietary compliance.
HLA-DQ2/HLA-DQ8	PCR-based assays	High negative predictive value; not affected by dietary gluten; found in 0.3% of general population

EIA, Enzyme immunoassay; *IFA,* indirect fluorescent antibody; *Ig,* immunoglobulin; *PCR,* polymerase chain reaction; *tTG,* tissue transglutaminase.
Adapted from Husby S, et al.: AGA clinical practice update on diagnosis and monitoring of celiac disease—changing utility of serology and histologic measures: expert review, *Gastroenterology* 156(4):885–889, 2019; Caio G, et al.: Celiac disease: a comprehensive current review, *BMC Medicine* 17(1):142, 2019.

specificity. AGA-IgG testing is particularly useful in the 2% of patients with CD who are IgA deficient. These tests, however, have largely been replaced by EMA. EMA binds to connective tissue surrounding smooth muscle cells. Serum EMA-IgA binds to the endomysium to produce a characteristic staining pattern seen on indirect immunofluorescence. This antibody is very sensitive and specific, and the titers fall quickly to undetectable levels after treatment (Volta et al., 1995). The epitope against which EMA is directed has been shown to be tissue transglutaminase (tTG). Use of anti-tTG-IgA assays has been shown to be highly sensitive and specific for the diagnosis of CD (Dieterich et al., 1998). EIAs for anti-tTG-IgA are widely available, less costly, and easier to perform than the older immunofluorescence assays for EMA-IgA.

Antigliadin antibody serology is best avoided for diagnosis of CD because of frequent false-positive results. A second generation of antigliadin antibody test based on the potentiation of toxic gliadin peptides by tTG enzymatic activity is used for monitoring dietary compliance. These IgA and IgG deamidated gliadin peptide (DGP) assays are not necessarily superior to other assays in diagnosis of CD. High sensitivity and specificity of anti-tTG-IgA and anti-tTG-IgG using purified human or recombinant human tTG have led to the belief that strongly positive tTG-IgA may obviate the need for tissue biopsy in diagnosing CD. Detections of EMA-IgA in conjunction with anti-tTG-IgA titers offers high diagnostic accuracy and tTG-IgA titers correlate well with mucosal inflammation and villous atrophy. Thus, these antibodies can be used to diagnose CD in symptomatic children and adults without the need for tissue biopsy and histologic examination (Tortora et al., 2014; Husby & Murray, 2014; Husby et al., 2019).

Although EMA-IgG and anti-tTG-IgG may be used for serologic diagnosis of CD in IgA-deficient patients, they are suitable to monitor the response to dietary modification. EMA-IgA antibody titers decline following treatment of CD with a gluten-free diet. Because of the ease of performance and better standardization, antigliadin antibodies are more useful in monitoring dietary compliance.

The HLA-DQ2 allele is identified in 90% to 95% of patients with CD and HLA-DQ8 in most of the remaining patients. These alleles occur in 30% and 40% of the general population, and the absence of these alleles is important for its high negative predictive value. Thus, the presence of HLA-DQ2 and HLA-DQ8 is important in determining which family members should undergo serologic testing (Kaukinen et al., 2002).

Whipple Disease

It is a rare multisystem disease that often presents with arthralgias, diarrhea, malabsorption, and weight loss. It is predominantly found in males; about 15% of the patients do not present with classical signs and symptoms of this disease (Fenollar et al., 2007). It is caused by *Tropheryma whipplei*, a bacillus that does not stain well with Gram stain, although classified with gram-positive bacteria based on 16S rRNA sequencing (Marth & Raoult, 2003). It can affect the central nervous system and cause endocarditis. Demonstration of periodic acid-Schiff (PAS)–positive material in the lamina propria and villous atrophy of the small intestine is diagnostic. A prothrombin time (PT) should be checked prior to biopsy because of the frequent occurrence of vitamin K malabsorption.

T. whipplei has been cultured from the stools of a patient with Whipple disease using a specific axenic medium and specific techniques (Raoult et al., 2006). Polymerase chain reaction (PCR) testing of infected tissue or cerebrospinal fluid has been used to confirm the diagnosis and monitor treatment (von Herbay et al., 1997). Biopsy of the duodenum with PAS staining had been considered pathognomonic for Whipple disease. It is now recognized that PAS-positive macrophages may be seen in AIDS patients with MAC. Thus, PCR has gained even more importance in the management of this entity. Long-term antibiotic therapy with central nervous system penetration is used to treat patients with Whipple disease (Ramzan et al., 1997; Singer, 1998).

TABLE 23.7
Markers for Inflammatory Bowel Disease

	FREQUENCY (%)	
Patients with:	**p-ANCA**	**ASCA**
Irritable bowel syndrome	<5	<5
Ulcerative colitis	70	15
Crohn disease	20	65

ASCA, Anti-*Saccharomyces cerevisiae* antibody; *p-ANCA,* perinuclear antineutrophil cytoplasmic antibody.
Adapted from Quinton JF, et al.: Anti-*Saccharomyces cerevisiae* mannan antibodies combined with antineutrophil cytoplasmic autoantibodies in inflammatory bowel disease: prevalence and diagnostic role. *Gut* 42(6):788-791, 1998; Mitsuyama K, et al.: Antibody markers in the diagnosis of inflammatory bowel disease. *World J Gastroenterol* 22(3):1304–1310, 2016.

Inflammatory Bowel Disease

Immunologic mechanisms within the colon are involved in the pathogenesis of inflammatory bowel disease. The underlying antigenic challenge to the immunologic response is not clearly understood. Over the last few years, two antibody tests have become available that assist in the laboratory evaluation of patients with inflammatory bowel disease (Rutgeerts & Vermeire, 2000). The combination of clinical findings, endoscopy, radiologic imaging, and blood work may help differentiate the subtypes of inflammatory bowel disease. Perinuclear-antineutrophil cytoplasmic antibody (p-ANCA) and anti-*Saccharomyces cerevisiae* antibody (ASCA) can be used to help distinguish irritable bowel syndrome from inflammatory bowel disease and ulcerative colitis from Crohn disease (Shanahan, 1994; Quinton et al., 1998) (Table 23.7) (see Chapter 55). These tests have limitations, and interpretation requires careful understanding of the tests. Whereas few normal persons with irritable bowel syndrome will have ANCA, 70% of persons with ulcerative colitis and 15% of persons with Crohn disease will have significant titers. In patients with inflammatory bowel disease, 70% of patients with Crohn disease will have ASCA, whereas only 15% of patients with ulcerative colitis will have significant titers (Bossuyt, 2006; Mitsuyama et al., 2016). Given the low sensitivity and specificity, the use of these tests should be dependent on the clinical circumstance. For example, a person with diarrhea and equivocal biopsy findings found to have a positive ANCA is more likely to have inflammatory bowel disease than irritable bowel syndrome. Likewise, if a person with what appears to be ulcerative colitis is found to have a positive ASCA, Crohn colitis may be present.

GASTROINTESTINAL BLEEDING

Throughout most of the GI tract, the lumen of the gut is separated from the capillary blood supply by only a single layer of epithelial cells. Thus, even minor injury to the epithelial lining may result in GI bleeding. Occult GI bleeding is unknown to the patient because the stools appear normal. Iron-deficiency anemia should be considered to be the result of GI bleeding until excluded (Rockey, 2010).

Hemoglobin and hematocrit are usually low, and their level may have some relation to the blood loss. A low mean cell volume (MCV) may indicate that the patient is iron deficient and that there has been chronic blood loss (see Chapter 9). An elevated MCV may mean that there is a folate or vitamin B_{12} deficiency with macrocytosis and raises the possibility of ethanol abuse, chronic liver disease, gastric cancer in association with pernicious anemia, or regional enteritis involving the terminal ileum. In addition to clinical peripheral neuropathy, hypersegmented leukocytes are more suggestive of vitamin B_{12} deficiency.

If a clotting defect exists, based on an abnormal international normalized ratio or PT, prompt correction of the deficiency is crucial. Extensive transfusion dilutes platelets and clotting factors, particularly factors V and VII. Also, a high proportion of patients who bleed while taking therapeutic anticoagulants do so from a clinically significant lesion. It is important to evaluate these patients for a GI pathologic condition in addition to correcting their clotting status. Leukocytosis may accompany acute GI bleeding, but it is usually not in excess of 15,000 leukocytes/mm^3. Leukocytosis should not be attributed to acute blood loss without first seeking sources of infection.

An elevated urea nitrogen in a patient whose urea nitrogen was recently normal or whose serum creatinine concentration is normal suggests an upper GI bleed. The urea nitrogen rise may be due to the hypovolemia of acute blood loss, but digestion of blood proteins in the small intestine and the absorption of nitrogenous products may be the cause.

Fecal Occult Blood Testing

The fecal occult blood test (FOBT) depends on the peroxidase activity of hemoglobin. Reagents used include guaiac, orthotoluidine, orthodianisidine, and benzidine (marketing restricted by federal regulation due to its carcinogenicity). The reagents differ in sensitivity, although all are associated with frequent false-positive and false-negative results mostly because of the specimen tested. Specimens collected by digital rectal examination have a high frequency of false-positives due to injury of the rectal mucosa.

The normal person loses 0.5 to 1.5 mL of blood into the GI tract daily in association with the normal shedding of epithelial cells. The commercial tests are designed to turn positive with a blood loss of greater than 5 to 10 mL per day. This corresponds to 5 to 10 mg of hemoglobin/g of feces, assuming a blood hemoglobin of 15 g/dL and an average daily 150 g stool.

Occult blood may arise anywhere along the intestinal tract and is often the first warning sign of GI malignancy. Other potential sources of occult blood may arise from bleeding esophageal varices, polyps, esophageal or gastric inflammation, peptic ulcer disease, inflammatory bowel disease, angiodysplasias of the colon, and hemorrhoids or fissures. Laboratory diagnosis of the presence of fecal occult blood has long depended on the guaiac-based tests, which are now being replaced with more specific and sensitive tests. Guaiac is a naturally occurring phenolic compound that is oxidized to quinone by hydrogen peroxidase, resulting in a detectable color change. These tests detect the pseudoperoxidase activity of heme, either as intact hemoglobin or as free heme (Allison et al., 1996). These tests are not specific for human hemoglobin; hemoglobin from red meat and peroxidase from fruits and vegetables and certain medications can lead to false-positive results. The presence of >5 to 10 mL/day of blood in the stool results in a positive guaiac smear.

Patient preparation and specimen collection are important in ensuring valid test results. The high rate of false-positive results is due to the lack of specificity of the reagents and the presence of peroxidase activity in other fecal constituents as well as the sensitivity of the different chromogens to peroxidase activity. The myoglobin and hemoglobin of ingested meat and fish have peroxidase activity that may produce a false-positive result. Bacteria in the bowel as well as ingested vegetables and fruits—such as horseradish, turnips, bananas, black grapes, pears, and plums—have peroxidase and can falsely elevate fecal peroxidase activity. False-negative tests occur in the presence of large amounts of vitamin C and other antioxidants. Certain medications also influence the FOBT. For example, drugs that can cause GI irritation and subsequent bleeding, such as anticoagulants, NSAIDs, or colchicine and reserpine, may lead to false-positive results. Oxidizing drugs (e.g., iodine) have also been implicated in producing false-positive results. Patients should avoid such medications or food products for at least 72 hours prior to stool collection for the FOBT. A positive FOBT prompts further evaluation for a GI lesion.

The limitations of the FOBT include the high number of false-positive and false-negative results. The sensitivity of the FOBT has been estimated to be between 30% and 50%. The true sensitivity of the FOBT is difficult to determine because individuals who test negative do not undergo further colonoscopic and upper GI and small-bowel evaluation to determine whether the FOBT result is a true negative. Only approximately 5% to 10% of positive reactions prove to be caused by an occult malignancy (Simon, 1998). A negative FOBT, however, cannot definitely rule out the presence of colonic neoplasia. If a patient is presenting with signs and symptoms suggestive of colon cancer, further evaluation is warranted even in the presence of a negative FOBT. Further evaluations usually include sigmoidoscopy with barium enema, virtual colonoscopy, or full colonoscopy, the latter being the most sensitive investigation.

Immunochemical fecal occult blood (iFOB) tests for human hemoglobin are more sensitive and specific, and give fewer false negatives. Some iFOB tests using mouse antihuman hemoglobin antibody are sensitive enough to detect 50 μg hemoglobin/g feces. These tests are not affected by diet, animal hemoglobin, human myoglobin, or peroxidase; thus, food restrictions are not necessary. They are useful only in screening for blood of the lower intestinal tract and are insensitive to upper GI bleeding since globin is destroyed in the small intestine. The iFOB tests are expensive and are not done at point of care.

Fecal DNA testing is a promising technique for colorectal cancer screening. This test involves collection of a single stool specimen, which is then screened for deoxyribonucleic acid (DNA) markers. PCR is used to amplify the fecal DNA. These tests are useful because DNA is shed continuously and remains stable in stool, and minute amounts are detectable. Clinical studies have shown that fecal DNA testing has high specificity and sensitivity for cancer detection, considerably more than chemical guaiac testing. Several markers have been investigated; however, further evaluation and improved specificity and sensitivity are needed for their widespread use (Itzkowitz et al., 2008; Lieberman, 2009; Imperiale et al., 2014).

Colon cancer is a leading cause of cancer-related deaths in the United States, accounting for approximately 55,000 deaths annually. According to recent cancer statistics, approximately 150,000 new colon cancer cases were diagnosed in 2003. Evidence has demonstrated the clinical usefulness of FOBT to detect these cancers at an earlier stage, potentially resulting in decreased mortality. Due to the generally favorable clinical biology of these tumors when detected earlier, with an 80% to 90% survival rate with local confined disease (Helm et al., 2003), and the relatively inexpensive, noninvasive nature of FOBTs, this may serve as a useful screening technique. Several professional organizations recommend annual or biennial FOBTs; however, universally accepted screening protocols have not been established. The U.S. Multi-Society Task Force of Colorectal Cancer guidelines for colorectal cancer screening recommend an annual iFOB test and colonoscopy every 10 years in asymptomatic average-risk individuals aged >50 years (Rex et al., 2017).

Blood in Newborn's Feces (Apt Test for Swallowed Blood)

When blood is found in the GI tract or stool of neonates, usually on the second or third day of life, a determination of whether it is swallowed blood of maternal origin or secondary to a primary GI disease in the newborn must be made (Guritzky & Rudnitsky, 1996). This distinction is made by Apt test, which is a qualitative test used to identify the presence of fetal hemoglobin in grossly bloody stools or vomitus (hematemesis) from a newborn. Infants may ingest maternal blood during birth and from a fissured or bleeding nipple. The sample is first mixed with water and centrifuged. The supernatant, which should be pink, is then mixed with 1% NaOH in a 5:1 ratio. If the blood is of maternal origin, the mixture turns yellow-brown after several minutes. Fetal blood remains pink since the HbF is more resistant to alkali denaturation than adult hemoglobin. The test has a relatively low sensitivity and the result must be interpreted with caution (McRury & Barry, 1994).

GASTROINTESTINAL AND PANCREATIC NEUROENDOCRINE NEOPLASMS

Pancreatic Adenocarcinoma

The laboratory findings in patients with pancreatic cancer are largely nonspecific and may include mild anemia and thrombocytopenia. Most patients have varying degrees of obstructive jaundice with elevations in

bilirubin (conjugated and total), alkaline phosphatase, gamma-glutamyl transpeptidase, and, to a lesser extent, aspartate aminotransferase and alanine aminotransferase. Five percent of the patients present initially with acute pancreatitis and uniform increases in amylase and lipase. This section is a brief summary of tumor markers that have been used to aid in the diagnosis of pancreatic cancer or its staging and follow-up. This topic is discussed more extensively in Chapters 77 and 78.

Carbohydrate Antigen 19-9 (CA 19-9)

CA 19-9 antigen, an oligosaccharide, is the sialylated form of the Lewis A (LeA) antigen (see Chapter 36) that is most commonly found on circulating mucins in cancer patients. It is normally present within the cells of the biliary tract and can be elevated in acute or chronic biliary disease. Elevated CA 19-9 levels are seen in 75% to 85% of patients with pancreatic carcinoma. In the absence of biliary obstruction, intrinsic liver disease, or benign pancreatic disease, a CA 19-9 value of greater than 100 U/mL (reference range: 0–37 U/mL) is highly specific for malignancy, usually pancreatic. About 5% to 10% of patients lack the enzyme necessary to produce CA 19-9; in these patients with low or absent levels of CA 19-9, monitoring disease with this tumor marker will not be possible. Evaluation of CA 19-9 levels has been used as an adjunct to imaging studies to determine the resectability potential of pancreatic carcinoma. Unfortunately, CA 19-9 is least sensitive for small, early-stage pancreatic carcinomas and thus has not proven to be effective for the early detection of pancreatic cancer or as a screening tool.

However, a new approach to the early detection of pancreatic cancer using CA 19-9 was achieved in a recent study (Cohen et al., 2017) on the sera of patients with early-stage (I, IIA, and 2B) pancreatic cancers that has resulted in significantly increased sensitivity of pancreatic cancer detection (see Chapter 77). In this study, CA 19-9 was used in conjunction with DNA probes for the k-ras oncogene that is expressed in over 90% of pancreatic cancers (Almoguera, 1988). In addition, enzyme-linked immunosorbent assays (ELISAs) for three potential serodiagnostic proteins, that is, hepatocyte growth factor (HGF), carcinoembryonic antigen (CEA), and the protein osteopontin (OPN), were performed on these sera. Expression of one or more of these markers was considered to indicate presence of tumor. This approach is promising and is being applied to an expanded cohort of patients.

CA 19-9 is useful in the staging and follow-up of patients with this disease. Patients presenting with low levels of CA 19-9 (<100 IU) are unlikely to have occult metastatic disease and therefore may not need a staging laparoscopy prior to resection if other imaging shows no advanced disease. Additionally, during surgical, chemotherapeutic, and/or radiotherapeutic treatment for pancreatic cancer, a falling CA 19-9 seems to be a useful surrogate for clinical response to the therapy. If biliary obstruction is not present, a rising CA 19-9 suggests progressive disease. Preoperative CA 19-9 levels may be of prognostic value, with high levels indicating poorer outcome and less chance of resectability. Preoperative values above 50 U/mL have been shown to be associated with higher chances of recurrence (see Chapter 77).

Carcinoembryonic Antigen

CEA is a high-molecular-weight glycoprotein found normally in fetal tissues. It has commonly been used as a tumor marker in other GI malignancies. Only 40% to 45% of patients with pancreatic carcinoma have elevated CEA levels (reference range: ≤2.5 mg/mL). Because benign and malignant conditions other than pancreatic cancer can lead to elevated CEA levels, it is not a sensitive or specific marker for pancreatic cancer. This protein is discussed further in Chapter 77.

Early Detection Markers

Many other tumor markers have been studied in pancreatic cancer using powerful techniques, such as gene expression microarrays and proteomics, but none has yet been shown to have general clinical utility. Recently, researchers have focused their attention to the detection of early pancreatic adenocarcinoma in high-risk patients, such as those with chronic pancreatitis, pancreatic cysts, family history, and new-onset type II diabetes utilizing a combination of tumor markers. Patients with some genetic syndromes have a greater risk of developing pancreatic cancer (Table 23.8; Shi, et al., 2009). A newly discovered glycan, sialylated tumor-related antigen (sTRA) has been found to be produced by a different subset of pancreatic adenocarcinomas than those that produce CA 19-9 (Staal et al., 2019). Whereas CA 19-9 testing detects only about 40% of carcinomas, combined CA 19-9 and sTRA detected around 70% of pancreatic adenocarcinomas in patients with benign conditions of the pancreas. Another study, utilizing a combination of thrombospondin-2 and CA 19-9, was able to discriminate resectable stage I pancreatic adenocarcinoma (Kim et al., 2017). Serodiagnostic markers for gastrointestinal tumors are discussed further in Chapters 77 and 78.

Neuroendocrine Neoplasms

GI and pancreatic neuroendocrine neoplasms (GIPanNENs) encompass two morphologically and biologically distinct groups of neuroendocrine neoplasms, one indolent and hormonally active and the other aggressive and hormonally inactive. They are relatively rare (< 4/100,000), although over the last 3 decades, the age-adjusted incidence has risen partly due to increased detection on radiographic imaging and endoscopy (Hemminki & Li, 2001; Dasari et al., 2017; Chauhan et al., 2018). The 2018 WHO classification distinguishes neoplasms as neuroendocrine if they exhibit the general neuroendocrine markers chromogranin and/or synaptophysin by immunohistochemistry and divides them into low-grade neuroendocrine tumors (NETs) and high-grade neuroendocrine carcinomas (NECs) by light microscopy (Rindi et al., 2018). NETs are further divided into low (G1), intermediate (G2), or high (G3) grade based on two grading parameters of prognostic significance: mitotic count and Ki-67 expression (Klöppel & La Rosa, 2018). As discussed in Chapter 76, recent studies have indicated that loss of the anti-oncogene PTEN (Phosphatase and TENsin homologue) protein that dephosphorylates IP_3 (phosphatidylinositol-3,4,5-trisphosphate) and increased pAKT (protein kinase B) expression may further distinguish more aggressive GI tumors from more indolent ones (Pitt et al., 2009; Estralla et al., 2014; Jayakumar et al., 2018).

Generally, NETs are indolent neoplasms that produce biogenic amines or peptide hormones and may be associated with recognizable paraneoplastic or hereditary tumor syndromes. They often contain alterations of the MEN1, DAXX/ATRX, and mTOR genes (Jiao et al., 2011; Scarpa et al., 2017) or manifest epigenetic dysregulation (Karpathakis et al., 2016). The majority are nonfunctional and present with localized symptoms or metastases. Radiographic imaging or endoscopy often fortuitously

TABLE 23.8
Pancreatic Cancer—Associated Genetic Syndromes

Genetic Syndrome	Gene(s)	Pancreatic Cancer Risk, -fold Increase	Histopathologic Features
Hereditary breast and ovarian cancer syndrome	*BRCA2*	3.5 to 10	Ductal adenocarcinoma
	BRCA1	2	
Peutz-Jeghers syndrome	*STK11/LKB1*	132	Intraductal papillary mucinous neoplasm
Familial adenomatous polyposis	*APC*	Up to 4	Ductal adenocarcinoma, intraductal papillary mucinous neoplasm, pancreatoblastoma
Familial atypical multiple mole melanoma	*CDKN2A*	13 to 22	Ductal adenocarcinoma
Hereditary nonpolyposis colorectal cancer syndrome	Mismatch repair genes	Increased	Medullary carcinoma
Hereditary pancreatitis	*PRSS1*	53	Ductal adenocarcinoma
	SPINK1		
Familial pancreatic cancer	Unknown	9 to 32	

Adapted from Shi C, et al.: Familial pancreatic cancer, *Arch Pathol Lab Med* 133:365–374, 2009.

discovers them. Even though NETs may secrete nonspecific neuroendocrine substances such as chromogranin or specific ones such as gastrin, they are not functional unless they cause a recognizable paraneoplastic syndrome, for example, carcinoid syndrome and ZE syndrome. Also, because NETs secrete a variety of substances, there are no general recommendations for assaying them. The diagnostic and prognostic value of hormonal NET secretion profiles is of limited value. In contrast, NECs are aggressive neoplasms not commonly associated with paraneoplastic or hereditary syndromes that often present with metastatic disease and contain TP53 and Rb1 mutations (Konukiewitz et al., 2017).

Laboratory Diagnosis

Functional Neuroendocrine Tumors

Carcinoid Syndrome. The secretion of excessive serotonin and other vasoactive substances into the systemic circulation produces the chronic flushing and/or diarrhea of the carcinoid syndrome. It is primarily associated with metastatic NETs most commonly originating in the appendix, distal small intestine and the proximal colon. The most sensitive (>90%) and specific (>90%) initial diagnostic test is measurement of 24-hour urinary excretion of the end-product of serotonin metabolism 5-hydroxyindoleacetic acid (5-HIAA) (Sjoblom, 1988; Mukerjee & Pincus, 1992). The normal rate of 5-HIAA secretion ranges from 2 to 8 mg/day (10–42 mmol/day). Patients with malabsorption or ingestion of tryptophan and serotonin-rich foods or certain medicine may have elevated levels (O'Toole et al., 2009). Certain gastroduodenal and distal colonic and rectal tumors lack DOPA decarboxylase and thus cannot convert 5-hydroxytryptophan into serotonin and 5-HIAA. Measurement of 5-hydroxytryptophan is challenging, as there are no commercially available assays available in the United States. A convenient test for plasma 5-HIAA concentration that correlates with 24-hour urinary 5-HIAA has recently been developed but has yet to be validated in large clinical series. The specificities and sensitivities of blood serotonin levels have not been well established and are not recommended (Allen et al., 2007; Tellez et al., 2013). Similarly, due to its relatively low specificity, the neuroendocrine marker chromogranin A is not recommended as a screening test for the carcinoid syndrome (Stridsberg et al., 2003).

Insulinoma. Insulinomas are rare, typically small, solitary (87%) pancreatic NETs derived from the ductular/acinar system that maintain high levels of insulin secretion in the presence of hypoglycemia, possibly by producing a variant of insulin messenger ribonucleic acid (mRNA) with increased translation efficiency (Service et al., 1991; Vortmeyer et al., 2004; Minn et al., 2004). Characteristically, they present with fasting and sometimes postprandial hypoglycemia. The laboratory evaluation of hypoglycemia in the nondiabetic patient protocol endorsed by the 2009 Endocrine Society guidelines is recommended (Cryer et al., 2009). High plasma levels of proinsulin, insulin, C-peptide, and low plasma β-hydroxybutyrate after a 72-hour fast or a mixed meal test establishes the diagnosis.

Gastrinoma. Gastrinomas are sporadic (80%) or associated with MEN-1 gastrin-secreting NETs that produce ZE syndrome. A quarter of these arise in the pancreas and the rest arise predominantly in the first part of the duodenum (Thom et al., 1991). Localizing the lesion can sometimes be challenging. The initial laboratory evaluation in a patient suspected with ZE syndrome is measurement of fasting serum gastrin. When elevated gastrin levels are not diagnostic (i.e., <10 times the upper limit of normal in the presence of gastric pH <2), the secretin stimulation test is performed; several criteria have been proposed to define a positive test. A calcium gluconate infusion study is performed in patients with a strong clinical suspicion of gastrinoma despite a negative secretin test (Berna et al., 2006). The secretin stimulation test should not be performed in severe ZE syndrome patients as they are particularly at risk for life-threatening consequences of discontinuing acid suppression. Biochemical studies to screen for MEN-1 are recommended because approximately 25% of MEN-1 patients present with ZE syndrome and up to 40% of MEN-1/ZE syndrome patients have no family history (Jensen et al., 2012).

Glucagonoma. Glucagonomas are rare, large, solitary, glucagon-secreting NETs located primarily in the distal pancreas and are metastatic at diagnosis (Wermers et al., 1996). The laboratory diagnosis of glucagonoma is made by measuring fasting plasma glucagon (Kindmark et al., 2007).

Somatostatinoma. Somatostatinomas are rare NETs arising in the head of the pancreas or the ampullary/periampullary region of the duodenum. The majority (75%) are malignant and present with metastatic disease (Doherty, 2005). The laboratory diagnosis of somatostatinoma is made by measuring fasting plasma somatostatin levels.

VIPoma. See the section on Diarrhea and Malabsorption.

Amyloidosis. GI amyloidosis is mainly of the reactive type (secondary or amyloid-associated [AA] amyloidosis), resulting from either mucosal or neuromuscular infiltration. It may result in GI bleeding from vascular friability. The patient may also have diarrhea from a combination of altered intestinal motility, bacterial overgrowth and protein-losing enteropathy. Liver involvement can be seen in either primary (amyloid light chain [AL]) or secondary (AA) amyloidosis. The common symptoms are involuntary weight loss, fatigue, and abdominal pain. The common physical findings are hepatomegaly, ascites, purpura, and splenomegaly. The most common laboratory abnormality is an elevated alkaline phosphatase. The diagnosis of multiple myeloma should be confirmed by tissue biopsy of duodenal or colorectal mucosa. Although the GI complications can result in significant morbidity, they are not usually the cause of death, which is most often due to renal failure, restrictive cardiomyopathy, or ischemic heart disease (Ebert & Nagar, 2008).

STOOL COLLECTION AND EXAMINATION

COLLECTION

Stool specimens are required for evaluation of diarrhea, malabsorption, detection of infectious agents and occult blood, and diagnosis of many other GI conditions, including cancer (see Table 23.4; Khare, et al., 2014; Shane, et al., 2017). Each of these indications have specific specimen requirements with regard to patient preparation, number of specimens, frequency of collection and testing, and special containers. It is prudent to check with the laboratory about test offerings and specimen requirements, including use and availability of collection kits. Stool specimen collection is also described elsewhere in this book (see Chapters 65, 66, and 76).

Stool sample collection at home is by no means simple and easy unless the patient has been instructed properly. Uninstructed patients sometimes exhibit considerable ingenuity in collecting stool specimens, but a few simple instructions are likely to produce more satisfactory specimens.

MACROSCOPIC EXAMINATION

The quantity, form, consistency, and color of the stool should be noted. Normally, 100 to 200 g of stool is passed per day. Diarrheic stool is watery. Passage of large amounts of mushy, foul-smelling, gray stool that floats on the water is characteristic of steatorrhea. Constipation may be associated with passage of small, firm, spherical masses of stool (scybala). Clay color suggests diminution or absence of bile or the presence of barium sulfate. Blood, especially blood originating from the lower gut, may cause the stool to be red; beets in the diet may mimic this. Bleeding from the upper GI tract is more likely to cause the stool to be black and have a tarry consistency. Bismuth, iron, and charcoal may also cause a black color. Stool that is allowed to stand in the air for a time may darken on the surface.

Mucus. The presence of recognizable mucus in a stool specimen is abnormal and should be reported. Translucent gelatinous mucus clinging to the surface of the formed stool suggests spastic constipation or mucous colitis. It is seen in stools of emotionally disturbed patients and may result from excessive straining. Bloody mucus clinging to the fecal mass suggests neoplasm or inflammatory processes of the rectal canal. Mucus associated with pus and blood is found in stools of patients with ulcerative colitis, bacillary dysentery, ulcerating diverticulitis, pseudomembranous colitis and intestinal tuberculosis. Patients with villous adenoma of the colon may pass copious quantities of mucus, amounting to 3 to 4 L in 24 hours. They frequently develop severe dehydration and electrolyte disturbances, especially hypokalemia.

Pus. Patients with chronic ulcerative colitis, infectious proctitis, and chronic bacillary dysentery frequently pass large quantities of pus with the stool, the recognition of which requires microscopic examination. This also occurs in patients with localized abscesses or fistulas communicating with the sigmoid colon, rectum, or anus. Large amounts of pus seldom accompany the stools of patients with amebic colitis and its presence is evidence against this diagnosis. No inflammatory exudate is seen in the watery stools of patients with viral gastroenteritis or irritable bowel syndrome.

MICROSCOPIC EXAMINATION

Fat. The simplest, most efficient, and most cost-effective method to screen for steatorrhea is microscopic stool examination using one of the Sudan stains. In our experience, results have correlated well with quantitative measurements when aliquots of the same homogenized stool have been analyzed. For this purpose, a small aliquot of stool suspension is placed on a slide and mixed with two drops of 95% ethanol. Then, two drops of

saturated ethanolic solution of Sudan III are added, with further mixing. A coverslip is then applied. Under these conditions, fatty acids appear as lightly stained flakes or as needle-like crystals that do not stain and therefore may be missed. Soaps also do not stain but appear as well-defined amorphous flakes or as rounded masses or coarse crystals. Neutral fats, however, appear as large orange or red droplets. When 60 or more stained droplets of neutral fats per high-power field (HPF) are seen, one may be reasonably certain that the patient has steatorrhea. Caution is advisable in interpretation, however, because mineral oil or castor oil may mimic neutral fat. The procedure is then repeated, adding several drops of 36% (v/v) acetic acid to the stool mixture and warming the slide several times over a flame until slight boiling occurs. This converts neutral fats and soaps to fatty acids and melts the fatty acids, causing them to form droplets that stain strongly with Sudan III. The slide is then examined while warm. After this procedure, the presence of up to 100 stained droplets per HPF is considered normal. Patients with steatorrhea of pancreatic origin are likely to have greater increases in fatty acids and soaps.

Meat Fiber. This procedure in no longer routinely utilized but is included for reference and for the rare instance of a special need. The stool sampling is identical to that used for Sudan preparations for detection of fecal fat. The stool is mixed thoroughly on a slide with a solution of eosin in 10% ethanol, allowed to stain for 3 min, and examined for muscle fibers. The entire area under the coverslip is examined, and only rectangular fibers with clearly evident cross-striations are counted. More than 10 fibers/HPF suggest maldigestion and/or hypermotility. It appears that examination for meat fibers correlates well with chemical determination of fat excretion (Moore et al., 1971). The clinician can then determine whether motility investigations or imaging studies are warranted.

Leukocytes. A small fleck of mucus or a drop of liquid stool is placed on a glass microscopic slide with a wooden applicator stick. Two drops of methylene blue are added and mixed thoroughly and carefully. A coverslip is placed on the mixture, which is allowed to stand for 2 to 3 minutes for good nuclear staining. Using low-power scanning, rough quantitative counts are made by approximating the average number of leukocytes and erythrocytes. All differential counts should be made under high power, counting 200 cells when possible. Only those cells clearly identified as either mononuclear or polymorphonuclear are included in the differential count. Macrophages and epithelial cells that cannot be clearly identified are ignored. The initial cell counts should be performed at the time of presentation of the specimen. Alternatively, fecal calprotectin (a neutrophil product) is measured in screening for inflammatory bowel disease (see Table 23.4).

ACKNOWLEDGMENT

This chapter is dedicated to the late Dr. Martin J. Salwen, who wrote and edited this chapter for many editions of this book.

SELECTED REFERENCES

Allison JE, Tekawa IS, Ransom LJ, et al.: A comparison of fecal occult-blood tests for colorectal-cancer screening, *N Engl J Med* 334:155–160, 1996.

Evaluation of three commonly used screening tests for fecal occult blood with regard to sensitivity, specificity, and predictive value related to colonoscopy and biopsy findings.

Djavan B, Zlotta A, Kratzik C, et al.: PSA, PSA density, PSA density of transition zone, free/total PSA ratio, and PSA velocity for early detection of prostate cancer in men with serum PSA 2.5 to 4.0 ng/mL, *Urology* 54:517–522, 1999.

The usage of PSA has changed the management of prostate cancer patients. This reference points out the dilemma using current PSA cutoff value and summarizes various PAS parameters to increase specificity of PSA.

Lipton A, Ali SM, Leitzel K, et al.: Elevated serum Her-2/neu level predicts decreased response to hormone therapy in metastatic breast cancer, *J Clin Oncol* 20:1467–1472, 2002.

Provides evidence that serum HER2/neu may be useful in prognosis and monitoring treatment of breast cancer patients.

National Committee for Clinical Laboratory Standards (NCCLS): Sweat testing: sample collection and quantitative analysis—Approved guidelines, Wayne, PA, 2000, National Committee for Clinical Laboratory Standards (now Clinical and Laboratory Standards Institute). NCCLS Document C34-A2.

Guideline for the performance of the sweat test for the diagnosis of cystic fibrosis. This document addresses issues pertaining to collecting, analyzing, reporting, and evaluating sweat test results. Sweat stimulation and collection and quantitative measurement of sweat chloride are described, along with quality assurance and result evaluation.

Rouprêt M, Hupertan V, Yates DR, et al.: Molecular detection of localized prostate cancer using quantitative methylation-specific PCR on urinary cells obtained following prostate massage, *Clin Cancer Res* 13:1720–1725, 2007.

Serves as an example and summary of the identification of biomarkers using current serum proteomics technology and will be the trend for future biomarkers.

Saghatchian M, Guepratte S, Hacene K, et al.: Serum HER-2 extracellular domain: Relationship with clinicobiological presentation and prognostic value before and after primary treatment in 701 breast cancer patients, *Int J Biol Markers* 19:14–22, 2004.

Provides evidence that serum HER2/neu may be useful in prognosis and monitoring treatment of breast cancer patients.

Sokoll LJ, Wians FH, Remaley AT: Rapid intraoperative immunoassay of parathyroid hormone and other hormones: a new paradigm for point-of-care testing, *Clin Chem* 50:1126–1135, 2004.

This study reviews the use of hormone-related intraoperative testing approaches, including parathyroid hormone, cortisol, gastrin, insulin, adrenocorticotropic hormone, and testosterone, regarding preoperative localization studies and/or assessment of the effectiveness of tumor resection during surgery.

Thomas PD, Forbes A, Green J, et al.: Guidelines for the investigation of chronic diarrhea, 2nd ed *Gut* 52(Suppl V):v1, 2003.

Provides guidelines to establish an optimal investigative scheme for patients presenting with chronic diarrhea to maximize positive diagnoses, while minimizing the number and invasiveness of investigations. Also features summary/recommendation tables with sections devoted to noninvasive testing.

Zhang Z, Bast Jr RC, Yu Y, et al.: Three biomarkers identified from serum proteomic analysis for the detection of early stage ovarian cancer, *Cancer Res* 64:5882–5890, 2004.

Serves as an example and summary of the identification of biomarkers using current serum proteomics technology and will be the trend for future biomarkers.

Access the complete reference list online at Elsevier eBooks for Practicing Clinicians.

REFERENCES

Adams PC, Barton JC, Hemochromatosis. *Lancet* 370:1855–1860, 2007.

Allen KR, Degg TJ, Anthoney DA, Fitzroy-Smith D: Monitoring the treatment of carcinoid disease using blood serotonin and plasma 5-hydroxyindoleacetic acid: three case examples, *Ann Clin Biochem* 44:300–3007, 2007.

Allison JE, Tekawa IS, Ransom LJ, et al.: A comparison of fecal occult-blood tests for colorectal-cancer screening, *N Engl J Med* 334:155–160, 1996.

Almoguera C, Shibata D, Forrester K, et al.: Most human carcinomas of the endocrine pancreas contain mutant c-K-ras genes, *Cell* 53:549–554, 1988.

Amarri S, Harding M, Coward WA, et al.: ^{13}C-mixed triglyceride breath test and pancreatic enzyme supplementation in children with cystic fibrosis, *Arch Dis Childhood* 76:349–351, 1997.

Andersen JM, Hedstrom J, Kemmpainen E, et al.: The ratio of trypsin-2-alpha(1)-antitrypsin to trypsinogen-1 discriminates biliary and alcohol-induced acute pancreatitis, *Clin Chem* 47:231–236, 2001.

Ashley SW, Evoy D, Daly JM: Stomach. In Schwartz SI, Shires GT, Spencer FC, et al.: *Principles of surgery*, New York, 1999, McGraw Hill, pp 1195–1196.

Atherton JC, Spiller RC: The urea breath test for *H. pylori*, *Gut* 35:723–725, 1994.

Bacon BR, Adams PC, Kowdley KV, et al.: Diagnosis and management of hemochromatosis: 2011 practice guideline by the American association for the study of liver diseases, *Hepatology* 54(1):328B343, 2011.

Baron EJ, Miller JM, Weinstein MP, et al.: A guide to utilization of the microbiology laboratory for diagnosis of infectious diseases: 2013 recommendations by the Infectious Diseases Society of America (IDSA) and the American Society for Microbiology (ASM), *Clin Infect Dis* 57:e22–e121, 2013.

Barr GD, Grehan MJ: Coeliac disease, *Med J Aust* 169:109–114, 1998.

Berna MJ, Hoffmann KM, Long SH, et al.: Serum gastrin in Zollinger-Ellison syndrome: II. Prospective study of gastrin provocative testing in 293 patients from the National Institutes of Health and comparison with 537 cases from the literature. evaluation of diagnostic criteria, proposal of new criteria, and correlations with clinical and tumoral features, *Medicine (Baltim)* 85:331–364, 2006.

Bossuyt X: Serologic markers in inflammatory bowel disease, *Clin Chem* 52(2):171–181, 2006.

Bulaj ZJ, Ajioka RS, Phillips JD, et al.: Disease-related conditions in relatives of patients with hemochromatosis, *N Engl J Med* 343:1529–1535, 2000.

Bytzer P, Stokholm M, Anderson I, et al.: Prevalence of surreptitious laxative abuse in patients with diarrhoea of uncertain origin: a cost benefit analysis of a screening procedure, *Gut* 30:1379–1384, 1989.

Cade A, Walters MP, McGinley N, et al.: Evaluation of fecal pancreatic elastase-1 as a measure of pancreatic exocrine function in children with cystic fibrosis, *Pediatr Pulmonol* 29:172–176, 2000.

Caio G, Volta U, Sapone A, et al.: Celiac disease: a comprehensive current review, *BMC Med* 17(1):142, 2019.

Capurso G, Carnuccio A, Lahner E, et al.: Corpus-predominant gastritis as a risk factor for false-negative ^{13}C-urea breath test results, *Aliment Pharmacol Ther* 24:1453–1460, 2006.

Chauhan A, Yu Q, Ray N, et al.: Global burden of neuroendocrine tumors and changing incidence in Kentucky, *Oncotarget* 9:19245–19254, 2018.

Cheng SH, Gregory RJ, Marshall J, et al.: Defective intracellular transport and processing of CFTR is the molecular basis of most cystic fibrosis, *Cell* 63:827–834, 1990.

Choi J, Kim CH, Kim D: Prospective evaluation of a new stool antigen test for the detection of *Helicobacter pylori*, in comparison with histology, rapid urease test, $^{(13)}$C-urea breath test, and serology, *J Gastroenterol Hepatol* 26:1053–1059, 2011.

Cohen JD, Javed AA, Thoburne C, Wong F, Tieg J, et al.: Combined circulating tumor DNA and protein biomarker-based liquid biopsy for the earlier detection of pancreatic cancers, *Proc Natl Acad Sci USA* 114:10202–10207, 2017.

Cohn JA, Mitchell RM, Jowell PS: The impact of cystic fibrosis and PSTI/SPINK1 gene mutations on susceptibility to chronic pancreatitis, *Clin Lab Med* 25:79, 2005.

Cryer PE, Axelrod L, Grossman AB, et al.: Evaluation and management of adult hypoglycemic disorders: an endocrine Society clinical practice guideline, *J Clin Endocrinol Metabol* 94, 2009. 709–28.

Cutler AF, Havstad S, Ma CK, et al.: Accuracy of invasive and noninvasive tests to diagnose *Helicobacter pylori* infection, *Gastroenterology* 109:136–141, 1995.

Dahlqvist A: Assay of intestinal disaccharides, *Anal Biochem* 22:99–107, 1968.

Dasari A, Shen C, Halperin D, et al.: Trends in the incidence, prevalence, and survival outcomes in patients with neuroendocrine tumors in the United States, *JAMA Oncol* 3:1335–1342, 2017.

Dechecchi MC, Tamanini A, Cabrini G: Molecular basis of cystic fibrosis: from bench to bedside, *Ann Transl Med* 6(17):334, 2018.

Dieterich W, Laag E, Schopper H, et al.: Autoantibodies to tissue transglutaminase as predictors of celiac disease, *Gastroenterology* 115:1317–1324, 1998.

DiMagno MJ, DiMagno EP: Chronic pancreatitis, *Curr Opin Gastroenterol* 21:544–554, 2005.

Ditchburn RK, Smith AH, Hayter CJ: Use of unabsorbed radioactive marker substances in a re-assessment of the radioactive triolein test of fat absorption, *J Clin Path* 24:506–514, 1971.

Doherty GM: Rare endocrine tumours of the GI tract, *Best Pract Res Clin Gastroenterol* 19, 2005. 807–17.

Duncan A: Screening for surreptitious laxative abuse, *Ann Clin Biochem* 37:1–8, 2000.

Duncan A, Hill PG: A UK survey of laboratory-based gastrointestinal investigations, *Ann Clin Biochem* 35:492–503, 1998.

Duncan A, Morris AJ, Cameron A, et al.: Laxative-induced diarrhoea - a neglected diagnosis, *J R Soc Med* 85:203–205, 1992.

Ebert EC, Nagar M: Gastrointestinal manifestations of amyloidosis, *Am J Gastroenterol* 103:776–787, 2008. 2008.

Elborn JS: Cystic fibrosis, *Lancet* 388:2519–2531, 2016.

Ensari A: Gluten-sensitive enteropathy (Celiac disease): controversies in diagnosis and classification, *Arch Pathol Lab Med* 134:826–836, 2010.

Estrella JS, Broaddus RR, Mathews A, et al.: Progesterone receptor and PTEN expression predict survival in patients with low- and intermediate-grade pancreatic neuroendocrine tumors, *Arch Pathol Lab Med* 138:1027–1036, 2014.

Etemad B, Whitcomb DC: Chronic pancreatitis. Diagnosis, classification, and new genetic developments, *Gastroenterology* 120:682–707, 2001.

Fasano A, Catassi C: Celiac disease, *N Engl J Med* 367:2419–2426, 2012.

Feldman RA, Deeks JJ, Evans SJW, et al.: Multi-laboratory comparison of eight commercially available *Helicobacter pylori* serology kits, *Eur J Clin Microbiol Infect Dis* 14:428–433, 1995.

Feldman RA, Evans SJW: Accuracy of diagnostic methods used for epidemiological studies of *Helicobacter pylori*, *Aliment Pharmacol Ther* 9(Suppl 2):21–31, 1995.

Fenner L, Widmer AF, Goy G, et al.: Rapid and reliable diagnostic algorithm for detection of *Clostridium difficile*, *J Clin Microbiol* 46:328–330, 2008.

Fenollar F, Puéchal X, Raoult D: Whipple's disease, *N Engl J Med* 356:55–66, 2007.

Fernandez R, Vizoso F, Rodriguez JC: Expression and prognostic significance of pepsinogen C in gastric carcinoma, *Ann Surg Oncol* 7:508–514, 2000.

Fine KD, Schiller LR: AGA technical review on the evaluation and management of chronic diarrhea, *Gastroenterology* 116:1464B1486, 1999.

Fordtran JS: Speculations on the pathogenesis of diarrhea, *Fed Proc* 26:1405–1414, 1967.

Forsmark CE, Baillie J: AGA Institute technical review on acute pancreatitis, *Gastroenterology* 132:2022–2044, 2007.

Forsmark CE, Vege SS, Wilcox CM: Acute pancreatitis, *N Engl J Med* 375(20):1972–1981, 2016.

Garza-González E, Perez-Perez GI, Maldonado-Garza HJ, Bosques-Padilla FJ: A review of *Helicobacter pylori* diagnosis, treatment, and methods to detect eradication, *World J Gastroenterol* 20:1438–1449, 2014.

Gisbert JP, de la Morena F, Abraira V: Accuracy of monoclonal stool antigen test for the diagnosis of *H. pylori* infection: a systematic review and meta-analysis, *Am J Gastroenterol* 101:1921–1930, 2006.

Goetze JP, Rehfeld JF: Impact of assay epitope specificity in gastrinoma diagnosis, *Clin Chem* 49:333–334, 2003.

Goff JS: Two-stage triolein breath test differentiates pancreatic insufficiency from other causes of malabsorption, *Gastroenterology* 83:44–46, 1982.

Graham DY: Can therapy ever be denied for *Helicobacter pylori* infection? *Gastroenterology* 113:S113–S117, 1997.

Green PHR, Cellier C: Celiac disease, *N Engl J Med* 357:1731–1743, 2007.

Gregg RE, Wetterau JR: The molecular basis of abetalipoproteinemia, *Curr Opin Lipidol* 5:81–86, 1994.

Guritzky RP, Rudnitsky G: Bloody neonatal diaper, *Ann Emerg Med* 27:662–664, 1996.

Halangk W, Lerch MM: Early events in acute pancreatitis, *Clin Lab Med* 25:1–15, 2005.

Han SW, Flamm R, Hachem CY, et al.: Transport and storage of *Helicobacter pylori* from gastric mucosal biopsies and clinical isolates, *Eur J Clin Microbiol Infect Dis* 14:349–352, 1995.

Helm J, Choi J, Sutphen R, et al.: Current and evolving strategies for colorectal cancer screening, *Cancer Control* 10:193–204, 2003.

Hemminki K, Li X: Incidence trends and risk factors of carcinoid tumors: a nationwide epidemiologic study from Sweden, *Cancer* 92:2204–2210, 2001.

Hernando D, Levin YS, Sirlin CB, Reeder SB: Quantification of liver iron with MRI: state of the art and remaining challenges, *J Magn Reson Imaging* 40(5):1003–1021, 2014.

Hill PG: Faecal fat: time to give it up, *Ann Clin Biochem* 38:164–167, 2001.

Hill PG: Gastric, pancreatic, and intestinal function. In Burtis CA, Ashwood ER, Bruns DE, editors: *Tietz Textbook of clinical Chemistry and molecular diagnostics*, 4th ed., Philadelphia, PA, 2006, Elsevier-Saunders.

Holmes GKT, Hill PG: Do we need to measure fecal fat? *Br Med J* 296:1552–1553, 1988.

Howes N, Greenhalf W, Stocken DD, Neoptolemos JP: Cationic trypsinogen mutations and pancreatitis, *Clin Lab Med* 25(39–59), 2005.

Hung PD, Schubert ML, Mihas AA: Zollinger-Ellison syndrome, *Curr Treat Options Gastroenterol* 6:163–170, 2003.

Husby S, Murray JA: Diagnosing coeliac disease and the potential for serological markers, *Nat Rev Gastroenterol Hepatol* 11, 2014. 655B663.

Husby S, Murray JA, Katzka DA: AGA clinical practice update on diagnosis and monitoring of celiac disease - changing utility of serology and histologic measures: expert review, *Gastroenterology* 156(4):885–889, 2019.

Imperiale TF, Ransohoff DF, Itzkowitz SH, et al.: Multitarget stool DNA testing for colorectal-cancer screening, *N Engl J Med* 370:1287–1297, 2014.

Itzkowitz S, Brand R, Jandorf L, et al.: A simplified, noninvasive stool DNA test for colorectal cancer detection, *Am J Gastroenterol* 103:2862–2870, 2008.

Jayakumar R, Lanjewar S, Axiotis CA: Loss of PTEN and increased pAKT expression distinguishes aggressive low-grade neuroendocrine tumors, *Ann Clin Lab Sci* 48:565–572, 2018.

Jensen RT: Gastrointestinal abnormalities and involvement in systemic mastocytosis, *Hematol Oncol Clin North Am* 14:579–623, 2000.

Jensen RT, Cadiot G, Brandi ML, et al.: ENETS Consensus Guidelines for the management of patients with digestive neuroendocrine neoplasms: functional pancreatic endocrine tumor syndromes, *Neuroendocrinology* 95:98–119, 2012.

Jiao Y, Shi C, Edil BH, et al.: DAXX/ATRX, MEN1, and mTOR pathway genes are frequently altered in pancreatic neuroendocrine tumors, *Science* 331:1199–1203, 2011.

Kapoor R, Moseley RH, Kapoor JR, et al.: Needle in a haystack, *N Engl J Med* 360:616–621, 2009.

Karpathakis A, Dibra H, Pipinikas C, et al.: Prognostic impact of novel molecular subtypes of small intestinal neuroendocrine tumor, *Clin Cancer Res* 22:250–258, 2016.

Kaukinen K, Partanen J, Mäki M, Collin P: HLA-DQ typing in the diagnosis of celiac disease, *Am J Gastroenterol* 97:695–699, 2002.

Kelly CP, LaMont JT: *Clostridium difficile* - more difficult than ever, *N Engl J Med* 359:1932–1940, 2008.

Khare R, Espy MJ, Cebelinski E, et al.: Comparative evaluation of two commercial multiplex panels for detection of gastrointestinal pathogens by use of clinical stool samples, *J Clin Microbiol* 52:3667–3673, 2014.

Kim J, Bamlet WR, Oberg AL, et al.: Detection of early pancreatic ductal adenocarcinoma with thrombospondin-2 and CA19-9 blood markers, *Sci Transl Med* 12(9), 2017. (eaah5583).

Kindmark H, Sundin A, Granberg D, et al.: Endocrine pancreatic tumors with glucagon hypersecretion: a retrospective study of 23 cases during 20 years, *Med Oncol* 24:330–337, 2007.

Kleinman DS, O'Brien JF: *Macroamylase*, *Mayo Clin Proc* 61:669–670, 1986.

Klöppel G, La Rosa S: Ki67 labeling index: assessment and prognostic role in gastroenteropancreatic neuroendocrine neoplasms, *Virchows Arch* 472:341–349, 2018.

Konukiewitz B, Schlitter AM, Jesinghaus M, et al.: Somatostatin receptor expression related to TP53 and RB1 alterations in pancreatic and extrapancreatic neuroendocrine neoplasms with a Ki67-index above 20, *Mod Pathol* 30:587–598, 2017.

Korkmaz H, Kesli R, Karabagli P, Terzi Y: Comparison of the diagnostic accuracy of five different stool antigen tests for the diagnosis of *Helicobacter pylori* infection, *Helicobacter* 18:384–391, 2013.

Krasilnikoff PA, Gudman-Hoyer E, Moltke HH: Diagnostic value of disaccharide tolerance tests in children, *Acta Paediatr Scand* 64:693–698, 1975.

Lankisch PG: Now that fecal elastase is available in the United States, should clinicians start using it? *Curr Gastroenterol Rep* 6:126–131, 2004.

Lankisch PG, Apte M, Banks PA: Acute pancreatitis, *Lancet* 386:85–96, 2015.

Lankisch PG, Mahlke R, Blum T, et al.: Hemoconcentration: an early marker of severe and/or necrotizing pancreatitis? A critical appraisal, *Am J Gastroenterol* 96:2081–2085, 2001.

LaSala PR, Svensson AM, Mohammad AA, Perrotta PL: Comparison of analytical and clinical performance of three methods for detection of *Clostridium difficile*, *Arch Pathol Lab Med* 136:527–531, 2012.

LeGrys VA, Yankaskas JR, Quittell LM, et al.: Diagnostic sweat testing: the cystic fibrosis Foundation guidelines, *J Pediatr* 151:85–89, 2007.

Leus J, Van Biervliet S, Robberecht E: Detection and follow up of exocrine pancreatic insufficiency in cystic fibrosis: a review, *Eur J Pediatr* 159:563–568, 2000.

Lewis JD, Kroser J, Bevan J, et al.: Urease-based tests for *Helicobacter pylori* gastritis. Accurate for diagnosis but poor correlation with disease severity, *J Clin Gastroenterol* 25:415–420, 1997.

Lieberman DA: Clinical practice: screening for colorectal cancer, *N Engl J Med* 361:1179–1187, 2009.

Liu AY, Lowe RC, Levy BD, et al.: Clinical problem-solving: a rash hypothesis, *N Engl J Med* 363:72–78, 2010.

Lüth S, Teyssen S, Forssmann K, et al.: Fecal elastase-1 determination: gold standard of indirect pancreatic function tests? *Scand J Gastroenterol* 36:1092–1099, 2001.

McRury JM, Barry RC: A modified Apt test: a new look at an old test, *Pediatr Emerg Care* 10:189–191, *Erratum: Pediatr Emerg Care* 10:248, 1994. 1994.

Malfertheiner P, Megraud F, O'Morain C, et al.: Current concepts in the management of *Helicobacter pylori* infection: the Maastricht III consensus report, *Gut* 56:772–781, 2007.

Malnick S, Zimhony O: Treatment of *Clostridium difficile*-associated diarrhea, *Ann Pharmacother* 36:1767–1775, 2000.

Marth T: Raoult D: Whipple's disease, *Lancet* 361:239–246, 2003.

Mitsuyama K, Niwa M, Takedatsu H, et al.: Antibody markers in the diagnosis of inflammatory bowel disease, *World J Gastroenterol* 22(3):1304–1310, 2016.

Miki K, Morita M, Sasajima M, et al.: Usefulness of gastric cancer screening using the serum pepsinogen test method, *Am J Gastroenterol* 98:735–739, 2003.

Minn AH, Kayton M, Lorang D, et al.: Insulinomas and expression of an insulin splice variant, *Lancet* 363:363–367, 2004.

Moore JG, Englert Jr E, Bigler AH, Clark RW: Simple fecal tests of absorption: a prospective study and critique, *Digestive Dis Sci* 16:97–105, 1971.

Mukerjee H, Pincus MR: A colorometric determination for 5-hydroxyindole acetic acid in urine, *Clin Chim Acta* 209:105–106, 1992.

Nandiwada SL, Tebo AE: Testing for antireticulin antibodies in patients with celiac disease is obsolete: a review of recommendations for serologic screening and the literature, *Clin Vaccine Immunol* 20:447–451, 2013.

NCCLS - National Committee for Clinical Laboratory Standards: Sweat testing: sample collection and quantitative analysis: Approved guidelines. *NCCLS document* C34-A2. Wayne, PA, 2000, National Committee for Clinical Laboratory Standards (now Clinical Laboratory Standards Institute).

Ndip RN, MacKay WG, Farthing MJ, Weaver LT: Culturing *Helicobacter pylori* from clinical specimens: review of microbiologic methods, *J Pediatr Gastroenterol Nutr* 36:616–622, 2003.

O'Toole D, Grossman A, Gross D, et al.: Mallorca consensus Conference participants, European neuroendocrine tumor Society: ENETS consensus guidelines for the standards of care in neuroendocrine tumors: biochemical markers, *Neuroendocrinology* 90:194–202, 2009.

Papachristou GI, Whitcomb DC: Inflammatory markers of disease severity in acute pancreatitis, *Clin Lab Med* 25:17–37, 2005.

Paulos S, Saugar JM, de Lucio A, et al.: Comparative performance evaluation of four commercial multiplex real-time PCR assays for the detection of the diarrhea-causing protozoa *Cryptosporidium hominis/parvum*, *Giardia duodenalis* and *Entamoeba histolytica*, *PloS One* 14, 2019. e0215068.

Peterson WL: *Helicobacter pylori* and peptic ulcer disease, *N Engl J Med* 324:1043–1048, 1991.

Phillips S, Rowe DJ, Dewar P, et al.: Fecal elastase 1: a marker of pancreatic insufficiency in cystic fibrosis, *Ann Clin Biochem* 36:739–742, 1999.

Pitt SC, Davis R, Kunnimalaiyaan M, Chen H: AKT and PTEN expression in human gastrointestinal carcinoid tumors, *Am J Transl Res* 1:291–299, 2009.

Powell LW: Diagnosis of hemochromatosis, *Semin Gasrointest Dis* 13:80–88, 2002.

Powell LW, Sekington RC, Deugnier Y: *Hemochromatosis*, *Lancet* 388:706–716, 2016.

Poutanen SM, Simor AE: *Clostridium difficile* - associated diarrhea in adults, *Can Med Assoc J* 171:51–58, 2004.

Quinton JF, Sendid B, Reumaux D, et al.: Anti-Saccharomyces cerevisiae mannan antibodies combined with antineutrophil cytoplasmic autoantibodies in inflammatory bowel disease: prevalence and diagnostic role, *Gut* 42(6):788–791, 1998.

Ramzan NN, Loftus Jr E, Burgart LJ, et al.: Diagnosis and monitoring of Whipple disease by polymerase chain reaction, *Ann Intern Med* 126:520–527, 1997.

Raoult D, Fenollar F, Birg M-L: Culture of *T. whipplei* from the stool of a patient with Whipple's disease, *N Engl J Med* 355:1503–1505, 2006.

Remaley AT, Wilding P: Macroenzymes: biochemical characterization, clinical significance, and laboratory detection, *Clin Chem* 35:2261–2270, 1989.

Rex DK, Boland CR, Dominitz JA: Colorectal cancer screening: recommendations for physicians and patients from the U.S. Multi-society Task Force on colorectal cancer, *Am J Gastroenterol* 112(7):1016–1030, 2017.

Rindi G, Klimstra DS, Abedi-Ardekani B, et al.: A common classification framework for neuroendocrine neoplasms: an International Agency for Research on Cancer (IARC) and World Health Organization (WHO) expert consensus proposal, *Mod Pathol* 31:1770–1786, 2018.

Rockey DC: Occult and obscure gastrointestinal bleeding: causes and clinical management, *Nat Rev Gastroenterol Hepatol* 7:265–279, 2010.

Rosenstein BJ, Cutting JR: The diagnosis of cystic fibrosis: a consensus statement, *J Pediatr* 132:589–595, 1998.

Rubio-Tapia A, Hill ID, Kelly CP, et al.: ACG clinical guidelines: diagnosis and management of celiac disease, *Am J Gastroenterol* 108, 2013. 656-576.

Rutgeerts P, Vermeire S: Serologic diagnosis of inflammatory bowel disease, *Lancet* 356:2117–2118, 2000.

Sabatino AS, Corazza GR: Coeliac disease, *Lancet* 373:1480–1493, 2009.

Samloff IM: Pepsinogens I and II: Purification from gastric mucosa and radioimmunoassay in serum, *Gastroenterology* 82:26–33, 1982.

Sanchez TH, Brooks JT, Sullivan PS, et al.: Bacterial diarrhea in persons with HIV infection, United States, 1992-2002, *Clin Infect Dis* 41:1621–1627, 2005.

Scarpa A, Chang DK, Nones K, et al.: Whole-genome landscape of pancreatic neuroendocrine tumours, *Nature* 543:65–71, 2017.

Schneider A: Serine protease inhibitor kazal type 1 mutations and pancreatitis, *Clin Lab Med* 25:61–78, 2005.

Schneider A, Barmada MM, Slivka A, et al.: Clinical characterization of patients with idiopathic chronic pancreatitis and SPINK1 mutations, *Scand J Gastroenterol* 39:903–904, 2004.

Service FJ, McMahon MM, O'Brien PC, Ballard DJ: Functioning insulinoma - incidence, recurrence, and long-term survival of patients: a 60-year study, *Mayo Clin Proc* 66:711–719, 1991.

Shanahan F: Neutrophil autoantibodies in inflammatory bowel disease: are they important? *Gastroenterology* 107:586–590, 1994.

Shane AL, Mody RK, Crump JA, et al.: Infectious Diseases Society of America clinical practice guidelines for the diagnosis and management of infectious diarrhea, *Clin Infect Dis* 65:e45–e80, 2017. 2017.

Shi C, Hruban RH, Klein AP: Familial pancreatic cancer, *Arch Pathol Lab Med* 133:365–374, 2009.

Simon JB: Fecal occult blood testing: clinical value and limitations, *Gastroenterol* 6:66–78, 1998.

Singer R: Diagnosis and treatment of Whipple's disease, *Drugs* 55:699–704, 1998.

Sjoblom SM: Clinical presentation and prognosis of gastrointestinal carcinoid tumours, *Scand J Gastroenterol* 23:779–787, 1988.

Smith SB, Snow AN, Perry RL, Qasem SA: *Helicobacter pylori*: to stain or not to stain? *Am J Clin Pathol* 137:733–738, 2012.

Smotkin J, Tenner S: Laboratory diagnostic tests in acute pancreatitis, *J Clin Gastroenterol* 34:459–462, 2002.

Sokoll LJ, Wians FH, Remaley AT: Rapid intraoperative immunoassay of parathyroid hormone and other hormones: a new paradigm for point-of-care testing, *Clin Chem* 50:1126–1135, 2004.

Staal B, Liu Y, Barnett D, et al.: The sTRA plasma biomarker: blinded validation of improved accuracy over CA19-9 in pancreatic cancer diagnosis, *Clin Cancer Res* 25:2745–2754, 2019.

Stridsberg M, Eriksson B, Oberg K, Janson ET: A comparison between three commercial kits for chromogranin A measurements, *J Endocrinol* 177:337–341, 2003.

Suerbaum S, Michetti P: *Helicobacter pylori* infection, *N Engl J Med* 347(15):1175–1186, 2002.

Surawicz CM, Brandt LJ, Binion DG, et al.: Guidelines for diagnosis, treatment, and prevention of *Clostridium difficile* infections, *Am J Gastroenterol* 108:478–498, 2013.

Svensson AM, LaSala PR: Pathology consultation on detection of *Clostridium difficile*, *Am J Clin Pathol* 13:10–15, 2012.

Tellez MR, Mamikunian G, O'Dorisio TM, et al.: A single fasting plasma 5-HIAA value correlates with 24-hour urinary 5-HIAA values and other biomarkers in midgut neuroendocrine tumors (NETs), *Pancreas* 42:405–410, 2013.

Thiede C, Morgner A, Alpen B, et al.: What role does *Helicobacter pylori* eradication play in gastric MALT and gastric MALT lymphoma? *Gastroenterology* 113:S61–S64, 1997.

Thom AK, Norton JA, Axiotis CA, Jensen RT: Location, incidence, and malignant potential of duodenal gastrinomas, *Surgery* 110:1086–1091, 1991. discussion: 1091–1093, 1991.

Thomas PD, Forbes A, Green J, et al.: Guidelines for the investigation of chronic diarrhea, 2nd ed *Gut* 52(Suppl V):v1–v15, 2003.

Tortora R, Imperatore N, Capone P: The presence of anti-endomysial antibodies and the level of anti-tissue transglutaminases can be used to diagnose adult coeliac disease without duodenal biopsy, *Aliment Pharmacol Ther* 40:1223–1229, 2014.

Treacy J, Williams A, Bais R, et al.: Evaluation of amylase and lipase in the diagnosis of acute pancreatitis, *ANZ J Surg* 71:577–582, 2001.

Turner JM, Lawrence S, Fellows IW, et al.: [^{14}C]-triolein absorption: a useful test in the diagnosis of malabsorption, *Gut* 28:694–700, 1987.

Van Deun A, Cobbaert C, Van Orshoven A, et al.: Comparison of some recent methods for the differentiation of elevated serum amylase and the detection of macroamylasaemia, *Ann Clin Biochem* 26:422–426, 1989.

van de Wouw BAM, de Boer WA, Jansz AR, et al.: Comparison of three commercially available enzyme-linked immunosorbent assays and biopsy-dependent diagnosis for detecting *Helicobacter pylori* infection, *J Clin Microbiol* 34:94–97, 1996.

Vantrappen GR, Rutgeerts PJ, Ghoos YF, Hiele MI: Mixed triglyceride breath test: a noninvasive test of pancreatic lipase activity in the duodenum, *Gastroenterology* 96:1126–1134, 1989.

Verner JV, Morrison AB: Islet cell tumor and a syndrome of refractory watery diarrhea and hypokalemia, *Am J Med* 25:374–380, 1958.

Volta U, Molinaro N, de Franceschi L, et al.: IgA anti-endomyseal antibodies on human umbilical cord tissue for celiac disease screening. Save both money and monkeys, *Dig Dis Sci* 40:1902–1908, 1995.

Von Herbay A, Ditton HJ, Schuhmacher F, Maiwald M: Whipple's disease: staging and monitoring by cytology and polymerase chain reaction analysis of cerebrospinal fluid, *Gastroenterology* 113:434–441, 1997.

Vortmeyer AO, Huang S, Lubensky I, Zhuang Z: Non-islet origin of pancreatic islet cell tumors, *J Clin Endocrinol Metab* 89:1934–1938, 2004.

Wang XI, Zhang S, Abreo F, Thomas J: The role of routine immunohistochemistry for *Helicobacter pylori* in gastric biopsy, *Ann Diagn Pathol* 14:256–259, 2010.

Wermers RA, Fatourechi V, Wynne AG, et al.: The glucagonoma syndrome. Clinical and pathologic features in 21 patients, *Medicine (Baltim)* 75:53–63, 1996.

West PS, Levin GS, Griffin GE, Mazwell JD: Comparison of simple screening tests for fat malabsorption, *Br Med J* 282:1501–1504, 1981.

WHO: http://www.who.int/topics/diarrhoea/en/, 2009.

Wilson C, Imire CW, Carter DC: Fatal acute pancreatitis, *Gut* 29:782–788, 1985.

Whitcomb DC: Genetic predispositions to acute and chronic pancreatitis, *Med Clin North Am* 84:531–547, 2000.

Wotherspoon AC: Gastric lymphoma of mucosa-associated lymphoid tissue and *Helicobacter pylori*, *Annu Rev Med* 49:289–299, 1998.

Wu BU, Johannes RS, Sun X, et al.: Early changes in blood urea nitrogen predict mortality in acute pancreatitis, *Gastroenterology* 137:129–135, 2009.

Xia HX, Keane CT, O=Morain CA: Pre-formed urease activity of *Helicobacter pylori* as determined by a variable cell count technique - clinical implications, *J Med Microbiol* 40:435–439, 1994.

Zimmer T, Stölzel U, Bäder M, et al.: Brief report: a duodenal gastrinoma in a patient with diarrhea and normal serum gastrin concentrations, *N Engl J Med* 333:634–636, 1995.

CHAPTER 24

TOXICOLOGY AND THERAPEUTIC DRUG MONITORING

Martin H. Bluth, Matthew R. Pincus, Naif Z. Abraham Jr.

BASIC TECHNIQUES FOR DETECTING DRUGS IN SERUM AND URINE, 347
Immunochemical Methods, 348
Drug Binding to Antibodies, 348
Chromatographic Techniques, 348
Screening For Drugs of Abuse, 354
THE DRUGS OF ABUSE, 354
General Aspects of the Mechanisms of Action, 354
Extent of Use of Drugs of Abuse, 354
Cocaine, 358
Amphetamines, 360
Tryptamines, 361
Piperazines, 361
Benzodiazepines, 361
Phencyclidine, 362
Barbiturates: Sedative-Hypnotics, 362
Propoxyphene (Darvon), 362
Methaqualone (Quaalude), 362
Marijuana (Cannabis), 362
Lysergic Acid Diethylamide (Lysergide), 363
Cathinones (Bath Salts; Class 8), 363
Sleep Aids (Class 9), 363
Muscle Relaxants (Class 10), 364
Other Drugs, 364
THERAPEUTIC DRUG MONITORING, 364
Pharmacokinetics, 364
Cardiotropics, 366
Anticonvulsants, 369
Antiasthmatics, 371
Antiinflammatory and Analgesic Drugs, 372
Immunosuppressives, 374
TOXINS AND ACUTE POISONING, 380
Environmental Carcinogens, 380
Cyanide, 380
Carbon Monoxide, 380
Alcohols and Glycols, 381
Arsenic, 382
Mercury, 382
Iron, 383
Lead, 383
Organophosphates and Carbamates, 384
Mycotoxins, 385
Nicotine and Metabolites, 385
CONCLUSION, 386
SELECTED REFERENCES, 386

KEY POINTS

- Testing for the presence of drugs in the blood and other body fluids of patients has undergone a vast increase over the past 20 years.
- Testing for the presence of drugs of abuse and/or poisons in patients has become mandatory both in the emergency department and in employment screening.
- Most drugs for which monitoring is standard can be assayed using homogeneous immunologic techniques.
- Gas and liquid chromatography–mass spectroscopy, which involve separation and identification of compounds in the gas phase from their mass/charge ratios and fragmentation patterns, are the gold standards for detection and quantitation of drugs in body fluids.
- The mechanisms of action of many therapeutic drugs have been at least partially elucidated. Many of these, such as the antiinflammatory, antiasthmatic, and immunosuppressive drugs, block specific points in signal transduction pathways.
- Ingestion of poisons causes life-threatening illness; poisons include cyanide, carbon monoxide, and a number of metals, such as lead, mercury, iron, and arsenic. If detected, the effects of these poisons can often be reversed.
- Interpretation of results for drugs of abuse must be made in conjunction with other signs and symptoms for appropriate patient management.

Toxicology is the study of substances introduced exogenously into the body. Elsewhere in this textbook, the analytic methods presented are concerned with determining the presence and levels of natural substances involved in normal body function. In this chapter, we discuss the biological effects and methods for detection of exogenous chemical compounds that profoundly influence bodily functions, often in a deleterious way but also for therapeutic benefit.

Toxicology has become divided into four areas. The first two areas are the detection of drugs of abuse and the determination of levels of therapeutic drugs being administered to patients. Also, it has been recognized that certain environmental compounds that are mutagens and carcinogens, such as benzopyrene and acetylaminofluorene, cause mutations in critical sequences of human DNA, leading to the frank development of cancer. In the ongoing revolution in molecular biology, this field has now expanded into the detection of certain markers such as abnormal DNA sequences, the presence of mutated proteins, or the presence of carcinogens bound to DNA. This rapidly expanding field is the subject of discussion in Parts 8 and 9, especially in the chapters concerning serum and solid-tissue diagnostic markers for cancer and pharmacogenomics. Finally, there are numerous toxins to which individuals become exposed, such as carbon monoxide, cyanide, metals, and so forth, for which detection is vital if physicians are to be able to reverse the adverse acute physiologic effects. In this chapter, we discuss each of these divisions of toxicology with special reference to the detection of drugs and toxins in body fluids In the course of this chapter, drug dosages for some therapeutic drugs are noted. These dosages are approximate and are noted only as examples, i.e., typical dosages that have been found to give levels of the drug in serum or in other body fluids that are usually, but not always, therapeutic. These listed doses are not in any way to be taken as endorsements of these doses and are not recommended doses. They serve merely as examples.

BASIC TECHNIQUES FOR DETECTING DRUGS IN SERUM AND URINE

The techniques involved in detecting the presence and/or the level of particular drugs, whether they are drugs of abuse or therapeutic drugs, are of two basic types: immunochemical and chromatographic.

IMMUNOCHEMICAL METHODS

Much drug testing today is performed using the so-called **homogeneous immunoassay**. The term *homogeneous* refers to the fact that these assays are all performed in solution, without any requirement for a phase separation that is traditionally used to separate bound from free ligand. This technology has revolutionized toxicology because it allows performance of rapid, stat analyses of blood and urine constituents. The technique is shown schematically in Figure 24.1. Here, we show examples of two types of assays. In the first, the enzyme-mediated (or multiplied) immunologic technique (EMIT), the drug itself is covalently attached to an enzyme such as glucose-6-phosphate dehydrogenase (Fig. 24.1A-1). When the drug-enzyme complex is incubated with an antibody to the drug, enzyme activity is markedly decreased as a result of blocking of the active site of the enzyme by the antibody. When, as in Figure 24.1A-2, exogenous drug (such as in serum) is added to the immune complex, this exogenous drug competes with the drug-enzyme complex for the antibody. Liberated drug-enzyme results in increased enzymatic activity. Increasing concentrations of drug in serum result in increased observed enzymatic activity. This method was pioneered largely by the Syva Corporation (now part of Siemens, Palo Alto, CA) and has been applied both to therapeutic drug monitoring and to detection of drugs of abuse.

Fluorescence polarization immunoassay (FPIA) is the second type of homogeneous drug assay, as shown in Figure 24.1B. Rather than being linked to an enzyme, as in Figure 24.1A, the drug is covalently attached to a fluorescent probe molecule. If a fluorescent molecule is excited with polarized light and is stationary (i.e., it does not "tumble" in solution), it will emit polarized light as a fluorophore. This emitted light has the same polarization as the exciting light. Thus, for example, if the exciting light is polarized to the left, the emitted light will also be polarized to the left. If a fluorophore tumbles freely in solution, however, the polarization is lost; that is, the emitted light is now polarized equally to the left and right. However, if the fluorophore is bound to a macromolecule such as an antibody, the polarization is strong because attached to the nontumbling antibody it remains relatively stationary. In these assays, the probe-labeled drug is incubated with the antibody. The fluorescence polarization of the probe-labeled drug is, of course, high because the fluorescence probe is relatively immobilized when bound to the antibody directed against it (Fig. 24.1B-1). Addition of exogenous drug, as in serum, to the incubated mixture results in displacement by the exogenous drug of some of the fluorescent probe-labeled drug molecules, as shown in Figure 24.1B-2. These displaced molecules can now tumble freely in solution. The result is a decrease in fluorescence polarization. This decrease is directly related to the concentration of drug in serum.

This assay can detect drug levels in the nanomolar range and is both highly sensitive and specific. Both Abbott Laboratories (Chicago), currently on the Architect Analyzer and formerly on the TDX, IMX, and AXSYM analyzers, and Roche Diagnostic Laboratories (Nutley, NJ), on the COBAS and INTEGRA analyzers, have pioneered this effective technique in monitoring a wide variety of therapeutic drugs and drugs of abuse.

DRUG BINDING TO ANTIBODIES

In both of the homogeneous methods discussed previously, a nonlinear relationship exists between the concentration of drug in serum and the response of the system—that is, the color that results from the enzymatic reaction (see Fig. 24.1A) or the decrease in fluorescence polarization (see Fig. 24.1B). This nonlinearity in response is due to the phenomenon of binding (i.e., the drug must bind to antibody before it is detected). This phenomenon may be expressed by the following equilibrium:

$$D + D\text{–}Ab \leftrightarrow D\text{–}Ab + D^* \qquad \text{(Eq. 24.1)}$$

where D is the drug concentration in serum, D* is the "marker" drug (i.e., drug labeled with an enzyme or a fluorescent probe), and Ab is the antibody. The concentration of free D* is a measure of D–Ab, because both are equimolar. The concentration of D–Ab is, in turn, related to D; the more D is present, the more D–Ab is formed. However, because the concentration of Ab is fixed in a given experiment, at sufficiently high concentrations of D, all of the Ab will be saturated so that at higher concentrations of D, no further D–Ab can form. The relationship between D and D–Ab is given by the Langmuir expression:

$$r = (D\text{–}Ab)/(Ab_0) = nkD/(kD + 1) \qquad \text{(Eq. 24.2)}$$

where (Ab_0) is the total concentration of antibody, k is the equilibrium constant for formation of the D–Ab complex, n is the number of antibody-binding sites per molecule of antibody, and D is free drug concentration as defined earlier in the chapter. Equation 24.2 is very similar to the Michaelis-Menten equation discussed in Chapter 21 (Eq. 21.10), except that there is no catalytic step here. This equation shows that the concentration of D–Ab is nonlinear in D, except where $Kd \ll 1$. Where $kD \gg 1$, saturation is achieved. This equation can be linearized in the form used for a Scatchard plot, that is,

$$r/D = kn - kr \qquad \text{(Eq. 24.3)}$$

where r/D is plotted versus r. Given the results for a set of experiments, a least-squares–best-fit line is drawn through the points. The slope of the line is –k, and the intercept is nk, so that n (the number of sites on the antibody) is equal to the intercept/slope. Thus, the values of n and k are readily determined. Once values for n and k are known, the value of D for any measured value of r can be directly computed from Equation 24.3.

Two problems that arise in using Equation 24.3 are that often the antibodies are nonhomogeneous so that the Scatchard plot is nonlinear, and possible blockage of free antibody sites by drug molecules is seen in solid-phase immunoassays. The first problem was solved by Rodbard and colleagues (1971), wherein the analysis mentioned previously was applied to multiple-binding equilibria. This analysis is used commonly in microprocessors that analyze the calibration curves in immunoassays. The second problem has been analyzed using a different theoretical approach (Pincus & Rendell, 1981). Equation 24.3 illustrates the basic principle of how the results of the drug immunoassay on serum are converted into drug concentrations in serum.

CHROMATOGRAPHIC TECHNIQUES

Chromatographic procedures (see Engelhardt, 2004, for an excellent brief history of liquid chromatography, and Chapter 4) have been applied mainly to the qualitative detection of drugs of abuse and toxins and less to the determination of levels of therapeutic drugs. The three major methods are thin-layer chromatography (TLC), high-performance liquid chromatography (HPLC), and gas chromatography–mass spectroscopy (GC-MS). Although GC-MS is considered the gold standard for detection and quantitation of volatile drugs and poisons, newer analytic techniques such as capillary electrophoresis (CE) and liquid chromatography–mass spectroscopy (LC-MS) and mass spectroscopy-mass spectroscopy (MS-MS) are available. These techniques are all discussed in turn.

Thin-Layer Chromatography

Many compounds can be separated from one another with this method based on their relative affinities for a polar solid stationary phase (usually a hydrated silicate) and a mobile liquid phase that is nonpolar (such as 10% methanol in chloroform). Depending on these affinities, different compounds adsorb to the hydrated silicate at different positions as the nonpolar solvent migrates up the stationary hydrated silicate. This principle is illustrated in Figure 24.2. For a given solvent system, the ratio of the distance traversed by the compound to the distance traversed by the solvent front is a constant for the compound and can be used to identify the compound in a mixture. This ratio is called the $\mathbf{r_f}$. This technique is central to identifying different drugs of abuse, many of which can be separated from one another using TLC. The method has been packaged in the form of Toxi-Lab kits (Irvine, CA) in which the user is supplied with discrete strips of silicate, extraction solvents, and color-developing solutions.

Toxi-Lab Procedures

The best specimen for drug detection by chromatography is urine because large quantities can be collected noninvasively. Once a urine specimen is collected, it is subjected to concentration and extraction procedures. In extraction procedures, acidic drugs are separated from basic ones. Almost all drugs of abuse are basic drugs, all of which are amine derivatives. The

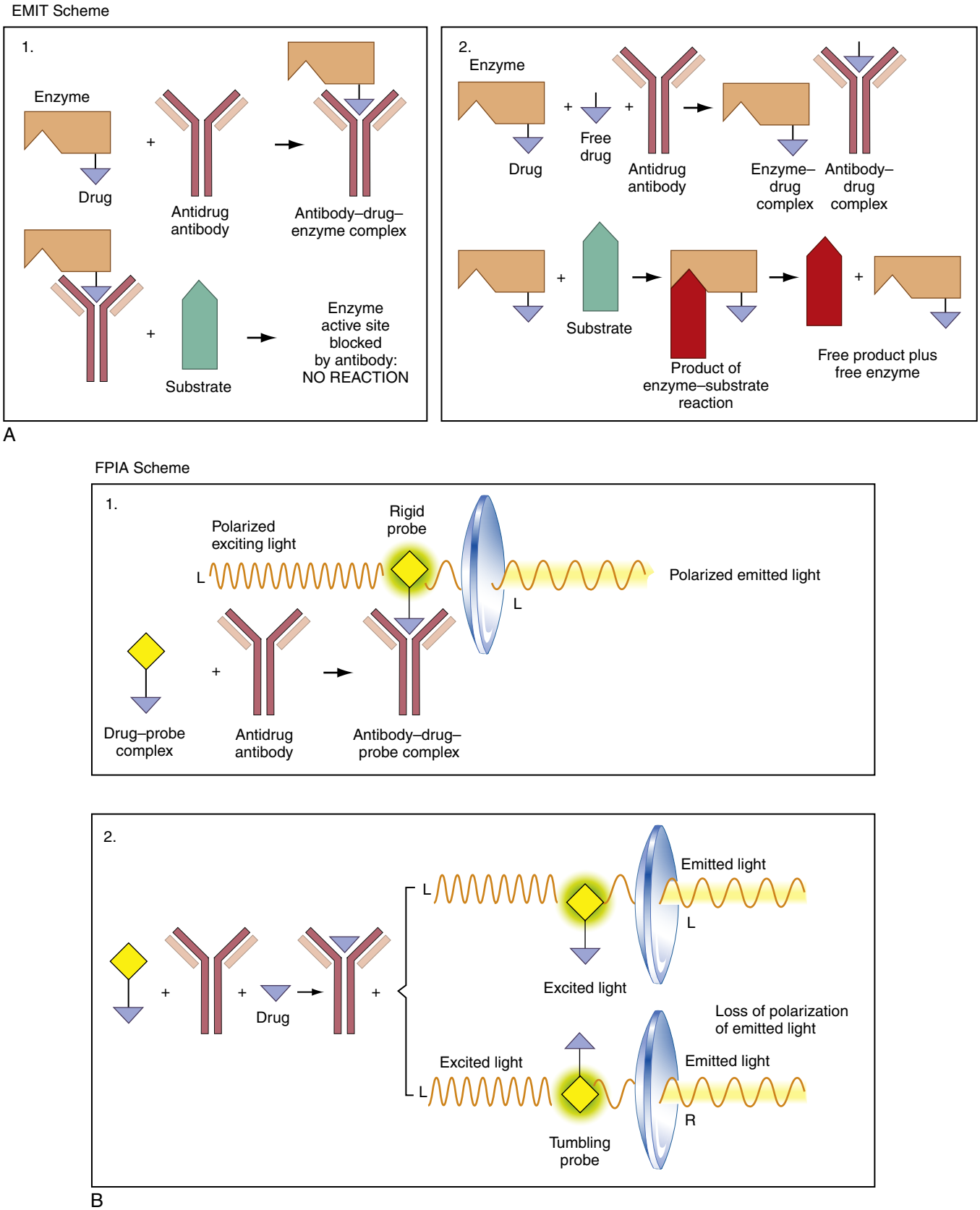

Figure 24.1 Homogeneous methods for detecting qualitatively or quantitatively the levels of drugs in body fluids. A, In the enzyme-mediated immunologic technique (EMIT), a drug-enzyme complex is used as the marker. When bound to the antidrug antibody, the active site of the enzyme (linked to the drug) is blocked. Therefore, when substrate is added, no reaction will occur, as is shown in Part 1. However, if free drug (as in serum) is present, some or most of the enzyme-drug complex is displaced from the antidrug antibody. Now the active sites of the liberated enzyme-drug complexes are free, and the substrate undergoes reactions as indicated in Part 2. B, In the fluorescence polarization immunoassay assay (FPIA), the same general approach is used as in A, except that, in this method, the drug is attached to a fluorescent label or fluorophore. As shown in the upper scheme, Part 1, when the drug-label complex is bound to the antidrug antibody, it becomes immobilized *("rigid probe")*. When excited with polarized light *(shown as polarized to the left, or "L")*, the fluorophore emits light, which is likewise polarized to the left *(also seen as "L" in the figure)*. As shown in the lower scheme, Part 2, when displaced by free drug, as in serum or urine, the drug-probe complex is displaced from the antidrug antibody. It is no longer immobilized and therefore tumbles freely in solution. This results in loss of polarization of the emitted light ("L" and "R," for left and right polarization), that is, in diminished fluorescence polarization.

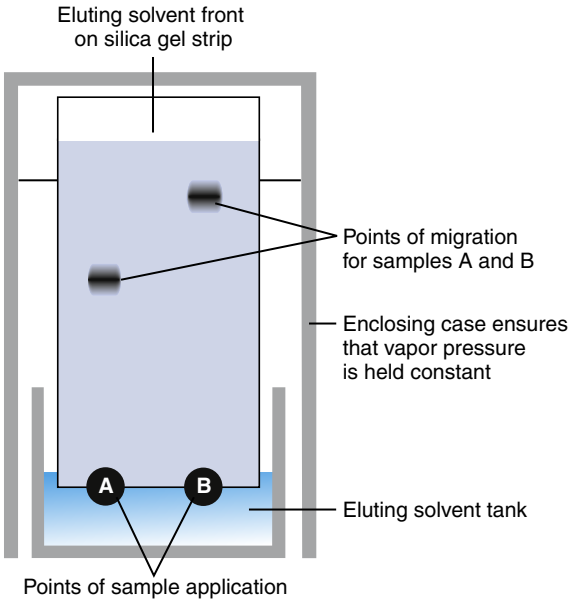

Figure 24.2 Illustration of the principle of thin-layer chromatography (TLC). Two solutes, A and B, are applied to the polar silicate strip. A is more polar than B and has a higher affinity, therefore, for the polar stationary phase than for the nonpolar mobile phase (usually methanol in chloroform). Moreover, this relative affinity of A is higher than the affinity of B for the polar phase. Therefore, A separates out first on the strip, and B migrates further on the strip.

important **acid drugs** comprise almost exclusively the barbiturates. In aqueous solution, the basic drugs are charged because of the equilibrium in Equation 24.4A:

$$R{-}NH_2 + H^+ \leftrightarrow R{-}NH_3^+ \qquad \text{(Eq. 24.4A)}$$

$$R{-}NH_3^+ + OH^- \leftrightarrow R{-}NH_2 + H_2O \qquad \text{(Eq. 24.4B)}$$

in which a primary amine (secondary and tertiary amines exhibit the same equilibrium) is represented by RNH_2. The ammonium ion form (right side of Eq. 24.4A) is soluble in water but not in nonpolar organic solvents. However, the amine-free base (left side of Eq. 24.4A) is soluble in nonpolar organic solvents. Extraction procedures to isolate the basic drugs are aimed at treating the urine with base so that significant amounts of the basic drugs will be uncharged as the amine-free base (Eq. 24.4B). This form can then be extracted into a nonpolar organic phase and applied to the silicate strip. The reverse process is carried out for acidic drugs (i.e., these are treated with acid and are extracted into nonpolar solvents). In practice, a small paper disk is added to the organic extraction mixture; the solvent is then evaporated so that all basic drugs adsorb onto the paper disk. This disk is then applied to one end of the silicate strip, and the strip is placed in the migrating nonpolar solvent. A separate strip is used for each extraction; the A strip is used for basic drugs and the B strip for acidic drugs. The chief utility of the B strip is in identifying the barbiturates, as is discussed subsequently.

Identification of Specific Drugs

After separation of the drugs on the plate, it is necessary to identify them. This objective is achieved by subjecting the drugs to standard color reactions for each separate compound. In this procedure for basic drugs, the strip is simply dipped successively in three different solvents, which results in characteristic color patterns for each drug. The strip is also subjected to ultraviolet (UV) light, which excites fluorescence in selected compounds. Similar procedures are used for the acidic drugs extracted onto the B strip. As shown in Figure 24.3, which is from the Toxi-Lab reference pattern book, each drug can be identified not only by its r_f but also by its color and characteristic color change in different reagents. These patterns are reinforced by the fluorescence characteristics. As an example, notice in Figure 24.3A on the Toxi-Lab A worksheet that morphine, the main metabolite of heroin, has a characteristic r_f of 0.14 and a characteristic dark-red or purple color in the first solvent that diminishes in intensity and changes color in the second solvent, water. It is nonfluorescent. If one or more of these characteristics differ(s) from this pattern, strong doubt about identification of the spot as morphine would exist. If all criteria are met, the sensitivity and specificity of the method are increased.

Reliability of the Method

Because the identification of each drug depends on the use of qualitative color changes and/or the presence of fluorescence, the sensitivity of the method is limited by the ability of the naked eye to detect these changes. Practically, the level of detection is on the order of 1 μg/mL of compound present on the strip. The chief value of the chromatographic method is confirmatory (i.e., confirmation of a positive immunoassay test result). The two methods are often performed together on a single specimen.

The major problems that occur with this method are that extraction procedures are occasionally inefficient so that insufficient amounts of drug are absorbed onto the disk. Also, the extraction and evaporation procedures are somewhat time-consuming, requiring approximately a half-hour for full processing. Furthermore, cocaine has a number of metabolites that are polar (e.g., ecgonine) and that barely migrate from the origin. Thus, it is sometimes difficult to detect the presence of this drug of abuse because it has been converted completely to the polar metabolites before excretion. Some difficulty may also be encountered in distinguishing among various opiates, such as between morphine and other opiates, because the r_f values of these drugs can be close to one another (see Fig. 24.3). However, experienced personnel can make this distinction in most cases. Also, some nontoxic drugs may give characteristic color changes and r_f values that are similar to those for the drug of abuse. A case in point is that certain antihistamines appear on the A strip to be very similar to amphetamines.

High-Performance Liquid Chromatography

TLC allows direct qualitative detection of drugs in a panoramic way. HPLC allows quantitative detection of drugs and allows sharper separation of these same drugs. In HPLC, the stationary phase, which can be either polar (silicic acid) or nonpolar (such as the C-18 columns), in reverse-phase chromatography is composed of uniform, ultrafine particles that vastly increase its adsorptive surface area. This stationary phase is packed into a column. The resistance to flow in this column is high so that large pressures are required to deliver constant reasonable flow rates. In the Waters HPLC instrument (Waters Corporation, Milford, MA), a constant pressure head is delivered to the column by the use of two pumps that operate so that as one withdraws, the other pushes forward (i.e., the two operate 180 degrees out of phase). The eluate from the column is monitored by a variety of detectors, ranging from UV multiwavelength detectors to redox potential electrode detectors. It is the usual practice in performance of quantitative HPLC to use an internal standard—that is, a compound similar in structure to the drug(s) of interest, which is added to the specimen to be analyzed in a known concentration. By knowing how much of this marker compound or internal standard is placed on the column and how much is recovered from the column in the eluate, the percentage recovery from the column can be calculated for this compound and, by extrapolation, for all of the drugs of interest for which concentrations are being quantitated. Thus, losses due to the column (in addition to losses in extraction procedures) can be corrected for using this technique. Generally, HPLC has been used for the quantitation of specific therapeutic drugs but has found use in detection of cocaine and heroin in urine. The sensitivity of the method is in the nanomolar to micromolar range.

One of the greatest uses of HPLC is in the separation and quantitation of the tricyclic antidepressants and their metabolites. These are among the most commonly prescribed drugs and are also used in excess as drugs of abuse in suicide attempts. It is often necessary to determine the levels not only of the parent tricyclic antidepressant but also of its active and inactive metabolites reviewed subsequently. Figure 24.4 shows a typical separation on a silicate column. Protriptyline, a less inactive tricyclic compound, is the internal standard. It is clear that the separation among the metabolites and parent compounds is quite sharp. This separation is completely reproducible.

A variant of TLC that includes the advantages of HPLC is capillary electrophoresis (CE) (Shihabi, 1993; Tagliaro et al., 1998). In this method, a capillary tube lined with silicate, 10 to 100 μm in internal diameter and 100 to 1000 mm in length, is used as the solid support in an electrophoresis apparatus. Here, the driving force for separation is the voltage (on the order of 25 kV) rather than pressure, as in HPLC. Because of the vast surface area, separations are

Toxi-lab A Worksheet

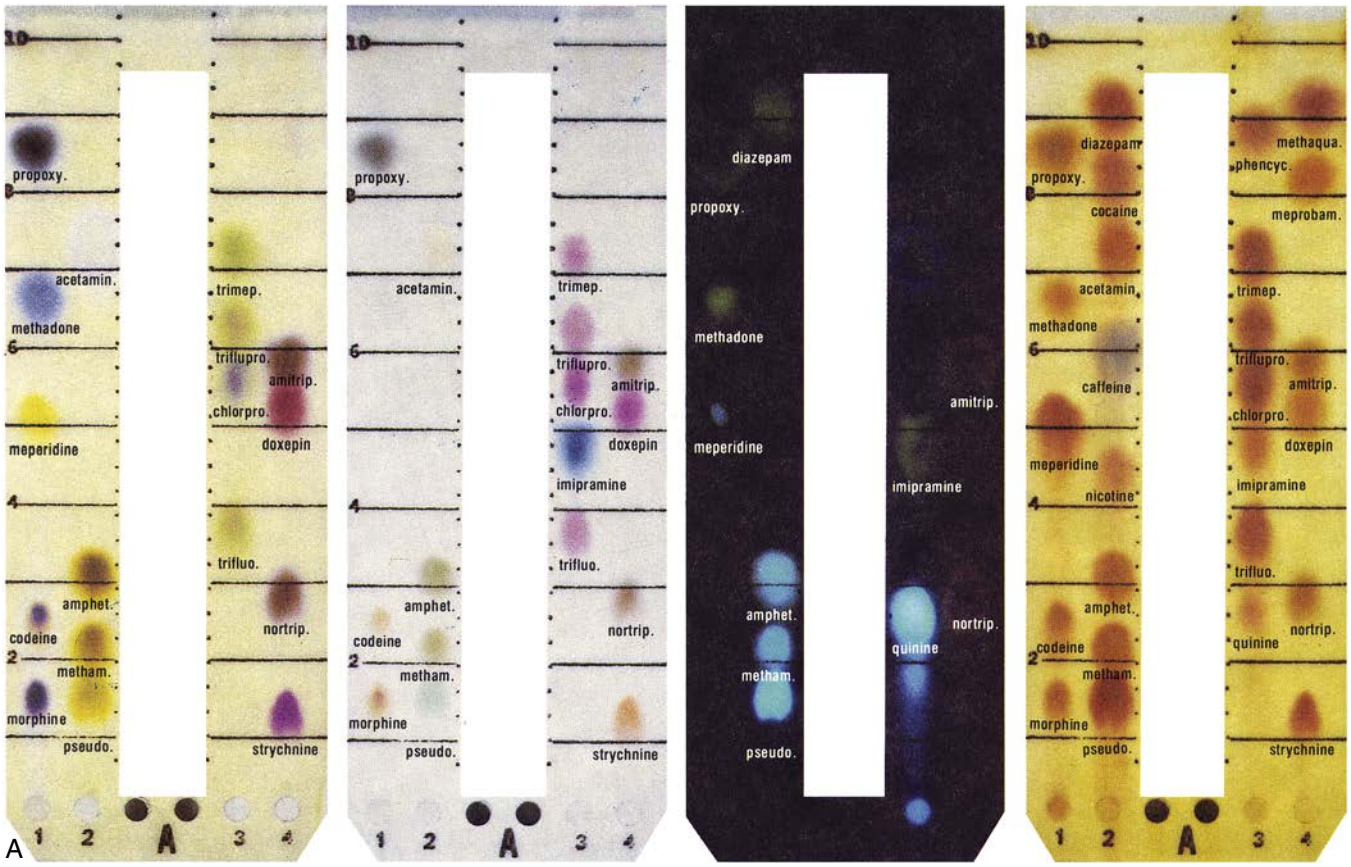

Toxi-lab B Worksheet

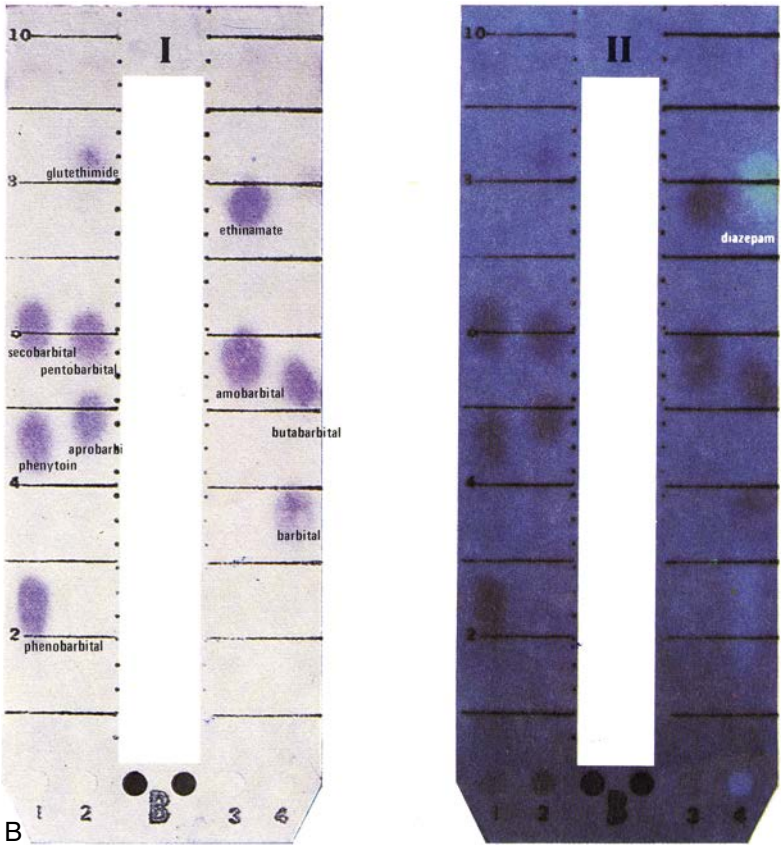

Figure 24.3 A set of typical separations of the major drugs of abuse (and some therapeutic drugs) on Toxi-Lab thin-layer chromatography. Toxi-Lab A worksheet: Typical separation of basic drugs on the A strip, together with characteristic color changes. The third Toxi-Lab A strip shows characteristic fluorescence of different drugs. Note that amphetamine and methamphetamine on the lower left are both fluorescent. Toxi-Lab B worksheet: *Left:* Typical separation of the more acidic drugs on the B strip with characteristic color changes. The major use of the B strip is to identify the presence of barbiturates. *Right:* Fluorescence patterns of drugs on the B strip.

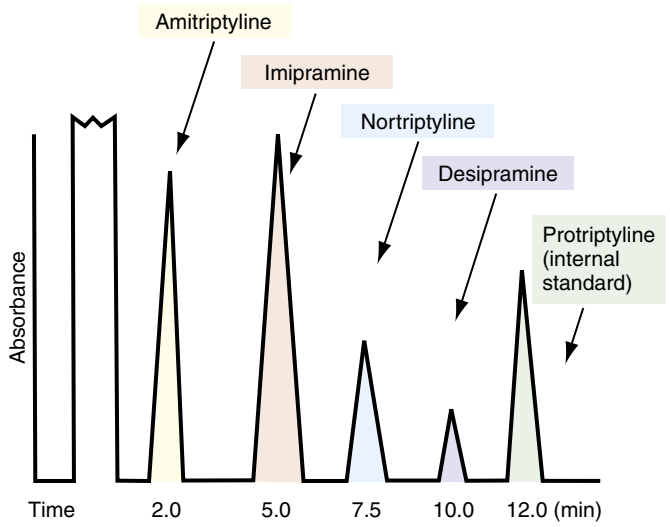

Figure 24.4 Sketch of a typical separation of the major tricyclic antidepressants on high-performance liquid chromatography. A complete separation can be effected in 12 minutes. The concentration of each drug is on the order of 100 μg/mL.

quite sharp. The system is highly versatile and can be used to separate serum proteins and small molecules. CE possesses a wide analytic spectrum (including biopolymers, pesticides, aromatic compounds, drugs, inorganic ions) because of high versatility in terms of separation modes. Different analyte selectivity is based on different physicochemical principles of separation without changes in instrumental hardware—a distinct advantage of this technique. Capillary zone electrophoresis, micellar electrokinetic capillary chromatography (MECK), capillary isotachophoresis, capillary isoelectric focusing, capillary electrochromatography, and capillary gel electrophoresis are different separation modes utilized in CE separations. For example, by adding a detergent to the buffer system, as with MECK, micelles will form. A neutral compound (such as a pesticide) will partition into the detergent, forming micelles, and the complex will separate out based on the mobility/charge of the micelle. In addition, new platforms such as chip-based CE and immunoaffinity CE are currently being developed. CE has not yet enjoyed as widespread use as the immunoassay techniques (discussed previously) in clinical toxicology but is commonly utilized in analytic forensic toxicologic studies as well as in molecular diagnostic studies and can easily be extended to other uses in clinical laboratory medicine (Boone & Ensing, 2003; Petersen et al., 2003; Chiesl et al., 2009). Recent studies have compared CE to HPLC in the determination of asialo-transferrin (Tf), a crucial marker for the reliable interpretation of carbohydrate-deficient transferrin (CDT), to serve as biomarkers in the study of alcohol abuse disorders (Porpiglia et al., 2018). CE allowed the identification of asialo-Tf in 108 out of 165 CDT "positive" cases, based on disialo-Tf measurement (cutoff, 1.8%), whereas HPLC showed a detectable asialo-Tf peak in only 2 cases. In addition, in some cases of disputed CDT increases, the quasi-absence of this Tf component in front of an important increase of disialo-Tf allowed the ruling out of a diagnosis of alcohol abuse, in agreement with all other clinical and laboratory data. These studies showed a superior performance of CE versus HPLC for the determination of asialo-Tf and the importance of this CDT component to avoid misinterpretation of non-alcohol–related CDT increases.

Gas Chromatography–Mass Spectroscopy

Testing for drugs of abuse has become one of the most rapidly developing areas in the clinical laboratory in view of the widespread and ever-expanding use of these drugs among large segments of the working population. In view of the increasing requirements for routine drug screening, it is necessary to have gold standard techniques to confirm the results obtained using screening methods such as EMIT and TLC.

GC-MS has proved to be such a gold standard because of its great sensitivity and reliability. This method, as its name implies, involves two techniques: gas-liquid chromatography and mass spectroscopy. In the former, compounds are directly heated into the gas phase or are derivatized to make them labile to facilitate heating them into the gas phase. They are then passed over a column containing the stationary phase, which often consists of a liquid, usually a hydrocarbon or silicone oil, that coats a solid support in the column and offers a large surface area for adsorption. Separation is based, much as in TLC, on the ability of each compound to adsorb to the stationary phase, which partially depends on the relative solubilities of the compound in the gas versus liquid phase. Normally, the compounds eluting from the column could be detected by conventional techniques, as discussed previously, except that once the compounds are in the gas phase, where they are heated, advantage can be taken of another feature of the system—the ability of compounds that are heated to high temperatures to lose or gain electrons.

The technique of mass spectroscopy is discussed comprehensively in Chapter 5. Here, we summarize briefly the salient features of this technique. At high temperatures, the highest energy electrons of a compound (i.e., the ones of lowest ionization potential) can be excited such that the molecule can lose electrons and become charged. This process may be aided by such techniques as electron bombardment in a specially designed chamber that directly creates molecule-ions. Most of these resulting molecule-ions are single cations. Different molecule-ions in general have different sizes and different molecular weights. These molecule-ions decompose into characteristic fragments whose ratios with respect to one another and whose positions of migration relative to one another are also constant. The molecule-ions are then passed through an electric field generated by four rods that are subjected to rapidly alternating currents, the so-called **quadrupole detector**. Depending on the frequency of the alternating current, certain molecule-ions with specific mass/charge ratios can pass through the field to a detector. Thus, the molecule-ions can be separated on the basis of molecular weight or, more exactly, on their mass/charge ratios. The overall design of GC-MS is shown in Figure 24.5.

The presence of the molecule-ion on the plate is detected by a charge multiplier detector system. The technique of GC-MS has become highly refined. Each molecule-ion created in the gas phase can undergo further changes, such as elimination reactions and rearrangements, and further degradation to small fragments that, in turn, ionize and give characteristic decomposition patterns. The patterns of thousands of compounds have now been determined. The position of the parent molecule-ion of the compound and the decomposition fragments give rise to a **fingerprint pattern** unique to the compound. These patterns are stored in a computer so that when a pattern for an unknown compound or group of compounds is obtained, the pattern is compared with the stored patterns to identify the compound(s) of interest. The entire method has been highly successful in detecting even low levels of cocaine and/or its metabolites in body fluids. A typical cocaine pattern is shown in Figure 24.6. Because single molecule-ion species give rise to significant currents in the detector, it is possible to detect very low levels of drugs, making this technique the ultimate reference method and the best confirmatory testing procedure available at present.

Liquid Chromatography–Mass Spectroscopy

As discussed previously, GC-MS is the gold standard for the identification of volatile compounds. Nonvolatile compounds, however, can be detected utilizing LC-MS (Davis et al., 1989; Maurer, 1998; Marquet, 2002; Niessen & Tinke, 1995, 2003). Unlike GC-MS, however, the coupling of LC with MS requires sophisticated interfaces between the LC and MS components. The interface must volatilize nonvolatile compounds that have been separated on the LC; must remove the liquid solvent from the LC; and must correct flow-rate incompatibility between the LC and MS. Two interface methods, electrospray (ES) and atmospheric pressure chemical ionization (APIC), appear to have become the gold standards for LC-MS. Both interface methods are utilized with atmospheric pressure ionization devices to facilitate removal of the mobile phase. They differ primarily in the range of analytes that can be accommodated and in how the solvent phase is nebulized. Ionizable analytes of high molecular weight and/or high polarity can be accommodated with ES, and APCI can be used for analytes of less polarity and lower molecular weight. At present, ES appears to have more clinical and forensic applications than APCI in toxicology.

LC-MS can be used to both screen and confirm positive test results from a screening assay. It has been used for confirmation of drugs-of-abuse assays, poisoning detection in acute or chronic intoxication, therapeutic drug identification and quantitation, and pharmacokinetic and drug metabolism studies. Although LC-MS has limitations when compared with GC-MS, it has become a powerful "mature and validated" (Marquet, 2002) technique in analytic toxicology and a complementary method to GC-MS. To this end, LC-MS/MS offers significant advantages over other traditional testing, such as immunoassay and gas chromatography–mass spectrometry (GC/MS) methodologies. Major strengths of LC-MS/MS include improvement in specificity, flexibility and sample throughput when compared with other technologies (Zhang et al., 2016).

LC-MS/MS offers much better specificity for a target molecule because the quadrupole recognizes not only the original ionized molecule but also all the fragments derived from the original ionized molecule. Combined with the HPLC technique, the separation of the analytes is much easier and the retention time is another characteristic factor that enhances the selectivity of the mass spectrum.

LC-MS/MS exhibits flexibility and versatility for the clinical labs to develop and validate new assays in house within a short time. LC-MS/MS

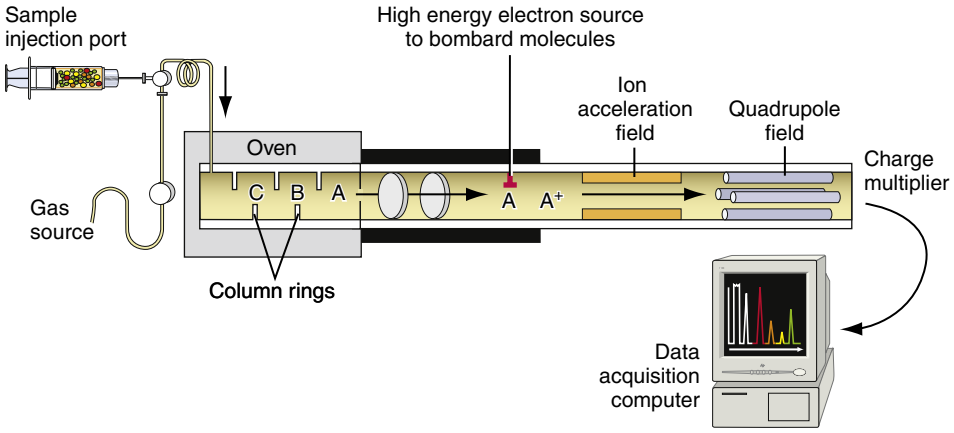

Figure 24.5 A schematic view of the components of gas chromatography–mass spectroscopy instrumentation. On the left of the figure is the gas chromatographic system, in which a volatilized compound is moved by an inert gas over a column consisting of rings coated with a liquid. Compounds C, B, and A separate on this column and are maintained in the gas phase by the oven that surrounds the column. The separated compounds then enter the mass spectrometer on the right side of the figure, where they are subjected to bombardment by electrons, resulting in molecule ion species. These ionic species then are accelerated in a field and are passed through an electric quadrupole field. Only those ions with a narrow range of mass/charge ratios (m/e ratios) will pass through the tuned field so that they strike the detector. The electric currents that result are digitalized and stored in a computer that analyzes the data (Davis et al., 1989).

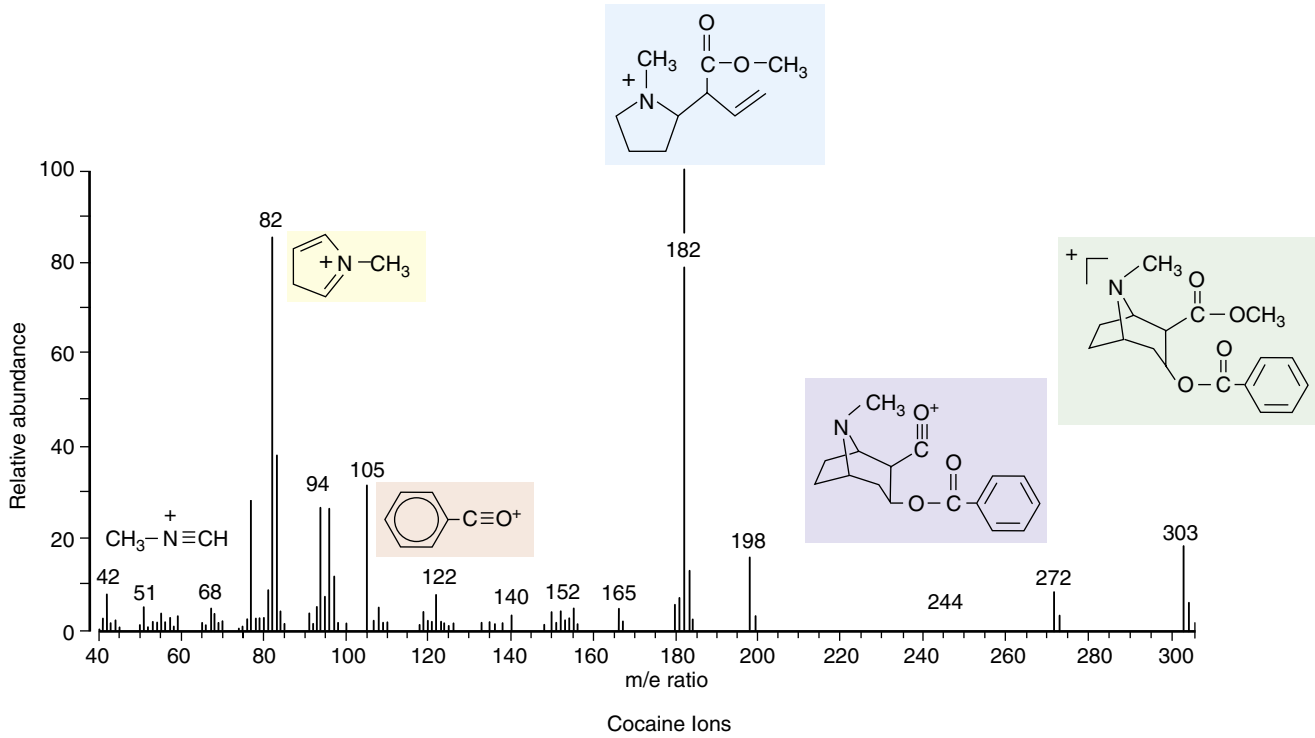

Figure 24.6 Fragmentogram for cocaine using gas chromatography–mass spectroscopy. The specimen is urine. This figure shows the characteristic peaks for cocaine metabolites. m/e is the mass-to-charge ratio, which for most ions is a measure of the molecular mass. (Courtesy of Dr. Chip Walls, Onondaga County, NY, Medical Examiner's Office).

assays, as laboratory-developed tests, are highly attractive for target analytes where no commercial immunoassays are available. In contrast to GC/MS, which is limited to volatile molecules, LC-MS/MS has a much wider range of applications since most biologically active molecules are polar, thermolabile, and nonvolatile. In addition, LC-MS/MS sample preparation is simpler and does not require derivatization techniques. Although LC-MS/MS offers the flexibility of developing assays to meet the clinical needs, the shortcoming of the flexibility is that method development, validation, and quality control may vary among different laboratories because most of the LC-MS/MS methods used in the clinical labs are often laboratory developed. Accuracy experiments are a prerequisite step in method validation to ensure that the interlaboratory result variance is less than 20% (Zhang et al., 2016).

Gas Chromatography Coupled with Infrared Spectroscopy

Infrared (IR), or Fourier-transformed infrared, spectroscopy (FTIR) utilizes light of high wavelength (low frequency), which excites vibronic states of molecules involved in bond stretching and bond angle bending. Every compound has a characteristic IR "fingerprint," that is, IR absorption pattern, so that even closely related compounds can be distinguished readily from one another by gas-phase IR. Thus, the fractions of patients' samples that elute from a GC or liquid chromatography column can be analyzed using this technique. As with mass spectroscopy, the FTIR spectra for different compounds can be stored in a computer attached to the GC-FTIR system. The spectra obtained from the eluates from the column are then analyzed for the presence of specific drugs of abuse. This method is particularly well suited for the detection of amphetamines (Belal et al., 2009).

Dried Blood Spot Testing

In addition to conventional blood and urine testing using fresh fluid samples such as blood and urine, dried blood spot (DBS) sampling is emerging as a minimally invasive microsampling technique. DBS testing provides advantages for analyte stability, transport, and ease of storage, making it an attractive matrix in forensic and clinical settings. Recent studies have demonstrated successful determination of various drugs, including illicits such as cocaine, amphetamine, methamphetamine, MDA, MDMA, morphine, codeine, 6-AM, cocaine, benzoylecgonine, methadone and EDDP, that were variably comparable to conventional testing (Ambach et al., 2019; Velghe, 2019a; Joye, 2019; Simões, 2018). These methods employ select aspects of DBS extraction systems coupled with standard LC-MS/MS configurations, high-resolution mass spectrometry (HRMS), and ultra-performance liquid chromatography (UPLC), among others. Concerns pertaining to DBS include hematocrit (Hct) levels, which can affect diffusion rates on the absorbent filter paper, matrix effects, and recovery bias that may impact on the accuracy of an analytic result, possibly leading to an under- or overestimation of the analyte being assessed (DeKesel, 2013). Various strategies have been designed that maintain the benefits of DBS but eliminate the Hct-based area bias, such as heated flow-through desorption, fixed volume capillary dispensation (HemaPEN) to filter paper spots, and precision volumetric absorptive microsampling (Mitra), among others (Velghe, 2019b; DeKesel, 2013).

SCREENING FOR DRUGS OF ABUSE

In most states of the United States, two levels of testing for drugs of abuse have become recognized: emergency department/point-of-care (POC) testing and employment screening/forensic testing. The former involves rapid, stat screening methods, in particular, EMIT (or FPIA) and TLC. The purpose of this type of screening test is to detect the presence of a drug or several drugs of abuse in the patient's urine. Rarely are the more sophisticated chromatographic procedures such as HPLC and GC-MS used for this purpose.

Forensic testing, on the other hand, requires not only a screen but also an independent confirmatory method, which is almost always chosen to be GC-MS or, less commonly, HPLC. It should be noted that, strictly by law, any confirmatory method is valid provided that it is a completely different method from the primary one. Thus, TLC can confirm EMIT, whereas FPIA cannot confirm it because both EMIT and FPIA are immunochemical methods. Another important legalistic consideration in forensic testing is the **chain of custody** (DeCresce et al., 1989; Poklis, 2001; Smith & Bluth, 2016a). This process is used in the collection of urine from the individual from whom the specimen is taken. It may begin by observation of specimen collection by one person. Then, that person or another specifically designated individual, usually a police officer (in the case of prisoners or suspects) or some other designated official, accompanies the messenger, who brings the specimen from the individual to the laboratory. This individual is a witness to the testing (and must sign a legal document to this effect) of the specific urine sample collected. More than one designated individual may be involved as the witness in this chain.

Specimen Validity Testing

Specimens submitted for urine toxicology testing may be manipulated during the preanalytic phase of collection (Smith & Bluth, 2016b). These can encompass metabolic "tricks" that a patient can incorporate prior to providing a urine sample as well as postvoiding to mask the presence of a substance that may cause clinical and/or legal issues if detected, including dilution, substitution, and adulteration.

Dilution

The simplest of these interferences involves diluting one's urine to the point that the concentration of the drug in question is below the detection limits of the test. The subject either adds liquid to the urine sample or drinks something that causes the urine to be very dilute. Though this is a very effective technique, it can be easily detected by the testing facility either by observing the collection process wherein any manipulation can be directly observed and/or by detection of abnormally low values for urine creatinine and specific gravity. A normal urine has a creatinine greater than 20 mg/dL, along with a specific gravity that is greater than 1.0030. If a urine specimen has both creatinine and specific gravity values below these cutoffs, the urine is considered to be dilute.

Substitution

Subjects can attempt to substitute their urine with either someone else's urine or with a urine-like liquid. This type of interference is detected with either an observed collection, recording the temperature of the urine immediately after collecting, and/or the testing facility testing the creatinine and specific gravity of the sample. A sample that is not between 90° F to 100° F is not humanly possible and should be questioned as to the source of the specimen (NRC Regulations Title 10, Code of Federal Regulations, Part § 26.111). Additionally, a creatinine that is less than 2 mg/dL with a specific gravity that is less than or equal to 1.0010 or greater than or equal to 1.0200 is not physiologically possible and is thus considered to be substituted.

Adulteration

Another way a sample can be tampered with is by the addition of a substance that interferes with screening test, causing the antibody to not bind to the drug in question. Specimen validity testing for oxidative substances and the pH of the sample usually detects these and other types of interference. A specimen will be reported as substituted when at least one of the following criteria is met:

- pH < 3 or ≥ 11
- Nitrite ≥ 500 μg/mL
- Chromium (VI) is present
- A halogen (e.g., bleach, iodine, fluoride) is present
- Glutaraldehyde is present
- Pyridine is present
- A surfactant is present

There is variability among clinical collection sites with regard to adherence to ascertaining whether strict collection protocols are part of a standard operating procedure and enforced. Thus, careful assessment of collection processes in light of an inconsistent laboratory toxicology result can often shed light as to whether adulteration or specimen mishandling, including accidental patient specimen mix-up, may have taken place.

THE DRUGS OF ABUSE

GENERAL ASPECTS OF THE MECHANISMS OF ACTION

The major drugs of abuse (Sweetman et al., 2002; Flomenbaum et al., 2006) are shown in Figure 24.7 (O'Neil et al., 2001; Haroz & Greenberg, 2006). As may be seen in this figure, these drugs, with the exception of the barbiturates and cannabinoids, are all basic amino group–containing compounds, most of which also contain benzene rings. The steric relationship of the amino group with respect to the aromatic benzene rings is rather similar, especially in cocaine, the opiates, and methadone. As might be expected, these compounds can cross-react, although with lower affinities, with each other's target receptors. The primary physiologic mechanisms of action of these drugs are not well understood, but some rudimentary knowledge has been gained as to some of the main targets of these drugs. Many of these drugs act directly on dopaminergic and norepinephrinergic neurotransmitter systems, especially the limbic system (sometimes referred to as the **smell brain**). This system is a more primitive one associated with pleasure seeking and is discussed further later.

In Figure 24.8, possible effects of several of the most important drugs on this system are shown. It appears that the amphetamines, closely related structurally to dopamine and the catecholamines, and cocaine cause release of dopamine from the vesicles at the axonal side of the synapse, which may partially be responsible for their producing a pleasant sensation (a so-called **high**) in many individuals (Hurd et al., 1988). The tricyclic antidepressants stimulate pathways that utilize norepinephrine as the neurotransmitter. These pathways, like the dopaminergic pathways, are involved in arousal and pleasure seeking. In this case, the tricyclic antidepressants, rather than promoting release of the neurotransmitters, block the reuptake of norepinephrine into the vesicles on the axonal side of the synapse. They also may exert nonspecific reuptake blockade of dopamine in the dopaminergic pathways (Baldessarini, 2006). It is of great interest that, paradoxically, the tricyclic antidepressants such as imipramine (Tofranil) have been used successfully to treat the effects of cocaine, although, as described later, benzodiazepine tranquilizers are now preferred. The major tranquilizers, such as haloperidol (Haldol) and chlorpromazine, used to treat psychotic states such as schizophrenia, appear to block attachment of dopamine to the dendritic receptors in the synapse, thereby blocking the stimulatory effects of dopamine. Associated with many dopaminergic neurons are inhibitory neurons that use γ-aminobutyric acid (GABA) as their neurotransmitter. It appears that many benzodiazepine receptors exist on these neurons, causing potentiation of GABA at the synapses in this system, reducing the dopaminergic effects of the stimulatory pathways on the limbic system. Thus, some of the tranquilizing effects of diazepam (Valium) and other benzodiazepines can be explained.

Widely distributed throughout the central nervous system and periphery are a variety of opioid receptors classified mainly as μ-, δ-, κ- and ε-receptors (Tseng, 2001; Snyder & Pasternak, 2003; Fujii et al., 2004). The μ-receptors appear to be specific for morphine and heroin, both of which produce a general analgesic state. These opioid receptors are discussed further in the following section.

Many of the drugs of abuse also act on two other major pathways in the brain: those using serotonin (serotonergic) and those utilizing *N*-methyl-D-aspartate (NMDA) and L-glutamate as their neurotransmitters. Neurotransmission by serotonin occurs by its binding to the 5-hydroxytryptamine (5-HT) receptor on the dendritic side of the synapse. There is a rather wide range of 5-HT receptors, not all of which produce the same physiologic effects. The major ones appear to be 5-HT_1 and 5-HT_2 receptors. The serotonin pathways encompass a rather wide swath of the brain and even the spinal cord. This neurotransmitter is the principal one for the limbic system and, in addition, for the basal ganglia, especially the amygdala, which is involved in aggressive behavior. As mentioned earlier, the limbic system is involved in pleasure seeking and pleasure reinforcement. Serotonergic pathways also extend to the hippocampus and are involved in memory. As a neurotransmitter in the spinal cord, serotonin induces muscle contraction. NMDA pathways are more involved in nociceptive (pain) pathways and are involved in memory and neuronal plasticity (Zhuo, 2009). They have been found to be involved in chronic pain reinforcement. Blockade of NMDA pathways by drugs of abuse can therefore remove this perceived undesirable effect.

EXTENT OF USE OF DRUGS OF ABUSE

Overall, in the U.S. population as of 2017, there has been a general increase in the use of all drugs of abuse in individuals 12 years of age and older, about 51.8

million individuals compared with 48.5 million in the previous year, representing an ≈6.6% increase (Substance Abuse and Mental Health Services Administration, 2017; www.cdcfoundation.org). Although these data refer mostly to cannabinoid (marijuana) use (≈79%), compared with other illicit drugs, misuse/abuse of other prescribed pharmacopeia, such as psychotherapeutics, account for another substantial group (≈18 million). The highest number of drug abusers (≈75%) occurs in 15 to 39 year old individuals. Whites and low-income adults have shown increased odds of lifetime prescription opioid use disorder. Interestingly, individuals in the 40- to 59-year-old bracket comprise most of the remainder, numbering over 20% of the overall number of drug abusers. Persons older than 26 years have a 20% to 25% lifetime probability of using cocaine whether they are working full-time, part-time, or are unemployed. Health care costs were ≈$80 billion in 2013, including ≈$29 billion in health care and substance abuse treatment as well as ≈$20 billion in lost productivity costs. Overdose deaths were >80,000 Americans in 2018 compared with >33,000 Americans in 2015, an increase of 2.5 times and 4 times the number in 2002. It is interesting to note that 3.8 million Americans reported nonmedical use of prescription opioids (2015 data) and that nearly one in every

1. OPIATES

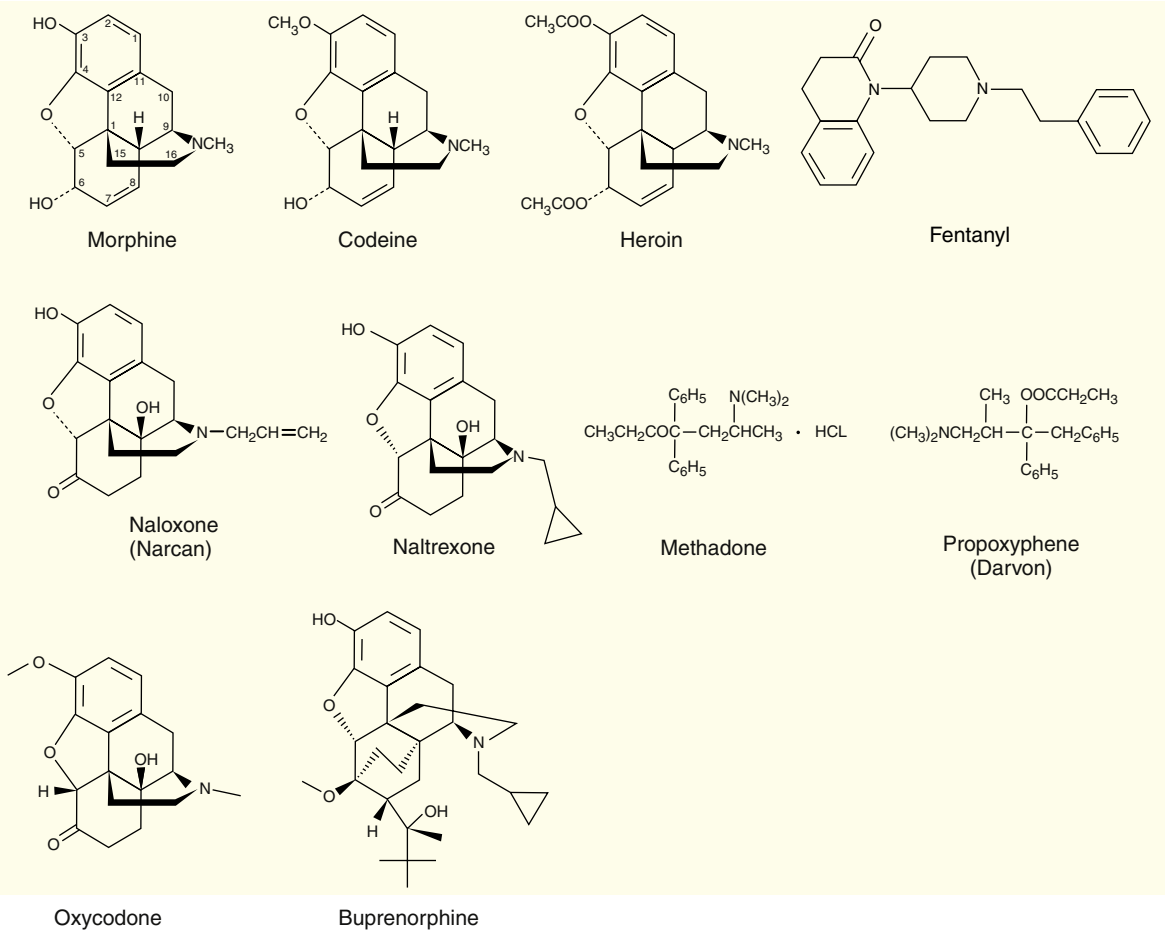

2. TRANQUILIZERS

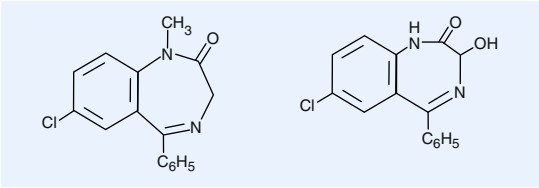

3. BARBITURATES; SEDATIVE - HYPNOTICS

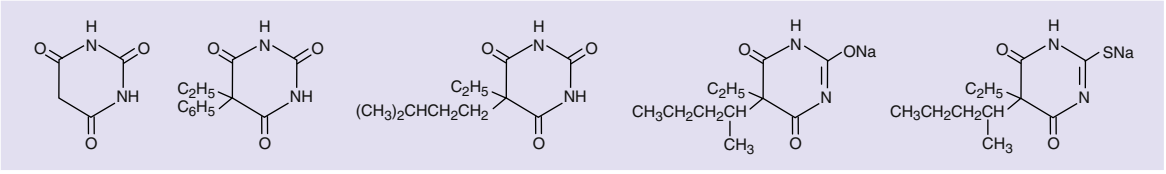

Figure 24.7 Chemical structures for the major drugs of abuse, divided into 10 classes labeled 1 to 10 in the figure. All of the opiates are seen to be basic compounds that are tertiary amines and that contain benzene rings. Notice that, in the barbiturate series, barbituric acid may be considered as a condensation product of urea and malonic acid. (Figures for carisoprodol and meprobamate are reprinted with permission from Wang, 2011.)

4. DOPAMINERGIC PATHWAY STIMULANTS

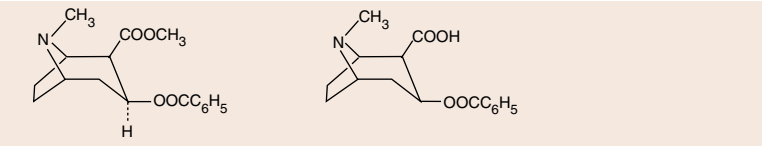

Cocaine

Benzoylecgonine
(less active metabolite)

AMPHETAMINES

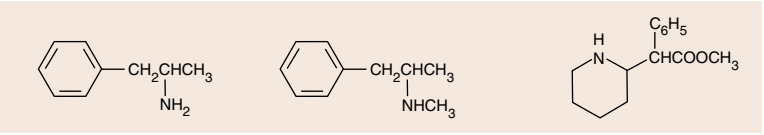

Amphetamine

Methamphetamine

Methylphenidate
(Ritalin - used to treat
hyperactive children)

4A. "DESIGNER" AMPHETAMINES/PHENYLETHYLAMINES

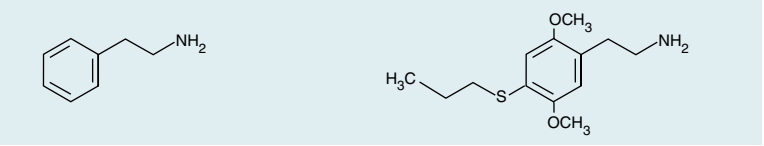

Phenylethylamine
Base compound

2,5-dimethyoxy-4(n)-propyl-
thiophenethylamine (2C-T-7)

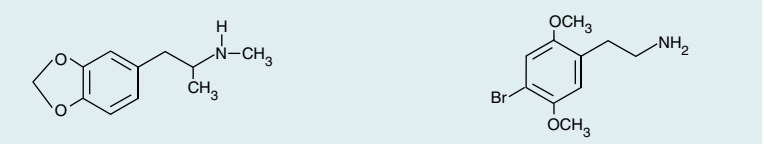

3,4-dimethyleneoxy-
methamphetamine
(MDMA or "Ecstasy")

5-Bromo-2,5-methoxy-
phenylethylamine (2CB)

5. HALLUCINOGENS

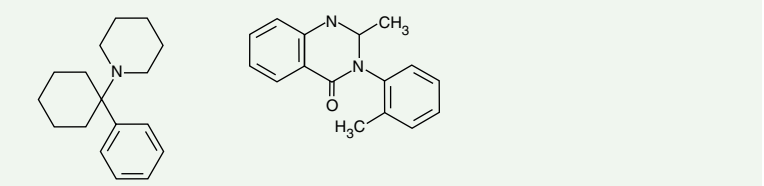

Phencyclidine

Methaquaalone

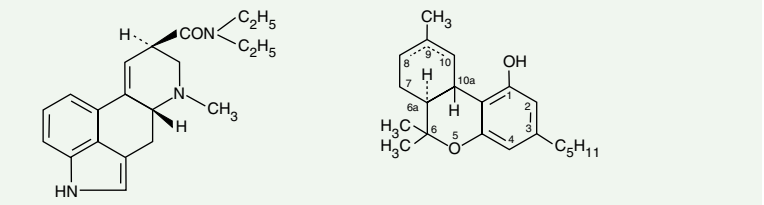

Lysergic acid
diethylamide
(LSD)

Tetrahydro
cannabinol

Figure 24.7—cont'd

6. TRYPTAMINES

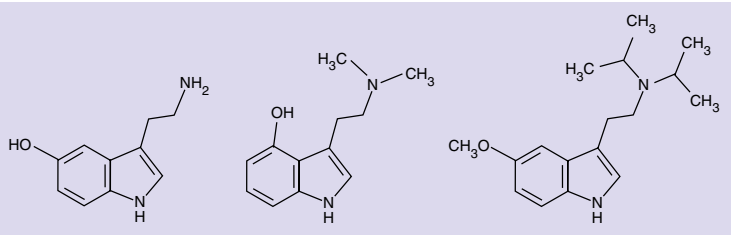

Serotonin-Base compound | Psilocin | 5-methoxy-N,N-diisopropyl tryptamine (5-Me)-DIPT

7. PIPERAZINES

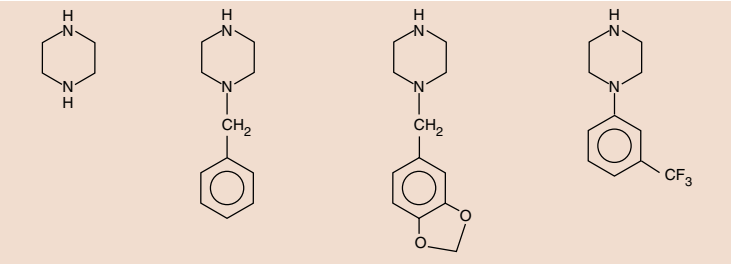

Piperazine | 1-Benzyl-piperazine ("BZP" or "A2") | 1-(3,4-Methylene-dioxybenzyl) piperazine ("MDBP") | 1-(3-Trifluoro methylphenyl) piperazine ("TFMPP" or "Molly")

8. BATH SALTS

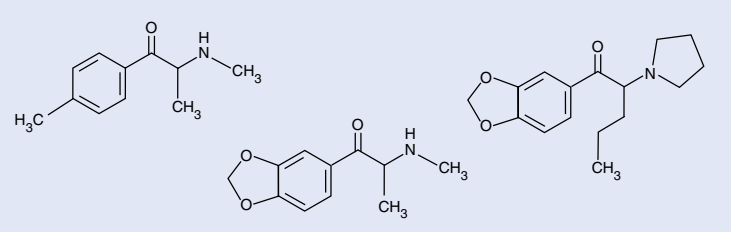

Mephedrone | Methylone | Methylenedioxypyrovalerone

9. SLEEP AIDS

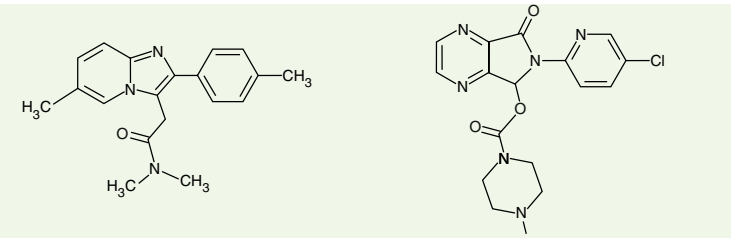

Zolpidem | Zopiclone

10. MUSCLE RELAXANTS

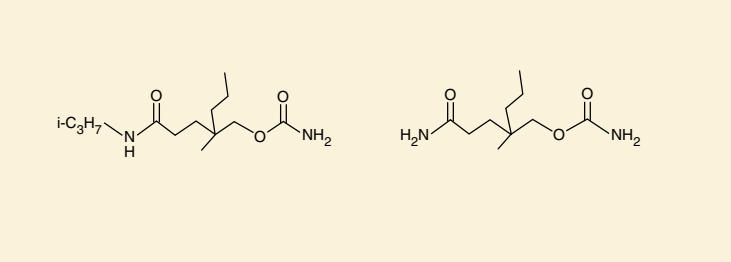

Carisoprodol | Meprobamate

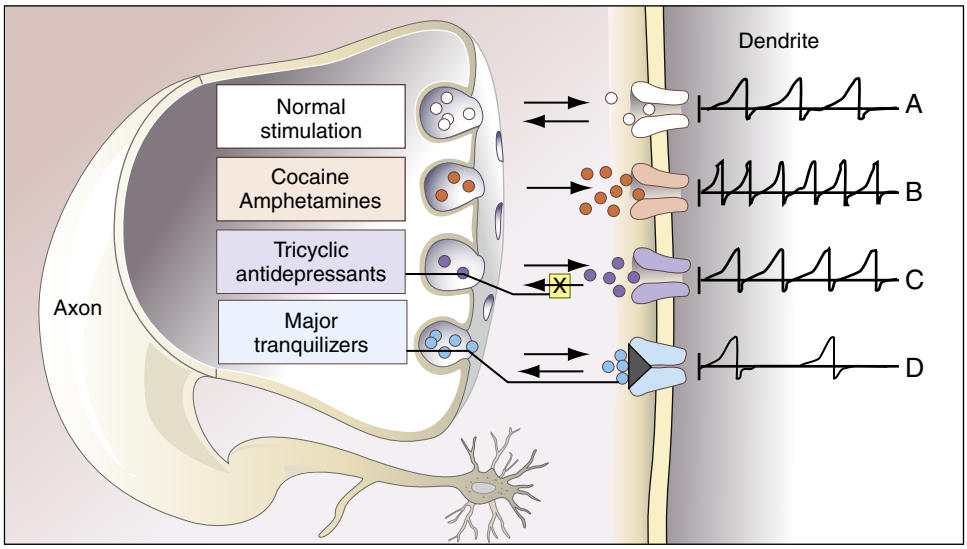

Figure 24.8 Illustration of the possible mechanisms of action of drugs of abuse and some therapeutic drugs on sympathomimetic amine (dopamine and norepinephrine) pathways. *A,* Normal neural transmission. A nerve impulse is conducted down the axon to the terminal boutons at the nerve ending. Vesicles, represented by the round gray structure, release their contents of neurotransmitter—here, dopamine—represented by small white circles. Dopamine molecules traverse the synaptic cleft and bind to dendritic receptors, initiating action potentials *(at right under "dendrite")* in the dendrites. Notice the *arrows* showing that dopamine is both released and taken up by the vesicles. *B,* In the presence of cocaine and amphetamines, enhanced release of neurotransmitter *(red circles)* from vesicles occurs, increasing the rate of firing in the dendrites. *C,* Tricyclic antidepressants block *(arrow with "X" in yellow box)* reuptake of the neurotransmitter *(purple circles)*, in this case, norepinephrine and, less specifically, dopamine, causing more neurotransmitter to "recycle" to the dendritic receptors, resulting in increased firing. *D,* Some of the neuroleptics act by blocking *(gray wedge)* postsynaptic dendritic receptors for dopamine *(blue circles)*, causing decreased firing.

two adolescents who reported the medical use of prescription opioids after initiating nonmedical use of prescription opiates had two or more substance use disorder symptoms at age 35 years (McCabe, 2019). It is also important to note that drug abuse does not spare any age, race, gender, or socioeconomic, employment, or educational status, demonstrating the scope of the issue.

COCAINE

Cocaine is derived from the coca plant and has enjoyed much popularity as an additive to certain foods. At the beginning of the 20th century, it was used in Coca-Cola, but owing to its addictive effects, this practice was discontinued. Cocaine is a derivative of the alkaloid ecgonine (i.e., the methyl ester of benzoylecgonine), as shown in Figure 24.7 (Group 4 drugs). The normal route of administration of cocaine is nasal (i.e., inhalation, called **snorting**), such that the drug passes through the nasal membranes. A particularly potent form of cocaine, called **crack,** is the free-base form that passes rapidly across the nasal membranes such that, for a given dose, most or all of it enters the bloodstream rapidly. The half-life of cocaine is 1 to 2 hours; the parent compound and its metabolites are usually cleared from the body within 2 days.

It is estimated that as many as 25 million people in the United States have used cocaine at least once (Jones & Wie, 2006); fortunately, most of these individuals do not continue. Fatalities from cocaine abuse are of two types: direct toxicity of the drug (Johanson & Fischman, 1989) and crime related to the illicit acquisition of the drug. Up to 25% of myocardial infarctions in patients between 18 and 45 years of age have been attributed to cocaine abuse (Jones & Wie, 2006).

Cocaine is used medically to induce local anesthesia during nasopharyngeal surgery. However, in large doses, it induces a euphoric state (the "high" experienced by the user) and may also induce hallucinatory states. It can also promote violent behavior (Flomenbaum et al., 2006; Hoffman, 2006). Many of these results can be explained by cocaine's dopaminergic effects. One study (Azmitia et al., 1990) suggests that cocaine induces increased calcium ion influx in dopaminergic neurons. The increased intracellular calcium activates phospholipases that possibly act as second messengers in causing ultimate release of dopamine in synapses. Prolonged action of phospholipases, however, ultimately causes cell death. In the previously mentioned study, in fact, cocaine was found to be neurotoxic. It also has a general cytotoxic effect from formation of an *N*-oxide free-radical produced in the metabolism of this compound in the liver. It appears then that, over time, cocaine induces neuronal loss. In addition, binding of cocaine to cell receptors in the limbic system induces synthesis of cyclic adenosine monophosphate (cAMP) that appears to be critical in activating cell processes involved in dopamine release (Cami & Farre, 2003). Cocaine may also block the reuptake of dopamine at the axonal side of the synapse. As if becoming toxic from cocaine abuse were not sufficient, many cocaine abusers consume this drug together with alcohol. Ethanol becomes esterified to cocaine in the liver to form cocaethylene, which blocks reuptake of dopamine in dopaminergic pathways more effectively than does cocaine and causes pronounced vasoconstriction of the coronary arteries, inducing increased myocardial oxygen demand. This cocaine derivative is deadlier than either cocaine or ethanol alone (Jones & Wie, 2006).

Studies (Lange et al., 1989; Lange & Hillis, 2001; Frishman et al., 2003; Jones & Wie, 2006) further indicate that prolonged use of cocaine results in cardiotoxicity—that is, cocaine can cause progressive atherosclerosis and causes constriction of the coronary arteries that can, in turn, induce myocardial ischemia and sometimes frank infarction. Cocaine has been found to induce sympathomimetic effects on the myocardium by increasing heart rate. At the same time, it induces increased vasoconstriction. The net effect is increased chronotropy and afterload, resulting in increased oxygen demand by the myocardium. At the same time, cocaine induces platelet aggregation and stimulates production of plasminogen activator inhibitor (Jones & Wie, 2006). These events all predispose to development of myocardial infarction.

One highly disturbing aspect of cocaine abuse is the fact that cocaine passes readily across the placenta and into the lactating mammary gland, thus is readily passed from mothers to nursing infants. Often in the hospital setting, mothers receive the drug from dealers and breastfeed their newborn babies, who are therefore maintained on this drug. Cocaine causes mental retardation, delayed development, and strong drug dependence in newborns. It can also produce malformations in utero.

Cocaine has not been considered classically to be an addictive drug, as it does not cause the true physical dependence typical of abusers of barbiturates and opiates. However, the high produced by the drug is extraordinarily reinforcing so that the drug-seeking behavior of the cocaine and opiate abuser is similar. Evidence in experimental animals suggests that cocaine can induce the release of β-endorphins that bind to μ-receptors in the limbic system (Gianoulakis, 2004). This induces a pleasant and positive feeling of reinforcement. Clinically, patients who are overdosed with cocaine may become violent and irrational, requiring sedation. The treatment of choice for patients in hyperexcitable states with cardiac symptoms such as palpitations is one of the benzodiazepines. Thus, it is not uncommon to find cocaine and Valium in the urine of cocaine addicts. Occasionally, overdosed patients will become obtunded or comatose. The treatment for these patients is usually supportive. As noted in the previous section, antidepressants, including the tricyclics, and selective serotonin reuptake inhibitors (SSRIs), such as fluoxetine (Prozac), have been found to inhibit some of the undesirable effects of cocaine and have been used in the treatment of cocaine abuse.

Metabolism

The half-life of cocaine, as stated previously, is approximately 1 to 2 hours. It is metabolized to more polar compounds that have significantly less potency than the parent compound. These metabolites have longer half-lives and, with techniques such as GC-MS, can be detected up to 48 hours after administration of the drug. The immunoassay methods can detect the drug for about

24 to 36 hours after administration. If a patient has inhaled cocaine free-base ("crack"), it is possible to detect the parent compound, cocaine, by TLC up to several hours after administration owing to the high doses of drug present.

THE OPIATES: HEROIN, MORPHINE, CODEINE, OXYCODONE, BUPRENORPHINE, AND FENTANYL

The primary medicinal use of opiates such as codeine and morphine is to diminish or eliminate pain in a patient. As noted earlier, there are several classes of opiate receptors that are involved in the modulation of pain. These receptors are classified as μ, κ, δ, and ε. The endogenous ligands for each of these receptors are the antinociceptive peptides: endomorphin (Tyr-Pro-Trp-Phe-NH_2 and Tyr-Pro-Phe-Phe-NH_2) for μ-receptors, dynorphins A (Tyr-Gly-Gly-Phe-Leu-Arg-Arg-Ile-Arg-Pro-Lys-Leu-Lys) and B (Tyr-Gly-Gly-Phe-Leu-Arg-Arg-Gln-Phe-Lys-Val-Val-Thr) for κ-receptors, Met- and Leu-enkephalin (Tyr-Gly-Gly-Phe-Met and Tyr-Gly-Gly-Phe-Leu) for ε-receptors, and deltorphin (Tyr-D-Met-Phe-His-Leu-Met-Asp-NH_2) and Met and Leu-enkephalin for δ-receptors. Note that the first five amino acids of dynorphin are identical to those of Leu-enkephalin, suggesting a possible reason for the binding of enkephalin to κ-receptors. The exogenous opiates (e.g., morphine, codeine, fentanyl) whose structures are shown in Group 1 of Figure 24.7, are known to be agonists, primarily, for μ-receptors. As can be seen in this figure, morphine, codeine, heroin, oxycodone, and buprenorphine have quite similar structures. In fact, morphine is a metabolite of heroin, the diacetyl precursor of morphine.

A major target for each of the endogenous opiate peptides and for the exogenous agents shown in Figure 24.7 is the main pain pathway (i.e., the spinothalamic tract). This neural pathway carries nerve impulses from peripheral pain receptors to the peripheral nerves that innervate them to the posterior horn of the spinal cord where the nerves synapse to ascending fibers in the spinothalamic pathway. These nerves travel to the next spinal level where they cross the midline and then travel to the medulla as the lateral lemniscus that synapses in the thalamus (mainly in the ventroposterior nucleus [VPN]) and then projects to the cortex where pain perception takes place. Activation of the opioid receptors that occurs at these synapses results in hyperpolarization of the dendritic side of the synapses, blocking nerve conduction, thereby diminishing the sensation of pain.

In addition, it appears that the opioid receptors also play another major role in pain modulation via the activation of descending tracts that emanate from the midbrain in the periaqueductal gray area and travel to nuclei in the median raphe of the medulla. After synapsing with these nuclei, these tracts synapse at interneurons in the posterior horn of the spinal cord where they activate the release of GABA, resulting in inhibition of nerve conduction in the spinothalamic tract. Normally, these pathways are quiescent, but release of any of the endogenous antinociceptive peptides or introduction of exogenous drugs (e.g., morphine or codeine) results in removal of inhibition of these pathways, again resulting in inhibition of nerve conduction in the spinothalamic pathway with diminished perception of pain.

Morphine and Heroin

Morphine, a μ-receptor agonist, in addition to acting on pain pathways as described earlier, further acts by binding to μ-receptors in the limbic system (central nervous system [CNS]), mainly in the nucleus accumbens and the ventral tegmental area, resulting in an analgesic state. Binding of morphine and the other opiates to the μ-receptor inhibits the release of GABA from the nerve terminal, reducing the inhibitory effect of GABA on dopaminergic neurons. The resulting increased activation of dopaminergic neurons results in sustained activation of the postsynaptic membrane, causing a sense of euphoria. On the molecular level, binding of morphine to these receptors activates a cell-signaling cascade via G-protein activation that results in elevated expression of many transcriptionally active proteins such as ERK, jun, and fos, and superactivation of adenyl cyclase, resulting in high intracellular levels of cAMP (Tso & Wong, 2003). Besides being used as a major analgesic, morphine (Dilaudid) is important in treating acute congestive heart failure by lowering venous return to the heart (i.e., it is a powerful preload reducer by causing increased splanchnic pooling of blood).

Heroin induces a pleasant, euphoric state and is highly addictive both physically and psychologically. As can be seen in Figure 24.7, heroin is a diacetyl form of morphine. This characteristic facilitates heroin's crossing the blood-brain barrier, allowing it to reach higher concentrations in the CNS. Withdrawal from this drug is exceedingly difficult, with a myriad of symptoms such as hypothermia, palpitations, cold sweats, and nightmares. This is a true physical dependence, the molecular basis for which is not fully understood. It appears that the dependence is strongly linked to the number of cell surface μ-receptors (Tso & Wong, 2003).

This class of compounds exhibits certain important paradoxical effects on the parasympathetic nervous system. These drugs exert a procholinergic effect on the eyes and on blood vessels in the periphery (i.e., they cause constriction of pupils [**pin-point pupils**] and peripheral vasodilatation). In contrast, in the gut they lower gastrointestinal (GI) motility (i.e., they exhibit anticholinergic effects in the GI tract). This fact enables rapid diagnosis of heroin or, in general, opiate abuse in a patient brought to the emergency department in an obtunded or comatose state. These patients typically have severe miosis (pupillary constriction). Although the sign is not useful in acute diagnosis, constipation commonly occurs.

Administration of heroin occurs via the intravenous route. Addicts are readily recognized by the presence of needle tracks on their arms and hands and by extensive thrombosis of their peripheral veins. The half-life of heroin via the intravenous route is about 3 minutes, and the effects of the drug last approximately 3 hours. The major metabolites are *N*-acetylmorphine and morphine. The half-life of morphine is about 3 hours. Overdoses of heroin are extremely dangerous and can cause severe obtundation, coma, respiratory arrest, hypotension (secondary to histamine release), and cardiac arrhythmias. One of the most common acute therapeutic modalities for heroin overdose is intravenous treatment with naloxone (Narcan; see Fig. 24.7), a strong competitive antagonist to the action of heroin. Heroin addiction, as a chronic problem, is treated pharmacologically with a partial agonist of heroin—methadone (shown in the Group 1 structures in Fig. 24.7), which is discussed later.

Another opiate antagonist is naltrexone, whose structure is shown in the Group 1 structures in Figure 24.7. The primary effect of this drug is to lower the euphoria experienced by opiate abusers. However, it has no effect on opiate craving by drug abusers. On the other hand, it has been found to be effective in reducing the physical dependence of patients treated with the drug. However, to achieve abstinence, psychosocial support of the patient is required. Surprisingly, naltrexone has been found to be effective in the treatment of alcohol dependence; in particular, it has been found to reduce relapse rates after abstinence and to reduce heavy drinking to lower levels of consumption. The half-life of naltrexone is about 4 hours. Treatment of opiate abuse requires daily administration of one 50-mg tablet per day (often missed by opiate drug abusers). Excretion is via urine.

Codeine and Analogs

The structure of codeine is similar to that of morphine and heroin (Group 1 structures in Fig. 24.7). Codeine acts in a manner similar to that of morphine and is used as a milder analgesic and as an antitussive. The codeine analog, dextromethorphan (D-3-methoxy-*N*-methylmorphine), is an antitussive agent that is a component of cough-suppressive medications.

Dextromethorphan, an analog of codeine, is the active component of cough syrups because of its antitussive effects. Recently, there has been a "run" on cough medicines by addicts, who can obtain them legally and then consume quantities sufficient to reach their desired euphoric state. Unlike codeine, dextromethorphan is believed generally not to be addictive, although cases of drug dependency have been documented. For therapeutic use, the recommended dose of dextromethorphan is 15 to 30 mg given three to four times per day. **Moderate intoxication** is achieved at about 100 to 200 mg, and **heavy intoxication** is reached at around 1500 mg (Haroz & Greenberg, 2006). It is surprising to note that dextromethorphan does not have analgesic properties because of its lack of affinity for μ-, κ-, and δ-receptors. It has been found to induce the release and to block the reuptake of serotonin. Similar to the action of phencyclidine (PCP), discussed later, dextromethorphan has also been found to block NMDA receptors that are critical for neuronal plasticity and memory and are involved in central pain pathways in the brain, as discussed earlier (Zhuo, 2009). Dextromethorphan is readily absorbed from the GI tract and, in about 85% of individuals, is rapidly metabolized to dextrophan, an active metabolite, and D-hydroxymorphinane via the 2D6 cytochrome P450 isozyme (Haroz & Greenberg, 2006). It is dextrophan that has a high affinity for NMDA receptors, so that most individuals experience PCP-like effects (i.e., euphoria; tactile, auditory, and visual hallucinations; paranoia; altered time perception; and general disorientation). For the 15% of individuals who are slow metabolizers of dextromethorphan, these effects are much less pronounced and are replaced by sedation and dysphoria (Haroz & Greenberg, 2006). Overdoses of dextromethorphan can result in mainly neurologic effects, such as lethargy, or, conversely, hyperexcitability; ataxia; slurred speech; tremors and fasciculations; hypertonia and hyperreflexia; and nystagmus, as well as either pupillodilation or pupilloconstriction. Diaphoresis may also occur. In addition, cardiovascular sequelae include tachycardia and hypertension. Unfortunately, a number of antitussives contain, in addition to dextromethorphan, anticholinergic agents such as chlorpheniramine. Thus, abuse of antitussive medication can give rise to such symptoms as tachycardia, mydriasis, flushed skin, urinary retention, and constipation.

Oxycodone

This drug is effective in reducing pain, especially pain associated with malignancy. Its structure is shown in the Group 1 compounds in Figure 24.7, where it can be seen to be similar in structure to codeine, with the difference that there is a keto rather than a hydroxyl group at the 6– position (lower cyclohexone ring in Fig. 24.7) and a hydroxyl group rather than a hydrogen atom at the carbon between the two bridgehead carbons. On an empty stomach, pain diminution commences within about 15 minutes after oral drug administration. Peak serum levels are achieved in about 1 hour. The slow release form of oxycodone is Oxycontin, which achieves peak serum levels in about 3 hours. Although there is some controversy about the site of action of oxycodone, i.e., primary action on κ-receptors rather than μ-receptors (Smith, 2008), oxycodone does bind to μ-receptors and one of its metabolites, oxymorphone, is known to have a high affinity for μ-receptors (Smith, 2008). The half-life for oxycodone is about 3.2 hours and for Oxycontin is 4.5 hours. Metabolites of oxycodone are α- and β-oxycodol, oxymorphone, α- and β-oxymorphol and noroxymorphone, noroxycodone, and α- and β-noroxycodol and noroxymorphone (N-desmethyloxycodone). Most of the parent compound and its metabolites are excreted in the urine.

As with morphine and codeine, oxycodone, especially at high doses, can induce euphoria and a sense of well-being. Like the other opiates, it also induces a true physical dependence. At high doses, side effects are particularly pronounced, which include fatigue, dizziness, constipation, vomiting, anxiety, shallow breathing and apnea, hypotension, meiosis, circulatory collapse, and death. Withdrawal from oxycodone includes such symptoms as myositis, anxiety, nausea, insomnia, fever, hypogonadism, and hormonal imbalance. Given the side effects and the physical consequences of withdrawal, it is difficult to fathom the appeal of abuse of this drug. Nonetheless, abuse of oxycodone has grown to the point where it has now been added to the roster of drugs of abuse that are routinely assayed for mainly in urine.

Buprenorphine

Although, like oxycodone, this prescription drug has become a drug of abuse, buprenorphine is a mixed agonist-antagonist on opiate receptors. It has some opiate activity on μ-receptors, but it is purely an antagonist on κ- and δ-receptors. Its major use is the same as for methadone, as discussed later, in treating addiction to opiates, but it is also used in the treatment of pain. Since it has partial agonist activity, it does not cause life-threatening respiratory depression, as is true of agonists such as morphine. It undergoes extensive metabolism in the liver; therefore, excretion is via the hepatobiliary system in contrast to oxycodone, whose excretion is almost completely via the urinary tract. Thus, renal failure does not result in accumulation of buprenorphine in serum while it does cause increased levels of oxycodone. Treatment of patients with buprenorphine for addiction is carried out in programs in which the patient has access to private and group counseling during and after the treatment period. Suboxone is a combination of buprenorphine and naloxone (see Fig. 24.7). As described earlier, naloxone is an antagonist at μ-receptors and is administered with buprenorphine to block its toxic effects in patients who try to inject suboxone intravenously as a drug of abuse. The antagonism is limited due to the fact that the affinity of buprenorphine for the μ-receptor is about five times that of naloxone. Buprenorphine is also available as a transdermal patch (Butrans) that is used to treat chronic, rather than acute, pain and has been found to be effective for this purpose. However, the transdermal patch route has posed some challenges with regard to urine and oral drug testing as it does not require the same first-pass metabolism through the liver as with sublingual (Subutex, Suboxone) ingestion and releases microdoses compared with the pill form (Meyer & Maurer, 2011). Buprenorphine is metabolized via CYP3A4 enzyme to norbuprenorphine via the liver; both analytes are often included in a standard urine drug test to demonstrate ingestion of the parent drug. The presence of both buprenorphine and its metabolite norbuprenorphine in the urine can help obviate suspicion of diversion in a patient suspected of adding straight buprenorphine directly to the urine, which would not yield norbuprenorphine in such a case. Buprenorphine has been found to be more effective than methadone in treating patients with depressive traits (Gerra et al., 2004), a phenomenon that is thought to be associated with its pure antagonistic effects on κ-receptors. Since it, like oxycodone, has become popular as a drug of abuse, screening for its presence in urine has become common. Toxic effects of this drug include nausea, vomiting, drowsiness, dizziness, headaches, memory loss, perspiration, dry mouth, miosis, orthostatic hypotension, impotence, decreased libido, and urinary retention. Constipation can occur but is less frequent than with morphine. Hepatic necrosis and hepatitis with jaundice, as with the major tranquilizers/neuroleptic drugs, have further been observed in patients with high levels of buprenorphine. The half-life of buprenorphine is 23 to 42 hours, while that of naloxone is 2 to 12 hours. This difference between the two drugs again limits the antagonistic effect of naloxone on buprenorphine.

Fentanyl

This opiate analgesic (Group 1 drugs in Fig. 24.7) is about 80 times more potent than morphine in blocking pain. It can be taken orally as so-called **fentanyl lollipops**, smoked, inhaled, or administered by transdermal fentanyl patches (Haroz & Greenberg, 2006). Overdose effects of this drug are the usual ones seen for opiate abuse and include respiratory depression and miosis. Treatment may involve irrigation of the bowel, and anti-opiates such as naloxone may be administered. Hypotension is less common than with other opiates, such as morphine, because of the lack of histamine release.

Carfentanil

Generally used in veterinary medicine to tranquilize large animals (e.g., rhinoceros), carfentanil has made its way into street drug applications and has been responsible for dozens of deaths (Fomin et al., 2018). Carfentanil is metabolized in hepatocytes via *N*-dealkylation and monohydroxylation of the piperidine ring. Carfentanil is 4-anilidopiperidine, structurally similar to fentanyl, and acts primarily on the μ opioid receptors as an agonist. Carfentanil is purported to have a clinical potency up to 10,000 times that of morphine and 100 times that of fentanyl, such that it is anticipated that 1 mg of carfentanil is approximately equivalent to 8 to 10 g of morphine. Carfentanil induces similar effects to other opioids; however, due to its potency, it also induces strong side effects such as sedation, respiratory depression, rise in systemic blood pressure and temperature, and decrease in heart and respiratory rates. Naltrexone is the antidote of carfentanil, eliminating its effects.

Methadone

This interesting compound, whose structure is shown in the Group 1 drugs in Figure 24.7, is a nonbicyclic drug that binds competitively with morphine to μ-receptors in the brain. However, although it can become addictive, the addictive effects are less than those of equivalent concentrations of heroin, possibly because its binding affinity is lower, so that it induces less of an effect than heroin. Thus, administration of methadone to heroin addicts allows them to experience the effects of heroin but in a modulated manner. By gradually lowering the methadone dose, physical dependence becomes reduced, and it appears that a trough serum methadone level greater than 100 ng/mL is adequate for effective methadone maintenance (Bell et al., 1988). However, it should be noted that addiction to methadone can also occur. In toxicology laboratories, the most common request received for methadone screens comes from methadone clinics to test whether a patient is administering methadone or has relapsed into taking heroin. As can be seen in Figure 24.3, it is a simple matter to distinguish methadone from the opiates by TLC. Similarly, EMIT or FPIA detects each drug with high specificity. Confirmation via GC/LC-MS is also utilized and can detect methadone in urine approximately 3 to 5 days postingestion. Methadone is further metabolized to 2-ethylidene-1,5-dimethyl-3,3-diphenylpyrrolidine (EDDP). Recent studies have reported the utility of methadone-to-EDDP ratios to monitor for patient compliance (Diong et al., 2014).

AMPHETAMINES

These compounds, as can be seen in Figure 24.7 (Group 4 drugs), bear a close resemblance to the adrenergic amines such as epinephrine and norepinephrine and may be expected to exert sympathomimetic effects. They also resemble dopamine and may be expected to have effects on dopaminergic pathways. The amphetamines cause euphoria and increased mental alertness that may be attributed to their effects on these pathways. This group of drugs, however, also exerts pronounced stimulatory effects on γ- and β-receptors in the cardiovascular system and in the kidney to cause pronounced adrenergic effects such as increased heart rate, increased blood pressure, palpitations, bronchodilation, anxiety, pallor, and tremulousness. Studies indicate that amphetamines are also competitive inhibitors of the enzyme monoamine oxidase, which inactivates adrenergic neurotransmitters by oxidatively removing their amino groups. Blockage of this enzyme prolongs the effects of epinephrine and norepinephrine, with the attendant neurologic and cardiovascular sequelae. One particular amphetamine, 3,4-methylenedioxymethamphetamine (MDMA or **ecstasy**), a derivative of methamphetamine (see Group 4A drugs in Fig. 24.7), has become popular as a recreational drug of abuse because it has euphoric and psychedelic effects but minimal hallucinogenic effects (Gill et al., 2002; Haroz & Greenberg, 2006).

Clinical Symptoms

The pharmacologic action of amphetamines includes CNS and respiratory stimulation and sympathomimetic activity (e.g., bronchodilation, pressor

response, mydriasis). Loss of weight may also occur as the result of an anorectic effect. Psychic stimulation and excitability, leading to a temporary increase in mental and physical activity, can occur. Anxiety and nervousness can also be produced.

Acute Toxicity

Initial manifestations of an overdose may be cardiovascular in nature. Symptoms may include flushing or pallor, tachypnea, palpitation, tremor, labile pulse rate and blood pressure (hypertension and hypotension), cardiac arrhythmia, heart block, circulatory collapse, and angina. Mental disturbances such as delirium, confusion, delusions, disorientation, and hallucinations may occur. Acute psychotic syndromes may be characterized by vivid auditory and visual hallucinations, restlessness, homicidal or suicidal tendencies, panic state, paranoid ideation, loosening of associations, combativeness, and changes in affect. A frequent and potential sign of acute intoxication is hyperpyrexia; rhabdomyolysis has also been associated with acute amphetamine overdose. Cardiovascular collapse is the usual cause of death.

Chronic Usage

Tolerance may be produced within a few weeks; physical or psychic dependence may occur with prolonged usage. Symptoms of chronic abuse include emotional lability, somnolence, loss of appetite, occupational deterioration, mental impairment, and social withdrawal. Trauma and ulcer of the tongue and lip may occur as a result of continuing chewing or teeth-grinding movements. A syndrome with the characteristics of paranoid schizophrenia can occur with prolonged high-dosage use. Aplastic anemia and fatal pancytopenia are rare complications.

Treatment

No specific antidote for amphetamine overdose is known. Treatment of overdose is symptomatic, with general physiologic supportive measures immediately implemented. When cardiovascular symptoms are noted, propranolol (Inderal), discussed subsequently under therapeutic drugs, can be used as an antidote.

Detection

Both Toxi-Lab and EMIT (Syva, San Jose, CA) procedures are effective in detecting these drugs of abuse. Occasionally, on the Toxi-Lab A strip, amphetamines may be confused with antihistamines such as diphenhydramine.

"Designer" Amphetamines and Related Drugs of Abuse

The quest for euphoria-producing drugs has resulted in the advent of synthetic phenylethylamines, so-called **designer drugs**, such as MDMA, several further examples of which are shown in Category 4A of Figure 24.7. With all of these drugs, the consequences of the sought-after effects of euphoria and hallucinations are headaches, nausea, vomiting, anxiety, agitation, violent behavior, tachycardia, hypertension, respiratory depression, and seizures, as discussed previously in the case of standard amphetamines.

Other phenylethylamine derivatives shown in Figure 24.7, especially 2C-T-7 and 2CB, bind to 5-HT_2 receptors and induce hallucinogenic effects (Haroz & Greenberg, 2006). These drugs have been taken orally or have been insufflated, smoked, administered intravenously, and even taken rectally. Death from overdose of these designer drugs has been reported but is uncommon. Unfortunately, thus far, no specific assays are available for most of these drugs in urine. Their presence must be ascertained by history and/or symptoms reported in the absence of positive urine tests for standard amphetamines. On occasion, GC-MS is used to detect their presence.

TRYPTAMINES

These drugs are derivatives of serotonin, whose structure is shown in the Group 6 drugs in Figure 24.7. These tryptamines, some of which occur in plants, are relatively simple to obtain and were not proscribed until relatively recently. An example is *N,N*-dimethyltryptamine (DMT), which has strong hallucinogenic properties. Smoking DMT results in the rapid onset of hallucinogenic effects that are short-lived, giving rise to the term **businessman's lunch**. Other tryptamines contain modifications of the indole ring, as shown in the Group 6 drugs in Figure 24.7. These also allows them to interact with 5-HT receptors (Haroz & Greenberg, 2006); this interaction is thought to result in their hallucinogenic effects. However, the mechanism of action of this class of drugs is not well understood. Psilocin shown in this figure is a component of the so-called **Psilocybe**, called **magic mushrooms** because of their hallucinogenic effects. The hallucinogenic effects of these drugs are enhanced by the presence of monoamine oxidase inhibitors such as β-carbolines (Haroz & Greenberg, 2006). The mixture of these two compounds is present in a South American tea called **ayahuasca**, which combines two plants—one containing DMT and the other carbolines, which themselves can induce nausea and vomiting. Like the amphetamines and other phenylethylamine derivatives, the tryptamines cause, in addition to the desired effects of euphoria and empathy, auditory and visual hallucinations, nausea, vomiting, diarrhea, and emotional distress. Symptoms further include agitation, tachycardia, hypertension, diaphoresis, salivation, dystonia, mydriasis, tremors, confusion, seizures, and, in a few cases, rhabdomyolysis and paralysis. Currently, no routine assays are available for these compounds. As with the amphetamines, many of the psychogenic and physiologic effects of the tryptamines can be countered with supportive therapy and the administration of benzodiazepines.

PIPERAZINES

The structure of the parent compound, piperazine, is shown in Group 7 of Figure 24.7. Several of the derivatives of piperazine are also shown in this figure. Many of these piperazines were used as antihelminthics during the 1950s but were subsequently discontinued. However, their euphoria-producing effects were discovered, leading to a "legal" way of obtaining drugs of abuse. Two classes of piperazine derivatives have been identified: *N*-benzylpiperazines, the parent compound of which is *N*-benzylpiperazine (BZP) and phenylpiperazines. The former group includes 1-(3,4-methylenedioxybenzyl)piperazine. The latter group includes 1-(3-chlorophenyl)piperazine, 1-(4-methoxyphenyl)piperazine, and 1-(3-trifluoromethylphenyl)piperazine (TFMPP). BZP (known as **A2**) and TFMPP (known as **Molly**) are among the most popular piperazines. Studies have shown that these piperazines produced effects that were similar to those of the amphetamines, suggesting that the target receptors of these drugs are the same. Both classes of piperazines have been found to increase dopamine and serotonin levels. TFMPP has been found to act as a partial agonist at 5-HT_{2A} receptors and is a full agonist at other 5-HT receptors. Although TFMPP is three times less potent than MDMA, it produces a full MDMA effect when combined with BZP, with which it is synergistic (Haroz & Greenberg, 2006). The TFMPP-BZP combination at low doses induces euphoria with decreased motor action, making the euphoric experience more pleasurable. The acute undesirable effects of piperazines are similar to those of the amphetamines and MDMA (i.e., hallucinations, psychomotor agitation, increased heart rate and blood pressure, and increased body temperature). Two deaths from BZP have been reported when combined with another drug such as MDMA (Haroz & Greenberg, 2006). Both TFMPP and BZP have skin-irritant properties, causing sore nasal passages and throats. As with the tryptamines and designer amphetamines, no standard assay method detects these drugs in urine at this time. Treatment is supportive, as described in the preceding section.

BENZODIAZEPINES

Among this group of drugs, shown in Figure 24.7 (Group 2), the most prominent is Valium (diazepam). Benzodiazepines are used therapeutically, as so-called **minor tranquilizers**. Their mechanisms of action appear to be potentiation of GABA, a neurotransmitter that *inhibits* conduction in dopaminergic neurons, and facilitation of its binding to GABA receptors (Campo-Soria et al., 2006). Benzodiazepines bind to the α subunit of the so-called **$GABA_A$ receptor** at a site that is distinct from that for GABA itself and cause an increase in the frequency of chloride ion channel opening at the $GABA_A$ receptor. Usually used as a therapeutic drug to produce calming effects at doses between 2.5 and 10 mg and to produce muscle-relaxing effects at higher doses, Valium has been used by drug addicts in high doses to counter the excitatory effects of other drugs of abuse or as a means of inducing tranquil states. Among some drug abusers, benzodiazepines are used to potentiate the effects of heroin (Fraser, 1998). A number of drug abusers have become addicted to Valium when using high doses several times each day. Acutely, benzodiazepine overdose may produce somnolence, confusion, seizures, and coma. Rarely, hypotension, respiratory depression, and cardiac arrest may occur. Chronically, physical and psychological dependence occur. Sudden discontinuance of the drug may lead to anxiety, sweating, irritability, hallucinations, diarrhea, and seizures. Treatment is supportive. Gradual diminution of the benzodiazepine removes physical dependence. The half-life for Valium is 20 to 70 hours, but the half-life of one of its active metabolites is 50 to 100 hours.

PHENCYCLIDINE

This interesting tricyclic compound, shown in Figure 24.7 (Group 5), has numerous effects on a variety of different neural pathways. Used almost exclusively as a drug of abuse, this drug is traded on the streets under the name of **angel dust** or **angel hair**. It is peculiar that the use of this drug appears to be periodic. The physiologic effects of PCP appear to be analgesic and anesthetic and, paradoxically, stimulatory. This drug has been found to interact with cholinergic, adrenergic, GABA-secreting, serotonergic, and opiate neuronal receptors. It has also been found to block NMDA receptors (Hevers et al., 2008). Thus, a wide variety of bizarre and apparently paradoxical symptoms can be seen in the same patient. This drug has been shown to bind to specific regions of the inner chloride channels of neurons, apparently profoundly affecting chloride transport. It has also been found to bind strongly to a class of neural receptors called **sigma receptors** (Schuster et al., 1994). This receptor binds strongly to the neuroleptic, antipsychotic drug haloperidol (Haldol)—a finding that may implicate the sigma receptor in some of the clinical findings of severe psychosis in patients suffering from overdose with PCP.

Because of its varied actions, clinically acute manifestations vary from depression to euphoria and can involve catatonia, violence, rage, and auditory and visual hallucinations. Vomiting, hyperventilation, tachycardia, shivering, seizures, coma, and death are among the common occurrences that result from abuse of this drug. Most fatalities occur from the hypertensive effects of the drug, especially on the large cerebral arteries (Bayorh et al., 1984). As can be inferred from this spectrum of possible symptoms, diagnosis based on clinical findings is impossible. Only the results of a drug screen can be diagnostic. Treatment of drug abuse with PCP is supportive, with the patient kept in isolation in a darkened, quiet room. Acidification of the urine increases the rate of PCP excretion. As might be expected from findings regarding the sigma receptor, treatment with Haldol results in sedation of the violent, hallucinating patient.

BARBITURATES: SEDATIVE-HYPNOTICS

An almost bewildering variety of these major sedative drugs is available. However, all are derivatives of barbituric acid, which may be regarded as the condensation product of urea and malonic acid, as indicated in Figure 24.7 (Group 3 drugs). Depending on the substituents of the $-CH_2$ group of the malonic acid portion, the particular drug may be long acting, as is phenobarbital, with a benzene ring and ethyl group substituents on this carbon; short acting, as is pentobarbital, with neopentyl and ethyl groups at this position; or ultra-short acting, as is the case with thiopental. The long-acting barbiturate phenobarbital is a therapeutic drug that is used as an anticonvulsant, unlike the short- and ultra–short-acting drugs, and is discussed in the Therapeutic Drug Monitoring section later in the chapter. All of the barbiturates are fat soluble and therefore pass easily across the blood-brain barrier. All of them seem to stabilize membranes such that depolarization of the membranes becomes more difficult.

As with the benzodiazepines, the barbiturates are known to interact with GABA receptors. In particular, they bind to the α subunit of the $GABA_A$ receptor at a site that is distinct both from the GABA binding site and from the benzodiazepine binding site. Their effect is to increase the *duration* of chloride ion channel opening at the $GABA_A$ receptor, potentiating the GABA effect (i.e., inhibition of dopamine-dependent nerve conduction). It is thought that this action of chloride channel opening, called **direct gating** of the chloride channel, is the basis for barbiturate toxicity, which is greater than for the benzodiazepines, which do not increase the **duration** of chloride channel opening but rather increase the **frequency** of channel opening, as discussed in the Benzodiazepines section earlier in the chapter. In addition, at higher doses, barbiturates have been found to inhibit a subtype of glutamate receptors, called **AMPA receptors**. Glutamate is a major excitatory neurotransmitter. More generally, barbiturates have been found to block calcium ion–induced release of neurotransmitters.

For unknown reasons, the short-acting and ultra–short-acting barbiturates seem to inhibit selectively the reticular activating system, which is involved with arousal, hence their sedative and hypnotic effects. The ultra–short-acting barbiturates rapidly diffuse out of the CNS, accounting for their rapid action. Phenobarbital, however, selectively reduces the excitability of rapidly firing neurons and is therefore a highly effective anticonvulsant. It may be more than coincidental that phenobarbital and the equally effective anticonvulsant phenytoin (Dilantin) bear structural resemblance to one another and may exert similar effects on rapidly firing neurons. The mechanism of action of phenytoin is discussed subsequently.

Clinically, at low doses, the short-acting and ultra–short-acting barbiturates produce sedation, drowsiness, and sleep. They also impair judgment. At higher doses, anesthesia is produced. At very high doses, these drugs can cause stupor, coma, and death. The toxic manifestations of these drugs are depression, Cheyne-Stokes respirations, cyanosis, hypothermia, hypotension, tachycardia, areflexia, and pupillary constriction. Treatment of drug overdose is supportive and includes the standard treatment for shock. When administered within 30 minutes of drug ingestion, activated charcoal is an effective barbiturate chemoadsorbent.

Diagnosis of drug abuse with short-acting and ultra–short-acting barbiturates is done by immunoassay and TLC screening procedures. HPLC has found some use in this regard but is not a standard method. The barbiturates are weak acids, the N-H protons being somewhat acidic. Thus, they are acid extracted and placed on the B strip in Toxi-Lab procedures. Their presence is easily detected by Toxi-Lab TLC, as shown in Figure 24.3, Worksheet B. Immunoassays for those drugs are also excellent, the one caveat being that high levels of phenobarbital in urine cross-react with antibodies against the short-acting barbiturates. Thus, it is important that TLC confirms a positive immunoassay result for sedative-hypnotic barbiturates.

PROPOXYPHENE (DARVON)

This analgesic drug, whose structure is shown in the Group 1 drugs in Figure 24.7, has pharmacologic properties very similar to those of the opiates, such as morphine. As can be seen in Figure 24.7 (drug Group 1), the structure of propoxyphene is quite similar to that of methadone. This drug can be taken orally so that the feelings of pleasant sedation induced by opiates can be obtained without the intravenous apparatus needed for infusion of heroin. A major cause of drug-related death is propoxyphene overdose alone or in combination with CNS depressants such as barbiturates and alcohol. Toxic symptoms are similar to those seen with overdoses of opiates (namely, respiratory depression, cardiac arrhythmias, seizures, pulmonary edema, and coma). Nephrogenic diabetes insipidus may also occur. In addition, propoxyphene has been found to cause cardiac arrhythmias (Barkin et al., 2006). Treatment for propoxyphene overdose is mainly supportive. Administration of naloxone (Narcan) reverses the toxic effect of the drug.

METHAQUALONE (QUAALUDE)

Methaqualone is a 2,3-disubstituted quinazoline (Group 5 drugs in Figure 24.7). Although not structurally similar to the barbiturates, it has many of the same sedative-hypnotic properties as the barbiturates. This compound also possesses anticonvulsant, antispasmodic, local anesthetic, antitussive, and weak antihistamine actions. Oral administration leads to rapid and complete absorption of the drug, with approximately 80% bound to plasma protein. Peak plasma concentrations are reached in approximately 2 to 3 hours. Almost all of the drug appears to be metabolized by the hepatic cytochrome P450 microsomal enzyme system, with only a small percentage (<5%) excreted unchanged in the urine. The serum half-life ranges from 20 to 60 hours. The dosages used for its hypnotic-sedative actions range from 150 to 300 mg daily. Toxic serum concentrations are generally reached at 10 μg/mL. Tolerance to as well as dependence on some of its actions occurs, such that abusive dosages can be up to six to seven times greater than those employed therapeutically. Symptoms of overdose can be similar to barbiturate toxicity and produce CNS depression with lethargy, respiratory depression, coma, and death. However, unlike barbiturate overdose, muscle spasms, convulsions, and pyramidal signs (hypertonicity, hyperreflexia, and myoclonus) can result from severe methaqualone intoxication. Treatment for overdose includes supportive therapy, as well as delaying absorption of remaining drug with activated charcoal and drug removal by gastric lavage.

MARIJUANA (CANNABIS)

This is one of the oldest and most widely used of the mind-altering drugs. Marijuana is a mixture of cut, dried, and ground portions of the hemp plant *Cannabis sativa*. Hashish refers to a more potent product produced by extraction of the resin from the plant. The principal psychoactive agent in marijuana is considered to be δ-9-tetrahydrocannabinol (δ-9-THC; Group 5 drugs in Fig, 24.7), a lipid-soluble compound that readily enters the brain and may act by producing cell membrane changes. δ-9-THC binds to the presynaptic neural cannabinoid receptor CB1, which releases the inhibitory neurotransmitter GABA in the hippocampus, amygdala, and cerebral cortex (Iversen, 2003). Different forms of THC have been found to cause distinctly different physiologic effects (Fusar-Poli et al., 2009). δ-9-THC induces an increase in anxiogenic effects, and cannabidiol produces a diminution in anxiety. The latter derivative was found to attenuate blood oxygenation levels in the amygdala and the anterior and posterior cingulate cortex; δ-9-THC was found to modulate activation in frontal and parietal regions of the brain.

Marijuana may be introduced through the lungs by smoking or through the gastrointestinal tract by oral ingestion in food. Once THC enters the body, it is readily stored in body fat and has a half-life of approximately 1 week. Biotransformation is complex and extensive; less than 1% of a dose is excreted unchanged. About one-third is excreted in the urine, primarily as δ-9-carboxy-THC and 11-hydroxy-δ-9-THC. These metabolites may be detected in the urine from 1 to 4 weeks after the last ingestion depending on both dosage and frequency of ingestion.

In general, marijuana does not appear to cause physiologic dependence, although a proportion of chronic users of this drug can develop physiologic dependence (Iversen, 2003). Tolerance (Martin et al., 2004) and psychological dependence do seem to occur. Two major physiologic effects of marijuana are reddening of the conjunctivae and increased pulse rate. Muscle weakness and deterioration in motor coordination can also occur. The preponderant changes seen with cannabis intoxication are perceptual and psychic changes. These range from euphoria, relaxation, passiveness, and altered time perception, seen at low doses, to adverse reactions such as paranoia, delusions, and disorientation, which can be seen at high doses in psychologically susceptible individuals.

The dosage, the route of administration, the individual's psychological makeup, and the setting are important determinants in each individual's reaction to cannabis intoxication. Thus, high doses in an individual unprepared for or unaware of drug consumption may produce a disturbing experience. More commonly, experienced users report mild euphoria, enhancement or alteration of the physical senses, introspection with altered emphasis or importance of ideas, and heightening of subjective experiences. Heavy chronic use may produce bronchopulmonary disorders. Although the relative safety of chronic use is controversial, acute panic reactions, delirium, and psychoses occur rarely (Bryson, 1989). Few users seek treatment; when a distressed user does seek treatment, medical intervention is generally conservative. However, following an acute episode, psychological evaluation may be necessary in an individual with an underlying psychiatric disturbance. Rarely, marijuana may be ingested by intravenous infusion of a boiled concentrate. Severe multisystem toxicity may be produced by this route of administration. Symptoms may include acute renal failure, gastroenteritis, hepatitis, anemia, and thrombocytopenia.

LYSERGIC ACID DIETHYLAMIDE (LYSERGIDE)

Lysergic acid diethylamide (LSD; Group 5 in Fig. 24.7) is a semisynthetic indolalkylamine and a hallucinogen. It is one of the most potent pharmacologic materials known, producing effects at doses as low as 20 μg, and is equally effective by injection or oral administration. Comparison of the structure of LSD with that of 5-hydroxytryptamine (serotonin), as shown in the Group 6 drugs in Figure 24.7, reveals that LSD has a tryptamine-like nucleus, but it lacks the 5-hydroxyl group of serotonin. LSD has multiple complex effects in the CNS. In the locus coeruleus and the median raphe of the midbrain, which utilize serotonergic pathways, it has the paradoxical effect of **inhibiting** both the firing of neurons in these structures and the release of serotonin at the axonal sides of synapses (Passie et al., 2008). This process, in turn, may produce a state of CNS hyperarousal. On the other hand, it actually acts as a serotonin **agonist** on postsynaptic HT_{1A} receptors. It is a pure agonist on 5-HT_2 receptors in other serotonergic pathways. Recently, it has been found that the hallucinogenic effect of LSD is due to its agonistic effect on 5-HT_2 receptors, and that it behaves very much like the tryptamines (Group 6 drugs; see Fig. 24.7) and phenylethylamines (Groups 4 and 4A drugs; see Fig. 24.7), discussed previously, in producing this effect. In addition, it has been found to have both agonistic *and* antagonistic effects on dopaminergic pathways. Thus, it acts at multiple sites in the CNS in complex ways. LSD further affects both the sympathetic and parasympathetic nervous systems. However, the sympathetic effect appears to be greater; initial symptoms include hypertension, tachycardia, mydriasis, and piloerection.

The usual dosage of LSD is 1 to 2 μg/kg; LSD produces an experience that begins within 1 hour of ingestion, usually peaks at 2 to 3 hours, and generally lasts 8 to 12 hours after ingestion. Metabolism occurs in the liver, whereas excretion occurs mainly in the bile.

LSD is the most commonly abused drug in its class and is believed by its users to provide insights and new ways of solving problems. The psychic effects are usually intense and vary depending on the user's personality, expectations, and circumstances. LSD acts on all body senses, but visual effects are the most intense. Common perceptual abnormalities include changes in the sense of time, organized visual illusions or hallucinations, blurred or **undulating** vision, and synesthesias. Mood may become very labile, and dissolution and detachment of ego may occur. LSD toxicity levels are low, and deaths are generally due to trauma secondary to errors in the user's judgment. Panic reactions—a **bad trip**—are the most common adverse reactions. These may occur in any user and cannot be reliably predicted or prevented. Borderline psychotic and depressed individuals are at risk for the precipitation of suicide or a prolonged psychotic episode by the usage of LSD. Flashbacks, which are poorly understood, occur days to months after ingestion. This occurs when the user experiences recurrences of a previous hallucinogenic experience in the absence of drug ingestion.

Acute panic reactions may be treated by frequent reassurance and a quiet and calm environment; diazepam may also be effective. However, except for treating specific complications, LSD abuse has no systematic program of treatment.

CATHINONES (BATH SALTS; FIG. 24.7, CLASS 8)

Synthetic cathinones (i.e., "bath salts"—see Fig. 24.7, Class 8) are a type of psychoactive designer drug that produces amphetamine- or cocaine-like subjective effects by activating monoamine systems in the brain and periphery (Banks et al., 2014). Bath salts produce the expected desirable effects at lower doses. However, high doses as well as chronic exposure can foster psychosis, violent behaviors, tachycardia, hyperthermia, and even death. There are three main synthetic cathinones: 4-methyl-N-methylcathinone (mephedrone), 3,4-methylenedioxy-N-methylcathinone (methylone), and 3,4-methylenedioxypyrovalerone (MDPV). These compounds are structurally related to the parent compound cathinone, which is a naturally occurring β-keto amphetamine with known psychostimulant properties. Bath salts enhance sympathetic nervous system activity and are thought to act by increasing the concentration of dopamine in the synaptic cleft that results in increased activation of postsynaptic dopamine receptors (see Fig. 24.8). Furthermore, bath salts such as methcathinone is a substrate for the dopamine transporter, thereby blocking the ability of dopamine to bind to the transporter and subsequently reducing one of the main mechanisms of dopaminergic neurotransmission termination.

The diagnosis of bath salt ingestion requires a high index of suspicion when evaluating a patient presenting with intoxication or overdose as there are no commonly available laboratory drug screening testing approaches that can be employed at a point-of-care or office setting at the time of presentation. They may precipitate a false-positive methamphetamine drug screening result. Laboratory detection of synthetic cathinones requires high-complexity GC/MS or LC/MS confirmatory testing with a detection window for urine sample of 2 to 3 days postingestion. Serum and urine toxicologic studies can also identify potential coingestion of other toxic agents. Treatment of synthetic cathinone overdose is primarily supportive care, as a specific antidote does not exist. The most common treatments used in emergency departments are intravenous fluids, benzodiazepines, oxygen, and sedatives. Specific metabolic sequelae (hyponatremia, myocarditis, and necrotizing fasciitis) should be treated by medical and/or surgical interventions as required (Thornton & Baum, 2014).

SLEEP AIDS (FIG. 24.7, CLASS 9)

It is estimated that one in six adults with a diagnosed sleep disorder and one in eight adults with trouble sleeping reported using sleep aids, that 50 to 70 million Americans suffer from sleep disorders or deprivation, and that 4% of adults aged 20 years and over reported using a prescription sleep aid in the past month, with greater use in the elderly. Furthermore, sleep aids include sedative/hypnotic agents and are also subject to dependency and abuse. Prescription sleep aids include barbiturates and benzodiazepines in addition to other agents. The imidazopyridine zolpidem (Ambien), represents a chemically novel nonbenzodiazepine hypnotic agent (see Fig. 24.7, Class 9) which binds to the σ-1 receptor in the brain. Unlike benzodiazepines, zolpidem does not contain myorelaxant or anticonvulsant effects, and its effects on anxiety appear to be minor. It does not appear to affect sleep stages but does appear to reduce the latency to and to prolong the duration of sleep in patients with insomnia owing to its rapid onset of action and short elimination half-life (Langtry et al., 1990). In contrast, the cyclopyrrolone zopiclone/eszopiclone (Lunesta), another nonbenzodiazepine hypnotic agent (see Fig. 24.7, Class 9), modulates the GABA(A) receptor through allosteric mechanisms (Döble et al, 1995). Although its receptor binding is not facilitated directly by GABA, its interaction with the GABA(A) receptor can potentiate responses to GABA. As such, coadministration of benzodiazepines, which is not uncommon in those with sleep disorders, can have deleterious potentiating effects. The detection window for these sleep aids is generally 1 to 7 days postingestion when conventionally assessed via GC/MS or LC/MS confirmatory testing approaches.

MUSCLE RELAXANTS (FIG. 24.7, CLASS 10)

Pain management of musculoskeletal conditions includes carisoprodol (Soma; see Fig. 24.7, Class 10), a CNS depressant with an unknown mechanism of pharmacologic action. Its sedative effects are generally attributed to the actions of its primary metabolite, meprobamate, at GABA(A) receptors (GABA(A)R). Interestingly, although its primary metabolite meprobamate (Miltown, Equanil; see Fig. 24.7, Class 10) is classified as a controlled substance at the federal level, carisoprodol is not (Gonzalez, et al. 2009). These agents are available in varying doses and ingestion recommendations, and the general detection window in a urine sample postingestion is 1 to 3 days. There have been reports of carisoprodol-related abuse, diversion, and death, thus deeming it a drug of concern for the U.S. Department of Justice Drug Enforcement Agency, Office of Diversion Control. In Florida, the number of carisoprodol/meprobamate-related deaths in 2005 exceeded those attributed to opioids, including heroin and fentanyl. In fact, abuse of carisoprodol has become an international problem. Recently, the Committee for Medicinal Products for Human Use (CHMP) concluded that the abuse potential associated with carisoprodol outweighs its benefits as a therapeutic drug.

OTHER DRUGS

There is no lack of ingenuity when it comes to conjuring up new synthetic drugs of abuse. There have been a number of new synthetic cannabinoids available to the clinical marketplace, many of which have deleterious health effects that are more severe than that of marijuana. These have brand names like "Spice" or "K2" and their effects can be physical, affecting cardiovascular, neurologic, renal, pulmonary, or metabolic systems. Effects can be psychological as well, altering cognitive and behavioral functions (Castellanos, et al. 2016). These synthetic cannabinoids, propagated by "street" chemists, can be of the benzoyl, naphthoyl, alkyl, or phenylacetyl derivatives among others and comprise >50 different types (Debruyne & Le Boisselier, 2015). For example, the aminoalkylindole cannabinoid derivative JWH-018 (1-penthyl-3-(1-napthoyl)indole), one of the first derivatives detected in K2 preparations seized in the United States, is thought to exert its effects via G protein–coupled cannabinoid type 1 (CB-1) receptors. The affinity of JWH-018 for the CB-1 receptor is about 15 times greater than conventional δ^9-THC. Although the general detection window for urine testing is about 3 to 5 days postingestion of JWH-018 and similar analogs, there are no quality control and manufacturing standards for such illicit drugs.

THERAPEUTIC DRUG MONITORING

It has now become recognized that serum levels of many of the therapeutic drugs administered to patients must be frequently determined both because of the possible toxic side effects of many of these medications and because, often, lack of patient compliance results in subtherapeutic levels of the drug, requiring intervention. Recent data suggest that the lack of adherence to medical therapeutic recommendations is a major cause of morbidity and mortality in multiple disease processes among all age groups (Lieber et al., 2015). Furthermore, it is important for the physician, when initiating drug therapy, to ascertain when the serum levels of the drug have achieved a stable therapeutic level. Therefore, it is important to understand the principles, called **pharmacokinetics**, on which drug therapy is based. Some of the basic principles of pharmacokinetics and the physiologic effects of specific classes of therapeutic drugs are presented in this section. The ones discussed are those whose specific levels are most commonly followed by clinicians and are most commonly assayed for in clinical laboratories. It should be noted that virtually all therapeutic drugs are assayed from specimens of serum, not urine, most commonly using immunoassay techniques such as FPIA.

PHARMACOKINETICS

Figure 24.9 summarizes the two ways in which a therapeutic drug is administered to a patient: discontinuously or continuously (Gerson, 1987a,b). The former method is the most common. Most patients are treated with medications taken orally at fixed periods. For example, to achieve antiinflammatory effects, two aspirin tablets of 350 mg each are taken every 4 to 6 hours. In this case, the aspirin is taken at discrete times, between which a certain amount will be metabolized and/or excreted before the next dose is given. For continuous administration, a patient will be infused with a drug intravenously, such as with lidocaine (Xylocaine) in the intensive care unit for a cardiac arrhythmia or with heparin to prevent thromboembolic events. In this case, while the drug is metabolized, a constant amount of the drug is being infused continuously. Eventually, with continuous infusion of a drug, a steady-state concentration of the drug is reached once the amount of drug infused in a unit of time equals

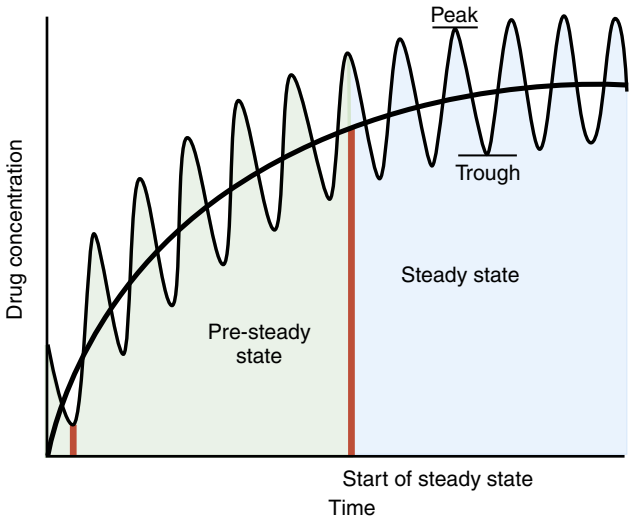

Figure 24.9 Illustration of the time course of drug levels as a function of method of administration. In the discontinuous method, represented by the *curve* showing peaks and troughs, a constant dose of a drug is administered at regular intervals. After each drug dose, the drug level increases to a peak value, followed by a fall that continues to a trough level, at which time the next regular drug dose is given, resulting in another peak level. After approximately 4 to 5 half-lives, the drug levels achieve the steady state, as labeled in the figure, when constant peak and trough levels occur. Note that, if a loading dose can be given to the patient that is equal to the peak steady-state value, the entire left portion (pre–steady state) of the curve is eliminated. After the loading dose, the steady state is maintained by giving periodic maintenance doses. The *black smooth curve* shows a typical time course for drugs that are administered continuously, mainly by the intravenous route. The steady state is achieved as a continuing constant value rather than as peaks and troughs, as in the discontinuous method.

the amount of drug eliminated in the same unit of time. A steady-state concentration of a drug that is discontinuously infused is also reached. However, repeated dosing (equal doses spaced equally apart) produces peak and trough serum concentrations that vary around a steady-state or average concentration.

For both discontinuous and continuous infusions, the ultimate drug level is determined by a battle between the amount infused and the amount excreted. All drugs are eventually excreted. They can be excreted unchanged in the urine or may be excreted in urine as metabolites of the parent drug. These metabolic conversions occur predominantly in the liver. Occasionally, some drugs enter the enterohepatic circulation and are excreted in stool. Regardless of their mode of excretion, many but not all drugs have a half-life that is more or less independent of their concentrations. The half-life of a drug is the time taken for half the drug that was initially present in serum to be consumed. The reason that the half-life of a drug is independent of its concentration is that many drugs are excreted according to so-called **first-order kinetics**, as discussed in Chapter 21 (Eqs. 21.22 and 21.23). This process may be summarized as follows:

$$D \xrightarrow{k} E \qquad \text{(Eq. 24.5)}$$

where D is the drug concentration and E is the excreted and/or inactivated form of the drug. The constant, k, is the rate constant for the disappearance of D. The half-life, called $t_{1/2}$, is related to the rate constant, k, by the following relationship:

$$t_{1/2} = 0.693 / k \qquad \text{(Eq. 24.6)}$$

As can be seen from this equation, $t_{1/2}$ is a constant and does not depend on drug concentration. Thus, the half-life of the drug determines the time to reach the steady-state or average concentration.

The object of all drug therapy is to achieve a constant serum level of the drug that will be therapeutic. If the half-life for a drug is known, it is possible to compute the divided dose of the drug that should be given and the time interval between doses so that this level will be achieved. As can be seen in Figure 24.9, at the beginning of drug administration, wide fluctuations in the drug level occur until, after a given period, the fluctuations give the same maxima (peaks) and the same minima (troughs), and the mean level of the drug becomes constant. The problem in dosing is to ensure that the maximum level of the drug will be in the therapeutic range and will not reach toxic levels and, at the same time, to ensure that the minimum level of the drug will remain in the therapeutic range and will not be subtherapeutic.

In general, for discontinuous doses, the drug level at the end of the nth dosing period can be expressed as the sum of a geometric series:

$$D = (D_0 r^N - D_0)/(r - 1) \quad \text{(Eq. 24.7)}$$

where D_0 is the constant dose given at each regular time period, r is the fraction of drug remaining after the constant time interval between doses, and N is the number of the dose (e.g., the second dose, the third dose). Note that, because r is a fraction less than 1, as N becomes large, the first term in Equation 24.7, $D_0 r^N$, becomes small, so that

$$D = D_0/(1 - r) \quad \text{(Eq. 24.8)}$$

For example, if the time interval between doses is chosen as the $t_{½}$, then r = ½. If the time interval is chosen to be that for ¾ of the drug to remain, then r = ¾. (This time can be calculated directly from the $t_{½}$ as ½ × $t_{½}$.) Suppose we take r = ½. Then, after four timed doses, the first term in the numerator of Equation 24.7 is $D_0 \times (½)^4 = D_0/16$ or approximately 0.06 × D_0, which is small compared with D_0, and, in effect,

$$D = 2D_0 \quad \text{(Eq. 24.9)}$$

This level is the maximum (peak) level shown in Figure 24.9. It is the level achieved just after the dose, D_0, is given. Note that at the end of the dosing period, just before the next dose, D_0, is given, the drug level decreases to r × ($2D_0$). If r = ½, then this level becomes D_0. The problem in pharmacokinetics is to determine what dose, D_0, and what period, r, to choose such that the peak and trough values lie within the therapeutic range for the drug. Frequently, it is found that to achieve the right peak and trough levels, the time required to achieve the steady state is too long, especially where the need for drug therapy is urgent. In these cases, a **loading dose** can be administered. Here, the peak level is administered; for the above example, this level would be $2D_0$. Then, after the usual time period, defined by r, elapses, a **maintenance dose**, D_0, is given. This process is repeated every r-defined time period so that the peaks and troughs are maintained. This process obviates the entire dosing schedule shown in Figure 24.9 (i.e., the entire left side of the curve is eliminated, leaving only the steady-state portion). The reason that this process is not performed uniformly is that not all patients can tolerate large initial doses of specific drugs. Therefore, giving loading doses may not always be possible.

For continuous infusions (see Fig. 24.9), for the simplest case in which drug distribution is instantaneous, the rate of drug infusion is constant, and the drug is excreted in a first-order manner, the rate law is

$$dD/dt = k_1 - k_2 D \quad \text{(Eq. 24.10)}$$

where D is the drug concentration, k_1 is the constant rate of infusion, and k_2 is the first-order rate constant for excretion/inactivation of D. This equation can be solved for D:

$$D = (k_1/k_2)\left(1 - e^{-k_2 t}\right) \quad \text{(Eq. 24.11)}$$

From Equation 24.11, if t is large, the term $e^{-k_2 t}$ becomes small, and D approaches its steady-state value, k_1/k_2. This value is approached when the rate of drug infusion equals the rate of drug disappearance. Another way to obtain this value is to note that, at steady state, as in the formation and disappearance of the enzyme-substrate complex in Michaelis-Menten kinetics (see Chapter 21, Equation 21.4), dD/dt must = 0. Then, from Equation 24.10,

$$dD/dt = k_1 - k_2 D = 0 \quad \text{(Eq. 24.12)}$$

so that

$$D_{steadystate} = k_1/k_2 \quad \text{(Eq. 24.13)}$$

As in the case of periodic drug administration at constant intervals, 4 half-lives are sufficient to reach the steady-state condition. Because, as shown previously in Equation 24.6, $k_2 = 0.693/(t_{½})$, after 4 half-lives when $t = 4t_{½}$

$$D = (k_1/k_2) \cdot \left(1 - e^{-2.772}\right) \quad \text{(Eq. 24.14)}$$

where, in effect, D is close to k_1/k_2. Thus, for continuous infusions, the ratio of k_1 (the rate of drug infused per unit of time) to k_2 (the rate constant for the first-order disappearance of the drug) is the desired steady-state level of the drug (i.e., where the amount of drug delivered equals the amount of drug eliminated over the same unit of time). Unlike the situation with discontinuous infusion, the only parameter that is needed to achieve the steady-state level in a given time is k_1, which includes drug concentration and infusion rates, whereas with discontinuous administration of the drug, both D_0 and r are needed.

There are two major points from this presentation. First, it is a good rule of thumb to wait for 4 or more half-lives to achieve the steady-state level of a drug. Second, results of an assay for a drug level in the time period during which this steady state is being achieved should be interpreted with extreme caution—a rule often forgotten in clinical practice. Notice from Figure 24.9 that if assays are performed in the pre–steady-state period (before achievement of 4 or more half-lives), erratic results are obtained owing to fluctuations in drug concentrations for the discontinuous case and rising but persistently low values for the continuous case. It is also important to note that the pharmacokinetics of many drugs may be altered in patients with varied disease states as different diseases can affect blood flow to organs involved in drug elimination as well as the protein or carrier binding kinetics in plasma, fluid, and tissue compartments (Ogawa et al., 2013).

Volume of Distribution

When one is administering drugs, it is of vital importance to know whether the drug is stored in fat or other tissue or whether it is all present in serum. Because a given dose of a drug is known and the concentration of the drug in serum can be determined, one can measure the total volume of body fluid in which the drug is dissolved by the following relation:

$$D = D_0/V_d, \text{ or } V_d = D_0/D \quad \text{(Eq. 24.15)}$$

where D is the concentration of drug in serum, D_0 is the amount of drug administered, and V_d is the volume in which D_0 must be dissolved to give the concentration D. This volume, V_d, is referred to as the volume of distribution. If all of the drug is present in serum, V_d is the blood volume that can be determined from conversion tables relating body weight to blood volume. If, however, some of the drug is stored in body tissue, a smaller amount is present in serum so that the denominator in Equation 24.15 ($V_d = D_0/D$) is reduced and V_d will be larger than the expected blood volume, indicating that some drug is being stored in tissue. If this result occurs, it means that the drug will very likely be released continuously from storage depots (i.e., tissues), which can raise anomalously the level of drug in serum, potentially to toxic levels. Thus, before any drug is administered, the volume of distribution should be known.

Metabolism in the Liver

Many drugs are converted to metabolites, some of which are pharmacologically active and some inactive. Much of this conversion occurs in the extramitochondrial, microsomal system present in hepatocytes. This metabolic system is mainly oxidative, which utilizes a series of oxidative enzymes that, in turn, utilize a special cytochrome system: cytochrome P450 (Gonzalez & Tukey, 2006). This extremely critical cytochrome system has now been strongly implicated as predisposing particular individuals to develop cancer by metabolizing certain environmental compounds, such as benzopyrene, into frank carcinogens (see later discussion). In addition, genetic polymorphism of the cytochrome P450 enzymes affects an individual's particular response to a drug, including toxicity and an adverse drug reaction (Ingelman-Sundberg, 2004). As described in Chapter 75, it is now possible to test individuals for their abilities to metabolize specific drugs by amplification of their genes encoding cytochrome P450. Certain amino acid substitutions in this protein cause it to be very active in drug metabolism (i.e., rapid inactivation of the drug). This implies that the patient may need substantially higher doses to achieve a therapeutic level or that it may be necessary to use another less rapidly metabolized drug.

Because the excretion of many drugs depends on the integrity of the liver and the cytochrome P450 system, in patients with liver failure due to passive congestion, hepatitis, cirrhosis, and the like, the effective half-life of the drug is increased, making it necessary to lower the divided dose of the drug. Conversely, some drugs induce the intracellular synthesis of the microsomal enzymes, leading to diminished half-life values; thus, it may be necessary to raise the divided dose.

One example of drug induction of microsomal enzymes is phenobarbital. (Dilantin is another example of this phenomenon.) This drug induces its own metabolism (so that its concentration levels do not obey first-order kinetics). In instances in which the levels of a drug metabolized in the liver are higher than the highest therapeutic value, reductions in the levels may be induced by administering low levels of phenobarbital to induce the microsomal system.

This summary of some of the general principles of drug administration should be helpful in the interpretation of values clinically and should permit a better understanding of the subsequent discussion of specific therapeutic drugs most commonly measured or determined in the laboratory.

TABLE 24.1
Digoxin

Purpose	Treatment of Congestive Heart Failure and Atrial Fibrillation-Flutter
General adult dose	Oral: 0.75–1.5 mg for digitalization, 0.125–0.5 mg/day for maintenance
Usual bioavailability	Approximately 60%–85% for tablet or elixir; 90%–100% for liquid-filled capsules
Half-life	Approximately 35–40 hours; however, prolonged in patients with decreased renal function
General therapeutic range	0.5–2 ng/mL
General toxic level	>2 ng/mL, but somewhat variable
Transport	Approximately 20%–25% plasma protein bound
Metabolism	Generally, only small amounts are metabolized (liver, lumen of large intestine)
Elimination	Approximately 50%–75% unchanged in urine
Steady state	Approximately 7 days in undigitalized patients with normal renal function
Mechanism of action	Causes release of calcium ions in T-system of myocardium; slows AV node conduction
Toxic effects	Gastric disturbances, nausea, vomiting, atrial and ventricular arrhythmias, irregular pulse

AV, Atrioventricular.

TABLE 24.2
Procainamide

Purpose	Treatment of Supraventricular or Ventricular Arrhythmias
General adult dose	Oral: 1.5 g/day, in divided doses, for maintenance therapy
Usual bioavailability	75%–95%
Half-life	Approximately 3.5 hours in patients with normal renal function
General therapeutic range	4-10 μg/mL
General toxic level	>12 μg/mL
Transport	Approximately 15% plasma protein bound
Metabolism	Hepatic: N-acetylprocainamide (active), with $t_{½}$ approximately 7 hours in patients with normal renal function
Elimination	Approximately 50%–60% unchanged in urine
Steady state	Minimum of 12 hours
Mechanism of action	Prolongation of atrial refractory period and decreased myocardial excitability
Toxic effects	Reversible lupus erythematosus-like syndrome, irregular pulse, hypotension, rash, agranulocytosis

TABLE 24.3
Phenobarbital

Purpose	Treatment of Generalized Tonic-Clonic Seizures, Simple Partial Seizures, Anxiety, Insomnia
General adult dose	Oral: 100–200 mg/day for seizure control; 30–120 mg/day for anxiety; 100–320 mg for sleep induction
Usual bioavailability	Approximately 90%–100%
Half-life	Approximately 5–6 days in adults; approximately 3–4 days in children
General therapeutic range	15–30 μg/mL for epilepsy control
General toxic level	>40 μg/mL, although tolerance may develop
Transport	Approximately 40%–60% plasma protein bound
Metabolism	Approximately 75% hepatic: *p*–hydroxyphenobarbital, inactive
Elimination	Approximately 25% unchanged in urine
Steady state	Approximately 14–21 days
Mechanism of action	Stabilizes damaged membranes and raises threshold for neuronal membrane depolarization
Toxic effects	Drowsiness, depression, respiratory depression, coma, sedation, hypotension. Respiratory depression may be caused by rapid intravenous administration.

TABLE 24.4
Phenytoin (Dilantin)

Purpose	Treatment of Generalized Tonic-Clonic Seizures, Simple Partial Seizures, Complex Partial Seizures
General adult dose	Oral: 300–400 mg/day maintenance dose
Usual bioavailability	Variable: 30%–95%
Half-life	24 ± 12 hours, and dose dependent
General therapeutic range	10–20 μg/mL
General toxic level	>20 μg/mL
Transport	Approximately 90%–95% plasma protein bound
Metabolism	Hepatic: 5-(p-hydroxyphenyl)5-phenylhydantoin, inactive
Elimination	Approximately 5% unchanged in urine
Steady state	Approximately 7–8 days
Mechanism of action	Appears to block sodium and calcium ion influxes into repeatedly depolarizing CNS neurons
Toxic effects	Nystagmus, ataxia, diplopia, drowsiness, coma; rapid intravenous administration may produce cardiovascular collapse and/or CNS depression

CNS, Central nervous system.

Tables 24.1 to 24.6 summarize the critical pharmacologic data for a number of commonly assayed drugs.

In the following presentation, seven classes of the drugs most commonly assayed for are discussed: cardiotropic, anticonvulsant, antiasthmatic, anti-inflammatory, immunosuppressive, psychotropic, and chemotherapeutic. (Antibiotics are discussed in Part 7.) The emphasis in this discussion is on the mechanisms of action of these drugs. Common to most of these drugs is the fact that they interfere with specific steps in signal transduction pathways in cells, which are often remarkably similar to one another. Despite these similarities, specific drugs block signal transduction pathway steps that affect only specific cells and seem not to affect signal transduction in other cells.

CARDIOTROPICS

These drugs are the ones most commonly used to treat congestive heart failure and cardiac arrhythmias (Opie & Gersh, 2001; Roden, 2006; Frishman & Sica, 2011).

Despite differences in the structures and properties of the drugs and their specific uses, all of them act on one or another phase of the action potentials in cells that are in the conduction system and in myocytes. Their net effect is to slow down electrical conduction. In addition, it is important to remember that the conduction tissue is innervated by both the sympathetic and parasympathetic (mainly vagal) nervous systems. The former increases the conduction rate, and the latter tends to slow conduction. The actions of each of the cardiotropic drugs are summarized in Figure 24.10. As shown in this figure, several major ion currents control the action potentials of the cells making up the pacemaker tissue of the atrioventricular (AV) node and the ventricular conduction bands (composed of Purkinje cells): first, rapid sodium influx current, and then decreased flux (shutoff of sodium conductance channels), as outlined in the red area in Figure 24.10; second, a calcium ion influx that prolongs the action potential and then calcium channel shutoff, as outlined in the blue area in Figure 24.10; and third, potassium ion efflux that promotes repolarization of the cell. As shown in Figure 24.10, there are four classes of drugs that act on one or more of these phases of the action potential, resulting in its prolongation. Class I

TABLE 24.5

Carbamazepine (Tegretol)

Purpose	Treatment of Generalized Tonic-Clonic Seizures, Simple Partial Seizures, Complex Partial Seizures, Trigeminal Neuralgia, and Glossopharyngeal Neuralgia
General adult dose	Oral: 0.8–1.2 g/day maintenance for seizure control; 0.2–1.2 g/day for neuralgia
Usual bioavailability	70%
Half-life	Initially, approximately 35 hours; approximately 8–20 hours after 3–4 weeks of administration
General therapeutic range	4–12 μg/mL
General toxic level	>12 μg/mL
Transport	60%–70% plasma protein bound
Metabolism	Hepatic: carbamazepine-10,11-epoxide (active); carbamazepine-10,11-transdihydrodiol (inactive)
Elimination	1%–2% unchanged in urine
Steady state	3–7 days
Mechanism of action	Decreases sodium and calcium ion influx into repeatedly depolarizing CNS neurons; reduces excitatory synaptic transmission in the spinal trigeminal nucleus
Toxic effects	Drowsiness, ataxia, dizziness, nausea, vomiting, involuntary movements, abnormal reflexes, irregular pulse

CNS, Central nervous system.

TABLE 24.6

Theophylline

Purpose	Treatment and Prevention of Moderate to Severe Asthma
General adult dose	Depends on body weight, route of administration, and age and condition of patient
Usual bioavailability	Varies according to form, with about 100% for oral liquids and uncoated tablets
Half-life	Varies: 8–9 hours in nonsmoking adults, 5–6 hours in adults who smoke, and 3–4 hours in children, but may vary widely
General therapeutic range	10–20 μg/mL
General toxic level	>20 μg/mL
Transport	60% plasma protein bound
Metabolism	Hepatic: caffeine; 1,3-dimethyluric acid; 1-methyluric acid; 3-methylxanthine
Elimination	10% unchanged in urine
Steady state	5 half-lives; 90% of steady state reached in 3 half-lives
Mechanism of action	Increases intracellular cAMP by inhibiting phosphodiesterase; this causes the smooth muscle of the bronchial airways and pulmonary blood vessels to relax
Toxic effects	Hypotension, syncope, tachycardia, arrhythmias, seizures, gastrointestinal bleeding

cAMP, Cyclic adenosine monophosphate.

drugs block sodium influx in phase I and include quinidine, procainamide, and lidocaine. These agents, especially lidocaine, act by blocking the rapid sodium influx of phase I, decreasing the rate of ventricular diastolic depolarization. Class II drugs include β-receptor blockers such as propranolol (Inderal) that inhibit the chronotropic effects of adrenergic neurotransmitters such as epinephrine and norepinephrine. Class III drugs, such as amiodarone, block repolarizing potassium currents, increasing the length of the action potential (represented by the black curve over the yellow area in Figure 24.10) and increase the length of the refractory period. Class IV drugs, of which verapamil is an important member, slow calcium ion influx, resulting in action potential prolongation. In addition to these classes of drugs, digitalis cardiac glycosides have parasympathetic-like effects on the

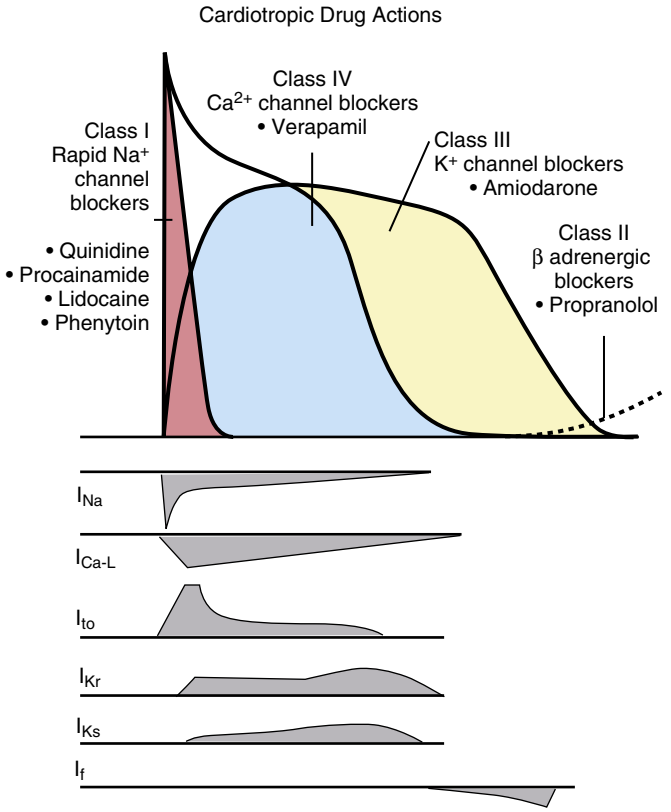

Figure 24.10 Overview of the effects of different antiarrhythmic agents on the myocardial conduction system. X-axis is time (msec); Y-axis is voltage. The normal action potential is shown as the *black line* that first spikes to a high voltage, mainly because of a rapid sodium influx into cells in the conduction system. This component of the action potential, caused by sodium ion influx, is shown enclosed in the *red area.* The actual action potential is prolonged by a succeeding influx of calcium ions shown enclosed under the *blue area* that overlaps somewhat with the red (sodium influx) area. Termination of the calcium ion influx and efflux of potassium ions results in repolarization, shown by the *curve bordered by the blue area.* Class I channel blockers, as listed in the figure, block sodium influx, thereby diminishing the rate of depolarization. Class II blockers, like propranolol, block β-adrenergic (epinephrine and norepinephrine) stimuli, diminishing the rate of diastolic depolarization. Class III blockers, like amiodarone, block potassium channels, resulting in reduction in potassium efflux and slowing down repolarization. This results in prolongation of the action potential, as shown by continuation of the voltage curve over the *yellow area.* Class IV blockers, like verapamil, block calcium channels, again prolonging the action potential (*blue*), although this prolongation is not explicitly shown. By prolonging the action potential, Class III and IV agents slow down nodal conduction through prolonged refractoriness of the affected cells. Various ion currents induce the action potentials. The time courses for different ion currents that occur during the action potential are shown below the colored graph. I^{Na}, sodium influx current; IC^{a-L}, calcium influx current; IT^{O}, transient outward current; I^{Kr} and I^{Ks}, potassium efflux currents; I^{f}, hyperpolarization current. (Redrawn from Opie LH, Gersh BJ: *Drugs for the heart,* ed 5. Philadelphia, 2001, WB Saunders.)

cells of the AV node, resulting in slowing of conduction. Both digitalis and amiodarone also have marked inotropic effects on the myocardium. Thus, both are used in the treatment of congestive heart failure. In damaged myocardium, digitalis blocks sodium-potassium adenosine triphosphatase (ATPase), resulting in transient increases in sodium ion around the sarcolemma, which leads to the release of cytosolic calcium ion to the T-system. This allows increased myocardial contractility. We now discuss the key properties and actions of these cardiotropic drugs.

Cardiac Glycosides (Digitalis and Its Derivatives)

Digoxin

Because they slow conduction in the AV node, digoxin (also referred to as *digitalis*, of which digoxin and the longer-lasting digitoxin are derivatives) and the other cardiac glycosides are often used to treat atrial arrhythmias, in particular, atrial flutter and atrial fibrillation. However, there is recent support for their use in cancer treatment (Slingerland et al., 2013). The mechanism of action for their antiarrhythmic effect in heart disease is to block rapid atrial conduction signals to the ventricles, thereby slowing ventricular response. This is due to their proparasympathetic effects, which include enhancement of blockade of depolarizing calcium currents and increased hyperpolarizing potassium currents in the AV node. These effects result in shortening action potential duration and increasing AV nodal refractoriness (Roden, 2006).

Their direct positive inotropic effect increases cardiac output in cardiac failure. This effect has been found to be due to increased intrasarcolemmal concentration of calcium, allowing it to activate proteins such as troponin C that are important in the contractile apparatus (Rocco & Fang, 2006; McMurray et al., 2012). This increase in calcium concentration is due to the binding of digoxin to the α subunit of sodium-potassium–activated ATPase, causing its inhibition and the consequent reduction of sodium efflux and diminution of the transmembrane potential. As this potential increases, more calcium efflux occurs, resulting in less activation of muscle contraction. Blockade of sodium efflux therefore allows accumulation of intrasarcolemmal calcium and increased activation of contractile proteins (Rocco & Fang, 2006).

Digoxin (see Table 24.1) has a rapid onset of action (within 1–2 hours when given orally) and a relatively short half-life (35–40 hours). Most patients will excrete approximately 50% to 75% of a dose unchanged in the urine. The general range of therapeutic serum levels is from 0.5 to 2 ng/mL. High concentrations of the drug are found in skeletal and cardiac muscle, as well as in liver, brain, and kidneys. It is important to note the recent impact of pharmacogenetics on the biology of digoxin as well as other drugs (Talameh & Lanfear, 2012). Reports by Neuvonen and colleagues (2011) showed that the *ABCB1* 3435T polymorphism provided higher serum drug concentrations of digoxin with a higher frequency among females, thus providing a possible explanation regarding the increased morbidity of females treated with digoxin compared with placebo. Digoxin is available as oral tablets, elixir, oral capsules, and intravenous solution, which have bioavailabilities of 70%, 80%, 90%, and 100%, respectively (Ehle et al., 2011). Understanding the formulation administered in conjunction with patient compliance and comorbidities can alert the clinician of suspected toxicity.

Digitoxin

In contrast, digitoxin has a longer half-life (4 to 6 days) with a relatively slower onset of action (within 1 to 4 hours when given orally, with maximal effect in 8 hours); 90% to 100% of a dose is absorbed, with approximately 95% bound to plasma protein. The general range of therapeutic serum levels is from 9 to 25 ng/mL. The drug is extensively metabolized in the liver (90%), with digoxin being the active metabolite.

Toxic side effects of the digitalis glycosides include gastric disturbances, nausea, vomiting, and atrial and ventricular arrhythmias. It is crucial that levels of digoxin (or digitoxin) be monitored closely and accurately while the patient is initially being given this drug. As mentioned previously, the therapeutic range for digoxin is from 0.5 to 2 ng/mL (i.e., the range is narrow). Toxic levels exceed 2 ng/mL; thus, the difference between therapeutic and toxic doses is small. This difference necessitates careful digoxin assay.

Digoxin toxicity is often treated with Digibind (GlaxoSmithKline, Research Triangle Park, NC), consisting of ovine Fab fragments. This antidote can interfere with determination of digoxin serum levels (Valdes et al., 1998). Some assays have been reported to determine only the "free" digoxin level (i.e., that not bound to Digibind Fab), which inactivates digoxin. For other assays that determine total digoxin (i.e., free plus Fab-bound digoxin), it is recommended that an ultrafiltrate of serum be employed to determine the level of free or active digoxin. Alternatively, given that Digibind can cause spurious and erroneous results, it has been recommended that, because the half-life of Digibind is 15 to 20 hours, therapeutic levels of digoxin should be determined 2 to 4 days after the last Digibind dose.

Procainamide (Pronestyl)

Procainamide (see Table 24.2) is a class I antiarrhythmic drug that is useful in treating supraventricular or ventricular arrhythmias. One of its major effects includes increased refractoriness of the atrium and decreased myocardial excitability by blocking open sodium channels and outward potassium currents, both of which prolong action potentials and increase refractoriness (Roden, 2006). Because there is an effect on potassium currents, some of its effects resemble those of the Class III potassium current blockers. The bioavailability of procainamide is 75% to 95%. Approximately 15% is bound to plasma protein, and approximately 50% is excreted by the kidneys. The half-life is approximately 3.5 hours, with a general range of therapeutic serum level of 4 to 10 μg/mL. *N*-acetylation to the major active metabolite *N*-acetylprocainamide (NAPA) is the major metabolic pathway of biotransformation. NAPA, however, does not block open sodium channels but effectively prolongs action potentials (Roden, 2006). Both drugs prolong the QRS and Q-T intervals on electrocardiography over time.

Toxic side effects include a reversible lupus-like syndrome (Zimetbaum et al., 2011) with elevated antinuclear antibody titers, urticaria, rash, agranulocytosis, and nephrotic syndrome. The lupus-like syndrome may be initiated by leukocyte metabolism of procainamide to a chemically reactive metabolite that could then covalently bind to monocyte/macrophage membrane proteins to stimulate production of autoantibodies. In addition, the tertiary amino moiety of the covalently bound procainamide metabolite might mimic a portion of histone protein, resulting in the production of antihistone antinuclear antibody (Uetrecht, 1988).

Quinidine

Quinidine, also a class I antiarrhythmic, like procainamide, is used to treat supraventricular and ventricular arrhythmias and tachyarrhythmias. The prevention of ventricular tachycardia or frequent premature ventricular contractions and the maintenance of sinus rhythm after the conversion of atrial flutter or atrial fibrillation are its two major uses (Valdes et al., 1998). Like procainamide, quinidine blocks sodium channels and outward potassium currents, especially the I_{Kr} rectifier current (see Figure 24-10), resulting in prolongation of action potentials and increased refractoriness, leading to prolongation of both the QRS complex and the Q-T interval (Roden, 2006).

The bioavailability of quinidine is 90% to 100%, with approximately 85% of the drug bound to plasma protein. Quinidine is 60% to 85% metabolized in the liver via hydroxylation reactions, with some metabolites being active. Urinary excretion is approximately 20%. The half-life of quinidine is 5 to 12 hours, and the general therapeutic range is 2.3 to 5 μg/mL. Maximal serum levels are reached in 1 to 3 hours. Toxic side effects of quinidine include cinchonism (vertigo, tinnitus, headache, visual disturbances, and disorientation), fever, hepatitis, and blood dyscrasia. Ventricular arrhythmias, AV block, and ventricular fibrillation leading to syncope and sudden death can occur.

Lidocaine

Lidocaine (Xylocaine), another class I antiarrhythmic, can also be used as a local anesthetic. Its major use as an antiarrhythmic is in the acute control and prevention of ventricular arrhythmias after acute myocardial infarction. Its effect is to block sodium channels mainly in ventricular but not atrial tissue. Unlike procainamide and quinidine, lidocaine does not cause QRS and Q-T prolongation (Roden, 2006). A loading intravenous dose of 50 to 100 mg is given over 2 to 3 minutes to treat ventricular arrhythmias in adults. Further dosages may be administered in 5- to 10-minute intervals of 25 to 50 mg, up to a maximum of 300 mg in a 1-hour period. Following loading, infusion is then continued at a rate of 1.4 to 3.5 mg/minute for a 70-kg male. In children, 0.5 to 1 mg/kg can be given every 5 minutes for a maximum of three doses. Unfortunately, lidocaine can cause heart block and congestive heart failure, limiting its use in critical care patients (Roden, 2006).

Lidocaine is neither highly protein bound nor appreciably stored in body tissues; it has a half-life of approximately 2 hours and a therapeutic serum range of 1.2 to 5.5 μg/mL. The time to reach a maximum serum level is generally 5 to 8 hours. Ninety percent of a dose of lidocaine is metabolized in the liver via *N*-dealkylation. Urinary excretion is 10%. Toxic side effects include convulsions, coma, and respiratory depression (CNS effects) as well as bradycardia and hypotension.

Propranolol

Propranolol, a class II antiarrhythmic β-receptor–blocking drug that antagonizes the effects of epinephrine on the heart, on the arteries and arterioles of skeletal muscles, and on the bronchus, exerts its effects largely on the AV node and is used to treat sinus tachycardia, atrial tachycardia, and ventricular arrhythmias. Overall, blockade of β-1 receptors increases AV conduction time and reduces heart rate, myocardial contractility and output, and cardiac automaticity. Because it is a vasodilator, it is also used in the treatment of angina pectoris; hypertension; and symptomatic coronary artery disease, particularly after an acute myocardial infarction. Oral dosages vary from 40 to 320 mg daily in adults for antiarrhythmic activity to as high as 480 mg daily in the control of hypertension. Both supine and standing blood pressures are also reduced. Bioavailability of propranolol is approximately 30%. The half-life of propranolol is 3 hours, with a therapeutic serum range of 50 to 100 ng/mL, and with maximum serum levels reached in approximately 6 hours. Approximately 93% is protein bound. Propranolol is metabolized in the liver, with 0.5% excreted in the urine unchanged. Toxic effects include bradycardia, arterial insufficiency (Raynaud type), hypotension, AV block, nausea, vomiting, pharyngitis, bronchospasm, and thrombotic thrombocytopenic purpura. Marrow suppression occurs rarely.

Amiodarone

Amiodarone, a structural analog of thyroid hormone, is chiefly a class III antiarrhythmic drug, which markedly prolongs the action potential mainly by blocking potassium channels in cardiac muscle (see Figure 24.10). Its activity is complex in that it significantly blocks inactivated sodium

channels by a poorly understood mechanism, thus exhibiting class I action, and also exhibits weak adrenergic- and calcium channel–blocking effects (Roden, 2006). All of these actions prolong the effective refractory period along the conduction bands. Its indication for use is with life-threatening ventricular arrhythmias. The oral loading dose is 1200 to 1600 mg/day with a maintenance dose of 200 to 400 mg/day. Bioavailability is ≈35% to 65%. Amiodarone has two components in its half-life: a rapid component of 3 to 10 days (involving ≈50% of the drug) and a slow component of 25 to 110 days. The general therapeutic range is 1 to 2.5 μg/mL, although this is not well defined, and the toxic level is >2.5 μg/mL, again not well defined. Approximately 96% is plasma protein bound; the drug undergoes liver metabolism and shows extensive body distribution because of its hydrophobic (lipid-soluble) structure. Excretion is very slow by skin, biliary tract, and lacrimal glands. Toxic effects can be profound and include symptomatic bradycardia, heart block, fatal pulmonary fibrosis, hepatitis, visual field disturbances, optic nerve neuropathy (Passman et al., 2012), photodermatitis, and mainly hypothyroidism but sometimes hyperthyroidism. New variations of antiarrhythmic medications—including dronedarone, dofetilide, vernakalant, and ranolazine, among others—are being investigated for their selective atrial specific activity as well as decreased extracardiac side effects (for review, see Saklani & Skanes, 2012).

Verapamil

Verapamil is a class IV antiarrhythmic drug that blocks activated and inactivated calcium channels that are especially prominent in nodal tissue (particularly the AV node). Indications include angina, hypertension, and supraventricular arrhythmias. Unlike β-adrenergic receptor blockers, calcium channel blockers have not been found to reduce mortality after a myocardial infarction (Roden, 2006). The oral dose is 120 to 480 mg/day in three to four divided doses. Bioavailability is ≈10% to 20%. The half-life is 2 to 8 hours but increases to 4.5 to 12 hours after repeated oral doses. The general therapeutic range is 80 to 400 ng/mL, although this is not well defined. Approximately 90% is plasma protein bound, and the drug undergoes extensive metabolism in the liver, where norverapamil, an active metabolite, is produced. Approximately 75% of the active components are eliminated by the kidney and ≈25% through the GI tract. Toxic effects include hypotension, ventricular fibrillation, constipation, and peripheral edema.

ANTICONVULSANTS

Anticonvulsants are used in the treatment of seizure disorders, in particular, grand mal, petit mal, and psychomotor seizures and other specialized seizure disorders such as tic douloureux (trigeminal neuralgia). Although the mechanisms of action of these drugs are incompletely understood, it appears that all of these agents, with the possible exception of phenobarbital, block sodium influx into neurons that have damaged membranes, as schematized in Figure 24.11. In addition, several of these agents, especially phenytoin, block secondary calcium influxes into such cells, which also seem to inhibit the rapid firing of these cells. Another effect of phenobarbital, and possibly also of phenytoin, is membrane stabilization through intercalation, as shown in Figure 24.11. Many of the anticonvulsants are effective against grand mal seizures but have no effects or adverse effects on petit mal seizures. Only drugs such as ethosuximide (Zarontin) and valproic acid (Depakote) are effective against this condition. Thus, although the mechanism of action of these drugs appears to be similar, they differ in specificities.

Phenobarbital

Phenobarbital (see Table 24.3), a long-acting barbiturate, is used in the treatment of generalized grand mal tonic-clonic seizures and simple partial seizures with motor or somatosensory symptoms as well as for anxiety and insomnia. It is not used in the treatment of absence seizures (i.e., petit mal), which may be exacerbated by phenobarbital, or for complex partial seizures, which do not respond well. As discussed previously in the Barbiturates section, phenobarbital increases the duration of chloride ion channel opening at the $GABA_A$ receptor, thereby potentiating the GABA effect and raising the threshold for neuronal membrane depolarization, resulting in the diminished frequency of firing of action potentials (Löscher & Rogawski, 2012). In addition, it can stabilize damaged neuronal membranes (see Figure 24.11).

Phenobarbital is also given for withdrawal symptoms in infants born to opiate- or barbiturate-addicted mothers. Because phenobarbital enhances the metabolism of bilirubin by induction of cytochrome P450–dependent enzymes in the hepatic microsomal system, it has been used to treat patients with congenital hyperbilirubinemia (familial nonhemolytic, nonobstructive jaundice). The oral dose of phenobarbital for anxiety in adults is 30 to 120 mg daily in divided doses; for sleep induction in adults, 100 to 320 mg daily is generally used. For seizure control, divided doses of 100 to 200 mg/day in adults or 30 to 100 mg/day in children are generally used.

Phenobarbital has a long half-life of 4 to 6 days. Oral doses are almost completely absorbed (90% to 100% bioavailability), and the optimal serum concentration for seizure control is generally 15 to 30 μg/mL; 40% to 60% is metabolized in the liver, whereas 10% to 40% may be eliminated unchanged in the urine. Approximately 40% to 60% is plasma protein bound, and the main site of storage is the brain. A steady state is reached in 14 to 21 days. Importantly, phenobarbital and, as discussed in the next section, phenytoin (Dilantin), induce a number of the cytochrome P450 systems. Cytochrome P450 2B6 (CYP2B6) is specifically induced by phenobarbital via the CAR/RXR nuclear receptor heterodimer. This system is described at length in Chapter 75 on pharmacogenomics.

Toxic side effects include nystagmus, ataxia, stupor, respiratory depression, coma, and hypotension. Barbiturates are contraindicated in patients with acute intermittent porphyria (i.e., partial porphobilinogen deaminase deficiency), because barbiturates enhance the synthesis of δ-aminolevulinic acid synthetase and thus the synthesis of heme pathway intermediates in the liver.

Phenytoin (Dilantin)

Phenytoin is used to treat generalized tonic-clonic, simple partial, and complex partial seizures (see Table 24.4). It is ineffective in treating myoclonus, absence (petit mal), and atonic seizures. It is usually given intravenously in addition to intravenous diazepam to terminate status epilepticus. Remarkably, phenytoin has no apparent effects on resting neurons or on normally firing neurons. It is thus specific for epileptogenic foci in the CNS (Yaari et al., 1986). It is interesting to note that carbamazepine (Tegretol) exerts similar effects, as discussed later. Data on the mechanism of action of this drug strongly suggest that phenytoin blocks sodium and calcium influxes into repeatedly depolarizing neurons in the CNS and also into neurons that are partially depolarized. Reducing sodium and calcium influx into these cells reduces their excitability and prolongs their refractory period (Yaari et al., 1986). In fact, phenytoin appears to bind selectively to fast-firing sodium channels in their refractory states, thereby prolonging their refractory periods (Bazil & Pedley, 1998); that is, it slows the rate of recovery of inactivated sodium channels (McNamara, 2006). This finding helps explain the ability of phenytoin to block only neurons that are firing rapidly and repetitively.

Although the average daily maintenance dose in adults is 300 to 400 mg, the dosage must be tailored to the patient's response and serum drug concentrations. The usual therapeutic serum concentration is 10 to 20 μg/mL, with a steady state reached in 5 to 10 days (for plateau; see Figure 24.9). The serum half-life is generally 24 hours, but it is dose dependent. Thus, its excretion is not a first-order process. Phenytoin is stored in the brain, is metabolized in the liver (95%), and is approximately 90% to 95% bound to plasma protein. Both aspirin and phenylbutazone can displace phenytoin from serum albumin and can significantly increase the serum concentration of phenytoin. Because phenytoin, like phenobarbital, is a relatively potent hepatic microsomal enzyme inducer and inducer of the CYP3A4 and CYP2C19 families of the P450 enzyme responsible for the hepatic degradation of various drugs, certain antibiotics, oral anticoagulants, quinidine, and oral contraceptives may be more rapidly metabolized, thus decreasing their effectiveness.

Because the relationship between serum concentrations and daily dosage is not linear, small increases in dosage can greatly increase therapeutic serum concentrations. Symptoms of toxicity generally occur at serum concentrations greater than 20 μg/mL. Toxic side effects include nystagmus, ataxia, stupor, and coma. Arrhythmias can be produced by rapid intravenous administration.

Fosphenytoin is a water-soluble parenteral formulation of phenytoin that is rapidly converted (half-life of 8–15 minutes) in vivo to phenytoin. The half-life is independent of plasma concentration, and it has identical pharmacodynamic, pharmacokinetic, and clinical properties to phenytoin. This prodrug offers improved flexibility and tolerability for the patient as compared with intravenous phenytoin and is indicated for the treatment of partial and generalized seizures in adults in whom intravenous administration is indicated (Bazil & Pedley, 1998).

Primidone (Mysoline)

Primidone is used to treat generalized tonic-clonic, simple partial, and complex partial seizures. Its chemical structure is closely related to the basic structure of the barbiturates, and it is metabolized in the liver into two active metabolites: phenobarbital and phenylethylmalonamide. Thus, some of its anticonvulsant effects are due to phenobarbital activity. Unlike

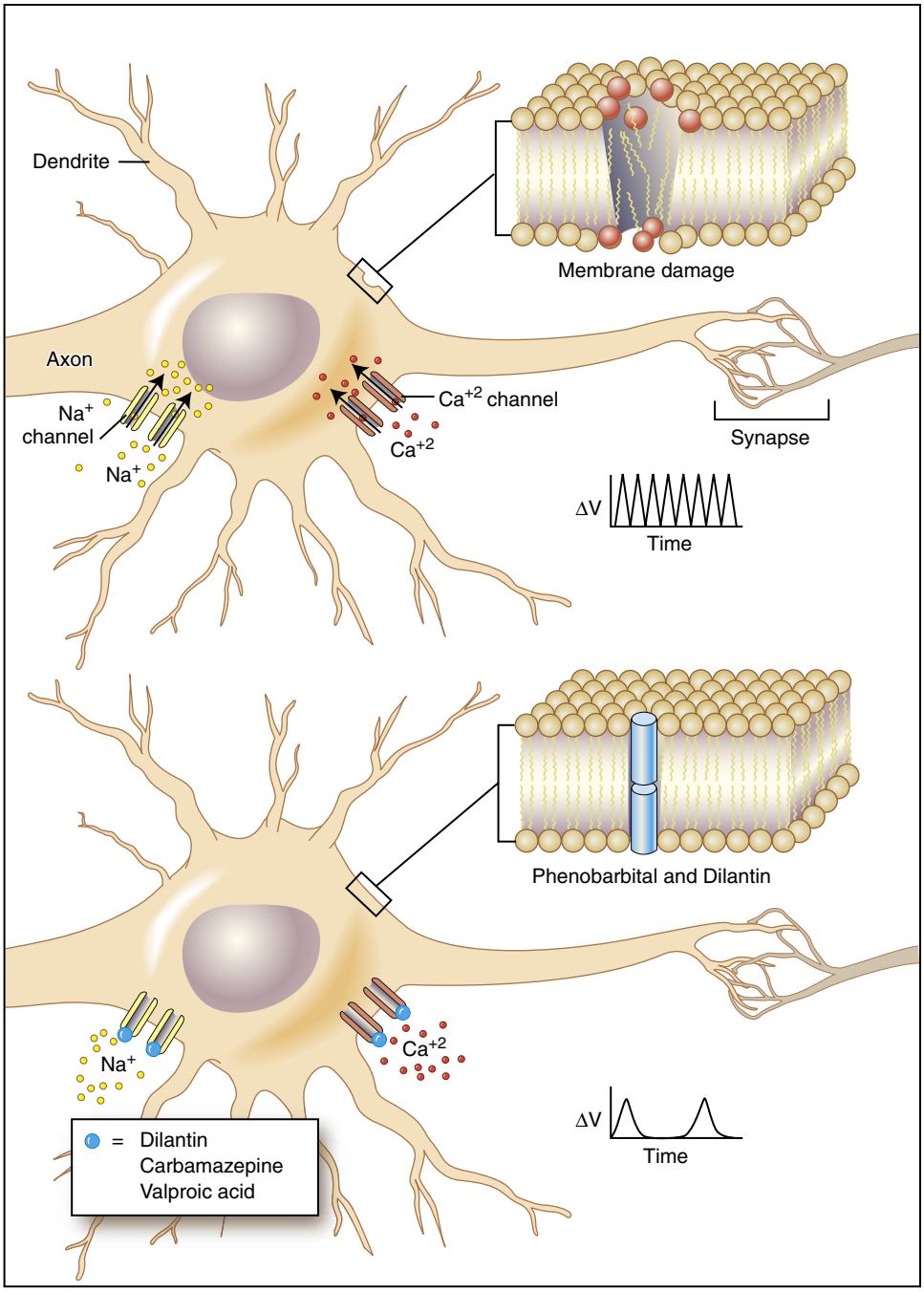

Figure 24.11 Effects of anticonvulsants on neurons. *Top,* Damaged neuronal membranes, as shown in the section in the *upper right* of the figure, result in sodium *(yellow circles)* and calcium *(red circles)* influxes via their respective channels that cause repeated firing, as shown in the voltage-time curve to the right of the figure. *Bottom,* Anticonvulsants such as phenytoin (Dilantin), carbamazepine (Tegretol), and valproic acid (Depakote; *represented by blue circles*) block sodium and calcium channels, resulting in a substantially diminished rate of firing, as shown in the voltage-time curve to the right of the figure. Both phenytoin and phenobarbital, shown as blue cylinders, are also thought to stabilize the damaged neuronal membrane, as shown in the membrane section schematized in the upper-right drawing.

phenobarbital, however, primidone may increase the threshold of membrane depolarization within the CNS.

This drug is usually given in increasing doses. Initially, a dose of 100 to 125 mg orally is given at bedtime each night for 3 days. The dose is then increased to 100 to 125 mg twice daily for 3 days, then to 100 to 125 mg three times daily for 3 days, and finally 250 mg three or four times daily but not to exceed 2 g/day. Absorption is rapid and complete (100%), with a usual therapeutic serum concentration of 5 to 21 μg/mL. A steady state is reached in 4 to 7 days, and the half-life is approximately 12 hours. Plasma protein binding is relatively low (20%), with most of the drug remaining free in the serum, and with little drug being stored in body tissues.

Sedation is a common toxic side effect. Dizziness, ataxia, and skin rashes have also been observed. Primidone, like phenobarbital, is contraindicated in patients with acute intermittent porphyria.

Ethosuximide (Zarontin)

Ethosuximide is the drug of choice for absence (petit mal) seizures unaccompanied by other types of seizures. It is preferred over valproic acid (see later discussion), at least initially, because hepatotoxicity is a rare but serious side effect of valproic acid. Ethosuximide may depress the motor cortex and may reduce the frequency of neuronal firing. It also inhibits T-current spikes on the electroencephalogram that underlie bursts of action potentials in the thalamus but does not affect normal electrical conduction (McNamara, 2006). The basis for its specificity, however, is not well understood.

The oral dosage in adults is generally 500 to 1000 mg daily. Absorption is fairly rapid and complete (100%), with peak serum concentrations occurring in 1 to 4 hours. A steady state is reached in 8 to 10 days. The usual therapeutic serum concentration is 40 to 100 μg/mL, but it can be as high as 170 to 190 μg/mL in children. The serum half-life is generally 60 hours in adults and 30 hours in children. Ethosuximide is essentially free in serum and not protein bound. It is mainly metabolized in the liver (60%–90%) to desmethylmethsuximide. Gastrointestinal disturbances are among the most common toxic effects and include nausea, vomiting, and gastric distress. Other effects include drowsiness and ataxia. Rare serious side effects, such as systemic lupus erythematosus, aplastic anemia, and pancytopenia have been reported.

Carbamazepine (Tegretol)

Carbamazepine (see Table 24.5) is a primary antiepileptic drug that is used in the treatment of generalized tonic-clonic seizures and simple partial and complex partial seizures, as well as in combinations of these seizure types.

Absence (petit mal), myoclonic, and atonic seizures may be exacerbated by this drug. This drug is also used to treat tic douloureux (trigeminal neuralgia) and glossopharyngeal neuralgia. It is, in fact, the drug of choice in the treatment of these neuralgias.

Carbamazepine is a tricyclic compound (i.e., iminostilbene) that is chemically related to imipramine, a tricyclic antidepressant. It is believed that a reduction in excitatory synaptic transmission in the spinal trigeminal nucleus is the basis for this drug's antineuralgic action. Its antiepileptic action is quite similar to that of phenytoin; that is, it decreases sodium and calcium influx into hyperexcitable neurons (Yaari et al., 1986; Bazil & Pedley, 1998). Like phenytoin, carbamazepine slows the rate of recovery of voltage-activated sodium channels from inactivation (McNamara, 2006).

Oral doses of carbamazepine are completely absorbed, and the usual adult maintenance dose is 0.8 to 1.2 g/day. Ninety-eight percent is biotransformed in the liver into two active metabolites: a 10,11-epoxide form, which is active (McNamara, 2006), and a 10,11-dihydroxy form of carbamazepine. The usual therapeutic serum concentration is 4 to 12 μg/mL, and steady state is reached in 3 to 4 days. The serum half-life of Tegretol is 8 to 20 hours (after 3–4 weeks of administration), and 60% to 70% is plasma protein bound. The more common toxic reactions seen with this drug include drowsiness, ataxia, dizziness, nausea and vomiting, and lightheadedness. Rare hematologic reactions may occur and can be quite serious; they include aplastic anemia, thrombocytopenia, and agranulocytosis.

Valproic Acid (Depakene)

Valproic acid is commonly used in the treatment of generalized tonic-clonic seizures, absence seizures, myoclonic seizures, and atonic seizures. It is not effective for the treatment of infantile spasms. Although the mechanism of action is not definitely known, valproic acid is thought to enhance the activity of the GABA-mediated inhibitory system. In addition, its action is similar to that of phenytoin and carbamazepine in that it inhibits sustained, repetitive firing of depolarized neurons by prolongation of the refractory state of sodium channels (Hardman et al., 2001; McNamara, 2006). Like ethosuximide, it decreases T-current–induced action potentials (McNamara, 2006). Absorption of valproic acid is rapid and complete. The recommended initial dose is 15 mg/kg/day, increasing at 1-week intervals by 5 to 10 mg/kg/day until therapy is judged sufficient, or undesirable side effects occur, or the maximum allowable dose is reached at 60 mg/kg/day. Any daily dose >250 mg should be given in divided doses. Usually the therapeutic serum concentration is 50 to 100 μg/mL, and a steady state is reached in 1 to 4 days. Most (90%–100%) of the drug is metabolized in the liver and a high percentage (90%) is plasma protein bound. The serum half-life is 8 to 15 hours.

Valproic acid has been shown to produce teratogenic effects in experimental animals; these included developmental abnormalities and skeletal defects. Thus, valproic acid should be used with caution in pregnant women. Toxic side effects include sedation, gastric disturbances, hematologic reactions, ataxia, somnolence, and coma. Rare fatal hepatotoxicity has occurred, and severe or fatal pancreatitis has been reported (Sztajnkrycer, 2002).

Newer Anticonvulsants

Topiramate, lamotrigine (Lamictal), gabapentin (Neurontin), pregabalin (Lyrica), levetiracetam (Keppra), and felbamate (Felbatol) are additional anticonvulsant agents that are approved for use in the United States for patients whose response to the more established anticonvulsants is less than optimal. Therapeutic ranges and toxic concentrations for these drugs have not been determined. Topiramate and lamotrigine are utilized as adjunctive treatment for partial seizures in adults. Topiramate is a substituted sulfamate monosaccharide that induces hyperpolarizing potassium currents and enhances $GABA_A$ receptor currents at synapses (McNamara, 2006). Lamotrigine is a triazine derivative that acts much in the same manner as phenytoin and carbamazepine. However, because it has broader antiseizure activity than either of these other two anticonvulsants, other mechanisms may be involved, one of which appears to be blockade of glutamate release at synapses using this amino acid as a neurotransmitter (McNamara, 2006).

Topiramate has a half-life of approximately 21 hours, with approximately 15% of the drug bound to protein. Lamotrigine has a variable half-life, depending on whether the drug is used as monotherapy or with an inducer. Approximately 55% of lamotrigine is protein bound.

Gabapentin is also utilized as adjunctive treatment for partial seizures and for migraines, chronic pain, and bipolar disorder (McNamara, 2006). As its name suggests, it was designed to act as a GABA-like drug. However, it has been found that it does not have this effect but rather seems to induce cortical release of GABA from synaptic vesicles by a poorly understood mechanism (McNamara, 2006). It has a half-life of 5 to 7 hours, with less than 3% protein binding. The mechanism of action is thought to include the activity as a ligand at the α_2-δ subunit of voltage-gated calcium channels by calcium influx at nerve terminals. This interaction reduces the release of neurotransmitters, such as glutamate norepinephrine and substance P. To this end, gabapentin has recently been reported to facilitate cannabis abstinence by producing effects that overlap with those of cannabinoids (Lile et al., 2016) and recent animal studies show synergistic pain reduction effects when coadministered with morphine and its metabolites (Papathanasiou et al., 2016). This has propagated abuse potential both in synergy with other agents to potentiate their effects and for this drug class in its own right (Bossard et al., 2016). The general detection window (urine) for gabapentin and pregabalin is 1 to 4 days postingestion.

Levetiracetam is used in benzodiazepine-resistant status epilepticus or where patients have allergic side effects to phenytoin. It does not appear to act through classical anticonvulsant pathways, including voltage-dependent Na^+ channels, GABAergic transmission, or affinity for either GABAergic or glutamatergic receptors. Rather, it is thought that the antiepileptic mechanism of action involves inhibitory effects on depolarization-induced and Ca^{2+}-induced Ca^{2+} release–associated neurotransmitter releases, GABA turnover rate in the striatum, removal of Zn^{2+}-induced suppression of $GABA_A$-mediated presynaptic inhibition (resulting in a presynaptic decrease in glutamate-mediated excitatory transmission), and decreased levels of the amino acid taurine (a low-affinity agonist for $GABA_A$ receptors) in the hippocampus (Deshpande & Delorenzo, 2014).

Felbamate is a phenyl-substituted dicarbamate that not only inhibits NMDA-evoked responses but also enhances GABA-evoked responses (McNamara, 2006).

Common side effects of topiramate include fatigue, psychomotor slowing, somnolence, and difficulty with concentration and speech. Acute-angle glaucoma can also occur (Asconape, 2002). Common side effects of lamotrigine include ataxia, CNS depression, diplopia, dizziness, abnormal thinking, nausea, nervousness, rash, and somnolence. An additional major toxic effect reported for lamotrigine is Stevens-Johnson syndrome (Brodtkorb, 1998; Warner et al., 1998). Common side effects of gabapentin include ataxia, dizziness, fatigue, and somnolence. Felbamate has been found to produce a relatively high incidence of aplastic anemia and hepatic failure (Asconape, 2002). Thus, the drug is utilized in patients failing other treatments only when the potential clinical benefits outweigh the potential clinical risks (Bazil & Pedley, 1998; Brodtkorb, 1998; Asconape, 2002; McNamara, 2006). Attention to emerging anticonvulsants and the differences in their bioavailability may sensitize the clinician to variability of their side effects in infants, children, and pregnant women (Tricco et al., 2014).

ANTIASTHMATICS

Asthma is a form of chronic obstructive pulmonary disease that has a variety of causes, some of them allergenic in nature. As indicated in Figure 24.12, at the heart of asthma is bronchoconstriction due to contraction of smooth muscle fibers in bronchioles. This may be induced by allergenic causes that trigger inflammatory processes that, in turn, result in the release of histamine from mast cells. Histamine, when it binds to H_1 receptors in smooth muscle cells, induces second messengers such as inositol triphosphate and diacylglycerol that ultimately stimulate muscle contraction (see Fig. 24.12). Opposing this process is the binding of epinephrine to β_2 receptors, resulting in stimulation of adenylate cyclase that induces synthesis of cAMP, a second-messenger molecule that induces blockade of muscle contraction. As part of a regulatory process, phosphodiesterase induces hydrolysis of cAMP and thus helps to remove inhibition of smooth muscle contraction.

As indicated in Figure 24.12, there are at least three different therapeutic strategies for blocking bronchiolar smooth muscle contraction. The first is blockade of release of histamine from mast cells by drugs such as cromolyn. This is not the only inflammatory process that can induce the bronchoconstriction of asthma. Other components of the inflammatory process may also be active in provoking bronchoconstriction. These are summarized in Figure 24.13, which shows that, among the agents promoting bronchoconstriction, the leukotrienes and prostaglandins are quite prominent. To counter these effects, oral antiinflammatory agents, such as the leukotriene inhibitors zileuton and zafirlukast, have been found to be effective in asthma because they interrupt the leukotriene/arachidonic acid pathways involved in inflammation and bronchial reactivity. It is important to note that steroids have been found to be highly effective in blocking inflammation-induced bronchospasm. As indicated in Figure 24.13, these agents potently inhibit leukotriene, prostaglandin, and platelet-activating factor production (not shown in Fig. 24.13) by inhibiting phospholipase A2 and the inducible cyclo-oxygenase-2 isoform. Lipid-soluble steroids, especially in aerosolized form, avoiding adverse systemic effects, have been

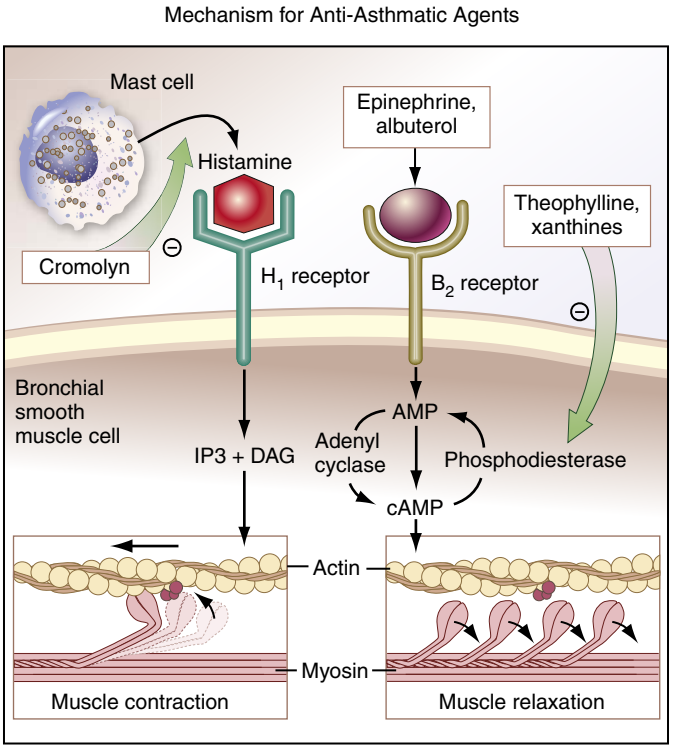

Figure 24.12 Summary of the mechanisms of action of antiasthmatic agents. Three basic mechanisms are shown. Note that all three mechanisms result in promotion of smooth muscle relaxation in the small airways (i.e., fewer actin-myosin cross-bridges*; arrows show loss of cross-bridges),* as shown at lower right of the figure. On the left, release of histamine from mast cells in response to allergenic stimulation results in histamine–H_1 receptor complexes that promote a signal transduction pathway in which inositol triphosphate (IP_3) and diacylglycerol (DAG), both second messengers, are induced and promote smooth muscle contraction. Histamine release is blocked *(minus sign in circle, next to green arrow)* by the drug cromolyn. In the middle of the figure, epinephrine and albuterol are shown to form complexes with β receptors. These complexes induce adenyl cyclase activity such that cyclic adenosine monophosphate (cAMP) is synthesized; this second messenger blocks smooth muscle contraction. On the right, xanthines, such as theophylline, are shown to block the enzyme phosphodiesterase, resulting in prolonged lifetimes of cAMP, allowing it to function for prolonged periods in blocking smooth muscle contraction.

found to be among the most effective agents against asthma. These agents include beclomethasone, flunisolide, and triamcinolone. Longer-acting lipid-soluble β_2 agonists, such as formoterol and salmeterol, are also available and appear to be long acting because of their ability to dissolve into the bronchial smooth muscle membrane.

Second, for severe asthmatic attacks, subcutaneous injection of epinephrine is effective in relieving bronchoconstriction on an acute basis via the mechanism shown in Figure 24.12. For more long-term treatment, β_2 receptor–binding agonist drugs, including albuterol (Proventil, Ventolin) and terbutaline (Brethine), are effective in reversing this process by the same mechanism. Both of these agents stimulate production of cAMP, as shown in the central pathway of Figure 24.12. Third, as shown in Figure 24.12, blockade of phosphodiesterase by such drugs as theophylline and the xanthines prevents hydrolysis of cAMP, allowing for continuous inhibition of bronchoconstriction.

Although still a commonly prescribed antiasthmatic drug, theophylline is being replaced with other antiasthmatics such as steroid and β-adrenergic bronchial inhalers, used mainly for acute and subacute asthmatic attacks in adults. These latter agents have fewer toxic side effects (Pesce et al., 1998). However, laboratory assays for therapeutic levels of antiasthmatics have been performed only for theophylline, predominantly because its therapeutic range is narrow, and potential side effects are serious, as discussed in the following section.

Theophylline

Theophylline (see Table 24.6) is used as a bronchodilator for the treatment of moderate or severe asthma, both for the prevention of attacks and for the treatment of symptomatic exacerbations. Besides its main effect of inhibiting a variety of phosphodiesterases, theophylline also inhibits the bronchoconstrictive action of adenosine and activates histone deacetylases. The latter action may result in decreases in the transcription of proinflammatory genes. It also inhibits the release of proinflammatory agents, such as histamine, from a variety of inflammatory cells (Undem, 2006).

Theophylline exerts additional actions such as vasodilatation, diuresis, positive cardiac inotropic effects, and stimulation of diaphragmatic contraction. Owing to the latter stimulating effect, theophylline may be of benefit to some patients with emphysema. Theophylline has also been effective in the treatment of primary apnea of prematurity, in which the absence of respiratory effort lasts longer than 20 seconds in newborn infants. This latter effect is thought to be due to medullary stimulation by the drug. It has been found that caffeine is more effective for this purpose because it has diminished toxicity (Pesce et al., 1998).

In the treatment of asthma, the dosage is calculated on the basis of body weight and depends on the route of administration and the age of the patient. Because the therapeutic index (i.e., the closeness of toxic levels to therapeutic levels) of theophylline is low, cautious dosage determination is essential. Careful monitoring of patient response and serum theophylline levels is required because theophylline is metabolized at different rates for each patient. Theophylline levels can be estimated 1 hour after intravenous administration, 1 to 2 hours after oral administration, or generally 3 to 8 hours after extended-release administration from appropriately drawn blood samples.

The therapeutic serum level is 10 to 20 μg/mL, and the mean half-life is approximately 8.7 hours in nonsmoking adults (5.5 hours in smoking adults). However, the half-life may vary widely among individuals, again indicating the need for close supervision of the patient and appropriate monitoring of serum concentrations in each patient. Approximately 60% of the drug is protein bound, and about 90% is metabolized in the liver, with caffeine being one of the metabolites produced. Theophylline crosses the placenta and may be teratogenic in pregnant females. Other common side effects include tachycardia, arrhythmias, seizures, and gastrointestinal bleeding. Newer antiasthmatic options, such as the nonsedating H_1 receptor inverse agonist, bilastine, as well as additional emerging pharmacopeia (Braido et al., 2014) will provide additional treatment opportunities and may require drug monitoring by the clinical laboratory.

ANTIINFLAMMATORY AND ANALGESIC DRUGS

As noted in the preceding section, and as shown in Figure 24.13, membrane damage resulting from immune complexes, trauma, or other stress induces the release of phospholipids, among other events,. These, in turn, become substrates for phospholipase A_2, which results in the production of arachidonic acid. This centrally important compound may be converted into leukotrienes via lipoxygenase, or thromboxanes and prostaglandins via cyclooxygenase (COX). All of these agents provoke chemotaxis of neutrophils, resulting in their activation and, ultimately, in inflammation. In addition, they increase vascular permeability (inducing more influx of neutrophils) and smooth muscle contraction. As noted in the preceding section, and as shown in Figure 24.13, corticosteroids are powerful antiinflammatory agents that work through the blockade of COX in addition to blocking the formation of arachidonic acid.

Although steroids are highly effective antiinflammatory agents, they provoke a number of undesirable side effects, including fluid retention, weight gain, osteoporosis, gastrointestinal bleeding, and mental changes. Other nonsteroidal drugs, including **nonsteroidal antiinflammatory drugs (NSAIDs)**, have been found to be effective in blocking inflammation by similar mechanisms, as shown in Figure 24.13, without the undesirable side effects of the corticosteroids. These agents, most of which block COX specifically, include such drugs as naproxen (Naprosyn, Aleve), ibuprofen (Advil, Motrin), indomethacin (Indocin), and piroxicam (Feldene). These agents inhibit two forms of COX: COX-1 and COX-2. The former is involved in maintaining membrane integrity of mucosal cells in the gastrointestinal tract; the latter is involved in the inflammatory process. Because all of these agents inhibit both forms of COX, they have the undesirable side effect of gastrointestinal tract toxicity and induce GI bleeding. Newer agents that more selectively inhibit COX-2 have recently become available, including celecoxib (Celebrex) and rofecoxib (Vioxx). Because some patients treated with Vioxx have been diagnosed with myocardial infarction, this drug was withdrawn. Other NSAIDs such as diflunisal (Dolobid) inhibit prostaglandin synthetase, but the exact mechanism of action is not clear.

Acetylsalicylic acid (aspirin), a potent COX inhibitor, is an effective antiinflammatory agent that also has antipyretic and analgesic effects, which also result from COX inhibition. The latter two effects are thought possibly to be due to inhibition of COX in the CNS (**COX-3**), mainly in the hypothalamus, although this is not certain (Burke et al., 2006).

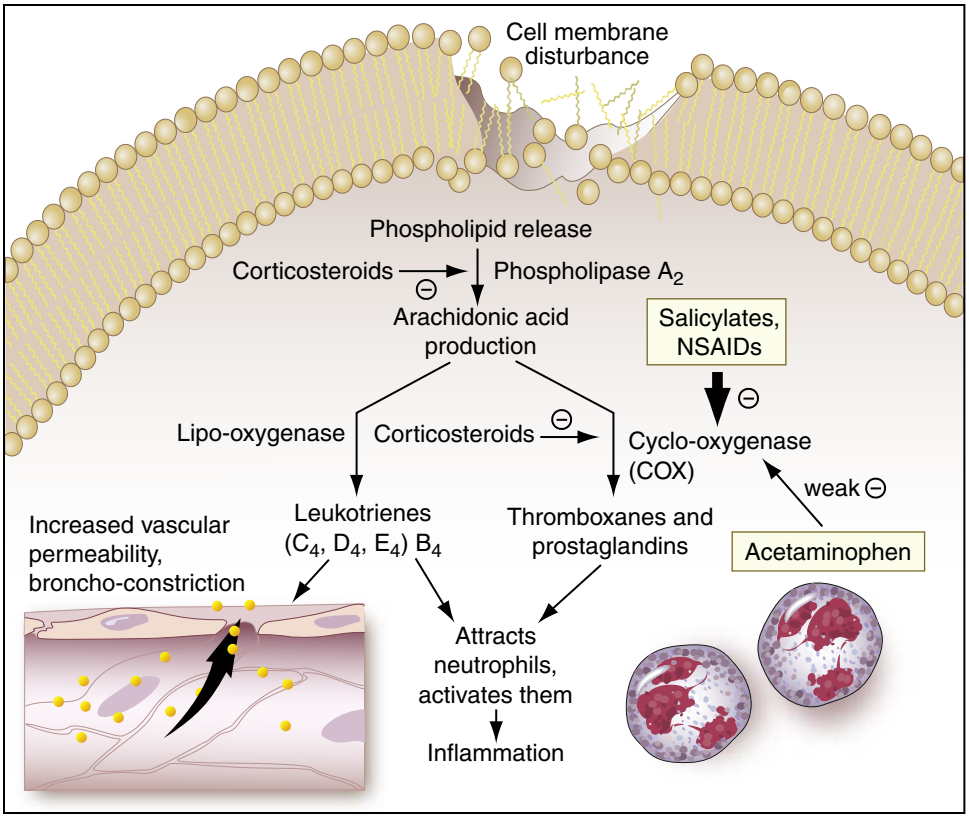

Figure 24.13 Mechanisms of action of anti-inflammatory drugs. The figure shows that the fundamental event in inflammation-induced cell death is membrane damage in cells that results in activation of phospholipase A_2. This enzyme promotes the synthesis of arachidonic acid. This is a substrate for two critical enzymes: lipoxygenase, which promotes synthesis of leukotrienes, and cyclooxygenase (COX), which promotes synthesis of thromboxanes and prostaglandins. Both classes of compounds promote neutrophil chemotaxis *(lower right)* with resulting phagocytosis of damaged cells and a further destructive inflammatory response. Leukotrienes themselves promote increased vascular permeability, causing increased migration of neutrophils to damaged cells, and smooth muscle contraction *(lower left)*. In this figure, corticosteroids such as prednisone and cortisone are shown to block *(black minus signs in circles, next to arrows)* two key enzymes in this signal transduction inflammatory cascade: phospholipase A_2 and cyclooxygenase. Corticosteroids are also thought to stabilize damaged membranes. Nonsteroidal antiinflammatory drugs (NSAIDs) block predominantly cyclooxygenase; acetaminophen (Tylenol) blocks mainly COX in the central nervous system and only weakly blocks peripheral COX and is therefore more of an antipyretic than an antiinflammatory drug.

Acetaminophen (Tylenol) inhibits COX-3 but exerts little effect on COX-1 and COX-2. Thus, it is not an antiinflammatory, does not result in gastrointestinal tract bleeding, and is an effective analgesic and antipyretic.

Of all of these drugs, therapeutic drug monitoring is performed only with acetylsalicylic acid and acetaminophen. We will therefore discuss these two drugs further.

Aspirin

Acetylsalicylic acid (aspirin) is a nonsteroidal antiinflammatory compound that is used as an analgesic, an antipyretic, and, in larger doses, an antiinflammatory agent. In lower doses, it exhibits its anticoagulant activity due to its antiplatelet activity through inhibition of COX in platelets, resulting in blockade of platelet plug formation. It can be effective in the treatment of fever, neuralgia, headache, myalgia, and arthralgia, and in the management of some rheumatic diseases.

Oral dosages of aspirin that are generally used for analgesia and antipyresis in adults range from 500 mg as necessary, to a maximum of 4 g/day. Usual doses for rheumatoid arthritis include 500 mg every 4 to 6 hours, or 650 mg every 4 hours, or 1 g every 4 to 6 hours, or 1.95 g twice daily. For juvenile rheumatoid arthritis in children, the usual dose is 3.5 g/day.

The small intestine is the primary site of aspirin absorption, which usually occurs rapidly following oral administration, with peak plasma levels established within 1 to 2 hours. Before entering the systemic circulation, aspirin is rapidly hydrolyzed to acetic acid and salicylic acid. Hydrolysis occurs partially by plasma esterase and partially by the liver. Both aspirin and salicylic acid enter the CNS.

Approximately 70% to 90% of salicylic acid is plasma protein bound. The serum half-life is dose dependent and increases with the dose—from approximately 3 hours with 500 mg to approximately 15 hours with 4 g. Salicylic acid is cleared not only by metabolism but also by urinary excretion; as the half-life increases, the rate of urinary excretion decreases. This can produce toxic effects if the dosage interval is not increased appropriately. However, the rate of elimination can vary widely with the patient, necessitating individualization of dosage for large amounts of drug. Tinnitus, muffled hearing, and a sensation of fullness in the ears are the most common signs of chronic aspirin toxicity. In infants, young children, and patients with preexisting hearing loss, otic symptoms will not occur, and hyperventilation is the most common sign of overdose.

As discussed in Chapter 15, overdoses of aspirin can cause metabolic acidosis. Because salicylate itself stimulates central respiratory centers, overdose causes an increased breathing rate, leading to a respiratory alkalosis that can predominate so that the patient exhibits respiratory alkalosis subsequent to initial metabolic acidosis. Acute aspirin intoxication is a common cause of fatal drug poisoning in children. Toxic doses produce acid-base disturbances, direct CNS stimulation of respiration, hyperpyrexia and hypoglycemia, gastrointestinal bleeding, and nausea and vomiting. Acute renal failure, CNS dysfunction with stupor and coma, and pulmonary edema may develop. Figure 24.14 summarizes the toxic levels of aspirin in children as a function of time after the toxic dose was taken.

A serious toxic effect of aspirin, mainly in children but also recognized in adults, is hepatotoxicity leading to fulminant hepatic failure (i.e., Reye syndrome). This occurs when a patient is treated with aspirin for fever during a viral illness. After apparent recovery, the patient becomes seriously ill from hepatic failure with signs and symptoms, including hepatic encephalopathy (described in Chapters 9 and 22). Although once almost always fatal, newer supportive measures have resulted in a significant increase in survival from this life-threatening condition, the basic cause of which is as yet undetermined.

Acetaminophen

Acetaminophen (Tylenol), or *N*-acetyl-*p*-aminophenol, is used as an analgesic and antipyretic to treat fever, headache, and mild to moderate myalgia and arthralgia. Acetaminophen is as effective as aspirin in its analgesic and antipyretic actions and is preferred over aspirin in patients with a bleeding/coagulation disorder or in children requiring only antipyretics or analgesics, because no association between acetaminophen and Reye syndrome has been demonstrated. Furthermore, an accidental overdose in children may be less toxic than with aspirin; hepatotoxicity is rarely associated with acetaminophen overdose in children younger than 6 years of age.

Oral doses of acetaminophen are rapidly and essentially completely absorbed from the GI tract. Generally, 325 to 650 mg at 4-hour intervals is prescribed for adults and children older than 12 years of age, with a maximum of 4 g daily. The plasma half-life is approximately 2 hours, with peak plasma levels of 5 to 20 μg/mL occurring in 30 to 60 minutes. Plasma protein binding is about 20% with therapeutic doses. The major metabolites of acetaminophen produced by the liver are glucuronide and sulfate conjugates, with minor metabolites being deacetylated and hydroxylated derivatives. The latter metabolite is thought to produce hepatotoxicity with overdose.

At therapeutic levels, about 90% of acetaminophen is conjugated as glucuronides or sulfates in the liver. About 5% is converted to a toxic metabolite, *N*-acetyl-*p*-aminobenzoquinoneimime (NAPQI), which is hepatotoxic at high concentrations (Rowden et al., 2006). It is this metabolite that causes toxic liver effects at high doses of acetaminophen in the

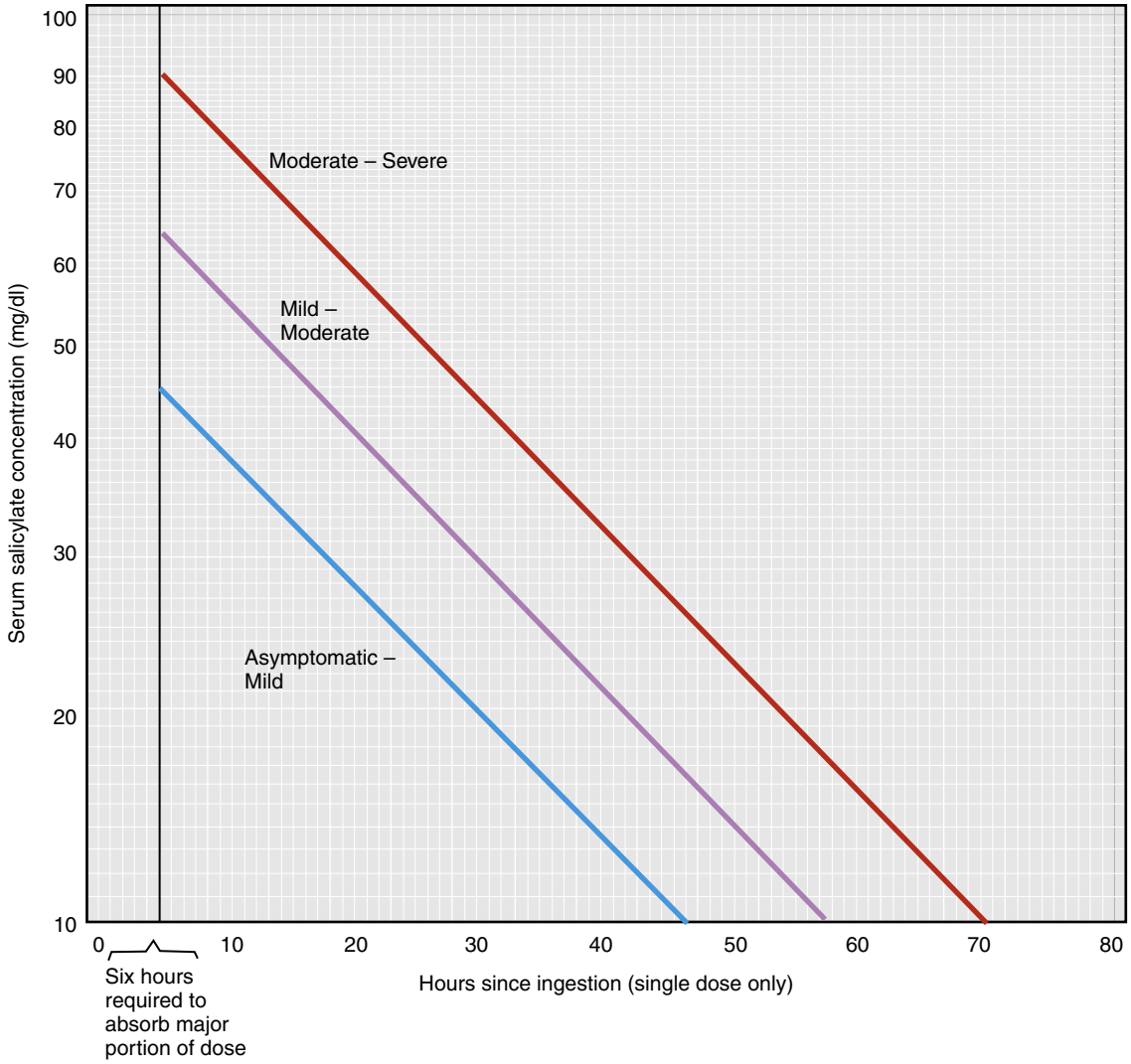

Figure 24.14 Aspirin toxicity levels in children as a function of time. (Howanitz & Howanitz, 1984; modified with permission from Done AK: Salicylate intoxication: significance of measurements of salicylate in blood in cases of acute ingestion, *Pediatrics* 1960;26:800.)

liver by the cytochrome P450 mixed oxidase system. This metabolite is normally cleared by conjugation to glutathione (GSH) by glutathione-S-transferase (GST) in the liver. In cases of toxic levels of NAPQI, in which the NAPQI levels overwhelm the GST system, acetylcysteine is administered. This compound conjugates to NAPQI, detoxifying it.

Toxic doses of acetaminophen occur at acute ingestion levels of 140 mg/kg (White & Wong, 1998). Acute manifestations of toxic doses generally occur within 2 to 3 hours after ingestion and include nausea, vomiting, and abdominal pain. A characteristic sign of toxicity is cyanosis of the skin, mucosa, and fingernails due to methemoglobinemia. However, this is seen more frequently with phenacetin poisoning. CNS stimulation followed by CNS depression may occur in severe poisoning, with vascular collapse, shock, and total seizures. Coma usually precedes death. At very high doses (as with suicide attempts), fulminant hepatic failure may occur, with maximum liver damage not becoming apparent until 2 to 4 days after drug ingestion (Sunheimer et al., 1994). Chronic acetaminophen abuse may produce chronic toxicity and death. Anemia, renal damage, and gastrointestinal disturbances are usually associated with chronic toxicity. Toxic effects can be treated effectively with NAC (acetylcysteine) (Rowden et al., 2006).

IMMUNOSUPPRESSIVES

Although intact humoral and cell-mediated immunity is essential in preventing infection, it becomes vital to suppress functioning of these systems in some circumstances. These include aberrations of the immune system, such as autoimmune disease (e.g., lupus erythematosus, Sjögren syndrome) and normal functioning of the immune system (e.g., in tissue transplantation). In the latter circumstance, the most important component of the immune system is cell-mediated immunity. As shown in Figure 24.15, in host-versus-graft or in graft-versus-host disease, CD4+ T cells become activated when a foreign antigen binds to the major histocompatibility class (II) Ia protein on the surface of macrophages (antigen-presenting cells). Specific T cell clones bind to the antigen using their T cell receptors (CD3), which recognize the antigen-Ia complex. Activation of the T cell receptor results in a signal transduction cascade that ultimately ends in engulfment via receptor-mediated endocytosis of the antigen by the macrophage and destruction in lysosomes. In this cascade, calcium ions are mobilized, resulting in the activation of calcineurin, a phosphatase that forms a complex with calmodulin. Activated calcineurin dephosphorylates cytosolic nuclear factor of activated T cells $(NF\text{-}AT)^C$, resulting in its activation, whereupon it translocates to the nucleus and binds to NF-AT from the nucleus $(NF\text{-}AT)^N$. This transcriptionally active complex results in the synthesis of interleukin (IL)-2, which becomes secreted as an extracellular mitogen (i.e., an autocrine factor). It binds to the IL-2 receptor of the T cell, activating it toward the binding of a protein, called **target of rapamycin (TOR)**, which serves to activate cyclin kinases that promote progression of the cell cycle from G1 to S and stimulate nucleotide synthesis. This ends in differentiation and proliferation of the T cell and ultimate antigen destruction.

As shown in Figure 24.15, there are specific agents (Hess et al., 1988; Kahan, 1989; Isoniemi, 1997; Braun et al., 1998; McEvoy et al., 2004: Krensky et al., 2006) that block one or more of these steps and, by so doing, inhibit antigen destruction. The drugs cyclosporine and tacrolimus are cyclic polypeptides that bind to intracellular proteins called **immunophilins**. Cyclosporine (CsA) binds to the immunophilin cyclophilin, while tacrolimus binds to the immunophilin called **FKBP12**. These complexes then block calcineurin-induced activation of NF-AT and therefore block IL-2 synthesis so that antigen destruction cannot occur. On the other hand, another immunosuppressive agent, rapamycin (Sirolimus), has

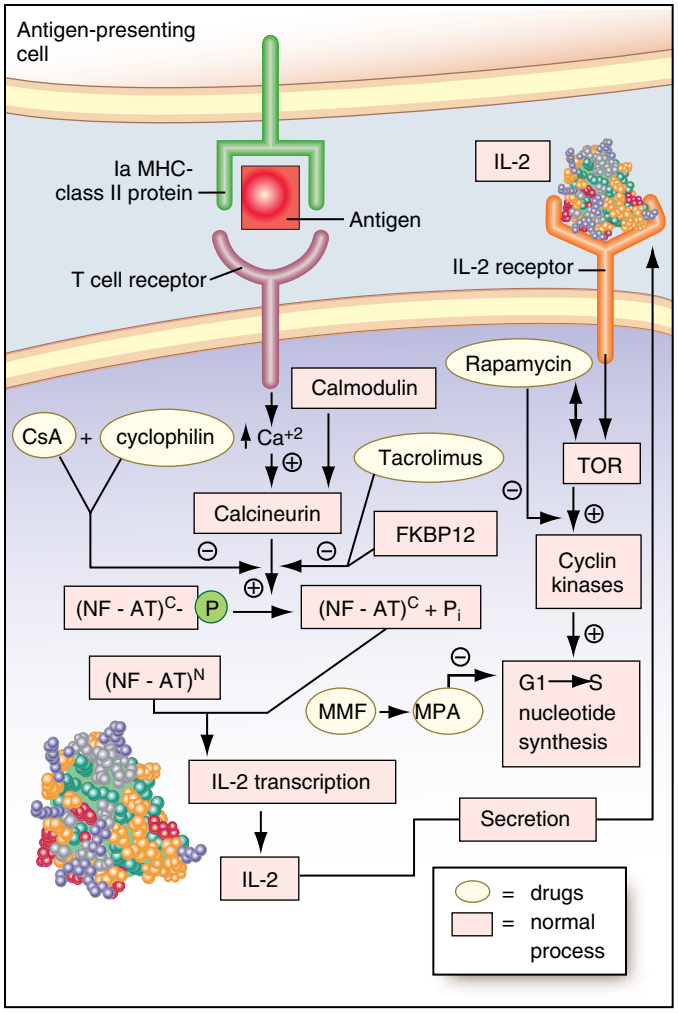

Figure 24.15 Mechanisms and sites of action of immunosuppressive drugs. This figure shows two linked, centrally important signal transduction pathways induced by antigen—in this case, foreign transplanted cells, for activation of cell-mediated immunity. In the first pathway, antigen is "presented" to antigen-specific (clonal) T cells by attachment of the antigen to the Ia molecule (major histocompatibility class [MHC] II—or DR in humans—protein). The formation of a ternary complex of antigen *(red box)*, Ia *(green receptor on the antigen-presenting cell; i.e., macrophage)*, and the T cell receptor *(purple receptor, upper left)* results in a signal transduction cascade that causes the synthesis of IL-2, shown as a space-filling model in the *lower-left* part of the figure. Critical to this pathway is activation, by calcium-activated calmodulin, of the phosphatase, calcineurin, which dephosphorylates cytosolic nuclear factor of activated T cells $(NF\text{-}AT)^C$, resulting in its activation. It then translocates to the nucleus and binds to NF-AT from the nucleus $(NF\text{-}AT)^N$, which directly promotes transcription of interleukin (IL)-2. In the second, linked, signal transduction pathway *(right side)*, newly synthesized IL-2 is then secreted by the T cell and acts as an autocrine factor in binding to the extracellular domain of the IL-2 receptor of the T cell to form a complex, as shown in the *upper-right* part of the figure. This complex induces activation of a second signal transduction cascade in which target of rapamycin (TOR) protein is stimulated and, in turn, activates cyclin kinases that promote activation of cyclins, which, in turn, promote progression of the cell cycle from G1 to S necessary for blast transformation of clonal T cells that, with macrophages, engulf and destroy the antigen. All elements of the normal signal transduction pathways are shown as *pink boxes*. The immunosuppressive drugs and their target proteins block different parts of these two pathways and are shown as *yellow ellipses*. Cyclosporine (CsA) and tacrolimus complex, respectively, with cyclophilin and FKBP12 to form inhibitory complexes that block calcineurin in the first pathway. On the other hand, rapamycin blocks TOR, thereby blocking IL-2–induced blast transformation in the second pathway; mycophenolate mofetil (MMF) blocks nucleotide synthesis, thereby blocking G1-S progression in the second pathway.

no such effect on T cells but rather binds to the critical TOR protein, disenabling activation of cyclin kinases so that T cell activation cannot proceed. Finally, mycophenolate mofetil, an antibiotic, is hydrolyzed to free mycophenolic acid in the cell. This agent is a powerful inhibitor of inosine monophosphate dehydrogenase and guanosine monophosphate synthetase, disenabling deoxypurine nucleotide synthesis, which, in turn, disables DNA synthesis uniquely in lymphocytes. Other cells have rescue pathways that circumvent this blockade, making the effects of this drug selective for lymphocytes (Krensky et al., 2006). In the same vein, some alkylating agents that are generally used as chemotherapeutic agents, such as cyclophosphamide (Cytoxan), can be used to suppress DNA synthesis in T cells, but these are not selective for lymphocytes.

It should be noted that the corticosteroids also have immunosuppressive effects on cell-mediated immunity but are much less specific and, as noted in the previous section, have multiple undesirable side effects. They are, therefore, not the drugs of choice for use in transplantation. In the following section, we discuss the properties of the more specific immunosuppressive drugs, most of which require monitoring of serum (plasma) levels (Dunn et al., 2001; Dancey, 2002; Drosos, 2002; Scott et al., 2003; Mueller, 2004).

Cyclosporine (CsA)

Cyclosporine (CsA) is a cyclic polypeptide containing 11 amino acids, five of which are methylated. Maximum suppression with CsA occurs during the first 24 hours of antigen stimulation by the allograft. Thus, CsA must be administered in the early phase of the immune response for optimal suppression of T cell function and increased success of transplantation (McEvoy et al., 2004).

CsA is indicated to prevent organ rejection in kidney, heart, and liver allogeneic transplants and is the drug of choice for maintenance of kidney, liver, heart, and heart-lung allografts. CsA may also be utilized as a first- or second-line drug in the treatment of acute graft-versus-host disease following bone marrow transplantation, in the active stage of severe rheumatoid arthritis, and for severe, recalcitrant plaque psoriasis. It may also be used in the treatment of other autoimmune diseases and in organ transplantation.

Because CsA is variably absorbed from the GI tract, the optimal dose must be carefully determined for each patient individually, and blood levels should be monitored frequently. It has been occasionally found that, although serum levels of the parent drug are low, the metabolites, some of which are active, maintain a therapeutic drug level. Therefore, in patients with apparently low levels of the parent drug, it is necessary to determine the levels of metabolites. Peak blood concentrations occur at approximately 3.5 hours after administration. About 20% to 40% of a given dose of CsA is absorbed, and it is metabolized on the first pass through the liver. Human cytochrome P450 III A3 (CYP3A) of the P450 III gene family appears to be the primary enzyme responsible for CsA metabolism. Because a number of drugs may induce or may be metabolized by this cytochrome P450 isoenzyme, coadministration of these drugs may be responsible for alterations in CsA levels that can complicate CsA therapy (Kronbach et al., 1988). Agents that inhibit the CYP3A system include calcium channel blockers (e.g., verapamil, discussed earlier), antimicrobials, and human immunodeficiency virus protease inhibitors. Grapefruit and grapefruit juice are also known to exert inhibitory effects on this system (Krensky et al., 2006). Trough whole blood or plasma concentrations, at 24 hours, of 250 to 800 ng/mL or 50 to 300 ng/mL, respectively (as determined by immunoassay), are believed to minimize graft rejection and, concurrently, toxic effects.

Adverse effects of CsA may occur in all organ systems of the body. Trough serum levels greater than 500 ng/mL are associated with CsA-induced nephrotoxicity, which is the most frequent toxic reaction seen with CsA. CsA-induced nephrotoxicity is accompanied by hyperkalemia and hyperuricemia, hypertension, and gingival hyperplasia.

Other toxic effects include neurologic effects (tremors, seizures, headache, paresthesia, flushing, confusion), dermatologic effects (hirsutism, hypertrichosis, rash), hepatotoxicity, GI effects (diarrhea, nausea, vomiting, anorexia, abdominal discomfort), infectious complications, hematologic effects (leukopenia, anemia, thrombocytopenia), and sensitivity reactions, including anaphylaxis (Philip & Gerson, 1998). It is important to note that the risk for immunosuppressed states is increased, and the occurrence of lymphoma, especially CNS lymphoma, may be associated with immunosuppression by CsA. It has also been found that CsA induces immune system–independent increased invasiveness of adenocarcinoma cells in culture, apparently by activating transforming growth factor-β (TGF-β) (Hojo et al., 1999). This behavior is blocked by monoclonal antibodies to TGF-β.

Both oral and intravenous preparations of CsA are available. Interpatient and intrapatient absorption of the oral preparation is variable, and absorption can be affected by many factors. It is generally recommended that whole blood be used for drug level monitoring and that an assay method with high specificity for unchanged drug (vs. metabolites) be used. Thus, the optimal dose must be carefully determined for each patient individually, and blood levels should be monitored frequently, with CsA blood concentrations qualified by biological fluid (whole blood vs. plasma vs. serum) and assay method (immunoassay vs. HPLC) used. At present, any currently available immunoassay (FPIA, EMIT) is acceptable for routine monitoring, although it is important that consistent laboratories and methods be used (McEvoy et al., 2004).

Neoral is a microemulsion formulation of CsA that is miscible in water; it increases the solubility of CsA in the small bowel (Frei et al., 1998). This preparation has shown superior pharmacokinetics with improved bioavailability and equivalent safety with no apparent increase in toxicity. It appears to offer advantages over oral solutions of CsA by decreasing intrapatient and interpatient blood level variability. Intravenous CsA is reserved for patients unable to tolerate oral administration. This route of administration carries a low but definite (0.1%) risk for anaphylaxis, which does not occur following oral administration of the drug.

Tacrolimus (FK-506)

Tacrolimus is a macrolide lactone antibiotic with a mechanism of action similar to that of cyclosporine; it is more potent than CsA in its inhibitory effect (McEvoy et al., 2004). It is currently being utilized in transplant surgery to prevent organ rejection. As is the case with CsA, higher trough concentrations of tacrolimus appear to increase the relative risk for toxicity, and therapeutic drug monitoring is recommended. The same monoclonal antibody is used in the two methods available for monitoring. One method is a microparticle enzyme immunoassay, and the other method is an enzyme-linked immunosorbent assay. Whole blood is the specimen of choice. The toxic potential appears to be similar to the toxic effects of CsA. The most common include nephrotoxicity, neurotoxicity (such as tremor and headache), gastrointestinal effects such as diarrhea and nausea, hypertension, alterations in glucose metabolism (diabetes mellitus), hyperkalemia, and infectious complications. However, unlike with CsA, gingival hyperplasia and hirsutism do not occur. Anaphylaxis may occur with intravenous administration, and oral therapy is recommended whenever possible. Tacrolimus appears to be best suited for use in combination with other new immunosuppressive agents.

Rapamycin (Sirolimus)

Rapamycin is an antibiotic similar to tacrolimus. Peak concentrations are reached after about 1 hour after a single oral dose or after about 2 hours after multiple doses for patients who have undergone renal transplantation (Krensky et al., 2006). The parent drug is the major active form, although several metabolites also have activity. About 40% of the drug is bound to serum proteins, especially albumin; it is metabolized predominantly in the liver by the CYP3A4 system (Krensky et al., 2006). Major side effects include GI symptoms, abnormalities in lipid levels, anemia, leukopenia, and thrombocytopenia. It can also cause delayed wound healing; however, it does not appear to be nephrotoxic. If used in combination with cyclosporine, because sirolimus aggravates CsA-induced renal dysfunction, administration of these two drugs must be separated in time (Krensky et al., 2006).

Mycophenolate Mofetil

Mycophenolate mofetil is a derivative of mycophenolate acid, a fungal antibiotic. The parent drug is metabolized to mycophenolic acid (MPA) within minutes of administration. The half-life of MPA is about 16 hours. Virtually all MPA is excreted in the urine as the glucuronide. This drug is used for prophylaxis of renal allograft rejection, usually in combination with a steroid or a calcineurin inhibitor (Krensky et al., 2006). Although this drug appears to decrease the rate of renal allograft rejection, differences in patient and allograft survival have not been demonstrated (Isoniemi, 1997). It may be of use in patients who do not tolerate CsA or tacrolimus (FK-506) well. Major side effects include GI symptoms such as diarrhea, nausea, and myelosuppression. Neither nephrotoxicity nor neurotoxicity has been demonstrated.

Leflunomide

Leflunomide (LFM) is an isoxazole derivative that inhibits lymphocyte proliferation by inhibiting dihydroorotic acid synthetase (Krensky et al., 2006), critical to deoxypyrimidine nucleotide synthesis. It is presently used in the treatment of rheumatoid arthritis, the only condition for which it has been approved for treatment, although it is being used increasingly for treatment of polyoma virus nephropathy seen in immunosuppressed renal transplant recipients (Krensky et al., 2006). LFM has not been demonstrated to cause nephrotoxicity or myelosuppression in humans.

DRUGS USED IN THE TREATMENT OF MANIA AND DEPRESSION

Both lithium and the antidepressants are used in the treatment of psychiatric affective disorders.

Lithium

Lithium is a monovalent cation, a member of the group of alkali metals, and is available commercially as citrate and carbonate salts. Lithium salts are considered to be antimanic agents and are used for the prophylaxis and treatment of bipolar disorder (manic-depressive psychosis) and as an adjunct to antidepressant therapy in melancholic depression (Baldessarini, 2006). In addition, lithium is considered by some investigators to be the drug of choice for the prevention of chronic cluster headache, and it may be effective in episodic or periodic forms of cluster headache. Initial oral dosages of lithium for acute mania range from 0.6 to 1.8 g daily (maximum, 2.4 g) and produce a therapeutic serum level of 0.75 to 1.5 mEq/L. Once the attack subsides, the dose is reduced rapidly to produce a serum concentration of 0.4 to 1.0 mEq/L. Oral adult dosages for cluster headaches generally range from 0.6 to 1.2 g daily in divided doses. In cases of acute mania, especially in agitated, uncooperative patients, because of the relatively slow onset of action of lithium, a benzodiazepine sedative (e.g., lorazepam, clonazepam) or the anticonvulsant valproate (Depakote; see previous section) is administered until some stabilization of the agitated state is achieved. Then, lithium is administered to achieve long-term stabilization. Alternatively, both drugs may be continued or, in some cases, the patient can be maintained on Depakote alone (Baldessarini & Tarazi, 2006).

In general, serum levels of and patient response to lithium are used to individualize dosage and must be monitored carefully. Complete absorption of lithium occurs 6 to 8 hours after oral administration. Plasma half-life varies from 17 to 36 hours, and onset of action is slow (5–10 days). Elimination occurs almost entirely by the kidneys, and about 80% of filtered lithium is reabsorbed. Lithium is not protein bound and is distributed in total body water, but it shows delayed and varied tissue distribution. Thus, symptoms of acute intoxication may not correlate well with serum levels because the distribution of the drug into different organs may be slow and/or varied.

The exact mechanism of action of lithium is unknown. However, lithium, as a monovalent cation, competes with other monovalent and divalent cations (such as sodium, potassium, calcium, and magnesium) at ion channels in cell membranes and at protein-binding sites such as membrane receptors and protein/peptide transport molecules and enzymes that are critical to the synthesis, storage, release, and uptake of central neurotransmitters. Lithium also has a marked inhibitory effect on inositol monophosphatase and on the synthesis of phosphatidylinositides, which are second messengers involved in neurotransmission, and on the synthesis of cAMP, also involved in neurotransmission (Phiel & Klein, 2001; Baldessarini, 2006, Baldessarini & Tarazi, 2006). These effects are exerted on the postsynaptic side of dopamine- and norepinephrine-utilizing tracts in the mesolimbic and mesocortical pathways that inhibit the mobilization of calcium ions required for postsynaptic depolarization. The effect, then, is to inhibit neurotransmission. In addition, lithium blocks release of dopamine from presynaptic vesicles, also resulting in diminished neurotransmission.

Toxicity may occur acutely, as the result of a single toxic dose, or chronically, from high and/or prolonged dosages or changes in lithium pharmacokinetics. Water loss (resulting from fever, decreased intake, abnormal gastrointestinal conditions such as diarrhea or vomiting, diuretics, or pyelonephritis) is the main contributing factor underlying chronic intoxication. Renal toxicity and hypothyroidism are also known possible side effects of lithium. Thus, it is advisable to monitor creatinine and thyroid-stimulating hormone periodically in patients who are under continuing treatment with this drug. Severity of intoxication is not clearly related to serum lithium levels. However, an imprecise prediction of severity of intoxication may be attempted from serum lithium levels obtained 12 hours after the last dose: slight to moderate intoxication with 1.5 to 2.5 mEq/L, severe intoxication with 2.5 to 3.5 mEq/L, and potentially lethal intoxication if greater than 3.5 mEq/L. Severity of lithium intoxication also depends on the length of time that the serum concentration remains toxic.

The most common symptoms of mild to moderate intoxication include nausea, malaise, diarrhea, and fine hand tremor. In addition, thirst, polydipsia, and polyuria—as well as drowsiness, muscle weakness, ataxia, and slurred speech—may occur. Symptoms of moderate to severe toxicity include hyperactive deep tendon reflexes, choreoathetoid movements, persistent nausea and vomiting, fasciculations, generalized seizures, and clonic movements of whole limbs. These may progress rapidly to generalized seizures, oliguria, circulatory failure, and death with serum levels greater than 3.5 mEq/L.

Antidepressants

Three classes of drugs are currently used in the treatment of clinical depression: classical tricyclic antidepressants (TCAs), SSRIs, and monoamine oxidase inhibitors (MAOIs) (Baldessarini, 2006). The rationale for use of the first class of drugs is their ability to block the uptake of norepinephrine at the axonal side of synapses in neural tracts from the brainstem to the forebrain that utilize this neurotransmitter, as indicated in Figure 24.8. This blockade allows longer stimulation times and higher concentrations

of norepinephrine at the dendritic side of the synapse, allowing them to bind to α_1 receptors in these tracts for prolonged times, resulting in prolonged and enhanced stimulation. Drugs in the second class produce the same effect in parallel neural pathways that utilize serotonin as the stimulatory neurotransmitter (see the General Aspects of the Mechanisms of Action section earlier in the chapter). Finally, MAOIs block the inactivating metabolism of both norepinephrine and serotonin neurotransmitters by inhibiting their oxidation by the enzyme monoamine oxidase, present in the mitochondria of the presynaptic (axonal) terminal, wherein their amino groups are oxidized to the corresponding aldehydes. This inhibition results in increased concentrations of these neurotransmitters.

Tricyclic Antidepressants

The structures of these related compounds are shown in Figure 24.16. Also shown are two other effective antidepressant drugs: doxepin and trazodone (Desyrel), a second-generation, so-called **atypical antidepressant**, which does not contain the fused-three-ring system of the TCAs. Besides blocking reuptake of norepinephrine at the axonal side of synapses, the TCAs have been found to *bind directly* to two classes of norepinephrine receptors: α_1, which occur on the postsynaptic side of the synapse, and α_2, so-called **autoreceptors**, which occur on the presynaptic side of the synapse. The postsynaptic α_1 receptors are involved in postsynaptic membrane depolarization involving calcium ion fluxes, resulting in nerve conduction. The presynaptic α_2 receptors, when bound to norepinephrine, induce its downregulation by causing decreased synthesis of tyrosine hydroxylase, the critical enzyme that catalyzes the rate-limiting step in norepinephrine biosynthesis (Baldessarini, 2006). This results in decreased levels of norepinephrine and in decreased secretion of this neurotransmitter into the synaptic cleft.

When the TCAs bind to α_1 receptors, they cause temporary blockade of these receptors. This effect is thought to cause the **observed side effect of initial hypotensive episodes** in patients who are treated with these

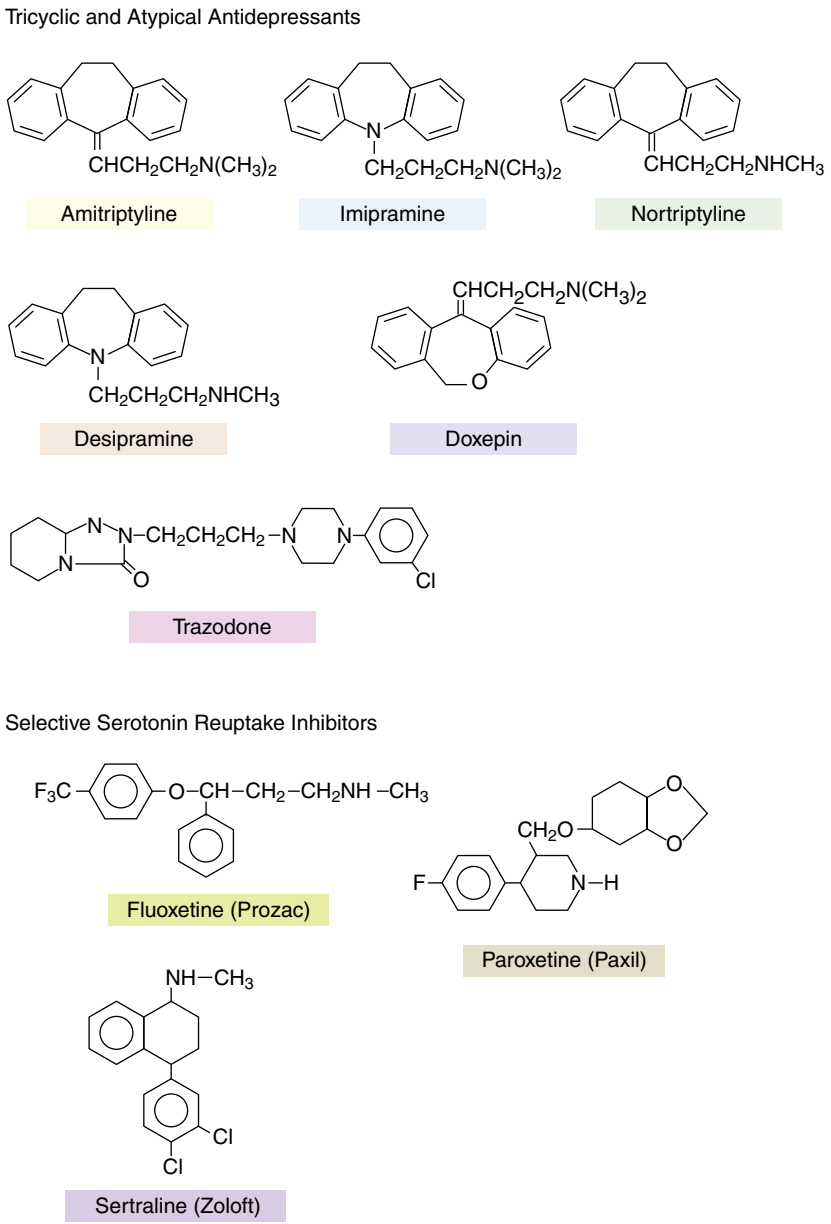

Figure 24.16 Structures of the most commonly used drugs in the three classes of antidepressants: tricyclic and atypical antidepressants, selective serotonin reuptake inhibitors, and monoamine oxidase inhibitors.

drugs. Over time, the binding of TCAs to these postsynaptic receptors apparently causes increased **sensitization** of the α_1 receptors to norepinephrine, overcoming the initial inhibition, while the presynaptic reuptake blockade of norepinephrine continues unimpeded. Concurrently, binding of the TCAs to presynaptic α_2 receptors has the opposite effect from their binding to the postsynaptic α_1 receptors, that is, desensitization with resulting loss of inhibition of epinephrine biosynthesis. Thus, the TCAs enhance norepinephrine-induced neurotransmission in the limbic system by blocking norepinephrine reuptake, sensitizing postsynaptic α_1 receptors and desensitizing inhibitory presynaptic α_2 receptors. In addition, TCAs appear to block, in a nonspecific manner, the reuptake of dopamine in the dopaminergic pathways in the limbic system (Baldessarini, 2006).

Besides stimulating dopaminergic pathways, the tricyclics, especially amitriptyline, have anticholinergic effects (Baldessarini, 2006). The pharmacologic side effects of the tricyclic antidepressants, in fact, reflect their anticholinergic activities. These include dry mouth, constipation, blurred vision, hyperthermia, adynamic ileus, urinary retention, and delayed micturition. Other CNS effects include drowsiness, weakness, fatigue, and lethargy, which are most common, as well as agitation, restlessness, insomnia, and confusion. Seizures and coma can also occur. Extrapyramidal symptoms may occur and include a persistent fine tremor, rigidity, dystonia, and opisthotonos. It is important to note that TCAs unfortunately have been used in suicide attempts by some depressed individuals who are being treated with them. The cardinal signs of TCA overdose are anticholinergic symptoms, such as dilated pupils and dry skin.

Toxicity

Overdose produces symptoms that are primarily extensions of common adverse reactions with excess CNS stimulation and anticholinergic activity. These include seizures, coma, hypotension, respiratory depression, areflexia, shock, and cardiorespiratory arrest. Agitation, confusion, hypertension, and the parkinsonian syndrome may also occur, as well as hallucinations and delirium. Occasional manifestations include ataxia, renal failure, dysarthria, and vomiting.

Treatment

Symptomatic and supportive care is the general mode of treatment. Gastric lavage, accompanied by instillation of activated charcoal, is usually recommended for removal of the tricyclic from the GI tract. Seizures are generally treated with intravenous diazepam. For overdoses with amitriptyline (see Fig. 24.16), use of cholinesterase inhibitors such as neostigmine has proved to be effective in reversing anticholinergic symptoms.

Selective Serotonin Reuptake Inhibitors

These are nontricyclic drugs with strong antidepressant activity that have been developed more recently. The most prominent of these is fluoxetine (Prozac), whose structure is shown in Figure 24.16. These drugs block the reuptake of serotonin in central serotonergic pathways as noted previously. Their effects on serotonin receptors parallel those of the TCAs on norepinephrine receptors, including ultimate downregulation of presynaptic autoreceptors. It is interesting to note that if the trifluoromethyl group of fluoxetine is placed at the ortho rather than the para position, the resulting drug behaves as a TCA (Baldessarini, 2006). It is important to note that fluoxetine and SSRIs in general do not appear to cause some of the side effects, such as the anticholinergic effects, associated with TCAs. For this reason, they have become the drugs of choice for treating clinical depression, although reports have described attempted suicide with some patients, especially adolescents, who are being treated with SSRIs. In addition, SSRIs have been reported to cause nausea and decreased libido and sexual function.

MAO Inhibitors

MAO is a flavin-containing oxidative enzyme that is encoded by two distinct genes. The two resulting enzymes, called **MAO-A** and **MAO-B,** have about 70% sequence identity. Each enzyme is found on the mitochondrial membrane. MAO-A deaminates epinephrine, norepinephrine, and serotonin, and MAO-B deaminates phenylethylamine. Both enzymes deaminate dopamine. Several MAOIs have been synthesized that inhibit either enzyme selectively. Thus, for example, MAO-A is inhibited selectively by clorgyline, and MAO-B is inhibited by selegiline (see Figure 24.16).

MAOIs are not used as the first line of treatment for depression because of their potential toxic effects and unfavorable interactions with TCAs and SSRIs. Toxic effects from overdoses include hypertension and/or hypotension, agitation, hallucinations, hyperreflexia, fever, and seizures (Baldessarini, 2006). The combination of an MAOI with an SSRI can lead to the so-called **serotonin syndrome**, which includes akathisia, myoclonus, hyperreflexia, diaphoresis, and shivering progressing to seizures and coma. In addition, MAOIs potentiate the action of over-the-counter anticold sympathomimetic amines such that they can cause hypertensive crises and intracerebral bleeding. Therefore, it is imperative to avoid use of these anticold medications in individuals treated with an MAOI. Their use is mostly for patients who do not respond to either SSRI or TCA therapy and who refuse electroconvulsant shock therapy.

Therapeutic Levels and Metabolism of Antidepressants

It is difficult to obtain reference ranges for the antidepressants because of their large numbers of metabolites, some of which may be active and others of which may be inactive, and which vary significantly in concentration from individual to individual—a problem that also exists for the neuroleptics discussed later. In addition, the volumes of distribution of these drugs are quite high because most are lipophilic and thus are stored in tissue and slowly released. For the TCAs, serum levels from 100 to 250 ng/mL generally are considered therapeutic; toxic effects may result at levels above 500 ng/mL and lethal doses above 1 μg/mL. Assays for the TCAs are performed by immunoassay (see the Immunochemical Methods section earlier and Fig. 24.1) or by HPLC (see the High-Performance Liquid Chromatography section earlier and Fig. 24.4).

Virtually all of these drugs are metabolized in the liver using the cytochrome P450–dependent oxidase system (Baldessarini, 2006). Different antidepressants require different isoforms of cytochrome P450. These isoforms include CYP2D6, CYP2C19, CYP3A3/4, and CYP1A2. In general, for both TCAs and SSRIs, oxidation, a modification that often includes glucuronidation and elimination of these drugs, occurs over several days. Most tricyclics are completely eliminated within 10 days. Secondary amine TCAs and *N*-demethylated derivatives of SSRIs have about twice the half-lives of their parent compounds. The **atypical TCA**, trazodone, is metabolized to mCPP, a piperazine that is discussed earlier under the Drugs of Abuse section. MAOIs have much shorter half-lives than TCAs and SSRIs, requiring frequent dosing to maintain therapeutic levels.

THE NEUROLEPTICS: ANTIPSYCHOTIC MAJOR TRANQUILIZERS

These drugs are used mainly in the treatment of acute schizophrenia and result in suppression of the agitated state. All neuroleptics appear to block the actions of dopamine and serotonin postsynaptically in the limbic system and motor cortex (see Fig. 24.8). Specific dopaminergic pathways, called the **mesolimbic-mesocortical pathways**, connect the substantia nigra of the midbrain to the limbic system and motor cortex (Baldessarini & Tarazi, 2006). In addition, the substantia nigra connects to the basal ganglia via the nigrostriatal pathway; depletion of dopamine in this pathway results in Parkinson disease. Thus, it may be expected that dopamine antagonists would affect the latter pathway in addition to the mesolimbic-mesocortical pathways. Indeed, many of the neuroleptics have, as side effects, dystonias, tardive dyskinesias, and frank parkinsonism, the latter fortunately being much less common. Originally, two classes of neuroleptics, the phenothiazines, typified by chlorpromazine, and the butyrophenones, typified by haloperidol (Haldol), were the drugs of choice. Besides postsynaptic blockade of dopamine, Haldol is known to bind with high affinity to sigma receptors in the CNS. This action may stimulate inhibitory pathways that modulate the activity of the dopaminergic pathways. All compounds in both classes have the undesired extrapyramidal side effects mentioned previously. In addition, the neuroleptics inhibit dopamine in the hypothalamic-pituitary tract, which inhibits release of prolactin by the pituitary gland. Therefore, the effect of the neuroleptics is to increase prolactin secretion by the pituitary gland, resulting in hyperprolactinemia. Treatment of patients with breast cancer with any neuroleptic that causes this effect is contraindicated (Baldessarini & Tarazi, 2006).

Newer neuroleptics have been developed that affect the nigrostriatal pathway to a lesser extent but are potent postsynaptic dopamine blockers in the mesolimbic-mesocortical pathways and therefore are effective, with fewer of the extrapyramidal side effects of the older drugs. These newer drugs (Burns, 2001) include risperidone (Risperdal; which does have some documented extrapyramidal side effects), olanzapine (Zyprexa), quetiapine (Seroquel), and aripiprazole (Abilify).

It has been difficult to monitor the levels of any of these drugs in serum because of the large number of metabolites for each drug resulting from extensive metabolism in the liver. Chlorpromazine, for example, has approximately 150 metabolites. The therapeutic efficacy of most of these metabolites is unknown. Reference ranges for serum levels therefore have not been established. Similar to the antidepressants, the neuroleptics, being lipophilic, have high volumes of distribution and are stored in tissues from which they are released over time.

Methods for assay include FPIA (see the Immunochemical Methods section earlier and Fig. 24.1) and HPLC (see the High-Performance Liquid Chromatography section earlier and Fig. 24.4). It is not clear in FPIA which, if any, metabolites cross-react with the antibody. For chlorpromazine, the estimated

therapeutic range is wide—between 50 and 300 ng/mL. The half-life of the drug is 16 to 30 hours and its bioavailability is 25% to 35%. Normal doses for chlorpromazine are 200 to 600 mg/day in divided doses. Other maintenance drugs in the phenothiazine series include thioridazine and fluphenazine (Prolixin).

Besides the extrapyramidal side effects, the phenothiazines can cause orthostatic hypotension, cholestasis, and, rarely, aplastic anemia. Occasionally, contact dermatitis has been reported to occur with phenothiazines. Of great importance is the subset of patients who have been chronically treated with these drugs and develop tardive dyskinesia. In most of these patients, the motor disturbances are irreversible.

Neuroleptics can cause a rare but important adverse reaction termed *neuroleptic malignant syndrome*. This can occur in patients who are extremely sensitive to the extrapyramidal effects of these drugs, and it may be fatal. Marked muscle rigidity, the first symptom to occur, may be followed by high fever, altered pulse and blood pressure, and leukocytosis. An excessively rapid inhibition of postsynaptic dopamine receptors is believed to be responsible for this syndrome. Treatment is cessation of the drug.

CHEMOTHERAPEUTIC AGENTS: METHOTREXATE AND BUSULFAN

Serum levels of both of these agents are monitored to assess whether therapeutic serum levels are present. Both agents are used in the treatment of different forms of cancer.

Methotrexate

Methotrexate, an antimetabolite consisting of a mixture containing no less than 85% 4-amino-10-methylfolic acid and related compounds, is a folic acid antagonist (Table 24.7). It inhibits the enzyme dihydrofolate reductase (Chabner et al., 2006). This results in blockade of the synthesis of tetrahydrofolic acid, which is needed for the formation of *N*-5,10-methylene-tetrahydrofolate, an intermediate in the transfer of a methyl group to deoxyuridylate to form thymidylate, needed in DNA synthesis. It has also been suggested that methotrexate may cause a rise in the intracellular levels of adenosine triphosphate (ATP), which blocks ribonucleotide reduction, also resulting in blocking of DNA synthesis. Methotrexate appears to inhibit polynucleotide ligase involved in DNA synthesis and repair. Furthermore, methotrexate and its analogs, like pemetrexed, a pyrrole-pyrimidine folate analog, accumulate in cells and are stored as polyglutamates, which allows them to inhibit other enzymes in DNA synthesis, including thymidylate synthase. Methotrexate polyglutamates also inhibit enzymes involved in purine nucleotide biosynthesis such as glycinamide ribonucleotide transformylase and aminoimidazole carboxamide transformylase in the synthesis of inosine monophosphate.

Methotrexate is used in the treatment of childhood acute lymphatic leukemia and a number of other hematologic malignancies, such as Hodgkin lymphoma, usually in combination with other antineoplastic agents. It has also been used successfully in the treatment of choriocarcinoma (Chabner et al., 2006). Pemetrexed is used to treat mesothelioma and refractory non–small-cell carcinoma of the lung.

Methotrexate is also an important immunosuppressive agent. Indications are severe, recalcitrant psoriasis and severe, active rheumatoid arthritis; in the latter, it may be used in combination with cyclosporine (Tugwell et al., 1995). Depending on the specific disease entity being treated, dosages given will vary, as will the therapeutic level of the drug. In Table 24.7, the doses and therapeutic drug levels for several different conditions are noted. The serum levels were determined by FPIA.

The kinetics of steady-state levels of this drug is triphasic: a rapid distribution phase followed first by a renal clearance phase with a $t_{1/2}$ of 2 to 3 hours, and then by a slow phase with a $t_{1/2}$ of 8 to 10 hours, in which methotrexate and its metabolites are filtered through the glomerulus and secreted in the renal tubules. If renal blood flow is compromised, the third phase is slowed, allowing toxic effects of the drug to occur. Excretion of the drug is biphasic: 92% is excreted within 24 hours and the remainder over a period of days. Approximately 50% of the drug in blood is bound to serum proteins. Based on these considerations, it is important, when treating with methotrexate, not to administer drugs that compromise renal blood flow and not to modify the drug regimen to account for reduced renal blood flow. The same considerations apply to patients with renal insufficiency. In both circumstances, it is important to monitor blood levels of methotrexate. Treatment with high-dose methotrexate and leucovorin (see later discussion) can itself be nephrotoxic because of the tendency of methotrexate to precipitate in acidic urine. Therefore, it is important to maintain high levels of hydration and to ensure alkalinization of the urine (Chabner et al., 2006).

As with most antineoplastic agents, methotrexate does not discriminate between transformed and normal cells. The rationale for using this drug is that it will kill rapidly dividing cancer cells that require rapid DNA synthesis but will not immediately affect normal cells, many of which are not dividing. Normal cells can be "rescued" from the effects of methotrexate and its analogs by treatment with *N*-5-formyltetrahydrofolate (called **leucovorin** or **citrovorum**), the product of dihydrofolate reductase. Leucovorin rescue is critical in cases in which it is necessary to administer high doses of methotrexate to individuals with tumors that do not respond to normal doses of this drug. In such cases, leucovorin is given 18 to 36 hours after the initial methotrexate dose, while serum levels of methotrexate are monitored. In addition, leucovorin should immediately be administered to a patient receiving low-dose methotrexate when methotrexate overdose is suspected (Roenigk et al., 1998). Serum methotrexate levels should be monitored during this time (Grem et al., 1995; Chabner et al., 2006).

The methotrexate/leucovorin strategy is compromised by the existence of many fast-growing normal cells in bone marrow, the gastrointestinal tract, the skin, and other epithelial lining cells. These cells are as susceptible to the cell-killing effects of methotrexate as neoplastic cells. Thus, the toxic effects of methotrexate include hematologic effects (e.g., leukopenia, thrombocytopenia) from bone marrow suppression, gastrointestinal effects (e.g., ulceration, glossitis, stomatitis, nausea, vomiting), and dermatologic effects (e.g., urticaria, vasculitis). They further include hepatic lesions such as cirrhosis; pulmonary lesions such as pulmonary fibrosis; and CNS effects from intrathecal methotrexate, including arachnoiditis, leukoencephalopathy, and increased cerebrospinal fluid pressure.

Toxicity of methotrexate can be treated using continuous flow hemodialysis. Alternatively, intravenous infusion of carboxypeptidase G2, a methotrexate-cleaving enzyme, results in rapid clearing of the drug (Chabner et al., 2006).

TABLE 24.7
Methotrexate

Condition	Usual Dose	Serum Level
Psoriasis	IM or IV: 7.5–50 mg/week Oral: 7.5–30 mg/week	<10 nM (Roenigk et al., 1998)
Refractory rheumatoid arthritis	IM: 5–25 mg/week Oral: 7.5–15 mg/week	(Tugwell et al., 1987a and b)*
Malignant neoplastic diseases†	IM or IV: 25 mg/m², 1–2 times/week Oral: 2.5–5 mg/day High-dose IV: 1.5 g/m² with rescue every 3 weeks (different regimens are available)	Strongly dependent on tumor type

IM, Intramuscular; *IV,* intravenous.
*Baseline monitoring of patient parameters (hemoglobin; white blood cell count; mean corpuscular volume; platelet count; urinalysis; blood urea nitrogen; and serum creatinine, transaminase, and alkaline phosphatase levels) is advocated. Highly dependent on type of cancer. The doses shown might apply to treatment of a non-Hodgkin lymphoma. Treatment of other cancers such as acute lymphoblastic leukemia may require different doses.
†With high-dose therapy, methotrexate levels are followed, and leucovorin doses are adjusted until serum methotrexate levels are less than 50 nM (Grem et al., 1995).

Busulfan

Busulfan is an alkylating agent used to treat a variety of leukemias and lymphomas before bone marrow transplantation. It is cytotoxic to marrow cells and is used in combination with cyclophosphamide, which is cytotoxic to mature lymphocytes that may be involved in a graft-versus-host reaction (Slattery & Risler, 1998). The therapeutic index of the drug is narrow. High plasma levels increase the possibility of development of hepatic venoocclusive disease (VOD), a potentially fatal complication. Therefore, therapeutic monitoring of busulfan levels, using HPLC or GC-MS, with measurement of the dose interval of this drug, is now routinely performed at bone marrow transplant centers. This decreases the incidence of VOD in patients whose initial serum levels of busulfan are too high and allows increasing doses for patients with too low an initial level of busulfan, thus optimizing therapeutic levels for each patient.

Therapeutic drug monitoring of chemotherapeutic agents has been hampered by the nonuniformity in establishing appropriate dosing, concentration, therapeutic versus toxic target ranges, administration of combination chemotherapies depending on tumor type, analytic challenges with prodrugs, intracellular compounds, as well as variability in published data from pharmacologic trials. Improvement in defining concentration-effect relationships and effective utilization of population PK/PD (pharmacokinetic/pharmacodynamic) models will likely foster more effective patient management (Paci et al., 2014).

TOXINS AND ACUTE POISONING

In this section, agents that cause chronic or acute injury to the patient are discussed. This injury can be direct, as with poisons such as cyanide and carbon monoxide, or indirect, as with carcinogens that induce mutations in genes that encode proteins that are critical in controlling the cell cycle.

ENVIRONMENTAL CARCINOGENS

Over the past decade or so, attention has been focused on the effects of chemical agents in the environment (carcinogens) that predispose individuals exposed to them to develop tumors in various tissues where these agents accumulate. Many of the individuals who are exposed to these agents work in industries where these agents are produced. Benzpyrene, an aromatic compound produced in cigarettes and in the exhaust of engines, is a known potent carcinogen and has been implicated in causing lung cancer. Nitrites, used as preservatives in red meats, have been associated with colon cancer. Aflatoxin, produced by the fungus *Aspergillus*, has been implicated in causing hepatocellular carcinoma. Aromatic hydrocarbons such as benzene and ionizing radiation have been implicated in causing acute leukemias. Vinyl chloride and the formerly used dye Thorotrast have been linked to angiosarcoma. Benzidine dyes, β-naphthylamine, dimethylbenzanthracene, and other aromatic compounds have been linked to multiple malignancies occurring in humans. Exposure to asbestos has been strongly implicated as a carcinogen in lung cancer and mesothelioma. In animal studies, polychlorinated biphenyls (PCBs) and dioxin, the former produced in fires, have been strongly implicated as causing a variety of cancers.

A number of carcinogens, like benzpyrene, are inactive in their native forms but are transformed into carcinogens through oxidative reactions catalyzed by cytochrome P450–dependent systems. Thus, to be an active carcinogen, benzpyrene must be converted into benzpyrene diol epoxide. Because only particular isoforms of cytochrome P450 react with particular carcinogens, only those individuals carrying the genes that encode these forms are susceptible (Caraco, 1998). A major effort is now being devoted to identifying those individuals with phenotypes who would be at risk (Peto, 2001).

Much interest has been focused on workers in occupations in which carcinogens are present in significant amounts. Steel foundries, shipbuilding and rubber plants, and other industrial plants may produce such carcinogens in significant amounts. In some of these industries, certain cancers occur at rates higher than in the general population (Brandt-Rauf & Pincus, 1998; Pincus & Friedman, 2003). Thus, in these exposed populations, it has become desirable to determine the levels of exposure to certain known carcinogens.

Carcinogens are thought to bind to DNA, leading ultimately to mutations in the genetic code, often resulting in synthesis of mutated proteins involved in control of the cell cycle (Brandt-Rauf & Pincus, 1998; Pincus & Friedman, 2003). These proteins are called **oncogene-encoded proteins** or **oncoproteins**. Mutagenesis, oncogenes, and oncoproteins are discussed in Chapter 77.

In populations with histories of exposure to carcinogens, assays have been developed to detect the presence of these carcinogens or of their DNA adducts. For detection of most unmodified carcinogens, the method of choice is currently GC-MS. For certain carcinogenic compounds such as PCBs, the method of electron capture is used. Halogenated compounds such as PCBs are separated on a GC column using an ionized gas as the carrier. Halogenated compounds "capture" electrons conducted through the carrier gas and thus are detected by the reduced currents.

Often, the presence of carcinogens in blood or urine is hard to detect directly. The carcinogens, however, may be bound to proteins or to DNA intracellularly. These adducts can be detected using Western blotting, which takes advantage of the existence of monoclonal antibodies to carcinogen–DNA adducts (Santella et al., 1987; Perera et al., 1988). This technique is sensitive to nanogram quantities of the nucleic acid adduct, which can be conveniently harvested from peripheral lymphocytes. It is also very useful in detecting oncoproteins in the body fluids of patients who have been exposed to carcinogens (De Vivo et al., 1994), as described in Chapter 77.

CYANIDE

The cyanide anion binds avidly to iron in the ferric or trivalent state. Because cyanide forms a relatively stable cyanoferric complex, it is able to inactivate iron-containing enzymes that cycle between the ferrous and ferric states in oxidation–reduction reactions. Cyanide produces tissue and cellular hypoxia primarily by reversibly binding to cytochrome A3 and by inhibiting its reoxidation. This inhibits the electron transport system and prevents cellular respiration and ATP (high-energy phosphate) formation. This blockade prevents the utilization of oxygen and aerobic metabolism, producing severe metabolic (lactic) acidosis. Although cyanide binds preferentially to the ferric form of iron, it can also bind to the ferrous iron of hemoglobin, producing cyanohemoglobin, which cannot transport oxygen. Cyanide will form complexes with other iron-containing enzymes, but its acute poisonous effect is attributable to the inhibition of electron transport and cell death, predominantly in the CNS.

The principal symptoms of cyanide overdose are tachypnea (initially), followed by respiratory depression and cyanosis, hypotension, convulsions, and coma. Death may occur in a matter of minutes because cyanide is a fast-acting toxin. Diagnosis may be difficult, and a high index of suspicion is needed to make the correct diagnosis. Clues include the odor of bitter almonds, the occurrence of an altered mental status and tachypnea in the absence of cyanosis, and an unexplained metabolic acidosis (with an increased anion gap).

Antidotal therapy has been based on a two-step strategy: First, to pull the CN^- ions away from cytochrome A3, hemoglobin is converted to methemoglobin (Fe^{3+} state) by using specific oxidants (i.e., amyl nitrite and sodium nitrite). The former is given first because it can be inhaled. Methemoglobin directly competes with ferricytochrome A3 to form a methemoglobin–CN^- complex. This cyanmethemoglobin complex is relatively nontoxic. In a second step, sodium thiosulfate is given intravenously. This reagent reacts with cyanmethemoglobin to form thiocyanate, which is harmless and is excreted in the urine. The first step is necessary simply to remove CN^- from the respiratory chain. Approximately 25% to 40% of the patient's total hemoglobin is converted to methemoglobin in this step; this methemoglobin is rapidly reconverted to oxyhemoglobin by red blood cell enzymes. The antidotes that are involved in each step are sold commercially as a cyanide antidote package by Eli Lilly and Company (Indianapolis, IN). Cyanide also binds tightly to cobalt ions, and hydroxocobalamin (a form of vitamin B_{12}) has recently been approved by the U.S. Food and Drug Administration as a cyanide antidote (Cyanokit, King Pharmaceuticals, Bristol, TN). It has the advantages of rapid onset of action and low toxicity at antidotal doses, making it suitable for prehospital administration to firefighters and others (Hall et al., 2009). Unfortunately, hydroxocobalamin has a different type of side effect that clinicians need to be aware of—that its deep red color can interfere in certain assays (Beckerman et al., 2009).

CARBON MONOXIDE

Carbon monoxide (CO) intoxication produces tissue hypoxia as a result of decreased oxygen transport. CO disrupts oxygen transport by binding to hemoglobin to form a reversible complex, carboxyhemoglobin (CO-Hb). It produces toxicity by decreasing or inhibiting oxyhemoglobin saturation by inducing a leftward shift of the oxyhemoglobin dissociation curve, causing a decrease in oxygen delivery to tissues, and by binding to other heme-containing proteins such as myoglobin and cytochrome A3 (Kao & Nanagas, 2006). Binding to cytochrome A3 inhibits cellular respiration and electron transport, as occurs with cyanide poisoning (see earlier discussion), and binding to hemoglobin decreases the oxygen reserve available to cardiac and skeletal muscle, with cardiac muscle being more severely affected.

However, binding of CO to hemoglobin cannot explain all of its toxic effects. Exchange transfusion into dogs of compatible blood that contained 57% to 64% CO-Hb (levels that are fatal) failed to induce any effect on the recipients (Goldbaum et al., 1975; Kao & Nanagas, 2006). The role of CO in inducing toxicity is therefore more complicated. In fact, numerous studies suggest that CO, in addition to its binding to hemoglobin and cytochrome A3, is involved in multiple other toxicity-inducing pathways. These include direct cellular toxicity caused by its binding to myoglobin, resulting in direct damage to skeletal and cardiac muscle. Further, it has been found that CO activates guanylyl cyclase in the CNS; this results in increased cyclic guanosine monophosphate that induces cerebral vasodilatation and can cause loss of consciousness. CO also induces the synthesis of nitric oxide (NO), a potent vasodilator that causes large decreases in systemic blood pressure. CO-induced damage to CNS structures such as the basal ganglia, white matter, and hippocampus correlates with the degree of systemic hypotension that it induces. Abnormally elevated levels of NO appear also to cause oxidative damage to the brain, resulting in delayed neurologic sequelae (DNS). This effect may be due to the ability of NO to enhance the ability of neutrophils to adhere to the endothelium via specific adherence molecules, such as β_2-integrin, which results in free-radical formation via activation of such enzymes as xanthine oxidase (Kao & Nanagas, 2006). These free radicals are thought to cause the oxidation of brain lipids that may serve as a basis for the observed DNS (Kao & Nanagas, 2006). Animal studies have further revealed that cerebrovascular vasodilatation is inhibited by NO inhibitors.

In addition, in several animal studies, it has been found that CO induces changes in myelin basic protein (MBP) that may cause an immunologic reaction. This effect is obviated in rats that have been made immunologically tolerant to MBP before exposure to CO (Kao & Nanagas, 2006).

Because the brain and the heart are most susceptible to CO poisoning, CO intoxication is commonly manifested through respiratory, neurologic, and cardiac symptoms, with dyspnea being a principal symptom. Others include headache, visual disturbances, tachycardia, syncope, tachypnea, coma, convulsions, and death. However, diagnosis is difficult because no pathognomonic sign occurs, except for a cherry red color of the face that is a strong clue to acute CO poisoning. However, this sign is not common in CO poisoning (Kao & Nanagas, 2006). Another problem is delayed neurologic symptoms that develop from days to months after apparent recovery. These include mental deterioration, mutism, memory impairment, gait disturbance, and urinary and fecal incontinence, which may be caused by NO-induced damage to CNS membrane lipids and cerebral vasodilatation as discussed previously (Kao & Nanagas, 2006).

CO poisoning should enter into the differential diagnosis of an acute encephalopathic state in the appropriate circumstances or setting. Car exhaust fumes cause more than 70% of known CO poisoning, including attempted suicides and chronic incidental exposure (e.g., auto repair). In addition, exposure to house fires, indoor heaters, and stoves predisposes to CO toxicity.

A CO-oximeter is utilized to make the definitive diagnosis by measuring the concentration of blood CO-Hb. This instrument is a dedicated spectrophotometer that measures total hemoglobin and the percentages of CO-Hb, oxyhemoglobin, and methemoglobin by screening at four different wavelengths simultaneously. This accurate and rapid analysis is mandatory to establish the diagnosis and should be performed with minimal delay after CO exposure. CO may also be quantitated by gas chromatography or GC-MS. Treatment is mainly with 100% oxygen, in some cases under hyperbaric conditions, with additional supportive treatment given as necessary.

ALCOHOLS AND GLYCOLS

Ethanol

Ethanol (Table 24.8) is probably the most common drug of abuse and is frequently responsible for the presentation of patients with altered mental status to hospitals and emergency departments. Ethanol is rapidly absorbed from the gastrointestinal tract, has a volume of distribution approximately equal to that of total body water, and diffuses freely in body tissues. It is predominantly metabolized by hepatic alcohol dehydrogenase to acetaldehyde and acetic acid/acetyl coenzyme A and then, by way of the Krebs cycle, to carbon dioxide and water. The fatal dose is generally 300 to 400 mL of pure ethanol (600 to 800 mL of 100-proof whiskey) consumed in less than 1 hour. Peak plasma concentrations are usually reached within 1 hour after ingestion. Table 24.8 summarizes the effects of different levels of ethanol in serum on human function.

TABLE 24.8

Influence of Acute Ethanol Ingestion on Ethanol Levels and Behavior

Ounces	Blood Concentration	Influence
1–2	10–50 mg/dL (2.2–10.9 mmol/L)	None to mild euphoria
3–4	50–100 mg/dL (10.9–21.7 mmol/L or greater)	Mild influence on stereoscopic vision and dark adaptation
	100 mg/dL (21.7 mmol/L)	Legally intoxicated
4–6	100–150 mg/dL (21.7–32.6 mmol/L)	Euphoria; disappearance of inhibition; prolonged reaction time
6–7	150–200 mg/dL (32.6–43.4 mmol/L)	Moderately severe poisoning; reaction time greatly prolonged; loss of inhibition and slight disturbances in equilibrium and coordination
8–9	200–250 mg/dL (43.4–54.3 mmol/L)	Severe degree of poisoning; disturbances of equilibrium and coordination; retardation of the thought processes and clouding of consciousness
10–15	250–400 mg/dL (54.3–86.8 mmol/L)	Deep, possibly fatal, coma

Ethanol acts as a sedative-hypnotic and depresses the CNS irregularly in descending order from cortex to medulla. Acute intoxication may be manifested by decreased inhibitions, incoordination, blurred vision, slurred speech, stupor, coma, seizures, and death. Most fatal intoxications occur at blood concentrations greater than 400 mg/dL. Capillary and arterial blood samples most accurately reflect brain ethanol concentrations. Serum ethanol concentrations are usually determined by enzymatic, gas chromatographic, or electrochemical oxidation techniques. In the most accurate assays for ethanol, serum is incubated with alcohol dehydrogenase, which oxidizes ethanol to acetaldehyde, and nicotinamide adenine dinucleotide (NAD) is converted to NADH (reduced form of NAD). Thus, simple monitoring for the absorbance of the incubated serum at 340 nm gives a direct determination of alcohol present. Acute poisoning is generally treated by supportive therapy, gastric lavage with tap water, or hemodialysis, if indicated (>500 mg/dL). Symptoms of chronic intoxication, such as acute alcoholic mania, may be treated with diazepam. Phenytoin may be utilized in patients with a history of seizures.

Detection of alcohol metabolites, ethyl sulfate (EtS) and ethyl glucuronide (EtG) have been purported to be able to detect alcohol consumption 40 to 80 hours post alcohol ingestion, availing a greater window of detection in patients that require such management. However, EtS and EtG are relatively comparable to detect alcohol consumption and are both minor metabolites subject to enzymatic conjugation of alcohol with sulfate or glucuronide, respectively. Each has its benefits and drawbacks. EtG may be affected by sample decay and biological conditions (infection) and EtS may be more applicable to acute alcohol intake. However, they are pretty similar in most respects and correlate with one another. It should be understood that results in the literature may differ depending on method (EIA vs. LCMS) and detection cutoff limits (500 vs. 250 ng/mL) and other factors. Therefore, they may not be superimposable (Nanau & Newman, 2015; Hellander & Beck, 2005).

Furthermore, certain studies claim that EtS is less subject to false positives from alcohol-based (inhaled) hand sanitizer, etc., and is less affected by cannabinoids and other components. However, EtS can be detected after consumption of nonalcoholic wine and both (EtS and EtG) can be detected after consuming nonalcoholic beer. These studies vary. As such, either of these analytes (as with any analyte) should be used as ancillary support and require coordination with the clinical history and findings for rendering appropriate clinical management.

Breathalyzer Testing. The clinical impairment that alcohol induces when consumed in elevated amounts places individuals who have consumed it at risk for causing accidents, especially if they are engaged in potentially high-risk activities such as driving. To screen such individuals who have been involved or who are at risk for being involved in accidents affecting themselves and others, the so-called **breathalyzer test** is administered. Since some alcohol that enters the circulation after it is imbibed is released in alveoli in the lungs, the presence of this gaseous alcohol can be quantitatively detected in a Breathalyzer device. This device traps the alcohol in an aqueous solution in a voltaic cell and subjects it to an oxidation reaction at an anode, converting it into acetic acid. The two electrons released from each alcohol molecule at the electrode are used to reduce one O_2 molecule in an adjoining electrode to two water molecules. The current generated by the flow of the electrons generates a voltage change that is directly related to the concentration of alcohol dissolved in the aqueous solution. (See Chapter 4 for a description of voltaic methods.) Alternatively, the level of gaseous alcohol can be directly detected by infrared spectroscopy by measuring the absorbance of its –OH stretching frequency. Using either method, the concentration of alcohol that is present in the aqueous solution or that is present in the gas phase of the collection device is then related to the alcohol concentration that was present in the blood of the individual being tested. Most breathalyzer testing is performed by law enforcement officials on individuals who have been driving or acting erratically and can be used as evidence to justify arrest of these individuals. Possible interfering compounds giving false-positive results can include acetone in diabetics and exposure of individuals to methyl tert-butyl ether, found in some gasoline preparations. Other reported interfering substances include compounds in lacquer, paint remover, cleaning fluids, and a variety of volatile compounds, especially ethers and alcohols other than ethanol.

In more recent developments, breathalyzers have been connected to the ignition system of cars. The drivers of these cars must breath into a conveniently placed breathalyzer device. Absence of breathing into the unit will result in failure of the ignition system to start. In addition, if, after breathing into the unit, the voltage change is above a predetermined value, the breathalyzer unit blocks the ignition system, resulting in the inability of the engine to start.

Methanol

Methanol (wood alcohol) poisoning occurs in patients who ingest methylated spirits or methanol-containing antifreeze. It is rapidly absorbed from the gastrointestinal tract and is metabolized and excreted at approximately 20% of the rate of ethanol. The toxic range is thought to be 60 to 250 mL, although as little as 15 mL has caused death. Alcohol dehydrogenase metabolizes methanol to formaldehyde and formic acid, which is responsible for ocular toxicity (diminished light sensation or frank blindness), and anion gap metabolic acidosis; these are the principal symptoms of intoxication. Other symptoms include nausea, vomiting, headache, seizures, and coma. GC-MS is used to measure blood methanol levels, with a peak level greater than 50 mg/dL considered to be toxic. In addition, serum osmolality levels are increased to levels greater than 300 mOsm. Methanol (or ethylene glycol) poisoning should be considered in acutely ill patients with hyperosmolarity, metabolic acidosis, and increased anion gap.

Osmolal Gap

For methanol, ethylene glycol, and isopropyl alcohol poisoning, because the molecular masses of these simple compounds are low, relatively small quantities in serum give rise to high serum osmolalities. As discussed in Chapter 9, serum osmolality can be estimated as Na × 2 + glucose/18 + blood urea nitrogen/2.8. This value should be close to the serum osmolality measured by freezing-point depression. If, however, any of these three compounds (or ethanol) is present in serum, the computed osmolality will be significantly less than the measured value (i.e., a so-called **osmolal gap** will exist), suggesting that a toxin is present. This is an effective screening method as a first step in detecting the presence of toxic compounds.

Ethylene Glycol

Ethylene glycol (1,2-ethanediol) is used in car radiator antifreeze. It has a half-life of around 3 hours and is metabolized to three major toxic compounds: glycolaldehyde, glycolic acid, and glyoxylic acid. The oxidation of ethylene glycol to glycolaldehyde is catalyzed by liver alcohol dehydrogenase. Both oxalic acid and formic acid are formed in smaller amounts. Oxalic acid itself is a highly toxic compound, which can rapidly precipitate as calcium oxalate crystals in various tissues as well as in urine. The formation of these crystals in urine, although not a constant finding, is an important diagnostic clue to ethylene glycol poisoning. The metabolite that accumulates in the highest concentrations in the blood is glycolic acid; its concentration in blood and urine appears to correlate directly with symptoms and mortality. It is the major contributor to the high anion gap seen in metabolic acidosis. The fatal dose of ethylene glycol is around 100 g, and anuria and necrosis are the principal symptoms of acute poisoning. Other symptoms include nausea and vomiting, myoclonus, seizures, convulsions, depressed reflexes, and coma. Definitive diagnosis of ethylene glycol intoxication can be made by measuring serum ethylene glycol and glycolic acid by HPLC.

Treatment of ethylene glycol and methanol toxicity is similar and is based on symptoms and serum level. The mainstay of treatment is inhibition of the alcohol dehydrogenase enzyme to minimize the formation of toxic metabolites, while the relatively nontoxic parent alcohol is eliminated renally. Although ethanol was originally used as a competitive inhibitor of alcohol dehydrogenase, the nonintoxicating agent fomepizole (4-methylpyrazole, Antizol, Paladin Labs, Montreal, Canada) is now generally preferred (Brent, 2009). Dialysis, either hemodialysis or peritoneal dialysis, is utilized to remove either parent compound and its corresponding toxic metabolic products.

Isopropyl alcohol has a half-life of approximately 3 hours and a volume of distribution similar to that of ethanol. It is readily absorbed through the GI tract and is metabolized at approximately 50% of the rate of ethanol. The metabolism of isopropanol occurs mainly by alcohol dehydrogenase to produce acetone, carbon dioxide, and water. The fatal dose of ingestion is 250 mL. Both isopropyl alcohol and its major metabolite, acetone, are CNS depressants.

CNS depression is the principal symptom of acute isopropanol intoxication. In addition, it produces significant GI irritation, which may be manifested by nausea and vomiting, including hematemesis and melena, abdominal pain, and gastritis. Other symptoms include confusion, coma, hypertension, respiratory failure, and death.

The diagnosis of isopropanol intoxication is difficult to make. Clues to the diagnosis include acetonuria, acetonemia, and hyperosmolarity without glycosuria, hyperglycemia, or acidosis. Gas chromatography is generally considered to be the best technique to determine isopropanol blood concentrations. Treatment includes supportive care, activated charcoal with gastric lavage, and hemodialysis in severe poisoning.

ARSENIC

Arsenic is used in ant poisons, rodenticides, herbicides and weed killers, insecticides, paints, wood preservatives, and ceramics, in the production of various metal alloys and livestock feed, as a tanning agent, and in medicines. Inorganic arsenicals, including sodium arsenate and lead or copper arsenite; organic arsenicals, such as carbarsone and tryparsamide; and arsine gas are the major toxicologic forms of arsenic. Arsine gas poisoning generally occurs in the industrial setting, where its production arises from the action of acid or water on arsenic-bearing metals. Arsenic compounds occur in three oxidation states: elemental, trivalent arsenite, and pentavalent arsenate.

Arsenic is readily absorbed through the GI tract and lungs, whereas absorption through the skin occurs more slowly. Twenty-four hours after ingestion, arsenic is distributed to all body tissues. The major route of excretion is through the kidneys. Arsenic can cross the placenta. The major concern with arsenic ingestion is systemic poisoning, presumably through its reversible interaction with multiple enzyme sulfhydryl groups. This, in turn, leads to the disruption of multiple metabolic systems. This phenomenon suggests that effective treatment of arsenic poisoning would be provided through administration of sulfhydryl-containing compounds that would compete with those of proteins for binding to the different forms of arsenic, as discussed later.

Arsine gas, the most dangerous of the three forms of arsenic, may irreversibly attach to sulfhydryl groups of hemoglobin, causing intravascular hemolysis, hemoglobinemia, and consequent acute renal failure, as well as direct nephrotoxicity. The acute fatal dosage of arsenic trioxide is approximately 120 mg, whereas less than 30 parts per million (ppm) of arsenic gas can produce poisoning. Organic arsenicals release arsenic slowly and have a fatal dose of approximately 0.1 to 0.5 g/kg.

Acute toxicity is usually manifested within the first hour of ingestion and generally reflects multiorgan involvement. Gastrointestinal symptoms are the most common presentation, with burning and dryness of the mouth and throat, difficulty swallowing, vomiting, and watery or bloody diarrhea containing shreds of intestinal lining or mucus. The odor of garlic may be on the breath, and a metallic taste in the patient's mouth. Cyanosis, hypotension, tachycardia, and ventricular arrhythmias may develop. Neuropathy usually occurs late (approximately 1–2 weeks) after ingestion or may become most intense during this time period. Severe volume depletion with resulting hypovolemic shock and acute renal tubular necrosis may occur, with death resulting from circulatory failure. Cutaneous manifestations of arsenic poisoning include hyperpigmentation of the skin and keratosis. The nail beds can show transverse white striations, called **Mees lines**, although this is not specific for arsenic poisoning (Ibrahim et al., 2006). Symptoms of poisoning with arsine gas usually manifest approximately 2 to 24 hours after exposure and may initially include nausea and vomiting, headache, anorexia, and paresthesias. Hematemesis and abdominal pain are also common, and acute renal failure, cardiac damage, anemia and hemolysis, or pulmonary edema may occur. The diagnosis of chronic intoxication is usually difficult; it should be considered in patients with a combination of GI symptoms, neuropathy, and cutaneous, cardiovascular, and renal disturbances.

Analysis of urine, hair, and nails, using ion emission spectroscopy, is important for the diagnosis of chronic arsenic poisoning.

Treatment of acute poisoning includes removal of residual arsenic by gastric lavage or emesis and treatment with dimercaprol, or British antilewisite (BAL), which combines with arsenic through its sulfhydryl groups to produce cyclic water-soluble complexes. However, the inherent toxicity of this compound limits its therapeutic usefulness. Less toxic derivatives of BAL are available, such as 2,3-dithioerythritol, which is less toxic in cell culture but shows greater efficacy than BAL at rescuing arsenic-poisoned cells in culture (Boyd et al., 1989). In severe poisoning, hemodialysis can be used to remove the arsenic-dimercaprol complexes.

MERCURY

Mercury compounds exist in four different forms with different toxicologic potential: elemental or metallic (Hg^o); mercurous (Hg^+); mercuric (Hg^{2+}); and alkyl mercury (i.e., organomercurials). Elemental mercury is poorly absorbed from the GI tract if mucosal integrity is preserved and shows no toxic effect unless it is converted to the divalent form. This may occur slowly by oxidation-reduction with water and chloride ion if a GI site for mercury stasis exists, but this is uncommon. Significant poisoning occurs with elemental mercury when it is inhaled or absorbed through the skin. It can pass through the blood-brain barrier and can accumulate in the CNS, where oxidation produces mercuric ion. Thus, primarily pulmonary and CNS toxicities are produced.

Of the two inorganic salts of mercury, mercurous (Hg^+) salts are poorly soluble and thus poorly absorbed. However, the mercuric (Hg^{2+}) salt is readily soluble and is readily absorbed after oral ingestion or inhalation. Severe inflammation of the mouth and other GI symptoms can result. The kidney is a preferred site of accumulation of inorganic mercuric compounds, where acute renal tubular and glomerular damage can ensue. Both

elemental mercury and the inorganic mercury compounds are excreted mainly in the urine.

In contrast to elemental and inorganic mercury, organic mercury compounds, containing alkyl, aryl, and alkoxyalkyl moieties, are environmental pollutants. These compounds contain at least one covalent mercury-carbon bond. Both the alkoxyalkyl and aryl mercurial compounds undergo metabolic breakdown and biotransformation to produce inorganic mercury, which toxicologically acts and manifests intoxication as would the previously mentioned inorganic mercury compounds. In contrast, the mercury-carbon bonds that occur within the methyl and ethyl forms are extremely stable and produce greater toxicity than the aryl and alkoxyalkyl forms. The alkyl forms are more lipid soluble, pass readily through biological membranes, and, on ingestion, show generally greater absorption into the body. Their major chemical effect is on the CNS, and they show a biological half-life of 70 to 90 days. A devastating effect of methylmercury, known as *congenital Minamata disease*, has been described in Japan in the children of mothers who were exposed to methylmercury and were born with many of the stigmata of cerebral palsy (Ibrahim et al., 2006).

Because bile is the major route of excretion, methylmercury can be reabsorbed into the blood via the enterohepatic system, accounting, in part, for its extended half-life. The major mechanism of action of mercury poisoning is through covalent bonding with protein sulfhydryl groups, producing widespread and nonspecific enzyme dysfunction, inactivation, and denaturation. Mercury inhibits the enzyme catecholamine-*O*-methyltransferase, a major enzyme in the metabolism of catecholamines, especially epinephrine and norepinephrine (see Chapter 25), resulting in hypertension, tachycardia, and sweating (Ibrahim et al., 2006). Thus, mercury poisoning can masquerade as a pheochromocytoma, which should be ruled out by performing 24-hour urine catecholamine determination (see Chapter 25). At the same time, blood mercury levels should be determined (reference range <10 μg/L). Unfortunately, the usefulness of this testing is limited by the short half-life of mercury in the blood.

Mercury, depending on its form, may cause systemic toxicity or local skin and mucous membrane lesions. Both organic and elemental mercury can cause CNS effects, whereas GI symptoms primarily occur with inorganic salts. Elemental mercury may produce severe pulmonary reactions. Chronic exposure to elemental mercury can give rise to two syndromes: acrodynia and erethism (Ibrahim et al., 2006). Acrodynia, also called **pink disease**, **Feer-Swift disease**, and **Feer syndrome**, occurs mainly in children but can also occur in adults, and involves a complex of symptoms that include a desquamating, erythematous rash of the palms and soles, sweating, hypertension, tachycardia, pruritus, poor muscle tone, and weakness of the proximal pelvic girdle. Erethism is a complex of neurologic symptoms that include, most prominently, personality changes involving memory loss, drowsiness, withdrawal, depression, and irritability. A fine-motor intention tremor of the hands also occurs. Inorganic mercury can induce severe renal tubular damage, especially in the proximal tubule; chronic exposure can cause membranous glomerulonephritis and nephrotic syndrome (Ibrahim et al., 2006).

In general, acute toxicity, with elemental, inorganic, or most organic forms, can be diagnosed from 24-hour urine levels. Blood levels may rise rapidly after acute exposure but fall rapidly and may not reflect total body burden. In contrast, because the short-chain alkyl organic mercuric compounds are mainly excreted in the bile, blood levels are better indicators of tissue levels and significant acute exposure. Hair analysis for mercury may help identify chronic mercury exposure, especially with organic mercury.

Treatment includes gastric lavage or emesis to remove the ingested poison as well as the use of dimercaprol and succimer. However, in methylmercury and alkylmercury poisoning, dimercaprol is contraindicated because it has been found to increase the concentrations of these compounds in the brain (Bryson, 1989). In these cases, treatment is symptomatic, although new agents are being evaluated clinically.

IRON

Acute iron poisoning is common in young children and is usually the result of ingestion of iron-containing products. Generally, iron overload that causes increased deposition of iron in tissues is termed *hemosiderosis*; if the excess iron induces tissue damage, the condition is termed *hemochromatosis*. Hemochromatosis can be inherited or acquired. Acquired hemochromatosis is caused by overingestion of iron or by leakage of iron from red blood cells, as may occur in a hemolytic crisis. Although ferric ions from food are usually reduced to ferrous ions and absorbed in the stomach, the large and small bowel can rapidly absorb toxic amounts (>30 mg/kg) of elemental iron. Once absorbed into the body, iron removal is difficult. Large doses of iron are thought to cause acute mucosal cell damage, and significant absorption of iron occurs once the binding capacity of transferrin is exceeded. Unbound iron in serum causes toxicity by hepatic cell damage, shock, and production of lactic acidosis. The hepatotoxicity seems to be dose related, occurs within 1 to 2 days of ingestion, and has been associated with levels equal to or greater than 1700 μg/dL (Tenenbein, 2001).

Iron absorption is tightly regulated by the *HFE* gene–encoded protein that is expressed mainly on hepatocytes and on epithelial cells in the gastrointestinal tract. This protein interacts with another protein synthesized in the liver called **hepcidin**. In addition, HFE protein interacts with transferrin receptors. In inherited or primary hemochromatosis, sometimes associated with other diseases, such as type 2 diabetes (Davis et al., 2008), mutations in the *HFE* gene that result in single amino acid substitutions at critical positions in the amino acid sequence, such as cysteine-to-tyrosine 282 (C282Y) and histidine-to-aspartic acid 63 (H63D), cause this protein to fail to regulate iron absorption in the gut, resulting in iron overload. The occurrence of hereditary hemochromatosis is on the order of 1 per 200 to 300 individuals, making this condition important as a cause of iron overload. Recent studies have further determined that patients who have received more than 10 transfusions with packed red blood cells are at risk for developing acquired hemochromatosis (Takatoku et al., 2007).

Assays for Serum Iron (see also Chapter 28)

Iron can be determined by specialized techniques for trace elements such as atomic absorption spectrophotometry, but in the modern clinical laboratory setting, it is almost always measured using a colorimetric indicator such as ferrozine. The Fe^{2+}-ferrozine complex has an intense purple color (absorption maximum, 562 nm) and other metal ions generally do not interfere, with the possible exception of copper, whose effects can be minimized through addition of thiourea or thioglycolate. It is necessary to use a reagent such as acid or detergent to release the serum iron from transferrin and another reagent such as ascorbate to reduce iron to the ferrous state.

Iron-Binding Capacity

Normally, all iron present in serum is bound to the iron-transporting protein, transferrin, which contains two iron-binding sites per transferrin molecule. In evaluating iron poisoning, it is important to measure iron-binding capacity, because toxicity will drastically increase as that capacity is exceeded. To obtain the total iron-binding capacity (TIBC), the method described in Chapter 28 can be used. Alternatively, saturating concentrations of iron can be added to a serum sample, excess iron is removed, for example, by adsorption with $MgCO_3$, and iron is remeasured. Alternatively, the amount of excess iron can be measured, and subtraction from the concentration of iron added gives the unsaturated iron-binding capacity.

Signs of Iron Intoxication

Vomiting appears to be an early manifestation of iron intoxication, along with severe gastroenteritis, melena, abdominal pain, and hematemesis. This occurs up to 6 hours after ingestion. For up to the next 10 hours, the patient may appear to improve. This is deceptive because manifestations of systemic toxicity (cyanosis, convulsions, shock, coagulopathy, renal and hepatic failure) may occur, leading to death. Patients who develop severe systemic symptoms and those who do not may develop late complications, including GI obstruction or stricture.

Definitive diagnosis is made with measurements of serum iron concentration and TIBC. In addition to supportive treatment, emesis or gastric lavage is used to prevent iron absorption. Chelation therapy with deferoxamine is also utilized if the acute intoxication is severe.

LEAD

Both organic and inorganic compounds of lead may be highly toxic, with their most serious effects occurring in the central and peripheral nervous systems. Absorption may occur by inhalation or ingestion. If more than 0.5 mg/day of lead is absorbed, lead accumulation and toxicity are believed to occur, whereas 0.5 g of absorbed lead is considered a fatal dose. However, acute toxicity is uncommon and is generally observed in patients who have been exposed to high concentrations of lead dusts. Lead poisoning is seen in children in large cities who consume lead in the form of paint (pica). Acute manifestations are primarily CNS symptoms (encephalopathy, convulsions, stupor) and GI symptoms such as colic. Chronic toxicity with lead accumulating in blood, soft tissues, and bone is more common. The largest body compartment of lead is bone, which contains approximately 96% of the total body burden. The half-life of lead in bone is 32 years, and bone may act as a reservoir for endogenous intoxication. Chronic toxicity may be manifested by a wide range of systemic effects, including general malaise, weight loss, anorexia, and constipation; lead encephalopathy exhibited by malaise with apathy, drowsiness, stupor, and seizures; peripheral

neuropathy with wrist drop or foot drop; and lead nephrosis with albuminuria, hematuria, and pyuria and anemia (hypochromic, microcytic, or normocytic) with basophilic stippling—the latter finding often a strong clue.

In addition, lead-induced pathologic changes may occur at even low levels of lead exposure. Needleman and Gatsonis (1990) reviewed 24 studies of childhood lead exposure to provide statistical evidence that low doses of lead may produce an intellectual deficit in children. However, the association of increased lead levels with decreased IQ has been called into question by the presence of confounding factors (Ibrahim et al., 2006). Schwartz and colleagues (1990) examined lead-induced anemia in children 1 to 5 years of age, using a cross-sectional epidemiologic study. They found a relationship between age, blood lead level, and hematocrit such that younger children had an increased risk for anemia at lower blood levels than children only a few years older. It thus appears that lead may produce deleterious effects, especially in children, at low levels of exposure. Generally, blood lead levels greater than or equal to 10 μg/dL indicate excessive lead absorption in children, and concentrations greater than 25 μg/dL indicate consideration of chelation therapy in the child. Several more recent studies suggest that no neurologic benefit is derived from chelation therapy among children with blood lead levels between 20 and 44 μg/dL (Ibrahim et al., 2006). The Centers for Disease Control and Prevention recommends universal screening of children beginning at 6 months of age (Klaassen, 2001; Bernard, 2003).

Organolead compounds such as tetraethyl and tetramethyl lead are lipid soluble and, similar to the organomercurials discussed previously, produce their major toxic effects on the CNS. Lead encephalopathy may occur early in the onset of intoxication and does not correlate well with blood lead concentrations. Hyperactive deep tendon reflexes, intention tremor, abnormal jaw jerk, and abnormalities of stance and gait are the most consistently observed neurologic manifestations of organolead toxicity.

Lead appears to interact with thiol, carboxylic, and phosphate groups to form stable complexes with enzymes and proteins (Bryson, 1989). This is particularly well known for heme synthesis, in which lead blocks the action of δ-aminolevulinic acid (ALA) synthetase, δ-ALA dehydratase (ALAD), coproporphyrinogen decarboxylase, and ferrochelatase, producing anemia. In addition, lead blocks two other enzymes—pyrimidine-5′-nucleotidase and Na-K–dependent ATPase, resulting in diminished energy supply for red blood cells, leading to decreased cell membrane integrity. Because pyrimidine-5′-nucleotidase is required for removal of clumped intracellular RNA, lead inhibition of this enzyme results in clumping of RNA complexes, giving rise to the observed basophilic stippling of red blood cells (Ibrahim et al., 2006). Lead-induced disruptions in heme synthesis allow for objective testing for inorganic lead exposure. Increased amounts of ALA in urine, decreased ALAD activity in red blood cells, increased amounts of free erythrocyte protoporphyrin, and elevated amounts of zinc protoporphyrin are found with inorganic lead poisoning. The assay for zinc protoporphyrin is a particularly simple fluorometric one that is widely used and is an excellent screening test for frank lead toxicity. However, the test is not sensitive to the low blood lead levels now regarded as harmful. The most sensitive screening test for organolead poisoning is decreased ALAD activity in urine because changes in the activities of other enzymes and in the levels of the products of heme synthesis are not consistent. Although whole-blood lead concentrations are a reliable indicator of recent lead exposure, the short half-life of circulating lead in blood makes estimates of total body burden unreliable. However, use of in vivo x-ray fluorescence of bone allows determination of cumulative lead burden (Kosnett et al., 1994). Treatment of poisoning includes supportive therapy as well as removal of soluble lead compounds by gastric lavage. Dilute magnesium sulfate or sodium sulfate solutions are commonly used. In addition, chelating agents such as dimercaprol, calcium disodium edetate, and succimer may be utilized, if necessary.

Quantitation of Lead in Blood

Unlike many other toxins, lead is generally measured in whole blood rather than in serum or plasma because most of the circulating lead is bound within the blood cells. Lead levels may be determined directly using atomic absorption spectroscopy, inductively coupled plasma/mass spectrometry (ICP/MS), or anode stripping voltammetry (ASV). In ICP/MS, a very hot source (the "inductively coupled plasma") atomizes the blood sample so that individual elements can be injected into and quantified by the mass spectrometer. In ASV, a voltaic cell is set up such that the anode consists of a mercury-coated graphite rod. When a negative potential is applied to this anode, cationic metals, such as lead, "plate out" in their metallic forms on the anode. The applied voltage is then stopped. Because an excess of electrons is present on the anode, current will flow to the cathode. Each of the metals plated on the anode therefore will become oxidized back to their respective ionic forms (i.e., be stripped from the anode). The metals with lowest oxidation potentials will strip first. Each metal will strip from the anode in the order of oxidation potential, recorded as the half-wave potential, which is a constant for a given metal. The total current associated with the stripping of each metal is proportional to the concentration of that metal.

ORGANOPHOSPHATES AND CARBAMATES

Pesticides generally contain organophosphates, which are esters of phosphoric acid or thiophosphoric acid, or carbamates, which are synthetic derivatives of carbamic acid. Although these are two distinctly different types of compounds, they both unfortunately interfere with neurotransmission. Both compounds inhibit the enzyme acetylcholinesterase (AChE), which normally hydrolyzes the neurotransmitter acetylcholine (ACh) after ACh has effected an action potential and has been released from its receptor site (see Chapter 21). Both compounds produce inhibition by reacting with the active site of AChE. This occurs by phosphorylation with the organophosphates to produce a relatively stable phosphate ester bond and by carbamoylation with the carbamates to form a more labile, and hence more easily reversible, carbamate ester bond. Both compounds thus cause accumulation of ACh at neuronal synapses and myoneural junctions to produce toxicity.

ACh is an important neurotransmitter in both the peripheral and central nervous systems. It is located at a number of different synapses in the CNS—at ganglionic synapses between the sympathetic and parasympathetic preganglionic and postganglionic fibers, at junctions between parasympathetic postganglionic fibers and effector organs, and at junctions between somatic motor neurons and skeletal muscle cells. Thus, signs and symptoms of organophosphate poisoning include parasympathetic manifestations such as salivation, lacrimation, urination, and defecation; pupillary constriction; bradycardia; and bronchoconstriction, which may predominate at low-dose poisoning. Autonomic ganglionic and somatic motor manifestations (e.g., muscular weakness, twitching, areflexia, tachycardia, and hypertension) and CNS manifestations (e.g., confusion, slurred speech, ataxia, convulsions, and respiratory and/or cardiovascular center depression) may predominate in severe intoxication. Death usually results from respiratory failure as the result of a combination of central depression, bronchospasm, excessive bronchial secretions, and respiratory muscle paralysis.

Morbidity and mortality due to carbamate poisoning are less severe because carbamates do not penetrate the CNS as effectively as organophosphates, and central cholinergic effects are thus minimal. In addition, the much greater lability of the carbamate ester bond allows spontaneous reactivation of AChE. This, in turn, decreases the slope of the toxicity dose-response curve as compared with that of the curve for organophosphates, such that small increments in carbamate dose are less likely to produce severe increases in toxicity.

In addition to acute poisoning, organophosphates may produce an intermediate syndrome occurring 1 to 4 days after poisoning and/or delayed neurotoxicity usually occurring 2 to 5 weeks after acute exposure. The former syndrome develops after acute cholinergic crisis and appears to involve cranial nerve palsies, proximal limb weakness, and respiratory paralysis, with the patient requiring ventilatory support (Senanayake & Karalliedde, 1987; Senanayake, 1998). In contrast, delayed neurotoxicity, which is not seen with all organophosphate compounds, appears to be due to neurotoxic esterase inhibition and usually produces a distal and symmetric sensorimotor polyneuropathy of the extremities (Davies, 1987; Tafuri & Roberts, 1987).

Diagnosis of organophosphate poisoning depends on a history of exposure shortly before the onset of illness, signs and symptoms of diffuse parasympathetic stimulation, and laboratory confirmation of exposure by measurement of erythrocyte acetylcholinesterase and plasma pseudocholinesterase activities (see Chapter 21). Whereas AChE is found primarily in nervous tissue and erythrocytes, pseudocholinesterase is found in plasma. The latter enzyme is much more nonspecific in its action than AChE in that, in addition to hydrolysis of ACh, pseudocholinesterase can hydrolyze many other natural and synthetic esters, as described in Chapter 21. Both activities may be decreased, and both activities can be measured in the laboratory. However, only inhibition of AChE is considered specific for organophosphate poisoning because a number of conditions may produce a low plasma pseudocholinesterase level (Tafuri & Roberts, 1987). Thus, the latter measurement is more sensitive but less specific than the red blood cell cholinesterase level for organophosphate poisoning. Generally, levels 30% to 50% of normal indicate exposure, and toxic manifestations occur with greater than 50% inhibition. However, symptoms may not appear until levels are 20% or less of normal. In actuality, confirmation of poisoning, rather than diagnosis, occurs by laboratory determinations. Because baseline values of cholinesterase levels before exposure are unlikely to be available, sequential postexposure cholinesterase determinations appear to be the best way to confirm organophosphate poisoning (Coye et al., 1987).

Treatment of acute poisoning includes respiratory support and, if necessary, decontamination of the patient and gastric lavage or emesis.

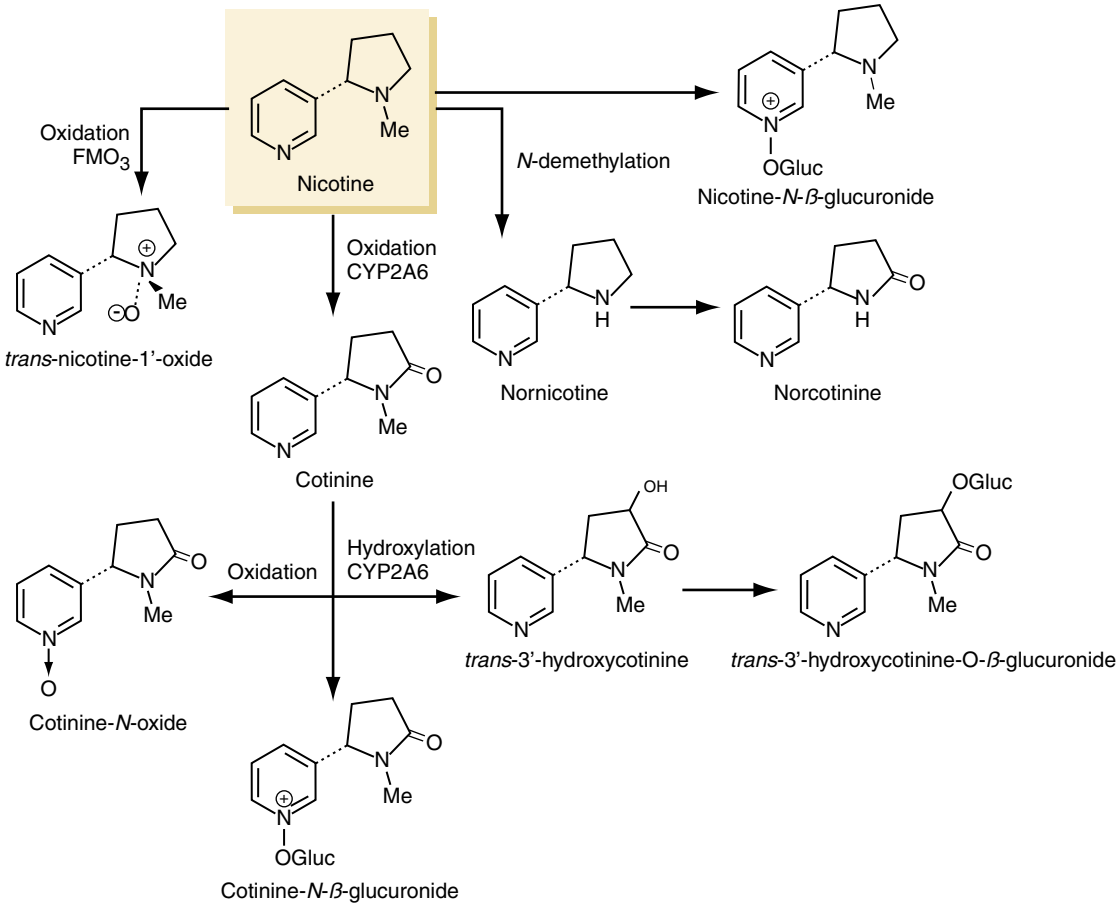

Figure 24.17 Nicotine metabolic pathway. In this figure cotinine is oxidized to cotinine-*N*-oxide *(left)*, cotinine-N-beta-glucuronide *(middle)*, or trans-3'-hydroxycotinine *(right)*. (Adapted from Miller EI, Norris HRK, Rollins DE,et al.: A novel validated procedure for the determination of nicotine, eight nicotine metabolites and two minor tobacco alkaloids in human plasma or urine by solid-phase extraction coupled with liquid chromatography-electrospray ionization-tandem mass spectrometry. J Chromatogr B Analyt Technol Biomed Life Sci 878:725–737, 2010.)

Administration of activated charcoal does not appear to be effective in removing the toxic agent (Eddleston et al., 2008). In the presence of symptoms, atropine is given to ameliorate excessive parasympathetic stimulation by competitively blocking the action of ACh at muscarinic receptors. Pralidoxime is also given as a specific antidote for organophosphate poisoning. If pralidoxime is given within 24 to 48 hours of exposure, it may reactivate phosphorylated cholinesterase by removing the covalently bound phosphate group from the enzyme's active site. However, this time period is variable, and utilization of pralidoxime after 48 hours may be indicated (Clark, 2006; Howland & Aaron, 2006). Chronic poisoning is usually treated by avoidance of further exposure until cholinesterase levels become normal.

MYCOTOXINS

Over the last 20 years, there has been an increase in the utility of medicinal plants to treat a number of human conditions. Much of this resurgence is thought to be due to rising costs of prescription drugs, interest in incorporating "natural" health and well-being regimens, multinational reform instituted by specific countries to utilize such crops as either facets of selected bioengineering initiatives and/or as export, as well as evidence-based medicine that demonstrates the benefit of using medicinal plants in certain disease states (Hoareau & DaSilva, 1999). However, toxic contamination of medicinal plants, plant-derived pharmaceutical products, animal feeds, and other foodstuffs have been reported (Ashiq et al., 2014; Pereira et al., 2014). Intake of such mold-derived "mycotoxins" can contribute to adverse human health problems and therefore represents a special hazard. Thus, in cases of suspected poisoning by medicinal plant preparations, detection of mycotoxins—such as aflatoxin, ochratoxin, zearalenone, fumonisins, deoxynivalenol, among others—is necessary. Clinical sequelae after exposure and/or ingestion of mycotoxins include liver cancer (aflatoxin), esophageal cancer and neural tube defects (fumonisins), gastroenteritis (deoxynivalenol), and renal diseases (ochratoxin A), among others (Wu et al., 2014).

In addition, detection of mycotoxins should be performed on preparations prior to their release for consumption.

Screening and identification of mycotoxins employ chemical extractive techniques such as QuEChERS or dispersive liquid-liquid microextraction, solid-phase extraction, or solid-liquid extraction using solvent mixtures such as acetonitrile/water; antibody-based immunochemical methods such as enzyme-linked immunosorbent assay (ELISA) and immunoaffinity column assay; and chromatographic techniques such as liquid chromatography (LC), gas chromatography (GC), LC/mass spectrometry (MS), GC-MS, capillary electrophoresis, supercritical fluid chromatography, and other related techniques. Mycotoxins are highly stable and therefore pose a concern during production but also in storage, transport, processing, and postprocessing steps of medicinal plant and foodstuff preparation.

NICOTINE AND METABOLITES

Nicotine is the major constituent of the *Nicotiana tabacum* (tobacco) plant and causes stimulation of the autonomic ganglia in the CNS. Smokers (active and passive) absorb nicotine through the skin, mucous membranes in the mouth, nose, and by the lungs during smoke inhalation. When smoked and inhaled into the lungs, nicotine is efficiently absorbed into the bloodstream and delivered to the brain in less than 20 seconds, where it interacts with multiple neurotransmitter systems to produce psychoactive effects, including reward. Although smoking remains socially prevalent, nicotine itself can be fatal with as minimal as 50 to 60 mg of nicotine for the conventional 70-kg male (WebMD, 2019). Further, although the body absorbs about one-tenth of the nicotine in a cigarette (≈1 mg), pets or small children can be poisoned with reduced concentrations by accidental consumption of cigarette butts or chewing tobacco (Miller et al., 2010). However, swallowing concentrated liquid nicotine, contained in the cartridges of e-cigarettes, can be toxic, with as little as a teaspoon inducing fatality in the average toddler (WebMD, 2019). Exposure to nicotine via recreational tobacco products or nicotine replacement therapy leads to the metabolism through Phase I (oxidation, hydroxylation and *N*-demethylation) and Phase II (conjugation with glucuronic acid) pathways that can be detected in body fluids (plasma, urine) (Fig. 24.17).

Nicotine has a short half-life in plasma of 1 to 2 hours. Cotinine and trans-3-hydroxycotinine have longer half-lives (6–22 hours and 4.6–8.3 hours, respectively) and are therefore considered as potentially more useful biomarkers for the assessment of exposure to nicotine. Quantitative GC/MS and LC-MS/MS methods have been employed to detect nicotine and its metabolites. Smokeless tobacco products, transdermal nicotine patches, and nicotine gum produce a more gradual and steadier delivery of nicotine to the bloodstream, resulting in a longer time period for the development of tolerance as well as less prominent pharmacologic effects. Various detection methods (GC/MS, LC-MS/MS) can distinguish whether an individual's nicotine exposure has occurred via active smoking (e.g. cigarette use) or from another route of administration (such as a transdermal nicotine patch).

CONCLUSION

Toxicology results are often central in determining whether patients are taking their prescribed medications or taking other nonprescribed medications and/or illicit substances (Bluth, 2016). While the detecting technologies and the inherent interferences have been discussed, there is also another layer of interrogation and thought that needs to be manifest to interpret a toxicology laboratory result. The laboratory's purpose is to detect or not detect and, where applicable, provide a concentration of the analyte in question. It is not the position of the routine (vs. forensic) clinical toxicology laboratory to render a unilateral decision regarding whether the patient diverted, surreptitiously administered, or overdosed on a medication or illicit substance. Such an assessment should be made in the context of integrating many other aspects of the patient-physician relationship. There is nothing that can replace the information that is obtained by taking a thorough history and background. Additionally, the laboratory cannot be tasked with carrying the entire burden of the drug testing result. It must be clearly understood that the clinical toxicology laboratory provides objective ancillary support that should be used in concert with other clinical parameters toward the effective management of the patient and should not be a standalone measurement in this regard. Consultation with the laboratory toxicologist can often provide clarification of results and clinical management strategies (scheduled vs. unscheduled testing, discontinuation of select drugs/interfering substances prior to retesting, etc.) as means to empower the doctor-patient relationship and provide optimal care.

SELECTED REFERENCES

Cami J, Farre M: Drug addiction, *N Engl J Med* 349:975–986, 2003.

This is a discussion of drug addiction and the various factors involved in drug abuse, the molecular mechanism of action of various drugs, and the neurobiology and neuroadaptation of drug addiction.

Engelhardt H: One century of liquid chromatography: from Tswett's columns to modern high speed and high performance separations, *J Chromatogr B* 800:3–6, 2004.

This is an excellent overview of the development and history of liquid chromatography in the 20th century, describing early successes of "adsorption biochemical analysis," as well as the recent modern revolution in analysis.

Ingelman-Sundberg M: Pharmacogenetics of cytochrome P450 and its applications in drug therapy: the past, present and future, *Trends Pharmacol Sci* 25:193–200, 2004.

An overview of cytochrome P450 pharmacogenetics, its clinical relevance, and possible future benefit for maximizing effective drug therapy.

Peto J: Cancer epidemiology in the last century and the next decade, *Nature* 411:390–395, 2001.

Reviews the effective use of cancer epidemiology in the 20th century for identification of various causes of cancer in humans.

Senanayake N: Organophosphorus insecticide poisoning, *Ceylon Med J* 43:22–29, 1998.

This is an excellent update on acute and chronic organophosphorus poisoning and the pathophysiology and behavioral effects of poisoning.

Snyder SH, Pasternak GE: Historical review: opioid receptors, *Trends Pharmacol Sci* 24:198–205, 2003.

Early molecular biology of opioid receptors is historically reviewed, including receptor localization, identification, and cloning.

Access the complete reference list online at Elsevier eBooks for Practicing Clinicians.

REFERENCES

General References

Bryson PD, editor: *Comprehensive review in toxicology*, Rockville, Md, 1989, Aspen Publishers.

Flomenbaum NE, Goldfrank LR, Hoffman R, et al.: *Goldfrank's toxicologic emergencies*, ed 8, New York, 2006, McGraw-Hill.

O'Neil MJ, Smith A, Heckelman PE, et al.: *The Merck index: an encyclopedia of chemicals, drugs, and biologicals*, ed 13, Merck and Co, 2001, Whitehouse Station, N.J.

Sweetman SC, Blake PS, McGlashan JM, et al.: *Martindale: the complete drug reference*, ed 33, London, 2002, The Pharmaceutical Press.

Basic Techniques for Detecting Drugs

Ambach L, Menzies E, Parkin MC, et al.: Quantification of cocaine and cocaine metabolites in dried blood spots from a controlled administration study using liquid chromatography-tandem mass spectrometry, *Drug Test Anal* 11:709–720, 2019.

Belal T, Awad T, DeRuiter J, et al.: CRGC-IRD methods for the identification of isomeric ethoxyphenethylamines and methoxymethcathinones, *Forensic Sci Int* 184:54–63, 2009.

Bluth MH: Drug testing and toxicology: redefining the Plague of Darkness, *Clin Lab Med* 36:xi–xx, 2016.

Boone CM, Ensing K: Is capillary electrophoresis a method of choice for systematic toxicological analysis? *Clin Chem Lab Med* 41:773–781, 2003.

Chiesl TN, Chu WK, Stocktom AM, et al.: Enhanced amine and amino acid analysis using pacific blue and the mars organic analyzer microchip capillary electrophoresis system, *Anal Chem* 81:2537–2544, 2009.

Davis IM, Bousquet RW, Childs PS: Gas chromatography/mass spectroscopy in clinical and forensic toxicology. In *Service training and continuing education*, Washington, DC, 1989, American Association for Clinical Pathology, pp 7–21.

De Kesel PM, Sadones N, Capiau S, Lambert WE, Stove CP: Hemato-critical issues in quantitative analysis of dried blood spots: challenges and solutions, *Bioanalysis* 5:2023–2041, 2013.

Joye T, Sidibé J, Déglon J, et al.: Liquid chromatography-high resolution mass spectrometry for broad-spectrum drug screening of dried blood spot as microsampling procedure, *Anal Chim Acta* 1063:110–116, 2019.

Marquet P: Progress of liquid chromatography–mass spectrometry in clinical and forensic toxicology, *Ther Drug Monit* 24:255–276, 2002.

Maurer HH: Liquid chromatography–mass spectrometry in forensic and clinical toxicology, *J Chromatogr B* 713:3–25, 1998.

Niessen WMA: Progress in liquid chromatography–mass spectrometry instrumentation and its impact on high-throughput screening, *J Chromatogr A* 1000:413–436, 2003.

Niessen WMA, Tinke AP: Liquid chromatography–mass spectrometry: general principles and instrumentation, *J Chromatogr A* 703:37–57, 1995.

Petersen JR, Okordudu AO, Mohammad A, et al.: Capillary electrophoresis and its application in the clinical laboratory, *Clin Chim Acta* 330:1–30, 2003.

Pincus MR, Rendell M: General quantitative treatment for the binding of divalent antibodies to antigens immobilized on a solid phase, *Proc Natl Acad Sci U S A* 78:5924–5927, 1981.

Porpiglia NM, Savchuk SA, Appolonova SA, Bortolotti F, Tagliaro F: Capillary Electrophoresis (CE) vs. HPLC in the determination of asialo-Tf, a crucial marker for the reliable interpretation of questioned CDT increases, *Clin Chim Acta* 486:49–53, 2018.

Rodbard D, Ruder HJ, Vaitukaitis J, et al.: Mathematical analysis of kinetics of radioligand assays: improved sensitivity obtained by delayed addition of labeled ligand, *J Clin Endocrinol Metab* 33:343–355, 1971.

Simões S, Ajenjo AC, Dias M: Dried blood spots combined to an UPLC–MS/MS method for the simultaneous determination of drugs of abuse in forensic toxicology, *J Pharmaceut Biomed Anal* 147:634–644, 2018.

Shihabi ZK: Applications of capillary electrophoresis in the clinical laboratory, check sample, vol. 33. Chicago, 1993, American Society of Clinical Pathologists. *Clinical Chemistry*, No. CC 94-4 (CC-242).

Smith MP, Bluth MH: (a): Forensic toxicology: an introduction, *Clin Lab Med* 36:753–759, 2016.

Smith MP, Bluth MH: (b): Common interferences in drug testing, *Clin Lab Med* 36:663–671, 2016.

Tagliaro F, Turrina S, Pisi P, et al.: Determination of illicit and/or abused drugs and compounds of forensic interest in biosamples by capillary electrophoretic/electrokinetic methods, *J Chromatogr B* 713:27–49, 1998.

Velghe S (a), Deprez S, Stove CP: Fully automated therapeutic drug monitoring of antiepileptic drugs making use of dried bloodspots. J Chromatogr A, 2019. pii: S0021-9673(19)30631-30634. doi: 10.1016/j.chroma.2019.06.022. [Epub ahead of print].

Velghe S (b), Delahaye L, Stove CP: Is the hematocrit still an issue in quantitative dried blood spot analysis? J Pharm Biomed Anal, 163:188–196, 2019.

Wang G, Huynh K, Barhate R, et al. Validation of a new homogeneous immunoassay for the detection of carisoprodol in urine. *J Anal Toxicol* 35(2):108–12, 2011.

Zhang YV, Wei B, Zhu Y, Zhang Y, Bluth MH: Liquid chromatography-tandem mass spectrometry: an emerging technology in the toxicology laboratory, *Clin Lab Med* 36:635–661, 2016.

Drugs of Abuse

Ashiq S, Hussain M, Ahmad B: Natural occurrence of mycotoxins in medicinal plants: a review, *Fungal Genet Biol* 66:1–10, 2014.

Azmitia EC, Murphy RB, Whitaker-Azmitia PM: MDMA (ecstasy) effects on cultured serotonergic neurons: evidence for Ca^{2+}-dependent toxicity linked to release, *Brain Res* 510:97–103, 1990.

Banks ML, Worst TJ, Rusyniak DE, Sprague JE: Synthetic cathinones ("bath salts"), *J Emerg Med* 46:632–642, 2014.

Barkin RL, Barkin SJ, Barkin DS: Propoxyphene (dextropropoxyphene): a critical review of a weak opioid analgesic that should remain in antiquity, *Am J Ther* 13:534–542, 2006.

Bayorh MA, Zokowska-Grojec Z, Palkovits M, et al.: Effect of phencyclidine (PCP) on blood pressure and catecholamine levels in discrete brain nuclei, *Brain Res* 321:315–318, 1984.

Bell J, Seres V, Bowron P, et al.: The use of serum methadone levels in patients receiving methadone maintenance, *Clin Pharmacol Ther* 43:623–629, 1988.

Bossard JB, Ponté C, Dupouy J, Lapeyre-Mestre M, Jouanjus: Disproportionality analysis for the assessment of abuse and dependence potential of pregabalin in the French Pharmacovigilance Database, *Clin Drug Investig*, 2016.

Campo-Soria C, Chang Y, Weiss DS: Mechanism of action of benzodiazepines on GABAA receptors, *Br J Pharmacol* 148:984–990, 2006.

Castellanos D, Gralnik LM: Synthetic cannabinoids 2015: an update for pediatricians in clinical practice, *World J Clin Pediatr* 5:16–24, 2016.

Debruyne D, Le Boisselier R: Emerging drugs of abuse: current perspectives on synthetic cannabinoids, *Subst Abuse Rehabil* 6:113–129, 2015.

DeCresce RP, Mazura AC, Lifshitz MS, et al.: Drug testing in the workplace, Chicago, 1989, *American Society of Clinical Pathology Press*.

Diong SH, Mohd Yusoff NS, Sim MS, et al.: Quantitation of methadone and metabolite in patients under maintenance treatment, *J Anal Toxicol* 38:660–666, 2014.

Döble A, Canton T, Malgouris C, et al.: The mechanism of action of zopiclone, *Eur Psychiatry* 10, 1995. 117s–28s.

Fraser AD: Use and abuse of the benzodiazepines, *Ther Drug Monit* 20:481–489, 1998.

Frishman WH, Del Vecchio A, Sanal S, et al.: Cardiovascular manifestations of substance abuse. Part 1: Cocaine, *Heart Dis* 5:187–201, 2003.

Fujii H, Narita M, Mizoquchi M, et al.: Drug design and synthesis of epsilon opioid receptor agonist: 17-(cyclopropylmethyl)-4,5alpha-epoxy-3,6beta-dihydroxy-6,14-endoethenomorphinan-7alpha-(N-methyl-N-phenethyl)carboxamide (TAN-821) inducing antinociception mediated by putative epsilon opioid receptor, *Bioorg Med Chem* 12:4133–4145, 2004.

Fusar-Poli P, Crippa JA, Bhattacharyya S, et al.: Distinct effects of Δ9-tetrahydrocannabinol and cannabidiol on neural activation during emotional processing, *Arch Gen Psychiatry* 66:95–105, 2009.

Gianoulakis C: Endogenous opioids and addiction to alcohol and other drugs of abuse, *Curr Top Med Chem* 4:39–50, 2004.

Gill JR, Hayes JA, deSouza IS, et al.: Ecstasy (MDMA) deaths in New York City: a case series and review of the literature, *J Forensic Sci* 47:121–126, 2002.

Gonzalez LA, Gatch MB, Forster MJ, Dillon GH: Abuse potential of soma: the GABA(A) receptor as a target, *Mol Cell Pharmacol* 1:180–186, 2009.

Haroz R, Greenberg MI: New drugs of abuse in North America, *Clin Lab Med* 26:147–164, 2006.

Hevers W, Hadley SH, Luddens H, et al.: Ketamine, but not phencyclidine, selectively modulates cerebellar GABAA receptors containing α6 and δ subunits, *J Neurosci* 28:5383–5393, 2008.

Hoffman RS: Cocaine. In Flomenbaum NE, Goldfrank LR, Hoffman RF, et al.: *Goldfrank's toxicologic emergencies*, ed 8, New York, 2006, McGraw-Hill, pp 1133–1147.

Hurd YL, Kehr J, Ungerstedt U: In vivo microdialysis as a technique to monitor drug transport: correlation of extracellular cocaine levels and dopamine outflow in the rat brain, *J Neurochem* 51:1314–1316, 1988.

Iversen L: Cannabis and the brain, *Brain* 126:1252–1270, 2003.

Johanson CE, Fischman MW: The pharmacology of cocaine related to its abuse, *Pharmacol Rev* 41:3–52, 1989.

Lange RA, Cigarroc RO, Yancy CW, et al.: Cocaine-induced coronary artery vasoconstriction, *N Engl J Med* 321:1557–1562, 1989.

Lange RA, Hillis LD: Cardiovascular complications of cocaine use, *N Engl J Med* 345:351–358, 2001.

Langtry HD, Benfield P: Zolpidem: a review of its pharmacodynamic and pharmacokinetic properties and therapeutic potential, *Drugs* 40:291–313, 1990.

Lile JA, Wesley MJ, Kelly TH, Hays LR: Separate and combined effects of gabapentin and [INCREMENT]9-tetrahydrocannabinol in humans discriminating [INCREMENT]9-tetrahydrocannabinol, *Behav Pharmacol* 27:215–224, 2016.

Martin BR, Sim-Selley LJ, Selley DE: Signaling pathways involved in the development of cannabinoid tolerance, *Trends Pharmacol Sci* 25:325–330, 2004.

Meyer MR, Maurer HH: Absorption, distribution, metabolism and excretion pharmacogenomics of drugs of abuse, *Pharmacogenomics* 12:215–233, 2011.

Papathanasiou T, Juul RV, Gabel-Jensen C, Kreilgaard M, Lund TM: *Population pharmacokinetic Modelling of morphine, gabapentin and their combination in the rat*, Pharm Res, 2016. [Epub ahead of print].

Passie T, Halpern JH, Stichtinoth DO, et al.: The pharmacology of lysergic acid diethylamide: a review, *CNS Neurosci Ther* 14:295–314, 2008.

Passman RS, Bennett CL, Purpura JM, et al.: Amiodarone-associated optic neuropathy: a critical review, *Am J Med* 125:447–453, 2012.

Poklis A: Analytic/forensic toxicology. In Klaassen CD, editor: *Casarett and Doull's toxicology: the basic science of poisons*, ed 6, New York, 2001, McGraw-Hill, pp 1089–1108.

Schuster DI, Ehrlich GK, Murphy RB: Purification and partial amino acid sequence of a 28 kDa cyclophilin-like component of the rat liver sigma receptor, *Life Sci* 55:PL151–PL156, 1994.

Smith MT: Differences between and combinations of opioids re-visited, *Curr Opin Anaesthesiol* 21:596–601, 2008.

Substance Abuse and Mental Health Services Administration: Results from the 2012 National Survey on drug Use and health: summary of National findings, NSDUH series H-46, Rockville, Md, 2013, Substance Abuse and Mental Health Services Administration. HHS Publication No. (SMA) 13-4795.

Thornton MD, Baum CR: Bath salts and other emerging toxins, *Pediatr Emerg Care* 30:47–52, 2014.

Tseng LF: Evidence for epsilon-opioid receptor-mediated beta-endorphin-induced analgesia, *Trends Pharmacol Sci* 22:623–630, 2001.

Tso PH, Wong YH: Molecular basis of opioid dependence: role of signal regulation by G-proteins, *Clin Exp Pharmacol Physiol* 30:307–316, 2003.

Zhuo M: Plasticity of NMDA receptor NR2B subunit in memory and chronic pain, *Mol Brain* 2:1–11, 2009.

Therapeutic Drugs

Asconape JJ: Some common issues in the use of antiepileptic drugs, *Semin Neurol* 22:27–39, 2002.

Baldessarini RJ: Drug therapy of depression and anxiety disorders. In Brunton LL, Lazo JS, Parker KL, editors: *Goodman and Gilman's the pharmacological basis of therapeutics*, ed 11, New York, 2006, McGraw-Hill, pp 429–459.

Baldessarini RJ, Tarazi FI: Pharmacotherapy of psychosis and mania. In Brunton LL, Lazo JS, Parker KL, editors: *Goodman and Gilman's the pharmacological basis of therapeutics*, ed 11, New York, 2006, McGraw-Hill, pp 461–500.

Bazil CW, Pedley TA: Advances in the medical treatment of epilepsy, *Annu Rev Med* 49:135–162, 1998.

Braido F, Sclifò F, Ferrando M, et al.: New therapies for allergic rhinitis, *Curr Allergy Asthma Rep* 14:422, 2014.

Braun F, Lort T, Ringe B: Update of current immunosuppressive drugs used in clinical organ transplantation, *Transpl Int* 11:77–81, 1998.

Brodtkorb E: Antiepileptic drug treatment: clinical considerations and concerns, *Prog Brain Res* 116:395–406, 1998.

Burke A, Smyth E, FitzGerald GA: Analgesic-antipyretic agents: pharmacotherapy of gout. In Brunton LL, Lazo JS, Parker KL, editors: *Goodman and Gilman's the pharmacological basis of therapeutics*, ed 11, New York, 2006, McGraw-Hill, pp 671–715.

Burns MJ: The pharmacology and toxicology of atypical antipsychotic agents, *J Toxicol Clin Toxicol* 39:1–14, 2001.

Chabner BA, Amrein PC, Druker BJ, et al.: Antineoplastic agents. In Brunton LL, Lazo JS, Parker KL, editors: *Goodman and Gilman's the pharmacological basis of therapeutics*, ed 11, New York, 2006, McGraw-Hill, pp 1335–1339.

Dancey JE: Clinical development of mammalian target of rapamycin inhibitors, *Hematol Oncol Clin N Am* 16:1101–1114, 2002.

Drosos AA: Newer immunosuppressive drugs: their potential role in rheumatoid arthritis therapy, *Drugs* 62:891–907, 2002.

Dunn CJ, Wagstaff AJ, Perry CM, et al.: Cyclosporin: an updated review of the pharmacokinetic properties, clinical efficacy and tolerability of a microemulsion-based formulation (Neoral) in organ transplantation, *Drugs* 61:1957–2016, 2001.

Frei UA, Neumayer H, Buchholz B, et al.: Randomized, double-blind, one-year study of the safety and tolerability of cyclosporine microemulsion compared with conventional cyclosporine in renal transplant patients, *Transplantation* 65(11):1455–1460, 1998.

Frishman WH, Sica DA, editors: *Cardiovascular pharmacotherapeutics*, ed 3, Minneapolis, 2011, Cardiotext Publishing.

Gerra G, Borella F, Zaimovic A, et al.: Buprenorphine versus methadone for opioid dependence: predictor variables for treatment outcome, *Drug Alcohol Depend* 75(1):37–45, 2004.

Therapeutic drug monitoring. I: pharmacokinetics, technology, and methodology, Gerson B, editor: *Clin Lab Med* 7:267–492, 1987a.

Therapeutic drug monitoring. II: patient care and applications, Gerson B, editor: *Clin Lab Med* 7:499–714, 1987b.

Grem JL, de Carvalho M, Wittes RE, et al.: Chemotherapy: the properties and uses of single agents: methotrexate. In Macdonald JS, Haller DG, Mayer RJ, editors: *Manual of oncologic therapeutics*, ed 3, Philadelphia, 1995, JB Lippincott, p 108.

Gonzalez J, Tukey RH: Drug metabolism. In Brunton LL, Lazo JS, Parker KL, editors: *Goodman and Gilman's the pharmacological basis of therapeutics*, ed 11, New York, 2006, McGraw-Hill, pp 71–91.

Hardman JG, Limbird LE, Gilman AG, editors: *Goodman & Gilman's the pharmacological basis of therapeutics*, ed 10, New York, 2001, McGraw-Hill.

Hess AD, Esa AH, Colombani PM: Mechanisms of action of cyclosporine: effect on cells of the immune system and on subcellular events in T cell activation, *Transplant Proc* 20(Suppl 2):29–40, 1988.

Hoareau L, DaSilva EJ: Medicinal plants: a re-emerging health aid, *Electron J Biotechnol* 2:56–70, 1999.

Hojo M, Morimoto T, Maluccio M, et al.: Cyclosporine induces cancer progression by a cell-autonomous mechanism, *Nature* 397:530–534, 1999.

Howanitz PJ, Howanitz JH: Therapeutic drug monitoring and toxicology. In Henry JB, editor: *Clinical diagnosis and management by laboratory methods*, vol. 17. Philadelphia, 1984, WB Saunders, pp 362–370.

Howland MA, Aaron CK: Pralidoxime. In Flomenbaum NE, Goldfrank LR, Hoffman RF, et al.: *Goldfrank's toxicologic emergencies*, ed 8, New York, 2006, McGraw-Hill, pp 1513–1519.

Isoniemi H: New trends in maintenance immunosuppression, *Ann Chir Gynaecol* 86:164–170, 1997.

Kahan BD: Pharmacokinetics and pharmacodynamics of cyclosporine, *Transplant Proc* 21(Suppl 1):9–15, 1989.

Krensky AM, Vincenti F, Bennett WM: Immunosuppressants, toleragens, and immunostimulants. In Brunton LL, Lazo JS, Parker KL, editors: *Goodman and Gilman's the pharmacological basis of therapeutics*, ed 11, New York, 2006, McGraw-Hill, pp 1405–1431.

Kronbach T, Fischer V, Meyer VA: Cyclosporine metabolism in human liver: identification of a cytochrome P-450 III gene family as the major cyclosporine-metabolizing enzyme explains interactions of cyclosporine with other drugs, *Clin Pharmacol Ther* 43:630–635, 1988.

Löscher W, Rogawski MA: How theories evolved concerning the mechanism of action of barbiturates, *Epilepsia* 53(Suppl 8):12–25, 2012.

McEvoy GK, Miller J, Litvak K, editors: *American hospital formulary Service drug information*, Bethesda, Md, 2004, American Society of Health-System Pharmacists, p 2004.

McMurray JJ, Adamopoulos S, Anker SD, et al.: ESC Guidelines for the diagnosis and treatment of acute and chronic heart failure 2012: the Task force for the diagnosis and treatment of acute and chronic heart failure 2012 of the European Society of Cardiology. Developed in collaboration with the heart failure association (HFA) of the ESC. ESC Committee for practice Guidelines, *Eur Heart J* 33:1787–1847, 2012.

McNamara JO: Pharmacotherapy of the epilepsies. In Brunton LL, Lazo JS, Parker KL, editors: *Goodman and Gilman's the pharmacological basis of therapeutics*, ed 11, New York, 2006, McGraw-Hill, pp 501–525.

Mueller XM: Drug immunosuppression therapy for adult heart transplantation. Part 1: immune response to allograft and mechanism of action of immunosuppressants, *Ann Thorac Surg* 77:354–362, 2004.

Opie LH, Gersh BJ: In *Drugs for the heart*, ed 5, Philadelphia, 2001, WB Saunders.

Paci A, Veal G, Bardin C, et al.: Review of therapeutic drug monitoring of anticancer drugs part 1—cytotoxics, *Eur J Cancer* 50:2010–2019, 2014.

Pesce AJ, Rashkin M, Kotagal U, et al.: Standards of laboratory practice: theophylline and caffeine monitoring. National Academy of Clinical Biochemistry, *Clin Chem* 44:1124–1128, 1998.

Phiel CJ, Klein PS: Molecular targets of lithium action, *Annu Rev Pharmacol Toxicol* 41:789–813, 2001.

Philip AT, Gerson B: Toxicology and adverse effects of drugs used for immunosuppression in organ transplantation, *Clin Lab Med* 18:755–765, 1998.

Rocco TP, Fang JC: Pharmacotherapy of congestive heart failure. In Brunton LL, Lazo JS, Parker KL, editors: *Goodman and Gilman's the pharmacological basis of therapeutics*, ed 11, New York, 2006, McGraw-Hill, pp 869–897.

Roden DM: Antiarrhythmic drugs. In Brunton LL, Lazo JS, Parker KL, editors: *Goodman and Gilman's the pharmacological basis of therapeutics*, ed 11, New York, 2006, McGraw-Hill, pp 899–932.

Roenigk Jr HH, Auerbach R, Maibach HI, et al.: Methotrexate in psoriasis: consensus conference, *J Am Acad Dermatol* 38:478–485, 1998.

Rowden AK, Norvell J, Eldridge DL, et al.: Acetaminophen poisoning, *Clin Lab Med* 26:49–65, 2006.

Scott LJ, McKeage K, Keam SJ, et al.: Tacrolimus: a further update of its use in the management of organ transplantation, *Drugs* 63:1247–1297, 2003.

Slattery JT, Risler LJ: Therapeutic monitoring of busulfan in hematopoietic stem cell transplantation, *Ther Drug Monit* 20:543–549, 1998.

Slingerland M, Cerella C, Guchelaar HJ, et al.: Cardiac glycosides in cancer therapy: from preclinical investigations towards clinical trials, *Invest New Drugs* 31:1087–1094, 2013.

Smith MP, Bluth MH: Forensic toxicology: an introduction, *Clin Lab Med* 36:753–760, 2016.

Sunheimer R, Capaldo G, Kashanian F, et al.: Serum analyte pattern characteristic of fulminant hepatic failure, *Ann Clin Lab Sci* 24:101–109, 1994.

Sztajnkrycer MD: Valproic acid toxicity: overview and management, *J Toxicol Clin Toxicol* 40:789–801, 2002.

Tugwell P, Bennett K, Gent M: Methotrexate in rheumatoid arthritis: indications, contraindications, efficacy, and safety, *Ann Intern Med* 107:358–366, 1987a.

Tugwell P, Bennett K, Gent M: Position paper: methotrexate in rheumatoid arthritis, *Ann Intern Med* 107:418–419, 1987b.

Tugwell P, Pincus T, Yocum D, et al.: Combination therapy with cyclosporine and methotrexate in severe rheumatoid arthritis, *N Engl J Med* 333:137–141, 1995.

Uetrecht JP: Mechanism of drug-induced lupus, *Chem Res Toxicol* 1:133–143, 1988.

Undem BJ: Pharmacotherapy of asthma. In Brunton LL, Lazo JS, Parker KL, editors: *Goodman and Gilman's the pharmacological basis of therapeutics*, ed 11, New York, 2006, McGraw-Hill, pp 717–736.

Valdes R, Jortani SA, Gheorghiade M: Standards of laboratory practice: cardiac drug monitoring. National Academy of Clinical Biochemistry, *Clin Chem* 44:1096–1109, 1998.

Warner A, Privitera M, Bates D: Standards of laboratory practice: antiepileptic drug monitoring. National Academy of Clinical Biochemistry, *Clin Chem* 44:1085–1095, 1998.

White S, Wong SHY: Standards of laboratory practice: analgesic drug monitoring. National Academy of Clinical Biochemistry, *Clin Chem* 44:1110–1123, 1998.

Yaari Y, Selzer ME, Pincus JH: Phenytoin: mechanism of its anticonvulsant action, *Ann Neurol* 20:171–184, 1986.

Zimetbaum P, Kowey PR, Michelson EL: Antiarrythmic drugs. In Frishman WH, Sica DA, editors: *Cardiovascular pharmacotherapeutics*, ed 3, Minneapolis, 2011, Cardiotext Publishing, pp 227–256.

Toxins and Poisons

Beckerman N, Leikin SM, Aitchinson R, et al.: Laboratory interferences with the newer cyanide antidote: hydroxocobalamin, *Semin Diagn Pathol* 26:49–52, 2009.

Bernard SM: Should the Centers for Disease Control and Prevention's childhood lead poisoning intervention level be lowered? *Am J Public Health* 93:1253–1260, 2003.

Boyd VL, Harbell JW, O'Connor RJ, et al.: 2,3-Dithioerythritol, a possible new arsenic antidote, *Chem Res Toxicol* 2:301–306, 1989.

Brandt-Rauf PW, Pincus MR: Molecular markers of carcinogenesis, *Pharmacol Ther* 77:135–148, 1998.

Brent J: Fomepizole for ethylene glycol and methanol poisoning, *N Engl J Med* 360:2216–2223, 2009.

Caraco Y: Genetic determinants of drug responsiveness and drug interactions, *Ther Drug Monit* 20:517–524, 1998.

Clark RF: Insecticides: organic phosphorus compounds and carbamates. In Flomenbaum NE, Goldfrank LR, Hoffman RF, et al.: *Goldfrank's toxicologic emergencies*, ed 8, New York, 2006, McGraw-Hill, pp 1497–1513.

Coye MJ, Barnett PG, Midtling JE, et al.: Clinical confirmation of organophosphate poisoning by serial cholinesterase analyses, *Arch Intern Med* 147:438–442, 1987.

Davies JE: Changing profile of pesticide poisoning, *N Engl J Med* 316:807–808, 1987.

Davis TME, Beilby J, Davis WA, et al.: Prevalence, characteristics and prognostic significance of HFE gene mutations in type II diabetes: the Fremantle Diabetes Study, *Diabetes Care* 31:1795–1801, 2008.

Deshpande LS, Delorenzo RJ: Mechanisms of levetiracetam in the control of status epilepticus and epilepsy, *Front Neurol* 5:11, 2014.

De Vivo I, Marion MJ, Smith SJ, et al.: Mutant c-K-ras-p21 in chemical carcinogenesis in humans exposed to vinyl chloride, *Cancer Causes Control* 5:273–278, 1994.

Eddleston M, Buckley NA, Senarathna L, et al.: Multiple-dose activated charcoal in acute self-poisoning: a randomised controlled trial, *Lancet* 371:579–587, 2008.

Ehle M, Patel C, Giugliano RP: Digoxin: clinical highlights: a review of digoxin and its use in contemporary medicine, *Crit Pathw Cardiol* 10:93–98, 2011.

Fomin D, Baranauskaite V, Usaviciene E, et al.: Human deaths from drug overdoses with carfentanyl involvement-new rising problem in forensic medicine: a STROBE-compliant retrospective study, *Medicine (Baltim)* 97, 2018. e13449.

Goldbaum LR, Ramirez RG, Absalon KB: What is the mechanism of carbon monoxide toxicity? *Aviat Space Environ Med* 46:1289–1291, 1975.

Hall AH, Saiers J, Baud F: Which cyanide antidote? *Crit Rev Toxicol* 39:541–552, 2009.

Helander A, Beck O: Ethyl sulfate: a metabolite of ethanol in humans and a potential biomarker of acute alcohol intake, *J Anal Toxicol* 29:270–274, 2005.

Ibrahim D, Froberg B, Wolf A, et al.: Heavy metal poisoning: clinical presentations and pathophysiology, *Clin Lab Med* 26:67–97, 2006.
Jones JH, Wie WB: Cocaine-induced chest pain, *Clin Lab Med* 26:127–146, 2006.
Kao LW, Nanagas KA: Toxicity associated with carbon monoxide, *Clin Lab Med* 26:99–125, 2006.
Klaassen CD, editor: *Casarett and Doull's toxicology: the basic science of poisons*, ed 6, New York, 2001, McGraw-Hill.
Kosnett MJ, Becker CE, Osterloh JD, et al.: Factors influencing bone lead concentration in a suburban community assessed by non-invasive x-ray fluorescence, *J Am Med Assoc* 271:197–203, 1994.
Lieber SR, Helcer J, Shemesh E: Monitoring drug adherence, *Transplant Rev* 29:73–77, 2015.
Miller EI, Norris HRK, Rollins DE, Tiffany ST, Wilkins DG: A novel validated procedure for the determination of nicotine, eight nicotine metabolites and two minor tobacco alkaloids in human plasma or urine by solid-phase extraction coupled with liquid chromatography-electrospray ionization-tandem mass spectrometry, *J Chromatogr B Analyt Technol Biomed Life Sci* 878:725–737, 2010.
Nanau RM, Neuman MG: Biomolecules and biomarkers used in diagnosis of alcohol Drinkingand in monitoring therapeutic interventions, *Biomolecules* 5:1339–1385, 2015, https://doi.org/10.3390/biom5031339.
Needleman HL, Gatsonis CA: Low-level lead exposure and the IQ of children: a meta-analysis of modern studies, *J Am Med Assoc* 263:673–678, 1990.
Neuvonen AM, JU P, Sajantila A: Post-mortem ABCB1 genotyping reveals an elevated toxicity for female digoxin users, *Int J Legal Med* 125:265–269, 2011.
Ogawa R, Stachnik JM, Echizen H: Clinical pharmacokinetics of drugs in patients with heart failure: an update (part 1, drugs administered intravenously), *Clin Pharmacokinet* 52:169–185, 2013.
Pereira VL, Fernandes JO, Cunha SC: Mycotoxins in cereals and related foodstuffs: a review on occurrence and recent methods of analysis, *Trends Food Sci Technol* 36:96–136, 2014.
Perera FP, Hemminki K, Young TL, et al.: Detection of polycyclic aromatic hydrocarbon–DNA adducts in white blood cells of foundry workers, *Cancer Res* 48:2288–2291, 1988.
Pincus MR, Friedman FK: Oncoproteins in the diagnosis of human malignancies, *Molec Diagn* 1:23–38, 2003.
Saklani P, Skanes A: Novel anti-arrhythmic medications in the treatment of atrial fibrillation, *Curr Cardiol Rev* 8:302–309, 2012.
Santella R, Hatch M, Pirastu R, et al.: Carcinogen evaluation: in vitro testing, in vivo testing, and epidemiology, *Semin Occup Med* 2:245–255, 1987.
Schwartz J, Landrigan PJ, Baker Jr EL, et al.: Lead-induced anemia: dose-response relationships and evidence for a threshold, *Am J Public Health* 80:165–168, 1990.
Senanayake N, Karalliedde L: Neurotoxic effects of organophosphorus insecticides: an intermediate syndrome, *N Engl J Med* 316:761–763, 1987.
Tafuri J, Roberts J: Organophosphate poisoning, *Ann Emerg Med* 16:193–202, 1987.
Takatoku M, Uchiyama T, Okamoto S, et al.: Retrospective nationwide survey of Japanese patients with transfusion-dependent MDS and aplastic anemia highlights the negative impact of iron overload on morbidity/mortality, *Eur J Haematol* 78:487–494, 2007.
Talameh JA, Lanfear DE: Pharmacogenetics in chronic heart failure: new developments and current challenges, *Curr Heart Fail Rep* 9:23–32, 2012.
Tenenbein M: Hepatotoxicity in acute iron poisoning, *J Toxicol Clin Toxicol* 39:721–726, 2001.
Tricco AC, Cogo E, Angeliki VA, et al.: Comparative safety of anti-epileptic drugs among infants and children exposed in utero or during breastfeeding: protocol for a systematic review and network meta-analysis, *Syst Rev* 3:68, 2014.
WebMD.com - https://www.webmd.com/smoking-cessation/nicotine-poisoning-can-you-overdose#1.
Wu F, Groopman JD, Pestka JJ: Public health impacts of foodborne mycotoxins, *Annu Rev Food Sci Technol* 5:351–372, 2014.

CHAPTER 25

EVALUATION OF ENDOCRINE FUNCTION

Helena A. Guber, Mihaela Oprea, Yan Xue Russell

PITUITARY FUNCTION, 387
Pituitary Tumors, 388
Prolactin, 389
Growth Hormone, 390
Posterior Pituitary Hormones, 392
THYROID FUNCTION, 395
Thyroid Hormone Synthesis and Metabolism, 396
Hypothalamic-Pituitary-Thyroid Axis, 398
Urinary Iodine Measurement, 401
Screening Programs for Detection of Neonatal Hypothyroidism, 402
Nonthyroidal Illness, 402
Physiologic Variables, 402
Medications and Thyroid Function Tests, 403
Thyroid Illness, 403
Screening for Thyroid Disease, 403
Uses Of L-Thyroxine, 403
Calcitonin, 404
ADRENAL FUNCTION, 404
Hormones of the Adrenal Medulla, 405
Hormones of The Adrenal Cortex, 407
Adrenal Insufficiency, 419
RENIN-ALDOSTERONE AXIS, 420
Renin and Hypertension, 421
Aldosterone Measurements, 423
Renin Measurements, 423
SELECTED REFERENCES, 424

KEY POINTS

- The endocrine system is finely integrated—the hypothalamus, pituitary gland, and target glands continually communicate through feedback inhibition and stimulation to control all aspects of metabolism, growth, and reproduction. By understanding this interplay and carefully manipulating these systems via provocative or suppressive stimuli, it is possible to characterize an underlying abnormality and provide directed treatment.
- Prolactin levels can be elevated as a result of a variety of pharmacologic and physiologic stimuli; values greater than 200 ng/mL are almost always associated with the presence of a pituitary tumor.
- The initial screening test for acromegaly is measurement of the serum insulin-like growth factor-1 (IGF-1).
- It is often unnecessary to perform provocative stimulation tests to document growth hormone deficiency in patients with a known history of pituitary disease or in those with evidence of three or more pituitary hormone deficiencies.
- Provided that the hypothalamic-pituitary-thyroid axis is intact, the ultrasensitive thyroid-stimulating hormone test is the best method for detecting clinically significant thyroid dysfunction.
- When measuring thyroglobulin as a tumor marker for thyroid cancer, always simultaneously check for thyroglobulin antibodies.
- The best screening test for pheochromocytoma is either the plasma free metanephrine or 24-hour urinary free metanephrines. The patient should avoid caffeine, alcohol, acetaminophen, monoamine oxidase inhibitors, and tricyclic antidepressants for at least 5 days before testing.
- It is frequently unnecessary to perform an adrenocorticotropic hormone (ACTH) stimulation test in critically ill patients. A random cortisol of greater than 25 μg/dL (700 nmol/L) during stress makes it highly unlikely that the patient is adrenally insufficient.
- Midnight salivary cortisol (MSC) is a highly sensitive, highly specific, and very simple way to screen for Cushing disease.

PITUITARY FUNCTION

The endocrine system is a finely tuned system in which the hypothalamus, pituitary gland, and various endocrine glands communicate through an intricate scheme of hormone-mediated feedback inhibition and stimulation stimuli. Hormones are classically defined as substances that act at sites distant from their place of origin. Included under the rubric of hormones are moieties that act in an autocrine (act directly on themselves), paracrine (act adjacent to the cells of origin), or intracrine (act within the cells of origin without ever exiting the cells) fashion. Through this intimate interplay of signals, the endocrine system serves to control metabolism, growth, fertility, electrolyte and water homeostasis, and responses to stress.

The pituitary gland, also known as the *hypophysis*, is located within the confines of the sella turcica. It is connected to the median eminence of the hypothalamus by the infundibular stalk and is divided into an anterior lobe (adenohypophysis) and a posterior lobe (neurohypophysis). It weighs about 0.6 g and measures about 12 mm in transverse and 8 mm in anteroposterior diameter. The anterior pituitary gland possesses five distinct hormone-synthesizing and hormone-secreting populations of cells. These cell groups include somatotrophs, which secrete growth hormone (GH); lactotrophs, which secrete prolactin (PRL); thyrotrophs, which secrete thyroid-stimulating hormone (TSH); gonadotrophs, which secrete the α and β subunits of follicle-stimulating hormone (FSH) and luteinizing hormone (LH); and corticotrophs, which secrete proopiomelanocortin (POMC). POMC is cleaved within the pituitary gland to form adrenocorticotropin (ACTH), β-endorphin, and β-lipotropin (β-LPH). The hypothalamus communicates with the anterior pituitary gland by secreting its own set of trophic hormones that are specific for each of the cell populations within the pituitary gland (Fig. 25.1). These trophic hormones travel along the infundibular stalk to the adenohypophysis through a system of portal vessels.

In contrast to the anterior pituitary gland, the posterior pituitary gland (neurohypophysis) does not synthesize hormones. The hormones that it does secrete, arginine vasopressin (AVP; also known as antidiuretic hormone [ADH]) and oxytocin, are synthesized within the magnicellular neurons of the paraventricular and supraoptic nuclei of the hypothalamus, transported along the axons, and stored in the nerve terminals that end in the neurohypophysis. A summary of the different hormones secreted by the pituitary gland can be found in Box 25.1.

Abnormalities of pituitary function fall within two broad categories: hormonal excess and hormonal deficiency. Hormonal excess usually occurs as the result of clonal expansion of a distinct population of cells. However, it can result from an increase in trophic hormones from the hypothalamus or ectopic sites. The causes of hormonal deficiency are more varied (Box 25.2) and can result in the deficiency of one or more hormones, often with continued and progressive loss of other hormones over time.

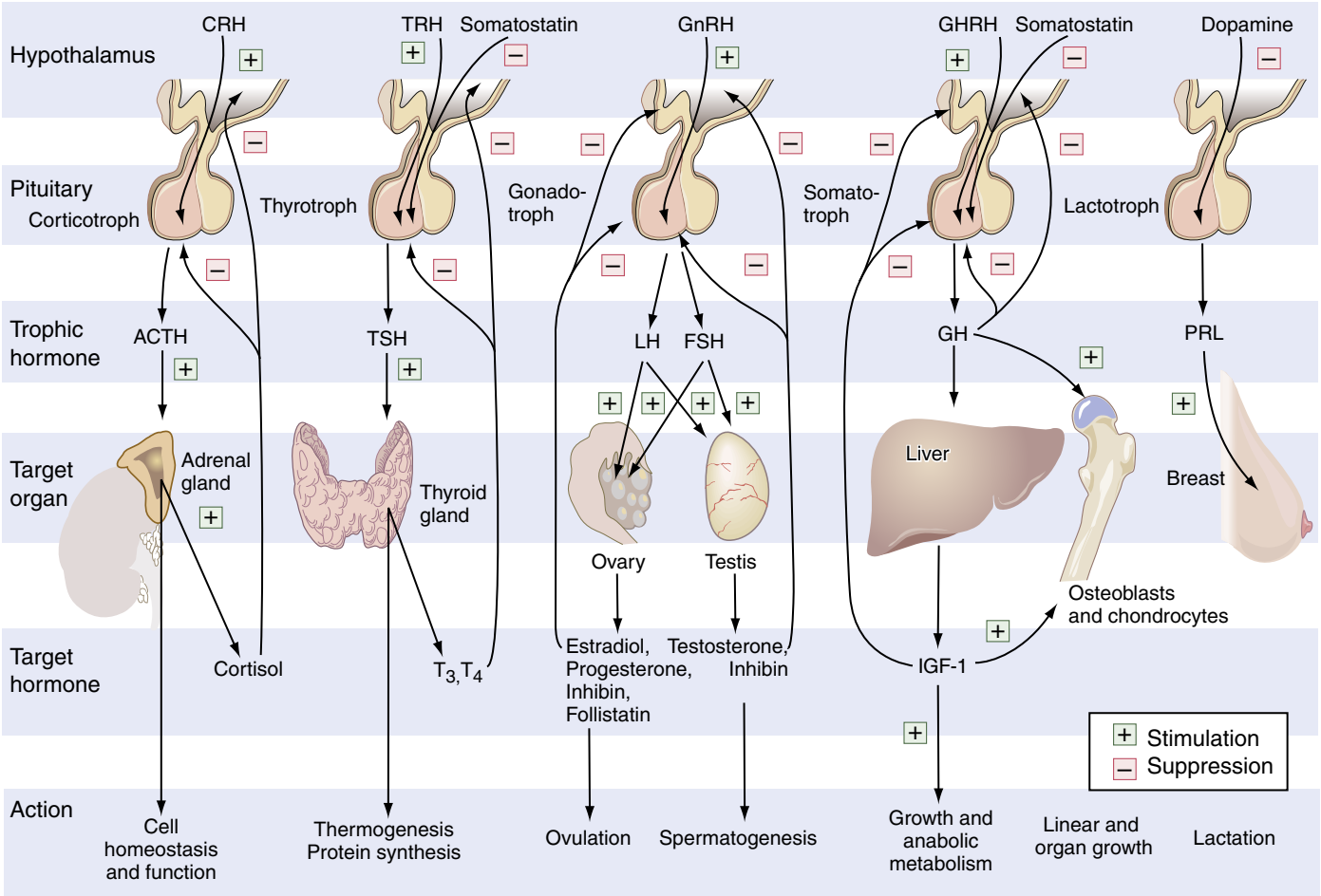

Figure 25.1 The hypothalamic-pituitary-target organ axis. *ACTH,* Adrenocorticotropin; *CRH,* corticotropin-releasing hormone; *FSH,* follicle-stimulating hormone; *GHRH,* growth hormone–releasing hormone; *GnRH,* gonadotropin-releasing hormone; *IGF-1,* insulin-like growth factor-1; *LH,* luteinizing hormone; *PRL,* prolactin; T_3, 3,5,3′-triiodothyronine; T_4, thyroxine; *TRH,* thyrotropin-releasing hormone; *TSH,* thyroid-stimulating hormone. (Redrawn from Melmed S, Kleinberg D: Anterior pituitary. In Larsen PR, Kronenberg HM, Melmed S, et al., editors: Williams textbook of endocrinology, ed 10, Philadelphia, 2003, Saunders, p 181, with permission.)

BOX 25.1

Hormones of the Pituitary Gland

Anterior Pituitary—Adenohypophysis

Growth hormone (GH; somatotropin)
Thyroid-stimulating hormone (TSH; thyrotropin)
Gonadotropins
- Follicle-stimulating hormone (FSH)
- Luteinizing hormone (LH)

Proopiomelanocortin (POMC)
- Adrenocorticotropin (ACTH)
- β-lipotropin
- β-endorphin

Prolactin (PRL)

Posterior Pituitary—Neurohypophysis

Arginine vasopressin (AVP) = Antidiuretic hormone (ADH)
Oxytocin

BOX 25.2

Causes of Pituitary Hormonal Deficiency

Pituitary neoplasm
Pituitary adenoma
Craniopharyngioma
Metastases or rarely primary carcinoma
Iatrogenic
Radiation
Hypophysectomy
Stalk resection
Granulomatous disease
Sarcoidosis
Infection
Tuberculosis
Syphilis
Fungi
Hemorrhage and infarction
Postpartum necrosis (Sheehan syndrome)
Head trauma
Apoplexy
Aneurysms of the internal carotid artery
Autoimmune lymphocytic hypophysitis
Hemochromatosis
Primary hypothalamic disorders
Tumor
Granulomas
Idiopathic or genetic deficiencies of hormones within the pituitary gland or hypothalamus

PITUITARY TUMORS

Pituitary tumors may be classified as microadenomas (<1 cm in greatest diameter and confined to the sella) or macroadenomas (≥ 1 cm in greatest diameter). They are further subcategorized into secretory and nonsecretory varieties (Table 25.1). All tumors have the potential to grow; in doing so, they can compress the optic chiasm, resulting in visual field defects, of which bitemporal hemianopia is the most frequent presentation. Invasion into the cavernous sinus can lead to compression of cranial nerves III, IV, VI, V1, and V2 and the intracavernous portion of the internal carotid artery. It can also lead to hydrocephalus caused by obstruction of the third ventricle. Aside from oversecretion of a particular hormone and extension into surrounding regions, these tumors can also cause hormonal deficiency due to compression of other cell lineages within the pituitary gland.

TABLE 25.1

Relative Frequency of Occurrence of Pituitary Tumors

Lactotroph (PRL)	30%
Somatotroph (GH)	15%
Combined GH/PRL	8%
Corticotroph (ACTH)	15%
Thyrotroph (TRH)	1%
Pleurihormonal	4%
Nonfunctioning	27%

ACTH, Adrenocorticotropin; *GH,* growth hormone; *PRL,* prolactin; *TRH,* thyrotropin-releasing hormone.

PROLACTIN

PRL is a polypeptide produced by the lactotrophs of the pituitary gland; it is responsible for the initiation and maintenance of lactation. Its secretion is normally kept at low levels by the inhibitory actions of dopamine produced by the hypothalamus. Similar to several pituitary hormones, PRL is secreted in a circadian fashion, with the highest levels attained during sleep and a nadir occurring between 10 AM and noon (Sassin et al., 1972). PRL is secreted in a pulsatile fashion, the amplitude and frequency of which not only vary throughout the day but are influenced by a variety of physiologic stimuli (e.g., stress, pregnancy, exercise). Because of these factors and a serum half-life of 26 to 47 minutes, it had been recommended that when screening for hyperprolactinemia three specimens be obtained at 20- to 30-minute intervals. Each sample could either be analyzed separately and their results averaged or an equal aliquot from each sample could be pooled into a single specimen for analysis. Current Endocrine Society guidelines recommend screening using a single determination, collected at any time of day, reserving the option to follow the aforementioned recommendations if the diagnosis is in doubt (Melmed et al., 2011). A single PRL level above the sex-matched upper limit of normal is diagnostic for hyperprolactinemia, with values above 250 μg/L usually indicating the presence of a prolactinoma. PRL is measured by immunometric assay.

The major circulating form of PRL is the nonglycosylated monomer. A number of other forms can occur, including "big" PRL and macroprolactin ("big, big" PRL), which are considered to be PRL coupled with immunoglobulin (Yazigi et al., 1997; Conner & Fried, 1998). Believed to be clinically inert, these forms can react with commonly utilized immunoassays, resulting in falsely elevated PRL levels in patients in whom pathologic elevation of PRL is not supported clinically. There are two laboratory approaches by which to detect macroprolactin. The gold standard—gel filtration chromatography (GFC)—separates and quantifies prolactin isoforms by size. The second method—precipitation by polyethylene glycol (PPEG)—removes macroprolactin from serum before quantification of monomeric PRL using a standard immunoassay (Diver et al., 2001; Amadori et al., 2003; Fahie-Wilson, 2003; Prazeres et al., 2003; Suliman et al., 2003; Toldy et al., 2003; Ram et al., 2008; Samson et al., 2015). Macroprolactinemia is considered significant if immunoreactive monomeric prolactin is <40% (Olukoga, 1999). The existence of macroprolactinemia should be entertained when the clinical picture is not concordant with the PRL level.

The degree of PRL elevation usually correlates well with tumor size. Under certain circumstances, the PRL may be falsely low or minimally elevated considering the size of the tumor. This discordance can be explained by the "hook effect," and it may result in the misdiagnosis of a patient having a nonfunctioning chromophobe adenoma instead of a prolactin-secreting adenoma.

This effect results when two antibodies to an antigen—in the current case, PRL—are used in an enzyme-linked immunosorbent assay (ELISA; see Chapter 45). One of these antibodies, called the *capture antibody*, is embedded on a solid surface, while the second, called the *secondary antibody*, is conjugated to a probe that is either an enzyme or a fluorescent or chemiluminescent moiety. If both antibodies are present in a so-called *one-step ELISA*, at high concentrations of antigen, excess antigen will bind to the secondary antibody in solution, blocking it from binding to any antigen captured by the capture antibody on the solid surface. Thus, the enzyme or fluorescent signal on the solid surface will be diminished, making it appear as if there is a low concentration of antigen (Barkan & Chandler, 1998; Petakov et al., 1998).

This effect does not occur if a wash step is performed prior to adding the secondary antibody; the wash step removes all excess antigen. Also, performance of homogeneous assays for PRL avoids the hook effect. If a hook effect is suspected, the sample should be diluted, often to levels of 1:1000, and then assayed. Typically, only a single dilution is performed when assaying for PRL in single-step ELISAs. It is preferable to utilize assays for PRL that avoid the hook effect.

BOX 25.3

Causes of Hyperprolactinemia

Physiologic
Sleep, stress, postprandially, pain
Coitus, pregnancy, nipple stimulation or nursing
Systemic disorders
Chest wall or thoracic spinal cord lesions
Primary or secondary hypothyroidism
Adrenal insufficiency
Chronic renal failure
Cirrhosis

Medications

Psychiatric medications: Phenothiazines, haloperidol, thioxanthenes, buspirone, olanzapine, risperidone, domperidone, monoamine oxidase inhibitors, fluoxetine, amitriptyline
Metoclopramide
Antihypertensives: labetalol, α-methyldopa, reserpine, verapamil
Antihistamines H_2: cimetidine, ranitidine
Estrogens, oral contraceptives, oral contraceptive withdrawal
Opiates: heroin, methadone, morphine, apomorphine
Thyrotroph (TRH)
Prolactin-secreting pituitary tumor: prolactinoma, acromegaly
Macroadenoma (compressing the pituitary stalk)
Macroprolactinemia
Pressure on or transection of the pituitary stalk, interrupting the transmission of dopamine to D_2 receptors on the lactotrophs: Surgery, traumatic transection, granulomas, metastases, meningioma, irradiation, histiocytosis X
Ectopic secretion of prolactin by nonpituitary tumors
Idiopathic
Polycystic ovarian disease
Epileptic seizures

If the pretest probability of the patient having a PRL-secreting tumor is high, it is recommended that the serum sample be subjected to serial dilutions or, at the least, a 1:100 dilution.

PRL acts on breast tissue where, in the setting of estrogen priming, it stimulates lactation. PRL also acts at the hypothalamus to inhibit the secretion of gonadotropin-releasing hormone (GnRH). Inhibition of GnRH results in a decrease in the release of LH and FSH from the anterior pituitary gland. In females, this leads to a decrease in estrogen and progesterone synthesis and secretion by the ovaries, along with failure of ovarian follicular maturation (ovulation). In males, a deficiency of FSH and LH causes a decrease in testicular production and synthesis of testosterone, along with a halt in spermatogenesis. It has also been suggested that hyperprolactinemia may stimulate adrenal androgen production and have an effect on immune responsiveness (Lobo et al., 1980; Walker et al., 1993).

The reference value for serum PRL is 1 to 25 ng/mL (1–25 μg/L) for women and 1 to 20 ng/mL (1–20 μg/L) for men. The higher PRL levels seen in females begin postpuberty and are presumably due to the stimulatory effect of estrogen (Eastman et al., 1996). During pregnancy, a progressive rise in serum PRL is observed, with levels reportedly reaching as high as 500 ng/mL by the third trimester (Rigg et al., 1977). This is largely due to an increase in the number of PRL-secreting cells and can be associated with a doubling or even greater increase in pituitary gland size (Scheithauer et al., 1990). PRL levels fall back to baseline about 3 weeks postpartum in women who are not breastfeeding. In nursing mothers, basal PRL levels remain moderately elevated, with episodic bursts in secretion in response to suckling.

PRL levels are increased by many physiologic and pathologic factors, as well as by a wide variety of medications (Box 25.3). Elevations in PRL resulting from physiologic and pharmacologic stimuli rarely exceed 200 ng/mL.

PRL deficiency can be seen with pituitary necrosis or infarction and in some cases of pseudohypoparathyroidism. In women with complete PRL deficiency, menstrual disorders and infertility have been found (Kauppila, 1997). It is PRL excess that is associated with clinical pathology. Hyperprolactinemia leads to inhibition of GnRH secretion, which typically manifests as sexual dysfunction and infertility in both men and women. Women may present with luteal phase abnormalities, oligomenorrhea, or frank amenorrhea, with or without galactorrhea. Men will present with hypoandrogenemia, decreased libido, and impotence. Pituitary adenomas are an important cause of hyperprolactinemia; however, any sellar or parasellar process that compresses the pituitary stalk and interrupts the tonic delivery of dopamine can lead to disinhibition of PRL secretion. Usually, the height of elevation of serum PRL levels correlates with the likelihood of the presence of a pituitary tumor; levels of

PRL in excess of 200 ng/mL almost always signify the presence of a prolactinoma (Kleinberg et al., 1977; Frantz, 1998; Freda & Wardlaw, 1999). Unlike other functioning pituitary tumors, the degree of elevation of PRL correlates fairly well with the size of the tumor.

Hyperprolactinemia exists in 20% to 40% of patients with acromegaly. This may be due to the presence of a mixed tumor (containing both lactotrophs and somatotrophs) or to interference with the normally active, PRL-inhibitory mechanisms (e.g., interruption of dopamine delivery owing to stalk compression by a tumor, resulting in disinhibition of PRL secretion). Another important cause of hyperprolactinemia is hypothyroidism. Thyrotropin-releasing hormone (TRH) not only stimulates TSH secretion but it also stimulates PRL secretion, thus explaining the mild hyperprolactinemia seen in both primary (thyroid) and secondary (pituitary) hypothyroidism. Therefore, thyroid function tests (free thyroxine [FT_4] and TSH) are always indicated to rule out hypothyroidism when a patient with hyperprolactinemia is evaluated. Thyroid hormone replacement therapy will usually return the PRL level to normal.

It is important to evaluate all patients discovered to have an abnormally elevated PRL. Since hyperprolactinemia can be found in upward of 40% of cases of acromegaly, it is appropriate to measure insulin-like growth factor (IGF)-1. Other hormones that may be assayed include FSH, LH, free testosterone, estradiol, and, if clinically indicated, tests of adrenal axis function. Rarely, hyperprolactinemia may be caused by ectopic hormone production. All patients should undergo computed tomography (CT) or magnetic resonance imaging (MRI) of the sella, performed with and without contrast. If there are no contraindications, MRI is preferred, as it provides better contrast and anatomic detail, is better for visualizing microadenomas, and is safer for serially monitoring patients since there is no exposure to radiation. A formal visual field examination is also a key monitoring tool in managing patients with pituitary tumors and should be done at least yearly in patients with stable disease.

GROWTH HORMONE

GH is a single-chain polypeptide of 191 amino acids synthesized, stored, and secreted by the somatotrophs of the pituitary gland in response to the secretion of growth hormone–releasing hormone (GHRH) by the hypothalamus. Somatostatin, also produced by the hypothalamus, inhibits GH synthesis and release. Although evidence exists for the direct action of GH on long bone growth in children, most of its anabolic and metabolic actions are mediated indirectly through an intermediary, IGF-1 (also called *somatomedin C*). IGF-1 is synthesized in the liver and in certain target tissues in response to stimulation by GH. IGF-1 circulates in the blood complexed to IGF-binding proteins (IGF-BPs); IGF-BP3 is the predominant circulating species. As with all hormones, it is the free, unbound form that is biologically active. Like somatostatin, IGF-1 negatively feeds back on the pituitary gland to inhibit GH secretion.

GH is secreted in a pulsatile fashion; the frequency and amplitude of the peaks are greatest during puberty, exhibiting a steady decline with increasing age (Casanueva, 1992). As up to 70% of GH secretion occurs during stage 4 (slow-wave) sleep, it has been suggested that the age-related decline in stage 4 sleep may account for the decline in GH seen with aging (Van Cauter, 2000; Van Cauter et al., 1998). In addition to GHRH and somatostatin, several other factors regularly mediate GH secretion (Fig. 25.2). Major stress (e.g., surgery, sepsis), fasting, sex steroids, chronic malnutrition, apomorphine, levodopa, uncontrolled diabetes mellitus, and high-protein meals all stimulate GH secretion. Women tend to have higher GH levels than men, perhaps because of estrogen sensitization of the hypothalamus to other GH stimuli (Eastman et al., 1996).

Serum GH is undetectable for most of the day in healthy, nonstressed individuals. This fact, along with the episodic nature of GH secretion, makes a single sampling difficult to interpret. As a result, the diagnosis of GH deficiency is

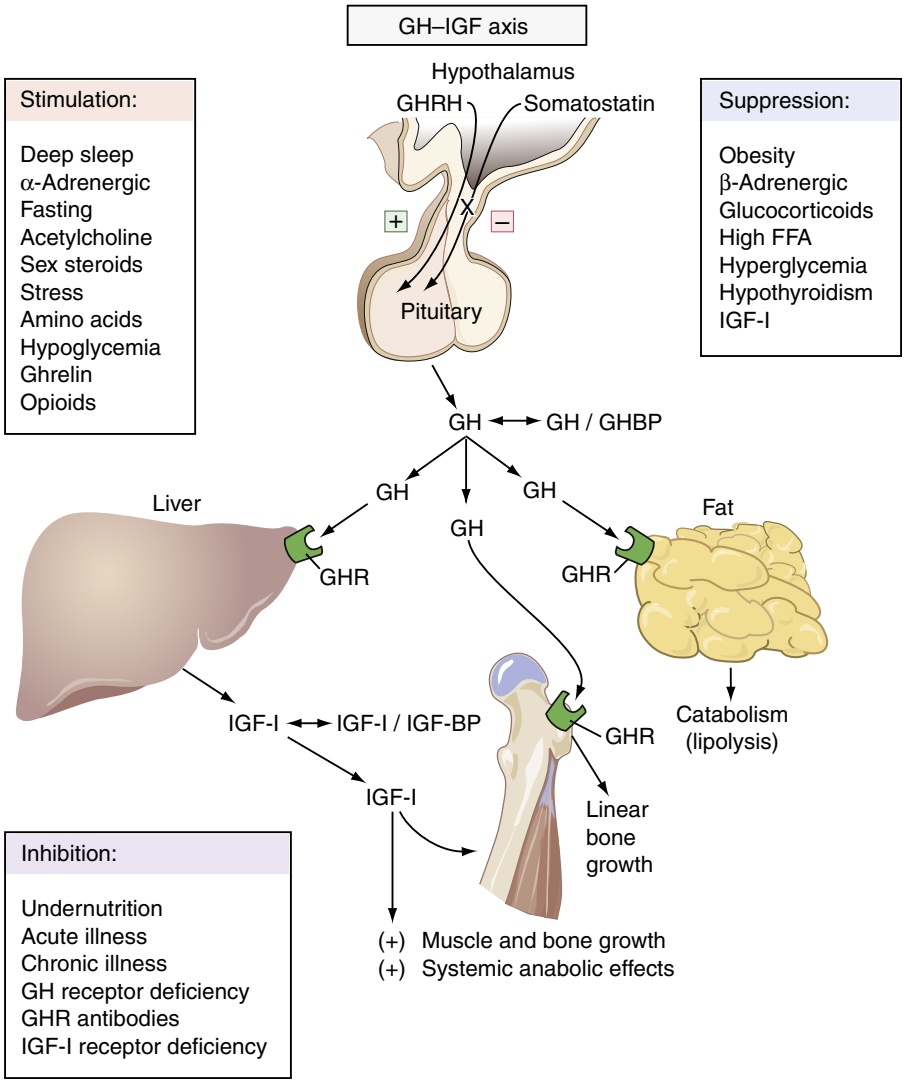

Figure 25.2 Hypothalamic-pituitary-growth hormone axis. Feedback loop influencing GH-IGF-1 secretion and action. *FFA,* Free fatty acid; *GH,* growth hormone; *GHBP,* growth hormone–binding protein; *GH-IGF,* growth hormone–insulin-like growth factor; *GHR,* growth hormone receptor; *GHRH,* growth hormone–releasing hormone; *IGF-1,* insulin-like growth factor-1; *IGF-BP,* IGF-binding proteins. (From Melmed S, Kleinberg D: Anterior pituitary. In Larsen PR, Kronenberg HM, Melmed S, et al., editors: Williams textbook of endocrinology, ed 10, Philadelphia, 2003, Saunders, p 221, with permission.)

made using GH measurements following pharmacologic stimulation, and GH excess is confirmed by failure of GH suppression following an oral glucose load. GH is commonly measured by chemiluminescent immunoassay.

Somatostatin is synthesized in the paraventricular and arcuate nuclei of the hypothalamus. It inhibits GH and TSH secretion. It also inhibits the secretion of insulin and several gut hormones (e.g., motilin, secretin, gastrin). Ghrelin, a 28–amino acid peptide produced by the gastric neuroendocrine cells and the hypothalamus, binds to the GH secretagogue receptor to stimulate the secretion of GHRH and GH.

Growth Hormone Deficiency

Idiopathic growth hormone deficiency is the most common cause of GH deficiency (GHD) in children, whereas a pituitary adenoma is the most common etiology in adult-onset GHD. No simple reproducible method for determining abnormal GH secretory patterns exists. In healthy normal individuals, 70% to 80% of GH results are below 1 ng/mL (<1 μg/L), and secretory peaks typically reach 20 to 40 ng/mL (20–40 g/L) (Baumann, 1987). Thus, in a child with decreased growth velocity, a low or nondetectable GH does not necessarily indicate GHD. Similar to GH, IGF-1 declines with age. IGF-1 is more diagnostically useful in patients younger than 40 years of age; however, it is still not sensitive enough to be used as a standalone test to make the diagnosis of GHD (Almeretti et al., 2003). Manipulation of the endocrine system through stimulation and suppression of the various axes is often required for diagnosing conditions of hormonal deficiency and surfeit. In this vein, GHD is diagnosed by showing failure of GH to increase adequately in response to pharmacologic stimulation. Several endocrine organizations have published guidelines on GH deficiency, detailing which patients to test, which test to utilize, and what cutoffs to apply (Ho & Ho, 2007; Casanueva et al., 2009). The insulin tolerance test (ITT) has long been considered the gold standard for diagnosing GHD. However, it is most unpleasant for the patient, requires the attendance of a physician throughout the testing period, and is contraindicated in those with a history of seizures or cardiac or cerebrovascular disease. Failure of GH to rise above 3 to 5 ng/mL in adults when glucose drops to <40 mg/dL (Melmed, 2019, Fleseriu M 2016) and above 10 ng/mL in children is considered to be abnormal. In patients unable to undergo an ITT and in those needing a second confirmatory test, arginine stimulation alone or in combination with GHRH is usually the next step. Combination testing with GHRH plus arginine was preferred, as many normal adults failed stimulation with arginine alone (Biller et al., 2002), however since GHRH is no longer commercially available in the United States, the glucagon stimulation test (GST) has become the accepted alternative. The mechanism by which glucagon stimulates GH release is not well understood. In this test, glucagon is administered IM to the patient, and GH serum levels are determined every 30 minutes over a 4-hour period. GH usually peaks after 120 to 180 minutes. The initial dose given depends on the BMI. For BMI ≤25 mg/M_2, a dose of 1 mg is given; for BMI values >25 mg/M_2, a dose of 1.5 mg is given. GHD is diagnosed by failure of GH to rise above 3 μg/L (a lower cut-point of 1 μg/L in overweight/obese patients improves sensitivity and specificity) (Yuen et al., 2019). Two caveats about this test should be noted: (1) glucagon is contraindicated in patients with pheochromocytoma, and (2) no studies have been performed in patients with diabetes or pre-diabetes (see Chapter 17), so the diagnostic accuracy of this test in these patients has not been established (Yuen, 2011). Common side effects of GST included nausea, vomiting, and delayed hypoglycemia. Glucagon is contraindicated in persons with pheochromocytoma. Other pharmacologic stimuli such as L-dopa, clonidine, and arginine are weak GH secretagogues requiring even lower cutoff points for diagnosis and are not widely recommended for use in the United States (Yuen, 2016). No studies have been performed in persons with diabetes or prediabetes, and therefore the diagnostic accuracy in these populations remains unclear (Yuen, 2011). Other methods to assess for GHD include 24-hour or nighttime monitoring of GH, and provocative tests using clonidine or L-dopa. All of these tests carry significant individual variability. They have not been systematically studied and are used mainly in the pediatric population (Rose et al., 1988).

Because body mass index (BMI) affects the GH response to stimulation with GHRH plus arginine, newer guidelines recommend the use of GH cutoffs based on BMI for interpretation of results (Cook et al., 2009). There are two settings in which an argument can be made against the need to test for GHD. The first is in patients with known pituitary disease who have a low IGF-1 level. The other scenario is in patients with evidence of three or more pituitary hormone deficiencies; studies have shown these patients to have a greater than 96% chance of having GHD (Hartman et al., 2002).

Because of perceived and actual deficiencies in these tests, the ghrelin-receptor agonist test is a current avenue of investigation. Ghrelin, sometimes called the "hunger hormone," is produced by the stomach. Release of ghrelin increases appetite, stimulates the release of GH, and regulates glucose metabolism. Ghrelin has been shown to stimulate growth hormone release through the growth hormone secretagogue receptor (GHSR)1a in the anterior pituitary and hypothalamus (Muller et al., 2015). Macimorelin acetate is an oral ghrelin receptor agonist. When administered in an oral form at 0.5 mg/kg, macimorelin is readily absorbed and stimulates GH secretion with good tolerability (Garcia, 2013). It has been shown to be a reproducible safe diagnostic test for adult growth hormone deficiency, with accuracy comparable to that of the ITT (Garcia, 2018). In a post hoc analysis, using a GH cutoff of 5.1 ng/mL, it showed 92% sensitivity and 96% specificity (Garcia, 2018). A GH cutoff of ≤2.8 μg/L is suggested by the AACE 2019 guidelines (Yuen et al., 2019).

For children, it is common to use exercise testing in screening for GHD. Further testing is not indicated if the results are normal. However, if GH fails to increase adequately, pharmacologic testing is warranted (Eddy et al., 1974). Healthy children may not respond to any single GH provocative test; therefore, GHD in childhood is defined by failure of serum GH to reach defined levels when at least two different pharmacologic stimuli are used. IGF-1 measurements have been used to screen for GHD in children; however, since a variety of factors can decrease IGF-1, it is not used to confirm the diagnosis of GHD. IGF-1 levels decline in malnutrition, hypothyroidism, hepatic disease, uncontrolled diabetes mellitus, renal disease, and with age. Levels of IGF-BP3 usually parallel those of IGF-1 and are often low in GHD. However, results falling within the reference range do not exclude the diagnosis of GHD. Up to 18% of subjects with GHD may have normal IGF-1 levels. Care should be taken when interpreting values for IGF-1, IGF-BP3, and GH because the assays themselves and the cutoffs used to define normal differ greatly between laboratories. To address these issues, there is a move to have laboratories utilize a World Health Organization international standard for GH and IGF-1 and to create a normative range from a statistically valid control group (Giustina et al., 2010).

It is important to understand the difference in the physiology behind testing with GHRH as compared to the other secretagogues. ITT and arginine stimulate the production of GHRH; clonidine increases GH secretion by inhibiting the release of somatostatin. For these stimuli to elicit a rise in GH, the hypothalamus must be intact. When GHRH is used for testing, the hypothalamus is bypassed and the pituitary gland is directly stimulated; therefore, it is possible to miss up to 50% of patients who have tertiary (hypothalamic) GHD.

Individuals with childhood-onset idiopathic GHD are less likely to have permanent GHD. It is recommended that unless they have a known genetic mutation, embryopathic lesion, or irreversible lesion/damage to the pituitary gland/hypothalamus, they should be taken off GH replacement and retested when they reach early adulthood (Molitch et al., 2006).

Growth Hormone Excess

Growth hormone overproduction can result in the condition called **acromegaly**. If the condition develops before closure of the epiphyses, these individuals may be exceedingly tall (**gigantism**). More commonly, it presents during adulthood, causing diffuse enlargement of soft tissues and organs throughout the body. Characteristic features include prognathism, frontal bossing, and spade-like hands. The screening test for clinically suspected acromegaly is a randomly collected IGF-1. A normal IGF-1 with respect to the appropriate age- and gender-matched reference ranges rules out the diagnosis of acromegaly (Katznelson et al., 2014). However, it should be noted that a physiologic increase in IGF-1 may be seen during pregnancy and late-stage adolescence (Katznelson et al., 2014). If the level of IGF-1 is elevated or borderline with respect to the appropriate age- and gender-related reference range, it becomes necessary to confirm the diagnosis using an oral glucose tolerance test (OGTT). The OGTT is performed by obtaining baseline blood samples for glucose and GH, administering 75 g of glucose orally, and then obtaining blood for glucose and GH every 30 minutes over the next 2 hours. A normal response is suppression of GH to <1 ng/mL (1 μg/L) at any time during the test. If GH fails to drop to below 1 ng/mL (1 μg/L), the patient is diagnosed as having acromegaly (American Association of Clinical Endocrinologists, 2004; Zahr, 2018, Katznelson, 2014). GH may fail to adequately suppress in the setting of puberty, uncontrolled diabetes mellitus, malnutrition, hepatic disease, and renal disease. However, all but puberty are associated with a normal serum IGF-1 (Katznelson et al., 2011).

The difficulty comes in diagnosing mild disease. Freda had studied 60 postoperative patients with acromegaly, 22 patients with active disease (elevated IGF-1), 38 patients in remission (normal IGF-1), and 25 healthy controls. The highest nadir GH was 0.13 μg/L in the controls and 0.3 μg/L in those with active disease. Of those with active disease, 50% had GH values <1 μg/L, leading to misclassification of these individuals as being normal when the criterion of a GH value <1 μg/L was applied (Freda et al., 1998; Trainer, 2002). In a more recent study of 16 patients with mild disease (the majority having microadenomas), Dimaraki and colleagues (2002) found that 50% of patients with acromegaly were able to suppress their GH levels to <1 μg/L following an OGTT. A proposed reason for these patients with

active disease showing normal suppression is that they may have subtle changes in GH secretion that are not elicitable using this short suppression test. To address this issue, the following suggestion has been proffered (Trainer, 2002). If the initial random IGF-1 is normal and GH is <0.3 μg/L, then acromegaly is excluded. If either test is abnormal, repeat the IGF-1 and proceed to an OGTT. Failure of GH to be suppressed below 0.3 μg/L, accompanied by an elevated IGF-1, is diagnostic of acromegaly. Suppression of GH below 0.3 μg/L with normal IGF-1 excludes acromegaly. For those who adequately suppress their GH but have an elevated IGF-1, close follow-up is recommended (Trainer, 2002). Oral, but not transdermal, estrogen can reduce IGF-1 concentrations (Giustina et al., 2010); therefore, temporarily withholding oral estrogen therapy during testing may be prudent.

Acromegalic patients may show a paradoxical rise, an absent response, or a partial decline in GH in response to an OGTT (Ezzat, 1997). Random GH sampling is not adequate to establish the diagnosis of acromegaly because considerable overlap in GH exists between healthy persons and patients with the disease. In addition, GH can be increased in patients with a number of disorders, including renal disease, cirrhosis, malnutrition, and uncontrolled diabetes mellitus, as well as in patients under physical or emotional stress. Although larger adenomas are generally associated with higher GH levels, the correlation between GH levels and acromegalic manifestations is poor. In most patients with untreated acromegaly, GH levels remain above basal levels throughout the day, ranging from 10 to 100 ng/mL (10–100 μg/L). Serum GH levels in excess of 50 to 100 ng/mL (50–100 μg/L) are virtually never seen in nonacromegalic persons (Barkan, 1989). Other diagnostic maneuvers using TRH, GnRH, and GHRH yield discordant results in about 50% of patients with acromegaly. Therefore, their use for diagnostic purposes or for monitoring disease activity is not recommended (American Association of Clinical Endocrinologists, 2004). In patients with documented acromegaly but no evidence of a pituitary tumor, GHRH should be measured to detect a hypothalamic or ectopic source for acromegaly.

Patients treated for acromegaly require lifelong monitoring for disease activity. Patients treated with surgery or radiation can be monitored by the GH response to OGTT and a random IGF-1 measurement. The goal of therapy is to normalize IGF-1 and suppress the GH response to OGTT to <1 ng/mL (<1 μg/L). Several studies have shown that when these goals are attained, mortality rates become comparable with those of the normal population (Swearingen et al., 1998; Holdaway et al., 2004; Rajasoorya et al., 1994; Orme et al., 1998). If an ultrasensitive assay is available, an OGTT GH nadir of <0.4 μg/L can be used. However, this lower cutoff has not been demonstrated to improve metabolic outcome or better diagnose remission (Melmed, 2018; Ku, 2016). As mentioned previously, caution is required in interpreting IGF-1 levels in women on oral but not topical estrogen treatment, as oral estrogens lower IGF-1 concentrations (Giustina et al., 2010). For patients on somatostatin receptor analogs, monitoring is performed by measuring GF-1 and GH just prior to the next treatment dose. Patients on GH receptor blockers are monitored by a random IGF-1 alone. In rare instances, acromegaly may be due to ectopic secretion of GHRH (e.g., bronchial carcinoid, pancreatic islet cell tumors, small cell lung cancer), in which case the measurement of GHRH may be useful.

POSTERIOR PITUITARY HORMONES

Oxytocin and vasopressin (see Chapters 9 and 15) are the two major hormones of the posterior pituitary gland. They each have distinct physiologic roles, with partially overlapping effects in stimulating smooth muscle contraction and in maintaining water homeostasis. They are small oligopeptides, each composed of nine amino acid residues with a total mass of about 1 kDa. They are synthesized in the nerve cell bodies within the hypothalamus and are transported along axons to the nerve terminals within the posterior pituitary gland, where they are stored in secretory granules. Neuronal action potentials originating in the hypothalamus are conducted along the axons, resulting in degranulation of the vesicles and release of oxytocin and vasopressin into the perivascular space and ultimately into the circulation. Unlike the anterior pituitary gland, the posterior pituitary gland is little more than a repository where hormones are held until they are secreted. Accordingly, disruption of the infundibular stalk or destruction or removal of the posterior pituitary gland does not necessarily result in complete loss of these hormones, as they are produced in the hypothalamus.

Oxytocin

Oxytocin secretion is stimulated by stretching of the cervix and vagina during parturition; this is known as the Fergusson reflex. Oxytocin contributes to uterine contractions late in labor both by direct action on the myometrium and by stimulation of prostaglandin secretion by the decidua (Fuchs et al., 1982). It also plays a role in hemostasis at the placental site following delivery. Throughout pregnancy, estrogen upregulates the numbers of oxytocin receptors on the uterus and decidua, resulting in increased sensitivity to oxytocin toward the end of the term.

Oxytocin stimulates the myoepithelial cells surrounding the mammary glands and lactiferous ducts to contract, resulting in milk ejection. In response to suckling, neurogenic stimuli are transmitted from the nipple to the third, fourth, and fifth thoracic nerves, to the spinal cord, to the midbrain, and on to the hypothalamus, where oxytocin release is triggered. Psychological stimuli can bypass this pathway, with bursts of oxytocin secretion occurring with anticipation of nursing or on hearing a baby cry (Jenkins & Nussey, 1991; Yokoyama et al., 1994). Stressful situations can inhibit its secretion, resulting in decreased milk ejection.

Pathologic conditions associated with oxytocin excess or deficiency are rare and are limited to case reports. Its function in males remains unknown. Clinical demand for the measurement of oxytocin levels is extremely rare. Because it has a half-life of 3 to 5 minutes and is subject to rapid degradation by oxytocinase, individual reference laboratory procedures for its collection must be strictly adhered to if meaningful results are to be obtained.

Arginine Vasopressin/Antidiuretic Hormone

AVP (ADH) is synthesized within the paraventricular and supraoptic nuclei of the hypothalamus. The major function of ADH is to maintain osmotic homeostasis by regulating water balance. It does this by stimulating the V2 receptors on principal epithelial cells that line the cortical collecting ducts of the kidney. As discussed in Chapter 15, ADH induces an increase in the production of cyclic adenosine monophosphate (cAMP), which, in turn, causes the water channels (aquaporins) to fuse with the apical membrane of the principal cells, increasing water permeability and reabsorption. At much higher blood concentrations, AVP also acts as a potent pressor by causing vasoconstriction (V1 receptor), stimulates ACTH secretion from the anterior pituitary gland, and stimulates the production of clotting factor VIII.

ADH secretion is modulated by changes in serum osmolality and by alterations in intravascular volume. Changes in plasma osmolality are detected by osmoreceptors located within the anterior hypothalamus. Plasma ADH rises and falls in direct proportion to the serum osmolality. A concordantly linear relationship exists between ADH and the urine osmolality (Uosm). The Uosm is capped at about 1200 mOsm/kg, the maximum Uosm allowed by the renal medullary concentration gradient.

ADH secretion is maximally stimulated at a serum osmolality greater than 295 mOsm/kg and is suppressed when the osmolality falls below 284 mOsm/kg. Thirst can be considered the fail-safe mechanism for fluid and osmotic homeostasis, as it is initiated at a greater plasma osmolality (Posm) than is needed to stimulate ADH secretion. The thirst receptors are located within the hypothalamus and are distinct from the osmoreceptors that stimulate ADH secretion.

Changes in intravascular volume are detected by baroreceptors. There are two sets of baroreceptors: low-pressure volume receptors located in the right atrium and pulmonary venous system, and high-pressure arterial baroreceptors located in the carotid sinus and aortic arch. These receptors are normally under tonic inhibition; a drop in intravascular volume removes the inhibition and results in a rise in ADH, leading to increased water reabsorption. ADH secretion is much more sensitive to changes in osmolality than to changes in intravascular volume. A 1% to 2% increase in osmolality will cause a rise in ADH secretion. A much greater stimulus, such as a 5% to 10% drop in blood volume or blood pressure, is needed before the baroreceptors trigger the release of ADH.

In addition to changes in osmolality and intravascular volume, other physiologic factors that can stimulate ADH secretion include nausea, cytokines, interleukin (IL)-6, hypoglycemia, hypercarbia, and nicotine (Reihman et al., 1985; Masrorakos et al., 1994).

Basal plasma vasopressin normally ranges from 0.5 to 2 pg/μL. In concert with atrial natriuretic hormone, thirst, and the renin-angiotensin-aldosterone axis, ADH works to maintain blood pressure, volume, and tonicity. Accordingly, when a patient is evaluated for a disorder of water homeostasis, these multiple interactive factors must be taken into consideration. Normal plasma osmolality ranges from 280 to 295 mOsm/kg and plasma sodium from 135 to 145 mmol/L. It can be determined directly by measuring the plasma freezing-point depression or the plasma vapor pressure. It can also be determined indirectly, by measuring the plasma sodium, blood urea nitrogen (BUN), and glucose, and applying the following formula (also, see Chapter 9):

$$plasma\ osmolality = \left\{2 \times [Na]\left(\frac{mmol}{L}\right)\right\} + \left\{Glucose\frac{\left(\frac{mg}{dL}\right)}{18}\right\} + \left\{BUN\frac{\left(\frac{mg}{dL}\right)}{2.8}\right\} \quad \text{(Eq. 25.1)}$$

This equation is discussed at length in Chapters 9 and 15.

Because sodium is the major plasma solute, hyponatremia is tantamount to hypoosmolality. There is usually excellent agreement between the

directly measured and calculated osmolality. However, there are two situations when this does not hold true: in pseudohyponatremia (also termed *factitious hyponatremia*), and in the presence of high concentrations of other effective solutes. In pseudohyponatremia, the plasma volume is displaced by the presence of high concentrations of lipids or proteins (e.g., hyperglobulinemia), resulting in a low plasma concentration of Na+, although the activity of Na+ in water is normal. In these instances, if Na+ is directly measured with an ion-specific electrode (ISE), the activity reading is normal. In order to extend electrode life, laboratories using high-throughput analyzers generally perform ISE measurements on diluted plasma (so-called indirect ISE measurement), making the resultant plasma concentration measurement vulnerable to pseudohyponatremia. The measured Posm is unaffected by the presence of hyperlipidemia or paraproteinemia, as the concentration of solute particles per volume of fluid is unchanged.

The presence of high concentrations of osmotically active solutes—such as glucose, radiographic contrast agents, mannitol, and ethylene glycol—causes a shift of water from the intracellular to the extracellular compartment, leading to dilutional hyponatremia (this situation, though quite different from that described earlier, is also sometimes referred to as *pseudohyponatremia*). Similar translocational hyponatremia occurs with the absorption of glycine during transurethral prostate resection as well as in gynecologic and orthopedic procedures (Ayus & Arieff, 1997; Hahn, 2001). The calculated Posm is unreliable in these situations; Posm must be measured directly instead. A difference between the calculated and measured Posm of greater than 10 mOsm/kg supports the presence of pseudohyponatremia or other osmolar solutes (Kumar & Berl, 1998). The most common situation causing a large "osmolal gap" is ethanol intoxication.

In hyperglycemia, the measured Na+ should be corrected by the addition of 1.6 mmol/L for each 100-mg/dL increase in serum glucose above normal (100 mg/dL). A more recent analysis suggested that this formula may underestimate the decrease in Na+ caused by hyperglycemia and supported the use of a 2.4-mmol/L correction factor (Hillier et al., 1999). True hyponatremia is present if, after the correction formula is applied, the serum Na+ is still <135 mmol/L.

During pregnancy, there is a resetting of the osmostat, with a drop in osmolality of approximately 10 mOsm/kg (Lindheimer & Davison, 1995). The precise mechanism for this is not known; however, studies have suggested a role for the hormone relaxin and for the enzyme oxytocinase. During pregnancy, there is a progressive increase in placental production of oxytocinase, which, in addition to breaking down oxytocin, breaks down vasopressin, possibly resulting in a change in the hypothalamic AVP osmolality feedback loop.

Diabetes Insipidus

Diabetes insipidus (DI) is classified as being either central (due to absent or decreased ADH secretion from the hypothalamus or neurohypophysis) or nephrogenic (due to renal resistance to the actions of ADH). Each is further subcategorized as being complete or partial. All variants are characterized by the passage of large volumes of dilute urine (>2.5 L/day) in the face of an inappropriately elevated Posm. Provided that the thirst mechanism is intact and there is free access to water, most individuals can avoid dehydration and maintain a normal Posm and serum sodium levels.

The water deprivation test is the preferred diagnostic test for identifying the presence of DI (Table 25.2). Central and nephrogenic DI can be distinguished by the response to either endogenous or exogenous vasopressin (Table 25.3). In neurogenic DI, ADH levels are low and the kidney rapidly acts to conserve water in response to exogenous ADH administration. In contrast, nephrogenic DI is associated with normal or increased levels of ADH, and administration of additional ADH has little or no effect on renal water reabsorption. Differentiating partial nephrogenic DI from primary polydipsia can be more difficult. Unlike DI, in which the underlying problem is difficulty in holding on to free water, in primary polydipsia the pathophysiology arises from increased intake of fluids. Primary polydipsia (PP) can be due to either dipsogenic DI or psychogenic polydipsia. In dipsogenic DI, the setpoint for ADH secretion is normal; however, a resetting of the thirst threshold occurs so that it is now below the threshold for ADH secretion. In psychogenic polydipsia, the osmostat for ADH secretion is normal. However, because of underlying psychiatric illness, the subject has a compulsion to drink excessive volumes of liquid. This intake of copious volumes of fluid as seen in PP leads to a washout in the medullary concentrating gradient within the kidney, resulting in a decreased ability to concentrate the urine in response to dehydration. Differentiating between nephrogenic DI and PP, as well as among those who have an equivocal response to ADH, is best achieved by plotting the basal and postdehydration Uosm and plasma ADH on nomograms created by Zerbe and Robertson (Figs. 25.3 and 25.4) (Zerbe & Robertson, 1981, 1987). Direct measurement of plasma ADH may be helpful in confirming the diagnosis of a pathologic ADH deficiency or excess in the presence of a known or suspected disorder of renal function or fluid and electrolyte homeostasis, or when a patient is unable to tolerate physiologic testing. In cases of congenital DI, family members who are heterozygote carriers of ADH gene mutations may be identified by demonstrating decreased ADH levels, which may be the only subclinical manifestation of ADH deficiency.

Due to instability of ADH (Morgenthaler, 2006), low accuracy (38%) in differentiation between DI and PP (Fenske, 2012), and the lack of a clinically useful description of the relationship between plasma AVP levels and osmolality (Zerbe, 1981), other avenues for diagnosing DI vs. PP have been sought. Among ADH biomarkers is copeptin, the 39 amino-acid C-terminal segment of pre-pro-arginine vaspression. It is secreted in response to the same stimuli as AVP and in equimolar amounts to AVP. Its high ex-vivo stability and ease of measurement make it an excellent surrogate for AVP. The normal range for copeptin is 1.0-13.8 pmol/L, with a higher median value seen in men (Morgenthaler, 2006). A baseline copeptin level of >21.4 pmol/L (without pre-thirsting) is considered diagnostic of nephrogenic DI (Timper, 2015). Measurement of copeptin in conjunction with the hypertonic infusion test has been shown to be superior to the standard water deprivation test in distinguishing PP from central DI, with a diagnostic accuracy of 97% when using a cutoff of >4.9pmol/L. In complete and partial DI the copeptin is ≤4.9 pmol/L and >4.9 pmol/L in PP with a sensitivity of 93.2% and specificity of 100% (Fenske, 2018). In CKD, P(cop) and P(vp) both increased with decreasing estimated glomerular filtration rate (eGFR), but

TABLE 25.2

Water Deprivation Test for Diagnosing and Classifying Diabetes Insipidus

Patients with mild polyuria may be instructed to withhold all fluid intake from 10 PM onward. For those with more severe polyuria (8 to 10 L/day), water deprivation should be started early in the morning under close observation.

1. During testing, the patient is forbidden to take in anything by mouth.
2. Obtain the following baseline parameters: urine volume (Uvol) and urinary osmolality (Uosm), plasma osmolality (Posm), and plasma sodium (PNa). Also, record the weight and blood pressure (BP)/pulse (P) seated and standing.
3. Urine and plasma are collected hourly for Uvol, Uosm, and Posm. Weight, BP, and P are also recorded. Record requests for fluid.
4. When the Uosm has plateaued (e.g., hourly increase <30 mOsm/kg for 3 consecutive hours), or when body weight has decreased by 3% to 5%, or the patient develops a >20–mmHg drop in systolic BP, obtain samples for Uvol, Uosm, Posm, PNa, and AVP (plasma).
5. Administer 1 μg of desmopressin IV or IM, or 5 μg of AVP SC Uosm; urine output and Posm are recorded at 30, 60, and 120 minutes after the injection. The highest Uosm value is used to evaluate the patient's response to AVP.

Precautions

When possible, discontinue any medications that can influence ADH secretion. Observe for hypotension and nausea, which may stimulate ADH secretion. The patient should not be permitted to smoke during the test.

Interpretation

Normal	Final Uosm before AVP challenge is higher than Posm. Following AVP challenge, the Uosm is less than 10% higher than the maximal Uosm achieved with water restriction alone.
Neurogenic DI	Final Uosm before AVP challenge is less than Posm. Following AVP administration, there is a greater than 50% increase in Uosm.
Nephrogenic DI	Final Uosm before AVP challenge is less than Posm. Following AVP administration, there is a less than 10% increase in Uosm.
Partial central DI	Uosm may be higher than Posm following dehydration; however, there is only a 10% to 50% increase in Uosm following administration of AVP.
Partial nephrogenic DI	Uosm may be higher than Posm following dehydration; however, there is a greater than 10% increase in Uosm following administration of AVP.

Plotting basal and postdehydration Uosm and plasma ADH on the nomograms from Zerbe and Robertson will permit further distinction between partial nephrogenic DI, partial central DI, and primary polydipsia (see Figs. 25.3 and 25.4).

ADH, Antidiuretic hormone; *AVP,* arginine vasopressin; *DI,* diabetes insipidus; *IM,* intramuscular; *IV,* intravenous; *SC,* subcutaneous.

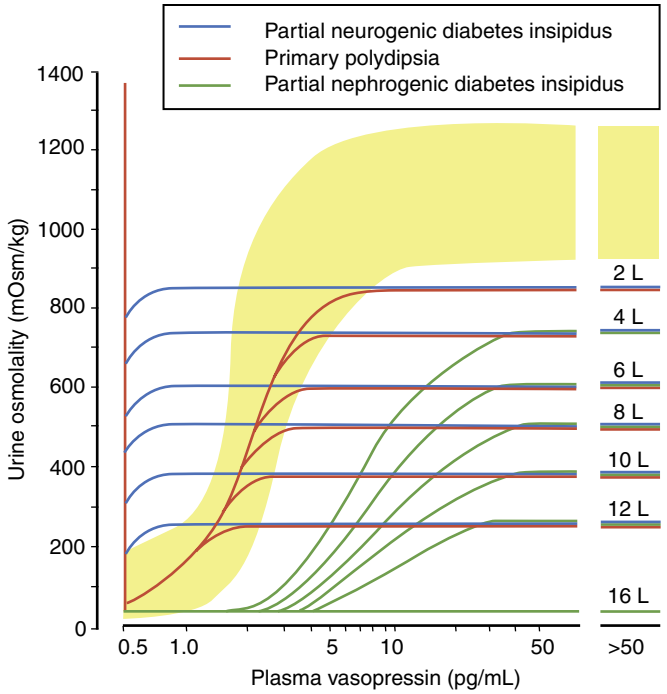

Figure 25.3 The relationship between urine osmolality (Uosm) and plasma arginine vasopressin (AVP/ADH) in patients with polyuria of diverse causes and severity. Each of the three categories of polyuria is described by its own family of sigmoid curves of differing heights. Differences in height within a family reflect differences in maximum concentrating capacity caused by "washout" of the medullary concentration gradient. They are proportional to the severity of the polyuria (indicated in liters per day at the right end of each plateau). The normal response is depicted in yellow. The three categories of polyuria differ principally in the ascending portion of the dose-response curve. In patients with partial neurogenic diabetes insipidus (DI), the curve lies to the left of normal, reflecting increased sensitivity to the antidiuretic effects of very low concentrations of plasma ADH. In contrast, in patients with partial nephrogenic DI, the curve lies to the right of normal, reflecting decreased sensitivity to ADH. In primary polydipsia, the relationship of Uosm to ADH remains relatively normal. (Redrawn from Bichet DG: Diabetes insipidus and vasopressin. In Moore WT, Eastman RC, editors: Diagnostic endocrinology, ed 2, St. Louis, 1996, Mosby, p 158, with permission.)

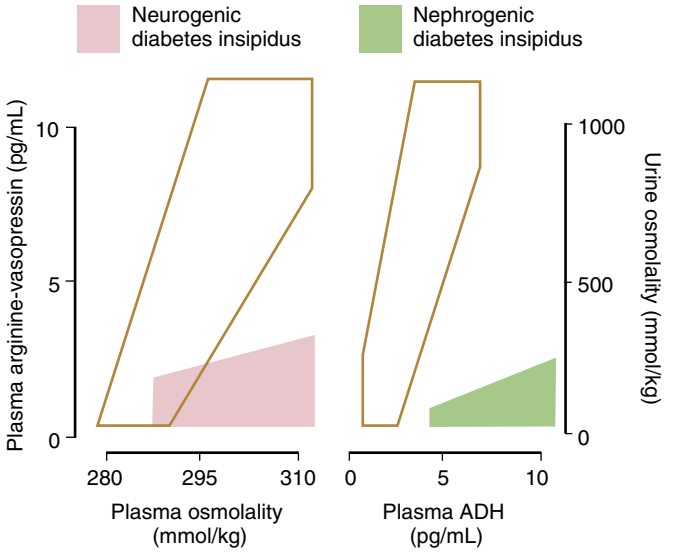

Figure 25.4 *Left,* Relationship between plasma arginine vasopressin (AVP/ADH) and plasma osmolality during the infusion of hypertonic saline. Patients with primary polydipsia and nephrogenic diabetes insipidus (DI) have values within the normal range *(open area)* in contrast to patients with neurogenic DI, who show a subnormal plasma ADH response to a rise in osmolality *(pink). Right,* Relationship between urine osmolality and plasma ADH during dehydration and water loading. Patients with primary polydipsia and neurogenic DI have values within the normal range *(open area)* in contrast to patients with nephrogenic DI, who have hypotonic urine despite high plasma ADH *(green).* (Redrawn from Bichet DG: Diabetes insipidus and vasopressin. In Moore TW, Eastman RC, editors: Diagnostic endocrinology, ed 2, St. Louis, 1996, Mosby, p 168, with permission.)

P(cop) increased much faster than P(vp) (Fenske, 2018; Ronan, 2014). Copeptin also rises in acute illness, myocardial infarction, and stroke. Another proposed approach is copeptin measurement following stimulation by arginine infusion, which has the advantage of already being a standard clinical test used to evaluate GHD and has been shown to differentiate between DI and PP with high accuracy (95%) (Winzeler 2019).

Nephrogenic DI is either congenital or acquired. An X-linked receptor defect is the most common etiology for congenital nephrogenic DI; medications are the most common cause of acquired nephrogenic DI (Holtzman & Ausiello, 1994). Medications known to be associated with acquired nephrogenic DI include lithium, demeclocycline, and methoxyflurane anesthetics. Other causes of acquired nephrogenic DI include hypercalcemia, hypokalemia, sickle cell disease, and postobstructive uropathy (Box 25.4).

Neurogenic DI may be congenital, the result of an autosomal-dominant mutation in the ADH signal peptide or in the exons that code for neurophysins (McLeod et al., 1993; Yuasa et al., 1993). More commonly, neurogenic DI is induced by lesions affecting the hypothalamus (metastatic tumors, trauma, granulomatous disorders) or medications. Drugs that may cause neurogenic DI by suppressing ADH release include phenytoin (Dilantin), chlorpromazine, and α-adrenergic agonists. It has been suspected that autoantibodies directed against the ADH-producing cells of the hypothalamus may be responsible for some cases of idiopathic neurogenic DI (De Bellis et al., 1994, 1999; Maghnie et al., 2000). These antibodies are detectable by indirect immunofluorescence antibody.

Another common condition in which decreased ADH levels have been found is primary nocturnal enuresis in children. Although these patients have ADH levels only slightly lower than controls (2.9 ng/L vs. 3.6 ng/L), the clinical symptoms are reliably ameliorated by vasopressin therapy (Willie et al., 1994). The determination of ADH levels in diagnosing this condition is not always helpful because of moderate overlap between enuretic and normal children. Measuring the specific gravity in the first morning urine is more reliable for identifying children who may benefit from ADH supplementation; they will have a urine specific gravity below 1.015 (Mevorach et al., 1995).

Syndrome of Inappropriate Secretion of ADH

The syndrome of inappropriate secretion of ADH (SIADH) is characterized by a euvolemic hypoosmolar hyponatremia associated with hyperosmolar urine (the result of continued inappropriate natriuresis). By definition, SIADH cannot be diagnosed until nonosmotic stimuli for ADH secretion and other pathologies that interfere with free water clearance have been excluded (Vistorina et al., 2002). Physiologic triggers of ADH secretion include nausea, pregnancy, hypoglycemia, intracranial hypertension, mechanical ventilation, and hypoxia. Hypothyroidism and glucocorticoid deficiency cause a decrease in free water clearance, leading to a dilutional hyponatremia. Mineralocorticoid deficiency can lead to hyponatremia caused by increased renal sodium loss. It is therefore extremely important to test for deficiencies of these axes and to institute appropriate hormonal replacement therapy before making a diagnosis of SIADH. Other confounding factors that can hamper the diagnosis of SIADH include renal disease, cardiac disease, and medications such as diuretics. In these situations, one can cautiously perform a water load test (Table 25.4). In the absence of medications or other conditions that may impair diuresis, failure to excrete 80% to 90% of the administered water load within 4 hours and to suppress the Uosm to <100 mOsm/kg is consistent with the diagnosis of SIADH.

In the right clinical setting, the diagnosis of SIADH often can be confidently made on the basis of serum and urine electrolyte determinations alone. A spot urine Na+ less than 30 mmol/L can generally distinguish those with hyponatremia due to volume depletion from those with SIADH, in whom urine Na+ is greater than 30 mmol/L (Chung et al., 1987). In contrast, differentiating the patient with euvolemia and SIADH from the one with hypovolemia and concomitant renal salt wasting (e.g., salt-losing nephropathy, diuretic use) can be much more difficult. In addition to hyponatremia, both have a spot UNa+ greater than 30 mmol/L and a fractional excretion of Na+ greater than 1. The fractional excretion of sodium (FENa [%]) is calculated as follows:

$$\frac{U_{[Na+]} \times P_{[Cr]}}{P_{[Na+]} \times U_{[Cr]}} \times 100 \qquad \text{(Eq. 25.2)}$$

where $U[Na^+]$ = urine sodium concentration, $P[Na^+]$ = plasma sodium concentration, $U[Cr]$ = urine creatinine concentration, and $P[Cr]$ = plasma creatinine concentration.

One way to distinguish between the two is to administer 1 L of 0.9% NaCl intravenously over 24 hours for 2 days. A rise in serum Na+ by more than 5 mmol/L is suggestive of hypovolemia. In SIADH, no change or an increase of less than 5 mmol/L occurs. Alternatively, fluid restriction to 600 to 800 mL/day for 2 to 3 days will lead to improvement in hyponatremia in SIADH but not in renal salt wasting (see Table 25.3).

TABLE 25.3

Tests in the Differential Diagnosis of Disorders of Water Homeostasis

	BASELINE			AFTER 12-HOUR FLUID RESTRICTION			
Disorder	**Serum Na+ and Osmolality**	**Urine Na+ and Osmolality**	**Serum ADH**	**Serum Na+ and Osmolality**	**Urine Na+ and Osmolality**	**Serum ADH**	**Urine Osmolality Post-AVP Challenge**
Normal control	N	N	N	N	High	High	Same
SIADH	Low	N–High	High	Low–N	High	High	—
Neurogenic DI	N-High	Low	Low	High	Low–N	Low	Increased
Nephrogenic DI	N–High	Low	N–High	High	Low–N	High	Same
Psychogenic polydipsia	Low–N	Low	Low	N	N–High	N–High	Same

ADH, Antidiuretic hormone; *AVP,* arginine vasopressin; *DI,* diabetes insipidus; *N,* normal; *SIADH,* syndrome of inappropriate secretion of ADH.

BOX 25.4

Causes of Diabetes Insipidus

Central

Primary
Familial
Idiopathic
Acquired
Tumors—craniopharyngioma, pituitary tumors, metastases (i.e., lung, breast), Rathke cleft cyst, nonlymphocytic leukemia
Granulomatous disorders—sarcoidosis, Langerhans cell histiocytosis, Wegener granulomatosis
Traumatic—head trauma, surgery
Infectious—tuberculosis, meningitis, encephalitis
Vascular—cerebral aneurysm, sickle cell anemia, Sheehan syndrome
Drugs—alcohol, diphenylhydantoin, chlorpromazine, and β-adrenergic agonists
Other—lymphocytic hypophysitis, hypoxic encephalopathy

Nephrogenic

Hereditary
Mutation in the V_2 receptor
Mutation in the aquaporin gene
Acquired
Drugs—lithium, phenytoin, demeclocycline, vinblastine, cisplatin, propoxyphene, colchicine, gentamicin, amphotericin, ethanol, atrial natriuretic hormone, norepinephrine, methoxyflurane anesthetics, furosemide
Electrolyte disorders—hypercalcemia, hypokalemia
Systemic illnesses—sickle cell, multiple myeloma, amyloidosis, sarcoidosis, Sjögren syndrome, polycystic kidney disease
Other—low-protein diet, postobstructive uropathy

TABLE 25.4

Water Load Test

1. Baseline: The patient must be euvolemic and have a serum Na^+ between 125 and 150 mmol/L and Posm >275 mOsm/kg.
2. The patient is given 20 mL of water per kilogram of body weight (max = 1500 mL) to drink over 30 minutes.
3. With the patient maintained in the recumbent position, urine output is collected every hour for the next 5 hours. Record the volume and osmolality of each specimen.

Interpretation

Normals	Excrete 80% to 90% of the administered water load within 4 hours and suppress the Uosm to <100 mOsm/kg.
SIADH	Failure to meet these criteria in the absence of medications or other conditions that may impair diuresis is consistent with the diagnosis of SIADH.

SIADH, Syndrome of inappropriate secretion of antidiuretic hormone.

The cause of renal salt wasting in SIADH is twofold. At the onset of the disease, there is volume expansion, which inhibits the renin-aldosterone axis and leads to greater improved delivery of sodium to the distal tubules. The continued sodium loss is due to secretion of atrial natriuretic protein (Kamoi et al., 1990), which also is stimulated by increased intravascular volume.

Because of hyperfiltration and the local actions of ADH on the renal V2 receptor, SIADH is one of the two states in which some of the lowest uric acid levels occur; the other is pregnancy. In SIADH, the serum levels of ADH may be variably increased, usually out of proportion to Posm. However, approximately 20% of cases meeting the physiologic diagnosis of SIADH will not have detectable levels of ADH (Zerbe & Robertson, 1980). This may be due to insensitivity of the assay to low levels of ADH, increased renal sensitivity to ADH, or perhaps the presence of another hormone with antidiuretic activity (Kamoi, 1997).

The diagnosis of SIADH is largely a diagnosis of exclusion, with the clinician having ruled out other causes of hyponatremia (Fig. 25.5). It most often occurs as a manifestation of the paraneoplastic syndrome. However, it may also occur in central nervous system trauma or infection, in lung disease, or as the result of medications (vinca alkaloids, tricyclic antidepressants, selective serotonin reuptake inhibitors; Box 25.5).

THYROID FUNCTION

The normal thyroid gland weighs about 15 to 25 g. It consists of two lobes connected in the middle by a narrow isthmus. It is divided into lobules, each composed of 20 to 40 follicles, separated by highly vascular connective tissue. The follicles are the site of thyroid hormone synthesis and storage. They are ring-shaped structures, formed by a single-cell band of follicular cells which surrounds a cavity containing colloid, thyroid hormone, thyroglobulin (Tg), and a variety of other glycoproteins. The follicular cells rest on a glycoprotein-rich basement membrane that separates the cells from surrounding capillaries. Microvilli at the apex of the follicular cells extend into the colloid, where iodination, exocytosis, and the initial phase of hormone secretion occur. The thyroid gland also contains parafollicular cells, or C cells, which are responsible for the synthesis and secretion of calcitonin, a hormone important in calcium metabolism (American Association of Clinical Endocrinologists, 2002; U.S. Preventive Services Task Force, 2015).

An intact hypothalamic-pituitary-thyroid (HPT) axis and a ready source of iodide are required for normal thyroid hormone synthesis. The hypothalamus secretes TRH, which, in turn, stimulates the thyrotrophs of the anterior pituitary gland to secrete TSH (thyrotropin, thyroid stimulating hormone). As implied by the name, TSH stimulates thyroid hormone synthesis and secretion by the thyroid gland. Thyroid hormone exerts negative feedback on both the hypothalamus and pituitary gland to maintain a TSH concentration within narrow limits; it also acts peripherally to mediate numerous metabolic activities.

Under TSH stimulation, iodine enters the follicular cells as inorganic iodide and through a series of metabolic steps is integrated, forming thyroid hormones, thyroxine (T_4), and 3,5,3′-triiodothyronine (T_3). The sequence of events as depicted in Figure 25.6 can be broken down into (1) active transport of iodide into the cell; (2) iodination of the tyrosyl residues on Tg (organification); (3) coupling of iodotyrosine molecules within Tg to form T_4 and T_3; (4) proteolysis of Tg with release of free iodotyrosine, T_4, and T_3, and secretion of iodothyronine into the circulation; (5) deiodination of iodotyrosines within the thyroid and reuse of liberated iodide; and (6) deiodination of T_4 to T_3.

One hundred percent of circulating T_4 is of thyroidal origin, whereas only 20% of T_3 is of thyroidal origin; 80% of T_3 is produced enzymatically in nonthyroidal tissues by 5′-monodeiodination of T_4 (Lum & Nicoloff, 1984). Approximately 110 nmol (85 μg) of T_4 and 10 nmol (8.5 μg) of T_3 are produced daily by the thyroid gland. The thyroid hormones circulate while attached to plasma proteins. About 70% of T_4 is bound to thyroxine-binding globulin (TBG), 20% to transthyretin (formerly called *thyroxine-binding prealbumin*), and 10% to albumin. Although most of the circulating T_3 is bound

to TBG, it does so with a 10-fold reduced affinity as compared with that of T_4 (Robbins, 1996; Braverman & Utiger, 2000). Small percentages of T_4 and T_3 remain unbound to protein—about 0.03% and 0.3%, respectively. As with other hormones, it is the free component that is metabolically active.

Thyroid disease may be classified functionally into hyperthyroidism, hypothyroidism, and euthyroidism. Signs and symptoms of hyperthyroidism include heat intolerance, tachycardia, weight loss, weakness, emotional lability, and tremor. The most common clinical syndrome associated with hyperthyroidism is Graves disease, caused by circulating antibodies to the TSH receptor. Other disorders that lead to hyperthyroidism include toxic multinodular goiter, toxic adenoma and, rarely, TSH-secreting pituitary tumors and thyroid carcinoma.

Hypothyroidism can result in hoarseness, cold sensitivity, dry skin, constipation, bradycardia, and muscle weakness. Myxedema coma is an advanced stage of thyroid hormone deficiency characterized by progressive stupor, hypothermia, and hypoventilation. Failure of the thyroid gland to secrete an adequate amount of thyroid hormone is called *primary hypothyroidism*. This is most commonly iatrogenic in origin, the result of ablation with radioactive iodine or thyroidectomy to treat hyperthyroidism, or radiation to the head and neck for malignancy. Central hypothyroidism occurs when TSH secretion is decreased as a result of a pituitary disorder. Tertiary hypothyroidism is the result of hypothalamic dysfunction.

Thyroid diseases such as goiter, thyroid adenoma, and thyroid carcinoma typically occur in individuals who are euthyroid (clinically and biochemically). Accurate TSH assays permit the diagnosis of subclinical hyperthyroidism and hypothyroidism. These patients appear clinically euthyroid; however, their TSH values are respectively suppressed or elevated. A number of clinical situations can lead to difficulties in the interpretation of thyroid function tests: the presence of abnormal protein–binding proteins (congenital or drug induced); alterations in thyroid hormone metabolism (as seen in those hospitalized with acute psychiatric illness); and alterations due to medications that affect thyroid hormone binding or the HPT axis directly and with substances causing assay interference (biotin).The most important and most common problem with thyroid function tests probably occurs in those patients with various illnesses that do not directly involve the thyroid gland, so-called *nonthyroidal illness*.

THYROID HORMONE SYNTHESIS AND METABOLISM

Iodine is a major component of thyroid hormone; the main source of iodine is dietary intake. Deiodination of organic iodine-containing moieties within the gland serves as another source. Inorganic iodide is transported into the follicular cell by the sodium-iodide symporter (NIS) located in the basolateral membrane

BOX 25.5

Causes of SIADH

CNS disease
Neoplasm, infection, trauma, cerebrovascular accident
Oat cell carcinoma and adenocarcinoma of the lung, pancreatic cancer, lymphoma
Pulmonary infection
TB, pneumonia, positive-pressure ventilation
Idiopathic

Medications

- Oral hypoglycemics—chlorpropamide, tolbutamide
- Antineoplastics—vincristine, cyclophosphamide
- Diuretics—hydrochlorothiazide
- Psychotropics—amitriptyline, phenothiazines, SSRIs, monoamine oxidase inhibitors
- Other—morphine, barbiturates, clofibrate, nicotine, acetylcholine, anesthetic agents, β-adrenergic stimulants, metoclopramide, desmopressin

CNS, Central nervous system; *SIADH*, syndrome of inappropriate secretion of antidiuretic hormone; *SSRIs*, selective serotonin reuptake inhibitors.

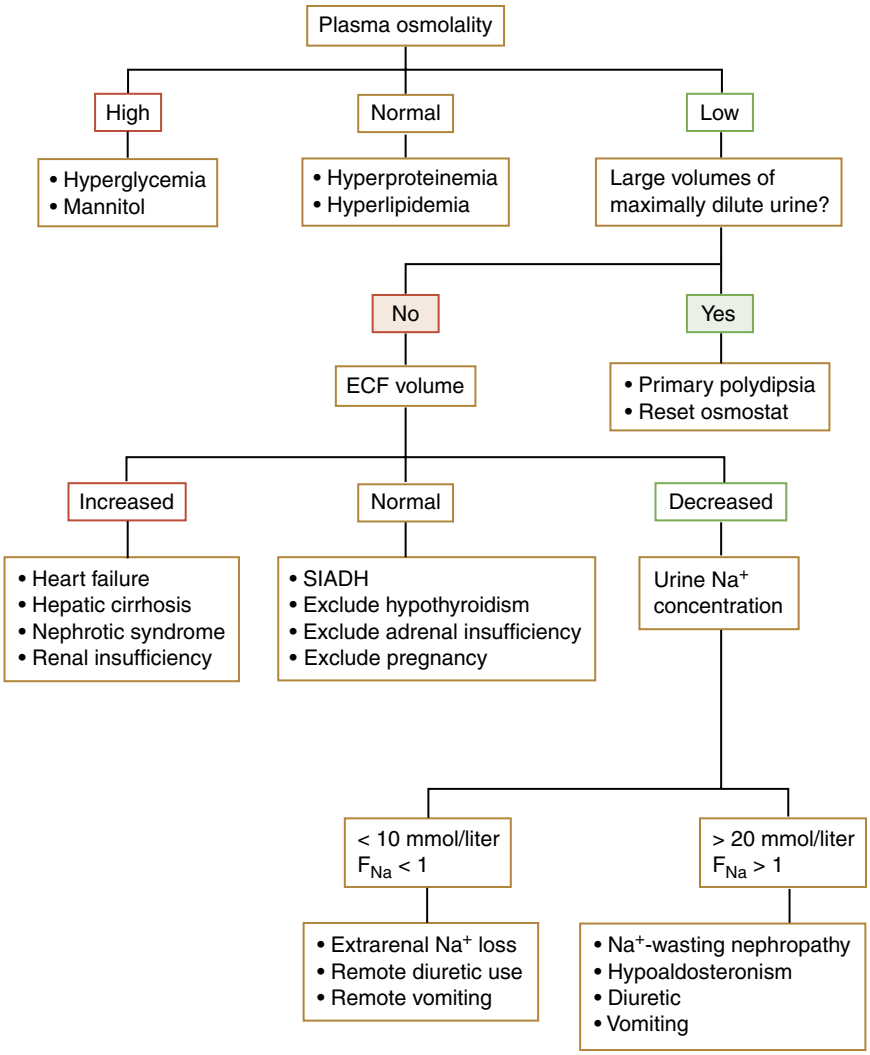

Figure 25.5 Algorithm for the evaluation of hyponatremia. *ECF,* Extracellular fluid; *SIADH,* syndrome of inappropriate secretion of ADH. From Singer GG: Fluid and electrolyte management. In Carey CF, Lee HH, Woeltje KF, editors: The Washington manual of medical therapeutics, ed 29, Philadelphia, 1998, Lippincott-Raven, p 44, with permission.

(Chambard et al., 1983). TSH modulates NIS activity: an increase in TSH secretion augments the uptake of iodide into the follicular cell. Iodide transport into the thyroid gland is also influenced by the serum iodide level; iodide deficiency increases pump activity, and iodide excess inhibits iodide uptake.

Thyroglobulin (Tg) is a glycoprotein synthesized by the rough endoplasmic reticulum in the basal and perinuclear regions of the follicular cell. It is acted on by the Golgi apparatus in the apical portion of the follicular cell, where iodination of the tyrosyl residues leads to the formation of monoiodotyrosyls and diiodotyrosyls (MITs and DITs). Tg is then transferred into the colloid for storage (Vassart & Dumont, 1973; Roth et al., 1985). The transformation of Tg into thyroid hormone requires two separate oxidative reactions, both catalyzed by thyroid peroxidase (TPO): the binding of iodide to Tg tyrosyl residues (iodination) to form the iodotyrosyls MIT and DIT, and the subsequent coupling of MIT and DIT to produce T_4 and T_3 (Deme et al., 1976; Bjorkman et al., 1981). T_4 and T_3 are released from Tg via lysosomal degradation and secreted into the circulation at the basal membrane. All of these reactions are under the control of TSH.

About half of all T_4 is monodeiodinated in at the 5′ position to form T_3, and about 40% undergoes deiodination of the inner ring of T_4 to form reverse T_3 (rT_3). The formation of rT_3, the third major circulating form of thyroid hormone, is catalyzed by the enzyme 5-deiodinase. Reverse T_3 has no biological activity, has a short half-life of 4 hours, and circulates bound to TBG; its formation is considered a disposal pathway in the peripheral metabolism of T_4 (LoPresti et al., 1989).

The Tg DIT/MIT ratio is influenced by iodide intake. DIT is the preferential iodotyrosine formed; thus, when iodide is abundant, T_4 is the predominant form of hormone synthesized and secreted, but when iodide sources are diminished, MIT is produced in greater quantities, leading to increased T_3 formation and release. In addition, the thyroid gland has a 5′-deiodinase that converts T_4 to T_3. This process is under the control of TSH, so that T_3 secretion is enhanced during periods of TSH stimulation (i.e., primary hypothyroidism) or the presence of TSH-stimulating immunoglobulin [TSI]) (Ishii et al., 1983).

The monodeiodination of T_4 to T_3 and rT_3 accounts for 70% of the peripheral metabolism of T_4 (LoPresti et al., 1989); the remainder of T_4 metabolism occurs by conjugation of T_4 to sulfate, deamination, and decarboxylation to form the acetic acid analog tetrac, and by ether link cleavage (Engler & Burger, 1984) (Table 25.5). T_3 but not rT_3 can be conjugated with sulfate to form T_3-sulfate, and can be converted to its acetic acid analog, triac (Engler & Burger, 1984). The enzymes responsible for these reactions are L-aminotransferase, located in the liver, and phenolsulfotransferases, which are present in many tissues throughout the body (Engler & Burger, 1984). After their formation from T_4, both T_3 and rT_3 can also undergo deiodination to form 3,3′-diiodothyronine (T_2).

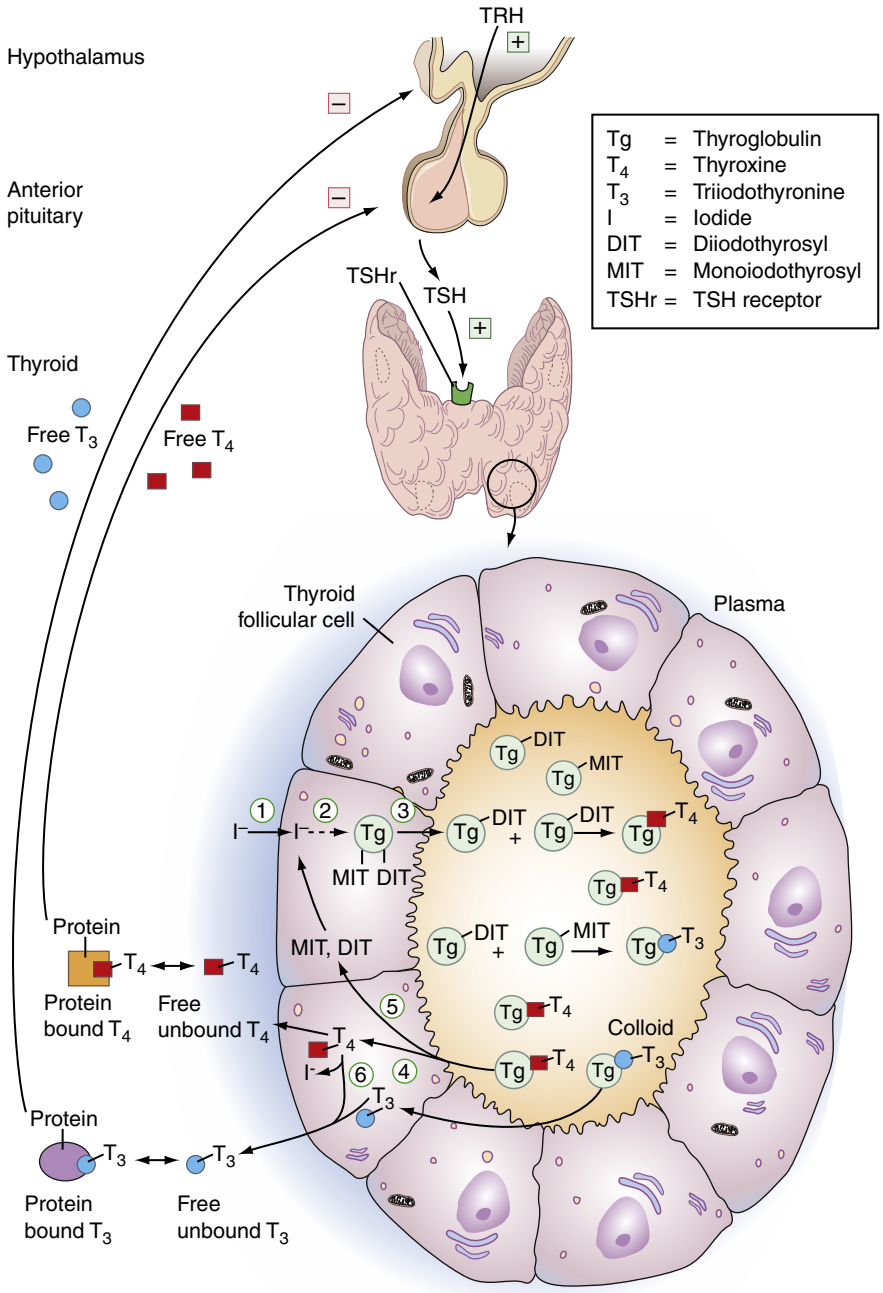

Figure 25.6 Hypothalamic-pituitary-thyroid axis and thyroid hormone synthesis. The steps for thyroid hormone synthesis and release are described in further detail in the text. *TRH,* Thyrotropin-releasing hormone; *TSH,* thyroid-stimulating hormone.

TABLE 25.5
Metabolic Dynamics of T_4 and T_3

	T_4	T_3
Production rate, nmol/day	110	50
Fraction of circulating hormone of thyroid origin	100%	20%*
Serum concentration		
Total, nmol/L	100	1.8
Free, pmol/L	20	5
Fraction of total hormone in free form	0.0002	0.003
Half-life, days	≈7	0.75
Relative metabolic potency	0.3	1.0

T_3, 3,5,3′-triiodothyronine; T_4, thyroxine.
*80% of circulating T_3 comes from the peripheral deiodination of T_4. To convert total T_4 from nmol/L to μg/dL or free T_4 from pmol/L to ng/dL, divide by 12.87. To convert total T_3 from nmol/L to ng/dL or free T_3 from pmol/L to pg/dL, multiply by 65.1.
From Larsen PR, Davies TF, Schlumberger MJ, et al.: Thyroid physiology and diagnostic evaluation of patients with thyroid disorders. In Larsen PR, Kronenberg HM, Melmed S, et al., editors: *Williams textbook of endocrinology,* ed 10, Philadelphia, 2003, Saunders, p 342.

Protein-bound thyroid hormone fractions are considered biologically inert, functioning as reservoirs for the formation of free thyroid hormone. Unbound T_3 is responsible for all of the metabolic effects of thyroid hormone. T_3 binds to the thyroid hormone receptor located on the nuclear membrane. This complex is transported to the thyroid hormone response elements (TREs) situated in the promoter regions of target genes, leading to increases in mRNA and protein synthesis. Four isoforms of the T_3 receptor have been described: α_1, α_2, β_1, and β_2 (Brent et al., 1991). α1 and β1 receptors are present in most tissues. The β_2 receptor is unique to the pituitary gland and is central in the negative-feedback regulation of TSH by thyroid hormone. The α_2 receptor is inhibitory and acts as a negative regulator of thyroid hormone action.

Mutations in the β receptors, which diminish the ability of T_3 to bind to the nucleus, have been described in the syndrome of impaired sensitivity to thyroid hormone (previously termed *thyroid hormone resistance syndrome*). Individuals with this syndrome have growth retardation and mental disabilities of varying degrees, as well as hypothyroidism (Refetoff, 1991).

HYPOTHALAMIC-PITUITARY-THYROID AXIS

The physiologic regulators responsible for integrating thyroid gland function with the periphery include hypothalamic hormone, TRH; pituitary hormone, TSH; thyroid hormones free T_4 (FT_4) and free T_3 (FT_3). TRH enhances TSH synthesis, stimulates the secretion of preformed TSH from the thyrotrophs, and modulates the bioactivity of TSH, resulting in the secretion of bioactive TSH (Beck-Peccos et al., 1985; Shupnik et al., 1986). TRH itself is under the negative-feedback influence of circulating thyroid hormones (TRH mRNA levels are inversely related to the circulating T_3 values) (Kakucska et al., 1992). The same feedback inhibition occurs at the level of the thyrotrophs.

Thyrotropin-Releasing Hormone

TRH is a modified tripeptide (pyroglutamyl-histidyl-proline-amide), released from the prepro molecule by a peptidase (Yamada et al., 1990). TRH is found in the hypothalamus, brain, C cells of the thyroid gland, δ cells of the pancreas, myocardium, prostate, testis, and spinal cord. The neuron bodies producing TRH are innervated by catecholamines, leptin, and somatostatin-containing axons, which ultimately influence the rate of TRH synthesis.

Thyroid hormone production is self-regulated through feedback inhibition at the level of the hypothalamus (TRH) and pituitary (TSH). TRH also affects the production of other pituitary hormones, for example, it stimulates the release of prolactin from the lactotrophs. Leptin plays a significant role in the regulation of the TRH gene (Bjorbeck & Kahn, 2004), affecting the individual's appetite for food intake. The precise interaction of leptin and the thyroid axis remains to be elucidated.

It is difficult to develop a specific antibody for TRH, and assays are not clinically useful.

Thyroid-Stimulating Hormone

TSH is a glycoprotein consisting of two mono-covalently linked α and β subunits. The α subunit shares the same amino acid sequences as LH, FSH, and human chorionic gonadotropin (hCG). It is the β subunit that carries specific information to the binding receptors for expression of hormonal activities.

The radioimmunoassay for measuring TSH was first developed by Odell and colleagues in 1965. This **first-generation assay** did not have sufficient sensitivity to distinguish normal TSH levels from the suppressed levels seen in primary hyperthyroidism. By the mid-1980s, a "sensitive" or second-generation immunometric TSH method using monoclonal or polyclonal antibodies was developed; sensitivity was improved to 0.1 to 0.2 mIU/L. Refinements in the immunometric method led to the third-generation assays now in common use, which allow measurement down to about 0.005 mIU/L. Fourth-generation TSH assays have been developed displaying sensitivities as low as 0.0004 mIU/L. However, they are not widely available and they fail to provide clinically useful information above and beyond that offered by third-generation assays. The American Thyroid Association (ATA) recommendations state that third-generation assays should be able to quantitate TSH in the 0.010- to 0.020-mIU/L range on an interassay basis with a coefficient of variation of 20% or less. In reporting assay results, the ATA recommends using functional sensitivity, defined as the point at which the interassay precision has a coefficient of variation equal to or less than 20% (Spencer et al., 1996).

Owing to improvements in the sensitivity of the TSH assay and the fact that TSH has an inverse log/linear relationship with FT_4 (e.g., small changes in FT_4 lead to large changes in TSH), this test alone can identify virtually all instances of hyperthyroidism and hypothyroidism. Exceptions exist in individuals with structural hypothalamic or pituitary disease, thyroid hormone resistance, disruption in HPT axis function due to medications, or when results are factitious as a result of substances causing assay interference (e.g., biotin, heterophile antibodies). Improved sensitivity of the third-generation assays facilitates distinguishing profound TSH suppression typical of frank Graves thyrotoxicosis (TSH <0.01 mIU/L) from modest degrees of TSH suppression (0.01–0.1 mIU/L) observed with mild (subclinical) primary hyperthyroidism and some cases of nonthyroidal illness. Although assay sensitivity has improved, the normal range has remained unchanged at approximately 0.35 and 5.0 mIU/L for most laboratories.

Serum TSH levels can be assayed using immunoassays and by mass spectroscopy, the latter being considered to be the gold standard with which all assays are compared. Reference intervals (RI) are specific for each methodology and manufacturer; this can prove problematic as patients move between doctors and different labs. To that end, the International Federation of Clinical Chemistry (IFCC) has formed a Committee for Standardization of Thyroid Function Tests. They are in the later stages of creating a process that harmonizes and standardizes TSH and FT_4 measurements. Until this is accomplished, it is recommended, when possible, to longitudinally adhere to using one particular lab for monitoring patients with thyroid disease (Thienpont, 2017; De Grande, 2017).

In hyperthyroidism, TSH is suppressed while FT_4 and/or FT_3 are elevated, while in hyperthyroidism caused by a TSH-producing tumor or pituitary resistance, the elevated FT_4 and/or FT_3 are accompanied by an inappropriately normal to slightly elevated TSH. In subclinical hyperthyroidism, the TSH is low, while both the FT_4 and FT_3 are in the normal range (Table 25.6).

In primary hypothyroidism, in which the problem lies with the thyroid gland itself, the TSH elevation is accompanied by low FT_4. In the setting of secondary (pituitary) and tertiary (hypothalamic) hypothyroidism the TSH is inappropriately normal for the low levels of T_4 and T_3. As the thyroid gland fails, the hypothalamus and pituitary compensate by increasing the synthesis and secretion of their respective hormones. This results in a state termed *subclinical hypothyroidism* in which the TSH is elevated while the T_4, T_3, and FT_4 remain normal.

An important cause of both increased and decreased TSH is nonthyroidal illness (NTI). Patients with NTI tend to have low TSH levels during the acute phase of their illness, rising to within or above the reference range with resolution of the underlying process and returning to normal once the acute illness has resolved. The interpretation of thyroid function tests (TFTs) in this setting is often confounded by the use of medications such as opioids, glucocorticoids, and dopamine, which suppress TSH secretion. New to this list of medications are checkpoint and tyrosine kinase inhibitors, which can cause secondary hypothyroidism (hypophysitis) as well as primary thyroid dysfunction.

The TSH-centered strategy has two primary limitations. First, it assumes that hypothalamic-pituitary function is intact and normal. Second, it assumes that the patient is stable (i.e., the patient has not had recent adjustments in therapy for hyperthyroidism or hypothyroidism) (Wardle et al., 2001). If either of these criteria is not met, the serum TSH result can be misleading (see Table 25.6). In these instances, measurement of FT_4 can often help clarify the diagnosis. In situations in which the TSH is low and

TABLE 25.6
Characterization of Thyroid Disorders According to Results of Thyroid Function Tests

Disorder	TSH	T_4	T_3	FT_4	Tg	TBG	rT_3	aTPO	ATG	TBII	TSI	TBA
Primary hypothyroidism	↑	↓	N or ↓	↓	N or ↓	N	↓	N or ↑	N or ↑	N or ↑	n	n or ↑
Transient neonatal hypothyroidism	↑	↓	↓	↓	N or ↓	N	↓	N	N	↑	n	↑
Hashimoto thyroiditis/hypothyroidism	↑	N or ↓	N or ↓	N or ↓	N or ↓	N	↓	↑	↑	n or ↑	n	n or ↑
Graves disease	↓	↑	↑	↑	↑	N	↑	↑	↑	↑	↑	n or ↑
Neonatal Graves disease	↓	↑	↑	↑	↑	N	↑	n or ↑	n or ↑	↑	↑	n or ↑
TSH deficiency	N or ↓	↓	↓	↓	↓	N	↓	n	n	N	n	n
Thyroid dyshormonogenesis	↑	↓	↓	↓	N, ↓ or ↑	N	↑	n	n	N	n	n
Thyroid hormone resistance	N or ↑	↑	↑	↑	↑	N	↑	n	n	N	n	n
TSH-dependent hyperthyroidism	↑	↑	↑	↑	↑	N	↑	n	n	n	n	n
T_4 protein-binding abnormalities*	N	V	V	N	N	V+	V	n	n	N	n	n
Nonthyroidal illness	V	N or ↓	↓	V	N	N	N or ↑	n	n	N	n	n
Subacute thyroiditis†	↓ or ↑	↑ or ↓	↑ or ↓	↑ or ↓	↑ or ↓	N	↑ or ↓	n	n	N	n	n

*The spectrum of binding protein abnormalities includes increased or decreased TBG binding, increased or decreased transthyretin binding, and ↑ albumin binding.
†Subacute thyroiditis involves a transient period of hyperthyroidism followed by a transient hypothyroid state.
ATG, Antithyroglobulin; *aTPO*, antithyroid peroxidase; *FT_4*, free thyroxine; *N*, normal; *n*, negative; *rT_3*, reverse triiodothyronine; *TBA*, TSH receptor–blocking antibody; *TBII*, TSH-binding inhibiting immunoglobulin; *Tg*, thyroglobulin; *T_3*, triiodothyronine; *T_4*, thyroxine; *TBG*, thyroxine-binding globulin; *TSH*, thyroid-stimulating hormone; *TSI*, thyroid-stimulating immunoglobulin; *V*, variable. From Fisher DA, editor: *Disorders of thyroid function,* online version of the Quest diagnostic manual, ed 3, p 268.

the FT_4 or TT_4 is normal, measurement of the total T_3 (TT_3) or FT_3 is fitting, as the patient may have T_3 thyrotoxicosis.

Thyroxine

After release from the follicles, T_4 binds to various proteins in the blood (thyroid-binding globulin, albumin, thyretin). T_4 can be measured by immunoassay after the hormone is separated from the carrier protein. The reference range is 5 to 12.5 μg/dL in adults, with slightly lower results for certain pediatric age groups. Although TSH is the principal test for assessing thyroid function, T_4 measurements are often used along with TSH and can be of importance in interpreting TSH results. The combination of a low T_4 and increased TSH is indicative of primary hypothyroidism, whereas elevated T_4 and/or T_3 combined with a decreased TSH is characteristic of primary hyperthyroidism. Hyperthyroidism, in which the T_4 is elevated while the serum T_3 is at or below the reference range, is termed *T_4 thyrotoxicosis*. This can occur in patients with iodine-induced thyrotoxicosis (e.g., patients on amiodarone or following iodine contrast media). A suppressed TSH in association with a normal to low-normal T_4 and a high T_3 characterizes *T_3 thyrotoxicosis*. This is more common in a toxic nodule and the elderly (see Table 25.6).

Severe NTI is associated with low T_4 and T_3 levels. This so-called low T_4 and T_3 syndrome, or euthyroid sick syndrome, is felt to be an adaptive response to reduce metabolic demands and conserve protein stores (LoPresti & Nicoloff, 1995) and is associated with a poor prognosis (Chopra, 1997). It is thought to arise from a maladjusted central inhibition of TRH (Van den Berghe et al., 1998; Van den Berghe 2000) (Fig. 25.7).

Euthyroid hyperthyroxinemia is distinguished by the presence of an increased serum T_4 in association with a normal TSH in an otherwise euthyroid individual. This entity has a variety of causes, including increased synthesis of binding proteins, as seen with certain drugs (e.g., estrogen) or medical conditions (e.g., liver disease), and decreased conversion of T_4 and T_3 (e.g., high doses of β blockers or steroids). It is also seen in patients who are acutely hospitalized for psychiatric illness, in those with familial dysalbuminemia, and in thyrotoxic patients with concomitant NTI. When medications or other factors cause increased protein binding, there is a consequent increase in serum total T_4; conversely, a decrease in binding capacity leads to a decrease in serum total T4. These perturbations do not have any physiologic effect in persons with a normal thyroid axis, as the bioactive, free hormone fraction remains unaffected. In these situations, free T_4 correlates better with thyroid functional status than does serum total T_4.

The T_3 uptake (T_3-UP) test is a classical method of adjusting the total T_4 measurement for alterations in binding protein. The T_3-UP test yields a relative measurement of unoccupied T_4 binding sites. It was performed by saturating available binding sites with radiolabeled T_3, then measuring the unbound T_3 by adsorbing it onto a resin (hence the term T_3 resin uptake). Procedures giving analogous results can be performed via nonisotopic methods on automated analyzers. The free thyroxine index (FTI) is then calculated as (T_3-UP of the patient)/(mean T_3-UP of the reference population) multiplied by the patient's total T_4. The FTI (reference range, 5.4–9.7) is only a relative estimate of the free T_4 concentration. In general, during thyrotoxicosis, both total T_4 and T_3-UP are elevated. Conversely, in hypothyroidism, both total T_4 and T_3-UP are decreased and, when there is a binding globulin abnormality, these two values diverge (e.g., total T_4 is elevated and the T_3-UP is decreased or the total T_4 is decreased and

the T_3-UP is increased). The FTI has been largely replaced by the direct measurement of free T_4 by immunoassay, dialysis, and ultrafiltration.

Free Thyroxine

FT_4 is the biologically active fraction of T_4. Equilibrium dialysis is the traditional reference technique for measuring FT_4. It is unaffected by changes in binding protein concentration. It is carried out by dialyzing serum against a nonprotein buffer using a membrane impermeable to proteins so that FT_4 will achieve equal concentrations on both sides of the membrane. The protein-free solution is then collected and analyzed for FT_4. Even this laborious method does not give a true measure of FT_4 in all cases because small molecules that may affect T_4 binding are diluted in the procedure. Refinement of this technique to include tandem mass spectroscopy (ED/MS-MS), has made this the new gold standard for measuring several hormones, including FT_4.

ED/MS-MS is costly, time-consuming, and ill-suited to meet the high-volume demands of clinical laboratories. Immunoassays performed on automated clinical chemistry platforms can rapidly provide appropriate results in most clinical circumstances and have become the mainstay for measuring all thyroid hormones. There are various circumstances in which immunoassays can be unreliable. Spurious results can occur with abnormal variants of the binding proteins (e.g., familial dysalbuminemic hyperthyroxinemia, a condition with high T_4 but normal FT_4, caused by an albumin variant that binds T_4 abnormally) or in the presence of T_4 or T_3 autoantibodies (Langsteger, 1997). Increases or decreases in serum FT_4 without concomitant changes in metabolic state have been reported in pregnancy, NTI, and in patients being treated with certain medications. For example, prolonged administration of phenytoin or carbamazepine results in a 15% to 30% decrease in both serum T_4 and FT_4. In these circumstances, dialysis or ultrafiltration methods are indicated.

Biotin, a commonly used supplement, has recently been documented to interfere with immunoassays that use streptavidin and biotinylated antibodies. Depending on whether a competitive or sandwich technique is used, the measured FT_4 or TSH will be falsely elevated or falsely low, respectively. Options to remedy this include having the patient stop biotin-containing supplements 3 to 5 days prior to testing or referring to a laboratory that does not use a streptavidin-biotin methodology (Bowen, 2019).

The RI for FT_4 is highly assay specific. In addition, RIs vary throughout pregnancy, infancy and childhood. It is therefore important to use the proper RI corresponding to each trimester of pregnancy and age range for infants and children. As with TSH, a process to harmonize FT_4 assays using the FT_4 obtained by ED/MS-MS as the universal standard, is currently under development (De Grande 2017). Until this standardization is finalized, it is recommended that one maintain consistency in the commercial lab and methodology utilized for measuring FT_4 and TSH.

Triiodothyronine

T_3, generally measured by immunoassay, has a reference interval typically in the range of 60 to 160 μg/dL (0.9–2.46 nmol/L). T_3 is much less bound to protein than is T_4; thus, a relatively greater proportion of T_3 than T_4 exists in a free, diffusible state. Since assays for FT_3 are less widely available and less widely standardized, the current practice is to measure total T_3 as opposed to FT_3. Total T_3 concentrations are measured by competitive immunoassay methods that are now mostly nonisotopic and use enzymes, fluorescence, or chemiluminescence molecules as signals (Nelson & Wilcox, 1996). The measurement of T_3 is useful in confirming the diagnosis of hyperthyroidism when TSH is suppressed but there is only minimal to no elevation in T_4.

In 90% of patients with hyperthyroidism, both T_4 and T_3 are increased, with the increase in T_3 usually greater than that of T_4. Serum T_3 can be normal or low in patients with hyperthyroidism in the setting of NTI or if they are taking medications that decrease the conversion of T_4 to T_3 (e.g., high-dose propranolol, amiodarone). Hyperthyroidism in association with an elevated T_3 but normal T_4 and FT_4 is termed *T_3 thyrotoxicosis* (Bitton & Wexler, 1990). Patients with this syndrome are a heterogeneous group with no distinctive signs or symptoms. Although most patients with T_3 thyrotoxicosis have Graves disease, it may also be seen with toxic multinodular goiter or toxic adenoma. T_3 thyrotoxicosis has been reported to occur in ≈1% to 4% of all thyrotoxic patients, with a much higher incidence in regions with iodine deficiency.

The measurement of T_3 is generally not useful in evaluating patients suspected of having hypothyroidism as levels fall within the RI in 15% to 30% of patients (Surks et al., 1990). However, decreased T_3 levels are seen in patients with severe hypothyroidism, whose $T_4 < 2$ μg/dL (32 nmol/L) (Bigos et al., 1978). In acute NTI, such as myocardial infarction, T_3 declines rapidly to about 50% of the reference value within a matter of days (Utiger, 1980). T_3 concentrations are also low in cord blood but increase rapidly during the first few hours of life.

Blood concentrations of T_3 rise rapidly following the ingestion of T_3-containing preparations (e.g. Cytomel, Amour thyroid), peaking within 2 to 4 hours. Clearance is also rapid, with a half-life of 0.68 to 1.38 days (Jonklaas et al., 2015). As a result, knowing both the time of hormone administration and consistency of blood test timing in relation to hormone ingestion is essential for proper interpretation of serum T_3 results. In contrast, the T_3 level is stable in patients treated with T_4 (levothyroxine). As in this situation, T_3 is derived from the peripheral conversion of T_4; stable levels are reached after only a few weeks of therapy.

A number of pharmacologic agents interfere with the conversion of T_4 to T_3 (i.e., glucocorticoids, amiodarone, large dosages of propranolol), causing low levels of T_3, low FT_3, and normal or even high levels of serum T_4 and FT_4, with normal TSH.

Reverse Triiodothyronine (rT_3)

rT_3 is a biologically inactive metabolite of thyroxine that is produced through 5-deiodination of T_4. T_3 and rT_3 tend to vary reciprocally. In NTI, rT_3 is elevated while T_3 is diminished. rT_3 is increased in healthy newborns, in patients with hyperthyroidism (including factitious hyperthyroidism), and in patients taking certain drugs, such as amiodarone and propranolol. Measurements of rT_3 are of little clinical utility and rarely if ever indicated.

Thyroglobulin

Tg is synthesized and secreted by thyroid follicular cells. It is present in the serum of normal individuals in the range of up to about 30 ng/mL

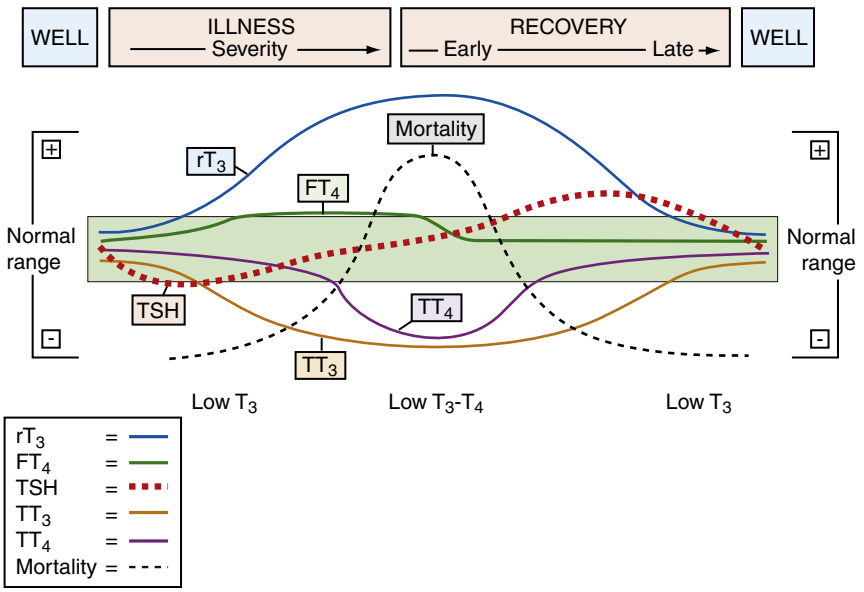

Figure 25.7 Changes in thyroid hormones during severe illness. *FT_4*, Free thyroxine; *rT_3*, reverse triiodothyronine; *TSH*, thyroid-stimulating hormone; *TT_3*, total triiodothyronine; *TT_4*, total thyroxine. (Redrawn from Demers LM, Spencer CA: NACB: Laboratory support for the diagnosis and monitoring of thyroid disease, 2003, p 11, with permission. Available at: www.nacb.org.)

(45 pmol/L). The serum Tg concentration reflects thyroid mass, thyroid injury, and TSH receptor stimulation (Spencer & Wang, 1995). Tg is increased in a variety of disorders, including Graves disease, thyroiditis, and nodular goiter. The routine measurement of Tg is never indicated. Its utility resides in monitoring for recurrence of certain variants of thyroid cancer, in the diagnosis of thyroid dysgenesis in congenital hypothyroidism, and in helping to distinguish thyrotoxicosis factitia from other forms of thyrotoxicosis.

While Tg is helpful in monitoring for recurrence/persistence of well-differentiated thyroid carcinoma, it is of no utility in patients with undifferentiated thyroid malignancies or medullary thyroid cancer. The clinical value of Tg measurement is limited in the presence of Tg antibodies (Tg Abs), found in 20% to 25% of patients with thyroid carcinoma. Tg Abs can interfere with Tg measurements by immunoassay, resulting in falsely low serum Tg concentrations (Spencer et al., 1999). It is therefore extremely important to always test for Tg Abs whenever measuring Tg. LC/MS-MS may eventually allow for accurate measurement of Tg in the presence of Tg Abs (Haugen, 2016). Even though the presence of Tg Abs may invalidate the value of Tg in monitoring recurrence and response to treatment in differentiated thyroid cancer, because Tg Ab reflects thyroid tissue mass, Tg Ab itself may be used as a surrogate marker (Spencer, 2013; Rosario, 2016; Haugen, 2016).

Recombinant human TSH (rhTSH) is commonly used to test patients with thyroid cancer for the presence of residual/recurrent disease. This is more practical, more convenient, and markedly less unpleasant for the patient than stopping thyroid hormone suppression over the span of several weeks to increase the TSH level; an elevated TSH is required for radioactive iodine (RAI) uptake to occur in remaining remnant or recurrent tumor. Measurement of Tg 72 hours following the last dose of rhTSH correlates highly with the presence of recurrence; some authorities support the use of this test alone without a concomitant whole-body scan (WBS) for iodine for those with "low-risk" tumors (<40 years of age, no distant metastases, size <1 cm, well differentiated). All other patients with thyroid cancer need to undergo WBS and measurement of Tg, which can either be accomplished using rhTSH or thyroid hormone withdrawal. Using a highly sensitive assay for Tg in patients who have undergone remnant ablation, a post-rhTSH Tg > 0.5 to 1.0 ng/mL, or Tg > 0.1 ng/mL while on suppression is suspicious for recurrence/persistence of disease and needs to be worked up accordingly (i.e., full restaging while hypothyroid off of suppressive therapy) (Haugen, 2016). Poorly differentiated tumors can cease production of Tg, in which case other modalities for monitoring—such as positron emission tomography scan and thyroid ultrasound—may be utilized.

In the early weeks post-thyroidectomy, serum Tg levels typically fall, with a half-life of 2 to 4 days. The pattern of change in serum Tg while on T_4 suppression is a better indicator of a change in tumor burden than any single serum Tg value (Spencer & Wang, 1995). Because of inter-assay variability, it is extremely important to use the same laboratory for monitoring TSH, Tg, and Tg Ab.

Thyroxine-Binding Globulin

TBG is the main serum carrier protein for both T_4 and T_3. Measurement of TBG may be helpful in patients who have serum T_4 and T_3 levels that do not agree with other laboratory parameters of thyroid function or that are not compatible with clinical findings. TBG is measured by immunoassay and ranges from 13 to 39 μg/dL (150–360 nmol/L) in healthy individuals. Inherited abnormalities in TBG include complete and partial deficiency, TBG variants with decreased affinity for T_4 or T_3, and TBG excess (Langsteger, 1997). Among the acquired causes of abnormalities in the TBG concentration are a variety of medications and medical conditions (Table 25.7). Medications such as salicylates, phenytoin, penicillin, and heparin can displace T_4 from binding to TBG.

TABLE 25.7
Some Causes of Alterations in Thyroxine-Binding Globulin

Increases	Decreases
Drugs	Drugs
Clofibrate	Androgens
Estrogens, oral contraceptives	Glucocorticoids
5-Fluorouracil	Genetic
Heroin	Complete deficiency
Methadone	Partial deficiency
Genetic	Liver failure
Acute or chronic active hepatitis	Malnutrition
Pregnancy	Nephrotic syndrome
Idiopathic	Idiopathic

Thyroid Autoantibodies

In autoimmune thyroid disease, cellular damage occurs as a result of autoantibodies and/or sensitized T lymphocytes binding to thyroid cell membranes, causing cell lysis, inflammatory reactions, and ultimately thyroid gland dysfunction. Three thyroid autoantigens are responsible for autoimmune thyroid disorders: TPO Ab, Tg Ab, and TSH receptor antibody (TRAb). TPO antibodies (TPO Abs) are involved in the tissue destructive process associated with Hashimoto thyroiditis and atrophic thyroiditis. Some studies suggest that TPO Abs may be cytotoxic to the thyroid gland (Chiovato et al., 1993; Guo et al., 1997). Longitudinal studies suggest that the presence of TPO Abs may be a risk factor for future thyroid dysfunction, including postpartum thyroiditis and autoimmune complications from treatment with amiodarone, interferon-α, and lithium (Feldt-Rasmussen et al., 1994; Johnson & Eegles, 1999; Martino et al., 2001).

Tg Ab is present in 10% to 15% of normals, 60% to 80% of patients with Hashimoto thyroiditis and 50% to 60% of those with Graves disease (Frolich, 2017). Even at low serum concentrations, Tg Ab can interfere with the anti-Tg antibody used in the immunoassay for measuring Tg. Thus, the Tg Ab concentration should be measured whenever measuring Tg. In iodide-deficient areas, serum Tg Ab measurement can be used to detect autoimmune thyroid disease in patients with a goiter and to monitor iodide therapy in endemic goiter.

TRAbs, previously known as *thyroid-stimulating immunoglobulin (TSI)* or *long-acting thyroid stimulators*, are classified as stimulating or blocking antibodies. Graves disease (GD) is an autoimmune condition in which goiter and hyperthyroidism are induced by thyroid-stimulating antibodies (TSI) that mimic the action of TSH on the thyrotropin receptor. Although both stimulating and blocking antibodies are present in GD, the latter usually do not cause symptoms; however, in a few cases, they may lead to the development of hypothyroidism. TRAbs are positive in 85% of patients with GD. Measurement of TRAbs has been used to predict the outcome of Graves patients treated with drug therapy; the lower the titer of the antibodies prior to treatment, the better the chance for remission following 6 to 12 months of therapy.

Measurement of TRAbs is used to predict the risk for thyroid dysfunction in newborns of mothers with GD as a result of transplacental passage of maternal TRAb (Heithorn et al., 1999; Radetti et al., 1999). In these patients, assays that distinguish blocking from stimulating antibodies are important clinically (Davies et al., 1998). In addition, TRAb, in particular thyroid stimulating antibody (TSI), is utilized to diagnose and monitor Graves ophthalmopathy.

URINARY IODINE MEASUREMENT

Iodine is required for normal thyroid hormone production. Iodine measurements are used mainly to assess the dietary iodine intake of certain populations. This is of great importance in that iodine deficiency disorders affect 2.2 billion persons throughout the world, including the United States (Delange, 1995; Dunn, 1998). Because most of the ingested iodine is excreted in the urine, measurement of urinary iodine (UI) excretion provides an accurate estimate of dietary iodine intake (Dunn, 1998). Suggested ranges for UI excretion are shown in Table 25.8.

TABLE 25.8
Urinary Iodine Excretion and Iodine Deficiency

Urinary Iodine Excretion, μg/L	>100	50–99	20–49	<20
Degree of deficiency*	None	Mild	Moderate	Severe
Goiter prevalence	<5%	5%–19.9%	2%–29.9%	>30%

*IDD Newsletter, August 1999;15:33–48.
From Demers LM, Spencer CA, editors: *NACB: Laboratory support for the diagnosis and monitoring of thyroid disease*, 2003, p 75. Available at: www.nacb.org.

SCREENING PROGRAMS FOR DETECTION OF NEONATAL HYPOTHYROIDISM

The prevalence of hypothyroidism in newborns is estimated from 1 in 3000 to 1 in 5000. It is higher in certain ethnic groups and is increased in iodine-deficient regions worldwide. Early detection of hypothyroidism during the neonatal period is critical for preventing severe mental disabilities associated with thyroid hormone deficiency. Screening is performed by collecting blood from a heel stick onto filter paper. Occasionally, cord blood is used in instances when the mother is on thyroid medications or when there is a family history of congenital hypothyroidism. Detection rates depend on the test used and the timing of specimen collection. Three strategies are utilized in screening, testing simultaneously for T_4 and TSH, testing for TSH with T_4 as a backup, and testing for T_4 with TSH as a backup. Testing is performed at 2 to 4 days of age or prior to discharge if the infant is being discharged before 48 hours of life (Rose, 2006). Premature infants, infants admitted to the neonatal intensive care unit, infants of multiple gestation, and those tested within the first 24 hours of birth should be retested at about 2 weeks of age or 2 weeks after the first screening test was carried out (Leger, 2014). Very-low-birth-weight infants should be retested at 2 and 4 to 6 weeks to detect late-onset transient hypothyroidism (Frank et al., 1996).

Measurement of only T_4 carries a high false-positive rate, necessitating recall of a large number of infants for retesting. Causes of false-positive results include congenital absence of TBG and transient low T_4 levels seen in premature infants. Screening with only T_4 may miss infants with compensated or partial thyroid insufficiency. Because about 15% of infants with primary thyroid disorders have compensated hypothyroidism (normal serum T_4 levels in association with elevated TSH), an elevated TSH is the most sensitive test for the diagnosis of congenital hypothyroidism. However, false-positive results are occasionally seen, for example, in premature or severely stressed infants. Screening with TSH alone also runs the risk of missing central hypothyroidism (e.g., pituitary or hypothalamic hypothyroidism). For newborns, if the initial TSH value is <10 mIU/L, no further action need be taken; if it lies in the 10- to 20-mIU/L range, then a repeat test needs to be performed in 2 to 6 weeks. Finally, if the initial blood spot TSH is greater than 20 mIU/L, endocrinologic evaluation is necessary to make the diagnosis of hypothyroidism.

NONTHYROIDAL ILLNESS

Seriously ill patients can have abnormal thyroid tests even without underlying thyroid pathology (DeGroot & Major, 1992; Kaptein, 1996). This usually reversible alteration in the hypothalamic-pituitary-thyroid axis is seen in situations such as starvation, sepsis, and acute myocardial infarction, and is characterized by a rapid decline in both total and free T_3 (Piketty et al., 1996). As the severity of the illness increases, the serum total T_4 falls because of T_4-binding protein disruption caused by inhibitors in the circulation as well as a concomitant drop in binding protein concentration (Wartofsky & Burman, 1982; Docter et al., 1993; Wilcox et al., 1994). Patients with NTI whose T_4 levels drop below 2 ng/dL have an exceptionally poor prognosis. These alterations in TFTs seen during NTI are termed *euthyroid sick syndrome* or *low T_4 syndrome*. Figure 25.7 shows the spectrum of changes in thyroid tests as they relate to the severity and stage of the illness. Patients with NTI tend to have low or low-normal TSH, normal to low-normal T_4, very low T_3, and elevated rT_3 during the acute phase of illness. As the underlying illness resolves, TSH rises to normal or above normal before finally returning to baseline (Faber et al., 1987). TSH may rise as high as 20 mIU/mL during the recovery phase. However, superimposed primary hypothyroidism is suspected if the TSH is ≥ 25 mIU/mL (Chopra, 1997). Interpretation of thyroid function tests during NTI can be complicated by medications. Glucagon, dopamine, and high doses of glucocorticoids can suppress TSH and mask hypothyroidism (Kaptein et al., 1980; Skamene & Patel, 1984; Brabant et al., 1989; Samuels et al., 1990). Many biologicals and checkpoint inhibitors can also affect the hypothalamic-pituitary-thyroid axis. In these situations, physical exam findings, thyroid antibody status, and thyroid function trends can often assist in clarifying the diagnosis.

In uremia, there is accumulation of indoleacetic acid, which interferes with thyroid hormone binding (Iitaka et al., 1998).

PHYSIOLOGIC VARIABLES

For practical purposes, variables such as age, gender, race, season, phase of menstrual cycle, cigarette smoking, exercise, fasting, and phlebotomy-induced stasis have minor effects on thyroid function tests in ambulatory adults (Hollowell et al., 2002). Studies have suggested that each individual has a genetically determined FT_4 setpoint (Meikle et al., 1988; Andersen et al., 2002); the pituitary gland will sense any deviation from this setpoint and cause reciprocal change in TSH secretion. In the early stages of thyroid dysfunction, changes in TSH precede alterations in FT_4; this is because TSH responds exponentially to subtle FT_4 changes, as shown in Figure 25.8.

Population studies suggest that normal aging is accompanied by a decrease in thyroid axis function, wherein TSH increases, FT_4 remains stable and T3 decreases (van den Beld, 2018). These alterations appear to have a survival benefit, as reports have linked mildly suppressed or elevated TSH with increased cardiovascular morbidity and mortality (Sawin et al., 1991; Parle et al., 2001). In children, the hypothalamic-pituitary-thyroid axis undergoes progressive maturation and modulation. There is a continuous decline in the TSH/FT_4 ratio from the time of mid-gestation until after puberty (Nilson et al., 1993; Adams et al., 1995; Lu et al., 1999; Zurakowski et al., 1999; Fisher et al., 2000a, 2000b); as a result, higher TSH concentrations are typically seen in children.

During pregnancy, estrogen production increases, progressively elevating the TBG concentration and resulting in an increase in the total T_4 and T_3 reference range to approximately 1.5 times the nonpregnancy upper reference level by 16 weeks' gestation (Weeke et al., 1982; Pedersen et al., 1993; Nohr et al., 2000). Although TBG excess leads to an increase in both T_4 and T_3 concentrations, the serum FT_4 and T_3 concentrations remain unchanged.

Placental hCG, which has structural similarity to TSH, has weak thyroid-stimulating activity (Talbot et al., 2001). The increase in hCG soon after fertilization results in a small increase in FT_4 and T_3 concentrations, usually within the normal reference range. These changes result in a fall in serum TSH during the first trimester; a subnormal serum TSH may be seen in about 20% of mothers who have normal pregnancies (Glinoer et al., 1990; Glinoer, 1997; Panesar et al., 2001). The peak rise in hCG and the nadir of TSH occur together at about 10 to 12 weeks' gestation. In 2% of pregnancies, the increase in FT_4 reaches supranormal levels and, if prolonged, may lead to a syndrome referred to as *gestational transient thyrotoxicosis*, which is characterized by more pronounced symptoms and signs of thyrotoxicosis. This condition is frequently associated with first-trimester hyperemesis gravidarum (Goodwin et al., 1992; Hershman, 1999).

The ATA recommends measurement of TSH as the principal determinant of thyroid status during pregnancy (Alexander, 2017) with the following trimester-specific reference ranges:

- First trimester TSH: 0.1 FT_4 and T_3 2.5 mIU/L
- Second trimester TSH: 0.2 to 2.5 mIU/L
- Third trimester TSH: 0.3 to 3.0 mIU/L

The optimal method to assess serum FT_4 during pregnancy is measurement in the dialysate or ultrafiltrate of the serum sample employing online extraction/liquid chromatography/tandem mass spectrometry (LC/MS/MS). If this method is not available, automated immunoassays using population-based trimester-specific RI may be used (Alexander, 2017).

Elevation of TSH during pregnancy could represent subclinical hypothyroidism (if the FT_4 is normal but TSH is 2.5 to 10.0 mIU/L) or overt

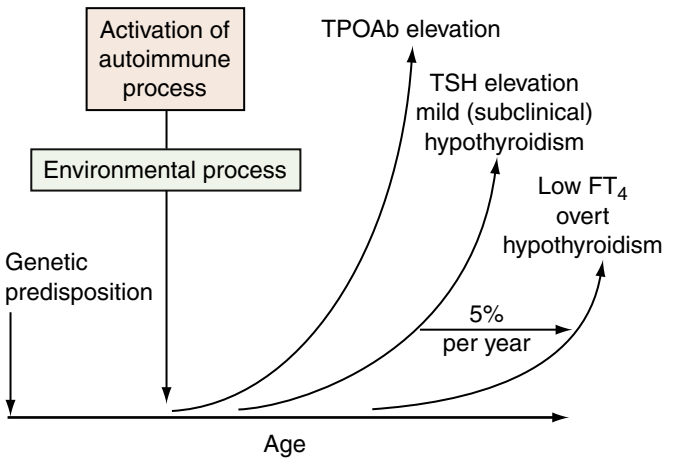

Figure 25.8 Depiction of the evolution of primary hypothyroidism of autoimmune origin. *FT_4*, Free thyroxine; *TPOAb*, thyroid peroxidase antibodies; *TSH*, thyroid-stimulating hormone. (From Demers LM, Spencer CA: NACB: Laboratory support for the diagnosis and monitoring of thyroid disease, 2003, p 47. Available at: www.nacb.org.)

hypothyroid (if the TSH is >10 mIU/L with low FT_4 or TSH 2.5 to 10 mIU/L with low FT_4).

All pregnant women with overt hypothyroid should be treated early to avoid fetal complications. When treating hypothyroid pregnant women, always use thyroxine, not T_3 or any other preparation.

MEDICATIONS AND THYROID FUNCTION TESTS

Drugs can cause both in vitro and in vivo effects on thyroid tests. This can lead to the misinterpretation of test results, inaccurate diagnoses, and further unnecessary tests and treatments (Surks & Sievert, 1995; Kailajarvi et al., 2000). Estrogen-induced TBG elevation causes abnormally high total T_4 and total T_3 but has no effect on TSH, FT_4, or free T_3. In normal individuals, the thyroid axis compensates for the increase in bound hormone by secreting more T_4 and T_3. However, patients with underlying hypothyroidism are incapable of this and instead require an increase in hormone replacement dose. Selective estrogen receptor modulators (SERMs), methadone, and heroin are among the other drugs that can increase TBG (Burch, 2019). Glucocorticoids in large doses suppress TSH secretion as well as decrease conversion of T_4 to T_3. Conversion of T_4 to T_3 is also suppressed by high doses of propranolol. Due to these effects, glucocorticoids and propranolol are utilized in the treatment of severe thyrotoxicosis (e.g., thyroid storm). Dopamine suppresses TSH and can temper the expected rise in TSH in hospitalized patients with primary hypothyroidism (Kaptein et al., 1980).

Iodide—found in iodide-containing contrast media used in CT scans and coronary angiography, solutions to sterilize the skin, radiopaque dyes, and some over-the-counter expectorants and supplements—can cause hyperthyroidism or hypothyroidism in susceptible individuals (Meurisse et al., 2000). When thyroid iodine stores are replete, exogenous iodine can induce hypothyroidism. This is referred to as the Wolff-Chaikoff effect. The converse occurs in states of iodine deficiency; Jod-Basedow phenomenon leads to hyperthyroidism. Amiodarone has complex effects on thyroid function and can cause hypothyroidism (10% of patients) or hyperthyroidism (1%–2%) in susceptible individuals with positive antibodies (TPO Abs) (Martino et al., 1987, 2001; Caron, 1995; Harjai & Licata, 1997; Daniels, 2001).

Lithium inhibits thyroid hormone synthesis and release and can cause hypothyroidism in about 15% to 50% of patients, especially those patients with positive TPO Abs (Lazarus, 1998; Kusalic & Engelsmann, 1999; Oakley et al., 2000). The mechanism of lithium action is similar to that of iodide. Lithium is concentrated by the thyroid gland and inhibits thyroid iodine uptake. It also inhibits iodotyrosine coupling, alters thyroglobulin structure, and inhibits thyroid hormone secretion. The latter effect is critical to the development of hypothyroidism and goiter (Lazarus, 1998).

Medications such as phenytoin, carbamazepine, salicylate, salsalate, and furosemide competitively inhibit T_4 binding to serum proteins, thereby causing the measured total T_4 levels to be depressed, and FT_4 estimated by FTI or direct assays to be artifactually low. FT_4 is maintained at its normal level, however. Therapeutic doses of phenytoin can accelerate the disposal of T_4 and perhaps directly suppress TSH centrally. All these mechanisms are responsible for the reduced T_4 seen with phenytoin (Surks et al., 1995).

Heparin can stimulate lipoprotein lipase, which liberates free fatty acids that inhibit T_4 binding to serum proteins, thereby falsely elevating FT_4 (Mendel et al., 1987). Phenobarbital, phenytoin, rifampin, and carbamazepine increase the rate of thyroid hormone clearance by increasing the deiodination of T_4 and T_3. Hypothyroid patients treated with any of these medications need to have their hormone levels monitored closely, as an increase in levothyroxine (L-T_4) dose may be required. Somatostatin or its analog, octreotide (Itoh et al., 1988), as well as dopamine (Kaptein et al., 1980), can inhibit TSH synthesis.

Owing to these various alterations in thyroid hormone parameters, the best indicator of thyroid status is the measurement of TSH along with FT_4. For those with pituitary disease or on phenytoin, T_4 by equilibrium dialysis should be used.

Checkpoint inhibitors are increasingly being utilized to treat a variety of malignancies. Currently, there are two main categories of inhibitors, one acting on programmed cell death 1 (PD-1) protein and the other on cytotoxic T-lymphocyte antigen 4 (CTLA-4). While both can cause thyroiditis and hypothyroidism, these sequelae are more often seen with PD-1 inhibitors, while hypophysitis is associated with the use of CTLA-4 inhibitors (Burch, 2019; Chalan, 2018). α-Interferon, IL-2, and tyrosine kinase inhibitors (TKIs) can also cause thyroiditis, resulting in hyperthyroidism and hypothyroidism. Bexarotene, used in treating T-cell lymphoma, has dual effects, causing central hypothyroidism and increasing the clearance of thyroid hormone.

It is important to be aware that changes in thyroid function (both hyperthyroidism and hypothyroidism) can, in turn, affect the metabolism and clearance of many medications, including insulin, sulfonylureas, digitalis, and Coumadin, as well as those drugs mentioned earlier. Close monitoring of drug levels or other parameters (e.g., blood glucose and international normalized ratio) is paramount under these circumstances.

THYROID ILLNESS

Hyperthyroid patients may present with one or all of the following signs and symptoms: weight loss, sweating, heat intolerance, palpitations, insomnia, increased bowel movement, tremors, infertility, or amenorrhea. They almost always have suppressed TSH levels, the exception being persons with secondary hyperthyroidism due to a TSH-producing pituitary tumor, or pituitary resistance to thyroid hormone. In all instances, the FT_4 and/or T_3 are elevated. Subclinical hyperthyroidism is defined as a suppressed TSH (<0.1 mIU/mL) with normal T_4 and T_3 levels and lack of signs or symptoms of hyperthyroidism (Ross, 1991). Detection of subclinical hyperthyroidism is particularly important in patients older than age 60 years, as they have an increased risk for atrial fibrillation, cardiovascular mortality (Sawin et al., 1994), and osteoporosis.

Patients with primary hypothyroidism can present with one or all the following signs and symptoms: cold intolerance, constipation, water retention, hypercholesterolemia, depression, bradycardia, pretibial myxedema or periorbital edema. In this instance, the TSH is elevated while the T_4 and T_3 are low. In patients with secondary or tertiary hypothyroidism due to pituitary or hypothalamic disorders, respectively, low T_4 and T_3 concentrations are accompanied by an inappropriately low TSH. Subclinical hypothyroidism is characterized by the ability to sustain normal T_4 and T_3 levels via increased secretion of TSH. In 2004, an expert panel recommended TSH reference limits of 0.4 to 4.5 mIU/mL, and against routinely treating individuals with a TSH in the range of 4.5 to 10 mIU/mL (Surks et al., 2004). The 2012 AACE guidelines (Garber, 2012) recommend treatment when the TSH is >10 mIU/mL. Treatment is suggested in patients with hypothyroid symptoms, goiter, positive TPO Abs, cardiovascular disease, heart failure, or associated risk factors for these diseases (e.g., hyperlipidemia). For TSH values that lie between the upper limit of a given laboratory and 10 mIU/mL, measurement of TPO Ab helps establish the presence of autoimmunity, which increases the probability of progression to overt hypothyroidism (Garber, 2012).

SCREENING FOR THYROID DISEASE

The ATA guidelines recommend screening at 35 years of age and every 5 years thereafter (Ladenson et al., 2000). This appears to be a cost-effective strategy, especially for women (Parle et al., 2001) and older adults (Vanderpump et al., 1995; Ladenson et al., 2000; Parle et al., 2001). Hashimoto thyroiditis is an autoimmune disease of the thyroid gland caused by binding of sensitized T lymphocytes and/or autoantibodies to cell membrane, causing cell lysis and an inflammatory reaction, resulting in cellular damage. This disease process is associated with high TSH and positive TPO Abs; its prevalence increases with increasing age (Vanderpump et al., 1995) and increased iodine intake. The incidence of low TSH is also increased in older adults (Vanderpump et al., 1995).

Mounting evidence indicates that a persistent TSH abnormality may lead to major health risks if left untreated. One study reported a higher cardiovascular mortality rate in patients with chronically low TSH (Parle et al., 2001), and numerous reports indicate that mild hypothyroidism in early pregnancy increases fetal loss and impairs the IQ of offspring (Pop et al., 1995, 1999; Haddow et al., 1999). It is important to always confirm any mild TSH abnormality before treating; the tests should be repeated within 2 to 3 weeks.

USES OF L-THYROXINE

The average replacement dose of L-thyroxine is 1.6 μg/kg body weight/day for adults. The replacement dose for infants and children depends on age and weight, and lower doses are given for older individuals (1.0 μg/kg body weight/day) (Sawin et al., 1983; Davis et al., 1984). The initial dose and the optimal time needed to establish the full replacement dose are dependent on the age, weight, and cardiac status of each patient. The requirement increases by 25% to 30% during pregnancy as well as in postmenopausal women starting hormonal replacement (Arafah, 2001). A serum TSH between 0.5 and 2.0 mIU/mL is the therapeutic goal level for L-T_4 replacement in primary hypothyroidism. A serum FT_4 concentration in the upper third of the reference interval is the therapeutic target in central hypothyroidism.

TSH is used to monitor treatment in those receiving thyroid hormone replacement therapy and to monitor the adequacy of suppression in patients with thyroid malignancy (Spencer, 1990). Both TSH and FT_4 should be used to monitor hypothyroid patients suspected of intermittent noncompliance. At least 6 weeks is needed before retesting of TSH following a change in the dose of L-T_4. Annual TSH measurement is recommended in patients on a steady dose of T_4. If FT_4 is being assayed, patients should withhold their L-T_4 dose on the day of the test, as serum FT_4 will be increased (about 13%) above baseline for 9 hours after the last dose is ingested (Ain et al., 1993); the TSH, however, is unlikely to be affected. Ideally, L-T_4 should be taken before meals, at the same time every day and at least 4 hours from any other medications or vitamins/dietary supplements.

L-T_4 is used to suppress TSH in patients with well-differentiated thyroid carcinoma, for which thyrotropin is considered a trophic factor (Dulgeroff & Hershman, 1994). TSH and FT_4 levels will vary in accordance with the time interval between ingestion of thyroid hormone and venipuncture. While this is usually a nonissue for patients being treated for hypothyroidism, for those on suppressive therapy for thyroid cancer, the smallest change in TSH may dictate a change in L-T_4 dose. To mitigate these fluctuations, it is recommended that the timing of L-T_4 to blood draw be kept as consistent as possible. It is recommended to use a TSH target of 0.05 to 0.1 mIU/mL for low-risk patients and a TSH value <0.1 mIU/mL for high-risk patients. If the thyroglobulin level is undetectable and no evidence of recurrence is noted 5 to 10 years after thyroidectomy, the dose of L-T_4 can be reduced to achieve low-normal TSH values (<0.4 mIU/mL).

CALCITONIN

Medullary thyroid carcinoma (MTC) originates from the parafollicular C cells of the thyroid gland. It accounts for 1% to 2% of thyroid cancers and 0.57% of thyroid nodules (Pacini et al., 1994). C cells secrete several hormones and biogenic amines, including calcitonin, carcinoembryonic antigen (CEA), chromogranin, and ACTH. Calcium and pentagastrin are potent calcitonin secretagogues (Abe et al., 1977; Williams et al., 1966; Wells et al., 1978). Both calcitonin and CEA are valuable tumor markers for patients with MTC; their serum concentration correlates directly with C-cell mass (Wells, 2015).

Among cases of MTC, 25% are inherited in an autosomal-dominant fashion as part of the multiple endocrine neoplasia (MEN) family, in particular MEN types 2A and 2B (Dunn, 1994; Brandi et al., 2001; Cobin et al., 2001).

The current ATA risk categories for hereditary MTC and the associated mutations are:

- Highest risk (patients with MEN 2B *and* RET codon M918T mutation)
- High risk (patients with MEN 2A *and* RET codon c634 mutation)
- Moderate risk (patients with hereditary MTC and RET codon mutations other than M918T and c634)

Calcitonin is a 32-amino acid monomeric peptide that is derived from cleavage and post-translational modification of larger precursors, preprocalcitonin and, subsequently, procalcitonin. Measurement of calcitonin is performed by two-site immunometric assays using monoclonal antibodies (Motte et al., 1988; van Heyningen, 1994; Becker et al., 1996). The newer immunochemiluminometric assays (ICMAs) are highly specific and sensitive for calcitonin, eliminating cross-reactivity with procalcitonin and calcitonin-related peptides, which can be elevated during sepsis and inflammatory conditions (Becker et al., 2004). Serum calcitonin levels are higher in men compared with women owing to the larger C-cell mass in men. It is markedly elevated in children under 3 years of age, particularly those younger than 6 months of age (Basuyau et al., 2004). The current revised ATA MTC guidelines do not specify reference ranges of basal or stimulated serum calcitonin levels. Rather, they encourage individual labs to set their own criteria based on studies of large numbers of normal and MTC-positive patients (Wells, 2015).

The use of calcitonin as a screening tool for MTC in patients with thyroid nodules is controversial in the United States. However, it is common practice in Europe (Elisei, 2004; Daniels, 2001; Vierhapper, 1997; Costante, 2007; Lai, 2019). Colombo et al. showed that basal CT (bCT) levels with the best accuracy to identify MTC were 18.7 pg/mL in women and 68 pg/mL in men, while the best stimulated CT (sCT) for distinguishing non-MTCs (normal controls and CCH) from MTCs were 184 pg/mL in women and 1620 pg/mL in men (Colombo et al., 2012). In a subsequent study they found that bCT had the same accuracy as sCT in the preoperative diagnosis of MTC at thresholds for MTC of 26 and 68 for bCT and 79 and 544 pg/mL for sCT in women and men, respectively (Mian et al., 2014).

Thyroid sonograms and fine-needle aspiration are the preferred diagnostic tests for MTC. In patients with inconclusive cytopathology, immunohistochemical staining or measurement of calcitonin in the washout fluid may be used for diagnosis (Trimboli, 2015). Serum calcitonin should be measured preoperatively and 3 to 6 months post-thyroidectomy (Wells, 2015; ATA guideline MTC). A detectable calcitonin level following thyroidectomy indicates the presence of remnant thyroid tissue or regional/distant metastasis (Engelbach, 2000). The serum doubling time of calcitonin is valuable to determine MTC progression rate, which is a significant predictor of survival (Barbet, 2005).

The presence of residual tissue or a recurrence of MTC can be ruled out only if both basal and post-pentagastrin or calcium-stimulated calcitonin are undetectable. Provocative stimuli, such as calcium and pentagastrin (Pg) or omeprazole, have been used to detect C cell abnormalities, as they increase calcitonin levels at all stages of MTC (Wells et al., 1978; Barbot et al., 1994; Gagel, 1996; Erdogan et al., 1997; Wion-Barbot et al., 1997; Vieira et al., 2002; Vitale et al., 2002).

In the Pg stimulation test for the diagnosis of MTC, an intravenous infusion of Pg (0.5 μg/kg body weight) is given over 5 seconds; blood samples are collected at baseline and 1, 2, 5, and 10 minutes after the start of the infusion. Interpretations of results are summarized in Table 25.9.

In the calcium stimulation test, intravenous injection of 2.5 mg/kg of calcium gluconate is given over 30 seconds; blood samples are then collected at baseline and at 1, 2, and 5 minutes. An increase in the plasma calcitonin level above 100 ng/L is an indication of C cell hyperplasia. The calcium infusion test has been reported to be less sensitive than the Pg test for the diagnosis of MTC. However, if combined with the Pg test, it enhances the sensitivity of the Pg test (Wells et al., 1978). Calcitonin may also be elevated in other conditions unrelated to thyroid neoplastic conditions, as summarized in Table 25.10.

ADRENAL FUNCTION

The adrenal glands are pyramidal structures located above each kidney, each weighing approximately 4 to 6 g. Anatomically, the adrenal gland is divided into two distinct parts, the medulla (inner layer) and the cortex (outer layer). The medulla, which is of neural crest origin (ectoderm), stores and secretes catecholamines. The cortex is of mesenchymal origin and is further divided into three zones: the outermost zona glomerulosa, which produces mineralocorticoids; the zona fasciculata, which is responsible for glucocorticoid production; and the inner zona reticularis, which synthesizes androgens. The cortex makes up about 80% to 90% of the adrenal gland. The glands have a very rich arterial supply that forms a subcapsular plexus and empties into a central vein. By weight, they have the

TABLE 25.9
Interpretation of the Pentagastrin (Pg) Test

Peak Calcitonin (CT) ng/L (pg/mL)	Interpretation
<10	Normal (80% of adults)
>30 but <50	5% of normal adults
>50 but <100	Possible MTC or other thyroid pathology
>100	Probable MTC
Basal or post-Pg CT value >10 pg/mL	C cell pathology or residual tissue in MEN 2 patients and MTC patients after surgery

MEN, Multiple endocrine neoplasia; *MTC*, medullary thyroid carcinoma.
From Demers LM, Spencer CA, editors: *NACB: Laboratory support for the diagnosis and monitoring of thyroid disease*, 2003, p 69. Available at: www.nacb.org.

TABLE 25.10
Conditions in Which Calcitonin May Be Elevated Other Than MTC

Neuroendocrine tumors	Small cell lung cancer, intestinal and bronchial carcinoid, all neuroendocrine tumors
Benign C cell hyperplasia (HCC)	Autoimmune thyroid disease, differentiated thyroid cancer
Other diseases	Kidney disease, hypergastrinemia, hypercalcemia

MTC, Medullary thyroid carcinoma.
From Demers LM, Spencer CA, editors: *NACB: Laboratory support for the diagnosis and monitoring of thyroid disease*, 2003, p 70. Available at: www.nacb.org.

highest perfusion of blood per gram of tissue—a feature that ensures rapid dissemination of hormones throughout the body in response to stress.

HORMONES OF THE ADRENAL MEDULLA

The adrenal medulla is part of the sympathoadrenal axis. Being of neural crest origin, it possesses the capability of synthesizing catecholamines through the process of amine precursor uptake and decarboxylation. The initial and rate-limiting step in catecholamine synthesis is the conversion of tyrosine to 3,4-dihydroxyphenylalanine (dopa) by the enzyme tyrosine hydroxylase. Through a series of steps, L-dopa is subsequently converted to dopamine (D), norepinephrine (NE), and epinephrine (E; Fig. 25.9). Epinephrine is almost exclusively produced and secreted by the adrenal medulla, where the ratio of NE/E is about 1 : 4. However, because all three catecholamines are also synthesized within the central and sympathetic nervous systems, the peripheral NE/E ratio is more like 9 : 1.

The catecholamines are metabolized by either catechol-O-methyltransferase (COMT) or monoamine oxidase (MAO). COMT converts D to methoxytyramine, E to metanephrine, and NE to normetanephrine, all of which, in turn, can be oxidized to vanillylmandelic acid (VMA) by MAO. MAO can also convert E and NE to 3,4-dihydroxymandelic acid, which is acted on by COMT to form VMA. 3-Methoxy-4-hydroxyphenylacetic acid (homovanillic acid [HVA]) is the final product of dopamine metabolism.

Pheochromocytoma and Paraganglioma

Catecholamine-producing tumors fall into two categories: pheochromocytomas and paragangliomas. Pheochromocytomas arise from the chromaffin cells of the adrenal medulla and account for 90% of these tumors. Paragangliomas are extra-adrenal in origin, arising in the paravertebral sympathetic ganglia of the chest, abdomen, and pelvis, and the parasympathetic chains along the vagus and glossopharyngeal nerves. Pheochromocytoma and paraganglioma will be collectively referred to as PPGL unless otherwise specified.

Pheochromocytomas have an incidence of about 500 to 1100 per year (Pacak et al., 2001a) and account for <1% of all secondary causes of hypertension. Although 90% of pheochromocytomas are benign, they are almost invariably lethal if not diagnosed and properly treated (Pacak et al., 2001a). Unlike pheochromocytomas, paragangliomas of the parasympathetic ganglia rarely produce a significant amount of catecholamines (<20% of cases) and therefore do not cause hypertension. Most pheochromocytomas are sporadic; however, 40% are familial, occurring as part of MEN 2A or MEN 2B, von Hippel–Lindau (VHL) disease, neurofibromatosis type 1 (NF-1), or familial paraganglioma (FP). The hereditary forms tend to present at a younger age and, except for FP, the tumors are usually intra-adrenal and bilateral.

Sustained or paroxysmal hypertension is the most common manifestation of this disease, present in about 90% of patients. Remarkably, 10% of patients are normotensive. More than 90% will present with paroxysmal attacks characterized by at least two of the three following symptoms: headache associated with palpitations and diaphoresis (Sheps et al., 1994; Young, 2016). Other symptoms include orthostatic hypotension, labile blood pressure, excessive sweating, anxiety, nervousness, weight loss, fatigue, pallor, and tremor. These symptoms can last from a few seconds to several hours, with the interval between attacks being highly variable—from several times a day to once every few months. Indications for screening for pheochromocytoma are listed in Box 25.6.

There is ongoing debate as to which test is the best for diagnosing PPGL. COMT is present in adrenal chromaffin cells and in tumors derived from these cells; it is absent from sympathetic nerves. As a result, the products of COMT, metanephrine (M) and normetanephrine (NM), serve as specific markers of chromaffin tumors (Lenders et al., 2014). Plasma metanephrine and normetanephrine (collectively referred to as metanephrines) are stable metabolites of E and NE and are produced continuously within tumors independent of catecholamine release. Thus, the most recent guidelines recommend the measurement of either plasma free metanephrines or 24-hour urine collection for fractionated metanephrines via high-pressure liquid chromatography with tandem mass spectrometry (HPLC/MS-MS) as the initial test (Lenders et al., 2014). Although less sensitive, fractionated catecholamines when clearly elevated (e.g., >2 times upper limit of the normal range) may also be diagnostic (Neumann et al., 2019).

The diagnosis of pheochromocytoma is made if the plasma concentration of either free metanephrine or normetanephrine is about four times the upper reference limit. Further testing is required in patients with high levels that are less than four times the upper reference limit (Sheps et al., 1994; Eisenhofer & Pacak, 2004; Eisenhofer et al., 2004). It is recommended that the samples be collected after the patient has been supine for at least 30 minutes. If a "seated" specimen returns as elevated, it should be confirmed by either repeating the test with the patient supine or obtaining a 24-hour urine sample for fractionated metanephrines. In centers where this assay is not available, the initial test should be the chromatographic measurement of a 24-hour urine collection for normetanephrine, metanephrine, fractionated free catecholamines (epinephrine, norepinephrine, dopamine), and creatinine (Lenders et al., 2002; Eisenhofer & Pacak, 2004; Eisenhofer et al., 2004). Metanephrine is the most sensitive and specific of these metabolites (Heron et al., 1996). Urinary creatinine should be measured in all 24-hour collections to assess for completion of the collection.

The diagnosis of pheochromocytoma can also be made by measuring plasma catecholamines; however, given their short half-life and episodic secretion, it is of use only if the sample is collected during a paroxysm. Values from the 24-hour urine collection or plasma catecholamines that are two to three times the upper limit of normal are usually diagnostic of pheochromocytoma.

BOX 25.6

Indications for Screening for Pheochromocytoma

1. Hypertension with episodic features suggestive of pheochromocytoma
2. Refractory hypertension
3. Prominent lability of blood pressure
4. Severe pressor response during anesthesia, parturition, surgery, or angiography
5. Unexplained hypotension due to anesthesia, surgery, or pregnancy
6. Family history of pheochromocytoma, MEN 2A or 2B, VHL disease, or neurofibromatosis
7. Incidentally discovered adrenal mass
8. Idiopathic dilated cardiomyopathy
9. Spells or attacks occurring during exertion, twisting and turning of the torso, straining, coitus, or micturition

MEN, Multiple endocrine neoplasia; *VHL*, von Hippel-Lindau.
From Dluhy RG, Lawrence JE, Williams G: Endocrine hypertension. In Larsen PR, Kronenberg HM, Melmed S, Polonsky KS, editors: *Williams textbook of endocrinology*, ed 10, Philadelphia, 2003, Saunders, p 557.

Biosynthetic Pathway for Catecholamines

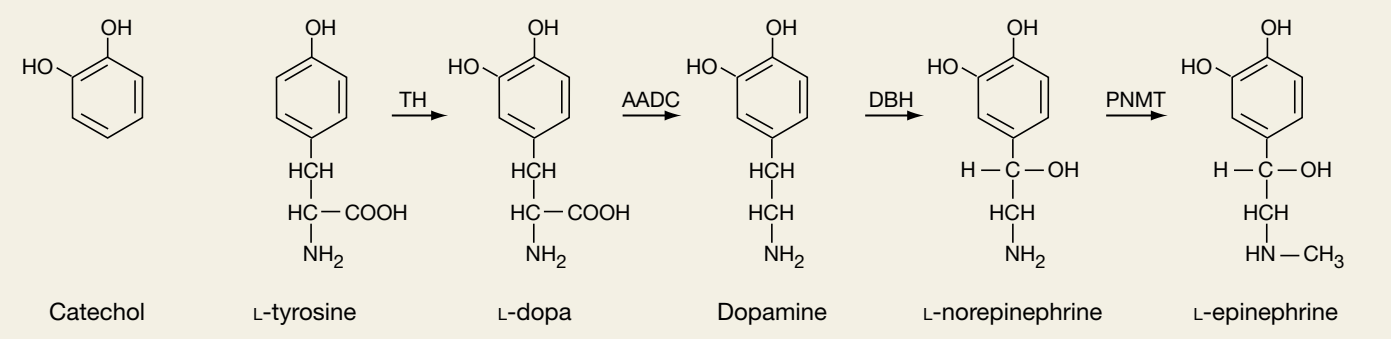

Figure 25.9 Catecholamines: biosynthetic pathway. The rate-limiting step is the conversion of L-tyrosine to L-3,4-dihydroxyphenylalanine (L-dopa) through the actions of tyrosine hydroxylase. *AADC*, aromatic L-amino acid decarboxylase; *DBH*, dopamine-β-hydroxylase; *PNMT*, phenylethanolamine N-methyltransferase; *TH*, Tyrosine hydroxylase. (Redrawn from Dluhy RG, Lawrence JE, Williams GH: Endocrine hypertension. In Larsen PR, Kronenberg HM, Melmed S, et al., editors: *Williams textbook of endocrinology*, ed 10, Philadelphia, 2003, Saunders, p 555, with permission.)

In cases of sporadic pheochromocytoma, the choice and interpretation of diagnostic tests depend on the pretest level of suspicion for disease. In this setting, the 24-hour urinary fractionated metanephrine and fractionated catecholamine measurements provide clinically acceptable sensitivity and significantly better specificity than fractionated plasma free metanephrine values (Sawka et al., 2003). Given the difficulties in collecting a complete 24-hour urine sample from pediatric patients, fractionated plasma free metanephrines should be considered the biochemical test of choice in that population (Weise et al., 2002) (Table 25.11).

Several factors can cause false-positive test results, either by stimulating catecholamine secretion and/or by interfering with the assay (Table 25.12). When assaying for plasma free metanephrines, patients should abstain from caffeinated beverages and alcohol for 24 hours before testing. They should also avoid acetaminophen, tricyclic antidepressants, phenoxybenzamine, α agonists (e.g., methyldopa [Aldomet]), and MAO inhibitors for at least 5 days before testing (Lenders et al., 1995). During testing for catecholamines, in addition to the list of items to avoid when testing for metanephrines, the patient should avoid nicotine, sympathomimetics (theophylline, pseudoephedrine), α agonists (e.g., albuterol), and levodopa/carbidopa. If antihypertensive medications are needed, angiotensin-converting enzyme inhibitors (ACEIs), angiotensin receptor blockers, and selective α_1-adrenoceptor blockers (e.g., prazosin) can be used without fear of causing false-positive results (Eisenhofer et al., 2003).

Although urinary catecholamine levels may be elevated in renal insufficiency and renal failure, the measurement of plasma free metanephrines can be used to reliably diagnose pheochromocytoma in both conditions (Eisenhofer et al., 2004). Stressors such as an acute myocardial infarction, congestive heart failure, surgery, and acute cerebrovascular accident are all associated with elevated levels of catecholamines. In these situations, one can treat empirically and test once the patient has stabilized. Plasma normetanephrine concentrations increase with age; as a result, older adult patients are particularly susceptible to having false-positive tests. The use of fractionated urinary metanephrines and catecholamines may be more suitable for this population (Sawka et al., 2003).

Plasma levels of normetanephrine less than 112 ng/L (0.61 nmol/L) and metanephrine less than 61 ng/L (0.31 nmol/L) virtually exclude pheochromocytoma; thus, no immediate further testing for the tumor should be necessary. With plasma concentrations of normetanephrine above 400 ng/L (2.19 nmol/L) or of metanephrine above 236 ng/L (1.20 nmol/L), the probability of pheochromocytoma is so high that the immediate task is to locate the tumor (Eisenhofer et al., 2003). More often than not, test results return as equivocal, requiring the need for confirmatory tests such as the clonidine suppression test or the glucagon stimulation test, or the measurement of urinary fractionated catecholamines. Clonidine is a centrally acting α-adrenergic agonist; it suppresses catecholamine release from the nervous system but has no effect on its release by the tumor (Bravo et al., 1981). In those with pheochromocytoma, clonidine fails to adequately suppress plasma levels of norepinephrine to less than 40% from baseline (Table 25.13).The clonidine suppression test is indicated only if the plasma catecholamines are greater than 1000 pg/mL (5.9 nmol/L). It is unreliable in those with normal or mildly elevated plasma catecholamines (Taylor et al., 1986; Elliott & Murphy, 1988; Sjoberg et al., 1992). Eisenhofer and colleagues (2003) showed that measuring plasma normetanephrines before and after clonidine testing increased the sensitivity and specificity of this test, especially in those who have only modest elevations of norepinephrine. The glucagon stimulation test can lead to dangerous rises in blood pressure; thus, it is no longer used. Unless the history is compelling or the patient falls into one of the categories of genetically inherited disorders, it is often unnecessary to repeat testing in those with slightly positive results.

TABLE 25.11

Sensitivity and Specificity of Hormone Levels for Diagnosing Pheochromocytoma

	SENSITIVITY		SPECIFICITY	
	Hereditary	**Sporadic**	**Hereditary**	**Sporadic**
Plasma				
Free metanephrines	97%	99%	96%	82%
Catecholamines	69%	92%	89%	72%
Urine				
Fractionated metanephrines	96%	97%	82%	45%
Catecholamines	79%	91%	96%	75%
Total metanephrines	60%	88%	97%	89%
Vanillylmandelic acid	46%	77%	99%	86%

Data from Pacak K, Eisenhofer G, Ilias I: Diagnostic imaging of pheochromocytoma, *Front Horm Res* 31:76–106, 2004; Lenders JW, Pacak K, Walther MM, et al.: Biochemical diagnosis of pheochromocytoma: Which test is best? *JAMA* 287:1427–1434, 2002.

TABLE 25.12

Effects of Medications on Testing for Pheochromocytoma

	PLASMA				URINE			
Medication Class	**NMN**	**NE**	**MN**	**E**	**NMN**	**NE**	**MN**	**E**
Tricyclics	+	+	–	–	+	+	–	–
Phenoxybenzamine	+	+	–	–	+	+	–	–
Buspirone	–	–	–	–	–	–	+	–
α-Adrenergic blockers	–	–	–	–	–	+	–	–
β-Adrenoceptor blockers	–	–	+	–	+	+	+	+
Calcium channel blockers	–	+	–	–	–	+	–	+
Sympathomimetics	+	+	–	–	+	+	–	–
Cocaine	+	+	+	+	+	+	+	+
α-methyldopa	+	–	–	–	+	–	–	–
Acetaminophen	+	–	+	–	+	–	+	–

E, Epinephrine; *MN,* metanephrines; *NE,* norepinephrine; *NMN,* normetanephrine. Diuretics, angiotensin-converting enzyme inhibitors, and angiotensin II receptor blockers have little influence on the frequency of false-positive results.
Data from Eisenhofer G, Goldstein DS, Walther, et al.: Biochemical diagnosis of pheochromocytoma: how to distinguish true from false-positive test results, *J Clin Endocrinol Metab* 88:2656–2666, 2003.

Among catecholamine-secreting tumors, 40% are familial. Genetic testing should be considered in all patients diagnosed with PPGLs, especially if the patient is younger than 50 years of age at presentation, has physical traits suggestive of one of the familial disorders, has multifocal disease, or has a positive family history (Lenders, 2014). Tests include assaying for mutations in the gene for menin in MEN 1, the RET oncogene in MEN 2A (Sipple disease) and MEN 2B, neurofibromin in NF-1, and VHL in von Hippel–Lindau syndrome. Familial paragangliomas are associated with various defects in the gene for succinate dehydrogenase. As with all genetic testing, pretest and posttest counseling is mandatory.

Chromogranin A (CgA) is a protein that is stored and secreted along with the catecholamines from the adrenal medulla and sympathetic nervous system. Although it is elevated in more than 80% of pheochromocytomas, it is not specific for this disorder, being secreted by other chromaffin tissues (Hsiao et al., 1991). CgA was initially thought to be useful in the diagnosis of pheochromocytoma, since medications typically used to treat it had no impact on CgA secretion or measurement. Despite a relatively high sensitivity of 86%, it has poor diagnostic specificity. This is due, in large part, to the fact that the kidneys play a major role in the clearance of CgA from the circulation so that even mild degrees of renal impairment (e.g., creatinine clearance [CrCl] <80 mL/min) can lead to significant increases in serum concentration of CgA (Bravo & Tagle, 2003). Among hypertensive patients with CrCl less than 80 mL/min, overall sensitivity, specificity, and accuracy and positive and negative predictive values (NPVs) of serum CgA dropped to 85%, 50%, 59%, 38%, and 90%, respectively. However, when combined with elevated plasma catecholamines in patients with CrCl of at least 80 mL/min, the diagnostic specificity and positive predictive values (PPVs) improved to 98% and 97%, respectively (Canale & Bravo, 1994). Its major use is in postoperative monitoring for recurrence of these tumors.

Testing Procedures

For 24-hour urine collections, creatinine is measured to verify the adequacy of the collection. To preserve the specimen adequately, urine should be collected in a container to which 25 mL of 6 N HCl has been added.

Plasma catecholamines are collected after an overnight fast (water permitted). The patient is placed in a reclining position in a quiet environment, and a heparin lock is inserted intravenously. After 20 to 30 minutes, blood is collected in a prechilled ethylenediaminetetraacetic acid (EDTA) lavender-top tube. The whole-blood sample should be kept in ice water until centrifuged (preferably at 4° C). Separation of plasma should take place within 2 hours of phlebotomy; the sample should then be frozen immediately.

Both urine and plasma specimens should be analyzed using HPLC/MS-MS, as this technique greatly eliminates problems caused by interfering substances (Taylor & Singh, 2002). For the urine metabolites, it is important to use age-appropriate reference ranges when interpreting the results. It is also important to be aware that reference ranges can vary widely not only from one laboratory to another but even within the same laboratory as newer methods are introduced.

TABLE 25.13

Pharmacologic Tests for Diagnosing Pheochromocytoma

Clonidine Suppression Test	
Indications	Patients with hypertension and clinical findings or family history that is highly suggestive of pheochromocytoma, and the catecholamines are elevated but not to the extent that is diagnostic of pheochromocytoma.
	Beta blockers should be withdrawn 48 hours prior to testing. Do not perform if BP <100/60 mmHg.
	IV cannula placed. Patient rests recumbent for 20 minutes. Blood for NE and NM is collected,* and 0.3 mg of clonidine is administered orally.
	BP and pulse are monitored closely. Blood for NE and NM are collected* after 3 hours.
Interpretation	Normal: Decrease in NE to below normal or a >50% decline from baseline. A decrease in NM to below normal or a 40% decline from baseline.
	Pheochromocytoma: Failure of NE to drop below normal or decrease by more than 50% from baseline. Failure of NM to drop below normal or decrease by more than 40% from baseline.

NE, Norepinephrine; *NM,* normetanephrines.
*Blood vials should be kept chilled on ice until processed.

Additional Follow-Up Testing

Once the diagnosis is confirmed biochemically, the tumor should be localized by a CT scan or MRI of the adrenal glands. If this is negative, imaging studies of the abdomen, chest, and pelvis should be performed. CT has greater sensitivity and MRI greater specificity. MRI is superior to CT in detecting extra-adrenal lesions and has the advantage of not requiring ionizing radiation or needing ionic contrast. If a tumor cannot be located by CT or MRI, or if metastatic disease is suspected, scanning with ^{131}I- or ^{123}I-labeled meta-iodobenzylguanidine should be performed. Octreoscanning and positron emission tomography are reserved for when the other techniques have failed. ^{18}F-FDG PET/CT scanning is especially useful in patients with paragangliomas or metastatic disease (Pacak et al., 2001b). MRI is preferred for evaluating PPGL metastases, detection of skull base and neck paragangliomas, and in patients in whom radiation exposure should be limited (children, pregnant women, patients with known germline mutations, and those with recent excessive radiation exposure).

Following successful tumor resection, the prognosis is generally excellent. Plasma or urinary metanephrines should be retested several weeks after surgery to ensure that the resection was complete and should be measured periodically thereafter as an early marker of disease recurrence (Werbel & Ober, 1995).

An algorithm to evaluate pheochromocytoma has been proposed by Eisenhofer and colleagues (2003) (Fig. 25.10).

Neuroblastoma

Similar to pheochromocytoma, neuroblastoma is of neural crest origin, arising within the adrenal glands or the sympathetic chain. It is the second most common solid malignant tumor in childhood, usually occurring before 3 years of age. Symptoms relate primarily to tumor mass rather than to hypertension, which is often mild or absent. At the time of diagnosis, 70% of cases will have distant metastases. About 90% of patients have elevated urinary HVA levels at the time of diagnosis, whereas almost 75% have increased urinary VMA levels (Tuchman et al., 1985). Both tests should be ordered when screening for the disease. In healthy children, at least up until about 15 years of age, urinary VMA and metanephrines tend to be higher (per mg of creatinine) and more variable than in adults. Urinary metanephrine can also be elevated in neuroblastoma patients but is not a sensitive measure of residual tumor. Urinary HVA is increased in familial dysautonomia (Riley-Day syndrome) and in some cases of pheochromocytoma.

HORMONES OF THE ADRENAL CORTEX

The adrenal cortex is composed of three distinct zones: the outermost zone, the zona glomerulosa, is followed by the intermediate zona fasciculata, which surrounds the innermost zona reticularis. In the broadest terms, each zone is responsible for the synthesis and secretion of a unique set of hormones: the zona glomerulosa—mineralocorticoids (aldosterone); the zona fasciculata—glucocorticoids (cortisol); and the zona reticularis—sex steroids (dehydroepiandrosterone sulfate and androgens). However, under certain pathologic and physiologic conditions, these distinctions become blurred.

Mineralocorticoid Axis

The chief mineralocorticoid is aldosterone, which promotes the reabsorption of sodium and water by the kidney to help maintain blood pressure and tonicity. Expression of the enzyme CYP11B2 (aldosterone synthetase) within the glomerulosa is site-specific. As a result, the synthesis of aldosterone and its intermediary 18-hydroxylated metabolites is restricted to the zona glomerulosa. The precursor molecules to aldosterone, 11-deoxycorticosterone (DOC) and 11-deoxycortisol, similarly possess mineralocorticoid activity. However, unlike aldosterone, they can be synthesized within the zona fasciculata as well as in the zona glomerulosa, which explains the hypertension and electrolyte disturbances seen in some forms of congenital adrenal hyperplasia. Although aldosterone will respond to acute changes in ACTH, it is mainly under the control of the renin-angiotensin system.

The zona fasciculata makes up 75% of the cortex and is responsible for the synthesis and secretion of glucocorticoids and, to a lesser extent, androgens and estrogens. The glucocorticoids are 21-carbon steroid compounds with a hydroxyl group on carbon 17, hence the synonym

17-hydroxycorticosteroids (17-OHCS). Cortisol is the key glucocorticoid, regulating its own secretion through negative feedback on the hypothalamic-pituitary-adrenal (HPA) axis and inhibiting corticotropin-releasing hormone (CRH) from the hypothalamus and ACTH release from the pituitary gland. Both CRH and AVP (ADH) are produced by the parvocellular neurons of the paraventricular nuclei of the hypothalamus. ACTH secretion is stimulated by CRH and, to a much lesser extent, by AVP. ACTH, in turn, stimulates cortisol production by the adrenal glands. Cortisol is needed in times of stress to maintain blood pressure and blood sugar, and to prevent shock. Although cortisol is the most important glucocorticoid, corticosterone, which is a hormone of the mineralocorticoid pathway, also possesses glucocorticoid activity.

Androgens and estrogens are produced by the zona reticularis. The androgens are 18-carbon steroids with saturated A rings, in contrast to the estrogens, which are 17-carbon steroids with unsaturated A rings.

The functions of these hormones are summarized in Table 25.14.

Congenital Disorders of Adrenal Cortical Enzyme Deficiencies

The hormones of the adrenal cortex are steroid derivatives, synthesized from low-density lipoprotein (LDL) cholesterol. LDL is delivered to the adrenal glands, where it is taken up by LDL receptors. Evidence also supports local synthesis of LDL from acetyl coenzyme A. Steroid acute regulatory protein (StAR) shuttles LDL across the mitochondrial membrane, where it begins its journey down the steroidogenic pathway (Fig. 25.11). The enzymes that catalyze these synthetic reactions are of four general types: hydroxylases, dehydrogenases, desmolases, and isomerases. Because most of the inborn errors of metabolism affecting steroid hormone synthesis in the adrenal cortex involve deficiencies of hydroxylases, they constitute the most clinically important group of enzymes.

At least eight different metabolic defects in the synthesis of cortisol and aldosterone have been described, each characterized by a deficiency of a

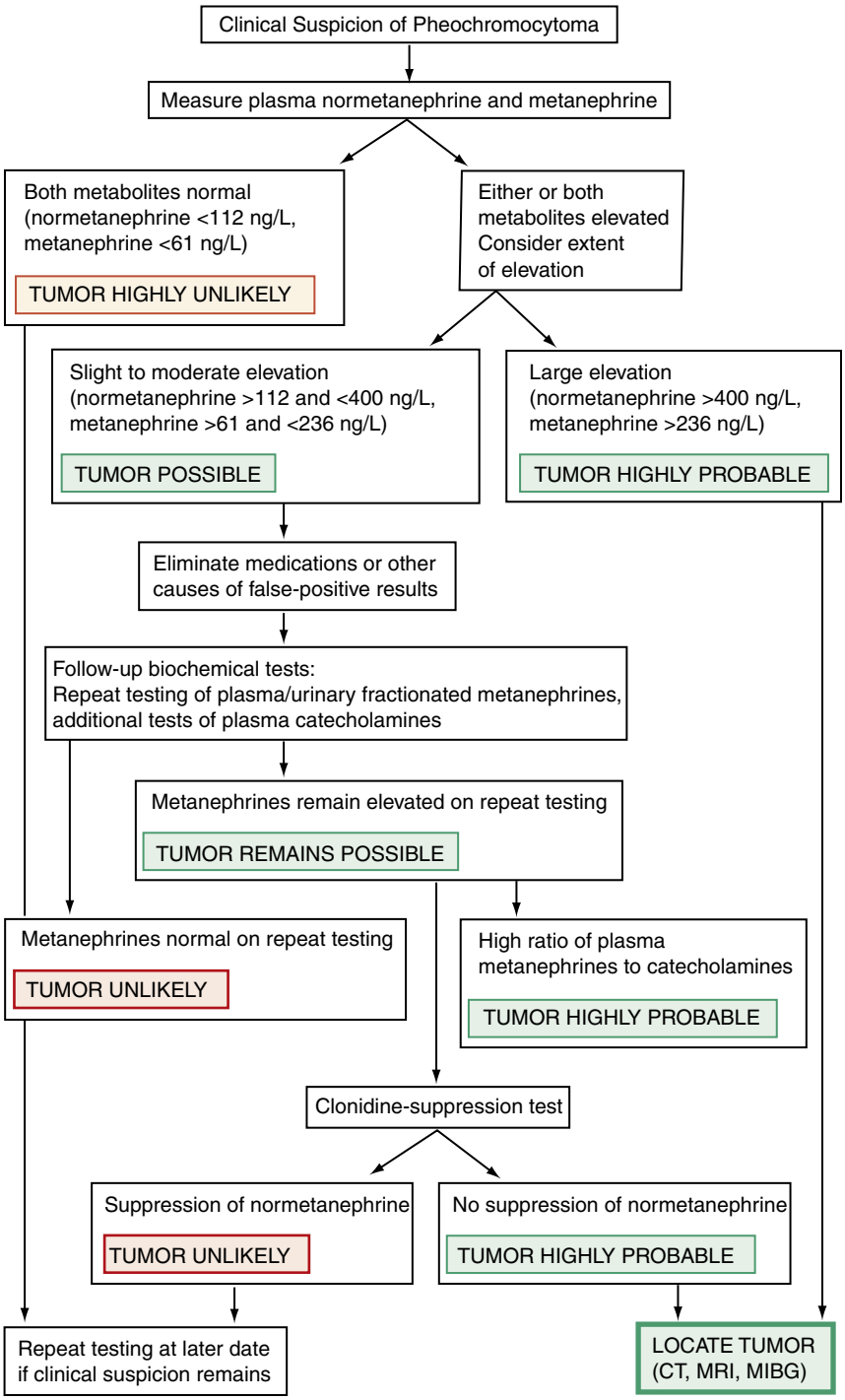

Figure 25.10 Algorithm for the evaluation of pheochromocytoma. *CT,* Computed tomography (scan); *MIBG,* metaiodobenzylguanidine (scan); *MRI,* magnetic resonance imaging. (Redrawn from Eisenhofer G, Goldstein DS, Walther MM, et al.: Biochemical diagnosis of pheochromocytoma: How to distinguish true- from false-positive test results, J Clin Endocrinol Metab 88:2656–2666, 2003, with permission.)

specific adrenal enzyme. A vast majority of these enzymatic deficiencies are inherited as autosomal-recessive traits with variable degrees of penetrance. Those enzymatic defects that uniquely affect the biosynthesis of cortisol are grouped under the rubric of congenital adrenal hyperplasia (CAH). These five enzymes are P450scc (defect in StAR), 3-β-hydroxysteroid dehydrogenase, 21-hydroxylase (21-OH), 11-hydroxylase, and 17-hydroxylase. CRH and ACTH synthesis and secretion are normally under the negative-feedback control of cortisol. In CAH, defects in the enzymes necessary for cortisol production lead to cortisol deficiency; cortisol deficiency, in turn, results in disinhibition of negative feedback on CRH and ACTH production. As a consequence, CRH and ACTH levels rise, inducing adrenal hyperplasia and a forward push in steroidogenesis as the body tries to compensate and normalize cortisol production. Not only does this result in a buildup of the hormonal precursors directly preceding the enzymatic defect, it also causes massive shunting of these precursors down the remaining functional pathways. The clinical manifestations of CAH are heterogeneous, depending on the severity and location of the enzymatic defects, which hormones are deficient, and which are produced in excess. Symptoms range from shock, salt wasting, and anomalous sexual development in infancy to hirsutism and infertility in the adult. Sometimes, as in partial enzymatic deficiencies of cortisol synthesis, near-adequate hormone synthesis is possible if hypersecretion of ACTH is able to stimulate adrenal hyperplasia to compensate for the deficiency. The clinical manifestations of various adrenal cortical enzyme deficiencies and their associated laboratory findings are summarized in Table 25.15.

The diagnosis is made by measuring the various serum hormone levels and assessing which steroids are produced in excess and which are deficient, and by calculating the precursor/product ratio and comparing these results to age- and sex-matched normative data. Levels of hormones distal to the block (product hormones) may be elevated as a result of peripheral conversion of the markedly elevated precursor hormones. The use of precursor/product ratios mitigates the risk for misdiagnosis due to misleading elevations of product hormones (Levine, 2002). If hormone levels return as borderline but the clinical suspicion for CAH remains high, the steroid levels should be remeasured 60 minutes after intravenous administration of 0.25 mg of ACTH. ACTH drives steroidogenesis forward, accentuating the block. When there is a proband, the diagnosis can be more accurately determined by genotyping.

CAH is categorized according to severity of disease into classic (neonatal, severe) and nonclassic (late-onset, cryptogenic) forms. The classic form is further subdivided into salt-losing and non–salt-losing (simple virilizing) variants.

TABLE 25.14
Physiologic Effects of Steroids

Representative Hormone	Biological Effects
Cortisol (as a representative glucocorticoid)	Protein nitrogen catabolism increased
	Gluconeogenesis
	Increased blood glucose concentration
	Decreased glucose tolerance
	Increased liver glycogen
	Increased liver glycogenolysis
	Decreased peripheral uptake and utilization of glucose
	Decreased synthesis of acid-sulfated mucopolysaccharides
	Fat synthesis and redistribution
	Cellular or tissue effects
	Anti-inflammatory
	Dissolution of lymphoid tissue
	Lymphopenia
	Eosinopenia
	Increased erythropoiesis
	Alteration of cellular permeability, especially decreased membrane permeability to water
	Increased gastric (HCl and pepsin) secretion
Aldosterone (as a representative mineralocorticoid)	Electrolyte regulation
	Sodium (Na^+) retention
	Potassium (K^+) excretion
	Retention of water and expansion of extracellular fluid volume
	Increases in blood pressure
Androgens (as representative sex hormones)	Protein nitrogen anabolism
	Growth and maturation—osseous and muscular
	Body hair (pubic and axillary)

21-Hydroxylase Deficiency

The enzyme 21-OH (also referred to as CYP21, CYP21A2, and P450c21) is located within the mitochondrial endoplasmic reticulum. 21-OH deficiency is the most common cause of CAH, accounting for about 95% of all cases. Screening of newborns using capillary heel blood on paper filter disks has identified this disorder in about 1 in 14,000 persons in North America, and in as many as 1 in 300 Yupik Eskimos of Alaska (Pang et al., 1988, 1982). The classic form is detected in about 1 in 16,000 live births; the nonclassic form is seen in about 0.2% of the general white population, and in 1% to 2% of those of Eastern European Jewish ancestry (Speiser et al., 1985; Therrell, 2001).

21-OH catalyzes the conversion of 17-hydroxyprogesterone (17-OHP) to 11-deoxycortisol (compound S), and progesterone to DOC. Thus, 21-OH deficiency leads to elevated levels of the steroid precursors 17-OHP and pregnanetriol in the urine and 17-OHP in the serum. These precursors are shunted toward the pathway, leading to excess androstenedione and testosterone production (Fig. 25.12). Clinical presentation often correlates with the severity of enzymatic dysfunction. The classic variety presents in the newborn period or in early childhood with adrenal insufficiency and virilization, with or without salt wasting. The nonclassic form presents in late childhood as early adrenarche or in young adulthood as hirsutism, amenorrhea, and infertility. The presentation in women is very similar to that of polycystic ovarian disease. Males may develop precocious puberty, adrenal rests within the testes, and infertility.

A close functional relationship exists between the adrenal cortex and the adrenal medulla. Dysplasia of the medulla and catecholamine hyposecretion have been described in classic 21-OH deficiency. In a study of 38 children with classic (CYP21A2) disease, levels of plasma epinephrine and metanephrine and urinary epinephrine were 40% to 80% lower in affected individuals than in normal persons (Merke et al., 2000). In another study, those with CYP21A2 showed a significantly decreased catecholamine response to exercise that was unaffected by the administration of stress doses of glucocorticoids (Weise et al., 2004). It has been suggested that the degree of medullary impairment may be a biomarker for CAH severity (Merke et al., 2002).

Diagnosis. Prenatal diagnosis is important because suppressive treatment with steroids can abrogate the development of virilization of the female fetus. Diagnosis is made by measuring the level of 17-OHP in amniotic fluid or by genotyping cells obtained by chorionic villous sampling. The genes responsible for 21-OH deficiency, *CYP21 (CYP21A2)* and *CYP21P (CYP21A)*, are located on chromosome 6. Of these two homologous genes, only *CYP21* is active; deleterious mutations within *CYP21P* interfere with normal gene expression. These mutations can be identified by PCR and Southern blotting on chorionic villous samples (White et al., 1994a; New, 1995). The 2010 consensus statement on the management of CAH due to 21-OH deficiency recommends that prenatal treatment of CAH be regarded as experimental and that the diagnosis should rest on clinical and hormonal data, with genotyping being reserved for equivocal cases and genetic counseling (Speiser et al., 2010).

Neonatal screening, which is now mandatory across the United States and in several other countries, is performed by measuring 17-OHP or by genotyping blood that has been obtained from a heel stick and collected on filter paper. 17-OHP can be measured by automated time-resolved Dissociation-Enhanced Lanthanide Fluoroimmunoassay (DELFIA) (Speiser et al., 2010). This is a modified two-step immunoassay in which the secondary antibody is conjugated to a chelate containing a lanthanide series element, e.g., Europium (Eu). Addition of a solution containing a high-affinity chelate to the complex causes the release of Eu to the second chelate. Excitation of the Eu chelated to this second chelating agent by monochromatic light at a wavelength that is between 320 and 340 nm results in a narrow, intense fluorescence band at 615 nm that, unlike most fluorescent probes, is stable over long time periods. Causes for false-positive screens include prematurity, illness, stress, and possibly the antenatal administration of glucocorticoids used to induce fetal lung maturation. The initial positive screen is followed up by checking the 17-OHP level by LC-MS/MS (Speiser et al., 2010). In regard to genotyping, aside from being the most definitive test for diagnosing CAH, the fact that the genotype correlates fairly well with disease severity means that it can also be used as a prognostic tool (Nordenstrom et al., 1999).

In the newborn with salt wasting, unstimulated 17-OHP levels are typically greater than 8000 ng/dL, rising to 100,000 ng/dL (3000 nmol/L) following administration of ACTH. Levels in the simple virilizing variant range from 10,000 to 30,000 ng/dL (300–1000 nmol/L). Those with nonclassic disease typically have 17-OHP levels ranging from 1500 to 10,000 ng/dL (50–300 nmol/L) (New et al., 1983). It is of note that randomly drawn hormone levels may be normal in those with nonclassic disease; therefore, it is important to test during the early morning. If the results are equivocal, the diagnosis can be confirmed by comparing serum 17-OHP levels before and 60 minutes after administration of 0.25 mg ACTH (Cortrosyn). ACTH acts to stimulate steroidogenesis, serving to dramatically increase the bottleneck at the site of the enzymatic block, resulting in a dramatic increase in precursors, in this case, 17-OHP. Post-ACTH 17-OHP values <330 ng/dL are normal, 330 to 1000 ng/dL indicates a heterozygote carrier, and levels greater than 2000 ng/dL are diagnostic for nonclassic CAH. If a proband is available, genotyping is superior to these older biochemical tests in identifying heterozygotes (Honour & Rumsby, 1993).

The goals of glucocorticoid and mineralocorticoid replacement therapy in children are the attainment of normal growth, weight, and pubertal development, and optimization of final adult height. In adults, the major treatment goals include lessening of signs of virilization and resumption of fertility. Glucocorticoid replacement is titrated to keep the 17-OHP level partially suppressed to between 100 and 1000 ng/dL (3–30 nmol/L) and the ACTH under 100 ng/L, thereby preventing shunting toward testosterone synthesis, and normalizing levels of androstenedione and testosterone. Normalization of 17-OHP should not be attempted because this requires supraphysiologic levels of glucocorticoids and may result in Cushing syndrome (Speiser & White, 2003).

Varying degrees of hypoaldosteronism accompany all forms of 21-OH deficiency. This is biochemically apparent as an elevated plasma renin activity (PRA) and a decreased aldosterone/PRA ratio. The objective of mineralocorticoid replacement is to normalize the PRA.

11-β-Hydroxylase Deficiency

The second most common enzyme deficiency of the adrenal cortex, accounting for about 7% of all cases of CAH, is the 11-β-hydroxylase (11-OH) deficiency. A defect in this enzyme blocks the final conversion of 11-deoxycortisol to cortisol and DOC to corticosterone. As with 21-OH deficiency, a compensatory increase in ACTH secretion leads to adrenal hyperplasia and a mass action shunting of precursor steroids toward testosterone synthesis, resulting in signs of virilization. This block also results in the accumulation of DOC; the mineralocorticoid activity of DOC leads to the development of hypertension and hypokalemia, similar to what is seen with hyperaldosteronism (Fig. 25.13).

11-OH deficiency is an autosomal-recessive disorder caused by mutations of the genes *CYP11B1* and *CYP11B2*, located on chromosome 8q21-q22 (White et al., 1994b). Diagnosis in the neonate is established by the presence of a high basal and high ACTH-stimulated 11-deoxycortisol.

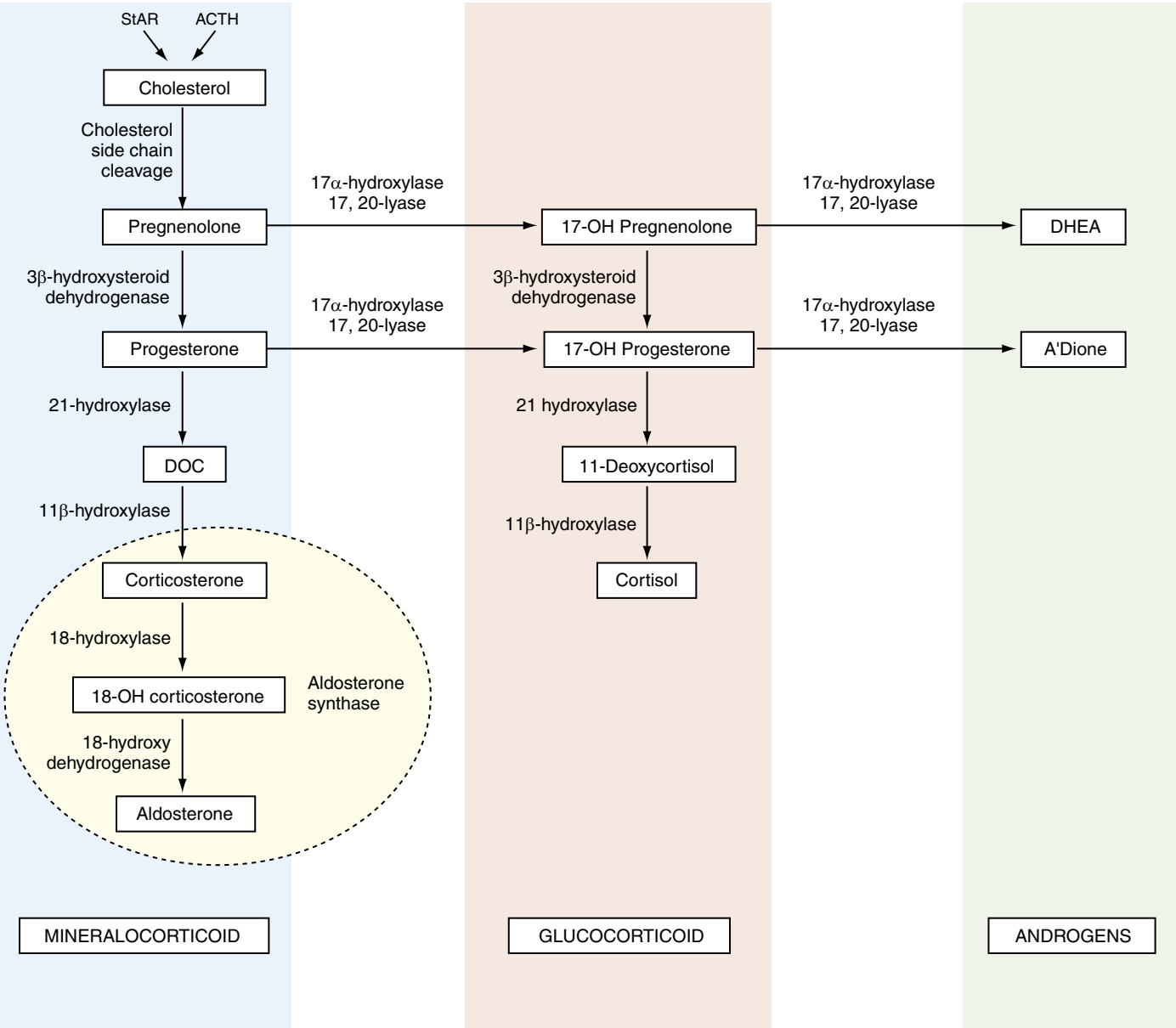

Figure 25.11 Steroidogenic pathways of the adrenal cortex. The adrenal steroids are categorized according to mineralocorticoid, glucocorticoid, or androgenic activity. The chemical structures for these steroids are shown in Figure 26.1 in Chapter 26. *ACTH,* Adrenocorticotropin; *DHEA,* dehydroepiandrosterone; *DOC,* deoxycorticosterone; *StAR,* steroidogenic acute regulatory (protein).

Concentrations of urinary tetrahydro-11-deoxycortisol in the urine are also elevated. During childhood and in young adults, the diagnosis of 11-OH deficiency is made by the presence of elevated early-morning and ACTH-stimulated serum levels of 11-deoxycortisol that are more than three times the upper limit for age-matched normals. Levels of DOC and adrenal androgens (androstenedione, dehydroepiandrosterone, and dehydroepiandrosterone sulfate) are also elevated. PRA and aldosterone are often suppressed as a result of salt and water retention induced by elevations of DOC. Unlike the heterozygotes with 21-OH deficiency, those with 11-OH deficiency often fail to show a rise in precursors following ACTH stimulation (Pang et al., 1980). However, an exuberant response was seen in those who had hirsutism (Gabrilove et al., 1965).

Prenatal diagnosis of 11-OH deficiency is made by measuring levels of tetrahydro-11-deoxycortisol (THS) in the maternal urine or amniotic

TABLE 25.15

Congenital Adrenal Hyperplasia: Clinical and Biochemical Features

Feature	21-Hydoxylase Deficiency	11-β-Hydoxylase Deficiency	17-β-Hydroxylase Deficiency	3-β-Hydroxysteroid Deficiency	Lipoid Hyperplasia	Aldosterone Synthase Deficiency
Defective gene	*CYP21*	*CYP11B1*	*CYP17*	*HSD3B2*	*StAR*	*CYP11B2*
Incidence	1:15,000	1:100,000	Rare	Rare	Rare	Rare
Ambiguous genitalia	+ (female)	+ (female)	+ (male) Absent puberty (female)	+ (male) Mild in female	+ (male) Absent puberty (female)	Normal
Acute adrenal insufficiency	+	Rare	No	+	++	Salt wasting only
Laboratory findings	↑ plasma 17-OHP and pregnanetriol Greatly ↑ urinary pregnanetriol and 17-KS	↑ serum DOC and 11-deoxycortisol ↑ urinary 17-OHCS and 17-KS	↑ serum DOC, 18-OH DOC, B, and 18-OHB	↑ serum 17-OH-pregnenolone, pregnenolone and DHEA ↑ urinary 17-KS ↑ Δ5/Δ4 serum and urinary steroids	All serum and plasma steroids are decreased	↑ serum B, 11-DOC, and 18-OHB
Glucocorticoids	↓	↓	↓	↓	↓	Normal
Mineralocorticoids	↓	↑	↓	↓	↓	↓
Androgens	↑	↑	↓	↓ male, ↑ female	↓	Normal

B, Corticosterone; *DHEA*, dihydroepiandrosterone; *11-DOC*, 11-deoxycorticosterone; *17-KS*, 17-ketosteroids; *18-OHB*, 18-hydroxycorticosterone; *17-OHP*, 17-α-hydroxyprogesterone. From Stewart PM: The adrenal cortex. In Larsen PR, Kronenberg HM, Melmed S, et al., editors: *Williams textbook of endocrinology,* ed 10, Philadelphia, 2003, Saunders, p 533.

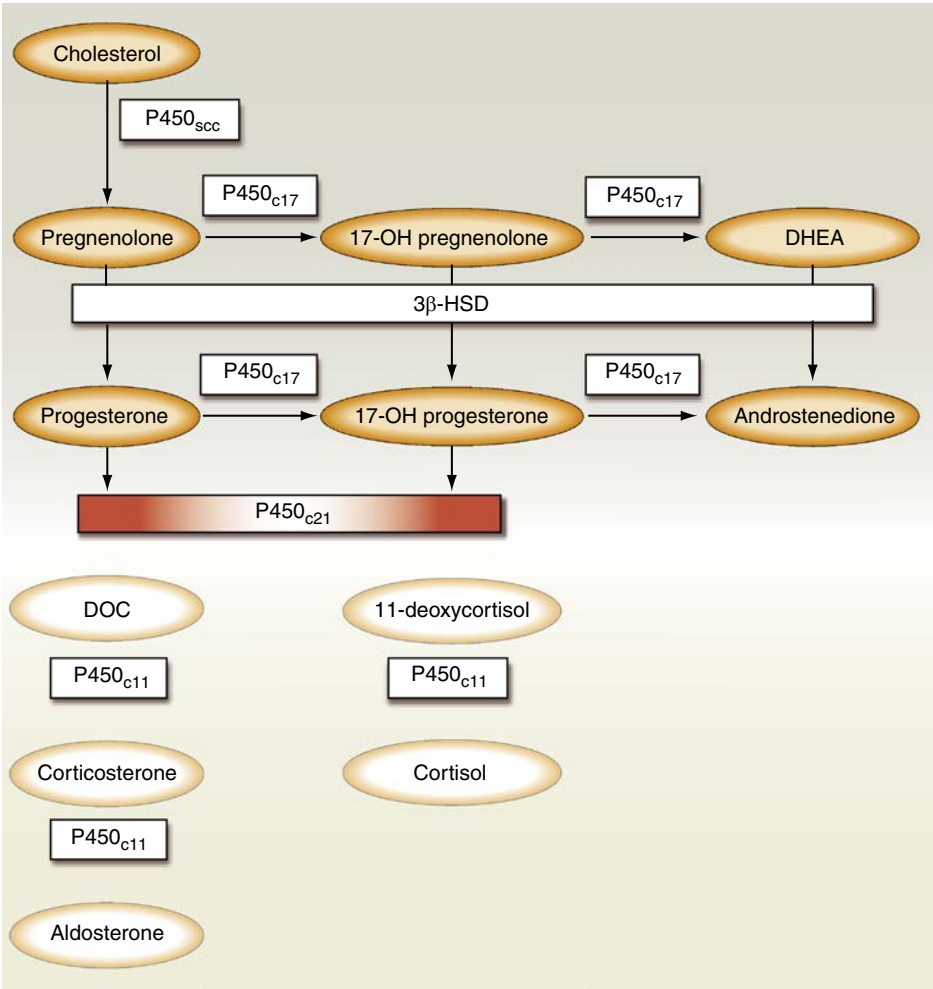

Figure 25.12 Defective steroidogenesis due to 21-hydroxylase deficiency. The relative increase in the hormones proximal to the block is depicted by more intense color. The more severe the enzymatic defect, the greater the concentration of the precursor hormones. *DHEA,* Dehydroepiandrosterone; *DOC,* deoxycorticosterone.

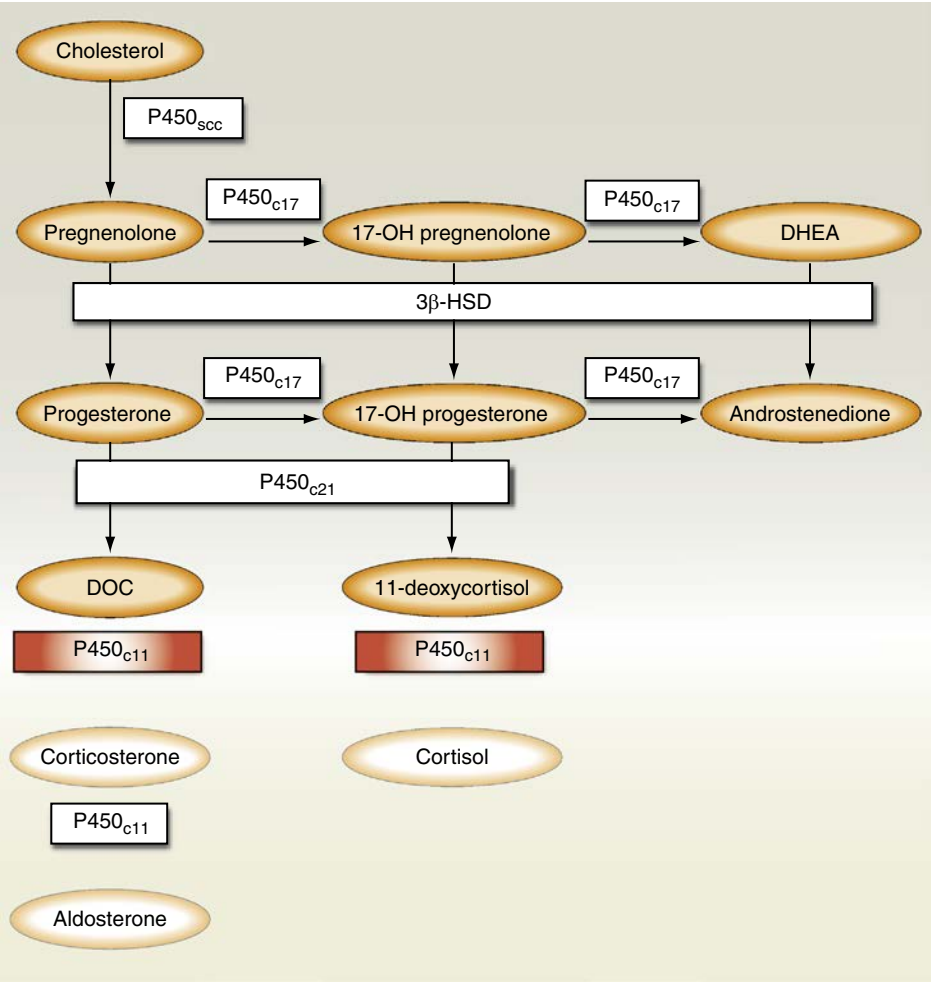

Figure 25.13 Defective steroidogenesis due to 11-β-hydroxylase deficiency. The relative increase in the hormones proximal to the block is depicted by more intense color. The more severe the enzymatic defect, the greater the concentration of the precursor hormones. High levels of 11-deoxycorticosterone (DOC) created by the block produce a state of mineralocorticoid excess. *DHEA,* Dehydroepiandrosterone.

fluid. These levels begin to rise in the first trimester. In addition to THS, elevation of 11-deoxycortisol levels and of the THS to tetrahydrocortisol plus tetrahydrocortisone ratio is seen (Rosler et al., 1988).

Treatment consists of the replacement of glucocorticoids, causing normalization of DOC and PRA.

3-β-Hydroxysteroid Dehydrogenase Deficiency

3-β-hydroxysteroid dehydrogenase (3-β-HSD), which catalyzes the second enzymatic step in steroidogenesis, is coded by two genes, *HSD3BI* and *HSD3BII*. *HSD3BII* is expressed in the adrenals and gonads; *HSD3BI* is expressed in placenta, skin, and other peripheral tissues and usually remains functionally intact at these sites in CAH. A defect in 3-β-HSD leads to a block in the conversion of Δ5 steroids (pregnenolone, 17-OH pregnenolone, and dihydroepiandrosterone) to Δ4 steroids (progesterone, 17-OHP, androstenedione), resulting in an increase in circulating levels of Δ5 steroids (Fig. 25.14). However, because *HSD3BI* is usually intact, levels of the Δ4 steroids may be normal or even elevated.

Patients with classic disease will have manifestations of glucocorticoid deficiency, with or without the accompaniment of salt wasting. Affected males have incomplete masculinization, and females may be normal or may have ambiguous genitalia. A late-onset variant has been described that is associated with features typical of polycystic ovarian disease, such as hirsutism, oligomenorrhea, and infertility (Pang et al., 1985).

Previous criteria for the diagnosis of 3-β-HSD deficiency examined the basal and ACTH-stimulated Δ4/Δ5 steroid ratios, 17-OH-pregnenolone (17-OHP)/cortisol, and levels of pregnenolone, 17-OH-pregnenolone, and dehydroepiandrosterone in urine and blood. The standard for diagnosing this disorder has been recently revised to correlate more closely with genotypic studies. The ACTH-stimulated Δ5-17 P levels and Δ5-17 P/cortisol ratios have been shown to be the best indices for definitively diagnosing 3-β-HSD deficiency (Lutfallah et al., 2002). Applicability of these new criteria to patients with the nonclassic variant is still debatable.

Treatment consists of glucocorticoids and mineralocorticoids, as well as sex steroids, in accordance with normal growth and development.

17-Hydroxylase Deficiency

17-Hydroxylase (CYP17, $P450_{c17}$) is expressed in the adrenal glands and the gonads and encodes two enzymes—17α-hydroxylase and 17,20-lyase. 17α-Hydroxylase catalyzes the conversion of pregnenolone and progesterone to their respective 17-OH derivatives. 17,20-Lyase converts 17-OH pregnenolone to dehydroepiandrosterone and 17-OH progesterone to androstenedione. CYP17 deficiency blocks the conversion of pregnenolone and progesterone to the 17-hydroxy derivatives, causing shunting from testosterone and cortisol synthesis to aldosterone (Fig. 25.15). Accordingly, these patients develop hypertension and hypokalemic alkalosis in association with incomplete masculinization (in the male) and decreased testosterone and cortisol levels. 17-OH deficiency is diagnosed by demonstrating high DOC, pregnenolone, and progesterone levels, along with decreased urinary 17-ketosteroids and 17-hydroxycorticosteroids. The gene associated with this condition (*CYP17*) has been located on chromosome 10q, the same gene as 17,20-desmolase (Kater & Biglieri, 1994).

Congenital Lipoid Adrenal Hyperplasia

Congenital lipoid adrenal hyperplasia (lipoid CAH) is the most severe form of CAH, in which the synthesis of all gonadal and adrenal cortical steroids is markedly impaired. Lipoid CAH may be caused by a defect in the StAR or the P450 side chain cleavage (scc) (Fujieda et al., 2003). StAR, located on chromosome 8p11, controls the rate-limiting step in steroidogenesis. It is responsible for the shuttling of cholesterol from the outer to the inner mitochondrial membrane. 20,22-Desmolase (CYP11A1, P450scc) converts cholesterol to pregnenolone (Fig. 25.16). Pathologically, the adrenal cortex shows marked accumulation of cholesterol and other lipids, which is the primary distinguishing feature from CAH.

The presentation of this extremely rare disorder is that of severe adrenal insufficiency with hypotension, salt wasting, and feminization of external genitalia in males. Occasionally, females may not present until the onset of puberty. Diagnosis is made by the presence of extremely low cortisol and aldosterone concentrations and elevated ACTH and plasma renin activity.

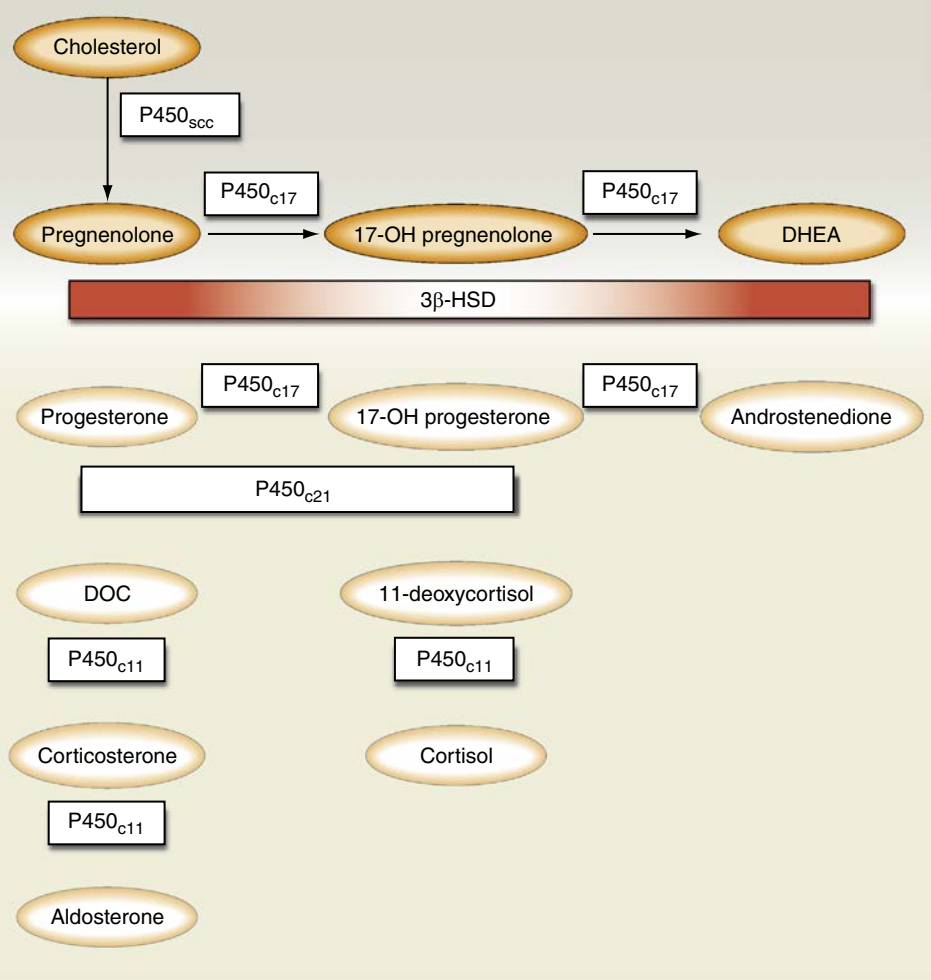

Figure 25.14 Defective steroidogenesis due to 3-β-hydroxysteroid dehydrogenase deficiency. The relative increase in the hormones proximal to the block is depicted by more intense color. The more severe the enzymatic defect, the greater the concentration of the precursor hormones. 17-α-hydroxyprogesterone levels may be elevated because of peripheral conversion of 17-α-hydroxy pregnenolone. *DHEA,* Dehydroepiandrosterone; *DOC,* deoxycorticosterone.

Aldosterone Synthetase Deficiency

Aldosterone synthetase (CYP11B2) is the final step in the steroid synthetic pathway leading to the production of aldosterone. It stimulates a multistep process: 11-hydroxylation of DOC to corticosterone, 18-hydroxylation of corticosterone to 18-hydroxycorticosterone, and, finally, 18-dehydrogenation to aldosterone. Isolated enzyme deficiency leads to salt wasting, hyperkalemia, and metabolic acidosis. This condition may be diagnosed by demonstrating the presence of metabolites of corticosterone and 11-deoxycorticosterone in the urine, elevated serum DOC, and deficiency of corticosterone, 18-hydroxycorticosterone, or aldosterone in the serum.

Cortisol and the Glucocorticoids

The adrenal cortex secretes cortisol in response to ACTH, a diurnal rhythm, and stress. ACTH, synthesized in the adenohypophysis, is formed from the cleavage of a much larger precursor molecule: POMC. In addition to ACTH, cleavage of POMC releases β-LPH, which, in turn, is cleaved to yield γ-LPH and β-endorphin. Within the ACTH sequence are α-MSH and the corticotropin-like intermediate lobe protein. Endorphins, which act on neurons in the brain, constitute a distinct peptidergic system related to pain perception. Although β-endorphin is secreted in parallel with ACTH, the significance of this remains unknown.

ACTH consists of 39 amino acid residues, of which residues 1 to 24 at the amino terminal possess full hormonal activity. Occasionally, POMC is incompletely processed; this leads to the formation of other forms of ACTH that usually have little biological activity, although they may retain immunoreactivity. These forms may predominate in malignant conditions such as ectopic production by primary or metastatic lung cancer and in some patients with Nelson syndrome, a disorder characterized by the occurrence of a pituitary tumor and skin hyperpigmentation following bilateral adrenalectomy. Defects in POMC cleavage enzymes may also be responsible for the formation of rare forms of isolated ACTH deficiency (Nussey et al., 1993).

ACTH is secreted in response to several factors, of which CRH and AVP are the most important. Among the other moieties reported to stimulate ACTH secretion are atrial natriuretic factor (ANF), angiotensin II, IL-6, IL-1, and tumor necrosis factor-α (Rivier & Vale, 1983; Chrousos, 1998).

CRH is synthesized and released from the hypothalamus; it acts to stimulate the synthesis and release of ACTH from the pituitary gland. CRH is released in a circadian pattern and in response to physiologic stimuli, such as stress and hypoglycemia. The HPA axis consists of various feedback loops that control cortisol synthesis and secretion. When plasma cortisol increases, it suppresses the release of CRH, ACTH, and AVP, which, in turn, leads to lowering of the cortisol level. Conversely, when serum cortisol reaches a nadir, the hypothalamus and pituitary gland respond by increasing CRH and ACTH production, leading to stimulation of cortisol formation and secretion. By this mechanism, ACTH and cortisol control the concentration of each other within a very narrow range; a small change in one results in a concomitant change in the other. When the adrenal gland is unable to respond to ACTH because of damage or disease, cortisol levels are low and ACTH levels are high. In those conditions in which the pituitary gland is destroyed, ACTH is not formed and cortisol levels are consequently low. Damage to the hypothalamus is also associated with low ACTH and cortisol levels; testing with CRH may permit the distinction between these two entities. Synthetic forms of CRH are used in testing the anterior pituitary gland's reserve of ACTH by comparing plasma ACTH and cortisol before and 1 hour after CRH stimulation (Grodum et al., 1993). This test is useful in distinguishing between lesions affecting the hypothalamus, pituitary gland, and adrenal glands (Fukata et al., 1993). If the lesion is in the hypothalamus, after a time delay, ACTH levels rise following CRH administration. If it is in the pituitary gland, no significant ACTH response occurs. With primary adrenal insufficiency, administration of CRH causes a further rise in an already elevated ACTH level but little or no rise in cortisol level.

If the HPA axis is interrupted by the administration of large quantities of exogenous glucocorticoids, they will exert an inhibitory effect on the hypothalamus and pituitary gland, suppressing CRH and ACTH secretion. If this suppression continues over a period of weeks, it leads to atrophy of

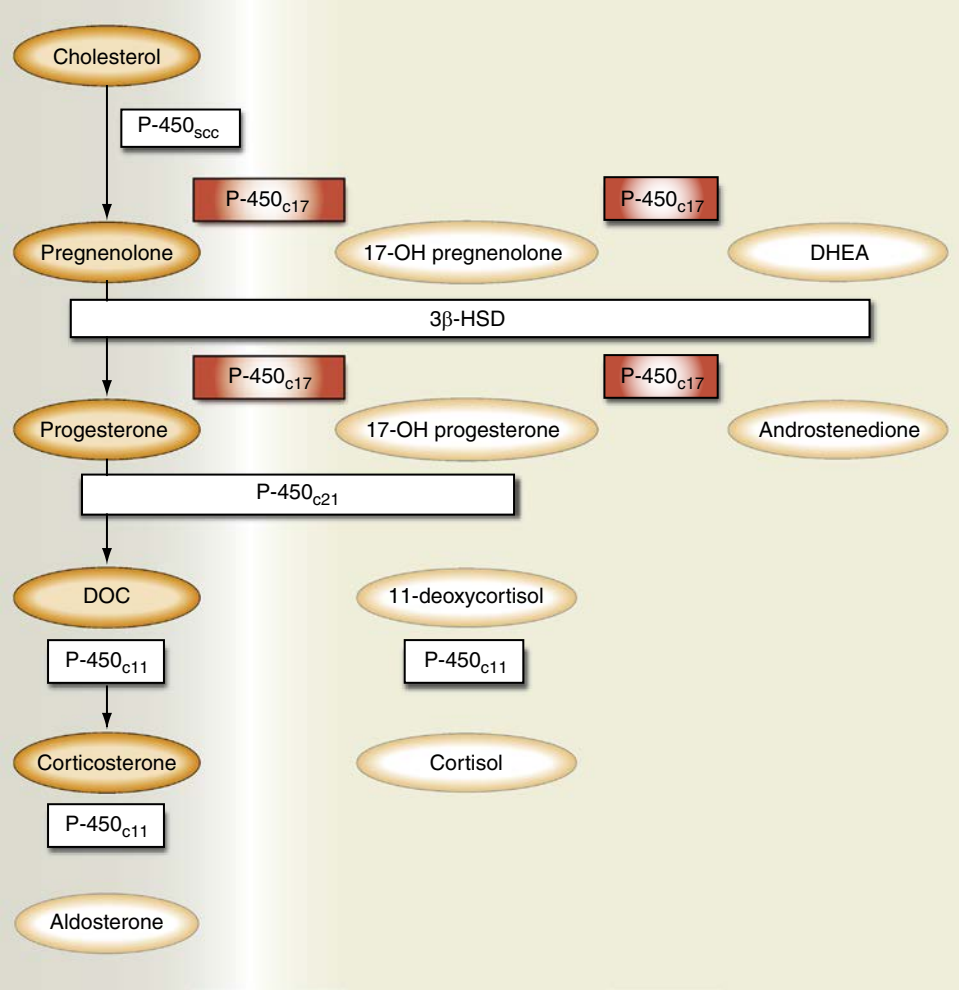

Figure 25.15 Defective steroidogenesis due to 17-hydroxylase deficiency. The relative increase in hormones proximal to the block is depicted by more intense color. The more severe the enzymatic defect, the greater the concentration of the precursor hormones. High levels of 11-deoxycorticosterone (DOC) and corticosterone created by the block produce a state of mineralocorticoid excess. *DHEA,* Dehydroepiandrosterone.

the adrenal glands. As a result, the HPA axis becomes unable to secrete cortisol in times of stress. The HPA axis can fully recover after tapering off of steroids.

The second influence on plasma cortisol levels is the diurnal pattern, which is due to the circadian pattern of ACTH release. Major increases in secretion occur at between 4 AM and 8 AM, followed by a decrease in ACTH during the rest of the day. In subjects with a normal sleep-wake cycle, the lowest ACTH concentrations are found shortly after midnight. Sudden changes in sleep-wake patterns have little effect on the diurnal pattern, but permanent changes in daily sleep habits result in a gradual change in diurnal secretory patterns. Superimposed on the circadian periodicity is an ultradian rhythm of 10 to 18 secretory bursts per 24 hours (Horrocks et al., 1990).

The third important influence on cortisol secretion is stress. Stimuli such as surgical trauma, pyrogens, hypoglycemia, and hemorrhage are capable of bringing about an acute increase in ACTH and cortisol secretion. This response to stress may be absent or decreased in magnitude in patients in whom large doses of steroids have been administered for some time. The initiation of any stress response is dependent on an intact nervous system. For example, trauma normally results in the acute release of ACTH and cortisol. However, in patients with spinal cord transections, the normal transmission of neurologic stimuli is interrupted. As a result, the same trauma applied to an extremity will not elicit any ACTH or cortisol response. Evidence suggests that the stress response of cortisol is mediated through excitatory and inhibitory inputs that integrate at the level of the hypothalamus and modulate CRH secretion. Cortisol levels also rise after meals, especially those high in protein; it also rises in depression (Linkowski et al., 1987).

Most disorders of cortisol secretion can be classified by the patterns of response of the following three hormones to suppression and stimulation: ACTH, plasma cortisol, and urinary free cortisol (Snow et al., 1992).

Laboratory Measurement of ACTH

Plasma ACTH is measured using a two-site chemiluminescence immunoassay. To prevent degradation of ACTH, it is best to collect the sample in a prechilled EDTA lavender-top tube. The specimen should be kept in an ice bath and should be processed as soon as possible. Following centrifugation in a refrigerated centrifuge, the specimen should be separated, transferred to a plastic tube, and kept frozen at –20° C until time of analysis. The normal reference range is 2 to 12 pmol/L (9–52 pg/mL) between 7 AM and 10 AM. Plasma ACTH is a useful tool for distinguishing primary (adrenal) from secondary (pituitary) or tertiary (hypothalamic) adrenal insufficiency. In primary adrenal insufficiency, low cortisol concentrations are found, along with increased ACTH levels. In secondary or tertiary adrenal insufficiency, both ACTH and cortisol are expected to be low. ACTH levels best discriminate between healthy individuals and those with adrenal insufficiency when specimens for ACTH are collected between 8 AM and 10 AM.

ACTH is less useful in diseases of cortisol excess. Up to 50% of patients may have normal ACTH levels in Cushing disease. Although the values tend to run higher (>20 pmol/L [>90 pg/mL]) in Cushing syndrome due to ectopic ACTH production, the values overlap with those seen in Cushing disease in 30% of cases (Findling, 1992). Because of the normal diurnal variation in ACTH and cortisol secretion, measurement of these values during their expected nadir, from 11 PM to 1 AM, is helpful in confirming the diagnosis of ACTH-dependent Cushing disease. An elevated midnight ACTH of greater than 5 pmol/L (23 pg/mL) in the face of an elevated serum cortisol confirms the diagnosis of ACTH-dependent Cushing disease. Those patients with ectopic ACTH-secreting tumors characteristically have markedly elevated plasma ACTH (usually >200 pg/mL) and elevated serum cortisol. Measurement of ACTH by plasma extraction, which detects ACTH precursors and fragments, may be useful in distinguishing patients with cancer-related syndromes or ACTH-secreting tumors from those with Cushing's disease, as the former entities are more likely to produce these other forms of ACTH (White & Clark, 1993). ACTH-secreting neoplasms may be occult, creating diagnostic difficulties. In this instance, ACTH measurement using selective venous sampling has proven useful in localization of the lesion.

In patients with increased levels of circulating glucocorticoids due to an adrenal adenoma or carcinoma and in those surreptitiously taking steroids,

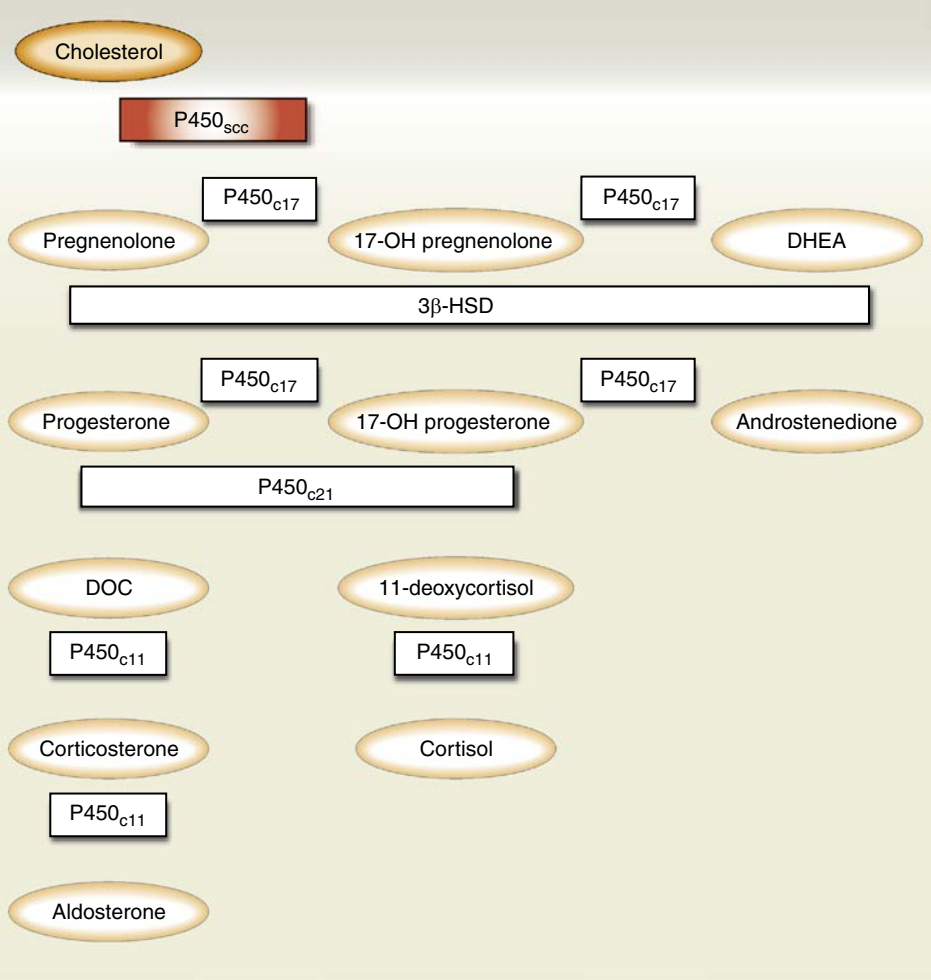

Figure 25.16 Defective steroidogenesis in congenital lipoid adrenal hyperplasia is due to a defect in steroidogenic acute regulatory protein or the side-chain cleavage enzyme (P450scc). The relative increase in hormones proximal to the block is depicted by more intense color. In this disorder, the synthesis of all classes of steroids is defective. *DHEA,* Dehydroepiandrosterone; *DOC,* deoxycorticosterone.

ACTH secretion is inhibited and levels are low or undetectable. In patients with pituitary-induced adrenal hyperplasia (Cushing disease), plasma ACTH may be at or above the upper reference interval at 9 AM and fail to show the expected fall after midnight. Another use of ACTH assays is in the determination of adequacy of cortisol replacement in CAH. When replacement therapy is optimal, ACTH values are similar to those seen in a reference population.

Plasma Corticotropin-Releasing Hormone

CRH measurements are performed by LC/MS-MS and remain largely a research tool. CRH circulates in one of two forms: free or bound to CRH-binding protein. The reference range for plasma CRH in men and nonpregnant women is <34 pg/mL. CRH is increased in Cushing syndrome due to ectopic production of CRH. CRH-binding protein increases during pregnancy. As a result, the normative range for CRH varies throughout pregnancy: first trimester <40 pg/mL; second trimester <153 pg/mL; and third trimester <847 pg/mL (Goland et al., 1986).

Serum Cortisol Measurements

About 90% of circulating cortisol is bound to serum protein, of which 10% to 20% is loosely bound to albumin. The remainder is bound to the glycoprotein transcortin (cortisol-binding globulin [CBG]). The remaining 10% of circulating cortisol is the unbound, free hormone. It is believed that only free cortisol is active and that the protein-bound fraction is metabolically inert, probably serving as a reservoir for free cortisol. Protein binding also may protect cortisol from deactivation by the liver or filtration by the kidney.

One of the earliest and simplest methods used to determine the serum cortisol concentration was a fluorometric assay developed by Nelson and Samuels that was based on a technique first developed by Porter and Silber (Porter & Silber, 1950; Nelson & Samuels, 1952). The subsequent development of antibody-based immunoassays provided a more specific method for cortisol estimation with the added advantages of requiring a smaller specimen volume and a more rapid turnaround time. The problem was that some of the antibodies used showed a large degree of cross-reactivity with other steroid species, resulting in spuriously elevated cortisol concentrations. In chronic renal disease, various steroids and their glucuronides accumulate in the blood. Cross-reactivity between these steroids and their conjugates with the antibodies used in the assay can yield significantly erroneous cortisol concentrations. Similarly, in CAH, high concentrations of cortisol precursors are seen in the serum because of an enzyme defect. Because these precursors cross-react with assay antibodies, artificial elevations of cortisol are found. The degree of interference varies with the assay used and cannot be easily predicted. Nonisotopic immunoassay methods using organometallic tracers, fluorescence polarization, and enzyme immunoassay techniques have also been developed for cortisol determinations (Bacarese-Hamilton et al., 1992; Lentjes et al., 1993; Philomin et al., 1994). The major disadvantage of all of these cortisol assays continues to be lack of specificity.

The measurement of cortisol by radioimmunoassay (RIA) and chemiluminescent techniques has largely been supplanted by HPLC/MS-MS, which appears to offer the ultimate in specificity. Serum cortisol is collected in a no-additive (red-top) tube. Reference values for serum cortisol for men and women roughly range from 5 to 25 μg/dL (140–690 nmol/L) at 8 AM to 10 AM, dropping to about 3 to 12 μg/dL (80–330 nmol/L) by 4 PM. Because of wide swings in basal cortisol levels resulting from its diurnal and ultradian pattern of secretion, serum cortisol assays are most useful when evaluated in the context of dynamic manipulation (i.e., adrenal stimulation or suppression).

Salivary Cortisol

Up to 30% of urinary free cortisol (UFC) and dexamethasone suppression screening tests may return an incorrect result. Recent studies have shown that the use of a midnight salivary cortisol (MSC) is a viable alternative. CBG is not present in saliva; therefore, the results may be more useful in situations in which CBG concentration is altered. Salivary cortisol is highly stable and easy to collect, making it a useful tool for screening and for diagnosing instances of increased cortisol secretion. It does not appear to be affected by the rate of saliva production and can reflect a change in serum cortisol as rapidly as a few minutes (Read et al., 1990). Because of alterations in circadian rhythm, it may not be an appropriate test for shift

workers or those with highly variable bedtimes. One study compared the sensitivity for the detection of Cushing syndrome by nighttime salivary cortisol levels versus that for simultaneous inpatient serum cortisol levels and urine glucocorticoid excretion. It was found that the salivary cortisol measurements worked as well as plasma measurements and better than urine glucocorticoid excretion. The authors concluded that measurement of bedtime salivary cortisol was a practical and accurate screening test for the diagnosis of Cushing syndrome (Papanicolaou et al., 2002). Another study compared the diagnostic performance of MSC measurement versus that of midnight serum cortisol (MNC) and UFC in differentiating 41 patients with Cushing syndrome from 33 with pseudo-Cushing states, 199 with simple obesity, and 27 healthy normal-weight volunteers. In the whole study population, no statistically significant differences in terms of sensitivity, specificity, diagnostic accuracy, and predictive values were observed among tests. In particular, the overall diagnostic accuracy for MSC was similar to those of UFC and MNC (Putignano et al., 2003; Elamin et al., 2008). A recent review of the literature has shown that elevated late-night (11 PM to 12 AM) salivary cortisol has greater than 90% sensitivity and specificity for the diagnosis of endogenous Cushing syndrome (Raff, 2009). It is recommended to have the patient avoid tobacco on the day of specimen collection.

Urinary Free Cortisol Measurements

Only 1% of total adrenal secretion appears in the urine as cortisol, but it is this fraction that provides valuable aid in the diagnosis of adrenal disease. In the kidney, glomerular filtration of free cortisol (unbound to CBG and albumin) is followed by passive tubular reabsorption without a demonstrable reabsorption maximum. At serum cortisol levels of about 20 to 25 μg/dL (the upper 8 AM reference value), the binding capacity of transcortin (CBG) is exceeded, leading to a very rapid and disproportionate increase in the unbound fraction compared with the total serum cortisol. Doubling of serum cortisol from 20 to 40 μg/dL results in at least a fivefold increase in unbound cortisol. At these levels, free cortisol clearance by the kidneys is directly proportional to the unbound serum cortisol concentration, and a steep rise in cortisol clearance is seen. Serum cortisol reflects the sum of free, CBG-bound and albumin-bound cortisol. Only free (unbound) cortisol is filtered by the kidneys. Therefore, unlike serum cortisol, UFC is not affected by conditions and medications that alter CBG and albumin concentrations. Thus, when UFC rather than serum cortisol is used, it is easier to differentiate patients with adrenal hyperfunction from a reference population.

UFC is the best specimen to submit because it provides an integrated profile of total cortisol secretion over a 24-hour period, which is most helpful in those with sporadic excess cortisol production. The collection should also be assayed for creatinine to ensure that an adequate specimen has been submitted. The reliability of the test may be further improved by submitting urine collected over 2 or 3 days because day-to-day fluctuations in cortisol excretion are known to occur. UFC levels are unaffected by alterations in hepatic metabolism of cortisol. Although total cortisol production and urinary 17-OHCS may be increased, serum cortisol and UFC remain within the reference interval. Because renal clearance of cortisol is dependent on normal kidney function, it is not surprising that patients with renal disease have low UFC values. UFC is unreliable when CrCl is <20 mL/min and is of reduced reliability when CrCl is <60 mL/min (Chan et al., 2004). Increased serum concentration of transcortin during pregnancy and with estrogen therapy results in increased serum cortisol levels. This increase is not reflected by an elevation of cortisol metabolites in urine, but UFC may be increased. Conditions in which spuriously elevated levels occur include starvation, use of topical steroids, and perhaps hydration in the form of water loading.

Method. HPLC with mass spectrometry is considered the current reference method for measuring UFC. It has diagnostic sensitivity of 100% and specificity of 98% for distinguishing patients with Cushing syndrome from normal individuals (Rudd, 1985). Prior assays (such as RIA) were less specific, with a tendency to overestimate the amount of cortisol present.

The normal range varies according to the assay technique used; however, values that are four times the upper reference limit are diagnostic for Cushing syndrome. A low UFC value is suggestive of adrenal hypofunction; however, because there is great overlap with the normal reference interval, this test is not used to make the diagnosis of adrenal insufficiency.

Hypercortisolism: Cushing Syndrome

Cushing syndrome is composed of a group of clinical and metabolic disorders resulting from prolonged exposure to elevated concentrations of glucocorticoids. The excessive levels of glucocorticoids may be of endogenous (secreted by the adrenal zona fasciculata), or far more commonly, of exogenous (e.g., pharmacologically administered steroids) origin. Patients with severe forms of the syndrome are easily recognizable by their florid presentation (e.g., striae, facial plethora, proximal muscle weakness, and stereotypical accumulations of fat). Many of the signs and symptoms due to hypercortisolism are common medical complaints (e.g., fatigue, weight gain, obesity, diabetes, and hypertension). However, it is important to suspect Cushing syndrome in certain situations, as these have an increase in morbidity and mortality. Persons who may fall into this category and who should undergo screening include those with osteoporosis, hypertension, or diabetes occurring at a younger-than-expected age; patients with multiple, progressive features suggestive of Cushing syndrome; and those with incidentally discovered adrenal adenomas (Nieman et al., 2008). Patients with ectopic ACTH-producing tumors have elevated ACTH and glucocorticoid levels. However, because of the rapid growth of these tumors, they usually die before clinical signs of the syndrome can manifest. Features most commonly appearing in this group include hypokalemia and proximal muscle weakness (Salgado et al., 2006).

Laboratory findings in Cushing syndrome include (1) excessive production of cortisol measured as elevated serum cortisol, UFC, or MSC, (2) loss of circadian rhythm of ACTH and cortisol, and (3) loss of suppression of cortisol production by administration of the synthetic glucocorticoid dexamethasone.

Cushing disease specifically refers to hypercortisolism due to an ACTH-secreting pituitary adenoma. Cushing syndrome is a global term that encompasses a wide variety of entities associated with hypercortisolemia.

Cushing syndrome is most commonly iatrogenic in origin; however, it may also be due to a primary adrenal malignancy or ectopic production of CRH or ACTH by a tumor. In adrenal Cushing syndrome, excess cortisol is autonomously produced by the adrenal glands, resulting in suppression of the hypothalamic-pituitary axis. Adrenal Cushing syndrome (adenoma or carcinoma) accounts for less than 20% of cases, whereas pituitary Cushing syndrome accounts for about 68%, and ectopic production of ACTH (outside the pituitary-adrenal axis) is the cause in about 12% of cases (Orth, 1995). Because the treatment and prognosis differ depending on the underlying etiology, it is important that a specific diagnosis be reached.

Evaluation of a patient suspected of having Cushing's syndrome begins with use of one of the three screening tests. If one of the tests returns as borderline or the suspicion for the diagnosis remains high, a different screening test should be performed. The second phase includes confirmation of the diagnosis and identification of the pathophysiologic process causing the hypercortisolism.

Tests Used for the Diagnosis of Cushing Syndrome

Screening Tests. Three screening tests are used in the evaluation of a patient suspected of having Cushing syndrome (Fig. 25.17): the 24-hour UFC, the overnight dexamethasone suppression test (DST), and the plasma or MSC level. The 24-hour UFC is a reflection of the unbound circulating cortisol that is freely filtered by the glomerulus. Unlike serum cortisol, it is unaffected by the level of circulating CBG. HPLC or gas chromatography coupled with tandem mass spectrometry provides the best specificity for measuring UFC. Unlike RIA or enzyme-linked immunosorbent assay, these techniques are not affected by cross-reactivity with steroid metabolites or synthetic glucocorticoids. The upper range of normal with these methods is 110 to 138 nmol/24 hours (40 to 50 μg/hour) (Raff & Findling, 2003). The creatinine should be measured in all collections to ensure the adequacy of the specimen. Urinary cortisol excretion is decreased when the glomerular filtration rate is <30 mL/minute, and thus may be normal despite the presence of excessive cortisol production (Arnaldi et al., 2003). It has been suggested that the 1-mg overnight DST should be the preferred screening test used for these individuals (Nieman et al., 2008). Because most pediatric patients being evaluated for Cushing syndrome are of adult weight (>45 kg), adult normal ranges may be used (Nieman et al., 2008).

As per the latest guidelines for the diagnosis of Cushing syndrome, any UFC concentration above the upper limit of normal for that particular assay should be considered a positive test (Nieman et al., 2008). Values greater than four times the upper limit of normal are diagnostic of Cushing syndrome. From 10% to 15% of patients with Cushing syndrome will have at least one in four 24-hour urine collections for free cortisol return as normal (Nieman & Cutler, 1990). If cortisol excretion is normal but clinical suspicion is high, the study should be repeated or a different screening method should be used. Milder elevations of UFC can be seen in pseudo-Cushing syndrome and during normal pregnancy. Pseudo-Cushing syndrome is an entity characterized by HPA axis overactivity but without true Cushing syndrome. It has been described in depression, anxiety disorders, alcoholism, poorly controlled diabetes, and morbid obesity. Refer to the Pseudo-Cushing

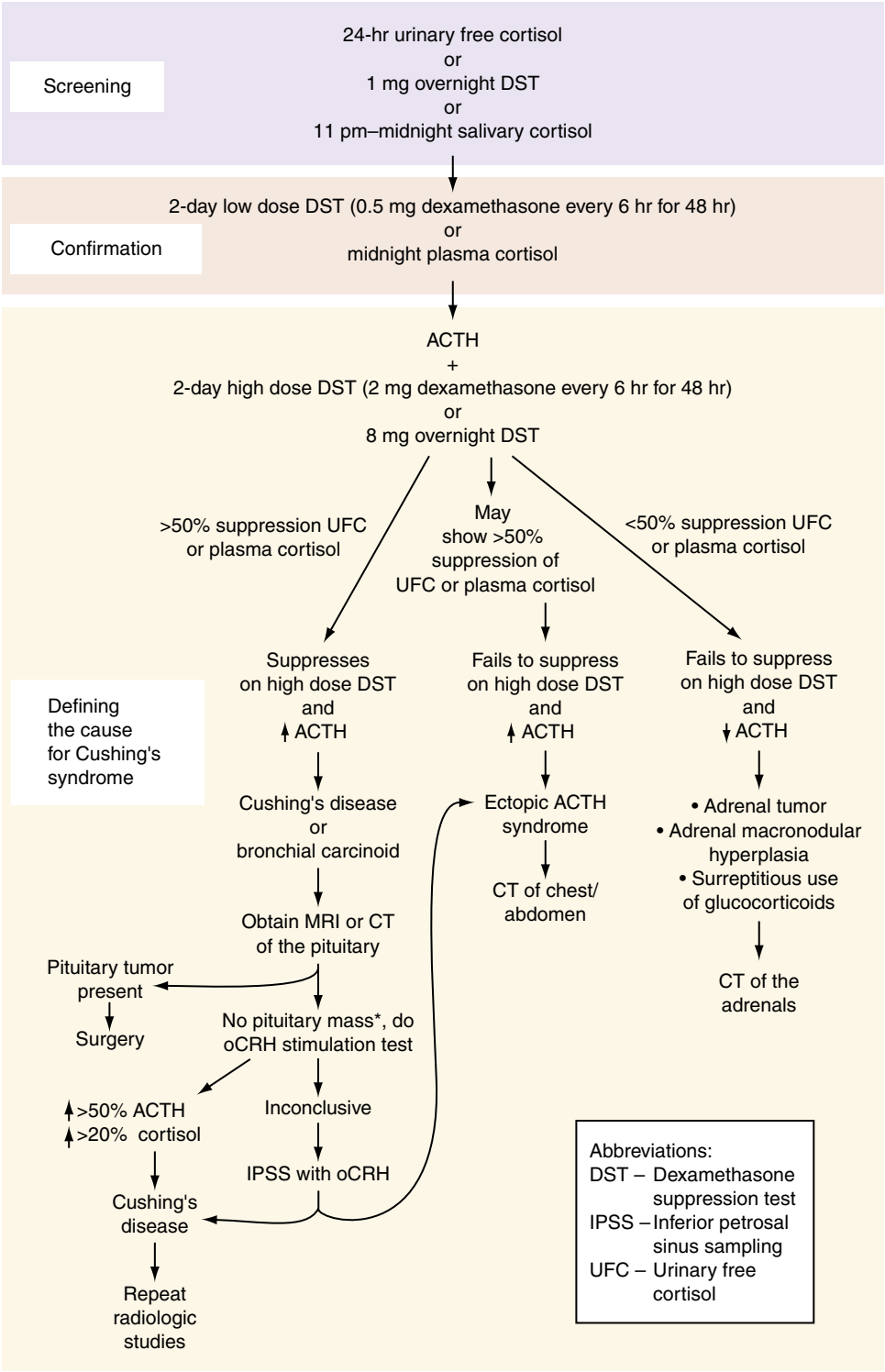

Figure 25.17 Algorithm for the evaluation of Cushing syndrome. All screening tests must be followed by a confirmatory test. *ACTH,* Adrenocorticotropin; *CT,* computed tomography; *oCRH,* ovine corticotropin-releasing hormone; *MRI,* magnetic resonance imaging. *If there is no pituitary mass, obtain a chest radiograph and chest CT to rule out bronchial carcinoid before proceeding to IPSS.

Syndrome section later in the chapter for more details. The overnight DST is a much simpler test to perform. The patient takes 1 mg of dexamethasone orally between the hours of 11 PM and midnight. The plasma cortisol is drawn the following morning between 8 AM and 9 AM. The original criterion for an abnormal response was failure to suppress the morning cortisol level to <5 μg/dL (138 nmol/L); this has been revised downward to <1.8 μg/dL (50 nmol/L) (Findling & Raff, 1999; Arnaldi et al., 2003; Nieman et al., 2008). Using the lower cutoff of <1.8 μg/dL (50 nmol/L) provides a greater than 95% sensitivity and 80% specificity and serves to minimize the number of false-positive results (Nieman et al., 2008). Failure to suppress could be due to Cushing syndrome or pseudo-Cushing syndrome and may even occur in some patients who are normal. The false-positive rate can be as high as 30% for a variety of reasons: dexamethasone was taken too early; the patient was on phenobarbital, phenytoin, or another medication known to accelerate the metabolism of dexamethasone; malabsorption; alcoholism; or morbid obesity. Pregnancy and drugs such as estrogen, which increase serum transcortin (aka CBG), may also result in elevated cortisol levels. Because of these and possibly other factors, about 1% of healthy individuals, 13% of obese patients, 50% of women on estrogen, and 25% of hospitalized and chronically ill patients show false-positive overnight DSTs. False-negative results, on the other hand, occur in less than 2% of patients. Patients with an adrenal adenoma unaccompanied by stigmata of hypercortisolism, whose serum cortisol fails to suppress below 5 μg/dL after 1 mg of dexamethasone, are considered as having subclinical Cushing syndrome (SCS). A low or suppressed level of ACTH or a low dehydroepiandrosterone sulfate (DHEA-S) concentration supports the diagnosis. In these patients, to establish the diagnosis, a second abnormal result of HPA axis function, such as a 2-day low-dose DST, may also be needed (Zeiger, 2009).

The MSC concentration is a simple, convenient, and accurate means by which to diagnose Cushing syndrome. MSC carries a high diagnostic

sensitivity and specificity and has been demonstrated to have an excellent correlation with the plasma free cortisol concentration (Papanicolaou et al., 2002; Yaneva et al., 2004; Alwani et al., 2014). Using a cutoff of 9.3 nmol/L on a commercial ELISA kit, MSC had a sensitivity of 100%, specificity of 83%, PPV of 94%, and NPV of 100% (Alwani et al., 2014). It performs slightly better than the 24-hour UFC in distinguishing patients with Cushing syndrome from obese subjects (Yaneva et al., 2004).

Several studies describe the use of a late-night (11 PM to 12 midnight) salivary cortisol (LNSC). Others use the terms MSC and LNSC interchangeably, although the methodologies describe the samples as being collected at midnight. There are no studies comparing MSC with LNSC; however, because the data for MSC is more robust, it is the preferred test.

The patient can collect the sample at home. Two methods can be used to collect the sample. The patient can chew on a cotton pledget for 2 to 3 minutes and then place the pledget into a plastic tube or the patient can passively drool directly into a test tube. The sample is then mailed to the reference laboratory. Because salivary cortisol is very stable, there is little concern about degradation during transport. The sample can be analyzed either by immunoassay or LC-MS/MS. While immunoassay is more widely used, LC-MS/MS is useful in evaluating for surreptitious use of steroids and for steroid excess in those using inhaled steroids (Raff, 2013). Normative values vary according to the reference laboratory. Results should be interpreted with caution in those who may have blunting of their circadian rhythm (e.g., shift workers, patients with depression, critical illness). Falsely elevated results may be seen in smokers and users of chewing tobacco, in which case refraining from use for 24 hours prior to collection is recommended.

Screening in special populations. The preferred screening test during pregnancy is for UFC. UFC levels normally rise during the second and third trimesters; therefore, UFC values greater than three times the upper limit of normal are considered consistent with Cushing syndrome (Nieman et al., 2008).

Because of the decrease in cortisol filtration with declining renal function, the 1-mg DST is the recommended screen in patients with renal failure. For those suspected of having cyclic Cushing syndrome, use of serial UFC or MSC is suggested. The diagnostic thresholds for MSC during pregnancy and in renal disease remain to be established.

For an incidentally discovered adrenal mass, the 1-mg DST has been shown to be superior to the UFC and MSC tests (Raff, 2013).

Confirmatory Tests for the Diagnosis of Cushing Syndrome. For equivocal screening results, one option is to repeat testing in 3 months. A more definitive way to confirm the diagnosis of Cushing syndrome is with a midnight plasma cortisol or 2-day low-dose DST performed alone or with the administration of CRH.

Midnight plasma cortisol requires hospital admission for at least 48 hours, insertion of a line for IV access before 10 PM, the patient sleeping at the time of the blood draw, and availability of staff to draw the blood at midnight. A midnight plasma cortisol greater than 7.5 μg/dL (207 nmol/L) is diagnostic of Cushing syndrome; this has a 100% specificity for normals and those with pseudo-Cushing syndrome (Newell-Price et al., 1995; Papanicolaou et al., 1998). The low-dose (2-day 2 mg) dexamethasone suppression test (LDDST) requires the collection of two baseline 24-hour urine samples for UFC. The patient is then given 0.5 mg dexamethasone orally every 6 hours, starting at 9 AM for 2 days. On day 2 of dexamethasone, another 24-hour urine sample is collected for UFC. All 24-hour urine collections should include the measurement of creatinine to assay for adequacy of the collection. A normal response is a decrease in UFC to less than 10 μg (27 nmol) per 24 hours on the second day of dexamethasone. This has a sensitivity of 97% to 100% for discriminating patients with Cushing syndrome from normal individuals (Newell-Price et al., 1998). Instead of measuring UFC, serum cortisol can be measured at baseline (9 AM day 1) and at 48 hours following the first dose of dexamethasone. A normal response consists of suppression of the plasma cortisol to less than 1.8 μg/dL (50 nmol/L), which has a sensitivity and specificity of more than 95% (Newell-Price et al., 1998). Performance of the LDDST with CRH has been purported to better distinguish Cushing syndrome from pseudo-Cushing syndrome (Yanovski et al., 1993). For this test, 1 μg/kg or 100 μg ovine CRH (oCRH) is administered IV 2 hours after the last dose of dexamethasone. Cortisol is measured prior to the first dose of dexamethasone on day 1 immediately prior to the administration of synthetic oCRH and then 15 minutes following oCRH. A dexamethasone level should be measured at the time of CRH administration to exclude false-positive results. Adherence to the time schedule is important for both LDDST and LDDST with CRH. The normal response for both tests is a serum cortisol of <1.8 μg/dL (<50 nmol/L).

TABLE 25.16

Differential Diagnosis of Hormonal Values Seen in Cushing Syndrome

Cause	Plasma ACTH	Plasma Cortisol (PM)	High-Dose or Overnight Dexamethasone Suppression
Pituitary-dependent	N—slightly ↑	↑	Yes
Adrenal disease	↓—undetectable	↑	No
Ectopic Cushing syndrome*	↑↑↑	↑↑	Usually no
Pseudo-Cushing syndrome	N—slightly ↑	N–↑	Usually yes

ACTH, Adrenocorticotropin; *N,* normal.
*ACTH levels may overlap with values seen in pituitary-dependent disease.

Tests for Defining the Cause of Cushing Syndrome. Once the diagnosis of Cushing syndrome is established, the next step is to determine its cause. Cushing syndrome is categorized as being ACTH dependent or ACTH independent; this is accomplished by measuring the plasma ACTH or by performing a high-dose DST or a CRH stimulation test (Table 25.16).

ACTH-independent Cushing syndrome results from autonomous production of cortisol, which would feed back on the hypothalamus and pituitary gland, causing suppression of CRH and ACTH secretion. The technique for measuring plasma ACTH has been described previously. Values below the level of detection or below 10 pg/mL (2 pmol/L) at 9 AM with concomitantly elevated cortisol support an ACTH-independent cause for Cushing syndrome. Plasma levels greater than 20 pg/mL (4 pmol/L) in the face of hypercortisolism are strongly suggestive of an ACTH-dependent cause. A CRH stimulation test with measurement of ACTH is indicated for values between 10 and 20 pg/mL (2–4 pmol/L) (Orth, 1995). Although patients with ectopic ACTH production tend to have markedly elevated ACTH levels, there is great overlap with the levels seen in Cushing disease. Therefore, it cannot be used to reliably distinguish between these entities.

The high-dose (2-day 8-mg) DST is useful for distinguishing Cushing disease from adrenal or ectopic Cushing syndrome. It is of note that cortisol levels in neuroendocrine tumors such as bronchial carcinoid may also suppress on high-dose dexamethasone. For the high-dose DST, a baseline 24-hour urine sample for UFC is collected. Beginning on day 1, the patient receives 1 mg of dexamethasone orally every 6 hours for 48 hours; urine for UFC is collected on days 1 and 2. Suppression of UFC or plasma cortisol by 50% or more from baseline is diagnostic of Cushing disease. As an alternative to measuring UFC, plasma cortisol can be collected before, during, and 6 hours after the last dose of dexamethasone. Most patients with adrenal adenomas, carcinomas, or ectopic ACTH syndromes do not show suppression. This test has a sensitivity and specificity of 60% to 85%; the greater the degree of suppression, the greater the specificity.

The 8-mg overnight DST has been reported by several authors to share similar sensitivity and specificity to the high-dose DST (Dicheck et al., 1994). An 8 AM plasma cortisol is obtained, and 8 mg of dexamethasone is administered orally at 11 PM. An 8 AM plasma cortisol is obtained the next morning. Reduction of cortisol to less than 5 μg/dL is strongly supportive of Cushing disease (see Fig. 25.17).

Most pituitary tumors and a few ectopic ACTH-secreting tumors will respond to CRH stimulation with an increase in plasma ACTH and cortisol, whereas little response is noted in those with primary adrenal Cushings. For the CRH stimulation test, two basal plasma cortisol and ACTH levels are collected about 5 minutes apart, and then 1 μg/kg of body weight or a single dose of 100 μg of oCRH (ovine CRH) is injected intravenously. Blood is sampled every 15 minutes for 1 to 2 hours for cortisol and ACTH. Normal subjects will show a rise in ACTH and cortisol of approximately 15% to 20%, while those with Cushing disease typically show a greater than 50% rise in ACTH and a greater than 20% rise in cortisol above baseline (Kaye & Crapo, 1990; Newell-Price et al., 2002; Stewart, 2016). Ovine CRH is superior to human CRH in distinguishing among the different causes of Cushing syndrome (Nieman et al., 1989). Vasopressin stimulates ACTH release through the V3 receptors in the anterior pituitary

gland. Administration of 10 units of vasopressin intramuscularly normally causes doubling of ACTH levels and an increase in serum cortisol of 150 μg/L over baseline. This offers no advantage over testing with CRH. It may prove useful, however, in differentiating Cushing disease from pseudo-Cushing syndrome and in the postoperative assessment of Cushing disease (Newell-Price et al., 2002).

In rare instances, it may be necessary to use selective sampling of inferior petrosal sinus blood to document that the pituitary gland is the source of excess ACTH. This invasive, technically difficult procedure carries a relatively high cost and complication rate and should be performed only at a center well experienced with this technique. The ACTH concentration in the petrosal sinus blood should exceed twice that of peripheral venous blood to ensure diagnostic sensitivity and specificity of 100% (Orth, 1995). In those with ectopic production, the ratio is usually less than 1.4:1. Use of CRH during sampling increases the sensitivity and specificity.

Given that the incidence of incidentaloma of the adrenal glands and pituitary gland has been reported to be as high as 10%, imaging studies should be performed only after the hormonal diagnosis of Cushing disease or syndrome has been made. In Cushing disease, visualization of the sella is performed by MRI or CT, with and without contrast, with MRI being the preferred study. For adrenal Cushing, the test of choice is a CT of the abdomen; for ectopic disease, a CT of the chest may also be needed.

Pseudo-Cushing Syndrome

Excess activity of the hypothalamic-pituitary axis, similar to that seen in pituitary Cushing syndrome, has been demonstrated in some patients with alcoholism, major depression, poorly controlled diabetes, and obesity. Resolution of the underlying problem results in normalization of the HPA axis. These patients may not suppress on a low-dose DST and may have elevated UFC. Depressed patients who fail to suppress cortisol secretion in response to dexamethasone also show an impaired ACTH response to exogenous CRH but will usually retain a normal cortisol response (Gold et al., 1986; Thalen et al., 1993). A single serum cortisol above 7.5 μg/dL at midnight has been shown to discriminate Cushing syndrome from pseudo-Cushing syndrome with 100% specificity (Papanicolaou et al., 1998). A more definitive test for distinguishing between these two entities is the combined dexamethasone-oCRH test. A dose of 1 μg/kg or 100 μg oCRH is infused 2 hours after a low-dose dexamethasone test. A plasma cortisol concentration greater than 38 nmol/L measured at 15 minutes following the administration of oCRH correctly identifies all cases of Cushing syndrome and all cases of pseudo-Cushing syndrome, with a specificity, sensitivity, and diagnostic accuracy of 100% (Yanovski et al., 1993).

ADRENAL INSUFFICIENCY

Adrenal insufficiency is categorized according to the key site of dysfunction within the HPA axis: primary (adrenal), secondary (pituitary), and tertiary (hypothalamic). A major distinction between primary adrenal insufficiency and either of the central causes is that primary disease is associated with mineralocorticoid deficiency. In the Western world, primary adrenal insufficiency, also known as *Addison disease*, is most commonly due to autoimmune adrenalitis (70%–90% of all cases). Other causes include tuberculosis (most common cause worldwide), granulomatous disorders, metastatic disease, hemorrhage, human immunodeficiency virus, acquired immunodeficiency syndrome, and infection. The most common cause of central adrenal insufficiency is HPA axis suppression due to prolonged treatment with pharmacologic doses of steroids.

Tests for the Diagnosis of Adrenal Insufficiency

Basal Hormone Measurements

An 8 AM to 9 AM plasma cortisol of less than 3 μg/dL (83 nmol/L) is indicative of adrenal insufficiency and obviates the need for further testing. Although most patients with hypocortisolism have low serum cortisol levels, a level drawn during a time of stress that falls within the reference range does not exclude the diagnosis. Rather, it may support this diagnosis, as a suboptimal cortisol level may have risen into the reference interval in response to the stress. During critical illness a random cortisol of greater than 25 μg/dL (700 nmol/L) makes it unlikely that the patient is adrenally insufficient (Burke, 1985), whereas a random cortisol of less than 10 μg/dL is strongly suggestive of adrenal insufficiency (Fleseriu & Loriaux, 2009).

ACTH Stimulation Test

The most convenient procedure for studying patients suspected of having hypocortisolism is the ACTH stimulation test. This test, which can be performed at any time of day, consists of drawing a baseline serum cortisol and then administering 250 μg of Cosyntropin (a commercially available ACTH analog) intravenously or intramuscularly. Serum for cortisol is again collected at 30 and 60 minutes post-Cosyntropin. A normal response is a cortisol level greater than 18 to 20 μg/dL (500–550 nmol/L) at either time point (Speckart et al., 1971; Burke, 1985). Drawing an ACTH level at baseline may help in distinguishing primary adrenal insufficiency (associated with an elevated ACTH usually greater than 50 to 100 pg/mL) from secondary or tertiary forms (which would have a low ACTH level less than 10 pg/mL; refer to the Laboratory Measurement of ACTH section earlier in the chapter) (Oelkers et al., 1992). The aldosterone response to ACTH may also help in making this distinction; failure of aldosterone to increase by more than 4 ng/dL over baseline suggests primary adrenal dysfunction.

Steroids should never be withheld from a critically ill patient suspected of having adrenal insufficiency. Instead, a random sample for cortisol and ACTH should be drawn and treatment initiated with dexamethasone, which does not interfere with the cortisol assay. Formal testing should take place within 72 hours, before HPA axis suppression occurs. About 90% of cortisol circulates bound to CBG and albumin, and approximately 10% circulates freely (unbound). CBG declines during critical illness, resulting in an increase in the fraction of unbound (free) cortisol compared with the bound fraction. Because the serum total cortisol concentration does not accurately reflect this alteration in free/bound cortisol, it is common to overdiagnose adrenal insufficiency in the critical care setting. Since access to laboratories that readily and reliably measure free cortisol is limited, some have advocated use of the free cortisol index (FCI) and calculated free cortisol (CFC) to better delineate those patients in true need of steroid replacement therapy (Beishuizen et al., 2001; Hamrahian et al., 2004; Ho et al., 2006). To obtain the FCI, it is necessary to measure the serum CBG. CFC is the total cortisol (nmol/L)/CBG (mg/L), with normal being a value above 12. Given that for the vast majority of institutions, determination of CBG requires that the sample be sent to a reference laboratory, it may be more prudent and certainly more expedient to simply send aliquots from t-0, t-+30, and t-+60 minutes post–ACTH administration for serum free cortisol and provide steroid coverage pending these results (Fleseriu & Loriaux, 2009). Checking the ACTH level at t-0 will help to further classify adrenal insufficiency as being primary versus secondary or tertiary. Salivary cortisol, which is unaffected by changes in CBG, may eventually prove useful in this setting (Raff, 2009).

Some have supported the use of a 1-μg dose of ACTH instead of the full 250-μg dose for diagnosing adrenal insufficiency. The premise is that the massively supraphysiologic dose of 250 μg will cause those with partial adrenal insufficiency to mount a normal response and that these individuals will fail to show an adequate rise in cortisol in response to a 1-μg test dose. This procedure has not gained wide acceptance, nor has the normal range been standardized; more importantly, the diagnosis of partial adrenal insufficiency remains in contention.

The ITT has long been considered the gold standard for assessing the HPA axis. Unlike the ACTH stimulation test, the ITT assesses the integrity of the entire HPA axis. If the HPA axis is intact, insulin-induced hypoglycemia stimulates the hypothalamus and the pituitary gland to secrete CRH and ACTH, respectively, which, in turn, leads to a rise in cortisol. This test is contraindicated in individuals with ischemic heart disease, in older adults (>70 years of age), during pregnancy, and in those with a history of seizures. Patients highly suspected of having central adrenal insufficiency (i.e., prior pituitary surgery or radiation therapy) should receive a lower dose (0.05 U/kg) of insulin rather than 0.1 to 0.15 U/kg. Glucose and cortisol are measured at –15 minutes, at baseline, and then at 15, 30, 45, 60, 90, and 120 minutes following insulin administration. For the test to be valid, adequate hypoglycemia must be attained (signs and symptoms of hypoglycemia and glucose less than 40 mg/dL [2.2 mmol/L]). A normal response is a rise in the cortisol level to greater than or equal to 18 μg/L or 20 μg/L at any time during the test (Nelson & Tindall, 1978; Burke, 1985; Grinspoon & Biller, 1994). Preliminary work suggests that there was no difference in peak GH or cortisol level attained when analog insulin was substituted for regular insulin for the ITT (Yuen et al., 2008).

The cortisol response to hypoglycemia can be predicted reliably by the response to acute ACTH stimulation—a safer, cheaper, and quicker test (Stewart, 2016). The ITT is used mainly as a second-line measure to further evaluate those patients who had a borderline response to the ACTH stimulation test.

In the days before the commercial availability of a reliable assay to measure ACTH, it was common to perform a prolonged ACTH stimulation test (ACTH infusion over a 2-day period) to distinguish central from primary adrenal insufficiency. In other hormone systems, lack of stimulation normally

leads to upregulation of the end-organ receptors. However, the adrenal glands downregulate their ACTH receptors in response to lack of stimulation. A short ACTH stimulation test would typically produce an inadequate response. By priming the system with prolonged exposure to ACTH, those with hypothalamic disease display a delayed but normal rise in cortisol.

Overnight Metyrapone Test

Metyrapone has also been used to assess the integrity of the HPA axis. Metyrapone inhibits 11-β-hydroxylase, preventing the conversion of 11-deoxycortisol (compound S) to cortisol. Under normal circumstances, the metyrapone-induced drop in cortisol is detected at the level of the hypothalamus and pituitary gland; a compensatory increase in CRH and ACTH secretion occurs, stimulating steroidogenesis and leading to a buildup of 11-deoxycortisol, the hormone preceding the block. Patients with central adrenal insufficiency fail to increase CRH and/or ACTH, steroidogenesis is not stimulated, and 11-deoxycortisol fails to increase. Metyrapone 30 mg/kg is administered orally at midnight; blood for cortisol and 11-deoxycortisol is collected the following morning at 8 AM. A rise in 11-deoxycortisol to greater than 7 μg/dL (200 nmol/L) is normal (Fiad et al., 1994; Grinspoon & Biller, 1994). An abnormal response is defined by 11-deoxycortisol less than 7 μg/dL accompanied by cortisol less than 5 μg/dL. This test should be performed with caution, as it may provoke an addisonian crisis in those with central hypocortisolism. Metyrapone is currently available only on a compassionate basis. As a result, this test is rarely performed.

Corticotropin-Releasing Hormone Test

The oCRH test can be used not only to diagnose hypocortisolism but to localize the site of damage (Schulte et al., 1984). It is a safe test; however, it is expensive. After blood is drawn for baseline ACTH and cortisol, 100 μg oCRH is administered intravenously. Blood is then collected for cortisol and ACTH every 15 minutes for 60 to 90 minutes. A normal response is seen as cortisol greater than 20 μg/dL. Basal ACTH levels and their change in response to oCRH are used to localize the site of pathology. Plasma corticotropin usually peaks at 15 to 30 minutes; cortisol usually peaks at around 30 to 40 minutes post–oCRH injection (Oelkers, 1996).

Both the bound and free cortisol concentrations show a progressive rise throughout pregnancy. With this in mind, it has been recommended that higher cutoffs be used to properly interpret the ACTH stimulation results in pregnancy (Jung et al., 2011). A random morning cortisol level less than 11 μg/dL, 16 μg/dL, and 22 μg/dL when measured during the first, second, and third trimester of pregnancy, respectively, should raise the suspicion of adrenal insufficiency (Jung et al., 2011). A serum cortisol 60 minutes post-ACTH of less than 25 μg/dL, 29 μg/dL, and 32 μg/dL for the first, second, and third trimester of pregnancy, respectively, is diagnostic of adrenal insufficiency (Lebbe & Arlt, 2013; Yuen et al., 2013).

Antibodies against 21-hydroxylase antigen should be assayed in those whose Addison disease (primary adrenal insufficiency) does not have an obvious explanation. Positive antibodies confirm autoimmune adrenalitis; these patients should be screened and monitored for the development of other autoimmune disorders. The absence of antibodies does not rule out an autoimmune etiology, as titers usually drop in concurrence with adrenal destruction.

The use of steroids in the treatment of malignant, inflammatory, and immunologic disorders is a common iatrogenic cause of adrenal insufficiency. The degree of adrenal suppression is dependent on the specific glucocorticoid dose, duration, frequency, and route of administration. Assessment of adrenal function in patients being tapered off of exogenous steroids can be performed once they are tapered to the equivalent of a daily dose of 10 mg hydrocortisone. Have them omit the morning glucocorticoid dose and measure the 8 AM cortisol level. If it is greater than 10 μg/dL, routine supplementation of steroids can be ended. Because the adrenal cortex lags behind the pituitary gland in recovery from steroid suppression, complete adrenal recovery can also be demonstrated by an appropriate rise in serum cortisol following an 8 AM Cosyntropin infusion.

RENIN-ALDOSTERONE AXIS

At least 20 million people in the United States have hypertension; 90% to 98% of cases are classified as essential hypertension. The mortality and morbidity from associated myocardial, cerebrovascular, and renal complications necessitate aggressive treatment of this disorder. Investigation into the etiology of hypertension revealed the importance of the renin-angiotensin-aldosterone system, not only in the origin and persistence of hypertension but also as a guide to its treatment. The role of the renin-aldosterone axis is to maintain blood pressure within normal limits by sensing and responding to changes in plasma volume, salt balance, and renal perfusion pressure.

Renin is a proteolytic enzyme that, although formed by other tissues throughout the body, is mainly formed and stored by juxtaglomerular (JG) cells within the macula densa of the kidney. Renin is synthesized from a larger precursor protein, prorenin (big renin), and is converted to its active form within the JG cells. The release of renin into the circulation occurs in response to a variety of triggers: a drop in renal hydrostatic pressure, hyponatremia, hypokalemia, or a decrease in catecholamines, angiotensin II, or atrial natriuretic hormone. Both suppression of plasma renin activity induced by potassium administration and stimulation of renin activity following potassium depletion occur independently of changes in aldosterone secretion or in sodium balance (Brunner et al., 1970).

Several isoenzymes of renin are known. Their release is regulated by cAMP. Renin acts on angiotensinogen (renin substrate), an α_2-globulin formed by the liver, converting angiotensinogen to angiotensin I. Angiotensin I, in turn, is converted into angiotensin II by the angiotensin-converting enzyme (ACE). ACE is found in the pulmonary and vascular endothelia as well as in cell membranes of the kidney, heart, and brain (Brewster & Perazella, 2004). It is believed that angiotensin II is the peptide responsible for the physiologic effects on target tissue. Angiotensin II not only stimulates the release of aldosterone, but it is also a very potent vasoconstrictor that can stimulate the release of catecholamines from the adrenal glands and norepinephrine from the sympathetic nervous system and stimulate the release of vasopressin. The octapeptide angiotensin II is further split to a heptapeptide, angiotensin III; in addition, angiotensin I may be changed directly to angiotensin III without being converted to angiotensin II. Although speculation about the functions of angiotensin III is ongoing, it appears to modulate aldosterone secretion in a similar manner to angiotensin II. The active angiotensins are rapidly cleared by various aminopeptidases (angiotensinases) within the circulation and during transit through tissues. These relationships are shown in Figure 25.18.

Renin, through its product, angiotensin II, directly stimulates the synthesis and secretion of aldosterone by the adrenal zona glomerulosa. Renin release, the rate-limiting step in the renin-aldosterone axis, is dependent on changes in effective plasma volume, which, in turn, are dependent on tubular reabsorption of sodium by the kidney. Low plasma volume and low serum sodium stimulate the secretion of renin, resulting in aldosterone

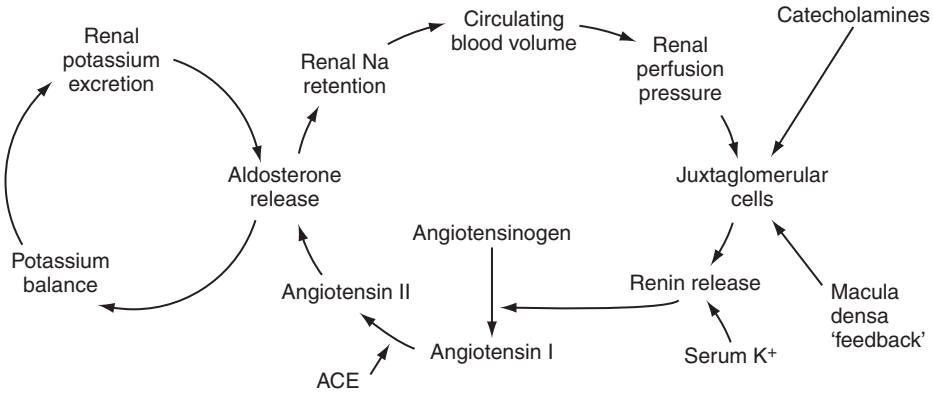

Figure 25.18 Renin-aldosterone axis. Elevated K^+ inhibits renin secretion but has a stimulatory effect on aldosterone. Catecholaminergic influence is variable; β-adrenergic activity stimulates and α-adrenergic activity inhibits renin secretion from the juxtaglomerular cells. *ACE,* Angiotensin-converting enzyme. (Redrawn from Braunwald E, Fauci AD, Kasper D, et al., editors: *Harrison's principles of internal medicine*, ed 15, New York, 2001, McGraw-Hill, p 2087.)

release, which, in turn, causes sodium retention along with an increase in plasma volume and blood pressure, and potassium loss. Conversely, an increase in effective blood volume or acute elevation in blood pressure results in low renin, low angiotensin, low aldosterone, and subsequent sodium loss. In contradistinction to aldosterone, renin secretion is inhibited by hyperkalemia (Fig. 25.19).

Aldosterone and glucocorticoids act at the mineralocorticoid receptor located in the cells lining the collecting ducts of the kidney to cause reabsorption of sodium, leading to an increase in intravascular volume. Aldosterone also causes renal potassium loss. Studies have suggested a role for aldosterone in the development and perpetuation of vasculopathy—it has been shown to stimulate genes for collagen synthesis, tissue growth factors, inflammatory factors, and plasminogen activator inhibitor type 1 (Brilla et al., 1994; Schunkert et al., 1997; Brown et al., 2000; Rocha et al., 2000; Luft, 2002). The synthesis of aldosterone is restricted to the zona glomerulosa; here, the enzyme aldosterone synthetase (CYP11B2) converts corticosterone to aldosterone. The major stimuli for aldosterone secretion are angiotensin II and hyperkalemia. ACTH is a much weaker stimulus. Somatostatin, atrial natriuretic hormone, dopamine, and heparin directly inhibit aldosterone synthesis. Cortisol circulates at a much higher concentration than aldosterone and, although it binds with equal affinity to the mineralocorticoid receptor, it does not normally function as a major mineralocorticoid. The reason is that the enzyme 11-β-hydroxysteroid dehydrogenase II (11-HSD-2, also known as CYP11B2), expressed by the mineralocorticoid target cells in the collecting tubules, acts to convert cortisol to cortisone, an inactive metabolite.

RENIN AND HYPERTENSION

The work of Laragh and colleagues has indicated that essential hypertension can be classified on the basis of renin measurements as high, low, or normal renin, and that drug selection can be based on this classification (Laragh et al., 1972; Laragh, 1993). About 15% of patients with essential hypertension have high-renin hypertension. Hyperreninemia resulting from renal parenchymal disease or renal vasculopathy leads to increased aldosterone production and the subsequent retention of sodium and enhanced potassium excretion. Patients with this condition are hypervolemic, intensely vasoconstrictive, and more prone to ischemic injury. Renin profiling has shown renin to be an independent risk factor for myocardial infarction. Even if pressures are controlled by antihypertensives, if they do not address plasma renin activity, such patients fare worse than individuals with lower renin levels (Alderman et al., 1991). Increased aldosterone (secondary aldosteronism) may contribute significantly to the symptoms and course of high-renin hypertension. Some of the causes of high-renin hypertension are listed in Box 25.7.

Renin-secreting tumors are extremely rare and can be difficult to diagnose. They can be benign or malignant, renal or extrarenal. The most common location is in the juxtaglomerular apparatus. A young patient with markedly elevated plasma renin activity, hyperaldosteronism, and hypokalemia in the absence of a renovascular lesion typifies the classic clinical presentation (Corvol et al., 1994). Malignant hypertension is also associated with high plasma renin activity and aldosterone. When such patients are given medications that interrupt the renin-aldosterone axis, such as ACEIs, blood pressure often normalizes. In renal vascular hypertension, the renin and aldosterone levels are also elevated. However, in contradistinction to malignant hypertension, treatment with ACEIs usually results in further deterioration of renal function. Patients suspected of having renal artery stenosis should undergo further testing (e.g., captopril-induced renogram, renal duplex ultrasound, magnetic resonance angiography). A positive test leads to renal vein angiography and catheterization for selective blood sampling. In unilateral renal disease, both plasma renin and aldosterone are elevated. Asymmetry in the renin levels obtained during renal vein catheterization offers one of the best measurements to judge the likelihood of blood pressure response to corrective surgery. When the ratio of plasma renin in the renal vein of the affected to the nonaffected side is at least 1.5 : 1, surgery may lead to improvement. With suppression of renin release from the nonaffected side, renal vein renin levels approximating those found in blood specimens obtained from the inferior vena cava also indicate probable success of curative surgery. Almost 40% of these patients have peripheral blood plasma renin activity that is within the reference interval (Streeten et al., 1979); consequently, peripheral plasma renin is a poor predictor of response to surgery. Renin secretion can be found in lung cancer, hepatic hamartoma, and other rare conditions (Anderson et al., 1989).

When an acceleration of hypertension occurs, renin is usually markedly increased. However, with chronic renal failure, almost any renin level can be expected. A small number of hypertensive patients on dialysis have intractable, accelerated hypertension. In those patients in whom dialysis cannot control the hypertension, markedly elevated plasma renin levels can be lowered by nephrectomy or, in the case of renal artery stenosis, angioplasty or revascularization (Whitehouse et al., 1981; Sonkodi et al., 1990; Tullis et al., 1999). ACEIs can be used to mitigate the rise in aldosterone; however, in the setting of renal disease, they can precipitate or worsen hyperkalemia. In renal transplant patients, elevated plasma renin may be indicative of renal ischemia and rejection.

Systemic hypertension occurs in patients with Cushing syndrome. Some of these patients have increased plasma renin and renin substrate. Other Cushing syndrome patients have hypokalemia associated with secretion of a minor mineralocorticoid (such as DOC or corticosterone) that causes hypertension (Krakoff et al., 1975). In still other patients, severely elevated cortisol levels overwhelm the capacity of 11-hydroxysteroid dehydrogenase (11-HSD) to convert cortisol to its metabolically inactive form, cortisone, leading to a picture of excess mineralocorticoid activity with suppressed plasma renin activity. Other causes of high-renin hypertension include treatment with medications such as diuretics, vasodilators, or other antihypertensives. Hormonal agents such as glucocorticoids, as well as some estrogen-containing oral contraceptives, have been found to increase renin substrate activity.

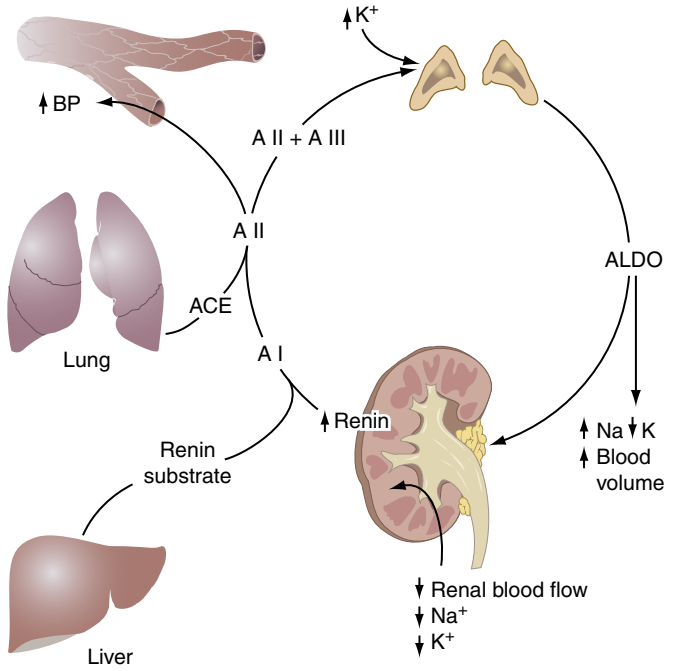

Figure 25.19 The normal renin-angiotensin-aldosterone axis. Renin, secreted by the kidney, cleaves angiotensin I from renin substrate (angiotensinogen) produced by the liver. Angiotensin I is converted to angiotensin II by angiotensin-converting enzyme (ACE), mainly in the lung. Angiotensin II increases peripheral vascular resistance and, together with angiotensin III, stimulates aldosterone (ALDO) secretion, which results in sodium retention and increased plasma volume. (Adapted from Stewart PM: The adrenal cortex. In Larsen PR, Kronenberg HM, Melmed S, et al., editors: *Williams textbook of endocrinology*, ed 10, Philadelphia, 2003, Saunders, p 499.)

BOX 25.7

Causes of Hypertension Associated with High Levels of Plasma Renin

- Renin-secreting tumor
- Malignant accelerated hypertension
- Renovascular hypertension
  - Major arterial lesions
  - Segmental lesions
- Chronic renal failure
  - End stage
  - Transplant rejection
- Cushing syndrome
- Iatrogenic
  - Volume-depleting agents
  - Vasodilating agents
  - Glucocorticoids
  - Estrogens

Even though plasma renin activity, aldosterone, and urinary sodium excretion may be normal in 60% of hypertensive patients, evidence indicates that renin-angiotensin plays a significant part in normal-renin hypertension. The response of many hypertensive patients with normal renin to ACEIs or angiotensin II antagonists (saralasin) has implicated renin and angiotensin II in sustaining hypertension in these patients. Moreover, Ames showed that once blood pressure was increased by angiotensin infusion, it could be maintained with only one-fifth of the original dose (Ames et al., 1965).

It was found that low-renin essential hypertension, which involves chronic expansion of plasma and extracellular fluid volume, is characterized by aldosterone oversecretion and responds to diuretic therapy. At least 25% of patients with essential hypertension are found to have low-renin hypertension. Most investigators have characterized this state as hyporesponsive, meaning that low-renin hypertensive patients fail to respond as well as healthy subjects do with upright posture, sodium restriction, diuretics, vasodilators, or a combination of these. Atrial natriuretic peptide may be elevated in these patients, and the response of aldosterone to renin may be exaggerated (Sergev et al., 1990). Renin suppression increases with age and appears to be more common in women and in the black population.

Listed in Box 25.8 are a group of syndromes associated with low levels of plasma renin. These have been divided into a subgroup that is of adrenal origin (primary) and a subgroup that is nonadrenal or secondary in origin. Primary aldosteronism is uncommon compared with renin hypertension. It is characterized by (1) systolic and diastolic hypertension caused by oversecretion of aldosterone by an adrenal adenoma (aldosterone-producing adenoma [APA]) or hyperplasia (idiopathic hyperaldosteronism [IHA]), (2) low renin or a high aldosterone/renin ratio (>50), (3) renal potassium wasting, and (4) sodium retention. It should be suspected in patients with hypertension and spontaneous or diuretic-induced hypokalemia, resistant hypertension requiring more than three medications, onset younger than 30 years of age, or an incidentally found adrenal mass. Several potential screening tests have been used to detect primary aldosteronism and to separate unilateral aldosterone-producing adenomas from other causes of primary aldosteronism. A low-salt diet (<2 g/day), stress, upright posture, and diuretics all increase plasma aldosterone, whereas a high-salt diet and lying in a supine position suppress aldosterone secretion in healthy subjects. Combinations of these maneuvers have been used in the diagnosis of excessive aldosterone secretion; however, they do not reliably distinguish APA from IHA. When healthy subjects are placed on a high-salt diet and lie in the supine position, they suppress their plasma aldosterone levels to less than 10 ng/dL (278 pmol/L).

Primary Hyperaldosteronism: Screening and Confirmation Tests

The algorithm proposed by Blumenfeld and colleagues for evaluating hypertensive patients suspected of having primary hyperaldosteronism is to initially measure the serum potassium (Blumenfeld et al., 1994). If it is less than 3.6 mmol/L, then plasma renin activity is measured. Plasma renin activity of less than 1.0 ng/mL/hour leads to 24-hour urine collection for aldosterone and potassium excretion. Findings of 24-hour urinary potassium greater than 30 mmol/24 hours in the face of hypokalemia and of aldosterone greater than 15 mg/24 hours lead to the localization of the underlying pathology to the adrenal gland.

BOX 25.8

Causes of Hypertension Associated with Low Levels of Plasma Renin

Primary Excess of Mineralocorticoids

Primary aldosteronism
Pseudoprimary (idiopathic) aldosteronism
Glucocorticoid-suppressible aldosteronism
11-Deoxycorticosterone excess (CAH due to 11-β-hydroxylase deficiency)
18-Hydroxy-11-deoxycorticosterone excess
Adrenal carcinoma (excess mineralocorticoids and/or glucocorticoids)

Secondary Excess of Mineralocorticoids

Licorice ingestion
Excess sodium intake
Hyporenin hypoaldosteronism
Long-standing essential hypertension
Diabetes mellitus

CAH, Congenital adrenal hyperplasia.

A more recent set of guidelines for the detection and diagnosis of primary hyperaldosteronism, as proffered by the Endocrine Society, include the following (Funder et al., 2008). Although patients with primary hyperaldosteronism classically present with spontaneous or easily provokable hypokalemia, many in fact will have serum potassium levels that are within the normal range. Thus, the preferred screening test is a plasma aldosterone concentration/plasma renin activity (PAC/PRA) ratio, PAC expressed in ng/dL, and PRA in ng/mL/hour. This is performed after the patient has remained upright for at least 2 hours. The patient should have stopped spironolactone and eplerenone for 4 to 6 weeks and other diuretics for at least 2 weeks before testing. Hypokalemia should be corrected (as it may suppress aldosterone secretion), and the patient should not be on a sodium-restricted diet. A PAC/PRA ratio greater than 30 is suggestive of primary hyperaldosteronism; a value greater than 50 is virtually diagnostic (Weinberger & Fineberg, 1993; Blumenfeld et al., 1994). It is of note that the lower limit of normal for the PRA assay varies by laboratory. Therefore, the diagnosis is supported only when both the PAC/PRA ratio and the PAC are elevated. The preferred technique for measuring PRA is a validated immunometric assay. HPLC/MS-MS is preferred for measuring plasma and urine aldosterone (Funder et al., 2008). The PAC/PRA ratio is highly dependent on the renin concentration; as such, it is important to use an assay with sufficient sensitivity in the lower ranges (e.g., <0.2–0.3 ng/mL/hour).

The diagnosis of primary hyperaldosteronism is confirmed by performing one of the four following confirmatory tests: oral sodium loading test, saline infusion test, fludrocortisone suppression test, or the captopril challenge test (Funder et al., 2008). Saline suppression can be accomplished by infusing 2 L of 0.9% saline over 4 hours or by administering sodium chloride tablets 10 to 12 g daily for 3 days. PAC at the end of the 4-hour infusion of less than 5 ng/dL (140 pmol/L) makes the diagnosis of hyperaldosteronism unlikely. A PAC greater than 10 ng/dL (280 pmol/L) strongly supports the diagnosis of primary hyperaldosteronism, whereas values greater than 5 ng/dL (140 pmol/L) but less than 10 ng/dL (280 pmol/L) are considered indeterminate and may be seen with IHA. On the last day of oral sodium administration, a 24-hour urine sample is collected for aldosterone, creatinine (to assess for adequacy of the collection), and sodium (>200 mmol/day confirms adequate sodium intake). An aldosterone greater than 10 mg/24 hours (28 nmol/24 hours) following 3 days of sodium loading confirms the diagnosis (Bravo et al., 1983, Bravo, 1994; Holland et al., 1984). For the fludrocortisone suppression test, 0.1 mg fludrocortisone is given orally every 6 hours for 4 days, together with slow-release potassium chloride supplements (in doses sufficient to maintain the plasma potassium close to 4.0 nmol/L) and slow-release sodium chloride (30 mmol three times a day) and liberalization of dietary sodium intake (enough to maintain a urinary sodium excretion of at least 3 mmol/kg). On day 4, an upright plasma cortisol is measured at 7 AM and 10 AM, and PAC and PRA are measured at 10 AM. A PAC greater than 6 ng/dL with a PRA less than 1 ng/mL/hour confirms the diagnosis, provided that the 10 AM cortisol is less than the 7 AM value. For the captopril challenge, baseline blood is collected for PRA, PAC, and cortisol; then, 25 to 50 mg of captopril is administered orally. PRA, PAC, and cortisol are again collected at 1 and 2 hours post-captopril. The patient is kept seated throughout the entire test. PAC is normally suppressed to greater than 30%; however, in primary hyperaldosteronism, the PAC remains elevated and the PRA suppressed. The choice of test depends on several factors, including patient compliance, presence of uncontrolled hypertension, renal insufficiency, congestive heart failure, and local expertise.

Differentiating Among the Different Causes of Primary Hyperaldosteronism

APA differs from IHA by more extreme blood pressures, greater potassium wasting, and higher atrial natriuretic peptide levels. Also, urinary and serum levels of 18-oxocortisol, 18-hydroxycortisol (serum >300 ng/dL), and 18-hydroxycorticosterone (serum >100 ng/dL) tend to be higher. A positive postural stimulation test (plasma aldosterone: ambulating rising to <130% of the supine level) has a moderate sensitivity and specificity for adenoma but not for hyperplasia. Once the diagnosis of primary hyperaldosteronism is confirmed, the next step is to image the adrenal glands by CT or MRI, looking for bilateral hyperplasia or a unilateral hypodense adenoma. The specificity of imaging to correctly categorize patients as having APA versus IHA varies from 67% to 84% (Doppmann et al., 1992; Gleason et al., 1993; Harpe et al., 1999; Magill et al., 2001). Removal of the adenoma is curative in 35% of cases and leads to improvement in another 55% (Blumenfeld et al., 1994). Surgery can cure or improve hypertension in patients with unilateral disease. For those in whom the disease is bilateral, medical treatment with drugs such as spironolactone leads to improvement in 76% of cases. Hyperplasia is not always bilateral.

As a result of multiple factors, including the increased incidence of nonfunctioning adrenal adenoma after 40 years of age, and the fact that hyperplasia may present as a unilateral adenoma on imaging, it is highly recommended that bilateral adrenal vein sampling be performed in individuals over 40 years of age who are contemplating surgery. Bilateral adrenal vein sampling is technically demanding and entails risk. However, as performed by an experienced radiologist, it is the gold standard for distinguishing adenoma from hyperplasia. An intravenous infusion of ACTH at 50 μg/hour is started 30 minutes before sampling and is continued throughout the procedure. This serves to mitigate any stress-induced fluctuations in aldosterone during the sampling, accentuate the gradient in cortisol from adrenal vein to inferior vena cava, and maximize the difference in secretion of aldosterone between the right and left adrenal glands in instances of APA. Samples for aldosterone and cortisol are obtained from each adrenal vein and from the periphery. An adrenal vein/peripheral vein cortisol of greater than 10 : 1 ensures that the samples are taken from the adrenal veins. There should be a less than 20% difference in cortisol measurements between both adrenal glands.

To correct for dilutional effects, the cortisol-corrected aldosterone ratio (i.e., aldosterone/cortisol) is utilized. In APA, the cortisol-corrected aldosterone ratio is usually at least fivefold higher on the side with the adenoma, and no gradient is seen in hyperplasia (Doppmann & Gill, 1996). As per the recent Endocrine Society guidelines, a cortisol-corrected aldosterone ratio from high side to low side of greater than 4 : 1 indicates APA, a ratio of less than 3 : 1 suggests IHA, and values between 4 : 1 and 3 : 1 are indeterminate and need to be interpreted in conjunction with imaging studies and clinical settings. Using these cutoffs, a sensitivity of 95% and a specificity of 100% are achieved (Funder et al., 2008).

Several studies have shown a discrepancy between radiologic findings and surgical findings in up to one-third of all cases. Kempers found that when compared with adrenal vein sampling, CT and MRI misdiagnosed the cause of primary hyperaldosteronism in 37.8% of patients (Kempers et al., 2009). Given the increased prevalence (5%–10%) of adrenal incidentalomas (nonfunctioning adrenal tumors) with increasing age, many authorities are recommending adrenal vein sampling for patients with hyperaldosteronism who are older than 40 years of age and have a unilateral hypodense adrenal nodule greater than 1 cm on CT scan (Young, 1999). Based on the findings of large prospective studies, others have suggested that the major strength of this technique may be its use in evaluating those patients with a high probability of APA but with normal findings or bilateral nodular disease on CT. It should be stressed that this test is technically difficult; even in the very best of hands, it is successful in only approximately 92% to 96% of cases (Doppmann et al., 1992; Radin et al., 1992; Young, 1999).

The syndrome of inapparent mineralocorticoid excess is due to dysfunction of 11-β-hydroxysteroid dehydrogenase type 2 (11-β-HSD2). Cortisol can function as a potent mineralocorticoid, binding to the mineralocorticoid receptor in the kidney with the same affinity as aldosterone. 11-β-HSD2 mitigates the mineralocorticoid action of cortisol by converting it to the metabolically inactive form, cortisone. When activity of this enzyme is decreased because of hereditary factors, the ingestion of large quantities of licorice (which has a high content of glycyrrhizic acid) or chewing tobacco, hypertension, hypokalemia, low PRA, and low PAC may result. An elevated cortisol/cortisone concentration on a 24-hour urine collection confirms the diagnosis.

TABLE 25.17
Differentiating the Various Causes of Hyperaldosteronism

Disorder	Aldosterone	Renin	Serum K^+
Primary hyperaldosteronism	↑	↓	↓
Renin-secreting tumor	↑	↑	↓—N
Dexamethasone-suppressible hyperaldosteronism	↑	↓	↓
Renovascular hypertension	N—↑	N—↑	↓—N
Bartter syndrome	↑	↑	↓
Diuretics, congestive heart failure, cirrhosis, nephrotic syndrome	↑	↑	N—↓

N, Normal.

Renin may be suppressed by excessive sodium intake. It is also suppressed in the syndrome of hyporenin-hypoaldosteronism, which is most commonly seen in patients with diabetes mellitus and renal disease. Secondary aldosteronism results from nonadrenal disease, in which both adrenal glands are stimulated (Table 25.17). Typically, these patients are not hypertensive.

Conditions such as nephrosis, cirrhosis, and heart failure are associated with decreased renal perfusion, causing a compensatory increase in renin and aldosterone levels (secondary hyperaldosteronism). The response of the renin-aldosterone system in pregnancy is especially complex; renin, renin substrate, angiotensin II, and aldosterone appear to be increased.

There are two variants of familial hyperaldosteronism (FH), FH-1, which is also known as *glucocorticoid remedial hyperaldosteronism* (*GRA*), and FH-2. GRA is an autosomal-dominant inherited disorder characterized by hyperaldosteronism, hyporeninemia, and severe, usually refractory, hypertension, with onset typically occurring in those younger than 20 years of age with a positive family history of early hypertension and/or hemorrhagic stroke. It is the result of translocation of aldosterone synthetase (CYP18, CYP11B2) onto the ACTH-sensitive promoter sequence of the 11-β-hydroxylase (CYP11B1) gene within the zona fasciculata. Thus, aldosterone synthesis is stimulated by ACTH. In addition to increased aldosterone, these individuals produce excess 18-OH cortisol and 18-oxycortisol. Diagnosis can be confirmed by normalization of aldosterone following 4 to 6 weeks of steroid suppression or by genetic testing using Southern blot or long polymerase chain reaction (Lifton et al., 1992; Kurtz & Spence, 1993). FH-2 is an autosomal-dominant condition that is associated with APA, IHA, or both. Unlike FH-1, aldosterone does not suppress in response to glucocorticoid treatment.

Liddle syndrome is a rare autosomal-dominant disorder characterized by hypertension and hypokalemia. However, unlike in primary hyperaldosteronism, PRA and PAC are both low. The defect is due to a mutation in the amiloride-sensitive sodium channel within the renal collecting ducts, leading to enhanced sodium reabsorption and increased potassium secretion. Liddle syndrome can be diagnosed by genetic testing or, if genetic testing is unavailable, by good clinical response to amiloride or triamterene, and by lack of response to dexamethasone or aldosterone antagonists.

ALDOSTERONE MEASUREMENTS

An isolated aldosterone measurement with no attention to patient preparation is of little clinical value. Even when time of sampling, posture, and dietary sodium and potassium are controlled, it is difficult to discriminate with certainty between primary aldosteronism and other forms of hypertension with the use of plasma aldosterone measurements alone. Interpretation of the aldosterone level must be done in the context of a simultaneously collected plasma renin and serum potassium.

Aldosterone assays are performed on plasma using extraction to remove aldosterone from plasma proteins, followed by chromatography and immunoassay or, preferably, LC-MS/MS. Urine is assayed following acid hydrolysis and extraction. Normative values exist for different age groups, postures, and sodium intakes (Table 25.18). HPLC-MS/MS affords greater consistency and is gradually replacing older methods.

RENIN MEASUREMENTS

Important technical differences have been noted in assessment of renin using current methods. Renin measurements are of two types: plasma

TABLE 25.18
Differentiating the Various Causes of Hypoaldosteronism

Disorder	Aldosterone	Renin	Serum K^+
Addison disease	↓	↑	↑
Cushing syndrome	↓	↓	N or ↓
Liddle syndrome	↓	↓	↓
Hyporenin hypoaldosteronism	↓	↓	↑
Apparent mineralocorticoid excess	↓	↓	↓
Isolated hypoaldosteronism	↓	↑	↑

N, Normal.

renin activity (PRA) and plasma renin concentration (PRC). The PRA is a bioassay wherein a plasma specimen containing renin is allowed to react with its substrate, angiotensinogen; after a specified period of time, the reaction is terminated, and generated angiotensin I is measured by RIA. For estimation of PRA, the endogenous substrate is not eliminated. Therefore, the rate of generation of angiotensin I is influenced by the concentrations of endogenous renin and its substrate. This type of assay is the most widely used method for the determination of renin. Comparison of results among laboratories is not possible because of procedural differences (e.g., variations in pH, ionic strength, length of the assay, the angiotensinase inhibitor, the conditions under which the specimen was obtained) and because of the lack of a specific reference preparation. In addition, the literature on renin assays reveals confusion regarding units of measurement employed. Even when an attempt is made to express the many arbitrary units in the same terms (nanograms of angiotensin liberated per milliliter per hour), wide ranges are reported for human PRA in reference populations.

When PRC rather than PRA is measured, the effect of substrate is eliminated. The PRC assay is an immunoassay directed to the renin molecule itself.

Assays of PRA and PRC provide similar information, except in a few clinical situations. With oral contraceptive administration, PRC remains within the reference interval, whereas PRA increases owing to the increase in substrate. Other procedures such as freezing, thawing, and acidification have been found to convert prorenin to renin, thereby increasing the values in PRC assays.

Because renin release is controlled by many physiologic and pharmacologic variables, it is extremely important to know the conditions under which the blood specimen was obtained. Such conditions as upright posture, the administration of diuretics, and low-sodium diets are potent stimuli of renin release and should be adequately controlled before plasma renin is measured. Renin also appears to be extremely labile; thus, the variables involved in specimen processing should be vigorously controlled. Blood should be drawn into an iced EDTA tube, which inactivates the enzymes (e.g., angiotensinases). It should be centrifuged at 4° C, and the plasma should be separated promptly from the cells, frozen immediately, and kept frozen until ready to be analyzed. With this technique, the specimen is stable for several months at –20° C.

Direct measurement of renin substrate, angiotensin I, or angiotensin II is not used widely in clinical practice because of tedious extraction or concentration steps as well as difficulty in eliminating formation or degradation of these compounds by proteases and other enzymes involved in the renin system. Although ACE levels can be measured easily, they are of little use in the diagnosis of hypertensive disorders.

SELECTED REFERENCES

American Association of Clinical Endocrinologists: Medical guidelines for clinical practice for the evaluation and treatment of hyperthyroidism and hypothyroidism, *Endocr Pract* 8:457–469, 2002.

An excellent reference for the diagnosis and treatment of commonly seen thyroid disorders, created by a consensus panel of experts in the field.

U.S. Preventive Services: Task Force screening for thyroid dysfunction: Recommendation statement, *Am Fam Physician* 91, 2015. 790A-790E.

Updated reference for diagnosis and treatment of thyroid disorders.

American Association of Clinical Endocrinologists: Medical guidelines for clinical practice for the diagnosis and treatment of acromegaly, *Endocr Pract* 10:213–225, 2004.

An excellent reference for the diagnosis and treatment of acromegaly, created by a consensus panel of experts in the field of acromegaly.

Zahr R, Fleseriu M: Updates in diagnosis and treatment of acromegaly, *Eur Endocrinol* 14:57–61, 2018.

A concise, updated summary of diagnosis and treatment of acromegaly.

Stewart PM, Newell-Price JDC: The adrenal cortex. In Melmed S, Polonsky KS, Larsen PR, Kronenberg HM, editors: *Williams textbook of endocrinology*, 13th ed., Philadelphia, PA, 2016, Elsevier.

One of the best written and most respected general endocrine reference textbooks; the chapter on the adrenal glands is concise, lucid, and well referenced.

Access the complete reference list online at Elsevier eBooks for Practicing Clinicians.

REFERENCES

Abe K, Adachi I, Miyakawa S, et al.: Production of calcitonin, adrenocorticotropic hormone, β-melanocyte stimulating hormone in tumors derived from amine precursor uptake and decarboxylation cells, *Cancer Res* 37:4190–4194, 1977.

Adams LM, Emery JR, Clark SJ, et al.: Reference ranges for new thyroid function tests in premature infants, *J Pediatr* 126:122–127, 1995.

Ain KB, Pucino F, Shiver T, et al.: Thyroid hormone levels affected by time of blood sampling in thyroxine-treated patients, *Thyroid* 3:81–85, 1993.

Alderman MH, Hadavan S, Oor WI, et al.: Association of the rennin-sodium profile with the risk of myocardial infarction in patients with hypertension, *N Engl J Med* 324:1098, 1991.

Alexander EK, Pearce NP, Brent GA, Brown RS, et al.: *Thyroid* 27(3), 2017. online ahead of printhttp doi.org/10.1089/thy.2016.0457.

Almeretti G, Corneli G, Baldelli R, et al.: Diagnostic reliability of a single IGF-I measurement in 237 adults with total anterior hypopituitarism and severe GH deficiency, *Clin Endocrinol* 59:56–61, 2003.

Alwani RA, Schmit Jongbloed LW, de Jong FH, et al.: Differentiating between Cushing's disease and pseudo-Cushing's syndrome: comparison of four tests, *Eur J Endocrinol* 170:477–486, 2014.

Amadori P, Dilberis C, Marcolla A, et al.: Macroprolactinemia: predictability on clinical basis and detection by PEG precipitation with two different immunometric methods, *J Endocrinol Invest* 26:148–156, 2003.

Ames RP, Borkpwski AJ, Sicinski AM, et al.: Prolonged infusion of angiotensin II and norepinephrine and blood pressure, electrolyte balance, aldosterone and cortisol secretion in normal man and in cirrhosis with ascites, *J Clin Invest* 44:1171, 1965.

Anderson PW, Macaulay L, Do S, et al.: Extrarenal renin-secreting tumors: insights into hypertension and ovarian renin production, *Medicine* 68:257, 1989.

Andersen S, Pedersen KM, Bruun NH, et al.: Narrow individual variations in serum T_4 and T_3 in normal subjects: a clue to the understanding of subclinical thyroid disease, *J Clin Endocrinol Metab* 87:1068–1072, 2002.

Arafah BM: Estrogen therapy may necessitate an increase in thyroxine dose for hypothyroidism, *N Engl J Med* 344:1743–1749, 2001.

Arnaldi G, Angeli A, Atkinson AB, et al.: Diagnosis and complications of Cushing's syndrome: a consensus statement, *J Clin Endocrinol Metab* 88:5593–5602, 2003.

Ayus JC, Arieff AI: Glycine induced hypo-osmolar hyponatremia, *Arch Intern Med* 157:223–226, 1997.

Bacarese-Hamilton T, Cattini R, Shandley C, et al.: A fully automated enzyme immunoassay for the measurement of cortisol in biologic fluids, *Eur J Clin Chem Clin Biochem* 30:531, 1992.

Barbot N, Calmettes C, Schuffenecker I, et al.: Pentagastrin stimulation test and early diagnosis of medullary carcinoma using an immunoradiometric assay of calcitonin: comparison with genetic screening in hereditary medullary thyroid carcinoma, *J Clin Endocrinol Metab* 78:114–120, 1994.

Barkan A: Acromegaly, diagnosis and therapy, *Endocrinol Metab Clin North Am* 18:277–310, 1989.

Barkan AL, Chandler WF: Giant pituitary prolactinoma with falsely low serum prolactin: the pitfall of the "high-dose hook effect" case report, *Neurosurgery* 42:913–915, 1998.

Basuvau JP, Mallet E, Leroy M, Brunelle P: Reference intervals for serum calcitonin in in men, women, and children, *Clin Chem* 50(10):1828–1830, 2004, https://doi.org/10.1373/clinchem.2003.026963.

Baumann G: Acromegaly, *Endocrinol Metab Clin North Am* 16:685–703, 1987.

Beck-Peccos P, Amr S, Menezes-Ferreira M, et al.: Decreased receptor binding of biologically inactive thyrotropin in central hypothyroidism: effect of treatment with thyrotropin releasing hormone, *N Engl J Med* 312:1085–1089, 1985.

Becker KL, Nylen ES, Cohen R, et al.: Calcitonin: structure, molecular biology and actions. In Beleziakin JP, Raisz LE, Rodan GA, editors: *Principle of bone biology*, San Diego, 1996, Academic Press, pp 471–474.

Becker KL, Nylen ES, Whir JC, et al.: Procalcitonin and calcitonin gene family of peptidase in inflammation, infection and sepsis: a journey from calcitonin back to its precursor, *JCEM* 89:1512–1525, 2004.

Beishuizen A, Thiis LG, Vermes I: Patterns of corticosteroid-binding globulin and the free cortisol index during septic shock and multitrauma, *Intensive Care Med* 27:1584–1601, 2001.

Bigos R, Ridgway EC, Kourides IA, et al.: Spectrum of pituitary alterations with mild and severe thyroid impairment, *J Clin Endocrinol Metab* 46:317, 1978.

Biller BMK, Samuels MH, Zagar A, et al.: Sensitivity and specificity of six tests for the diagnosis of adult GH deficiency, *J Clin Endocrinol Metab* 87:2067–2079, 2002.

Bitton RN, Wexler CI: Free triiodothyronine toxicosis: a distinct entity, *Am J Med* 88:531–533, 1990.

Bjorbeck C, Kahn BB: Leptin signalling in the central nervous system and the periphery, *Recent Prog Horm Res* 59:305–331, 2004.

Bjorkman U, Ekholm R, Denef J-F: Cytochemical localization of hydrogen peroxidase in isolated thyroid follicle, *J Utrastruct Res* 71:105–115, 1981.

Blumenfeld JD, Sealey JE, Schussel Y, et al.: Diagnosis and treatment of primary hyperaldosteronism, *Ann Intern Med* 121:877–885, 1994.

Bowen R, Benavides R, Colon-Franco JM, Katzman BM, et al.: Best practices in mitigating the risk of biotin interference with laboratory testing, *Clin Biochem*, 2019. Doi.org/10.1016/j.clinbiochem.2019.08.012.

Brabant A, Brabant G, Schuermeyer T, et al.: The role of glucocorticoids in the regulation of thyrotropin, *Acta Endocrinol* 121:95–100, 1989.

Brandi ML, Gagel RJ, Angeli A, et al.: Consensus guidelines for diagnosis and therapy of MEN type 1 and type 2, *J Clin Endocrinol Metab* 86:5658–5671, 2001.

Braverman LE, Utiger RD, editors: *Werner and Ingbar's the thyroid: a fundamental and clinical test*, Philadelphia, 2000, Lippincott-Raven.

Bravo EL: Primary aldosteronism, *Endocrinol Metab Clin North Am* 23:271, 1994.

Bravo EL, Tagle R: Pheochromocytoma: state-of-the-art and future prospects, *Endocr Rev* 24:539–553, 2003.

Bravo EL, Tarazi RC, Fouad FM, et al.: Clonidine-suppression: a useful aid in the diagnosis of pheochromocytoma, *N Engl J Med* 305:623, 1981.

Bravo EL, Tarazi RC, Dustan HP, et al.: The changing clinical spectrum of primary aldosteronism, *Am J Med* 74:641–651, 1983.

Brent GA, Moore DD, Larsen PR: Thyroid hormone regulation of gene expression, *Annu Rev Physiol* 53(17–35), 1991.

Brewster UC, Perazella MA: The renin-angiotensin-aldosterone system and the kidney: effects on kidney disease, *Am J Med* 116:263–272, 2004.

Brilla CG, Zhou G, Matsubara L, et al.: Collagen metabolism in cultured adult rat cardiac fibroblasts: response to angiotensin I and aldosterone, *J Mol Cell Cardiol* 26:809–820, 1994.

Brown NJ, Kim KS, Chen YQ, et al.: Synergistic effect of adrenal steroids and angiotensin II on plasminogen activator inhibitor-1 production, *J Clin Endocrinol Metab* 85:336–344, 2000.

Brunner HR, Baer L, Sealey JE, et al.: The influence of potassium administration and of potassium deprivation on plasma renin in normal and hypertensive subjects, *J Clin Invest* 49:2128–2138, 1970.

Burch HB: Drug effects on the thyroid, *N Engl J Med* 381(8):749–761, 2019.

Burke CW: Adrenal insufficiency, *Clin Endocrinol Metab* 14:947–976, 1985.

Canale MP, Bravo EL: Diagnostic specificity of serum chromogranin-A for pheochromocytoma in patients with renal dysfunction, *J Clin Endocrinol Metab* 78:1139–1144, 1994.

Caron P: Effect of amiodarone on thyroid function, *Press Med* 24:1747–1751, 1995.

Casanueva FF: Physiology of growth hormone secretion and action, *Endocrinol Metab Clin North Am* 21:483–517, 1992.

Casanueva FF, Castro AI, Micic D, et al.: New guidelines for the diagnosis of growth hormone deficiency in adults, *Horm Res* 71(Suppl 1):112–115, 2009.

Chalan P, Di Dalmazi G, Pani F, De Remigis A, Corsello A, Caturegli P: Thyroid dysfunctions secondary to cancer immunotherapy, *J Endocrinol Invest* 41(6):625–638, 2018, https://doi.org/10.1007/s40618-017-0778-8.

Chambard M, Verrier B, Gabrion J, et al.: Polarization of thyroid cells in cultures. Evidence for Baslateral localization of the iodide "pump" and of the TSH receptor-adenyl cyclase complex, *J Cell Biol* 96:1172–1177, 1983.

Chan KC, Lit LC, Law EL, et al.: Diminished free cortisol excretion in patients with moderate and severe renal impairment, *Clin Chem* 50:757–759, 2004.

Chiovato L, Bassi P, Santini F, et al.: Antibodies producing complement-mediated thyroid toxicity in patients with atrophic or goiterous autoimmune thyroiditis, *J Clin Endocrinol Metab* 77:1700–1705, 1993.

Chopra I: Euthyroid sick syndrome: is it a misnomer? *J Clin Endocrinol Metab* 82:329–334, 1997.

Chrousos GP: The hypothalamic-pituitary-adrenal axis and immune mediated inflammation, *N Engl J Med* 332:1351–1362, 1998.

Chung HM, Kluge R, Schrier RW, et al.: Clinical assessment of extracellular fluid volume in hyponatremia, *Am J Med* 83:905–908, 1987.

Cobin RH, Gharib H, Bergman DA, et al.: AACE/AAES medical/surgical guidelines for clinical practice: management of thyroid carcinoma, *Endocr Pract* 7:203–220, 2001.

Colombo C, Verga U, Mian C, et al.: Comparison of calcium and pentagastrin tests for the diagnosis and follow-up of medullary thyroid cancer, *J Clin Endocrinol Metab* 97:905–913, 2012.

Conner P, Fried G: Hyperprolactinemia: etiology, diagnosis and treatment alternatives, *Acta Obstet Gynecol Scand* 77:249–262, 1998.

Cook DM, Yuen KCJ, et al.: AACE medical guidelines for clinical practice for growth hormone use in growth hormone–deficient adults and transition patients—2009 update: executive summary of recommendations, *Endocr Pract* 15:580–586, 2009.

Corvol P, Pinet F, Plouin PF, et al.: Renin-secreting tumors, *Endocrinol Metab Clin North Am* 23:255, 1994.

Costante G, Meringolo D, Durante C, Bianchi D, et al.: Predictive value of serum calcitonin levels for preoperative diagnosis of medullary thyroid carcinoma in a cohort of 5817 Consecutive patients with thyroid nodules, *J Clin Endocrinol Metab* 92(2):450–455, 2007, https://doi.org/10.1210/jc.2006-1590.

Daniels GH: Amiodarone-induced thyrotoxicosis, *J Clin Endocrinol Metab* 86(3–8), 2001.

Davies T, Roli E, Braverman LE, et al.: Thyroid controversy: stimulating antibodies, *J Clin Endocrinol Metab* 83:3777–3780, 1998.

Davis FB, LaMantia RS, Spaulding FW, et al.: Estimation of a physiologic replacement dose of levothyroxine in elderly patients with hypothyroidism, *Arch Intern Med* 144:1752–1754, 1984.

De Bellis A, Bizzarro A, Amoresano Paglionico V, et al.: Detection of vasopressin cell antibodies in some patients with autoimmune endocrine diseases without overt diabetes insipidus, *Clin Endocrinol* 40:173–177, 1994.

De Bellis A, Colao A, Di Salle F, et al.: A longitudinal study of plasma vasopressin cell antibodies, posterior pituitary function and magnetic resonance imaging evaluations in subclinical autoimmune central diabetes insipidus, *J Clin Endocrinol Metab* 84:3047–3051, 1999.

De Grande LAC, Van Uytfanghe K, Reynders D, Das B, et al.: Standardization of free thyroxine measurements allows the Adoption of a more Uniform reference interval, *Clin Chem. Published online*, 2017, https://doi.org/10.1373/clinchem.2017.274407.

DeGroot LJ, Major G: Admission screening by thyroid function tests in an acute general care teaching hospital, *Am J Med* 93:558–564, 1992.

Delange F: Correction of iodine deficiency: benefits and possible side effects, *Eur J Endocrinol* 132:542–543, 1995.

Deme D, Pommier J, Nunez J: Kinetics of thyroglobulin iodination of hormone synthesis catalized thyroid peroxidase: role of iodide in the coupling reaction, *Eur J Biochem* 70:435–440, 1976.

Dicheck HL, Nieman LK, Oldfield EH, et al.: A comparison of the standard high-dose dexamethasone suppression test and the overnight 8 mg dexamethasone suppression test for the diagnosis of Cushing's syndrome, *J Clin Endocrinol Metab* 78:418–422, 1994.

Dimaraki EV, Jaffe CA, DeMott-Friberg R, et al.: Acromegaly with apparently normal GH secretion: implications for diagnosis and follow-up, *J Clin Endocrinol Metab* 87:3537–3542, 2002.

Diver MJ, Ewins DL, Worth RC, et al.: An unusual form of big, big (macro) prolactin in a pregnant patient, *Clin Chem* 47:346–348, 2001.

Docter R, Van Toor H, Krenning EP, et al.: Free thyroxine assessed with three assays in sera of patients with nonthyroidal illness and of subjects with abnormal concentrations of thyroxine-binding proteins, *Clin Chem* 39:1668–1674, 1993.

Doppmann JL, Gill Jr JR: Hyperaldosteronism: sampling the renal veins, *Radiology* 198:309–312, 1996.

Doppmann JL, Gill Jr JR, Miller DL, et al.: Distinction between hyperaldosteronism due to bilateral adrenal hyperplasia and unilateral aldosteronoma: reliability of CT, *Radiology* 184:677–682, 1992.

Dulgeroff AJ, Hershman JM: Medical therapy for differentiated thyroid carcinoma, *Endocr Rev* 15:500–515, 1994.

Dunn JT: When is thyroid nodule a sporadic medullary carcinoma? *J Clin Endocrinol Metab* 78:824–825, 1994.

Dunn JT: What happens to our iodine? *J Clin Endocrinol Metab* 83:3398–3400, 1998.

Eastman RC, Merriman GR, Moore WT, et al.: Acromegaly, hyperprolactinemia, gonadotropin-secreting tumors and hypopituitarism. In Moore WT, Eastman RC, editors: *Diagnostic endocrinology*, ed 2, St Louis, 1996, Mosby-Year Book, p 73.

Eddy RL, Gilliland PF, Ibarra JD, et al.: Human growth hormone release: comparison of provocative test procedures, *Am J Med* 56:179, 1974.

Eisenhofer G, Goldstein DS, Walther MM, et al.: Biochemical diagnosis of pheochromocytoma: how to distinguish true from false-positive test results, *J Clin Endocrinol Metab* 88:2656–2666, 2003.

Eisenhofer G, Lenders JW, Pacak K: Biochemical diagnosis of pheochromocytoma, *Front Horm Res* 31:76–106, 2004.

Eisenhofer G, Pacak K: Diagnosis of pheochromocytoma. In *Harrison's principles of internal medicine*, McGraw-Hill, 2004. online. Available at: http://www.accessmedicine.com/.

Elamin MB, Murad MH, Mullan R, et al.: Accuracy of diagnostic tests for Cushing's syndrome: a systematic review and meta-analysis, *J Clin Endocrinol Metab* 93:1553–1562, 2008.

Elisei R, Cosci B, Romei C, Agate L, et al.: Identification of a novel point mutation in the RET gene (Ala883Thr), which is associated with medullary thyroid carcinoma Phenotype only in Homozygous condition, *J Clin Endocrinology & Metabolism* 89(11):5823–5827, 2004, https://doi.org/10.1210/jc.2004-0312.

Elliott W, Murphy MB: Reduced specificity of the clonidine suppression test in patients with normal plasma catecholamine levels, *Am J Med* 84:419–424, 1988.

Engelbach M, Görges R, Forst T, Pfützner A, et al.: Improved diagnostic methods in the follow-up of medullary thyroid carcinoma by highly specific calcitonin measurements, *J Clin Endocrinol Metab* 85(5):1890–1894, 2000, https://doi.org/10.1210/jcem.85.5.6601.

Engler D, Burger AG: The deiodination of the iodothyronines and their derivatives in man, *Endocr Rev* 5:151–184, 1984.

Erdogan MF, Gullu S, Baskal N, et al.: Omeprazole: calcitonin stimulation test for the diagnosis follow-up and family screening in medullary carcinoma of the thyroid gland, *Ann Surg* 188:139–141, 1997.

Ezzat S: Acromegaly, *Endocrinol Metab Clin North Am* 26:703–723, 1997.

Faber J, Kirkegaard C, Rasmussen B, et al.: Pituitary-thyroid axis in critical illness, *J Clin Endocrinol Metab* 65:315–320, 1987.

Fahie-Wilson M: In hyperprolactinemia, testing for macroprolactin is essential, *Clin Chem* 49:1434–1436, 2003.

Feldt-Rasmussen U, Schleusner H, Carayon P: Meta-analysis evaluation of the impact of thyrotropin receptor antibodies on long-term remission after medical therapy of Grave's disease, *J Clin Endocrinol Metab* 78:98–102, 1994.

Fenske W, Refardt J, Chifu I, Schnyder I, Winzeler B, et al.: A copeptin-based approach in the diagnosis of diabetes insipidus, *N Engl J Med* 37(5):428–439, 2018.

Fiad TM, Kirby JM, Cunningham SK, et al.: The overnight single-dose metyrapone test is a simple and reliable index of the hypothalamic-pituitary axis, *Clin Endocrinol* 40:603–609, 1994.

Findling JW: Clinical application of a new immunoradiometric assay for ACTH, *Endocrinololgist* 2:360–365, 1992.

Findling JW, Raff H: Newer diagnostic techniques and problems in Cushing's disease, *Endocrinol Metab Clin North Am* 28:191–210, 1999.

Fisher DA, Nelson JC, Carlton EI, et al.: Maturation of human hypothalamic-pituitary-thyroid function control, *Thyroid* 10:229–234, 2000a.

Fisher DA, Schoen EJ, La Franchi S, et al.: The hypothalamic-pituitary-thyroid negative feedback control axis in children with treated congenital hypothyroidism, *J Clin Endocrinol Metab* 85:2722–2727, 2000b.

Fleseriu M, Loriaux DL: "Relative" adrenal insufficiency in critical illness, *Endocr Pract* 15:632–640, 2009.

Fleseriu M, Bodach ME, Tumialan LM, Bonert V, et al.: Congress of neurological Surgeons systematic review and evidence-based guideline for Pretreatment endocrine evaluation of patients with nonfunctioning pituitary adenomas, *Neurosurgery* 79(4):E527–E529, 2016.

Frank J, Faix J, Hermos RJ, et al.: Thyroid function in very low birth weight infants: effects on neonatal hypothyroidism screening, *J Pediatr* 128:548–554, 1996.

Frantz AG: Hyperprolactinemia. In Collu R, Brown GM, Van Loon GR, editors: *Clinical neuroendocrinology*, Boston, 1998, Blackwell Scientific, pp 311–332.

Freda PU, Post KD, Powell JS, et al.: Evaluation of disease status with sensitive measures of growth hormone secretion in 60 post-operative patients with acromegaly, *J Clin Endocrinol Metab* 83:3808–3816, 1998.

Freda PU, Wardlaw SL: Clinical review 110: diagnosis and treatment of pituitary tumors, *J Clin Endocrinol Metab* 84:3859–3866, 1999.

Frohlich E, Wahl R: Thyroid autoimmunity: role of anti-thyroid antibodies in thyroid and extra-thyroidal disease, *Front Immunol*(8)1–16, 2017. article 521.

Fuchs AR, Fuchs F, Husslein P: Oxytocin receptors and human parturition: a dual role for oxytocin in the initiation of labor, *Science* 215:1396, 1982.

Fujieda K, Okuhara K, Abe S, et al.: Molecular pathogenesis of lipoid adrenal hyperplasia and adrenal hypoplasia congenita, *J Steroid Biochem Mol Biol* 85:483–489, 2003.

Fukata J, Shimizu N, Imura H, et al.: Human corticotropin-releasing hormone test in patients with hypothalamo-pituitary-adrenocortical disorders, *Endocr J* 40:597, 1993.

Funder JW, Carey RM, Fardello C, et al.: Case detection, diagnosis, and treatment of patients with primary hyperaldosteronism: an Endocrine Society Clinical Practice Guideline, *J Clin Endocrinol Metab* 93:3266–3281, 2008.

Gabrilove JL, Sharma DC, Dorfman RI: Adrenocortical 11-β-hydroxylase deficiency and virilism first manifest in an adult woman, *N Engl J Med* 272:1189–1194, 1965.

Garber J, Cobin R, Gharib H, Hennessey J, et al.: Clinical practice guidelines for hypothyroidism in adults: cosponsored by the American association of clinical Endocrinologists and the American thyroid association, *Endocr Pract* 18(6):988–1028, 2012.

Garcia JM, Swerdloff R, Wang C, Kyle M, et al.: Macimorelin (AEZS-130)-stimulated growth hormone (GH) test: validation of a novel oral stimulation test for the diagnosis of adult GH deficiency, *J Clin Endocrinol Metab* 98(6):2422–2429, 2013, https://doi.org/10.1210/jc.2013-1157.

Garcia JM, Biller BMK, Korbonits M, Popovic V, et al.: Macimorelin as a diagnostic test for adult GH deficiency, *J Clin Endocrinol Metab* 103(8):3083–3093, 2018, https://doi.org/10.1210/jc.2018-00665.

Gagel RF: The abnormal pentagastrin test, *Clin Endocrinol* 44:221–222, 1996.

Giustina A, Chanson P, Bronstein MD, et al.: A consensus on criteria for cure of acromegaly, *J Clin Endocrinol Metab* 95:3141–3148, 2010.

Gleason PE, Weinberger MG, Pratt JH, et al.: Evaluation of diagnostic tests in the differential diagnosis of primary aldosteronism: unilateral adenoma versus bilateral micronodular hyperplasia, *J Urol* 150:1365–1368, 1993.

Glinoer D: The regulation of thyroid function in pregnancy: pathways of endocrine adaptation from physiology to pathology, *Endocr Rev* 18:404–433, 1997.

Glinoer D, De Nayer P, Bourdoux P, et al.: Regulation of maternal thyroid function during pregnancy, *J Clin Endocrinol Metab* 71:276–287, 1990.

Goland RS, Wardlaw SL, Stark RI, et al.: High levels of corticotropin-releasing hormone immunoactivity in maternal and fetal plasma during pregnancy, *J Clin Endocrinol Metab* 63:1199–1203, 1986.

Gold PW, Loriaux L, Roy A, et al.: Responses to corticotropin-releasing hormone in the hypercortisolism of depression and Cushing's disease, *N Engl J Med* 314:1329–1335, 1986.

Goodwin TM, Monotoro M, Mestman JH, et al.: The role of chorionic gonadotropin in transient hyperthyroidism of hyperemesis gravidarum, *J Clin Endocrinol Metab* 75:1333–1337, 1992.

Grinspoon SK, Biller BMK: Laboratory assessment of adrenal insufficiency, *J Clin Endocrinol Metab* 79:923–931, 1994.

Grodum E, Petersen PH, Hangaard J, et al.: Biological description of the cortisol response to corticotropin releasing hormone (CRH) stimulation: an optimization and simplification of the test, *Ups J Med Sci* 98:311–316, 1993.

Guo J, Jaume JC, Rapoport B, et al.: Recombinant thyroid peroxidase-specific Fab converted to immunoglobulin G (IgG) molecules: evidence for thyroid cell damage IgG, but not IgG4 autoantibodies, *J Clin Endocrinol Metab* 82:925–931, 1997.

Haddow JE, Palomaki GE, Allan WC, et al.: Maternal thyroid deficiency during pregnancy and subsequent neuropsychological development of the child, *N Engl J Med* 341:549–555, 1999.

Hahn RG: Natriuresis and "dilutional" hyponatremia after infusion of glycine 1.5%, *J Clin Anesth* 13:167–174, 2001.

Hamrahian AH, Oseni TS, Arafah BM: Measurements of serum free cortisol in critically ill patients, *N Engl J Med* 350:1629–1638, 2004.

Harjai KJ, Licata AA: Effects of amiodarone on thyroid function, *Ann Intern Med* 126:63–73, 1997.

Harpe R, Ferrett CG, McKnight JA, et al.: Accuracy of CT scanning and adrenal vein sampling in the pre-operative localization of aldosterone-secreting adrenal adenomas, *Q J Med* 92:643–650, 1999.

Hartman MC, Crowe BJ, Biller BM, et al.: Which patients do not require a GH stimulation test for the diagnosis of adult GH deficiency? *J Clin Endocrinol Metab* 87:477–485, 2002.

Haugen BR, Alexander EK, Bible KC, et al.: 2015 American thyroid association management guidelines for adult patients with thyroid nodules and differentiated thyroid cancer: the American thyroid association guidelines task Force on thyroid nodules and differentiated thyroid cancer, *Thyroid* 26(1):1–133, 2016, https://doi.org/10.1089/thy.2015.0020.

Heithorn R, Hauffa BP, Reinwein D: Thyroid antibodies in children of mothers with autoimmune thyroid disorder, *Eur J Pediatr* 158(24–28), 1999.

Heron E, Chatellier G, Billaud E, et al.: The urinary metanephrine-to-creatinine ratio for the diagnosis of pheochromocytoma, *Ann Intern Med* 125:300–303, 1996.

Hershman JM: Human chorionic gonadotropin and the thyroid: hyperemesis gravidarum and trophoblastic tumors, *Thyroid* 9:653–657, 1999.

Hillier TA, Abbott RD, Barrett EJ: Hyponatremia: evaluating the correction factor for hyperglycemia, *Am J Med* 106:399–403, 1999.

Ho JT, Al-Musalhi H, Chapman MJ, et al.: Septic shock and sepsis: a comparison of total and free plasma cortisol levels, *J Clin Endocrinol Metab* 91:105–114, 2006.

Ho KK, Ho KK: Consensus guidelines for the diagnosis and treatment of adults with GH deficiency II: a statement of the GH research Society in association with the European Society for pediatric endocrinology, Lawson Wilkins Society, European Society of endocrinology, Japan endocrine Society, and endocrine Society of Australia. 2007 GH deficiency consensus Workshop participants, *Eur J Endocrinol* 157:695–700, 2007.

Holdaway IM, Rajasoorya RC, Gamble GD: Factors influencing mortality in acromegaly, *J Clin Endocrinol Metab* 89:667–674, 2004.

Holland OB, Brown H, Kuhnert L, et al.: Further evaluation of saline infusion for the diagnosis of primary aldosteronism, *Hypertension* 6:717–723, 1984.

Hollowell JG, Staehling NW, Hannon WH, et al.: Serum TSH, T(4), and thyroid antibodies in the United States population (1988 to 1994): National health and Nutrition examination survey (NHANES III), *J Clin Endocrinol Metab* 87:489–499, 2002.

Holtzman EJ, Ausiello DA: Nephrogenic diabetes insipidus: causes revealed, *Hosp Pract* 29, 1994. 89–93, 97–98, 103–104.

Honour JW, Rumsby G: Problems in diagnosis and management of congenital adrenal hyperplasia due to 21-hydroxylase deficiency, *J Steroid Biochem Mol Biol* 45:69, 1993.

Horrocks PM, Jones AF, Ratcliffe WA, et al.: Patterns of ACTH and cortisol pulsatility over twenty four hours in normal males and females, *Clin Endocrinol* 32:127–134, 1990.

Hsiao RJ, Parmer RJ, Takiyyuddin MM, et al.: Chromogranin A storage and secretion: sensitivity and specificity for the diagnosis of pheochromocytoma, *Medicine (Baltim)* 70:33–45, 1991.

Iitaka M, Kawasaki S, Sakurai S, et al.: Serum substances that interfere with thyroid hormone assays in patients with chronic renal failure, *Clin Endocrinol* 48:739–746, 1998.

Ishii H, Inada M, Tanaka K, et al.: Induction of outer and inner ring monodeiodinases in human thyroid gland by thyrotropin, *J Clin Endocrinol Metab* 57:500–505, 1983.

Itoh S, Tanaka K, Kimagae M, et al.: Effect of subcutaneous injection of a long acting analogue of somatostatin (SMS 201-995) on plasma thyroid stimulating hormone in normal human objects, *Life Sci* 42:2691–2699, 1988.

Jenkins JS, Nussey SS: The role of oxytocin: present concepts, *Clin Endocrinol* 34:515–525, 1991.

Johnson AM, Eegles JM: Lithium associated clinical hypothyroidism: prevalence and risk factors, *Br J Psychiatry* 175:336–339, 1999.

Jonklaas J, Burman KD, Wang H, Latham KR: Single dose T3 administration: kinetics and effects on biochemical and physiologic parameters, *Ther Drug Monit* 37(1):110–118, 2015.

Jung C, Ho JT, Torpy DJ, et al.: A longitudinal study of plasma and urinary cortisol in pregnancy and postpartum, *JCEM* 96:1533–1540, 2011.

Kailajarvi M, Takala T, Gronroos P, et al.: Reminders of drug effects on laboratory test results, *Clin Chem* 64:1395–1400, 2000.

Kakucska I, Rand W, Lechan RM: Thyrotropin-releasing hormone gene expression in hypothalamic paraventricular nucleus is dependent upon feedback regulation by both triiodothyronine and thyroxine, *Endocrinology* 130:2845–2850, 1992.

Kamoi K: Syndrome of inappropriate antidiuresis without involving inappropriate secretion of vasopressin in an elderly woman: effect of intravenous administration of the nonpeptide vasopressin V2 receptor antagonist OPC-31260, *Nephron* 76:111–115, 1997.

Kamoi K, Ebe T, Kobayashi O, et al.: Atrial natriuretic peptide in patients with the syndrome of inappropriate antidiuretic hormone secretion and with diabetes insipidus, *J Clin Endocrinol Metab* 70:1385–1390, 1990.

Kaptein EM: Thyroid hormone metabolism and thyroid diseases in chronic renal failure, *Endocr Rev* 17:45–63, 1996.

Kaptein EM, Spencer CA, Kamiel MB, et al.: Prolonged dopamine administration and thyroid hormone economy in normal and critically ill subjects, *J Clin Endocrinol Metab* 51:387–393, 1980.

Kater CE, Biglieri EG: Disorders of steroid 17 alpha-hydroxylase deficiency, *Endocrinol Metab Clin North Am* 23:341, 1994.

Katznelson L, Atkinson JL, Cook DM, et al.: American Association of Clinical Endocrinologists medical guidelines for clinical practice for the diagnosis and treatment of acromegaly—2011 update, *Endocr Pract* 17(Suppl 4):1–44, 2011.

Katznelson L, Laws ER, Melmed S, et al.: Acromegaly: an endocrine Society clinical practice guideline, *J Clin Endocrinol Metab* 99(11):3933–3951, 2014.

Kauppila A: Isolated prolactin deficiency, *Curr Ther Endocrinol Metab* 6:31–33, 1997.

Kaye TB, Crapo L: The Cushing's syndrome: an update on diagnostic tests, *Ann Intern Med* 112:434–444, 1990.

Kempers MJE, Lenders JWM, Outheusden L, et al.: Systematic review: diagnostic procedures to differentiate unilateral from bilateral adrenal abnormality in primary aldosteronism, *Ann Intern Med* 151:329–337, 2009.

Kleinberg DL, Noel GL, Frantz AG: Galactorrhea: a study of 235 cases, including 48 with pituitary tumors, *N Engl J Med* 296:589–600, 1977.

Krakoff L, Nicolis G, Amsel B: Pathogenesis of hypertension in Cushing's syndrome, *Am J Med* 58:216, 1975.

Kumar S, Berl T: Sodium, *Lancet* 352:220–228, 1998.

Kurtz TW, Spence MA: Genetics of essential hypertension, *Am J Med* 94:77, 1993.

Kusalic M, Engelsmann F: Effect of lithium and maintenance therapy on thyroid and parathyroid function, *J Psychiatry Neurosci* 24:227–233, 1999.

Ladenson PW, Singer PA, Ain KB, et al.: American Thyroid Association guidelines of detection of thyroid dysfunction, *Arch Intern Med* 160:1573–1575, 2000.

Lai NB, Garg D, Heaney AP, Bergsneider M, Leung AM: *No benefit of dedicated thyroid nodule screening in patients with acromegaly*, Endoc Pract In-Press, 2019, https://doi.org/10.4158/EP-2019-0254.

Langsteger W: Clinical aspect and diagnosis of thyroid hormone transport protein anomalies, *Curr Top Pathol* 91:129–161, 1997.

Laragh JH: Renin profiling for the diagnosis, risk assessment and the treatment of hypertension, *Kidney Int* 44:1163, 1993.

Laragh JH, Baer L, Brunner HR, et al.: Renin, angiotensin and aldosterone system in pathogenesis and management of hypertensive vascular disease, *Am J Med* 52:633, 1972.

Lazarus JG: The effects of lithium therapy on thyroid and thyrotropin-releasing hormone, *Thyroid* 8:909–913, 1998.

Lebbe M, Arlt W: What is the best diagnostic and therapeutic management strategy for an Addison patient during pregnancy? *Clin Endocrinol* 78:497–502, 2013.

Leger J, Olivieri A, Donaldson M, Torresani T, et al.: European Society for Paediatric endocrinology consensus guidelines on screening, diagnosis, and management of congenital hypothyroidism, *J Clin Endocrinol Metab* 99(2):363–384, 2014.

Lenders JW, Duh Q-Y, Eisenhofer G, et al.: Pheochromocytoma and paraganglioma: an Endocrine Society clinical practice guideline, *J Clin Endocrinol Metab* 99(6):1915–1942, 2014.

Lenders JW, Keiser HR, Goldstein DS, et al.: Plasma metanephrines in the diagnosis of pheochromocytoma, *Ann Intern Med* 123:101–109, 1995.

Lenders JW, Pacak K, Walther MM, et al.: Biochemical diagnosis of pheochromocytoma: which test is best? *J Am Med Assoc* 287:1427–1434, 2002.

Lentjes EG, Romijn F, Massen RJ, et al.: Free cortisol in serum assayed by temperature-controlled ultra-filtration before fluorescence polarization immunoassay, *Clin Chem* 39:2518, 1993.

Levine LS: Congenital adrenal hyperplasia. In Lavin N, editor: *Manual of endocrinology and metabolism*, ed 3, Philadelphia, 2002, Lippincott, pp 147–162.

Lifton RP, Dluhy RG, Powers M: A chimaeric 11 beta-hydroxylase/aldosterone synthase gene causes glucocorticoid-remediable aldosteronism and human hypertension, *Nature* 355:262–265, 1992.

Lindheimer MD, Davison JM: Osmoregulation, the secretion of arginine vasopressin and its metabolism during pregnancy, *Eur J Endocrinol* 132:133–143, 1995.

Linkowski P, Medlwicz J, Kerlhofs M, et al.: 25-hr profiles of adrenocorticotropin, cortisol and growth hormone in major depressive illness: effect of anti-depressant treatment, *J Clin Endocrinol Metab* 65:141–152, 1987.

Lobo RA, Kletzky OA, Kaptein EM, et al.: Prolactin modulation of dehydroepiandrosterone sulfate secretion, *Am J Obstet Gynecol* 138:632, 1980.

LoPresti JS, Eigen A, Kaptein E, et al.: Alterations in 3,3′,5′-triiodothyronine metabolism in response to propylthiouracil, dexamethasone and thyroxine administration in man, *J Clin Invest* 84:1650–1656, 1989.

LoPresti JS, Nicoloff JT: *Non-thyroidal illness in endocrinology*, ed 3, Philadelphia, 1995, Saunders, pp 665–675.

Lu FL, Yau KI, Tsai KS, et al.: Longitudinal study of serum free thyroxine and thyrotropin levels by chemiluminescent immunoassay during infancy, *Taiwan Erh K'o I, Hseh Hui Tsa Chih* 40:225–227, 1999.

Luft FC: Proinflammatory effects of angiotensin II and endothelin: targets for progression of cardiovascular and renal disease, *Curr Opin Nephrol Hypertens* 11:59–66, 2002.

Lum SM, Nicoloff JT: Peripheral tissue mechanism for maintenance of serum triiodothyronine values in a thyroxine-deficient state in man, *J Clin Invest* 73:570–575, 1984.

Lutfallah C, Wang W, Mason JI, et al.: Newly proposed hormonal criteria via genotypic proof for type II 3-β-hydroxysteroid dehydrogenase deficiency, *J Clin Endocrinol Metab* 87:2611–2622, 2002.

McLeod JF, Kovacs L, Gaskill MB, et al.: Familial neurohypophyseal diabetes insipidus associated with a signal peptide mutation, *J Clin Endocrinol Metab* 77, 1993. 599A–G.

Maghnie M, Cosi G, Genovese E, et al.: Central diabetes insipidus in children and young adults, *N Engl J Med* 343:998–1007, 2000.

Magill SB, Raff H, Shaker JL, et al.: Comparison of adrenal vein sampling and computed tomography in the differentiation of primary aldosteronism, *J Clin Endocrinol Metab* 86:1066–1071, 2001.

Martino E, Aghini-Lombardi F, Mariotti S, et al.: Amiodarone: a common source of iodine-induced thyrotoxicosis, *Horm Res* 26:158–171, 1987.

Martino E, Bartalena L, Bogazzi F, et al.: The effects of amiodarone on the thyroid, *Endocr Rev* 22:240–254, 2001.

Masrorakos G, Weber JS, Magiakou MA: etal: hypothalamic-pituitary-adrenal axis and stimulation of systemic vasopressin secretion by recombinant interleukin-6 in humans: potential implications for the syndrome of inappropriate vasopressin secretion, *J Clin Endocrinol Metab* 79:934–939, 1994.

Meikle AW, Stringham JD, Woodward MG, et al.: Hereditary and environmental influences on the variation of thyroid hormones in normal male twins, *J Clin Endocrinol Metab* 66:588–592, 1988.

Melmed S, Casanueva FF, Hoffman AR, et al.: Diagnosis and treatment of hyperprolactinemia: an Endocrine Society Clinical practice guideline, *J Clin Endocrinol Metab* 96:273–288, 2011.

Melmed S: Pathogenesis and diagnosis of growth hormone deficiency in adults, *N Engl J Med* 380(26):2551–2562, 2019, https://doi.org/10.1056/NEJMra1817346.

Mendel CM, Frost PH, Kunitake ST, et al.: Mechanism of the heparin-induced increase in the concentration of free thyroxine in plasma, *J Clin Endocrinol Metab* 65:1259–1264, 1987.

Merke DP, Bornstein SR, Avila NA, et al.: Future directions in the study and management of congenital adrenal hyperplasia due to 21-hydroxylase deficiency, *Intern Med* 136:320–334, 2002.

Merke DP, Chrousos GP, Eisenhofer G, et al.: Adrenomedullary dysplasia and hypofunction in patients with classic 21-hydroxylase deficiency, *N Engl J Med* 343:1362–1368, 2000.

Meurisse M, Gollogly MM, Degauque C, et al.: Iatrogenic thyrotoxicosis: causal circumstances, pathophysiology and principles of treatment—review of the literature, *World J Surg* 24:1377–1385, 2000.

Mevorach RA, Bogaert GA, Kogan BA: Urine concentration and enuresis in healthy pre-school children, *Arch Pediatr Adolesc Med* 149:259–262, 1995.

Mian C, Perrino M, Colombo C, et al.: Refining calcium test for the diagnosis of medullary thyroid cancer: cutoffs, procedures, and safety, *J Clin Endocrinol Metab* 99(5):1656–1664, 2014.

Molitch ME, Clemmons DR, Malozowski S, et al.: Evaluation and treatment of adult growth hormone deficiency: an endocrine Society clinical practice guideline, *J Clin Endocrinol Metab* 91:1621–1634, 2006.

Morgenthaler NG, Struck J, Alonso C, Bergmann A: Assay for the measurement of copeptin, a stable peptide derived from the precursor of vasopressin, *Clin Chem* 52(1):112–119, 2006.

Motte P, Vauzelle P, Garder P, et al.: Construction and clinical validation of a sensitive and specific assay for mature calcitonin using monoclonal anti-peptide antibodies, *Clin Chim Acta* 174(35–54), 1988.

Nelson DH, Samuels LT: A method for the determination of 17-hydroxycorticosteroids in blood: 17-hydroxycorticosterone in the peripheral circulation, *J Clin Endocrinol Metab* 12:519–526, 1952.

Nelson JC, Tindall DJ: A comparison of the adrenal responses to hypoglycemia, metyrapone and ACTH, *Am J Med Sci* 275:165–172, 1978.

Nelson JC, Wilcox RB: Analytical performance of free and total thyroxine assays, *Clin Chem* 42:146–154, 1996.

Neumann HPH, Young WF, et al.: Pheochromocytoma and paraganglioma, *N Engl J Med* 381(16):552–564, 2019.

New MI: Steroid 21-hydroxylase deficiency (congenital adrenal hyperplasia), *Am J Med* 98(2S–8S), 1995.

New MI, Lorenzen F, Lerner AJ, et al.: Genotyping steroid 21-hydroxylase deficiency: hormonal reference data, *J Clin Endocrinol Metab* 57:320–326, 1983.

Newell-Price J, Morris DG, Drake WM, et al.: Optimal response criteria for the human CRH test in the differential diagnosis of ACTH-dependent Cushing's syndrome, *J Clin Endocrinol Metab* 87:1640–1645, 2002.

Newell-Price J, Trainer P, Besse M, et al.: The diagnosis and differential diagnosis of Cushing's syndrome and pseudo-Cushing's states, *Endocr Rev* 19:647–672, 1998.

Newell-Price J, Trainer PJ, Perry LA, et al.: Single sleeping mid-night cortisol has 100% sensitivity for the diagnosis of Cushing's syndrome, *Clin Endocrinol* 43:545–550, 1995.

Nieman LK, Biller BM, Findling JW, et al.: The diagnosis of Cushing's syndrome: an endocrine Society clinical practice guideline, *J Clin Endocrinol Metab* 93:1526–1540, 2008.

Nieman LK, Cutler Jr GB: The sensitivity of the urine free cortisol measurement as a screening test for Cushing's syndrome (abstract). In *Programs and abstracts of the Endocrine Society 72nd annual meeting*, Atlanta, 1990, Endocrine Society, p 822.

Nieman LK, Cutler Jr GB, Oldfield EH, et al.: The ovine corticotropin-releasing hormone (CRH) stimulation test is superior to the human CRH stimulation test for the diagnosis of Cushing's disease, *J Clin Endocrinol Metab* 69:165–169, 1989.

Nilson JC, Clarke SJ, Borat DI, et al.: Age-related changes in serum free thyroxine during childhood and adolescence, *J Pediatr* 123:899–905, 1993.

Nohr SB, Jorgensen A, Pedersen KM, et al.: Postpartum thyroid dysfunction in pregnant thyroid peroxidase antibody-positive women living in an area with mild to moderate iodine deficiency: is iodine supplementation safe? *J Clin Endocrinol Metab* 85:3191–3198, 2000.

Nordenstrom A, Thilen A, Hadenfeldt L, et al.: Genotyping is a valuable diagnostic complement to neonatal screening for congenital adrenal hyperplasia due to steroid 21-hydroxylase deficiency, *J Clin Endocrinol Metab* 84:1505, 1999.

Nussey SS, Soo SC, Gibson S, et al.: Isolated congenital ACTH deficiency: a cleavage enzyme defect? *Clin Endocrinol* 39:381, 1993.

Oakley PW, Dawson AH, Whyte IM: Lithium: thyroid effects and altered renal handling, *Clin Toxicol* 38:333–337, 2000.

Odell WD, Wilber JF, Paul WE: Radioimmunoassay of thyoglobulin in human serum, *J Clin Endocrinol Metab* 25:1179–1188, 1965.

Oelkers W: Adrenal insufficiency, *N Engl J Med* 335:1206–1212, 1996.

Oelkers W, Diederich S, Bahr V: Diagnosis and therapy surveillance in Addison's disease: rapid adrenocorticotropin (ACTH) test and measurement of plasma ACTH, renin activity and aldosterone, *J Clin Endocrinol Metab* 75:259–264, 1992.

Olukoga AO, Kane JW: Macroprolactinaemia: validation and application of the polyethylene glycol precipitation test and clinical characterization of the condition, *Clin Endocrinol* 51:119–126, 1999. doi.org/10.4158/EP-2019-0254.

Orme SM, McNally RJ, Cartwright RA, et al.: Mortality and cancer incidence in acromegaly: a retrospective cohort study. United Kingdom Acromegaly Study Group, *J Clin Endocrinol Metab* 83:2730–2734, 1998.

Orth DN: Cushing's syndrome, *N Engl J Med* 332:791, 1995.

Pacak K, Chrousos GP, Koch CA, et al.: Pheochromocytoma: progress in diagnosis, therapy and genetics. In Margioris A, Chrousos GP, editors: *Adrenal disorders (vol 1), Totawa, N.J.*, Humana Press, 2001a, pp 479–523.

Pacak K, Eisenhofer G, Carrasquillo JA, et al.: 6-[18F]-fluorodopamine positron emission tomography (PET) scanning for diagnostic localization of pheochromocytoma, *Hypertension* 38:6–8, 2001b.

Pacini F, Fontanelli M, Fugazzola L, et al.: Routine measurement of serum calcitonin in nodular thyroid diseases allows the preoperative diagnosis of unsuspected sporadic medullary thyroid carcinoma, *J Clin Endocrinol Metab* 78:826–829, 1994.

Panesar NS, Li CY, Rogers MS: Reference intervals for thyroid hormones in pregnant Chinese women, *Ann Clin Biochem* 38:329–332, 2001.

Pang S, Lerner AJ, Stoner E: Late-onset adrenal steroid 3-β-hydroxysteroid dehydrogenase deficiency. I. A cause of hirsutism in pubertal and postpubertal women, *J Clin Endocrinol Metab* 60:428–439, 1985.

Pang S, Levine LS, Lorenzen F, et al.: Hormonal studies in obligate heterozygotes and siblings of patients with 11-β-hydroxylase deficiency congenital adrenal hyperplasia, *J Clin Endocrinol Metab* 50:586–589, 1980.

Pang S, Murphey W, Levine LS, et al.: A pilot newborn screening for congenital adrenal hyperplasia in Alaska, *J Clin Endocrinol Metab* 55:413–420, 1982.

Pang SY, Wallace MA, Hofman L: Worldwide experience in newborn screening for classical congenital adrenal hyperplasia due to 21-hydroxylase deficiency, *Pediatrics* 81:866–874, 1988.

Papanicolaou DA, Mullen N, Kyrou I, et al.: Nighttime salivary cortisol: a useful test for the diagnosis of Cushing's syndrome, *J Clin Endocrinol Metab* 87:4515–4521, 2002.

Papanicolaou DA, Yanovski JA, Cutler Jr GB, et al.: A single midnight serum cortisol measurement distinguishes Cushing's disease from pseudo-Cushing state, *J Clin Endocrinol Metab* 83:1163–1167, 1998.

Parle JV, Masisonneuve P, Sheppard MC, et al.: Prediction of all-cause and cardiovascular mortality in elderly people from one low serum thyrotropin result: a 10-year study, *Lancet* 358:861–865, 2001.

Pedersen KM, Laurberg P, Iversen E, et al.: Amelioration of some pregnancy associated variation in thyroid function by iodine supplementation, *J Clin Endocrinol Metab* 77:1078–1083, 1993.

Petakov MS, Damjanovic SS, Nikolic-Durovic MM, et al.: Pituitary adenoma secreting large amounts of prolactin may give false low values in immunoradiometric assays: the hook effect, *J Endocrinol Invest* 21:184–188, 1998.

Philomin V, Vassieres A, Jaouen G: New applications of carbonylmetalloimmunoassay (CMIA): a non-radioisotopic approach to cortisol assay, *J Immunol Methods* 171:201, 1994.

Piketty ML, D'Herbomez M, Le Guillouzic D, et al.: Clinical comparison of three labeled-antibody immunoassays of free triiodothyronine, *Clin Chem* 42:933–941, 1996.

Pop VJ, De Vries E, van Baar AL, et al.: Maternal thyroid peroxidase antibodies during pregnancy: a marker of impaired child development? *J Clin Endocrinol Metab* 80:3561–3566, 1995.

Pop VJ, Kuijpens JL, van Baar AL, et al.: Low maternal free thyroxine concentrations during pregnancy are associated with impaired psychomotor development in infancy, *Clin Endocrinol* 50:147–148, 1999.

Porter CC, Silber RH: A quantitative color reaction for cortisone and related 17,21-dihydroxy-20-ketosteroids, *J Biol Chem* 185:201–207, 1950.

Prazeres S, Santos MA, Ferreira HG, et al.: A practical method for the detection of macroprolactinaemia using ultrafiltration, *Clin Endocrinol* 58:686–690, 2003.

Putignano P, Toja P, Dubini A, et al.: Midnight salivary cortisol versus urinary free and midnight serum cortisol as screening tests for Cushing's syndrome, *J Clin Endocrinol Metab* 88:4153–4157, 2003.

Radetti G, Persani L, Moroder W, et al.: Transplacental passage of anti-thyroid autoantibodies in a pregnant woman with auto-immune thyroid disease, *Prenat Diagn* 19:468–471, 1999.

Radin DR, Manoogian C, Nadler JL: Diagnosis of primary hyperaldosteronism: importance of correlating CT findings with endocrinologic studies, *AJR Am J Roentgenol* 158:553, 1992.

Ram S, Harris B, Fernando JR, Gama R, Fahie-Wilson M: False-positive polyethylene glycol precipitation tests for macroprolactin due to increased serum globulins, *Ann Clin Biochem* 45(3):256–259, 2008, https://doi.org/10.1258/acb.2008.007233.

Raff H, Findling JW: A physiologic approach to diagnosis of the Cushing syndrome, *Ann Intern Med* 138:980–991, 2003.

Raff H: Utility of salivary cortisol measurements in Cushing's syndrome and adrenal insufficiency, *J Clin Endocrinol Metab* 94:3647–3655, 2009. Review.

Raff H: Update on late-night salivary cortisol for the diagnosis of Cushing's syndrome: Methodological considerations, *Endocrine* 44:346–349, 2013.

Rajasoorya C, Holdaway IM, Wrightson P, et al.: Determinants of clinical outcome and survival in acromegaly, *Clin Endocrinol* 41:95–102, 1994.

Read GF, Walker RF, Wilson DW, et al.: Steroid analysis in saliva for the assessment of endocrine function, *Ann N Y Acad Sci* 595:260–274, 1990.

Refetoff S: Thyroid hormone resistance syndrome. In *The thyroid*, ed 6, Philadelphia, 1991, Lippincott.

Reihman DH, Farber MO, Heath DA: Effect of hypoxemia on sodium and water excretion in chronic obstructive lung disease, *Am J Med* 78(87–94), 1985.

Rigg LA, Lein A, Yen SSC: Pattern of increase in circulating prolactin levels during human gestation, *Am J Obstet Gynecol* 129:454–456, 1977.

Rivier C, Vale W: Effect of angiotensin II on ACTH release in vivo: role of corticotropin-releasing factor, *Regul Pept* 7:253–258, 1983.

Robbins J: Thyroid hormone transport protein and the physiology of hormone binding. In Gray CH, James VHT, editors: *Hormones in blood*, London, 1996, Academic Press, pp 96–110.

Rocha R, Steir CT, Kifor I, et al.: Aldosterone: a mediator of myocardial necrosis and renal arteriopathy, *Endocrinology* 141:3871–3878, 2000.

Ronan R, Fezeu L, Marre M, et al.: Comparison between copeptin and vasopressin in a population from the community and in people with chronic kidney disease, *J Clin Endocrinol Metab* 99(12):4656–4663, 2014.

Rosario PW, Carvalho M, Mourao GF, Calsolari MR: Comparison of antithyroglobulin antibody concentrations before and after ablation with ^{131}I as a predictor of structural disease in differentiated thyroid carcinoma patients with undetectable basal thyroglobulin and negative neck ultrasonography, *Thyroid* 26:525–531, 2016.

Rose SR, Brown RS, Foley T, et al.: American Academy of pediatrics, American thyroid association, and Lawson Wilkins pediatric endocrine Society. Update of newborn screening and therapy for congenital hypothyroidism, *Pediatrics* 117(6):2290–2303, 2006.

Rose S, Ross J, Uriarte M, et al.: The advantage of measuring stimulated as compared with spontaneous growth hormone levels in the diagnosis of growth hormone deficiency, *N Engl J Med* 319:201–207, 1988.

Rosler A, Weshler N, Leiberman E, et al.: 11 Beta-hydroxylase deficiency congenital adrenal hyperplasia: update of prenatal diagnosis, *J Clin Endocrinol Metab* 66:830–838, 1988.

Ross DS: Subclinical hyperthyroidism. In Braverman LE, Utiger RD, editors: *Werner and Ingbar's the thyroid: a fundamental and clinical text*, ed 6, Philadelphia, 1991, Lippincott, pp 1249–1255.

Roth J, Taatjes D, Lucocq J, et al.: Demonstration of an extensive trans-tubular network continuous with the Golgi apparatus stack that may function in glycosylation, *Cell* 43:287–295, 1985.

Rudd BT: Measurement of urine 17-oxogenic steroids, 17-hydroxycorticosteroids, and 17-oxosteroids has been superseded by better tests, *Br Med J* 291:805, 1985.

Salgado LR, Fragoso MC, Knoepfelmacher M, et al.: Ectopic ACTH syndrome: our experience with 25 cases, *Eur J Endocrinol* 155:725–733, 2006.

Samson SL, Hamrahian AH, Ezzat S: American Association of Clinical Endocrinologist, American College of Endocrinology disease state clinical review: clinical relevance of macroprolactin in the absence or presence of true hyperprolactinemia, *Endoc Pract* 21(12):1427–1435, 2015, https://doi.org/10.4158/EP15938.DSC.

Samuels MH, Veldhuis JD, Henry PM, et al.: Pathophysiology of pulsatile and copulsatile release of thyroid-stimulating hormone, and alpha subunit, *J Clin Endocrinol Metab* 71:425, 1990.

Sassin JF, Frantz AG, Weitzman ED, et al.: Human prolactin: 24-hour pattern with increased release during sleep, *Science* 177:120–127, 1972.

Sawin CT, Geller A, Kaplan MM, et al.: Low serum thyrotropin (thyroid stimulating hormone) in older persons with hyperthyroidism, *Arch Intern Med* 151:165–168, 1991.

Sawin CT, Geller A, Wolf PA, et al.: Low serum thyrotropin concentrations as a risk factor for atrial fibrillation in older persons, *N Engl J Med* 331:1249–1252, 1994.

Sawin CT, Herman T, Molitch ME, et al.: Aging and the thyroid: decreased requirement for thyroid hormone in older hypothyroid patients, *Am J Med* 75:206–209, 1983.

Sawka AM, Jaeschke R, Singh RJ, et al.: A comparison of biochemical tests for pheochromocytoma: measurement of fractionated plasma metanephrines compared with the combination of 24-hour urinary metanephrines and catecholamines, *J Clin Endocrinol Metab* 88:553–558, 2003.

Scheithauer BW, Sano T, Kovacs KT, et al.: The pituitary gland in pregnancy: a clinicopathologic and immunohistochemical study of 69 cases, *Mayo Clin Proc* 65:461–474, 1990.

Schunkert H, Hense HW, Muscholl M, et al.: Associations between circulating components of the renin-angiotensin-aldosterone system and left ventricular mass, *Heart* 77:24–31, 1997.

Schulte HM, Chrousos GP, Avgerinos P, et al.: The corticotropin-releasing hormone stimulation test: a possible aid in the evaluation of patients with adrenal insufficiency, *J Clin Endocrinol Metab* 58:1064–1067, 1984.

Sergev O, Racz K, Varga I, et al.: Atrial natriuretic peptide in normal and low renin essential hypertension, *Kidney Int* 30:S107–S108, 1990.

Sheps SG, Jiang NS, Klee GG, et al.: Recent developments in the diagnosis and treatment of pheochromocytoma, *Endo Rev* 15:356–368, 1994.

Shupnik MA, Greenspan SL, Ridgway EC: Transcriptional regulation of thyrotropin subunit genes by thyrotropin-releasing hormone and dopamine pituitary cell cultures, *J Biol Chem* 261:12675–12679, 1986.

Sjoberg RJ, Simcic KJ, Kidd GS: The clonidine suppression test for pheochromocytoma: a review of its utility and pitfalls, *Arch Intern Med* 152:1193–1197, 1992.

Skamene A, Patel YC: Infusion of graded concentrations of somatostatin in man: pharmaco-kinetics and differential inhibitory effects on pituitary and islet hormones, *Clin Endocrinol* 20:555–564, 1984.

Snow K, Jiang N, Kao PC, et al.: Biochemical evolution of adrenal dysfunction: the laboratory perspective, *Mayo Clin Proc* 67:1055, 1992.

Sonkodi S, Abraham G, Mohacsi G: Effects of nephrectomy on hypertension, renin activity and total renal function in patients with chronic renal artery occlusion, *J Hum Hypertens* 4:277–279, 1990.

Speckart PF, Nicoloff JT, Bethune JE: Screening for adrenocortical insufficiency with cosyntropin (synthetic ACTH), *Arch Intern Med* 128:761–763, 1971.

Speiser PW, Azziz R, Baskin LS, et al.: Congenital adrenal hyperplasia due to steroid 21-hydroxylase deficiency: an endocrine Society clinical practice guideline, *J Clin Endocrinol Metab* 95:4133–4160, 2010.

Speiser PW, Dupont B, Rubinstein P, et al.: High frequency of non-classical steroid 21-hydroxylase deficiency, *Am J Hum Genet* 37:650–667, 1985.

Speiser PW, White P: Congenital adrenal hyperplasia, *N Engl J Med* 349:776–788, 2003.

Spencer CA, LoPresti JS, Fatema S, et al.: Detection of residual and recurrent differentiated thyroid carcinoma by serum thyroglobulin measurement, *Thyroid* 9:435–441, 1999.

Spencer CA, Nicoloff JT: Serum TSH measurement: a 1990 status report, *Thyroid Today* 13(1–12), 1990.

Spencer CA, Wang CC: Thyroglobulin measurement: techniques, clinical benefits, and pitfalls, *Endocrinol Metab Clin North Am* 24:841–863, 1995.

Spencer CA, Takeuchi M, Kazarosyan M: Current status and performance goals for serum thyroglobulin (TSH) assays, *Clin Chem* 42:140–145, 1996.

Spencer C, Fatemi S: Thyroglobulin antibody (TgAb) methods – Strengths, pitfalls and clinical utility for monitoring TgAb-positive patients with differentiated thyroid cancer, *Best Pract Res Clin Endocrinol Metab* 27(5):701–712, 2013.

Streeten DHP, Tomycz N, Anderson GH: Reliability of screening methods for the diagnosis of primary aldosteronism, *Am J Med* 67:403, 1979.

Suliman AM, Smith TP, Gibney J, et al.: Frequent misdiagnosis and mismanagement of hyperprolactinemia in patients before the introduction of macroprolactin screening: application of a new strict laboratory definition of macroprolactinemia, *Clin Chem* 49:1504–1509, 2003.

Stewart PM, Newell-Price JDC: The adrenal cortex. In Melmed S, Polonsky KS, Larsen PR, Kronenberg HM, editors: *Williams textbook of endocrinology*, 13th ed., Philadelphia, PA, 2016b, Elsevier. (chap 15.

Surks MI, Chopra IJ, Maraish CN, et al.: American Thyroid Association guidelines for use of laboratory tests in thyroid disorders, *J Am Med Assoc* 263:1529–1532, 1990.

Surks MI, Ortiz E, Daniels GH, et al.: Subclinical thyroid disease: scientific review and guidelines for diagnosis and management, *J Am Med Assoc* 291:228–238, 2004.

Surks MI, Sievert R: Drugs and thyroid function, *N Engl J Med* 333:1688–1694, 1995.

Swearingen B, Barker II FG, Katznelson L, et al.: Long-term mortality after transsphenoidal surgery and adjunctive therapy for acromegaly, *J Clin Endocrinol Metab* 83:3419–3426, 1998.

Talbot JA, Lambert A, Anobile CJ, et al.: The nature of human chorionic gonadotrophin glycoforms in gestational thyrotoxicosis, *Clin Endocrinol* 55:33–39, 2001.

Taylor HC, Mayes D, Anton AH: Clonidine suppression test for pheochromocytoma: examples of misleading results, *J Clin Endocrinol Metab* 63:238–242, 1986.

Taylor RL, Singh RJ: Validation of liquid chromatography–tandem mass spectrometry method for analysis of urinary conjugated metanephrine and normetanephrine for screening of pheochromocytoma, *Clin Chem* 48:533–539, 2002.

Thalen BE, Kjellman BF, Ljunggren JG, et al.: Release of corticotropin after administration of corticotropin releasing hormone in depressed patients in relation to the dexamethasone suppression test, *Acta Psychiatr Scand* 87:133, 1993.

Therrell BL: Newborn screening for congenital adrenal hyperplasia, *Endocrinol Metab Clin North Am* 21:245–291, 2001.

Thienpont LM, Van Uyfanghe K, De Grande LAC, Reynders D, et al.: Harmonization of serum thyroid-stimulating hormone measurements Paves the way for the Adoption of a more Uniform reference interval, *Clin Chem* 63(7):1248–1260, 2017, https://doi.org/10.1373/clinchem.2016.269456. Epub 2017 May 18.

Timper K, Fenske W, Kuhn F, et al.: Diagnostic accuracy of copeptin in the differential diagnosis of the polyuria-polydipsia syndrome: a prospective multicenter study. *J Clin Endocrinol Metab* 100(6):2268–2274, 2015.

Toldy E, Locsei Z, Szabolcs I, et al.: Macroprolactinemia: the consequences of a laboratory pitfall, *Endocrine* 22:267–273, 2003.

Trimboli P, Treglia G, Guidobaldi L, Romanelli F, et al.: Detection rate of FNA cytology in medullary thyroid carcinoma: a meta–analysis, *Clin Endocrinol* 82:280–285, 2015, https://doi.org/10.1111/cen.12563. 2015.

Trainer P: Editorial: acromegaly—consensus, what consensus? *J Clin Endocrinol Metab* 87:3534–3536, 2002.

Tuchman M, Morris C, Ramnaraine ML, et al.: Value of random urinary homovanillic acid levels in the diagnosis and management of patients with neuroblastoma: comparison of 24-hour urine collections, *Pediatrics* 75:324–328, 1985.

Tullis MJ, Caps MT, Zierler RE: Blood pressure, antihypertensive medication, and atherosclerotic renal artery stenosis, *Am J Kidney Dis* 33:675–681, 1999.

US Preventive Services Task Force Screening for thyroid dysfunction: *Recommendation Statement American Family Physician* 91, 2015. 790A-790E.

Utiger R: Decreased extrathyroidal triiodothyronine production and nonthyroidal illness: benefits or harm? *Am J Med* 69:807–810, 1980.

Van Cauter E: Slow wave sleep and release of growth hormone, *J Am Med Assoc* 284:2717–2718, 2000.

Van Cauter E, Plat L, Copinschi G: Interrelations between sleep and the somatotropic axis, *Sleep* 21:553–566, 1998.

Van den Beld AW, Kaufman J-M, Zillikens MC, Lamberts SW, et al.: Ageing and Endocrinology 1: the physiology of endocrine systems with ageing, *Lancet* 6:647–658, 2018.

Van den Berghe G, De Zegher F, Bouillon R: Acute and prolonged critical illness as different neuroendocrine paradigms, *J Clin Endocrinol Metab* 83:1827–1834, 1998.

Van den Berghe G: Novel insights into the neuroendocrinology of critical illness, *Eur J Endocrinol* 143:1–3, 2000.

Van Heyningen V: One gene—four syndromes, *Nature* 367:319–320, 1994.

Vanderpump MPJ, Tunbridge WMG, French JM, et al.: The incidence of thyroid disorders in the community: a twenty year follow up of the Whickham survey, *Clin Endocrinol* 43:55–68, 1995.

Vassart G, Dumont JE: Identification of polysomes synthesizing thyroglobulin, *Eur J Biochem* 32:322–330, 1973.

Vierhapper H, Raber W, Bieglmayer C, Kaserer K, et al.: Routine measurement of plasma calcitonin in nodular thyroid diseases, *J Clin Endocrinol Metab* 82(5):1589–1593, 1997, https://doi.org/10.1210/jcem.82.5.3949.

Vieira AEF, Mello MP, Elias LLK, et al.: Molecular and biochemical screening for the diagnosis and management of medullary thyroid carcinoma in multiple endocrine neoplasia type 2A, *Horm Metab Res* 34:202–206, 2002.

Vistorina WM, Rydstedt LL, Sowers JR: Clinical disorders of vasopressin. In Lavin N, editor: *Manual of endocrinology and metabolism*, ed 3, Philadelphia, 2002, Lippincott, pp 68–82.

Vitale G, Ciccarelli A, Caraglia M, et al.: Comparison of two provocative tests for calcitonin in medullary thyroid carcinoma: omeprazole vs pentagastrin, *Clin Chem* 48:1505–1510, 2002.

Walker SE, Allen SH, McMurray RW: Prolactin and autoimmune disease, *Trends Endocrinol Metab* 4:47–151, 1993.

Wardle CA, Fraser WD, Squire CR: Pitfalls in the use of thyrotropin concentration as a first-line thyroid-function test, *Lancet* 357:1013–1014, 2001.

Wartofsky L, Burman KD: Alterations in thyroid function in patients with systemic illness: the "euthyroid sick syndrome", *Endocr Rev* 3:164–217, 1982.

Weeke J, Dybkjaer L, Granlie K, et al.: A longitudinal study of serum TSH and total and free iodothyronines during normal pregnancy, *Acta Endocrinol* 101:531–557, 1982.

Weinberger MH, Fineberg NS: The diagnosis of primary aldosteronism and separation of two major subtypes, *Arch Intern Med* 153:2125, 1993.

Weise M, Drinkard B, Mehlinger SL, et al.: Stress dose of hydrocortisone is not beneficial in patients with classic congenital adrenal hyperplasia undergoing short-term, high-intensity exercise, *J Clin Endocrinol Metab* 89:3679, 2004.

Weise M, Merke DP, Pacak K, et al.: Utility of plasma free metanephrines for detecting childhood pheochromocytoma, *J Clin Endocrinol Metab* 87:1955–1960, 2002.

Wells SA, Baylin SB, Linehan W, et al.: Provocative agents and the diagnosis of medullary carcinoma of the thyroid gland, *Ann Surg* 188:139–141, 1978.

Wells Jr SA, Asa SL, Dralle H, et al.: Revised American Thyroid Association guidelines for the management of medullary thyroid carcinoma, *Thyroid* 25(6):567–610, 2015, https://doi.org/10.1089/thy.2014.0335.

Werbel SS, Ober KP: Pheochromocytoma: update on diagnosis, localization, and management, *Med Clin North Am* 79:131–153, 1995.

White MC, Clark AJL: The cellular and molecular basis of the ectopic ACTH syndrome, *Clin Endocrinol* 39:131, 1993.

White PC, Curnow KM, Pascoe L: Disorders of steroid 11-beta-hydroxylase isoenzymes, *Endocr Rev* 15:421–438, 1994a.

White PC, Tusie-Lina MT, New MI, et al.: Mutations in steroid 21-hydroxylase (CYP21), *Hum Mutat* 3:373, 1994b.

Whitehouse Jr WM, Kazmers A, Zelenock GB: Chronic total renal artery occlusion: effects of treatment of secondary hypertension and renal function, *Surgery* 89:753–763, 1981.

Wilcox RB, Nelson JC, Tomei RT: Heterogeneity in affinities of serum proteins for thyroxine among patients with non-thyroidal illness as indicated by the serum free thyroxine response to serum dilution, *Eur J Endocrinol* 131(9–13), 1994.

Williams GA, Hargis GK, Galloway WB, Henderson WJ: Evidence for Thyrocalcitonin in man, *Proceedings of the Society for Experimental, Biol Medi* 122(4):1273–1276, 1966, https://doi.org/10.3181/00379727-122-31380(1966).

Willie S, Aili M, Harris A, et al.: Plasma and urinary levels of vasopressin in enuretic and non-enuretic children, *Scand J Urol Nephrol* 28:119–122, 1994.

Wion-Barbot N, Schuffenecker I, Niccoli P, et al.: Results of the calcitonin stimulation test in normal volunteers compared with genetically unaffected members of MEN 2A and familial medullary thyroid carcinoma families, *Ann Endocrinol* 58:302–308, 1997.

Yamada M, Radvick S, Wondisford FE, et al.: Cloning and structure of human genomic DNA and hypothalamic cDNA encoding human prepro TRH, *Mol Endocrinol* 4:551–556, 1990.

Yaneva M, Mosnier-Pudar H, Dugue MA, et al.: Midnight salivary cortisol for the initial diagnosis of Cushing's syndrome of various causes, *JCEM* 89:3345–3351, 2004.

Yanovski JA, Cutler Jr GB, Chrousos GP, et al.: Corticotropin-releasing hormone stimulation following low-dose dexamethasone administration: a new test to distinguish Cushing's syndrome from pseudo-Cushing's states, *J Am Med Assoc* 269:2232–2238, 1993.

Yazigi R, Quinero C, Sakameh WA: Prolactin disorders, *Fertil Steril* 7:215–225, 1997.

Yokoyama Y, Ueda T, Irahara M, et al.: Release of oxytocin and prolactin during breast massage and suckling in puerperal women, *Eur J Obstet Gynecol Reprod Biol* 53:17–20, 1994.

Young Jr WF: Primary aldosteronism: a common and curable form of hypertension, *Cardiol Rev* 7:207–214, 1999.

Young WF: Endocrine hypertension. In Melmed S, Polonsky KS, Larsen PR, Kronenberg H, editors: *Williams textbook of endocrinology*, ed 13, Philadelphia, 2016, Elsevier, pp 556–557.

Yuasa H, Ito M, Nagasaki H, et al.: Glu-47, which forms a salt bridge between neurophysin II and arginine vasopressin, is deleted in patients with familial central diabetes insipidus, *J Clin Endocrinol Metab* 77:600–604, 1993.

Yuen KC: Glucagon stimulation testing in assessing for adult growth hormone deficiency: current status and future perspectives, *ISRN Endocrinol*. 2011:608056, 2011.

Yuen KCJ, Chong LE, Koch CA: Adrenal insufficiency in pregnancy: challenging issues in diagnosis and management, *Endocrine* 44:283–292, 2013.

Yuen KCJ, Rakesh A, Cook MB, et al.: Evaluation of the pituitary function with insulin tolerance (hypoglycaemia) testing: are there any differences using insulin Lispro compared to regular insulin? *Horm Res* 69:233–239, 2008.

Yuen KCJ, Tritos NA, Samson SL, Hoffman AR, Katznelson L: American association of clinical Endocrinologists and American College of endocrinology disease state clinical review, *Update on growth hormone stimulation testing and propose revised cut-point for the glucagon stimulation test in the diagnosis of adult growth hormone deficiency* 22(10):1235–1244, 2016.

Yuen KCJ, Biller BMK, Radovick S, et al.: American Association of Clinical Endocrinologists and American College of Endocrinology Guidelines for Management of Growth Hormone Deficiency in Adults and Patients Transitioning from Pediatric to Adult Care, *Endocr Pract* 25(11):1191–1232, 2019.

Zahr R, Flerseriu M: Updates in diangosis and treatment of acromegaly, *Eurpean Endocrinol* 14:57–61, 2018.

Zeiger M, Thompson GB, Duh Q-Y, Hamrahian AH, et al.: American association of clinical Endocrinologists and American association of endocrine Surgeons medical guidelines for the management of adrenal incidentalomas, *Endocr Pract* 15(Suppl 1):1–20, 2009, https://doi.org/10.4158/EP.15.S1.1.

Zerbe RL, Robertson GL: Vasopressin function in the syndrome of inappropriate antidiuresis, *Annu Rev Med* 31:315–327, 1980.

Zerbe RL, Robertson GL: A comparison of plasma vasopressin measurements with a standard indirect test in the differential diagnosis of polyuria, *N Engl J Med* 304:1539–1546, 1981.

Zerbe RL, Robertson GL: Osmotic and nonosmotic regulation of thirst and vasopressin secretion. In Maxwell MH, Kleeman CR, Narins RG, editors: *Clinical disorders of fluid and electrolyte metabolism*, ed 4, New York, 1987, McGraw-Hill, pp 61–68.

Zurakowski D, Di Canzio J, Majzoub JA: Pediatric reference intervals for serum thyroxine, triiodothyronine, thyrotropin and free thyroxine, *Clin Chem* 45:1087–1091, 1999.

CHAPTER 26

REPRODUCTIVE FUNCTION AND PREGNANCY

Roohi Jeelani, Martin H. Bluth

NORMAL PHYSIOLOGY, 425
Sex Steroids, 425
Regulation of Male Reproduction, 427
Regulation of Female Reproduction, 427
Pregnancy, 428
LABORATORY EVALUATION OF REPRODUCTIVE FUNCTION, 429
Male Evaluation, 429
Female Evaluation, 431
Assisted Reproductive Technology, 433
LABORATORY EVALUATION OF PREGNANCY, 433
hCG and Early Pregnancy, 433
Neural Tube Defects, 434
Down Syndrome, 436
Erythroblastosis Fetalis, 436
Gestational Diabetes, 437
Fetal Lung Maturity, 437
Preeclampsia, 438
Premature Rupture of Membranes, 438
Preterm Labor, 439
Intrapartum Assessment of Fetal Status, 439
Other Evaluations, 439
SELECTED REFERENCES, 440

KEY POINTS

- Reproductive function and pregnancy are regulated by the complex interaction of a variety of hormones. They are synthesized and secreted by the testis (testosterone), ovary (estradiol and progesterone), pituitary (follicle-stimulating hormone [FSH] and luteinizing hormone [LH]), hypothalamus (gonadotropin-releasing hormone), and placenta (human chorionic gonadotropin [hCG], estrogens, and progesterone).
- Laboratory evaluation of reproductive function in the male typically begins with semen analysis. If the results are normal, further evaluation may be unnecessary. If the results are abnormal, then serum hormone measurements, particularly of testosterone, FSH, and LH, are important.
- Reproductive dysfunction in the female is often indicated by amenorrhea and/or infertility. Laboratory evaluation, as in the male, involves serum hormone measurements, particularly of hCG, prolactin, thyroid-stimulating hormone, free thyroxine, FSH, LH, and androgens.
- Infertility can be treated by several assisted reproductive technologies. These involve a variety of clinical manipulations, all of which are directed at externally controlling as much of the reproductive process as possible to achieve pregnancy and bring it to term. Laboratory monitoring of serum hormone levels (estradiol, progesterone, and hCG) plays an important role in these protocols.
- Early pregnancy is monitored by measuring serum hCG concentrations and determining that the pattern of dramatic increase during the first trimester is as expected.
- The risks for the most common birth defects, neural tube defects, and chromosomal aneuploidy are determined during the first- and second-trimester screenings.
- Fetal hemolytic disease is monitored by spectrophotometric estimation of the level of bilirubin in amniotic fluid or Doppler measurements of peak systolic velocity in the fetal middle cerebral artery.
- The status of fetal lung maturation is estimated from the evaluation of pulmonary surfactant in amniotic fluid. This can be accomplished by several methods, including determination of (1) the lecithin/sphingomyelin ratio and phosphatidyl glycerol by chromatography, or (2) microviscosity by fluorescence polarization.
- Pregnancy-induced hypertension, or preeclampsia, is characterized by hypertension and proteinuria; consequently, it can be monitored by urine protein measurements.
- Risk for preterm delivery and the need for medical intervention can be evaluated by checking levels of fetal fibronectin in the cervical secretions.

NORMAL PHYSIOLOGY

Normal reproductive function is mediated by a variety of hormones synthesized and secreted by the gonads (testes and ovaries), adrenals, pituitary, hypothalamus, and placenta. In addition, peripheral nonglandular tissues can contribute to hormone synthesis. Paracrine and autocrine mediators are also involved; however, in almost all cases, their exact roles are not well understood.

SEX STEROIDS

The testes and ovaries synthesize sex steroids (androgens and estrogens) from cholesterol via the same initial pathway used in the adrenal glands to synthesize mineralocorticoids, glucocorticoids, and androgens (Fig. 26.1). The specific hormone secreted by an endocrine gland depends on the presence and relative activities of various enzymes in the steroid pathway. Whereas the adrenal synthesizes androgens such as dehydroepiandrosterone (DHEA), DHEA-sulfate (DHEAS), and androstenedione, the testis metabolizes these steroids primarily to testosterone. The ovary converts testosterone to estradiol, and androstenedione to estrone. In addition, testosterone gets converted to estradiol in peripheral tissues such as adipose cells by the enzyme aromatase. Peripheral tissues (including those targeted by androgens) reduce testosterone to dihydrotestosterone (DHT). Because DHT is two to three times more potent than testosterone, this process yields an enhanced or activated androgenic effect. Peripheral tissues, such as liver, also hydroxylate estradiol to estriol, a metabolite with only one-hundredth the estrogenic potency of its precursor. Thus, this conversion is an inactivation process. During pregnancy, estriol is synthesized via a different pathway and may play a different role than estradiol (see later discussion). Peripheral tissues also convert adrenal androgens to testosterone and androgens to estrone and estradiol, the latter occurring in adipose tissue. Estrone is about one-tenth as potent as estradiol, which likely further modulates estradiol potency. Note that, although progesterone serves as an intermediate in the synthesis of all other steroid hormones, it also functions as a sex steroid in its own right in females.

As with any hormone, sex steroids act at tissue sites distant from their sites of synthesis and secretion. Once in the blood, most of the hydrophobic sex steroids become reversibly and noncovalently bound to plasma proteins. This interaction includes low-affinity, nonspecific binding to hydrophobic sites on albumin and high-affinity binding to specific transport proteins that are synthesized by the liver. Sex hormone–binding globulin (SHBG) transports androgens and estrogens, and corticosteroid-binding globulin (CBG) transports progesterone (as well as glucocorticoids). In blood, only about 1% to 2% of the sex steroids are free (unbound). About half of the remainder are bound to SHBG or CBG, and about half are bound to albumin. Only the

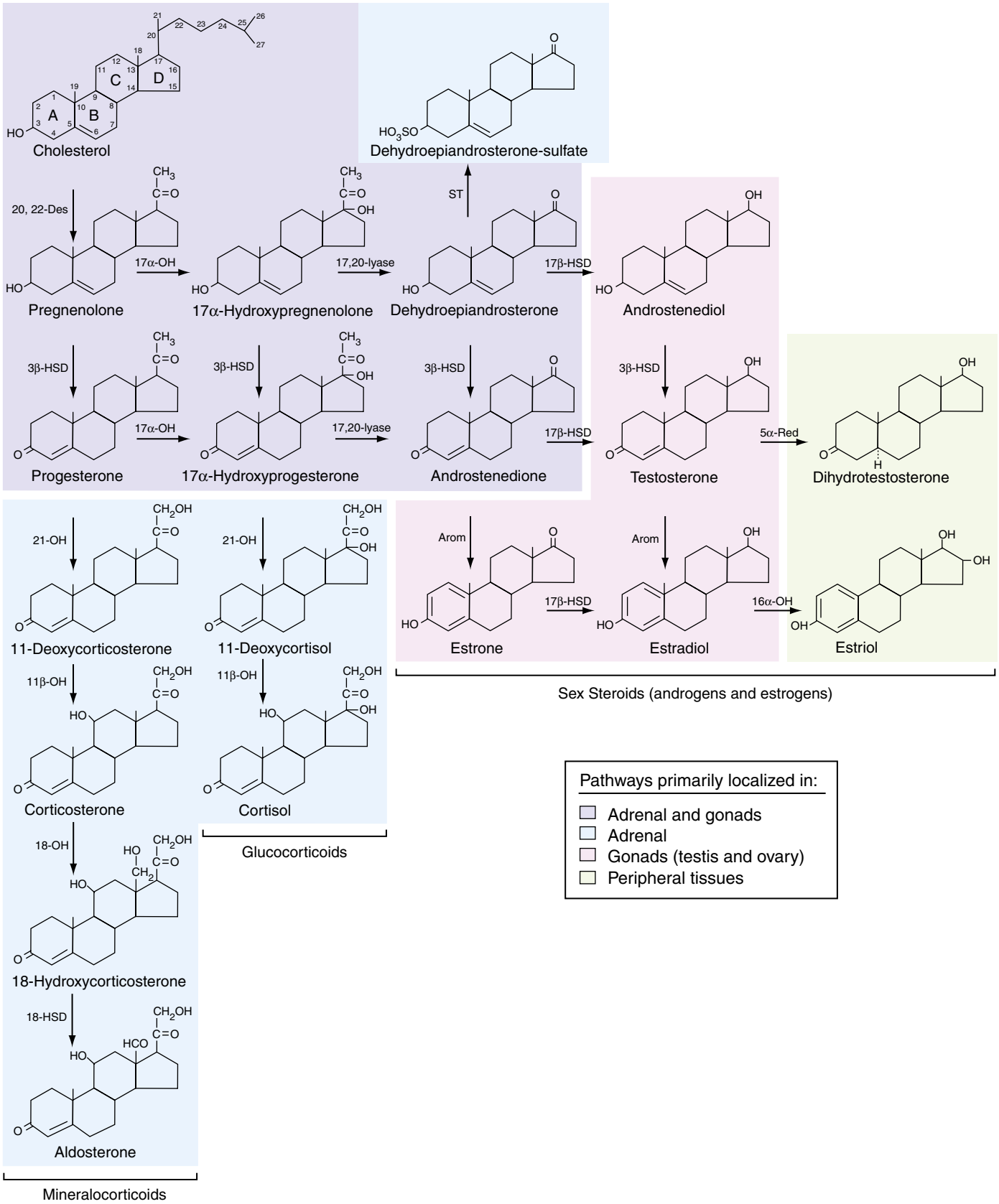

Figure 26.1 Steroid hormone synthesis. *Arom,* Aromatase; *16α-OH,* 16α-hydroxylase; *17-α-OH,* 17α-hydroxylase; *5α-Red,* 5α-reductase; *3β-HSD,* 3β-hydroxysteroid dehydrogenase; *17β-HSD,* 17β-hydroxysteroid dehydrogenase; *11-β-OH,* 11-β-hydroxylase; *20,22-Des,* 20,22 desmolase; *18-HSD,* 18-hydroxysteroid dehydrogenase; *18-OH,* 18-hydroxylase; *21-OH,* 21-hydroxylase; *ST,* sulfotransferase.

free fraction is biologically active because only the free hormone can exit the vascular system (by diffusion) and interact with target cells.

Each steroid binds with high affinity to specific receptor proteins that activate or inactivate genes in the target cell. Thus, the same hormone can elicit a different response in each type of target cell. The potency of a steroid's hormonal effect (e.g., androgenic effect) is primarily a function of its affinity for the specific receptor protein and the affinity of that complex for the chromatin acceptor sites. Thus, DHT is a more potent androgen than testosterone owing to its high-affinity binding to the target tissue. DHEA and androstenedione bind only weakly, if at all, to the

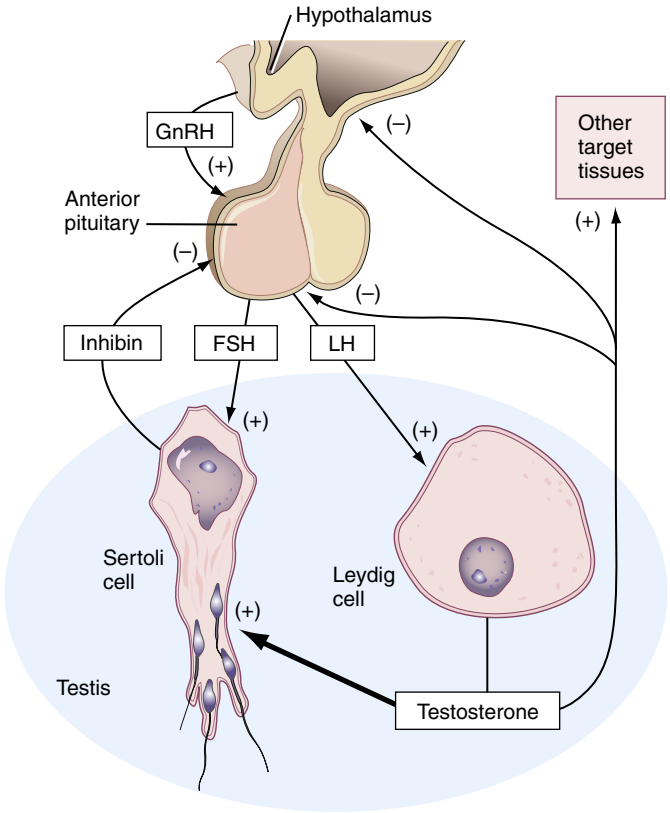

Figure 26.2 Regulation of reproduction in the male. *FSH,* Follicle-stimulating hormone; *GnRH,* gonadotropin-releasing hormone; *LH,* luteinizing hormone.

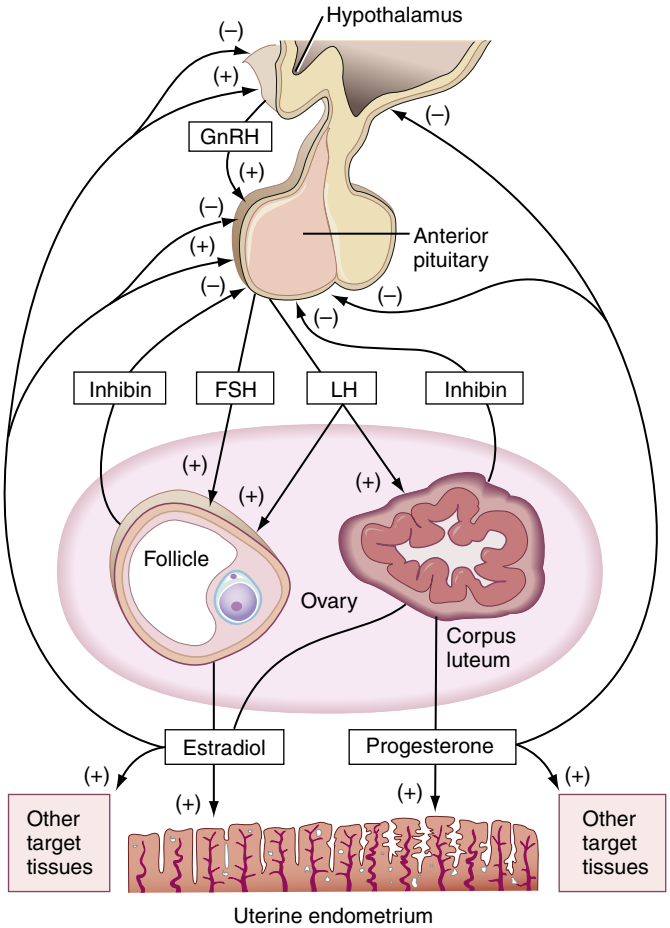

Figure 26.3 Regulation of reproduction in the female. *FSH,* Follicle-stimulating hormone; *GnRH,* gonadotropin-releasing hormone; *LH,* luteinizing hormone.

androgen receptor. Hence, their androgenic effect is low and most, if not all, of their androgenic activity derives from their peripheral conversion to testosterone.

REGULATION OF MALE REPRODUCTION

Figure 26.2 summarizes the regulation of reproduction in the human male. Gonadotropin-releasing hormone (GnRH) is a decapeptide that is synthesized and secreted by neuroendocrine cells of the hypothalamus, primarily in the arcuate nucleus. GnRH binds to specific cell membrane receptors on gonadotrophs in the anterior pituitary, resulting in the synthesis and secretion of two protein hormones—follicle-stimulating hormone (FSH) and luteinizing hormone (LH)—both named for their effects in females. Both FSH and LH are similar to thyroid-stimulating hormone (TSH) in that all three consist of two subunits and all share the same α subunit. Each has a different β subunit, however, which confers their functional specificity.

The seminiferous tubules of the testis contain cells in various stages of spermatogenesis (spermatogonia, spermatocytes, spermatids), along with Sertoli cells and Leydig cells. FSH induces Sertoli cells to synthesize and secrete androgen-binding protein into the lumen of the seminiferous tubule, which maintains the high testosterone concentration required for normal spermatogenesis. LH induces Leydig cells to synthesize testosterone; some enters the general circulation and is transported to other target tissues, such as skeletal muscle, where it has an anabolic effect. Some testosterone is also transported to the hypothalamus and anterior pituitary, where it has a negative-feedback effect—that is, it decreases and helps control the synthesis and secretion of GnRH, FSH, and LH. This, in turn, decreases testosterone synthesis by Leydig cells. Sertoli cells also synthesize and secrete another protein hormone—inhibin—which is a dimeric protein composed of an α and β subunit. It interacts with gonadotrophs in the anterior pituitary, where it also has a negative-feedback effect by decreasing the synthesis and secretion of FSH, but not LH. Androgens also stimulate inhibin production, which locally helps regulate spermatogenesis. However, the exact role of inhibin in the regulatory process is not understood.

REGULATION OF FEMALE REPRODUCTION

Figure 26.3 summarizes the regulation of reproduction in the human female. As in the male, GnRH from the hypothalamus increases the synthesis and secretion of FSH and LH from the anterior pituitary. Unlike in the male, however, the regulatory process in the female is cyclic and is referred to as the *menstrual cycle*. Pituitary, ovarian, and uterine changes that occur during the menstrual cycle are summarized in Figure 26.4. As illustrated, the cycle begins with menses, or shedding of the uterine endometrium, which is considered day one. During this period, FSH secretion from the anterior pituitary recruits a cohort of about 10 to 12 antral follicles to begin further growth and development within the ovaries. From this cohort, one to two (usually) antral follicles are selected to become the dominant follicle, continuing to grow and develop. The other recruited follicles undergo regression, or *atresia*. This process of follicular selection and maturation is known as *folliculogenesis* and occurs during the follicular phase (see Fig. 26.4). As the follicle grows, increasing amounts of estradiol are synthesized and secreted from the granulosa cells via FSH-induced aromatase activity. Estradiol acts to restore the endometrium via cell proliferation and growth—hence, the proliferative phase of the uterine endometrial cycle. Estradiol also has a negative-feedback effect on the hypothalamus and the anterior pituitary, decreasing FSH levels during the latter part of the follicular phase.

Near the end of the follicular phase, when estradiol levels are at their highest, around 200 to 300 IU, its feedback effect on the hypothalamus and anterior pituitary switches from negative to positive. The exact mechanism for this change to positive feedback is not understood. Its effect, however, is dramatic. It causes a surge in the secretion of GnRH, FSH, and particularly LH, which culminates in ovulation. The LH surge causes final oocyte maturation with the completion of meiosis in the ovaries before the follicle bursts, releasing the oocyte into the fallopian tubes. Owing to disruption of the growing follicle, estradiol synthesis and secretion drop dramatically. The disrupted follicle begins to differentiate into the corpus luteum; thus begins the luteal phase of the ovarian cycle. The corpus luteum synthesizes estradiol and progesterone as a result of the action of LH. The combination of the two steroids acts on the uterine endometrium to cause development of numerous exocrine glands, producing the secretory phase of the uterine endometrial cycle. This phase prepares the endometrium for implantation should fertilization and early development occur. LH levels decline gradually during the luteal phase, indicating restoration of negative-feedback regulation of the hypothalamus and anterior pituitary by estradiol and progesterone.

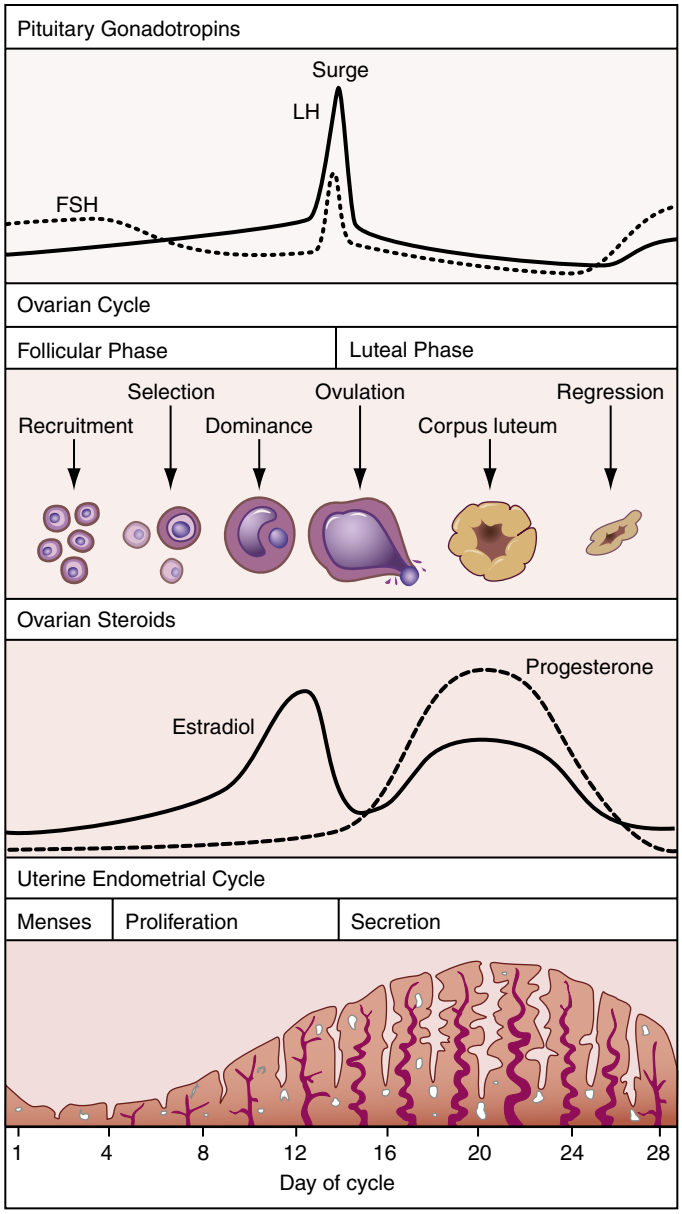

Figure 26.4 Pituitary, ovarian, and uterine changes during the human menstrual cycle. *FSH,* Follicle-stimulating hormone; *LH,* luteinizing hormone.

As in the male, inhibin has a selective negative-feedback effect on FSH. In the female, however, there are two different forms. One is synthesized and secreted by the developing follicles (inhibin B), and the other is from the corpus luteum (inhibin A) (Welt et al., 1999). Inhibin B reaches a peak in the early- to midfollicular phase and a second peak at ovulation. Inhibin A reaches its peak in the midluteal phase. Again, the exact regulatory roles they play are not understood.

In a normal fertile cycle, the corpus luteum begins to regress near the end of the luteal phase. This results in a decrease in estradiol and progesterone synthesis and secretion. Because these steroids are required for maintenance of the secretory endometrium, it begins to deteriorate and is ultimately shed during menstruation. With the drop in estradiol and progesterone, their negative-feedback effects decrease, and FSH and LH rise to begin another cycle.

PREGNANCY

If the oocyte is fertilized during its transit down the fallopian tubes, also known as the *oviduct*, it develops into a multicellular blastocyst by the time it reaches the uterus. Around the time of implantation (about 7–9 days after ovulation) and before the corpus luteum begins to regress, increasing amounts of an LH-like hormone, human chorionic gonadotropin (hCG), are found in maternal blood. hCG is synthesized and secreted by the syncytiotrophoblast cells of the developing placenta. It is a dimeric protein hormone that has the same α subunit as LH, FSH, and TSH, but a different β subunit. The β

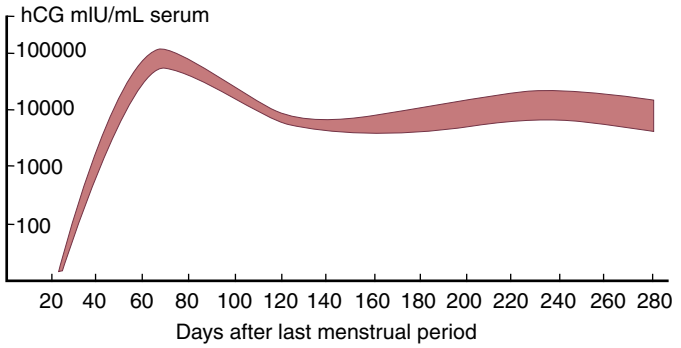

Figure 26.5 Serum hCG levels during normal pregnancy. *hCG,* Human chorionic gonadotropin. From Lau HL: Testing for pregnancy. In Practice of medicine, vol II. Hagerstown, MD, 1975, Harper & Row, Chapter 29; and Braunstein GD, Rasor J, Adler D, Danzer H, Wade ME: Serum human chorionic gonadotropin levels throughout normal pregnancy, Am J Obstet Gynecol 126:678, 1976.

subunit of hCG is very similar to that of LH, but larger. Hence, hCG can interact with LH receptors on luteal cells. This interaction prevents regression of the corpus luteum and allows it to continue synthesis and secretion of estradiol and progesterone, both of which are required for appropriate maintenance of the uterine endometrium throughout pregnancy.

During the first trimester of pregnancy, hCG increases from less than 5 mIU/mL serum to possibly more than 100,000 mIU/mL (Fig. 26.5). This increase is responsible for the similarly dramatic increases in the levels of estradiol and progesterone. By the end of the first trimester, however, hCG levels begin to plateau at first and then decline significantly. Estradiol and progesterone continue to increase because, by this time, the placenta has assumed most steroid synthesis, including significant amounts of estrone and estriol. Unlike hCG, these steroid levels increase as placental mass grows. Steroid intermediates from the fetal adrenal gland and the fetal liver also contribute to this process. For example, estriol is synthesized not by hydroxylation of estradiol (see Fig. 26.1) but rather by conversion from fetal 16-hydroxy-DHEAS. This is why maternal estriol measurements were historically used to assess fetal well-being in late pregnancy (Carr & Rehman, 2004). The estrogenic potency of estriol is only about one-hundredth that of estradiol and only one-tenth that of estrone. However, estriol promotes uteroplacental blood flow as potently as other estrogens, which may be the reason for its dramatic increase during the last two trimesters (Resnik et al., 1974).

Another hormone synthesized in large quantities by the placenta during the last two trimesters is human placental lactogen (HPL). It is structurally similar to both prolactin and growth hormone and has both lactogenic and growth-promoting activities, although both are relatively weak. In addition, HPL is an insulin antagonist and thus may play a role in maternal glucose utilization. However, its exact role is unclear because apparently normal pregnancies have been described in which HPL is not detectable in maternal blood or placenta (Sideri et al., 1983). Unlike hCG, the increase in HPL also parallels the steady increase in placental mass (Carr & Rehman, 2004).

The placenta also synthesizes inhibin. Whereas gonadal (testicular and ovarian) inhibin functions as an endocrine inhibitor of pituitary FSH secretion, placental inhibin may function as a paracrine or autocrine inhibitor of placental hCG secretion (Mesiano & Jaffe, 2013). Its exact regulatory role, however, has not been elucidated. It is also sometimes used as a marker in fetal testing (described later).

Parturition is the process by which the fetus is expelled from the internal environment of the maternal uterus to the external environment. This occurs as a result of a change in the activity of the uterine myometrium (smooth muscle), from irregular, long-lasting, low-frequency contractions to regular, high-intensity, high-frequency contractions. The initiation of this process in humans is not well understood and seems to differ from that in other mammals. It has been shown that progesterone inhibits uterine contractions during gestation in most other mammals and that the onset of parturition is preceded by a significant decrease in maternal plasma progesterone. In humans, however, this does not occur. In humans, it has been hypothesized that what is known as a parturition cascade may occur, which involves multiple and redundant endocrine, paracrine, and autocrine mediators. These mediators are thought to include fetal cortisol and DHEAS; placental estriol, oxytocin, prostaglandins, and corticotropin-releasing hormone; and maternal oxytocin. The effects of these mediators may also be modulated by changes in their receptor levels (Norwitz, 2013).

Parturition is followed by lactation. Initial development of the mammary gland occurs at puberty, when estradiol causes growth and branching of the ducts and progesterone causes formation of the alveoli. Similarly, during

TABLE 26.1

Changes in Reproductive Hormone Levels in Different Disease States

DISEASE STATE		HORMONE LEVEL			
Classification	**Example**	**FSH**	**LH**	**Testosterone**	**Estradiol**
Male					
Primary deficiency	Klinefelter syndrome	High	High	Low	–
Secondary deficiency	Panhypopituitarism	Low	Low	Low	–
Primary excess	Testicular tumor	Low	Low	High	–
Secondary excess	Precocious puberty	High	High	High	–
Other	Seminiferous tubule failure	High	Normal	Normal	–
Other	Partial androgen insensitivity	Normal	High	High	–
Female					
Primary deficiency	Menopause	High	High	–	Low
Secondary deficiency	Sheehan syndrome	Low	Low	–	Low
Primary excess	Feminizing ovarian tumor	Low	Low	–	High
Secondary excess	Gonadotropin-producing tumor (rare)	High	High	–	High
Other	Polycystic ovarian syndrome	Normal	High	High	–
Other	Masculinizing ovarian tumor	Low	Low	High	–

From Nickel KL: The gonads. In Kaplan LA, Pesce AJ, editors: *Clinical chemistry—Theory, analysis, and correlation*, ed 3. St. Louis, MO, 1996, Mosby, pp 892–911, with permission. *FSH*, Follicle-stimulating hormone; *LH,* luteinizing hormone.

pregnancy, the high concentrations of estrogens and progesterone cause further branching of the ducts and growth of the alveoli. The secretory capability of the alveolar epithelial cells is induced by prolactin, which increases during pregnancy, and by HPL. At parturition, the decrease in estrogen and progesterone eliminates their inhibitory effects on milk secretion, which still requires prolactin. Milk ejection, however, requires oxytocin, acting as part of a neuroendocrine reflex. This reflex is initiated by the suckling stimulus, which generates nerve impulses that travel from the nipple to the hypothalamus. There, they cause secretion of oxytocin from neuroendocrine cells in the posterior pituitary. The oxytocin travels to the mammary gland, where it stimulates the contraction of smooth muscle cells surrounding the alveoli, causing milk ejection. Prolactin also participates in this neuroendocrine reflex, in that nerve impulses reaching the hypothalamus also inhibit the synthesis and secretion of dopamine, which functions as a prolactin release–inhibiting hormone. This promotes the release of prolactin from the anterior pituitary, which then travels to the mammary gland, where it stimulates milk secretion, to replace that lost by ejection. As long as lactation continues, plasma prolactin concentrations remain elevated. This postpartum hyperprolactinemia causes postpartum amenorrhea due to interference with normal regulation by GnRH of FSH and LH secretion. Although this hypogonadotropic state will prevent pregnancy, it is not considered a reliable means of contraception, particularly in modern societies where breastfeeding is not consistent.

LABORATORY EVALUATION OF REPRODUCTIVE FUNCTION

Table 26.1 describes laboratory findings in various male and female reproductive disease states typically categorized according to (1) hormone deficiency or excess and (2) primary (gonad) or secondary (pituitary) dysfunction. In primary disease states, gonadal steroid levels are inversely related to pituitary gonadotropin levels, whereas in secondary disease states, they are directly related (e.g., both high or both low), as discussed in the endocrine section of Chapter 9 and in Chapter 25. These changes occur because gonadal steroids provide negative feedback to gonadotropins. For example, in primary ovarian failure or menopause, the decrease in estradiol reduces its negative-feedback effect on the hypothalamic-pituitary axis, resulting in increases in FSH and LH.

MALE EVALUATION

The evaluation of reproductive dysfunction in the male usually begins with semen analysis because it is a cost-effective and relatively simple procedure. In addition, if the results are normal, further evaluation is often unnecessary. If semen analysis is abnormal, then hormone analyses are performed, which include FSH, LH, and testosterone levels.

Semen Analysis

In addition to its use in the evaluation of reproductive dysfunction, particularly infertility, semen analysis is used to select donors for therapeutic insemination and to monitor the success of surgical procedures, such as varicocelectomy and vasectomy. Semen analysis consists of microscopic and macroscopic components; the latter include measuring physical (e.g., volume) and chemical (e.g., pH) properties. Useful guides and references for the procedure are available (Gilbert et al., 1992; Mortimer, 1994; Tomlinson et al., 1999; World Health Organization, 1999; Andrade-Rocha, 2003; Rylander et al., 2009).

Sample Collection

The patient should be instructed to collect semen after 2 to 5 days of sexual abstinence to ensure that the sperm count will be at its highest and improve the reliability of the test. Longer periods of abstinence usually result in a higher sperm concentration but reduced sperm motility. For semen collection, the laboratory should provide a sterile plastic (polypropylene) container with a screw top. The semen specimen should be delivered to the laboratory within 1 hour of collection and kept warm during transportation. A postejaculate urine sample may be collected at this time if retrograde ejaculation is suspected. Two specimens collected within 2- to 3-week intervals should be used for evaluation. If they are markedly different, additional specimens should be collected. Ideally, semen specimens should be collected in the privacy of a room adjacent to the laboratory, because some samples require sperm to be separated from seminal plasma as soon as possible. Assisted reproductive technologies (ARTs; see later discussion), such as in vitro fertilization (IVF), require that motile sperm be isolated from seminal plasma within 1 hour of ejaculation to protect sperm from the inhibitory effects of seminal plasma on fertilization. Semen should be obtained by masturbation; if circumstances preclude such collection, special Silastic condoms should be made available for semen collection with intercourse. Incomplete semen specimens should not be analyzed because they can give inaccurate values.

Examination

Macroscopic examination should be performed after liquefaction, which usually occurs in less than 20 minutes at room temperature. Failure to liquefy may indicate inadequate prostate secretion. Semen should be thoroughly mixed before examination and its viscosity recorded. The volume of ejaculate can be measured by weighing the collection cup before and after specimen collection. The appearance of a yellow hue in a semen specimen is associated with pyospermia; a rust color is due to small bleedings in the seminal vesicle. The pH ranges from 7.2 to 7.8; however, it may be 8.0 or higher with acute infection in the prostate, seminal vesicle, or epididymis. The pH will be 7.0 or lower if there is contamination with urine, an obstruction in the ejaculatory ducts, or if the specimen consists of mainly prostatic fluid.

Microscopic examination should be performed to obtain estimates of sperm concentration, motility, morphology, and agglutination. Other cellular elements, such as polygonal cells of the urethral tract and round cells such as spermatogenic cells and leukocytes, can also be observed when sperm are counted in a hemocytometer or Makler chamber. Because sperm

motility and velocity are temperature dependent, these parameters must be assessed on a microscope with a warm stage. At least four different fields of two specimen aliquots should be counted and the mean of the eight separate readings recorded. Total sperm count is then calculated by multiplying the dilution factor (normal concentration range, 15–50 million/mL) by its volume (normal range, 2–5 mL).

Total motility (normal range, 40% or above) is expressed as the percentage of sperm that move, including twitch. Progressive motility (normal range, 32% or above) is expressed as the percentage of sperm that move in a forward, linear motion. In addition, forward movement is graded. Sperm that move rapidly in a straight line with little yaw and lateral movement are grade 4 or, if they move more slowly, grade 3. Grade 2 sperm move even more slowly and with substantial yaw. Grade 1 sperm have no forward progression. Zero progression denotes absence of any motility. If motility is less than 30%, a viability stain of eosin Y with nigrosin as a counterstain is done. In bright-field microscopy, dead sperm will stain red, whereas live sperm will exclude the dye and appear unstained. In samples with no visible sperm, such as postvasectomy semen, the entire sample should be centrifuged and the pellet examined for intact or damaged sperm fragments. The analysis should be repeated in 4 to 6 months.

Agglutination occurs when motile sperm stick to one another in an orientation that is reproducible within a given specimen, such as head to head, tail to tail, midpiece to midpiece, or mixed ways, depending on the specificity of sperm antibodies. Agglutination suggests an immunologic cause of infertility, and a description of the type of agglutination should be recorded. This can usually be distinguished from clumping due to bacterial infection or tissue debris, which typically involves nonspecific orientation of the sperm.

Round cells should be differentiated into two classes: immature germ cells with a single or double highly condensed nucleus with a relatively large area of cytoplasm, and polymorphonuclear leukocytes, which are smaller than the germ cells and have a lower nuclear/cytoplasmic ratio. Peroxidase staining specifically identifies the polymorphonuclear leukocytes in the presence of lymphocytes and other cells that normally occur in semen. Bacterial contamination should be noted, as should the presence or absence of epithelial cells. If no sperm are seen in association with a low semen volume, a fructose test should be performed to confirm the presence of fluid from the seminal vesicle; the same test should be performed on postejaculate urine to rule out retrograde ejaculation. However, the significance of a fructose test result has declined over the years because of the availability of more direct diagnostic tools, such as transrectal ultrasonography.

Sperm morphology can predict fertility (Ombelet et al., 1997). In 2010, the World Health Organization (WHO) standardized the new normal values based on data from men with proven fertility. These men were defined as men who were known to help their partners conceive in the previous 12 months. Typically, more than 4% of the sperm in a semen specimen should exhibit normal morphology. Kruger and colleagues (1988) developed strict criteria for normal sperm morphology. Morphologically abnormal sperm usually have multiple defects; the average number of defects per sperm, designated as the *teratozoospermic index*, is a significant predictor of sperm function both in vivo and in vitro. A strict morphology score of greater than 4% of normal indicates excellent fertilizing capacity. Scores between 0% and 3% predict probable inability to fertilize. Wide variability in the size of the acrosomal cap is the most obvious characteristic of abnormal sperm. An acrosomal cap less than one-third of the head surface is considered abnormal, as are retention of a cytoplasmic droplet greater than one-half of the head size and a tail less than 45 μm long. Of particular note is the direct relationship between acrosome size and the frequency of fertilization or pregnancy.

Immunologic Tests

Sperm antibody binding to head or tail antigens is considered specific for immunologic infertility. The antibodies are usually of the immunoglobulin (Ig) A or IgG class and, rarely, the IgM class; IgA antibodies are the most clinically significant. Current methods detect sperm-bound antibodies by direct or indirect mixed agglutination reaction (MAR) tests for IgG and IgA, or by immunobead assay, which detects all classes but with varying sensitivity. Both tests require motile sperm. The direct MAR test can be performed on fresh semen, and the result can be read within a few minutes with a light microscope.

Semen is mixed with latex particles coated with nonspecific human IgG; then, monospecific antisera to human IgG is added. The anti-IgG bridges the sperm-bound IgG, if present, and the particle-bound IgG to form mixed agglutinates. In the absence of sperm-bound IgG, the anti-IgG agglutinates only the latex particles. Under light microscopy, localized binding of the particles identifies the antibody as specific to head, tail, or any other region of the sperm structure. An indirect test can also be done with this reagent to detect the presence of sperm antibody in semen, cervical mucus, or serum.

The immunobead assay can detect all three immunoglobulin classes when beads are coated with monospecific antisera to each class. Therefore, sperm are washed to remove all free immunoglobulin before the beads are added. An indirect assay can also be designed with this reagent. The test is best read under phase microscopy. Increased risk of men developing sperm antibody is associated with vasectomy, repeat prostate gland infections, obstruction of the ducts, cryptorchidism, varicocele, testicular biopsy, trauma, torsion, cancer, and genetic predisposition (Gilbert et al., 1992; Chamley & Clarke, 2007). In women, sperm antibody is usually associated with intense mucosal inflammation of the genital tract, but all causes are not fully understood.

Genital tract infections (see Part 7) may have significant adverse effects on male and female fertility (Pellati et al., 2008). For example, *Escherichia coli* can cause sperm agglutination and immobilization, and adherence of *E. coli* to sperm is mediated by mannose and mannose-binding cell surface structures present on both cell types (Sarkar et al., 1974; Wolff et al., 1993). Special precautions should be taken when collecting a semen specimen for detection of bacteria or yeast to eliminate the possibility of external sources of contamination. Seminal plasma cultures may help diagnose male accessory gland infection, particularly of the prostate. If the concentration of bacteria exceeds 1000 colony-forming units per milliliter, the colonies should be identified and tested for antibiotic sensitivity.

Accessory Glands

Seminal vesicle, prostate, and epididymis function can be evaluated by analyzing unique constituents of each. Prostate secretions, for example, are acidic and contain acid phosphatase. Seminal fluid that is more alkaline than normal (pH >8.0) and that has reduced acid phosphatase suggests prostate dysfunction. Fructose is a measure of seminal vesicle secretory function. In azoospermia caused by the congenital absence of vasa deferentia, a low fructose level may indicate an associated dysgenesis of the seminal vesicles, as in some patients born with cystic fibrosis. Ejaculatory duct obstruction, or agenesis of the vasa deferentia and seminal vesicles, may result in the production of semen with low volume, low pH, lack of coagulation, and absence of characteristic semen odor. Neutral α-glucosidase originates solely from the epididymis. Its measurement is of diagnostic value for distal ductal obstruction when considered with hormonal and testicular findings.

Image Analysis

Routine semen evaluation can be carried out by an automated image analysis system that uses sperm head movement to derive the magnitude of various swimming parameters. However, human sperm are extremely heterogeneous with respect to morphology, swimming characteristics, and sperm DNA content. Thus, no reference is made to evaluating specimens as normal or abnormal and fertile or infertile. Hence, semen evaluation by manual methods performed by trained technical staff remains a standard practice of andrology laboratories.

Hormone Analysis

If multiple semen analyses demonstrate azoospermia (no sperm), oligospermia (<15 million sperm/mL), or another abnormality, then hormone analyses are performed to help identify the specific dysfunction. An example of a diagnostic algorithm is shown in Figure 26.6.

Decreased testosterone accompanied by increased LH and FSH indicates primary testicular failure. This can be acquired or due to a genetic disease (Klinefelter syndrome; see Chapter 71). Decreased testosterone accompanied by decreased or inappropriately normal LH and FSH indicates hypothalamic-pituitary disease, resulting in secondary testicular failure. When LH and FSH levels are normal, secondary disease can be confirmed with an hCG stimulation test. hCG interacts with LH receptors; in the male, such interaction stimulates Leydig cells, if they are normal, to synthesize and secrete testosterone. Thus, administration of hCG should cause an increase in serum testosterone in secondary testicular failure but not in primary testicular failure.

If hypothalamic-pituitary disease is suspected, then prolactin (PRL) should also be measured. Hyperprolactinemia interferes with the normal regulation of FSH and LH secretion by GnRH, and prolactinomas are the most common type of pituitary tumor (see Chapter 25). However, if PRL is elevated, primary hypothyroidism must be excluded as a possible cause. In primary hypothyroidism, TSH and thyrotropin-releasing hormone (TRH) are elevated. Although the function of TRH is to stimulate the synthesis and secretion of TSH, TRH also stimulates the synthesis and secretion of prolactin. Thus, an elevated TSH suggests that primary hypothyroidism is the cause of the hyperprolactinemia, whereas a normal TSH suggests that a prolactinoma is the cause. If the latter were the case,

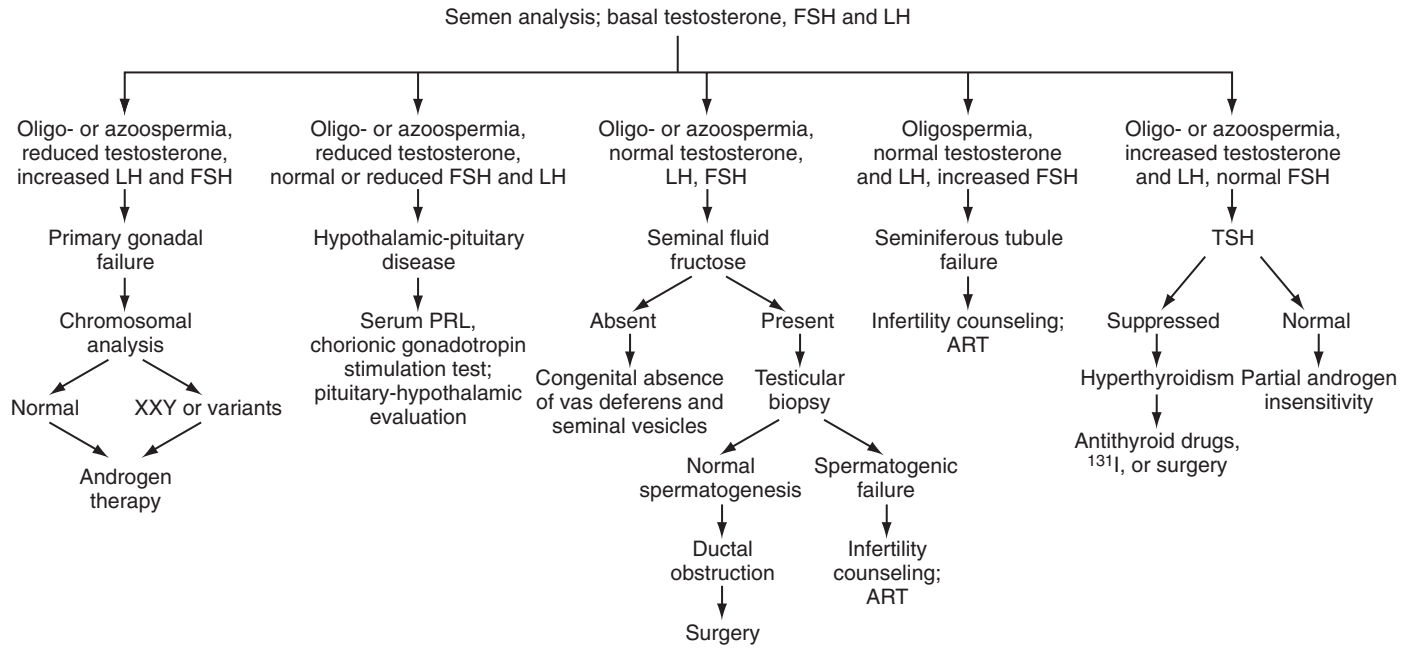

Figure 26.6 A diagnostic algorithm for male hypogonadism. *ART,* Assisted reproductive technology; *FSH,* follicle-stimulating hormone; *LH,* luteinizing hormone; *PRL,* prolactin; *TSH,* thyroid-stimulating hormone. (From Braunstein GD: Testes. In Greenspan FS, Gardner DG, editors: Basic and clinical endocrinology, ed 7, New York, 2004, Lange Medical Books/McGraw-Hill, pp 478–510, with permission.)

then imaging techniques with magnetic resonance imaging would be used to further evaluate the hypothalamic-pituitary axis.

If normal testosterone, LH, and FSH levels accompany oligospermia or azoospermia, then seminal fluid fructose should be evaluated. Its absence suggests the congenital absence of vasa deferentia and seminal vesicles. Its presence suggests ductal obstruction or spermatogenic failure, which can be distinguished using testicular biopsy. Oligospermia accompanied by normal testosterone and LH along with increased FSH suggests seminiferous tubule failure. The increase in FSH is likely due to reduced negative-feedback inhibition by decreased Sertoli cell inhibin. Increased testosterone and LH with normal/or elevated FSH suggest partial or complete androgen insensitivity. Testosterone provides negative feedback on GnRH secretion at the level of the hypothalamus through androgen receptors. Genetic mutations of androgen receptors in hypothalamic neurons result in increased pituitary release of LH, resistance to testosterone, hypogonadism, and oligospermia.

In evaluation protocols such as that shown in Figure 26.6, it is becoming more common to measure not just total testosterone but also free and/or bioavailable testosterone. The latter represents the sum of free testosterone plus that bound weakly to albumin. The remaining testosterone is bound tightly to SHBG. Free or bioavailable testosterone more accurately represents the biologically active hormone in conditions in which the concentration of SHBG is altered. For example, SHBG levels are increased with decreased testosterone, increased estrogen, hyperthyroidism, and liver disease, whereas they are decreased with increased testosterone, hypothyroidism, and acromegaly. Thus, if SHBG is high, total testosterone may be normal, but free or bioavailable hormone may be low. Conversely, if SHBG is low, total testosterone may be normal, but free or bioavailable hormone may be high (Ismail et al., 1986; Yeap, 2009). Methods for measuring total testosterone are readily available on automated immunoassay analyzers, but methods for measuring free and bioavailable testosterone are much more labor intensive. Consequently, free and bioavailable testosterone analyses are usually performed in a reference laboratory. The same considerations apply to testosterone measurements in females (see later discussion).

Gynecomastia, or breast development in males, is thought to be due to a relative imbalance of androgen (decreased) and estrogen (increased) acting at the mammary gland. The decrease in androgen action can be due to a concentration deficiency and/or a receptor deficiency (insensitivity). The condition is not uncommon during the neonatal and pubertal periods. A variety of other causes have been identified, including endocrine abnormalities, tumors, systemic diseases, and many drugs. Discontinuing or changing medications can exclude drug-induced disease, and liver or kidney disease can be identified through biochemical blood screens. Measuring serum testosterone, estradiol, LH, hCG, prolactin, and TSH can reveal an endocrine abnormality or hormone-secreting tumor. Results from these tests, together with imaging methods, can help differentiate among the following as possible causes of gynecomastia: primary or secondary testicular failure, hyperthyroidism, androgen resistance, prolactinoma, testicular or extratesticular germ cell tumor, Leydig or Sertoli cell tumor, or adrenal tumor (Braunstein, 2004).

FEMALE EVALUATION

Evaluation of the female reproductive system can be simplified to confirmation of ovulation and normal female reproductive anatomy (Strauss & Lessey, 2013). The abnormal menstrual cycle pattern is one of the best predictors of anovulation. Amenorrhea can be defined as the absence of menstrual flow by age 16 years, or by age 14 years if no breast development occurs (Speroff & Fritz Marc, 2010). In patients who have not exhibited menses by age 16 years, this is often due to a genetic and/or anatomic abnormality. In such cases, however, an endocrine abnormality is still a possible cause, and the presence or absence of secondary sexual characteristics (e.g., breast development) is an important indicator in the evaluation. An endocrine abnormality is a more likely cause in patients who have a history of menstruation but have not experienced menses for more than 3 months. A stepwise approach to evaluating amenorrhea (Fig. 26.7) is based on measuring hCG, PRL, TSH, free thyroxine (FT_4), FSH, LH, and androgen levels and assessing estrogen status.

Step 1: hCG is measured to exclude the most common cause of secondary amenorrhea—pregnancy. Although a result of greater than 5 mIU/mL is typically indicative of pregnancy, an elevated result can also be obtained with trophoblastic disease or an hCG-secreting tumor.

Step 2: PRL, TSH, and FT_4 are measured to exclude the endocrine disorders. Increased prolactin accompanied by normal TSH and FT_4 results suggests a prolactinoma, which would be further evaluated by imaging techniques. Hyperprolactinemia, however, can also be caused by primary hypothyroidism, as indicated by high TSH and low FT_4 (see earlier Male Evaluation section). The mechanism by which increased prolactin causes amenorrhea is the same as that discussed previously for postpartum amenorrhea in females and for hypogonadism in males. Low TSH and FT_4 suggest secondary hypothyroidism, in which case the patient should be evaluated for panhypopituitarism, a deficiency of all anterior pituitary hormones. Hyperthyroidism (increased FT_4) can also be associated with amenorrhea.

Step 3: If hCG, PRL, TSH, and FT_4 are all normal, then endogenous estrogen status is evaluated with the progestin withdrawal test. Progestin may be administered orally for 5 to 10 days or in one intramuscular injection (progestin dissolved in oil). The presence of withdrawal bleeding within 7 days after treatment indicates (1) that the outflow

tract is intact and (2) that sufficient estrogen was present at the outset to stimulate endometrial growth. If withdrawal bleeding is absent, the genital tract should be evaluated using imaging techniques.

Step 4: Serum FSH and LH levels should be determined. Elevated FSH and LH indicate primary ovarian failure, whereas low or inappropriately normal FSH and LH indicate secondary ovarian failure. The latter is of hypothalamic-pituitary origin and can result from a variety of clinical disorders, including Sheehan syndrome, eating disorders, weight loss, and stress. If withdrawal bleeding is present, then Step 5 is followed.

Step 5: Androgen excess should be evaluated. Elevated testosterone (>150 ng/mL) indicates a tumor or polycystic ovarian syndrome. The latter is a clinical entity often associated with enlarged ovaries and infertility as well as amenorrhea. Increased DHEAS suggests an adrenal tumor. 17-OH progesterone is an androgen precursor (see Fig. 26.1), and an increase in serum levels can indicate congenital or adult-onset adrenal hyperplasia due to 21-hydroxylase deficiency. These abnormalities may be accompanied by hirsutism (i.e., male pattern of hair growth in females).

The tests in Step 5 can also be used to evaluate hirsutism when it is the primary clinical presentation. Because amenorrhea or oligomenorrhea is often associated with infertility (Lobo et al., 1997; Speroff & Fritz Marc, 2010), the latter can be evaluated with the type of diagnostic algorithm shown in Figure 26.7. Evaluation of the ovulatory function is an important step in the infertility workup. One of the methods used to confirm ovulation is monitoring the basal body temperature. A rise in progesterone after ovulation increases basal body temperature by 0.4° F to 0.8° F, but it is not as reliable or used as often. More reliable are urinary ovulation predictor kits, which measure urinary LH by colorimetric assay.

Testing should be started 2 to 3 days before the LH surge and should be continued daily. LH has a short half-life and is rapidly excreted in the urine. In most cases, the test will be positive for only 1 day of the menstrual cycle. This test is not as reliable in patients who have polycystic ovarian syndrome because they have a baseline elevated LH that will cause a false-positive result. Another method that is reliable and widely available involves measurement of midluteal phase serum progesterone levels on day 21 of the menstrual cycle. Values above 3 ng/mL indicate ovulation and production of progesterone by the corpus luteum (Besser & Thorner, 2002). Inadequate progesterone levels result in luteal phase deficiency, in which maturation of the secretory endometrium is delayed; thus, implantation of the blastocyst does not occur. In many cases, but not all, such an out-of-phase endometrium can be demonstrated by histologic evaluation of an endometrial biopsy from the late luteal phase (Noyes et al., 1975). However, endometrial histologic dating is not a valid diagnostic tool and should not be considered in management of the infertile patient (Speroff & Fritz Marc, 2010).

When the diagnosis of ovarian failure is suspected, the level of FSH in the early follicular phase (on day 3) should be determined because, as mentioned earlier, it will be elevated. Concentrations greater than 10 mIU/mL are associated with diminished ovarian reserve, which is defined by low numbers of normal oocytes and the presence of poor-quality oocytes. Diminished ovarian reserve is associated with decreased probability of live birth with a natural or IVF cycle (Scott & Hofmann, 1995; Speroff & Fritz Marc, 2010). Additional information can be obtained by measurement of estradiol levels on the same day of each menstrual cycle (Buyalos et al., 1998). Levels greater than 80 pg/mL are considered abnormal and indicate ovarian stimulation of steroidogenesis by elevated FSH, which is typically seen in ovarian failure.

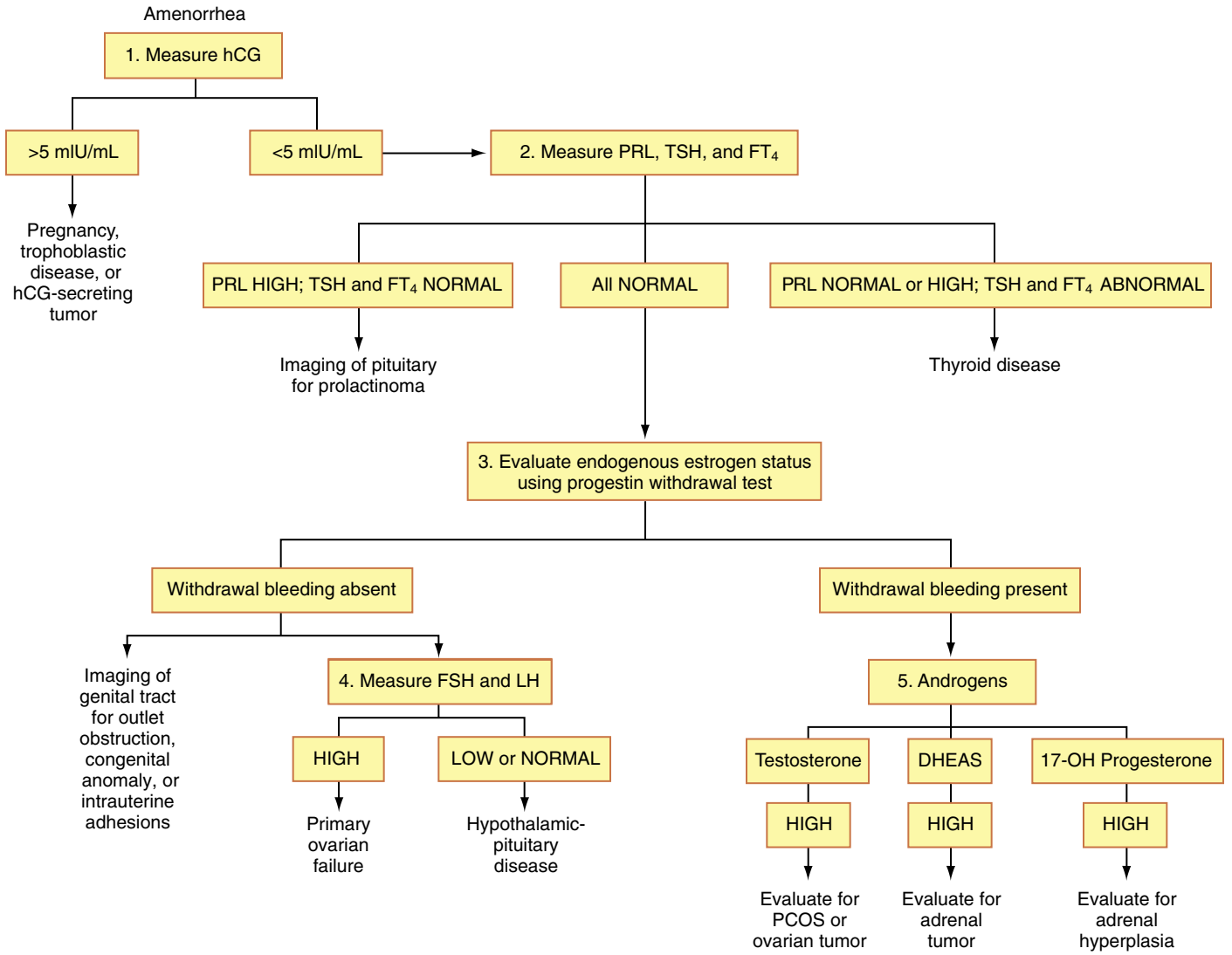

Figure 26.7 A diagnostic algorithm for amenorrhea. Sequential steps in the evaluation are numbered. *DHEAS,* Dehydroepiandrosterone sulfate; *FSH,* follicle-stimulating hormone; *FT_4,* free thyroxine; *hCG,* human chorionic gonadotropin; *LH,* luteinizing hormone; *PCOS,* polycystic ovarian syndrome; *PRL,* prolactin; *TSH,* thyroid-stimulating hormone.

Serum levels of Anti-Mullerian Hormone (AMH) have also been considered to be able to accurately predict ovarian reserve. AMH has recently been added as a new diagnostic assay during the initial female infertility evaluation. AMH is secreted by preantral and small antral follicles within the ovaries. As AMH is released, it inhibits FSH-induced aromatase activity (Mumford et al., 2016). It has been shown that when AMH is absent, faster rates of primordial follicular recruitment have been observed, resulting in premature ovarian failure (Dumont et al., 2015). Yet, it makes sense that as AMH levels increase, follicular recruitment is inhibited, resulting in disease states such as polycystic ovary syndrome (PCOS).

More extensive testing of ovarian reserve includes the clomiphene citrate challenge test. Among a number of effects, this drug, which is termed a *nonsteroidal estrogen receptor modulator*, stimulates production of GnRH which, in turn, stimulates the release of FSH and LH. In this test, serum FSH levels are determined on day 3 of the menstrual cycle. Clomiphene citrate is then administered on days 5 through 9 (or days 3–7) of the cycle. Serum levels of FSH and estradiol are then measured again on day 10. Women with a poor cohort and aging follicles cannot generate enough estradiol or inhibin B to suppress FSH. Therefore, FSH remains high.

ASSISTED REPRODUCTIVE TECHNOLOGY

Infertility is defined as 1 year of unprotected intercourse without conception (Speroff & Fritz Marc, 2010). Initial treatments may include artificial insemination with washed and concentrated sperm and/or ovulation induction with clomiphene citrate or letrozole, a nonsteroidal aromatase inhibitor. If these are unsuccessful, then one of several ARTs may be attempted. ARTs involve techniques of direct manipulation of oocytes that are performed to control as much of the reproductive process as possible to achieve pregnancy (Trounson & Gardner, 2000). Much of this external control requires significant monitoring through laboratory analyses.

Indications for ART include male infertility, ovarian failure, unexplained infertility, PCOS, tubal disease, uterine factor, and endometriosis. It is not uncommon for several causes of infertility to be present in one couple. ART can also be applied in infertile couples requiring donation. The latter involves two distinct groups of patients: (1) females without gonadal function because of gonadal dysgenesis, premature menopause (which may occur spontaneously or after surgical castration or castration induced by chemotherapy or radiotherapy), or resistant-ovary syndrome; and (2) women with functional ovaries who do not wish to use their own oocytes to become pregnant because of the risk of transmitting chromosomal abnormalities to the offspring (e.g., if there is a history of autosomal-dominant disease or X-linked disease, or when both partners are carriers of an autosomal-recessive disease) (Van Steirteghem et al., 1992; Pados et al., 1994). The most common form of ART is IVF; other forms involve gamete intrafallopian transfer, zygote intrafallopian transfer, or tubal embryo transfer, all performed with the use of laparoscopy, but they are rarely practiced.

A typical ART protocol has four steps: ovarian stimulation with exogenous gonadotropins, retrieval of oocytes from ovaries, fertilization in the laboratory, and transfer of embryos into the uterus. Controlled ovarian hyperstimulation (COH) begins with the exogenous stimulation of follicular growth using a synthetic human menopausal gonadotropin (hMG) preparation, which will have FSH and LH activity or predominantly FSH activity, depending on the specific material used. Unlike a normal reproductive cycle, in which typically only one dominant follicle matures, in an ART cycle, multiple follicles, upwards of 10 to 20, undergo growth and maturation. The number of follicles and their increase in size are monitored by regular transvaginal ultrasound analysis. The function of the developing follicles is monitored by sequential serum estradiol measurements. When sufficient follicular maturation is achieved, usually when the follicles have reached 18 mm in diameter or more, according to ultrasound and estradiol analyses, an exogenous bolus of hCG is administered. This hCG functions as a surrogate LH surge, interacting with follicular LH receptors to initiate the process of oocyte maturation and ovulation. However, this process is not allowed to progress to completion. Ovulation would normally occur approximately 48 hours after hCG administration. Therefore, 12 hours before induced ovulation, the oocytes are "retrieved" from the stimulated follicles. Under traditional IVF techniques, each oocyte is then mixed with sperm and allowed to incubate. A fertilization check is then reviewed 24 hours later. The presence of two polar nuclei indicate adequate fertilization by the sperm; its absence indicates fertilization has not occurred and the gametes are discarded. The resulting zygote is then incubated and monitored for proper development into the morula and blastocyst (day 5) stage before being either frozen (cryopreserved) for preservation and later use or transferred to the uterus for subsequent implantation. ART also includes methods for assisted fertilization by intracytoplasmic sperm injection (ICSI) obtained from ejaculate or extracted from the epididymis or testis. ICSI is the direct injection of sperm into the oocyte for manual fertilization.

Oocyte retrieval disrupts the follicles, as does normal ovulation; consequently, estradiol levels drop immediately afterward. As the follicles differentiate into corpora lutea, however, estradiol levels rebound and serum progesterone increases. This process may require "boosting," which is often achieved via exogenous progesterone support either orally, vaginally, or intramuscularly. As in a normal cycle, estradiol plus progesterone is required to prepare the uterine endometrium for implantation. Therefore, serum levels of the two steroids are monitored after transfer. If pregnancy is achieved, serum hCG will begin to be detected about 10 days after transfer. About 20 days after transfer, ultrasound examination can be used to confirm the presence of a gestational sac. If pregnancy is not achieved, confirmed by blood pregnancy test, exogenous progesterone administration should be halted, subsequently inducing menstruation.

Another type of ART is called *preimplantation genetic testing for aneuploidy* (*PGT-A*). PGT-A is most often performed using a biopsy of about 5 cells taken from the trophectoderm of the developing embryo. Preimplantation genetic testing may be indicated to detect chromosomal abnormalities in women of advanced maternal age and inherited single-gene disorders if it is known that both parents are carriers of the disease (preimplantation genetic testing for monogenic disorders [PGT-M]), as well as to determine gender. However, conventional prenatal diagnosis is still recommended later in pregnancy (Speroff & Fritz Marc, 2010).

LABORATORY EVALUATION OF PREGNANCY

On a patient's first visit to an obstetrician, ideally early in the first trimester, a number of clinical laboratory tests are routinely ordered to identify disorders that can be treated or prevented (Willett, 1994) (Table 26.2). Simple, inexpensive blood and urine tests are carried out for anemia, red cell alloimmunization, and suspected viral or bacterial infection. Sometimes, the clinical history, physical examination, or test results indicate additional studies for genetic disease, disorders of coagulation or thrombosis, causes of spontaneous abortion, and other conditions. Laboratory procedures used routinely to monitor pregnancy are summarized in Figure 26.8.

hCG AND EARLY PREGNANCY

Elevated hCG in maternal serum and urine is a reliable indicator of pregnancy. The first assays for urine hCG, developed in the early part of the twentieth century, were cumbersome bioassays. Starting in 1960, these were supplanted by simple immunoassays, usually based on agglutination inhibition. The discovery of monoclonal antibodies in the late 1970s led to the development of the current generation of quantitative hCG immunoassays, which typically use a pair of monoclonals to measure either the β subunit of hCG or the intact hCG α-β dimer. These assays can quantify hCG as low as 1 to 2 mIU/mL. Serum hCG increases above the reference interval (typically 4–6 mIU/mL) by implantation, 6 to 12 (mean, 9.1) days after ovulation (Wilcox et al., 1999). Urine hCG levels are commonly measured by qualitative immunoassay test kits with detection limits of approximately 20 mIU/mL. These methods can detect elevated urine hCG 2 to 3 days later than serum methods.

Serum hCG increases dramatically during the first trimester, reaching a peak at about 16 weeks' gestation (see Fig. 26.5). Throughout pregnancy, intact hCG is the predominant form present. However, a small quantity of free β subunit is present in the first trimester. Free α subunit appears in the second trimester and steadily increases in the last trimester (Ozturk et al., 1987).

Some cancers and medical conditions may be associated with increased levels of hCG. These include germ cell tumors and gestational trophoblastic disease. Tumor production often includes significant amounts of free β subunit, in addition to intact hCG. The use of hCG as a tumor marker is discussed more fully in Chapter 76. False-positive hCG is usually due to interference by heterophilic Ig antibodies; it is characterized by large molecular weight and is not filtered by renal glomeruli. Serum concentrations of hCG are typically less than 150 mIU/L with negative urine testing.

Quantitative measurements of hCG are indicated when a patient presents with early gestational vaginal bleeding or abdominal pain that may suggest the presence of ectopic pregnancy or spontaneous abortion. A simple protocol using only ultrasound and quantitative hCG examinations

TABLE 26.2
Prenatal Tests Ordered by Trimester and Visit

LABORATORY TESTS	VISIT TYPE			
	First Visit	First Trimester	Second Trimester	Third Trimester
Hematocrit or hemoglobin	X		X	
Blood type and Rh factor	X			
Antibody screen	X		X*	
Pap smear screening	X			
Fetal aneuploidy screening		X	X	
Neural tube defect screening		X	X	
Cystic fibrosis screening	X			
Urine culture	X			
Rubella serology	X			
Syphilis serology	X†			
HIV serology	X†			
Hepatitis B serology	X†			
Gonococcal screening	X			X
Chlamydial screening	X			X
Group B *Streptococcus* screening				X

HIV, Human immunodeficiency virus; *Pap,* Papanicolaou.
*Performed if indicated.
†Repeat in high-risk patients every trimester.

allows more accurate diagnosis and sound management than are obtained by clinical judgment alone (Koh & Yeo, 1997). Because hCG concentrations rise quickly in normal early pregnancy, serial measurements can be used to ensure that an intrauterine implantation has occurred. Doubling of hCG in 2 days provides a greater than 80% probability of intrauterine implantation of the fertilized ovum. Increases in serum hCG of less than 53% in 2 days indicate abnormal pregnancy with 99% sensitivity (Barnhart et al., 2004).

Because circulating hCG increases very rapidly in the first days postimplantation, it is important to consider diverse causes of low-level quantitative results, including normal production of hCG in the pituitary, especially in postmenopausal females (Odell & Griffin, 1987); early abortion ("microabortion") (Wilcox et al., 1988); use of hCG as a drug; and assay interference, as mentioned previously.

When hCG concentrations exceed discriminatory zone values of 1500 to 2000 mIU/mL, an intrauterine gestational sac becomes visible on ultrasound examination in a normal singleton pregnancy (Kadar et al., 1994). Multiple gestations have higher hCG levels than singletons, and hCG levels may rise above 2000 mIU/mL before ultrasound findings of intrauterine gestational sac are obtained (Goldstein et al., 1988). Absence of an intrauterine gestational sac and failure to double the serum hCG or the presence of an adnexal mass indicate a possible ectopic pregnancy. Furthermore, failure to double the serum hCG may suggest an ectopic pregnancy.

Estradiol and progesterone measurements may provide additional information. Low serum progesterone (<15 ng/mL) or estradiol (<200 ng/mL) indicates a blighted ovum with 90% likelihood. If hCG is less than 1000 mIU/mL in a patient with vaginal bleeding, a progesterone value of less than 5 ng/mL is 94% predictive of an abnormal pregnancy.

Progesterone measurements may provide additional information about abnormal pregnancy. Serum levels higher than 20 ng/mL usually are associated with normal intrauterine pregnancy. Low serum progesterone—less than 5 ng/mL—indicates an abnormal pregnancy with a specificity of 100% (Stovall et al., 1992). Serum progesterone levels are not helpful in assessment of the ectopic pregnancy because most of the time values range between 10 and 20 ng/mL.

Medical intervention using intramuscular methotrexate for compliant patients with unruptured ectopic pregnancy is less costly than surgery, may be a less complicated procedure, and may improve the patient's fertility. Cases may be selected for methotrexate treatment by using ultrasound to ascertain a tubal implantation and differentiate it from an interstitial one, for which methotrexate is not indicated. Ultrasound also ensures a small volume (<3 cm) of conceptual tissue with absent fetal heart motion. A serum progesterone decrease to less than 1.5 ng/mL may be a better predictor of resolution because hCG concentrations do not decline as rapidly after surgery (Saraj et al., 1998).

The laboratory can provide testing to help determine why an early pregnancy aborted spontaneously. For example, recurrent abortion caused by the antiphospholipid syndrome can be diagnosed by the presence of anticardiolipin and specific phospholipid antibodies in the first trimester. Recurrent abortion, defined as three or more, due to inherited thrombophilia may be diagnosed by detection of factor V Leiden gene mutation, β2 glycoprotein, antithrombin III, prothrombin gene mutation, levels of proteins C and S, and activated protein C activity.

NEURAL TUBE DEFECTS

Neural tube defects (NTDs) are among the most common congenital malformations in the United States and worldwide. The incidence of NTDs in the United States has been reported at approximately 1 per 1000 pregnancies. Whites in the United States have an average occurrence of 0.96 per 1000 and Hispanics 1.2 per 1000; the lowest prevalence was reported in African Americans, with an incidence of 0.75 per 1000 (Feuchtbaum et al., 1999). An increased risk of recurrence has been noted in families. For example, when a couple has had one offspring with an NTD, the risk in each subsequent pregnancy for any type of NTD increases to approximately 1% to 3% (Toriello & Higgins, 1983). However, data suggest a decline in these rates due to increased education within the medical community and toward women of childbearing age regarding the benefits of folic acid consumption along with the mandated fortification of grain products in certain states (New York State Department of Health, 2013; for review, see http://www.health.ny.gov/diseases/congenital_malformations/2013/docs/cmr_25.pdf).

NTDs result from failure of the neural tube to close by the 27th day after conception. Anencephaly comprises 50% of NTDs and involves absence of the calvarium, cranial vault, and cerebral hemispheres; it is incompatible with life. Abnormalities of the caudal portion of the neural tube, known as spina bifida, present as a lumbar (or cervical) meningomyelocele, with herniation of meninges, spinal cord, and nerve roots. The severity of complications—such as paralysis or muscle weakness, fecal and/or urinary incontinence, and intellectual impairment—is dependent on the vertebral level and extent of spina bifida, which may be open in 80% of cases (referring to whether the defect is completely uncovered or is covered only by a very thin membrane) or closed (covered by skin or a thick membrane). This distinction is important because maternal serum screening will detect only open defects.

Screening for fetal structural defects using maternal serum biochemical markers has become routine obstetric practice. NTDs are sporadic in 90% of cases and represent isolated defects with a multifactorial origin, involving both genetic and environmental factors. The incidence of NTD is associated with geographic region, ethnicity, diet, teratogen exposure (mainly from drugs, such as maternal valproic acid ingestion), maternal diabetes, and first-trimester maternal hyperthermia. Although NTDs are typically isolated defects, it is important to rule out fetal chromosomal abnormalities and single-gene disorders that may be associated with a different prognosis and a different recurrence risk.

Folic Acid Prevention

Of great interest is the finding that folic acid is a major preventive agent against NTD. Many clinical studies have established that folic acid supplementation before conception reduces the recurrence of fetal NTDs (Pitkin, 2007). The largest of these studies was a randomized prospective study by the British Medical Research Council (MRC Vitamin Research Group, 1991), which found that preconceptional folic acid supplementation decreased the recurrence of NTDs by 72%.

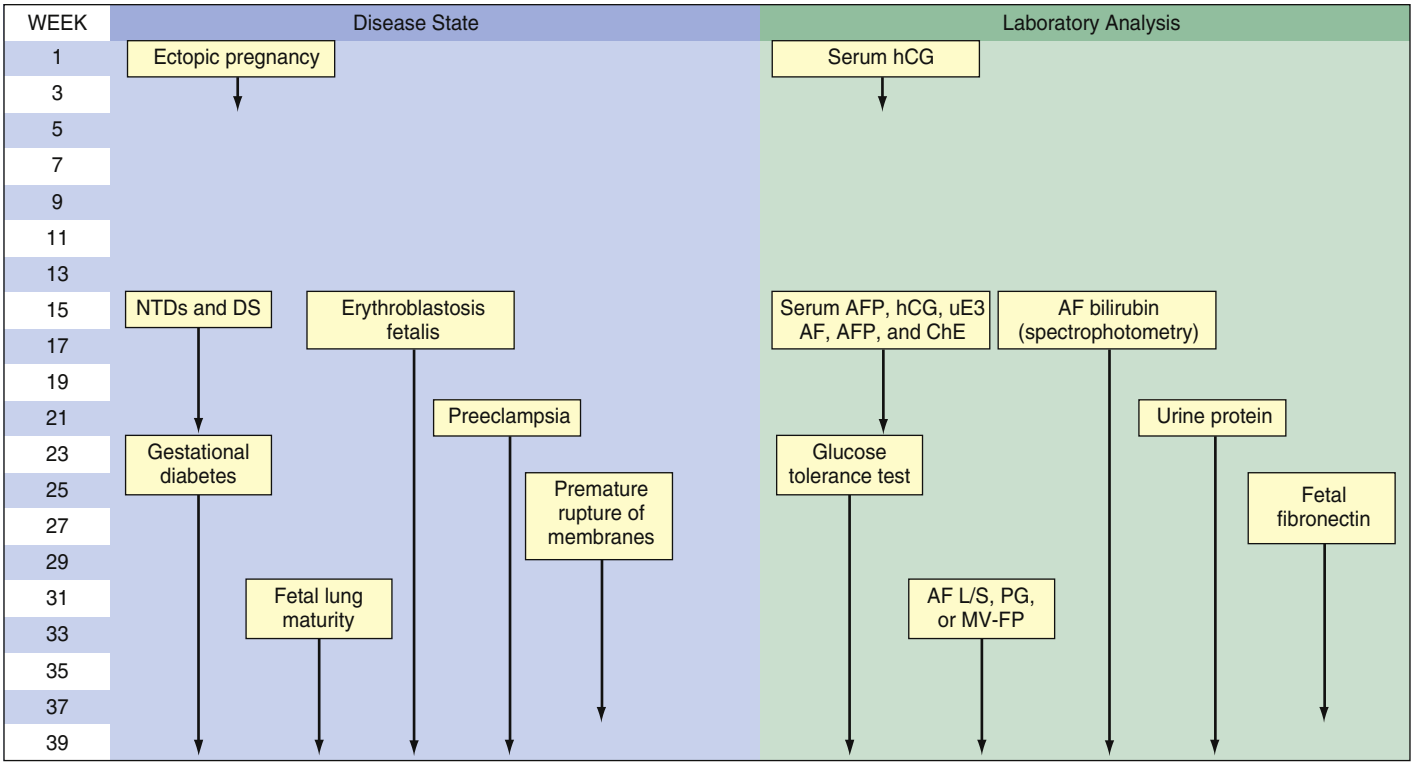

Figure 26.8 Approximate gestational weeks for laboratory evaluation of major disease states in pregnancy (when clinically indicated). *AChE,* Acetylcholinesterase; *AF,* amniotic fluid; *AFP,* α-fetoprotein; *ChE,* cholinesterase; *DS,* Down syndrome; *hCG,* human chorionic gonadotropin; *L/S,* lecithin/sphingomyelin ratio; *MV-FP,* microviscosity by fluorescence polarization; *NTDs,* neural tube defects; *PG,* phosphatidyl glycerol; *uE3,* unconjugated estriol.

Neural tube closures occur early in pregnancy and at least 50% of all pregnancies are unplanned. Thus, initiating folic acid supplementation at the time of missed menses is often insufficient, as neural tube development is already underway. For this reason, the American College of Obstetrics and Gynecology (ACOG, 2017) recommends that all women capable of becoming pregnant should take 400 μg of folic acid daily—supplementation should begin 1 month prior to pregnancy and through the first 12 weeks of pregnancy, at least.

Women at high risk of NTDs should supplement with higher doses of folic acid (Wilson et al., 2015). However, not all NTDs are preventable with folic acid supplementation. Folate-resistant NTDs include those associated with maternal obesity, hyperthermia, poor glucose control in the first trimester, and genetic factors.

Screening for Neural Tube Defects

The now well-established finding that α-fetoprotein (AFP) is a maternal serum marker for NTDs was first reported in 1974 (Brock et al., 1974). AFP, produced initially by the fetal yolk sac and later by the fetal liver, is the most abundant protein in fetal serum. Its concentration increases in both fetal serum and amniotic fluid until about 13 weeks' gestation, after which the liver gradually shifts to production of albumin. In NTDs, AFP becomes elevated because fetal serum from exposed neural membranes and blood vessels leaks into amniotic fluid (AF), producing a concentration in AF that is approximately 100-fold less than in fetal serum. Small amounts of AFP are also transferred across the placenta from fetal serum and across the amniotic membranes from AF to maternal serum (MS), where concentrations of AFP are nearly 1000-fold less than in AF. AF AFP peaks at 13 to 14 weeks and decreases in the second trimester by about 10% per week. Assays for AFP are based on immunochemical determinations using monoclonal antibodies against AFP and are available on autoanalyzers.

In the second trimester, when maternal screening is performed, MS AFP levels increase by approximately 15% per gestational week. This MS AFP increase, while AF levels are decreasing (see earlier discussion), is due to combined changes in transfer to MS and maternal clearance (Ashwood, 1999). This measurable increase serves as the basis of midtrimester MS AFP screening for open NTDs (UK Collaborative Study, 1977, Burton, 1988).

MS AFP screening is based on comparison of serum AFP levels from pregnant women in the midtrimester of pregnancy versus median AFP values from women with normal fetuses at comparable gestational ages. These comparisons are subsequently expressed as multiples of the median (MoM). Median values are based on data from the reference population that is screened. Expressing patient results as MoMs normalizes the values, allows for direct comparison of results between laboratories, and adjusts for the large changes in expected values with increasing gestational age. The goal of any maternal serum-screening program is to identify those women at sufficient risk for a fetal disorder to warrant further evaluation and follow-up. Large prospective trials of MS AFP screening showed that most affected pregnancies can be identified by elevated MS AFP levels greater than 2.5 times the normal median for singleton pregnancies. Most laboratories set the cutoff at 2.0 to 2.5 MoM, such that the detection rate is about 95% for anencephaly and 65% to 80% of open NTDs with a false-positive rate less than 5% (Wald et al., 1977; Milunsky, 1980). Only 2% of all women with positive test results are carrying affected fetuses. Thus, further evaluation and testing with genetic counseling should be considered.

Clinical factors must be considered when patient-specific results are calculated (Ashwood, 1999). Laboratories routinely adjust for the following factors:

1. Maternal weight: MS AFP concentration decreases with increasing maternal weight. Although the fetus itself produces a constant amount of AFP, the maternal blood volume will vary according to the weight of the mother. Failure to adjust for maternal weight causes increases in both false-positive and false-negative results and affects the sensitivity and specificity of the test (Johnson et al., 1990a).
2. Race: Although the reasons are not known, African American women have MS AFP values that are approximately 10% to 15% higher than those of white women (Johnson et al., 1990b).
3. Insulin-dependent diabetes mellitus (IDDM): MS AFP levels in otherwise normal women with IDDM are approximately 20% lower than in the general population. Therefore, the MoM values must be adjusted upward to reflect this phenomenon. This is typically accomplished by multiplying the initial MoM value by a factor, using a mathematical constant to increase the initial MoM result.
4. Multiple gestation: Multiple gestation (e.g., twins) will yield higher MS AFP levels because each fetus contributes its own AFP to the maternal blood. The MS AFP level is approximately proportional to the number of fetuses; this effect can be factored into the laboratory calculation and interpretation of the results. Screening for fetal defects is not as reliable as for single pregnancies in that one cannot determine the individual AFP contributions of each fetus. Therefore, the NTD detection rate is lower for multiple pregnancies than for single ones.
5. Gestational age determination: To establish a valid MoM value, a reliable estimate of gestational age is essential. The most common reason for abnormal MS AFP screening results is incorrect estimation of gestational age. If pregnancy is initially dated using ultrasound, the sensi-

tivity and specificity of the screening are accurate (Wald et al., 1994). Pregnancies with positive screening results that originally were dated by using the last menstrual period should have the gestational age verified by ultrasound. If the two estimated gestational ages differ by a defined amount (7 days for a first-trimester ultrasound, 10–14 days for a second-trimester ultrasound, and 3 weeks for a third-trimester ultrasound), then the results are recalculated based on the ultrasound results.

6. Fetal viability: Fetal demise raises the MS AFP levels. In cases of fetal demise, MS AFP does not have diagnostic value.

An algorithm for detection of NTD is summarized in Figure 26.9.

With advances in ultrasonography and the expansion of its use over the last decade, MS AFP has become a less important diagnostic tool for the detection of NTDs. In this case, the value of MS AFP lies more in its screening for other anatomic abnormalities and placental complications. In a study done in 2005, when compared with MS AFP alone, second-trimester two-dimensional ultrasonography showed a higher detection rate of NTDs by 21%, from 75% to 96% (Norem et al., 2005). Because of the high-sensitivity detection of NTDs, the findings of two-dimensional ultrasonography alone can be considered diagnostic of NTDs; additional studies are usually not necessary to confirm diagnosis. Thus, ACOG (2017) recommends second-trimester ultrasonography for all pregnant women. ACOG explains that the optimal time for single ultrasound examination is 18 to 22 weeks, allowing for confirmation of gestational age and screenings of physical anomalies, including NTDs. An earlier ultrasound may be indicated if the patient presented with abnormal MS AFP or another high-risk factor. Although it is possible to detect NTDs in the first trimester, the detection rate has been shown to be much lower than with second-trimester screening.

DOWN SYNDROME

All women should be offered screening for fetal chromosomal abnormalities before fetal age 20 weeks, regardless of maternal age (ACOG, 2007). Many multicenter trials have evaluated the different approaches to screening for aneuploidy in the first and second trimesters. First-trimester screening, performed between 12 and 13 weeks, includes nuchal translucency measurement combined with two maternal serum analytes: free β subunit of hCG with pregnancy-associated plasma protein A (PAPP-A) and maternal age. An increase in the size of nuchal translucency, which refers to a fluid collection at the back of the fetal neck in the first trimester, is characteristic of fetal chromosomal and structural abnormalities. Patient data are converted to MoM based on population and gestational age. PAPP-A is a glycoprotein produced by the trophoblast; its levels are reduced to 0.48 MoM in affected pregnancies, whereas levels of free β subunit are elevated to 1.98 MoM in comparison with normal pregnancies (Spencer et al., 1999). Nuchal translucency, as a single ultrasonographic marker, has a detection rate of 64% to 70% for Down syndrome, trisomy 18, trisomy 13, and Turner syndrome. Adding the calculation of MS PAPP-A and β-hCG improves the detection rate to 82% to 87%. Women with increased risk of aneuploidy or advanced maternal age (age 35 years or greater at the time of delivery) on first-trimester screening should be offered genetic counseling and the option of diagnostic testing, such as chorionic villous sampling or second-trimester amniocentesis (ACOG, 2007). In 2012, ACOG released guidelines for noninvasive fetal testing called cell-free fetal DNA. This test is done on maternal plasma and is used as a screening test. Indications for offering this test include maternal age 35 years or greater at delivery, increased risk for aneuploidy on another screening test, history of previous pregnancy with aneuploidy, and parental balanced robertsonian translocation with increased risk of fetal trisomy 13 or 21 (ACOG, 2012; see Chapter 71.)

Other approaches to screening for fetal chromosomal abnormalities include the second-trimester triple screen with MS AFP, hCG, and unconjugated estriol (uE3) performed between 15 and 20 weeks. The level of MS AFP in pregnancies with Down syndrome is reduced to 0.74 MoM and the uE3 level to 0.75 MoM, whereas hCG is increased to 2.06 MoM (Wald et al., 2003). The detection rate of triple screen can be improved from 69% to 81% by adding the inhibin A (quadruple screen) dimeric protein produced by placenta and fetus. The level of inhibin A shows the same trend as hCG and is increased in pregnancies with Down syndrome at 1.77 MoM (Spencer et al., 1999).

Adjustments can be made to the MoM for special populations in which analytes are affected differently. For example, serum concentrations of each biomarker are approximately double in twin pregnancy but cannot be interpreted in higher-order multiples. In pregestational diabetes, MS AFP, estriol (E3), and inhibin A levels are reduced. As body weight increases, analyte levels decrease. In smokers, MS AFP and inhibin A levels are higher, while E3 and hCG levels are lower. An algorithm for detecting Down syndrome is shown together with that for NTD in Figure 26.9.

Several strategies incorporating the results of first- and second-trimester screening have been proposed by ACOG. The highest sensitivity rate with the lowest false-positive rates is achieved by using integrated first- and second-trimester screening with a detection rate of 94% to 96% and a 5% false-positive rate (Malone et al., 2005). Cell free fetal DNA can identify approximately 98% of cases of Down syndrome with a false-positive rate of less than 0.5% (ACOG, 2012). Results of the first- and second-trimester screening are reported to the patient after first- and second-trimester screening is completed. Those found to have increased risk of aneuploidy should be offered amniocentesis. With another approach, called *sequential screening*, the patient is informed about first-trimester results. Early diagnostic testing (chorionic villous sampling) is offered after a positive result, whereas patients with negative results may undergo additional second-trimester screening and may benefit from its higher sensitivity. The advantage of integrated and sequential screening is a lower false-positive rate that leads to fewer diagnostic procedures. Additionally, all patients who elected to have only first-trimester screening for chromosomal abnormalities should undergo neural tube defect screening in the second trimester (ACOG, 2007).

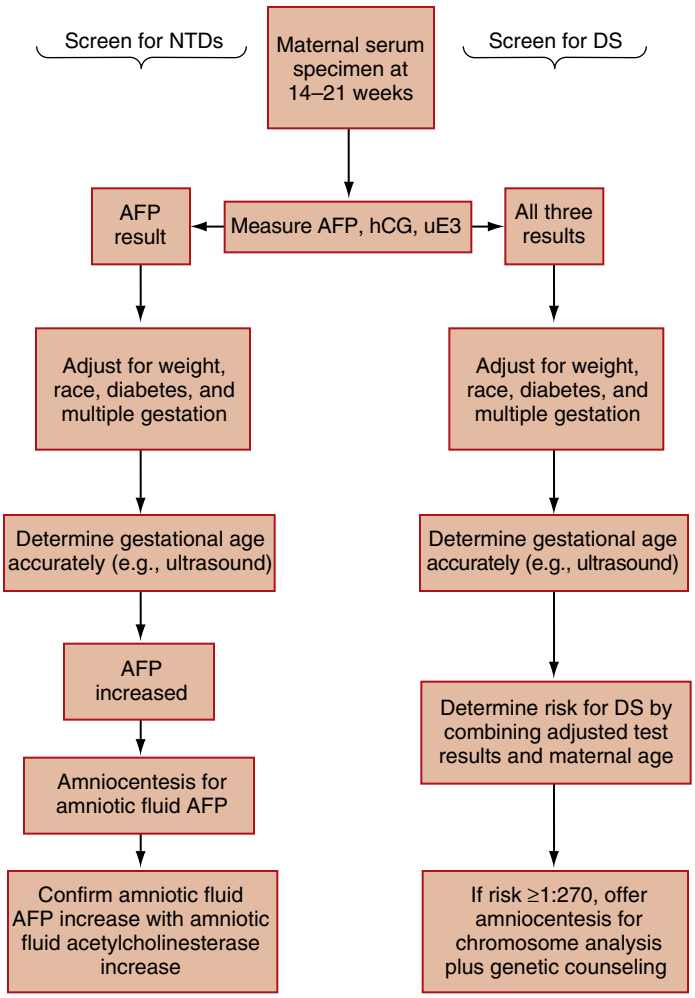

Figure 26.9 A diagnostic algorithm for the simultaneous screening of fetuses for neural tube defects (NTDs) and Down syndrome (DS). *AFP,* α-Fetoprotein; *hCG,* human chorionic gonadotropin; *uE3,* unconjugated estriol.

ERYTHROBLASTOSIS FETALIS

Severe hemolytic disease in a fetus is marked by anemia accompanied by normoblastic hyperplasia (erythroblastosis) and may be followed by congestive heart failure (hydrops) and intrauterine death. The role of transfusion medicine in the management of immunized (sensitized) RhO-negative mothers is reviewed in Chapter 37. Detection of fetal blood in maternal circulation has conventionally been identified by Kleihauer-Betke testing in the setting of incompatibility (i.e., Rh-negative mother carrying an Rh-positive fetus). However, flow cytometry has been reported as an effective alternative in this regard (Kim & Makar, 2012).

Hemoglobin (Hb), released by hemolysis, is catabolized to unconjugated bilirubin. A fetus with hemolytic disease does not develop hyperbilirubinemia or become jaundiced because the placenta normally removes the bilirubin. However, some bilirubin appears in the amniotic fluid. The measurement of amniotic fluid bilirubin levels using spectral analysis at 450 nm (ΔOD_{450}) was introduced to clinical practice by Liley in 1961 and has been the accepted method of assessing the severity of erythroblastosis in utero. This has been predominantly replaced by assessing MCA Doppler responses for fetal anemia as a screening test first and, in the rare event that confirmation is needed, the Liley test is utilized. Bilirubin absorbs light maximally at a wavelength of 450 nm and imparts a yellow color to AF. Some of the absorbance at this wavelength is due to Hb. Both bilirubin and Hb can be maternal and fetal in origin; thus, pigmentation will not discriminate between a hemolytic process in the mother and one in the child.

In erythroblastosis, the net absorbance of light at 450 nm (A or ΔOD) due to bilirubin correlates with the severity of anemia (or hemolytic rate). Bilirubin is bound to albumin; its concentration is dependent on the turnover of the protein, and its concentration in AF does not change rapidly. To determine whether the net bilirubin concentration in amniotic fluid is elevated, a specimen of AF (5 mL) is collected, protected from light, and centrifuged or filtered. Light absorbance of the AF is scanned continuously between wavelengths of 350 nm and 700 nm. The resulting spectrophotometric curve can be used to determine whether the fluid contains bilirubin and/or other pigmented products of hemolysis and to quantify the bilirubin pigment that is present as follows.

Because the absorbance at 450 nm is due to both bilirubin and Hb, if hemolysis occurs, both of these molecules will be elevated in concentration above the background values for their combined absorbance at 450 nm. To determine whether the bilirubin in AF is elevated, both background absorbances at 450 nm must be determined, and the contribution of Hb must also be computed.

To determine the background absorbance of the AF (i.e., what the absorbance would have been with no hemolysis and hyperbilirubinemia), a straight line is drawn between the two absorbances from the scan—at 350 nm and 700 nm. Absorbances at these two wavelengths are not affected by bilirubin or Hb, and, in normal AF, absorbance changes linearly with wavelengths between 350 and 700 nm. The absorbance from the straight line at 450 nm is therefore subtracted as the background value from the observed absorbance at 450 nm. This net absorbance still contains a contribution from Hb.

To correct for Hb absorbance, use is made of the fact that Hb uniquely absorbs at 410 nm—a wavelength at which bilirubin does not absorb. From scans of the absorbance of Hb versus wavelength, it is known that the absorbance of Hb at 450 nm is 0.05 of its absorbance at 410 nm. Thus, by knowing the net absorbance of Hb at 410 nm, its absorbance at 450 nm can be calculated as 0.05 × absorbance at 410 nm. To obtain the net absorbance of Hb at 410 nm, the background absorbance at 410 nm must be subtracted from the observed absorbance. This value, similar to the one at 450 nm, is obtained from the straight line drawn between the absorbances at 350 and 700 nm. The net absorbance at 410 nm is then multiplied by 0.05 to obtain the Hb contribution at 450 nm. The resulting value is subtracted from the net absorbance at 450 nm to obtain the net absorbance of bilirubin in AF. These computations may be summarized in the following equation:

$$A_{Bili450} = (A_{450} - A_{450background}) - 0.05\,(A_{410} - A_{410background}),$$

where the background values are determined from the straight line between 350 nm and 700 nm, as described previously.

The net bilirubin absorbance is recorded on a Liley graph (Fig. 26.10), which denotes weeks of gestation on the linear abscissa and net absorbance on the log scale ordinate (Ashwood, 1999). Spectrophotometry of aspirated fluid is most accurate after 26 to 28 weeks. Net absorbance at 450 nm decreases as the duration of an unaffected pregnancy increases after 28 weeks (before 26 weeks, background absorbance is relatively constant). Decreasing absorbance reflects fluid dilution by fetal urine and accounts for the negative slopes of lines demarcating Liley's prediction zones (lower = zone 1, mid = zone 2, upper = zone 3) for mild, moderate, and severe hemolysis, respectively, as shown in Figure 26.10. The greater the net absorbance at 450 nm, the greater the hemolysis. Although Liley's method originally applied only to the third trimester of pregnancy, a modified curve for the second trimester has been proposed by Queenan and colleagues (1993) and involves four zones instead of three (see Fig. 26.10). Serial testing (every 14 days or less often) allows for trending of net absorbance values.

Trends are usually unidirectional, either paralleling the negatively sloped lines on Liley's graph or showing a positive slope. A rising or plateauing trend of ΔOD_{450} values that reaches the 80th percentile of zone 2 on the Liley curve or enters the intrauterine transfusion zone of the Queenan curve necessitates investigation by fetal blood sampling. Cordocentesis is performed with blood readied for intrauterine transfusion if the fetal hematocrit is found to be less than 30%, or delivery is indicated if gestational age is 35 weeks or greater. If no rise in ΔOD_{450} values is detected, the last amniocentesis should be performed at 37 weeks with testing for fetal lung maturity and anticipated induction of labor (Moise, 2002).

Maternal and fetal acid-base imbalances can alter AF pH and shift the wavelengths of pigment absorbance maxima. Pigments that may be present other than bilirubin and that may affect the results include Hb, methemalbumin, and meconium. Each produces a characteristic spectrophotometric effect. Blood contamination (with interference by hemolysis) is encountered frequently. Less often, in vivo maternal jaundice or hemolysis can cause misinterpretation. The presence of fetal red cells in AF indicates worsening of anemia by blood loss, or it may explain a rise in maternal antibody titer (anamnestic response to a new fetomaternal hemorrhage), development of new antibodies, and subsequent increase in the net absorbance of AF at 450 nm. Exposure of AF to light and maternal use of steroids, markedly increased AF Hb concentration, or poor calibration of a spectrophotometer may cause inaccurate net absorbance measurements.

The current trend in the management of Rh immunization is the use of Doppler measurements of peak systolic velocity in the fetal middle cerebral artery (MCA). This has proved to be an accurate noninvasive method of assessing and monitoring the degree of fetal anemia in pregnancies complicated by Rh immunization (ACOG, 2006a). Based on one study, a value above 1.5 MoM for gestational age detects all cases of anemia, with a false-positive rate of only 12% (Mari et al., 2000). A rise in peak velocity of fetal MCA greater than 1.5 MoM is an indication for fetal blood sampling. If Doppler measurements were used as the method of fetal monitoring during pregnancy, ΔOD_{450} spectrophotometry with fetal lung maturity testing should be considered after 35 weeks to assess fetal status, because higher false-positive rates have been reported with determination of MCA blood flow after 35 weeks' gestation, followed by induction of labor at 37 to 38 weeks (Moise, 2002).

GESTATIONAL DIABETES

Any glucose intolerance in a pregnant woman is termed gestational diabetes (see Chapter 17) regardless of the state of glucose tolerance antepartum or postpartum. Prompt diagnosis and treatment of gestational diabetes may help to avoid maternal and fetal complications such as preeclampsia, fetal congenital malformation, fetal macrosomia (abnormally large body size), and fetal demise. In addition, for a patient who is a known diabetic, an HbA_{1c} level assessment should be ordered preconception and maintained at a level of 6.0% or below for healthy pregnancy outcomes.

FETAL LUNG MATURITY

Fetal lung maturation is marked by production of surface-active phospholipid compounds called *surfactant*. The presence of surfactant decreases

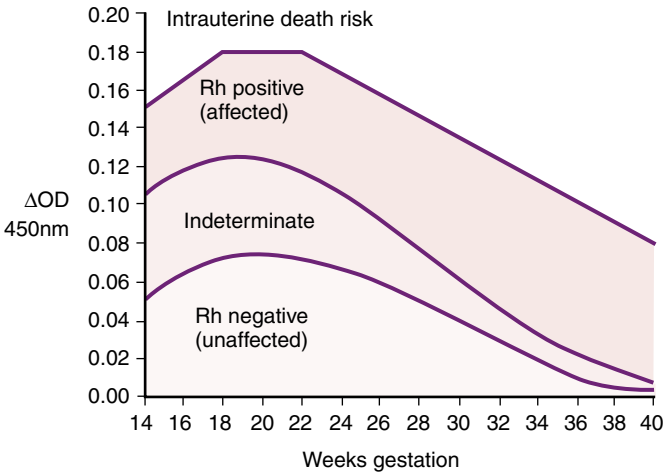

Figure 26.10 Graph for interpretation of net absorbance at 450 nm of amniotic fluid. The four zones are indicative of the relative level of fetal hemolytic disease. (From Queenan JT, Tomai TP, Ural SH, et al.: Deviation in amniotic fluid optical density [OD] at a wavelength of 450nm in Rh-immunized pregnancies from 14–40 weeks gestation: A proposal for clinical management, *Am J Obstet Gynecol* 168:1370–1376, 1993, with permission.)

surface tension within the alveolar space during inspiration, allows continuous and effective gas exchange, and prevents alveolar collapse during expiration. It is produced by type II pneumocytes in the form of lamellar bodies. Deficiency of surfactant leads to neonatal respiratory distress syndrome (RDS), a disorder that results in hypoxia, acidemia, and vascular protein transudation into alveolar air spaces (hyaline membrane disease). Fetal lung maturity testing should be performed before scheduled delivery at less than 39 weeks and uncertain gestational age. It is contraindicated when delivery is necessary for maternal or fetal indications, or before 32 weeks, when most results show immaturity (ACOG, 2008). Although exogenous surfactant is available for prophylaxis and therapy in newborn RDS, the incidence and severity of the disease can be prevented by maternal antenatal steroid administration to enhance fetal lung maturity.

In the third trimester, fetal respiratory activity allows the passage of surfactant into amniotic fluid, and its quantity may be evaluated using tests of amniotic fluid samples. Before 35 weeks' gestation, the major component of surfactant is α-palmitic β-myristic lecithin. After that time, dipalmitic lecithin predominates, and phosphatidyl glycerol (PG) appears about a week later. PG increases until term and maintains alveolar stability. Minor phospholipid components of surfactant include phosphatidyl inositol, phosphatidyl ethanolamine, phosphatidyl serine, and sphingomyelins. The concentrations of components of surfactant are determined by biochemical tests that measure the PG presence and the lecithin/sphingomyelin ratio. Biophysical tests, such as fluorescence polarization, lamellar body counts, foam stability index, and optical density, use the surface-active properties of the phospholipids. The lecithin/sphingomyelin (L/S) ratio test was the first practical chemical test to assess fetal pulmonary status (Gluck et al., 1971). It estimates the ratio of lecithin to sphingomyelin in amniotic fluid. Concentrations of sphingomyelin remain constant throughout the pregnancy, and levels of lecithin are increasing. Following extraction and purification with solvents, amniotic fluid surfactant lipids are chromatographed on thin-layer silica (see Chapter 26 for discussion of this technique). The phospholipids are made visible by heat charring or staining. Densitometric quantification determines the L/S ratio. L/S ratios greater than 2.0 usually indicate maturity; ratios less than 1.5 indicate immaturity. In the presence of newer tests, assessment of L/S ratios becomes less cost-effective with longer turnaround time; hence, it is of importance only if the lamellar body count is shown to be immature. It uses the standard hematologic counter to establish lamellar body concentrations. The most commonly accepted cutoffs with high negative predictive value for RDS are 50,000 or higher. Some believe that the test is unsatisfactory in diabetic women, in whose neonates RDS can occur when L/S ratios are greater than 2.0 (Dubin, 1992).

The presence of PG on the thin-layer chromatogram, in addition to an L/S ratio greater than 2.0, indicates fetal pulmonary maturity with virtual certainty in any patient. The presence of PG can be determined using a newer slide agglutination test with antisera specific to PG.

Overall, the following factors may affect fetal lung maturity tests:

1. Blood contamination appears to increase the number of false-positive test results (Carlan et al., 1997), except for those using PG presence.
2. Meconium does not affect lamellar body counts and determination of PG.
3. Amniotic fluid volumes: L/S ratios, lamellar body counts, and PG levels are lower in polyhydramnios (Piazze et al., 1998).
4. Diabetes mellitus: Studies have shown delayed production of PG in the fetuses of pregnant women with diabetes; however, the same thresholds apply to pregnancies of diabetic and nondiabetic women (Melanson et al., 2007). Recent guidance by ACOG, though, states that amniocentesis for the purpose of fetal lung maturity testing—including L/S ratio, PG, disaturated lecithin, and lamellar body count—no longer have clinical utility and are not recommended (Johnson et al., 2019). Rather, the decision to deliver should be more broadly based on multiple maternal and fetal parameters, and not just the fetal lung status.
5. Method of collection of AF: Comparing the AF collected vaginally with that collected by amniocentesis shows whether results of fluid collected vaginally are mature. The test is more reliable (Edwards et al., 2000).

Comparison of previous tests in many studies has shown similar characteristics, with high sensitivity between 81% and 92%, and typical negative predictive value from 95% to 100% (Neerhof et al., 2001; Winn-McMillan & Karon, 2005; Haymond et al., 2006).

PREECLAMPSIA

Preeclampsia is a syndrome characterized by hypertension of 140 mm Hg or greater systolic or 90 mm Hg or greater diastolic on two separate occasions four hours apart, or 160 mm Hg or greater systolic or 110 mm Hg or greater diastolic minutes apart. In addition, proteinuria greater than 0.3 g/L in a 24-hour urine specimen that occurs after 20 weeks' gestation in previously normotensive women, protein/creatinine ratio greater than or equal to 0.3, or urine protein dipstick of +1 when other resources are unavailable (National High Blood Pressure Education Program Working Group, 2000; ACOG, 2013) is diagnostic. If there is an absence of proteinuria, then the presence of new-onset elevation of BP along with (1) thrombocytopenia of 100,000/μL or less, (2) renal insufficiency defined as serum creatinine of 1.1 mg/dL or doubling of serum creatinine in the absence of other renal disease, (3) elevated liver aminotransferases of twice the normal concentrations, (4) pulmonary edema, or (5) cerebral or visual defects is diagnostic.

The incidence of preeclampsia is 5% to 8% of all pregnant women. Preconceptional risk factors associated with preeclampsia include first pregnancy, chronic hypertension, renal disease, antiphospholipid syndrome, diabetes, obesity, advanced maternal age, thrombophilia, partner who fathered preeclamptic pregnancy in another woman, and history of preeclampsia in previous pregnancies.

Conditions that can mimic preeclampsia include systemic lupus erythematosus, idiopathic thrombocytopenic purpura, thrombotic thrombocytopenic purpura, hemolytic-uremic syndrome, cholestasis of pregnancy, and fatty liver disease (Sibai, 2004).

Life-threatening manifestations of preeclampsia that remain a cause of maternal mortality are eclampsia and HELLP syndrome (hemolytic anemia, elevated liver enzymes, low platelet count). Eclampsia, which is defined as new-onset grand mal seizures in women with preeclampsia, may result in intracranial hemorrhage.

The cause of preeclampsia remains unknown. Pathophysiologic abnormalities include abnormal trophoblastic invasion by the placenta, resulting from an imbalance between proangiogenic and angiogenic factors (Barton & Sibai, 2008). Impaired uteroplacental flow causes intrauterine growth restriction, oligohydramnios, and placental abruption (abruptio placenta). The interaction of various vasoactive agents—such as prostacyclin, thromboxane A_2, nitric oxide, and endothelins—causes the vasospasm that leads to depleted intravascular volume and hepatic and renal changes. Hematologic changes usually are seen as hemoconcentration, thrombocytopenia, and hemolysis. Hepatic involvement manifests as elevation of aminotransferases, usually twice above the normal limit. Lactate dehydrogenase (LD) is increased primarily because of hepatic disease (mostly LD_5) or as the result of hemolysis with increases in LD_1 and LD_2. Hyperbilirubinemia occurs in the presence of hemolysis as well. The proteinuria in preeclampsia is of a glomerular type (mostly albumin), and the urine sediment contains hyaline and finely granular casts. Mild to moderate increases in urea and creatinine are noted, as is a marked increase in uric acid.

Preeclampsia or gestational hypertension with severe features is diagnosed if one or more of these criteria are met: blood pressure systolic of 160 or greater, diastolic of 110 or greater, proteinuria of 5 g or higher in a 24-hour urine specimen, oliguria (<500 mL/24 hours), cerebral or visual disturbances, pulmonary edema, right upper quadrant pain, impaired liver function, thrombocytopenia (<100 K/μL), or fetal growth restriction (ACOG, 2013).

In the past decade, many biophysical and biochemical markers have been proposed to predict which women are likely to develop preeclampsia, but none of the screening tests has been found to be reliable and cost-effective. Several studies have analyzed the levels of angiogenic factors in preeclampsia. Results revealed decreased levels of placental growth factor, placental protein-13, and pregnancy-associated plasma protein A, along with elevation of fms-like tyrosine kinase-1, endoglin (a transmembrane receptor that is vital for angiogenesis), and dimethylarginine (a marker for atherosclerotic heart disease) (Levine et al., 2006). However, because of differences in study design and methods of analysis, these markers have poor predictive value and specificity. A more promising test is Doppler velocimetry of the uterine arteries (Espinoza et al., 2007).

Preeclampsia can be managed expectantly and followed by delivery at 37 weeks. Delivery at any gestational age is indicated for eclampsia, HELLP, placental abruption, nonreassuring fetal heart pattern, pulmonary edema, severe hypertension, worsening of renal function, persistent symptoms of headaches, visual disturbances, and epigastric pain.

PREMATURE RUPTURE OF MEMBRANES

Premature rupture of membranes is rupture of membranes before the onset of labor. It may be followed by a variety of complications, including chorioamnionitis, fetal pulmonary hypoplasia, placental abruption, and neonatal respiratory distress. The diagnosis of membrane rupture is made upon visualization of fluid passing from the cervical canal on the sterile

speculum examination. Amniotic fluid constitutes part of the posterior vaginal fluid pool; identification of the amniotic component is optimally carried out within 2 hours of membrane rupture. Unlike vaginal secretions, whose pH is acidic (pH, 4.5–5.5), amniotic fluid is alkaline, with pH of 7.0 to 7.5. The vaginal pool aspirate can be tested with nitrazine paper to estimate pH visually. A positive test is indicated by a blue color and a negative one by a yellow-green color. Among false-positives, 5% are related to the presence of blood, mucus, semen, bacterial vaginosis, alkaline urine, or soap. False-negatives are less likely (1%) but may be seen with membrane rupture that occurred more than 24 hours earlier or if sampling was inadequate. The nitrazine test is usually performed at the bedside and is said to have an overall accuracy of about 90% in the absence of bloody show, vaginal discharge, or prolonged membrane rupture (Friedman & McElin, 1969). An aliquot of the aspirated fluid can be applied to a glass microscope slide, dried for 5 minutes, and examined microscopically for arborization (ferning), which indicates the presence of amniotic fluid in the vaginal fluid pool. False-positive ferning occurs in less than 2% of cases and is associated with the presence of blood, urine, or cervical mucus. False-negatives occur in less than 5% of cases. An alternative method for detecting amniotic fluid in vaginal secretions is rapid immunoassay of proteins present in amniotic fluid. A test for placental α-1 microglobulin is currently marketed as the AmniSure test (Qiagen, Hilden, Germany), whereas a test for AFP and placental protein 12 is marketed as ROM Plus (Clinical Innovations, Murray, UT).

PRETERM LABOR

Numerous biochemical markers and biophysical tools have been evaluated for predicting preterm delivery. In 1991, Lockwood and colleagues discovered an association between the presence of fetal fibronectin (fFN) in cervical secretions and the risk of preterm delivery. fFN is a glycoprotein produced by fetal membranes found in the choriodecidual junction amniotic fluid. It is released as cervical secretions at up to 20 weeks' gestation. It has been identified in malignant cell lines and is recognized by antibody FDC-6 (Lockwood et al., 1991). Fibronectin is responsible for the cellular adhesiveness of placenta and membranes to the decidua. Disruption of the chorion from the decidual layer of the uterus leads to the release of intact or degraded chorionic components of the extracellular matrix into the cervical and vaginal secretions. The fFN enzyme immunoassay is a U.S. Food and Drug Administration–approved test for assessment of the risk for preterm delivery in women between 24 and 35 weeks' gestation. The purposes of the test are to identify asymptomatic women who are at risk for preterm delivery and to predict the risk of delivery in symptomatic women with preterm contractions. The specimen is collected during sterile speculum examination with a swab from the posterior fornix of the vagina or the region of the external cervical os for 10 seconds. Concentrations of fFN in the cervicovaginal fluid greater than 50 ng/mL are considered positive (Garite & Lockwood, 1996). The swab should be performed before procedures that may disrupt the cervix, such as the digital examination, Papanicolaou smear, cervical culture, and vaginal ultrasound. The following criteria should be met: cervical dilation less than 3 cm, intact membranes, absence of uterine bleeding, sexual intercourse more than 24 hours before, and absence of cervical cerclage. A meta-analysis of many studies on patients with symptoms suggestive of preterm labor showed that cervicovaginal fFN is an effective predictor of preterm delivery (Leitich et al., 1999). Testing for fFN can reduce unnecessary hospitalization and avoid intervention in symptomatic pregnant women. Detection of fFN can also help in the management of pregnancy in asymptomatic women who have known risk factors for preterm labor, such as previous preterm delivery or short cervix.

It appears to be most valuable in ruling out imminent delivery in patients with symptoms with negative predictive values for delivery within 7, within 14, and at less than 37 weeks (99.5%, 99.2%, and 84.5%, respectively) (Peaceman et al., 1997). The test is often performed with sonographic assessment of cervical length. An fFN test has limited application for screening of asymptomatic women and those with no risk factors because of the low incidence of preterm labor in this population (Leitich et al., 1999). Currently, it is used in conjunction with cervical length; when the cervical length is less than 20 mm, fFN is the more indicative test.

INTRAPARTUM ASSESSMENT OF FETAL STATUS

The goal of intrapartum fetal surveillance is to recognize whether the fetus with a nonreassuring fetal heart tracing on external monitoring is acidotic and at risk for neurologic impairment or death. Usually, episodes of hypoxemia are transient and well tolerated by the fetus. However, prolonged or repeat episodes may lead to hypoxic-ischemic encephalopathy. Available tests can help to ensure fetal well-being and reduce false-positive findings on external fetal heart monitoring. Noninvasive and preferred tests, such as digital scalp stimulation and vibroacoustic stimulation of the fetus, followed by the presence of reassuring fetal heart monitoring, indicate that the fetus is not acidotic. The direct method for evaluation of fetal acid-base status is fetal scalp blood sampling. This test is performed using the amnioscope with a light source; blood is collected from a punctured fetal scalp and is transferred in a heparinized capillary tube. A pH value of less than 7.20 identifies fetal acidosis. However, the test has low sensitivity (36%) and poor predictive value (9%) in predicting fetal acidemia of pH less than 7.0 (Kruger et al., 1999). The use of fetal scalp pH assessment is decreasing in many institutions because of the difficulty involved in obtaining and processing samples and in obtaining standardized laboratory equipment.

Another method of predicting fetal acidosis involves the measurement of fetal lactate concentrations with the use of rapid enzymatic assays. Blood samples are collected by using techniques similar to those used in fetal scalp pH. A large multicenter, randomized trial compared the effectiveness of pH analysis of fetal scalp blood versus use of lactate levels in identifying hypoxia at birth and showed no differences between the two groups in obstetric and neonatal outcomes (Wiberg-Itzel et al., 2008).

The most objective tool for determining intrapartum fetal status and obtaining information related to obstetric management is umbilical cord sampling. Immediately after delivery, arterial blood is drawn from a segment of clamped umbilical cord to a heparinized capillary syringe and is analyzed for cord blood pH and blood gas values. ACOG (2006b) recommends analysis of umbilical cord blood in neonates with low Apgar scores to differentiate hypoxia from metabolic acidemia and other causes of low Apgar scores. Significant metabolic acidosis is defined by umbilical cord blood pH values of less than 7.0; base deficits of 12 mmol/L or greater are predictive of adverse neurologic outcomes and are included in the criteria for an acute intrapartum hypoxic event.

OTHER EVALUATIONS

Infection During Pregnancy

Viral, bacterial, and parasitic infections can have a significant impact on the mother, fetus, or both. Important examples are human immunodeficiency virus, hepatitis virus (A, B, and C), rubella virus, varicella virus, parvovirus B19, cytomegalovirus, *Chlamydia trachomatis*, group B *Streptococcus*, *Neisseria gonorrhoeae*, syphilis, tuberculosis, toxoplasmosis, and malaria. These are discussed in Part 7 of this text.

Hematologic and Coagulation Disorders

Various disorders can have a negative effect on mother, fetus, or both, including maternal anemias (nutritional, sickle cell), maternal and fetal thrombocytopenias (idiopathic thrombocytopenic purpura, fetal alloimmune thrombocytopenia, thrombotic thrombocytopenic purpura), maternal coagulopathies (acute disseminated intravascular coagulation, von Willebrand disease), and maternal thrombophilias. These are described in Parts 4 and 5.

Testosterone Replacement Therapy

Unique categories of medicine are continuously emerging to address specific needs. One such category falls under the rubric of "Life Extension" and includes testosterone replacement therapy (TRT). As sildenafil (Viagra) has captured a significant market share for patients with erectile dysfunction (ED), so too is TRT maturing to address deficiencies in male-related health care. Testosterone deficiency has been purported to be etiologically responsible for male depression, cardiovascular risk, fatigue, cognition, vitality, metabolism, as well as ED (Kovak, 2014; Yeap, 2015; Hua, 2016; Hui, 2019). To this end, TRT clinics have been opening to provide diagnosis and treatment for testosterone-deficient men; however, their services are not covered by insurance. The determination that TRT is needed is made based on conventional criteria from the American Urological Society Guidelines (Mulhall, 2018) and the Endocrine Society Clinical Practice Guidelines (Bhasin, 2018) and includes total testosterone levels below 300 ng/mL on two separate morning blood draws. A low testosterone level would prompt assessment of LH levels. A low or low/normal LH level points to a secondary (central) hypothalamic-pituitary defect (hypogonadotropic hypogonadism), while an elevated LH level indicates a primary testicular defect (hypergonadotropic hypogonadism) (Bhasin, 2010). Additional diagnostic algorithms also include testing for levels of prostate-specific antigen, PRL,

free testosterone, HbA_{1c}, SHBG, estradiol, and FSH (Mulhall, 2018). Further, hematocrit determinations are required since TRT can be associated with polycythemia. While certain reports show that TRT is safe and does not promote increased incidence of prostate cancer and that any increased risk of thromboembolism occurs in patients with underlying coagulation issues (thrombophilia) rather that general elevated hematocrit, other studies suggest that TRT can increase the risk of such negative events (Mulhall, 2018; Houghton, 2018). Future studies are needed to better understand the risk-benefit ratio and clinical implementation of TRT in the male population.

SELECTED REFERENCES

Ashwood ER: Clinical chemistry of pregnancy. In Burtis CA, Ashwood ER, editors: *Tietz textbook of clinical chemistry*, ed 3, Philadelphia, 1999, WB Saunders.

This overview includes detailed descriptions of amniotic fluid spectrophotometry of bilirubin for erythroblastosis fetalis (Liley's test).

Mortimer D: *Practical laboratory andrology*, New York, 1994, Oxford University Press.

Descriptive guide and reference for clinical evaluation of reproductive function in the male.

Speroff L, Fritz Marc A: *Clinical gynecologic endocrinology and infertility*, ed 8, Philadelphia, 2010, Lippincott Williams & Wilkins.

General reference for female reproductive endocrinology and ART.

Strauss JF, Barbieri RL, editors: *Yen and Jaffe's reproductive endocrinology*, ed 7, Philadelphia, 2013, WB Saunders.

Comprehensive reference for all aspects of reproductive function and pregnancy.

Trounson AO, Gardner DK: *Handbook of in vitro fertilization*, ed 2, Boca Raton, FL, 2000, CRC Press.

General reference for ARTs.

Willett GD, editor: *Laboratory testing in ob/gyn*, Boston, 1994, Blackwell Scientific Publications.

Comprehensive and concise summary of laboratory evaluation of the female.

Access the complete reference list online at Elsevier eBooks for Practicing Clinicians.

REFERENCES

ACOG (American College of Obstetricians and Gynecologists): Neural tube defects. ACOG practice bulletin No. 187, *Obstet Gynecol* 130(6):e279–e290, 2017.

ACOG (American College of Obstetricians and Gynecologists): *Prevention of Rh D alloimmunization. ACOG practice bulletin No. 75*, Washington, DC, 2006a, ACOG (reaffirmed 2014).

ACOG (American College of Obstetricians and Gynecologists): Umbilical cord blood gas and acid-base analysis. ACOG Committee Opinion No. 348, *Obstet Gynecol* 108:1319–1322, 2006b.

ACOG (American College of Obstetricians and Gynecologists): Screening for fetal chromosomal abnormalities. ACOG practice bulletin No. 77, *Obstet Gynecol* 109:217–227, 2007 (reaffirmed 2013).

ACOG (American College of Obstetricians and Gynecologists): Fetal lung maturity. ACOG practice bulletin No. 97, *Obstet Gynecol* 112:717–726, 2008.

ACOG (American College of Obstetricians and Gynecologists): Hypertension in pregnancy. ACOG Task Force, *Obstet Gynecol* 122(5), 2013.

ACOG (American College of Obstetricians and Gynecologists): Noninvasive prenatal testing for fetal aneuploidy. ACOG Committee Opinion No. 545, *Obstet Gynecol* 120:1532–1534, 2012.

Andrade-Rocha FT: Semen analysis in laboratory practice: an overview of routine tests, *J Clin Lab Anal* 17:247–258, 2003.

Barnhart KT, Sammel MD, Rinaudo PF, et al.: Symptomatic patients with an early viable intrauterine pregnancy: HCG curves redefined, *Obstet Gynecol* 104:50–55, 2004.

Barton JR, Sibai BM: Prediction and prevention of recurrent preeclampsia, *Obstet Gynecol* 112:359–372, 2008.

Besser GM, Thorner MO: *Comprehensive clinical endocrinology*, ed 3, Edinburgh, 2002, Mosby.

Bhasin S, Cunningham GR, Hayes FJ, et al.: Testosterone therapy in men with androgen deficiency syndromes: an endocrine society clinical practice guideline, *J Clin Endocrinol Metab* 95:2536, 2010.

Bhasin S, Brito JP, Cunningham GR, et al.: Testosterone therapy in men with hypogonadism: an endocrine society clinical practice guideline, *J Clin Endocrinol Metab* 103(5):1715–1744, 2018, https://doi.org/10.1210/jc.2018-00229.

Braunstein GD: Testes. In Greenspan FS, Gardner DG, editors: *Basic and clinical endocrinology*, ed 7, New York, 2004, Lange Medical Books/McGraw-Hill, pp 478–510.

Brock DJ, Bolton AE, Scringeour RA: Prenatal diagnosis of spina bifida and anencephaly through maternal plasma α-fetoprotein, *Lancet* 767–769, 1974. i.

Burton BK: Outcome of pregnancy in patients with unexplained elevated or low levels of maternal serum α-fetoprotein, *Obstet Gynecol* 72:709–713, 1988.

Buyalos RP, Ghosh K, Daneshmand ST: Infertile women of advanced reproductive age: variability of day 3 FSH and E2 levels, *J Reprod Med* 43:1023–1026, 1998.

Carlan SJ, Gearity D, O'Brien WF: The effect of maternal blood contamination on the TDx-FLM II assay, *Am J Perinatol* 14:491–494, 1997.

Carr BR, Rehman KS: Fertilization, implantation, and endocrinology of pregnancy. In Griffin JE, Ojeda SR, editors: *Textbook of endocrine physiology*, ed 5, New York, 2004, Oxford University Press, pp 249–273.

Chamley LW, Clarke GN: Antisperm antibodies and conception, *Semin Immunopathol* 29:169–184, 2007.

Dubin S: Assessment of fetal lung maturity by laboratory methods, *Clin Lab Med* 12:603, 1992.

Dumont A, et al.: Role of anti-Müllerian hormone in pathophysiology, diagnosis and treatment of polycystic ovary syndrome: a review, *Reprod Biol Endocrinol: RBE (Rev Bras Entomol)* 13:137, 2015, https://doi.org/10.1186/s12958-015-0134-9.

Edwards RK, Duff P, Ross KC: Amniotic fluid indices of fetal pulmonary maturity with preterm premature rupture of membranes, *Obstet Gynecol* 96:102–105, 2000.

Espinoza J, Romero R, Nien JK, et al.: Identification of patients at risk for early onset and/or severe preeclampsia with the use of uterine artery Doppler velocimetry and placental growth factor, *Am J Obstet Gynecol* 196:326, 2007.

Feuchtbaum LB, Currier RJ, Riggle S, et al.: Neural tube defect prevalence in California (1990–1994): Eliciting patterns by type of defect and maternal race/ethnicity, *Genet Test* 3:265–272, 1999.

Friedman ML, McElin TW: Diagnosis of ruptured fetal membranes: clinical study and review of the literature, *Am J Obstet Gynecol* 104:544–550, 1969.

Garite TJ, Lockwood CJ: Fetal fibronectin (fFN): a new test for diagnosis and prediction of impending preterm delivery, *Contemp Obstet Gynecol* 41:77–93, 1996.

Gilbert BR, Cooper GW, Goldstein M: Semen analysis in the evaluation of male factor subfertility, *AUA Update Series* 11:250–255, 1992.

Gluck L, Kulovich MV, Borer R, et al.: Diagnosis of the respiratory distress syndrome by amniocentesis, *Am J Obstet Gynecol* 109:440–445, 1971.

Goldstein SR, Snyder JR, Watson C, et al.: Very early pregnancy detection with endovaginal ultrasound, *Obstet Gynecol* 72:200–204, 1988.

Haymond S, Luzzi VI, Parvin CA, et al.: A direct comparison between lamellar body counts and fluorescent polarization methods for predicting respiratory distress syndrome, *Am J Clin Pathol* 126:894–899, 2006.

Houghton DE, Alsawas M, Barrioneuvo P, et al.: Testosterone therapy and venous thromboembolism: a systematic review and meta-analysis, *Thromb Res* 172:94–103, 2018. Epub 2018 Oct 28. https://doi.org/10.1016/j.thromres.2018.10.023.

Hua JT, Kerry L, Hildreth KL, Pelak VS: Effects of testosterone therapy on cognitive function in aging: a systematic review, *Cogn Behav Neurol* 29, 2016. 122–113.

Hui J, He S, Liu R, Zeng Q, Zhang H, Wei A: Trends in erectile dysfunction research from 2008 to 2018: a bibliometric analysis, *Int J Impot Res*, 2019.

Ismail AA, Astley P, Burr WA, et al.: The role of testosterone measurement in the investigation of androgen disorders, *Ann Clin Biochem* 23:113–134, 1986.

Johnson AM, Palomaki GE, Haddow JE: Maternal serum alpha-fetoprotein levels in pregnancies among black and white women with fetal open spina bifida. A United States Collaborative Study, *Am J Obstet Gynecol* 162:328–331, 1990a.

Johnson LM, Johnson C, Karger AB: End of the line for fetal lung maturity testing, *Clin Biochem* 71:74–76, 2019.

Johnson AM, Palomaki GE, Haddow JE: The effect of adjusting maternal serum α-fetoprotein levels for maternal weight in pregnancies with fetal open spina bifida. A United States Collaborative Study, *Am J Obstet Gynecol* 163:9–11, 1990b.

Kadar N, Bohrer M, Kemmann E, et al.: The discriminatory human chorionic gonadotropin zone for endo-vaginal sonography: a prospective, randomized study, *Fertil Steril* 61:1016–1020, 1994.

Kim YA, Makar RS: Detection of fetomaternal hemorrhage, *Am J Hematol* 87:417–423, 2012.

Koh GH, Yeo GS: Diagnosis of ectopic pregnancy—why we need a protocol, *Singapore Med J* 38:369–374, 1997.

Kovac JR, Pastuszak AW, Lamb DJ, Lipshultz LI: Testosterone supplementation therapy in the treatment of patients with metabolic syndrome, *Postgrad Med* 126(7):149–156, 2014.

Kruger TF, Acosta AA, Simmons KF, et al.: Predictive value of abnormal sperm morphology in in vitro fertilization, *Fertil Steril* 49:112, 1988.

Kruger K, Hallberg B, Blennow M: Predictive value of fetal scalp blood lactate concentration and pH as markers of neurologic disability, *Am J Obstet Gynecol* 181:1072, 1999.

Leitich H, Egarter C, Kaider A, et al.: Cervicovaginal fetal fibronectin as a marker for preterm delivery: a meta-analysis, *Am J Obstet Gynecol* 180:1169–1176, 1999.

Levine RJ, Lam C, Qian C, et al.: Soluble endoglin and other circulating antiangiogenic factors in preeclampsia, *N Engl J Med* 355:992–1005, 2006.

Liley AW: Liquor amnii analysis in the management of pregnancy complicated by rhesus sensitization, *Am J Obstet Gynecol* 82:1359–1370, 1961.

Lobo RA, Mishell DR, Paulson RJ, et al.: In Malden M, editor: *Mishell's textbook of infertility, contraception and reproductive endocrinology*, ed 4, Blackwell Science, 1997.

Lockwood CJ, Senyei AE, Dische MR, et al.: Fetal fibronectin in cervical and vaginal secretions as a predictor of preterm delivery, *N Engl J Med* 325:669–674, 1991.

Malone F, Canick JA, Ball RH, et al.: First-trimester or second-trimester screening, or both, for Down's syndrome. First- and second-trimester evaluation of risk (FASTER) research Consortium, *N Engl J Med* 353:2001–2011, 2005.

Mari G, Deter RL, Carpenter RL, et al.: Noninvasive diagnosis by Doppler ultrasonography of fetal anemia due to maternal red-cell alloimmunization. Collaborative Group for Doppler Assessment of the Blood Velocity of Anemic Fetuses, *N Engl J Med* 342:9–14, 2000.

Melanson SE, Jarolim P, McElrath TF, et al.: Fetal lung maturity testing in diabetic mothers, *Lab Med* 38:553–555, 2007.

Mesiano S, Jaffe RB: The endocrinology of human pregnancy and fetal-placental neuroendocrine development. In Strauss JF, Barbieri RL, editors: *Yen and Jaffe's reproductive endocrinology*, ed 7, Philadelphia, 2013, WB Saunders, pp 327–366.

Milunsky A: Prenatal detection of neural tube defects. VI. Experience with 20,000 pregnancies, *J Am Med Assoc* 244:27–31, 1980.

Moise Jr KJ: Management of rhesus alloimmunization in pregnancy, *Obstet Gynecol* 100:600–611, 2002.

MRC Vitamin Study Research Group: Prevention of neural tube defects: results of the medical research Council Vitamin study, *Lancet* 338:131–137, 1991.

Mulhall JP, Trost LW, Brannigan RE, et al.: Evaluation and management of testosterone deficiency, *AUA Guideline J Urol* 200(2):423–432, 2018. Epub 2018 Mar 28. https://doi.org/10.1016/j.juro.2018.03.115.

Mumford SL, Legro RS, Diamond MP, et al.: Baseline AMH level associated with ovulation following ovulation induction in women with polycystic ovary syndrome, *J Clin Endocrinol Metab* 101:3288-3296, 2016.

National High Blood Pressure Education Program Working Group: Report on high blood pressure in pregnancy, *Am J Obstet Gynecol* 183:S1–S22, 2000.

Neerhof MG, Haney EI, Silver RK, et al.: Lamellar body counts compared with traditional phospholipid analysis as an assay for evaluating fetal lung maturity, *Obstet Gynecol* 97:305–309, 2001.

New York State Department of Health: *Congenital Malformations Registry summary report: Statistical summary of children born in 1983–2007*, 2013. Published.

Norwitz ER: Endocrine diseases of pregnancy. In Strauss JF, Barbieri RL, editors: *Yen and Jaffe's reproductive endocrinology*, ed 7, Philadelphia, 2013, WB Saunders, pp 735–785.

Noyes RW, Hertig AT, Rock J: Dating the endometrial biopsy, *Am J Obstet Gynecol* 122:262–263, 1975.

Norem CT, Schoen EJ, Walton DL, et al.: Routine ultrasonography compared with maternal serum alpha-fetoprotein for neural tube defect screening, *Obstet Gynecol* 106(4):747–752, 2005.

Odell WD, Griffin J: Pulsatile secretion of human chorionic gonadotropin in normal adults, *N Engl J Med* 317:1688–1691, 1987.

Ombelet W, Bosmans E, Janssen M, et al.: Semen parameters in a fertile versus subfertile population: a need for a change in the interpretation of semen testing, *Hum Reprod* 12:987–993, 1997.

Ozturk M, Bellet D, Manil L, et al.: Physiological studies of human chorionic gonadotropin (hCG), αhCG, and βhCG as measured by specific monoclonal immunoradiometric assays, *Endocrinology* 120:549–558, 1987.

Pados G, Camus M, Van Steirteghem A: The evolution and outcome of pregnancies from oocyte donation, *Hum Reprod* 9:538–542, 1994.

Peaceman AM, Andrews WW, Thorp JM, et al.: Fetal fibronectin as a predictor of preterm birth in patients with symptoms: a multicenter trial, *Am J Obstet Gynecol* 177:13–18, 1997.

Pellati D, Mylonakis I, Bertoloni G, et al.: Genital tract infections and infertility, *Eur J Obstet Gynecol Reprod Biol* 140:3–11, 2008.

Piazze JJ, Maranghi L, Cosmi EV, et al.: The effect of polyhydramnios and oligohydramnios on fetal lung maturity indexes, *Am J Perinatol* 15:249–252, 1998.

Pitkin RM: Folate and neural tube defects, *Am J Clin Nutr* 85:285S–288S, 2007.

Queenan JT, Tomai TP, Ural SH, et al.: Deviation in amniotic fluid optical density at a wavelength of 450 nm in Rh-immunized pregnancies from 14-40 weeks gestation: a proposal for clinical management, *Am J Obstet Gynecol* 168:1370–1376, 1993.

Resnik R, Killam AP, Battaglia FC, et al.: The stimulation of uterine blood flow by various estrogens, *Endocrinology* 94:1192, 1974.

Rylander L, Wetterstrand B, Haugen TB, et al.: Single semen analysis as a predictor of semen quality: clinical and epidemiological implications, *Asian J Androl* 11:723–730, 2009.

Saraj AJ, Wilcox JH, Najmabadi S, et al.: Resolution of hormonal markers of ectopic gestation: a randomized trial comparing single-dose intramuscular methotrexate with salpingostomy, *Obstet Gynecol* 92:989–994, 1998.

Sarkar S, Jones OW, Shioura N: Constancy in human sperm DNA content, *Proc Natl Acad Sci U S A* 71:3512–3516, 1974.

Scott RT, Hofmann GE: Prognostic assessment of ovarian reserve, *Fertil Steril* 63:1–11, 1995.

Sibai BM: Imitators of severe preeclampsia/eclampsia, *Clin Perinatol* 31:835–852, 2004.

Sideri M, De Virgiliis G, Guidobono F, et al.: Immunologically undetectable human placental lactogen in a normal pregnancy, *Br J Obstet Gynaecol* 90:771, 1983.

Spencer K, Souter V, Tul N, et al.: A screening program for trisomy 21 at 10-14 weeks using fetal nuchal translucency, maternal serum free beta-human chorionic gonadotropin and pregnancy-associated plasma protein-A, *Ultrasound Obstet Gynecol* 13:231–237, 1999.

Stovall TG, Ling FW, Carson SA, et al.: Serum progesterone and uterine curettage in differential diagnosis of ectopic pregnancy, *Fertil Steril* 57:456–457, 1992.

Strauss JF, Lessey BA: The structure, function, and evaluation of the female reproductive tract. In Strauss JF, Barbieri RL, editors: *Yen and Jaffe's reproductive endocrinology*, ed 7, Philadelphia, 2013, WB Saunders, pp 255–305.

Mumford SL, Legro RS, Diamond MP, et al.: Baseline AMH level associated with ovulation following ovulation induction in women with polycystic ovary syndrome, *J Clin Endocrinol Metabol* 101(Issue 9):3288–3296, 2016, https://doi.org/10.1210/jc.2016-1340.

Tomlinson MJ, Effrossini K, Barratt CR: The diagnostic and prognostic value of traditional semen parameters, *J Androl* 20:588–593, 1999.

Toriello HV, Higgins JV: Occurrence of neural tube defects among first-, second-, and third-degree relatives of probands: results of a United States study, *Am J Med Genet* 15:601–606, 1983.

UK Collaborative: Study on Alpha-Fetoprotein in Relation to Neural Tube Defects: maternal serum alpha-fetoprotein measurement in antenatal screening for anencephaly and spina bifida in early pregnancy, *Lancet*1323–1332, 1977, i.

Van Steirteghem AC, Pados G, Devroey P: Oocyte donation for genetic indications, *Reprod Fertil Dev* 4:681–688, 1992.

Wald NJ, Cuckle H, Brock JH, et al.: Maternal serum alpha-fetoprotein measurement in antenatal screening for anencephaly and spina bifida in early pregnancy, *Lancet* 1(8026):1323–1332, 1977.

Wald NJ, Kennard A, Smith D: First trimester biochemical screening for Down's syndrome, *Ann Med* 26:23–29, 1994.

Wald NJ, Rodeck C, Hackshaw AK, et al.: First and second trimester antenatal screening for Down's syndrome: the results of the Serum, Urine and Ultrasound Screening Study (SURUSS). [published erratum appears in J Med Screen 2006;13:51–2], *J Med Screen* 10:56–60, 2003.

Welt CK, McNicholl DJ, Taylor AE, et al.: Female reproductive aging is marked by decreased secretion of dimeric inhibin, *J Clin Endocrinol Metab* 84:105–111, 1999.

Wiberg-Itzel E, Lipponer C, Norman M, et al.: Determination of pH or lactate in fetal scalp blood in management of intrapartum fetal distress: Randomised controlled multicentre trial, *BMJ* 336:1284–1287, 2008.

Wilcox A, Baird DD, Weinberg CR: Time of implantation of the conceptus and loss of pregnancy, *N Engl J Med* 340:1796–1799, 1999.

Wilcox AJ, Weinberg CR, O'Connor JF, et al.: Incidence of early loss of pregnancy, *N Engl J Med* 319:189–194, 1988.

Winn-McMillan T, Karon BS: Comparison of the TDx-FLM II and lecithin to sphingomyelin ratio assays in predicting fetal lung maturity, *Am J Obstet Gynecol* 193:778–782, 2005.

Wolff H, Panhans A, Stolz W, et al.: Adherence of *Escherichia coli* to sperm: a mannose mediated phenomenon leading to agglutination of sperm and *E* coli, *Fertil Steril* 60:154–158, 1993.

World Health Organization: *WHO laboratory manual for the examination of human semen and sperm–cervical mucus interaction*, London, 1999, Cambridge University Press.

Yeap BB: Testosterone and ill-health in aging men, *Nat Clin Pract Endocrinol Metab* 5:113–121, 2009.

Yeap BB: Testosterone and cardiovascular disease risk, *Curr Opin Endocrinol Diabetes Obes* 22:193–202, 2015.

CHAPTER 27

VITAMINS AND TRACE ELEMENTS

Mariana Markell, Haseeb A. Siddiqi

INTRODUCTION, 441
VITAMINS, 442
Water-Soluble Vitamins, 443
Fat-Soluble Vitamins, 446
TRACE ELEMENTS, 447
Chromium, 448
Cobalt, 449
Copper, 449
Fluoride, 450
Iodine, 450
Iron, 450
Manganese, 451
Molybdenum, 451
Selenium, 451
Zinc, 451
SELECTED REFERENCES, 452

KEY POINTS

- Vitamins and trace elements are grouped because of the very small amount required to satisfy their extensive metabolic activity.
- Vitamins are essential organic substances that the body cannot synthesize or does not consistently synthesize sufficient for the metabolic needs. This is species specific.
- Vitamins may function variously as enzymatic cofactors, antioxidants, or like hormones, and are active in energy metabolism, protein metabolism, blood cell maturation, and bone formation.
- Vitamins may play a key role in chromatin rearrangement and methyl donation underlying epigenetic modification.
- Vitamins are unrelated chemically and have different physiologic activities.
- Vitamins may be single chemicals (e.g., ascorbic acid) or include a family of closely related compounds (e.g., vitamins A, D, E, and K and cobalamin).
- Vitamins may be classified according to water or lipid solubility, which affects absorption and transport, storage, toxicity, excretion, and the disease conditions that cause deficiencies even when there is sufficient nutritional intake.
- Assessing both dietary intake and body stores requires different test strategies for diagnosis of deficiency or toxicity.
- Deficiencies are especially important at the age extremes of life, in malnutrition of whatever cause and in people who take certain pharmacologic agents.
- Often, a therapeutic trial of the nutrient considered deficient is the most reliable approach to diagnosis and treatment.
- Essential trace elements have specific metabolic functions that cannot be replaced by other minerals.
- Deficiencies of trace elements may result from insufficient ingestion because the soil, water, or plants in the region are inadequate in a specific element, because of interference by another dietary ingestant, because of the lack of a necessary protein needed for the absorption or metabolism of the element, or because of a failure to supplement an element for those receiving total parenteral nutrition.
- The functions of trace elements include structural, signal transduction, and catalytic. Some are components of metalloenzymes or function as enzyme cofactors, provide electron and oxygen transport, or are active in the maintenance of macromolecule conformation or vitamin or hormonal activity.
- To avoid contamination, trace elements must be analyzed with considerable care. Because they are widely distributed in the environment, there is a risk of contamination. For many, the very minute concentration in body fluids and tissues necessitates analytic techniques that are sensitive in concentrations of μg/L or even ng/L.
- Trace element concentration in body fluids correlates poorly with the amount in body stores. Serum levels are unreliable because of the influence of unrelated conditions. There are no particularly good assays for trace element dietary status. Test results need be interpreted with caution.
- The only definitive test of human trace element deficiency is assessment of the clinical response to controlled supplementation with the element considered deficient.
- The intake required to cause toxicity is very variable for the different trace elements.

INTRODUCTION

Twenty-three vitamins and trace elements are a collection of dietary heterogeneous ingredients necessary for health, development, and longevity. They are collectively described as essential micronutrients because of the very small amounts required to satisfy their diverse physiologic roles, and their functions are as varied as their compositions (Mason, 1996). These micronutrients are unrelated organic catalysts and elements that are not endogenously synthesized (Rubin & Strayer, 2005). They are critically needed in small amounts for metabolism of proteins, carbohydrates, and fats, and for the body's structure (e.g., vitamin K in bone matrix). Many micronutrients are important antioxidants (e.g., vitamins C and E) or are cofactors for antioxidant enzymes (e.g., selenium in glutathione peroxidase). Recommended allowances reconcile optimum nutrition and the prevention of deficiency symptoms or diseases. The requirements for most essential nutrients to maintain health are now fairly well characterized (Mason, 1996). Deficiency and toxicity states are often insidious for both and may be attributable to an inappropriate intake or to defective utilization. Deficiencies are most often due to malnutrition (McLaren, 1994). Initially, the interest was the prevention of deficiency diseases and elucidation of the biochemical roles of these micronutrients as coenzymes and cofactors. Research in the assessment of vitamin and trace element nutriture has further identified their many other important functions, such as antioxidant activity, hormone-like stimulation, and their role in epigenetic modification (Machlin, 1992; Sies et al., 1992; Anderson et al., 2012).

Dietary Reference Intakes (DRIs), introduced by the Food and Nutrition Board and Institute of Medicine (1997), provide four types of reference values. These reference values provide quantitative estimates of the dietary level of each of the essential nutrients and are primarily intended for nutritionists (Barr et al., 2002). The *Recommended Dietary Allowance* (RDA) is the average daily nutrient amount sufficient for the nutrient requirements of nearly all (97%–98%) healthy people categorized by age, gender, and physiologic need. The RDA is derived from the *Estimated Average Requirement* (EAR). The *Adequate Intake* (AI) is a recommended average daily nutrient intake level based on observed or experimentally determined approximations or estimates of nutrient intake by a group (or groups) of apparently healthy people that are assumed to be adequate; they are used when an RDA cannot be determined. The *Tolerable Upper Intake Level* (UL) is the highest level of daily nutrient

intake likely to pose no risk of adverse health effects for most individuals in the general population (Institute of Medicine, 1998; Ross et al., 2011).

Several groups warrant selective micronutrient supplementation. These include pregnant women, neonates, and infants; the aged; patients receiving long-term parenteral nutrition or hyperalimentation; individuals who take certain pharmacologic agents, individuals who follow strict vegan diets, and individuals with altered gastrointestinal absorption. Poverty and food insecurity are continued sources of deficiencies, as are so-called "fad diets," defined by the Federal Trade Commission as diets that are deficient in one or more nutrients.

This chapter reviews micronutrients that include vitamins and the essential trace mineral elements. The 13 vitamins are outlined in Table 27.1, along with their functions and deficient and toxic states. The 10 essential trace mineral elements are presented in Table 27.4, along with their functions and the effects of deficiency and toxicity.

VITAMINS

Vitamins are organic molecules that are required in microgram to milligram amounts for health, growth, and reproduction (McCormick & Greene, 1994). With the exception of vitamin D, the body depends completely on dietary intake for vitamins, although there is some enteric bacterial production of vitamin K, nicotinic acid, riboflavin, biotin, cobalamin, and folic acid (Eastwood, 2003; Grodner et al., 2004). However, these syntheses occur mostly in the colon and are not nutritionally significant because they are poorly absorbed. Lack of each vitamin results in a clearly definable metabolic deficit. This is species specific, because different species have different synthesizing capabilities. For example, many lower animals can produce their own ascorbic acid, but humans cannot and require ascorbate to prevent scurvy (Combs, 1998).

Vitamins may be classified according to their properties, such as function, nutritional source, or their solubility in water (see Table 27.1). In this discussion, vitamins are divided into two groups based on solubility. Solubility affects absorption and transport. Water-soluble vitamins are easily absorbed, which allows for minimal storage. However, deficiencies can develop quickly, even within weeks (Grodner et al., 2004). Thiamine, riboflavin, niacin, pyridoxine, cobalamin, vitamin C, folate, pantothenic acid, and biotin are water soluble. Vitamins A, D, E, and K are considered water insoluble or fat soluble, and depend on normal lipid digestion and micellar solubilization for absorption, such as the presence of bile and pancreatic lipase. Malabsorption of fat may result in deficiencies of the fat-soluble vitamins despite an adequate dietary intake.

TABLE 27.1

Vitamins: Functions, Deficiency Syndromes, and Toxicity

	Functions	Deficiency Syndromes	Toxicity
Water-Soluble Vitamins			
Ascorbate (vitamin C)	Many redox reactions Hydroxylation of collagen	Scurvy	Chronic megadoses of 10 to 150 times the RDA (1–15 g) may cause cramps, diarrhea, nausea, kidney stones. Abrupt stoppage of megadoses may result in scurvy, as its metabolism is accelerated with megadoses.
Biotin	Cofactor in carboxylation reactions	Rare. Caused by lack of biotin in total parenteral nutrition. Also, avidin in raw egg whites binds biotin in gut, preventing absorption. Dermatitis, glossitis, hair loss, anorexia, depression, and hypercholesterolemia.	No known toxicity.
Cobalamin (vitamin B_{12})	Folate metabolism and DNA synthesis, maintenance of myelinization of spinal tracts	Megaloblastic anemia, peripheral neuropathy	No appreciable toxicity.
Folate (folic acid)	Transfer and use 1-carbon units in DNA and amino acid synthesis	Megaloblastic anemia, neural tube defects	Teratogenic effect in rodent model. No adverse effects at high oral doses.
Niacin (nicotinic acid)	Incorporated into NAD and NAD phosphate, redox reactions	Pellagra: dementia, dermatitis, diarrhea	Excess preformed niacin and nicotinic acid cause vascular dilatation, "flushing"; hepatotoxic.
Thiamine (vitamin B_1)	As pyrophosphate, is coenzyme in decarboxylation reactions	Dry (neuromuscular) and wet (cardiac failure) beriberi, Wernicke-Korsakoff syndrome	Only when given parenterally. Headache, muscle weakness, cardiac arrhythmia, convulsions.
Pantothenic acid (vitamin B_5)	Incorporated in coenzyme A	No syndrome recognized	Very high doses: diarrhea.
Pyridoxine (vitamin B_6)	Derivatives are coenzymes in many intermediary reactions; amino acid, phospholipid and glycogen metabolism	Cheilosis, glossitis, dermatitis, peripheral neuropathy, convulsions	Long-term megadose supplementation causes ataxia and sensory neuropathy. The UL is 100 mg/day.
Riboflavin (vitamin B_2)	Converted to flavin coenzymes, cofactor for many enzymes in intermediary metabolism	Ariboflavinosis, cheilosis, angular stomatitis, glossitis, dermatitis, corneal vascularization.	Toxicity to riboflavin has not been reported. Absorption limited normally.
Fat-Soluble Vitamins			
Vitamin A (retinol)	A component of retinal rod pigment. Role in vision in dim light, growth; reproduction. Maintenance of resistance to infection	Squamous metaplasia, especially glandular, follicular hyperkeratosis; xerophthalmia; night blindness, reproductive disorders, vulnerability to infection.	Livers of polar bears and large animals have very high levels of vitamin A. Acute: can cause drowsiness, headache, vomiting, stupor, skin peeling, and papilledema. Chronic: teratogenic, osteoporosis, hepatotoxicity. Carotenoids in excess, distinct orange-yellow skin color.
Vitamin D (cholecalciferol)	Promotes absorption of calcium and phosphorus; mineralization of bones and teeth	Rickets in children, osteomalacia in adults, hypocalcemia, tetany	High intake of vitamin D causes hypercalcemia and its sequelae: hypercalciuria, bone demineralization, constipation, muscle weakness, renal calculi.
Vitamin E (tocopherol)	Antioxidant, scavenges free radicals; cellular respiration, primarily in muscle, RBC integrity	Spinocerebellar degeneration, ataxia	Mild GI distress, nausea; coagulopathies in patients receiving anticonvulsants.
Vitamin K (phytomenadione)	Cofactor of procoagulants—hepatic factors II (prothrombin), VII and X, protein C and protein S	Defective clotting, bleeding disorder	Foods containing vitamin K cause no toxicity problems. Excess amounts of vitamin K may decrease clotting time.

Data after Berdanier, 1998; Combs, 1998; Eastwood, 2003; Grodner et al., 2004; Kane & Kumar, 2005; Katz, 2001.

Determining the extent to which metabolic demands for micronutrients have been met is complex and very difficult. The preferred method for dietary intake assessment is repeat 24-hour recall, which is less prone to error than food frequency questionnaires (Freedman et al., 2017).

Disease conditions, infections, or trauma can alter metabolism and significantly change the requirements for vitamins and trace elements in multiple ways (Gidden & Shenkin, 2000; Elia, 2001). Laboratory studies help somewhat to improve the assessment of balance of supply and demand, but they are seriously limited (Gidden & Shenkin, 2000). Subclinical deficiencies are known to occur, but the extent of depletion before significant biochemical, physiologic, or histologic changes can only be surmised. Interpreting the results of tests of nutritional status requires reference intervals with provision for relevant factors such as ethnicity, geographical variation, and the time of sample collection.

Vitamins exist in almost all foods, but no one food group is a good source of all vitamins (Grodner et al., 2004; Table 27.2). The vitamin B complex includes thiamine, riboflavin, niacin, biotin, pyridoxine, and cobalamin. Cobalamin is present only in animal products, including meat (especially liver), milk, cheese, eggs, and other animal proteins. The other members of the vitamin B complex are found in leafy green vegetables, milk, and liver. Vitamin A and niacin have precursor substances that can be converted to the active vitamin form in humans. Vitamin K and biotin are produced by the gut microflora but in insufficient quantities to sustain metabolism. Niacin and vitamin D can be synthesized in the human body (Williams, 2002).

Deficiencies are particularly important at the extremes of life and are a concern for developing fetuses, infants, and the elderly (Seymour, 2000). Deficiencies are also frequent for those with protein energy malnutrition in developing nations. In developed countries, the conditions resulting in vitamin deficiencies include decreased intake, absorption, or production. Decreased intake characteristically occurs in patients suffering from alcoholism (thiamine); vegans (vitamin D, cobalamin); and the elderly (vitamin D, folate). Conditions resulting in decreased absorption include liver and biliary tract disease (vitamins A, D, E, and K), small bowel disease (folate and the fat-soluble vitamins A, D, E, and K), and ileal disease or resection (cobalamin). Conditions that cause decreased production include kidney disease (vitamin D). Folate deficiency can be caused by drugs that act as antagonists, reducing the activity of dihydrofolate reductase (aminopterin, methotrexate [amethopterin], pyrimethamine, trimethoprim, and triamterene); act as folate antagonists and produce folate deficiency by inhibiting this enzyme; anticonvulsants and antituberculosis drugs; alcohol; and oral contraceptives that alter serum levels through other mechanisms (Lambie & Johnson, 1985). Deficiencies also occur in those with long-term chronic disease associated with decreased oral intake, including acquired immunodeficiency syndrome (AIDS) and patients receiving hemodialysis, in whom loss of water-soluble vitamins through dialysate may occur. The assessment of body stores and the chronic nutritional state for the micronutrients continues to present difficulties. Tests often indicate only the recent nutritional intake. A therapeutic trial of the nutriment considered deficient is often the easiest and most reliable approach. Specific diagnostic strategies are also helpful (Feldman, 1994; Gibson, 2002; see Table 27.2).

Toxicity rarely results from excessive dietary intake but may occur due to overdoses of vitamin supplements. Single large doses of the water-soluble vitamins are rarely toxic because they are rapidly excreted, but repeated doses can cause toxicity, especially pyridoxine. Vitamin A has a toxic potential greater than that for the other hypervitaminoses, although the actual incidence is low. Intakes as low as 25 times the RDA are considered potentially toxic for vitamin A. Carotenoids have a low toxicity. Vitamin D toxicity is a concern, especially in children (Vogiatzi et al., 2014).

WATER-SOLUBLE VITAMINS

Thiamine

Thiamine pyrophosphate (TPP; vitamin B_1) is an essential cofactor of enzymes involved in carbohydrate and amino acid intermediary metabolism and is important in brain function. Good sources include yeast, legumes, enriched grain products, and pork. Early signs of deficiency include anorexia, weight loss, muscle weakness, apathy, confusion, and irritability. Later consequences include edema and high-output cardiac failure (wet beriberi), polyneuropathy with depressed reflexes, paresthesias, weakness and muscle atrophy (dry beriberi), and a distinctive neurologic sequela (Wernicke-Korsakoff syndrome) characterized initially by agitation and psychosis followed by ataxia, ophthalmoplegia, and a dementia in which confabulation is a prominent finding. Lesions of the mammillary bodies and the area that abuts the third ventricle are distinctive findings (Rubin & Strayer, 2005). The infantile form is rare in developed countries but has been seen when thiamine was inadvertently left out of infant formula, as occurred in Israel in 2005. Pediatric beriberi can present with aphonia or weak crying initially but cardiac failure may be sudden and rapidly fatal.

In adults, thiamine deficiency is often associated with alcohol abuse in part due to the effect of alcohol on thiamine uptake by intestinal carriers (Subramanya et al., 2010). Thiamine deficiency is also seen in those with poor nutrition from any cause. No toxicity is described from high oral doses. Antithiamine factors are present in betel, tea, and some foods. In the United States, all breads and flour are enriched with thiamine. There is a significant loss of thiamine when foods are cooked in water, and it is unstable at high temperatures. Thiamine is produced in the colon by normal enteric bacteria, although the contribution is apparently slight, and it is absorbed throughout the small intestine. It is bound to albumin in the plasma. At high thiamine intakes, the excess is excreted in the urine (Kohlmeier, 2003). Thiamine deficiency is most often diagnosed clinically, and the response to parenteral thiamine administration provides the most reliable evidence for thiamine deficiency (Rubin & Strayer, 2005; Olsen & Regis, 2010). The available assays for thiamine and related compounds require fasting blood samples and lack standardization and reproducibility (Crook, 2019).

Riboflavin

Vitamin B_2 normally forms two coenzymes: flavin mononucleotide and flavin adenine dinucleotide. These have an important role in electron transport in several oxidative systems. Dietary sources include milk and dairy products, meat, poultry, fish, and green vegetables. Bread and cereals are fortified with riboflavin. Absorption is mostly in the jejunum. Riboflavin is so prevalent in the diet that deficiency severe enough to cause marked debilities is not known. Mild riboflavin deficiencies are likely common. Deficiency frequently occurs in association with a lack of thiamine and/or niacin (Guyton & Hall, 1997). With prolonged deficiency, cracking and swelling of the lips (cheilosis); cracking and inflammation of the angles of the mouth (angular stomatitis); deep-red smooth tongue, called magenta tongue (glossitis, atrophy); a greasy scaling of the cheeks and the areas behind the ears (seborrheic dermatitis); and normocytic anemia can appear (Kohlmeier, 2003). Interstitial keratitis of the cornea is the most troubling lesion. It results in corneal opacification and ulceration (Rubin & Strayer, 2005). Deficiencies during infancy and childhood impair growth. There is little danger of toxicity because excess riboflavin is rapidly lost. A 24-hour urine screen will indicate recent riboflavin intake (Kohlmeier, 2003).

Niacin

Vitamin B_3 (nicotinic acid) plays a major role in the formation of nicotinamide adenine dinucleotide (NAD) and its phosphate NADP, which are important in intermediary metabolism and a large number of oxidation-reduction reactions. NAD is important in catabolism of fat, carbohydrate, protein, and alcohol, as well as cell signaling and DNA repair. NADP is important mostly in anabolism reactions, such as fatty acid and cholesterol synthesis (Jacobson et al., 2012). Animal proteins are foods high in tryptophan, such as meat, eggs, and milk. They are good sources for endogenously synthesized niacin. Urine is the main excretory path for niacin metabolites. Niacin is in many grains. Deficiency causes pellagra, which is now uncommon in the developed world but can be seen in malnourished alcoholics.

Malabsorption of tryptophan, as seen in Hartnup disease, or the carcinoid syndrome, in which tryptophan is consumed to make serotonin, may produce mild symptoms of pellagra. Pyridoxine and riboflavin deficiencies increase the requirement for niacin because they are both cofactors and are required for the synthesis of niacin by the liver. Corn is a poor source of tryptophan, and the niacin in corn is bound and poorly available. Pellagra is prevalent in areas where corn (maize) is the staple food, such as in certain parts of Africa (Guyton & Hall, 1997).

Pellagra is characterized by the 4 "Ds": dermatitis, diarrhea, dementia, and, if untreated, death. A scaly dermatitis can form on areas exposed to light or pressure, such as the knees and elbows and, more commonly, the neck (called Casal's necklace). The hands show a rough, scaly dermatitis with a glove-like distribution and a pattern of hyperkeratosis, vascularization, and chronic inflammation. Similar lesions are seen in the mouth and vaginal mucous membranes (Rubin & Strayer, 2005). Niacin supplements at doses over 500 mg can cause flushing, itching, and gastric irritation. They can cause transient, asymptomatic elevations in serum aminotransferase levels in up to 20% of people. The elevations are rarely greater than 3 times the upper limit of the reference range and usually resolve spontaneously even with continuation of the drug. The effect is partially dose related and is common with doses above 3 g/day. Liver damage has been reported after use of certain formulations, especially sustained-release formulations that were used in the past to treat elevated cholesterol.

Pyridoxine

Vitamin B_6 is a coenzyme that participates in more than 100 transamination, decarboxylation, and other reactions, including the initial step of porphyrin

TABLE 27.2

Vitamins: RDA, Food Sources, and Analysis of Body Levels

	RDA	Food Sources	Laboratory Assessment for Subclinical Deficiency States
Water-Soluble Vitamins			
Ascorbic acid, vitamin C	M: 90 mg F: 75 mg Smokers: 125 mg	Fruits and vegetables: citrus fruits, red and green peppers, strawberries, tomatoes, broccoli, potatoes, leafy green vegetables	Fasting specimen required. S—ascorbic acid, deficient <11.4 μmol/L. WBC—ascorbic acid by HPLC, reflects tissue stores, preparation, and assay difficult. <11.4 nmol/10^8 cells associated with scurvy. 24-h U-ascorbic acid, reflects recent dietary intake. Vitamin C load test U.
Biotin	AI 30 μg	Liver, kidneys, peanut butter, egg yolks, yeast	Microbiological assay.
Cobalamin, vitamin B_{12}	M/F: 2.4 μg	Meat, fish, poultry, eggs, dairy products	S—vitamin B_{12} by RIA, deficiency <125 pmol/L; U—methylmalonic acid
Folate, folic acid	M/F: 400 μg Pregnancy: 600 μg Lactation: 500 μg	Leafy green vegetables, legumes, cereals, some fruits and juices	Hemolysis interferes. RBC-folate; S-folate; S—methyltetrahydrofolate, reflects recent intake, not stores. Cutoff point, negative folate balance <6.8 nmol/L. Polyglutamate forms of folate present, reflect body folate stores. Folate (nmol/L): depleted <368; deficient <322; anemia <227. U—formiminoglutamic acid (FIGLU). Histidine load test U.
Niacin, nicotinic acid, B_3	Niacin equivalent = 1 mg niacin or 60 mg tryptophan. M: 16 mg NE/d F: 14 mg NE/d	Protein-containing foods are good sources for both niacin and tryptophan. Meats, poultry, fish, legumes, enriched cereals, milk, coffee, tea	Ratio of RBC—nicotinamide adenine dinucleotide (NAD) and NADP nucleotide, <1 may indicate risk of niacin deficiency. Ratio 2—pyridine (40%–60%): N′-methyl nicotinamide (20%–30%); deficiency of niacin when ratio <1.
Pantothenic acid	AI 5 mg	Whole-grain cereals, legumes, meat, fish, poultry	Whole blood—pantothenic acid, inadequate intake <100 μg /dL. 24-h U—pantothenic acid, abnormally low <1 mg/day.
Pyridoxine, vitamin B_6	M/F: 1.3 mg	Whole grains, cereals, legumes, chicken, fish, pork, eggs	P-pyridoxal-5′-phosphate, cation exchange HPLC, assay by fluorometry. B_6 status: >30 nmol/L adequate, ≥0.8 acceptable, <0.5 marginal or inadequate. RBC—aminotransferases, reflect long-term pyridoxine status; AST more sensitive to B_6 deficiency than ALT. U—4-pyridoxic acid, dietary intake of B_6. U—xanthinuric acid, tryptophan metabolite. Tryptophan load test U.
Riboflavin, vitamin B_2	M: 1.3 mg F: 1.1 mg Riboflavin destroyed by light	Milk, enriched grains, broccoli, asparagus, dark leafy greens, whole grains, enriched breads, cereals. Also, dairy products, meats, fish, poultry, eggs.	RBC—glutathione reductase, expressed as ratio of assays with and without flavin adenine dinucleotide. 24-h U—riboflavin measures recent intake, not body stores, nonspecific; varies with physical activity.
Thiamine, vitamin B_1	M: 1.2 mg F: 1.1 mg	Whole or enriched grains, flour, lean pork, legumes, seeds, nuts.	RBC—transketolase activity, expressed as ratio of assays with and without thiamine pyrophosphate. 24-h U—thiamine measures recent dietary intake, not body stores.
Fat-Soluble Vitamins			
Vitamin A, retinol	Retinol activity equivalents = (RAE) M: 900 μg RAE F: 700 μg RAE	Natural preformed vitamin A only in fat of animal-related foods: whole milk, butter, liver, egg yolks, fatty fish Carotenoids are found in deep green, yellow, and orange fruits and vegetables: broccoli, cantaloupe, sweet potato, carrots, tomatoes, spinach.	Hemolysis interferes. Liver retinol stores: S-retinol, insensitive test. Dose response: S-retinol and dehydroretinol by HPLC 4–6 h after oral 3,4-didehydroretinylacetate (100 μg/kg), more sensitive index than S-retinol of marginal retinol status. RBP—index of retinol, low specificity. In vitamin A deficiency, RBP accumulates in liver as apo RBP (RBP not bound to retinol). After retinol dose, retinol binds to apo. RBP in liver, holo RBP (RBP bound to retinol) released from liver, causing increased S-retinol. Blood sample at baseline and 5 h after oral vitamin A. Calculate RDR (%) > 14%–20%, marginal vitamin A status. S—carotenoids indicate current intake of carotenoids. Rapid dark adaptation (RDA) for night blindness.
Vitamin D, cholecalciferol	AI M/F: 10 μg Ages: 51–70 y 15 μg >70 y 20 μg	Butter, egg yolks, liver, fatty fish. Vitamin D–fortified milk. Sunlight exposure converts precursor to active vitamin D.	S—25-hydroxyvitamin D: Deficiency: <3 nmol/L Toxicity: >500 nmol/L Separate S—25(OH)D by HPLC, assay by CPBA, indicates total endogenous and exogenous vitamin D, reflects vitamin D content of liver.

TABLE 27.2

Vitamins: RDA, Food Sources, and Analysis of Body Levels—cont'd

Vitamin E, tocopherol	α-tocopherol equivalents = α-TE M/F: 15 mg α-TE	Vegetable oils, corn, soy, safflower. Whole grains, seeds, nuts, wheat germ, green leafy vegetables.	Ratio S—tocopherol; S—lipids; reverse phase HPLC with high-sensitivity fluorescence detector; levels correlate with S—cholesterol deficiency when ratio <0.6 mg total tocopherol/g serum lipids.
Vitamin K, phytomenadione	AI M: 120 μg F: 90 μg	Vitamin K synthesized by bacteria in jejunum and ileum; dietary intake is still required. Dark green leafy vegetables.	Prothrombin time

Data from: McCormick et al., 1994; Gibson, 2002; Grodner et al., 2004; Brewster, 1996.
AI, Adequate intake; *ALT,* alanine aminotransferase; *CPBA,* competitive protein binding assay; *F,* female; *FIGLU,* formiminoglutamic acid; *HPLC,* high-performance liquid chromatography; *M,* male; *M/F,* male/female; *NAD,* nicotinamide adenine dinucleotide; *NE,* niacin equivalent; *P,* plasma; *PT,* prothrombin time; *RAE,* retinol activity equivalents; *RBC,* erythrocyte; *RBP,* retinol-binding protein; *RDA,* recommended dietary allowance; *RDR,* relative dose response; *S,* serum; *U,* urine; *WBC,* leukocyte.

synthesis, glycogen mobilization, amino acid transsulfuration, aminotransferases, and neurotransmitter synthesis. Good food sources include fortified cereals, organ meats, muscle foods, potatoes, and fruits other than citrus. Cooking results in leaching of the pyridoxine. Urine is the major excretory pathway. Deficiencies are usually seen along with other vitamin or protein deficiencies, and they can occur in alcoholics. Isolated deficiency of pyridoxine is uncommon and may cause a microcytic hypochromic anemia in which the iron stores are saturated, epileptic seizures, EEG abnormalities, depression, confusion, seborrheic dermatitis, and possibly platelet and clotting abnormalities. Several inborn errors of amino acid metabolism respond to very high doses of pyridoxine. Homocystinuria—a disorder of methionine metabolism that leads to increased levels of homocysteine and its metabolites (homocystine, homocysteine-cysteine complex, and others) in blood and urine—may respond to supplements of folate, cobalamin, and sometimes pyridoxine.

Plasma pyridoxal 5-phosphate (PLP) is the major coenzyme form in the body and the primary form of circulating vitamin B_6 in plasma (Truswell, 2002). Normal >30 nmol/L indicates adequate status in adults. Urinary 24-hour 4-pyridoxic acid level reflects recent dietary intake of vitamin B_6. Levels vary with age, sex, and pregnancy. Urinary xanthurenic acid after a tryptophan (or methionine) oral load is an indirect measure of functional vitamin B_6 deficiency. Activity of erythrocyte alanine aminotransferase can be used to detect B6 deficiency. Pyridoxine is one of the B vitamins that is toxic at high doses. Ingestion of >100 mg/day in adults over months to years has been reported to cause a peripheral sensory neuropathy and possibly skin lesions (Kohlmeier, 2003).

Cobalamin

Cobalamin is a complex cobalt-containing molecule, synthesized only by bacteria. It comprises several "vitamers." Cyanocobalamin and hydroxycobalamin are pharmacologic forms, whereas adenosylcobalamin and methylcobalamin are the main biological forms. The main known cofactor roles of cobalamin are in the synthesis of succinate from methylmalonate and the synthesis of methionine from homocysteine. Thus, cobalamin deficiency results in increased levels of methylmalonate and homocysteine. Clinically, many manifestations of deficiency are similar to those of folate deficiency and can be overcome by large amounts of folate. These include impaired DNA synthesis, which results in megaloblastic anemia. Cobalamin deficiency also causes neuropsychiatric damage, largely related to demyelination in the posterior columns of the spinal cord, peripheral nerves, and even the cerebrum. Neurologic damage is not relieved, and may even be worsened, by treatment with folate.

Absorption of cobalamin is unique. When vitamin B_{12} is ingested in its nonprotein-bound form, it is bound to a carrier protein known as *R-binder* or *transcobalamin I*, secreted by both salivary glands. If the vitamin B_{12} bound to protein is ingested, it must undergo proteolytic cleavage in the stomach or duodenum, where it then binds to R-binder. When bound R-cobalamin enters the second segment of the duodenum, it is freed from the binder by pancreatic proteases. It is then complexed to intrinsic factor, which is secreted by the gastric parietal cells, for absorption in the terminal ileum. Inadequate dietary intake is not the usual cause of cobalamin deficiency except in strict vegans who do not supplement, because cobalamin in not present in plants. Elderly patients may be at risk for deficiency due to decreased intestinal transport. Pharmacologic agents, including proton pump inhibitors and metformin, have been associated with cobalamin deficiency. The most common cause of severe deficiency is autoimmune atrophic gastritis, also known as pernicious anemia, which results from decreased production and activity of intrinsic factor due to autoantibodies against intrinsic factor (observed in 60% of case) and parietal cells (observed in 90% of cases) (Stabler, 2013; Bizarro & Antico, 2014).

Normal body stores of cobalamin are sufficient to last for 3 to 6 years. Food sources include liver, shellfish, fish, meat, eggs, milk, cheese, and yogurt. Plasma levels of less than 125 pmol/L indicate a cobalamin deficiency, but the test does not have good sensitivity and specificity. Elevated serum or urinary methylmalonate and raised plasma homocysteine also indicate that cobalamin is low. The classical Schilling test uses radiolabeled cobalamin to measure its absorption on different days, with and without intrinsic factor (West, 2002), but it is not generally available today. Only about one-fourth of circulating cobalamin is bound to the transport protein transcobalamin and thus available for transport into cells. Measurement of this holotranscobalamin fraction may provide a better assessment of B_{12} status, but it has not yet been well validated (also see Chapter 33).

Folate

Folate is the generic name for compounds related to folic acid (pteroylglutamic acid). Like cobalamin, it plays a coenzyme role in one-carbon transfer reactions; deficiency leads to impaired synthesis of purines and pyrimidines and thus of deoxyribonucleic acid (DNA) (Guyton & Hall, 1997). It is also involved in methylation reactions that alter gene transcription. It is widely available in plants and, to a lesser extent, organ meats. However, dietary folate is present in polyglutamate forms and must be hydrolyzed to be absorbed. The absorption of folate is complex: after hydrolysis, it can be absorbed through the brush border of the duodenum via facilitated anion exchange or use of folate receptors via endocytosis (Nazki et al., 2014). More than half of the folate content of food is lost during boiling but not during steaming of foods. Deficiency results in megaloblastic anemia and leukopenia. In pregnancy, fetal neural tube defects are associated with low folate levels—periconceptual supplementation markedly reduces the incidence (Wildman & Medeiros, 2000). Central to the physiologic roles of folate is its role as a methyl donor—a role that is facilitated by multiple enzymes, including methyltetrahydrofolate reductase (MTHR). Recently, polymorphisms of the MTHR gene have been associated with increased risk of certain cancers and leukemias (Nazki et al., 2014) (also see Chapter 33).

Pantothenic Acid

Pantothenic acid is part of coenzyme A (CoA) and acyl carrier protein (ACP). Both are carriers of acyl groups. Acetyl-CoA is involved in the tricarboxylic acid cycle, and CoA is involved in the synthesis of lipids. It is transported in erythrocytes as CoA. The highest tissue concentrations are found in the liver, adrenals, kidneys, brain, heart, and testes. CoA and ACP are metabolized to free pantothenic acid and excreted in the urine. Urine levels indicate dietary intake and range from 2 to 7 mg/day. Pantothenic acid is widely present in foods; dietary deficiency occurs only in severe malnutrition with other nutrient deficiencies. The "burning feet syndrome" that was seen in malnourished prisoners of war during World War II responded to large doses of Ca-pantothenate (Truswell & Milne, 2002; Huisjes & Card, 2019).

Biotin

Biotin is a coenzyme for several carboxylase enzymes that include pyruvate carboxylase (provides oxaloacetate for the tricarboxylic acid cycle), acetyl CoA, and carboxylase (fatty acid synthesis). Biotin deficiency is rare because it is found in many foods, and bacterial production in the large intestine supplements the dietary intake. Avidin, an antivitamin, is found in uncooked egg whites and can produce a deficiency of biotin when large amounts are ingested because avidin binds biotin in the gut, preventing absorption. Biotin deficiency in humans has resulted from the failure to include biotin in total parenteral nutrition and is characterized by a scaly dermatitis, glossitis, hair loss, anorexia, depression, and hypercholesterolemia (Truswell & Milne, 2002; Carling & Turner, 2019).

Ascorbate

Ascorbic acid (vitamin C) is an essential cofactor for α-ketoglutarate-dependent dioxygenases. Examples are prolyl hydroxylases, which play a role in the biosynthesis of collagen and in downregulation of hypoxia-inducible factor (HIF)-1, a transport factor that regulates many genes responsible for tumor growth, energy metabolism, and neutrophil function and apoptosis (Traber & Stevens, 2011). It is necessary for maintaining the integrity of gums, arteries, and other soft tissues; bone (collagen synthesis); brain and nerve function (neurotransmission and hormone synthesis); nutrient metabolism (especially iron, protein, and fat); and antioxidant defense and free radical scavenging. That may occur directly or via reduction of the tocopheroxyl radical (vitamin E). Ascorbic acid is found in high concentration in leukocytes, adrenal glands, pituitary glands, and the brain. Most common food sources are fruits, including citrus; berries; tomatoes; and many vegetables. Prolonged storage and overcooking can cause significant vitamin loss. Deficiency results in *scurvy*, which manifests as bleeding gums, painful swollen joints, poor wound healing, confusion, fatigue, and diminished immune function. Today, it is rarely seen in the developed world, being seen in alcoholics and in elderly individuals who eat a diet lacking in fruits and vegetables. The signs of scurvy have been described since antiquity. The disease was widespread among sailors in the 16th to 18th centuries. The typical pattern involved bleeding gums; painful, swollen joints; and muscle weakness. Onset was within months of the start of a voyage. British expeditions had devastating losses of men due to scurvy. The carnage prompted the Admiralty to seek a cure; in 1747, James Lind, a Scottish surgeon, performed a clinical nutrition experiment on a ship in which he gave six different dietary supplements to six pairs of scorbutic sailors. He found that oranges and lemons cured scurvy, which he reported in his book *Treatise of The Scurvy* (Jacob, 1994). He believed that scurvy was caused by dampness and the crowded conditions on ships. Only subsequently was it discovered that scurvy was due to ascorbate deficiency.

Daily ingestion of 3000 mg or more of vitamin C has been associated with gastric and intestinal irritation and kidney stones; it can also interfere with copper metabolism. Unlike other vertebrates, humans are not able to complete the synthesis of ascorbate (Kohlmeier, 2003). Tests to assess ascorbate status can be performed using serum or leukocytes. Both correlate well with dietary intake. Urine assays, however, tend to reflect recent dietary intake (Skeaff, 2002).

FAT-SOLUBLE VITAMINS

Vitamin A and Retinol

Vitamin A activity is obtained from compound classes that include preformed vitamin A, retinol and related compounds retinal and retinoic acid, and the precursors β-carotene and related carotenoids. The latter are provitamins found in yellow and red pigments in vegetables and some fruits. Retinol is essential for vision as a precursor for retinal, the pigment that combines with opsin to form rhodopsin, which is necessary for both low-light and color vision. Retinoic acid also plays a part in cellular differentiation, morphogenesis, synthesis of glycoproteins, gene expression, immunity, growth, reproduction, and the prevention of cancer and heart disease (Truswell, 2002). Vitamin A is needed to maintain certain specialized cell membranes; for skeletal maturation; for the formation of the light-sensitive rods of the retina; and for the structure of cell membranes. Vitamin A deficiency is unusual in developed countries, but it continues to be a frequent cause of blindness due to corneal damage in the poorer regions of the world, particularly parts of Africa, the Middle East, and Southeast Asia. Retinol is in high concentration in fish liver, and leafy green vegetables are a rich source of carotene (Rubin & Strayer, 2005). Hippocrates (466–377 BCE) recognized that consuming liver could cure night blindness (West, 2002). Vitamin A deficiency is usually seen where the diet includes few dairy products and vegetables for long periods of time or in malabsorption syndromes (Eastwood, 2003). Deficiency results in squamous metaplasia, which causes the sweat and tear ducts to be blocked by squamous debris. The epithelia of the trachea, bronchi, renal pelvis, pancreatic ducts, uterus, and salivary glands are often affected. The earliest sign of vitamin A deficiency is vision loss in dim light (night blindness). Toxicity is usually the result of excessive vitamin A intake in the form of supplements, especially in children. It does not occur at intakes of less than 10,000 U/day. Vitamin A toxicity occurred in explorers who ate polar bear livers, which have an exceptionally high concentration of vitamin A. In toxicity, the liver and spleen are enlarged with lipid-laden macrophages. Vitamin A is concentrated in the hepatocytes, and prolonged toxicity causes cirrhosis. Headache, hyperexcitability, and bone pain are early symptoms. The lesions are mostly reversible, early in the course, upon discontinuation of the excessive dosing. High doses of synthetic derivatives of retinoic acid are teratogenic. Excessive carotene is benign and causes a jaundice-like discoloration of the skin (Rubin & Strayer, 2005).

Circulating retinol concentrations do not consistently correlate with retinol total body stores. The relative dose–response test (Loerch et al., 1979) indirectly assesses the stores. Two blood samples are collected—one before and one 5 hours after a physiologic dose of vitamin A. In vitamin A–depleted subjects, a rapid, sustained rise in serum retinol concentration occurs compared with a lower, shallow rise in those who are vitamin A sufficient (Loerch et al., 1979).

Vitamin D

Vitamin D (cholecalciferol) plays an essential role as a hormone in the control of calcium and phosphorus metabolism. Exposure of the skin to ultraviolet light converts naturally occurring 7-dehydrocholesterol to cholecalciferol, or vitamin D_3. It is actually a hormone because it acts at the cell nucleus via a steroid response element. D_3 is diet derived from animal sources, particularly fish liver and oils. Ergocalciferol, or vitamin D_2, which is of equal potency in humans, is derived from its provitamin ergosterol, which occurs in fungi and plants and is the major synthetic form used to fortify milk and margarine. Both vitamins D_2 and D_3 require two hydroxylation steps to achieve the active form—1,25-dihydroxyvitamin D [25(OH) D], or calcitriol. The first hydroxylation occurs at the 25 position in the liver and the second at the 1 position in the kidney. Calcitriol promotes absorption of calcium and phosphate from the small intestine (Truswell, 2002; Lamberg-Allardt, 2013). Deficiency results from inadequate dietary intake; insufficient sunlight reaching the skin; inadequate absorption, such as what occurs in fat malabsorption syndromes; or failure of conversion to the active metabolite due to chronic liver or kidney disease. In children before the epiphyses have closed, the bone lesion secondary to hypovitaminosis D is called rickets; in adults, it is called osteomalacia.

Hypervitaminosis D is extremely rare and is usually due to the ingestion of excessive vitamin D preparations. In sarcoidosis and other granulomatous disease, abnormal 1-hydroxylase activity in macrophages of the granulomata can cause increased formation of calcitriol. Hypervitaminosis D causes hypercalcemia. Early symptoms are weakness, constipation, frequent urination, and headache. The sequelae of hypercalcemia include hypercalciuria, nephrocalcinosis, nephrolithiasis, and ectopic calcification of the blood vessels, heart, and lungs (Rubin & Strayer, 2005).

Recently, there has been extensive discussion of data indicating that various nonskeletal diseases—including cancer, autoimmune diseases, and others—are more prevalent in individuals with low 25(OH)D levels. However, a review examining 137 health outcomes did not find convincing evidence for a clear role of vitamin D in any of them owing to inconsistencies in randomized trials, concluding that vitamin D may be a marker rather than the cause of disease (Theodoratou et al., 2014).

Plasma calcium and phosphate fall in vitamin D deficiency, and plasma alkaline phosphatase (bone isoenzyme) is increased in rickets and osteomalacia. The most direct way to determine vitamin D status is by an assay of plasma 25(OH)D (Truswell, 2002), which may be performed either by immunoassay or mass spectrometric methods. Immunoassays for 25(OH)D are also available but are more appropriate for evaluating states of calcium dysregulation than nutritional status. The actual level for optimal 25(OH)D plasma levels is controversial. At this time, the target levels vary by age but are in the vicinity of 30 ng/mL, whereas levels less than 20 ng/mL may be regarded as deficient (Bischoff-Ferrari, 2014; Carter & Card, 2019).

Vitamin E

Vitamin E (tocopherol) is a fat-soluble antioxidant that prevents free radical damage by peroxyl radicals. Although there are eight naturally occurring tocopherols and tocotrienols, only α-tocopherol is recognized by the α-tocopherol transfer protein, which may make it the only variant that meets human requirements (Leonard & Traber, 2019). Nuts, wheat germ, corn and soy beans are rich in vitamin E. Deficiency is very uncommon, but it may occur as a result of fat malabsorption, in total parenteral nutrition, or in premature infants. The clinical findings in deficiencies have been inconsistent, with reports of anemia, ataxia, and lost reflexes. High-dose (>1500 U) vitamin E ingestion has been reported to cause bleeding by altering platelet reactivity. This effect is enhanced in patients taking anticoagulants such as warfarin (Eastwood, 2003; Amrein et al., 2014).

Measurement of vitamin E is not routinely performed. Plasma α-tocopherol levels <12 μmol/L vitamin E are considered indicative of vitamin E deficiency (Institute of Medicine, 2000; Leonard & Traber, 2019).

Vitamin K

The vitamin K family is a group of 3 fat soluble vitamins involved in carboxylation reactions of glutamate residues. The vitamin K–dependent proteins include the coagulation factors, prothrombin (II), factor VII, factor IX, and factor X, Protein C, Protein S, as well as osteocalcin and Matrix

Gla protein (Górska, 2019). Deficiency of the clotting factors listed can result in a bleeding disorder. Effects on osteocalcin may contribute to osteoporosis and abnormal Gla protein to cardiovascular disease. In each reaction, vitamin K, an active hydroquinone, is oxidized to vitamin K epoxide, an inactive form. It is then reduced back to its active hydroquinone form by the enzyme vitamin K epoxide reductase (VKOR).

Vitamin K occurs in three forms: phylloquinone (K_1), menaquinone-n (K_2), and menadione (K_3). Vitamin K_1 is present in fresh green vegetables—such as broccoli, cabbage, and spinach—and in beef liver. Vitamin K_2 is produced by intestinal bacteria. Dietary deficiency is uncommon. It does occur in fat malabsorption. Also, antibiotic sterilization of the intestinal flora may result in vitamin K deficiency. Warfarin antagonizes the actions of VKOR, the enzyme that recycles oxidized vitamin K back to the active hydroquinone (Górska, 2019). Vitamin K deficiency in the newborn is prevented by routine administration at birth.

Laboratory assessment of vitamin K status is technically challenging and is performed only by specialized laboratories (Górska, 2019). Prothrombin time (PT) is not a good surrogate because it is not elevated until deficiency is quite advanced, as undercarboxylated prothrombin must fall >50% before PT elevates.

TRACE ELEMENTS

Trace mineral elements are metals, except for selenium and the halogens—fluoride and iodine. Individually, they are present in tissue concentrations of less than 1 μg/g of wet tissue (Kane & Kumar, 2005) and constitute less than 0.01% of dry body weight (Gibson, 1990; Taylor, 1996). They are referred to as "trace elements" because quantitation was not possible with the analytic methods available at the time they were discovered (O'Dell & Sunde, 1997). Essential trace elements are those that result in an impairment of normal health, function, or development when there is a deficiency that is corrected when supplemented with physiologic levels of that element (Mertz, 1981a, 1981b; Gibson, 1990) and have specific in vivo metabolic functions that cannot be effectively replaced by other similar elements (Milne, 1994).

The various essential trace elements were discovered by several different means. Deficiencies of some of these elements were found in areas where the soil, water, or plants were inadequate in a specific element, such as iodine, fluorine, cobalt, or copper. Deficiencies were also identified when essential elements became biologically unavailable because of interference by other dietary ingestants. One example is the zinc deficiency seen in males in the Middle East and in Hispanics in Denver, Colorado, as a result of eating unleavened bread high in phytate and low-fiber and low-meat diets (Wildman & Medeiros, 2000). Other deficiencies were caused by a mutation that resulted in a lack of a protein needed to absorb or metabolize the element. The symptoms of still other deficiencies were identified in patients whose diets lacked a necessary element or in those on total parenteral nutrition not supplemented with an essential trace element (O'Dell & Sunde, 1997).

Ten trace mineral elements have been generally recognized as essential in humans (Table 27.3). Only copper, iodine, iron, selenium, and zinc are associated with well-characterized deficiency states (Kane & Kumar, 2005). A necessary biochemical role has not been conclusively demonstrated in humans for boron, manganese, nickel, silicon, and vanadium, although signs of deficiency have been described (Gropper et al., 2018). It is difficult to create a deficient model because of the ubiquitous distribution of these elements in the environment and food supply, which frequently causes contamination of the testing system, and because only minute amounts are needed to support physiologic processes. It remains uncertain whether any of the other trace mineral elements are essential in animals and humans. Some authors have concluded that arsenic, boron, fluoride, lithium, manganese, nickel, silicon, and vanadium, which have been shown to have essential biochemical roles in some animal species, are presumptively essential in humans as well (Gropper et al., 2018).

TABLE 27.3
Classification of Trace Mineral Elements

Essential in Humans and Animals	Essential in Some Animals and Possibly in Humans	Possibly Essential in Some Animals	Not Essential
Chromium	Arsenic	Bromine	Aluminum
Cobalt	Boron	Cadmium	Antimony
Copper	Lithium	Lead	Bismuth
Fluorine	Nickel	Strontium	Germanium
Iodine	Silicon	Tin	Mercury
Iron	Vanadium		Silver
Manganese			Thallium
Molybdenum			Titanium
Selenium			
Zinc			

Data from Gibson, 1990; O'Dell & Sunde, 1997

The roles of the trace mineral elements include structural, signal transduction, and especially catalytic properties (Table 27.4). Some of the trace mineral elements are components of metalloenzymes, function as enzyme cofactors, provide electron and oxygen transport, and are active in the maintenance of macromolecule conformation or vitamin and hormonal activity. These trace minerals are avidly accumulated by cells under the control of several families of proteins (Finney & O'Halloran, 2003). Normally, homeostasis of these elements is tightly controlled.

Deficiencies of trace elements are usually due to poor oral intake, inadequate supplementation in total parenteral nutrition, or a disease state in which there is insufficient intestinal absorption or increased excretion or utilization. Deficiencies can also be due to interaction between trace elements (e.g., zinc and copper) and with other nutrients (e.g., zinc and vitamin A) interfering with absorption or adversely affecting metabolic utilization. Large amounts of dietary zinc interfere with intestinal copper absorption and result in copper deficiency and anemia (Milne, 1994; Willis et al., 2005). Genetic defects in trace element metabolism include Menkes kinky hair syndrome (copper), Wilson disease (copper), congenital atransferrinemia (iron), hereditary hemochromatosis (iron), acrodermatitis enteropathica (zinc), and xanthine and sulfite oxidase deficiencies (molybdenum) (Gropper et al., 2018).

Trace elements are widely distributed in the environment. Considerable care is required for their analysis without contamination since they are often present in needles, syringes, stoppers, water, and air. Special collection and handling are necessary. Clean room techniques and ultrapure reagents must be used. Reference materials and strict quality control are requisite with each assay run to ensure analytic accuracy. It is especially important that trained technical personnel perform the testing (Mertz, 1975; Veillon, 1986). Improved materials are now available for collecting, processing, and analyzing trace elements that reduce contamination. These include trace element–free syringes, evacuated tubes with fitted siliconized needles, acid-washed glassware, and standard reference materials with certified values (Casey & Robinson, 1983; Gibson, 1990; WHO, 1996).

The major advances in understanding and managing the dynamics of trace mineral elements during the past 2 decades have been achieved by the extraordinary precision and sensitivity of improved analytic instruments. Atomic absorption spectrometry (AAS) is the most widely used instrument for clinical trace element analysis in biological samples. Graphite furnace AAS (GFAAS) has improved the limit of quantitation (LOQ) to parts per billion (ppb, μg/L) and permits the simultaneous measurement of multiple elements. Zeeman effect background correction improves the element signal measurement when testing in complex specimens such as serum, plasma, or blood. Other specimen handling enhancements have further improved sensitivity and precision. Flame AAS (FAAS) has an LOQ in the ppm (mg/L) range. Atomic emission spectrometry (AES) consists of flame AES and plasma source emission spectrometry, which measures photon output rather than photon absorption, as in AAS. The emission line(s) of the excited electrons are measured. The LOQ is ppm (mg/L). The sample in neutron activation analysis (NAA) is irradiated with low-energy neutrons for the production of radioactive nuclides. In NAA, there is excitation of the atomic nucleus; thus, the trace element is determined independent of its physical or chemical state. The newly formed radionuclide emits x-rays or γ-rays. The LOQ is ppb (μg/L) to ppt (ng/L) with multielement detection, but with a limited dynamic range. This technique is especially suited for in vitro trace element determination in biological matrices. In instrumental neutron activation analysis (INAA), there is direct measurement of the emitted x- or γ-radiation. Inductively coupled plasma/mass spectroscopy (ICP/MS) is a highly sensitive and specific method for the measurement of multiple trace elements in a single run over an especially broad dynamic range with low background interference and LOQs of ppb (μg/L) to ppt (ng/L). An internal standard is used for enhanced precision (Milne, 1994; Chan et al., 1998a).

Testing for the assessment of trace element status requires either measurement of the concentration in accessible tissues (hair, nails) and body fluids (serum, urine) or the activity of a trace element–dependent enzyme. There are no particularly good indicators for the determination of trace element dietary status because of the poor correlation with total body stores. The only definitive test of human trace mineral element deficiency is the clinical response to controlled supplementation with the element of concern,

TABLE 27.4
Function, Deficiency, and Toxicity of Essential Trace Mineral Elements

Element	Function/Enzyme Component	Effects of Deficiency	Effects of Toxicity
Chromium (Cr)	Potentiates insulin action, glucose and lipid metabolism, Cr(III) low toxicity, poorly absorbed. Component of glucose tolerance factor.	No method to determine deficiency in humans; impaired glucose tolerance in type 2 diabetes, insulin resistance, hyperglycemia, peripheral neuropathy, hyperlipidemia	Cr(VI) toxic, oxidative damage, skin ulcers, contact dermatitis, asthma, renal and hepatic necrosis, lung cancer
Cobalt (Co)	Hemoglobin synthesis. Component of vitamin B_{12}.	Cobalt deficiency, as such, not in humans; symptoms due to lack of vitamin B_{12}: Anemia, anorexia, growth depression	Cardiomyopathy, heart failure, goiter, hypothyroidism; warm sensation, vomiting, diarrhea
Copper (Cu)	Cellular respiration, neurotransmitter regulator, oxidation reaction, electron transport, collagen synthesis, development of vascular and skeletal structures and CNS, antioxidant. Component of $CuZnSO_4$, metallothionein, cytochrome C, tyrosinase, dopamine β-hydroxylase, lysyl oxidase.	Menkes kinky hair syndrome, X-linked, congenital failure of Cu absorption; abnormal collagen cross-linking, muscle weakness, iron refractory hypochromic anemia, leukopenia, neurologic defects, hypopigmentation. In prematurity: Bone fractures, skeletal defects. Occurs in malnourished children and premature infants not supplemented.	Relatively nontoxic Wilson disease: Autosomal recessive, failure to excrete Cu in bile; excess Cu in liver, kidneys, brain, eyes; hepatic necrosis, hypertension, Kayser-Fleischer rings in eyes. Cu interferes with absorption of iron and zinc.
Fluorine (F)	Prevents tooth decay.	Increased dental caries	Mottled enamel, fluorosis
Iodine (I)	Component of thyroid hormone.	Goiter, hypothyroidism, cretinism in infants, myxedema in adults	Goiter, thyrotoxicosis
Iron (Fe)	Oxygen transport, respiration, amino acids and free-radical metabolism, lipids, oxidative phosphorylation. Component of hemoglobin, metalloenzymes, vitamin A.	Hypochromic microcytic anemia, glossitis, angular stomatitis, cheilosis, koilonychia Blood loss or inadequate iron intake; iron deficiency anemia:<7 g/100 mL blood	Hemochromatosis: Genetic, primary, autosomal recessive; acquired, secondary, iron overload Iron deposition in liver, pancreas, heart, and skin
Manganese (Mn)	Bone and connective tissue. Component of metalloenzymes: hydrolases, oxidoreductases and lipases, pyruvate carboxylase, superoxide dismutase, and arginase.	Not well defined in humans; skeletal and cartilage defects	Least toxic of trace elements Psychiatric disorders: Memory, speech, hallucinations; syndrome resembles Parkinson and Wilson diseases
Molybdenum (Mo)	DNA metabolism, essential for uric acid production. Component of sulfite and xanthine oxidase.	Naturally occurring deficiency not known, growth depression, hypercuprinemia, defective keratin form, goiter, cretinism	Anemia, goiter, thyrotoxicosis, hypouricemia, hyperoxypurinemia
Selenium (Se)	Protects against oxidative damage of lipid, gene expression, thyroxine deiodinase. Component of glutathione peroxidase.	Keshan disease: cardiomyopathy, cardiomegaly, heart failure, cataracts, osteoarthritis in children, myopathy, discolored/thickened nails, impaired growth	Hair and nail loss, selenosis, tooth decay, neuropathy, liver failure, garlic odor on breath
Zinc (Zn)	Protein synthesis, zinc finger proteins—gene expression, immunity, needed for normal skin, bones, and hair. Component of metallothionein ≈300 enzymes.	Acrodermatitis enteropathica; causes cardiomyopathy in children. In children, low height, hypogeusia, growth retardation, infertility, immune deficits, delayed wound healing, glossitis, seborrheic-like dermatitis, osteoporosis.	Relatively nontoxic: Nausea, vomiting, and GI irritation; causes copper deficiency

Data from: Fausto da Silva & Williams, 1991; Alcock, 1996; Kane & Kumar, 2005.
CNS, Central nervous system; *DNA,* deoxyribonucleic acid; *GI,* gastrointestinal.

followed by an evaluation of improvement of an impaired function (Milne, 1994; Eastwood, 2003). A combination of tests is usually more reliably interpretable, especially when the findings are concordant. The interpretation of plasma or serum levels can be deceptive because of the response to stress or when there is expansion of the blood volume or a decrease in serum albumin as what occurs, for example, in the third trimester of pregnancy. Also, hemolysis interferes. Serum zinc, copper, manganese, chromium, and molybdenum levels are not reliable for assessing nutritional status or dietary intake because the results do not reflect body stores. Trace element assays in blood, serum, or urine usually reflect the current nutriture (Table 27.5).

Hair, fingernail, or toenail analyses provide a retrospective window or an assessment of chronic exposure for the period of hair or nail growth (Gibson, 2002). Hair and nail clippings must be collected with care and washed to avoid surface contamination. The first morning void urine is less affected by recent dietary intake. Load tests measure the change in urine concentration following a loading dose of the mineral element. When tissue levels are low, the deficiency will cause retention of the element. Similarly, tolerance tests measure the change in plasma concentration following a challenge dose. Usually, the dose is in the pharmacologic range rather than the physiologic level normally experienced. Because of the risk of environmental contamination, hair and nail clippings are of limited use in determining dietary intake or body status, except when reduced (Eastwood, 2003).

Each of the essential and nonessential trace mineral elements can be toxic when present in high concentrations. Toxicity is quite variable for the different trace elements. Some have a high toxicity. The toxic effects of selenium are produced by intakes of only 10 times the nutritional requirement. In contrast, trivalent chromium toxicity has never been reported after oral pharmacologic doses up to 1000 μg, above which there is a theoretical risk of damage to DNA (Bogden & Klevay, 2000).

CHROMIUM

Clinical signs of chromium (Cr) deficiency were first described in patients receiving parenteral nutrition and in preterm infants. Chromium sources include meats, whole grains, green beans, broccoli, and some spices. After its absorption in low quantities in the intestine, chromium binds to plasma transferrin and then concentrates in the liver, spleen, other soft tissues, and bone. Chromium at pharmacologic doses has been shown to enhance the action of insulin in animals (Vincent, 2013). It is no longer believed that oral supplementation in chromium-replete people improves insulin-resistance, glucose intolerance, weight loss, or neurologic deficits (Vincent, 2013).

TABLE 27.5

Properties of Essential Trace Mineral Elements

Element	Tissue Distribution	Body Content	Transport (Reference Value)	Excretion
Chromium (Cr)	Spleen, heart	4–6 mg Cr(III)	Transferrin-P 0.15 μg/mL Cr (0.12–2.1 μg/L)	Urine 100–200 ng/day
Cobalt	Muscle, liver, fat	1.1 mg	Albumin (0.11–0.45 μg/L)	Urine 80%
Copper (Cu)	Muscle and liver Liver 30–50 μg/g dry; 50%–70% of body Cu	50–80 mg (1.2–2.5 μg/g fat-free tissue)	Ceruloplasmin 60%–95%, albumin, transcuprein (Cu-S 70–140 μg/dL)	Feces includes bile and unabsorbed dietary Cu
Iodine (I)	Thyroid: 70%–80% of total body I in thyroxine bound to thyroglobulin	15–20 mg (11–15 mg in thyroid)	Thyroxine-binding protein 80% thyroxine-binding prealbumin (transthyretin)	Urine 100–150 μg/day
Iron (Fe)	RBC Hb 400–600 mg/L, liver, spleen, bone marrow 25%, myoglobin	4–5 g (¾ in Hb) 50 mg/kg 2.5 g in RBCs	Transferrin-P (2–2.5 g/L) Ferritin-S 1 μg/L = 10 mg tissue iron stores Hemosiderin 1 g iron	Bile 84 μg/kg, blood loss, menses, GI mucosal cells
Manganese (Mn)	Liver, bone, pancreas	12–20 mg	Mn-Blood 200 nmol/L	Bile and intestinal secretions
Molybdenum (Mo)	Liver, kidney, bone, adrenal	Blood 30–700 nmol/L	RBC protein, α_1-macroglobulin (S: 8–34 μg/L)	Urine 90%, bile 10%
Selenium (Se)	Liver, kidney, muscle	15 mg	Protein (Se-P: 7–30 μg/dL)	Urine 60%, feces 40%
Zinc (Zn)	Muscle 60%, bone 30%, liver, prostate, semen	1.2–2.3 g	Albumin 60%–70%, α_2-macroglobulin (Zn-P 11–22 μmol/L)	Feces, gut secretions, GI mucosal cells

Data from Fausto da Silva & Williams, 1991; Milne, 1994; O'Dell & Sunde, 1997; Kohlmeier, 2003.
GI, Gastrointestinal; *Hb,* hemoglobin; *RBC,* red blood cell.

Hexavalent chromium is a recognized carcinogen. Industrial exposure to metal fumes and dust is associated with lung cancer, kidney failure, dermatitis, and skin ulcers. Health risks are caused by soil contamination by Cr^{6+} waste disposal sites left by leather tanning and dyestuff industries. Chromium is used extensively in the manufacture of stainless steel, chrome plating, leather tanning, printing, and as an anticorrosive in cooling systems. Increased chromium in urine confirms recent occupational or environmental exposure to excess chromium (Halls & Fell, 1988).

COBALT

Cobalt (Co) is essential for humans as an integral part of vitamin B_{12} (cobalamin). Cobalt has no other known function in humans. Cobalt in cobalamin is present only in animal products; thus, vegetarians and vegans must take vitamin B_{12} supplements. Microflora of the human intestine are not able to use cobalt to synthesize cobalamin; thus, free cobalt does not impact the body's vitamin B_{12} pool.

Cobalt toxicity has been reported in patients receiving metal-on-metal hip implants as well as following industrial exposure (Leyssens et al., 2017). The syndrome is characterized by neurologic deficits (hearing and visual impairment) as well as hypothyroidism and cardiac effects (heart failure).

COPPER

Copper (Cu) was one of the first identified trace elements (Bogden & Klevay, 2000) and is the third most abundant trace element in the human body, following zinc and iron. It participates in reactions that involve electron transfer and binding to organic molecules (Samman, 2002).

Biochemistry

Copper is present in all living cells (Marston, 1952). It is a cofactor required for many metalloenzymes involved in electron transport and oxidation reactions and is essential for cellular respiration, neurotransmitter regulation, collagen synthesis, nutrient metabolism, and in the antioxidant defense against free radicals (Kohlmeier, 2003). Copper-containing plasma amine oxidases catabolize some active amines such as tyramine, histidine, and polyamines, and they inactivate the catecholamines (norepinephrine, tyramine, dopamine, and serotonin). Another cuproenzyme, lysyl oxidase, helps collagen proteins cross-link into larger fibers. Also, copper is a component of cytochrome C oxidase, which catalyzes the cellular utilization of oxygen (Wildman & Medeiros, 2000). Extracellular superoxide dismutase is found in high concentrations in the lungs, thyroid, and uterus. Copper/zinc dismutases are found in the cytosol of most cells, especially brain, thyroid, liver, pituitary, and erythrocytes. Both dismutases scavenge and reduce superoxide radicals. Copper-containing proteins include ceruloplasmin, albumin, and transcuprein, which transport copper; metallothionein, which sequesters and stores copper; and clotting factor V (Chan et al., 1998b).

Dietary Sources

Rich sources of copper include liver, shellfish, chocolate, nuts, and seeds. Copper pipes or vessels do not increase the copper content of water unless they are exposed to acids (Kohlmeier, 2003). The average daily copper intake of American adults is about 1.6 mg in males and 1.2 mg in females. Adults should get at least 0.9 mg/day (Institute of Medicine, 2001). Smoking, strenuous exercise, infections, and injuries increase the need for copper.

Metabolism

Copper concentrations in the body are tightly regulated and depend on dietary intake. Its absorption occurs in the stomach and especially in the small intestine (Wapnir, 1998; Turnlund, 1998). Bile adds about 5 mg/day to the ingested copper. Absorption is decreased by excessive zinc or iron intake. Too much copper may cause iron deficiency. Histidine, gluconate, and citrate enhance copper absorption (Wildman & Medeiros, 2000). Ascorbate decreases copper absorption by reducing Cu^{++} to Cu^{+} (Kohlmeier, 2003).

Newly absorbed copper is transported bound to albumin and transcuprein and is rapidly cleared from the blood circulation by the liver. When copper reenters the circulation, it is bound to ceruloplasmin, which transports 65% to 90% of the plasma copper, and metallothionein and other copper-containing proteins. Ceruloplasmin is not a classical transport protein because the copper is not exchangeable (Eastwood, 2003). Metallochaperones are specific binding proteins that provide targeted intracellular copper transport to shuttle copper for metabolic needs (Kohlmeier, 2003). Copper is imported into cells through the cell membrane by a transport protein known as copper transporter 1 (Ctr1). Ctr1 then binds to intracellular copper chaperone proteins. One of these proteins, Atox1, delivers copper to the secretory pathway and docks with either copper-transporting adenosine triphosphatase (ATPase) ATP7B in the liver or ATP7A in other cells. ATP7B then directs copper to plasma ceruloplasmin or to biliary excretion in concert with a newly discovered chaperone, Murr1 (Stern, 2010). Excess copper is bound to thionein, decreasing the potential for copper toxicity (Wildman & Medeiros, 2000). Free copper ions are pro-oxidants and can create oxygen free radicals, and intracellular free copper is kept at a very low concentration.

Testing

The total copper in an adult human is 50 to 80 mg, mainly concentrated in muscle and liver. The liver has the highest copper concentration, averaging

between 30 and 50 μg/g dry tissue. Reference ranges for serum copper concentration are age and sex dependent and are higher in pregnancy. There is diurnal variation, with peak values in the morning. The gender reference ranges include the following: women, 49 to 184 μg/dL (7.7–29.0 μmol/L) and men, 59 to 118 μg/dL (9.3–18.6 μmol/L) by ICP/MS (Chan et al., 1998b). Two commonly used clinical analytic methods are FAAS and ICP/MS. In the latter method, metal ions in a sample are vaporized in a carrier gas that itself is partially ionized. Mostly small cations, such as metal cations, are then detected in the quadrupole field of the mass spectrometer (see Chapter 5). Serum or plasma copper levels are insensitive to the diagnosis of copper deficiency and are decreased only in severe deficiency (Gibson, 2002). Lower concentrations may be indicative of depleted copper stores. However, circulating copper levels are affected by factors unrelated to nutriture. Reduced serum proteins due to nephrosis, malabsorption, and malnutrition may cause the serum copper to be low without reflecting inadequate liver copper stores. Ceruloplasmin is a useful indicator of copper status. It acts as an α_2-globulin acute-phase reactant. Ceruloplasmin is sensitive to the same factors that affect plasma copper and may be measured immunochemically or by its oxidase activity (Milne, 1994). It is increased in patients with infections, neoplasms, pregnancy, and hormonal contraception use (Kohlmeier, 2003). Measurement of erythrocyte Cu-Zn superoxide dismutase is also useful for assessing copper status. The activity is reduced in copper-deficient states.

Copper is excreted primarily in the feces, which includes unabsorbed dietary copper and biliary and gastrointestinal secretions, although small amounts are also lost in sweat, urine, and saliva.

Genetic Diseases

Menkes syndrome and Wilson disease are genetic defects in copper metabolism. Menkes syndrome is a rare X-linked recessive congenital defect of copper absorption. Onset usually occurs by 3 months of age. There is poor mental development, failure to keratinize hair, skeletal problems, and degenerative changes in the aorta. The brittle hair (steely) is kinky or twisted, and there is poor skin and hair pigmentation, hypothermia, and seizures. The hair is like the wool of sheep who grazed in pastures lacking copper. The affected infants have decreased serum and liver copper but red blood cell (RBC) copper is normal (Wildman & Medeiros, 2000).

Wilson disease (hepatolenticular degeneration), also discussed in Chapter 22, is an autosomal-recessive disease that results from impaired biliary copper excretion. It presents in individuals between 6 and 40 years of age. Excess copper is deposited in the liver and the basal nuclei of the brain, causing sclerosis. There are also abnormalities of the kidney, cornea, and brain. Presentation includes neurologic disorders, cirrhosis of the liver, and Kayser-Fleischer rings due to the deposition of copper in the cornea. The latter can be seen initially only on slit lamp examination, but as copper overload progresses they can sometimes be seen by the naked eye. Urinary copper is increased to greater than 100 μg/24 hours, and serum ceruloplasmin is usually decreased. Clinical severity of the disease correlates poorly with the ceruloplasmin level, because ceruloplasmin may be normal or increased in response to hepatic inflammation. Serum copper is generally decreased because of the low ceruloplasmin, and serum copper levels are not useful diagnostically. Serum ceruloplasmin of less than 20 mg/dL with increased hepatic copper of greater than 250 μg/g dry weight is diagnostic. Treatment of Wilson disease includes chelation by D-penicillamine and trientene, other secondary agents and occasionally zinc supplementation (Li et al., 2016). Wilson and Menkes syndromes are caused by various mutations in the *ATP7B* and *ATP7A* genes, respectively, located on chromosome 13q, which both code for ATPases involved in copper transport.

In the absence of Menkes syndrome, deficiency is rare. Deficiencies have been observed in premature babies, malnourished infants and adults, long-term hyperalimentation with infusates deficient in copper, patients with sickle cell disease receiving zinc therapy, and those treated with copper-chelating agents such as penicillamine (Milne, 1994). It has also been reported following Roux-en-Y bariatric surgery (Kumar et al., 2016). Denture adhesive can be a source of excess dietary zinc that induces copper deficiency (Hedera et al., 2009). Symptoms of copper deficiency include hypochromic anemia, ataxia, neutropenia, osteoporosis and bone and joint abnormalities, decreased skin pigmentation, and neurologic abnormalities. Body stores last only a few weeks when intake is low.

Copper toxicity has not been reported from food intake. Doses in excess of 10 mg/day can cause nausea, vomiting, abdominal cramps, and diarrhea, and may even cause hemolytic anemia, kidney dysfunction, and liver injury, especially in infants. Acute poisoning may present with hemolysis and brain and hepatic cellular damage (Eastwood, 2003). Higher doses can cause coma and death. Excess supplements or ingestion of contaminated water are the usual sources. Ingestion of fungicides containing copper sulfate or industrial exposure sometimes causes acute copper poisoning (Williams, 1982).

FLUORIDE

Fluoride (Fl) is used to prevent dental caries. Fluoridation of drinking water now reduces the incidence of tooth decay for more than 60% of the U.S. population and reduces the incidence of tooth decay by more than 60%. Dental fluorosis is the unsightly mottling of dental enamel and is seen in erupting teeth of children due to excessive fluoride, possibly from ingestion of fluoride-containing toothpastes. Occupational exposure to inhaled fluoride dust during aluminum refining causes severe bone abnormalities; safety equipment now limits such exposure. No cases are attributable to the controlled fluoridation of water supplies.

IODINE

Dietary iodine (I) is normally ingested as iodide and is required for the synthesis of thyroid hormones. It is transported to the thyroid follicles, where it is trapped and concentrated. The gland is stimulated by the pituitary hormone, thyroid-stimulating hormone (TSH), to incorporate iodide into tyrosine to form thyronines within the thyroglobulin in the follicular lumen. Proteolytic cleavage of the thyroglobulin releases the iodothyronine hormones into the circulation. With blockade of iodine uptake by antithyroid drugs such as propylthiouracil, the glandular iodide concentration can reach 800 times the plasma iodide concentration. A tightly controlled feedback system among the thyroid, the hypothalamus, and the pituitary maintains the thyroid hormone concentration within physiologic limits.

Deficiency results in inadequate thyroid hormone and hypothyroidism. Iodine deficiency in pregnancy can result in congenital hypothyroidism, which manifests as intellectual disability and the syndrome of cretinism. Adults with myxedema hypothyroidism have mental status changes and hypotension. Patients often develop a goiter.

IRON

Body iron (Fe) is present in hemoglobin, myoglobin, storage iron, and tissue iron. Iron is stored as ferritin and hemosiderin. Normally, very small amounts of iron are present in most cells and in body fluids. Ferritin and transferrin are the main transport proteins that carry iron in the blood, while regulation of absorption and utilization are controlled by peptides such as the iron regulatory proteins (IRPs), hepcidin, and matriptase (Mt2). Other proteins, including divalent metal transporter-1 (DMT1), ferroportin (FPN1), and transferrin receptors (Tfrs) in association with ferroxidases such as duodenal cytochrome B, ceruloplasmin (Cp), and heme carrier protein (HCP1), are also involved.

Hepcidin is the main regulatory protein that controls iron transport across membranes. In the presence of hepcidin, iron transport is inhibited. It is produced in the liver as a prohormone, which must be cleaved by proteases for activation. Biosynthesis of hepcidin is induced in the face of inflammation and underlies the anemia of "ineffective erythropoiesis" observed in that state.

Iron absorption occurs in the duodenum and proximal jejunum. Iron in food exists in two states, heme and nonheme iron. Nonheme iron itself can exist as Fe^{2+} or Fe^{3+}, but it can only be absorbed in the Fe^{2+} state. As is true of copper, phytates in food can interfere with absorption of iron. Transport of iron from the enterocyte into the blood requires the action of ferroportin. Ferroportin is also present in macrophages. In the presence of hepcidin, ferroportin is degraded and iron transport inhibited both across the enterocyte and from macrophage storage. Once iron reaches the plasma, it is transported by transferrin. Transferrin saturation can be used to measure iron stores. Intracellular iron is stored in association with ferritin (Waldvogel-Abramowski et al., 2014).

Iron overload can be either primary, as in hereditary hemochromatosis, or secondary, as occurs in sickle cell disease, thalassemia, and other "iron-loading" anemias, iatrogenic due to multiple blood transfusions or intravenous iron (most commonly in hemodialysis patients), and chronic liver disease. As discussed in Chapter 22, the majority of patients with hereditary hemochromatosis are homozygous for HFE mutation C282Y. Patients with hemochromatosis present with progressive liver disease, diabetes, and darkening of the skin (bronze diabetes). The mechanism by which the HFE mutation induces iron overload involves downregulation of hepcidin with inappropriate storage of iron in various tissues (Bacon et al., 2011). Treatment of hemochromatosis involves judicious use of phlebotomy. Secondary iron overload is treated with chelating agents, including deferoxamine

or deferasirox. In all cases, use of vitamin C should be avoided because of its permissive effect on iron absorption (also see Chapter 33).

MANGANESE

Manganese (Mn) is an important cofactor for enzymes associated with the formation of connective and bony tissue and carbohydrate and lipid metabolism. Food sources include whole-grain foods, nuts, leafy vegetables, soy, and teas. Manganese is absorbed from the small intestines and transported to the liver, bound to albumin. Excretion occurs via bile into feces. Manganese is a constituent of many important metalloenzymes, including Fe/Mn-superoxide dismutase, pyruvate carboxylase, arginase, and glycosyl transferases. On a normal diet, deficiency has not been documented. Dietary deficiency results in low plasma cholesterol, impaired glucose tolerance, skeletal abnormalities, dermatitis, color changes in hair, and reduced blood-clotting function not responsive to vitamin K.

Toxic exposure to manganese-containing dust produces neurologic symptoms (manganism) resembling Parkinson disease. Manganese deposition in the brain is seen with biliary atresia in children. Serum manganese and brain magnetic resonance imaging are used to detect excessive exposure. Plastic cannulas prevent sample contamination.

MOLYBDENUM

Molybdenum (Mo) is incorporated into metalloenzymes and several important enzymes, including sulfite oxidase and xanthine oxidase, an enzyme that has a major role in purine biosynthesis. Grains, nuts, and legumes such as peas, lentils, and beans are good sources. Regulation at the level of the kidney occurs, and urine concentration reflects dietary intake. Deficiency has not been observed in healthy people on a normal diet. There is one report of intolerance to intravenous molybdenum in a patient receiving parenteral nutrition during treatment for Crohn disease. It suggests that, for most, there is sufficient molybdenum as a contaminant in total parenteral nutrition fluids. Diagnosis of molybdenum deficiency is based on demonstration of excess sulfite in the urine. Toxicity of molybdenum has not been studied in humans. However, animal models suggest that long-term ingestion of more than 10 mg/day can cause kidney and liver damage as well as infertility, diarrhea, and gout. Excess intake interferes with copper absorption, increases urinary copper excretion, and inhibits binding of copper to plasma proteins. It has been used as a treatment for copper toxicosis in animals.

SELENIUM

Selenium (Se) is present in foods as both inorganic (selenates and selenites) and organic (selenomethionine and selenocysteine) forms. Selenium is present in the body as the amino acid selenomethionine as well as a constituent of glutathione peroxidase, an important enzyme in the defense against oxidant stress. In China, prior to the 1970, when selenium supplementation became routine, selenium deficiency was associated with endemic cardiomyopathy (Keshan disease) as well as skeletal muscle disorders with proximal weakness in patients who were infected with Coxsackie virus (Sunde, 2014). Immunodeficiency can result from selenoprotein deficiency. Toxicity from selenium includes hair loss, garlic breath, irritability, and mild nerve and nail damage. Oral selenium supplementation eliminated Keshan disease in areas where it was endemic (Loscalzo, 2014). Selenium can be measured in the plasma or serum to estimate short-term intake, or in hair or nail clippings, which more reliably reflects long-term intake (Sunde, 2014). Whole-blood selenium can be quantified by graphite furnace atomic absorption GFAAS.

ZINC

Zinc (Zn) is second to iron as the most abundant trace element in the body. It is the most common catalytic metal ion in the cytoplasm of cells. Total body stores of zinc are 1.5 g in adult women and 2.5 g in men, which are distributed in all tissues. It is almost entirely intracellular (King & Keen, 1994). Most zinc is found in skeletal muscle (≈60%) and bone (≈30%) (Wildman & Medeiros, 2000). It is a cofactor for more than 100 enzymes and is involved in wound healing, immune function, DNA synthesis, and in almost all aspects of metabolism (Kohlmeier, 2003). It is also essential for the synthesis and action of insulin (Samman, 2002). Zinc is present in the divalent state in biological systems, and participation in oxidation-reduction reactions is not possible. Important zinc-containing metalloenzymes include carbonic anhydrase, alkaline phosphatase, RNA and DNA polymerases, reverse transcriptase, thymidine kinase, carboxypeptidases, alcohol dehydrogenase, and Cu/Zn superoxide dismutase.

Dietary Sources

Zinc is ubiquitous in food. Oysters are especially rich in zinc, and other shellfish and meats are good sources. As mentioned earlier with other trace elements, the presence of phytates in plants and whole grains can reduce zinc bioavailability (Kohlmeier, 2003), while ingestion of protein can enhance absorption (Lönnerdal, 2000). The estimated average requirement to maintain adequate stores is 8 mg/day for women eating a mixed diet and 11 mg/day for men (Institute of Medicine, 2001). Vegetarians and pregnant or nursing women need slightly more. Zinc is excreted primarily by the intestine and is not stored in the body; thus, daily intake is required.

Metabolism

Zinc is mainly absorbed from the duodenum, although some is absorbed in the jejunum. Some zinc enters the intestinal lumen with pancreatic secretions. Intraluminal digestion by proteases, DNAses, and RNAses frees zinc, which complexes with histidine, cysteine, and nucleotides. High dietary calcium and possibly iron will also reduce zinc absorption (Samman, 2002). The transport of zinc across the enterocyte and into portal blood is incompletely understood. It includes metallothionein as well as recently described zinc transport proteins and divalent cation transporter-1 (DCT-1) (Roohani et al., 2013). In blood, the zinc is bound to albumin and α_2-macroglobulin, with zinc blood concentrations of 10 to 17 μmol/L.

Muscle and bones, which contain most of the body's zinc, have a slow turnover, with a half-life of 300 days (Wastney et al., 2000). The half-life of the metallothionein-bound zinc in the liver is about 2 weeks; this pool can be readily mobilized and cover for an insufficient dietary intake. However, the liver pool is small and contains less than 170 mg. Zinc deficiency can become functionally significant within a week (Miller et al., 1994).

Almost all blood zinc is complexed to the large proteins albumin or α_2-macroglobulin; thus, there is little zinc in the glomerular filtrate. Urine losses are about 0.5 mg/day (Kohlmeier, 2003), and the primary route of excretion is gastrointestinal, through biliary and intestinal secretion (Roohani et al., 2013). About 1 mg/day is lost in sweat, skin, and hair. Fecal losses, which include unabsorbed dietary zinc and endogenous secretions, can be less than 1 mg/day (Sian et al., 1996). Another potential source of zinc loss in males is seminal fluid. Each ejaculate contains about 0.5 mg, probably from prostatic secretions.

Certain medications can alter zinc homeostasis. The fluoroquinolone antibiotics can inhibit gastrointestinal absorption, and thiazide diuretics can enhance urinary losses by as much as 60%.

Zinc fingers are ubiquitous looped sequence-specific DNA-binding proteins with functions that are extraordinarily diverse and include DNA recognition, RNA packaging, transcriptional activation, regulation of apoptosis, protein folding and assembly, and lipid binding (Wildman & Medeiros, 2000; Laity et al., 2001).

Deficiency

Zinc deficiency is observed in patients who abuse alcohol and in malabsorption syndromes, as well as in populations with high phytate intake and poor soil zinc levels. Symptoms are nonspecific because of the many enzymes and tissues affected. In severe deficiencies there is hypogonadism, dwarfism, deformed bones, poor wound healing, abnormal hair and nails, loss of taste, gastrointestinal disturbances, poor chylomicron formation, central nervous system abnormalities, immunodeficiencies, and malabsorption. Zinc deficiency may cause teratogenicity during pregnancy, with congenital malformations, fetal dysmaturity, prematurity, neural tube defects, and spina bifida (Chan et al., 1998b). Zinc deficiency observed in alcoholics and in patients with cirrhosis is manifested by low serum zinc concentrations and increased urinary excretion (Prasad, 1982; Eastwood, 2003).

Acrodermatitis enteropathica is a rare autosomal-recessive disorder secondary to impaired intestinal absorption and transport of zinc. Symptoms include hyperpigmented skin lesions, pustular and bullous dermatitis, alopecia, growth retardation, diarrhea, secondary infection, irritability, lethargy, and depression. Plasma or serum zinc is below 40 μg/mL. Oral zinc therapy results in rapid and complete remission (Chan et al., 1998b).

Zinc toxicity is rare in humans. Animals that were given high levels of supplementation exhibited weight loss attributed to reduced food intake. Inhalation of zinc oxide fumes is the most common cause of zinc overdose in humans, and manifests as "metal fume fever." Symptoms are a flu-like illness, with onset 4 to 6 hours after exposure to the fumes. Fatigue, chills, myalgias, cough, dyspnea, leukocytosis, thirst, metallic taste, and salivation characterize this self-limited illness, with resolution of symptoms in 36 hours after removal from the contaminated area.

Testing

The two groups of tests include analysis of zinc in a body tissue or body fluid, such as plasma, serum, blood cells, or urine, and testing a zinc-dependent function, such as taste acuity or the measurement of the activity of zinc-containing enzymes. In most instances, the assays will show a decrease with zinc deficiency. Test results need be interpreted with caution because the levels may be affected by unrelated conditions. There is a complex diurnal variation of zinc levels, with levels highest in the morning after fasting, rising slightly after meals, and then falling for about 4 hours (Roohani et al., 2013). Albumin levels significantly affect the circulating zinc level, as do pregnancy and any significant infection or inflammatory state. Also, many steroids, including adrenocortical and gonadal, depress the zinc level. Erythrocyte levels are 10 times that of serum, and hemolysis is a serious problem affecting the usefulness of the results.

ICP/MS is the reference testing method used for zinc testing in serum, plasma, and other clinical specimens. Zinc plasma level reference value is 70 to 120 μg/dL (10.7–18.4 μmol/L), of which one-third is bound to α_2-macroglobulin and the rest to albumin. From 10% to 20% of the blood zinc is in the plasma; the remainder is associated with carbonic anhydrase in the erythrocytes. Hemolysis must be avoided. Fasting morning levels of zinc below 70 μg/dL (10.7 μmol/L) suggest marginal deficiency. Serum zinc values are 5% to 10% higher than plasma.

Zinc levels in erythrocytes and hair provide a long-term assessment of body zinc status. Lowered hair zinc has been demonstrated in several different zinc-deficient conditions. Care must be taken to avoid environmental contamination and to sample hair grown during the condition under study and not the time period just prior (Milne, 1994). The urinary zinc excretion reference value is 0.15 to 1.00 mg/day (2.3–15.3 μmol/day). Urinary zinc excretion is usually decreased in zinc deficiency. In some conditions associated with zinc deficiency, such as cirrhosis, severe alcoholism, sickle cell anemia, postsurgical periods, and total parenteral nutrition, increased urinary zinc excretion is often present (Jacob & Milne, 1993).

Hyperzincemia is a familial disorder that results in elevated serum zinc levels but does not cause any apparent toxicity. Zinc overdoses that result in similar plasma zinc levels have been known to be fatal (Wildman & Medeiros, 2000).

ACKNOWLEDGMENT

This chapter is dedicated to the late Dr. Martin J. Salwen, who wrote or edited this chapter for many editions of this book.

SELECTED REFERENCES

Kohlmeier M: *Nutrient metabolism*, San Diego, CA, 2015, Academic Press.

This text provides a systematic presentation of the metabolism of the vitamins and trace elements, with masterful integration of the vast subject of nutritional metabolism and biochemistry, in the context of normal human physiology. Extensive current references are provided.

Mann J, Truswell AS, editors: *Essentials of human nutrition*, ed 4, Oxford, 2012, Oxford University Press.

The trace elements and vitamins are presented with a focus on deficiencies, toxicity, and biochemical testing. An appendix is included that assesses numerous standard and newly introduced static and dynamic biochemical tests, and load and tolerance tests, the findings, utility, and their interpretability.

Taylor A: Detection and monitoring of disorders of essential trace elements, *Ann Clin Biochem* 33:486–510, 1996.

Presented are the findings in deficiencies of essential trace elements due to metabolic disorders, with descriptions of the clinical disorders, the clinical signs and test results for the assessment of trace element status, the findings, interpretability, and utility of the data; nonoccupational disorders associated with accumulation of essential trace elements; and protocols for testing in genetic, therapeutic, and disease states, including nonanalytic factors affecting interpretation and analytic techniques.

Wildman REC, Medeiros DM: *Advanced human nutrition*, ed 4, Boca Raton, FL, 2019, CRC Press.

Presents the biochemistry and physiology of the vitamins and the essential trace elements, including tables of functions, tissue content and excretion, deficiency and toxicity symptoms, and the food sources with their micronutrient content.

Access the complete reference list online at Elsevier eBooks for Practicing Clinicians.

REFERENCES

Alcock NW: Trace elements. In Kaplan LA, Pesce AJ, editors: *Clinical Chemistry*, ed 3, St. Louis, MO, 1996, Mosby, pp 746–759.

Amrein K, Schnedl C, Holl A, et al.: Effect of high-dose vitamin D3 on hospital length of stay in critically ill patients with vitamin D deficiency. The VITdAL-ICU Randomized Clinical Trial, *J Am Med Assoc* 312:1520–1530, 2014.

Anderson OS, Sant KE, Dolinoy DC: Nutrition and epigenetics: an interplay of dietary methyl donors, one-carbon metabolism, and DNA methylation, *J Nutr Biochem* 23:853–859, 2012.

Bacon BR, Adams PC, Kowdley KV, Powell LW, Tavill AS: American association for the study of liver diseases: diagnosis and management of hemochromatosis: 2011 practice guideline by the American association for the study of liver diseases, *Hepatology* 54:328–343, 2011.

Barr SI, Murphy SP, Poos MI: Interpreting and using the dietary references intakes in dietary assessment of individuals and groups, *J Am Diet Assoc* 102:780–788, 2002.

Berdanier CD: *CRC desk reference for nutrition*, Boca Raton, FL, 1998, CRC Press.

Bischoff-Ferrari HA: Optimal serum 25-hydroxyvitamin D levels for multiple health outcomes, *Adv Exp Med Biol* 810:500–525, 2014.

Bizarro N, Antico A: Diagnosis and classification of pernicious anemia, *Autoimmun Rev* 13:565–568, 2014.

Bogden JD, Klevay LM: Clinical nutrition of the essential trace elements and minerals. In Bogden JD, Klevay LM, editors: *The Guide for health Professionals*, Totowa, NJ, 2000, Humana Press, p 397.

Brewster MA: Vitamins. In Kaplan LA, Pesce AJ, editors: *Clinical Chemistry*, ed 3, St. Louis. MO, 1996, Mosby, pp 760–792.

Carling RS, Turner C: Methods for assessment of biotin (Vitamin B_7). In Harrington D, editor: *Laboratory assessment of vitamin status*, London, UK, 2019, Academic Press, pp 193–217.

Carter G, Card DJ: Methods for assessment of vitamin D. In Harrington D, editor: *Laboratory assessment of vitamin status*, London, UK, 2019, Academic Press, pp 49–77.

Casey CE, Robinson MF: Some aspects of nutritional trace element research. In Siegel H, editor: *Metal Ions in Biological Systems*, vol. 16. New York, 1983, Marcel Dekker, pp 1–26.

Chan S, Gerson B, Reitz RE, Sadjadi SA: Technical and clinical aspects of spectrometric analysis of trace elements in clinical samples, *Clin Lab Med* 18:615–629, 1998a.

Chan S, Gerson B, Subramaniam S: The role of copper, molybdenum, selenium, and zinc in nutrition and health, *Clin Lab Med* 18:673–685, 1998b.

Combs Jr GF: *The vitamins*, 2nd ed, San Diego, CA, 1998, Academic Press.

Crook MA: Methods for assessment of thiamine (Vitamin B_1). In Harrington D, editor: *Laboratory assessment of vitamin status*, London, UK, 2019, Academic Press, pp 149–164.

Eastwood M: *Principles of human nutrition*, ed 2, Oxford, UK, 2003, Blackwell.

Elia M: Metabolic response to starvation, injury and sepsis. In Payne-James J J, Grimble G, Silk D, editors: *Artificial nutrition support in clinical Practice*, London, UK, 2001, Greenwich Medical Media, pp 1–24.

Fausto da Silva JJR, Williams RJP: *The biological Chemistry of the elements*, Oxford, UK, 1991, Clarendon Press.

Feldman EB: Assessment of nutritional status. In Noe DA, Rock RC, editors: *Laboratory medicine*, Baltimore, MD, 1994, Williams & Wilkins.

Finney LA, O'Halloran TV: Transition metal speciation in the cell: insights from the chemistry of metal ion receptors, *Science* 300:931–936, 2003.

Freedman LS, Commins JM, Willett W, et al.: Evaluation of the 24-hour recall as a reference instrument for calibrating other self-report instruments in nutritional cohort studies: evidence from the validation studies pooling project, *Am J Epidemiol* 186:73–82, 2017.

Gibson RS: *Principles of nutritional assessment*, Oxford, UK, 1990, Oxford University Press.

Gibson R: Determining nutritional status. In Mann J, Truswell AS, editors: *Essentials of human nutrition*, ed 2, Oxford, UL, 2002, Oxford University Press, pp 467–497.

Gidden F, Shenkin A: Laboratory support of the clinical nutrition service, *Clin Chem Lab Med* 38:683–714, 2000.

Górska RM: Methods for assessment of vitamin K. In Harrington D, editor: *Laboratory assessment of vitamin status*, London, UK, 2019, Academic Press, pp 107–147.

Grodner M, Long S, DeYoung S: *Foundations and clinical Applications of nutrition*, ed 3, St. Louis, MO, 2004, Mosby.

Gropper SS, Smith JL, Carr TP: *Advanced nutrition and human metabolism*, ed 7, Boston, MA, 2018, Cengage Learning.

Guyton AC, Hall JE: *Human physiology and mechanisms of disease*, ed 6, Philadelphia, PA, 1997, WB Saunders.

Halls DJ, Fell GS: Faster determination of chromium in urine by atomic absorption spectrometry, *J Anal Atom Spectrom* 3:105–109, 1988.

Hedera P, Peltier A, Fink JK, et al.: Myelopolyneuropathy and pancytopenia due to copper deficiency and high zinc levels of unknown origin II. The denture cream is a primary source of excessive zinc, *Neurotoxicology* 30:996–999, 2009.

Huisjes R, Card DJ: Methods for assessment of pantothenic acid (Vitamin B_5). In Harrington D, editor: *Laboratory assessment of vitamin status*, London, UK, 2019, Academic Press, pp 173–179.

Institute of Medicine: *Dietary reference intakes for calcium, phosphorus, magnesium, vitamin D, and fluoride*, Washington, DC, 1997, National Academies Press.

Institute of Medicine: *Dietary reference intakes for thiamin, riboflavin, niacin, vitamin B_6, folate, vitamin B_{12}, pantothenic acid, biotin, and choline*, Washington, DC, 1998, National Academies Press.

Institute of Medicine: *Dietary reference intakes for vitamin C, vitamin E, selenium, and carotenoids*, Washington, DC, 2000, National Academies Press.

Institute of Medicine: *Dietary reference intakes for vitamin A, vitamin K, arsenic, boron, chromium, copper, iodine, iron, manganese, molybdenum, nickel, silicon, vanadium, and zinc (micronutrients)*, Washington, DC, 2001, National Academies Press.

Jacob RA: Vitamin C. In Shils ME, Olsen JA, Shike M, editors: *Modern nutrition in health and disease*, 8th ed, Philadelphia, PA, 1994, Lea & Febiger, pp 432–448.

Jacob RA, Milne DB: Biochemical assessment of vitamins and trace metals, *Clin Lab Med* 13:371–385, 1993.

Jacobson EL, Kim H, Kim M, Jacobson MK: Niacin: vitamin and antidyslipidemic drug, *Subcell Biochem* 56:37–47, 2012.

Kane AB, Kumar V: Environmental and nutritional pathology. In Kumar V, Abbas AK, Fausto N, editors: *Robbins and Cotran Pathologic Basis of disease*, ed 7, Philadelphia, PA, 2005, Elsevier, pp 415–468.

Katz DL: *Nutrition in clinical Practice*, Philadelphia, PA, 2001, Lippincott, Williams & Wilkins.

King JC, Keen CL: Zinc. In Shils ME, Olsen JA, Shike M, editors: *Modern nutrition in health and disease*, ed 8, Philadelphia, PA, 1994, Lea & Febiger, pp 214–239.

Kumar P, Hamza N, Madhok B, et al.: Copper deficiency after gastric bypass for morbid obesity: a systematic review, *Obes Surg* 26:1335–1342, 2016.

Laity JH, Lee BM, Wright PE: Zinc finger proteins: new insights into structural and functional diversity, *Curr Opin Struct Biol* 11:39–46, 2001.

Lamberg-Allardt C, Brustad M, Meyer HE, Steingrimsdottir L: Vitamin D - a systematic literature review for the 5th edition of the Nordic Nutrition Recommendations, *Food Nutr Res* 57, 2013, https://doi.org/10.3402/fnr.v57i0.22671.

Lambie DG, Johnson RH: Drugs and folate metabolism, *Drugs* 30:145–155, 1985.

Leonard SW, Traber MG: Methods for assessment of vitamin E. In Harrington D, editor: *Laboratory assessment of vitamin status*, London, UK, 2019, Academic Press, pp 79–105.

Leyssens L, Vinck B, Van Der Straeten C, et al.: Cobalt toxicity in humans - a review of the potential sources and systemic health effects, *Toxicology* 387:43–56, 2017.

Li WJ, Chen C, You ZF, et al.: Current drug Managements of Wilson's disease: from west to East, *Curr Neuropharmacol* 14:322–325, 2016.

Loerch JD, Underwood BA, Lewis KC: Response of the plasma levels of vitamin A to a dose of vitamin A an indicator of hepatic vitamin A reserves in rats, *J Nutr* 109:778–786, 1979.

Lönnerdal B: Dietary factors influencing zinc absorption, *J Nutr* 130(Suppl 5S):1378S–1383S, 2000.

Loscalzo J: Keshan disease, selenium deficiency, and the selenoproteome, *N Eng J Med* 370:1756–1760, 2014.

Machlin LJ: Introduction. In HE S, Machlin LJ, editors: *Beyond deficiency*, vol. 669. Ann NY Acad Sci, 1992, pp 1–6.

Marston HR: Cobalt, copper and molybdenum in the nutrition of animals and plants, *Physiol Rev* 32:153–157, 1952.

Mason JB: Consequences of altered micronutrient status. In Bennett JC, Plum F, editors: *Cecil Textbook of medicine*, ed 20, Philadelphia, PA, 1996, WB Saunders, pp 1144–1154.

McCormick DB, Greene HL: Vitamins. In Burtis CA, Ashwood ER, editors: *Tietz Textbook of clinical Chemistry*, ed 2, Philadelphia, PA, 1994, WB Saunders, pp 1275–1316.

McLaren DC: Clinical manifestations of human vitamin and mineral disorders: a resume. In Shils ME, Olsen JA, Shike M, editors: *Modern nutrition in health and disease*, ed 8, Philadelphia, PA, 1994, Lea & Febiger, pp 909–923.

Mertz W: Trace-element nutrition in health and disease: contributions and problems of analysis, *Clin Chem* 21:468–475, 1975.

Mertz W: The essential trace elements, *Science* 213:1332–1338, 1981a.

Mertz W: The scientific and practical importance of trace elements, *Phil Trans R Soc Lond B* 294:9–18, 1981b.

Miller LV, Hambidge KM, Naake VL, et al.: Size of the zinc pools that exchange rapidly with plasma zinc in humans: alternative techniques for measuring and relation to dietary zinc intake, *J Nutr* 124:268–276, 1994.

Milne DB: Trace elements. In Burtis CA, Ashwood ER, editors: *Tietz Textbook of clinical Chemistry*, ed 2, Philadelphia, PA, 1994, WB Saunders, pp 1317–1353.

Nazki FH, Sameer AS, Ganaie BA: Folate: metabolism, genes, polymorphisms and the associated diseases, *Gene* 533:11–20, 2014.

O'Dell BL, Sunde RA: *Handbook of nutritionally essential mineral elements*, New York, NY, 1997, Marcel Dekker.

Olsen RQ, Regis JT: Delirious deficiency, *Lancet* 376:1362, 2010.

Prasad AS: Clinical and biochemical spectrum of zinc deficiency in human subjects. In Prasad AS, editor: *Clinical, biochemical, and nutritional aspects of trace elements*, New York, NY, 1982, Alan R. Liss, pp 3–62.

Roohani N, Hurrell R, Kelishadi R, Schulin R: Zinc and its importance for human health: an integrative review, *J Res Med Sci* 18:144–157, 2013.

Ross AC, Taylor CL, Yaktine AL, Del Valle HB: *Dietary reference intakes for calcium and vitamin D. Institute of medicine (US) Committee to review dietary reference intakes for vitamin D and calcium*, Washington, DC, 2011, National Academies Press (US).

Rubin E, Strayer DS: Environmental and nutritional pathology. In Rubin E, Gorstein F, Rubin R, et al.: *Rubin's Pathology: Clinicopathologic Foundations of medicine*, ed 4, Philadelphia, PA, 2005, Lippincott Williams & Wilkins, pp 312–355.

Samman S: Trace elements. In Mann J, Truswell AS, editors: *Essentials of human nutrition*, ed 2, Oxford, UK, 2002, Oxford University Press, pp 159–188.

Seymour CA: Trace metal disorders. In Ledingham JGG, Warrell DA, editors: *Concise Oxford Textbook of medicine*, Oxford, UK, 2000, Oxford University Press, pp 710–718.

Sian L, Mingyan X, Miller LV, et al.: Zinc absorption and intestinal losses of endogenous zinc in young Chinese women with marginal zinc intakes, *Am J Clin Nutr* 63:348–353, 1996.

Sies H, Stahl W, Sunquist AR: Antioxidant functions of vitamins, HE S, Machlin LJ, editors: *Beyond Deficiency*, *Ann NY Acad Sci* 669:7–20, 1992.

Skeaff M: Vitamins C and E. In Mann J, Truswell AS, editors: *Essentials of human nutrition*, ed 2, Oxford, UK, 2002, Oxford University Press, pp 231–247.

Stabler SP: Vitamin B_{12} deficiency, *N Engl J Med* 368:149–160, 2013.

Stern BR: Essentiality and toxicity in copper health risk assessment: Overview, update and regulatory considerations, *J Toxicol Environ Health* 73:114–127, 2010.

Sunde RA: Selenium. In Ross AC, Caballero B, Cousins RJ, et al.: *Modern nutrition in health and disease*, ed 11, Baltimore, MD, 2014, Lippincott Williams & Wilkins, pp 265–276.

Subramanya SB, Subramanian VS, Said HM: Chronic alcohol consumption and intestinal thiamin absorption: effects on physiological and molecular parameters of the uptake process, *Am J Physiol Gastrointest Liver Physiol* 299:G23–G31, 2010.

Theodoratou E, Tzoulaki I, Zgaga L, Ioannidis JP: Vitamin D and multiple health outcomes: umbrella review of systematic reviews and meta-analyses of observational studies and randomised trials, *BMJ* 348, 2014. g20352014.

Traber MG, Stevens JF: Vitamins C and E: beneficial effects from a mechanistic perspective, *Free Radic Biol Med* 51:1000–1013, 2011.
Truswell S: Vitamins D and K. In Mann J, Truswell AS, editors: *Essentials of human nutrition*, ed 2, Oxford, UK, 2002, Oxford University Press, pp 249–258.
Truswell S, Milne R: The B vitamins. In Mann J, Truswell AS, editors: *Essentials of human nutrition*, ed 2, Oxford, UK, 2002, Oxford University Press, pp 209–230.
Turnlund JR: Human whole-body copper metabolism, *Am J Clin Nutr* 67(Suppl 5):960S–964S, 1998.
Veillon C: Trace element analysis of biological samples, *Anal Chem* 58:851A–866A, 1986.
Vincent JB: *The Bioinorganic Chemistry of chromium*, Chichester, UK, 2013, John Wiley & Sons.
Vogiatzi MG, Jacobson-Dickman E, DeBoer MD: Drugs, and Therapeutics Committee of the Pediatric Endocrine Society: vitamin D supplementation and risk of toxicity in pediatrics: a review of current literature, *J Clin Endocrinol Metab* 99:1132–1141, 2014.
Waldvogel-Abramowski S, Waeber G, Gassner C, et al.: Physiology of iron metabolism, *Transfus Med Hemother* 41:213–221, 2014.
Wapnir RA: Copper absorption and bioavailability, *Am J Clin Nutr* 67(Suppl):10545–10605, 1998.
Wastney ME, House WA, Barnes RM, et al.: Kinetics of zinc metabolism: variation with diet, genetics and disease, *J Nutr* 130(Suppl 5S):1355S–1359S, 2000.
West CE: Vitamin A and carotenoids. In Mann J, Truswell AS, editors: *Essentials of human nutrition*, ed 2, Oxford, UK, 2002, Oxford University Press, pp 188–207.
WHO: *Trace elements in human nutrition and disease*, Geneva, Switzerland, 1996, World Health Organization.
Williams DM: Clinical significance of copper deficiency and toxicity in the world population. In Prasad AS, editor: *Clinical, biochemical, and nutritional aspects of trace elements*, New York, NY, 1982, Alan R. Liss, pp 277–299.
Williams P: Food toxicity and safety. In Mann J, Truswell AS, editors: *Essentials of human nutrition*, ed 2, Oxford, UK, 2002, Oxford University Press, pp 416–432.
Willis MS, Monaghan SA, Miller MI, et al.: Zinc-induced copper deficiency, *Am J Clin Path* 123:125–131, 2005.

CHAPTER 28

CHEMICAL BASIS FOR ANALYTE ASSAYS AND COMMON INTERFERENCES

Matthew R. Pincus, Richard A. McPherson, Jay Bock

INTRODUCTION, 453
ION-SELECTIVE ELECTRODES, 453
SPECTROPHOTOMETRIC DETERMINATIONS USING SIMPLE REAGENTS, 454
Beer's Law, 454
End-Point Versus Rate Method, 454
Interferences, 455
Quantitation of Analytes, 456
USE OF ENZYMES AS REAGENTS TO DETERMINE ANALYTE CONCENTRATIONS, 458
General Features, 458
Analytes Whose Concentrations are Determined by Enzyme Reactions, 458
Assays for Enzymes, 462
SELECTED REFERENCES, 466

KEY POINTS

- The clinical chemistry metabolic profile gives important quantitative information for over 25 serum analytes, often facilitating diagnosis of disease.
- Serum electrolyte concentrations for sodium, potassium, chloride, and sometimes calcium are most commonly assayed using ion-selective electrodes.
- Assays for other analytes, including total protein, albumin, bilirubin, creatinine, calcium, iron and iron-binding capacity, magnesium, and phosphate, are performed using spectrophotometry on complexes that each analyte forms with simple reagents. These complexes absorb light at wavelengths at which there is minimal absorbance by both the analyte itself and by the reagent. The concentration of the analyte is determined using Beer's law.
- Assays for a number of serum analytes—including ammonia, bicarbonate, cholesterol, glucose, lactate, triglycerides, urea, and uric acid—utilize enzymes that catalyze reactions in which the analytes are converted into products whose concentrations can be measured conveniently.
- Spectrophotometric assays can be performed by waiting for the point at which the increase or decrease in absorbance of a complex at a particular wavelength ceases to change (end-point method) or by the initial rates of complex formation (rate method).
- Assays for specific enzymes are performed using substrates that are specific for these enzymes. The concentrations of the products of the enzyme-catalyzed reactions are determined spectrophotometrically as described in Chapter 21, allowing for direct determination of enzyme activity.
- Often, the products of enzyme-catalyzed reactions are measured in coupled reactions in which the product of the enzyme-catalyzed reaction is the substrate for another enzyme added at high concentration, allowing for the rapid conversion of the product of the first reaction to another product whose concentration can be easily determined.
- Interferences with spectrophotometric methods most commonly include hemolysis, bilirubinemia, lipemia, and some drugs. Hematocrit effect and volume displacement are interferences that can affect point-of-care testing as well as main laboratory chemistry analyzers, sometimes with extreme bias.

INTRODUCTION

In many of the preceding chapters, we have discussed the chemical bases for the assays employed for the diagnosis of specific diseases. In this chapter, we present a consolidation of the methods that are used in the typical so-called "metabolic panel" in Clinical Chemistry, a panoply of chemical assays that are often requested for patients undergoing outpatient annual checkups or who are being admitted to the hospital. We summarize and discuss the chemical bases for these assays in a concise manner so that the reader can refer to these methods conveniently and understand the assays and their limitations. Understanding of the assays further enables an understanding of why certain substances interfere with particular assays and can give rise to misleading results. It should be kept in mind that, for many of the assays described here, more than one method can be used. Since it is impossible to cover all variations of methods used to quantitate each analyte, we describe the principles that underlie commonly employed methods and refer, where possible, to alternate approaches.

Metabolic panels consist of serum electrolytes (sodium, potassium, and chloride), bicarbonate, calcium, phosphate, magnesium, blood urea nitrogen (BUN), creatinine, glucose, uric acid, total protein, albumin, total and direct bilirubin, cholesterol, high-density lipoprotein (HDL) and low-density lipoprotein (LDL), triglycerides, ammonia, iron and iron-binding capacity, and the enzymes: creatine kinase (CK), aspartate aminotransferase (AST), alanine aminotransferase (ALT), alkaline phosphatase (ALP), lactate dehydrogenase (LD), γ-glutamyl transferase (GGT), amylase, and lipase. The reader may recognize various panels that measure the functioning of specific tissues, including the kidney, such as the renal "profile" (i.e., BUN, creatinine, calcium, and phosphate). These panels are of great use in diagnosing disease states, as discussed in Chapter 9.

We divide the basic assays for these analytes functionally into four method-based groups:

1. Ion-selective electrodes
2. Spectrophotometric assays based on color complexes for specific molecules: for example, the color noncovalent complex of albumin with bromcresol green dye and bilirubin covalently reacted with diazotized sulfanilic acid to give azo-derivatized forms of the indole rings of bilirubin
3. Analyte concentrations using enzymes as reagents. In Chapter 21, we discussed how small molecule substrates are used to determine serum enzyme concentrations. In a similar manner, this process can be reversed; enzymes can be used to determine the concentrations of small or large molecules (like proteins). If an analyte is a specific substrate for an enzyme and if the formation of product or disappearance of the substrate can be conveniently followed, this method can be used quite effectively.
4. Enzyme assays, that is, use of substrates to determine enzyme concentrations as described in Chapter 21. Almost all of these assays are also based on spectrophotometric measurements. These depend on the substrates employed in the assays and, in many cases, the need for the use of indicator enzymes in so-called "coupled reactions."

ION-SELECTIVE ELECTRODES

As explained in Chapter 4, this technique is used to measure the concentrations of specific ions, using an electrochemical method. This method is nonspecific in that it does not discriminate between ions in causing voltage differences between the measuring electrode and the standard electrode. It is the presence of an ion perm-selective membrane barrier on the measuring electrode that allows only a specific ion to pass through

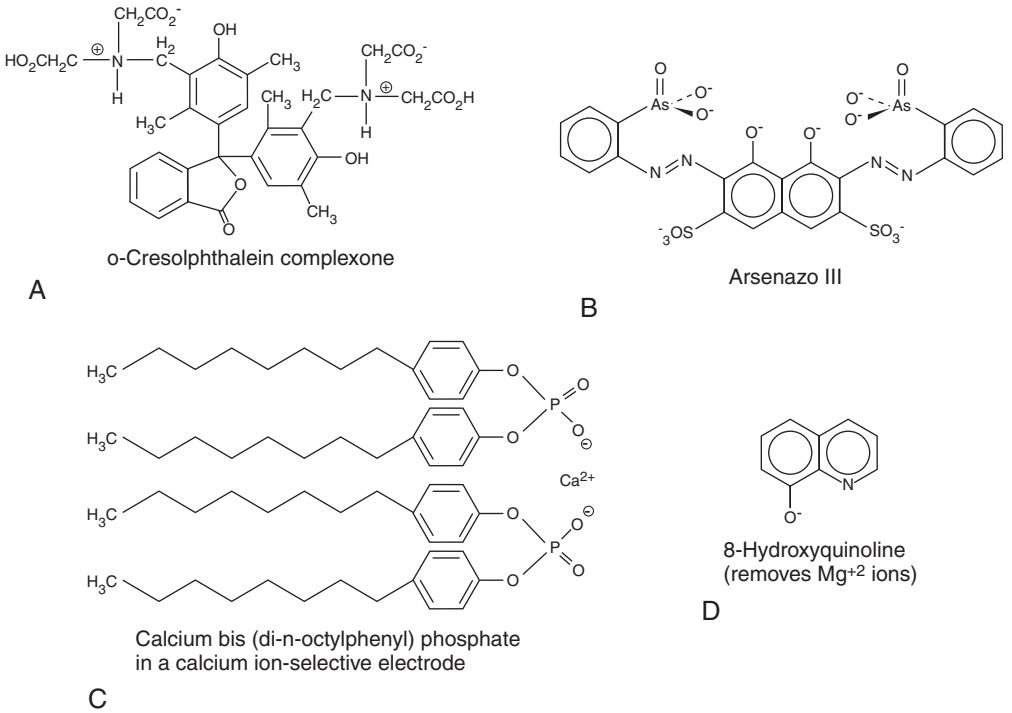

Figure 28.1 Structures of agents that bind selectively to Ca^{+2} ions with the exception of 8-hydroxyquinolone, which binds and precipitates Mg^{+2} ions.

and allow contact with the measuring electrode. Each ion requires a different material that will be selectively permeable to this ion and to this ion only. Thus, glass is perm-selective to hydrogen ion. A special polymer of the polyamino acid antibiotic, valinomycin, is perm-selective to potassium ions. A polymer resin of polyvinylchloride (PVC) is perm-selective to sodium ions. Recently, an anodized indium tin oxide membrane was found to be even more perm-selective to sodium ions (Lin & Hsu, 2010). Similarly, calcium-chelating organic molecules impregnated into PVC membranes serve as perm-selective membranes for calcium ions. In addition, dioctylphenyl phosphates, as shown in Figure 28.1C, have been found to chelate calcium ions selectively and to serve as effective ion-selective electrodes.

There are three basic causes of malfunctions of ion-selective electrodes. The first and most common is defects in the perm-selective membrane itself. This allows the presence of ions other than the one whose concentration is being measured to be present at the measuring electrode. The result is ion concentrations that are falsely elevated. This defect is almost always detected in routine quality control that shows a strong upward drift in the controls despite frequent calibrations.

The second cause of inaccuracies in ion-selective electrodes is buildup of counter-voltages from liquid junction potentials present at the salt bridge connecting the measuring electrode with the reference electrode. Since these voltages oppose the voltage between the two electrodes, the voltages are diminished, giving lower-than-expected ion concentrations. Buildup of liquid junction potentials occurs over time and affects the lifetime of electrodes. Therefore, it is vital to change electrodes at the times specified by the manufacturer to avoid erroneous results.

The third cause of malfunctioning electrodes is buildup of proteins on the electrodes, resulting in alteration of the voltage between the testing and reference electrodes. This phenomenon gives rise to erratic results and lack of reproducibility of ion concentrations in a single specimen. This problem can be avoided by performing washes of the electrodes at manufacturer-specified times.

Volumetric Effect. Although it is not caused by any malfunctioning of the electrode or ion-selective membrane, the effect of serum (or other body fluid) volumes may cause inaccuracies of results. If a serum sample is directly incubated with the ion-selective membrane and electrode, the concentration of an ion can be accurately determined. This is referred to as a direct determination. However, analyzers commonly dilute the sample with buffer prior to incubation with the electrode in a process referred to as an *indirect determination*. If the sample contains significant amounts of lipids and/or proteins, the volume of the sample is partitioned into an aqueous phase in which the ions are dissolved and a separate lipid/protein phase. In this case, the addition of buffer to the sample will dilute the whole sample, but the ions are dissolved only in the aqueous phase. This phase has a smaller volume than the volume of the whole sample. Therefore, addition of buffer will dilute the aqueous phase of the sample more. When the ion concentration in the diluted sample is determined, the result must be multiplied by the dilution factor. If the result is multiplied by this factor, it may underestimate the ion concentration in the sample because the dilution factor was for the whole sample and not for the aqueous phase, which requires a higher factor. When this occurs for sodium ion concentration, the artifactually low concentration is referred to as *pseudohyponatremia*. This occurrence is an uncommon one but can affect the determinations of any analytes where volume partitioning can occur.

SPECTROPHOTOMETRIC DETERMINATIONS USING SIMPLE REAGENTS

These are by far the most common types of assays. We discuss each analyte measured by this method.

BEER'S LAW

We remind the reader that all spectrophotometric determinations are made using the Beer-Lambert Law (see Chapter 4), which states that the absorbance, A, of an analyte at a particular wavelength is proportional to its concentration, C, and the length of the light path, L, in the cuvette in which the analyte is dissolved in a solvent (usually water or aqueous buffer), that is,

$$A = \varepsilon \times C \times L \qquad \text{(Eq. 28.1)}$$

where ε is the proportionality constant, also called the *extinction coefficient*.

END-POINT VERSUS RATE METHOD

As we now describe, the spectrophotometric determination of the concentration of an analyte requires the addition of another compound or reagent with which the analyte of interest reacts either covalently or noncovalently. The reagent is always added in excess. The resulting complex absorbs light at a wavelength at which neither the free analyte nor the unbound reagent absorbs or at which each species absorbs only minimally. If the reaction is allowed to proceed to completion and the absorbance is then determined, the method is referred to as an *end-point method*. In some cases, the rate of formation of the complex is slow.

To avoid long waiting periods, the rate of the reaction over a short time period is determined and is used to compute the concentration of the analyte. In Chapters 21 and 24, we discussed the order of reactions. In the case

of formation of colored complexes, the analyte, A, reacts with the reagent, R, to form the measured product, that is, the color complex, or AR:

$$A + R \rightarrow AR \qquad \text{(Eq. 28.2)}$$

The rate equation describing the rate of formation of AR, that is, d(AR)/dt, is

$$d(AR)/dt = k(A)(R) \qquad \text{(Eq. 28.3)}$$

where k is the rate constant for this reaction. This is referred to as a *second-order rate* process because the rate depends on the concentrations of both A and R. However, since R is added in excess of A, at least initially, the concentration of R does not change appreciably so that it may be considered constant. The reaction then becomes a *pseudo–first-order* reaction. In this case,

$$d(AR)/dt = kR_0(A) \qquad \text{(Eq. 28.4)}$$

where R_0 is the defined added concentration of reagent so that

$$d(AR)/dt = k'(A) \qquad \text{(Eq. 28.5)}$$

where k' is kR_0.

Thus, the rate of formation of AR is proportional to the concentration of A. Plots of AR versus time should be linear for the initial time periods (which can range from seconds to minutes). The slope is $k' = kR_0$, whose value is known. Therefore, A must be equal to the slope of the initial straight line divided by k'. This process is quite similar to the one described to compute enzyme concentrations in serum at low substrate concentrations, as described in Chapter 21.

In the same manner in which we determine the concentration of enzymes in serum by observing the *initial* rate of the enzyme-catalyzed reaction in the presence of saturating concentrations of substrate, where the concentration of the substrate is known, we can likewise determine the initial concentration of A by measuring the initial rate at which AR forms. This rate is proportional to the initial concentration of A, the desired quantity.

INTERFERENCES

Compounds that interfere with assays for analytes can cause either significantly higher or lower values than the true value. There is great variability in the reasons for interference. For example, for analytes that bind to dyes to form complexes that absorb at unique wavelengths, the presence of exogenous molecules—such as drugs, especially antibiotics, that may also absorb at the same unique wavelengths as for the complexes—will render higher values than for the analyte being assayed alone. The presence of exogenous agents—such as immunoglobulins, that can bind to an analyte being assayed for—may block the binding of the analyte to a dye or to an enzyme in the assay, resulting in artifactually lower values. In some assays involving electron transfers from the compound being assayed to an acceptor molecule, the presence of high levels of even endogenous analytes that can serve as electron acceptors can cause spuriously lower values for the level of the assayed analyte. Fortunately, these types of occurrence are not common. For example, in the case of small molecule interference of the absorbances of color complexes, many of the color complex absorbances are determined at wavelengths higher than 500 nm, where most small molecules—such as drugs, cofactors such as NADH, FADH, pyridoxal phosphate, and so on—do not absorb. However, because these interferences sometimes do occur, they must be acknowledged.

More common as causes of interferences are three types of nonspecific agents: hemolysis, resulting in the release of hemoglobin from lysed red blood cells that can affect the absorbances in certain assays; icteremia from both direct and indirect bilirubin; and lipemia from elevated levels of triglycerides and/or lipoprotein complexes. In general, these three agents cause spuriously elevated results. In the case of lipemia, this elevation is due to light scattering that increases the absorbance of a sample over many wavelengths. As discussed earlier in the ion-selective electrode section and further later, lipemia can also cause a spurious decrease in absorbance due to the fact that most assays involve dilution of serum or plasma. Since elevated levels of lipids in serum or plasma consume significant volumes, errors in estimation of the actual dilutions occur such that the dilution factor is lower than it should be, resulting in computation of spuriously lower values.

Because these three latter agents—hemoglobin, bilirubin, and lipids—are the most common causes of spurious assay results, most commercial assays evaluate each to determine at what concentration interference of a given assay can occur. This involves the addition of different concentrations of the agent to serum that has been assayed for a given analyte in the presence of increasing concentrations of each potential interfering agent. The agents are hemoglobin for hemolysis, bilirubin for icterus, and a lipid preparation called Intralipid, a 20% fat emulsion used to simulate extremely turbid samples. At its highest concentration, Intralipid is the equivalent of approximately 1500 mg/dL serum triglyceride, for lipemia. The results are reported as the highest concentration of each agent assayed for which there was no change in the assay result. No change in the result is usually defined as an assay result that is within ±10% to 12% of the value determined in the absence of this compound.

It should be noted that multiple methods are used to determine analyte levels in body fluids; these methods may differ in sensitivity to potential interfering agents. Thus, it is not possible to discuss interferences for all methods for each analyte. In general, we discuss interferences for the most commonly used methods for each analyte. In addition, there are numerous possible interferences from drugs used to treat different conditions, all of which would consume voluminous discussions. Since these interferences are rare but voluminous, we refer the reader to a compendium of potential drug interferences for further references (Young, 2000) and discuss only those that are commonly observed.

Common Interferences with Point-of-Care Testing

The most common point-of-care testing (POCT) is for glucose, done both in hospitals and more extensively for self-monitoring of outpatients. Because medical personnel and patients themselves naturally have a strong belief that the results obtained with their own hands are correct despite potential bias, it is valuable for laboratorians to understand how some common interferences can lead to discrepant and inaccurate results by POCT.

Hematocrit Effect and Volume Displacement

Biologically and medically important measurements of chemical constituents in blood are largely made in serum or plasma as representative of concentrations that perfuse the organs and tissues of the body. POCT typically utilizes specimens of whole blood, which consists of almost one-half cellular elements. The impact of erythrocytes on measurements can be enormous, as they occlude the surface of dipstick-style systems. In this *hematocrit effect*, higher hematocrits let less plasma pass to react with POCT reagents, leading to falsely low results. Lower hematocrits (more typical of hospitalized patients) allow more plasma to pass, leading to falsely elevated results. Only systems that separate cells from plasma before the plasma moves on to reagent strips can avoid the hematocrit effect.

Patients should calibrate results from their own POCT meter with simultaneous measurements on a plasma or serum specimen performed with standard laboratory analyzers. Any major discrepancy due to hematocrit effect or other phenomenon should be taken into account for a patient to use POCT for long-term self-monitoring.

As stated earlier, another potential source or error in POCT and even main laboratory testing is volume displacement of plasma in a specimen due to extremely high triglycerides. The physiologically important measurement is that in plasma, but high levels of triglycerides can displace the plasma on its path to reagent strips, leading to falsely low results. Similarly high triglycerides can displace plasma or serum in samples aspirated for analysis on a main laboratory instrument. A conventional approach to this problem has been to separate plasma or serum from high triglycerides by ultracentrifugation, although this additional maneuver might not be available at all institutions.

A very successful way to solve the problem of high triglycerides for measurement of electrolytes, including calcium, is to utilize ion-selective electrodes, which directly measure the physiologically active ions. Some instrument configurations use a standard volume aspirate of sample that is diluted in a larger quantity of buffer prior to measurement with ion-selective electrodes. This latter approach is inadequate for specimens with high triglycerides because, as described above, plasma containing the analytes to be measured is displaced in part during the sample aspiration, leading to falsely low results. Especially for calcium measurements, it is important to have available an ion-selective electrode method for use in undiluted specimens.

A new development in diabetes care is continuous glucose monitoring (CGM) for subcutaneous sampling of interstitial fluid every 15 minutes using devices that are mounted on the skin. Results are used for controlling glucose with an insulin pump (e.g., artificial pancreas). These electrochemical devices are still undergoing widespread evaluation for

oxidation-reduction interferences, such as from acetaminophen, which can cause markedly false-positive results (Basu, 2016).

As an internal control for presence of excess reducing substances that can interfere with urine dipstick measurement of glucose, a pad for detecting ascorbic acid has been introduced by some manufacturers. The use of this result is not to determine that the patient has been taking high levels of vitamin C but rather to detect what might be a serious false negative for glucose due to high level of the reducing substance that reacts with hydrogen peroxide at the chromogen step of the glucose detection reagents.

QUANTITATION OF ANALYTES

We will now discuss commonly used methods to determine the concentrations of analytes by formation of color complexes.

Albumin and Total Protein

Albumin

As noted in Chapter 20, albumin is the most anionic of the major serum proteins and migrates toward the anode on serum protein electrophoresis. It binds with high affinity to bromcresol green (BCG), a derivative of triphenyl methane, and bromcresol purple (BCP). The reaction with BCG is shown in Equation 28.6.

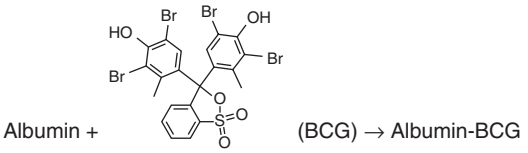

(Eq. 28.6)

The amount of albumin present in the sample is measured as an endpoint reaction at 628 nm. A similar reaction with BCP gives a color complex whose absorbance is read at 603 nm. BCG reacts also to some extent with α-1 and α-2 proteins, sometimes tending to overestimate the concentration of albumin. BCP does not react with these proteins; thus, it is considered to be more specific in quantitation of albumin.

Interferences. Lipemic samples (triglycerides >10 g/L), also can result in higher values. Hyperbilirubinemia or hemolysis does not affect the assay since the absorption maximum of the complex is at a wavelength distinct from those at which bilirubin and hemoglobin interfere. Heparin interferes positively with the BCG method. This effect does not occur at therapeutic levels of heparin but rather with specimens collected through a line containing heparin, resulting in high concentration of the drug in the blood specimen. Specimens containing dextran should also be avoided.

Total Protein

As discussed in Chapter 20, all proteins are polyamino acids linked by peptide (CONH) bonds. These peptide bonds form complexes with cupric ions in cupric sulfate to form a color complex in alkaline solution, the so-called *biuret reaction* as shown in Equation 28.7.

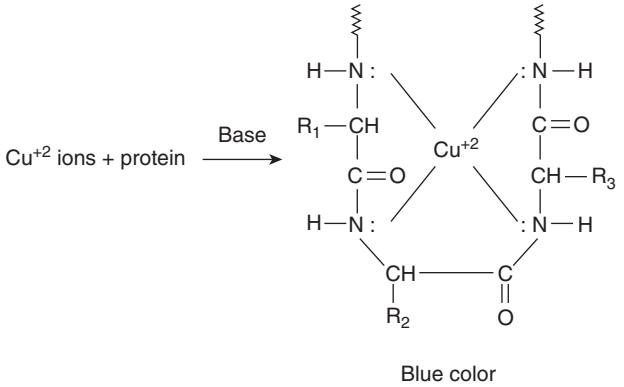

(Eq. 28.7)

Note that this occurs for every four consecutive peptide units. Since most proteins contain at least 150 to 200 amino acid residues, and many of them more than 300 amino acid residues, many of these complexes are formed for each protein. Since there are large numbers of proteins in serum, this reaction is multiplied manyfold, making the biuret method quite sensitive. The absorbance of the colored complex is determined at 540 nm.

Interferences. Hemolysis causes no significant interference. Bilirubinemia has been reported not to cause positive interference at levels of ≤30 mg/dL, although in dog sera, this level was found to be 10 mg/dL. Lipemia causes negative interference. The antibiotics carbenicillin and methylbenzethonium have been found to cause positive and negative interferences, respectively.

Bilirubin

As discussed in Chapter 22, the most common method for measuring serum bilirubin is the Jendrassik-Grof method. In this method, diazotized sulfanilic acid reacts with two pyrrole rings of bilirubin to give two phenylazo adducts, as shown in Equation 28.8 (Natelson, 1971).

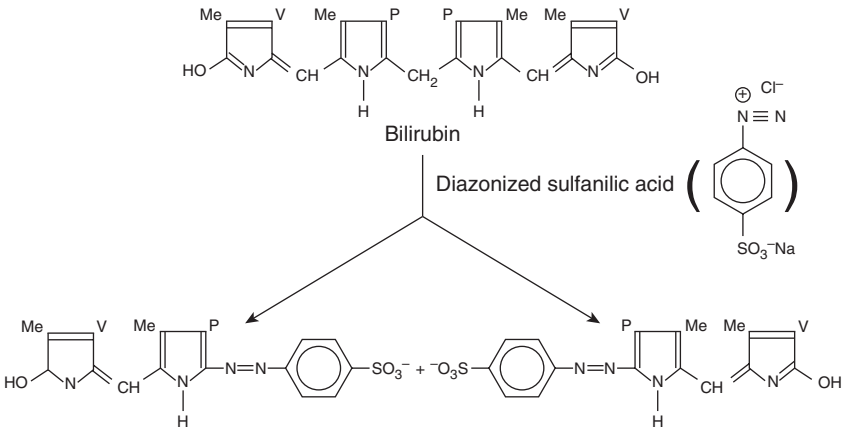

(Eq. 28.8)

In this equation, Me is the methyl group, V is the vinyl group, and P is the 3-substituted propionic acid moiety. Note that, interestingly, electrophilic aromatic substitution occurs on the pyrrole rings such that the central methylene carbon is removed altogether, giving the two sets of phenylazo adducts, which absorb at 600 nm.

As discussed in Chapter 22, bilirubin is conjugated to glucuronic acid at either or both propionic acid (P) moieties. Unconjugated bilirubin is much less soluble than are the conjugated forms. Most of the unconjugated bilirubin is bound tightly to albumin, making it largely unavailable for reaction with the diazotized sulfanilic acid reagent.

However, addition of agents such as ethanol, methanol, or caffeine-benzoate induces the dissociation of unconjugated bilirubin from albumin, allowing it to react with the reagent. Caffeine-benzoate is the preferable agent since methanol and ethanol can induce protein precipitation and increased turbidity. Interference by hemoglobin resulting from hemolysis can also occur. The soluble bilirubins (mostly conjugated, but see later discussion) that react in the absence of dissociating reagents are termed *direct bilirubin*, while the bilirubin that reacts in the presence of the dissociating agent is *total bilirubin*. So-called *indirect bilirubin* (mostly unconjugated bilirubin bound to albumin) is obtained by subtraction of direct bilirubin from total bilirubin (Tolman & Rej, 1999). As noted in Chapter 22, not all conjugated bilirubin is detected as direct bilirubin, and a small amount of unconjugated bilirubin may be detected as direct bilirubin.

Interferences. Studies on Beckman AU analyzers indicate that there is no interference on total bilirubin levels as a result of hemolysis up to 25 mg/dL hemoglobin in serum and, as a result of lipidemia, up to 500 mg/dL of Intralipid.

Calcium

Most methods rely on the formation of a color complex of Ca^{+2} ions with an appropriate chelating agent with which it forms a color complex. Since approximately half of total calcium is bound to protein, mainly to albumin, lowering the pH of the sample liberates calcium ions. The calcium ions are then reacted with a strong chelating compound with which they form a color complex. The two major calcium chelating compounds that are currently used are ortho-cresolphthalein (forms a red-colored complex) and Arsenazo III (Rowatt & Williams, 1989; Morgan et al., 1993), whose structures are shown in Figures 28.1A and 28.1B, respectively. The reaction is shown in the following equation:

$$\text{Dye} + Ca^{+2} \rightarrow \text{Dye} - Ca^{+2} \qquad \text{(Eq. 28.9)}$$

where dye is either ortho-cresolphthalein or Arsenazo III.

Use of ortho-cresolphthalein is often accompanied by a further step in which the reaction solution is treated with the compound 8-hydroxyquinoline, whose structure is also shown in Figure 28.1D, at alkaline pH to prevent any possible complex from forming with magnesium ion. The amount of complex that forms is rather strongly dependent on the temperature, which must be carefully maintained. At low calcium concentrations, a one-to-one complex forms, whereas at higher calcium concentrations, two moles of calcium bind to one mole of dye. Since the extinction coefficients of mono- and di-calcium dye complexes differ, the absorbance is nonlinear with respect to calcium concentration. However, use of a modified Beer's law equation can be employed to compute concentration from absorbance; nonlinear methods can likewise be used for this purpose. The only major potential interfering compound for this assay is magnesium ion, which can be removed with 8-hydroxyquinoline, as noted earlier.

Arsenazo III has a high affinity for calcium ions, but the amount of complex formed is strongly pH dependent, Usually, imidazole buffers at pH 6.0 are employed for this reaction. Importantly, citrate, which is a tricarboxylic acid that can chelate calcium ions, has been found to interfere with this reaction. It has been found that determination of absorbance at 650 nm is the optimal wavelength for determination of the concentration of calcium ion complex with Arsenazo III at which there is little interference by other analytes, other than in hemolyzed samples.

Ion-Selective Electrodes for Calcium Determinations

Since calcium can be released from its normally bound states by acidification, addition of acid to a serum sample will convert all calcium to readily measurable ionic forms. Thus, total calcium can be measured voltammetrically. The electrode is a specific calcium ion exchanger of which there are several types, including ETH 1001 and bis-di-(n-octylphenyl) phosphate. The structure of the latter is shown in Figure 28.1C (Endres & Rude, 1999). Ionized calcium (i.e., calcium that is not bound to protein or in complex formation with strong chelators) can be measured directly with ion-selective electrodes without the prior acid treatment step. As with other ion-selective electrode methods, protein that can coat the electrodes can cause interference.

Creatinine

Creatinine has been found to form a complex with picric acid (2,4,6-trinitrophenol) under alkaline conditions, as shown in Equation 28.10, which illustrates the Jaffe reaction.

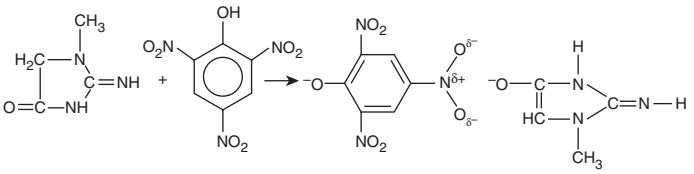

(Eq. 28.10)

The actual structure of the complex is not completely known. Most studies suggest that it is a noncovalent ionic complex, as shown in Equation 28.10 (Vasillades, 1976). However, there is some evidence that the carbonyl oxygen (in its enolate form) of creatinine can attack the 1-carbon of picric acid to form a covalent (so-called *Janovsky-like*) adduct (Kroli et al., 1987). Irrespective of the structure(s) of this complex, its absorbance is determined between 490 and 500 nm. The reaction is sensitive to temperature.

Possible Interferences of the Jaffe Reaction for Creatinine. Hemolysis, lipemia, and icteremia can all cause interferences. Hemolysis releases Jaffe-reacting chromogens and therefore will falsely increase results. Lipemia and icteremia (elevated bilirubin) can inhibit optical readings and falsely decrease values. Reaction of picric acid with bilirubin can be minimized by treatment with ferricyanide or small amounts of surfactant.

Other possible interferences include ketones and α-keto acids, such as acetoacetate, as found in uncontrolled diabetes, bilirubin, and other organic compounds. Elevated serum levels of protein, glucose, ascorbic acid, guanidine, and antibiotics—including cephalosporins and aminoglycosides (mainly streptomycin)—can also cause falsely elevated creatinine values. Ammonia can also be an interferent. Therefore, if the sample is plasma, it is important to determine whether ammonium heparinate was used as an anticoagulant. In general, these interferences are minimized in urine samples since urine creatinine levels are much higher than in serum or plasma, and urine does not contain significant levels of interfering chromogens. In view of the false elevations of creatinine that occur due to the presence of elevated serum glucose levels, acetoacetate, and acetone in patients with poorly controlled diabetes who are at risk for developing renal disease, diagnosis of renal disease or of progressive severity of renal disease may be compromised.

Iron

Serum iron levels can be readily determined by a specific reaction of ferrous iron (Fe^{+2}) with the compound ferrozine, the structure of which is shown in Equation 28.11.

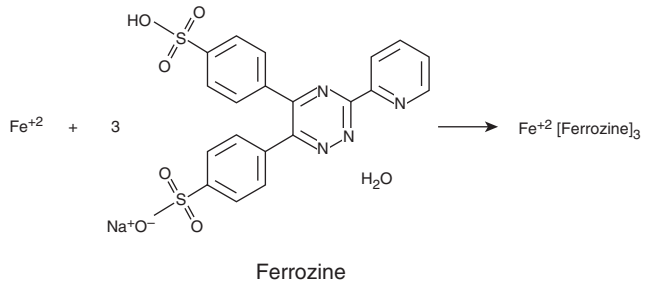

(Eq. 28.11)

The reaction is performed in an acid medium so that ferrous ions can be dissociated from transferrin and maintained in the reduced state. Actually, each ferrous ion complexes with three ferrozine molecules to form a magenta-colored complex, remarkably insensitive to pH, whose absorbance can be determined at 562 nm, although some assays (such as on the Siemens Advia 1650) are performed at 571 nm. As might be expected, hemolysis can cause major interferences with this assay due to red blood cell iron and release of hemoglobin that can compete with ferrozine for binding to serum iron. In addition, zinc and copper can interfere with this assay. This interference can be removed by use of thioglycolate, which complexes these two ions.

Total Iron-Binding Capacity

This is a measure of the total number of functional ferrous ion binding sites in transferrin. As discussed in Chapter 24, the basic approach is to strip serum transferrin of all bound iron and then to add an excess of iron to the serum sample to determine the concentration of transferrin-bound iron. To accomplish this, the serum sample is added to an acidic buffer,

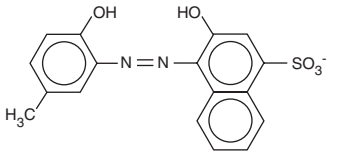

Calmagite for Mg^{+2} determination

Figure 28.2 Structure of calmagite, an agent that forms a selective color complex with Mg^{+2} ions.

which dissociates all transferrin-bound iron, containing excess ferric chloride and ferrozine. All of the iron is then bound to ferrozine. Then, the pH of the solution is raised into the neutral range where the affinity of iron for transferrin is greatly increased over that for ferrozine. All iron that can bind to available sites on transferrin does so. This results in a decrease in the magenta color at 562 (or 571) nm. This decrease is proportional to the total concentration of functional transferrin binding sites. This set of reactions is summarized in Equation 28.12.

$$\text{Iron-transferrin} + \text{buffer 1} \xrightarrow{\text{low pH}} \text{transferrin} + \text{colored iron-dye complex} \quad \text{(Eq. 28.12A)}$$

$$\text{transferrin} + \text{colored iron-dye complex} + \text{buffer 2} \xrightarrow{\text{increase pH}} \text{iron-transferrin} + \text{decreased colored iron-dye complex} \quad \text{(Eq. 28.12B)}$$

Interferences. These include bilirubin, which does not cause interference up to approximately 40 mg/dL; copper, which causes no significant interference up to 1 mg/dL; hemoglobin, which causes no significant interference up to 200 mg/dL in a hemolysate; and lipemia, which causes no significant interference in up to 1000 mg/dL of Intralipid. Abnormally elevated concentrations of trace metals may result in interference with this assay.

Magnesium

Several dyes that form specific complexes with Mg^{+2} ions are used to determine the serum concentrations of this metal ion. They include calmagite (530 to 550 nm), shown in Figure 28.2, methylthymol blue (600 nm), and xylidyl blue (600 nm). The numbers in parentheses in the preceding sentence indicate the wavelengths at which complex concentration is determined for each dye (Endres & Rude, 1999). In the case of calmagite, the calcium-chelating compound ethylene glycol tetraacetic acid (EGTA) can be used to remove interference from calcium ions, potassium cyanide can be added to remove interference from heavy metal ions, and polyvinylpyrrolidone can be added to the reaction solution to minimize interference from proteins.

Phosphate

Phosphate occurs as both inorganic, mainly orthophosphate, and organic phosphate, such as in glucose-6-phosphate, nucleic acids, phosphoproteins, and so on. Most phosphates in serum are inorganic phosphates; the organic phosphates are mainly intracellular. As discussed in Chapter 9, there are three forms of inorganic phosphate, the most common ones occurring at usual blood pH being $H_2PO_4^{-1}$ and HPO_4^{-2}. The most commonly used method to measure total serum inorganic phosphate is the phosphomolybdate method, in which ammonium molybdate is reacted with inorganic phosphate to form an ammonium phosphomolybdate complex (Endres & Rude, 1999). The unreduced form of this complex can be determined readily by the increase in absorbance at 340 nm. The pH must be maintained in the acid range because alkaline conditions can result in reduction of the complex. In fact, reduction of this complex gives a blue-colored product whose absorbance can be determined in the 600- to 700-nm range (the Fiske-Subbarow method). Reducing agents used include ascorbic acid, stannous chloride, ferrous ammonium sulfate, 1-amino-2-naphthol-4-sulfonic acid (used originally), and many others. Most methods use the direct 340-nm determination because of its speed and the fact that it involves only one step.

Interferences. It should be noted that, while no interference from partially hemolyzed samples has been found to occur in the Fiske-Subbarow assay up to hemoglobin levels of 350 mg/dL, there is the risk that phosphates can be split from labile phosphoesters in lysed erythrocytes, thereby yielding falsely elevated phosphate levels. Therefore, this assay should not be performed on hemolyzed samples. No significant interference up to 40 mg/dL bilirubin has been found for this assay, and no significant interference has been found to occur with up to 900 mg/dL of Intralipid. Two other interferences for the inorganic phosphate assay have been described: mannitol and immunoglobulin (Ig) G and IgM paraproteins. The former is used therapeutically and has short half-lives (see Chapter 24) so that simply withholding this agent for brief periods will result in its rapid excretion. The latter can be removed by deproteinizing methods, such as ultrafiltration of serum, in these rare cases.

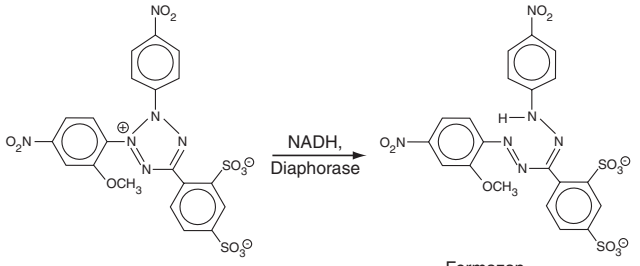

Figure 28.3 Reduction of a tetrazolium to a formazan in which NADH or NADPH is converted to NAD or NADP, respectively, in the presence of a catalyst—either the enzyme diaphorase or phenazine methosulfate. The formazan strongly absorbs at 500 nm. This reaction can be used to enhance the sensitivity of reactions in which either NADH or NADPH is generated.

USE OF ENZYMES AS REAGENTS TO DETERMINE ANALYTE CONCENTRATIONS

GENERAL FEATURES

Rate Versus End-Point Methods

These are quite similar to the methods discussed in the section on spectrophotometric determinations earlier in the chapter. For rate methods, the total amount of enzyme is added to the serum sample so that, unlike in enzyme assays, total enzyme concentration is known. Note, though, that the substrate concentration is not known (we seek to determine this). It is not known whether saturation conditions prevail. Therefore, to compute the substrate concentration for an observed initial rate, the Michaelis-Menton equation is solved for substrate concentration. This is possible since K_m and V_{max} are known for the enzyme reagent used. As with dye-based methods, end-point methods using enzymes are based on the determination of the point at which product concentration remains constant. This concentration is the total substrate or analyte concentration.

NADH and NADPH as Quantitative Indicators

In this section and the following section, it will be seen that a common approach in determining the serum concentrations of analytes and enzymes is to follow the reduction of NAD or NADP to NADH or NADPH, respectively. NAD[P]H have strong absorbances at 340 nm, while the oxidized forms (i.e., NAD[P]) have no absorbance. Thus, determination of the *increase* in absorbance at 340 nm for an enzyme-catalyzed reaction in which NAD[P] is converted to NAD[P]H or of the *decrease* in absorbance at 340 nm for an enzyme-catalyzed reaction in which NAD[P]H is converted to NAD[P] is a very convenient means of measuring analyte concentration.

In some assays, in which NAD[P]H is an end product, the sensitivity of the level of NAD[P]H produced is enhanced by adding another step wherein a dye reagent, a tetrazolium derivative, is reduced by NAD[P]H to yield a formazan that strongly absorbs at wavelengths around 500 nm. This reaction can be catalyzed by an electron transfer agent, including the enzyme diaphorase (lipoamide dehydrogenase, EC 1.6.4.3) or phenazine methosulfate. A prototypical reaction is shown in Figure 28.3. In principle, this reaction can be used for any reaction in which NAD[P]H is generated.

ANALYTES WHOSE CONCENTRATIONS ARE DETERMINED BY ENZYME REACTIONS

Ammonia

Ammonia is measured by use of the versatile enzyme glutamate dehydrogenase (GLDH). In this reaction, ammonia reacts with α-ketoglutarate to form glutamate in a reductive amination reaction. In the first step of this reaction, a Schiff base forms between ammonia and the α-keto group of α-ketoglutarate. In the second step, the resulting double bond is then reduced by NADPH, giving the primary amine in glutamate, plus NADP. The overall reaction is shown in Figure 28.4. Therefore, ammonia concentration can be determined by the decrease in absorbance at 340 nm as NADPH is converted to NADP. This enzyme can be used in any reaction in which ammonia is generated. Ammonia samples are stable for 3 hours at 2°C to 4°C or 24 hours at –20°C.

Interferences. Hemolysis precludes accurate ammonia determination since erythrocytes contain levels of ammonia approximately 3 times that of plasma. Although pyruvate can negatively interfere with this assay, no interference from pyruvate has been observed up to a level of 0.01 mg/dL (0.75 mmol/L). ALT can also interfere with the serum ammonia assay, but no interference from ALT has been observed up to a level of 2400 U/L. Since cigarette smoke contains substantial levels of ammonia that can contaminate samples to be assayed for ammonia, these samples should not be stored or exposed to any areas where smoke may be present.

Bicarbonate Ions (HCO^{3-})

One of the glycolytic enzymes, phosphoenolpyruvate carboxykinase (PEPCK), utilizes bicarbonate ion to carboxylate phosphoenol pyruvate to form oxaloacetate (OAA), a Krebs cycle intermediate, with attendant dephosphorylation (Eq. 28.13).

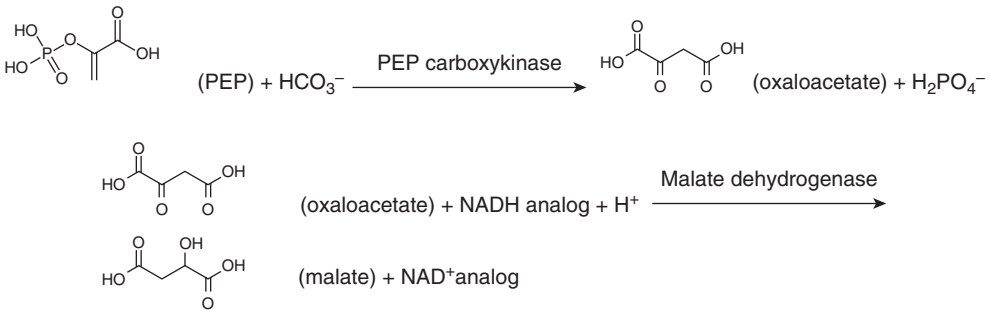

(Eq. 28.13A)

(Eq. 28.13B)

Thus, advantage can be taken of this reaction to consume serum bicarbonate in this reaction, thereby enabling us to determine its concentration. PEPCK is added to serum. The resulting OAA is then reduced by adding malate dehydrogenase to form malate. In this second reaction, NADH is oxidized to NAD so that the decrease in absorbance of NADH can be monitored at 340 nm. Often, an NAD analog is used so that the decreased absorbance at 410, rather than 340, nm is monitored.

Interferences. Hemolysis: No significant interference occurs up to 500 mg/dL hemoglobin. Bilirubinemia (icterus): No significant interference occurs up to 40 mg/dL bilirubin. Lipemia: No significant interference occurs up to 1000 mg/dL Intralipid. There is also a report that markedly elevated serum LDH levels can cause falsely elevated bicarbonate levels (Saleem, 2013).

Cholesterol

As discussed in Chapter 18, cholesterol circulates as both free (mainly in LDL particles) and cholesterol ester (mainly in HDL particles). To determine the serum concentration of total cholesterol, therefore, all cholesterol ester is first converted to free cholesterol using cholesterol esterase (Eq. 28.14A). The resulting total free cholesterol is then oxidized to 7-α-hydroxy-cholesten-3-one with cholesterol oxidase, as also shown in Equation 28.14A. As can be seen, hydrogen peroxide (H_2O_2) a strong oxidizing agent, is generated in this reaction. Advantage can be taken of this property to generate strongly absorbing chromophores, as we now describe.

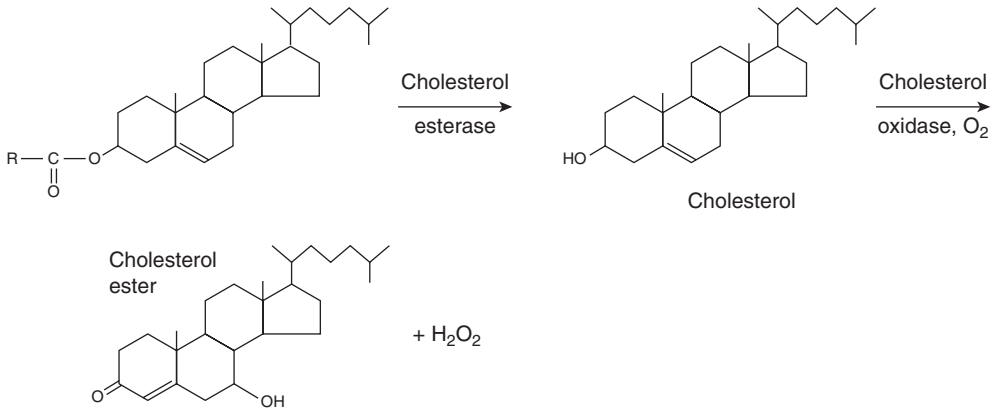

(Eq. 28.14A)

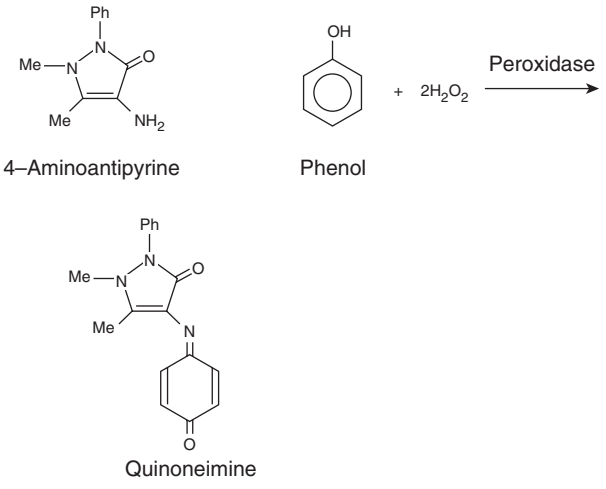

(Eq. 28.14B)

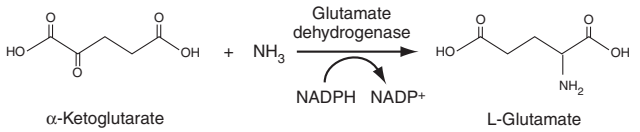

Figure 28.4 Reductive amination reaction, catalyzed by glutamate dehydrogenase (GLDH), in which ammonia reacts with α-ketoglutarate to form the amino acid glutamic acid. In this reaction, NADPH is converted to NADP, allowing ammonia concentration to be determined by the total decrease in absorbance of light at 340 nm, the wavelength at which NADH absorbs.

The Quinoneimine Strategy

H_2O_2 can be reacted, in the presence of a peroxidase, with a phenazone, mainly 4-aminoantipyrene, which forms a highly colored quinoneamine dye with phenol, as shown in Equation 28.14B. This is a prototypical reaction in which the phenol is oxidized to the quinone and in which the exocyclic $-NH_2$ group of 4-aminoantipyrene then adds to the quinone to form a strongly absorbing color complex. Phenol is one of many compounds that can be used to form a quinone or an oxidized aromatic ring, known collectively as *Trinder reagents.* Several of these are aniline derivatives and include N-ethyl-N-(2-hydroxy-3-sulfopropyl)m-toluidine (TOPS) (absorbance is determined at 545 nm), N-(2-hydroxy-3-sulfopropyl)-3,5-dimethoxyaniline (HDAOS), and TOOS (N-ethyl-N-[2-hydroxy-3-sulfo-n-propyl]-3-methylaniline) among a number of other similar compounds. We will have occasion to refer to this set of reactions in the determination of the concentrations of a number of analytes in addition to cholesterol, as described in the following section.

For cholesterol determination, H_2O_2 is generated and is reacted with 4-aminoantipyrine and, generally, *phenol* in the presence of a peroxidase to yield the quinoneimine, shown in the next section, whose absorbance is determined at 505 nm.

Interferences. Hemolysis: There is no significant interference up to 500 mg/dL hemolysate. Bilirubin: There is no significant interference up to 8 mg/dL bilirubin. Lipemia: There is no significant interference up to 1000 mg/dL Intralipid. Other potential interference, ascorbate: No significant interference up to 8 mg/dL.

HDL Cholesterol (Jensen et al., 2002; Sugiuchi et al., 1995)

Until relatively recently, methods have been employed in which either LDL or HDL fractions are selectively precipitated, centrifuged, and the cholesterol in the supernatant assayed. For example, to assay HDL cholesterol, fractions containing apo-B proteins as in LDL and very-low-density lipoprotein (VLDL) particles (see Chapter 18) were precipitated using a polyanion and a divalent cation such as dextran sulfate-$MnCl_2$ or phosphotungstate-$MgCl_2$ combinations. The remaining cholesterol in the supernatant, presumably only HDL cholesterol, is then assayed using the method described in the next section. These methods are somewhat time-consuming and, of course, require manual procedures that cannot be automated.

It was found that the enzymes used in the two assays shown in Equation 28.14 could be made relatively specific for reacting with HDL cholesterol by the relatively simple expedient of adding polyethylene glycol (PEG 6000) to the free amino groups of basic amino acids of the polypeptide chains of these enzymes. Also, addition of α-cyclodextran sulfate (average of six glucose units with an average of two sulfates per glucose unit) in the presence of Mn^{+2} ions greatly reduces the reactivity of the cholesterol in LDL (LDL-C), VLDL, and chylomicron fractions. Thus, addition of the two PEGylated enzymes with sulfated cyclodextran and $MnCl_2$ allows direct determination of HDL cholesterol (HDL-C). The indicator reaction with H_2O_2 is the same as in Equation 28.14B. The overall method is summarized in Equation 28.15A.

$$\text{LDL}-\text{C} + \text{cyclodextran sulfate} + \text{MnCl}_2 + \text{PEG}-\text{cholesterol esterase/cholesterol oxidase} \rightarrow \text{NR}$$

$$\text{HDL}-\text{C} + \text{cyclodextran sulfate} + \text{MnCL}_2 + \text{PEG}-\text{cholesterol esterase/cholesterol oxidase} \rightarrow \text{H}_2\text{O}_2 + 7-\alpha-\text{hydroxy}-4-\text{cholesten}-3-\text{one}$$

$$2\text{H}_2\text{O}_2 + 4-\text{aminoantipyrene} + \text{phenol or other Trinder reagent} \rightarrow \text{quinoneimine}, \qquad \text{(Eq. 28.15A)}$$

where NR is no reaction.

Interferences. Hemolysis: No significant interference has been found up to 500 mg/dL hemolysate. Bilirubin: no significant interference has been determined, individually, up to 40 mg/dL direct and 40 mg/dL indirect bilirubin. Lipemia: No significant interference has been found up to 1500 mg/dL Intralipid and, independently, with up to 900 mg/dL added triglyceride and with up to 1000 mg/dL of endogenous triglyceride. Ascorbate: No significant interference has been noted up to 20 mg/dL ascorbate. In rare cases, IgM in Waldenstrom macroglobulinemia has been found to interfere with HDL cholesterol determinations. However, in tests with up to 5 g/dL of added gammaglobulin, no significant interference has been found.

LDL Cholesterol (Nauck et al., 2002)

The basic strategy for direct determination of LDL-C is first to add a reagent that protects LDL-C from reacting with the two enzymes, cholesterol esterase and cholesterol oxidase, and then to react cholesterol from all of the other fractions so that it is completely consumed, and finally to add a deprotecting agent that allows LDL-C to undergo reaction with the two enzymes. Charged surfactants have been found to block cholesterol in LDL from reacting with the two enzymes, cholesterol esterase and oxidase. The release agent is also a surfactant that, in contradistinction to the protecting agent, is neutral.

In practice, two composite reagents are added to serum sequentially. The first contains protective surfactant and polyanions, which block the reaction of LDL-C with cholesterol esterase and oxidase, and catalase, which consumes the H_2O_2 generated in the reaction of all of the non-LDL-C, summarized in Equation 28.15B. Then, a second reagent is added that consists of 4-aminoantipyrene as described earlier, sodium azide, which blocks catalase, the deprotecting surfactant that releases LDL-C, and an appropriate Trinder agent, that is, chromophore-producing compound that reacts with the 4-aminoantipyrene to form the color complex. These reactions are summarized in Equations 28.15B and 28.15C.

$$\text{LDL}-\text{C} + \text{charged surfactant/polyanions} + \text{cholesterol esterase/cholesterol oxidase} \rightarrow \text{NR}$$

$$\text{HDL}-\text{C} + \text{charged surfactant} + \text{cholesterol esterase/cholesterol oxidase} \rightarrow \text{H}_2\text{O}_2 + 7-\alpha-\text{hydroxy}-4-\text{cholesten}-3-\text{one}$$

$$2\text{H}_2\text{O}_2 + \text{catalase} \rightarrow 2\text{H}_2\text{O} + \text{O}_2 \qquad \text{(Eq. 28.15B)}$$

$$\text{LDL}-\text{C/charged surfactant/polyanion} + \text{neutral releasing surfactant} + \text{cholesterol esterase/cholesterol oxidase} + \text{sodium azide}-\text{catalase} \rightarrow \text{H}_2\text{O}_2 + 7-\alpha-\text{hydroxy}-4-\text{cholesten}-3-\text{one}$$

$$2\text{H}_2\text{O}_2 + 4\text{-aminoantipyrene} + \text{phenol or other Trinder reagent} \rightarrow \text{quinoneimine} \qquad \text{(Eq. 28.15C)}$$

There are multiple variations of this set of reactions, but all of them are based on the overall strategy described here.

Interferences. These are the same as described in the preceding section of methods for determination of HDL cholesterol.

Glucose

The most commonly used method to determine serum glucose levels is to induce phosphorylation of glucose by hexokinase and adenosine triphosphate (ATP) to yield glucose-6-phosphate. By adding glucose-6-phosphate dehydrogenase (G6PD), glucose-6-phosphate is converted into gluconolactone-6-phosphate (first step in the pentose phosphate pathway). This is an oxidation reaction. NADP is reduced to NADPH, whose absorbance can be determined directly at 340 nm. These reactions are summarized in Equation 28.16.

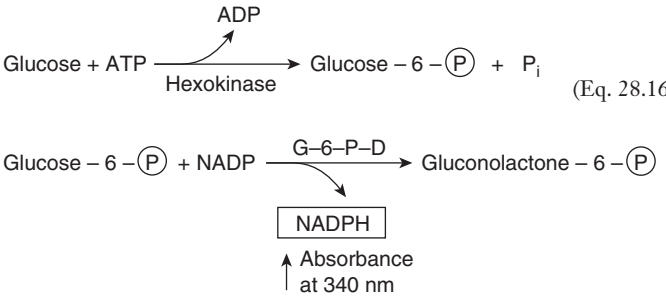

(Eq. 28.16A)

(Eq. 28.16B)

In Equation 28.16, the circled P represents the phosphate moiety. This reaction sequence is perhaps the one most commonly used. Other methods for glucose determination are also available and are used most

commonly in POCT (Yoo & Lee, 2010). In these reactions, glucose oxidase is used to convert glucose to gluconolactone. In this reaction, flavine adenine dinucleotide, FAD, is reduced to $FADH_2$. In the presence of oxygen, FAD is regenerated, and oxygen is reduced to H_2O_2. The latter is oxidized in the presence of a platinum electrode to yield $2H^+ + O_2 + 2e$ (electrons). The electrons flow through a circuit giving rise to a current, which is proportional to the glucose concentration. There are several variants of this strategy. In one of these, glucose dehydrogenase bound to the dye pyrroquinolinequinone (PQQ) oxidizes glucose to gluconolactone plus the reduced form of PQQ, which has an intense red color that can be measured spectrophotometrically. Most commonly, the reduced dye is reoxidized and the released electrons measured as current electrochemically, as described earlier. The electrochemical methods for POCT use whole blood for glucose determination. Thus, the hematocrit has an effect on the concentration of glucose that must be included in obtaining the whole blood glucose value (D'Orazio, 2009; Yoo & Lee, 2010).

Interferences. For the glucose assay based on treatment of serum samples with ATP, hexokinase, and G6PD and measurement of the absorbance of NADPH, interference by hemoglobin is less than 3% up to a hemoglobin level of 5 g/dL; interference by bilirubin is <10% up to 40 mg/dL; and interference by lipemia is <10% up to 700 mg/dL Intralipid. Other interferences include ascorbate, which is less than 3% up to 20 mg/dL ascorbate. For the electrochemical determinations of glucose levels in serum or whole blood, there are three major possible interferences: triglycerides, oxygen, and uric acid (Ginsberg, 2009). Triglycerides tend to cause negative interference due to putative volume displacement effects, as described earlier. In methods that use electron transfer from glucose to electron acceptor molecules such as FAD or PQQ, higher than normal oxygen pressures may result in competition of oxygen with the electron acceptor, leading to artifactually lower glucose values. Similarly, uric acid can undergo oxidation, giving erroneously elevated values, but only at high levels.

Lactate

As discussed in Chapter 21, lactate reacts almost exclusively with LD, as shown in Equation 28.17.

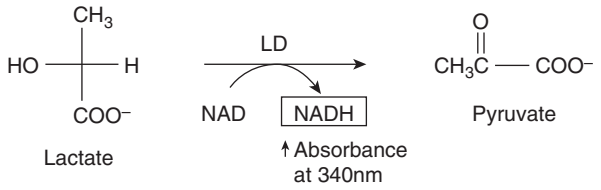

(Eq. 28.17)

Since NAD is converted to NADH, shown in the box, the increase in absorbance of NADH at 340 nm is followed until it becomes constant. After subtraction of a blank for background absorbance of the serum sample at 340 nm, the total absorbance is used to compute directly the increased concentration of NADH due to lactate oxidation.

Interferences. Hemolysis: Hemoglobin causes no interference up to 500 mg/dL. Icterus: There is no significant interference of bilirubin up to 16 mg/dL. Lipemia: No significant interference up to 1000 mg/dL of Intralipid. Ascorbate: No significant interference up to 10 mg/dL ascorbic acid. Glycolic acid from ethylene glycol intoxication gives falsely low values of lactate (Porter, 2000).

Triglycerides

These are a heterogenous group of triesters of fatty acids with glycerol (see Chapter 18). The nature of the fatty acid esters can differ widely in chain length, presence, and number of unsaturated bonds in the aliphatic chains, and chain arrangement. The strategy for determining triglyceride concentration is to hydrolyze all of the fatty acid esters of triglycerides to produce glycerol. It is then the resulting total concentration of glycerol that is taken as the total triglyceride concentration. Technically, this requires the use of a serum blank to determine the level of endogenous glycerol, but the level of glycerol in serum has been found to be quite low. Thus, these blank determinations are not usually performed (Rifai et al., 1999).

In the reference method for determining triglyceride concentration, the triglycerides are first extracted into chloroform; the extract is then treated with silicic acid to extract phospholipids from the chloroform extract. The chloroform extract is then treated with strong potassium hydroxide base to hydrolyze all of the fatty acid esters of glycerol in a process referred to as *saponification*. The resulting glycerol is treated with sodium periodate, resulting in the formation of 2 moles of formaldehyde and 1 mole of formic acid. The formaldehyde is then treated with chromotropic acid to give a chromogen whose structure has not been proved as yet but that contains two chromotropic acid molecules linked by a formaldehyde carbon bridge. This adduct absorbs strongly at 580 nm. Of course, this is a time-consuming manual method that serves only as a reference method and cannot be automated.

In the automated methods performed directly on serum, triglycerides are hydrolyzed to glycerol plus free fatty acids using lipase. Here, we point out that lipase cleaves the fatty acid esters of glycerol at positions 1 and 3 of glycerol but not position 2. However, the 2-acid esters of glycerol spontaneously rearrange to form the 1- or 3-fatty acid esters that are then hydrolyzed by lipase. This allows complete hydrolysis of the fatty acid esters of glycerol.

To determine the total glycerol concentration, the glycerol is converted by the enzyme α-glycerokinase to form 1-phosphoglycerol. This product is converted, in turn, to dihydroxyacetone by glycerophosphate oxidase in the presence of oxygen. This is an oxidation-reduction reaction that generates H_2O_2. This is used to oxidize phenol or m-chlorophenol in the presence of 4-aminoantipyrene to form a conjugated adduct, as described in the cholesterol assay section earlier in the chapter. The absorbance (usually at

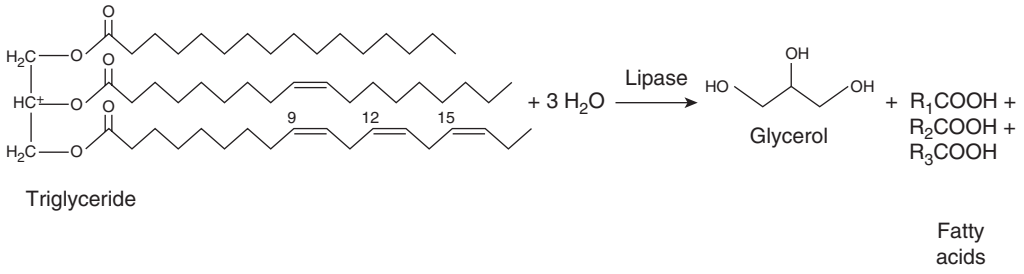

(Eq. 28.18A)

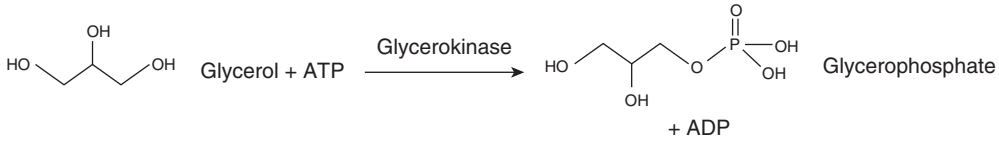

(Eq. 28.18B)

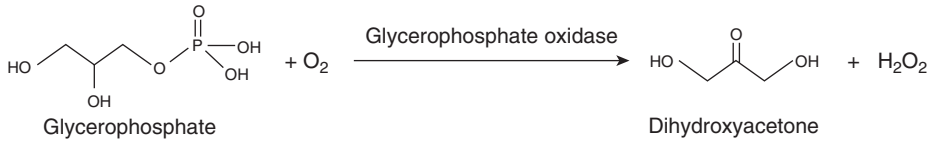

(Eq. 28.18C)

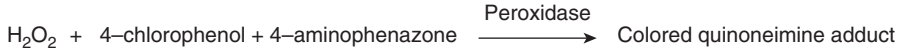

(Eq. 28.18D)

505 nm) of this adduct is proportional to the concentration of generated glycerol. These reactions are summarized in Equation 28.18.

Variants of this basic approach include subjecting the glycerophosphate shown in Equation 28.18B to glycerophosphate dehydrogenase to produce dihydroxyacetone phosphate in a reaction in which NAD is converted into NADH. The NADH can be directly determined at 340 nm.

Interferences. There are no significant interferences from hemolysis up to 500 mg/dL hemoglobin (hemoglobin up to 500 mg/dL); icterus (bilirubin levels up to 40 mg/dL). Ascorbate: There is no significant interference up to 20 mg/dL ascorbate.

Urea or Blood Urea Nitrogen

The reactions here use ultimately the same GLDH enzyme as used for ammonia determination, as described in the earlier section entitled The Quinoneimine Strategy. Here, urea is hydrolyzed into CO_2 and NH_3 in a reaction catalyzed by the enzyme urease. The resulting ammonia is then reacted with α-ketoglutarate to give glutamate in the reductive amination reaction shown in Equation 28.19.

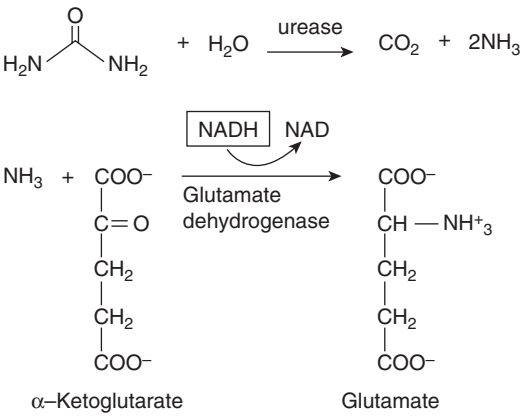

(Eq. 28.19A)

(Eq. 28.19B)

Interferences. There is no significant interference from hemolysis up to 500 mg/dL hemoglobin; from icterus up to 40 mg/dL bilirubin; or from lipemia up to 500 mg/dL Intralipid.

Uric Acid

As shown in Equation 28.20A, uric acid is converted into allantoin by the enzyme uricase. In this reaction, H_2O_2 is generated. As shown in Equation 28.20B, the resulting H_2O_2 can then be used to oxidize a Trinder reagent, in this case TOOS (see the earlier section The Quinoneimine Strategy), which reacts with 4-aminoantipyrene to form a quinoneimine. Another is to use the resulting H_2O_2 to oxidize a convenient substrate such as ethyl alcohol to acetaldehyde by the enzyme catalase. The resulting acetaldehyde can then be further oxidized to acetate by the enzyme alcohol dehydrogenase. In this reaction, NADP is converted to NADPH, resulting in an increased absorbance at 340 nm.

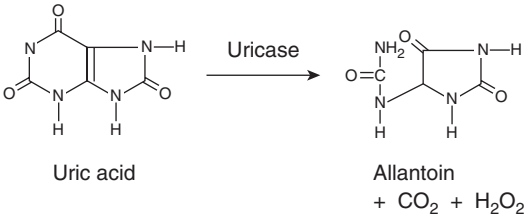

(Eq. 28.20A)

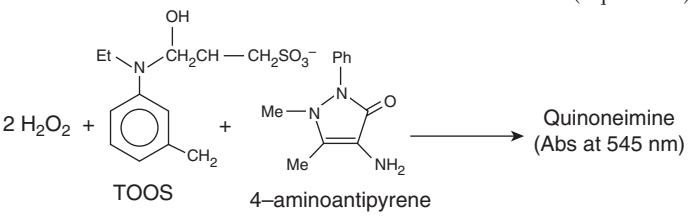

(Eq. 28.20B)

Interferences. There is no interference from hemolysis up to 500 mg/dL hemoglobin; icterus up to 40 mg/dL bilirubin; or lipemia up to 1000 mg/dL Intralipid. There is no interference from ascorbic acid up to 20 mg/dL ascorbate.

ASSAYS FOR ENZYMES

Enzyme assays are discussed in Chapter 21. As discussed in that chapter, most enzyme reactions are carried out under saturating conditions in which the substrate concentration is significantly greater than K_M. This ensures that the initial rate of the reaction is proportional to the total enzyme concentration. Most enzyme assay results are expressed in activities, that is, international units (IU), the slopes of the plots of product formed versus time, as described in Chapter 21.

Alanine Aminotransferase (ALT) and Aspartate Aminotransferase (AST)

ALT

As described in Chapter 22, this enzyme, which is expressed mainly in liver, reversibly catalyzes the transamination reaction between alanine and α-ketoglutarate to give pyruvate and glutamate. As discussed in Chapter 22, it is vital that the cofactor B_6, pyridoxal phosphate, be present since it is the moiety that is involved in the actual reaction. As shown in Equation 28.21, the pyruvate that is produced is then reacted with LD in the presence of

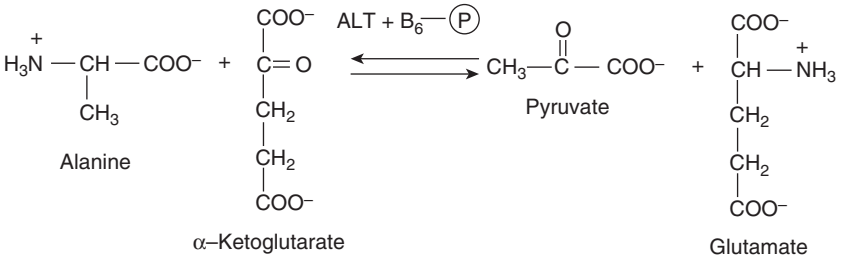

(Eq. 28.21A)

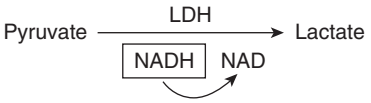

(Eq. 28.21B)

NADH to produce lactate. Since NADH is converted to NAD in this reaction, the decrease in absorbance of NADH at 340 nm is measured.

Interferences. Hemolysis: No interference with this reaction up to 500 mg/dL hemoglobin; Icterus: No significant interference up to 40 mg/dL bilirubin. Lipemia: No significant interference to 300 mg/dL Intralipid. Pyruvate does not cause negative interference at levels <1 mmol/L (8.7 mg/dL).

AST

As is also described in Chapter 22, this enzyme—which, like ALT, requires cofactor B_6 (pyridoxal phosphate)—reversibly catalyzes the reaction of aspartic acid with α-ketoglutarate to yield OAA and glutamate. The resulting OAA is then reacted with malate dehydrogenase, which converts the OAA to malate. As in the detection reaction for

ALT described earlier, NADH is converted to NAD, resulting in a decreased absorbance at 340 nm. These reactions are summarized in Equation 28.22.

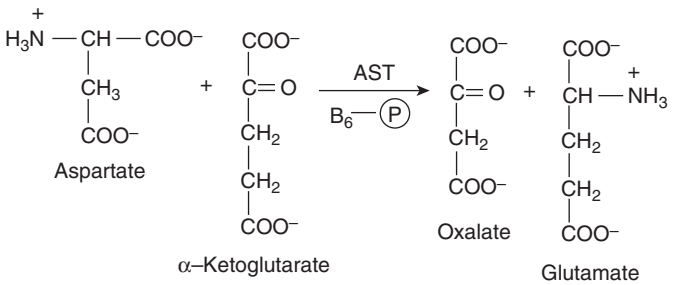

(Eq. 28.22A)

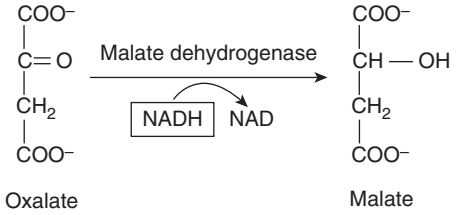

(Eq. 28.22B)

Interferences. Hemolysis can interfere with this determination; icterus does not induce interference at bilirubin levels up to 30 mg/dL; lipemia does not result up to levels of Intralipid of 500 mg/dL. Pyruvate demonstrates positive interference at levels ≥2.4 mg/dL. Heparin may also cause negative interference (Harr, 1987).

Alkaline Phosphatase (ALP)

As discussed in Chapter 21, the quantitative determination of serum ALP is based on colorimetric measurement of the rate of formation of p-nitrophenol (pNP), as the p-nitrophenoxide anion, a yellow compound, at 410 nm, from hydrolysis of para-nitrophenylphosphate (pNPP) by ALP, as shown in Equation 28.23. P_i represents inorganic phosphate cleaved from the substrate.

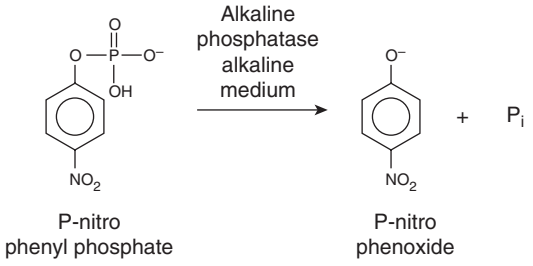

(Eq. 28.23)

Interferences. Hemolysis: Although hemoglobin has not been found to cause significant interference of this assay up to a concentration of 450 mg/dL, hemoglobin absorbs strongly at 410 nm, the wavelength at which the assay is performed, making hemolysis a risk factor for interference. Icterus: There is no significant interference up to 32 mg/dL bilirubin. Lipemia: No significant interference occurs up to 1000 mg/dL Intralipid. Recent studies suggest that citrate, oxalate, fluoride, EDTA, glycine, monoethanolamine, and high concentrations of phosphate and chloride can interfere with ALP assays.

Amylase (Moss & Henderson, 1999)

This enzyme hydrolyzes poly α-1,4-linked glucose polymers found in starch, amylopectin, and glycogen such that hydrolysis occurs at every second glucose residue. There are two types of amylases: α and β. β-Amylase cleaves maltose unit—glucosyl(α-1,4)glucose—from the reducing to the nonreducing end, as an exo-amylase, while α-amylase cleaves internally in addition to its cleaving from the reducing end of the α-1,4,-linked glucose polymer. Serum amylase is of the α type. The two major sources of this enzyme are pancreas and salivary glands. Thus serum amylase levels can be used as markers for pancreatic and salivary gland function. Both strongly homologous isozymes are present in serum. Over 200 methods for assaying for these enzymes have been described. Older methods used starch as the substrate. The glucose polymer forms a well-defined helix in solution. Iodine can bind within this helical structure to form a colored complex. In the presence of amylase, the polymer is degraded, resulting in lower iodine binding and hence less color complex formation. This decrease in color over time can be followed. In addition, as starch is hydrolyzed by amylase, the turbidity of the solution decreases, allowing turbidimetry (see Chapter 4) to be used to measure amylase activity.

Chromogenic substrate polymers of glucose have been synthesized in which a dye is bound covalently to the polymer. In the presence of amylase, the polymer is hydrolyzed, releasing small dye-labeled oligosaccharides. In the Johnson & Johnson slide technology system, the oligosaccharide is bound to an anionic dye, drimarene red Z2B. The dye-labeled oligosaccharides from amylase cleavage diffuse into the reagent layer where they are bound to a cationic polymer, where their concentrations can be determined spectrophotometrically. The parent polysaccharide cannot diffuse into this layer and is thus excluded. On Abbott analyzers, the parent polymer is labeled with a fluorescent probe. Since the structure of the long polymer is rigid (a helical structure), the fluorescence is polarized when the probe is stimulated with polarized light. (See Chapter 24 for a description of fluorescence polarization.) When the polymer is hydrolyzed by amylase, probe-bound fragments are released that are much smaller than the parent polymer and whose "tumbling times" are much faster, resulting in a major decrease in fluorescence polarization. Thus, the decreased fluorescence polarization can be followed over time to determine the enzyme activity.

Digestion of glucose polymers by amylase results in the formation of oligosaccharides like maltose and maltotriose (three glucose units in α-1,4 linkage). Oligosaccharides with three or fewer glucose units can be hydrolyzed to glucose with α-glucosidase. The resulting glucose formed can be assayed as described in the glucose assay section earlier in the chapter. A problem with this approach is the presence of endogenous glucose. This provides a high blank background. Endogenous glucose can be removed with a gel filtration column, although this does not lend the method to automation.

These methods use natural polymers of starch or amylopectin as substrates. This has the problem of standardization of the substrate material from lot to lot. In addition, the inhomogeneous substrate forms sols in aqueous solution that are easily contaminated. They are also temperature-sensitive and have limited stability. Newer methods involve use of synthetic substrates.

In one such method, synthetic maltopentaose (5α-1,4-linked glucose residues) is hydrolyzed by amylase to yield maltotriose and maltose. These are directly hydrolyzed to glucose by α-glucosidase. Since there is a high endogenous glucose background, this glucose is removed by a gel filtration column, as mentioned earlier.

To obviate the endogenous glucose problem, synthetic maltotetraose (4α-1,4-linked glucose residues) is used as the substrate. Amylase cleaves this substrate into 2 maltose units. These are then treated with the enzyme maltose phosphorylase and inorganic phosphate to form glucose-1-phosphate + glucose. Glucose-1-phosphate is then converted to glucose-6-phosphate by phosphoglucomutase. The resulting glucose-6-phosphate is then treated with G6PD, as described earlier in the glucose assay section, so that the formation of NADPH at 340 nm can be followed over time. It may be noted that, since the glucose-6-phosphate is generated from maltose and not from any endogenous glucose, endogenous glucose does not interfere with this reaction. However, amylase is not completely specific for generating 2 maltose sugars from maltotetraose and also cleaves the substrate, to a more minor extent, to glucose and maltotriose. Thus, the assay somewhat underestimates the level of amylase.

More recently, chromogenic substrates have been synthesized. These contain oligo-α-1,4-linked glucose units with 4 (or p)-nitrophenol (4-NP) in α-acetal linkage to the reducing sugar of the oligosaccharide. In one assay, maltoheptaose (7 glucose units in α-1,4 linkage) attached to 4-NP at its reducing end, is used as the substrate, as illustrated in Figure 28.5. Amylase hydrolyzes this substrate mainly into $(glucose)_4$-NP, $(glucose)_3$-NP, and $(glucose)_2$-NP plus $(glucose)_3$, $(glucose)_4$, and $(glucose)_5$, respectively. These reactions are summarized in Equation 28.24.

$$\text{NP-(glucose)}_7 \xrightarrow{\text{Amylase}} \text{NP-(glucose)}_{4,3,2} + \text{(glucose)}_{3,4,5} \qquad \text{(Eq. 28.24A)}$$

$$\text{NP-(glucose)}_{4,3,2} \xrightarrow{\alpha\text{-glucosidase}} (4\ \text{glucose} + \text{NP}) + (3\ \text{glucose} + \text{NP}) + (2\ \text{glucose} + \text{NP}) \qquad \text{(Eq. 28.24B)}$$

As shown in Equation 28.24B, the –NP-linked fragments are then further degraded with α-glucosidase to yield 4- (or p)-nitrophenol, which, at alkaline pH, forms the p-nitrophenoxide anion that absorbs strongly at 405 to 410 nm, as discussed earlier in the alkaline phosphatase section.

Note that Equation 28.24 assumes that a limit digest occurs for the tetra-, tri-, and disaccharides, always liberating one mole of p-nitrophenoxide anion per mole of each saccharide. In practice, this does not occur. In fact, hydrolysis of $(\text{glucose})_4$-NP by α-glucosidase is slow, although the rate can be enhanced by blocking OH-groups of the terminal nonreducing glucose unit. Thus, 4,6-ethylidene, 4,6-benzylidene, and other blocking groups have been found to enhance α-glucosidase activity.

Other problems with this approach include the consideration that the pKa of nitrophenol is close to the pH of the assay reactions. Thus, only about half of the released p-nitrophenol will be present as the oxyanion. In addition, the method is sensitive to ionic strength effects and the concentration of protein present in the assay mixture, both of which affect the pKa of the p-nitrophenol. It may also be subjected to interference by hemoglobin.

It has been found that these problems are largely removed by use of 2-chloro,4-nitrophenol (CNP) in place of 4-NP. Because of the ortho electron-withdrawing property of the o-Cl group, the pKa of the liberated phenol is lowered so that 100% of it exists as the colored phenoxide anion. It also minimizes the other complications listed earlier (except hemoglobin interference) and, because it is a better cleaving group in the mechanism of α-glucosidase–induced hydrolysis, higher yields of the smaller saccharides, and thus of CNP, are obtained, allowing for higher yields of the colored final product.

Interferences. Hemolysis: While hemolysis does not cause interference with some assays for amylase at hemoglobin levels up to 500 mg/dL, the assays that use liberation of p-nitrophenoxide anion monitored at 405 to 410 nm are subject to interference from hemoglobin, which absorbs significantly at these wavelengths. Icterus: There is no interference at bilirubin levels to 30 mg/dL. Lipemia: There is no interference by Intralipid up to 1000 mg/dL. Heparin may also cause negative interference (Harr, 1987).

Creatine Kinase

As discussed in Chapter 21, creatine kinase reversibly catalyzes the reaction between creatine and ATP to yield creatine phosphate and ADP. This reaction occurs prominently in muscle tissue, allowing for storage of the so-called *high-energy phosphate bond* as creatine phosphate. For the purposes of the enzyme assay, the reaction is reversed, that is, ADP and creatine phosphate are added to the sample to generate ATP + creatine. The product, ATP, is coupled into hexokinase/G6PD reactions and generates NADPH as shown in Equation 28.25. The CK activity is proportional to the absorbance increase of NADPH at 340 nm.

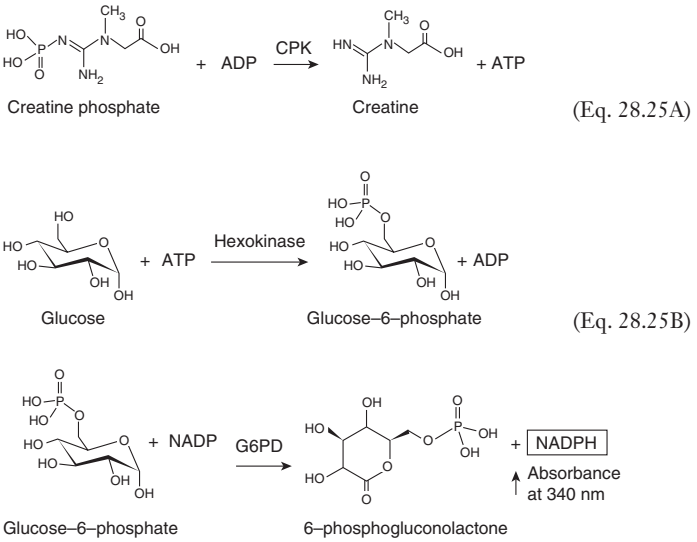

Interferences. Hemolysis: No significant interference occurs up to a hemoglobin concentration of 100 mg/dL. Icterus: No significant interference occurs up to a bilirubin concentration of 60 mg/dL. Lipemia: No significant interference occurs up to an Intralipid concentration of 1000 mg/dL. Drugs: Cyanokit (hydroxocobalamin) may cause interferences. In very rare cases, an IgM gammopathy, such as in Waldenström macroglobulinemia, may cause unreliable results.

γ-Glutamyl Transferase

As discussed in Chapter 22, this enzyme occurs on the canalicular surface of the hepatocyte (see Figure 22.9) and catalyzes the transfer of the γ-glutamyl residue of glutathione (γ-glutamyl-cysteinyl-glycine) to another amino acid or to an exogenous agent, such as a drug. As it happens, GGT transfers the γ-glutamyl residue from the synthetic substrate L-γ-glutamyl-3-carboxy-4-nitroanilide to glycylglycine to yield γ-glutamyl-glycylglycine and free 5-amino-2-nitro-benzoate (ANB) as shown in Equation 28.26.

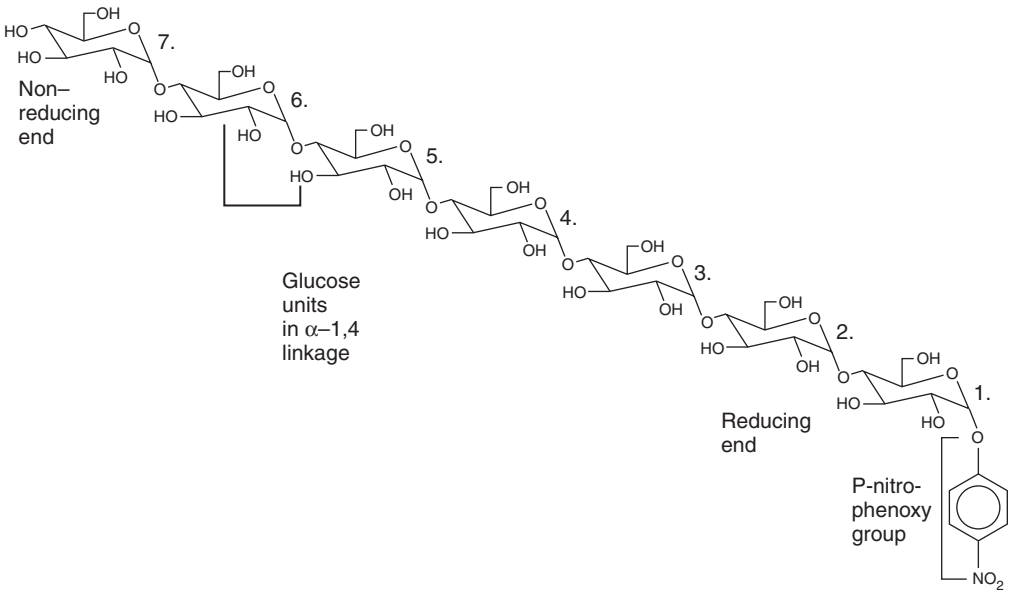

Figure 28.5 Structure of a synthetic substrate for amylase assays. This is the p-nitrophenyl glycoside of maltoheptaose. In practice, to enhance reaction specificity and to ensure more efficient cleavage by α-glucosidase, a protecting 4,6-ethylidene or benzylidene group is introduced on the seventh glucose unit on the nonreducing end.

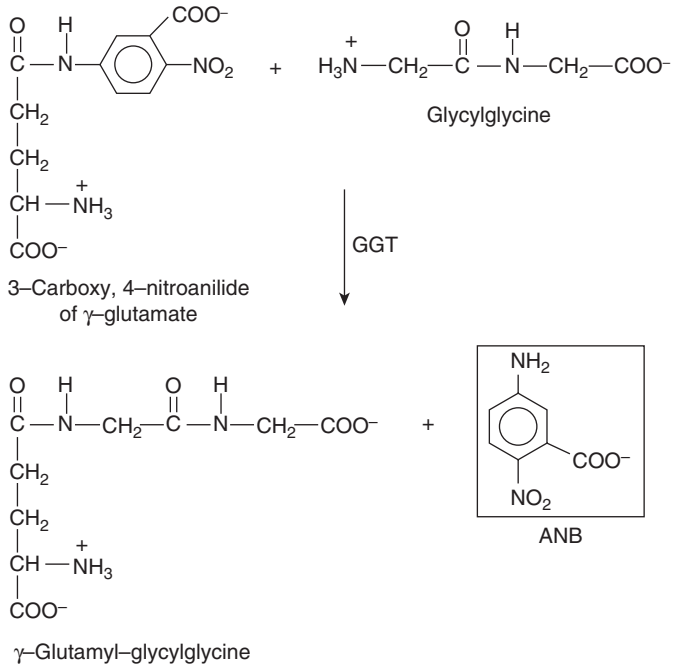

(Eq. 28.26)

Free ANB, which is a substituted aniline, absorbs at 410 nm. The rate of formation of ANB is measured as the increase in absorbance at 410 nm divided by the time interval over which it is measured, directly giving GGT activity.

Interferences. Hemolysis: There is no interference of hemoglobin up to concentrations of 350 mg/dL; Icterus: There is no interference of bilirubin up to a concentration of 40 mg/dL; Lipemia: There is no interference of Intralipid up to a concentration of 1000 mg/dL. It has also been found that some antiepileptic drugs (phenytoin, phenobarbital) and other barbiturates may result in falsely elevated GGT values. High levels of serum alcohol may likewise falsely elevate serum GGT.

Lactate Dehydrogenase

This enzyme, the reactions that it catalyzes, and assays for this enzyme are discussed in Chapter 21. Here, we note that the reaction scheme shown in Equation 28.17 for the assay for lactate is the same scheme as for the assay of LD. In this case, lactate is added to the serum sample at a concentration above its K_M, and the activity determined by the rate of increase of NADH absorbance at 340 nm.

Interferences. Because even minimal hemolysis causes significant increase in serum LD due to high levels of this enzyme in red cells (mainly LD1), positive interference will occur, giving falsely elevated values. Thus, hemolyzed samples should not be assayed for this enzyme.

Icterus: there is no significant interference from bilirubin at concentrations up to 40 mg/dL; Lipemia: There is no significant interference up to 1000 mg/dL Intralipid.

Lipase

As discussed earlier in the triglycerides assay section, lipases cleave fatty esters of glycerol. As discussed in Chapters 18 and 23, there are several isozymes of lipase, including pancreatic lipase, intestinal lipase, lipoprotein lipase, and gastric lipase. The first three of these forms have strong homology to one another and significantly less homology to the gastric isozyme. These lipases hydrolyze triglycerides that are long-chain fatty acid esters of glycerol. In addition, there are arylesterases and aliesterases that hydrolyze short-chain fatty acid esters and such simple esters as ethylacetate (aliesterase) and phenyl acetate (arylesterase) (Moss & Henderson, 1999). In serum, pancreatic lipase is very much the predominant form. Thus, assays for lipase are for the purpose of evaluating pancreatic function.

To be active, all lipases require a water-fat emulsion interface, the emulsion containing the substrate triglycerides. To attach to this interface, lipase requires the presence of a detergent, such as cholate, and another protein to which it binds, co-lipase. The latter binds both to lipase and to the detergent-emulsion complex, allowing lipase to interact with the triglycerides. Thus, all assay mixtures for lipase must contain both the detergent and co-lipase.

Assays for lipase can be performed by adding long-chain fatty acid esters to serum and the reaction monitored titrimetrically. In this case, dilute sodium hydroxide solution is added to serum to neutralize the long-chain fatty acids that are released, but the pH of the reaction mixture is maintained constant. The amount of base added over a given time period is a measure of the increased concentration of fatty acids over the time period, giving a rate that should be proportional to the total lipase concentration. The long-chain fatty acids used are contained in olive oil that has been treated to remove contaminating substances. This approach is also used with the pure triglyceride triolein as the substrate.

Although this is a reference method, it is difficult to adapt to continuously used autoanalyzers. Thus, other approaches have been devised. In one of these, 1-oleoyl-2,3-diacetyl glycerol is hydrolyzed by lipase to yield oleic acid and diacetylglycerol. The latter is reacted with an enzyme called diacetinase that hydrolyzes the two acetyl esters to yield glycerol and 2 moles of acetate. The glycerol generated in this reaction sequence is then treated with α-glycerol kinase + ATP. The reaction sequences shown in Equations 28.18B to 28.18D are then carried out. In a variant of this sequence, a 1,2-diacylglycerol is used as the substrate to yield the 2-acylglycerol that is then hydrolyzed by monoglyceride lipase (to accelerate the reaction) to yield glycerol that is subjected to the reactions described earlier.

A more recently developed assay for lipase that is being used successfully utilizes the artificial substrate for lipase, 1,2-O-dilauryl-rac-glycero-3-glutaric acid-(6′-methylresorufin) ester (DGGMR), as shown in Figure 28.6. Lipase cleaves this substrate such that it generates 1,2-O-dilauryl-rac-glycerol and an unstable intermediate, the hemiglutaric acid-(6′-methylresorufin) ester, which, spontaneously degrades to glutaric acid and methylresorufin. The oxyanion of this dye that forms under basic conditions is red colored and strongly absorbs at 580 nm. Thus, the absorbance increase of the red methylresorufin at 580 or 581 nm is proportional to the lipase activity. The reactions are summarized in Figure 28.6.

In order to obtain soluble substrates for lipase, artificial substrates with shorter-chain fatty acids are used. One of these is butyrin, the triester of n-butyric acid with glycerol. The glycerol generated by

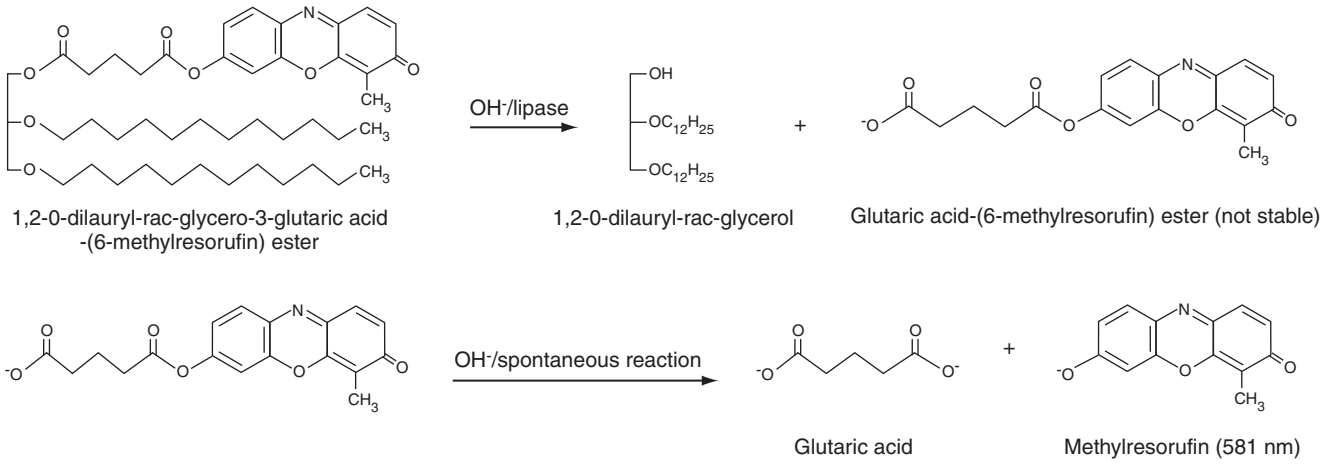

Figure 28.6 Artificial substrate for serum lipase resulting in liberation of methylresorufin, whose absorbance can be determined at 580 nm.

lipase is subjected to the reactions described earlier. In a variant of this approach, the n-butyric acid ester of 2,3-dimercapto-1-ol (i.e., a dithioester) is used. The limit digest of this substrate by lipase is 2,3-dimercapto-1-propanol. The two vicinal –SH groups can then be reacted with Ellman reagent, 5,5′-dithio-bis-(2-nitrobenzoic acid), to form a color complex that absorbs strongly at 412 nm. A problem with the use of these shorter-chain substrates is that they are also substrates for the ali- and arylesterases in serum (Moss & Henderson, 1999). To block the reaction of these enzymes, the covalent inhibitor phenylmethylsulfonylfluoride is added. This compound is a strong esterase (but not lipase) inhibitor.

Interferences. Hemolysis: There is no significant interference by hemoglobin up to 500 mg/dL. Icterus: There is no interference by bilirubin up to 12 mg/dL. Lipemia: There is no significant interference by Intralipid up to 500 mg/dL. Ascorbate: There is no significant interference up to 20 mg/dL ascorbate.

SELECTED REFERENCES

Jensen T, Truong Q, Frandsen M, et al.: Comparison of a homogeneous assay with a precipitation method for the measurement of HDL cholesterol in diabetic patients, *Diabetes Care* 25:1914–1918, 2002.

This is an important study that compares a homogeneous method with an immunoprecipitation method for determination of LDL cholesterol.

Kroli MH, Roach NA, Poe B, et al.: Mechanism of interference with the Jaffe reaction for creatinine, *Clin Chem* 33:1129–1132, 1987.

This is an interesting paper that presents possible structures for the creatinine-picrate complex and explains how ketones can interfere with this reaction.

Lin J-LJ, Hsu H-Y: Study of sodium ion selective electrodes and differential structures with anodized indium tin oxide, *Sensors* 10:1798–1809, 2010.

This paper presents a highly selective ion-selective electrode for sodium and illustrates how ion-selective electrodes are developed.

Nauck M, Warnick GR, Rifai N: Methods for measurement of LDL-cholesterol: a critical assessment of direct measurement by homogeneous assays versus calculation, *Clin Chem* 48:236–254, 2002.

Sugiuchi H, Uji Y, Okabe H, et al.: Direct measurement of high-density lipoprotein cholesterol in serum with polyethylene glycol-modified enzymes and sulfated α-cyclodextrin, *Clin Chem* 41:717–723, 1995.

This paper explains the basis for the homogenous (direct) determination of HDL cholesterol.

Access the complete reference list online at Elsevier eBooks for Practicing Clinicians.

REFERENCES

Basu A, Veettil S, Dyer R, Peyser T, Basu R: Direct evidence of acetaminophen interference with subcutaneous glucose sensing in humans: a pilot study, *Diabetes Technol Therapeut* 18, 2016. S2-43 - S2-47.

D'Orazio PD: Variability among methods for measuring glucose in whole blood: the influence of hematocrit. American Society of Clinical Pathology Check Sample, *Clin Chem* 49(CC 09–4 [CC-378]):43–55, 2009.

Endres DB, Rude RK: Mineral and bone metabolism. In ed 4, Burtiss CA, Ashwood ER, editors: *Tietz Textbook of clinical chemistry*Philadelphia, 1999, Saunders, pp 1397–1403.

Ginsberg B: Factors affecting blood glucose monitoring: sources of errors in measurement, *J Diabetes Sci Technol* 3:903–913, 2009.

Harr R, Bond L, Trumbull D: A Comparison of results for serum versus Heparinized plasma for 30 common analytes, *Lab Med* 18:449–455, 1987.

Morgan BR, Artiss JD, Zak B: Calcium determination in serum with stable alkaline Arsenazo III and triglyceride clearing, *Clin Chem* 39:1608–1612, 1993.

Moss DW, Henderson AR: Clinical enzymology. In ed 3, Burtiss CA, Ashwood ER, editors: *Tietz textbook of clinical chemistry*Philadelphia, 1999, Saunders, pp 617–721.

Natelson S: In *Techniques of clinical chemistry*, ed 3, Springfield, IL, 1971, Charles C. Thomas, p 176.

Porter WH, Crellin M, Rutter PW, Oeltgen P: Interference by glycolic acid in the Beckman Synchron method for lactate: a useful clue for unsuspected ethylene glycol intoxication, *Clin Chem* 46:874–875, 2000.

Rifai N, Bachorik PS, Albers JJ: Lipids, lipoproteins and apolipoproteins. In Burtiss CA, Ashwood ER, editors: *Tietz textbook of clinical chemistry*, ed 3, Philadelphia, 1999, Saunders, pp 809–861.

Rowatt E, Williams RJP: The interaction of cations with the dye Arsenazo III, *Biochem J* 259:295–298, 1989.

Saleem M, Dimeski G, Bourne L, et al.: Artifactually elevated serum bicarbonate results caused by elevated serum lactate dehydrogenase concentrations, *Ann Clin Biochem* 50:365–367, 2013.

Tolman KG, Rej R: Liver function. In Burtiss CA, Ashwood ER, editors: *Tietz textbook of clinical chemistry*,, ed 3, Philadelphia, 1999, Saunders, pp 1133–1137.

Vasillades J: Reaction of alkaline sodium picrate with creatinine: I. Kinetics and mechanism of formation of the mono-creatinine picric acid complex, *Clin Chem* 22:1664–1671, 1976.

Yoo E-H, Lee S-Y: Glucose biosensors: an overview of use in clinical practice, *Sensors* 10:4558–4576, 2010.

Young DS: In *Effects of drugs on clinical laboratory tests*, 5th Edition, AACC Press, 2000.

PART 3

Urine and Other Body Fluids

EDITED BY | Donald S. Karcher, Richard A. McPherson, Matthew R. Pincus

CHAPTER 29

BASIC EXAMINATION OF URINE

Roger S. Riley, Richard A. McPherson

URINE FORMATION, 468
COMPONENTS OF BASIC (ROUTINE) URINALYSIS, 468
Specimen Evaluation, 469
Gross/Physical Examination, 469
Chemical Screening, 472
Examination of Urine Sediment, 486
METHODS FOR URINALYSIS, 499
Basic (Routine) Urinalysis Procedure, 499
Automated Urinalysis, 500
Automated Microscopy Analyzers, 503
Integrated, Fully Automated Urinalysis Systems, 505
SPECIAL TESTING AND MONITORING TECHNIQUES, 505
Urinary Calculi, 505
Laboratory Tests used to Investigate Stone Formers, 507
Urinary Screening for Inherited Metabolic Diseases, 507
Additional Urine Testing Modalities, 509
SELECTED REFERENCES, 509

KEY POINTS

- Many different diseases can display abnormalities in the urine. Therefore, examination of the urine is an important laboratory function.
- Basic urinalysis consists of gross examination of the urine as well as a dipstick analysis for blood, white blood cells, sugar, and other substances. The dipstick may be read manually or by an automated instrument.
- A microscopic analysis of urine may be necessary in many cases. This is done to detect cellular elements, casts, and crystals. Each of these items can be caused by several different disease states.
- Although microscopic examination of the urine is usually performed manually, several automated instruments can perform this analysis.
- Red blood cells within the urine can come from any point along the urinary tract. Dysmorphic red blood cells are often a sign of glomerular disease.
- The first voided morning urine, because it is the most concentrated, is often the best specimen for analysis. Some procedures may require a 12- or 24-hour urine sample.
- Specific gravity and osmolality measurements reflect the concentrating ability of the kidneys. After a period of dehydration, the osmolality should be three to four times that of plasma.
- Proteinuria greater than 4 g/day is seen in nephrotic syndrome. Although nephrotic syndrome is usually seen in primary renal disease, it is occasionally seen in a systemic disease that affects the kidneys.
- Ketonuria can be seen in diabetic individuals. It can also be seen in other states, such as febrile illness and cachexia.
- The dipstick nitrite and leukocyte esterase tests are used to help diagnose urinary tract infection. Positive results should be confirmed by microscopic analysis of the urine.
- Urinary calculi are most commonly formed from calcium. Workup of habitual stone formers should include analysis of both the urine and the stone.

A significant amount of information can be obtained through the examination of urine. Careful examination enables the detection of disease processes intrinsic to the urinary system, both functional (physiologic) and structural (anatomic), and sometimes unsuspected (Echeverry, Hortin, & Rai, 2010; Haber, 1988; Takemura, Ishida, Inoue, Kobayashi, & Beck, 2000). The progression or regression of various lesions can be monitored with only minimal distress to the patient. Furthermore, systemic disease processes, such as endocrine or metabolic abnormalities, can be detected through the recognition of abnormal quantities of disease-specific metabolites excreted in the urine. Laboratory urine tests will continue to play an essential role in clinical medicine.

The purpose of this chapter is to highlight the pertinent information that can be provided by the most common urine tests. Two main types of urinalysis are currently performed. These include (1) the dipstick (reagent strip) urinalysis, which is commonly performed in screening laboratories, in physician offices, and as patient home testing; and (2) the basic (routine) urinalysis, which adds a microscopic examination of urine sediment to the reagent strip urinalysis. These examinations utilize various laboratory disciplines, particularly chemistry and microscopy. In addition to these front-line diagnostic procedures, new technologies—including immunocytochemistry, molecular diagnostics, deoxyribonucleic acid (DNA) ploidy, and cell cycle analysis—are constantly evolving to provide additional diagnostic and prognostic information. Urine microbiology studies, crucial to the diagnosis of infectious pathogens of the urinary tract, are addressed elsewhere in this textbook. It is important to remember that each of these modalities has a certain clinical utility. Table 29.1 lists the benefits of commonly ordered urine laboratory examinations.

URINE FORMATION

In the normal adult, approximately 1200 mL of blood perfuses the kidneys each minute, which accounts for about 25% of the cardiac output. The glomeruli (normally numbering at least 1 million per kidney) receive blood through afferent arterioles, and an ultrafiltrate of the plasma passes through each glomerulus into the Bowman space. From here, the filtrate is passed through the tubules and collecting ducts, where reabsorption or secretion of various substances and the concentration of urine can occur (Scott & Quaggin, 2015). Ultimately, the original glomerular filtrate volume of about 180 L in 24 hours is reduced to about 1 to 2 L depending on the status of hydration. This urine formed in the kidneys passes from the collecting ducts into the renal pelvis, ureters, bladder, and urethra to be voided.

The kidneys take part in several regulatory functions. Through glomerular filtration and tubular secretion, numerous waste products—including nitrogenous products of protein catabolism, and both organic and inorganic acids and bases—are eliminated from the body. Fluid, electrolytes (including sodium, potassium, calcium, and magnesium), and acid-base status are regulated in homeostasis. Furthermore, the kidneys provide important hormonal regulation with erythropoietin and renin production as well as vitamin D activation. Any derangement of these functions by renal or systemic disease can be reflected as chemically or cytologically altered urine.

COMPONENTS OF BASIC (ROUTINE) URINALYSIS

The basic (routine) urinalysis consists of four parts: specimen evaluation, gross/physical examination, chemical screening, and sediment examination.

TABLE 29.1

Benefits of Common Urine Laboratory Tests

Type of test	Aims	CLINICAL UTILITY			
		Screen	Diagnosis	Monitor	Prognosis
Urine chemistry (reagent strip)	Glucosuria	+++	+	+	+
	Proteinuria				
	Hematuria				
	Leukocyturia				
	Infection				
Wet urinalysis (routine)	Diabetes	++++	++	++	+
	Proteinuria				
	Hematuria				
	Leukocyturia				
	Infections				
	Cylindruria				
	Crystalluria				
Urine microbiology	Infections	++	++++	++	+
Urine cytology (conventional)	Cancer	+	++	+	–
	Inflammation				
	Viral infections				
Cytodiagnostic urinalysis	Glomerular and renal tubular disorders	+	++++	+++	++
	LUT disorders				
	Nonbacterial infections				
	Lithiasis				
Image cytometry and DNA analysis	Urothelial cancer	–	++	+++	+++
Flow cytometry	Urothelial cancer	–	+	+++	++

From Schumann GB, Schumann JL, Marcussen N: *Cytodiagnostic urinalysis of renal and lower urinary tract disorders*, New York, 1995, Igaku-Shoin Medical Publishers, with permission.
LUT, Lower urinary tract; –, negative; +, low positive; ++++, strongly positive.

SPECIMEN EVALUATION

Before one proceeds with any examination, the urine specimen must be evaluated in terms of its acceptability. Considerations include proper labeling, proper specimen for the requested examination, proper preservative, visible signs of contamination, and whether any transportation delays may have caused significant deterioration (Delanghe & Speeckaert, 2016; Stankovic & DiLauri, 2008). Each laboratory should have written and enforced guidelines for the acceptance or rejection of specimens. A properly labeled specimen must have the patient's full name and the date and time of collection. Additional information may be required by the institution, but these three essentials constitute minimum labeling requirements.

The first voided morning urine, which is the most concentrated, is best for routine urinalysis. At times, a catheterized specimen or suprapubic collected urine specimen is received. If a single specimen is submitted for multiple measurements, bacteriologic examination should be done first provided that the urine has been properly collected. With pediatric patients and persons in acute renal failure, only a small volume of urine may be available for processing. In such cases, a notation should be made and the measurements most pertinent to the diagnosis should be performed first. For quantitative measurements, timed (12- or 24-hour) urinary collection is preferred to random specimens.

GROSS/PHYSICAL EXAMINATION

Appearance

Some of the more important changes in the gross appearance of urine are described in this section. A comprehensive list is provided in Table 29.2.

Color

The yellow color of urine is due largely to the pigment urochrome, excretion of which is generally proportional to the metabolic rate. It is increased during fever, thyrotoxicosis, and starvation. Small quantities of urobilins and uroerythrin (pink pigment) also contribute to urine coloration. In normal individuals, both pale and dark yellow urine can be produced; these differences are rough indicators of hydration and urine concentration. Pale urine, typically of low specific gravity, is excreted following high fluid intake; darker urine is seen when fluids are withheld. Note that pale urine of high specific gravity may be found in diabetes mellitus. An abnormal color to the urine is usually due to an ingested food or medication but may also be a clue to a specific disease state (Aycock & Kass, 2012). For color changes of urine in pediatric patients, see Cone (1968). Table 29.3 lists the urine color changes associated with commonly used drugs.

Red Urine. The most common abnormal color for urine is red or red-brown. When seen in females, menstrual flow contamination should be considered. Hematuria (presence of red blood cells [RBCs]), hemoglobinuria, and myoglobinuria may produce pink, red, or red-brown coloration. All three of these conditions are easily detectable on reagent strip testing; however, further evaluation is necessary for absolute differentiation (see the Blood, Hemoglobin, Hemosiderin, and Myoglobin in Urine section later in the chapter).

In the porphyrias, urine coloration is variable. It is usually red in congenital erythropoietic porphyria and porphyria cutanea tarda; however, in lead porphyrinuria, the urine color is generally normal. In acute intermittent hepatic porphyria, it is normal but darkens on standing. Red urine also may be associated with the use of drugs and dyes in diagnostic tests—for example, phenolsulfonphthalein, which is sometimes used in assessing renal function, will cause a red color in alkaline urine. Patients with an unstable hemoglobin may produce urine with red-brown color that does not give a positive indication of hemoglobin or bilirubin. The pigment is probably a dipyrrole or bilifuscin. An innocuous red urine associated with ingestion of beets is seen in genetically susceptible persons.

Yellow-Brown or Green-Brown Urine. Yellow-brown or green-brown urine is generally associated with bile pigments, chiefly bilirubin. On shaking the urine specimen, a yellow foam may be seen, which distinguishes bilirubin from a normal, dark, concentrated urine, which will have white foam. In severe obstructive jaundice, the urine may be dark green.

Orange-Red or Orange-Brown Urine. Excreted urobilinogen is colorless but is converted in the presence of light and low pH to urobilin, which is dark yellow to orange. Urobilin will not color the foam on shaking; in this way, it may be confused with a concentrated normal urine. Reagent strip testing would be confirmatory in this situation.

Dark Brown or Black Urine. Acid urine containing hemoglobin will darken on standing because of the formation of methemoglobin. "Cola-colored" urine may be seen with rhabdomyolysis (Keverline, 1998) and in some patients taking L-dopa. Rarer causes of dark-brown urine are homogentisic acid (alkaptonuria) and melanin. Urine-containing homogentisic acid will darken more rapidly when alkaline.

TABLE 29.2
Appearance and Color of Urine

Appearance	Cause	Remarks
Colorless	Very dilute urine	Polyuria, diabetes insipidus
Cloudy	Phosphates, carbonates	Soluble in dilute acetic acid
	Urates, uric acid	Dissolve at 60° C and in alkali
	Leukocytes	Insoluble in dilute acetic acid
	Red blood cells ("smoky")	Lyse in dilute acetic acid
	Bacteria, yeasts	Insoluble in dilute acetic acid
	Spermatozoa	Insoluble in dilute acetic acid
	Prostatic fluid	
	Mucin, mucous threads	May be flocculent
	Calculi, "gravel"	Phosphates, oxalates
	Clumps, pus, tissue	
	Fecal contamination	Rectovesical fistula
	Radiographic dye	In acid urine
Milky	Many neutrophils (pyuria)	Insoluble in dilute acetic acid
	Fat	Nephrosis, crush injury—soluble in ether
	Lipiduria, opalescent	
	Chyluria, milky	Lymphatic obstruction—soluble in ether
	Emulsified paraffin	Vaginal creams
Yellow	Acriflavine	Green fluorescence
Yellow-orange	Concentrated urine	Dehydration, fever
	Urobilin in excess	No yellow foam
	Bilirubin	Yellow foam if sufficient bilirubin
Yellow-green	Bilirubin-biliverdin	Yellow foam
Yellow-brown	Bilirubin-biliverdin	"Beer" brown, yellow foam
Red	Hemoglobin	Positive } Reagent strip for blood
	Erythrocytes	Positive } Reagent strip for blood
	Myoglobin	Positive } Reagent strip for blood
	Porphyrin	May be colorless
	Fuscin, aniline dye	Foods, candy
	Beets	Yellow alkaline, genetic
	Menstrual contamination	Clots, mucus
Red-purple	Porphyrins	May be colorless
Red-brown	Erythrocytes	
	Hemoglobin on standing	
	Methemoglobin	Acid pH
	Myoglobin	Muscle injury
	Bilifuscin (dipyrrole)	Result of unstable hemoglobin
Brown-black	Methemoglobin	Blood, acid pH
	Homogentisic acid	On standing, alkaline; alkaptonuria
	Melanin	On standing, rare
Blue-green	Indicans	Small intestine infections
	Pseudomonas infections	
	Chlorophyll	Mouth deodorants

TABLE 29.3
Urine Color Changes with Commonly Used Drugs*

Drug	Color
Alcohol, ethyl	Pale, diuresis
Anthraquinone laxatives (senna, cascara)	Reddish, alkaline; yellow-brown, acid
Chlorzoxazone (Paraflex; muscle relaxant)	Red
Deferoxamine mesylate (Desferal; chelates iron)	Red
Ethoxazene (Serenium; urinary analgesic)	Orange, red
Fluorescein sodium (given IV)	Yellow
Furazolidone (Furoxone, Tricofuron; an antibacterial, antiprotozoal nitrofuran)	Brown
Indigo carmine dye (renal function, cystoscopy)	Blue
Iron sorbitol (Jectofer; possibly other iron compounds forming iron sulfide in urine)	Brown on standing
Levodopa (L-dopa; for parkinsonism)	Red then brown, alkaline
Mepacrine (Atabrine; antimalarial, intestinal worms, *Giardia*)	Yellow
Methocarbamol (Robaxin; muscle relaxant)	Green-brown
Methyldopa (Aldomet; antihypertensive)	Darkens; if oxidizing agents present, red to brown
Methylene blue (used to delineate fistulas)	Blue, blue-green
Metronidazole (Flagyl; for *Trichomonas* infection, amebiasis, *Giardia*)	Darkening, reddish brown
Nitrofurantoin (Furadantin; antibacterial)	Brown-yellow
Phenazopyridine (Pyridium; urinary analgesic), also compounded with sulfonamides (e.g., Azo Gantrisin)	Orange-red, acid pH
Phenindione (Hedulin; anticoagulant. Important to distinguish from hematuria)	Orange, alkaline; color disappears on acidifying
Phenol poisoning	Brown; oxidized to quinones (green)
Phenolphthalein (purgative)	Red-purple, alkaline pH
Phenolsulfonphthalein (also sulfobromophthalein)	Pink-red, alkaline pH
Rifampin (Rifadin, Rimactane; tuberculosis therapy)	Bright orange-red
Riboflavin (multivitamins)	Bright yellow
Sulfasalazine (Azulfidine; for ulcerative colitis)	Orange-yellow, alkaline pH

*Other commonly used drugs have been noted to produce color change once or occasionally: amitriptyline (Elavil)—blue-green; phenothiazines—red; triamterene (Dyrenium)—pale blue (blue fluorescence in acid urine).

Blue, Green, or Blue-Green Urine. A blue, green, or blue-green discoloration of the urine is most commonly due to food dyes or additives, some foods, or medications, including amitriptyline, doxorubicin, cimetidine, flutamide, indomethacin, methocarbamol, mitoxantrone, phenylbutazone, phenergan, propofol, promethazine, triamterene, rinsapin, and sildenafil (Aycock & Kass, 2012; Brunzel, 2012; Strasinger & Di Lorenzo, 2014). Rare causes of blue or green urine include *Pseudomonas* infection and some inherited diseases, such as Hartnup disease, indicanemia, indicanuria, and familial hypercalcemia. In cancer patients receiving chemotherapy, the methylene blue included in several dysuria medications, including Prosed DS, Trac Tabs, Urised, and Uroblue, may cause green or bluish-green urine discoloration (Cotten & McCudden, 2011; Meng et al., 2013).

Purple Urine. Urine with a bright purple color has been reported in association with long-term urinary catheterization with coexistent urinary tract infection (Demelo-Rodríguez et al., 2016).

Clarity (Character)

Urine is normally clear; thus, the presence of particulate material in an unspun specimen warrants further investigation. The differential diagnosis for cloudy urine is broad and includes several nonpathologic entities. Turbidity may simply be due to the precipitation of crystals or nonpathologic salts referred to as *amorphous*. Phosphate, ammonium urate, and carbonate can precipitate in alkaline urine; these redissolve when acetic acid is added. Uric acid and urates cause a white, pink, or orange cloud in acid urine and redissolve on warming to 60°C.

Cloudy urine can be attributed to the presence of various cellular elements. Leukocytes may form a white cloud similar to that caused by phosphates, but the cloud remains after acidification. Likewise, bacterial growth may cause a uniform opalescence that is not removed by acidification or filtration. It has been suggested that turbidimetric assessment using a double-beam turbidimeter may be useful for urine infection screening (Livsey, 1995). Turbidity may also be due to RBCs, epithelial cells, spermatozoa, or prostatic fluid. Prostatic fluid normally contains a few leukocytes and other formed elements.

Miscellaneous causes for cloudy urine include mucus from the lower urinary tract or genital tract, blood clots, menstrual discharge, and other particulate material such as pieces of tissue, small calculi, clumps of pus, and fecal material. Fecal material in urine may occur with a fistulous connection between the colon or rectum and bladder. Contamination with powders or with antiseptics that become opaque with water (phenols) will also cause a turbid urine.

Chyluria. This is a rare condition in which the urine contains lymph. It is associated with obstruction to lymph flow and rupture of lymphatic vessels into the renal pelvis, ureters, bladder, or urethra (Guttilla et al., 2017). Although parasitic infection with *Wuchereria bancrofti* (filariasis) is the prevailing cause (Cortvriend et al., 1998), abdominal lymph node enlargement, tumors, scoliosis surgery, and pregnancy have also been associated with chyluria. Even with filariasis, this condition is rare.

The appearance of the urine varies with the amount of lymph present, ranging from clear to opalescent or milky. Clots may form and, if sufficient lymph is present, the urine may layer with the chylomicrons on top and fibrin and cells beneath. Chylomicrons may not be apparent microscopically unless they have coalesced as microglobules. This fatty material can be extracted from urine using an equal volume of ether or chloroform. Urine phosphates, in contradistinction, will not clear with this method. Pseudochyluria occurs with the use of paraffin-based vaginal creams for the treatment of *Candida* infection.

Lipiduria. Fat globules appear in the urine most often with nephrotic syndrome; these consist of neutral fats (triglycerides) and cholesterol (Streather et al., 1993). Lipiduria can also be present in patients who have sustained skeletal trauma with fractures to major long bones or the pelvis. Presumably, the source of lipid is exposed fatty marrow. Keep in mind that in addition to these endogenous lipids, oily contaminants such as paraffin may float on the urine surface. Microscopic examination of the urine may be required to classify fatty materials as Oil Red O–positive droplets or cholesterol esters with polarization.

Odor

Urine normally will have a faint, aromatic odor of undetermined source. Specimens with extensive bacterial overgrowth can be recognized by an ammoniacal, fetid odor. Additionally, ingestion of asparagus or thymol produces distinctive odors in urine.

Characteristic urine odors associated with amino acid disorders include the following:

Cystinuria	Rotten eggs
Hawkinsinuria	Swimming pool
Ketoacidosis	Sweet, fruity
Isovaleric acidemia and glutaric acidemia	Sweaty feet
Maple syrup urine disease (MSUD)	Maple syrup
Methionine malabsorption	Cabbage, hops
Phenylketonuria	Mousy, musty
Trimethylaminuria	Rotting fish
Tyrosinemia	Rancid

Lack of odor in urine from patients with acute renal failure suggests acute tubular necrosis (ATN) rather than prerenal failure.

Urine Volume

Under ordinary conditions, the main determinant of urine volume is water intake. The average adult produces from 600 to 2000 mL of urine per day, with night urine generally not in excess of 400 mL. In pregnancy, the usual diurnal variation may be reversed. Young children, compared with adults, may excrete about three to four times as much urine per kilogram of body weight. Measurement of urine output during timed intervals may be valuable in clinical diagnosis.

Increases in Urine Volume

Production of more than 2000 mL of urine in 24 hours is termed *polyuria*; *nocturnal polyuria* (*nocturia*) is excretion of more than 500 mL of urine at night with a specific gravity of less than 1.018. In general, high volumes of urine tend to result in a low specific gravity.

Excessive intake of water (polydipsia) will result in polyuria, as will consumption of certain drugs with a diuretic effect, such as caffeine, alcohol, thiazides, and other diuretics. Intravenous solutions may increase the urine output. Increased salt intake and high-protein diets will require more water for excretion. Nocturia is common in elderly individuals, with a prevalence of 80% to 90% by 80 years of age in both sexes (Weiss & Blaivas, 2000).

Pathologic states that result in excess renal fluid loss/urine excretion can be divided into three groups.

Defective Hormonal Regulation of Volume Homeostasis. Diabetes insipidus can be due to a deficiency (central/pituitary variety) of, or renal unresponsiveness (nephrogenic) to, antidiuretic hormone. In either situation, excessive thirst and water intake occur, together with marked polyuria and nocturia. Up to 15 L of urine per day may be produced.

Defective Renal Salt/Water Absorption. This can be due to the administration of diuretic agents or an abnormality of the renal tubules, resulting in sodium wasting or impairment of the countercurrent mechanism. In progressive chronic renal failure, functioning renal tissue is diminished and the ability to concentrate urine is gradually lost. To excrete the daily renal water and solute load, an increase in urine volume per residual nephron results and the urine eventually becomes isoosmotic with the plasma ultrafiltrate.

Osmotic Diuresis. In diabetes mellitus with hyperglycemia, an excessive amount of glucose is excreted, causing a solute diuresis.

Decreases in Urine Volume

Oliguria is the excretion of less than 500 mL of urine per 24 hours, and anuria is the near-complete suppression of urine formation. Water deprivation will cause a decrease in urine volume even before signs of dehydration appear. Oliguria can be rather abrupt in onset, as can acute renal failure, or it may be due to a chronic progressive renal disease. In either case, retention of nitrogenous waste products (azotemia) can occur (see Chapter 15). The causes of acute renal failure are classically categorized as follows.

Prerenal. Loss of intravascular volume may result from hemorrhage or from dehydration associated with prolonged diarrhea, vomiting, excess sweating, or severe burns. So-called *third spacing* is the shifting of intravascular fluids to extracellular spaces. Additionally, conditions such as congestive heart failure, sepsis, anaphylaxis, or renal artery embolic occlusion may result in a decrease in renal blood flow.

Postrenal. Bilateral hydronephrosis, resulting from high-grade or long-standing obstruction of the urinary tract, may be associated with a marked decrease in urine flow and even anuria. This can occur with prostatic hyperplasia and carcinoma. Bilateral ureteral obstruction due to stones, clots, and sloughed tissue, and urethral obstruction due to stricture or valves, are other forms of obstruction. The anuria associated with sulfonamide therapy and dehydration is due to obstruction caused by the precipitation of crystals in the renal tubules when the urinary pH is acidic.

Renal Parenchymal Disease. This should be considered after other prerenal and postrenal causes of oliguria have been ruled out. The list of conditions is extensive and includes various vascular disorders, glomerulonephritis, interstitial nephritis, and ATN. A common cause of ATN is renal ischemia due to heart failure or hypotension. Numerous nephrotoxic agents may produce ATN, including several antibiotics, mercury, cadmium, carbon tetrachloride, and glycerol. Other causes include hemoglobinuria and myoglobinuria, associated with hemolysis and muscle damage, respectively, as well as excessive quantities of intratubular proteins or crystals.

Chronic renal failure, a progressive and irreversible loss of renal function, results from several disease entities. These include hypertensive and diabetes-associated nephrosclerosis, chronic glomerulonephritis, polycystic kidney disease, and other urologic disorders. Urinary specific gravity is low and proteinuria, casts, and renal cells may be evident. Pyelonephritis or interstitial nephritis will cause predominantly tubular dysfunction with polyuria early in the disease, but later oliguria of chronic renal failure supervenes.

Specific Gravity and Osmolality

The volume of excreted urine and the concentrations of its solutes are varied by the kidney to maintain the homeostasis of body fluid and electrolytes. Specific gravity and osmolality measurements reflect the relative degree of concentration or dilution of a urine specimen. This, in turn, aids in evaluating the concentrating and diluting abilities of the kidneys. Both of these indices, as well as urine color, have been found to be reliable indicators of hydration status (Armstrong et al., 1998; McKenzie et al., 2017).

The specific gravity of a specimen indicates the relative proportions of dissolved solid components to total volume of the specimen; in other words, it reflects the density of the specimen. Osmolality, on the other hand, indicates the number of particles of solute per unit of solution. Larger particles, such as proteins and sugars, tend to elevate the specific gravity more than smaller electrolytes. In critical circumstances, the measurement

of osmolality of urine (and plasma) is preferred to the measurement of specific gravity (Imran et al., 2010; Voinescu et al., 2002).

Specific Gravity

Urea (20%), sodium chloride (25%), sulfate, and phosphate contribute most of the specific gravity of normal urine. Normal adults with adequate fluid intake will produce urine of specific gravity 1.016 to 1.022 over a 24-hour period. However, normal kidneys have the ability to produce urine with a specific gravity that ranges from 1.003 to 1.035. If a random specimen of urine has a specific gravity of 1.023 or more, the concentrating ability can be considered normal. Minimum specific gravity after a standard water load should be less than 1.007.

Urines of low specific gravity are called *hyposthenuric*, with the specific gravity less than 1.007. In diabetes insipidus, loss of concentrating ability (as described earlier) results in production of large volumes of urine with a specific gravity as low as 1.001 (specific gravity of water is 1.000). Prolonged excretion of urine with low specific gravity can also be seen with various renal abnormalities, including pyelonephritis and glomerulonephritis. High specific gravity can be seen after excess water loss/dehydration, adrenal insufficiency, hepatic disease, or congestive heart failure. When little or no variability is noted between several specimens from a patient and the specific gravity is fixed at about 1.010, this is known as *isosthenuria*. This finding is indicative of severe renal damage with disruption of both concentrating and diluting abilities.

Methods. Several methods are available to measure specific gravity—reagent strip, refractometer, urinometer, and the falling drop method.

Reagent Strip. This is an indirect method for measuring specific gravity. The reagent area has three main ingredients present: polyelectrolyte, indicator substance, and buffer. The principle of this method is based on the pKa change of pretreated polyelectrolytes in relation to the ionic concentration of the urine. When the ionic concentration is high, the pKa (acid dissociation constant) is decreased, as is the pH. The indicator substance then changes color relative to ionic concentration, which is translated to specific gravity values. The results obtained by this method should be used with caution, since it is not affected by high amounts of glucose, protein, or radiographic contrast material, all of which tend to elevate the specific gravity readings obtained from refractometers and urinometers, described in the following sections. The reagent strip assay for urine pH must be performed carefully to avoid runover from adjacent test areas, which can cause false readings.

Refractometer (see Chapter 4). This is also an indirect method. The refractive index of a solution is related to the content of dissolved solids present. The index is the ratio of the velocity of light in air to the velocity of light in a solution. It varies directly with the proportion of particles in solution and, therefore, with the specific gravity.

The optical analog handheld clinical refractometer is a device that requires only a few drops of urine (unlike the 15 mL of urine necessary with the urinometer). Although the refractometer measures the refractive index of a solution, the scale used is valid only for urine and cannot be used to indicate the specific gravity of salt or sugar solutions. This should be kept in mind if salt solutions are to be used for calibration. Special graphs or tables are required to convert refractive index scale numbers to solute concentrations in aqueous solutions if this should be required (American Optical Catalog Number 10403). The specific gravity reading on the refractometer is generally slightly lower than a urinometer reading on the same urine specimen by about 0.002. Digital refractometers are now available for human clinical applications.

Procedure. A temperature-compensated hand model is widely used. The instrument is temperature compensated between 60°F and 100°F (15°C to 38°C). It is damaged by heat above 150°F (66°C) and by immersion of the eyepiece and focusing ring in water. It should read zero with distilled water; the zero reading can be reset if necessary by breaking the seal over the setscrew, turning it with a small screwdriver, and resealing. Check calibration daily. Copper sulfate solutions can be adjusted to monitor a high specific gravity level as an additional check.

To make a specific gravity determination of urine, clean the surfaces of the cover and prism with a drop of distilled water and a damp cloth, and allow them to dry. Close the cover. Hold horizontally and apply a drop of urine at the notched bottom of the cover so that it flows over the prism surface by capillary action. Point the instrument toward a light source at an angle that gives optimal contrast. Rotate the eyepiece until the scale is in focus. Read directly on the specific gravity scale the sharp dividing line between light and dark contrast. The entire procedure should be repeated with a second drop of urine from the same sample.

Urinometer. This is a hydrometer that is adapted to directly measure the specific gravity of urine at room temperature. It should be checked each day by measuring the specific gravity of distilled water. If the urinometer does not give a reading of 1.000, an appropriate correction must be applied to all readings taken with that urinometer. The accuracy of a urinometer may be further checked with solutions of known specific gravity. An automated urinometer using a capacitive sensor has been described (Eklund et al., 2015; Slettengren et al., 2019).

Because temperature influences the specific gravity, urine samples should be allowed to come to room temperature before a reading is made or a correction of 0.001 should be made for each 3°C above or below the calibration temperature indicated on the urinometer. Corrections must also be made for protein or glucose present; subtract 0.003 for every 1 g/dL of protein and 0.004 for every 1 g/dL of glucose.

Procedure. The urinometer vessel is filled three-fourths full with urine (minimum volume required is about 15 mL). The urinometer is inserted with a spinning motion to make sure that it is floating freely. (When reading the urinometer, be sure that it is not touching the sides or the bottom of the cylinder. Avoid surface bubbles, which obscure the meniscus.) Read the bottom of the meniscus.

Falling Drop Method. This is a direct method for measuring specific gravity. It is more accurate than the refractometer and is more precise than the urinometer. This method utilizes a specially designed column filled with water-immiscible oil. A measured drop of urine is introduced into the column; as this drop falls, it encounters two beams of light. Breaking the first beam starts a timer and breaking the second turns it off. The falling time is measured electronically and is expressed as a specific gravity (Marable, 1963). Despite its accuracy and use of small specimen volume, this method is not widely practiced.

Osmolality

The normal adult with a normal fluid intake will produce urine of about 500 to 850 mOsm/kg water. The normal kidney is able to produce a urine osmolality in the range of 800 to 1400 mOsm/kg water in dehydration, and a minimal osmolality of 40 to 80 mOsm/kg water during water diuresis. After a period of dehydration, the osmolality of the urine should be three to four times that of the plasma (e.g., with a plasma osmolality of 285 mOsm/kg water, the urine osmolality should be at least 855 mOsm/kg water). The influence of age and gender on urine osmolality is poorly documented; however, in one study, males of all ages had higher urine osmolality and total osmole excretion than females (Perinpam, 2016).

Methods. The freezing-point depression method is commonly employed. A solution containing 1 osmol or 1000 mOsm/kg water depresses the freezing point 1.86°C below the freezing point of water. For methods, see Chapter 4.

CHEMICAL SCREENING

Reagent strips are the primary method used for the chemical examination of urine. Although easily used, they represent multiple complex, state-of-the-art chemical reactions (Pugia, 2000). Box 29.1 lists recommendations for both storage and use of reagent strips. Although reading of the strips has traditionally been done manually, automated instruments, such as the Bayer Atlas (Siemens Medical Solutions Diagnostics, Tarrytown, NY) and Beckman Coulter Diagnostics iChemVELOCITY (Beckman Coulter, Inc., Brea, CA), are now available that will aspirate a precise amount of urine, deposit it on the dipstick, and read the chemical reactions on the reagent strip by reflectance (Lyon et al., 2003; Penders et al., 2002; Wu, 2010). These systems provide excellent reproducibility of results and are not prone to some of the inconsistencies that occur when human hands try to time the reactions and when human eyes attempt to discriminate different shades of color reactions.

It should be noted that reagent strip methods are changed periodically, sensitivities and color reactions altered, and new measurements added. Manufacturers supply tables of common interfering substances, which should be consulted. Interference with ascorbic acid and drugs producing colored urine, such as phenazopyridine (Pyridium) and other azo compounds as well as methylthioninium chloride (methylene blue), may be encountered.

The chemical measures most commonly found on reagent strips will be discussed first, with less commonly measured chemical parameters following. A discussion on the clinical application of each analyte will precede reagent strip and other methods. Confirmatory methods will be included when available and necessary.

BOX 29.1

Recommendations for Reagent Strips

Storage

Protect from moisture and excessive heat.
Store in cool, dry area but not in a refrigerator.
Check for discoloration with each use; discoloration may indicate loss of reactivity.
Do not use discolored strips or tablets.
Keep container tightly stoppered.
Check manufacturer's directions with each new lot number for changes in procedure.

Testing

Test urine as soon as possible after receipt.
Remove only enough strips for immediate use; recap tightly.
Test a well-mixed, unspun urine sample.
Urine samples must be at room temperature before testing.
Do not touch the test area with fingers.
Do not use reagent strips in the presence of volatile acids or alkaline fumes.
Dip reagent strip into urine briefly—no longer than 1 second.
Drain excess urine off—run edge of strip along rim of tube, or blot edge on absorbent paper.
Do not allow reagents to run together.
Do not lay reagent strip directly on workbench surface.
Follow exact timing recommendations for each chemical test.
Hold reagent strip close to the color chart and read under good lighting.
Know sources of error, sensitivity, and specificity of each test on the reagent strip.
Think! Make correlations between patient history and individual test, and then follow through.

Urine pH

The kidneys and lungs normally work in concert to maintain acid-base equilibrium. The lung excretes carbon dioxide, whereas the renal contribution is that of reclaiming and generating bicarbonate and secreting ammonium ions. The proximal renal tubule is responsible for the bulk of the bicarbonate reabsorption/generation, and the distal tubule provides the remaining function.

The tubular cells exchange hydrogen ions for sodium of the glomerular filtrate. The metabolic activity of the body produces nonvolatile acids, principally sulfuric, phosphoric, and hydrochloric acids, but also small amounts of pyruvic, lactic, and citric acids and ketone bodies. These are excreted by the glomerulus as salts (sodium, potassium, calcium, and ammonium salts) and, together with ammonia produced by the proximal tubules, can then go on to trap secreted hydrogen ions for elimination in the urine (see Chapter 15).

Normal pH

The average adult on a normal diet excretes about 50 to 100 mEq of hydrogen ions in 24 hours to produce urine of about pH 6. In healthy individuals, urine pH may vary from 4.6 to 8.

Acid Urine

Acid urine may be produced by a diet high in meat protein and with some fruits, such as cranberries. During the mild respiratory acidosis of sleep, a more acid urine may be formed. Also, therapeutic acidification of the urine by various pharmacologic agents—including ammonium chloride, methionine, and methenamine mandelate—is used in the treatment of some calculi. This would include phosphate and calcium carbonate stones, which tend to develop in alkaline urine.

In acid-base disturbances, the pH of the urine reflects attempts at compensation by the kidneys. Patients with metabolic or respiratory acidosis should produce acid urine with increased titratable acidity and ammonium ion concentration. In diabetic ketoacidosis, large quantities of hydrogen ions are excreted, much as ammonium ion. In potassium depletion, such as in hypokalemic alkalosis of prolonged vomiting or in hypercorticism, or with prolonged use of diuretics, paradoxical aciduria with slightly acid urine may occur in the presence of a metabolic alkalosis. Low urine pH is associated with metabolic syndrome, chronic kidney disease, and an increased incidence of nephrolithiasis (Nakanishi et al., 2012).

Alkaline Urine

Alkaline urine may be induced by a diet high in certain fruits and vegetables, especially citrus fruits (Welch, Mulligan, Bingham, & Khaw, 2008). The urine tends to become less acid following a meal (the so-called *alkaline tide*). This was long believed to be a urinary compensation for gastric acid secretion; however, recent studies do not support this view (Johnson et al., 1995). Sodium bicarbonate, potassium citrate, and acetazolamide may be used to induce alkaline urine in the treatment of some calculi, particularly those composed of uric acid, cystine, or calcium oxalate. These agents may also be used in some urinary tract infections (the antibiotics neomycin, kanamycin, and streptomycin are more active in alkaline urine), in sulfonamide therapy, and in the treatment of salicylate poisoning.

The capacity to exchange hydrogen ion for cation and the formation of ammonia are decreased when tubular function is impaired. In classic renal tubular acidosis, glomerular filtration is normal, but the distal tubular ability to form ammonia and exchange hydrogen ions for cations is defective. Systemic acidosis results. The urine is relatively alkaline, and the pH cannot be lowered below 6 to 6.5, even with administration of an acid-loading substance. Additionally, titratable acidity and the concentration of ammonium are decreased (Singh et al., 1995). In proximal renal tubular acidosis, bicarbonate wasting occurs. This can also be seen in Fanconi syndrome.

In metabolic alkalosis, an alkaline urine with higher levels of urinary bicarbonate is produced, and ammonia production is decreased. The kidney may produce urine with a pH as high as 7.8. In respiratory alkalosis, an alkaline urine is produced that is associated with increased excretion of bicarbonate.

Methods

Reagent Strip. Indicators methyl red and bromothymol blue give a range of orange, green, and blue colors as the pH rises, permitting estimation of pH values to within half a unit within the range of 5 to 9. It should be read immediately, but time is not critical. Care should be taken not to have excessively wet strips where acid buffer from the protein patch runs into the pH patch, causing it to become orange.

Measurement of urine pH and acidity must always be made on freshly voided specimens. If precise measurements are required, the container should be filled to minimize the amount of dead space, and the urine covered tightly. The container should be kept cold, preferably on ice, but not frozen (Cook et al., 2007). On standing, the pH tends to rise because of loss of carbon dioxide and because bacterial growth produces ammonia from urea.

pH Electrode. Although the estimate of the pH obtainable by indicator strip is usually sufficient, more accurate measurement with a pH meter and glass electrode may be indicated in some clinical circumstances, such as the diagnosis and treatment of patients with disturbances of acid-base balance or monitoring urine alkalinization in patients receiving high-dose methotrexate therapy or undergoing treatment for nephrolithiasis (Kwong et al., 2013; Wockenfus et al., 2013).

Because the pH meter may tend to drift, it must be standardized with three buffers of known pH immediately before use. After standardization, spray the electrodes with distilled water, clean, and dry with a tissue. Immerse the electrode in the urine sample and report the pH of urine at the temperature of measurement.

Titratable Acidity of Urine. The pH of the urine is largely dependent on the amounts of monobasic and dibasic phosphate present. Titratable acidity is measured by titrating an aliquot of 24-hour urine (collected on ice) with 0.1 N NaOH, with pH 7.4 as an end point. Measurement may be used, together with urinary ammonia determination, in patients with chronic acidosis of obscure origin. Normal titratable acidity is in the range of 200 to 500 mL 0.1 N NaOH (or 6 mL 0.1 N NaOH per kg of body weight) or 20 to 40 mEq/24 hours. This procedure is described in previous editions of this textbook.

Protein in Urine

Normally, up to 150 mg of protein is excreted in the urine daily, with the average urine protein concentration varying from 2 to 10 mg/dL depending on urine volume. Anderson has demonstrated more than 200 urinary proteins, derived from both plasma and the urinary tract (Anderson et al., 1979). About one-third is albumin, and the remaining plasma proteins include small globulins, such as α-, β-, and γ-globulins. Plasma proteins with a molecular weight less than 50,000 to 60,000 pass through the glomerular basement membrane and are normally reabsorbed by proximal tubular cells. Albumin (molecular weight 69,000) is apparently filtered, but only in very small amounts. Retinol binding, β_2-microglobulin, immunoglobulin (Ig) light chains, and lysozyme are excreted in small amounts. Tamm-Horsfall glycoprotein (uromucoid), secreted by distal tubular cells and cells of the ascending loop of Henle, constitutes one-third or more of the total normal protein loss (Devuyst

et al., 2017). IgA in secretions of the urinary tract, enzymes, and proteins from tubular epithelial cells, other desquamated cells, and leukocytes also contribute to urine protein.

Detection of an abnormal amount of protein in urine is an important indicator of renal disease because protein has a very low maximal tubular rate of reabsorption; increased filtration of protein quickly saturates the reabsorptive mechanism. Screening methods are routinely used to differentiate normal protein excretion from abnormal and, therefore, should not detect less than about 8 to 10 mg/dL in a normal adult with a normal rate of urine flow. The reagent strip method is sensitive to albumin while acid precipitation methods detect all proteins and, therefore, will indicate the presence of globulins as well as albumin. It should be noted that a very dilute random urine specimen may have a falsely low protein value. Because a positive result for protein is significant, it should be confirmed by a second method and on repeated specimens. Depending on the history and examination, confirmatory measurements for elevated protein should be accompanied by the evaluation of renal function, examination of the urine sediment, and urine culture.

Functional proteinuria is usually less than 0.5 g/day and can be seen in various situations in which dehydration contributes to the level of protein measured in urine. With strenuous exercise, a mixture of high- and low-molecular-weight proteins appears in the urine, and many casts, both hyaline and granular, can be seen. Functional proteinuria may also accompany congestive heart failure, cold exposure, and fever. In any event, the proteinuria resolves with appropriate treatment or rest within 2 to 3 days.

Intermittent, transient proteinuria can occasionally be seen in patients with a normal history, normal physical examination findings, and otherwise normal renal function. Except for the occasional proteinuria, urinalysis is also normal. These patients are typically followed every 6 months to check for hypertension or other abnormalities, and the overall prognosis is good. A transient proteinuria may also occur in normal pregnancy, but any proteinuria in pregnancy is an important finding and requires investigation. Persistent proteinuria of 1 to 2 g/day in an asymptomatic person, or when accompanied by hematuria, has a poorer prognosis than intermittent (transient) or postural proteinuria.

Recent interest has focused on the importance of proteinuria in determining risk for adverse outcomes in chronic kidney disease (CKD) (Krstic et al., 2016; Levey et al., 2003; Sarnak & Astor, 2011). Current guidelines for classifying stages of CKD are based on estimated glomerular filtration rate; however, heavy proteinuria was found to be independently associated with a twofold or greater increase in all-cause mortality, myocardial infarction, and progression to renal failure (Hemmelgarn et al., 2010). A systematic review and meta-analysis of 26 cohort studies involving 169,949 individuals showed a strong and continuous association between proteinuria and risk for coronary artery disease, leading those authors to suggest the routine incorporation of testing for proteinuria into assessment of cardiovascular risk (Perkovic et al., 2008).

Hereditary proteinuria syndromes are rare and have heterogeneous forms, ranging from congenital nephrotic syndrome with severe proteinuria to focal segmental glomerulosclerosis with moderate proteinuria (Benoit et al., 2010; Caridi et al., 2010). Progression to end-stage renal disease is a common outcome. Specific diagnosis is possible with genetic testing for mutations in the genes for various structural proteins of the glomerulus (Joshi et al., 2013; Machuca et al., 2009; Tryggvason et al., 2006).

Postural Proteinuria

Postural (orthostatic) proteinuria occurs in 3% to 5% of apparently healthy young adults. In this condition, proteinuria is found during the day but not at night, when a recumbent position is assumed. Persistent proteinuria may develop in some of these healthy subjects at a later date; renal biopsies have shown abnormalities of the glomerulus or obstruction of the left renal vein in a few cases (Milani et al., 2010; Robinson et al., 1961). Proteinuria is apparently related to an exaggerated lordotic position and may result from renal congestion or ischemia. The total daily excretion of protein rarely exceeds 1 g and, in most instances, no other evidence of renal disease is apparent.

To evaluate the possibility of postural proteinuria, the patient is instructed to empty the bladder upon going to bed in the evening. Immediately upon arising in the morning, the patient voids and saves this specimen. After 2 hours of standing and walking about, the patient voids again and saves the specimen. The two urine specimens are assessed for protein; if the first is negative and the second positive, the patient may have postural proteinuria. Frequent examination of the patient should be made to reevaluate this condition.

Proteinuria in Older Adults

The incidence of significant proteinuria found on urinalysis in the older adult population is substantially increased when compared with patients younger than 60 years of age (Verma et al., 2012). It has been estimated that the older adult population in general has a threefold to fourfold greater incidence of glomerulonephritis, and approximately one-quarter of those affected have a minimal change–like disorder that may respond to steroid therapy. Occult malignancies in this population may also give rise to membranous glomerulonephritis, with resultant proteinuria (Threatte, 1986).

Proteinuria Quantification

More useful information for the diagnosis of kidney disease and for following the response to treatment is obtained by quantitatively analyzing the amount of protein excreted over a 24-hour period. It should be noted that the accuracy of measurements of any quantitative urine determination depends on the adequacy and completeness of the timed urine collection. Erroneous results are often related to collection problems. Repeat measurements may be needed to decide whether the proteinuria is intermittent or persistent. Due to the difficulty in collecting timed urine specimens, a random untimed (i.e., "spot") urine specimen for the determination of the urine albumin-to-creatinine ratio (ACR) or total urinary protein-to-creatinine ratio (PCR) is recommended as an acceptable alternative specimen by the Laboratory Working Group of the National Kidney Disease Education Program and other authorities (Group KDIGOKCW, 2013; Rodby, 2016). To determine the PCR, the urine protein (mg/dL) reading from the dipstick is divided by the urine creatinine (mg/mL) (Ginsberg et al., 1983). The ratio is normally less than 0.2 g protein/g creatinine in adults and children over 2 years of age, and less than 0.5 g protein/g creatinine in children under 2 years of age. Since the creatinine excretion rate is proportional to the patient's age, sex, and weight and can be predicted from the serum creatinine (Cockcroft & Gault, 1976), an estimated 24-hour protein excretion rate can be obtained by multiplying the PCR by the creatinine excretion rate. The result is usually normalized for body surface area and expressed as the 24-hour protein excretion in g/day per 1.73 m^2 body surface area. The ACR is recommended by some authorities as an alternative to the PCR in untimed urine specimens, with an ACR greater than 30 mg albumin/g creatinine considered abnormal (Lamb et al., 2009).

Heavy Proteinuria (>4 g/day). Heavy protein loss is characteristically seen with nephrotic syndrome. Classically, a low serum albumin level, generalized edema, and increased serum lipids (cholesterol, triglycerides, and phosphatides) accompany this disorder. Lipoproteins, low-density and very-low-density, are increased in serum, whereas high-density lipoprotein, a smaller molecule, has been demonstrated in the urine (de Mendoza et al., 1976). It has been suggested that loss of lipoprotein lipase in urine contributes to the rise in serum lipid levels. γ-Globulin is also lost in the urine, which may contribute to susceptibility to bacterial infections commonly found in nephrotic patients. When lipid is lost in urine, many granular casts, fatty casts, and fat-filled renal tubular epithelial cells (oval fat bodies) are found in the sediment. Cholesterol ester droplets may be demonstrable by polarization.

Nephrotic syndrome is principally associated with glomerular dysfunction/damage due to (1) primary renal diseases, including idiopathic disease, and (2) systemic diseases with renal involvement (Certikova-Chabova & Tesar, 2013). Transient or mechanical causes include severe congestive heart failure, constrictive pericarditis, and renal vein thrombosis. The last can be a consequence of nephrotic syndrome because of losses of anticlotting factors in urine and elevation of serum fibrinogen. In children, a common cause of nephrotic syndrome is minimal change disease (also known as *nil lesion*), a steroid-responsive glomerular disorder. Acute, rapidly progressive, and chronic types of glomerulonephritis are causes of heavy proteinuria and may be accompanied by urinary erythrocytes or erythrocyte casts. Diabetes mellitus and lupus erythematosus are systemic diseases that frequently cause glomerular injury and heavy proteinuria. Urine sediment may be "telescoped," that is, may display all types of cells and casts in lupus nephritis or with a hypersensitivity reaction (Schreiner, 1955). Malaria, malignant hypertension, toxemia of pregnancy, heavy metals (gold, mercury), drugs (penicillamine), neoplasia in general, amyloidosis, sickle cell disease, renal transplant rejection, and, rarely, primary antiphospholipid syndrome (Levy et al., 1998) are additional causes of heavy proteinuria.

Moderate Proteinuria (1.0–4.0 g/day). Moderate proteinuria may be found in the vast majority of renal diseases, including those mentioned previously, as well as nephrosclerosis, multiple myeloma, and toxic nephropathies. Also included are degenerative, malignant, and

inflammatory conditions of the lower urinary tract, including irritative conditions such as the presence of calculi.

Minimal Proteinuria (<1.0 g/day). Minimal proteinuria may be noted in chronic pyelonephritis, in which case it may be intermittent, and in relatively inactive phases of glomerular diseases. It is also seen with nephrosclerosis, chronic interstitial nephritis, congenital diseases such as polycystic disease and medullary cystic disease, and renal tubular diseases. In tubular diseases, the urinary sediment usually is not abnormal, but erythrocytes, leukocytes, and tubular cells may be seen with interstitial nephritis. However, significant sediment findings may sometimes accompany trace protein results. Minimal proteinuria is also present in postural proteinurias and transient proteinuria.

Qualitative Categories of Proteinuria

Detection of the types of protein present in urine requires electrophoretic separation of urine proteins. Based on these and on clinical findings, proteinuria may be separated into a glomerular pattern and a tubular pattern, indicating which part of the nephron is primarily involved. However, these anatomic entities tend to merge as disease progresses.

Glomerular Pattern. Glomerular disease causes proteinuria, which may be heavy (>3–4 g/day). Loss or reduction of the fixed negative charge on the glomerular basement membrane allows albumin to permeate into the Bowman space in large quantities, more than can be reabsorbed by the proximal tubular cells. When serum albumin is lost in urine, other proteins of similar size or charge are also lost (e.g., antithrombin, transferrin, prealbumin, α_1-acid glycoprotein, α_1-antitrypsin). Because tubular function may still be normal, very small plasma proteins are largely reabsorbed. Large proteins, in contradistinction, are not seen in urine while the glomerulus is still selective (e.g., α_2-macroglobulin, β-lipoprotein). As larger proteins appear, the proteinuria is less selective, indicating greater damage to the glomerulus (e.g., with membranous nephropathy and proliferative glomerulonephritis).

Mechanisms of proteinuria in diabetic kidney disease with specific attention to glomerular damage were recently reviewed, with special recognition that CKD is actually a multifactorial, complex disease involving a combination of both glomerular and tubulointerstitial scarring (Baines & Brunskill, 2011; Erkan, 2013; Garg & Rabelink, 2011; Han et al., 2017; Magee et al., 2017).

Tubular Pattern. This is associated with loss of a small amount of urinary protein that would otherwise be largely reabsorbed. These proteins most often are of low molecular weight (e.g., α_1-microglobulin, N-acetyl-β-D-glucosaminidase [NAG], β-globulins such as β_2-microglobulin, light-chain immunoglobulins, cystatin C, and lysozyme), usually without a clear predilection for albumin-sized molecules. By radioimmunoassay, β_2-microglobulin excretion has been measured in microgram amounts in urine as an indication of tubular damage; its normal excretion is about 100 μg/day. A tubular pattern proteinuria occurs with renal tubular diseases such as Fanconi syndrome, cystinosis, Wilson disease, and pyelonephritis, and with renal transplantation rejection. The amount of proteinuria is typically lower than that seen with glomerular disease, at about 1 to 2 g/day. Tubular proteinuria may be missed by the reagent strip test because of the absence or very low amounts of albumin, but it may be detected by an acid precipitation method (Skoberne et al., 2017). In addition, urinary tubular indexes comparing tubular proteins to albumin, particularly the ratios of α-1-m to albumin and NAG to albumin, reportedly have a high sensitivity and specificity in the differentiation between primary tubulointerstitial diseases and primary glomerular diseases (Skoberne et al., 2017). There is also interest in the utilization of specific molecules released into the urine during tubular injury as monitors of renal insufficiency in patients with diabetic nephropathy. The biomarkers under study include neutrophil-gelatinase–associated lipocalin (NGAL), kidney injury molecule 1 (KIM-1), liver–fatty-acid–binding protein (L-FABP), calprotectin, inflammatory cytokines, and others (Azimi, 2017; Kim et al., 2018; Lowenstein & Grantham, 2016; Tramonti & Kanwar, 2013; Tummalapalli et al., 2016).

Overflow Proteinuria. Overflow proteinuria is due to the overflow of excess levels of a protein in the circulation, and can be seen with hemoglobin, myoglobin, or immunoglobulin loss into the urine. These proteins are not initially associated with glomerular or tubular diseases but may themselves cause renal damage. Myoglobin may cause ATN (see the Blood, Hemoglobin, Hemosiderin, and Myoglobin in Urine section, and case 4 in Chapter 9). Hemoglobin in low amounts is not thought to be toxic unless hypovolemia is present.

Bence Jones Proteinuria. Bence Jones protein is the light chain from a monoclonal immunoglobulin that is filtered in the kidney. Bence Jones proteinuria is associated with multiple myeloma, macroglobulinemia, primary (AL) amyloidosis, and malignant lymphomas. The incidence of Bence Jones proteinuria in multiple myeloma has been estimated as 50% to 80%; however, its demonstration depends greatly on the technique used. Bence Jones protein may be missed altogether if only a reagent strip test for protein is used. Electrophoresis and immunofixation electrophoresis methods (see Chapter 20) are the best detection and quantification methods, along with the immunoassay measurement of free light chains (Olivieri & Rai, 2010) (see Chapter 45).

Excretion of Bence Jones protein in large amounts, sometimes several grams in 24 hours, causes the tubular cells to deteriorate because of the high levels of protein reabsorbed. Inclusions may form in the cells, and desquamated cells may form casts in the tubular lumen. Casts also form from immunoglobulin and Tamm-Horsfall protein mixtures. With renal failure, less protein is reabsorbed and more Bence Jones protein and other proteins appear in the urine. The damaged kidney is sometimes called a *myeloma kidney*, and the nephrotic syndrome may follow.

Microalbuminuria. Microalbuminuria is the presence of albumin in urine above the normal level but below the detectable range of conventional urine dipstick methods. Several authors have suggested that these lower urine albumin levels ranging from 20 to 200 mg/L (or an approximate rate of excretion of 20 to 200 μg/min) are an indicator of early and possibly reversible glomerular damage (Mogensen, 1984; Viberti et al., 1982). In diabetic patients, microalbuminuria is associated with a fourfold to sixfold increase in cardiovascular mortality and is an independent risk factor for renal mortality (Bakris, 1996; Roshan & Stanton, 2013; Zelmanovitz et al., 1998). It is also more prevalent in hypertensive subjects and may be an indicator of subclinical renal and extrarenal organ damage (Gerber et al., 1998; Viazzi et al., 2016). Various analytic methods have been introduced, including immunologic test systems and dye-binding chemical test strips, both of which are discussed in the next section.

Methods

Several screening and quantitative methods are available for the analysis of protein in urine (Hay-Lombardie et al., 2018; Viswanathan & Upadhyay, 2011). Because a positive screening test may have serious implications, it is important to be able to confirm results by a second, different method. Common screening tests include the qualitative/semiquantitative colorimetric reagent strip test and precipitation-based testing (Table 29.4).

Accurate results are obtained with reagent strips only when albumin is increased (White et al., 2011). Because of the lack of sensitivity of the reagent strip to globulins, it may be necessary to use an acid precipitation method for screening purposes. This will depend on the patient population and the diseases being screened. Reagent strips do have the advantage of avoiding false-positive reactions with organic iodides, such as those used for radiographic contrast, and tolbutamides or other drugs.

Most other qualitative screening methods rely on protein precipitation (e.g., with heat and acetic acid, with nitric acid, with sulfosalicylic acid [SSA] and trichloroacetic acid). These methods will precipitate globulins as well as albumin. In practice, negative reagent strips with positive SSA methods in urine specimens are attributable to radiographic dye, to penicillins, and, rarely, to an isolated increase in globulins. Sulfosalicylic and trichloroacetic acids are used to precipitate protein in the cold and are used as a convenient screening method. The sensitivity may be as low as 0.25 mg/dL depending on the technique used.

With the intense interest in utilizing proteinuria as a risk stratifier for both diabetic and nondiabetic nephropathy, as well as other

TABLE 29.4
Screening Test for Detection of Proteinuria

Urine Constituents or Condition	Reagent Strip	Acid Precipitation
Highly buffered alkaline urine	May cause FP	May cause FN
Drug metabolites	No effect	May cause FP
Radiocontrast media	No effect	May cause FP
Turbidity	No effect	May cause FP
Quaternary ammonium groups or chlorhexidine	May cause FP	No effect

FN, False negative; *FP,* false positive.

conditions such as preeclampsia and coronary artery disease, recommendations for measurement have centered on methods for urine albumin quantification rather than total protein (Benz-de Bretagne et al., 2018; Lamb et al., 2009; Lamb et al., 2013). Urine albumin measurements are considered much more standardized and reliable than total protein at low concentrations, where assessment of risk for progression in chronic kidney disease is important for diagnosis and planning therapy.

Reagent Strip. This method takes advantage of the protein error of pH indicators. Because proteins carry a charge at physiologic pH, their presence will elicit a pH change. The reagent strip is impregnated with tetrabromophenol blue buffered to an acid pH of 3, or tetrachlorophenol-tetrabromosulfophthalein. In the absence of protein, the strip is yellow; 30 to 60 seconds following urine application, variable shades of green develop depending on the type and concentration of protein present. Results may be read in a "plus" system as negative, trace, and 1+ to 4+. Most methods will detect 5 to 20 mg of albumin per deciliter.

As stated previously, reagent strips tend to be more sensitive to albumin than to globulins, Bence Jones protein, or mucoprotein. "Trace" results may be seen with physiologic normal excretion of protein in concentrated urine specimens from healthy individuals. High salt levels will lower results. Exceptionally alkaline and/or highly buffered urine samples may give positive results in the absence of significant proteinuria (e.g., with a patient on alkaline medication or with bacterial contamination). False-positive results can occur with highly pigmented urine, quaternary ammonium compounds, amidoamines in fabric softeners, chlorhexidine, and excessive leaching of the acid buffer of the test strip by excessive wetting. The method is unaffected by urine turbidity, radiographic media, and most drugs or their metabolites.

Sulfosalicylic Acid Method—Qualitative. This method depends on formation of a precipitate for determination of the presence of protein.

Procedure. Specimens should be centrifuged and a clear supernatant used. To approximately 3 mL of supernatant urine in a clean test tube, aliquot an equal amount of 3% SSA. Invert to mix. Let stand exactly 10 minutes. Invert again twice. Using ordinary room light (not a lamp), observe the degree of turbidity and/or precipitation, and grade the results according to the following descriptions:

Negative—no turbidity (≈5 mg/dL or less)
Trace—perceptible turbidity (≈20 mg/dL)
1+ —Distinct turbidity, but no discrete granulation (≈50 mg/dL)
2+ —Turbidity with granulation, but no flocculation (≈200 mg/dL)
3+ —Turbidity with granulation and flocculation (≈500 mg/dL)
4+ —Clumps of precipitated protein or solid precipitate (≈1.0 g/dL or more)

This method will detect about 5 to 10 mg/dL. Albumin, globulins, glycoproteins, and Bence Jones proteins are all detected (Ndamase & Freercks, 2014). High levels of detergents may decrease the result. When radiographic dye is present, SSA precipitate will increase on standing, and typical crystals are seen on microscopic examination of the precipitate. In this situation, another urine specimen from the patient should be assayed. However, the effects of the radiographic media may persist for up to 3 days. A reagent strip test may be substituted or heat and the acetic acid method may be used. In the acetic acid method, radiographic contrast media will clear with heat, whereas protein will increase turbidity.

Quantitative Protein Determinations and Confirmatory Methods. Quantitative measurements of urine protein are typically adaptations of one of the various precipitation methods or are colorimetric in nature. SSA and trichloroacetic acid (TCA) are commonly used as precipitants; the resultant turbidity can be measured by a photometer or a nephelometer. If a visual interpretation is performed, a set of gelled commercial standards that correspond to 10, 20, 30, 40, 50, 75, and 100 mg/dL may be used, with results reported in milligrams per deciliter as opposed to the "plus" method of screening precipitation tests. With SSA, the turbidity produced with albumin is 2.4 times that produced with globulin; polypeptides, glycoproteins, and Bence Jones proteins are also precipitated with this method. Of historic note, Exton reagent contains SSA, sodium sulfate, and an indicator—bromphenol blue. TCA, in contradistinction, will cause γ-globulin to be precipitated with greater turbidity than albumin; however, the difference is not marked.

More precise measurements suitable for smaller amounts of protein are available. In these methods, a TCA precipitate is dissolved in sodium hydroxide and measured by use of the biuret reaction. The quantitative TCA-biuret method is tedious but gives good precision. A color correction blank is used. For a comparison of biuret methods with the SSA turbidity method, see Lizana and colleagues (Lizana et al., 1977).

Several dye-binding colorimetric methods are available to quantitate urine protein. These include Coomassie blue, Ponceau S, and benzethonium chloride turbidity methods (McElderry et al., 1982). Pyrogallol Red-Molybdate will also react with protein to form a blueish-purple complex that absorbs at 600 nm.

Methods used to quantitate urinary protein have not been satisfactory. Participants in the College of American Pathologists proficiency testing surveys will be aware that the mean values reported vary twofold between methods, with the SSA method producing high values. Precision is poor, with the SSA turbidimetric method showing the poorest coefficient of variation. The TCA-biuret, Coomassie blue, and TCA turbidity methods show closer agreement and about half the coefficient of variation of the SSA method. Problems arise from nonstandardized methods. With turbidity methods, these include different acid concentrations and timing, along with variation in the protein standard.

Microalbuminuria Determination Methods. Very small amounts of proteins, such as albumin and β_2-microglobulin, are measured by immunologic means using antibodies to the proteins, nephelometric methods, immunoassay, protein strip electrophoresis, high-performance liquid chromatography (HPLC), or other means (Benz-de Bretagne et al., 2018). The Micral II test strip (Boehringer Mannheim, Indianapolis, IN) is an immunologic test system that gives an almost immediate, reliable semiquantitative determination of low urine albumin concentrations (Kutter, 1998). Oxytetracycline may interfere with this method, causing higher readings. There is no interference with pH. A newer method, Clinitek microalbumin (Bayer Diagnostics, Tarrytown, NY), is a highly sensitive dye-binding method (Graziani et al., 2009; Guy et al., 2009). It has the further advantage of an additional test pad for simultaneous measurement of creatinine concentration. This method is not absolutely specific for albumin, for the dye compound also reacts with Tamm-Horsfall mucoprotein. HPLC is a highly sensitive method for the early detection of microalbuminuria but is not widely utilized at this time (Horikoshi et al., 2013).

Bence Jones Proteinuria Determination Methods. Methods for detection of Bence Jones protein in urine include protein electrophoresis, immunofixation electrophoresis, capillary zone electrophoresis, and immunoassay for free light chains (Basile et al., 2016) (see Chapter 47). The traditional electrophoretic procedure employs the Amido black stain on a 200-fold concentrated urine. Newer methods, performed on less concentrated urine, including a modified Coomassie brilliant blue stain, are comparably sensitive and specific (Graziani et al., 2003; Wong et al., 1997). The presence of Bence Jones globulin or clonal production of immunoglobulin is indicated by a single sharp peak in the globulin region on protein electrophoresis. Bence Jones globulin represents either the κ or the λ immunoglobulin light chain.

Bence Jones protein precipitates at temperatures between 40°C and 60°C and redissolves at near 100°C. Other methods depend on precipitation in the cold with salts, ammonium sulfate, and acids. In the presence of marked Bence Jones proteinuria, most methods yield positive results. When only a small amount of Bence Jones protein is present or when other globulins are present, results may be doubtful. False-positive reactions are seen when other globulins are precipitated by acetic acid in the heat precipitation method. A false-negative reaction may occur if the Bence Jones protein is too concentrated and the precipitate does not redissolve on boiling.

Glucose and Other Sugars in Urine

Various sugars may be found in the urine under certain circumstances, both pathologic and physiologic. These include glucose, fructose, galactose, lactose, maltose, pentose, and sucrose. Glucose is by far the most common and will be discussed in the next section.

Glucose

The presence of detectable amounts of glucose in urine is termed *glycosuria*. This condition occurs whenever the glucose level in the blood surpasses the renal tubule capacity for reabsorption. Glucose may appear in the urine at different blood glucose levels; yet, there is not always a concomitant hyperglycemia. Glomerular blood flow, tubular reabsorption rate, and urine flow also will influence its appearance. When hyperglycemia is present, however, glycosuria usually occurs when the blood level is greater than 180 to 200 mg/dL. Glycosuria may be seen in several different conditions described in the following sections.

Diabetes Mellitus. Although hyperglycemia alone is not necessarily indicative of diabetes mellitus, the appearance of glucose in the urine necessitates further workup. When glycosuria is present, it is typically accompanied by polyuria and thirst. Inadequate carbohydrate utilization in these patients results in elevated ketone levels in the blood and urine due to increased fat metabolism (Zaccardi et al., 2016).

For diabetic individuals, the advantage of a urine method over a blood test for glucose is that it is painless and inexpensive. Urine glucose measurements are most useful for well-controlled diabetic individuals who do not have to make frequent adjustments in their insulin/hypoglycemic agents. In insulin-dependent diabetes, a negative urine measurement could correspond to a wide range of serum glucose levels; this is attributed to the great variation in renal threshold for glucose in diabetic patients. Therefore, urine measurements may be misleading, and home blood glucose monitoring is preferred.

Monitoring for glycosuria in diabetic patients is not without problems. Reagent strips may be difficult to interpret at the 1-g/dL (1%) and 2-g/dL (2%) glucose levels. Copper reduction tests or newer, more sensitive reagent strips may be more efficacious. With the Clinitest tablet method, diabetic patients are able to estimate reducing substance levels in urine to about 10 g/dL, using one drop of specimen rather than two or five drops. In some clinics, the 24-hour urine glucose measurement is found to be useful for monitoring patients. It represents a defined longer time period, and, with blood levels of glycated hemoglobin, it contributes to the regular overall long-term management of the disease.

Several studies have looked at the usefulness of urine dipstick testing for glycosuria as a screening method for diabetes, and the results have been mixed. Bullimore and Keyworth (1997) concentrated on patients over 50 years of age in a general practice setting and found this method to be practical and effective, whereas Friderichsen and Maunsbach (1997) came to an opposing conclusion. The latter authors suggest that if diabetes screening is carried out in general practice, blood glucose measurements should be utilized for patients in selected risk groups. The primary role of blood glucose and HbA_{1c} measurements in the diagnosis and management of diabetes mellitus was later endorsed by the American Association for Clinical Chemistry and other organizations (Sacks et al., 2011). However, Dallosso and colleagues (2014) found that both blood glucose and urine glucose self-monitoring resulted in improved HbA_{1c} levels at 18 months in newly diagnosed patients with type 2 diabetes if structured education was provided. Routine dipstick glucose analysis can identify gravidas at increased risk for gestational diabetes (Gribble et al., 1995).

Other Causes of Glycosuria. Glycosuria with concomitant hyperglycemia is seen in several endocrine disorders. These include pituitary and adrenal disorders such as acromegaly, Cushing syndrome, hyperadrenocorticism, functioning α- or β-cell pancreatic tumors, hyperthyroidism, and pheochromocytoma. Pancreatic disease with loss of functioning islet cells is also associated with glycosuria—for example, carcinoma, pancreatitis, and cystic fibrosis.

Numerous other causes of glycosuria with hyperglycemia have been recognized, among them being central nervous system disorders, including brain tumor or hemorrhage, hypothalamic disease, and asphyxia. Disturbances of metabolism associated with burns, infection, fractures, myocardial infarction, and uremia, as well as liver disease, glycogen storage disease, obesity, and feeding after starvation, may all be associated with glycosuria, as are certain drugs (e.g., thiazides, corticosteroids, adrenocorticotropic hormone, and birth control pills).

In pregnancy, an increase in glomerular filtration rate occurs and all of the filtered glucose may not be reabsorbed. In this situation, glycosuria may appear at relatively low blood glucose levels. Persistent or greater than trace amounts of glycosuria should be investigated. In some patients, diabetes occurs only during pregnancy. Glycosuria after a glucose challenge has been used during pregnancy, but its predictive value for gestational diabetes, preeclampsia, and low birth weight has been questioned (Coolen & Verhaeghe, 2010). Glucose tolerance may also be decreased in older adults, especially when patients have a poor intake of carbohydrates, but this is not necessarily accompanied by glycosuria.

Glycosuria without hyperglycemia is usually associated with renal tubular dysfunction. True inherited renal glycosuria is uncommon and is associated with reduced glucose reabsorption. In renal tubular transport diseases, glycosuria may be accompanied by impaired reabsorption of water, amino acid, bicarbonate, phosphate, and sodium—a pattern seen in Fanconi syndrome. Galactosemia, cystinosis, lead poisoning, and myeloma are additional examples of conditions associated with renal tubular dysfunction and possible glycosuria.

Other Sugars in Urine

Small quantities of disaccharides are normally excreted in the urine—about 50 mg in 24 hours. With intestinal diseases such as severe sprue or acute enteritis, the level may rise to 250 mg or more. Fructose, galactose, lactose, maltose, and L-xylulose are found in urine in patients with inherited metabolic disorders (Scriver et al., 1989). If an inherited disorder is suspected, the sugar may be identified by thin-layer chromatography. Qualitative confirmatory tests generally are not satisfactory for sugars.

Fructose. Fructose appears in urine in association with inherited enzyme deficiencies that cause benign essential fructosuria and serious fructose intolerance associated with severe vomiting and liver and kidney disease (Tran, 2017). Fructosuria may also be seen with parenteral feedings that include fructose. Urinary fructose has been used as a marker of sucrose intake in dietary intervention studies (Luceri et al., 1996).

Galactose. Galactose is found in the urine in genetic disorders of galactose metabolism associated with a deficiency of galactose-1-phosphate uridyl transferase or galactokinase (Demirbas et al., 2018). In these diseases, galactose derived from dietary lactose is not converted to glucose. Early detection followed by dietary restriction may control the disease.

Lactose. Lactose may appear in the urine late in normal pregnancy or during lactation. In lactose intolerance, high levels of sugars accumulate in the gut; lactose will be absorbed and excreted unchanged in the urine.

Pentose. Pentosuria may follow the ingestion of large amounts of fruit, causing the excretion of L-xylulose and L-arabinose in amounts up to 0.1 g/day. It may also be seen with certain drug therapies and with benign essential pentosuria.

Sucrose. Sucrose may appear in the urine after the ingestion of very large amounts of sucrose. Sucrase deficiency is associated with intestinal diseases such as sprue in the same manner as lactase deficiency. Sucrose intolerance is an inherited disorder associated with sucrase and α-dextrinase (isomaltase) deficiencies. Symptoms are similar to those seen with lactase deficiency and occur in the first few weeks of life when sweetened food is ingested. Tolerance may develop, but sucrose may have to be avoided permanently. Factitious sucrosuria may create a high specific-gravity urine with negative glucose oxidase and negative copper reduction tests.

Methods

Reagent Strip. This method is based on a specific glucose oxidase and peroxidase method, a double sequential enzyme reaction; reagent strips differ only in the chromogen used. The method is specific for glucose—no reaction is seen with lactose, galactose, fructose, or reducing metabolites of drugs. The reagent strips may be used for semiquantitative results, which should be reported as approximate grams per deciliter. Combination glucose and ketone reagent strips detect not only ketonuria but also suppression of the glucose reaction by ketones seen with some reagent strips.

False-positive readings may be produced by strongly oxidizing cleaning agents in the urine container. Low specific gravity may falsely elevate results. Sodium fluoride used as a preservative will cause false-negative readings, as can high specific gravity and occasionally ascorbic acid. Glycolytic enzymes from cells and bacteria will reduce glucose levels in urine on standing; prompt refrigeration or testing is essential.

Chemistry

$$\text{Glucose} + O_2 \xrightarrow{\text{Glucose oxidase}} \text{Gluconic acid} + H_2O_2 \quad \text{(Eq. 29.1A)}$$

$$H_2O_2 + \text{Chromogen} \xrightarrow{\text{peroxidase}} \text{Oxidized chromogen} + H_2O \quad \text{(Eq. 29.1B)}$$

Chromogens utilized in some common dipstick tests include the following:

Clinistix—o-toluidine chromogen. Color changes from pink to purple. This formulation detects 100 mg/dL of glucose and is more sensitive to interfering substances, such as ascorbic acid, than the following.

Multistix—potassium iodide chromogen. Color changes from blue to brown at 30 seconds.

Chemstrip—an aminopropyl-carbazole chromogen. Color changes from yellow to orange-brown at 60 seconds.

Copper Reduction Tests

As a screening test, the glucose oxidase method will not detect increased levels of galactose or other sugars in urine. It is therefore important that a copper reduction method be used, especially for young pediatric patients. A policy to screen for reducing sugars should be made by the individual laboratory, after consultation with its clinical staff. In many instances, policies related to performing this screening were instituted in the 1960s, before the widespread mandatory screening of newborns for inborn errors of metabolism became routine. With this state-mandated newborn

screening, detection of an unsuspected reducing substance in the urine is rare; thus, the routine performance of this test without a specific request by the patient's physician may have outlived its usefulness (Naumova, Schappert, & Kaplan, 2006).

The copper reduction method will detect sufficient quantities of any reducing substances in the urine, including reducing sugars such as lactose, fructose, galactose, maltose, and the pentoses. In those instances in which the copper method is positive and the glucose oxidase method is negative, glycosuria is ruled out. However, before investigation for other sugars is begun, the clinical findings and drug history should be evaluated. Although the copper reduction method will detect nonglucose reducing sugars, the yield for these sugars is extremely low.

Normal neonatal infants during the first 10 to 14 days of life may excrete urine that yields a positive reaction because of glucose, galactose, fructose, and lactose. Normal pregnant and postpartum women may also have positive reactions because of the presence of lactose.

Of the copper reduction methods used for screening purposes, the qualitative Benedict method is more sensitive to reducing substances in urine than is the single-tablet (Clinitest) copper reduction method. Many substances in urine, metabolites, and drug-related metabolites will influence urinary sugar methods (Table 29.5). Strong reducing substances—such as ascorbic acid, gentisic acid, or homogentisic acid—may inhibit the enzyme method while contributing to the positivity of the copper reduction method. The tablet method is not affected as much as the Benedict method. Very large doses of ascorbic acid do not affect the two-drop copper reduction method. Drugs, especially the cephalosporins, and radiographic media will give false-positive or unusual colors with Clinitest. Although large doses of ascorbic acid do not affect the two-drop Clinitest for sugars (i.e., do not cause false-positive results), delays in color development may be noted with the glucose oxidase method.

Chemistry. Copper sulfate, sodium hydroxide, sodium carbonate, and citric acid are incorporated into each Clinitest tablet. Copper sulfate reacts with reducing substances in the urine, converting cupric sulfate to cuprous oxide. Based on Benedict's copper reduction reaction,

$$\begin{aligned} &Cu^{2+} \xrightarrow{\text{Hot alkaline solution}} Cu^{+} \\ &Cu^{+} + OH^{-} \rightarrow CuOH\ (\text{yellow}) \\ &2CuOH \xrightarrow{\text{Heat}} Cu_2O\ (\text{red}) + H_2O \end{aligned} \qquad \text{(Eq. 29.2)}$$

Heat is caused by the reaction of sodium hydroxide with water and citric acid.

Procedure. Clinitest reagent tablets will detect 250 mg of reducing substance per deciliter of urine. Both five-drop and two-drop Clinitest methods can be used; corresponding color charts are available (Belmonte et al., 1967). The two-drop method was developed in response to a so-called *pass-through phenomenon* that may occur if more than 2 g/dL of sugar is present in the urine. In the pass-through phenomenon, the solution that results after addition of the Clinitest tablet goes through the entire range of colors and back to a dark-greenish brown. This final color does not compare with any section of the color chart; however, it corresponds most closely to a significantly lower result. It is important to observe the entire reaction and to continue to observe for 15 seconds after boiling inside the tube has stopped so that reversion to a different color is not missed and a falsely low result reported.

Five-Drop Method. Place five drops of urine in a dry test tube and add 10 drops of water. Add one Clinitest tablet by easing it into the tube without touching it—it contains strong alkali. Watch while boiling takes place, but do not shake or touch the bottom of the tube—it is hot. Wait for 15 seconds after boiling stops, then shake the tube gently and immediately compare the color of the solution with the color scale. Results correspond to the following approximate concentrations: Negative, 0.25 g/dL, 0.5 g/dL, 0.75 g/dL, 1.0 g/dL, 2.0 g/dL, and pass-through. It is important to watch the solution carefully while it is boiling. If the solution passes through orange to a dark shade of greenish-brown, this indicates that more than 2 g/dL sugar is present. This should be recorded as greater than 2 g/dL without reference to the color scale. Urine samples showing this pass-through phenomenon should be retested with the two-drop method.

Two-Drop Method. Place two drops of urine in a test tube and add 10 drops of water. Add one Clinitest tablet. Watch while boiling takes place, but do not shake. Wait 15 seconds after the boiling stops, then shake the tube gently. Compare the color of the solution with the color scale supplied for the two-drop method. The pass-through phenomenon may also occur with the two-drop method with large concentrations of sugar—over 5 g/dL. Report results as 1 g/dL, 2 g/dL, 3 g/dL, 5 g/dL, and more than 5 g/dL if a pass-through reaction occurs. With negative or low-level results, the five-drop method should be performed.

TABLE 29.5
Reactions of Substances to Test for Glucosuria

Constituent	Glucose Oxidase Reagent Strip	Copper Reduction Tablet Test
Glucose	Positive	Positive
Sugars other than glucose		
Fructose, Galactose, Lactose, Maltose, Pentose	No effect	Positive
Sucrose	No effect	No effect
Ketones (large quantities)	May depress color	No effect
Creatine	No effect	May cause false-positive
Uric acid		
Homogentisic acid (alkaptonuria)	No effect	Positive
Drugs*		
Ascorbic acid (large amounts)	May delay color	Trace positive
Cephalosporins (e.g., Keflin)	No effect	Positive, brown color
L-Dopa (large amounts)	False-negative	No effect
Nalidixic acid glucuronide	No effect	Positive
Probenecid	No effect	Positive
Pyridium	Orange color may affect result	
Salicylate (large amounts)	May lower reading	No effect
X-ray dye (diatrizoates)	No effect	Black color
Contaminants		
Hydrogen peroxide	False-positive	May inhibit positive test
Hypochlorite (bleach)	False-positive	
Sodium fluoride	False-negative	No effect

*Other drugs implicated in copper reduction are amino acids, caronamide, chloral hydrate, chloroform, chloramphenicol, formaldehyde, hippuric acid, isoniazid, thiazides, oxytetracycline, *p*-aminosalicylic acid, penicillin, phenols, streptomycin, phenothiazines, and sulfonamides.

Precautions. Observe the precautions in the literature supplied with the Clinitest tablets. The bottle must be kept tightly closed at all times to prevent absorption of moisture and kept away from direct heat and sunlight in a cool, dry place. The tablets normally have a spotted bluish white color. If not stored properly, they will absorb moisture or deteriorate from heat, turning dark blue or brown. In this condition, they will not give reliable results. They are also available individually packaged in aluminum foil to help prevent this absorption of moisture. Although more expensive, such packaging is useful when a limited number of measurements are performed.

Additional Tests for Sugars. As stated earlier, the copper reduction method will detect the majority of nonglucose sugars that might be present in urine, apart from sucrose, which is not a reducing sugar. It does not, however, differentiate between these sugars, therefore necessitating more complicated testing. Additional confirmatory testing will be discussed here.

Fructose. Fructose is identified by thin-layer chromatography. A qualitative measurement, a resorcinol test, is useful. Fructose will also reduce Benedict reagent at low temperatures.

Galactose. Thin-layer chromatography is used to identify galactose in urine. However, the disease is usually identified by erythrocyte enzyme assay when suspected.

Lactose. Lactose is identified by thin-layer chromatography or a qualitative lactose test, such as described later.

Procedure. To 15 mL urine in a test tube, add 3 g lead acetate. Shake and filter. Boil filtrate, add 2 mL concentrated NH_4OH (ammonium hydroxide), and boil. Lactose will cause the formation of a brick-red solution and then a red precipitate with clear supernatant.

Pentose. At concentrations of 250 to 300 mg/dL, L-xylulose will reduce Benedict's qualitative reagent at 50°C (water bath) within 10 minutes or at room temperature in several hours. Generally, the pentoses are identified by thin-layer chromatography.

Sucrose. Sucrose will ferment yeast and can be separated by chromatography but needs to be stained with a substance not dependent on reducing properties.

Ketones in Urine

Whenever a defect in carbohydrate metabolism or absorption or an inadequate amount of carbohydrate is present in the diet, the body compensates by metabolizing increasing amounts of fatty acids. When this increase is large, ketone bodies, the products of incomplete fat metabolism, begin to appear in the blood and are excreted in the urine. In ketonuria, the three ketone bodies present in the urine are acetoacetic (diacetic) acid (20%), acetone (2%), and 3-hydroxybutyrate (about 78%). Acetone is formed nonreversibly from acetoacetic acid; β-hydroxybutyric acid (3-hydroxybutyrate) forms reversibly from acetoacetic acid.

$$\begin{aligned} &\text{Acetoacetic acid} \xrightarrow{-CO_2} \text{Acetone} \\ &\text{Acetoacetic acid} \xleftrightarrow{+2H} 3-\text{Hydroxybutyrate} \end{aligned} \qquad \text{(Eq. 29.3)}$$

Depending on the methods used, total ketone bodies (as acetone) can range as high as 17 to 42 mg/dL. According to Killander and colleagues (1962), up to 2 mg acetoacetic acid/dL is normal. Ketonemia and ketonuria are commonly seen in uncontrolled diabetes mellitus as well as several other conditions to be discussed here.

Diabetic Ketonuria

Ketonuria implies the presence of ketoacidosis (ketosis) and may provide a warning of impending coma. Up to 50 mg of acetoacetic acid/dL may be present without clinical evidence of ketosis. Type 1 diabetic patients are more prone to episodes of ketosis, often associated with infection, stress, or other problems in management. Whereas large amounts of ketones and glucose are present in urine in diabetic ketoacidosis, ketonuria is not found with the hyperosmolar hyperglycemic coma that sometimes occurs in type 2 diabetes (Karslioglu French et al., 2019). Ketoacidosis with mild to moderate glucose elevations (euglycemic ketoacidosis) is a reported complication of the newer antisodium-glucose cotransporter 2 (SGLT2) inhibitor antidiabetic drugs (Goldenberg et al., 2016; Qiu et al., 2017).

Nondiabetic Ketonuria

In infants and children, ketonuria commonly occurs in a variety of conditions, such as acute febrile diseases and toxic states accompanied by vomiting or diarrhea. Inherited metabolic disease should be suspected when there is severe persistent neonatal ketosis (Ponzi et al., 2018; Weinstein et al., 2018). Ketonuria may be present in hyperemesis of pregnancy, in cachexia, and following anesthesia. In these cases, ketonuria is likely related to increased tissue (especially fat) catabolism in the face of limited food intake. In pregnancy, a normal patient may have a low fasting blood glucose level and mild ketonuria. Occasionally, ketonuria is seen in patients with hyperthyroidism, following exposure to cold or severe exercise, or with a low-carbohydrate (ketogenic) diet for weight reduction (Ullah, 2018).

Lactic Acidosis

Lactic acidosis may coexist with many acquired conditions—including shock, diabetes mellitus, renal failure, liver disease, and infection—and in response to certain drugs, especially phenformin and salicylate poisoning (Kraut & Madias, 2014). Hyperlactatemia has also been reported in certain inherited metabolic diseases, including glycogen storage disorder (GSD) type I, pyruvate dehydrogenase (PDH) deficiency, and many of the mitochondrial disorders (Tchan, 2018). Acetoacetate and 3-hydroxybutyrate may both be highly elevated, although usually the butyrate is high and acetoacetate low. Under these circumstances, ketonuria may not be detected by the usual nitroprusside test.

Methods. Because acetone, acetoacetic acid, and 3-hydroxybutyrate are all present in the urine with ketonuria, methods that indicate the presence of any one of these three ketone bodies are generally satisfactory to detect this condition. Commonly used nitroprusside strip and tablet tests based on the Rothera method detect acetoacetic acid and acetone (Misra & Oliver, 2015). Different methods measure acetoacetic acid alone, or both acetone and acetoacetic acid. Ferric chloride (Gerhardt test) detects acetoacetic acid. These methods do not measure 3-hydroxybutyrate, the predominant ketone body.

In urine and plasma, reagent strips and tablets react to 10 mg of acetoacetic acid/dL and are less sensitive to acetone. The blood level of ketone bodies may be estimated by the urine ketone dipstick at the bedside. This is especially helpful in determining the severity of ketosis for the treatment of diabetic acidosis.

When a patient is being followed with qualitative determinations of acetone and acetoacetic acid, repeated reports of marked elevations would not reflect the change that is actually taking place. In such an instance, semiquantitative results can be obtained with either the reagent strip or the Rothera tablet test by measuring several dilutions of each specimen.

Problems can occur with false-negative results because of unstable reagents and labile ketones. Bacterial action will cause loss of acetoacetic acid, which can happen in vivo as well as in vitro. Acetone is lost at room temperature but not if kept in a closed container in a refrigerator. Refrigerated samples should be brought to room temperature for testing. Preservatives do not prevent decay of ketones. If results are unexpected, fresh reagents, checked against known positive and negative controls, should be used.

Reagent Strip. This method is based on a nitroprusside (sodium nitroferricyanide) reaction for ketones. Different formulations are available. Reagent strips without alkali react to acetoacetic acid and not to acetone. With large (3+) results, urine may be diluted and remeasured, reporting a "moderate" result and the dilution factor.

Chemstrip reagent strips contain sodium nitroferricyanide and glycine, which react with acetoacetic acid and acetone in an alkaline medium to form a violet dye. A positive result is indicated by a color change from beige to violet, which is read at 60 seconds. The method detects about 10 mg/dL of acetoacetic acid and 70 mg/dL of acetone; the sensitivity and reaction of the reagent strip are similar to those of the tablet (Acetest), described later.

Multistix contains buffers and sodium nitroferricyanide, which react with acetoacetic acid, producing a pink-maroon color in 15 seconds. The reagent area detects 5 to 10 mg acetoacetic acid/dL of urine. It does not react with acetone.

Reagent strips correlate only moderately well with quantitative acetoacetate in plasma and poorly with total blood ketones. Color reactions (false-positives) occur after the use of phthaleins (sulfobromophthalein [BSP] or phenolsulfonphthalein [PSP] dye) or in the presence of extremely large quantities of phenylketones and the preservative 8-hydroxyquinoline, or L-dopa metabolites. Acetylcysteine (aerosol) produces a strong red color. The antihypertensive drugs methyldopa and captopril give positive results as well as the chemotherapy adjuvant mercaptoethane sulfonate sodium (MESNA). False-negative results occur because of loss of reagent reactivity.

Nitroprusside Tablet Test. A tablet test method may be useful if the urine has an interfering color. However, the routine utilization of the nitroprusside tablet test to confirm a positive dipstick result for ketones is unnecessary (Meng et al., 2013). These tablets are very sensitive to humidity and will deteriorate if not stored properly. The Acetest tablet contains sodium nitroprusside, glycine, and a strongly alkaline buffer. It can be used to assay whole blood, plasma, serum, or urine.

Acetest will detect 5 to 10 mg of acetoacetic acid per deciliter of urine and 20 to 25 mg of acetone per deciliter of urine. Like the reagent strips, it does not react with 3-hydroxybutyrate. It will give positive results with L-dopa and large amounts of phenylketones and with BSP and PSP dyes, which react with the alkali in the tablets.

Procedure. Place the tablet on a clean surface, preferably a piece of white paper. Place one drop of urine, serum, plasma, or whole blood on the tablet. For urine measurements, compare the color of the tablet with a color chart at 30 seconds. For serum or plasma measurements, compare the color of the tablet with the color chart at 2 minutes. For whole-blood measurements, remove clotted blood from the tablet and compare the color of the tablet with the color chart 10 minutes after application of the specimen.

If acetone and acetoacetic acid are present, the tablet will show a color varying from lavender to deep purple. Report the results as negative, small, moderate, or large. If large, a dilution may be made. Report these analyses in a form such as this: undiluted "large," 1:2 dilution "large," 1:4 dilution "moderate," and so forth.

Other Tests for Ketones. The Gerhardt ferric chloride test has been used for many years as a measurement for acetoacetic acid. However, ferric chloride methods are not very specific and the sensitivity is low, at about 25 to 50 mg/dL. The ferric chloride method gives positive results with salicylate and L-dopa. The test tube nitroprusside method of Rothera is sensitive to acetoacetic acid, at about 1 to 5 mg/dL, and to acetone with a sensitivity of 10 to 25 mg/dL.

Blood, Hemoglobin, Hemosiderin, and Myoglobin in Urine

The presence of an abnormal number of blood cells in urine is known as *hematuria*, whereas the term *hemoglobinuria* refers to the presence of free hemoglobin in solution in urine. Hematuria is relatively common, hemoglobinuria uncommon, and *myoglobinuria* rare.

Hematuria

Gross hematuria is the presence of an increased number of red blood cells in a properly collected urine specimen visible to the naked eye, while

TABLE 29.6
Some Causes of Hemolysis and Hemoglobinuria

Erythrocyte trauma	Prosthetic cardiac valves (especially aortic)
	Ostium primum repair with patch causing turbulence
	Extensive burns
	Severe exercise
	Marching
	Severe trauma to muscle and other vascular tissues
Organisms	Malaria
	Bartonella
	Clostridium welchii toxin
	Brown recluse spider bite
Erythrocyte enzyme deficiencies	Glucose-6-phosphate dehydrogenase subjects in the following situations: Exposure to oxidant drugs (acetanilid, sulfamethoxazole, nitrofurantoin), antimalarials (e.g., primaquine), fava beans (*Vicia fava*) in susceptible groups, with diabetic acidosis, and with infection
Unstable hemoglobin diseases	With exposure to oxidant drugs
Immune-mediated (see Chapter 36)	Hemolytic-uremic syndrome
	Thrombotic thrombocytopenic purpura
	Incompatible blood transfusions
	Warm antibodies (autoimmune—transient after infection, drug-induced)
	Cold antibodies
	IgM—viral anti-i mycoplasma anti-I
	IgG—paroxysmal, Donath–Landsteiner anti-P
	Membrane sensitivity, complement-mediated (paroxysmal nocturnal hemoglobinuria)
	Drugs
	Acting as haptens (penicillins)
	Immune complex (quinidine, phenacetin)
	α-Methyldopa
Normal factors	Oxidative hemolysis due to drugs, large doses or exposure to naphthalene (mothballs), some sulfonamides, sulfones, nitrofurantoin

microscopic hematuria is defined by the presence of three or greater red blood cells per high-powered field. Although asymptomatic microscopic hematuria may be detected by dipstick testing in up to 16% of screening populations (Courtemanche et al., 2019; Rockall et al., 1997), many serious diseases of the urinary tract release red blood cells into the urine (Kazi & Benz, 2014; Peterson & Reed, 2019). A retrospective investigation of microscopic hematuria by renal biopsy disclosed several histopathologic findings, including membranous nephropathy, IgA nephropathy, non-IgA mesangioproliferative glomerulonephritis, focal glomerulosclerosis, and mild glomerular abnormalities. More than 15% of patients in this study showed normal histology (McGregor et al., 1998). Hematuria can occur with disease (neoplastic and nonneoplastic) or trauma (including calculi) anywhere in the kidneys or urinary tract as well as with bleeding disorders and anticoagulant usage, and with the use of other drugs such as cyclophosphamide (Sharp et al., 2013). Hematuria may also be seen in healthy persons undertaking excessive exercise (e.g., marathon runners) in whom bleeding originates from the bladder mucosa.

Because of the diagnostic importance of small amounts of hematuria and because of the tendency of erythrocytes to undergo lysis in urine, a screening test for hemoglobin is a useful adjunct to microscopic examination of the sediment. Some studies suggest that reagent strip hemoglobin screening may be more sensitive than urine microscopy in detecting hematuria, while others have found reagent strips unreliable for this purpose (Ooi et al., 1998; Rothschild, 2016). However, a common problem with the method is the inhibition of the hemoglobin reagent strip by interfering substances, commonly ascorbic acid. This problem emphasizes the need for a routine microscopic examination to screen for hematuria and confirm the presence of hematuria in patients with a positive reagent strip hemoglobin test (Davis et al., 2012; Margulis & Sagalowsky, 2011). A positive test for hemoglobin with a normal urinary sediment suggests that a fresh urine sample should be examined for erythrocytes because an alkaline pH or urine specific gravity of less than 1.010 may cause lysis of erythrocytes. Genetic testing has been advocated to assist in the diagnosis of children with isolated microscopic hematuria (Gale, 2013).

TABLE 29.7
Urine and Plasma Findings with Intravascular Hemolysis

Test	Moderate Hemolysis	Marked Hemolysis
Urine		
Bilirubin (conjugated)	Absent	Absent
Urobilinogen	Normal or elevated	Elevated
Hemoglobin	Absent	Present
Hemosiderin	Absent	Present (late)
Plasma		
Bilirubin (unconjugated)	Elevated	Elevated
Haptoglobin	Decreased	Absent
Hemoglobin	Elevated	Elevated (marked)

Hemoglobinuria

Any cause of hemolysis has the potential of causing hemoglobinuria, but the presence of hemoglobinuria indicates significant intravascular hemolysis as opposed to extravascular hemolysis. Hemoglobin binds to plasma haptoglobin, and free hemoglobin will pass through the glomerulus as αβ dimers (molecular weight [MW], 32,000) once this binding capacity is saturated. Some hemoglobin is reabsorbed by proximal tubular cells and the remaining hemoglobin is excreted.

Hemoglobinuria may follow severe exertion in which there is direct trauma to small blood vessels; many other causes of acute erythrocyte lysis are summarized in Table 29.6. Plasma appears pink at levels of about 50 mg/dL of hemoglobin and, with marked hemolysis, plasma levels may reach 1 g/dL. The plasma hemoglobin level is more often increased in severe acquired hemolytic anemias than in hereditary hemolytic anemias. However, moderately elevated levels occur with sickle cell disease and homozygous thalassemias. Note that unstable hemoglobins can cause a brown-pigmented urine. This is thought to be due to a dipyrrole or bilifuscin, and no reaction occurs with the reagent strip test for heme. A comparison of expected urine and plasma findings with moderate and marked hemolysis is shown in Table 29.7.

Hemosiderin in Urine

Free hemoglobin is readily filtered by the glomeruli and can be subsequently reabsorbed by proximal tubular cells, where it can be catabolized into ferritin and hemosiderin. Hemosiderin will be present 2 to 3 days after an acute hemolytic episode that caused hemoglobinuria. At this time, the reagent strip method for hemoglobin is often negative. However, hemosiderin can be found as yellow-brown granules that are free or in epithelial cells and occasionally in casts (Fig. 29.1). Hemosiderin also appears in the urine sediment in diseases with a true siderosis of kidney parenchyma (hemochromatosis). Although the existence of hemosiderinuria indicates a chronic hemolytic state, its presence is rarely needed to make the diagnosis of hemolysis. Other tests—such as serum bilirubin, lactate dehydrogenase, and haptoglobin levels—will usually point to the correct diagnosis.

Because of the intermittent presence of hemosiderinuria, urinary iron levels may be quantitated to establish the presence of chronic intravascular hemolysis. Normal urinary iron excretion is about 0.1 mg/day; this is increased with hemochromatosis and in association with erythrocytes traumatized by prosthetic heart valves. Urinary iron levels are normal with pernicious anemia and in hereditary spherocytosis.

Myoglobinuria

When acute destruction of muscle fibers (rhabdomyolysis) occurs, as with trauma, myoglobin is released, rapidly cleared from the blood, and excreted in the urine as a red-brown pigment (Cervellin et al., 2010). Free myoglobin, a monomer with a MW of 17,000, is excreted quickly, whereas the hemoglobin-haptoglobin complex is more slowly removed. Myoglobinuria has been seen following a number of strenuous exercises, such as marathon running and karate. Other less common conditions associated with sustained or recurrent myoglobinuria include dermatomyositis (Rose et al., 1996), defects of muscle phosphofructokinase and adenosine monophosphate deaminase (Bruno et al., 1998), mitochondrial trifunctional protein

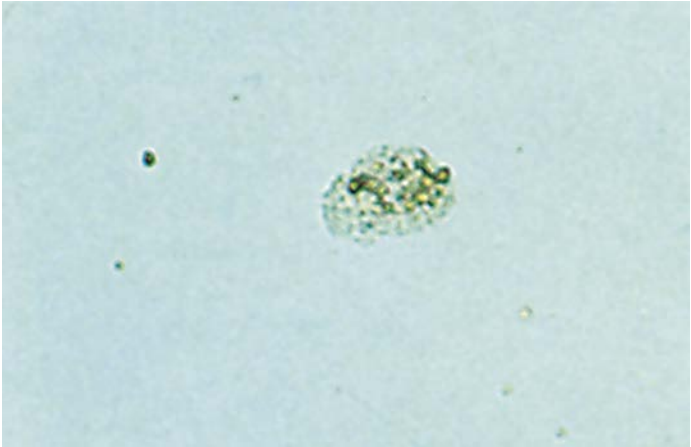

Figure 29.1 Renal tubular epithelial cell (unstained) containing brown pigment, iron (×260).

deficiency (Miyajima et al., 1997), and the metabolic myopathies (Angelini, 2014; Sharp & Haller, 2014).

The diagnosis of rhabdomyolysis and myoglobinuria is usually made from the history and other laboratory findings as follows. Typically, the patient with rhabdomyolysis has muscle tenderness or cramps and voids red-brown urine within 1 or 2 days after exertion (Zimmerman & Shen, 2013; Zutt et al., 2014). The reagent strip urine test for hemoglobin is markedly positive, and protein and a few red blood cells are present (Schifman & Luevano, 2019). Serum is clear and has a markedly elevated creatine kinase (CK), aldolase, and a normal haptoglobin level. Serum creatinine may be increased. The urine usually clears in 2 to 3 days, and the serum CK level declines. The serum measurements and history help to distinguish myoglobinuria from hemoglobinuria.

The distinction between hematuria, hemoglobinuria, and myoglobinuria may be difficult to make on examination of the urine. In all three cases, the urine can be dark red to brown, and some erythrocytes are seen in the sediment (to a much greater degree with hematuria). The reagent strip test for blood is also positive in all three cases. If serum can be examined, it will often be pink with hemoglobinemia but a normal color with myoglobinemia because this pigment is cleared so rapidly. Accurate quantitative measurement of urine myoglobin can also be performed by immunoassay. Although some slight interference by hemoglobin may occur, this is an excellent way to detect and quantify the presence of myoglobinuria (Loun et al., 1996). Table 29.8 compares hematuria, hemoglobinuria, and myoglobinuria.

Methods

Reagent Strip for Heme Compounds (Hemoglobin, Myoglobin). This method is based on the liberation of oxygen from peroxide in the reagent strip by the peroxidase-like activity of heme in free hemoglobin, lysed erythrocytes, or myoglobin. Intact erythrocytes are lysed on the strip, causing the hemoglobin to react. Therefore, well-mixed urine must be tested, as intact erythrocytes may be missed if only supernatant urine is used. The reagent area is impregnated with a buffered mixture of an organic peroxide and the chromogen tetramethylbenzidine.

$$H_2O_2 + \text{Chromogen} \xrightarrow{\text{Heme peroxidase activity}} \text{Oxidized chromogen (color change)} + H_2O \qquad \text{(Eq. 29.4)}$$

Heme catalyzes the oxidation of tetramethylbenzidine to produce a green color. The strip is read at 60 seconds following sample application.

Multistix and Chemstrip detect 0.05 to 0.3 mg of hemoglobin/dL urine. Note that 0.3 mg of hemoglobin/dL is equivalent to that from 10 lysed erythrocytes/μL. Normal erythrocytes contain approximately 30 pg of hemoglobin/cell.

Sensitivity is reduced in urine specimens with high specific gravity, in which erythrocyte lysis may not occur, and when protein levels are high. Ascorbic acid in large concentrations may cause a false-negative result, as can formalin when used as a urine preservative, and the antihypertensive drug captopril. The presence of nitrite in large amounts will delay the reaction. Oxidizing contaminants such as hypochlorites (bleach) or iodine from skin-cleansing preparations may produce false-positive results. Microbial peroxidase, associated with urinary tract infection, potentially causes a false-positive reading.

TABLE 29.8
Differentiation of Hematuria, Hemoglobinuria, and Myoglobinuria

Condition	Plasma Findings	Urine Findings
Hematuria	Color—normal	Color—normal, smoky, pink, red, brown Erythrocytes—many Renal—red blood cell casts Protein—marked increase Lower urinary tract—no casts Protein—present or absent
Hemoglobinuria	Color—pink (early) Haptoglobin—low	Color—pink, red, brown Erythrocytes—occasional Pigment casts—occasional Protein—present or absent Hemosiderin—late
Myoglobinuria	Color—normal Haptoglobin—normal Creatine kinase—marked increase Aldolase—increased	Color—red, brown Erythrocytes—occasional Dense brown casts—occasional Protein—present or absent

Other Tests for Hemoglobin and Myoglobin. Qualitative tests have been generally unsatisfactory in separating myoglobin and hemoglobin, and both conditions may be present following crush injuries. Hemoglobin and myoglobin can be bound to proteins in urine, which contributes to the difficulty of separating them by salt precipitation or electrophoresis. The salt precipitation method of Blondheim and colleagues (1958) is described next (Blondheim et al., 1958).

Qualitative Test for Myoglobin

1. Use a fresh urine specimen. Observe the color. Characteristically, urine with myoglobinuria is red when fresh and turns brown on standing, but some myoglobin may be present without color change. Myoglobin is less stable at an acid pH. Neutralize and refrigerate specimen pending testing.
2. Mix 1 mL of urine and 3 mL of 3% sulfosalicylic acid to assay for protein. If the pigment is precipitated, it is a protein. Filter. If the filtrate is a normal color, no abnormal nonprotein pigment is present. (Note: The heat and acetic acid test does not precipitate myoglobin or hemoglobin.)
3. To 5 mL of urine in a test tube, add 2.8 g of ammonium sulfate. Dissolve by mixing. The urine is now 80% saturated with ammonium sulfate. This is optimal for precipitation of hemoglobin. Filter or centrifuge. If the supernatant shows a normal color, the precipitated pigment is hemoglobin. If the supernatant fluid is colored, this is presumptive evidence of myoglobin.

This precipitation test has been largely replaced with specific immunoassays for myoglobin.

Capillary electrophoresis has been shown to successfully separate urinary hemoglobin from myoglobin based on differing electrophoretic mobility (Shihabi, 1995).

Detection of Hemosiderin in Urine. The Prussian blue reaction is used to demonstrate iron in hemosiderin (Fig. 29.2). A dry smear and an alternative wet preparation are described next.

Dry Procedure. When stained with Prussian blue reagent, hemosiderin appears as blue granules, 1 to 3 μm, singly or in groups, in renal tubular epithelial cells, as amorphous sediment, or as blue granules in casts. An iron stain used for the detection of siderocytes in blood or bone marrow is also suitable. Urine is collected in an iron-free glass container overnight. Let stand for 2 hours. Decant three-fourths of it and centrifuge the remainder. Make a smear(s) of the sediment and allow to air dry. (Note: All glassware, slides, coverslips, and so on, should be iron free. Water should be demineralized.)

Reagents

The Prussian blue reagent is made fresh.

Prussian blue stain: Add concentrated hydrochloric acid (HCl) to an aliquot of the potassium ferrocyanide solution (20% in demineralized water) until a white precipitate forms that remains stable on shaking. Filter through No. 5 filter paper.

Working counterstain: Dilute 1 mL safranin O stain (0.5 g in 100 mL distilled water) to 50 mL with phosphate buffer (pH, 6.4 to 4.7).

Procedure

1. Fix the smear in methyl alcohol for 10 minutes.
2. Rinse with iron-free water (demineralized) and air dry.
3. Stain with Prussian blue reagent for 30 minutes.
4. Wash gently for at least 4 minutes with iron-free water and air dry.
5. Counterstain with safranin O for 1 to 5 minutes.
6. Rinse with iron-free water. Air dry.
7. Mount coverslip.

Wet Procedure

1. Centrifuge a complete morning specimen or random urine sample for 5 minutes and pool the sediment. Examine several drops of sediment microscopically, searching for coarse yellow-brown granules, especially within renal tubular epithelial cells or casts.
2. If such granules are seen, suspend the rest of the sediment in a fresh mixture of 5 mL of 2% potassium ferrocyanide solution and 5 mL of 1% HCl, and allow to stand for 10 minutes.
3. Centrifuge and discard the supernatant. Examine the sediment microscopically. Coarse granules of hemosiderin appear blue in this preparation in cells, casts, and amorphous material. If granules do not stain, reexamine after 30 minutes (occasionally, the reaction is delayed).

Bilirubin in Urine

Bilirubin is a breakdown product of hemoglobin that is formed in the reticuloendothelial cells of the spleen, liver, and bone marrow (Andrews, 1999, 2005; Levitt & Levitt, 2014; Waldvogel-Abramowski et al., 2014). It is initially carried in the blood linked to albumin; this unconjugated bilirubin (or indirect bilirubin) is water insoluble and therefore is unable to pass through the glomerular barrier of the kidney. Unconjugated bilirubin is transported to the liver, where it is conjugated with glucuronic acid to form bilirubin glucuronide. This conjugated form of bilirubin (direct bilirubin) is water soluble and able to pass through the glomerulus of the kidney into the urine. Conjugated bilirubin is normally excreted in the bile into the duodenum; normal adult urine contains only 0.02 mg of bilirubin/dL. This small amount is not detected by the usual testing methods. Excretion of bilirubin is enhanced by alkalosis.

As discussed in Chapter 22, conjugated bilirubin appearing in urine generally indicates that there is excess conjugated bilirubin in the bloodstream. This can occur when there is either (1) obstruction to bile outflow from the liver (intrahepatic or extrahepatic) or (2) hepatocellular disease with resultant inability of hepatocytes to sufficiently excrete conjugated bilirubin into the bile. For example, bilirubinuria may be present when intracanalicular pressure rises secondary to periportal inflammation, fibrosis, or hepatocyte swelling. Gallstones in the common bile duct and carcinoma of the head of the pancreas are possible sources of extrahepatic biliary obstruction leading to bilirubinuria. Bilirubinuria is often seen with acute viral hepatitis or drug-induced cholestasis before the appearance of jaundice; it typically accompanies jaundice of acute alcoholic hepatitis. In persons exposed to potentially hepatotoxic drugs or toxins, a positive test for bilirubinuria may be an early indication of cholestasis or liver damage. In congenital hyperbilirubinemias, bilirubin will appear in the urine in the Dubin-Johnson and Rotor types. Bilirubin is not present with Gilbert disease or Crigler-Najjar disease (Erlinger et al., 2014; Levitt & Levitt, 2014).

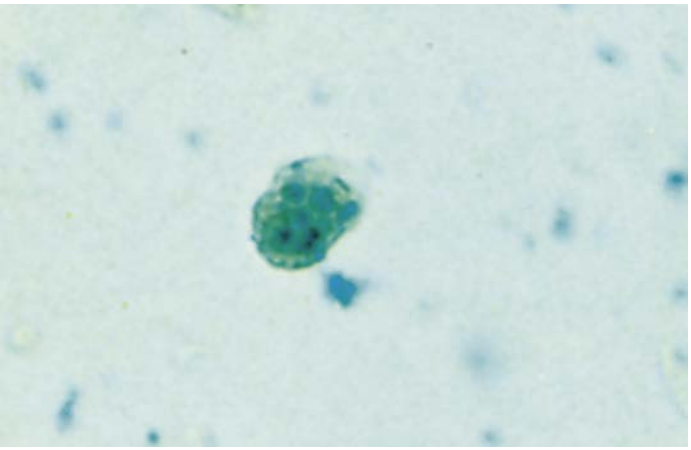

Figure 29.2 Renal tubular epithelial cell positive with Prussian blue stain, hemosiderin (×260).

Bilirubinuria is associated with yellow-brown to greenish-brown urine that may have a yellow foam, elevated serum bilirubin (conjugated), jaundice, and pale-colored feces. These acholic stools are so called because of the absence of bilirubin-derived pigment. A positive test for urinary bilirubin with a negative test for urobilinogen in urine is indicative of intrahepatic or extrahepatic biliary obstruction. This test is valuable in the differential diagnosis of jaundice because bilirubinuria is not found with hemolytic jaundice. Table 29.9 summarizes typical urine and fecal findings in jaundice of various causes.

Methods

Reagent Strip. This test is based on the coupling reaction of bilirubin with a diazonium salt in acid medium. When this method is used, normal urine contains no detectable bilirubin. Specific tests differ in the diazonium salt utilized. Multistix uses diazotized 2,4-dichloroaniline as the diazo salt, with a color change from cream-buff to tan at 20 seconds. This system will detect 0.8 mg/dL of urine; however, the color change may be difficult to read. Chemstrip uses 2,6-dichlorobenzene-diazonium tetrafluoroborate, and the color changes from pink to violet at 30 to 60 seconds. This test detects 0.5 mg/dL of urine.

Urine must be fresh because bilirubin glucuronide in urine quickly hydrolyzes to less reactive free bilirubin. Oxidation of bilirubin in specimens that have stood too long, especially when exposed to light, will result in false-negative findings. Large amounts of ascorbic acid and nitrite can also lower bilirubin results. Metabolites of drugs such as phenazopyridine give a reddish color at the low pH of the strip and mask the result. Rifampin, indican, Lodine, and large amounts of chlorpromazine metabolites may cause false positives, whereas salicylates do not interfere. Urobilinogen does not affect the result.

Confirmatory Bilirubin Tests. The diazo test method, in which bilirubin is coupled to *p*-nitrobenzene diazonium *p*-toluene sulfonate to form a blue or purple color (in the form of a tablet or reagent strip), is commonly used. The reagent strip test is much less reactive to free bilirubin than is the tablet test, so that a difference in results becomes more apparent as the urine ages. Another test employs a ferric chloride reagent to oxidize bilirubin to a green biliverdin. The diazo tablet method is described next.

Diazo Tablet Method. Tablets contain *p*-nitrobenzene diazonium *p*-toluene as well as sulfosalicylic acid and sodium bicarbonate. The latter substances provide an acid medium for the reaction and an effervescent mixture that will ensure the solution of a portion of the tablet when water is added. (The Ictotest kit, including absorbent mats and reagent tablets, is available through Siemens Healthcare Diagnostics Inc., Deerfield, IL.)

Note: Reagent tablets are hygroscopic; thus, they should be protected from moisture or high humidity. The tablets are packed in a brown bottle because prolonged direct exposure to strong light results in decomposition of the stabilized diazonium compound. Prolonged exposure over several weeks to temperatures of 100°F or more may also result in deterioration of the tablets. A brown discoloration indicates deterioration; when each new bottle is opened, tablets should be checked for positive and negative reactions.

Procedure

1. Place 10 drops of specimen on an asbestos-cellulose mat provided with the kit. Bilirubin, if present, will be adsorbed onto the mat surface.

TABLE 29.9
Urine and Fecal Findings in Jaundice

Finding	Normal	Obstruction to Bile Flow	Hemolysis, Hemolytic Anemia	Liver Damage, Hepatitis, Cholestasis
Urinary bilirubin	Absent	Increased, dark urine	Absent	Increased early
Urinary urobilinogen	Present	Neoplasm—low or absent; gallstones—variable	Increased	Decreased early; increased late
Fecal color	Dark	Pale; intermittent with gallstones in common bile duct; persistent with neoplasm in duct or pancreas	Dark	Pale early and dark late in hepatitis; pale with cholestasis

2. Place a reagent tablet on the moistened area of the mat.
3. Place one drop of water onto the tablet. Wait 5 seconds, and then place a second drop so that the water runs off the tablet onto the mat. If bilirubin is present, there will be a coupling of bilirubin with *p*-nitrobenzene diazonium *p*-toluene sulfonate from the tablet, as shown by the formation of a blue to purple color within 30 seconds. The tablet should be moved to reveal the purple color. A pink or red color is negative.

The diazo test reacts positively to bilirubin in amounts as low as 0.05 to 0.1 mg/dL. No purple reaction is seen with urobilin or other pigments, although high levels of urobilin or indican give a red color. Azo compounds (e.g., phenazopyridine) cause an atypical color. Rifampin may also interfere. Chlorpromazine metabolites in large amounts produce a purple color, and the metabolites of the anti-inflammatory drugs mefenamic and flufenamic acid cause false-positive results.

Wash-Through Tablet Method. When false-positive reactions are suspected (e.g., with chlorpromazine), the contaminant can be diluted out with water in the mat.

Procedure. Prepare duplicate mats with 10 drops of urine on each. Add 10 drops of water to one mat. Place a reagent tablet on each mat and then two drops of water onto each tablet. Bilirubin, if present, is adsorbed into the mat fibers and will appear the same on each mat; an interfering substance produces a light color or no color on the mat with the extra water.

Urobilinogen in Urine

Conjugated bilirubin from the liver eventually reaches the duodenum complexed with cholesterol, bile salts, and phospholipids within the bile (Andrews, 1999, 2005). The conjugated bilirubin is not absorbed from the small intestine but instead passes on into the colon, where resident bacteria hydrolyze the conjugate. The free bilirubin is then reduced to urobilinogen, mesobilirubinogen, and stercobilinogen. Up to 50% of the urobilinogen is reabsorbed into the portal circulation and is reexcreted, unconjugated, into the bile. The vast majority of remaining urobilinogen is excreted in feces as colored urobilins or stercobilin, which are formed after further removal of hydrogen. A small amount is excreted in the urine.

Urobilinogen represents a group of closely related tetrapyrrole compounds; because a mixture of substances is actually measured, the term *units* is frequently used instead of the more precise milligrams-per-deciliter terminology. These are roughly equivalent. Normal output of urobilinogen in the urine is 0.5 to 2.5 mg or units/24 hours. These substances are colorless and labile, as opposed to the urobilins, the oxidation products of urobilinogen that impart a yellow-orange color to normal urine. Output of urobilinogen is increased in alkaline urine; the level is decreased in acid urine.

Whenever the liver is unable to efficiently remove the reabsorbed urobilinogen from the portal circulation, more urobilinogen than normal is routed through the kidney and hence is excreted in the urine. This can occur when there is hepatocellular damage due to viral hepatitis, drugs, or toxic substances, or in some cases of cirrhosis. With congestive heart failure, liver congestion prevents effective urobilinogen handling, and reexcretion into the bile is impaired. If an infection is present, such as cholangitis associated with obstruction, large amounts of urobilinogen are excreted in urine together with bilirubin.

In contradistinction, an excess of urobilinogen in urine together with absent bilirubin is typically associated with hemolysis. This can be seen following acute lysis of erythrocytes as well as with destruction of erythrocyte precursors in the bone marrow with megaloblastic anemias. Increased urobilinogen also accompanies bleeding into tissues and the subsequent formation of excess bilirubin. These jaundiced patients have dark-colored stools because excess urobilinogen is also excreted into the feces. Urinary urobilinogen may be increased when fever is associated with dehydration and concentrated urine.

Persistent absence of urinary urobilinogen occurs with complete obstruction of the outflow of bile into the intestine, accompanied by pale stools. In infants, biliary atresia leads to markedly decreased urinary urobilinogen. One study revealed that urinary urobilinogen measured by the modified Ehrlich method had a sensitivity of 80% and specificity of 100% in the differentiation of biliary atresia from other causes of cholestasis when combined with measurements of serum γ-glutamyltransferase (GGT) (El-Guindi et al., 2016). Broad-spectrum antibiotics, which suppress the normal intestinal flora, may prevent the conversion of bilirubin to urobilinogen and therefore may reduce its excretion in feces and urine.

The brown pigment mesobilifuscin is a dipyrrole that normally contributes to fecal and urine color. It does not react with tests for blood or bilirubin. Although it is not derived from bilirubin, as is urobilinogen, it is a likely byproduct of heme synthesis. Its excess causes a dark-brown urine that can be seen with homozygous β-thalassemia or whenever Heinz bodies form in erythrocytes (e.g., with the unstable hemoglobins).

Methods

Reagent Strip. Testing is based on the Ehrlich aldehyde reaction or on the formation of a red azo dye from a diazonium compound.

Multistix utilizes the former method; its test area is impregnated with an acid buffer solution and *p*-dimethylaminobenzaldehyde, which produces a reddish-brown color with urobilinogen. Color varies from light yellow to shades of red-brown, and values from 0.2 to 1 mg/dL are considered normal. This test method is not specific for urobilinogen and will detect substances known to react with the Ehrlich reagent, including porphobilinogen, *p*-aminosalicylic acid metabolites, sulfonamides, procaine, 5-hydroxyindoleacetic acid, indole, and methyldopa (Aldomet). It is not a reliable method for the detection of porphobilinogen.

The Chemstrip urobilinogen test area is impregnated with 4-methoxybenzene-diazonium-tetrafluoroborate, which couples with urobilinogen in an acid medium to form a red azo dye. Results are read at 10 to 30 seconds, and the test can detect approximately 0.4 mg/dL. This test, unlike the Ehrlich reagent–based methods, is specific for urobilinogen.

A freshly voided sample is best for testing given that urobilinogen is quite labile and will potentially form nonreactive urobilin in acid urine. Both reagent strips are affected by the metabolites of drugs such as phenazopyridine, which colors the urine orange-red in an acid medium, and other compounds such as Azo-Gantrisin. These may mask the reaction with urobilinogen or give a false-positive result. Bilirubin and blood do not usually affect the test, but bilirubin may occasionally cause a green color.

Other Urobilinogen and Porphobilinogen Tests. Qualitative testing for urobilinogen and porphobilinogen may be performed when reagent strip testing indicates more than 1 mg/dL of Ehrlich-reacting substance present in the urine (see the Porphyrins section later in the chapter for more information on these testing modalities).

Quantitative tests for urobilinogen in urine are seldom performed. Consult Henry (1979) for a 2-hour quantitative urobilinogen method, and Davidsohn and Henry (1974) or Schwartz and colleagues (1944) for 24-hour quantitation. For quantitative comparative purposes in the same patient, a 2-hour test is used in which urine is collected from 2 PM to 4 PM after lunch. This period after the meal coincides with heightened excretion of urobilinogen, as the pH of the urine is more nearly neutral. Other 2-hour periods may be tested for comparison.

Indirect Tests for Urinary Tract Infection

It is not uncommon for significant urinary tract infections to be present in patients who do not experience typical symptoms. Given that these infections if untreated can cause severe renal damage, many physicians are finding it prudent to request tests for bacteriuria in high-risk individuals (Foxman, 2014; Nicolle, 2014). These would include patients who are older adults, pregnant, or diabetic, and those with a previous history of urinary tract infections (Chu & Lowder, 2018; Froom & Shimoni, 2018). The two most commonly utilized testing modalities for indirect assessment of bacteriuria and leukocyturia are the reagent strip nitrite and leukocyte esterase, respectively. These tests are best used to rule out urinary tract infections (St John et al., 2006; Wright & Safranek, 2006) and are discussed in the next sections. Microscopic urinalysis serves as a rapid confirmatory test for the presence of leukocytes and bacteria, with bacteriologic culture remaining the "gold standard" for detecting bacteriuria. However, some studies have shown that the urine reagent strip examination is highly sensitive for urinary infection, and microscopic examination can be safely excluded in patients with negative findings to improve laboratory efficiency and reduce cost (Miler & Nikolac, 2018). Many other methods are also under investigation. In this regard, an immunochromatographic test strip for the measurement of urinary lactoferrin released from leukocytes may prove useful for the rapid diagnosis of urinary tract infection (Arao et al., 1999). Other potential urinary markers include Tamm-Horsfall protein, myeloperoxidase, xanthine oxidase, neutrophil gelatinase-associated lipocalin, neprilysin, and α-1-microglobulin (Ciragil et al., 2014; Lubell et al., 2017; Masajtis-Zagajewska & Nowicki, 2017; Wu et al., 2018).

Nucleic Acid Methods

Bacteriuria can be detected by dipstick analysis for nitrites (converted from dietary nitrate to nitrite) by many species of common bacteria causing urinary tract infections (UTIs). Microscopic examination provides confirmation of bacterial presence; however, conventional culture, isolation, identification, and antibiotic susceptibility testing requires two to

three days. Emerging technologies on the molecular level, such as multiplex polymerase chain reaction or mass spectroscopy, can provide direct pathogen detection/identification from primary culture but do not generally provide antibiotic susceptibility information, although testing for antibiotic resistance genes can be done with nucleic acid testing (Davenport et al., 2017). Optimization of direct urine testing will promote correct prescribing of antibiotics instead of empirical use of antibiotics that can be incorrect and costly and result in overuse of antibiotics with the risk of developing multidrug-resistant organisms.

Shotgun and next-generation sequencing of urinary cell free DNA (cfDNA) have been useful for monitoring the dynamics between host and uropathogens and for detecting pathogens of different types in urine, including BK virus, JC polyoma virus, Zika virus, Lyme disease, and leptospira (Burnham et al., 2018). Fragments of cfDNA that derive from dying cells and bacteria as they break down are an attractive target for direct testing because their small size allows them to pass readily from blood into urine, where they can be easily accessed. Thus, cfDNA of *Mycobacterium tuberculosis* can be found in the urine of patients with pulmonary and other sites of tuberculosis (Fernández-Carballo et al., 2019).

Nitrite

Many bacteria that are urinary tract pathogens are able to reduce nitrate to nitrite. Thus, they will generate a positive urine nitrite test when present in significant numbers (>10^5 to 10^6/mL bladder urine). Common organisms include *Escherichia coli*, *Klebsiella*, *Enterobacter*, *Proteus*, *Staphylococcus*, and *Pseudomonas* species; *Enterococcus*, yeasts, and some gram-positive bacteria are unable to reduce nitrate to nitrite. If the nitrite test is positive, a culture should be considered provided that the specimen was properly collected and stored prior to testing. A first morning clean-voided midstream specimen is best.

According to Kunin and DeGroot (1975), self-administered repeated nitrite tests (three tests) in a small group of patients revealed about 70% overall positive results when compared with cultures. When only *E. coli* was present, bacteriuria detected by a positive nitrite test in any of the three first morning specimens showed 93% agreement with culture results. No significant false-positive nitrite results were reported in this large test group. Other authors report more disappointing results with nitrite dipstick screening for urinary tract infection, particularly in hospital inpatients and with pregnancy (Rogozinska et al., 2016; Zaman et al., 1998). In children with UTIs, nitrite negativity has been reported to predict potential resistance to cephalosporin treatment (Weisz et al., 2010).

Screening for asymptomatic bacteriuria (ASB) has been recommended for pregnant women who generally suffer from urinary retention due to obstruction from the gravid uterus as well as for persons having invasive urologic procedures in the 2005 guidelines of the Infectious Diseases Society of America (Nicolle et al., 2019). These guidelines were expanded in 2019 specifically not to recommend or to recommend against screening for ASB in children, healthy nonpregnant women, functionally impaired older women or men, diabetic patients, kidney transplant patients, and patients with other solid-organ transplants, neutropenia, spinal cord injury, indwelling urethral catheters, elective nonurologic surgery, and implantation of urologic devices.

Methods. The test depends on the conversion of nitrate to nitrite by bacterial action in the urine. Because overnight (minimum of 4 hours) bladder incubation is typically required for the infecting bacterial population to convert urinary nitrate to nitrite, a first morning specimen is best. A positive result is an indication for culture unless the specimen has been improperly stored after collection, allowing contaminant bacterial growth.

Reagent Strip. The nitrite testing area of Multistix is impregnated with *p*-arsanilic acid, which forms a diazonium salt when it reacts with nitrite present in the urine. This compound is then able to couple with benzoquinoline to form a pink azo dye. This method detects 0.075 mg of nitrite/dL in solution and is read at 40 seconds. Chemstrip contains a benzoquinoline and sulfanilamide, which produce a pink azo dye with nitrite at 30 seconds, and is able to detect 0.05 mg of nitrite/dL. Note that pink spots or edges are interpreted as negative.

False-positive results most commonly occur with poorly collected/stored specimens as the result of contaminants and postcollection bacterial proliferation. False positives may also be produced by medications that color the urine red or turn red in an acid medium (e.g., phenazopyridine).

False-negative nitrite results may be due to ascorbic acid, urobilinogen, or low pH (<6). Random specimens collected during the day and urine from patients with draining catheters do not show good correlation between the nitrite test and significant bacteriuria, presumably because of the time required for the chemical reduction to nitrite in the bladder urine. Additionally, some false-negative results occur because some nitrate-reducing organisms form compounds other than nitrite, such as ammonia, nitric and nitrous oxide, hydroxylamine, and nitrogen, and therefore give a negative nitrite test result. Lack of dietary nitrate may also produce false-negative results even when a significant number of organisms are present.

Leukocyte Esterase

Extracts of human neutrophil azurophilic (primary) granules contain up to 10 proteins showing esterolytic activity; this esterase activity is commonly used as a marker for these cells. Because neutrophils and other cells are labile in urine, leukocyte esterase activity can be indicative of remnants of cells that are not visible microscopically.

The presence of significant numbers of neutrophils in the urine suggests a UTI; however, difficulty has arisen in determining suitable cutoff points for normal and abnormal numbers of these cells. Because quantitative counts are so low, precision is poor. Positive leukocyte esterase results correlate with "significant" numbers of neutrophils, either intact or lysed. With the use of a chamber count of about 10 neutrophils/μL of fresh urine as a cutoff point, the numbers of false-negative and false-positive results are low. Likewise, when a concentrated (10 : 1) urine sediment and a cytocentrifuged stained preparation are used, a negative reagent strip test is associated with fewer than 100 neutrophils in 10 high-power fields (hpf) (450×). Multiple clinical studies have also confirmed the high negative predictive value of simultaneously negative reagent strip nitrite and leukocyte esterase assays for the presence of a UTI in both older children and adults (Kayalp et al., 2013; Mody & Juthani-Mehta, 2014; Mori et al., 2010). The leukocyte esterase test may also be useful in the workup of suspected urethritis in male patients; it has a high negative predictive value in this diagnostic setting (Bowden, 1998).

Methods

Reagent Strip. This test is similar in principle to the naphthol chloroacetate reaction used for granulocyte esterase detection in hematology. Neutrophilic esterases catalyze the hydrolysis of esters to produce their respective alcohols and acids. For example, Multistix utilizes 3-hydroxy-5-phenyl-pyrrole-*N*-tosyl-L-alanine ester as a substrate, which reacts in the presence of leukocyte esterase to form pyrrole alcohol. The alcohol then reacts with a diazonium salt to produce a purple color. The intensity of the color produced is proportional to the amount of enzyme present, which is related to the number of neutrophils present.

Cells originating from the urinary tract (i.e., urothelium) and erythrocytes do not contribute to the esterase level. Elevated urine specific gravity, protein, and glucose may all decrease test results, as can the presence of boric acid and certain antibiotics, such as tetracycline, cephalexin, and cephalothin. Very large amounts of ascorbic acid may inhibit the reaction.

Contamination of urine with vaginal fluid may give positive results, and large numbers of squamous epithelial cells and bacteria would be seen on microscopic evaluation. Also, *Trichomonas* and eosinophils may represent alternative cellular sources of esterases, causing false-positive results. Oxidizing agents and formalin may give false-positive colors, and nitrofurantoin and other strong colors may affect color interpretation. High concentrations of protein, glucose, oxalic acid, and ascorbic acid may produce false-negative results (Strasinger & Di Lorenzo, 2014).

Miscellaneous Chemical Screening Tests

Ascorbic Acid

Large quantities of ascorbic acid may occasionally be found in the urine of individuals taking therapeutic doses of vitamin C or other preparations containing abundant ascorbic acid. Because of its reducing properties, ascorbic acid may inhibit several reagent strip reactions (i.e., glucose, blood, bilirubin, nitrite, and leukocyte esterase) (Lee et al., 2017; Unic et al., 2018). Reagent strips from various manufacturers differ in their susceptibility to this substance; suspicious results should be investigated. For example, when the microscopic examination of urine sediment shows more than two erythrocytes per high-power field but heme is not detected by the reagent strip method, it may be useful to check for the presence of ascorbic acid.

Urine tests for ascorbic acid have also been used as an indication of adequate ascorbic acid therapy. With the usual Western diet, 2 to 10 mg/dL is excreted daily, but after ingestion of large amounts of ascorbic acid, levels in urine may rise to 200 mg/dL. Oxalate and sulfate are the metabolites of ascorbic acid; with ingestion of large quantities (1 g or more per day), oxalate stones may form in susceptible persons.

Methods. Several manufacturers have developed reagent strip methods for detecting ascorbic acid, discussed next. Gas chromatographic/mass spectrometric measurement is a more accurate quantitative method (Deutsch, 1997).

Reagent Strip. The ascorbic acid testing area of C-Stix reagent strips is impregnated with phosphomolybdates buffered in an acid medium. The phosphomolybdates are reduced by ascorbic acid to molybdenum blue. This test detects 5 mg/dL of ascorbic acid in urine after 10 seconds. Gentisic acid and L-dopa may cause false-positive results.

Stix reagent strips are not as sensitive as C-Stix; they can detect about 25 mg/dL of ascorbic acid at 60 seconds. The reagent in Stix is methylene green, which is reduced to its colorless form with ascorbic acid. Neutral red provides a background color, and the overall color changes from blue to purple at levels of 150 mg/dL. This same testing method is also incorporated into Multistix multiple reagent strips. Large amounts of bilirubin and pH greater than 7.5 interfere with the color. False-positive results are not seen with urates, salicylates, gentisic acid, or creatinine.

5-Hydroxyindoleacetic Acid

Serotonin (5-hydroxytryptamine) is produced by the argentaffin cells of the intestines from tryptophan and is carried in the blood by platelets. Carcinoid tumors (argentaffinoma) can produce excessive amounts of serotonin, especially when metastatic. Characteristic symptoms include intestinal and vasomotor disturbances and bronchoconstriction; edema, right-sided valvular heart disease, and neurologic symptoms may also be present.

Although serotonin in the urine can be analyzed directly by HPLC methods (Panholzer et al., 1999), screening tests that detect the serotonin metabolite 5-hydroxyindoleacetic acid in the urine are more commonly used. The quantitative method is more sensitive because it eliminates the interfering keto acids and indoleacetic acid. The normal excretion of 5-hydroxyindoleacetic acid in 24 hours is 1 to 5 mg.

Screening Test. A random urine specimen is usually sufficient for screening purposes; if a 24-hour collection is made, it should be acidified with HCl. Boric acid may also be used as a preservative. Patients should be instructed not to take any drugs for 72 hours before the test; phenothiazines, acetanilid drugs, and mephenesin, a muscle relaxant, will interfere with this test.

The principle of the test is based on the development of a purple color specific for 5-hydroxyindoles with nitrous acid and 1-nitroso-2-naphthol. Ethylene dichloride is used to remove interfering chromogens. For the procedure, see Henry (1984).

Melanin

Normal melanocytes convert tyrosine to dihydroxyphenylalanine (DOPA), then to dopaquinone, and by oxidative steps to melanin. The enzyme tyrosinase is required for the first conversion step and is found in specific organelles in melanocytes called *melanosomes*. Its formation is increased by melanin-stimulating hormone. Melanosomes with pigment are normally transferred from melanocytes to skin and mucous membrane cells. Enlarged melanosomes are found in some neoplastic cells (e.g., nevus, melanoma).

Increased urinary excretion of melanin metabolites occurs as malignant melanoma metastasizes, although it is unusual to find dark-colored urine in these patients even when the specimen stands at room temperature for 24 hours. These urinary melanogens include indoles, catechols, and catecholamines. DOPA does not appear in large amounts in urine from melanotic patients.

No simple specific test is available for melanuria. Screening tests for melanin should be made on fresh specimens of urine and include tests based on nonspecific color reactions produced with ferric chloride, Ehrlich aldehyde reagent, and nitroferricyanide. Procedures for the ferric chloride and nitroferricyanide tests for melanin can be found in Henry (1984).

A column cation-exchange chromatographic method allows detection of melanin metabolites in urine. Another approach is to measure DOPA oxidase levels in urine. The enzyme is increased in the urine of patients with melanoma and is markedly increased with liver metastases.

Rarely, cells containing melanin pigment are seen in urine sediment when melanuria with pigment uptake by renal tubular cells or metastatic melanoma to the bladder is present. A ferrous ion uptake stain can be used to color the melanin in cells dark blue.

Porphyrins

The porphyrias are a group of diseases resulting from defects in the synthesis of heme (Balwani & Desnick, 2012; Besur et al., 2014). These are inherited enzyme deficiencies in which the enzyme substrate is usually excreted in excess in urine and/or feces. During the acute porphyric attack, high levels of porphobilinogen are excreted; between attacks, levels of porphobilinogen may be increased or normal. The patterns of excretion of the various porphyrins vary with the different diseases and, together with the clinical findings, help to establish the diagnosis. In addition, genetic testing is increasingly being used in the diagnosis of the porphyrias (Whatley & Badminton, 2013).

The porphyrins are excreted in most of the porphyrias and in lead poisoning. Additionally, porphyrin metabolism may be abnormal in patients with established human immunodeficiency virus infection, particularly when there is a concomitant hepatitis C virus infection (O'Connor et al., 1996; Ryan Caballes et al., 2012).

Skin photosensitivity and cutaneous lesions frequently accompany high levels of porphyrins. The one entity without skin lesions is acute intermittent porphyria. In patients presenting with neurologic disease and acute abdominal pain—the hepatic group—production and excretion of δ-aminolevulinic acid (ALA) and porphobilinogen are increased during the acute porphyric attack. This is likely due to increased activity of ALA synthase and subsequent increased production of the precursors. Exacerbations of the hepatic diseases are precipitated by drugs known to induce liver enzyme activity (e.g., barbiturates, certain steroids).

Methods. In patients suspected of having an acute porphyric attack, porphobilinogen is sought in urine specimens. The Watson-Schwartz test is used to separate causes of a positive Ehrlich-reacting test and to give an indication of large amounts of urobilinogen or the presence of porphobilinogen. A positive result for porphobilinogen in the Watson-Schwartz test can be further confirmed by the Hoesch test because the former may show false-positive results for porphobilinogen as a result of drugs such as methyldopa. When a qualitative porphobilinogen test is specifically requested or a known porphyric patient is being followed, the simpler Hoesch test may be used instead of the Watson-Schwartz test.

Urine specimens for urobilinogen or porphobilinogen must be fresh. If testing will be delayed, the pH should be adjusted to near neutral (pH 7) and the specimen stored in a refrigerator, where it is stable for about 1 week. Urine may darken if the patient has porphyria, especially if left at room temperature.

Watson-Schwartz Test. The Ehrlich aldehyde reaction and Watson-Schwartz tests are based on solubility differences between urobilinogen and porphobilinogen. Urobilinogen can be extracted by chloroform and/or butanol, whereas porphobilinogen will remain in an aqueous phase.

Procedure.

1. To 2.5 mL fresh urine, add 2.5 mL Ehrlich reagent and mix.
2. Add 5 mL saturated sodium acetate and mix. Check with pH paper to confirm that the solution is in the pH range of 4 to 5. Adjust pH if necessary.
3. Add 5 mL chloroform; insert a stopper and shake vigorously for 1 minute. Permit the phases to separate.
4. Examine the upper (aqueous) phase. If the color is absent, consider the result of the screening test to be negative and stop.
5. If color is present, separate the upper (aqueous) phase and add 5 mL of butanol. Insert a stopper and shake vigorously for 1 minute. Allow phases to separate.
6. A "pink to rose red" color in the lower aqueous layer indicates a positive result and suggests a concentration of porphobilinogen that is several times normal. A color in the upper butanol layer indicates an increase in urobilinogen concentration (Fig. 29.3).

Hoesch Test. The Hoesch test is based on the inverse Ehrlich reaction (i.e., of maintaining an acid solution by adding a small urine volume to a relatively large reagent volume), eliminating the problem of urobilinogen reactivity. The sensitivity is similar to that of the Watson-Schwartz test, but the reaction is for porphobilinogen. This test will detect about 20 to 100 mg/L of porphobilinogen; urobilinogen in amounts up to 200 mg/L does not give a positive result (red color). A yellow color may be caused by urea.

The urorosein urinary pigment related to indoleacetic acid will produce a positive Hoesch test (in response to strong HCl), and the rose color may be confused with a positive porphobilinogen result. Some of the false-positive problems may be excluded by testing the specimen with concentrated HCl (6 mol/L) separately in conjunction with the Hoesch test. Urine from a patient having an acute porphyric attack may be dark red in color, necessitating a 1 : 10 dilution with water before testing.

The Watson-Schwartz test detects greater than 6 mg/L and the Hoesch test greater than 11 mg/L of porphobilinogen. The Watson-Schwartz test is more sensitive than the Hoesch test for porphobilinogen and may yield a positive result between attacks of acute intermittent porphyria. Large doses of methyldopa (Aldomet) gave positive results, as did indoles in some patients with intestinal ileus and the drug phenazopyridine, which becomes orange with HCl. A quantitative porphobilinogen test is necessary if the Watson-Schwartz test or the Hoesch test result is questionable. This situation may arise because of the instability of porphobilinogen.

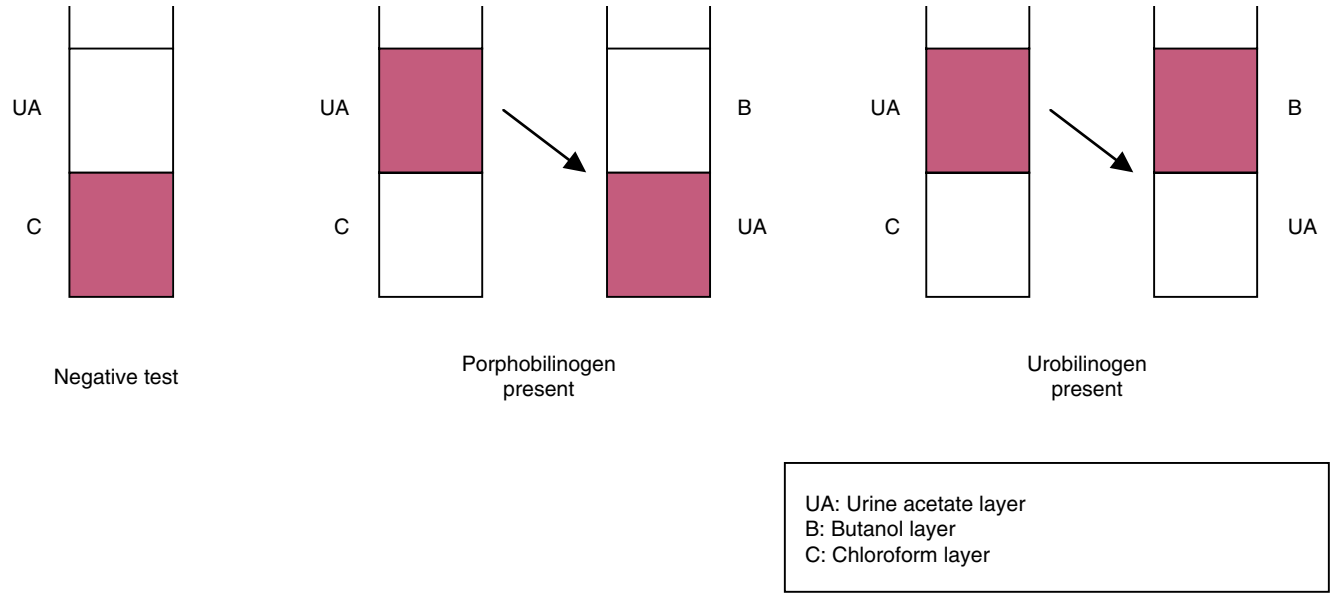

Figure 29.3 Watson-Schwartz test. Interpretation of screening method for urine urobilinogen and porphobilinogen.

Alternative urine screening tests for porphobilinogen have been described. These include a micellar electrokinetic capillary chromatographic method (Chen et al., 2015; Luo et al., 1996) as well as a semiquantitative kit in which urine is pretreated with ion-exchange resin, and the color of the Ehrlich-porphobilinogen adduct is compared to a set of standards (Deacon & Peters, 1998; Vogeser & Stauch, 2011).

Uroporphyrin and coproporphyrin can be detected by fluorescence. An orange-red fluorescence is seen if a positive specimen is placed near an ultraviolet light source.

Fluorescence Screening Procedure for Porphyrin. In this method, the urine is acidified and the extracted porphyrin exposed to ultraviolet light.

1. Place 5 mL urine in a stoppered glass centrifuge tube. Add 3 mL of a mixture of one part glacial acetic acid with four parts ethyl acetate.
2. Shake and allow to separate. Centrifuging will accelerate the separation.
3. Using a Wood's lamp, observe the upper layer for fluorescence. Inspect the tube in a dark room with ultraviolet reflected light. A lavender-to-violet color indicates the presence of porphyrins; pink-to-red fluorescence indicates higher levels of porphyrin. Pale blue with no pink color is negative. Normal urine may fluoresce blue.

To increase the sensitivity of the test and remove interfering drug metabolites, transfer the upper layer to a glass tube and acidify with 0.5 mL of 3 M HCl (25 mL concentrated HCl diluted to 100 mL with water). Shake. Porphyrins are extracted into the lower aqueous layer and will produce a red-orange fluorescence.

An alternative screening method utilizes an anion-exchange resin column. Porphyrins are adsorbed, eluted, and exposed to fluorescent light. This method removes interfering substances and is similar in principle to the quantitative method for total porphyrins and for coproporphyrin and uroporphyrin.

Screening tests together with the clinical findings will indicate whether quantitative tests should be done. The latter are usually performed by reference or research laboratories.

Urine specimens for quantitative porphobilinogen should be kept at a near neutral pH (between 6 and 7) and protected from light. Frozen specimens are fairly stable, although ALA is more stable if the urine is acidic. If the urine is to be tested for both substances, the near neutral pH is preferred and the urine aliquot is frozen. These substances are quantitated by eluting from different columns and reacting with Ehrlich reagent. A micellar electrokinetic capillary chromatographic method has been described that allows separation of ALA and porphobilinogen (Luo et al., 1996).

Urine specimens for quantitative porphyrins must be collected in a dark container containing 5 g sodium carbonate for a 24-hour specimen to give a concentration of 0.1% sodium carbonate or to produce urine of neutral pH. Coproporphyrin and uroporphyrin can be separated by thin-layer chromatography or by extraction and fluorometry and quantitated using ion-exchange columns. Additional methods include the Bio-Rad (porphyrin) column test, spectrophotometry (Zuijderhoudt & Dorresteijn-de Bok, 1998), capillary electrophoresis (Chiang & Li, 1997), fast atom bombardment mass spectrometry (Luo et al., 1997), and laser desorption/ionization time-of-flight mass spectrometry (Jones et al., 1995).

Fecal porphyrins can be qualitatively estimated using extraction and ultraviolet (UV) light, or quantitated. In some porphyrias, erythrocytes may show fluorescence when an unstained blood smear is examined microscopically. The nucleated bone marrow erythrocytes give greater fluorescence.

EXAMINATION OF URINE SEDIMENT

Microscopic examination of urine, in conjunction with dipstick chemical analysis, has been used for decades to assist in the detection of renal and urinary tract disease processes (Cameron, 2015; Cavanaugh & Perazella, 2019; Magiorkinis & Diamantis, 2015; Perazella, 2015). With microscopy, one can detect those cellular and noncellular elements of urine that do not give distinct chemical reactions. Microscopy can also serve as a confirmatory test in some circumstances (e.g., erythrocytes, leukocytes, bacteria) and yields new information 66% of the time (Tworek et al., 2008). In the routine laboratory, examination of the urine sediment is best reserved and most useful for those samples with abnormal dipstick results (European Confederation of Laboratory Medicine, 2000).

To perform a microscopic evaluation of urine with competence, one must be knowledgeable of numerous morphologic entities (e.g., organisms, hematopoietic and epithelial cells, crystals, casts). Also, microscopists must be aware of the clinical relevance of urine findings as well as the common chemical abnormalities associated with microscopic interpretations. Discrepancies should be investigated before a report is issued. The quality of the manual microscopic analysis of urine is dependent on the expertise and experience of the examiner (Tsai et al., 2005).

Centrifuged urine sediment should contain all the insoluble materials (commonly referred to as *formed elements*) that have accumulated in the urine following glomerular filtration and during passage of fluid through the renal tubules and lower urinary tract. Cellular elements are derived from two sources: (1) desquamated/spontaneously exfoliated epithelial lining cells of the kidney and lower urinary tract, and (2) cells of hematogenous origin (leukocytes and erythrocytes). Cellular and noncellular casts may be seen; these are formed in the renal tubules and collecting ducts. Crystals of variable clinicopathologic significance may also be present. Organisms (bacteria, fungi, viral inclusion cells, parasites) and neoplastic cells represent elements that are typically foreign to urine; when detected, further investigation is required.

"Normal" or reference values for formed elements will vary from one laboratory to another because of (1) the variation in concentration of random urine specimens and (2) the different methods used to concentrate the sediment by centrifugation. No specific standardized procedure is used. Individual laboratories have established their own reference values, often in conjunction with nephrologists and nephropathologists.

Methods for Examining Urine Sediment

In general, randomly collected urine specimens are satisfactory for microscopic evaluation; however, it is recommended that examination take place

when the sample is fresh, particularly if no preservative has been added. Cells and casts begin to lyse within 2 hours of collection. Refrigeration (2°C–8°C) helps prevent the lysis of pathologic entities; however, this may increase the precipitation of various amorphous and crystalline materials. Midstream collection is recommended for females to reduce contamination from vaginal elements.

Bright-Field Microscopy

Although bright-field microscopy can be performed to a limited extent on unstained urine preparations, identification of leukocytes, histiocytes, epithelial cells, and cellular casts may be difficult. Subdued light is more effective in delineating translucent structures of the urine, such as hyaline casts, crystals, and mucous threads. A crystal-violet safranin stain is commonly used to aid in delineation of formed elements in urine.

Supravital Stain Reagents

Solution I:	Crystal violet	3.0 g
	Ethyl alcohol (95%)	20.0 mL
	Ammonium oxalate	0.8 g
Solution II:	Safranin O	1.0 g
	Ethyl alcohol (95%)	40.0 mL
	Distilled water	400.0 mL

Three parts of solution I and 97 parts of solution II are mixed and filtered. The mixture should be clarified by filtering every 2 weeks and discarded after 3 months. Separately, solutions I and II can be kept indefinitely at room temperature.

Several commercially available staining reagents are available. A 2% solution of methylene blue and toluidine blue may be used as a simple, quick supravital stain.

Procedure. Add one or two drops of stain to approximately 1 mL of concentrated urine sediment. Mix with a pipet and place a drop of this suspension on a slide and coverslip.

Phase-Contrast Microscopy

Phase-contrast microscopy is beneficial for the detection of more translucent formed elements of the urinary sediment—notably, casts that may escape detection under ordinary bright-field microscopy. Phase-contrast microscopy has the advantage of hardening the outlines of even the most transparent formed elements, making detection simple (Fig. 29.4) (Fogazzi & Delanghe, 2018). Scanning time is decreased and the yield increased. Several microscopes have been designed to allow the operator to perform bright-field or phase-contrast examinations, depending on which objectives or condensors are utilized.

Polarized Microscopy

This is used to distinguish crystals and fibers from cellular or protein cast material. Lipid droplets or spherocrystals containing cholesterol esters are anisotropic in polarized light, show up brightly against a dark field, and form Maltese crosses with crossed polars. Visible evidence of anisotropy depends on the orientation of the crystal in the field; not all will be seen. If a red retardation plate is inserted, the cholesterol droplet will show typical blue and yellow quadrants against a red background. Starch granules will have a similar appearance when polarized but are much larger. Crystals, hair, and clothing fibers also show up brightly but do not exhibit Maltese cross forms. Fatty acids and triglycerides do not form liquid spherocrystals and do not show anisotropy, but glycosphingolipids in Fabry disease are birefringent and may be seen in urinary sediments. Unique fat bodies with whorled or "mulberry" appearance that show a Maltese cross with polarization have been reported in patients with Fabry disease (Yano et al., 2017).

Quantitative Counts

The hemocytometer is used in many laboratories to quantify the elements of urine sediment. Cells and casts from undiluted well-mixed urine are counted and reported as the number of cells per microliter. Normal values for neutrophils vary from 5 to 30/μL according to different workers; upper limits for erythrocytes range from 3 to 20/μL and for casts as few as 1 to 2/μL. Counting cells from an unspun sample of urine in a hemocytometer has advantages over the examination of cytocentrifuged-spun urine. These include decreased variability caused by centrifugation and suspension, a fixed volume of urine for examination, and a marked visual field for accurate counting. Kesson and colleagues (1978) provided evidence that chamber counts on centrifuged urine sediments are more reliable in predicting renal functional abnormalities than is a conventional method using cells per high-power field. Recovery of cells may vary depending on centrifuge speed, specific gravity, and pH.

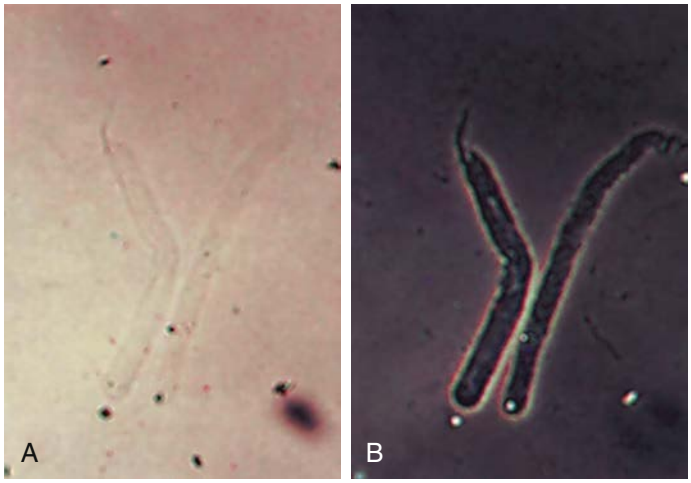

Figure 29.4 A, Hyaline casts. Bright-field (×100). B, Hyaline casts. Phase-contrast microscopy (×100).

Microscopic Components in Urine Sediment

Cells

Erythrocytes. Under high power, unstained erythrocytes (RBCs) appear as pale biconcave disks that may vary somewhat in size but are usually about 7 μm in diameter. If the specimen is not fresh when it is examined, erythrocytes may appear as faint, colorless circles ("shadow cells") because the hemoglobin may dissolve out. They may become crenated in hypertonic urine and appear as small, rough cells with crinkled edges. In dilute urine, the cells will swell and rapidly lyse, releasing hemoglobin and leaving only empty cell membranes, referred to as *ghost cells*.

On occasion, erythrocytes may be confused with oil droplets or yeast cells. However, oil droplets exhibit greater variation in size and are highly refractile, and yeast cells usually show budding. If identification is difficult, two preparations may be made and a few drops of acetic acid added to one. Erythrocytes are lysed in the acidified preparation.

Erythrocytes are found in small numbers (0–2 cells/hpf) in normal urine; more than 3 cells/hpf is considered abnormal. The presence of increased numbers of erythrocytes in the urine may indicate a variety of urinary tract and systemic conditions. These include (1) renal disease—glomerulonephritis, lupus nephritis, interstitial nephritis associated with drug reactions, calculus, tumor, acute infection, tuberculosis, infarction, renal vein thrombosis, trauma (including renal biopsy), hydronephrosis, polycystic kidney, and, occasionally, ATN and malignant nephrosclerosis; (2) lower urinary tract disease—acute and chronic infection, calculus, tumor, stricture, and hemorrhagic cystitis following cyclophosphamide therapy; (3) extrarenal disease—acute appendicitis, salpingitis, diverticulitis, acute febrile episodes, malaria, subacute bacterial endocarditis, polyarteritis nodosa, malignant hypertension, blood dyscrasias, scurvy, and tumors of the colon, rectum, and pelvis; (4) toxic reactions due to drugs, such as sulfonamides, salicylates, methenamine, and anticoagulant therapy; and (5) physiologic causes, including exercise. When increased numbers of erythrocytes are found in the urine in conjunction with erythrocyte casts, bleeding may be assumed to be renal in origin.

Dysmorphic Erythrocytes. Numerous studies have concentrated on the variable morphology of urinary erythrocytes, attempting to localize the site of origin of hematuria. RBCs with cellular protrusions or fragmentation are termed *dysmorphic* (Fig. 29.5). Some authors have suggested that their presence in urine samples is strongly suggestive of renal glomerular bleeding (Dong et al., 2016; Fogazzi et al., 2008; Fracchia et al., 1995). Others have not found dysmorphic morphology reliable in predicting primary renal hematuria (Crop et al., 2010; Favaro et al., 1997; Ward et al., 1998; Zaman & Proesmans, 2000). The so-called *G1 cell*, which has a doughnut shape with one or more membrane blebs, may be more specific than dysmorphic cells for diagnosing glomerular hematuria (Dinda et al., 1997; Nagahama et al., 2005). Another study describes immunocytochemical staining of urinary erythrocytes with Tamm-Horsfall protein in renal hematuria; this appears to be even more reliable than cellular morphology in terms of separating renal from nonrenal sources of erythrocytes

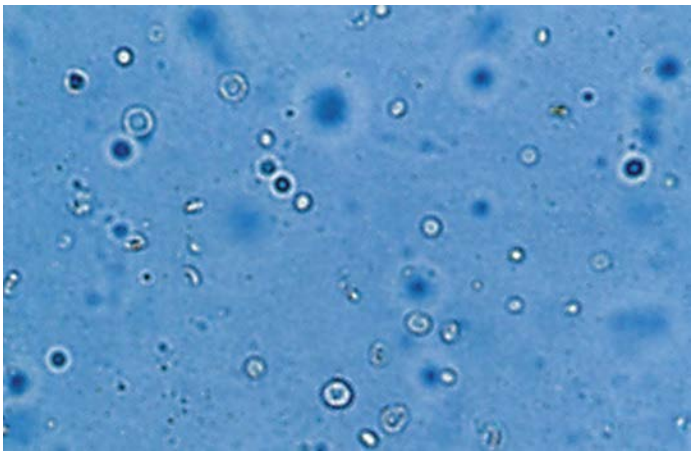

Figure 29.5 Dysmorphic erythrocytes (×160).

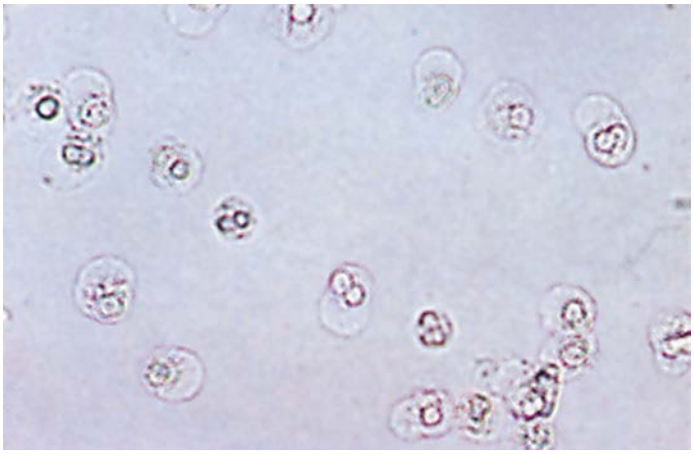

Figure 29.6 Neutrophils with dilute acetic acid (×100).

(Fukuzaki et al., 1996). Normal persons may also have a mixture of distorted and undistorted (isomorphic) erythrocytes in urine.

Leukocytes

Neutrophils. The polymorphonuclear leukocyte (neutrophil) is the predominant type of leukocyte (white blood cell [WBC]) that appears in the urine. Under high power, these cells appear as granular spheres about 12 μm in diameter with multilobated nuclei. Nuclear segments may sometimes appear as small, round, discrete nuclei. When cellular degeneration has begun, nuclear detail may be lost, and neutrophils may then become difficult to distinguish from renal tubular epithelial cells. Dilute acetic acid may enhance nuclear detail so that definition may still be possible (Fig. 29.6). Ultimately, however, with continued degeneration, neutrophilic nuclear segments fuse, making distinction from mononuclear cells difficult or impossible. Supravital staining may also be helpful in emphasizing nuclear detail. With crystal-violet safranin, neutrophilic nuclei appear reddish purple and cytoplasmic granules violet. The peroxidase cytochemical reaction is also useful in distinguishing neutrophils from tubular cells.

In dilute or hypotonic urine, neutrophils swell and their cytoplasmic granules exhibit brownian movement. Because of the refractility of the moving granules, neutrophils in this setting are known as *glitter cells*. These cells stain poorly with supravital stains and will show loss of nuclear segmentation. The leukocyte esterase reagent strip is valuable in the confirmation of pyuria in hypotonic urine specimens.

Additionally, leukocytes are rapidly lysed in hypotonic or alkaline urine. Approximately 50% are lost following 2 to 3 hours of standing at room temperature. This necessitates prompt examination of the urinary sediment following collection.

Pyuria. Typically, fewer than 5 leukocytes/hpf are seen in normal urine, although females not uncommonly will have somewhat higher quantities present. Increased numbers of leukocytes (principally neutrophils) in the urine constitute pyuria and indicate the presence of infection or inflammation in the urinary tract. When accompanied by leukocyte casts or mixed leukocyte–epithelial cell casts, increased urinary leukocytes are considered to be renal in origin.

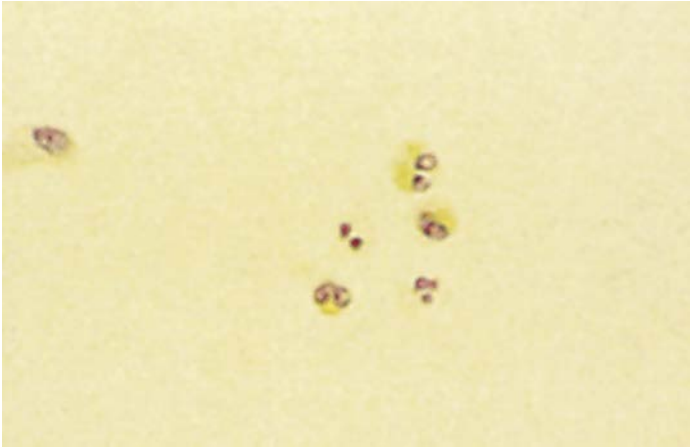

Figure 29.7 Eosinophils (×500).

Infection, either bacterial or nonbacterial, may be centered in the renal parenchyma (pyelonephritis) or may be localized as cystitis, prostatitis, urethritis, or balanitis. In women, the acute urethral syndrome (dysuria-pyuria syndrome) is regularly associated with greater than 8 neutrophils/μL in clean-catch urine specimens; however, bacterial colony counts are lower than expected. *Chlamydia trachomatis*, staphylococci, and coliforms are causative agents. Urinary neutrophil counts greater than 30 cells/hpf suggest acute infection; repeated sterile cultures in this setting may indicate tuberculosis or nephritis. Gross pyuria may reflect rupture of a renal or urinary tract abscess. It should be noted that the common finding of leukocytes in urine is not as reliable an indication of urinary tract infection as the detection of bacteriuria by Gram stain or culture of a fresh midstream specimen.

Increased leukocytes may be found in a variety of other urinary tract diseases, including glomerulonephritis, systemic lupus erythematosus (SLE), and interstitial nephritis. Calculous disease at any level may give rise to increased numbers of urinary leukocytes caused by stasis-induced ascending infection or localized mucosal inflammatory response. Bladder tumors, as well as a variety of acute or chronic localized inflammatory processes, may also cause leukocytes to be increased in the urine. Urine leukocytes may be transiently increased during fevers and following strenuous exercise.

Eosinophils. These cells are not normally seen in urine, and the finding of more than 1% eosinophils among the leukocyte population present is considered significant (Fig. 29.7). Evaluation of a concentrated stained urine is necessary for proper evaluation of urine for the presence of eosinophils. A cytocentrifuge preparation with Wright, Diff-Quik, or Papanicolaou stain is commonly used, and the Hansel secretion stain (methylene blue and eosin-Y in methanol, Libe Labs, Florissant, MO) has been shown to be an excellent stain for recognition of eosinophiluria. Appropriately stained, bilobed eosinophils may be noted in patients with tubulointerstitial disease associated with hypersensitivity to drugs such as penicillin and its analogs, although some studies have questioned the diagnostic significance of this finding (Muriithi et al., 2013). The cellular pattern in allergic interstitial nephritis typically includes many erythrocytes and some renal tubular epithelial cells. Eosinophiluria is also seen in other acute disorders of the genitourinary tract, with small numbers seen in UTIs and renal transplant rejections.

Lymphocytes and Mononuclear Leukocytes. Small lymphocytes are normally present in urine and, along with histiocytes, are easily differentiated in stained smears. When mononuclear cells (histiocytes, lymphocytes, or plasma cells) constitute 30% or more of a differential count, chronic inflammation is indicated. Many small lymphocytes may be found in urine during renal transplant rejection. Plasma cells and atypical lymphocytes should be noted when present, in which case further investigation is warranted.

Epithelial Cells

Squamous Epithelial Cells. These cells are the most frequent epithelial cells seen in normal urine and the least significant. The distal one-third of the urethra is lined by squamous epithelial cells; in the urine, these cells are large and flat, with abundant cytoplasm and small round central nuclei (Fig. 29.8). Their margins are often folded. When stained with crystal-violet safranin, nuclei are purple and cytoplasm pink to violet. Many of the squamous cells present in female urine may be derived from the vagina or vulva.

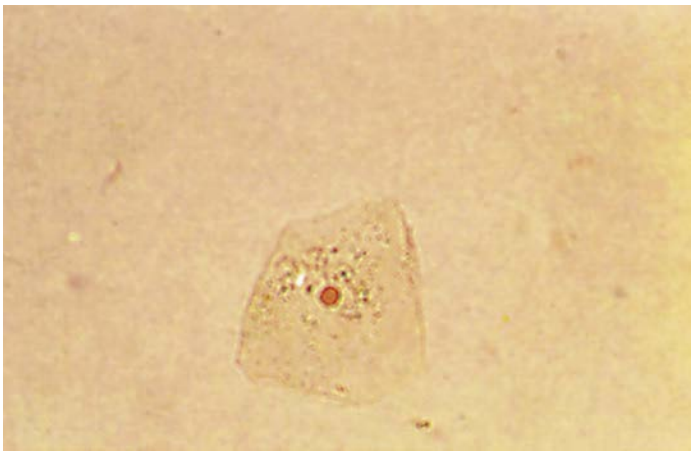

Figure 29.8 Squamous epithelial cell. Pyridium stained (×200).

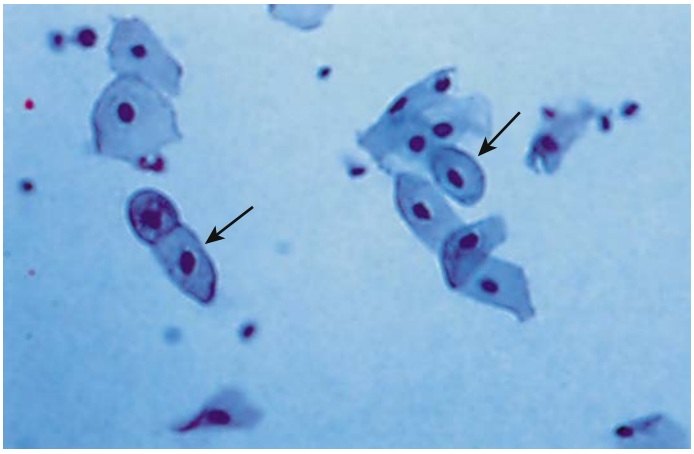

Figure 29.9 Transitional epithelial cells. Papanicolaou stained (×430).

Transitional (Urothelial) Epithelial Cells. Transitional epithelial cells line the urinary tract from the renal pelvis to the lower third of the urethra. These cells are smaller than squamous cells, ranging from 40 to 200 μm. They are round or pear shaped, with a round, centrally located nucleus. Occasional binucleate forms may be seen. When stained, transitional cells have dark-blue nuclei with variable amounts of pale-blue cytoplasm (Fig. 29.9). Another helpful clue to the proper identification of transitional cells is a characteristic *endo-ecto cytoplasmic rim*.

A few urothelial cells are present in normal urine, reflecting normal desquamation; similar to squamous cells, they are rarely of pathologic significance. The exception is the presence of large clumps or sheets of transitional cells in the absence of instrumentation (i.e., catheterization). This situation necessitates cytologic examination with the Papanicolaou stain to evaluate for possible transitional cell carcinoma (Fogazzi et al., 2015).

Renal Tubular Epithelial Cells. These are the most significant types of epithelial cells found in urine because the finding of an increased number indicates tubular damage (Figs. 29.10 and 29.11). Small numbers of tubular cells may be seen in normal urine, reflecting the normal sloughing of aging cells. They may be present in somewhat larger numbers in the urine of normal newborns.

The Papanicolaou stain has been shown to be especially useful in distinguishing renal tubular cells from other mononuclear cells in urine (Barkan & Wojcik, 2014). Renal epithelial cells from the proximal and distal convoluted tubules occur singly and are large (14–60 μm), oblong cells with characteristic coarsely granular eosinophilic cytoplasm. Nuclei may be multiple but are small with dense chromatin and rare nucleoli. Increased numbers of proximal and distal convoluted renal epithelial cells and renal epithelial cell casts are seen in cases of ATN and with certain drug or heavy metal toxicities. The quantitation of renal tubule epithelial cells, granular casts, and other urine sediment elements was used by Bagshaw and later by other investigators to develop a diagnostic scoring system to differentiate ATN from prerenal acute kidney injury in patients with acute renal failure (Bagshaw et al., 2006; Chawla et al., 2008; Perazella et al., 2010; Perazella et al., 2008; Poloni et al., 2019).

Epithelial cells from the collecting ducts measure 12 to 20 μm and are identified by their characteristic cuboidal or polygonal shape and large, usually slightly eccentric nucleus. Cytoplasmic properties include a basophilic endo-ecto cytoplasmic rim commonly found in transitional epithelial cells. Increased numbers of collecting duct epithelial cells are found in renal transplant rejection, ATN (diuretic phase), and other ischemic injuries to the kidney. They may also be found in increased numbers in malignant nephrosclerosis as well as in cases of acute glomerulonephritis accompanied by tubular damage. Ingestion of various drugs and chemicals may cause significant tubular desquamation. Collecting duct tubular cells are easily found in the urine following salicylate intoxication.

Renal epithelial fragments of collecting duct origin have been described. Three or more renal cells of collecting duct origin constitute a renal epithelial fragment and indicate a more severe form of renal tubular injury with basement membrane disruption. Renal epithelial fragments are indicative of ischemic necrosis and are usually found accompanying varying degrees of renal tubular injury and pathologic casts. Proximal and distal convoluted tubular cells are not found in fragment form. Proper identification of renal epithelial fragments is essential not only in diagnosing a more severe form of renal tubular injury but also in avoiding a false-positive diagnosis of low-grade transitional cell carcinoma.

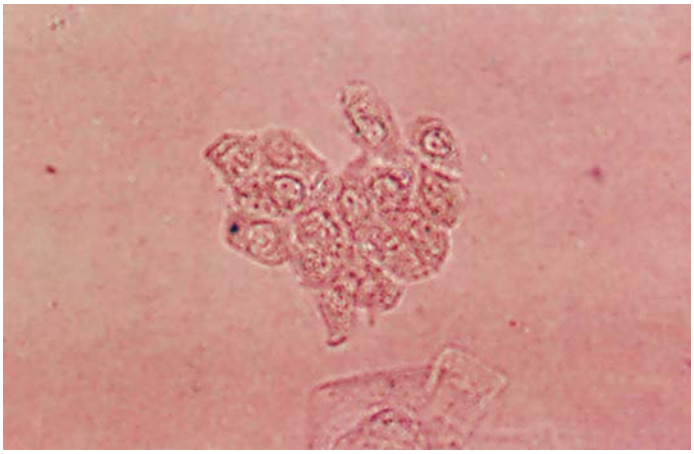

Figure 29.10 Renal tubular epithelial cells (×200).

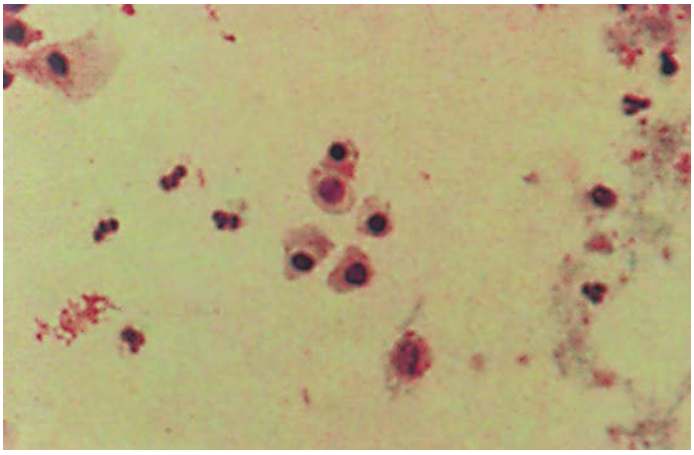

Figure 29.11 Renal tubular epithelial cells and neutrophils. Papanicolaou stained (×430).

Lipids in Renal Tubular Epithelial Cells. Oval fat bodies are tubular cells that have absorbed lipoproteins with cholesterol and triglycerides leaked from nephrotic glomeruli (Fig. 29.12). Therefore, oval fat bodies constitute one form of lipiduria. Lipids may also appear in the urine as free fatty droplets or within histiocytes as ingested material. The presence of any or all of these lipid forms accompanied by marked proteinuria is characteristic of nephrotic syndrome.

Positive identification of lipid is required before lipiduria is reported. When free or incorporated droplets contain large amounts of cholesterol, they exhibit a Maltese cross formation under polarized light (Figs. 29.13 and 29.14). When they contain large quantities of triglycerides, fat stains (Oil Red O or Sudan III) are required for positive lipid identification.

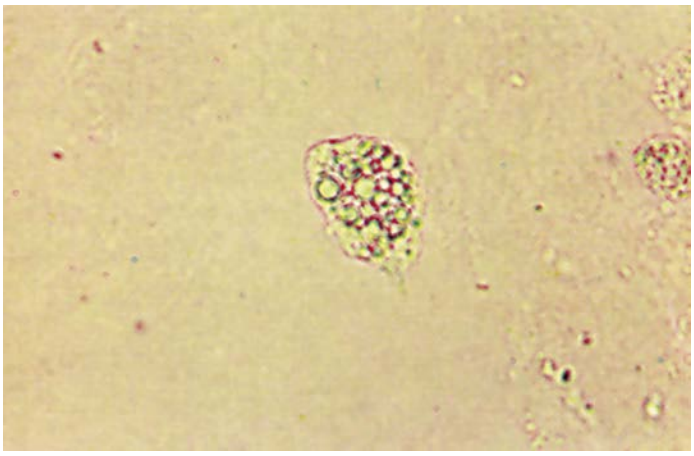

Figure 29.12 Oval fat body (×160).

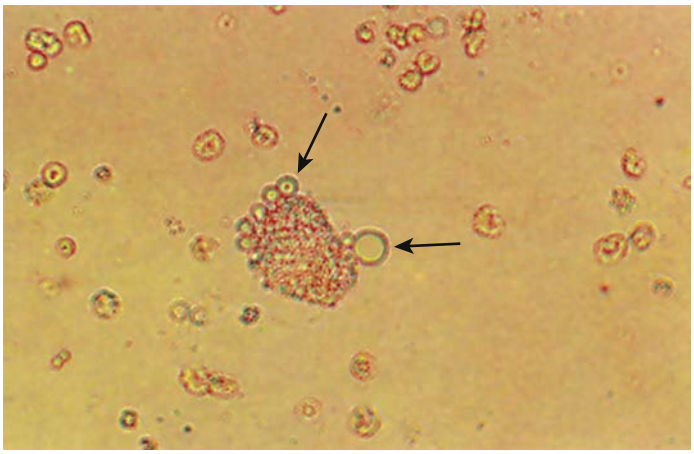

Figure 29.13 Oval fat body with attached fat droplets. Bright field (×160).

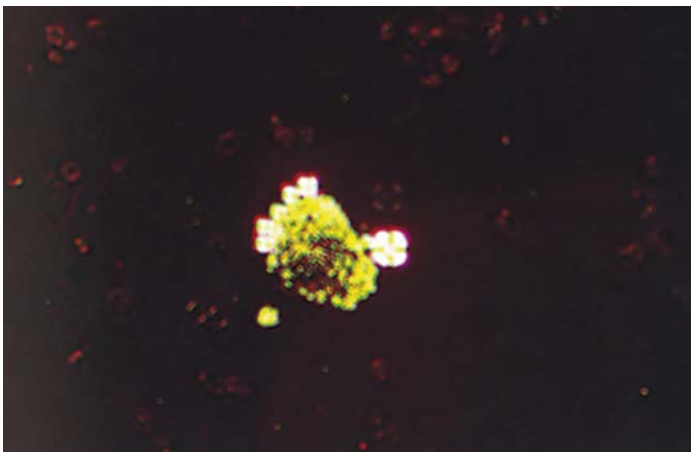

Figure 29.14 Oval fat body with attached fat droplets. Polarized (×160).

Pigment in Renal Tubular Epithelial Cells. With hemoglobinuria or myoglobinuria, heme pigment is absorbed into the cells and converted to hemosiderin. The iron-laden cells are desquamated and found in the urine sediment. The cytoplasmic granules appear yellow-brown and stain for iron with Prussian blue. These cells may also be incorporated into casts (see Figs. 29.1 and 29.2).

Melanin granules are absorbed into the tubular cells in rare cases of melanuria. The desquamated pigmented cells may be demonstrated in the sediment. Pigmented tumor cells are also found in cases of melanoma metastasis to the bladder.

Bilirubin pigment colors all of the elements of the sediment, including renal tubular epithelial cells and casts. Note that urobilin does not color cells and casts.

BOX 29.2

Classification of Casts

Matrix

Hyaline—variable size
Waxy—often broad in use

Inclusions

Granules—proteins, cell debris
Fat globules—triglycerides, cholesterol esters
Hemosiderin granules
Crystals—uncommon
Melanin granules—rare

Pigments

Hemoglobin, myoglobin, bilirubin, drugs

Cells

Erythrocytes and red blood cell remnants
Leukocytes—neutrophils, lymphocytes, monocytes, and histiocytes
Renal tubular epithelial cells
Mixed cells—erythrocytes, neutrophils, and renal tubular cells
Bacteria

Casts

Casts are the only formed elements of urine that have the kidney as their sole site of origin. Tamm-Horsfall protein is the glycoprotein secreted by the thick part of the ascending loop of Henle (and possibly the distal tubule), which constitutes about one-third of the total urinary protein in normal individuals (El-Achkar & Wu, 2012; Rampoldi et al., 2011). It is generally held that Tamm-Horsfall protein forms the matrix of all casts. The protein forms a meshwork of fibrils that can potentially trap any elements present in the tubular filtrate, including cells, cell fragments, or granular material.

Casts can be quite variable in their appearance, size, shape, and stability. Perhaps this variability is one factor in the apparent low precision of cast identification in some laboratories (Rasoulpour et al., 1996; Yoo et al., 1995). The width of a cast depends on the size of the tubule in which it was formed. Broad casts are seen in dilated tubules or with stasis in collecting ducts. Thin casts occur in tubules compressed by swollen interstitial tissue or as the result of disintegration. Casts may be short and stubby, or long and convoluted. The latter variety appears when diuresis occurs after urinary stasis. Casts typically have parallel sides and blunt ends, but with age they may begin to disintegrate and show thinning and irregularities. Fibrils may separate, causing a frayed appearance. Tails and tapering ends can be seen; these disintegrating forms are referred to as *cylindroids*.

In the normal person, very few casts are seen in the urinary sediment. In kidney diseases, they may appear in large numbers and in many forms. Increased numbers of casts usually indicate that kidney disease is widespread and that many nephrons are involved. Large numbers of casts may also be seen in healthy persons after strenuous exercise accompanied by proteinuria.

Cast formation increases with lower pH or increased ionic concentration and with stasis or obstruction of the nephron by cells or cell debris. It is increased when larger than normal quantities of plasma proteins enter the tubules. The protein in excess is usually albumin, but globulins such as the Bence Jones immunoglobulin cause cast formation, as do hemoglobin and myoglobin. The plasma proteins possibly react or combine with Tamm-Horsfall protein to form less translucent casts and granular casts.

Casts may be classified according to their matrix, inclusions, pigments, and cells present, as shown in Box 29.2. A detailed discussion, including clinical significance, follows.

Hyaline Casts

These are the most frequently observed casts, consisting almost entirely of Tamm-Horsfall protein; zero to two hyaline casts per low-power field is considered normal. Hyaline casts are translucent with bright-field microscopy and pink with supravital staining and are more easily visualized with phase-contrast microscopy (see Fig. 29.4). Increased numbers are seen with renal diseases and transiently with exercise, heat exposure, dehydration, fever, congestive heart failure, and diuretic therapy.

Waxy Casts

With chronic renal diseases, some casts become denser in appearance and are known as *waxy*. These differ from hyaline casts in that they are easily visualized because of their high refractive index. Waxy casts are uncommon

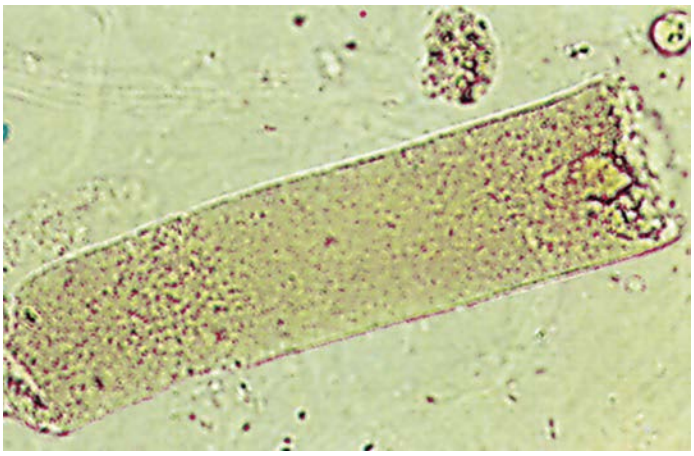

Figure 29.15 Waxy cast (×200).

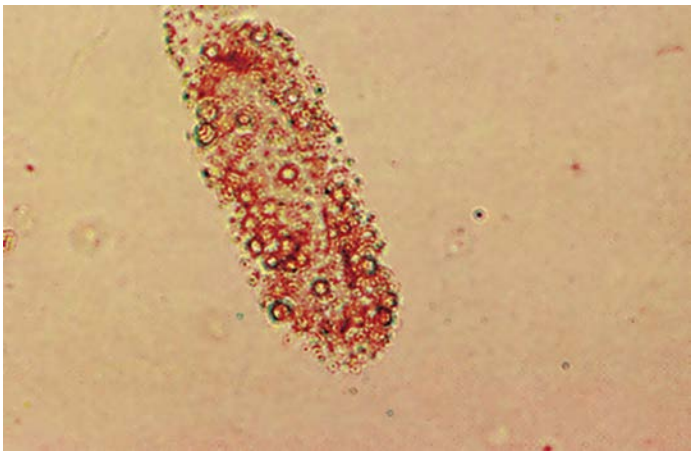

Figure 29.17 Erythrocyte cast (×200).

Figure 29.16 Fine granular cast becoming waxy (×200).

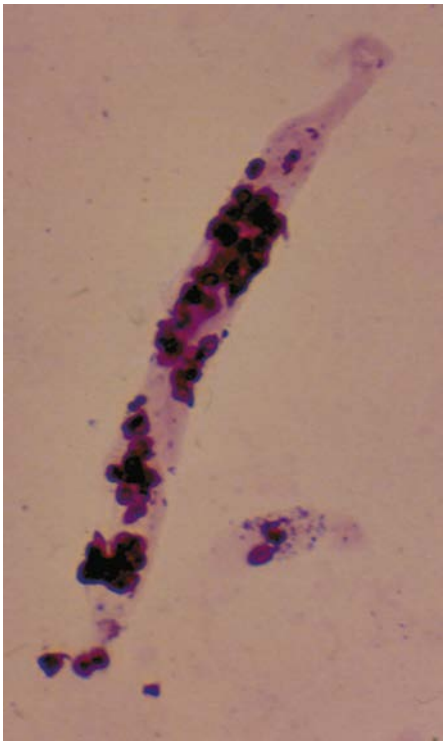

Figure 29.18 Leukocyte cast. IRIS urinalysis stain (×200).

in glomerular diseases, with the reported exception of postinfectious glomerulonephritis and renal amyloidosis (Spinelli et al., 2013). With bright-field microscopy, waxy casts are homogeneously smooth in appearance with sharp margins, blunted ends, and cracks or convolutions frequently seen along the lateral margins, indicating a measure of brittleness (Fig. 29.15).

Waxy casts are commonly associated with tubular inflammation and degeneration. They are observed most frequently in patients with chronic renal failure and are found during acute and chronic renal allograft rejection. Early waxy casts are believed by some investigators to reflect the final phase of dissolution of the fine granules of granular casts (Fig. 29.16). Because time is required for granules to undergo lysis, waxy casts imply localized nephron obstruction and oliguria. When waxy casts are unusually broad, they are known as *renal failure casts*. These casts imply advanced tubular atrophy and/or dilation, in turn, reflecting end-stage renal disease and extreme stasis of urine flow.

Cellular Casts

Erythrocyte (Red Blood Cell) Casts. Finding these casts in the urine is significant because they are an indication of bleeding within the nephron. Glomerular damage allows erythrocytes to escape into the tubule; if there is concomitant proteinuria and if conditions are optimal for cast formation, RBC casts form in the distal nephron. In urine, these casts appear yellow under low-power objectives. A prerequisite for the identification of an erythrocyte cast is that RBC outlines should be sharply defined in at least part of the cast (Fig. 29.17). The amount of matrix material that may be visible ranges from scant to a prominent delicate hyaline matrix with only one or two visible RBCs. These casts are better visualized with phase-contrast microscopy or with supravital staining, in which case the erythrocytes are colorless or lavender in a pink matrix. With prolonged stasis, red cell casts may degenerate and appear in the urine as reddish brown, coarsely granular hemoglobin (blood) casts.

Pathologic disorders in which erythrocyte casts appear in the sediment include many acute glomerulonephritides, IgA nephropathy, lupus nephritis, subacute bacterial endocarditis, and renal infarction. Rarely, tubulointerstitial disease may allow transtubular entry of erythrocytes with subsequent incorporation into a cast. This may occur in severe pyelonephritis. Additionally, the appearance of erythrocyte and leukocyte casts has been found to coincide with renal relapse in patients with SLE (Hebert et al., 1995; Martinez-Martinez et al., 2017).

Leukocyte (White Blood Cell) Casts. WBC casts are refractile and exhibit granules; frequently, multilobated nuclei will be visible (Fig. 29.18), unless disintegration has begun. Phase-contrast microscopy may be helpful in delineating nuclear segmentation. Supravital stains also enhance visualization.

Leukocytes usually enter tubular lumina from the interstitium and, for the most part, leukocyte casts (Fig. 29.19) reflect tubulointerstitial disease with neutrophilic exudates and interstitial inflammation. The most common disease of this category is pyelonephritis. Leukocyte casts may be present in glomerular disease owing to the chemotactic effect of complement. They are also seen in interstitial nephritis, lupus nephritis, and even the nephrotic syndrome.

Renal Tubular Epithelial Cell Casts. Renal tubular epithelial cell casts may be difficult to distinguish from leukocyte casts, particularly in unstained preparations viewed with bright-field microscopy. Supravital staining, phase-contrast microscopy, and Papanicolaou staining (see Figs. 29.19 and 29.20) are helpful in delineating between these two cast types.

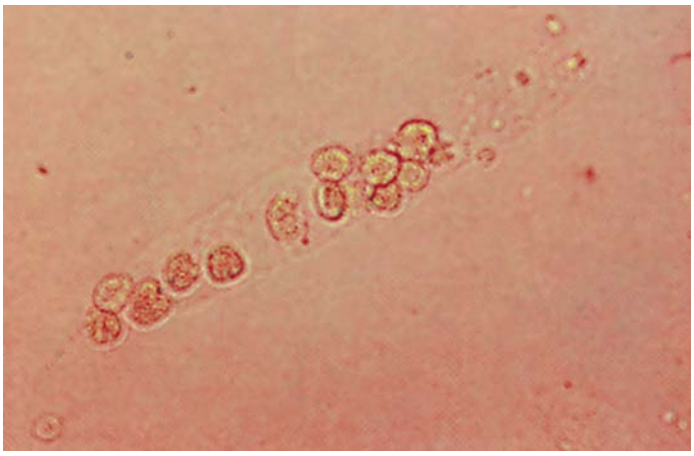

Figure 29.19 Cellular cast (×200).

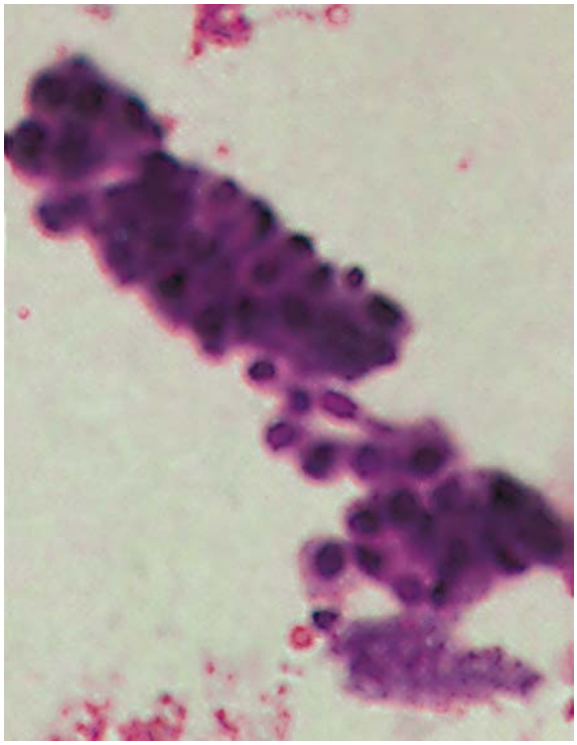

Figure 29.20 Renal tubular epithelial cell cast. Papanicolaou stained (×430).

Figure 29.21 Mixed (leukocyte and renal epithelial tubular cell) cast (×200).

Figure 29.22 Cellular cast (×200).

The most reliable distinguishing characteristic of renal tubular cells is their singular round nuclei.

Renal tubular epithelial cell casts are seen in urine with ATN, viral disease (e.g., cytomegalovirus), or exposure to a variety of drugs. Heavy metal poisoning and ethylene glycol and salicylate intoxication may cause tubular cells and casts to appear in the urine. In transplant units, these cells and casts constitute some of the more reliable criteria for detecting acute allograft rejection after the third postoperative day.

Mixed Cellular Casts. Not infrequently, two distinct cell types may be present within a single cast. This has been referred to as a *mixed cast*. Examples might include leukocyte/renal, erythrocyte/leukocyte, and eosinophil/renal (Fig. 29.21). When cell types cannot be established with certainty, the resulting cast is known as a *cellular cast* (Fig. 29.22). Some inferences as to cell type may be drawn from the dominant population of free cells in the surrounding sediment.

Inclusion Casts

Granular Casts. Granular casts are fairly common and may appear in both pathologic and nonpathologic conditions (Fig. 29.23). Granules may be small or large and may originate from plasma protein aggregates that pass into the tubules from damaged glomeruli, as well as from cellular remnants of leukocytes, erythrocytes, or damaged renal tubular cells. Fine salt precipitates and lysosomes may also be granular components. Protein aggregates include fibrinogen, immune complexes, and globulins. With prolonged stasis, large granules in casts may become smaller, and there appears to be no advantage to separating types of granular casts.

Granular casts appear with glomerular and tubular diseases but are also a feature of tubulointerstitial disease and renal allograft rejection. They may accompany pyelonephritis, viral infections, and chronic lead poisoning. Coarsely granular casts occur, with hematuria, in cases of renal papillary necrosis. It is possible that some fine granules represent calcium phosphate precipitants in hyperparathyroidism. Granular casts may also be seen following periods of extreme stress or strenuous exercise.

Fatty Casts. Fatty material is incorporated into the cast matrix from lipid-laden renal tubular cells. These are commonly seen when heavy proteinuria is present and are a feature of nephrotic syndrome and nonproliferative glomerular diseases (Fogazzi et al., 2005) (Figs. 29.24 and 29.25).

Crystal Casts. Casts containing urates, calcium oxalate, and sulfonamides (sulfamethoxazole) are occasionally seen. A matrix is visible in a true crystal cast, and the crystals may polarize. These casts indicate deposition of crystals in the tubule or collecting duct. Hematuria, possibly related to tubular damage, regularly accompanies crystal casts. These casts should be carefully distinguished from clumps of crystals forming at room or refrigerator temperatures.

Pigmented Casts

Hemoglobin (Blood) Casts. Hemoglobin casts typically appear yellow to red, although sometimes the color is pale (Fig. 29.26). Most often, hemoglobin casts, also known as *blood casts*, are seen with erythrocyte casts

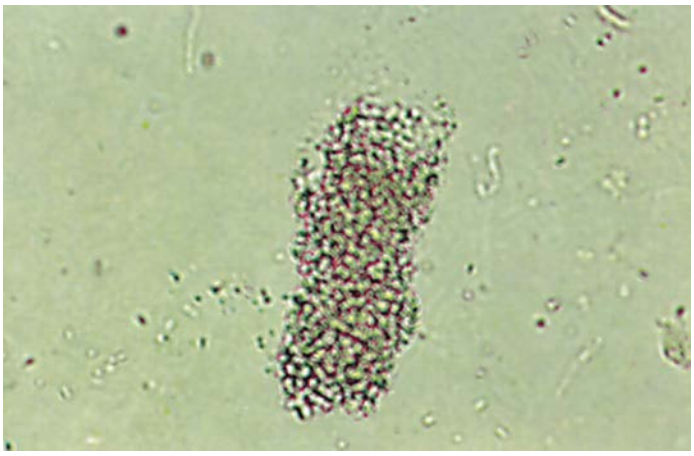

Figure 29.23 Granular cast (×200).

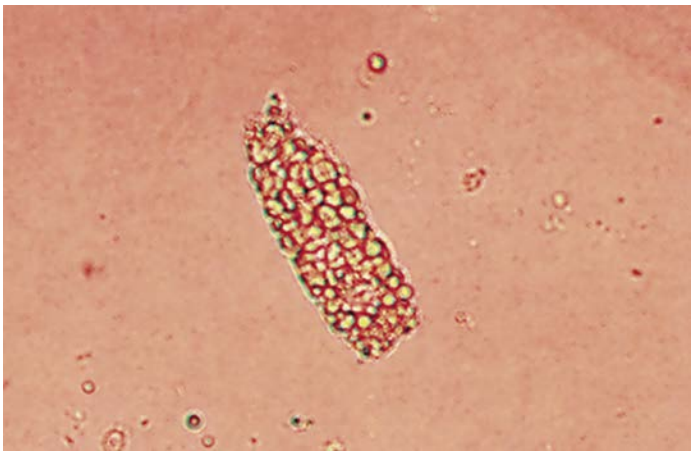

Figure 29.24 Fatty cast. Bright field, nonpolarized (×160).

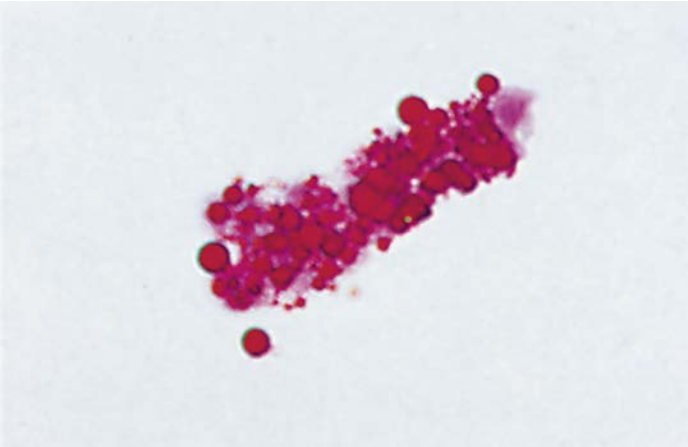

Figure 29.25 Fatty cast. Positive Oil Red O (×200).

and glomerular disease. Less commonly, they are seen with tubular bleeding and rarely with hemoglobinuria.

Hemosiderin Casts. Hemosiderin granules in casts derive from pigment-laden renal tubular cells.

Myoglobin Casts. These casts are red-brown in color and occur with myoglobinuria following acute muscle damage. They may be associated with acute renal failure.

Bilirubin and Other Drug Casts. Bilirubin is seen in urine when obstructive jaundice is present and will color casts a deep yellow-brown. Drugs such as phenazopyridine cause a bright-yellow to orange color in acid urine and color casts and cells as well.

Broad Casts

Broad casts are defined as those with a diameter two to six times that of normal casts. They indicate tubular dilation and/or stasis in the distal collecting duct. All types of casts may occur in broad forms, typically seen in individuals with chronic renal failure. They portend a poor prognosis.

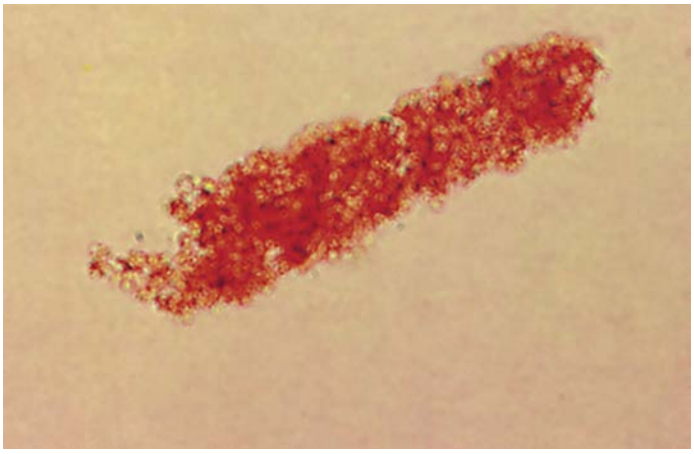

Figure 29.26 Hemoglobin cast (×200).

Other Miscellaneous Casts or Castlike Structures

Bacteria may become embedded in cast matrices; on supravital staining, they appear dark purple with a pale-pink matrix. Mucous threads are commonly confused with casts. However, these are larger, long, and ribbonlike, with poorly defined edges and pointed or split ends, in contradistinction to casts, which tend to have well-defined edges and blunt ends.

Telescoped Sediment

This term is used to describe the simultaneous occurrence of elements of glomerulonephritis and those of nephrotic syndrome in the same urine specimen. Therefore, a telescoped sediment might include RBCs, RBC casts, cellular casts, broad waxy casts, lipid droplets, oval fat bodies, and fatty casts. Such sediment may be found in collagen vascular disease (notably, lupus nephritis) and subacute bacterial endocarditis.

Crystals

Crystals form by the precipitation of urinary salts when alterations in multiple factors affect their solubilities (Verdesca et al., 2011). These include changes in pH, temperature, and concentration. Precipitates can appear in the urine in the form of true crystals or amorphous material. Most crystal formation takes place in refrigerated specimens and those allowed to sit at room temperature for several hours. Increased solute concentration is typically responsible for crystal formation.

Although most crystals in the urine are of limited clinical significance, proper identification is essential so as not to miss the relatively few abnormal crystals that are associated with various pathologic conditions (Daudon & Frochot, 2015). Knowledge of urine pH is a valuable aid in crystal identification because it is the pH that determines which chemical will precipitate. Many of the commonly seen crystals have characteristic morphologies. However, variability does exist, sometimes leading to confusion between pathologic and nonpathologic crystal structures. For the purpose of separating abnormal from more commonly occurring *nuisance crystals*, a summary of crystal morphology is presented in Table 29.10.

Crystals Found in Normal Acid Urine

Amorphous Urates (Calcium, Magnesium, Sodium, and Potassium Urates). Amorphous urates will precipitate upon standing in concentrated urine of a slightly acid pH. When large quantities are present, the urine sediment may appear pink-orange to reddish brown on macroscopic examination; this appearance has been referred to as *brick dust*. Microscopically, this amorphous material appears as yellow-brown small granules that can form clumps and adhere to fibers and mucous threads. Amorphous urates will convert to uric acid crystals with acidification with acetic acid and will dissolve with heat (60°C) and with dilute alkali.

Crystalline Urates (Sodium, Potassium, and Ammonium). These biurates and acid urates form small brown spheres (Fig. 29.27) or colorless needles in slightly acid urine. The spheres may cluster in pairs and triplets. Similar to amorphous urates, these crystalline forms will slowly revert to uric acid plates on acidification with acetic acid.

Crystalline Uric Acid. Uric acid crystals occur at low pH (5.0–5.5) and are seen in a variety of shapes, including rhombic or four-sided flat plates, prisms, oval forms with pointed ends (lemon-shaped), wedges,

TABLE 29.10

Characteristics of Amorphous and Crystalline Urinary Sediments

Substance	Description	URINE PH WHERE FOUND: Acid	Neutral	Alkaline	Solubility Characteristics and Comments
Ampicillin	Uncommon—from high dose; colorless; long prisms that form clusters, sheaves	+	–	–	
Bilirubin	Reddish brown; amorphous needles, rhombic plates, or cubes; may color uric acid crystals	+	–	–	Soluble in alkali, acid, acetone, and chloroform
Cholesterol	Rare; colorless; flat plate with corner notch; accompanies fatty casts and oval fat bodies	+	+	–	Very soluble in chloroform, ether, and hot alcohol
Calcium carbonate	Colorless; small granules in pairs, fours; spheres; rarely needles	–	+	+	Soluble in acetic acid with effervescence
Calcium oxalate	Dihydrate—common; colorless; small refractile octahedron	+	+	–	Soluble in dilute HCl
	Monohydrate—uncommon; dumbbell and ovoid rectangle				
Cystine	Colorless; hexagonal plates, often laminated; rapidly destroyed by bacteria; may be confused with uric acid, but cystine is soluble in dilute hydrochloric acid	+	–	–	Soluble in alkali (especially ammonia) and dilute HCl; insoluble in boiling water, acetic acid, alcohol, ether; apply cyanide-nitroprusside reaction
Hematin	Small, biconvex "whetstone" seen with hemoglobinuria	+	–	–	
Hemosiderin	Golden brown; granules in clumps, in cells, casts	+	+	–	Blue with Prussian blue
Hippuric acid	Rare; colorless, needles, rhombic plates and four-sided prisms; distinguish from phosphates	+	+	+	Soluble with hot water and alkali; insoluble in acetic acid
Indigotin	Rare; blue; amorphous or small crystals; colors other crystals	+	+	+	Very soluble in chloroform; soluble in ether; insoluble in acetone
Phosphates					
Amorphous phosphate (magnesium, calcium)	Colorless; fine, granular precipitate	–	+	+	Insoluble with heat; soluble with acetic acid, dilute HCl
Calcium hydrogen phosphate	Less common; colorless, star-shaped or long, thin prisms or needles; form rosettes	sl	+	sl	Slightly soluble in dilute acetic acid, soluble in dilute HCl
Triple phosphate (ammonium, magnesium)	Common form: colorless; three- to six-sided prisms, "coffin lids"	–	+	+	Soluble in dilute acetic acid
	Less often: Flat, fern leaf form, sheets, flakes				
Radiographic media (meglumine diatrizoate)	Intravenous: Colorless; thin, rhombic plates, some with notch, resemble cholesterol plates; elongated crystals	+	–	–	Soluble in 10% NaOH: Insoluble in ether and chloroform; high specific gravity in urine: polarizes with interference colors
	Retrograde: Colorless; long, pointed crystals				
Sulfonamides					
Acetylsulfadiazine	Wheat sheaves with eccentric binding	+	–	–	
Acetylsulfamethoxazole	Brown; dense spheres or irregular divided spheres	+	–	–	
Sulfadiazine	Brown; dense globules	+	–	–	Soluble in acetone
Tyrosine	Rare; colorless or yellow, appears black with focusing; fine silky needles in sheaves or rosettes	+	–	–	Soluble in alkali, dilute mineral acid, relatively heat soluble; insoluble in alcohol, ether
Urates					
Amorphous (calcium, magnesium, sodium, potassium)	Common; colorless to yellow-brown; amorphous, granular precipitate	+	+	–	Soluble in dilute alkali; soluble at 60°C or lower; change to uric acid crystal with concentrated HCl or acetic acid
Monosodium urate	Colorless; needles or amorphous precipitate	+	–	–	
Urates (sodium, potassium, ammonium)	Brown; small, spherical; clusters resemble biurates	sl	+	–	Soluble at 60°C; change to uric acid with glacial acetic acid
Ammonium biurate	Common in "old" urine; dark yellow or brown; spheres or "thorn apples" (spheres with horns)	–	+	+	Soluble at 60°C with acetic acid; soluble strong alkali; change to uric acid with concentrated hydrochloric or acetic acid
Uric acid	Common; yellow, red-brown, brown; large variety of shapes—rhombic, four-sided plates, rosettes, "whetstones," lemon shapes; rarely, colorless hexagonals	+	–	–	Soluble in alkali; insoluble in alcohol and acids; polarizes with interference colors
Xanthine	Rare; colorless; small, rhombic plates	+	+	–	Soluble in alkali; soluble with heat; insoluble in acetic acid

sl, Slight.

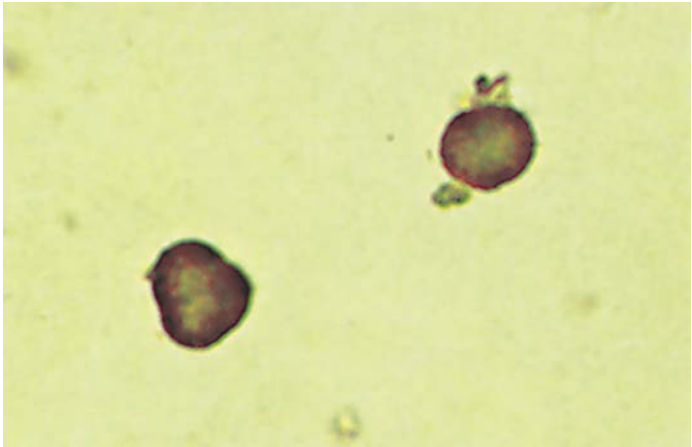

Figure 29.27 Acid urates (×160).

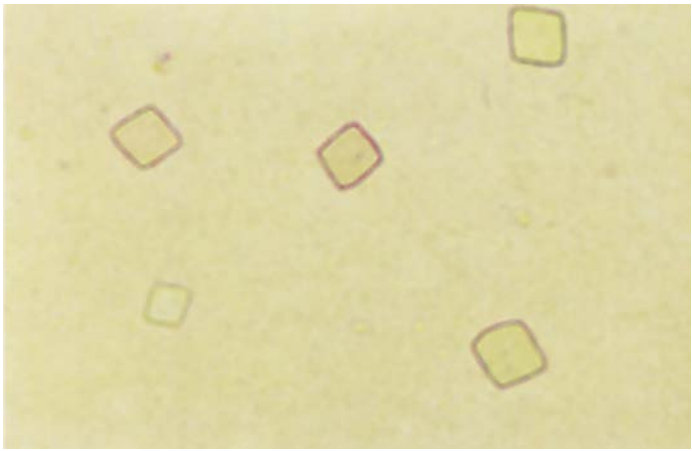

Figure 29.28 Uric acid crystals (×160).

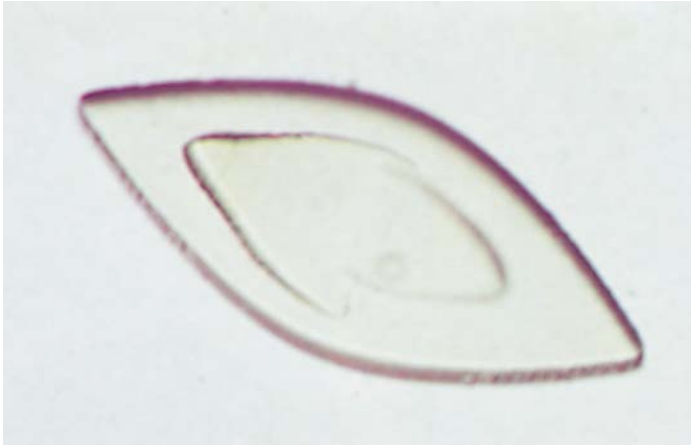

Figure 29.29 Large uric acid plate, laminated (×160).

rosettes, and irregular plates (Figs. 29.28 and 29.29). Most are colored, typically yellow or reddish brown. Rarely, they are colorless and hexagonal, resembling cystine (Fig. 29.30). Needle- and pencil-like forms have also been described (Baroni et al., 2018). Unlike cystine, they show birefringence with polarized light (Fig. 29.31).

Large numbers of uric acid crystals and urates may reflect increased nucleoprotein turnover, especially during chemotherapy of leukemia or lymphoma. Increased quantities may be seen with Lesch-Nyhan syndrome and may provide circumstantial evidence of the nature of small stones lodged in the ureters, especially when radiolucent and found in conjunction with raised serum uric acid levels. They may also herald the urate nephropathy of gout.

Calcium Oxalates. Dihydrates may appear at pH 6 or in neutral urine. Their classic form is that of a small, colorless octahedron that resembles an envelope (Fig. 29.32). Dumbbell shapes and ovoid forms

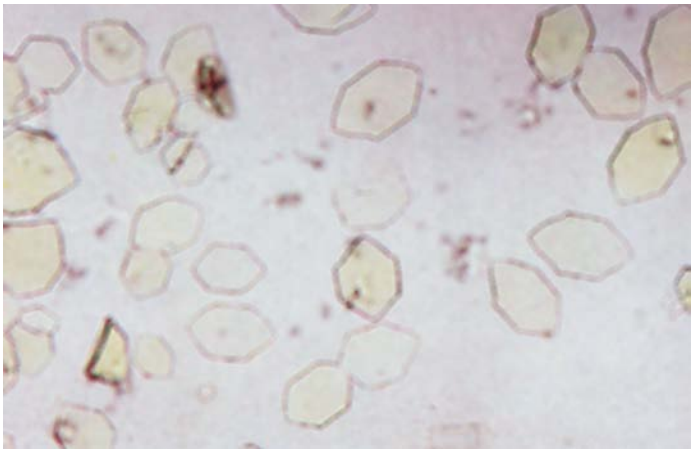

Figure 29.30 Hexagonal uric acid crystals. Bright field (×50).

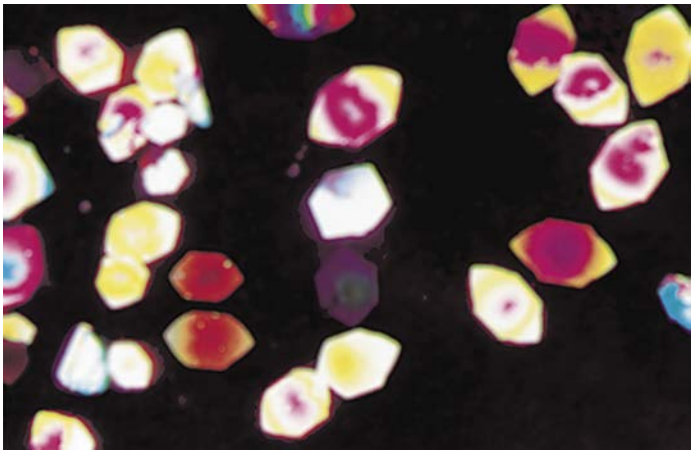

Figure 29.31 Hexagonal uric acid crystals. Polarized (×50).

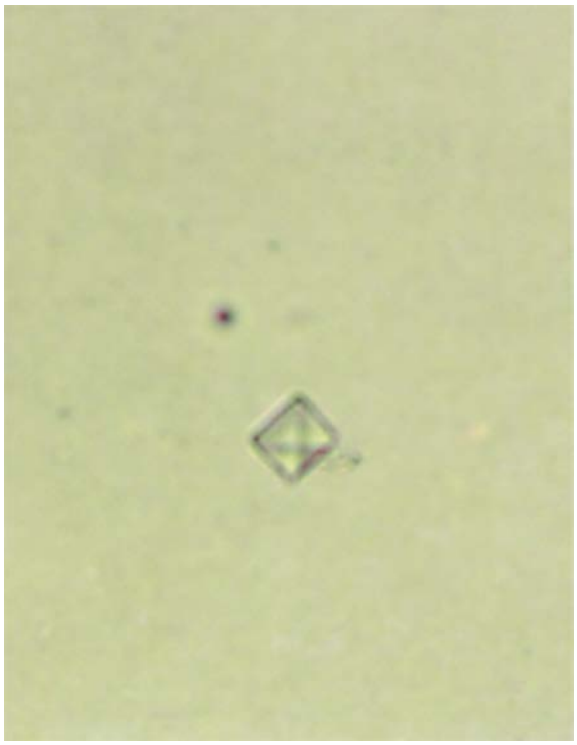

Figure 29.32 Calcium oxalate crystals (×200).

Figure 29.33 Calcium oxalate. Unusual oval form (×200).

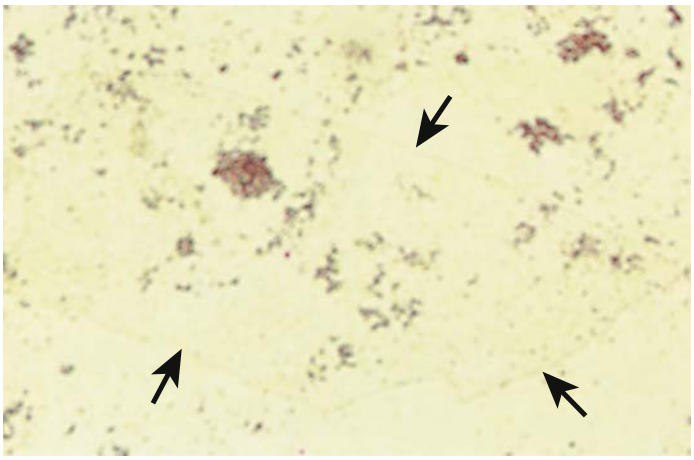

Figure 29.34 Calcium phosphate (large clear plate). Almost amorphous phosphates (×64).

may occur (Fig. 29.33). Longer forms occur in calcium oxalate monohydrate. Oxalate crystals are insoluble in acetic acid.

Oxalate crystals in large numbers may reflect severe chronic renal disease or ethylene glycol or methoxyflurane toxicity. Oxaluria has come into prominence as a reflection of the increased absorption of oxalates from food following small bowel disease and resection, notably for Crohn disease. Oxaluria may also be present in genetically susceptible persons following large doses of ascorbic acid.

Crystals Found in Normal Alkaline Urine

Amorphous Phosphates (Calcium and Magnesium). Similar to amorphous urates, amorphous phosphates have a granular appearance microscopically. Unlike the former, they tend to be colorless and will produce a fine or lacy white precipitate macroscopically. Clumps or masses can often be seen by light microscopy (Fig. 29.34). Large amounts of this material may precipitate out upon prolonged standing at room temperature or in a refrigerator.

Calcium and magnesium monohydrogen phosphates are the least soluble in alkaline urine, although the dihydrogen phosphates may be soluble at a similar pH. Phosphates, in general, will dissolve in acids such as dilute hydrochloric and nitric acids and vary in solubility in acetic acid. They do not dissolve in dilute sodium hydroxide solutions or alcohol.

Crystalline Phosphates. Triple phosphate (ammonium magnesium phosphate) crystals are one of the most easily identified urine crystals,

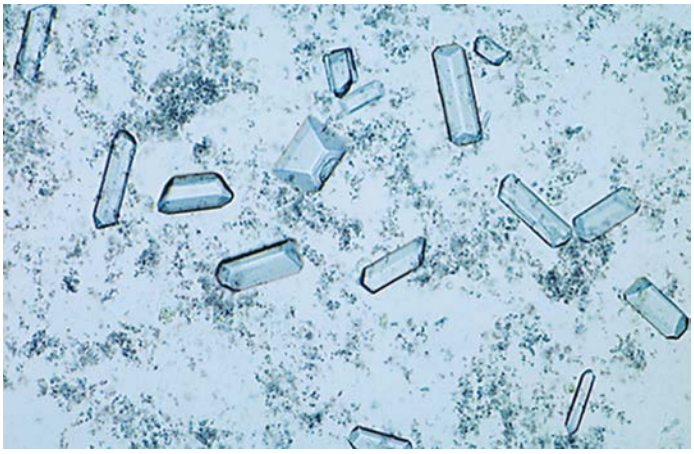

Figure 29.35 Triple phosphate (×50).

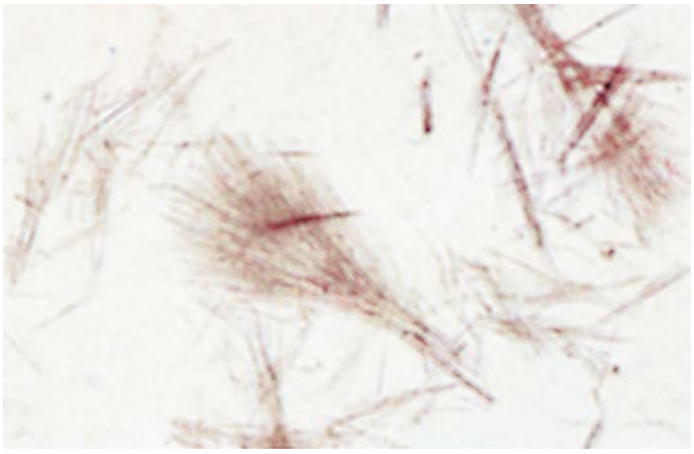

Figure 29.36 Calcium phosphate (fine sheaves) (×160).

although they commonly show variation in size. They are colorless, three- to six-sided prisms with oblique ends referred to as coffin lids (Fig. 29.35). They may form colorless sheets, flakes, or fine sheaves (Fig. 29.36). Magnesium phosphate forms colorless rhomboids, some with notched ends or corners. These are seldom recognized. Dicalcium hydrogen phosphate crystals, on the other hand, may be seen in neutral or slightly acidic urine, and are long, three-sided prisms with pointed ends. They may form clusters or rosettes. Overall, phosphate crystals have little if any clinical significance. They are often seen in infected urine of alkaline pH.

Calcium Carbonate. These uncommon crystals are small and colorless, with dumbbell or spherical shapes. They may form pairs, fours, or clumps. They are distinguished from other crystals/amorphous material by their production of carbon dioxide in the presence of acetic acid.

Ammonium Biurate. Similar to typical urate crystals, ammonium biurate crystals have a yellow-brown color and appear as spheres with radial or concentric striations and irregular projections or thorns (Fig. 29.37). Referred to as *thorn apples*, they may also be seen in neutral and occasionally in slightly acidic urine. They dissolve with heat at 60°C and with acetic acid, reappearing as typical uric acid crystals after about 20 minutes.

Crystals Found in Abnormal Urine

Cystine. Cystine crystals are colorless, refractile, hexagonal plates (Fig. 29.38), which appear in acid urine. They are soluble in water at pH less than 2 or greater than 8, and they may be confused with hexagonal forms of uric acid (see Fig. 29.30). Whereas uric acid crystals polarize (see Fig. 29.31), thin cystine crystals do not, although thick laminated forms may polarize. Furthermore, both cystine and uric acid are soluble in ammonia water, but cystine will also dissolve in dilute hydrochloric acid and uric acid will not.

Cystine crystals are among the most important crystals identified in urine sediment. They occur in patients with cystinuria and may be associated with cystine calculi (Sahota et al., 2019; Saravakos et al., 2014; Thomas, Wong et al., 2014). Confirmatory testing consists of the cyanide-nitroprusside reaction (see the Cystinuria section later in the chapter).

Tyrosine. In acidic urine, tyrosine forms fine silky needles that may be arranged in sheaves or clumps, especially after refrigeration. These may

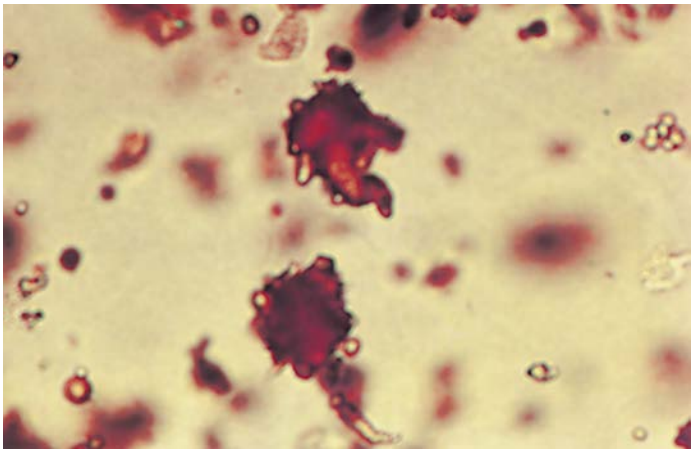

Figure 29.37 Ammonium biurate (×160).

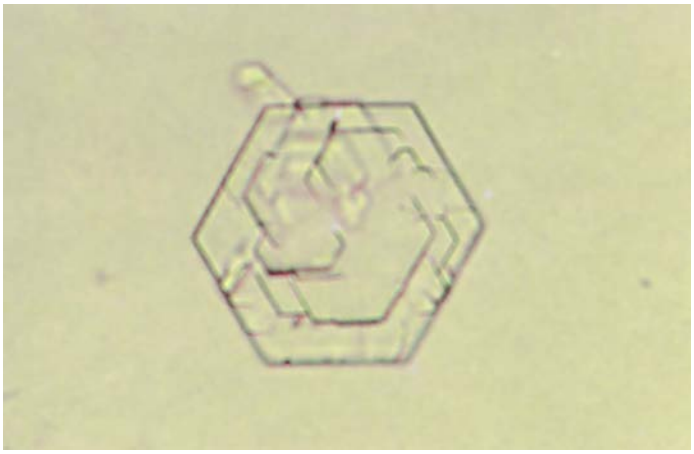

Figure 29.38 Cystine (hexagonal, laminated) (×200).

Figure 29.39 Tyrosine crystals (×160).

be colorless or yellow, appearing black as the microscope is focused (Fig. 29.39). They are soluble in alkali (ammonia and potassium hydroxide) and in dilute hydrochloric acid; they are not soluble in alcohol or ether.

These crystals, which are uncommon, are less soluble than leucine, and therefore are more often precipitated in urine (see the Tyrosinuria section later in the chapter). Tyrosine and leucine crystals are occasionally seen in the urine of patients with severe liver disease (see the Urinary Screening for Inherited Metabolic Diseases section later in the chapter).

Leucine. These crystals are also rare, occurring as yellow, oily-appearing spheres with radial and concentric striations (Fig. 29.40). They are soluble in both acids and alkalis. Leucine and tyrosine crystals may occur together; leucine may be precipitated with tyrosine crystals if alcohol is added to the urine.

Sulfonamide (Sulfadiazine) Crystals. These crystals may be seen in urine of acid pH and may take on various morphologies, depending on the

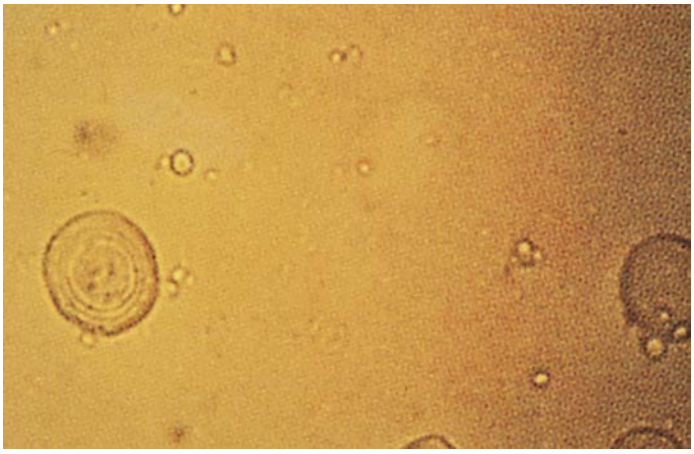

Figure 29.40 Leucine crystals (×160).

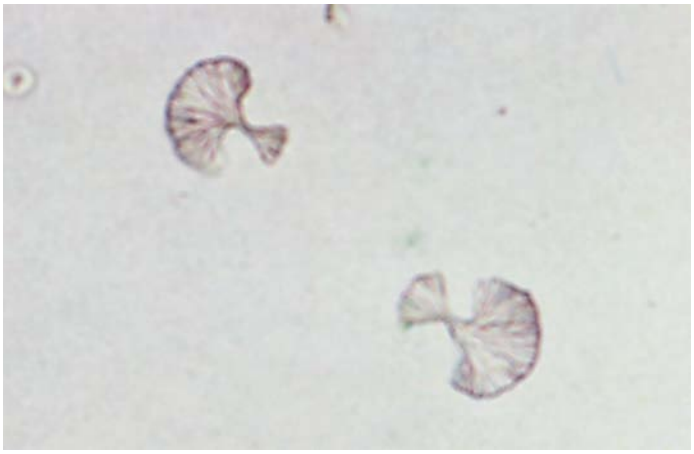

Figure 29.41 Sulfadiazine (×160).

form of drug involved. They may be seen as fan-shaped yellow-brown sheaves of wheat with central bindings, striated sheaves with eccentric bindings (Fig. 29.41), rosettes, arrowheads, petals, needles, and round forms with radial striations. They are occasionally colorless. Confirmatory testing is by the diazo reaction. High-performance liquid chromatographic and colorimetric methods have also been described (Mount et al., 1996; Simo-Alfonso et al., 1995).

With the advent of soluble sulfonamides, sulfa crystals are not as frequently found in urine, especially when urine is examined at 37°C. Before this development, these crystals could be seen in the urine of patients on sulfonamide therapy who were inadequately hydrated. This could result in renal tubular damage if crystal formation occurred within the nephron. Currently, sulfamethoxazole (Bactrim, Septra) is seen with some regularity.

Ampicillin (High Dosage). Ampicillin may crystallize in the urine under conditions of high dosage. These crystals appear in urine of acid pH as long, fine, colorless , needle-like structures (Fig. 29.42). They may form coarse sheaves after refrigeration.

Radiographic Media (Meglumine Diatrizoate). Urinary crystals form after radiographic examinations using diatrizoate dyes. They may be found in urine of acid pH shortly after intravenous radiographic studies (particularly if the patient has not been well hydrated), appearing as flat, clear, colorless, notched rhombic plates, or longer, slender rectangles. They are easily polarized, showing interference colors (Figs. 29.43 and 29.44). They may also be seen after retrograde cystograms as long, colorless needles, forming clusters after refrigeration. The presence of radiographic crystals should correlate with a high specific gravity (>1.040).

Other Drugs. One must always remember to check the patient's drug therapy when unusual crystals are found in the urine. Several drugs have been reported to cause crystalluria when administered in high-dosage schedules or following overdose. Examples include high-dosage 6-mercaptopurine therapy, primidone overdosage, and dihydroxyadenine from massive blood transfusion.

Abnormal Cells and Other Formed Elements

Tumor Cells. Malignant tumor cells exfoliated from the renal pelvis, ureter, bladder wall, and urethra are best identified using cytologic

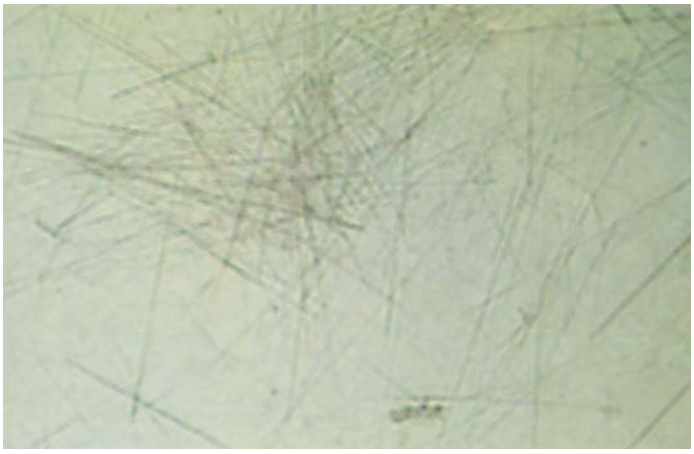

Figure 29.42 Ampicillin (×160).

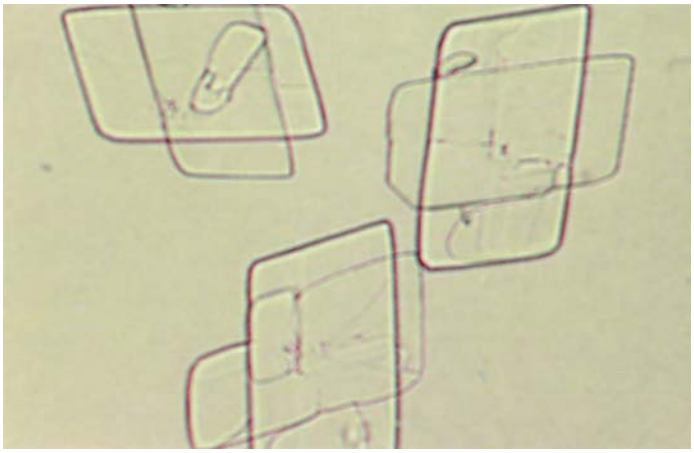

Figure 29.43 Renografin (meglumine diatrizoate). Bright field (×160).

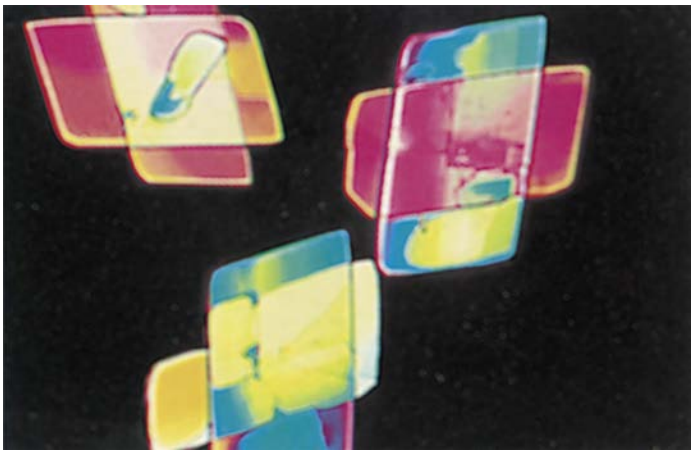

Figure 29.44 Renografin (meglumine diatrizoate). Polarized (×160).

Figure 29.45 Bacteria and leukocytes (×600).

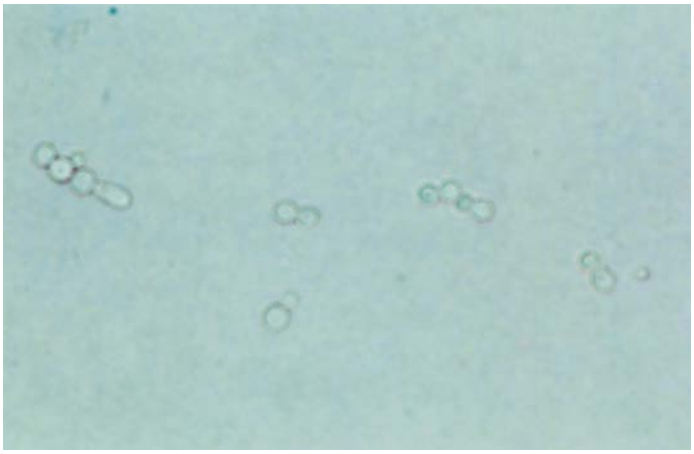

Figure 29.46 *Candida.* Budding yeasts (×200).

techniques. Myeloma cells have also been noted in urine, both with and without apparent renal involvement. For a comprehensive discussion of disease types and cytologic morphologies, the reader is directed to standard urinary cytology references (Ali et al., 2009; Brimo et al., 2009; Koss & Hoda, 2012).

Viral Inclusion Cells. Epithelial cells containing inclusion bodies may be found in the urine sediment in various viral infections involving the urinary tract. Syncytial giant cells containing eosinophilic, intranuclear inclusions are seen in patients during herpetic infections. In children or immunosuppressed patients with cytomegalovirus infection, affected cells are enlarged and contain basophilic intranuclear inclusions and/or cytoplasmic bodies. Polyomavirus (e.g., BK virus)-infected cells contain dense, basophilic, homogeneous intranuclear inclusions that often completely fill the nucleus. Cytologic techniques are far more sensitive in detecting all of the aforementioned viral cytopathic effects. Renal epithelial cells with intranuclear inclusions can be identified in unstained urine sediment specimens by bright field or phase-contrast microscopy in patients infected with cytomegalovirus or polyomavirus (Poloni et al., 2016; Poloni et al., Pinto et al., 2013; Singh et al., 2006). These cells have been termed *decoy cells* because of their resemblance to malignant cells. Clinically, decoy cells are of greatest significance in immunocompromised patients, especially renal transplant recipients, in whom they have been used as a marker for polyomavirus BK-associated nephropathy (BKVAN) (D'Alessandro et al., 2019; Yamada et al., 2018).

Platelets. These have been demonstrated in urine. Up to 30,000/μL have been demonstrated by phase-contrast microscopy and confirmed by electron microscopy in the urine of patients with hemolytic-uremic syndrome.

Bacteria. Finding bacteria in urine may or may not be significant depending on the method of urine collection and how soon after collection of the specimen the examination takes place. If bacteria are identified with Gram stain in an uncentrifuged urine specimen under an oil-immersion lens, this suggests that more than 100,000 organisms/mL are present (i.e., significant bacteriuria). Most commonly, rod-shaped bacteria are seen because the enteric organisms are the causative agents in the majority of UTIs (Fig. 29.45). Leukocytes will usually be seen in the sediment as well.

Acid-fast bacilli may be seen in urine sediment, but because the urethral flora may contain nonpathogenic acid-fast organisms, the presence of tuberculosis in urine must be substantiated by culture and/or polymerase chain reaction methods.

Fungi. Yeasts (most commonly, *Candida* species) may be causative agents in UTIs (e.g., in diabetes mellitus), but yeasts are also common contaminants from the skin, the female genital tract, and the air. On microscopic examination, they may be confused with erythrocytes; the presence of budding helps to identify them as yeast cells (Fig. 29.46). Pseudohyphae of *Candida* are occasionally found (Fig. 29.47).

Parasites. Parasites and parasitic ova may be seen in urine sediments as a result of fecal or vaginal contamination. When noted, repeat examination

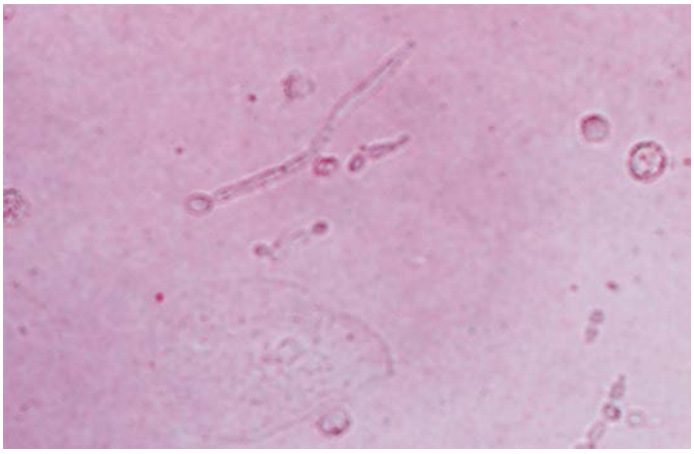

Figure 29.47 *Candida.* Pseudohyphae (×160).

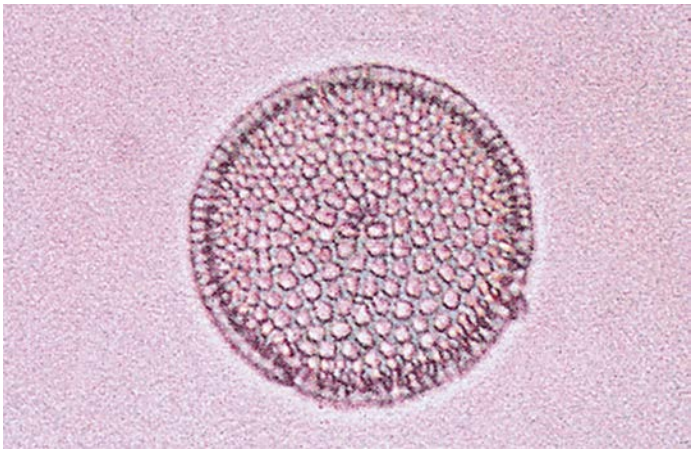

Figure 29.49 Pollen grain (×160).

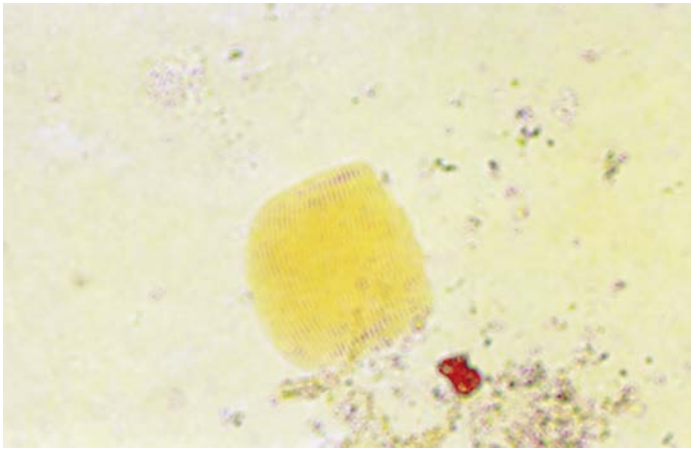

Figure 29.48 Muscle fiber (×200).

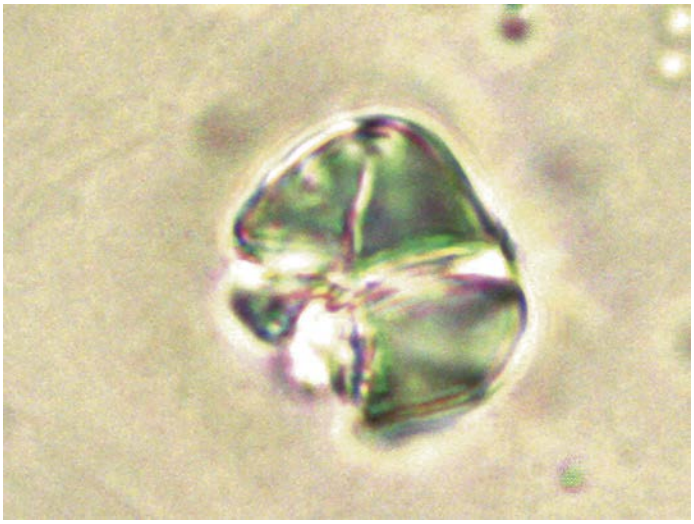

Figure 29.50 Starch granule (×160).

should be performed on a fresh, clean-voided urine specimen. Although *Trichomonas vaginalis* may be present in urine as a result of vaginal contamination, urethral or bladder infection can occur. When suspected, the protozoa should be searched for immediately in a wet preparation of the sediment. Motility of the organism is helpful in making the appropriate identification. In patients with schistosomiasis due to *Schistosoma haematobium*, typical ova are shed directly into the urine accompanied by erythrocytes from the urinary bladder. Amebas are rarely seen in the urine; they may reach the bladder from lymphatics or more likely from fecal contamination of the urethra. The pathogenic *Entamoeba histolytica* is usually accompanied by erythrocytes and leukocytes.

Contaminants and Artifacts

Partially digested muscle fibers or vegetable cells may be found when fecal contamination occurs (Fig. 29.48). Spermatozoa are occasionally present, and pollen grains contaminate specimens seasonally (Fig. 29.49). Fibers from many different sources may be seen, including cotton, hair, wood fibers from applicator sticks, and synthetic fibers from disposable diapers. Unlike casts, these fibers polarize brightly.

Starch granules from surgical gloves are the most common contaminants of urine and other body fluids. Microscopically, they appear bright and faintly striated with an irregular outline and a central depression (Fig. 29.50). With crossed polarizing filters, starch granules exhibit a typical Maltese cross pattern, and because of their large size (several times larger than an erythrocyte), they are not likely to be confused with cholesterol droplets. Oil droplets from catheter lubricants may be confused with cells, especially RBCs. Lipid material from vaginal creams also forms droplets in urine and may form large amorphous aggregates.

METHODS FOR URINALYSIS

BASIC (ROUTINE) URINALYSIS PROCEDURE

1. Pour 10 to 15 mL of a well-mixed urine specimen into a graduated disposable centrifuge tube. Perform physical examination and reagent strip chemical evaluations. Centrifuge at 450 g for 5 minutes.
2. Carefully remove and save the supernatant. The final volume used to resuspend the sediment may vary with the standardized system used but should remain constant within any given laboratory. Use a disposable pipet, specialized tube, or pipet system to concentrate the sediment.
3. Gently resuspend the sediment in the remaining supernatant and add one drop of supravital stain if desired. Using an appropriate pipet, load/charge the examination chamber of a standardized slide. Allow the urine to settle for 30 to 60 seconds.
4. Examine with low- and high-power objectives. Subdued light or phase-contrast illumination will be required to detect sediment entities with a low refractive index. The fine focus should be varied continuously while scanning. Systematically progress around the entire examination chamber, being careful to examine along the edges for casts.
5. Count the number of casts in at least 10 low-power fields (lpf), average, and report the number of casts per lpf. A reasonable range may be used in reporting (e.g., 0–2, 2–5, 5–10). Use high power to identify casts by type. Casts will not be missed if phase-contrast microscopy is used (see Fig. 29.4).
6. Identify and count erythrocytes, leukocytes, and renal epithelial cells using the high-power objective. Count at least 10 hpf, average, and report as cells/hpf. A reasonable range may be used for reporting.
7. Comment on the following:
   a. Squamous and transitional cells if present in large numbers or as fragments (transitional cells).
   b. Bacteria, yeast, and microorganisms. Bacteriuria detectable on low power should be reported as at least 2+.
   c. Crystals (quantitated under low power). The presence of abnormal crystals should be confirmed chemically and correlated with the patient history.
   d. Large amounts of mucus.
8. The authors recommend confirming the following results with cytopathologic examination or specific chemical tests (crystals):

a. More than two renal epithelial cells/hpf
b. Pathologic casts
c. Atypical mononuclear cells, particularly urothelial cells
d. Tissue fragments
e. Pathologic crystals

Review the entire report, including physical, chemical, and microscopic data, and correlate with available clinical information. Discrepancies should be resolved before the report is released. Normal values for the procedure include the following: 0 to 10 RBCs/hpf, 0 to 10 WBCs/hpf, and 0 to 2 hyaline casts/lpf. Values will vary, depending on the standardized system used.

Routine urinalysis is a helpful diagnostic tool in the workup and follow-up of various urinary system disorders. Table 29.11 summarizes the macroscopic, reagent strip, and microscopic findings typical for the most commonly encountered entities.

AUTOMATED URINALYSIS

The automation of laboratory assays has rapidly progressed during the recent past in order to standardize procedures, streamline efficiency, and minimize cost and turnaround time. Automated instruments can also be interfaced with laboratory information systems, facilitating reporting and result retrieval as well as quality control and quality assurance. The automation of urinalysis was heralded in the early 1980s by the development of the Yellow IRIS, an automated urine microscopy analyzer (Oyaert & Delanghe, 2019). Since that time, several new generations of urine microscopy analyzers have been released as well as partially or completely automated instruments that read urine reagent strips and measure the physical properties of urine specimens. Many of the automated urine chemistry and urine microscopy instruments are available separately or combined into completely automated urinalysis systems. Automated urinalysis technology is dynamic, with new instruments and improved versions of current instruments constantly developed to fulfill the market demand for improved accuracy and efficiency (Ahmed et al., 2016). The most widely used automated urinalysis instruments available at the time of this writing are discussed in this section.

Several instruments are available to automate the macroscopic evaluation and chemical component of the routine urinalysis. These instruments include compact, portable, semi-automated and fully automated dipstick readers designed for point-of-care (POC) testing in the emergency department, intensive care wards, physician offices, and clinics, as well as larger, fully automated urine chemistry reagent strip analyzers with a higher throughput designed for central clinical laboratories. These instruments improve the accuracy and reproducibility of reagent strip analysis by standardizing the timing of the procedure and eliminating the subjective error inherent in visual interpretation of the color change. Most also flag abnormal findings, store previous results, print results, and include an interface to an electronic health record system that eliminates the error associated with manual result transcription.

Automated reagent strip analyzers were first introduced in 1972, with the Aution Analyzer AU-6 (Arkray, Kyoto, Japan), and considerably advanced since that time with the incorporation of computerization and other technologies. However, all automated reagent strip analyzers utilize the principle of reflectance photometry to measure the color intensity of the reaction pads of the dipstick. An object illuminated by an incident light source absorbs some of the light and scatters the remaining light (termed *diffuse reflectance*) in all directions. In a reagent strip reader, incident light generated by a monochromatic light source (usually a light-emitting diode [LED]) or polychromatic light source and filter is directed at a specific angle to the reaction pad for each analyte. The chromophore in the reaction pad absorbs a quantity of light proportional to the intensity of the specific color of the pad. The nonabsorbed, reflected light at a specific defined wavelength for the reaction pad is directed to a photodiode, converted into an analog electrical signal, and changed into digital form by an analog-to-digital (ADC) converter. A microprocessor converts the signal to a reflectance value and compares it to calibration standards of known concentration to determine the final concentration of the urine analyte.

Nearly all automated reagent strip readers provide measurements of urine leukocyte, nitrite, protein, blood, glucose, ketone, bilirubin, urobilinogen, pH, specific gravity, and color. However, the analytic capability can vary with different instruments, reagent strips, and testing markets. Measurements of microalbumin, creatinine, PCR, ACR, and/or urine human chorionic gonadotropin (hCG) may also be available from some manufacturers.

Semi-automated urine chemistry analyzers read reagent strips but require the operator to measure and enter the color and clarity of the specimen. They also require the operator to activate the instrument, manually dip and blot the reagent strip, and place the strip on a platform in the strip reader. The instrument moves the strip under a detector, reads the reflectance of each reaction pad at the proper time, and displays the results for verification, printing, or electronic reporting. Patient information is entered by the operator or obtained by a barcode reader integrated into the system. Many include memory to store patient and quality control results, an integrated printer or printer interface, and an interface for a laboratory information system. Many semi-automated urine chemistry analyzers are available from manufacturers in the United States, Europe, and Asia. The instruments are calibrated only for specific reagent strips, usually from the instrument manufacturer, and include quality control reagents. Information on several widely used semi-automated readers follows.

Semi-automated urine chemistry analyzers available at this writing include the Clinitek Status+ Analyzer (Siemens Healthcare Diagnostics, Inc., Tarrytown, NY), Clinitek Advantus UC-1000 Semi-Automated Urine Chemistry Analyser (Sysmex, Kobe, Japan), Urisys 1100 Urine Analyzer (Roche Diagnostics, Indianapolis, IN), Cobas u411 Urinalysis Test System (Roche Diagnostics, Indianapolis, IN), Accustrip URS Urinalysis Reader (Jant Pharmacal Corp., Encino, CA), Uri-Trak 120 Urine Analyzer (Stanbio, Boerne, TX), the Aution 11 AE-4022 Semi-Automated Urine Chemistry Analyzer (Arkray, Edina, MN), the DocUReader 2 Pro (77 Elektronika Kft., Budapest, Hungary), the Mission U120 Urine Analyzer (Acon Laboratories, San Diego, CA), and the Uryxxon 500/Uryxxon Relax Urine Strip Readers (Macherey-Nagel GmbH & Co. KG, Düren, Germany).

The Clinitek Status+ Analyzer is the latest generation of a widely used series of semi-automated reagent strip analyzers. In addition to urine reagent strips, it is also designed to read immunoassay cartridges. It is a CLIA-waived, small, portable, bench-top instrument powered by batteries or by an electrical outlet for bench top use. The optical system consists of a series of six LEDs, each at a different wavelength, that illuminates the entire strip or cassette length. Reflected light from the strip passes through a lens focused on a charge-coupled device (CCD), which converts the light intensity into an electronic signal for processing by an A/D converter and decoding by a microprocessor. The decoded values are compared to lookup tables containing specific decode ranges for each reagent and their respective clinical values. Results are reported to the operator via touch screen display, onboard printer, and/or computer interface. The instrument has internal automatic calibration; additional quality control is provided by automatic checks for proper strip identification, humidity exposure, and common sample interferences. Patient and operator information can be entered manually together with the color and clarity of the specimen. Using Multistix 10SG urine test strip, Multistik Pro or other compatible test strips, the instrument can measure albumin, bilirubin, occult blood, creatinine, glucose, ketone, leukocytes, nitrite, pH, protein, PCR, ACR, specific gravity, and urobilinogen. Urine hCG can also be measured using an hCG immunoassay cassette.

The Urisys 1100 urine analyzer is a compact, bench-top, CLIA-waived, semi-automated reflectance photometer designed to read Chemstrip 10MD*, Chemstrip 7, and Chemstrip 5 OB urine test strips for the determination of specific gravity, pH, leukocytes, nitrite, protein, glucose, ketones, urobilinogen, bilirubin, and blood. Each test pad is read photometrically in less than 70 seconds. The Urisys 1100 has a throughput of up to 100 samples/hour, corrects for specific gravity in highly alkaline samples, and compensates for urine color. Data entry is through a barcode reader or keyboard, and there is an integrated printer and advanced data connectivity for transmission of results. In conjunction with an associated POC data management system, advanced operator access and password protection is provided to enhance the security of POC urinalysis.

The Cobas u 411 urinalysis test system is a bench-top semi-automated reflectance photometer for small and medium-sized laboratories. It is designed to read the commonly used Chemstrip 10 UA reagent test strip for the measurement of bilirubin, blood, glucose, ketones, leukocytes, nitrite, pH, protein, specific gravity, and urobilinogen. The analyzer has a high throughput of up to 600 test strips/hour with continuous strip loading. The optical unit contains 4 LEDs that emit light at wavelengths of 470 nm, 555 nm, and 620 nm. The reflected light is detected by 11 wide-range photosensors using automatic strip detection by two sensors. The analyzer compensates for urine color and permits multiple user-defined microscopic parameters for flagging abnormal results and further microscopic follow-up testing. Calibration verification is performed using a calibration strip included with the analyzer. Sample identification is by manual entry, barcode reader, or download from the host computer. There is an integrated thermal printer and serial interfaces to a barcode reader, sediment terminal and/or personal computer/LIS. There is also a USB port to allow data archiving and easy updating of instrument software via memory stick.

TABLE 29.11

Various Urinary System Diseases and Corresponding Urinalysis Abnormalities

Diseases	Macroscopic Urinalysis	Microscopic Urinalysis
Acute glomerulonephritis	Gross hematuria "Smoky" turbidity Proteinuria	Erythrocyte and blood casts Epithelial casts Hyaline and granular casts Waxy casts Neutrophils Erythrocytes
Chronic glomerulonephritis	Hematuria Proteinuria	Granular and waxy casts Occasional blood casts Erythrocytes Leukocytes Epithelial casts Lipid droplets
Acute pyelonephritis	Turbid Occasional odor Occasional proteinuria	Numerous neutrophils (many in clumps) Few lymphocytes and histiocytes Leukocyte casts Epithelial casts Renal epithelial cells Erythrocytes Granular and waxy casts Bacteria
Chronic pyelonephritis	Occasional proteinuria	Leukocytes Broad waxy casts Granular and epithelial casts Occasional leukocyte casts Bacteria Erythrocytes
Nephrotic syndrome	Proteinuria Fat droplets	Fatty and waxy casts Cellular and granular casts Oval fat bodies and/or vacuolated renal epithelial cells occurring singly or as cellular clusters
Acute tubular necrosis	Hematuria Occasional proteinuria	Necrotic or degenerated renal epithelial cells Neutrophils and erythrocytes Granular and epithelial casts Waxy casts Broad casts Epithelial tissue fragments
Cystitis	Hematuria	Numerous leukocytes Erythrocytes Transitional epithelial cells occurring singly or as fragments Histiocytes and giant cells Bacteria Absence of casts
Dysuria-pyuria syndrome	Slightly turbid	Numerous leukocytes, bacteria Erythrocytes No casts
Acute renal allograft rejection (lower nephrosis)	Hematuria Occasional proteinuria	Renal epithelial cells Lymphocytes and plasma cells Neutrophils Renal epithelial casts Renal epithelial fragments Granular, bloody, and waxy casts
Urinary tract neoplasia	Hematuria	Atypical mononuclear cells with enlarged, irregular hyperchromatic nuclei and sometimes containing prominent nucleoli that occur singly or as tissue fragments Neutrophils Erythrocytes Transitional epithelial cells
Viral infection	Hematuria Occasional proteinuria	Enlarged mononuclear cells and/or multinucleated cells with prominent intranuclear and/or cytoplasmic inclusions Neutrophils Lymphocytes and plasma cells Erythrocytes

The Uryxxon Relax and Urilyzer (Analyticon Biotechnologies AG, Lichtenfels, Germany) are other urine chemistry analyzers that measure blood, urobilinogen, bilirubin, protein, nitrite, ketones, glucose, pH, specific gravity, and leukocytes. The Aution 11 (Menarini Diagnostics, Florence, Italy) also measures albumin and creatinine.

The performance of semi-automated urine chemistry analyzers with manual urinalysis, similar semi-automated instruments, and fully automated urine chemistry analyzers in laboratory and clinical settings has been evaluated in a few published studies. In one study of analytic performance and user friendliness, Schot and collaborators compared the analytic performance of six semi-automated analyzers (Clinitek Status, Uryxxon Relax, Urisys 1100, Aution 11, Aution Micro, and Urilyzer) with the Urisys 2400 automated urine analyzer (Schot et al., 2015). All of the semi-automated analyzers showed good user-friendliness and analytic performance, with five of the six showing perfect agreement with the laboratory standard for the nitrite test. The sensitivity for leukocytes and erythrocytes was lower than the automated findings, but the specificity was high.

The most recent technological innovation in CLIA-waived urinalysis assays is the smartphone-based dipstick reader (Barnes et al., 2018; Karlsen & Dong, 2017; Ra et al., 2018). Smartphones are widely used in medicine for communication and data storage and manipulation, but urinalysis is one of the first diagnostic applications. The three smartphone-based urinalysis systems receiving U.S. Food and Drug Administration (FDA) clearance for at-home testing in 2018 and 2019 are technically similar in principle. The operator immerses a dipstick into a urine specimen, waits for a specified period, blots the specimen, places it on a special plastic plate with colored spots, and photographs the plate and dipstick with a complementary smartphone app. The software program compensates for lighting conditions and compares each reaction pad to standards to produce an analytic result for transmission to a health care provider. These systems include the Dip.io (Healthy.io, Tel Aviv, Israel), the Inui In-home Urine Analysis (Inui Health, Sunnyvale, VA), and the Scanostics UTI Check Application Test SystemTestCard (Teco Diagnostics, Anaheim, CA). Other systems, including the TestCard (TestCard Diagnostics, London, UK) are not yet available in the United States.

Fully automated urine chemistry analyzers are usually part of an integrated system in a high-volume laboratory that also performs urine sediment analysis. In these instruments, multiple barcoded tubes of urine are loaded into a rack or carousel for sample identification by barcode reading and automatic pipetting of a precisely measured urine aliquot directly onto a reagent strip. The reagent strip is advanced to a reflectance photometer that measures the color change of each reaction pad at the proper time and at the appropriate wavelength. Most instruments use the manufacturer's standard reagent strips to determine leukocytes, ketones, protein, glucose, nitrite, blood, urobilinogen, pH, bilirubin, creatinine, and protein. The instruments also use measurements of light transmission or light scatter to determine urine clarity and refractive index to measure specific gravity. Urine color is determined by multiple wavelength spectrophotometry or by reflectance photometry, using a pad on the reagent strip. Abnormal results are flagged to identify specimens requiring microscopic sediment examination or further testing. An interface with the laboratory information system permits transmission of patient results and quality control measurements for storage and further analysis. The reagent strip is automatically disposed of when the analysis is complete. A microprocessor collates the results for verification and transmission to the laboratory information system. Fully automated chemistry analyzers that are part of an integrated system may apply rules to identify specimens requiring urine microscopy and pass the specimen to the microscopy analyzer for further evaluation.

Current models of fully automated urine chemistry analyzers include the Clinitek Novus Urine Chemistry Analyzer (Siemens Healthcare Diagnostics, Inc., Tarrytown, NY), iChemVelocity (Beckman Coulter Inc., Brea, CA), UC-3500 Fully Automated Urine Chemistry Analyser (Sysmex Corporation, Kobe, Japan), Cobas u 601 urine analyzer (Roche, Indianapolis, IN), LabUMed 2 (77 Elektronika Kft., Budapest, Hungary), the AUTION MAX AX-4030 (Arkray, Edina, MN), the Mission Expert U500 Ultra Urine Analyzer (Acon Laboratories, San Diego, CA), and the NUA-1500 Fully Automated Urine Biochemistry Analyzer (NeoMedica Bioscience Technology, Nis, Serbia).

The Clinitek Novus Automated Urine Chemistry Analyzer uses conventional reaction strips to provide a qualitative measure of urine nitrite and semi-quantitative measurements of bilirubin, blood, glucose, ketone, leukocytes, pH, protein, color, and urobilinogen. However, instead of loose reaction strips placed in a storage well, the analyzer uses cassettes that contain reagent test pads organized in strips on test cards. The reaction pads are illuminated by two pairs of LED lights and a complementary metal oxide semiconductor (CMOS) digital imager is used to measure reflected light. Since the refractive index and specific gravity of urine are measures of the amount of solute, the refractive index of the specimen is measured by a fiber optic refractive sensor system and converted to a quantitative specific gravity result. Urine clarity is determined by projecting light into the sample through a series of optical fibers and measuring the transmitted and scattered light. The Clinitek Novus system can batch test up to 20 sample racks of 10 samples each using barcoded tubes and also has STAT testing capabilities. The calibration process uses baseline adjustments for each test pad, clarity, and specific gravity. Special features to improve accuracy include an algorithm to decrease the number of false-positive bilirubin results and compensation for nonspecific color changes of the reaction pads from colored urine specimens.

The iChemVELOCITY is a fully automated urine chemistry analyzer that reads test strips with a dual wavelength reflectance system. The plastic strips contain nine pads impregnated with chemicals specific for the determination of glucose, protein, bilirubin, urobilinogen, pH, blood, ketones, nitrite, leukocyte esterase, and ascorbic acid. A color compensation pad is included on the strip to compensate for the natural color of urine and its effect on the color of the reaction pads. Test strips are placed onto a strip conveyor system by a mechanical extractor. A sample probe mixes the sample, aspirates an aliquot of urine and dispenses it onto each reagent pad. At defined wavelengths, the iChemVELOCITY analyzes the color changes and the intensity of reflected light from the reaction pads. These measurements are used to calculate clinically meaningful results. Specific gravity is determined with an electronic refractometer assembly. Color is measured by transmitted light and clarity is measured by scattered light. The instrument has a throughput of up to 210 samples per hour.

The Cobas u 601 is a modular analyzer that performs fully automated urine strip testing with a throughput of up to 240 samples/hour. The instrument consists of a computer with touchscreen display, rack transport system, liquid handling system, test strip cassette compartment, automated test strip processing area, test strip reflectance photometer, and physical measurement cell (PMC) for clarity and specific gravity. Patient identification is entered either manually using the touch screen or scanned with a barcode reader. Urine sample tubes are manually placed into a rack, which is loaded into the analyzer. The rack is automatically moved within the analyzer fluid handling station using a rack conveyor. During a run, the urine sample is aspirated into the fluid system and pipetted onto test pads of a test strip. The test strips are stored in a cassette that holds 400 test strips. Each cassette is identified by a unique radiofrequency identification (RFID) tag that also contains information on expiration date and lot number. The instrument uses reagent strips with an iodate-impregnated mesh layer that provides resistance to ascorbic acid and ensures uniform color development by ensuring uniform penetration of the urine into the test area. This technology helps to prevent false-negative results for glucose and hemoglobin and permits the detection of low concentrations of glucose and erythrocytes/hemoglobin (5–10 erythrocytes/mL) in the presence of high levels of ascorbic acid. A color compensation pad on the reagent strips reduces false readings in the presence of highly colored urine specimens, and strip analysis is facilitated with a consistent reading time of 60 seconds for all parameters. A reference plate is measured along with each test strip measurement, and the assay reflectance measurements are normalized to the reference plate when calculating the results.

The AUTION MAX AX-4030 urinalysis system provides comprehensive measurements of urine color/tone turbidity, abnormal coloration, specific gravity, glucose, protein, bilirubin, pH, blood, urobilinogen, ketones, nitrite, and leukocytes. Creatinine can also be measured with the use of AUTION STICKS 10PA. The instrument incorporates an internal turbidity/color measurement module that uses transmitted and scattered light. Turbidity is determined mathematically from scattered light when the urine specimen in a cylindrical cell is illuminated with light at a wavelength of 635 nm. The turbidity measurement is reported as clear, turbid, or dense turbid. Urine color (hue and tone) is evaluated by illuminating the specimen with red (635 nm), green (525 nm), and blue (470 nm) light and measuring the amount of transmitted light. The data are compared against 23 standard colors to determine the hue (i.e., yellow, orange, brown, red, violet, blue, green, colorless, and other) and tone (light, normal, dark). Specific gravity is obtained by measuring the refraction of the sample using a prism and subjecting results to a calculation formula (reflection refractometry). The light from an LED passes through the prism and is reflected on the prism face contacting the sample. The light reflected off the prism is collimated into a thin beam by passing through a slit and directed to a detector (CCD image sensor). At this point, the refractive index at the interface between the prism face and sample will change according to the specific gravity; therefore, the position of the incident light from the slit will change. The refractive index is obtained by detecting the position of

the incident light and, after correcting it for temperature effects, it is converted into a Brix value. The specific gravity of the sample is then obtained using this Brix value and a conversion formula. Reagent strip analysis is automatic and consists of test strip picking, sample transport, sample aspiration, test strip staining, measurement, and test strip disposal. The measurement unit irradiates the reagent pad with two wavelengths of light from a five-wavelength LED and picks up the reflected light with a single detector. The reflectivity of the color correction pad of the test strip is also measured to correct the readings of colored urine specimens. Destabilizing factors such as the amount of reflected light and colored samples are corrected. Reflectivity is calculated mathematically and compared against calibration curves stored in the instrument. A thermal compensation feature minimizes error caused by temperature changes outside of the optimal temperature range for measurement. The instrument automatically detects false-positive reactions of reagent pads caused by drugs administered and flags these specimens. The instrument incorporates a large color LCD screen to facilitate operation, has both integrated and hand-held barcode readers, and a memory capacity for measurement results of 2500 samples. A unique feature of the instrument is the incorporation of dual test strip feeders for multiple test strips, permitting two types of test strips to be used.

The LabUMat 2 (77 Elektronika Kft., Budapest, Hungary) is one of the latest fully automated urine chemistry analyzers, used in 80 countries but not yet cleared for use in the United States. It is a desktop instrument designed for ease of use, with operation via a color touch screen. The operator fills the instrument with distilled water, fills the strip feeder with urine reagent strips and puts the racks with samples on the rack conveyor. Test strip evaluation with LabStrip 11 Plus urine test strips is performed by a patented detection technique using four discrete wavelengths. A separate measurement cell is used for specific gravity, color, and turbidity. It has a throughput of 240 tests per hour and internal memory large enough to store 10,000 records. Automated QC analysis and self-check is provided; software and language upgrades can be performed via USB stick. The test strips provide analysis of bilirubin, urobilinogen, ketones, ascorbic acid, glucose, protein, blood, pH, nitrite, and leukocytes.

The UC-3500 is a modular, fully automated urine chemistry analyzer marketed by Sysmex Corporation (Tokyo, Japan) under a business alliance with Eiken Chemical Company (Tokyo, Japan). The instrument prioritizes operator usability with simple operating panels. It has a high throughput of 276 urine specimens/hour using a sample handler that can hold 8 tube racks with 10 tubes each. The instrument uses reflectance photometry with a color CMOS sensor to measure urobilinogen, occult blood, proteins, glucose, ketone bodies, bilirubin, nitrites, leukocytes, and pH using MEDITAPE UC-9A and Meditape UC-11A urine chemistry test papers. The advanced CMOS sensor distinguishes RBCs and free hemoglobin. Albumin and creatinine can also be measured with the MEDITAPE UC-11A test strip. The instrument is highly sensitive for albumin, with a low detection limit of 5.5 mg/L (Delanghe et al., 2017). Specific gravity, color tone and turbidity are determined by a refractometry measurement method. The instrument automatically detects the position of the test strip pads, recognizing wrong strips and abnormal urine color. Detailed diagnostic performance evaluations of the UC-3500 in comparison to reference methods showed good correlation for all measured parameters (Oyaert & Delanghe, 2019; Oyaert et al., 2018).

AUTOMATED MICROSCOPY ANALYZERS

Microscopic examination of urine sediment is a labor-intensive and time-consuming procedure subject to subjective interpretation and clerical errors (Tworek et al., 2008). In contrast, automated microscopic analysis of uncentrifuged urine provides many benefits, including decreased labor costs and improved laboratory productivity, improved turnaround time, reduced observer-associated error and bias, improved accuracy and precision, elimination of centrifugation, reduced operator exposure to biohazardous material, minimization of clerical errors, and local archival of results for quality assurance, competency assessment, and education (Brunzel, 2018). The Yellow IRIS urinalysis workstation, introduced by International Remote Imaging Systems (IRIS) Inc. (Chatsworth, CA), was the first commercial instrument to perform "automated intelligent microscopy." An evaluation of the Yellow IRIS system, published in 1985, showed significantly increased sensitivity and precision as well as a 300% improvement in urinalysis productivity by CAP standards compared with manual urine microscopy (Deindoerfer et al., 1985). Since that time, many technological advances have been incorporated into several additional generations of urine microscopy analyzers using flow or cuvette-based digital imaging or laser flow cytometry. Generally, these systems do not replace manual microscopy for all specimens but rather provide quantitative results with small coefficients of variation for most routine urine specimens. Manual analysis of the urine sediment by light microscopy is still recommended for specimens with suspicious findings and for patients with known or suspected renal disease or infection. The latest of these instruments are discussed next.

Flow Imaging Particle Analysis

Flow imaging particle analyzers capture magnified digital images of particles in a fluid during passage through a flow cell. The particles are quantitated, measured, and identified using image recognition software. This technology, termed *flow imaging microscopy*, *digital flow microscopy* and *digital flow morphology*, has been widely used in the medical and biological sciences, and for counting and classifying plankton and other particles (Doan et al., 2018; Han et al., 2016; Vembadi et al., 2019).

The Yellow IRIS was the first urine analyzer to use flow imaging microscopy; the IRIS iQ200 (Beckman Coulter, Inc., Brea, CA) is the latest version of this instrument. The iQ200 is a bench-top automated urine microscopy analyzer that provides a quantitative or qualitative count of cells, casts, crystals, organisms, and other formed elements in a urine specimen as they are passed in hydrodynamic flow in front of a digital camera. The analyzer counts and auto-identifies the particles and stores the images for verification by the operator. The iQ200 analyzer consists of a microscopy module, computer workstation module, and optional load/unload stations. Tubes of urine are placed in sample racks on the front of the microscopy unit and transported to the barcode reader and pipetting station. A pipettor mixes the sample and aspirates approximately 1 mL of sample. Peristaltic pumps pass the urine sample through a flowcell surrounded by a buffered, isotonic fluid called iQ lamina. The geometry of the flow cell and the streamlined flow of iQ lamina hydrodynamically position the specimen, with any contained particles, within the focal depth of the lens of a microscope. A CCD video camera coupled to the microscope captures 500 frames per sample. The flash of a strobe lamp illuminates each field. Auto-particle neural network recognition software isolates individual particles in a single frame and uses the size, shape, contrast, and texture of the particles to assign them to one of 12 auto-classified categories (i.e., RBCs, WBCs, WBC clumps, hyaline casts, unclassified casts, squamous epithelial cells, nonsquamous epithelial cells, bacteria, yeast, crystals, mucus, and sperm). Any images that do not classify into one of these 12 categories are placed in a category designated "unknown." The particle concentration is calculated from the number of images, normalization factor, and the volume scanned. User-defined criteria for the auto-release of results is checked and results are sent either directly to the host computer and/or printer or to the system monitor for verification. The images from abnormal non–auto-released specimens appear on the system screen for verification. The operator may manually reclassify the digital images when necessary and in accordance with the laboratory's policy. Unclassified crystals (UNCX), unclassified casts (UNCCs), and nonsquamous epithelial cells (NSEs) may be further subclassified during the verification process. Free text comments can be entered by the operator. Once the verification process has been completed, the results can be sent to the laboratory information system and/or printer. The reported accuracy and precision of the IRIS microscopy system for cell counting and identification is equivalent or better than manual microscopy, although verification and validation for individual laboratories is necessary, with performance criteria for microscopic confirmation in specimens with dysmorphic erythrocytes, casts, and crystals (Boven et al., 2012; Cui et al., 2017; Du et al., 2015; Ince et al., 2016). Cell counts can also be performed on body fluids other than urine, with the exception of cerebrospinal fluids and other specimens with very low cell counts (Butch et al., 2008).

Cuvette-Based Particle Analysis

Urine microscopy using cuvette-based particle analysis is a recent innovation, with two commercial systems available at present. In these analyzers, an aliquot of the urine specimen is centrifuged in a specially designed cuvette for a brief period of time at a low g force. Multiple images are acquired by a high-resolution digital camera coupled to a microscope focused on the monolayer of particles on the bottom of the cuvette. The images are nearly identical to those visualized through an optical microscope and can be displayed on a monitor for manual interpretation and verification by the operator. However, the instruments also have image processing software with algorithms and an image reference library that can automatically count and classify the particles for auto-validation or further evaluation by the operator.

The UriSed (77 Elektronika Kft., Budapest, Hungary) and Cobas u 701 (Roche Diagnostics, Basel, Switzerland) urine analyzers are the only

cuvette-based urine analyzers at this time. They are used in Europe and other markets but are not yet available in the United States. The UriSed 3 (also called the Sedimax 3) is the latest version of the instrument developed by 77 Elektronika. In this instrument, 200 µL aliquots of urine from bar-coded tubes are dispensed into a specially designed disposable cuvette and centrifuged for 10 seconds at 260 g. The cuvette is then forwarded to a microscope table for automatic focusing and imaging at a magnification of 400×. The analyzer acquires a user-defined number of bright-field images (usually 15) of each sample, corresponding to approximately 10 manual microscopy fields (Brunzel, 2018). Phase contrast microscopy is also available in the UriSed 3 to improve the visualization of urine casts and other translucent particles. Particle identification and quantitation into 15 categories can be automatically performed in real time by incorporated software using neural network technology. The zoomable images acquired by the instrument are also available for manual review by the operator, who can correct or verify the instrument interpretation or place particles into 28 additional categories. The images and data are archived for further use. The throughput is approximately 100 specimens per hour. In a comparison of three automated urine sediment analyzers with manual analysis, Akin and collaborators found that the UriSed and iQ200 analyzers were in agreement with manual analysis for red cells, leukocytes, and epithelial cells, but produced more reproducible results (Akin et al., 2009).

The Cobas u 701 is a similar urine analyzer using cuvette-based technology. A recent evaluation of the Cobas u 701 for screening 2046 urine specimens for bacteria in a routine pathology laboratory showed excellent sensitivity and negative predictive value (>99%) (Waterhouse et al., 2019).

A recent urine particle analyzer, the Sysmex UD-10, uses a slightly different approach. Uncentrifuged urine is aspirated into an imaging cell and permitted to settle to the bottom of the cell by gravity. Using stage scanning technology with automatic focus, a moving CCD camera captures images of the sediment with pulsed LED lighting. The instrument captures 40 images in a normal mode and 80 in a precise mode. The integrated software classifies the particles into eight categories based on size. The operator can view the images for further classification. The instrument has a reported throughput of 50 samples per hour in normal mode and 30 in the precise mode. The UD-10 was developed as part of a modular system for integration with the Sysmex urine flow cytometers and analytic software to permit automated particle imaging.

Flow Cytometric Particle Analysis

In urine flow cytometers, aliquots of urine are stained with fluorescent dyes specific for DNA and cell membrane components and then passed through a flow cell that orients the cells and other particles into single file by hydrodynamic focusing. The particle stream is illuminated by a laser beam, which excites fluorescent dyes attached to the particles and scatters light. The present instruments use two flow channels, one for bacteria and the other for cells and all other particles. Sensors detect impedance, fluorescence, and scattered light at forward and side angles (Fig. 29.51). The data is then passed to a computer with specialized analytic software for analysis and display. As with other types of flow cytometers, the data output from a urine flow cytometer is displayed as scattergrams denoting particle populations identified as RBCs, WBCs, squamous epithelial cells, hyaline cells, or bacteria (Brunzel, 2018). Other particles, including nonhyaline casts, small round cells, crystals, mucus, sperm, yeasts, and other particles, are not identified by the current urine flow cytometers, but the instruments report a "flag" denoting their presence (Brunzel, 2018). Therefore, urine flow cytometry cannot replace manual urine microscopy, especially in advanced medical facilities.

The UF-100 analyzer (Sysmex Corporation, Kobe, Japan), released in 1995, was the first commercially available urine particle analyzer using laser flow cytometry. The UF-100 analyzes urine by flow cytometry and gives quantitative results for RBCs and WBCs, epithelial cells, casts, and bacteria (Fig. 29.52). It can detect yeast, crystals, dysmorphic RBCs, and pathologic casts (Fig. 29.53) in the urine (Ben-Ezra et al., 1998; Ottiger & Huber, 2003). This technology may be useful in decreasing the number of urine specimens requiring routine microscopy (Fenili & Pirovano, 1998). Normal values are fewer than 20 RBCs/µL, fewer than 25 WBCs/µL, and fewer than 2000 bacteria/µL. Similar to the microscopic examination of urine on unspun specimens, the automated systems are not prone to the artifacts that characterize examination of spun urine sediment. Second generations of this machine released in 2006, the UF-500i and UF-1000i, provided better enumeration of bacteria with fewer artifacts due to interfering debris. A later version, the UX-2000, combined urine chemistry and sediment analysis into a single compact system and provided enhanced detection of WBCs and bacteria as well as other benefits (Jiang et al., 2011; Kadkhoda et al., 2011; Khejonnit et al., 2015; Laiwejpithaya et al., 2018; Manoni et al., 2010; Sanchez-Mora et al., 2017). The Sysmex instruments also have a body fluid counting mode (Fleming et al., 2014).

The UF-1000i was succeeded in 2015 by a series of third-generation instruments, the UF-3000, UF-4000, and UF-5000. Another instrument, the AUTION HYBRID AU-4050, released in 2012 by Arkray, Inc. (Kyoto, Japan) is a compact, integrated urinalysis that combines a reagent strip reader with a flow cytometric urine particle analyzer. The UF-5000 has two different flow analysis chambers, designated surface (SFch) and core (CRch), uses a blue semi-conductor laser at 488 nm wavelength, and detects signals of forward scattered light (FSC), side scattered light (SSC), side fluorescent light (SFL), as well as a new parameter, depolarized side scattered light (DSS), to improve the differentiation of RBCs and crystals. The maximal throughput is 105 urine specimens per hour and the instrument can measure 17 diagnostic parameters of cells and formed elements, including transitional and renal tubular cells. The approved parameters are RBCs, nonlysed RBCs, WBCs, WBC clumps, epithelial cells, squamous epithelial cells, nonsquamous epithelial cells, transitional epithelial cells, renal tubular epithelial cells, casts, hyaline casts, nonhyaline casts, bacteria, crystals, yeast-like cells, spermatozoa, and mucus. An integrated body fluid mode (BF) can classify and count seven diagnostic parameters. An important innovation is the "Bact Info" parameter, which distinguishes gram-negative and gram-positive bacteria. Normal automatic and STAT operating modes are available, with a minimum volume of 2.0 mL uncentrifuged native urine in the normal mode and 0.6 mL in the STAT mode

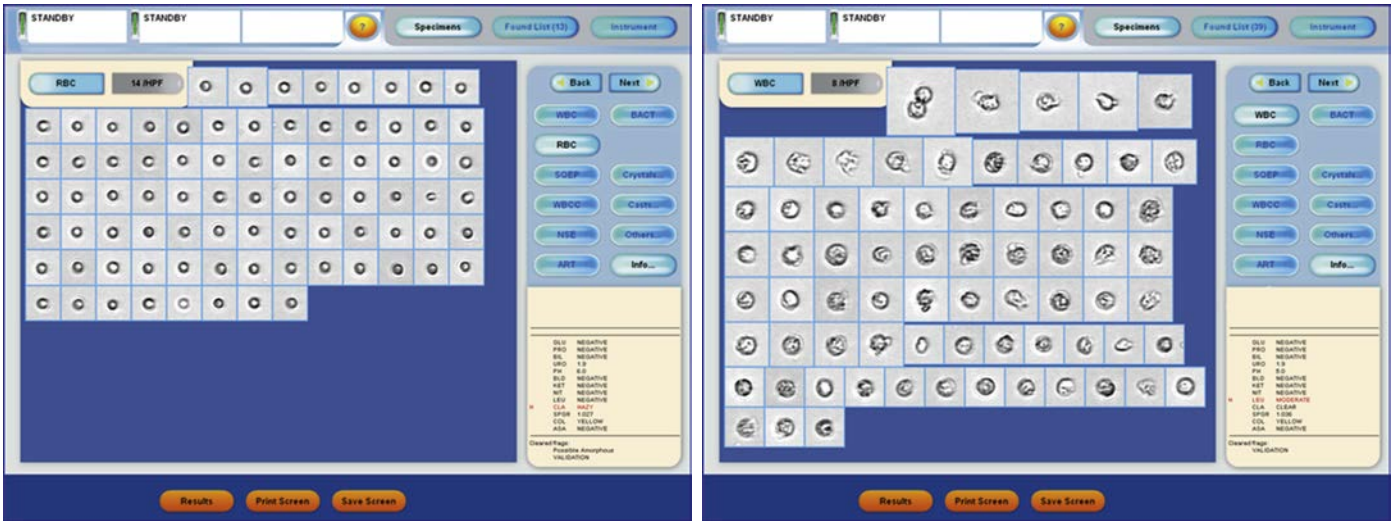

A B

Figure 29.51 Operator screens of IRIS iRICELL 2000 iQ200ELITE microscopy module. A, Red blood cell panel showing images of erythrocytes identified in the specimen. B, White blood cell panel demonstrating images of leukocytes in the specimen.

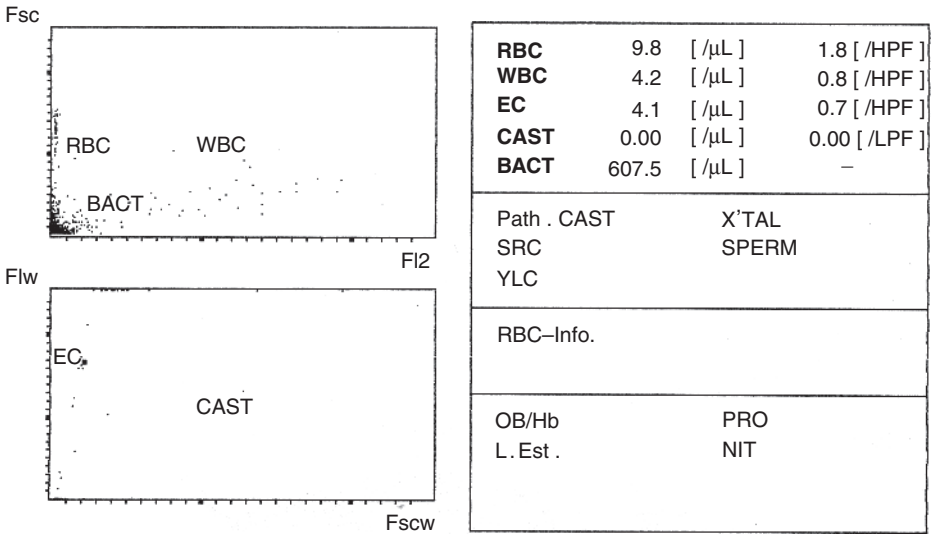

Figure 29.52 Printout from UF-100 automated urine analyzer, showing normal urine. Note the lack of RBCs, WBCs, bacteria, and casts. *RBCs,* Red blood cells; *WBCs,* white blood cells.

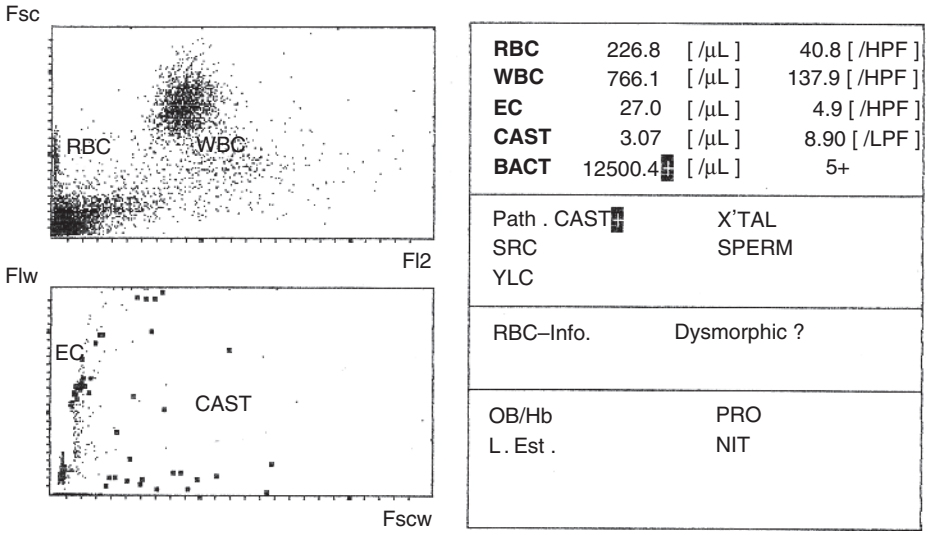

Figure 29.53 Printout from UF-100 automated urine analyzer, showing abnormal urine. Compare with Figure 29.52. Note the sizable numbers of RBCs, WBCs, bacteria, and casts. *ECs,* Squamous epithelial cells; *NIT,* nitrite; *PRO,* protein; *RBCs,* red blood cells; *SRC,* small round cells; *WBCs,* white blood cells; *X'TAL,* crystals; *YLC,* yeast-like cells.

(Previtali et al., 2017). The performance of the UF-5000 was evaluated by Previtali and coworkers, who compared the automated finding in 736 uncentrifuged urine specimens with those obtained with the Fuchs-Rosenthal counting chamber (Previtali et al., 2017). The negative predictive value was very good for all parameters; the authors concluded that the instrument could accurately and rapidly exclude UTI. The sensitivity and specificity for all parameters also exceeded the reported values for urine microscopy analyzers using image-based technology. Several additional studies have confirmed the diagnostic accuracy of the UF-5000 in screening urine specimens for infection (De Rosa et al., 2018; Ren et al., 2018). Its ability to differentiate gram-positive and gram-negative bacteria was also reported to be very good but not accurate enough to replace culture (Kim et al., 2018).

INTEGRATED, FULLY AUTOMATED URINALYSIS SYSTEMS

Fully automated urinalysis systems that provide integrated analysis of urine chemistry and microscopy are optimal for larger, high-volume laboratories. In these systems, barcoded urine specimen tubes are loaded into the analyzer, patient identification and test orders are obtained from the laboratory information system, chemical and/or microscopic analysis is automatically performed, and the results are autoverified or held for further evaluation by the system operator. Typically, chemical analysis is performed first, and the specimen is automatically transported to the microscopy unit if indicated by user-defined criteria. These systems optimize laboratory productivity and have a high throughput. The integrated urinalysis systems available at present include (1) the iRICELL Automated Urinalysis System, consisting of the iChem Velocity urine chemistry analyzer integrated with the iQ200 microscopy analyzer; (2) the CLINITEK AUWi System, and ATLAS urine chemistry analyzer connected to a UF-1000i flow cytometer; (3) the combination of a LabUMat chemistry analyzer with a UriSed microscopy unit; and (4) the AUTION HYBRID System. The AUTION HYBRID System is the only completely integrated urinalysis system presently on the market, consisting of an AUTION MAX chemistry module combined with a flow cytometric sediment module in a single compact unit. Barcoded sample tubes are loaded into the instrument, and dual sample probes acquire separate aliquots for macroscopic/chemical and sediment analysis.

SPECIAL TESTING AND MONITORING TECHNIQUES

URINARY CALCULI

Nephrolithiasis is a common condition, affecting nearly 1 in 11 individuals in the United States (Khan et al., 2016; Mayans, 2019; Scales et al., 2012; Sorokin et al., 2017; Ziemba & Matlaga, 2017). It is a heterogeneous disorder, with stones developing from a wide variety of metabolic, environmental, and genetic disturbances (Shin et al., 2018). Although most studies have concentrated on nonorganic components, many stones have been found to be associated with an organic matrix containing lipids and protein, suggesting the involvement of cellular membranes in the nucleation and growth of crystals (Bagga et al., 2013; Baumann & Affolter, 2014; Khan et al., 1996; Wiener et al., 2018). Many substances act as promoters or inhibitors of this process (Aggarwal et al., 2013).

Upper (renal) stones are common in Western industrialized countries, whereas bladder stones are uncommon. The passage of stones down the ureter produces renal colic, which is characterized by severe pain in the

flank radiating to the groin. Hematuria frequently accompanies stone passage. If stones obstruct the pelvis of the kidney or ureter, hydronephrosis can result, and infection is a common consequence. Recurrences are frequent, but with appropriate identification of the stones and the risk factors associated with them, stone formation may be greatly reduced.

Calcium oxalate or a mixture of oxalate and calcium phosphate is often found in stones (≈80%) (Alelign & Petros, 2018). Mixed calcium phosphate, magnesium ammonium phosphate, and uric acid are the next most common constituents (3%–10% each); these are followed by cystine stones (1%–2%). Carbonate, which is frequently detected in chemical analysis, probably results from adsorption of carbon dioxide to the calcium phosphate crystal. Males are more often affected with calcium stones than females, and children are not often affected with calcium stones.

Calcium oxalate precipitates at an acid or neutral pH, and calcium phosphate—hydroxyapatite $Ca_{10}(PO_4)_6(OH)_2$—forms calculi at the normal urinary pH of 6.0 to 6.5. Uric acid, which is not very soluble, will crystallize at a low pH (5.3) and form stones. Magnesium ammonium phosphate (struvite) forms stones at alkaline pH, where the ammonium level is high. These tend to form in the pelvis of the kidney but apparently are not attached to papillae, as are the calcium stones. However, they may develop on preexisting nuclei when infection from organisms such as *Proteus* causes alkalization of the urine (Flannigan et al., 2014; O'Kell et al., 2017). Struvite stones may become large, forming casts of the kidney pelvis and showing staghorns. Mixed stones may form when calcium or uric acid crystals (or stones) cause obstruction followed by infection and the subsequent deposition of ammonium salts.

Hypercalciuria and Calcium Stones

Calcium homeostasis is maintained by parathyroid hormone (PTH) and 1,25-dihydroxycholecalciferol ($1,25[OH]_2D$). Both affect bone resorption by osteoclasts. PTH causes a diminution of phosphorus reabsorption and an increase in calcium reabsorption by renal tubular cells. It also causes increased synthesis of $1,25(OH)_2D$, which acts on the small intestinal mucosa, causing increased absorption of calcium and phosphorus. Low serum ionized calcium levels cause increased PTH secretion, and low serum phosphorus stimulates $1,25(OH)_2D$ synthesis.

About 40% of patients with calcium stones will have hypercalciuria, defined as a daily urinary excretion of calcium in excess of 0.1 mmol/kg (Houillier & Boulanger, 1998). Increased calcium in urine may result from an increase in intestinal calcium absorption, lack of appropriate renal tubular reabsorption of calcium, resorption or loss of calcium from bone, or a combination of these factors. Vitamin D supplementation has also been identified as a contributing factor (Letavernier & Daudon, 2018; Malihi et al., 2016). In a few instances of hypercalciuria, an underlying disease process can be identified. In most cases, however, it is primary or idiopathic hypercalciuria (IH). Although the exact mechanism of hypercalciuria is still unknown in this disorder, it most likely comprises a combination of factors, including those listed previously (Coe et al., 2016). Three hypotheses to account for IH pathophysiology have been proposed. These include possible defects in the fatty acid content of cell membranes, increased expression of the vitamin D or calcium receptors of the 25-hydroxyvitamin D_1 α-hydroxylase, or a disease of monocytes (Bataille et al., 1998). Recent studies have revealed that polymorphisms in genes for proteins regulating tubular phosphate and calcium reabsorption, preventing calcium salt precipitation, and coding a proximal tubule water channel are associated with calcium nephrolithiasis (Arcidiacono et al., 2014; Oliveira et al., 2019; Vezzoli, Macrina et al., 2019).

Excess loss of calcium in urine and the possibility of stone formation may occur secondary to a variety of other conditions. For instance, hypercalciuria may result from increased absorption of calcium from the gut. This may occur following excessive loss of phosphorus from the kidney and low serum phosphorus levels or when increased serum $1,25(OH)_2D$ is seen with normal serum phosphorus levels. Increased resorption of bone may occur with immobilization of the skeleton, rapidly progressive bone disease, thyrotoxicosis, and Cushing disease, leading to hypercalciuria. Calcium may be lost from bone as a result of osteolytic tumors as well as in the presence of renal disease, such as distal renal tubular acidosis and medullary sponge kidney. Sarcoidosis, vitamin D excess, and furosemide may also cause renal hypercalciuria.

About 5% to 10% of calcium stones are associated with primary hyperparathyroidism (Cong et al., 2018). In this disorder, increased mineral turnover in bone and hypercalcemia are important causes of hypercalciuria. Affected patients often present with stone symptoms, and calcium phosphate deposits may be found in the renal tissue, cornea, and other organs.

Dietary hypercalciuria is an uncommon cause of calcium stones; it is associated with a large calcium intake, on the order of 3 to 4 g/day, together with a high-protein intake. About 800 mg/day is the normal recommended adult intake.

As stated previously, calcium oxalate stones are the most common. They may form with excess oxalate and uric acid in the urine, the latter sometimes providing a nidus for stone formation. Newly formed calcium oxalate aggregates are about 20 to 25 μm in diameter, much smaller than the outlet of the collecting ducts. Adherence to the epithelial surface apparently allows stones to continue growth rather than be excreted. Calcium phosphate stone formation is favored by a less acid urine, as is seen in renal tubular acidosis, with infection, and in persons consuming large amounts of alkali. These stones are also seen in primary hyperparathyroidism, although the urine is in the normal pH range. In a patient exposed to heat and dehydration, these may contribute to a rise in urinary solute levels followed by crystallization and stone formation.

Hyperoxaluria

A majority of calcium stones (70%–80%) contain oxalate. Some of the oxalate in urine is dietary in origin from beverages (tea, cocoa, coffee, cola), vegetables (beans, rhubarb, spinach), nuts, berries, and citrus fruits. Oxalate is also derived from ascorbic acid.

The gastrointestinal system plays an important role in oxalate homeostasis. Oxalate absorption increases when calcium and magnesium intake decreases. Disorders of the small bowel—such as Crohn disease, ileal resection, and intestinal bypass surgery—may result in excessive oxalate absorption, with subsequent excretion in the urine. Malabsorption with steatorrhea causes loss of calcium due to soap formation of calcium with fatty acids, and malabsorption with increased bile salts remaining in the gut is thought to promote oxalate absorption in the colon. Additionally, absence of *Oxalobacter formigenes* from the intestinal tract of patients with cystic fibrosis appears to lead to increased absorption of oxalate, thereby increasing the risk for hyperoxaluria (Sidhu et al., 1998; Young, 2018).

Other causes of hyperoxaluria include pyridoxine deficiency and primary hyperoxaluria. The latter is a rare inherited autosomal-recessive disease with oxoglutarate carboligase deficiency (Cochat & Rumsby, 2013; Dindo et al., 2019). Systemic oxalosis and renal failure may be seen in young adulthood. Renal transplantation and large doses of pyridoxine or nicotinamide have been tried for the treatment of these patients.

Hyperuricuria

Excessive excretion of uric acid may be due to excessive dietary intake of purines (liver, dried beans, some fish, meat) or various disease processes. Endogenous uric acid production is increased in gout, glycogen storage diseases, Lesch-Nyhan syndrome, many leukemias, and treated tumors with associated cell necrosis. Chemotherapy and irradiation can lead to increased breakdown of tumor cells (nucleotide/purine forms uric acid), which may cause acute renal failure secondary to tubular and ureteral obstruction by masses of uric acid crystals.

In gout, about 20% of patients form stones, most of which are pure uric acid or mixed uric acid and calcium. Heat, dehydration, and unusually acid urine contribute to stone formation. Gouty nephropathy occurs with sodium urate deposits in the medulla, even when stones are not present, and masses of crystals may cause obstruction of terminal collecting ducts in the kidney. Uricosuric drugs cause potential problems with massive uric acid output in the first 3 to 4 days of treatment.

Normally, about one-third of the uric acid formed is degraded by bacteria in the colon. Absence of bacteria or intestinal diversion may cause increased absorption of uric acid from the gut. Because ileostomy patients lose large amounts of alkaline fluid from the intestine, they excrete concentrated acidic urine and are likely to produce uric acid stones.

The average uric acid excretion by adults is 500 to 600 mg/24 hours. Solute concentration as well as pH appears to be important in the solubility of uric acid and urate (Shekarriz & Stoller, 2002). Uric acid, a weak acid, forms free, insoluble, undissociated uric acid and a urate (which is more soluble with some sodium and potassium present) at pH 5.5. The amount of free uric acid present in urine will decrease as the pH rises and, at pH 7, uric acid is more soluble as urate. With high salt concentrations, the urate becomes less soluble. If urine volume is low, the solubility of uric acid at acid pH will be exceeded.

Whereas large quantities of uric acid crystals are regularly seen in urinary sediment, uric acid stone formation is relatively uncommon, accounting for 10% to 15% of urinary stones (Ma et al., 2018). Uric acid crystals form a sludge that may obstruct the nephron without forming a stone. On the other hand, uric acid and sodium acid urate crystals are found as nuclei for calcium stones. Most normal persons with a pH of 6 have urine saturated with uric acid but do not form stones. Further acidity or dehydration is apparently required to engender stone formation.

Cystine Stones

Cystine stones form in patients with an inherited amino acid transport disorder (see the Cystinuria section later in the chapter). Cystine, ornithine, lysine, and arginine are subsequently excreted in large amounts in the urine. Of these, only cystine forms crystals and stones. Cystine does not become soluble until the urine pH is 7.4, and stones form over a range of normal urinary pH values. Heterozygous carriers for the disease will have increased amounts of cystine in urine but do not form stones; homozygotes are stone formers. A 24-hour quantitative urine cystine measurement is needed to detect potential stone formers; this should always be done when cystine crystals are found in random specimens.

Rare Calculi

Calculi containing sulfonamides have been described, and silica calculi have been reported in patients ingesting silica gel over a long period of time. Triamterene (Dyazide, Dyrenium), a relatively insoluble diuretic, may contribute to stone formation. It can form 1- to 2-mm mustard-colored stones, giving a bright-blue fluorescence when dissolved in butanol and with exposure to ultraviolet light. Rare adenine stones have been described in children with an inherited enzyme deficiency disorder and hyperuricemia. Xanthine stones are uncommon and may be associated with a genetic disorder with an absence of xanthine oxidase.

LABORATORY TESTS USED TO INVESTIGATE STONE FORMERS

Urine Examinations

1. Routine urinalysis, qualitative test for cystine, and urine culture. Hematuria is a constant finding when stones are present, even when they are asymptomatic. Proteinuria is usually not a feature of calculous disease, but with renal tubular damage, excretion of low molecular weight plasma proteins such as β_2-microglobulin, and some albumin, may be increased. Erythrocyte casts usually are not found, and other casts are unusual. Leukocytes are increased when infection is present, and the reagent strip nitrite and leukocyte esterase may be elevated. Multiple clusters of nonmalignant transitional cells may be found in urine of patients with calculous disease and may be helpful in the diagnosis of unsuspected calculi.
2. Twenty-four–hour urine specimen: Sodium, calcium, phosphorus, uric acid, oxalate, and creatinine clearance (Ennis & Asplin, 2016). Supersaturation values from 24-hour urine collections have been shown to accurately reflect stone composition (Asplin et al., 1998). Some authors suggest that spot urine samples are sufficient for the metabolic evaluation of stone formers, although because of day-to-day variation, three samples should be obtained to overcome the doubtful significance of a single result (Strohmaier et al., 1997).
3. Urine pH determination on a fresh specimen is important in determining the types of crystals likely to be precipitated, for example, uric acid with low pH (5.0–5.5), and triple phosphate with alkaline urine.

Serum Chemistry

Appropriate tests include calcium, phosphorus, uric acid, and electrolytes.

Stone Analysis

Calculi may be of various sizes, commonly described as sand, gravel, or stone. The physical characteristics of the various calculi rarely will suffice for their identification, but a few points are worth noting. Uric acid and urate stones are typically yellow to brownish red and are moderately hard. Phosphate stones are usually pale and friable. Calcium oxalate stones are very hard, often of a dark color, and typically have a rough surface. Cystine stones are yellow-brown and feel somewhat greasy.

Several methods are available for the analysis of calculi, such as optical crystallography, radiographic diffraction, and infrared spectroscopy (Ennis & Asplin, 2016). Electron beam analysis and mass spectroscopy are also used. A simplified method for analysis of renal calculi is presented by Farrington and colleagues (1980). A quantitative method for five of eight frequently measured substances using available clinical chemistry methods has been described: calcium, phosphorus, magnesium, ammonium, and uric acid. Cystine, oxalate, and carbonate are detected by qualitative means and are interpreted with the quantitative results to characterize the stones. Most laboratories refer calculi specimens to more specialized laboratories for chemical analysis, where both chemical and specialized tests should be used to determine the composition of the stones.

Method for Gross Examination of Calculi

1. Wash the stone(s) free of blood, mucus, preservation solution, and so forth. Place stones in a beaker, cover with several thicknesses of gauze held firmly in place with rubber bands, and wash under cold running water. Drain, remove gauze carefully, and dry beaker and stones in an oven. Rinse tiny stones with water from a squeeze bottle (not running water).
2. Record the dimension of the stone.
3. Describe briefly the color and texture of the stone's exterior surface. The stone may be photographed for recording purposes.
4. Cut, saw, or break the stone to examine the interior. Note whether a foreign body may have acted as a nucleus for its formation. Describe the color and texture of the interior and layers, if present.
5. Reduce small stones to a fine powder by pulverizing with a mortar and pestle.
6. If possible, when a stone is very large, it may be advisable to make separate analyses of layers that appear to have different constituents.

Because most small calculi consist of calcium oxalate, the best way to analyze them is to put all available powder in one test tube. (If the stone is very tiny, it may be placed directly in the test tube and crushed with a spatula.) Reagents used for the chemical determination of rare stones may be found in an earlier edition of this textbook (Henry, 1996). It is important to have known positive material to test the reagents.

Radiologic Examination

Asymptomatic stones are sometimes found. Most stones are radiopaque, except for pure uric acid and the rare xanthine; cystine stones are opaque because of their sulfur content.

URINARY SCREENING FOR INHERITED METABOLIC DISEASES

Urine has been used for many years to screen for metabolic diseases, particularly those resulting from a genetic predisposition. In many of these diseases, an abnormal metabolite or a larger than normal amount of a normal metabolite is excreted in the urine. Because these conditions are uncommon and their symptoms often nonspecific, and because some may be treatable if early diagnosis is confirmed, blood and urine should be analyzed using techniques that are highly selective and sensitive. Numerous inborn errors of metabolism have been identified; this section will describe some of the more common disease entities.

Aminoacidurias

Excretion of one or more amino acids in the urine may be due to a block in a major metabolic pathway (overflow type) or a deficiency in renal tubular function (renal type). Phenylketonuria is an example of overflow aminoaciduria in which an enzyme substrate and other metabolites in the pathway accumulate, causing increased body fluid levels and increased substrate excretion in urine. Unlike the overflow-type diseases, renal-type aminoacidurias do not have high levels of the amino acid in the blood because the primary defect is in the renal tubular reabsorption mechanism. An example of renal transport aminoaciduria is cystinuria.

Phenylketonuria

Phenylketonuria is an autosomal-recessive inherited disorder in which there is absence of the enzyme phenylalanine hydroxylase (Blau, 2016). Both sexes are affected equally, with an incidence of about 1 in 11,000. Allelic heterogeneity can be extensive, particularly in the United States (Guldberg et al., 1996). Mental retardation is the major clinical finding, and dietary restriction of phenylalanine has proven efficacious in these patients.

Because they are not converted to tyrosine in this disorder, phenylalanine and other normal metabolites accumulate in abnormal amounts. Plasma phenylalanine and phenylpyruvic acid levels are elevated; urinary phenylpyruvic acid (highest), phenylacetic acid, and phenylalanine are increased. Urinary indoleacetic acid and other indoles arising from altered tryptophan metabolism and indican (an indole) are also increased. The excretion of 5-hydroxyindoleacetic acid is diminished, paralleling the low level of serum 5-hydroxytryptamine. The urine and sweat of these patients have a characteristic mousy/musty odor due to phenylacetic acid.

Methods. Phenistix reagent strips contain ferric ammonium sulfate, magnesium sulfate, and cyclohexylsulfamic acid. At 30 seconds following immersion into urine, the color of the test area is compared with the color chart provided. A positive test result shows a gray to gray-green color. The test detects 5 to 10 mg/dL. Salicylates and metabolites of phenothiazine

derivatives may cause a pink-to-purple color. Ion-exchange HPLC has been found suitable for quantitative confirmatory testing of abnormal specimens (Reilly et al., 1998).

Alkaptonuria

Normally, phenylalanine and tyrosine are metabolized to homogentisic acid (dihydroxyphenylacetic acid), which is then oxidized to maleylacetoacetic acid. In alkaptonuria, the enzyme homogentisic acid oxidase is deficient, and homogentisic acid is excreted in urine in large quantities. The urine characteristically turns brown-black on standing or with alkaline pH. Patients with alkaptonuria develop dark-blue to black pigmentation in cartilage and connective tissue. Frequently, the disease is not diagnosed until arthritis has already developed.

Methods. Screening methods include ferric chloride and silver nitrate tests. A transient, dark-blue color appears as two drops of 10% ferric chloride solution are added to about 2 mL of urine containing homogentisic acid. The silver nitrate test involves adding 4 mL of 3% silver nitrate to 0.5 mL urine, mixing, and then adding several drops of 10% NH_4OH. Homogentisic acid will cause a black color to develop. Confirmatory methods include paper or thin-layer chromatography, as well as capillary electrophoresis. These methods should distinguish homogentisic acid from gentisic acid, an aspirin metabolite.

Tyrosinuria

Tyrosinemia with tyrosinuria occurs when the metabolism of tyrosine derived from the diet or from phenylalanine is abnormal. This may be part of a generalized amino acid disorder associated with liver disease or may represent one of the various genetic disorders involving tyrosine metabolism. Tyrosine crystals may appear in the urine as fine, silky crystals scattered singly or aggregated to form sheaves. They appear brown to black, precipitate at an acid pH, and are soluble in alkali. Small quantities of tyrosine may appear in the urine of normal individuals.

Transitory hypertyrosinemia may occur in low-birthweight and premature infants as a benign condition. Typically, these infants are asymptomatic, and no liver or renal disease is present. The elevated tyrosine levels may be accompanied on occasion by transiently elevated phenylalanine levels. Tyrosine and the phenolic acids *p*-hydroxyphenyllactic and *p*-hydroxyphenylpyruvic acids are excreted in larger than normal amounts in the urine. The nature of the enzymatic defect has not been well characterized, and the tyrosine level of these patients usually returns to normal within a few weeks to months.

Type I hereditary tyrosinemia (tyrosinosis) is an autosomal-recessive disorder characterized by defects in fumarylacetoacetate hydrolase and maleylacetoacetate hydrolase (Chinsky et al., 2017). Succinylacetoacetone and succinylacetone accumulate and inhibit renal function, various hepatic enzymes, and porphobilinogen synthetase. Patients may experience liver failure, renal dysfunction, rickets, and acute intermittent porphyria–like symptoms. Hepatoma is a late complication. Generalized aminoaciduria, phosphaturia, glycosuria, and uricosuria may occur. A low-tyrosine/phenylalanine diet is the mainstay of therapy.

Type II tyrosinemia (Richner-Hanhart syndrome) is an autosomal-recessive inherited deficiency of tyrosine aminotransferase. Patients will have tyrosinemia, tyrosinuria, and increased urinary phenolic acids. The metabolism of other amino acids, renal function, and hepatic function are otherwise normal. Erosions of the cornea, soles, and palms are common, and mental retardation sometimes occurs. Therapy centers on a low-tyrosine/phenylalanine diet.

Methods. The nitrosonaphthol test for tyrosine is a nonspecific screening method and should be confirmed by chromatography or quantitative serum assay of tyrosine. Tyrosine and tyramine form soluble red complexes with nitrosonaphthol.

Maple Syrup Urine Disease

MSUD is one of a group of diseases associated with abnormal branched-chain amino acid metabolism (Blackburn et al., 2017). These include hypervalinemia, isovaleric acidemia causing "sweaty feet" odor, and other rare diseases. Several different clinical forms of MSUD have been described, together with various sites of biochemical derangement. The classic type of MSUD, inherited as an autosomal-recessive trait, is marked by severe neonatal vomiting, seizures, stupor, irregular respirations, and, often, hypoglycemia. Left untreated, patients become rapidly comatose and die. Leucine, isoleucine, valine, and their corresponding keto acids are elevated in the plasma and excreted in the urine. Deficient decarboxylases and other enzymes are thought to prevent the conversion of keto acids to fatty acids. Intermittent, intermediate, thiamine-responsive, and dihydrolipoyl dehydrogenase (E3) deficiency forms of MSUD have been described (Holmes et al., 1997).

The urine of patients with MSUD has an odor resembling maple syrup, caramelized sugar, or curry, the source of which is not certain. The urinary keto acids are demonstrable by the first week of life.

Methods. The dinitrophenylhydrazine screening test indicates the presence of α-keto acids in the urine. Insoluble hydrazones are formed from the reaction of carbonyl groups with dinitrophenylhydrazine. A positive result is seen with MSUD and possibly in phenylketonuria (phenylpyruvic acid), histidinemia (imidazole pyruvic acid), and methionine malabsorption (oasthouse syndrome). The test is positive with ketonuria due to other inherited diseases and other causes. A preliminary screening test for ketones should be performed.

Procedure.

1. Reagent and control (ketoglutaric acid, 25 mg in 100 mL of normal urine) should be at room temperature.
2. Add 10 drops of reagent (100 mg of 2,4-dinitrophenylhydrazine in 100 mL of 2N HCl) to 1 mL of clear urine.
3. Within 10 minutes, a yellow or chalky white precipitate indicates a positive reaction. It should be the same as or greater than the control precipitate.

Gas or thin-layer chromatographic analysis and nuclear magnetic resonance spectroscopy of the urine may be used as confirmatory methods (Holmes et al., 1997).

Cystinuria

Cystinuria is a common amino acid disorder that occurs equally in both sexes, with an incidence estimated at about 1 per 10,000 (homozygous; larger numbers for heterozygotes) (Sahota et al., 2019). In mass screening programs for infants, the homozygous form is detected at about the same rate as phenylketonuria. Defective transport of cystine by the epithelial cells of the renal tubules and gut is transmitted as an autosomal-recessive trait. The basic defect is not known. Although large amounts of the dibasic acids ornithine, lysine, and arginine are also excreted in this disease, cystine is the only one that crystallizes out, with stone formation as a clinical manifestation.

Cystinosis is a rare, recessively inherited disorder caused by a mutation in the *CTNS* gene encoding the integral transmembrane protein cystinosin, which functions in the transport of cystine from the lysosome (David et al., 2019). A deficiency of cystinosin leads to cystine crystal deposition within lysosomes throughout the body, including the kidney, eye, bone marrow, and spleen (Ivanova et al., 2014). The severe form of this disorder is characterized by photophobia, renal failure, rickets, and growth failure. With renal tubular involvement, Fanconi syndrome develops with generalized aminoaciduria and glucosuria. Benign and intermediate varieties of cystinosis have been described. Unlike in cystinuria, the cystine loss in cystinosis parallels the loss of other amino acids in the urine.

Urinary cystine is sometimes detected in patients with various renal tubular diseases. Cystine is excreted with other amino acids in Wilson disease, Lowe disease, and with the aminoaciduria of Hartnup disease.

Methods. Examine a first morning urine specimen for colorless, hexagonal crystals of cystine. Cystine may not always crystallize in a concentrated urine, although it may be present in large amounts.

The cyanide-nitroprusside test used for the qualitative determination of urine cystine is Brand's modification of the Legal nitroprusside reaction. Cystine is reduced to cysteine by sodium cyanide; the free sulfhydryl groups then react with nitroprusside to produce a red-purple color. Cysteine, cystine, homocystine, and ketones (dark red) all will give positive reactions. The qualitative test separates normal, heterozygote, and homozygote ranges of excretion. The lower limit of the test was 35 to 60 μmol of cystine/mol of creatinine, which corresponded to the heterozygote range. Homozygous stone formers usually excrete more than 300 mg/g of creatinine and are also detected by this test.

Procedure.

1. Place 3 to 5 mL of urine in a test tube and add 2.0 mL of sodium cyanide solution (5 g/dL water); allow to stand for 10 minutes. Timing is important. Treat a control solution in the same way. For a positive control, use 5 mg of cystine dissolved in 10 mL of 0.1 N HCl, diluted to 100 mL with normal urine.
2. Add fresh, aqueous sodium nitroprusside solution (5 g/dL) dropwise (about five drops), and mix.
3. Read immediately as positive or negative. A stable red-purple color will develop with cystine. "Trace" results may also be reported. A concentrated normal specimen could give a weakly positive trace result.

Further identification and quantification of cystine may be accomplished by thin-layer or quantitative ion-exchange chromatography or high-voltage electrophoresis.

Homocystinuria

The classic form of homocystinuria is due to deficiency of cystathionine β-synthase, which catalyzes the formation of cystathionine from homocystine and serine in the methionine pathway (Mudd, 2011). Homocysteine

is rapidly oxidized to homocystine, which accumulates along with methionine and is excreted in the urine. Children with this disease may have seizures, thromboses, mental retardation, arachnodactyly, and kyphoscoliosis. Connective tissue manifestations are thought to result from accumulation of the intermediate homocysteine, which interferes with collagen cross-linking.

Urine for testing must be fresh because homocystine is labile. The cyanide-nitroprusside test, described earlier, is positive. Quantitative chemical analysis reveals high levels of homocystine, methionine, and cysteine-homocysteine disulfide. Urine levels are monitored to follow the effects of the methionine-restricted diet used to treat this disease.

ADDITIONAL URINE TESTING MODALITIES

A latex agglutination nephelometric immunoassay has been developed to measure urinary basic fetoprotein (BFP). Levels of this substance may be elevated with ureter stones, infection, and prostate and bladder cancers, making BFP a nonspecific marker of inflammation or tumor (Itoh et al., 1998).

The urine Trinder spot test, performed by emergency department physicians, is a sensitive screen for salicylates.

Rendl and colleagues (1998) described a semiquantitative rapid urinary iodide test, suitable for epidemiologic surveys of iodine deficiency, particularly in developing countries.

Lastly, a monoclonal antibody assay for the detection of free urinary pyridinium cross-links can help to identify bone resorption in patients with osteoporosis, hyperthyroidism, hyperparathyroidism, and Paget disease of bone (Gomez et al., 1996).

Cytopathologic examination of the urine is commonly performed to detect malignancies. Enzyme-linked immunosorbent assay and fluorescence in situ hybridization tests can be used to detect carcinoma of the urinary bladder. These tests are discussed in greater detail in Chapter 77.

SELECTED REFERENCES

Aggarwal KP, Narula S, Kakkar M, et al.: Nephrolithiasis: molecular mechanism of renal stone formation and the critical role played by modulators, *BioMed Res Int* 292953, 2013.

Comprehensive review of renal stone formation emphasizing the role of inhibitors/promoters in calcium oxalate crystallization.

Arcidiacono T, Mingione A, Macrina L, et al.: Idiopathic calcium nephrolithiasis: a review of pathogenic mechanisms in the light of genetic studies, *Am J Nephrol* 40:499–506, 2014.

A review of the potential contribution of genetic polymorphisms to nephrolithiasis, including genes coding for proteins regulating tubular phosphate and calcium reabsorption, preventing calcium salt precipitation, and coding for a water channel in the proximal tubule.

Ben-Ezra J, Bork L, McPherson RA: Evaluation of the Sysmex UF-100 automated urinalysis analyzer, *Clin Chem* 44:92–95, 1998.

In this study, the authors compare the Sysmex UF-100 automated urinalysis analyzer with manual microscopy. The UF-100 showed good correlation with microscopy for detection of cellular elements and casts in the urine.

Besur S, Hou W, Schmeltzer P, et al.: Clinically important features of porphyrin and heme metabolism and the porphyrias, *Metabolites* 4:977–1006, 2014.

A comprehensive review of the genetic, clinical, and laboratory features of the porphyrias.

Cavanaugh C, Perazella MA: Urine sediment examination in the diagnosis and management of kidney disease: core curriculum, *Am J Kidney Dis* 73(2):258–272, 2019.

Comprehensive review of urine sediment examination and its role in the diagnosis and management of renal disease.

David D, Princiero Berlingerio S, Elmonem MA, et al.: Molecular basis of cystinosis: Geographic distribution, functional consequences of mutations in the CTNS gene, and potential for repair, *Nephron* 141(2):133–146, 2019.

A detailed review of the CTNS gene mutations, including their correlation with the clinical phenotypes and possible implications for gene therapy.

Davis R, Jones JS, Barocas DA, et al.: Diagnosis, evaluation and follow-up of asymptomatic microhematuria (AMH) in adults: AUA guideline, *J Urol* 188:2473–2481, 2012.

The authors present a systematic approach to the diagnostic evaluation and monitoring of patients with asymptomatic microhematuria.

Dinda AK, Saxena S, Guleria S, et al.: Diagnosis of glomerular haematuria: role of dysmorphic red cell, G1 cell, and bright-field microscopy, *Scand J Clin Lab Invest* 57:203–208, 1997.

This study shows that the presence of dysmorphic red blood cells in the urine has excellent sensitivity (82%) and specificity (100%) in the diagnosis of glomerular disease.

Dindo M, Conter C, Oppici E, et al.: Molecular basis of primary hyperoxaluria: clues to innovative treatments, *Urolithiasis* 47(1):67–78, 2019.

A review of primary hyperoxalurias, the basic principles of new therapeutic strategies, and their possible treatment applications.

Echeverry G, Hortin GL, Rai AJ: Introduction to urinalysis: historical perspectives and clinical application, *Methods Mol Biol* 641:1–12, 2010.

A review of the process and clinical significance of urinalysis from a historical perspective.

Fogazzi GB, Pallotti F, Garigali G: Atypical/malignant urothelial cells in routine urinary sediment: worth knowing and reporting, *Clin Chim Acta* 439:107–111, 2015.

The authors demonstrate the feasibility of identifying bladder carcinoma by routine urine sediment examination and review the criteria for the identification of neoplastic cells.

Foxman B: Urinary tract infection syndromes: occurrence, recurrence, bacteriology, risk factors, and disease burden, *Infect Dis Clin North Am* 28:1–13, 2014.

A comprehensive review of the pathogenesis and clinical features of urinary tract infections.

Gale DP: How benign is hematuria? Using genetics to predict prognosis, *Pediatr Nephrol* 28:1183–1193, 2013.

A review of microscopic hematuria in children, emphasizing the importance of genetic testing in the identification of patients with Alport syndrome and other diseases.

Garg P, Rabelink T: Glomerular proteinuria: a complex interplay between unique players, *Adv Chronic Kidney Dis* 18:233–242, 2011.

A review of the pathophysiology of proteinuria in light of new discoveries regarding genetic changes that affect the structure and function of the components of the glomerular filtration barrier.

Gerber LM, Johnson K, Alderman MH: Assessment of a new dipstick test in the screening for microalbuminuria in patients with hypertension, *Am J Hypertens* 11:1321–1327, 1998.

The authors examine the applicability of a urine dipstick method in detecting microalbuminuria. Specificity with this test was 90%, with a negative predictive value of 93% to 97%. Comparison between random and 24-hour urines showed good correlation.

Hay-Lombardie A, Pallet N, Bigot-Corbel E, et al.: Quantitative measurement of urinary proteins in 2018: advantages, disadvantages, limits, *Ann Biol Clin* 76(6):627–631, 2018.

A comprehensive review of the current methodogy of urine protein quantitation.

Hemmelgarn BR, Manns BJ, Lloyd A, et al.: Relation between kidney function, proteinuria, and adverse outcomes, *J Am Med Assoc* 303:423–429, 2010.

This article shows a strong association between proteinuria and the adverse outcomes of mortality, myocardial infarction, and progression to kidney failure independent of the commonly used estimated glomerular filtration rate.

Jefferson JA, Shankland SJ, Pichler RH: Proteinuria in diabetic kidney disease: a mechanistic viewpoint, *Kidney Int* 74:22–36, 2008.

This comprehensive review describes the pathophysiology of proteinuria through damage to the glomerulus with emphasis on the glomerular filtration barrier at the cellular level.

Lamb EJ, MacKenzie F, Stevens PE: How should proteinuria be detected and measured? *Ann Clin Biochem* 46:205–217, 2009.

This review covers current guidelines for measurement of protein in urine, emphasizing the merits of assays for albumin over total protein to assess glomerular protein loss in chronic kidney disease but with consideration for loss of other proteins in tubular proteinuria.

Lamb EJ, McTaggart MP, Stevens PE: Why albumin to creatinine ratio should replace protein to creatinine ratio: it is not just about nephrologists, *Ann Clin Biochem* 50:301–305, 2013.

A review of the diagnostic advantages of the albumin-to-creatinine ratio in comparison with the protein-to-creatinine ratio of the diagnosis of microalbuminuria.

Nicolle LE: Urinary tract infections in special populations: diabetes, renal transplant, HIV infection, and spinal cord injury, *Infect Dis Clin North Am* 28:91–104, 2014.

A review of the unique problems of diagnosing and treating urinary tract infections in immunosuppressed patients and other special patient populations.

Ma Q, Fang L, Su R, et al.: Uric acid stones, clinical manifestations and therapeutic considerations, *Postgrad Med J* 94(1114):458–462, 2018.

A comprehensive review of the pathophysiology, diagnosis, and treatment of uric acid stones.

Oyaert M, Delanghe J: Progress in automated urinalysis, *Ann Lab Med* 39(1):15–22, 2019.

laser desorption ionization–time-of-flight mass spectrometry (MALDI-TOF MS) for the identification of urinary pathogens.

Perkovic V, Verdon C, Ninomiya T, et al.: The relationship between proteinuria and coronary risk: a systematic review and meta-analysis, *PLoS Med* 5, 2008. e207.

This meta-analysis of 26 cohort studies demonstrated a strong and continuous association between proteinuria and risk for coronary artery disease, suggesting that proteinuria should be used in the risk assessment of cardiovascular disease.

Rockall AG, Newman-Sanders AP, al-Kutoubi MA, et al.: *Haematuria, Postgrad Med J* 73:129–136, 1997.

This is a review article on hematuria from a clinical perspective. It proposes a rational algorithm for the laboratory and clinical workup of patients with hematuria.

Sahota A, Tischfield JA, Goldfarb DS, et al.: Cystinuria: genetic aspects, mouse models, and a new approach to therapy, *Urolithiasis* 47(1):57–66, 2019.

A comprehensive review of the pathophysiology and treatment of cystinuria, with an emphasis on recent discoveries.

Strohmaier WL, Hoelz KJ, Bichler KH: Spot urine samples for the metabolic evaluation of urolithiasis patients, *Eur Urol* 32:294–300, 1997.

This study describes the clinical and laboratory workup of urolithiasis patients. Spot urines were equally as informative as 24-hour urines in the evaluation of these patients.

Wiener SV, Ho SP, Stoller ML: Beginnings of nephrolithiasis: insights into the past, present and future of Randall's plaque formation research, *Curr Opin Nephrol Hypertens* 27(4):236–242, 2018.

A review of the pathogenesis of kidney stone formation based on Randall's plaque research and the Anderson-Carr-Randall progression.

Yoo YM, Tatsumi N, Kirihigashi K, et al.: Inaccuracy and inefficiency of urinary sediment analysis, *Osaka City Med J* 41:41–48, 1995.

In this study, the authors examined the laboratory characteristics of manual urine microscopy. Counts of cellular elements, but not casts, showed good reproducibility, even by inexperienced technologists. Most of the casts found were nonpathologic hyaline casts.

Access the complete reference list online at Elsevier eBooks for Practicing Clinicians.

REFERENCES

Aggarwal KP, NarulaS, Kakkar M, Tandon C: Nephrolithiasis: molecular mechanism of renal stone formation and the critical role played by modulators, *BioMed Res Int* 292953, 2013, https://doi.org/10.1155/2013/292953.

Ahmed AI, Baz H, Lotfy S, Urinalysis: The automated versus manual techniques; is it time to change?, *Clin Lab* 62(1–2):49–56, 2016. Retrieved from: https://www.ncbi.nlm.nih.gov/pubmed/27012033.

Akin OK, Serdar MA, Cizmeci Z, GencO, Aydin S: Comparison of LabUMat-with-UriSed and iQ200 fully automatic urine sediment analysers with manual urine analysis, *Biotechnol Appl Biochem* 53(Pt 2):139–144, 2009, https://doi.org/10.1042/BA20080188.

Alelign T, Petros B: Kidney Stone Disease: an update on current concepts, *Adv Urol* 3068365, 2018, https://doi.org/10.1155/2018/3068365.

Ali SZ, Rosenthal DL, Ali TZ: *Epstein JI: Atlas of urinary Cytopathology with histopathologic correlations*, First ed., New York, 2009, Demos Medical Publishing.

Anderson NG, Anderson NL, Tollaksen SL: Proteins of human urine, I, Concentration and analysis by two-dimensional electrophoresis, *Clin Chem* 25(7):1199–1210, 1979. Retrieved from: http://www.ncbi.nlm.nih.gov/pubmed/455639.

Andrews NC: Disorders of iron metabolism, *N Engl J Med* 341(26):1986–1995, 1999, https://doi.org/10.1056/NEJM199912233412607.

Andrews NC: Molecular control of iron metabolism, *Best Pract Res Clin Haematol* 18(2):159–169, 2005, https://doi.org/10.1016/j.beha.2004.10.004.

Angelini C: Spectrum of metabolic myopathies, *Biochim Biophys Acta*, 2014, https://doi.org/10.1016/j.bbadis.2014.06.031.

Arao S, Matsuura S, Nonomura M, Miki K, Kabasawa K, Nakanishi H: Measurement of urinary lactoferrin as a marker of urinary tract infection, *J Clin Microbiol* 37(3):553–557, 1999. Retrieved from: http://www.ncbi.nlm.nih.gov/pubmed/9986811.

Arcidiacono T, Mingione A, Macrina L, Pivari F, Soldati L, Vezzoli G: Idiopathic calcium nephrolithiasis: a review of pathogenic mechanisms in the light of genetic studies, *Am J Nephrol* 40(6):499–506, 2014, https://doi.org/10.1159/000369833.

Armstrong LE, Soto JA, Hacker Jr FT, Casa DJ, Kavouras SA, Maresh CM: Urinary indices during dehydration, exercise, and rehydration, *Int J Sport Nutr* 8(4):345–355, 1998. Retrieved from: http://www.ncbi.nlm.nih.gov/pubmed/9841955.

Asplin J, Parks J, Lingeman J, Kahnoski R, Mardis H, Lacey S, Coe F: Supersaturation and stone composition in a network of dispersed treatment sites, *J Urol* 159(6):1821–1825, 1998. Retrieved from: http://www.ncbi.nlm.nih.gov/pubmed/9598467.

Aycock RD, Kass DA: Abnormal urine color, *South Med J* 105(1):43–47, 2012, https://doi.org/10.1097/SMJ.0b013e31823c413e.

Azimi A: Could "calprotectin" and "endocan" serve as "Troponin of Nephrologists"? *Med Hypotheses* 99:29–34, 2017, https://doi.org/10.1016/j.mehy.2016.12.008.

Bagga HS, Chi T, Miller J, Stoller ML: New insights into the pathogenesis of renal calculi, *Urol Clin North Am* 40(1):1–12, 2013, https://doi.org/10.1016/j.ucl.2012.09.006.

Bagshaw SM, Langenberg C, Bellomo R: Urinary biochemistry and microscopy in septic acute renal failure: a systematic review, *Am J Kidney Dis* 48(5):695–705, 2006, https://doi.org/10.1053/j.ajkd.2006.07.017.

Baines RJ, Brunskill NJ: Tubular toxicity of proteinuria, *Nat Rev Nephrol* 7(3):177–180, 2011, https://doi.org/10.1038/nrneph.2010.174.

Bakris GL: Microalbuminuria: prognostic implications, *Curr Opin Nephrol Hypertens* 5(3):219–223, 1996. Retrieved from: http://www.ncbi.nlm.nih.gov/pubmed/8737856.

Balwani M, Desnick RJ: The porphyrias: advances in diagnosis and treatment, *Hematology Am Soc Hematol Educ Program*19–27, 2012, https://doi.org/10.1182/asheducation-2012.1.19.

Barkan GA, Wojcik EM: Genitourinary cytopathology (kidney and urinary tract), *Cancer Treat Res* 160:149–183, 2014, https://doi.org/10.1007/978-3-642-38850-7_7.

Barnes L, Heithoff DM, Mahan SP, Fox GN, Zambrano A, Choe J, Mahan MJ: Smartphone-based pathogen diagnosis in urinary sepsis patients, *EBioMedicine* 36:73–82, 2018, https://doi.org/10.1016/j.ebiom.2018.09.001.

Baroni S, Garigali G, Primiano A, Gervasoni J, Fogazzi GB: Very unusual "needle- and pencil-like" uric acid crystals in the urine unmasked by infrared spectroscopy investigation, *Clin Chim Acta* 479:72–73, 2018, https://doi.org/10.1016/j.cca.2018.01.018.

Basile U, Gulli F, Torti E, Napodano C, Dell'Abate MT, De Santis E, Cigliana G: Evaluation of screening method for Bence Jones protein analysis, *Clin Chem Lab Med* 54(11):e331–e333, 2016, https://doi.org/10.1515/cclm-2015-1239.

Bataille P, Fardellone P, Ghazali A, Cayrolle G, Hottelart C, Achard JM, Fournier A: Pathophysiology and treatment of idiopathic hypercalciuria, *Curr Opin Rheumatol* 10(4):373–388, 1998. Retrieved from: http://www.ncbi.nlm.nih.gov/pubmed/9725102.

Baumann JM, Affolter B: From crystalluria to kidney stones, some physicochemical aspects of calcium nephrolithiasis, *World J Nephrol* 3(4):256–267, 2014, https://doi.org/10.5527/wjn.v3.i4.256.

Belmonte MM, Sarkozy E, Harpur E: Urine sugar determination by the two drop Clinitest method, *Diabetes* 16:557, 1967.

Ben-Ezra J, Bork L, McPherson RA: Evaluation of the Sysmex UF-100 automated urinalysis analyzer, *Clin Chem* 44(1):92–95, 1998. Retrieved from: http://www.ncbi.nlm.nih.gov/pubmed/9550564.

Benoit G, Machuca E, Antignac C: Hereditary nephrotic syndrome: a systematic approach for genetic testing and a review of associated podocyte gene mutations, *Pediatr Nephrol* 25(9):1621–1632, 2010, https://doi.org/10.1007/s00467-010-1495-0.

Benz-de Bretagne I, Roger C, Carlier MC, groupe de travail Sfbc SS: Urinary albumin measurement methods, *Ann Biol Clin* 76(6):633–637, 2018, https://doi.org/10.1684/abc.2018.1390.

Besur S, Hou W, Schmeltzer P, Bonkovsky HL: Clinically important features of porphyrin and heme metabolism and the porphyrias, *Metabolites* 4(4):977–1006, 2014, https://doi.org/10.3390/metabo4040977.

Blackburn PR, Gass JM, Vairo FPE, Farnham KM, Atwal HK, Macklin S, Atwal PS: Maple syrup urine disease: mechanisms and management, *Appl Clin Genet* 10:57–66, 2017, https://doi.org/10.2147/TACG.S125962.

Blau N: Genetics of phenylketonuria: then and now, *Hum Mutat* 37(6):508–515, 2016, https://doi.org/10.1002/humu.22980.

Blondheim SH, Margoliash E, Shafrir E: A simple test for myohemoglobinuria (myoglobinuria), *J Am Med Assoc* 167(4):453–454, 1958. Retrieved from: http://www.ncbi.nlm.nih.gov/pubmed/13538723.

Boven LA, Kemperman H, Demir A: A comparative analysis of the Iris iQ200 with manual microscopy as a diagnostic tool for dysmorphic erythrocytes in urine, *Clin Chem Lab Med* 50(4):751–753, 2012, https://doi.org/10.1515/CCLM.2011.813.

Bowden FJ: Reappraising the value of urine leukocyte esterase testing in the age of nucleic acid amplification, *Sex Transm Dis* 25(6):322–326, 1998. Retrieved from: http://www.ncbi.nlm.nih.gov/pubmed/9662768.

Brimo F, Vollmer RT, Case B, Aprikian A, Kassouf W, Auger M: Accuracy of urine cytology and the significance of an atypical category, *Am J Clin Pathol* 132(5):785–793, 2009, https://doi.org/10.1309/AJCPPRZLG9KT9AXL.

Bruno C, Minetti C, Shanske S, Morreale G, Bado M, Cordone G, DiMauro S: Combined defects of muscle phosphofructokinase and AMP deaminase in a child with myoglobinuria, *Neurology* 50(1):296–298, 1998. Retrieved from: http://www.ncbi.nlm.nih.gov/pubmed/9443500.

Brunzel NA: Physical examination of urine. In *Fundamentals of urine and body fluid analysis*, 3rd ed., Saunders, 2012, pp 91–108.

Brunzel NA: *Fundamentals of urine & body fluid analysis*, Fourth edition, St. Louis, Missouri, 2018, Elsevier.

Bullimore SP, Keyworth C: Finding diabetes—a method of screening in general practice, *Br J Gen Pract* 47:371–374, 1997.

Burnham P, Dadhania D, Heyang M, et al.: Urinary cell-free DNA is a versatile analyte for monitoring infections of the urinary tract, *Nat Commun* 9:2412, 2018.

Butch AW, Wises PK, Wah DT, Gornet TG, Fritsche HA: A multicenter evaluation of the Iris iQ200 automated urine microscopy analyzer body fluids module and comparison with hemacytometer cell counts, *Am J Clin Pathol* 129(3):445–450, 2008, https://doi.org/10.1309/WR1C5WNT6UFXNC6J.

Cameron JS: A history of urine microscopy, *Clin Chem Lab Med* 53(Suppl 2):s1453–1464, 2015, https://doi.org/10.1515/cclm-2015-0479.

Caridi G, Trivelli A, Sanna-Cherchi S, Perfumo F, Ghiggeri GM: Familial forms of nephrotic syndrome, *Pediatr Nephrol* 25(2):241–252, 2010, https://doi.org/10.1007/s00467-008-1051-3.

Cavanaugh C, Perazella MA: Urine sediment examination in the diagnosis and management of kidney disease: core curriculum 2019, *Am J Kidney Dis* 73(2):258–272, 2019, https://doi.org/10.1053/j.ajkd.2018.07.012.

Certikova-Chabova V, Tesar V: Recent insights into the pathogenesis of nephrotic syndrome, *Minerva Med* 104(3):333–347, 2013. Retrieved from: http://www.ncbi.nlm.nih.gov/pubmed/23748287.

Cervellin G, Comelli I, Lippi G: Rhabdomyolysis: historical background, clinical, diagnostic and therapeutic features, *Clin Chem Lab Med* 48(6):749–756, 2010, https://doi.org/10.1515/CCLM.2010.151.

Chawla LS, Dommu A, Berger A, Shih S, Patel SS: Urinary sediment cast scoring index for acute kidney injury: a pilot study, *Nephron Clin Pract* 110(3):c145–c150, 2008, https://doi.org/10.1159/000166605.

Chen M, Eintracht S, MacNamara E: Successful protocol for eliminating excessive urine microscopies: quality improvement and cost savings with physician support, *Clin Biochem* 50(1–2):88–93, 2017, https://doi.org/10.1016/j.clinbiochem.2016.06.016.

Chen YL, Huang YC, Wang CC: Direct assay of uroporphyrin and coproporphyrin in human urine by reverse-mode field amplified sample injection-sweeping and micellar electrokinetic chromatography, *Talanta* 143:27–34, 2015, https://doi.org/10.1016/j.talanta.2015.04.086.

Chiang SC, Li SF: Separation of porphyrins by capillary electrophoresis in fused-silica and ethylene vinyl acetate copolymer capillaries with visible absorbance detection, *Biomed Chromatogr* 11(6):366–370, 1997. doi:10.1002/(SICI)1099-0801(199711)11:6<366::AID-BMC708>3.0.CO;2-G.

Chinsky JM, Singh R, Ficicioglu C, van Karnebeek CDM, Grompe M, Mitchell G, Scott CR: Diagnosis and treatment of tyrosinemia type I: a US and Canadian consensus group review and recommendations, *Genet Med* 19(12), 2017, https://doi.org/10.1038/gim.2017.101.

Chu CM, Lowder JL: Diagnosis and treatment of urinary tract infections across age groups, *Am J Obstet Gynecol* 219(1):40–51, 2018, https://doi.org/10.1016/j.ajog.2017.12.231.

Ciragil P, Kurutas EB, Miraloglu M: New markers: urine xanthine oxidase and myeloperoxidase in the early detection of urinary tract infection, *Dis Markers* 269362, 2014, https://doi.org/10.1155/2014/269362.

Henry JB, editor: *Clinical diagnosis and management by laboratory methods*, 16th ed, Philadelphia, 1979, WB Saunders.

Henry JB, editor: *Clinical diagnosis and management by laboratory methods*, 17th ed, Philadelphia, 1984, WB Saunders.

Henry JB, editor: *Clinical diagnosis and management by laboratory methods*, 19th ed, Philadelphia, 1996, WB Saunders.

Cochat P, Rumsby G: Primary hyperoxaluria, *N Engl J Med* 369(7):649–658, 2013, https://doi.org/10.1056/NEJMra1301564.

Cockcroft DW, Gault MH: Prediction of creatinine clearance from serum creatinine, *Nephron* 16(1):31–41, 1976. Retrieved from: http://www.ncbi.nlm.nih.gov/pubmed/1244564.

Coe FL, Worcester EM, Evan AP: Idiopathic hypercalciuria and formation of calcium renal stones, *Nat Rev Nephrol* 12(9):519–533, 2016, https://doi.org/10.1038/nrneph.2016.101.

Cone Jr TE: Diagnosis and treatment: some syndromes, diseases, and conditions associated with abnormal coloration of the urine or diaper, A clinician's viewpoint, *Pediatrics* 41(3):654–658, 1968. Retrieved from: http://www.ncbi.nlm.nih.gov/pubmed/5641785.

Cong X, Shen L, Gu X: Current opinions on nephrolithiasis associated with primary hyperparathyroidism, *Urolithiasis* 46(5):453–457, 2018, https://doi.org/10.1007/s00240-018-1038-x.

Cook JD, Strauss KA, Caplan YH, Lodico CP, Bush DM: Urine pH: the effects of time and temperature after collection, *J Anal Toxicol* 31(8):486–496, 2007. Retrieved from: http://www.ncbi.nlm.nih.gov/pubmed/17988463.

http://jat.oxfordjournals.org/content/31/8/486.full.pdf.
Coolen JC, Verhaeghe J: Physiology and clinical value of glycosuria after a glucose challenge during pregnancy, *Eur J Obstet Gynecol Reprod Biol* 150(2):132–136, 2010, https://doi.org/10.1016/j.ejogrb.2010.02.032.
Cortvriend J, Van Nuffel J, Van den Bosch H, Van Erps P: Non-parasitic chyluria: a case report and review of the literature, *Acta Urol Belg* 66(3):11–15, 1998. Retrieved from: http://www.ncbi.nlm.nih.gov/pubmed/9864871.
Cotten SW, McCudden CR: What is your guess? The case of the blue-green urine, *Clin Chem* 57(4):646–647, 2011, https://doi.org/10.1373/clinchem.2011.161919.
Courtemanche K, Chan P, Kassouf W: Prevalence and associated factors for dipstick microscopic hematuria in men, *BMC Urol* 19(1):76, 2019, https://doi.org/10.1186/s12894-019-0505-1.
Crop MJ, de Rijke YB, Verhagen PC, Cransberg K, Zietse R: Diagnostic value of urinary dysmorphic erythrocytes in clinical practice, *Nephron Clin Pract* 115(3):c203–212, 2010, https://doi.org/10.1159/000313037.
Cui M, Ju S, Shi Y, Jing R: Performance verification of the Iris iQ200 Sprint automated urine microscopy analyzer in a hospital routine laboratory, *Clin Lab* 63(10):1607–1612, 2017, https://doi.org/10.7754/Clin.Lab.2017.170318.
D'Alessandro M, Poli L, Lai Q, Gaeta A, Nazzari C, Garofalo M, Pretagostini R: Automated intelligent microscopy for the recognition of decoy cells in urine samples of kidney transplant patients, *Transplant Proc* 51(1):157–159, 2019, https://doi.org/10.1016/j.transproceed.2018.05.030.
Dallosso HM, Bodicoat DH, Campbell M, Carey ME, Davies MJ, Eborall HC, Heller S: Self-monitoring of blood glucose versus self-monitoring of urine glucose in adults with newly diagnosed Type 2 diabetes receiving structured education: a cluster randomized controlled trial, *Diabet Med*, 2014, https://doi.org/10.1111/dme.12598.
Daudon M, Frochot V: Crystalluria, *Clin Chem Lab Med* 53(Suppl 2):s1479–1487, 2015, https://doi.org/10.1515/cclm-2015-0860.
Davenport M, Mach KE, Shortliffe LMD, et al.: New and developing diagnostic technologies for urinary tract infections, *Nat Rev Urol* 14:296–310, 2017.
David D, Princiero Berlingerio S, Elmonem MA, Oliveira Arcolino F, Soliman N, van den Heuvel B, Levtchenko E: Molecular basis of cystinosis: Geographic distribution, functional consequences of mutations in the CTNS gene, and potential for repair, *Nephron* 141(2):133–146, 2019, https://doi.org/10.1159/000495270.
Davis R, Jones JS, Barocas DA, Castle EP, Lang EK, Leveillee RJ, American Urological A: Diagnosis, evaluation and follow-up of asymptomatic microhematuria (AMH) in adults: AUA guideline, *J Urol* 188(6 Suppl):2473–2481, 2012, https://doi.org/10.1016/j.juro.2012.09.078.
de Mendoza SG, Kashyap ML, Chen CY, Lutmer RF: High density lipoproteinuria in nephrotic syndrome, *Metabolism* 25(10):1143–1149, 1976. Retrieved from: http://www.ncbi.nlm.nih.gov/pubmed/184367.
De Rosa R, Grosso S, Lorenzi G, Bruschetta G, Camporese A: Evaluation of the new Sysmex UF-5000 fluorescence flow cytometry analyser for ruling out bacterial urinary tract infection and for prediction of Gram negative bacteria in urine cultures, *Clin Chim Acta* 484:171–178, 2018, https://doi.org/10.1016/j.cca.2018.05.047.
Deacon AC, Peters TJ: Identification of acute porphyria: evaluation of a commercial screening test for urinary porphobilinogen, *Ann Clin Biochem* 35(Pt 6):726–732, 1998. Retrieved from: http://www.ncbi.nlm.nih.gov/pubmed/9838985.
Deindoerfer H, Gangwer JR, Laird CW, Ringold RR: "The Yellow IRIS" urinalysis workstation—the first commercial application of "automated intelligent microscopy", *Clin Chem* 31(9):1491–1499, 1985. Retrieved from: https://www.ncbi.nlm.nih.gov/pubmed/4028398.
Delanghe J, Speeckaert M: Preanalytics in urinalysis, *Clin Biochem* 49(18):1346–1350, 2016, https://doi.org/10.1016/j.clinbiochem.2016.10.016.
Delanghe JR, Himpe J, De Cock N, Delanghe S, De Herde K, Stove V, Speeckaert MM: Sensitive albuminuria analysis using dye-binding based test strips, *Clin Chim Acta* 471:107–112, 2017, https://doi.org/10.1016/j.cca.2017.05.032.
Demelo-Rodríguez P, Galán-Carrillo I, Del Toro-Cervera J: Purple urine bag syndrome, *Eur J Intern Med* 35:e3–e4, 2016, https://doi.org/10.1016/j.ejim.2016.05.005.
Demirbas D, Coelho AI, Rubio-Gozalbo ME, Berry GT: Hereditary galactosemia, *Metabolism* 83:188–196, 2018, https://doi.org/10.1016/j.metabol.2018.01.025.
Deutsch JC: Gas chromatographic/mass spectrometric measurement of ascorbic acid and analysis of ascorbic acid degradation in solution, *Methods Enzymol* 279:13–24, 1997. Retrieved from: http://www.ncbi.nlm.nih.gov/pubmed/9211252.
Devuyst O, Olinger E, Rampoldi L: Uromodulin: from physiology to rare and complex kidney disorders, *Nat Rev Nephrol* 13(9):525–544, 2017, https://doi.org/10.1038/nrneph.2017.101.
Dinda AK, Saxena S, Guleria S, Tiwari SC, Dash SC, Srivastava RN, Singh C: Diagnosis of glomerular haematuria: role of dysmorphic red cell, G1 cell and bright-field microscopy, *Scand J Clin Lab Invest* 57(3):203–208, 1997. Retrieved from: http://www.ncbi.nlm.nih.gov/pubmed/9238755.
Dindo M, Conter C, Oppici E, Ceccarelli V, Marinucci L, Cellini B: Molecular basis of primary hyperoxaluria: clues to innovative treatments, *Urolithiasis* 47(1):67–78, 2019, https://doi.org/10.1007/s00240-018-1089-z.
Doan M, Vorobjev I, Rees P, Filby A, Wolkenhauer O, Goldfeld AE, Hennig H: Diagnostic potential of imaging flow cytometry, *Trends Biotechnol* 36(7):649–652, 2018, https://doi.org/10.1016/j.tibtech.2017.12.008.
Dong ZY, Wang YD, Qiu Q, Hou K, Zhang L, Wu J, Chen XM: Dysmorphic erythrocytes are superior to hematuria for indicating non-diabetic renal disease in type 2 diabetics, *J Diabetes Investig* 7(1):115–120, 2016, https://doi.org/10.1111/jdi.12371.
Du J, Xu J, Wang F, Guo Y, Zhang F, Wu W, Cui W: Establishment and development of the personalized criteria for microscopic review following multiple automated routine urinalysis systems, *Clin Chim Acta* 444:221–228, 2015, https://doi.org/10.1016/j.cca.2015.02.022.
Echeverry G, Hortin GL, Rai AJ: Introduction to urinalysis: historical perspectives and clinical application, *Methods Mol Biol* 641:1–12, 2010, https://doi.org/10.1007/978-1-60761-711-2_1.
Eklund A, Slettengren M, van der Linden J: Performance and user evaluation of a novel capacitance-based automatic urinometer compared with a manual standard urinometer after elective cardiac surgery, *Crit Care* 19:173, 2015, https://doi.org/10.1186/s13054-015-0899-4.
El-Achkar TM, Wu XR: Uromodulin in kidney injury: an instigator, bystander, or protector? *Am J Kidney Dis* 59(3):452–461, 2012, https://doi.org/10.1053/j.ajkd.2011.10.054.
El-Guindi MA, El-Said HH, Hussein MH: Nassar Rel S, Sira AM: urinary urobilinogen in biliary atresia: a missed, simple and cheap diagnostic test, *Hepatol Res* 46(2):174–182, 2016, https://doi.org/10.1111/hepr.12558.
Ennis JL, Asplin JR: The role of the 24-h urine collection in the management of nephrolithiasis, *Int J Surg* 36(Pt D):633–637, 2016, https://doi.org/10.1016/j.ijsu.2016.11.020.
Erkan E: Proteinuria and progression of glomerular diseases, *Pediatr Nephrol* 28(7):1049–1058, 2013, https://doi.org/10.1007/s00467-012-2335-1.
Erlinger S, Arias IM, Dhumeaux D: Inherited disorders of bilirubin transport and conjugation: new insights into molecular mechanisms and consequences, *Gastroenterology* 146(7):1625–1638, 2014, https://doi.org/10.1053/j.gastro.2014.03.047.
European Confederation of Laboratory Medicine: European urinalysis guidelines, *Scand J Clin Lab Invest Suppl* 231:1–86, 2000. Retrieved from: http://www.ncbi.nlm.nih.gov/pubmed/12647764.
Farrington CJ, Liddy ML, Chalmers AH: A simplified sensitive method for the analysis of renal calculi, *Am J Clin Pathol* 73(1):96–99, 1980. Retrieved from: http://www.ncbi.nlm.nih.gov/pubmed/7352431.
Favaro S, Bonfante L, D'Angelo A, Giacomini A, Normanno M, Calo L, Borsatti A: Is the red cell morphology really useful to detect the source of hematuria?, *Am J Nephrol* 17(2):172–175, 1997. Retrieved from: http://www.ncbi.nlm.nih.gov/pubmed/9096449.
Fenili D, Pirovano B: The automation of sediment urinalysis using a new urine flow cytometer (UF-100), *Clin Chem Lab Med* 36(12):909–917, 1998, https://doi.org/10.1515/CCLM.1998.158.
Fernández-Carballo BL, Broger T, Wyss R, et al.: Toward the development of a circulating free DNA-based *in vitro* diagnostic test for infectious diseases: a review of evidence for tuberculosis, *J Clin Micro* 57, 2019. e01234–18.
Flannigan R, Choy WH, Chew B, Lange D: Renal struvite stones—pathogenesis, microbiology, and management strategies, *Nat Rev Urol* 11(6):333–341, 2014, https://doi.org/10.1038/nrurol.2014.99.
Fleming C, Brouwer R, van Alphen A, Lindemans J, de Jonge R: UF-1000i: validation of the body fluid mode for counting cells in body fluids, *Clin Chem Lab Med* 52(12):1781–1790, 2014, https://doi.org/10.1515/cclm-2014-0512.
Fogazzi GB, Delanghe J: Microscopic examination of urine sediment: phase contrast versus bright field, *Clin Chim Acta* 487:168–173, 2018, https://doi.org/10.1016/j.cca.2018.09.036.
Fogazzi GB, Edefonti A, Garigali G, Giani M, Zolin A, Raimondi S, Messa P: Urine erythrocyte morphology in patients with microscopic haematuria caused by a glomerulopathy, *Pediatr Nephrol* 23(7):1093–1100, 2008, https://doi.org/10.1007/s00467-008-0777-2.
Fogazzi GB, Pallotti F, Garigali G: Atypical/malignant urothelial cells in routine urinary sediment: worth knowing and reporting, *Clin Chim Acta* 439:107–111, 2015, https://doi.org/10.1016/j.cca.2014.10.021.
Fogazzi GB, Saglimbeni L, Banfi G, Cantu M, Moroni G, Garigali G, Cesana M: Urinary sediment features in proliferative and non-proliferative glomerular diseases, *J Nephrol* 18(6):703–710, 2005. Retrieved from: http://www.ncbi.nlm.nih.gov/pubmed/16358228.
Foxman B: Urinary tract infection syndromes: occurrence, recurrence, bacteriology, risk factors, and disease burden, *Infect Dis Clin North Am* 28(1):1–13, 2014, https://doi.org/10.1016/j.idc.2013.09.003.
Fracchia JA, Motta J, Miller LS, Armenakas NA, Schumann GB, Greenberg RA: Evaluation of asymptomatic microhematuria, *Urology* 46(4):484–489, 1995. Retrieved from: http://www.ncbi.nlm.nih.gov/pubmed/7571215.
Friderichsen B, Maunsbach M: Glycosuric tests should not be employed in population screenings for NIDDM, *J Public Health Med* 19(1):55–60, 1997. Retrieved from: http://www.ncbi.nlm.nih.gov/pubmed/9138218.
Froom P, Shimoni Z: The uncertainties of the diagnosis and treatment of a suspected urinary tract infection in elderly hospitalized patients, *Expert Rev Anti Infect Ther* 16(10):763–770, 2018, https://doi.org/10.1080/14787210.2018.1523006.
Fukuzaki A, Kaneto H, Ikeda S, Orikasa S: Determining the origin of hematuria by immunocytochemical staining of erythrocytes in urine for Tamm-Horsfall protein, *J Urol* 155(1):248–251, 1996. Retrieved from: http://www.ncbi.nlm.nih.gov/pubmed/7490846.
Gale DP: How benign is hematuria? Using genetics to predict prognosis, *Pediatr Nephrol* 28(8):1183–1193, 2013, https://doi.org/10.1007/s00467-012-2399-y.
Garg P, Rabelink T: Glomerular proteinuria: a complex interplay between unique players, *Adv Chronic Kidney Dis* 18(4):233–242, 2011, https://doi.org/10.1053/j.ackd.2011.06.001.
Gerber LM, Johnston K, Alderman MH: Assessment of a new dipstick test in screening for microalbuminuria in patients with hypertension, *Am J Hypertens* 11(11 Pt 1):1321–1327, 1998. Retrieved from: http://www.ncbi.nlm.nih.gov/pubmed/9832175.
Ginsberg JM, Chang BS, Matarese RA, Garella S: Use of single voided urine samples to estimate quantitative proteinuria, *N Engl J Med* 309(25):1543–1546, 1983, https://doi.org/10.1056/NEJM198312223092503.
Goldenberg RM, Berard LD, Cheng AYY, Gilbert JD, Verma S, Woo VC, Yale JF: SGLT2 inhibitor-associated diabetic ketoacidosis: clinical review and recommendations for prevention and diagnosis, *Clin Ther* 38(12):2654–2664, 2016, https://doi.org/10.1016/j.clinthera.2016.11.002. e2651.
Gomez Jr B, Ardakani S, Evans BJ, Merrell LD, Jenkins DK, Kung VT: Monoclonal antibody assay for free urinary pyridinium cross-links, *Clin Chem* 42(8 Pt 1):1168–1175, 1996. Retrieved from: http://www.ncbi.nlm.nih.gov/pubmed/8697572.
Graziani M, Merlini G, Petrini C: Proteins ICoP, proteins SISGo: guidelines for the analysis of bence Jones protein, *Clin Chem Lab Med* 41(3):338–346, 2003, https://doi.org/10.1515/CCLM.2003.054.
Graziani MS, Gambaro G, Mantovani L, Sorio A, Yabarek T, Abaterusso C, Rizzotti P: Diagnostic accuracy of a reagent strip for assessing urinary albumin excretion in the general population, *Nephrol Dial Transplant* 24(5):1490–1494, 2009, https://doi.org/10.1093/ndt/gfn639.

Gribble RK, Meier PR, Berg RL: The value of urine screening for glucose at each prenatal visit, *Obstet Gynecol* 86(3):405–410, 1995, https://doi.org/10.1016/0029-7844(95)00198-Z.

Group KDIGOKCW: KDIGO 2012 clinical practice guideline for the evaluation and manage- ment of chronic kidney disease, *Kidney Int Suppl* 3:1–150, 2013.

Guldberg P, Levy HL, Hanley WB, Koch R, Matalon R, Rouse BM, Guttler F: Phenylalanine hydroxylase gene mutations in the United States: report from the Maternal PKU Collaborative Study, *Am J Hum Genet* 59(1):84–94, 1996. Retrieved from: http://www.ncbi.nlm.nih.gov/pubmed/8659548.

Guttilla A, Beltrami P, Bettin L, Galantini A, Dal Moro F, Ficarra V, Zattoni F: Chyluria: the state of the art, *Urologia* 84(2):65–70, 2017, https://doi.org/10.5301/uj.5000225.

Guy M, Newall R, Borzomato J, Kalra PA, Price C: Diagnostic accuracy of the urinary albumin: creatinine ratio determined by the CLINITEK Microalbumin and DCA 2000+ for the rule-out of albuminuria in chronic kidney disease, *Clin Chim Acta* 399(1–2):54–58, 2009, https://doi.org/10.1016/j.cca.2008.09.006.

Haber MH: Pisse prophecy: a brief history of urinalysis, *Clin Lab Med* 8(3):415–430, 1988. Retrieved from: http://www.ncbi.nlm.nih.gov/pubmed/3048852.

Han Q, Zhu H, Chen X, Liu Z: Non-genetic mechanisms of diabetic nephropathy, *Front Med* 11(3):319–332, 2017, https://doi.org/10.1007/s11684-017-0569-9.

Han Y, Gu Y, Zhang AC, Lo YH: Review: imaging technologies for flow cytometry, *Lab Chip* 16(24):4639–4647, 2016, https://doi.org/10.1039/c6lc01063f.

Hay-Lombardie A, Pallet N, Bigot-Corbel E, groupe de travail Sfbc SS: Quantitative measurement of urinary proteins in 2018: advantages, disadvantages, limits, *Ann Biol Clin* 76(6):627–631, 2018, https://doi.org/10.1684/abc.2018.1389.

Hebert LA, Dillon JJ, Middendorf DF, Lewis EJ, Peter JB: Relationship between appearance of urinary red blood cell/white blood cell casts and the onset of renal relapse in systemic lupus erythematosus, *Am J Kidney Dis* 26(3):432–438, 1995. Retrieved from: http://www.ncbi.nlm.nih.gov/pubmed/7645551.

Hemmelgarn BR, Manns BJ, Lloyd A, James MT, Klarenbach S, Quinn RR: Alberta Kidney Disease N: relation between kidney function, proteinuria, and adverse outcomes, *J Am Med Assoc* 303(5):423–429, 2010, https://doi.org/10.1001/jama.2010.39.

Holmes E, Foxall PJ, Spraul M, Farrant RD, Nicholson JK, Lindon JC: 750 MHz 1H NMR spectroscopy characterisation of the complex metabolic pattern of urine from patients with inborn errors of metabolism: 2-hydroxyglutaric aciduria and maple syrup urine disease, *J Pharm Biomed Anal* 15(11):1647–1659, 1997. Retrieved from: http://www.ncbi.nlm.nih.gov/pubmed/9260660.

Horikoshi S, Okuda M, Nishimura E, Ohsawa I, Suzuki Y, Shimizu Y, Tomino Y: Usefulness of HPLC assay for early detection of microalbuminuria in chronic kidney disease, *J Clin Lab Anal* 27(4):333–338, 2013, https://doi.org/10.1002/jcla.21608.

Horikoshi S, Eva G, Christopher S, Flynn E, Henner D: Is specific gravity a good estimate of urine osmolality? *J Clin Lab Anal* 24(6):426–430, 2010, https://doi.org/10.1002/jcla.20424.

Ince FD, Ellidag HY, Koseoglu M, Simsek N, Yalcin H, Zengin MO: The comparison of automated urine analyzers with manual microscopic examination for urinalysis automated urine analyzers and manual urinalysis, *Pract Lab Med* 5:14–20, 2016, https://doi.org/10.1016/j.plabm.2016.03.002.

Itoh Y, Sakabe K, Kawai T: Basic fetoprotein in normal and pathologic urine, *Ren Fail* 20(2):235–241, 1998. Retrieved from: http://www.ncbi.nlm.nih.gov/pubmed/9574448.

Ivanova E, De Leo MG, De Matteis MA, Levtchenko E: Cystinosis: clinical presentation, pathogenesis and treatment, *Pediatr Endocrinol Rev* 12(Suppl 1):176–184, 2014. Retrieved from: https://www.ncbi.nlm.nih.gov/pubmed/25345100.

Jiang T, Chen P, Ouyang J, Zhang S, Cai D: Urine particles analysis: performance evaluation of Sysmex UF-1000i and comparison among urine flow cytometer, dipstick, and visual microscopic examination, *Scand J Clin Lab Invest* 71(1):30–37, 2011, https://doi.org/10.3109/00365513.2010.535011.

Johnson CD, Mole DR, Pestridge A: Postprandial alkaline tide: does it exist?, *Digestion* 56(2):100–106, 1995. Retrieved from: http://www.ncbi.nlm.nih.gov/pubmed/7750662.

Jones RM, Lamb JH, Lim CK: Urinary porphyrin profiles by laser desorption/ionization time-of-flight mass spectrometry without the use of classical matrices, *Rapid Commun Mass Spectrom* 9(10):921–923, 1995, https://doi.org/10.1002/rcm.1290091011.

Joshi S, Andersen R, Jespersen B, Rittig S: Genetics of steroid-resistant nephrotic syndrome: a review of mutation spectrum and suggested approach for genetic testing, *Acta Paediatr* 102(9):844–856, 2013, https://doi.org/10.1111/apa.12317.

Jou WW, Powers RD: Utility of dipstick urinalysis as a guide to management of adults with suspected infection or hematuria, *South Med J* 91(3):266–269, 1998. Retrieved from: http://www.ncbi.nlm.nih.gov/pubmed/9521367.

Kadkhoda K, Manickam K, Degagne P, Sokolowski P, Pang P, Kontzie N, Alfa M: UF-1000i flow cytometry is an effective screening method for urine specimens, *Diagn Microbiol Infect Dis* 69(2):130–136, 2011, https://doi.org/10.1016/j.diagmicrobio.2010.09.013.

Karlsen H, Dong T: Smartphone-based rapid screening of urinary biomarkers, *IEEE Trans Biomed Circuits Syst* 11(2):455–463, 2017, https://doi.org/10.1109/TBCAS.2016.2633508.

Karslioglu French E, Donihi AC, Korytkowski MT: Diabetic ketoacidosis and hyperosmolar hyperglycemic syndrome: review of acute decompensated diabetes in adult patients, *BMJ* 365:l1114, 2019, https://doi.org/10.1136/bmj.l1114.

Kayalp D, Dogan K, Ceylan G, Senes M, Yucel D: Can routine automated urinalysis reduce culture requests? *Clin Biochem* 46(13–14):1285–1289, 2013, https://doi.org/10.1016/j.clinbiochem.2013.06.015.

Kazi SN, Benz RL: Work-up of hematuria, *Prim Care* 41(4):737–748, 2014, https://doi.org/10.1016/j.pop.2014.08.007.

Kesson AM, Talbott JM, Gyory AZ: Microscopic examination of urine, *Lancet* 2(8094):809–812, 1978. Retrieved from: http://www.ncbi.nlm.nih.gov/pubmed/81363.

Keverline JP: Recurrent rhabdomyolysis associated with influenza-like illness in a weight-lifter, *J Sports Med Phys Fitness* 38(2):177–179, 1998. Retrieved from: https://www.ncbi.nlm.nih.gov/pubmed/9763805.

Khan SR, Atmani F, Glenton P, Hou Z, Talham DR, Khurshid M: Lipids and membranes in the organic matrix of urinary calcific crystals and stones, *Calcif Tissue Int* 59(5):357–365, 1996. Retrieved from: http://www.ncbi.nlm.nih.gov/pubmed/8849402.

Khan SR, Pearle MS, Robertson WG, Gambaro G, Canales BK, Doizi S, Tiselius HG: Kidney stones, *Nat Rev Dis Primers* 2:16008, 2016, https://doi.org/10.1038/nrdp.2016.8.

Khejonnit V, Pratumvinit B, Reesukumal K, Meepanya S, Pattanavin C, Wongkrajang P: Optimal criteria for microscopic review of urinalysis following use of automated urine analyzer, *Clin Chim Acta* 439:1–4, 2015, https://doi.org/10.1016/j.cca.2014.09.027.

Killander J, Sjolin S, Zaar B: Rapid tests for ketonuria. A comparative study, *Scand J Clin Lab Invest* 14:311–314, 1962. Retrieved from: http://www.ncbi.nlm.nih.gov/pubmed/14037075.

Kim SY, Jeong TD, Lee W, Chun S, Sunwoo S, Kim SB, Min WK: Plasma neutrophil gelatinase-associated lipocalin as a marker of tubular damage in diabetic nephropathy, *Ann Lab Med* 38(6):524–529, 2018, https://doi.org/10.3343/alm.2018.38.6.524.

Kim SY, Park Y, Kim H, Kim J, Koo SH, Kwon GC: Rapid screening of urinary tract infection and discrimination of gram-positive and gram-negative bacteria by automated flow cytometric analysis using Sysmex UF-5000, *J Clin Microbiol* 56(8), 2018, https://doi.org/10.1128/JCM.02004-17.

Koss LG, Hoda RS: *Koss's cytology of the urinary tract with histopathologic correlations (2012 ed.)*, Heidelberg, 2012, Springer.

Kraut JA, Madias NE: Lactic acidosis, *N Engl J Med* 371(24):2309–2319, 2014, https://doi.org/10.1056/NEJMra1309483.

Krstic D, Tomic N, Radosavljevic B, Avramovic N, Dragutinovic V, Skodric SR, Colovic M: Biochemical markers of renal function, *Curr Med Chem* 23(19):2018–2040, 2016. Retrieved from: https://www.ncbi.nlm.nih.gov/pubmed/26769095.

Kunin CM, DeGroot JE: Self-screening for significant bacteriuria. Evaluation of dipstrip combination nitrite/culture test, *J Am Med Assoc* 231(13):1349–1353, 1975. Retrieved from: http://www.ncbi.nlm.nih.gov/pubmed/1091747.

Kutter D: A chemical test strip to determine low concentrations of albumin and creatinine in urine, *Lab Med* 29:769–772, 1998.

Kwong T, Robinson C, Spencer D, Wiseman OJ, Karet Frankl FE: Accuracy of urine pH testing in a regional metabolic renal clinic: is the dipstick accurate enough? *Urolithiasis* 41(2):129–132, 2013, https://doi.org/10.1007/s00240-013-0546-y.

Laiwejpithaya S, Wongkrajang P, Reesukumal K, Bucha C, Meepanya S, Pattanavin C, Chuntarut A: UriSed 3 and UX-2000 automated urine sediment analyzers vs manual microscopic method: a comparative performance analysis, *J Clin Lab Anal* 32(2), 2018, https://doi.org/10.1002/jcla.22249.

Lamb EJ, MacKenzie F, Stevens PE: How should proteinuria be detected and measured? *Ann Clin Biochem* 46(Pt 3):205–217, 2009, https://doi.org/10.1258/acb.2009.009007.

Lamb EJ, McTaggart MP, Stevens PE: Why albumin to creatinine ratio should replace protein to creatinine ratio: it is not just about nephrologists, *Ann Clin Biochem* 50(Pt 4):301–305, 2013, https://doi.org/10.1177/0004563212473284.

Lee W, Kim Y, Chang S, Lee AJ, Jeon CH: The influence of vitamin C on the urine dipstick tests in the clinical specimens: a multicenter study, *J Clin Lab Anal* 31(5), 2017, https://doi.org/10.1002/jcla.22080.

Letavernier E, Daudon M: Vitamin D, hypercalciuria and kidney stones, *Nutrients* 10(3), 2018, https://doi.org/10.3390/nu10030366.

Levey AS, Coresh J, Balk E, Kausz AT, Levin A, Steffes MW, Eknoyan G: National Kidney Foundation practice guidelines for chronic kidney disease: evaluation, classification, and stratification, *Ann Intern Med* 139(2):137–147, 2003. Retrieved from: http://www.ncbi.nlm.nih.gov/pubmed/12859163.
http://annals.org/data/Journals/AIM/20044/0000605-200307150-00013.pdf.

Levitt DG, Levitt MD: Quantitative assessment of the multiple processes responsible for bilirubin homeostasis in health and disease, *Clin Exp Gastroenterol* 7:307–328, 2014, https://doi.org/10.2147/CEG.S64283.

Levy Y, George J, Ziporen L, Cledes J, Amital H, Bar-Dayan Y, Shoenfeld Y: Massive proteinuria as a main manifestation of primary antiphospholipid syndrome, *Pathobiology* 66(1):l49–52, 1998. Retrieved from: http://www.ncbi.nlm.nih.gov/pubmed/9577967.

Livsey SA: Turbidimetric urine screening, *Br J Biomed Sci* 52(1):71–73, 1995. Retrieved from: http://www.ncbi.nlm.nih.gov/pubmed/7549609.

Lizana J, Brito M, Davis MR: Assessment of five quantitative methods for determination of total proteins in urine, *Clin Biochem* 10(2):89–93, 1977. Retrieved from: http://www.ncbi.nlm.nih.gov/pubmed/862182.

Loun B, Astles R, Copeland KR, Sedor FA: Adaptation of a quantitative immunoassay for urine myoglobin. Predictor in detecting renal dysfunction, *Am J Clin Pathol* 105(4):479–486, 1996. Retrieved from: http://www.ncbi.nlm.nih.gov/pubmed/8604691.

Lowenstein J, Grantham JJ: The rebirth of interest in renal tubular function, *Am J Physiol Renal Physiol* 310(11):LF1351–1355, 2016, https://doi.org/10.1152/ajprenal.00055.2016.

Lubell TR, Barasch JM, XuK IM, Cabrera KI, Dayan PS: Urinary neutrophil gelatinase-associated lipocalin for the diagnosis of urinary tract infections, *Pediatrics* 140(6), 2017, https://doi.org/10.1542/peds.2017-1090.

Luceri C, Caderni G, Lodovici M, Spagnesi MT, Monserrat C, Lancioni L, Dolara P: Urinary excretion of sucrose and fructose as a predictor of sucrose intake in dietary intervention studies, *Cancer Epidemiol Biomarkers Prev* 5(3):167–171, 1996. Retrieved from: http://www.ncbi.nlm.nih.gov/pubmed/8833616.

Luo J, Lamb JH, Lim CK: Analysis of urinary and faecal porphyrin excretion patterns in human porphyrias by fast atom bombardment mass spectrometry, *J Pharm Biomed Anal* 15(9–10):1289–1294, 1997. Retrieved from: http://www.ncbi.nlm.nih.gov/pubmed/9226555.

Luo JL, Deka J, Lim CK: Determination of 5-aminolaevulinic acid dehydratase activity in erythrocytes and porphobilinogen in urine by micellar electrokinetic capillary chromatography, *J Chromatogr A* 722(1–2):353–357, 1996. Retrieved from: http://www.ncbi.nlm.nih.gov/pubmed/9019304.

Lyon ME, Ball CL, Lyon AW, Walpole E, Church DL: A preliminary evaluation of the interaction between urine specific gravity and leukocyte esterase results using Bayer Multistix and the Clinitek 500, *Clin Biochem* 36(7):579–581, 2003. Retrieved from: http://www.ncbi.nlm.nih.gov/pubmed/14563454.

Ma Q, Fang L, Su R, Ma L, Xie G, Cheng Y: Uric acid stones, clinical manifestations and therapeutic considerations, *Postgrad Med J* 94(1114):458–462, 2018, https://doi.org/10.1136/postgradmedj-2017-135332.

Machuca E, Benoit G, Antignac C: Genetics of nephrotic syndrome: connecting molecular genetics to podocyte physiology, *Hum Mol Genet* 18(R2):R185–194, 2009, https://doi.org/10.1093/hmg/ddp328.

Magee C, Grieve DJ, Watson CJ: Brazil DP: diabetic nephropathy: a Tangled Web to Unweave, *Cardiovasc Drugs Ther* 31(5–6):579–592, 2017, https://doi.org/10.1007/s10557-017-6755-9.

Magiorkinis E, Diamantis A: The fascinating story of urine examination: from uroscopy to the era of microscopy and beyond, *Diagn Cytopathol* 43(12):1020–1036, 2015, https://doi.org/10.1002/dc.23370.

Malihi Z, Wu Z, Stewart AW, Lawes CM, Scragg R: Hypercalcemia, hypercalciuria, and kidney stones in long-term studies of vitamin D supplementation: a systematic review and meta-analysis, *Am J Clin Nutr* 104(4):1039–1051, 2016, https://doi.org/10.3945/ajcn.116.134981.

Manoni F, Tinello A, Fornasiero L, Hoffer P, Temporin V, Valverde S, Gessoni G: Urine particle evaluation: a comparison between the UF-1000i and quantitative microscopy, *Clin Chem Lab Med* 48(8):1107–1111, 2010, https://doi.org/10.1515/CCLM.2010.233.

Marable H: Falling drop method for urine specific gravity, *Am J Med Technol* 29:20–24, 1963. Retrieved from: https://www.ncbi.nlm.nih.gov/pubmed/13932740.

Margulis V: Sagalowsky AI: assessment of hematuria, *Med Clin North Am* 95(1):153–159, 2011, https://doi.org/10.1016/j.mcna.2010.08.028.

Martinez-Martinez MU, Llamazares-Azuara LM, Martinez-Galla D, Mandeville PB, Valadez-Castillo F, Roman-Acosta S, Abud-Mendoza C: Urinary sediment suggests lupus nephritis histology, *Lupus* 26(6):580–587, 2017, https://doi.org/10.1177/0961203316669241.

Masajtis-Zagajewska A, Nowicki M: New markers of urinary tract infection, *Clin Chim Acta* 471:286–291, 2017, https://doi.org/10.1016/j.cca.2017.06.003.

Mayans L: Nephrolithiasis, *Prim Care* 46(2):203–212, 2019, https://doi.org/10.1016/j.pop.2019.02.001.

McElderry LA, Tarbit IF, Cassells-Smith AJ: Six methods for urinary protein compared, *Clin Chem* 28(2):356–360, 1982. Retrieved from: http://www.ncbi.nlm.nih.gov/pubmed/7055959.

McGregor DO, Lynn KL, Bailey RR, Robson RA, Gardner J: Clinical audit of the use of renal biopsy in the management of isolated microscopic hematuria, *Clin Nephrol* 49(6):345–348, 1998. Retrieved from: http://www.ncbi.nlm.nih.gov/pubmed/9696429.

McKenzie A, Muñoz C, Ellis L, Perrier E, Guelinckx I, Klein A, Armstrong L: Urine color as an indicator of urine concentration in pregnant and lactating women, *Eur J Nutr* 56(1):355–362, 2017, https://doi.org/10.1007/s00394-015-1085-9.

Meng QH, Handy B, Wagar E: Confirmatory testing of urine ketones and bilirubin: still necessary? *Arch Pathol Lab Med* 137(8):1028–1029, 2013, https://doi.org/10.5858/arpa.2013-0054-LE.

Meng QH, Handy B, Wagar EA: It's not easy being blue-green, *Ann Lab Med* 33(6):457–458, 2013, https://doi.org/10.3343/alm.2013.33.6.457.

Milani GP, Mazzoni MB, Burdick L, Bianchetti MG, Fossali EF: Postural proteinuria associated with left renal vein entrapment: a follow-up evaluation, *Am J Kidney Dis* 55(6):e29–31, 2010, https://doi.org/10.1053/j.ajkd.2010.03.004.

Miler M, Nikolac N: Patient safety is not compromised by excluding microscopic examination of negative urine dipstick, *Ann Clin Biochem* 55(1):77–83, 2018, https://doi.org/10.1177/0004563216687589.

Misra S, Oliver NS: Utility of ketone measurement in the prevention, diagnosis and management of diabetic ketoacidosis, *Diabet Med* 32(1):14–23, 2015, https://doi.org/10.1111/dme.12604.

Miyajima H, Orii KE, Shindo Y, Hashimoto T, Shinka T, Kuhara T, Kaneko E: Mitochondrial trifunctional protein deficiency associated with recurrent myoglobinuria in adolescence, *Neurology* 49(3):833–837, 1997. Retrieved from: http://www.ncbi.nlm.nih.gov/pubmed/9305349.

Mody L, Juthani-Mehta M: Urinary tract infections in older women: a clinical review, *J Am Med Assoc* 311(8):844–854, 2014, https://doi.org/10.1001/jama.2014.303.

Mogensen CE: Microalbuminuria predicts clinical proteinuria and early mortality in maturity-onset diabetes, *N Engl J Med* 310(6):356–360, 1984, https://doi.org/10.1056/NEJM198402093100605.

Mori R, Yonemoto N, Fitzgerald A, Tullus K, Verrier-Jones K, Lakhanpaul M: Diagnostic performance of urine dipstick testing in children with suspected UTI: a systematic review of relationship with age and comparison with microscopy, *Acta Paediatr* 99(4):581–584, 2010, https://doi.org/10.1111/j.1651-2227.2009.01644.x.

Mount DL, Green MD, Zucker JR, Were JB, Todd GD: Field detection of sulfonamides in urine: the development of a new and sensitive test, *Am J Trop Med Hyg* 55(3):250–253, 1996, https://doi.org/10.4269/ajtmh.1996.55.250.

Mudd SH: Hypermethioninemias of genetic and non-genetic origin: a review, *Am J Med Genet C Semin Med Genet* 157C(1):3–32, 2011, https://doi.org/10.1002/ajmg.c.30293.

Muriithi AK, Nasr SH, Leung N: Utility of urine eosinophils in the diagnosis of acute interstitial nephritis, *Clin J Am Soc Nephrol* 8(11):1857–1862, 2013, https://doi.org/10.2215/CJN.01330213.

Nagahama D, Yoshiko K, Watanabe M, Morita Y, Iwatani Y, Matsuo S: A useful new classification of dysmorphic urinary erythrocytes, *Clin Exp Nephrol* 9(4):304–309, 2005, https://doi.org/10.1007/s10157-005-0380-9.

Nakanishi N, Fukui M, Tanaka M, Toda H, Imai S, Yamazaki M, Nakamura N: Low urine pH Is a predictor of chronic kidney disease, *Kidney Blood Press Res* 35(2):77–81, 2012, https://doi.org/10.1159/000330487.

Naumova NN, Schappert J, Kaplan LA: Reducing substances in urine: a paradigm for changes in a standard test, *Ann Clin Lab Sci* 36(4):447–448, 2006. Retrieved from: http://www.ncbi.nlm.nih.gov/pubmed/17127733.

Ndamase S, Freercks R: The utility of urine sulphosalicylic acid testing in the detection of non-albumin proteinuria, *S Afr Med J* 105(2):153, 2014, https://doi.org/10.7196/samj.9270.

Nicolle LE: Urinary tract infections in special populations: diabetes, renal transplant, HIV infection, and spinal cord injury, *Infect Dis Clin North Am* 28(1):91–104, 2014, https://doi.org/10.1016/j.idc.2013.09.006.

Nicolle LE, Gupta K, Bradley SF, et al.: Clinical practice guideline for the management of asymptomatic bacteriuria: 2019 update by the Infectious Diseases Society of America, *Clin Infect Dis* 68:e83–e110, 2019.

O'Connor WJ, Murphy GM, Darby C, Fogarty J, Mulcahy F, O'Moore R, Barnes L: Porphyrin abnormalities in acquired immunodeficiency syndrome, *Arch Dermatol* 132(12):1443–1447, 1996. Retrieved from: http://www.ncbi.nlm.nih.gov/pubmed/8961872.

O'Kell AL, Grant DC, Khan SR: Pathogenesis of calcium oxalate urinary stone disease: species comparison of humans, dogs, and cats, *Urolithiasis* 45(4):329–336, 2017, https://doi.org/10.1007/s00240-017-0978-x.

Oliveira B, Unwin R, Walsh SB: Inherited proximal tubular disorders and nephrolithiasis, *Urolithiasis* 47(1):35–42, 2019, https://doi.org/10.1007/s00240-018-01103-z.

Olivieri B, Rai AJ: A primer on clinical applications and assays using urine: focus on analysis of plasma cell dyscrasias using automated electrophoresis and immunofixation, *Methods Mol Biol* 641:13–26, 2010, https://doi.org/10.1007/978-1-60761-711-2_2.

Ooi SB, Kour NW, Mahadev A: Haematuria in the diagnosis of urinary calculi, *Ann Acad Med Singapore* 27(2):210–214, 1998. Retrieved from: http://www.ncbi.nlm.nih.gov/pubmed/9663312.

Ottiger C, Huber AR: Quantitative urine particle analysis: integrative approach for the optimal combination of automation with UF-100 and microscopic review with KOVA cell chamber, *Clin Chem* 49(4):617–623, 2003. Retrieved from: http://www.ncbi.nlm.nih.gov/pubmed/12651815.

Oyaert M, Delanghe J: Progress in automated urinalysis, *Ann Lab Med* 39(1):15–22, 2019, https://doi.org/10.3343/alm.2019.39.1.15.

Oyaert M, Delanghe JR: Semiquantitative, fully automated urine test strip analysis, *J Clin Lab Anal* 33(5), 2019, https://doi.org/10.1002/jcla.22870. e22870.

Oyaert MN, Himpe J, Speeckaert MM, Stove VV, Delanghe JR: Quantitative urine test strip reading for leukocyte esterase and hemoglobin peroxidase, *Clin Chem Lab Med* 56(7):1126–1132, 2018, https://doi.org/10.1515/cclm-2017-1159.

Panholzer TJ, Beyer J, Lichtwald K: Coupled-column liquid chromatographic analysis of catecholamines, serotonin, and metabolites in human urine, *Clin Chem* 45(2):262–268, 1999. Retrieved from: http://www.ncbi.nlm.nih.gov/pubmed/9931050.

Penders J, Fiers T, Delanghe JR: Quantitative evaluation of urinalysis test strips, *Clin Chem* 48(12):2236–2241, 2002. Retrieved from: http://www.ncbi.nlm.nih.gov/pubmed/12446482.

Perazella MA: The urine sediment as a biomarker of kidney disease, *Am J Kidney Dis* 66(5):748–755, 2015, https://doi.org/10.1053/j.ajkd.2015.02.342.

Perazella MA, Coca SG, Hall IE, Iyanam U, Koraishy M, Parikh CR: Urine microscopy is associated with severity and worsening of acute kidney injury in hospitalized patients, *Clin J Am Soc Nephrol* 5(3):402–408, 2010, https://doi.org/10.2215/CJN.06960909.

Perazella MA, Coca SG, Kanbay M, Brewster UC, Parikh CR: Diagnostic value of urine microscopy for differential diagnosis of acute kidney injury in hospitalized patients, *Clin J Am Soc Nephrol* 3(6):1615–1619, 2008, https://doi.org/10.2215/CJN.02860608.

Perinpam M, Ware EB, Smith JA, et al.: Key influence of sex on urine volume and osmolality, *Biol Sex Differ* 7:12, 2016, https://doi.org/10.1186/s13293-016-0063-0.eCollection2016.

Perkovic V, Verdon C, Ninomiya T, Barzi F, Cass A, Patel A, Huxley R: The relationship between proteinuria and coronary risk: a systematic review and meta-analysis, *PLoS Med* 5(10), 2008, https://doi.org/10.1371/journal.pmed.0050207. e207.

Peterson LM, Reed HS: *Hematuria*, *Prim Care* 46(2):265–273, 2019, https://doi.org/10.1016/j.pop.2019.02.008.

Poloni JA, Pinto GG, Giordani MS, Keitel E, Inocente N, Voegeli CF, Rotta LN: Bright field microscopy to detect decoy cells due to BK virus infection in the fresh and unstained urine sediment in kidney allograft recipients, *J Clin Lab Anal* 30(6):1044–1050, 2016, https://doi.org/10.1002/jcla.21978.

Poloni JA, Pinto GG, Pasqualotto AC, Rotta LN: Decoy cells due to polyomavirus BK infection in the urine sediment of a patient with lupus nephritis, *Lupus* 22(14):1547–1548, 2013, https://doi.org/10.1177/0961203313504635.

Poloni JAT, Perazella MA, Keitel E, Marroni CA, Leite SB, Rotta LN: Utility of a urine sediment score in hyperbilirubinemia/hyperbilirubinuria, *Clin Nephrol* 92(3):141–150, 2019, https://doi.org/10.5414/CN109673.

Ponzi E, Maiorana A, Lepri FR, Mucciolo M, Semeraro M, Taurisano R, Dionisi-Vici C: Persistent hypoglycemia in children: Targeted gene panel improves the diagnosis of hypoglycemia due to inborn errors of metabolism, *J Pediatr* 202:272–278, 2018, https://doi.org/10.1016/j.jpeds.2018.06.050. e274.

Previtali G, Ravasio R, Seghezzi M, Buoro S, Alessio MG: Performance evaluation of the new fully automated urine particle analyser UF-5000 compared to the reference method of the Fuchs-Rosenthal chamber, *Clin Chim Acta* 472:123–130, 2017, https://doi.org/10.1016/j.cca.2017.07.028.

Pugia MJ: Technology behind diagnostic reagent strips, *Lab Med* 31:92–96, 2000.

Qiu H, Novikov A, Vallon V: Ketosis and diabetic ketoacidosis in response to SGLT2 inhibitors: basic mechanisms and therapeutic perspectives, *Diabetes Metab Res Rev* 33(5), 2017, https://doi.org/10.1002/dmrr.2886.

Ra M, Muhammad MS, Lim C, Han S, Jung C, Kim WY: Smartphone-based point-of-care urinalysis under variable illumination, *IEEE J Transl Eng Health Med* 6:2800111, 2018, https://doi.org/10.1109/JTEHM.2017.2765631.

Rampoldi L, Scolari F, Amoroso A, Ghiggeri G, Devuyst O: The rediscovery of uromodulin (Tamm-Horsfall protein): from tubulointerstitial nephropathy to chronic kidney disease, *Kidney Int* 80(4):338–347, 2011, https://doi.org/10.1038/ki.2011.134.

Rasoulpour M, Banco L, Laut JM, Burke GS: Inability of community-based laboratories to identify pathological casts in urine samples, *Arch Pediatr Adolesc Med* 150(11):1201–1204, 1996. Retrieved from: http://www.ncbi.nlm.nih.gov/pubmed/8904863.

Reilly AA, Bellisario R, Pass KA: Multivariate discrimination for phenylketonuria (PKU) and non-PKU hyperphenylalaninemia after analysis of newborns' dried blood-spot specimens for six amino acids by ion-exchange chromatography, *Clin Chem* 44(2):317–326, 1998. Retrieved from: http://www.ncbi.nlm.nih.gov/pubmed/9474031.

Ren C, Wu J, Jin M, Wang X, Cao H: Rapidly discriminating culture-negative urine specimens from patients with suspected urinary tract infections by UF-5000, *Bioanalysis*, 2018, https://doi.org/10.4155/bio-2018-0175.

Rendl J, Bier D, Groh T, Reiners C: Rapid urinary iodide test, *J Clin Endocrinol Metab* 83(3):1007–1012, 1998, https://doi.org/10.1210/jcem.83.3.4633.

Robinson RR, Glover SN, Phillippi PJ, Lecocq FR, Langelier PR: Fixed and reproducible orthostatic proteinuria. I. Light microscopic studies of the kidney, *Am J Pathol* 39:291–306, 1961. Retrieved from: http://www.ncbi.nlm.nih.gov/pubmed/13742344.

Rockall AG, Newman-Sanders AP, al-Kutoubi MA: Vale JA: haematuria, *Postgrad Med J* 73(857):129–136, 1997. Retrieved from: http://www.ncbi.nlm.nih.gov/pubmed/9135826.

Rodby RA: Timed urine collections for albumin and protein: "the king is dead, long live the king!", *Am J Kidney Dis* 68(6):836–838, 2016, https://doi.org/10.1053/j.ajkd.2016.06.025.

Rogozinska E, Formina S, Zamora J, Mignini L, Khan KS: Accuracy of onsite tests to detect asymptomatic bacteriuria in pregnancy: a systematic review and meta-analysis, *Obstet Gynecol* 128(3):495–503, 2016, https://doi.org/10.1097/AOG.0000000000001597.

Rose MR, Kissel JT, Bickley LS, Griggs RC: Sustained myoglobinuria: the presenting manifestation of dermatomyositis, *Neurology* 47(1):119–123, 1996. Retrieved from: http://www.ncbi.nlm.nih.gov/pubmed/8710064.

Roshan B, Stanton RC: A story of microalbuminuria and diabetic nephropathy, *J Nephropathol* 2(4):234–240, 2013, https://doi.org/10.12860/JNP.2013.37.

Rothschild B: Sole dependence on urine testing strips and the ability to identify clinically significant disease: Challenging the current paradigm for heme detection in general clinical situations, *Lab Med* 47(2):e18–20, 2016, https://doi.org/10.1093/labmed/lmv031.

Ryan Caballes F, Sendi H, Bonkovsky HL: Hepatitis C, porphyria cutanea tarda and liver iron: an update, *Liver Int* 32(6):880–893, 2012, https://doi.org/10.1111/j.1478--3231.2012.02794.x.

Sacks DB, Arnold M, Bakris GL, Bruns DE, Horvath AR, Kirkman MS, Nathan DM: Guidelines and recommendations for laboratory analysis in the diagnosis and management of diabetes mellitus, *Clin Chem* 57(6):e1–e47, 2011, https://doi.org/10.1373/clinchem.2010.161596.

Sahota A, Tischfield JA, Goldfarb DS, Ward MD, Hu L: Cystinuria: genetic aspects, mouse models, and a new approach to therapy, *Urolithiasis* 47(1):57–66, 2019, https://doi.org/10.1007/s00240-018-1101-7.

Sanchez-Mora C, Acevedo D, Porres MA, Chaques AM, Zapardiel J, Gallego-Cabrera A, Maesa JM: Comparison of automated devices UX-2000 and SediMAX/AutionMax for urine samples screening: a multicenter Spanish study, *Clin Biochem* 50(12):714–718, 2017, https://doi.org/10.1016/j.clinbiochem.2017.02.005.

Saravakos P, Kokkinou V, Giannatos E: Cystinuria: current diagnosis and management, *Urology* 83(4):693–699, 2014, https://doi.org/10.1016/j.urology.2013.10.013.

Sarnak MJ, Astor BC: Implications of proteinuria: CKD progression and cardiovascular outcomes, *Adv Chronic Kidney Dis* 18(4):258–266, 2011, https://doi.org/10.1053/j.ackd.2011.04.002.

Scales Jr CD, Smith AC, Hanley JM, Saigal CS: Urologic diseases in America P: prevalence of kidney stones in the United States, *Eur Urol* 62(1):160–165, 2012, https://doi.org/10.1016/j.eururo.2012.03.052.

Schifman RB, Luevano DR: Value and Use of urinalysis for myoglobinuria, *Arch Pathol Lab Med*, 2019, https://doi.org/10.5858/arpa.2018-0475-OA.

Schot MJ, van Delft S, Kooijman-Buiting AM, de Wit NJ, Hopstaken RM: Analytical performance, agreement and user-friendliness of six point-of-care testing urine analysers for urinary tract infection in general practice, *BMJ Open* 5(5), 2015, https://doi.org/10.1136/bmjopen-2014-006857. e006857.

Schreiner GE: Some observations on telescoped urinary sediments, *Ann Intern Med* 42(4):826–838, 1955, https://doi.org/10.7326/0003-4819-42-4-826.

Schwartz S, Shorov V, Watson CJ: Studies of urobilinogen. IV. Quantitative determination of urobilinogen by means of Evelyn photoelectric colorimeter, *Am J Clin Pathol* 14:598–604, 1944.

Scott RP, Quaggin SE: Review series: the cell biology of renal filtration, *J Cell Biol* 209(2):199–210, 2015, https://doi.org/10.1083/jcb.201410017.

Sharp LJ, Haller RG: Metabolic and mitochondrial myopathies, *Neurol Clin* 32(3):777–799, 2014, https://doi.org/10.1016/j.ncl.2014.05.001. ix.

Sharp VJ, Barnes KT, Erickson BA: Assessment of asymptomatic microscopic hematuria in adults, *Am Fam Physician* 88(11):747–754, 2013. Retrieved from: http://www.ncbi.nlm.nih.gov/pubmed/24364522.
http://www.aafp.org/afp/2013/1201/p747.pdf

Shekarriz B, Stoller ML: Uric acid nephrolithiasis: current concepts and controversies, *J Urol* 168(4 Pt 1):1307–1314, 2002. Retrieved from: http://www.ncbi.nlm.nih.gov/pubmed/12352383.

Shihabi ZK: Myoglobinuria detection by capillary electrophoresis, *J Chromatogr B Biomed Appl* 669(1):53–58, 1995. Retrieved from: http://www.ncbi.nlm.nih.gov/pubmed/7581887.

Shin S, Srivastava A, Alli NA, Bandyopadhyay BC: Confounding risk factors and preventative measures driving nephrolithiasis global makeup, *World J Nephrol* 7(7):129–142, 2018, https://doi.org/10.5527/wjn.v7.i7.129.

Sidhu H, Hoppe B, Hesse A, Tenbrock K, Bromme S, Rietschel E, Peck AB: Absence of Oxalobacter formigenes in cystic fibrosis patients: a risk factor for hyperoxaluria, *Lancet* 352(9133):1026–1029, 1998, https://doi.org/10.1016/S0140-6736(98)03038-4.

Simo-Alfonso EF, Ramis-Ramos G, Garcia-Alvarez-Coque MC, Esteve-Romero JS: Determination of sulphonamides in human urine by azo dye precolumn derivatization and micellar liquid chromatography, *J Chromatogr B Biomed Appl* 670(1):183–187, 1995, https://doi.org/10.1016/0378-4347(95)00158-f.

Singh HK, Bubendorf L, Mihatsch MJ, Drachenberg CB, Nickeleit V: Urine cytology findings of polyomavirus infections, *Adv Exp Med Biol* 577:201–212, 2006, https://doi.org/10.1007/0-387-32957-9_15.

Singh PP, Pendse AK, Ahmed A, Ramavataram DV, Rajpurohit SK: A study of recurrent stone formers with special reference to renal tubular acidosis, *Urol Res* 23(3):201–203, 1995. Retrieved from: http://www.ncbi.nlm.nih.gov/pubmed/7483148.

Skoberne A, Borstnar S, Avgustin N, Kovac D, Rigler AA, Veceric-Haler Z, Lindic J: Tubular urinary indexes reliably distinguish between primary tubulointerstitial and primary glomerular diseases in patients referred for kidney biopsy, *Clin Nephrol* 88(13):1–6, 2017, https://doi.org/10.5414/CNP88FX01.

Slettengren M, Wetterfall H, Eklund A, van der Linden J: A pilot evaluation of a capacitance-based automatic urinometer in a pediatric intensive care setting, *Pediatr Crit Care Med*, 2019, https://doi.org/10.1097/PCC.0000000000002000.

Sorokin I, Mamoulakis C, Miyazawa K, Rodgers A, Talati J, Lotan Y: Epidemiology of stone disease across the world, *World J Urol* 35(9):1301–1320, 2017, https://doi.org/10.1007/s00345-017-2008-6.

Spinelli D, Consonni D, Garigali G, Fogazzi GB: Waxy casts in the urinary sediment of patients with different types of glomerular diseases: results of a prospective study, *Clin Chim Acta* 424:47–52, 2013, https://doi.org/10.1016/j.cca.2013.05.009.

St John A, Boyd JC, Lowes AJ, Price CP: The use of urinary dipstick tests to exclude urinary tract infection: a systematic review of the literature, *Am J Clin Pathol* 126(3):428–436, 2006, https://doi.org/10.1309/C69RW1BT7E4QAFPV.

Stankovic AK, DiLauri E: Quality improvements in the preanalytical phase: focus on urine specimen workflow, *Clin Lab Med* 28(2):339–350, 2008, https://doi.org/10.1016/j.cll.2007.12.011. viii.

Strasinger SK, Di Lorenzo MS: Physical examination of urine. In *Urinalysis and body fluids*, 6th ed., Philadelphia, PA: F.A., 2014, Davis Company, pp 59–70.

Streather CP, Varghese Z, Moorhead JF, Scoble JE: Lipiduria in renal disease, *Am J Hypertens* 6(11 Pt 2):353S–357S, 2014, https://doi.org/10.1093/ajh/6.11.353s.

Strohmaier WL, Hoelz KJ, Bichler KH: Spot urine samples for the metabolic evaluation of urolithiasis patients, *Eur Urol* 32(3):294–300, 1997. Retrieved from: http://www.ncbi.nlm.nih.gov/pubmed/9358216.

Takemura Y, Ishida H, Inoue Y, Kobayashi H, Beck JR: Opportunistic discovery of occult disease by use of test panels in new, symptomatic primary care outpatients: yield and cost of case finding, *Clin Chem* 46(8 Pt 1):1091–1098, 2000. Retrieved from: http://www.ncbi.nlm.nih.gov/pubmed/10926888.

Tchan M: Hyperammonemia and lactic acidosis in adults: differential diagnoses with a focus on inborn errors of metabolism, *Rev Endocr Metab Disord* 19(1):69–79, 2018, https://doi.org/10.1007/s11154-018-9444-5.

Thomas K, Wong K, Withington J, Bultitude M, Doherty A: Cystinuria-a urologist's perspective, *Nat Rev Urol* 11(5):270–277, 2014, https://doi.org/10.1038/nrurol.2014.51.

Threatte GA: Laboratory evaluation of renal function in the elderly. In Michelis MF, Davis BB, Preuss HG, editors: *Geriatric nephrology*, vol. 1. New York: Field, 1986, Rich and Associates, Inc, pp 18–21.

Davidsohn I, Henry JB, editors: *Todd-Sanford clinical diagnosis by laboratory methods*, 15th ed, Philadelphia, 1974, WB Saunders.

Tramonti G, Kanwar YS: Review and discussion of tubular biomarkers in the diagnosis and management of diabetic nephropathy, *Endocrine* 43(3):494–503, 2013, https://doi.org/10.1007/s12020-012-9820-y.

Tran C: Inborn errors of fructose metabolism. What can We Learn from them? *Nutrients* 9(4), 2017, https://doi.org/10.3390/nu9040356.

Tryggvason K, Patrakka J, Wartiovaara J: Hereditary proteinuria syndromes and mechanisms of proteinuria, *N Engl J Med* 354(13):1387–1401, 2006, https://doi.org/10.1056/NEJMra052131.

Tsai JJ, Yeun JY, Kumar VA, Don BR: Comparison and interpretation of urinalysis performed by a nephrologist versus a hospital-based clinical laboratory, *Am J Kidney Dis* 46(5):820–829, 2005, https://doi.org/10.1053/j.ajkd.2005.07.039.

Tummalapalli L, Nadkarni GN, Coca SG: Biomarkers for predicting outcomes in chronic kidney disease, *Curr Opin Nephrol Hypertens* 25(6):480–486, 2016, https://doi.org/10.1097/MNH.0000000000000275.

Tworek JA, Wilkinson DS, Walsh MK: The rate of manual microscopic examination of urine sediment: a College of American Pathologists Q-Probes study of 11,243 urinalysis tests from 88 institutions, *Arch Pathol Lab Med* 132(12):1868–1873, 2008, https://doi.org/10.1043/1543-2165-132.12.1868.

Unic A, Nikolac Gabaj N, Miler M, Culej J, Lisac A, Horvat A, Vrkic N: Ascorbic acid-A black hole of urine chemistry screening, *J Clin Lab Anal* 32(5), 2018, https://doi.org/10.1002/jcla.22390. e22390.

Vembadi A, Menachery A, Qasaimeh MA: Cell cytometry: review and perspective on Biotechnological advances, *Front Bioeng Biotechnol* 7:147, 2019, https://doi.org/10.3389/fbioe.2019.00147.

Verdesca S, Fogazzi GB, Garigali G, Messa P, Daudon M: Crystalluria: prevalence, different types of crystals and the role of infrared spectroscopy, *Clin Chem Lab Med* 49(3):515–520, 2011, https://doi.org/10.1515/CCLM.2011.078.

Verma V, Kant R, Sunnoqrot N, Gambert SR: Proteinuria in the elderly: evaluation and management, *Int Urol Nephrol* 44(6):1745–1751, 2012, https://doi.org/10.1007/s11255-012-0252-7.

Vezzoli G, Macrina L, Magni G, Arcidiacono T: Calcium-sensing receptor: evidence and hypothesis for its role in nephrolithiasis, *Urolithiasis* 47(1):23–33, 2019, https://doi.org/10.1007/s00240-018-1096-0.

Viazzi F, Cappadona F, Pontremoli R: Microalbuminuria in primary hypertension: a guide to optimal patient management? *J Nephrol* 29(6):747–753, 2016, https://doi.org/10.1007/s40620-016-0335-0.

Viberti GC, Hill RD, Jarrett RJ, Argyropoulos A, Mahmud U, Keen H: Microalbuminuria as a predictor of clinical nephropathy in insulin-dependent diabetes mellitus, *Lancet* 1(8287):1430–1432, 1982. Retrieved from: http://www.ncbi.nlm.nih.gov/pubmed/6123720.

Viswanathan G, Upadhyay A: Assessment of proteinuria, *Adv Chronic Kidney Dis* 18(4):243–248, 2011, https://doi.org/10.1053/j.ackd.2011.03.002.

Vogeser M, Stauch T: Evaluation of a commercially available rapid urinary porphobilinogen test, *Clin Chem Lab Med* 49(9):1491–1494, 2011, https://doi.org/10.1515/CCLM.2011.605.

Voinescu GC, Shoemaker M, Moore H, Khanna R, Nolph KD: The relationship between urine osmolality and specific gravity, *Am J Med Sci* 323(1):39–42, 2002. Retrieved from: http://www.ncbi.nlm.nih.gov/pubmed/11814141.

Waldvogel-Abramowski S, Waeber G, Gassner C, Buser A, Frey BM, Favrat B, Tissot JD: Physiology of iron metabolism, *Transfus Med Hemother* 41(3):213–221, 2014, https://doi.org/10.1159/000362888.

Ward JF, Kaplan GW, Mevorach R, Stock JA, Cilento Jr BG: Refined microscopic urinalysis for red blood cell morphology in the evaluation of asymptomatic microscopic hematuria in a pediatric population, *J Urol* 160(4):1492–1495, 1998. Retrieved from: http://www.ncbi.nlm.nih.gov/pubmed/9751402.

Waterhouse N, Nichol G, Kasapic D: An evaluation of the automated Cobas u 701 microscopy analyzer for the routine screening of urine to identify negative samples, *Clin Lab* 65(1), 2019, https://doi.org/10.7754/Clin.Lab.2018.180612.

Weinstein DA, Steuerwald U, De Souza CFM, Derks TGJ: Inborn errors of metabolism with hypoglycemia: glycogen storage diseases and inherited disorders of Gluconeogenesis, *Pediatr Clin North Am* 65(2):247–265, 2018, https://doi.org/10.1016/j.pcl.2017.11.005.

Weiss JP: Blaivas JG: nocturia, *J Urol* 163(1):5–12, 2000. Retrieved from: https://www.ncbi.nlm.nih.gov/pubmed/10604303.

Weisz D, Seabrook JA, Lim RK: The presence of urinary nitrites is a significant predictor of pediatric urinary tract infection susceptibility to first- and third-generation cephalosporins, *J Emerg Med* 39(1):6–12, 2010, https://doi.org/10.1016/j.jemermed.2008.01.010.

Welch AA, Mulligan A, Bingham SA, Khaw KT: Urine pH is an indicator of dietary acid-base load, fruit and vegetables and meat intakes: results from the European Prospective Investigation into Cancer and Nutrition (EPIC)-Norfolk population study, *Br J Nutr* 99(6):1335–1343, 2008, https://doi.org/10.1017/S0007114507862350.

Whatley SD, Badminton MN: Role of genetic testing in the management of patients with inherited porphyria and their families, *Ann Clin Biochem* 50(Pt 3):204–216, 2013, https://doi.org/10.1177/0004563212473278.

White SL, Yu R, Craig JC, Polkinghorne KR, Atkins RC, Chadban SJ: Diagnostic accuracy of urine dipsticks for detection of albuminuria in the general community, *Am J Kidney Dis* 58(1):19–28, 2011, https://doi.org/10.1053/j.ajkd.2010.12.026.

Wiener SV, Ho SP, Stoller ML: Beginnings of nephrolithiasis: insights into the past, present and future of Randall's plaque formation research, *Curr Opin Nephrol Hypertens* 27(4):236–242, 2018, https://doi.org/10.1097/MNH.0000000000000414.

Wockenfus AM, Koch CD, Conlon PM, Sorensen LD, Cambern KL, Chihak AJ, Karon BS: Discordance between urine pH measured by dipstick and pH meter: implications for methotrexate administration protocols, *Clin Biochem* 46(1–2):152–154, 2013, https://doi.org/10.1016/j.clinbiochem.2012.10.018.

Wong WK, Wieringa GE, Stec Z, Russell J, Cooke S, Keevil BG, Lockhart S: A comparison of three procedures for the detection of Bence-Jones proteinuria, *Ann Clin Biochem* 34(Pt 4):371–374, 1997. Retrieved from: http://www.ncbi.nlm.nih.gov/pubmed/9247668.

Wright OR, Safranek S: Urine dipstick for diagnosing urinary tract infection, *Am Fam Physician* 73(1):129–130, 2006. Retrieved from: http://www.ncbi.nlm.nih.gov/pubmed/16417075.

Wu TH, Li KJ, Yu CL, Tsai CY: Tamm-horsfall protein is a potent Immunomodulatory molecule and a disease biomarker in the urinary system, *Molecules* 23(1), 2018, https://doi.org/10.3390/molecules23010200.

Wu X: Urinalysis: a review of methods and procedures, *Crit Care Nurs Clin North Am* 22(1):121–128, 2010, https://doi.org/10.1016/j.ccell.2009.10.012.

Yamada Y, Tsuchiya T, Inagaki I, Seishima M, Deguchi T: Prediction of early BK virus infection in kidney transplant recipients by the number of cells with intranuclear inclusion bodies (decoy cells), *Transplant Direct* 4(2), 2018, https://doi.org/10.1097/TXD.0000000000000759. e340.

Yano T, Takahashi R, Yamashita T, Nagano N, Ishikawa A, Sakurai A, Miura T: Detection of urinary mulberry bodies leads to diagnosis of Fabry Cardiomyopathy: a simple clue in the urine sediment, *Circ Heart Fail* 10(12), 2017, https://doi.org/10.1161/CIRCHEARTFAILURE.117.004538.

Yoo YM, Tatsumi N, Kirihigashi K, Narita M, Tsuda I, Kawamoto T, Takubo T: Inaccuracy and inefficiency of urinary sediment analysis, *Osaka City Med J* 41(2):41–48, 1995. Retrieved from: http://www.ncbi.nlm.nih.gov/pubmed/8778645.

Young JG: Urinary tract stones in cystic fibrosis, *Paediatr Respir Rev* 27:21–23, 2018, https://doi.org/10.1016/j.prrv.2018.03.007.

Zaccardi F, Webb D, Yates T, Davies M: Pathophysiology of type 1 and type 2 diabetes mellitus: a 90-year perspective, *Postgrad Med J* 92(1084):63–69, 2016, https://doi.org/10.1136/postgradmedj-2015-133281.

Zaman Z, Borremans A, Verhaegen J, Verbist L, Blanckaert N: Disappointing dipstick screening for urinary tract infection in hospital inpatients, *J Clin Pathol* 51(6):471–472, 1998. Retrieved from: http://www.ncbi.nlm.nih.gov/pubmed/9771448.

Zaman Z, Proesmans W: Dysmorphic erythrocytes and G1 cells as markers of glomerular hematuria, *Pediatr Nephrol* 14(10–11):980–984, 2000. Retrieved from: http://www.ncbi.nlm.nih.gov/pubmed/10975311.

Zelmanovitz T, Gross JL, Oliveira J, de Azevedo MJ: Proteinuria is still useful for the screening and diagnosis of overt diabetic nephropathy, *Diabetes Care* 21(7):1076–1079, 1998. Retrieved from: http://www.ncbi.nlm.nih.gov/pubmed/9653598.

Ziemba JB, Matlaga BR: Epidemiology and economics of nephrolithiasis, *Investig Clin Urol* 58(5):299–306, 2017, https://doi.org/10.4111/icu.2017.58.5.299.

Zimmerman JL, Shen MC: Rhabdomyolysis, *Chest* 144(3):1058–1065, 2013, https://doi.org/10.1378/chest.12-2016.

Zuijderhoudt FM, Dorresteijn-de Bok J: Comparison of the Bio-Rad Porphyrin Column Test with a simple spectrophotometric test for total urine porphyrin concentration, *Ann Clin Biochem* 35(Pt 3):418–421, 1998. Retrieved from: http://www.ncbi.nlm.nih.gov/pubmed/9635109.

Zutt R, van der Kooi AJ, Linthorst GE, Wanders RJ, de Visser M: Rhabdomyolysis: review of the literature, *Neuromuscul Disord* 24(8):651–659, 2014, https://doi.org/10.1016/j.nmd.2014.05.005.

CHAPTER 30

CEREBROSPINAL, SYNOVIAL, SEROUS BODY FLUIDS, AND ALTERNATIVE SPECIMENS

Donald S. Karcher, Richard A. McPherson

CEREBROSPINAL FLUID, 510
Specimen Collection and Opening Pressure, 510
Indications and Recommended Tests, 511
Gross Examination, 511
Microscopic Examination, 512
Chemical Analysis, 515
Microbiological Examination, 521

SYNOVIAL FLUID, 522
Specimen Collection, 523
Recommended Tests, 523
Gross Examination, 523
Microscopic Examination, 524
Chemical Analysis, 526
Lipids, 526
Immunologic Studies, 527
Microbiological Examination, 527

PLEURAL FLUID, 527
Specimen Collection, 527
Transudates and Exudates, 527
Recommended Tests, 527
Gross Examination, 528
Microscopic Examination, 528
Chemical Analysis, 529
Immunologic Studies, 531
Microbiological Examination, 531

PERICARDIAL FLUID, 531
Specimen Collection, 531
Gross Examination, 532
Exudates And Transudates, 532
Microscopic Examination, 532
Chemical Analysis, 532
Immunologic Studies, 533
Microbiological Examination, 533

PERITONEAL FLUID, 533
Transudates and Exudates, 533
Specimen Collection, 533
Recommended Tests, 534
Gross Examination, 534
Microscopic Examination, 534
Chemical Analysis, 535
Microbiological Examination, 536

ALTERNATIVE SPECIMENS, 536
Saliva, 536
Meconium, 536
Hair and Nails, 536
Breath Testing, 537
Tissue Aspirates, 537

CHEMICAL MEASUREMENTS IN BODY FLUIDS, 537

SELECTED REFERENCES, 538

KEY POINTS

- Cerebrospinal fluid is an essential part of a neurologic examination, comprising special attention to cell counts, basic chemical analyses, and microbiological cultures with specific antibody titers.
- Determining the etiologic cause of fluid accumulation in various body cavities (synovial fluid in joints, pleural fluid in the chest, pericardial fluid around the heart, and peritoneal fluid in the abdomen) is critical for proper treatment of these disorders.
- Serous fluids can be distinguished as either transudates that arise due to an imbalance of hydrostatic pressures or exudates caused by an inflammatory process.
- Appropriate laboratory examination of these fluids is critical for the diagnosis of numerous diseases (bacterial, viral, and fungal infections; distinction between various arthritides; primary [e.g., mesothelioma] and metastatic malignancies; among others).
- Accurate test interpretation depends on appropriate specimen collection, physician/laboratory communication, analytically sound laboratory methods, and reliable reference values.
- Alternative or nonstandard specimens can have an important role in diagnostic or forensic testing; however, performing these tests may require additional method validation to ensure their appropriateness and accuracy.

CEREBROSPINAL FLUID

In adults, approximately 500 mL of cerebrospinal fluid (CSF) is produced each day (0.3–0.4 mL/min). The total adult volume varies from 90 to 150 mL, about 25 mL of which is in the ventricles and the remainder in the subarachnoid space. In neonates, the volume varies from 10 to 60 mL. Thus, the total CSF volume is replaced every 5 to 7 hours (Wood, 1980). An estimated 70% of CSF is derived by ultrafiltration and secretion through the choroid plexuses. The ventricular ependymal lining and the cerebral subarachnoid space account for the remainder. CSF leaves the ventricular system through the medial and lateral foramina, flowing over the brain and spinal cord surfaces within the subarachnoid space. CSF resorption occurs at the arachnoid villi, predominantly along the superior sagittal sinus.

The CSF has several major functions: (1) It provides physical support because a 1500-g brain weighs about 50 g when suspended in CSF; (2) it confers a protective effect against sudden changes in acute venous (respiratory and postural) and arterial blood pressure or impact pressure; (3) it provides an excretory waste function because the brain has no lymphatic system; (4) it is the pathway whereby hypothalamus releasing factors are transported to the cells of the median eminence; and (5) it maintains central nervous system (CNS) ionic homeostasis.

The blood-brain barrier (BBB) consists of two morphologically distinct components: a unique capillary endothelium held together by intercellular tight junctions; and the choroid plexus, where a single layer of specialized choroidal ependymal cells connected by tight junctions overlies fenestrated capillaries. The CSF ionic components (e.g., H^+, K^+, Ca^{++}, Mg^{++}, bicarbonate) are tightly regulated by specific transport systems, whereas glucose, urea, and creatinine diffuse freely but require 2 hours or longer to equilibrate. Proteins cross by passive diffusion at a rate dependent on the plasma-to-CSF concentration gradient and inversely proportional to their molecular weight and hydrodynamic volume (Fishman, 1992). Thus, the BBB maintains the relative homeostasis of the CNS environment during acute perturbations of plasma components.

SPECIMEN COLLECTION AND OPENING PRESSURE

CSF may be obtained by lumbar, cisternal, or lateral cervical puncture or through ventricular cannulas or shunts. Details of the performance of lumbar puncture are described elsewhere (Herndon & Brumback, 1989; Ward & Gushurst, 1992).

A manometer should be attached before fluid removal to record the opening pressure. CSF pressure varies with postural changes, blood pressure, venous return, Valsalva maneuvers, and factors that alter cerebral blood flow. The normal opening adult pressure is 90 to 180 mm of water in the lateral decubitus position with the legs and neck in a neutral position.

It may be slightly higher if the patient is sitting up and varies up to 10 mm with respiration. However, the pressure may be as high as 250 mm of water in obese patients. In infants and young children, the normal range is 10 to 100 mm of water, with the adult range attained by 6 to 8 years of age (Fishman, 1992). Opening pressures above 250 mm H_2O are diagnostic of intracranial hypertension, which may be due to meningitis, intracranial hemorrhage, and tumors (Seehusen et al., 2003). If the opening pressure is greater than 200 mm H_2O in a relaxed patient, no more than 2.0 mL should be withdrawn.

Idiopathic intracranial hypertension is most commonly seen in obese women during their childbearing years. When an elevated opening pressure is noted, CSF must be removed slowly and the pressure carefully monitored. Additional CSF should not be removed if the pressure reaches 50% of the opening pressure (Conly & Ronald, 1983).

Elevated pressures may be present in patients who are tense or straining and in those with congestive heart failure, meningitis, superior vena cava syndrome, thrombosis of the venous sinuses, cerebral edema, mass lesions, hypoosmolality, or conditions inhibiting CSF absorption. Opening pressure elevation may be the only abnormality in cryptococcal meningitis and pseudotumor cerebri (Hayward et al., 1987). Decreased CSF pressure may be present in spinal-subarachnoid block, dehydration, circulatory collapse, and CSF leakage. A significant pressure drop after removal of 1 to 2 mL suggests herniation or spinal block above the puncture site, in which case no further fluid should be withdrawn.

Up to 20 mL of CSF may normally be removed. Prior to collecting the sample, the clinician should be aware of the quantity of CSF required for the requested tests to ensure that a sufficient sample is submitted. In addition, the clinician should always provide an appropriate clinical history to the laboratory. The sample site (e.g., lumbar, cisternal) should be noted because cytologic and chemical parameters vary at different sites. The necessity for a simultaneous serum glucose should also be considered. This is best obtained 2 to 4 hours before lumbar puncture because of the delay in serum-CSF equilibrium.

The CSF specimen is usually divided into three serially collected sterile tubes: tube 1 for chemistry and immunology studies; tube 2 for microbiological examination; and tube 3 for cell count and differential. An additional tube may be inserted in the No. 3 position for cytology if a malignancy is suspected. Under certain conditions, some variations are critical. For example, if tube 1 is hemorrhagic because of a traumatic puncture, it should not be used when protein studies are the most important aspect of the analysis (i.e., suspected multiple sclerosis). Indeed, tube 3 should be examined for the major purpose of CSF collection. Perhaps the only definite statement one can make is that tube 1 should never be used for microbiology because it may be contaminated with skin bacteria. If questions arise, communication between the laboratory and clinician before CSF analysis is critical.

Glass tubes should be avoided because cell adhesion to glass affects the cell count and differential. Specimens should be delivered to the laboratory and processed quickly to minimize cellular degradation, which begins within 1 hour of collection. Refrigeration is contraindicated for culture specimens because fastidious organisms (e.g., *Haemophilus influenza*, *Neisseria meningitidis*) will not survive. It is also contraindicated for samples in which flow cytometry is likely to be needed for detection of leukemia or lymphoma cells, as refrigeration may affect expression and/or detection of certain surface antigens on these cells.

INDICATIONS AND RECOMMENDED TESTS

Indications for lumbar puncture can be divided into four major disease categories: meningeal infection, subarachnoid hemorrhage, primary or metastatic malignancy, and demyelinating diseases (American College of Physicians, 1986). Identification of infectious meningitis, particularly bacterial, is the most important indication for CSF examination (Box 30.1). Recommended laboratory tests are directed toward identification of these disorders (Box 30.2). CSF examination for other diseases is generally less helpful but often provides supportive evidence of a clinical diagnosis or helps to rule out other diseases (Irani, 2009). Limited routine studies followed by reflexive ordering of more focused tests (as needed) on the stored specimen have been advocated as a way of improving test efficiency (Albright et al., 1988).

GROSS EXAMINATION

Normal CSF is crystal clear and colorless and has a viscosity similar to that of water. Abnormal CSF may appear cloudy, frankly purulent, or pigment tinged. Turbidity or cloudiness begins to appear with leukocyte (white blood cell [WBC]) counts over 200 cells/μL or red blood cell (RBC) counts of 400/μL. However, grossly bloody fluids have RBC counts greater than 6000/μL. Microorganisms (bacteria, fungi, amebas), radiographic contrast material, aspirated epidural fat, and a protein level greater than 150 mg/dL (1.5 g/L) may also produce varying degrees of cloudiness. Experienced observers may be able to detect cell counts of less than 50 cells/μL with the unaided eye by observing for the Tyndall effect (Simon & Abele, 1978). Here, direct sunlight directed on the tube at a 90-degree angle from the observer will impart a "sparkling" or "snowy" appearance as suspended particles scatter the light.

Clot formation may be present in patients with traumatic taps, complete spinal block (Froin syndrome), or suppurative or tuberculous meningitis. It is not usually seen in patients with subarachnoid hemorrhage. Fine surface pellicles may be observed after refrigeration for 12 to 24 hours. Clots may interfere with cell count accuracy by entrapping inflammatory cells and/or by interfering with automated instrument counting.

Viscous CSF may be encountered in patients with metastatic mucin-producing adenocarcinomas, cryptococcal meningitis due to capsular polysaccharide, or liquid nucleus pulposus resulting from needle injury to the annulus fibrosus.

Pink-red CSF usually indicates the presence of blood and is grossly bloody when the RBC count exceeds 6000/μL. It may originate from a subarachnoid hemorrhage, intracerebral hemorrhage, or cerebral infarct, or from a traumatic spinal tap.

BOX 30.1

Diseases Detected by Laboratory Examination of CSF

High Sensitivity, High Specificity*

Bacterial, tuberculous, viral, and fungal meningitis
Viral encephalitis

High Sensitivity, Moderate Specificity

Subarachnoid hemorrhage
Multiple sclerosis
Central nervous system syphilis
Infectious polyneuritis
Paraspinal abscess

Moderate Sensitivity, High Specificity

Meningeal malignancy

Moderate Sensitivity, Moderate Specificity

Intracranial hemorrhage
Subdural hematoma

CSF, Cerebrospinal fluid.
* Sensitivity is the ability of a test to detect disease when it is present; specificity is the ability of a test to exclude disease when it is not present (see Chapter 8).
Modified from American College of Physicians, Health and Public Policy Committee: The diagnostic spinal tap, *Ann Intern Med* 104:880, 1986, with permission.

BOX 30.2

Recommended CSF Laboratory Tests

Routine

Opening CSF pressure
Total cell count (WBC and RBC)
Differential cell count (stained smear)
Glucose (CSF/plasma ratio)
Total protein

Useful Under Certain Conditions

Cultures (bacteria, fungi, viruses, *Mycobacterium tuberculosis*)
Gram stain, acid-fast stain
Fungal and bacterial antigens
Enzymes (LD, ADA, CK-BB)
Lactate
Multiplex polymerase chain reaction (PCR) assay (bacteria, fungi, TB, viruses)
Cytology
Isoelectric focusing and IgG immunoblotting
Proteins (C-reactive, 14-3-3, τ, β-amyloid, transferrin)
VDRL test for syphilis
Fibrin-derivative D-dimer
Tuberculostearic acid

ADA, Adenosine deaminase; *CK-BB,* creatine kinase-BB; *CSF,* cerebrospinal fluid; *LD,* lactate dehydrogenase; *RBC,* red blood cell; *TB,* tuberculosis; *VDRL,* venereal disease research laboratory; *WBC,* white blood cell.
Modified from Kjeldsberg CR, Knight JA: *Body fluids: laboratory examination of amniotic, cerebrospinal, seminal, serous, and synovial fluids,* ed 3, Chicago, 1993, © American Society for Clinical Pathology, with permission.

TABLE 30.1
Xanthochromia and Associated Diseases/Disorders

CSF Supernatant Color	Associated Diseases/Disorders
Pink	RBC lysis/hemoglobin breakdown products
Yellow	RBC lysis/hemoglobin breakdown products
	Hyperbilirubinemia
	CSF protein >150 mg/dL (1.5 g/L)
Orange	RBC lysis/hemoglobin breakdown products
	Hypervitaminosis A (carotenoids)
Yellow-green	Hyperbilirubinemia (biliverdin)
Brown	Meningeal metastatic melanoma

CSF, Cerebrospinal fluid; *RBC,* red blood cell.

Xanthochromia

Xanthochromia commonly refers to a pale pink to yellow color in the supernatant of centrifuged CSF, although other colors may be present (Table 30.1). To detect xanthochromia, the CSF should be centrifuged and the supernatant fluid compared with a tube of distilled water. Xanthochromic CSF is pink, orange, or yellow owing to RBC lysis and hemoglobin breakdown. Pale pink to orange xanthochromia from released oxyhemoglobin is usually detected by lumbar puncture performed 2 to 4 hours after the onset of subarachnoid hemorrhage, although it may take as long as 12 hours. Peak intensity occurs in about 24 to 36 hours and then gradually disappears over the next 4 to 8 days. Yellow xanthochromia is derived from bilirubin. It develops about 12 hours after a subarachnoid bleed and peaks at 2 to 4 days but may persist for 2 to 4 weeks.

Visible CSF xanthochromia may also be due to the following: (1) oxyhemoglobin resulting from artifactual RBC lysis caused by detergent contamination of the needle or collecting tube, or a delay of longer than 1 hour without refrigeration before examination; (2) bilirubin (bilirachia) in jaundiced patients; (3) CSF protein levels over 150 mg/dL, which are also present in bloody traumatic taps (>100,000 RBCs/μL) or in pathologic states such as complete spinal block, polyneuritis, and meningitis; (4) disinfectant contamination; (5) carotenoids (orange) in people with dietary hypercarotenemia (i.e., hypervitaminosis A); (6) melanin (brownish) from meningeal metastatic melanoma; and (7) rifampin therapy (red-orange).

Although careful gross CSF inspection has good sensitivity (Britton et al., 1983), spectrophotometry can also help to differentiate hemoglobin-derived substances from other xanthochromic pigments with different maximal absorption peaks (Smith et al., 2013).

Differential Diagnosis of Bloody CSF

A traumatic tap occurs in about 20% of lumbar punctures. Therefore, distinction of a traumatic puncture from a pathologic hemorrhage is of vital importance. Although the presence of crenated RBCs is not useful, the following observations may be helpful in distinguishing the two forms of bleeding.

1. In a traumatic tap, the hemorrhagic fluid usually clears between the first and third collected tubes but remains relatively uniform in subarachnoid hemorrhage.
2. Xanthochromia, microscopic evidence of erythrophagocytosis, or hemosiderin-laden macrophages indicate a subarachnoid bleed in the absence of a prior traumatic tap. RBC lysis begins as early as 1 to 2 hours after a traumatic tap. Thus, rapid evaluation is necessary to avoid false-positive results.
3. A commercially available latex agglutination immunoassay test for cross-linked fibrin derivative D-dimer is specific for fibrin degradation and should theoretically be negative in traumatic taps (Lang et al., 1990). However, it has been shown to not effectively distinguish subarachnoid hemorrhage from traumatic lumber puncture (Eclache et al., 1994).

MICROSCOPIC EXAMINATION

Total Cell Count

Although the traditional manual method for cell counting in CSF samples, using undiluted CSF in a manual counting chamber, continues to be a useful approach, because of the low cell counts frequently encountered in CSF, the precision of manual counting in these samples is inherently limited (Barnes et al., 2004, Zimmerman et al., 2011). Improvements in the hardware and software in flow cytometers now allow reliable use of these instruments in performing automated total WBC counts and WBC differential counts (Hoffman & Janssen, 2002; Aune et al., 2004), and even in detecting bacteria (Nanos & Delanghe, 2008) in CSF samples. Although these instruments are increasingly used clinically to perform these counts on CSF samples, the low clinical decision levels for total WBC count in CSF and persistent technical limitations of flow cytometers at low WBC levels and with certain WBC types continue to be cause for concern (Hoffman & Janssen, 2002; Andrews et al., 2005; Glasser et al., 2009; Kleine et al., 2009). When issues of turnaround time and cost are considered, however, automated total WBC and WBC differential counts in CSF samples is a reasonable alternative to manual counting (Zimmerman et al., 2011; Li et al., 2014), with added manual examination of the sample to avoid missing pathologic cell types as a useful cross-check (Strik et al., 2005). When considering use of automated cell counters with CSF samples, laboratories should carefully follow manufacturer and Clinical and Laboratory Standards Institute guidelines (CLSI Approved Guideline H56-A, 2006) when implementing these automated methods.

The normal leukocyte cell count in adults is 0 to 5 cells/μL. It is higher in neonates, ranging from 0 to 30 cells/μL, with the upper limit of normal decreasing to adult values by adolescence. No RBCs should be present in normal CSF. If numerous (except with a traumatic tap), a pathologic process is probable (e.g., trauma, malignancy, infarct, hemorrhage). Although RBC counts have limited diagnostic value, they may give a useful approximation of the true CSF WBC count or total protein in the presence of a traumatic puncture by correcting for leukocytes or protein introduced by the traumatic puncture. To be valid, all measurements (WBC, RBC, protein) must be performed on the same tube. This procedure also assumes that the blood is derived exclusively from the traumatic tap. The corrected WBC count is as follows:

$$WBC_{corr} = WBC_{obs} - WBC_{added}$$

where

$$WBC_{added} = WBC_{BLD} \times RBC_{CSF} / RBC_{BLD}$$

and

$$WBC_{obs} = \text{CSF leukocyte count}$$

$$WBC_{added} = \text{leukocytes added to CSF by traumatic tap}$$

$$WBC_{BLD} = \text{peripheral blood leukocyte count}$$

$$RBC_{CSF} = \text{CSF erythrocyte count}$$

$$RBC_{BLD} = \text{peripheral blood erythrocyte count}$$

An analogous formula may be used to correct for **added total protein** (TP):

$$TP_{added} = [TP_{serum} \times (1 - HCT)] \times RBC_{CSF}/RBC_{BLD}$$

In the presence of a normal peripheral blood RBC count and serum protein, these corrections amount to about 1 WBC for every 700 RBCs and 8 mg/dL protein for every 10,000 RBCs/μL. This latter RBC correction factor is reasonably accurate as long as the peripheral WBC count is not extremely high or low.

An observed/expected (added) WBC count ratio greater than 10 has a sensitivity of 88% and a specificity of 90% for bacterial meningitis. When the predicted WBC count is below the observed count, the probability of bacterial meningitis appears to be low (Mayefsky & Roughmann, 1987; Bonadio et al., 1990).

Differential Cell Count

Suggested differential count reference ranges are presented in Table 30.2. A differential performed in a counting chamber is unsatisfactory because the low cell numbers give rise to poor precision and identifying the cell type beyond granulocytes and "mononuclears" is difficult in a wet preparation. Direct smears of the centrifuged CSF sediment are also subject to significant error from cellular distortion and fragmentation.

The **cytocentrifuge method** is rapid, requires minimal training, and allows Wright staining of air-dried cytospins. It is the recommended method for differential cell counts in all body fluids (Rabinovitch & Cornbleet, 1994). Cell yield and preservation are better than with simple centrifugation. From 30 to 50 cells can be concentrated from 0.5 mL of "normal"

TABLE 30.2

CSF Reference Values for Differential Cytocentrifuge Counts

Cell type	Adults, %	Neonates, %
Lymphocytes	62 ± 34	20 ± 18
Monocytes	36 ± 20	72 ± 22
Neutrophils	2 ± 5	3 ± 5
Histiocytes	Rare	5 ± 4
Ependymal cells	Rare	Rare
Eosinophils	Rare	Rare

CSF, Cerebrospinal fluid.

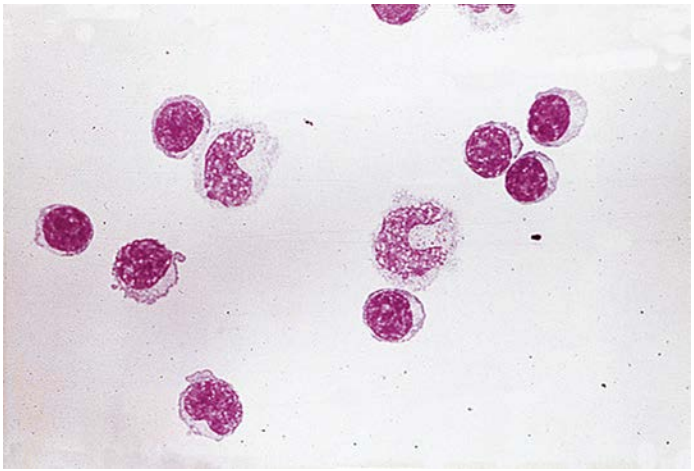

Figure 30.1 Cerebrospinal fluid cytology (lymphocyte to monocyte distribution ratio 70:30).

CSF. Variable artifactual distortions may be seen, but they are minimized when the specimen is fresh, albumin is added to the specimen (2 drops of 22% bovine serum albumin), and the cell concentration is adjusted to about 300 WBCs/L prior to centrifugation (Kjeldsberg & Knight, 1993). Manual differential cell counting on a cytocentrifuge preparation of CSF continues to be the most reliable method, even with low cell numbers. Although automated differential counts may be safely performed on CSF samples using flow cytometers (Hoffman & Janssen, 2002; Aulesa et al., 2003; Li et al., 2014), confirmation of the automated differential count by manual examination of a cytocentrifuged smear is recommended with some instruments (Aune et al., 2004; Strik et al., 2005) and is a requirement with specimens at risk for containing neoplastic cells. Effective detection of neoplastic cells, such as leukemic cells, using the cytocentrifuge method on CSF appears to be highly instrument dependent (Huppmann et al., 2012).

Filtration and sedimentation methods are too cumbersome for routine use. However, filtration does allow concentration of large volumes of CSF for cytologic examination or culture while retaining the fluid filtrate for additional studies.

In adults, normal CSF contains small numbers of **lymphocytes** and **monocytes** in an approximate 70:30 ratio (Fig. 30.1). A higher proportion of monocytes is present in young children, in whom up to 80% may be normal (Pappu et al., 1982). Erythrocytes due to minor traumatic bleeding are commonly seen, especially in infants. Small numbers of neutrophils (polymorphonuclear leukocytes [PMNs]) may also be seen in "normal" CSF specimens, most likely as a result of minor hemorrhage (Hayward & Oye, 1988) and improved cell concentration methods. No general consensus regarding an upper limit of normal for PMNs has been established. Many laboratories accept up to 7% neutrophils with a normal WBC count. Over 60% neutrophils has been reported in high-risk neonates without meningitis (Rodriguez et al., 1990). The number of PMNs may be decreased by as much as 68% within the first 2 hours after lumbar puncture owing to cell lysis (Steele et al., 1986).

Traumatic puncture may result in the presence of bone marrow cells, cartilage cells, squamous cells, ganglion cells, and soft-tissue elements. In addition, ependymal and choroid plexus cells may rarely be seen (Fig. 30.2). Moreover, blastlike primitive cell clusters, most likely of germinal matrix origin, are sometimes found in premature infants with intraventricular hemorrhage (Fig. 30.3).

Increased CSF **neutrophils** occur in numerous conditions (Box 30.3). In early bacterial meningitis, the proportion of PMNs usually exceeds 60%. However, in about one-quarter of cases of early viral meningitis, the proportion of PMNs also exceeds 60%. Viral-induced neutrophilia usually changes to a lymphocytic pleocytosis within 2 to 3 days. A total PMN count of over 1180 cells/μL (or more than 2000 WBCs/μL) has a 99% predictive value for bacterial meningitis (Spanos et al., 1989). Persistent

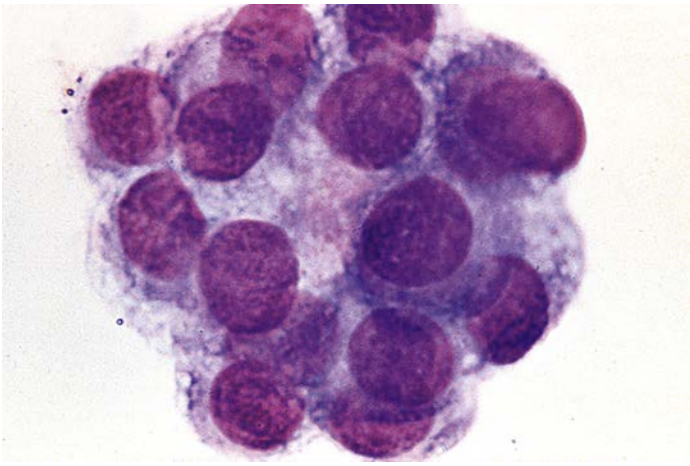

Figure 30.2 Choroid plexus cells in cerebrospinal fluid.

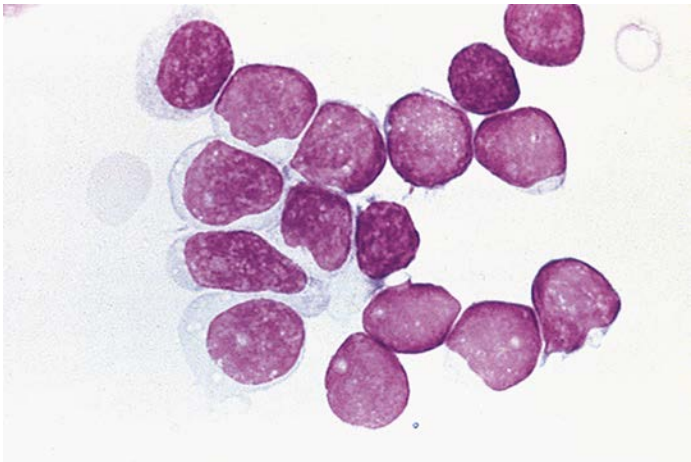

Figure 30.3 Cluster of blastlike cells in cerebrospinal fluid from a premature newborn. (From Kjeldsberg CR, Knight JA: *Body fluids: laboratory examination of amniotic, cerebrospinal, seminal, serous and synovial fluids,* ed 3, Chicago, 1993, © American Society for Clinical Pathology, with permission.)

BOX 30.3

Causes of Increased CSF Neutrophils

Meningitis

Bacterial meningitis
Early viral meningoencephalitis
Early tuberculous meningitis
Early mycotic meningitis
Amebic encephalomyelitis

Other infections

Cerebral abscess
Subdural empyema
AIDS-related CMV radiculopathy

Following seizures

Following CNS hemorrhage
Subarachnoid
Intracerebral

Following CNS infarct

Reaction to repeated lumbar punctures
Injection of foreign material in subarachnoid space (e.g., methotrexate, contrast media)
Metastatic tumor in contact with CSF

AIDS, Acquired immunodeficiency syndrome; *CMV,* cytomegalovirus; *CNS,* central nervous system; *CSF,* cerebrospinal fluid.

BOX 30.4

Causes of CSF Lymphocytosis

Meningitis

Viral meningitis
Tuberculous meningitis
Fungal meningitis
Syphilitic meningoencephalitis
Leptospiral meningitis
Bacterial due to uncommon organisms
Early bacterial meningitis where leukocyte counts are relatively low
Parasitic infestations (e.g., cysticercosis, trichinosis, toxoplasmosis)
Aseptic meningitis due to septic focus adjacent to meninges

Degenerative Disorders

Subacute sclerosing panencephalitis
Multiple sclerosis
Drug abuse encephalopathy
Guillain-Barré syndrome
Acute disseminated encephalomyelitis

Other Inflammatory Disorders

Handl syndrome (headache with neurologic deficits and CSF lymphocytosis)
Sarcoidosis
Polyneuritis
CNS periarteritis

CNS, Central nervous system; *CSF,* cerebrospinal fluid.

BOX 30.5

Inflammatory and Infectious Causes of CSF Plasmacytosis

Acute viral infections
Guillain-Barré syndrome
Multiple sclerosis
Parasitic CNS infestations
Sarcoidosis
Subacute sclerosing panencephalitis
Syphilitic meningoencephalitis
Tuberculous meningitis

CNS, Central nervous system; *CSF,* cerebrospinal fluid.

neutrophilic meningitis (over 1 week) may be noninfectious or due to less common pathogens such as *Nocardia*, *Actinomyces*, *Aspergillus*, and the zygomycetes (Peacock et al., 1984).

Increased CSF **lymphocytes** have been reported in various diseases/disorders (Box 30.4). Lymphocytosis (>50%) may occur in early acute bacterial meningitis when the CSF leukocyte count is under 1000/μL (Powers, 1985). Reactive lymphoplasmacytoid and immunoblastic variants may be present, particularly with viral meningoencephalitis. Blastlike lymphocytes may be seen admixed with small and large lymphocytes in the CSF of neonates.

Plasma cells, not normally present in CSF, may appear in a variety of inflammatory and infectious conditions (Box 30.5), along with large and small lymphocytes, and in association with malignant brain tumors (Fishman, 1992). Multiple myeloma may also rarely involve the meninges (Varga et al., 2018).

Although **eosinophils** are rarely present in normal CSF, they may be increased in a variety of CNS conditions (Box 30.6). For example, eosinophilia is frequently mild (1%–4%) in a general inflammatory response, but in children with malfunctioning ventricular shunts, it may be marked (Fig. 30.4). A suggested criterion for eosinophilic meningitis is 10% eosinophils (Kuberski, 1981); parasitic invasion of the CNS is the most common cause worldwide. *Coccidioides immitis* is a significant cause of CSF eosinophilia in endemic regions of the United States (Ragland et al., 1993).

Increased CSF **monocytes** lack diagnostic specificity and are usually part of a "mixed-cell reaction" that includes neutrophils, lymphocytes, and plasma cells. This pattern is seen in tuberculous and fungal meningitis, chronic bacterial meningitis (i.e., *Listeria monocytogenes* and others), leptospiral meningitis, ruptured brain abscess, *Toxoplasma* meningitis, and amebic encephalomeningitis. A mixed-cell pattern without neutrophils is characteristic of viral and syphilitic meningoencephalitis. **Macrophages** with phagocytosed erythrocytes (**erythrophages**) appear from 12 to 48 hours following a subarachnoid hemorrhage or traumatic tap. Hemosiderin-laden macrophages (**siderophages**) appear after about 48 hours and may persist for weeks (Fig. 30.5). Brownish yellow or red hematoidin crystals may form after a few days.

BOX 30.6

Causes of CSF Eosinophilic Pleocytosis

Commonly associated with:

Acute polyneuritis
CNS reaction to foreign material (drugs, shunts)
Fungal infections
Idiopathic eosinophilic meningitis
Idiopathic hypereosinophilic syndrome
Parasitic infections

Infrequently associated with:

Bacterial meningitis
Leukemia/lymphoma
Myeloproliferative disorders
Neurosarcoidosis
Primary brain tumors
Tuberculous meningoencephalitis
Viral meningitis

CNS, Central nervous system; *CSF,* cerebrospinal fluid.
Modified from Kjeldsberg CR, Knight JA: *Body fluids: laboratory examination of amniotic, cerebrospinal, seminal, serous and synovial fluids*, ed 3, Chicago, 1993, © American Society for Clinical Pathology, with permission.

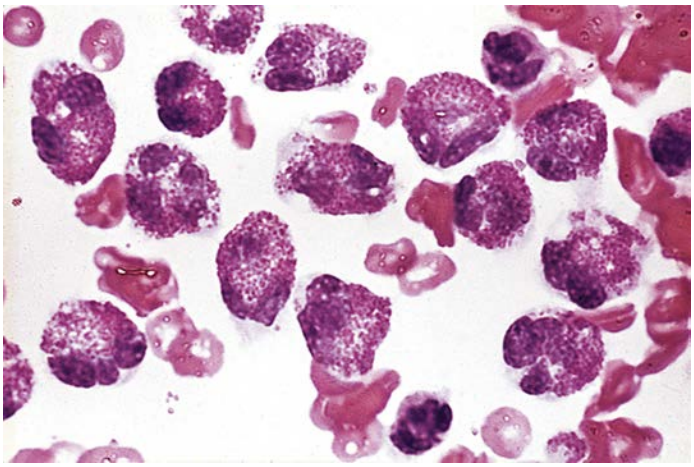

Figure 30.4 Eosinophils in cerebrospinal fluid from a child with a malfunctioning ventricular shunt.

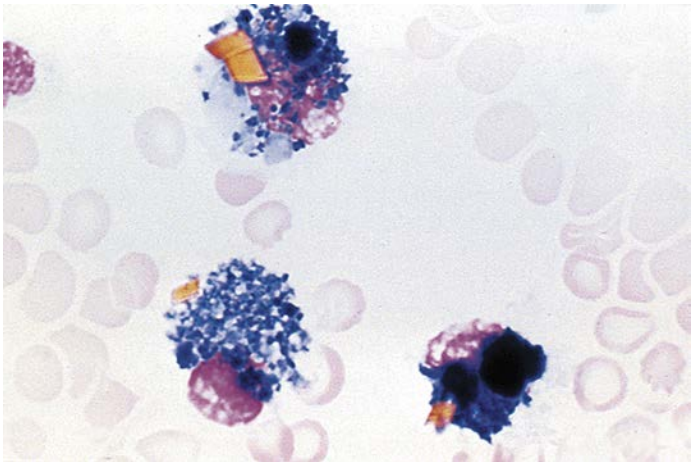

Figure 30.5 Hemosiderin-laden macrophages (siderophages) from the cerebrospinal fluid of a patient with a subarachnoid hemorrhage. Hemosiderin crystals (golden-yellow) are also present. (From Kjeldsberg CR, Knight JA: *Body fluids: laboratory examination of amniotic, cerebrospinal, seminal, serous and synovial fluids,* ed 3, Chicago, 1993, © American Society for Clinical Pathology, with permission.)

Morphologic CSF examination for tumor cells has moderate sensitivity and high specificity (97%–98%) (Marton & Gean, 1986). Sensitivity depends on the type of neoplasm. CSF examination of leukemic patients has the highest sensitivity (about 70%), followed by metastatic carcinoma (20%–60%) and primary CNS malignancies (30%). Sensitivity may be optimized by using filtration methods with larger fluid volumes or by

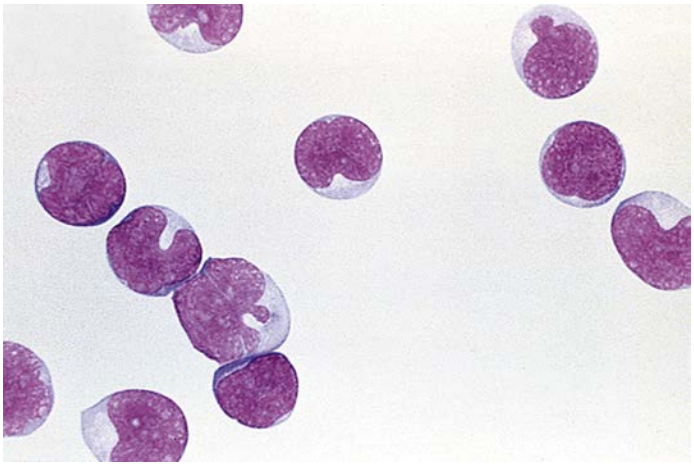

Figure 30.6 Acute lymphoblastic leukemia in cerebrospinal fluid. Note the uniformity of the blast cells.

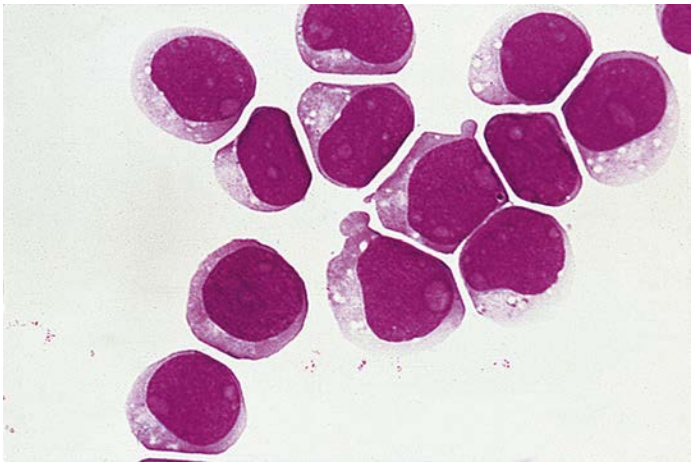

Figure 30.7 Acute myeloid leukemia in cerebrospinal fluid.

performing serial punctures in patients in whom a neoplasm is strongly suspected. Processing of CSF samples using liquid-based thin-layer methods also increases sensitivity in the detection of neoplastic cells and enhances preservation of these cells for potential immunocytochemical analysis (Sioutopoulou et al., 2008). These liquid-based methods are now commonly used for cytopathologic examination of CSF and other body cavity fluid specimens.

Leukemic involvement of the meninges is more frequent in patients with acute lymphoblastic leukemia (Fig. 30.6) than in those with acute myeloid leukemia (Fig. 30.7). Both are significantly more common than CNS involvement in the chronic leukemias. A leukocyte count over 5 cells/μL with unequivocal lymphoblasts in cytocentrifuged preparations is commonly accepted as evidence of CSF involvement. The incidence of CNS relapse in children with lymphoblasts but cell counts lower than 6 cells/μL appears to be low and is not significantly different from cases in which no blasts are identified (Odom et al., 1990; Gilchrist et al., 1994; Tubergen et al., 1994). As noted previously, the ability to detect leukemic cells in CSF using the cytocentrifuge method is highly instrument dependent; low levels of these cells may be missed with certain instruments (Huppmann et al., 2012).

Non-Hodgkin lymphomas involving the leptomeninges are usually high-grade tumors (lymphoblastic, large-cell immunoblastic, and Burkitt lymphomas; Fig. 30.8); low-grade lymphomas and Hodgkin lymphoma are significantly less common (Bigner, 1992; Walts, 1992). T cells predominate in normal and inflammatory conditions, whereas most lymphomas, especially those occurring in immunocompromised hosts, are of B-cell lineage. Lymphoblastic lymphoma, the most common T-cell lymphoma to involve the CSF, can be detected by terminal deoxynucleotidyl transferase stain.

Multiparameter flow cytometric immunophenotypic studies, deoxyribonucleic acid (DNA) analysis by polymerase chain reaction (PCR), and, more recently, DNA sequence analysis have been shown to significantly improve diagnostic sensitivity and specificity in CSF samples involved by leukemic or lymphoma cells (Rhodes et al., 1996; Finn et al., 1998; Scrideli & Queiroz, 2004; Bromberg et al., 2007; Quijano et al., 2009; Martinez-Laperche et al., 2013; Lacayo et al., 2013, Bento et al., 2018). Considering their greater sensitivity in detecting leukemia or lymphoma cells in CSF samples, whenever available, these advanced technologies should be part of the complete evaluation in patients being worked up for these conditions.

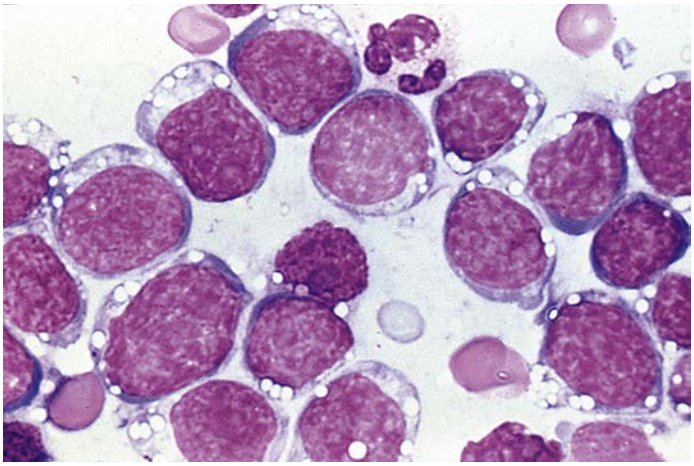

Figure 30.8 Burkitt lymphoma in cerebrospinal fluid. The cells are characterized by blue cytoplasm with vacuoles and a slightly clumped chromatin pattern. (From Kjeldsberg CR, Knight JA: *Body fluids: laboratory examination of amniotic, cerebrospinal, seminal, serous and synovial fluids,* ed 3, Chicago, 1993, © American Society for Clinical Pathology, with permission.)

Amebas, fungi (especially *Cryptococcus neoformans*), and *Toxoplasma gondii* organisms may be present on cytocentrifuge specimens but may be difficult to recognize without confirmatory stains.

CHEMICAL ANALYSIS

Reference values for lumbar CSF in adults are listed in Table 30.3.

Proteins

Total Protein

More than 80% of the CSF protein content is derived from blood plasma in concentrations of less than 1% of the plasma level (Table 30.4).

Prealbumin (transthyretin), transferrin, and small quantities of nerve tissue–specific proteins are the major qualitative differences that normally exist between CSF and plasma proteins. Although some authors have argued against routine measurement of total protein (American College of Physicians, 1986), it is the most common abnormality found in CSF. Thus, an increased CSF protein serves as a useful, albeit nonspecific, indicator of meningeal or CNS disease.

Reference Values. CSF total protein reference values vary considerably among laboratories owing to differences in methods, instrumentation, and type of reference standard used. CSF protein levels of 15 to 45 mg/dL have long been accepted as the "normal" reference range (Silverman & Christenson, 1994). Other studies using different methods have shown generally higher reference ranges, approximately 15 to 60 mg/dL (Lott & Warren, 1989).

Although discrepancies in gender and in those older than 60 years of age have been reported, the differences are probably not significant. However, infants have significantly higher CSF protein levels than older children and adults. Thus, mean levels of 90 mg/dL for term infants and 115 mg/dL for preterm infants were reported; the upper levels were 150 mg/dL and 170 mg/dL, respectively (Sarff et al., 1976). Others have noted that the CSF protein concentration falls rapidly from birth to 6 months of age (mean levels, 108 mg/dL to 40 mg/dL), plateaus between 3 and 10 years of age (mean, 32 mg/dL), and then rises slightly from 10 to 16 years of age (mean, 41 mg/dL) (Biou et al., 2000).

Elevated CSF protein levels may be caused by increased permeability of the BBB, decreased resorption at the arachnoid villi, mechanical obstruction of CSF flow due to spinal block above the puncture site, or an increase in intrathecal immunoglobulin (Ig) synthesis. Common conditions associated with elevated lumbar CSF protein values (>65 mg/dL) are summarized in Box 30.7.

Low lumbar CSF total protein levels (<20 mg/dL) normally occur in some young children between 6 months and 2 years of age and in patients with conditions associated with increased CSF turnover. These include (1) removal of large CSF volumes; (2) CSF leaks induced by trauma or lumbar puncture; (3) increased intracranial pressure, probably due to an increased rate of protein resorption by the arachnoid villi; and (4) hyperthyroidism (Fishman, 1992).

TABLE 30.3
Adult Lumbar CSF Reference Values

Analyte	Conventional Units	SI Units
Protein	15–60 mg/dL	0.15–0.60 g/L
Prealbumin	2%–7%	
Albumin	56%–76%	
α_1-Globulin	2%–7%	
α_2-Globulin	4%–12%	
β-Globulin	8%–18%	
γ-Globulin	3%–12%	
Electrolytes		
Osmolality	280–300 mOsm/L	280–300 mmol/L
Sodium	135–150 mEq/L	135–150 mmol/L
Potassium	2.6–3.0 mEq/L	2.6–3.0 mmol/L
Chloride	115–130 mEq/L	115–130 mmol/L
Carbon dioxide	20–25 mEq/L	20–25 mmol/L
Calcium	2.0–2.8 mEq/L	1.0–1.4 mmol/L
Magnesium	2.4–3.0 mEq/L	1.2–1.5 mmol/L
Lactate	10–22 mg/dL	1.1–2.4 mmol/L
pH		
Lumbar fluid	7.28–7.32	
Cisternal fluid	7.32–7.34	
pCO_2		
Lumbar fluid	44–50 mm Hg	
Cisternal fluid	40–46 mm Hg	
pO_2	40–44 mm Hg	
Other Constituents		
Ammonia	10–35 μg/dL	6–20 μmol/L
Glutamine	5–20 mg/dL	0.3–1.4 mmol/L
Creatinine	0.6–1.2 mg/dL	45–92 μmol/L
Glucose	50–80 mg/dL	2.8–4.4 mmol/L
Iron	1–2 μg/dL	0.2–0.4 μmol/L
Phosphorus	1.2–2.0 mg/dL	0.4–0.7 mmol/L
Total lipid	1–2 mg/dL	0.01–0.02 g/L
Urea	6–16 mg/dL	2.0–5.7 mmol/L
Urate	0.5–3.0 mg/dL	30–180 μmol/L
Zinc	2–6 μg/dL	0.3–0.9 μmol/L

CSF, Cerebrospinal fluid; *pCO_2*, partial pressure of carbon dioxide; *pO_2*, partial pressure of oxygen.

TABLE 30.4
Mean Concentrations of Plasma and CSF Proteins

Protein	CSF, mg/L	Plasma/CSF Ratio
Prealbumin	17.3	14
Albumin	155.0	236
Transferrin	14.4	142
Ceruloplasmin	1.0	366
Immunoglobulin (Ig) G	12.3	802
IgA	1.3	1346
α_2-Microglobulin	2.0	1111
Fibrinogen	0.6	4940
IgM	0.6	1167
β-Lipoprotein	0.6	6213

CSF, Cerebrospinal fluid.
Modified from Felgenhauer K: Protein size and cerebrospinal fluid composition, *Klin Wochenschr* 52:1158, 1974, with permission.

Protein electrophoresis of concentrated normal CSF reveals two distinct differences from serum: a prominent transthyretin (prealbumin) band and two transferrin bands. Transthyretin is relatively high because of its dual synthesis by the liver and choroid plexus. The second transferrin band, referred to as β_2-transferrin, migrates more slowly than its serum equivalent owing to cerebral neuraminidase digestion of sialic acid residues.

BOX 30.7
Conditions Associated with Increased CSF Total Protein

Traumatic Spinal Puncture
Increased Blood-CSF Permeability
Arachnoiditis (e.g., following methotrexate therapy)
Meningitis (bacterial, viral, fungal, tuberculous)
Hemorrhage (subarachnoid, intracerebral)
Endocrine/metabolic disorders
- Milk-alkali syndrome with hypercalcemia
- Diabetic neuropathy
- Hereditary neuropathies and myelopathies
- Decreased endocrine function (thyroid, parathyroid)
- Other disorders (uremia, dehydration)

Drug Toxicity
Ethanol, phenothiazines, phenytoin

CSF Circulation Defects
Mechanical obstruction (tumor, abscess, herniated disk)
Loculated CSF effusion

Increased Immunoglobulin (Ig) G Synthesis
Multiple sclerosis

Neurosyphilis
Subacute sclerosing panencephalitis

Increased IgG Synthesis and Blood-CSF Permeability
Guillain-Barré syndrome
Collagen vascular diseases (e.g., lupus, periarteritis)
Chronic inflammatory demyelinating polyradiculopathy

CSF, Cerebrospinal fluid.

Methods. Turbidimetric methods, commonly based on trichloroacetic acid (TCA) or sulfosalicylic acid and sodium sulfate for protein precipitation, are popular because they are simple, rapid, and require no special instrumentation. However, they are temperature sensitive and require much larger specimen volumes (about 0.5 mL). A false protein elevation may be observed using TCA methods in the presence of methotrexate (Kasper et al., 1988). Benzethonium chloride and benzalkonium chloride have been used as precipitating agents in automated methods and micromethods (Luxton et al., 1989; Shephard & Whiting, 1992).

Colorimetric methods include the Lowry method, dye-binding, methods using Coomassie brilliant blue (CBB) or Ponceau S, and the modified Biuret method. The CBB method is rapid and highly sensitive and can be used with small sample sizes. Immunochemical methods measure specific proteins, require only 25 to 50 μL of CSF, and are relatively simple to perform once conditions and reagents have been standardized. Automated methods are now almost always used and show good correlation with traditional standard methods (Lott & Warren, 1989).

Albumin and IgG Measurements

The permeability of the BBB may be assessed by immunochemical quantification of the CSF albumin/serum albumin ratio in grams per deciliter (g/dL). The normal ratio of 1:230 (Tourtellotte et al., 1985) yields an unwieldy decimal of 0.004, which prompted the use of the **CSF/serum albumin index**, which is arbitrarily calculated as follows:

$$\text{CSF/Serum albumin index} = \frac{\text{CSF albumin (mg/dL)}}{\text{Serum albumin (g/dL)}} \qquad \text{(Eq. 30.1)}$$

An index value less than 9 is consistent with an intact barrier. Slight impairment is considered with index values of 9 to 14, moderate impairment with values of 14 to 30, and severe impairment with values greater than 30 (Silverman & Christenson, 1994). The index is slightly elevated in infants up to 6 months of age, reflecting the immaturity of the BBB, and increases gradually after 40 years of age. A traumatic tap invalidates the index calculation.

Increased intrathecal IgG synthesis is reflected by an increase in the CSF/serum IgG ratio:

$$\text{CSF/Serum IgG ratio} = \frac{\text{CSF IgG (mg/dL)}}{\text{Serum IgG (g/dL)}} \qquad \text{(Eq. 30.2)}$$

The normal ratio is 1/390 or 0.003 (Tourtellotte et al., 1985). Similar to the albumin index, the CSF/serum IgG index may be obtained by using milligrams per deciliter for the CSF IgG value. The CSF/serum IgG index normal range is 3.0 to 8.7.

The **CSF/serum IgG index** can be elevated by intrathecal IgG synthesis or increased plasma IgG crossover from breakdown of the BBB. Ig

derived from plasma crossover may be corrected by dividing the CSF/serum IgG index by the CSF/albumin index to yield the CSF IgG index.

$$\text{CSF IgG index} = \frac{\text{CSF IgG (mg/dL)} / \text{Serum IgG (g/dL)}}{\text{CSF albumin (mg/dL)} / \text{Serum albumin (g/dL)}} \quad \text{(Eq. 30.3)}$$

or

$$\text{CSF IgG index} = \frac{\text{CSF IgG (mg/dL)} \times \text{Serum albumin (g/dL)}}{\text{Serum IgG (g/dL)} \times \text{CSF albumin (mg/dL)}} \quad \text{(Eq. 30.4)}$$

The reference range for the IgG index varies, reflecting variations in determination of the four index components. A reasonable normal upper limit is 0.8 (Souverijn et al., 1989). However, each laboratory should determine its own critical ratio.

The **IgG synthesis rate** is calculated by an empirical formula (Tourtellotte et al., 1985):

$$\begin{aligned}\text{IgG synthesis rate (mg/day)} = [&(\text{CSF IgG} - \text{Serum IgG}/369)\\ &- (\text{CSF albumin} - \text{Serum albumin}/230)\\ &\times (\text{Serum IgG}/\text{Serum albumin})\\ &\times 0.43 \times 5\ \text{dL/day}]\end{aligned} \quad \text{(Eq. 30.5)}$$

All protein concentrations are expressed in milligrams per deciliter. The first bracketed term represents the difference between measured CSF IgG and the IgG expected from diffusion across a normal BBB; 369 is the normal serum/CSF ratio. The second bracketed term represents the difference between measured CSF albumin and expected albumin if the blood-brain barrier is intact; 230 is the normal serum/CSF albumin ratio. The CSF albumin excess is multiplied by the IgG/albumin ratio and the molecular weight ratio of IgG to albumin (0.43) to correct for changes in CSF IgG due to increased barrier permeability. The number 5 converts the result from a concentration to a daily amount, assuming an average daily CSF production of 500 mL (i.e., 5 dL). The formula does not consider variations in CSF production or Ig consumption. It assumes that the IgG/albumin ratio remains constant over various degrees of BBB impairment—a concept that may lead to variable error (Lefvert & Link, 1985). The reference interval for the synthesis rate is –9.9 to +3.3 mg/day. Values greater than 8.0 mg/day indicate an increased rate (Silverman & Christenson, 1994).

CSF IgG is normally 3% to 5% of total CSF protein. However, in multiple sclerosis (MS), the concentration approaches that of plasma (15%–18%) (Hersey & Trotter, 1980). The CSF IgG index and the IgG synthesis rate have a sensitivity of 90% in patients with definite MS, but the sensitivity is lower in patients with possible MS, in whom accuracy is most needed (Marton & Gean, 1986). In addition, the specificity for MS is only moderate because increased intrathecal IgG synthesis occurs in many other inflammatory neurologic diseases.

The Ig index and synthesis rate calculations may also be applied to IgM, IgA, Ig light chains, and specific antibodies to infectious microorganisms. For example, increased synthesis of IgM and free κ light chains have been suggested as markers for MS (Rudick et al., 1989; Lolli et al., 1991).

Electrophoretic Techniques. Although the diagnosis of MS is ultimately a clinical one, significant advances have been made in laboratory testing for this disorder. CSF total protein is increased in less than 50% of patients with MS. Indeed, if the CSF protein exceeds 100 mg/dL, the patient probably does not have MS. However, the γ-globulin fraction, as determined by CSF electrophoresis, is often increased in MS. Thus, the CSF total protein/γ-globulin ratio exceeds 0.12 in about 65% of cases (Johnson & Nelson, 1977). Using **electroimmunodiffusion**, a CSF IgG/albumin ratio greater than 0.25 is present in about 75% of cases (Tourtellotte et al., 1971). Levels greater than the mean CSF IgG index + 3SD are present in 80% to 85% of MS cases, although the upper reference level varies significantly among laboratories.

High-resolution agarose gel electrophoresis of concentrated CSF from patients with MS often shows discrete populations of IgG, the **oligoclonal bands**. Although these discrete IgG populations are normally absent, two or more bands are necessary to support the diagnosis of MS; a single band is not considered a positive result. Using this technique, oligoclonal bands have been reported in 83% to 94% of patients with definite MS, 40% to 60% of those with probable MS, and 20% to 30% of possible MS cases. However, they are also frequently present in patients with subacute sclerosing panencephalitis, various viral CNS infections, neurosyphilis, neuroborreliosis, cryptococcal meningitis, Guillain-Barré syndrome, transverse myelitis, meningeal carcinomatosis, glioblastoma multiforme, Burkitt lymphoma, chronic relapsing polyneuropathy, Behçet disease, cysticercosis, and trypanosomiasis, among others (Trotter & Rust, 1989; Chalmers et al., 1990; Fishman, 1992; Hall & Snyder, 1992). Subsequent studies have shown that agarose gel electrophoresis sensitivity for MS is less than previously reported (see later discussion).

Oligoclonal light chains (both κ and λ) are present in about 90% of MS patients (Gallo et al., 1989; Sindie & Laterte, 1991). They have also occasionally been identified in the CSF of those who are negative for IgG oligoclonal bands. Detection of free light chains in CSF and comparison to serum has been shown to be a sensitive marker for intrathecal immunoglobulin synthesis (Fischer et al., 2004).

Coomassie brilliant blue or paragon violet stains can resolve oligoclonal bands in only 5 μg of IgG (Silverman & Christenson, 1994). However, **silver staining** is 20 to 50 times more sensitive than CBB and can be used on unconcentrated CSF. It is important to note that these electrophoretic techniques must be simultaneously carried out on the patient's serum to be certain that a polyclonal gammopathy is not present (e.g., liver disease, systemic lupus, rheumatoid arthritis [RA], chronic granulomatous disease) because these disorders may be accompanied by Ig diffusion into the CSF, yielding false-positive results.

Immunofixation electrophoresis (IFE) is more sensitive than agarose gel electrophoresis and does not require CSF concentration (Cawley et al., 1976). Another study reported a sensitivity of 74% using this technique compared with 57% for agarose gel electrophoresis (Cavuoti et al., 1998). More recently, using a semiautomated immunofixation-peroxidase technique, the sensitivity was 83% and the specificity was 79% in patients with clinically definite MS (Richard et al., 2002).

Isoelectric focusing and IgG immunoblotting (IgG-IEF) performed on paired CSF and serum samples is the most sensitive and now the recommended method for the detection of oligoclonal bands (Andersson et al., 1994; Fortini et al., 2003; Keren, 2003). One study showed that IgG-IEF detected 100% of definite MS, but only about 50% were positive by agarose electrophoresis (Lunding et al., 2000). Others detected 91% of MS cases but only 68% with agarose (Seres et al., 1998). Similarly, a semiautomated IgG-IEF technique identified 90% of MS cases compared with 60% for agarose electrophoresis (Fortini et al., 2003). In 2005, an international consensus standard for the diagnosis of MS established IgG-IEF as the method of choice for qualitative detection of oligoclonal IgG bands as evidence of intrathecal synthesis of IgG (Freedman et al., 2005). More recent studies have reinforced the utility of IgG-IEF in diagnosing MS and distinguishing this disease from other disorders (Dobson et al., 2013). Figure 30.9 shows the different patterns seen on IgG-IEF in paired CSF and serum samples from patients with MS and other conditions.

Oligoclonal bands (OCBs) in CSF have a high sensitivity but low specificity for MS; thus, they are useful for screening but not for diagnosis. The overlap of positive OCB findings in infectious and other inflammatory conditions has stimulated the search for new biomarkers in CSF that are more specific for MS (Gastaldi et al., 2017) and that have potential prognostic relevance. Candidate markers showing promise include the following:

- Immunoglobulin free light chains (FLCs) as an indicator of B-cell activity are found in serum as well as other body fluids and could potentially be useful for diagnosing true MS patients who happen to be OCB negative. Early studies indicate utility for FLC measurements in CSF (especially because such measurements are automated); however, larger patient groups should be evaluated for wide acceptance (Presslauer et al., 2016).
- Oligoclonal IgM bands in CSF appear to be a very powerful marker for more severe and more aggressive MS (Villar et al., 2005). Unfortunately, hydrophobicity of IgM requires its chemical reduction prior to electrophoresis, which may still be affected by artifacts from reassociation of monomeric IgM. Nevertheless, oligoclonal IgM in CSF (which is directed against myelin lipid, usually phosphatidylcholine) is considered a very promising prognostic test for MS but will require more developmental work for standardization (Thangarijh et al., 2008).
- The measles-rubella-zoster (MRZ) reaction consists of measuring antibody titers to those viruses in CSF and serum. The MRZ reaction is positive if at least two of those indexes (CSF titer/serum titer) are positive. MRZ is considered highly specific for MS and could be recommended for patients with suspected MS who are OCB negative (Brettschneider et al., 2009).
- Neurofilaments are released into CSF following neuron and axon injury. They are also found in serum and, as such, could be used to monitor progression of MS as a highly prognostic marker once measurements become well established and are widely practiced (Petzold, 2015).

Further advances in CSF proteomic testing whereby literally hundreds of individual protein species can be identified is likely to provide more diagnostic power for neurologic diseases in coming years (Núñez Galindo et al., 2019; Jankovska et al., 2019).

In summary, the diagnosis of MS, as with many other neurologic disorders, is ultimately a clinical one based on neurologic history and physical

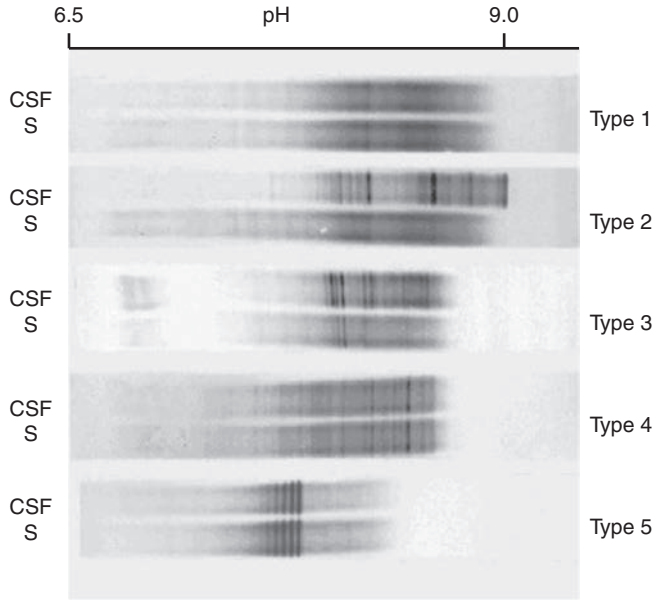

Figure 30.9 Immunoglobulin G isoelectric focusing (IgG-IEF) analysis of cerebrospinal fluid (CSF) illustrating the different patterns seen in paired CSF and serum (S) samples from patients with multiple sclerosis (MS) and other conditions. The 5 classic patterns are: Type 1, no bands in CSF or S samples; Type 2, oligoclonal IgG bands in CSF and none in the S sample, indicative of intrathecal IgG synthesis; Type 3, oligoclonal bands in CSF (like Type 2) and additional identical oligoclonal bands in CSF and S samples, still indicative of intrathecal IgG synthesis; Type 4, identical oligoclonal bands in CSF and S samples, indicative of a systemic and not intrathecal immune reaction with a normal or abnormal blood–CSF barrier and passive transfer of oligoclonal bands from S to CSF; and Type 5, identical monoclonal bands in CSF and S samples, indicative of the presence of a paraprotein (monoclonal IgG component). (Modified from Freedman MS, Thompson EJ, Deisenhammer F, et al.: Recommended standard of cerebrospinal fluid analysis in the diagnosis of multiple sclerosis: a consensus statement, *Arch Neurol* 62:865, 2005; used with permission.)

examination. Nevertheless, advanced laboratory results in CSF—such as elevated IgG indices, particularly the detection of oligoclonal IgG bands and neuroimaging techniques—have proved invaluable in the diagnosis of MS.

Other CSF Proteins

Approximately 300 different proteins have been identified in CSF using two-dimensional electrophoresis, the first dimension being isoelectric focusing and the second polyacrylamide gel in the presence of sodium dodecyl sulfate (Harrington et al., 1986). Using this technique, four abnormal proteins were identified in patients with Creutzfeldt-Jakob disease (CJD). Two of these proteins (molecular mass about 40 kilodaltons [kDa] each) were present in some, but not all, patients with herpes simplex encephalitis, Parkinson disease, Guillain-Barré syndrome, and schizophrenia. They were not present in various other neurologic disorders or in 100 normal CSF control specimens. However, these and two other proteins (molecular masses about 26 and 29 kDa) were present in all cases of CJD and in 5 of 10 cases of herpes simplex encephalitis. Neither of these latter proteins was present in any other neurologic disease or in controls.

Increased concentrations of various specific CSF proteins have been associated with several CNS diseases (Table 30.5).

Myelin Basic Protein. Myelin basic protein (MBP), a component of the myelin nerve sheath, is released during demyelination as a result of various neurologic disorders, especially MS. Thus, MBP has been shown to positively correlate with CSF leukocyte count, intrathecal IgG synthesis, and the CSF/serum albumin concentration quotient (Sellebjerg et al., 1998). These results supported the use of MBP in CSF as a surrogate disease marker during acute MS exacerbations. Others have found that analysis of antibody against MBP in patients with a clinically isolated syndrome is a rapid and precise method for predicting early conversion to clinically definite MS (Berger et al., 2003). However, increased CSF levels have also been reported in Guillain-Barré syndrome, lupus erythematosus (LE), subacute sclerosing panencephalitis, and various brain tumors, and following CNS irradiation and chemotherapy (Mahoney et al., 1984; Brooks, 1989). Measurement of CSF MBP levels has also been proposed as a prognostic marker in patients with serious head injury (Noseworthy et al., 1985). More recently, the clinical utility of MBP measurement in patients with MS has been questioned based on similarity of abnormal results to other established laboratory methods, such as presence of OCBs on protein electrophoresis, for diagnosing MS (Greene et al., 2012).

TABLE 30.5
CSF Proteins and Central Nervous System Diseases

Protein	Major Diseases/Disorders
α_2-Macroglobulin	Subdural hemorrhage, bacterial meningitis
β-Amyloid and τ proteins	Alzheimer disease
β_2-Microglobulin	Leukemia/lymphoma, Behçet syndrome
C-reactive protein	Bacterial and viral meningitis
Fibronectin	Lymphoblastic leukemia, AIDS, meningitis
Methemoglobin	Mild subarachnoid/subdural hemorrhage
Myelin basic protein	Multiple sclerosis, tumors, others
Protein 14-3-3	Creutzfeldt-Jakob disease
Transferrin	CSF leakage (otorrhea, rhinorrhea)

AIDS, Acquired immunodeficiency syndrome; *CSF*, cerebrospinal fluid.

α2-Macroglobulin. Except for a small amount transported across the BBB in pinocytic vesicles, α_2-macroglobulin (A2M) is normally excluded from the CSF because of its large size. The number of these vesicles is increased in certain polyneuropathies, resulting in an increased CSF A2M level. Significant elevation reflects subdural hemorrhage or breakdown of the BBB, as occurs in bacterial meningitis. A2M measurement alone, or in relationship to albumin and IgG, may assist in the evaluation of neurologic disorders and increased CSF protein, and in the rapid differentiation between bacterial and aseptic meningitis (Meucci et al., 1993; Kanoh & Ohtani, 1997).

β2-Microglobulin. This protein is part of the human leukocyte antigen class I molecule on the surfaces of all nucleated cells. CSF levels above 1.8 mg/L are associated with leptomeningeal leukemia and lymphoma but are not highly specific (Weller et al., 1992) in that they have a maximal positive predictive value of 78% in cases with a positive cytology (Jeffrey et al., 1990). β_2-Microglobulin (B2M) has also been shown to be a marker for neuro-Behçet syndrome (Kawai & Hirohata, 2000). Viral infections, including human immunodeficiency virus (HIV)-1, other inflammatory conditions, and various malignancies have also been associated with elevated levels. The measurement of B2M remains primarily investigational.

C-Reactive Protein. Early studies indicated that CSF C-reactive protein (CRP) is useful in differentiating viral (aseptic) meningitis from bacterial meningitis (Corral et al., 1981; Abramson et al., 1985; Stearman & Southgate, 1994). Others reported that CSF CRP is a more useful screening test for viral versus bacterial meningitis, especially in children (Sormunen et al., 1999). A meta-analysis of CRP studies since 1980 suggested that a normal CSF or serum CRP has a high probability of ruling out bacterial meningitis (i.e., negative predictive value about 97%) (Gerdes et al., 1998). Another study found not only that CSF CRP levels were increased in bacterial meningitis, but that these levels were significantly higher in patients with gram-negative bacterial meningitis than in those with gram-positive bacterial meningitis (Rajs et al., 2002). This assay has been found to be more specific than blood CRP levels in the laboratory diagnosis of meningitis in children (Malla et al., 2013).

Fibronectin. This large glycoprotein (molecular mass ≈420 kDa) is normally present in essentially all tissues and body fluids. Its primary function is its role in cell adhesion and phagocytosis (Ruoslahti et al., 1981). Thus, cell adhesion allows leukocytes to adhere to and pass through the vascular endothelia and migrate to the inflammatory site.

In children with acute lymphoblastic leukemia, elevated CSF fibronectin levels are associated with a poor prognosis, presumably due to leukemic involvement of the CNS (Rautonen et al., 1989). Significant CSF elevations have also been reported in Burkitt lymphoma (Rajantie et al., 1989), some metastatic solid tumors, astrocytomas, and bacterial meningitis (Weller et al., 1990; Torre et al., 1991). Decreased levels have been reported in viral meningitis and in the acquired immunodeficiency syndrome (AIDS)–dementia complex (Torre et al., 1991, 1993). Detection of fibronectin with alternatively spliced extra domain A is found in lower amounts in CSF from children with bacterial meningitis as opposed to viral meningitis or without meningitis (Pupek et al., 2013).

β-Amyloid Protein 42 and Tau (τ) Protein. The diagnosis of Alzheimer disease (AD) is based on the presence of dementia and a specific clinical profile (i.e., from medical history, clinical examination) suggestive of AD, together with the exclusion of other causes of dementia.

Pathologically, the disease is characterized by the presence of neurofibrillary tangles and amyloid plaques.

Studies indicate that measurement of biochemical markers increases diagnostic accuracy, especially early in the course of the disease, when clinical symptoms are mild and vague and overlap with cognitive changes that accompany aging and ischemic dementia. Thus, increased CSF levels of microtubule-associated tau (τ) protein and decreased levels of β-amyloid protein ending at amino acid 42 (β-amyloid protein 42) have been shown to significantly increase the accuracy of AD diagnosis (Andreasen et al., 2001; Riemenschneider et al., 2002; Sunderland et al., 2003). The positive predictive value for early AD is greater than 90% (Andreasen et al., 2001). Others have found that the calculated ratio of phosphorylated τ protein (P-tau) to β-amyloid peptide is superior to either measure alone (Maddalena et al., 2003). The results were as follows: distinguishing patients with AD from healthy controls—sensitivity 96%, specificity 97%; patients with AD from those with non-AD dementia—sensitivity 80%, specificity 73%; and patients with AD from those with other neurologic disorders—sensitivity 80%, specificity 89%. These assays all appear to have a place in the biochemical diagnosis of early AD (Blennow & Zetterberg, 2009), although development of a highly effective CSF assay to diagnose AD remains elusive.

Protein 14-3-3. The transmissible spongiform encephalopathies constitute a group of uniformly fatal neurodegenerative diseases. Of these, CJD is the major spongiform disease in humans. Two proteins, designated 130 and 131, have been detected in low concentrations in CSF from CJD patients. These proteins have the same amino acid sequence as protein 14-3-3 (Hsich et al., 1996). In patients with dementia, a positive immunoassay for the 14-3-3 protein in CSF strongly supports a diagnosis of CJD. In a subsequent study of patients with suspected CJD, the sensitivity of the 14-3-3 protein determined by immunoassay was 97%, and the specificity was 87% (Lemstra et al., 2000). False-positive results were seen primarily in patients with stroke and meningoencephalitis.

Others, using a modified Western blot technique, reported a 94.7% positive predictive value and a 92.4% negative predictive value for CJD (Zerr et al., 1998). False-positive results were seen in patients with herpes simplex encephalitis, atypical encephalitis, metastatic lung cancer, and hypoxic brain damage.

Detecting elevation of protein 14-3-3 in combination with elevation of other brain-derived proteins, such as τ protein, in CSF appears to be useful in the diagnosis of CJD (Sanchez-Juan et al., 2006, Muayqil et al., 2012).

Transferrin and CSF Leakage. CSF leakage usually presents as otorrhea or rhinorrhea following head trauma, in some cases beginning months to years after the injury. Recurrent meningitis is a serious complication, making accurate identification of the leaking fluid very important. In this regard, protein and glucose measurements are too nonspecific to be of value. Transferrin, an iron-binding glycoprotein with a molecular mass of about 77 kDa, is synthesized primarily in the liver. However, two transferrin isoforms are present in the CSF; the major isoform (β_1-transferrin) is present in all body fluids. The second isoform (β_2-transferrin), present only in the CNS, is produced in the CNS by the catalytic conversion of β-1-transferrin by neuraminidase. Immunofixation electrophoresis readily identifies both isoforms (see Chapter 20).

Detection of β_2-transferrin in CSF by protein electrophoresis with transferrin immunofixation is a noninvasive, rapid, and inexpensive test of high sensitivity and specificity that requires as little as 0.1 mL of fluid (Ryall et al., 1992; Normansell et al., 1994). Several reports have demonstrated the value of this technique in the diagnosis of CSF otorrhea and rhinorrhea—conditions in which both isoforms are readily identified (Irjala et al., 1979; Rouah et al., 1987; Zaret et al., 1992). Others have stressed the importance of β_2-transferrin identification in both CSF and inner ear perilymphatic leakage, as well as possible sources of error due to the presence of a transferrin allelic variant (Skedros et al., 1993a, 1993b; Sloman & Kelly, 1993). β_2-transferrin is sufficiently stable in CSF stored at room temperature and/or when mixed with nasal mucus that a negative result in a patient-collected nasal fluid specimen up to 1 week old is a reliable negative finding for CSF leakage (Bleier et al., 2011).

Methemoglobin and Bilirubin. Although most cases of subarachnoid and intracerebral hemorrhage are readily identified by computed tomography (CT), patients with mild subarachnoid hemorrhage, small subdural or cerebral hematomas, and blood seepage from an aneurysm or neoplasm and from small cerebral infarcts often are not identified by this technique. In these cases, CSF spectrophotometric analysis has been shown to detect methemoglobin in colorless CSF (<0.3 μmol/L) (Trbojevic-Cepe et al., 1992). An increase in CSF bilirubin is also recognized as a key finding supporting the diagnosis of subarachnoid hemorrhage (UK National External Quality Assessment Scheme for Immunochemistry Working Group, 2003). A single net bilirubin absorbance cutoff point of >0.007 absorbance units is recommended in the decision tree for interpretation and reporting of results. Guidelines for the use of CSF spectrophotometric analysis in the detection of hemoglobin breakdown products have been developed (Beetham, 2009).

Glucose

Derived from blood glucose, fasting CSF glucose levels are normally 50 to 80 mg/dL (2.8–4.4 mmol/L)—about 60% of plasma values. Rigorous evaluation of CSF and serum glucose levels in a large number of children confirmed that the CSF glucose level is normally approximately 60% of the serum glucose level during childhood (Nigrovic et al., 2012). Results should be compared with plasma levels, ideally following a 4-hour fast, for adequate clinical interpretation. The normal CSF/plasma glucose ratio varies from 0.3 to 0.9, with fluctuations in blood levels caused by the lag in CSF glucose equilibration time. A good rule of thumb is that CSF glucose is about two-thirds of the level of serum glucose. This enables the detection of low CSF glucose in patients with abnormal glucose levels. Thus in a diabetic patient with a serum glucose level of 250 mg/dL, the expected CSF glucose would be around 167 mg/dL in CSF. If the patient were found to have a CSF glucose of, say, 100 mg/dL, there would be evidence for a possible microorganism-induced lowering of CSF glucose even though the absolute value of CSF glucose is elevated.

CSF values below 40 mg/dL (2.2 mmol/L) or ratios below 0.3 are considered to be abnormal. Hypoglycorrhachia is a characteristic finding of bacterial, tuberculous, and fungal meningitis. However, sensitivity can be as low as 55% for bacterial meningitis (Hayward et al., 1987); thus, a normal level does not exclude these conditions. Some cases of viral meningoencephalitis also have low glucose levels but generally not to the degree seen in bacterial meningitis. Meningeal involvement by a malignant tumor, sarcoidosis, cysticercosis, trichinosis, ameba (*Naegleria*), acute syphilitic meningitis, intrathecal administration of radioiodinated serum albumin, subarachnoid hemorrhage, symptomatic hypoglycemia, and rheumatoid meningitis may also produce low CSF glucose levels (Fishman, 1992).

Decreased CSF glucose results from increased anaerobic glycolysis in brain tissue and leukocytes and from impaired transport into the CSF. Bacteria are usually present in insufficient quantities to be a major contributor to the use of glucose in CSF. CSF glucose levels normalize before protein levels and cell counts during recovery from meningitis, making it a useful parameter in assessing response to treatment.

Increased CSF glucose is of no clinical significance, reflecting increased blood glucose levels within 2 hours of lumbar puncture. A traumatic tap may also cause a spurious increase in CSF glucose.

Lactate

CSF and blood lactate levels are largely independent of each other. The reference interval for older children and adults is 9.0 to 26 mg/dL (1.0–2.9 mmol/L) (Knight et al., 1981). Newborns have higher levels, ranging from about 10 to 60 mg/dL (1.1–6.7 mmol/L) for the first 2 days and from 10 to 40 mg/dL (1.1–4.4 mmol/L) for days 3 to 10 (McGuinness et al., 1983). Elevated CSF lactate levels reflect CNS anaerobic metabolism due to tissue hypoxia.

Lactate measurement has been used as an adjunctive test in differentiating viral meningitis from bacterial, partially treated bacterial, mycoplasma, fungal, and tuberculous meningitis, in which routine parameters yield equivocal results (Cunha, 2012). In patients with viral meningitis, lactate levels are usually below 25 mg/dL (2.8 mmol/L) and are almost always less than 35 mg/dL (3.9 mmol/L), whereas bacterial meningitis typically has levels above 35 mg/dL (Bailey et al., 1990; Cameron et al., 1993). Using 30 to 36 mg/dL as the cutoff value for bacterial meningitis, the sensitivity and specificity are about 80% and 90%, respectively. Viral meningitis, partially treated bacterial meningitis, and tuberculous meningitis often have intermediate lactate levels that overlap each other, limiting the use of lactate measurements in this differential diagnosis.

Persistently elevated ventricular CSF lactate levels are associated with a poor prognosis in patients with severe head injury (DeSalles et al., 1986).

F2-Isoprostanes

Isoprostanes are prostaglandin-like compounds resulting from nonenzymatic free radical-initiated peroxidation of arachidonic acid. A subclass of these compounds have a characteristic so-called F2 ring structure and are therefore called F2-isoprostanes. F2-isoprostanes are increased in diseased regions of the brain in patients with AD (Pratico et al., 1998) and are markers of free radical brain injury associated with advanced age and latent AD (Montine et al., 2011). Compared with age-matched controls, CSF F2-isoprostanes are elevated in patients with probable AD (Montine et al., 1999). Therefore, in conjunction with CSF τ and β-amyloid protein, the measurement of CSF F2-isoprostanes appears to enhance the accuracy of the laboratory diagnosis of AD (Montine et al., 2001) and by itself appears to correlate with the degree of cognitive decline in some AD patients (Duits et al., 2013).

Enzymes

A wide variety of enzymes derived from brain tissue, blood, or cellular elements have been described in the CSF. Although CSF enzyme assays are not commonly used in the diagnosis of CNS diseases, there are diseases/disorders in which they may prove useful.

Adenosine Deaminase

Adenosine deaminase (ADA) catalyzes the irreversible hydrolytic deamination of adenosine to produce inosine. Because ADA is particularly abundant in T lymphocytes, which are increased in tuberculosis, its measurement has been recommended in the diagnosis of pleural, peritoneal, and meningeal tuberculosis. Higher ADA levels are present in tuberculous infections than in viral, bacterial, and malignant diseases (Blake & Berman, 1982; Mann et al., 1982, Choi et al., 2002), and measuring ADA in CSF appears to be a sensitive and specific assay in diagnosing tuberculous meningitis (Xu et al., 2010, Saini et al., 2017). ADA appears to have limited utility in HIV-associated neurologic disorders (Corral et al., 2004).

Creatine Kinase

Brain tissue is rich in creatine kinase (CK) because it participates in maintaining an adequate supply of adenosine triphosphate. Increased CSF CK activity has been reported in numerous CNS disorders, including hydrocephalus, cerebral infarction, various primary brain tumors, and subarachnoid hemorrhage, among others (Savory & Brody, 1979). In patients with head trauma, CSF CK levels correlate directly with the severity of the concussion (Florez et al., 1976).

CSF CK-MM and CK-MB are not normally present; when identified, they are due to blood contamination (CK-MM) and an equilibrium between CK-BB and CK-MM to produce CK-MB. Because the CK-BB isoenzyme accounts for about 90% of brain CK activity and mitochondrial CK (CKmt) the other 10%, CK isoenzyme measurements are more specific than total CK for CNS disorders (Chandler et al., 1984).

CSF CK-BB is increased about 6 hours following an ischemic or anoxic insult. Global brain ischemia following respiratory or cardiac arrest results in diffuse cerebral injury with peak CK-BB levels in about 48 hours (Chandler et al., 1986). Here, CSF CK-BB activity less than 5 U/L (upper normal level) indicates minimal neurologic damage; 5 to 20 U/L indicates mild to moderate CNS injury; and levels between 21 and 50 U/L are commonly correlated with death. Death occurs in essentially all patients with levels above 50 U/L.

Increased CSF CK-BB levels also correlate with the outcome following a subarachnoid hemorrhage (Coplin et al., 1999). A CK-BB level greater than 40 U/L increases the chance of an unfavorable early or late outcome to 100%.

Lactate Dehydrogenase

Lactate dehydrogenase (LD) activity is high in brain tissue, with a predominance of the electrophoretically fast-moving isoenzyme fractions LD_1 and LD_2. Total LD activity of 40 U/L is a reasonable upper limit of normal for adults and 70 U/L for neonates (Donald & Malan, 1986; Engelke et al., 1986). LD is useful in differentiating a traumatic tap from intracranial hemorrhage because a current traumatic tap with intact RBCs does not significantly elevate the LD level (Engelke et al., 1986). Sensitivity and specificity are about 70% to 85% depending on the cutoff value. As with lactate, LD activity is significantly higher in bacterial meningitis than in aseptic meningitis (Donald & Malan, 1986; Engelke et al., 1986). Using a cutoff of 40 U/L, the sensitivity is about 86% and the specificity about 93%.

Total CSF LD levels are also increased in patients with CNS leukemia, lymphoma, metastatic carcinoma, bacterial meningitis, and subarachnoid hemorrhage (Kjeldsberg, 1993). CSF LD isoenzymes have been shown to add considerable specificity in the evaluation of various metastatic brain tumors (Fleisher et al., 1981). The LD_5/total LD ratio is increased (i.e., above 10%–15%) in patients with leptomeningeal metastases from carcinoma of the breast and lung and malignant melanoma. LD isoenzyme analysis is also useful in detecting CNS involvement by leukemias and lymphomas (Lossos et al., 2000). Isoenzyme analysis shows a distinct pattern in young children with infantile spasms (Nussinovitch et al., 2003a) and febrile convulsions (Nussinovitch et al., 2003b). Compared with controls, both disorders are characterized by decreased LD_1, increased LD_2 and LD_3, and no changes in LD_4 and LD_5.

CT is of limited value in estimating recovery potential and neurologic outcome during the early stages of ischemic brain injury. However, compared with controls (mean LD, 11.2 U/L), patients with an early stroke had a mean level of 40.9 U/L, and those with a transient ischemic attack (TIA) had a mean value of 11.8 U/L (Lampl et al., 1990). In patients with hypoxic brain injury, an increased LD level 72 hours following resuscitation indicates a poor prognosis (Karkela et al., 1992).

Lysozyme

Lysozyme (muramidase) catalyzes the depolymerization of mucopolysaccharides. Because the enzyme is particularly rich in neutrophil and macrophage lysosomes, its activity is very low in normal CSF. However, CSF lysozyme activity is significantly increased in patients with both bacterial and tuberculous meningitis. Thus, discriminant analysis demonstrated that 97% of patients with bacterial meningitis had increased lysozyme levels (Ribeiro et al., 1992). Others found that patients with tuberculous meningitis had significantly higher CSF lysozyme levels than those with bacterial meningitis, partially treated bacterial meningitis, and controls (Mishra et al., 2003). The diagnostic sensitivity and specificity for tuberculous meningitis were 93.7% and 84.1%, respectively. Increased levels are also present in cerebral atrophy, various CNS tumors, multiple sclerosis, intracranial hemorrhage, and epilepsy (Kjeldsberg, 1993).

Ammonia, Amines, and Amino Acids

CSF ammonia levels vary from 30% to 50% of blood values. Elevated levels are generally proportional to the degree of existing hepatic encephalopathy but are difficult to quantify. Moreover, because hepatic encephalopathy generally correlates with blood ammonia levels, the measurement of CSF ammonia has little, if any, clinical value. However, cerebral glutamine, synthesized from ammonia and glutamic acid, serves as the means for CNS ammonia removal. Thus, CSF glutamine levels reflect the concentration of brain ammonia. Glutamine reference intervals are method dependent; the upper reference level is about 20 mg/dL. Values over 35 mg/dL are usually associated with hepatic encephalopathy (Fishman, 1992). Elevated CSF glutamine levels have also been reported in patients with depression (Levine et al., 2000) and encephalopathy secondary to hypercapnia and sepsis (Mizock et al., 1989). Measurement of a variety of biogenic amines in CSF has been shown to assist in the diagnosis of bacterial and viral meningitis (Taj et al., 2018).

A major etiologic theory of schizophrenia involves dopamine. The cornerstone for this theory is the fact that neuroleptic drugs that block dopamine receptors are effective in the treatment of this disorder. Thus, it has been reported that CSF levels of homovanillic acid (HVA), a metabolite of the biogenic amines, are related to the severity of schizophrenic psychosis (Maas et al., 1997). However, HVA concentration varied as a function of psychosis rather than being related to the diagnosis of schizophrenia per se. Others have reported decreased CSF levels of 5-hydroxyindoleacetic acid, a metabolite of serotonin, in schizophrenic patients with suicidal behavior (Cooper et al., 1992). This report adds support for a possible relationship between suicide and CNS serotonin metabolism.

Although free CSF amino acids are relatively high in infants younger than 30 days of age, their concentration is further increased in those with febrile convulsions and bacterial meningitis. γ-Aminobutyric acid (GABA), a major inhibitory brain transmitter, is significantly decreased in basal ganglia neurons and is very low or undetectable in the CSF of patients with AD and Huntington disease (Achar et al., 1976; Dubowitz et al., 1992). CSF GABA was detected in all patients with migraine attacks, but not in those with tension headaches or in the control group without headaches (Welch et al., 1975). Infants with startle disease, a rare inherited autosomal-dominant disorder characterized by seizures or the so-called **stiff baby syndrome**, have significantly decreased CSF GABA levels (Dubowitz et al., 1992; Berthier et al., 1994).

Electrolytes and Acid-Base Balance

There are no clinically useful indications for the measurement of CSF sodium, potassium, chloride, calcium, or magnesium. Measurements of CSF pH, partial pressure of carbon dioxide (pCO_2), and bicarbonate are also not practical for patient care (Fishman, 1992).

Tumor Markers

Numerous studies have shown that various tumor markers are increased in the CSF of patients with both primary and metastatic tumors.

Carcinoembryonic Antigen

Carcinoembryonic antigen (CEA) is an oncofetal protein produced by a variety of carcinomas. An early study found increased CEA levels in 44% of patients with metastatic brain tumors (Suzuki & Tanaka, 1980). Others reported that CSF levels of CEA have a sensitivity of only about 31%, although the specificity is about 90% for detecting metastatic carcinoma of the leptomeninges (Klee et al., 1986; Twijnstra et al., 1986). CSF levels of CEA in patients with benign, primary malignant, and metastatic brain tumors are approximately 0.31 ng/mL, 0.92 ng/mL, and 6.3 ng/mL, respectively (Batabyal et al., 2003). CSF CEA levels are particularly sensitive in detecting leptomeningeal carcinoma metastasis (Kang et al., 2010).

Other oncofetal proteins include **human chorionic gonadotropin** (hCG), produced by choriocarcinoma and malignant germ cell tumors with a trophoblastic component, and **α-fetoprotein,** a glycoprotein produced by yolk sac

TABLE 30.6

Typical Lumbar CSF Findings in Meningitis

Test	Bacterial	Viral	Fungal	Tuberculous
Opening pressure	Elevated	Usually normal	Variable	Variable
Leukocyte count	≥1000/μL	<100/μL	Variable	Variable
Cell differential	Mainly neutrophils*	Mainly lymphocytes†	Mainly lymphocytes	Mainly lymphocytes
Protein	Mild to marked increase	Normal to mild increase	Increased	Increased
Glucose	Usually ≤40 mg/dL	Normal	Decreased	Decreased: may be <45 mg/dL
CSF/serum glucose ratio	Normal to marked decrease	Usually normal	Low	Low
Lactic acid	Mild to marked increase	Normal to mild increase	Mild to moderate increase	Mild to moderate increase

Data from Body BA, Oneson RH, Herold DA: Use of cerebrospinal fluid lactic acid concentration in the diagnosis of fungal meningitis, *Ann Clin Lab Sci* 17:429, 1987; Tang LM: Serial lactate determinations in tuberculous meningitis, *Scand J Infect Dis* 20:81, 1988; Arevalo CE, Barnes PF, Duda M, Leedom JM: Cerebrospinal fluid cell counts and chemistries in bacterial meningitis, *South Med J* 82:1122, 1989; Fishman RA: *Cerebrospinal fluid in diseases of the nervous system,* ed 2, Philadelphia, 1992, Saunders; Wubbel L, McCracken GH Jr: Management of bacterial meningitis, *Pediatr Rev* 19:78, 1998; Zunt JR, Marra CM: Cerebrospinal fluid testing for the diagnosis of central nervous system infection, *Neurol Clin* 17:675, 1999.
CSF, Cerebrospinal fluid.
*Lymphocytosis present in about 10% of cases.
†Neutrophils may predominate early in disease.

elements of germ cell tumors. Both β-hCG and α-fetoprotein may be useful in the diagnosis and monitoring of the response to therapy in patients with CNS germ cell tumors (Seregni et al., 2002; Ferguson et al., 2008, Tian et al., 2011).

Elevation of CSF **ferritin** is a sensitive indicator of CNS malignancy but has very low specificity because it is also increased in patients with inflammatory neurologic diseases (Zandman-Goddard et al., 1986). This assay has greater diagnostic utility in detecting subarachnoid hemorrhage in patients presenting late (Petzold et al., 2011).

As discussed in Chapter 21, assay for placental alkaline phosphatase (PLAP) in CSF is useful in determining whether a tumor in the pineal body is a germ cell tumor or a pinealoma. Elevated levels of PLAP in CSF are indicative of germ cell tumors, which are radio-sensitive, thereby obviating the need for invasive surgery for tumor removal.

MICROBIOLOGICAL EXAMINATION

A thorough and prompt examination of CSF is essential for the diagnosis of CNS infection because an inaccurate or delayed report may result in significant mortality or morbidity. Although changes in opening pressure, total cell and differential counts, total protein, and glucose suggest an infectious origin (Table 30.6), Gram stain, culture, and other relevant studies are critical for a definitive diagnosis.

Bacterial Meningitis

The most common agents of bacterial meningitis are group B streptococcus (neonates), *Neisseria meningitidis* (3 months and older; Fig. 30.10), *Streptococcus pneumoniae* (3 months and older), *Escherichia coli* and other gram-negative bacilli (newborn to 1 month), *Haemophilus influenzae* (3 months to 18 years), and *Listeria monocytogenes* (neonates, older adults, alcoholics, and immunosuppressed) (Graves, 1989; Wenger et al., 1990). *H. influenzae*, once the most common bacterial cause of meningitis in young children, has decreased dramatically from widespread use of *H. influenzae* type b vaccine. CSF shunts, head trauma, and neurosurgery place patients at risk for CNS infections from *Staphylococcus* species, gram-negative bacilli, and *Propionibacterium* species.

The Gram stain remains an accurate, rapid method by which to diagnose CNS infection. All specimens should be concentrated by centrifugation before Gram stain and culture. Depending on the type of infecting microorganism and its concentration in the CSF, Gram stain sensitivity ranges from 60% to 90%, with the greatest sensitivity corresponding to higher concentrations of bacteria (about 10^5 colony-forming units/mL). For example, the sensitivity of the Gram stain for detecting *Listeria monocytogenes* and gram-negative bacilli is 50% or less (Greenlee, 1990). For patients with many polymorphonuclear leukocytes but no organisms seen on Gram stain, the more sensitive acridine orange stain may be helpful. Cultures have a sensitivity of 80% to 90% but are about 30% less sensitive in partially treated cases (Greenlee, 1990).

Although standard culture-based methods remain the mainstay for diagnosis, the BinaxNOW *Streptococcus pneumoniae* antigen test, an immunochromatographic membrane assay that detects the presence of the C polysaccharide cell wall antigen common to all pneumococcal serotypes, has been proven to be a valuable tool for the rapid diagnosis of pneumococcal meningitis from CSF. Latex agglutination bacterial antigen tests performed on CSF to detect *H. influenzae*, *N. meningitidis*, *S. pneumoniae*, and β-hemolytic group B streptococci have historically been used as adjuncts to Gram stain and culture.

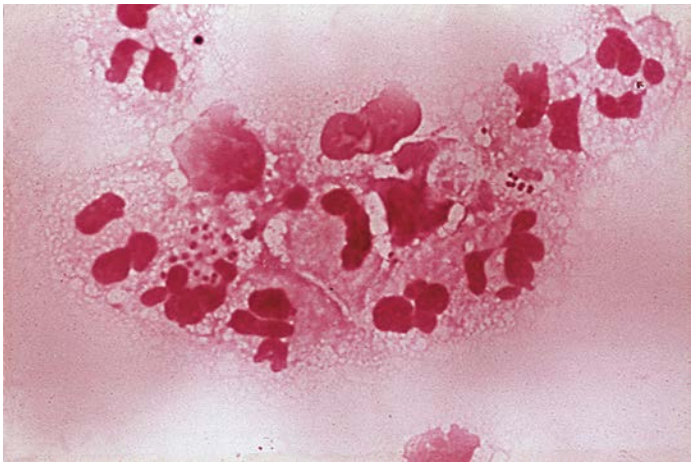

Figure 30.10 Cerebrospinal fluid Gram stain showing gram-negative diplococci characteristic of *N. meningitidis*.

However, the sensitivity is approximately the same as the Gram stain. Perhaps the best application of latex agglutination antigen tests is seen in partially treated, community-acquired meningitis that is negative for microorganisms by Gram stain (Perkins et al., 1995; Wilson, 1997, Mohammadi et al., 2013).

The PCR and sequencing of 16S ribosomal ribonucleic acid (RNA) in CSF have been shown to be very useful in the diagnosis of bacterial meningitis (Schuurman et al., 2004). Compared with bacterial culture, the assay shows a sensitivity of 86%, a specificity of 97%, a positive predictive value of 80%, and a negative predictive value of 98%. Nucleic acid amplification tests may also be helpful in patients already receiving antimicrobial therapy and in detecting more fastidious pathogens such as *N. meningitidis* (Porritt et al., 2000; Seward & Towner, 2000; Baethgen et al., 2003). Significant advances have been made over the past few years in the rapid diagnosis of bacterial, fungal, and viral meningitis and viral encephalitis using multiplex PCR-based assays, such as the Cepheid Xpert (Sunnyvale, CA) and Biofire FilmArray (Salt Lake City, UT) systems (Slika et al., 2013; Leber et al., 2016; Liesman et al., 2018). This approach to rapid diagnosis has revolutionized how bacterial, fungal, and viral infection is detected in the CNS and other sites.

Spirochetal Meningitis

The incidence of neurosyphilis increased in the 1980s and 1990s, particularly in patients with HIV infection. In one report, 44% of patients with neurosyphilis had AIDS (Flood et al., 1998). The diagnosis of CNS infection in patients with syphilis relies primarily on CSF parameters and serologic testing, although molecular DNA testing may now represent another approach. Abnormalities in CSF protein and cell counts are common in syphilitic meningitis but are nonspecific. CSF serologic testing to diagnose neurosyphilis is difficult. The standard nontreponemal test performed on CSF is the venereal disease research laboratory (VDRL) test. If few erythrocytes are contaminating the CSF, the VDRL specificity is high, but its sensitivity is only 50% to 60% (Davis & Schmitt,

1989). Treponemal tests, such as the treponemal antibody absorption (FTA-ABS) test, are both sensitive and specific for syphilis; however, their use in CSF for neurosyphilis is controversial. The CSF FTA-ABS is highly sensitive, but false-positive results may occur. In the absence of CSF abnormalities or clinical suspicion, it should not be used as a screening test. Thus, the following generalizations have been proposed (Davis & Schmitt, 1989): (1) a nonreactive serum FTA-ABS test rules out neurosyphilis; (2) a reactive serum FTA-ABS test with a nonreactive CSF FTA-ABS test essentially rules out neurosyphilis; (3) a reactive CSF VDRL test makes a diagnosis of neurosyphilis likely; and (4) a reactive CSF FTA-ABS test may indicate active neurosyphilis, asymptomatic neurosyphilis, treated neurosyphilis, or a false-positive reaction. Other studies have demonstrated the utility of PCR-based assays as a potentially sensitive and specific means of diagnosing neurosyphilis (Leslie et al., 2007); although these tests may not represent a clear advance over CSF serologic assays (Marks et al., 2018).

Diagnosis of Lyme meningitis represents another challenge for the laboratory. The mainstay of diagnosis remains serologic analysis performed on a serum specimen, using an enzyme-linked immunosorbent assay (ELISA)–based screening assay followed by confirmation with Western blot. PCR-based analysis may be performed on CSF specimens; however, the sensitivity of this approach may be low, particularly in patients with chronic neuroborreliosis (Steere, 2010).

Rapid diagnosis of leptospiral and other bacterial infections is now possible using genomic methods, including next-generation DNA sequencing analysis. Studies have shown that patients with neuroleptospirosis in whom a diagnosis could not be established by conventional methods may be successfully diagnosed using next-generation sequencing analysis of CSF (Wilson et al., 2014; Wilson et al., 2019). This methodology offers another approach to rapid diagnosis of a range of infections, as well as a way to rapidly track infection outbreaks (Sherry et al., 2013).

Viral Meningitis

Enteroviruses (echoviruses, coxsackieviruses, polioviruses) and arboviruses are responsible for the majority of meningitis cases. A seasonal peak in spring to autumn has been noted for these agents. As an example, echoviruses 9 (E9) and 30 (E30) were found to be mainly responsible for an increase in cases of aseptic meningitis (Morbidity and Mortality Weekly Report, 2003). Most patients present with a CSF pleocytosis; although neutrophils may be observed early in the infection, patients soon develop a predominance of lymphocytes.

Before molecular diagnostic testing, viral meningitis was a diagnosis of exclusion because the sensitivity of viral cultures can be low. Thus, in an early study, a specific etiologic diagnosis by viral cultures varied from 72% for enteroviruses to 5% for herpes simplex virus (HSV) (Marton & Gean, 1986).

Reverse transcriptase polymerase chain reaction (RT-PCR) is significantly more sensitive than cell culture (Dumler & Valsamakis, 1999; Hausfater et al., 2004). In recent years, PCR-based assays have evolved as the gold standard for the increasingly rapid diagnosis of viral meningitis secondary to enterovirus, HSV, cytomegalovirus, varicella zoster, and JC virus. The use of RT-PCR may result in significant cost savings by shortening hospital stays and eliminating unnecessary diagnostic and therapeutic interventions (Ramers et al., 2000). For patients with arbovirus-associated meningitis, acute and convalescent serologic testing in serum remains the cornerstone for diagnosis, with CSF testing a possible adjunct. Presumptive diagnosis of West Nile viral meningitis may be made on a CSF specimen using an IgM antibody-capture ELISA. PCR testing for West Nile virus and other arboviruses may also be done on CSF specimens. Although these assays have low sensitivity because of the short-lived nature of the viremia in these diseases, they may still be useful in diagnosing arbovirus infections (Vaughn et al., 2010; Vanichanan et al., 2016).

PCR amplification of HSV DNA has revolutionized the testing for HSV infection in CSF and has replaced brain biopsy as the primary method used in the early diagnosis of HSV meningoencephalitis (Tunkel, 2008). False negatives might occur in very early infections and with bloody taps, necessitating analysis of a second CSF specimen (Tyler, 2004).

Human Immunodeficiency Virus

A wide variety of CSF abnormalities may be found in HIV-positive patients with or without neurologic disease, including lymphocytic pleocytosis, elevated IgG indexes, and OCBs (Chalmers et al., 1990; Hall & Snyder, 1992). Identifying opportunistic infection is the most important indication for examining the CSF. Serious fungal infections may exist in the presence of few or no CSF parameter abnormalities.

Fungal Meningitis

Cryptococcus neoformans is the most frequently isolated fungal pathogen from CSF. India ink or nigrosin stains for cryptococcus capsular halos have a sensitivity of about 25%, increasing to 53% with multiple lumbar punctures, and to greater than 90% in untreated HIV-infected patients (Marton & Gean, 1986). Detection of cryptococcal antigen from sera or CSF using latex agglutination has higher sensitivity, ranging from 60% to 95%. False-negatives due to a prozone effect or low concentration of polysaccharide antigen may occur. Early disease, intraparenchymal infection, infection with nonencapsulated *C. neoformans* variants, and immune complexes (corrected with pronase treatment) may also produce false negatives. Conversely, sera or CSF from patients with rheumatoid factor or *Trichosporon asahii* infection may be falsely positive. If clinical suspicion for dimorphic or filamentous fungi is high, large volumes of CSF (approximately 15–20 mL) are optimal for culture to improve the recovery of fungal organisms. PCR-based assays have so far not been shown to reliably detect *C. neoformans* infection in CSF (O'Halloran et al., 2017).

Tuberculous Meningitis

Abnormal CSF with elevated protein and lymphocytic predominance are the hallmark features of tuberculous meningitis. The sensitivity of CSF acid-fast stains for the diagnosis of tuberculous meningitis is highly variable, ranging from 10% to 12% (Greenlee, 1990) to greater than 50% (Thwaites et al., 2004). Large volumes of CSF, often obtained from multiple lumbar punctures with the use of concentration techniques, are recommended to improve the sensitivity of both acid-fast stain and culture (Marton & Gean, 1986).

PCR nucleic acid amplification for detecting *Mycobacterium tuberculosis* DNA-specific sequences have shown great promise in the rapid and accurate diagnosis of tuberculous meningitis (Lin et al., 1995; Desai & Pal, 2002), but PCR methods using a single primer are associated with relatively low sensitivity (Pai et al., 2003). Multiplex PCR analysis, using primers to multiple relevant tubercular genes, appears to be a significantly more sensitive method in the rapid diagnosis of tuberculous meningitis (Kusum et al., 2011; DiDiodato et al., 2019).

Dot-ELISA has been standardized to detect tuberculosis antigens and antibodies against *M. tuberculosis* in CSF. Using this technique, a positive reaction was present in 86% of cases with suspected tuberculous meningitis (Kashyap et al., 2003). Only 5% of patients with other disorders, mainly pyogenic meningitis, were positive.

Other tests have been shown to be useful in some cases of tuberculous meningitis. ADA levels are significantly higher in tuberculous meningitis than in other types of meningitis and CNS disorders (Pettersson et al., 1991; Choi et al., 2002; Solari et al., 2013), although the degree of increase indicative of tuberculous infection varies depending on the specific assay used.

Primary Amebic Meningoencephalitis

This rare disease is caused by the free-living ameba *Naegleria fowleri*, *Acanthamoeba* species, and *Balamuthia mandrillaris*. *Naegleria* and *Balamuthia* are more likely to cause an acute inflammatory response with a neutrophilic pleocytosis, decreased glucose level, elevated protein concentration, and the presence of erythrocytes. Gram stain is always negative. *Acanthamoeba* more often produces a granulomatous meningitis. Motile *Naegleria* trophozoites may be visualized by light or phase-contrast microscopy in direct wet mounts, allowing rapid diagnosis. Intact and degenerating organisms may be identified on Wright- or Giemsa-stained cytospins but must be distinguished from macrophages (dos Santos, 1970; Benson et al., 1985). Acridine orange stain is useful in differentiating amebas (brick red) from leukocytes (bright green). Immunocytochemical staining of CSF specimens using an antibody to *Naegleria fowleri* has been shown to improve microscopic detection of this organism (Visvesvara, 2010). Multiplex PCR-based methods are an even more sensitive modality for detecting multiple amebic organisms in CSF (Qvarnstrom et al., 2006).

SYNOVIAL FLUID

Synovium refers to the tissue lining synovial tendon sheaths, bursae, and diarthrodial joints, except for the articular surface. It is composed of one to three cell layers that form a discontinuous surface overlying fatty, fibrous, or periosteal joint tissue.

Synovial fluid (SF) is an ultrafiltrate of plasma combined with hyaluronic acid produced by the synovial cells or synoviocytes. Small ions and

TABLE 30.7

Synovial Fluid Findings by Disease Category

Finding	Normal	CATEGORY			
		Group I Noninflammatory	Group II Inflammatory	Group III Infectious	Group IV Hemorrhagic
Clarity	Transparent	Transparent	Transparent/opaque	Opaque	Opaque
Color	Clear to pale yellow	Xanthochromic	Xanthochromic to white/bloody	White	Red-brown or xanthochromic
WBCs/mL	0–150	<3000	3000–75,000	50,000–200,000	50–10,000
PMNs, %	<25	<30	>50	>90	<50
RBCs	No	No	No	Yes	Yes
Glucose (blood/SF difference, mg/dL)	0–10 (0–0.56 mmol/L)	0–10 (0–0.56 mmol/L)	0–40 (0–2.2 mmol/L)	20–100 (1.11–5.5 mmol/L)	0–20 (0–1.11 mmol/L)

Modified from Kjeldsberg CR, Knight JA: *Body fluids: laboratory examination of amniotic, cerebrospinal, seminal, serous and synovial fluids,* ed 3, Chicago, 1993, © American Society for Clinical Pathology, with permission.
PMNs, Polymorphonuclear cells, neutrophils; *RBCs,* red blood cells; *SF,* synovial fluid; *WBCs*, white blood cells.

molecules (e.g., Na^+, K^+, glucose, urea) readily pass into the joint space and therefore are similar in concentration to plasma. Large molecules are absent or present only in trace amounts. Resorption of synovial molecules is by lymphatics and is not size dependent. SF acts as a lubricant and provides nutrients for the avascular articular cartilage.

Examination of the SF is essential to distinguish infectious from noninfectious arthritis. Results from gross and microscopic examination of SF have traditionally been divided into "reaction types," as depicted in Table 30.7. These groupings are largely descriptive, and considerable overlap among them is evident. Except for Gram stain, culture, and crystal examination, SF parameters can be nonspecific and must be integrated into the clinical context.

Noninflammatory effusions (Group I) typically have leukocyte counts less than 3000/μL, with a minority of neutrophils. Osteoarthritis, traumatic arthritis, neuropathic osteoarthropathy, pigmented villonodular synovitis, and early rheumatic fever usually present with little inflammatory response. Early rheumatoid arthritis, early bacterial infection, and viral arthritis may also present as noninflammatory effusions.

Inflammatory effusions (Group II) have leukocyte counts between 3000 and 75,000/μL, with neutrophils accounting for more than 50% of the population. RA, systemic lupus erythematosus (SLE), Reiter syndrome, rheumatic fever, acute crystal-induced arthritis, arthritis associated with inflammatory bowel disease, psoriatic arthritis, and fat droplet synovitis are examples of this reaction group.

Purulent (infectious) effusions (Group III) typically have leukocyte counts greater than 50,000/μL, of which 90% or more are neutrophils. Bacterial, fungal, and tuberculous joint infections constitute this group.

Hemorrhagic effusions (Group IV) may be seen in association with traumatic arthritis, pigmented villonodular synovitis, synovial hemangioma, neuropathic osteoarthropathy, joint prostheses, and hematologic disorders (hemophilia, anticoagulant therapy, sickle cell disease or trait).

SPECIMEN COLLECTION

Joint fluid aspiration (arthrocentesis) should be confined to patients with an undiagnosed effusion or a significant clinical change related to a known effusion. It should be performed by an experienced operator using good sterile technique. Caution is necessary to avoid aspirating a sterile joint in someone with bacteremia or through a cutaneous or periarticular soft-tissue infection into a sterile joint. Large joints such as the knee normally contain no more than 4.0 mL of SF; thus, small sample size is common unless an effusion is present.

Synovial fluid must be collected with sterile, disposable needles and plastic syringes to avoid contamination by birefringent particulates. The syringe may be heparinized with 25 U of sodium heparin/mL of SF in routine arthrocentesis. Oxalate, lithium heparin, and powdered ethylenediaminetetraacetic acid (EDTA) anticoagulants should be avoided because they form crystal artifacts that may be misleading during the microscopic examination. Before aspiration, the joint should be turned or otherwise manipulated to ensure mixing of its contents.

Ideally, the specimen should be separated into three parts: 3 to 10 mL into a sterile heparinized tube or syringe for microbiological studies; 2 to 5 mL in an anticoagulant tube (sodium heparin or liquid EDTA) for microscopic examination; and about 5 mL into a plain (no anticoagulant) tube for chemical analysis (normal SF does not clot because fibrinogen is absent).

BOX 30.8

Recommended Synovial Fluid Tests

Routine tests
Gross examination (color, clarity)
Total and differential leukocyte counts
Gram stain and bacterial culture (aerobic and anaerobic)
Crystal examination with polarizing microscope and compensator
Useful tests in certain circumstances
Fungal and acid-fast stains and cultures
Multiplex PCR assay for bacterial, fungal, and mycobacterial DNA
Serum–synovial fluid glucose differential
Lactate and other organic acids
Complement
Enzymes
Uric acid

DNA, Deoxyribonucleic acid; *PCR,* polymerase chain reaction.
Modified from Kjeldsberg CR, Knight JA: *Body fluids: laboratory examination of amniotic, cerebrospinal, seminal, serous and synovial fluids,* ed 3, Chicago, 1993, © American Society for Clinical Pathology, with permission.

Heparin concentrations greater than 125 U/mL have an inhibitory effect on some pathogenic bacteria (Rosett & Hodges, 1980). Specimens for culture, therefore, should be at least 1 to 2 mL in volume if they are submitted in green-top sodium heparin tubes (Becton Dickinson, Rutherford, NJ) containing 143 U/tube of heparin, or submitted in recapped syringes after removal of the needle and excess air.

Dry taps may still have fluid within the needle, which may be sufficient for the most critical tests. Such specimens should be submitted with the needle still on the syringe and carefully recapped or with its tip stuck into a sterile cork. Good communication with the laboratory is crucial to the appropriate processing of such specimens. Saline injection and reaspiration is also effective in collecting SF following a dry tap (Partridge et al., 2018).

RECOMMENDED TESTS

Laboratory examination of SF is of major importance in the differential diagnosis of joint disease, especially in crystal-induced and infectious arthritis. When either is suspected, arthrocentesis and a systematic examination of the SF are imperative and, when examination is carried out properly, are usually diagnostic. In other joint diseases, a specific diagnosis may not be possible. Nevertheless, fluid examination is still important if only to rule out infectious arthritis, which is a critical diagnosis to make in that a joint may be irreversibly damaged within 2 to 3 days if not properly treated. This is especially true when *Staphylococcus aureus* is the infectious organism. Therefore, routine tests should be directed toward the diagnosis of these two disorders (Box 30.8). Although other tests are not of practical value for routine use, they may provide important diagnostic information under certain circumstances.

GROSS EXAMINATION

Total volume should be recorded at the bedside, especially if the sample is to be divided for submission to different laboratory sections.

Color should be evaluated in a clear glass tube against a white background. Normal SF is colorless but is often pale yellow because of diapedesis of a few RBCs associated with even mild trauma. Noninflammatory and inflammatory disorders impart a straw to yellow color (xanthochromia). Septic fluid may be yellow, brown, or green depending on the chromogens produced by the offending organism and the host response, including the presence of WBCs and RBCs.

A **traumatic tap** produces an uneven distribution of blood during arthrocentesis or streaking in the syringe. Although pale yellow xanthochromia is difficult to distinguish from normal, a red-brown color following centrifugation is good evidence of pathologic hemarthrosis.

Clarity relates to the number and type of particles within the SF. Because normal SF is transparent, newsprint is easily read through the tube. Although translucent fluid obscures details, black and white areas can be distinguished, but opaque fluid completely obscures the background.

Leukocytes are most commonly responsible for changes in clarity. However, very large numbers of crystals may produce an opaque, milky, opalescent fluid without leukocytes. A shimmering, oily-appearing specimen suggests an abundance of cholesterol crystals, which may grossly resemble pus.

Increased turbidity is less often due to concentrations of fibrin, free-floating **rice bodies** (fragments of degenerating proliferative synovial cells or microinfarcted synovium), metal and plastic particles from patients with joint prostheses, or cartilage fragments in osteoarthritis. A **ground pepper** appearance from pigmented cartilage fragments may be the result of a metabolic disorder (i.e., ochronosis).

MICROSCOPIC EXAMINATION

Total Cell Count

Total leukocyte counts should be performed promptly to avoid degenerative cell loss, which begins as soon as 1 hour following arthrocentesis. Cell counts may still be performed using a standard hemocytometer in smaller laboratories. However, automated cell counting now offers more reliable results (Ottink et al., 2019). Leukocyte counts over 50,000/μL require dilution, which should be done with saline, not acetic acid, to avoid mucin clot formation and cell clumping. Flow cell–based automated cell counters may be used, but their use risks clogging the machine aperture or obtaining spuriously high cell counts from non-WBC particles (e.g., crystals, fat globules). Pretreatment of highly viscous SF samples with hyaluronidase improves automated cell counting using these instruments (Aulesa et al., 2003). Automated cell counting in SF samples using digital image–based technology avoids the clogging and spurious count problems and offers a reliable method for these counts (Walker et al., 2009; Scott, 2014).

Leukocyte counts greater than 10,000/μL, and often greater than 50,000/μL, are characteristic of crystal-induced arthritis (e.g., gout, pseudogout), chronic inflammatory arthritis (e.g., RA, SLE, ankylosing spondylitis), and septic arthritis (Kjeldsberg, 1993). Osteoarthritis, osteochondritis dissecans, trauma, and synovioma usually have total WBC counts less than 10,000/μL.

Erythrocytes should be routinely counted unless it is an obvious traumatic tap. If a large number of RBCs interferes with the leukocyte count, they may be lysed by dilution with 0.3 normal saline or 1% saponin in saline.

The upper reference level for SF leukocytes is 150 to 200/μL (Kjeldsberg, 1993). Elevated cell counts are used to help divide findings into different disease categories but are nonspecific for any particular disease because of extensive overlap.

Differential Leukocyte Count

Cytospin preparations are preferred over smears from centrifuged SF because the cell morphology is significantly better preserved. Treatment with hyaluronidase may be necessary to produce thin smears in viscous specimens. Liquid-based thin-layer processing instruments may also be used effectively to produce good-quality preparations of SF for microscopic examination (Policarpio-Nicolas & Valente, 2013). Automated leukocyte differential counts utilizing flow cytometers may be reliably performed on SF samples (Aulesa et al., 2003), with even better performance, including detection of crystals, using digital image–based instruments (Walker et al., 2009; Scott, 2014).

Neutrophils normally account for about 20% of SF leukocytes. Neutrophils generally exceed 50% in urate gout, pseudogout, and RA; they most often exceed 75% in acute bacterial arthritis. When 75% is used as a cutoff, the sensitivity for an inflammatory process is about 75% and the specificity is 92% (Shmerling et al., 1990). These cells frequently exhibit degenerative changes and may contain bacteria, crystals, lipid droplets, vacuoles, or dark blue to black granular inclusions thought to consist of immune complexes (ragocytes, RA cells). The presence of ragocytes in patients with RA may indicate a poorer outcome (Davis et al., 1988).

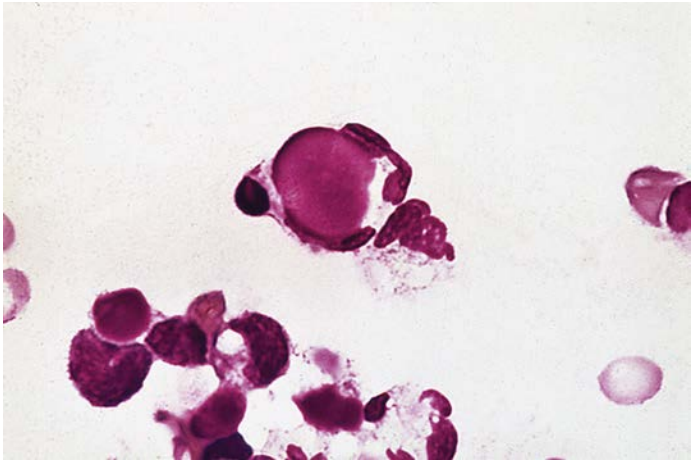

Figure 30.11 Lupus erythematosus cell in the synovial fluid from a patient with systemic lupus erythematosus.

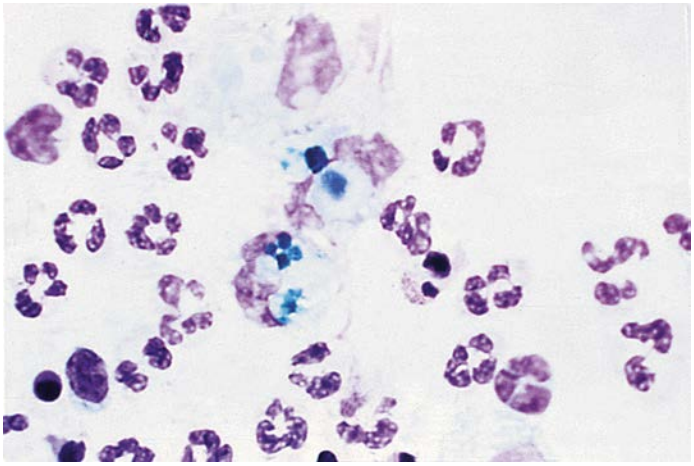

Figure 30.12 Reiter cells in the synovial fluid from a patient with Reiter syndrome.

Lupus erythematosus (LE) cells, sometimes present in patients with lupus arthritis, are most often neutrophils that have phagocytosed the nuclei of degenerating cells (Fig. 30.11). However, LE cells are not pathognomonic for SLE because they have also been identified in the SF of RA patients (Hunder & Pierre, 1970).

Lymphocytes, normally constituting about 15% of SF cells, are prominent in early RA and other autoimmune disorders, as well as in chronic infections. Reactive forms, including immunoblasts, are occasionally present.

Monocytes and **macrophages** are the most common cells present in normal SF, accounting for approximately 65% of the cell count. Monocytosis may be self-limited in viral arthritis or serum sickness, or more chronic in SLE or undifferentiated connective tissue disorders. Reiter cells, originally believed to be specific for Reiter syndrome, are macrophages containing degenerating neutrophils (Fig. 30.12).

Eosinophilia, defined as more than 2% of the leukocyte count, has been reported in Lyme disease, RA, rheumatic fever, metastatic carcinoma, parasitic infection, chronic urticaria, and angioedema, and following arthrography (allergic reaction to dye) and irradiation (Podell et al., 1980; Kay et al., 1988).

Synovial cells, termed *synoviocytes*, have no pathologic significance. They appear similar to mesothelial cells and may be difficult to distinguish from monocytes and macrophages.

Lipid bodies are associated with trauma, aseptic necrosis, and RA. These droplets often form Maltese crosses under polarized light, can be associated with a leukocyte response, and may cause spurious elevations of the automated WBC count (Wise et al., 1987).

Crystal Examination

Crystals in SF lead to acute inflammation with increased WBC counts and a neutrophil-predominant infiltrate. Crystal identification, especially if intracellularly in neutrophils or macrophages, is pathognomonic for a crystal-induced arthritis (Judkins & Cornbleet, 1997).

Gout refers to the process of crystal deposition in articular tissue. Common usage typically implies urate gout; an inflammatory response to crystal deposition is referred to as *gouty arthritis*. The most common types of endogenous crystals responsible for gouty arthritis are **monosodium urate monohydrate** (urate gout), **calcium pyrophosphate dihydrate** (pyrophosphate gout, chondrocalcinosis, or "pseudogout"), apatite and other **basic calcium phosphates** (BCPs; apatite gout), **calcium oxalate** (oxalate gout), and **lipids** (lipid gout).

Except for BCP, all of the above crystals can be detected by polarized light microscopy. A high-quality polarizing microscope with a first-order red plate compensator should be used. The **polarizer** filter is placed directly above the light source. The **analyzer** (another polarizing filter) is placed between the specimen slide and the microscope oculars, oriented 90 degrees from the polarizer to produce a dark background. The **compensator** is placed between the polarizer and analyzer, usually oriented 45 degrees (halfway) between the planes of the two polarizing filters.

Initial examination should be performed on a wet preparation using polarized light. Phase-contrast microscopy enhances crystal detection. The slide and coverslip must be cleaned and carefully dried immediately before use to avoid birefringent dust particulate artifacts. The coverslip edges are sealed with nail polish or other sealant, which retards but does not prevent evaporation. The coverslip edge is used to find the proper plane of focus; however, crystals in this location should be ignored because they are most likely artifacts. Most crystals are scanned with a 10× objective and are evaluated with at least a 40× objective, concentrating especially on cellular areas. Complete examination requires 100× oil immersion, however, because apparently negative fluids on scanning may contain a large population of small crystals (Gatter & Schumacher, 1991). Aligning the crystals' orientation to the compensator by rotating the microscope stage or the compensator facilitates recognition and identification. Crystal morphology, the extinction angle, strength, and signs of any birefringence (i.e., the ability to refract light and split the incident light into two rays: a fast ray and a slow ray) are noted. The sensitivity and specificity of polarized microscopy for crystals are 78% and 79%, respectively, for monosodium urate (Hasselbacher, 1987), and 12% and 67% for calcium pyrophosphate dihydrate (McGill & York, 1991). Repeat examination following 24 hours of refrigeration at 4°C may result in a significant increase in the number of crystal-positive fluids (Yuan et al., 2003). Cytospin preparations are also used effectively in the detection of crystals in SF samples (Theiler et al., 2014).

The Diff-Quik staining method may be a reliable alternative to polarized microscopy. Overall specificity, sensitivity, and accuracy are 87.5%, 94.4%, and 91.9%, respectively. The overall positive predictive value is 92.7%; the negative predictive value is 90.3% (Selvi et al., 2001). Other more sophisticated and reliable methods, such as X-ray crystallography and Fourier transform infrared spectroscopy, have been described for identifying and characterizing crystals in biological specimens but are seldom used clinically (Rosenthal & Mandel, 2001).

Monosodium urate (MSU) crystals appear as needle-shaped rods 5 to 20 μm long, but they may be only 1 to 2 μm in length or, rarely, may appear as rounded spherolites. They are strongly birefringent (Fig. 30.13): yellow when oriented parallel to the compensator and blue with perpendicular orientation (negative birefringence or elongation; Fig. 30.14). A control slide of MSU crystals should always be used for comparison. Alternatively, betamethasone, a steroid that appears as a strongly negative birefringent rod, can be used to prepare a reference slide for the polarizing microscope (Judkins & Cornbleet, 1997).

MSU crystals are found in 90% of acute urate gout and in about 75% of patients between attacks. Intracellular MSU crystals are characteristic of acute urate gout. They may also occasionally be observed as a result of inflammation in septic arthritis (McCarty, 1988).

Calcium pyrophosphate dihydrate (CPPD) crystals are found in a group of conditions collectively known as *CPPD crystal deposition disease* or *pseudogout*. These crystals appear as rhomboids, rods, or rectangles 1 to 20 μm in length. CPPD crystals are weakly birefringent with positive elongation (blue when aligned with the compensator axis; Fig. 30.15). Many are too small to polarize the light, making them difficult to detect without phase-contrast microscopy.

CPPD crystals are associated with degenerative arthritis and are seen in arthritides associated with hypomagnesemia, hemochromatosis, hyperparathyroidism, and hypothyroidism (Jones et al., 1992).

Calcium hydroxyapatite and the other BCP crystals are typically too small and nonbirefringent (isotropic) to see with light microscopy unless they are clumped into 1- to 50-μm spherical microaggregates. **Alizarin red S dye** may be used to stain these and other calcium-containing crystals (Lazcano et al., 1993). At present, identification of BCP crystals is not important for diagnosis or prognosis, or as a guide in treatment.

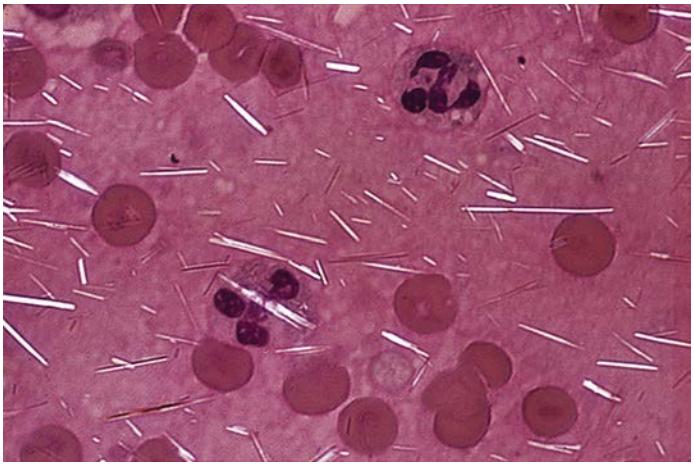

Figure 30.13 Monosodium urate crystals under polarized light from a patient with urate gout.

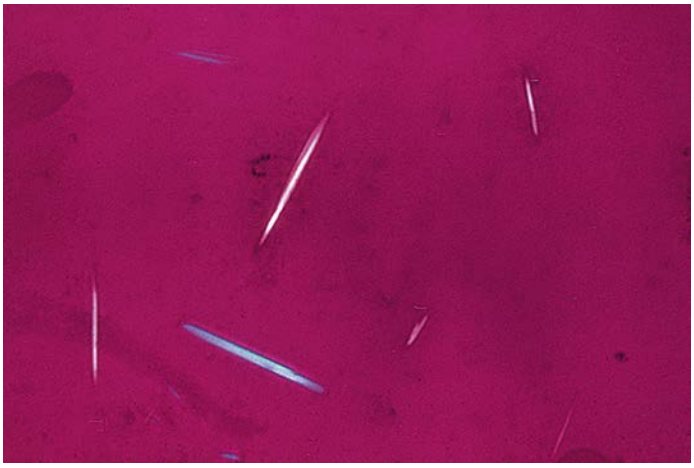

Figure 30.14 Monosodium urate crystals in synovial fluid. Compensated polarized light. (From Kjeldsberg CR, Knight JA: *Body fluids: laboratory examination of amniotic, cerebrospinal, seminal, serous and synovial fluids,* ed 3, Chicago, 1993, © American Society for Clinical Pathology, with permission.)

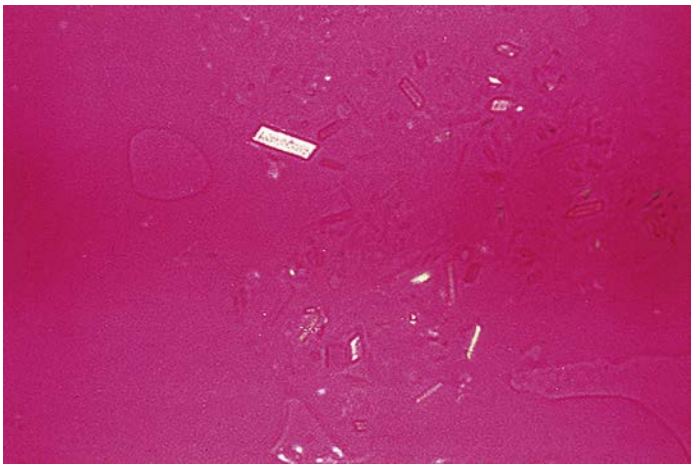

Figure 30.15 Calcium pyrophosphate dihydrate crystals in synovial fluid from a patient with pseudogout. Compensated polarized light. (From Kjeldsberg CR, Knight JA: *Body fluids: laboratory examination of amniotic, cerebrospinal, seminal, serous and synovial fluids,* ed 3, Chicago: © American Society for Clinical Pathology; 1993, with permission.)

Calcium oxalate dihydrate crystals are 5- to 30-μm bipyramidal octahedral "envelopes" with variable birefringence and positive elongation. They are seen in arthropathy associated with chronic renal dialysis and primary oxalosis, a rare inborn error of metabolism. The monohydrate form is birefringent but nondescript in shape.

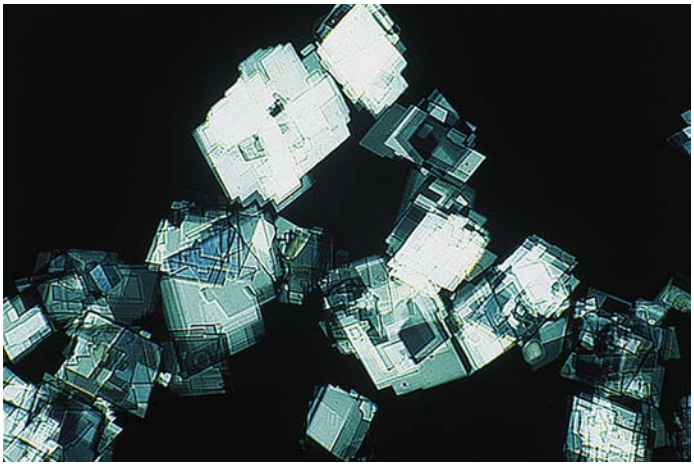

Figure 30.16 Cholesterol crystals in synovial fluid. Polarized light.

TABLE 30.8
Reference Intervals for Synovial Fluid Constituents

Constituent	Synovial Fluid	Plasma
Total protein	1–3 g/dL	6–8 g/dL
Albumin	55%–70%	50%–65%
α_1-Globulin	6%–8%	3%–5%
α_2-Globulin	5%–7%	7%–13%
β-Globulin	8%–10%	8%–14%
γ-Globulin	10%–14%	12%–22%
Hyaluronic acid	0.3–0.4 g/dL	
Glucose	70–110 mg/dL	70–110 mg/dL
Uric acid	2–8 mg/dL	2–8 mg/dL
Lactate	9–29 mg/dL	9–29 mg/dL

Modified from Kjeldsberg CR, Knight JA: *Body fluids: laboratory examination of amniotic, cerebrospinal, seminal, serous and synovial fluids,* ed 3, Chicago, 1993, © American Society for Clinical Pathology, with permission.

Lipid crystals or particles are 1- to 20-μm spheres with a Maltese cross appearance and positive birefringence under compensated polarized light. They have been implicated as a cause of acute arthritis (McCarty, 1988).

Crystalline corticosteroids from intraarticular injection may have an appearance similar to MSU or CPPD crystals and persist up to 1 month following injection. Most often, they have blunt, jagged edges without clear crystal structure because they are prepared by grinding up larger crystalline forms. Triamcinolone hexacetonide is negatively birefringent, but most others show positive birefringence.

Cholesterol crystals typically appear as irregular birefringent plates, often with notched corners (Fig. 30.16). In chronic effusions (e.g., tuberculous arthritis, RA, SLE), needle- or rhomboid-shaped crystals similar to MSU or CPPD may be present (Ettlinger & Hunder, 1979). Very small (1–5 microns) irregular, rod- and needle-shaped cholesterol crystals have been identified by X-ray diffraction analysis and by ultrastructural studies in osteoarthritis effusions (Fam et al., 1981). Cholesterol crystals are ethanol and ether soluble and are not phagocytosed by leukocytes. If cholesterol crystals are detected, quantitative analysis should show that the SF cholesterol level exceeds the plasma level.

Glove powder (modified cornstarch) introduced during joint surgery appears as round, strongly birefringent particles 5 to 30 μm in diameter, with a central notch and a Maltese cross appearance when polarized.

A variety of other crystals or particulates may be present in SF. These include monoclonal Ig crystals or cryoglobulins, Charcot-Leyden crystals, amyloid fragments, cartilage fragments, collagen fibrils and fibrin strands, hematoidin crystals from prior hemorrhage, crystals from certain anticoagulants, nail polish, prosthetic fragments, and dust particles (Gatter & Schumacher, 1991).

CHEMICAL ANALYSIS

Chemical analyses of SF generally offer only supportive information to the routine tests. High viscosity may be remedied by dilution with normal saline, sonication, or hyaluronidase treatment. Reference intervals for the more important chemical analytes are shown in Table 30.8.

Mucin Clot Test

Addition of acetic acid to SF precipitates hyaluronate into a mucin clot, which may be graded as good, fair, or poor. A fair to poor mucin clot test reflects dilution and depolymerization of hyaluronic acid—a nonspecific finding of several inflammatory arthritides. Although of historic interest, the mucin clot test has minimal clinical utility today and is rarely used (Baker, 1991).

Glucose

Proper interpretation of SF glucose values requires comparison with serum levels, ideally preceded by a fast of 8 hours to allow glucose to equilibrate across the synovial membrane. The serum-synovial differential is less than 10 mg/dL in normal and many noninflammatory conditions. In septic arthritis, this difference ranges from 20 to 60 mg/dL but overlaps significantly with other inflammatory conditions, thereby limiting its clinical usefulness. When a cutoff value of 75 mg/dL is used, the sensitivity of low glucose for detecting an inflammatory joint disease is only 20%; the specificity is 84% (Shmerling et al., 1990).

In vitro glycolysis by large numbers of leukocytes may falsely reduce SF glucose values unless testing is performed within 1 hour of collection. Tubes containing sodium fluoride, an inhibitor of glycolysis, prevent the loss of glucose.

Protein

The mean normal protein concentration is 1.38 g/dL in living volunteers (Weinburger & Simkin, 1989) and a reliable reference interval is 1.0 to 3.0 g/dL. With increasing inflammation, larger proteins (e.g., fibrinogen) enter the synovial space. Spontaneous clot formation may be detected in nonanticoagulated specimen tubes. Although elevation of the SF protein level may be associated with inflammatory and infectious conditions, measurement of SF protein is highly nonspecific; the sensitivity is about 52% and the specificity 56% for inflammatory disorders (Shmerling et al., 1990).

Enzymes

Numerous enzymes have been studied in SF, including lactate dehydrogenase, aspartate aminotransferase, adenosine deaminase, acid and alkaline phosphatase, and lysozyme, among others (Kjeldsberg, 1993). **Lactate dehydrogenase** is elevated in RA, gout, failed arthroplasties, and infectious arthritis. This increase most likely reflects the neutrophil infiltrate. Elevated **acid phosphatase** may have negative prognostic value in RA but is not specific (Luukkainen et al., 1989).

Organic Acids

When compared with nonseptic monoarticular arthritis, SF **lactic acid** levels are usually increased in patients with septic arthritis (Kjeldsberg, 1993). Levels significantly greater than 30 mg/dL (3.7 mmol/L) are commonly associated with septic arthritis due to gram-positive cocci and gram-negative bacilli. Measurement of D-lactate levels in SF appears to be a useful method for rapid diagnosis of bacterial synovitis (Gratacos et al., 1995). In other studies, however, normal or intermediate lactate levels neither rule in nor rule out infection. Moreover, gonococcal arthritis is notorious for having normal SF lactate levels (Curtis et al., 1983).

When gas-liquid chromatography is used, the presence of other organic acids not normally present in SF (e.g., **n-valeric**, **n-hexanoic**, and **succinic acids**) may be very helpful in differentiating septic from nonseptic arthritis (Borenstein et al., 1982).

Uric Acid

Synovial fluid uric acid levels generally, although not always, parallel serum levels in gout and noninflammatory arthropathies. This assay provides little clinical value in SF analysis except in some cases in which gout is suspected but crystals are not identified or when microscopic crystal analysis is not available (Reeves, 1965; Vaidya et al., 2018). Increased SF uric acid levels in these cases support a diagnosis of gout.

LIPIDS

In contrast to plasma, normal SF contains extremely low concentrations of lipids. Synovial fluid lipid abnormalities include (1) rare cholesterol-rich pseudochylous effusions typically associated with chronic RA; (2) lipid droplets, usually the result of trauma; and (3) extremely rare chylous effusions seen in association with RA, SLE, filariasis, pancreatitis, and trauma (Wise et al., 1987). These diseases can usually be differentiated clinically and by

gross and microscopic examination; quantification of lipids currently has no clinical value in joint fluid analysis, except in cases in which cholesterol crystals may resemble MSU or CPPD. In these cases, a cholesterol level that exceeds the plasma level supports the presence of cholesterol crystals.

IMMUNOLOGIC STUDIES

Rheumatoid factor (RF) is found in the SF of about 60% of RA patients, usually at a titer equal to or slightly lower than the serum titer. **Antinuclear antibodies** (ANAs) are found in the SF of about 70% of patients with SLE and 20% of patients with RA. Neither is specific enough for practical use. SF **complement** levels, normally about 10% of serum levels, increase to 40% to 70% of serum activity with inflammation, proportional to the increase in protein exudation. Complement consumption in SLE, and RA in particular, results in levels less than 30% of serum complement.

MICROBIOLOGICAL EXAMINATION

Immediate transportation of joint fluid and good communication of clinical suspicions to the laboratory are extremely important in the rapid identification of an infectious agent.

Septic arthritis may be acute or chronic; Gram stain and culture should be performed as part of the routine SF evaluation. Gram stain sensitivity varies from about 75% for staphylococcal infections and 50% for most gram-negative organisms to less than 25% for gonococcal infections (Goldenberg & Reed, 1985). Concentration methods, including cytocentrifugation, may increase the sensitivity of the Gram stain.

Culture sensitivity ranges from 75% to 95% for nongonococcal joint infections in patients who have not received antibiotics. For patients with gonorrhea, the sensitivity is only 10% to 50% (Shmerling, 1994). In partially treated patients, the use of resin-containing blood culture bottles for culturing SF may improve isolation and identification of the responsible organism.

The use of PCR with primers to detect bacterial DNA is helpful, particularly for the more fastidious, uncultivable pathogens (e.g., *Borrelia burgdorferi*, *Chlamydia* spp., *Mycoplasma* spp.) (Nocton et al., 1994; Li et al., 1996; Jalava et al., 2001; Pons et al., 2018). Viruses are often associated with acute infectious arthritis; depending on the putative virus, serology, viral culture, and detection of viral DNA by nucleic acid amplification should be performed.

Depending on the clinical history, infectious arthritis may be associated with particular exposures and their associated pathogens. Arthritis develops in approximately 60% of patients with Lyme disease resulting from exposure to ticks infected with *Borrelia burgdorferi* (Golightly, 1993). The PCR test for detecting *B. burgdorferi* DNA in SF is positive in 96% of untreated cases (Nocton et al., 1994; Exner & Lewinski, 2003).

In patients with a travel history or outdoor occupations, SF/tissue should be examined for fungal pathogens by KOH/calcofluor white stain and cultured on selective fungal media. For example, a patient with a recent travel history to Arizona may present with a monoarticular arthritis secondary to *Coccidioides immitis*.

Patients with chronic arthritis and risk factors for *Mycobacterium tuberculosis* or nontuberculous infections should undergo a synovial biopsy (Verettas et al., 2003; Titov et al., 2004). Ziehl-Neelsen or Kinyoun stains for acid-fast organisms have a sensitivity of about 20%. Cultures for *M. tuberculosis* are positive in about 80% of proven cases. Because conventional culture methods for *M. tuberculosis* are often very time-consuming, applying PCR in SF for the detection of *M. tuberculosis* is a useful technique for more rapid diagnosis (Fujimoto et al., 2010).

PLEURAL FLUID

The pleural cavity is a potential space lined by mesothelium of the visceral and parietal pleurae. The pleural cavity normally contains a small amount of fluid that facilitates movement of the two membranes against each other. This fluid is a plasma filtrate derived from capillaries of the parietal pleura. It is produced continuously at a rate dependent on capillary hydrostatic pressure, plasma oncotic pressure, and capillary permeability. Pleural fluid is reabsorbed through the lymphatics and venules of the visceral pleura.

An accumulation of fluid, called an **effusion**, results from an imbalance of fluid production and reabsorption. This fluid accumulation in the pleural, pericardial, and peritoneal cavities is known as a **serous effusion**.

SPECIMEN COLLECTION

Thoracentesis is indicated for any undiagnosed pleural effusion or for therapeutic purposes in patients with massive symptomatic effusions.

BOX 30.9

Classification of Pleural Effusions

Transudates: Increased Hydrostatic Pressure or Decreased Plasma Oncotic Pressure

Congestive heart failure
Hepatic cirrhosis
Hypoproteinemia (e.g., nephrotic syndrome)

Exudates: Increased Capillary Permeability or Decreased Lymphatic Resorption

Infections
- Bacterial pneumonia
- Tuberculosis, other granulomatous diseases (e.g., sarcoidosis, histoplasmosis)
- Viral or mycoplasma pneumonia

Neoplasms
- Bronchogenic carcinoma
- Metastatic carcinoma
- Lymphoma
- Mesothelioma (increased hyaluronate content of effusion fluid)

Noninfectious inflammatory disease involving pleura
- Rheumatoid disease (low pleural fluid glucose in most cases)
- Systemic lupus erythematosus (LE cells are occasionally present)

Pulmonary infarct (may be associated with hemorrhagic effusion)

Fluid from Extrapleural Sources

Pancreatitis (elevated amylase activity in effusion fluid)
Ruptured esophagus (elevated amylase activity and low pH)
Urinothorax (elevated creatinine and low pH)

LE, Lupus erythematosus.

Pleural fluid samples are frequently collected, handled, and/or analyzed in a less than satisfactory manner. Indeed, improper collection/handling and undertesting or inappropriate testing are more common than with other body fluids. The laboratory often receives a large syringe or vacuum bottle, which must be circulated through the various laboratory sections. Moreover, a large blood or fibrin clot may be present as the result of inadequate anticoagulation or mixing.

Except for an EDTA tube for total and differential cell counts, the specimen should be collected in heparinized tubes to avoid clotting. Aliquots for aerobic and anaerobic bacterial cultures are best inoculated into blood culture media at the bedside. If malignancy, fungal infection, or mycobacterial infection is suspected, all remaining fluid (≥100 mL) should be submitted to maximize the yield of stains and culture. Because serous effusions are more forgiving than CSF in maintaining cellular integrity, fresh specimens for cytology may be stored for up to 48 hours in the refrigerator with satisfactory results. For pH measurements, the fluid should be collected anaerobically in a heparinized syringe and submitted to the laboratory on ice. Grossly purulent specimens do not require pH measurement and may clog the analyzer.

TRANSUDATES AND EXUDATES

It has long been recognized that the initial classification of a pleural fluid as a **transudate** or an **exudate** greatly simplifies the process of arriving at a correct final diagnosis. Moreover, it determines whether further testing is needed.

Transudates are usually bilateral owing to systemic conditions leading to increased capillary hydrostatic pressure or decreased plasma oncotic pressure (Box 30.9). Malignant effusions may infrequently be transudative as the result of a simultaneous confounding clinical condition, such as congestive heart failure (Ashchi et al., 1998). Exudates are more often unilateral, associated with localized disorders that increase vascular permeability or interfere with lymphatic resorption (see Box 30.9).

RECOMMENDED TESTS

The evaluation of serous body fluids (pleural, pericardial, peritoneal) is directed first toward differentiating transudative from exudative effusions. Transudates generally require no further workup. However, the fluid should be retained for 7 to 10 days in case further testing is needed. To separate the two, several chemical parameters have been proposed, although none is 100% accurate (Table 30.9).

Classical teaching stressed that exudates and transudates can be distinguished on the basis of total protein concentrations above (exudates) or

TABLE 30.9
Laboratory Criteria for Pleural Fluid Exudate

Pleural fluid/serum protein ratio	≥0.50
Pleural fluid/serum LD ratio	≥0.60
Pleural fluid LD	≥2/3 upper limit of normal serum LD
Pleural fluid cholesterol	>45 mg/dL
Pleural fluid/serum cholesterol ratio	≥0.30
Serum–pleural fluid albumin gradient	≤1.2 g/dL
Pleural fluid/serum bilirubin ratio	≥0.60

LD, Lactate dehydrogenase.

below (transudates) 3.0 g/dL. However, using total protein alone misclassifies both exudates and transudates by about 30% (Melsom, 1979). It is now well accepted that test combinations increase sensitivity, improve accuracy, and serve as the basis for well-established diagnostic criteria (Light et al., 1972; Light, 2002). According to Light's criteria, an exudate meets one or more of the following criteria: (1) pleural fluid/serum protein ratio greater than 0.5; (2) pleural fluid/serum LD ratio greater than 0.6; and (3) pleural fluid LD level greater than two-thirds of the serum upper limit of normal. Using these criteria, the sensitivity and specificity are about 98% and 80%, respectively.

Several alternative measurements have been proposed to differentiate exudates from transudates. Testing for total cholesterol, the albumin gradient, or a combination of LD and total cholesterol may discriminate effusions with equivocal Light's criteria results. For example, the albumin gradient is recommended to confirm a clinical transudate misclassified as an exudate by Light's criteria (Light, 1997, 2002), that is, a serum albumin level greater than 1.2 g/dL higher than the pleural fluid level indicates that the fluid is a transudate (Burgess et al., 1995). In many such cases, the patient is being diuresed. Other test combinations have equaled but not surpassed the performance of Light's criteria. In most cases, the same categorization of pleural fluids as exudates or transudates may be achieved using measurements of protein and LD alone without comparison with a blood sample, as was accomplished with application of Light's criteria (Light, 2002; Murphy & Jenkinson, 2008). The traditional use of Light's criteria for distinguishing between transudates and exudates has recently been recommended for simplification based on measurements of LD and cholesterol only in the fluid and not in comparison with simultaneous values in serum (Lépine et al., 2019). In that study of 400 consecutive thoracenteses, values in pleural fluid of LD greater than 0.6 times the upper limit of normal for serum and of cholesterol greater than 40 mg/dL (1.04 mmol/L) showed the best sensitivity and negative likelihood ratio for classifying an effusion as exudative. This approach spares additional blood draws and testing without adversely impacting diagnostic sensitivity.

Some tests, such as the combination of pleural fluid LD and cholesterol or cholesterol alone, may be more convenient and cost-effective by avoiding the need for simultaneous blood tests (Costa et al., 1995; Hamal et al., 2013). Bilirubin measurement is not a strong discriminator of effusions (Heffner et al., 1997).

Further analysis of exudates is directed toward ruling out malignancy and infection. Cytology and appropriate bacterial stains and cultures or PCR-based microbial assays are the most useful tests in this regard. Moreover, given that pleural fluid DNA levels are significantly increased in exudates, quantitative analysis may be an effective method to evaluate the causes of serous effusion (Chan et al., 2003). Recommended tests for the evaluation of pleural effusions are summarized in Box 30.10. The types of tests ordered and the interpretation of test results should always be correlated with clinical findings and differential diagnosis. Total leukocyte, differential, and RBC counts are of limited use in the evaluation of serous effusions.

GROSS EXAMINATION

Transudates are typically clear, pale yellow to straw colored, and odorless, and do not clot. Approximately 15% of transudates are blood tinged. A bloody pleural effusion (hematocrit >1%) suggests trauma, malignancy, or pulmonary infarction (Jay, 1986). A traumatic tap is suggested by uneven blood distribution, fluid clearing with continued aspiration, or formation of small blood clots. A pleural fluid hematocrit greater than 50% of the blood hematocrit is good evidence for a hemothorax (Light, 1995).

Exudates may grossly resemble transudates, but most show variable degrees of cloudiness or turbidity, and they often clot if not heparinized. A feculent odor may be detected in anaerobic infections. Turbid, milky, and/or bloody specimens should be centrifuged and the supernatant examined. If the supernatant is clear, the turbidity is most likely due to cellular elements or debris. If the turbidity persists after centrifugation, a chylous or pseudochylous effusion is likely.

True chylous effusions are produced by leakage from the thoracic duct resulting from obstruction by lymphoma, carcinoma, or traumatic disruption. A creamy top layer of chylomicrons may form in the specimen on standing. Idiopathic congenital chylothorax is the most common form of pleural effusion in the newborn.

Pseudochylous or chyliform effusions may have a milky, greenish, or "gold paint" appearance. They accumulate gradually through the breakdown of cellular lipids in long-standing effusions such as rheumatoid pleuritis, tuberculosis, or myxedema. Features that distinguish true chylous from pseudochylous effusions are summarized in Table 30.10.

BOX 30.10
Pleural Effusion: Recommended Tests

Routine Tests
Gross examination
Pleural fluid/serum protein ratio (used for Light's criteria)
Pleural fluid/serum LDH ratio (used for Light's criteria)
Examination of Romanowski-stained smear (malignant cells, LE cells)

Useful Tests in Most Patients
Stains and cultures for microorganisms
Cytology

Useful Tests in Selected Cases
Pleural fluid cholesterol
Pleural fluid/serum cholesterol ratio
Albumin gradient
pH
Lactate
Enzymes (ADA, amylase)
Interferon-γ
C-reactive protein
Lipid analysis
Multiplex PCR assay for bacterial, fungal, viral, and mycobacterial DNA
Tumor markers
Immunologic studies
Tuberculostearic acid
Pleural biopsy

ADA, Adenosine deaminase; *LD,* lactate dehydrogenase; *LE,* lupus erythematosus.
Modified from Kjeldsberg CR, Knight JA: *Body fluids: laboratory examination of amniotic, cerebrospinal, seminal, serous and synovial fluids,* ed 3, Chicago, 1993, © American Society for Clinical Pathology, with permission.

MICROSCOPIC EXAMINATION

Cell Counts

Total cell counts may be performed using manual hemocytometer methods. However, automated cell counts are increasingly used with pleural and other serous fluid specimens (Aulesa et al., 2003; Conner et al., 2003; Yang et al., 2013). Leukocyte counts have limited utility in separating transudates (<1000/μL) from exudates (>1000/μL). Although RBC counts above 100,000/μL are highly suggestive of malignancy, trauma, or pulmonary infarction, they are not specific for these conditions.

Differential Leukocyte Count and Cytology

Examination is commonly performed on a stained smear, preferably prepared by cytocentrifugation and with the air-dried smear stained with a Romanowski stain. Examination by the hematology laboratory can be highly effective in the rapid detection of malignant cells, especially hematologic malignancies (Kendall et al., 1997). Filtration or automated concentration methods with Papanicolaou stain may also be used, especially if cell loss is a matter of concern. Automated WBC differential counts may be done on pleural fluid samples, with increasingly reliable results using more recent technology (Conner et al., 2003; Fuster et al., 2018). Liquid-based thin-layer methods are often used to prepare pleural and other serous fluid specimens for cytopathologic examination and show good performance in the detection of malignant cells (Moriarity et al., 2008).

Cytologic analysis will establish the diagnosis of metastatic carcinoma in 70% or more of cases when both smears and cell blocks are examined (Light, 2002). The sensitivity is significantly lower if the patient has mesothelioma (10%), squamous cell carcinoma (20%), lymphoma (25%–50%),

TABLE 30.10

Characteristic Features of Chylous and Pseudochylous Effusions

Feature	Chylous	Pseudochylous
Onset	Sudden	Gradual
Appearance	Milky-white, or yellow to bloody	Milky or greenish, metallic sheen
Microscopic examination	Lymphocytosis	Mixed cellular reaction, cholesterol crystals
Triglycerides*†	≥110 mg/dL (≥1.24 mmol/L)	<50 mg/dL (<0.56 mol/L)
Lipoprotein electrophoresis	Chylomicrons present	Chylomicrons absent

Modified from Kjeldsberg CR, Knight JA: *Body fluids: laboratory examination of amniotic, cerebrospinal, seminal, serous and synovial fluids,* ed 3, Chicago, 1993, © American Society for Clinical Pathology, with permission.
*Values in parentheses are SI units.
†Triglyceride levels between 50 mg/dL and 110 mg/dL are equivocal and require electrophoresis to confirm chylothorax.

or sarcoma (25%). Preparation of cell blocks is unnecessary, except for effusions in which malignancy is an important consideration (Sumedha, 2017; Jonasson et al., 1990). Well-differentiated carcinoma cells may be easily recognized (Figs. 30.17 and 30.18) or may be highly undifferentiated (Fig. 30.19). A panel of immunocytochemical or immunohistochemical stains may be necessary for confirmation. These studies are enhanced by the use of liquid-based preparation methods or cell block technology (Sioutopoulou et al., 2008; Dey et al., 2017).

Mesothelial cells are common in pleural fluids from inflammatory processes (see Fig. 30.17). However, they are conspicuously scarce in patients with tuberculous pleurisy and rheumatoid pleuritis and in patients who have had pleurodesis. Fibrin deposition and fibrosis occurring in these conditions prevent mesothelial cell exfoliation.

Neutrophils predominate in pleural fluid from patients with pleural inflammation (Box 30.11). More than 10% of transudates will also have a predominance of neutrophils, but this has limited clinical significance.

Lymphocytes predominate in the disorders summarized in Box 30.11. Most are small, but medium, large, and reactive (transformed) variants may be seen. Nucleoli and nuclear cleaving are more prominent in effusions than in the peripheral blood; these features may be particularly prominent in cytocentrifuge preparations. **Plasma cells** may also be observed. Lymphocytosis associated with transudates is of limited clinical significance.

Low-grade non-Hodgkin lymphoma and chronic lymphocytic leukemia (CLL) may be difficult to distinguish from benign lymphocyte-rich serous effusion (Fig. 30.20). Immunophenotyping by flow cytometry or immunocytochemistry in conjunction with cellular morphology is usually helpful in making a correct diagnosis. The relative proportions of T and B cells are not definitive by themselves for separating benign from malignant exudates (Ibrahim et al., 1989). However, the pattern of expression of Ig light chains and/or other distinctive cell marker combinations may allow specific diagnosis of lymphoproliferative disorders. Molecular DNA analysis may be another useful adjunct to morphologic analysis. An unusual form of high-grade B-cell non-Hodgkin lymphoma, called *primary effusion lymphoma*, may be seen in pleural, peritoneal, and/or pericardial fluid specimens, typically from immunocompromised patients, with a characteristic highly anaplastic and immunoblastic morphologic appearance and without expression of most B cell–associated antigens (Karcher & Alkan, 1997). The diagnosis is usually confirmed by demonstrating in the neoplastic cells the presence of human herpesvirus-8 (HHV-8)–associated antigens and/or DNA by immunophenotypic and/or molecular analysis.

An eosinophilic effusion is one that has 10% or more **eosinophils.** The most common causes are related to the presence of air or blood in the pleural cavity (see Box 30.11). Most of these are exudates; however, in about 35% of patients, the cause is unknown (Adelman et al., 1984). A small number of **mast cells** or **basophils** often accompany eosinophils. Eosinophil-derived **Charcot-Leyden crystals** may also be seen.

CHEMICAL ANALYSIS

Protein

The measurement of pleural fluid total protein or albumin has little clinical value except when combined with other parameters to differentiate exudates from transudates. Protein electrophoresis shows a pattern similar to serum, except for a higher proportion of albumin; it has little value for differential diagnosis (Light, 1995).

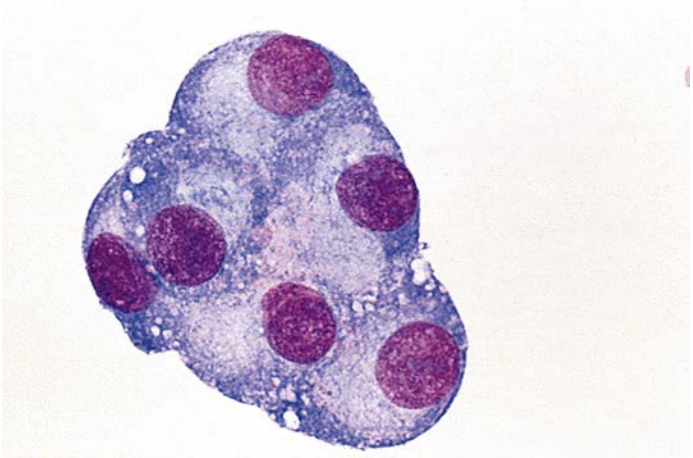

Figure 30.17 Mesothelial cells in pleural fluid.

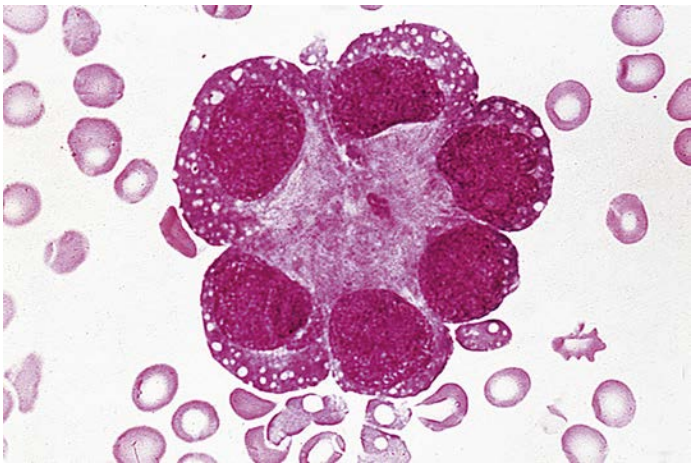

Figure 30.18 Well-differentiated breast carcinoma cells in pleural fluid.

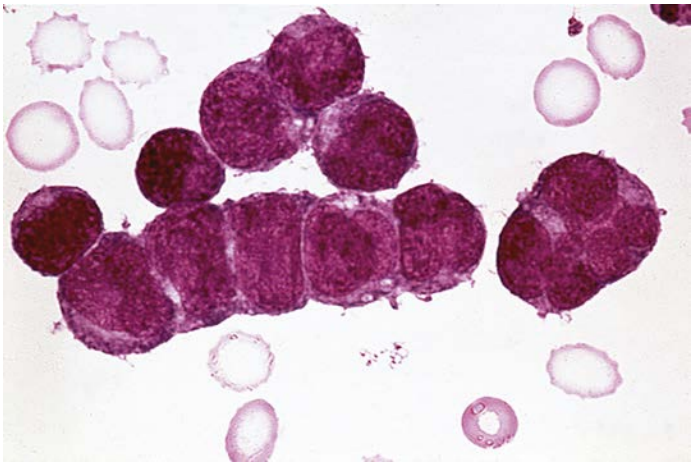

Figure 30.19 Small-cell carcinoma of the lung showing typical molding of nuclei.

Glucose

The glucose level of normal pleural fluid, transudates, and most exudates is similar to serum levels. Decreased pleural fluid glucose, accepted as a level below 60 mg/dL (3.33 mmol/L) or a pleural fluid/serum glucose ratio less than 0.5, is most consistent and dramatic in rheumatoid pleuritis and grossly purulent parapneumonic exudates (Sahn, 1982). Low pleural fluid glucose may also be present in malignancy, tuberculosis, nonpurulent bacterial infection, lupus pleuritis, and esophageal rupture.

Lactate

Pleural fluid lactate levels can be a useful adjunct in the rapid diagnosis of infectious pleuritis. Levels are significantly higher in bacterial and

BOX 30.11

Cellular Differential of Pleural Effusions

Neutrophilia (>50%)
Bacterial pneumonia (parapneumonic effusion)
Pulmonary infarction
Pancreatitis
Subphrenic abscess
Early tuberculosis
Transudates (>10%)

Lymphocytosis (>50%)
Tuberculosis
Viral infection
Malignancy (lymphoma, other neoplasms)
True chylothorax
Rheumatoid pleuritis
Systemic lupus erythematosus
Uremic effusions
Transudates (≈30%)

Eosinophilia (>10%)
Pneumothorax (air in pleural space)
Trauma
Pulmonary infarction
Congestive heart failure
Infection (especially parasitic, fungal)
Hypersensitivity syndromes
Drug reaction
Rheumatologic diseases
Hodgkin disease
Idiopathic

tuberculous pleural infections and other complicated parapneumonic pleural effusions than in other pleural conditions (Santotoribio et al., 2016). Values greater than 90 mg/dL (10 mmol/L) have a positive predictive value for infectious pleuritis of 94% and a negative predictive value of 100% (Gastrin & Lovestad, 1988).

Enzymes

Amylase elevations above the serum level (usually 1.5–2.0 or more times greater) indicate the presence of pancreatitis, esophageal rupture, or malignant effusion (Light & Ball, 1973). Elevated amylase derived from esophageal rupture or malignancy is the salivary isoform, which differentiates it from pancreatic amylase (Kramer et al., 1989).

Pleural fluid LD levels rise in proportion to the degree of inflammation. In addition to their use in separating exudates from transudates, declining LD levels during the course of an effusion indicate that the inflammatory process is resolving. Conversely, increasing levels indicate a worsening condition requiring aggressive workup or treatment.

ADA, which is particularly rich in T lymphocytes, is significantly increased in tuberculous pleuritis. At a level of 50 U/L, the sensitivity, specificity, positive predictive value, negative predictive value, and efficiency for tuberculosis are 91%, 81%, 84%, 89%, and 86%, respectively (Burgess et al., 1996). When the lymphocyte/neutrophil ratio is 0.75 or greater, the percentages are 88%, 95%, 95%, 88%, and 92%, respectively. ADA levels of 40 U/L or greater are present in about 99.6% of patients with verified tuberculous pleuritis (Lee et al., 2001). However, in patients with lymphocyte-rich pleural fluids from nontuberculous causes, ADA levels less than 40 U/L are present in 97.1% of cases. Factors such as patient age may impact ADA levels in pleural fluid, with lower levels and the need for a lower cutoff value for tuberculous effusions in older patients (Tay et al., 2013).

Interferon-γ

Pleural fluid interferon (IFN)-γ levels are significantly increased in the pleural fluid of patients with tuberculous pleuritis. The sensitivity of levels of 3.7 IU/L or greater is 99%, and the specificity is 98% (Villena et al., 1996a). Test sensitivity does not differ in HIV-positive and HIV-negative patients. Only about 20% of patients with effusions due to hematologic malignancies have IFN-γ levels slightly above 3.7 IU/L (Villena et al., 2003a).

pH

Pleural fluid pH measurement has the highest diagnostic accuracy in assessing the prognosis of parapneumonic effusions (Heffner et al., 1995).

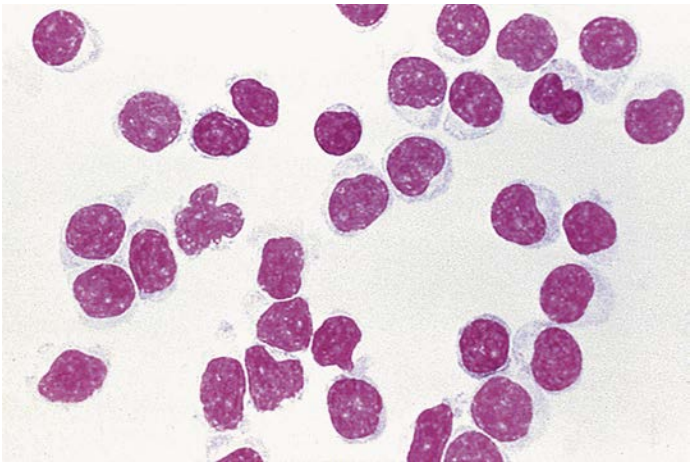

Figure 30.20 Pleural effusion in patient with non-Hodgkin lymphoma, small lymphocytic type. The cells are small round forms, difficult to distinguish from benign lymphocytes. (From Kjeldsberg CR, Knight JA: Body fluids: *Laboratory examination of amniotic, cerebrospinal, seminal, serous and synovial fluids,* ed 3, Chicago, 1993, © American Society for Clinical Pathology, with permission.)

A parapneumonic exudate with a pH greater than 7.30 generally resolves with medical therapy alone. A pH less than 7.20 indicates a complicated parapneumonic effusion (loculated or associated with empyema), requiring surgical drainage.

Patients with borderline complicated exudates (pH 7.20–7.30) may be closely watched with repeat measurements. A concomitant pleural glucose level below 60 mg/dL (3.33 mmol/L), however, strongly suggests impending empyema. Rheumatoid pleuritis and malignant effusions with a poor response to pleurodesis also have pH values below 7.20 and a low glucose level (Rodriquez-Panadero & Mejias, 1989). A pH below 6.0 is characteristic of **esophageal rupture**, although the pH in severe empyema may be 6.0 or less (Good et al., 1980).

Urinothorax, a collection of urine presumably produced by lymphatic drainage of perirenal accumulations into the pleural cavity, is also associated with a pleural fluid pH less than 7.30. These effusions are transudative, because of their low protein content, and smell of urine. They have a creatinine level greater than in simultaneously drawn serum (Miller et al., 1988).

Lipids

Some serous effusions appear to be chylous (i.e., a milky appearance) but are not (pseudochylous), whereas others may not look chylous but are (Maldonado et al., 2009). Although pseudochylous fluids may be partially due to increased leukocytes and necrotic debris, they are primarily due to the presence of increased lecithin-globulin complexes. A true chylous effusion has chylomicrons on lipoprotein electrophoresis. Lipid measurements are also helpful in identifying chylous effusions (Staats et al., 1980). Thus, pleural fluid triglyceride levels above 110 mg/dL indicate a chylous effusion; values from 60 to 110 mg/dL (0.68–1.24 mmol/L) are less certain and require lipoprotein electrophoresis to confirm a chylothorax, particularly in fasting and postoperative patients (Maldonado et al., 2009). Nonchylous and pseudochylous effusions generally have triglyceride levels below 50 mg/dL (0.56 mmol/L) and no chylomicrons on electrophoresis (see Table 30.10).

Cholesterol measurements may be useful in separating transudates from exudates, especially when there is a question regarding Light's criteria (Hamal et al., 2013). A total cholesterol value of 54 mg/dL or more and a pleural fluid/serum cholesterol ratio of 0.32 or higher have sensitivity and specificity values similar to Light's criteria (Suay et al., 1995). Elevated levels and the presence of cholesterol crystals may be seen with pleural effusions that have been present for several years.

C-Reactive Protein

Pleural fluid CRP is a clinically useful screening test for organ disease, index of disease activity, and measure of response to therapy (Castano & Amores, 1992). Pleural fluid CRP levels >30 mg/L reportedly have a sensitivity of 93.7%, a specificity of 76.5%, and a positive predictive value of 98.4% in parapneumonic infections (Turay et al., 2000). In a more recent study, mean CRP values were ≥138 mg/L in parapneumonic infections compared with <64 mg/L in other types of exudative effusions (Izhakian et al., 2016). Measurement of pleural fluid CRP contributes to both the

diagnosis and assessment of severity of parapneumonic effusions (Porcel et al., 2012).

Tuberculostearic Acid (10-Methyloctadecanoic Acid)

Tuberculostearic acid (TSA) was first isolated from the bacillus *Mycobacterium tuberculosis*. This fatty acid is a structural component of mycobacteria and is not normally present in human tissue. Using gas chromatography–mass spectroscopy, TSA was measured in sputum, bronchial washings, and pleural fluid from patients with pulmonary tuberculosis (Muranishi et al., 1990). Here, pleural fluid TSA was identified in 24 of 32 (75%) patients with active tuberculosis; bronchial washings were positive for TSA in 15 of 22 cases. In patients with other pulmonary disorders, only 4 of 46 pleural fluids and 3 of 69 bronchial washings had detectable levels. A later smaller study reported the following for pleural fluid TSA: Sensitivity 54%, specificity 80%, positive predictive value 75%, negative predictive value 61%, and efficacy 66% (Yorgancioglu et al., 1996). Combining TSA and ADA analysis in pleural fluid samples appears to increase the diagnostic sensitivity for tuberculous pleuritis (Muranishi et al., 1992).

Tumor Markers

Although not recommended as a routine test, various tumor markers are often a useful adjunct in enigmatic noninflammatory exudates with negative cytology. Several tumor markers—especially CEA, CA 15-3, CA 549, CA 72-4, CA 125, and CYFRA 21-1, among others—have been studied in pleural fluids. CEA is probably the most useful single marker for adenocarcinomas, but reported cutoff values vary considerably. The sensitivity of CEA for malignant effusions varies depending on tumor origin and is about 50% overall. Although complicated parapneumonic effusions may result in elevated CEA levels (Garcia-Pachon et al., 1997), they are usually not a problem to distinguish clinically.

A combination of tumor markers increases the accuracy of diagnosis of malignant effusions. Thus, a combination of CEA, CA 15-3, and CA 72-4 had an accuracy of 90% with 78% sensitivity, 95% specificity, 88% positive predictive value, and 91% negative predictive value (Villena et al., 1996b). Similarly, CA 15-3 and CEA combined had an accuracy of 87% (Romero et al., 1996); a combination of CA 549, CEA, and CA 15-3 had a sensitivity of 65%, specificity 99%, and accuracy 85% (Villena et al., 2003b). The use of the cytokeratin 19 fragment (CYFRA 21-1) may also be useful in combination with other tumor markers. Complicating the use of these tests, different tumor markers may be positive in both malignant and inflammatory pleural effusions (Topolcan et al., 2007). Pleural fluid tumor marker levels may be particularly useful in specimens with inconclusive cytologic results (Antonangelo et al., 2015).

Other tumor markers may also be useful in the diagnosis of unexplained effusions. For example, a marked increase in pleural fluid prostate-specific antigen (PSA) can lead to the correct diagnosis of metastatic prostate cancer in pleural and pericardial effusions, even when negative by cytologic examination (Chin et al., 1999).

MicroRNA (miRNA)

A new adjunctive approach to diagnosis of serous cavity fluids is the analysis of microRNA (miRNA), which has great stability in such a fluid environment and can be detected and examined even in fluids in which malignant cells can be rare or degenerated and, thus, not fit for standard cytologic evaluation (Nicolè et al., 2019). Using miRNA has the potential for greatly enhancing examination of serous fluids and diagnosing malignancy.

IMMUNOLOGIC STUDIES

Approximately 5% of patients with RA and 50% with SLE develop pleural effusions sometime during the course of their disease.

RF is commonly present in pleural effusions associated with seropositive RA. Although a pleural fluid titer of 1:320 or greater in a patient with known RA is reasonable evidence of rheumatic pleuritis (Halla et al., 1980), elevated RF titers up to 1:1280 have been identified in 41% of patients with bacterial pneumonia, 20% of patients with malignant effusions, and 14% of patients with tuberculosis, making this test of little value (Levine et al., 1968).

ANA titers once appeared to be useful in the diagnosis of effusion due to lupus pleuritis; (Good et al., 1983). Later studies have indicated no benefit of this testing in pleural fluid specimens over and above serum testing (Porcel et al., 2007).

Decreased **complement** levels (CH50 <10 U/mL or C4 level below 10×10^{-5} U/g protein) are present in most patients with rheumatoid or lupus pleuritis (Hunder et al., 1972; Halla et al., 1980). However, decreased complement is not highly specific for these diseases and is of little value for routine diagnosis, although it may be helpful in the diagnosis of otherwise enigmatic effusions.

MICROBIOLOGICAL EXAMINATION

Bacteria most commonly associated with parapneumonic effusions are *Staphylococcus aureus*, *Streptococcus pneumoniae*, β-hemolytic group A streptococci, enterococci, and some gram-negative bacilli. Anaerobic bacteria are isolated in a significant proportion of cases; thus, both anaerobic and aerobic cultures should be performed. The sensitivity of the Gram stain is approximately 50% (Ferrer et al., 1999); concentration methods, such as cytocentrifugation, may increase the sensitivity. Use of resin-containing blood culture bottles may improve the isolation of certain bacteria in partially treated patients.

For patients with suspected *M. tuberculosis*, direct staining of tuberculous effusions for acid-fast bacteria has a sensitivity of 20% to 30%, and positive cultures are found in 50% to 70% of cases (Baer & Smith, 2001). Pleural biopsy yields the highest culture sensitivity (50%–75%) and may provide a rapid presumptive diagnosis of tuberculosis by histopathologic demonstration of granulomas or acid-fast bacteria. Combining culture and acid-fast stains with pleural biopsy increases the sensitivity to about 95% (Jay, 1986). Real-time PCR analysis of pleural fluid specimens shows good sensitivity and specificity for the diagnosis of *M. tuberculosis* and may provide an effective less invasive alternative method for rapid diagnosis (Rosso et al., 2011; Saeed et al., 2017).

ADA can provide rapid chemical evidence for tuberculous effusions independent of HIV status (Burgess et al., 1996; Riantawan et al., 1999; Lee et al., 2001). Although the ADA-2 isoenzyme form is elaborated by activated lymphocytes in tuberculosis, only mild elevations occur in lymphocyte-rich pleural effusions from nontuberculous causes. However, the relatively low prevalence of tuberculous pleurisy in North America anticipates a lower positive predictive value rate compared with the excellent results reported in the Asian and European literature, where tuberculosis is more common. Combining ADA measurement and real-time PCR analysis provides good diagnostic efficiency in tuberculous pleural effusions (Kaur et al., 2012).

Pleural fluid interferon-γ is significantly increased in tuberculous pleuritis and may be helpful in some cases because it is independent of HIV status and is only modestly increased in about 20% of hematologic malignancies (Villena et al., 2003a).

PERICARDIAL FLUID

From 10 to 50 mL of fluid is normally present in the pericardial space, produced by a transudative process similar to pleural fluid. Pericardial effusions are most often caused by viral infection; enterovirus is the most common etiologic agent. They may also develop as a result of bacterial, tuberculous, or fungal infection, or in association with autoimmune disorders, renal failure, myocardial infarction, mediastinal injury, or the effects of various drugs, or they may be idiopathic (Box 30.12). HIV-infected patients commonly have asymptomatic pericardial effusions, which may become large in more advanced disease (Silva-Cardosa et al., 1999), or they may be associated with primary effusion lymphoma (Karcher & Alkan, 1997). Many of the recommended laboratory tests described for pleural fluid also pertain to pericardial effusions (see Box 30.10).

The **postpericardiotomy syndrome** is a fairly common but nonspecific complication of cardiac surgery (or other cardiac damage) that develops days to weeks following the initial injury. It is characterized by the development of fever, pleuritic chest pain, and other signs of pleural, pericardial, and, less often, lung inflammation (Tamarappoo et al., 2016). Exudative pleural effusions develop in more than 80% of cases. These are often serosanguineous to hemorrhagic and typically have a pH greater than 7.4 and a normal glucose level (Stelzner et al., 1983). No specific tests are available for diagnosing this syndrome. Diagnosis, therefore, remains one of clinical exclusion. Although the cause is uncertain, the time course, presence of antimyocardial antibodies, and response to antiinflammatory therapy suggest an immune-mediated process. Increased levels of antimyocardial antibodies relative to serum, decreased complement levels, and immune complexes have been documented in pleural fluid from a single patient with the syndrome (Kim & Sahn, 1996).

SPECIMEN COLLECTION

Pericardial effusions of unknown origin or large effusions with signs of cardiac tamponade are generally submitted for laboratory examination. Fluid

BOX 30.12
Causes of Pericardial Effusions

Idiopathic (most often viral)
Infection
Bacteria
Tuberculosis
Fungi
Viruses
AIDS-related (usually viral)
Neoplasm
Metastatic carcinoma
Lymphoma
Drugs
Hydralazine
Procainamide
Phenytoin
Renal failure
Hemorrhage
Trauma
Anticoagulant therapy
Leakage of aortic aneurysm
Autoimmune disorders
Hypothyroidism
Rheumatoid arthritis
Systemic lupus erythematosus
Inflammatory bowel disease
Wegener's granulomatosis
Acute myocardial infarction
Radiation therapy

AIDS, Acquired immunodeficiency syndrome.

may be obtained by pericardiotomy following limited thoracotomy, or by pericardiocentesis (sterile needle aspiration).

GROSS EXAMINATION

Normal pericardial fluid is pale yellow and clear. Large effusions (>350 mL) are most often caused by malignancy or uremia, or they may be idiopathic. In HIV-associated cardiac tamponade, 45% of cases are idiopathic, and tuberculous and bacterial effusions each account for about 20% of cases (Chen et al., 1999). Infection or malignancy typically produces turbid effusions, whereas effusions due to uremia are usually clear and straw colored. These and several other disorders may produce hemorrhagic effusions.

Blood-like fluid obtained by pericardiocentesis might represent a hemorrhagic effusion or inadvertent aspiration of blood from the heart. Blood obtained from the heart chamber will have a hematocrit comparable with that of peripheral blood, and blood gas analysis yields results similar to venous or arterial blood. In contrast, the hematocrit of a hemorrhagic effusion is usually lower than that of peripheral blood. Blood from a cardiac puncture clots, but a hemorrhagic effusion usually does not.

A milky appearance suggests the presence of a chylous or pseudochylous effusion. Identification and differentiation of these effusions are discussed in the Pleural Fluid section earlier in the chapter.

EXUDATES AND TRANSUDATES

According to Light's criteria, a pleural exudate has one or more of the following: pleural fluid/serum protein ratio >0.5; pleural fluid/serum LD ratio >0.6; and pleural fluid LD level >200 U/L. Light's criteria have also been shown to be the most reliable diagnostic tool for identifying pericardial exudates and transudates (Burgess et al., 2002a).

Routine testing of pericardial effusions should probably be limited to cell count, glucose, total protein, LD, bacterial culture, and cytology (Meyers et al., 1997). Other more specific tests are appropriate only when there is a high clinical suspicion of unusual causes of pericardial effusion.

MICROSCOPIC EXAMINATION

The hematocrit and RBC count document the presence of a hemorrhagic effusion but are of limited value for differential diagnosis. Total leukocyte counts over 10,000/μL suggest bacterial, tuberculous, or malignant pericarditis; however, low counts may be encountered in these conditions, limiting the value of this measurement (Agner & Gallis, 1979). Leukocyte differential counts may be helpful in determining the cause of certain pericardial effusions, particularly when combined with other pericardial fluid findings (Reuter et al., 2006). Even when the differential count is not helpful, examination of a stained smear should always be performed to evaluate for atypical or malignant cells.

Cytologic identification of malignant cells is usually not difficult. Metastatic carcinomas of the lung and breast are most frequently observed in malignant pericardial effusion. Cytology has a sensitivity of 95% and a specificity of 100% (Meyers et al., 1997).

CHEMICAL ANALYSIS

Chemical parameters for the diagnosis of pericardial effusions have not been studied to the same extent as in other body fluids. Although pericardial effusions are very similar to pleural fluids, routine application of these tests requires additional studies to fully appreciate their diagnostic importance.

Protein

A value greater than 3.0 g/dL has a sensitivity of 97% for exudative effusions but a specificity of only 22%, which significantly limits its usefulness. Thus, total protein has no discriminating power in pericardial diagnosis (Meyers et al., 1997).

Glucose

Pericardial glucose levels less than 60 mg/dL have a diagnostic accuracy of only 36% in identifying pericardial exudates (Meyers et al., 1997). Values less than 40 mg/dL (<2.22 mmol/L) are common in bacterial, tuberculous, rheumatic, or malignant effusions.

pH

Pericardial fluid pH may be markedly decreased (<7.10) in rheumatic or purulent pericarditis. Malignancy, uremia, tuberculosis, and idiopathic disorders may have moderate decreases in the range of 7.20 to 7.30 (Kindig & Goodman, 1983).

Lipids

Separation of true chylous from pseudochylous effusions may be facilitated by triglyceride and cholesterol measurements, as well as by lipoprotein electrophoresis for chylomicrons (see Table 30.10). See the section on Lipids in the Pleural Fluid section earlier in the chapter for further details on the diagnosis of chylous effusions.

Enzymes

A pericardial fluid LD level greater than 200 U/L has been suggested as a cutoff for pericardial exudates (Burgess et al., 2002a). Moreover, the measurement of LD and creatine kinase in postmortem pericardial fluid within 48 hours of death may be useful in establishing acute myocardial injury when such injury is suspected but cannot be established by the usual histologic methods (Luna et al., 1982; Stewart et al., 1984). Pericardial fluid levels of CK-MB, myoglobin, and troponin I in postmortem pericardial fluid are significantly increased in patients with myocardial injury (Perez-Carceles et al., 2004).

ADA activity is a useful adjunctive test for tuberculous pericarditis in suspicious cases with negative acid-fast stains. The median ADA level in tuberculous pericarditis is significantly higher than in other pathologic effusions (Burgess et al., 2002b). Using a cutoff of 30 U/L, the sensitivity is 94%, specificity 68%, and positive predictive value 80%. Using a cutoff of 40 U/L, the sensitivity and specificity are 93% and 97%, respectively (Koh et al., 1994). Combining pericardial ADA levels with other findings adds to the diagnostic utility of measuring this analyte (Reuter et al., 2006).

Interferon-γ

Increased IFN-γ levels have been reported in tuberculous serous effusions, including tuberculous pericarditis (Burgess et al., 2002b). Here, the IFN-γ level was greater than 1000 pg/L, which was significantly higher than in effusions from other pathologic conditions. A cutoff value of 200 pg/L results in a sensitivity and specificity of 100% for the diagnosis of tuberculous pericarditis. As with ADA, combining IFN-γ levels with other pericardial fluid findings improves the diagnostic utility of this assay (Reuter et al., 2006).

Polymerase Chain Reaction

PCR is a sensitive technique and may be more specific than adenosine deaminase in the diagnosis of tuberculous pericarditis (Lee et al., 2002). However, a negative test does not rule out tuberculous pericarditis because some pericardial fluids from patients with large tuberculous effusions may not contain *M. tuberculosis*. PCR-based analysis is superior to ADA levels in

diagnosing tuberculous pericarditis (Pandie et al., 2014) and provides high sensitivity and specificity in the rapid diagnosis of this condition (Saeed et al., 2017).

IMMUNOLOGIC STUDIES

A negative ANA test makes the diagnosis of lupus serositis highly unlikely. Conversely, high ANA titers in pericardial effusions lack specificity, even when they are as high as 1 : 5120 (Leventhal et al., 1990; Wang et al., 2000). If a high ANA titer is unexplained, malignancy should be considered.

MICROBIOLOGICAL EXAMINATION

The sensitivity of the Gram stain and culture for bacterial pericarditis is similar to other serous body fluids (i.e., about 50% and 80%, respectively). Important aerobic bacteria include *S. aureus*, *S. pneumoniae*, *S. pyogenes*, and gram-negative bacilli. Although infectious pericarditis due to anaerobic bacteria may be encountered rarely, the bacteria are sometimes not recognized because of inconsistent methods used for their isolation and identification (Brook, 2002). For this reason, proper laboratory technique is of particular importance when infection with an anaerobic organism is suspected. The major anaerobic organisms are the *Bacteroides fragilis* group, anaerobic streptococci, *Clostridium* species, *Fusobacterium* species, and *Bifidobacterium* species.

Identification of a specific etiologic agent in viral pericarditis is difficult because the viruses (e.g., coxsackieviruses, influenza virus, mumps) are rarely isolated from pericardial fluid. Obtaining acute and convalescent sera for antibody response to suspected viral pathogens may help support the diagnosis (Bellinger & Vacek, 1987). Viral infection probably accounts for most idiopathic HIV-associated pericardial effusions.

The sensitivity of acid-fast stains and culture for tuberculous pericarditis is about 50% (Agner & Gallis, 1979). PCR-based assays now provide high sensitivity (84.3%) and specificity (100%) in the rapid diagnosis of tuberculous pericarditis and pleuritis (Saeed et al., 2017) and are superior to ADA levels in making this diagnosis (Pandie et al., 2014).

PCR-based assays may aid in the rapid diagnosis of a variety of other bacterial and other infections in the pericardial space (Tenenbaum et al., 2005; Levy et al., 2006).

PERITONEAL FLUID

Ascites is the pathologic accumulation of excess fluid in the peritoneal cavity. Up to 50 mL of fluid is normally present in this mesothelial-lined space. As with pleural and pericardial fluids, it is produced as an ultrafiltrate of plasma dependent on vascular permeability and on hydrostatic and oncotic pressure.

TRANSUDATES AND EXUDATES

Common causes of peritoneal effusions are listed in Box 30.13. The laboratory criteria for classifying ascitic fluid as a transudate or an exudate are not as well defined as they are for pleural and pericardial fluids. For example, infected or malignancy-related samples are not uncommonly reported with protein concentrations in the transudative range (i.e., <3.0 g/dL), and many patients with cirrhotic or heart failure ascites have protein values in the exudative range (>3.0 g/dL) (Runyon et al., 1992).

The **serum-ascites albumin gradient (SAAG)**, defined as the serum albumin concentration minus the ascitic fluid albumin concentration, is widely considered to be the most reliable method to differentiate peritoneal transudates from exudates (Runyon et al., 1992; Tarn et al., 2010). Ascites caused by portal hypertension has a gradient of at least 1.1 g/dL (>11 g/L; transudate), whereas ascites produced by other causes has a gradient less than 1.1 g/dL (exudate) (Runyon et al., 1992). The diagnostic accuracy is 98% for the SAAG compared with only 52% to 80% for four other markers: ascitic fluid total protein, ascites/serum total protein ratio, ascitic fluid LD concentration, and ascites/serum LD ratio (Akriviadis et al., 1996).

An ascitic fluid/serum bilirubin ratio of 0.6 or greater is also significantly associated with exudates (Elis et al., 1998). Indeed, the accuracies of the SAAG, bilirubin ratio, and Light's criteria were 84%, 81.5%, and 80.2%, respectively. Others have suggested that if the ascitic fluid LD is >130 U/L and the ascitic fluid/serum total protein ratio is >0.4, the fluid should be regarded as an exudate (Paramothayan & Barron, 2002).

Although the serum-ascites albumin gradient is probably the best single method to differentiate an ascitic exudate from a transudate, other methods compare favorably and no ideal biochemical markers allow complete discrimination between ascitic fluid exudates and transudates.

BOX 30.13

Causes of Peritoneal Effusions

Transudates: Increased Hydrostatic Pressure or Decreased Plasma Oncotic Pressure

Congestive heart failure
Hepatic cirrhosis
Hypoproteinemia (e.g., nephrotic syndrome)

Exudates: Increased Capillary Permeability or Decreased Lymphatic Resorption

Infections
- Primary bacterial peritonitis
- Secondary bacterial peritonitis (e.g., appendicitis, bowel rupture)
- Tuberculosis

Neoplasms
- Hepatoma
- Lymphoma
- Mesothelioma
- Metastatic carcinoma
- Ovarian carcinoma
- Prostate cancer
- Colonic adenocarcinoma
- Pancreatic carcinoma

Trauma
Pancreatitis
Bile peritonitis (e.g., ruptured gallbladder)

Chylous Effusion

Damage to or obstruction of thoracic duct (e.g., trauma, lymphoma, carcinoma, tuberculosis and other granulomas [e.g., sarcoidosis, histoplasmosis], parasitic infestation)

SPECIMEN COLLECTION

Paracentesis

Diagnostic paracentesis is performed in most patients with new ascites or if there is a change in the clinical picture of a patient with ascites, such as rapid fluid accumulation or fever development. A minimum of 30 mL is needed for complete evaluation. If possible, at least 100 mL should be provided for cytologic examination. Samples for cell counts should be placed in an EDTA-anticoagulated venipuncture tube. Culture specimens should include blood culture bottles that have been inoculated at the bedside with ascitic fluid (10 mL per culture bottle).

Diagnostic Peritoneal Lavage

This procedure is no longer recommended as a routine technique for the evaluation of abdominal trauma. Concerns of oversensitivity and nonspecificity, and improvements in noninvasive diagnostic procedures such as computed tomography and ultrasound, have limited its common use to (1) rapid screening for significant abdominal hemorrhage in hemodynamically unstable patients and (2) evaluation of hollow viscous injuries (Pryor et al., 2004; Whitehouse et al., 2009).

A catheter is placed through a small incision into the abdominal cavity. If less than 15 mL of gross blood can be aspirated, diagnostic peritoneal lavage (DPL) is performed by infusing 1.0 L of saline or Ringer's solution (20 mg/kg in children) and retrieving the fluid by gravity drainage. At least 600 mL should be recovered to avoid falsely low counts (Sullivan et al., 1997). The catheter is sometimes left in place so that DPL may be repeated in 2 to 3 hours if initial results are negative or indeterminate.

Commonly accepted criteria for DPL interpretation after trauma are shown in Box 30.14. The positive predictive value is only 23% for an isolated (no other abnormal criteria) leukocyte count of 500/μL or greater (Soyka et al., 1990).

The conventional DPL criteria may be unreliable in detecting hollow viscous injury when blood is present from a simultaneous solid-organ injury not requiring surgical repair, resulting in unnecessary exploratory laparotomies. Suggested modifications of DPL criteria to adjust for this source of bleeding include either of the following: (1) WBC count greater than or equal to RBC count divided by 150, where RBC is $10 \times 10^4/mm^3$ or greater (Otomo et al., 1998); or (2) cell count ratio greater than 1.0 (Fang et al., 1998). The cell count ratio is defined as the ratio between WBC and RBC counts in the lavage fluid divided by the WBC/RBC ratio in the peripheral blood. These criteria have a reported specificity of 97% for hollow-organ injury, especially if DPL is performed at least 3 hours following injury.

Other applications of DPL include the evaluation of patients with suspected acute peritonitis or pancreatitis. A WBC count in the lavage fluid

BOX 30.14

Criteria for Evaluation of Peritoneal Lavage

Positive Result

Aspiration of >15 mL gross blood on catheter placement
Grossly bloody lavage fluid
RBC >100,000/μL after blunt trauma
RBC >50,000/μL after penetrating trauma
WBC >500/μL
Amylase >110 U/dL

Indeterminate Result

Small amount of gross blood on catheter placement
RBC 50,000–100,000/μL after blunt trauma
RBC 1000–50,000/μL after penetrating trauma
WBC 100–500/μL

Negative Result

RBC <50,000/μL after blunt trauma
RBC <1000/μL after penetrating trauma
WBC <100/μL

RBC, Red blood cells; *WBC,* white blood cells.
Modified from Feied CF: Diagnostic peritoneal lavage, *Postgrad Med* 85:40, 1989, with permission.

of 200 cells/mm^3 is associated with a 99% probability of acute peritonitis (Larson et al., 1992).

Peritoneal Dialysis

Dialysate fluid from renal patients undergoing chronic ambulatory peritoneal dialysis should be submitted to the laboratory to check for infection.

Peritoneal Washings

This procedure is performed intraoperatively to document early intraabdominal spread of gynecologic and gastric carcinomas. Samples are generally sent for cytologic examination only.

RECOMMENDED TESTS

The most important tests for the evaluation of ascitic fluid are listed in Box 30.15. Relative importance varies depending on the type of sample and the clinical findings. For example, RBC and WBC counts are more important than cytology or the SAAG in the evaluation of abdominal effects of trauma. Gross examination may provide immediate information in the clinical and laboratory triage.

GROSS EXAMINATION

Whereas transudates are generally pale yellow and clear, exudates are cloudy or turbid because of the presence of leukocytes, tumor cells, or increased protein levels. The presence of food particles, foreign material, or green-yellow bile staining in a DPL specimen suggests perforation of the gastrointestinal or biliary tract. Acute pancreatitis and cholecystitis may also cause greenish discoloration.

Blood-tinged or grossly bloody fluid must be distinguished from a traumatic tap in which the blood usually clears with continued paracentesis. As little as 15 mL of blood per liter of fluid produces a bright red opaque color such that newsprint cannot be read through the lavage tubing. In most cases, the ability to read newsprint through the tubing results in a negative DPL. Opaque specimens require cell counts because newsprint readability is lost well below the 100,000 RBCs/μL criterion for a positive DPL (Bellows et al., 1998). Bloody ascites is also seen in malignancy and tuberculosis.

Milky fluid that does not clear with centrifugation suggests a chylous or pseudochylous effusion. True chylous peritoneal effusions are significantly less common than chylous pleural effusions. They are caused by disruption or blockage of lymphatic flow by trauma, lymphoma, carcinoma, tuberculosis, other granulomatous diseases (e.g., sarcoidosis), hepatic cirrhosis, adhesions, or parasitic infestation. Differentiation of true chylous and pseudochylous effusions is discussed in the Gross Examination section in the Pleural Fluid section later in the chapter.

MICROSCOPIC EXAMINATION

The total leukocyte count is useful in distinguishing ascites due to uncomplicated cirrhosis from spontaneous bacterial peritonitis (SBP), which is

BOX 30.15

Recommended Tests in Peritoneal Effusions

Useful in Most Patients

Gross examination
Cytology
Stains and culture for microorganisms
Serum-ascites albumin gradient (SAAG)

Useful in Selected Disorders

Total leukocyte and differential cell counts
RBC count (lavage)
Bilirubin
Creatinine/urea nitrogen
Enzymes (ADA, ALP, amylase, LD, telomerase)
Lactate
Cholesterol (malignant ascites)
Fibronectin
Multiplex PCR assay for bacterial, fungal, and mycobacterial DNA
Tumor markers (CEA, PSA, CA 19-9, CA 15-3, CA-125)
Immunocytology/flow cytometry
Tuberculostearic acid

ADA, Adenosine deaminase; *ALP,* alkaline phosphatase; *CEA,* carcinoembryonic antigen; *LD,* lactate dehydrogenase; *PSA,* prostate-specific antigen; *RBC,* red blood cell.
Modified from Kjeldsberg CR, Knight JA: *Body fluids: Laboratory examination of amniotic, cerebrospinal, seminal, serous and synovial fluids*, ed 3, Chicago, 1993, © American Society for Clinical Pathology, with permission.

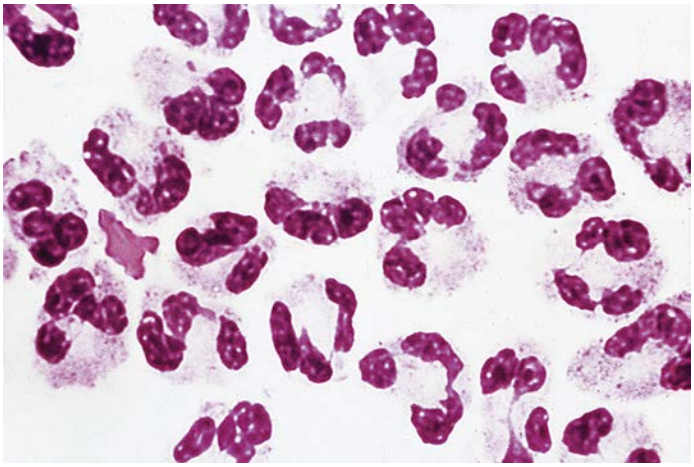

Figure 30.21 Neutrophils in a patient with bacterial peritonitis.

caused by migration of bacteria from the intestine into the ascitic fluid. Approximately 90% of patients with SBP will have leukocyte counts greater than 500/μL, more than 50% of which are neutrophils (Fig. 30.21) (Runyon & Hoefs, 1984; Stewart et al., 1986).

The ascitic fluid total neutrophil count is the preferred method for the diagnosis of SBP. Cutoff values of 250 and 500 neutrophils/μL have been recommended, with a diagnostic accuracy of about 94% for 500 neutrophils/μL and about 90% for 250 neutrophils/μL (Stassen et al., 1986; Albillos et al., 1990).

Cell counts, total protein, and albumin gradient values vary with fluid shifts associated with ascites formation and resolution. For example, diuresis may cause the WBC count to increase from 300/μL to 1000/μL or more. When obtained by DPL, a leukocyte count of 200/μL or more is reported to be associated with a 99% probability of acute peritonitis (Alverdy et al., 1988; Larson et al., 1992).

Eosinophilia (>10%) is most commonly associated with the chronic inflammatory process associated with chronic peritoneal dialysis. It has also been reported in congestive heart failure, vasculitis, lymphoma, and ruptured hydatid cyst.

Cytology has an overall sensitivity of 40% to 65% for malignant ascites. Peritoneal carcinomatosis accounts for about two-thirds of malignant effusions; cytology has a sensitivity of over 95% when confined to these cases (Runyon et al., 1988). Liquid-based thin-layer preparations of peritoneal effusions and pelvic washings have been shown to be superior to standard cytologic preparations in the detection of carcinoma (Moriarity

et al., 2008). Immunocytochemical stains are useful in characterizing atypical cells in equivocal cases.

CHEMICAL ANALYSIS

Protein

The SAAG is superior to total protein content in differentiating cirrhosis from other causes of peritoneal effusions (Runyon et al., 1992). SBP is commonly associated with low total protein (<3.0 g/dL) and a high SAAG (>1.1 g/dL), making total protein measurements of little value in this disorder. Extracellular fluid shifts associated with ascites formation and resorption also cause variations in protein content.

Glucose

Early reports indicated that peritoneal fluid glucose levels of 50 mg/dL or less are present in 30% to 60% of cases of tuberculous peritonitis and in about 50% of patients with abdominal carcinomatosis (Polak & Torres da Costa, 1973; Brown & An, 1976). Another study found decreased glucose levels in most cases of tuberculous ascites (Bansal et al., 1998). Still, glucose measurements are of little value because the sensitivity and specificity are generally too low to be of practical value (Tarn et al., 2010).

Enzymes

Amylase activity in normal peritoneal fluid is similar to plasma levels. A level greater than three times the plasma value is good evidence of pancreas-related ascites, including acute pancreatitis and pancreatic pseudocyst (Runyon, 1987a). Amylase is not recommended in the routine evaluation of ascites, however, because the prevalence of pancreatic ascites is low. Retrospective amylase measurement on a stored specimen is indicated if initial studies are not diagnostic. Amylase levels in peritoneal lavage fluid may be valuable in patients following blunt and penetrating abdominal trauma (McAnena et al., 1991). Here, amylase levels greater than or equal to 20 U/L have a sensitivity of 87%, a specificity of 75%, and a positive predictive value of 46% for significant intraabdominal injury. In these cases, laparotomy should be considered. Gastroduodenal perforation, acute mesenteric vein thrombosis, intestinal strangulation, or necrosis may also produce elevated amylase levels. Although various nonpancreatic malignancies may rarely produce amylase elevations, isoenzyme evaluation usually identifies the salivary isoform in these latter cases (Kosches et al., 1989).

Elevated **alkaline phosphatase** (**ALP**) levels greater than 10 U/L in DPL fluid are useful in predicting hollow visceral injury in patients who would otherwise not undergo laparotomy (specificity 99.8%, sensitivity 94.7%) (Jaffin et al., 1993). Ascitic fluid ALP measurements may also be helpful in the differentiation of primary bacterial peritonitis from secondary bacterial peritonitis due to bowel perforation. Secondary peritonitis has significantly higher mean ALP levels than SBP. ALP levels >240 U/L were present in 92% of patients with secondary peritonitis versus 12% with SBP (Wu et al., 2001). The sensitivity and specificity for differentiating secondary peritonitis from SBP were 92% and 88%, respectively.

LD activity is often increased in malignant effusions (Gerbes et al., 1991; Tarn et al., 2010). An ascitic fluid/serum LD ratio greater than 0.6 has a reported sensitivity of 80% (Boyer et al., 1978). Combined measurement of ascitic fluid LD and cholesterol totally discriminated peritoneal carcinomatosis from cirrhosis and hepatocarcinoma-related ascites (Castaldo et al., 1994; Halperin et al., 1999). Although both serum and peritoneal fluid LD levels are significantly higher in patients with ovarian cancer than in those with benign ovarian tumors or other gynecologic malignancies, peritoneal fluid LD has higher diagnostic sensitivity (87%) and diagnostic accuracy (90%) than serum LD (60% and 77%, respectively) (Schneider et al., 1997). LD has also been used for the early diagnosis of SBP, in which it has a diagnostic accuracy of about 74% using an ascitic fluid/serum ratio cutoff of 0.4 (Lee et al., 1987).

The presence of **telomerase** is a specific discriminatory marker in malignant ascites (Tangkijvanich et al., 1999; Hess et al., 2002). Telomerase activity was detected in 81% of malignant peritoneal effusions with a sensitivity of 76% and a specificity of 95.7%.

ADA is commonly used in high-prevalence areas to identify patients with tuberculous peritonitis (Burgess et al., 2001). Using receiver operating characteristic curves and a cutoff value of 30 U/L, the sensitivity and specificity were 94% and 92%, respectively. Using a cutoff value of 33 U/L, the sensitivity, specificity, positive and negative predictive values, and overall diagnostic accuracy for diagnosing tuberculous peritonitis were 100%, 96.6%, 95%, 100%, and 98%, respectively (Dwivedi et al., 1990). ADA is not thought to be helpful in low-prevalence areas (Tarn et al., 2010).

Fibronectin

Using a cutoff value of 85 μg/mL (85 mg/L), fibronectin was more reliable in differentiating malignant from sterile ascites (diagnostic accuracy, 79%) than were total protein, LD, γ-glutamyltransferase, pH, amylase, triglycerides, leukocyte count, and cytologic examination (Colli et al., 1986). In a subsequent study using a cutoff of 94.6 μg/mL, the sensitivity, specificity, positive accuracy, negative accuracy, and overall diagnostic accuracy in the diagnosis of malignant ascites were 100%, 95%, 93.8%, 100%, and 97.1%, respectively (Sood et al., 1997). Further studies have supported the utility of fibronectin measurement in the diagnosis of malignant ascites (Lee et al., 2006). However, this measurement is still not used routinely for this purpose (Tarn et al., 2010).

Lactate

Ascitic fluid lactate has been used with pH measurements to differentiate SBP from uncomplicated ascites. Sensitivity and specificity for lactate levels are approximately 90% using a cutoff of 40 mg/dL (4.44 mmol/L), with a positive predictive value of 62% (Stassen et al., 1986). Although not as accurate as leukocyte counts, the high specificity of lactate in hepatic ascites suggests that it has some value in the diagnosis of SBP in otherwise equivocal cases. Malignant and tuberculous ascites are also associated with elevated lactate levels.

Patients with hollow viscous perforation, gangrenous intestine, peritonitis, or intraabdominal abscess have a peritoneal fluid minus plasma lactate level of at least 13.5 mg/dL (1.5 mmol/L), which reportedly separates these patients completely from those with other conditions producing acute abdominal problems (DeLaurier et al., 1994). The peritoneal-serum lactate ratio is also useful in identifying postoperative patients in need of reintervention (Bini et al., 2014).

Creatinine and Urea

Measurement of creatinine and urea nitrogen is useful to differentiate between peritoneal fluid and urine (Tarn et al., 2010). Elevated peritoneal fluid urea nitrogen and creatinine, in association with elevated serum urea but normal serum creatinine (due to back-diffusion of urea), suggests urinary bladder rupture.

Bilirubin

The mean (±SD) ascitic fluid bilirubin concentration in various types of ascites has been reported as 0.7 ± 0.8 mg/dL, and the mean ascitic fluid/serum bilirubin ratio as 0.38 ± 0.44 (Runyon, 1987b). An ascitic fluid bilirubin greater than 6.0 mg/dL and an ascitic fluid/serum bilirubin ratio over 1.0 suggest choleperitoneum from a ruptured gallbladder. A ratio of 0.6 or greater has been advocated as an additional marker for an exudative process, although its accuracy is not as high as that of the SAAG (Elis et al., 1998).

pH

Ascitic fluid pH has been thought to be helpful in the diagnosis of SBP in patients with cirrhotic ascites, especially if it is used in conjunction with the leukocyte count (Attali et al., 1986; Stassen et al., 1986). A pH less than 7.32 or a blood–ascitic fluid pH difference of more than 0.1 has a reported sensitivity and specificity of about 90% for SBP, with the pH differential being slightly more accurate. However, peritoneal fluid pH appears useless in detecting SBP in the absence of neutrophils (Runyon & Antillon, 1991). Patients with an ascitic fluid pH of less than 7.15 have a poor prognosis (Attali et al., 1986). Low pH is also found in patients with malignant and pancreatic ascites and tuberculous peritonitis. Overall, however, peritoneal fluid pH is not thought to contribute significantly to clinical decision-making (Tarn et al., 2010).

Cholesterol

The ascitic fluid cholesterol level is a moderately useful index in separating malignant ascites (>45–48 mg/dL) from cirrhotic ascites (Mortensen et al., 1988; Castaldo et al., 1994). The sensitivity and specificity average just over 90% using a cutoff value of 45 to 48 mg/dL (1.2 mmol/L). Thus, using a cutoff value of 48 mg/dL, the sensitivity, specificity, positive and negative predictive value, and overall diagnostic accuracy for differentiating malignant from nonmalignant ascites were reported as 96.5%, 96.6%, 93.3%, 98.3%, and 96.6%, respectively (Garg et al., 1993).

Interleukin-8

Interleukin-8, a cytokine produced by a variety of cells in response to stimuli such as bacterial lipopolysaccharide, is significantly higher in SBP compared with sterile ascites (Martinez-Bru et al., 1999). Using a cutoff value of 100 ng/L, the sensitivity and specificity were both 100% in cirrhotic

patients. Interleukin-8 levels also correlate with the stage of disease in patients with endometriosis (Malhotra et al., 2007).

Tuberculostearic Acid (10-Methyloctadecanoic Acid)

As noted in the Pleural Fluid section, TSA was detected in pleural fluid in 75% of patients with pulmonary tuberculosis using gas chromatography–mass spectroscopy (Muranishi et al., 1990). Using quantitative chemical ionization gas chromatography–mass spectrometry, the measurement of TSA is a valuable technique to identify tuberculous peritonitis as well as tuberculous meningitis (spinal fluid) and pneumonia (pleural fluid) (Brooks et al., 1998).

Tumor Markers

Because of their reportedly low sensitivity and specificity, the measurement of tumor markers in peritoneal fluid is generally considered to be of little value. However, they are often useful in selected cases, such as in following a patient's response to therapy and in the early detection of tumor recurrence. They may also be very useful in cases in which cytology is negative but suspicion of malignant ascites is high. In one study, cytologic examination was positive in only 40% (35 of 89 patients) of malignant cases, while tumor markers were positive in 80% (Cascinu et al., 1997). Moreover, excluding small-cell lung and renal cancers, for which specific tumor markers are lacking, tumor markers (i.e., CEA, CA 19-9, CA 15-3, PSA) in ascitic fluid for other carcinomas were positive in 97% of cases. These tumor markers, as well as α-fetoprotein, were also found to be highly specific (over 90%) for serous fluid malignancies, although their sensitivities were low (19%–38%) (Sari et al., 2001). The measurement of **PSA** may also be a valuable marker for the diagnosis of malignant effusions due to prostate cancer (Appalaneni et al., 2004).

CEA has a sensitivity of 40% to 50% and a specificity of about 90% for malignant effusions, using a cutoff value of 3.0 ng/mL (Mezger et al., 1988). In a similar study using a 5-mg/mL cutoff, the specificity was about 97% (Gulyas et al., 2001). Elevated CEA levels in peritoneal washings suggest a poor prognosis in gastric carcinoma (Irinoda et al., 1998).

Ascitic fluid **CA-125** is elevated to some degree in a variety of nonmalignant conditions. Indeed, cardiovascular and chronic liver disease may be the most frequent diagnoses in patients with increased CA-125 levels (Miralles et al., 2003), thereby supporting the general opinion that CA-125 in ascitic fluid lacks adequate specificity as a marker for malignancy. Extremely high levels are likely to be caused by epithelial carcinomas of the ovary, fallopian tubes, or endometrium. The sensitivity for ovarian carcinoma depends on the tumor's stage (range, 40% to 95%) and histologic subtype (mucinous adenocarcinomas have lower values) (Molina et al., 1998).

DNA ploidy analysis by flow cytometry or image analysis may provide useful complementary diagnostic information in cases with equivocal cytology results when the malignant cells carry an aneuploid karyotype, although the added value of DNA ploidy analysis over cytology is small (Bisht et al., 2014). Image analysis appears to be more practical than flow cytometry when the tumor cells are scarce (Rijken et al., 1991).

MICROBIOLOGICAL EXAMINATION

Primary peritonitis occurs at any age and is seen in children with nephrotic syndrome and in adults with cirrhotic liver disease. SBP occurs in patients with ascites in the absence of recognized secondary causes such as bowel perforation or intraabdominal abscess. The bacteria in SBP are most often normal intestinal flora, and more than 92% are monomicrobial. Aerobic gram-negative bacilli (e.g., *E. coli*, *Klebsiella pneumoniae*) are responsible for two-thirds or more of all cases (Gilbert & Kamath, 1995), followed by *S. pneumoniae*, *Enterococcus* spp., and, rarely, anaerobes. The Gram stain has a sensitivity of 25% in SBP (Lee et al., 1987), and routine cultures are positive in only about 50% of cases (Castellote et al., 1990). Inoculation of blood culture bottles at the bedside and concentration of large volumes of fluid can improve sensitivity, but up to 35% of infected patients may still have negative ascitic fluid cultures (Marshall, 1988). Use of resin-containing blood culture bottles may improve the isolation of certain bacteria in partially treated patients.

Ascitic fluid total neutrophil count is the preferred method for the diagnosis of SBP (see the Microscopic Examination section earlier in the chapter). As noted earlier, in difficult cases, several analytes may be useful in differentiating SBP from secondary bacterial or tuberculous peritonitis. Because of the low number of bacteria in many cases of SBP, sensitive methods for detection of bacteria in these specimens are often needed. PCR has been successfully used in the detection of bacterial DNA in culture-negative ascitic fluid (Such et al., 2002; Soriano et al., 2011). More recently, in situ hybridization performed on leukocytes suspended in peritoneal fluid has been used to detect bacteria in SBP (Enomoto et al., 2014). Multiplex PCR-based detection systems have been shown to be effective in the rapid diagnosis of SBP (Almuhayawi et al., 2014).

The sensitivity of acid-fast stains for *M. tuberculosis* is no more than 20% to 30%, and cultures have a sensitivity of only 50% to 70% (Reimer, 1985). Application of PCR to detect *M. tuberculosis* DNA may be used, but a negative result does not exclude the diagnosis (Schwake et al., 2003). In a patient with a high clinical suspicion for tuberculous peritonitis, laparoscopic examination with biopsy may be indicated.

ALTERNATIVE SPECIMENS

SALIVA

Saliva is generally easily collected by noninvasive means; thus, its acquisition is well accepted by patients. Because it is a filtrate of plasma, saliva has concentrations of some small molecules that are in equilibrium with the free (unbound) active fractions of those substances in plasma. This property has been especially useful for measuring free cortisol, which is the physiologically important fraction that reflects the secretion rate of cortisol and, thus, is important for diagnosis. Salivary cortisol measurements have been used to assess adrenal function in critically ill subjects (Arafah et al., 2007) and in those with Cushing syndrome and adrenal insufficiency (Raff, 2009), with late-night (or midnight) salivary cortisol being an effective screening test for Cushing syndrome (Raff et al., 1998). Unfortunately, salivary concentrations of several other steroid hormones are not reliable measures of plasma free levels because of rapid fluctuations in their salivary concentrations (e.g., estradiol, progesterone, testosterone, dehydroepiandrosterone, aldosterone) (Wood, 2009).

Saliva also contains some antibody molecules that apparently derive from plasma. Thus, measurements are sometimes performed on saliva to detect antibodies against infectious agents in circumstances when collection of saliva is much more convenient or acceptable to patients. Testing of saliva for antibodies against HIV has been practiced widely in sexually transmitted disease clinics, although episodes of false-positive results have diminished confidence in these point-of-care tests (Cummiskey et al., 2008).

Genetic testing requires DNA from the patient that can be obtained conveniently from leukocytes in blood specimens or even more conveniently from buccal cells in saliva or from swabs of the interior of the mouth.

Drug testing has also been performed in saliva to provide evidence of ingestion of illicit substances. Although drugs such as amphetamines, cocaine, and opioids are present in oral fluid at concentrations similar to those in plasma, local absorption of these drugs in the mouth can increase their concentration in saliva after use (Drummer, 2006).

MECONIUM

The analysis of body fluids can provide unique information based on anatomic location (often remote or not readily accessible) or sequences of metabolic processes and normal clearance of chemical constituents from the body. An example of this clinical utility is the examination of meconium from newborns for the detection of illicit drugs such as cocaine and amphetamines that the mother might have abused while pregnant. The drugs cross the placenta from maternal circulation into that of the fetus, which excretes the drug or its metabolites in bile that remains in the meconium until birth (Concheiro et al., 2013). This window of drug detection in meconium is much broader than that for testing of urine or blood by several weeks and covers second and third trimesters of pregnancy. Such testing is considered more reliable than self-reporting by mothers due to fear of reprisal and possible loss of custody. These results can be used both for medical management of the mother and baby as well as for medical-legal purposes. Recently, measurement of ethyl glucuronide in meconium was found to be an objective measure of maternal alcohol use (Himes et al., 2015).

HAIR AND NAILS

Drug testing has time limitations of detection in blood for periods of minutes to hours after ingestion. The need to detect illicit drug use over longer periods of time has prompted analysis of other body sources. Concentrations of drugs in saliva follow the same time course as blood of minutes to hours after ingestion. Detection in urine can be as soon as minutes up to many days after drug use. Sweat concentrations also rise in minutes

but may persist for weeks. True long-term detection is possible in hair and nails, where drugs of abuse can be detected days to even years after ingestion. Although numerous companies offer drug testing of hair or nail specimens, there has not been official adoption of this strategy by government agencies, largely because of issues of uncertainty as to whether the substances detected from hair or nail specimens were actually "in" the hair following ingestion and incorporation into that tissue, or whether the detected drug was simply "on" the surface of the specimen because of incidental contact that did not involve ingestion (Curtis & Greenberg, 2008).

Cerumen

Forensic analysis of drugs can include nonstandard specimens that are convenient to collect or might have an accumulation of drugs for an extended period of time. For example, a recent study has shown potential utility of earwax (cerumen) as an alternative forensic specimen to detect psychotropic drugs such as antiepileptics, anxiolytics, antipsychotics, and drugs of abuse as well as metabolic disorders with long-term representation of metabolites (Shokry & Filho, 2017; Shokry et al., 2017). Collection of earwax is relatively noninvasive and presumably also free of contamination, which can be advantageous for acceptance of its use in forensic testing. Analysis of this type of specimen was done by liquid chromatography–mass spectrometry (LC-MS).

Fingerprints

Fingerprints have also been explored as alternative specimens for detection of drugs such as acetaminophen, dihydrocodeine, and methylephedrine using LC-MS (Kuwayama et al., 2016). Fingerprint fluid could potentially be used for drug testing when sample collection of standard fluids such as blood, urine, or even saliva might be delayed or not feasible.

BREATH TESTING

Exhaled Nitric Oxide and Exhaled Breath Condensate

Inflammatory disorders of the lungs—including asthma, chronic obstructive pulmonary disease, and chronic cough—have largely been evaluated in the past by bronchoscopy, lavage, biopsy, and analysis of induced sputum. Noninvasive techniques for monitoring these disorders are now available as detection of chemical constituents in exhaled breath. **Exhaled nitric oxide** (NO) is an inflammatory mediator that is unstable in tissues but is much more stable in the gas phase, in which it can be measured in single breath exhalations by specialized devices expressing NO content in parts per billion. This use is currently considered investigational but theoretically has great potential for monitoring pulmonary inflammation by noninvasive means with much greater frequency than by invasive procedures (Dweik et al., 2011).

A second approach to monitoring pulmonary disease is to measure nonvolatile inflammatory markers in **exhaled breath condensate** (EBC) collected from exhaled breath that is condensed by passage through a cooling device. Such specimens of respiratory fluid are scant, but they contain a rich assortment of substances such as cytokines, leukotrienes, oxidants, antioxidants, and so on that can reveal inflammatory activity by noninvasive means (Horvath et al., 2005). Even pH of EBC has been found useful in assessing lung disease; EBC tends to be slightly alkaline (mean pH 7.7 ± 0.49) in health, but it becomes more acidic with disease changes in the lower airways (Vaughan et al., 2003). EBC analysis is currently considered investigational.

Carbon-13-Urea Breath Test

Diagnosis of infection with *Helicobacter pylori* may be aided by the carbon-13-urea breath test in which the patient drinks a solution of ^{13}C-urea. *H. pylori* has the enzyme urease, which breaks down urea, releasing $^{13}CO_2$ into the patient's breath. Samples of breath taken in a balloon or other specialized collection devices are analyzed by mass spectrometry (Patel et al., 2014) (see Chapters 4, 5, and 24). Detection of $^{13}CO_2$ indicates infection with *H. pylori*. An alternative procedure utilizes ^{14}C in place of ^{13}C, although ^{14}C detection is based on low-level radioactivity. ^{13}C has the advantage of not being radioactive but the disadvantage of not being measured in most local laboratory facilities. The ^{13}C-urea breath test has special utility for pediatric patients (Frenck et al., 2006).

Opportunities for analysis of additional body fluid types will increase as collection methodologies expand, particularly in collaboration with invasive radiologic approaches. Some problems expected with these new unique specimens include scant specimen volumes, unknown protein and other chemical composition that might adversely affect measurements, and lack of reference ranges to distinguish normal healthy results from those in disease.

TISSUE ASPIRATES

Breast nipple aspirate fluid can be obtained by noninvasive means such as massage or with automated collection devices to yield material suitable for cytologic examination for early detection of breast cancer. This new collection approach may lead to other effective applications of cancer detection using modalities such as proteomics or still to be discovered biomarkers (Alexander et al., 2004).

Fine-needle aspiration for cytologic examination is frequently used to evaluate head and neck masses. Rapid identification of a mass of parathyroid tissue has been done by measuring parathyroid hormone (PTH) in saline, into which the needle aspirate is flushed (Conrad et al., 2006). This method was shown to be 99% accurate for diagnosis of parathyroid tissue because the measured values of PTH are orders of magnitude higher in parathyroid aspirates than in those from other tissues such as thyroid, adipose, or lymphatic. This type of specimen is truly unusual and would not likely be included in any manufacturer's claims for assay performance. However, the use of this specimen is well recognized by endocrine surgeons who now consider it a standard of practice.

Another diagnostic application of tumor markers is for aspirates collected from pancreatic cysts during surgery, although such fluids might also be collected by direct aspiration with a needle guided through ultrasound. High levels of CA19-9 in pancreatic cyst fluid suggest malignancy, whereas low levels are more consistent with benign processes (Khalid & Brugge, 2007). CA19-9 measurement in pancreatic cyst fluid is an aid to diagnosing malignancy in conjunction with cytology and other studies. The advantage of CA19-9 in this context is its relatively fast turnaround time by immunoassay that might be completed during the time period of surgical procedure. CEA has also been used for this purpose (Rockacy & Khalid, 2013).

BILLING FOR TESTS IN NONSTANDARD SPECIMENS

Although considerations of medical necessity provide strong motivation for performing tests in unusual specimen types to provide unique information that could not be obtained by other means, reporting of the results and subsequent billing may lead to confusion. Most laboratory computer systems have strictly defined specimen types, such as blood, serum, urine, and CSF. When dealing with an unusual specimen type that is not individually coded or recognized in a computer system, laboratories should take care not to enter these results as though they were serum or other commonly tested fluid. For both medical needs and reimbursement, some disclaimer should be included to indicate the specimen type so that it is not confused with serum or other conventional fluid.

CHEMICAL MEASUREMENTS IN BODY FLUIDS

Plasma, serum, CSF, and urine are standard fluids that are often submitted for chemical analysis. Manufacturers generally provide product claims for their assays in one or more of these body fluids, but they have not established assay behavior in other specimen types, such as pleural fluid, peritoneal fluid, SF, and other accumulations of abnormal fluids, such as drainage or lavage fluids. These types of fluids are not normally present in health but rather can form as the result of various pathologic processes, such as hemodynamic imbalance, infection, inflammation, malignancy, or other organ dysfunction. Consequently, the composition of these fluids can range widely, thereby leading to unpredictable effects on laboratory measurements. Matrix effects from variations in protein concentration can alter fluid surface tension, viscosity, and miscibility in a reaction mixture. All of these variations might cause differences in measurements because of errors in pipetting fixed volumes or in speed and completeness of mixing with reagents in an assay. Other constituents present in these pathologic fluids (e.g., hyaluronic acid in SF) but not in serum also have the potential to alter measurements in assays intended for use in serum. This potential for erroneous measurements in body fluids due to matrix effects should be recognized when such requests for analysis are received.

A second issue concerning chemical measurements in pathologic fluids is what reference range to use for comparison in an interpretive report. Because abnormal fluid accumulations do not exist in a state of health, they cannot, of course, be collected from a normal healthy population to establish reference ranges.

These two issues of potential interferences and lack of reference ranges for analysis of body fluids fly in the face of Clinical Laboratory

Improvement Act requirements for assay validation. In fact, the lack of manufacturers' claims for body fluid testing might actually place a greater burden on a laboratory to validate these assays than for use in serum for which manufacturer claims are typically cleared by the U.S. Food and Drug Administration. Without such validation, measuring chemical constituents in body fluids could be considered an off-label use of commercial assays.

In recognition of these difficulties faced by laboratories, the Clinical and Laboratory Standards Institute (CLSI) has developed the document C49-A, Analysis of Body Fluids in Clinical Chemistry, to provide guidance in this situation (CLSI, 2007). The specific recommendations from the CLSI are as follows:

1. Review performance claims of the manufacturer for the possibility of extending a commercial assay to body fluids with special attention to accuracy, precision, analytic measurement range, reference interval (usually in comparison with simultaneous measurement in serum, in addition to the patient's body fluid), and interferences from substances in the body fluid.
2. Existing methods may be suitably modified for body fluid analysis when necessary to obtain medically relevant information. Matrix effects that could alter the accuracy of measurement must be recognized. Furthermore, lack of a reference range for the analyte in body fluids should be compensated for by interpretation of results in comparison with a simultaneously collected serum specimen.
3. The preconditions for using a routine assay for an alternate body fluid are that the measurement system in another specimen type (serum plasma, urine)
   a. Has acceptable test characteristics.
   b. Has a reference method by which to ascertain bias.
   c. Has calibrators and controls.
   d. Undergoes external proficiency testing whenever available.
4. Specimen collection of body fluid and its handling, processing, and storage should follow guidelines for specimens of plasma or serum collected for that measurement. Special attention should be directed to the possibility of interference from anticoagulants into which a body fluid might be collected (e.g., heparin, EDTA, citrate).
5. Unusual properties of a body fluid such as high viscosity should be given consideration if they have the potential to alter the analyte concentration in the final solution of the reaction mixture (e.g., inaccurate pipetting, inadequate mixing).
6. The presence of an interferent in a body fluid can be assessed by testing the fluid neat and at 1:2 and 1:4 dilutions. Recovery of similar concentrations suggests lack of interference. Low concentrations can be checked for interference by mixing with a routine (serum) sample with a high measurable value to measure recoverability.
7. Result reporting should include the measured value and the type of fluid analyzed plus a statement that accuracy might be affected by sample type and that results should be interpreted in the clinical context. The laboratory is urged to contact ordering physicians to explain these limitations.

A key point is that to be useful clinically, measurements in body fluids need not necessarily be highly accurate but instead must be within a clinically acceptable range of the true value. This CLSI document provides an extensive list of applications of many different chemical analytes that may provide medically unique information about the source of a body fluid (e.g., creatinine in peritoneal fluid to evaluate urinary tract injury, amylase in peritoneal fluid to evaluate for pancreatitis, triglycerides in pleural fluid as an indicator of chylous effusion from lymphatic damage).

SELECTED REFERENCES

Blennow K, Zetterberg H: Cerebrospinal fluid biomarkers for Alzheimer's disease, *J Alzheimers Dis* 18:413, 2009.

This article describes the use of biochemical markers in the diagnosis of Alzheimer disease.

Clinical and Laboratory Standards Institute (CLSI): *Analysis of body fluids in clinical chemistry: approved guideline*, Wayne, PA, 2007, Clinical and Laboratory Standards Institute. CLSI Document C49-A.

This document provides guidance on acceptable practices for chemical analysis in body fluids for which extensive method validation is not feasible but that have the potential to contribute valuable or even unique diagnostic information.

Clinical and Laboratory Standards Institute (CLSI): *Body fluid analysis for cellular composition: approved guideline*, Wayne, PA, 2006, Clinical and Laboratory Standards Institute. CLSI Document H56-A.

This document provides guidance on the examination of cellular components of body fluids.

Conrad DN, Olson JE, Hartwig HM, et al.: A prospective evaluation of novel methods to intraoperatively distinguish parathyroid tissue utilizing a parathyroid hormone assay, *J Surg Res* 133:38, 2006.

This article provides a useful method to prepare fine-needle tissue aspirates for measurement of parathyroid hormone to assist in the rapid evaluation of tissue masses.

Curtis J, Greenberg M: Screening for drugs of abuse: hair as an alternative matrix: a review for the medical toxicologist, *Clin Toxicol* 46:22, 2008.

This review article provides excellent background information regarding the physiology and toxicology of drug testing in hair, along with a description of many of the legal and practical issues surrounding this application.

Freedman MS, Thompson EJ, Deisenhammer F, et al.: Recommended standard of cerebrospinal fluid analysis in the diagnosis of multiple sclerosis: a consensus statement, *Arch Neurol* 62:865, 2005.

This article is a consensus statement commissioned by the Consortium of Multiple Sclerosis Clinics that establishes the "minimum standard" for evaluation of CSF in patients suspected of having multiple sclerosis.

Hussong JW, Kjeldsberg CR: *Kjeldsberg's body fluid analysis*, Chicago, 2014, American Society for Clinical Pathology.

This is an updated version of a classic reference book on body fluid analysis.

Irani DN, editor: *Cerebrospinal fluid in clinical practice*, Philadelphia, 2009, Saunders.

This book provides a description of findings in CSF with different neurologic disorders.

Leber AL, Everhart K, Balada-Llasat, et al.: Multicenter evaluation of BioFire FilmArray meningitis/encephalitis panel for detection of bacteria, viruses, and yeast in cerebrospinal fluid specimens, *J Clin Microbiol* 54:2251, 2016.

This article summarizes the utility of a multiplex PCR-based detection system in the diagnosis of meningitis/encephalitis caused by multiple organism types.

Light RW: Clinical practice: pleural effusion, *N Engl J Med* 346:1971, 2002.

This article provides a step-by-step approach to the clinical evaluation of pleural fluids and the use of laboratory examinations in that process.

Raff H: Utility of salivary cortisol measurements in Cushing's syndrome and adrenal insufficiency, *J Clin Endocrinol Metab* 94:3647, 2009.

This article is a comprehensive and useful review of the clinical applications of cortisol measurements in saliva.

Tarn AC, Lapworth R: Biochemical analysis of ascitic (peritoneal) fluid: what should we measure? *Ann Clin Biochem* 47:397, 2010.

This article provides an overview of biochemical analysis of peritoneal fluid.

Wilson MR, Naccache SN, Samayoa E, et al.: Actionable diagnosis of neuroleptospirosis by next-generation sequencing, *N Eng J Med* 370:2408, 2014.

This article describes the use of next-generation DNA sequencing, a powerful new laboratory modality, in the detection of an infectious agent in cerebrospinal fluid.

Zimmermann M, Ruprecht K, Kainzinger F, et al.: Automated vs. manual cerebrospinal fluid cell counts: a work and cost analysis comparing the Sysmex XE-5000 and the Fuchs-Rosenthal manual counting chamber, *Int J Lab Hematol* 33:629, 2011.

This article discusses the pros and cons of automated cell counting in cerebrospinal fluid specimens.

Access the complete reference list online at Elsevier eBooks for Practicing Clinicians.

REFERENCES

Abramson JS, Hampton KD, Babu S, et al.: The use of C-reactive protein from cerebrospinal fluid for differentiating meningitis from other central nervous system diseases, *J Infect Dis* 151:854, 1985.

Achar VS, Welch KM, Chabi E, et al.: Cerebrospinal fluid gamma-aminobutyric acid in neurologic disease, *Neurology* 26:777, 1976.

Adelman M, Albelda S, Gottlieb J, et al.: Diagnostic utility of pleural fluid eosinophilia, *Am J Med* 77:915, 1984.

Agner RC, Gallis HA: Pericarditis: differential diagnosis considerations, *Arch Intern Med* 139:407, 1979.

Akriviadis EA, Kapnias D, Hadjigavriel M, et al.: Serum/ascites albumin gradient: its value as a rational approach to the differential diagnosis of ascites, *Scand J Gastroenterol* 31:814, 1996.

Albillos A, Cuervas-Mons V, Millan L, et al.: Ascitic fluid polymorphonuclear cell count and serum to ascites albumin gradient in the diagnosis of bacterial peritonitis, *Gastroenterology* 98:134, 1990.

Albright RE, Christenson RH, Habig RL, et al.: Cerebrospinal fluid (CSF) TRAP: a method to improve CSF laboratory efficiency, *Am J Clin Pathol* 90:707, 1988.

Alexander H, Stegner AL, Wagner-Mann C, et al.: Proteomic analysis to identify breast cancer biomarkers in nipple aspirate fluid, *Clin Cancer Res* 10:7500–7510, 2004.

Almuhayawi M, Ullberg M, Ozenci V: Identification of microorganisms from sterile body fluids by use of FilmArray, *J Clin Microbiol* 53:710, 2014.

Alverdy JC, Saunders J, Chamberlin WH, et al.: Diagnostic peritoneal lavage in intra-abdominal sepsis, *Am Surg* 54:456, 1988.

American College of Physicians: The diagnostic spinal tap, *Ann Intern Med* 104:880, 1986.

Andrews J, Setran E, McDonnel L, et al.: An evaluation of the Cell-Dyn 3200 for counting cells in cerebrospinal and other body fluids, *Lab Hematol* 11:98, 2005.

Andersson M, Alvarez-Cermeno J, Bernardi G, et al.: Cerebrospinal fluid in the diagnosis of multiple sclerosis: a consensus report, *J Neurol Neurosurg Psychiatry* 57:897, 1994.

Andreasen N, Minthon L, Davidsson P, et al.: Evaluation of CSF-tau and CSF-Abeta42 as diagnostic markers for Alzheimer disease in clinical practice, *Arch Neurol* 58:373, 2001.

Antonangelo L, Sales RK, Cora AP, et al.: Pleural fluid tumour markers in malignant pleural effusion with inconclusive cytologic results, *Curr Oncol* 22:e336, 2015.

Appalaneni V, Yellinedi S, Baumann MA: Diagnosis of malignant ascites in prostate cancer by measurement of prostate specific antigen, *Am J Med Sci* 327:262, 2004.

Arafah BM, Nishiyama FJ, Tlaygeh H, et al.: Measurement of salivary cortisol concentration in the assessment of adrenal function in critically ill subjects: a surrogate marker of the circulating free cortisol, *J Clin Endocrinol Metab* 92:2965, 2007.

Arevalo CE, Barnes PF, Duda M, et al.: Cerebrospinal fluid cell counts and chemistries in bacterial meningitis, *South Med J* 82:1122, 1989.

Ashchi M, Golish J, Eng P, et al.: Transudative malignant pleural effusions: prevalence and mechanisms, *South Med J* 91:23, 1998.

Attali P, Turner K, Pelleteir G, et al.: pH of ascitic fluid: diagnostic and prognostic value in cirrhotic and noncirrhotic patients, *Gastroenterology* 90:1255, 1986.

Aulesa C, Mainar I, Prieto M, et al.: Use of the Advia 120 hematology analyzer in the differential cytologic analysis of biological fluids (cerebrospinal, peritoneal, pleural, pericardial, synovial, and others), *Lab Hematol* 9:214, 2003.

Aune M, Becker J, Brugnara C, et al.: Automated flow cytometric analysis of blood cells in cerebrospinal fluid, *Am J Clin Pathol* 121:690, 2004.

Baer KE, Smith GP: Serous body cavity fluid examination, *Lab Med* 32:85, 2001.

Baethgen LF, Moraes C, Weidlich L, et al.: Direct-test PCR for detection of meningococcal DNA and its serogroup characterization: standardization and adaptation for use in a public health laboratory, *J Med Microbiol* 52:793, 2003.

Bailey EM, Domenico P, Cunha BA: Bacterial or viral meningitis? Measuring lactate in CSF can help you know quickly, *Postgrad Med* 88:217, 1990.

Baker DG: Chemistry, serology and immunology. In Gatter RA, Schumacher HR, editors: *A practical handbook of joint fluid analysis*, 2nd ed, Philadelphia, 1991, Lea & Febiger, p 70.

Bansal S, Kaur K, Bansal AK: Diagnosing ascitic etiology on a biochemical basis, *Hepato-Gastroenterology* 45:1673, 1998.

Barnes P, Eby C, Shimer G: An evaluation of the utility of performing body fluid counts on the Coulter LH 750, *Lab Hematol* 10:127, 2004.

Batabyal SK, Ghosh B, Sengupta S, et al.: Cerebrospinal fluid and serum carcinoembryonic antigen in brain tumors, *Neoplasma* 50:377, 2003.

Beetham R: CSF spectrophotometry for bilirubin-why and how? *Scand J Clin Lab Invest* 69(1), 2009.

Bellinger RL, Vacek JL: A review of pericarditis. 2. Specific pericardial disorders, *Postgrad Med* 82:105, 1987.

Bellows CF, Salomone JP, Nakamura SK, et al.: What's black and white and red (read) all over? The bedside interpretation of diagnostic peritoneal lavage fluid, *Am Surg* 64:112, 1998.

Benson RL, Ansbacher L, Hutchison RE, et al.: Cerebrospinal fluid centrifuge analysis in primary amebic meningoencephalitis due to *Naegleria fowleri*, *Arch Pathol Lab Med* 109:668, 1985.

Bento LC, Correia RP, Alexandra AM, et al.: Detection of central nervous system infiltration by myeloid and lymphoid hematologic neoplasms using flow cytometry analysis: diagnostic accuracy study, *Frontiers Med* 5(1), 2018.

Berger T, Rubner P, Schautzer F, et al.: Antimyelin antibodies as a predictor of clinically definite multiple sclerosis after a first demyelinating event, *N Engl J Med* 349:139, 2003.

Berthier M, Bonneau D, Desbordes JM, et al.: Possible involvement of a gamma-hydroxybutyric acid receptor in startle disease, *Acta Paediatr* 83:678, 1994.

Bigner SH: Cerebrospinal fluid (CSF) cytology: current status and diagnostic applications, *J Neuropathol Exp Neurol* 51:235, 1992.

Bini R, Ferrari G, Apra F, et al.: Peritoneal lactate as a potential biomarker for predicting the need for reintervention after abdominal surgery, *J Trauma Acute Care Surg* 77:376, 2014.

Biou D, Benoist J-F, Huong CN-TX, et al.: Cerebrospinal fluid protein concentrations in children: age-related values in patients without disorders of the central nervous system, *Clin Chem* 46:399, 2000.

Bisht B, Handa U, Mohan H, et al.: Complimentary value of DNA flow cytometry and image morphometry in detection of malignant cells in effusion fluids, *Malaysian J Pathol* 36:83, 2014.

Blake J, Berman P: The use of adenosine deaminase in the diagnosis of tuberculosis, *S Afr Med J* 62:19, 1982.

Bleier BS, Debnath I, O'Connell BP, et al.: Preliminary study on the stability of beta-2 tranferrin in extracorporeal cerebrospinal fluid, *Otolaryngology* 144:101, 2011.

Blennow K, Zetterrberg H: Cerebrospinal fluid biomarkers for Alzheimer's disease, *J Alzheimers Dis* 18:413, 2009.

Body BA, Oneson RH, Herold DA: Use of cerebrospinal fluid lactic acid concentration in the diagnosis of fungal meningitis, *Ann Clin Lab Sci* 17:429, 1987.

Bonadio WA, Smith DS, Goddard S, et al.: Distinguishing cerebrospinal fluid abnormalities in children with bacterial meningitis and traumatic lumbar puncture, *J Infect Dis* 162:251, 1990.

Borenstein DG, Gibbs CA, Jacobs RP: Gas-liquid chromatographic analysis of synovial fluid, *Arthritis Rheum* 25:947, 1982.

Boyer TD, Kahn AM, Telfer BR: Diagnostic value of ascitic fluid lactic dehydrogenase, protein, and WBC levels, *Arch Intern Med* 138:1103, 1978.

Brettschneider J, Tumani H, Kiechle U, et al.: IgG antibodies against measles, rubella, and varicella zoster predict conversion to multiple sclerosis in clinically isolated syndrome, *PloS One* 4, 2009. e7638.

Britton C, Hultman E, Murray V, et al.: The diagnostic accuracy of CSF analyses in stroke, *Acta Med Scand* 214:3, 1983.

Bromberg J, Breems D, Kraan J, et al.: CSF flow cytometry greatly improves diagnostic accuracy in CNS hematologic malignancies, *Neurology* 68:1674, 2007.

Brook I: Pericarditis due to anaerobic bacteria, *Cardiology* 97:55, 2002.

Brooks BR: Nonimmunoglobulin proteins in human cerebrospinal fluid. In Herndon RM, Brumback RA, editors: *Cerebrospinal fluid*, Boston, 1989, Kluwer Academic Publishers, p 167.

Brooks JB, Syriopoulou V, Butler WR, et al.: Development of a quantitative chemical ionization gas chromatography–mass spectrometry method to detect tuberculostearic acid in body fluids, *J Chromatogr B Biomed Sci Appl* 712:1, 1998.

Brown KD: An ND: tuberculous peritonitis. Low ascitic fluid glucose concentration as a diagnostic aid, *Am J Gastroenterol* 66:277, 1976.

Burgess LJ, Maritz FJ, LeRoux I, et al.: Combined use of pleural adenosine deaminase with lymphocyte/neutrophil ratio: increased specificity for the diagnosis of tuberculous pleuritis, *Chest* 109:414, 1996.

Burgess LJ, Maritz FJ, Taljaard JJ: Comparative analysis of the biochemical parameters used to distinguish between pleural transudates and exudates, *Chest* 107:1604, 1995.

Burgess LJ, Reuter H, Carstens ME, et al.: The use of adenosine deaminase and interferon-gamma as diagnostic tools for tuberculous pericarditis, *Chest* 122:900, 2002a.

Burgess LJ, Reuter H, Taljaard JJ, et al.: Role of biochemical tests in the diagnosis of large pericardial effusions, *Chest* 121:495, 2002b.

Burgess LJ, Swanepoel CG, Taljaard JJ: The use of adenosine deaminase as a diagnostic tool for peritoneal tuberculosis, *Tuberculosis* 8:243, 2001.

Cameron PD, Boyce JM, Ansari BM: Cerebrospinal fluid lactate in meningitis and meningococcaemia, *J Infect* 26:245, 1993.

Cascinu S, Del Ferro E, Barbanti I, et al.: Tumor markers in the diagnosis of malignant serous effusions, *Am J Clin Oncol* 20:247, 1997.

Castaldo G, Oriani G, Cimino L, et al.: Total discrimination of peritoneal malignant ascites from cirrhosis and heptocarcinoma-associated ascites by assays of ascitic cholesterol and lactate dehydrogenase, *Clin Chem* 40:478, 1994.

Castano VJL, Amores AC: Use of pleural fluid C-reactive protein in laboratory diagnosis of pleural effusions, *Eur J Med* 1:201, 1992.

Castellote J, Xiol X, Verdaguer R, et al.: Comparison of two ascitic fluid culture methods in cirrhotic patients with spontaneous bacterial peritonitis, *Am J Gastroenterol* 85:1605, 1990.

Cavuoti D, Baskin L, Jialal I: Detection of oligoclonal bands in cerebrospinal fluid by immunofixation electrophoresis, *Am J Clin Pathol* 109:585, 1998.

Cawley LP, Minard BJ, Tourtellotte WW, et al.: Immunofixation electrophoresis techniques applied to identification of proteins in serum and cerebrospinal fluid, *Clin Chem* 22:1262, 1976.

Chalmers AC, Aprill BS, Shephard H: Cerebrospinal fluid and human immunodeficiency virus: findings in healthy, asymptomatic, seropositive men, *Arch Intern Med* 150:1538, 1990.

Chan MHM, Chow KM, Chan ATC, et al.: Quantitative analysis of pleural fluid cell-free DNA as a tool for the classification of pleural effusions, *Clin Chem* 49:740, 2003.

Chandler WL, Clayson KJ, Longstreth Jr WT, et al.: Creatine kinase isoenzymes in human cerebrospinal fluid and brain, *Clin Chem* 30:1801, 1984.

Chandler WL, Clayson KJ, Longstreth Jr WT, et al.: Mitochondrial and BB isoenzymes of creatine kinase in cerebrospinal fluid from patients with hypoxic-ischemic brain damage, *Am J Clin Pathol* 86:533, 1986.

Chen Y, Brennessel D, Walters J, et al.: Human immunodeficiency virus-associated pericardial effusions: report of 40 cases and review of the literature, *Am Heart J* 137:516, 1999.

Chin NW, Sinay LJ, Taylor J, et al.: Metastatic prostate cancer presenting as pleural and pericardial effusions, *Fed Pract* 16:19, 1999.

Choi SH, Kim YS, Bae IG, et al.: The possible role of cerebrospinal fluid adenosine deaminase activity in the diagnosis of tuberculous meningitis in adults, *Clin Neurol Neurosurg* 104:10, 2002.

Colli A, Buccino G, Cocciolo M, et al.: Diagnostic accuracy of fibronectin in the differential diagnosis of ascites, *Cancer* 58:2489, 1986.

Concheiro M, González-Colmenero E, Lendoiro E, et al.: Alternative matrices for cocaine, heroin, and methadone in utero drug exposure detection, *Ther Drug Monit* 35:502–509, 2013.

Conly JM, Ronald AR: Cerebrospinal fluid as a diagnostic body fluid, *Am J Med* 75:102, 1983.

Conner B, Lee Y, Branca P, et al.: Variations in pleural fluid WBC count and differential counts with different sample containers and different methods, *Chest* 123:1181, 2003.

Cooper SJ, Kelly CB, King DJ: 5-Hydroxyindoleacetic acid in cerebrospinal fluid and prediction of suicidal behaviour in schizophrenia, *Lancet* 340:940, 1992.

Coplin WM, Longstreth Jr WT, Lam AM, et al.: Cerebrospinal fluid creatine kinase-BB isoenzyme activity and outcome after subarachnoid hemorrhage, *Arch Neurol* 56:1348, 1999.

Corral CJ, Pepple JM, Moxon ER, et al.: C-reactive protein in spinal fluid of children with meningitis, *J Pediatr* 99:365, 1981.

Corral I, Quereda C, Navas E, et al.: Adenosine deaminase activity in cerebrospinal fluid of HIV-infected patients: limited value for diagnosis of tuberculous meningitis, *Eur J Clin Microbiol Infect Dis* 23:471, 2004.

Costa M, Quiroga T, Cruz E: Measurement of pleural fluid cholesterol and lactate dehydrogenase: a simple and accurate set of indicators for separating exudates from transudates, *Chest* 108:1260, 1995.

Cummiskey J, Mavinkurve M, Patneth-Pollak R, et al.: False-positive oral fluid rapid HIV tests—New York City, 2005-2008, *MMWR Morb Mortal Wkly Rep* 57:1–5, 2008.

Cunha BA: Cerebrospinal fluid (CSF) lactic acid levels: a rapid and reliable way to differentiate viral from bacterial meningitis or concurrent viral/bacterial meningitis, *J Clin Microbiol* 50:211, 2012.

Curtis GDW, Newman RJ, Slack MPE: Synovial fluid lactate and the diagnosis of septic arthritis, *J Infect* 6:239, 1983.

Davis MJ, Denton J, Freemont AJ, et al.: Comparison of serial synovial fluid cytology in rheumatoid arthritis: delineation of subgroups with prognostic implications, *Ann Rheum Dis* 47:559, 1988.

Davis LE, Schmitt JW: Clinical significance of cerebrospinal fluid tests for neurosyphilis, *Ann Neurol* 25:50, 1989.

DeLaurier GA, Ivey RK, Johnson RH: Peritoneal fluid lactate and diagnostic dilemmas in acute abdominal disease, *Am J Surg* 167:302, 1994.

Desai MM, Pal RB: Polymerase chain reaction for the rapid diagnosis of tuberculous meningitis, *Indian J Med Sci* 56:546, 2002.

DeSalles AAF, Kontos HA, Becker DP, et al.: Prognostic significance of ventricular CSF lactic acidosis in severe head injury, *J Neurosurg* 65:615, 1986.

DiDiodato G, Bradbury N: Cerebrospinal fluid analysis with the BioFire FilmArray meningitis/encephalitis molecular panel reduces length of hospital stay in patients with suspected central nervous system infections, *Open Forum Infect Dis* 6:1, 2019.

Dobson R, Ramagopalan S, Davis A, et al.: Cerebrospinal fluid oligoclonal bands in multiple sclerosis and clinically isolated syndromes: a meta-analysis of prevalence, prognosis and effect of latitude, *J Neurol Neurosurg Psychiatry* 84:909, 2013.

Donald PR, Malan C: Cerebrospinal fluid lactate and lactate dehydrogenase activity in the rapid diagnosis of bacterial meningitis, *S Afr Med J* 69:39, 1986.

dos Santos JGN: Fetal primary amebic meningoencephalitis: a retrospective study in Richmond, Virginia, *Am J Clin Pathol* 54:737, 1970.

Drummer OH: Drug testing in oral fluid, *Clin Biochem Rev* 27:147, 2006.

Dubowitz LM, Bouza H, Hird MF, et al.: Low cerebrospinal fluid concentration of free gamma-aminobutyric acid in startle disease, *Lancet* 340:80, 1992.

Duits FH, Kester MI, Scheffer PG, et al.: Increase in cerebrospinal fluid F2-isoprostanes is related in cognitive decline in APOE ε4 carriers, *J Alzheimers Dis* 36:563, 2013.

Dumler JS, Valsamakis A: Molecular diagnosis for existing and emerging infections: complementary tools for a new era of clinical microbiology, *Am J Clin Pathol* 112:533, 1999.

Dweik RA, Boggs PB, Erzurum SC, et al.: An official ATC clinical practice guideline: interpretation of exhaled nitric oxide levels (FENO) for clinical applications, *Am J Respir Crit Care Med* 184:602–615, 2011.

Dwivedi M, Misra SP, Misra V, et al.: Value of adenosine deaminase estimation in the diagnosis of tuberculous ascites, *Am J Gastroenterol* 85:1123, 1990.

Eclache V, Vu T, Le Roux G: D-dimer in the cerebrospinal fluid: a marker of central nervous system involvement in neoplastic disease, *Nouv Rev Fr Hematol* 36:321, 1994.

Elis A, Meisel S, Tishler T, et al.: Ascitic fluid serum bilirubin concentration ratio for the classification of transudates or exudates, *Am J Gastroenterol* 93:401, 1998.

Engelke S, Bridgers S, Saldanha RL, et al.: Cerebrospinal fluid lactate dehydrogenase in neonatal intracranial hemorrhage, *Am J Med Sci* 291:391, 1986.

Enomoto H, Inoue S, Matsuhisa A: Diagnosis of spontaneous bacterial peritonitis and an *in situ* hybridization approach to detect an "unidentified" pathogen, *Int J Hepatol*7, 2014, https://doi.org/10.1155/2014/634617. ID 634617 . [Accessed 26 January 2015].

Ettlinger RE, Hunder GC: Synovial effusions containing cholesterol crystals, *Mayo Clin Proc* 54:366, 1979.

Exner MM, Lewinski MA: Isolation and detection of *Borrelia burgdorferi* DNA from cerebral spinal fluid, synovial fluid, blood, urine, and ticks using the Roche MagNA Pure system and real-time PCR, *Diagn Microbiol Infect Dis* 46:235, 2003.

Fam AG, Pritzker KP, Cheng PT, et al.: Cholesterol crystals in osteoarthritic joint effusions, *J Rheumatol* 8:273, 1981.

Fang J-F, Chen R-J, Lin B-C: Cell count ratio: new criterion of diagnostic peritoneal lavage for detection of hollow organ perforation, *J Trauma* 45:540, 1998.

Ferguson AM, Ford B, Gronowski A: Method validation for cerebrospinal fluid human chorionic gonadotropin measurement with the Advia Centaur, *Clin Chem* 54:1408, 2008.

Ferrer A, Osset J, Alegre J, et al.: Prospective clinical and microbiological study of pleural effusions, *Eur J Clin Microbiol Infect Dis* 18:237, 1999.

Finn WG, Peterson LC, James C, et al.: Enhanced detection of malignant lymphoma in cerebrospinal fluid by multiparameter flow cytometry, *Am J Clin Pathol* 110:341, 1998.

Fischer C, Arneth B, Koehler J, et al.: Kappa free light chains in cerebrospinal fluid as markers of intrathecal immunoglobulin synthesis, *Clin Chem* 50:1809, 2004.

Fishman RA: *Cerebrospinal fluid in diseases of the nervous system*, ed 2, Philadelphia, 1992, Saunders.

Fleisher M, Wasserstrom WRT, Schold SC, et al.: Lactic dehydrogenase isoenzymes in the cerebrospinal fluid of patients with systemic cancer, *Cancer* 47:2654, 1981.

Flood J, Weinstock HS, Guroy M, et al.: Neurosyphilis during the AIDS epidemic, san Francisco, 1985-1992, *J Infect Dis* 177:931, 1998.

Florez G, Cabeza A, Gonzalez JM, et al.: Changes in serum and cerebrospinal fluid enzyme activity after head injury, *Acta Neurochir* 35:3, 1976.

Fortini AS, Sanders EL, Weinshenker BG, et al.: Cerebrospinal fluid oligoclonal bands in the diagnosis of multiple sclerosis, *Am J Clin Pathol* 120:672, 2003.

Frenck RW, Fathy HM, Sherif M, et al.: Sensitivity and specificity of various tests for the diagnosis of *Helicobacter pylori* in Egyptian children, *Pediatrics* 118:195–202, 2006.

Fujimoto N, Gemba K, Yao A, et al.: Tuberculosis diagnosis by PCR analysis of synovial fluid, *J Infect Chemother* 16:53, 2010.

Fuster O, Andino B, Pardo A, et al.: Continuous ambulatory peritoneal dialysis, ascitic and pleural body fluids evaluation with the Mindray BC-6800 hematology analyzer, *J Clin Lab Anal* 32:1, 2018.

Gallo P, Tavolato B, Bergenbrant S, et al.: Immunoglobulin light chain patterns in the cerebrospinal fluid: a study with special reference to the occurrence of free light chains in cerebrospinal fluid with and without oligoclonal immunoglobulin G, *J Neurol Sci* 94:241, 1989.

Garcia-Pachon E, Padilla-Navas I, Dosda ME, et al.: Elevated level of carcinoembryonic antigen in nonmalignant pleural effusions, *Chest* 111:643, 1997.

Garg R, Sood A, Arora S, et al.: Ascitic fluid cholesterol in differential diagnosis of ascites, *J Assoc Physicians India* 41:644, 1993.

Gastrin B, Lovestad A: Diagnostic significance of pleural fluid lactate concentration in pleural and pulmonary disease, *Scand J Infect Dis* 20:85, 1988.

Gatter RA, Schumacher HR: *A practical handbook of joint fluid analysis*, ed 2, Philadelphia, 1991, Lea & Febiger.

Gerbes AL, Jungst D, Xie Y, et al.: Ascitic fluid analysis for the differentiation of malignancy-related and nonmalignant ascites, *Cancer* 68:1808, 1991.

Gerdes LU, Jorgensen PE, Nexo E, et al.: C-reactive protein and bacterial meningitis: a meta-analysis, *Scand J Clin Lab Invest* 58:383, 1998.

Gilbert JA, Kamath PS: Spontaneous bacterial peritonitis: an update, *Mayo Clin Proc* 70:365, 1995.

Gilchrist GS, Tubergen DG, Sather HN, et al.: Low numbers of CSF blasts at diagnosis do not predict for the development of CNS leukemia in children with intermediate-risk acute lymphoblastic leukemia. A Children's Cancer Group report, *J Clin Oncol* 12:2594, 1994.

Glasser L, Murphy C, Machan J: The clinical reliability of automated cerebrospinal fluid cell counts on the Beckman-Coulter LH750 and IRIS iQ200, *Am J Clin Pathol* 131:58, 2009.

Goldenberg DL: Reed JI: bacterial arthritis, *N Engl J Med* 312:764, 1985.

Golightly MG: Laboratory considerations in the diagnosis and management of lyme borreliosis, *Am J Clin Pathol* 99:168, 1993.

Good JT, King TE, Antony VB, et al.: *Lupus pleuritis*, *Chest* 84:714, 1983.

Good JT, Taryle DA, Maulitz RM, et al.: The diagnostic value of pleural fluid pH, *Chest* 78:55, 1980.

Gratacos J, Vila J, Moya F, et al.: D-lactic acid in synovial fluid: a rapid diagnostic test for bacterial synovitis, *J Rheumatol* 22:1504, 1995.

Graves M: Cerebrospinal fluid infections. In Herndon RM, Brumback RA, editors: *The cerebrospinal fluid*, Boston, 1989, Kluwer Academic Publishers, p 143.

Greene DN, Schmidt R, Wilson AR, et al.: Cerebrospinal fluid myelin basic protein is frequently ordered but has little value, *Am J Clin Pathol* 138:262, 2012.

Greenlee JE: Approach to diagnosis of meningitis: cerebrospinal fluid examination, *Infect Dis Clin North Am* 4:583, 1990.

Gulyas M, Kaposi AD, Elek G, et al.: Value of carcinoembryonic antigen (CEA) and cholesterol assays of ascitic fluid in cases of inconclusive cytology, *J Clin Pathol* 54:831, 2001.

Hall CD, Snyder CR, Robertson KR, et al.: Cerebrospinal fluid analysis in human immunodeficiency virus infection, *Ann Clin Lab Sci* 22:139, 1992.

Halla JT, Schrohenloher RE, Volankis JE: Immune complexes and other laboratory features of pleural effusions, *Ann Intern Med* 92:748, 1980.

Halperin R, Hadas E, Bukovsky I, et al.: Peritoneal fluid analysis in the differentiation of ovarian cancer and benign ovarian tumor, *Eur J Gynecol Oncol* 20:40, 1999.

Hamal AB, Yogi KN, Bam N, et al.: Pleural fluid cholesterol in differentiating exudative and transudative pleural effusion, *Pulm Med*1, 2013. 2013.

Harrington MG, Merrill CR, Asher DM, et al.: Abnormal proteins in the cerebrospinal fluid of patients with Creutzfeldt-Jacob disease, *N Engl J Med* 315:279, 1986.

Hausfater P, Fillet AM, Rozenberg F, et al.: Prevalence of viral infection markers by polymerase chain reaction amplification and interferon-alpha measurements among patients undergoing lumbar puncture in an emergency department, *J Med Virol* 73:137, 2004.

Hayward RA, Oye RK: Are polymorphonuclear leukocytes an abnormal finding in cerebrospinal fluid? Results from 225 normal cerebrospinal fluid specimens, *Arch Intern Med* 148:1623, 1988.

Hayward RA, Shapiro MF, Oye RK: Laboratory testing on cerebrospinal fluid: a reappraisal, *Lancet* 1:8523, 1987.

Heffner JE, Brown LK, Barbieri CA: Diagnostic value of tests that discriminate between exudative and transudative pleural effusions, *Primary Study Investigators*, *Chest* 111:970, 1997.

Heffner JE, Brown LK, Barbieri C, et al.: Pleural fluid chemical analysis in parapneumonic effusions: a meta-analysis, *Am J Respir Crit Care Med* 151:1700, 1995.

Herndon RM, Brumback RA, editors: *The cerebrospinal fluid*, Boston, 1989, Kluwer Academic Publishers.

Hersey LA, Trotter JL: The use and abuse of the cerebrospinal fluid IgG profile in the adult: a practical evaluation, *Ann Neurol* 8(126), 1980.

Hess JL, Highsmith WE: Telomerase detection in body fluids, *Clin Chem* 48:18, 2002.

Himes SK, Dukes KA, Tripp T, et al.: Clinical sensitivity and specificity of meconium fatty acid ethyl ester, ethyl glucuronide, and ethyl sulfate for detecting maternal drinking during pregnancy, *Clin Chem* 61:523–532, 2015.

Hoffman J, Janssen W: Automated counting of cells in cerebrospinal fluid using the Cell Dyn-4000 haematology analyser, *Clin Chem Lab Med* 40:1168, 2002.

Horvath I, Hunt J, Barnes PJ, et al.: Exhaled breath condensate: methodological recommendations and unresolved questions, *Eur Respir J* 26:523–548, 2005.

Hsich G, Kenney K, Gibbs CJ, et al.: The 14-3-3 protein in cerebrospinal fluid as a marker for transmissible spongiform encephalopathies, *N Engl J Med* 335:924, 1996.

Hunder GG, McDuffie FC, Hepper NGG: Pleural fluid complement activity in systemic lupus erythematosus and rheumatoid arthritis, *Ann Intern Med* 76:357, 1972.

Hunder GG, Pierre RV: In vivo LE cell formation in synovial fluid, *Arthritis Rheum* 13:448, 1970.

Huppmann AR, Rheingold SR, Bailey LC, et al.: Detection of leukemic lymphoblasts in CSF is instrument-dependent, *Am J Clin Pathol* 137:795, 2012.

Ibrahim RE, Teich D, Smith ER, et al.: Flow cytometric surface light chain analysis of lymphocyte-rich effusions, *Cancer* 63:2024, 1989.

Irinoda T, Terashima M, Takagane A, et al.: Carcinoembryonic antigen level in peritoneal washing is prognostic factor in patients with gastric cancer, *Oncol Rep* 5:661, 1998.

Irjala K, Suorpaa J, Laurent B: Identification of CSF leakage by immunofixation, *Arch Otolaryngol* 105:447, 1979.

Izhakian S, Wasser WG, Fox BD, et al.: The diagnostic value of the pleural fluid C-reactive protein in parapneumonic effusions, *Dis Markers* 1:2016, 2016.

Jaffin JH, Ochsner MG, Cole FJ, et al.: Alkaline phosphatase levels in diagnostic peritoneal lavage as a predictor of hollow visceral injury, *J Trauma* 34:829, 1993.

Jalava J, Skurnik M, Toivanen A, et al.: Bacterial PCR in the diagnosis of joint infection, *Ann Rheum Dis* 60:287, 2001.

Jankovska E, Svitek M, Holada K, Petrak J: Affinity depletion versus relative protein enrichment: a side-by-side comparison of two major strategies for increasing human cerebrospinal fluid proteome coverage, *Clin Proteomics* 16:9, 2019.

Jay SJ: Pleural effusions. 2: definitive evaluation of the exudate, *Postgrad Med* 80:181, 1986.

Jeffrey GM, Frampton CM, Legge HM, et al.: Cerebrospinal fluid β2-microglobulin levels in meningeal involvement by malignancy, *Pathology* 22:20, 1990.

Johnson KP, Nelson BJ: Multiple sclerosis: diagnostic usefulness of cerebrospinal fluid, *Ann Neurol* 2:425, 1977.

Jonasson JG, Ducatman BS, Wang HH: The cell block for body cavity fluids: do the results justify the cost? *Mod Pathol* 3:667, 1990.

Jones AC, Chuck AJ, Arie EA, et al.: Diseases associated with calcium pyrophosphate deposition disease, *Semin Arthritis Rheum* 22:188, 1992.

Judkins SW, Cornbleet PJ: Synovial fluid crystal analysis, *Lab Med* 28:774, 1997.

Kanoh Y, Ohtani H: Levels of interleukin-6, CRP and alpha 2 macroglobulin in cerebrospinal fluid (CSF) and serum as indicators of blood-CSF barrier damage, *Biochem Mol Biol Int* 43:269, 1997.

Kang SJ, Kwang SK, Yoon SH, et al.: Diagnostic value of cerebrospinal fluid level of carcinoembryonic antigen in patients with leptomeningeal carcinomatous metastasis, *J Clin Neurol* 6:33, 2010.

Karcher D, Alkan S: Human herpesvirus-8-associated body cavity-based lymphoma in human immunodeficiency virus-infected patients: a unique B-cell neoplasm, *Hum Pathol* 28:801, 1997.

Karkela J, Pasanen M, Kaukinen S, et al.: Evaluation of hypoxic brain injury with spinal fluid enzymes, lactate, and pyruvate, *Crit Care Med* 20:378, 1992.

Kashyap RS, Kainthla RP, Biswas SK, et al.: Rapid diagnosis of tuberculous meningitis using simple DOT ELISA method, *Med Sci Monit* 9:123, 2003.

Kasper LM, Moorehead WR, Oel TO, et al.: An alternative method assaying cerebrospinal fluid protein in the presence of methotrexate, *Clin Chem* 34:2091, 1988.

Kaur C, Menon B: Evaluation of real time polymerase chain reaction, adenosine deaminase and interferon gamma in tubercular pleural effusions, *Euro Resp J* 40:P1408, 2012.

Kawai M, Hirohata S: Cerebrospinal fluid beta(2)-microglobulin in neuro-Behçet's syndrome, *J Neurol Sci* 179:132, 2000.

Kay J, Eichenfield AH, Athreya BH, et al.: Synovial fluid eosinophilia in Lyme disease, *Arthritis Rheum* 31:1384, 1988.

Kendall B, Dunn C, Solanki P: A comparison of the effectiveness of malignancy detection in body fluid examination by the cytopathology and hematology laboratories, *Arch Pathol Lab Med* 121:976, 1997.

Keren DF: Optimizing detection of oligoclonal bands in cerebrospinal fluid by use of isoelectric focusing with IgG immunoblotting, *Am J Clin Pathol* 120:649, 2003.

Khalid A, Brugge W: ACG practice guidelines for the diagnosis and management of neoplastic pancreatic cysts, *Am J Gastroenterol* 102:2339–2349, 2007.

Kim S, Sahn SA: Postcardiac injury syndrome: an immunologic pleural fluid analysis, *Chest* 109:570, 1996.

Kindig JR, Goodman MR: Clinical utility of pericardial fluid pH determination, *Am J Med* 75:1077, 1983.

Kjeldsberg CR, Knight JA: *Body fluids: laboratory examination of amniotic, cerebrospinal, seminal, serous, and synovial fluids*, ed 3, Chicago, 1993, American Society for Clinical Pathology.

Klee GG, Tallman RD, Goellner JR, et al.: Elevation of carcinoembryonic antigen in cerebrospinal fluid among patients with meningeal carcinomatosis, *Mayo Clin Proc* 61(9), 1986.

Kleine T, Nebe C, Lower C, et al.: Modifications of haematology analyzers to improve cell counting and leukocyte differentiating in cerebrospinal fluid controls of the Joint German Society for Clinical Chemisty and Laboratory Medicine, *Cytometry* 75A:688, 2009.

Knight JA, Dudek SM, Haymond RE: Early (chemical) diagnosis of bacterial meningitis—cerebrospinal fluid glucose, lactate, and lactate dehydrogenase compared, *Clin Chem* 27:1431, 1981.

Koh KK, Kim EJ, Cho CH, et al.: Adenosine deaminase and carcinoembryonic antigen in pericardial effusion diagnosis, especially in suspected tuberculous pericarditis, *Circulation* 89:2728, 1994.

Kosches DS, Sosnowik D, Lendvai S, et al.: Unusual anodic migrating isoamylase differentiates selected malignant from nonmalignant ascites, *J Clin Gastroenterol* 11:43, 1989.

Kramer MR, Saldana MJ, Cepero RJ, et al.: High amylase levels in neoplasm-related pleural effusion, *Ann Intern Med* 110:567, 1989.

Kuberski T: Eosinophils in cerebrospinal fluid: criteria for eosinophilic meningitis, *Hawaii Med J* 40:97, 1981.

Kusum S, Aman S, Pallab R, et al.: Multiplex PCR for rapid diagnosis of tuberculous meningitis, *J Neurol* 258:1781, 2011.

Kuwayama K, Miyaguchi H, Yamamuro T, et al.: Effectiveness of saliva and fingerprints as alternative specimens to urine and blood in forensic drug testing, *Drug Test Anal* 8:644–651, 2016.

Lacayo NJ, Weng L, Gawad C, et al.: Use of rearranged immune receptor sequencing to measure minimal residual disease (MRD) in bone marrow, cerebrospinal fluid and testes in relapsed childhood acute lymphoblastic leukemia, *Blood* 122:4984, 2013.

Lampl Y, Paniri Y, Eshel Y, et al.: Cerebrospinal fluid lactate dehydrogenase levels in early stroke and transient ischemic attacks, *Stroke* 21:854, 1990.

Lang DT, Berberian LB, Lee S, et al.: Rapid differentiation of subarachnoid hemorrhage from traumatic lumbar puncture using the d-dimer assay, *Am J Clin Pathol* 91:403, 1990.

Larson FA, Haller CC, Delcore R, et al.: Diagnostic peritoneal lavage in acute peritonitis, *Am J Surg* 164:449, 1992.

Lazcano O, Li CY, Pierre RV, et al.: Clinical utility of the Alizarin Red S stain on permanent preparations to detect calcium-containing compounds in synovial fluid, *Am J Clin Pathol* 99:90, 1993.

Leber AL, Everhart K, Balada-Llasat, et al.: Multicenter evaluation of BioFire FilmArray meningitis/encephalitis panel for detection of bacteria, viruses, and yeast in cerebrospinal fluid specimens, *J Clin Microbiol* 54:2251, 2016.

Lee C-M, Changchien C-S, Shyu W-C, et al.: Serum-ascites albumin concentration gradient and ascites fibronectin in the diagnosis of malignant ascites, *Cancer* 70:2057, 2006.

Lee HH, Carlson RW, Bull DM: Early diagnosis of spontaneous bacterial peritonitis: values of ascitic fluid variables, *Infection* 15:232, 1987.

Lee J-H, Lee CW, Lee S-G, et al.: Comparison of polymerase chain reaction with adenosine deaminase activity in pericardial fluid for the diagnosis of tuberculous pericarditis, *Am J Med* 113:519, 2002.

Lee YCG, Rogers JT, Rodriguez RM, et al.: Adenosine deaminase levels in nontuberculous lymphocytic pleural effusions, *Chest* 120:356, 2001.

Lefvert AK, Link H: IgG production within the central nervous system: a critical review of proposed formulae, *Ann Neurol* 17:13, 1985.

Lemstra AW, van Meegen MT, Vreyling JP, et al.: 14-3-3 testing in diagnosing Creutzfeldt-Jakob disease: a prospective study in 112 patients, *Neurology* 55:514, 2000.

Lépine P-A, Thomas R, Nguyen S, et al.: Simplified criteria using pleural fluid cholesterol and lactate dehydrogenase to distinguish between exudative and transudative pleural effusions, *Respiration* 98:48–54, 2019.

Leslie DE, Assato F, Karapanagiotidis T, et al.: Development of a real-time PCR assay to detect *Treponema pallidum* in clinical specimens and assessment of assay comparison with serological testing, *J Clin Microbiol* 45:93, 2007.

Leventhal LJ, DeMarco DM, Zurier RB: Antinuclear antibody in pericardial fluid from a patient with primary cardiac lymphoma, *Arch Intern Med* 150:1113, 1990.

Levine J, Panchalingam K, Rapoport A, et al.: Increased cerebrospinal fluid glutamine levels in depressed patients, *Biol Psychiatry* 47:586, 2000.

Levine H, Szanto M, Grieble HG, et al.: Rheumatoid factor in nonrheumatoid pleural effusions, *Ann Intern Med* 69:487, 1968.

Levy PY, Fournier PE, Charrel R, et al.: Molecular analysis of pericardial fluid: a 7-year experience, *Eur Heart J* 27:1942, 2006.

Li F, Bulbul R, Schumacher HRJ, et al.: Molecular detection of bacterial DNA in venereal-associated arthritis, *Arthritis Rheum* 39:950, 1996.

Li A, Gronlund E, Brattsand G: Automated white blood cell counts in cerebrospinal fluid using the body fluid mode on the platform Sysmex XE-5000, *Scan J Clin Lab Invest* 74:673, 2014.

Liesman RM, Strasburg AP, Heitman AK, et al.: Evaluation of a commercial multiplex molecular panel for diagnosis of infectious meningitis and encephalitis, *J Clin Microbiol* 56(1), 2018.

Light RW: In *Pleural diseases*, ed 3, Baltimore, 1995, Williams & Wilkins.

Light RW: Diagnostic principles in pleural disease, *Eur Respir J* 10:476, 1997.

Light RW: Clinical practice. pleural effusion, *N Engl J Med* 346:1971, 2002.

Light RW, Ball Jr WC: Glucose and amylase in pleural effusions, *J Am Med Assoc* 225:257, 1973.

Light RW, MacGregor MI, Luchsinger PC, et al.: Pleural effusions: the diagnostic separation of transudates and exudates, *Ann Intern Med* 77:507, 1972.

Lin JJ, Harn HJ, Hsu YD, et al.: Rapid diagnosis of tuberculous meningitis by polymerase chain reaction assay of cerebrospinal fluid, *J Neurol* 242:147, 1995.

Lolli F, Siracusa G, Amato MP, et al.: Intrathecal synthesis of free immunoglobulin light chains and IgM in initial multiple sclerosis, *Acta Neurol Scand* 83:239, 1991.

Lossos IS, Breuer R, Intrator O, et al.: Cerebrospinal fluid lactate dehydrogenase isoenzyme analysis for the diagnosis of central nervous system involvement in hematooncologic patients, *Cancer* 88:1599, 2000.

Lott JA, Warren P: Estimation of reference intervals for total protein in cerebrospinal fluid, *Clin Chem* 35:1766, 1989.

Luna A, Villanueva E, Castellano M, et al.: The determination of CK, LDH and its isoenzymes in pericardial fluid and its application to the post-mortem diagnosis of myocardial infarction, *Forensic Sci Int* 19:85, 1982.

Lunding J, Midgard R, Vedeler CA: Oligoclonal bands in cerebrospinal fluid: a comparative study of isoelectric focusing, agarose gel electrophoresis and IgG index, *Acta Neurol Scand* 102:322, 2000.

Luukkainen R, Kaarela K, Huhtala H, et al.: Prognostic significance of synovial fluid analysis in rheumatoid arthritis, *Ann Med* 21:269, 1989.

Luxton RW, Patel P, Keir G, et al.: A micro-method for measuring total protein in cerebrospinal fluid by using benzethonium chloride in microliter plate wells, *Clin Chem* 35:1731, 1989.

Maas JW, Bowden CL, Miller AL, et al.: Schizophrenia, pyschosis, and cerebrospinal fluid homovanillic acid concentrations, *Schizophr Bull* 23:147, 1997.

Maldonado F, Hawkins FJ, Daniels CE, et al.: Pleural fluid characteristics of chylothorax, *Mayo Clin Proc* 84:129, 2009.

Malla KK, Malla T, Rao KS, et al.: Is cerebrospinal fluid C-reactive protein a better tool than blood C-reactive protein in laboratory diagnosis of meningitis in children? *Sultan Qaboos Univ Med J* 13:93, 2013.

Marks M, Lawrence D, Kositz C, et al.: Diagnostic performance of PCR assays for the diagnosis of neurosyphilis: a systematic review, *Sex Transm Infect* 94:585, 2018.

McAnena OJ, Marx JA, Moore EE: Peritoneal lavage enzyme determinations following blunt and penetrating abdominal trauma, *J Trauma* 31:1161, 1991.

McCarty DJ: Crystal identification in human synovial fluids, *Rheum Disease Clin North Am* 14:253, 1988.

McGill NW, York H: Reproducibility of synovial fluid examination for crystals, *Aust N Z J Med* 34:710, 1991.

McGuinness GA, Weisz SC, Bell WE: CSF lactate levels in neonates, *Am J Dis Child* 137:48, 1983.

Maddalena A, Papassotiropoulos A, Muller-Tillmanns B, et al.: Biochemical diagnosis of Alzheimer disease by measuring the cerebrospinal fluid ratio of phosphorylated tau protein to β-amyloid peptide 42, *Arch Neurol* 60:1202, 2003.

Mahoney Jr DH, Fernbach DJ, Glaze DG, et al.: Elevated myelin basic protein levels in cerebrospinal fluid of children with acute lymphoblastic leukemia, *J Clin Oncol* 2:58, 1984.

Malhotra N, Gupta S, Agarwal A, et al.: Peritoneal fluid interleukin (IL-8) in patients with endometriosis—is there a correlation with severity or symptoms of disease? *Fertil Steril* 88(suppl 1):S213, 2007.

Mann AD, Macfarlane CM, Verburg CJ, et al.: The bromide partition test and CSF adenosine deaminase activity in the diagnosis of tuberculous meningitis in children, *S Afr Med J* 62:432, 1982.

Marshall JB: Finding the cause of ascites: the importance of accurate fluid analysis, *Postgrad Med* 83:189, 1988.

Martinez-Bru C, Gomez C, Cortes M, et al.: Ascitic fluid interleukin-8 to distinguish spontaneous bacterial peritonitis and sterile ascites in cirrhotic patients, *Clin Chem* 45:2027, 1999.

Martinez-Laperche C, Gomez-Garcia AM, Lassaletta A, et al.: Detection of occult cerebrospinal fluid involvement during maintenance therapy identifies a group of children with acute lymphoblastic leukemia at high risk for relapse, *Am J Hematol* 88:359, 2013.

Marton KI, Gean AD: The spinal tap: a new look at an old test, *Ann Intern Med* 104:840, 1986.

Mayefsky JH, Roughmann KJ: Determination of leukocytosis in traumatic spinal tap specimens, *Am J Med* 82:1175, 1987.

Melsom RD: Diagnostic reliability of pleural fluid protein estimation, *J Royal Soc Med* 72:823, 1979.

Meucci G, Rossi G, Bertini R, et al.: Laser nephelometric evaluation of albumin, IgG and alpha2-macroglobulin: applications to the study of alterations of the blood-brain barrier, *J Neurol Sci* 118:73, 1993.

Meyers DG, Meyers RE, Prendergast TW: The usefulness of diagnostic tests on pericardial fluid, *Chest* 111:1213, 1997.

Mezger J, Permanetter W, Gerbes AL, et al.: Tumour associated antigens in diagnosis of serous effusions, *J Clin Pathol* 41:633, 1988.

Miller KS, Wooten S, Sahn SA: Urinothorax: a cause of low pH transudative pleural effusions, *Am J Med* 85:448, 1988.

Miralles C, Orea M, Espana P, et al.: Cancer antigen 125 associated with multiple benign and malignant pathologies, *Ann Surg Oncol* 10:150, 2003.

Mishra OP, Batra P, Ali Z, et al.: Cerebrospinal fluid lysozyme level for the diagnosis of tuberculous meningitis in children, *J Trop Pediatr* 49:13, 2003.

Mizock BA, Rackow EC, Burke GS: Elevated cerebrospinal fluid glutamine in septic encephalopathy, *J Clin Gastroenterol* 11:362, 1989.

Mohammadi SF, Patil AB, Nadagir SD, et al.: Diagnostic value of latex agglutination test in diagnosis of acute bacterial meningitis, *Ann Indian Acad Neurol* 16:645, 2013.

Molina R, Filella X, Jo J, et al.: CA 125 in biological fluids, *Int J Biol Markers* 13:224, 1998.

Morbidity and Mortality Weekly Report: Outbreaks of aseptic meningitis associated with echoviruses 9 and 30 and preliminary surveillance reports on enterovirus activity—United States, *J Am Med Assoc* 290:1444, 2003. 2003.

Montine TJ, Beal MF, Cudkowicz ME, et al.: Increased cerebrospinal fluid F2-isoprostane concentration in probable Alzheimer's disease, *Neurology* 52:562, 1999.

Montine TJ, Kaye JA, Montine KS, et al.: Cerebrospinal fluid Abeta42, tau, and F2-isoprostane concentrations in patients with Alzheimer disease, other dementias, and in age-matched controls, *Arch Pathol Lab Med* 125:510, 2001.

Montine TJ, Peskind ER, Quinn JF, et al.: Increased cerebrospinal fluid F2-isoprostanes are associated with aging and latent Alzheimer's disease as identified by biomarkers, *NeuroMolecular Med* 13:37, 2011.

Moriarity A, Schwartz M, Ducatman B, et al.: A liquid concept—do classic preparations of body cavity fluid perform differently than ThinPrep cases? *Arch Pathol Lab Med* 132:1716, 2008.

Mortensen PB, Kristensen SD, Bloch A, et al.: Diagnostic value of ascitic fluid cholesterol levels in the prediction of malignancy, *Scand J Gastroenterol* 23:1085, 1988.

Muayqil T, Gronseth G, Camicioli R: Evidence-based guideline: diagnostic accuracy of CSF 14-3-3 protein in sporadic Creutzfeldt-Jakob disease, *Neurology* 79:1499, 2012.

Muranishi H, Nakashima M, Hirano H, et al.: Simultaneous measurements of adenosine deaminase activity and tuberculostearic acid in pleural effusions for the diagnosis of tuberculous pleuritis, *Internal Med* 31:752, 1992.

Muranishi H, Nakashima M, Isobe R, et al.: Measurement of tuberculostearic acid in sputa, pleural effusions, and bronchial washings: a clinical evaluation for diagnosis of pulmonary tuberculosis, *Diagn Microbiol Infect Dis* 13:235, 1990.

Murphy MJ, Jenkinson F: Categorisation of pleural fluids in routine clinical practice: analysis of pleural fluid protein and lactate dehydrogenase alone compared with modified Light's criteria, *J Clin Pathol* 61:684, 2008.

Nanos N, Delanghe J: Evaluation of Sysmex UF-1000i for use in cerebrospinal fluid analysis, *Clin Chimica Acta* 392:30, 2008.

Nicolè, Cappello F, Cappellesso R, et al.: MicroRNA profiling in serous cavity specimens: diagnostic challenges and new opportunities, *Caner Cytopathol*, 2019. https://doi.org/10.1002/cncy.22143.

Nigrovic LE, Shah SS, Neuman MI: Relationship between cerebrospinal fluid glucose and serum glucose, *N Eng J Med* 366:576, 2012.

Nocton JJ, Dressler F, Rutledge RJ, et al.: Detection of *Borrelia burgdorferi* DNA by polymerase chain reaction in synovial fluid from patients with lyme arthritis, *N Engl J Med* 330:229, 1994.

Normansell DE, Stacy EK, Booker CF, et al.: Detection of beta-2-transferrin in otorrhea and rhinorrhea in a routine clinical laboratory setting, *Clin Diagn Lab Immunol* 1:68, 1994.

Noseworthy TW, Anderson BJ, Noseworthy AF, et al.: Cerebrospinal fluid myelin basic protein as a prognostic marker in patients with head injury, *Crit Care Med* 13:743, 1985.

Núñez Galindo A, Macron C, Cominetti O, Dayon L: Analyzing cerebrospinal fluid proteomes to characterize central nervous system disorders: a highly automated mass spectrometry-based pipeline for biomarker discovery, *Methods Mol Biol* 1959:89–112, 2019.

Nussinovitch M, Avitzur Y, Finkelstein Y, et al.: Lactic dehydrogenase isoenzyme in cerebrospinal fluid of children with febrile convulsions, *Acta Paediatr* 92:186, 2003a.

Nussinovitch M, Harel D, Eidlitz-Markus T, et al.: Lactic dehydrogenase isoenzyme in cerebrospinal fluid of children with infantile spasms, *Eur Neurol* 49:231, 2003b.

Odom LF, Wilson H, Cullen J, et al.: Significance of blasts in low-cell count cerebrospinal fluid specimens from children with acute lymphoblastic leukemia, *Cancer* 66:1748, 1990.

O'Halloran JA, Franklin A, Lainheart W, et al.: Pitfalls associated with the use of molecular diagnostic panels in the diagnosis of Cryptococcal meningitis, *Open Forum Infect Dis* 4:1, 2017.

Otomo Y, Henmi H, Mashiko K, et al.: New diagnostic peritoneal lavage criteria for diagnosis of intestinal injury, *J Trauma* 44:991, 1998.

Ottink KD, Strahm C, Muller-Kobold A, et al.: Factors to consider when assessing the diagnostic accuracy of synovial leukocyte count in periprosthetic joint infection, *J Bone Joint Infect* 4:167, 2019.

Pai M, Flores L, Pai N, et al.: Diagnostic accuracy of nucleic acid amplification tests for tuberculous meningitis: a systematic review and meta-analysis, *Lancet Inf Dis* 3:633, 2003.

Pandie S, Peter JG, Kerbelker ZS, et al.: Diagnostic accuracy of quantitative PCR (Xpert MTB/RIF) for tuberculous pericarditis compared to adenosine deaminase and unstimulated interferon-gamma in a high burden setting: a prospective study, *BMC Med* 12:101, 2014.

Pappu ID, Purolit DM, Levkoff AH: CSF cytology in the neonate, *Am J Dis Child* 136:297, 1982.

Paramothayan NS, Barron J: New criteria for the differentiation between transudates and exudates, *J Clin Pathol* 55:69, 2002.

Partridge DG, Winnard C, Townsend R, et al.: Joint aspiration, including culture of reaspirated saline after a 'dry tap', is sensitive and specific for the diagnosis of hip and knee prosthetic joint infection, *Bone Joint J 100–B*749, 2018.

Patel SK, Pratap CB, Jain AK, et al.: Diagnosis of *Helicobacter pylori:* what should be the gold standard? *World J Gastroenterol* 28:12847–12859, 2014.

Peacock JEJ, McGinnis MR, Cohen MS: Persistent neutrophilic meningitis: report of four cases and review of the literature, *Medicine* 63:379, 1984.

Perez-Carceles MD, Noguera J, Jimenez JL, et al.: Diagnostic efficacy of biochemical markers in diagnosis postmortem of ischaemic heart disease, *Forensic Sci Int* 142:1, 2004.

Perkins MD, Mirrett S, Reller LB: Rapid bacterial antigen detection is not clinically useful, *J Clin Microbiol* 33:1486, 1995.

Pettersson T, Klockars M, Weber TH, et al.: Diagnostic value of cerebrospinal fluid adenosine deaminase determination, *Scand J Infect Dis* 23:97, 1991.

Petzold A: The prognostic value of CSF neurofilaments in multiple sclerosis at 15-year follow-up, *J Neurol Neurosurg Psychiatry* 86:1388–1390, 2015.

Petzold A, Worthington V, Appleby I, et al.: Cerebrospinal fluid ferritin level: a sensitive diagnostic test in late-presenting subarachnoid hemorrhage, *J Stroke Cerebrovasc Dis* 20:489, 2011.

Podell TE, Ault M, Sullam P, et al.: Synovial fluid eosinophilia, *Arthritis Rheum* 23:1060, 1980.

Polak M, Torres da Costa AC: Diagnostic value of the estimation of glucose in ascitic fluid, *Digestion* 8:347, 1973.

Policarpio-Nicolas ML, Valente PT: Monosodium urate (gout) crystals: an uncommon finding in ThinPrep synovial fluid cytology, *Diagn Cytopathol* 41:93, 2013.

Pons B, Jay C, Martin T, et al.: Identification of pathogens in synovial fluid samples with an automated multiplexed molecular detection system, *Open Forum Infect Dis* 5(suppl):S678, 2018.

Porcel JM, Bielsa S, Esquerda A, et al.: Pleural fluid C-reactive protein contributes to the diagnosis and assessment of severity of parapneumonic effusions, *Eur J Internal Med* 23:447, 2012.

Porcel JM, Ordi-Ros J, Esquerda A, et al.: Antinuclear antibody testing in pleural fluid for the diagnosis of lupus pleuritis, *Lupus* 16:25, 2007.

Porritt RJ, Mercer JL, Munro R: Detection and serogroup determination of *Neisseria meningitidis* in CSF by polymerase chain reaction (PCR), *Pathology* 32:42, 2000.

Powers W: Cerebrospinal fluid lymphocytosis in acute bacterial meningitis, *Am J Med* 79:216, 1985.

Pratico D, Lee VM, Trojanowski JQ, et al.: Increased F2-isoprostanes in Alzheimer's disease: evidence for enhanced lipid peroxidation in vivo, *FASEB J* 12:1777, 1998.

Presslauer S, Milosavljevic D, Huebl W, et al.: Validation of kappa free light chains as a diagnostic biomarker in multiple sclerosis and clinically isolated syndrome: a multicenter study, *Mult Scler* 22:502–510, 2016.

Pryor JP, Reilly PM, Dabrowski GP, et al.: Nonoperative management of abdominal gunshot wounds, *Ann Emerg Med* 43:344, 2004.

Pupek M, Jasonek J, Katnik-Prastowska I: EDA-containing fibronectin levels in the cerebrospinal fluid of children with meningitis, *Ann Clin Lab Sci* 43:257, 2013.

Quijano S, Lopez A, Sancho J, et al.: Identification of leptomeningeal disease in aggressive B-cell non-Hodgkin's lymphoma: improved sensitivity of flow cytometry, *J Clin Oncol* 27:1462, 2009.

Qvarnstrom Y, Visvesvara GS, Sriram R, et al.: Multiplex real-time PCR for simultaneous detection of *Acanthamoeba* spp., *Balamuthia mandrillaris*, and *Naegleria fowleri*, *J Clin Microbiol* 44:3589, 2006.

Rabinovitch A, Cornbleet PJ: Body fluid microscopy in US laboratories: data from two College of American Pathologists surveys, with practice recommendations, *Arch Pathol Lab Med* 118:13, 1994.

Raff H, Raff JL, Findling JW: Late-night salivary cortisol as a screening test for Cushing's syndrome, *J Clin Endocrinol Metab* 83:2681, 1998.

Ragland SA, Arsura E, Ismail Y, et al.: Eosinophilic pleocytosis in coccidioidal meningitis: frequency and significance, *Am J Med* 95:254, 1993.

Rajantie J, Koskiniemi M, Siimes MA, et al.: CSF fibronectin concentration in Burkitt's lymphoma: an early marker for CNS involvement, *Eur J Haematol* 42:313, 1989.

Rajs G, Finzi-Yeheskel Z, Rajs A, et al.: C-reactive protein concentrations in cerebral spinal fluid in gram-positive and gram-negative bacterial meningitis, *Clin Chem* 48:591, 2002.

Ramers C, Billman G, Hartin M, et al.: Impact of a diagnostic cerebrospinal fluid enterovirus polymerase chain reaction test on patient management, *J Am Med Assoc* 283:2680, 2000.

Rautonen J, Koskiniemi M, Siimes MA, et al.: Elevated cerebrospinal fluid fibronectin concentration indicates poor prognosis in children with acute lymphoblastic leukemia, *Int J Cancer* 43:32, 1989.

Reeves B: Significance of joint fluid uric acid levels in gout, *Ann Rheum Dis* 24:569, 1965.

Reimer LG: Approach to the analysis of body fluids for the detection of infection, *Clin Lab Med* 5:209, 1985.

Reuter H, Burgess L, Van Vurren W, et al.: Diagnosing tuberculous pericarditis, *QJM* 99:827, 2006.

Rhodes CH, Glantz MJ, Glantz L, et al.: A comparison of polymerase chain reaction of cerebrospinal fluid and conventional cytology in the diagnosis of lymphomatous meningitis, *Cancer* 77:543, 1996.

Riantawan P, Chaowalit P, Wongsangiem M, et al.: Diagnostic value of pleural fluid adenosine deaminase in tuberculous pleuritis with reference to HIV coinfection and a Bayesian analysis, *Chest* 116:97, 1999.

Ribeiro MA, Kimura RT, Irulegui I, et al.: Cerebrospinal fluid levels of lysozyme, IgM and C-reactive protein in the identification of bacterial meningitis, *J Trop Med Hyg* 95:87, 1992.

Richard S, Miossec V, Moreau J-F, et al.: Detection of oligoclonal immunoglobulins in cerebrospinal fluid by an immunofixation-peroxidase method, *Clin Chem* 48:167, 2002.

Riemenschneider M, Lautenschlager N, Wagenpfeil S, et al.: Cerebrospinal fluid tau and beta-amyloid 42 proteins identify Alzheimer disease in subjects with mild cognitive impairment, *Arch Neurol* 59:1729, 2002.

Rijken A, Dekker A, Taylor S, et al.: Diagnostic value of DNA analysis in effusions by flow cytometry and image analysis: a prospective study on 102 patients as compared with cytologic examination, *Am J Clin Pathol* 95:6, 1991.

Rockacy M, Khalid A: Update on pancreatic cyst fluid analysis, *Ann Gastroenterol* 26:122–127, 2013.

Rodriguez AF, Kaplan SL, Mason Jr EO: Cerebrospinal fluid values in the very low birth weight infant, *J Pediatr* 116:971, 1990.

Rodriquez-Panadero F, Mejias JL: Low glucose and pH levels in malignant pleural effusions, *Am Rev Respir Dis* 139:663, 1989.

Romero S, Fernandez C, Arriero JM, et al.: CEA, CA 15-3 and CYFRA 21-1 in serum and pleural fluid of patients with pleural effusions, *Eur Respir J* 9:17, 1996.

Rosenthal AK, Mandel N: Identification of crystals in synovial fluids and joint tissues, *Curr Rheumatol Rep* 3:11, 2001.

Rosett W, Hodges GR: Antimicrobial activity of heparin, *J Clin Microbiol* 11:30, 1980.

Rosso F, Michelon C, Sperhacke R, et al.: Evaluation of real-time PCR of patient pleural effusion for diagnosis of tuberculosis, *BMC Res Notes* 4:279, 2011.

Rouah E, Rogers BB, Buffone GJ: Transferrin analysis by immunofixation as an aid in the diagnosis of cerebrospinal fluid otorrhea, *Arch Pathol Lab Med* 111:756, 1987.

Rudick RA, French CA, Breton D, et al.: Relative diagnostic value of cerebrospinal fluid kappa chains in MS: comparison with other immunoglobulin tests, *Neurology* 39:964, 1989.

Runyon BA: Amylase levels in ascitic fluid, *J Clin Gastroenterol* 9:172, 1987a.

Runyon BA: Ascitic fluid bilirubin concentration as a key to choleperitoneum, *J Clin Gastroenterol* 9:543, 1987b.

Runyon BA, Antillon MR: Ascitic fluid pH and lactate: insensitive and nonspecific tests in detecting ascitic fluid infection, *Hepatology* 13:929, 1991.

Runyon BA, Hoefs JC: Ascitic fluid analysis in the differentiation of spontaneous bacterial peritonitis from gastrointestinal tract perforation into ascitic fluid, *Hepatology* 4:447, 1984.

Runyon BA, Hoefs JC, Morgan TR: Ascitic fluid analysis in malignancy-related ascites, *Hepatology* 8:1104, 1988.

Runyon BA, Montano AA, Akriviadis EA, et al.: The serum-ascites albumin gradient is superior to the exudate-transudate concept in the differential diagnosis of ascites, *Ann Intern Med* 117:215–220, 1992.

Ruoslahti E, Engvall E, Hayman EG: Fibronectin: current concepts of its structure and function, *Coll Res* 1:95, 1981.

Ryall RG, Peacock MK, Simpson DA: Usefulness of beta 2-transferrin assay in the detection of cerebrospinal fluid leaks following head injury, *J Neurosurg* 77:737, 1992.

Sahn SA: The differential diagnosis of pleural effusions, *West J Med* 137:99, 1982.

Saeed M, Ahmad M, Iram S, et al.: GeneXpert technology: a breakthrough for the diagnosis of tuberculous pericarditis and pleuritis in less than 2 hours, *Saudi Med J* 38:699, 2017.

Saini PA, Chakrabarti PR, Shilpi D, et al.: Raised adenosine deaminase in the cerebrospinal fluid: a tool for the diagnosis of tuberculous meningitis in developing countries, *Niger Postgrad Med J* 24:56, 2017.

Sanchez-Juan P, Green A, Ladogana A, et al.: CSF tests in the differential diagnosis of Creutzfeldt-Jacob disease, *Neurology* 67:637, 2006.

Santotoribio JD, Alnayef-Hamwie H, Batalha-Caetano P, et al.: Evaluation of pleural fluid lactate for diagnosis and management of parapneumonic pleural effusion, *Clin Lab* 62:1683, 2016.

Sarff LD, Platt LH, McCracken Jr GH: Cerebrospinal fluid evaluation in neonates: comparison of high risk infants with and without meningitis, *J Pediatrics* 88:473, 1976.

Sari R, Yildirim B, Sevinc A, et al.: The importance of serum and ascites fluid alpha-fetoprotein, carcinoembryonic antigen, CA 19-9, and CA 15-3 levels in differential diagnosis of ascites etiology, *Hepato-Gastroenterology* 48:1616, 2001.

Savory J, Brody JP: Measurement and diagnostic value of cerebrospinal fluid enzymes, *Ann Clin Lab Sci* 9:68, 1979.

Schneider D, Halperin R, Langer R, et al.: Peritoneal fluid lactate dehydrogenase in ovarian cancer, *Gynecol Oncol* 66:399, 1997.

Schuurman T, de Boer RF, Kooistra-Smid AMD, et al.: Prospective study of use of PCR amplification and sequencing of 16S ribosomal DNA from cerebrospinal fluid for diagnosis of bacterial meningitis in a clinical setting, *J Clin Microbiol* 42:734, 2004.

Schwake L, von Herbay A, Junghanss T, et al.: Peritoneal tuberculosis with negative polymerase chain reaction results: report of two cases, *Scand J Gastroenterol* 38:221, 2003.

Scott G: *An automated approach to body fluid analysis*, Medical Laboratory Observer, 2014. http://www.mlo-online.com/articles/201406. [Accessed 25 January 2015].

Scrideli C, Queiroz R: Molecular diagnosis of leukemic cerebrospinal fluid cells in children with newly diagnosed acute lymphoblastic leukemia, *Haematologica* 89:1013, 2004.

Seehusen DA, Reeves MM, Fomin DA: Cerebrospinal fluid analysis, *Am Family Physician* 68:1103, 2003.

Sellebjerg F, Christiansen M, Nielsen PM, et al.: Cerebrospinal fluid measures of disease activity in patients with multiple sclerosis, *Mult Scler* 4:475, 1998.

Selvi E, Manganelli S, Catenaccio M, et al.: Diff-Quik staining method for detection and identification of monosodium urate and calcium pyrophosphate crystals in synovial fluids, *Ann Rheum Dis* 60:194, 2001.

Seregni E, Massimino M, Nerini Molteni S, et al.: Serum and cerebrospinal fluid human chorionic gonadotropin (hCG) and alpha-fetoprotein (AFP) in intracranial germ cell tumors, *Int J Biol Markers* 17:112, 2002.

Seres E, Bencsik K, Rajda C, et al.: Diagnostic studies of cerebrospinal fluid in patients with multiple sclerosis [in Hungarian], *Orv Hetil* 139:1905, 1998.

Seward RJ, Towner KJ: Evaluation of a PCR-immunoassay technique for detection of *Neisseria meningitidis* in cerebrospinal fluid and peripheral blood, *J Med Microbiol* 49:451, 2000.

Shephard MD, Whiting MJ: Nephelometric determination of total protein in cerebrospinal fluid and urine using benzalkonium chloride as precipitation reagent, *Ann Clin Biochem* 29:411, 1992.

Sherry NL, Porter JL, Seemann T, et al.: Outbreak investigation using high-throughput genome sequencing within a diagnostic microbiology laboratory, *J Clin Microbiol* 51:1396, 2013.

Shmerling RH: Synovial fluid analysis: a critical reappraisal, *Rheum Dis Clin North Am* 20:503, 1994.

Shmerling RH, Delbanco TL, Tosteson ANA, et al.: Synovial fluid tests. What should be ordered? *J Am Med Assoc* 264:1009, 1990.

Shokry E, Filho NRA: Insights into cerumen and application in diagnostics: past, present and future perspective, *Biochem Med* 27, 030503 2017. https://doi.org/10.11613/BM.2017.030503.

Shokry E, Marques JG, Ragazzo PC, et al.: Earwax as an alternative specimen for forensic analysis, *Forensic Toxicol* 35:348–358, 2017.

Silva-Cardosa J, Moura B, Martins L, et al.: Pericardial involvement in human immunodeficiency virus infection, *Chest* 115:418, 1999.

Silverman LM, Christenson RH: Amino acids and proteins. In Burtis CA, Ashwood ER, editors: *Tietz textbook of clinical chemistry*, ed 2, Philadelphia, 1994, Saunders, p 625.

Simon RP, Abele JS: Spinal-fluid pleocytosis estimated by the Tyndall effect, *Ann Intern Med* 89:75, 1978.

Sindie CJ, Laterte EC: Oligoclonal free kappa and lambda bands in the cerebrospinal fluid, *J Neuroimmunol* 33:63, 1991.

Sioutopoulou D, Kampas L, Gerasimidou K, et al.: Diagnosis of metastatic tumors in cerebrospinal fluid samples using thin-layer cytology, *Acta Cytol* 52:304, 2008.

Skedros DG, Cass SP, Hirsh BE, et al.: Beta-2-transferrin assay in clinical management of cerebral spinal fluid and perilymphatic fluid leaks, *J Otolaryngol* 22:341, 1993a.

Skedros DG, Cass SP, Hirsh BE, et al.: Sources of error in the use of beta-2 transferrin analysis for diagnosing perilymphatic and cerebral spinal fluid leaks, *Otolaryngol Head Neck Surg* 109:861, 1993b.

Slika S Abbas F, Mahfouz R: Implementation of the Cepheid Xpert EV assay for rapid detection of enteroviral meningitis: experience of a tertiary care center and a technical review, *Genet Test Mol Biomarkers* 17:232, 2013.

Sloman AJ, Kelly RH: Transferrin allelic variants may cause false positives in the detection of cerebrospinal fluid fistulae, *Clin Chem* 39:1444, 1993.

Smith A, Wu AHB, Lynch KL, et al.: Multi-wavelength spectrophotometric analysis for detection of xanthochromia in cerebrospinal fluid and accuracy for the diagnosis of subarachnoid hemorrhage, *Clin Chim Acta* 424:231, 2013.

Solari L, Soto A, Agapito J, et al.: The validity of cerebrospinal fluid parameters for the diagnosis of tuberculous meningitis, *Int J Infectious Dis* 17:e1111, 2013.

Sood A, Moudgil A, Sood N, et al.: Role of fibronectin in diagnosis of malignant ascites, *J Assoc Physicians India* 45:283, 1997.

Soriano G, Esparcia O, Montemayor M, et al.: Bacteral DNA in the diagnosis of spontaneous bacterial peritonitis, *Aliment Pharmacol Ther* 33:275, 2011.

Sormunen P, Kallio MJ, Kilpi T, et al.: C-reactive protein is useful in distinguishing Gram stain-negative bacterial meningitis from viral meningitis in children, *J Pediatr* 134:725, 1999.

Souverijn JHM, Smit WG, Peet R, et al.: Intrathecal Ig synthesis: its detection by isoelectric focusing and IgG index, *J Neurol Sci* 93:211, 1989.

Soyka JM, Martin M, Sloan EP, et al.: Diagnostic peritoneal lavage: is an isolated WBC count >500/mm^3 predictive of intra-abdominal injury requiring celiotomy in blunt trauma patients? *J Trauma* 30:874, 1990.

Spanos A, Harrell FEJ, Durack DT: Differential diagnosis of acute meningitis: an analysis of the predictive value of initial observations, *J Am Med Assoc* 262:2700, 1989.

Staats BA, Ellefson RD, Budahn LL, et al.: The lipoprotein profile of chylous and nonchylous pleural effusions, *Mayo Clin Proc* 55:700, 1980.

Stassen WN, McCullough AJ, Bacon BR, et al.: Immediate diagnostic criteria for bacterial infection of ascitic fluid, *Gastroenterology* 90:1247, 1986.

Stearman M, Southgate HJ: The use of cytokine and C-reactive protein measurements in cerebrospinal fluid during acute infective meningitis, *Ann Clin Biochem* 31:255, 1994.

Steele RW, Marmer DJ, O'Brien MD, et al.: Leukocyte survival in cerebrospinal fluid, *J Clin Microbiol* 23:965, 1986.

Steere AC: Borrelia burgdorferi. In Mandell GL, Bennett JE, Dolin R, editors: *Principles and practice of infectious diseases*, ed 7, Philadelphia, 2010, Churchill-Livingstone, p 3077.

Stelzner TJ, King TEJ, Antony VB, et al.: The pleuropulmonary manifestations of the postcardiac injury syndrome, *Chest* 84:383, 1983.

Stewart RJ, Gupta RK, Purdie GI, et al.: Fine catheter aspiration cytology of peritoneal cavity improves decision-making about difficult cases of acute abdominal pain, *Lancet* 2:1414, 1986.

Stewart RV, Zumwalt RE, Hirsch CS, et al.: Postmortem diagnosis of myocardial disease by enzyme analysis of pericardial fluid, *Am J Clin Pathol* 82:411, 1984.

Strik H, Luthe H, Nagel I, et al.: Automated cerebrospinal fluid cytology: limitations and reasonable applications, *Analyt Quant Cytol Histol* 27(1), 2005.

Suay VG, Moragon EM, Viedma EC, et al.: Pleural cholesterol in differentiating transudates and exudates, *Respiration* 62:57, 1995.

Such J, Frances R, Munoz C, et al.: Detection and identification of bacterial DNA in patients with cirrhosis and culture-negative nonneutrocytic ascites, *Hepatology* 36:135, 2002.

Sullivan KR, Nelson MJ, Tandberg D: Incremental analysis of diagnostic peritoneal lavage fluid in adult abdominal trauma, *Am J Emerg Med* 15:277, 1997.

Sumedha D, Nag D, Nandi A, et al.: Utility of cell block to detect malignancy in fluid cytology: adjunct or necessity? *J Cancer Research Therapeutics* 13:425, 2017.

Sunderland T, Linker G, Mirza N, et al.: Decreased beta-amyloid1-42 and increased tau levels in cerebrospinal fluid of patients with Alzheimer disease, *J Am Med Assoc* 289:2094, 2003.

Suzuki Y, Tanaka R: Carcinoembryonic antigen in patients with intracranial tumors, *J Neurosurg* 53:355, 1980.

Taj A, Jamil N: Cerebrospinal fluid concentrations of biogenic amines: potential biomarker for diagnosis of bacterial and viral meningitis, *Pathogens* 7:39, 2018.

Tamarappoo BK, Klein AL: Post-pericardiotomy syndrome, *Curr Cardiol Rep* 18:116, 2016.

Tang LM: Serial lactate determinations in tuberculous meningitis, *Scand J Infect Dis* 20:81, 1988.

Tangkijvanich P, Tresukolos D, Sanpatamukul P, et al.: Telomerase assay for differentiating between malignancy-related and nonmalignant ascites, *Clin Cancer Res* 5:2470, 1999.

Tarn AC, Lapworth R: Biochemical analysis of ascitic (peritoneal) fluid: what should we measure? *Ann Clin Biochem* 47:397, 2010.

Tay TR, Tee A: Factors affecting pleural fluid adenosine deaminase level and the implication on the diagnosis of tuberculous pleural effusion: a retrospective cohort study, *BMC Infect Dis* 13:546, 2013.

Tenenbaum T, Heusch A, Henrich B, et al.: Acute hemorrhagic pericarditis in a child with pneumonia due to *Chlamydophila pneumoniae*, *J Clin Microbiol* 43:520, 2005.

Thangarajh M, Gomez-Rial J, Hedstrom AK, et al.: Lipid-specific immunoglobulin M in CSF predicts adverse long-term outcome in multiple sclerosis, *Mult Scler* 14:1208–1213, 2008.

Theiler G, Quehenberger F, Rainer F, et al.: The detection of calcium pyrophosphate crystals in the synovial fluid of patients with rheumatoid arthritis using the cytospin technique: prevalence and clinical correlation, *Rheumatol Int* 34:137, 2014.

Thwaites GE, Chau TT, Farrar JJ: Improving the bacteriological diagnosis of tuberculous meningitis, *J Clin Microbiol* 42:378, 2004.

Tian C, Shi Q, Pu C, et al.: Re-evaluation of the significance of cerebrospinal fluid human chorionic gonadotropin in detecting intracranial ectopic germinomas, *J Clin Neurosci* 18:223, 2011.

Titov AG, Vyshnevskaya EB, Mazurenko SI, et al.: Use of polymerase chain reaction to diagnose tuberculous arthritis from joint tissues and synovial fluid, *Arch Pathol Lab Med* 128:205, 2004.

Topolcan O, Holubec L, Polivkova V, et al.: Tumor markers in pleural effusions, *Anticancer Res* 27:1921, 2007.

Torre D, Zeroli C, Ferrario G, et al.: Cerebrospinal fluid concentration of fibronectin in HIV-1 infection and central nervous system disorders, *J Clin Pathol* 46:1039, 1993.

Torre D, Zeroli C, Issi M, et al.: Cerebrospinal fluid concentration of fibronectin in meningitis, *J Clin Pathol* 44:783, 1991.

Tourtellotte WW, Staugaitis SM, Walsh MJ, et al.: The basis of intra-blood–brain barrier IgG synthesis, *Ann Neurol* 17:21, 1985.

Tourtellotte WW, Tavolato B, Parker JA, et al.: Cerebrospinal fluid electroimmunodiffusion, *Arch Neurol* 25:345, 1971.

Trbojevic-Cepe M, Vogrinc Z, Brinar V: Diagnostic significance of methemoglobin determination in colorless cerebrospinal fluid, *Clin Chem* 38:1401, 1992.

Trotter JL, Rust RS: Human cerebrospinal fluid immunology. In Herndon RM, Brumback RA, editors: *The cerebrospinal fluid*, Boston, 1989, Kluwer Academic Publishers, p 179.

Tubergen DG, Cullen JW, Boyett JM, et al.: Blasts in CSF with a normal cell count do not justify alteration of therapy for acute lymphoblastic leukemia in remission. A Children's Cancer Group study, *J Clin Oncol* 12:273, 1994.

Tunkel AR: The management of encephalitis: clinical practice guidelines by the Infectious Diseases Society of America, *Clin Infect Dis* 47:303, 2008.

Turay UY, Yildirim Z, Turkoz Y, et al.: Use of pleural fluid C-reactive protein in diagnosis of pleural effusions, *Respir Med* 94:432, 2000.

Twijnstra A, Nooyen WJ, van Zanten AP, et al.: Cerebrospinal fluid carcinoembryonic antigen in patients with metastatic and nonmetastatic neurological diseases, *Arch Neurol* 43:269, 1986.

Tyler KL: Herpes simplex virus infections of the central nervous system: encephalitis and meningitis, including Mollaret's, *Herpes* 11(Suppl 2):57A, 2004.

UK National External Quality Assessment Scheme for Immunochemistry Working Group: National guidelines for the analysis of cerebrospinal fluid for bilirubin in suspected subarachnoid hemorrhage, *Ann Clin Biochem* 40:481, 2003.

Vaidya B, Bhochhibhoya M, Nakarmi S: Synovial fluid uric acid level aids diagnosis of gout, *Biomed Rep* 9:60, 2018.

Vanichanan J, Salazar L, Wootton SH, et al.: Use of testing for West Nile virus and other arboviruses, *Emerg Infect Dis* 22:1587, 2016.

Varga G, Mikala G, Gopcsa L, et al.: Multiple myeloma of the central nervous system: 13 cases and review of the literature, *J Oncol* 1:2018, 2018.

Vaughn DW, Barrett A, Solomon T: Flaviviruses. In Mandell GL, Bennett JE, Dolin R, editors: *Principles and practice of infectious diseases*, ed 7, Philadelphia, 2010, Churchill-Livingstone, p 2148.

Vaughan J, Ngamtrakulpanit L, Pajewski TN, et al.: Exhaled breath condensate pH is a robust and reproducible assay of airway acidity, *Eur Respir J* 22:889–894, 2003.

Verettas D, Kazakos C, Tilkeridis C, et al.: Polymerase chain reaction for the detection of *Mycobacterium tuberculosis* in synovial fluid, tissue samples, bone marrow aspirate and peripheral blood, *Acta Orthop Belg* 69:396, 2003.

Villar L, Sabada MC, Roldan E, et al.: Intrathecal synthesis of oligoclonal IgM against myelin lipids predicts an aggressive disease course in MS, *J Clin Invest* 115:187–194, 2005.

Villena V, Lopez-Encuentra A, Echave-Sustaeta J, et al.: Diagnostic value of CA 72-4, carcinoembryonic antigen, CA 15-3, and CA 19-9 assay of pleural fluid: a study of 207 patients, *Cancer* 78:736, 1996a.

Villena V, Lopez-Encuentra A, Echave-Sustaeta J, et al.: Interferon-gamma in 388 immunocompromised and immunocompetent patients for diagnosing pleural tuberculosis, *Eur Respir J* 9:2635, 1996b.

Villena V, Lopez-Encuentra A, Echave-Sustaeta J, et al.: Diagnostic value of CA 549 in pleural fluid: comparison with CEA, CA 15-3 and CA 72-4, *Lung Canc* 40:289, 2003a.

Villena V, Lopez-Encuentra A, Pozo F, et al.: Interferon gamma levels in pleural fluid for the diagnosis of tuberculosis, *Am J Med* 115:365, 2003b.

Visvesvara GS: Amebic meningoencephalitides and keratitis: challenges in diagnosis and treatment, *Curr Opin Infect Dis* 23:590, 2010.

Walker TJ, Nelson LD, Dunphy BW, et al.: Comparative evaluation of the IRIS iQ200 body fluid module with manual hemacytometer count, *Am J Clin Pathol* 131:333, 2009.

Walts AE: Cerebrospinal fluid cytology: selected issues, *Diagn Cytopathol* 8:394, 1992.

Wang DY, Yang PC, Yu WL, et al.: Serial antinuclear antibodies titre in pleural and pericardial fluid, *Eur Respir J* 15:1106, 2000.

Ward E, Gushurst CA: Uses and techniques of pediatric lumbar puncture, *Am J Dis Child* 146:1160, 1992.

Weinburger A, Simkin PA: Plasma proteins in synovial fluids of normal human joints, *Semin Arthritis Rheum* 19:66, 1989.

Welch KM, Chabi E, Bartosh K, et al.: Cerebrospinal fluid gamma aminobutyric acid level in migraine, *Br Med J* 30:516, 1975.

Weller M, Sommer N, Stevens A, et al.: Increased intrathecal synthesis of fibronectin in bacterial and carcinomatous meningitis, *Acta Neurol Scand* 82:138, 1990.

Weller M, Stevens A, Sommer N, et al.: Humoral CSF parameters in the differential diagnosis of hematologic CNS neoplasia, *Acta Neurol Scand* 86:129, 1992.

Wenger JD, Hightower AW, Broome CV, et al: Bacterial meningitis in the United States: report of a multistate surveillance study, 1986, J Infect Dis 162:1316, 1990.

Whitehouse JS, Weigelt JA: Diagnostic peritoneal lavage: a review of indications, technique, and interpretation, *Scad J Trauma Resusc Emerg Med* 17:13, 2009.

Wilson ML: Clinically relevant, cost-effective clinical microbiology: strategies to decrease unnecessary testing, *Am J Pathol* 107:154, 1997.

Wilson MR, Naccache SN, Samayoa E, et al.: Actionable diagnosis of neuroleptospirosis by next-generation sequencing, *N Eng J Med* 370:2408, 2014.

Wilson MR, Sample HA, Zorn KC, et al.: Clinical metagenomic sequencing for diagnosis of meningitis and encephalitis, *N Engl J Med* 380:2327, 2019.

Wise CM, White RE, Agudelo CA: Synovial fluid lipid abnormalities in various disease states: review and classification, *Semin Arthritis Rheum* 16:222, 1987.

Wood JH: *Neurobiology of CSF*, New York, 1980, Plenum Press.

Wood P: Salivary steroid assays—research or routine? *Ann Clin Biochem* 46:183, 2009.

Wu SS, Lin OS, Chen YY, et al.: Ascitic fluid carcinoembryonic antigen and alkaline phosphatase levels for the differentiation of primary from secondary bacterial peritonitis with intestinal perforation, *J Hepatol* 34:215, 2001.

Wubbel L, McCracken Jr GH: Management of bacterial meningitis, *Pediatr Rev* 19:78, 1998.

Xu HB, Jiang RH, Li L, et al.: Diagnostic value of adenosine deaminase in cerebrospinal fluid for tuberculous meningitis: a meta-analysis, *Int J Tuberc Lung Dis* 14:1382, 2010.

Yang D, Zhou Y, Chen B: Performance evaluation and result comparison of the automated hematology analyzers Abbott CD 3700, Sysmex XE 2100 and the Coulter LH 750 for cell counts in serous fluids, *Clin Chim Acta* 419:113, 2013.

Yorgancioglu A, Akin M, Dereli S, et al.: The diagnostic value of tuberculostearic acid in tuberculous pleural effusions, *Monaldi Arch Chest Dis* 51:108, 1996.

Yuan S, Bien C, Wener MH, et al.: Repeat examination of synovial fluid for crystals: is it useful? *Clin Chem* 49:1562, 2003.

Zandman-Goddard G, Matzner Y, Konijn AM, et al.: Cerebrospinal fluid ferritin in malignant CNS involvement, *Cancer* 58:1146, 1986.

Zaret DL, Morrison N, Gullbranson R, et al.: Immunofixation to quantify beta-2-transferrin in cerebrospinal fluid from skull injury, *Clin Chem* 38:1909, 1992.

Zerr I, Bodemer M, Gefeller O, et al.: Detection of 14-3-3 protein in the cerebrospinal fluid supports the diagnosis of Creutzfeldt-Jakob disease, *Ann Neurol* 43:32, 1998.

Zunt JR, Marra CM: Cerebrospinal fluid testing for the diagnosis of central nervous system infection, *Neurol Clin* 17:675, 1999.

PART 4

Hematology and Transfusion Medicine

EDITED BY | Robert E. Hutchison, Katalin Banki, Richard A. McPherson

CHAPTER 31

BASIC EXAMINATION OF BLOOD AND BONE MARROW

Neerja Vajpayee, Susan S. Graham, Sylva Bem

HEMATOLOGY PRINCIPLES AND PROCEDURES, 540
Hemoglobin, 540
Hematocrit (Packed Cell Volume), 542
Erythrocyte Indices, 543
Manual Blood Cell Counts, 544
Instrument Technology, 549

BLOOD FILM EXAMINATION, 551
Examination of Wet Preparations, 551
Making and Staining Blood Films, 551
Erythrocytes, 552
Erythrocyte Sedimentation Rate, 562

BONE MARROW EXAMINATION, 563
Indications For Marrow Study, 564
Preparation of The Aspirate and Biopsy Section, 564
Staining Marrow Preparations, 564
Examination of Marrow, 565

SELECTED REFERENCES, 569

KEY POINTS

- Assessment of erythrocyte, leukocyte, and platelet counts from manual and automated particle counters is central to the diagnosis and management of hematologic disease.
- With few exceptions, manual methods have been replaced by automated hematology analyzers. The selection of analyzers is varied and voluminous enough to meet the needs of any hematology laboratory setting.
- Hematology automation combined with sophisticated algorithms for data interpretation has led to dramatic improvement in the utility of automated analyzers in patient care. Newer instrumentation has progressed far beyond the screening tools of the past.
- Examination of peripheral blood with bone marrow smear/biopsy represents the cornerstone of hematologic diagnosis. Bone marrow examination provides a semiquantitative and qualitative assessment of the state of hematopoiesis and aids in the diagnosis of several hereditary and acquired benign and malignant diseases.

Hematology includes the study of blood cells and coagulation. It encompasses analyses of the concentration, structure, and function of cells in blood; their precursors in the bone marrow; the chemical constituents of plasma or serum intimately linked with blood cell structure and function; and the function of platelets and proteins involved in blood coagulation. Advancement of molecular biological techniques and their increased use in hematology have led to the detection of several genetic mutations underlying the altered structure and function of cells and proteins that may result in hematologic disease.

HEMATOLOGY PRINCIPLES AND PROCEDURES

HEMOGLOBIN

Hemoglobin (Hb), the main component of the red blood cell (RBC), is a conjugated protein that serves as the vehicle for the transportation of oxygen (O_2) and carbon dioxide (CO_2). When fully saturated, each gram of Hb holds 1.34 mL of O_2. The red cell mass of the adult contains approximately 600 g of Hb, capable of carrying 800 mL of O_2. A molecule of Hb consists of two pairs of polypeptide chains ("globins") and four prosthetic heme groups, each containing one atom of ferrous iron. Each heme group is precisely located in a pocket or fold of one of the polypeptide chains. Located near the surface of the molecule, the heme reversibly combines with one molecule of O_2 or CO_2. The main function of Hb is to transport O_2 from the lungs, where O_2 tension is high, to the tissues, where it is low. At an O_2 tension of 100 mm Hg in the pulmonary capillaries, 95% to 98% of the Hb is combined with O_2. In the tissues, where O_2 tension may be as low as 20 mm Hg, the O_2 readily dissociates from Hb; in this instance, less than 30% of the O_2 would remain combined with Hb.

Reduced Hb is Hb with iron unassociated with O_2. When each heme group is associated with one molecule of O_2, the Hb is referred to as *oxyhemoglobin (HbO_2)*. In both Hb and HbO_2, iron remains in the ferrous state. When iron is oxidized to the ferric state, methemoglobin (hemiglobin [Hi]) is formed, and the molecule loses its capacity to carry O_2 or CO_2.

Anemia is a decrease to below normal Hb concentration, erythrocyte count, or hematocrit (Hct). It is a very common condition and is frequently a complication of other diseases. Clinical diagnosis of anemia or of high Hb based on estimation of the color of the skin and of visible mucous membranes is highly unreliable. The correct estimation of Hb is important and is one of the routine tests performed on practically every patient.

Hemoglobin Derivatives

Hemiglobin (Methemoglobin)

Methemoglobin (Hi) is a derivative of Hb in which the ferrous iron is oxidized to the ferric state, resulting in the inability of Hi to combine reversibly with O_2. The polypeptide chains are not altered. A normal individual has up to 1.5% methemoglobin. Methemoglobinemia will cause chocolate-brown discoloration of blood, cyanosis, and functional "anemia" if present in high enough concentrations. Cyanosis becomes obvious at a concentration of about 1.5 g Hi/dL (i.e., 10% of Hb). Comparable degrees of cyanosis will be caused by 5 g Hb/dL of blood, 1.5 g Hi/dL of blood, and 0.5 g sulfhemoglobin (SHb)/dL of blood. The degree of cyanosis, however, is not necessarily correlated with the concentration of Hi. A small amount of Hi is always being formed but is reduced by enzyme systems within the erythrocyte. The most important is the NADH (reducing agent derived from nicotinamide adenine dinucleotide)-dependent methemoglobin reductase system (NADH-cytochrome-b_5 reductase). Others, which may function mainly as reserve systems, are ascorbic acid, reduced glutathione, and reduced nicotinamide adenine dinucleotide phosphate (NADPH)–methemoglobin reductase. The latter requires a natural cofactor or an auto-oxidizable dye such as methylene blue for activity. NADPH is an essential cofactor for maintaining intracellular glutathione in the reduced state so that hemoglobin iron remains in the ferrous state.

Methemoglobinemia, an increased amount of Hi in the erythrocytes, may result from increased production of Hi or decreased NADH-cytochrome-b_5 reductase activity, and may be hereditary or acquired (Jaffé & Hultquist, 1989). The hereditary form is divided into two major categories. In the first, methemoglobinemia is due to a decrease in the capacity of the erythrocyte to reduce the Hi that is constantly being formed back to Hb. This is most often due to *NADH-cytochrome-b_5 reductase deficiency*, which is inherited as an autosomal-recessive characteristic. The homozygote has methemoglobin levels of 10% to 50% and is cyanotic. Only occasionally is polycythemia present as a compensating mechanism.

Hi concentrations of 10% to 25% may give no apparent symptoms; levels of 35% to 50% result in mild symptoms, such as exertional dyspnea and headaches; and levels exceeding 70% are probably lethal. Therapy with ascorbic acid or methylthioninium chloride (methylene blue) in this form of hereditary methemoglobinemia will reduce the level of Hi, the latter apparently by activation of the NADPH–methemoglobin reductase system. Heterozygotes have intermediate levels of NADH-cytochrome-b_5 reductase activity and normal blood levels of Hi. They may become cyanotic because of methemoglobinemia after exposure to oxidizing chemicals or drugs in amounts that will not affect normal individuals.

In the second major category of hereditary methemoglobinemia, the reducing systems within the erythrocyte are intact but the structure of the Hb molecule itself is abnormal. A genetically determined alteration in the amino acid composition of α- or β-globin chains may form a Hb molecule that has an enhanced tendency toward oxidation and a decreased propensity of the methemoglobin formed to be reduced back to Hb. Their principal consequence is asymptomatic cyanosis as a result of methemoglobinemia; they are designated as various forms of *hemoglobin M (Hb M)*. In six of the seven Hb M variants, tyrosine is substituted for histidine in the heme pocket of the proximal or distal globin chain. Nagai & Mawatari (1995) showed by spectroscopy that a considerable proportion of the mutant subunits of Hb M Saskatoon and Hb M Boston stay in the fully reduced form under circulation conditions. They are inherited as autosomal-dominant traits (Lukens, 2004). Methylthioninium chloride therapy in these individuals is without effect and treatment is not necessary.

Most cases of methemoglobinemia are classified as secondary or acquired, due mainly to exposure to drugs and chemicals that cause increased formation of Hi. Chemicals or drugs that directly oxidize HbO_2 to Hi include nitrites, nitrates, chlorates, and quinones. Other substances, which are aromatic amino and nitro compounds, probably act indirectly through a metabolite because they do not cause Hi formation in vitro. These include acetanilid, phenacetin, sulfonamides, and aniline dyes. Ferrous sulfate may produce methemoglobinemia after ingestion of very large doses. Levels of drugs or chemicals that would not cause significant methemoglobinemia in a normal individual may do so in someone with a mild reduction in NADH-cytochrome-b_5 reductase activity that, under ordinary circumstances, is not cyanotic. Such individuals are newborn infants and persons heterozygous for NADH-cytochrome-b_5 reductase deficiency (Bunn & Forget, 1986). Hi is reduced back to Hb by the erythrocyte enzyme systems. It can also be reduced (slowly) by the administration of reducing agents, such as ascorbic acid or sulfhydryl compounds (glutathione, cysteine); these, as well as methylthioninium chloride, are of value in cases of hereditary NADH-cytochrome-b_5 reductase deficiency. In cases of acquired or toxic methemoglobinemia, methylthioninium chloride is of great value; its rapid action is based not on its own reduction capacity but on its acceleration of the normally slow NADPH–methemoglobin reductase pathway. Hi can combine reversibly with various chemicals (e.g., cyanides, sulfides, peroxides, fluorides, azides). Because of the strong affinity of Hi for cyanide, the therapy of cyanide poisoning is to administer nitrites to form Hi, which then combines with the cyanide. Thus, the free cyanide (which is extremely poisonous to the cellular respiratory enzymes) becomes less toxic when changed to HiCN.

Hi is quantitated by spectrophotometry. If Hi is elevated, drugs or toxic substances must first be eliminated as a cause. Congenital methemoglobinemia due to NADH-cytochrome-b_5 reductase deficiency is determined by assay of the enzyme. An abnormal hemoglobin (Hb M) may also be responsible for methemoglobinemia noted at birth or in the first few months of life.

Sulfhemoglobin

SHb is a mixture of oxidized, partially denatured forms of Hb that form during oxidative hemolysis (Jandl, 1996). During oxidation of Hb, sulfur (the source of which may vary) is incorporated into heme rings of Hb, resulting in a green hemochrome. Further oxidation usually results in the denaturation and precipitation of Hb as Heinz bodies (Fig. 31.1). SHb cannot transport O_2, but it can combine with carbon monoxide (CO) to form carboxysulfhemoglobin. Unlike methemoglobin, SHb cannot be reduced back to Hb, and it remains in the cells until they break down. The blood is mauve-lavender in sulfhemoglobinemia. SHb has been reported in patients receiving treatment with sulfonamides or aromatic amine drugs (phenacetin, acetanilid), as well as in patients with severe constipation, in cases of bacteremia due to *Clostridium perfringens* and in a condition known as *enterogenous cyanosis*. The concentration of SHb in vivo normally is less than 1%, and in these conditions it seldom exceeds 10% of the total Hb. It results in cyanosis and is usually asymptomatic. The reason why some patients develop methemoglobinemia, some sulfhemoglobinemia, and others Heinz bodies and hemolysis is not well understood. SHb is quantitated by spectrophotometry.

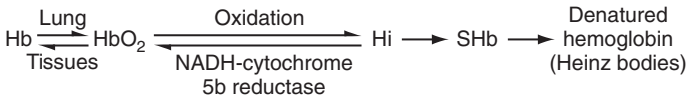

Figure 31.1 Simplified concept of oxidation of hemoglobin (Hb) to methemoglobin (Hi), as proposed by Jandl (1996). Reversible binding and release of oxygen occur in lungs and tissues; oxidation of ferrous ions and formation of Hb are reversible in the red cell to a limited extent; continued oxidation leads to irreversible conformational changes and sulfhemoglobin; still further oxidation results in denaturation of the Hb and precipitation within the erythrocyte as Heinz bodies. *HbO_2,* Oxyhemoglobin; *NADH,* reduced nicotinamide adenine dinucleotide; *SHb,* sulfhemoglobin.

Carboxyhemoglobin

Endogenous CO produced in the degradation of heme to bilirubin normally accounts for about 0.5% of carboxyhemoglobin (HbCO) in the blood and is increased in hemolytic anemia. Hb has the capacity to combine with CO with an affinity 210 times greater than for O_2. CO will bind with Hb even if its concentration in the air is extremely low (e.g., 0.02%–0.04%). In those cases, HbCO will build up until typical symptoms of poisoning appear. HbCO cannot bind and carry O_2. Furthermore, increasing concentrations of HbCO shift the Hb-O_2 dissociation curve increasingly to the left, thus adding to the anoxia. If a patient poisoned with CO receives pure O_2, the conversion of HbCO to HbO_2 is greatly enhanced. HbCO is light sensitive and has a typical brilliant cherry-red color.

Acute CO poisoning is well known. It produces tissue hypoxia as a result of decreased O_2 transport. Chronic poisoning, a result of prolonged exposure to small amounts of CO, is less well recognized but is of increasing importance. The chief sources of the gas are gasoline motors, illuminating gas, gas heaters, defective stoves, and the smoking of tobacco. Exposure to CO is thus one of the hazards of modern civilization. The gas has even been found in the air of busy streets of large cities in sufficient concentration to cause mild symptoms in persons such as traffic police officers, who are exposed to it over long periods of time. Chronic exposure through tobacco smoking may lead to chronic elevation of HbCO and an associated left shift in the Hb-O_2 dissociation curve; smokers tend to have higher Hcts than nonsmokers and may have polycythemia. Healthy persons exposed to various concentrations of the gas for 1 hour do not experience definite symptoms (headache, dizziness, muscular weakness, and nausea) unless the concentration of gas in the blood reaches 20% to 30% of saturation; however, it appears that in chronic poisoning, especially in children, serious symptoms may occur with lower concentrations. HbCO may be quantitated by differential spectrophotometry or by gas chromatography.

Measurement of Hemoglobin Concentration (Manual Technique of Hemoglobinometry)

The cyanmethemoglobin (hemiglobincyanide; [HiCN]) method has the advantages of convenience and a readily available, stable standard solution.

Hemiglobincyanide Method

Principle. Blood is diluted in a solution of potassium ferricyanide and potassium cyanide. The potassium ferricyanide oxidizes Hb to Hi (methemoglobin), and potassium cyanide provides cyanide ions (CN^-) to form HiCN, which has a broad absorption maximum at a wavelength of 540 nm (Fig. 31.2; Table 31.1). The absorbance of the solution is measured in a spectrophotometer at 540 nm and is compared with that of a standard HiCN solution.

Reagent. The diluent is detergent-modified Drabkin reagent:

0.20 g Potassium ferricyanide ($K_3Fe[CN]_6$)
0.05 g Potassium cyanide (KCN)
0.14 g Dihydrogen potassium phosphate (anhydrous; KH_2PO_4)
Nonionic detergent, for example,
0.5 mL Sterox S.E. (Harleco) *or*
1.0 mL Triton X-100 (Rohm and Haas)
Distilled water to 1000 mL

The solution should be clear and pale yellow, have a pH of 7.0 to 7.4, and give a reading of zero when measured in the photometer at 540 nm against a water blank.

Substituting dihydrogen potassium phosphate (KH_2PO_4) in this reagent for sodium bicarbonate ($NaHCO_3$) in the original Drabkin reagent shortens the time needed for complete conversion of Hb to HiCN from 10 minutes to 3 minutes. The detergent enhances lysis of erythrocytes and decreases turbidity from protein precipitation.

Care must be taken with KCN in the preparation of the Drabkin solution, as salts or solutions of cyanide are poisonous. The diluent itself contains only 50 mg KCN/L—less than the lethal dose for a 70-kg person. However, because hydrogen cyanide (HCN) is released by acidification, exposure of the diluent to acid must be avoided. Disposal of reagents and samples in running water in the sink is advised. The diluent keeps well in a dark bottle at room temperature but should be prepared fresh periodically.

Method. To 5.0 mL of diluent, 20 µL of blood is added (1:251), mixed well, and allowed to stand at room temperature for at least 3 minutes (Dacie & Lewis, 1991). The absorbance is measured against the reagent blank in the photoelectric colorimeter at 540 nm or with an appropriate filter. A vial of HiCN standard is then opened and the absorbance measured, at room temperature, in the same instrument in a similar fashion. The test sample must be analyzed within a few hours of dilution. The standard must be kept in the dark when not in use and discarded at the end of the day.

$$\text{Hb (g/dL)} = \left[A^{540}\text{ test sample}/A^{540}\text{ standard}\right] \times [\text{Concentration of standard (mg/dL)}/100\text{ mg/g}] \times 251$$

It is usually convenient to calibrate the photometer to be used for hemoglobinometry by preparing a standard curve or table that will relate absorbance to Hb concentration in grams per deciliter. The absorbance of fresh HiCN standard is measured against a reagent blank. Absorbance readings are made of fresh HiCN standard and of dilutions of this standard in the reagent (1 in 2, 1 in 3, and 1 in 4) against a reagent blank. Hb values in grams per deciliter are calculated for each solution as described previously. When the absorbance readings are plotted on linear graph paper as the ordinates against Hb concentration as the abscissa, the points should describe a straight line that passes through the origin. An advantage of the HiCN method is that most forms of hemoglobin (Hb, HbO_2, Hi, and HbCO, but not SHb) are measured.

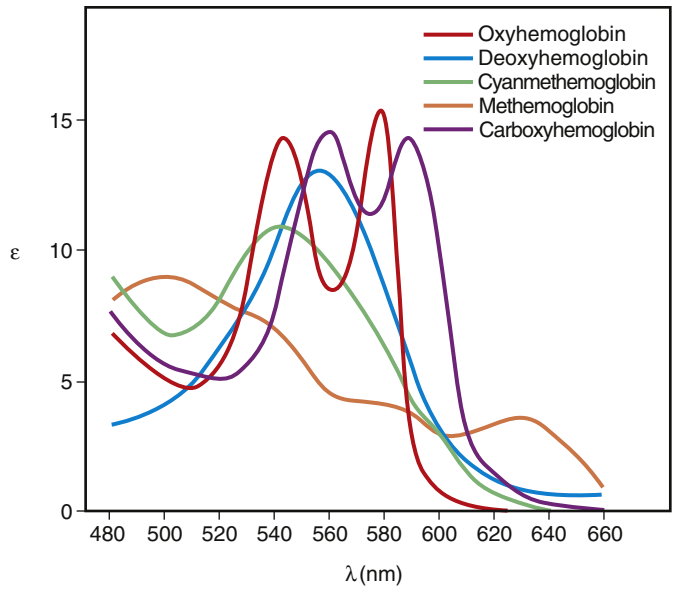

Figure 31.2 Absorption spectra of oxyhemoglobin (HbO_2), deoxyhemoglobin (Hb), methemoglobin (hemiglobin [Hi]), and cyanmethemoglobin (hemiglobincyanide [HiCN]) (From Morris MW, Skrodzki Z, Nelson DA: Zeta sedimentation ratio [ZSR], a replacement for the erythrocyte sedimentation rate [ESR], *Am J Clin Pathol* 64:254–256, 1975. © 1975 American Society for Clinical Pathology.)

The test sample can be directly compared with the HiCN standard, and the readings can be made at the convenience of the operator because of the stability of the diluted samples. Increased absorbance not due to Hb may be caused by turbidity due to abnormal plasma proteins, hyperlipemia, large numbers of leukocytes (counts >30 × 10^9/L), or fatty droplets, any of which may lead to increased light scattering and apparent absorbance.

Errors in Hemoglobinometry

Sources of error may be those of the sample, the method, the equipment, or the operator.

Errors Inherent in the Sample. Improper venipuncture technique may introduce hemoconcentration, which will make Hb concentration and cell counts too high. Improper technique in fingerstick or capillary sampling can produce errors in either direction.

Errors Inherent in the Method. The HiCN method is the method of choice. Use of the HiCN standard for calibration of the instrument and for the test itself eliminates a major source of error. The broad absorption band of HiCN in the region of 540 nm makes it convenient to use both in filter-type photometers and in narrow-band spectrophotometers. With the exception of SHb, all other varieties of hemoglobin are converted to HiCN. Since the total non-sulfohemoglobin concentration is known and since the molar extinction coefficient for each type of hemoglobin is known at a number of different wavelengths, the concentration of sulfohemoglobin can be directly determined at any one of these wavelengths using Beer's Law (Chapter 4).

Errors Inherent in the Equipment. The accuracy of equipment is not uniform. A good grade of pipet with a guaranteed accuracy of greater than 99% is desirable. Calibration of pipets will lessen errors. Significant error can be introduced by the use of unmatched cuvets; therefore, flow-through cuvets are preferred. The wavelength settings, filters, and meter readings require checking. The photometer must be calibrated in the laboratory before its initial use and must be rechecked frequently to reduce the method's error to 2% (±CV).

Automated equipment is now widely used and eliminates most errors associated with manual techniques of hemoglobinometry.

Spectrophotometric Identification of Hemoglobins

The various Hbs have characteristic absorption spectra, which can be determined easily with a spectrophotometer. Useful absorbance maxima are given in Table 31.1. The maxima for Hi vary considerably with pH. The maxima given in the two right-hand columns are useful for distinguishing among these forms of Hb. Absorbance between 405 and 435 nm (the Soret band) is considerably greater and may be used when small concentrations of Hb are to be measured.

HEMATOCRIT (PACKED CELL VOLUME)

The Hct of a sample of blood is the ratio of the volume of erythrocytes to that of the whole blood. It may be expressed as a percentage (conventional) or as a decimal fraction (SI units). The units L/L are implied. Dried heparin and ethylenediaminetetraacetic acid (EDTA) are satisfactory anticoagulants. Before taking a sample from a tube of venous blood for a hematologic determination, it is important to mix the blood thoroughly. If the tube has been standing, this requires at least 60 inversions of the tube, or 2 minutes on a mechanical rotator; less than this leads to unacceptable deterioration in precision (Fairbanks et al., 1971). The number of inversions required to achieve homogeneity of a specimen depends on the dimensions of the container. Standard 10 to 14 × 75-mm tubes, containing 5 mL of blood

TABLE 31.1
Nomenclature and Absorption Maxima of Hemoglobins

		ABSORPTION PEAK 1		ABSORPTION PEAK 2		ABSORPTION PEAK 3	
Term	**Symbol**	λ*	ε	λ	ε	λ	ε
Hemoglobin	Hb	431	(140)	555	(13.04)		
Oxyhemoglobin	HbO_2	415	(131)	542	(14.37)	577	(15.37)
Carboxyhemoglobin	HbCO	420	(192)	539	(14.36)	568.5	(14.31)
Hemiglobin (methemoglobin)	Hi	406	(162)	500	(9.04)	630	(3.70)
Hemiglobincyanide (cyanmet Hb)	HiCN	421	(122.5)	540	(10.99)		

Data from van Assendelft OW (1970).The wavelength (λ) in nanometers for each maximum is followed by the extinction coefficient (ε)in parentheses.
*These wavelengths are not shown in the absorption spectrum in Fig. 31.2. because the hemoglobins have much higher absorbances (i.e., the Soret band region).

and an air bubble that constitutes at least 20% of the tube volume, require at least eight inversions (National Committee for Clinical Laboratory Standards [NCCLS], 1993). The venous Hct agrees closely with the Hct obtained from a skin puncture; both are greater than the total body Hct. The Hct may be measured directly by centrifugation with macromethods or micromethods, or indirectly as the product of the mean corpuscular volume (MCV) times RBC count in automated instruments. In blood kept at room temperature, swelling of erythrocytes between 6 and 24 hours raises Hct and MCV. Cell counts and indices are stable for 24 hours at 4°C (Brittin et al., 1969).

Gross Examination

Hct determination is performed by centrifugation. Inspection of the specimen after spinning may furnish valuable information. The relative heights of the red cell column, buffy coat, and plasma column should be noted. The buffy coat is the red-gray layer between the red cells and the plasma; it includes platelets and leukocytes.

An orange or green color of the plasma suggests increased bilirubin; pink or red suggests hemoglobinemia. Poor technique in collecting the blood specimen is the most frequent cause of hemolysis. If specimens are not obtained within 1 or 2 hours after a fat-rich meal, cloudy plasma may point to nephrosis or certain abnormal hyperglobulinemias, especially cryoglobulinemia.

Hematocrit Measurement by Micromethod

Equipment

A capillary Hct tube about 7 cm long with a uniform bore of about 1 mm is used. For blood collection directly from a skin puncture, heparinized capillary tubes are available.

Procedure

The microhematocrit tube is filled by capillary attraction from a free-flowing puncture wound or a well-mixed venous sample. The capillary tube should be filled to at least 5 cm. The empty end is sealed with modeling clay. The filled tube is placed in the radial grooves of the microhematocrit centrifuge head with the sealed end away from the center. Place the bottom of the tube against the rubber gasket to prevent breakage. Centrifugation for 5 minutes at 10,000 to 12,000 g is satisfactory unless the Hct exceeds 50%; in that case, an additional 5 minutes of centrifugation should be employed to ensure minimal plasma trapping. The capillary tubes are not graduated. The length of the blood column, including the plasma, and of the red cell column alone must be measured in each case with a millimeter rule and a magnifying lens, or with one of several commercially available measuring devices. The manufacturer's instructions must be followed.

Interpretation of Results

Typical reference values for adult males are 0.41 to 0.51, and for females, 0.36 to 0.45. A value below an individual's normal value or below the reference interval for age and sex indicates anemia, and a higher value, polycythemia. The Hct reflects the concentration of red cells—not the total red cell mass. The Hct is low in hydremia of pregnancy, but the total number of circulating red cells is not reduced. The Hct may be normal or even high in shock accompanied by hemoconcentration, although the total red cell mass may be decreased considerably owing to blood loss. The Hct is unreliable as an estimate of anemia immediately after loss of blood or immediately following transfusions.

Sources of Error

Centrifugation. Adequate duration and speed of centrifugation are essential for a correct Hct. The red cells must be packed so that additional centrifugation does not further reduce the packed cell volume. In the course of centrifugation, small proportions of the leukocytes, platelets, and plasma are trapped between the red cells. The error resulting from the former is, as a rule, quite insignificant. The amount of trapped plasma is larger in high Hcts than in low Hcts. Trapped plasma accounts for about 1% to 3% of the red cell column in normal blood (about 0.014 in a Hct of 0.47) and slightly more in macrocytic anemia, spherocytosis, and hypochromic anemia (Dacie & Lewis, 1991). Even greater amounts of trapped plasma are noted in the Hcts of patients with sickle cell anemia; these vary depending on the degree of sickling and consequent rigidity of the cells. In using the microhematocrit as a reference method for calibrating automated instruments, correction for trapped plasma is recommended (International Committee for Standardization in Hematology [ICSH], 1980).

Sample. Posture, muscular activity, and prolonged tourniquet-stasis can cause the same order of changes in Hct and cell concentrations as they do in nonfilterable soluble constituents. Unique to the Hct is error due to excess EDTA (inadequate blood for a fixed amount of EDTA): The Hct will be falsely low as a result of cell shrinkage, but the Hb and cell counts will not be affected. There is no uniformity as to which EDTA salt is used for anticoagulation (O'Broin et al., 1997). The tripotassium (K_3-EDTA) salt shrinks red cells about 2% and lowers packed cell volume compared with the dipotassium salt (K_2-EDTA) (Koepke et al., 1989). Also, because K_3-EDTA is a liquid, measured Hb and red and white cell counts are decreased by 1% to 2%. Although the ICSH and the Clinical Laboratory Standards Institute recommend the K_2-EDTA salt (powder), the K_3-EDTA is more often used, perhaps because of its increased miscibility and fewer instances of specimen clotting (Geller, 1996).

Other Errors. Technical errors include failure to mix the blood adequately before sampling, improper reading of the levels of cells and plasma, and inclusion of the buffy coat as part of the erythrocyte volume. With good technique, the precision of the Hct, expressed as ±2 CV (coefficient of variation), is ±1%. With low Hct values, the CV is greater because of reading error.

ERYTHROCYTE INDICES

Wintrobe introduced calculations for determining the size, content, and Hb concentration of red cells; these erythrocyte indices have been useful in the morphologic characterization of anemias. They may be calculated from the red cell count, Hb concentration, and Hct.

Mean Cell Volume

The MCV, the average volume of red cells, is calculated from the Hct and the red cell count. MCV = Hct × 1000/RBC (in millions per μL), expressed in femtoliters or cubic micrometers. If the Hct = 0.45 and the red cell count = 5 × 10^{12}/L, 1 L will contain 5 × 10^{12} red cells, which occupy a volume of 0.45 L.

$$\text{MCV} = 0.45\ \text{L} / 5 \times 10^{12} = 90 \times 10^{-15}\ \text{L}$$

$$\text{One femtoliter (fL)} = 10^{-15}\ \text{L} = 1\ \text{cubicmicrometer}\ (\mu\text{m}^3).$$

Mean Cell Hemoglobin

The mean cell hemoglobin (MCH) is the content (weight) of Hb of the average red cell; it is calculated from the Hb concentration and the red cell count.

$$\text{MCH} = \text{Hb (in g/L)} / \text{RBC (in millions}/\mu\text{L)}$$

The value is expressed in picograms. If the Hb = 15 g/dL and the red cell count is 5 × 10^{12}/L, 1 L contains 150 g of Hb distributed in 5 × 10^{12} cells.

$$\text{MCH} = 150 / \left(5 \times 10^{12}\right) = 30 \times 10^{12}\ (\text{pg})$$

$$\text{One picogram (pg)} = 10^{-12}\ \text{g}$$

Mean Cell Hemoglobin Concentration

The mean cell (corpuscular) hemoglobin concentration (MCHC) is the average concentration of Hb in a given volume of packed red cells. It is calculated from the Hb concentration and the Hct.

$$\text{MCHC} = \text{Hb in } \frac{\frac{\text{g}}{\text{dL}}}{\text{Hct}}, \text{ expressed in g/dL (SI units are g/L)}$$

If the Hb = 15 g/dL and the Hct = 0.45,

$$\text{MCHC} = 15 \frac{\frac{\text{g}}{\text{dL}}}{0.45} = 33.3 \frac{\text{g}}{\text{dL}}.$$

Indices are determined in the electrical impedance instruments somewhat differently. The MCV is derived from the mean height of the voltage pulses formed during the red cell count, and the Hb is measured by optical density of HiCN. The other three values are calculated as follows:

$$\text{Hct} = \text{MCV} \times \text{RBC};\ \text{MCH} = \text{Hb}/\text{RBC};\ \text{MCHC} = (\text{Hb}/\text{Hct}) \times 100$$

The reference values for the indices will depend on whether they are determined from the centrifuged Hct or the cell counters. The values in

normal individuals will be similar if both are corrected for trapped plasma. However, because of increased trapped plasma in hypochromic anemias and sickle cell anemia, the MCHC calculated from the microhematocrit will be significantly lower than the MCHC derived from the electrical impedance counters.

The 95% reference intervals for normal adults are as follows: MCV = 80 to 96 fL; MCH = 27 to 33 pg; and MCHC = 33 to 36 g/dL (Ryan, 2001). In a healthy person, there is very little variation—no more than ±1 unit in any of the indices. Deviations from the reference value for an individual or outside the reference intervals for normal persons are useful, particularly in characterizing morphologic types of anemia.

In *microcytic anemias*, the indices may be as low as an MCV of 50 fL, an MCH of 15 pg, and an MCHC of 22 g/dL; rarely do any become lower.

In *macrocytic anemias*, the values may be as high as an MCV of 150 fL and an MCH of 50 pg, but the MCHC is normal or decreased (Dacie & Lewis, 1991). The MCHC typically increases only in spherocytosis, and rarely is over 38 g/dL.

MANUAL BLOOD CELL COUNTS

Except for some platelet counts and low leukocyte counts, the hemocytometer is no longer used for routine blood cell counting. However, it is still necessary for the technologist to be able to use this method effectively and to know its limitations. Any cell-counting procedure includes three steps: dilution of the blood, sampling of the diluted suspension into a measured volume, and counting of the cells in that volume. Counts of erythrocytes, leukocytes, and platelets are each expressed as concentrations, that is, cells per unit volume of blood. The unit of volume was expressed as cubic millimeters (mm^3) because of the linear dimensions of the hemocytometer (cell counting) chamber:

$$1\ mm^3 = 1\ \mu L$$

Although there is no consistency in the literature in the use of traditional/conventional units versus Système International d'Unites (SI) units, the ICSH recommends that the unit of volume be the liter (SI units), as on the right in the following examples:

Erythrocytes :
$5.00 \times 10^6 / mm^3 = 5.00 \times 10^6 / \mu L$ (conventional) $= 5.00 \times 10^{12} / L$ (SI units)

Leukocytes :
$7.0 \times 10^3 / mm^3 = 7.0 \times 10^3 / \mu L$ (conventional) $= 7.0 \times 10^9 / L$ (SI units)

Platelets :
$300 \times 10^3 / mm^3 = 300 \times 10^3 / \mu L$ (conventional) $= 300 \times 10^9 / L$ (SI units)

Erythrocyte Counts: Manual

Systems for manual dilutions combine a microcapillary tube with a plastic vial containing a premeasured volume of diluent. After the capillary tube is filled, it is pushed into the container and the sample is washed out by squeezing the soft plastic vial. This system is especially convenient for microsampling. Unopettes are available with diluents for counts of RBCs, white blood cells (WBCs), platelets, eosinophils, and reticulocytes.

Semiautomated Methods

Instruments are available for precise and convenient diluting that both aspirate the sample and wash it out with the diluent. The dilutor should perform a 1:250 or a 1:500 dilution with a coefficient of variation of less than 1%.

Reticulocyte Count: Manual

Principle

Reticulocytes are immature nonnucleated red cells that contain ribonucleic acid (RNA) and continue to synthesize Hb after loss of the nucleus. When blood is briefly incubated in a solution of new methylene blue or brilliant cresyl blue, the RNA is precipitated as a dye-ribonucleoprotein complex. Microscopically, the complex appears as a dark-blue network (reticulum or filamentous strand) or at least two dark-blue granules that allow reticulocytes to be identified and enumerated (ICSH, 1998). A proposed reference method for reticulocyte counting based on determination of the reticulocyte/red cell ratio has been published (ICSH, 1998) expanding on the 1994 ICSH red cell count reference method.

Reagent. One percent new methylene blue in a diluent of citrate/saline (1 part 30 g/L sodium citrate plus 4 parts 9 g/L sodium chloride).

Controls. Although commercial controls are available, Ebrahim and Ryan (1996) describe a method requiring about 2 hours that produces a multilevel control that is stable for several months. Hypotonic dialysis of RBCs in the presence of RNA followed by a short period of hypertonic dialysis to reseal the pores of the RBC membrane results in about 20% of the RBCs as "synthetic reticulocytes" with various amounts of encapsulated RNA.

Procedure

Three drops each of reagent and blood are mixed in a test tube, incubated 15 minutes at room temperature, and remixed. Two wedge films are made on glass slides and air dried.

Viewed microscopically with an oil immersion lens, reticulocytes are pale blue and contain dark blue reticular or granular material, and red cells stain pale blue or blue-green. The percentage of reticulocytes is determined in at least 1000 red cells. A Miller disk inserted into the eyepiece allows rapid estimation of large numbers of red cells by imposing two squares (one square is nine times the area of the other) onto the field of view (Brecher & Schneiderman, 1950). Reticulocytes are counted in the large square and red cells in the small square in successive microscopic fields until at least 300 red cells are counted. This provides an estimate of reticulocytes among at least 2700 red cells, as follows:

$$\text{Reticulocytes (percent)} = [\text{No. reticulocytes in large squares} / (\text{No. red cells in small squares} \times 9)] \times 100$$

The absolute reticulocyte count is determined by multiplying the reticulocyte percentage by the red cell count.

Reference Values

Normal adults have a reticulocyte count of 0.5% to 1.5%, or 24 to 84 × 10^9/L. In newborn infants, the percentage is 2.5% to 6.5%. This falls to the adult range by the end of the second week of life.

Interpretation

Because reticulocytes are immature red cells that lose their RNA a day or so after reaching the blood from the marrow, a reticulocyte count provides an estimate of the rate of red cell production. An absolute reticulocyte count or reticulocyte production index is more helpful than the percentage (see Chapter 33).

Sources of Variation

Because such a small number of actual reticulocytes are counted, the sampling error in the manual reticulocyte count is relatively large. The 95% confidence limits may be expressed as follows:

$$R \pm 2\sqrt{[R\ (100 - R)\ / N]}$$

where *R* is the reticulocyte count in percent, and *N* is the number of erythrocytes examined. This means that if only 1000 erythrocytes are evaluated, the 95% confidence limits for a 1% count are 0.4% to 1.6%; for a 5% count, 3.6% to 6.4%; and for a 10% count, 8.1% to 11.9%.

Physiologic Variation in Erythrocytes. Changes in red cell values are greatest during the first few weeks of life (Fig. 31.3). At the time of birth, as much as 100 to 125 mL of placental blood may be added to the newborn if tying the cord is postponed until its pulsation ceases. In a study of newborns whose cords had been clamped late, average capillary red cell counts were 0.4 × 10^{12}/L higher 1 hour after and 0.8 × 10^{12}/L higher 24 hours after birth compared with newborns whose cords had been clamped early. Capillary blood (obtained by skin puncture) gives higher RBC and Hb values than venous blood (cord). The differences may amount to about 0.5 × 10^{12} RBC/L and 3 g Hb/dL. Slowing of capillary circulation and the resulting loss of fluid may be the responsible factors. Examination of venous blood furnishes more consistent results than are obtained by examination of capillary blood.

In the full-term infant, nucleated red cells average about 0.5 × 10^9/L. The normoblast count declines to about 200/μL at 24 hours, 25/μL at 48 hours, and less than 5/μL at 72 hours. By 7 days, it is rare to find circulating normoblasts (Barone, 1999).

The normal reticulocyte count at birth ranges from 3% to 7% during the first 48 hours, during which time it rises slightly. After the second

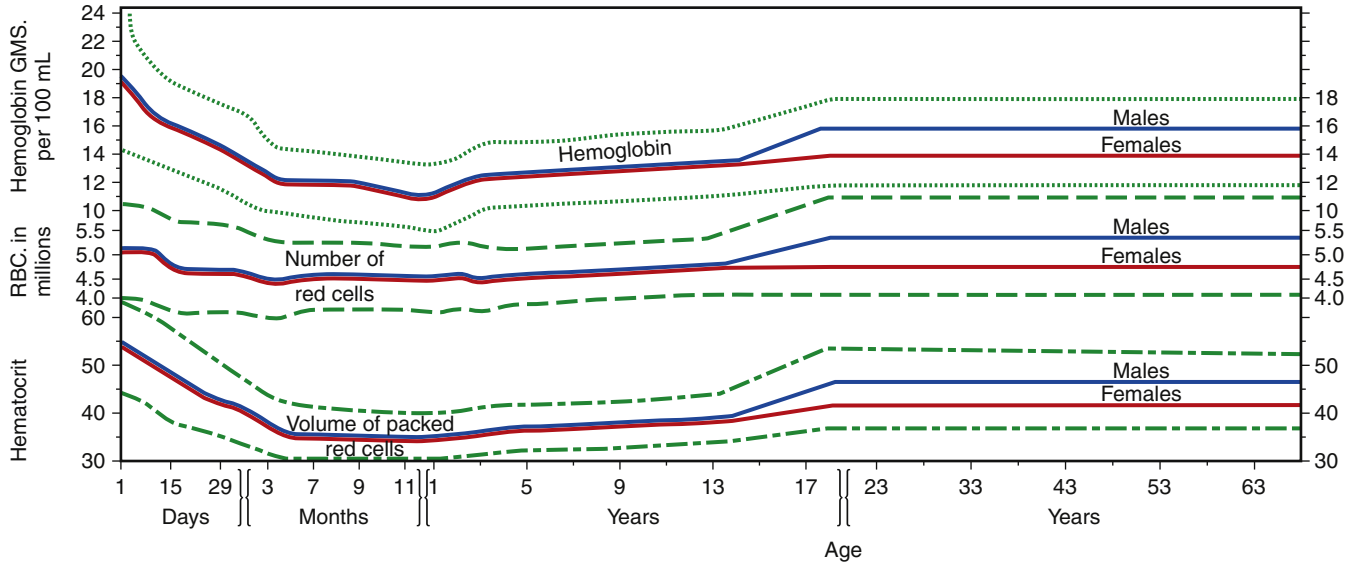

Figure 31.3 Values for hemoglobin (Hb), hematocrit (Hct; volume of packed red cells), and red cell count from birth to old age. Mean values are heavy lines. Reference interval for Hb is indicated by dotted lines, for red cell counts by dashed lines, and for Hct by dotted and dashed lines. The scales on the ordinate are similar, so that relative changes in Hb, red cell count, and Hct are apparent on inspection. The scale for age, however, is progressively altered (Wintrobe, 1974).

day, it falls rather rapidly to 1% to 3% by the seventh day of life. Hb concentration in capillary blood during the first day of life averages 19.0 g/dL, with 95% of normal values falling to between 14.6 and 23.4 g/dL. In cord blood, the average is 16.8 g/dL, with 95% of normal between 13.5 and 20 g/dL. Frequently, an initial increase in the Hb level of venous blood is seen at the end of 24 hours compared with that of cord blood. At the end of the first week, the level is about the same as in cord blood, and it does not begin to fall until after the second week. During the first 2 weeks, the lower limit of normal is 14.5 g/dL for capillary blood and 13.0 g/dL for venous blood. The Hct in capillary blood on the first day of life averages 0.61, with 95% of normal values between 0.46 and 0.76. In cord blood, the average is 0.53. Changes during the first few weeks parallel the Hb concentration. The Hb and Hct are highest at birth but fall rather steeply in the first days and weeks of life to a minimum at 2 months of age, at which time the lower limit of the 95% reference values and the mean value for the Hb are 9.4 and 11.2 g/dL, and for the Hct are 0.28 and 0.35, respectively. After 4 months of age, the lower limit for the Hb is 11.2 g/dL and 0.32 for the Hct. These values rise gradually until about 5 years of age and somewhat more steeply in boys than in girls thereafter (Shannon & Pearson, 2002). The normal MCV at birth ranges from 104 to 118 fL compared with the adult reference interval of 80 to 96 fL. Because the RBC count does not fall to the degree that the Hb and Hct counts fall, the MCV decreases abruptly, then gradually, during the first few months of life. The lowest value is reached at about 1 year. In studies in which iron deficiency and thalassemia are excluded, the lower reference limit (95% reference values) for the MCV gradually rises between 1 year and 15 years of age—from 70 to 76 fL in boys and from 70 to 78 fL in girls (Shannon & Graef, 1996). Reference intervals for RBC values in sexually mature adults are given in Table 31.2. The indices are similar in males and females, but the Hb is 1 to 2 g/dL higher in males, with commensurate increments in Hct and RBCs (see Fig. 31.3). This is believed to be mainly the effect of androgen in stimulating erythropoietin production and its effect on the marrow. In older men, the Hb tends to fall; in older women, the Hb tends to fall to a lesser degree (in some studies) or even rise slightly (in other studies). In older individuals, therefore, the sex difference is less than 1 g Hb/dL (Dacie & Lewis, 1991). Posture and muscular activity change the concentration of the formed elements. The Hb, Hct, and RBC counts increase by several percent in going from recumbency to standing, and strenuous muscular activity causes a further increase, presumably owing primarily to loss of plasma water. Diurnal variation that is not related to exercise or to analytic variation also occurs. The Hb is highest in the morning, falls during the day, and is lowest in the evening, with a mean difference of 8% to 9% (Dacie & Lewis, 1991). In persons living at a higher altitude, the Hb, Hct, and RBC counts are elevated over what they would be at sea level. The difference is about 1 g Hb/dL at 2 km altitude and 2 g Hb/dL at 3 km. Increased erythropoiesis is secondary to anoxic stimulation of erythropoietin production. People who are smokers also tend to have a mild erythrocytosis.

TABLE 31.2
Typical Blood Cell Values in a Normal Population of Young Adults

	Men		Women
White cell count ($\times 10^9$/L blood)		7.8 (4.4–11.3)	
Red cell count ($\times 10^{12}$/L blood)	5.21 (4.52–5.90)		4.60 (4.10–5.10)
Hemoglobin (g/dL blood)	15.7 (14.0–17.5)1		13.8 (12.3–15.3)
Hematocrit (%)	46 (41.5–50.4)		40.2 (35.9–44.6)
Mean cell volume (fL/red cell)		88.0 (80.0–96.1)	
Mean cell hemoglobin (pg/red cell)		30.4 (27.5–33.2)	
Mean cell hemoglobin concentration (g/dL RBC)		34.4 (33.4–35.5)	
Red cell distribution width (CV, %)		13.1 (11.6–14.6)	
Platelet count ($\times 10^9$/L blood)		311 (172–450)	

The mean and reference intervals (normal range) are given. Because the distribution curves may be nongaussian, the reference interval is the nonparametric central 95% confidence interval. Results are based on 426 normal adult men and 212 normal adult women. Studies were performed on the Coulter model S-Plus IV. From Morris MW, Skrodzki Z, Nelson DA: Zeta sedimentation ratio (ZSR), a replacement for the erythrocyte sedimentation rate (ESR), *Am J Clin Pathol* 164:254–256, 1975.
CV, Cell values; *RBC,* red blood cell.

Leukocyte Counts: Manual

Specimen Collection

EDTA should be used; heparin is unsatisfactory as an anticoagulant.

Hemocytometer Method. Although this method is used only occasionally in leukocyte counting, the technologist should be able to perform it in these circumstances:

1. As a check on the validity of electronic methods for calibration purposes
2. As a check on the validity of electronic counts in patients with profound leukopenia or thrombocytopenia
3. For blood specimens with platelet counting interference (i.e., very microcytic RBCs)
4. As a backup method

It is also commonly used as a method for counting cells in cerebrospinal fluid (CSF).

Counting Chamber. The hemocytometer is a thick glass slide with inscribed platforms of known area and precisely controlled depth under the coverslip. Counting chambers and cover glasses should be rinsed in lukewarm water immediately after use; wiped with a clean, lint-free cloth; and allowed to air dry. The surfaces must not be touched with gauze or linen because these materials may scratch the ruled areas.

Diluting Fluid. The diluting fluid lyses the erythrocytes so that they will not obscure the leukocytes. The fluid must be refrigerated and filtered frequently to remove yeasts and molds.

Procedure

1. Well-mixed blood is diluted 1:20 in diluting fluid and the vial rotated for about 5 minutes. The chamber is loaded with just enough fluid to fill the space beneath the cover glass.
2. The cells are permitted to settle for several minutes, and the chamber is surveyed with a low-power (10×) objective lens to verify uniform cell distribution.
3. Counting is performed. The condenser diaphragm of the microscope is partially closed to make the leukocytes stand out clearly under a low-power objective lens. The leukocytes are counted in each of the four large (1-mm^2) corner squares (A, B, C, and D in Fig. 31.4). A total of eight large corner squares from two sides of a chamber are counted.
4. Each large square encloses a volume of 1/10 mm^3, and the dilution is 1:20. A general formula is as follows:

$$\text{Leukocyte count } (\text{cells}/\text{mm}^3) = (\text{cc}/\text{lsc}) \times \text{d} \times 10$$

where *cc* is the total number of cells counted, *d* is the dilution factor, 10 is the factor transforming value over one large square (1/10 mm^3) to the volume in mm^3, and *lsc* is the number of large squares counted.

In leukopenia, with a total count below 2500, the blood is diluted 1:10. In leukocytosis, the dilution may be 1:100 or even 1:200.

Sources of Error

Errors may be due to the nature of the sample, to the operator's technique, and to inaccurate equipment. Errors that are inherent in the distribution of cells in the counting volume are called "field" errors and can be minimized only by counting more cells.

Hemocytometer leukocyte counts show a CV of about 6.5% for normal and increased counts and about 15% in leukopenic blood. Utilizing electronic counters, on the other hand, results in CVs of approximately 1% to 3%.

Errors Due to the Nature of the Sample. Partial coagulation of the venous blood causes changes in the distribution of the cells and/or decreases their number. Failure to mix the blood thoroughly and immediately before dilution introduces an error, which depends on the degree of sedimentation.

Operator's Errors. Errors caused by faulty technique may occur during dilution, when the chamber is loaded, and when the cells are counted.

Errors Due to Equipment. Equipment errors can be diminished by using pipets and hemocytometers certified by the U.S. Bureau of Standards.

Inherent or Field Errors. Even in a perfectly mixed sample, variation occurs in the number of suspended cells that are distributed in a given volume (i.e., come to rest over a given square). This "error of the field" is the minimal error. Another error is the "error of the chamber," which includes variations in separate fillings of a given chamber and in sizes of different chambers. Still another is the "error of the pipet," which includes variations in filling a given pipet and in the sizes of different pipets. In performing a WBC count, if 200 cells are counted using two chambers and one pipet, the CV = 9.1%, corresponding to 95% confidence limits of ±18.2% (twice the CV). Using four chambers and two pipets and counting twice as many cells reduces the 95% confidence limits to ±12.8%. This relatively large percentage error is of little practical consequence because of the physiologic variation of the leukocyte count.

Nucleated Red Blood Cells. Nucleated red blood cells (NRBCs) will be counted and cannot be distinguished from leukocytes with the magnification used. If their number is high, as seen on the stained smear, a correction should be made according to the following formula:

$$\text{True leukocyte count} = (\text{Total count} \times 100) \;/\; (100 + \text{No. of NRBCs})$$

where the *No. of NRBCs* is the number of nucleated red cells that are counted during the enumeration of 100 leukocytes in the differential count.

Reference Value. In the total leukocyte count, no distinction is made among the six normal cell types (neutrophils and bands, lymphocytes, monocytes, eosinophils, and basophils). The reference interval for adults is 4.5 to 11.0 × 10^9/L.

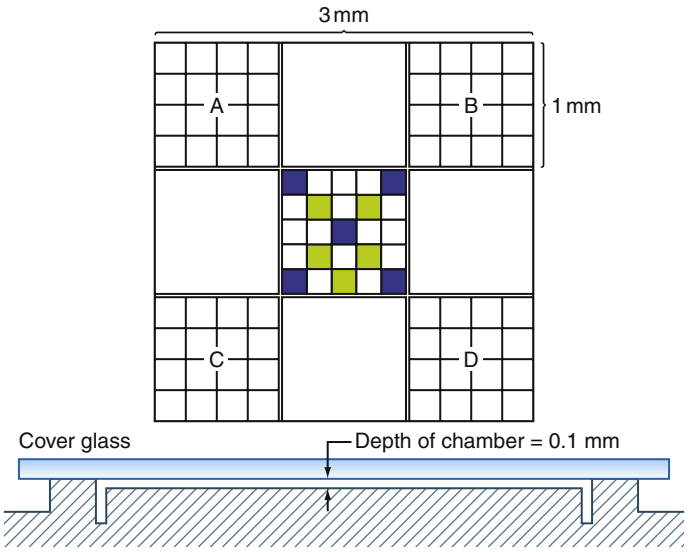

Figure 31.4 The upper figure is a diagram of the improved Neubauer ruling; this is etched on the surface of each side of the hemocytometer. The large corner squares, A, B, C, and D, are used for leukocyte counts. The five blue squares in the center are used for red cell counts or for platelet counts, and the 10 green plus blue squares for platelet counts. Actually, each of the 25 squares within the central sq mm has within it 16 smaller squares for convenience in counting (not shown). The lower figure is a side view of the chamber with the cover glass in place.

Physiologic Variation in Leukocytes

The total white cell count at birth and during the first 24 hours varies within wide limits. Neutrophils are the predominant cell, varying from 6 to 28 × 10^9/L; about 15% of these are band forms (Altman & Dittmer, 1974), and a few myelocytes are present. Neutrophils drop to about 5 × 10^9/L during the first week of life and remain at about the same level thereafter. Lymphocytes are about 5.5 × 10^9/L at birth and change little during the first week. They become the predominant cell, on average, after the first week of life and remain so until about 7 years of age, when neutrophils again predominate. The upper limit of the 95% reference interval for lymphocytes at 6 months of age is 13.5, at 1 year of age 10.5, at 2 years of age 9.5, at 6 years of age 7.0, and at 12 years of age 6.0 × 10^9/L. For neutrophils at the same ages, the values are 8.5, 8.5, 8.5, 8.0, and 8.0 × 10^9/L, respectively—all somewhat higher than those for adults (Table 31.3).

Example

The blood smear shows 25 NRBCs per 100 leukocytes. The total nucleated cell count is 10,000.

True leukocyte count = 10,000 × 100/125 = 8000/μL (8.0 × 10^9/L)

Diurnal variation has been recognized in the neutrophil count, with highest levels in the afternoon and lowest levels in the morning at rest. Exercise produces leukocytosis, which includes an increased neutrophil concentration as a result of a shift of cells from the marginal to the circulating granulocyte pool. Increased lymphocyte drainage into the blood also appears to contribute to the total increase. Both average and lower reference values for neutrophil concentration in the black population are lower than in the white population; this difference must be taken into account in assessing neutropenia. Cigarette smokers have higher average leukocyte counts than nonsmokers. The increase is greatest (about 30%) in heavy smokers who inhale and affects neutrophils, lymphocytes, and monocytes.

Mild changes occur during the menstrual cycle. Neutrophils and monocytes fall and eosinophils tend to rise during menstruation. Basophils have been reported to fall during ovulation.

Platelet Counts

Platelets are thin disks, 2 to 4 μm in diameter and 5 to 7 fL in volume (in citrated blood). They function in hemostasis, in maintenance of vascular integrity, and in the process of blood coagulation.

In EDTA-blood, the mean platelet volume (MPV) increases with time up to 1 hour in vitro, is relatively stable between 1 and 3 hours, and then increases further with time. Change from a discoid to a spherical shape accounts for this increase in apparent volume in EDTA compared with citrate (Rowan & Fraser, 1982). For reproducible results, platelet volume

TABLE 31.3

Normal Leukocyte Count, Differential Count, and Hemoglobin Concentration at Various Ages

	LEUKOCYTES*								
Age	**Total Leukocytes**	**Total Neutrophils**	**Band Neutrophils**	**Segmented Neutrophils**	**Eosinophils**	**Basophils**	**Lymphocytes**	**Monocytes**	**Hemoglobin (g/dL Blood)**
12 months	11.4 (6.0–17.5)	3.5 (1.5–8.5) *31*	0.35 *3.1*	3.2 (1.0–8.5) *28*	0.30 (0.05–0.70) *2.6*	0.05 (0–0.20) *0.4*	7.0 (4.0–10.5) *61*	0.55 (0.05–1.1) *4.8*	12.6 (11.1–14.1)
4 years	9.1 (5.5–15.5)	3.8 (1.5–8.5) *42*	0.27 (0–1.0) *3.0*	3.5 (1.5–7.5) *39*	0.25 (0.02–0.65) *2.8*	0.05 (0–0.2) *0.6*	4.5 (2.0–8.0) *50*	0.45 (0–0.8) *5.0*	12.7 (11.2–14.3)
6 years	8.5 (5.0–14.5)	4.3 (1.5–8.0) *51*	0.25 (0–1.0) *3.0*	4.0 (1.5–7.0) *48*	0.23 (0–0.65) *2.7*	0.05 (0–0.2) *0.6*	3.5 (1.50–7.0) *42*	0.40 (0–0.8) *4.7*	13.0 (11.4–14.5)
10 years	8.1 (4.5–13.5)	4.4 (1.8–8.0) *54*	0.24 (0–1.0) *3.0*	4.2 (1.8–7.0) *51*	0.20 (0–0.60) *2.4*	0.04 (0–0.2) *0.5*	3.1 (1.5–6.5) *38*	0.35 (0–0.8) *4.3*	13.4 (11.8–15.0)
21 years	7.4 (4.5–11.0)	4.4 (1.8–7.7) *59*	0.22 (0–0.7) *3.0*	4.2 (1.8–7.0) *56*	0.20 (0–0.45) *2.7*	0.04 (0–0.2) *0.5*	2.5 (1.0–4.8) *34*	0.30 (0–0.8) *4.0*	15.5 (13.5–17.5) 13.8 (12.0–15.6)

From Altman PL, Dittmer DS, editors: *Blood and other body fluids,* Washington, DC, 1961, Federation of American Societies for Experimental Biology (for leukocyte and differential count); Dalman PR: Developmental changes in red blood cell production and function. In: Rudolph AM, Hoffman JIE, editors: *Pediatrics,* ed 18, Norwalk, CT, 1987, Appleton & Lange, pp 1011–1012 (for hemoglobin concentrations).

*Values are expressed as mean (95% reference) values. For leukocytes and differential count cell types, the units are cells × $10^9/\mu L$; the numbers in italics are mean percentages.

measurements obtained with multichannel instruments should be made between 1 and 3 hours after the blood is drawn. The frequency distribution of platelet volumes in an individual is log normal. However, a nonlinear inverse relationship has been noted between the MPV and the platelet count within normal individuals (Fig. 31.5). Therefore, reference values for the MPV appear to vary with the platelet count (Bessman et al., 1981). The MPV is generally increased in hyperthyroidism (Ford et al., 1988) and myeloproliferative disease (Small & Bettigole, 1981). Platelets are more difficult to count because they are small (must be distinguished from debris) and have a tendency to adhere to glass, any foreign body, and particularly to one another. It is often possible to recognize a significant decrease in the number of platelets by careful inspection of stained films. With capillary blood, films must be made evenly and very quickly after the blood is obtained to avoid clumping and to minimize the decrease due to adhesion of platelets to the margins of the injured vessels. A better estimate is possible by examining stained films made from venous blood with EDTA as an anticoagulant (EDTA-blood), in which platelets are evenly distributed and where clumping normally does not occur. The visual method of choice employs the phase-contrast microscope. Once considered the gold standard, it has been largely replaced as the reference method by the RBC/platelet ratio. This method employs monoclonal antibodies to platelet-specific targets on the glycoprotein IIb/IIa complex (CD41 and Cd61) to enumerate platelets using flow cytometry. This method helps to differentiate platelets from interfering substances such as microcytic RBCs, WBC fragments, microorganisms, and debris (Table 31.4) (ICSH, 2001).

Hemocytometer Method—Phase-Contrast Microscope

Specimen. Venous blood is collected with EDTA as the anticoagulant. Blood from skin puncture wounds gives more variable results but is satisfactory if the blood is flowing freely and if only the first few drops are used.

Diluent Solution. One percent ammonium oxalate is mixed in distilled water. The stock bottle is kept in the refrigerator. The amount needed for the day is filtered before use, and the unused portion is discarded at the end of the day.

Procedure.

1. Well-mixed blood is diluted 1:100 in diluting fluid, and the vial containing the suspension is rotated on a mechanical mixer for 10 to 15 minutes.
2. The hemocytometer is filled in the usual fashion, using a separate capillary tube for each side.
3. The chamber is covered with a Petri dish for 15 minutes to allow settling of the platelets in one optical plane. A piece of wet cotton or filter paper is left beneath the dish to prevent evaporation.

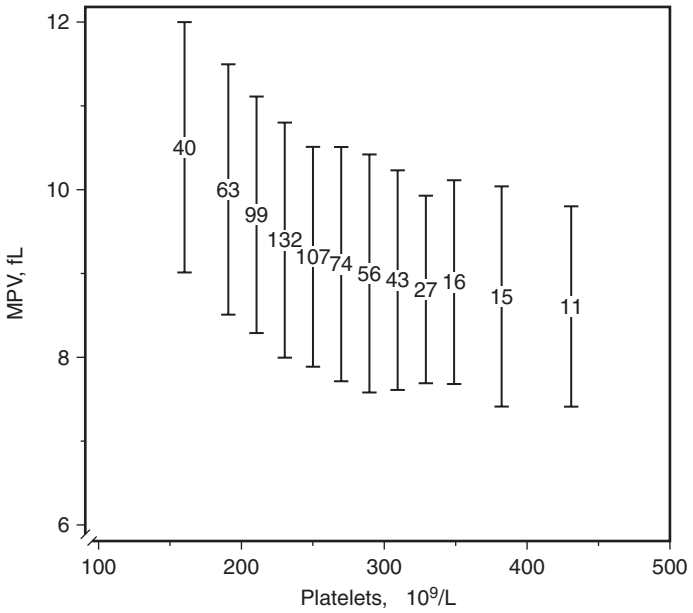

Figure 31.5 Mean platelet volume (MPV) related to platelet count in 683 normal subjects. Each group is shown as mean (number) ±2 SD (bar) of subjects grouped by platelet counts of 128 to 179, 180 to 199, 200 to 219, 220 to 239, 240 to 259, 260 to 279, 280 to 309, 310 to 319, 320 to 339, 340 to 359, 360 to 403, 404 to 462 × 10^9/L. The number of the mean position is the number of subjects in the group (Bessman et al., 1981).

4. The platelets appear round or oval and frequently have one or more dendritic processes. Their internal granular structure and a purple sheen allow the platelets to be distinguished from debris, which is often refractile. Ghosts of red cells that have been lysed by the ammonium oxalate are seen in the background.
5. Platelets are counted in 10 small squares (the black squares in Fig. 31.4), five on each side of the chamber. If the total number of platelets counted is less than 100, more small squares are counted until at least 100 platelets have been recorded—10 squares per side (black plus shaded squares; see Fig. 31.4) or all 25 squares in the large central square on each side of the hemocytometer, if necessary. If the total number of platelets in all 50 of these small squares is less than 50, the count should be repeated with a 1:20 or a 1:10 dilution of blood.

TABLE 31.4

Potential Causes of Erroneous Results with Automated Cell Counters

Parameter	Causes of Spurious Increase	Causes of Spurious Decrease
WBC	Cryoglobulin, cryofibrinogen	Clotting
	Heparin	Smudge cells
	Monoclonal proteins	Uremia plus immunosuppressants
	Nucleated red cells	
	Platelet clumping	
	Unlysed red cells	
RBC	Cryoglobulin, cryofibrinogen	Autoagglutination
	Giant platelets	Clotting
	High WBC (>50,000/mL)	Hemolysis (in vitro)
		Microcytic red cells
Hb	Carboxyhemoglobin (>10%)	Clotting
	Cryoglobulin, cryofibrinogen	Sulfhemoglobin
	Hemolysis (in vitro)	
	Heparin	
	High WBC (>50,000/μL)	
	Hyperbilirubinemia	
	Lipemia	
	Monoclonal proteins	
Hct (automated)	Cryoglobulin, cryofibrinogen	Autoagglutination
	Giant platelets	Clotting
	High WBC (>50,000/μL)	Hemolysis (in vitro)
	Hyperglycemia (>600 mg/dL)	Microcytic red cells
Hct (microhematocrit)	Hyponatremia	Excess EDTA
	Plasma trapping	Hemolysis (in vitro)
		Hypernatremia
MCV	Autoagglutination	Cryoglobulin
	High WBC (>50,000/μL)	Cryofibrinogen
	Hyperglycemia	Giant platelets
	Reduced red cell deformability	Hemolysis (in vitro)
		Microcytic red cells
		Swollen red cells
MCH	High WBC (>50,000/μL)	Spuriously low Hb
	Spuriously high Hb	Spuriously high RBC
	Spuriously low RBC	
MCHC	Autoagglutination	High WBC (>50,000/μL)
	Clotting	Spuriously low Hb
	Hemolysis (in vitro)	Spuriously low Hct
	Hemolysis (in vivo)	
	Spuriously high Hb	
	Spuriously high Hct	
Platelets	Cryoglobulin, cryofibrinogen	Clotting
	Hemolysis (in vitro and in vivo)	Giant platelets
	Microcytic red cells	Heparin
	Red cell inclusions	Platelet clumping
	White cell fragments	Platelet satellitosis

From Cornbleet J: Spurious results from automated hematology cell analyzers, *Lab Med* 14:509, 1983.
EDTA, Ethylenediaminetetraacetic acid; *Hb,* hemoglobin; *Hct,* hematocrit; *MCH,* mean cell hemoglobin; *MCHC,* mean cell hemoglobin concentration; *MCV,* mean corpuscular volume; *RBC,* red blood cell; *WBC,* white blood cell.

Calculation

Each of the 25 small squares defines a volume of 1/250 μL (1/25 mm^2 area × 1/10 mm depth): Platelet count (per μL) = (Number of cells counted/Number of squares counted) × Dilution × 250.

By adjusting the number of squares so that at least 100 platelets are counted, the field error (the statistical error caused by counting a limited number of platelets in the chamber) can be kept in the same range for low platelet counts as for high platelet counts. It has been shown that the CV due to combined field, pipet, and chamber errors is about 11% when at least 100 platelets are counted, and 15% when 40 platelets are counted.

Platelet counts tend to be the least reproducible of the blood cell counts; the technologist must be vigilant to ensure their accuracy. This includes the readiness to confirm suspicious or abnormal results with a freshly drawn sample. Whenever the platelet count is in question, such as with an instrument flag, the blood film (prepared from EDTA-blood) must be checked to corroborate the count and to detect abnormalities in platelets or other blood elements that may give a false value. Further, because of the low number of platelets counted in the manual method and the high degree of imprecision with severe thrombocytopenia (CV >15%), 7×10^9 platelets/L is the lowest count that should be reported from manual quantitation (Hanseler et al., 1996).

Sources of Error

Blood in EDTA is satisfactory for 5 hours after collection at 20°C and for 24 hours at 4°C provided that no difficulty was encountered in collection. Platelet clumps present in the chamber imply a maldistribution and negate the reliability of the count; in this case, a new sample of blood must be collected. The causes of platelet clumping are likely to be initiation of platelet aggregation and clotting before the blood reaches the anticoagulant; imperfect venipuncture; delay in the anticoagulant contacting the blood; or, in skin puncture technique, delay in sampling. Capillary blood gives similar mean values, but errors are about twice those with venous blood, probably because the platelet level varies in successive drops of blood from the skin puncture wound.

Falsely Elevated Counts. Fragments of leukocyte cytoplasm that are sometimes numerous in leukemias may falsely elevate the count. The phase-contrast hemocytometer method must be employed in these cases, with a correction made based on the ratio of fragments to platelets determined from the blood film.

Falsely Low Counts. These can occur if platelets adhere to neutrophils (platelet satellitism) or if there is platelet clumping due to agglutinins (Lombarts & deKieviet, 1988), spontaneous aggregation, or incipient clotting due to faulty blood collection. The first two of these phenomena appear to depend on EDTA (Dacie & Lewis, 1991). The reported incidence of EDTA-induced in vitro platelet clumping and pseudothrombocytopenia has ranged from 0.1% (Bartels et al., 1997) to 2% (Lippi et al., 1990). Alterations in platelet histograms or in quantitative cutoff measures derived from them should be used to screen for pseudothrombocytopenia (Bartels et al., 1997).

Reticulated Platelets

Reticulated platelets are those newly released circulating platelets that have residual RNA. Reticulated platelet counts are an estimate of thrombopoiesis (Rapi et al., 1998), analogous to the use of reticulocyte count as an estimate of erythropoiesis. Matic and colleagues (1998) describe an optimized flow-cytometric analysis method after incubating whole blood with thiazole orange, which has a 3000-fold increase in fluorescence after binding to RNA. Phycoerythrin-labeled antibodies directed against GPIb on the surface of the platelet are also in the incubation mixture to distinguish platelets from other cells or debris. Recombinant human erythropoietin seems to improve platelet function in uremia not only by correcting the anemia but also by increasing young platelets, detected as reticulated platelets (Tassies et al., 1998). Significantly lower median levels of reticulated platelets in frequent plateletpheresis donors than in new donors suggest that repeat platelet donation might lead to relative exhaustion of thrombopoiesis (Stohlawetz et al., 1998). Depending on the conditions of the measurement, published normal values for reticulated platelets vary tremendously from 3% to 20% (Matic et al., 1998).

Increased reticulated platelet values have been reported in idiopathic thrombocytopenic purpura (Koike et al., 1998; Saxton et al., 1998) and hyperthyroidism (Stiegler et al., 1998). In neonates younger than 30 weeks' gestation, the reticulated platelet count was about twice that seen in full-term infants (Peterec et al., 1996). Bone marrow recovery after chemotherapy for acute myeloid leukemia (AML) showed an increase in reticulated platelets after about day 20 (Stohlawetz et al., 1999). *Decreased* reticulated platelet values have been reported in association with aplasia and liver cirrhosis (Koike et al., 1998; Saxton et al., 1998). Sysmex 9 (Lincolnshire, IL) has developed an automated method to quantify reticulated platelets using a nucleic acid–specific dye. The immature platelet fraction (IPF) is useful in demonstrating thrombocytopenia due to increased platelet destruction (Briggs et al., 2004).

Reference values for platelet counts are 150 to 450 × 10^9/L. Reference values for MPV are approximately 6.5 to 12 fL in adults.

Physiologic Variation in Platelets

The average platelet count is slightly lower at birth than in older children and adults, and may vary from 84 to 478 × 10^9/L (Barone, 1999). After the first week of life, the reference intervals are those of the adult. In women, the platelet count may fall at the time of menstruation. Women have higher platelet (and WBC and neutrophil) counts than men, and Africans (and less so Afro-Caribbeans) have lower platelet, WBC, and neutrophil counts than whites (Bain, 1996). Reported means (95% reference ranges) for platelet counts were 218 (143–332) for white men and 183 (115–290) for African men versus 246 (169 to 358) for white women and 207 (125 to 342) for African women. Among Australians west of Sydney and 49 years of age or older, Tsang and colleagues (1998) list 247 (128–365) for mean platelet counts for men and 275 (147–403) for women.

INSTRUMENT TECHNOLOGY

Because of the relatively low cost, reduced time (for labor and results), and increased accuracy of the automated analyzers, semiautomated instruments are rarely used in clinical practice these days. Speed of performance, elimination of visual fatigue of the technician, and improved precision are decisive advantages of the electronic cell counter over the hemocytometer/manual methods of performing blood cell counts. Electronic counting instruments are discussed in the following section.

Hematology Analyzers

The multichannel instruments used in the modern laboratory for performing cell counts are based on the principles of electrical impedance, light scattering, radiofrequency conductivity, and/or cytochemistry (Ward, 2000). The principles of these techniques are discussed in the following section. Combining hematology instrumentation with laboratory automation allows for reduction in preanalytic and postanalytic variables and positive identification of samples for processing and analysis, storage, and retrieval.

Electrical Impedance

Cells passing through an aperture through which a current is flowing cause changes in electrical resistance, which is counted as voltage pulses. This principle, illustrated in Fig. 31.6, is used in instruments marketed by Coulter (e.g., LH series, GEN-S, HmX, A-T; Beckman Coulter Inc., Brea, CA), Sysmex (e.g., XE and XT series; Sysmex America Inc., Mundelein, IL), Abbott (e.g., Cell-Dyn, 3700, Ruby, Sapphire; Abbott Diagnostics, Santa Clara, CA, ABX (e.g., Micros 60, Pentra series; ABX Diagnostics Inc., Irvine,CA), and others. An accurately diluted suspension of blood (CS) is made in an isotonic conductive solution that preserves the cell shape. The instrument has a glass cylinder (GC) that can be filled with the conducting fluid and has within it an electrode (E2) and an aperture (A) of 100 μm diameter in its wall. Just outside the glass cylinder is another electrode (E1). The cylinder is connected to a U-shaped glass tube that is partially filled with mercury (M), and that has two electrical contacts (EC1 and EC2). The glass cylinder is immersed in the suspension of cells to be counted (CS) and is filled with conductive solution and closed by a valve (V). A current now flows through the aperture between E1 and E2. As mercury moves up the tube, the cell suspension is drawn through the aperture into the cylinder. Each cell that passes through the aperture displaces an equal volume of conductive fluid, increasing the electrical resistance and creating a voltage pulse, because its resistance is much greater than that of the conductive solution. The pulses, which are proportional in height to the volume of the cells, are counted. This is the Coulter principle.

In the simplest system, the counting mechanism is started when the mercury contacts EC1 and stopped when it contacts EC2. During this time, the cells are counted in a volume of suspension exactly equal to the volume of the glass tubing between contact wires EC1 and EC2. If two or more cells enter the aperture simultaneously, they will be counted as one pulse; this produces a coincidence error for which corrections are now automatically made by analyzers. A threshold setting or pulse discriminator allows the exclusion of pulses below an adjustable height on certain counters. On others, a second threshold also excludes the counting of pulses above a certain height. One therefore counts only the cells in the "window" between the two settings. By systematically changing each threshold by given increments, one can determine a frequency distribution of relative cell volumes. Such cell size distributions can be automatically plotted and are valuable in the study of red cells, white cells, or platelets when two or more changing populations of cells are present. This is the basis for determination of the blood cell histograms, which are now routinely produced by the multichannel hematology analyzers.

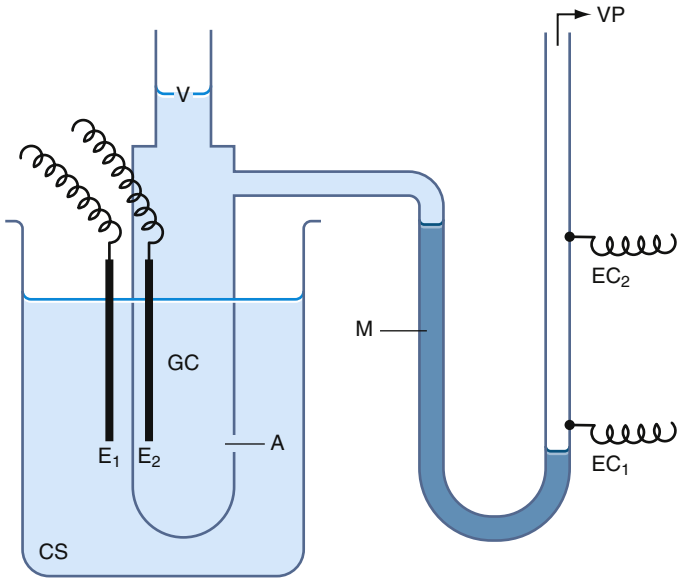

Figure 31.6 Schematic diagram of particle counter in which changes in electrical resistance are counted as voltage pulses. *A,* Aperture; *CS,* cell suspension; E_1 and E_2, platinum electrodes; EC_1 and EC_2, electrical contacts; *GC,* glass cylinder; *M,* mercury column; *V,* valve; *VP,* vacuum pump. (Adapted from Ackerman P: Electronic instrumentation in the clinical laboratory, Boston, 1972, Little, Brown, p 140.)

Radiofrequency Conductivity

Conductivity is determined using a high-frequency electromagnetic probe that provides information on the cells' internal constituents (chemical composition, nuclear characteristics, and granular constituents) by permeating the lipid layer of a cell's membrane. Conductivity is especially helpful in differentiating between cells of like size, such as small lymphocytes and basophils (Burns et al., 1992; Bentley et al., 1993). This principle is utilized in instruments marketed by Coulter (e.g., LH series, GENfi-S, HmX, A-T; Beckman Coulter Inc., Brea, CA) and Sysmex (XE-2100, XT 2000i, HST-N; Sysmex America Inc., Mundelein, IL).

Light Scattering

In the electro-optical analyzers (Fig. 31.7), a light-sensitive detector measures light scattering. All major multichannel analyzers now employ optical methods, at least to some extent. The size of the pulse detected is proportional to the size of the particle (WBC, RBC, or platelet). Although the precision of the instruments employing optical methods is equivalent to that of systems utilizing electrical impedance, some systems use a combination of the two methods to supply an internal comparison. Forward-angle scatter of a laser-generated monochromatic light determines cell surface characteristics, morphology, and granulation. Measurement of light scatter at multiple angles allows enhanced differentiation of cell types. For example, in the Abbott Cell Dyn, four simultaneous light-scattering measurements are made on each white cell. Zero-degree forward angle is primarily affected by, and thus determines, cell size. Ten-degree light scatter is an indicator of cell structure or complexity and is especially helpful in resolving basophils and separating all cell populations. Ninety-degree light scatter separates granulated cells and is termed *lobularity*. Depolarized 90-degree light scattering resolves eosinophils because of their large crystalline granularity. Abnormal cells can have distinctive locations in the size-versus-complexity scatterplot and help to determine WBC suspect flags (Cornbleet et al., 1992), such as for blasts, variant lymphs, bands, and immature granulocytes. Fluorescent deoxyribonucleic acid (DNA) dyes are used in the Abbott automated hematology systems to enumerate nucleated RBCs and identify populations of atypical lymphocytes and nonviable WBCs. Adaptive gating technology permits better separation of overlapping clusters of cell types. Suspect flags are generated when the distinction cannot be clearly delineated, as is often the case in the presence of abnormal WBC populations or interfering substances.

Cytochemistry

A method unique to the Siemens automated hematology series (Siemens Healthcare Diagnostics, Deerfield, IL) is the use of a cytochemical reaction to determine the peroxidase activity of WBCs. The mean peroxidase index (MPXI), a measure of neutrophil-staining intensity, is determined for each specimen. The relative positivity seen in neutrophils, eosinophils, and monocytes is used in conjunction with data derived from light

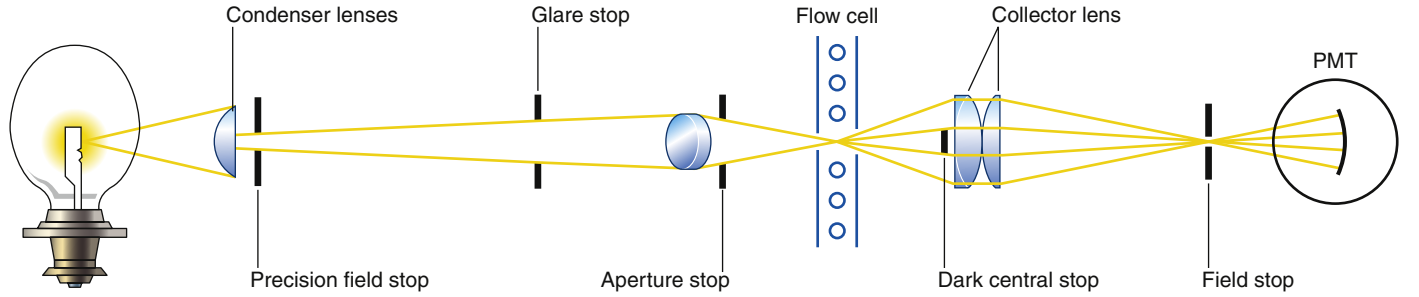

Figure 31.7 Schematic diagram of the electro-optical cell counter. Light is focused on the flow cell. Only light scattered by a cell reaches the photomultiplier tube (PMT), which converts to an electrical pulse (see Chapter 4). (From Mansberg HP: Optical techniques of particle counting. *In Advances in automated analysis, vol 1*, Technicon International Congress, New York, 1970, Mediad, with permission. Reprinted courtesy of Technicon Instrument Corporation, Tarrytown, NY.)

scatter to determine the WBC differential (Simson, 1986). ABX Diagnostics utilizes a cytochemical reagent that fixes the WBCs in their native state and subsequently stains their intracellular and plasmic membranes with chlorazol black E (Clinical Case Studies: Interpretation Guide for ABX 5-Part Diff Hematology Analyzers, ABX Horiba Diagnostics, Montpelier, France).

Reporting/Flagging

Each instrumentation system combines the data generated by these methods in their own configuration to provide a five- or six-part WBC differential along with RBC morphology and platelet parameters (Fig. 31.8). The principles of measurement specific to selected systems are detailed in Table 31.5. Data generated by the instrument that are not acceptable based on instrument- or user-defined criteria are flagged to alert the technologist that reporting the sample requires further investigation. Data management systems now include sophisticated programs that utilize user-defined criteria to determine reflex and repeat testing, including automated slide making and staining. Extreme care must be taken when defining these criteria, as the addition of each lessens the advantage provided by automating the process. The best configurations are developed with the patient population in mind. In addition, follow-up should be tailored to minimize the extended time necessary to derive the correct result.

Sources of Error

Table 31.4 lists various causes of erroneous results obtained from automated cell counters.

Automated Differential Leukocyte Counting

Because the differential leukocyte count is nonspecific, nonprecise, error prone, usually labor intensive, expensive to perform, and of limited clinical significance as a screening test, some investigators have suggested that it may be prudent to discontinue use of the differential count as an inpatient screening test for adults (Connelly et al., 1982). Automation of the differential count eliminates some of the detractions. Ideally, requirements for the automated differential leukocyte counting system should include the following:

1. The distribution of cells analyzed should be identical to that in the blood.
2. All leukocytes usually found in blood diseases should be accurately identified or detected and flagged in some way.
3. The speed of the process should enable a large number of cells to be counted to minimize statistical error.
4. The instrument should be cost-effective (Bentley & Lewis, 1977).

Impedance counters and flow cytometer systems and their differential counts are discussed in the Instrument Technology section earlier in the chapter.

The automated systems have the advantage of rapidly analyzing larger numbers of cells and significantly reducing the statistical error of counting.

Disadvantages include that the categories of cells are not completely consonant with those with which we are familiar on Romanowsky's-stained films. An "unclassified" category is difficult to interpret. When an abnormal result occurs, a film must be made and examined. Because of concern regarding the instrument flags, each laboratory should devise a policy for blood film examination and visual counting when indicated. Camden (1993) provides guiding questions to be asked in selecting a new hematology analyzer for your laboratory. The ICSH (1984b) also published a protocol for evaluation of automated blood cell counters.

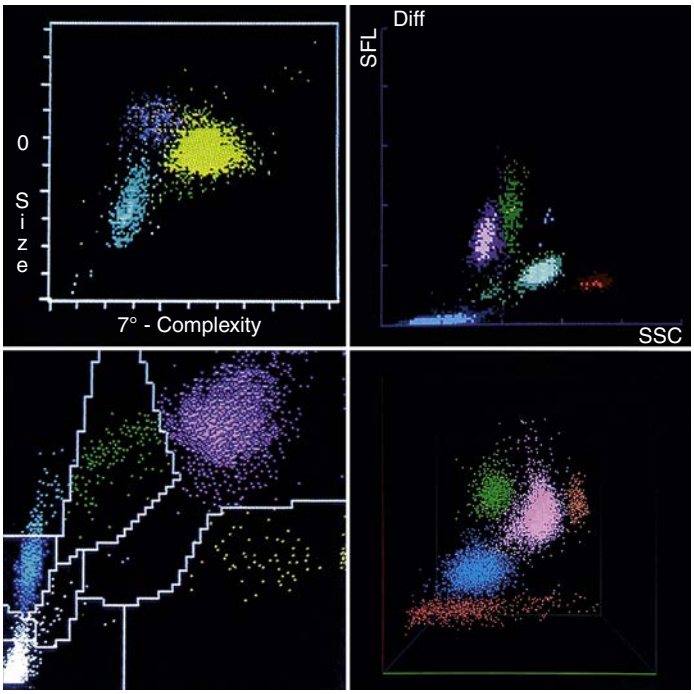

Figure 31.8 White blood cell (WBC) scattergrams/cytograms. *Top left,* Abbott CELL-DYN 4000 WBC scatterplot, light scatter versus volume. *Top right,* Sysmex XT 2000i, WBC scattergram, side-scattered light versus side fluorescence. *Bottom left,* Siemens Advia 120, WBC peroxidase cytogram. *Bottom right,* Coulter LH 750, WBC scattergram, light scatter versus volume.

TABLE 31.5
Principles Used by Various Multichannel Instruments in the Clinical Laboratory

	METHOD			
Instrument	**Impedance**	**Conductivity**	**Light Scatter**	**Cytochemistry**
Abbott	X	X	X	
ABX	X		X	X
Siemens			X	X
Coulter	X	X	X	
Sysmex	X	X	X	

Digital Image Processing

A uniformly made and stained blood film is placed on a motor-driven microscope stage. A computer controls scanning the slide and stopping it when leukocyte(s) are in the field. The optical details (e.g., nuclear and cytoplasmic size, density, shape, color) are recorded by a camera in digital form; these characteristics are compared with a memory bank of such characteristics for the different cell types. If the pattern fits that of a normal cell type, it is identified as such; otherwise, the cell is classified as other or unknown. The coordinates of the unknown cells are kept by the instrument and relocated at the end of the count so that the technologist

can classify them (Lapen, 1982; Parthenis & Metaxaki-Kossionides, 1992; Mukherjee et al., 2004).

In a review conducted by a committee on behalf of the ICSH, accuracy of preclassification was reported to be between 81.2% and 96.4% for all normal leukocytes with the exception of eosinophils (63.2%) (Kratz et al., 2005). Preclassification of immature granulocytes, plasma cells and blasts was unreliable and required review by a skilled morphologist (Rollins-Raval et al., 2012). Software applications make it possible to classify RBCs morphologically into categories with high sensitivity, but mixed specificity, making review necessary but more efficient than manual microscopic review. Similarly, images for platelet estimation and morphology expedite the review process. Due to the area captured by digital imaging, detection of platelet clumps varies (Gulati et al., 2014). ICSH recommendations for the appropriate use of digital imaging in conjunction with automated cell counters include developing adequate flagging criteria based on the specific needs of the laboratory, always reconciling the flags generated by the automated cell counter, and training operators on the different staining characteristics of slides prepared by automated slide makers and stainers versus manual methods (Kratz et al., 2019).

Automated Reticulocyte Counting

Many of the same principles applied in determination of the WBC differential may be utilized to determine reticulocyte counts, resulting in enhanced precision and increased accuracy in routine practice (Metzger & Charache, 1987). Depending on the specific model of analyzer, this process may be semiautomated or fully automated. All methods rely on the addition of a stain or dye to detect the RNA content of the RBC. Such stains include new methylene blue (NMB), oxazine, auramine O, polymethine, and thiazole orange. Methods of detection include impedance, light scatter, absorption, and fluorescence intensity. Reticulocyte fractions are separated based on RNA content, with the more immature cells containing the highest amount of reticulum. The immature reticulocyte fraction (IRF) quantitatively describes the youngest reticulocytes with the greatest staining intensity. This parameter allows early detection of an increased erythropoietic response, important in determining the response of the bone marrow recovering from chemotherapy or transplant or the response to erythropoietin therapy. It may also be used in conjunction with the absolute reticulocyte count to classify anemias (Davis & Biegelow, 1994; Davis, 1996; d'Onofrio et al., 1996). The reticulocyte Hb content (CHr) provides a sensitive index by which to identify hypochromic RBCs. The reticulocyte hemoglobin content, CHr and RET-He, reported by Siemens (Tarrytown, NY) and Sysmex (Lincolnshire, IL) provides a sensitive index by which to identify hypochromic RBCs. It has also been shown to be useful in evaluating iron deficiency in cancer patients (Peerschke et al., 2014).

BLOOD FILM EXAMINATION

Microscopic examination of the blood spread on a glass slide or coverslip yields useful information regarding all formed elements of the blood. The process of making thin blood film causes mechanical trauma to the cells. Also, the cells flatten on the glass during drying, and fixation and staining involve exposure to methanol and water. Some artifacts are inevitably introduced, but these can be minimized by good technique.

EXAMINATION OF WET PREPARATIONS

It is sometimes advantageous to examine fresh blood under the microscope to avoid artifacts of fixation or staining. This is readily accomplished by sealing a small drop of blood diluted with isotonic sodium chloride beneath a coverslip on a glass slide. Buffered glutaraldehyde will preserve the cells for reexamination at a later time. Petroleum jelly or xipamide (Aquaphor) may be used to seal the edges of the coverslip to the slide. Wet preparations are used to detect sickling, and spherocytes may be readily detected in this manner. Wet preparations may be examined to ensure that the erythrocyte abnormalities seen on fixed films are not artifacts of drying or staining.

MAKING AND STAINING BLOOD FILMS

Examination of the blood film is an important part of the hematologic evaluation. The reliability of the information obtained depends heavily on well-made and well-stained films that are systematically examined. Blood films should be prepared immediately if possible. Three methods of making films are described: the two-slide or wedge method, the cover glass method, and the spinner method.

Wedge Method

Place a drop of blood 2 to 3 mm in diameter about 1 cm from the end of a clean, dust-free slide that is on a flat surface. With the thumb and forefinger of the right hand, hold the end of a second (spreader) slide against the surface of the first slide at an angle of 30 to 45 degrees and draw it back to contact the drop of blood. Allow the blood to spread and form the angle between the two slides. Push the "spreader slide" at a moderate speed forward until all the blood has been spread into a moderately thin film. The spreader slide should be clean, dry, and slightly narrower than the first slide so that the edges can be easily examined with the microscope.

The slides should be rapidly air dried by waving the slides or using an electrical fan. The thickness of the film can be adjusted by changing the angle of the spreader slide or the speed of spreading, or by using a smaller or larger drop of blood. At a given speed, increasing the angle of the spreader slide will increase the thickness of the film. At a given angle, increasing the speed with which the spreader slide is pushed will also increase the thickness of the film. The film should not cover the entire surface of the slide. A good film includes a thick portion and a thin portion and a gradual transition from one to the other. The film should have a smooth, even appearance and be free from ridges, waves, or holes. The edge of the spreader must be absolutely smooth. If it is rough, the film has ragged tails containing many leukocytes. In films of optimal thickness, some overlap of red cells is seen in much of the film, but with even distribution and separation of red cells toward the thin tail. The faster the film is air dried, the better is the spreading of individual cells on the slide. Slow drying (e.g., in humid weather) results in contraction artifacts of the cells. The slide may be labeled with a lead pencil on the frosted end or directly on the thicker end of the blood film.

Cover Glass Method

No. 1 or 1.5 cover glasses 22 mm square are recommended. Touch a cover glass to the top of a small drop of blood without touching the skin and place it, blood side down, crosswise on another cover glass so that the corners appear as an eight-point star. If the drop is not too large and the cover glasses are perfectly clean, the blood will spread out evenly and quickly in a thin layer between the two surfaces. Just as it stops spreading, pull the cover glasses quickly but firmly apart on a plane parallel to their surfaces. The blood usually is much more evenly spread on one of the cover glasses than it is on the other. Cover glasses should be placed film side up on clean paper and allowed to dry in the air or they may be inserted back to back in slits made in a cardboard box. Films from venous blood may be prepared similarly by placing a drop of blood on a coverslip and proceeding as described.

Spinner Method

Blood films that combine the advantages of easy handling of the wedge slide and uniform distribution of cells of the cover glass preparation may be made with special types of centrifuges known as *spinners* (Rogers, 1973). The spinner slide produces a uniform blood film in which all cells are separated (a monolayer) and randomly distributed. White cells can be easily identified at any spot in the film. On a wedge smear, disproportions (1) of monocytes occur at the tip of the feather edge, (2) of neutrophils are seen just in from the feather edge, and (3) of both occur at the lateral edges of the film (Rogers, 1973). This has little practical and perhaps some historic significance.

Most manufacturers of automated hematology analyzers now offer slide maker-stainers. Details are available from the vendors.

Blood Stains

The aniline dyes used in blood work are of two general classes: basic dyes, such as methylene blue; and acid dyes, such as eosin. Nuclei and certain other structures in the blood are stained by the basic dyes and, hence, are called *basophilic*. Structures that take up only acid dyes are called *acidophilic*, or *eosinophilic*. Other structures stained by a combination of the two are called *neutrophilic*.

Polychrome methylene blue and *eosin* stains are the outgrowth of the original time-consuming Romanowsky's method and are widely used. They stain differentially most normal and abnormal structures in the blood. The basic components of thiazine include methylene blue (tetramethylthionine) and, in varying proportions, its analogs produced by oxidative demethylation: azure B (trimethylthionine); azure A (asymmetric dimethylthionine); symmetric dimethylthionine; and azure C (monomethylthionine) (Lillie, 1977). The acidic component eosin is derived from a xanthene skeleton. Most Romanowsky's stains are dissolved in methyl alcohol and combine fixation with staining. Among the best known methods are the Giemsa and Wright's stains.

Wright's Stain

This is a methyl alcoholic solution of eosin and a complex mixture of thiazines, including methylene blue (usually 50%–75%), azure B (10%–25%), and other derivatives (Lubrano et al., 1977). Wright's stain, certified by the Biological Stain Commission, is commercially available as a solution ready for use or as a powder. The buffer solution (pH 6.4) contains primary (monobasic) potassium phosphate (KH_2PO_4), anhydrous 6.63 g; secondary (dibasic) sodium phosphate (Na_2HPO_4), anhydrous 2.56 g; and distilled water to make 1 L. A more alkaline buffer (pH 6.7) may be prepared by using 5.13 g of the potassium salt and 4.12 g of the sodium salt.

Procedure.

1. To prevent the plasma background of the film from staining blue, blood films should be stained within a few hours of preparation or fixed if they must be kept without staining.
2. Fixation and staining may be accomplished by immersing the slides in reagent-filled jars or by covering horizontally supported slides or coverslips with the reagents. With the latter method, covering the film with copious stain avoids evaporation, which leads to precipitation.
3. Fixation is provided for 1 to 2 minutes with absolute methanol.
4. The slide is next exposed to undiluted stain solution for 2 minutes. Then, without removing the stain from the horizontal slide, an equal amount of buffer is carefully added and is mixed by blowing gently.
5. The stain is flushed from the horizontal slide with water. Washing for longer than 30 seconds reduces the blue staining. The back of the slide is cleaned with gauze.
6. The slide is allowed to air dry in a tilted position.
7. Cover glasses are mounted film side down on a slide with Canada balsam or another mounting medium.

Films stained well with Wright's stain have a pink color when viewed with the naked eye. Under low power, the cells should be evenly distributed. The red cells are pink, not lemon yellow or red. There should be a minimum of precipitate. The color of the film should be uniform. The blood cells should be free from artifacts, such as vacuoles. The nuclei of leukocytes are purple, the chromatin and parachromatin clearly differentiated, and the cytoplasmic neutrophilic granules tan in color. The eosinophilic granules are red-orange, and each is distinctly discernible. The basophil has dark-purple granules. Platelets have dark-lilac granules. Bacteria (if present) are blue. The cytoplasm of lymphocytes is generally light blue; that of monocytes has a faint blue-gray tinge. Malarial parasites have sky-blue cytoplasm and red-purple chromatin. The colors are prone to fade if the preparation is mounted in balsam of poor quality or is exposed to the light.

Staining Problems.

Excessively blue stain. Thick films, prolonged staining time, inadequate washing, or too high an alkalinity of stain or diluent tends to cause excessive basophilia. In such films, the erythrocytes appear blue or green, the nuclear chromatin is deep blue to black, and the granules of the neutrophils are deeply overstained and appear large and prominent. The granules of the eosinophils are blue or gray. Staining for a shorter time or using less stain and more diluent may correct the problem. If these steps are ineffective, the buffer may be too alkaline, and a new one with a lower pH should be prepared.

Excessively pink stain. Insufficient staining, prolonged washing time, mounting the coverslips before they are dry, or too high an acidity of the stain or buffer may cause excessive acidophilia. In such films, the erythrocytes are bright red or orange, the nuclear chromatin is pale blue, and the granules of the eosinophils are sparkling brilliant red. One of the causes of the increased acidity is exposure of the stain or buffer to acid fumes. The problem may be a low pH of the buffer or it may be the methyl alcohol, which is prone to develop formic acid as a result of oxidation on standing.

Other staining problems. Inadequately stained red cells, nuclei, or eosinophilic granules may be due to understaining or excessive washing. Prolonging the staining or reducing the washing may solve the problem.

Precipitate on the film may be due to unclean slides; drying during the period of staining; inadequate washing of the slide at the end of the staining period, especially failure to hold the slide horizontally during the initial washing; inadequate filtration of the stain; or permitting dust to settle on the slide or smear.

Other Stains

Besides Wright's stain, Romanowsky-type stains include a number of others: Giemsa, Leishman's, Jenner's, May-Grünwald, MacNeal's, and various combinations. Some have been particularly recommended for certain purposes, such as Giemsa stain for excellence in staining malarial parasites and protozoa.

Reference Method

Studies have demonstrated the ability of the combination of just two dyes—azure B and eosin Y—to give the full range of colors provided by ideal Romanowsky's staining of blood and marrow cells. This is the reference method for Romanowsky's staining (ICSH, 1984a).

Automated Slide Stainer

Automated slide stainers are being used in several laboratories for routine hematology and microbiology slides. The stainer is a compact instrument with microprocessor control for flexibility in staining applications. Several slides can be stained uniformly in minutes. Typically, any automated stainer has several user-definable programs to choose from. Staining problems are encountered even with the use of automatic stainers and must be dealt with on an individual basis.

Review of Peripheral Smear

Practicing pathologists may be called upon to review peripheral blood smears, to confirm or compare their assessment with that of the technologist, and to review the findings with clinical colleagues at the multihead microscope. Although this is a daily task for the hematopathologist, the general pathologist examines the peripheral smear less frequently and the bone marrow preparation even less so. Following is a summary of the main features that the general pathologist should evaluate.

ERYTHROCYTES

In the blood from a healthy person, the erythrocytes, when not crowded together, appear as circular, homogeneous disks of nearly uniform size, ranging from 6 to 8 μm in diameter (Fig. 31.9). However, even in normal blood, individual cells may be as small as 5.5 μm and as large as 9.5 μm. The center of each is somewhat paler than the periphery. In disease, erythrocytes vary in their Hb content, size, shape, staining properties, and structure.

Color

Hemoglobin Content

The depth of staining furnishes a rough guide to the amount of Hb in red cells. The terms *normochromic*, *hypochromic*, and *hyperchromic* are used to describe this feature of red cells. Normochromic refers to normal intensity of staining (see Fig. 31.9). When the amount of Hb is diminished, the central pale area becomes larger and paler. This is known as *hypochromia*. The MCH and MCHC are usually decreased (Fig. 31.10). In megaloblastic anemia, because the red cells are larger and, hence, thicker, many stain deeply and have less central pallor (Fig. 31.11). These cells are hyperchromic because they have an increased MCH, but

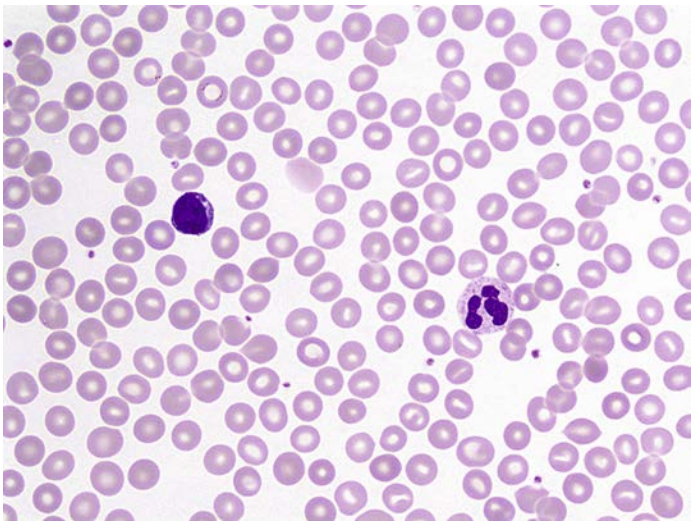

Figure 31.9 Normal peripheral smear. Erythrocytes appear as circular, homogeneous disks of nearly uniform size, ranging from 6 to 8 μm in diameter, with central pallor not exceeding more than one-third of the cell. On average, the red cells are approximately the same size as the nucleus of a small lymphocyte (500×).

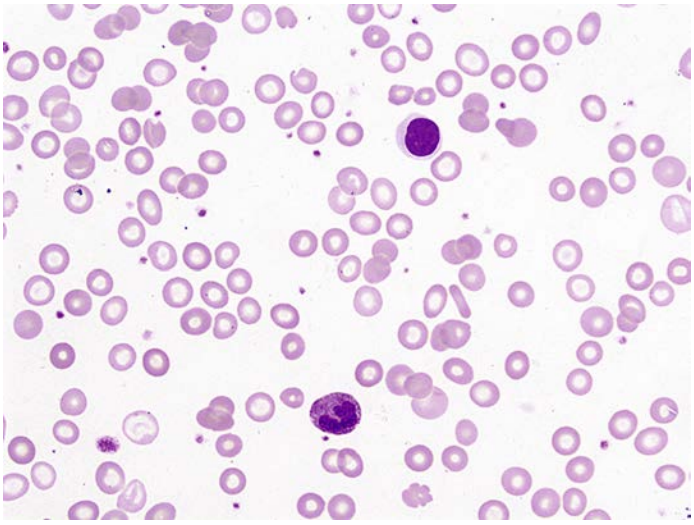

Figure 31.10 Microcytic hypochromic red cells in iron deficiency anemia. Red cells are hypochromic—the amount of hemoglobin per cell is decreased, and the central pale area becomes larger (more than one-third) (500×).

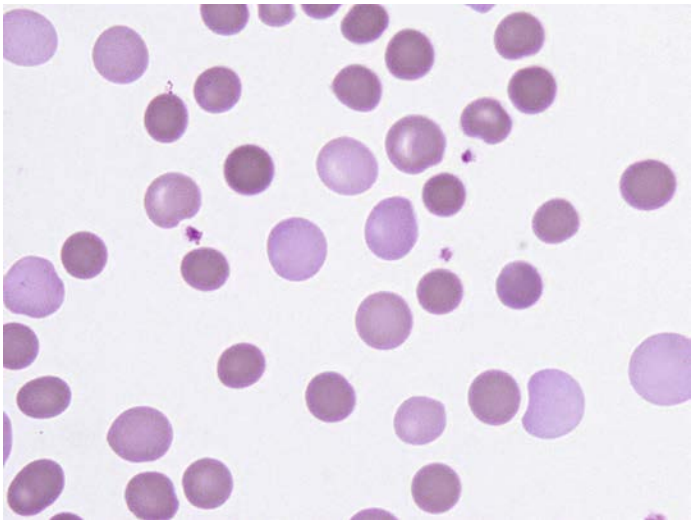

Figure 31.12 Hereditary spherocytosis. Spherocytes are nearly perfectly round, smaller than normal red cells, and lack central pallor (hyperchromic) (1000×).

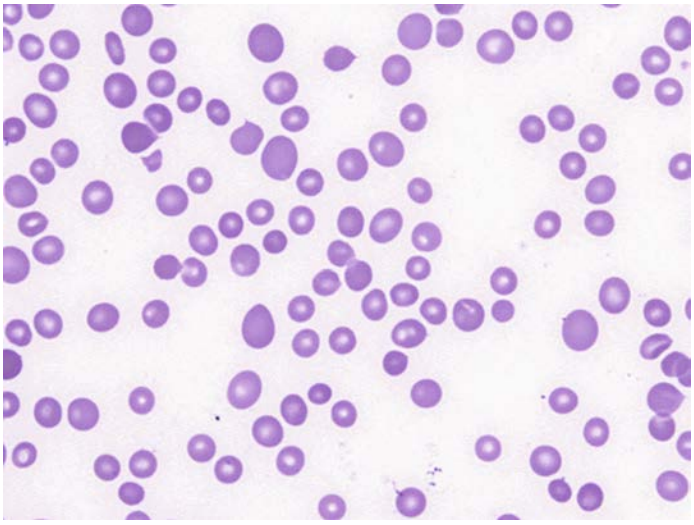

Figure 31.11 Macrocytes. Red cells are larger and thicker, stain deeply, and lack central pallor (500×).

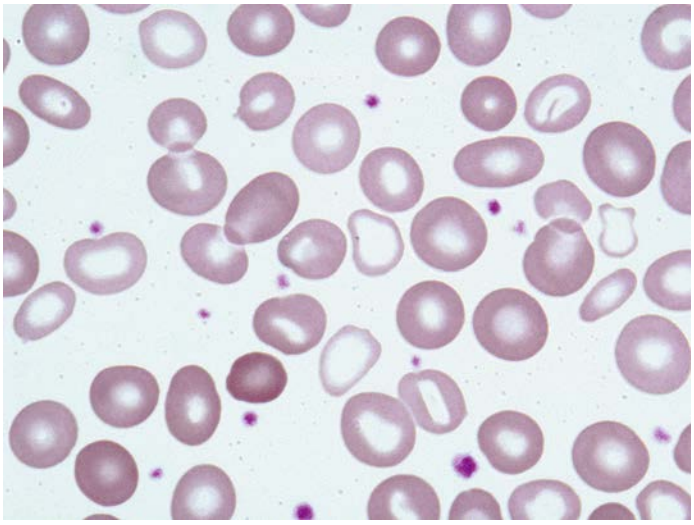

Figure 31.13 Dimorphic anemia. Anisocytosis and anisochromia characterized by the presence of microcytic hypochromic cells, normocytic cells, and few macrocytes (1000×).

the MCHC is normal. In hereditary spherocytosis (Fig. 31.12), the cells are also hyperchromic; although the MCH is normal, the MCHC is usually increased because of a reduced surface/volume ratio. The presence of hypochromic cells and normochromic cells in the same film is called *anisochromia* or, sometimes, a *dimorphic anemia* (Fig. 31.13). This is characteristic of sideroblastic anemias but also is found some weeks after iron therapy for iron deficiency anemia or in a hypochromic anemia after transfusion with normal cells.

Polychromatophilia

A blue-gray tint to the red cells (polychromatophilia or polychromasia) is a combination of the affinity of Hb for acid stains and the affinity of RNA for basic stains. The presence of residual RNA in the red cell indicates that it is a young red cell that has been in the blood for 1 to 2 days. These cells are larger than mature red cells and may lack central pallor (Fig. 31.14). Young cells with residual RNA are polychromatophilic red cells on air-dried films stained with Wright's stain but are reticulocytes when stained supravitally with brilliant cresyl blue. Therefore, increased polychromasia implies reticulocytosis; it is most marked in hemolysis and in acute blood loss.

Size

The red cells may be abnormally small, or microcytes (see Fig. 31.10), or abnormally large, or macrocytes (see Fig. 31.11), or they may show abnormal variation in size (anisocytosis) (see Fig. 31.13). Anisocytosis is a feature of most anemias; when it is marked in degree, both macrocytes and microcytes are usually present. In analyzing causes of anemia, the terms

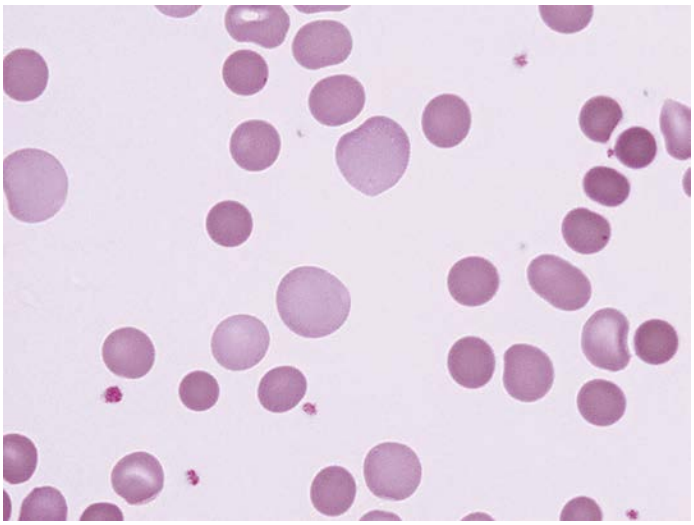

Figure 31.14 Polychromatophilia. Polychromatophilic red cells are young red cells, larger than mature red cells; they lack central pallor and appear slightly basophilic on Wright's stain. They are called *reticulocytes* when stained supravitally with brilliant cresyl blue (1000×).

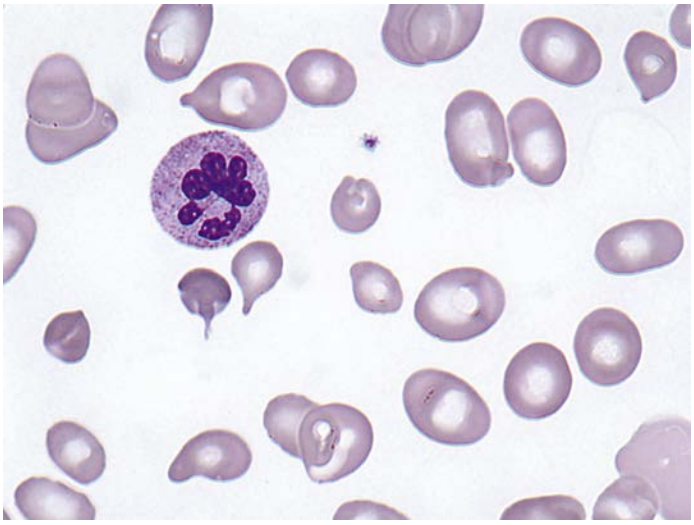

Figure 31.15 Poikilocytosis. Variation in shape of red cells. Abnormally shaped cells include oval, pear-shaped, and other irregularly shaped cells (1000×).

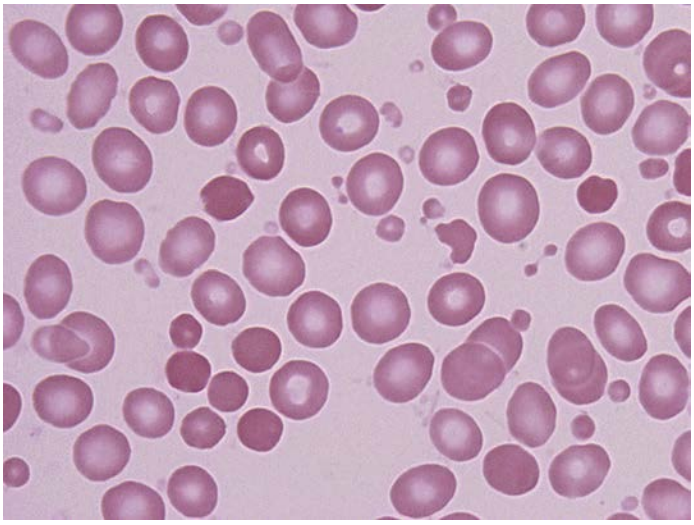

Figure 31.17 Thermal injury. Tiny bits of membrane (in excess of hemoglobin) are removed from the red cell surface, leading to formation of spherocytes (1000×).

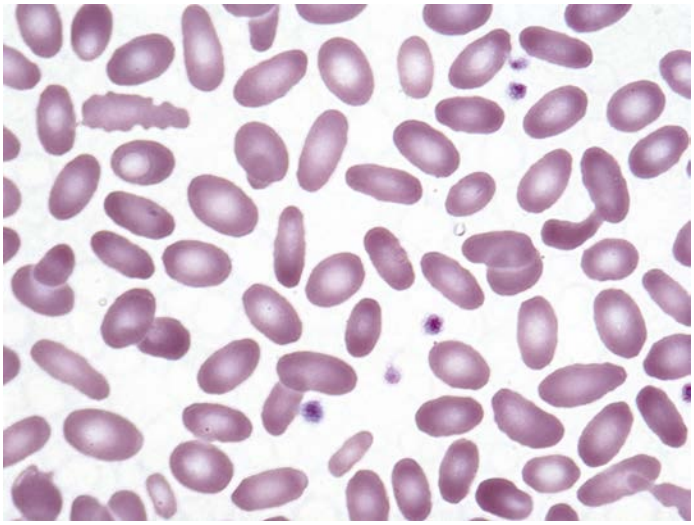

Figure 31.16 Hereditary elliptocytosis. Most cells are elliptocytes. They are seen in a normal person's blood but usually account for less than 10% of cells. They are also common in iron deficiency anemia, myelofibrosis, megaloblastic anemia, and sickle cell anemia (1000×).

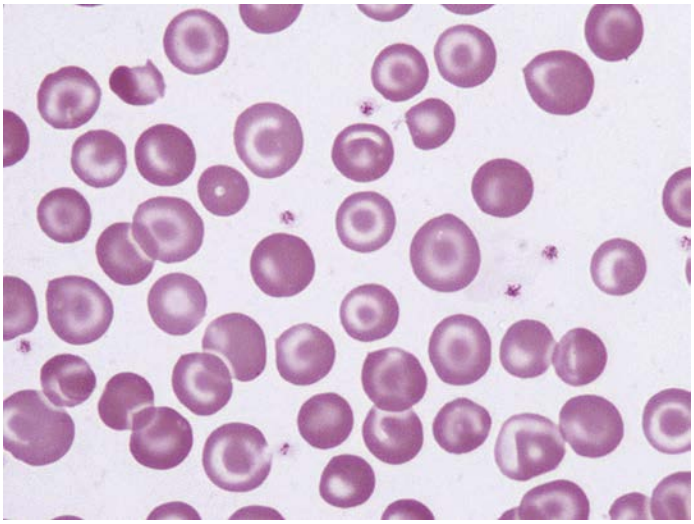

Figure 31.18 Target cells. Red cells with a thin membrane, peripheral rim of hemoglobin (Hb), and dark, central, Hb-containing area. They are frequently seen in Hb C disease, in hypochromic anemia, and in liver disease (1000×).

microcytic and *macrocytic* have greatest meaning when considered as cell volume rather than cell diameter. The mean cell volume is measured directly on a multichannel analyzer. We perceive the diameter directly from the blood film and infer volume (and the Hb content) from it. Thus, the red cells in Figure 31.10 are microcytic; because they are hypochromic, they are thinner than normal and the diameter is not decreased proportionately to the volume. Also, the mean cell volume in the blood of the patient with spherocytosis (see Fig. 31.12) is in the normal range; although many of the cells have a small diameter, their volume is not decreased because they are thicker than normal.

Shape

Variation in shape is called *poikilocytosis*. Any abnormally shaped cell is a poikilocyte. Oval, pear-shaped, teardrop-shaped, saddle-shaped, helmet-shaped, and irregularly shaped cells may be seen in a single case of anemia, such as megaloblastic anemia (Fig. 31.15).

Elliptocytes are most abundant in hereditary elliptocytosis (Fig. 31.16), in which most cells are elliptical; this is a dominant condition that is only occasionally associated with hemolytic anemia. Elliptocytes are seen in normal persons' blood but account for less than 10% of the cells. They are more common, however, in iron deficiency anemia (see Fig. 31.10), myelofibrosis with myeloid metaplasia, megaloblastic anemia, and sickle cell anemia.

Spherocytes are nearly spherical erythrocytes, in contradistinction to normal biconcave disks. Their diameter is smaller than normal. They lack the central pale area or have a smaller, often eccentric, pale area (because the cell is thicker and can come to rest somewhat tilted instead of perfectly flattened on the slide). They are found in hereditary spherocytosis (HS) (see Fig. 31.12), in some cases of autoimmune hemolytic anemia (AHA), and in some conditions in which a direct physical or chemical injury has occurred to the cells, such as from heat (Fig. 31.17). In each of these three instances, tiny bits of membrane (in excess of Hb) are removed from the adult red cells, leaving the cells with a decreased surface/volume ratio. In HS and AHA, this occurs in the reticuloendothelial system; in other instances (e.g., in the patient with body burns), this may occur intravascularly.

Target cells are erythrocytes that are thinner than normal (leptocytes) and when stained show a peripheral rim of Hb with a dark, central, Hb-containing area. They are found in obstructive jaundice (Fig. 31.18), in which there appears to be an augmentation of the cell surface membrane; in the postsplenectomy state, in which there is a lack of normal reduction of surface membrane as the cell ages; in any hypochromic anemia, especially thalassemia; and in Hb C disease.

Schistocytes (cell fragments) indicate the presence of hemolysis, whether in megaloblastic anemia, severe burns (see Fig. 31.17), or microangiopathic hemolytic anemia (Fig. 31.19). The latter process may be associated with small blood vessel disease or with fibrin in small blood vessels and results in intravascular fragmentation; particularly characteristic are helmet cells and triangular cells.

Acanthocytes are irregularly spiculated red cells in which the ends of the spicules are bulbous and rounded (Fig. 31.20). They are seen in abetalipoproteinemia, hereditary or acquired, and in certain cases of liver disease. Burr cells, or echinocytes (Fig. 31.21), are regularly

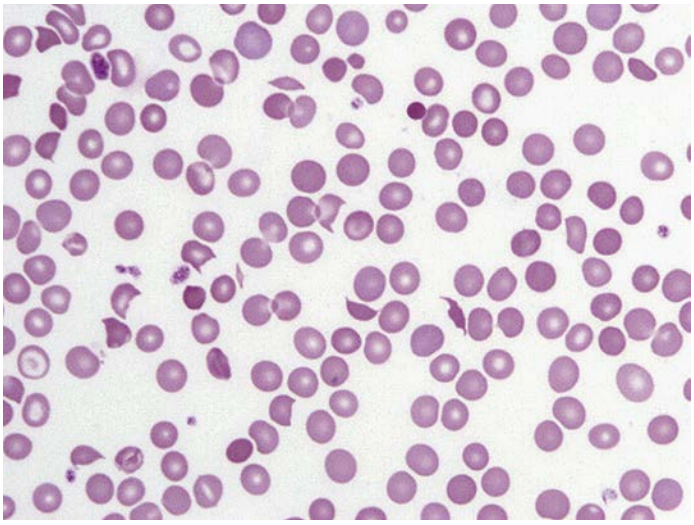

Figure 31.19 Schistocytes. Presence of cell fragments is indicative of hemolysis. Schistocytes can be seen in several conditions, including microangiopathic hemolytic anemia, megaloblastic anemia, burns, and disseminated intravascular coagulation (500×).

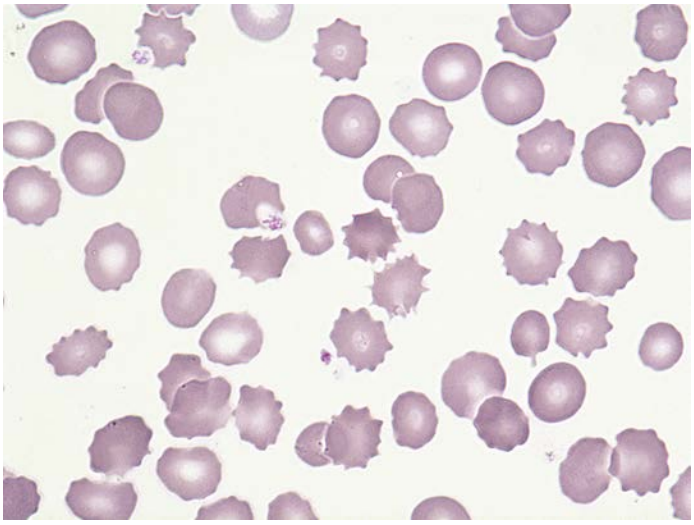

Figure 31.21 Echinocytes. Regularly contracted cells with sharp ends; may occur as an artifact during film preparation or as the result of hyperosmolarity or decreased adenosine triphosphate due to several causes (1000×).

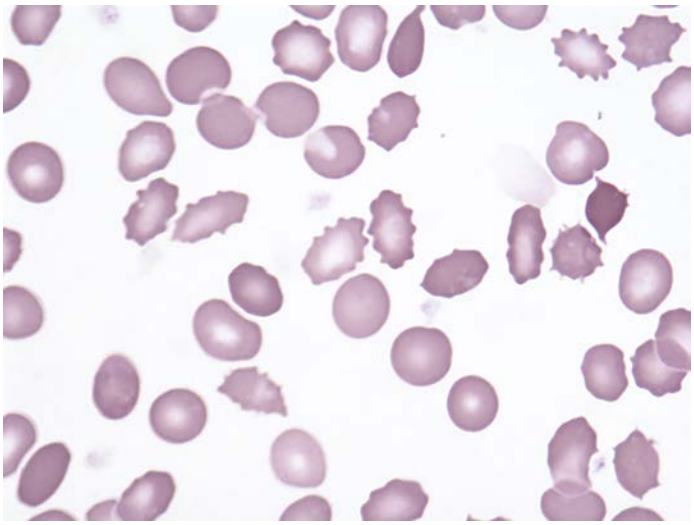

Figure 31.20 Acanthocytes. Irregularly spiculated cells with bulbous and rounded ends, frequently seen in abetalipoproteinemia or certain cases of liver disease (1000×).

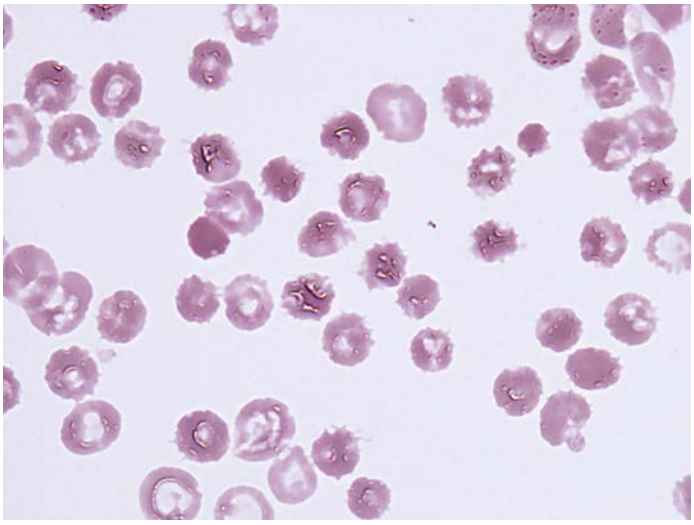

Figure 31.22 Artifact. Tiny pits or bubbles in the red cells. They can be caused by a small amount of water contaminating the Wright's stain or by insufficient slide drying (500×).

contracted cells that may commonly occur as an artifact during preparation of films (Dalal, 2002). They may also be present due to hyperosmolarity or to the discocyte-echinocyte transformation. In vivo, the latter may be associated with decreased red cell adenosine triphosphate (ATP) resulting from any of several causes. Artifacts resembling crenated cells consisting of tiny pits or bubbles indenting the red cells (Fig. 31.22) may be caused by a small amount of water contaminating the Wright's stain (or absolute methanol, if this is used first as a fixative).

Structure

Basophilic Stippling (Punctate Basophilia)

This is characterized by the presence, within the erythrocyte, of irregular basophilic granules, which vary from fine to coarse (Fig. 31.23). They stain deep blue with Wright's stain. The erythrocyte containing them may stain normally in other respects or it may exhibit polychromatophilia. Fine stippling is commonly seen when there is increased polychromatophilia and, therefore, with increased production of red cells. Coarse stippling may be seen in lead poisoning or other diseases with impaired Hb synthesis, in megaloblastic anemia, and in other forms of severe anemia. It is attributed to an abnormal instability of the RNA in the young cell. Red cells with inorganic iron-containing granules (as demonstrated by stains for iron) are called *siderocytes*. Sometimes, these granules stain with Wright's stain; if so, they are called *Pappenheimer bodies*.

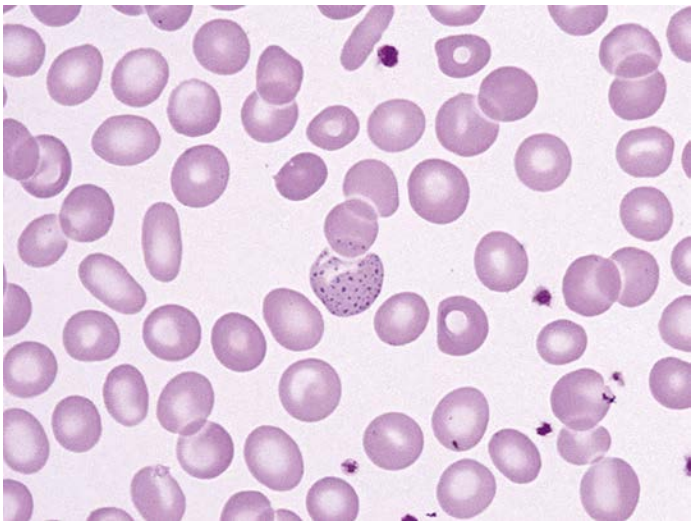

Figure 31.23 Basophilic stippling. Presence of irregular basophilic granules, either fine or coarse; commonly seen in increased red cell production. Coarse stippling is usually seen in lead poisoning or other anemias due to impaired hemoglobin synthesis, such as megaloblastic anemia (1000×).

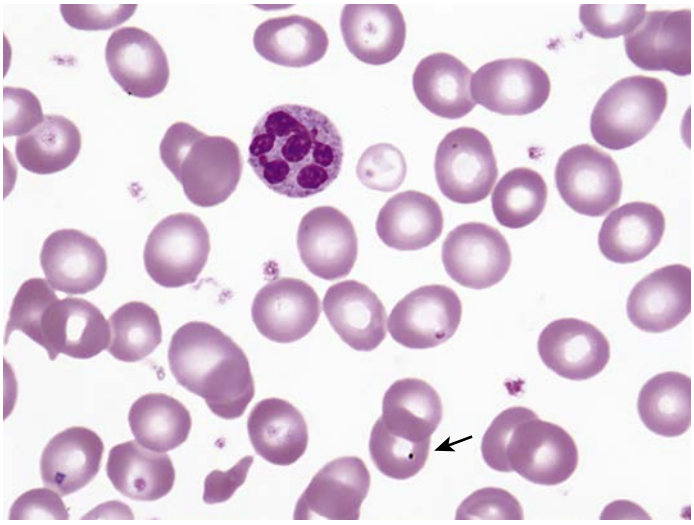

Figure 31.24 Howell-Jolly bodies. Smooth, round remnants of nuclear chromatin. Seen in postsplenectomy states and hemolytic and megaloblastic anemias (a hypersegmented neutrophil is also seen) (1000×).

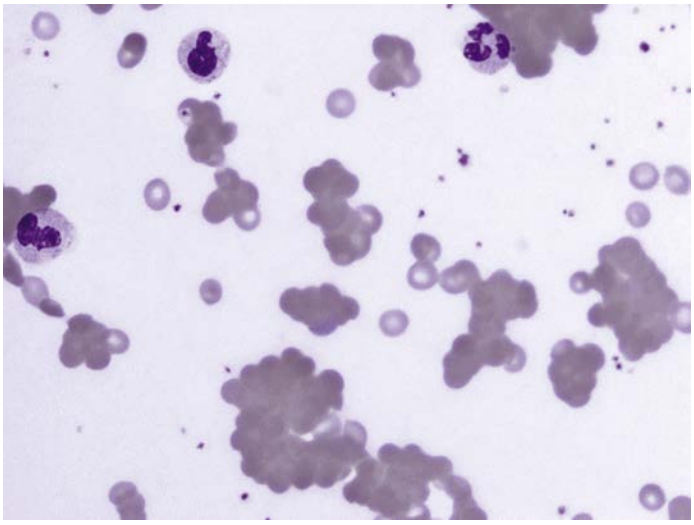

Figure 31.26 Agglutination. Clumping of red cells, which is more irregular than linear rouleaux formation. It is caused by cold agglutinins (500×).

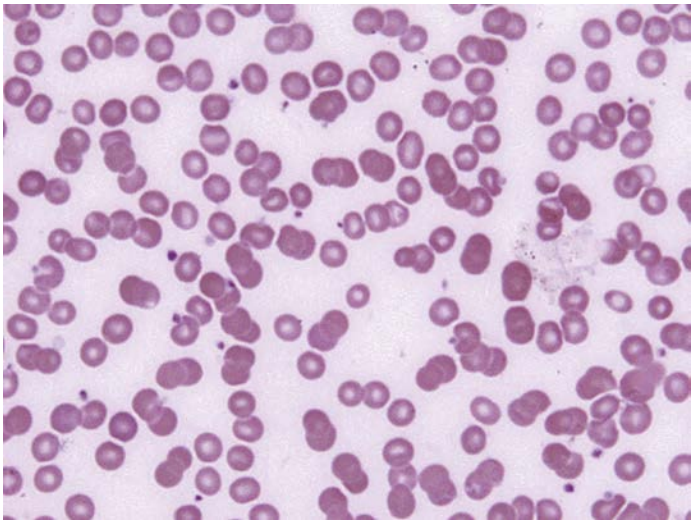

Figure 31.25 Rouleaux formation. Alignment of red cells one upon another so that they resemble a stack of coins. It is usually caused by elevated plasma fibrinogen or globulins (500×).

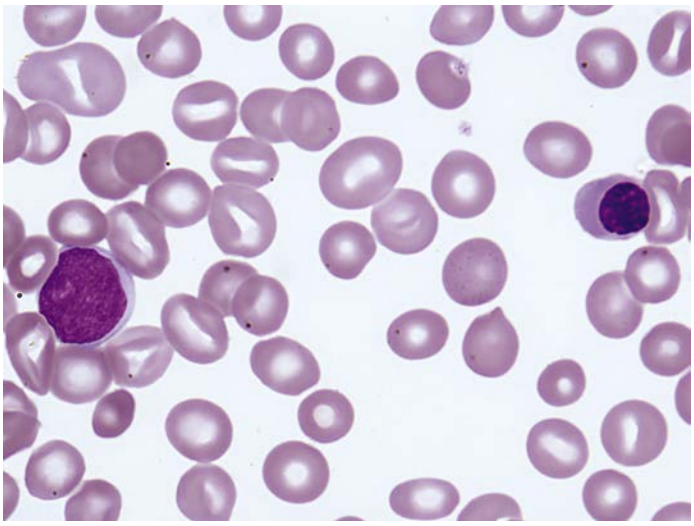

Figure 31.27 Nucleated red cell/normoblasts. Precursors of mature red cells, normoblasts are usually present only in the bone marrow. Their presence in blood is usually associated with increased red cell production or infiltrative bone marrow disorders (1000×).

In contrast to basophilic stippling, Pappenheimer bodies are few in number in a given red cell and are rarely seen in the peripheral blood except after splenectomy.

Howell-Jolly Bodies

These particles are smooth, round remnants of nuclear chromatin. Single Howell-Jolly bodies may be seen in megaloblastic anemia (Fig. 31.24), in hemolytic anemia, and after splenectomy. Multiple Howell-Jolly bodies in a single cell usually indicate megaloblastic anemia or some other form of abnormal erythropoiesis.

Cabot Rings

These are ring-shaped, figure-of-eight, or loop-shaped structures. Occasionally, they are formed by double or several concentric lines. They are observed rarely in erythrocytes in pernicious anemia, lead poisoning, and certain other disorders of erythropoiesis. They stain red or reddish purple with Wright's stain and have no internal structure. The rings are probably microtubules remaining from a mitotic spindle (Bessis, 1977). They are interpreted as evidence of abnormal erythropoiesis.

Malarial Stippling

Fine granules may appear in erythrocytes that harbor *Plasmodium vivax*. With Wright's stain, the minute granules, "Schüffner's granules," stain purplish red. They are sometimes so numerous that they almost hide the parasites. These red cells are, as a rule, larger than normal.

Rouleaux Formation

This is the alignment of red cells one upon another so that they resemble stacks of coins. On air-dried films, rouleaux appear as in Figure 31.25. Elevated plasma fibrinogen or globulins cause rouleaux to form and also promote an increase in the erythrocyte sedimentation rate. Rouleaux formation is especially marked in paraproteinemia (monoclonal gammopathy). *Agglutination*, or clumping, of red cells is more surely separated from rouleaux in wet preparations and on air-dried films tends to show more irregular and round clumps than linear rouleaux. Cold agglutinins are responsible for this appearance (Fig. 31.26).

Nucleated Red Blood Cells

In contrast to erythrocytes of lower vertebrates and to most mammalian cells, the mammalian erythrocyte lacks a nucleus. NRBCs (normoblasts; Fig. 31.27, and see Fig. 31.48) are precursors of nonnucleated mature red cells in the blood. In the human, normoblasts are normally present only in the bone marrow. Stages in their production (see Chapter 32) from the earliest to the latest include pronormoblast, basophilic normoblast, polychromatophilic normoblast, and orthochromatic normoblast. In general, NRBCs that might appear in the blood in disease are polychromatic normoblasts. In some, however, the cytoplasm is so basophilic that it is difficult to recognize the cell as erythroid except by the character of the nucleus, intensely staining chromatin, and sharp separation of chromatin

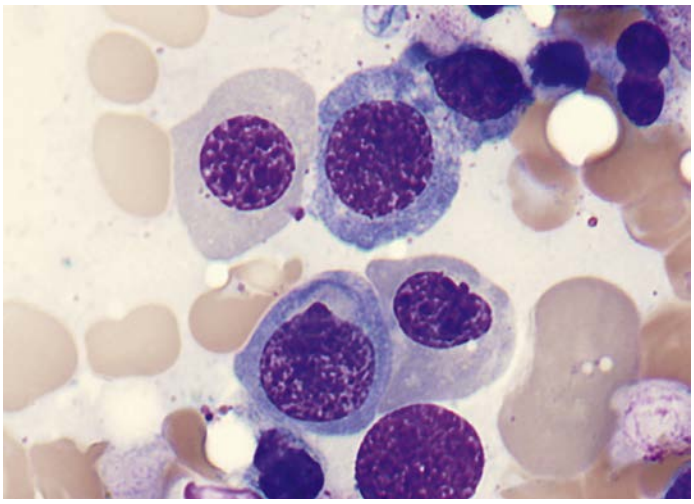

Figure 31.28 Megaloblast. Large nucleated red cell with abnormal "open" nuclear chromatin. They are frequently seen in the bone marrow in myelodysplastic syndrome or other megaloblastic anemia. Occasionally, these can also be seen in the peripheral blood (1000×).

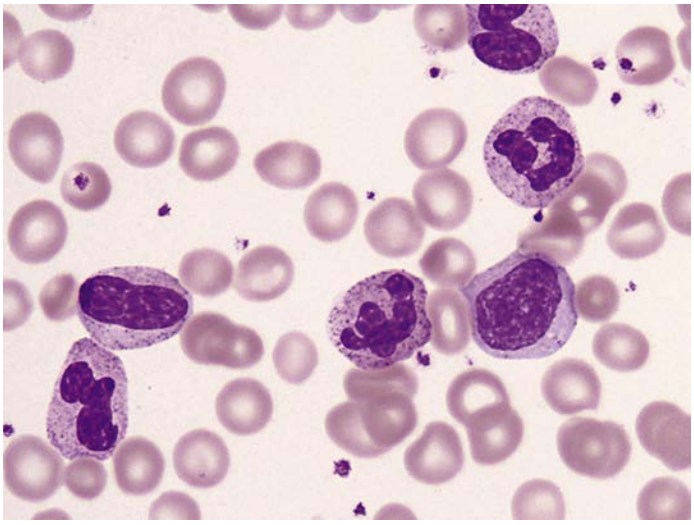

Figure 31.29 Leukemoid reaction. Left-shifted neutrophilic series with neutrophils, bands, and myelocytes. The neutrophils also show coarse toxic granulation (1000×).

from parachromatin. Such erythroid cells are often mistaken for lymphocytes—an error that usually can be prevented by careful observation of the nucleus. The megaloblast (Fig. 31.28) is a distinct, nucleated erythroid cell—not merely a larger normoblast. It is characterized by large size and an abnormal "open" nuclear chromatin pattern. Cells of this series are not found in normal marrow but are characteristically present in the marrow and sometimes in the blood of patients with pernicious anemia or other megaloblastic anemias.

Significance of Nucleated Red Blood Cells

Normoblasts are present normally only in the blood of the fetus and of very young infants. In the healthy adult, they are confined to the bone marrow and appear in the circulating blood only in disease, in which their presence usually denotes an extreme demand made on the marrow, extramedullary hematopoiesis, or marrow replacement. Large numbers of circulating NRBCs are found particularly in hemolytic disease of the newborn (erythroblastosis fetalis) and thalassemia major.

Leukoerythroblastic Reaction

The presence of normoblasts and immature cells of the neutrophilic series in the blood is known as a *leukoerythroblastic reaction* (Fig. 31.29). This often indicates space-occupying disturbances of the marrow, such as myelofibrosis with myeloid metaplasia, metastatic tumor, leukemias, multiple myeloma, Gaucher disease, and others. Nonetheless, in the study of Weick and colleagues (1974), more than one-third of patients with a leukoerythroblastic reaction did not have malignant or potentially malignant disease (Table 31.6).

TABLE 31.6
Conditions Associated with Leukoerythroblastosis

0.63	0.26	Solid tumors and lymphomas
	0.24	Myeloproliferative disorders, including chronic myeloid leukemia (CML)
	0.13	Acute leukemias
0.37	0.03	Benign hematologic conditions
	0.08	Hemolysis
	0.26	Miscellaneous, including blood loss

Data from Weick JK, Hagedorn AB, Linman JW: Leukoerythroblastosis: diagnostic and prognostic significance, *Mayo Clin Proc* 49:110, 1974.
Proportions are based on a series of 215 cases discovered in a study of 50,277 blood film examinations in a 6-month period—a proportion of 0.004.

LEUKOCYTES ON PERIPHERAL BLOOD SMEAR EXAMINATION

Before evaluating leukocytes on the Romanowsky's-stained blood film, one should first determine that the film is well made, the distribution of the cells is uniform, and the staining of the cells is satisfactory. One first scans the counting area of the slide and, in wedge films, the lateral and feather edges, where monocytes, neutrophils, and large abnormal cells (if present) tend to be disproportionately represented. With coverslip preparations, this uneven distribution is less likely to occur. Suspicious cells are detected at 10× magnification and are confirmed at high power. Because nucleated red cells, macrophages, immature granulocytes, immature lymphoid cells, megakaryocytes, and abnormal cells are not normally found in blood, they should be recorded if present.

While scanning under low power, it is advisable to estimate the leukocyte count from the film. Even though it is a crude approximation, it sometimes enables one to detect errors in total count. One then proceeds to determine the percentage distribution of the different types of leukocytes, which is known as the *differential leukocyte count*. In patients with leukopenia, it may be necessary to concentrate the leukocytes by centrifuging blood anticoagulated with EDTA and preparing films from the top layer of the packed cells. This buffy coat contains primarily leukocytes and platelets. In the crenellation technique of counting, the field of view is moved from side to side across the width of the slide in the *counting area*, just behind the feather edge, where the red cells are separated from one another and are free of artifacts. As each leukocyte is encountered, it is classified, until 100, 200, 500, or 1000 leukocytes have been counted. The greater the number of cells counted, the greater is the precision. However, for practical reasons, 100-cell counts are usually made. A record of the count may be kept by using a mechanical or electronic tabulator. Leukocytes that cannot be classified should be placed together in an unidentified group. In some conditions, notably leukemia, many of these unidentified leukocytes may be present. During the differential leukocyte counting procedure, the morphology of erythrocytes and platelets is examined, and the number of platelets is estimated. The absolute concentration of each variety of leukocyte is its percentage times the total leukocyte count. An increase in absolute concentration is an absolute increase; an increase in percentage only is a relative increase. Reference intervals are more useful if given as absolute concentrations rather than percentages (see Table 31.3).

Leukocytes Normally Present in Blood

Neutrophil (Polymorphonuclear Neutrophilic Leukocyte; Segmented Neutrophilic Granulocyte)

Neutrophils average 12 μm in diameter; they are smaller than monocytes and eosinophils and slightly larger than basophils. The nucleus stains deeply; it is irregular and often assumes shapes comparable to such letters as E, Z, and S. What appear to be separate nuclei normally are segments of nuclear material connected by delicate filaments.

A filament has length but no breadth as one focuses up and down. A *segmented neutrophil* (Fig. 31.30, and see Fig. 31.50) has at least two of its lobes separated by a filament. A *band neutrophil* (see Figs. 31.30 and 31.50) has either a strand of nuclear material thicker than a filament connecting the lobes or a U-shaped nucleus of uniform thickness. The nucleus in both types of neutrophils has coarse blocks of chromatin and rather sharply

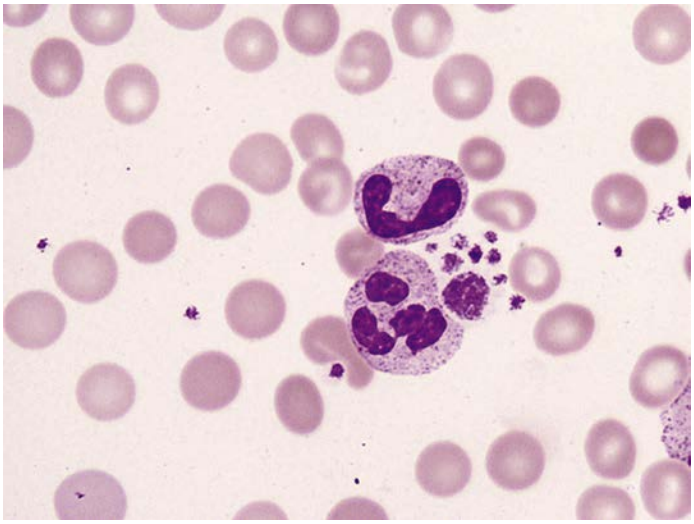

Figure 31.30 Neutrophil and band form. Neutrophil and band form depicting separation of nuclear lobes in the mature neutrophil versus horseshoe-shaped nucleus in the band form. A giant platelet is also seen (1000×).

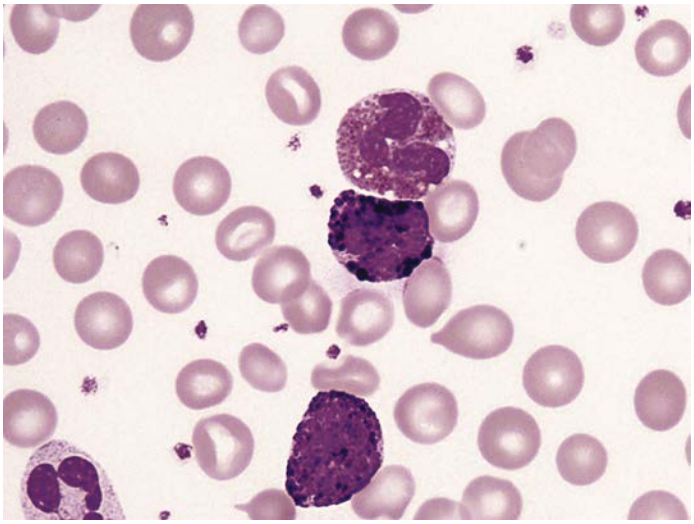

Figure 31.32 Basophil *(below)* and eosinophil *(above)*. Eosinophilic granules are coarser and bigger and often do not overlie the nucleus, unlike the basophil, which has large, deeply basophilic granules, often obscuring nuclear details (1000×).

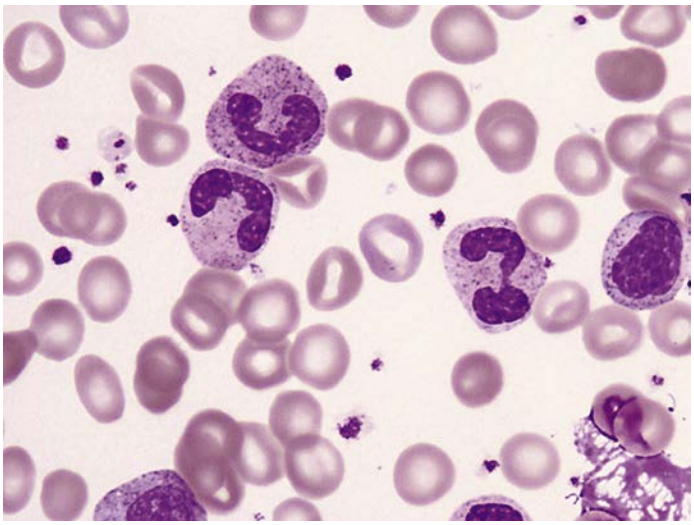

Figure 31.31 Neutrophilic granules. Cytoplasmic granules in myelocytes and mature neutrophils (1000×).

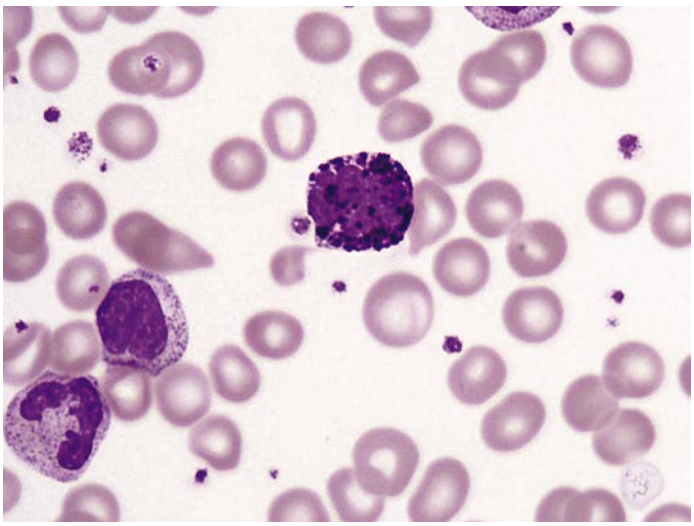

Figure 31.33 Basophil *(center)* and neutrophilic myelocyte and band *(left)*. The granules in the basophil are much bigger and coarser compared with the fine azurophilic granules of the neutrophil and precursors (1000×).

defined parachromatin spaces. If, because of overlapping of nuclear material, it is not possible to be certain whether a filament is present, the cell should be placed in the segmented category (Mathy & Koepke, 1974). The number of lobes in normal neutrophils ranges from two to five, with a median of three. The cytoplasm itself is colorless and has tiny granules (0.2–0.3 μm) that stain tan to pink with Wright's stain. About two-thirds of these are specific granules and one-third azurophil granules. With light microscopy, the two types of granules often cannot be distinguished in the mature cell (Fig. 31.31). Segmented neutrophils average 56% of leukocytes; reference intervals are 1.8 to 7.0 × 10^9/L in white adults but have a lower limit of about 1.1 × 10^9/L in black adults. Band neutrophils average 3% of leukocytes; the upper reference value is about 0.7 × 10^9/L in whites and slightly lower in blacks (using the preceding definition and counting 100 cells in the differential; see Table 31.3).

Normally, about 10% to 30% of segmented neutrophils have two lobes, 40% to 50% have three lobes, and 10% to 20% have four; no more than 5% have five lobes. A "shift to the left" occurs when increased bands and less mature neutrophils are present in the blood, along with a lower average number of lobes in segmented cells (see Figs. 31.29 and 31.31).

Neutrophilia, or neutrophilic leukocytosis, is an increase in the absolute count, and neutropenia is a decrease.

Eosinophil (Eosinophilic Granulocyte)

Eosinophils average 13 μm in diameter. The structure of these cells is similar to that of polymorphonuclear neutrophils, with the striking difference that, instead of neutrophilic granules, their cytoplasm contains larger round or oval granules that have a strong affinity for acid stains (Fig. 31.32). They are easily recognized by the size and color of the granules, which stain bright red with eosin. The cytoplasm is colorless. The nucleus stains somewhat less deeply than that of the neutrophils and usually has two connected segments (lobes), rarely more than three. Eosinophils average 3% of the leukocytes in adults, and the upper reference value is 0.6 × 10^9/L when calculated from the differential count. If allergic individuals are excluded, the upper limit is probably 0.35 × 10^9/L or 350/μL. The lower reference value is probably 40/μL; a decrease in eosinophils (eosinopenia) can be detected only by counting large numbers of cells, as in direct hemocytometer counts (Dacie & Lewis, 1991) or with a flow cytometer–automated differential counter.

Basophil (Basophilic Granulocyte)

In general, basophils resemble neutrophils, except that the nucleus is less segmented (usually merely indented or partially lobulated), and granules are larger and have a strong affinity for basic stains (Figs. 31.32 and 31.33). In some basophils, most of the granules may be missing because they are soluble in water, leaving vacuoles or openings in the cytoplasm. The granules then are a mauve color. In a well-stained film, the granules are deep purple and the nucleus is somewhat paler and often nearly hidden by the granules so that its form is difficult to distinguish. Unevenly stained granules of basophils may be ring shaped and resemble *Histoplasma capsulatum* or protozoa.

Basophils are the least numerous of the leukocytes in normal blood and average 0.5%. The 95% reference values for adults are 0 to 0.2 to 10^9/L when derived from the differential count.

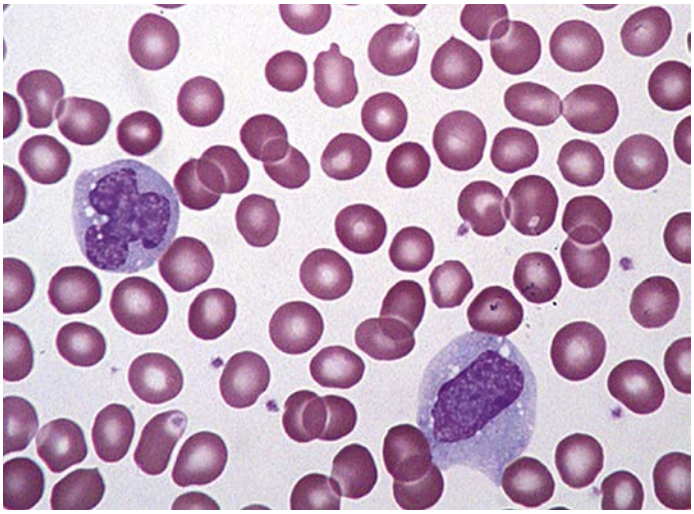

Figure 31.34 Monocyte. Among the normal blood cells, the monocyte is the largest and has the most delicate nuclear chromatin pattern. A moderate amount of light-gray cytoplasm with fine granularity and vacuolation is noted (500×).

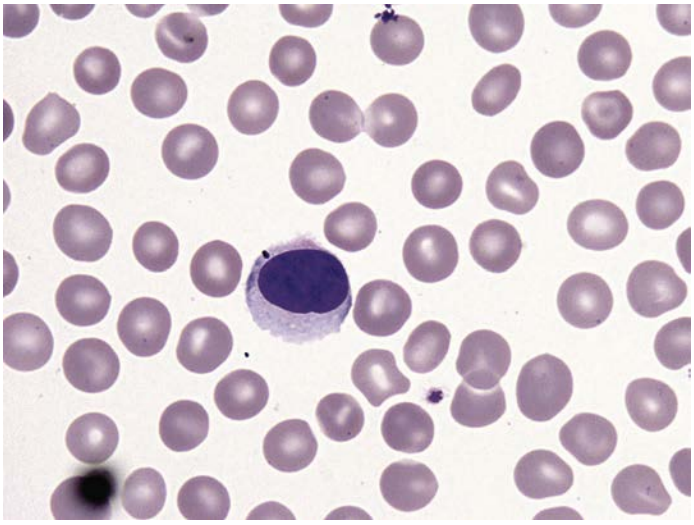

Figure 31.36 Reactive large lymphocyte with moderately abundant gray-blue cytoplasm (1000×).

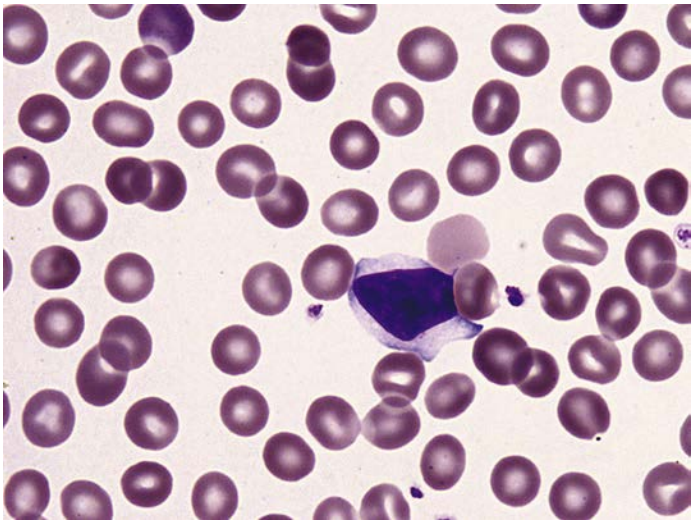

Figure 31.35 Lymphocyte. This is a benign reactive lymphocyte with moderately abundant pale-gray cytoplasm hugging the surrounding red cells and distinct separation of chromatin/parachromatin (1000×).

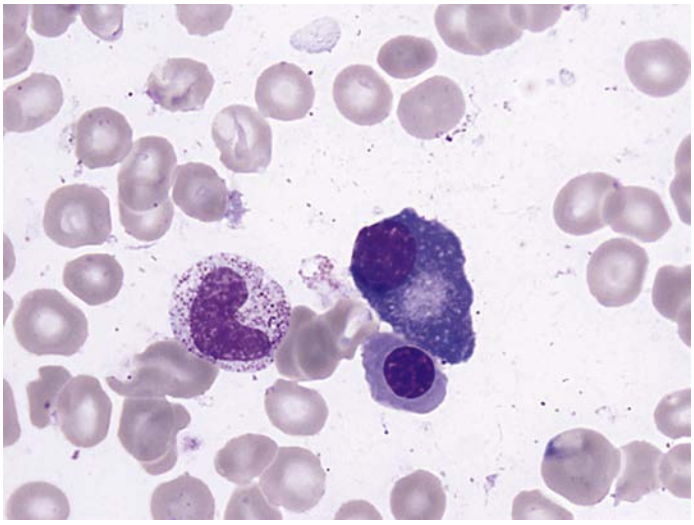

Figure 31.37 Plasma cell. Eccentric round nucleus with clumped nuclear chromatin and moderate amount of basophilic cytoplasm with prominent nuclear hof, or clear zone (1000×).

Monocyte

The monocyte is the largest cell of normal blood (Fig. 31.34). It generally has about two to three times the diameter of an erythrocyte (14–20 μm), although smaller monocytes sometimes are encountered. It contains a single nucleus, which is partially lobulated, deeply indented, or horseshoe shaped. Occasionally, the nucleus of a monocyte may appear round or oval. The cytoplasm is abundant. The nuclear chromatin often appears to be in fine, parallel strands separated by sharply defined parachromatin. The nucleus stains less densely than that of other leukocytes. The cytoplasm is blue-gray and has a ground-glass appearance. It often contains fine red to purple granules that are less distinct and smaller than the granules of neutrophils. Occasionally, blue granules may be seen. When the monocyte transforms into a macrophage, it becomes larger (20–40 μm); the nucleus may become oval and the chromatin more reticular or dispersed so that nucleoli may be visible. A perinuclear clear zone (Golgi) may be evident. The fine red or azurophil granules are variable in number or may have disappeared. The more abundant cytoplasm tends to be irregular at the cell margins and to contain vacuoles. These are phagocytic vacuoles, which may contain ingested red cells, debris, pigment, or bacteria. Evidence of phagocytosis in monocytes or the presence of macrophages in directly made blood films is pathologic and often indicates the presence of active infection.

Monocytes average 4% of leukocytes, and the reference interval for adults is approximately 0 to 0.8×10^9/L depending on the method used to perform the differential count (see Table 31.3).

Lymphocyte

Lymphocytes are mononuclear cells without specific cytoplasmic granules. Small lymphocytes are about the size of an erythrocyte or slightly larger (6–10 μm; see Fig. 31.9). The typical lymphocyte has a single, sharply defined nucleus containing heavy blocks of chromatin. The chromatin stains dark blue with Wright's stain, whereas the parachromatin stands out as lighter-stained streaks; at the periphery of the nucleus, the chromatin is condensed. Characteristically, a gradual transition or smudging is seen between the chromatin and the parachromatin. The nucleus is generally round but is sometimes indented at one side. The cytoplasm stains pale blue except for a clear perinuclear zone. Larger lymphocytes (Figs. 31.35 and 31.36), 12 to 15 μm in diameter, with less densely staining nuclei and more abundant cytoplasm, are frequently found, especially in the blood of children, and may be difficult to distinguish from monocytes. The misshapen, indented cytoplasmic margins of lymphocytes are due to pressure of neighboring cells. In the cytoplasm of about one-third of large lymphocytes, a few round, red-purple granules are present. They are larger than the granules of neutrophilic leukocytes. There is a continuous spectrum of sizes between small and large lymphocytes and, indeed, there can be a transition from small to large to blast forms as well as the reverse. It is not meaningful to classify small lymphocytes and large lymphocytes separately. The presence of significant proportions of atypical lymphocytes must be noted; these indicate transformation of lymphoid cells as a response to antigenic stimulation. Plasma cells have abundant blue cytoplasm, often with light streaks or vacuoles, an eccentric round nucleus, and a well-defined clear (Golgi) zone adjacent to the nucleus (Fig. 31.37). The nucleus of the

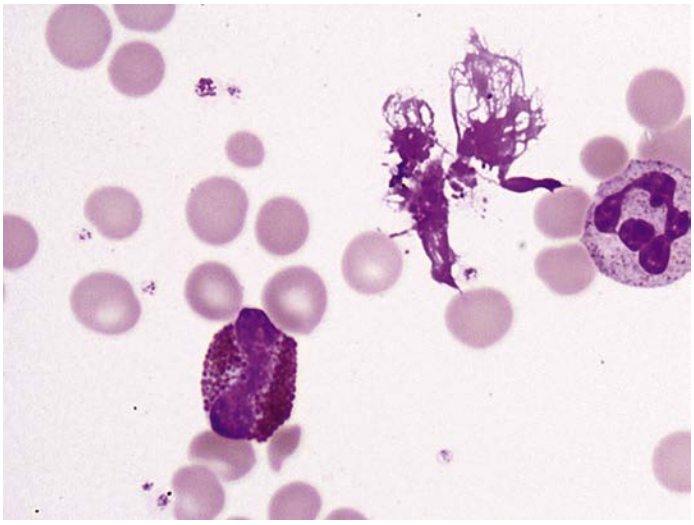

Figure 31.38 Broken cell. A broken cell of the myeloid series with ruptured cell membrane and disintegration of cytoplasmic contents (1000×).

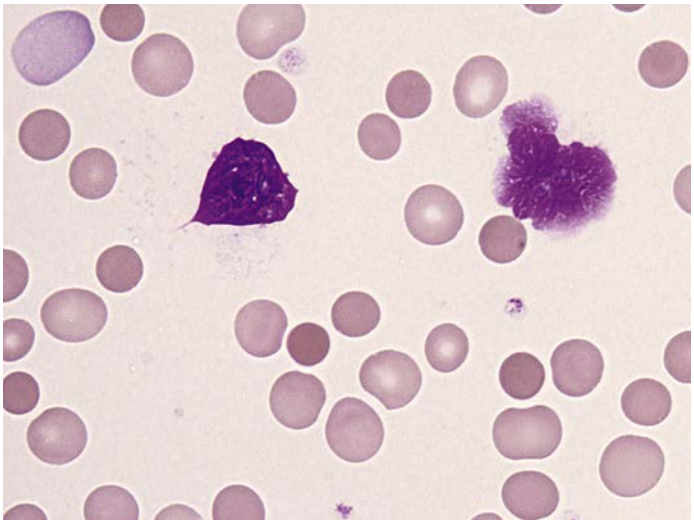

Figure 31.40 Smudge cell. Nuclear remnant from a damaged/broken white cell (1000×).

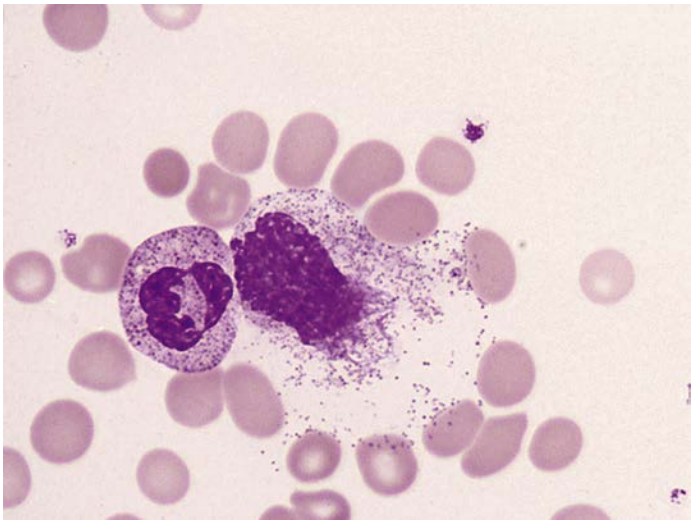

Figure 31.39 Ruptured cell. Ruptured/disintegrating leukocyte (1000×).

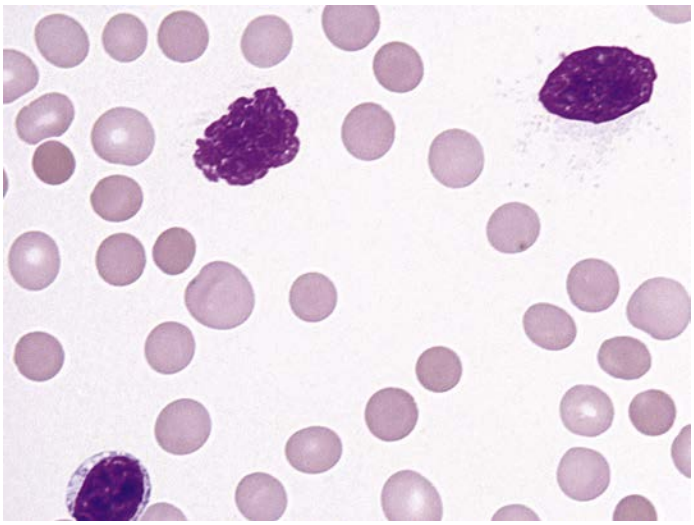

Figure 31.41 Basket cells (1000×).

plasma cell has heavily clumped chromatin, which is sharply defined from the parachromatin and is often arranged in a radial or wheel-like pattern. Plasma cells are not present normally in blood.

Lymphocytes average 34% of all leukocytes and range from 1.5 to 4 × 10^9/L in adults. The lymphocytes and their derivatives, the plasma cells, operate in the immune defenses of the body.

Artifacts

Broken Cells

Damaged or broken leukocytes (Figs. 31.38 and 31.39) constitute a small proportion of the nucleated cells in normal blood. Bare nuclei from ruptured cells (Figs. 31.40 and 31.41) vary from fairly well-preserved nuclei without cytoplasm to smudged nuclear material, sometimes with strands arranged in a coarse network, the so-called *basket cells*. They probably represent fragile cells, usually lymphocytes that have been broken in preparing the film. They are numerous in chronic lymphocytic leukemia and in acute leukemias.

Degenerative Changes

As EDTA-blood ages in the test tube, changes in leukocyte morphology begin to take place (Sacker, 1975). The degree of change varies among cells and in different individuals. Within a half hour, the nuclei of neutrophils may begin to swell, with some loss of chromatin structure. Cytoplasmic vacuoles appear, especially in monocytes and neutrophils. Nuclear lobulation appears in mononuclear cells; deep clefts may cause the nucleus to resemble a cloverleaf (radial segmentation of the nuclei; Rieder cells). Finally, loss of the cytoplasm and a smudged nucleus may be all that remains of the cell (see Fig. 31.40). Prolonged storage can also produce changes resembling toxic granulation (Dalal, 2002). Degenerative changes occur more rapidly in oxalated blood than in EDTA-blood. They arise more rapidly with increasing concentrations of EDTA, such as occur when evacuated blood collection tubes are incompletely filled.

Contracted Cells

In the thicker part of wedge films, drying is slow. Obvious changes in the film include rouleaux of the erythrocytes and shrinkage of the leukocytes. Because the leukocytes are contracted and heavily stained, mononuclear cells are difficult to distinguish. Optimal cell identification is usually impossible in these areas.

Endothelial Cells

Endothelial cells from the lining of the blood vessel may appear in the first drop of blood from a fingerstick specimen or, rarely, in venous blood. They have an immature reticular chromatin pattern and may be mistaken for histiocytes or for tumor cells.

Radial Segmentation of the Nuclei

Use of oxalated blood results in the appearance of abnormal segmentation of the nuclei of leukocytes on the blood film. This segmentation differs from that of the granulocytes in that the lobes appear to radiate from a single point, giving a cloverleaf or cartwheel picture. Extensive changes can occur within 1 or 2 hours in oxalated blood. Less extensive changes occur with other anticoagulants, including EDTA.

Vacuolation

Vacuoles may develop in the nucleus and cytoplasm of leukocytes, especially monocytes and neutrophils from blood anticoagulated with EDTA.

TABLE 31.7

Ninety-Five Percent Confidence Limits for Various Percentages of Blood Cells of a Given Type as Determined by Differential Counts*

a	n = 100	n = 200	n = 500	n = 1000	n = 10,000
0	0.0–3.6	0.0–1.8	0.0–0.7	0.0–0.4	0.0–0.1
1	0.0–5.4	0.1–3.6	0.3–2.3	0.5–1.8	0.8–1.3
2	0.0–7.0	0.6–5.0	1.0–3.6	1.2–3.1	1.7–2.3
3	0.6–8.5	1.1–6.4	1.7–4.9	2.0–4.3	2.6–3.4
4	1.1–9.9	1.7–7.7	2.5–6.1	2.9–5.4	3.6–4.5
5	1.6–11.3	2.4–9.0	3.3–7.3	3.7–6.5	4.5–5.5
6	2.2–12.6	3.1–10.2	4.1–8.5	4.6–7.7	5.5–6.5
7	2.9–13.9	3.9–11.5	4.9–9.6	5.5–8.8	6.5–7.6
8	3.5–15.2	4.6–12.7	5.8–10.7	6.4–9.9	7.4–8.6
9	4.2–16.4	5.4–13.9	6.6–11.9	7.3–10.9	8.4–9.6
10	4.9–17.6	6.2–15.0	7.5–13.0	8.2–12.0	9.4–10.7
15	8.6–23.5	10.4–20.7	12.0–18.4	12.8–17.4	14.3–15.8
20	12.7–29.2	14.7–26.2	16.6–23.8	17.6–22.6	19.2–20.8
25	16.9–34.7	19.2–31.6	21.3–29.0	22.3–27.8	24.1–25.9
30	21.2–40.0	23.7–36.9	26.0–34.2	27.2–32.9	29.1–31.0
35	25.7–45.2	28.4–42.0	30.8–39.4	32.0–38.0	34.0–36.0
40	30.3–50.3	33.2–47.1	35.7–44.4	36.9–43.1	39.0–41.0
45	35.0–55.3	38.0–52.2	40.6–49.5	41.9–48.1	44.0–46.0
50	39.8–60.2	42.9–57.1	45.5–54.5	46.9–53.1	49.0–51.0
55	44.7–65.0	47.8–62.0	50.5–59.4	51.9–58.1	54.0–56.0
60	49.7–69.7	52.9–66.8	55.6–64.3	56.9–63.1	59.0–61.0
65	54.8–74.3	58.0–71.6	60.6–69.2	62.0–68.0	64.0–66.0
70	60.0–78.8	63.1–76.3	65.8–74.0	67.1–72.8	69.0–70.9
75	65.3–83.1	68.4–80.8	71.0–78.7	72.2–77.7	74.1–75.9
80	70.8–87.3	73.8–85.3	76.2–83.4	77.4–82.4	79.2–80.8
85	76.5–91.4	79.3–89.6	81.6–88.0	82.6–87.2	84.2–85.7
90	82.4–95.1	85.0–93.8	87.0–92.5	88.0–91.8	89.3–90.6
91	83.6–95.8	86.1–94.6	88.1–93.4	89.1–92.7	90.4–91.6
92	84.8–96.5	87.3–95.4	89.3–94.2	90.1–93.6	91.4–92.6
93	86.1–97.1	88.5–96.1	90.4–95.1	91.2–94.5	92.4–93.5
94	87.4–97.8	89.8–96.9	91.5–95.9	92.3–95.4	93.5–94.5
95	88.7–98.4	91.0–97.6	92.7–96.7	93.5–96.3	94.5–95.5
96	90.1–98.9	92.3–98.3	93.9–97.5	94.6–97.1	95.5–96.4
97	91.5–99.4	93.6–98.9	95.1–98.3	95.7–98.0	96.6–97.4
98	93.0–99.9	95.0–99.4	96.4–99.0	96.9–98.8	97.7–98.3
99	94.6–99.9	96.4–99.9	97.7–99.7	98.2–99.5	98.7–99.2
100	96.4–100.0	98.2–100.0	99.3–100.0	99.6–100.0	99.9–100.0

Courtesy of Rümke CL: The imprecision of the ratio of two percentages observed in differential white blood cell counts: a warning, *Blood Cells* 11:137–140, 1985.
**n* is the number of cells counted; a, the observed percentage of cells of the given type. The limits for n = 100, 200, 500, and 1000 are exact; for n = 10,000, they have been determined with Freeman and Tukey's approximation, as described in the Geigy tables.

Vacuoles may be associated with swelling of the nuclei and loss of granules from the cytoplasm.

"Pseudophagocytosis"

Occasionally, a small lymphocyte, or more often an erythrocyte, will lie atop a granulocyte or a monocyte and, thus, will appear to have been ingested. The true positions of such cells can be suspected because they will come into sharp focus in a plane above that of the larger cell.

Sources of Error in the Differential Leukocyte Count

Even in perfectly made blood films, the differential count is subject to the same errors of random distribution. For interpretation of day-to-day or slide-to-slide differences in the same patient, it is helpful to know how much of the variation is ascribable to chance alone. Table 31.7 gives 95% confidence limits for different percentages of cells in differential counts performed, classifying a total of 100 to 10,000 leukocytes. In comparing the percentages from two separate counts, if one number lies outside the confidence limits of the other, it is probable that the difference is significant (i.e., not due to chance). Thus, on the basis of a 100-cell differential count, if the monocytes were 5% one day and 10% the next, it is probable that the difference is due solely to sampling error. Although the difference could be real, one cannot be sure of this because of the small number of cells counted. If, on the other hand, the differential count totaled 500 cells, the difference between 5% and 10% is significant; one can be reasonably certain (with a 5% chance of being wrong) that the difference is a real one and is not due to chance alone. Of course, this is a minimal estimate of the error involved in differential counts because it does not include mechanical errors (due to variations in collecting blood samples, inadequate mixing, irregularities in distribution depending on the type and quality of the blood films, and poor staining) or errors in cell identification, which depend on the judgment and experience of the observer. Therefore, meticulous technique, as well as accurate and consistent cell classification, is required. The physician who interprets the results must be aware of possible sources of error, especially error due to chance in the distribution of cells. Table 31.3 shows the distribution of the various types of leukocytes in the blood of normal persons. Absolute concentrations are given, as these have considerably greater significance than percentages alone.

PLATELETS ON PERIPHERAL BLOOD SMEAR EXAMINATION

In films made from EDTA-blood and stained with Romanowsky's stains, platelets are round or oval, 2 to 4 μm in diameter, and separated from one another (Fig. 31.42). The platelet count may be estimated from such films. On average, if the platelet count is normal, about one platelet is found per 10 to 30 red cells. At 1000× magnification, this is equivalent to

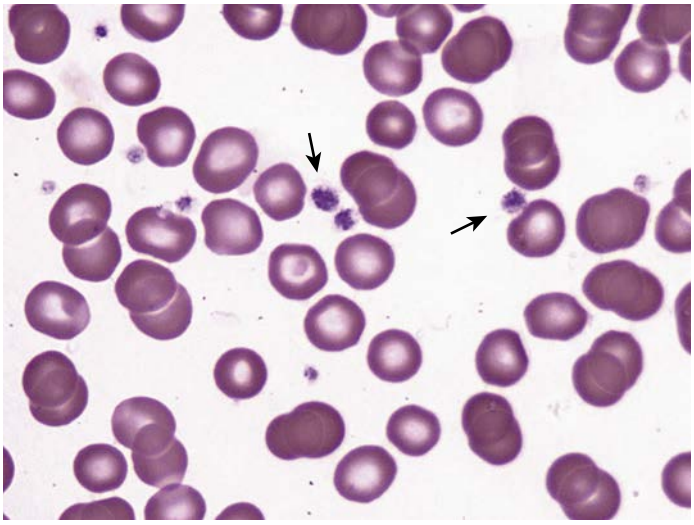

Figure 31.42 Platelet. Platelets are round to oval, 2 to 4 μm in diameter, and separated from one another (1000×).

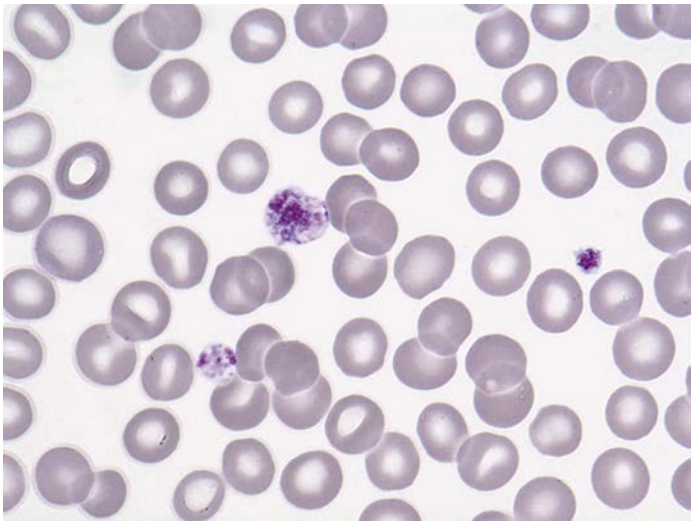

Figure 31.43 Platelet/giant platelet. Platelets show fine granularity; an occasional larger (giant) form is noted (1000×).

about 7 to 20 platelets per oil immersion field in the areas where red cell morphology is optimal (Fig. 31.43). Platelets contain fine purple granules that usually fill the cytoplasm. Occasionally, granules are concentrated in the center (the "granulomere") and surrounded by a pale cytoplasm (the "hyalomere"). These are probably activated platelets, the appearance resulting from contraction of the microtubular band. A few platelets may have decreased concentrations of granules (hypogranular platelets). In EDTA-blood from normal individuals, the fraction of platelets that exceed 3 μm in diameter and the fraction of platelets that are hypogranular are both less than 5% if the films are made at 10 minutes or 60 minutes after the blood is drawn. If films are made immediately or at 3 hours after blood drawing, the fraction of large platelets and the fraction of hypogranular or activated platelets are increased (Zeigler et al., 1978). These artifacts make it necessary to standardize time of film preparation when evaluating platelet size from films. In patients with immune thrombocytopenia, large platelets/giant platelets (see Fig. 31.30) are increased in number. They are also increased in patients with the rare Bernard-Soulier syndrome and in those with myelophthisis or myeloproliferative syndrome. In the latter, the platelets are frequently hypogranular or have a distinct granulomere and hyalomere. In blood films made from skin puncture wounds, platelets assume irregular shapes with sharp projections and tend to clump together.

ERYTHROCYTE SEDIMENTATION RATE

Erythrocyte sedimentation rate (ESR) is a useful but nonspecific marker of underlying inflammation. Recently, high-sensitivity C-reactive protein and other inflammatory markers have been used to detect or monitor disease, particularly cardiovascular disease and metabolic syndrome (Pearson et al., 2003; Rifai, 2005). When well-mixed venous blood is placed in a vertical tube, erythrocytes will tend to fall toward the bottom. The length of fall of the top of the column of erythrocytes over a given interval of time is called the ESR. Several factors are involved.

Plasma Factors

An accelerated ESR is favored by elevated levels of fibrinogen and, to a lesser extent, α_2-, β-, and γ-globulins. These asymmetric protein molecules have a greater effect than other proteins in decreasing the negative charge of erythrocytes (zeta potential) that tends to keep them apart. The decreased zeta potential promotes the formation of rouleaux, which sediment more rapidly than single cells. Removal of fibrinogen by defibrination lowers the ESR. No absolute correlation has been noted between the ESR and any of the plasma protein fractions. Albumin and lecithin retard sedimentation, and cholesterol accelerates the ESR.

Red Cell Factors

Anemia increases the ESR because the change in the erythrocyte/plasma ratio favors rouleaux formation independently of changes in the concentrations of plasma proteins. By any method of measurement, ESR is most sensitive to altered plasma proteins in the Hct range of 0.30 to 0.40 (Bull, 1975). The sedimentation rate is directly proportional to the weight of the cell aggregate and inversely proportional to the surface area. Microcytes sediment slower than macrocytes, which have decreased surface area/volume ratios. Rouleaux also have a decreased surface area/volume ratio and accelerate the ESR. Red cells with an abnormal or irregular shape, such as sickle cells or spherocytes, hinder rouleaux formation and lower the ESR.

Stages in the ESR

Three stages can be observed: (1) In the initial 10 minutes, little sedimentation occurs as rouleaux forms; (2) for about 40 minutes, settling occurs at a constant rate; and (3) sedimentation slows in the final 10 minutes as cells pack at the bottom of the tube.

Methods

Westergren Method

The Westergren method is widely used, as the method is very simple. The ICSH (1993) has recommended it as the reference method when undiluted whole blood is used. The ICSH states that the patient's Hct should not exceed 35% because reproducibility of sedimentation may be poorer in narrow tubes. A formula to convert between diluted and undiluted blood ESR is as follows:

$$\text{Diluted blood ESR} = (\text{Undiluted ESR} \times 0.86) - 12$$

Equipment. The Westergren tube is a straight pipet 30 cm long, 2.55 mm in internal diameter, and calibrated in millimeters from 0 to 200. It holds about 1 mL. The Westergren rack is also used, with levelers as needed for a vertical tube position.

Reagent. A 0.105 molar solution (range, 0.10–0.136) of sodium citrate is used as the anticoagulant-diluent solution (31 g of $Na_3C_6H_5O_7 \cdot H_2O$ added to 1 L of distilled water in a sterile glass bottle). This is filtered and kept refrigerated without preservatives.

Procedure.

1. Two milliliters of whole blood are added to 0.5 mL of sodium citrate and mixed by inversion.
2. A Westergren pipet is filled to the 0 mark and is placed exactly vertical in the rack at room temperature without vibration or exposure to direct sunlight.
3. After exactly 60 minutes, the distance from the 0 mark to the top of the column of red cells is recorded in millimeters as the ESR value. If the demarcation between plasma and the red cell column is hazy, the level is taken where the full density is first apparent.

Modified Westergren Method

A modification of the Westergren method produces the same results but employs blood anticoagulated with EDTA rather than with citrate. This is more convenient because it allows the ESR to be performed from the same tube of blood as is used for other hematologic studies. Two milliliters of well-mixed EDTA-blood is diluted with 0.5 mL of 3.8% sodium citrate or with 0.5 mL of 0.85% sodium chloride. Undiluted blood anticoagulated with EDTA gives poor precision (ICSH, 1977). The ESR gradually increases with age. Westergren's original upper limits of normal (10 mm/hour for men and 20 mm/hour for women) appear to be too low. According

to studies by Böttiger and Svedberg (1967) and Zauber and Zauber (1987), upper limits of reference values for the Westergren method should be as follows:

	Men	Women
Below 50 years of age	15 mm/hour	20 mm/hour
Above 50 years of age	20 mm/hour	30 mm/hour
Above 85 years of age	30 mm/hour	42 mm/hour

Smith and Samadian (1994) state that the rise in ESR with age likely reflects higher disease prevalence in older adults. Therefore, for practical purposes, it may be advisable to use the standard normal range in older adult patients.

Sources of Error

If the concentration of the anticoagulant is higher than recommended, the ESR may be elevated. Sodium citrate or EDTA does not affect the rate of sedimentation if used in the proper concentration. Heparin, however, alters the membrane zeta potential and cannot be used as an anticoagulant. It can also increase the ESR when used as a medication in vivo (Penchas, 1978). Bubbles left in the tube when it is filled will affect the ESR. Hemolysis may modify the sedimentation. The cleanliness of the tube is important. Tilting the tube accelerates the ESR. The red cells aggregate along the lower side, while the plasma rises along the upper side. Consequently, the retarding influence of the rising plasma is less effective. An angle of even 3 degrees from the vertical may accelerate the ESR by as much as 30%. Plastic ESR pipets have slightly higher (1–2 mm/hour) values than glass pipets (Schneiderka et al., 1997).

Temperature should be within the range of 20°C to 25°C. Lower or higher temperatures in some cases alter the ESR. If the blood has been kept refrigerated, it should be permitted to reach room temperature and be mixed by inversion a minimum of eight times before the test is performed. The test should be set up within 2 hours after the blood sample is obtained (or within 12 hours if EDTA is used as the anticoagulant and the blood is kept at 4°C). Otherwise, some samples with elevated ESRs will be falsely low (Morris et al., 1975). On standing, erythrocytes tend to become spherical and less readily form rouleaux.

No effective method is known for correcting for anemia in the Westergren method, although this can be done with the Wintrobe method.

Alternative Methods and Technologies to Measure ESR

The **VES-MATIC 20** instrument is a bench-top analyzer designed to measure the ESR in 20 blood samples (Plebani et al., 1998; Caswell & Stuart, 1991). It is completely automated. The blood is collected in special cuvets and is carefully mixed by the instrument; the samples are then left to sediment for a certain period. The 18-degree slant of the tubes with respect to the vertical axis causes acceleration of the sedimentation, allowing results comparable with those of Westergren at the first hour to be obtained in only 25 minutes; those comparable with Westergren at the second hour require only 45 minutes. The optoelectrical sensors automatically read the erythrocyte sedimentation level. The data are elaborated and then are printed or visualized on the display.

The **Micro-ESR method** has greater utility in pediatric patients. Barrett and Hill (1980) described a micro-ESR method using 0.2 mL blood to fill a plastic disposable tube 230 mm long with a 1-mm internal bore. Capillary blood values correlated well with venous blood micro-ESR and Westergren ESR values. Kumar and Singhi (1994) refer to a micro-ESR that utilizes whole blood to completely fill a 75-mm heparinized microhematocrit capillary tube.

Another instrument used to measure ESR is ESR STAT PLUS, which is a centrifugation-based method. The sample is placed in the centrifuge, and an infrared laser tracks the erythrocyte-plasma interface and makes multiple measurements from which the linear portion of the sedimentation curve is identified and is used by the software algorithm to determine the ESR result. This method requires smaller volumes of specimen than the Westergren method and is faster. The pitfall is correlation with the reference Westergren method, especially in the 0 to 20 mm/hour range. It can also be prone to human error because it requires a minimum of 15 mixing intervals followed by a 5-minute limit before drawing into the capillary tube (Shelat, 2008).

Application

The ESR is one of the oldest laboratory tests still in use. Although some of its usefulness has decreased as more specific methods of evaluating disease (such as C-reactive protein [CRP]) have been developed (Zlonis, 1993), new clinical applications are being reported (Saadeh, 1998). Recently, the ESR has been reported to be of clinical significance in sickle cell disease (low value in the absence of painful crisis, moderately increased 1 week into the crisis), osteomyelitis (elevated, helpful in following therapy), stroke (ESR ≥28 mm/hour has a poorer prognosis), prostate cancer (ESR ≥37 mm/hour has a higher incidence of disease progression and death), and coronary artery disease (ESR >22 mm/hour in white men had a high risk for coronary artery disease) (Saadeh, 1998). In pregnancy, the ESR increases moderately, beginning at the 10th to 12th week, and returns to normal about 1 month postpartum. The ESR tends to be markedly elevated in monoclonal blood protein disorders such as multiple myeloma or macroglobulinemia, in severe polyclonal hyperglobulinemia due to inflammatory disease, and in hyperfibrinogenemia.

Moderate elevations are common in active inflammatory disease such as rheumatoid arthritis, chronic infection, collagen disease, and neoplastic disease. The ESR has little diagnostic value in these disorders but can be useful in monitoring disease activity. It is simpler than measurement of serum proteins, which has tended to replace ESR. Because the test is often normal in patients with neoplasm, connective tissue disease, and infection, a normal ESR cannot be used to exclude these diagnostic possibilities. In patients with known cancer, however, when the value exceeds 100 mm/hour, metastases are usually present (Sox & Liang, 1986). The ESR is of little value in screening asymptomatic patients for disease; history and physical examination will usually disclose the cause of an elevated ESR (Sox & Liang, 1986). The ESR is useful and indicated in establishing the diagnosis and in monitoring polymyalgia rheumatica and temporal arteritis, for which the rate typically exceeds 90 mm/hour (Zlonis, 1993). Emergency physicians continue to use the ESR in evaluating temporal arteritis, septic arthritis, pelvic inflammatory disease, and appendicitis (Olshaker & Jerrard, 1997). Freeman (1997) urges immediate quick ESR estimation if giant cell arteritis is clinically indicated, as a delay of even a few hours in starting steroid therapy may result in irreversible visual failure. Harrow and colleagues (1999) conclude that an ESR of 5 mm or less at 30 minutes correctly identifies most patients with normal ESRs without misclassifying elevated ESRs.

In Hodgkin disease, the ESR may be a very useful prognostic blood measurement in the absence of systemic ("B") symptoms (fever, weight loss, night sweats). In one study (Vaughan Hudson et al., 1987), one-third of asymptomatic patients had both an ESR of less than 10 mm/hour and an excellent survival rate regardless of age, stage, or histopathology. Asymptomatic patients with an ESR of 60 mm/hour or greater had a survival rate as poor as those with systemic symptoms.

Iversen and colleagues (1996) reported that 70% of renal cell carcinoma patients had an increased ESR, which had been significantly rising for up to 6 years before diagnosis. They argued for a systematic graphing and baseline determination of the ESR over time, which showed a marked elevation in ESR 1 year before diagnosis. Such a trend of increasing ESR should lead to further investigation, as with renal ultrasound, which may then lead to curative nephrectomy before metastases occur.

BONE MARROW EXAMINATION

The bone marrow examination provides a semiquantitative and qualitative assessment of the state of hematopoiesis and aids in the diagnosis of several hereditary and acquired benign and malignant diseases. Marrow aspiration and biopsy can be carried out as an office procedure on ambulatory patients with minimal risk (Ryan, 2015). It compares favorably with ordinary venipuncture and is less traumatizing than a lumbar puncture. A battery-powered device was developed to capture bone marrow biopsy. Bone marrow biopsies performed with this device were significantly faster and superior in quality (Reed et al., 2011). As for any other special procedure, however, the clinical indications for marrow examination should be clear. In each instance, the physician should have in mind some reasonable prediction of its result and consequent benefit to the patient. An adequate bone marrow specimen is essential for reaching the correct diagnosis and avoiding sampling error (Merzianu et al., 2018). Without exception, the peripheral blood should be examined carefully first. It is a relatively uncommon circumstance to find hematologic disease in the bone marrow without evidence of it in the peripheral blood. It is estimated that the weight of the marrow in the adult is 1300 to 1500 g. The marrow can undergo complete transformation in a few days and, occasionally, even in a few hours. As a rule, this rapid transformation involves the whole organ, as evidenced by the fact that a small sample represented by a biopsy or aspiration is usually fairly representative of the whole marrow. This conclusion is in accord with results of studies of biopsy samples simultaneously removed from several sites. According to these observations, the various

sites chosen for removal of marrow for studies are in most instances equally good. Consequently, the difficulty of access, the risks involved, the ease of obtaining a good biopsy specimen, and discomfort to the patient are the main reasons for selection of a site in the particular patient. Within a given site, the cellular distribution may vary in apparently hyperplastic or hypoplastic areas. This is particularly the case immediately below the cortex. Occasionally, failure to obtain quantitatively or qualitatively adequate material in one site may be followed by success in another location. Also, the need for repeated aspirations or biopsies may indicate the use of several different sites. We regard the posterior iliac crest as the preferred site. The large marrow space allows both aspiration and biopsy to be performed with ease at one time. The techniques of marrow aspiration and biopsy have been adequately reviewed (Hyun et al., 1988). Bone marrow biopsy needle type can affect specimen length and quality (Brestoff, 2019). Both operator techniques and specimen processing play a vital role in improving the quality of bone marrow assessment (Odejide et al., 2013).

INDICATIONS FOR MARROW STUDY

Bone marrow biopsy and aspiration should be performed only when there is a clear clinical indication (Bain, 2001a, 2001b). While widely accepted criteria for assessing adequacy of bone marrow samples for establishing a diagnosis do not exist at this time, there are some disease-specific guidelines (Merizanu et al., 2014; National Comprehensive Cancer Network [NCCN], 2014). Both bone marrow aspiration and biopsy are performed routinely together. Besides increasing the yield of diagnostic tissue, each specimen also provides unique information (Kaur et al., 2014). Biopsy provides information about the bone marrow architecture, whereas cellular details are much better appreciated on the aspirate smears.

In microcytic anemia, evaluation of iron stores and sideroblasts allows categorization of the anemia (i.e., iron deficiency, anemia of chronic disease, sideroblastic).

In macrocytic anemia, marrow examination will confirm whether the process is megaloblastic; in some cases, changes in the blood are minimal, yet the marrow is megaloblastic. In normocytic anemia (or macrocytic anemia) without an increased reticulocyte production index, the marrow is evaluated for quantitative or qualitative abnormalities in erythropoiesis (e.g., pure red cell aplasia, myelodysplasia).

In neutropenia, thrombocytopenia, or pancytopenia, marrow study is helpful in assessing the presence and normality of the precursor cells in each series. This enables one to assess the probability of decreased production, impaired maturation, or increased destruction as the mechanism of the disorder. In cytopenias, marrow examination sometimes will reveal the presence of leukemia or another hematologic neoplasia.

In immunoglobulin abnormalities, the diagnosis of plasma cell myeloma or macroglobulinemia may be confirmed if infiltrations of abnormal plasma cells or lymphocytes are present. Marrow examination is essential for the diagnosis and classification of acute leukemia. It is frequently performed to assist in the diagnosis and staging of other neoplasms, including lymphomas (Cheson et al., 2014) and metastatic tumors, and to assess response to therapy for hematologic disorders. If the marrow cannot be aspirated ("dry tap"), biopsy is essential. Marrow biopsy should also be performed if blood changes suggest myelofibrosis with myeloid metaplasia or if granulomatous disease or metastatic tumor is suspected.

PREPARATION OF THE ASPIRATE AND BIOPSY SECTION

Marrow Films

Delay, no matter how brief, is undesirable. Films can be made in a manner similar to that used for ordinary blood counts. Gray particles of marrow are visible with the naked eye. They are the best material for the preparation of good films and serve as landmarks for the microscopic examination of stained smears.

Direct Films

A drop of marrow is placed on a slide a short distance away from one end. A film 3 to 5 cm long is made with a spreader, not wider than 2 cm, dragging the particles behind but not squashing them. A trail of cells is left behind each particle.

Imprints

Marrow particles can also be used for preparation of imprints. One or more visible particles are picked up with a capillary pipet, the broken end of a wooden applicator, or a toothpick, and are transferred immediately to a slide and made to stick to it by a gentle smearing motion. The slide is air dried rapidly by waving, and then it is stained.

Crush Preparations

Marrow particles in a small drop of aspirate may be placed on a slide near one end. Another slide is carefully placed over the first. Slight pressure is exerted to crush the particles, and the slides are separated by pulling them apart in a direction parallel to their surfaces. All films should be dried rapidly by whipping them through the air. As the aspirated material is being spread, the appearance of fat as irregular holes in the films gives assurance that marrow and not just blood has been obtained.

Special Studies

It is recommended that, for evaluation of most hematologic diseases, an additional bone marrow aspirate specimen should be collected for ancillary testing, including flow cytometry analysis, karyotype, and fluorescent in situ hybridization (FISH) assays and molecular studies. Flow cytometry is best performed on a heparin- or EDTA-anticoagulated aspirate specimen, which is stable for at least 24 hours at room temperature. For cytogenetic or cell culture analysis, anticoagulated marrow should be added to tissue culture medium and analyzed as soon as possible to maintain optimal cell viability. Cytogenetic specimens are generally not adversely affected by overnight incubation. DNA is relatively stable and can be extracted and analyzed from paraffin-embedded tissue sections. However, decalcification of the biopsy specimens during processing results in some degree of DNA denaturation and precludes optimum molecular testing. Further, reverse transcriptase polymerase chain reaction (RT-PCR) assays, involving amplification of complementary DNA (cDNA) prepared from cellular messenger RNA (mRNA), are often needed for molecular diagnosis of translocations associated with leukemia and lymphoma. mRNA has a variable half-life in an intact cell and is degraded rapidly (on the order of seconds to minutes) in a cell lysate by ubiquitous RNases. For maximal mRNA recovery, cell suspensions, mostly buffy coat or mononuclear cell preparations, should be lysed in an appropriate RNase inhibitor–containing buffer as soon as possible after sampling. Molecular assays are best performed on an EDTA-anticoagulated bone marrow specimen, as heparin can interfere with some PCR-based assays (Ryan & Cohen, 2000).

Histologic Sections

The needle biopsy and clotted marrow particles (fragments) are fixed in Zenker's acetic solution (5% glacial acetic acid; 95% Zenker's) for 6 to 18 hours or in B-5 fixative for 1 to 2 hours (Hyun et al., 1988). Excessive time in either fixative makes the tissue brittle. Although these fixatives, particularly B-5, provide the best histology, they contain toxic mercuric chloride and are gradually being replaced by fixatives such as zinc formalin and other preparations. The tissue is processed routinely for embedding in paraffin, cut at 4 μm, and stained routinely with hematoxylin and eosin (H&E). Giemsa and periodic acid–Schiff (PAS) stains are frequently useful. Embedding the tissue in plastic material allows thinner sections to be examined and better survival of protein structure so that enzyme histochemistry and immunocytochemistry are practical for identification of cell lineages.

Sections provide the best estimate of cellularity and a picture of marrow architecture but are somewhat inferior for the study of cytologic details. Another disadvantage is that particles adequate for histologic sections are not always obtained, especially in conditions in which the diagnosis depends on marrow evidence (e.g., myelofibrosis, metastatic cancer).

STAINING MARROW PREPARATIONS

Romanowsky's Stain

Marrow films should be stained with Romanowsky's stain (e.g., Wright-Giemsa) in a manner similar to that used for blood films. A longer staining time may be necessary for marrows with greater cellularity. Several special stains may be performed on peripheral blood smears, bone marrow aspirate, and touch imprint smears and bone marrow biopsy sections, besides the usual Romanowsky's and H&E stains. These include cytochemical stains (myeloperoxidase, Sudan black B, naphthol As-D chloroacetate esterase, nonspecific esterases, acid phosphatases, leukocyte alkaline phosphatase, periodic acid–Schiff stain, toluidine blue, and iron stain) and immunocytochemical stains, depending on the disease and the preliminary morphologic examination of the smear and/or section (Perkins, 2004).

Perls Test for Iron

Procedure

One film containing marrow particles is fixed for 10 minutes in formalin vapor, immersed for 10 minutes in a freshly prepared solution that contains

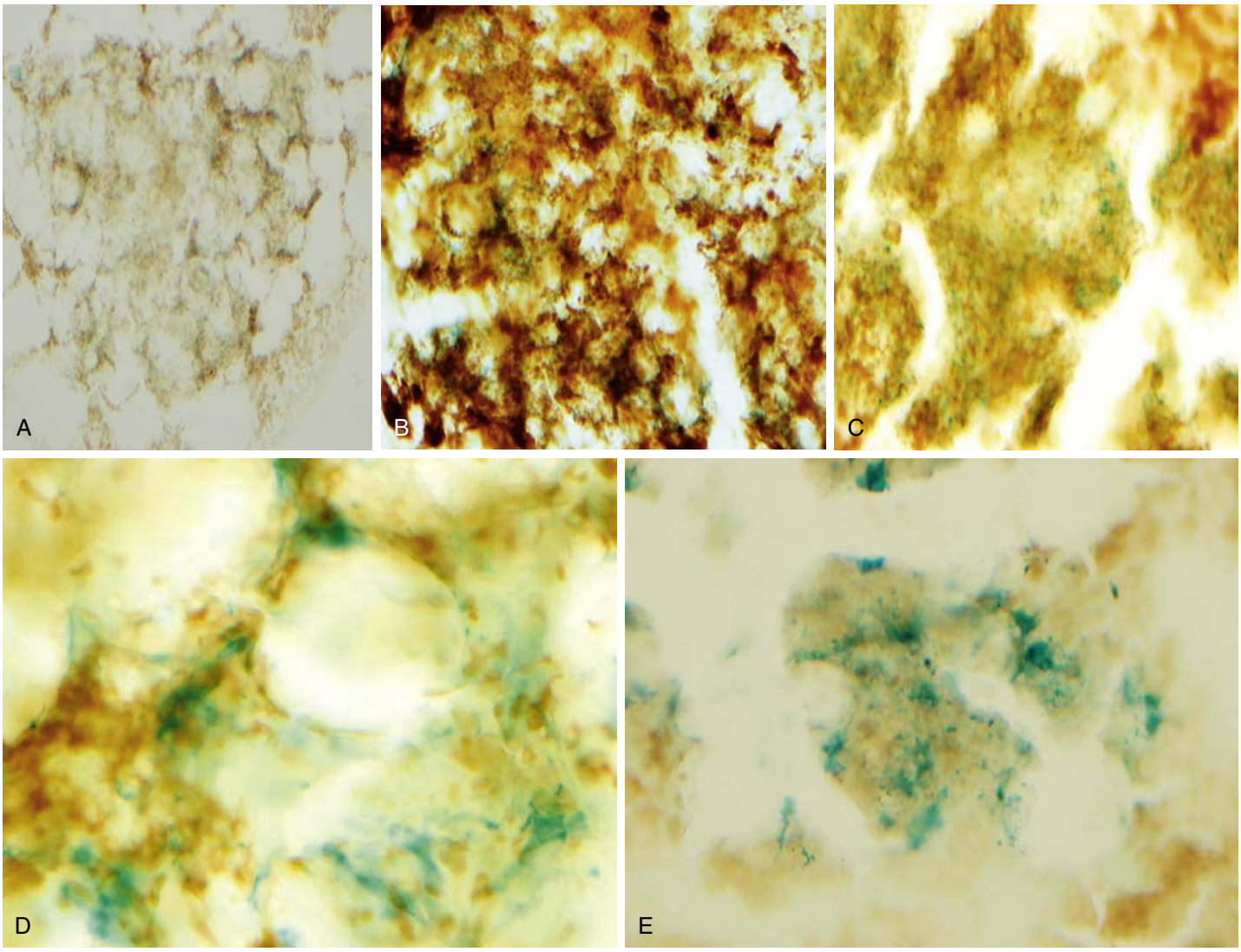

Figure 31.44 Bone marrow storage iron located in macrophages. A, Iron stores 1+ (1000×). B, Iron stores 2+ (1000×). C, Iron stores 3+ (1000×). D, Iron stores 4+ (1000×). E, Iron stores 5+ (500×).

0.5% potassium ferrocyanide and 0.75% hydrochloric acid, rinsed, dried, and counterstained with Nuclear Fast Red.

Interpretation

The Prussian blue reaction is produced when hemosiderin or ferritin is present; iron in Hb is not stained. It is reported as negative or 1+ to 5+. Storage iron, which is contained in macrophages, can be evaluated only in marrow particles on the film. In adults, 2+ is normal, 3+ is slightly increased, 4+ is moderately increased, and 5+ is markedly increased (Fig. 31.44). Storage iron in the marrow is located in macrophages. Normally, a small number of blue granules are seen. In iron deficiency, blue-staining granules are absent or extremely rare. Storage iron is increased in most other anemias, infections, hemochromatosis, hemosiderosis, hepatic cirrhosis, uremia, and cancer, and after repeated transfusions. Sideroblasts (Fig. 31.45) are normoblasts that contain one or more particles of stainable iron. Normally, from 20% to 60% of late normoblasts are sideroblasts; in the remainder, no blue granules can be detected. The percentage of sideroblasts is decreased in iron deficiency anemia (in which storage iron is decreased) as well as in the common anemias associated with infection, rheumatoid arthritis, and neoplastic disease (anemia of chronic disease/anemia of inflammation in which storage iron is normal or increased). The number of sideroblasts is increased when erythropoiesis is impaired for other reasons (sideroblastic anemia, myelodysplastic syndrome); it is roughly proportional to the degree of saturation of transferrin. The Prussian blue reaction can also be performed on slides previously stained with a Romanowsky's stain to identify sideroblasts or to determine whether iron is present in other cells of interest. Iron stain is used to evaluate for the presence of abnormal sideroblasts and ring sideroblasts (Fig. 31.46), as seen in various hematologic diseases.

Sections

Routine H&E stains are satisfactory for most purposes. Romanowsky's stains can be used to good advantage with fixed material. Iron stains are best performed on films that contain particulate marrow tissue. They are less sensitive in sections of marrow because some iron is lost in processing, and a lesser thickness of tissue is examined in sections.

EXAMINATION OF MARROW

It is desirable to establish a routine procedure to obtain maximum information from examination of the marrow. Pathology-driven algorithmic testing with integrated reporting improves the pathologist's ability to render a specific World Health Organization diagnosis and improves test utilization. The College of American Pathologists has published guidelines recommending bone marrow synoptic reporting for hematologic neoplasms (Pearson et al., 2019).

Peripheral Blood

The complete blood cell count, including platelet count and reticulocyte count, should be performed on the day of the marrow study and the results incorporated in the report. The pathologist or hematologist who examines the marrow should also carefully examine the blood film as previously described and should incorporate the observations in the marrow report.

Cellularity of the Marrow

Marrow cellularity is expressed as the ratio of the volume of hematopoietic cells to the total volume of the marrow space (cells plus fat and other stromal elements). Cellularity varies with the age of the subject and the site. For example, at 50 years of age, the average cellularity in the vertebrae is

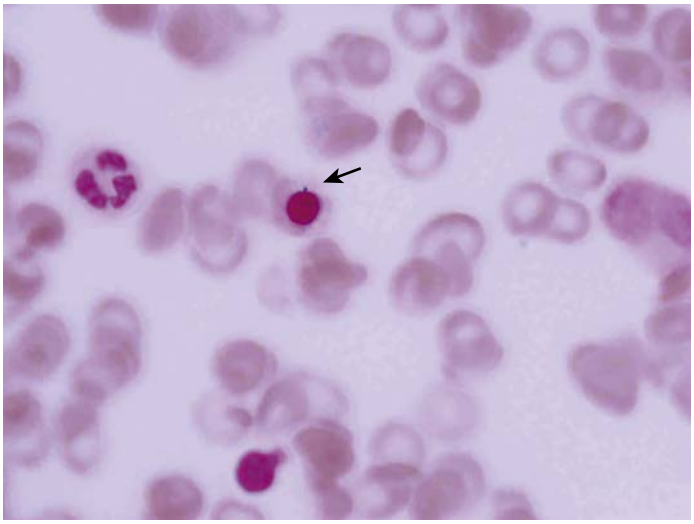

Figure 31.45 Normal sideroblast. Single iron granule seen in the cytoplasm of a maturing normoblast. Identification requires high magnification and bright illumination while focusing up and down (1000×).

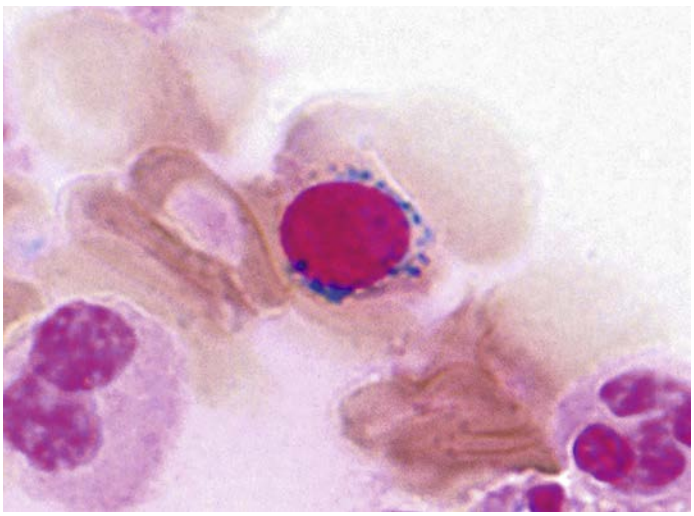

Figure 31.46 Ring sideroblast. Siderotic granules form a perinuclear ring spanning more than half of the nuclear diameter (Prussian blue stain, 1000×).

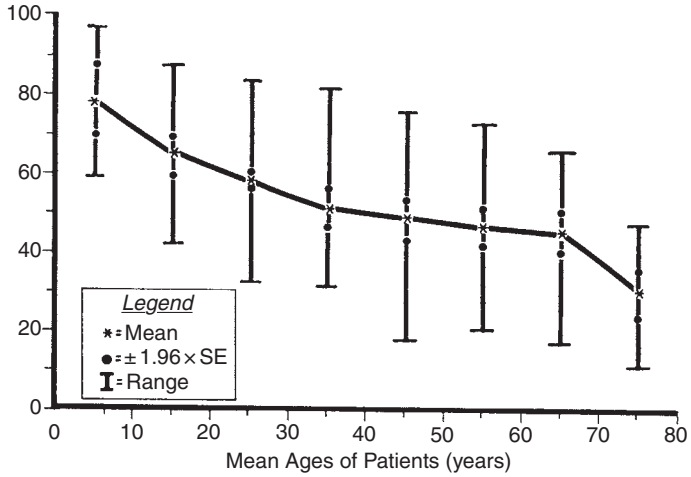

Figure 31.47 Marrow cellularity in hematologically normal individuals. Percent cellularity on the ordinate versus age, grouped by decade, on the abscissa (From Hartsock RJ, Smith EB, Petty CS: Normal variations with aging of the amount of hematopoietic tissue in bone marrow from the anterior iliac crest, *Am J Clin Pathol* 43:326–331, 1965, with permission.)

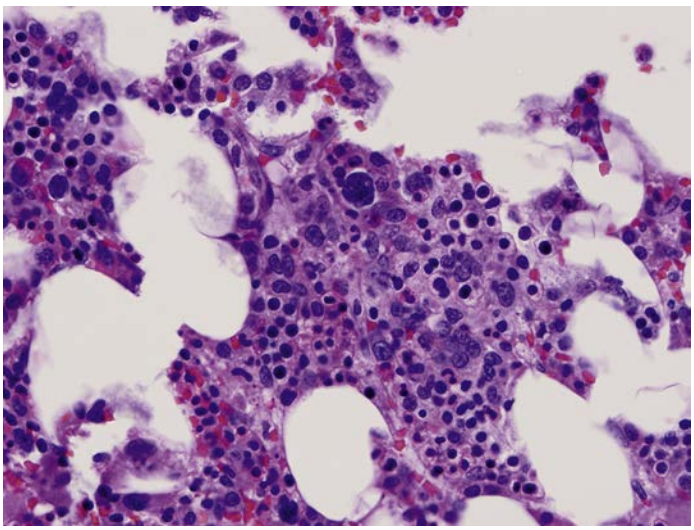

Figure 31.48 Marrow biopsy (500×). Cellularity here is between 50% and 60%, which is normal for an adult. Megakaryocytes, myeloid, and erythroid precursors are present. (Normoblasts have intensely staining nuclei and tend to occur in clusters.)

75%; sternum, 60%; iliac crest, 50%; and rib, 30%. Normal cellularity of the iliac bone at different ages has been well defined by Hartsock and colleagues (1965), as summarized in Figure 31.47. If the percentage is increased for the patient's age, the marrow is hypercellular, or hyperplastic; if decreased, the marrow is hypocellular, or hypoplastic. Marrow cellularity is best judged by histologic sections of biopsy or aspirated particles (Fig. 31.48) but should also be estimated from the particles present in marrow films. This is done by comparing the areas occupied by fat spaces and by nucleated cells in the particles as well as the density of nucleated cells in the "tail" or fallout of the particles. Comparison of films and sections on each marrow specimen will enable the observer to estimate cellularity reasonably well from films—a skill that is useful when sectioned material is unavailable.

Distribution of Cells

Distribution of various cell types can be ascertained in two ways. First, one scans several slides under low, then high, magnification. On the basis of previous experience, one then estimates the number and distribution of cells. Second, one actually makes a differential count of 300 to 500 cells and calculates the percentage of each type of cell. A combination of both methods is preferred. The second of these methods, careful differential counting, is an essential part of training in this work, without which accuracy in the first method may be difficult to achieve. The differential count also affords an objective record from which future changes may be measured.

One first scans the marrow film under low power (100× or 200× magnification) while looking for irregularities in cell distribution, numbers of megakaryocytes, and the presence of abnormal cells. Then, one selects areas on the film where marrow cells are both undiluted with blood cells and separated and spread out sufficiently to allow optimal identification. These areas are usually just behind marrow particles on direct films or near the particles on crushed films. The differential count is performed at 400× or 1000× magnification. Examples of reference intervals for differential counts of marrow at selected different ages are given in Table 31.8.

Changes in marrow cell distribution are most dramatic in the first month of life, during which a predominance of granulocytic cells at birth changes to a predominance of lymphocytes. This predominance of lymphocytes characterizes the bone marrow during infancy. A small proportion of "immature" or transitional lymphoid cells (fine nuclear chromatin, high nuclear/cytoplasmic ratio, small to intermediate cell size) is normally present; it may be that these cells include stem cells and progenitor cells. These cells probably include cells designated as "hematogones"; they may be increased in iron deficiency anemia, immune thrombocytopenic purpura, and other disorders, especially in infancy. Normoblasts fall after birth, rise to a maximum at 2 months, then fall to a stable, relatively low level by 4 months, remaining there during most of infancy. The myeloid/erythroid (M/E) ratio is the ratio of total granulocytes to total normoblasts. In newborns and infants, it is somewhat higher than in older children or adults (see Table 31.8). In adults, the range is broad, varying from about 1.2 : 1 to 5 : 1. Both the differential count and the M/E ratio are relative values that must be interpreted with respect to cellularity or with respect to other evidence that one of the systems is normal. An **increased** M/E ratio (e.g., 6 : 1) may be found in infection, chronic myelogenous leukemia, or erythroid hypoplasia. A **decreased** M/E ratio (i.e., <1.2 : 1) may mean a depression of leukopoiesis or a normoblastic hyperplasia, depending on

TABLE 31.8

Differential Cell Counts of Bone Marrow in Percent of Total Nucleated Cells

	ROSSE ET AL. (1977)			MAUER (1969)	JANDL (1987)
Cell Types	**Birth (Mean, SD)**	**1 Month (Mean, SD)**	**18 Months (Mean, SD)**	**Childhood (Mean, Range)**	**Adult (Mean, Range)**
Normoblasts, total	4.48 ± 7.24	8.04 ± 5.00	8.21 ± 3.71	23.1	21.5 (14.2–30.4)
Pronormoblasts	0.02 ± 0.06	0.10 ± 0.14	0.08 ± 0.13	0.5 (0.0–1.5)	0.6 (0.2–1.4)
Basophilic n.	0.24 ± 0.25	0.34 ± 0.33	0.50 ± 0.34	1.7 (0.2–4.8)	2.0 (0.7–3.7)
Polychromatophilic n.	13.06 ± 6.78	6.90 ± 4.45	6.97 ± 3.56	18.2 (4.8–34.0)	12.4 (12.2–24.2)
Orthochromatic n.	0.69 ± 0.73	0.54 ± 1.88	0.44 ± 0.49	2.7 (0.0–7.8)	6.5 (2.0–22.7)
Neutrophils, total	60.37 ± 8.66	32.35 ± 7.68	36.06 ± 7.40	57.1	56.0 (45.1–66.5)
Myeloblasts	0.31 ± 0.3	10.62 ± 0.50	0.06 ± 0.08	1.2 (0.0–3.2)	1.0 (0.5–1.8)
Promyelocytes	0.79 ± 0.9	10.76 ± 0.6	50.64 ± 0.59	1.4 (0.0–4.0)	3.4 (2.6–4.6)
Myelocytes	3.95 ± 2.93	2.50 ± 1.48	2.49 ± 1.39	18.3 (8.5–29.7)	11.9 (8.1–16.9)
Metamyelocytes	19.37 ± 4.8	411.30 ± 3.59	12.42 ± 4.15	23.3 (14.0–34.2)	18.0 (9.8–25.3)
Bands	28.89 ± 7.56	14.10 ± 4.63	14.20 ± 5.23		11.0 (8.5–20.8)
Segmented	7.37 ± 4.64	3.64 ± 2.97	6.31 ± 3.91	12.9 (4.5–29.0)	10.7 (8.0–16.0)
Eosinophils	2.70 ± 1.27	2.61 ± 1.40	2.70 ± 2.16	3.6 (1.0–9.0)	3.2 (1.2–6.2)
Basophils	0.12 ± 0.20	0.07 ± 0.16	0.10 ± 0.12	0.06 (0.0–0.8)	<0.1 (0.0–0.2)
Lymphocytes, total	15.6	49.0	45.5	16.0 (4.8–35.8)	15.8 (10.8–22.7)
Transitional	1.18 ± 1.13	1.95 ± 0.94	1.99 ± 1.00		
Small	14.42 ± 5.54	47.05 ± 9.24	43.55 ± 8.56		
Plasma cells	0.00 ± 0.02	0.02 ± 0.06	0.06 ± 0.08	0.4 (0.2–0.6)	1.8 (0.2–2.2)
Monocytes	0.88 ± 0.85	1.01 ± 0.89	2.12 ± 1.59		1.8 (0.2–2.8)
Megakaryocytes	0.06 ± 0.15	0.05 ± 0.09	0.07 ± 0.12		<1.0 (0.0–0.2)
Reticulum cells					0.3 (0.0–0.5)
M/E ratio	4.2	4.0	4.4	2.9 (1.2–5.2)	2.5 (1.2–5.0)

M/E, Myeloid/erythroid ratio.
Data from Rosse C, Kraemer MJ, Dillon TL, et al: Bone marrow cell populations of normal infants: the predominance of lymphocytes, *J Lab Clin Med* 89:1225–1240, 1977; Mauer AM: *Pediatric hematology,* New York, 1969, McGraw-Hill; Jandl JH: *Blood: textbook of hematology,* Boston, 1987, Little, Brown.

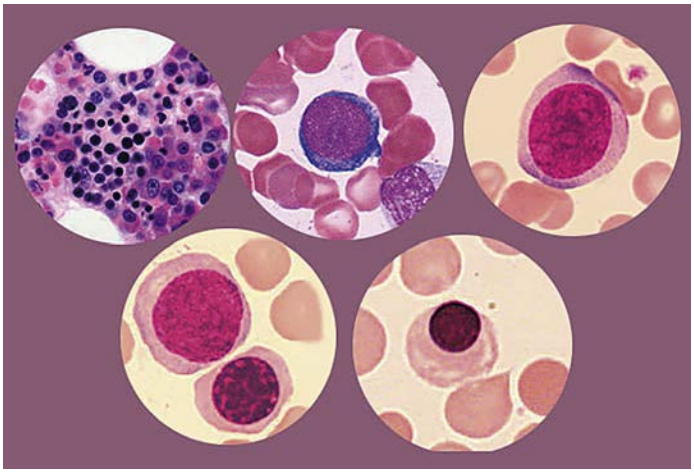

Figure 31.49 Normal erythroid maturation. Various stages of normoblastic erythroid maturation (1000×).

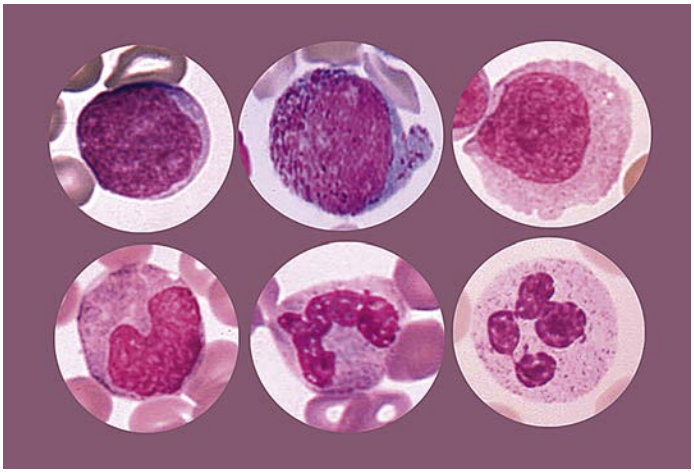

Figure 31.50 Normal myeloid (neutrophilic) maturation. Various stages of normal myeloid maturation from the blast to the mature neutrophil.

the marrow cellularity. The number of megakaryocytes is estimated more reliably in sections than in marrow films. In scanning areas of films with good cellularity under low power (100×), an average of one to three megakaryocytes should be found in each field in normal marrow.

Maturation

While examining cells during the differential count, one should evaluate whether maturation is normal (Figs. 31.49 and 31.50), that is, whether nuclear and cytoplasmic development is in balance. Impaired cytoplasmic maturation in normoblasts, for example, occurs when Hb synthesis is impaired; impaired nuclear maturation occurs in megaloblastic anemias. Bizarre or dysplastic maturation occurs as a result of certain drugs, in some leukemias, and in dysmyelopoietic syndromes.

Presence of Rare Cell Types or Abnormal Cells

In scanning the marrow, one looks for the presence of rare or unexpected cell types.

Tissue mast cells (Fig. 31.51) are normally very infrequent. They are increased in number in aplastic or refractory anemias and in lymphoproliferative disorders.

Osteoblasts (Fig. 31.52) are cells that synthesize the collagen matrix of bone. **Osteoclasts** are cells that resorb bone and are thought to result from the fusion of histiocytes. Both cell types are normally present in small numbers in the aspirates of infants and children. They are uncommonly seen in adult marrow, except when bone destruction or repair is occurring, as in hyperparathyroidism, Paget disease, metastatic tumor, or a recent biopsy at the same site.

Osteoblasts are large cells with a single eccentric nucleus that has reticular chromatin and a prominent nucleolus. The cytoplasm is moderately basophilic; a large, pale Golgi zone is separated from the nucleus, rather than abutting it as in plasma cells. Osteoblasts are often present in clusters and may be confused with immature plasma cells or myeloma cells. Osteoclasts (Fig. 31.53) are large, multinucleated cells up to 100 μm diameter that may be mistaken for megakaryocytes. They have multiple nuclei that

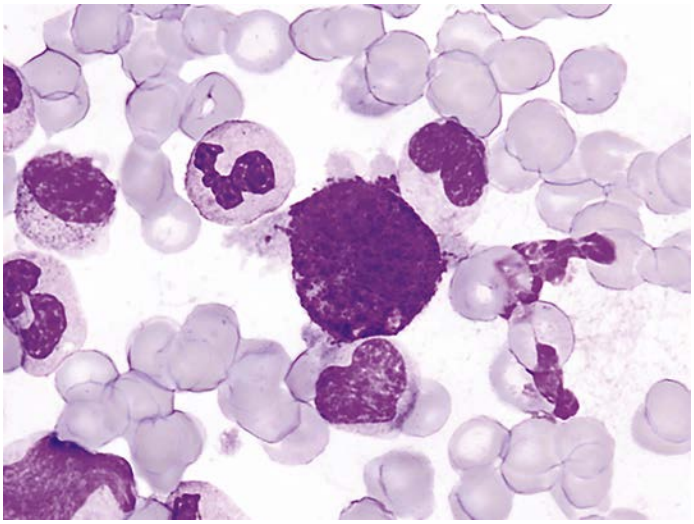

Figure 31.51 Tissue mast cell. Mast cells contain numerous dense dark-purple cytoplasmic granules that can completely cover the round nucleus (1000×).

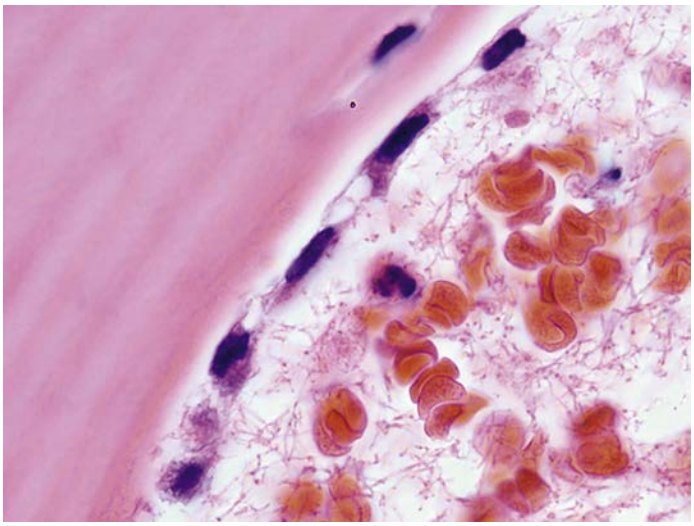

Figure 31.52 Osteoblast. Frequently found in pediatric patients, osteoblasts line the bone trabeculae. In smears, they appear as cells with eccentrically placed nuclei, resembling plasma cells, but the cytoplasmic clearing is more centrally located and is not found in the Golgi area, as in plasma cells (1000×).

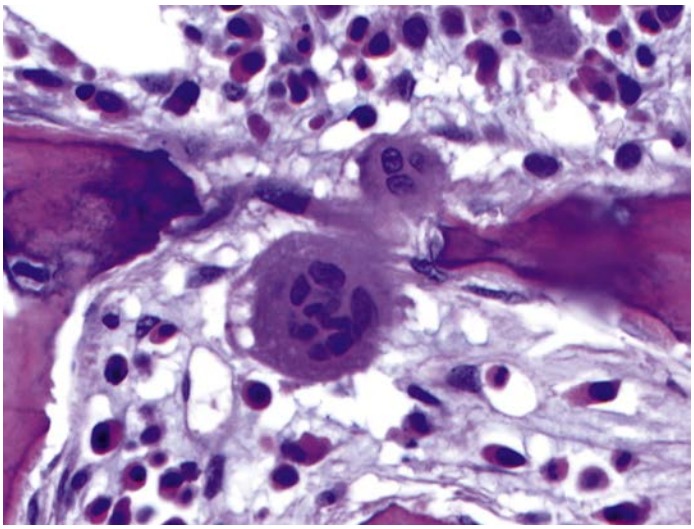

Figure 31.53 Osteoclast. Osteoclasts resorb bone and participate in bone remodeling (1000×).

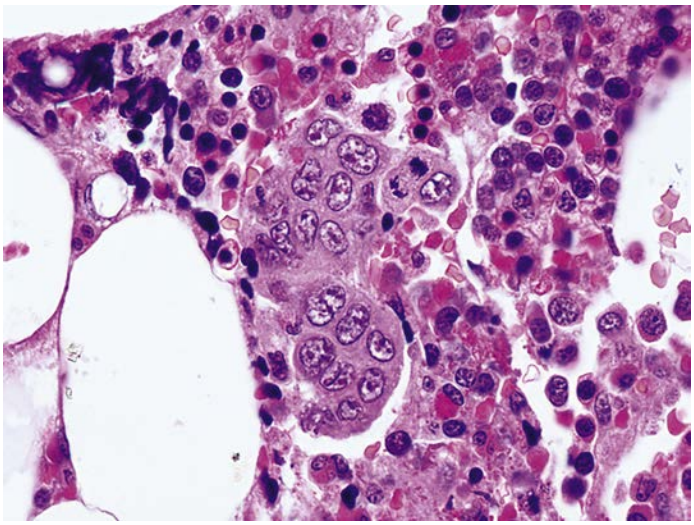

Figure 31.54 Metastatic tumor. Bone marrow biopsy with islands of metastatic gastric adenocarcinoma (1000×).

are separate (not joined, as in megakaryocytes). The chromatin is reticular, and a prominent nucleolus is usually present. The cytoplasm may be basophilic but usually has pink-purple granules that resemble megakaryocyte granules. Coarse fragments of purple-staining material are often present. Clusters of **metastatic neoplastic cells** (Fig. 31.54) may be found in one or more marrow films of patients with metastatic tumor in the bone sampled. They may be found in biopsy sections and not in films, in both, or, less commonly, in one or more films and not in the biopsy. Some metastatic neoplastic cells resemble myeloblasts or other primitive blasts. The clue to recognizing them is that they almost always appear in clusters or clumps of cells; this is not true of hematopoietic blast cells.

Evaluation of the Biopsy Specimen

Histologic sections allow better estimates of marrow cellularity and of the number of megakaryocytes than do marrow films (see Fig. 31.48). Normally, immature myeloid precursors lie along bone trabeculae, erythroid precursors are in discrete interstitial islands, and megakaryocytes are scattered in the interstitium. In good histologic preparations, cell distribution and maturation abnormalities can be quite reliably determined. In addition to more reliable detection of the presence of lymphomas or metastatic tumor, the histologic pattern can often be diagnostic of the type of neoplasm. Other focal lesions not found in films include granulomas, abscesses, and vascular lesions. In some conditions, such as myelofibrosis and hairy cell leukemia, the bone marrow cannot be aspirated and biopsy is necessary to establish a diagnosis. Trabeculae should always be examined to detect bone abnormalities. Osteosclerosis with thickened bone trabeculae may accompany myelofibrosis or may be congenital. In osteoporosis, the bone trabeculae are thin. Osteomalacia is characterized by a recognizable osteoid seam. Osteitis fibrosa occurs in hyperparathyroidism and is characterized by irregular osteoclastic bone resorption, endosteal fibrosis, and some osteoblastic activity in areas of bone regeneration. Irregularly widened trabeculae with a "mosaic" pattern are typical findings in Paget disease of bone.

Interpretation

The summary of the marrow report includes an estimate of cellularity, an estimate of the number of megakaryocytes, the M/E ratio, statements about any cytologic or maturation abnormalities, an estimate of the storage iron and proportion of sideroblasts, and statements about any other abnormal findings present (see Fig. 31.46). Abnormalities in blood cell counts and morphology are also summarized. An interpretation of observed findings is made, which includes a diagnosis if this is possible. In making such an interpretation, one should include an integration of marrow and blood observations with clinical findings and other laboratory data. Alterations in blood and marrow cells are discussed, with reference to the diseases and disorders considered, in subsequent chapters.

SELECTED REFERENCES

Cornbleet J: Spurious results from automated hematology cell analyzers, *Lab Med* 14:509, 1983.

Extremely useful reference for analysis of spurious results obtained from automated cell counters. It discusses reasons for spurious results with each parameter in a nicely tabulated format.

International Committee for Standardization in Haematology (ICSH): Protocol for evaluation of automated blood cell counters, *Clin Lab Haematol* 6:69–84, 1984b.

This protocol evaluates automated blood cell counters to assess the performance, advantages, and limitations of such instruments.

Ryan DH: Examination of the blood. In Kaushansky K, Prchal JT, Press OW, et al.: *Williams hematology*, vol. 9. New York, 2015, McGraw Hill.

Extensive review of bone marrow examination, including discussion of marrow aspiration technique.

Smock KJ: Examination of the blood and bone marrow. In Greer JP, Arber DA, Appelbaum FR, et al.: *Wintrobe's clinical hematology*, vol. 14. Philadelphia, 2019, Wolters Klower.

Comprehensive review of blood and bone marrow examination, including detailed discussion of various ancillary studies that can be done for establishing the diagnosis of hematologic diseases.

Ward P: The CBC at the turn of the millennium: an overview, *Clin Chem* 46:1215–1220, 2000.

This review article effectively summarizes current methods utilized by automated hematology analyzers. It also offers comments on advantages and limitations of selected CBC and differential parameters.

Access the complete reference list online at Elsevier eBooks for Practicing Clinicians.

REFERENCES

Ackerman P: *Electronic instrumentation in the clinical laboratory*, Boston, 1972, Little, p 140. Brown.

Altman PL, Dittmer DS, editors: *Blood and other body fluids*, Washington, DC, 1961, Federation of American Societies for Experimental Biology.

Altman PL, Dittmer DS: 2, *Biology data book*, vol. III. Bethesda, Md, 1974, Federation of American Societies for Experimental Biology, p 1856.

Bain BJ: Ethnic and sex differences in the total and differential white count and platelet count, *J Clin Pathol* 49:664–666, 1996.

Bain BJ: Bone marrow aspiration, *J Clin Pathol* 54:657–663, 2001a.

Bain BJ: Bone marrow trephine biopsy, *J Clin Pathol* 54:737–742, 2001b.

Barone MA: Lab values. In 3, McMillan JA, Deangelis CD, Feigin RD, et al.: *Oski's pediatrics, principles and practice*Philadelphia, 1999, Lippincott, p 2224.

Barrett BA, Hill PI: A micromethod for the erythrocyte sedimentation rate suitable for use on venous or capillary blood, *J Clin Pathol* 33:1118, 1980.

Bartels PC, Schoorl M, Lombarts AJ: Screening for EDTA-dependent deviations in platelet counts and abnormalities in platelet distribution histograms in pseudothrombocytopenia, *Scand J Clin Lab Invest* 57:629–636, 1997.

Bentley SA, Johnson A, Bishop CA: A parallel evaluation of four automated hematology analyzers, *Am J Clin Pathol* 100:626–632, 1993.

Bentley SA, Lewis SM: Automated differential leukocyte counting: the present state of the art, *Br J Haematol* 35:481–485, 1977.

Bessis M: *Blood smears reinterpreted, translated by Brecher G.*, New York, 1977, Springer-Verlag, p 60.

Bessman JD, Williams LJ, Gilmer Jr PR: Mean platelet volume: the inverse relation of platelet size and count in normal subjects, and an artifact of other particles, *Am J Clin Pathol* 76:289–293, 1981.

Böttiger LE, Svedberg CA: Normal erythrocyte sedimentation rate and age, *Br Med J* 2:85–87, 1967.

Brecher G, Schneiderman M: A time-saving device for the counting of reticulocytes, *Am J Clin Pathol* 20:1079–1093, 1950.

Brestoff JR, Toland A, Afaneh K, et al.: Bone marrow biopsy needle type affects core biopsy specimen length and quality and aspirate hemodilution, *Am J Clin Pathol* 151:185–193, 2019.

Briggs C, Kunka S, Hart D, et al.: Assessment of an immature platelet fraction(IPF) in peripheral thrombocytopenia, *Br J Haematol* 126(1):93, 2004.

Brittin GM, Brecher G, Johnson CA, et al.: Stability of blood in commonly used anticoagulants: use of refrigerated blood for quality control of the Coulter Counter Model S, *Am J Clin Pathol* 52:690–694, 1969.

Bull BS: Is a standard ESR possible? *Lab Med* 6:31, 1975.

Bunn HF, Forget BG: *Hemoglobin: molecular, genetic and clinical aspects*, Philadelphia, 1986, Saunders, p 623.

Burns ER, Lampasso J, Kowatch N, et al.: Performance characteristics of state-of-the-art hematology analyzers, *Clin Lab Sci* 5:181–185, 1992.

Camden TL: How to select the ideal hematology analyzer, *MLO Med Lab Obs* 25:29–33, 1993.

Caswell M, Stuart J: Assessment of Diesse Ves-matic automated system for measuring erythrocyte sedimentation rate, *J Clin Pathol* 44:946–949, 1991.

Cheson BD, Fisher RI, Barrington SF, et al.: Recommendations for initial evaluation, staging and response assessment of Hodgkin and non Hodgkin lymphoma: the Lugano classification, *J Clin Oncol* 32(27):3059–3068, 2014.

Connelly DP, McClain MP, Crowson TW, et al.: The use of the differential leukocyte count for inpatient case finding, *Hum Pathol* 13:294–300, 1982.

Cornbleet PJ, Myrick D, Judkins S, et al.: Evaluation of the cell-Dyn 3000 differential, *Am J Clin Pathol* 98:603–614, 1992.

Dacie JV, Lewis SM: In *Practical haematology*, 7, Edinburgh, 1991, Churchill Livingstone, p 33.

Dalal BI, Brigden ML: Artifacts that may be present on a blood film, *Clin laborat medi* 22:81–100, 2002.

Dalman PR: Developmental changes in red blood cell production and function. In Rudolph AM, Hoffman JIE, editors: *Pediatrics, ed 18, Norwalk, Conn.*, Appleton & Lange, 1987, pp 1011–1012.

Davis BH: Immature reticulocyte fraction (IRF): by any name, a useful clinical parameter of erythropoietic activity, *Lab Hematol* 2:2–8, 1996.

Davis BH, Biegelow NC: Automated reticulocyte analysis: clinical practice and associated new parameters, *Hematol Oncol Clin North Am* 8:617–630, 1994.

d'Onofrio G, Tichelli A, Foures C, et al.: Indicators of haematopoietic recovery after bone marrow transplantation: the role of reticulocyte measurements, *Clin Lab Haematol* 18:45–53, 1996.

Ebrahim A, Ryan WL: Encapsulation of ribonucleic acid in human red cells for use as a reticulocyte quality control material for flow cytometric analysis, *Cytometry* 25:156–163, 1996.

Fairbanks VF, Fahey JL, Beutler E: In *Clinical disorders of iron metabolism*, 2, New York, 1971, Grune & Stratton, p 178.

Ford HC, Toomath RJ, Carter JM, et al.: Mean platelet volume is increased in hyperthyroidism, *Am J Hematol* 27:190–193, 1988.

Freeman AG: Is the erythrocyte sedimentation rate outdated? *J R Soc Med* 90:179–180, 1997.

Geller A: *Vacutainer systems*, Franklin Lakes, NJ, 1996, Becton Dickinson.

Gulati G, Uppal G, Florea AD, et al.: Detection of platelet clumps on peripheral blood smears by CellaVision DM96 system and microscopic review, *Lab Med* 45(4):368–371, 2014.

Hanseler E, Fehr J, Keller H: Estimation of the lower limits of manual and automated platelet counting, *Am J Clin Pathol* 105:782–787, 1996.

Harrow C, Singer AJ, Thode HC: Facilitating the use of the erythrocyte sedimentation rate in the emergency department, *Acad Emerg Med* 6:658–660, 1999.

Hartsock RJ, Smith EB, Petty CS: Normal variations with aging of the amount of hematopoietic tissue in bone marrow from the anterior iliac crest, *Am J Clin Pathol* 43:326–331, 1965.

Hyun BH, Gulati GL, Ashton JK: Bone marrow examination: techniques and interpretation, *Hematol Oncol Clin North Am* 2:513–523, 1988.

International Committee for Standardization in Haematology (ICSH): Recommendation for measurement of erythrocyte sedimentation rate of human blood, *Am J Clin Pathol* 68:505, 1977.

International Committee for Standardization in Haematology (ICSH): Expert Panel on Blood Cell Sizing: recommendation for reference method for determination of packed cell volume of blood, *J Clin Pathol* 33:1–7, 1980.

International Committee for Standardization in Haematology (ICSH): ICSH reference method for staining of blood and bone marrow films by azure B and eosin Y (Romanowsky stain), *Br J Haematol* 57:707–710, 1984a.

International Committee for Standardization in Haematology: Reference method for the enumeration of erythrocytes and leucocytes, *Clin Lab Haematol* 20:77–79, 1994.

International Council for Standardization in Haematology (Expert Panel on Blood Rheology): ICSH recommendations for measurement of erythrocyte sedimentation rate, *J Clin Pathol* 46:198–203, 1993.

International Council for Standardization in Hematology: Expert Panel on Cytometry: proposed reference method for reticulocyte counting based on the determination of the reticulocyte to red cell ratio, *Clin Lab Haematol* 20:77–79, 1998.

International Council for Standardization in: Hematology Expert Panel on cytometry and International Society of laboratory hematology task Force on platelet counting: platelet counting by the RBC/platelet ratio method: a reference method, *Am J Clin Pathol* 115:460–464, 2001.

Iversen OH, Roger M, Solberg HE, et al.: Rising erythrocyte sedimentation rate during several years before diagnosis can be a predictive factor in 70% of renal cell carcinoma patients: the benefit of knowing subject-based reference values, *J Int Med* 240:133–141, 1996.

Jaffé ER, Hultquist DE, et al.: Cytochrome b5 reductase deficiency and enzymopenic hereditary methemoglobinemia. In Scriver CR, Beaudet al, Sly WS, et al.: *The metabolic basis of inherited disease*, 6, New York, 1989, McGraw-Hill.

Jandl JH: In *Blood: textbook of hematology*, 1, Boston, 1987, Little. (Brown.

Jandl JH: In *Blood: textbook of hematology*, 2, Boston, 1996, Little, Brown, p 505.

Kaur M, Singh Rana AP, Kapoor S, et al.: Diagnostic value of bone marrow aspiration and biopsy in routine hematology practice, *J Clin Diagn Res* 8:FC13–FC16, 2014.

Koepke JA, van Assendelft OW, Bull BS: Standardisation of EDTA anticoagulation for blood counting procedures, *Lab Medica* 5:15–17, 1989.

Koike Y, Yoneyama A, Shirai J: Evaluation of thrombopoiesis in thrombocytopenic disorders by simultaneous measurement of reticulated platelets of whole blood and serum thrombopoietin concentrations, *Thromb Haemost* 79:1106–1110, 1998.

Kratz A, Bengtsson HI, Casey JE, et al.: Performance evaluation of the CellaVison DM96 system: WBC differentials by automated digital image analysis supported by an artificial neural network, *Am J Clin Pathol* 124(5):72–79, 2005.

Kratz A, Lee S, Zini G, et al.: Digital morphology analyzers in hematology: ICSH review and recommendations, *Int J Lab Hematol* 41:437–447, 2019.

Kumar V, Singhi S: Predictors of serious bacterial infection in infants up to 8 weeks of age, *Indian J Pediatr* 32:171–180, 1994.

Lapen D: A standardized differential stain for hematology, *Cytometry* 2:309–315, 1982.

Lillie RD, editor: *HJ Conn's biological stains*, 9, Baltimore, 1977, Williams & Wilkins, p 416.

Lippi U, Schinella M, Nicoli M: EDTA-induced platelet aggregation can be avoided by a new anticoagulant also suitable for complete blood count, *Haematology* 75:38–41, 1990.

Lombarts AJ, deKieviet W: Recognition and prevention of pseudothrombocytopenia and concomitant pseudoleukocytosis, *Am J Clin Pathol* 89:634–639, 1988.

Lubrano GJ, Dean WW, Heinsohn HG, et al.: The analysis of some commercial dyes and Romanowsky stains by high-performance liquid chromatography, *Stain Technol* 52:13–23, 1977.

Lukens JN: Hemoglobins associated with cyanosis: methemoglobinemia and low affinity hemoglobins. In *Wintrobe's clinical hematology*, 11, Philadelphia, 2004, Lippincott, p 1487.

Mathy KA, Koepke JA: The clinical usefulness of segmented vs. stab neutrophil criteria for differential leukocyte counts, *Am J Clin Pathol* 61:947–958, 1974.

Matic GB, Chapman ES, Zaiss M: Whole blood analysis of reticulated platelets: improvements of detection and assay stability, *Cytometry* 34:229–234, 1998.

Mauer AM: *Pediatric hematology*, New York, 1969, McGraw-Hill.

Merzianu M, Cheney R, Groman A, et al.: Bone marrow core biopsy adequacy and variability in the Unites States and Canada: a multicenter retrospective study, *Blood* 124:1376, 2014.

Merzianu M, Groman A, Hutson A, et al.: Trends in bone marrow sampling and core biopsy specimen adequacy in the United States and Canada: a multicenter study, *Am J Clin Pathol* 150(5):393–405, 2018.

Metzger DK, Charache S: Flow cytometric reticulocyte counting with thioflavin T in a clinical hematology laboratory, *Arch Pathol Lab Med* 111:540–544, 1987.

Morris MW, Skrodzki Z, Nelson DA: Zeta sedimentation ratio (ZSR), a replacement for the erythrocyte sedimentation rate (ESR), *Am J Clin Pathol* 164:254–256, 1975.

Mukherjee DP, Ray N, Acton ST: Level set analysis for leukocyte detection and tracking, *IEEE Trans Image Process* 13:562–572, 2004.

Nagai M, Mawatari K: Studies of the oxidation states of hemoglobin M Boston and hemoglobin M Saskatoon in blood by EPR spectroscopy, *Biochem Biophys Res Commun* 210:483–490, 1995.

National Comprehensive Cancer Network (NCCN): *Clinical practice guidelines in Oncology, Non Hodgkin lymphoma vs.* at nccn.org on . [Accessed 23 November 2014], 2014.

National Committee for Clinical Laboratory Standards (NCCLS): Methods for the erythrocyte sedimentation rate test. In *Candidate standard for approval. Villanova, Pa*, 3, 1993. (NCCLS. NCCLS Document H2-A3.

O'Broin S, Kelleher B, O'Connor G: Uniformity of anticoagulation for full blood counting, *Clin Lab Haematol* 19:159–160, 1997.

Odejide OO, Cronin AM, DeAngelo DJ, et al.: Improving the quality of bone marrow assessment: Impact of operator techniques and use of a specimen preparation checklist, *Cancer* 119:3472–3478, 2013.

Olshaker JS, Jerrard DA: The erythrocyte sedimentation rate: clinical laboratory in emergency medicine, *J Emerg Med* 15:869–874, 1997.

Parthenis K, Metaxaki-Kossionides C: Blood analysis using black and white digital images, *J Biomed Eng* 14:287–292, 1992.

Pearson TA, Mensah GA, Alexander RW, et al.: Markers of inflammation and cardiovascular disease: application to clinical and public health practice. A statement for health care professionals from the Centers for Disease Control and Prevention and the American Heart Association, *Circulation* 107:499–511, 2003.

Pearson LN, Miller JM, Lunde JH, et al.: Combined Pathology-driven algorithmic testing and integrated reporting for bone marrow examination, *Arch Pathol Lab Med* 143:732–737, 2019.

Peerschke EIB, Pessin MS, Maslak P: Using the hemoglobin content of reticulocytes (RET-He) to evaluate anemia in patients with cancer, *Am J Clin Pathol* 142:506–512, 2014.

Penchas S: Heparin and the ESR, *Arch Intern Med* 138:1865–1866, 1978.

Peterec SM, Brennan SA, Rinder HM: Reticulated platelet values in normal and thrombocytopenic neonates, *J Pediatr* 129:269–274, 1996.

Plebani M, DeToni S, Sanzari MC, et al.: The TEST 1 automated system: a new method for measuring erythrocyte sedimentation rate, *Am J Clin Pathol* 110:334–340, 1998.

Rapi S, Ermini A, Bartolini L: Reticulocytes and reticulated platelets: simultaneous measurement in whole blood by flow cytometry, *Clin Chem Lab* 36:211–214, 1998.

Reed LJ, Raghupati R, Strakhan M, et al.: The powdered bone marrow biopsy technique is superior to the standard manual technique for hematologists-in-training; a prospective, randomized comparison, *Blood* 118, 2011. Abstract 3133.

Rifai N: High-sensitivity C-reactive protein: a useful marker for cardiovascular disease risk prediction and the metabolic syndrome, *Clin Chem* 51:504–505, 2005.

Rogers CH: Blood sample preparation for automated differential systems, *Am J Med Technol* 39:435–442, 1973.

Rollins-Raval MA, Raval JS, Contis L: Experience with CellaVision DM96 for peripheral blood differentials in a large multi-center academic hospital system, *J Pathol Inform* 3:29, 2012.

Rosse C, Kraemer MJ, Dillon TL, et al.: Bone marrow cell populations of normal infants: the predominance of lymphocytes, *J Lab Clin Med* 89:1225–1240, 1977.

Rowan RM, Fraser C: Platelet size distribution analysis. In van Assendelft OW, England JM, editors: *Advances in hematological methods: the blood count*, Boca Raton, Fla, 1982, CRC Press, p 125.

Rümke CL: The imprecision of the ratio of two percentages observed in differential white blood cell counts: a warning, *Blood Cell* 11:137–140, 1985.

Ryan DE: In *Examination of the blood*, 6, New York, 2001, McGraw Hill.

Ryan DH, Cohen HJ: Bone marrow aspiration and morphology. In Hoffman R, Benz EJ, Shattil SJ, et al.: *Hematology: basic principles and practice*, 3, New York, 2000, Churchill Livingstone, pp 2460–2479.

Saadeh C: The erythrocyte sedimentation rate: old and new clinical applications, *South Med J* 91:220–225, 1998.

Sacker LS: Specimen collection. In Lewis SM, Coster JF, editors: *Quality control in haematology*, New York, 1975, Academic Press, p 211.

Saxton BR, Blanchette VW, Butchart S: Reticulated platelet counts in the diagnosis of acute immune thrombocytopenic purpura, *J Pediatr Hematol Oncol* 20:44–48, 1998.

Schneiderka P, Dohnal L, Shachova J: Erythrocyte sedimentation rate in glass and plastic pipettes, *Sb Lek* 98:301–315, 1997.

Shannon K, Pearson HA: Blood and blood forming tissues. In Rudolph CD, Rudolph AM, Hostetter MK, et al.: *Rudolph's pediatrics*, 21, New York, 2002, McGraw Hill, p 1521.

Shannon M, Graef JW: Lead intoxication in children with pervasive developmental disorders, *J Toxicol Clin Toxicol* 34:177–181, 1996.

Shelat SG: Differences in erythrocyte sedimentation rates using the Westergren method and a centrifugation method, *Am J Clin Pathol* 130:127–130, 2008.

Simson E: *Proceedings of the Technicon H-1 hematology Symposium*. In Tarrytown NY, editor: Technicon Instruments, 1986.

Small BM, Bettigole RE: Diagnosis of myeloproliferative disease by analysis of platelet volume distribution, *Am J Clin Pathol* 76:685–691, 1981.

Smith EM, Samadian S: Use of the erythrocyte sedimentation rate in the elderly, *Br J Hosp Med* 51:394–397, 1994.

Sox Jr HC, Liang MH: The erythrocyte sedimentation rate: guidelines for rational use, *Ann Intern Med* 104:515–523, 1986.

Stiegler G, Stohlawetz P, Brugger S: Elevated numbers of reticulated platelets in hyperthyroidism: direct evidence for an increase of thrombopoiesis, *Br J Haematol* 101:656–658, 1998.

Stohlawetz P, Stiegler G, Jilma B: Measurement of the levels of reticulated platelets after plateletpheresis to monitor activity of thrombopoiesis, *Transfusion* 38:454–458, 1998.

Stohlawetz P, Stiegler P, Knobl P: The rise of reticulated platelets after intensive chemotherapy for AML reduces the need for platelet transfusions, *Ann Hematol* 78:271–273, 1999.

Tassies D, Reverter JC, Cases A: Effect of recombinant human erythropoietin treatment on circulating reticulated platelets in uremic patients: associations with early improvement in platelet function, *Am J Hematol* 59:105–109, 1998.

Tsang CW, Lazarus R, Smith W: Hematological indices in an older population sample: derivation of healthy reference values, *Clin Chem* 44:96–101, 1998.

van Assendelft OW: *Spectrophotometry of haemoglobin derivatives*, Assen, The Netherlands, 1970, Royal Van Gorcum Ltd.

Vaughan Hudson B, Maclennan KA, Bennett MH, et al.: Systemic disturbance in Hodgkin's disease and its relation to histopathology and prognosis, *Clin Radiol* 38:257, 1987.

Weick JK, Hagedorn AB, Linman JW: Leukoerythroblastosis: diagnostic and prognostic significance, *Mayo Clin Proc* 49:110–113, 1974.

Wintrobe MM: In *Clinical hematology*, 7, Philadelphia, 1974, Lea & Febiger.

Zauber NP, Zauber AG: Hematologic data of healthy very old people, *J Am Med Assoc* 257:2181–2184, 1987.

Zeigler Z, Murphy S, Gardner FH: Microscopic platelet size and morphology in various hematologic disorders, *Blood* 51:479–486, 1978.

Zlonis M: The mystique of the erythrocyte sedimentation rate: a reappraisal of one of the oldest laboratory tests still in use, *Clin Lab Med* 13:787–800, 1993.

CHAPTER 32

HEMATOPOIESIS

Sharad C. Mathur, Robert E. Hutchison, Golam Mohi

STEM CELLS, 570
Hematopoietic Stem Cells and Progenitors, 570
Hematopoietic Growth Factors, 572
HEMATOPOIETIC TISSUES, 572
Embryonic and Fetal Hematopoiesis, 572
Postnatal Hematopoiesis, 572
ERYTHROCYTE PRODUCTION, 572
Normoblastic Maturation, 572
Megaloblastic Maturation, 574
Regulation of Erythrocyte Production, 574
Synthesis of Hemoglobin, 574
Structure and Function of Hemoglobin, 574
ERYTHROCYTE DESTRUCTION, 576
Degradation of Hemoglobin, 576
ERYTHROKINETICS, 576
Measurements of Total Production of Erythrocytes or Hemoglobin, 576
Measurements of Total Destruction of Erythrocytes or Hemoglobin, 577
Measurements of Effective Production of Erythrocytes: Reticulocyte Count, 577
Measurements of Effective Survival of Erythrocytes In Blood, 577
Summary, 578
NEUTROPHILS, 578
Morphology of Neutrophil Precursors, 578
Distribution and Kinetics, 579
Function, 579
EOSINOPHILS, 579
Morphology of Eosinophil Precursors, 580
Distribution and Kinetics, 580
Function, 580
BASOPHILS AND MAST CELLS, 580
Morphology, 580
Distribution and Kinetics, 581
Function, 581
MONOCYTES AND MACROPHAGES, 581
Morphology, 581
Distribution and Kinetics, 582
Function, 582
MEGAKARYOCYTES, 582
Morphology, 582
Megakaryocytes in Blood, 583
Distribution and Kinetics, 583
Function, 583
LYMPHOCYTES, 583
Primary Lymphoid Tissue, 583
Secondary Lymphoid Tissue, 586
Lymphocyte Function and Physiology, 586
SELECTED REFERENCES, 587

KEY POINTS

- Hematopoietic stem cells are a rare population of cells in the adult bone marrow that sustains hematopoiesis and gives rise to all kinds of blood cells, including granulocytes, monocytes, lymphocytes, megakaryocytes, and erythrocytes.
- Differentiation and maturation of hematopoietic cells are influenced by soluble factors, including growth factors and cytokines, by interaction with the bone marrow stroma, and are mediated in part through interaction of adhesion molecules.
- The primary function of erythrocytes is delivery of oxygen from lungs to tissues. This is dependent on the particular properties and adequate production of hemoglobin and is regulated by oxygen tension in the kidneys, where erythropoietin is produced.
- Neutrophils and monocytes are derived from a common progenitor cell under the influence of growth factors and are the major phagocytic cells. They and the other granulocytic cells (eosinophils, basophils, and mast cells) respond to soluble factors, eliminate microorganisms, and modulate immunity.
- Megakaryocytes, stimulated by thrombopoietin, give rise to platelets and thus effect primary hemostasis.
- Lymphocytes arise from bone marrow stem cells, developing and proliferating in thymus and peripheral lymphoid tissue as well as in bone marrow. They are made up of complex populations of genetically distinct individual B cells, T cells, natural killer (NK) cells, and related subtypes. These interact with other cells, secrete soluble factors—including, principally, cytokines and immunoglobulins—and effect both humoral and cellular immunity.

STEM CELLS

Stem cells are defined as cells that are capable of self-renewal and differentiation into multilineage cells. Embryonic stem cells are pluripotent and have the ability to generate all tissues in the body. Tissue-specific stem cells are multipotent and can give rise to mature cells of a particular tissue. It is suggested that each tissue of our body arises from a tissue-specific stem cell. Stem cells are rare in most tissues. Several tissue-specific stem cells have been identified and prospectively purified based on their surface markers. Hematopoietic stem cells (HSCs) are the best characterized stem cell population.

HEMATOPOIETIC STEM CELLS AND PROGENITORS

Hematopoietic stem cells (HSCs) are characterized by their ability to self-renew and differentiate into committed hematopoietic progenitors. HSCs differentiate into multipotent progenitors (MPPs), which do not have the capacity to self-renew but can generate lineage-committed progenitors, including common lymphoid progenitors (CLPs) and common myeloid progenitors (CMPs) (Kondo et al., 1997; Akashi et al., 2000). CLPs differentiate into T-lymphocytes, B-lymphocytes, and natural killer (NK) cells. CMPs give rise to granulocyte/macrophage progenitors (GMPs) and megakaryocyte/erythrocyte progenitors (MEPs). GMPs differentiate into mature granulocytes, monocytes, and macrophages, whereas MEPs differentiate into platelets and erythrocytes (Reya et al., 2001). Thus, HSCs give rise to all mature blood cells of the hematopoietic system (Fig. 32.1).

Human HSCs are immunophenotypically defined as $Lin^-CD34^+CD38^-CD90^+CD45RA^-CD49f^+$ (Doulatov et al., 2012). They lack lineage-commitment markers (Lin-), such as CD2, CD3, CD4, CD7, CD8, CD10, CD11b, CD14, CD19, CD20, CD56, CD71, and glycophorin A (GPA). As HSCs differentiate into MPPs, the expression of CD90 (Thy1) and CD49f is downregulated (Doulatov et al., 2012). MPPs are defined as $Lin^-CD34^+CD38^-CD90^-CD45RA^-CD49f^-$. CMPs (defined as $Lin^-CD34^+CD38^+CD123^{+/low}CD45RA^-$), GMPs (defined as $Lin^-CD34^+CD38^+CD123^+CD45RA^+$), and MEPs (defined as $Lin^-CD34^+CD38^+CD123^-CD45RA^-$) are distinguishable based on the expression of interleukin-3 (IL-3) receptor α chain (CD123) and CD45RA (Manz et al., 2002; Bryder et al., 2006). CLPs are identified as $Lin^-CD34^+CD38^+CD10^+$ or $Lin^-CD34^+CD38^+CD127^+$ (Bryder et al., 2006; Pang et al., 2011). When committed progenitors differentiate into lineage-restricted progenitors/precursors, they express lineage-specific antigens such as CD33, CD11b, and CD14 for myeloid precursors, CD71

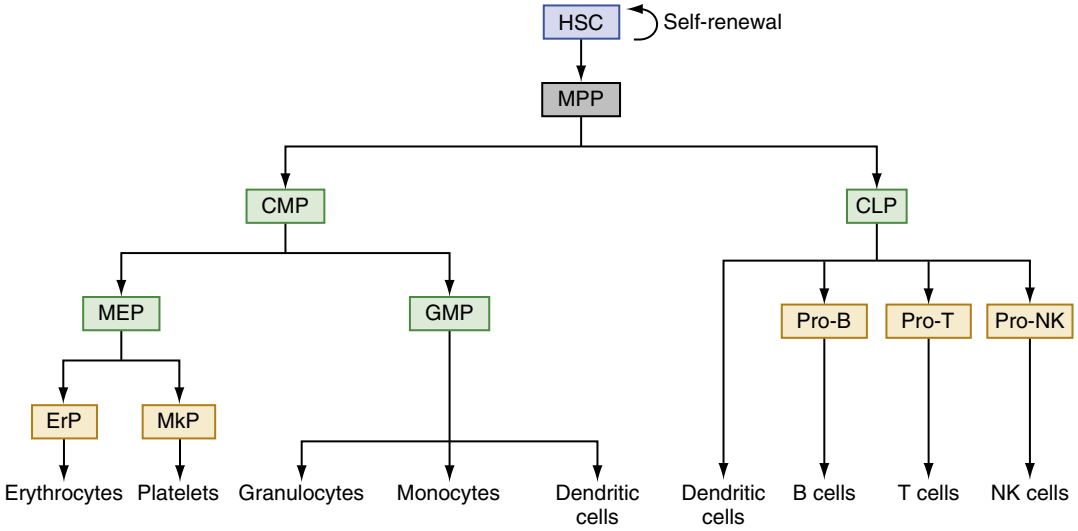

Figure 32.1 A scheme of hematopoietic development hierarchy. *CLP,* Common lymphoid progenitors; *CMP,* common myeloid progenitors; *ErP,* erythroid precursors; *GMP,* granulocyte/macrophage progenitors; *HSC,* hematopoietic stem cells; *MEP,* megakaryocyte/erythrocyte progenitors; *MkP,* megakaryocyte precursors; *MPP,* multipotent progenitors.

BOX 32.1

Lineage-Specific Markers

Myeloid—CD33, CD11b, CD14
Erythroid—CD71, GPA
Megakaryocytic—CD41, CD61
B-lymphoid—CD10, CD19
T-lymphoid—CD3, CD7

and GPA for erythroid precursors, CD41 and CD61 for megakaryocytic precursors, CD10 and CD19 for B-lymphoid precursors, and CD3 and CD7 for T-lymphoid precursors (Box 32.1).

In adults, HSCs are mainly contained in the bone marrow. HSCs are also present in small numbers in the peripheral blood and are increased with administration of growth factors and/or some chemotherapeutic agents, allowing the use of peripheral blood as well as bone marrow to obtain HSCs for stem cell transplantation. In some pathologic conditions, such as in hematologic malignancies, extramedullary hematopoiesis is observed and HSCs can be found in other tissues, including the spleen and liver. Most of the HSCs remain in a quiescent state (G_0 stage of the cell cycle) to prevent rapid exhaustion of HSCs. Since G_0 is a relatively metabolically inactive phase of the cell cycle, HSCs are exposed to less DNA damage induced by metabolic by-products and reactive oxygen species (ROS) than more metabolically active differentiated cells (Rossi et al., 2005; Bryder et al., 2006). FoxO family transcription factors protect HSCs from oxidative damage and extend their life span by increasing the expression of genes required for the detoxification of ROS as well as genes that promote quiescence (Tothova et al., 2007). ATM, a serine/threonine kinase that is activated in response to DNA damage and is required for normal DNA repair, plays an important role in the maintenance of HSC quiescence by regulating the ROS levels (Ito et al., 2006). HSCs also express high levels of multidrug-resistant (MDR) genes (Rossi et al., 2005; Bryder et al., 2006), whose products may play roles in the protection of HSCs from stress or genotoxic agents.

The most important property of stem cells is self-renewal. Self-renewal is the process by which stem cells divide to generate more daughter stem cells. Self-renewal of HSCs is crucial to HSC function and to maintain a long-term steady-state pool of HSCs in adult bone marrow. The function of HSCs is controlled by both cell-intrinsic and cell-extrinsic regulators, including transcription factors, signal transduction pathways, and niche factors. Using gene targeting experiments in mice, several transcription factors have been found critical for the maintenance and function of HSCs. These include stem cell leukemia/T-cell acute lymphoblastic leukemia 1 (SCL/TAL1), LIM-domain-only protein 2 (LMO2), GATA family of transcription factor 2 (GATA2), growth factor independent 1 (GFI1) and growth factor independent 1B (GFI1B). Deletion of these transcription factors severely impairs the HSC function in mice (Shivdasani et al., 1995; Lacombe et al., 2010; Yamada et al., 1998; Tsai et al., 1994; Ling et al., 2004; van der Meer et al., 2010). Several signaling pathways have been identified to regulate HSC self-renewal. The Notch, Sonic hedgehog (Shh), Wnt/β-catenin, transforming growth factor-β (TGF-β) and Janus kinase 2 (JAK2) signaling pathways have been shown to regulate HSC self-renewal (Varnum-Finney et al., 2000; Bhardwaj et al., 2001; Reya et al., 2003; Blank & Karlsson, 2015; Akada et al., 2014). Recent studies also suggest important roles for epigenetic regulators in the maintenance of HSCs. Bmi1, a component of the polycomb repressive complex 1 (PRC1), regulates transcription of target genes through epigenetic silencing and is required for HSC self-renewal (Park et al., 2003). DNMT1 and DNMT3A, which regulate DNA methylation, play important roles in HSC self-renewal and differentiation (Trowbridge et al., 2009; Challen et al., 2011; Challen et al., 2014). TET2, which catalyzes the conversion of 5-methyl-cytosine (5mC) to 5-hydroxymethyl-cytosine (5hmC) of DNA, is frequently found mutated in hematologic malignancies and has been implicated in HSC self-renewal (Moran-Crusio et al., 2011; Ko & Rao, 2011).

The stem cell niche also plays a crucial role in the maintenance and self-renewal of HSCs (Morrison & Scadden, 2014). HSCs are mainly localized in the sinusoids of the bone marrow, where perivascular stromal cells and endothelial cells produce multiple factors that are important components of the HSC niche. Stem cell factor (SCF), CXC-chemokine ligand 12 (CXCL12) and thrombopoietin (TPO) are important niche factors that are required for HSC maintenance (Ding et al., 2012; Ding & Morrison, 2013; Greenbaum et al., 2013; Yoshihara et al., 2007). Sympathetic nerves (Katayama et al., 2006), nonmyelinating Schwann cells (Yamazaki et al., 2011), macrophages (Winkler et al., 2010), and osteoclasts (Mansour et al., 2012) may also contribute to HSC niche and promote HSC maintenance in the bone marrow. It is suggested that HSCs physically attach to the niche and, when they divide, one daughter cell remains attached to the niche whereas the other daughter cell is displaced away from the niche to proceed to a differentiation pathway (Clarke & Fuller, 2006). Oncogenic mutations associated with leukemia and other malignancies usually exploit the self-renewal mechanisms of normal stem cells. These mutations often originate in normal HSCs and transform them into leukemic stem cells (LSCs) with increased self-renewal capacity.

Self-renewal and differentiation potentials of human HSCs can be assessed by serial transplantation of HSCs into immune-deficient NSG (NOD/SCID/γ-chain deficient) mice and by hematopoietic progenitor colony assays, respectively. Purified HSCs from human bone marrow or peripheral blood are transplanted into sublethally irradiated NSG mice, which permit long-term engraftment of human cells without graft versus host disease. The repopulating human cells, termed *severe-combined immunodeficiency mouse-repopulating cells (SRCs)*, are assessed using flow cytometry. Hematopoietic progenitor colony assay is used to determine the differentiation capacity of HSCs/progenitors. The earliest undifferentiated myeloid progenitor colony that expresses CD34 and CD33 is called the *colony-forming unit-granulocyte, erythrocyte, macrophage, megakaryocyte* (*CFU-GEMM*). In the presence of different cytokines, CFU-GEMM cells can differentiate into colony-forming unit-granulocyte (CFU-G), colony-forming unit-macrophage (CFU-M), burst-forming unit-erythroid (BFU-E), colony-forming unit-erythrocyte (CFU-E), and colony-forming unit-megakaryocyte (CFU-Mk). In addition, evidence suggests that HSCs can transdifferentiate into nonhematopoietic cells (Zubair et al., 2002).

HEMATOPOIETIC GROWTH FACTORS

Soluble or membrane-bound factors contributing to control of hematopoiesis include hematopoietic growth factors and cytokines. They regulate the proliferation, survival, and differentiation of hematopoietic precursor cells and facilitate the function of mature blood cells. Hematopoietic growth factors/cytokines may act locally near the site at which they are produced or they may circulate in the blood. They are produced by different types of hematopoietic or nonhematopoietic cells and usually affect more than one lineage (Metcalf, 2008). They often act synergistically with other growth factors and may act on normal cells as well as neoplastic cells. There are specific receptors for each cytokine that transmits signals from the cell surface to the nucleus following interaction with the cytokine.

Genes associated with hematopoietic growth factors/cytokines have been identified, cloned, and sequenced. Purified recombinant cytokines have been generated and utilized experimentally. Several of these cytokines have been in clinical use to stimulate hematopoietic cell production. Erythropoietin (EPO) is critical for the production of erythrocytes, whereas TPO is required for the production of megakaryocytes (Metcalf, 2008). Other important growth factors/cytokines involved in hematopoiesis include SCF, FLT-3 ligand, granulocyte/macrophage colony stimulating factor (GM-CSF), granulocyte colony stimulating factor (G-CSF), macrophage colony stimulating factor (M-CSF), interleukins (IL-3, IL-4, IL-5, IL-6, IL-7, IL-11, IL-13, and IL-15), and interferons (IFN-α and IFN-γ).

Another class of factors, called *chemokines*, is important in regulating hematopoietic cell trafficking and homing. The chemokine CXCL12 (also known as SDF-1) is expressed by bone marrow stromal cells and microvascular endothelial cells. HSCs express CXCR4, the receptor for CXCL12. CXCL12-CXCR4 chemokine signaling is involved in HSC maintenance and engraftment (Sugiyama et al., 2006). G-CSF–induced mobilization of HSCs is likely due to disruption of the interaction between CXCL12 and CXCR4 (Papayannopoulou & Scadden, 2008). Several other chemokines and their receptors also play roles in T- and B-cell development, inflammation, and immune surveillance (Moser et al., 2004).

HEMATOPOIETIC TISSUES

EMBRYONIC AND FETAL HEMATOPOIESIS

Beginning in the first month of prenatal life, primitive hematopoiesis starts outside the embryo in the mesenchyme of the yolk sac as **blood islands**. These contain predominantly **primitive erythroblasts**, which are large and megaloblastic, are formed intravascularly, and retain their nuclei. Definitive hematopoiesis in mammals takes place in the aorta-gonad-mesonephros (AGM) region of the embryo, from which hematopoietic cells migrate to the placenta, liver, and spleen. At the sixth week, hematopoiesis begins in the liver, which becomes the major hematopoietic organ of early and midfetal life. **Definitive erythroblasts**, which become nonnucleated red cells, are formed extravascularly in the liver; granulopoiesis and megakaryocytes are present to a lesser degree. In the middle part of fetal life, the spleen and, to a lesser extent, lymph nodes have a minor role in hematopoiesis, but the liver continues to dominate. In the latter half of fetal life, the bone marrow becomes progressively more important as a site of blood cell production. As this occurs, the liver's role diminishes.

POSTNATAL HEMATOPOIESIS

Shortly after birth, hematopoiesis in the liver ceases. The marrow is then the only site for the production of erythrocytes, granulocytes, and platelets. Hematopoietic stem cells and committed progenitor cells are maintained in the marrow. Lymphocytes (of the B-cell type) continue to be produced in the marrow and in the secondary lymphoid organs, whereas T lymphocytes are produced in the thymus and in the secondary lymphoid organs (see the Lymphocytes section later in the chapter).

At birth, the total marrow space is occupied by active hematopoietic (red) marrow. As body growth progresses and marrow space increases during infancy, only part of that space is needed for hematopoiesis; the remaining space is occupied by fat cells. Later in childhood, only the flat bones (the skull, vertebrae, thoracic cage, shoulder, and pelvis) and the proximal parts of the long bones of the upper and lower limbs are sites of blood cell formation. The remaining marrow space is fatty or yellow marrow that can be replaced by hematopoietic cells if continuous, intensive stimulation exists.

The marrow circulation is closed, that is, arterioles deriving from central longitudinal arteries (i.e., in long bones) connect directly with broad venous sinuses that anastomose and eventually empty into central longitudinal veins. The flattened endothelium of the sinuses is partially covered by adventitial reticular cells, a form of fibroblast that elaborates argentophilic reticulin fibers. These reticular cells and fibers form the supporting meshwork of the marrow stroma, where the hematopoietic cells reside. The reticular cells are minimally phagocytic; they may swell and take up water, become fat cells, and induce hematopoietic stem cells to become committed progenitor cells. After proliferation and maturation have occurred in the marrow stroma, blood cells gain entrance to the blood through or between the endothelial cells of the sinus wall. This requires displacement of adventitial cells. Stromal mesenchymal cells and sinusoidal endothelial cells produce a variety of cytokines and chemokines involved in hematopoiesis.

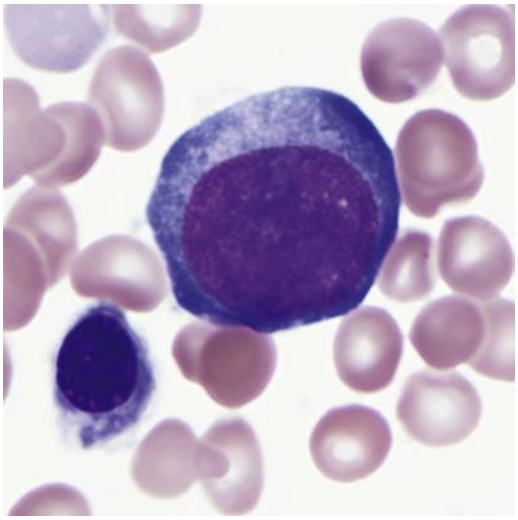

Figure 32.2 Pronormoblast with a large round nucleus, fine chromatin, and basophilic cytoplasm (Wright-Giemsa, 1000×).

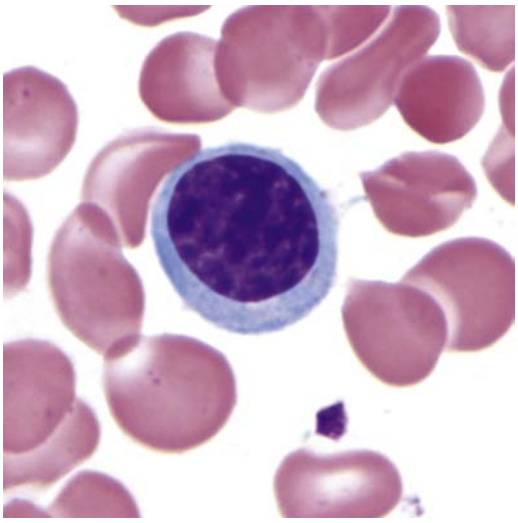

Figure 32.3 Basophilic normoblasts with chromatin condensation and deeply basophilic cytoplasm (Wright-Giemsa, 1000×).

ERYTHROCYTE PRODUCTION

The erythrocyte is a vehicle for the transport of hemoglobin, which is produced in precursor cells of the erythrocytes, the normoblasts. The function of hemoglobin is the transport of oxygen and carbon dioxide. The erythrocyte is also metabolically capable of keeping hemoglobin in a functional state.

NORMOBLASTIC MATURATION

The earliest recognizable erythroid precursor is the **pronormoblast** (Fig. 32.2). At about 20 μm diameter, it is the largest of the erythroid precursors. The nucleus has a fine, uniform chromatin pattern that is somewhat more distinct and more intensely stained than that of the myeloblast. The nuclear membrane is prominent. One or more prominent nucleoli are present. The cytoplasm has a heterogeneous quality and is moderate in amount and basophilia; no granules are present. The pronormoblast undergoes mitosis and forms two basophilic normoblasts.

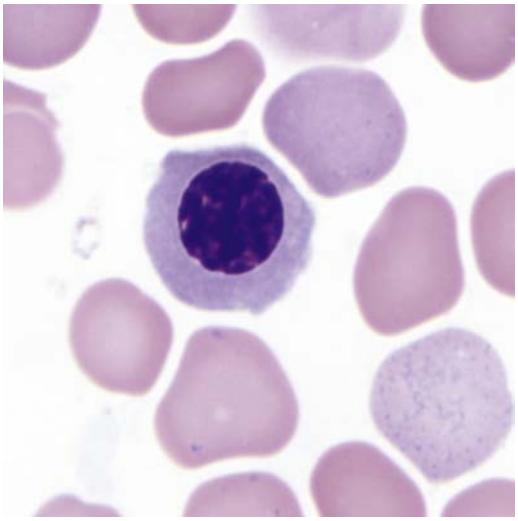

Figure 32.4 Polychromatophilic normoblast with light-blue cytoplasm due to accumulation of hemoglobin (Wright-Giemsa, 1000×).

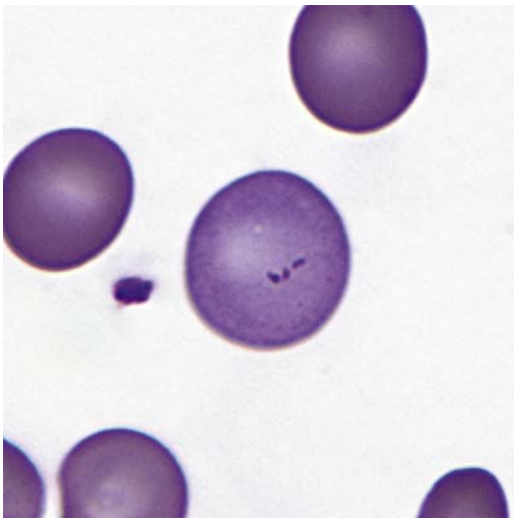

Figure 32.6 Reticulocyte (polychromatophilic erythrocyte) with pink-gray cytoplasm due to residual RNA (Wright-Giemsa, 1000×). *RNA,* Ribonucleic acid.

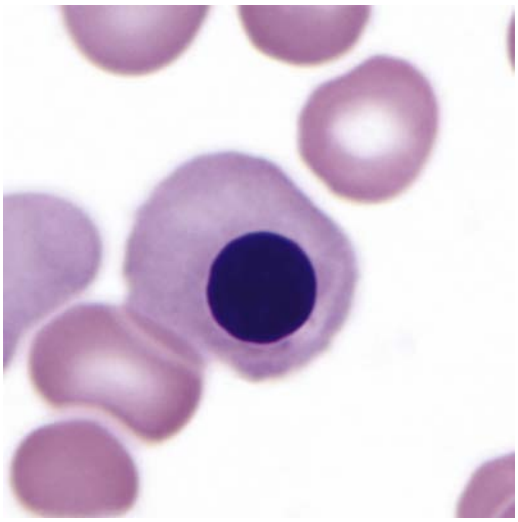

Figure 32.5 Orthochromatic normoblast with pyknotic nucleus and pink-gray cytoplasm (Wright-Giemsa, 1000×).

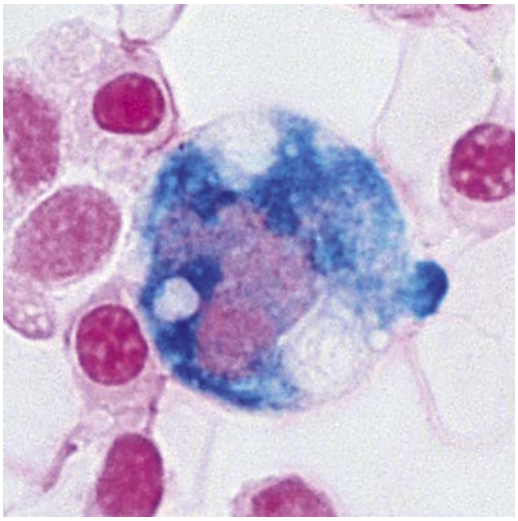

Figure 32.7 Siderophage with associated normoblasts (part of an erythroblastic island) in the bone marrow (Prussian blue, 1000×).

The **basophilic normoblast** (Fig. 32.3) is somewhat smaller and has slightly coarser chromatin that stains intensely. The chromatin may be partially clumped, and the pattern may suggest a wheel with broad spokes. The parachromatin (the nonchromatin part of the nucleus) is distinct and stains pink. Nucleoli are present but are not often visible. The nuclear/cytoplasmic (N/C) ratio is moderate; about one-fourth of the total cell area appears to be cytoplasm. The cytoplasm is deeply basophilic, owing to the abundance of ribonucleic acid (RNA); much of this is evident as polyribosomes on electron micrographs. The cell borders of early normoblasts frequently appear irregular owing to the presence of pseudopodia.

After mitosis of the basophilic normoblast, evidence of continuing hemoglobin production becomes visible in the cytoplasm of the two daughter cells as polychromasia, that is, mixtures of the red-staining of hemoglobin with the blue of RNA in varying shades of gray. This cell is the **polychromatophilic normoblast** (Fig. 32.4), which is slightly smaller than the basophilic normoblast. The nucleus occupies about half of the area of the cell, stains intensely, and has moderately condensed chromatin that is sharply distinct from the pink parachromatin. The polychromatophilic normoblast undergoes one or two mitotic divisions.

After the last mitosis, the nucleus becomes small and dense (pyknotic), and the **orthochromatic normoblast** stage is reached (Fig. 32.5). Mitosis is no longer possible. The cell is smaller than the polychromatophilic normoblast and has a lower N/C ratio. The cytoplasm contains more abundant hemoglobin and fewer polyribosomes and remains slightly polychromatophilic.

Finally, accompanied by cytoplasmic contractions and undulations, the nucleus and a small rim of cytoplasm are ejected from the orthochromatic normoblast, forming the **reticulocyte** (Fig. 32.6). On air-dried films with Romanowsky-type stains, the reticulocyte is polychromatophilic as a result of the retention of RNA.

In the marrow, developing erythroid cells are usually in contact with macrophages in what are termed *erythroblastic islands* (Fig. 32.7). These erythroblastic islands are usually broken up when aspirated marrow is spread on slides, but fragments of macrophage cytoplasm may sometimes be seen attached to the separated normoblasts, especially on Prussian blue–stained films.

During proliferation and maturation, iron is transferred from plasma transferrin into the cells in the normoblastic series. The pronormoblast and the basophilic normoblast have the highest content of RNA, which begins to decline in the polychromatophilic normoblasts as hemoglobin increases in amount. Synthesis of RNA gradually decreases in each stage through the orthochromatic normoblasts. When the nucleus is no longer present (in the reticulocyte), RNA synthesis ceases, yet the RNA already present remains for a few days, and protein and heme synthesis continue in the reticulocyte until the cell loses its RNA and mitochondria.

During this maturation process, three or four mitotic divisions occur in a period of 3 days, resulting in the potential production of 16 reticulocytes from each pronormoblast. The reticulocytes are larger than mature red blood cells and remain in the marrow stroma for 1 to 2 days before being released into the blood.

In the marrow, the reticulocytes are about equal in number to the nucleated erythrocytes and slightly greater in number than the reticulocytes in the circulating blood. If sufficiently severe hypoxia is present, this marrow pool of reticulocytes can be released. This approximately doubles the number of circulating reticulocytes.

Normally, reticulocytes remain as such, slowly synthesizing hemoglobin, for 2 to 3 days in the marrow and for 1 day in the blood. Residual ribosomes, mitochondria, and other organelles are then removed, and the

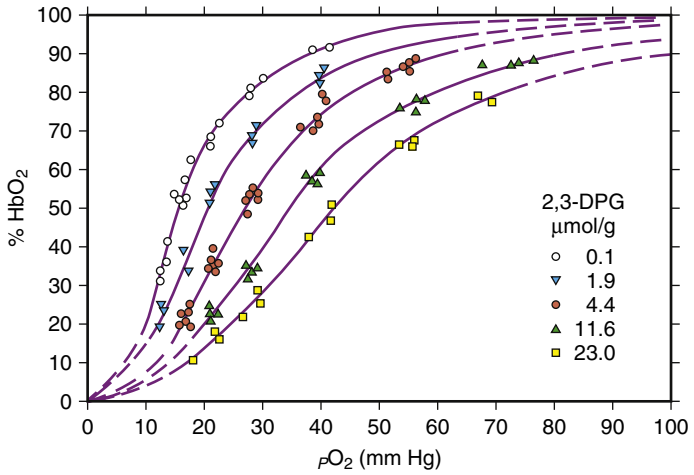

Figure 32.8 Oxygen dissociation curves of hemoglobin at different concentrations of 2,3-DPG. The curve is sigmoidal and shifts to the right with increasing concentrations of 2,3-DPG. This results in decreased affinity of hemoglobin for oxygen and increased delivery of oxygen to the tissues. *DPG,* diphosphoglycerate. (Reprinted from Duhm J: *Oxygen affinity of hemoglobin and red cell acid base status,* p 583, Copyright 1972, with permission from Elsevier.)

mature erythrocytes circulate for about 120 days. During this time, they gradually age, certain enzymatic activities diminish, and they are finally destroyed within phagocytic cells of the mononuclear phagocyte system (reticuloendothelial system).

MEGALOBLASTIC MATURATION

Abnormal maturation of erythroid precursors that occurs in vitamin B_{12} deficiency or folic acid deficiency is known as *megaloblastic maturation*, and the abnormal erythroid cells are called *megaloblasts*. Because of impaired ability of the cells to synthesize DNA, the intermitotic and mitotic phases are prolonged. This results in enlarged cells, with nuclear maturation lagging behind cytoplasmic maturation (nuclear-cytoplasmic dissociation). The nuclear chromatin pattern is more delicate and more "open," with prominent parachromatin. Karyorrhexis, or breaking up of the nucleus, and Howell-Jolly bodies are frequently noted. Megaloblastic development parallels normoblastic maturation; the stages of promegaloblast, basophilic megaloblast, polychromatophilic megaloblast, and orthochromatic megaloblast may be recognized.

REGULATION OF ERYTHROCYTE PRODUCTION

The number of erythrocytes in the blood may be regulated by changing the rate of production. The rate of erythrocyte destruction does not vary appreciably in normal individuals. Increased production of erythrocytes occurs when oxygen transport to the tissues is impaired, as in anemia, in cardiac or pulmonary disorders, and in the low oxygen tension of high altitudes. Erythrocyte production decreases when an individual is hypertransfused or exposed to high oxygen tension.

Oxygen affinity of hemoglobin is modulated by the concentration of phosphates, in particular, 2,3-diphosphoglycerate (2,3-DPG) in the red blood cell. These phosphates combine with the β-chains of reduced hemoglobin and diminish its affinity for oxygen (Fig. 32.8). In areas of tissue hypoxia, as oxygen moves from hemoglobin into the tissues, the amount of reduced hemoglobin in the red blood cells increases, binding more 2,3-DPG, further reducing its oxygen affinity so that more oxygen can be delivered to the tissues. If hypoxia persists, depletion of free 2,3-DPG leads to increased glycolysis, production of more 2,3-DPG, and a persistently lower oxygen affinity of the hemoglobin.

Tissue hypoxia induces formation of EPO via production of the transcriptional factor, hypoxia-inducible factor-1 (HIF-1). HIF-1 is a heterodimer consisting of α- and β-subunits, of which the α-subunit is regulated by hypoxia. Under conditions of normal oxygen tension, HIF-1α undergoes proteosomal degradation, but it is stable under hypoxic conditions. EPO effects the production of more red blood cells in the bone marrow. It acts by inducing committed progenitor cells (CFU-E and BFU-E) in the marrow to proliferate and differentiate into pronormoblasts by shortening the generation time of normoblasts and by promoting early release of reticulocytes into the blood. The result is increased numbers of marrow normoblasts in a normal ratio of cell types, a condition known as *normoblastic hyperplasia.* Increased cellular expression of HIF-1α can result from a 598C→T mutation in the von Hippel-Lindau gene (the von Hippel-Lindau protein is involved in HIF-1α degradation). This results in elevation of EPO levels and an autosomal-recessive form of hereditary polycythemia known as *Chuvash polycythemia* (Gordeuk et al., 2004).

Measurement of EPO is accomplished by in vitro immunologic methods utilizing serum or plasma, with ethylenediaminetetraacetic acid (EDTA) plasma providing greater sensitivity (Lindstedt & Lundberg, 1998). Elevated levels are detected in patients with secondary polycythemia and in those with aplastic anemia. Decreased levels below the normal range are found in normal individuals after transfusion and in those with primary polycythemia (polycythemia vera). However, considerable overlap exists; normal EPO levels may be found in both primary and secondary polycythemia (Spivak, 2002). Anti-EPO antibodies have been described in pure red blood cell aplasia and systemic lupus erythematosus (Casadevall et al., 1996; Schett et al., 2001). These may interfere with immunoassays for EPO and may contribute to anemia.

SYNTHESIS OF HEMOGLOBIN

Heme Synthesis

Heme synthesis occurs in most cells of the body except for the mature erythrocytes, but most abundantly in the erythroid precursors. Succinylcoenzyme A condenses with glycine to form the unstable intermediate α-amino β-ketoadipic acid, which is readily decarboxylated to δ-aminolevulinic acid (ALA; Fig. 32.9). This condensation requires pyridoxal phosphate (vitamin B_6) and occurs in mitochondria.

ALA is excreted normally in small amounts in the urine, but in certain abnormalities of heme synthesis (e.g., lead poisoning), excretion is increased. Two molecules of ALA condense to form the monopyrrole porphobilinogen, catalyzed by the enzyme ALA-dehydrase. Porphobilinogen is also normally excreted in small amounts in the urine. Markedly elevated amounts appear in the urine in acute intermittent porphyria and are easily detected by a color reaction with Ehrlich's aldehyde reagent.

Four molecules of porphobilinogen react to form uroporphyrinogen III or I (Fig. 32.10). The type III isomer is converted, by way of coproporphyrinogen III and protoporphyrinogen, to protoporphyrin. In certain diseases when this pathway is partially blocked, the type I isomers of uroporphyrinogen and coproporphyrinogen are formed, and their oxidized excretion products, uroporphyrin I and coproporphyrin I, are increased in amount.

Protoporphyrin is normally found in mature erythrocytes. In lead poisoning and in iron deficiency, levels of free erythrocyte protoporphyrin (FEP) are increased. Iron is inserted into protoporphyrin by the mitochondrial enzyme ferrochelatase to form the finished heme moiety.

Globin Synthesis

Globin synthesis occurs in the cytoplasm of the normoblast and reticulocyte. The polypeptide chains are manufactured on the ribosomes. Specific small soluble RNA (sRNA) molecules determine the placement of each amino acid according to the code in the messenger RNA (mRNA). Progressive growth of the polypeptide chain begins at the amino end. This process of protein synthesis occurs on ribosomes clustered into polyribosomes, which are held together by the mRNA. Because the reticulocyte can synthesize hemoglobin for at least 2 days after loss of its nucleus, it appears that the mRNA for hemoglobin is quite stable. The polypeptide chains released from the ribosomes are folded into their three-dimensional configurations spontaneously.

Control of hemoglobin synthesis is exerted primarily through the action of heme. Increased heme inhibits further heme synthesis by inhibiting the activity and synthesis of ALA synthase. Heme also promotes globin synthesis, mainly at the site of chain initiation, and the interaction of ribosomes with mRNA.

STRUCTURE AND FUNCTION OF HEMOGLOBIN

In each hemoglobin (Hb) molecule, one heme group is inserted into a hydrophobic pocket of one folded polypeptide chain (Bunn & Forget, 1986). Normal adult HbA consists of four heme groups and four polypeptide chains (two α-chains and two β-chains), which form a roughly globular hemoglobin molecule (Fig. 32.11). The ferrous iron atoms have six coordination bonds: four to the pyrrole nitrogens of heme, one to the imidazole nitrogen of histidine of the globin chain (87-α or 92-β), and one that is reversibly bound to oxygen. As the oxygen partial pressure increases, each of the four heme groups sequentially binds one molecule of oxygen. In the

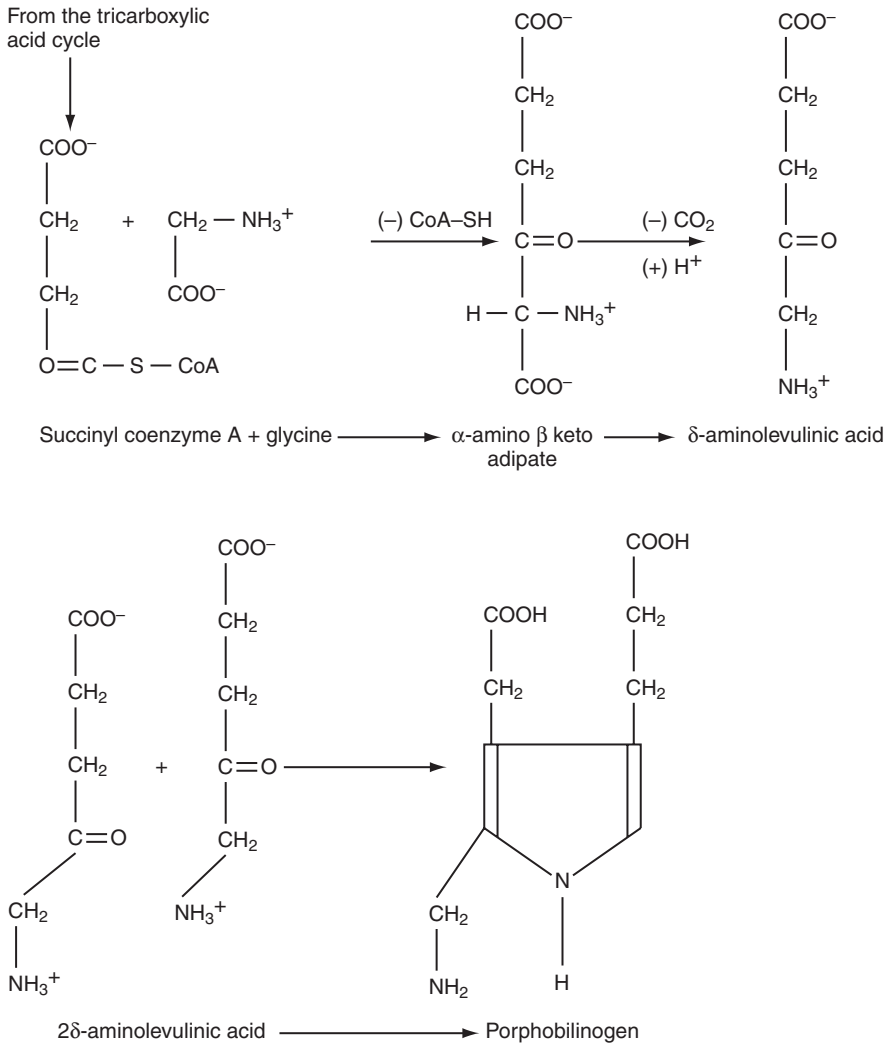

Figure 32.9 Formation of porphobilinogen from succinyl-coenzyme A and glycine. (From Leavell BS: *Fundamentals of clinical hematology*, ed 4, Philadelphia, 1976, Saunders, with permission.)

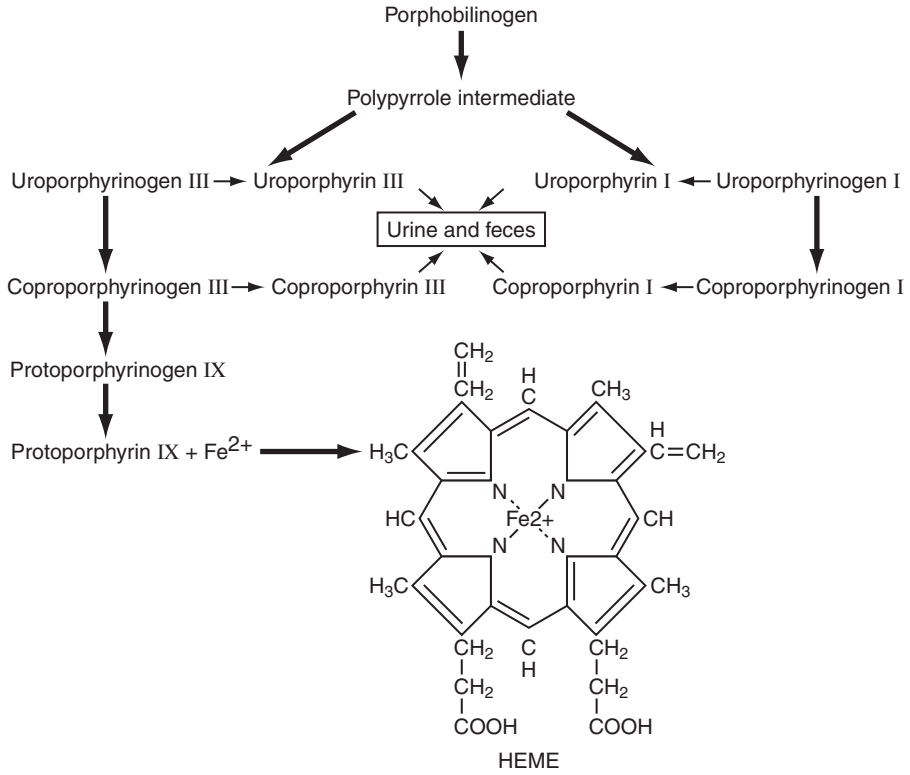

Figure 32.10 Formation of heme from porphobilinogen. (From Leavell BS: *Fundamentals of clinical hematology*, ed 4, Philadelphia, 1976, Saunders, with permission.)

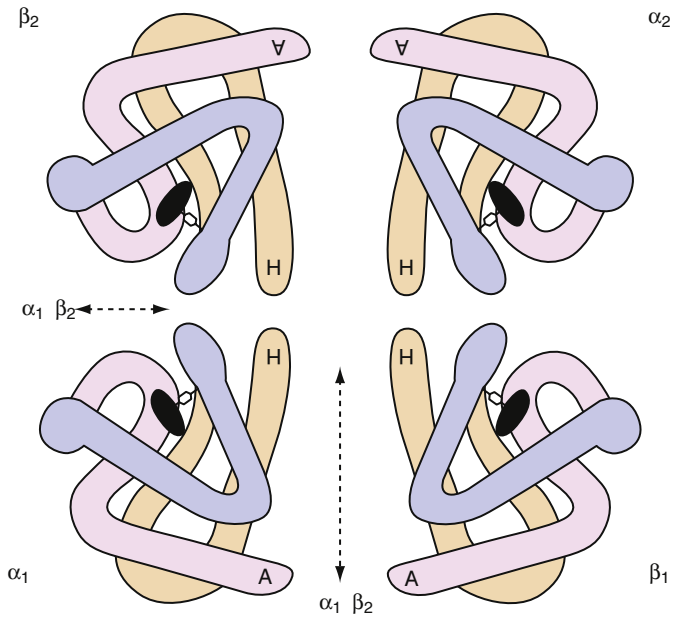

Figure 32.11 The hemoglobin molecule (tetramer, molecular weight 64,500 Da). The heme group for each monomeric polypeptide chain is depicted as a black disk, connected to an imidazole group of histidine and located near the surface of the molecule in a "pocket" formed by the polypeptide chain. The letters *A* and *H* designate α-helix segments of each polypeptide chain: A is the amino-terminal segment and H is the carboxy-terminal segment. The four monomers are separated in this drawing but actually make contact along a relatively large area ($\alpha_1\beta_1$), which is thought to be the relatively fixed or stabilizing contact area, and a smaller ($\alpha_1\beta_2$) area thought to be the functional contact area, where movement occurs during oxygenation and deoxygenation, changing the molecular configuration. (Redrawn from White JM, Dacie JV: The unstable hemoglobins—molecular and clinical features, *Prog Hematol* 7:69, 1971, with permission.)

process, a change in the overall configuration of the hemoglobin molecule occurs, which favors the additional binding of oxygen.

The sigmoid-shaped oxygen dissociation curve of hemoglobin reflects this increasing affinity for oxygen with increasing partial pressure of oxygen in the lungs (see Fig. 32.8). In the tissues, conversion of oxygenated Hb to Hb, decreasing pH, and increasing temperature produced by metabolic processes, as well as the binding of more 2,3-DPG to Hb, result in a shift of the Hb-oxygen dissociation curve to the right, favoring the release of oxygen from hemoglobin.

Carbon dioxide (CO_2) is transported in erythrocytes as well as in plasma. A small part of red blood cell CO_2 is dissolved and is bound to amino groups of hemoglobin as carbamino-CO_2, but most is in the bicarbonate form. The enzyme carbonic anhydrase catalyzes the transformation of carbon dioxide to bicarbonate in the red blood cell while in the tissue capillary bed and catalyzes the reverse reaction (the release of carbon dioxide from bicarbonate) in the erythrocyte when it is in the capillary bed of the lungs.

The porphyrias (Fig. 32.12), abnormalities of heme synthesis, are described in Chapter 33.

ERYTHROCYTE DESTRUCTION

The erythrocyte gradually undergoes metabolic changes over the course of its 120-day life span, at which time the less viable senescent cell is removed from the circulation. Certain glycolytic enzymes diminish in activity as the cell ages. Older red blood cells have a smaller surface area and an increased mean cell hemoglobin concentration (MCHC) compared with younger cells. Furthermore, aged red blood cells lose sialic acid from their membranes, exposing an asialoglycophorin. This senescent antigen is recognized and an autoantibody is synthesized by the host. After binding of the autoantibody, the senescent cell is removed from the circulation by the mononuclear phagocyte system, primarily within the spleen. About 3 million cells are normally removed from the blood per second with no demonstrable histologic evidence of erythrophagocytosis.

In some pathologic states, the mononuclear phagocyte system removes younger sensitized or abnormal red blood cells at a rapid rate. Subsequently, erythrophagocytosis is often evident. In autoimmune hemolytic anemia, the mononuclear phagocyte system removes red blood cells following the binding of autoantibodies or complement to reticulocytes and young red blood cells. In other pathologic states, red blood cells are removed because of structural defects that interfere with their normal passage through the microcirculation of the mononuclear phagocyte system.

DEGRADATION OF HEMOGLOBIN

After removal of the red blood cell from the circulation, hemoglobin is broken down within the macrophages of the mononuclear phagocyte system into its three constituents: iron, protoporphyrin, and globin. The iron goes into storage and may be completely reutilized. The globin may be degraded and returned to the amino acid pool of the body. In contrast, the protoporphyrin ring is split, converted to bilirubin, and excreted from the body.

In the macrophage, the protoporphyrin ring is cleaved by a heme oxidase enzyme at the α-methene bridge, yielding 1 mol of carbon monoxide (CO) and 1 mol of biliverdin. The CO appears in the blood as carboxyhemoglobin (HbCO) and is eventually exhaled. Biliverdin is reduced to bilirubin in the macrophage, and bilirubin is transported to the liver by plasma albumin. It is removed from the plasma by the liver cell, conjugated mainly with glucuronide, and excreted in the bile. In the intestine, reduction by bacteria occurs, and bilirubin is transformed into urobilinogen, mesobilirubinogen, and stercobilinogen, compounds that are collectively designated urobilinogens.

Estimation of exhaled CO, HbCO, or fecal urobilinogen can be used as a measure of hemoglobin breakdown. When production of red blood cells is diminished and the level of circulating hemoglobin is low, as in aplastic anemia, urobilinogen excretion is reduced. When destruction of erythrocytes is increased, as in hemolytic anemia, all three are increased in amount.

In normal humans, about 80% to 90% of the excreted bile pigment measured as fecal urobilinogen is derived from breakdown of senescent erythrocytes that have lived 100 to 120 days. However, about 10% to 20% of the pigment is excreted within the first few days. This early labeled bile pigment comes from nonhemoglobin heme formed in the liver as well as from the breakdown of newly formed hemoglobin in the bone marrow. Much of the latter may represent hemoglobin from the pieces of cytoplasm of the orthochromatic normoblast that are lost during the process of nuclear extrusion.

In certain hematologic diseases—notably, thalassemia, megaloblastic anemia, myelodysplasia, and erythropoietic porphyria—this early labeled bile pigment fraction may be markedly increased. This intramedullary destruction of hemoglobin, which never appears in circulating erythrocytes, is known as *ineffective erythropoiesis*.

ERYTHROKINETICS

The balance between delivery of erythrocytes to the blood and removal of erythrocytes from the blood results in a relatively constant hemoglobin mass in the circulation. Anemia occurs when removal of erythrocytes from the blood is increased and cannot be compensated for by increased production, when delivery of erythrocytes to the blood is decreased, or when both processes exist together.

When anemia develops, tissue hypoxia leads to elevated levels of erythropoietin in the plasma. Resultant normoblastic hyperplasia produces more erythrocytes for delivery to the circulation. The marrow in a normal individual is capable of six to eight times the normal output of erythrocytes with extreme stimulation. This capacity must be compared with the output actually attained when one is evaluating the marrow response of a given patient.

Measurements that assess **effective erythropoiesis** (production and delivery of erythrocytes to the circulation), **ineffective erythropoiesis**, and destruction of erythrocytes may be necessary to determine the mechanism and cause of anemia.

MEASUREMENTS OF TOTAL PRODUCTION OF ERYTHROCYTES OR HEMOGLOBIN

The **total mass of erythropoietic cells** in the body cannot be easily measured. An estimate is made by examining a sample of bone marrow from a normally active site and determining the cellularity and percentage of total nucleated cells that are erythropoietic (see the Bone Marrow Examination section in Chapter 31). When marrow activity increases, usually the additional hematopoietic cells replace the fat in the red marrow sites before extension occurs into the yellow marrow of the long bones. One assumes that the sample is representative of the marrow as a whole—an assumption that usually is valid.

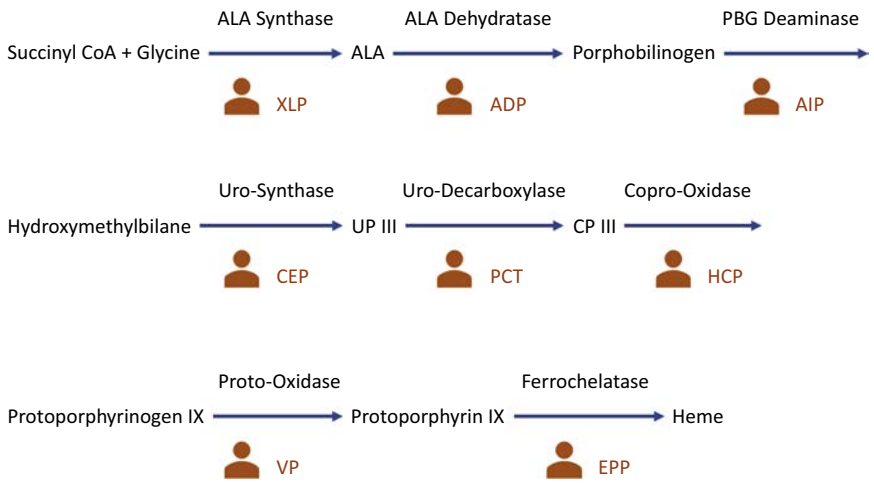

Figure 32.12 Biosynthetic pathway of heme and pathogenesis of the porphyrias. *ADP,* Aminolevulinic acid dehydratase deficiency porphyria; *AIP,* acute intermittent porphyria;*ALA,* Aminolevulinic acid; *CEP,* congenital erythropoietic porphyria; *CP III,* coproporphyrinogen III; *EPP,* erythropoietic protoporphyria; *HCP,* hereditary coproporphyria; *HMB,* hydroxymethylbilane; *PCT,* porphyria cutanea tarda; *UP III,* uroporphyrinogen III; *VP,* variegate porphyria; *XLP,* X-linked protoporphyria.

The **plasma iron turnover** is calculated from the serum iron level and the rate of removal of injected radioactive iron from the plasma. About 25% to 30% of the iron is not used in erythropoiesis and is primarily taken up by the liver. The remaining 70% to 75% is taken up by erythropoietic cells; therefore, it is a measure of total erythropoiesis, both effective and ineffective.

MEASUREMENTS OF TOTAL DESTRUCTION OF ERYTHROCYTES OR HEMOGLOBIN

Determination of **fecal urobilinogen** is an estimate of the total excretion of bile pigments—the breakdown products of heme. This measurement includes pigment derived from hemoglobin formed and destroyed in the marrow without ever reaching the circulating erythrocytes. Limitations include diminished conversion of bilirubin to urobilinogen caused by oral administration of broad-spectrum antibiotics, and failure of pigment to reach the intestine in obstructive jaundice.

A portion (up to 50%) of the excreted urobilinogen is reabsorbed into the portal circulation and is re-excreted into the bile, without conjugation, by the liver. Only a small amount is normally excreted in the urine. Increased urinary urobilinogen is seen with severe liver disease as well as with conditions associated with increased heme catabolism that overwhelm the metabolic capacity of the liver. Thus, hepatocellular damage, cirrhosis, hepatic congestion due to congestive heart failure, obstructive liver disease, cholangitis, hemolytic anemia, and ineffective erythropoiesis are all associated with elevation of urinary urobilinogen.

MEASUREMENTS OF EFFECTIVE PRODUCTION OF ERYTHROCYTES: RETICULOCYTE COUNT

Because the RNA of the reticulocyte disappears about 1 day after its entry into the blood, enumeration of reticulocytes will be a measure of the number of cells being delivered by the marrow to the blood each day, that is, a measure of effective erythropoiesis. The absolute reticulocyte count is calculated by multiplying the reticulocyte percentage by the erythrocyte count. To give a meaningful expression of erythropoiesis, the absolute reticulocyte count, or some estimate of it, and not simply the percentage, must be used. The normal absolute reticulocyte count is approximately 50×10^9/L, or 1% of circulating erythrocytes. Because the normal maturation time for reticulocytes in the blood is 1 day, production of reticulocytes is 50×10^9/L per day.

A second consideration is an adjustment for increased maturation time of reticulocytes in the blood as a result of accelerated release from the marrow, an effect of erythropoietin. The need for this is recognized by the presence of large, polychromatic cells or nucleated red blood cells in the blood film, indicating a shift of excessively immature reticulocytes from the marrow into the blood. To avoid an overestimate of daily erythrocyte production, a correction factor is used that is based on estimated maturation time of reticulocytes in the blood. This varies inversely with hematocrit as follows (Hillman & Finch, 1996):

Hematocrit, %	Reticulocyte maturation time, days
45	1.0
35	1.5
25	2.0
15	2.5

If a patient has an Hct of 0.25, a red blood cell count of 2.89×10^{12}/L, and a reticulocyte count of 7%, the patient will have an absolute reticulocyte count of 202×10^9/L. Because the average normal absolute reticulocyte count is 50×10^9/L, the patient has

$$(202 \times 10^9/\text{L}) / (50 \times 10^9/\text{L})$$

or four times as many reticulocytes as normal. However, this must be corrected for the increased maturation time: $4 \times {}^1/_2 = 2$. Therefore, two times as many reticulocytes are entering the blood per day as in a normal individual, that is, red cell production is two times normal.

If only the hematocrit is available, the same correction can be made as follows:

Correction for anemia:

Patient's reticulocyte count (7%)/Normal reticulocyte count (1%) × Patient's Hct (0.25)/Normal Hct (0.45) = 4

Correction for shift:

Corrected reticulocyte index (4) ×1/Maturation time (2) = 2

These corrections are necessary to assess the degree of red blood cell production in response to anemia.

A normal individual with a normal supply of iron can increase red blood cell production by two times normal within 1 week if the hematocrit drops to 0.35, or by three times normal if the hematocrit drops to 0.25. Only if there is a parenteral supply of iron (such as in hemolysis) can the maximal red blood cell production of six to eight times normal be achieved.

If an appropriate marrow response to anemia has not been reached in 1 to 2 weeks, some impairment of red blood cell production exists.

The **erythrocyte utilization of iron** is a measure of the amount of an injected dose of iron that appears in the hemoglobin of circulating erythrocytes. It is derived from the plasma iron turnover and the percentage of radioactive iron that has been injected and that appears in the circulating erythrocytes after 2 weeks, assuming that none of the newly formed cells has been destroyed in that time interval. This, too, is a measure of effective erythropoiesis.

MEASUREMENTS OF EFFECTIVE SURVIVAL OF ERYTHROCYTES IN BLOOD

The **erythrocyte survival** can be determined by removing a sample of blood, labeling the erythrocytes with chromium-51 (^{51}Cr), inactivating the excess ^{51}Cr remaining in the plasma, and reinjecting the labeled erythrocytes into the patient. The ^{51}Cr is bound to the β-chain of the hemoglobin molecule and, for the most part, is not released until the red blood cell is removed from

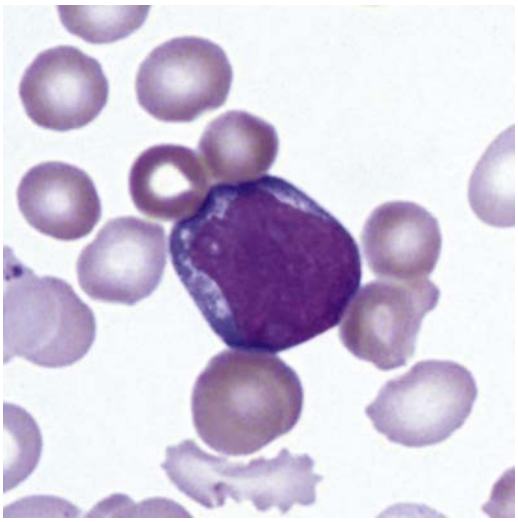

Figure 32.13 Myeloblast with high nuclear/cytoplasmic ratio, fine chromatin, visible nucleoli, and basophilic cytoplasm (Wright-Giemsa, 1000×).

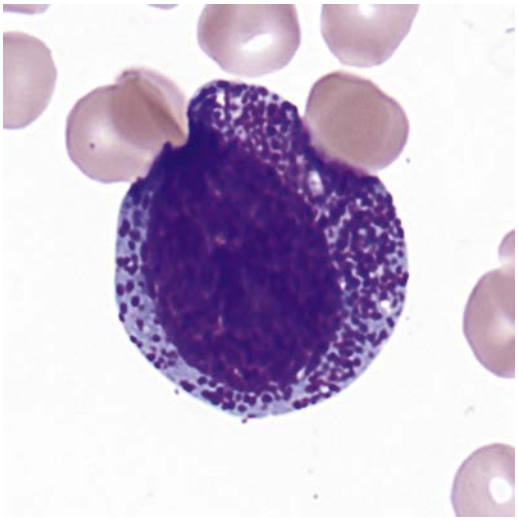

Figure 32.14 Promyelocyte *(center)* with azurophilic granules in the cytoplasm; the nuclear chromatin is still fine (Wright-Giemsa, 1000×).

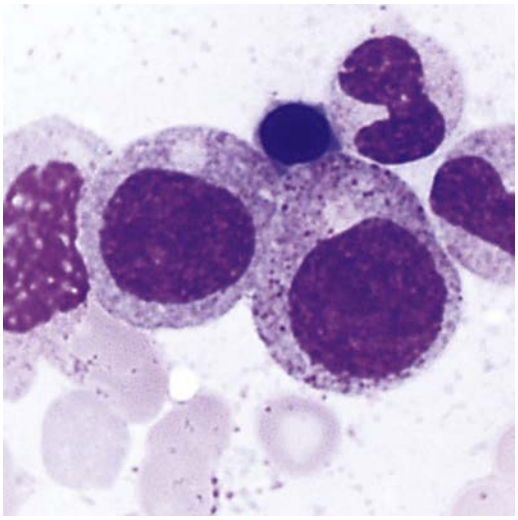

Figure 32.15 Myelocytes have secondary granules in the cytoplasm and show condensation of nuclear chromatin. Persistent primary granules are seen in early myelocytes *(center-right)* and are lost as myelocytes mature. A band neutrophil and an orthochromatic normoblast are also seen (Wright-Giemsa, 1000×).

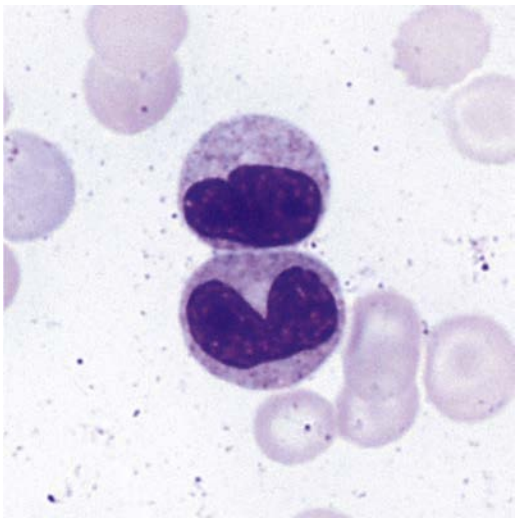

Figure 32.16 Metamyelocytes show nuclear indentation and increased chromatin clumping (Wright-Giemsa, 1000×).

the circulation and the hemoglobin is degraded. Measurements of radioactivity in the red blood cells are made at 2 hours or 24 hours (the zero time, or 100% level) and at 1- to 3-day intervals until over 50% of the activity has disappeared. The results are usually expressed as the ^{51}Cr half-survival time. The normal range is 28 to 38 days. (The reason it is not 60 days is that ^{51}Cr is eluted from the hemoglobin at the rate of about 1% per day.) If production of erythrocytes equals destruction (i.e., if a steady state exists), the erythrocyte survival is also a measure of effective production of erythrocytes.

SUMMARY

Total erythropoiesis refers to the total production of hemoglobin or red cells; *effective erythropoiesis* refers to production of hemoglobin or red blood cells that reach the circulation; and *ineffective erythropoiesis* refers to production of hemoglobin or red blood cells that never reach the circulating blood. These concepts of the **erythrokinetic** approach to the study of anemia are useful, especially in anemias that defy easy classification.

NEUTROPHILS

The common progenitor cell for neutrophils and monocytes (GMP) divides and gives rise to the progenitor cells for granulocytes (CFU-G) and for monocytes (CFU-M). CFU-G and CFU-M cells give rise to myeloblasts and monoblasts, respectively, under stimulation of colony-stimulating factors for granulocytes and monocytes (see Fig. 32.1).

MORPHOLOGY OF NEUTROPHIL PRECURSORS

The **myeloblast** (Fig. 32.13) is a cell about 15 μm in diameter with a moderately high N/C ratio; a large oval to quadrangular nucleus; a very fine, uniform chromatin pattern; a delicate nuclear membrane; and two to five nucleoli. The cytoplasm is pale, clear blue, and without granules. The appearance of azurophilic (primary) granules (≈0.5-μm diameter) heralds the earliest promyelocyte (Fig. 32.14) and indicates that the cell is to be a neutrophil. The **promyelocyte** stage encompasses the entire period of production of azurophilic granules. The promyelocyte is slightly larger than the myeloblast. The nuclear chromatin begins to condense, and the nucleoli are less obvious. The cytoplasm is basophilic and is filled by an increasing number of azurophilic granules. The **neutrophil myelocyte** stage begins with the appearance of specific neutrophil (secondary) granules, at first only in the Golgi region. As more specific granules develop, they spread throughout the cytoplasm (Fig. 32.15). With successive mitoses, the number of azurophilic granules (whose production has ceased at the end of the promyelocyte stage) is diminished. Therefore, the early neutrophil myelocyte has a rather fine, dispersed nuclear chromatin pattern, many azurophilic granules, and few specific granules. The late neutrophil myelocyte has a somewhat more condensed chromatin pattern, a cytoplasm well filled with specific granules, and rather few azurophilic granules. The myelocyte is the latest stage capable of cell division. The next stage, the **neutrophil metamyelocyte**, is distinguished by an indented, kidney-shaped nucleus with more condensed chromatin (Fig. 32.16). From this stage on, changes in the cytoplasm are

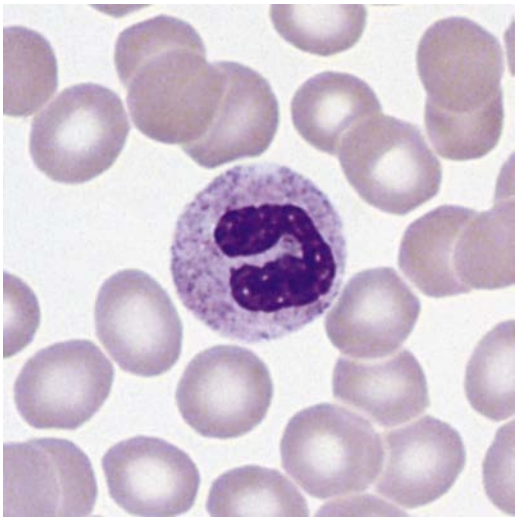

Figure 32.17 Band neutrophil with mature nucleus with clumped chromatin but without segmentation (Wright-Giemsa, 1000×).

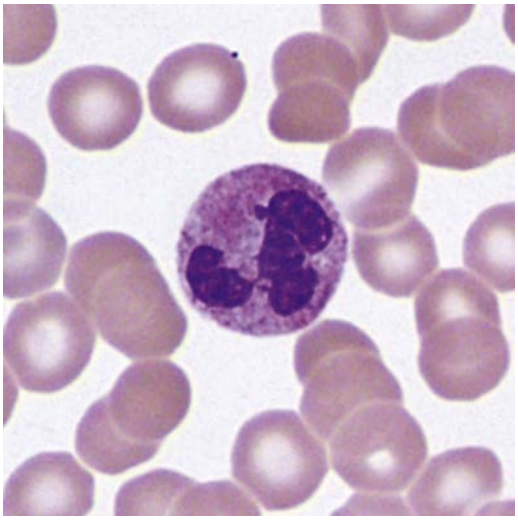

Figure 32.18 Segmented neutrophil with multiple nuclear lobes joined by fine chromatin filaments (Wright-Giemsa, 1000×).

insignificant. In the **band neutrophil** (stab form), the nucleus has more condensed chromatin and a rather uniform elongated shape (Fig. 32.17). Partial constriction of the nucleus occurs in the band stage, until a fine filament (length but no breadth) is formed between two of the lobes, at which point the cell is classified as a **segmented neutrophil** (Fig. 32.18).

During development and maturation, neutrophilic precursors express various cell surface markers that can be used for immunophenotypic recognition. Myeloblasts express the HSC marker CD34, as well as HLA-DR and myeloid lineage specific markers CD13, CD33, CD15, and CD117. Mature neutrophils express CD13, CD15, CD16, and CD11b, but lose HLA-DR and CD33.

The mature human neutrophil has twice as many specific granules as azurophilic granules (Box 32.2). The azurophilic granules (formed in the promyelocyte stage) contain lysosomal enzymes (e.g., acid hydrolases: acid phosphatase, β-glucuronidase), myeloperoxidase, elastase, arylsulfatase, and cationic antibacterial proteins, along with other enzymes and proteins. The specific granules (formed in the myelocyte stage) contain lysozyme, lactoferrin, collagenase, plasminogen activator, aminopeptidase, and vitamin B_{12}–binding protein, as well as other enzymes and proteins. Tertiary granules, similar in size to the specific granules, contain gelatinase. Alkaline phosphatase is located in yet another type of cytoplasmic organelle lighter in density than specific granules. These organelles first appear during the late myelocyte stage.

BOX 32.2

Neutrophil Constituents and Functions

Azurophilic granules (formed in promyelocyte stage)

Lysosomal enzymes: acid hydrolases, acid phosphatase, β-glucuronidase
Myeloperoxidase
Elastase
Arylsulfatase
Cationic antibacterial proteins

Specific granules (formed in myelocyte stage)

Lysozyme
Lactoferrin
Collagenase
Plasminogen activator
Aminopeptidase

Tertiary granules

Gelatinase

Cytoplasmic organelles

Alkaline phosphatase

Neutrophil functions

Phagocytosis
Bactericidal activity

DISTRIBUTION AND KINETICS

For each neutrophil in the blood vessels, about 16 precursors are present in the marrow. From the time of differentiation into a myeloblast, through about five mitotic divisions (three of which occur at the myelocyte stage), it takes about 14 days until the progeny of that cell reach the blood. The last 6 to 7 days are spent in the maturation and storage pool. When a neutrophil enters the blood, it moves readily between a circulating granulocyte pool, which is sampled in the leukocyte count, and a marginal granulocyte pool, which is not, but is either marginated along vessel walls or sequestered in capillary beds. In less than 1 day after it arrives, the neutrophil emigrates from the circulation in a random manner and enters the tissues. Migration into tissues is dependent on adhesion molecules of the selectin family (and their corresponding ligands) expressed on neutrophils and endothelial cells. From there, if not utilized in an inflammatory exudate, neutrophils leave the body within a few days via secretions in bronchi, saliva, the gastrointestinal tract, and urine, or they are destroyed by the mononuclear phagocyte system.

FUNCTION

Neutrophils are able to move in a zigzag manner, but their motion changes to a straight-line path if a chemotactic attractant or factor (e.g., a bacterium coated with certain components of complement) is within a certain distance. Neutrophils express chemokine receptors CXCR1 and CXCR2, which are responsible for neutrophil migration in response to chemokines. Neutrophils also have receptors for the Fc portion of IgG as well as for complement (C3) and bind and phagocytose the coated particle. Phagocytosis occurs with the formation of a phagocytic vacuole that contains the ingested particle; accompanying this process is an increase in metabolic activity and energy production. Specific granules, followed shortly by azurophilic granules, empty their contents into the phagocytic vacuoles—a process known as *degranulation*. Bactericidal activity occurs within the vacuole, mediated by hydrogen peroxide (H_2O_2), superoxide anion (O_2^-), myeloperoxidase, and a halide ion generating free halogen, or by other enzymatic activity. Other substances can act as chemotactic factors as well. The C5a fragment is a chemotactic factor and is also an anaphylatoxin that causes smooth muscle contraction. Substances liberated by bacteria and metabolic products of arachidonic acid may also act as chemotactic factors for neutrophils. Neutrophils are thus important in defense against infectious disease. If their enzymes are activated and released outside the cell, neutrophils can cause tissue necrosis, tissue injury, and inflammation.

EOSINOPHILS

Eosinophils are produced in the bone marrow. In vitro culture studies show that there is a separate eosinophilic committed progenitor cell (CFU-Eo) in the marrow that is distinct from CFU-GM, CFU-G, and CFU-M. Three growth factors (GM-CSF, IL-3, IL-5) produced by T lymphocytes influence eosinophil development. IL-5 promotes terminal maturation, functional activation, and prevention of apoptosis of eosinophils.

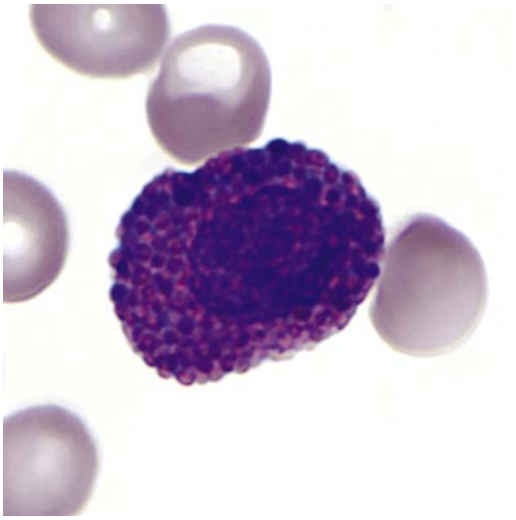

Figure 32.19 Eosinophil myelocyte with ovoid nucleus and eosinophilic secondary granules in the cytoplasm (Wright-Giemsa, 1000×).

BOX 32.3

Eosinophil Constituents and Functions

Eosinophil-specific granules

Larger granules

Major basic protein
Acid hydrolases
Peroxidase
Phospholipase
Cathepsin
Eosinophil cationic protein
Eosinophil-derived neurotoxin

Smaller granules

Arylsulfatase
Peroxidase
Acid phosphatase

Eosinophil functions

Anthelmintic activity—major basic protein, eosinophilic cationic protein, peroxidase
Phagocytosis
Allergic response
Dampen inflammatory reactions

MORPHOLOGY OF EOSINOPHIL PRECURSORS

The cell that is the precursor for the earliest recognizable eosinophil, the eosinophil myelocyte, is morphologically indistinguishable from that which gives rise to neutrophils and monocytes or to basophils (see Figs. 32.1 and 32.13). In the early eosinophil myelocyte, the granules are large and take the basophilic stain. As the cell matures, the granules appear olive-green and, finally, the characteristic red-orange color (Figs. 32.19 and 32.20). Nuclear maturation is similar to that of the neutrophil. Eosinophils are slightly larger than neutrophils and have fewer nuclear lobes. Mature eosinophils express CD16 and CD32.

Electron micrographs of eosinophils show characteristic granules that have a dense crystalloid core in a less dense matrix. Immature granules, appearing in the myelocyte, at first have no crystalloids but develop them as maturation proceeds. Mature granules are of two types: a larger granule (0.5–1.5 μm in largest diameter) with a dense crystalloid and a smaller granule (0.1–0.5 μm diameter) without a crystalloid. The smaller granules appear later during maturation, after the myelocyte stage.

Eosinophil-specific granules (Box 32.3) contain major basic protein (MBP) in the crystalloid core; MBP is toxic to parasites and cells, neutralizes heparin, and induces histamine release from basophils. Granule constituents in the matrix include acid hydrolases, peroxidase, phospholipase, and cathepsin. The specific granules also contain eosinophil cationic protein (ECP), eosinophil-derived neurotoxin (EDN), and eosinophil peroxidase (EPO). ECP shortens coagulation time and alters fibrinolysis; it also inhibits lymphocyte proliferation and is a potent neurotoxin. EDN is a strong neurotoxin (Gleich & Adolphson, 1986). The smaller granules contain arylsulfatase; both granule types contain peroxidase and acid phosphatase. EPO is different from the type of peroxidase present in neutrophils and monocytes; also, eosinophils contain no alkaline phosphatase or muramidase. Eosinophils secrete IL-1, IL-3, IL-6, IL-8, tumor necrosis factor-α (TNF-α), and GM-CSF. TNF-α appears to be the cause of fibrosis in Hodgkin disease (Roberts et al., 1999).

DISTRIBUTION AND KINETICS

The kinetics of eosinophils are similar to those of neutrophils. They are stored in the bone marrow for several days after going through various maturational stages. The half-life in the blood is approximately 18 hours before entering the tissues, where they survive for at least 6 days. Eosinophils in the tissues, however, are at least 100 times as numerous as the total number of eosinophils in the blood; they are located primarily in skin, lung, and gastrointestinal tract (i.e., the epithelial barriers to the outside world).

FUNCTION

Eosinophils act as phagocytes and modulate inflammatory responses (see Box 32.3). Eosinophils leave the blood when adrenal corticosteroid hormones increase. They proliferate in response to immunologic stimuli. This proliferative response is mediated, at least with some antigens, by T lymphocytes, monocytes, and mast cells. Eosinophils destroy helminths by generating potent oxidants and releasing cationic proteins. Eosinophils participate in some inflammatory conditions, particularly allergic reactions, asthma, and certain myocardial diseases (Gleich & Adolphson, 1986). Although eosinophils phagocytose foreign particles and antigen-antibody complexes, this is not their only activity. Another major function of eosinophils is to dampen hypersensitivity and inflammatory reactions. Evidence indicates that eosinophils modulate reactions that occur when tissue mast cells and basophils degranulate. Eosinophils express the chemokine receptor CCR3. Among the chemotactic factors that attract eosinophils, eosinophil chemotactic factor of anaphylaxis (ECF-A) is present in basophils and mast cells; also, eosinophils contain substances that inactivate factors released by mast cells and basophils, such as histamine, slow-reacting substances of anaphylaxis, and platelet-activating factor (PAF).

When an intense or prolonged eosinophilic inflammatory reaction occurs, there is often the formation of Charcot-Leyden crystals. These hexagonal bipyramidal crystals are composed of lysophospholipase localized in the cytoplasm of eosinophils.

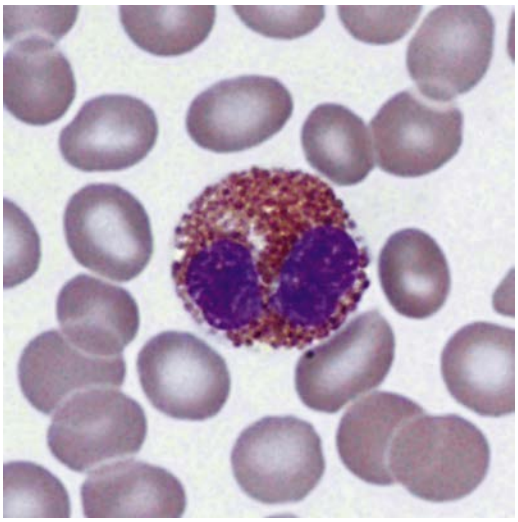

Figure 32.20 Mature eosinophil with bilobed nucleus and large eosinophilic cytoplasmic granules (Wright-Giemsa, 1000×).

BASOPHILS AND MAST CELLS

Basophils and mast cells are derived from hematopoietic precursors and probably share a common precursor with other granulocytes and monocytes.

MORPHOLOGY

Basophils develop from a cell resembling a myeloblast. The first recognizable stage is a **basophil myelocyte**, with the appearance of specific basophil

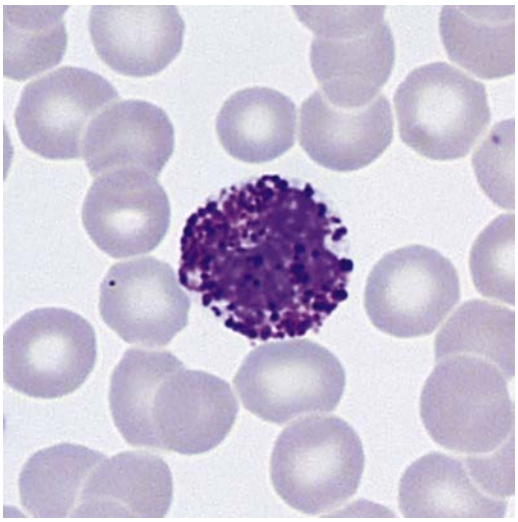

Figure 32.21 Mature basophil with large dark red-purple basophilic granules that partially obscure the nucleus (Wright-Giemsa, 1000×).

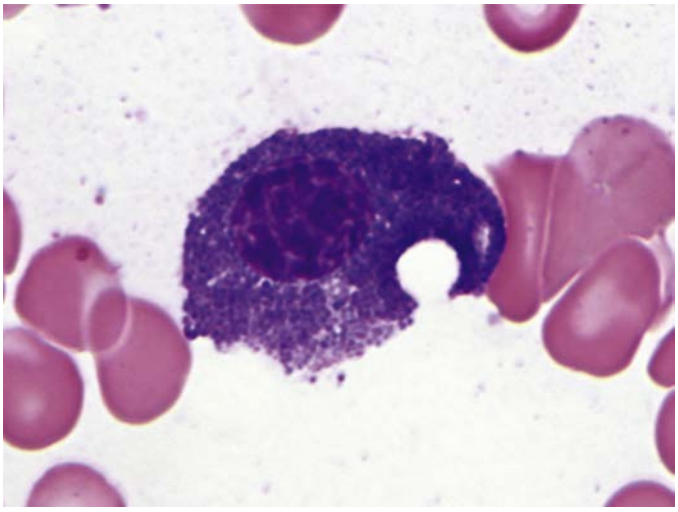

Figure 32.22 Bone marrow mast cell shows numerous uniform purple granules in the cytoplasm that partially obscure the nucleus (Wright-Giemsa, 1000×).

granules. These granules (about 0.2–1 μm in diameter) are larger than the azurophilic granules of the promyelocyte and often are irregular in shape. As the cell matures, the granules become more metachromatic (red-purple) because of increasing acid mucopolysaccharide (heparin) content. During maturation, cytoplasmic RNA decreases and the nucleus partially segments. Because of incomplete nuclear segmentation, stages analogous to the neutrophil are not readily identified. In mature basophils, the nucleus has condensed but smudged chromatin, and the background cytoplasm lacks basophilia (residual RNA; Fig. 32.21). Mature basophils express CD32.

In contrast, **tissue mast cells** are connective tissue cells of mesenchymal origin that contain metachromatic cytoplasmic granules. They are widely distributed throughout the body, including bone marrow, thymus, and spleen, but they do not normally appear in blood. On Romanowsky-stained films (Fig. 32.22), they are usually larger than basophils and have a low N/C ratio and a round or oval reticular nucleus that is usually obscured by abundant red-purple granules. The granules are smaller, more round and regular, and less soluble than basophil granules. The cytoplasmic granules are often spindle-shaped rather than round.

DISTRIBUTION AND KINETICS

Basophils have a life span similar to eosinophils. The maturation time in the marrow is approximately 7 days. Basophils circulate in the blood and are not normally found in tissues, in contrast to mast cells, which can spend 9 to 18 months in connective tissue. GM-CSF, IL-3, and IL-5 influence basophil production. However, IL-3 is the principal growth factor for basophilic growth, whereas *c-kit* ligand enhances the number and activation state of mast cells (Lyman, 1998).

FUNCTION

With regard to circulating numbers, basophils respond to adrenal corticosteroids in similar fashion to eosinophils. Basophil granules contain histamine, heparin, and peroxidase (Box 32.4). Basophils synthesize and store histamine and ECF-A. They synthesize and release slow-reacting substance of anaphylaxis (SRS-A) and probably PAF at the time of stimulation but do not store them. Basophils lack hydrolytic enzymes such as alkaline and acid phosphatase, at least in cytochemically demonstrable amounts. Glycogen is abundant outside the granules. Although ultrastructurally different, mast cells have similar cytochemical characteristics, except for the presence of proteolytic enzymes and serotonin, which basophils lack. In tissues, the two cell types appear to function in a similar manner.

Basophils (as well as mast cells) appear to be involved in immediate hypersensitivity reactions, such as allergic asthma. Immunoglobulin E (IgE) binds readily to basophil and mast cell membranes. When a specific antigen reacts with the membrane-bound IgE, degranulation occurs with the release of mediators of immediate hypersensitivity (e.g., histamine, SRS-A, PAF, heparin, ECF-A). The latter leads to the accumulation of eosinophils, which contain substances that tend to counteract these mediators. Basophils are also involved in some delayed hypersensitivity reactions, or **cutaneous basophil hypersensitivity**, such as contact allergies, in which they appear to undergo a different type of degranulation response.

BOX 32.4

Basophil Constituents and Functions

Basophil-specific granules
Histamine
Heparin
Peroxidase
Eosinophilic chemotactic factor A

Other cellular constituents
Slow-reacting substance of anaphylaxis
Platelet-activating factor

Basophil functions
Immediate hypersensitivity reactions
Some delayed hypersensitivity reactions

MONOCYTES AND MACROPHAGES

Monocytes and macrophages share the same committed progenitor cell as neutrophils, the GMP (see Fig. 32.1).

MORPHOLOGY

In normal marrow, it is not possible morphologically to distinguish the "monoblast" from the myeloblast. The earliest recognizable cell in this series is the **promonocyte**, which is 15 to 20 μm in diameter—somewhat larger than the myeloblast. The N/C ratio is moderate and the nucleus may be oval or indented, with a fine uniform or slightly streaked chromatin pattern and two to five nucleoli. The cytoplasm is basophilic, with a ground-glass appearance and a variable number of fine azurophilic granules (Fig. 32.23). The **monocyte**, which is present in both blood and marrow, is only slightly smaller; it has a moderate to low N/C ratio and an indented or lobed nucleus with a finely streaked, only slightly condensed, delicate chromatin pattern. Nucleoli are indistinct or obscured. The cytoplasm is opaque, more gray than blue, and contains an abundance of fine azurophilic granules (Fig. 32.24).

Macrophages, the tissue component of the monocyte system, arise from emigrated blood monocytes. Macrophages are larger than monocytes and measure 15 to 80 μm in diameter. They have irregular cell membranes, often with blebs and pseudopodia. The N/C ratio is high, with an oblong and/or indented nucleus. Although macrophages are located in virtually all tissues of the body, the greatest numbers are found in the bowel, liver, bone marrow, and spleen.

In promonocytes, monocytes, and macrophages, the granules (Box 32.5) contain acid hydrolase, arylsulfatase, nonspecific esterase, and peroxidase. More than one type of granule may be present. As the cell matures, peroxidase activity diminishes, and acid phosphatase, arylsulfatase, and nonspecific esterase activity increases. The enzyme activity occurs in the rough endoplasmic reticulum, Golgi zone, coated vesicles, and digestive vacuoles. This suggests that, in the macrophages, the coated vesicles are a second form of primary lysosome that shuttles hydrolytic enzymes from the Golgi to the digestive vacuoles.

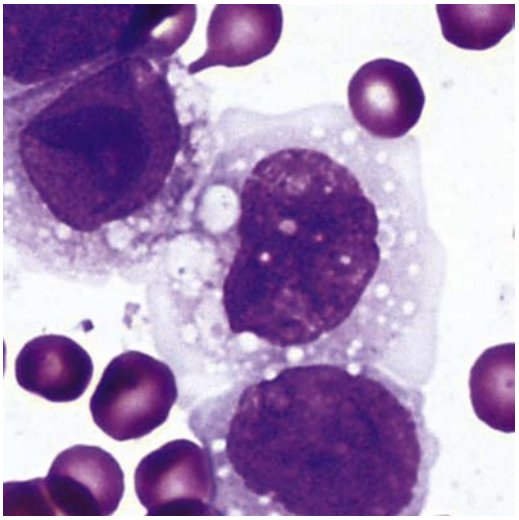

Figure 32.23 Promonocytes have fine nuclear chromatin, often with visible folds and basophilic cytoplasm that may contain vacuoles (Wright-Giemsa, 1000×).

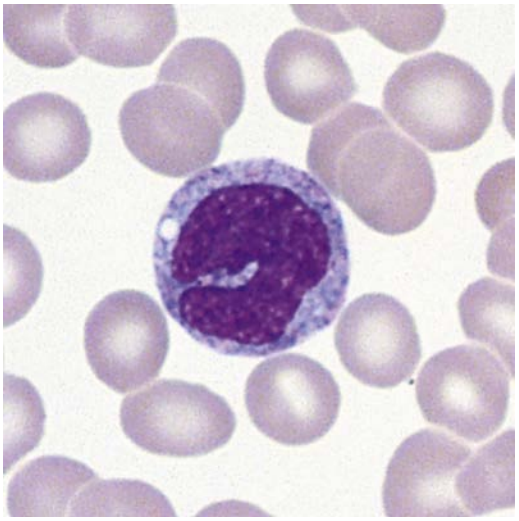

Figure 32.24 Mature monocyte with an indented nucleus, delicate chromatin, basophilic cytoplasm, and fine azurophilic granules (Wright-Giemsa, 1000×).

In addition to these enzymes, monocytes and macrophages possess numerous surface receptors and surface antigens. Monocytes and macrophages possess class I (HLA-A, B, C) antigens and class II (HLA-DR, DP, DQ) gene complex molecules. The CD4 T-cell antigen (molecule) not only is present on T-helper cells but is also present on monocytes and macrophages. Because the CD4 molecule acts as a receptor for the human immunodeficiency virus type-1 (HIV-1), the virus infects monocytes and macrophages along with T-helper cells. Monocytes and macrophages express CD11 (CD11a, b, c) antigens, markers that define surface adhesion glycoproteins. CD14, CD64, and CD68 antigens are also present on monocytes and macrophages. These surface molecules are often used to identify the lineage of mononuclear cells in hematologic malignancies.

DISTRIBUTION AND KINETICS

After promonocytes are formed, they respond to M-CSF and undergo two or three mitotic divisions in a period of about 50 to 60 hours before being released into the blood. Under conditions of increased demand, the cycle time can shorten, with earlier release of more immature cells into the blood. Blood monocytes are distributed in a circulating monocyte pool and a marginal monocyte pool in a ratio of 1:3.5. Once monocytes enter the blood, they leave randomly with a half-time of 8.4 hours. This time period is shortened in splenomegaly or acute infection and may be prolonged in monocytosis. After monocytes leave the blood, they spend several months, perhaps longer, as tissue macrophages.

BOX 32.5

Monocyte/Macrophage Constituents and Functions

Granules and other constituents

Acid hydrolase
Arylsulfatase
Nonspecific esterase
Peroxidase
Acid phosphatase

Monocyte/macrophage functions

Phagocytosis—bacteria, cellular debris, senescent cells
Antigen processing
Cell-mediated immunity—antibody-dependent cellular cytotoxicity
Synthesis of bioactive molecules

FUNCTION

The monocyte is formed in the marrow and transported by the blood. It then migrates into the tissues, where it transforms into a histiocyte or a macrophage to spend most of its life span. Blood monocytes and tissue macrophages make up a mononuclear phagocyte system (reticuloendothelial system).

The mononuclear phagocyte system has an important role in defense against microorganisms, including mycobacteria, fungi, bacteria, protozoa, and viruses (see Box 32.5). The cells are motile and respond to chemotactic factors (complement components as well as lymphokines and γ-interferon from activated T lymphocytes). They become immobilized by migration-inhibition factor from activated lymphocytes. They engage in phagocytosis, a process that is enhanced if the particle is coated by IgG or complement for which the macrophages have membrane receptors. After phagocytosis, they kill ingested microorganisms.

These mononuclear phagocytes are an integral part of both humoral and cell-mediated immunity. They handle or process antigens, providing contact of the antigen (or antigenic information) with lymphocytes. They also respond to various lymphokines and monokines and act as effector (e.g., cytotoxic) cells in the cell-mediated immune response. Monocytes and macrophages function in antibody-dependent cellular cytotoxicity. They have the ability to kill a variety of malignant cells (Weinberg, 2004) by promoting both cytostasis and cytolysis. Some of the ability of macrophages to destroy malignant cells may be attributed to the production of H_2O_2, nitrous oxide, and reactive oxygen intermediates.

Macrophages remove and process senescent cells and debris through phagocytosis and digestion. For example, erythrocytes, leukocytes, and megakaryocyte nuclei are removed by macrophages in the marrow; inhaled particulate material is removed by alveolar macrophages in the lungs.

Macrophages may be activated by specific factors (e.g., cytophilic antibody) or nonspecific factors (e.g., in response to phagocytosed material). Activation results in enlargement of the cell and enhanced metabolism, phagocytosis, microbicidal activity, cytotoxicity, secretion of cytolytic proteins (including TNF-α), and the like.

Macrophages synthesize and secrete a large number of biologically active molecules, including enzymes, complement components, binding proteins, coagulation factors, cytokines and growth factors, chemotactic factors, angiogenesis factors, and bioactive lipids. Therefore, this system has multiple functions, including host defense, control of hematopoiesis, and policing of the environment within the body (Johnston, 1988).

MEGAKARYOCYTES

Platelets originate from polyploid megakaryocytes, the largest of all hematopoietic cells, which account for less than 1% of the total nucleated marrow cells. Megakaryocytes arise from megakaryocyte-erythrocyte progenitors (MEP) and then from a megakaryocyte precursor (MkP) cell (see Fig. 32.1). Megakaryocyte proliferation is largely regulated by thrombopoietin. Additional growth factors, including kit-ligand, IL-3, IL-6, and IL-11, support megakaryocytic development in the presence of TPO (Kaushansky, 1995). Serum TPO levels are generally inversely proportional to platelet count. However, levels are elevated in liver disease and inflammatory states, probably through hepatocyte or marrow stromal cell responses (Kaushansky, 2003).

MORPHOLOGY

Committed progenitor cells are not morphologically distinguishable from lymphocytes. Megakaryocyte development is characterized by **endomitosis**,

nuclear division without cytoplasmic division, which results in ploidies varying from 2N to 64N. Most are 8N and 16N, with smaller numbers on either side. Nuclear lobes do not correlate precisely with ploidy. Nuclear chromatin is intensely staining, rather dispersed early, and more compact and dense later. Nucleoli are small at all stages of megakaryocyte development.

The earliest recognizable **megakaryoblast** has overlapping nuclear lobes and a small amount of basophilic cytoplasm. During the course of maturation, nuclear lobes increase and spread out, and red-pink granules become visible, first in the center of the cell. In the **mature megakaryocyte**, the nucleus is more compact, basophilia has disappeared, and the granules are clustered into small aggregates (Fig. 32.25).

The formation of individual platelets is a complex process. Megakaryocytes develop invaginated surface membranes (demarcation membranes) that provide a membrane reserve for proplatelet formation (Italiano & Shivdasani, 2003). Proplatelets are pseudopodial extensions of megakaryocytes that progressively branch and thin out. Microtubular action is important in the formation of proplatelets and in bringing granule and organelle constituents into the proplatelets. Platelets are formed at the ends of proplatelets and are released by microtubular action (Hartwig & Italiano, 2003).

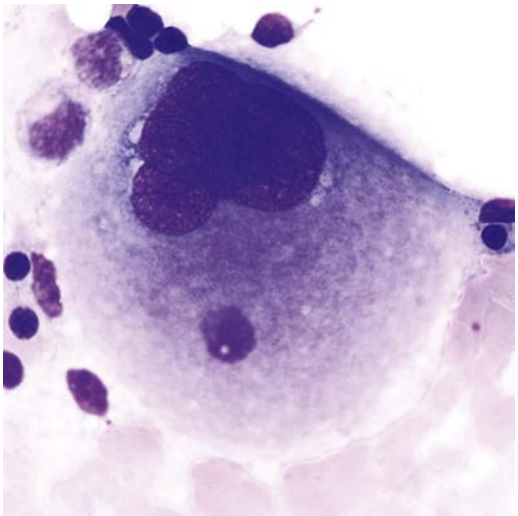

Figure 32.25 Megakaryocyte with a large, lobated nucleus and abundant granular cytoplasm (Wright-Giemsa, 1000×).

MEGAKARYOCYTES IN BLOOD

Whole megakaryocytes or fragments may occasionally be found in normal blood films. If buffy coat films are examined, they are consistently present. Megakaryocyte fragments in blood films may be as small as lymphocytes and are recognized by the deeply stained chromatin (with a sharper chromatin-parachromatin separation than in lymphocyte nuclei) and by fragments of attached megakaryocyte cytoplasm. They are found more frequently than normal in myelophthisic processes and myeloproliferative neoplasms or after stress or injury to the marrow.

Dwarf or micromegakaryocytes (Fig. 32.26) show evidence of abnormal megakaryopoiesis: agranular cytoplasm with hyaloplasmic zones or pseudopods, and association with large atypical platelets having similar cytoplasmic characteristics. These abnormal dwarf megakaryocytes are rarely found in any condition except myeloproliferative neoplasms or myelodysplastic syndromes.

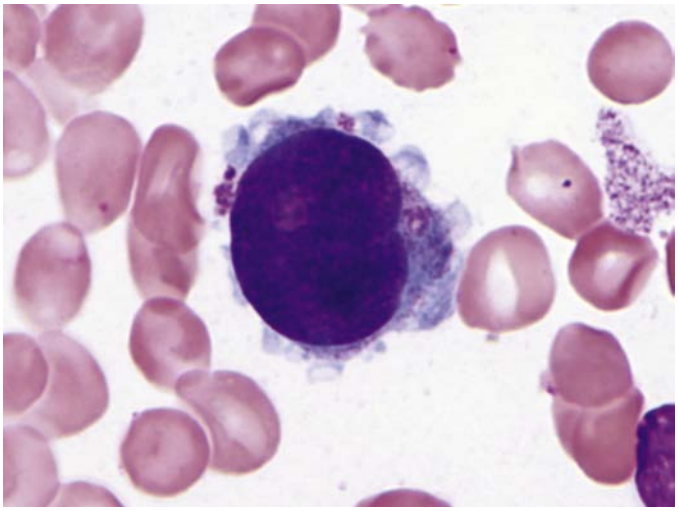

Figure 32.26 Dwarf megakaryocyte with bilobed nucleus and scant granular cytoplasm; a few giant platelets are also seen. These cells are most often associated with myeloproliferative neoplasms or myelodysplastic syndromes (Wright-Giemsa, 1000×).

DISTRIBUTION AND KINETICS

The maturation time for megakaryocytes in the marrow is about 5 days in humans. Platelets are released into the marrow sinuses over a period of several hours (Hartwig & Italiano, 2003), and the megakaryocyte nuclei are phagocytosed by macrophages. Newly released platelets appear larger, more active metabolically, and more effective hemostatically. Platelets circulate at a stable concentration that averages 275×10^9/L. At any one time, about two-thirds of the total platelets are in the circulation, and the remaining one-third are present in the spleen. In asplenic individuals, all platelets are circulating. In diseases characterized by splenic enlargement, 80% to 90% of platelets may be sequestered in the spleen, resulting in decreased concentrations of circulating platelets (thrombocytopenia).

Platelets survive for 8 to 11 days in the circulation. Some platelets are utilized in maintaining vascular integrity and in plugging small vascular injuries (random loss); others are removed by the mononuclear phagocytic system when they become senescent.

FUNCTION

Platelets normally function in (1) maintaining the integrity of blood vessels, and (2) forming hemostatic plugs to stop blood loss from injured vessels and, in the process, promoting coagulation of plasma factors.

LYMPHOCYTES

PRIMARY LYMPHOID TISSUE

During fetal life, lymphocyte precursors originate in the bone marrow and undergo antigen-independent lineage commitment. Maturation and selection of T cells occur primarily in the thymus and, of B cells, in the marrow and peripheral lymphoid organs. The T-cell population is largely self-renewable following thymic involution. B cells are capable of only limited self-renewal. They are dependent on recruitment from marrow stem cells to replenish programmed B cells and plasma cells that are incapable of self-renewal.

B-Cell Development: Bone Marrow

A distinct organ, the bursa of Fabricius, is present in birds and serves as the primary site of B-cell development, thus, the term *B cell* for bursa cells (Table 32.1). In the human, B cells develop in the bone marrow after the hematopoietic stem cells have populated that organ. During adult life, generation of B cells occurs in the bone marrow.

B-cell differentiation can be divided conveniently into two stages. The initial stage of B-cell differentiation involves the antigen-independent generation of diversity through rearrangement of the Ig heavy- and light-chain genes. The second stage is regulated by antigen triggering, T-cell interaction, macrophages, and various growth factors (Fig. 32.27). This stage occurs predominantly in the secondary lymphoid organs (LeBien & Tedder, 2008).

A progenitor cell gives rise to the first recognizable B cell in humans and mammals. This cell in humans is the pro-B (progenitor) cell that is characterized by receptor CD19 and terminal deoxynucleotidyl transferase (TdT) but contains no cytoplasmic or surface bound Ig (Hagman & Grosschedl, 1994). Differentiation of pro-B cells requires Ig gene rearrangement, induced by recombination enzymes (RAG1 and RAG2) and TdT, and triggered by pre–B cell antigen receptor (pre-BCR) as well as other signaling molecules and transcription factors, leading to a functional BCR (Ichii et al., 2014). Proliferation and survival of B-cell progenitors depends on bone marrow stroma–derived IL-7 signaling through the IL-7 receptor (IL-7R) to JAK1 and JAK3, and activation of STAT5 and STAT3. This also involves signaling of the PI3k-Akt pathway, FOXO1, and cyclins D2 and D3 (Clark et al., 2014). The pre–B cell is characterized by the presence of intracytoplasmic μ heavy chains with no surface-bound immunoglobulin ($sIg^-c\mu^+$). It also contains HLA-DR antigens, CD19, CD79a, and other surface markers.

In becoming a pre–B cell, a lymphoid stem cell undergoes *DJ* and *VDJ* gene segment rearrangement to form a functional *V* gene for the μ heavy chain (Fig. 32.28). A productive heavy-chain gene rearrangement is then

followed by a rearrangement of the *VJ* gene segment of the light chain. Rearrangement of the κ light-chain gene on chromosome 2 occurs first. If the κ rearrangements at both loci are nonproductive, rearrangement of the λ light-chain gene on chromosome 22 follows. Only one productive *VH* and *VL* gene emerges, limiting each B cell to one unique antibody structure (Bertoli & Burrows, 1988). The pre–B cell generates an intact Ig molecule and expresses surface IgM. Isotype switching (e.g., changing from IgM/IgD to IgG1) and constant heavy gene deletions occur in pre–B cells and more differentiated B cells. Switching occurs by the formation of a DNA loop in which all intervening constant heavy genes are deleted (Fig. 32.29). IgD can be coexpressed with IgM through alternative RNA processing.

IgM/IgD coexpressing mature B cells were first described in chronic lymphocytic leukemia, in which both antigen receptors were shown to have the same idiotype specificity (Fu et al., 1974). Similar cells were later found in human fetal spleens and also express CD5 (Antin, 1986). These are frequently referred to as *virgin* or *naïve* B cells and lack expression of CD27, a TNF receptor family member (Klein et al., 1998). Naïve B cells (IgD+/CD27–) are frequent in the blood, although most lack CD5. After antigen activation in the presence of T cells and macrophages, they are recruited into germinal centers, where they undergo somatic hypermutation. Maturation and expansion of antigen-specific mature B cells is orchestrated in a complex manor by Bcl-6 (Basso et al., 2010). Germinal center B cells express Bcl-6 and CD10 and are polymorphic in terms of size and nuclear outlines.

Eventually, high-affinity B cells are selected and differentiate into plasma cells or memory B cells. Memory B cells express CD27 and either IgM or another heavy chain (rarely IgD alone), and some show IgM/IgD/CD27 coexpression (Klein et al., 1998). Memory B cells also express CD45RA (isoform of CD45) and a specific epitope (MEM55) of CD45RB, while naïve B cells express CD45RO (Muraro et al., 2000; Koethe et al., 2011).

Plasma cells are characterized by abundant cytoplasmic Ig and expression of CD38 and CD138. They express either IgM, IgG, or IgA.

TABLE 32.1

Key Cell Surface Markers in Lymphocyte Development

Cell Name	CD Markers
Progenitor B cell	CD19, TdT, CD79a, HLA-DR
Pre–B cell	CD19, TdT, CD10, CD20, cytoplasmic μ
Naïve mature B cell	CD19, CD20, Bcl-2, surface IgM
Germinal center B cell	CD19, CD20, CD10, Bcl-6
Mature B cells (peripheral blood)	CD19, CD20, CD21, CD22, CD24, CD38
Plasma cells	CD38, CD138, cytoplasmic Ig

T-Cell Development: Thymus

The microenvironment of the thymus is necessary for the differentiation of T cells (Table 32.2). The human thymus has two parts: the cortex and the medulla. The cortex is subdivided into two portions—the subcapsular cortex and the inner cortex—and is populated predominantly by small lymphocytes with a few scattered epithelial cells. Fibrous septa extend from the capsule to the medullary region. The medulla is composed mostly of epithelial cells with a small component of lymphocytes. In the medulla, Hassall's corpuscles, small islands of partially hyalinized epithelial cells, are present.

Pro–T cells from the bone marrow or fetal liver migrate to the thymus, where they undergo T-cell receptor (TCR) gene rearrangement and are processed into functionally mature T cells for circulation in the blood and to the peripheral or secondary lymphoid tissues.

TCR genes are organized in a similar manner to Ig genes. They possess V, D, J, and C regions and undergo rearrangement during early T-cell maturation. In addition to the heterodimeric glycoproteins (α/β or γ/δ), the TCR/CD3 complex also contains CD3—epsilon, -zeta, and -eta subunits (Blumberg et al., 1990). The TCR recognizes foreign peptides held in an association with self-MHC molecules. In early T-cell development, the γ- and β-chain genes rearrange simultaneously, with TCR commitment dependent

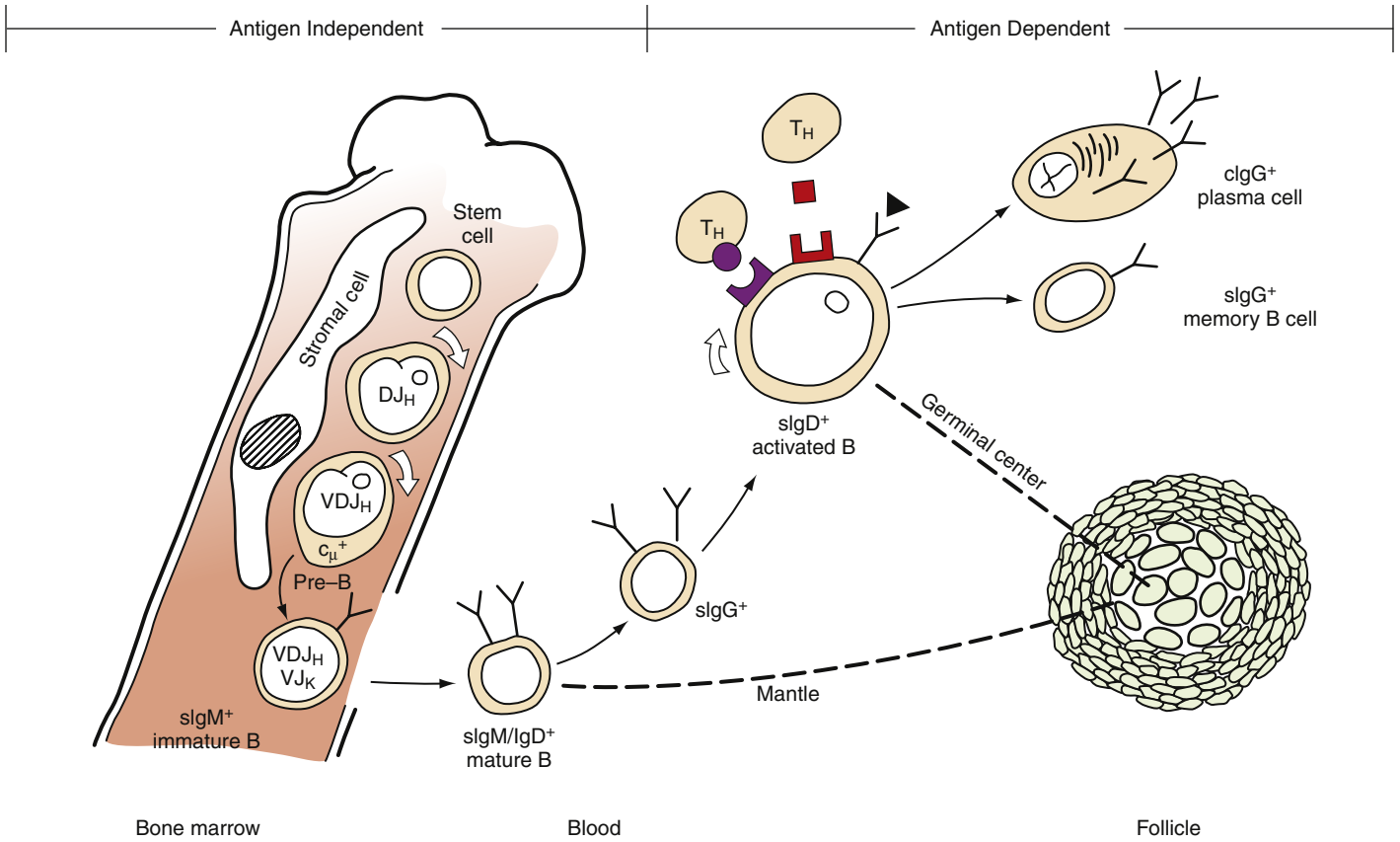

Figure 32.27 Differentiation of pre–B cells into B cells occurs independently of antigen, whereas proliferation and terminal differentiation of B cells are antigen driven. Hematopoietic stem cells with stromal cell help give rise to pre–B cells. These proliferate *(open arrow denotes cell cycling),* rearrange *DJ* and *VDJ* gene segments, and then express μ chains in the cytoplasm (cμ+). A small, resting pre–B cell *(not shown)* with rearranged *VJk* gene assembles a complete IgMk molecule, becoming an immature B cell and leaving the bone marrow. Expression of sIgD marks entry of the cell into the mature, resting phase (or G_0) characteristic of most blood and mantle zone B cells. Switching to an alternative isotype (IgG in this case) may occur before an encounter with antigen or afterward. Antigen triggers the resting B cell to enlarge (in the G_1 phase of the cell cycle) and present processed antigen and DR to the antigen-specific T cell receptor–CD3 complex. T-helper cells (T_H) secrete growth factors that bind to newly expressed receptor, further enhancing proliferation (S and M phases) in germinal centers. The activated B cell can be induced to differentiate into plasma cells, which secrete their abundant cytoplasmic IgG. Alternatively, it can become a memory B cell with refined specificity poised to deliver an anamnestic immune response on its next encounter with antigen. *IgG,* Immunoglobulin G. (From Bertoli LF, Burrows PD: Normal B-lineage cells: their differentiation and identification, *Clin Lab Med* 8:15, 1988, with permission.)

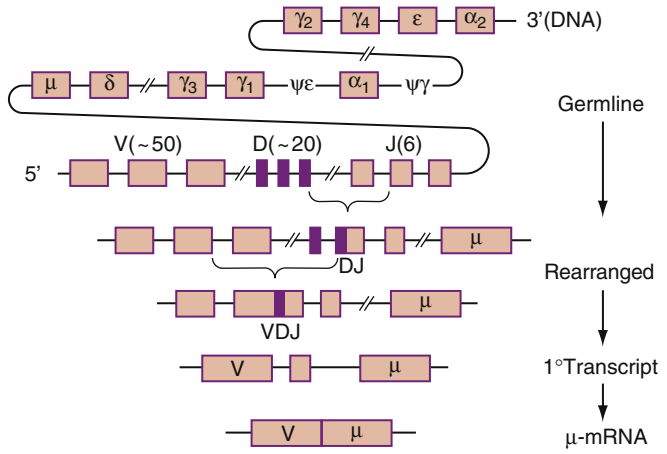

Figure 32.28 Generation of a functional *Ig* gene requires DNA rearrangement. In the germline and in somatic nonlymphoid cells, *V, D,* and *J* gene segments are widely separated in the DNA of chromosome 14. A cell committed to the B lineage first undergoes D to J rearrangement, juxtaposing the D and J segments and deleting intervening DNA sequences. This is followed by V to DJ rearrangement, generating a complete VDJ exon. The primary RNA transcript is processed to yield a contiguous V (VDJ) mRNA. *DNA,* Deoxyribonucleic acid; *Ig,* immunoglobulin. (From Bertoli LF, Burrows PD: Normal B-lineage cells: their differentiation and identification, *Clin Lab Med* 8:15, 1988, with permission.)

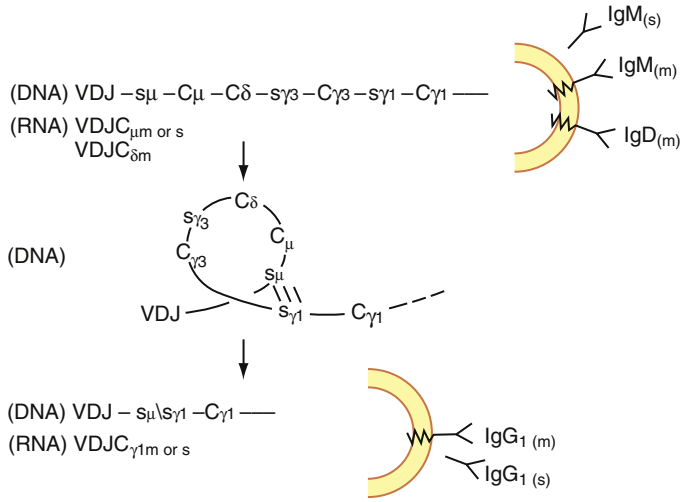

Figure 32.29 Alternative strategies for expression of non-IgM isotypes. IgD can be coexpressed with IgM by alternative processing of a primary RNA transcript of VDJ-Cμ-Cδ, to yield μ membrane (m), μ secretory (s), and δm RNAs. The production of IgG, IgA, or IgE isotypes involves DNA rearrangement. During the switch from IgM to IgG, for example, intrachromosomal recombination between homologous switch (s) regions results in deletions of C_μ, C_δ, and $C_{\gamma3}$, so that $C_{\gamma1}$ is now the first *C* gene 3′ of the VDJ exon. Thus, the same variable region is expressed with a different constant region. *Ig,* Immunoglobulin; *RNA,* ribonucleic acid. (From Bertoli LF, Burrows PD: Normal B-lineage cells: their differentiation and identification, Clin Lab Med 8:15, 1988, with permission.)

on expression of surrogate α-chain and development of a pre-TCR (Haks et al., 1998; Kang et al., 2001). Successful passage of thymocytes with β-chain–containing pre-TCR through a developmental checkpoint is followed by rearrangement of the TCR α-chain and formation of α/β T cells. During this process, developing T cells first coexpress both CD4 and CD8 (double positive cells), with subsequent downregulation of one or the other. In the thymic medulla, pre–T cells lose the ability to make TdT as they convert to mature T cells and then circulate in the blood and peripheral lymphoid tissues. Initially, pro–T cells migrate from the bone marrow or the fetal liver to the cortex of the thymus. Pro–T cells migrate from the subcapsular cortex to the inner cortex and then to the thymic medulla (see Table 32.2).

Monoclonal antibodies against functional epitopes on thymic cells were first used by Reinherz, Schlossman, and others to describe a distinct T-cell maturation pattern that is now well known (Reinherz et al., 1980). T lymphoblasts mature to common (cortical) thymocytes, then to medullary thymocytes, and finally to mature peripheral T cells of CD4 or CD8 phenotype.

Cells that express high levels of CD34 are double negative for CD4 and CD8, and as CD34 expression diminishes, CD4 and CD8 emerge together

TABLE 32.2
Summary of T-Cell Maturation

Stage	Maturation Events	Cell Surface Markers
Pro–T cell	Migration from marrow to thymic cortex	CD2, CD44
α/β Pre–T cell	Migration from thymic cortex to medulla, elimination of self-recognizing T cells, α/β TCR rearrangement (for T cells destined for the helper or suppressor subset)	TdT, CD1, CD2, CD3, CD4, CD5, CD7, CD8
γ/δ Pre–T cell	Migration from thymic cortex to medulla, elimination of self-recognizing T cells, γ/δ TCR rearrangement (for T cells destined for the cytotoxic subset)	TdT, CD1, CD2, CD3, CD7
Mature T cell	Loss of ability to make TdT, circulation in peripheral blood as helper, suppressor, or cytotoxic subset	Helper T: CD2, CD3, CD4, CD5, CD7 Suppressor T: CD2, CD3, CD5, CD7, CD8 Cytotoxic T: CD2, CD3, CD7

and then alone, while CD1 and CD10 also become expressed (Terstappen et al., 1992). Surface CD3 also arises.

A majority of postthymic (peripheral) T cells express α/β TCR; a small minority do not, but rather express γ/δ chains. NK cells express only ε chains with cytoplasmic CD3. Mature T cells are of at least three types. CD4 (helper) T cells possess α/β TCR chains and express CD2, CD3, CD4, CD5, and CD7 cell markers. CD8 (suppressor or cytolytic) T cells have α/β TCR chains and express CD2, CD3, CD5, CD7, and CD8 cell markers. Mature T cells with γ/δ TCR chains exhibit CD2, CD3, and CD7, lack CD4 and CD8, and function as cytotoxic cells.

CD4 T cells can develop into at least four subgroups with different functions (Zhu & Paul, 2008). Th1 cells produce IFN- γ, TNF-β, and IL-2 and mediate an immune response against intracellular pathogens. Th2 cells produce IL-4 and IL-5 and are important in defense against extracellular parasites. Th17 cells produce IL-17, IL-21, and IL-22 and mediate immune responses against extracellular bacteria and fungi. Induced regulatory T (iTreg) cells produce TGF-β, IL-10, and IL-35 and are involved in maintaining self-tolerance and regulating immune responses. Antigen-independent development of T cells is controlled by interaction with thymic epithelial cells and thymic fibroblasts as well as by the influences of cytokines, growth factors, and thymic hormones. IL-1, IL-2, IL-3, IL-4, IL-7, and SCF are critical in the growth and differentiation of thymic lymphocytes. Thymic hormones produced by thymic epithelial cells also induce T-cell function.

In the T-zone area of the peripheral lymphoid system, the T-cell antigen–dependent pathway occurs through the binding of the TCRs to antigen peptides associated with appropriate MHC I and MHC II molecules on macrophages or interdigitating dendritic cells (IDCs). This results in the release of IL-1 by the activated macrophages, which, in turn, leads to the formation of IL-2 receptors on T cells and the subsequent synthesis and release of IL-2 by these activated T cells. In this activation process, many other cytokines (including IL-4, IL-6, IL-10, TNF, and interferon) are released, and appropriate cytokine receptors are upregulated. These events result in the activation and maturation of T-helper cells, T-suppressor cells, T-cytotoxic cells, and other immunoregulatory cells. This activation process not only increases the number of antigen-specific T cells, it also alters the immunophenotype and changes the expression of certain adhesion molecules on T cells. For example, LFA-1 (a heterodimer formed from CD11a and CD18) and VLA-4 (a heterodimer of CD29 and CD49d, CD44, and CD2) are upregulated, and L-selectin (CD62L) is downregulated. Changes in the expression of adhesion markers allow for the proper circulation of T cells in the body.

Natural Killer Cells: Bone Marrow

Immunophenotypic and functional data suggest that NK cells and T cells have a close developmental relationship. Expression of CD3 proteins has been found in human fetal NK cells. Thus, it is likely that NK cells and T cells have a common precursor cell. Although NK cells can develop in the thymus, the thymic environment is not required for NK cell differentiation. NK cells can develop in secondary lymphoid tissues and bone marrow

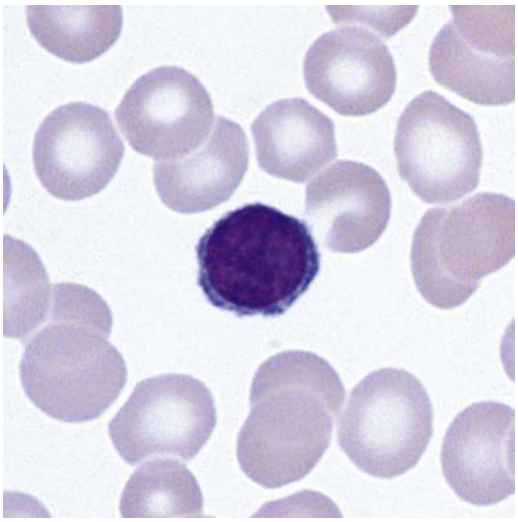

Figure 32.30 Small lymphocyte with high nuclear/cytoplasmic ratio, condensed chromatin, and scant basophilic cytoplasm (Wright-Giemsa, 1000×).

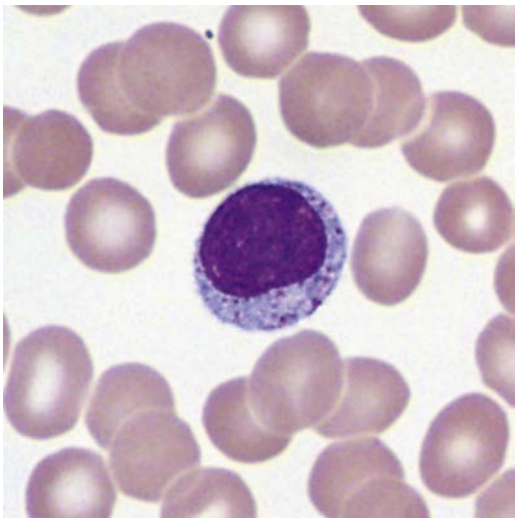

Figure 32.32 Large granular lymphocyte with azurophilic cytoplasmic granules (Wright-Giemsa, 1000×).

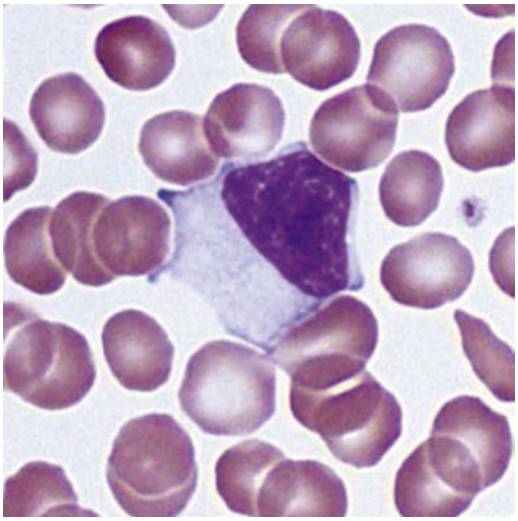

Figure 32.31 Atypical lymphocyte with a large nucleus, finer chromatin, and abundant basophilic cytoplasm scalloping around adjacent red blood cells (Wright-Giemsa, 1000×).

(Caligiuri, 2008). Fetal NK cells possess CD3γ, δ, ε, and CD28; adult NK cells express CD2, CD3ξ, CD7, CD8α, CD16, and CD56. SCF, IL-7, and IL-2 are critical in the development of NK cells (Spits et al., 1995). NK cells proliferate in the presence of IL-2, and their activity can be augmented by exposure to IFN-γ. NK cells appear to be targeted against virus-infected cells unable to signal cytotoxic T cells (usually as a result of low expression of class I MHC molecules). Because NK cells possess the Fc portion of IgG, they participate in antibody-dependent cell lysis (MacLennan, 1999).

SECONDARY LYMPHOID TISSUE

In late fetal and postnatal life, lymphocytes are produced in the secondary lymphoid tissue: spleen, lymph nodes, and intestine. Lymphocytes of the secondary lymphoid organs are progeny from stem cells that have been influenced by primary lymphoid organs. The secondary lymphoid organs are thus composed of a mixture of B cells and T cells. Lymphopoiesis in secondary lymphoid organs depends solely on antigenic stimulation. B cells and T cells tend to localize in anatomically distinct parts of the lymphoid tissues, where proliferation can take place.

LYMPHOCYTE FUNCTION AND PHYSIOLOGY

T cells and their progeny function in cell-mediated immunity, which includes delayed hypersensitivity, graft rejection, graft-versus-host reactions, defense against intracellular organisms (such as tubercle bacillus and *Brucella*), and defense against neoplasms. B cells and their progeny perform in humoral immunity, or in the production of antibodies, either as a lymphocyte or after transformation into a plasma cell.

A majority of circulating lymphocytes are T cells that have a life span of months to years. The B cells are a minor population (10%–20% of the lymphocytes), probably have a short life span measured in days (with the exception of memory B cells), and are distinguished by the presence of considerable Ig on their surface membranes.

Lymphocytes circulate in the blood and home to appropriate lymphoid organs. During fetal development, lymphocytes migrate from fetal liver to bone marrow or thymus. Later, pro–T cells migrate from the bone marrow to the thymus, and immature B cells home to secondary lymphoid tissues. After thymic processing, virgin T cells also home to specific areas in the peripheral lymphoid tissues. The circulation of lymphocytes is regulated by multiple cell surface adhesion molecules and chemokines, including integrins, selectins, and leukocyte (L) selectin. The circulation and homing of lymphocytes is a very complex, multistep phenomenon, reviewed elsewhere (Springer, 1994; Paraskevas, 2014). However, in the postcapillary venule of lymphoid tissue, the lymphocyte travels from the blood through the endothelium and into the lymphoid tissue, where it may stay or percolate through and return to the blood via the thoracic duct lymph. Small lymphocytes (Fig. 32.30) have little cytoplasm and, in electron micrographs, few organelles and relatively little RNA. After antigenic stimulation, small lymphocytes (B cells or T cells, depending on the nature of the antigen) become activated, increase their RNA synthesis, and undergo blast transformation. On Romanowsky-stained films, these blasts are large cells (15–25 μm) with abundant, rather deep-blue cytoplasm, a large reticular nucleus with uniform chromatin, and prominent nucleoli. This cell is called the **reticular lymphocyte** (nonleukemic lymphoblast; **immunoblast**). If the blasts are derived from B cells, the new lymphocytes function in the production of antibodies (B cells, plasma cells). If the blasts are derived from T cells, the progeny act in cellular immune response. The latter is mediated by several soluble factors produced by the activated T cell, including IL-2, which induces the proliferation of T cells; IL-3, which is a multipotential colony-stimulating factor; IL-4, which promotes the proliferation of B cells; IL-5, which enhances the proliferation of eosinophils as well as B cells; IL-6, which promotes differentiation of B cells; lymphotoxin, which is directly toxic to cells; and migratory inhibitory factor, which promotes adherence of macrophages and keeps them at the site. Atypical lymphocytes (Fig. 32.31) are seen in certain viral infections such as infectious mononucleosis. These cells have large nuclei with fine chromatin and more abundant cytoplasm that often scallops around adjacent red blood cells. Large granular lymphocytes (Fig. 32.32) contain azurophilic granules in their cytoplasm; these cells most often represent cytotoxic T cells or NK cells.

Plasma cells have abundant blue cytoplasm, often with light streaks or vacuoles, an eccentric round nucleus, and a well-defined clear (Golgi) zone adjacent to the nucleus. The nucleus of the plasma cell has heavily clumped chromatin, which is sharply defined from the parachromatin and is often arranged in a radial or wheel-like pattern (Fig. 32.33). Plasma cells are immunoglobulin secreting cells that are derived from activated B-cells (lineage-switched and mutated), initially as plasmablasts (PB), in both germinal center (GC) and extrafollicular settings. Antibody production and affinity are variable, with a portion of plasma cells being long-lived. Antibody responses are complex and vary with antigenic stimuli (Elsner & Shlomchik, 2020).

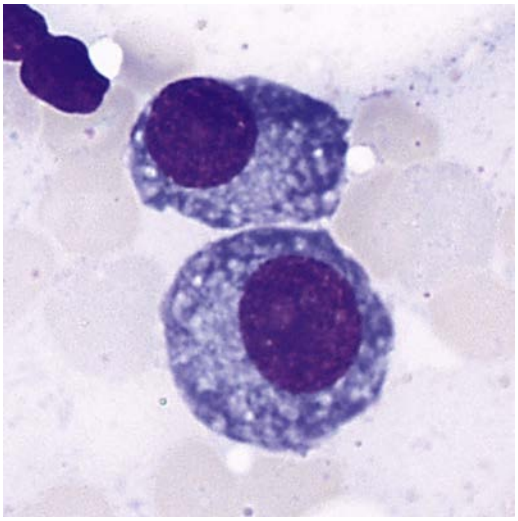

Figure 32.33 Plasma cells with an abundant basophilic cytoplasm, eccentric nucleus, and perinuclear clear Golgi zone (Wright-Giemsa, 1000×).

SELECTED REFERENCES

Davé UP, Koury MJ: Structure of the marrow and the hematopoietic microenvironment. In Kaushansky K, Lichtman MA, Prchal JT, Levi M, et al.: *Williams hematology*, 9, New York, 2015, McGraw-Hill.

This reference puts hematopoiesis into the essential context of the bone marrow microenvironment.

Doulatov S, Notta F, Laurenti E, et al.: Hematopoiesis: a human perspective, *Cell Stem Cell* 10:120–136, 2012.

Excellent review of recent advances in the knowledge of human hematopoiesis, with the contribution of experimentation in the mouse.

Hillman RS, Finch CA: In *Red cell manual*, 7, Philadelphia, 1996, FA Davis.

Updated classic work illustrating the morphology of red blood cells, with descriptions of red blood cell disorders and pathophysiology, diagnosis, and treatment of anemias.

Kaushansky K: Thrombopoietin: a tool for understanding thrombopoiesis, *J Thromb Haemost* 1:1587, 2003.

A review of the effects of the primary hormonal regulator of platelet production and the underlying mechanisms through which it works.

Park C: Lymphocytes and lymphatic organs. In Greer JP, Arber DA, Glader B, List AF, et al.: *Wintrobe's clinical hematology*, 14, Philadelphia, 2018, Wolters Kluwer.

This provides an excellent basic discussion of post–bone marrow lymphopoiesis.

Quigley JG, Means RT, Glader B: The erythrocyte—the birth, life, and death of red blood cells: erythropoiesis, the mature red blood cell, and cell destruction. In Greer JP, Arber D, Glader B, List AF, et al.: *Wintrobe's clinical hematology*, 14, Philadelphia, 2018, Wolters Kluwer.

Essentials of erythroid commitment, colony formation and development, heme and globin, and control of erythropoiesis.

Sieff CA, Daley GQ, Zon LI: Anatomy and physiology of hematopoiesis. In *Nathan and Oski's hematology of infancy and childhood*, 8, Philadelphia, 2014, Elsevier-Saunders.

A thorough but readable reference on hematopoiesis from marrow anatomy through progenitor cells, molecular signaling, growth factors and receptors, differentiation, clinical disorders, and treatment considerations.

Access the complete reference list online at Elsevier eBooks for Practicing Clinicians.

REFERENCES

Akada H, Akada S, Hutchison RE, et al.: Critical role of Jak2 in the maintenance and function of adult hematopoietic stem cells, *Stem Cell* 32:1878–1889, 2014.

Akashi K, Traver D, Miyamoto T, et al.: A clonogenic common myeloid progenitor that gives rise to all myeloid lineages, *Nature* 404:193–197, 2000.

Antin JH, Emerson SG, Martin P, et al.: Leu-1+ (CD5+) B cells. A major lymphoid subpopulation in human fetal spleen: phenotypic and functional studies, *J Immunol* 136:505–510, 1986.

Basso K, Saito M, Sumazin P, et al.: Integrated biochemical and computational approach identifies BCL6 direct target genes controlling multiple pathways in normal germinal center B cells, *Blood* 115:975–984, 2010.

Bertoli LF, Burrows PD: Normal B-lineage cells: their differentiation and identification, *Clin Lab Med* 8:15–30, 1988.

Bhardwaj G, Murdoch B, Wu D, et al.: Sonic hedgehog induces the proliferation of primitive human hematopoietic cells via BMP regulation, *Nat Immunol* 2:172–180, 2001.

Blumberg RS, Ley S, Sancho J, et al.: Structure of the T cell antigen receptor: evidence for two CD3 epsilon subunits in the T cell receptor-CD3 complex, *Proc Natl Acad Sci U S A* 87:7220–7224, 1990.

Blank U, Karlsson S: TGF-β signaling in the control of hematopoietic stem cells, *Blood* 125:3542–3550, 2015.

Bryder D, Rossi DJ, Weissman IL: Hematopoietic stem cells: the paradigmatic tissue-specific stem cell, *Am J Pathol* 169:338–346, 2006.

Bunn HF, Forget BG: *Hemoglobin: molecular, genetic and clinical aspects*, Philadelphia, 1986, Saunders, p 13.

Caligiuri MA: Human natural killer cells, *Blood* 112:461–469, 2008.

Casadevall N, Dupuy E, Molho-Sabatier P, et al.: Autoantibodies against erythropoietin in a patient with pure red-cell aplasia, *N Engl J Med* 334:630–633, 1996.

Challen GA, Sun D, Jeong M, et al.: Dnmt3a is essential for hematopoietic stem cell differentiation, *Nat Genet* 44:23–31, 2011.

Challen GA, Sun D, Mayle A, et al.: Dnmt3a and Dnmt3b have overlapping and distinct functions in hematopoietic stem cells, *Cell Stem Cell* 15:350–364, 2014.

Clarke MF, Fuller M: Stem cells and cancer: two faces of eve, *Cell* 124:1111–1115, 2006.

Clark MR, Mandal M, Ochiai K, et al.: Orchestrating B cell lymphopoiesis through interplay of IL-7 receptor and pre-B receptor signaling, *Nat Rev Immunol* 14:69–80, 2014.

Ding L, Morrison SJ: Haematopoietic stem cells and early lymphoid progenitors occupy distinct bone marrow niches, *Nature* 495:231–235, 2013.

Ding L, Saunders TL, Enikolopov G, et al.: Endothelial and perivascular cells maintain haematopoietic stem cells, *Nature* 481:457–462, 2012.

Doulatov S, Notta F, Laurenti E, et al.: Hematopoiesis: a human perspective, *Cell Stem Cell* 10:120–136, 2012.

Elsner RA, Shlomchik MJ: Germinal center and extrafollicular B cell responses in vaccination, immunity, and autoimmunity. Immunity 53:1136-1150, 2020.

Fu SM, Winchester RJ, Feizi T, et al.: Idiotypic specificity of surface immunoglobulin and the maturation of leukemic bone-marrow-derived lymphocytes, *Proc Natl Acad Sci U S A* 71:4487–4490, 1974.

Gleich GJ, Adolphson CR: The eosinophilic leukocyte: structure and function, *Adv Immunol* 39:177–253, 1986.

Gordeuk VR, Sergueeva AI, Miasnikova GY, et al.: Congenital disorder of oxygen sensing: association of the homozygous Chuvash polycythemia VHL mutation with thrombosis and vascular abnormalities but not tumors, *Blood* 103:3924–3932, 2004.

Greenbaum A, Hsu YM, Day RB, et al.: CXCL12 in early mesenchymal progenitors is required for haematopoietic stem-cell maintenance, *Nature* 495:227–230, 2013.

Hagman J, Grosschedl R: Regulation of gene expression at early stages of B-cell differentiation, *Curr Opin Immunol* 6:222–230, 1994.

Haks MC, Krimpenfort P, Borst J, et al.: The CD3gamma chain is essential for development of both the TCRalphabeta and TCRgammadelta lineages, *EMBO J* 17:1871–1882, 1998.

Hartwig J, Italiano J: The birth of the platelet, *J Thromb Haemost* 1:1580–1586, 2003.

Ichii M, Oritani K, Kanakura Y: Early B lymphocyte development: similarities and differences in human and mouse, *World J Stem Cells* 6:421–431, 2014.

Italiano JE, Shivdasani A: Megakaryocytes and beyond: the birth of platelets, *J Thromb Haemost* 1:1174–1182, 2003.

Ito K, Hirao A, Arai F, et al.: Reactive oxygen species act through p38 MAPK to limit the lifespan of hematopoietic stem cells, *Nat Med* 12:446–451, 2006.

Johnston Jr RB: Current concepts: immunology. Monocytes and macrophages, *N Engl J Med* 318:747–752, 1988.

Kang J, Volkmann A, Raulet DH: Evidence that gammadelta versus alphabeta T cell fate determination is initiated independently of T cell receptor signaling, *J Exp Med* 193:689–698, 2001.

Katayama Y, Battista M, Kao WM, et al.: Signals from the sympathetic nervous system regulate hematopoietic stem cell egress from bone marrow, *Cell* 124:407–421, 2006.

Kaushansky K: Thrombopoietin: the primary regulator of platelet production, *Blood* 86:419–431, 1995.

Klein U, Rajewsky K, Kuppers R: Human immunoglobulin (IgM+IgD+ peripheral blood B cells expressing the CD27 cell surface antigen carry somatically mutated variable region genes: CD27 as a general marker for somatically mutated (memory) B cells, *J Exp Med* 188:1679–1689, 1998.

Ko M, Rao A: TET2: epigenetic safeguard for HSC, *Blood* 118:4501–4503, 2011.

Koethe S, Zander L, Koster S, et al.: Pivotal advance: CD45RB glycosylation is specifically regulated during human peripheral B cell differentiation, *J Leukoc Biol* 90(5–19), 2011.

Kondo M, Weissman IL, Akashi K: Identification of clonogenic common lymphoid progenitors in mouse bone marrow, *Cell* 91:661–672, 1997.

Lacombe J, Herblot S, Rojas-Sutterlin S, et al.: Scl regulates the quiescence and the long-term competence of hematopoietic stem cells, *Blood* 115:792–803, 2010.

LeBien TW, Tedder TF: B lymphocytes: how they develop and function, *Blood* 112:1570–1580, 2008.

Lindstedt G, Lundberg PA: Are current methods of measurement of erythropoietin (EPO) in human plasma or serum adequate for the diagnosis of polycythaemia vera and the assessment of EPO deficiency? *Scand J Clin Lab Invest* 58:441–458, 1998.

Ling KW, Ottersbach K, van Hamburg JP, et al.: GATA-2 plays two functionally distinct roles during the ontogeny of hematopoietic stem cells, *J Exp Med* 200:871–882, 2004.

Lyman SD, Jacobsen SE: c-Kit ligand and Flt3 ligand: stem/progenitor cell factors with overlapping yet distinctive activities, *Blood* 91:1101–1134, 1998.

Mansour A, Abou-Ezzi G, Sitnicka E, et al.: Osteoclasts promote the formation of hematopoietic stem cell niches in the bone marrow, *J Exp Med* 209:537–549, 2012.

Manz MG, Miyamoto T, Akashi K, et al.: Prospective isolation of human clonogenic common myeloid progenitors, *Proc Natl Acad Sci U S A* 99(18):11872–11877, 2002.

Metcalf D: Hematopoietic cytokines, *Blood* 111:485–491, 2008.

Morrison SJ, Scadden DT: The bone marrow niche for haematopoietic stem cells, *Nature* 505:327–334, 2014.

Moser B, Wolf M, Walz A, et al.: Chemokines: multiple levels of leukocyte migration control, *Trends Immunol* 25:75–84, 2004.

Muraro PA, Pette M, Bielekova B, et al.: Human autoreactive CD3+ T cells from naïve CD45RA+ and memory CD45RO+ subsets differ with respect to epitope specificity and functional antigen avidity, *J Immunol* 164:5474–5481, 2000.

Pang WW, Price EA, Sahoo D, et al.: Human bone marrow hematopoietic stem cells are increased in frequency and myeloid-biased with age, *Proc Natl Acad Sci U S A* 108:20012–20017, 2011.

Papayannopoulou T, Scadden DT: Stem-cell ecology and stem cells in motion, *Blood* 111:3923–3930, 2008.

Park IK, Qian D, Kiel M, et al.: Bmi-1 is required for maintenance of adult self-renewing haematopoietic stem cells, *Nature* 423:302–305, 2003.

Reinherz EL, Kung PC, Goldstein G, et al.: Discrete stages of human intrathymic differentiation: analysis of norma thymocytes and leukemic lymphoblasts of T-cell lineage, *Proc Natl Acad Sci U S A* 77:1588–1592, 1980.

Reya T, Duncan AW, Ailles L, et al.: A role for Wnt signalling in self-renewal of haematopoietic stem cells, *Nature* 423:409–414, 2003.

Reya T, Morrison SJ, Clarke MF, et al.: Stem cells, cancer, and cancer stem cells, *Nature* 414:105–111, 2001.

Roberts PJ, Linch DC, Webb DKH: Phagocytes. In Hoffbrand AV, Lewis SM, Tuddenham EGD, editors: *Postgraduate haematology*, 4, Oxford, 1999, Butterworth Heinemann, p 235.

Rossi DJ, Bryder D, Zahn JM, et al.: Cell intrinsic alterations underlie hematopoietic stem cell aging, *Proc Natl Acad Sci U S A* 102:9194–9199, 2005.

Schett G, Firbas U, Füreder W, et al.: Decreased serum erythropoietin and its relation to anti-erythropoietin antibodies in anaemia of systemic lupus erythematosus, *Rheumatology* 40:424–431, 2001.

Shivdasani RA, Mayer EL, Orkin SH: Absence of blood formation in mice lacking the T-cell leukaemia oncoprotein tal-1/SCL, *Nature* 373:432–434, 1995.

Spits H, Lanier L, Phillips JH: Development of human T and natural killer cells, *Blood* 85:2654–2670, 1995.

Spivak JL: Polycythemia vera: myths, mechanisms, and management, *Blood* 100:4272–4290, 2002.

Springer TA: Traffic signals for lymphocyte recirculation and leukocyte emigration: the multistep paradigm, *Cell* 76:301–314, 1994.

Sugiyama T, Kohara H, Noda M, et al.: Maintenance of the hematopoietic stem cell pool by CXCL12-CXCR4 chemokine signaling in bone marrow stromal cell niches, *Immunity* 25:977–988, 2006.

Terstappen LW, Huang S, Picker LJ: Flow cytometric assessment of human T-cell differentiation in thymus and bone marrow, *Blood* 79:666–677, 1992.

Tothova Z, Kollipara R, Huntly BJ, et al.: FoxOs are critical mediators of hematopoietic stem cell resistance to physiologic oxidative stress, *Cell* 128:325–339, 2007.

Trowbridge JJ, Snow JW, Kim J, et al.: DNA methyltransferase 1 is essential for and uniquely regulates hematopoietic stem and progenitor cells, *Cell Stem Cell* 5:442–449, 2009.

Tsai FY, Keller G, Kuo FC, et al.: An early haematopoietic defect in mice lacking the transcription factor GATA-2, *Nature* 371:221–226, 1994.

van der Meer LT, Jansen JH, van der Reijden BA: Gfi1 and Gfi1b: key regulators of hematopoiesis, *Leukemia* 24:1834–1843, 2010.

Varnum-Finney B, Xu L, Brashem-Stein C, et al.: Pluripotent, cytokine-dependent, hematopoietic stem cells are immortalized by constitutive Notch1 signaling, *Nat Med* 6:1278–1281, 2000.

Weinberg JB: Mononuclear phagocytes. In Foerster J, Lukens J, Rogers GM, et al.: *Wintrobe's clinical hematology*, 11, Baltimore, 2004, Williams & Wilkins, pp 349–386.

Winkler IG, Sims NA, Pettit AR, et al.: Bone marrow macrophages maintain hematopoietic stem cell (HSC) niches and their depletion mobilizes HSCs, *Blood* 116:4815–4828, 2010.

Yamada Y, Warren AJ, Dobson C, et al.: The T cell leukemia LIM protein Lmo2 is necessary for adult mouse hematopoiesis, *Proc Natl Acad Sci U S A* 95:3890–3895, 1998.

Yamazaki S, Ema H, Karlsson G, et al.: Nonmyelinating Schwann cells maintain hematopoietic stem cell hibernation in the bone marrow niche, *Cell* 147:1146–1158, 2011.

Yoshihara H, Arai F, Hosokawa K, et al.: Thrombopoietin/MPL signaling regulates hematopoietic stem cell quiescence and interaction with the osteoblastic niche, *Cell Stem Cell* 1:685–697, 2007.

Zhu J, Paul WE: CD4 T cells: fates, functions, and faults, *Blood* 112:1557–1569, 2008.

Zubair AC, Silberstein L, Ritz J: Adult hematopoietic stem cell plasticity, *Transfusion* 42:1096–1101, 2002.

CHAPTER 33

ERYTHROCYTIC DISORDERS

M. Tarek Elghetany, Katalin Banki

ANEMIAS, 588
General manifestations, 588
Impaired Production—Iron Deficiency Anemia, 588
Impaired Production—Megaloblastic Anemia, 592
Impaired Production—Other, 597
Blood Loss Anemia, 603
Hemolysis—General, 603
Hemolysis—Membrane Disorders, 605
Hemolysis—Hemoglobin Disorders, 607
Thalassemias, 616
Hemolysis—Metabolic Disorders, 621
Hemolysis—Acquired, 623
Laboratory Investigations of Anemia, 628
POLYCYTHEMIA, 630
Relative Polycythemia, 630
Absolute Polycythemia, 630
THE PORPHYRIAS, 631
Physiology, 631
Approach to the Porphyrias, 633
Neurovisceral Symptoms in Isolation, 633
Neurovisceral Symptoms Plus Photosensitivity, 634
Photosensitivity Plus Hemolytic Anemia, 634
Photosensitivity in Isolation, 634
Analytic Techniques, 634
SELECTED REFERENCES, 635

KEY POINTS

- Anemia may result from decreased marrow production or shortened red cell survival.
- Nonmarrow diseases, such as endocrine, renal, and inflammatory disorders, significantly influence bone marrow function.
- Anemias associated with nutritional deficiencies may affect tissues other than the bone marrow.
- Stem cell disorders, such as inherited and acquired aplastic anemias, and paroxysmal nocturnal hemoglobinuria usually affect more than one cell line.
- Hemolytic anemia may be caused by extrinsic factors, usually acquired, such as chemical agents or antibodies, or intrinsic factors, usually inherited, such as disorders of the red cell membrane or enzymes, or hemoglobinopathy.
- Polycythemia is defined by laboratory parameters and may be absolute with an increase in total red cell mass or relative as a result of a decrease in plasma volume.
- Porphyrias are inherited and acquired disorders of heme biosynthetic pathways with clinical manifestations resulting from accumulation of intermediate heme synthetic products.

ANEMIAS

GENERAL MANIFESTATIONS

Anemia is considered to be present if the hemoglobin (Hb) concentration or the hematocrit (Hct) is below the lower limit of the 95% reference interval for the individual's age, sex, and geographic location (altitude; Table 33.1). This means that 2.5% of normal individuals will be classified as anemic. Conversely, individuals whose Hb falls within the reference intervals for age and sex yet significantly below their own usual values should be considered anemic.

Anemia may be absolute when red blood cell (RBC) mass is decreased or relative when associated with a higher plasma volume. Causes of absolute anemia fall into two major pathophysiologic categories: impaired red cell production and increased erythrocyte destruction (or loss in excess of the ability of the marrow to replace these losses). Several authors have included anemia following acute blood loss in the latter category (Hillman, 1996; Prchal, 2010). The presence of anemia may be a sign of an underlying disorder of which the cause should be identified because correction may be very important to the health of the individual. Relative anemia may occur with pregnancy, with macroglobulinemia, and in postflight astronauts. Recent studies suggest that prolonged exposure to weightlessness, which causes hemoconcentration due to decreased plasma volume, as well as the return to sea level after a period of high-altitude acclimatization, are associated with selective loss of young red cells, also known as *neocytes*, as a result of erythropoietin (EPO) withdrawal, a process known as neocytolysis. It is thought that EPO withdrawal may cause decreased expression of certain molecules, such as CD55 and CD59, which are protective against red cell destruction by macrophages (Mairbäurl, 2018).

Anemia may also be classified by red cell morphology as macrocytic, normocytic, or microcytic—an approach that is useful in differential diagnosis (see later discussion). Both pathophysiologic and morphologic classifications should be understood. Some anemias (e.g., blood loss anemia) have more than one pathogenetic mechanism and go through more than one morphologic stage.

Clinical signs and symptoms result from diminished delivery of oxygen (O_2) to the tissues; therefore, they are related to the lowered Hb concentration and blood volume and are dependent on the rate of these changes. Modifying factors include compensatory adjustments in cardiac output, respiratory rate, and O_2 affinity of Hb. When anemia develops slowly in a patient who is not otherwise severely ill, Hb concentrations as low as 6 g/dL may develop without producing any discomfort or physical signs as long as the patient is at rest.

In general, the anemic patient complains of easy fatigability and dyspnea on exertion, and often of faintness, vertigo, palpitations, and headache. The more common physical findings are pallor, a rapid bounding pulse, low blood pressure, slight fever, some dependent edema, and systolic murmurs. In addition to these general signs and symptoms, certain clinical findings are characteristic of the specific type of anemia.

IMPAIRED PRODUCTION—IRON DEFICIENCY ANEMIA

Iron Metabolism (Muckenthaler, 2017; Camaschella, 2018)

Iron is an essential component of Hb, of myoglobin (in muscle cells), and of certain enzymes (in most body cells). The major "pools" of iron in the body are illustrated in Figure 33.1. Two-thirds or more of the body's total iron is in the erythron (normoblasts and erythrocytes); each milliliter of red cells contains about 1 mg of iron. Storage iron is present in macrophages of the reticuloendothelial system in two forms: ferritin and hemosiderin. Ferritin is a water-soluble complex of ferric salt and a protein, apoferritin. Apoferritin has a molecular weight of approximately 450,000 Da and consists of 24 subunits with a variable ratio of H (heavy) and L (light) types. Apoferritin forms a shell around a crystalline core of predominantly ferric oxyhydroxide (FeOOH). The genes for the H and L subunits have been located on chromosomes 11 and 19,

TABLE 33.1
Reference Values Below Which Anemia Is Considered to Exist at Sea Level

Age, Years	Hb, g/dL
Both Sexes	
1–2	11
3–5	11.2
6–11	11.8
Females	
12–15	11.9
16–69	12
≥70	11.8
Males	
12–15	12.6
16–19	13.6
20–49	13.7
50–69	13.3
≥70	12.4

From Looker AC, Dallman PR, Carroll MD, et al.: Prevalence of iron deficiency in the United States. *JAMA* 277:973–976, 1997.
Hb, Hemoglobin.

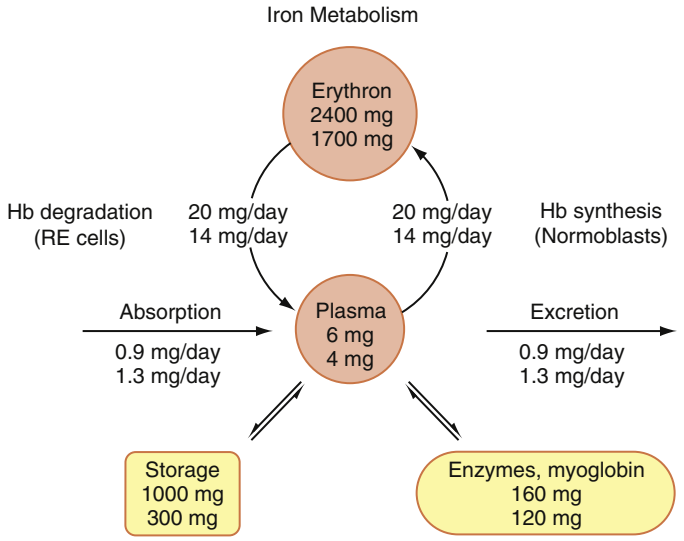

Figure 33.1 Scheme of iron metabolism. The upper figure in each position is average for an 80-kg man; the lower figure is for a 65-kg woman. (Data from Hillman and Finch, 1974.) The plasma iron, bound largely to transferrin, is central in this scheme. It completely turns over several times a day in supplying iron for heme synthesis. Each day, about 1% of total circulating red cells are destroyed, and the same number of new red cells is delivered to the blood. That proportion of the total erythron iron enters the plasma from the site of hemoglobin (Hb) degradation, the macrophages of the reticuloendothelial (RE) system, and travels (bound to transferrin) to the normoblasts in the marrow. Storage iron largely resides also in the macrophages of the RE system. Absorbed iron enters the plasma pool, bound to transferrin. Iron is largely excreted by loss of cells.

respectively. The H monomers have ferroxidase activity, allowing them to become more efficient in taking up and releasing iron. Hemosiderin is water insoluble and consists mostly of aggregates of FeOOH core crystals with partially or completely degraded protein shells. Protein degradation usually occurs in lysosomes. The iron in hemosiderin is much more difficult to release than that of ferritin. Most of the iron utilized in Hb synthesis is that recently released from degraded Hb in macrophages and transported to the normoblasts by plasma transferrin (a β-globulin, molecular weight 80,000 Da, gene located on chromosome 3). Each molecule of apotransferrin binds two atoms of ferric iron. Subsequently, transferrin binds to transferrin receptor-1 (TfR-1) (CD71) on the cell membrane of erythroid precursors, reticulocytes, and most body cells. The transferrin–transferrin receptor complex is rapidly internalized as an endosome, iron is released following pH decline of the endosome, and apotransferrin returns to the circulation and binds more iron. The freed iron is reduced to the ferrous form by STEAP3 (six-transmembrane epithelial antigen of prostate 3) and transported into the cytosol by DMT1 (divalent metal transporter 1, also known as NRAMP2, SLC11A2). Iron is imported into the mitochondria by a solute carrier known as mitoferrin-1, where iron is used to synthesize heme, iron-sulphur clusters, and other proteins (Camaschella, 2018). Experimental studies in mice indicate that TfR-1 is essential for brain, heart, gut, and skeletal muscle development as well as immune system function. While TfR-1 is widely expressed, only hepatocytes and erythroid precursors express a related molecule designated as transferrin receptor-2 (TfR-2). Recent evidence suggests that TfR-2 may work in concert with HFE protein in hepatocytes to control iron absorption. Mutations in the *TfR-2* gene have been associated with type 3 hemochromatosis (see later discussion).

In humans, approximately 20 mg of iron is needed daily in order to generate in excess of 200 billion RBCs. The majority of the daily iron needs (80%–90%) is provided by recycling of iron from senescent red cells and the remainder through daily intake of iron. Very little iron is lost from the body; this small iron loss occurs mainly as loss of cells from the gastrointestinal (GI) tract and to a lesser extent from the skin and through the urine. The iron lost in women averages more, because of menstrual blood loss, than that excreted in men. About 1 mg is lost each day, except in menstruating females, whose iron loss averages about 2 mg/day. Iron balance is maintained by control of absorption. In the United States, dietary iron averages 15 mg/day with 7% absorption in men and 11 mg/day with 13% absorption in women. Absorption can be increased in iron deficiency, but only to about 20% of ingested iron in meat-containing diets and less in vegetarian diets (Hillman, 1996). Absorption takes place largely in the small intestine, most efficiently in the duodenum and upper jejunum, with heme iron absorbed more efficiently than inorganic iron. Iron absorption is facilitated by ascorbate and citrate and is inhibited by phytates and tannins. Acid production by the stomach lowers the pH in the duodenum, thus enhancing the solubility and uptake of nonheme ferric iron. Iron entry into mucosal cells of the upper GI tract seems to involve more than one pathway, including an independent mechanism for heme absorption. A heme carrier protein 1 (HCP1) has been described. However, recent evidence suggests that it is identical to proton-coupled folate transporter (PCFT), which is involved rather exclusively in folate transport (Beutler, 2010; Visentin, 2014). A dual role of PCFT in folate and heme iron uptake is being investigated.

Nonheme iron is transported across the mucosal membrane through a channel called the *divalent metal transporter*, which is regulated by iron regulatory proteins 1 and 2 (IRP-1 and IRP-2). These regulatory proteins, particularly IRP-2, affect the translation of several proteins that are involved in iron metabolism, with a net result of increasing intracellular iron. Messenger RNA (mRNA) of these proteins have IREs (internal ribosome entry sites), which may increase or decrease translation when bound to IRPs. For example, iron deficiency increases the translation of DMT1 and TfR-1 while it decreases the translation of erythroid aminolevulinic acid synthetase and apoferritin (Zhang, 2014). DMT1 regulates iron transport from intestinal surface to inside the cell. This process is aided by duodenal cytochrome *b*–like ferroreductase, which reduces iron to the ferrous form. DMT1 also transports other metals, such as lead, cobalt, and nickel. The export of iron from enterocytes, macrophages, and hepatocytes to plasma involves another transport system, which includes ferroportin-1 and hephaestin (Fleming, 2008). Ferroportin-1 is located at the basolateral membrane of apical enterocytes and functions as a transport protein delivering iron in the ferrous state to the plasma. Ferroportin-1 is also expressed on macrophages. Hephaestin, named after the Greek god **Hephaestus**, who forged iron, has a ferroxidase activity that contributes to iron transport by transforming iron to the ferric form to enable its uptake by circulating apotransferrin. Ceruloplasmin also has ferroxidase activity and is involved as well in the release of iron from the cells. Because both ceruloplasmin and hephaestin are copper-containing ferroxidases, copper deficiency affects iron release and can produce iron deficiency anemia. Another 25-amino-acid antimicrobial peptide, hepcidin, has been shown to play a major role in iron homeostasis through a hormonal effect. Hepcidin is produced by the liver, is filtered by the kidney, and accumulates in urine. Hepcidin negatively controls the release of iron from cells, such as intestinal epithelium and macrophages, to the plasma. Hepcidin combines with ferroportin-1, leading to internalization and lysosomal degradation of both proteins. Thus, it limits the release of intracellular iron into the plasma (Fleming, 2008). It has been recently reported that hepcidin also physically occludes the site of iron export in the central cavity

of ferroportin (Wang, 2019). Hepcidin is the product of the *HAMP* (hepcidin/hepatic antimicrobial peptide) gene located on chromosome 19q13.1. At least 4 mechanisms are involved in the regulation of hepcidin secretion: inflammation, systemic iron availability through hepatocyte iron-sensing system, erythropoietic activity, and hypoxia. Increased marrow erythropoietic activity has been associated with decreased hepcidin and increased iron absorption. A hormone named erythroferrone (ERFE) has been recently identified. ERFE is secreted by erythroblasts in response to erythropoietin and causes suppression of hepcidin release (Kautz, 2014). The current evidence suggests that human hemochromatosis protein (HFE), TfR-2, and hemojuvelin (HJV) interact with each other to form a hepatocyte "iron-sensing complex." When transferrin is highly saturated, HFE is displaced from TfR-1 and interacts with TfR-2 and HJV to activate *HAMP* transcription pathways. Matriptase-2 (MT-2) is a membrane serine protease expressed predominantly in hepatocytes. It acts to cleave and inactivate HJV, producing a lower level of hepcidin (Wang, 2019). Recent studies suggest that the early steps of iron sensing actually occur in the liver sinusoidal endothelial cells, which transmit signals to the hepatocytes for further steps of control (Camaschella, 2019). In the plasma, total iron averages 110 μg/dL (19.7 μ mol/L). The great majority of this is bound to the transferrin, which has a capacity to bind 330 μg of iron per deciliter (or 59.1 μmol/L) and, therefore, is about one-third saturated. A very small amount of iron in plasma is in ferritin. Plasma (or serum) ferritin averages about 100 μg/L in men (less in women—about 50 μg/L).

Iron Deficiency Anemia (IDA)

When iron loss exceeds iron intake for a time long enough to deplete the body's iron stores, insufficient iron is available for normal Hb production. When well developed, iron deficiency is characterized by a hypochromic microcytic anemia.

Iron deficiency typically results when the need for iron is increased (e.g., during rapid growth in infancy and childhood, during pregnancy) or when excessive loss of blood has reduced the body's reserves of iron (e.g., following repeated hemorrhages, excessive menstruation, or multiple pregnancies).

Iron deficiency is probably the most common cause of anemia, affecting at least 1.2 billion individuals worldwide (Camaschella, 2019). Children between the ages of 6 and 24 months are particularly susceptible. It is caused by insufficient dietary iron to meet the needs of rapid growth. After the first 4 to 6 months of life, the iron stores present from birth have been exhausted, and the infant depends on dietary iron. An infant maintained on milk and carbohydrates without supplements of iron-containing foods is likely to develop iron deficiency anemia—one component of the "milk anemia" of infancy. This anemia is also frequently related to intestinal blood loss due to cow's milk protein intolerance in young children when cow's milk is introduced too early. In a study in the United States, IDA was reported in 3% of toddlers aged 1 to 2 years and in 2% to 5% of adolescent girls and women of childbearing age, with iron deficiency (absent anemia) noted in higher (>9%) proportions (Looker, 1997). IDA also affects 2% to 5% of pregnant women. Defective absorption of iron and eventual IDA occur after total gastrectomy or even subtotal gastrectomy. Prolonged treatment of peptic ulcer and acid reflux by H_2 blockers and acid pump blockers may cause defective iron absorption. Except for the sprue syndrome, causes of malabsorption of iron are extremely rare. Because iron deficiency increases the rate of absorption of both iron and lead, lead intoxication may accompany iron deficiency.

If an adult male had absolutely no iron intake or absorption (which would be extremely unlikely), his body iron stores of 1000 mg would last for 3 to 4 years before he would even begin to become iron deficient. Therefore, almost all cases of IDA in adult males are due to chronic blood loss. Hemorrhagic lesions—such as benign and malignant tumors, chronic ingestion of some medications, and helminthic infections—are common causes of iron deficiency in males and postmenopausal females.

The sequence of events in developing IDA is usually as follows (Hillman, 1996): When blood loss exceeds absorption, a negative iron balance exists. Iron is mobilized from stores, storage iron decreases, plasma ferritin decreases, iron absorption increases, and plasma iron-binding capacity (transferrin) increases. This stage is known as **iron depletion**. After iron stores are depleted, the plasma iron concentration falls, saturation of transferrin falls below 15%, and the percentage of sideroblasts decreases in the marrow. As a result of lack of iron for heme synthesis, red cell protoporphyrin increases. This second stage is **iron-deficient erythropoiesis**; anemia may not yet be present. The third stage is **IDA**; in addition to the abnormalities just discussed, anemia is detectable. The anemia at first is normochromic and normocytic, gradually becomes microcytic, and finally becomes microcytic and hypochromic.

Clinical Features

Clinical findings may be due to the underlying cause of the blood loss itself, to the general manifestations of anemia (see previous discussion), or to iron deficiency. Those that are probably attributable to lack of tissue iron include paresthesias, such as numbness and tingling; restless leg syndrome; atrophy of epithelium of the tongue with burning or soreness; fissures or ulcers at the corners of the mouth (angular stomatitis); chronic gastritis, which leads to decreased gastric secretions but few symptoms; "pica," which is the craving to eat unusual substances such as dirt or ice; concave or spoon-shaped nails (koilonychia); and difficulty swallowing due to "webs" of tissue or partial strictures at the junction of the esophagus and hypopharynx. The latter two findings are relatively uncommon. The combination of glossitis, sore mouth, dysphagia, and iron deficiency is called Plummer-Vinson syndrome. Splenomegaly may occur in iron deficiency but is uncommon. In young children, lower test scores and delayed motor development have been reported in association with IDA.

Laboratory Features

Blood. In early IDA, the stained blood film often shows normochromic normocytic erythrocytes (Hillman, 1996). In later stages, the picture is one of microcytosis, anisocytosis, poikilocytosis (including elliptical and elongated cells), and varying degrees of hypochromia. The thin red cells (leptocytes) have faint red color compared to normal. The plasma membranes of iron-deficient cells are abnormally stiff. This abnormality contributes to the development of poikilocytes, particularly elongated hypochromic elliptocytes (pencil cells). Anisocytosis may be identified by automated blood counters as increased red cell distribution width (RDW). This finding, however, is not specific for IDA. A high RBC count is commonly encountered in children under the age of 4 years. Reticulocytes are usually decreased in absolute numbers, except following iron therapy. Also, reticulocyte hemoglobin content (Ret-He, CHr) is reduced. The mean corpuscular volume (MCV) is low, and Hb and Hct are relatively lower than the erythrocyte count. Osmotic fragility may be decreased because the red cells are thinner than normal (see Figs. 31.10 and 33.2).

The leukocyte count is normal or slightly lowered. Granulocytopenia and a small number of hypersegmented neutrophils may be present. Megaloblastic changes in severe iron deficiency may be related to decreased activity of the enzyme ribonucleotide reductase, which contains an essential nonheme iron atom (Beck, 1991). However, the detection of hypersegmented neutrophils should raise suspicion for a mild folate deficiency, which may become more overt after iron therapy (Dallman, 1993). Platelets may be increased whether the lack of iron is due to blood loss or dietary deficiency, but tend to be decreased in severe anemia. When microcytosis is severe, automated platelet count may not be accurate due to some degree of interference by very small erythrocytes.

Marrow. Erythroid hyperplasia occurs early; however, in later stages, the limiting effect of severe iron deficiency restricts erythropoiesis to the basal level. The erythroblasts are smaller than normal, deficient in the amount of Hb in the cytoplasm, and irregular in shape, with frayed margins (Fig. 33.3). Giant neutrophil bands or metamyelocytes, if present, are rarely due to iron deficiency per se; usually, they indicate an associated cobalamin or folate deficiency (see later discussion under Megaloblastic Anemia). Iron stains should be performed routinely on marrow aspirate films (Figs. 33.4 and 33.5). **Storage iron** is absent, unless iron has recently been administered in some form. The proportion of erythroblasts that are **sideroblasts** is decreased (<20%). This proportion is usually about the same as the percent saturation of transferrin (or total iron-binding capacity [TIBC]) and is a measure of iron delivery to the erythroblasts.

Serum Iron. The reference interval is 50 to 160 μg/dL (9–29 μmol/L) in adults. The level is lower in iron deficiency and in infection and anemia of chronic disease.

Serum (Total) Iron-Binding Capacity. The reference interval for adults is 250 to 400 μg/dL (45–72 μmol/L). In IDA, the serum TIBC is increased. It is normal or decreased in the anemia of chronic disease. If chronic infection coexists with chronic blood loss, the TIBC may not be increased even though the patient is iron deficient. Some laboratories measure transferrin level as an alternative.

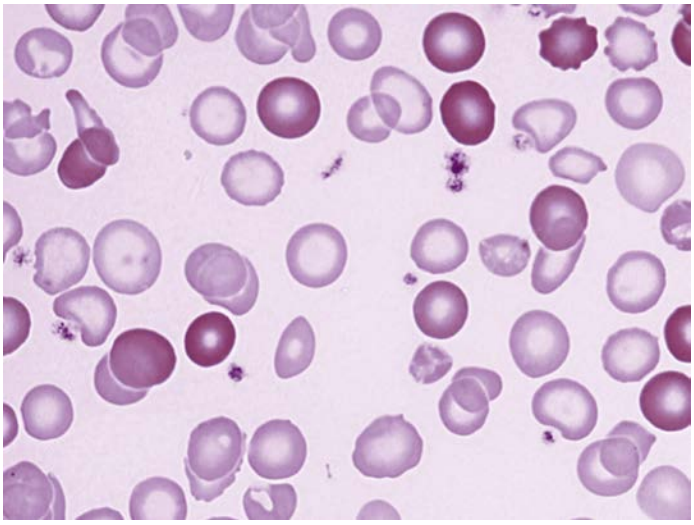

Figure 33.2 Iron deficiency anemia, posttransfusion. The cells are pale with an enlarged central pallor, variation in size, and tendency for elliptocytic formation, in sharp contrast to the transfused normochromic cells.

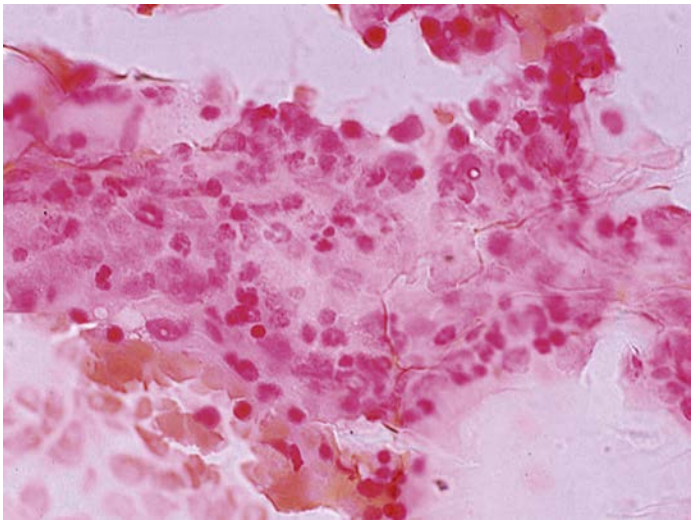

Figure 33.4 Marrow film, Prussian blue reaction. Depleted iron stores: No blue-green staining iron is visible. On a scale of 0–5+, the iron is normal from 1+ to 3+ for women and from 2+ to 3+ for men.

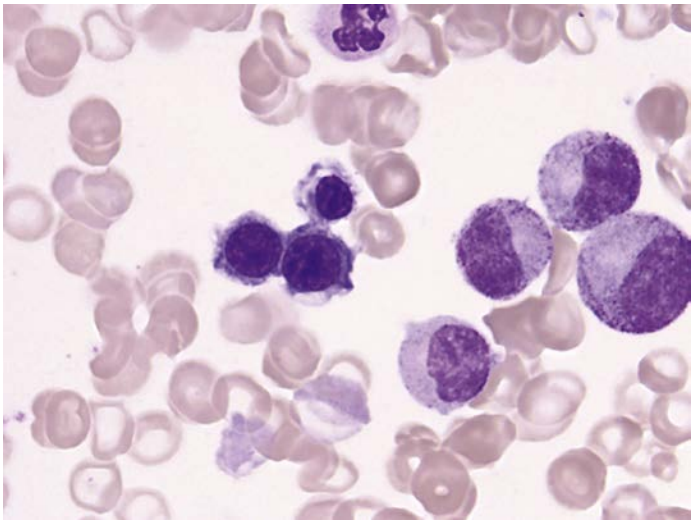

Figure 33.3 Marrow film, iron deficiency anemia. The three normoblasts have irregular margins and irregular clear spaces, reflecting lack of adequate hemoglobin synthesis (i.e., defective cytoplasmic maturation).

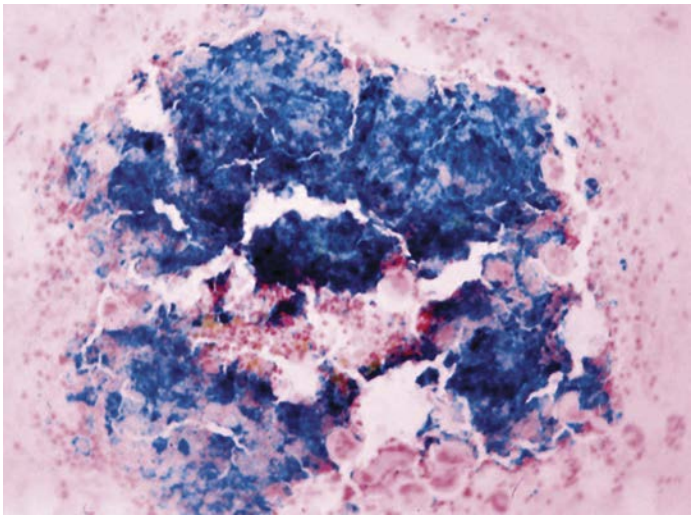

Figure 33.5 Marrow film, Prussian blue reaction. On a scale of 0 to 5+, the amount of storage iron is judged at 5+, which is markedly increased.

Percent Saturation of TIBC. The ratio of serum iron to TIBC is the percent saturation of the TIBC. Normally, this is 20% to 55%; values below 15% indicate iron-deficient erythropoiesis.

A marked diurnal variation in serum iron by as much as 30% normally occurs, with highest values in the morning and lowest values late in the day. Consequently, fasting morning blood specimens are preferred for the diagnosis of iron deficiency. The TIBC remains relatively constant in a normal individual. Pregnancy and oral contraceptives increase TIBC.

Serum iron is usually higher in the first 90 days of life. It then dips to somewhat lower reference intervals for the second month of life, and the value gradually increases with age until it reaches the adult range approximately at the age of 15 years (Ritchie, 2002b; Soldin, 2004). On the other hand, the TIBC gradually rises with age until it reaches values that are comparable to those of adults at the age of 15 years (Soldin, 2004). Similarly, percent saturation in children is less than in adults; it reaches the adult value between the ages of 15 and 18 years (Ritchie, 2002b).

Serum Ferritin. In adults, the reference values are 12 to 300 μg/L, with higher values in men than in women. Serum ferritin appears to be in equilibrium with tissue ferritin and is a good reflection of storage iron in normal subjects and in most disorders. The equivalence of 1 μg/L of serum ferritin with 8 to 10 mg storage iron has been suggested. In patients with some hepatocellular diseases, malignancies, and inflammatory diseases, serum ferritin provides a disproportionately high estimate of storage iron because serum ferritin is an acute-phase reactant. In such disorders, IDA may exist with a normal serum ferritin concentration. In the presence of inflammation, persons with a serum ferritin level of less than 50 to 60 μg/L are likely to respond to iron therapy. On the other hand, hypothyroidism and ascorbate deficiency may lower plasma ferritin levels independent of iron stores (Brittenham, 2009).

In infancy and childhood, between the ages of 6 months and 15 years, the reference interval for serum ferritin is somewhat lower than in early infancy or adult life (Soldin, 2004). In men, serum ferritin gradually rises between the ages of 18 and 30 years, whereas in women, it does not. However, postmenopausal women have a much higher ferritin level than premenopausal women, and it is comparable with that of men (Van den Bosch, 2001). Serum ferritin levels do not display diurnal variation.

Erythrocyte Porphyrins. Because heme is formed by insertion of iron into protoporphyrin IX, the latter is increased in iron-deficient erythropoiesis, whether owing to iron deficiency or to anemia of chronic disease. It is also increased in lead poisoning and in some cases of sideroblastic anemia but is normal in thalassemia. Zinc usually becomes attached to protoporphyrin, forming zinc protoporphyrin (ZPP). A relatively simple micromethod measuring ZPP in whole blood has been shown to be useful in distinguishing microcytosis due to iron deficiency from that due to β-thalassemia minor (Labbé, 2004). The normal reference interval was 10 to 99 μg/dL of erythrocytes; in iron deficiency, erythrocyte porphyrins became elevated before the development of anemia, which may be one of the earliest indicators of iron deficiency (Labbé, 2004).

Serum Transferrin Receptors. TfRs also exist in a soluble form in the circulation. Serum TfRs (STfRs) are produced by shedding of membrane

TfRs during erythrocyte maturation. STfRs vary with the rate of erythropoiesis. Patients with aplastic anemia (AA) have lower than normal levels of STfRs, and patients with autoimmune hemolytic anemia have higher values. IDA is associated with increased serum levels of TfRs, probably as a result of increased membrane TfR synthesis and expression secondary to iron starvation. Unlike serum ferritin, STfRs are usually not affected by inflammation (Clark, 2009).

Serum Transferrin Receptor–to–Serum Ferritin Ratio. The serum transferrin receptor–to–serum ferritin (STfR/F) ratio has been suggested as a new approach to estimate total body iron stores. However, it appears to have limited value in identifying anemia of chronic disease (ACD). The STfR/F ratio may be better utilized in identifying IDA coexisting with ACD (Clark, 2009).

Reticulocyte Hemoglobin Content. Some automated hematology analyzers offer an assay of Hb content within reticulocytes (Ret-He, CHr; in pg/cell). By measuring this parameter, the status of erythropoiesis in the previous 3 to 4 days may be assessed using reticulocytes as a guide (Clark, 2009).

Hepcidin Level. Measuring plasma hepcidin may serve as a valuable tool in the study of abnormalities of iron metabolism, hemochromatosis, anemia of inflammation, and iron deficiency. Hepcidin level measurement is currently undergoing numerous studies.

Differential Diagnosis

Anemia due to iron deficiency usually needs to be distinguished from other causes of microcytosis with or without anemia. These include the thalassemia traits, long-standing ACD, and the sideroblastic anemias (see later discussions of these entities). Bone marrow storage iron and serum ferritin will be decreased in iron deficiency and normal or elevated in all others. In **thalassemia trait**, the anemia, if present, is very mild, the ZPP is normal, serum iron is normal, and the condition is present in family members. In β-thalassemia trait, HbA_2 and sometimes fetal hemoglobin (HbF) are increased. Yet, HbA_2 is often decreased in iron deficiency. In **ACD** (chronic infection, inflammatory conditions such as rheumatoid arthritis, or neoplastic disease), although the serum iron is low, as in iron deficiency, the TIBC is low or normal. In the **sideroblastic anemias**, which include chronic lead poisoning, the serum iron and percent TIBC saturation are increased, and pathologic "ring" sideroblasts are present in the marrow.

Management

The first principle in therapy of IDA is that the underlying cause can be identified and corrected. Ferrous iron is given orally—at about 200 mg/day—in three doses between meals. This will provide 40 to 60 mg of absorbed iron per day, which, with the iron produced by turnover of senescent red cells, will be sufficient to increase production to two or three times normal (Hillman, 1996). The reticulocyte count will reach a maximum at 5 to 10 days and then will gradually decrease toward normal. Monitoring the Hb is best; Hb should increase by 0.1 to 0.2 g/dL per day after the fifth day and by at least 2 g/dL for each of the subsequent 3 weeks. After the Hb has returned to normal, iron therapy should be continued for at least 2 months to replenish storage iron. Patients refractory to treatment need to be investigated for continued underlying diseases, particularly chronic gastritis and *Helicobacter pylori* gastritis (Clark, 2009). In recent years, there has been significant improvement in iron supplements available through intravenous route. Some of these products, such as low-molecular-weight iron dextran, have a stable carbohydrate shell that prevents the release of free iron and enhances their safety (Camaschella, 2019).

Iron-Refractory Iron Deficiency Anemia (IRIDA)

This is a recently described hereditary recessive microcytic anemia, which does not respond to oral iron therapy. Initial studies suggest that IRIDA is caused by a mutation in the *TMPRSS6* gene (mapped to chromosome 22q12-13) encoding a transmembrane serine protease known as matriptase-2 (MT-2). As mentioned before, MT-2 is involved in the downregulation of hepcidin through modulating the HJV pathway. IRIDA patients have inappropriately high hepcidin levels, preventing iron absorption and release. Patients may show a slow or partial response to parenteral iron (Wang, 2019).

IMPAIRED PRODUCTION—MEGALOBLASTIC ANEMIA

Macrocytosis with Normoblastic Marrow

Macrocytic anemias that are not megaloblastic may be due to early release of erythrocytes from the marrow, so-called *shift reticulocytes*. This may occur in response to acute blood loss, hemolysis, bone marrow infiltration, and high levels of EPO associated with bone marrow failure diseases such as aplastic anemia, refractory anemia, and inherited bone marrow failure syndromes, including Diamond-Blackfan anemia. Nonmegaloblastic macrocytosis is also found in hypothyroidism, in individuals with excessive alcohol intake, and in liver disease (Hillman, 1996).

Megaloblastic Anemia

Blood

Macrocytic anemias associated with megaloblastosis differ from nonmegaloblastic macrocytic anemia in that macro-ovalocytes and giant hypersegmented neutrophils are present in the blood (Figs. 31.11, 31.15, and 33.6). Pancytopenia is the rule. The anemia is macrocytic with an elevated MCV and is characterized by macro-ovalocytes and often extreme degrees of anisocytosis and poikilocytosis, including red cell fragments. Microcytes and dacrocytes are common. Basophilic stippling, multiple Howell-Jolly bodies, nucleated red cells with karyorrhexis, and even megaloblasts may be seen in the peripheral blood. Leukopenia is present. Granulocytes have increased numbers of lobes (hypersegmentation), presumably as a result of abnormal nuclear maturation. Five lobes in more than 5% of the neutrophils constitute hypersegmentation (Herbert, 1985), as do any neutrophils with six or more lobes. Thrombocytopenia is usually encountered and on rare occasions is sufficiently severe to be responsible for bleeding. It is worth noting that significant morphologic changes may occur in the blood in the absence of anemia and that neurologic symptoms may be present in the absence of anemia.

Marrow. Megaloblastic anemia is characterized by enlargement of all rapidly proliferating cells of the body, including marrow cells. The major abnormality is the diminished capacity for deoxyribonucleic acid (DNA) synthesis. In cobalamin or folate deficiency, there is marked reduction in intracellular 5,10-methylene tetrahydrofolate, which is required to transform deoxyuridine monophosphate to deoxythymidine monophosphate. This reaction is mediated by thymidylate synthase and is essential to maintain the normal rate of DNA synthesis (Green, 2017). With such deficiency, the cells have both a prolonged intermitotic resting phase and a block early in mitosis. The number of mitotic figures is increased. Ribonucleic acid (RNA) synthesis is less impeded than DNA synthesis; hence, cytoplasmic maturation and growth continue, accounting for enlargement of the cells. The delicate chromatin and the prominent parachromatin result in a distinctly more "open" chromatin pattern than is seen in the erythroid precursors (Figs. 31.28 and 33.6). The nuclei undergo karyorrhexis readily, and multiple Howell-Jolly bodies may be present. Usually, more cells analogous to the pronormoblast and basophilic normoblast are noted (i.e., promegaloblast and basophilic megaloblast) than are seen in normal erythropoiesis. This has sometimes been termed *maturation arrest*, or *nuclear-cytoplasmic asynchrony*. Giant polychromatic megaloblasts are especially distinctive. The same general features are seen in the other cell lines. In the granulocytic series, the cells are larger, with retarded nuclear maturation and large cytoplasmic mass. Often, the specific granules themselves are distinctly larger. The chromatin pattern is less condensed (more "open"). As a result, the nucleus appears to stain poorly. Abnormally contorted nuclear configurations are common. The giant metamyelocyte is the most characteristic of the abnormal granulocytes. Megakaryocytes, too, are large, polylobated, and have separated nuclear lobes or nuclear fragments (Green, 2017).

The bone marrow is hyperplastic (Fig. 33.7). The fat is replaced, and red marrow extends into the long bones. The number of erythroid precursors (megaloblasts) is increased, and the myeloid/erythroid ratio is decreased. If the megaloblastic process is incompletely developed or if the patient has been inadequately treated, the findings may be only partial. Because they persist longer, granulocytic alterations are especially helpful in assessing recently treated megaloblastic anemia. Marrow findings result from the effects of impaired nucleic acid synthesis, leading to megaloblastosis and hypoxic stress, giving rise to increased numbers of erythroid cells. If the patient is transfused with packed red cells, the number of erythroid precursors diminishes but the cytologic abnormalities persist.

Erythrokinetics. In megaloblastic anemias, the mass of erythroid tissue is increased, plasma iron turnover is rapid, and urine and fecal urobilinogen are increased. These measures indicate an **increase in total erythropoiesis** that may be up to three times normal. The decreased rate of appearance of iron in the Hb of circulating erythrocytes and reticulocytopenia indicate **ineffective erythropoiesis**. In addition to increased destruction of defective erythroid precursors in the marrow, survival of circulating erythrocytes is short, indicating hemolysis. Indirect serum

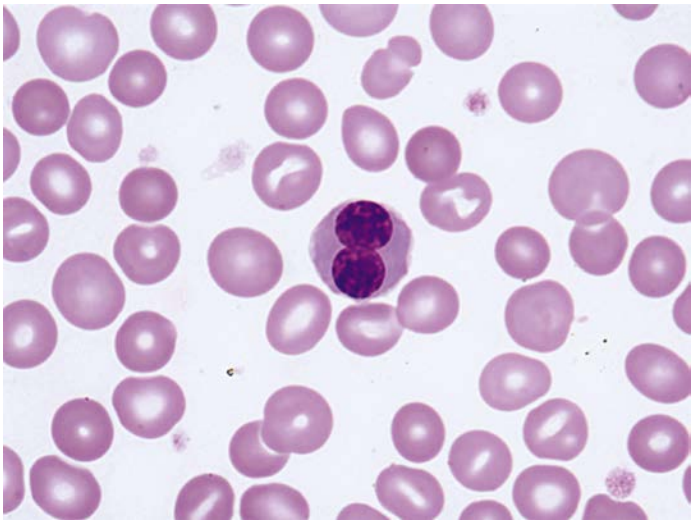

Figure 33.6 Blood film, megaloblastic anemia. Macrocytosis and a circulating megaloblast with abnormal, binucleated nucleus and open chromatin.

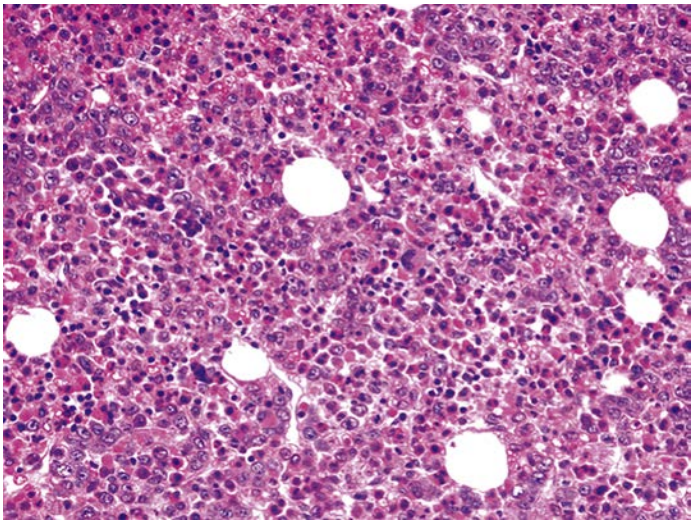

Figure 33.7 Hypercellular marrow in megaloblastic anemia. Cellularity is over 95%.

bilirubin is increased, serum iron is increased, endogenous carbon monoxide (CO) production is increased, and serum lactate dehydrogenase (LD) is usually greatly elevated. Serum muramidase may be elevated, implying ineffective granulocytopoiesis.

Megaloblastic anemia is nearly always due to cobalamin or folic acid deficiency. The aforementioned findings are similar for either.

Cobalamin (Vitamin B_{12}) Metabolism

Vitamin B_{12} (cyanocobalamin) has a molecular weight of 1355 Da. The molecule's two major parts are (1) a **planar group** (the corrin nucleus), a ring structure surrounding a cobalt atom; and (2) a **nucleotide group**, which consists of the base, 5,6-dimethylbenzimidazole, and a phosphorylated ribose esterified with 1-amino,2-propanol. A cyanide group is in coordinate linkage with the trivalent cobalt. Different forms of vitamin B_{12} result from replacement of the cyanide by hydroxy, adenosyl, or methyl groups; generically, these are termed **cobalamins**.

Cobalamin is the only vitamin exclusively synthesized by microorganisms. It is found in practically all animal tissues and is stored primarily in the liver in the form of adenosylcobalamin. The human liver contains approximately 1 μg/g of liver. Cobalamin is released from food by gastric acid and peptic digestion and then becomes bound to R binders (cobalamin-binding proteins with *R*apid electrophoretic mobility compared with intrinsic factor) present in saliva. The R proteins belong to the same family of isoproteins as the plasma haptocorrin (HC) binder (Green, 2017). Salivary HC protects vitamin B_{12} from the acidic environment in the stomach. On entering the duodenum, cobalamin is released from salivary HC by pancreatic enzymes to finally bind to gastric intrinsic factor (IF), a 44-kDa glycoprotein produced in the parietal cells of the stomach. The gene for IF is located on chromosome 11. This cobalamin–IF complex, which is highly resistant to digestion, then adheres to specific receptor sites on the epithelial cells of the ileum, at which site the cobalamin is absorbed. The cobalamin–IF receptor is a combination of two proteins: a 460-kDa protein called *cubilin* (CUBN) and a 45- to 50-kDa protein called *amnionless* (AMN). CUBN lacks both transmembrane and cytoplasmic domains and its internalization depends on other transmembrane proteins, particularly AMN. Both proteins are also present in renal tubules. Mutation of any of the two genes can produce megaloblastic anemia with proteinuria, also known as *Imerslund-Gräsbeck syndrome* (Kozyraki, 2013). The concentration of the receptor in the ileum increases progressively until it reaches its maximum near the terminal ileum. The cobalamin–IF complex is taken into the cell, where cobalamin is released and the IF is destroyed. The receptor recycles to the surface of the cell (Kozyraki, 2013). Cobalamin is exported from the enterocyte with multidrug resistance protein 1 (Green, 2017).

Cobalamin is transported in the plasma as methylcobalamin, with 10% to 30% bound to transcobalamin (TC), formerly known as *transcobalamin II* and 70% to 90% bound to HC (variously called TC I, TC III, R binder, cobalophilin; see later discussion). Ninety percent of *newly absorbed* cobalamin is bound to TC, which serves as the chief transport protein, rapidly delivering the vitamin to the liver, hematopoietic cells, and other dividing cells, which express transcobalamin receptors (CD320). The HC-bound cobalamine is not immediately available for body cells but it acts as a passive reservoir in equilibrium with body stores in the liver but not taken up by other body cells. The reference values for plasma cobalamin depend on the method of assay, but they commonly are 200 to 900 ng/L (150–670 pmol/L). The relative importance of the transcobalamins is illustrated by the clinical effects of congenital deficiency. Lack of TC results in severe megaloblastic anemia in infancy; yet, the serum cobalamin level is normal. Lack of HC is not accompanied by anemia or megaloblastosis; yet, the serum cobalamin level is decreased.

HCs are found in milk, plasma, saliva, gastric juice, and other body fluids. HC may arise from granulocytes, salivary glands, and liver, as well as from other tissues. HC may help clear nonphysiologic cobalamin analogs. Elevation of HC accounts for the elevation of total cobalamin-binding proteins in myeloproliferative neoplasms. TC is also synthesized by a variety of cells, including renal cells, enterocytes, and hepatocytes, and acts as an acute-phase reactant; its levels are increased in inflammatory and infectious conditions (Carmel, 1999; Green, 2017). In humans, cobalamins are involved in two important enzymatic reactions: a mitochondrial reaction involves the formation of succinyl coenzyme A (CoA) from methylmalonyl CoA utilizing adenosyl cobalamin; the second is a cytosolic reaction involving the acquisition of a methyl group from N^5-methyl tetrahydrofolate through the conversion of homocysteine to methionine and, thus, forming tetrahydrofolate. The latter reaction allows tetrahydrofolate to change to 5,10-methylene tetrahydrofolate, which is the most important methyl donor for the formation of deoxythymidine from deoxyuridine. Therefore, to be useful to the cell, cyanocobalamin and hydroxocobalamin must be converted to adenosyl and methyl forms through reduction and alkylation (Green, 2017; Zheng, 2019). In the absence of a sufficient amount of deoxythymidine, deoxyuridine will be incorporated in DNA, which will ultimately result in DNA strand breaks, fragmentation, and apoptotic cell death (Green, 2017). The daily requirement for cobalamin is 0.4 μg/day for infants and 2.4 μg/day for adults (Salinas, 2018). The body's stores of 2 to 5 mg will last for several years if intake is cut off, as is the case when total gastrectomy is performed (Beck, 1991).

Cobalamin Deficiency

Although the true prevalence of cobalamin deficiency in the general population is unknown, it increases with age. Approximately 15% of adults older than 65 years have laboratory findings of vitamin B_{12} deficiency. This prevalence may be attributed to the high frequency of hypochlorhydria of 25% to 50%, which has been reported in the elderly population. The widespread use of proton pump inhibitors to control gastric secretion, inflammatory bowel disease, and gastric and small intestinal resections are contributing factors (Salinas, 2018). Cobalamin deficiency is produced by any of several mechanisms that are not always exclusive of each other and involve inadequate intake and reduced absorption.

Inadequate Intake

A dietary deficiency is an *extremely rare* cause of megaloblastic anemia in the United States and is seen only in persons who completely abstain from

animal food, including milk and eggs. Only strict vegetarians are known to develop this form of cobalamin deficiency.

Defective Production of Intrinsic Factor

This is the most common cause of cobalamin deficiency.

Pernicious Anemia

Pernicious anemia (PA) is a "conditioned" nutritional deficiency of cobalamin that is caused by failure of the gastric mucosa to secrete intrinsic factor. This abnormality is genetically determined but usually is not manifested until late in life; less than 10% of cases occur in persons younger than age 40 years. The annual incidence of PA is approximately 25 new cases per 100,000 individuals over the age of 40 years and the prevalence is higher in women (Salinas, 2018). Positive family history is obtained in approximately 30% of patients. Modern surveys indicate that PA is as common in blacks as in whites (Carmel, 1999).

Clinical Features

Symptoms of **anemia** and the combination of skin pallor and jaundice giving a lemon-yellow appearance to the skin are often present. The tongue may be sore, smooth, and pale (atrophic glossitis) or red and raw (acute glossitis). **GI symptoms** may be prominent and include episodic abdominal pain, constipation, and diarrhea. Diffuse and irregular degeneration of the white matter of the **central nervous system (CNS)** characteristically involves the posterior and lateral columns of the spinal cord (subacute combined degeneration) and sometimes other sites. Symmetric sensations of "pins and needles" of the distal extremities, numbness and tingling, loss of position sensation (difficulty with balance and gait), and loss of vibratory sensation (perhaps the most constant sign) are indicative of peripheral neuropathy and posterior column lesions. Lateral column involvement gives rise to weakness, spasticity, and increased deep tendon reflexes. Sometimes, the brain may be affected, and the patient shows irritability, emotional instability, or a change in personality. Neuropsychiatric disorders may be associated with cobalamin deficiency even without accompanying hematologic manifestations (Lindenbaum, 1988). Recent studies suggest that cobalamin is essential for the maintenance of certain levels of cytokines and growth factors in the CNS. Cobalamin deficiency has been reported to cause an increase in CSF levels of myelinotoxic cytokines, such as tumor necrosis factor-α, while decreasing myelinotrophic cytokines, such as interleukin (IL)-6 (Scalabrino, 2009).

Gastric Findings

Atrophic gastritis of varying degrees is found in most adults with PA, and gastric atrophy involving all coats of the wall in the remainder. IF and hydrochloric acid (HCl) are secreted by gastric parietal cells in the human. In adult PA, IF secretion is absent, and almost always histamine-refractory achylia and achlorhydria—decreased volume of gastric juice and lack of HCl secretion—are present.

Immune Abnormalities

Autoantibodies have been found in the serum of patients with pernicious anemia (Green, 2017). **Anti–parietal cell antibodies** react with gastric parietal cells, which secrete both HCl and IF, and are present in more than 90% of patients. These anti–parietal cell antibodies are also present in patients with chronic gastritis, such as that associated with iron deficiency, and in some patients with thyroiditis and myxedema; they are seen in 4%–5% of age-matched healthy individuals. When these antibodies are chronically injected into rats, they decrease gastric HCl, IF, and pepsin secretion and produce gastric atrophy. The major antigen to which these antibodies are produced is the acid-producing enzyme H^+, K^+-ATPase, a 92-kDa protein present on the luminal membrane of parietal cells, which is the target of proton pump inhibitors. A recent study suggests that antibodies to *H. pylori* are common in PA, particularly in young patients. Infection may be the first step toward initiation of an autoimmune response (Hershko, 2007).

Another type of autoantibody is directed against intrinsic factor. **Anti–intrinsic factor antibodies** occur in the serum, saliva, and gastric juice of about 75% of patients with PA. Two types of anti-IF antibodies occur: "blocking" antibodies, which block the binding of cobalamin to IF; and "binding" antibodies, which bind to the cobalamin–IF complex and prevent the complex from binding to receptors in the terminal ileum. Although these antibodies can cause some functional impairment in vivo, it is not clear whether the antibodies are the cause or an effect of the disease. IF antibodies in the absence of PA occur in a small percentage of individuals with hyperthyroidism (Graves disease) and similarly in persons with insulin-dependent diabetes. Therefore, IF antibodies are considered highly specific and confirmatory for PA although their absence does not exclude the diagnosis (Green, 2017).

Family studies in patients with PA have shown an increased incidence of the disease in relatives, and many relatives have achlorhydria and partial defects of cobalamin absorption. Relatives of patients with PA also have a higher incidence of gastric parietal cell antibodies and of thyroid antibodies than normal individuals.

It is possible that adult PA is a genetically determined autoimmune gastritis. However, the relationship of the gastric lesion to the antibodies remains unclear. Patients with PA have an annual incidence of gastric cancer at 0.1% to 0.5% (Salinas, 2018).

Pernicious Anemia in Children

Two forms of PA are known to occur in children. **Congenital or infantile pernicious anemia** usually appears early in the second year of life. IF secretion may be lacking or the secreted IF may be functionally defective, but acid secretion and the appearance of the gastric mucosa are normal. Antibodies to parietal cells and to IF are absent. These cases are caused by mutations in the IF gene (*GIF*) mapped to chromosome 11q12. **Juvenile pernicious anemia** occurs usually in older children and is like that of adults, with gastric atrophy, achlorhydria, and serum antibody to IF and parietal cells, although the latter may be absent in a subset of patients (Whitehead, 2006).

Gastrectomy

Surgical removal of the stomach (total or even subtotal occasionally) will remove the source of IF. This will lead to megaloblastic anemia after the body's stores of cobalamin have been exhausted—in 3 to 6 years—if cobalamin therapy has not been given. Frequently, the anemia is due in part to iron deficiency.

Defective Absorption of Cobalamin

Malabsorption Syndromes. Celiac disease, tropical sprue, resection of the small bowel, or inflammatory disease of the small bowel may be associated with multiple defects of absorption, including other vitamins. Folic acid deficiency (absorbed principally in the upper small bowel) is more commonly seen than cobalamin deficiency (absorbed principally in the lower small bowel) in diseases leading to malabsorption. The reason for this is probably the lesser time necessary for depletion of body stores of folic acid.

Imerslund-Gräsbeck syndrome is an autosomally recessive inherited defect in the intestinal absorption of cobalamin that occurs in the presence of normal IF. In many patients, proteinuria of the tubular type is also found. Most reported cases are from Northern Europe. As mentioned earlier, the syndrome is caused by a defect in the CUBN/AMN receptor (Kozyraki, 2013).

Lack of Availability of Cobalamin. In certain countries, infestation with the fish tapeworm *Diphyllobothrium latum* is common enough that cobalamin deficiency may occur occasionally when it is present. The worm successfully competes with the host for the ingested cobalamin. Most common in Finland, it is rarely seen in the United States.

Bacteria in a blind loop of intestine may also preferentially utilize ingested cobalamin to the detriment of the host.

As mentioned earlier, inherited TC deficiency leads to megaloblastic anemia accompanied by neurologic symptoms in early childhood.

Another cause of inactivation of vitamin B_{12} is the use of nitrous oxide (N_2O) gas as an anesthetic and sometimes as a recreational drug. It affects mostly individuals who have low levels of vitamin B_{12} (Green, 2017).

Vitamin B_{12} or folate deficiency may exert indirect cardiovascular effects. Both deficiencies are associated with hyperhomocystinemia, which is an independent factor for atherosclerosis and vascular thrombosis (Green, 2017).

Diagnosis of Cobalamin Deficiency

Recognition of megaloblastic anemia indicates the likelihood of cobalamin deficiency or folic acid deficiency. In addition, evidence of neurologic involvement favors cobalamin deficiency. This diagnosis can be established by one of four methods.

Therapeutic Trial. With the patient on a diet low in cobalamin and folate, a parenteral physiologic dose of cobalamin (10 μg/day) is given. Optimal hematologic response indicates deficiency and consists of reticulocytosis beginning on the third or fourth day, reaching a peak on the seventh day. Erythropoiesis becomes normoblastic by 2 days, and leukopoiesis becomes normal by 12 to 14 days. Within a week, leukocyte and platelet counts have returned to normal, and the Hb concentration begins to rise.

Serum Cobalamin Assay. This is the usual method of detecting a cobalamin-deficient state. The original microbiological assay of serum cobalamin employed an organism (e.g., *Euglena gracilis*) that requires cobalamin for growth. Although the microbiological method is precise and reliable, it requires at least 48 hours of incubation and is subject to the inhibitory effects of antibiotics. These microbiological assays have been largely abandoned and replaced by immunochemical assays measuring serum vitamin B_{12}. Reference values are 200 to 900 ng/L. In megaloblastic anemia due to cobalamin deficiency, serum cobalamin is usually less than 100 ng/L. Individuals with folate deficiency and mild cobalamin deficiency and who are pregnant have borderline values between 100 and 200 ng/L. Patients with human immunodeficiency virus (HIV) infection or multiple myeloma and those receiving megadose vitamin C therapy often have low serum cobalamin levels in the absence of clinical manifestations (Ward, 2002; Green, 2017). Spuriously normal cobalamin levels have been recorded in patients with cobalamin deficiency associated with overgrowth of intestinal bacteria, which produce biochemically inert B_{12} analogs, and in patients with autoimmune disorders, myeloproliferative neoplasms, and active liver disease (Ward, 2002). Measurement of TC–bound cobalamin (holotranscobalamin) may provide additional information in that its levels fall below the normal range long before total serum cobalamin does and probably represent a state of negative cobalamin balance (Zittoun, 1999). This marker is considered to be more accurate in assessing the biologically active fraction of vitamin B_{12} and has been proposed to be used also in assessing the absorption of vitamin B_{12} when measured before and after an oral dose of nonradiolabeled cobalamin (Green, 2017). Individuals with TC polymorphism 67A>G have abnormally low levels of holoTC in the absence of vitamin B_{12} deficiency (Salinas, 2018).

Methylmalonic Acid and Homocysteine Assays. Because a cobalamin coenzyme is essential for the isomerization of methylmalonate to succinate, urine excretion of increased amounts of methylmalonate is found in cobalamin deficiency. Provided that the rare inborn error of metabolism, methylmalonic aciduria, is not present, this is a sensitive test for cobalamin deficiency, but it is not usually necessary for the diagnosis. In addition, plasma levels of methylmalonic acid and homocysteine are increased in more than 90% of patients and their rise usually precedes the drop in serum vitamin B_{12} level. Plasma levels of methylmalonate are normal in folate deficiency in the absence of cobalamin deficiency (Green, 2017). Following several weeks of therapy, their plasma concentration returns to normal. Plasma levels of these metabolites should be interpreted with caution in patients with chronic renal failure because of the tendency of these metabolites to accumulate (Zittoun, 1999).

Deoxyuridine Suppression Test. This measures the ability of marrow cells in vitro to utilize deoxyuridine in DNA synthesis. Normally, in marrow cells, the major source of thymidine for DNA is de novo synthesis from deoxyuridine, which requires intact cobalamin and folate enzymes. Therefore, less than 10% of added tritium-labeled thymidine (^{3}H-Tdr) is incorporated into DNA. In megaloblastic marrows due to cobalamin or folate deficiency, deoxyuridine cannot be efficiently converted to thymidine, and more ^{3}H-Tdr is taken up into DNA. An abnormal deoxyuridine suppression test indicates cobalamin or folate deficiency. This test is very sensitive and produces abnormal results before anemia or macrocytosis is observed (Zittoun, 1999). It currently is seldom used as a diagnostic test.

Detecting the Cause of Cobalamin Deficiency

Clinical history is useful in suggesting whether cobalamin or folate deficiency is the cause of megaloblastic anemia. Clinical associations of PA include a family history of PA in one-third of patients, along with certain endocrine deficiencies (thyroid disease, diabetes mellitus, hypothyroidism, and Addison disease) and immune disorders (immune thrombocytopenic purpura, autoimmune hemolytic anemia, and acquired hypogammaglobulinemia). Cobalamin deficiency is likely to occur in strict vegetarians and in patients with paresthesias, neuropathy, or a previous gastrectomy.

In cobalamin-deficient patients, it is important to determine whether IF is lacking. To do so, the ability of the patient to absorb an oral dose of radioactive cobalamin may be measured. The Schilling test, which measures radioactivity in a 24-hour sample of urine, is now rarely used. Two hours after oral administration of 0.5 to 2.0 μg of radioactive cobalamin, a large "flushing" dose of nonlabeled cobalamin is given parenterally. Normal individuals will excrete more than 7% of a 1-μg dose of ingested cobalamin in the urine in 24 hours, whereas patients lacking IF will excrete less. If excretion is low, the test must be repeated using the same procedure, except that hog IF is given orally, along with labeled cobalamin. If 24-hour excretion is normal, the low value in the first part was due to IF deficiency. If excretion remains abnormal in the second part of the procedure, an explanation for malabsorption of cobalamin on the basis of intestinal disease must be sought. The test may be repeated after 7 to 10 days of antibiotic administration if bacterial overgrowth is suspected, and pancreatic extracts may be added to investigate the possibility of pancreatic dysfunction. The validity of the results depends on good renal function and accurate urine collection. The Schilling test will be abnormal in PA even after the patient is treated with cobalamin and is in remission. Some patients may absorb vitamin B_{12} in water (as given in the original Schilling test) but fail to absorb vitamin B_{12} bound to protein in food. A modification of the Schilling test is being introduced to include protein-bound B_{12} using egg yolk or chicken serum (Zittoun, 1999).

Other tests that will establish the diagnosis of PA include direct assay of IF in gastric juice. The combination of megaloblastic anemia, decreased serum cobalamin, and the presence of serum antibodies to IF is essentially diagnostic of PA, obviating the need for the Schilling test (Lindenbaum, 1983). As mentioned earlier, the use of holoTC before and after oral dose of vitamin B_{12} may be an alternative to test vitamin B_{12} absorption defects. The combined assessment of antibodies to IF and parietal cells increase diagnostic sensitivity for PA to 73% and diagnostic specificity to almost 100% (Salinas, 2018).

Folic Acid Metabolism

Folic acid (or pteroylmonoglutamic acid) contains three parts: pteridine, *p*-aminobenzoate, and L-glutamic acid (Babior, 2001). In nature, folic acid occurs mainly as less soluble polyglutamates, with multiple glutamic acid residues attached to one another by peptide bonds. Folic acid is present in a wide variety of foods, such as eggs, milk, leafy vegetables, yeast, liver, and fruits, and is formed by intestinal bacteria as well. Folates are extremely thermolabile; prolonged cooking (>15 minutes) in large quantities of water in the absence of reducing agents destroys folate.

Polyglutamates are hydrolyzed to monoglutamate by folate hydrolase, which is present in the brush border of proximal jejunum and has maximal exopeptidase activity at pH 6.5 (Visentin, 2014). Folate monoglutamates are transported across the intestinal membrane by a variety of carriers, including reduced folate carrier (Solute Carrier [SLC] 19A1) and PCFT (SLC46A1). The latter has been shown to be the most important folate transporter. It is highly expressed at the upper region of the small intestine and is most active at acidic pHs (Zheng, 2019). PCFT is also present in colonic mucosa but at a much lower concentration. In the plasma, one-third of the folate is free and two-thirds is nonspecifically and loosely bound to serum proteins. A small amount of folate is specifically bound to folate-binding proteins, the physiologic significance of which is unclear. Folate is rapidly removed from plasma to cells and tissues for utilization. The principal form of folate in serum, erythrocytes, and liver is 5-methyltetrahydrofolate (5-methyl-FH_4); the liver is the chief storage site. Uptake of folate by the cells is dependent on three folate receptors (FOLR1 to FOLR3), one of which has been shown to be deficient in a condition known as *cerebral folate deficiency* (Baumgartner, 2013, Zheng, 2019). Intracellular folates exist primarily as polyglutamates. A significant enterohepatic circulation is present, and bile contains 2 to 10 times the folate concentration of normal serum. Moreover, folates that are filtered in the renal glomeruli are extensively reabsorbed back into the renal circulation (Visentin, 2014). The minimal daily requirement is about 50 μg of pteroylmonoglutamate or 400 μg of total folate; a typical reference interval for serum folate is 5 to 21 μg/L (11–48 nmol/L), and for red cell folate, 150 to 600 μg/L (340–1360 nmol/L) of RBCs.

The Folate–Cobalamin Relationship

Anemia of cobalamin deficiency is partially corrected by folate even in the absence of cobalamin supplementation, but the reverse is not true. This is because folic acid will be reduced to dihydrofolate and tetrahydrofolate, partially and temporarily alleviating the anemia component. Therefore, some of the megaloblastic manifestations in cobalamin deficiency are actually caused by abnormalities in folate metabolism. The most accepted theory for their interrelationship is the methylfolate trap theory. This theory is based on the observation that the methyl form of tetrahydrofolate (FH_4) would leak out of cells unless conjugated to form polyglutamates. Methyl FH_4 is a poor substrate for the conjugating enzyme. Cobalamin is essential for the process of conversion of methyl FH_4 to FH_4 through the conversion of homocysteine to methionine. Absence of cobalamin causes accumulation of methyl FH_4, which is followed by its leakage out of the cells (Zheng, 2019).

Folic Acid Deficiency

Inadequate Intake of Folate

Evolution of Laboratory Abnormalities. Herbert delineated the sequence of events in the onset of folate-deficient megaloblastic anemia. After a folate-deficient diet was initiated, various abnormalities were established as follows: 3 weeks, low serum folate; 5 weeks, hypersegmented neutrophils in bone marrow; 7 weeks, hypersegmented neutrophils in peripheral blood, with bone marrow showing increased and abnormal mitoses and basophilic intermediate megaloblasts; 10 weeks, bone marrow showing some large metamyelocytes and polychromatophilic intermediate megaloblasts; 13 weeks, high excretion of formiminoglutamic acid (FIGLU) in urine; 17 weeks, low erythrocyte folate; 18 weeks, macroovalocytosis of erythrocytes with many large metamyelocytes in bone marrow; 19 weeks, overtly megaloblastic bone marrow; and 20 weeks, anemia (Herbert, 1985).

At this time, changes in the intestinal epithelium have not yet appeared. Therefore, in the human, with no dietary intake of folic acid, anemia will appear in 3 to 6 months. The peripheral blood and bone marrow features of megaloblastic anemia due to folic acid deficiency are similar to those of cobalamin deficiency; however, leukopenia and thrombocytopenia are less constant. Folic acid deficiency has usually been found in association with some complicating factor.

Nutritional Folate Deficiency. Megaloblastic anemia due to lack of folate is most commonly associated with insufficient dietary intake. The usual diet does not contain much above the minimal requirements, and body stores in the adult are sufficient for only about 3 months' needs. Dietary folate deficiency is especially common in the tropics and in India and, even in those locations, it is usually associated with increased demand for folate in pregnancy, rapid growth in infancy, infection, or hemolytic anemia. Elderly persons on inadequate diets in the United States may develop folate-deficient megaloblastic anemia.

Folate deficiency in infancy is uncommon in the United States. Human milk or fresh cow's milk contains sufficient folate; heated milk, powdered milk, and goat's milk do not. If the infant's milk lacks folate, if the diet is low in ascorbic acid, or if infection or diarrhea is a problem, megaloblastic anemia may occur.

Megaloblastic anemia in pregnancy is not uncommon because of the fetal requirements for folate. The mother's plasma folate level gradually falls during pregnancy, and at birth the plasma level in the newborn averages five times that of the mother. Megaloblastic anemia is more frequent in multipara, may be precipitated by infection, and is usually due to folate deficiency rather than cobalamin deficiency. Pregnant women should receive, in addition to iron, folic acid supplements. Recent studies indicate that folate supplementation for pregnant women reduces the risk of giving birth to babies with neural tube defects, with anencephaly and spina bifida being the most common defects. It has been estimated that more than 50% of neural tube defects in babies are related to maternal folate deficiency in the periconceptual period (Baumgartner, 2013).

Liver Disease. Liver disease associated with alcoholism may be associated with folate-deficient megaloblastic anemia because of the grossly inadequate diet of the alcoholic and because the liver is the major site for folate storage and metabolism. With adequate dietary folic acid intake, however, the anemia that is found with liver disease is macrocytic and normoblastic—not megaloblastic.

Defective Absorption of Folate

Defective absorption of folic acid occurs in association with malabsorption syndromes discussed previously and in the blind loop syndrome, in which bacteria preferentially utilize folate.

Nontropical sprue, or adult celiac disease, is an important cause of malabsorption in adults or children that is related to dietary gluten (wheat protein). Included among the signs of malabsorption may be megaloblastic anemia due to folic acid deficiency (Beck, 1991). Jejunal biopsy shows villous atrophy. The folate deficiency, as well as the malabsorption, responds to a gluten-free diet. Folic acid therapy (parenteral) corrects the folate deficiency but not the general malabsorption.

Tropical sprue is a poorly understood malabsorptive disorder that is common in the Caribbean, India, and Southeast Asia. It can be acquired by travelers to those regions and persists for many years after the travelers return. Evidence of malabsorption includes megaloblastic anemia due to folate deficiency. Treatment with folic acid brings considerable improvement in general malabsorption, as well as in the anemia, but additional antimicrobial treatment is recommended.

Megaloblastic anemia or decreased serum and red cell folate without anemia has been associated with the long-term use of anticonvulsant drugs such as phenytoin, phenobarbital, and primidone. The problem appears to be a drug-induced malabsorption of pteroylpolyglutamate. Oral contraceptives cause malabsorption of folate in a small proportion of women owing to impaired deconjugation of pteroylpolyglutamate (Beck, 1991).

Hereditary folate malabsorption is a rare autosomal-recessive condition caused by mutation affecting the gene encoding the PCFT (SLC46A1) molecule (Visentin, 2014).

As mentioned earlier, cerebral folate deficiency is caused by a defective cerebral folate transport system, caused in most cases by mutation in FOLR1. Patients present in late infancy with severe developmental delay, motor dysfunction, and epilepsy. Oral folinic acid may improve the symptoms (Baumgartner, 2013, Zheng, 2019).

Increased Requirement for Folate

The increased need for folate in pregnancy and in infants has been mentioned. Increased cell turnover that occurs in neoplasia and in the markedly stimulated hematopoiesis of hemolytic anemias may result in megaloblastic erythropoiesis. The basis for this is the increase in need for a marginal supply of folate.

Inadequate Utilization of Folate

Inadequate utilization of folic acid is relatively rare. Folic acid antagonists such as methotrexate block folic acid metabolism—because of this, they are used in therapy of some malignant neoplasms. In addition to inhibiting growth of the tumor, they induce megaloblastic hematopoiesis.

In addition to the previously mentioned nutritional problem in alcoholics, **alcohol** may exert a direct effect in suppressing hematopoiesis by blocking the metabolism of folate. In addition, alcohol can interfere with folate absorption and folate enterohepatic circulation, usually resulting in increased loss of folate in urine. Animal studies suggest that alcohol may decrease the expression of PCFT (Visentin, 2014). Plasma homocysteine is usually elevated in alcoholics.

Diagnosis of Folate Deficiency

Folic acid deficiency or cobalamin deficiency is suspected when the blood and bone marrow show findings characteristic of megaloblastic anemia. Usually, serum folate and cobalamin levels are then determined. Some cases may be associated with marked red cell fragmentation simulating microangiopathic hemolytic anemia. Severe folate deficiency in pregnancy may mimic the syndrome of hemolysis, elevated liver enzymes, and low platelets (HELLP syndrome; see later discussion).

Serum and Red Cell Folate. A microbiological assay for folic acid activity employing *Lactobacillus casei* is a reliable method for definitive diagnosis (Beck, 1991). However, these assays are laborious, have poor precision, and are affected by antibiotics. Radioisotopic and chemiluminescence methods employing different folate binders are widely used because of their rapidity and greater convenience. Commonly used assays utilize folate-binding protein to capture serum folate. Unlike serum folate (which is entirely 5-methyltetrahydrofolate), red cell folates are a heterogeneous mixture of different forms with varying polyglutamate chain lengths, which pose challenges to nonmicrobiological assays.

The serum folate level is decreased (<3 μg/L) in megaloblastic anemia due to folate deficiency but is usually normal or increased in cobalamin deficiency. A low serum folate level precedes a decrease in red cell or tissue folate. It indicates a negative folate balance but does not by itself indicate tissue folate deficiency. Serum folate is highly sensitive to folate intake and may normalize after a single adequate meal despite the presence of true underlying deficiency. In cobalamin deficiency, serum folate is decreased in 10% of cases, increased in 20%, and normal in the remainder (Tietz, 1990).

Red cell folate is a better test of body folate stores and is decreased in megaloblastic anemia due to folate deficiency. In cobalamin deficiency, however, red cell folate is low in almost two-thirds of cases; thus, this needs to be excluded before a low red cell folate is taken as proof of severe folate deficiency. Therefore, three measurements are often useful in distinguishing between deficiencies of folic acid and cobalamin (Table 33.2).

Physiologic doses of folic acid (parenteral, 50–200 μg/day) will allow an adequate reticulocyte response in patients with folic acid deficiency, but not with cobalamin deficiency. On the other hand, the usual therapeutic doses of folic acid (5–15 mg/day) or larger doses of cobalamin (500–1000 μg) may induce a partial response in a patient with megaloblastic anemia due to the other deficiency. Treatment of cobalamin deficiency with folic acid is hazardous in that, although a reticulocyte response may occur, neurologic damage will progress.

Urinary Formiminoglutamic Acid (FIGLU)

Folic acid coenzymes are required for the conversion of FIGLU to glutamic acid in the catabolism of histidine. When oral histidine is given, FIGLU will appear in increased amounts in the urine if folate deficiency is present. The test is useful in patients with megaloblastic anemia due to antifolate drugs; these patients have normal serum folate levels but greatly decreased tissue coenzyme levels (Beck, 1991).

Deoxyuridine Suppression Test. See earlier discussion.

Plasma Homocysteine Assay. As with cobalamin deficiency, total plasma homocysteine is increased in approximately 75% of patients with folate deficiency. The level of methylmalonic acid is normal (Green, 2017).

Acute Megaloblastic Anemia

Acute megaloblastic anemia may develop over the course of only a few days. The most common cause has been related to N_2O anesthesia. N_2O rapidly destroys methylcobalamin, causing a rapidly progressive megaloblastic anemia. Acute folate deficiency may occur in some patients in intensive care units because of a combination of factors (decreased intake, total parenteral nutrition, dialysis, surgery, sepsis, medications). These patients may present with rapidly progressive thrombocytopenia in the absence of hypersegmented neutrophils. Serum folate may be normal (Green, 2017).

Therapy for Megaloblastic Anemia

Although it may be necessary to treat severely anemic patients with both vitamins, it is usually possible to determine which deficiency is the cause and treat only for that.

The maximal reticulocyte response occurs in 5 to 7 days. Within 4 to 6 hours after the initial therapy (if parenteral), the marrow shows decreased early megaloblasts and the appearance of pronormoblasts. Within 2 to 4 days, the marrow is predominantly normoblastic. Granulocytic abnormalities return to normal more slowly, and hypersegmented neutrophils disappear from the blood only after 12 to 14 days.

PA is treated parenterally with 1000 μg of cyanocobalamin daily for 1 week, once weekly for 1 month, then monthly for the lifetime of the patient (Salinas, 2018). High concentrations of oral cobalamin (e.g., 1000 μg per day) force absorption of approximately 1% through an alternate system. Some reports recommend the use of oral cobalamin therapy instead of injections (Green, 2017).

In folate deficiency, oral therapy is generally used at a dosage of 1 to 2 mg/day. Cobalamin deficiency must be excluded and corrected if present to avoid the occurrence of neuropathies of cobalamin deficiency. Supplemental dietary folic acid during pregnancy is reported to reduce the incidence of neural tube defects in infants.

Other Defects of Nucleoprotein Synthesis

Other defects of nucleoprotein synthesis may lead to megaloblastic anemias that do not respond to cobalamin or folic acid.

Congenital Defects

Orotic aciduria is a very rare autosomal-recessive condition in which certain enzymes required for pyrimidine synthesis are absent. Findings include excessive urinary excretion of orotic acid, failure of normal growth and development, and megaloblastic anemia that is refractory to cobalamin and folate but that responds to uridine.

Inborn defects in enzymes involved in folate metabolism, including methyltetrahydrofolate reductase and glutamate formiminotransferase deficiencies, have been described. Similarly, disorders of enzymes responsible for converting cobalamin to its methyl or adenosyl forms causing methylmalonic aciduria, homocystinuria, or both have also been described (Baumgartner, 2013).

Synthetic Inhibitors

Synthetic inhibitors of purine synthesis (6-mercaptopurine, thioguanine, azathioprine), of pyrimidine synthesis (5-fluorouracil), or of deoxyribonucleotide synthesis (cytosine arabinoside or hydroxyurea) are used in chemotherapy for neoplasia and may concomitantly produce megaloblastosis.

Myelodysplastic Syndromes

Some macrocytic anemias are caused by myelodysplastic syndromes (see Chapter 34). They are associated with certain dysplastic features in the marrow or blood and will show no response to cobalamin or folate therapy.

IMPAIRED PRODUCTION—OTHER

Anemia of Inflammation (AKA Anemia of Chronic Disease)

Anemia of inflammation (AI) (Weiss, 2019) is an anemia syndrome typically found in patients with chronic infections or inflammatory or neoplastic disorders. It is characterized by reduced reticulocyte response accompanied by low serum iron despite adequate iron stores. It is also termed *anemia of chronic disease*, or *cytokine response*, although the term *anemia of inflammation* is now a more common term. Estimates suggest that up to 40% of all anemias worldwide can be considered AI or combined anemia with a significant AI component. The frequency is higher in the elderly population. AI has also been observed in acute trauma and critical care patients.

The anemia is mild to moderate, with Hb level rarely below 8 g/dL. Erythrocytes are usually normocytic and normochromic, although in 20% to 50% of patients, the anemia is microcytic and hypochromic. Anisocytosis and poikilocytosis are slight. The reticulocyte count usually is not elevated. Leukocytes and platelets are not distinctively altered, except by the causative disease.

The marrow is normocellular or minimally hypocellular or hypercellular, and the cell distribution is not greatly disturbed. The normoblasts may have frayed hypochromic cytoplasm, and the appearance of Hb in the cells may be delayed (as in IDA). Sideroblasts are decreased, but storage of iron is normal or increased.

The serum iron concentration is characteristically decreased, the TIBC is decreased or normal (in contrast to IDA, in which the TIBC is elevated), and the percent saturation is decreased. Erythrocyte protoporphyrin and serum ferritin are elevated.

The most important pathogenetic mechanism of AI is the presence of high levels of cytokines, which may result in decreased red cell survival, altered iron metabolism, direct inhibition of hematopoiesis, and decreased EPO secretion. Tumor necrosis factor-α (TNF-α) plays a significant role in inflammation and immune response. TNF-α levels are increased in patients with cancer, rheumatoid arthritis, infection, and the acquired immunodeficiency syndrome. In vitro inhibition of human erythroid colony formation, burst forming units-erythroid (BFU-E), and colony forming units-erythroid (CFU-E) by TNF-α has been reported. Similarly, an inhibitory action of IL-1 and interferon-γ (IFN-γ) on erythropoiesis has been implicated. Ceramide, a product of cytokine-induced enzymatic hydrolysis of cell membrane sphingomyelin, plays a role as a messenger in the inhibitory effects of IFN-γ (Weiss, 2019).

TABLE 33.2

Correlation of Vitamin B_{12} and Folate Levels With Clinical Status: Three Laboratory Tests Needed to Separate Four Clinical Situations

Clinical Situation	Serum Vitamin B_{12}, pg/mL	Serum Folate, ng/mL	Red Cell Folate, ng/mL
Normal*	Normal (200–900)	Normal (5–16), indeterminate (3–5), or low (<3)	Normal (>150)
Vitamin B_{12} deficiency	Low (<100)	Normal (5–16) or high (>16)	Low (<150)
Folic acid deficiency	Normal	Low	Low
Deficiency of both	Low	Low	Low

From Herbert V: Megaloblastic anemias. *Lab Invest* 52:3–19, 1985.
*Normal includes transient states of negative folate balance.

EPO levels, although above normal, have been disproportionate to the degree of anemia, indicating relative EPO deficiency in AI. Inhibitory effects of cytokines on EPO synthesis sites such as renal and liver cells have been suggested. The relative deficiency of EPO induces neocytolysis (i.e., selective hemolysis of the youngest RBCs). Thus, a mild hemolytic event usually accompanies AI although shortened red cell survival may be more significant in acute conditions, such as acute infections and severe sepsis. In addition, macrophage activation by inflammatory cytokines may play an additional role in shortened red cell survival (Weiss, 2019).

Recently, hepcidin has been shown to be elevated in AI through induction by IL-6 and is considered an acute-phase reactant. As mentioned earlier, hepcidin interferes with the release of intracellular iron. Recent evidence also suggests that hepcidin may exert an inhibitory effect on erythroid colony formation at certain levels of EPO and, thus. may provide a bone marrow inhibitory effect.

The anemia usually fails to respond to iron therapy. However, patients treated with EPO have shown improvement.

Anemia of Renal Insufficiency

A normocytic normochromic anemia is commonly encountered in patients with chronic renal failure (CRF). The correlation between severity of anemia and degree of elevation of blood urea nitrogen (BUN) is positive but not strictly linear. When creatinine clearance falls below 20 mL/min, the Hct is usually below 0.30 (Caro, 2010).

Several factors are often involved in the anemia of CRF. Decreased production of EPO by the damaged kidney is probably the important factor in most cases in which the BUN exceeds 100 mg/dL. Both ineffective erythropoiesis and impaired ability of the marrow to respond to EPO appear to be present to some degree.

Inhibitors of erythropoiesis have been demonstrated in the plasma of patients with CRF. The nature of these inhibitory factors is not known; however, parathyroid hormone and spermine have been implicated as inhibitors of erythropoiesis. Recent studies indicate the presence of a high level of inflammatory cytokines, such as IL-1, IL-4, IL-6, and TNF-α, in patients with CRF. As discussed under Anemia of Inflammation, these cytokines exert a bone marrow suppressive effect and probably contribute to the development of anemia (Weiss, 2019). The role of hepcidin in this type of anemia is also being investigated.

Hemolysis is a significant feature in many cases of CRF. There appears to be an extracorpuscular factor in uremic plasma that has a detrimental effect on red cell metabolism and results in morphologically deformed cells (echinocytes and spiculated red cells). Numerous irregularly contracted and fragmented cells are seen in the hemolytic-uremic syndrome (HUS) and in malignant hypertension as a result of traumatic damage incurred by the red cells in traversing damaged small blood vessels. Changes in red cell membrane adenosine triphosphatase (ATPase) and transketolase may render the red cells more sensitive to oxidant drugs or chemicals.

In addition, bleeding is a common problem in chronic renal disease, probably owing to thrombocytopenia in some patients, or to platelet functional defects, which are present in most patients. Anemia due to iron deficiency from blood loss should always be suspected. Folic acid deficiency may be a problem in patients in a dialysis program in that folic acid is readily moved into the dialysis bath. Aluminum in dialysis water may interfere with iron incorporation in erythroid cells producing microcytic anemia (Caro, 2010). A novel therapeutic approach is the potential use of prolyl hydroxylase inhibitors, which stabilize hypoxia-inducible factors and increase the level of endogenous EPO (Weiss, 2019).

Anemia in Liver Disease

Anemia of liver disease is multifactorial and is very common, affecting approximately 75% of patients with chronic liver disease (Means, 2019). Associated pathologies include IDA, congestive splenomegaly, chronic posthemorrhagic anemia, and folate-deficient megaloblastic anemia due to poor nutrition in alcoholic cirrhosis. Hypoplastic anemia secondary to viral-induced marrow suppression, acquired hemolytic anemia associated with Coombs-positive red cells and anemia due to lipid disturbances or drug interactions also occur (Gallagher, 2009). Iron deficiency is most common, occurring in approximately 50% of patients, followed by hypersplenism in approximately 25% (Ozatli, 2000).

IFN-α and ribavirin (Rbv) are common therapies for hepatitis C infection. Anemia (hemoglobin <11 g/dL) is seen in 30% to 40% of patients. Rbv induces suppression of erythropoiesis, possibly through downregulation of EPO receptors, and can also cause dose-dependent hemolytic anemia, particularly in patients with impaired renal function. IFN-α can produce anemia through suppression of hematopoietic progenitor cell proliferation and induction of apoptosis of erythroid progenitor cells (Gonzalez-Casas, 2009).

Another type of anemia uniquely associated with liver disease is characterized by shortened red cell survival and relatively inadequate red cell production. It is exaggerated by an increased blood volume that appears to correlate with the degree of portal hypertension. The red cells are normocytic or macrocytic (thin macrocytes). Frequently, target cells are present, especially in obstructive jaundice. These cells have increased surface membrane with increased cholesterol and lecithin content. However, phospholipid/cholesterol ratio is normal. Reticulocytes may be slightly increased and platelets may be normal or decreased depending on the level of thrombopoietin production. The bone marrow may be slightly hypercellular, and erythropoiesis is macronormoblastic rather than megaloblastic. Changes in leukocytes such as those seen in megaloblastic anemias are not seen, and this type of anemia does not respond to cobalamin (vitamin B_{12}) or folic acid. The anemia is of unknown origin. However, abnormal erythrocyte oxidative metabolism, including decreased pentose phosphate shunt and reduced ATP, may contribute to decreased red cell survival (Means, 2019).

Approximately 10% to 30% of patients with severe cirrhosis have a hemolytic anemia associated with "spur cells," which are red cells with thorny projections similar to acanthocytes in more than 5% of red cells. As with target cells, the spur cells occur secondary to lipid abnormalities in the plasma. They have increased surface membrane with increased cholesterol, but normal phospholipid content in the membrane. The increased membrane cholesterol tends to associate with the outer membrane leaflet, making it more rigid. The spleen attempts to remodel the membrane, resulting in characteristic membrane projections (Means, 2019).

Anemia in Endocrine Disease

Uncomplicated anemia in hypothyroidism is mild to moderate, with Hb concentration rarely less than 8 to 9 g/dL; it is normochromic and normocytic without reticulocytosis and with normal red cell survival. Anemia is observed in 21% to 60% of hypothyroid patients (Means, 2019). It reflects decreased marrow production due to a smaller tissue O_2 requirement and subsequent reduced EPO secretion. Because plasma volume is decreased in hypothyroidism, the apparent degree of anemia may not be proportional to the decrease in red cell mass.

Hypothyroidism may be complicated by IDA, producing microcytic anemia. This is most often seen in females as a result of menorrhagia, although in males it may occur due to achlorhydria and diminished iron absorption.

Macrocytosis is frequently observed and, although the incidence of PA in patients with hypothyroidism may be increased, the exact etiology of macrocytosis remains unknown. A mild anemia occurs in 10% to 25% of patients with hyperthyroidism. The anemia may be slightly microcytic. Plasma volume may be increased, suggesting dilution.

In adrenal cortical hormone deficiency, a mild normochromic normocytic anemia is present although the decreased plasma volume may mask the degree of anemia. The cause is unclear, but the condition is corrected by hormone replacement.

Deficient testosterone secretion in men results in a decrease in red cell production of 1 to 2 g Hb/dL (to a value comparable with that of women). This appears to be due to a stimulatory effect of androgens on EPO secretion, occurring through enhanced EPO action on the marrow and possibly as a direct effect on a subset of marrow cells, such as stromal cells, macrophages, and myeloid precursors.

Pituitary deficiency also causes moderately severe normocytic anemia, which is associated with marrow hypoplasia. The mechanism is probably complex and related to loss of function of multiple endocrine glands and possibly loss of growth hormone effect.

A small number of patients with hyperparathyroidism have a normocytic, normochromic anemia. Earlier studies suggested that the parathyroid hormone may suppress normal erythropoiesis but more recent studies failed to support this theory. The cause of the anemia is unknown but is likely related to marrow fibrosis (Means, 2019).

Anemia Associated With Bone Marrow Infiltration (Myelophthisic Anemia)

This anemia is associated with marrow replacement by (or involvement with) abnormal cells or tissue component, such as metastatic carcinoma, multiple myeloma, leukemia, lymphoma, lipidoses or storage diseases, and certain other conditions.

Normochromic and normocytic (occasionally macrocytic) anemia of varying severity is present. Reticulocytes are often increased, and normoblasts are present in a number that is usually out of proportion to the severity of the anemia. The leukocyte count is normal or reduced (occasionally elevated), and immature neutrophils and even myeloblasts may be found. Platelets are normal or decreased, and bizarre, atypical platelets can sometimes be seen.

Examination of the marrow will usually reveal the condition responsible for this reaction. Mechanical crowding out of the hematopoietic tissue by the pathologic process has been assumed but not proved and probably is not the usual cause. Often, the amount of erythropoietic tissue in the marrow as determined by morphologic and kinetic studies is normal or increased. The mechanism described earlier under Anemia of Inflammation may often play a role, but the reason for the outpouring of immature cells into the blood is not clear.

In addition to myelophthisic anemias, circulating normoblasts and immature neutrophils can be seen in hemolytic anemias, severe anemias due to other causes, severe infections, recovering marrow, and congestive heart failure, but usually the normoblasts are not as numerous.

The **leukoerythroblastotic (or leukoerythroblastic) reaction** associated with myelophthisic anemias cannot always be distinguished from the blood picture of primary myelofibrosis, which is one of the myeloproliferative neoplasms. In primary myelofibrosis, particularly the fibrotic phase, enlargement of the spleen and liver is almost always found. In the blood film, more severe red cell abnormalities, such as tear-drop shapes (dacrocytes), leukocytosis, myeloblasts and immature granulocytes of all varieties (not just neutrophils), increased basophils, more atypical platelets, more numerous megakaryocyte fragments, and dwarf megakaryocytes are all findings more characteristic of primary myelofibrosis than of a leukoerythroblastotic reaction of some other cause. Examination of the bone marrow biopsy is necessary for the final diagnosis.

Aplastic Anemia

AA usually refers to pancytopenia associated with a severe reduction in the amount of hematopoietic tissue that results in deficient production of blood cells in the absence of a bone marrow infiltrative process or increased reticulin (Clucas, 2019). Usually two of the following three blood parameters are needed to diagnose AA: Hgb less than 100 g/L, granulocyte count less than 1.5×10^9/L, and platelet count less than 50×10^9/L. The marrow, although hypocellular, may have patchy areas of normocellularity, or even hypercellularity. The diagnosis of **severe AA** is made in pancytopenic patients when at least two of the following three peripheral blood values—granulocyte count less than 0.5×10^9/L, platelet count less than 20×10^9/L, or reticulocyte count less than 20×10^9/L, or 1% (corrected for Hct)—are present and the bone marrow is less than 25% cellular. With the pervasive use of automated reticulocyte counts, the threshold for severe AA stands at 60×10^9/L using automated counts (Dezern, 2019). The term *very severe AA* is used when the granulocyte count is less than 0.2×10^9/L (Clucas, 2019). Otherwise, the AA would be classified as moderate or nonsevere. AA is usually classified as inherited (see later discussion) or acquired. The incidence of acquired AA is 2 per million per year based on retrospective studies in Europe and North America, and is about 2 to 3 times higher in East Asia, with the highest being in Japan and estimated at 14 per million per year (Dezern, 2019). There is a bimodal age of peak presentation, with the first occurring in patients aged 15 to 25 years and the second in patients over 60 years old.

Clinical Features

The clinical course may be acute and fulminating, with profound pancytopenia and a rapid progression to death, or the disorder may have an insidious onset and a chronic course. The symptoms and signs depend on the degree of the deficiencies: bleeding from thrombocytopenia, infection from neutropenia, and signs and symptoms of anemia. As a rule, splenomegaly and lymphadenopathy are absent. Bleeding is the most common presentation of acquired AA, occurring in approximately 40% of patients (Young, 2009). Bleeding usually manifests as easy bruisability, gum bleeds, and episodic nosebleeds. Less than 5% of patients present with infection.

Etiology

Acquired aplastic anemias are of diverse origin. Since 1980, in approximately 70% of cases, no specific etiologic agent could be correlated with the disease; such cases are considered idiopathic. Drug- and chemical-related AAs account for 11% to 20%, and those associated with infectious hepatitis account for 2% to 9% of cases (Young, 2009).

Pathogenesis

Hematopoietic failure may occur at any level in the differentiation of bone marrow precursor cells, whether pluripotential or committed stem (progenitor) cells. The CD34+ cells in the bone marrow, which contain most of the stem cells and committed progenitor cells, are markedly decreased in patients with AA, with a percentage of marrow CD34+ cells of <0.3% (Dezern, 2019).

The mechanism of acquired AA is suggested to fall under two main categories: direct damage and immune-mediated destruction of marrow cells. Direct damage to the hematopoietic stem and progenitor cells could be caused by a known agent, such as cytotoxic drugs, irradiation, and viruses, or an unknown agent that in some way alters the ability of the cell to proliferate or differentiate. Immune-mediated destruction of stem and progenitor cell compartments results from cytotoxic lymphocyte activation, cytokine production, and specific cell elimination. Most studies indicate that stem cell destruction results from T-cell autoimmunity. An unidentified antigenic exposure leads to polyclonal expansion of CD4+ T cells with overproduction of proinflammatory cytokines, such as INF-γ and TNF-α. There is also oligoclonal expansion of a CD8+ cytotoxic cell population. AA patients have increased T helper 17 (Th17) cells secreting IL-17. The stem cell destructive process is augmented by deficits in regulatory T cells (Tregs), which normally suppress autoreactivity (Shallis, 2018). Recent studies favor immune-mediated mechanisms for AA and suggest that chemical and viral antigens may initiate the destructive immune process (Young, 2009). A role for intrinsic stem cell defects and abnormal bone marrow microenvironment may be contributory. For example, approximately 35% of AA patients are found to have leukocytes with short telomeres, suggesting a stem cell defect (Shallis, 2018). In addition, the role of thrombopoietin and the thrombopoietin signaling pathway in stem cell homeostasis and survival is also being investigated to the extent of using thrombopoietin agonists as potential therapeutic agents. However, the immune destruction of stem cells is the most important factor and most patients with acquired AA are now viewed as suffering from an immune-mediated disease.

Prognosis

Complications of AA are infection, bleeding, and problems of iron overload from repeated transfusions. The prognosis appears to depend on the severity of marrow damage; however, the initial blood count and response to therapy during the first few months of treatment are important prognostic factors (Young, 2009). Usually, the age of the patient influences the decision regarding which therapy the patient should receive. In some survivors, partial recovery is common. With the introduction of modern treatment protocols utilizing immunosuppressive therapy and bone marrow transplantation, long-term survival rates greater than 60% are reported. Survivors have a much higher risk of developing myelodysplastic syndrome, paroxysmal nocturnal hemoglobinuria (PNH), acute leukemia, and solid tumors. Clonal evolution to myelodysplastic syndromes and acute myeloid leukemia occurs in 10% to 20% of patients with acquired AA. Cytogenetic abnormalities, such as monosomy 7 and trisomy 8, occur in 13% and 7% of acquired AA, respectively. Uniparental disomy in the short arm of chromosome 6 (6pUPD) occurs in approximately 13% (Shallis, 2018). Genetic mutations in myeloid malignancy-associated genes, such as *ASXL1*, *DNMT3A*, and *BCOR* are reported in up to half of acquired AA patients and may be related to progression (Clucas, 2019). PNH clones occur in 50% to 70% of acquired AA patients, representing somatic mutation in the *PIGA* gene. PNH clone size is usually small and of uncertain clinical significance, although some studies suggest that it may indicate a favorable response to immunosuppressive therapy (Dezern, 2019, Clucas, 2019).

Management

Treatment of acquired AA includes bone marrow transplantation for patients younger than 40 years of age with severe disease if there is a human leukocyte antigen (HLA)–matched sibling. Children and young adults have a much higher survival probability compared with older adults (Young, 2009). Immunosuppression using horse antilymphocyte globulin (ATG) and cyclosporin A produces hematologic remission in 60% to 80% of patients. Rabbit ATG produces slightly lower remission rates in some studies (Scheinberg, 2012). Androgens appear to be least helpful in the stimulation of any residual marrow. Supportive care must be used with caution. Certainly, appropriate antibiotics should be used to combat infection; however, the risk for sensitization should be considered with the administration of blood products. Single-donor platelets or platelets from HLA-matched donors are preferred (Alter, 1998).

Idiopathic Acquired Aplastic Anemia

In patients with pancytopenia and a hypocellular marrow, a search should be made for evidence of exposure to radiation, drugs, and chemicals of known or possible propensity to injure the marrow so that further exposure can be eliminated. Nevertheless, in approximately 70% of cases of AA, no suspected causal relationship to toxic agents can be found. These cases are designated as idiopathic with a presumed immunologic mechanism, as mentioned earlier. The symptoms and signs do not differ, but the onset is commonly more insidious than in toxic or hypersensitive AAs.

Blood

The red cells are usually normal to increased in size with a varying degree of anisocytosis and poikilocytosis, particularly oval macrocytes. Macrocytosis may be a prominent feature, particularly in response to high levels of EPO. The RDW may be increased, even without transfusion (Elghetany, 1997). Polychromasia, stippling, and normoblasts are most often conspicuously absent. Leukopenia with marked decrease in granulocytes and a relative lymphocytosis are observed. In severe leukopenia, there is often absolute lymphocytopenia. Neutrophil granules may be larger than normal and may stain dark red (unlike the "toxic" granules found in infections), and the neutrophil alkaline phosphatase may be elevated. However, neutrophil left shift is not seen in the absence of infection (Elghetany, 1997). Thrombocytopenia is part of the picture. Monocytopenia may be present. The serum iron is usually increased, and serum cobalamin and folate levels are usually normal. Although an occasional patient is hypogammaglobulinemic, most patients have normal levels of serum immunoglobulins.

Bone Marrow

In most cases, the aspirate consists of red cells, lymphocytes, some plasma cells, mast cells, and fatty particles. Marrow sections will show fatty tissue with inconspicuous fibrosis and islands of lymphocytes and plasma cells (Fig. 33.8). Although focal areas of predominantly erythroid normocellularity or hypercellularity (hot spots) may sometimes be present, the overall cellularity is decreased. The hot spots usually show erythroid precursors with delayed nuclear maturation at a high proliferative rate. Vascularity may be prominent with occasional ectatic sinuses. Storage iron is increased. Rare cases may show lymphoid aggregates.

Erythrokinetics

An increased serum iron concentration is a valuable early sign of erythroid hypoplasia and reflects decreased plasma iron turnover. In addition, erythrocyte utilization of iron is decreased. Therefore, both effective and total erythropoiesis are decreased in AA.

Acquired Aplastic Anemia Associated With Chemical or Physical Agents

Toxic Aplastic Anemias. A number of physical and chemical agents produce marrow damage in all humans and animals exposed to a sufficient dose. Examples include ionizing radiation, mustard compounds, benzene, and antineoplastic agents such as busulfan, urethane, and antimetabolites. Benzene, although strongly linked to AA, is now considered less of a problem than in the past because of reduction in exposure.

Ionizing Radiation. Effects depend on the radiosensitivity of the cells and the capacity of the cells to regenerate, as well as the survival rate of cells in the blood. Erythroid cells are most sensitive, granulocytes have intermediate sensitivity, and megakaryocytes are the least sensitive of the three. Stromal cells are relatively insensitive.

After acute exposure to radiation, the reticulocyte count falls, but the red cells decline slowly because of their long survival. Within the first few hours, neutrophilic leukocytosis occurs as the result of a shift from marginal and probably marrow storage pools. A fall in lymphocytes occurs after the first day and is responsible for the early leukopenia, because lymphocytes are sensitive to irradiation and are directly killed. After 5 days or so, granulocytes begin to fall. The platelets decrease later. Platelets are often the last to return to normal in the recovery phase. Quiescent marrow stem cells are remarkably resistant to a single dose of irradiation. However, chronic exposure to low-dose irradiation, including localized radiation for ankylosing spondylitis, is associated with delayed increased risk for AA because of its impact on the stem cell replicating pool (Young, 2009).

Hypersensitive Aplastic Anemias. A large number of drugs produce marrow damage in some individuals after single or repeated exposures. Effects are not dose related as they are in the previously discussed toxic aplasia. Agents include antimicrobial drugs (salvarsan, chloramphenicol, sulfonamides, chlortetracycline, streptomycin), anticonvulsants (mephenytoin, trimethadione), analgesics (phenylbutazone, indomethacin), antithyroid drugs (carbimazole), antihistaminics (tripelennamine), H_2-histamine receptor antagonists (cimetidine), insecticides (dichlorophenyltrichloroethane [DDT]), and other chemicals—some known (gold compounds, quinacrine, chlorpromazine, hair dyes, bismuth, mercury) and others unknown. The nonsteroidal antiinflammatory medications are becoming more linked to an increased risk for developing AA following marked reduction in the use of chloramphenicol.

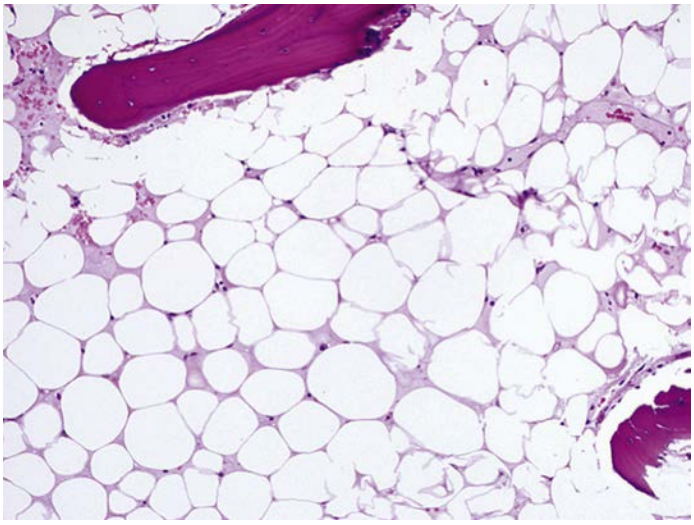

Figure 33.8 Section of hypocellular marrow, aplastic anemia. Cellularity is less than 5%.

Chloramphenicol is an important drug in this category. This antibiotic was considered to be the most common cause of AA at the peak of its use, which began in 1949. Reactions of the marrow to chloramphenicol are of two types, which are possibly unrelated (Alter, 1998).

In about half of patients who receive chloramphenicol, increased serum iron, reticulocytopenia with anemia, neutropenia, and thrombocytopenia are found. The marrow may show decreased erythroid cells and vacuolization of primitive erythroid and granulocyte precursors. These changes are dose related, time dependent, and reversible.

In a very small proportion of persons receiving chloramphenicol, an irreversible AA develops that may be fatal. Pancytopenia occurs 3 weeks to 5 months from the last dosage. No relationship has been established between the reversible erythropoietic lesion and the development of AA; it may be that individual susceptibility is responsible for the latter. For this reason, it is essential that restraint be employed in using the drug; monitoring its administration with blood cell counts is not an effective preventive measure.

Acquired Aplastic Anemia Associated With Other Disease

Infection. Viral infections are frequently associated with limited marrow suppression, typically neutropenia and less commonly thrombocytopenia. Marrow aplasia has been described as a rare sequela to viral hepatitis, occurring two to three months after an episode of acute hepatitis. As mentioned earlier, hepatitis-associated AA represents approximately 5% of cases of acquired AA (Dezern, 2019). Almost all cases are seronegative for hepatitis A, B, C, and G. These patients are usually males younger than age 20 years. The prognosis is usually grave, with severe AA; bone marrow transplantation is considered early in the course of the disease (Espinoza, 2017). After orthotopic liver transplantation for fulminant seronegative hepatitis, up to 30% of patients develop hepatitis-associated AA (Dezern, 2019). Parvovirus has been associated with transient erythroid aplastic crisis in patients with chronic hemolytic disorders although some cases of AA have been reported with such infection. Human immunodeficiency virus, dengue virus, cytomegalovirus, and Epstein-Barr virus may also cause hematopoietic depression. Several immunologic abnormalities have been documented in patients with hepatitis-associated AA, including increased soluble IL-2 receptor, low ratios of CD4+/CD8+ cells, high percentages of CD8+ cells, and reduced proportions of CD4+CD25+ Tregs. Clonal expansion of T cells with conserved antigen specificity has been found in these patients, suggesting that abnormal immune responses underlie the disease and viral antigens may elicit T-cell responses that cross-react with antigens expressed by the stem cells (Espinoza, 2017).

Paroxysmal Nocturnal Hemoglobinuria. This rare clonal disorder (see later discussion) may be followed by AA. Usually, in PNH, a variable degree of marrow hypofunction coexists. Alternatively, in some patients who present with AA, the red cell defect of PNH may be present or may appear during the course of the disease. As mentioned earlier, PNH defect may be detected in as many as 50% to 70% of patients with AA. However, hemolytic disease occurs in approximately one-third of these patients.

Pregnancy. Pregnancy occurring in a patient with acquired AA may make the pancytopenia more severe. Occasionally, however, AA occurs during pregnancy and remits following delivery. In some such cases, aplasia recurs during a second pregnancy. Infants may be anemic, thrombocytopenic, or leukopenic. Survival rates for AA in pregnancy have been relatively high for the mother (83%) and the baby (75%). Hemorrhage is the most common cause of death in these patients (Young, 2009).

Thymoma. Although thymomas are usually associated with pure red cell aplasias, other bone marrow elements may also become depressed. Pancytopenia, often with hypoplastic bone marrow, occurs in rare cases with thymoma. AA may occur as a late complication after the treatment of thymoma (Ritchie, 2002a).

Immunologic Diseases. AA occurs in approximately 10% of cases of eosinophilic fasciitis. The prognosis of AA in this setting is usually poor. AA may be associated with systemic lupus erythematosus (SLE) and rheumatoid arthritis (RA), although the role of drug therapy in the pathogenesis of AA has been considered (Young, 2009). AA may also complicate multiple sclerosis, congenital immunodeficiency syndromes, and immune thyroid disease.

Inherited Bone Marrow Failure Syndromes

The term *inherited bone marrow failure syndromes* (*IBMFS*) designates individuals with a genetic predisposition to chronic bone marrow failure, which may be associated with other congenital anomalies. IBMFS may involve a single cell line, such as Diamond-Blackfan anemia, or multiple cell lines, such as Fanconi anemia. Several of these syndromes are associated with increased risk for hematologic and solid organ malignancies. Between 30% and 35% of childhood AA cases are inherited. In a study of 134 children with AA, 40 patients were diagnosed with inherited AA. Twenty-six had Fanconi anemia (FA), 10 patients had familial AA without classic signs of FA, and 4 patients presented with amegakaryocytic thrombocytopenia that later developed into complete aplasia (Alter, 1998). The current literature and large-center studies suggest an annual incidence of IBMFS of approximately 65 per million live births (Dror, 2018).

Fanconi Anemia. FA is an autosomal-recessive disorder with a carrier frequency of 1/300 in the United States and Europe and is higher in individuals of Ashkenazi Jewish descent (Furutani, 2019). Rare cases are X linked or autosomal dominant. Often, more than one member of a family is affected. The pancytopenia becomes obvious after infancy and is usually significant in early childhood, with median age at diagnosis of 6.5 years. The anemia is usually normochromic and may be macrocytic; increased levels of HbF and i antigen may be observed; the marrow is generally hypocellular. Developmental anomalies are present in approximately 60% of patients and may include hyperpigmentation, short stature, hypogonadism, malformations of the extremities (e.g., aplasia of the radius, frequent abnormalities of the thumbs), microcephaly, and malformation of other organs (e.g., heart, kidneys). Chromosomal defects consisting of random breaks and rearrangements characteristically are present in blood lymphocytes as well as in marrow cells. Chromosomal breakage becomes more evident when the cultured cells are challenged with alkylating and DNA cross-linking agents such as mitomycin C and diepoxybutane. Some mosaic cases may be difficult to diagnose; studying skin fibroblasts may be better than blood cells. A breakthrough in investigating FA evolved from the observation that hybrid cells from FA and normal cells resulted in correction of the abnormal chromosome fragility, a process known as *complementation*. At least 21 complementation groups have been distinguished to date. The most common is complementation group A (FANCA), which occurs in approximately 70% of FA patients. Several FA proteins form a nuclear complex that is involved in DNA repair. The FA/BRCA DNA repair pathway repairs covalently cross-linked strands of DNA that will not separate and will interfere with DNA replication. The DNA cross-linking may result from endogenous reactive aldehydes or exogenous cross-linking agents. The predicted median survival in FA is 39 years. Patients with FA are at higher risk of developing myelodysplastic syndromes, acute leukemia, and nonhematologic tumors, particularly in the head and neck, liver, lower esophagus, vulva, and anus, with an overall cumulative incidence of neoplasia of 15% (Alter, 2018). The median age for all cancers in patients with FA was 30 years (Alter, 2018).

Other Inherited Aplastic Anemias. A few children present with bleeding manifestations during their neonatal period secondary to amegakaryocytic thrombocytopenia. As their disease progresses, they develop a pancytopenia and a hypocellular marrow. Chromosome breakage studies are usually normal. The mode of inheritance is autosomal recessive. The molecular defect is related to a mutation in the gene for thrombopoietin receptor, *c-MPL*, which maps to 1p35 (Furutani, 2019).

Pancytopenic anaplastic anemia may develop in a subset of patients with other familial disorders. Some patients with dyskeratosis congenita (DC; reticulated hyperpigmentation of skin, dystrophic nails, and mucous membrane leukoplakia) and Shwachman-Diamond syndrome (SDS; exocrine pancreatic insufficiency and neutropenia) develop AA during the course of their disease (Alter, 2002). Recent studies indicate that DC results from abnormalities in telomere maintenance system and is now considered one of the telomere biology disorders. SDS results from biallelic mutation of the SBDS gene, which interacts with molecules responsible for ribosomal subunit assembly, resulting in abnormal ribosome biogenesis (Furutani, 2019). Both DC and SDS are associated with increased risk for hematologic malignancies and solid tumors (Alter, 2018).

Pure Red Cell Aplasia

Transitory Arrest of Erythropoiesis (Transient Aplastic Crisis)

This may occur during the course of a hemolytic anemia (often preceded by an infection). The combination of aplasia and hemolysis becomes a life-threatening situation due to rapidly progressing anemia. Red cell production may occasionally cease during or following rather minor infections in normal children or adults, at which time the marrow will show absence of all but a few of the most immature erythroid precursors. Aplastic episodes in chronic hemolytic anemias often appear to be due to parvovirus B19 infection. This virus inhibits erythropoiesis by infecting mature CFU-Es. The morphologic hallmark of the disease is the presence of scattered giant pronormoblasts in the bone marrow aspirate with marked reduction in the more mature erythroid precursors. Nuclear inclusion may be difficult to identify with Wright's stain. The aplastic crises resulting from parvovirus infection are transient, with erythroid marrow recovery in 1 to 2 weeks after onset (Erslev, 2001a).

Transient Erythroblastopenia of Childhood

Transient erythroblastopenia of childhood (TEC) occurs in previously healthy children, usually younger than 8 years of age, with most affected children between 1 and 3 years of age. It is characterized by a moderate to severe normocytic anemia that develops gradually, severe reticulocytopenia, transient neutropenia (20%), and increased platelet counts (60% of patients). Macrocytosis is usually observed during recovery because of the effects of reticulocytes. A history of a viral infection within the previous 3 months is frequently elicited. The bone marrow is generally normocellular and shows virtual absence of erythroid precursors, except for a few early forms. Granulocytic maturation arrest may occur in some neutropenic patients. Patients recover within 1 to 2 months without therapy except in rare occasions in which RBC transfusions may be needed for symptomatic anemia. TEC can occur in siblings simultaneously and in seasonal clusters. Transient neurologic manifestations, such as hemiparesis and seizures, may accompany TEC. In most cases, the pathogenesis involves humoral inhibition of erythropoiesis; cell-mediated immunosuppression was identified in about 25% of cases, but parvovirus has not been proven to be the cause of TEC (Narla, 2019).

Congenital Red Cell Aplasia (Diamond-Blackfan Anemia; Congenital Hypoplastic Anemia)

Diamond-Blackfan anemia (DBA) is a rare, congenital red cell aplasia that usually becomes obvious during the first year of life, with the median age of presentation being 2 months and more than 90% of cases being identified during the first year of life (Narla, 2019). Abnormal physical findings, such as short stature, craniofacial abnormalities, and thumb anomalies, are seen in more than 50% of patients. Severe anemia is usually macrocytic, reticulocyte level is low, leukocytes are normal or slightly decreased, platelets are normal or increased, and the marrow usually shows a reduction in all developing erythroid cells, except normal granulocytic and megakaryocytic cell lines. In a small number of cases, residual erythroid precursors are detected. These precursors are mostly pronormoblasts. HbF is elevated (5%–25%) to a degree not expected for the patient's age, and the antigen i is often present. Red cell adenosine deaminase (ADA) is usually increased. These findings contrast with TEC,

in which the red cells are normocytic, the HbF is normal, the antigen i is absent, and red cell enzymes are at a lower level (characteristic of an older cell population) (Narla, 2019).

DBA has an autosomal-dominant pattern of inheritance with variable penetrance. The defect appears to be in the erythroid-committed progenitor cells. CFU-Es and BFU-Es are decreased in the marrow, and BFU-Es, which normally circulate, are absent or decreased in the blood. In addition, these progenitor cells exhibit acceleration in programmed cell death (apoptosis) and fail to respond in in vitro culture systems to normal T cells and to usual levels of EPO, suggesting a qualitative defect. DBA results from defects in ribosomal proteins, whether small (S) or large (L) units. The most common is a mutation in the *RPS19* gene, which was detected in 25% of patients (Narla, 2019). Rare cases have been caused by mutations in the *GATA1* gene. About 75% of patients respond at least partially to corticosteroids. Approximately 20% of patients experience spontaneous remission by the age of 25 years. The overall long-term survival is about 65%, although many patients require long-term steroid use. DBA is also associated with a higher risk of developing solid tumors, acute myeloid leukemia, and myelodysplastic syndrome (Alter, 2018; Narla, 2019).

Acquired Pure Red Cell Aplasia

Among middle-aged adults, selective failure of red cell production occurs rarely. Reticulocytopenia and a cellular marrow devoid of all but the most primitive erythroid precursors are characteristic. Leukocyte and platelet production is normal. About half of reported cases have been associated with thymoma, usually a noninvasive spindle cell type. However, only 5% to 10% of patients with thymoma have the anemia. Remission of the anemia occurs in about one-fourth of cases following surgical removal of the thymoma. Chronic acquired red cell aplasia has also been associated with other conditions, such as drugs, collagen vascular disorders, viral infections such as HIV, lymphoproliferative disorders of granular lymphocytes, or other disorders with immunologic aberrations. Most of these anemias appear to be part of a spectrum of autoimmune cytopenias in which the target cells are erythroid stem cells or normoblasts. In some patients, antibodies that react with these cells have been identified. Corticosteroids and immunosuppressive drugs have been used as therapy, but less than half of patients achieve satisfactory remission (Erslev, 2001a).

Sideroblastic Anemia

Sideroblastic anemia is characterized by accumulation of iron in the mitochondria, which appears as ring distribution around the nucleus of erythroid precursors on iron stain. The red cells are usually microcytic in the hereditary forms and often macrocytic in the acquired forms of the disease (Bottomley, 2014). The red cells may be mixed with normochromic cells so that the appearance is dimorphic (see Fig. 31.13). The serum iron concentration is increased, the TIBC is decreased, and the percent saturation of the iron-binding protein is greatly elevated. The marrow shows markedly increased storage iron (see Fig. 33.5), erythroid hyperplasia with evidence of defective hemoglobinization, and increased numbers of sideroblasts. In addition, increased numbers of siderotic granules per cell and granules surround the nucleus (with most authors requiring five or more iron granules encircling at least one-third of the circumference), forming "ring sideroblasts" (Swerdlow, 2017) (see Figs. 31.45 and 33.19). In the latter case, iron loading of mitochondria is seen by electron microscopy. These findings are associated with defective synthesis of heme, which may be due to any of several possible enzyme defects. Occasionally, megaloblast-like changes are seen in the erythroid cells, but changes typical of cobalamin or folate deficiency are not seen in granulocytes unless folate deficiency coexists.

Hereditary Sideroblastic Anemias

Hereditary sideroblastic anemias include several modes of inheritance (i.e., X-linked, autosomal dominant, and autosomal recessive). They may be caused by defective heme synthesis (nonsyndromic), abnormal iron-sulfur cluster biogenesis (mostly nonsyndromic), or abnormal mitochondrial proteins (mostly syndromic affecting organs other than hematopoietic tissue). The X-linked forms are the most common, constituting about 40% of cases, and generally exhibit low levels of δ-aminolevulinic acid synthase (ALAS) enzyme. This occurs in males and may not appear until adolescence. It is rare, but a few family studies have been well documented. In contrast to acquired sideroblastic anemia, the ring sideroblast abnormality is usually found in late, nondividing erythroblasts (Bottomley, 1982). The gene for ALAS-2 isoenzyme (erythroid ALAS) has been localized to the X chromosome, and a point mutation of this gene (*Xp11.21*) seems to occur in most X-linked sideroblastic anemias (Bottomley, 2014). Mutations of the *ALAS-2* gene may result in enzyme with low affinity for pyridoxal phosphate, structural instability, an abnormal catalytic site, or increased susceptibility to mitochondrial proteases. The degree of anemia improves with pyridoxine supplementation when the mutation disrupts the catalytic association between the enzyme and pyridoxal phosphate (Alcindor, 2002). Hereditary sideroblastic anemias may be due to a defect in the mitochondrial proteins (i.e., mitochondrial cytopathy). Most of these disorders are produced by deletions in the mitochondrial genome, which may account for as much as 30% of the entire mitochondrial genome (Bottomley, 2014). These rare diseases are usually associated with systemic manifestations such as Pearson syndrome (pancreatic insufficiency, vacuolation of bone marrow cells, ring sideroblasts, and a variable degree of marrow failure). However, the anemia of Pearson syndrome is usually macrocytic and occasional patients may exhibit pure red aplasia being mistaken for DBA. Pearson syndrome is caused by deletions in the mitochondrial genome (Ducamp, 2019).

Acquired Sideroblastic Anemias

Myelodysplastic Syndrome With Ring Sideroblasts. Myelodysplastic syndrome with ring sideroblasts (MDS-RS) is a category of myelodysplastic syndromes (Swerdlow, 2017; see also Chapter 34). The dimorphic anemia has both hypochromic-microcytic and macrocytic RBCs, and the MCV is usually high (see Fig. 31.13). At least 15% of erythroblasts (early and late forms) in bone marrow are ring sideroblasts. Other manifestations of dysplasia in the erythroid cell line may be seen. Most cases are associated with somatic mutations affecting mRNA splicing, particularly *SF3B1* (Ducamp, 2019).

Secondary (Drug- or Toxin-Induced) Sideroblastic Anemia

This form of sideroblastic anemia is secondary to some agent that interferes with heme synthesis; recognition is important because hematologic improvement occurs if the agent is removed.

The **antituberculosis drugs** isoniazid, cycloserine, and pyrazinamide cause sideroblastic abnormalities in some patients on long-term therapy.

Lead poisoning is an important member of this group because environmental exposure to lead is usually unrecognized and needs to be detected. Lead interferes with heme synthesis by blocking the enzymes ALAS, ALA dehydratase, and heme synthase. These blocks are only partial and of different degrees; ALA and coproporphyrin are increased in the urine. **Chloramphenicol** also results in ring sideroblast formation, probably by inhibiting mitochondrial protein synthesis. **Copper deficiency** or **zinc overload** can produce sideroblastic anemia, vacuolated marrow cells, and neutropenia. Large quantities of ingested zinc interfere with copper absorption and produce manifestations of copper deficiency. Copper chelators in large doses, such as penicillamine, can produce sideroblastic anemia.

Ethanol-induced anemia is perhaps the most common of the reversible sideroblastic anemias. Folate deficiency, hypomagnesemia, and hypokalemia are concomitant findings. Alcohol may produce ring sideroblasts through decreased plasma levels of pyridoxal phosphate, along with decreased activity of ALA dehydratase and ferrochelatase and possible inhibition of mitochondrial protein synthesis (Bottomley, 2014). After withdrawal of alcohol intake, abnormal sideroblasts usually disappear within a few days.

Primary pyridoxine deficiency, often associated with malnutrition, is occasionally associated with sideroblastic anemia. However, other manifestations, such as peripheral neuropathy and dermatitis, dominate the clinical presentation. Sideroblastic anemia as the sole manifestation of pyridoxine deficiency has not been reported in humans, although it occurs in animals (Alcindor, 2002).

Myelodysplastic Syndrome with Single or Multilineage Dysplasia

This is a clonal bone marrow disorder, which usually occurs in individuals over the age of 50 years. Normocytic or macrocytic anemia, reticulocytopenia, often pancytopenia, and a hypercellular marrow showing erythroid hyperplasia with a variable degree of dyshematopoiesis are present. Often, the patient has been treated with cobalamin, folic acid, and iron without response. The process is usually unremitting, and in a small proportion of cases additional dysplastic changes in marrow cells and increased blast cells evolve into an acute leukemia (see Chapter 34).

Congenital Dyserythropoietic Anemias

Congenital dyserythropoietic anemias (CDAs) represent a family of inherited refractory anemias characterized by ineffective erythropoiesis, marrow erythroid multinuclearity, and secondary hemosiderosis.

At least three types have thus far been separated on the basis of marrow and serologic findings, with some patients not meeting any of the three types (Iolascon, 2013). CDA-I is autosomal recessive and has megaloblastic changes with some binucleation in approximately 5% of marrow erythroblasts, internuclear chromatin bridges, and a macrocytic anemia, which is usually mild to moderate. It presents early in life with neonatal anemia and sometimes jaundice. Approximately 80% of patients require blood transfusion in the first month of life (Dror, 2018). Electron microscopy (EM) studies of bone marrow erythroid precursors demonstrated that heterochromatin is denser than normal and forms sharply delineated clumps with small translucent vacuoles, giving rise to the description of a "Swiss cheese" appearance, and cytoplasm may penetrate through widened pores of the nuclear envelope. Most cases have an abnormality in the *CDAN1* gene located on the long arm of chromosome 15, which encodes a ubiquitous protein called codanin-1 (Iolascon, 2013). CDA-II is also autosomal recessive and more common than the others. It shows binuclearity and multinuclearity of 10% to 40% of erythroid precursors with pluripolar mitoses and karyorrhexis. The anemia is normocytic. CDA-II is distinguished from the others in that it has a positive acidified serum test (with some but not all normal sera) and a negative sucrose hemolysis test. It is known as *hereditary erythroblastic multinuclearity with positive acidified serum test* (*HEM-PAS*). The red cells have an antigen not present on normal or PNH cells, and about one-third of normal sera contain the corresponding immunoglobulin (Ig) M antibody. In addition, red cells in CDA-II react strongly with anti-i and anti-I. Electron microscopy demonstrates an excess of endoplasmic reticulum parallel to the cell membrane, which gives the appearance of a double membrane in late erythroblasts and some erythrocytes. CDA-II is thought to be related to abnormal membrane glycosylation. The gene for CDA-II has been identified as *SEC23B* (*CDAN2*), which maps to 20q11.2 (Iolascon, 2013). CDA-III has giant erythroid precursors, with more pronounced multinuclearity (gigantoblasts) in 10% to 40% of erythroid precursors, along with a macrocytic anemia. The gene for CDA-III (*KIF23*) has been recently localized on chromosome 15q23. In contrast to CDA-I and CDA-II, which are autosomal recessive, CDA-III has autosomal-dominant inheritance. Other variants involving transcription factors *GATA1* and *KLF1* have been described in a small number of families.

BLOOD LOSS ANEMIA

Acute Posthemorrhagic Anemia

Blood may be lost from the circulation externally or internally into a tissue space or body cavity. If blood is lost over a short time in amounts sufficient to cause anemia, **acute posthemorrhagic anemia** occurs. Normal healthy individuals are able to compensate for rapid blood loss of up to 20% of circulating blood volume with few symptoms (Hillman, 1996). After a single episode of excessive bleeding, the major manifestations are those due to depletion of blood volume (hypovolemia). After a day or so, blood volume is returned to previous levels by movement of fluid into the circulation, and anemia becomes evident.

The earliest hematologic change is a transient fall in the platelet count, which may rise to elevated levels within an hour. The next development is a moderate neutrophilic leukocytosis with a shift to the left; a maximum leukocyte count of 10 to 35 × 10^9/L may occur in 2 to 5 hours. Hb and Hct do not fall immediately; rather, they fall slowly as tissue fluids move into the circulation to compensate for lost blood volume. The fall in Hb and Hct may not reveal the full extent of red cell loss until 2 or 3 days after the hemorrhage.

The anemia that develops at first is normochromic and normocytic, with a normal MCV and mean cell hemoglobin concentration (MCHC) and only minimal anisocytosis and poikilocytosis. Increased EPO secretion stimulates erythroid proliferation in the marrow and reticulocytes begin to reach the circulation in 3 to 5 days, reaching a maximum by 10 days or so. During this period, transient macrocytosis (increased MCV), increased polychromasia, and normoblasts may appear in the blood. It takes about 2 to 4 days after blood loss for the leukocyte count to return to normal and about 2 weeks for the morphologic changes to disappear. Return of red cell values is slower.

Chronic Posthemorrhagic Anemia

If blood is lost in small amounts over an extended period, both clinical and hematologic features that characterize acute posthemorrhagic anemia are lacking. Regeneration of red cells occurs at a slower rate.

The reticulocyte count may be normal or slightly increased. Significant anemia does not usually develop until after storage iron is depleted; therefore, the anemia is one of iron deficiency. The anemia is at first normochromic and normocytic. Gradually, the newly formed red cells become microcytic, then hypochromic. The leukocyte count is normal or slightly decreased owing to neutropenia. Platelets are commonly increased; only later, in severe iron deficiency, are they likely to be decreased.

The cause of blood loss must be identified because a hidden malignancy, particularly of the GI tract, may be the cause of the anemia.

HEMOLYSIS—GENERAL

Anemias that are due primarily to increased red cell destruction are **hemolytic anemias.** Therefore, a shortened red cell survival proves that hemolysis is present; this measurement is usually unnecessary in practice.

Hemolytic anemias may be due to a defect of the red cell itself, an **intrinsic hemolytic anemia**. These are usually hereditary and are commonly grouped as **membrane**, **metabolic**, and **hemoglobin** defects. Alternatively, hemolysis may be due to a factor outside the red cell and acting on it. This is **extrinsic hemolytic anemia**, almost always acquired. The terms *intravascular hemolysis* and *extravascular hemolysis* refer to the **site** of destruction of the red cell—within the circulating blood and outside it, respectively.

Erythrocyte Survival Studies

Shortened red cell survival defines hemolysis. If the hemolytic process is moderate or severe, evidence of increased red cell turnover will suffice to show that hemolysis is present. If the hemolytic process is mild or obscure, red cell survival studies may be necessary.

Radioactive chromium (^{51}Cr) is convenient and widely used for red cell survival studies. Labeled chromate is added to a blood sample in vitro and binds to β-chains of Hb. The chromated red cells are injected intravenously; their disappearance is measured by counting blood, which is sampled every 1 to 2 days for 10 to 14 days. Residual activity is an index of the intravascular life span of the labeled red cells. Because ^{51}Cr emits γ-rays, external scanning can detect sites of red cell destruction.

The erythrocyte life span is usually expressed as the period during which one-half of the radioactivity remains in the blood (the $T_{½}$ ^{51}Cr; Fig. 33.9). Chromium normally elutes from the red cells at a rate of 1% per day. Thus, the half-life of the ^{51}Cr-labeled erythrocytes in normal individuals is 25 to 32 days instead of 60 days. Blood loss, changes in Hct, and recent blood transfusions significantly complicate the interpretation of survival data; therefore, a steady state is necessary for usable results.

In autoimmune hemolytic anemias, the slope of red cell survival produces a straight line when plotted on semilogarithmic paper (see Fig. 33.9). In other hemolytic anemias, two cell populations may exist. In these situations, the survival curve may be composed of an initial steep slope followed by a flatter component (Fig. 33.10) (Bentley, 1977). This type of curve has been seen in hereditary enzyme-deficiency hemolytic anemias, sickle cell anemia, and PNH (Dacie, 1991).

CO production measures heme catabolism immediately before and during the time of the assay. This is the only available method to study short-term fluctuations in red cell destruction (Franco, 2009).

Flow cytometry has been applied in some centers to measure red cell survival. Most techniques use ex vivo labeling of red cells by biotin. The rate of cell disappearance is then measured using fluorochrome-conjugated avidin or streptavidin. With multicolor flow cytometry, additional parameters—such as reticulocytes and HbF content—may be monitored simultaneously (Franco, 2009).

Hemoglobin Destruction

Laboratory findings differ depending on the site of blood destruction, the amount of destroyed blood, and the rate of destruction. If the destruction is **intravascular** and the quantity of destroyed blood is large, free Hb and methemalbumin will be present in the plasma (hemoglobinemia and methemalbuminemia). The urine may contain free Hb and hemosiderin.

Free Hb readily dissociates into αβ-dimers ($\alpha_2\beta_2 \rightarrow 2\alpha\beta$). These are bound to haptoglobin, an α_2-globulin, and the Hb–haptoglobin complex is rapidly removed from the circulation and catabolized by the liver parenchymal cells. This process prevents Hb from appearing in the urine. However, when the plasma Hb level exceeds 50 to 200 mg/dL (8–31 μmol/L), which is the capacity of haptoglobin to bind Hb, the free αβ-dimers of Hb readily pass through the glomerulus of the

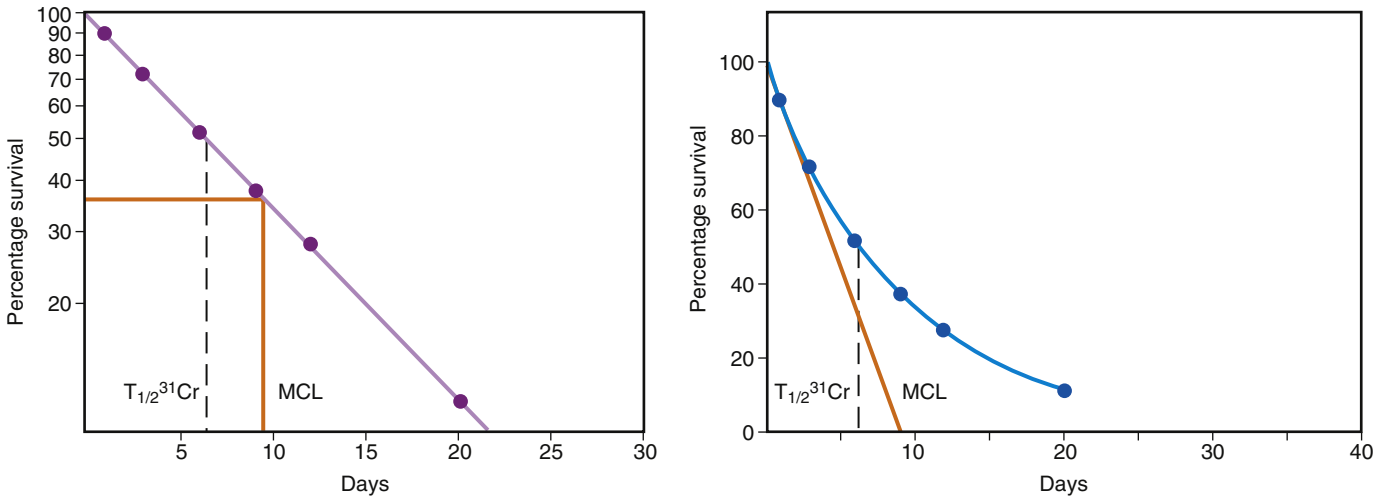

Figure 33.9 Results of ^{51}Cr erythrocyte survival curve in patients with autoimmune hemolytic anemia. The results are plotted on semilogarithmic graph paper. The mean cell life span (MCL) was 9 to 10 days and was recorded at a period when 37% of cells were still circulating. The time of 50% survival ($T_{1/2}$ ^{51}Cr) was 6 to 7 days. (From Dacie JV, Lewis SM. *Practical haematology*, ed 7, Edinburgh, Churchill Livingstone, 1991, p. 386.)

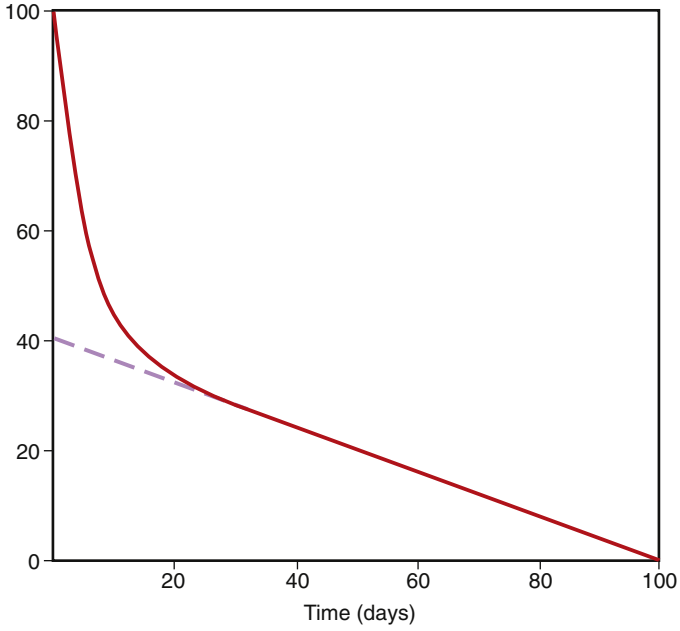

Figure 33.10 Results of radioactive chromium (^{51}Cr) erythrocyte survival curve in a patient with hemolytic anemia containing two cell populations. The percent survival is on the ordinate. By extrapolating the flatter curve to time 0, it can be estimated that 40% of the cells have a mean life span of 100 days. Sixty percent of cells have a mean life span of 5 days. (From Bentley SA. Red cell survival studies reinterpreted. *Clin Haematol* 6:601–623. 1977.)

kidney. Part of the Hb is then absorbed by the proximal tubular cells, where the Hb iron is converted to hemosiderin. When these tubular cells are shed into the urine later, **hemosiderinuria** results. If the amount of Hb in the tubular lumen exceeds the capacity of the tubular cells to absorb it, it reaches the urine (**hemoglobinuria**). In the process, it may be oxidized to methemoglobin (hemiglobin). Plasma Hb not bound to haptoglobin or removed by the kidney is oxidized to hemiglobin. The oxidized heme groups (hemin) are bound to **hemopexin**, a β-globulin, and the complex is rapidly cleared by the hepatic parenchymal cells. If hemopexin is depleted, hemin groups bind to albumin, forming methemalbumin. Once hemopexin again becomes available, it removes the hemin groups from albumin for hepatic clearance (Hillman, 1996).

LD is released from red cells and is increased in serum in hemolysis, especially in intravascular hemolysis; it is cleared more slowly than Hb. If the upper reference value is 207 IU/L, the LD in hemolytic anemia may be increased by as much as 800 IU/L. In megaloblastic anemia, associated with marked ineffective erythropoiesis, the LD is greatly increased—to several thousand units. Serum LD is also increased in other forms of cellular injury. In hemolytic anemias, reversal of the LD isoenzyme pattern is seen, with LD_1 exceeding LD_2.

The normal plasma Hb level is 0.5 to 5.0 mg/dL (0.08–0.78 μmol/L). A rise to 10 mg/dL imparts to the plasma a yellow to orange color. With further increase, the color becomes pink. Levels up to 25 to 30 mg/dL are common in hemolytic anemia. Higher levels usually indicate intravascular hemolysis and are seen in hemolytic transfusion reactions and in paroxysmal cold and nocturnal hemoglobinurias.

If hemolysis is primarily **extravascular**, no hemoglobinemia, hemoglobinuria, or hemosiderinuria is present. Hemolysis is detected by measuring an increase in one of the products of heme catabolism (see Chapter 32):

1. An increase in CO expired or in the blood carboxyhemoglobin level.
2. An increase in indirect-reacting serum bilirubin; because this is bound to albumin, it will not appear in the urine.
3. An increase in urine urobilinogen or, more consistently, in fecal urobilinogen.

The normal urobilinogen in a 24-hour specimen is 0.5 to 4.0 mg (0.8–6.75 μmol) in urine and 40 to 280 mg (0.068–0.470 mmol) in the stool. Following excessive hemolysis, it may increase to 5 to 200 mg in the urine and to 300 to 400 mg in the stool. Examination of feces is more dependable than examination of urine because feces may show an increase when the urine shows none. It may show an increase even when the serum bilirubin concentration is not raised because the normal liver can remove large amounts of (indirectly reacting) bilirubin and of reabsorbed urobilinogen from the blood.

Hemolytic anemia is characterized also by increased red cell production (see Chapter 32). Because of the availability of maximal amounts of iron for Hb formation, red cell production reaches the maximal degree possible (about eight times normal) in severe chronic hemolytic anemia if complicating factors such as folate deficiency do not intervene. If red cell destruction exceeds the capacity of the marrow to replace red cells at the same rate, hemolytic anemia occurs. With less severe hemolysis, the marrow may be able to produce enough red cells that anemia does not occur; this is called *compensated hemolysis*.

Sudden worsening of the degree of anemia may occur in chronic hemolytic anemia and may be due to either of two basic mechanisms. Occasionally, episodes of bone marrow failure (transient arrest of erythropoiesis; see earlier discussion) characterized by erythroid hypoplasia and reticulocytopenia may upset the equilibrium between production and destruction of red cells. In most instances, these **aplastic crises** are probably due to parvoviral infection (Erslev, 2001c). On the other hand, an increased rate of red cell destruction may occur associated with infection or other illness that increases splenic size. This is not associated with erythroid aplasia and is called a *hemolytic crisis*.

Blood Film

The anemia is normocytic or macrocytic. Macrocytosis is due to the presence of increased reticulocytes, which are larger than normocytes. Polychromasia is usually prominent; it may be excessively basophilic and normoblasts may be present, both of which indicate a "shift" of marrow reticulocytes into the blood. Other red cell abnormalities may give a clue

to the nature of the hemolytic process. Spherocytes suggest hereditary spherocytosis (HS) or autoimmune hemolysis (see Fig. 31.12); schistocytes imply microangiopathic hemolytic anemia (see Fig. 31.19); sickle cells, target cells, or crystals suggest a hemoglobinopathy. When hemolytic anemia is acute, increased numbers and younger forms of leukocytes and platelets are often released from the marrow together with erythrocytes. The result is leukocytosis with a "shift to the left" and thrombocytosis with both normal and giant platelets.

Bone Marrow

Erythroid hyperplasia is present and may be striking in degree. With rapidly proliferating erythroid precursors, some degree of dysplasia may also be seen in erythroid precursors. Storage iron is usually increased and sideroblasts are normal or increased in number, reflecting the abundance of available iron for Hb synthesis.

HEMOLYSIS—MEMBRANE DISORDERS

The red cell membrane is made of a lipid bilayer anchored to the spectrin/actin membrane skeleton by two major protein complexes: ankyrin complex and the 4.1R complex. Numerous other transmembrane proteins of various functions, including transport, adhesion, and signaling, are also identified. Some of these proteins are involved in ion exchange, such as Na,K-ATPase and calcium-dependent K^+ channel, also known as *Gardos channel*. These ion channels, pumps, and transporters are essential in maintaining normal RBC hydration, deformability, and shape (Andolfo, 2016).

Hereditary Spherocytosis

HS affects 1 in 5000 of the U.S. population, occurring predominantly in those of Northern European ancestry. Prevalence in other ethnic groups is unknown, although HS has been reported worldwide, particularly in Japanese and African populations. The reported prevalence may be an underestimation in that milder forms may be clinically asymptomatic (Da Costa, 2013). HS is characterized by spherocytic red cells that are intrinsically defective, splenomegaly, and familial occurrence (most often autosomal dominant). In about 15% to 30% of cases, however, neither parent is affected. The hemolytic process is variable in severity and is corrected by splenectomy, although the spherocytosis remains. Cholelithiasis is a relatively common complication, particularly if patients with HS co-inherited Gilbert syndrome (Andolfo, 2016).

The laboratory findings are those of a chronic extravascular hemolytic process: evidence of increased pigment catabolism, erythroid hyperplasia, and reticulocytosis. The direct antiglobulin test is negative. The red cells characteristically have increased osmotic fragility. On the blood film, spherocytes have a smaller diameter and are more intensely stained than normal cells. They have no central pallor, which may be eccentric if present (see Fig. 31.12). The MCV is low-normal and the MCHC is often increased, reflecting a decrease in cell surface. In compensated cases, reticulocytosis may be a sensitive indicator.

Osmotic Fragility Test

Red cells are suspended in a series of tubes containing hypotonic solutions of NaCl, varying from 0.9% to 0.0%, incubated at room temperature for 30 minutes, and centrifuged. The percent hemolysis in the supernatant solutions is measured and plotted for each NaCl concentration. Cells that are more spherical, with a decreased surface/volume ratio, have a limited capacity to expand in hypotonic solutions and lyse at a higher concentration of NaCl than do normal biconcave red cells. They are said to have increased osmotic fragility. Conversely, cells that are hypochromic and flatter have a greater capacity to expand in hypotonic solutions, lyse at a lower concentration than normal cells, and are said to have decreased osmotic fragility (Fig. 33.11).

The osmotic fragility of freshly drawn blood is usually increased in HS but may be normal in mildly affected patients. In blood that is incubated at 37°C for 24 hours before the test is performed, the osmotic fragility is almost always increased (Fig. 33.12).

The increased osmotic fragility of freshly drawn blood is characteristic but not specific; it may occur in acquired spherocytic anemias, such as immune-mediated hemolytic anemia. A greater difference in median fragility (after incubation from before incubation) occurs in HS cells than in control normal cells; this is an important diagnostic feature in HS. A tail of very fragile cells conditioned by the spleen is usually seen. The tail usually disappears after splenectomy. Cells with increased surface/volume ratio, such as target cells, are osmotic resistant. These cells are seen in iron deficiency, thalassemia, liver disease, and reticulocytosis.

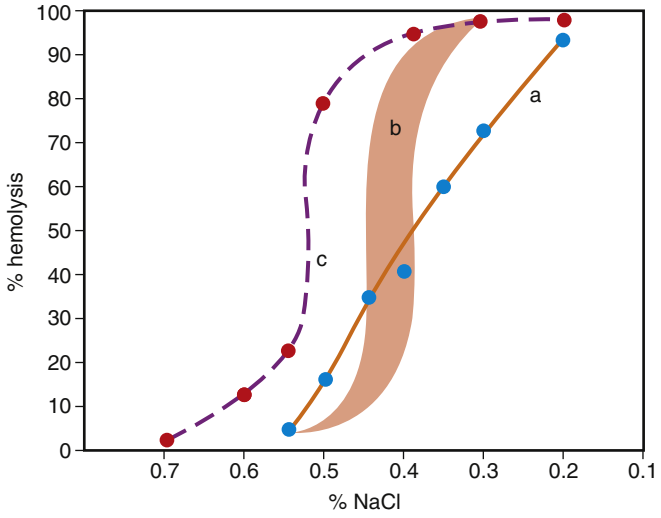

Figure 33.11 Erythrocyte osmotic fragility. *a,* Thalassemia, showing a small fraction of cells with increased fragility *(lower left)* and a larger fraction of cells with decreased fragility *(upper right). b,* Normal curves fall in the shaded area. *c,* Hereditary spherocytosis, showing increased osmotic fragility.

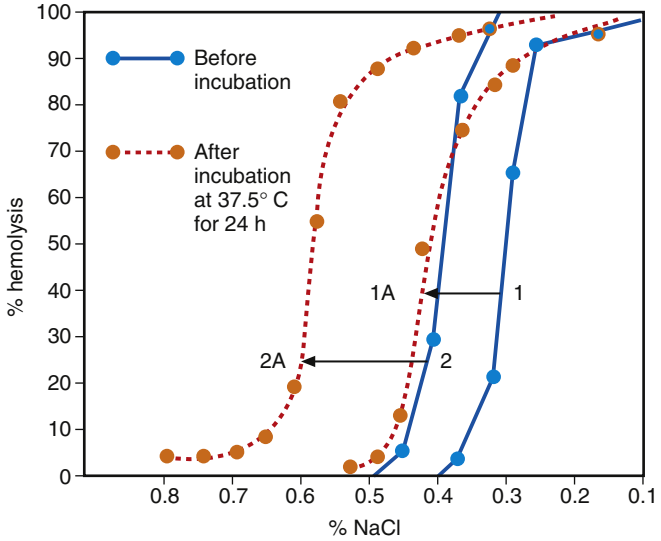

Figure 33.12 The effect of incubation on erythrocyte osmotic fragility. The change in the osmotic fragility curve from "before incubation" to "after incubation" is illustrated for normal blood (1→1A) and for blood from a patient with hereditary spherocytosis (HS) (2→2A). Blood in HS characteristically shows a greater increase in fragility with incubation than does normal blood or even blood of acquired spherocytosis (e.g., autoimmune hemolytic anemia).

Autohemolysis Test

Sterile, defibrinated blood is incubated at 37°C for 48 hours (Dacie, 1991). During this time, red cells undergo a complex series of changes, lose membrane, and become more spherocytic. In normal blood, without added glucose, the amount of autohemolysis at 48 hours is 0.2% to 2.0%. In normal blood, incubated with added glucose, the amount of autohemolysis is less—0% to 0.9%.

In HS, autohemolysis is virtually always increased; with glucose, the lysis is diminished to a variable extent. This test is being used less frequently and is probably no more sensitive than the incubated osmotic fragility test (Dacie, 1991).

Additional Tests

Several additional tests have been employed. The most common is the flow cytometry dye binding assessment using eosin-5′-maleimide (EMA) dye. The test has sensitivity and specificity exceeding 90%, although positive results may be seen in other conditions, such as CDA II (Da Costa, 2013; Andolfo, 2016).

RBCs in HS are characterized by an unstable lipid bilayer, which facilitates the release of lipids from the membrane, resulting in loss

of surface area and formation of poorly deformable spherocytes that are selectively retained and damaged in the spleen (the mechanism is sometimes referred to as a vertical defect since it affects the association between the lipid bilayer and the red cell skeleton). The erythrocytes are abnormally permeable to sodium, and there is no defect in energy metabolism, which is, in fact, increased. The increased metabolic activity has been explained as an attempt to compensate for a membrane defect that leaks cations, with degenerative changes and loss of cell membrane accelerated by the metabolic and physical stresses of passage through the spleen.

The genetic defects in HS are heterogeneous but affect the skeletal proteins of the red cell membrane. The ankyrin-1 defect is the most common in Europe and the United States, affecting 40% to 65% and causing low expression of ankyrin associated with mild to moderate disease. Band 3 (*SLC4A1* gene) is the next in prevalence, affecting 20% to 35% of patients and causing mild to moderate disorder. Mutation of α spectrin (*SPTA1* gene) is autosomal recessive and rare, affecting <5%, but usually causes a severe form of HS (Da Costa, 2013).

Hereditary Elliptocytosis

This autosomal-dominant condition probably includes more than one genetic variant. In the U.S. population, the prevalence is approximately 3 to 5 per 10,000. It is more common in individuals of African and Mediterranean ancestry. All cases of hereditary elliptocytosis (HE) are associated with weakening of the membrane skeleton and defective association of proteins that hold the skeleton together, which is sometimes referred to as a horizontal defect (Da Costa, 2013). On the basis of red cell morphology, HE can be divided into three groups: (1) common HE (including hereditary pyropoikilocytosis [HPP]), with elliptocytes that may be rod shaped, (2) spherocytic HE, and (3) Southeast Asian ovalocytosis. The most commonly defined abnormality appears to be a defect in spectrin, resulting in impaired association of spectrin dimers into spectrin tetramers and spectrin oligomers. Other abnormalities include a defect in spectrin-actin-protein 4.1R junctional complex. HPP is associated with two abnormalities: a mutation in spectrin that disrupts spectrin heterodimer self-association and a partial deficiency of spectrin that results in a decreased spectrin/band 3 ratio.

Common Hereditary Elliptocytosis

Most persons with the common form of HE (≈90% of cases) are nonanemic; a minority of this group (perhaps 10%–20%) have mild hemolysis. Nonhypochromic elliptocytes are abundant in the blood film, numbering approximately 15% (see Fig. 31.16), whereas in normal individuals less than 5% of the red cells are elliptical (Gallagher, 2009). The deformity is increased in sealed, moist preparations.

In a subgroup of common HE, especially in black families, affected neonates transiently have moderate poikilocytosis, red cell fragmentation, and budding, with hemolytic anemia. During the first year of life, hemolysis declines and typical HE emerges. Worsening of hemolysis in the neonatal period has been attributed to the presence of fetal hemoglobin, which binds poorly to 2,3-diphosphoglycerate (2,3-DPG). Higher levels of the latter exert a destabilizing effect on spectrin-protein 4.1-actin interaction (Gallagher, 2009).

Hereditary Pyropoikilocytosis

HPP is a severe congenital hemolytic anemia characterized by microcytosis, striking micropoikilocytosis and fragmentation, and autosomal-recessive inheritance caused by homozygous or compound heterozygous mutations. HPP represents a subtype of common HE. It occurs primarily in blacks. In contrast to normal red cells, which show budding and fragmentation when heated to 49°C, HPP red cells fragment at 45°C to 46°C. In white European populations, one parent may carry an asymptomatic polymorphism causing low expression of the α spectrin known as *low-expression Lyon* (α^{LELY}). This polymorphism may be detected in the heterozygous state in 42% and in the homozygous state in 9% of the European population (Da Costa, 2013). This hypomorphic haplotype alone causes minimal damage in both heterozygous and homozygous states since the α chains are produced in excess. However, when inherited with other mutations, the resulting phenotype is HPP (Andolfo, 2016).

Spherocytic Hereditary Elliptocytosis

This subgroup accounts for 10% of cases. A mild to moderate hemolytic anemia and splenomegaly are present, with both elliptocytes and spherocytes, along with abnormal osmotic fragility and autohemolysis tests. Poikilocytes and fragments are usually absent. The molecular basis of this subtype is unknown.

Southeast Asian Ovalocytosis

This subgroup is also autosomal dominant and occurs with high frequencies (20%–30%) in certain populations of the Far East, particularly Malaysia. Hemolysis is usually absent or mild although it may be more pronounced in neonates (Da Costa, 2013). The erythrocytes are less elongated, and some have the appearance of stomatocytic ovalocytes. Many cells contain one or two transverse ridges or a longitudinal slit. This condition is associated with increased resistance to malaria. The underlying defect is related to a deletion of 27 bases from the band 3 gene, resulting in the loss of amino acids 400 to 408 (Andolfo, 2016). Since the function of band 3 is anion exchange ($Cl^-/HCO3^-$), this disorder affects red cell permeability.

Primary Red Cell Hydration Disorders (Permeability Defects)

At the steady state, the erythrocytes contain a very high concentration of K^+ and very low concentration of Na^+ compared with that of the plasma. The regulation of ionic and water content is a dynamic process affected by several mechanisms, including passive leak through ion channels, gradient-driven active transport, and active exchange through Na^+/K^+ pump and Ca^{++} pump. Water passively follows the ionic movements (Caulier, 2018). Primary red cell hydration disorders include hemolytic disorders, such as hereditary stomatocytosis, and predominantly nonhemolytic disorders, such as cryohydrocytosis (may cause mild hemolysis) and familial pseudohyperkalemia.

Hereditary Stomatocytosis

This is an autosomal-dominant disorder that is commonly divided into dehydrated stomatocytosis (DHst) and the rare entity of overhydrated stomatocytosis (OHst). The phenotype varies from asymptomatic to severe hemolytic anemia. In DHst, there is red cell dehydration due to loss of cations, predominantly K^+ and water. MCV is normal or slightly increased despite increased MCHC with stomatocytes seen on blood smears. Red cell survival is not significantly compromised. Recent studies suggest that most cases of DHst are caused by gain of function mutations in the *PIEZO1* gene encoding PIEZO1 protein, which is a cation channel activated by mechanical stimuli. When the PIEZO1 channel is activated, there is a significant Na^+ uptake, which is counteracted by K^+ loss without net water movement. However, it also drives Ca^{++} influx, causing activation of the Gardos channel and loss of K^+ with cell dehydration (Caulier, 2018). In the rare OHst, there is massive cation leak, causing markedly increased MCV (usually above 110 fL) and decreased MCHC. The phenotype is severe, with hemolytic anemia and reticulocytosis. Recent studies suggest that this form is caused by mutations in the Rh-associated glycoprotein, which is a member of the band 3 complex and is involved in ammonium or gas transport (Da Costa, 2013; Caulier, 2018). Individuals with Rh deficiency syndrome, either absent (Rh_{null}) or markedly reduced (Rh_{mod}), usually have hemolytic anemia with stomatocytosis.

Familial pseudohyperkalemia (FP) and cryohydrocytosis (CHC) are additional forms of red cell hydration disorders causing stomatocytosis. CHC is associated with band 3 mutation, causing cation leak at low temperature. It may be associated with mild hemolytic anemia due to minimal leak at 37°C. FP is associated with increased in vitro K^+ leak at cold temperature, affecting mostly specimens and blood components stored at low temperature. It is caused by mutations in the ABC6 transporter (Caulier, 2018).

Paroxysmal Nocturnal Hemoglobinuria

PNH is an acquired clonal stem cell disorder characterized by the production of abnormal erythrocytes, granulocytes, and platelets (Brodsky, 2009). The red cell defect renders them more susceptible to complement-mediated intravascular lysis. Three types of erythrocytes have been described according to their in vitro sensitivity to lysis by complement: type I with normal sensitivity, type II with medium sensitivity (three to five times normal), and type III with extreme sensitivity (15–25 times normal). Several complement defense proteins are decreased or absent in PNH. These proteins include decay accelerating factor (DAF, CD55), membrane inhibitor of reactive lysis (MIRL, CD59), and C8-binding protein (a homologous restriction factor). DAF is a glycoprotein that antagonizes the convertase complexes of complement. MIRL is a protein that controls the membrane attack complex, C5b-9. Other proteins that are deficient in PNH include CD58 (leukocyte function antigen 3), CD14 (endotoxin-binding protein receptor), CD24, and CD16a (Fcγ receptor). Membrane-associated enzymes, such as acetyl cholinesterase and leukocyte alkaline phosphatase, may be deficient

as well. Recent work indicates that deficient proteins and enzymes are attached to the cell membrane by a common glycolipid anchor called GPI. Deficiency of GPI results in secondary deficiency of the attached proteins. Therefore, PNH can be redefined as partial or complete lack of GPI-linked proteins on a population of cells of the hematopoietic system.

PNH is a rare disease with an estimated annual incidence of 4 per million (Brodsky, 2009). The disease is characterized by chronic intravascular hemolysis with or without obvious hemoglobinuria. However, hemosiderinuria is almost constantly present. Typical nocturnal or sleep-related hemoglobinuria is present in a minority of patients. Bouts of hemolysis could be initiated by infection, surgery, whole blood transfusion, injection of contrast dyes, or even severe exercise. The proposed relationship between mild drop in pH during sleep and nocturnal hemoglobinuria has not been confirmed (Brodsky, 2009).

The blood usually shows a normocytic anemia with a reticulocytosis that is often less than expected for the degree of anemia. Hypochromic microcytic anemia is not uncommon, however, and is due to loss of iron in the urine. Neutropenia occurs in three-fifths and thrombocytopenia in two-thirds of patients at some time during the course of disease so that pancytopenia is common. The direct antiglobulin test is usually negative.

The marrow may be hypercellular with erythroid hyperplasia, but it may be hypocellular. PNH clinical categories include classic PNH, PNH in the setting of another bone marrow disorder, such as AA and MDS, and subclinical PNH (Devos, 2018).

Complement-mediated hemolysis is the central mechanism underlying the mortality and morbidity associated with classic PNH. Thrombotic complications are also common, occurring in approximately 40% of patients, and represent a major cause of mortality. Thrombosis occurs in veins in 85% of cases and commonly occurs in unusual sites, such as hepatic (Budd-Chiari syndrome), cerebral, and abdominal veins (Devos, 2018). The absence of CD59 on platelets results in externalization of phosphatidylserine, a site for prothrombinase complexes, thus increasing the propensity for thrombosis. Abdominal pain occurs in approximately one-third of patients and is likely related to reduction of available nitric oxide (NO) being scavenged by free hemoglobin. AA and MDS are frequently associated with subclinical PNH clones in 50% to 60% and 15% to 20%, respectively (Devos, 2018). In these patients, the size of the PNH clone is usually small and cytopenias rather than hemolysis are the predominant feature. The disease may undergo partial remissions and exacerbations. In more than half of patients, both the proportion of abnormal cells and the clinical severity decrease with time. Abnormal cytogenetics can be found in up to 20% of PNH patients. In approximately 3% to 5% of PNH patients, the disease progresses to acute leukemia.

Laboratory Diagnosis. Previous manual tests for the diagnosis of PNH, such as sucrose hemolysis and Ham's tests, have been largely replaced by flow cytometry studies. Markers of hemolysis, such as LD, are commonly elevated in classic PNH.

Flow cytometry using immunofluorescent staining of red cells with a monoclonal antibody against deficient proteins such as CD55, CD58, and CD59 is gradually becoming the standard method of diagnosing PNH. Granulocytes and monocytes provide excellent diagnostic targets for flow cytometry, with CD24 and CD14 being excellent GPI-linked surface antigens, respectively. A fluorescein-labeled proteolysin variant (FLAER) is increasingly being used for the diagnosis of PNH. It binds selectively to the GPI anchor. Guidelines for high-sensitivity flow cytometry detection of minor clones of PNH has been published and are being adopted by many laboratories (Sutherland, 2012).

The gene responsible for the PNH phenotype has been identified on the X chromosome and designated *phosphatidyl inositol glycan A* (*PIG-A*). More than 120 somatic mutations of the *PIG-A* gene have been described. Over the last few years, a humanized monoclonal antibody against the terminal complement protein C5 (eculizumab; Alexion, Cheshire, CT) has been approved for the treatment of patients with hemolytic PNH. This drug significantly reduces hemolysis, transfusion requirements, and thrombosis, and has improved the quality of life for PNH patients (Devos, 2018).

HEMOLYSIS—HEMOGLOBIN DISORDERS

There are two main groups of inherited disorders of Hb: (1) structural variants, with defects in the structure, and (2) thalassemias, with defects in the synthesis of a globin chain. There is an overlap between these groups. A handful of structural variants also have a thalassemic phenotype with decreased synthesis and, hence, level of the abnormal globin chain. Hereditary persistence of fetal hemoglobin (HPFH) is related to the thalassemias, although the phenotype is not clearly thalassemic. Most thalassemias involve the α- or β-globin chain. δ- and γ-Thalassemias are known, but are clinically less significant.

Normal Hemoglobins

The heme group is identical in all Hbs. The globin part of the molecule is a tetramer, made up of two dimers; each dimer contains an α-like and β-like globin. Beyond the embryonic period, there is one type of α-like globin that forms three distinct Hbs with the three different β-like globins. There are also three embryonic Hbs, which are expressed only in the first 3 months of gestation (Fig. 33.13).

Hemoglobin A (α2β2)

HbA is the major normal adult Hb, accounting for about 97% of the total. It consists of two identical α-chains, each with 141 amino acids, and two identical β-chains, with 146 amino acids each. Each chain is linked with one heme group. The molecule is ellipsoidal, with the four heme groups at the surface of the molecule, where they function by combining reversibly with O_2.

Hemoglobin F (α2γ2)

HbF is the major Hb of the fetus and newborn infant. The increased O_2 affinity of fetal blood versus adult blood is due to its lower affinity for 2,3-DPG. The two α-chains are identical to those of HbA, and the two γ-chains, with 146-amino-acid residues, differ from β-chains. In normal individuals, HbF has two types of γ-chains, which differ by one amino acid, having either alanine (Aγ) or glycine (Gγ) at position 136. There is a common polymorphism of the Aγ gene, in which threonine replaces isoleucine at position 75. This HbF variant is called *HbF Sardinia* and is without functional abnormalities. Approximately 10% of total HbF is a negatively charged variant, designated *HbF1*, owing to posttranslational acetylation of the amino-terminal end of γ-chains.

During fetal life, HbF predominates, as γ-chain production is high. β-Chain production begins before the 20th week of prenatal life so that HbA is 10% of the total between 20 and 35 weeks and 15% to 40% at the time of birth. Around birth, the production of HbF is turned down; by 6 months, HbF is usually less than 8%, and by 12 months it is less than 5% in about 90% of infants. Between 12 and 24 months of age, HbF is usually less than 3% but varies from 3% to 10% in about 20% of infants. After the age of 2 years, HbF is normally less than 2% and only traces of HbF (<0.8%) are present in most adults. During fetal life, all red cells produce and contain HbF, whereas in adults only 3% to 5% do so; these are termed *F cells*. Adult production of HbF is regulated by multiple genetic loci, including the Xmn1-HBG2 site in the β-globin locus, the HMIP locus at 6q23, and the bcl11A locus on chromosome 2 (Thein, 2009). Polymorphic variants at these loci cause a modest increase (up to 5%) in HbF in 3% to 5% of healthy adults and underlie most cases of Swiss-type or heterocellular HPFH.

F cells may increase in number when reactivation of HbF synthesis occurs in normal pregnancy and in disorders of erythropoiesis, particularly chronic bone marrow failure syndromes. HbF may be elevated in megaloblastic anemia, myelofibrosis, aplastic anemia, paroxysmal nocturnal hemoglobinuria, refractory anemias, leukemias, and solid tumors (up to 5%–10%). In the second trimester of pregnancy, there could be a slight increase and in hydatidiform moles, a more significant increase—up to 6%.

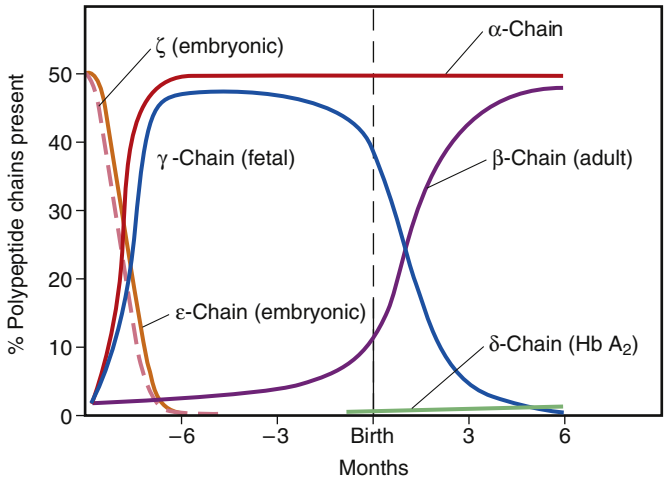

Figure 33.13 Relative proportions of polypeptide chains of hemoglobin present during fetal and neonatal life. (From Bentley SA. Red cell survival studies reinterpreted. *Clin Haematol* 16:601–623, 1977.)

The highest levels of HbF are found in juvenile myelomonocytic leukemia, Fanconi anemia, and erythroleukemia (30%–50%). Elevated HbF is found in a few hemoglobinopathies, in β- and δβ-thalassemias, and in HPFH. The switch from γ-globin to β-globin and the decrease in HbF are delayed in sickle cell disease and in thalassemia trait, each in which a stable HbF level is not reached until adolescence.

Hemoglobin A_2 ($\alpha_2\delta_2$)

HbA_2 accounts for 1.5% to 3.5% of normal adult Hb. Its two α-chains are the same as in HbA; its two δ-chains differ from β-chains in only 10 of their 146 amino acids. Due to its inefficient promoter, the transcription of the δ-globin gene is low and HbA_2 always remains a minor Hb. δ-Chain synthesis begins late in fetal life. The level of HbA_2 gradually increases during the first few years of life, at which time the adult level is reached.

Increased HbA_2 is seen almost exclusively in β-thalassemias. It rarely reaches 6% and never more than 12%. HbA_2 is occasionally increased in hyperthyroidism and megaloblastic anemia. It might be increased in sickle cell trait and sickle cell disease, but the increase is only modest and the level stays below 4.0%. Its level decreases in iron deficiency and α-thalassemia. If the patient with β-thalassemia trait has concomitant severe iron deficiency, the increase in HbA_2 might be dampened down and appear equivocal. In these instances, retesting should be performed after the iron deficiency is corrected. Because of its developmental delay, HbA_2 might not be useful in diagnosing β-thalassemia trait in young infants.

Embryonic Hemoglobins. The zeta (ζ) chain is the embryonic analog of the α-chain and combines with epsilon (ε) chains to form Hb Gower-1 (ζ2ε2) or with γ-chains to form Hb Portland (ζ2γ2). The ε-chain is the embryonic counterpart of the γ-, β-, and δ-chains and combines with α-chains to form Hb Gower-2 (α2ε2). These embryonic Hbs are found at the gestational age of less than 3 months.

The Globin Gene Clusters. Globin synthesis is controlled by two separate gene clusters. The ζ-gene and two α-genes (α-like globins), together with nonfunctioning pseudogenes, are on chromosome 16. Genes for the ε-, two γ-, δ-, and β-chains (β-like globins), and a pseudogene are located on chromosome 11 (Fig. 33.14). Note that there are two functioning α-genes on a haploid chromosome (balanced by only one β-gene). The different globin genes evolved from a common ancestor by gene duplication. There is considerable polymorphism of regulatory sequences within these clusters, accounting for normal variations and wide phenotypic differences in hemoglobinopathy and thalassemia syndromes.

Glycosylated Hemoglobins. The terms *glycation* and *glycosylation* imply the linkage of a sugar to a protein. Approximately 5% of HbA undergoes posttranslational glycosylation, resulting in linkage of sugars to serine, asparagine, and hydroxylysine residues. Glycosylation of Hb increases linearly over the 120-day life span of the red cell. The glycosylated Hbs have been designated HbA_{1a}, HbA_{1b}, and HbA_{1c}. HbA_{1c} contains a molecule of glucose attached nonenzymatically by a ketoamine linkage to the amino-terminal amino group of each β-chain. HbA_{1c} level correlates with the serum glucose level and is used for the diagnosis of diabetes and as an index of metabolic control during the preceding 2 to 3 months. HbA_{1c} may be falsely decreased in conditions associated with rapid red cell turnover, such as hemolytic anemia.

Laboratory Investigation of Hemoglobinopathies and Thalassemias

Current practices include automated complete blood count (CBC); ferritin or free erythrocyte protoporphyrin to rule out iron deficiency; and high-performance liquid chromatography (HPLC) or capillary electrophoresis for HbA_2 and HbF measurement and detection of Hb variants; followed by alkaline and acid electrophoresis when a variant is found and additional studies (Sickledex, molecular studies), as necessary.

Cation-Exchange HPLC and Capillary Electrophoresis. Numerous automated systems have been developed in the last 20 years for initial screening of Hb variants and for separation and determination of percentages of HbA, HbA_2, and HbF. A cation-exchange HPLC system, such as Bio-Rad Variant by Bio-Rad Laboratories (Philadelphia, PA), is commonly used. Resolution of this system is claimed to be similar to that of isoelectric focusing, and data banks of retention times are available (Figs. 33.15 and 33.16) (Bain, 2010; Riou, 1997). Variants detected by HPLC are confirmed by an alternative technique, such as electrophoresis. Capillary electrophoresis is a rapidly developing automated system with a performance similar to that of HPLC (Keren, 2008).

Hemoglobin Electrophoresis and Isoelectric Focusing. Hb molecules in an alkaline solution have a net negative charge and move toward the anode in an electrophoretic system. A practical method for routine Hb electrophoresis is cellulose acetate at alkaline pH. It is rapid and reproducible and separates the major Hb variants S, D, G, C, and E from HbA (Figs. 33.17 and 33.18). Quantification of the major bands is easily accomplished. Those with an electrophoretic mobility greater than that of HbA at pH 8.6 are known as the "fast Hbs"; these include, in order of increasing mobility, Hbs K, J, Bart's, N, I, and H. Hbs A_2, C, E, and O Arab at the slow end are unresolved from each other, as are S, D, G, and Lepore. Citrate agar electrophoresis at an acidic pH provides ready separation of Hbs that migrate together on cellulose acetate: S from D and G, and C from E and O (Fig. 33.19). Isoelectric focusing separates Hbs based on their isoelectric point along a pH gradient, with high resolution (Fig. 33.20) (Basset, 1982).

Acid Elution Slide Test for F Cells. Modification of the original method of Kleihauer and Betke is useful for analyzing the distribution of HbF among red cells. Hemoglobins other than HbF are eluted from the red cells on an air-dried blood film by a citric acid–phosphate buffer (pH 3.3). Only HbF remains in the fixed red cells, and the distribution can be determined after staining. In normal adults, almost all red cells appear as ghosts; 1% to 5% of red cells contain residual Hb and appear pink (F cells). In most types of HPFH, HbF is distributed evenly among red cells (pancellular distribution). In all other conditions, such as thalassemia or a hemoglobinopathy, and in Swiss-type HPFH, the distribution of HbF is heterogeneous or uneven among red cells (heterocellular distribution).

Detection of F cells by Flow Cytometry. This is more accurate than the acid elution slide test. Most adult cells are negative, F cells show moderate fluorescence and fetal cells of neonates show bright fluorescence when stained with an anti–HbF antibody.

HbA_2 Quantitation. HbA_2 quantitation is challenging for two reasons: (1) Its level is low with a narrow range and only a modest increase in disease, requiring a high degree of precision, and (2) Hb variants with similar charge or retention time interfere with its estimation. Several laboratory methods of varying accuracy and precision are being used (Stephens, 2012). Cation-exchange HPLC (Head, 2004) and capillary electrophoresis are considered to be sufficiently precise. Densitometry of electrophoretic bands on cellulose acetate membrane is unreliable. In the HPLC method, HbA_2 level is falsely elevated in the presence of HbS, because aged HbS has a similar retention time and cannot be measured in the presence of HbE as they elute together. Capillary zone electrophoresis, however, can separate HbA_2 from HbE (Borbely, 2013). HbA_2 estimation is used principally in diagnosis of β-thalassemia trait, in which it is elevated up to 7%. HbA_2 values of normals (<3.3%) do not overlap with those of β-thalassemia trait patients (>3.8%), when performed by HPLC.

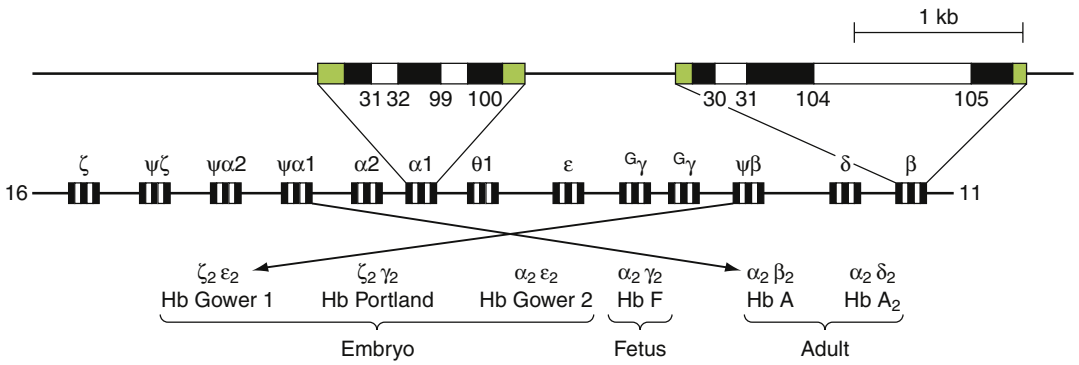

Figure 33.14 The α- and β-globin gene clusters on chromosomes 16 and 11, respectively. In the extended α- and β-globin genes, the introns are shaded dark, the 5′ and 3′ noncoding regions are hatched, and the exons are unshaded. (From Weatherall DJ, Clegg JB. *The thalassemia syndromes*, ed 4, Oxford, Blackwell Scientific Publications, 2001.)

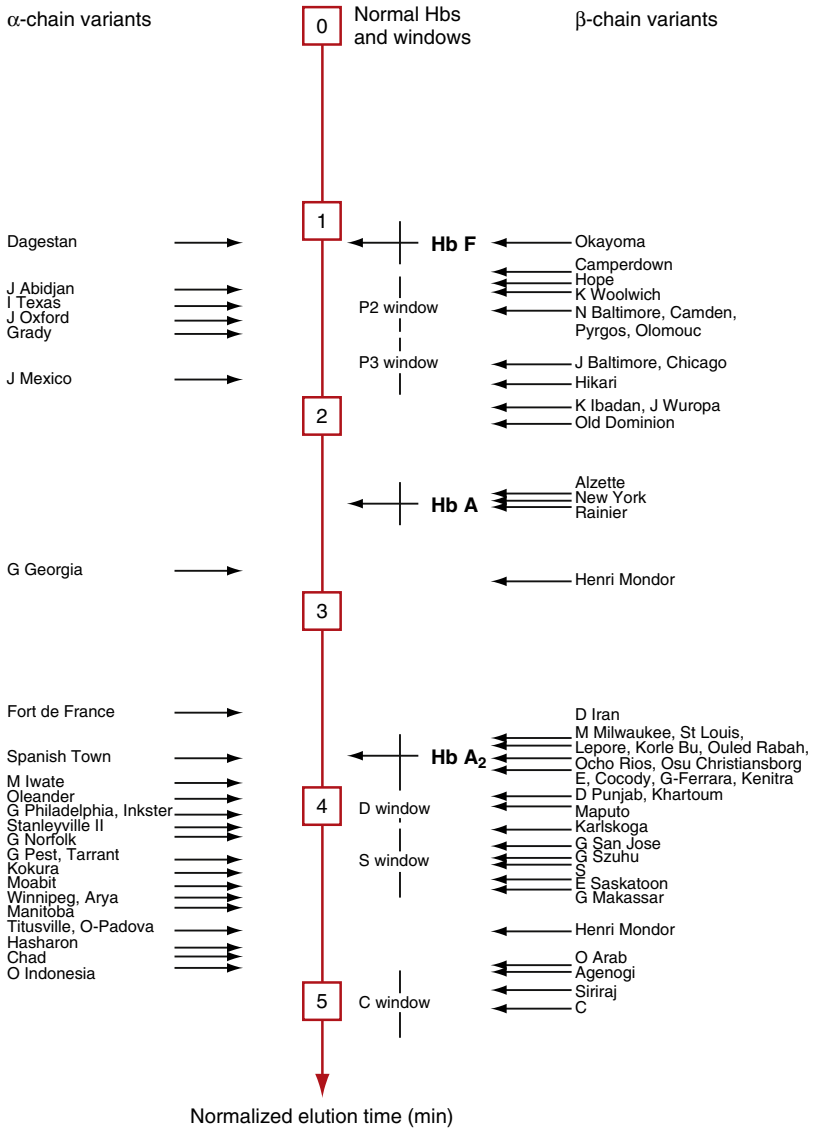

Figure 33.15 Elution times of 74 hemoglobins. Elution times were normalized to a reference value of 3.8 minutes for HbA_2. Cation-exchange high-performance liquid chromatography (HPLC) separation by the Bio-Rad Variant system, using the β Thalassemia Short Program. (From Riou J, Godart C, Hurtrel D, et al.: Cation-exchange HPLC evaluated for presumptive identification of hemoglobin variants. *Clin Chem* 43:34–39, 1997.)

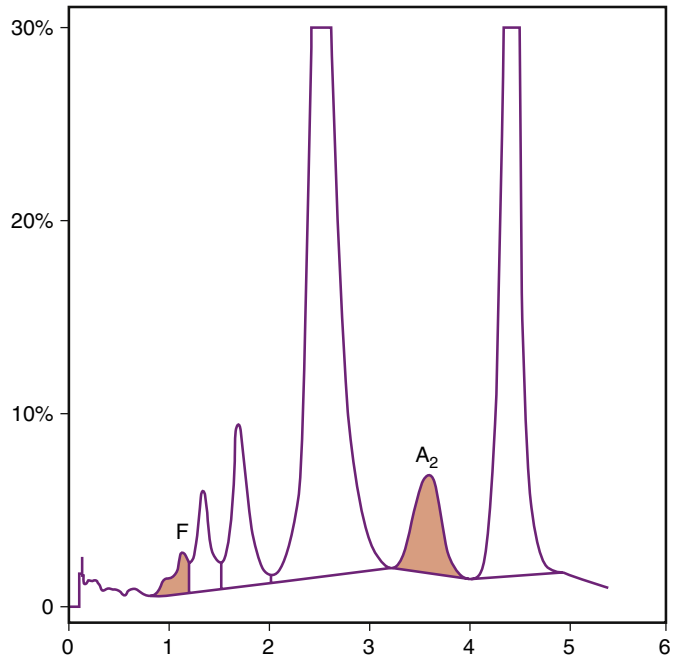

Figure 33.16 Ion-exchange high-performance liquid chromatography (HPLC) separation of hemoglobins (Hbs): patient with sickle cell trait: Hbs F, A, and A_2 and an abnormal Hb in the S window are detected. Hemoglobin A_2 cannot be quantified because of the presence of HbS. (Bio-Rad Variant Classic Hb Testing System, Bio-Rad Laboratories, Philadelphia, PA.)

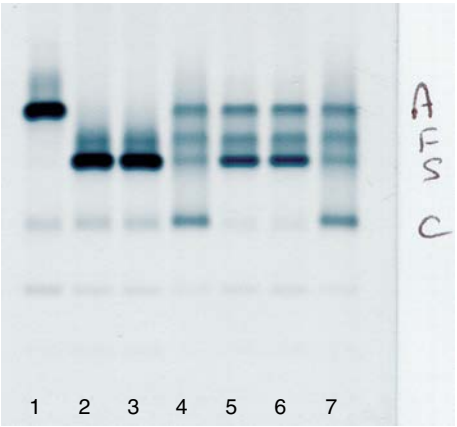

Figure 33.17 Electrophoretic separation of hemoglobins at alkaline pH. 1, Normal adult; 2 and 3, 17-year-old with sickle cell anemia; 5 and 6, patient with sickle cell anemia, recently transfused; 4 and 7, Hbs A/F/S/C standard (Hydragel 7 Hemoglobin/Hydrasys System, Sebia Electrophoresis, Norcross, GA).

Sickling Test—Metabisulfite Slide Test. Adding sodium metabisulfite, a reducing substance, to blood enhances deoxygenation of Hb and sickling of HbS (Fig. 33.21). The test does not distinguish sickle cell anemia from sickle trait or other HbS syndromes because all red cells sickle, although sickling occurs more rapidly with greater amounts of HbS in the cells. Positive tests may occur with other rare sickling hemoglobins (Hbs S Travis, C Harlem), HbI, and high concentrations

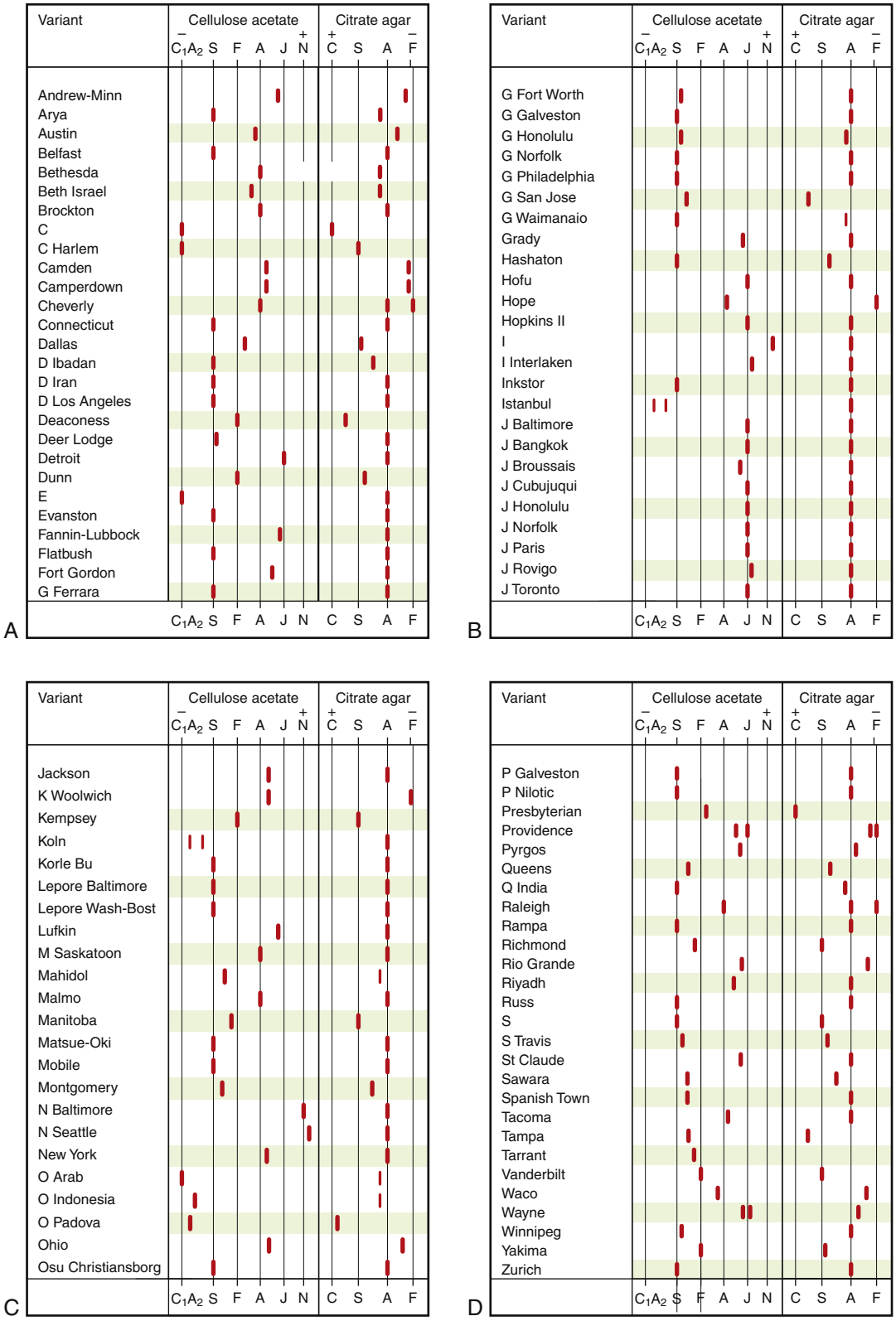

Figure 33.18 Electrophoretic mobility of 102 hemoglobin variants at alkaline (cellulose acetate) and acidic (citrate agar) pH. (Courtesy of Winston Moo-Penn and Danny Jue.)

of Hb Bart's. Hb I, an α-chain variant, has normal functional properties. False-negative tests may occur if HbS concentration is less than 10% (as in very young infants) or if deoxygenation is inadequate (e.g., deterioration of reagent).

Sickle Solubility Test. In this nonquantitative test, red cells are lysed with saponin, and Hb is reduced by dithionite (sodium hydrosulfite). Reduced HbS is insoluble in concentrated inorganic buffer (2.3 M phosphate buffer), and the polymers of deoxy-HbS obstruct light rays to produce opacity. The test is useful in screening large numbers of people for the presence of HbS or other sickling Hbs. False-positive reactions (turbid solution) occur also in the presence of many Heinz bodies, as in unstable Hb disorders after splenectomy and in blood protein disorders due to precipitation of plasma proteins. False-negative reactions (clear solution) occur if the amount of HbS is too small, as in severe anemia.

DNA Analysis. Gap–polymerase chain reaction (gap-PCR) is used for the detection of large deletions in α-thalassemias or, less often, in other thalassemia syndromes. In gap-PCR, primers bind to regions flanking common deletions and generate specifically sized PCR products. The six most common α-deletions can be detected in one reaction using multiplex

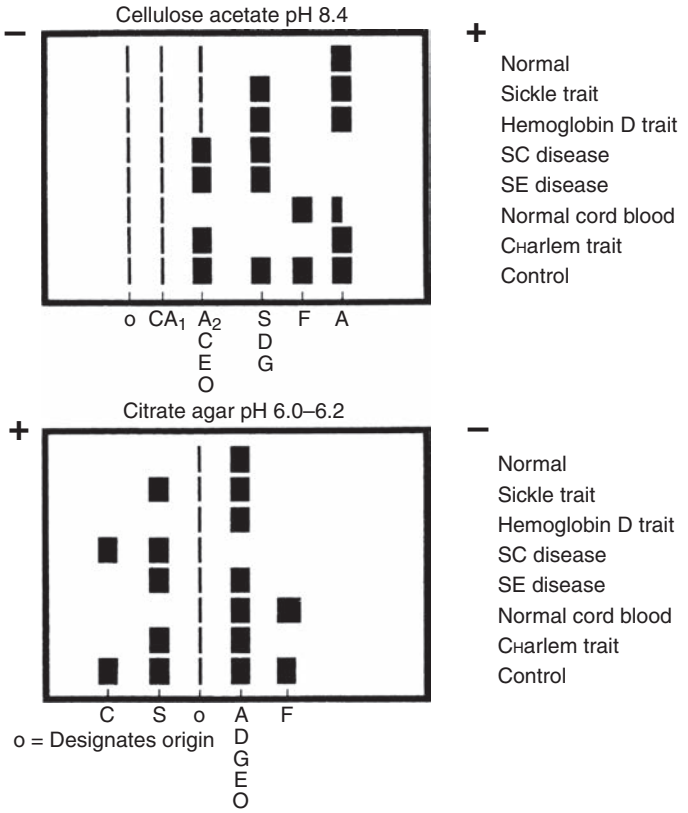

Figure 33.19 Hemoglobin (Hb) electrophoresis. Comparison of various Hb samples on cellulose acetate (at pH 8.4) and citrate agar (at pH 6), showing relative mobilities. The control is a composite sample. The relative amounts of Hb are not necessarily proportional to the size of the band. (From Schmidt RM, Brosious EF: *Basic laboratory methods of hemoglobinopathy detection*, ed 6, Atlanta, U.S. Department of Health, Education and Welfare, Centers of Disease Control and Prevention, 1976. HEW Publ. No. CDC 77-8266.)

PCR primers (Liu, 2000). As mild α-thalassemia is often a diagnosis of exclusion by other methods, DNA analysis should now be offered when evaluating risk to offspring (Sabath, 2017). DNA sequencing is utilized to detect single-nucleotide mutations and small deletions that are responsible for most β-thalassemias and hemoglobinopathies.

Structural Hemoglobin Variants

As of 2019, 1351 Hb variants had been identified (http://globin.cse.psu.edu/ Globin Gene Server). Of these variants, 90% are due to single amino acid substitutions. In the remaining 10%, the polypeptide chain is abnormally long or short as a result of termination errors, frameshift mutations, insertions, deletions, or fused or hybrid chains.

A majority affect the α- or β-globin chains. Involvement of the γ-chain and the δ-chain occurs, but because of the small amount of Hb involved, their variants are less often detected and are rarely of clinical significance. A large number of Hb variants that do not cause disease have been discovered in surveys.

New Hbs were assigned letters of the alphabet, then geographic names—usually to distinguish different Hbs with similar electrophoretic mobilities. Several variants of HbD, HbG, and HbJ, for example, are known. Sometimes, a variant is known by multiple names, based on independent discoveries. HbM indicates a variant that forms methemoglobin. Amino acid substitutions in some of the known Hb variants are listed and classified by functional characteristics in Table 33.3.

Hbs S, C, E, and D are, by far, the most important variants (Table 33.4), as shown for African Americans. Together with the thalassemias, they reached polymorphic frequencies in regions where falciparum malaria was/is endemic, owing to partial protection against this parasite by mechanisms still not fully understood. It is estimated that more than 300,000 children are born each year with a severe hemoglobin disorder, either a sickling disorder or thalassemia (Weatherall, 2010).

Abnormal Hemoglobin Syndromes

In homozygous β-chain structural variants, both allelic genes for the abnormal β-chain are present so that no normal β-chain (hence, no HbA) is produced. Because α-, γ-, and δ-genes are normal, HbF and HbA_2 are structurally normal, although they may be increased in amount.

In heterozygous β-chain structural variants, the abnormal Hb is present, in addition to HbA, HbF, and HbA_2. Its level depends on its rate of synthesis and stability but also on its readiness to form dimers with α-chains. This latter process is driven by electrostatic forces between the positively charged α-globin and the negative β-globin. Because most β-globin variants acquire a positive charge, their assembly with the positive α-chain is slower. As a result, the percentage of abnormal Hb is usually less than that of HbA. In the presence of a coexistent α-thalassemia, when β-chains compete for an insufficient number of α-globins, these effects are exaggerated and the level of structural variant decreases further. Similar forces influence the levels of HbA_2. The δ-chain subunit of HbA_2 has a significant positive charge, not favorable for dimer formation. Positively charged β-chain variants also have little affinity for α-chains, leaving excess α-chains for assembly with δ-globin and resulting in a slight increase in HbA_2. This has been described in Hbs S and C trait, but the increase is so minimal that its existence was always questioned.

Compound heterozygotes for a β-chain structural variant and β^+-thalassemia are well known. Here, the quantity of abnormal Hb exceeds that of HbA in contrast to the heterozygous β-structural hemoglobinopathies, in which the reverse is true.

In heterozygous α-chain structural variants, the abnormality in the α-chain will affect all three Hb types. Therefore, six different hemoglobins are found—the three normal hemoglobins and the three abnormal forms.

Compound heterozygotes for two β-chain abnormalities produce two different abnormal β-chains. Therefore, there are two abnormal Hbs and no HbA. An example of this is HbSC disease. Compound heterozygotes for β- and δ-chain abnormalities and for α- and β-chain abnormalities are rare but have provided important information. The latter will have four major Hb types on electrophoresis.

Hemoglobin S

Sickle Cell Trait (HbAS)

The heterozygous state for HbS is the most common hemoglobinopathy in the United States. It is present in about 8% of African Americans and in as many as 45% of the population in certain areas of West Africa. The gene is found throughout sub-Saharan Africa and, at a much lower frequency, in the Mediterranean, Middle East, and India. HbS trait is a benign condition without clinical symptoms or hematologic abnormalities. Added risk associated with sickle cell trait is minimal at most and is seen only in very rare circumstances. Extreme low O_2 tensions can trigger sickling, and a few people have sustained splenic infarction when flying at very high altitude in unpressurized airplanes. Slightly increased incidences of hematuria, impaired ability to concentrate urine, and bacteriuria in women have been reported. Sickle cell trait confers protection to children from the lethal effects of falciparum malaria, which accounts for the major distribution of HbS in Central Africa.

The stained blood film appears normal, except perhaps for a few target cells. Blood cell counts are normal. The sickle cell slide preparation is positive, and almost all red cells eventually sickle. The Sickledex solubility test is positive.

Hemoglobin separation typically shows 60% HbA, 40% HbS, normal HbF, and normal to slightly increased HbA_2, up to 4.0%.

The proportion of HbS is decreased in the presence of α-thalassemia; HbS is less than 35% when one α-gene is deleted and less than 29% when two genes are lost (Head, 2004). In the latter, cells are hypochromic and microcytic. Because 27% of African Americans carry an α^+-thalassemia gene, it is not surprising that their coexistence is quite common. HbS level may also be diminished in iron and folate deficiency. Clinically, the combination of sickle cell trait and α-thalassemia trait is benign, with possible mild microcytic anemia due to the thalassemia trait.

Sickle Cell Disease (HbSS)

Homozygous HbS disease is a severe chronic hemolytic anemia, first manifested in early childhood and often fatal before the age of 30 years. With modern medical care, many patients live longer, but the median age of death in the United States is still only in the 40s. HbS is found mostly in the black population; 1 of every 600 black persons in the United States has sickle cell anemia (Steinberg, 1999).

In HbS (β6 glu→val), the glutamic acid in the sixth position on the β-chain is replaced by valine. HbS is freely soluble when fully oxygenated; when O_2 is removed, HbS polymerizes, with formation of tactoids (fluid crystals) that are rigid and deform the cell into the shape that gave the disease its name. A strong interaction between the side chain of β6 valine and

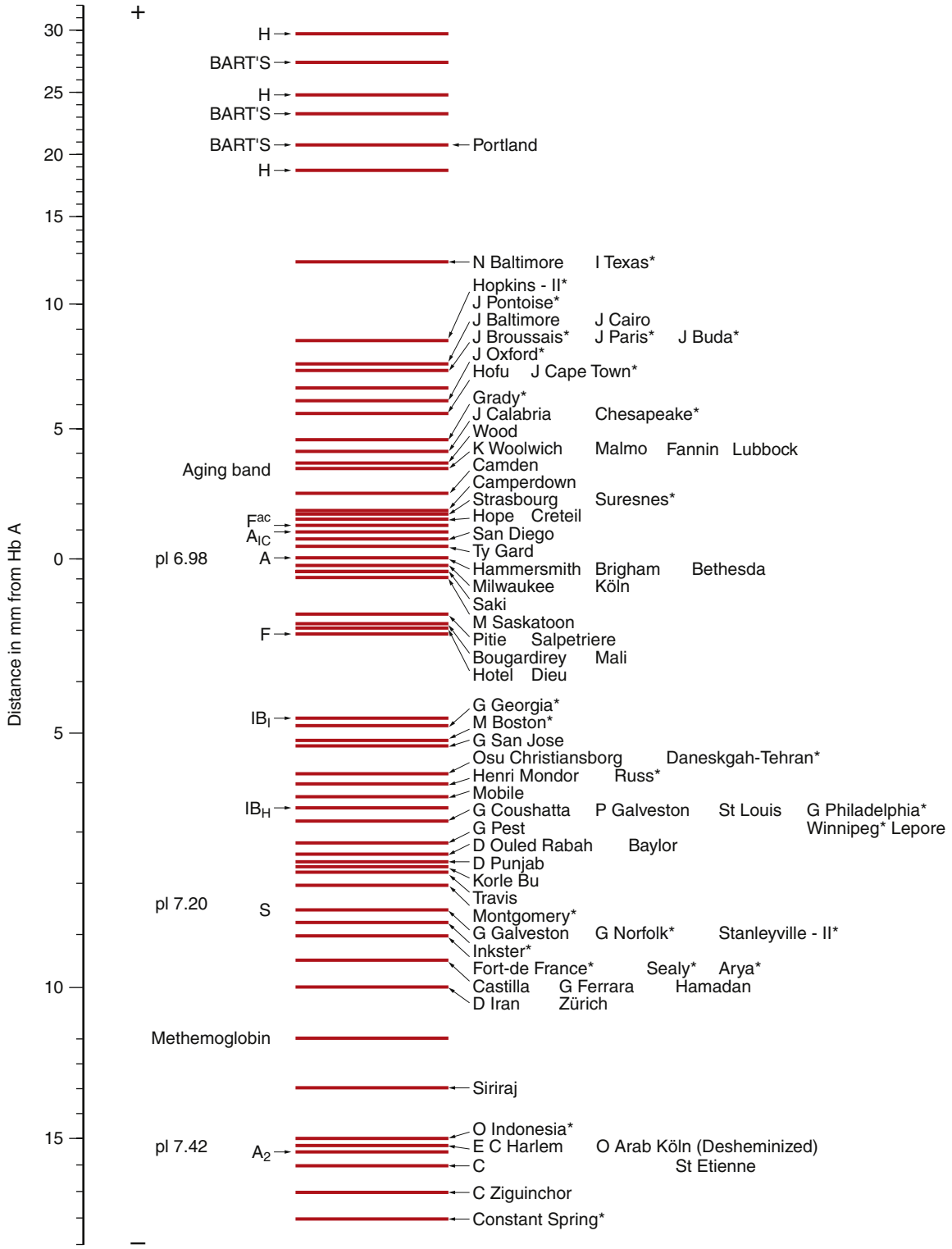

Figure 33.20 Comparison of 57 hemoglobin variants by isoelectric focusing. Asterisk denotes α-chain variants. (From Basset P, Braconnier F, Rosa J: An update on electrophoretic and chromatographic methods in the diagnosis of hemoglobinopathies. *J Chromatogr Biomed Appl* 227:267–304, 1982.)

the hydrophobic pocket of β85 phenylalanine and 88 leucine of another HbS molecule is probably the basis of polymer formation. In homozygous HbS disease, sickling occurs in the peripheral microcirculation at physiologic O_2 tensions, and the rigidity of the red cells is responsible for the hemolysis as well as for most of the complications. These irreversibly sickled cells result from membrane reorganization during repeated episodes of sickling and unsickling in addition to cell dehydration that markedly reduces cellular deformability. Sickle cells contain high calcium levels, which stimulate potassium and water loss and exaggerate cell dehydration (Weatherall, 1999). The hemolytic component is mostly extracellular and is caused by clustering of band 3 of the cell membrane, with the consequence of increased IgG binding and recognition by macrophages. Integrins (α4β1) on the sickle cell surface attach to fibronectin and adhesion molecules expressed on endothelial cells; this is enhanced by inflammatory cytokines, von Willebrand factor, and platelet activation. Together, these interactions cause vaso-occlusion.

Complications. In early childhood, bilateral painful swelling of the dorsa of the hands or feet occurs as a result of sickling and capillary stasis. This is known as the *hand-foot syndrome* or *sickle cell dactylitis*. It lasts about 2 weeks, is accompanied by changes of periostitis as observed by X-ray, and does not occur after the age of 4 years.

The spleen is central to three complications: A **sequestration crisis** refers to sudden pooling of blood and rapid enlargement of the spleen, resulting in hypovolemic shock. This may occur in early

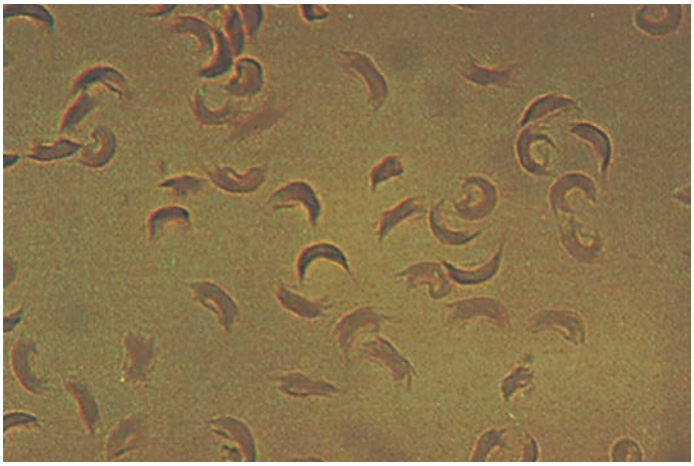

Figure 33.21 Sickle cell preparation, in sodium metabisulfate; sickle cell anemia. Even in sickle cell trait, all cells eventually sickle.

childhood when splenomegaly is present and is often preceded by infection. **Functional asplenia** consists of inadequate antibody responses under some conditions and an impaired ability of the reticuloendothelial system to clear bacteria and particulate material from the blood, probably owing to reticuloendothelial blockade. This may explain in part the increased risk of infection in children with the disease. Salmonellal and pneumococcal infections are unusually prevalent in children with sickle cell anemia. Vaso-occlusive episodes result in progressive infarction, fibrosis, and contraction of the spleen—so-called *autosplenectomy*. Although splenomegaly is present in childhood, a small fibrotic remnant is the rule in the adult.

From early childhood, patients cannot produce concentrated urine, apparently as a result of anoxic damage in the medullae of the kidneys. Hematuria as a result of papillary necrosis is common. Renal insufficiency occurs in 5% to 20% of adults.

Vaso-occlusive crises are debilitating episodes of abdominal and bone or joint pain accompanied by fever, which are probably due to plugging of small blood vessels by masses of sickled cells. Bone necrosis occurs in 10% to 50% of patients and may be a focus for salmonella osteomyelitis. Acute chest syndrome represents episodes of acute chest pain often associated with a new infiltrate in the chest film. Approximately 40% of patients experience at least one episode of acute chest syndrome. Although an infectious origin has been suspected in earlier studies, fat embolism is now considered to play a major role in this syndrome. The various complications that result from recurring vaso-occlusive crises involve many body organs (Steinberg, 2009).

Aplastic crises occasionally can afflict any patient with chronic hemolytic anemia. Temporary failure of red cell production that would not be noticed in a person with a normal red cell life span will cause a serious fall in Hb concentration in chronic hemolytic anemia. This may be the result of infection, particularly parvovirus B19, exposure to toxic drugs, or folic acid deficiency; sometimes no cause can be found. Hemolytic crises due to a further increase in hemolysis are rare.

Diagnosis. The anemia is normochromic and normocytic; polychromasia is increased and nucleated RBCs are present. Sickle cells are almost always found in the stained smear (Fig. 33.22). Target cells are numerous, and Howell-Jolly and Pappenheimer bodies are regularly seen in older children and adults as a result of asplenia. The microhematocrit as an estimate of degree of anemia is unreliable because of excessive plasma trapping. Neutrophilia and thrombocytosis are usual. The marrow shows erythroid hyperplasia.

No HbA is found if the patient has not been transfused recently; more than 80% of the hemoglobin is HbS, 1% to 20% HbF, and 2% to 4.5% HbA_2. The fetal hemoglobin is distributed unevenly among the red cells. HbS and several D and G hemoglobins have the same electrophoretic mobility at alkaline pH, but of these, only HbS gives a positive sickling test.

Hemoglobin SC Disease

The frequency of HbSC disease is almost the same as that of HbSS disease in African Americans. It causes a mild hemolytic anemia. Crises are less frequent and less painful than in sickle cell anemia. Onset is usually in childhood, but the disease might be undetected until later in life. The life expectancy is only modestly shortened. The body habitus is normal or stocky in contrast to the asthenic features in sickle cell anemia.

TABLE 33.3

Functional Classification of Hemoglobin Variants

I. Homozygous: hemoglobin (Hb) polymorphisms: the variants that are most common

HbS	$\alpha_2\beta_2^{6Val}$	Severe hemolytic anemia: sickling
HbC	$\alpha_2\beta_2^{6Lys}$	Mild hemolytic anemia
HbD	Punjab $\alpha_2\beta_2^{121Gln}$	No anemia
HbE	$\alpha_2\beta_2^{26Lys}$	Mild microcytic anemia

II. Heterozygous: hemoglobin variants causing functional aberrations or hemolytic anemia in the heterozygous state

A. Hemoglobins associated with methemoglobinemia and cyanosis
- HbM Boston $\alpha_2^{58Tyr}\beta_2$
- HbM Iwate $\alpha_2^{87Tyr}\beta_2$
- HbM Saskatoon $\alpha_2\beta_2^{63Tyr}$
- HbM Milwaukee $\alpha_2\beta_2^{67Glu}$
- HbM Hyde Park $\alpha_2\beta_2^{92Tyr}$
- HbFM Osaka $\alpha_2\gamma_2^{63Tyr}$
- HbFM Fort Ripley $\alpha_2\gamma_2^{92Tyr}$

B. Hemoglobins associated with altered oxygen affinity
1. Increased affinity and polycythemia
   - Hb Chesapeake $\alpha_2^{92Leu}\beta_2$
   - HbJ Capetown $\alpha_2^{92Gln}\beta_2$
   - Hb Malmo $\alpha_2\beta_2^{97Gln}$
   - Hb Yakima $\alpha_2\beta_2^{99His}$
   - Hb Kempsey $\alpha_2\beta_2^{99Asn}$
   - HbY psi (Ypsilanti) $\alpha_2\beta_2^{99Tyr}$
   - Hb Hiroshima $\alpha_2\beta_2^{146Asp}$
   - Hb Rainier $\alpha_2\beta_2^{145Cys}$
   - Hb Bethesda $\alpha_2\beta_2^{145His}$
2. Decreased affinity—may have mild anemia or cyanosis
   - Hb Kansas $\alpha_2\beta_2^{102Thr}$
   - Hb Titusville $\alpha_2^{94Asn}\beta_2$
   - Hb Providence $\alpha_2\beta_2^{82Asn}$
   - Hb Agenogi $\alpha_2\beta_2^{90Lys}$
   - Hb Beth Israel $\alpha_2\beta_2^{102Ser}$
   - Hb Yoshizuka $\alpha_2\beta_2^{108Asp}$

C. Unstable hemoglobins
1. Hb may precipitate as Heinz bodies after splenectomy: "congenital Heinz body anemia"
   a. Severe hemolysis: no improvement after splenectomy
      - Hb Bibba $\alpha_2^{136Pro}\beta_2$
      - Hb Hammersmith $\alpha_2\beta_2^{42Ser}$
      - Hb Bristol $\alpha_2\beta_2^{67Asp}$
        - Hb Olmsted $\alpha_2\beta_2^{141Arg}$
   b. Severe hemolysis: improvement after splenectomy
      - Hb Torino $\alpha_2 43Val\beta_2$
      - Hb Ann Arbor $\alpha_2 80Arg\beta_2$
      - Hb Genova $\alpha_2\beta_2^{28Pro}$
      - Hb Shepherd's Bush $\alpha_2\beta_2^{74Asp}$
      - Hb Koln $\alpha_2\beta_2^{98Met}$
        - Hb Wein $\alpha_2\beta_2^{130Asp}$
   c. Mild hemolysis: intermittent exacerbations
      - Hb L-Ferrara $\alpha_2^{47Gly}\beta_2$
      - Hb Hasharon $\alpha_2^{47His}\beta_2$
      - Hb Leiden $\alpha_2\beta_2^{6\text{ or }7}$ (Glu deleted)
      - Hb Freiburg $\alpha_2\beta_2^{23}$ (Val deleted)
      - Hb Seattle $\alpha_2\beta_2^{70Asp}$
      - Hb Louisville $\alpha_2\beta_2^{42Leu}$
      - Hb Zürich $\alpha_2\beta_2^{63Arg}$
        - Hb Gun Hill $\alpha_2\beta_2^{91\text{-}97}$ (5 a. a. deleted)
   d. No disease
      - Hb Etobicoke $\alpha_2^{84Arg}\beta_2$
      - Hb Dakar $\alpha_2^{112Gln}\beta_2$
      - Hb Sogn $\alpha_2\beta_2^{14Arg}$
        - Hb Tacoma $\alpha_2\beta_2^{30Ser}$
2. Tetramers of normal chains: appear in thalassemias
   - Hb Bart's γ_4
   - HbH β_4
     - Hb α_4

Data from Winslow RM, Anderson WF: The hemoglobinopathies. In Stanbury JB, Wyngaarden JB, Fredrickson DS, et al., editors. The metabolic basis of inherited disease, ed 5, New York: McGraw-Hill, 1983, pp 2281–2317.

TABLE 33.4

Prevalence of Common Hemoglobin Disorders Among African Americans

	%
Traits	
Silent α-thalassemia (αα/–α)	24
HbAS	8.6
α-Thalassemia trait (–α/–α)	5.7
HbAC	2.4
β-Thalassemia trait	1.5
HPFH	0.1
Hbs D and G	0.026
All others	0.3
Sickling Disorders	
HbSS	0.16
HbS/C	0.13
HbS/thal	0.06
HbS/HPFH	0.004
Other Disorders	
HbCC	0.02
HbC/β-thalassemia	0.02
Homozygous β-thalassemia	0.005

Data from Motulsky (1973), Schneider (1976), and Pierce (1977).
Hb, Hemoglobin; *HPFH,* hereditary persistence of fetal hemoglobin.

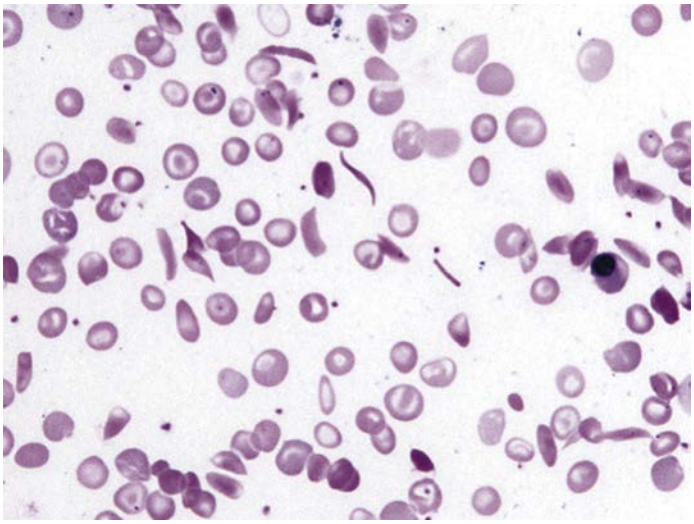

Figure 33.22 Blood film, sickle cell anemia. The erythrocytes are far from one another, suggesting a severe anemia. Numerous pointed sickle cells and target cells are present. Close to the nucleated red blood cell, elliptical cells are seen. These cells have a dense center instead of the usual central pallor, suggesting that they are incipient sickle cells (500 ×).

Splenomegaly might be the only finding on physical examination. Fatigue, dyspnea on effort, frequent upper respiratory infections, attacks of mild jaundice, and arthralgias are seen. Constant hip and low back pain may be present with aseptic necrosis of the head of the femur. Hematuria from renal medullary infarction and splenic infarcts has been described. In pregnancy, crises are more frequent and there is an increase in thrombotic tendency, which can cause massive thromboembolism and sudden death following childbirth. A higher incidence of retinopathy is seen in HbSC disease than in HbSS disease.

Anemia varies from moderate to very mild and is normochromic-normocytic. Anisocytosis and poikilocytosis are mild to severe, and target cells are numerous—up to 85% of the erythrocytes. Plump and angulated sickled cells are often present on the film. The sickling test is positive. HbS is 50% and HbC is slightly less. HbF is usually under 2%. The proportions of Hbs are the same in patients with coexistent α-thalassemia

HbS/β-Thalassemia

This is the third most common sickling disorder after HbSS and HbSC in African Americans, and the most common one in people from the Mediterranean. It usually runs a milder course in black people (usually S/β^+-thalassemia) but causes a severe sickling disorder with manifestations similar to those of sickle cell anemia in people of Italian, Turkish, or Greek descent.

In HbS/β^0-thalassemia, HbA is absent; HbS is 75% to 90%, HbF is 5% to 20%, and HbA_2 is 4% to 6%. This disorder clinically and hematologically resembles sickle cell disease, except for the spleen, which remains enlarged after childhood and into adult life. The main difference is that in HbS/β^0-thalassemia, the MCV and MCH are decreased, and the HbA_2 might be significantly increased. Family study is often necessary for a clear distinction. On the blood smear, pronounced microcytosis, variable hypochromia, and many target cells are present. As a consequence of reduced cellular hemoglobin, HbS polymers are formed more slowly, and fewer sickled cells are present on the smear.

In HbS/β^+-thalassemia, HbA is 15% to 30%; HbS is over 50%, HbF is 1% to 20%, and HbA_2 is 4% to 6%. Although these individuals clinically may resemble those with sickle trait (HbAS), in S/β^+-thalassemia, the amount of HbS always exceeds HbA, while in sickle cell trait HbA always exceeds HbS.

Hb SS/α-Thalassemia

Of patients with sickle cell anemia, 30% to 40% are heterozygous and 2% to 3% are homozygous for α^+-thalassemia. The MCV (83 fL in heterozygotes and 72 fL in homozygotes) and MCH are decreased. The Hb level is higher and reticulocyte count is significantly lower as compared with sickle cell anemia. On the smear, sickled cells are uncommon, similarly to HbS/β^0-thalassemia. Although the anemia is less severe, the vaso-occlusive disease is not; some studies even show increased morbidity and mortality. As described earlier, δ-chains successfully compete with positively charged S-chains for a limited number of α-chains, and HbA_2 levels increase. Hematologically, this cannot be separated from HbS/β^0-thalassemia (Table 33.5). Whenever microcytosis and increased HbA_2 are present in sickle cell anemia, family or molecular studies are to be done to differentiate these entities.

Hemoglobin SD Disease (HbS/D–Los Angeles). SD disease simulates but is less severe than sickle cell anemia and, thus, may also resemble SC disease. It is occasionally seen in the African American population. On routine (alkaline) electrophoresis, the pattern is indistinguishable from sickle cell anemia because HbS and HbD cannot be separated. Agar gel electrophoresis at pH 6.2 will separate HbS and HbD.

HbS/O Arab. Compound heterozygotes of HbS and HbO Arab (β121 glu→lys) have a severe sickling disorder. HbO Arab is found in black and Arabic people.

Other Compound Heterozygosities with HbS. HbE and a few other, less frequent β-variants also cause sickling disorders with HbS. Coexistence of an α-chain variant and a sickle cell trait does not cause a sickling disorder.

Other Common β-Chain Variants

HbC Trait (β6 glu→lys). Hemoglobin C is prevalent in West Africans and in about 2% to 3% of black people. The heterozygous state (HbAC) is asymptomatic, without anemia, with normal or minimally reduced MCV and normal red cell life span. The MCHC might be slightly elevated. Target cells are present on blood film. HbC makes up about 40% of the total hemoglobin. When significant microcytosis is present, it is usually caused by coexistent α-thalassemia, and HbC is reduced to 38%, 32%, and 24% in patients with three, two, and one α -gene, respectively (Weatherall, 2001).

HbC Disease. Homozygous HbC disease is a mild hemolytic anemia with splenomegaly that is often asymptomatic but occasionally results in jaundice and abdominal discomfort. Life expectancy is normal. In the United States, 0.02% of black people have HbC disease (Schneider, 1976). Reticulocytosis is low for the degree of anemia. The anemia is largely a consequence of low O_2 affinity of HbC (Bunn, 1986) and should not be treated. The MCV is usually decreased, and the MCHC is normal or increased. Numerous target cells with an admixture of microspherocytes and minimal polychromasia are seen in the blood. Hexagonal or rod-shaped crystals may be seen in erythrocytes in the stained smear, especially after splenectomy or after slow drying of the smear (Fig. 33.23). As opposed to HbS, crystals of HbC tend to melt at low partial pressure of oxygen (pO_2) and do not cause vaso-occlusive disease. The red cells are dehydrated (causing the increased MCHC) owing to loss of cations and water as a result of interaction of HbC with the red cell membrane. As a consequence, the cells are more rigid and less deformable than normal, increasing their likelihood of being trapped and destroyed in the spleen. HbF is elevated at 2% to 4%, and HbA_2, when measured by HPLC, might be slightly increased; the remainder of hemoglobin is HbC.

TABLE 33.5

Differential Diagnosis of Sickle Cell/Thalassemia Syndromes

Genotype	Clinical Expression	Hb	MCV	HbF	HbA_2	HbA
SS	Severe	7–8	85–95	2–20	2–4	
S/β^0 thal	Moderate to severe	8–10	65–75	5–20	4–6	
SS/α thal	Moderate to severe	8–10	70–85	2–20	3–5	
S/HPFH	Asymptomatic to mild	13–14	75–85	20–30	1–3	
S/β^+ thal	Mild to moderate	11–12	70–80	1–13	3–6	10–30

Data from Bunn (1986) and Steinberg (2001).
Hb, Hemoglobin; *HbA,* accounts for 97% of normal adult hemoglobin; *HbA_2,* accounts for the remaining 3% of normal adult hemoglobin; *HbF,* fetal hemoglobin; *HPFH,* hereditary persistence of fetal hemoglobin; *MCV,* mean corpuscular volume.

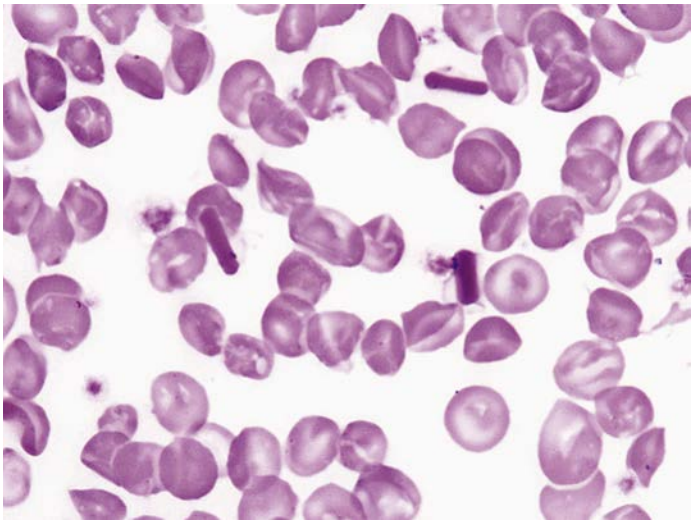

Figure 33.23 Hemoglobin (Hb) C disease, after splenectomy. Before splenectomy, the only morphologic abnormality was the presence of target cells. After splenectomy, Howell-Jolly bodies and Hb crystals, such as those in the center, were present. Note that almost all of the Hb in this particular cell is in the dark bar, and the membrane is still visible. Some such crystals are distinctly hexagonal (1000 ×).

HbC/β^+-Thalassemia. This occurs mainly in black people, in whom it tends to result in little disability, except for anemia in pregnancy. Red cell indices are typical of β-thalassemia trait, but there is anisocytosis and 20% to 50% target cells. Usual values are 65% to 80% for HbC, 16% to 30% for HbA, and 2% to 5% for HbF.

HbC/β^0-thalassemia. People of Mediterranean extraction usually have a moderately severe hemolytic anemia with β^0 or a severe β^+ genotype. This combination is extremely rare in the African population. HbC/β^0-thalassemia may be difficult to distinguish from HbC disease in that HbA is absent in both, and there is an overlap in HbA_2 and HbF levels. HbA_2 is elevated to about twice normal, and HbF is elevated at 3% to 10%.

HbE (β 26 glu→lys). This is probably the most prevalent hemoglobin variant worldwide and the third most common in the United States, behind HbS and HbC. It is found primarily in Southeast Asia, especially in people of Thai and Burmese extraction, but is also found in blacks and whites. HbE is associated with a β-thalassemia phenotype and with a structurally abnormal globin chain. The mutation that causes amino acid substitution also activates a cryptic splice site that competes with the normal RNA splice donor site, and normally processed RNA is decreased. In the laboratory, HbE can be demonstrated to be unstable. It precipitates abnormally in the heat denaturation test and with isopropanol, yet this has no in vivo significance; the red cell survival is normal.

HbE Trait (HbAE). HbAE is asymptomatic, with borderline microcytosis (MCV = 84 ± 5) and no anemia. HbA is 65% to 70% of the total hemoglobin, HbE is 30%, and HbF is normal. Coexistence of one α-thalassemia gene does not change any of these parameters and can be proven only by DNA analysis. If two or three α-thalassemia genes are also present, the proportion of HbE decreases to 21% and 14%, respectively. The proportion of HbE is also significantly lower in iron deficiency.

Hemoglobin E Disease. This is also asymptomatic; it resembles a thalassemia trait, with microcytosis (average MCV = 70 fL), erythrocytosis, normal MCHC, and slight anemia. Thus, HbE behaves as an extremely mild thalassemia. The reticulocyte count is normal, but 20% to 80% target cells are evident on the blood film. HbE accounts for more than 90% of the hemoglobin, with HbF from 1% to 10% and no HbA.

HbE β-Thalassemia. In sharp contrast with HbE disease, this is a severe condition. It is one of the most important thalassemia syndromes, comprising close to half of the severe β-thalassemia cases (Weatherall, 2010). It is most common in Southeast Asia. The clinical variability is marked; rarely, there are very few symptoms, but the usual picture is that of thalassemia intermedia or thalassemia major. Most of the thalassemia alleles are of the β^0 or severe β^+ variety. Ineffective erythropoiesis, a consequence of excess α-globins, red cell indices, red cell morphology, and clinical manifestations, are similar to those in homozygous β-thalassemia. Hbs E, F, and A_2 are present. HbF shows extreme variation, from 5% to 85%; the mean HbF is 42%, and HbE is usually 40% to 60% (Weatherall, 2001).

HbD Los Angeles (Punjab) (β121 glu→gln). This constitutes the most common D variant in African Americans (<0.02%). In the Punjab region of India, heterozygosity reaches 3%. Homozygotes have normal red cell indices, no evidence of hemolysis, and 95% HbD with normal HbF and HbA_2 (Bunn, 1986). Double heterozygotes for HbD Punjab/β-thalassemia have a mild hemolytic anemia with thalassemic red cell indices and increased HbF and HbA_2.

The significance of HbD Punjab is that compound heterozygosity with HbS produces a moderately severe sickling disorder (see earlier discussion of HbSD disease). Other, less frequent D hemoglobins (D Iran, D Ibadan) and G hemoglobins do not cause sickling—a major difference for genetic counseling. D and G hemoglobins migrate with HbS on alkaline electrophoresis but are separated from HbS at acidic pH, migrating with HbA. It is more difficult to separate them from each other. Careful analysis of isoelectric focusing and HPLC are helpful in most cases.

Common α-Chain Variants

HbG Philadelphia (α 68asn→lys). This is the most common α-chain variant in black people. Almost invariably, the linked α-gene is deleted ($-\alpha^G$). Simple heterozygotes ($-\alpha^G/\alpha\alpha$) have 30% HbG and normal red cell indices, but double heterozygotes with α-gene deletion on the other chromosome as well ($-\alpha^G/-\alpha$) have 45% HbG and a thalassemia trait phenotype. As with other α-chain variants, a minor hemoglobin representing a combination of α^G with δ is present close to HbA_2 and helps to differentiate HbG Philadelphia from β-chain variant G and D hemoglobins (sometimes called *G_2 hemoglobin*).

Disorders of Hemoglobin Function and Stability

A number of amino acid substitutions occur in the heme pocket, where they may cause oxidation of ferrous iron to ferric form, producing the methemoglobin form (HbM) or alter the affinity of the heme for O_2. The latter usually alters the stability of the molecule as well. Other substitutions affect the αβ contact sites; these also can change stability and O_2 affinity of the molecule (Bunn, 1994).

These functionally significant hemoglobinopathies are heterozygous; usually, the concentration of the abnormal Hb is less than 50%. Generally, Hbs with abnormal α-chains form a smaller proportion of the total (10%–25%) than those with abnormal β-chains (35%–50%).

Hemoglobins Associated With High Oxygen Affinity and Polycythemia

A total of 101 abnormal Hbs with high O_2 affinity that are associated with familial erythrocytosis are known today (Globin Gene Server). Some are listed in Table 33.3. The O_2 dissociation curve is shifted to the left. The p_{50}, the pO_2 at which Hb is 50% saturated, is decreased. Under physiologic conditions, the normal p_{50} of whole blood is 26 mm Hg; in this disorder, it has ranged from 5 to 23 mm Hg. Because the Hb has high affinity for O_2, it cannot unload the oxygen and the tissues are relatively hypoxic, resulting in increased EPO production and polycythemia. These disorders are autosomal dominant; only heterozygotes have been described. The Hb concentration has ranged from 15.0 to 23.8 g/dL. Measurement of O_2 affinity is required to establish the diagnosis. Because the amino acid substitution is inside the molecule, often the abnormal hemoglobin is indistinguishable from HbA on electrophoresis or HPLC.

Hemoglobins Associated With Low Oxygen Affinity

There are fewer variants with decreased O_2 affinity (see Table 33.3). The O_2 dissociation curve is shifted to the right (increased p_{50}). These individuals

have mild "anemia," as they can unload more O_2 to the tissues and they simply do not need that much Hb. A handful of variants with markedly decreased affinity are associated with cyanosis. In these, O_2 uptake is impaired in the lung and the level of deoxyhemoglobin is more than 5 g/dL, causing cyanosis. The skin and mucous membranes have a slate-gray color. There is no anemia. Many of the unstable Hbs also have decreased O_2 affinity; however, the hemolytic state dominates the clinical picture.

M Hemoglobins: Pseudocyanosis

Thirteen abnormal Hbs are associated with clinical methemoglobinemia and cyanosis that do not respond to methylthioninium chloride (methylene blue) (Globin Gene Server). The color is similar to cyanosis—a brownish color, caused by methemoglobin. The common feature is that all have an amino acid substitution at or near the heme group so that methemoglobin is unusually stable, and reduction to ferrous heme and hence reversible binding of O_2 are prevented. Methemoglobin constitutes no more than 3% of the total Hb in normal humans.

Cyanosis from birth is seen in HbM disease with α-chain abnormalities, or in fetal HbM (HbFM Osaka). In the latter, cyanosis will disappear after the γ-chains have been replaced by β-chains by 6 months of age. Cyanosis does not appear until nearly 6 months of age in HbM variants with β-chain abnormalities for the same reason. Of course, the cyanosis is not associated with enzyme abnormalities in the red cell, toxic drugs, or cyanotic heart disease—conditions that must be considered in the differential diagnosis. Patients usually have no other symptoms.

All HbM disorders thus far discovered have been reported in heterozygotes, probably because homozygosity is lethal. Some types of HbM do not separate from HbA on alkaline electrophoresis. If the hemolysate is first converted to methemoglobin, the HbM will migrate differently from normal methemoglobin at pH 7.1. The absorption spectra of the eluted HbM, which may be distinctive, can be compared with those of normal methemoglobin (Bunn, 1994).

Unstable Hemoglobins

More than 100 Hbs, mostly β-chain variants, have been described in which the stable tetrameric structure is not maintained and Hb precipitates within the red cell as Heinz bodies (Bunn, 1998). Some are listed in Table 33.3. Rare unstable hemoglobins such as HbF Poole are γ-chain variants. The precipitated Hb attaches to the cell membrane, making the cells inflexible. Heinz bodies are removed by the spleen that further damages the cells and causes shortened survival. The O_2 affinity is usually abnormal but may be increased or decreased. Some of these unstable Hbs cause "congenital Heinz body hemolytic anemias."

All patients have been heterozygous. Clinical features have shown considerable variation, from severe hemolytic anemia in the first year of life (e.g., Hb Hammersmith, Hb Bristol) to a very mild chronic hemolytic anemia (e.g., Hb Louisville, Hb Hasharon) that may be exacerbated by drugs (e.g., Hb Zurich). A few unstable Hbs have been discovered incidentally in clinically normal individuals (e.g., Hb Tacoma, Hb Sogn).

Jaundice and splenomegaly are common, as in other hemolytic anemias. More distinctive in some cases is the excretion of darkly pigmented urine (only during hemolytic crises in mild variants). Cyanosis is present in some patients and is due to methemoglobinuria and sulfhemoglobinemia or to low O_2 affinity.

The anemia is normocytic and normochromic to hypochromic, the latter because of the removal of precipitated Hb from aging red cells by macrophages of the spleen and other reticuloendothelial organs. Prominent basophilic stippling, probably related to excessive clumping of ribosomes, is a common feature. Occasional "bite cells" may be seen. Patients with relatively high Hb concentrations in the steady state usually have Hb variants with a high O_2 affinity and an unexpectedly high reticulocyte count (e.g., Hb Köln, Hb Gun Hill). On the other hand, patients with rather low Hb concentrations may be relatively asymptomatic if their Hb has a low O_2 affinity; their reticulocyte counts are unexpectedly low for the Hb concentration (e.g., Hb Hammersmith). Heinz bodies are rarely seen in circulating red cells before splenectomy, although sometimes they may be generated by incubating the red cells with brilliant cresyl blue or new methylene blue. After splenectomy, Heinz bodies are readily demonstrable in a large proportion of cells; the blood film shows irregularly contracted cells and basophilic stippling that may be pronounced.

In splenectomized patients, the Heinz bodies may interfere with Hb determinations and with electronic platelet and white cell counts. Before the absorbance of the hemolysate is measured, it should be centrifuged to remove the Heinz bodies. Platelet and leukocyte counts should be performed by visual methods. Hb electrophoresis is normal in about one-fourth of patients. HbA_2 may be elevated in β-chain variants because of the loss of abnormal Hb from the cells; this phenotype may resemble thalassemia intermedia. HbF may be increased to a level of 10% to 15%. Key laboratory determinations include heat instability and isopropanol precipitation tests.

Heat Instability Test. Most unstable Hbs precipitate more rapidly than normal Hbs when incubated at 50°C (Dacie, 1991). In a hemolysate in Tris buffer, an easily visible precipitate forms within an hour if unstable Hb is present; the control sample is clear or slightly cloudy. Slight precipitation is equivocal; the test should be repeated and the isopropanol precipitation test performed as well. Precipitates accounting for 10% to 40% of the total Hb are found in unstable Hb disorders.

Isopropanol Precipitation Test. A relatively nonpolar solvent weakens the internal bonds of Hb and decreases its stability (Carrell & Kay, 1972). Unstable hemoglobins precipitate within 20 minutes in the nonpolar solvent isopropanol, whereas a normal hemolysate remains clear for 30 to 40 minutes. False-positive results occur with high levels of HbF.

THALASSEMIAS

In thalassemias, globin chains, usually of normal structure, are produced at a decreased rate. *β-Thalassemia* refers to decreased production of β-chains; α-thalassemia, δβ-, δ-, and γδβ-thalassemias refer to reduced synthesis of the respective polypeptide chains. As a result, there is an overall deficit of Hb tetramers in the red cells, and MCV and MCH are reduced. However, it is not the lack of the affected globin chain but rather the accumulation of the unaffected one that causes hemolysis and, primarily in β-thalassemia, ineffective hematopoiesis in severe forms of the disease.

Thalassemia occurs predominantly in persons of Mediterranean, African, and Asian ancestry as, similarly to Hb variants or glucose-6-phosphate dehydrogenase (G6PD) deficiency, thalassemia genes are under selective pressure by malaria. In Greece and Southern Italy, the prevalence of β-thalassemia is around 10%, and that of α-thalassemia is 5%. Between 25% and 30% of black people and 20% of Thai people carry an α-thalassemia gene. Because structural variants and thalassemias occur in the same population, a wide variety of diseases emerge from their interactions.

Several classifications are used. The clinical classification defines *thalassemia major*, a severe and transfusion-dependent form; *thalassemia intermedia*, with less severe symptoms and generally transfusion independent; and *thalassemia minor* (carrier state or trait), without clinical symptoms but with hematologic abnormalities. The genetic classification is based on gene(s) affected by the mutation, heterozygous/homozygous state, absent/reduced rate of globin synthesis, and so forth. Finally, specific mutations cause well-defined syndromes and can be used for classification.

Molecular Defects

In β-thalassemia, there is considerable heterogeneity in the molecular defects. Almost 300 different mutations have been identified as the cause of β-thalassemia. Most are associated with single base substitutions that produce nonsense codons, frameshift, or defects in promoter activity, RNA processing/splicing, or translation, resulting in decreased or unstable mRNA (Thein, 2013). Large deletions are uncommon. In rare structural variants, the production of highly unstable β-chains results in the phenotype of β-thalassemia. Despite this diversity, 20 common mutations account for 80% of β-thalassemia alleles in the world population (Weatherall, 1999). In β^0-thalassemia, β-chain synthesis is absent on the affected chromosome. mRNA is absent or may be present but nonfunctional. In β^+-thalassemia, β-globin chains are present but reduced in quantity.

In $\delta\beta^0$-thalassemia, large deletions involve the δβ– or Aγδβ–gene complex. As a result, no HbA or HbA_2 synthesis is supported from the affected chromosome, but the γ-gene is upregulated and HbF production is increased. Lepore Hbs have δβ-fusion globins that are the result of unequal crossover between δ- and β-globin genes during meiosis.

The α-thalassemias are generally due to gene deletion of various lengths. Two α-globin genes are present on each chromosome 16, surrounded by two highly homologous duplication units, each containing three homologous segments (Z, X, and Y). Unequal crossing over between the Z segments produces a chromosome with one α-gene ($-\alpha^{3.7}$) and another with three (ααα). Similar nonreciprocal crossing over between X boxes causes another common deletion ($-\alpha^{4.2}$; Fig. 33.24). This recombination has a high probability, and chromosomes with missing or extra α-genes are found in every civilization. Nonetheless, only the thalassemic alleles became frequent in certain populations, under pressure from malaria. These defects, affecting only one of the genes, are called *α^+-thalassemia*. The heterozygous genotype can be written (–α/αα). Nondeletion defects are less common ($\alpha^T\alpha/\alpha$). α^0-Thalassemia results from deletion of both α-globin genes on the chromosome (Fig. 33.25), which leads to no α-chain synthesis (– –/αα).

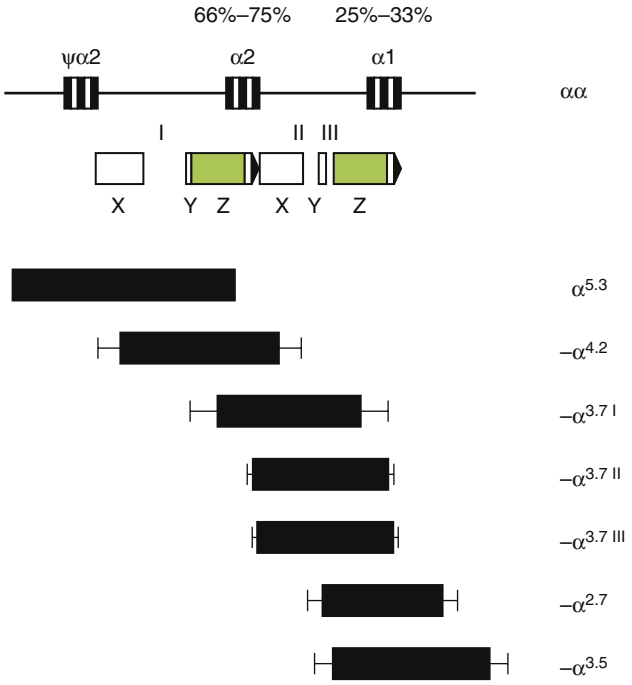

Figure 33.24 Deletions that cause α^+ thalassemia. The homologous boxes (X, Y, and Z) are interrupted by nonhomologous segments (I, II, and III). Black bars show the extent of each deletion and thin bars show the breakpoint areas. In each case, only one α-gene is deleted.

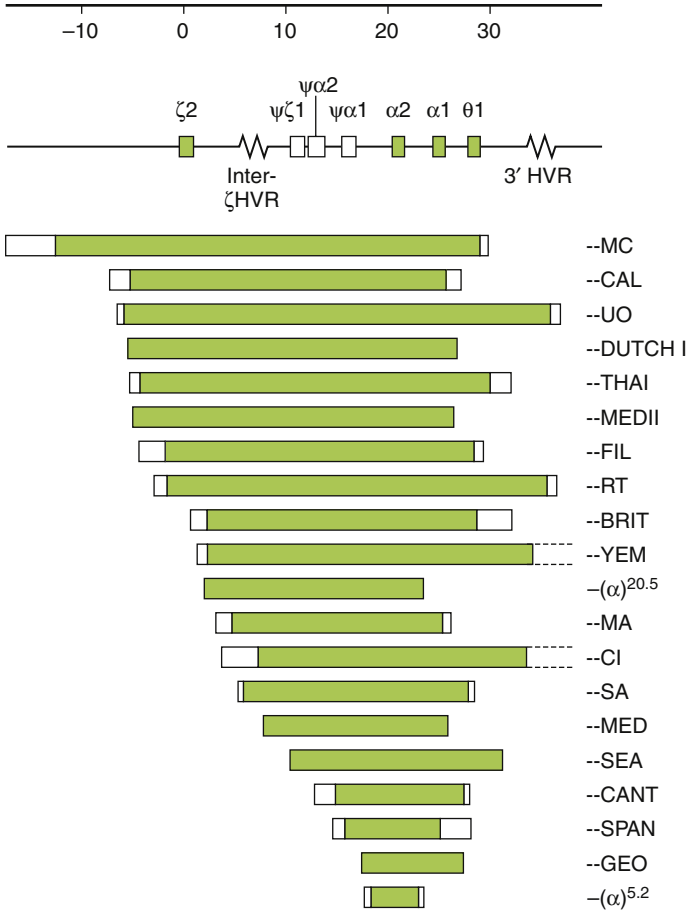

Figure 33.25 Large deletions of the α-gene complex cause α^0-thalassemia. No α-chain synthesis is directed from the chromosome. MED (Mediterranean) and SEA (South East Asian) deletions are the most frequent.

Hb Constant Spring is due to an abnormal termination codon that results in an elongated α-chain with 31 extra amino acids. Because of marked reduction in mRNA stability, the clinical phenotype of α-thalassemia is seen.

β-Thalassemias

Clinical and Hb findings in the β-thalassemias are summarized in Tables 33.6 and 33.7 (Forget, 1982). The disorders are very heterogeneous phenotypically as well as at the level of the molecular defects. The terms *thalassemia major*, *thalassemia intermedia*, and *thalassemia minor* refer to clinical severity and are not genetic designations.

Homozygous β-Thalassemia (Thalassemia Major; Cooley Anemia)

In the absence (β^0) or a marked decrease (β^+) of β-chain production, there is an excess of α-chains. Aggregates of α-chains are unstable and precipitate in the normoblast or erythrocyte and damage the cells. Excess α-chains and their degradation products—heme, hemin, and iron, which serve as foci for the generation of reactive O_2 species—result in the partial oxidation of band 4.1 and a reduced spectrin/band 3 ratio in RBC precursors. Precipitates and cells are removed, causing ineffective erythropoiesis and severe hemolytic anemia. Furthermore, clustering of band 3 in the membrane may be followed by opsonization with autologous IgG and complement and removal by macrophages (Weatherall, 1999).

Clinical findings include jaundice and splenomegaly, which become evident early in childhood. Prominent frontal bones, cheekbones, and jaws impart a mongoloid appearance. These changes and X-ray findings of a thinned cortex of the long and flat bones and thickening of the skull with osteoporosis ("hair-on-end" appearance) reflect extreme bone marrow hyperplasia. Growth is stunted and puberty is delayed. Most patients require regular transfusions and develop problems caused by iron loading. Iron overload commonly develops, and the major cause of death is cardiac failure due to myocardial siderosis by the end of the third decade.

Unlike most hemolytic diseases, the anemia is hypochromic and microcytic. Extreme poikilocytosis with bizarre shapes, target cells, ovalocytosis, Cabot rings, Howell-Jolly bodies, nuclear fragments, siderocytes, anisochromia, anisocytosis, and often extreme normoblastosis are present (Fig. 33.26). Poikilocytosis is more striking in patients with intact spleen, while nucleated RBCs are more numerous after splenectomy. Nucleated RBCs have hypochromic cytoplasm and, especially after splenectomy, aggregates of densely staining Hb, which probably represent precipitated α-chains. Incubation of the blood with methyl violet stains these precipitates in both red cells and erythroblasts. The reticulocyte count is less elevated than expected for the degree of anemia because of destruction of erythroid precursors in the marrow. Serum iron and indirect-reacting bilirubin are increased.

In the marrow, marked erythroid hyperplasia is present. Many late normoblasts show inclusion bodies, as in the blood. Gaucher-like cells are present. Storage iron and sideroblasts are increased.

In β^0-thalassemia, HbA is absent, HbF is as high as 98%, and HbA_2 is about 2%. In β^+-thalassemias (Mediterranean), HbF is 60% to 95%, with HbA present. Although HbA_2 may or may not be increased, the ratio of HbA_2 to HbA is always increased. In black people with β^+-thalassemia, the clinical features are less severe (thalassemia intermedia), and transfusion is usually unnecessary; HbF is 20% to 40%, HbA_2 is 2% to 5%, and the rest is HbA (Table 33.7).

Heterozygous β-Thalassemia (β-Thalassemia Trait; Thalassemia Minor; Cooley's Trait)

This is caused by the β^0-thalassemia gene with absent, or the β^+-thalassemia gene with reduced, β-globin chain synthesis from the affected allele. There are usually no symptoms or abnormal physical signs. The only clinical presentation might be a refractory anemia of pregnancy (Weatherall, 2001).

Most β-thalassemia heterozygotes have a mild anemia but, occasionally, Hct and Hb might be normal. Those of African origin have higher Hb levels than people from the Mediterranean region, reflecting their milder genotype. Characteristically, the RBC count is elevated (5–7 M/μL), the MCH is low (usually <22 pg), and the MCV is low (between 55 and 70 fL). The MCHC is sometimes low but often normal. The reticulocyte count is twice the normal value. On stained films, the cells have a moderate degree of microcytosis, hypochromia, and poikilocytosis; target cells and basophilic stippling are often, but not always, present (Fig. 33.27). In the marrow, there is mild erythroid hyperplasia with ragged cytoplasmic borders—a sign of defective hemoglobinization.

HbA_2 is elevated in the 3.5% to 7% range and HbF is slightly elevated (1%–3%) in about half of cases. In the few cases in which HbF exceeds 4%, it is likely that a gene for HPFH is also present. The relatively rare deletional forms tend to have higher levels of HbF (up to 9%) and in a few families, in which the deletion included the promoter region, HbF was

TABLE 33.6

β-Thalassemias and Their Associated Biochemical and Molecular Defects

	Typical DNA Defect	β-Chain	δ-Chain	γ-Chain	HbF distribution	α: Non–α-globin imbalance
β^+ thalassemia	Mutation	↓	+	+	Heterocellular	+++
β^0 thalassemia	Mutation	0	+	+	Heterocellular	++++
ββ thalassemia	Deletion	0	0	+++	Heterocellular	++
HPFH	Deletion	0 or ↓	0	++++	Pancellular	+

DNA, Deoxyribonucleic acid; *Hb,* hemoglobin; *HbF,* fetal hemoglobin; *HPFH,* hereditary persistence of fetal hemoglobin.
Data from Forget BG: Molecular studies of genetic disorders affecting the expression of the human β-globin gene: a model system for the analysis of inborn errors of metabolism. *Recent Prog Horm Res* 38:257–277, 1982.

TABLE 33.7

Major Categories of β-Thalassemia Syndromes

Syndrome	Genotype	Clinical Features	Hemoglobin Pattern
Homozygous States			
β^+-thalassemia	β^+/β^+	Thalassemia major or intermedia	↓↓HbA, ↑↑HbF, variable HbA_2
β^0-Thalassemia	β^0/β^0	Thalassemia major	>95% HbF, rest HbA_2
$\delta\beta^0$-Thalassemia	$\delta\beta^0/\delta\beta^0$	Thalassemia intermedia	100% HbF
Hb Lepore	Lepore/Lepore	Thalassemia major	85% HbF, 15% Hb Lepore
Heterozygous States			
β^+-Thalassemia	β^+/β	Thalassemia minor	HbA, ↑HbA_2, ±↑HbF
β^0-Thalassemia	β^0/β	Thalassemia minor	HbA, ↑HbA_2, ±↑HbF
$\delta\beta^0$-Thalassemia	$\delta\beta^0/\delta\beta$	Thalassemia minor	HbA, 5%–20% HbF, ±↓HbA_2
Hb Lepore	Lepore/β	Thalassemia minor	HbA, ↑HbF, ↓HbA_2, 10% Hb Lepore

Modified from Orkin SH, Nathan DG: The thalassemias. *N Engl J Med* 295:710–714, 1976.
Hb, Hemoglobin.

found to be unusually high (up to 14%) (Weatherall, 2001). In infants, a slower than normal decline in HbF level is observed, and the adult steady-state level is not reached until adolescence. This is a particularly important consideration in double heterozygosity for β-thalassemia and HbS when HbF level is used to predict prognosis.

β-Thalassemia Trait with Normal HbA_2

In a few cases, both HbA_2 and HbF are normal. These are difficult to distinguish from α-thalassemia trait; only molecular studies might be definitive. The bulk of these cases results from the coinheritance of δ-thalassemia (Weatherall, 2001), either in *trans* or in *cis*, to the β-thalassemia gene. In other patients with normal Hb pattern, only minimal hematologic changes are noted (the "silent" β-thalassemia gene), and only a more severe β-thalassemia syndrome in a family member suggests the presence of a very mild β-thalassemia mutation.

Iron studies are little different from normal (Weatherall, 2001), although iron deficiency often complicates thalassemia trait in childhood and during pregnancy. In severe iron deficiency, the level of HbA_2 may fall into the normal range, thus obscuring the diagnosis of β-thalassemia trait, but this is unusual. Most often, although the level of HbA_2 falls, it remains elevated above the normal range (Weatherall, 2001). Nevertheless, when iron deficiency is present, repeat measurement of HbA_2 is recommended after replenishment of iron.

The differential diagnosis between iron deficiency and β- or α-thalassemia trait can be difficult. Increased RBCs in the presence of decreased MCV is the hallmark of thalassemia trait. An MCV/RBC ratio <13 suggests thalassemia trait; a ratio >13 is more consistent with iron deficiency, but this and other formulas are not conclusive enough for diagnosis.

$\delta\beta^0$-Thalassemia

This is sometimes called *F-thalassemia*, a helpful name, as you have to think of it when there are thalassemic indices and significantly increased levels of HbF. β- and δ-chains are not produced; this is nearly, although not completely, compensated for by increased output of γ-chains. The heterozygous state is similar to a mild β-thalassemia trait, except that HbA_2 is not increased or even slightly reduced (mean level is 2.4%), and HbF is significantly increased (5.4%–20%). In the homozygous state, hemoglobin consists of only HbF.

Clinically, $(\delta\beta)^0$-thalassemia behaves as a mild form of β-thalassemia. In the heterozygous state, the Hb is normal or slightly reduced, the MCH is between 21 and 26 pg, and the MCV is 65–79 fL. There are no clinical symptoms. Homozygotes have a mild form of thalassemia intermedia with Hb level of 10 to 13 g/dL, mildly thalassemic red cell indices, and only minimal hepatosplenomegaly. It is most common in the Mediterranean

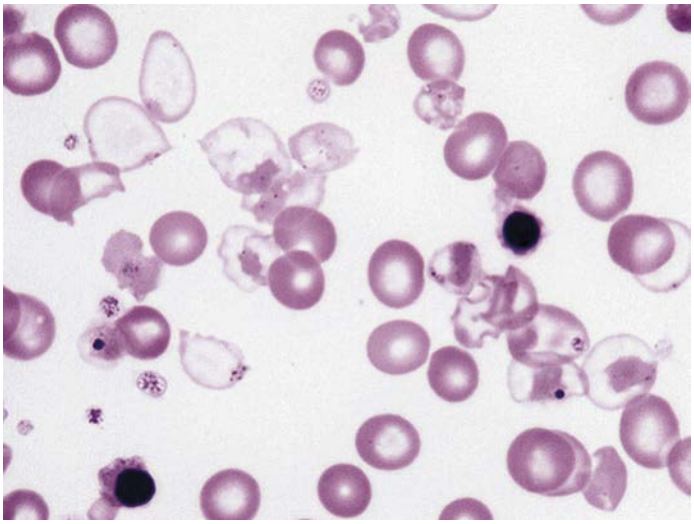

Figure 33.26 Homozygous β-thalassemia. A few cells contain hardly any hemoglobin (Hb), and the Hb is often precipitated at the membrane. Bizarre target cells, Howell-Jolly bodies, and poorly hemoglobinized nucleated red blood cells are seen.

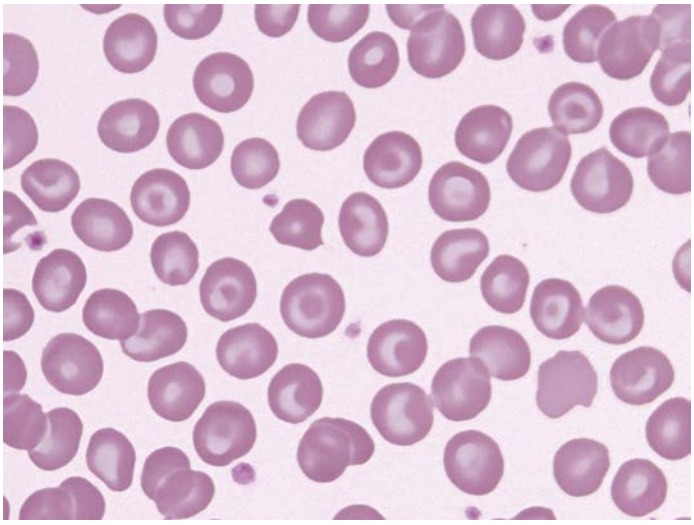

Figure 33.27 β-Thalassemia trait. Hypochromic, microcytic red blood cells with frequent targeting. Mild anemia.

population. The mild phenotype is the result of increased production of γ-chains, which compensate to some degree for the lack of β-chains.

The molecular defect is a long deletion involving the β- and δ- and often also the Aγ-gene. Twenty-one different deletions have been described but the hematologic findings are essentially the same. When the Aγ-gene is also deleted, the accurate nomenclature is $(A\gamma\delta\beta)^0$-thalassemia; homozygotes have a somewhat more severe phenotype.

δβ⁺-Thalassemia: Lepore Hemoglobins

In the Lepore hemoglobins, an abnormal δβ-fusion chain is produced, a result of chromosome crossing-over and fusion of genetic material at the δβ-genes. No normal δ- or β-chain synthesis is directed from the affected chromosome. Because HbF production is only slightly increased and the composite δβ-chain is synthesized at a very slow rate, a severe thalassemic phenotype is produced. Hematologic abnormalities are similar to those seen in β^0-thalassemia. Hb Lepore migrates slightly faster than HbS on alkaline electrophoresis and usually constitutes about 10% of total Hb in the heterozygotes; HbA_2 averages 2%, and HbF is 2% to 3% In homozygotes, Hb Lepore is 10% to 15%, and the rest is HbF. Different Hb Lepores have been described, depending on the point of fusion, but they behave similarly. This is a much more severe thalassemia than the $(\delta\beta)^0$ with transfusion-dependent thalassemia major in the homozygous state.

In a similar mechanism, anti-Lepore hemoglobins have a βδ-fusion gene. Several of these hemoglobins have been described, including P-Nilotic.

Hereditary Persistence of Fetal Hemoglobin

A group of conditions with persistence of fetal hemoglobin production beyond infancy, but without significant hematologic abnormalities, is known as HPFH. There are two major types: pancellular and heterocellular (or Swiss) HPFH.

The pancellular form of HPFH is closely related to β- and δβ-thalassemias, with which it forms a continuous spectrum. At one end of the spectrum is minimal γ-chain production with no compensation for deficiency of β-chains in β-thalassemia. At the other end, HbF production is up and almost entirely compensates for the deficit in HPFH (Weatherall, 2001). As a result, at least in heterozygotes, there is no clear evidence of thalassemia (except maybe borderline microcytosis in a few cases); this serves as a criterion in diagnosis. In clinical practice, a patient with significantly elevated HbF and reduced HbA_2 is suspected to have HPFH if the red cell indices are normal but is diagnosed with $\delta\beta^0$-thalassemia if the indices are thalassemic. Nevertheless, there is a slight α/non–α-chain imbalance, and HPFH could be considered an extremely mild thalassemia. HbF is homogeneously (evenly) distributed among the red cells (pancellular). This is in contrast to β- or δβ-thalassemia, in which the distribution is heterocellular. Pancellular HPFH is relatively rare. It is found in about 0.1% of African Americans and even less frequently in other ethnic groups.

Deletional Pancellular HPFH. In the six deletional forms, the δβ-gene complex is deleted. The black and Ghanaian forms are the most common, but Indian, Italian, and Southeast Asian forms are also well documented. Homozygotes have slightly microcytic, hypochromic red cells, but no anemia. HbF is 100%; no HbA or HbA_2 is present. The Hct can even be high—a result of high O_2 affinity of HbF. In the heterozygote, no hematologic abnormalities are found. HbF is 15% to 30%, and HbA_2 is decreased at 1% to 2.1%.

Hb Kenya. This is a fusion Hb analogous to the Lepore Hbs. It contains a γβ-fusion gene and is associated with an HPFH phenotype. In the heterozygote, Hb Kenya is around 10%, HbF is 7%, and HbA_2 is reduced.

Nondeletional Pancellular HPFH. A mutation in the promoter region of one of the γ-genes results in increased synthesis of HbF. Output from the δ- and β-genes in *cis* is reduced. Levels of HbF range from 3% to 31%, HbA_2 is invariably low, and the red cell indices are close to normal. There are two particulars to keep in mind. First, β-chain synthesis is decreased, but not absent, from the affected chromosome: compound heterozygotes of this form of HPFH and HbS on the other chromosome do have HbA (≈30%). The hemoglobin composition is similar to that seen in HbS/β^+-thalassemia, except that HbA_2 is reduced. Second, it is not rare to find it together with an α-thalassemia gene, which is highly prevalent in African Americans.

Heterocellular or Swiss-type HPFH has less HbF, ranging from 2% to 5%. The distribution of HbF is uneven (heterocellular): Both HbF cells and erythrocytes completely lacking HbF are present. It was first described among healthy Swiss army recruits but is present in other populations and is quite common. It is caused by polymorphic variations at three well-known and other lesser known loci that regulate adult HbF production (Thein, 2009). In normals or in carriers of β-thalassemia or HbS, there is only a minimal increase in HbF. When inherited with HbSS or homozygous β-thalassemia, however, the result could be an unusually high level of HbF and milder disease.

α-Thalassemias

α-Thalassemia is probably the most common single-gene disorder in humans. Its distribution is largely limited to tropical and subtropical regions of Asia and Africa and the Mediterranean, where it reaches extremely high frequencies.

Two α-globin genes are present on each chromosome 16. α-Thalassemias are classified according to the total output of these two linked α-globin genes. In α^0-thalassemia, both genes are inactive (– –/), but in α^+-thalassemia, only one gene is defective as the result of deletion (–α/) or, less frequently, of mutation ($\alpha^T\alpha$/). Nondeletional forms usually result in less globin output from the linked α-gene and more severe phenotypes. Rarely, the chromosome has a deletion and a separate mutation (α^T–/). Previously, α^0 and α^+ were called *α-thalassemia 1* and *α-thalassemia 2*. This was rather confusing, as the milder defect with one affected gene was called *α-thalassemia 2*, and the more severe genotype with two defective genes was called *α-thalassemia 1*. These terms were also used to describe clinical phenotypes.

Unlike the extremely unstable α-chains in β-thalassemia, excess β- and γ-chains can form stable tetramers, hemoglobin H (β_4), and Bart's (γ_4). These precipitate in aging red cells and, through interaction with the cell membrane, cause hemolysis. This is mostly a hemolytic anemia, whereas in β-thalassemia, ineffective erythropoiesis predominates.

α-Thalassemia Syndromes

Four α-thalassemia syndromes result from the combination of these genotypes, which roughly correspond to the loss of 4, 3, 2, or 1 genes from the normal complement (αα/αα; Table 33.8). In the following discussion, nondeletion forms are not always depicted separately for the sake of simplicity.

Hemoglobin Bart's Hydrops Fetalis (– –/– –). Complete absence of α-chains is incompatible with life. Infants are stillborn with severe edema, marked anemia, and marked hepatosplenomegaly. The blood shows marked anisocytosis, poikilocytosis, microcytosis, and erythroblastosis. ABO or Rh incompatibility is absent. Because of the absence of α-chains, no HbA or HbF is present. Large quantities of Hb Bart's (γ_4), a variable amount of Hb Portland, and traces of HbH (β_4) are present; all of these migrate faster than HbA on alkaline electrophoresis. Hb Bart's is functionally useless for O_2 transfer, causing extreme intrauterine hypoxia.

TABLE 33.8
α-Thalassemia Syndromes

Syndrome	Defective Genes	Genotype	Clinical Features	Newborn	After First Year
Hydrops fetalis	4	—/—	Fetal or neonatal death with severe anemia	Hb Bart's >80% HbH, Hb Portland	
HbH disease	3	—/–α (—/αα^{CS})	Chronic hemolytic anemia	Hb Bart's 20%–40% (HbCS)	HbH 5%–30% (HbCS 2%–3%)
Thalassemia minor	2	—/αα –α/–α $\alpha^T\alpha$/–α	Asymptomatic, mild anemia, thalassemic indices	Hb Bart's 5%–10%	None
Silent carrier	1	–α/αα (αα/αα^{CS})	No clinical or hematologic abnormality	Hb Bart's ±1%–2% (HbCS)	None (HbCS 1%)

Modified from Wintrobe MM, Lee GR, Boggs DR, et al.: Clinical hematology, ed 8. Philadelphia, Lea & Febiger; 1981.
Hb, Hemoglobin.

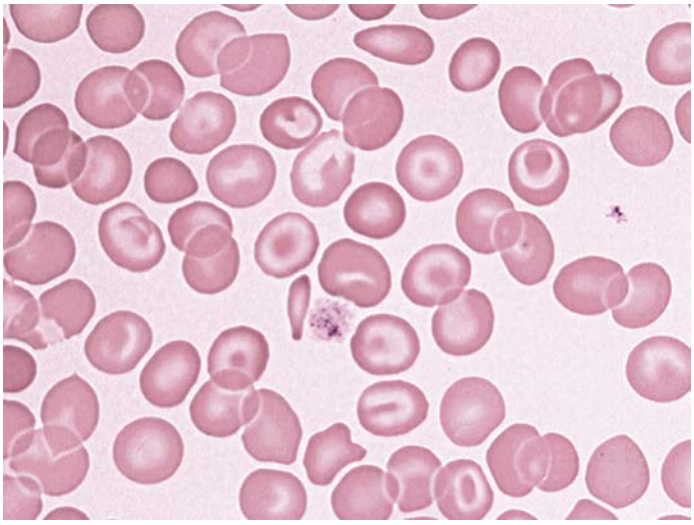

Figure 33.28 Hemoglobin H disease. Mild anemia and target cells.

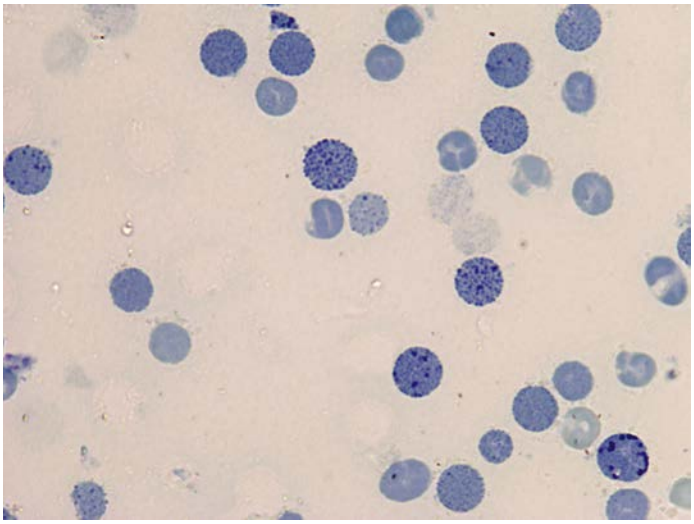

Figure 33.29 Hemoglobin H preparation. Film made after incubation of blood with brilliant cresyl blue. Several red cells contain multiple small, pale-blue inclusions.

Hemoglobin H Disease (–α/– –). Three of the four α-genes are absent. A chronic hemolytic anemia occurs with the clinical picture of thalassemia intermedia in a minority of cases, although the severity varies and most patients do well. Hb H disease is very common in Southeast Asia but is also seen in the Mediterranean and the Middle East. It is very rare, however, in black people, as α^0-thalassemia is uncommon in this group. Splenomegaly and sometimes hepatomegaly are present. Hb values average 3 g/dL less than in age- and sex-matched controls. Transfusion is rarely needed. The anemia may become more severe during pregnancy, but Hb rarely falls below 7 g/dL. The MCV (60–70 fL) and MCH (17–21 pg) are decreased and the RBC count is increased (6.0–6.2 M/μL). The blood film shows hypochromia, basophilic stippling, and anisopoikilocytosis with target cells (Fig. 33.28). Reticulocytes range from 4% to 5%.

Hemoglobin electrophoresis shows a rapidly migrating band of HbH (β4), accounting for 1% to 40% (average 9%) of the hemoglobin, and the slightly less rapidly migrating Hb Bart's in half of the cases. HbH can precipitate and can be lost from the hemolysate in vitro by careless handling or prolonged storage. In old hemolysates, HbH appears as a series of bands on electrophoresis. The percentage of Hb Bart's is 2% to 40% at birth; it gradually falls thereafter, averaging 4.8%, but the level in adults is variable. As in other α-thalassemia syndromes, more Hb Bart's is present at birth than HbH in adult life. HbA_2 is diminished.

Hemoglobin H Preparation. Vital staining of the blood with an oxidizing dye such as brilliant cresyl blue induces inclusion bodies (HbH precipitates) in many of the red cells. During incubation of two parts of blood in one part of 1% brilliant cresyl blue stain, the unstable HbH (β_4) gradually precipitates as uniformly distributed multiple small pale-blue inclusions (Fig. 33.29). HbH inclusions must be distinguished from (1) the granules and reticular networks of reticulocytes, which are darker blue in color, and (2) preformed Heinz bodies, which are larger, also darker blue, and are often attached to the membrane. After 20 minutes of incubation at room temperature, HbH inclusions are present in at least half of the red cells in HbH disease and in rare red cells in α-thalassemia trait. The larger, single Heinz bodies may be found after splenectomy in HbH disease.

α-Thalassemia Trait: Heterozygous α^0-Thalassemia (– –/αα) or Homozygous α^+-Thalassemia (–α/–α). Absence of two α-genes results in clinical features similar to β-thalassemia trait with very mild anemia and thalassemic indices, with MCV ranging from 65 to 75 fL. The α-chain/β-chain synthesis ratio is decreased (≈0.6). Diagnosis is best made at birth by finding 5% to 10% Hb Bart's in cord blood; in normals, only trace amounts (<0.5%) are present. In adults, Hb Bart's is undetectable and Hb studies are perfectly normal, except that HbA_2 might be slightly reduced. HbH inclusions are found in α^0-thalassemia, but rarely in heterozygous or homozygous α^+-thalassemia, and only in a very small percentage of red cells if exhaustively sought after and if the sample is enriched for HbH-containing red cells. Otherwise, no evidence of Hb imbalance is detectable by standard techniques, and the diagnosis is one of excluding iron deficiency, anemia of chronic disease, and β-thalassemia trait. In contrast to β-thalassemia, HbF is normal and HbA_2 is normal or decreased. This condition is absolutely benign, and most patients are diagnosed on routine screening. Hematologic findings are identical in the two distinct genotypes found in different populations: (– –/αα), common in Southeast Asia and the Mediterranean and exceedingly rare in black people; and (–α/–α), most common in those of African descent.

Silent Carrier α-Thalassemia (Heterozygous α^+-Thalassemia) (αα/–α). In this condition, one of four α-globin genes is absent. Hematologic findings are normal, except that the MCV might be slightly reduced, with a mean value of 81 fL and a range of 75 to 85 fL, and the MCH might be minimally decreased. However, the red cell indices often are perfectly normal. During the neonatal period, heterozygous α^+-thalassemia can be diagnosed by a raised level of Hb Bart's (1%–2%) in the cord blood. Hb Bart's disappears by the age of 6 months, and the diagnosis can be made only by molecular studies. Because only 40% of newborns with the heterozygous α^+-thalassemia genotype have detectable Hb Bart's in their cord blood, failure to detect Hb Bart's in the newborn does not rule out silent carrier α-thalassemia, and newborn screening should not be used to rule out this entity.

From large studies comparing hematologic findings of different genotypes, it became apparent that there is a continuum between normal, silent carrier, and α-thalassemia trait. Because there is no clear separation between one- and two-gene defects, some authors group these together as milder α-thalassemia phenotypes. None of the α-thalassemia genes or their combinations can be identified with certainty without molecular studies.

Hemoglobin Constant Spring ($\alpha^{CS}\alpha$/). Hb Constant Spring is due to an abnormal termination codon that results in an elongated α-chain with 31 extra amino acids. It is by far the most common of the elongated α-chain variants. Because of marked reduction in mRNA stability, the clinical phenotype of α-thalassemia is seen. Similar to other nondeletional α^+-thalassemia genes, it causes a more severe phenotype. The homozygous state appears as an asymptomatic, mild hemolytic anemia, with a Hb level of 9 to 11 g/dL. The red cell indices are unusual for thalassemia: The MCV is normal (88 fL) and the RBC count is low (3.9 M/μL). Hemoglobin consists of HbA, normal HbA_2, 5% to 8% HbCS, and trace amounts of Hb Bart's (Weatherall, 2001). Heterozygotes have a silent carrier phenotype with no hematologic abnormality and about 1% HbCS. HbCS undergoes proteolysis and appears as 1 to 4 faint bands migrating either slightly slower or slightly faster than HbA_2 at alkaline pH and is easily missed. HbCS is common in Southeast Asia, where it is found in about 50% of cases of HbH disease ($\alpha^{CS}\alpha$/– –).

Screening and Prenatal Diagnosis of Hemoglobin Disorders

In populations in which there is a significant incidence of severe forms of thalassemia or sickle cell anemia, women should be screened early in pregnancy for thalassemia and the sickle cell trait (Weatherall, 2010). If both parents are carriers, prevention of severe disease is possible through genetic counseling and offering prenatal diagnosis with the option of therapeutic abortion. In many high-frequency regions, successful screening of schoolchildren or premarital counseling has been implemented. Initial tests include MCV (<80 fL), MCH (<27 pg), and HPLC to estimate HbA_2 (>3.5% cutoff values are in parentheses) and to detect common Hb variants.

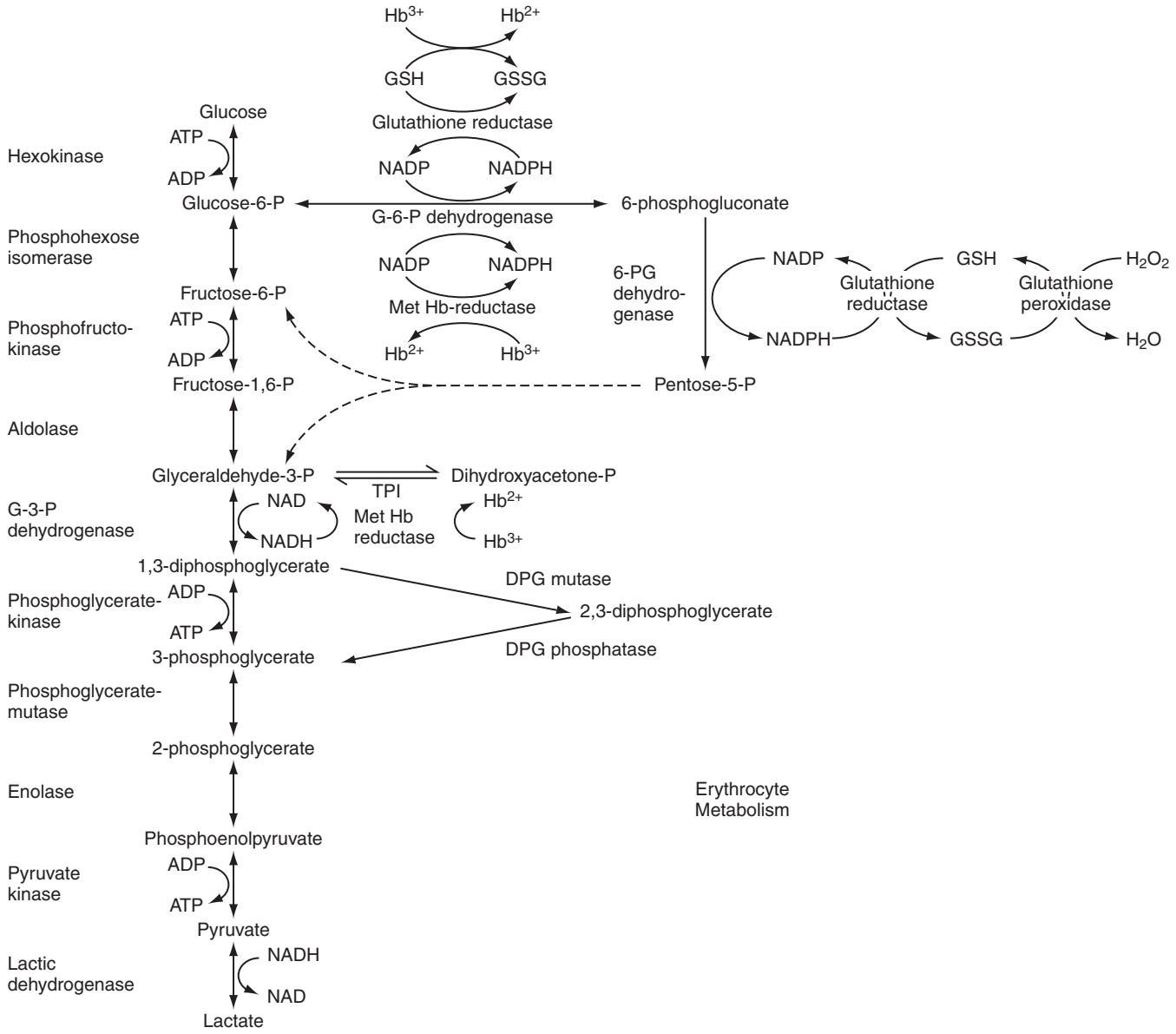

Figure 33.30 Erythrocyte metabolism is discussed in the text. Normally, most hemiglobin (methemoglobin, Hb⁺++) is reduced to hemoglobin (Hb⁺+) by nicotinamide adenine dinucleotide–linked methemoglobin reductase (NAD, Met Hb reductase). Nicotinamide adenine dinucleotide phosphate (NADP)-linked methemoglobin reductase requires methylene blue for activation and is more effective in drug-induced methemoglobinemia than the normal cell mechanism. *GSH,* Reduced glutathione; *GSSG,* oxidized glutathione.

HEMOLYSIS—METABOLIC DISORDERS

Deficient enzyme activity in the erythrocyte may result in abnormalities that lead to premature destruction and hemolytic anemia; these disorders are usually inherited. However, interference with, or oxidative stress on, erythrocyte metabolism can sometimes result in hemolysis in individuals who have normal erythrocytes.

Erythrocyte Metabolism

The mature red cell lacks mitochondria and, therefore, lacks oxidative phosphorylation and Krebs cycle activity. The two main RBC metabolic pathways are the energy-producing glycolytic pathway and the antioxidant-supporting pentose phosphate pathway. Energy production is mainly glycolytic, 90% of which occurs through the Embden-Meyerhof pathway, as glucose goes to lactic acid with the net production of 2 mol of adenosine triphosphate (ATP) per one molecule of glucose (Fig. 33.30). ATP is needed for energy-requiring reactions in the cell: for active cation transport across the membrane, for maintaining membrane deformability, and for preserving the cell's biconcave shape. Glucose uptake by red cells is independent of insulin. Approximately 90% of glucose is consumed in the glycolytic pathway, while 10% is utilized in the pentose phosphate pathway (hexose monophosphate [HMP] shunt). In addition to energy production, one step of the glycolytic pathway replenishes NADH (reducing agent derived from nicotinamide adenine dinucleotide [NAD]), which plays a major role in protecting Hb from oxidative stress. Most of the hemiglobin (methemoglobin, oxidized Hb) produced in the normal cell (about 3% of the total per day) is reduced by NAD-linked methemoglobin (MetHb) reductase. The HMP shunt generates nicotinamide adenine dinucleotide phosphate (NADPH) in the first two steps through the enzymes G6PD and 6-phosphogluconate. NADPH production is linked to glutathione reduction and, through this mechanism, to preservation of vital enzymes and Hb from oxidation. Small amounts of oxidized hemoglobin (MetHb) are reduced by glutathione (GSH). The activity of the HMP shunt increases when the cell is exposed to an oxidant drug, probably as a result of increased NADP production. If an enzyme in this pathway lacks activity, GSH cannot be regenerated and it will remain in its oxidized form as GSSG. Thus, Hb and other cellular structures will not be protected from the oxidant stress. Oxidation in the red cells is mediated by high-energy derivatives of O_2, referred to collectively as *activated* O_2 (van Solinge, 2010). Oxidized globin chains denature and precipitate as Heinz bodies, which adhere to the membrane, inducing rigidity and a tendency to lyse. Moderate enzyme deficiencies in this pathway (e.g., in G6PD) may not be associated with anemia under normal conditions. However, an acute hemolytic episode occurs if the cells are challenged by oxidant stress (e.g., drugs, infection).

Deficiencies in the Embden-Meyerhof pathway result in impaired ATP generation and a chronic hemolytic anemia. The mechanism of red cell destruction here is less clear. Heinz bodies are not formed. Lack of cell

deformability and impaired cation pumping are important in the hemolytic process. However, ATP deficiency is difficult to demonstrate in many patients, and other disorders associated with more severe ATP deficiency are not associated with significant hemolysis (van Solinge, 2010).

The Rapoport-Luebering shunt provides for the conversion of 1,3-diphosphoglycerate (1,3-DPG) to 2,3-DPG instead of directly to 3-phosphoglycerate (3-PG; see Fig. 33.30). If this shunt is operating, generation of 2 mol of ATP (per mole of glucose) is bypassed; the result is no net energy production in glycolysis. However, 2,3-DPG combines with the β-chain of adult Hb and decreases the affinity of Hb for O_2. At a given pO_2, therefore, increased 2,3-DPG allows more O_2 to leave Hb and go to the tissues; the O_2 dissociation curve is shifted to the right. Increased activity of this shunt is apparently stimulated by hypoxia.

Glucose-6-Phosphate Dehydrogenase Deficiency

About 10% of male American blacks who were given the antimalarial drug primaquine during the Korean War in the 1950s developed a self-limited, acute hemolytic anemia (Beutler, 1994). The relationship between antimalarial drugs and hemolysis had been observed earlier, in the 1920s (Beutler, 1999). Only the older red cells were destroyed, and it was eventually determined that the deficiency in susceptible red cells was in G6PD. Reticulocytes have five times higher enzyme activity than the oldest erythrocyte population (van Solinge, 2010). It has since been found that G6PD deficiency is widespread throughout the world. Among whites, the highest incidence is in Kurdish Jews; the deficiency is common in the Middle East, in Mediterranean countries, and in Asia. G6PD deficiency is the most common human enzyme defect, present in more than 400 million people worldwide, and is thought to have conferred a selective advantage against infection by falciparum malaria (Glader, 2019).

G6PD is present in all cells; however, its concentration varies in different tissues. In healthy red cells, the enzyme operates at only 1% to 2% of its maximal potential, allowing for a large reserve of reductive potential. Because G6PD is determined by a gene on the X chromosome, full expression of the deficiency is found in the male hemizygote. Partial expression may be found in the heterozygous female, who has two populations of red cells—one normal and one deficient. The deficiency of G6PD limits the regeneration of NADPH, which renders the cell vulnerable to oxidative denaturation of Hb. Because, normally, G6PD is highest in young cells and decreases as the cell ages, in persons with G6PD deficiency, the older cells are preferentially destroyed.

Hemolytic susceptibility in affected persons can increase greatly during intercurrent illness or upon exposure to various drugs that have oxidant properties (Box 33.1) (Beutler, 1978).

The monomeric form of G6PD contains 515 amino acids and has a molecular weight of 59 kDa. The genetic heterogeneity is great; approximately 400 biochemical variants have been defined. This genetic heterogeneity is expressed as variations in stability and the electrophoretic and catalytic properties of the enzymes, in the degree of deficiency, in the types of cells in the body affected, in the types of drugs that will produce hemolysis, and in susceptibility to chronic hemolysis or to neonatal jaundice. The most common ("normal") G6PD isoenzyme in all population groups is designated as B. In blacks, an electrophoretically more rapid variant, A^+, is prevalent and has almost the same activity; 20% of black males have this variant. Eleven percent of black males have the A^- type of G6PD, which has only 5% to 15% of normal enzyme activity. It is these individuals who are susceptible to hemolysis after ingesting oxidant drugs or during infection. The most common variant in whites is G6PD-Mediterranean, found in Mediterranean populations. The level of enzyme activity in affected males is low—often less than 1%. These individuals usually are not anemic but may have somewhat more severe and non–self-limited hemolytic anemia with infection, and with a wider variety of drugs than the black variant. In a subgroup of G6PD-deficient subjects, severe hemolysis may occur within hours after eating fava beans ("favism"). Although the vast majority of G6PD-deficient subjects worldwide are not anemic, a small proportion of persons with G6PD-Mediterranean (and persons with some rarer variants) have a chronic nonspherocytic hemolytic anemia. G6PD deficiency is a common cause of neonatal jaundice, occurring in approximately one-third of all male neonates with jaundice (Glader, 2019). Jaundice is usually evident by 1 to 4 days of age and is more severe in premature babies than in full-term infants. In a very small fraction of G6PD patients, chronic lifelong hemolysis occurs in the absence of infection or drug exposure and is one of the diagnostic possibilities of congenital nonspherocytic hemolytic anemia.

Laboratory findings during active hemolysis are those of hemolytic anemia in general. In the blood film, one finds poikilocytes, some spherocytes, bite cells, and irregularly contracted cells that stain densely and have contraction of Hb from a part of the cell membrane. These probably are cells from which Heinz bodies have been removed by the spleen. After supravital staining with methyl violet, Heinz bodies may be present early in an acute hemolytic episode. G6PD deficiency may be detected by one of the screening tests: the dye reduction test, ascorbate cyanide test, or a fluorescent spot test. Confirmation is made with a quantitative assay.

BOX 33.1

Drugs and Chemicals That Have Clearly Been Shown to Cause Clinically Significant Hemolytic Anemia in G6PD Deficiency

Acetanilid
Methylene blue
Nalidixic acid (NegGram)
Naphthalene
Niridazole (Ambilhar)
Nitrofurantoin (Furadantin)
Pamaquine
Pentaquine
Phenylhydrazine
Primaquine
Sulfacetamide
Sulfanilamide
Sulfamethoxazole (Gantanol)
Sulfapyridine
Thiazolesulfone
Toluidine blue
Trinitrotoluene (TNT)

From Beutler E: *Hemolytic anemia in disorders of red cell metabolism.* New York, Plenum Medical Book Company, 1978.
G6PD, Glucose-6-phosphate dehydrogenase.

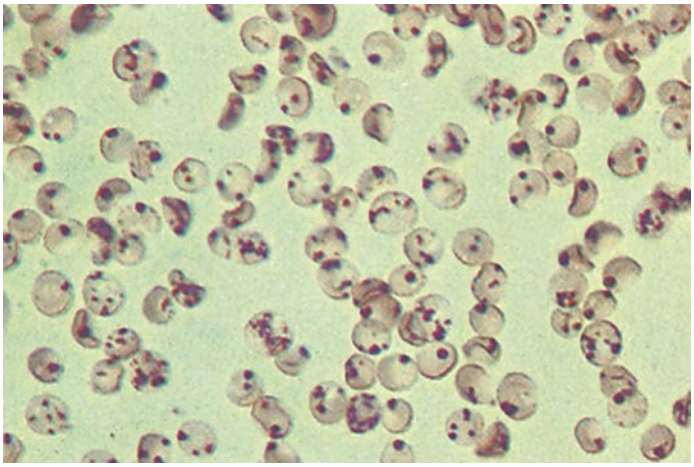

Figure 33.31 Heinz bodies. Normal red cells incubated with an oxidant drug and stained while in suspension with methyl violet; finally, an air-dried film was made and stained with Wright's stain. Purple-staining Heinz bodies are precipitates of denatured hemoglobin that tend to attach to the cell membrane.

Heinz Bodies

When a globin chain denatures, it forms precipitates that are known as *Heinz bodies* (Dacie, 1991). These precipitates cannot be detected in Romanowsky's-stained, air-dried blood films, but after vital staining with methyl violet or crystal violet, Heinz bodies stain deep purple. They vary from 1 to 4 μm in diameter and often attach to the red cell membrane. They also stain, but less intensely, as pale-blue inclusions in reticulocyte stains (e.g., new methylene blue; Fig. 33.31).

The presence of Heinz bodies in freshly drawn blood indicates that (1) an oxidizing drug or chemical (e.g., phenylhydrazine, chlorate, naphthalene, dapsone) has been ingested in Hb; (2) a drug such as primaquine has been ingested by an individual with G6PD deficiency (or another defect resulting in a deficiency of reduced glutathione) so that Hb is not protected from oxidative denaturation; or (3) the subject has an unstable Hb.

Ascorbate Cyanide Test

When blood is incubated with a solution of sodium cyanide and sodium ascorbate, hydrogen peroxide is generated from the coupled oxidation of ascorbate and oxyhemoglobin (Dacie, 1991). Cyanide inhibits catalase,

hydrogen peroxide is available to oxidize Hb, and the brown color of methemoglobin is discernible. This occurs more rapidly in G6PD-deficient cells than in normal cells.

The ascorbate cyanide test is not specific in that abnormalities in the glutathione synthesis or maintenance pathways can produce positive results.

Fluorescent Spot Test

Whole blood is added to a mixture of glucose-6-phosphate (G6P), NADP, saponin, and buffer. A spot of this mixture is placed on filter paper and is observed for fluorescence with ultraviolet light. If G6PD is present, NADP is converted to NADPH. Because phosphogluconate dehydrogenase is present in most hemolysates, further NADP is converted to NADPH (see Fig. 33.30). NADPH fluoresces, but NADP does not. The normal control sample fluoresces brightly; lack of fluorescence indicates G6PD deficiency. By reoxidizing any small amounts of NADPH formed, oxidized glutathione (GSSG) enhances the ability of the test to detect mild G6PD deficiency. This is the recommended screening test for G6PD deficiency (Beutler, 1979).

Quantitative Assay of G6PD. For G6PD, most assays are based on the rate of reduction of NADP to NADPH, measured spectrometrically at 340 nm, when a hemolysate is incubated with G6P (Beutler, 1984). In heterozygotes or in acute hemolysis in black subjects with G6PD deficiency, the diagnosis may be obscured even with the assay because of increased levels of G6PD in reticulocytes and younger erythrocytes. Usually, however, the ascorbate cyanide screening test will be positive in these instances.

Pyruvate Kinase (PK) Deficiency

The most common red cell enzyme deficiency involving the Embden-Meyerhof glycolytic pathway, PK deficiency results in mild to moderately severe nonspherocytic chronic hemolytic anemia with splenomegaly. The prevalence of PK deficiency is estimated to be 1:20,000 in the general white population (Grace, 2019). PK deficiency is one of the causes of congenital nonspherocytic hemolytic anemia. The anemia may be detected in infancy or not until adult life in milder cases and varies from mild to transfusion dependent, with hemoglobin ranging from 6.5 to 11 g/dL. Splenomegaly occurs in 80% to 85% of patients and gallstones in 30% to 45% (Grace, 2019). Cases of hydrops fetalis have been reported. Neonatal jaundice occurs in more than half of cases, which may require exchange transfusion. Patients tend to tolerate the anemia rather well because of high levels of 2,3-DPG, which occur as a result of the block in glycolysis. The blood film may show no notable red cell abnormalities until after splenectomy, when echinocytes, irregularly contracted cells, and crenated red cells may be prominent. Reticulocyte counts are elevated and increase further after splenectomy to as high as 70%.

PK isoenzymes are produced by two separate genes: one on chromosome 15, encoding the M (muscle) isoforms, and the other on chromosome 1, encoding the L (liver) and R (red cell) isoforms. The complexity of PK isoforms is further complicated by the fact that functional enzyme is a tetramer. Inheritance is autosomal recessive, but this is probably true only in consanguineous families. *PKLR* mutants comprise over 300 mutations and are not detected in phenotypically normal heterozygotes that have one half the normal PK activity. Most individuals with PK-deficient hemolytic anemias are therefore probably double heterozygotes for two mutant genes. Acquired PK deficiency occurs occasionally in myelodysplastic disorders and leukemias.

The autohemolysis test gives variable results. Some patients show only a mild increase in autohemolysis that is partially prevented by glucose (type I), and others have a greater increase that is not prevented by glucose (type II). Heinz bodies are not found. The diagnosis is made by a specific screening test or enzyme assay.

The reticulocyte count in unsplenectomized patients is usually increased, although not proportional to the degree of anemia, because younger PK-deficient erythrocytes are selectively sequestered in the spleen. Splenectomy is indicated in cases requiring transfusions. After splenectomy, the Hb concentration usually increases by 1 to 2 g/dL and the reticulocytes increase sharply, although hemolysis persists. An oral drug that activates numerous PK mutants is currently under study for potential use in many patients (Grace, 2019).

Fluorescent Spot Test. Pyruvate kinase catalyzes the phosphorylation of adenosine diphosphate (ADP) to ATP by phosphoenolpyruvate (PEP) with the formation of pyruvate (Beutler, 1984). Pyruvate then reduces any NADH present to NAD with the formation of lactate (see Fig. 33.30). Loss of fluorescence of NADH under ultraviolet light is observed as evidence of the presence of PK.

Leukocytes must be removed from the sample because they normally contain about 300 times as much PK as red cells do, and in PK deficiency, the red cells but not the leukocytes are deficient.

Quantitative Assay of PK. The same principle is employed as in the screening test, but the rate of decrease of absorbance at 340 nm is measured. A negative screening test or a normal PK assay (using the standard high substrate [PEP] concentrations) does not rule out PK-deficient hemolytic anemia. Because mutant PK enzymes may have normal activity at high PEP concentrations and decreased activity at low PEP concentrations, it is necessary to perform the assay both ways (Beutler, 1984).

Other Glycolytic Enzyme Deficiencies

Other enzyme deficiencies in the **Embden-Meyerhof pathway**, such as hexokinase, glucose phosphate isomerase, and phosphofructokinase, are very rare (Beutler, 1994; van Solinge, 2010, Glader, 2019). When severe, they produce hemolytic anemia, with two exceptions: (1) LD deficiency has no clinical manifestations; and (2) deficiencies of 2,3-DPG mutase and 2,3-DPG phosphatase activities occur together and result in erythrocytosis as a result of lack of 2,3-DPG, shifting the O_2 dissociation curve of Hb to the left and relative tissue hypoxia.

Other enzyme deficiencies in the **hexose monophosphate shunt** are rare. They include the two enzymes involved in glutathione synthesis: γ-glutamyl cysteine synthase and glutathione synthetase. As in G6PD deficiency, hemolysis increases with oxidant drug exposure or infection.

No good evidence is available, however, for the causation of chronic hemolytic anemia by 6-phosphogluconate deficiency, catalase, enolase, glutathione reductase (GR) deficiency, or glutathione peroxidase (GP_x) deficiency (Beutler, 1994; van Solinge, 2010). GR contains flavine-adenine dinucleotide and is often partially deficient because of dietary riboflavin deficiency. GP_x is one-half normal in about 30% of the Jewish population as a result of homozygosity for a gene with low GP_x activity. In addition, GP_x activity is dependent on selenium intake in the diet. In neither case is there an association with a hematologic disorder.

Pyrimidine-5′-Nucleotidase Deficiency

When RNA is degraded in the reticulocyte, pyrimidine nucleotides must be dephosphorylated by pyrimidine-5′-nucleotidase (PN) to cross the red cell membrane (Gregg, 2018). PN requires Mg^{++} for its activity and is inhibited by a number of heavy metals, such as lead. Autosomal-recessive PN deficiency results in accumulation of pyrimidines, and the impaired degradation of RNA results in pronounced basophilic stippling in red cells on the blood film. This is probably one of the more common enzyme deficiencies responsible for nonspherocytic hereditary hemolytic anemia once G6PD and PK deficiencies are excluded (Rees, 2003). More than 20 PK mutations have been reported and most patients are homozygous (Gregg, 2018).

The disorder is characterized by mild to moderate chronic hemolysis, jaundice, reticulocytosis (≈10%), marked basophilic stippling (about 5% of the red cells), and splenomegaly without notable improvement after splenectomy. However, no cases of transfusion dependency associated with PN deficiency have been reported (Rees, 2003). A screening test compares the ultraviolet absorption of deproteinized extracts of red cells at 260 nm with that at 280 nm. In PN deficiency, the major absorption peak is shifted from the normal 260 nm to 280 nm, which is the maximum for the pyrimidines uridine diphosphate and cytidine diphosphate. Confirmation requires an assay showing decreased nucleotidase activity (Beutler, 1984).

Acquired PN deficiency occurs in lead poisoning and is probably responsible for the basophilic stippling in that condition. It has been also reported in β-thalassemia trait, acute leukemias, chronic myeloid leukemia, chronic lymphocytic leukemia, and lymphomas (Rees, 2003).

HEMOLYSIS—ACQUIRED

Extrinsic Chemical Agents

Agents Hemolytic to Normal Cells

The action of chemical agents depends on the dose and on other factors, many of which are known only vaguely. They range from simple substances, such as water, to some that are highly complex. When used as irrigating fluid, distilled water may be found responsible for acute hemolytic anemia as a result of entry into venous channels during transurethral resection. Also, drowning in fresh water may be associated with red cell hemolysis, particularly in the lungs, although drowning in salt water could cause profound red cell hydration (Mentzer, 2018).

In addition to anemia, some chemicals produce methemoglobinemia, which can manifest as cyanosis (toluene, trinitrotoluene, nitrobenzene, acetanilide, and phenacetin). Some may lead to AA (toluene and trinitrotoluene). Promin, a sulfone derivative, makes blood turn chocolate brown because of the formation of sulfhemoglobins. As mentioned earlier, ribavirin, a drug used in the treatment of hepatitic C virus infection, may produce a dose-dependent hemolytic anemia in about one-third of patients.

Lead toxicity may produce progressive anemia, with basophilic stippling, reticulocytosis, normoblastemia, Cabot rings, Howell-Jolly bodies, and leukocytosis. Lead not only causes damage to the red cell and hemolysis but also produces defects in the heme synthetic pathway. In cases of chronic exposure to lead, basophilic stippling, more in the marrow than in the peripheral blood, ring sideroblasts, and coproporphyrinuria are the characteristic findings. These changes produce defective erythrocytes, which are removed by the spleen.

Agents Hemolytic to Abnormal Cells

Certain drugs and chemicals that have oxidizing activity may produce hemolytic anemia in individuals with G6PD deficiency or other defects, resulting in glutathione deficiency. In addition, unstable hemoglobins, such as Hb Zürich, have a propensity for drug-induced hemolytic anemia. Premature infants, although they have high levels of G6PD, have glutathione instability and low levels of glutathione and may develop hemolytic anemia when given large doses of synthetic water-soluble analogs of vitamin K.

It must be remembered that, if exposure to these oxidant substances is great enough, acute hemolytic anemia may be produced in normal individuals.

During the acute hemolytic episode, Heinz bodies can be demonstrated frequently by direct staining of blood with methyl violet. Red cells with Heinz bodies are removed from the circulation by the spleen or the Heinz bodies are extracted from the red cells by splenic action. Therefore, Heinz bodies may not be found in the blood if the spleen is effectively removing them or after the acute hemolytic process has abated.

Tests for G6PD deficiency, the most common underlying cause of drug-sensitive hemolytic anemia were described earlier in this chapter.

Physical Agents

Heat

Normal red cells undergo budding and fragmentation when exposed to a temperature of 49°C (120°F) in vitro (Mentzer, 2018). Extensive burns produce hemolytic anemia, probably because of direct damage to red cells. Gross hemoglobinuria may occur in patients with severe burns. The blood film may show remarkable morphologic abnormalities of the red cells, including budding fragmentation of the membrane and microspherocytosis. The most severe abnormalities are often found immediately after extensive burns before a reticulocyte response has had time to develop. Badly damaged cells are rapidly removed from the circulation.

Traumatic Hemolysis

Hemolytic anemias characterized by striking morphologic abnormalities of the red cells, which include fragments (schistocytes, triangular cells, helmet cells), have been attributed to physical trauma to the red cells. The International Council for Standardization in Hematology (ICSH) recommends the classification of schistocytes into four categories: crescentic/triangular, keratocytes, helmet cells, and microspherocytes. It also recommends the use of a 1% threshold to designate increased schistocytes (Zini, 2012). The basis of the hemolytic process is probably damage to the red cells in their contact with loose fibrin meshworks (intravascular coagulation) or with pathologic vascular lesions. Two general categories are recognized in this group of disorders, aptly termed the *red cell fragmentation syndrome*: macroangiopathic and microangiopathic.

Macroangiopathic Hemolytic Anemia (Cardiac Valvular Disease and Prostheses). Chronic intravascular hemolysis associated with low serum haptoglobin, hemosiderinuria, reticulocytosis, and red cell abnormalities (e.g., various forms of schistocytes) may occur after surgical replacement of a diseased heart valve with a prosthesis or after surgical repair of a septal defect with a plastic patch (Erslev, 2001b). This has been attributed to mechanical damage of red cells in the turbulent environment of a leaky valve or of a roughened surface uncovered by endothelial cells. Repair of the valve or coverage of the patch by endothelium has improved the hemolytic process. Other studies have shown that some patients with cardiac valvular disease have a hemolytic process that may be altered by surgery. Postperfusion syndrome occurs in some patients after cardiopulmonary bypass. The syndrome includes febrile inflammatory illness accompanied by acute intravascular hemolysis and leukopenia. Presumably, complement is activated as blood passes through the oxygenator (Mentzer, 2018).

External mechanical trauma has been reported in **march hemoglobinuria,** a condition that is seen in soldiers after a long march and in joggers and other athletes following long practices, particularly on hard surfaces. In this condition, anemia and reticulocytosis are uncommon. The chronic intravascular hemolysis may lead to iron deficiency as a result of loss of Hb in the urine.

Thrombotic Microangiopathy (Microangiopathic Hemolytic Anemia [MHA]). Thrombotic microangiopathies (TMAs) are microvascular occlusive disorders characterized by systemic or intrarenal aggregation of platelets, thrombocytopenia, and mechanical injury to erythrocytes. Fragmented red cells (e.g., schistocytes, irregularly contracted cells) are probably produced when blood flows through turbulent areas in the microcirculation that are partially occluded by platelet aggregates (Moake, 2002). TMA may be idiopathic or precipitated by drugs such as mitomycin C, transplantation, malignancy, pregnancy, collagen vascular disease, or HIV (Kottke-Marchant, 2017). Most TMAs have clinical symptoms that include microangiopathic hemolysis, thrombocytopenia, and signs of organ damage ranging from fever, mental status changes, and renal dysfunction to atypical presentations, such as cardiac damage.

The classification of TMA has been controversial for many years. In routine clinical practice, the term *thrombotic thrombocytopenic purpura* (*TTP*) is often used for adult cases with predominant neurologic symptoms, whereas the term *hemolytic-uremic syndrome* (*HUS*) has been used to describe childhood cases with thrombotic microangiopathy and predominant renal involvement (Moake, 2002). However, the distinction is not always possible, and overlapping symptoms may be observed. Authors suggested the inclusion of both entities under TTP/HUS, presuming a similar pathogenetic mechanism with variable organ tropism. However, recent studies indicate a difference in pathogenetic mechanisms between HUS and TTP, as discussed later.

Hemolytic-Uremic Syndrome

HUS is classified into diarrhea-associated (D+) or typical form, and diarrhea-negative (D–) or atypical form. D+ HUS constitutes approximately 95% of cases in children and is less common in adults (Shatzel, 2017). D+ HUS occurs most commonly in infants younger than 2 years of age, but it affects all ages. It is caused by one of several serotypes of *Escherichia coli* that produce a verotoxin (named for its toxicity against African green monkey kidney [vero] cells). The most common is *E. coli* O157:H7, which produces Shiga toxins 1 and 2. This microorganism is one of the cattle gut commensals. *E. coli* O104:H4 has been associated with epidemic infection in Europe. The annual incidence of infection with *E. coli* O157 is approximately 8 per 100,000 people in North America. The percentage of cases with bloody diarrhea that progress to HUS is 3% to 7% for sporadic cases and 20% to 30% for some outbreaks. HUS usually occurs 4 to 6 days after the onset of diarrhea. Shiga toxins cause bloody diarrhea, then enter the circulation and travel in the plasma on the surface of platelets or monocytes (Moake, 2002). Recent studies suggest that these toxins become attached to glomerular capillary endothelium and other renal epithelial cells. It causes direct cell damage by binding to globotriaosylceramide (Gb3, ceramide trihexoside, CD77) on these cells, producing apoptosis (Shatzel, 2017). Shiga toxins, together with locally secreted cytokines, also cause the release of unusually large multimers of von Willebrand factor (vWF), which promote platelet aggregation in renal vasculature (Kottke-Marchant, 2017). Endothelial cell damage is the hallmark of D+ HUS in children, and endothelial swelling may be severe enough to occlude the capillary lumen. The thrombi of D+ HUS are composed predominantly of fibrin with few platelets and little vWF. Hemolytic anemia with schistocytes (due to interaction of red cells with microvascular thrombotic lesions), variable thrombocytopenia, and uremia are the cardinal features. Death formerly occurred in almost half of cases; the renal pathology has included acute glomerulonephritis and thrombotic and necrotic vascular lesions associated with patchy, bilateral renal cortical necrosis. However, with advanced supportive therapy, including transfusions and dialysis, some investigators have reported mortality reduced to 5% to 15%. Nonetheless, minor to major renal impairment has been reported in approximately 50% of patients. Some 5% to 10% of patients with HUS have D– HUS, with no antecedent diarrhea of Shiga toxin–producing organisms, and some of these patients have familial history of the disease. First presentations are more common in children, including neonates, although some cases present in adulthood. Infections and pregnancy may trigger hemolytic crises. It is now known that atypical HUS is caused by activation or abnormal regulation of the alternate pathway of the complement (Kottke-Marchant, 2017). Approximately 50% of patients with D– HUS have inherited mutations in one of the complement regulatory proteins: factor H, factor I, membrane cofactor protein (MCP, CD46), or factor B, mostly heterozygous mutations. These patients have a much higher mortality rate and high risk of relapse after renal transplant (Shatzel, 2017). The complement C5 inhibitor eculizumab has been shown effective in improving renal function and controlling the disease process in both native and transplanted kidneys in patients with complement-mediated HUS. Approximately 5%

of D– HUS patients have antibodies against factor H, raising the possibility of using plasma exchange or immunosuppressants for therapeutic strategy.

Thrombotic Thrombocytopenic Purpura

TTP may occur at any age but has a peak incidence in the third decade; it occurs more often in females than in males. It was initially described by Elie Moschcowitz in 1924 in a young woman. The annual incidence is 3.7 cases per 100,000. The acquired form is more common, with an incidence of 0.2 to 1.0 per 100,000 compared with the much less common familial form, which has an incidence of 0.05 to 0.40 per 100,000 (Shatzel, 2017). The triad of clinical manifestations present in most patients includes hemolytic anemia, thrombocytopenia, and neurologic symptoms. In addition, fever and renal diseases are often present. This constitutes the classic pentad. Pathologically, microvascular occlusive lesions with hyaline thrombi and endothelial proliferation are widespread throughout the body. Until 1997, the origin was unknown. Different theories included endothelial injury by oxidant stress, antiendothelial antibodies, anti-CD36 (glycoprotein IV located on microvasculature) antibodies, platelet aggregating factors, and release of large vWF multimers into the plasma. In 1996, a protease that cleaves vWF subunits was identified in normal plasma. In 1997 and the following years, several reports indicated deficient vWF-cleaving protease in patients with TTP due to low enzyme levels (in familial cases) or to the presence of IgG enzyme inhibitor (in nonfamilial cases). These observations were confirmed by additional studies, which showed normal levels of vWF-cleaving protease in HUS (Moake, 2004). The enzyme has been further characterized as number 13 in a family of 19 distinct ADAMTS-type enzymes identified to date (a disintegrin and metalloprotease with eight thrombospondin-1-like domains). Therefore, the vWF-cleaving metalloprotease is now referred to as ADAMTS13 (Moake, 2004). In the absence of vWF-cleaving protease, ultra-large vWF multimers secreted by endothelial cells would not be processed normally. These highly adhesive multimers may induce platelet clumping in the microcirculation under shear stress, resulting in the clinical manifestation of TTP. The disease is acute and until the 1980s was fatal in well over half of cases. With the therapy of plasma exchange by plasmapheresis and plasma transfusions (in addition to platelet inhibitors), the remission rate has improved, and long-term survival now approaches 90% (Moake, 2004). TTP can now be classified into three main categories: familial, idiopathic, and secondary. The familial form (Upshaw-Schulman syndrome) results from a mutation in the *ADAMTS13* gene and is associated with very low activity of the enzyme. More than 50 mutations have been described to date. Approximately 50% of patients with familial TTP experience their first episode during childhood, and exacerbations may occur in association with minor infections. The familial form represents a minority of cases, approximately 5% (Shatzel, 2017). Most TTP cases are caused by antibodies to ADAMTS13, which inhibit the proteolytic function of the metalloprotease and increase its clearance from the circulation. The secondary form may occur along the course of other conditions, such as malignancies, organ transplantation, chemotherapy, infection, and certain medications, such as cyclosporine, quinine, ticlopidine, and clopidogrel. The mechanism of TTP under these circumstances is unknown, although direct endothelial cytotoxicity and drug-induced autoimmunity are possible mechanisms. TMA after organ transplantation is a well-recognized entity occurring as a complication of renal, lung, and allogeneic hematopoietic stem cell transplant. In this setting, medications, such as sirolimus and cyclosporin, infections, and graft-versus-host as well as complement dysregulation disease are important factors. The outcome is usually poor, with a high rate of mortality (Shatzel, 2017).

Preeclampsia/Eclampsia

Preeclampsia and eclampsia are microangiopathic disorders occurring with pregnancy and sharing some features of HUS or TTP. Approximately 4% to 39% of patients with severe preeclampsia develop HELLP syndrome: hemolysis, elevated liver enzymes, and low platelet count. The syndrome becomes manifest usually during the third trimester, although some patients may develop it during the postpartum period. Most patients recover within a few days after delivery. In a small subset of patients, severe persistent multisystem disease requires plasma exchange (McMinn, 2001). ADAMSTS13 has been reported to be low in 10% to 20% of cases. HELLP syndrome can result in multiple maternal and fetal complications, such as disseminated intravascular coagulopathy, renal dysfunction, hepatic infarction, cerebral hemorrhage, and fetal cytopenias, particularly thrombocytopenia (Shatzel, 2017).

Infectious Agents

Destruction of erythrocytes by plasmodia is responsible for the anemia in malaria. This is supported by the observation that the osmotic and mechanical fragility of parasitized erythrocytes is increased. Inhibition of marrow activity may be an additional factor. Fulminant hemoglobinuria (blackwater fever) is a complication of *P. falciparum* malaria.

Oroya fever, a frequently fatal disease that occurs in Peru, is characterized by a hemolytic anemia and leukocytosis. *Bartonella bacilliformis* is the responsible agent.

Babesiosis, a protozoan infection transmitted by ticks from rodents or cattle, is associated with hemolysis; parasites may be seen in red cells in Romanowsky's-stained blood films.

Hemolytic anemia with cold agglutinins may complicate mycoplasmal pneumonia and infectious mononucleosis. This is due to the effect of antibody on the red cells.

Hemolytic anemia of varying severity is frequent in some bacterial infections. A notable example is *Clostridium perfringens* septicemia following septic abortion or biliary tract surgery, which may be accompanied by a dramatic and life-threatening hemolytic crisis.

BOX 33.2

Classification of Immune Hemolytic Anemias

Autoimmune hemolytic anemias
Associated with warm antibodies
Associated with cold antibodies
Combined warm and cold antibodies
Alloimmune hemolytic anemias
Transfusion-associated hemolytic anemia
Hemolytic disease of newborn
Rh incompatibility
ABO incompatibility
Drug-induced hemolytic anemia
Drug adsorption
Autoantibody induction
Neoantigen formation

Immune Hemolytic Anemias

Immune hemolytic anemias are disorders in which erythrocyte survival is reduced because of the deposition of immunoglobulin and/or complement on the red cell membrane and subsequent enhanced red cell destruction or elimination by the immune system. The immune hemolytic anemias can be grouped according to the presence of autoantibodies, alloantibodies, or drug-related antibodies (Box 33.2).

Autoimmune Hemolytic Anemia

The autoimmune hemolytic anemias (AIHAs) are due to an altered immune response, resulting in the production of antibody against the host's own erythrocytes, with subsequent hemolysis. The incidence of AIHA is estimated at 170 cases per 1 million population with 0.2 to 1.0 per million in children and teenagers (Michel, 2018). AIHAs can be classified according to serologic or clinical characteristics (Table 33.9). Some AIHAs are mediated by antibodies with maximum binding affinity at 37°C, and other AIHAs are mediated by antibodies with maximum binding affinity at 4°C. In addition, AIHAs could be viewed according to their association with other disorders. In a study of 1834 patients, approximately 40% of cases of AIHA have been associated with an underlying disease, while the remainder were idiopathic (Sokol, 1992). Lymphoproliferative disorders account for approximately half of cases of both warm and cold AIHA (Gehrs, 2002).

Etiology and Pathophysiology. The cause of the production of autoantibody in patients with AIHA is unknown. However, several mechanisms have been suggested. Autoimmune antibodies, particularly cold-reacting antibodies, are sometimes produced following an infection. This is typically seen with the elaboration of anti-I in patients with *Mycoplasma pneumoniae* infections and anti-i in patients with infectious mononucleosis. The cold agglutinins of anti-I and anti-i specificity are strikingly similar to one another in the structure of antigen binding sites. These antibodies react with antibodies that also identify the product of the *VH4-34* gene segment in B cells. It has been hypothesized that infections can cause the production of antibodies of B cells, utilizing this gene segment. These antibodies will also have cold agglutinins activity against the I/i antigens (Rosse, 2004).

The amount of antibody, its avidity for the erythrocyte autoantigen, and its ability to fix complement are significant variables. Opsonization of red cells can destroy them in the circulation (intravascular hemolysis) or can cause their accelerated removal from the circulation by tissue macrophages (extravascular hemolysis). Major sites for these macrophages are the spleen and, to a lesser extent, the liver (Gehrs, 2002).

TABLE 33.9
Autoimmune Hemolytic Anemia (AIHA)*

Condition	Warm AIHA	COLD AIHA		Mixed AIHA
		CHAD	PCH	
Idiopathic	282 (23)	194 (16)	5 (<1)	47 (4)
Drug-induced disorders	184 (15)	0	0	2 (<1)
Neoplasia	165 (14)	81 (7)	0 (0)	26 (2)
Non-Hodgkin lymphoma	27	25	0	8
Chronic lymphocytic leukemia	65	4	0	8
Hodgkin lymphoma	11	7	0	5
Carcinomas	37	30	0	4
Miscellaneous	25	15	0	1
Infections	9 (<1)	76 (6)	14 (1)	2 (<1)
Pneumonia—*Mycoplasma*	0	21	0	0
Viral pneumonia	2	19	0	0
Infectious mononucleosis	0	11	1	0
Miscellaneous	7	25	13	2
Collagen diseases	30 (2)	15 (1)	0 (0)	20 (2)
Systemic lupus erythematosus	7	4	0	16
Rheumatoid arthritis	21	6	0	4
Others	2	5	0	0
Miscellaneous disorders	45 (4)	20 (2)	0	6 (<1)
Totals	715 (58)	386 (32)	19 (2)	103 (8)

Data from Sokol RJ, Hewitt S: Autoimmune hemolysis: a critical review. *Crit Rev Oncol Hematol* 4:125–154, 1985.
CHAD, Cold hemagglutinin disease; *PCH,* paroxysmal cold hemoglobinuria.
*Numbers in parentheses are percentages.

The development of AIHA in patients with lymphoproliferative disorders or with autoimmune disorders may relate to some abnormality with B cells, T cells, or macrophages, or the interaction among these cells. Perhaps loss of T-cell suppressor function could result in unrestrained production of red cell antibody by B cells. This hypothesis is strengthened by the observation that methyldopa, a drug known to cause the development of anti–red cell antibodies, inhibits the activation of suppressor T lymphocytes (Gehrs, 2002). Antibodies in primary warm AIHA are frequently polyreactive and polyclonal, with no clonal B cells detected by PCR (Michel, 2018). While in cold agglutinin disease, oligoclonal or monoclonal B-cell population is commonly detected.

In AIHA associated with warm-type antibody, there is IgG coating of erythrocytes with or without complement fixation. Clearance of red cells occurs mostly in the spleen. In the absence of complement fixation, it appears that the Fc portion of the red cell–bound IgG interacts with the Fc receptor present on the membrane of splenic macrophages located along the cords of Billroth. Thus, sensitized erythrocytes are retained, phagocytosed, or fragmented by splenic macrophages during their passage through the spleen (mostly extravascular hemolysis).

In AIHA associated with the production of cold-type autoantibody, erythrocytes are usually coated with IgM. Under these circumstances, the fixation of complement frequently occurs. In paroxysmal cold hemoglobinuria, the offending antibody is an IgG that fixes complement. If the entire complement sequence is activated, there may be intravascular hemolysis. This phenomenon may occur in cases of cold hemagglutinin disease as well as in paroxysmal cold hemoglobinuria. If complement activation fails to proceed to completion but is halted at an intermediate stage, intravascular lysis of the erythrocytes may not occur. However, extravascular hemolysis can still continue. In this situation, sensitized cells with C3b on the membrane are bound in the liver by the interaction of C3b and its receptors on Kupffer's cells. Erythrocytes may be phagocytosed entirely or portions of the cells may be removed, resulting in fragmentation and spherocyte formation.

Approximately 7% of patients with AIHA satisfy diagnostic criteria for both warm and cold autoantibodies (Sokol, 1992). In these cases, IgG and C3d sensitize the erythrocytes. The serum contains IgM cold autohemagglutinins (optimally reactive at 4°C but with a high thermal amplitude to 37°C) and IgG warm autoantibodies.

AIHA Associated With Warm Antibody. The warm antibody type of AIHA is slightly more frequent in females than in males and is most likely to occur in individuals 40 years or older; peak incidence occurs around the seventh decade. This age distribution may be related to the higher frequency of lymphoproliferative disorders with age (Packman, 2010). Idiopathic warm-antibody AIHA accounts for approximately 50% of cases. Chronic lymphocytic leukemia and lymphomas account for about half of secondary warm-antibody AIHAs; autoimmune disorders, such as SLE, account for most of the remaining cases (Packman, 2010). Clinical signs and symptoms frequently are those of an underlying disorder. However, the patient with idiopathic AIHA may have noted the presence of a mild upper respiratory tract infection just before the onset of hemolysis. As the disorder progresses, weakness, dizziness, and fever may be noted. Jaundice can be a presenting complaint. Pregnancy carries a fivefold risk of developing autoantibodies compared with the control population (Gehrs, 2002).

Laboratory findings include the presence of moderate to severe anemia. The neutrophil count may be increased. In a small proportion of cases, thrombocytopenia can exist and if severe should raise the possibility of concomitant immune thrombocytopenia (Evans syndrome). The peripheral film frequently shows spherocytosis, red cell fragmentation, polychromasia, and a few normoblasts. Reticulocyte percentage is high in approximately 50% of patients and is often associated with increased MCV. However, as many as one-third of patients have transient reticulocytopenia despite the presence of normal or hyperplastic erythroid precursors in the marrow (Packman, 2010). The lack of reticulocytosis should not keep one from making a diagnosis of AIHA. The bone marrow exhibits erythroid hyperplasia, sometimes with mild megaloblastic changes. Reticulocytopenia may be related to immune destruction of reticulocytes or bone marrow suppression caused by marrow infiltration, infection, nutritional deficiencies, or chemicals (Packman, 2010).

There is usually a decrease in serum haptoglobin and an increase in unconjugated bilirubin and LD. The osmotic fragility and autohemolysis test can be normal or increased.

Direct and indirect antiglobulin tests indicate the presence of erythrocyte antibodies. The specificity of the autoantibodies is usually directed against antigens of the Rh system, membrane protein band 3 and band 4.1, and glycophorin A. However, activity against U, LW, Kell, jk^a, and Fy^a antigens may also occur. The warm antibody is most likely an IgG with subclass IgG1 and less frequently with IgG3. When IgG2 or IgG4 is present on the red cells alone, no hemolytic reaction is associated (Packman, 2001a). Occasionally, the antibody may be an IgA immunoglobulin or, rarely, an IgM immunoglobulin. Complement may be detected on the erythrocyte membrane in slightly more than half of cases. Although many warm antibodies fix complement, intravascular complement–mediated hemolysis and hemoglobinuria are unusual, possibly because of the ability of complement regulatory proteins in plasma and on red cell surfaces to abort fixation of terminal complement components (Packman, 2010).

In some cases, sensitized red cells contain less immunoglobulin than can be detected using commercially prepared antiglobulins, which are normally sensitive to 250 to 500 molecules of IgG per red cell. Under these circumstances, the autoantibody at times can be detected with an antiglobulin consumption test or more automated enhanced agglutination techniques (Packman, 2010).

The clinical course of AIHA associated with warm antibody is characterized by periods of remission and relapse. In secondary AIHA, the course and prognosis are related to the nature of the underlying disorder. In idiopathic AIHA, complications of the hemolytic disorder may be severe, leading to the demise of the patient. Pulmonary emboli, infection, and cardiovascular collapse are causes of death, and deep vein thrombosis and splenic infarcts are common complications during active hemolysis (Packman, 2010).

AIHA Associated With Cold Antibody. AIHA associated with cold antibody can be mediated by IgM and less frequently by IgG. The IgM autoantibody is associated with a syndrome known as cold agglutinin disease, whereas the IgG autoantibody is seen with paroxysmal cold hemoglobinuria.

Cold Agglutinin Disease

Cold agglutinin disease occurs in individuals usually over the age of 50 years and in females more often than in males. In some cases, cold agglutinin disease is associated with a lymphoproliferative disorder or infection (especially with *M. pneumoniae* or infectious mononucleosis). Cases unassociated with an underlying disorder are listed as idiopathic. Virtually all sera from healthy individuals contain low-titer cold agglutinins, regarded as benign or harmless, and are polyclonal. Postinfectious cold agglutinins are usually polyclonal. By contrast, monoclonal cold agglutinins are generally pathogenetic and may arise from B-cell lymphoma (Gehrs, 2002). Cold agglutinin disease represents approximately 20% of AIHA.

Symptoms and signs vary widely. Some individuals may present with indications of acrocyanosis or Raynaud's phenomenon. Others will have episodes of hemolysis, including hemoglobinuria, following exposure to cold. Temperatures of 30°C and lower are normally attained in the superficial skin vessels of those body parts exposed to cold. The thermal range of the antibody is clinically more important than the agglutination titer (Petz, 2008).

Laboratory findings usually indicate an anemia. Spherocytes and polychromatophilic erythrocytes are present to a variable degree in the blood film. There may be marked red cell agglutination, which should be differentiated from rouleaux formation (see Figs. 31.25 and 31.26). A mild leukocytosis can exist. Red cell agglutination may interfere with automated hematology counts, particularly MCHC, which tends to be high.

The cold antibody is usually IgM with anti-I or, less frequently anti-i, specificity. Rarely do other specificities exist. In the chronic idiopathic form of cold agglutinin disease, the antibody tends to be monoclonal IgM, *k* with anti-I specificity (Gehrs, 2002). The autoantibody is also capable of fixing complement. When the titer of cold antibody is very high, the thermal range of antibody activity may extend up to 37°C. The direct antiglobulin test is positive only if the reagents contain anticomplement activity. Thus, one usually observes a positive antiglobulin reaction with broad-spectrum and non–γ-reagents, but no agglutination with only the γ-reagent. On cold exposure and antibody binding to red cells, the complement may be activated to the stage of C3b, which adheres to the red cells after entering the systemic circulation. In the hepatic circulation, macrophages carry specific receptors for C3b. However, cells usually escape hepatic destruction. Most patients experience chronic mild to moderate anemia, which they tolerate well, and patient outcome is significantly better than with warm-antibody AIHA (Petz, 2008). Some authors remain with the opinion that chronic cold agglutinin disease is a variant of Waldenström's macroglobulinemia in which the IgM M-component has cold agglutinin activity.

Paroxysmal Cold Hemoglobinuria

Paroxysmal cold hemoglobinuria is a very rare disorder that can occur in an individual of any age. However, more cases are now being reported in young children (Petz, 2008). Females are as frequently involved as males. Patients have symptoms of acute hemolysis following exposure to the cold. Chills, fever, pain in the back and legs, and hemoglobinuria are reported. The acute form may follow an acute upper respiratory illness or immunization by 1 to 2 weeks, but the chronic form is associated with congenital syphilis. Hemoglobinuria following exposure to cold is rare in the acute form.

Laboratory features consist of anemia, elevated reticulocyte count, increased concentration of indirect bilirubin, and the presence of Hb in the urine. Anemia is frequently severe and rapidly progressive.

The serum contains a cold hemolysin with biphasic activity. This antibody, first described by Donath and Landsteiner (1904), is IgG that fixes the first components of complement (C1–C4) in the cold (4°C). As the temperature rises to 25°C to 37°C, the antibody dissociates but the remainder of the complement proteins are activated and erythrocyte lysis results. This biphasic hemolysis is the basis for the Donath-Landsteiner autohemolysis test for the diagnosis of this condition. The direct antiglobulin test is positive with anti-C3 but is generally negative with anti-IgG unless performed at colder temperatures. The specificity of the antibody is directed against the P antigen. In general, the prognosis is good.

AIHA Associated With Warm and Cold Antibodies

AIHA associated with both warm and cold autoantibodies is mediated by IgG warm antibodies and complement as well as IgM cold hemagglutinins. Females are more likely involved than males. There appears to be an association between the combined warm and cold antibody AIHA and SLE in that 15% to 42% of patients have SLE (Shulman, 1985; Sokol, 1985). In one study (Shulman, 1985), 6 of 12 patients (50%) had idiopathic AIHA and 4 of these (33%) had concomitant thrombocytopenia (Evans syndrome; see later discussion). All 12 patients had severe hemolysis that responded dramatically to corticosteroid therapy.

Evans Syndrome

Evans syndrome is the combination of warm AIHA and immune thrombocytopenia (ITP). Platelet antibodies are usually against glycoprotein IIB/IIIA (Michel, 2018). Neutropenia occurs in 25%. There is no sex predilection, but half the cases are secondary. Evans syndrome is more common in patients with SLE, antiphospholipid antibodies, and autoimmune lymphoproliferative syndrome (ALPS). In young individuals with Evans syndrome, ALPS should be considered as a diagnostic possibility (Michel, 2018).

Alloimmune Hemolytic Disease of the Newborn

Alloimmune hemolytic disease of the newborn (HDN) usually occurs following the transplacental passage of maternal antifetal red cell antibodies. HDN most frequently results from incompatibility in Rh and ABO erythrocyte antigens between mother and fetus. In rare cases, some other red cell antigen may be responsible for this disorder.

In HDN due to **Rh incompatibility**, prior sensitization is necessary to initiate the disease process. This sensitization usually occurs during pregnancy when Rh(D)-positive fetal red cells cross the placenta and enter the circulation of a mother with Rh-negative cells. Most women have less than 1 mL of fetal blood in their circulation following delivery. However, intrapartum fetomaternal hemorrhage of more than 30 mL occurs in approximately 1% of pregnancies (Ramasethu, 2010). Maternal sensitization can also occur by a previous incompatible transfusion. Under either of these circumstances, maternal IgG antibodies are produced against the fetal cells. If a subsequent pregnancy occurs in a sensitized mother, fetal erythrocytes again reach the maternal circulation and restimulate an antibody response, resulting in transfer of anti-Rh(D) antibody across the placenta and reduced fetal red cell survival.

In the **ABO system**, anti-A or anti-B antibodies of the IgG class may arise spontaneously in the mother; their presence does not require prior transfusion or pregnancy. As a result, firstborn children may suffer from HDN when ABO incompatibility exists. Although ABO incompatibility occurs in 15% of group O pregnancies, ABO hemolytic disease is estimated to occur in only 3% of all births (Ramasethu, 2010).

The clinical features of HDN due to Rh incompatibility vary greatly. Some newborns experience only mild jaundice. Others initially appear markedly pale and then develop jaundice. They can have prominent hepatosplenomegaly. The disease may be complicated by a bleeding diathesis, marked acid-base abnormalities, and kernicterus. In very severe cases, patients can present with hydrops fetalis.

Early examination of the blood usually reveals an increase in nucleated erythrocytes, which may include forms as immature as pronormoblasts. Although this finding gave the disease its name, *erythroblastosis fetalis*, erythroblastosis is not always present, especially if the examination is not performed immediately after birth.

Up to 2.0×10^9 nucleated red cells per liter in term infants and up to 5.0×10^9/L in premature infants are commonly seen in this disorder. Normally, nucleated red cells average 0.5×10^9/L in term infants and 1.0 to 1.5×10^9/L in premature infants. Blood from the umbilical vein for early examination is more reliable than peripheral (capillary) blood because the erythrocyte count and the Hb may be significantly altered between birth and ligation of the cord.

Generally, there is macrocytic anemia of varying severity and an increase in reticulocytes. Occasionally, anemia may develop suddenly on the second or third day. The leukocyte count is frequently elevated, with immature leukocytes. Normoblastic hyperplasia of the marrow is pronounced.

In severely affected infants, thrombocytopenia, depression of prothrombin complex procoagulants, or diffuse intravascular coagulation may occur.

A direct antiglobulin test on fetal erythrocytes indicates the presence of an IgG antibody. When the maternal serum and an eluate from the fetal erythrocytes are incubated separately with a panel of O cells, one can usually demonstrate the presence of antibody with Rh(D) specificity. In Rh-negative pregnant women known to be sensitized to Rh(D), the titer of anti-Rh(D) antibody is measured periodically during pregnancy to serve as a guide for performing amniocentesis.

HDN associated with **ABO incompatibility** is less severe than that observed with Rh incompatibility. Occasionally, the diagnosis is suggested by the presence of unexplained hyperbilirubinemia in a group A or B newborn infant from a group O mother.

Laboratory findings usually show a mild anemia and modest reticulocytosis. In contrast to Rh isoimmune disease, spherocytosis in ABO isoimmune disease may be prominent. However, there may be no anemia. Fetal cells are usually weakly positive with the antiglobulin reagents. Serum from the newborn and eluates from the cells should contain anti-A or anti-B antibody. In addition, maternal serum should contain high titers of anti-A or anti-B antibodies of the IgG subclass.

Drug-Induced Immune Hemolytic Anemia

Immune hemolytic anemia may occur following the administration of drugs. Most cases in the 1970s were associated with methyldopa or high-dose intravenous penicillin therapy. Recently, this picture has changed,

BOX 33.3

Examples of Drugs Implicated in Causing Immune Hemolytic Anemia and Their Mechanism of Action

Hapten or Drug Adsorption Mechanism

Penicillins
Cephalosporins
Tetracyclines
Tolbutamide

Ternary Complex Mechanism

Stibophen
Quinidine
Quinine
Cephalosporins
Rifampicin
Diethylstilbestrol
Chlorpropamide
Amphotericin B

Possible Autoantibody Mechanism

α-Methyldopa
L-Dopa
Procainamide
Cephalosporins
Mefenamic acid
Fludarabine

Modified from Packman CH: Hemolytic anemia resulting from immune injury. In Kaushansky K, Lichtman MA, Beutler E, Kipps TJ, Seligsohn U, Prchal JT, editors. *Williams hematology*, ed 8, New York, McGraw-Hill, 2010, p. 780.

with second- and third-generation cephalosporins being the most common causative agent and accounting for more than 80% of drug-induced immune hemolytic anemia (Garratty, 2007). Four mechanisms appear to mediate immune hemolysis (Packman, 2010).

Formation of Ternary Complexes (Neoantigen Formation). Numerous drugs are known to weakly bind to red cell membrane, even when given in small doses (Box 33.3). Antibodies recognize the combined drug and red cell membrane components as antigen and bind to them, forming a ternary complex. The drug-induced antibody is usually IgM and tends to fix complement, resulting in lysis of cells. In addition, red cells may be sequestered in the liver and spleen because of their coating with C3b.

Patients present with acute intravascular hemolysis, hemoglobinemia, and hemoglobinuria. The direct antiglobulin reaction is positive if the reagents contain anticomplement activity. The reaction usually is negative with the γ-reagent because it contains little anti-IgM or complement specificity.

The diagnosis can be determined by incubating the patient's serum with the offending drug in the presence of target erythrocytes while observing agglutination, lysis, or sensitization of the erythrocytes.

Adsorption of Drug to Red Cell Membrane. Penicillin and cephalosporin, particularly in high doses, bind firmly to proteins, including red cell membrane. These drugs induce an antibody response to them, but the antibody specificity is not directed against a red cell membrane. Both IgM and IgG antibodies are made, but only the IgG antibodies are associated with immune hemolysis. Complement is not involved. The erythrocytes, coated with IgG antibody, are presumably removed via the Fc receptors on macrophages in the spleen.

The direct antiglobulin test is strongly positive. Antibody eluted from patients' erythrocytes will react only with red cells previously treated with penicillin or cephalosporins.

Induction of Autoantibody by Drugs. In approximately 15% of patients using the antihypertensive drug methyldopa, a positive direct antiglobulin reaction is present. The antibody is of the IgG class and in some studies appears to have Rh specificity (Packman, 2010). The actual mechanism of autoantibody production is not known. However, it has been hypothesized that methyldopa causes activation of T cells and increased secretion of γ-IFN, which upregulates MHC class I and class II molecules on antigen-presenting cells and induces antibody production by B cells. The drug may also bind to hemoglobin-free proerythroblasts, producing a neoantigen followed by the production of autoantibody (Packman, 2010).

Development of the positive antiglobulin reaction occurs after a lag period of 3 to 6 months and is dose dependent. Thirty-six percent of patients have a positive antiglobulin reaction when consuming 2 g or more of methyldopa per day and 11% have a positive reaction when taking only 1 g daily. An immune hemolytic anemia occurs in less than 1% of patients and is not dose dependent. Methyldopa also decreases mononuclear phagocytic activity, which may explain the rarity of hemolytic anemia despite the common presence of autoantibodies (Sokol, 1992). Levodopa, procainamide, fludarabine, and mefenamic acid are additional drugs that have been reported to cause an autoimmune hemolytic anemia (AIHA) in a fashion similar to methyldopa.

Nonimmunologic Adsorption of Immunoglobulins to Red Cell Membrane. Drugs such as cephalosporins and cisplatin appear to alter the erythrocyte membrane, resulting in the nonspecific adsorption of plasma protein to its surface. As a result, IgG and IgM may be loosely bound to red cell membrane. This phenomenon can then cause a positive direct antiglobulin reaction. It is now believed that this mechanism can cause hemolytic anemia (Garratty, 2007).

LABORATORY INVESTIGATIONS OF ANEMIA

The diagnosis and study of anemia require the proper use and interpretation of laboratory measurements. Prerequisites for the efficient use of the laboratory are a careful history and physical examination, both of which lead to initial laboratory measurements and provide important guidance in determining the nature of the anemia. Anemias that are of acute onset and rapidly progressive course are likely hemolytic in origin while slowly progressive anemias are likely caused by bone marrow production defects.

Whether the patient is anemic can be ascertained by determining whether the Hb, Hct, or erythrocyte count lies below (1) the reference intervals for age, sex, and altitude or (2) the patient's previous values, even though these are within the reference intervals. The task then is to define the underlying cause or mechanism for the anemia.

Usually, complete blood count (WBC, RBC, Hb, Hct, MCV, MCH, MCHC, platelets) and examination of a Wright's-stained film are part of the routine examination of blood. It is possible that all of these values could be normal in the presence of a mild macrocytic anemia, in which the RBC count does not fall below the normal range and the macrocytes present (and detectable on the blood film) do not elevate the MCV above the normal range.

Once anemia is discovered, the basic examination of the blood should include the following: (1) Hb, Hct, RBC count, and erythrocyte indices; (2) blood film examination; (3) leukocyte count; (4) platelet count; and (5) reticulocyte count.

With current multichannel instruments, all red cell values and their indices have comparable precision. Indices are **mean** values, however, and will not detect different populations of cells that balance each other. For example, combined deficiencies of folate and iron may give rise to populations of macrocytic and hypochromic microcytic cells, which could yield normal indices. Careful examination of the blood film is essential, and red cell volume RDW is very useful in defining this type of abnormality (see Chapter 31).

The size of the erythrocytes, determined by the MCV and by examination of the blood film, will determine the morphologic type of anemia. In addition, certain findings on the blood film will suggest mechanisms that are involved.

Increased numbers of **polychromatic** macrocytes, with or without normoblasts, suggest increased erythropoiesis. In the untreated patient, this is usually due to recent hemorrhage or hemolysis. In this situation, the history (of blood loss) or physical examination (jaundice or splenomegaly) will help. It is to be remembered that repeat or chronic hemorrhage may result in IDA, which is typically microcytic.

Findings suggestive of hemolysis are **poikilocytes** (abnormally shaped red cells), **sickle cells**, **schistocytes**, and **spherocytes**. Sometimes, it is difficult to detect spherocytes in HS because of minimal anisocytosis. Morphologic findings in red cells that are helpful in this situation include the presence of a low mean cell diameter (MCD), between 6.0 and 6.5 μm (normal = 7.0–7.4 μm), red cells with small eccentric or no pallor, and red cells with slightly more intense staining due to Hb density.

Target cells may be found in hemoglobinopathies, especially in the presence of HbC, HbD, and HbE, and in the thalassemias. They may be present in any **hypochromic** anemia, although usually in smaller numbers. Target cells without microcytosis are also found in liver disease and in the absence of the spleen or of splenic function.

Fine **basophilic stippling** (which is due to precipitation of RNA) may be found in polychromatic red cells associated with a significant increase in the generation of erythrocytes, as in response to hemorrhage or hemolysis. **Coarse basophilic stippling** suggests an abnormality in Hb synthesis. It is found in megaloblastic anemias, thalassemias, refractory anemias, some red cell enzyme deficiencies, unstable Hbs, and lead poisoning. In particular, hypochromasia or microcytosis with significant stippling is against the diagnosis of IDA and is more suggestive of thalassemia or lead poisoning. As mentioned earlier, some cases of iron deficiency may be associated with lead poisoning (see Iron Metabolism).

TABLE 33.10

Laboratory Features in Microcytic Hypochromic Anemias

				MARROW					
	Serum iron	**Serum TIBC**	**% saturation**	**% sideroblasts**	**Iron stores**	**Serum ferritin**	**ZPP**	**HbA_2**	**HbF**
Iron deficiency	↓	↑	↓	↓	↓	↓	↑	N-↓	N
β-Thalassemia trait	N (↑)	N	N	N	N-↑	N-↑	N	↑	N-↑
ACD	↓	N-↓	↓	↓	N-↑	N-↑	↑	N	N
Sideroblastic anemia	↑	↓	↑	↑	↑	↑	↑ (↓)	N	N-↑

ACD, Anemia of chronic disease; *N,* normal; *TIBC,* total iron-binding capacity; *ZPP,* zinc protoporphyrins; ↓, decreased; ↑, increased.

The combination of **oval macrocytes** (especially egg-shaped macrocytes) and **hypersegmented neutrophils** indicates the very likely existence of megaloblastic anemia.

Finally, examination of the blood film allows the evaluation of **qualitative abnormalities in leukocytes and platelets** as well as an estimate of their numbers. Blood diseases that may be first suspected or detected in this manner are many and include compensated hemolytic anemia; early megaloblastic anemia; and anomalies of red cells, such as hereditary elliptocytosis, or of leukocytes, such as the Pelger-Hüet nuclear anomaly.

After the basic studies just mentioned, the choice of additional procedures depends on the morphologic type of the anemia as determined by the indices and the blood film.

Macrocytic Anemia (Increased MCV)

The macrocytic anemias are normochromic, as determined by appearance on the film and by the MCHC. The first step is to ascertain whether the anemia is megaloblastic. Clues from the film have been mentioned. A **bone marrow aspiration** should be performed to confirm the presence of megaloblastosis.

Megaloblastic Marrow

If the marrow is **megaloblastic,** with characteristic changes in both red cell and white cell precursors, the anemia in all likelihood is due to folate or cobalamin deficiency.

See earlier sections on diagnosis of cobalamin deficiency and of folate deficiency. Once the type of deficiency is defined, the cause must be determined.

Nonmegaloblastic Marrow

If the marrow is not megaloblastic, conditions that can be associated with macrocytosis should be investigated. These include liver disease, hemolytic anemias, hypothyroidism, excessive alcohol intake, aplastic anemias, and myelodysplastic syndromes. Anemias associated with these disorders, although they *may* be macrocytic, usually are more normocytic and, thus, are considered with the normocytic anemias as well.

Microcytic and Hypochromic Anemias (Decreased MCV and MCH)

If the counts are performed on a multichannel instrument, the MCHC is likely to be in the normal range, with slight to moderate degrees of hypochromia. Consequently, MCV has assumed the leading role in the detection of microcytic hypochromic anemias. These anemias reflect a quantitative defect in Hb synthesis. Major causes of microcytic anemia include the following:

1. **Iron deficiency anemias** are due to increased requirement or blood loss not balanced by intake.
2. **Anemia of inflammation** (AI; also, anemia of chronic disease) is associated with infection, neoplasia, or collagen disease. This anemia may be normochromic and normocytic, but in long-standing disease is often hypochromic and microcytic.
3. **Thalassemia** is a genetically determined impairment in the rate of globin synthesis.
4. **Sideroblastic anemia** is that group of refractory anemias with erythroid hyperplasia of the marrow in which a defect in Hb synthesis creates a population of hypochromic microcytic cells. The blood film is dimorphic and macrocytes may prevail, making the MCV normal or high, particularly in acquired forms of sideroblastic anemia. Microcytic anemia is common in the inherited form.

Because **iron deficiency** is the most common anemia, the first step is to determine whether the body lacks iron.

When blood loss cannot be documented, serum ferritin, serum iron and iron-binding capacity, or bone marrow study for iron should be performed. These will usually discriminate between the two most common anemias in this category: iron deficiency and simple chronic anemia associated with some other disease—frequently, chronic infection or cancer. In both, the serum iron concentration is low. However, in iron deficiency, the TIBC is elevated whereas in simple AI it is normal or decreased. Storage iron in the marrow is depleted in iron deficiency but is normal or elevated in anemia of chronic disease. IDA in an adult male almost always means chronic blood loss; the source must be found and corrected, if necessary. If no obvious source for iron loss is identified, PNH should be considered, particularly when there is associated neutropenia or thrombocytopenia.

Hypochromic anemias (or hypochromic erythrocytoses) with basophilic stippling and normal or increased serum iron are most likely **thalassemias**, in which case the next examinations to perform are Hb electrophoresis and determination of HbA_2 and HbF. Family studies are often necessary.

Sideroblastic anemias include myelodysplastic syndrome with ring sideroblasts (see Chapter 34) and anemias that occur after therapy with certain drugs (e.g., isoniazid) or in chronic lead poisoning. Coarse basophilic stippling is common in this group of anemias.

Table 33.10 summarizes some laboratory distinctions within the microcytic anemias.

Normocytic and Normochromic Anemias (Normal MCV)

This large group of anemias has many causes. A useful approach is evaluation of the erythrokinetics in a given patient (see Chapter 32). Often, the reticulocyte production index (RPI) and examination of the bone marrow will suffice. The RPI is the simplest measure of effective erythropoiesis.

Optimal Marrow Response: Reticulocyte Production Index Greater Than Two

If the output of reticulocytes has exceeded two times normal as determined by the absolute reticulocyte count, or RPI, it can be assumed that the marrow has reached an optimal response. The cause for the anemia is then **acute blood loss** or **hemolysis**. If blood loss cannot be proved, evidence that hemolysis is in fact present must be sought.

Erythroid hyperplasia of the marrow, serum bilirubin, and urine or fecal urobilinogen will indicate whether erythropoietic activity and destruction are increased. Red cell survival determination may be needed to prove hemolysis in some cases. Low serum haptoglobin and high LD point to hemolysis, but a normal level does not exclude it. LD may also be markedly elevated in megaloblastic anemia, particularly in association with vitamin B_{12} or folate deficiency. None of these measurements will specify whether hemolysis is intravascular or extravascular, but elevated plasma Hb, hemoglobinuria, and hemosiderinuria indicate intravascular hemolysis.

Once it is determined that excessive hemolysis is occurring, the type of hemolytic mechanism must be ascertained.

Direct Antiglobulin (Coombs) Test. If the direct antiglobulin reaction is *positive* using broad-spectrum reagents, tests to determine the presence of IgG, IgM, or complement on the red cells should be undertaken. If immunoglobulin is present on the red cells, tests for antibody specificity, cold agglutinins, Donath-Landsteiner antibody, and serum protein electrophoresis may help to define the process.

If the direct antiglobulin reaction is *negative*, the examinations performed next will depend on the clinical findings and the results of measurements already made.

If HS is suspected, osmotic fragility before and after 24-hour incubation at 37°C and family studies will be necessary. Alternative tests include flow cytometry for EMA binding.

If a nonspherocytic congenital hemolytic anemia is suspected, screening for G6PD and PK deficiencies, and Hb electrophoresis will be helpful. If these are negative, the heat instability test, isopropanol solubility test, and autohemolysis test should be considered.

If thalassemia seems likely, determinations of HbA_2 and HbF and perhaps looking for HbH inclusions are appropriate. Thalassemias are usually microcytic and hypochromic anemias; β-thalassemia major, β-thalassemia intermedia, and HbH disease are hemolytic disorders and may have an increased RPI.

If drug-induced hemolysis is suspected, a test for Heinz bodies, a screening test for G6PD, and, if possible, tests for a drug-dependent autoantibody are indicated.

If the nature of the hemolytic anemia is obscure, a flow cytometry test for PNH should be performed.

Inadequate Marrow Response: Reticulocyte Production Index Less Than Two

The mechanism of the anemia may be ineffective erythropoiesis. Conditions with the greatest degree of ineffective erythropoiesis appear in other categories (e.g., megaloblastic anemia, thalassemia), but most of the myelodysplastic syndromes have a hyperplastic bone marrow and impaired delivery of cells to the blood. In some of these, morphologic changes in erythroid precursors may overlap with megaloblastic anemia, but granulocytic and megakaryocytic changes usually seen in megaloblastic anemia are lacking.

A low reticulocyte count may indicate decreased production caused by inadequate stimulation of the marrow. Chronic renal disease may result in impaired production of EPO. Certain endocrinopathies, such as hypopituitarism or hypothyroidism, may result in regulation of Hb production at a lower level as a result of decreased tissue need for O_2.

A large group of normochromic anemias associated with various chronic diseases form a heterogeneous group characterized by failure of the marrow to meet the need for slightly decreased red cell survival. Some of these are AIs associated with infection, cancer, or rheumatoid arthritis; they have the defect in iron metabolism noted previously in the section on hypochromic microcytic anemias.

Inability of the marrow to respond to EPO may be due to damage to the marrow by drugs or toxic chemicals, to unknown causes, or to infiltration of the marrow by neoplastic cells or fibrous tissue.

In those conditions with low reticulocyte counts in which the marrow is not effectively producing erythrocytes, it is usually helpful to examine the bone marrow. Other studies conducted to determine the underlying disease process can then proceed according to the marrow picture, the assessment of erythrokinetics, and the clinical findings.

POLYCYTHEMIA

Polycythemia (erythrocytosis) is classically defined as an elevated Hct level above the normal range. In the clinical setting, polycythemia exists when Hb and red cell count are increased, reflecting an elevation of the total red cell volume (Maran, 2004). Yet, the recent World Health Organization (WHO) classification of hematologic malignancies has defined polycythemia as Hgb >16.5 g/dL for men and >16.0 g/dL for women, as one of the three major criteria for the diagnosis of polycythemia cera (Swerdlow, 2017).

Absolute polycythemia refers to an increase in the total red cell mass in the body; in **relative polycythemia**, the total red cell mass is normal, but the Hct is elevated because the plasma volume is decreased. Polycythemia may be classified as in Box 33.4. Some classifications are based on EPO response (Cazzola, 2004) and others are based on the underlying mechanism (i.e., primary or secondary and congenital or acquired) (Bento, 2018).

RELATIVE POLYCYTHEMIA

Relative polycythemia refers to an increase in Hct or red cell count as a result of decreased plasma volume; total red cell mass is not increased. This occurs in acute dehydration (e.g., severe diarrhea, burns) and in patients on diuretic therapy.

In **spurious polycythemia** (apparent polycythemia, Gaisböck syndrome), the red cell mass is often high normal and the plasma volume is low normal; these patients have been regarded as an extreme of the normal physiologic state. Almost all are men; they have a high incidence of tobacco smoking and tend to be obese and to have hypertension. Sleep apnea and diuretics may be contributory factors. Serum EPO level is normal (Cazzola, 2004).

BOX 33.4

Pathophysiologic Classification of Polycythemia

Relative Polycythemia

1. Diminished plasma volume: dehydration; shock
2. Spurious polycythemia (stress polycythemia; Gaisböck syndrome)

Absolute Polycythemia

1. Secondary polycythemia with appropriately increased EPO production
   a. Decreased oxygen (O_2) loading: hypoxia, high altitude, pulmonary disease, cyanotic heart disease, carboxyhemoglobinemia, methemoglobinemia, HbM
   b. Decreased O_2 unloading: high O_2 affinity hemoglobinopathy, biphosphoglycerate deficiency
2. Secondary polycythemia with inappropriately increased EPO production
   a. Neoplasms: Wilms tumor, renal carcinoma, cerebellar hemangioma, hepatoma
   b. Localized tissue hypoxia: polycystic kidney, renal artery stenosis
   c. Postrenal transplant
   d. Acute hepatitis
3. Genetic polycythemia
   a. Primary familial congenital polycythemia (mutated EPO receptor)
   b. Chuvash and Croatian polycythemia (mutated *VHL* gene)
4. Primary marrow disorders
   a. Polycythemia vera

Modified from Cazzola M: Serum erythropoietin concentration as a diagnostic tool for polycythemia vera. *Haematologica* 89:1159–1160, 2004.
EPO, Erythropoietin; *HbM,* methemoglobin.

ABSOLUTE POLYCYTHEMIA

Appropriately Increased Erythropoietin Production Due to Hypoxia

Cellular response to hypoxia is controlled by a family of α-β heterodimeric transcription factors known as *hypoxia-inducible factors* (*HIFs*), which regulate the transcription of EPO. There are three HIF isoforms—HIF1α, HIF2α, and HIF3α—with HIF2α being the major isoform regulating EPO expression. In the presence of normoxia, HIF1α is rapidly destroyed by the collaborative effect of O_2, prolyl hydroxylase domain–containing enzymes (PHD), and the von Hippel–Lindau tumor suppressor protein (VHL), which facilitates ubiquitin-mediated proteosomal degradation of HIF1α, thus reducing transcription of EPO. Under hypoxic conditions, degradation of HIFα is slowed, resulting in increased transcription of its target genes, which include EPO. Binding of EPO to its receptor results in autophosphorylation of the receptor-associated Janus kinase 2 (JAK 2), which has tyrosine kinase activity (Patnaik, 2009).

Arterial Oxygen Unsaturation

Lack of O_2 reaching the blood for whatever reason results in arterial unsaturation, impaired O_2 delivery to the tissues, increased production of EPO, erythroid hyperplasia in the marrow, and resultant erythrocytosis. The red cell mass is increased. As a response to the hypoxia, the red cell 2,3-DPG and the p_{50} are increased. In contrast to polycythemia vera, there is usually no leukocytosis or thrombocytosis, and the neutrophil alkaline phosphatase is normal. Arterial O_2 unsaturation may be the cause of polycythemia in persons living at high altitudes; in patients with chronic pulmonary disease and a block in diffusion of O_2 into the blood; in cyanotic heart disease in which there is right-to-left shunt; and in carboxyhemoglobinemia mostly related to cigarette smoking. In the case of CO poisoning, hypoxia is caused by two mechanisms: direct reduction of O_2 saturation and interference with O_2 release from Hb (Landaw, 1990). Approximately 5% to 10% of individuals living in high altitudes (above 2500 m) develop chronic mountain sickness (CMS), sometime referred to as *Monge's disease*. CMS is characterized by excessive erythrocytosis with Hb > 21 g/dL for men and >19 g/dL for women, and three or more of the following symptoms: shortness of breath, palpitations, sleep disturbance, cyanosis, headaches, paresthesia, tinnitus, and dilation of veins (Villafuerte, 2015). Recent studies suggest that a large population of South Americans experiencing a CMS phenotype has single-nucleotide polymorphism in the Sentrin-specific Protease 1 (SENP1) gene, which upregulates the gene and protects HIF1α from degradation causing erythrocytosis (Villafuerte, 2015).

High Oxygen Affinity Hemoglobinopathy

Another cause of tissue hypoxia is the presence of structurally abnormal Hb that has a high affinity for O_2 (Prchal, 2003) (see earlier under Hemoglobins Associated With High Oxygen Affinity and Polycythemia). As in other functional hemoglobinopathies, the disorder occurs in the heterozygote. More than 100 Hb mutations associated with increased O_2 affinity have been identified (Prchal, 2003). Abnormal Hb releases less O_2 to the tissues than does normal Hb at the same pO_2; the O_2 dissociation curve is shifted to the left, and the p_{50} is decreased. The red cell 2,3-DPG is not increased. With this relative tissue hypoxia, EPO production and erythrocytosis are increased. It must be emphasized that routine Hb electrophoresis often does not detect these Hb variants because the amino acid substitution occurs at one of the αβ-contact sites or near the heme pocket. Therefore, a low p_{50} is presumptive evidence for a hemoglobinopathy. Some high-affinity Hbs associated with polycythemia are unstable; in these instances, the heat instability test is positive.

Other causes of altered O_2 affinity include HbM and deficiency of red cell enzyme 2,3-DPG mutase, which is involved in the generation of 2,2-DPG (Gordeuk, 2005).

Inappropriate Erythropoietin Production

Neoplasms

Neoplasms, benign or malignant, have been associated with polycythemia. Renal neoplasms account for the majority. In almost all cases, erythrocytosis has disappeared after resection of the tumor. These neoplasms have been shown to express high levels of EPO mRNA. These tumors include cerebellar hemangiomas, renal cell carcinomas, Wilms tumors, some hepatomas, uterine leiomyomas, pheochromocytoma, parathyroid adenomas, and meningiomas (Patnaik, 2009).

Renal Disorders

In other neoplasms or growths (e.g., renal cysts, hydronephrosis, ovarian carcinoma, some hepatomas), it appears that the mass impinging on the kidney induces increased renal production of EPO as a result of increased pressure or local hypoxia within the kidney. Renal artery stenosis is also associated with polycythemia. Posttransplant erythrocytosis occurs in 10% to 20% of renal transplant recipients. The prevalence is much higher in patients who receive a renal transplant without removing their original kidneys. The therapeutic effects of angiotensin-converting enzyme inhibitors in this condition suggest a role for angiotensin II in regulating erythropoiesis (Prchal, 2003).

Familial Polycythemia

The most common familial polycythemia is due to the presence of a **high oxygen affinity hemoglobin**, which is inherited as an autosomal-dominant trait. Congenital polycythemia may be due to a defect in the hypoxia-sensing mechanism, including HIF, PHD, and VHL in addition to EPO receptors. Von Hippel–Lindau syndrome is an autosomal-dominant disorder associated with mutations in the *VHL* gene. These mutations result in increased levels of HIF-α and increased levels of EPO (Prchal, 2003; Gordeuk, 2005). Chuvash polycythemia is an autosomal-recessive congenital polycythemia that is endemic in the Chuvash population of the Russian federation and caused by autosomal-recessive loss-of-function mutation of the *VHL* gene. It has been reported to be associated with a high mortality rate caused by thrombotic and hemorrhagic complications. *VHL* gene mutations have also been recently described in the Croatian population as well.

Congenital polycythemia may occur secondary to a defect in the EPO receptor in the presence of a normal hypoxia-sensing mechanism. Primary familial and congenital polycythemia (PFCP) is an autosomal-dominant disorder that is present at birth. PFCP is associated with low serum EPO levels and in vitro hypersensitivity of erythroid progenitors to EPO. Approximately 20 germline mutations in the EPO receptor gene *(EPOR)* with resulting truncated receptors have been described in PFCP (Patnaik, 2009; Pasquier et al., 2018). As mentioned earlier, marked decrease in red cell 2,3-DPG associated with **deficiency of 2,3-DPG mutase** activity results in polycythemia and appears to be inherited as an autosomal-recessive condition.

Polycythemia Vera

Polycythemia vera is a myeloproliferative neoplasm characterized by panmyelosis, that is, a condition in which excessive proliferation occurs in megakaryocytes and granulocytes, as well as in erythrocytes. It is manifested by erythrocytosis, leukocytosis, and thrombocytosis of varying degrees. Mutation in the *JAK2* gene is now described as a constant finding. Polycythemia vera is discussed with the myeloproliferative neoplasms.

MEASUREMENT OF ERYTHROCYTE AND PLASMA VOLUME

The diagnosis of absolute polycythemia depends on reliable measurements of erythrocyte and plasma volumes. Erythrocyte and plasma volumes are measured with the use of radioactive isotopic tracers and the dilution principle. The most commonly employed tracers are ^{51}Cr in the form of sodium chromate bound to erythrocytes for measurement of erythrocyte volume. ^{125}I or ^{131}iodine is bound to albumin and can be used to measure plasma volume.

For a detailed description of measurement of red cell and plasma volume, see the report of the International Committee for Standardization in Hematology (1980).

Erythrocyte Volume

In brief, blood is collected from the patient, and the erythrocytes are labeled with ^{51}Cr. The chromated erythrocytes are washed in saline. An aliquot of the ^{51}Cr erythrocytes diluted in saline is injected intravenously into the patient. After a period of equilibration, usually 10 to 20 minutes, a sample of blood is withdrawn from the opposite arm. In cases in which the equilibration time is likely to be prolonged (as in splenomegaly, heart failure, or shock), another sample should be withdrawn 60 minutes after injection.

Radioactivity of each sample is recorded by a scintillation counter. The erythrocyte volume (EV) is calculated using the following formula:

$$\text{EV (mL)} = I\,\text{(cpm)}/C\ \text{(cpm/mL)} \qquad \text{(Eq. 33.1)}$$

where I is the total injected radioactivity (counts/minute) and C is the radioactivity in erythrocytes after mixing is complete (counts/minute/mL of erythrocytes).

Plasma Volume

Approximately 20 mL of blood is withdrawn from a patient. After centrifugation, the plasma is removed, and radioiodine-labeled albumin is added. After mixing, the labeled plasma is injected intravenously into the patient. At 10, 20, and 30 minutes following injection, 5 mL of blood is removed and radioactivity is counted in a well-type scintillation counter. The radioactivity at zero time (P_0) is determined by plotting the three points on semilogarithmic graph paper and extrapolating to zero time. A standard is prepared by diluting an aliquot of the radioiodine-labeled albumin with saline containing a small amount of detergent.

The plasma volume (PV) is calculated using the following formula:

$$\text{PV (mL)} = S\ \text{(cpm/mL)} \times D \times V\ \text{(mL)}/P_0\ \text{(cpm/mL)} \qquad \text{(Eq. 33.2)}$$

where
S = counting rate of standard (counts/minute/mL)
D = dilution of diluted standard solution
V = volume of radioiodine-labeled albumin solution injected
P_0 = counting rate of plasma sample corrected to zero time (counts/minute/mL).

Interpretation

The normal erythrocyte volume for men is 20 to 36 mL/kg; for women, it is 19 to 31 mL/kg. The plasma volume for men is 25 to 43 mL/kg; for women, it is 28 to 45 mL/kg. In newborns and premature infants, the red cell volume and plasma volume in milliliters per kilogram are higher than in adults.

Patients with polycythemia have red cell volumes exceeding 36 mL/kg for men and 32 mL/kg for women. Changes in erythrocyte volume and plasma volume in a variety of conditions are recorded in Table 33.11.

THE PORPHYRIAS

PHYSIOLOGY

Heme biosynthesis is an essential pathway that occurs in all metabolically active cells containing mitochondria and is most prominent in bone marrow and liver. The erythroid marrow is the major heme-forming tissue in the body, producing 85% of the daily heme requirement. Heme complexed with globin forms hemoglobin, which is kept in normal circulating red blood cells for approximately 120 days, which is the average life expectancy of a red cell, whereas heme produced in liver for cytochromes and enzymes, such as catalase and tryptophan pyrrolase, is subject to much more rapid turnover, measurable in hours. A brief sequence of the heme biosynthesis pathway, with the disease states associated with specific enzyme deficiencies along the pathway, is shown in Figure 33.32.

TABLE 33.11

Clinical Effect of Variable Relationship Between Red Cell Volume and Plasma Volume

Red Cell volume	Plasma Volume	Cause	Effect
Normal	High	Pregnancy Cirrhosis Nephritis Congestive cardiac failure	Pseudoanemia
Normal	Low	Stress Peripheral circulatory failure Dehydration Edema Prolonged bed rest	Pseudopolycythemia
Low	Normal	Anemia	Accurate reflection of degree of anemia
Low	High	Anemia	Anemia less severe than indicated by blood count
Low	Low	Hemorrhage Severe anemia (when hematocrit <0.2)	Anemia more severe than indicated by blood count
High	Normal to low	Polycythemia	Accurate reflection of polycythemia or polycythemia less severe than apparent
High	High	Polycythemia (when hematocrit >0.5)	Polycythemia more severe than apparent
Normal or even high	High	Marked splenomegaly	Pseudoanemia

From Dacie JV, Lewis SM: *Practical haematology,* ed 5, Edinburgh, Churchill Livingstone, 1975.

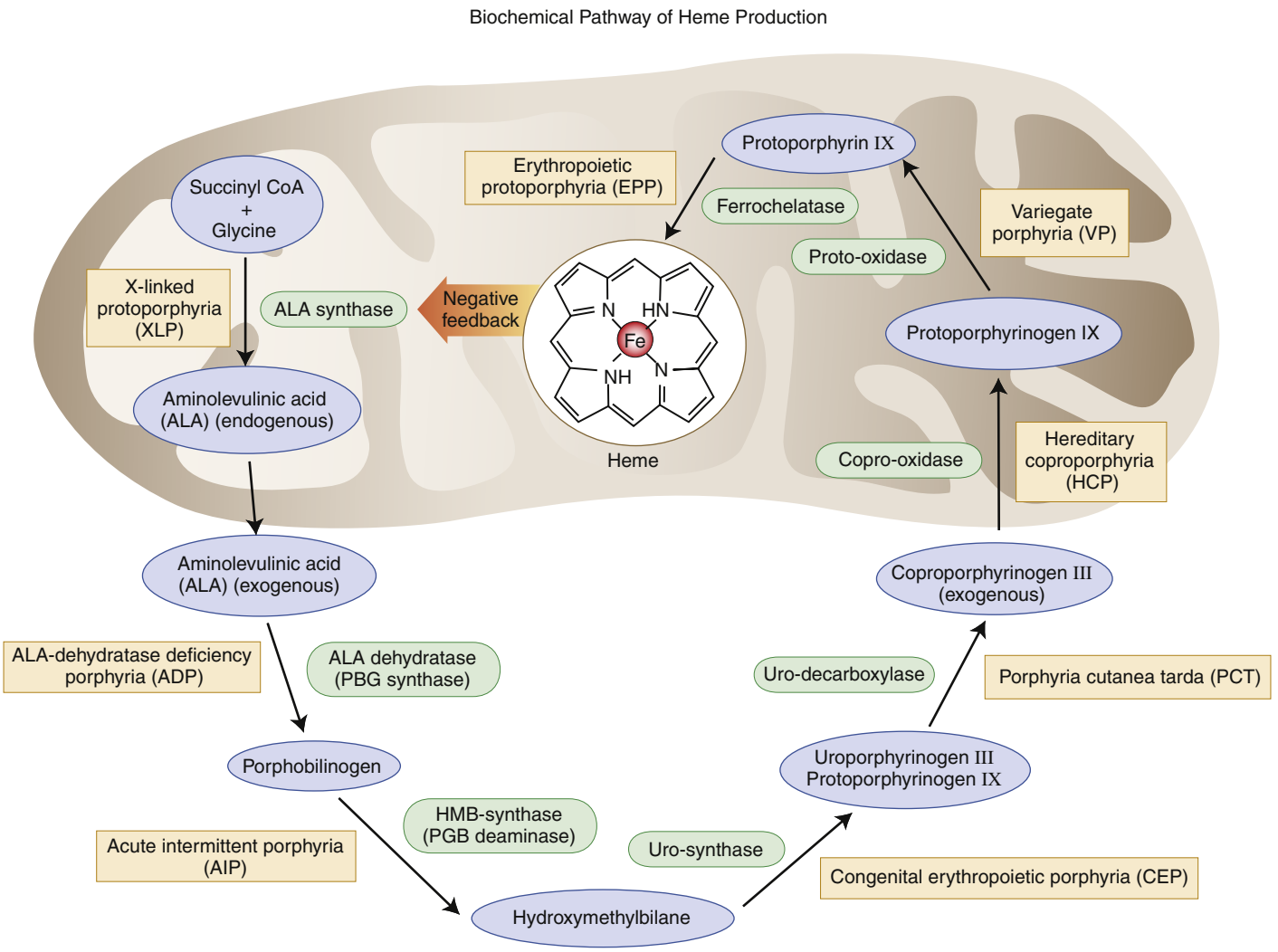

Figure 33.32 Porphyria biochemical pathway of heme production. *ADP,* Aminolevulinic acid dehydratase; *AIP,* Acute intermittent porphyria; *ALA,* aminolevulinic acid; *CEP,* congenital erythropoietic porphyria; *CP III,* coproporphyrinogen III; *EPP,* erythropoietic protoporphyria. *HCP,* hereditary coproporphyria; *HMB,* hydroxymethylbilane; *PCT,* porphyria cutanea tarda; *UP III,* uroporphyrinogen III; *VP,* variegate porphyria; *XLP,* X-linked protoporphyria.

Porphyrins are compounds composed of four pyrrole rings connected by methene bridges, differentiated by substituents found in the eight peripheral positions. The arrangement of four nitrogen atoms in the center of the porphyrin ring enables porphyrins to chelate various metal ions, such as iron, or in disease states, zinc. The biosynthetic intermediates between porphobilinogen (PBG) and protoporphyrin are not porphyrins but rather their reduced, precursor forms: the porphyrinogens. Their name is derived from the Greek word *porphyra*, meaning purple. The porphyrias make up a group of inherited and acquired disorders of heme biosynthesis caused by a deficiency or loss of function mutation of a specific enzyme in the biosynthetic pathway, culminating in the excess production and increased excretion of precursors formed in the steps before the enzyme defect. The only exception is the recently described X-linked-dominant erythropoietic protoporphyria, which results from a gain-of-function mutation of ALAS2, which is expressed exclusively in erythroid cells (Fuller, 2018). Porphyrins that leak out of capillaries into the skin are the cause of photosensitivity, and the precursor substances have been linked to the neurovisceral manifestations. δ-Aminolevulinic acid seems to be the chief offender here (Sassa, 2006).

APPROACH TO THE PORPHYRIAS

The overproduction of porphyrins and their precursors is mainly hepatic or erythropoietic in origin. In the acute porphyrias and porphyria cutanea tarda, the liver is the main source of overproduction; in congenital erythropoietic porphyria, the marrow is the main source while in erythropoietic protoporphyria, porphyrins are produced by both the liver and marrow (Fuller, 2018). Consulting pathologists may take a three-step approach to this diverse group of uncommon diseases. First, review the clinical manifestations described by the referring provider. Classifying porphyrias by their clinical presentation is a helpful starting point, as clinicians will call with information about their patients' signs and symptoms and then will ask for help with ordering laboratory studies (Tables 33.12 and 33.13). Second, suggest biochemical studies, as outlined in Table 33.12 and to follow. A rapid diagnostic test for urine porphobilinogen is now available as a first step. Finally, coordinate genetic testing as guided by biochemical test results. Great strides have been made in identifying the genes and many mutations causing the porphyrias; patients will likely wish to know this information as they discuss their diagnosis with family members. Websites helpful to both providers and patients include those of the Porphyrias Consortium of the National Institutes of Health Rare Disease Clinical Research Network (https://www.rarediseasesnetwork.org/cms/porphyrias), the American Porphyria Foundation (www.porphyriafoundation.com) and the Drug Database for Acute porphyrias (www.porphyriadrugs.com).

NEUROVISCERAL SYMPTOMS IN ISOLATION

Acute Intermittent Porphyria (AIP)

AIP is the most common acute and probably the most common inherited porphyria (Chemmanur, 2004). It is inherited in an autosomal-dominant fashion with incomplete penetrance, making family studies more challenging, and over 375 mutations have been identified (Balwani, 2012). In northern Europe and North America, approximately 1 in 10,000

TABLE 33.12
Key Features of Major Porphyrias

Porphyria	Clinical Features	Excess Metabolites	Rapid Test Enzyme Deficiency Genetic Mutations
Acute intermittent porphyria	Abdominal pain; psychiatric symptoms	PBG (U) ALA (U) Darkened urine on standing	✔ HMB synthase HMBS (>375 mutations)
Congenital erythropoietic porphyria	Photosensitivity; red urine, teeth; hemolysis	UP (U) CP (U) UP (E) Red, fluorescent pigment in urine	UP I synthase, UROS UPG III cosynthase (>35 mutations)
Hereditary coproporphyria	Photosensitivity	CP III (F, U) PBG (U) ALA (U) Red, fluorescent pigment in urine	✔ Copro'ogen oxidase CPOX (>60 mutations)
Variegate porphyria	Photosensitivity	PBG (U) ALA (U) UP (U, F) CP (U, F) Red, fluorescent pigment in urine	✔ Proto'ogen oxidase PPOX (>165 mutations)
Porphyria cutanea tarda	Photosensitivity	UP I (U) UP III (U) Acid induces pink fluorescence	Uro'ogen decarboxylase UROD (>105 mutations)

ALA, aminolevulinic acid; *CP*, coproporphyrin; *E*, erythrocyte; *F*, feces; *PBG*, porphobilinogen; *U*, urine; *UP*, uroporphyrin; *UPG*, uroporphyrinogen.

TABLE 33.13
Test Results for the Porphyrias

Porphyria	Urine	RBC	Feces
Acute intermittent porphyria	↑ PBG, ALA	↓ PBGD activity	Noncontributory
ALA dehydratase deficiency porphyria	↑ porphyrins (ALA alone is increased) Note: Rule out organic acids and heavy metals in urine.	↓ D-aminolevulinic acid dehydratase activity	Noncontributory
Variegate porphyria	↑ porphyrins, PBG	Noncontributory	↑ coproporphyrin III/I ratio (<10)
Hereditary coproporphyria	↑ porphyrins, PBG	Noncontributory	↑ coproporphyrin III/I ratio (>10)
Porphyria cutanea tarda	↑ porphyrins	↓ UROD in Type II, UROD WNL in Types I, III	Noncontributory
Congenital erythropoietic porphyria	↑ porphyrins	↓ UPG III cosynthase	Noncontributory
Erythropoietic protoporphyria	Noncontributory	↑ free protoporphyrin	Noncontributory

ALA, Aminolevulinic acid; *PBG,* porphobilinogen; *PBGD,* porphobilinogen deaminase; *UPG,* uroporphyrinogen; *UROD,* uroporphyrinogen decarboxylase; *WNL,* within normal limits.

individuals carries the gene with only about 10% manifesting clinical symptoms (Fuller, 2018). PBG deaminase deficiency has been demonstrated in all examined tissues at levels of about 50% during attacks and quiescent periods. Diagnosis may be made most easily with demonstration of elevated levels of ALA and PBG in urine during acute attacks (with PBG greater in amount than ALA), but the PBG enzyme assay can be performed at any time on RBCs. Frequently, patients have urine metabolite levels at or near the reference range during quiescent periods. Characteristically, the urine of AIP patients turns dark red upon exposure to air and light, as PBG is oxidized to a porphyrin spontaneously. The patient may be hyponatremic (20% of cases) or hypomagnesemic during acute attacks (Anyaegbu, 2012). Common symptoms include colicky abdominal pain (74%), nausea and vomiting (73%), mental confusion, severe anxiety, depression, tachycardia, and motor weakness usually causing symmetric limb weakness (63%) (Bonkovsky, 2014). Symptoms typically begin at the time of puberty, reflecting the influence of steroid hormones on the disease, but the disease can present in children (Anyaegbu, 2012). Prevention is the mainstay of management, with avoidance of particular drugs (barbiturates and sulfonamides among many others), hormonal changes, and fasting. Specifically, a low-carbohydrate diet may trigger an attack. A recent study identified an increased risk of malnutrition in AIP patients compared with matched controls (Garcia-Diz, 2012). In the postoperative period, patients with AIP must be managed carefully to avoid hypoglycemia (Benassi, 2012).

Aminolevulinic Acid Dehydratase Deficiency Porphyria (ADP)

ADP is the rarest of the porphyrias, with just 10 reported cases (Balwani, 2012). Clinically indistinguishable from AIP, it may be differentiated in the laboratory by the presence of excess ALA alone in the urine and decreased D-aminolevulinic acid dehydratase in the red blood cells of affected patients. Of note, this type of porphyria must be distinguished from tyrosinemia and heavy metal intoxication.

NEUROVISCERAL SYMPTOMS PLUS PHOTOSENSITIVITY

Variegate Porphyria (VP)

Similar to AIP and hereditary coproporphyria (HCP), VP is inherited as an autosomal-dominant disorder with low penetrance. It is sometimes referred to as South African porphyria because of its prevalence in the white population in this region. It is called **variegate** because of the spectrum of patient presentations. Some have only the cutaneous manifestations, others just the neurovisceral, and others both features. Thus, the clinician need not check both boxes to entertain this diagnosis, especially in patients of Afrikaner descent. Patients have approximately 50% activity of protoporphyrinogen oxidase. Thus, they excrete fecal protoporphyrins and coproporphyrins and urine ALA, PBG, and coproporphyrins. Induction of hepatic ALA synthase I by precipitating factors, such as barbiturates, oral contraceptives, or a low-carbohydrate diet, specifically results in increased ALA and PBG during acute attacks (Chemmanur, 2004). Cutaneous manifestations in the form of erosions or bullae following trauma to sun-exposed skin are seen at a younger age than is observed with porphyria cutanea tarda. Diagnosis is made by conventional measurements of metabolites, family history, and DNA analysis. Avoidance of triggering factors remains the major approach to patient care.

Hereditary Coproporphyria

Also inherited in an autosomal-dominant fashion with incomplete penetrance, HCP is less common than AIP. It is due to a deficiency of coproporphyrinogen oxidase. Clinically, HCP combines the clinical features of acute porphyria with photosensitive skin manifestations but overall resembles a milder form of AIP with its neurovisceral attacks, and cutaneous manifestations are seen in roughly a third of patients (Chemmanur, 2004). Fecal coproporphyrinogen III is excreted both during and between attacks, and ALA and PBG are seen in urine during an acute crisis. ALA excretion usually exceeds that of PBG; this, coupled with the cutaneous findings (if present) helps to differentiate HCP from AIP. Prevention, including sunscreen, is central to management.

PHOTOSENSITIVITY PLUS HEMOLYTIC ANEMIA

Porphyria Cutanea Tarda (PCT)

PCT is the most common of the porphyrias in the United States. Type 1 is sporadic; type 2 is inherited in autosomal-dominant fashion. The deficient enzyme is uroporphyrinogen decarboxylase (UROD), and researchers have postulated the presence of an inhibitor of UROD, possibly secondary to iron and metabolites of uroporphyrinogen. Over 105 mutations have been inherited in the UROD gene (Balwani, 2012). It is interesting to note that patients with hemochromatosis are at increased risk for acquired PCT (Chemmanur, 2004). Patients present with cutaneous findings alone, which are due to mild trauma to sun-exposed areas, not simple photosensitivity. The most striking clinical feature is bullous dermatosis, which starts as vesicles that become confluent to form bullae (Fuller, 2018). Diagnostic laboratory findings include increased uroporphyrins with smaller increases in urine coproporphyrins. Exacerbating factors—such as alcohol, an inducer of hepatic ALA synthase I, and estrogens—should be avoided. Additional management strategies involve phlebotomy to reduce the hepatic iron load, chloroquine to complex porphyrins for urinary excretion, and the use of sunscreen (Chemmanur, 2004).

Congenital Erythropoietic Porphyria (CEP)

CEP (Günther disease) is distinct from the other porphyrias discussed earlier in both its inheritance (it is a recessive disorder) and its severity. Patients present shortly after birth with red-pigmented urine, hemolytic anemia, and severe cutaneous photosensitivity. Pink-brown deposits in bones and erythrodontia are striking and may be a useful clue if the diagnosis has not already been made. Needle-like inclusions of porphyrin in circulating RBCs may occur after splenectomy (Fuller, 2018). The deficient enzyme is uroporphyrinogen III synthase, with over 35 mutations identified, and ALA synthase activity is increased. Coproporphyrin I and uroporphyrin I are present in urine. The prognosis for CEP is significantly worse than for the other porphyrias, with death occurring at an early age in many cases.

PHOTOSENSITIVITY IN ISOLATION

Erythropoietic Protoporphyria (EPP) and X-linked Porphyria (XLP)

EPP is due to a partial deficiency of the enzyme ferrochelatase, the final enzyme in the heme biosynthetic pathway. An autosomal-recessive disorder, it is caused by one of over 135 mutations of the FECH gene (Balwani 2012). Clinical symptoms begin in childhood, earlier than in other porphyrias (which have their onset at puberty); painful, itching erythema occurs within a short time (minutes) of sun exposure. Neuropsychiatric symptoms are absent, but a recent case series described a child who was sent for psychiatric care after screaming in pain when outside (Wahlin, 2006). This article makes a useful point regarding the emotional sequelae of painful skin lesions. Emotional distress follows many diseases and must be carefully distinguished from the specific, although myriad, neurovisceral symptoms that characterize other porphyrias. Uniquely among the porphyrias, EPP has a normal urine profile—RBC testing must be performed to render a diagnosis. XLP is newly described and clinically indistinguishable from EPP. It is due to a gain-of-function of the ALAS2 gene (Balwani, 2012).

ANALYTIC TECHNIQUES

Diagnosis in the clinic or hospital laboratory may begin with the Trace PBG Kit (Trace America/Trace Diagnostics) to identify urine porphobilinogens. Table 33.12 shows which porphyrias will have elevated levels. After an initial test, analysis of urine, red blood cells, and feces for various porphyrins typically increased in the porphyrias, and for specific enzymes of the heme biosynthetic pathway, takes place in reference laboratories. The pathologist should select a laboratory that is well familiar with the porphyrias, and that follows a logical algorithm so that disease, if present, can be properly classified. Neither the ordering clinician nor the general pathologist needs to attempt classification of the porphyria by selecting one or two specific assays. The algorithmic approach is the rational one and begins with a quantitative evaluation of porphyrins: PBG and ALA in the urine, and porphyrins and PBGD (porphobilinogen deaminase) measurement in the erythrocytes. HPLC and fluorometry are the mainstays of analytic technique. HPLC can separate individual porphyrins; this, combined with measurement of total fecal porphyrins, reliably distinguishes between AIP and HCP (Deacon, 2001). VP may be diagnosed by measurement of fecal and urine metabolites and by the fluorescence emission peak of 624 to 627 nm, which is unique among the porphyrias (Poh-Fitzpatrick, 1980). The proper samples to submit for testing are urine (a 24-hour sample is strongly preferred, with the appropriate preservative dictated by the reference laboratory) and blood. A stool sample should be provided if VP or HCP is being considered but is less critical for the other porphyrias. Genetic testing for specific mutations should be performed on patients diagnosed by clinical signs and urine/RBC/feces analysis. Recall that the porphyrias are characterized by incomplete penetrance. Family history may or may not suggest the diagnosis; an absence of family history in no way precludes the presence of a porphyria. Once a specific mutation is identified, testing of kindreds can follow in a targeted fashion.

SELECTED REFERENCES

Andolfo I, Russo R, Gambale A, et al.: New insights on hereditary erythrocyte membrane defects, *Haematologica* 101:1284–1294, 2016.

An excellent review of red cell membrane structure and membrane disorders.

Balwani M, Desnick RJ: The porphyrias: advances in diagnosis and treatment, *Blood* 120(23):4496–4504, 2012.

Comprehensive review of the diagnosis, classification, and treatment of the porphyrias.

Bunn HF, Forget BG: *Hemoglobin: molecular, genetic and clinical aspects*, Philadelphia, 1986, WB Saunders.

This classic book provides elegant descriptions of major hemoglobinopathies and includes essential clues to differential diagnosis in a concise manner.

Garratty G, Arndt PA: An update on drug-induced immune hemolytic anemia, *Immunohematol* 23:105–119, 2007.

A detailed review about the prevalence and mechanism of cephalosporin-induced hemolytic anemia.

Hoyer JD, Kroft SH, editors: *Color atlas of hemoglobin disorders. A compendium based on proficiency testing*, College of American Pathologists, 2003.

A practical approach to diagnosis of common hemoglobin disorders.

Kottke-Marchant K: Diagnostic approach to microangiopathic hemolytic anemia, *Int J Lab Hematol* 39(Suppl 1):69–75, 2017.

An excellent review of pathophysiologic mechanisms, clinical presentation, and management of thrombotic microangiopathy. The accompanying algorithm is exceptionally well designed and simple.

Kozyraki R, Cases O: Vitamin B12 absorption: mammalian physiology and acquired and inherited disorders, *Biochimie* 95:1002–1007, 2013.

An excellent review of recent advances in the physiology of vitamin B_{12} absorption and its disorders.

Steinberg MH, Forget BG, Higgs DR, Weatherall DJ, editors: *Disorders of hemoglobin* ed 2, New York, 2009, Cambridge University Press.

Comprehensive reference book on disorders of hemoglobin; detailed account of hemoglobin variants.

Weatherall DJ, Clegg JB: *The thalassaemia syndromes*, ed 4, Oxford, 2001, Blackwell Scientific Publications.

A complete study of thalassemias and their interaction with variant hemoglobins.

Weiss G, Ganz T, Goodnough LT: Anemia of inflammation, *Blood* 133:40–50, 2019.

A concise and informative review of anemia of inflammation.

Alcindor T, Bridges KR: Sideroblastic anaemias, *Br J Haematol* 116:733–743, 2002.

Access the complete reference list online at Elsevier eBooks for Practicing Clinicians.

REFERENCES

Alter BP, Giri N, Savage S, Rosenberg PS: Cancer in the National Cancer Institute inherited bone marrow failure syndrome cohort after fifteen years of follow-up, *Haematologica* 103:30–39, 2018.

Alter BP, Young NS: The bone marrow failure syndromes. In Nathan DG, Orkin SH, editors: *Oski's hematology of infancy and childhood*, 5th ed., Philadelphia, 1998, WB Saunders, p 237.

Andolfo I, Russo R, Gambale A, et al.: New insights on hereditary erythrocyte membrane defects, *Haematologica* 101:1284–1294, 2016.

Anyaegbu E, Goodman M, et al.: Acute intermittent porphyria: a diagnostic challenge, *J Child Neurol* 917–921, 2012.

Babior BM: Metabolic aspects of folic acid and cobalamine. In Beutler E, Lichtman MA, Coller BS, Kipps TJ, Seligsohn U, editors: *Williams hematology*, 6th ed., New York, 2001, McGraw-Hill, p 305.

Bain BJ, Wild BJ, Stephens AD, Phelan LA: *Variant Haemoglobins: a guide to identification*, 1st edition, Wiley-Blackwell, 2010.

Balwani M, Desnick RJ: The porphyrias: advances in diagnosis and treatment, *Blood* 120(23):4496–4504, 2012.

Basset P, Braconnier F, Rosa J: An update on electrophoretic and chromatographic methods in the diagnosis of hemoglobinopathies, *J Chromatogr Biomed Appl* 227:267–304, 1982.

Baumgartner MR: Vitamin-reposive disorders: cobalamin, folate, biotin, vitamins B1 and E, *Handb Clin Neurol* 113:1799, 2013. –1810.

Beck WS, editor: *Hematology*, 5th ed., Cambridge, Mass, 1991, The MIT Press.

Benassi F, Righi E, Cimato P, et al.: Cardiac surgery in patients with acute intermittent porphyria, *J Card Surg* 27:331–334, 2012.

Bentley SA: Red cell survival studies reinterpreted, *Clin Haematol* 6:601–623, 1977.

Bento C: Genetic basis of congenital erythrocytosis, *Int J Lab Hematol* 40(Suppl 1):62–67, 2018.

Beutler E: *Hemolytic anemia in disorders of red cell metabolism*, New York, 1978, Plenum Medical Book Company.

Beutler E, Blume KG, Kaplan JC, et al.: International committee for standardization in haematology: recommended screening test for glucose-6-phosphate dehydrogenase (G-6-PD) deficiency, *Br J Haematol* 43:465–467, 1979.

Beutler E: *Red cell metabolism: a manual of biochemical methods*, 3rd ed., Orlando, Fla, 1984, Grune & Stratton.

Beutler E: The molecular biology of enzymes and erythrocyte metabolisms. In Stamatoyannopoulos G, Nienhuis AW, Majerus PW, Varmus H, editors: *The molecular basis of blood diseases*, 2nd ed., Philadelphia, 1994, WB Saunders, p 331.

Beutler E, Luzzatto L: Hemolytic anemia, *Semin Hematol* 36:38–47, 1999.

Bonkovsky HL, Maddukuri VC, et al.: Acute porphyrias in the USA: features of 108 subjects from Porphyria Consortium, *Am J Med*, 2014. epub ahead of print.

Borbely N, Phelan L, Szydlo R, et al.: Capillary zone electrophoresis for haemoglobinopathy diagnosis, *J Clin Pathol* 66:29–39, 2013.

Bottomley SS: Sideroblastic anaemia, *Clin Haematol* 11:389–409, 1982.

Bottomley SS, Fleming MD: Sideroblastic anemia: diagnosis and management, *Hematol Oncol Clin N Am* 28:653–670, 2014.

Brodsky RA: Paroxysmal nocturnal hemoglobinuria. In Hoffman R, Benz EJ, Shattil SJ, et al.: *Hematology: basic principles and practice*, 5th ed., Philadelphia, 2009, Churchill Livingstone, p 385.

Bunn HF, Forget BG: *Hemoglobin: molecular, genetic and clinical aspects*, Philadelphia, 1986, WB Saunders.

Bunn HF: Sickle hemoglobin and other hemoglobin mutants. In Stamatoyannopoulos G, Nienhuis AW, Majerus PW, Varmus H, editors: *The molecular basis of blood diseases*, 2nd ed., Philadelphia, 1994, WB Saunders, p 207.

Bunn HF: Human hemoglobins: normal and abnormal. In Nathan DG, Orkin SH, editors: *Oski's hematology of infancy and childhood*, 5th ed., Philadelphia, 1998, WB Saunders, p 729.

Camaschella C, Pagani A: Advances in the understanding of iron metabolism and its crosstalk with erythropoiesis, *Br J Haematol* 182:481–494, 2018.

Camaschella C: Iron deficiency, *Blood* 133:30–39, 2019.

Carmel R: Ethnic and racial factors in cobalamin metabolism and its disorders, *Semin Hematol* 36:88–100, 1999.

Caro J, Outschoorn UM: Anemia of chronic renal disease. In Kaushansky K, Lichtman MA, Beutler E, Kipps TJ, Seligsohn U, Prchal JT, editors: *Williams hematology*, 8th ed., New York, 2010, McGraw-Hill, p 495.

Carrell RW, Kay R: A simple method for the detection of unstable haemoglobins, *Br J Haematol* 23:615–619, 1972.

Caulier A, Rapetti-Mauss R, Guizouarn H, et al.: Primary red cell hydration disorders: pathogenesis and diagnosis, *Int J Lab Hematol* 40(Suppl 1):68–73, 2018.

Cazzola M: Serum erythropoietin concentration as a diagnostic tool for polycythemia vera, *Haematologica* 89:1159–1160, 2004.

Chemmanur AT, Bonovsky HL: Hepatic porphyries: diagnosis and management, *Clin Liver Dis* 4:807–838, 2004.

Clark SF: Iron deficiency anemia: diagnosis and management, *Curr Opin Gastroenterol* 25:122–128, 2009.

Clucas DB, Fox LC, Wood EM, et al.: Revisiting acquired aplstic anemia: current concepts in diagnosis and management, *Intern Med J* 49:152–159, 2019.

Dacie JV, Lewis SM: *Practical haematology*, 7th ed., Edinburgh, 1991, Churchill Livingstone.

Da Costa L, Galimand J, Fenneteau O, et al.: Hereditary spherocytosis, elliptocytosis, and other red cell membrane disorders, *Blood Rev* 27:167–178, 2013.

Dallman PR, Yip R, Oski FA: Iron deficiency and related nutritional anemias. In Nathan DG, Oski FA, editors: *Hematology of infancy and childhood*, 4th ed., Philadelphia, 1993, WB Saunders, p 413.

Deacon AC, Elder GH: Best Practice No. 165: front line tests for the investigation of suspected porphyria, *J Clin Pathol* 54:500–507, 2001.

Devos T, Meers S, Boeckx N, et al.: Diagnosis and management of PNH: review and recommendations from a Belgian expert panel, *Eur J Hamatol* 101:737–749, 2018.

Dezern AE, Brodsky RA: Acquired aplastic anemia. In Greer JP, Rodgers GM, Glader B, Arber DA, Means Jr RT, List AF, Appelbaum FR, Dispenzieri A, Fehniger TA, editors: *Wintrobes's clinical hematology*, 14th Ed, Philadelphia, 2019, Wolters Kluwer.

Donath J, Landsteiner K: Uber paroxysmale Haemoglobinurie, *Munch Med Wschr* 51:1590, 1904.

Dror Y: Inherited bone marrow failure syndromes. In Hoffman RB, Benz Jr EJ, Silberstain LE, Heslop H, Weitz J, Anastasi J, Salama ME, editors: *Hematology: basic principles and practice*, 7th Ed., Philadelphia, 2018, Elsvier Health Sciences.

Ducamp S, Fleming MD: The molecular genetics of sideroblastic anemia, *Blood* 133:59–69, 2019.

Elghetany MT, Hudnall SD, Gardner FH: Peripheral blood picture in primary hypocellular refractory anemia and idiopathic acquired aplastic anemia: an additional tool for differential diagnosis, *Haematologica* 82:21–24, 1997.

Erslev AJ: Pure red cell aplasia. In Beutler E, Lichtman MA, Coller BS, Kipps TJ, Seligsohn U, editors: *Williams hematology*, 6th ed., New York, 2001a, McGraw-Hill, p 391.

Erslev AJ: Traumatic cardiac hemolytic anemia. In Beutler E, Lichtman MA, Coller BS, Kipps TJ, Seligsohn U, editors: *Williams hematology*, 6th ed., New York, 2001b, McGraw-Hill, p 619.

Espinoza JL, Kotecha R, Nakao S: Microbe-induced inflammatory signals triggering acquired bone marrow failure syndromes, *Front Immunol* 8:186, 2017.

Fleming MD: The regulation of hepcidin and its effect on systemic and cellular iron metabolism, Hematology 151. In *Annual meeting of the American Society of hematology, san Francisco, December 2008*, 2008.

Forget BG: Molecular studies of genetic disorders affecting the expression of the human β-globin gene: a model system for the analysis of inborn errors of metabolism, *Recent Prog Horm Res* 38:257–277, 1982.

Franco RS: The measurement and importance of red cell survival, *Am J Hematol* 84:109–114, 2009.

Fuller SJ, Wiley JS: Heme biosynthesis and its disorders: porphyrias and sideroblastic anemias. In Hoffman RB, Benz Jr EJ, Silberstain LE, Heslop H, Weitz J, Anastasi J, Salama ME, editors: *Hematology: basic principles and practice*, 7th Ed., Philadelphia, 2018, Elsvier Health Sciences.

Furutani E, Shimamura A: Inherited aplastic anemia syndromes germline. In Greer JP, Rodgers GM, Glader B, Arber DA, Means Jr RT, List AF, Appelbaum FR, Dispenzieri A, Fehniger TA, editors: *Wintrobes's clinical hematology*, 14th Ed, Philadelphia, 2019, Wolters Kluwer.

Gallagher PG, Jarolim P: Red cell membrane disorders. In Hoffman R, Benz EJ, Shattil SJ, et al.: *Hematology: basic principles and practice*, 5th ed., Philadelphia, 2009, Churchill Livingstone, p 623.

Garcia-Diz L, Murcia AM, Gris JL, et al.: Assessing nutritional status of acute intermittent porphyria patients, *Eur J Clin Invest* 42:943–952, 2012.

Garratty G, Arndt PA: An update on drug-induced immune hemolytic anemia, *Immunohematology* 23:105–119, 2007.

Gehrs BC, Friedberg RC: Autoimmune hemolytic anemia, *Am J Hematol* 69:258, 2002.

Globin Gene Server: . Available from http://globin.cse.psu.edu/.

Glader B, Grace RF: Hereditary hemolytic anemias due to RBC enzyme disorders. In Greer JP, Rodgers GM, Glader B, Arber DA, Means Jr RT, List AF, Appelbaum FR, Dispenzieri A, Fehniger TA, editors: *Wintrobes's clinical hematology*, 14th Ed, Philadelphia, 2019, Wolters Kluwer.

Gonzalez-Casas R, Jones EA, Moreno-Otero R: Spectrum of anemia associated with chronic liver disease, *World J Gastroenterol* 15:4653–4658, 2009.

Grace RF, Layton DM, Barcellini W: How we manage patrients with pyruvate kinase deficiency, *Br J Haematol* 184:721–734, 2019.

Green R: Vitamin B12 deficiency from the perspective of a practicing hematologist, *Blood* 129:2603–2611, 2017.

Head CE, Conroy M, Jarvis M, et al.: Some observations on the measurement of haemoglobin A2 and S percentages by high performance liquid chromatography in the presence and absence of alpha thalassaemia, *J Clin Pathol* 57:276–280, 2004.

Herbert V: Megaloblastic anemias, *Lab Invest* 52(3–19), 1985.

Hershko C, Patz J, Ronson A: The anemia of achylia gastrica revisited, *Blood Cells Mol Dis* 39:178–183, 2007.

Hillman RS, Finch CA: *Red cell manual*, 4th ed., Philadelphia, 1974, FA Davis.

Hillman RS, Finch CA: *Red cell manual*, 7th ed., Philadelphia, 1996, FA Davis.

International Committee for Standardization in Haematology: Recommended methods for measurement of red-cell and plasma volume, *J Nucl Med* 21:793, 1980.

Iolascon A, Heimpel H, Wahlin A, et al.: Congenital dyserythropoietic anemias: molecular insights and diagnostic approach, *Blood* 122:2162–2166, 2013.

Kautz L, Jung G, Valore EV, et al.: Identification of eythroferrone as an erythroid regulator of iron metabolism, *Nat Genet* 46:678–684, 2014.

Keren DF, Hedstrom D, Gulbranson R, et al.: Comparison of Sebia Capillarys capillary electrophoresis with the Primus high-pressure liquid chromatography in the evaluation of hemoglobinopathies, *Am J Clin Pathol* 130:824–831, 2008.

Kottke-Marchant K: Diagnostic approach to microangiopathic hemolytic anemia, *Int J Lab Hematol* 39(Suppl 1):69–75, 2017.

Kozyraki R, Cases O: Vitamin B12 absorption: mammalian physiology and acquired and inherited disorders, *Biochimie* 95:1002–1007, 2013.

Labbé RF, Dewanji A: Iron assessment tests: transferrin receptor vis-a-vis zinc protoporphyrin, *Clin Biochem* 37:165–174, 2004.

Landaw SA: Polycythemia vera and other polycythemic states, *Clin Lab Med* 10:857–871, 1990.

Lindenbaum J: Status of laboratory testing in the diagnosis of megaloblastic anemia, *Blood* 61:624–627, 1983.

Lindenbaum J, Healton EB, Savage DG, et al.: Neuropsychiatric disorders caused by cobalamin deficiency in the absence of anemia or macrocytosis, *N Engl J Med* 318:1720–1728, 1988.

Liu YT, Old JM, Miles K, et al.: Rapid detection of α-thalassemia deletions and α-globin gene triplication by multiplex polymerase chain reactions, *Br J Haematol* 108:295–299, 2000.

Looker AC, Dallman PR, Carroll MD, et al.: Prevalence of iron deficiency in the United States, *J Am Med Assoc* 277:973–976, 1997.

Mairbäurl H: Neocytolysis: how to get rid of the extra erythrocytes formed by stress erythropoiesis upon descent from high altitude, *Front Physiol* 9:345, 2018.

Maran J, Prchal J: Polycythemia and oxygen sensing, *Pathol Biol* 52:280–284, 2004.

McMinn JR, George JN: Evaluation of women with clinically suspected thrombotic thrombocytopenic purpura-hemolytic uremic syndrome during pregnancy, *J Clin Apheresis* 16:202–209, 2001.

Means Jr RT: Anemias secondary to inflammation/chronic disease and systemic disorders. In Greer JP, Rodgers GM, Glader B, Arber DA, Means Jr RT, List AF, Appelbaum FR, Dispenzieri A, Fehniger TA, editors: *Wintrobes's clinical hematology*, 14th Ed, Philadelphia, 2019, Wolters Kluwer.

Mentzer WC, Schrier S: Extrinsic nonimmune hemolytic anemias. In Hoffman RB, Benz Jr EJ, Silberstain LE, Heslop H, Weitz J, Anastasi J, Salama ME, editors: *Hematology: basic principles and practice*, 7th Ed., Philadelphia, 2018, Elsvier Health Sciences.

Michel M, Jäger U: Autoimmune hemolytic anemia. In Hoffman RB, Benz Jr EJ, Silberstain LE, Heslop H, Weitz J, Anastasi J, Salama ME, editors: *Hematology: basic principles and practice*, 7th Ed., Philadelphia, 2018, Elsvier Health Sciences.

Moake JL: Thrombotic microangiopathies, *N Engl J Med* 347:589–600, 2002.

Moake JL: Idiopathic thrombotic thrombocytopenic purpura, Hematology. In *Annual meeting of the American Society of hematology, san Diego, December 2004*, vol. 408. 2004.

Motulsky AG: Frequency of sickling disorders in US Blacks, *N Engl J Med* 288:31–33, 1973.

Muckenthaler MU, Rivella S, Hentze MW, et al.: A red carpet for iron metabolism, *Cell* 168:344–361, 2017.

Narla A, Lipton JM: Means Jr RT: red cell aplasia: acquired and congenital. In Greer JP, Rodgers GM, Glader B, Arber DA, Means Jr RT, List AF, Appelbaum FR, Dispenzieri A, Fehniger TA, editors: *Wintrobes's clinical hematology*, 14th Ed, Philadelphia, 2019, Wolters Kluwer.

Ozatli D, Koksal AS, Haznedaroglu IC, et al.: Erythrocytes: anemias in chronic liver diseases, *Hematology* 5:69–76, 2000.

Packman CH: Hemolytic anemia resulting from immune injury. In Kaushansky K, Lichtman MA, Beutler E, Kipps TJ, Seligsohn U, Prchal JT, editors: *Williams hematology*, 8th ed., New York, 2010, McGraw-Hill, p 777.

Pasquier F, Marty C, Balligand T, et al. New pathogenetic mechanisms induced by germline erythropoietin receptor mutations in primary erythrocytosis. *Haematologica* 103:575–586, 2018.

Patnaik MM, Tefferi A: The complete evaluation of erythrocytosis: congenital and acquired, *Leukemia* 23:834–844, 2009.

Petz LD: Cold antibody autoimmune hemolytic anemias, *Blood Rev* 22(1–15), 2008.

Pierce HI, Sumiko KK, Sofroniadou K, et al.: Frequencies of thalassemia in American blacks, *Blood* 49:981–986, 1977.

Poh-Fitzpatrick MB: A plasma porphyrin fluorescence marker for variegate porphyria, *Arch Dermatol* 116:543–547, 1980.

Prchal JT: Classification and molecular biology of polycythemias (erythrocytoses) and thrombocytosis, *Hematol Oncol Clin North Am* 17:1151–1158, 2003.

Prchal JT: Clinical manifestations and classification of erythrocytic disorders. In Kaushansky K, Lichtman MA, Beutler E, Kipps TJ, Seligsohn U, Prchal JT, editors: *Williams hematology*, 8th ed., New York, 2010, McGraw-Hill, p 445.

Ramasethu J, Luban NLC: Alloimmune hemolytic anemia of the fetus and newborn. In Kaushansky K, Lichtman MA, Beutler E, Kipps TJ, Seligsohn U, Prchal JT, editors: *Williams hematology*, 8th ed., New York, 2010, McGraw-Hill, p 799.

Rees DC, Duley JA, Marinaki AM: Pyrimidine 5′ nucleotidase deficiency, *Br J Haematol* 120:375–383, 2003.

Riou J, Godart C, Hurtrel D, et al.: Cation-exchange HPLC evaluated for presumptive identification of hemoglobin variants, *Clin Chem* 43:34–39, 1997.

Ritchie DS, Underhill C, Grigg AP: Aplastic anemia as a late complication of thymoma in remission, *Eur J Haematol* 68:389–391, 2002a.

Ritchie RF, Palomaki GE, Neveux LM, et al.: Reference distributions for serum iron and transferrin saturation: a practical, simple, and clinically relevant approach in a large cohort, *J Clin Lab Anal* 16:237–245, 2002b.

Rosse WF: Cold-induced immune hemolytic anemia, Hematology. In *Annual meeting of the American Society of hematology, san Diego, December 2004*, vol. 58. 2004.

Sabath DE: Molecular diagnosis of thalassemias and hemoglobinopathies, *Am J Clin Pathol* 148(6–15), 2017.

Salinas M, Flores E, López-Garrigós M, et al.: Vitamin B12 deficiency and clinical laboratory: lessons revisited and clarified in seven questions, *Int J Lab Hematol* 40(Suppl 1):83–88, 2018.

Sassa S: Modern diagnosis and management of the porphyrias, *Br J Haematol* 135:281–292, 2006.

Scalabrino G: The multi-faceted basis of vitamin B12 (cobalamin) neurotrophism in adult central nervous system: lessons learned from its deficiency, *Prog Neurobiol* 88:203–220, 2009.

Scheinberg P, Young NS: How I treat acquired aplastic anemia, *Blood* 120:1185–1196, 2012.

Shallis RM, Ahmad R, Zeidan AM: Aplastic anemia: etiology, molecular pathogenesis, and emerging concepts, *Eur J Haematol* 101:711–720, 2018.

Shatzel JJ, Taylor JA: Syndromes of thrombotic microangiopathy, *Med Ckin N Am* 101:395–415, 2017.

Shulman IA, Branch DR, Nelson JM, et al.: Autoimmune hemolytic anemia with both cold and warm autoantibodies, *J Am Med Assoc* 253:1746–1748, 1985.

Sokol RJ, Hewitt S: Autoimmune hemolysis: a critical review, *Crit Rev Oncol Hematol* 4:125–154, 1985.

Sokol RJ, Booker DJ, Stamps R: The pathology of autoimmune haemolytic anaemia, *J Clin Pathol* 45:1047–1052, 1992.

Soldin OP, Bierbower LH, Choi JJ, et al.: Serum iron, ferritin, transferrin, total iron binding capacity, hs-CRP, LDL cholesterol and magnesium in children; new reference intervals using the Dade dimension clinical chemistry system, *Clin Chim Acta* 342:211–217, 2004.

Steinberg MH: Management of sickle cell disease, *N Engl J Med* 340:1021–1030, 1999.

Steinberg MH, Forget BG, Higgs DR, Weatherall DJ, editors: *Disorders of hemoglobin*, 2nd ed., New York, 2009, Cambridge University Press.

Stephens AD, Angastiniotis M, Baysal E, et al.: ICSH recommendations for the measurement of Hemoglobin A2, *Int J Lab Hematol* 1–13, 2012.

Sutherland DR, Keeney M, Illingworth A: Practical guidelines for the high-sensitivity detection and monitoring of paroxysmal nocturnal hemoglobinuria clones by flow cytometry, *Cytometry B* 82B:195–208, 2012.

Swerdlow SH, Campo E, Harris NL, et al.: *WHO classification of tumours of haematopoietic and lymphoid tissues*, Lyon, 2017, IARC Press.

Tietz NW, editor: *Clinical guide to laboratory tests*, 2nd ed., Philadelphia, 1990, WB Saunders.

Thein SL, Menzel S: Discovering the genetics underlying foetal haemoglobin production in adults, *Br J Haematol* 145:455–467, 2009.

Thein SL: The molecular basis of β-thalassemia, *Cold Spring Harb Perspect Med* 3:a011700, 2013.

Van den Bosch G, Van den Bossche J, Wagner C, et al.: Determination of iron metabolism—related reference values in a healthy adult population, *Clin Chem* 47:1465–1467, 2001.

Van Solinge WW, van Wijk R: Disorders of red cells resulting from enzyme abnormalities. In Kaushansky K, Lichtman MA, Beutler E, Kipps TJ, Seligsohn U, Prchal JT, editors: *Williams hematology*, 8th ed., New York, 2010, McGraw-Hill, p 647.

Villafuerte FC: New genetic and physiological factors for excessive erythrocytosis and chronic mountain sickness, *J Appl Physiol* 119:1481–1486, 2015.

Visentin M, Diop-Bove N, Zhao R, et al.: The intestinal absorption of folates, *Annu Rev Physiol* 76:251–274, 2014.

Wahlin S, Floderus Y, Ros A-M, et al.: The difficult clinical diagnosis of erythropoietic protoporphyria, *Physiol Res* 55(suppl 2):S155–S157, 2006.

Wang C-Y, Babitt JL: Liver iron sensing and body iron homeostasis, *Blood* 133:18–29, 2019.

Ward PC: Modern approaches to the investigation of vitamin B12 deficiency, *Clin Lab Med* 22:435–445, 2002.

Weatherall DJ, Clegg JB: Genetic disorders of hemoglobin, *Semin Hematol* 36:24–37, 1999.

Weatherall DJ, Clegg JB: *The thalassaemia syndromes*, 4th ed., Oxford, 2001, Blackwell Scientific Publications.

Weatherall DJ: The inherited diseases of hemoglobin are an emerging global health burden, *Blood* 115:43316, 2010.

Weiss G, Ganz T, Goodnough LT: Anemia of inflammation, *Blood* 133:40–50, 2019.

Winslow RM, Anderson WF: The hemoglobinopathies. In Stanbury JB, Wyngaarden JB, Fredrickson DS, et al.: *The metabolic basis of inherited disease*, 5th ed., New York, 1983, McGraw-Hill, pp 2281–2317.

Wintrobe MM, Lee GR, Boggs DR, et al.: *Clinical hematology*, 8th ed., Philadelphia, 1981, Lea & Febiger.

Young NS, Maciejewski JP: Aplastic anemia. In Hoffman R, Benz EJ, Shattil SJ, et al.: *Hematology: basic principles and practice*, 5th ed., Philadelphia, 2009, Churchill Livingstone, p 359.

Zhang D-L, Ghosh MC, Rouault TA: The physiological functions of iron regulatory proteins in iron homeostasis – an update, *Front Pharamcol* 5:124, 2014.

Zheng Y, Cantley LC: Toward a better understanding of folate metabolism in health and disease, *J Exp Med* 216:253–266, 2019.

Zini G, D'Onofrio G, Briggs C, et al.: ICSH recommendations for identification, dignoastic value, and quantification of schistocytes, *Int J Lab Hematol* 34:107–116, 2012.

Zittoun J, Zittoun R: Modern clinical testing strategies in cobalamin and folate deficiency, *Semin Hematol* 36:35–46, 1999.

CHAPTER 34

LEUKOCYTIC DISORDERS

Michel R. Nasr, Robert E. Hutchison

LEUKOCYTES, 636

NONNEOPLASTIC DISORDERS, 636
Granulocytic and Monocytic Disorders, **636**
Lymphocytic and Plasmacytic Disorders, 641
Leukemoid Reactions, 645

NEOPLASTIC DISORDERS PRIMARILY INVOLVING LEUKOCYTES, 646
Myeloproliferative Neoplasms, 646
Precursor Lymphoid Neoplasms, 663
Mature B-Cell Neoplasms, 664
Mature T-Cell and Natural Killer Cell Neoplasms, 676
Hodgkin Lymphoma, 683
Immunodeficiency-Associated Lymphoproliferative Disorders, 685
Histiocytic and Dendritic Cell Neoplasms, 686

SELECTED REFERENCES, 688

KEY POINTS

- Leukocytes are regulated by complex homeostatic mechanisms that direct their responses to infection and inflammation.
- Leukocytosis often reflects an underlying abnormality; leukopenia, especially neutropenia, places a patient at risk for infection.
- Hematopoietic neoplasms have been categorized by a World Health Organization classification according to cell of origin, cytogenetic and molecular abnormalities, immunophenotype, and clinical features.
- Acute leukemias are rapidly progressing neoplasms of precursor myeloid or lymphoid cell origin. An understanding of biology is associated with improvements in therapy.
- Myeloproliferative neoplasms and myelodysplastic syndromes are heterogeneous disorders of differentiated myeloid cells. They often are initially indolent but ultimately progress.
- Non-Hodgkin lymphomas most often arise from mature B cells. They are pathologically and clinically heterogeneous. T-cell lymphomas are less common, also heterogeneous, and often difficult to treat successfully.
- Hodgkin lymphoma is a neoplasm of defective B cells. Much of its pathology is due to an associated inflammatory milieu.

LEUKOCYTES

Leukocytes, or white blood cells (WBCs), are found within the bone marrow (BM), the peripheral blood, and the tissues. They protect the body from infection and other foreign insults and include granulocytes, lymphocytes (B cells, T cells, and natural killer [NK] cells), monocytes, eosinophils, and basophils. Leukocyte function and homeostasis are highly complex areas of biology that span several disciplines.

NONNEOPLASTIC DISORDERS

Laboratory examination of leukocytes occurs as part of the automated complete blood count (CBC) for almost every patient. The total leukocyte (or WBC) count—as well as the relative and absolute concentrations of neutrophils, lymphocytes, monocytes, eosinophils, and basophils—is determined and compared with normal values for the patient's age and sex. The absolute concentrations (i.e., the product of the WBC count and the percentage of the respective cell series, such as lymphocytes or neutrophils) are of most value in determining abnormalities. Abnormal results from the automated count are flagged and then reviewed by a skilled laboratory technologist.

These abnormalities include leukocytosis, or increase in the total WBC count, and leukopenia, a decrease in the total WBC count, each compared with normal values for age and sex. The differential count, usually first performed on an automated instrument, quantifies the relative and absolute concentrations of the various forms of leukocytes and the maturation state for neutrophils. An increase in the absolute concentration of cells in each series is termed *neutrophilia* (*neutrophilic leukocytosis*), *lymphocytosis*, *monocytosis*, *eosinophilia* (*eosinophilic leukocytosis*), and *basophilia* (*basophilic leukocytosis*). A decrease in the absolute concentration is termed *neutropenia*, *lymphopenia* (or *lymphocytopenia*), *monocytopenia*, *eosinopenia*, and *basopenia*. Increased numbers of band neutrophils and/or presence of immature neutrophils (metamyelocytes and earlier) are noted and enumerated and often confirmed or modified by a manual differential count.

Nucleated red blood cells (RBCs) are also counted and subtracted from the WBC count by automated or manual method. Abnormalities may occur in both neoplastic conditions (e.g., leukemia or marrow infiltration by metastatic tumor) and nonneoplastic conditions (e.g., infection, drug effect or nutritional deficiency). An increase in any cell type may be clinically important, but a decrease is most important for neutrophils. Lymphocytopenia is important in immunodeficiency syndromes. Isolated monocytopenia, eosinopenia, or basopenia is not usually considered pathologic. Functional neutrophil abnormalities occasionally occur.

GRANULOCYTIC AND MONOCYTIC DISORDERS

Neutrophilia

Neutrophilic leukocytosis or *neutrophilia* refers to an absolute concentration of neutrophils in the blood above normal for age. The normal reference interval (established for each laboratory separately) is approximately 1.8 to $7.0 \times 10^3/\mu L$ for adults, with a slightly wider range ($1.0–8.5 \times 10^3/\mu L$) in young children. The neutrophilias are acquired disorders; key causes are listed in Box 34.1.

Mechanisms

The primary factors influencing the neutrophil count are (1) the rate of inflow of cells from the bone marrow; (2) the proportion of neutrophils in the marginal granulocyte pool (MGP; cells adhering to vessel walls) and the circulating granulocyte pool (CGP) of the blood—MGP and CGP are approximately equal in size and in equilibrium in health; and (3) the rate of outflow of neutrophils from the blood.

Physiologic leukocytosis is produced by factors or situations that are not related to underlying tissue pathology. Severe exercise, hypoxia, stress, or the injection of epinephrine will result in a decrease in the MGP and a corresponding increase in the CGP, resulting in "pseudoneutrophilia" (i.e., no change in total blood granulocyte pool [TBGP]). This simple redistribution of cells between the CGP and MGP, also known as *demargination*, is the release and detachment of leukocytes from receptors on vessel luminal walls. Stress of greater severity and presence of endotoxin or corticosteroids also results in an increased inflow of cells to the blood from the marrow maturation/storage pool.

Pathologic leukocytosis is an increased WBC count that occurs as a result of disease, usually in response to infection or tissue damage, and is most often neutrophilia. When attracted to a focus of inflammation, neutrophils leave the blood and migrate in response to chemotactic molecules and gradients (Petri, 2018; Liew, 2019). There is compensatory flow of

neutrophils from the marrow storage compartment into the blood; the result is neutrophilia. Usually, production and storage compartments are able to sustain the increased CGP (neutrophilia) and MGP in the face of the increased flow of neutrophils from the blood into the inflammatory site. The marrow will show granulocytic hyperplasia (increased myeloid to erythroid [M/E] ratio and increased cellularity), with intact maturation. An increase in immature peripheral blood granulocytes is often termed a "shift to the left." Increased WBCs with left shift and toxic features (see later discussion) may resemble leukemia and is often termed a "leukemoid" reaction (Fig. 34.1).

If the demand for neutrophils is extremely great, as in severe infection, there may be depletion of the marrow storage pool with decreased CGP (neutropenia) and MGP because the supply of cells is insufficient for the demand. In these instances, the marrow will show increased early neutrophil precursors through the myelocyte stage, but decreased metamyelocytes, bands, and neutrophils.

Determinants

Host factors modify the degree of neutrophilic response, with children responding more intensely than adults. The degree of neutrophilia may be impaired by iron, folate, or cobalamin deficiency, or marrow failure due to other causes.

Pyogenic bacteria especially induce neutrophilia. More virulent agents result in higher neutrophil counts; when the infection is overwhelming, toxic neutropenia with a shift to the left can occur, more commonly in the elderly.

Antibiotics modify the response to infection and, while steroid therapy causes neutrophilia by demargination, it tends to impair the host response to infection.

Neutrophilia, sometimes pronounced, is occasionally seen in patients with primary or metastatic nonhematologic neoplasms, including gastrointestinal and hepatic tumors, Hodgkin lymphoma (HL) and renal cell carcinoma (Granger & Kontoyiannis, 2009; Hernandez, 2002).

Neutropenia

Neutropenia is a reduction of the absolute neutrophil count (ANC) below ≈1.5–2 × 10^9/L for white adults and below ≈1.2–1.3 × 10^9/L for black adults. The ANC is the product of the WBC count and the percentage of mature as well as immature neutrophils in the WBC differential count. "Agranulocytosis" refers to severe neutropenia, usually <0.5 × 10^9/L, and is often associated with depletion of eosinophils and basophils as well. Severe chronic neutropenia (SCN) refers to patients with ANC <0.5× 10^9/L for months or years, due to inherited or acquired rare disorders. (Welte & Zeidler, 2009) If the neutrophil count is less than 1× 10^9/L, the risk of infection is increased, and greater still if less than 0.5× 10^9/L.

Mechanisms by which neutropenia occurs include (1) decreased or ineffective production (proliferation or maturation defect); (2) increased removal from the blood (survival defect); (3) altered distribution between CGP and MGP; or (4) combinations of these mechanisms. Neutropenias may be inherited, autoimmune, toxic, or drug associated. Drug-induced neutropenia occurs through several mechanisms and is always an important consideration in the differential diagnosis of leukopenia. A partial list of causes associated with neutropenia are shown in Box 34.2.

Constitutional disorders associated with neutropenia frequently present in early infancy and are of complex molecular origin (Hauck, 2013; Wegman-Ostrosky, 2017). Those due to myeloid hypoplasia or a proliferation defect include Fanconi anemia (FA), Kostmann syndrome, Shwachman-Diamond syndrome, and cyclic neutropenia. Those that are due to maturation defects include severe congenital neutropenia (SCN), myelokathexis, and Chédiak-Higashi syndrome.

FA is an inherited BM failure syndrome that usually occurs in childhood and rarely presents in adulthood. This condition is heterogeneous in its clinical manifestations but was classically defined by the presence of aplastic anemia and congenital physical malformations. The aplastic anemia of FA patients appears to be indistinguishable from acquired aplasia. FA patients are also susceptible to hematopoietic and certain solid organ malignancies. Diagnosis is usually made by cytogenetic analysis while looking for chromosome breakage after exposure to diepoxybutane or mitomycin C. The underlying molecular pathology is complex and involves multiple and varied DNA repair and signaling pathways (Auerbach, 2009; Kupfer, 2013; Wegman-Ostrosky, 2017).

Severe congenital neutropenia (Kostmann syndrome) is a rare severe (ANC typically <200/μL) congenital neutropenia appearing in early infancy, usually with an autosomal-recessive pattern of inheritance. The marrow usually shows the presence of early granulocytes (promyelocyte/myelocyte arrest), but few maturing forms are seen; neutrophil survival is normal. Mutations in *ELANE/ELA2*, encoding neutrophil elastase, are present in about 50% of cases and are autosomal dominant; mutations of the anti-apoptotic gene *HAX-1* are sometimes present and are recessive. Autosomal-dominant negative mutations in *GFL1* or *G6PC3* are causative in some cases; most recently, mutations of *CSF3R*, encoding the granulocyte colony stimulating factor (G-CSF) receptor, have been identified and may be associated with increased risk of acute myeloid leukemia (AML) and myelodysplastic syndromes (MDS). Additionally, some patients have mutations in *GATA2*, with neutropenia and sometimes monocytopenia, and familial tendency to AML/MDS. Screening for these mutations may be important, especially if monocytopenia is also present (Carlsson, 2007; Pasquet, 2013).

Cyclic neutropenia typically presents with recurrent episodes of symptomatic infection (fatigue, mouth ulcers, cervical lymphadenopathy, fever) due to cyclic episodes of severe neutropenia related to periodicity or cycling of neutrophil production. This disease usually presents in childhood but may present in adulthood and is usually not life-threatening. Typically, oscillations of neutrophil and monocyte levels (between near normal levels and very low levels) occur over an approximately 21-day period. Mutations in *ELA2*, similar to those seen in Kostmann syndrome, have been identified in many patients (Dale & Welte, 2011).

Chronic familial neutropenia or benign familial neutropenia refers to a lower than normal neutrophil count, as found in some ethnic populations. It may be an incidental and clinically stable finding with no predisposition to infection in many families. However, screening for *GATA2* mutations may also be indicated when there is family history of AML/MDS.

Common causes of congenital neutropenia are neutropenia of pregnancy-induced hypertension (PIH; most common) and overwhelming bacterial infection. Typical signs of infection, including a granulocytic left shift, toxic granulation, and Döhle bodies, accompany the latter. However, these changes are not seen in PIH, although its pathophysiology is due to an inflammatory state (Marins, 2019). Neither usually continues beyond the first week of life. Other causes should be searched for in infants with persistent neutropenia (Christensen, 2004). Neonatal alloimmune neutropenia (NAIN or NAN) is rare and occurs due to maternal alloantibodies against human neutrophil antigens (HNAs) that the mother lacks and that are inherited from the father (Porcelijn, 2018).

Patients with congenital or primary immunodeficiency diseases may exhibit some degree of neutropenia. Males with X-linked agammaglobulinemia (XLA) are often neutropenic; XLA should be considered in the differential diagnosis of chronic neutropenia in an infant. An abnormal nonreceptor tyrosine kinase, associated with signal transduction and differentiation of hematopoietic cells, appears to be involved. This is due to various mutations in the gene *BTK* (Bruton's or B lymphocyte tyrosine kinase) on the long arm of the X chromosome (q22). Other congenital syndromes having a prominent association with neutropenia include selective immunoglobulin (Ig) A deficiency, common variable immunodeficiency, and hyper IgM syndrome (Dotta & Badolato, 2014).

Certain autoimmune diseases can also be associated with chronic neutropenia. Both rheumatoid arthritis (RA) and systemic lupus erythematosus (SLE) show this association (Starkebaum, 2002). The combination of chronic neutropenia and RA is termed Felty syndrome (FS). Patients develop symptoms owing to both RA (e.g., subcutaneous nodules, contractures, erythema, warmth, tenderness, symmetric involvement of large and small joints, musculoskeletal pain) and chronic neutropenia (symptoms of recurrent bacterial and fungal infections). A portion of these cases are associated with large granular lymphocyte (LGL) leukemia that may be indistinguishable from FS (Liu & Loughran, 2011). In some cases of FS, a neutrophil-specific antibody may be involved. SLE may present with multisystem involvement, making presenting symptoms highly variable. Alterations in neutrophil proliferation and survival with neutropenia due, at least in part, to immune-mediated destruction, occur in both SLE and FS, and increased neutrophil apoptosis may be noted in SLE.

Autoimmune myelofibrosis is a rare cause of isolated neutropenia (Chalayer et al., 2014). Prognosis of these patients appears to be very good with corticosteroid therapy.

Drugs are the most common cause of acute neutropenia (agranulocytosis) and typically show a lack of granulocytic cells in the marrow. However, progenitor hyperplasia may be present and is often termed *promyelocytic hyperplasia* or *maturation arrest*. Most classes of drugs have been implicated,

BOX 34.1

Key Causes of Neutrophilia

- Acute inflammatory—collagen vascular, vasculitis
- Acute infectious—bacterial, some viral, fungal, parasitic
- Drugs, toxins, metabolic—corticosteroids, growth factors, uremia, ketoacidosis
- Tissue necrosis—burns, trauma, MI, RBC hemolysis
- Physiologic—stress, exercise, smoking, pregnancy
- Neoplastic—carcinomas, sarcomas, myeloproliferative disorders

MI, Myocardial infarction; *RBC,* red blood cell.

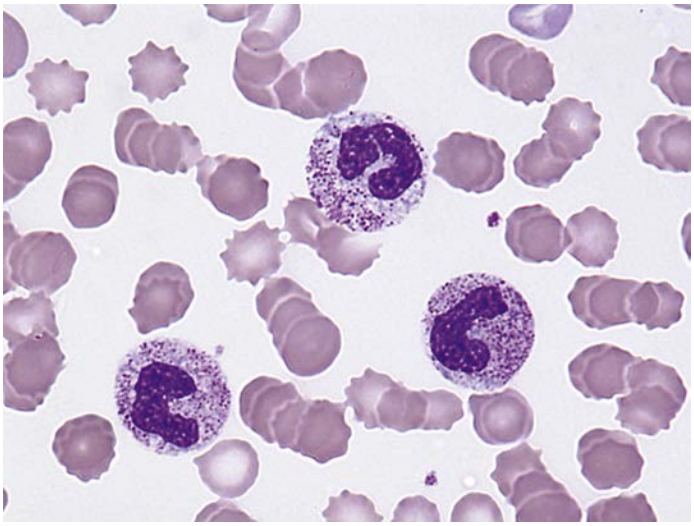

Figure 34.1 A neutrophil with toxic granulation is pictured, along with two bands. Basophilic inclusions (Döhle bodies) are present as well (× 1000).

with clozapine, trimethoprim-sulfamethoxazole, and methimazole most commonly associated. Pathogenesis is not well understood for individual cases (Tesfa et al., 2009). Mortality is about 5% and management includes cessation of medication, use of antibiotics, and consideration of G-CSF (Pick & Nystrom, 2014).

Inhibition of granulopoiesis or myeloid toxicity occurs with chemotherapeutic agents, chlorpromazine and others. These effects tend to be dose dependent and reversible. Important and limiting side effects of cancer chemotherapy are severe neutropenia, with its risk of infection, and severe thrombocytopenia, with risk of bleeding. Anemia is more readily controlled with transfusion.

Radiation damages bone marrow progenitor cells as well as marrow stromal elements. Radiation type, dose, and duration are all factors that determine the extent of bone marrow damage, such as aplasia or hypoplasia. Lymphocytes are most sensitive and are directly killed by exposure. The lymphocyte count correlates with and has been used to assess dose and severity of exposure (Dainiak, 2002). In addition, hematopoietic precursors undergoing mitosis are very sensitive to injury and death.

Isolated neutropenia or agranulocytosis is fairly uncommon in adults. When a myelophthisic process—such as metastatic carcinoma, disseminated tuberculosis, or Gaucher disease—infiltrates the BM, the damage is not limited to granulopoiesis but rather affects normoblasts and megakaryocytes as well. Because of the short life span of granulocytes, however, neutropenia is the earliest recognizable effect in the blood. It may take weeks before damage to the erythropoietic tissue becomes manifest because of the usually long life span of erythrocytes. Platelets have a rather short life span; on the other hand, megakaryocytes are more resistant to damage.

Neutropenia due to increased ineffective granulocytopoiesis occurs in megaloblastic anemias and with drugs that have an antifolate effect. In these conditions, anemia and thrombocytopenia are usually associated. The marrow is usually hyperplastic. In megaloblastic anemia due to nutritional deficiency, drug-induced suppression of deoxyribonucleic acid (DNA) synthesis, or an inborn error of metabolism asynchronous nuclear/cytoplasmic maturation (megaloblastic change or megaloblastosis) is identified in marrow progenitor cells. Ineffective granulocytopoiesis may also occur in myelodysplasia.

BOX 34.2

Key Causes of Neutropenia*

- Drugs—cancer chemotherapy, chloramphenicol, sulfas/other antibiotics, phenothiazines, benzodiazepines, antithyroids, anticonvulsants, quinine, quinidine, indomethacin, procainamide, thiazides
- Radiation
- Toxins—alcohol, benzene compounds
- Intrinsic defects—Fanconi, Kostmann, cyclic neutropenia, Chédiak-Higashi
- Immune mediated—collagen vascular disorders, RA, AIDS
- Hematologic—megaloblastic anemia, myelodysplasia, marrow failure, marrow replacement
- Infectious—any overwhelming infection
- Others—starvation, hypersplenism

AIDS, Acquired immunodeficiency syndrome; *RA,* rheumatoid arthritis.
*Brief, partial list.

In starvation, cellularity tends to be decreased, and a morphologic marrow change termed *serous fat atrophy* or *gelatinous transformation of the bone marrow* is present. This change shows a loss of hematopoietic cells within the marrow stroma replaced by small or shrunken fat cells expanded by an intercellular, homogeneous, eosinophilic material. BM hypocellularity is typically seen with advanced disease.

Transient neutropenia may occur early in some infections, followed by leukocytosis once the marrow production catches up with the demand. Some bacterial infections—notably, brucellosis and *Salmonella* infections—are associated with neutropenia. They may have some depressing effects on the marrow as well. Patients with measles and rubella have neutropenia for several days after appearance of the rash. Hepatitis, infectious mononucleosis and influenza may also cause acute neutropenia. Lymphocytosis is present and persists after the neutropenia subsides.

The neutropenia of hypersplenism has been attributed to selective removal of neutrophils by the spleen. It is associated with neutrophilic hyperplasia of the marrow and is corrected by splenectomy. Splenomegaly due to many causes may result in shortened neutrophil survival and neutropenia. These include congestive splenomegaly, FS, Gaucher disease, and lymphoma.

Pseudo-neutropenia may be caused by increased margination of neutrophils in some individuals without a decrease in total granulocyte count. Rather than showing an equal distribution between MGP and CGP, an increased proportion of neutrophils appear to be present in the MGP. Small doses of endotoxin will cause a shift of neutrophils into the MGP from the CGP, resulting in an apparent neutropenia before causing leukocytosis.

Morphologic Alterations in Neutrophils

In addition to quantitative changes, qualitative morphologic alterations occur in neutrophils. These, too, may be inherited or acquired. Some of these, such as toxic granules or cytoplasmic vacuoles, are acquired and disappear after the stimulus that provoked them is gone. Others are hereditary and persist through life, with or without functional impairment (Box 34.3). These were reviewed by Brunning (1970) and later by Kroft (2002).

It should be noted that disorders of leukocyte function may exist with no structural abnormality detectable with the usual modes of morphologic examination.

Toxic Granulation

Toxic granules are dark-blue to purple cytoplasmic granules in the metamyelocyte, band, or neutrophil stage. They are peroxidase positive and may be numerous or few in number; less peroxidase activity may be seen in toxic than in normal neutrophils. Toxic granulation is noted in infections or other toxic conditions but may also be seen in noninfectious reactive conditions (Figs. 34.1 and 34.2).

Döhle Inclusion Bodies

These small, oval inclusions in the peripheral cytoplasm of polymorphonuclear neutrophils stain pale blue with Wright's stain (see Fig. 34.1). They are remnants of free ribosomes or rough-surfaced endoplasmic reticulum, persisting from an earlier stage of development.

May-Hegglin Anomaly

This is characterized by pale-blue inclusions resembling Döhle bodies in neutrophils, by giant platelets and, in some persons, by thrombocytopenia

(Fig. 34.3). The inclusions are larger and more prominent than the Döhle bodies found in infections. They have been described in eosinophils, basophils, and monocytes as well as in neutrophils. The blue staining of the inclusions is due to RNA. Granulocyte function is normal. May-Hegglin is a rare autosomal-dominant condition involving the nonmuscle myosin heavy chain 9 gene (*MYH9*) linked to chromosome 22q12-13. The mutations appear to alter the assembly and stability of myosin and may be responsible for the underlying pathophysiology and changes seen in leukocyte and platelet structure and function. Varied mutations in *MYH9* are responsible for a phenotypic spectrum of illness, including May–Hegglin anomaly, Sebastian, Fechtner, and Epstein platelet syndromes (Pecci et al., 2014; Saposnik et al., 2014).

Alder-Reilly Anomaly

Dense, prominent, larger than normal azurophilic granulation in all white blood cells was described by Alder in 1939 (Fig. 34.4) (Alder, 1939). In neutrophils, it may resemble toxic granulation; however, it is unrelated to infection and is not transient. In 1941, Reilly described similar granulocytes in some but not all patients with gargoylism, Hurler syndrome, or, more generally, the genetic mucopolysaccharidoses (Reilly, 1941). Other observations have shown that the heavy granulation in neutrophils can occur as a feature of the genetic mucopolysaccharidoses or independently in otherwise healthy persons (Brunning, 1970).

Occurring more often than the Alder-Reilly anomaly in the genetic mucopolysaccharidoses is a metachromatic inclusion in the lymphocytes surrounded by a clear space (Fig. 34.5). Macrophages in the marrow frequently contain similar granulation. This group of disorders is inherited and is characterized by deficiencies or derangement in various lysosomal enzymes required for degrading mucopolysaccharides. The result is abnormal deposition and storage of mucopolysaccharides in multiple organs. Skeletal abnormalities are prominent.

Pelger-Huët Anomaly

This hereditary autosomal-dominant condition involves failure of normal segmentation of granulocytic nuclei. Most nuclei are bilobed and rounded, with a characteristic spectacle or pince-nez shape (Fig. 34.6). The chromatin is quite coarse, and these are not normal young band forms. When a large number of band-like neutrophils appear in the differential count in a patient without infection or other cause, careful analysis of the blood films of the patient and family members will occasionally establish the presence of the Pelger-Huët anomaly. The cells are functionally normal, and the underlying abnormality is mutation of the lamin B-receptor gene (Colella & Hollensead, 2012).

A similar-appearing acquired disorder of nuclear segmentation in granulocytes may be found in cases of granulocytic leukemia, myelodysplastic and some myeloproliferative disorders, in some infections, and after exposure to certain drugs. This is called the *pseudo–Pelger-Huët anomaly*. In addition to band forms and neutrophils with only two segments, mature cells with round, nonsegmented nuclei and coarse chromatin are common. In contrast to the congenital Pelger-Huët anomaly, ring-shaped and other abnormal nuclei may be seen, and the cytoplasm is usually hypogranular.

Chédiak-Higashi Syndrome

Partial oculocutaneous albinism, photophobia, immunodeficiency, abnormally large granules in leukocytes and other granule-containing cells, neurologic defects, and frequent pyogenic infections characterize this rare autosomal-recessive disorder (Introne, 1999). An accelerated lymphoma-like phase occurs, with lymphadenopathy, hepatosplenomegaly, and pancytopenia. Lymphoid infiltrates are widespread, and death ensues at an early age. Granulocytes, monocytes, and lymphocytes contain giant granules (Fig. 34.7), which appear to be abnormal lysosomes. The pathogenesis of this disorder is linked to an abnormality of granule maturation, causing enlargement and apparent fusion of granules and vesicles (such as lysosomes, melanosomes, and platelet dense granules) in all cell types. Leukocyte functional abnormalities exist.

Myelokathexis applies to peripheral neutropenia with the presence of BM neutrophils. WHIM (warts, hypogammaglobulinemia, infection, and myelokathexis) syndrome is a rare autosomal-dominant disease of leukocyte trafficking involving chromosome 2q21. The disease appears to be due to mutations in the chemokine receptor gene *CXCR4* and altered leukocyte response to its functional ligand CXCL12. Hematologic changes include severe peripheral neutropenia with lymphopenia also common, but with granulocytic hyperplasia of the BM (Dotta et al., 2011; Gulino et al., 2004).

BOX 34.3

Morphologic Alterations in Neutrophils

- Toxic granulation—azurophilic cytoplasmic granules seen in severe infections, other toxic conditions, and reactive conditions
- Cytoplasmic vacuoles—seen in infection, indicating phagocytosis
- Döhle bodies—pale-blue, oval cytoplasmic remnants of ribosomes seen in infection and other toxic conditions
- May-Hegglin anomaly—rare autosomal-dominant condition with pale-blue cytoplasmic ribosomal inclusions resembling Döhle bodies
- Alder-Reilly anomaly—prominent azurophilic granulation not related to infection
- Pelger-Huët anomaly—bilobed or rounded nuclei with pince-nez shape
- Chédiak-Higashi syndrome—autosomal-recessive disorder with giant granules, likely representing giant fused lysosomes, and abnormal leukocyte function

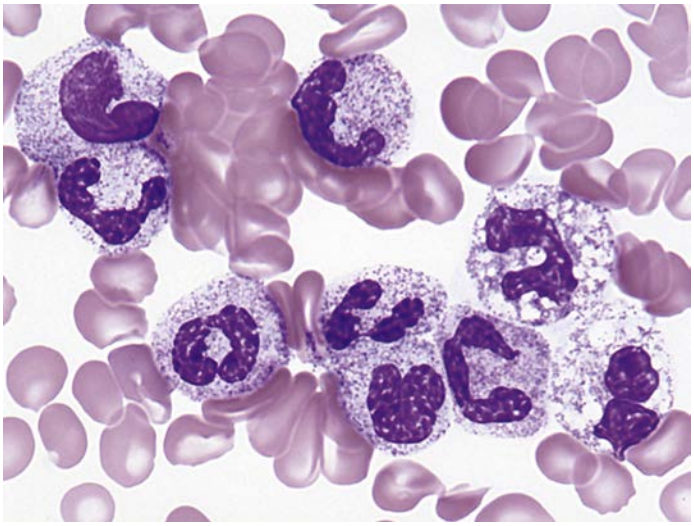

Figure 34.2 Leukemoid toxic neutrophilia with left shift and toxic vacuolization (×1000).

Functional Disorders of Neutrophils

Inherited and acquired disorders affecting neutrophils and other leukocytes may result in abnormal function and susceptibility to infections. Deficiencies of humoral factors (antibodies, components of complement) may result in defective chemotaxis or opsonization. As described previously, some inherited disorders, such as the May-Hegglin, Alder-Reilly, and Pelger-Huët anomalies, have altered morphologic appearances but apparently normal granulocytic function. Other inherited conditions, such as the Chédiak-Higashi syndrome and specific granule deficiency (SGD), display alterations in both morphology and function. Inherited conditions such as chronic granulomatous disease (CGD), myeloperoxidase deficiency (MYD), and leukocyte adhesion deficiency (LAD) exhibit functional disorders with essentially normal morphology on Wright's- and Giemsa-stained films (Dinauer, 2019).

CGD (Holland, 2013) is a rare primary immunodeficiency affecting neutrophils, eosinophils, macrophages, and monocytes. It results from the inability of these phagocytic cells to kill intracellular microorganisms. Patients present with recurrent bacterial and fungal infections (skin, liver, mouth, lymph nodes). These lead to chronic granulomatous lesions (a hallmark of the disease) that may, in turn, obstruct vital organ systems and ultimately lead to death. Symptoms occur early in life, and both autosomal-recessive (≈66%) and X-linked (≈33%) modes of inheritance are known. The disease results from genetic defects in any of the membrane-bound or cytoplasmic components of nicotinamide adenine dinucleotide phosphate (NADPH) oxidase.

Primary MYD is a congenital disorder that is not uncommon and is easily identifiable with automated cell counters incorporating measurement of MPO activity in the differential count. Secondary MYD, which can be transient and corrected with treatment of the underlying disease, may occur secondary to conditions such as myeloid neoplasms, drugs, severe infectious diseases, diabetes mellitus, and pregnancy. Primary MYD may be total or partial and does not show

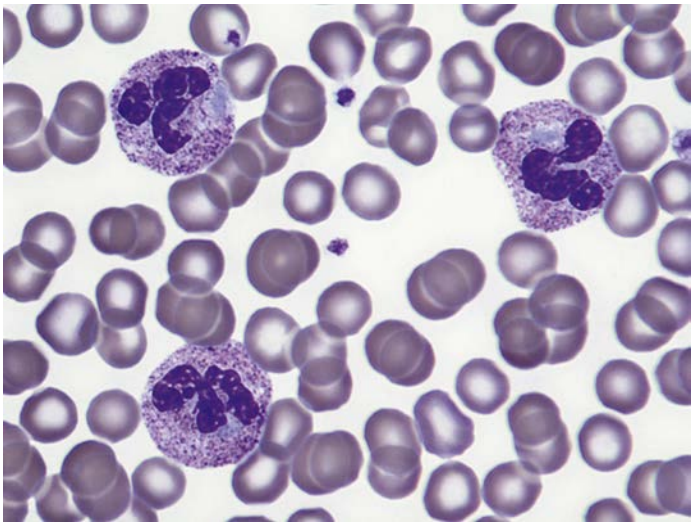

Figure 34.3 May-Hegglin anomaly, showing Döhle-like inclusions (×1000).

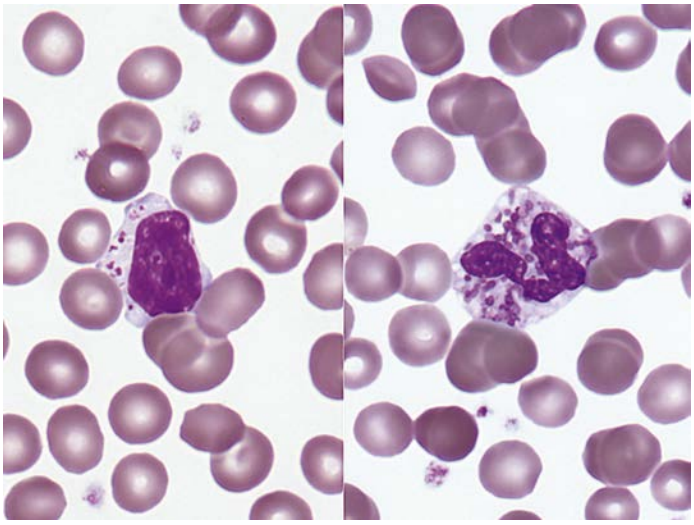

Figure 34.5 Genetic mucopolysaccharidoses often show abnormal lymphocyte granules with surrounding halos. In these cells from the same blood film, neutrophils showed similar changes (×1000).

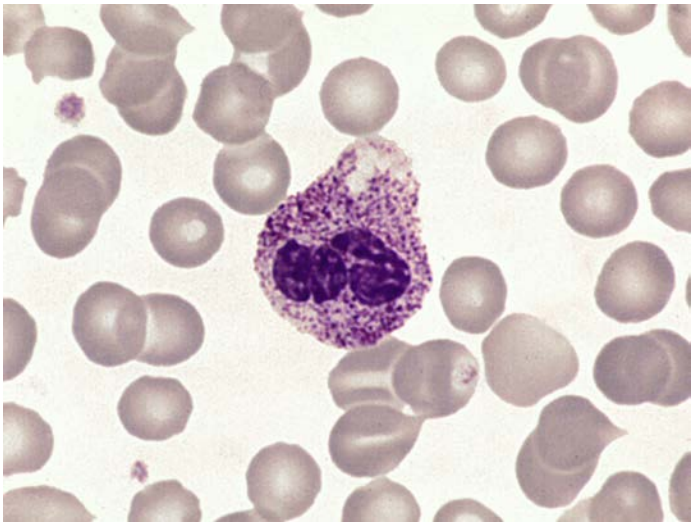

Figure 34.4 The Alder-Reilly anomaly may be found in healthy individuals or in those with mucopolysaccharidoses, in which granules are metachromatic (×1000).

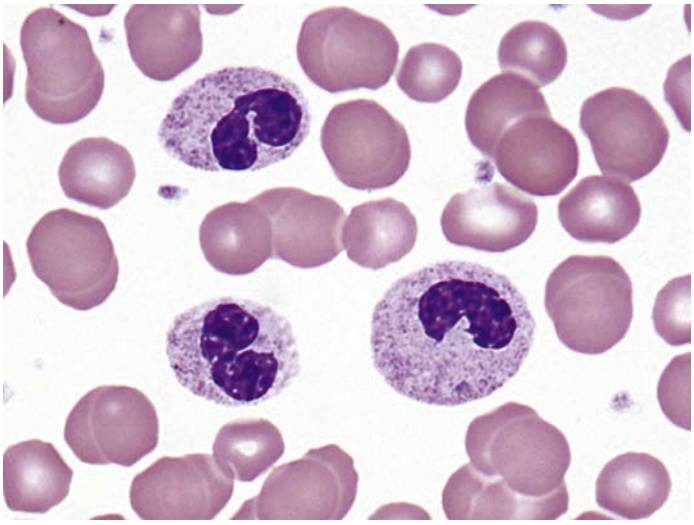

Figure 34.6 Inherited Pelger-Huët anomaly (×1000).

the severity of CGD but can increase frequency and severity of infections (Nauseef, 2014).

Human eosinophil peroxidase is structurally related to MPO but is not identical and is encoded by a different gene. Deficiency is thought to be extremely rare, is unrelated to MYD, may show autosomal-recessive inheritance, and appears to be without clinical symptoms. Eosinophil peroxidase largely functions by neural signaling (Akasheh et al., 2014).

SGD is an extremely rare condition that presents with multiple bacterial infections, atypical bilobed nuclei within neutrophils, and lack of secondary/specific cytoplasmic granules within neutrophils on Wright's-stained peripheral blood films. SGD also affects eosinophils. In addition to granule deficiencies and impaired bactericidal activity, neutrophils are defective in chemotaxis, receptor upregulation, and disaggregation (Gombart, 2001).

Leukocyte Adhesion Deficiency Diseases

Proper neutrophil function is dependent on cell–cell adhesion via the integrins, nonadhesive surface molecules in circulating leukocytes, which, upon proper stimulation, become adhesive or develop increased binding properties for their specific ligands (van de Vijver et al., 2013). In LAD, defective leukocyte adhesion and migration occur, resulting clinically in recurrent infection and leukocytosis. Delayed separation of the umbilical cord often occurs. Several types (LAD-I, -II, and -III) are described. Some forms of LAD can be diagnosed by flow cytometry, with lack of expression of CD18 or CD15a on neutrophils. Hematopoietic stem cell transplantation is the only cure.

Eosinophilia

Eosinophilia exists if blood eosinophils exceed ~0.35 to 0.5 × 10^9/L. Reactive eosinophilia is typically associated with allergic processes and parasitic infections. Classically, the major function of eosinophils appeared to be the release of granule contents or reactive oxygen species to damage the target organism or offending cell. Immunoregulatory and proinflammatory signaling roles also exist; thus, eosinophils are both effector and regulatory cells. Causes of eosinophilia have been reviewed (Furuta et al., 2014; Helbig, 2014; Montgomery et al., 2013).

Eosinophil production is stimulated by interleukin-5 (IL-5), migration is influenced by the chemokine eotaxin, and the two factors interact in producing eosinophilia. Causes and conditions associated with eosinophilia are shown in Box 34.4.

Eosinophilia is frequent in a variety of hematologic neoplasms, including clonal myeloproliferative diseases (described later in this chapter). It also occurs with a broad spectrum of nonhematopoietic primary or metastatic neoplasms, usually associated with advance-stage disease. Paraneoplastic eosinophilia occurs in Hodgkin lymphoma and peripheral T-cell lymphomas. In some other lymphomas and leukemias of other lineages, it is clonal and part of the neoplastic process, such as B lymphoblastic leukemia with t(5;14) (*IL3-IgH*), while in lymphocytic variant

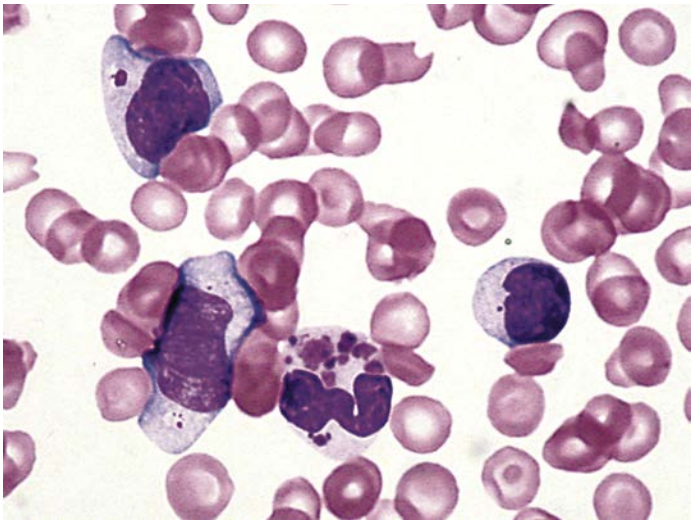

Figure 34.7 Chédiak-Higashi neutrophils and lymphocytes with large granules (×1000).

hypereosinophilic syndrome (HES), it may be secondary to an abnormal lymphoid proliferation.

Moderate to severe peripheral blood eosinophilia is most commonly associated with infection by helminthes, including nematodes, trematodes, and cestodes. Eosinophilia is more pronounced if tissues are invaded (e.g., trichinosis) than when parasites inhabit the lumen of a viscus (e.g., tapeworm). Some parasites, such as *Taenia solium* (cysticercosis) produce little inflammatory response while alive, but trigger an inflammatory response upon degeneration of the organism. Other parasites, such as *Trichinella spiralis* (trichinosis) incite peripheral eosinophilia upon larval invasion of the muscles and encystment. Leukocytosis and eosinophilia extending over months are seen in toxocariasis (*Toxocara canis* or *T. catis*) or visceral larva migrans. Cutaneous larva migrans caused by larvae of the dog (*Ancylostoma braziliense*) or cat (*A. caninum*) hookworm also cause eosinophilia.

Loeffler syndrome (simple eosinophilic pneumonia) affects all age groups and is characterized by repeated, transient pulmonary exudates accompanied by fever and clinical symptoms of bronchitis, often producing sputum that contains eosinophils. It may be caused by a variety of exposures, including certain drugs, inhaled antigens, or helminth (see earlier discussion) infestation. The latter occurs during periods of dissemination or migration when the parasites pass from the blood into the alveoli of the lung. Loeffler syndrome may also be idiopathic. Tropical pulmonary eosinophilia is a syndrome of paroxysmal cough and bronchospasm associated with marked eosinophilia and often associated with *Wuchereria bancrofti* in India, Africa, Southeast Asia, and the South Pacific.

Many drugs are also associated with blood or pulmonary eosinophilia and pulmonary infiltrates. Implicated drugs include: pilocarpine, physostigmine, digitalis, *p*-aminosalicylic acid, sulfonamides, chlorpromazine, phenytoin, some antidiabetic drugs, some anticancer agents, and many others.

Idiopathic HES (Fig. 34.8) is a heterogeneous syndrome composed of a number of different disorders of varying severity, after myeloproliferative neoplasms with abnormalities of *PDGFRA*, *PDGFRB*, and *FGFR1*, and CMML with eosinophilia are excluded.

The organ most consistently affected in HES is the heart, with mural thrombi formation, myocarditis, endocardial and myocardial fibrosis, constrictive pericarditis, and fibroplastic endocarditis (Brito-Babapulle, 2003). Hepatosplenomegaly is common. Other organ systems may be involved, including the central nervous system (CNS) and retina, lungs, skin, gastrointestinal (GI) tract, and kidney.

Basophilia

Basophilia is an increase in the absolute basophil count above 0.2×10^9/L. Causes of basophilia are listed in Box 34.5. Basophilia is seen most frequently in hypersensitivity and allergic reactions, chronic myeloid leukemia (Fig. 34.9), myeloid metaplasia (extramedullary myelopoiesis), and polycythemia vera. Relative basophilia may be transient following irradiation. Basophilia may be present in hypothyroidism, in chronic hemolytic anemia, and following splenectomy. Reactive basophilia is an uncommon finding overall, sometimes seen in patients combating helminth infections (Voehringer, 2013).

BOX 34.4

Key Causes of Eosinophilia

- Allergic—urticaria, hay fever, asthma
- Inflammatory—eosinophilic fasciitis, Churg-Strauss syndrome
- Parasitic—trichinosis, filariasis, schistosomiasis
- Nonparasitic infections—systemic fungal, scarlet fever, chlamydial pneumonia of infancy
- Respiratory—pulmonary eosinophilic syndromes (Loeffler, tropical pulmonary eosinophilia), Churg-Strauss syndrome
- Neoplastic— MPN with translocation of *PDGFRA/B* or *FGFR1*, CML, mastocytosis, Hodgkin lymphoma, T-cell lymphomas, lymphocytic HES
- Idiopathic hypereosinophilic syndromes—affecting heart, liver, spleen, CNS, other organs
- Others—certain drugs, hematologic and visceral malignancies, GI inflammatory diseases, sarcoidosis, Wiskott-Aldrich syndrome

CML, Chronic myelogenous leukemia; *CNS,* central nervous system; *GI,* gastrointestinal; *HES,* hypereosinophilic syndrome; *MPN,* myeloproliferative neoplasm; *PDGFRA/B,* platelet-derived growth factor α/β.

Monocytosis

Monocytosis is an increase in monocytes above the upper reference value, especially when greater than 1.0×10^9/L. The most common causes are recovery from neutropenia and indolent infections. Causes and associations of monocytosis are shown in Box 34.6.

Monocytosis is present during the recovery stage from acute infection and from agranulocytosis, in which it is considered a favorable sign. Monocytosis may be present in subacute bacterial endocarditis. In this condition, monocytes may show phagocytosis of other blood cells, red blood cells, and leukocytes. It may be present in mycotic, rickettsial, protozoal, and viral infections.

Infectious disease, however, is an uncommon cause of monocytosis. In a classic study of 160 successive cases of absolute monocytosis (Maldonado, 1965), more than half (85) were associated with hematologic neoplasms. These included acute monocytic and granulocytic leukemias, lymphoma (HL most frequently), multiple myeloma, and myeloproliferative disorders.

Monocytopenia

Monocytopenia is a decrease in circulating monocytes below the lower reference value of 0.2×10^9/L. During therapy with prednisone, monocytes fall during the first few hours after the first dose but return to above original levels by 12 hours. Monocytopenia has been observed in hairy cell leukemia (HCL), in congenital complex immunodeficiency involving monocytopenia and susceptibility to mycobacterial infection (MonoMac syndrome) due to *GATA2* mutation, other rare immunodeficiencies, and in B-lymphoblastic leukemia (Dotta & Badolato, 2014; Hsu, 2011; Kraut, 2003; Park & Rogers, 2013). Monocytopenia is uncommon as an isolated finding.

LYMPHOCYTIC AND PLASMACYTIC DISORDERS

In these disorders, the pathologist should consider neoplastic conditions, which are covered in the later sections of this chapter, as well as the benign causes, immediately following.

Lymphocytes in Normal Individuals

In normal individuals, the absolute numbers of lymphocytes and T cells are highest in young children. The percentage of lymphocytes in the blood is normally up to about 50% for the first 5 years. During the first decade of life, the absolute lymphocyte counts and the absolute number of T cells decrease but remain higher than observed in the adult. By the time of adolescence, the absolute lymphocyte count and absolute number of T cells have leveled off to values observed throughout adulthood. The absolute number of B lymphocytes remains stable during all stages of life (Davey, 1977; Perkins, 2004). In adolescence and adulthood, lymphocytes constitute about 20% to 40% of all leukocytes, or 1.5 to 4.0×10^9/L cells/L.

The normal CD4/CD8 ratio is between 1.0 and 3.4, but we have seen values as high as 12.0 in reactive conditions. In the neonate, the numbers of total T cells and CD8+ T cells may be similar or decreased compared with adults, whereas CD4+ T cells may be similar or increased.

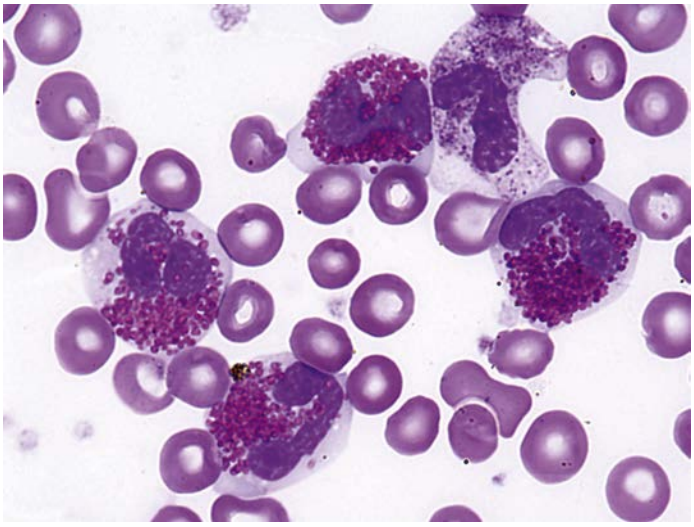

Figure 34.8 Marked eosinophilia of unknown cause, suggesting hypereosinophilic syndrome, peripheral blood (×1000).

Lymphocytosis

Lymphocytosis is an increase in the number of lymphocytes in the peripheral blood; reference intervals are ≈1.5 to 4.0 × 10^9/L in the adult and ≈1.5 to 8.8 × 10^9/L in the child. Relative lymphocytosis (an increase in the percentage of lymphocytes) is present in various conditions and is especially prominent in disorders with neutropenia. Lymphocytosis is unusual in acute bacterial infections but is commonly associated with viral infection (Epstein-Barr virus [EBV], hepatitis; Box 34.7).

Lymphocytosis Associated With Viral Infection

Lymphocytosis is a frequent finding in children with viral infection and may be marked. Lymphocytic leukemoid reactions were previously referred to as acute infectious lymphocytosis (AIL), often lasting 3 to 5 weeks but without other blood changes in most patients. Lymph node enlargement is rare and minimal when present. The spleen and liver are rarely, if ever, enlarged. Lymph node biopsy may show reactive follicular hyperplasia but no characteristic changes. In some cases, there has been an increase in white cells in the cerebrospinal fluid (CSF), with about 40% lymphocytes.

A chronic form of infectious lymphocytosis also occurs in children. The leukocyte count is 10 to 25 × 10^9/L, with 60% to 80% lymphocytes of normal appearance.

Pertussis

Whooping cough (pertussis), although reduced by routine immunization, still occurs in unimmunized children and is most severe in infants in whom most disease-associated deaths occur. The disease has been resurgent in the United States in recent years in part due to vaccine factors (Clark, 2014). It also occurs in adults with immunity reduced since childhood vaccination. The etiologic agent is *Bordetella pertussis*, a highly infectious agent that produces an inflammatory reaction of the entire respiratory tract. The incubation period is approximately 6 to 20 days. Symptoms begin as a head cold, progressing to paroxysms of coughing productive of thick sputum. Paroxysms typically end with a "whooping" sound due to deep inspiration, giving the disease its descriptive name. There is frequently pain over the trachea and bronchi. The disease typically lasts 6 to 12 weeks.

Patients frequently develop significant lymphocytosis, with counts higher than 30 × 10^9/L recorded. The lymphocytes are small, mature T cells with a normal CD4/CD8 ratio (Hudnall, 2000). The lymphocyte count is highest during the first 3 weeks of the illness, decreasing during the fourth and subsequent weeks (Lagergren, 1963). The lymphocytosis is at least partially due to the release of lymphocytosis-promoting factor (LPF) or pertussis toxin (PT) from the organism. PT inhibits chemokine signaling through G-coupled protein receptors, reducing lymphocyte retention in bone marrow and spleen, inhibits LFA-1–mediated arrest on lymph node venules, and reduces CD62L expression on circulating leukocytes, inhibiting extravasation (Carbonetti, 2016). Thus, the lymphocytosis is due to redistribution of lymphocytes into the peripheral circulation without increased lymphopoiesis.

BOX 34.5

Key Causes of Basophilia

- Myeloproliferative disease
- Allergic—food, drugs, foreign proteins
- Infectious—variola, varicella
- Chronic hemolytic anemia—especially postsplenectomy
- Inflammatory—collagen vascular disease, ulcerative colitis

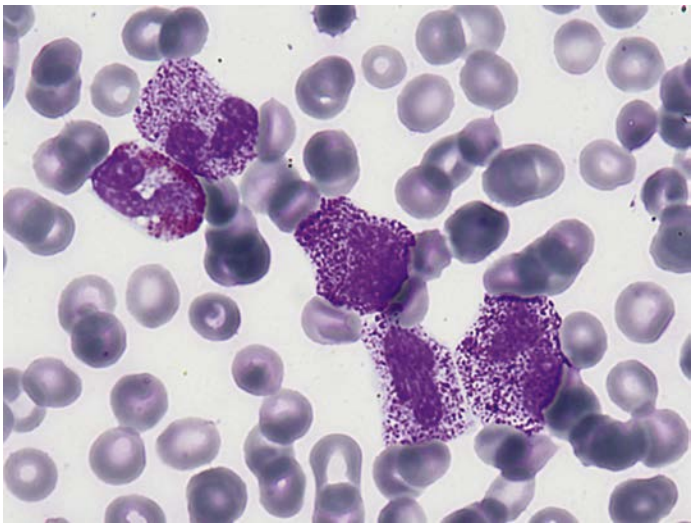

Figure 34.9 Marked basophilia and an eosinophil in a patient with Philadelphia chromosome positivity (×1000). (Courtesy of Robin Abaya, MD.)

BOX 34.6

Key Causes of Monocytosis

- Infectious—tuberculosis, subacute bacterial endocarditis, syphilis, protozoan, rickettsial
- Recovery from neutropenia
- Hematologic—leukemias, myeloproliferative disorders, lymphomas, multiple myeloma
- Inflammatory—collagen vascular disease, chronic ulcerative colitis, sprue, myositis, polyarteritis, temporal arteritis
- Others—solid tumor, immune thrombocytopenic purpura, sarcoidosis

Chronic Lymphocytosis/Persistent Polyclonal B Cell Lymphocytosis

Persistent reactive lymphocytosis is an uncommon event in adults. Significant lymphocytosis should raise suspicion of neoplastic disease, such as chronic lymphocytic leukemia. Coexistence of neutropenia or classic FS suggests large granular lymphocyte (LGL) leukemia. Often, tissue biopsy and/or immunophenotyping of peripheral blood will point to a specific disease or diagnosis. Mononucleosis or lymphocytosis due to other viruses occasionally presents later in life, however.

A rare condition, persistent polyclonal lymphocytosis, has been reported in adults, predominantly in female smokers, and in the postsplenectomy state (Himmelmann et al., 2001; Lairmore et al., 2012). It is a benign polyclonal B-cell proliferation with binucleated atypical lymphocytes in the blood. However, the possibility of incipient lymphoma has been considered (Troussard et al., 2008).

Retrovirus-Associated Diseases and Conditions

Human T lymphotropic virus type 1 (HTLV-1), discovered in 1980, is a retrovirus associated with adult T-cell leukemia/lymphoma (ATL) (Poiesz, 1980). It is endemic in areas of Japan, the Caribbean basin, and the southeastern United States. HTLV-2, a second human retrovirus, was first found in a patient with hairy cell leukemia (HCL) (Kalyanaraman, 1982). A third human retrovirus, human immunodeficiency virus type 1 (HIV-1), was recognized and confirmed as the cause of acquired immunodeficiency syndrome (AIDS [discussed further later]) in 1983 (Barre-Sinoussi, 1983; Gallo, 1983). Subsequently, a second but distinct type of HIV—now called HIV-2—was identified (Alizon, 1984). More recently,

BOX 34.7

Key Causes of Lymphocytosis

- Infectious—many viral, pertussis, tuberculosis, toxoplasmosis, rickettsial
- Chronic inflammatory—ulcerative colitis, Crohn
- Immune mediated—drug sensitivity, vasculitis, graft rejection, Graves, Sjögren
- Hematologic—ALL, CLL, lymphoma
- Stress—acute, transient

ALL, Acute lymphoblastic leukemia; *CLL,* chronic lymphocytic leukemia.

additional retroviruses, HTLV-3/4 and simian foamy retrovirus, have also been found to infect humans (Gessain et al., 2013).

HIV-1 infects both monocytes/macrophages and T cells (both essential cells for normal immune system function) using cell surface chemokine receptors (CCR5 on the former and CXCR4 on the latter). Infection ultimately causes progressive loss of CD4+ lymphocytes, disrupts normal immune function, and produces immunodeficiency and disease. Disease not only includes many different types of infections, but also an increase in neoplastic disease, including lymphomas. HIV-1 plays an indirect role (through immune dysregulation and not by direct induction) in the development of lymphoma. HIV-2 is less widespread and somewhat less virulent (Nyamweya et al., 2013).

HTLV-1 and HTLV-2 also infect and transform T cells: primarily CD4+ cells with HTLV-1 and CD8+ cells with HTLV-2. HTLV-1 infects 15 to 20 million people worldwide, with endemic areas in Japan, the Caribbean, and Africa. It is usually transmitted by breast milk or exposure to blood. Acute infection shows few clinical symptoms, consisting of fever, limited lymphadenopathy, and occasional skin rash. Lymphocytosis occurs, usually less than 20×10^9/L. Most (90%–95%) of patients with antibodies against HTLV-1 are symptom free. After a years-long latency, 3% to 5% manifest ATL or tropical spastic paraparesis (Lairmore et al., 2012).

Infectious Mononucleosis and Epstein-Barr Virus Infection

Infectious mononucleosis (IM) is usually a self-limited infectious disease characterized by sore throat, prolonged malaise, atypical lymphocytosis with the presence of large transformed lymphocytes (Fig. 34.10), lymphadenopathy (most often posterior cervical), and often splenomegaly (Vouloumanou et al., 2012). In immunocompromised patients, EBV is associated with benign B-cell hyperplasia, malignant lymphoma, and posttransplantation lymphoproliferative disease.

Etiology and Pathophysiology. IM is a disorder that occurs secondary to infection with EBV. When the primary infection occurs in healthy individuals during early childhood, the disease often goes unnoticed. However, when the infection involves healthy adolescent individuals or adults, the resultant disorder is the IM syndrome. In most cases, the virus gains entry into the body through the oropharyngeal epithelial and lymphoid tissues, and the virus appears to infect both tissues. The virus attaches to C3d complement receptors (CD21) on B lymphoid cells and enters into the cells. The EBV then stimulates DNA synthesis in these B cells and induces the formation of several new antigens, including the viral capsid antigen (VCA), the membrane antigen (MA), early antigen (EA)—both diffuse (EA-D) and restricted (EA-R) subtypes—Epstein-Barr nuclear antigens (EBNA), and the lymphocyte-detected membrane antigen (LYDMA) (Harrington, 1988). Thus, the earliest phase of this disease is characterized by an infection of B cells that proliferate, develop neoantigens, circulate, stimulate an immune response, and synthesize immunoglobulin (Sixbey, 1984). VCA, EA, and EBNA are the viral proteins most important for serodiagnosis in immunocompetent patients. Clinical and laboratory features are summarized in Box 34.8.

Typically, the humoral immune response is characterized by the rise in titer of IgG and IgM viral capsid antibodies during the incubation and early prodrome periods. The titer of IgM capsid antibody starts to fall during the second and third weeks of illness and then diminishes to undetectable levels within the following several months. The IgG viral capsid antibody decreases during convalescence but remains detectable for life. Approximately 2 to 3 weeks after the onset of illness, EBV antibodies against the early antigens appear and then decline over the succeeding 2 months. The titer of the EBV nuclear antigen antibodies rises during the latter portion of convalescence and is apparently detectable throughout life.

The cellular immune response in IM is characterized by proliferation and activation of T cells, usually during the second week of illness, in response to EBV-induced B-cell infection and activation. Because these activated T cells are derived mostly from the cytotoxic/suppressor cell subpopulation, marked suppression and destruction of EBV-infected B cells occur. Indeed, most of the atypical lymphocytes observed in the peripheral blood of patients with IM during the second week of illness possess the CD8 antigen. These cytotoxic/suppressor T cells kill infected B cells and diminish polyclonal antibody production induced by the EBV. In addition to T-cytotoxic cells, the activity of NK cells has a profound effect on limiting the proliferation of EBV-infected B cells in patients with IM.

Most (over 90%) immunocompetent adults have serologic evidence of past EBV infection. EBV has the capacity not only to infect cells (many of which are destroyed by an intact immune system) but to produce a latent infection in resting memory B cells and, in some cases, produce transformation of lymphocytes to malignant lymphoma. However, a majority of latently infected individuals show no disease manifestations throughout their lifetimes.

The resting memory B cells can act as a reservoir of EBV, because viral antigens are not expressed on the lymphocyte surface. In IM, a spectrum of EBV expression patterns (programs) is found in different cells (Klein, 2007). In type III latency-growth program, cells express a full set of EBV-encoded proteins, including six nuclear proteins (EBNA1–6) and three latent membrane proteins (LMP1, LMP2 and LMP3).

LMP1 has strong immunogenic activity and is present only in acute infection, except in immunocompromised hosts. The type I latency program involves expression of only one nuclear protein, EBNA-1, and is found in some memory B cells. Type IIa latency involves expression of EBNA-1, LMP-1, and LMP-2. Type IIb latency expresses all EBNAs (EBNA1–6) but not LMP-1.

Tumor cells in posttransplant lymphoproliferative disorders (PTLDs) correspond to latency type III, BL cells to latency type I, and cells in EBV+ HL and EBV+ nasopharyngeal carcinoma (NPC) to latency type IIa, with LMP-1 expression. EBV-encoded ribonucleic acids (RNAs) EBER-1 and EBER-2 are reliably expressed at high levels in virtually all latent EBV infections and are detected with high sensitivity by in situ hybridization assays that are currently the standard for EBV identification (Gulley, 2008).

Clinical Features. IM has been observed in patients from 3 months to 70 years of age but is most common in adolescents and young adults. A 2- to 5-week incubation period prior to onset of symptoms usually occurs. Patients usually have vague symptoms. including fever, sore throat with ulcerative pharyngitis, and lymphadenopathy.

Complications. Hemolytic anemia related to anti-I antibodies occurs in 1% to 3% of cases. Mild thrombocytopenia occurs in about half of cases. Splenic rupture may also occur. Neutropenia, pancytopenia, chronic active EBV infection (CAEBV) and EBV hemophagocytic syndrome (EBVHS) occur rarely.

Abnormal liver function tests indicative of hepatitis occur in 85% to 100% of patients with IM. Clinical jaundice is rare, but occasionally jaundice and acute pharyngitis are the only clinical manifestations of IM. Although uncommon, complications may also involve the nervous system, heart, kidney, and lungs.

Approximately one-third of patients with IM carry β-hemolytic streptococci in the pharynx. Thus, one should pay attention to strict clinical, hematologic, and serologic criteria in distinguishing IM from streptococcal pharyngitis.

Hematologic Features. Leukocytes are increased, ranging from 12 to 25×10^9/L. Rarely, counts as high as 80×10^9/L have been recorded. The leukocytosis is usually due to lymphocytosis (60%–90%) composed of a variety of atypical lymphocytes. The total leukocyte count, as a rule, returns to normal within 3 weeks. The atypical lymphocytes have nuclear alterations and an increase in the amount and basophilia of cytoplasm.

Lymphocytes include "monocytoid" lymphocytes, which likely correspond to immunoblasts in lymph nodes (see Fig. 34.10). Other atypical lymphocytes, which are more numerous, include plasmacytoid lymphocytes and those with small nuclei but abundant cytoplasm.

Often, the number of monocytes rises transiently. The term *mononucleosis* refers to an increase in lymphocytes, not in monocytes ("mononuclear" cells include both lymphocytes and monocytes).

Cytologic alterations are not pathognomonic of IM. Similar cells are found in a variety of disorders, including cytomegalovirus mononucleosis, toxoplasmosis, and infectious hepatitis, and usually to a lesser extent in viral pneumonia, varicella, mumps, and viral exanthemas of children.

Neutrophils are relatively and absolutely decreased in most cases during the first week of illness. During this time, a shift to the left may

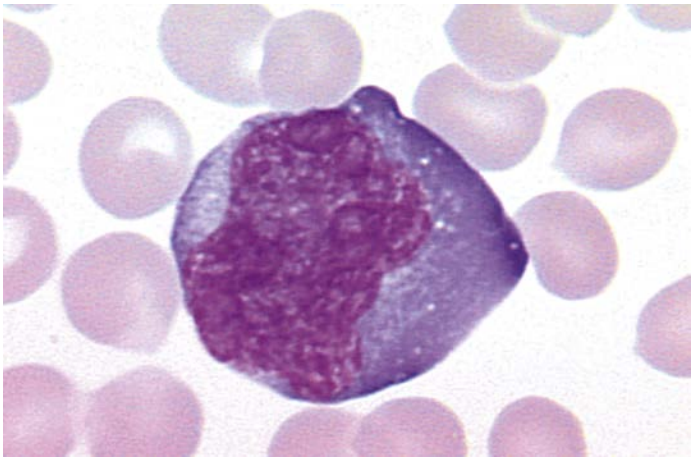

Figure 34.10 Infectious mononucleosis, showing a large activated lymphoid cell in the blood (×1000).

BOX 34.8

Summary of Features of Infectious Mononucleosis (IM) in Immunocompetent Patients

Epstein-Barr Virus (Human Herpesvirus-4)

Pathophysiology
- Virus enters through oropharyngeal epithelial and lymphoid cells
- Virus attaches to CD21 on B cells
- Viral antigens—viral capsid antigen (VCA), early antigen (EA), Epstein-Barr nuclear antigen (EBNA)—are produced and elicit antibody production

Humoral Immune Response
- Immunoglobulin (Ig) M against VCA rises during incubation and prodrome, falls over few weeks to months
- IgG against VCA rises during incubation, decreases during convalescence, remains detectable for life
- Antibodies to EA rise 2–3 weeks after onset of illness, then fall
- Antibodies to EBNA rise during convalescence, detectable for life

Cellular Immune Response
- T cells activated during second week of illness
- CD8-positive cytotoxic T cells kill infected B cells
- Natural killer cells kill infected B cells
- Some resting memory B cells remain latently infected

Clinical Features
- 2- to 5-week incubation period
- Vague onset of symptoms
- Fever, sore throat, lymphadenopathy
- Adolescents, young adults more often symptomatic than younger children

Laboratory Features
- Leukocytosis with absolute lymphocytosis and atypical lymphocytes
- Transient monocytosis
- Relative and absolute neutropenia early on
- Mild thrombocytopenia in half of cases
- Hemolytic anemia in 1%–3% of cases, often with anti-I specificity
- Elevated transaminases in 85%–100% of cases, but clinical jaundice rare
- Spot test is simple, rapid, specific, based on agglutination of horse red blood cells (RBCs)
- Heterophil antibody (HA) test is based on differential absorption of IM-specific HA by beef RBC stroma and guinea pig kidney

occur, with an increase in band cells and metamyelocytes. Toxic granules and Döhle bodies may be seen. The eosinophils are within normal limits.

The BM from patients with IM usually shows increased cellularity. Numbers of lymphocytes, macrophages, plasma cells, megakaryocytes, and erythroid cells are increased. The neutrophilic series appears decreased. About half of cases may have collections of mononuclear cells forming loose granulomas.

Serologic Findings in Immunocompetent Patients

The spot test for IM is based on the principle that horse erythrocytes are more sensitive than sheep erythrocytes in testing for IM. A positive test for IM shows agglutination of horse erythrocytes by serum absorbed with guinea pig kidney but not by serum absorbed with beef erythrocyte stroma. The spot test has proved to be a simple, rapid, highly specific, and sensitive test for the heterophil antibodies of IM. False-positive tests occur but are very rare. The spot test is still in use, as are other similarly performing immunoassays and latex-based detection tests for heterophil antibody. False-negative tests occur particularly in young children who produce heterophil antibodies (IgM) in limited amounts. In heterophil-negative IM, the diagnosis may be substantiated by assay for antibody to EBV.

As previously mentioned, several antibodies are produced by the host in response to a variety of EBV antigens (see Box 34.8). Antibody to the viral capsid antigen arises within the first 2 weeks of onset. This antibody, measured by an immunofluorescent or other method, is used for determining exposure to EBV. Assaying for the presence of EBV antibody is usually limited to the few cases of heterophil-negative IM.

In addition to heterophil and EBV antibodies, patients with IM frequently produce antibodies to a wide variety of antigens. Antibodies against human erythrocytes, leukocytes, and platelets have been described. Patients with IM have an increased frequency of cold agglutinins. Positive tests for rheumatoid factor and antinuclear factor have been reported.

In immunocompromised patients, serologic tests are of limited value; direct detection methods are considered more reliable. Determination of EBV viral load by polymerase chain reaction (PCR) appears to be one of the better tests for this patient population (Hess, 2004).

Differential Diagnosis. Clinical, hematologic, and serologic features of IM permit an accurate diagnosis to be made in more than 90% of cases. When the heterophil test is negative, one must consider several possibilities. The patient could still have EBV antibody–positive but heterophil-negative IM. Cytomegalovirus infection, however, is the most common cause of heterophil-negative mononucleosis. Other possibilities include toxoplasmosis, infectious hepatitis, human herpesvirus 6, HIV-1 and HIV-2, and ingestion of drugs (*p*-aminosalicylic acid, phenytoin [Dilantin], and diaminodiphenylsulfone).

Course. Classic IM is a benign disorder, with complications occurring in less than 5% of patients. The disorder usually resolves in 3 to 4 weeks. Fatalities are extremely rare but tend to occur in X-linked lymphoproliferative disease (XLP). EBV infection can produce any one of three severe complications in XLP: fulminant IM, life-threatening lymphoproliferative disease and B-cell lymphoma, and dysgammaglobulinemia. Although classically associated with EBV infection, XLP can occur in patients seronegative for EBV. In addition to XLP, EBV-associated lymphoproliferative disorders can occur in individuals with congenital and acquired immunodeficiencies.

Cytomegalovirus Infection

Some individuals infected with cytomegalovirus develop a syndrome similar to IM (Boeckh, 2011). This disorder can occur following massive blood transfusion (posttransfusion mononucleosis) or spontaneously (cytomegalovirus mononucleosis).

Leukocytosis is characteristic with absolute lymphocytosis. Usually, 20% or more of the leukocytes are atypical lymphocytes. BM aspirates have shown increased numbers of normal lymphocytes and atypical lymphocytes. Abnormal liver function test results are the most frequent abnormal laboratory finding. In a small percentage of patients, titers of cold agglutinins, rheumatoid factor, or antinuclear antibodies may be increased. No rise in heterophil, EBV, or *Toxoplasma gondii* antibodies occurs. The diagnosis is usually made by isolating the cytomegalovirus from urine, saliva, blood, or tissue biopsy, or by serology.

Toxoplasmosis

Toxoplasma gondii, a protozoan parasite, can produce in both young and old a disease (toxoplasmosis) similar to IM. Diagnosis is critical in congenitally infected fetuses and newborns, women infected during pregnancy, immunocompromised patients, and patients with chorioretinitis.

Only a small proportion (≈10%) of immunocompetent individuals are symptomatic. These patients typically present with lymphadenopathy, commonly cervical. Some patients may also present with fever, headache, sore throat, hepatosplenomegaly, chorioretinitis, and an increased number of atypical lymphocytes in the peripheral blood. In immunocompromised patients, disease commonly involves the CNS and eyes but may also involve the lungs and heart.

The histopathology of lymph nodes is usually distinctive, with scattered epithelioid histiocytes that often blur the germinal center/mantle zone border, and with sinus monocytoid B-cell hyperplasia (Fig. 34.11). Morphology correlates closely with elevated *Toxoplasma* antibody titers (Dorfman, 1973). BM biopsy specimens have no specific pathologic lesion.

The diagnosis is established by demonstrating an elevation of *Toxoplasma* antibodies in immunocompetent patients. In immunocompromised patients, serologic tests are not sensitive, and direct detection of the organism from blood, from body fluids, or in tissue is necessary for definitive diagnosis (Remington et al., 2004; Torres et al., 2013).

Autoimmune Lymphoproliferative Syndrome

Autoimmune lymphoproliferative syndrome (ALPS) is an uncommon cause of lymphadenopathy, splenomegaly, and autoimmune cytopenias, with onset in childhood that is caused by an inheritable genetic defect, a mutation in one of the genes encoding FAS, or CD95, or occasionally a caspase gene. FAS is a key component of apoptosis. The disease has variable penetrance and is characterized by chronic lymphoid hyperplasia with presence of CD4/CD8 double negative T cells, and the symptoms mentioned earlier (Shah et al., 2014).

Other Nonneoplastic Causes of Lymphadenopathy

Other causes of benign or reactive lymphadenopathy include autoimmune disease and infection, Castleman disease, Rosai-Dorfman disease (sinus histiocytosis with massive lymph node hyperplasia), Kikuchi histiocytic necrotizing lymphadenitis, Kawasaki disease, and others.

Lymphocytopenia

Lymphocytopenia is present when the absolute lymphocyte count is below $\approx 1.8 \times 10^9$/L in adults and below $\approx 2.0 \times 10^9$/L in children. Normally, about 80% of circulating peripheral blood lymphocytes are CD3+ T cells, and a majority (≈65%) of these cells are CD4+ helper T cells. A number of immunologic deficiency disorders that are genetically determined have lymphocytopenia, along with various other immunologic defects of humoral or cell-mediated immunity. Lymphocytopenia in these disorders is due to impaired lymphopoiesis. Increased levels of adrenocortical hormones, administration of chemotherapeutic drugs, or irradiation will result in lymphocytopenia. Impaired drainage of the intestinal lymphatics with loss of lymphocytes into the intestines due to a number of causes has been implicated as a mechanism for lymphocytopenia. In advanced cases of non-Hodgkin lymphoma (NHL) and HL, as well as in terminal cases of carcinoma, lymphocytopenia is often observed. Causes and conditions associated with lymphocytopenia include those listed in Box 34.9.

Acquired Immunodeficiency Syndrome

Acquired immunodeficiency syndrome (AIDS), once a progressively fatal infectious disorder with characteristic clinical, hematologic, and serologic abnormalities, can now be controlled in most patients with antiretroviral therapy (ART).

Etiology. AIDS is a disorder secondary to infection with HIV-1 and HIV-2—RNA retroviruses that are cytotropic for CD4+ T cells and for other cells, including macrophages, monocytes, megakaryocytes, and CNS microglial cells. Viral entry into a cell results from interaction with the CD4 receptor and with chemokine coreceptors that determine target cell tropism (Starr-Spires, 2002). HIV is responsible for both direct killing of infected cells and indirect killing of neighboring cells, utilizing both apoptotic-dependent and apoptotic-independent mechanisms of cell destruction (Garg et al., 2012).

HIV infection is spread by contamination with secretions, excretions, blood, and tissues that contain the virus. Because of the cytotropic effect of the AIDS viruses for CD4+ cells, there is a marked decrease in the number of T-helper cells and an imbalance in T-suppressor/cytotoxic cells in the blood and lymphoid tissues of the body. As a result, a profound cellular immune depression occurs, characterized by infection with a variety of opportunistic organisms. Initially, B cells are not involved and immunoglobulin levels are normal or increased. However, as the disease progresses, the frequency of malignancy in these patients is increased. AIDS-associated cancers include Kaposi sarcoma, NHL, and cervical cancer (all AIDS-defining cancers), as well as HL and anogenital cancers (Bellan, 2003; Mbulaiteye, 2003). Although the cause of these malignancies is undoubtedly multifactorial, recent studies suggest that HIV may possess oncogenic potential (Borges et al., 2014). In addition, the functions of monocytes and NK cells are abnormal.

Hematologic Features. The most common hematologic abnormality in patients with AIDS is anemia of chronic disease and lymphopenia (80%–85% of cases), particularly of the T-helper/inducer (CD4) subset.

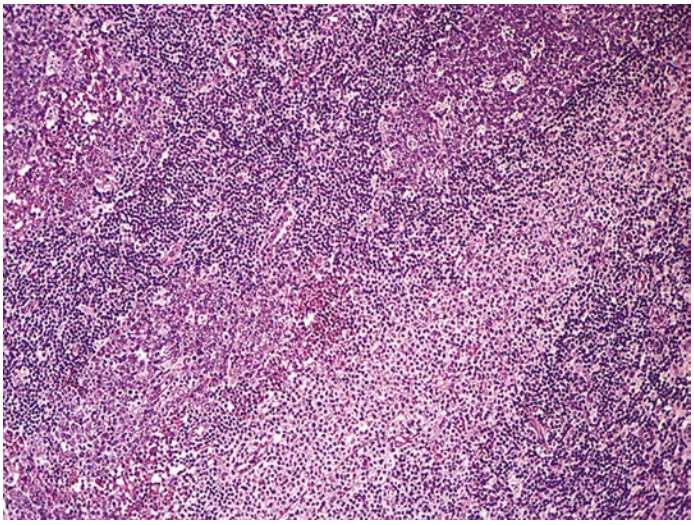

Figure 34.11 Toxoplasmosis lymphadenitis shows follicular hyperplasia with monocytoid B-cell hyperplasia *(lower right-center)* and scattered individual and aggregates of histiocytes, often impinging on the germinal center/mantle zone border (×200).

Thrombocytopenia occurs in approximately 30% of cases and neutropenia in 40%, often with a left shift; the former is often immune mediated (Hoxie, 1995).

The peripheral blood film usually displays atypical lymphocytes that have a plasmacytoid appearance. Monocytes are often large, with a fine nuclear chromatin and cytoplasmic vacuoles. Immune-mediated anemia, thrombocytopenia, and neutropenia in AIDS have also been described.

The BM is usually normocellular to hypercellular (Castella, 1985). Often, increased numbers of immature myeloid precursor cells, macrophages laden with iron, and plasma cells occur. Defects occur in BM progenitor cells, such as colony-forming unit-granulocyte, monocyte (CFU-GM); colony-forming unit-granulocyte, erythrocyte, monocyte, megakaryocyte, pluripotential stem cell (CFU-GEMM); colony-forming unit-megakaryocyte (CFU-MK); and burst-forming unit-erythrocyte (BFU-E). Many drugs used to treat AIDS and its infectious complications are also myelosuppressive. Suppression of the marrow is, in many patients, multifactorial, resulting from an interaction of direct HIV cytopathic effect, dysregulation of the immune system and of apoptosis, possible complicating infection and/or nutritional imbalance, and drug effect. The most clinically valuable information of BM biopsy is usually the identification of infection or malignancy in the marrow. The disease course has been converted to a relatively indolent chronic course in those who receive and adhere to ART, but AIDS remains a tragic illness in disadvantaged populations and in those not treated.

Plasmacytosis

Plasma cells are not normally present in circulating blood. They are increased in a variety of chronic infections, in allergic states, in the presence of neoplasms, and in other conditions in which the serum γ-globulin concentration is elevated. Plasma cells have also been recorded in the blood of patients with viral disorders, including rubella, measles, chickenpox, and mumps. They are moderately increased in cutaneous exanthemas, IM, syphilis, subacute bacterial endocarditis, sarcoidosis, and collagen disease. Rarely, bacterial sepsis may show a peripheral plasmacytosis mimicking plasma cell leukemia. Their increase is usually linked with increases in lymphocytes, monocytes, and eosinophils. Causes and conditions associated with plasmacytosis include those listed in Box 34.10.

In the marrow, an average of 1% to 2% of plasma cells are present in adults. An increase beyond 4% is significant; lower values are found in children. Increases of up to 20% of plasma cells may be found in a variety of conditions other than multiple myeloma, including metastatic carcinoma, chronic granulomatous infection, conditions linked with hypersensitivity, and following administration of cytotoxic drugs. They are often increased in aplastic anemia, but this is probably just a relative increase. On the other hand, they are decreased or absent in agammaglobulinemia.

LEUKEMOID REACTIONS

A leukemoid reaction is an excessive leukocytic response in the peripheral blood. It includes leukocytosis of 50×10^9/L or higher with a shift to the

BOX 34.9

Key Causes of Lymphocytopenia

- Destructive—radiation, chemotherapy, corticosteroids
- Debilitative—starvation, aplastic anemia, terminal cancer, collagen vascular disease, renal failure
- Infectious—viral hepatitis, influenza, typhoid fever, TB
- AIDS associated—HIV cytopathic effect, nutritional imbalance, drug effect
- Congenital immunodeficiency—Wiskott-Aldrich syndrome
- Abnormal lymphatic circulation—intestinal lymphangiectasia, obstruction, thoracic duct drainage/rupture, CHF

AIDS, Acquired immunodeficiency syndrome; *CHF,* congestive heart failure; *HIV,* human immunodeficiency virus; *TB,* tuberculosis.

BOX 34.10

Key Causes of Plasmacytosis

- Viral—infectious mononucleosis, measles, rubella, HIV
- Bacterial—tuberculosis, syphilis, streptococcus, staphylococcus
- Parasitic—malaria, trichinosis
- Inflammatory—SLE, RA, inflammatory bowel disease, alcoholic liver disease
- Neoplastic—plasma cell leukemia, myeloma
- Immune stimulation—immune complex disease (serum sickness), drug sensitivity, transfusion
- Trauma

HIV, Human immunodeficiency virus; *RA,* rheumatoid arthritis; *SLE,* systemic lupus erythematosus.

left; lower counts, even below normal, with considerable numbers of immature granulocytes; and similar quantitative or qualitative changes in lymphocytes or monocytes. Depending on the predominant cell, leukemoid reactions may be neutrophilic, eosinophilic, lymphocytic, or monocytic.

Congenital Neutrophilia

A rare family with chronic congenital neutrophilia has been described with a mutation of *CSF3R* (T617N), activated GCSF receptor, and increased response to GCSF (Plo et al., 2009).

Neutrophilic Leukemoid Reactions

Excessive neutrophilia may occur in many situations, including hemolysis, hemorrhage, malignancy with bone involvement, HL, myelofibrosis, infection (especially tuberculosis), severe burns, eclampsia, and certain toxins.

Examination of the blood is usually more helpful than marrow examination. Leukemoid reactions lack the characteristic differential count that is seen in CML, including the myelocyte "peak," eosinophilia, and basophilia (Fig. 34.12).

Eosinophilic Leukemoid Reactions

Cells as immature as eosinophilic myelocytes rarely appear in the blood in reactive eosinophilia, in which the leukocyte count may exceed 50×10^9/L (see Fig. 34.8). Eosinophilic leukemoid reactions usually occur in children and are frequently caused by parasitic infection. Hypereosinophilia is discussed later in this chapter.

Leukoerythroblastosis

In patients with or without anemia, circulating normoblasts frequently are accompanied by a neutrophilic leukemoid reaction; this, then, is a **leukoerythroblastotic reaction.** A moderate anemia with normoblasts in the peripheral blood is fairly common in metastatic carcinoma involving BM. Leukoerythroblastosis may also be associated with marrow infection and/or fibrosis, and may be seen in benign conditions such as GI bleeding and hemolytic anemia.

Lymphocytic Leukemoid Reactions

Extremely high counts of normal-appearing lymphocytes may occur in infectious lymphocytosis and in pertussis (see earlier discussion). When atypical lymphocytes are strikingly increased or immature (which may occur in conditions such as IM), the distinction from leukemia may be difficult.

Examination of the marrow may be useful because lymphocytes are minimally increased, if at all, in most leukemoid reactions in contrast to leukemia. Flow cytometric studies of peripheral blood and/or BM would reveal a nonclonal population of lymphocytes with a normal combination of cell surface markers in benign proliferations.

NEOPLASTIC DISORDERS PRIMARILY INVOLVING LEUKOCYTES

MYELOPROLIFERATIVE NEOPLASMS

The myeloproliferative neoplasms recognized by the WHO are chronic myeloid leukemia, *BCR-ABL1* positive (CML); chronic neutrophilic leukemia (CNL); polycythemia vera (PV); primary myelofibrosis (PMF); essential thrombocythemia (ET); chronic eosinophilic leukemia, not otherwise specified (NOS); and myeloproliferative neoplasm, unclassifiable (Swerdlow, 2017). These are clonal proliferations of a pluripotential stem cell that can differentiate along granulocytic, erythroid, and megakaryocytic lines. Each has a chronic course that may terminate as acute leukemia, myelofibrosis, or a coagulopathy. One, CML, has a characteristic 9;22 translocation; another, PV, exhibits a mutation of *JAK2* V617F that is shared with approximately 50% each of ET and PMF, most of the remainder of which carry calreticulin or other mutations. Key features of the major disorders and of myelodysplastic/myeloproliferative diseases are summarized in Table 34.1.

Chronic Myeloid Leukemia, *BCR-ABL1*-Positive

Clinical and Laboratory Features

Blood. The leukocyte count is usually over 5×10^9/L and may exceed 30×10^9/L. The differential count is characteristic. There is a complete spectrum of granulocytic cells, from a few myeloblasts to mature neutrophils, with myelocyte and neutrophil "peaks" (see Fig. 34.12). Myeloblasts account for less than 10% of the cells. The relative percentage of neutrophil myelocytes increases as the total leukocyte count increases. Basophilia is consistently present and eosinophilia is almost always noted, along with the presence of eosinophil myelocytes. Monocytes are also absolutely increased in most patients.

Course. A synthetic tyrosine kinase inhibitor (TKI; imatinib mesylate [Gleevec]) specifically targets the BCR-ABL1 protein and results in long-term remission for most patients (Druker et al., 2001). Treatment failures occur due to secondary mutations; newer-generation TKIs are often helpful (Jabbour & Kantarjian, 2014; Soverini et al., 2014). In the past, treatment (busulfan or hydroxyurea) controlled the disease only in the chronic phase.

Prior to TKI therapy and in patients who fail treatment, the disease changes after a variable period into a more aggressive or accelerated phase. This is characterized by one or more features of progressive myeloproliferation: increased blood or marrow blasts of 10% to 19%; peripheral blood basophilia >20%; persistent thrombocytopenia unrelated to therapy $<10 \times 10^9$/L; thrombocytosis $>100 \times 10^9$/L; increasing leukocytosis and splenomegaly unresponsive to therapy; or cytogenetic clonal evolution. Granulocytic dysplasia, increased small dysplastic megakaryocytes and reticulin fibrosis are also suggestive.

Blast phase is essentially a progression to acute leukemia and is defined by >20% blasts in the blood or BM and large aggregates of blasts in the marrow or in extramedullary locations. Blast lineage is myeloid in 70% of cases and may include any myeloid cell types (neutrophilic, eosinophilic, basophilic, monocytic, erythroid, or megakaryocytic), although Auer rods are rarely found. In approximately one-third of cases, however, the appearance is that of acute lymphoblastic leukemia (ALL). Usually, these are of precursor B-lineage. Occasional cases are precursor T-lineage. Myeloid antigens are often coexpressed, and bilineal myeloid/lymphoid cases are rarely found. Occasionally, a patient will initially present in blast phase.

Chronic Neutrophilic Leukemia

CNL is a rare myeloproliferative disorder characterized by persistent and unexplained neutrophilia of $>25 \times 10^9$/L mature granulocytes resembling reactive neutrophilia (Elliott, 2001; Bain, 2008). It typically affects older adults and presents with splenomegaly and sometimes hepatomegaly, often with mucocutaneous bleeding, pruritus, or gout. There may be a left shift with bands present and toxic granulation. BM findings include hypercellularity with granulocytic hyperplasia showing a myeloid/erythroid ratio of up to 20:1 and a predominance of mature neutrophils to myelocytes. Erythroid cellularity and megakaryocytes may be increased, but dysplasia is not present. Cytogenetics are usually (90%) normal, with some cases showing abnormalities, including +8, +9, del(20q), and del(11q). Cases with variant Ph′-positive chromosome and neutrophilia are considered CML.

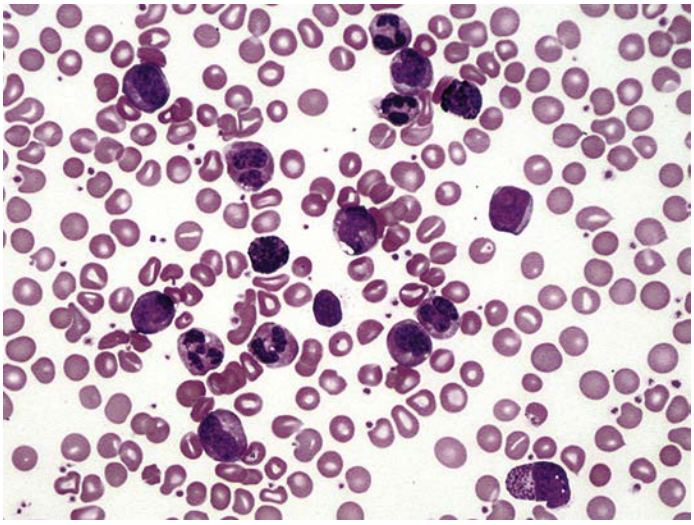

Figure 34.12 Chronic myeloid leukemia with increased segmented neutrophils, myelocytes, and basophils and an occasional blast (×500).

Mutations of *CSF3R* (T618I and T615A) have been associated with CNL, often together with *ASXL1* or *SETBP1* mutations (Elliott & Tefferi, 2014; Gotlib et al., 2013; Maxson et al., 2013). *JAK2* mutation has been reported in some cases. Reactive processes due to occult malignancy or other causes of inflammation may induce marked neutrophilia mimicking CNL (Swerdlow, 2017).

Polycythemia Vera

Polycythemia vera is a clonal stem cell proliferation affecting primarily the erythroid series, characterized by excessive proliferation of erythroid and usually granulocytic and megakaryocytic elements in the marrow (panmyelosis). It is genetically characterized by mutation of Janus 2 kinase, *JAK2*V617F, or another functionally similar mutation such as *JAK2* exon 12 mutation (Levine, 2008). *JAK2* mutation occurs in essentially all patients with PV but is also present in approximately 50% of patients with thrombocythemia and primary myelofibrosis. The disease is manifested in the blood by an absolute increase in red cell mass, leukocytosis, and thrombocytosis. Serum and urine erythropoietin are decreased. The production of erythrocytes is autonomous with **endogenous erythroid colonies (EECs)** growing in vitro without erythropoietin. There is initially a proliferative phase and eventually a spent phase with iron depletion and associated anemia, marrow fibrosis, increased splenomegaly, and extramedullary hematopoiesis.

Clinical Features

The disease is slightly more frequent in men than in women. It usually begins in middle age. Affected patients exhibit ruddy cyanosis, and splenomegaly is present in two-thirds. Thrombotic or hemorrhagic phenomena occur in about half of patients, and thrombosis is most common. Myocardial infarction, cerebral thrombosis, splenic or pulmonary infarcts, and thrombophlebitis account for the most frequent thrombotic episodes; upper GI bleeding, often from peptic ulcer, is the most common bleeding problem. Pruritus, especially after bathing, is common.

Laboratory Features

Blood. Erythrocytes exceed 6 to 12 × 10^{12}/L, and the hemoglobin is >18.5 g/dL (males) or >16.5 g/dL (females). Mean cell volume (MCV), mean cell hemoglobin (MCH), and mean cell hemoglobin concentration (MCHC) are normal or low. The erythrocytes become hypochromic and microcytic if chronic blood loss has occurred. Macrocytes, polychromatic cells, and normoblasts may be found but are not a prominent feature of the disease. Red cell production is increased. Red cell destruction is normal during the period of erythrocytosis. Later in the disease, as splenomegaly develops, red cell survival diminishes. The total blood volume is increased, primarily because of increased red cell mass, and the plasma volume may also be elevated to a lesser degree. Blood viscosity is high, and it may be difficult to prepare good blood films. The erythrocyte sedimentation rate (ESR) is reduced.

The platelet count is increased in about two-thirds of patients, often to levels exceeding 1000 × 10^9/L. In 80% of untreated patients, functional platelet abnormalities are present with decreased aggregation in response to adenosine diphosphate (ADP) and epinephrine. No consistent abnormality of secondary hemostasis is present.

Moderate neutrophilic leukocytosis in the range of 10 to 30 × 10^9/L is common. Immature granulocytes are seen in about one-half of cases, and basophils are often absolutely increased. The neutrophil alkaline phosphatase (NAP) is markedly elevated in 80% of patients.

The arterial oxygen saturation is normal. Hyperuricemia appears in many patients with PV as a result of increased nucleic acid metabolism. In some patients, secondary gout or renal uric acid stones occur.

Marrow. The marrow is moderately to markedly hypercellular, with prominent normoblastic erythroid hyperplasia in panmyelosis. Megakaryocytes show an increase in and clustering of variable small and large megakaryocytes associated with an increase in dilated sinuses and frequently cluster around sinusoids (Fig. 34.13). Increased reticulin is often present, and storage iron is decreased or absent in 95% of cases.

Diagnosis

Criteria of the WHO for the diagnosis of PV (Swerdlow, 2017):

Major Criteria

1. Elevated Hb >16.5 (males) or 16 (females) g/dL or hematocrit or other evidence of increased red cell volume.
2. Bone marrow biopsy showing hypercellularity with panmyelosis with granulocytic, erythroid, and megakaryocytic proliferation with pleomorphic megakaryocytes.
3. Presence of *JAK2* V617F or similar mutation such as *JAK2* exon 12 mutation.

Minor Criterion

1. Low serum erythropoietin level

Major criterion number 2 (bone marrow biopsy) may not be required in cases with persistent erythrocytosis (hemoglobin levels > 18.5 g/dL in males or 16.5 g/dL in females) if major criterion number 3 and the minor criterion are present.

In addition to *JAK2* V617F or exon 12 mutations, there is emerging information on other genetic abnormalities, including mutations of *TET2*, expression of STAT5B, and varied signaling abnormalities (Levine, 2009; Rampal et al., 2014; Rice et al., 2011; Tefferi et al., 2009).

PV is a chronic disease; patients usually live 10 to 20 years under good control. Phlebotomy, chlorambucil, radioactive phosphorus (^{32}P), and hydroxycarbamide (hydroxyurea) have been used to control the manifestations of the disease.

In about 20% to 40% of patients, the spent or postpolycythemic phase occurs with progressive anemia, gradual splenic enlargement, and further elevation of the leukocyte count, with more immature granulocytes and more circulating nucleated red cells. Many erythrocytes become oval, and teardrop cells (dacryocytes) become prominent. BM aspiration becomes impossible because of myelofibrosis, and splenomegaly increases, owing to extramedullary hematopoiesis. Manifestations at this stage of the disease are indistinguishable from those of myelofibrosis with myeloid metaplasia. Another late complication of PV is acute leukemia or MDS associated with ^{32}P and alkylators but not with hydroxyurea (Bjorkholm et al., 2011).

Primary Myelofibrosis

This is a chronic, progressive clonal panmyelosis characterized by megakaryocytic and often granulocytic hyperplasia with varying degrees of reactive fibrosis of the marrow and extramedullary hematopoiesis (Swerdlow, 2017). Typically, leukoerythroblastic anemia occurs with marked red cell abnormalities, circulating normoblasts, immature granulocytes, and atypical platelets. Chronic idiopathic myelofibrosis (CIM) is an uncommon disease with an incidence one-third that of CML. It occurs typically in persons over the age of 50 years and has an insidious onset, with weight loss, anemia, and abdominal discomfort due to the large spleen. Often, the liver is enlarged as well, and the patient may be slightly jaundiced. Radiography shows patchy osteosclerosis in up to half of patients, but osteoporosis may also be seen.

A prefibrotic stage in 20% to 30% of cases is characterized by mild normocytic anemia with poikilocytosis, including dacryocytes, nucleated RBCs, thrombocytosis, and mild leukocytosis with some immature forms. The marrow is hypercellular and contains abnormal megakaryocytes, which cluster around sinuses and trabeculae. The histopathology of the BM is dominated by atypical, enlarged, and immature megakaryocytes with cloud-like immature nuclei, and small megakaryocytes (Michiels et al., 1999; Michiels et al., 2014). Fibrosis may be minimal initially. Intrasinusoidal hematopoiesis is often present (Fig. 34.14).

Characteristic findings in the fibrotic stage include moderate normochromic, normocytic anemia (often with some hypochromic cells and basophilic stippling), moderate anisocytosis, and marked poikilocytosis, including prominent teardrop forms (dacryocytes) and elliptocytes. Normoblasts are often increased out of proportion to the degree of anemia

TABLE 34.1

Key Features of Major Myeloproliferative and Myelodysplastic/Myeloproliferative Neoplasms

Disorder	Demographics	Laboratory Features, Morphology	Cytogenetics	Prognosis
CML	Middle-aged	*BCR-ABL1* present	t(9:22)(q34;q11) *BCR-ABL1*	Dependent on response to TKI
CNL	Older adults	Neutrophilia > 25K/μL	*CSF3R* mutation	Indolent
PV	Middle-aged, M > F	Major criteria: Hb >16.5 g/dL in M or >16.0 g/dL in F; *JAK2* V617F (or Exon 12); hypercellular marrow with panmyelosis Minor criterion:↓EPO; all three major criteria, or first 2 major plus minor criterion	*JAK2* V617F (or Exon 12) negative t(9;22)	10–20 years
PMF	>50 years	Major criteria: megakaryocyte proliferation/atypia with marrow fibrosis; CML, PV, MDS ruled out; *JAK2* V617F, *CALR*, *MPL* mutation or other clonal marker Minor criteria: leukoerythroblastosis, ↑LD, anemia, leukocytosis ≥11 × 10^9/L splenomegaly; all 3 major plus at least one minor criterion	*JAK2* V617F, *CALR, MPL;* *TET2, ASXL1, EZH2, CBL, IDH1/IDH2, TP53, SF3B1, and SRSF2* mutations; +8, +9, del(20q), del(13q), del(1p), negative t(9;22)	Dependent on phase: ≈10 years in early prefibrotic phase; ≈5 years in fibrotic phase
ET	5th decade (M = F), second peak in 30′ s (F > M)	Major criteria: platelet count >450 K; BM with proliferation of mature megakaryocytes; PV, PMF, CML, MDS ruled out; *JAK2 V617F, CALR*, or *MPL* mutation Minor criterion: clonal marker or absence of reactive thrombocytosis NOTE: All four criteria must be met.	*JAK2* V617F in 50%; *CALR* 30%; *MPL* 3% del(13q22), +8, +9 seen in 5%–10% of cases; negative t(9;22)	Stable for many years (most cases)
CMML	Median, 65–75 years, M > F	Monocytosis >1000 with monocytes accounting ≥10% of WBC, cytopenias, myeloid dysplasias, <20% blasts	+8, –7, 12p abn in 20%–40% of cases; negative t(9;22)	20–40 months with progression to AML in 15%–30%
JMML	Younger than 3 years, M > F	Monocytosis >1000, blasts <20%, plus 2 of ↑Hb F, splenomegaly, immature grans, clonal abn, GM-CSF hypersensitivity, hyperphosphorylation of STAT5	Monosomy 7, negative t(9;22)	Poor; possible benefit from BMT
Myeloid/lymphoid neoplasms w/↑eos and *PDGFR/FGFR1/PCM1-JAK2*	M 25–55 years	PB w/inc eos, BM eos with mast cells	*FIP1L1-PDGFRA, PDGFRB, FGFR1, PCM1-JAK2*	Variable response to TKI
Mastocytosis	All ages	Mononuclear w/central nuclei, variable basophilic granules (often not seen in fixed tissue); dense aggregates of spindle cells	*KIT* D816V	Cutaneous, indolent; systemic, variable; leukemia, aggressive
CEL NOS, idiopathic HES	Usually adult M; any age or sex	PB ≥1.5 K eos/μL, <20% blasts	+8, i(17q) 8p11 w/various partners	Indolent, 80% 5-year survival

Abn, Abnormalities; *AML,* acute myelogenous leukemia; *BM,* bone marrow; *BMT,* bone marrow transplant; *CEL,* chronic eosinophilic leukemia; *CML,* chronic myeloid leukemia; *CMML,* chronic myelomonocytic leukemia; *eos,* eosinophils; *EPO,* erythropoietin; *ET,* essential thrombocythemia; *F,* female; *GM-CSF,* granulocyte-macrophage colony-stimulating factor; *grans,* granulocytes; *Hb,* hemoglobin; *HES,* hypereosinophilic syndrome; *inc,* increased; *JMML,* juvenile myelomonocytic leukemia; *LD,* lactate dehydrogenase; *M,* male; *MDS,* myelodysplastic syndrome; *NAP,* neutrophil alkaline phosphatase; *NOS,* not otherwise specified; *PB,* peripheral blood; *PMF,* primary myelofibrosis; *PV,* polycythemia vera; *TKI,* tyrosine kinase inhibitor; *WBC,* white blood cell.

with slight reticulocytosis. The anemia may have a complicated origin, with components of marrow failure, ineffective erythropoiesis, and hemolysis. Splenomegaly due to extramedullary hematopoiesis is typical.

The leukocyte count is moderately increased; immature neutrophils and occasionally myeloblasts are present. Basophils are often increased. Platelets are normal or decreased in number (rarely increased) and often atypical, with distinct clear "zones." Micromegakaryocytes the size of lymphocytes with both nucleus and cytoplasm or small megakaryoblasts may usually be found if searched for; on rare occasions, they are present in considerable numbers.

In vitro blood cell culture shows increased colonies (CFU-GM) similar to those in CML. Serum GM-CSF is high, serum uric acid is frequently increased, and cobalamin is normal or elevated.

It is usually impossible to aspirate marrow; thus, biopsy is necessary. The marrow is fibrotic, with residual islands of atypical megakaryocytes, erythroid, and granulocytic precursors. The fibrosis is of loose connective tissue with scanty collagen, but reticulin fibers are abundant. Foci of osteoid and/or new bone formation in endophytic plaques may be found, and bony trabeculae may be irregularly thickened (myelosclerosis). The marrow may show a mixture of hyperplasia and fibrosis in one sample or may vary in different sites of the body. Megakaryocytes with abnormal nuclei cluster or form sheets that may be found in sinuses with other marrow precursors. Extramedullary hematopoiesis is found in the spleen and liver.

Biology

Although the proliferating megakaryocytes are neoplastic, the stromal proliferation is reactive because of inappropriate release of megakaryocyte/platelet-derived growth factors, including platelet-derived growth factor (PDGF), transforming growth factor (TGF)-β, basic fibroblast growth factor (bFGF) and calmodulin (Reilly, 1998).

Approximately 50% to 60% of patients show *JAK2* V617F mutation; 30% show mutation of *CALR* (calreticulin) (Tefferi et al., 2014). A small number, up to 5%, have an *MPL* W515K/L gene mutation. Testing for these is important for prognostication. *TET2* may be a predisposing mutation and modifying mutations include *ASXL1*, *EZH2*, *CBL*, *IDH1/IDH2*, *TP53* and *SRSF2*. Chromosomal studies show absence of *BCR-ABL1*, but variable cytogenetic changes; +8, +9, del(20q), del(13q)(q12-22), partial trisomy 1q, del(5q) and der(6)t(1;6)(q21-23;p21.3). Additional cytogenetic abnormalities may be associated with cytotoxic therapy and/or progression of disease.

Course

The natural course is increasing fibrosis with progressive anemia and enlargement of the spleen. Hemolysis frequently becomes an increasing element in the anemia, and infection may be a serious problem. Portal hypertension occurs in 10% to 20% of cases and may result in bleeding esophageal varices. Hypertension may be due to portal vein thrombosis

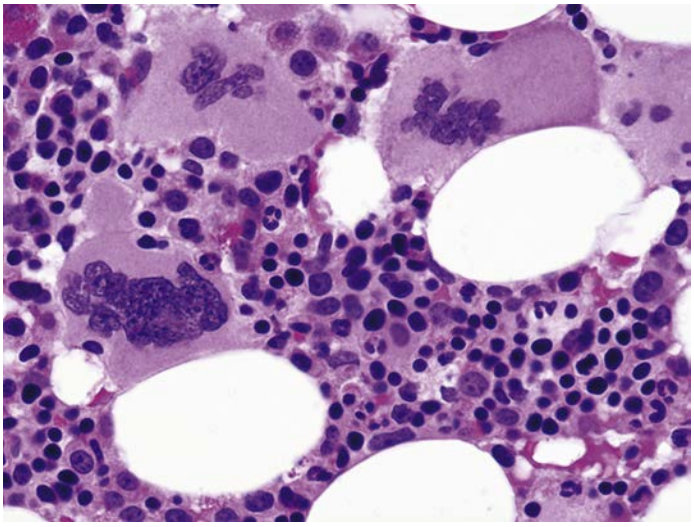

Figure 34.13 Bone marrow biopsy in polycythemia vera shows panmyelosis with normoblastic hyperplasia (×500).

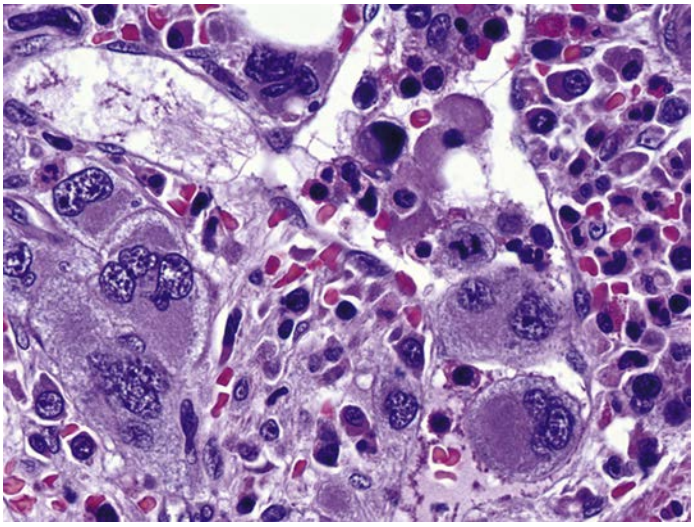

Figure 34.14 Bone marrow biopsy in primary myelofibrosis, with increased spacing between cells suggesting fibrosis and intrasinusoidal hematopoiesis (×500).

or intrahepatic obstruction as a result of myeloid metaplasia coupled with increased portal blood flow.

The median survival has been about 5 years, considerably less than that of PV. However, some patients live longer—in those patients, the terminal event is frequently acute leukemia. Therapy has been largely palliative but JAK kinase inhibitors may alter the disease course.

Occasionally, patients exhibit cytopenias and marrow fibrosis due to other causes, some of which may show favorable response to specific therapies. These include metastatic tumors, primary hematopoietic tumors such as HCL or plasma cell dyscrasia, damage from radiation, and, rarely, autoimmune myelofibrosis. Malnourished children with vitamin D deficiency (rickets) sometimes show myelofibrosis. Solvent exposure may be a factor; benzene has been most often suspected and is a known inducer of AML at threshold levels of exposure. Current environmental exposure appears much lower than levels likely to be associated with hematologic malignancies (Duarte-Davidson, 2001; Courage, 2001). Peritrabecular marrow fibrosis occurs in primary hyperparathyroidism or secondary hyperparathyroidism of chronic renal failure.

Essential Thrombocythemia (ET)

Thrombocythemia is a clonal myeloproliferative neoplasm primarily affecting the megakaryocytic lineage with the principal manifestation of sustained thrombocytosis. Of ET cases, 50% to 60% carry a *JAK2* V617F mutation, 30% of cases have *CALR* mutation and 3% *MPL*. It most often occurs in the fifth decade, with equal sex distribution, with another peak of incidence in females in their 30s (Tefferi et al., 2014).

Clinical Features

Patients often (50%) present with asymptomatic thrombocytosis, but up to half of patients present with hemorrhage or thrombosis. The latter occurs as arterial or venous thrombosis or as microvascular occlusion resulting in transient ischemic attacks (TIAs) or digital ischemia. Characteristic recurrent, spontaneous mucosal hemorrhages are most common in the GI tract or the upper airway. Hemorrhages are occasionally preceded or accompanied by thrombosis. Mild splenomegaly occurs in 50% of cases.

Laboratory Features

Blood. The most striking feature is the marked increase in platelets ($\geq 450 \times 10^9$/L; usually $>1000 \times 10^9$/L), often with abnormal and giant forms and usually accompanied by fragments of megakaryocytes. Neutrophilic leukocytosis is sometimes present. Hypochromic microcytic anemia due to chronic blood loss is present in many cases. Platelet function defects in thrombocythemia are frequently demonstrable. The most typical finding is decreased aggregation in response to epinephrine.

Marrow. The marrow shows increased and enlarged megakaryocytes with mature cytoplasm and multilobulated nuclei and a tendency to cluster in a normal or only slightly hypercellular BM (Michiels, 1999) (Fig. 34.15). Megakaryocyte nuclei are not described as atypical but often are distinctive and resemble other myeloproliferative neoplasms (MPNs). Erythroid proliferation may be present secondary to blood loss. Biopsy features may be indistinguishable from those of PV, but usually with less erythroid prominence. Splenic extramedullary hematopoiesis may be present.

Diagnosis

Criteria of the WHO for the diagnosis of thrombocythemia (Swerdlow, 2017):

Major criteria

1. Sustained platelet count $\geq 450 \times 10^9$/L.
2. BM biopsy showing proliferation of mainly megakaryocytes with enlarged mature nuclei, no increase or left shift of granulopoiesis or erythropoiesis.
3. Not meeting WHO criteria for polycythemia vera, PMF, *BCR-ABL1*–positive CML, MDS, or other myeloid neoplasm.
4. Demonstration of *JAK2* V617F, *CALR*, or *MPL* mutation.

Minor criterion

Demonstration of a clonal marker or absence of evidence for reactive thrombocytosis.

The diagnosis of ET requires that either all major criteria or the first 3 major criteria plus the minor criterion are met.

Genetics

From 40% to 50% of cases carry a *JAK2* V617F mutation. Most other cases carry a mutation of calreticulin (*CALR*) that is mutually exclusive to *JAK2* mutation and carries reduced or no risk of transformation to PV (Cazzola & Kralovics, 2014). *BCR-ABL1* translocations must be ruled out to exclude CML. Some cases show +8, abnormalities of 9q or del(20q). Mutations seen in PMF are seen in reduced frequency in ET (Cazzola & Kralovics, 2014; Martinez-Aviles et al., 2012), although this raises the possibility of early PMF mimicking ET.

Most cases are stable for many years, but a small proportion may merge into other chronic myeloproliferative neoplasms or, rarely, develop into acute leukemia. Current treatment recommendations are based on clinical risk stratification to guide cytoreduction, platelet inhibition and anticoagulation (Tefferi & Barbui, 2013).

Myeloproliferative Neoplasm, Unclassifiable

These are cases with features of MPN but do not meet criteria for a specific entity or have intermediate features (Swerdlow, 2017). Examples of MPN-U include prefibrotic/early PMF, masked/prepolycythemic PV, and early-phase ET, as well as cases with features of MPN but presenting with some dysplasia or increased blasts, and those with convincing evidence of MPN that is obscured, however, by a concurrent inflammatory or neoplastic condition. *BCR-ABL1* and other specific cytogenetic abnormalities are absent. This category overlaps with myelodysplastic/myeloproliferative disease, unclassifiable. Often, with follow-up, characteristic findings develop that allow definitive diagnosis.

Chronic Eosinophilic Leukemia, NOS, and Idiopathic Hypereosinophilic Syndrome

CEL is a clonal proliferation of eosinophils with chronic increase in the blood and often organ damage due to tissue infiltration. The blood contains

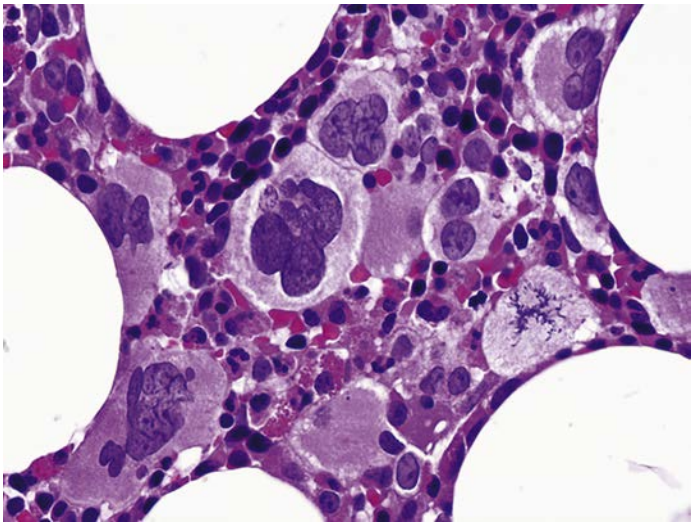

Figure 34.15 Bone marrow biopsy in essential thrombocythemia, with increased and clustered megakaryocytes (×500). Nuclei in this case are unusual, resembling primary myelofibrosis.

>1.5 × 10^9/L mostly mature eosinophils and often increased but fewer than 20% blasts in the blood or marrow. A working conference on eosinophil disorders has recommended that the term *hypereosinophilia* (*HE*) be used for these cases, subcategorized as HE_{FA} for familial cases, HE_{US} for cases of undetermined significance, HE_N for those due to clonal neoplasms and HE_R for reactive eosinophilias (Valent et al., 2012). A lymphocyte variant of HE is associated with clonal T cells showing abnormal antigen expressions (Gotlib, 2014). Some other neoplasms, including T-cell lymphoma and HL, are often causes of secondary eosinophilia due to cytokine production (IL2, IL3, IL5, GM-CSF). When associated with a defined MPN, the eosinophilia is considered a component of that disease and not termed *CEL*. MPNs with eosinophilia and *PDGFRA*, *PDGFRB*, or *FGFR1* gene abnormalities are classified separately.

Some cases of CEL have clonal cytogenetic abnormalities; +8, i(17q) or 8p11 translocations, including t(8;13)(p11;q12), t(8;9)(p11;q32-34), and t(6;8)(q27;p11). The 8p11 translocation may also occur in AML, precursor B- or precursor T-ALL. Other abnormalities, including *JAK2* V617F mutation and trisomy 10, may occur. The clinical outcome of CEL and HES is usually indolent, with 5-year survival of about 80%.

Mastocytosis

Mastocytosis is a clonal neoplastic proliferation of mast cells involving skin, BM, lymph nodes, and/or spleen (Akin, 2014; Swerdlow, 2017), with variable degrees of malignancy. Subtypes are described based on distribution of disease and clinical manifestations. Symptoms are complex and arise from secretion of vasoactive amines, including histamine and serotonin, as well as from mass effects.

Mastocytosis is associated with mutations of the *KIT* proto-oncogene that encodes the tyrosine kinase receptor for stem cell factor (SCF), most frequently, *KIT* D816V with CD117 expression. Morphologically, increased mast cells are found in involved organs, often with associated fibrosis. Mast cells normally are mononuclear cells with central nuclei, clumped chromatin, and dense basophilic granules. They are frequently difficult to identify, however, as mast cell granules are not well preserved in fixed tissue and cells may appear like bland clear cells, histiocytes, fibroblasts, or others. Mast cells may be identified in tissue using Giemsa or toluidine blue stain and immunohistochemistry. Mast cell tryptase is the most specific marker, but cells also express CD117, as well as CD45, CD33, CD68, CD2, and CD25. Mast cells lack myeloperoxidase but often express chloroacetate esterase. Diagnostic testing should include immunologic assays (immunohistochemistry and/or flow cytometry) for CD117, CD2, CD25, and tryptase, as well as assays for *KIT* D816V mutation in marrow, blood, or other extracutaneous organs for systemic disease.

Urticaria with melanin pigmentation is common with skin involvement and is referred to as *urticaria pigmentosa* (*UP*) or *maculopapular cutaneous mastocytosis* (*MPCM*). This form occurs in both children and adults. In children, lesions are often large and papular or are associated with blistering in children younger than 3 years old. It is often self-limited or may spontaneously regress. Histology shows aggregates of spindle-shaped mast cells filling the papillary dermis and extending into the reticular dermis (Swerdlow, 2017). A diffuse cutaneous variant is referred to as *diffuse cutaneous mastocytosis* and a localized variant as *mastocytoma of skin*.

Systemic mastocytosis is defined by involvement of at least one extracutaneous organ with or without skin involvement. It presents with variable cutaneous and constitutional symptoms, including urticaria, pruritus and dermatographism, symptoms of systemic histamine release, bone pain, arthralgia and fractures, splenomegaly, hepatomegaly, or lymphadenopathy.

BM involvement is sometimes difficult to identify, with paratrabecular and perivascular aggregates of increased lymphocytes, eosinophils, neutrophils, mast cells, and fibroblasts. Marrow biopsy of most cases shows multifocal, sharply demarcated compact aggregates of mast cells. These may be spindle shaped and lacking in apparent granules on hematoxylin and eosin (H&E) stain, or may consist of mixed infiltrates of mast cells, lymphocytes, eosinophils, histiocytes, and fibroblasts, with a peripheral rim or central core of lymphocytes. Compact infiltrates of hypergranular mast cells also occur and are referred to as *tryptase-positive round cell infiltrates*, or TROCI. The latter may also be seen in basophilic leukemia or AML. Mast cells are frequently increased in hematologic neoplasms such as HCL, lymphoplasmacytic lymphoma, and myeloid neoplasm and are most apparent around BM particles on aspirate smears. Reactive mast cells do not typically show compact aggregates.

In addition, systemic mastocytosis (SM) not infrequently presents simultaneously with or in close temporal relationship with other hematopoietic neoplasms, including acute leukemia, myeloproliferative and/or myelodysplastic neoplasms, and, occasionally, other hematopoietic neoplasia. SM is sometimes detected only after treatment for an acute process (Figs. 34.16 and 34.17). These cases are referred to as *systemic mastocytosis with associated hematologic neoplasm* (*SM-AHN*). The associated hematologic neoplasm (AHN) is categorized by criteria for the same disorder without SM.

Mast cell leukemia also occurs and is defined by the presence of atypical mast cells constituting more than 20% of a marrow aspirate. More than 10% of the circulating cells are usually mast cells (Swerdlow, 2017). Chronic forms and a prephase with 5% to 29% mast cells in the BM occur. Myelomastic leukemia (MML) is a related entity in which mastocytic differentiation in advanced myeloid neoplasms occurs without SM (Valent, 2014).

Mast cell sarcoma refers to localized, destructive extramedullary tumors of highly atypical mast cells, occurring in the larynx, bowel, meninges, bone, and skin. Extracutaneous mastocytoma of mature granulated mast cells occurs rarely in the lung.

The outcome is highly variable, with cutaneous disease usually indolent. In children, it usually regresses. Systemic disease without skin involvement is more aggressive than with skin disease, and mast cell leukemia and sarcoma are highly aggressive.

Myeloid/Lymphoid Neoplasms with Eosinophilia and Rearrangement of *PDGFRA, PDGFRB, FGFR1*, or with *PCM1-JAK2*

This disease category contains a group of myeloid/lymphoid neoplasms associated with eosinophilia that have genetic abnormalities resulting in abnormal tyrosine kinases that may be successfully treated with TKIs, the first two of which are responsive to imatinib and/or similar TKIs (Gotlib, 2014; Swerdlow, 2017).

MPN with rearrangement of *PDGFRA* is most often associated with a *FIP1L1-PDGFRA* fusion protein resulting from a cryptic deletion at 4q12. The disease usually presents as CEL with peripheral eosinophil counts >1.5 × 10^9/L, with multisystem involvement and organ damage. BM eosinophilia is often accompanied by increased mast cells that are considered part of the disease. It usually occurs in men between 25 and 55 years but may occur in others as well. Presentation also occurs as AML and as T-lymphoblastic lymphoma/leukemia (T-LBL). Diagnosis and appropriate therapy depend on identification of the genetic abnormality by reverse transcriptase polymerase chain reaction (RT-PCR) or by cytogenetic fluorescent in situ hybridization (FISH) assay for deletion of the *CHIC2* gene, or use of a break-apart probe encompassing *FIP1L1* and *PDGFRA*. Other genetic variants have been described and are generally imatinib sensitive (Swerdlow, 2017).

Rearrangement of *PDGFRB* at 5q32, usually due to t(5;12)(q32;p13.2) with production of *ETV6-PDGFRB*, resembles chronic myelomonocytic leukemia (CMML) with eosinophilia. Variant translocations involving *PDGFRB* may be associated with other morphologies, including CEL, MPN, and others. This disease occurs most often in middle age, but with a wide age range and a 2:1 M/F ratio. Diagnosis of MPN with *PDGFRB* (rather than a morphologic diagnosis as MPN, NOS, or CMML)

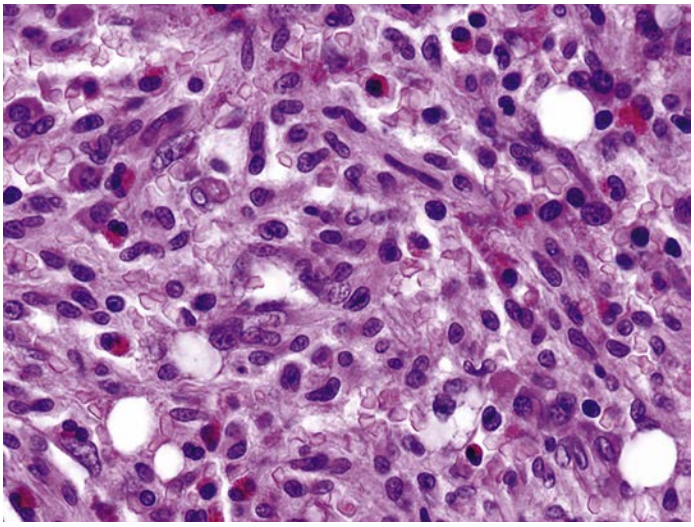

Figure 34.16 Mastocytosis in the bone marrow, presenting after treatment for acute myeloid leukemia (×500).

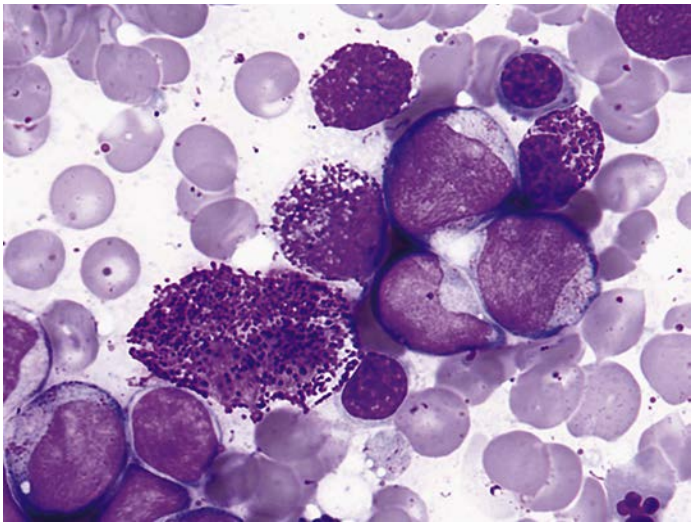

Figure 34.17 Acute leukemia with early mast cell disease before therapy (earlier specimen from case shown in Fig. 34.16) (×1000).

is imperative because it is sensitive to TKI therapy (Cheah et al., 2014). Diagnostic testing is by cytogenetics to detect t(5;12) and/or by RT-PCR. Secondary trisomy 21 is frequent.

Myeloid and lymphoid neoplasms involving *FGFR1* at chromosome region 8p11 are heterogeneous and may present as CEL, AML, T- or, less often, B-lymphoblastic leukemia/lymphoma, or mixed phenotype acute leukemia (MPAL). Eosinophilia is present in 90% of cases overall. Although an abnormal tyrosine kinase is produced, it is not imatinib sensitive. The genetic abnormalities are most often translocations and karyotyping may be diagnostic. It was formerly called *8p11 stem cell syndrome* or a similar name. Prognosis is currently poor (Gotlib, 2014; Swerdlow, 2017). Hematologic neoplasms associated with t(8;9) (p22;p24.1) resulting in *PCM1-JAK2* share characteristic features, often including eosinophilia and left shifted neutrophils in the peripheral blood. These cases may have the hematologic features of CEL, MDS/MPN, AML, B- or T-ALL. Prognosis is quite variable.

Myelodysplastic and Myelodysplastic/Myeloproliferative Neoplasms

Myeloproliferative diseases, in general, are neoplasms in which proliferation of hematopoietic cells outpaces apoptosis, and cellular elements in the blood are increased while the morphology of hematopoiesis is near normal. Myelodysplastic diseases or syndromes are disorders in which apoptosis predominates, hematopoiesis is ineffective, and cytopenias occur. The myelodysplastic/myeloproliferative disorders show features of both, with variable increases in cells, as well as cytopenias and morphologic dysplasia. These include chronic myelomonocytic leukemia (CMML), atypical chronic myeloid leukemia (aCML), *BCR-ABL1* negative, juvenile myelomonocytic leukemia (JMML), myelodysplastic/myeloproliferative neoplasm with ring sideroblasts and thrombocytosis, and myelodysplastic/myeloproliferative neoplasm, unclassifiable.

MDS occurs primarily in persons over age 50 years and usually presents as an anemia refractory to hematinics (iron, folate, B_{12}), with or without neutropenia and thrombocytopenia. Liver, spleen, or lymph nodes are not usually enlarged. The marrow is hypercellular, with abnormal maturation in one or more of the three hematopoietic cell lines, and blast cells are often increased. These disorders have also been called *dysmyelopoietic syndromes* or "preleukemias" because of the high proportion of cases that ultimately progress to overt acute leukemia (Bennett, 1976, 1982; Swerdlow, 2017). A scoring system for predicting survival and risk of acute leukemic transformation has been developed based on percentage of blasts, cytogenetics, and extent of cytopenias. In general, a blast count >5% elevates risk and >10% increases risk further; complex chromosomal abnormalities or chromosome 7 abnormalities are high risk; del(5q), isolated del(2q), -Y, and normal cytogenetics are low risk; other cytogenetic findings are intermediate risk; and more than one cytopenia increases risk.

Genetics and Epigenetics

Molecular genetic analyses suggest that MDS occurs due to initial oncogenic driver mutations and that progression occurs with accumulating mutations. Most patients have 2 to 3 driver mutations occurring in genes of RNA splicing (*SF3B1*, *SRSF2*, *U2AF1*, *ZRSR2*), DNA methylation (*TET2*, *DNMT3A*, *IDH1/2*), chromatin modification (*ASXL1*, *EZH2*), transcription regulation (*RUNX1*), DNA repair (*TP53*), signal transduction (*CBL*, *NRAS*, *KRAS*) and/or cohesin *(STAG2)* (Cazzola et al., 2013; Papaemmanuil et al., 2013; Lin et al., 2014). Abnormalities of the "spliceosome" and of DNA methylation lead to epigenetic disruption.

Types of Abnormal Cellular Maturation

Dyserythropoiesis resembles megaloblastic change and includes nuclear fragmentation or karyorrhexis, multinuclearity, nuclear budding or bridging, basophilic stippling, and ring sideroblasts. These features may also be seen in toxicity due to drugs, chemotherapy, heavy metals, alcohol, and other toxins (Figs. 34.18 and 34.19). Erythroid cells may be decreased or increased in number. Erythrocytic abnormalities in the blood film include presence of oval macrocytes, anisochromia, basophilic stippling, dacryocytes, and reticulocytopenia.

Dysgranulopoiesis includes nuclear/cytoplasmic asynchrony, hypogranulation, nuclear hyposegmentation with increased chromatin condensation, occasionally abnormal large azurophilic granules, inappropriately prominent nucleoli, or other abnormalities. Neutrophil precursors and monocytes often resemble one another. Neutrophils with mature chromatin but with decreased granulation and bilobed or unilobed nuclei resemble the cells of Pelger-Huët anomaly and are termed *pseudo–Pelger-Huët* cells (Figs. 34.20 and 34.21).

Dysmegakaryocytopoiesis includes large megakaryocytes with unsegmented nuclei, micro megakaryocytes, and megakaryocytes with two or more small, unconnected nuclei (Fig. 34.22). Megakaryocytes may be decreased in number. In the blood film, giant hypogranular platelets are frequent, and micro megakaryocytes are seen rarely.

Myelodysplastic/Myeloproliferative Neoplasms

Chronic Myelomonocytic Leukemia. CMML is a clonal stem cell malignancy in which the predominant feature is persistent monocytosis (>1 × 10^9/L with monocytes accounting for ≥10% of the leukocytes) for longer than 3 months and all other causes have been excluded (Swerdlow, 2017). Typically, cytopenias are present in the blood (anemia, thrombocytopenia, and/or neutropenia), but neutrophilia with morphologic abnormalities also occurs. There is absence of a Philadelphia chromosome or *BCR-ABL1*, dysplasia of one or more myeloid lineages, and less than 20% blasts plus promonocytes in the marrow (Fig. 34.23). The marrow also shows monocytosis and often has increased promonocytes, which may be distinguished from abnormal myelocytes by nonspecific esterase (α-napthyl acetate, or α-napthyl butyrate esterase) staining or strong labeling with anti-lysozyme or CD68. Eosinophilia or basophilia may be present, and plasmacytoid-appearing monocytes are seen frequently. When eosinophils exceed 1.5 × 10^9/L, the WHO recommends the subcategory of CMML with eosinophilia.

In CMML and in the AMLs with monocytic differentiation, promonocytes are considered equivalent to blasts and are included with them for determining the blast percentage. Promonocytes are monocytic precursors that have recognizable monocyte morphology but immature chromatin

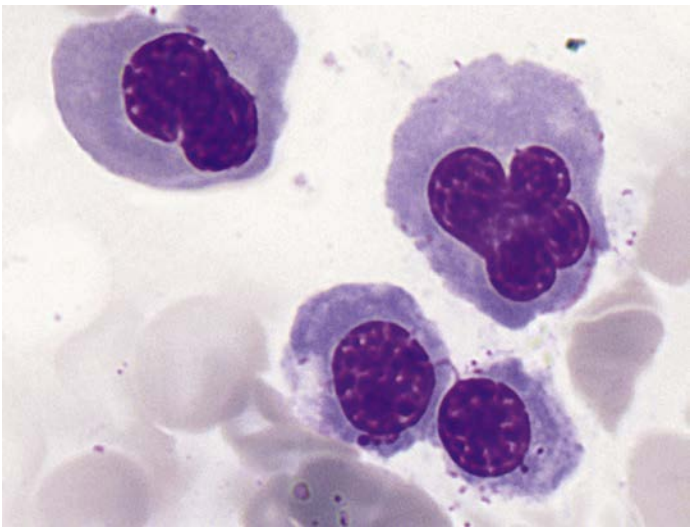

Figure 34.18 Drug-induced dyserythropoiesis, with irregular nuclear lobation in the cells above right, compared with two relatively normal normoblasts (×1000).

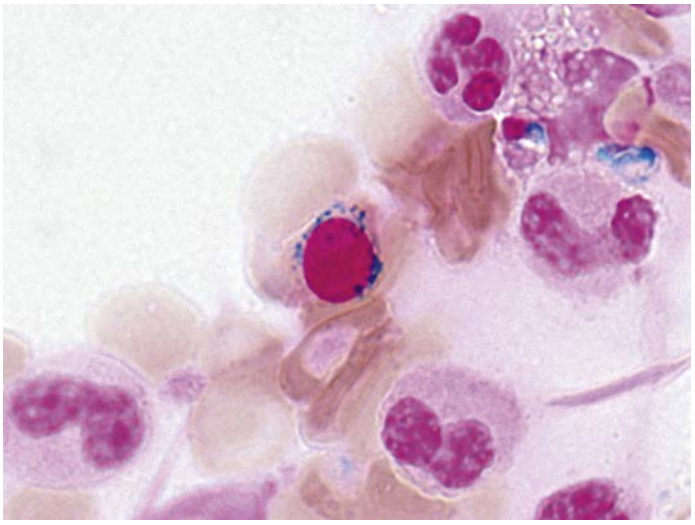

Figure 34.19 A ring sideroblast is present in the center of the field (×1000).

and finely convoluted or cerebriform nuclei (Fig. 34.24). CMML cases are divided into three subcategories: CMML-0, CMML-1, and CMML-2. Cases with <2% blasts in the blood and <5% in the marrow are referred to as *CMML-0*. The subcategory CMML-1 refers to cases with 2% to 4% blasts in the blood, with 5% to 9% in the marrow. *CMML-2* refers to cases with 5% to 19% blasts in the blood, 10% to 19% in the marrow, or with the presence of Auer rods. This indicates aggressive disease with likely impending transformation to acute leukemia.

The immunophenotype is CD13/CD33+, with variable CD14/CD68/CD64/CD4-positive. Plasmacytoid monocytes may be seen and may express CD14, CD43, CD56, CD68, and CD4, with variable CD2/CD5. Cytogenetic abnormalities in 20% to 40% of cases include +8, −7/del, and abnormalities of 12p. *ASXL1*, *TET2*, *RUNX1*, *NRA1*, *SETBP1*, and *SRSF2* comutation are associated with CMML (Cazzola et al., 2013; Itzykson et al., 2013; Itzykson et al., 2013).

CMML occurs most often in older age (median, 65–75 years) with a male predominance. Symptoms are usually those related to cytopenias (fatigue, infection, bleeding) or hypermetabolic state (fever, weight loss, night sweats). Hepatosplenomegaly may be present, particularly in patients with elevated WBCs. Lymphadenopathy may be associated with granulocytic sarcoma and evolution to acute leukemia. Median survival is 20 to 30 months, with progression to AML in 15% to 30%.

Atypical Chronic Myeloid Leukemia, *BCR-ABL1*-Negative. This disease shows myelodysplastic and myeloproliferative features, a predominant component of increased neutrophils and precursors with dysplastic features, and dysplasia of other cell lines (Swerdlow, 2017). Ph′ chromosome or *BCR-ABL1* is absent. These cases were previously considered along with CML or CMML, but they are Ph′ chromosome and *BCR-ABL1* negative and, although monocytosis is often present, it is less prominent than neutrophilia. Clinical features may include anemia, thrombocytopenia, or splenomegaly. The marrow is hypercellular, with variable features of each lineage. A variant, "syndrome of abnormal chromatin clumping," shows exaggerated chromatin condensation as well as other dysplastic features.

Cytogenetics show +8, +13, del(20q), i(17q), or del(12p) in up to 80% of cases. *SETBP1* mutation is found in 25% (Piazza et al., 2013). There is no *BCR-ABL1* fusion gene, and cases with *PDGFRA* or *PDGFRB* rearrangements are excluded. This disease usually occurs in later years, although with a wide reported age distribution down to the teen years. It has a generally poor outcome with median survival of 20 months, and a 25% to 40% transformation to acute leukemia.

Criteria for diagnosis of aCML include the following (Swerdlow, 2017):

- Leukocytosis (WBC ≥13 × 10^9/L) due to increased neutrophils and precursors with prominent dysgranulopoiesis
- Prominent dysgranulopoiesis
- No Ph′ chromosome or *BCR-ABL1* fusion gene
- No rearrangement of *PDGFRA*, *PDGFRB*, *FGFR1*, or *PCM1-JAK2*
- Neutrophil precursors (promyelocytes, myelocytes, metamyelocytes) ≥10% of WBCs
- Minimal absolute basophilia; basophils usually <2% of leukocytes
- No or minimal absolute monocytosis; monocytes <10% of WBCs

Figure 34.20 Pseudo–Pelger-Huët neutrophil (×1000).

- Hypercellular marrow with granulocytic proliferation and granulocytic dysplasia, with or without dysplasia of erythroid and megakaryocytic lineages
- Less than 20% blasts in blood or marrow

Juvenile Myelomonocytic Leukemia. JMML is a clonal disorder of predominantly granulocytic and monocytic lineages, with dysplasia in these and frequently other lineages, occurring in children or young adolescents (Swerdlow, 2017). *BCR-ABL1* is absent, and *RAS/MAPK* pathway mutations are characteristic. The occurrence is 1.3 cases per million children younger than 14 years, and most affected children are younger than 3 years of age, with a 2:1 male predominance. JMML is frequent in children with neurofibromatosis type 1.

In all, 25% of patients show monosomy 7, 35% exhibit mutations of *PTPN11* (encoding *SHP2* or *KRAS*), and 20% each have mutations in *NRAS*, *KRAS2*, and *NF1*. Some infants with Noonan syndrome and *PTPN11* mutation may have spontaneous recovery or accelerated disease. Patients with normal karyotype often have markedly increased hemoglobin F. Immune phenomena of hypergammaglobulinemia and autoantibodies are frequent.

Blood shows leukocytosis, thrombocytopenia, and, often, anemia. The WBC count is relatively high, usually 25 to 30 × 10^9/L, and mature neutrophils predominate, while monocytosis is also present. Circulating nucleated red blood cells (NRBCs) are frequent. The marrow is hyperplastic with granulocytic hyperplasia, variable erythroid cellularity, and, often, decreased megakaryocytes. Cutaneous leukemic infiltrates are common.

The prognosis is poor; death is usually due to organ failure from leukemic infiltrates, although some patients benefit from BM transplant.

Criteria for diagnosis of JMML follow (Swerdlow, 2017).

Clinical and hematologic criteria (all four criteria are required)

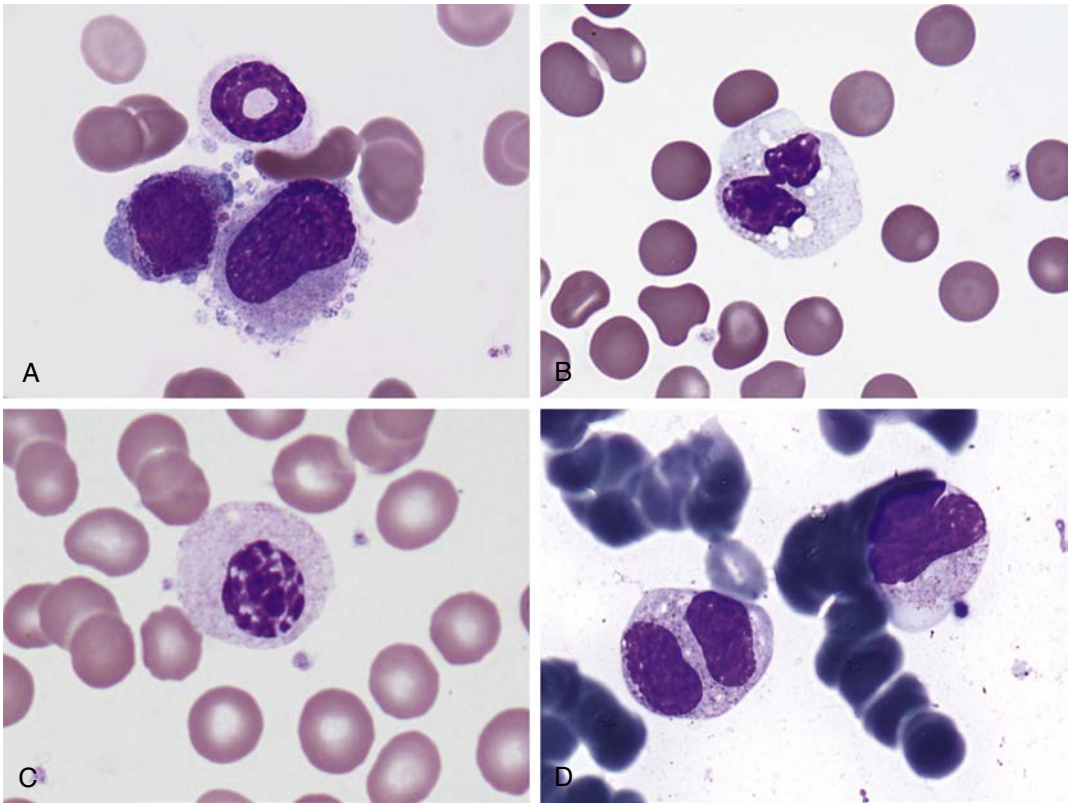

Figure 34.21 Other forms of neutrophil dysplasia. A, Ring neutrophil along with dysplastic erythroid and megakaryocytic cells in the marrow (×1000). B, Pelger-Huët neutrophil resembling a monocyte (×1000). C, Mononuclear Pelger-Huët cell (×1000). D, Large, irregularly lobulated and granulated neutrophil precursors (×1000).

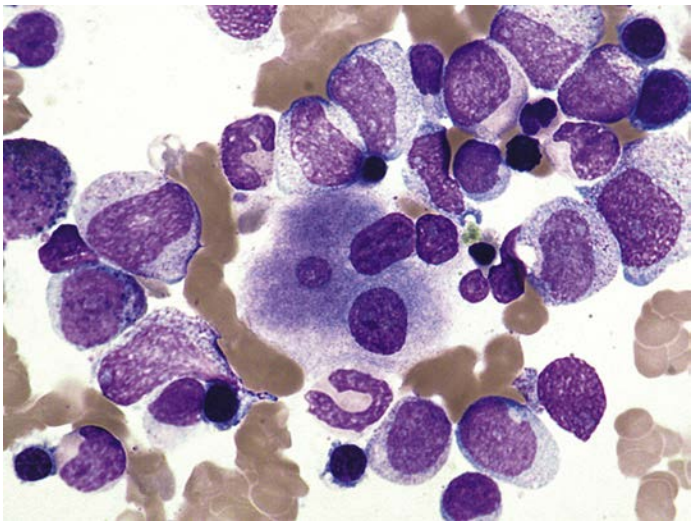

Figure 34.22 A dysplastic megakaryocyte showing unconnected nuclear lobes. Mononuclear forms are also frequent in myelodysplasia (×500).

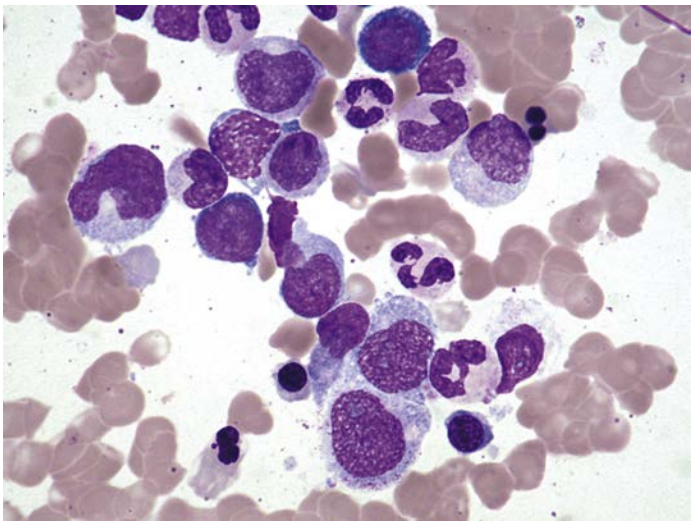

Figure 34.23 This case of chronic myelomonocytic leukemia shows moderate trilineage dysplasia and monocytosis (×500).

- Peripheral blood monocytosis >1 × 10^9/L
- Absence of Ph′ chromosome or *BCR-ABL-1*
- Blasts and promonocytes less than 20% of blood and marrow
- Splenomegaly

Plus one of the following genetic criteria:

- Somatic mutation in *KRAS*, *NRAS*, or *PTPN11*
- Clinical diagnosis of neurofibromatosis type 1 *or NF1* mutation
- Germline mutation of *CBL* and loss of heterozygosity of *CBL*

Other criteria:

Cases that do not meet any of these genetic criteria must meet the following criteria in addition to the clinical and hematologic criteria.

- Monosomy 7 or any other chromosomal abnormality

or

≥2 of the following:

- Hemoglobin F increased for age
- Immature granulocytes or erythroid precursors in the blood
- Hyperphosphorylation of STAT5
- GM-CSF hypersensitivity of myeloid progenitors in vitro

Myelodysplastic/Myeloproliferative Neoplasm, Unclassifiable

This category of the WHO classification is used for those cases with features of myelodysplastic syndrome but with the addition of prominent myeloproliferative features, including thrombocytosis ≥450 × 10^9/L with megakaryocytic hyperplasia or WBC >13 × 10^9/L, with or without splenomegaly, no previous CMPD or MDS, and absence of a chromosomal abnormality specific to another disease (no *BCR-ABL1* or rearrangement of *PDGFRA*, *PDGFRB*, or *FGFR1*; no *PCM1-JAK2*, del[5q], t[3;3][q21;q26] or inv[3][q21;q26]) (Swerdlow, 2017).

Myelodysplastic/Myeloproliferative Neoplasm with Ring Sideroblasts and Thrombocytosis

This disorder is a subtype of MDS/MPN characterized by features of myelodysplastic syndrome with ≥15 ring sideroblasts (MDS with ring sideroblasts; see later description), along with features similar to essential thrombocythemia, with peripheral thrombocytosis ≥450 × 10^6/L, and

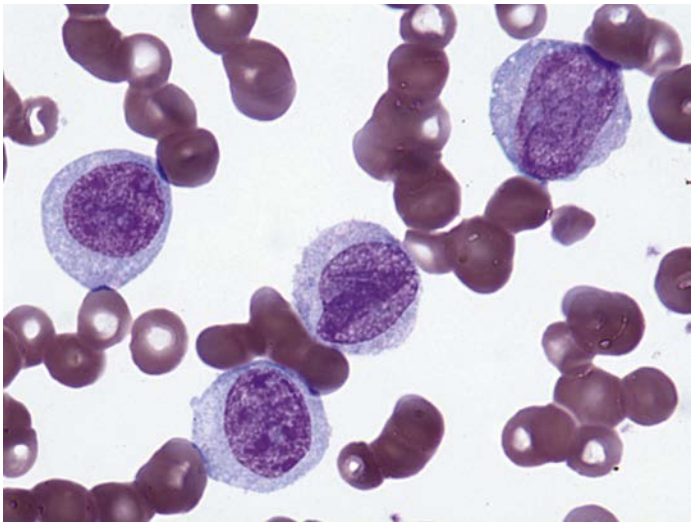

Figure 34.24 Promonocyte *(center)* shows immature chromatin and finely convoluted nuclear folds in comparison with monoblasts.

increased, large atypical BM megakaryocytes. A majority of cases (60%–90%) carry *SF3B1* mutations, which are often associated with the *JAK2* V617F mutation and less commonly with *CALR* or *MPL* W515K/L mutation. It is hypothesized that *SF3B1* mutation is the driver and that *JAK2* V617F, *CALR*, or *MLP* mutations are secondary events leading to thrombocytosis (Malcovati & Cazzola, 2013; Swerdlow, 2017).

Myelodysplastic Syndromes

Myelodysplastic syndromes are clonal hematopoietic neoplasms characterized by cytopenias due to ineffective hematopoiesis and increased apoptosis. They show morphologic dysplasia of at least one and usually more lineages and have varied cytogenetic findings (but not typically those associated with myeloproliferative neoplasms), and many have a propensity to progress to acute leukemia (Table 34.2).

Myelodysplastic Syndrome with Single Lineage Dysplasia

This category consists of neoplasms, with dysplasia affecting >10% of one myeloid cell lineage, and single-lineage cytopenia or bicytopenia, with <10% dysplasia of other lineages.

This clonal disorder can involve primarily the erythroid lineage with ineffective erythropoiesis but without increased blasts. Anemia (Hb <10 g/dL) with reticulocytopenia and abnormal erythrocytes are the presenting findings. Abnormal granulocytes are rare, and blasts are less than 1% in the blood. The marrow is normocellular to hypercellular with erythroid hyperplasia and/or dyserythropoiesis and less than 5% blasts.

Some patients can present with persistent neutropenia with absolute neutrophil count of $<1.8 \times 10^9$/L. Dysplasia usually consists of nuclear hypolobation and hypogranulation. Toxic/secondary neutropenia is excluded.

Occasionally, patients can present with persistent thrombocytopenia with platelet count of $<100 \times 10^9$/L. More than 10% of at least 30 megakaryocytes evaluated in smears and sections show dysplastic features of hypolobation, binucleation or multinucleation, and/or micro megakaryocytes. Survival is relatively good (>5 years), and progression to acute leukemia (AL) is low (6%).

Myelodysplastic Syndrome with Ring Sideroblasts

Myelodysplastic syndrome with ring sideroblasts (MDS-RS) involves two categories, including MDS-RS with single-lineage dysplasia (MDS-RS-SLD) and MDS-RS with multilineage dysplasia (MDS-RS-MLD). In MDS-RS-SLD, in addition to the findings of anemia and dyserythropoiesis, ring sideroblasts are present and constitute ≥15% of marrow erythroid precursors or ≥5% if *SF3B1* mutation has been identified. These are nucleated RBC precursors in which stainable iron particles (iron-encrusted mitochondria) form a ring of 10 or more closely associated with and encircling at least one-third of the nucleus (see Fig. 34.19). Defective cytoplasmic maturation and anisochromic erythrocytes are associated abnormalities. Survival is similar to MDS-SLD, with a lower progression to AL (≤2%). Mutation of *SF3B1* is found in more than 80% to 90% of cases, usually with mutations of additional genes including *DNMT3* and *RUNX1* (Lin et al., 2014; Swerdlow, 2017).

Myelodysplastic Syndrome with Multilineage Dysplasia

Myelodysplastic syndrome with multilineage dysplasia (MDS-MLD) is a clonal disorder with bicytopenias or pancytopenia and dysplasia of 10% or more of the precursors of two or more lineages. Blasts are not increased, with <1% in the blood and <5% in the marrow. Ring sideroblasts may be present; when ≥15% ring sideroblasts or ≥5% ring sideroblasts and SF3B1 mutation, the cases are classified as MDS with ring sideroblasts and multilineage dysplasia.

This disease usually occurs in older individuals (median age, ≈70 years). In contrast to MDS-SLD and MDS-RS-SLD, which infrequently show cytogenetic abnormalities (<10%), MDS-MLD and MDS-RS-MLD show them in up to 50%. These include trisomy 8, monosomy 7, del(7q), monosomy 5, del(5q), del(20q), and complex karyotypes. Survival is approximately 36 months, and AL conversion is 15% at 2 years and 28% at 5 years (Swerdlow, 2017).

Myelodysplastic Syndrome with Excess Blasts

Myelodysplastic syndrome with excess blasts (MDS-EB) includes two subcategories: MDS-EB1 and MDS-EB2. In MDS-EB1, the blood shows cytopenia in two or three of the cell lines and less than 5% circulating blasts. The marrow is hypercellular, with variable erythroid or granulocytic hyperplasia. Dyspoietic changes are present in all three cell lines, and 5% to 9% of marrow cells are blasts. Less than 5% blasts are present in the blood, and no Auer rods are found. Clusters of 5 to 8 blasts and promyelocytes in the marrow interstitium are frequently seen on sections and have been referred to as *abnormal localization of immature precursors* (*ALIP*). Hypocellular marrow is seen in a minority of cases (10%–15%). These may be difficult to interpret, as the patients are often older, with decreased cellularity to begin with, and because marrow stress in hypoplastic anemia often causes some dysplasia. A diagnosis of MDS should be made cautiously when the marrow is hypoplastic.

Cases of MDS-EB with concurrent myelofibrosis are referred to as *MDS-EB with fibrosis* (*MDS-EB-F*). Megakaryocytes are increased and dysplastic, and reticulin fibrosis is significant, often resulting in a dry tap.

MDS-EB2 has findings similar to MDS-EB1, but with any of the following: (1) greater than 5% blasts in the blood, (2) 10% to 19% blasts in the marrow, or (3) the presence of Auer rods. Cytogenetic abnormalities include +8, −5, del(5q), −7, del(7q), and del(20q). Survival is usually less than 2 years in MDS-EB1 or -EB2, with progressive marrow failure and cytopenias or progression to AL in 25% for MDS-EB1 and in 33% for MDS-EB2.Cases with 5% to 19% blasts in blood or bone marrow and ≥50% erythroid precursors in bone marrow are referred to as *MDS-EB and erythroid predominance*. The previously classified erythroleukemia (with ≥50% erythroid precursors and ≥20% myeloblasts of nonerythroid nucleated marrow cells) are now categorized based on blasts as percentage of all marrow cells irrespective of the percentage of the marrow erythroid precursors.

Myelodysplastic Syndrome with Isolated del(5q)

This disorder is characterized by anemia and/or thrombocytosis with increased megakaryocytes and isolated deletion of chromosome region 5q. Some cases may exhibit one additional cytogenetic abnormality other than monosomy 7 or del(7q). A subset of cases have *JAK2* V617F mutation. Blasts are <5% in the marrow and <1% in blood; lymphoid aggregates are often present. Megakaryocytes are usually small and hypolobulated. Anemia may be severe and macrocytic, and an otherwise normocellular to hypercellular marrow may have erythroid hypoplasia. Outcome is relatively favorable.

Myelodysplastic Syndrome, Unclassified

The myelodysplastic syndrome, unclassified category is used when clinical and hematologic findings of myelodysplasia exist, but without specific features to allow placement in one of the other categories. Patients usually have neutropenia or thrombocytopenia with a hypercellular BM and dysplasia of granulocytic or megakaryocytic lineage. Less than 5% blasts are found in the BM, and they are not increased in the blood.

Childhood Myelodysplastic Syndrome; Refractory Cytopenia of Childhood

In the WHO classification, it is recognized that MDS, although rare in children, does occur but tends to show different features than in adults. Refractory cytopenia of childhood (RCC) is defined as MDS with persistent cytopenia with <5% blasts in the BM and <2% in the blood, and dysplasia. The marrow is also frequently hypocellular. Pancytopenia is frequent, with macrocytic anemia showing anisopoikilocytosis. The cytogenetic

abnormality of monosomy 7 is the most common genetic abnormality and is associated with progressive disease. Cases with trisomy 8 may show a long stable period. This disorder may be morphologically indistinguishable from results of infection, vitamin deficiency (B_{12}, folate, vitamin E), metabolic or autoimmune disease, paroxysmal nocturnal hemoglobinuria (PNH), or acquired aplastic anemia.

ACUTE MYELOID LEUKEMIA

AML is the most common form of acute leukemia during the first few months of life, but during childhood and adolescence it accounts for approximately one-third of AL. In the middle and later years of life, it becomes the most frequent AL, with a median age of 60 years, and an occurrence of 10/100,000 per year in those older than 60 years. Viruses, radiation, cytotoxic chemotherapy, benzene, and smoking have been linked to increased incidence, but most cases are not known to be associated with such factors.

The onset often resembles acute infection and includes signs of granulocytic insufficiency, with ulcerations of mucous membranes (especially of the mouth and throat) and fever. Enlargement of lymph nodes, spleen, and liver is not pronounced. Marked prostration and general malaise may be present. In untreated cases, the course is rapidly progressive.

AML classification currently utilizes a multilayered approach that recognizes recurrent acquired cytogenetic abnormalities associated with specific types, history of predisposing factors (prior cytotoxic therapy), association with MDS or related abnormalities, and morphologic stratification for those for which none of these can be appreciated. This approach requires, or at least encourages, attempts to define the morphology, cytogenetics, and immunophenotype of each case. With advances in molecular cytogenetics and FISH, and with widespread adoption of these and other methods, it is likely that most cases will eventually be categorized by their genetic abnormalities. See Box 34.11 and Tables 34.3 and 34.4.

The French-American-British Cooperative Group (FAB) published proposals in 1976 for the classification of acute leukemias (Bennett, 1976) based on morphology of cells in Romanowsky's-stained blood and marrow films and certain supplemental cytochemical reactions or serum lysozyme levels. These criteria have been superseded by the current WHO classification (Swerdlow, 2017), but basic morphologic tenets remain, and FAB criteria serve as the basis for subtyping AML, not otherwise specified.

The diagnosis of AML requires the presence of 20% blasts in the marrow or blood. Myeloblasts generally have central nuclei with fine, uncondensed chromatin and often prominent nucleoli (usually three to five) but have variable cytoplasm and may have some cytoplasmic granules. Primitive myeloblasts are identified by monoclonal antibodies against myeloid-associated antigens (MPO, CD13, CD33, CD117). More mature myeloblasts can also be identified by cytochemical reactions with granulocyte-associated enzymes using MPO, Sudan black B (SBB), and chloroacetate esterase (CAE) assays, although flow cytometric assays are utilized more often in current practice. Monoblasts are frequently large with abundant cytoplasm, diffuse chromatin, and often prominent nucleoli. Monoblasts are characterized by strong reaction with α-napthyl acetate esterase (ANA), which is inhibited in monocytes by sodium fluoride, or with α-napthyl butyrate esterase (ANB), or antibodies including antilysozyme, CD68, CD64, and CD36. For cases with monocytic differentiation, promonocytes are considered equivalent to blasts (see Fig. 34.24). Promonocytes are immature recognizable monocytes with some chromatin condensation but with fine nuclear convolutions. Abnormal promyelocytes are also considered blast equivalents for the diagnosis of acute promyelocytic leukemia. Megakaryoblasts are identified by antibodies against platelet-associated antigens or electron microscopy for platelet peroxidase.

Initial assessment for suspected AML is based on a differential WBC count of the blood and a 500-cell count of the marrow aspirate. Acute leukemia is diagnosed when blasts exceed 20% of the marrow or blood. MDS is suggested when less than 20% of the nucleated marrow cells are myeloblasts.

A helpful finding in the diagnosis of AML is the presence of Auer rods, eosinophilic rod–like cytoplasmic inclusions derived from myeloperoxidase-positive primary granules. Phi bodies, which appear as strings of eosinophilic bead-like granules, are derived from catalase-positive microperoxisomes and are seen in larger numbers in AML and also in MDS. However, they generally are not given the same diagnostic import as Auer rods. With Romanowsky's stains, Auer rods are linear or spindle-shaped, red-purple inclusions in myeloblasts or promyelocytes (Fig. 34.25). Less commonly, they may be seen in more mature neutrophils, as in AML with t(8;21). Auer rods, derivatives of azurophilic granules, stain positively for SBB, MPO, CAE, and acid phosphatase. Auer rods can be found in any of the subtypes of AML, but they are especially associated with those with granulocytic differentiation.

The main categories of AML in the WHO classification are (1) AML with recurrent cytogenetic abnormalities; (2) AML with myelodysplasia-related changes; (3) AML, therapy related; and (4) AML, not otherwise specified (subclassified by morphology and immunophenotype). Many biological factors vary the risk of adverse outcome, but few are definitive (Liersch, 2014).

Acute Leukemia with Recurrent Genetic Abnormalities (Swerdlow, 2017)

AML with Balanced Translocations/Inversions

AML with t(8;21)(q22;q22.1), *RUNX1-RUNX1T1*. The morphology usually corresponds to AML with neutrophilic maturation, and these represent 5% to 12% of AML, with predominance in young patients. Blasts are 20% or greater in the marrow (or blood), and maturing neutrophilic precursors constitute more than 10% of marrow nucleated cells (not including NRBCs, lymphocytes, and plasma cells). Morphologic findings are characteristic but variable: large blasts with abundant basophilic cytoplasm; maturing neutrophil precursors with peripheral cytoplasmic basophilia; frequent Auer rods, often long, sharp, and tapered, and sometimes present in myelocytes and mature forms up to segmented neutrophils; abnormal granulation, including giant Chédiak-Higashi–like or secondary granules or homogenous waxy-appearing secondary granulation; and

TABLE 34.2
Key Features of the Major Myelodysplastic Syndromes (MDS)

Disorder	Demographics	Laboratory Features, Morphology	Cytogenetics	Risk Group
MDS with single-lineage dysplasia, anemia, thrombocytopenia, or neutropenia	Median age, 65–70 years	Peripheral blood (PB) with unicytopenia or bicytopenia, blasts <1%; bone marrow (BM) with >10% unilineage dysplasia and <5% blasts	Del (20q), +8, abnormalities of chromosome 5 or 7	Low
MDS with ringed sideroblasts	Median age, 60–73 years	Similar to RA with >15% ringed sideroblasts (or ≥5 ring sideroblasts and SF3B1 mutation) in BM	Rare abnormalities of single chromosome	Low
MDS with multilineage dysplasia	Median age, 70 years	PB with cytopenias of ≥2 cell lines, <1% blasts, <1 × 10^9/L monocytes; BM with dysplasia of ≥10% of precursors of ≥2 cell lines, <5% blasts	+8, –5, –7, del(7q), del(20q), complex in up to 50%	Intermediate
MDS with excess blasts (MDS-EB)	Over age 50 years	MDS-EB1: PB with <5% blasts, <1 × 10^9/L monocytes; BM with hypercellularity, dyspoiesis, 5%–9% blasts without Auer rods; MDS-EB2: PB with 5%–9% blasts, or 10%–19% BM blasts, or Auer rods	+8, –5, del(5q), –7, del(7q), del(20q)	MDS-EB1, intermediate; MDS-EB2, high
5q– syndrome	Middle-aged to older females	PB with thrombocytosis, <5% blasts; BM with increased, hypolobulated megakaryocytes, <5% blasts	5q– with or without one additional cytogenetic abnormality other than monosomy 7 or del(7q)	Low

nuclear dysplasia with bilobed nuclei that may be widely separated (Fig. 34.26). Monocytosis is not prominent, and monocytes are less than 20% of the marrow. Eosinophilia is common, and basophils or mast cells may be increased. The immunophenotype is distinctive with high-intensity CD34 along with myeloid markers MPO and CD13, but relatively weak CD33 and sometimes CD56. One or more B-cell markers—CD19, PAX5, and cytoplasmic CD79a—are often coexpressed.

The presence of t(8;21) is diagnostic of AML, even when blasts appear to be less than 20%. This disease is referred to as a *core binding factor leukemia* because *RUNX1*, also known as AML1 or *core binding factor α* (*CBFA*), encodes a transcription factor required for hematopoieses. The outcome of AML with t(8;21) is generally more favorable than AML without recurrent genetic abnormalities or with MDS-associated abnormalities. Additional genetic abnormalities also occur, including *KIT* mutations associated with less favorable outcome and mutations of *ASXL1/2* (Micol et al., 2014; Wichmann et al., 2014).

AML with inv(16)(p13.1q22) or t(16;16)(p13.1;q22), *CBFβ-MYH11*. These correspond to acute myelomonocytic leukemia with abnormal eosinophils. Occurrence and outcome are similar to AML with t(8;21). These cases show >20% blasts (or occasionally lower) in marrow and/or blood with differentiation to monocytic and neutrophilic lineages (≥20% each). The presence of inv(16)(p13.1q22) or t(16;16)(p13.1;q22) is diagnostic of AML irrespective of blast count. Eosinophils are characteristically increased (Fig. 34.27), including those with large basophilic granules (as in eosinophil promyelocytes), and cytoplasmic positivity is often weak for chloroacetate esterase. This type is associated with the chromosomal abnormality inv(16)(p13.1q22) or its variant t(16;16)(p13.1;q22) with fusion of the *CBFB* gene on 16q and *MYH11* on 16p and variable resultant chimeric messenger RNA (mRNAs; due to differing breakpoints) and a *BCGB-MYH11* fusion protein. This additional core binding factor leukemia generally has relatively favorable outcomes compared with other AMLs. In addition to karyotyping, RT-PCR or FISH is useful for timely diagnosis. Secondary genetic abnormalities are common, including trisomy 22, trisomy 8, *KIT*, *FLT3*, *WT1*, and *RAS* mutations (Krauth et al., 2014; Paschka et al., 2013).

The immunophenotype typically shows both granulocytic (CD13, CD15, CD33, CD65, MPO) and monocytic (CD4, CD14, CD64, CD36, CD11b, CD11c, and lysozyme) markers, sometimes with CD2 coexpression.

Acute Promyelocytic Leukemia with t(15;17)(q22;q11-12), *PML-RARA*, and Variants. Promyelocytes instead of myeloblasts predominate in the marrow in hypergranular promyelocytic leukemia (PML) (M3) (McKenna, 1982) (Fig. 34.28). Azurophilic granules are abundant and intensely stained. Auer rods are found in most cases and frequently are multiple (10 or more) in a given cell (see Fig. 34.28). Hemorrhagic complications are frequent as the result of disseminated intravascular coagulation (DIC), apparently initiated by procoagulant material from leukemic cell granules.

The characteristic chromosomal abnormality t(15;17)(q22;q21) shows fusion of the retinoid acid receptor gene-α (*RARA*) on chromosome 17 with the *PML* gene on chromosome 15. The *RARA-PML* fusion gene is transcribed as a chimeric mRNA. Leukemia usually responds to therapy with all-*trans* retinoic acid (ATRA), which is usually given in addition to chemotherapy, and the prognosis is relatively favorable (Huang et al., 1988). The molecular genetic abnormality may be detected in the laboratory by cytogenetics, RT-PCR, or FISH. Achievement of remission often occurs as a slow "maturation" process, rather than therapy-induced aplasia followed by remission as seen in treatment of other acute leukemias.

Variant translocations include t(11;17)(q23.2;q21.2), t(5;17)(q35.1q21.2), and t(11;17)(q23.2;q21.2). Some variants, such as t(11;17)(q23.2;q21.2), do not respond to ATRA. *FLT3* mutations are frequent and are associated with decreased survival, and *WT1* mutations occur in about 6% (Krauth et al., 2014).

Hypogranular or microgranular variants of M3 (M3V) occur in which cytoplasmic granules appear sparse by light microscopy and numerous but smaller by electron microscopy (Bennett, 1980; Golomb, 1980). Nuclei of most leukemic cells are bilobed or reniform; confusion with an atypical monocytic leukemia is frequent. Cytochemical staining reactions are somewhat less positive than in the hypergranular M3. Auer rods, single or

BOX 34.11

Clinical and Laboratory Features of Acute Myeloid Leukemia

- Affects all ages, but increases with older age (>60 years)
- May resemble acute infection at presentation
- Usually requires 20% blasts in blood or marrow for diagnosis
- Key myeloid antigens: myeloperoxidase, CD13, CD33, CD117, and CD14/CD64
- Recurrent cytogenetic abnormalities that characterize defined subtypes
- Classification made by morphology, cytogenetics, flow cytometry, cytochemistry

TABLE 34.3

Key Features of the Major Acute Myeloid Leukemias

Category	Cell Morphology	Cell Surface Markers	Cytogenetics	Prognosis
AML with t(8;21)	≥20% blasts (rare cases with <20% occur), ≥10% maturing granulocytes, Auer rods, dysplasia, abnormal granules	CD13, CD33, CD117, CD19, CD34	t(8;21)(q22;q22.1) *RUNX1-RUNX1T1*	More favorable
AML with inv(16)	Blasts with both monocytic and neutrophilic differentiation, increased eosinophils/immature eosinophils	CD13, CD33, CD14, CD4, 64	inv(16)(p13;q22) or t(16;16)(p13.1;q22)	More favorable
APL with t(15;17)	Promyelocytes with azurophilic granules, Auer rods	CD13, CD33 CD2, ± CD117	t(15;17)(q22;q11-12) *PML-RARα;* Variants all involve 17q21.2	More favorable if responsive to ATRA
AML with t(9;11)	Monoblasts and promonocytes predominate	CD33, CD65, CD4, HLA-DR	t(9;11)(p21.3;q23.3) *KMT2A-MLLT3*	Intermediate
AML, therapy related	Multilineage dysplasia, RS, increased basophils	CD13, CD33, CD34, ± CD56, CD57	11q23 abnormality seen with topoisomerase II inhibitor–associated AML	Less favorable
AML with t(6;9)	Any morphology may be seen but myelomonocytic is most common	CD13, CD33, CD38, HLA-DR, CD117	*DEK-NUP214;* t(6;9)(p23;q34.1)	Less favorable
AML with inv(3) or t(3;3)	Any morphology may be seen except APL	CD13, CD33, HLA-DR, CD34, CD38	Inv(3)(q21.3;q26.2) or t(3;3)(q21.3;q26.2) *GATA2, MECOM*	Less favorable
AML with t(1;22)	Megakaryoblastic morphology with small and large megakaryocytes	CD41, CD61, ± CD13, CD33	t(1;22)(p13.3;q13.1) *RBM15-MKL1*	Less favorable
AML with *NPM1* mutation	Myelomonocytic and monocytic features	CD13, CD33, CD34 is negative	*NPM1* mutation, cytoplasmic expression	More favorable in absence of *FLT3*
AML with *CEBPA* mutation	Variable, generally similar to less differentiated AMLs in FAB scheme (M1, 2)		CD13, CD33, CD65, CD11b, CD15	More favorable

AML, Acute myeloid leukemia; *APL,* acute promyelocytic leukemia; *ATRA,* all-*trans* retinoic acid; *PML*, promyelocytic leukemia*; RARα,* retinoid acid receptor gene-α.

TABLE 34.4

Key Features of the Acute Myeloid Leukemias, Not Otherwise Specified

Category	Cell morphology	Cell surface markers
All categories	≥20% blasts in BM and/or blood	Myeloid differentiation, any lineage
AML, minimally differentiated	Myeloblasts, <3% positive for SBB, MPO, or ANA	CD13, CD33, CD117
AML without maturation	Myeloblasts ≥90% of nonerythroids in BM, ≥3% positive for MPO	CD13, CD33, CD117
AML with maturation	Same as for AML with t(8;21)	CD13, CD33, CD117
Acute myelomonocytic leukemia	Monocytic and granulocytic cells, each 20%–80%	Variable CD13, CD33, CD14, CD4, CD11b, CD11c, CD64, CD36, CD68
Acute monoblastic/monocytic	≥80% of nonerythroids monoblasts (M5a) or differentiating monos (M5b)	CD13, CD33, CD117, CD14, CD4, CD11b, CD11c, CD64, CD68, CD36
Pure erythroleukemia	≥80% erythroid precursors with ≥30% proerythroblasts and rare myeloid blasts	Glycophorin A in erythroids; CD13, CD33, CD117 in myeloblasts
Acute megakaryoblastic leukemia	Blasts with cytoplasmic blebs, often clusters; PB may show megakaryocytic fragments; MPO negative	CD41, CD61, CD36, often CD13, CD33

AML, Acute myeloid leukemia; *ANA,* antinuclear antibody; *BM,* bone marrow; *MPO,* myeloperoxidase; *PB,* peripheral blood; *SBB,* Sudan black B.

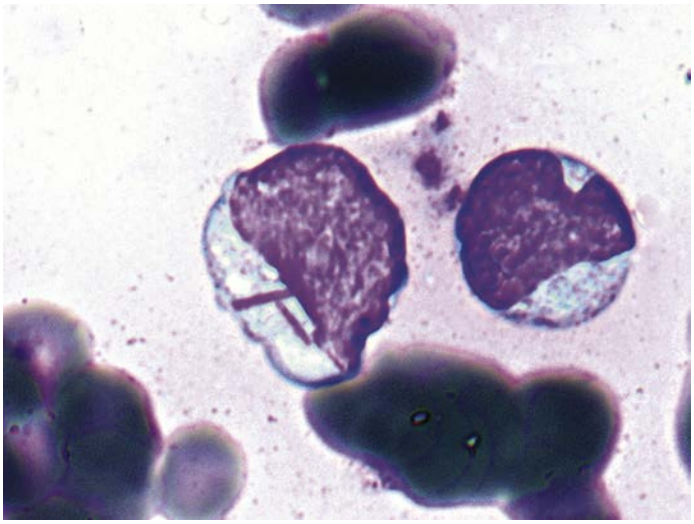

Figure 34.25 Auer rods vary from prominent, as in this cell, to thin and delicate.

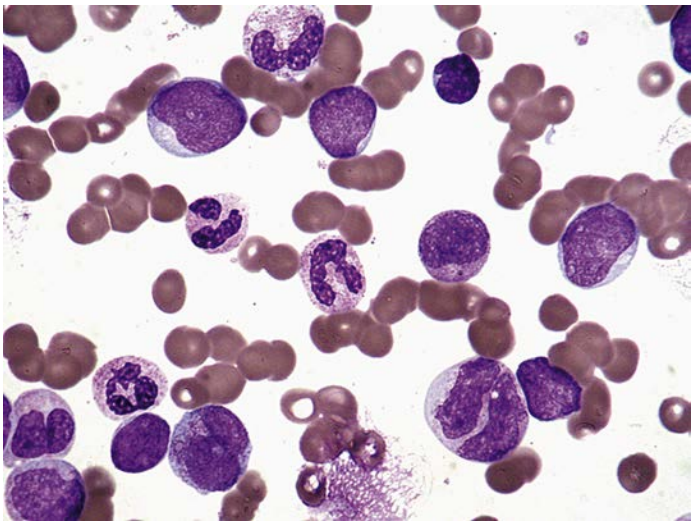

Figure 34.26 This case of acute myelogenous leukemia with t(8;21) shows granulocyte maturation with abnormal granulation and bilobed precursors (×500).

multiple, and typical hypergranular promyelocytes are found in variable numbers, and there appears to be a spectrum between typical and hypogranular types. The WBC count may be high.

In acute promyelocytic leukemia, a majority of leukemic cells stain for MPO, SBB, and CAE, along with ANA in 25%. The immunophenotype is typically bright CD33; heterogeneous CD13, CD64, and CD117; and dim to absent HLA-DR, CD34, CD11a, CD11b, CD15, CD18, and CD64.

AML with t(9;11)(p21.3;q23.3); *KMT2A-MLLT3*. The 11q23.3 abnormalities are present in a more diverse group of leukemias than other recurrent genetic abnormalities. Chromosome band 11q23.3 abnormalities, which involve the *KMT2A* gene (previously called *MLL*), are not specific for AML but are also found in ALL, mixed lineage leukemias, and occasionally in lymphomas. The most common *KMT2A* translocation in AML involving *MLLT3* is t(9;11)(p21.3;q23.3). Others include t(6;11)(q27;q23.3), t(10;11)(p12;q23.3), t(11;17)(q23.3;q21.2), and t(11;19)(q23.3;p13.1). Most cases of t(9;11) show monocytic differentiation (monoblastic or myelomonocytic) (Fig. 34.29). In general, the prognosis of AML with 11q23.3 abnormalities is less favorable than that of other AML with standard chemotherapy, but cases with t(9;11)(p21.3;q23.3) may have intermediate prognosis (Chen et al., 2013).

AML with t(6;9)(p23;q34.1); *DEK-NUP214*. This disease shows variable morphology and granulocytic and/or monocytic differentiation but is usually associated with multilineage dysplasia and basophilia of marrow and blood (≥2%). Immunophenotype includes usual MPO, CD13, CD33, CD38, and HLA-DR, with variably positive CD117, CD34, CD64, and TdT, but not lymphoid lineage-associated antigens. A *DEK-NUP214* fusion protein acts as an abnormal transcription and nuclear transport factor. *FLT3-ITD* mutations are present in most cases. Prognosis is generally poor (Gupta et al., 2010; Tarlock et al., 2014).

AML with inv(3)(q21.3q26.2) or t(3;3)(q21.3;q26.2); *GATA2, MECOM*. This disease shows multilineage dysplasia, increased atypical megakaryocytes with monolobed or bilobed nuclei, and normal to increased platelet counts. Pseudo–Pelger-Huët cells are common, and differentiation may be granulocytic and/or monocytic. Marrow eosinophils, basophils, and/or mast cells are often increased. The inv(3) or t(3;3) usually activates *MECOM* expression by repositioning a distal *GATA2* enhancer. Monosomy 7 is a frequent secondary event, and t(3;3) variants show increased *N-RAS* mutations. This is an aggressive disease with short survival and adverse prognosis is enhanced by monosomy 7 (Lugthart et al., 2010).

AML (Megakaryoblastic) with t(1;22)(p13.3;q13.1); *RBM15-MKL1*. This is an acute leukemia of infants and young children, more often reported in girls, presenting as acute megakaryoblastic leukemia with hepatosplenomegaly. This form is not associated with Down syndrome. Blasts are usually medium-sized to large with fine reticular chromatin, one to three nucleoli, and basophilic cytoplasm with blebs or pseudopods. Cytochemistry/immunophenotype shows absence of MPO and SBB and expression of platelet markers CD41 and CD61 (best demonstrated by cytoplasmic labeling techniques), CD36, and variable CD13, CD33, and CD34. Micro megakaryocytes are often found, and biopsy sections show reticulin fibrosis. Patients may respond well to chemotherapy.

AML with *BCR-ABL1*. AML with *BCR-ABL1* is a provisional entity in the current WHO classification of myeloid neoplasm and acute leukemia. This disease is a de novo AML in patients with no evidence of an underlying CML and without recurrent genetic abnormalities. It is a rare neoplasm, accounting for <1% of all AMLs. It occurs in adults, with possibly higher incidence in males than in females. The disease appears to have a poor prognosis and is often refractory to chemotherapy. Some data

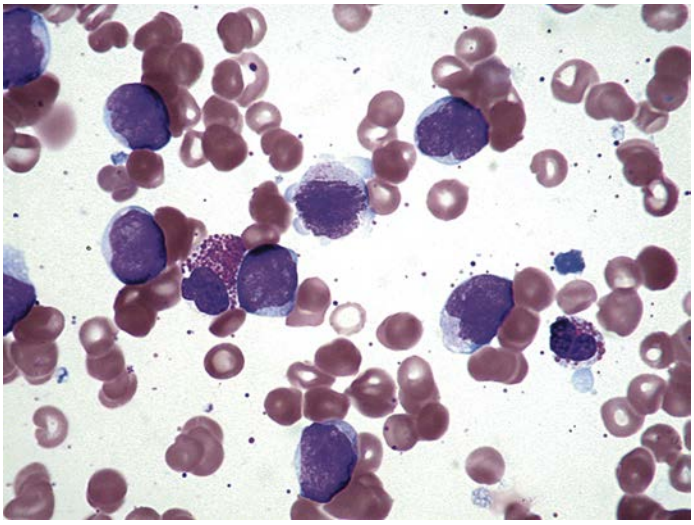

Figure 34.27 Acute myelogenous leukemia with inv16 shows myelomonocytic differentiation with eosinophilia. (Two eosinophils are present in this view.)

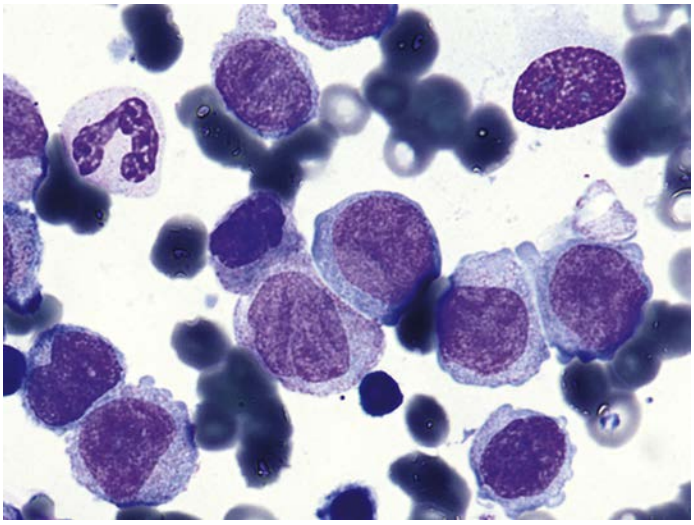

Figure 34.29 Acute myelogenous leukemia with monocytic differentiation and 11q23 abnormality (×1000).

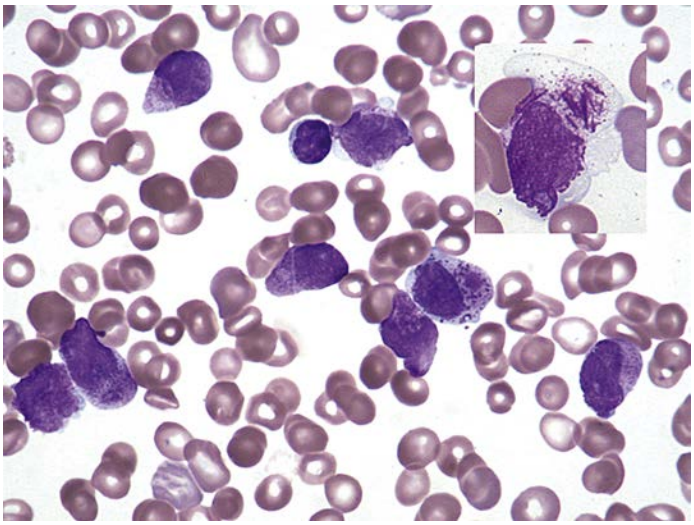

Figure 34.28 Acute promyelocytic leukemia with t(15;17) shows predominantly abnormal promyelocytes (×500). *Inset (top right):* Abnormal promyelocytes with bundles of Auer rods are known as faggot cells from their resemblance to bundles of firewood, or faggots (×1000).

suggest that treatment with TKIs followed by allogenic stem cell transplantation may improve patient survival (Swerdlow, 2017).

AML with Gene Mutations

Although many cases of AML have been associated with recurring translocations or inversions, many have shown normal karyotype. Most if not all of these carry genetic mutations not detectable by Giemsa banding morphology; mutations are also found in cases with karyotypic abnormalities. Several carry prognostic implications. As these continue to be investigated, new specific categories of AML are certain to be described. Biological and clinical associations are available for some common AML-associated mutations.

AML with *NPM1* Mutation. *NPM1*, encoding the nuclear shuttle protein nucleophosmin, is a primary driver mutation in AML. It is found in half of cases with normal karyotype and is associated with a favorable prognosis. This favorable association is especially noted in cases with normal karyotype and without *FLT3* mutation. *NPM1* mutation may be detected by immunohistochemical assay of sections, in which the affected cells show abnormal cytoplasmic localization of NPM protein, or it may be detected by PCR assays. Most cases have monocytic or myelomonocytic differentiation, but cases with multilineage dysplasia, erythroid differentiation, and other patterns are also found (Falini et al., 2011).

AML with Biallelic *CEBPA* Mutation. *CEBPA* encodes the CCAAT/enhancer binding protein-α, another hematopoietic proliferation- and differentiation-inducing transcription factor. Similar to *NPM1* mutation, it is associated with improved prognosis in AML with normal karyotype and without *FLT3* mutation. It is found in less than 20% of cases of AML. The morphology is most often AML without differentiation or AML with differentiation, although monocytic differentiation may also occur. Immunophenotype includes usually CD34, frequently CD7, with myeloid markers HLA-DR, CD11b, CD13, CD15, CD33, and CD65.

AML with *RUNX1* Mutation. AML with *RUNX1* mutation is a provisional entity in the current WHO classification. It is a de novo leukemia that occurs primarily in older adults. Cases meeting the diagnostic criteria for AML with recurrent genetic abnormalities, AML with myelodysplasia-related changes, and therapy-related myeloid neoplasms are excluded from this category. In general, *RUNX1* mutation in AML is reported to be associated with a poor prognosis. It has been reported that treating patients with allogenic stem cell transplantation may improve outcome (Swerdlow, 2017).

KIT **mutations** are also seen in cases of AML as well as in GI stromal tumors and mast cell disease. In core binding factor leukemias, *KIT* mutation has shown adverse but variable prognostic effect (Foran, 2010).

Acute Myeloid Leukemia with Myelodysplasia-Related Changes (Swerdlow, 2017)

These leukemias show morphologic features of myelodysplasia or history of prior MDS or MDS/MPN, or they have MDS-related cytogenetic abnormalities. Patients with a history of cytotoxic chemotherapy or radiation for another malignancy are not included. These cases are characterized by 20% or more blasts in blood and/or marrow as well as dysplasia in ≥50% of cells of at least two lineages. Dysplastic features are similar to those of MDS of various types (Fig. 34.30).

Cytogenetic abnormalities qualifying for this disorder include 7/del(7q), del(5q)/t, i(17q)/t(17p), −13/del(13q), del(11q), del(12p)/t(12p), idic(X)(q13), t(11;16)(q23.3;p13.3), t(3;21)(q26.2;q22.1), t(1;3(p36.3;q21.2), t(2;11)(p21;q23.3), t(5;12)(q32;p13.2), t(5;7)(q32;q11.2), t(5;17)(q32;p13.2), t(5;10)(q32;q21), and t(3;5)(q25.3;q35.1). The immunophenotype often includes primitive blasts with myeloid phenotype and CD34 expression, CD56, and/or CD7. The prognosis is generally poor.

Therapy-Related Myeloid Neoplasms

These disorders are related to prior radiation or cytotoxic chemotherapy utilizing alkylating agents or topoisomerase inhibitors. They include cases of AML, MDS, and MDS/MPN. Most patients have been treated for prior malignancies, but some have been treated for nonneoplastic conditions.

Most commonly, disease is related to mutagenic effects of alkylating agents (including chlorambucil, cyclophosphamide, thiotepa, and busulfan) or radiation. These effects usually occur 5 to 10 years postexposure and most often present as MDS. Cytogenetic features are similar to those of MDS and AML with multilineage dysplasia. Loss of portions of chromosome 5 or 7 is common. Response to therapy and outcomes is poor.

Cases secondary to prior chemotherapy with topoisomerase II inhibitors (including epipodophyllotoxins etoposide and teniposide, and doxorubicin) occur after a shorter latency period of 1 to 5 years and most often are associated with overt AML with balanced chromosomal translocations involving 11q23 *KMT2A*, previously called *MLL*) or 21q22.1 (*RUNX1*).

These most often show AML with maturation, monocytic or myelomonocytic morphology.

Acute Myeloid Leukemia, Not Otherwise Specified

These cases do not fulfill criteria for the previous categories or cytogenetic studies were unsuccessful or could not be performed. Categorization is similar to French-American-British Cooperative Group criteria (Bennett, 1976, 1985; Swerdlow, 2017).

Genomic Variation in AML With Normal Karyotype

AML with normal karyotype, considered intermediate risk—or AML, NOS in the WHO classification—represents up to 50% of AML cases. While genomic studies have tended to support prior discoveries and clinical correlates associated with genetic subtypes in AML, additional mutations have been identified that may narrow this group and provide targets for new therapies (Abdel-Wahab & Levine, 2013; Cagnetta et al., 2014; Cancer Genome Atlas Research Network, 2013). These include recurrent mutations in *TET2*, *DNMT3A*, *IDH1/2*, and *ASXL1*, involved in epigenetic regulation, and others, including *WT1*. Incorporation of genomic and epigenetic analyses into clinical settings is ongoing.

Acute Myeloblastic Leukemia, Minimally Differentiated

In acute myeloblastic leukemia, minimally differentiated, myeloblasts display less than 3% positivity with SBB, MPO, or ANA (Bennett, 1991). When examined for myeloid and lymphoid markers using flow cytometry or immunocytochemistry, however, at least 20% of the blasts exhibit myeloid-associated antigens (CD13, CD33, CD117, and/or MPO). Stem cell antigens CD34, CD38, HLA-DR, and TdT are often expressed, while lineage-specific lymphoid markers cCD3, cCD20, and cCD79a are absent. Some primitive markers often associated with lymphoid lineage, including CD2, CD7, and CD19, are not lineage specific and are sometimes expressed (Fig. 34.31).

Acute Myeloblastic Leukemia without Maturation

In this category, myeloblasts represent at least 90% of nonerythroid cells in the BM (Bennett, 1985a, 1985b) and at least 3% of blasts labeled with MPO or SBB. Positive staining for CAE is sometimes also present but is less sensitive. CD13, CD33, CD117, and/or MPO antigens are usually detectable, as are other less specific markers. CD3, CD20, and CD79a are usually absent (Fig. 34.32).

Acute Myeloblastic Leukemia with Maturation

Myeloblasts represent 20% (per WHO) to 89% of total marrow cells, granulocytes from promyelocytes to neutrophils are greater than 10% of nonerythroid cells, and monocytes and their precursor cells are less than 20% (Fig. 34.33). Most blasts stain with MPO, SBB, and CAE.

Cases with t(8;21) (q22;q22.1) are categorized as AML with recurrent cytogenetic abnormality t(8;21).

Acute Myelomonocytic Leukemia

In acute myelomonocytic leukemia, myeloblasts constitute more than 20% of total marrow cells. The sum of the monoblasts, promonocytes, and monocytes is greater than 20% but is less than 80% of nonerythroid cells. Cells of the granulocytic series (myeloblasts, promyelocytes, myelocytes, and other more mature forms) also represent 20% to 80% of nonerythroid cells (Fig. 34.34). Peripheral blood monocytosis ($\geq 5 \times 10^9$/L) is usually present.

In myelomonocytic leukemia, variable staining of leukemic cells with MPO, SBB, CAE, and periodic acid–Schiff (PAS) has been noted. In most cases, leukemic cells exhibit diffuse and intense staining with ANA and ANB. In some cases, these nonspecific esterases cannot be demonstrated, and the diagnosis may be made on the basis of Romanowsky's stains and/or immunophenotyping.

Immunologic markers are variable but usually show myeloid antigens CD13 and/or CD33, as well as variable expression of monocytic markers CD14, CD4, CD11b, CD11c, CD64, CD36, CD68, and lysozyme. Some pure myeloblasts may be present, including those with CD34 and CD117 expression, and a second population of variably mature monocytes. Cases with recurrent cytogenetic abnormalities are categorized separately.

Acute Monoblastic and Acute Monocytic Leukemia

In this disorder, 80% or more of marrow nonerythroid cells are monoblasts, promonocytes, or monocytes (see Figs. 34.24 and 34.35). Two subtypes are recognized. The monoblastic subtype is characterized by large blasts accounting for 80% or more of marrow monocytic cells.

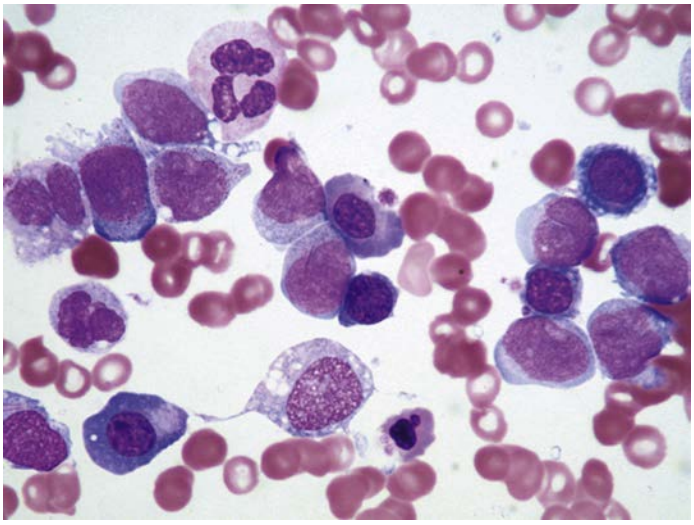

Figure 34.30 Acute myelogenous leukemia with multilineage dysplasia showing dysgranulopoiesis and dyserythropoiesis (×1000).

The monocytic subtype has fewer monoblasts (<80% of marrow monocytic cells) and greater numbers of promonocytes and monocytes (Bennett, 1985b). In both, ANA and ANB label the leukemic cells diffusely and intensely (80% or more of leukemic cells). Occasional cases fail to show nonspecific esterases, and the diagnosis is made from Romanowsky's stains and/or immunophenotypic techniques. Antilysozyme and CD68 are particularly useful on slides. Both myeloid and monocytic markers are frequently expressed, as in acute myelomonocytic leukemia. The translocation t(8;16)(p11.2;p13.3) has been associated with AML-M5 (or M4) with erythrophagocytosis.

Pure Erythroid Leukemia

The previous category of erythroleukemia, with ≥50% erythroid precursors of marrow cells and ≥20% myeloblasts of nonerythroid marrow cells, is now classified based on the total blast percentage of all marrow cells irrespective of percentage of nonerythroid nucleated marrow cells. These cases are classified as AML with myelodysplasia-related changes (if blasts are ≥20% of total marrow cells) or MDS with excess blasts (if blasts are <20% of all marrow cells).

Very rarely, there is virtually no granulocytic involvement in the neoplastic process and primitive erythroblasts predominate. This has been known as *erythremic myelosis* and is now known as *pure erythroid leukemia*. Morphologic abnormalities of erythroblasts are often pronounced, with atypical megaloblastic features, bizarre nuclear shapes, and multinucleated giant forms. The cytoplasm may contain pseudopods and/or vacuoles, particularly in the probasophilic and basophilic erythroblasts. Sometimes, abnormal monocytic and megakaryocytic elements are present as well (Fig. 34.36). CD71 (dim), hemoglobin A, glycophorin A, spectrin, ABH blood group antigens, and HLA-DR are frequently expressed with absence of myeloid-associated markers, including MPO. Complex karyotypes are frequent, often including monosomy 5 or del(5q), monosomy 7 or del(7q), trisomy 8, 11q abnormalities, 17p abnormalities, del(20q), and/or +13.

In some cases, erythroid cells may show strong cytoplasmic PAS positivity (Fig. 34.37). This is granular in early erythroid precursors and diffuse in later stages. Erythroid precursors are PAS negative in normal individuals and in most diseases, including nutritional megaloblastic anemia. They are sometimes positive, however, in iron deficiency anemia, thalassemia, and MDS with ring sideroblasts. Ring sideroblasts may be seen in erythroleukemia, and myeloblasts usually stain with SBB, MPO, and CAE. A nonspecific esterase-positive monocytic component may also be present. Neoplastic erythroid precursors are sometimes positive for ANA and ANB.

Acute Megakaryoblastic Leukemia

The diagnosis of acute megakaryoblastic leukemia, like other forms of AML, requires ≥20% blasts in the marrow. Megakaryoblasts are highly polymorphic; some blasts simulate lymphoblasts, while others are larger and have pseudopods or stringy cytoplasmic projections. The cytoplasm is usually light blue and may or may not possess granules (Fig. 34.38). The nuclei often have one to three nucleoli. Micro megakaryocytes may be present and are not counted as blasts.

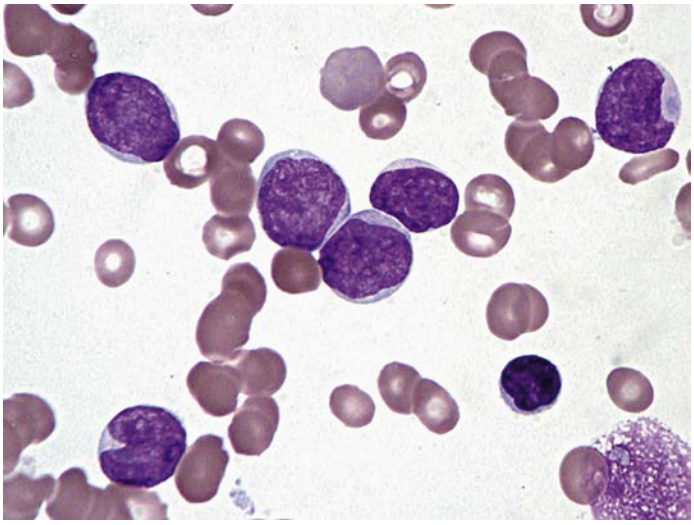

Figure 34.31 Acute myelogenous leukemia, minimally differentiated, resembles acute lymphoblastic leukemia and requires immunophenotyping for diagnosis (×500).

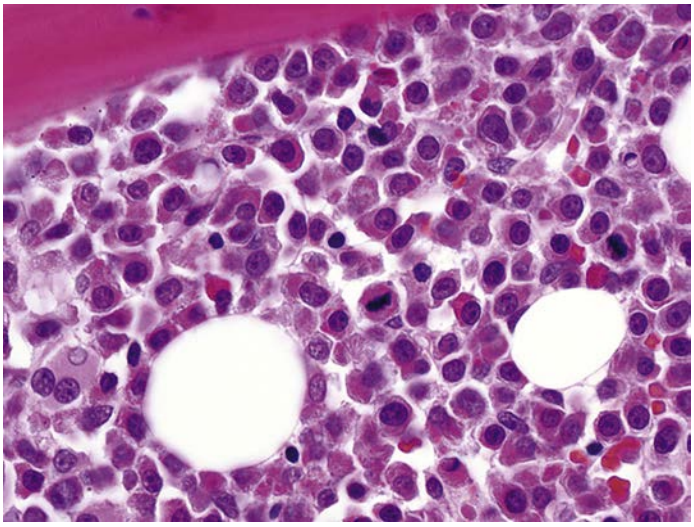

Figure 34.33 Acute myelogenous leukemia with maturation shows maturing granulocytic cells on this biopsy (×200).

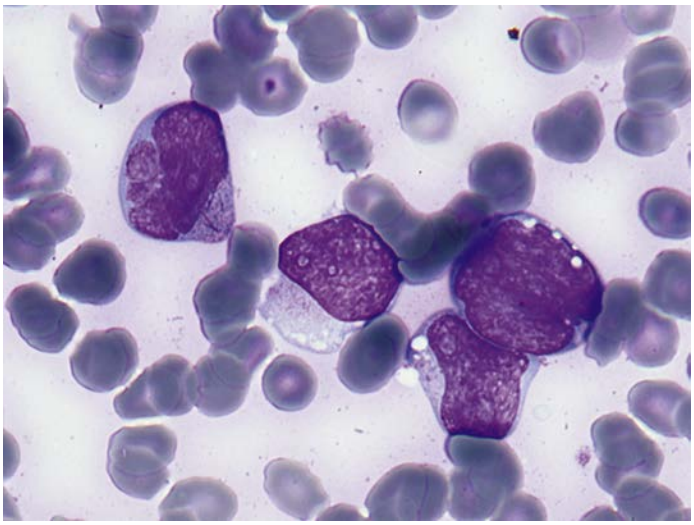

Figure 34.32 Acute myelogenous leukemia without maturation shows blasts with less than 10% maturing neutrophils. Auer rods are present in the cell at upper left.

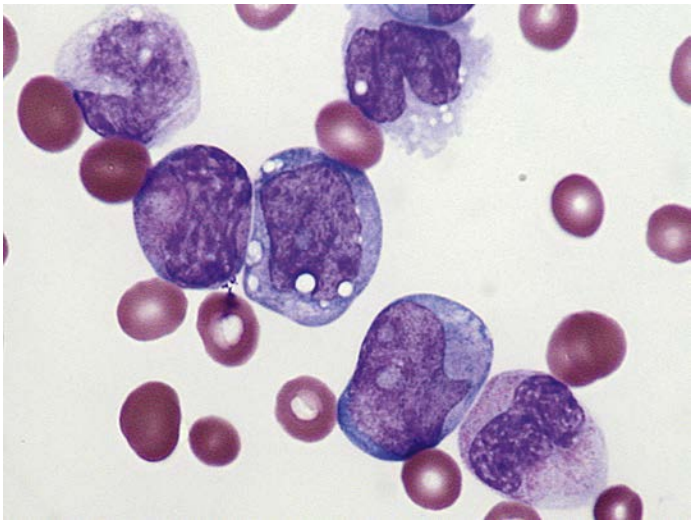

Figure 34.34 Acute myelomonocytic leukemia shows blasts and dual differentiation to granulocytes and monocytes (×1000). Acute monocytic leukemia shows monoblasts and maturing monocytes. Promonocytes are counted as blasts and show finely convoluted nuclei (×1000).

The blasts are cytochemically undifferentiated. They do not stain with SBB, MPO, CAE, or ANB. However, ANA is usually positive in a focal cytoplasmic pattern (Fig. 34.39). The PAS reaction shows diffuse and peripheral granular (often in large blocks) staining.

Megakaryocytic lineage is most often demonstrated by immunophenotyping using monoclonal antibodies against platelet glycoprotein Ib (CD41) or IIb/IIIa (CD61) (Bennett, 1985a). Blasts are often also positive for myeloid antigens CD13 and CD33, and characteristically for CD36. Care must be taken to differentiate this disease from AML with minimal differentiation by flow cytometry, which may show artifactual positivity for platelet markers due to adherence of platelets to blasts. This can be done by immunochemical examination of cytospins or bone marrow trephine biopsy section.

In the peripheral blood, there is usually pancytopenia with marked leukopenia and anemia. Megakaryocytic fragments are sometimes present in the blood. The BM shows variable and sometimes pronounced myelofibrosis.

Clumping of blasts may simulate metastatic tumors, such as neuroblastoma or small cell carcinoma. Infants with t(1;22)(p13.3;q13.1) often show marrow infiltration mimicking neuroblastoma.

Young children (through 4 years of age) with Down syndrome (trisomy 21) have an increased incidence of megakaryoblastic leukemia, preceded in 30% by transient myeloproliferative disorder/transient abnormal myelopoiesis (TMD/TAM) of Down syndrome and by a dysplastic prephase in 70%. See also later discussion.

Acute Basophilic Leukemia

Acute basophilic leukemia is a rare form of AML in which the blastic cells differentiate along the basophil lineage. The peripheral blood usually demonstrates anemia and thrombocytopenia with leukocytosis. The BM is infiltrated by blastic cells simulating lymphoblasts or myeloblasts. Blasts are generally negative for SBB and myeloperoxidase. An increase in mature basophils or in blasts staining with toluidine blue may occur. Diagnosis historically rests on the identification of blasts with basophilic granules by ultrastructural methods and the literature consists of isolated reports with a variety of AML genotypes. The blasts usually express CD13, CD33, and CD123, and are negative for CD117. The differential diagnosis includes myelomastic leukemia.

Acute Panmyelosis with Myelofibrosis

This is a rare form of acute leukemia with panmyeloid proliferation and marrow fibrosis. Pancytopenia is typically seen. Red blood cells show minimal poikilocytosis, but dysplastic features in myeloid cells are often seen, as are atypical platelets.

The BM sample frequently shows a dry tap; on biopsy, clusters of blasts, late erythroid precursors, and dysplastic megakaryocytes are seen in a variably fibrotic background (Fig. 34.40). This is differentiated from acute megakaryoblastic leukemia by involvement of all three myeloid lineages rather than only the megakaryocytic.

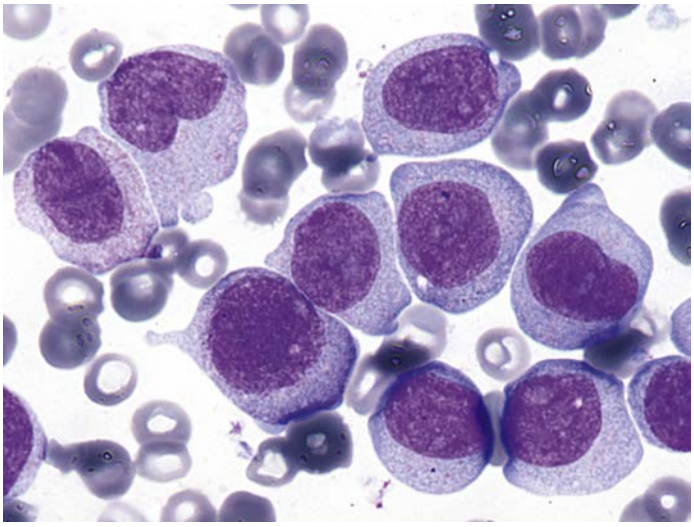

Figure 34.35 Acute monoblastic leukemia shows predominantly monoblasts (×1000).

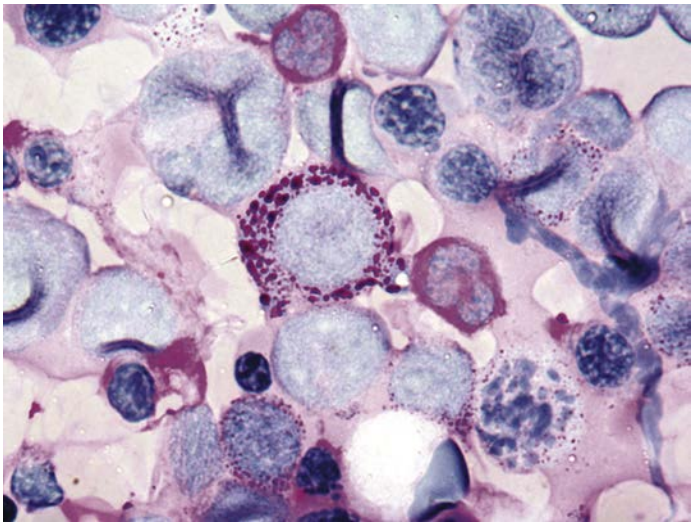

Figure 34.37 Coarse periodic acid–Schiff-positive granules are often seen in erythroid precursors in erythroleukemia (×1000).

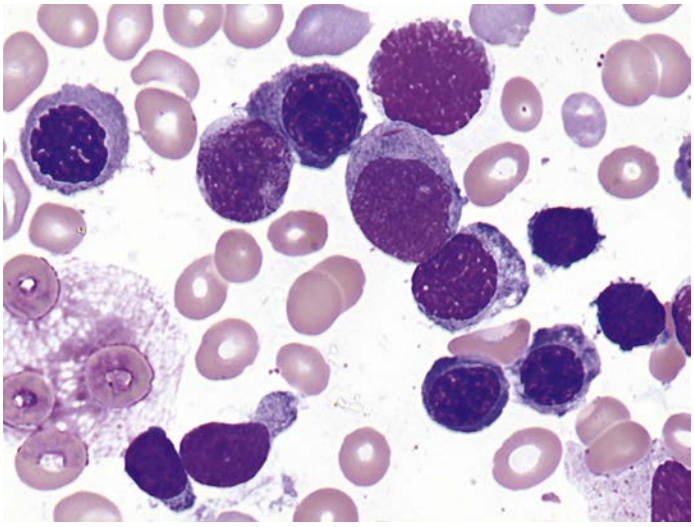

Figure 34.36 Erythroleukemia, erythroid/myeloid, shows predominance of erythroid precursors with increased myeloblasts. An Auer rod is seen in the blast at upper center (×1000).

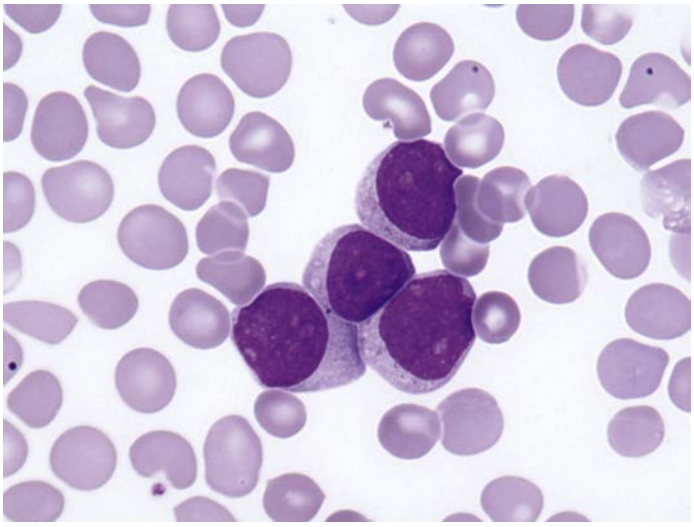

Figure 34.38 Blasts sometimes cluster in acute megakaryocytic leukemia (×1000).

Myeloid Sarcoma

This neoplasm has been called *myeloblastic sarcoma*, *granulocytic sarcoma*, *extramedullary myeloid cell tumor*, and *chloroma*. It represents a localized tumor of myeloblasts or monoblasts, with or without maturation, infiltrating extramedullary sites (Fig. 34.41). Myeloid sarcomas may occur at any age in patients with AML or any other known myeloproliferative disorder, or de novo. The diagnosis is equivalent to that of AML, and marrow involvement usually follows if it is not antecedent. These tumors occur in the skin, lymph nodes, nasopharyngeal and upper respiratory tract tissues, breast, ovary, bone, perineural and epidural structures, and the eye and other orbital structures, as well as in a variety of soft tissues.

The diagnosis depends on recognizing the nature of the primitive cells that can often be mistaken for solid tumors, including non-HLs, amelanotic melanomas, or undifferentiated carcinoma (Hutchison, 1990). The diagnosis is facilitated by making touch imprint preparations of cut sections of the tumor and staining them with Romanowsky's stains, by cytochemical reactions, and by immunophenotyping. Anti-MPO and CD68 are particularly useful for granulocytic or monocytic lineage in paraffin sections.

Myeloid Proliferations Associated with Down Syndrome

Children and adults with Down syndrome have a much higher frequency of leukemia than those without the syndrome. This includes ALL and AML, and diagnostic considerations for most are similar to leukemia occurring outside the syndrome. In addition, two specific and likely related disorders are unique to this group of patients.

Transient Abnormal Myelopoiesis Associated with Down Syndrome

Transient abnormal myelopoiesis (TAM) occurs in 10% of neonates with Down syndrome and in a small number who are phenotypically normal but have trisomy 21 mosaicism. It presents as acute megakaryoblastic leukemia, frequently with thrombocytopenia and leukocytosis, often with higher blast proportions in blood than in marrow, and hepatosplenomegaly. It is characterized by mutations of *GATA1*. Blasts may express CD34, CD13, CD33, CD117 and/or CD7. Uniquely, this disorder resolves spontaneously in the vast majority of cases. However, 20% to 30% subsequently develop nonremitting AML, as discussed later.

Myeloid Leukemia Associated with Down Syndrome

AML of Down syndrome occurs most often in the first 3 to 5 years at an incidence greater than 50 times that of others. It is usually of megakaryocytic lineage and may be preceded by a preleukemic phase similar to RCC or by TAM. Blasts are of megakaryocytic/myeloid lineage, and express CD41 and CD61 as well as CD34, CD117, CD13, CD33, CD7, CD4, CD42, CD36, and/or CD71. Genetics show trisomy 21 and *GATA1* mutations, often with additional copies of chromosome 8 and/or 21 (Roy, 2009). AML also occurs with less frequency in older patients with Down syndrome. However, in older patients, *GATA1* mutations are usually absent.

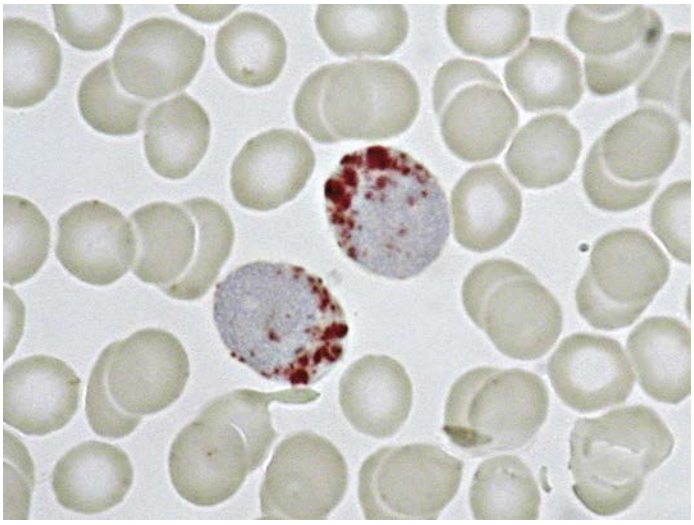

Figure 34.39 Alpha naphthyl acetate esterase-positive granules in megakaryoblasts.

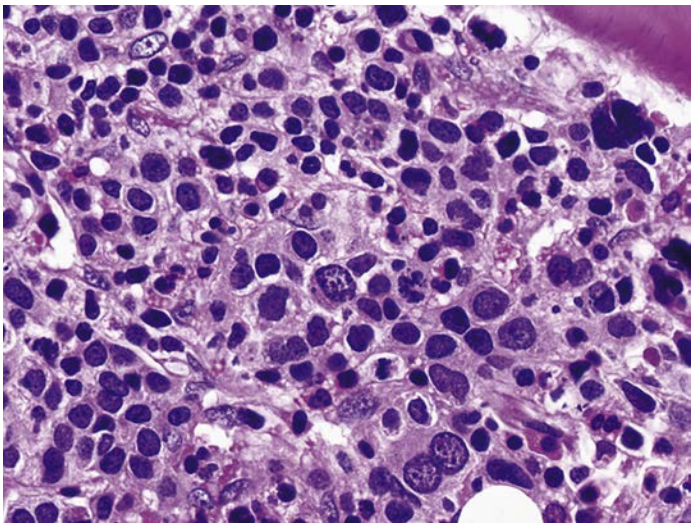

Figure 34.40 Acute panmyelosis with myelofibrosis shows involvement of all three myeloid lineages, with fibrosis (×200).

Blastic Plasmacytoid Dendritic Cell Neoplasm

This tumor used to be included in the WHO classification with the lymphomas and was called *blastic NK-cell lymphoma* or *CD4+ CD56+ hematodermic neoplasm*. It is now known to be derived from plasmacytoid dendritic cell precursors and presents in skin with frequent involvement of blood and marrow, and often lymph nodes. Skin lesions may be nodules, plaques, or patches. Tumors resemble lymphoblastic lymphomas with monomorphic dermal infiltrates of blasts with fine chromatin and irregular nuclei, along with agranular cytoplasm. Cytochemical stains for myeloid precursors are absent, and immunohistochemistry shows characteristic findings of CD4, CD56, CD43, and CD45RA. Plasmacytoid dendritic cell markers CD123, TCL1A, and BDCA-2/CD303 are positive. CD99 is reported positive. CD7, CD68, and CD33 are often expressed; CD3, CD5, CD13, CD34, CD117, CD20, CD16, LAT, lysozyme, MPO, and CD19 are negative. Cytotoxic T-cell markers are also negative in tissue sections. Immunoglobulin and usually T-cell receptor genes are germline. The disease is aggressive, usually relapsing after initial therapy, but occasionally responding well to aggressive therapy.

Acute Leukemias of Ambiguous Lineage (Swerdlow, 2017)

Some cases of acute leukemia have features that are indeterminate between lymphoid and myeloid lineage or have features of more than one lineage (Swerdlow, 2017; Bene, 2012). This is a controversial area of difficult-to-classify leukemia. Many leukemias that appear to be of defined lineage have one or more immunologic markers that are aberrant or show lineage infidelity. A single such marker is usually insignificant. ALL with myeloid markers responds similarly to other types of ALL, and lymphoid markers in AML are primarily important if they help suggest a subtype, such as CD19 expression in AML with t(8;21).

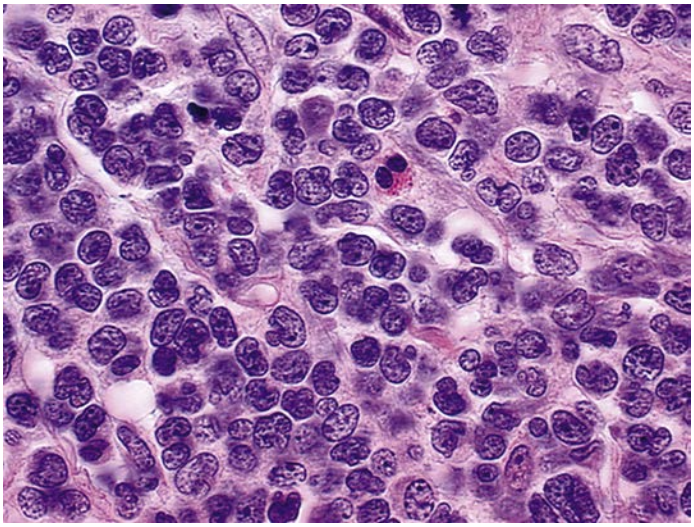

Figure 34.41 Myeloid sarcoma, in this case presenting in the skin, resembles lymphoma but with large blastic or monocytoid cells. Eosinophils or precursors are frequently present (×500).

Ambiguous acute leukemias fall into two main categories per the WHO classification: acute undifferentiated leukemia (AUL) and mixed phenotype acute leukemia (MPAL). MPAL is divided into several entities. The term *bilineal acute leukemia* has been applied to rare disorders in which there are distinct blast populations of more than one lineage. Biphenotypic leukemia has referred to those with one population of leukemic cells showing multiple lineage expression (Box 34.12). Subcategories of MPAL are listed in the following sections.

Acute Undifferentiated Leukemia

These are rare acute leukemias in which the predominant cells are blast forms that cannot be classified using morphologic, cytochemical, ultrastructural, immunologic, or DNA analytic methods. CD34, CD38, and HLA-DR are frequently expressed; CD7 and TdT may be expressed as well.

Mixed Phenotype Acute Leukemia with t(9;22)(q34.1;q11.2); BCR-ABL1

These are cases of MPAL with t(9;22) translocation and associated *BCR-ABL1*. They are rare disorders, more common in adults than in children. Cases with prior CML are excluded.

Mixed Phenotype Acute Leukemia with t(v;11q23.3); KMT2A-Rearranged

This disease is more common in children than in adults. Dimorphic blast populations are frequent and consist of monoblasts and lymphoblasts. The prognosis is generally poor.

Mixed Phenotype Acute Leukemia, B/Myeloid, NOS

Myeloperoxidase or monocytic differentiation and CD19 with CD79a, cCD22, and/or CD10; neither t(9;11) nor 11q23.3 translocation occurs.

Mixed Phenotype Acute Leukemia, T/Myeloid, NOS

Myeloperoxidase or monocytic differentiation and cytoplasmic or surface CD3; neither t(9;11) or 11q23.3 translocation.

Mixed Phenotype Acute Leukemia, NOS—Other Rare Types

This category includes T- and B-lineage disease and cases with trilineage differentiation.

Acute Leukemia of Ambiguous Lineage, NOS

The neoplastic cells in this leukemia express combinations of markers with no specific lineage differentiation. This leukemia has a poor prognosis. Patients with acute leukemia of ambiguous lineage, NOS are usually treated with myeloid-specific therapy (Swerdlow, 2017).

Natural Killer Cell Lymphoblastic Leukemia/Lymphoma

This category considers the possibility of bilineage NK and T-lineage lymphoblastic leukemia/lymphoma, but such an entity remains ambiguous.

BOX 34.12

Lineage Requirements in Mixed Phenotype Acute Leukemia

Myeloid lineage
Myeloperoxidase or ≥2 of the monocyte differentiation markers (NSE, lysozyme, CD14, CD64, CD11c)
T lineage
Cytoplasmic or surface CD3
B lineage
Strong CD19 with strong CD79a, cytoplasmic CD22, or CD10
or
Weak CD19 with at least two: strong CD79a, cytoplasmic CD22, or CD10

From Swerdlow (2017).
NSE, Neuron-specific enolase.

PRECURSOR LYMPHOID NEOPLASMS

Historically, lymphoid leukemias and lymphomas were classified separately. Leukemias are hematopoietic malignancies primarily involving BM and blood and have been most extensively categorized by the FAB group. Lymphomas are those primarily involving lymphoid organs or other soft tissues; they have been subject to numerous classification schemes that evolved rapidly because of advances in immunology, oncology, and genetics. Since publication of the Revised European–American Lymphoma (REAL) classification, lymphoid leukemias and lymphomas have been classified by biological features of the disease rather than by the anatomic distribution, and an international consensus in classification has generally been attained (Berard, 1997; Harris, 1994, 2000). The WHO classification deals with neoplasia of bone marrow, blood, and lymphoid tissues and focuses on cytogenetic and molecular findings whenever possible (Swerdlow, 2017).

B Lymphoblastic Leukemia/Lymphoma

Clinical Features

This category of malignancy most often presents as leukemia and is the prototype of ALL. The other major type of ALL is T lymphoblastic, which is less common and tends to present as lymphoma or concurrently as both leukemia and lymphoma. ALL is the most common malignancy of children and adolescents. In the United States, 6000 new cases are reported per year, two-thirds of which affect children. The evolution of treatment with combination chemotherapy, CNS treatment, intensified therapy for high-risk categories with identification of minimal residual disease (MRD), and increasing understanding of molecular and genetic risk categories has led to cure rates of greater than 80% in children (Pui et al., 2011; Pui & Evans, 2013; Zhou et al., 2012). Favorable factors include age 5 to 10 years, hyperdiploidy (best, 54–62 with trisomy 4, 10, and/or 17), and t(12;21). Poor risk factors include age younger than 1 year, t(9;22), t(4;11), MRD after therapy, and ancestry factors that have varied with therapies. Proper therapy has reduced some adverse risk factors and molecular genetic characterization has identified targets for therapy, such as genotypes sensitive to ABL1 inhibitors.

Among adults, only 30% to 40% are cured, in part because of the higher frequency of adverse genetic abnormalities. Adult ALL incidence increases in middle to older age, similarly to genetically high-risk AML. Individuals with this disorder often present with symptoms of fatigue, fever, and bleeding. Generalized lymphadenopathy, splenomegaly, and hepatomegaly are common findings. Because leukemic cells infiltrate many tissues of the body, other symptoms may occur. Leg pain can be associated with periosteal infiltrates, as well as headache, nausea, and vomiting with meningeal leukemia. Rapid onset of unconsciousness may indicate subarachnoid hemorrhage.

Presentation occurs occasionally in skin, bone, and/or lymph node without BM involvement (<25% blasts in the marrow). These cases are referred to as lymphoma. They most often occur in young people (<18 years) and show overlapping features with precursor B-ALL, with TdT and B-lineage markers. Morphology in tissue sections shows diffuse infiltrations of small cells (nuclei smaller than histiocyte nuclei) with diffuse chromatin, inconspicuous nucleoli, scant cytoplasm, high mitotic rate, and frequently a "starry-sky" pattern of admixed histiocytes (indicating high apoptotic rate).

Anemia, usually normocytic, is present in precursor B-ALL when clinical manifestations are fully developed. Frequently, nucleated red cells are present. Thrombocytopenia of moderate to marked degree is the rule. The leukocyte count occasionally is very high (>100 × 10^9/L), often is slightly elevated, but is perhaps most frequently normal or decreased. The predominant cell is the lymphoblast.

Marrow

By the time the patient is symptomatic, hematopoietic cells and fat are usually replaced by a diffuse infiltration of lymphoblasts. Blast percentage is usually greater than 50%. Predominance of small blasts with high nuclear/cytoplasmic (N/C) ratios and inconspicuous nucleoli (L1 type in the FAB classification) is most common in childhood ALL (Fig. 34.42). Chromatin is diffuse in some cells but may show variable condensation, and blasts may be difficult to distinguish from the normal lymphocytes of young children. Larger blasts with more abundant cytoplasm, prominent nucleoli, and often irregular nuclei (FAB L2) also occur and tend to predominate in adult ALL.

The blasts are negative for SBB, peroxidase, and naphthol ASD CAE. Azurophilic granules may be present, but they are SBB and peroxidase negative. In other cases, ALL blasts may exhibit some SBB reactivity, but peroxidase is negative.

Blasts characteristically express TdT, cytoplasmic CD22 and CD79a, CD19, and HLA-DR. CD10 (common ALL antigen) is expressed in many, and expression of CD34 is variable. Cytoplasmic μ immunoglobulin heavy chain (cyt-μ) indicates a slightly more mature state, but surface immunoglobulin is negative. Myeloid-associated antigens CD13, CD33, and CD15 may be expressed.

Cytogenetics

Cytogenetic findings are increasingly important in diagnosis and prognostication in ALL and have been previously reviewed (Mrozek, 2004). The current WHO classification divides B-ALL into groups based on frequently found (recurrent) cytogenetic findings (Swerdlow, 2017).

B Lymphoblastic Leukemia/Lymphoma with t(9;22)(q34.1;q11.2); BCR-ABL1

The Ph′ chromosome t(9;22) with production of a fusion *BCR-ABL1* occurs in about 25% of cases of adult ALL and 2% to 4% of cases of childhood ALL. The t(9;22) is the most frequent adult ALL translocation and is associated with a poor prognosis. Two types are found: that identical to CML, involving the bcr region of BCR with resultant p210 kD fusion protein, occurring in half of adult cases of Ph′-positive ALL; and another with breakpoint upstream of bcr, producing a smaller chimeric message and p190 kD protein. The latter occurs in most childhood Ph′-positive cases. Ph′-positive ALL is most often of precursor B cell lineage but also may present with biphenotypic myeloid differentiation.

B Lymphoblastic Leukemia/Lymphoma with t(v;11q23.3); KMT2A-Rearranged

Abnormalities of the *KMT2A* gene at chromosome region 11q23.3 are seen in 5% to 7% of cases of ALL (Le Beau, 2000) as well as in AML, and are often associated with *FLT3* overexpression. ALL with t(4;11)(q21;q23.3) is associated with a poor prognosis, high WBC count, and immature B-lineage phenotype with lack of CD10 or CD24 but with CD15 expression. It involves *KMT2A* and the partner gene *AFF1* (*AF4*). It is most common in infants, and many cases of ALL with this abnormality are biphenotypic. Translocation t(11;19)(q23.3;p13.3) is the next most frequent *KMT2A* abnormality in ALL but also occurs in AML (monocytic). Overall, 11q23.3 (*KMT2A*) abnormalities, with the possible exception of t(9;11) in AML, confer poor prognosis.

B Lymphoblastic Leukemia/Lymphoma with t(12;21)(p13.2;q22.1); ETV6-RUNX1

This constitutes approximately 25% of B-ALL, correlates with high-density CD10 and CD34 expression with negative CD9 and CD20, and is associated with good prognosis. The *ETV6* (also called *TEL*) gene at 12p13.2 is fused with the *RUNX1* (also called *AML1*) gene at 21q22.1 with a resultant fusion protein. *RUNX1* is a transcription factor involved in hematopoietic differentiation/proliferation. The abnormality is difficult to detect by karyotyping but can be detected by RT-PCR analysis for the chimeric mRNA or by FISH.

B Lymphoblastic Leukemia/Lymphoma with t(1;19)(q23;p13.3); TCF3-PBX1

Another translocation, t(1;19)(q23;p13), and variants are associated with pre-B cell ALL (with cytoplasmic μ Ig). It involves the *TCF3* (also called *E2A*) gene at 19p13.3, which encodes transcription factors, and *PBX1* at 1q23. This has also been associated with increased relative risk for CNS relapse.

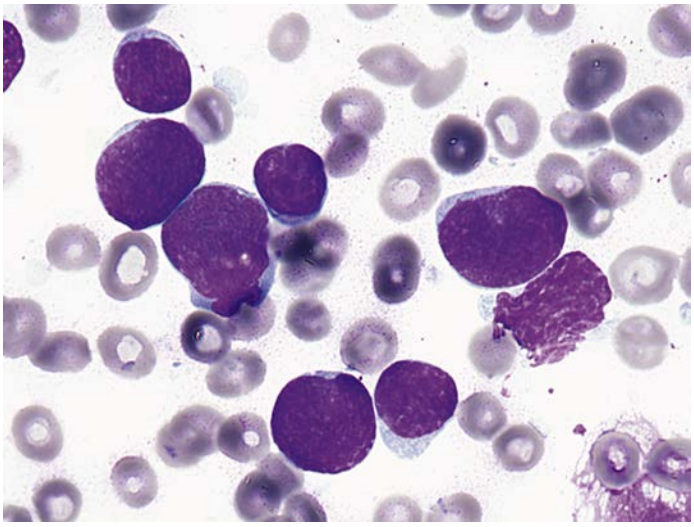

Figure 34.42 Acute lymphoblastic leukemia of B-lineage, with small to medium-sized blasts and lack of conspicuous nucleoli (×1000).

B Lymphoblastic Leukemia/Lymphoma with t(5;14) (q31.1;q32.1); IGH/IL3

This rare variant of B-ALL is associated with eosinophilia. The rearrangement results in constitutive expression of *IL3* and interleukin effects. Immunophenotype is CD19+, CD10+.

B Lymphoblastic Leukemia/Lymphoma with Hyperdiploidy

B-ALL with multiple trisomies and between 50 and 66 chromosomes (normal = 46) is referred to as hyperdiploid. This usually occurs in children and implies favorable prognosis. Trisomies of chromosome 4,10, and 17 are considered markers for low-risk disease in pediatric leukemia protocols. Blasts usually express CD19, CD10, and CD34 but often are CD45 negative.

B Lymphoblastic Leukemia/Lymphoma with Hypodiploidy

Hypodiploid B-ALL shows fewer than the normal 46 chromosomes. Prognosis is unfavorable, especially when chromosomes are fewer than 45, and even more so when fewer than 44.

B Lymphoblastic Leukemia/Lymphoma, BCR-ABL1-Like

B-lymphoblastic leukemia/lymphoma with *BCR-ABL1*-like is a provisional entity in the 4th edition of the WHO classification. These leukemias lack *BCR-ABL1* gene fusion, but usually have a gene expression profile similar to that seen in ALL with *BCR-ABL1*. Multiple different translocations, rearrangements, and mutations are associated with this entity, including translocations of other tyrosine kinases or *CRLF2*, and which are potentially responsive to targeted therapy by TKIs. The disease is relatively common and has a poor prognosis. Therefore, it is important to screen for *BCR-ABL1*-like ALL, especially in high-risk patients (Swerdlow, 2017).

B Lymphoblastic Leukemia/Lymphoma with iAMP21

This disease is characterized by intrachromosomal amplification of chromosome 21. It occurs mostly in older children and accounts for approximately 2% of pediatric B-ALL. It is associated with a poor prognosis and patients usually need to be treated with more intensive chemotherapy (Swerdlow, 2017).

B Lymphoblastic Leukemia/Lymphoma, Not Otherwise Specified (Refers to All Other B-ALLs)

Other genetic factors in B-ALL. *IKZF1* deletion in B-ALL is associated with a high risk of relapse. *PAX5* deletions or mutations are observed in approximately 30% of cases. Deletion or mutation of *CDKN2A/B* occurs in 21% to 36% of pediatric B-ALL and 50% of adult cases. Abnormalities in JAK-STAT signaling occur with various *JAK* mutations (excluding *JAK2* V617F) as well as increased expression of cytokine receptor CRLF2; mutations of *PAX5* and *RAS* are also frequent (Zhou et al., 2012).

T Lymphoblastic Leukemia/Lymphoma

T lymphoblastic leukemia (T-ALL), which accounts for 10% to 20% of cases of ALL, occurs predominantly in boys who tend to be slightly older than children with B lymphoblastic leukemia (B-ALL). Patients with T-lineage ALL often have a high leukocyte count and mediastinal involvement. Blast morphology is heterogeneous, similar to B-ALL, and immunophenotyping is required for diagnosis. The immunophenotype reflects thymic T cells, which have a distinct maturation pattern (Reinherz, 1980), and the blasts show varying maturity. Most cases exhibit TdT, CD7, and cytoplasmic CD3 with variable CD1a, CD2, and CD5. Some cases, of early thymic phenotype, lack CD4 or CD8, but most (midcortical thymic phenotype, particularly in lymphoma presentation) coexpress CD4 and CD8. In late cortical thymic phenotype, CD4 or CD8 alone may be present. In these, TdT and/or CD1a is particularly helpful for diagnosis. Myeloid markers such as CD13, CD33, and/or CD117 may be present, and CD79a may be present occasionally.

T lymphoblastic lymphoma (T-LBL), which accounts for 85% to 90% of all LBLs, often shows a more mature thymic phenotype than leukemic presentation (Crist, 1988). These are relatively common lymphomas of adolescents and young adults (one-third of pediatric NHLs) and also occur later in life. They typically present in the mediastinum and/or peripheral lymph nodes, and pleural effusions are common. Airway compromise or superior vena cava syndrome is frequently present, resulting in emergent need for therapy and limiting diagnostic procedures.

Morphology. T-LBL usually shows diffuse tissue involvement by blasts with nuclei smaller than those of histiocytes or reactive endothelial cells (Fig. 34.43), although some show nuclei similar in size to Burkitt lymphoma (BL). Chromatin is usually finely dispersed to slightly clumped, but rarely as much as Burkitt lymphoma. Mitotic rates are high, and there is often a "starry-sky" pattern similar to Burkitt. Neoplastic cells sometimes show selective T-zone involvement of lymph nodes and/or a leukemia-like infiltration pattern in soft tissue.

The differential diagnosis of T-LBL in young patients primarily involves it, BL, and occasionally large B-cell lymphoma (LBCL). Mediastinal location favors T-LBL over BL, but not LBCL. In adults, the differential diagnosis includes blastoid and blastic variants of mantle cell lymphoma. Myeloid sarcoma is also in the differential in any age group. Expression of TdT and lineage-specific T-cell markers without B or myeloid markers is usually diagnostic.

Genetics. T-cell receptor genes are frequently rearranged, but Ig heavy-chain genes may also be rearranged (Racke, 2011). Patients with T-cell ALL frequently show translocations of α and δ T-cell receptor loci at 14q11.2, the β locus at 7q35, or the γ locus at 7p14-15, usually with genes encoding transcription factors. Partner genes include *MYC* (8q24.1), *TAL1* (1p32), *RBTN1* (11p15), *RBTN2* (11p13), *HOX11* (10q24), *HOX11L2* (5q35), and *LCK* (1p34.3-35). TAL1 regulatory gene deletions occur in 25% of cases, and del(9p) involving *CDKN2* is also frequent (Mrozek, 2004).

Early T-Cell Precursor Lymphoblastic Leukemia

Early T-cell precursor lymphoblastic leukemia (ETP-ALL) is a unique category with a poor prognosis, comprises approximately 15% of T-ALL, lacks expression of CD1a and CD8 with weak or absent CD5, and displays aberrant expression of one or more of the myeloid and hematopoietic stem cell markers CD13, CD33, CD34, and CD117. A mutational spectrum resembles AML (Zhang, 2012). ETP-ALL shows activating mutations in genes regulating cytokine receptor and RAS signalling (*NRAS*, *KRAS*, *FLT3*, *IL7R*, *JAK3*, *JAK1*, *SH2B3*, and *BRAF*), inactivating lesions disrupting hematopoietic development (*GATA3*, *ETV6*, *RUNX1*, *IKZF1* and *EP300*), histone-modifying genes (*EZH2*, *EED*, *SUZ12*, *SETD2*, and *EP300*) and/or recurrent mutations (*DNM2*, *ECT2L*, and *REL*) (Zhang, 2012).

MATURE B-CELL NEOPLASMS

These constitute the most numerous and possibly the most diverse group of hematopoietic neoplasms. Overall rates vary geographically, with 15/100,000 in the United States. There is also geographic variation in histologic types, with follicular and diffuse large B cells predominating in Western developed countries, constituting 50% of NHLs; myeloma is also common. The cells affected in mature B-cell malignancies are those making up the humoral immune system, which is characterized by innumerable clones of B lymphocytes with genetically distinct immunoglobulin gene rearrangements, many states of maturation, and interaction with regulatory pathways. Clinical behaviors relate to clonal escape from regulation, the balance of proliferation and apoptosis, and modulation by therapy. Features of major categories are shown in Table 34.5 (Swerdlow, 2017).

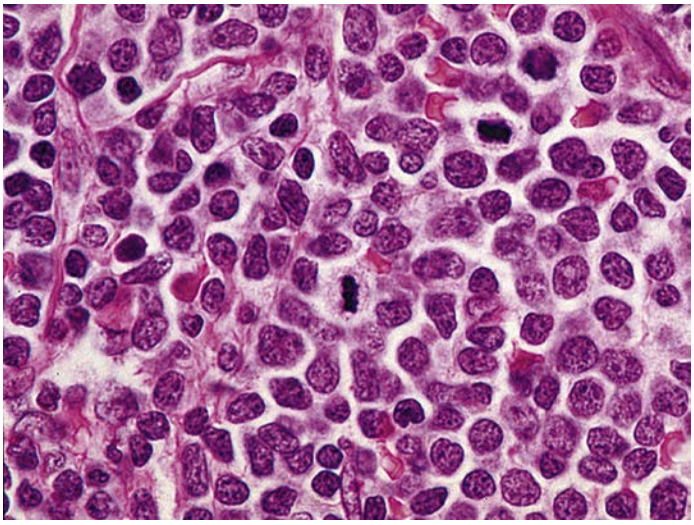

Figure 34.43 T lymphoblastic lymphoma (×500).

Monoclonal B-Cell Lymphocytosis

Diagnosis of chronic lymphocytic leukemia requires the presence of leukocytosis of ≥5 × 10^9/L monoclonal lymphocytes with chronic lymphocytic leukemia (CLL) phenotype (see later discussion) for at least 3 months or lower counts with the presence of cytopenias and/or disease-related symptoms. Otherwise, a diagnosis of monoclonal B-cell lymphocytosis is made, analogous to the concept of monoclonal gammopathy of unknown significance (MGUS) (Swerdlow, 2017).

Chronic Lymphocytic Leukemia/Small Lymphocytic Lymphoma

This is a clonal proliferation of small B lymphocytes involving BM, blood, and lymph nodes. It is common, usually indolent, at least initially, but difficult if not impossible to cure (Muller-Hermelink, 2008). Cases with predominant involvement in the marrow and blood are traditionally called CLL, and lymphomas are called small lymphocytic lymphoma (SLL), but these are considered manifestations of a single entity. A majority of cases are leukemic and constitute 90% of chronic lymphoid leukemias in the United States and Europe. It is rare in those younger than age 40 years; most cases occur over the age of 60 years, and the condition is more than twice as common in men as in women. Onset is insidious, and the disease is commonly discovered by chance during the investigation of another problem. Most patients are >50 years of age.

The tumors show diffuse infiltrates of small mature lymphocytes with clumped chromatin and scant to moderate cytoplasm (Fig. 34.44). Admixed prolymphocytes and proliferation centers (containing increased prolymphocytes and lymphocytes with increased cytoplasm) are characteristic. Mitotic rates are very low.

CLL/SLL shows a characteristic phenotype of monoclonal B cells (CD19/CD20/CD79a) with dim surface Ig (single light chain with IgM or IgM and IgD), coexpression of usual T-cell marker CD5, and expression of CD23 and CD200 (Alapat, 2012; Sandes, 2013). CLL/SLL cells usually express LEF1, which is considered a reliable marker to differentiate CLL/SLL from other small B-cell lymphomas. CD10, BCL-6 and cyclin D1 are negative. This pattern is very useful in distinguishing CLL/SLL from mantle cell, follicular, and marginal zone lymphomas.

Ig heavy and (monotypic) light-chain genes are rearranged and IGH genes have undergone somatic hypermutation of V regions as occurs in germinal centers (GC or memory-like) in 50-60%. Unmutated (naïve) *IGHV* is associated with adverse prognosis and with expression of the tyrosine kinase ZAP-70, normally expressed in T-cells. ZAP-70 can be detected by flow cytometry, but the protein undergoes degradation in vitro and is technically variable. DNA methylation profiles can also be used to separate CLL into naïve B-cell-like, intermediate, and memory B-cell-like groups with prognostic significance (Queiros et al., 2014). A prior concept that CLLs with mutated *IGHV* have experienced the germinal center (GC) environment while CLL with unmutated *IGHV* (naïve B-cell) have not has been recently challenged by gene expression profiling (GEP) studies showing similar profiles for both (Gaidano, Foa, & Dalla-Favera, 2012). It has been suggested that unmutated *IGHV* may be associated with other adverse factors, such as *NOTCH1* mutation. *SF3B1* and *BRC3* mutations are also negative indicators of prognosis. Aberrant methylation may deregulate *BCL2*, *TCL1*, and *ZAP-70* (Rodriguez-Vicente et al., 2013).

Cytogenetic studies show del 13q14.3 in 50%, with disruption of the tumor suppressor locus DLEU2/MIR15A/MIR16A, trisomy 12 in 20%, del(11q22-23) affecting the ataxia telangiectasia mutated (ATM) gene in 20%, del(17p13) at the p53 locus in 10%, and del(6q21) in 5%. The first of these is associated with a favorable outcome, and the latter three with an adverse outcome. Cytogenetic abnormalities vary with mutation status. These abnormalities often cannot be detected by karyotype because CLL cells are minimally proliferative in culture, but are detectable by FISH probes. Other adverse features include expression of CD38, CD49d, doubling of lymphocyte count in <12 months, and elevated β_2-microglobullin.

In the typical type of CLL, 90% or more of the cells are small lymphocytes that are monotonously similar in appearance and usually look normal. Nuclear chromatin may be coarsely condensed and more sharply separated by parachromatin than in normal lymphocytes or, in some cases, the chromatin is less condensed than normal. Nucleoli are evident in many of the lymphocytes. Size variation is minimal, and the amount of cytoplasm is slight to moderate. Less than 10% of lymphocytes are prolymphocytes or reticular lymphocytes (transformed lymphocytes).

Often, there is neither anemia nor thrombocytopenia at the time of diagnosis. Anemia due to impaired production does develop as the marrow is replaced by leukemic cells. In addition, erythrocyte life span in some patients with CLL may be reduced. This is especially true when there is marked splenomegaly. Autoimmune hemolytic anemia develops in about 10% of patients. Thrombocytopenia is often slight and occasionally becomes severe as the disease progresses so that hemorrhagic manifestations appear. Thrombocytopenia is usually due to hypoproliferation but may also be secondary to an immune process or splenic sequestration. Patchy, nodular, or interstitial involvement of the BM by neoplastic lymphocytes is associated with a relatively good outcome. A diffuse infiltrate of the BM, however, usually correlates with a poor prognosis and/or advanced disease. An increasing proportion of prolymphocytes (between 10% to 55%; mixed CLL/PLL) may indicate aggressive disease. Atypical morphology with nuclear irregularities is associated with trisomy 12 (Swerdlow, 2017).

B-Cell Prolymphocytic Leukemia

Prolymphocytic leukemia (PLL) was originally described as a variant of CLL (Galton, 1974). The male/female ratio is approximately 1:1, and mean age is 65 years. PLL is characterized by a very marked lymphocytosis (usually greater than 100 × 10^3/μL), massive splenomegaly, moderate hepatomegaly, and inconspicuous lymphadenopathy. The malignant lymphoid cells have a large vesicular nucleolus, condensed nuclear chromatin, and a moderate amount of cytoplasm (Fig. 34.45). More than 55% of blood leukemic cells are prolymphocytes. Immunophenotype varies from SLL/CLL by bright surface Ig (monoclonal IgM with or without IgD), lack of CD5 in two-thirds of cases, and usually lack of CD23 and presence of FMC-7. Abnormalities of *p53* are frequent, and deletions at 11q23 and 13q14 occur. *MYC* amplification or translocation with deregulation appears to be frequent (Flatley et al., 2014; Put et al., 2012). PLL is usually less responsive to treatment than CLL in general, and it has a poorer prognosis.

Splenic Marginal Zone Lymphoma

Splenic marginal zone lymphoma (SMZL) has many clinical, laboratory, and morphologic features similar to hairy cell leukemia (HCL) and features similar to SLL/CLL (Swerdlow, 2017). The disease incidence rates in males and females are similar. Patients are often in their seventh decade of life when they present with splenomegaly.

In the spleen, the neoplastic infiltrate expands from the white pulp into the red pulp. Some patients show a small monoclonal gammopathy, usually IgM. The BM may demonstrate patchy infiltrates or massive involvement. The tumor arises from splenic marginal zones, which in reactive processes are seen as an outer zone of pale lymphocytes with moderately abundant cytoplasm surrounding the white pulp and imparting a target-like appearance. In some cases, reactive follicles with GCs are present, and an expanded marginal zone surrounds the white pulp and involves the red pulp. Marginal zone hyperplasia may mimic this disorder. Other cases show predominantly red pulp involvement (Figs. 34.46 and 34.47). Red cell lakes are not present, and lymph nodes are not characteristically involved. The tartrate-resistant acid phosphatase (TRAP) stain is usually negative, although positive reactions have been recorded.

The immunophenotype is mature B cell with surface IgM/IgD (similar to SLL/CLL), positive CD20, CD79, and other pan–B-cell markers. CD5, CD10, CD23, cyclin D1, LEF1CD103, annexin A1, and CD43 are characteristically negative.

TABLE 34.5

Key Features of Major Mature B-Cell Neoplasms

Lymphoma	Demographics, clinical and laboratory presentations	Morphology	CELL SURFACE MARKERS		Cytogenetics
			Positive	Negative	
CLL/SLL	M > F, over 60 years; insidious onset of fatigue, lymphadenopathy; WBC >5 K/μL, anemia, thrombocytopenia, occasionally AIHA	Small lymphocytes with condensed chromatin	CD19, CD20, CD5, CD22, CD23, CD79a, dim sIg, LEF1	CD10, bcl-6, FMC-7	+12, del(13q14.3), del(11q22-23), del(17q)(TP53)
B-cell PLL	M = F, mean age 65 years; massive splenomegaly, minimal lymphadenopathy, WBC >100 K	Prolymphocytes ≥55%	CD19, CD20, FMC-7, bright sIg	CD5, CD23, often negative	Occ del(17p), del(13q14)
Hairy cell leukemia	M > F, median age 50 years; insidious onset with splenomegaly, leukopenia with monocytopenia	Medium-sized cells with round to oval indented nuclei, reticular chromatin, frayed cytoplasmic borders	CD20, CD22, CD79a, CD103, CD25, CD11c, CD123	CD5, CD10, CD23	***BRAF*** (V600e) mutation
Lymphoplasmacytic lymphoma	M > F, mean age 63 years; BM, nodal and splenic involvement, symptomatic IgM paraprotein	Plasmacytoid lymphocytes and plasma cells with PAS-positive inclusions (Dutcher bodies)	CD19, CD20, CD22, CD25, CD38, CD79a, bright sIgM, cIgM	CD5, CD10, CD23, CD103, bcl-6	***MYD88*** mutation del(6q), +3, +4, +18, none specific
Heavy chain disease (α-HCD, immunoproliferative small intestinal disease, prototype)	Younger adults in poorer Mediterranean communities with malabsorption, diarrhea	Lymphoplasmacytic infiltrate of intestinal mucosa, variant of MALT	NA	NA	
Marginal zone lymphomas: splenic, nodal, MALT	F = M, median age 61 years; indolent course involving stomach, other mucosal sites, spleen, or nodes	Lymphocytes with condensed chromatin and moderate cytoplasm; lymphoepithelial lesions in MALT type	CD20, CD79a, sIgM, bcl-2	CD5, CD10, CD23, bcl-6	+3, t(11;18)(q21;q21) in MALT type, 7q abnormalities
Follicular lymphoma	F > M, median age 59 years; lymphadenopathy, BM and splenic involvement frequent	Follicle-like structures with centrocytes and varying numbers of centroblasts	CD19, CD20, CD22, CD23, CD79a, CD10, bcl-2, bcl-6, sIgM	CD5, CD43	t(14;18)(q32;q21)
Mantle cell lymphoma	M > F, median age 60 years; lymphadenopathy, splenomegaly, BM involvement; typically refractory	Atrophic germinal centers, prominent mantle zones, small lymphs with irregular nuclei; blastoid/pleomorphic variants	CD5, CD43, FMC-7, bcl-2, cyclin D1, sIgM	CD10, CD23, bcl-6	t(11;14)(q13;q32)
Diffuse large B-cell lymphoma	M > F, all ages, moderately aggressive but responds to chemo and anti-CD20	Diffuse infiltrate of large B cells, variable morphology	CD19, CD20, CD22, CD79a, sIg, bcl-2±, bcl-6±, CD30±, MUM1 in post-GC types	CD5 (usually)	t(14;18) in 20%, 3q27 (bcl-6) abn in 30%, C-MYC translocation
Mediastinal large B-cell lymphoma	F > M, young to middle-aged adults; airway compression, superior vena cava syndrome	Sclerotic lesions with clear, multilobulated, or RS-like cells	CD19, CD20, CD22, CD79a, CD30	CD5, CD10	Amplifications of 9p24, 2p15, others
Primary effusion lymphoma	Rare, associated with HHV-8 in immunosuppressed younger gay men; pleural effusion	Immunoblastic or anaplastic cells	CD45, CD30, CD38, CD138	CD19, CD20, CD79a, sIg, bcl-6	
Plasmablastic lymphoma	Rare, associated with EBV in immunosuppressed	Plasmacytoid	CD45, CD38, CD138, CD79a	CD45, CD20, PAX-5 negative or weak	
EBV associated; DLBCL, NOS, chronic inflammation, lymphomatoid granulomatosis, post-transplant	Immunosuppressed, elderly, others	Variable	CD20, EBV-EBER		
Burkitt lymphoma	1. Endemic: children in Africa, jaw mass M > F 2. Sporadic: children to young adults, worldwide, M > F 3.Immunodeficiency-associated: HIV patients	Uniform cells with round to oval nuclei, multiple nucleoli, high mitotic rate	CD19, CD20, CD10, bcl-6, sIg	TdT, bcl-2	t(8;14)(q24;q32), t(2;8)(p12;q24), t(8:22)(q24;q11)
High-grade B cell lymphoma, double/triple hit	M=F, elderly	Variable morphology with variable mitotic and apoptotic figures	CD19, CD20, CD79a, CD10, bcl-6, sIg, Bcl2		8q24/***MYC*** and, t(8;14)(q24;q32)and/or 3q23/***BCL6*** rearrangement

AIHA, Autoimmune hemolytic anemia; *BL,* Burkitt lymphoma; *BM,* bone marrow; *cIg,* cytoplasmic immunoglobulin; *CLL,* chronic lymphocytic leukemia; *EBER,* EBV-encoded RNA; *DLBCL,* diffuse large B-cell lymphoma; *EBV,* Epstein-Barr virus; *F,* female; *GC,* germinal center; *HHV,* human herpesvirus; *HIV,* human immunodeficiency virus; *Ig,* immunoglobulin; *M,* male; *MALT,* mucosa-associated lymphoid tissue; *MYC, c-Myc* gene; *NA,* not applicable; *PAS,* periodic acid–Schiff; *PLL,* prolymphocytic leukemia; *RS,* Reed-Sternberg; *sIg,* surface immunoglobulin; *SLL,* small lymphocytic lymphoma; *TdT,* deoxyribonucleotidyl transferase; *WBC,* white blood cell.

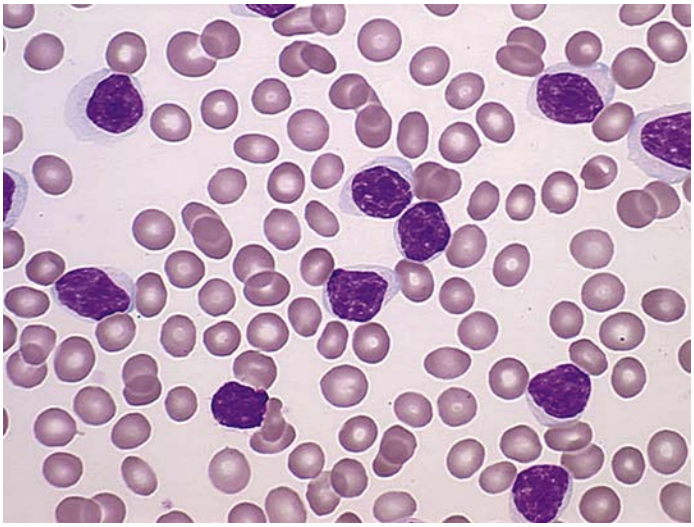

Figure 34.44 Chronic lymphocytic leukemia (×1000).

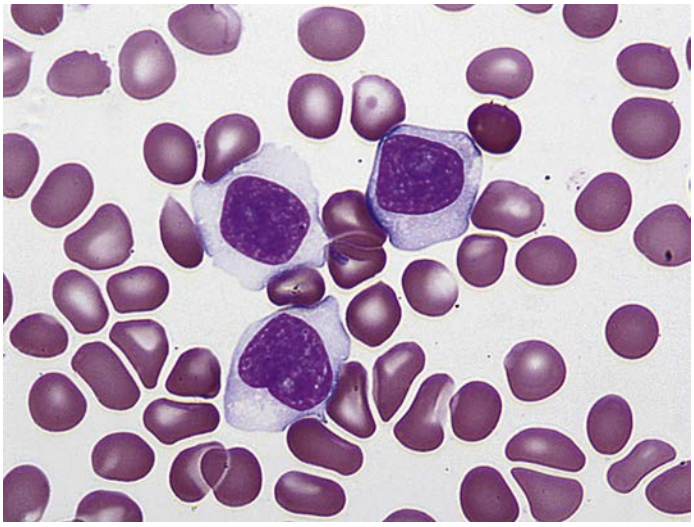

Figure 34.45 B-cell prolymphocytic leukemia typically shows high white blood cell count, large lymphocytes with moderately abundant cytoplasm, and prominent nucleoli, although variability is noted (×1000).

Immunoglobulin genes are clonally rearranged, and half of cases show somatic mutations, most frequently in *NOTCH2* (Baliakas et al., 2014; Mian et al., 2014; Parry et al., 2013). Translocation/loss of 7q21-32 is noted in 40% of cases, and trisomy 3q in some. Bcl-2 is variable.

SMZL is indolent but has shown poor response to therapy. Treating patients using chemotherapy combined with anti-CD20 therapy appears promising (Arcaini, 2004).

Hairy Cell Leukemia

Bouroncle (1958) initially described this disorder, which is clinically variable in its manifestations. HCL occurs more frequently in males than in females. The mean age of afflicted patients is 50 years. It has an insidious onset and is characterized by proliferation of abnormal cells in the reticuloendothelial organs and blood. Splenomegaly is the predominant physical finding (Foucar, 2008). Pancytopenia or depression of only two cell lines is the usual finding, with variable numbers of hairy cells. Monocytopenia is characteristic and hairy cells are usually infrequent in the blood, although they may result in leukocytosis. In most cases, BM aspiration is difficult. Marrow biopsy shows a marrow that varies in cellularity, often having both hypocellular and hypercellular areas and reticulin fibrosis. Hypocellular cases of HCL occur and mimic aplastic anemia. Morphologically, the cells are medium sized (10–20 μm in diameter) with round to oval nuclei, although many are notched or dumbbell or bean shaped. The chromatin pattern is usually uniformly reticular, and nucleoli are small and inconspicuous. In some cells, chromatin is more condensed, resembling that of a lymphocyte. The cytoplasm is moderate in amount, is light blue-gray, and exhibits numerous hair-like projections and frayed borders, most prominent on electron micrographs (Fig. 34.48).

In marrow sections, cells with small central nuclei, abundant cytoplasm, and reticulin fibrosis produce a characteristic fried-egg appearance, which may resemble erythroid islands when involvement is not extensive (Fig. 34.49). Chromatin is usually more delicate and nuclei more irregular than in erythroid precursors. In small or poorly preserved biopsies, HCL may be mistaken for large B-cell lymphoma.

Splenectomy specimens are usually diagnostic, with red pulp infiltrates of cells similar to those in the marrow. In addition, the cells tend to line splenic sinuses, obliterating the endothelium and producing red cell "lakes," which lack visible endothelium. Lymph nodes may show paracortical infiltrates, and the liver may show sinus infiltration.

Cytochemically, these cells contain acid phosphatase, which is resistant to inhibition by tartrate-resistant acid phosphatase; this is in contrast to the isoenzymes of acid phosphatase present in other hemic cells (Yam, 1971).

Immunophenotype is mature B cell (CD19, CD20, CD22, CD79a, DBA.44, FMC-7, and surface membrane immunoglobulin [SMIg]) with expression of hairy cell–associated markers CD103, CD25, CD11c, CD123, annexin A1 (ANXA1), and (dim) cyclin D1 (Falini, 2004). Cells are negative for CD5, CD10, and CD23. Immunoglobulin heavy- and light-chain genes are rearranged, with somatic mutation of V gene regions. HCL shows consistent *BRAF* V600E mutation (Tiacci et al., 2011; Waterfall et al., 2014).

The clinical course is usually chronic but may be acute or subacute. Median survival is between 5 and 6 years. Traditionally, splenectomy has offered significant benefit to many patients. Treatment with α-interferon provided the first chemotherapy remissions, but pentostatin (2′-deoxycoformycin) and cladribine (2-chlordeoxyadenosine) now produce more durable remissions. BRAF inhibitors can be used to treat refractory or relapsed cases.

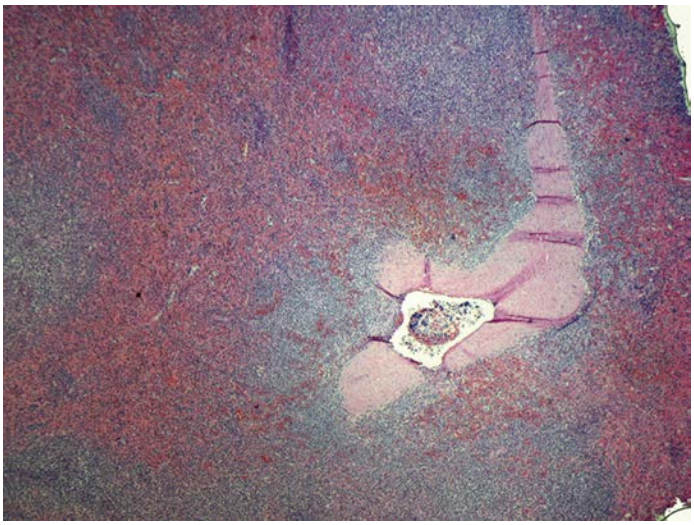

Figure 34.46 Splenic marginal zone lymphoma showing mild white pulp expansion and patchy red pulp involvement (×100).

Splenic B-Cell Lymphoma/Leukemia, Unclassifiable

Splenic Diffuse Red Pulp Small B-Cell Lymphoma

This is a lymphoma of small B cells with diffuse splenic red pulp involvement and involvement of BM sinusoids and blood. At least some cases were previously referred to as splenic lymphoma with circulating villous lymphocytes due to circulating neoplastic cells with short cytoplasmic villi, often with a polar distribution (Fig. 34.50). Neoplastic lymphocytes show clumped chromatin and moderate basophilic cytoplasm. Patients have massive splenomegaly but often low levels of lymphocytosis. Neoplastic cells may circulate in the blood, even in the absence of marrow involvement. The phenotype is B cell with expression of DBA.44 and surface IgG, but usually absent CD103 and absent annexin A1.

Hairy Cell Leukemia Variant

Most cases of hairy cell variant are described as lymphoproliferative disorders resembling HCL but with a high WBC count and the presence of prominent nucleoli (Sainati, 1990), and not closely related biologically. These cases have morphology and clinical features intermediate between HCL and PLL (Fig. 34.51). Response to chemotherapy is poor, but the

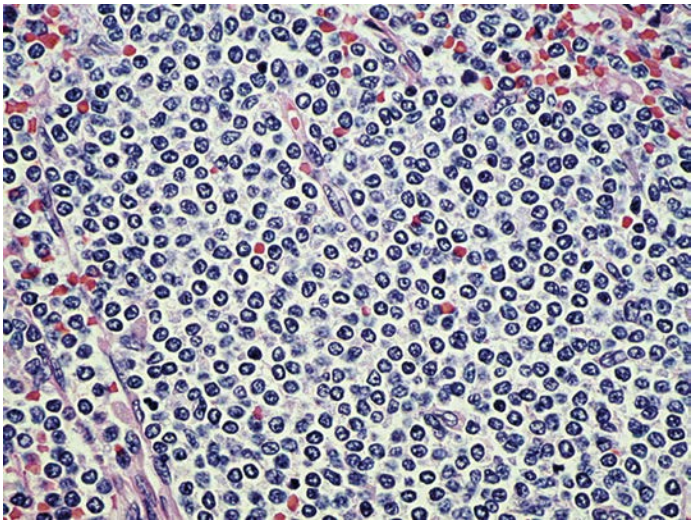

Figure 34.47 Higher-power view of splenic red pulp involvement by monocytoid splenic marginal zone cells in splenic marginal zone lymphoma (×200).

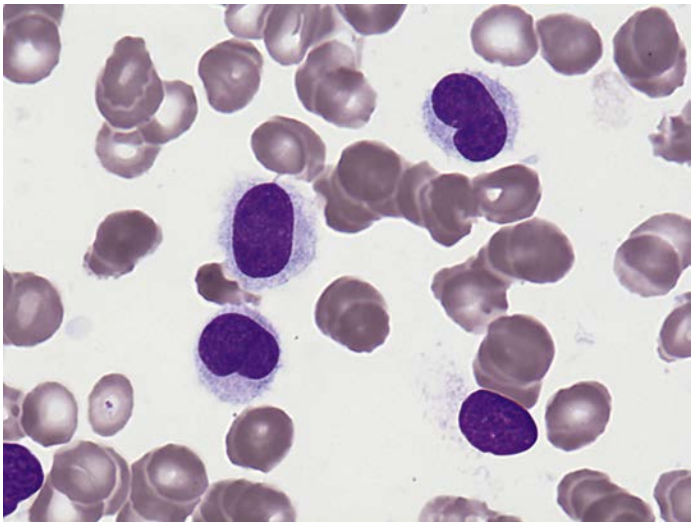

Figure 34.48 Hairy cell leukemia shows lymphoid cells with foamy cytoplasm and cytoplasmic projections, and oval or indented nuclei with reticular chromatin (×1000).

clinical course is chronic, and remission may be attained with splenectomy. TRAP and CD103 are variable, and CD25 and annexin A1 are usually negative. A very rare form of variant HCL has been described, mostly in Japanese patients, and is referred to as *Japanese variant*. This disorder shows slightly more prominent nucleoli than typical HCL, but less so than prolymphocytoid variants, also variable CD103 and TRAP, negative CD25, and usually lack of surface Ig. It shows clonal rearrangement of Ig genes and must be distinguished from polyclonal B-cell lymphocytosis with similar morphology. Many cases of HCL-v exhibit *MAP2K1* mutations (Waterfall et al., 2014).

Lymphoplasmacytic Lymphoma

Lymphoplasmacytic lymphomas (*LPLs*), a term derived from the Kiel classification (Stansfeld, 1988), refers to tumors of small lymphocytes with plasmacytoid differentiation and plasma cells, secretion of a monoclonal IgM paraprotein, and lack of CD5 expression. They usually involve BM, lymph nodes, and spleen (Fig. 34.52).

Lymph nodes show diffuse infiltrates of lymphocytes, plasmacytoid lymphocytes, and plasma cells. Proliferation centers are not present, and monocytoid B cells are not seen. The infiltrate may be paracortical, with sparing of sinuses. PAS-positive inclusions are often seen in the cytoplasm, and Golgi-centered inclusions frequently invaginate into the nucleus of the lymphoid cells, forming **Dutcher bodies**. Tissue mast cells are frequently increased.

The BM usually shows nodular and/or diffuse interstitial infiltrates of similar cells. Blood involvement may be present, but with lower WBC counts than CLL.

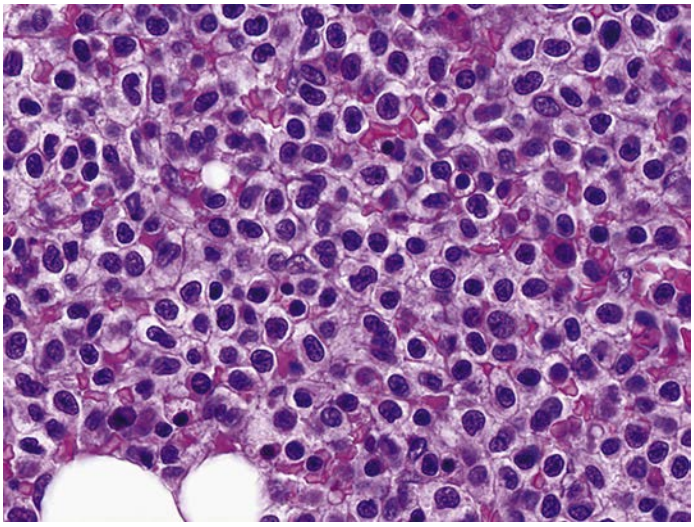

Figure 34.49 Hairy cell leukemia in a bone marrow biopsy shows small nuclei with moderate cytoplasm and distinct cytoplasmic boundaries (×500).

The immunophenotype shows B cell markers CD19, CD20, CD22, and CD79a with bright surface and cytoplasmic IgM (occasionally IgG or IgA) but not IgD, and a monoclonal κ or λ light chain. It differs from CLL by absence of CD5 and bright immunoglobulin expression. CD10 and CD23 are also negative; CD38 is positive, and CD43 is variable.

Ig heavy- and light-chain genes are clonally rearranged, and there is somatic mutation of variable regions, consistent with a post-antigen selection (post-GC) state of maturation and differing from CLL (Swerdlow, 2017).

MYD88 L265P mutation has emerged as a defining genetic feature of LPL and *CXCR4* mutations also occur (Hamadeh, 2014; Patkar, 2014; Treon, 2014; Varettoni, 2013). Del6q21 and trisomy 4 are frequent in LPL, and trisomies 3 and 18 and other abnormalities are sporadically reported.

The term *Waldenström's macroglobulinemia* (*WM*) refers to LPL with BM involvement and a monoclonal IgM paraprotein. It has a peak incidence between the ages of 60 and 70 years. Symptoms of increased viscosity include visual disturbances, neurologic symptoms, impaired kidney function, and congestive heart failure. Hemorrhagic phenomena may occur as the result of interference of complexes with platelets and clotting factors. Cryoglobulinemia occurs somewhat more frequently than with myeloma and often results in Raynaud phenomenon.

Normochromic, normocytic anemia is sometimes associated with thrombocytopenia or pancytopenia. Relative or slight absolute lymphocytosis is usually found. Marked rouleaux formation is evident on the blood film, and the sedimentation rate is usually extremely rapid, although it may be low if macrocryoglobulins are present and the test is carried out at a lower temperature. Anemia is occasionally hemolytic with a positive Coombs test. Some cases of WM may be due to marginal zone lymphoma but diagnostic test for *MYD88* mutation will likely clarify this possibility.

Heavy-Chain Diseases

A small number of patients produce and excrete heavy-chain fragments without associated light chains (Bianchi, 2014). Some of these proteins show structural mutations. The classification of associated lymphoproliferative disorders is somewhat ambiguous. Lymphoproliferative disorders associated with γ heavy-chain disease often resemble LPL or plasmacytoma; μ heavy-chain disease may resemble CLL, and α heavy-chain disease is associated with mucosa-associated lymphoid tissue (MALT) lymphoma.

γ Heavy-Chain Disease

γ heavy chain disease (HCD) is a lymphoproliferative disorder characterized by secretion of a truncated γ-chain without light-chain binding sites. It presents with lymphadenopathy, hepatosplenomegaly, fever, and propensity to infection. Anemia is constantly present, often with leukopenia and thrombocytopenia. Atypical lymphocytes or plasma cells are frequently present in the blood, and a few cases have terminated in plasma cell leukemia. The marrow is usually abnormal, with increased plasma cells, lymphocytes, and eosinophils. A rather broad serum protein "spike" has been found in the βγ-region in most patients, accompanied by hypogammaglobulinemia. The diagnosis is made by showing that the protein reacts on immunoelectrophoresis with antisera to γ-chains but not to light chains.

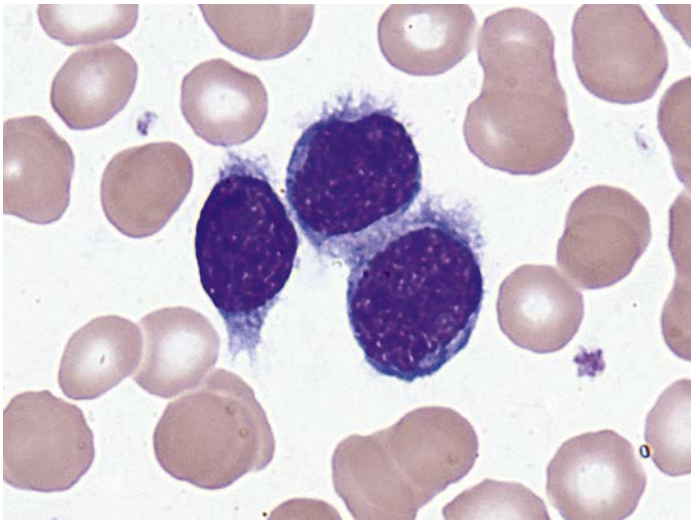

Figure 34.50 Villous lymphocytes (×1000).

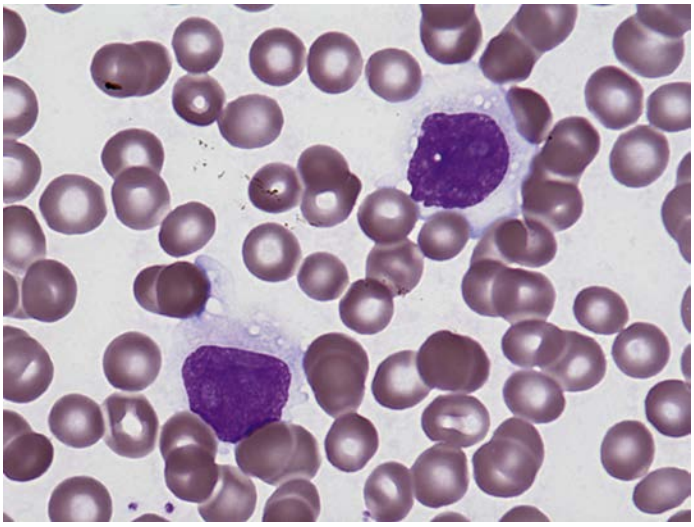

Figure 34.51 Hairy cell leukemia (HCL) variant shows morphology intermediate between usual HCL and prolymphocytic leukemia.

The protein is also found in the urine in varying amounts, although concentration techniques may be necessary to demonstrate it.

α Heavy-Chain Disease

α Heavy-chain disease (HCD) appears to be more common than γ HCD and involves a younger age group. The uniform clinical pattern in most patients is malabsorption and diarrhea accompanying a massive lymphoplasmacytic infiltration of intestinal mucosa, sometimes evolving to large B-cell lymphoma. It has also been referred to as *Mediterranean abdominal lymphoma* and *immunoproliferative small intestinal disease* (*IPSID*). In a few patients, the respiratory tract has been involved instead. BM and other lymphoid organs have not been involved. Usually, routine protein electrophoresis is negative, but small amounts of α chain may be detected in the serum and sometimes in the urine with immunoelectrophoresis. The abnormal protein does not contain light chains. It is most common in Mediterranean areas and is associated with poor living conditions in low socioeconomic groups. Similar to MALT lymphoma, many cases may initiate an infectious antigen-driven proliferation.

μ Heavy-Chain Disease

The few patients who have been described with μ HCD have had chronic lymphocytic leukemia with vacuolated plasma cells in the marrow. Routine serum electrophoresis showed only hypogammaglobulinemia. The μ heavy chain was detected by serum immunoelectrophoresis; it was not found in the urine. In most patients, however, the urine contained κ light chain in large amounts (Franklin, 1975).

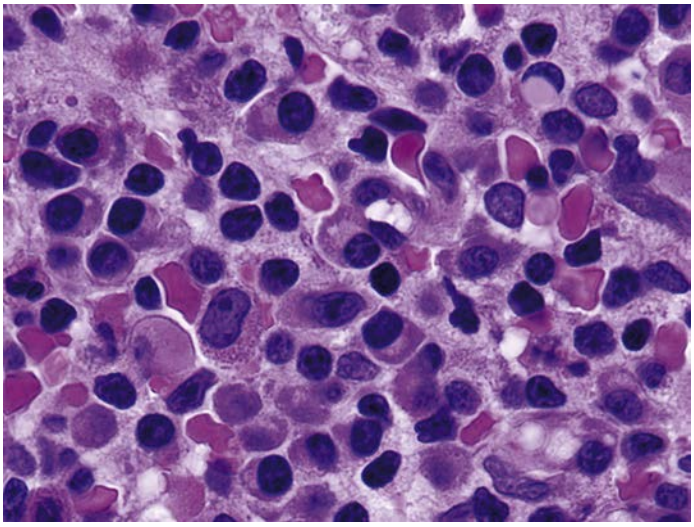

Figure 34.52 Lymphoplasmacytic lymphoma involving the marrow, with associated Waldenström macroglobulinemia. Lymphocytes, plasma cells, plasmacytoid lymphocytes, and a rare Dutcher body *(upper right)* can be seen (×1000).

Plasma Cell Neoplasms

Clonal neoplasms of mature plasma cells are common neoplasms that have been difficult to treat and are greatly feared. They are now known, however, to consist of a spectrum of disease varying from indolent and nonprogressive to highly aggressive and refractory to therapy. The best measures of disease course are the clinical findings themselves. Treatments using new agents are rapidly evolving to increase efficacy and improve outcome. Major categories now are monoclonal gammopathy of undetermined significance, smoldering or asymptomatic myeloma, and symptomatic myeloma (Box 34.13).

Monoclonal Gammopathy of Undetermined Significance

Monoclonal gammopathy of undetermined significance is the term utilized when a monoclonal serum immunoglobulin is present but no myeloma is detectable. Most cases (75%) are IgG, with smaller proportions of IgM (15%) and IgA (10%). It is a preneoplastic condition with progression to myeloma in about 1% of affected patients per year. The condition consists of a monoclonal Ig (M-component) of <30 g/L IgG, <10% clonal plasma cells in the marrow, absence of lytic bone lesions, no myeloma-related organ or tissue impairment (CRAB: hypercalcemia, renal insufficiency, anemia, or bone lesions), and no evidence of other B-cell lymphoproliferative disorders. Cytogenetic and immunophenotypic abnormalities are similar to those in myeloma, and none is known to be predictive of progression (Landgren, 2013).

Plasma Cell Myeloma

Plasma cell myeloma is a neoplastic proliferation of plasma cells, occurring primarily in the BM. Although plasma cells also proliferate in lymph nodes and spleen, these organs are rarely enlarged.

Multiple myeloma is rare in those younger than 40 years of age. The mean age at the time of diagnosis is 62 years, with an equal sex distribution. Bone pain is the most common symptom, and pathologic fractures are frequent. Neurologic symptoms may be prominent from encroachment of tumor that has broken through the bony cortex on spinal nerves or spinal cord. Bone destruction leads to calcium mobilization, with increased calcium in the serum and metastatic calcification. Growth of myeloma cells in the marrow produces multiple tumors, which appear on a radiograph as multiple punched-out osteoporotic lesions. Occasionally, the growth is diffuse and appears as diffuse osteoporosis. A propensity to infection is common because of impaired production of antibodies.

There is usually normochromic, normocytic anemia, and normoblasts may be present in the blood. The leukocyte count is slightly decreased, normal, or slightly increased. Occasional myeloid left shift to the myeloblast may be noted. The platelet count is usually normal but may be decreased. The most striking feature of the blood film is the marked degree of rouleaux formation.

The BM shows the presence of plasma cells or myeloma cells, ranging from less than 1% to over 90% depending on the degree of involvement at the site of the aspirated marrow. Diagnosis of myeloma and its variants is based on both pathology and clinical findings, including serum monoclonal

BOX 34.13

Diagnostic Criteria for Monoclonal Gammopathy of Undetermined Significance, Smoldering Myeloma, and Plasma Cell Myeloma

Monoclonal Gammopathy of Undetermined Significance

M-protein in serum <30 g/L
Marrow plasmacytosis <10%
No lytic bone lesions
No myeloma-related symptoms (no CRAB)

Smoldering (asymptomatic) Myeloma

Serum M-component >30 g/L
Marrow plasmacytosis >10%
No end-organ impairment (no CRAB) or amyloidosis

Plasma Cell Myeloma

M-protein in serum or urine (no specific level needs be met)
Bone marrow clonal plasma cells
Organ or tissue impairment (CRAB)

CRAB, Hyper***c***alcemia, ***r***enal insufficiency, ***a***nemia, or ***b***one lesions.

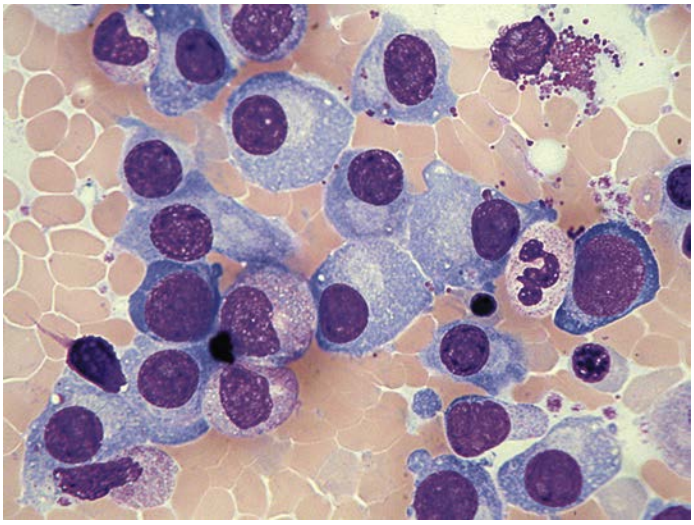

Figure 34.53 Myeloma in the bone marrow showing large plasma cells with nucleoli (×1000).

immunoglobulin and radiologic evidence of lytic bone lesions. Lytic bone lesions are associated with increased osteoclastic activity, hypercalcemia, and neurologic changes. This may be related to activity of the receptor activator for NF-κB (RANK) ligand.

Cytologically, the cells may be indistinguishable from normal plasma cells, but they usually show abnormal chromatin, with less clumping of nuclear chromatin, large nucleoli, lack of perinuclear clear zones, lighter blue cytoplasm, or varying degrees of anaplasia (Fig. 34.53). Immature, plasmablastic, and anaplastic variants are described.

The immunophenotype is variable, most typically with expression of CD38 and CD138, loss of CD19 expression (normally present on plasma cells), and absence of CD20, but with abnormal acquisition of CD56 and, often, CD117. Immunohistochemical labeling or mRNA in situ hybridization of BM sections for κ and λ usually identifies monoclonal plasma cells. Cyclin D1 expression is associated with t(11;14).

Cytogenetic analysis divides myeloma into two main groups: hyperdiploid with multiple trisomies involving odd-numbered chromosomes and associated with good prognosis; and hypodiploid associated with adverse prognosis. Karyotype and FISH studies show frequent del13q14 (50% of cases), translocations t(4;14) with associated overexpression of *MMSET* and *FGFR3*, t(14;16) with associated *MAF* overexpression, t(14;20), or deletion of TP53 (del 17p13) that, along with aneuploidy, are unfavorable. In contrast, t(11;14) or t(6;14) are favorable. Losses of 8, 13, 14, and X are common. Biological features may be used for prognostic grouping and to identify therapeutic targets (Landgren & Morgan, 2014; Vincent Rajkumar, 2014; Zhou, Barlogie, & Shaughnessy, 2009).

Serum globulin is usually increased, often strikingly so. This increase is responsible for the tendency toward rouleaux formation and an elevated ESR. Serum protein electrophoresis usually shows an M spot, a homogeneous band in the γ or β region; less commonly, there is hypogammaglobulinemia (when only light chains are produced by the neoplastic plasma cells). Immunoelectrophoresis indicates that the monoclonal protein is IgG in over 50% of cases, IgA in about 20%, IgD in less than 1%, and IgE very rarely. Roughly 5% of myeloma proteins are cryoglobulins, that is, proteins that precipitate from cooled serum and redissolve on warming. Some tumors secrete free monoclonal light chains (Bence Jones protein), in addition to the whole immunoglobulin molecule, and in about 25%, only light chains are produced. Hypogammaglobulinemia is found in the latter group because light chains are filtered through the renal glomerulus, leaving little or none in the serum, in addition to the fact that immunoglobulin production by nonmalignant plasma cells is greatly reduced. If renal damage has occurred, albumin and whole immunoglobulin molecules are also found in the urine. Excretion of light chains sometimes results in obstruction and loss of nephrons and so-called myeloma kidney. Renal insufficiency is common and is the presenting feature of multiple myeloma in some cases. Amyloidosis, which is present in about 10% to 15% of cases of multiple myeloma, may be a factor in renal failure.

Median survival after diagnosis of multiple myeloma has been approximately 3 to 4 years, but new drugs are likely altering this.

Clinical Variants. Smoldering (Asymptomatic) Myeloma. Smoldering myeloma shows M protein at myeloma levels (>30 g/L) and/or 10% or more clonal plasma cells in the marrow with no related organ/tissue impairment (CRAB). Patients with solitary plasmacytoma and bone lesions detected only by magnetic resonance imaging (MRI) are included. These asymptomatic patients differ from those with MGUS primarily by a higher rate of progression: 10% per year for the first 5 years, 3% per year for the next 5 years, and then 1% per year thereafter (Landgren, 2013).

Nonsecretory Myeloma. These patients are similar to others with myeloma, except that tumor cells do not produce (15%) or secrete (85%) immunoglobulin. The incidences of renal insufficiency, hypercalcemia, and depression of normal Ig are less.

Plasma Cell Leukemia. Often in multiple myeloma, a few plasma cells are found in the peripheral blood. Only in the rare instances of myeloma in which large numbers of plasma cells circulate (either >20% of blood leukocytes, or $>2 \times 10^9$/L) is the term *plasma cell leukemia* used (Fig. 34.54). Patients with plasma cell leukemia tend to have tissue infiltration, advanced-stage disease, and poor survival (Fernandez de Larrea et al., 2013). The immunophenotype varies from usual myeloma in that CD56 is often absent.

Solitary Plasmacytoma of Bone. These patients show no clinical features of myeloma but may have a monoclonal immunoglobulin without suppression of normal immunoglobulin. Tumors are controlled by radiation, but two-thirds of cases eventually progress to myeloma.

Extraosseous Plasmacytoma. Extramedullary solitary plasmacytomas occur in the GI tract, bladder, CNS, breast, thyroid, testis, parotid gland, lymph nodes, or skin and are irradiated. They recur in one-quarter of patients but progress to myeloma in only about 15%.

Monoclonal Immunoglobulin Deposition Diseases

Primary Amyloidosis

Primary amyloidosis, an uncommon presentation of plasma cell neoplasms of various types, results from abnormal polymerization of immunoglobulin into β-pleated sheets in connective tissue. A variety of amyloid types occur, including hereditary, secondary associated with chronic inflammation, the type associated with Alzheimer disease, and others. All amyloid is biochemically composed of an A protein component and a P component. In plasma cell dyscrasia, the A component is derived from immunoglobulin light (L) chains and is referred to as *AL amyloid*. It may be detected by homogeneous pink staining of thickened blood vessels in abdominal fat, BM, rectum, or other tissues. Congo Red stain shows characteristic apple-green birefringence under polarized light. It may also be detected by thioflavin T, antibodies against amyloid P, and antibodies against immunoglobulin light chains. It may involve the heart, with subsequent congestive failure, liver with hepatomegaly, kidney with nephrotic syndrome or renal failure, nerves with sensory/motor loss, and other organs. It may occur in overt myeloma (20%), but most often it is seen in patients with disease otherwise fulfilling criteria for MGUS.

Monoclonal Light- and Heavy-Chain Deposition Diseases

Nonamyloid immunoglobulin deposition may result in organ dysfunction in rare disorders known as light-chain deposition disease (LCDD) or heavy-chain deposition disease (HCDD) (Swerdlow, 2017).

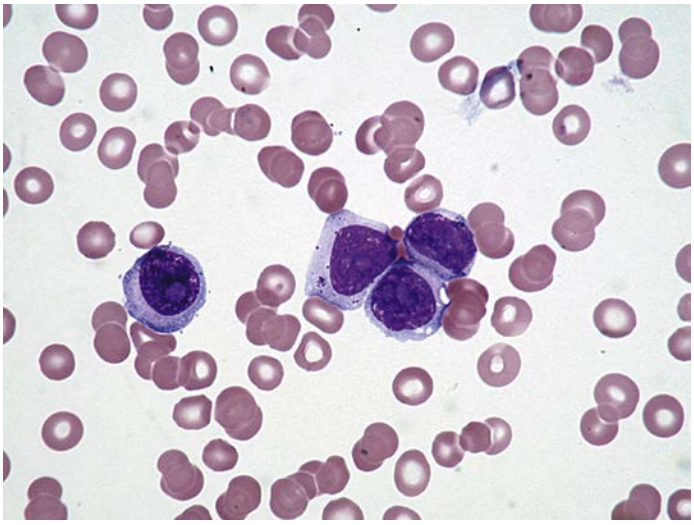

Figure 34.54 Plasma cell leukemia with cells resembling immunoblasts (×1000).

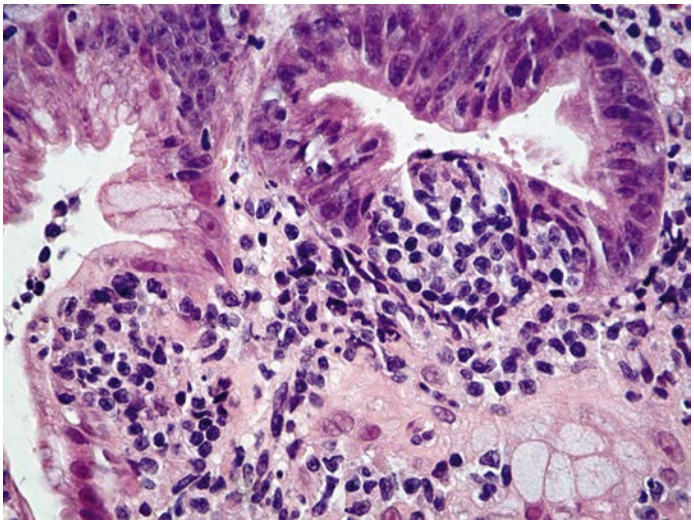

Figure 34.55 Mucosa-associated lymphoid tissue lymphoma with nests in lymphocytes in gastric epithelium (×500).

Plasma Cell Neoplasms with Associated Paraneoplastic Syndrome

POEMS Syndrome

This is a syndrome of polyneuropathy, organomegaly, endocrinopathy, monoclonal gammopathy, and skin changes (POEMS) associated with osteosclerotic multiple myeloma showing marrow fibrosis and sclerosis and with lymph node changes resembling plasma cell Castleman disease. The plasma cells usually express λ light chain, and heavy chain is IgG or IgA.

TEMPI Syndrome

This is a syndrome of telangiectasias, elevated erythropoietin and erythrocytosis, monoclonal gammopathy, perinephric fluid collection, and intrapulmonary shunting associated with plasma cell neoplasm. The clonal plasma cells are most commonly IgG κ, and usually <10% of the total bone marrow cells.

Extranodal Marginal Zone Lymphoma of Mucosa-Associated Lymphoid Tissue

Extranodal marginal zone B-cell lymphoma of mucosa-associated lymphoid tissue (MALT lymphoma) is an indolent lymphoma of mucosal tissue, including the stomach, other GI tract, bronchi, salivary glands, thyroid, skin, and other areas. MALT lymphoma of the stomach is in many cases an antigen-driven clonal B-cell proliferation related to infection by *Helicobacter pylori*, which is also associated with gastric ulcer; early cases may respond to antibacterial therapy. Other patients have autoimmune disorders such as Sjögren syndrome or Hashimoto thyroiditis. The terminology of MALT lymphomas refers only to those of predominantly small cells, although large-cell and other aggressive lymphomas may arise in the same tissues. α Heavy chain disease, or IPSID, is considered a special subtype of this disease (see earlier discussion).

Gastric or other mucosa is infiltrated by small lymphocytes that form clusters within the epithelium, referred to as *lymphoepithelial lesions* (Fig. 34.55). Submucosa contains diffuse infiltrates of small lymphocytes, centrocytes, monocytoid lymphocytes, and plasma cells. GCs, apparently reactive to the entire process, are usually present. Plasma cells often are abundant at the periphery of the lesions and generally are monoclonal.

The immunophenotype is B cell (CD19, CD20, CD22, CD79a) with surface Ig. CD5, CD10, bcl-6, and usually CD23 are negative. Bcl-2 is frequently positive, and CD43 is variable. Follicular dendritic cell–associated markers CD21 and CD35 often reveal expanded follicular meshworks and colonized GCs. Ig genes are clonal with somatic mutations. Trisomies 3 and 18 occur frequently. Translocation 11;18 creates an *BIRC3-MALT1* fusion and occurs in gastric MALT tumors not responsive to *H. pylori* treatment. Translocations 1;14 and 14;18 deregulate *BCL10* and *MALT1*, respectively. Each translocation deregulates NF-κB (Isaacson, 2005). These tumors are typically indolent, with good response to radiation therapy.

Nodal Marginal Zone Lymphoma

These tumors are derived from post-GC marginal zone B cells and show small lymphocytes surrounding reactive follicles and expanding in the interfollicular zones. They may resemble nodal involvement by MALT lymphoma or splenic marginal zone lymphoma (Fig. 34.56). GC colonization is frequent, as are plasma cell differentiation and occasional eosinophilia. Increased large cells may be present and do not apparently affect prognosis, although transformation to diffuse large B-cell lymphoma may occur.

The immunophenotype is similar to MALT or SMZL, with surface Ig (IgM/IgD, IgM, less often IgA or IgG), B-cell markers (CD19, CD20, CD22, CD79a), expression of CD23, variable CD43, and absence of CD5 or CD10. Bcl-2 is expressed in a majority of cases, and survivin is overexpressed in about 50%, suggesting activation of anti-apoptotic pathways. Nodal MZL is heterogeneous at the molecular and immunohistochemical levels (Camacho, 2003). Ig heavy-chain and (monotypic) light-chain genes are rearranged. Trisomies 3, 7, and 18 may occur, and 5-year survival is greater than 50%.

Pediatric Nodal Marginal Zone Lymphoma

A clinical subtype of nodal marginal zone lymphoma occurs in the pediatric age group, usually in boys, with localized lymphadenopathy of the head and neck. Tumors contain a progressively transformed GC and resemble reactive lymphadenopathy, but show clonal immunoglobulin gene rearrangement. Children have excellent outcomes with conservative treatment.

Follicular Lymphoma

Follicular lymphoma (FL) is a group of related lymphomas of GC-derived B cells. Morphologic distinction between the subgroups is based on the numbers of centroblasts in the neoplastic follicles (Harris, 2011).

The overall morphologic pattern (Fig. 34.57) shows recapitulation of lymph node follicles but with limited diversity of cell type and lack of proliferation of other lymph node structures. The tumors generally show crowded follicles of more than usual uniformity, lacking distinct mantles and with little intervening paracortex, and lacking normal GC **tingible body** macrophages and polarization. Most often, small irregular cells (small cleaved cells or centrocytes) predominate, with variable numbers of admixed large cells (large cleaved and noncleaved cells or centroblasts). There may be diffuse infiltrates as well. The term *follicular* indicates a greater than 75% follicular pattern; *follicular and diffuse* refers to cases that are 25% to 75% follicular; *focally follicular* refers to cases with less than 25% follicular pattern; and *diffuse* indicates that no follicular component is present (Table 34.6). BM involvement is frequent and usually first involves the paratrabecular regions, often in a spotty fashion.

Cytologic grading is based on the average number of centroblasts (CBs) per high-power field (hpf) within neoplastic follicles (Figs. 34.58 and 34.59). It is now recommended that grades 1 and 2 be combined into grade 1-2. An hpf is defined as that with a 40× lens and a 10× ocular with

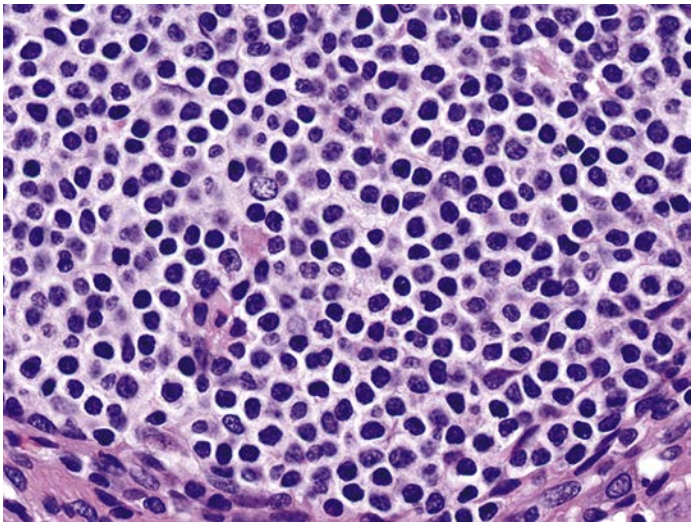

Figure 34.56 Nodal marginal zone lymphoma showing a nodule of monocytoid B cells (×200).

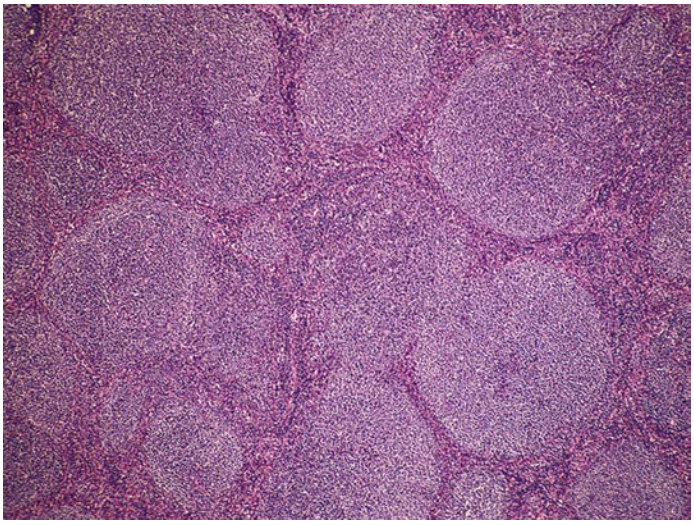

Figure 34.57 Low-power view of follicular lymphoma, recapitulating lymph node germinal centers (×200).

an 18-mm field of view. A 50× lens with a 22-mm 10× ocular, often used in wet hematology, provides a nearly equivalent field of view.

Marginal zone or monocytoid B-cell differentiation occurs in up to 10% of cases. It usually appears around follicles and in interfollicular areas and resembles a composite lymphoma. FL shows an immunophenotype of mature B cells with bright monoclonal surface Ig, CD19, CD20, CD22, CD23, CD79a, and CD10 expression. Bcl-2 (cytoplasmic) and bcl-6 (nuclear) are both usually expressed, which helps to separate FL from reactive hyperplasia (bcl-2–negative/bcl-6–positive) and other lymphomas not of germinal center cell (GCC) derivation (bcl-6–negative). CD5 and CD43 are typically absent.

IgH is clonally rearranged along with a light-chain Ig gene, and there is t(14;18)(q32;q21) with juxtaposition of IgH and *BCL-2*. Bcl-2 protein is inappropriately expressed, and subsequent inhibition of apoptosis is considered a primary pathogenic mechanism of FL. Deletions of 9p or 17p13 involving TP53 (both associated with large cell transformation) may be seen, and rearrangements or mutations of *BCL6* at 3q27, and abnormalities of X, 1, 2, 4, 5, 7, 12, 13, and 18. Genomic studies show driver mutations of chromatin regulators *KREB2*, *EZH2*, *KMT2D* (*MLL2*), and mutations occurring at time of transformation in *EBF1*, *MYD88*, and *TNFAIP3* (Okosun et al., 2014).

Prognosis is variable, with grades 1 and 2 disease generally showing an indolent course but lack of cure. Grade 3 is more aggressive but likely more curable. Attempts to identify patients requiring aggressive therapy have led to a follicular lymphoma international prognostic index (FLIPI) based on age, stage, hemoglobin, number of nodal areas involved, and LD. Diffuse large B-cell lymphoma (DLBCL) is considered by WHO authors to be a different entity even when it arises in FL (Swerdlow, 2017). In these situations, two diagnoses are recommended, such as "follicular lymphoma, grade 3/3 (75%), with diffuse large B cell lymphoma (25%)," when the DLBCL occupies 25% of the sampled tumor. Leukemic involvement by FL may also occur and is sometimes known as *lymphosarcoma cell leukemia*. Flow cytometry is helpful to distinguish between that, CLL, and leukemic mantle cell or marginal zone lymphomas.

Diffuse FL is essentially a diffuse transformation of grade 1 or 2 FL. Diagnosis requires phenotyping and/or cytogenetic studies to rule out mantle cell or marginal zone lymphoma, and includes previous categories of diffuse small cleaved cell, centrocytic diffuse, diffuse mixed small cleaved, and large cell and centrocytic/centroblastic diffuse.

FL occurring in the pediatric age group (pediatric-type FL) is a distinct entity that usually lacks t(14;18) or bcl-2 expression and behaves in an indolent fashion. Most cases are grade 3. Primary intestinal FL may occur in duodenal polyps (duodenal-type FL) and is usually indolent, as are many other extranodal FL s. In situ follicular neoplasia of bcl-2–positive follicle cells has been described.

Large B-Cell Lymphoma with IRF4 Rearrangement

This is a rare subtype of large B-cell lymphoma characterized by *IRF4* rearrangement, which exhibits variable histomorphologic patterns, including entirely diffuse, follicular and diffuse, or entirely follicular. The neoplastic cells usually show strong IRF4/MUM1 expression. It occurs more frequently in children and tends to have good outcomes with immunotherapy with or without radiation.

TABLE 34.6

Follicular Lymphoma: Grading and Variants

Grading	Definition
Grade 1-2 (low grade)	
1	0–5 centroblasts per hpf
2	6–15 centroblasts per hpf
Grade 3	>15 centroblasts per hpf
3A	Centrocytes present
3B	Solid sheets of centroblasts
Reporting of Pattern	**Proportion Follicular**
Follicular	>75%
Follicular and diffuse	25%–75%
Focally follicular	<25%*
Follicular Lymphoma: Variants	
Diffuse large B-cell lymphoma with follicular lymphoma	Presence of diffuse areas with >15 centroblasts/hpf

From Swerdlow (2017).
hpf, High-power field of 40 × lens with 10 × 18-mm eyepiece or 50 × lens with 10 × 22-mm eyepiece (average of 10 fields within follicles).
*Give approximate percentage in report.

Primary Cutaneous Follicle Center Lymphoma

This is the most common primary cutaneous B-cell lymphoma and consists of variably distinct follicular to diffuse lesions in the dermis composed of bcl-6/CD20/CD79a–positive centrocytes and admixed centroblasts, with a background of CD21/CD35–positive follicular dendritic cells. Bcl-2 is usually negative, and CD10 is associated with more distinct follicular patterns. A bcl-2–positive FL in the skin suggests extension of disease from another location. Prognosis is excellent with typical response to radiation.

Mantle-Cell Lymphoma

Since the REAL classification was published, it has become recognized that mantle-cell lymphoma (MCL) is a dangerous form that combines refractoriness to therapy with an aggressive clinical course and poor survival. Refractoriness is likely due in part to strong expression of Bcl-2, also seen in normal mantle cells, FLs, and some other leukemias, lymphomas, and solid tumors. Bcl-2 inhibits apoptotic pathways.

The tumor usually shows a diffuse or sometimes mantle zone pattern (Swerdlow, 2017). In the mantle zone pattern, atrophic GCs are often seen in the center of nodules. These may be seen as occasional small

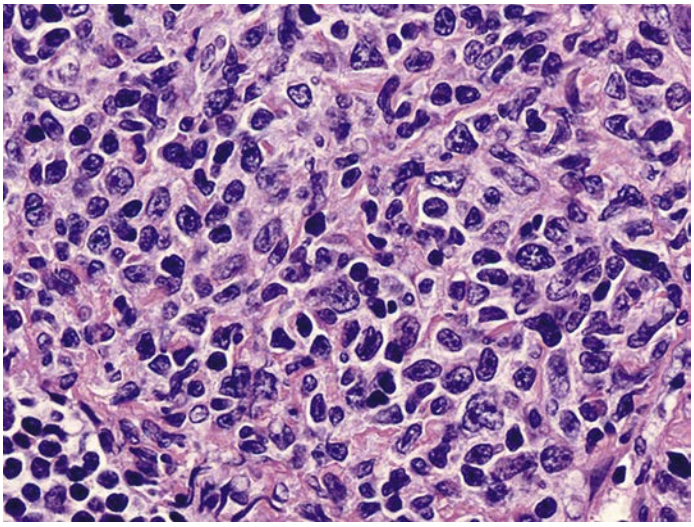

Figure 34.58 Follicular lymphoma, grade 2, showing centrocytes with 5–15 centroblasts per high-power field (hpf). Grade 1 shows <5 centroblasts per hpf.

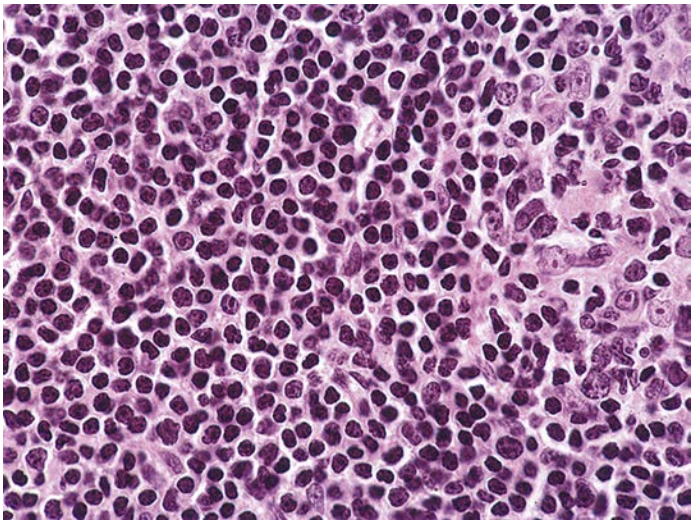

Figure 34.60 Mantle cell lymphoma, showing an expanded mantle around residual germinal center, which can be seen to the right in the figure

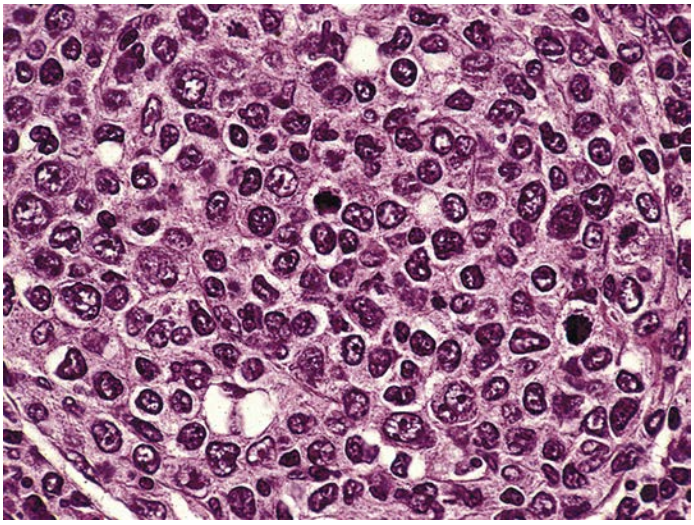

Figure 34.59 Follicular lymphoma, grade 3a, shows centrocytes with >15 centroblasts per high-power field (hpf) (×500).

naked follicles within a diffuse infiltrate. Nuclei are small to medium sized with clumped to moderately dispersed chromatin and a moderately increased mitotic rate. Nuclear membranes are typically slightly irregular, with occasional small round and cleaved nuclei also present. Scattered histiocytes with lightly eosinophilic cytoplasm are often present. A blastic or "blastoid" variant shows slightly larger nuclei with blast-like chromatin and a higher mitotic rate, simulating lymphoblastic lymphoma (Fig. 34.60).

These are monoclonal (monotypic surface IgM and IgD) B cells (CD19, CD20, CD22) with characteristic coexpression of CD5 (and CD43) and absence of CD23 or CD200. Bcl-2 and cyclin-D1 are expressed, while bcl-6 and CD10 are negative. Rare cases occur without CD5 expression or without cyclin D1. SOX11 is a useful marker for cyclin D1–negative cases and SOX11-negative MCL may be more indolent than usual MCL.

Immunoglobulin heavy and (monotypic) light-chain genes are rearranged. A majority of cases have t(11;14)(q13;q32) involving the Ig heavy-chain gene and *CCND1*. The t(11;14) translocation is usually detected by FISH. Complex karyotype, p16 deletion, or p53 deletion is often seen in advanced, blastoid, or pleomorphic variants. Secondary 8q24 abnormalities are associated with blastic/blastoid morphology and leukemic presentation (Setoodeh et al., 2013; Vose, 2013). BCL-2 rearrangements are absent. In situ mantle-cell neoplasm with cyclin D1–positive lymphoid cells restricted to the mantle zone of reactive lymphoid tissue has been described. These cases often have indolent clinical course, but a rare case may progress to overt MCL.

Diffuse Large B-Cell Lymphoma, NOS

DLBCL includes a variety of morphologies, all of which share a diffuse pattern, large cells, and mature B-cell phenotype (Swerdlow, 2017). It occurs in both nodal and extranodal sites and at all ages. It is frequent in immunosuppressed patients (often in association with EBV in these) and is the most common lymphoma of the CNS. Various morphologies are mimicked by peripheral T-cell lymphomas; thus, phenotyping is required for diagnosis.

DLBCL presents with diffuse infiltration by large B cells (nuclei larger than histiocytes or endothelial cell nuclei) with variable morphology. They may be centroblasts and/or centrocytes with scant cytoplasm and multiple nucleoli (centroblastic morphologic variant; Fig. 34.61). Some cases show plasmacytoid immunoblasts with large nuclei, one or more prominent nucleoli, and abundant amphophilic cytoplasm that may be eccentric (immunoblastic variant). Other cases of DLBCL show polymorphic cell morphology with large and small cells and Reed-Sternberg–like giant cells (anaplastic variant; Fig. 34.62). Still others occasionally show large cells with clear cytoplasm.

Neoplastic cells show surface Ig, sometimes cytoplasmic Ig, and B-cell markers (CD19, CD20, CD22, CD79a). CD30 is occasionally present in variable numbers of cells. CD20 expression by immunohistochemistry (IHC) is usually very helpful in paraffin-section diagnosis. CD10 and/or BCL6 suggests GC differentiation, and IRF4/MUM1 suggests post-GC differentiation.

In DLBCL, Ig heavy-chain and (monotypic) light-chain genes are rearranged. Bcl-2 and/or bcl-6 abnormalities and protein expression are frequent (Skinnider, 1999; Capello, 2000).

Gene array studies have separated DLBCL into at least four major expression groups: germinal center B-cell (GCB), activated B-cell (ABC)-like, type 3, and mediastinal large B-cell (MLBC) lymphoma. Of the first three, GCB shows better response to therapy than ABC or type 3. *BCL2* and *BCL6* are in the gene cluster of GCC-like tumors, and may be surrogates for this category. GC cases frequently show the t(14;18) translocation, deletion of *PTEN*, amplification of the miR-17-92 cluster, and/or TP53 mutations. *EZH2*, *MLL2*, and *CREBBP* mutations are found in over 20% and *MEF2* mutations in 12% (Jardin, 2014). ABC type often shows t(3;14) translocation, trisomy 3, deletion of the *INK4A-ARF* locus, and ***BCL2*** amplification, and shares *MLL2* mutations with GCB in about 30%. Genomic studies in DLBCL also show frequent abnormalities of DNA methyltransferases (*DNMT1-3*), histone deacetylases and methyltransferases, and transcription repressor *EZH2* that are targetable with azacytidine, histone deacetylase inhibitors (HDACs) and other targeted drugs (Cerchietti & Leonard, 2013).

Subgrouping by immunophenotyping roughly follows expression grouping. Cases with CD10 expression (>30% of cells) or CD10–, BCL-6+, and IRF4/MUM1– are considered GC types. All others are non-GC types. A variety of other specific types of DLBCL are also described by the WHO classification, as follows (Swerdlow, 2017).

T-Cell/Histiocyte-Rich Large B-Cell Lymphoma

T-cell/histiocyte-rich large B-cell lymphoma (TCHRLBCL) is characterized by a diffuse infiltrate of a limited number of large B cells

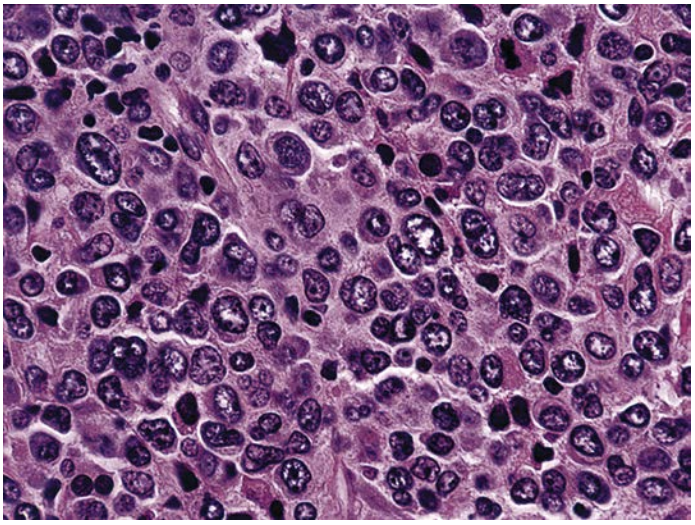

Figure 34.61 Diffuse large B-cell lymphoma with centroblasts and admixed centrocytes (×500).

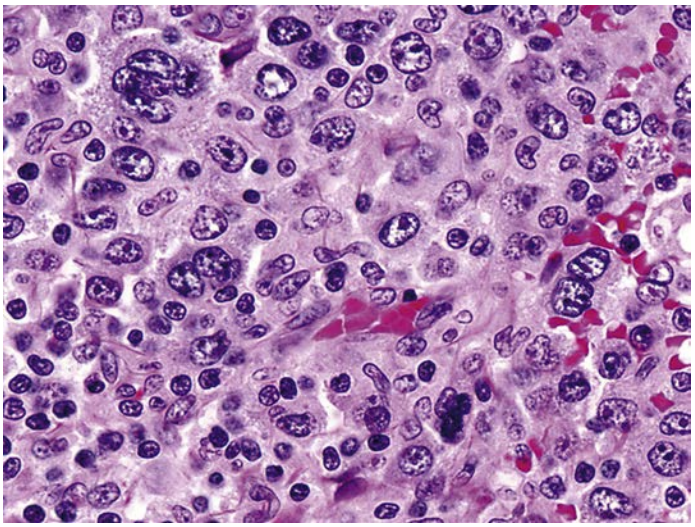

Figure 34.62 Diffuse large B-cell lymphoma, with polymorphism and Reed-Sternberg–like cells (×1000).

scattered among histiocytes and T cells. Large B cells usually constitute 10% or less of total cells, while T cells constitute the majority (Tousseyn & De Wolf-Peeters, 2011). The neoplastic cells may appear as centroblasts or immunoblasts or resemble lymphocyte and histiocytic (L&H) cells of lymphocyte-predominant HL (LPHL), and include Reed-Sternberg–like cells (Fig. 34.63). It is often difficult to distinguish it from nodular lymphocyte-predominant HL (NLPHL). However, the distinction is important as this is a usually aggressive tumor that presents with advanced stage, while LPHL is often localized and indolent and requires less therapy. The phenotype is similar to LPHL, with CD20, CD79a, and epithelial membrane antigen (EMA) positivity. J-chain, Oct-2, and Bob-1 are also expressed. Surface/cytoplasmic Ig, if monoclonal, is somewhat helpful, but LPHL is also now considered a clonal B-cell disease. Helpful distinctions are the diffuse infiltrate, T-cell background, lack of CD3/CD57 rosettes around neoplastic cells in a nodular B-cell background as seen in nodular LPHL, lack of residual IgD-positive mantle cells, and lack of a follicular dendritic meshwork by CD21/CD23/D35 staining. Advanced-stage presentation also suggests TCHRLBCL, but rare cases of NLPHL may present with disseminated disease.

Primary DLBCL of the Central Nervous System

CNS DLBCL usually presents in middle age as supratentorial tumors with various neurologic symptoms. Homogeneous to focally necrotic on MRI, they frequently show characteristic perivascular tumor cell accumulations on biopsy. These express pan-B-cell markers with BCL-6 and strong IRF4/MUM1 positivity in most and variable BCL-2 expression,

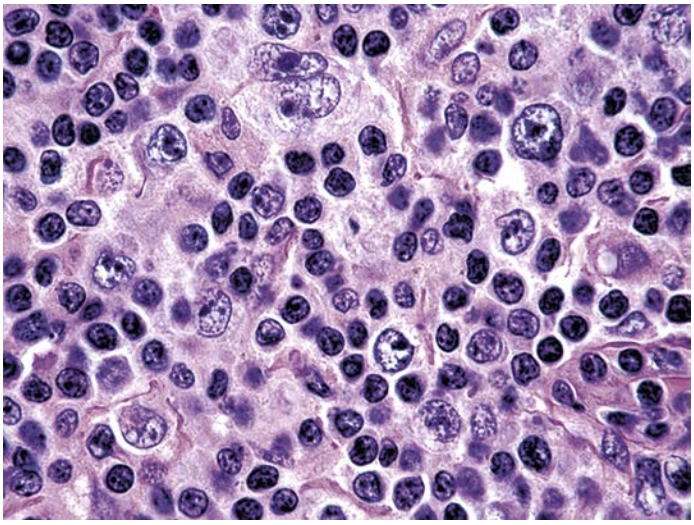

Figure 34.63 T-cell and histiocyte-rich large B-cell lymphoma resembles lymphocyte-predominant Hodgkin lymphoma, but most small cells are T cells (×500).

and they are typically EBV negative. Tumors typically respond to modern chemotherapy. MYD88 mutations are present in more than 35% (Jardin, 2014).

Primary Cutaneous DLBCL, Leg Type

These are aggressive B-cell lymphomas that typically arise in older adults, women more often than men, and often on the lower legs, although they may occur anywhere in the skin. They are composed of monotonous sheets of large B cells with expression of pan-B-cell markers, with monotypic Ig, strong BCL2, IRF4/MUM1, and FOX-P1. BCL-6 is usually positive, and CD10 negative. Next-generation sequencing (NGS) studies show mutations in the **CD79B**, **MYD88**, and **CARD11** genes (Jardin, 2014).

EBV-Positive DLBCL, NOS

Although EBV-positive DLBCLs usually occur in patients older than 50 years of age, they can occasionally arise in younger patients. Histology varies from mostly large cells to a more polymorphic distribution of cell sizes, often geographic necrosis, with EBV demonstrable by antibody staining for EBV LMP-1 and by ISH for EBV-encoded ribonucleotides. CD10 and BCL6 are negative, IRF4/MUM1 is usually positive, and CD30 is frequently expressed. Nf-κB is generally activated (Ok et al., 2013). These aggressive tumors are similar to DLBCL arising in immunosuppressed patients, and a form of age-related immunosuppression is surmised. There is, correspondingly, a spectrum of age-related EBV-associated lymphoid proliferations varying from reactive hyperplasia to overt lymphoma (Dojcinov et al., 2011).

EBV-Positive Mucocutaneous Ulcer

EBV-positive mucocutaneous ulcer is usually seen in patients with age-related immunosenescence and iatrogenic immunosuppression. The disease commonly occurs in the oral cavity and can involve the GI tract or skin. The lesion is typically unifocal and shows EBV-positive cells with Hodgkin and Reed-Sternberg–like morphology and polymorphic inflammatory infiltrate in the background. The disease has an indolent clinical course and usually regresses spontaneously (Swerdlow, 2017).

DLBCL Associated with Chronic Inflammation

This is another EBV-associated tumor that arises in situations with protracted chronic inflammation, the prototype being pyothorax-associated lymphoma (PAL). Features are similar to EBV+ DLBCL, NOS.

Lymphomatoid Granulomatosis

This is an angiocentric lymphoproliferative disorder involving the lung and/or other sites, including the brain, kidney, liver, skin, upper respiratory tract, and GI tract (Katzenstein, 2010). It is considered to be an EBV-driven B-cell neoplasm with a prominent reactive T-cell component, sometimes in a setting of immunosuppression (Katzenstein, 2010; Wilson, 1996). It has histologic features similar to NK/T-cell lymphoma of nasal type (Pittaluga, 2008).

Presentation is usually cough, dyspnea, and chest pain with constitutional symptoms, including fever, malaise, weight loss, GI symptoms,

myalgias, and neurologic symptoms. Bilateral mid- to lower-lung nodules are most commonly seen, often with nodules in the brain, kidney, skin, and subcutaneous tissue.

Histology shows an angiocentric and angiodestructive infiltrate of polymorphic lymphocytes, plasma cells, immunoblasts, and histiocytes, with inconspicuous neutrophils and eosinophils and without well-formed granulomas (Colby, 2012). Fibrinoid necrosis of vessels is often seen (Fig. 34.64), as is tissue infarction.

Immunophenotyping shows variable numbers of CD79a, usually CD20-positive B cells with EBV LMP-1 and EBER expression, variable CD30, and lack of CD15. A majority of background cells are reactive T cells with CD4 predominance. Higher-grade lesions (with more B cells) show clonal rearrangement of the IgH receptor genes. T-cell receptor genes are not clonally rearranged.

Grading is related to the number of clonal EBV-positive lymphocytes. Grade I lesions are polymorphic with only occasional large cells. Grade II is mixed with large pleomorphic cells in a mixed inflammatory background. Grade III is essentially DLBCL.

Outcome is variable, with waxing and waning, sometimes spontaneous remissions, and often progression to pulmonary failure in a median of 2 years. Appropriate therapy is related to determination of grade. Grade III lesions are treated with systemic chemotherapy, and grades I and II may be treated with α-interferon.

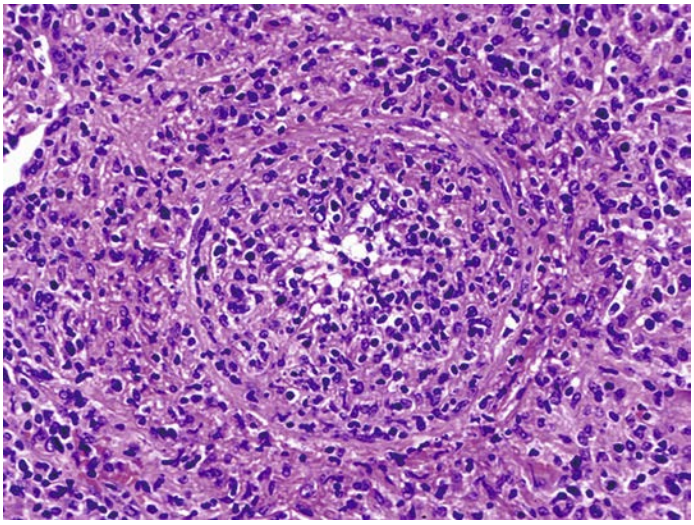

Figure 34.64 Lymphomatoid granulomatosis, showing a polymorphous angiodestructive pulmonary infiltrate (×200). Courtesy Dr. Anna-Luise Katzenstein.

Primary Mediastinal (Thymic) Large B-Cell Lymphoma

Primary mediastinal (thymic) large B-cell lymphoma (PMBL) often appears in young adulthood to middle age and is more frequent in women. Histology is variable, but diffuse or compartmentalizing sclerosis is frequent, and clear cells, multilobulated cells, or Reed-Sternberg–like cells may be present (Fig. 34.65). Symptoms are often related to location, with airway compression or superior vena cava syndrome and often local invasion and local recurrence after therapy. CD45, CD19, and CD20 are expressed, but not CD5 or CD10 (Swerdlow, 2017). CD30 is expressed in some cases, but not with the phenotype of classical HL. Ig genes are clonally rearranged; *IgV* and *Bcl-6* gene hypermutations are consistent with GCC derivation but occur similarly to normal thymic B cells (Csernus, 2004). Gene expression array analysis shows PMBL to be similar to nodular sclerosis classical HL (Savage, 2003). Mutations of *PTPN1* are frequent (Jardin, 2014).

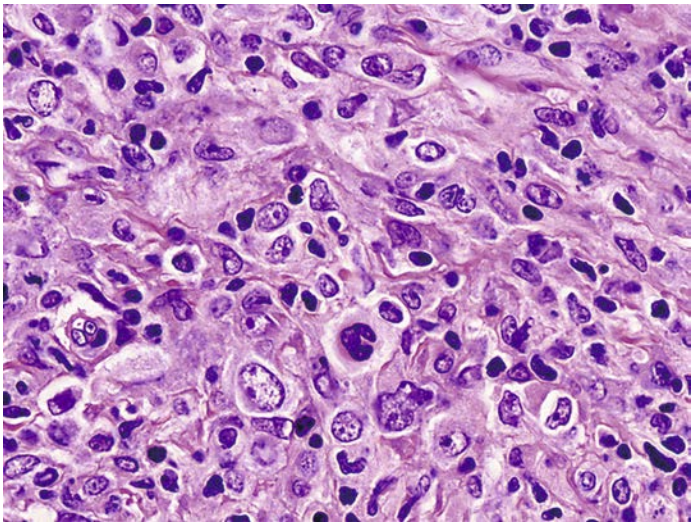

Figure 34.65 Mediastinal large B-cell lymphoma with sclerosis (×500).

Intravascular Large B-Cell Lymphoma

Intravascular large B-cell lymphoma is a rare tumor largely restricted to the intravascular lumina of small vessels (Swerdlow, 2017). It is very aggressive, widely disseminated at diagnosis, and often undiagnosed until autopsy. Findings often include hemorrhage, thrombosis, and/or necrosis of tissues throughout the body, with tumor only inconspicuously present in the small vessels. B-cell markers are expressed (CD19, CD20, CD22, D79a) and CD5 in some. Rare T-cell cases are described. Diagnosis is difficult but may be made from blood by morphology and flow cytometry (Patel et al., 2014).

ALK-Positive Large B-Cell Lymphoma

These are diffuse large B-cell lymphomas with expression of full-length ALK protein and plasmablastic or anaplastic morphology. Most described cases show t(2;17)(p23;q23) with clathrin gene involvement (*CLTL-ALK*); other rare abnormalities include t(2;5)(p23;q35), as in typical anaplastic large cell lymphoma (ALCL). They are of B-cell derivation with expression of CD79a but absent CD20 and frequently lack CD30 expression (Chikatsu et al., 2003; De Paepe et al., 2003; Gascoyne et al., 2003). Molecular studies show constitutive STAT3 activation with a plasmablastic differentiation program of *BLIMP1*, *XBP1*, and *C-MYC* expression, but not *PAX-5* and without *MYC* translocation (Valera et al., 2013).

Plasmablastic Lymphoma

Plasmablastic lymphoma shows immunoblastic morphology with expression of plasma cell antigens CD38 and CD138 and is frequently but not always associated with EBV. CD20, CD45, and PAX5 are weak to absent, but CD79a and IRF4/MUM1 are positive. There is cytoplasmic IgG. It has an aggressive behavior and has been reported primarily in the oral cavity of HIV patients, but is now known to occur in other patients and other locations as well. Patients with HIV, immunocompetent patients, and posttransplant patients show different frequency levels or frequency of EBV, CD45 expression and *C-MYC* aberrations (Morscio et al., 2014).

HHV8-Positive DLBCL, NOS

This tumor, arising in multicentric Castleman disease and frequently in patients with HIV, resembles an IgM-producing plasmablastic lymphoma. CD20 and CD38 are variably expressed, CD79a and CD138 are negative, and EBER is negative. HHV-8 is detectable by IHC. The disease is aggressive.

Primary Effusion Lymphoma

This is another rare tumor presenting in serous effusions but without tumors. Cytology is usually immunoblastic or anaplastic. It is associated with the Kaposi sarcoma virus human herpesvirus-8 (HHV-8) in immunodeficient patients. Tumor cells label as B cells and have Ig rearrangements, though T-cell varieties have been reported. EBV can usually be detected using in situ hybridization (ISH) (Swerdlow, 2017).

Burkitt Lymphoma

BL was first described in the jaws of African children by Dennis Burkitt in 1958 (Burkitt, 1958; Ferry, 2006). It represents approximately one-third of pediatric NHL, but also occurs in adults. Several epidemiologic types of BL exist. The prototype is **endemic** BL, which occurs predominantly in children in Africa and other equatorial regions and is associated with EBV. **Sporadic** BL occurs worldwide in children and adults and is not usually associated with EBV. Patients with HIV or other immunosuppression often have EBV-related BL, which is, however, different from the endemic form at the molecular level. BL is a highly proliferative tumor that grows very rapidly.

The tumor shows a diffuse infiltrate with pushing borders of medium-sized relatively uniform cells with round to oval nuclei containing three to five moderately prominent nucleoli in relatively clear parachromatin (Fig. 34.66). Cytoplasm is moderate and basophilic, and tends to square off between adjacent cells. Lipid-laden cytoplasmic vacuoles are seen in imprints (Figs. 34.67 and 34.68). Both high mitotic and high apoptotic rates are noted, along with a prominent pattern of "starry sky" macrophages. In most cases, the histology is distinctive, but some overlap is seen with both DLBCL and, occasionally, lymphoblastic lymphoma.

Burkitt leukemia/lymphoma exhibits leukemic cells with moderately clumped chromatin and basophilic vacuolated cytoplasm (see Fig. 34.66) with surface immunoglobulin restricted to one light chain. Typically, they show lack of TdT, presence of B-cell antigens CD19, CD22, CD20, CD79a, and often CD10, and expression of monoclonal surface Ig. Rare cases show lack of surface membrane immunoglobulin or expression of TdT; these require cytogenetic confirmation. Burkitt leukemia/lymphoma shows very high proliferative rates and rapid disease progression. Although the condition is rapidly fatal if untreated, recent results of therapy in pediatric patients have shown long-term survival of better than 90% (Patte, 2001). Outcome in adults has also improved (Rizzieri et al., 2014).

Burkitt leukemia/lymphoma shows characteristic cytogenetic abnormalities consisting of translocation of *C-MYC* on chromosome region 8q24 to one of the immunoglobulin genes (heavy chain-14q32, κ-2q12, or λ-22q11) to give t(8;14), t(2;8), or t(8;22). Most cases show t(8;14)(q24;q32). *C-MYC* promotes both proliferation and apoptosis and presumably causes uncontrolled proliferation of immunoglobulin-bearing B cells. Genomic studies show additional involvement of *TCF3* activation, with downstream effects on *PTPN6* (*SHP1*), tonic B-cell receptor (BCR) stimulation of *PI3K* signaling and *CCND3* transactivation (Schmitz et al., 2014). BL is sensitive to chemotherapy, however.

High-Grade B-Bell Lymphoma with *MYC* and *BCL2* and/or *BCL6* Rearrangements

High-grade B-cell lymphoma (HGBL) double-hit (DH) or triple-hit (TH) is a newly defined category in the current WHO classification that harbors *MYC* and *BCL2* and/or *BCL6* rearrangements. All B-cell lymphoma with these molecular features are included in this category except FLs and B-lymphoblastic leukemia/lymphomas. It occurs mostly in elderly patients, with slightly male predominance. The overall prognosis of this lymphoma is poor, with a median survival of 5 to 19 months (Swerdlow, 2017).

High-Grade B-Cell Lymphoma, NOS

HGBL, NOS is an aggressive lymphoma that lacks *MYC* and *BCL2* and/or *BCL6* rearrangements. This lymphoma has morphologic features intermediate between DLBCL and BL or mature B-cell lymphoma with blastoid morphology. It occurs predominantly in elderly patients usually presenting with advanced disease (Swerdlow, 2017).

B-Cell Lymphoma, Unclassifiable, with Features Intermediate Between DLBCL and Classical Hodgkin Lymphoma

These are essentially **gray-zone tumors** with overlap features that prevent precise diagnosis. Mediastinum is often involved, and the differential diagnosis is usually between PMBL and classical HL. These disorders have shown overlap by gene expression studies; thus, it is not surprising that morphologic overlap occurs.

MATURE T-CELL AND NATURAL KILLER CELL NEOPLASMS

T-cell and NK cell lymphomas and leukemias are a diverse group of neoplasms that are uncommon to rare compared with B-cell lymphomas. Although they account for only about 12% of lymphomas overall, an approximately equal number of categories is recognized by the WHO. Most of these are typified by clonal rearrangement of genes encoding CD3. True NK cell neoplasms do not, however, show clonal rearrangement of T-cell receptor genes by clinical methods. Features of major T/NK neoplasms are summarized in Table 34.7. Most are highly malignant, although some indolent diseases are also in this category (Gaulard, 2014).

A majority of postthymic (peripheral) T cells express αβ-chains of the T-cell receptor (TCR); a small minority do not, but rather express γδ-chains. NK cells express only ε-chains with cytoplasmic CD3. T-cell clonality studies in the laboratory usually focus on γδ-receptor rearrangement, which is present in all or most T cells. This is because in early T-cell development, the γ- and β-chain genes rearrange simultaneously, with TCR commitment dependent on expression of surrogate α-chain and development of a pre-TCR (Kang et al., 1998; Kreslavsky et al., 2010).

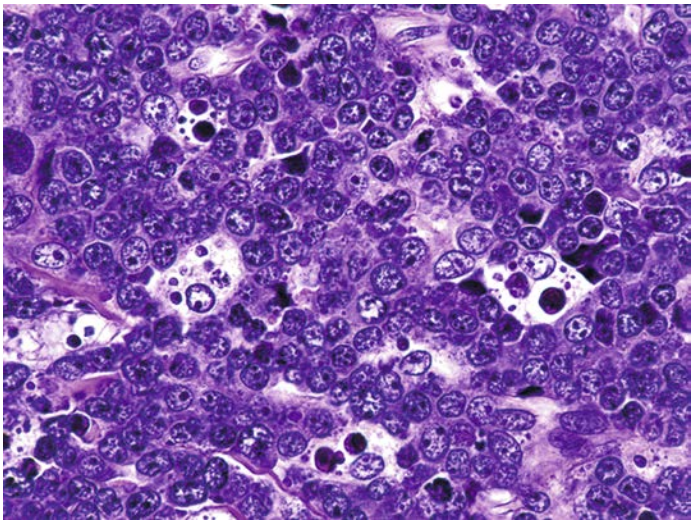

Figure 34.66 Burkitt lymphoma (×500).

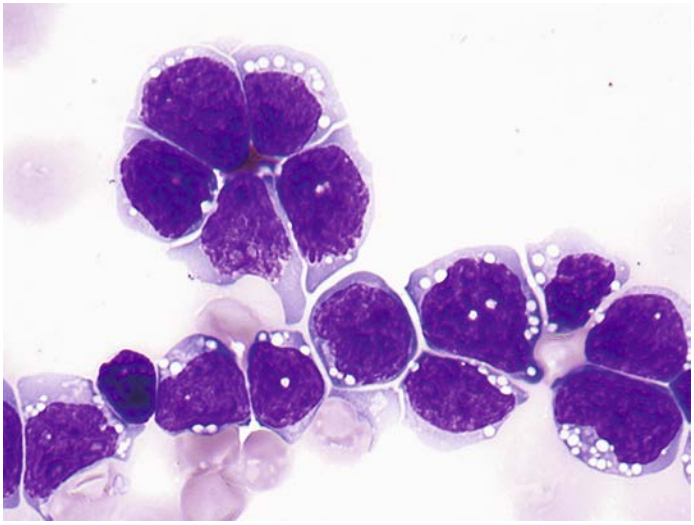

Figure 34.67 Burkitt lymphoma cytology (×1000).

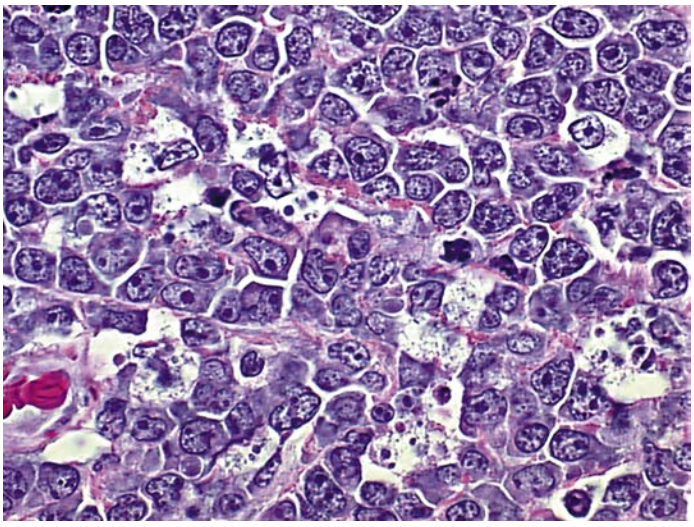

Figure 34.68 Atypical Burkitt or Burkitt-like lymphoma, with moderate pleomorphism and increased numbers of prominent nucleoli (×500).

Flow cytometry assays using antibodies for each TCR V β family is also useful and rapid (Tembhare et al., 2011).

Mature αβ T cells express CD2, CD3, CD5, CD7, and either CD4 or CD8. They are negative for TdT and CD1. Normal resting lymphoid tissue usually shows a CD4/CD8 ratio of 2:1. Differentiation to one or the other in the thymus involves activation or silencing of CD4 or CD8 from CD4+CD8+ cells but is poorly understood (Yasutomo, 2000). Primarily mature CD4 cells proliferate in the postthymic environment (Foa, 1980). The CD4/CD8 ratio drops in acute inflammation and rises to often high levels in recovery and chronic inflammation; thus, these are not good markers of clonality. Peripheral T-cell neoplasms often lose expression of a normal pan-T-cell antigen such as CD7 and show predominance of CD4 or CD8 (Knowles, 1989). Care must be taken to distinguish abnormal αβ T cells from normal NK cells.

γδ T cells typically are doubly negative for CD4 and CD8 and are also often CD5 negative with CD2 expression and show a maturation sequence of CD7. Because they usually account for only 1% to 2% of normal T cells, an increase in these cells is a suspicious finding in itself. NK cells are highly variable in expression of pan-T-cell antigens CD2 and CD7, are often CD5 negative, and typically express CD16 (a low-affinity Fc receptor also found on monocytes and granulocytes), with variable CD56 and CD57. CD3 is detectable in the cytoplasm with polyclonal antibodies but is also present on the surface in some NK neoplasms. Cytotoxic granule constituents TIA-1, granzyme-B, and perforin are usually present in NK cells and cytotoxic T cells.

T-Prolymphocytic Leukemia

T-prolymphocytic leukemia is an uncommon disorder with a median age of 69 years, and the disease is slightly more frequent in males than in females. Patients present with a marked lymphocytosis (>100 × 10^9/L), anemia, and thrombocytopenia. In most cases, the neoplastic cell is a prolymphocyte with a prominent **punched-out** nucleolus showing distinct perinucleolar chromatin and moderately abundant cytoplasm. In approximately 20% of patients, however, the lymphocytes lack distinctive features and do not possess a prominent nucleolus. Hepatosplenomegaly, lymphadenopathy, and skin involvement are common.

The immunophenotype is most often CD4+ peripheral T cell (60%), with CD4/CD8 coexpression in 25%, and CD8+ in 15%. CD7 is strong, and surface CD3 weak.

There is clonal TCR αβ (and γδ) rearrangement. In all, 80% show inv(14)(q11;q32) and 10% t(14;14)(q11;q32) involving TCR αβ locus and oncogenes *TCL1A* and *TCL1B*. Chromosome 8 abnormalities t(8;8)(p11-12;q12) or trisomy 8q is seen in 70%. Other abnormalities include t(X;14)(q28;q11) and deletions at 11q23.

T-prolymphocytic leukemia is a rapidly progressive malignancy with survival usually less than 1 year. Recent progress has been made with new therapies, including alemtuzumab (Campath-1H) (Dearden, 2012).

Large Granular Lymphocyte Leukemia

This is a clonal proliferation of CD3(+) cytotoxic T-lymphocytes, and sometimes CD3(-) NK cells (Zhang & Loughran, 2012). The median age is 63 years and 60% to 70% of patients are symptomatic with recurrent infections due to neutropenia. Anemia or rheumatoid arthritis is also common. Lymphocytosis is usually mild (up to 20 × 10^9/L), and the lymphocyte number may be normal. LGL cells are usually at least 2 × 10^9/L. Chronic neutropenia is frequent, splenomegaly may be present, and there may be anemia and/or thrombocytopenia. LCLs are at least relatively increased and show moderate size with abundant light-blue cytoplasm and condensed chromatin. Azurophilic cytoplasmic granules vary in number and size (Fig. 34.69). The BM exhibits a moderate interstitial infiltrate of granulated lymphocytes. Erythroid and myeloid elements may be normal or hypoplastic in occasional cases. The spleen typically shows red pulp infiltrates. The common variant is CD3/CD8/CD57/TCR αβ+, CD4-negative. Benign LGL lymphocytosis following bone marrow transplantation is not unusual.

TCR γ-gene rearrangement is usually clonal by PCR, and TCR-β is also usually rearranged. Although a single clonal band usually confirms a suspicious diagnosis, PCR assays may show a dominant clone emerging from an oligoclonal population of autoimmune origin. This, along with a typically indolent course, makes cases with low WBC counts very difficult to diagnose. Therapy is generally based on low-dose methotrexate or cyclophosphamide.

Chronic Lymphoproliferative Disorders of NK Cells

Chronic lymphocytosis of LCLs of NK phenotype occurs rarely. These are generally indolent asymptomatic processes that come to light as incidental findings or may be associated with neutropenia and/or anemia. They resemble LGL leukemia but are CD3 negative, with expression of CD16, dim CD56, cytotoxic granule markers TIA-1 and granzyme B and M, and variable CD2, CD7, and CD57. CD5 and CD8 are often expressed. KIR NK-receptors (NKRs) are often expressed in restricted fashion, possibly related to exogenous antigens such as from viral infections, but are not frequently assayed in clinical laboratories (Zambello et al., 2014). T-cell receptors are not clonally rearranged and there are no characteristic cytogenetic abnormalities. EBV is not associated.

Aggressive NK Cell Leukemia

This is a rare aggressive leukemia of NK cells associated with EBV and usually occurring in Asian teens and young adults. It usually presents with constitutional symptoms. The WBC count is variable and hepatosplenomegaly is common; it sometimes shows lymphadenopathy, hepatosplenomegaly, coagulopathy, hemophagocytic syndrome, and/or multiorgan failure (Swerdlow, 2017).

Morphology of leukemic cells is variable, sometimes resembling LGL leukemia, sometimes showing larger lymphoid cells with condensed chromatin and basophilic cytoplasm, and sometimes showing blastic or transformed cells.

The immunophenotype is surface CD3 negative and cytoplasmic CD3 ε/CD2/CD56 positive, and it expresses cytotoxic molecules (TIA-1, granzyme-B, and/or perforin). CD16 is variable, and CD57 negative.

TCR genes are not rearranged. Clonality may be established by detecting clonal episomal EBV (analyzing tandem repeats by Southern blot) or finding clonal cytogenetic abnormalities such as del(6)(q21;q25).

Indolent NK cell proliferation also occurs and is characterized by adult onset, lack of constitutional symptoms, lack of EBV, and a CD57+ phenotype (along with CD2, CD16, and CD56, with negative surface CD3; Fig. 34.70).

EBV-Positive T Cell and NK Cell Lymphoproliferative Diseases of Childhood

These are rare lymphomas occurring most often in Asians or Native Americans from Central or South America that are associated with EBV (Swerdlow, 2017). These appear to be unique clinicopathologic and geographically related disorders but may overlap with other more usual forms of chronic EBV-associated disorders (Hong, 2013; Rodriguez-Pinilla, 2011; Wang, 2014).

Systemic EBV-Positive T-Cell Lymphoproliferative Disease of Childhood

This is an aggressive, often fulminant disease following acute or chronic EBV infection and characterized by indistinct monoclonal infiltrates of small T cells, occasionally with some pleomorphism, associated with hepatosplenomegaly and hemophagocytic syndrome involving these organs and BM. Cells are mature T cells with CD2, CD3, and TIA-1 expression, variable CD4 (chronic EBV) or CD8 (acute EBV), and negative CD56.

Chronic Active EBV Infection of T- and NK-Cell Type, Systemic Form

Chronic active EBV infection of T-cell and NK-cell type is a systemic EBV+ T-cell and/or NK-cell proliferation with no morphologic changes suggestive of a neoplastic lymphoproliferation. It occurs predominantly in children and young adults from Asia. The clinical behavior is variable, with some patients having an indolent clinical course and others developing rapidly progressive disease (Swerdlow, 2017).

Hydroa Vacciniforme-Like Lymphoma

This is an EBV-positive cutaneous T-cell lymphoma of sun-exposed skin (Quintanilla-Martinez, et al., 2013b). The infiltrate is that of CD56+ cytotoxic T or NK cells predominantly involving the dermis. The disease course is variable and tends to be initially indolent but more aggressive following dissemination.

Adult T-Cell Leukemia-Lymphoma

Adult T-cell leukemia-lymphoma (ATLL) is a highly variable but often clinically aggressive T-cell leukemia/lymphoma associated with HTLV-1 retrovirus infection (Ishitsuka & Tamura, 2014; Poiesz et al., 1980; Qayyum & Choi, 2014; Tobinai et al., 2012; Yoshie & Matsushima, 2014). It is most endemic in southwestern Japan but also in the Caribbean basin, southeastern United States, and central Africa. Transmission of HTLV-1 may occur vertically (from mother to child), or through sexual

TABLE 34.7

Key Features of the Major Mature T-Cell and NK-Cell Neoplasms

Lymphoma	Demographics; Clinical and Laboratory Presentations	Morphology	CELL SURFACE MARKERS (TYPICAL PROFILE)		Gene Rearranged, Involved
			Positive	Negative	
T-cell PLL	M > F; median age, 65 years; lymphocytosis >100 × $10^3/\mu L$, anemia, thrombocytopenia, HSM, skin lesions	Prolymphocyte	CD7; CD4 (60%), CD4/8 (25%), CD8 (15%)		TCR-γδ TCR-αβ inv(14) (q11;q32)
LGL leukemia	Median age, 63 years; neutropenia causing infection, anemia, mild lymphocytosis (usually >2 × $10^3/\mu L$)	Moderately sized cell with condensed chromatin, abundant pale-blue cytoplasm, azurophilic granules	CD3, CD8, CD57, TCR-γδ; some variants are CD4+ or CD4/8+ or CD4/8–	CD4	TCR-γδ TCR-αβ
Aggressive NK-cell leukemia	Asian teens to young adults; constitutional symptoms, HSM, variable WBC count	Variable, may resemble LGL cells or appear blastic	cCD3ε, CD2, CD56	sCD3, 57	Clonal EBV, del(6) (q21;q25), del11q
Adult T-cell leukemia/lymphoma	Associated with HTLV-1, frequent in Japan, Caribbean, Central Africa; acute variant with skin, lymph node involvement, hypercalcemia	Moderately large blastic cells with convoluted nuclei (floret cells), agranular, basophilic cytoplasm	CD2, CD3, CD4, CD5, CD25, often CD30	CD7, CD8	TCR-γδ TCR-αβ
Extranodal NK-/T-cell lymphoma, nasal type	Most prevalent in Asia, Native Americans of Mexico and Central and South America	Angiocentric and destructive, involving upper aerodigestive tract	CD2, CD56, cytotoxic granules, cyto CD3ε	Surface CD3	Germline receptor genes
Enteropathy-associated T-cell lymphoma	All ages and regions; increased in celiac disease (may present concurrently), jejunum and ileum	Large cells with inflammatory background	CD3, CD7, CD103; CD3, CD8	CD4, CD5	TCR-γδ TCR-αβ
Hepatosplenic T-cell lymphoma	Rare, increased in adolescents and young adults and with chronic immunosuppressive therapy; involves liver/spleen/marrow	Medium-sized cells involving splenic red pulp and sinuses of liver and marrow	CD3, CD8±, CD56±	CD4, CD5, often CD4/CD8 double negative	TCR-γδ
Subcutaneous panniculitis-like T-cell lymphoma	Rare, F > M; subcutaneous panniculitis with neoplastic cells	Involves fat lobules, spares septa, variable-sized monomorphic cells, rimming of fat cells, histiocytes	CD3, βF1, CD8, cytotoxic granules	CD4, CD56	TCR-γδ TCR-αβ
PTCL, NOS	Peripheral nodes, disseminated disease, sometimes cutaneous	Varies in cell size and from polymorphic to monomorphous	Variable with CD3, CD4, other pan-T-cell markers	CD7, CD5, others often lost	TCR-γδ TCR-αβ
Angioimmunoblastic T-cell lymphoma	Middle-aged and elderly; generalized disease, systemic symptoms, hypergammaglobulinemia	Partial nodal effacement involving paracortex, increased venules, clear-cell clusters, EBV+ B cells	CD3, CD2, CD5, CD4, (reactive CD8), CD10, CXCL13, Bcl6	CD8	TCR-γδ TCR-αβ +3, +5, +X
Mycosis fungoides/Sézary syndrome (SS)	M > F, middle-aged to older; dermatitis progressing to ulcerated lesions; PB involvement in SS	Dermal band-like infiltrates of lymphocytes with cerebriform nuclei, microabscesses	CD2, CD3, CD4	CD7, CD8	TCR-γδ TCR-αβ
Primary cutaneous CD30-positive	M > F, adults to elderly; limited to skin lesions	Polymorphic lymphoid cells, some anaplastic	CD4, CD30	Often CD2, CD3, CD5, ALK	TCR-γδ TCR-αβ
Anaplastic large-cell lymphoma, ALK-positive	M > F, teens, young adults; peripheral, abdominal adenopathy, extranodal and BM involvement, frequent B symptoms	Pleomorphic large cells, wreath-like nuclei, multiple nucleoli, abundant cytoplasm	CD30 (cytoplasmic and Golgi), CD2, CD4, CD5	CD3, CD7, EBV	TCR-γδ TCR-αβ t(2;5) (p23;q35) Other variants involve 2p23

BM, Bone marrow; *EBV,* Epstein-Barr virus; *HSM,* hepatosplenomegaly; *HTLV,* human T lymphotropic virus type 1; *LGL,* large granular lymphocyte; *NK,* natural killer; *NOS,* not otherwise specified; *PB,* peripheral blood; *PLL,* prolymphocytic leukemia; *PTCL,* peripheral T-cell lymphoma; *TCR,* T-cell receptor; *WBC,* white blood cell.

contact, intravenous drug abuse, or blood transfusion. Only a minority of individuals infected with HTLV-1 (2.5%) develop ATLL, typically after a latent period of many years. Acute infection results in a flu-like syndrome.

The acute variant typically shows leukemia, skin involvement, generalized lymphadenopathy, lytic bone lesions, and hypercalcemia. The blood film demonstrates anemia and thrombocytopenia with the presence in blood and marrow of moderately large blastic cells with convoluted or clover-leafed nuclei and condensed chromatin (**floret cells**). Nucleoli are small or absent, and the cytoplasm is agranular and basophilic. Admixed blast-like cells are present. Marrow involvement is often patchy, with increased osteoclastic activity. Skin lesions resemble mycosis fungoides, including the presence of Pautrier microabscesses, but often with more pleomorphic cells.

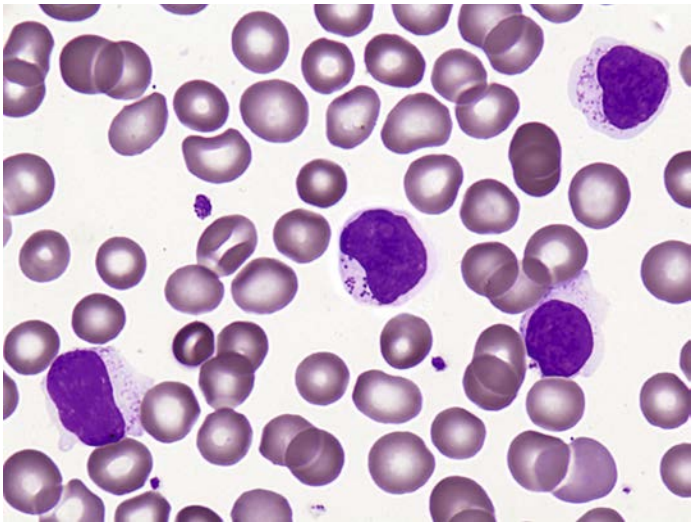

Figure 34.69 Large granular lymphocytic leukemia (×1000).

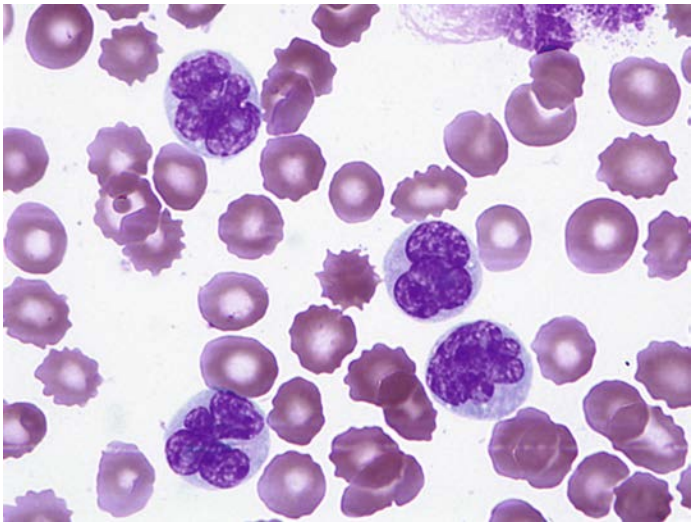

Figure 34.70 Natural killer cell leukemia in an adult, with floret cells resembling adult T-cell leukemia.

Lymph nodes in acute or lymphomatous variants show highly variable morphology, often with features and diversity reminiscent of ALCL. Histology may resemble common ALCL, small cell variant, HL, or typical large cell lymphoma (Fig. 34.71).

The chronic variant often resembles mycosis fungoides, and the smoldering variant shows low-level leukemic involvement with <5% circulating neoplastic cells. Clonal integration of HTLV-1 is an invariable finding and is essentially diagnostic (Yamaguchi, 2002). However, it should be noted that HTLV-1 infection is chronic and that these patients may have other hematologic diseases, just as other people do.

The immunophenotype of ATLL is CD2/CD3/CD5/CD25 positive, usually CD4+ and CD7 negative. CD30 is often positive, but ALK is negative. Cytotoxic markers are negative. *TCR* genes are clonally rearranged. Occasional patients with smoldering disease show a Hodgkin-like lymphoproliferative disorder of EBV-infected B cells with CD30 and CD15 expression, likely related to chronic immunosuppression. It may be noted that both HTLV-1 and EBV are potent inducers of CD30. New therapies include those targeting chemokine receptor CCR4, which is highly expressed on these cells that show T regulatory (Treg) features.

Extranodal NK/T-Cell Lymphoma, Nasal Type

These lymphomas have been referred to as lethal midline granulomas, polymorphic reticulosis, and angiocentric T-cell lymphoma. They are extranodal lymphomas, usually of NK-cell derivation or T-cell lineage, which are associated with EBV and are most common in Asia and Latin America. They typically involve the nasopharynx, palate, skin, GI tract, testes, or other sites. The hemophagocytic syndrome is sometimes associated (Swerdlow, 2017).

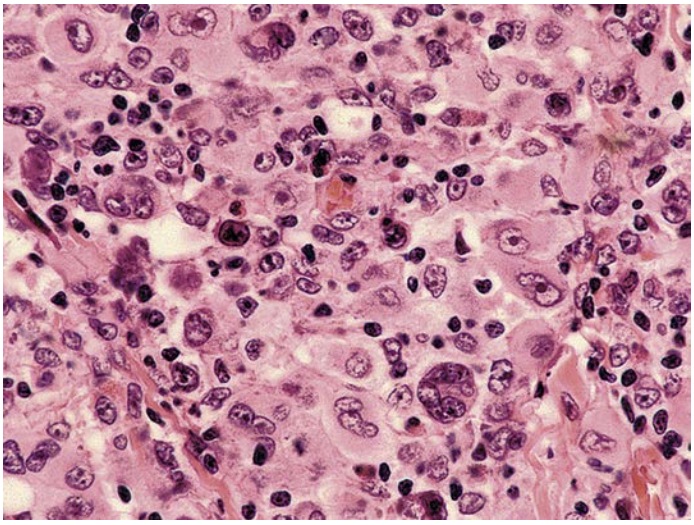

Figure 34.71 Adult T-cell leukemia/lymphoma, with anaplastic features (×500).

The histology shows diffuse infiltrates of lymphoid cells of varying, often polymorphic, cytology—from small lymphocytes to large cells, immunoblasts, and/or anaplastic cells. Typically, mucosal ulcerations are present and some areas show an angiocentric and angioinvasive pattern (Fig. 34.72) with fibrinoid necrosis of vessels and associated infarction-like necrosis.

Immunophenotype is usually CD2/CD56 positive, with cCD3-ε and expression of cytotoxic molecules. CD43, CD45Ro, HLA-DR, CD25, CD95, and FAS ligand are also expressed, but CD4, CD8, CD5, CD16, and CD57 are negative.

TCR αβ and γδ and IgH genes are germline in most cases, but clonal episomal EBV is present. EBER ISH is positive. Del(6)(q21;q25) or i(6)(p10) is occasionally described. Prognosis is variable.

Enteropathy-Associated T-Cell Lymphoma

This is a clonal T-cell malignancy of intraepithelial T cells. It is associated with celiac disease, but patients often present simultaneously with malabsorption and lymphoma (Swerdlow, 2017). It usually occurs in the jejunum or ileum, with other locations in or outside of the GI tract reported.

Morphology shows variable small and medium-sized to large neoplastic cells, often with pale to eosinophilic cytoplasm and eccentric angulated nuclei. In some cases, the cytology is similar to ALCL with wreath-like multinucleation and horseshoe nuclei (Fig. 34.73). Other cases have bland-appearing small lymphocytes. Histiocytes and eosinophils are often abundant.

The phenotype is CD3, CD7, CD103 positive, CD8 variable, CD4 negative, often with double-negative CD4/CD8. Small-cell variants are CD8/CD56 positive. Cytotoxic molecules are expressed. *TCR* genes are clonally rearranged, and patients with celiac disease typically have HLA DQA1*0501 and DQB1*0201. This is usually an aggressive disease.

Monomorphic Epitheliotropic Intestinal T-Cell Lymphoma

Monomorphic epitheliotropic intestinal T-cell lymphoma is a rare and aggressive primary intestinal T-cell lymphoma. This lymphoma mostly affects Asian populations and has no association with celiac disease. The neoplastic lymphocytes are medium-sized and usually express CD3, CD8, and CD56. The prognosis of this lymphoma is very poor, with a median survival of 7 months (Swerdlow, 2017).

Hepatosplenic T-Cell Lymphoma

This is a rare neoplasm, usually of γδ T cells, which shows sinusoidal infiltration of spleen, liver, and BM. It is most common in adolescent or young adult males. Patients present with massive splenomegaly, hepatomegaly, pronounced thrombocytopenia, and, sometimes, leukocytosis and anemia (Swerdlow, 2014, 2017).

Histology shows diffuse splenic red pulp involvement by small to medium-sized lymphoid cells with slightly dispersed chromatin and moderate cytoplasm. The liver shows similar cells in sinuses. Diagnosis is best made in the BM with presence of a characteristic infiltration of sinuses but otherwise intact architecture and hematopoiesis (Fig. 34.74).

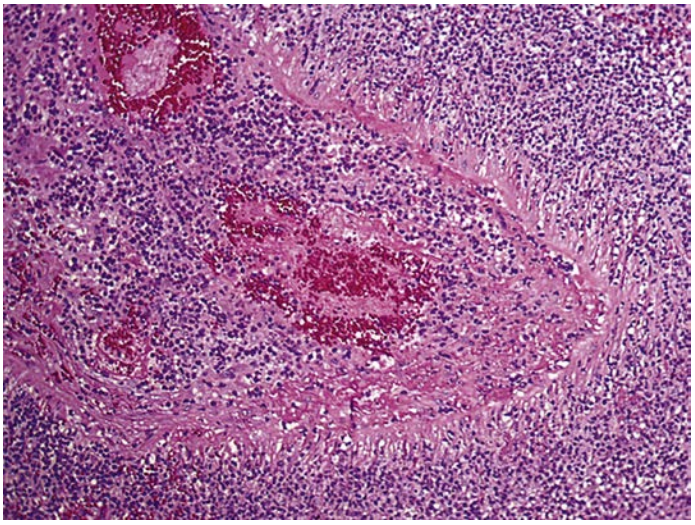

Figure 34.72 Nasal-type T-cell/natural killer cell lymphoma, showing angioinvasion and destruction (×200).

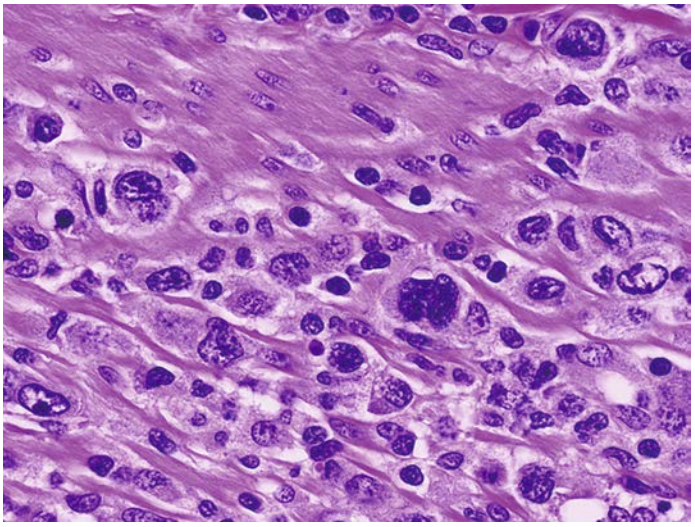

Figure 34.73 Enteropathy-associated T-cell lymphoma infiltrating the muscularis of the small bowel (×500).

Immunophenotyping of sections is extremely helpful because of inconspicuous morphology on H&E.

The immunophenotype is CD3 and TIA-1 positive, with double-negative CD4 and CD8, negative CD5, granzyme B, and perforin (Belhadj, 2003). TCR δ1 antibodies are positive and TCR αβ negative, although some cases of αβ type occur.

TCR γ PCR is positive, and TCR β occasionally positive. Most cases are EBV negative, but EBV-positive cases may occur (Taguchi, 2004). Isochromosome 7q is usually described, with occasional trisomy 8. The disease is aggressive, with early responses to therapy but usual relapse and progression.

Subcutaneous Panniculitis-like T-Cell Lymphoma

Subcutaneous panniculitis-like T-cell lymphoma (SPTCL) is a neoplasm of cytotoxic T cells that usually occurs as multiple nodules in the subcutaneous fat of the trunk or extremities and mimics benign panniculitis. The overlying epidermis and dermis are not involved, but the septa of subcutaneous adipose are infiltrated. The lymphoid infiltrate is polymorphic and may be deceptively bland, although some large cells are usually present (Fig. 34.75). There is rimming of fat cells by lymphocytes and usually vascular involvement, with areas of necrosis and histiocytic infiltrates. Acute inflammatory cells are not typically present as they are in benign panniculitis, and multinucleated giant cells usually are not seen.

The immunophenotype is usually mature CD8+ T cell with expression of granzyme B, perforin, and TIA-1, with a genotype of clonal αβ T-cell type (Go et al., 2004). The disease prognosis is typically good, but it is usually poor when hemophagocytic syndrome is present. Median 5-year survival is approximately 80% (Swerdlow, 2017).

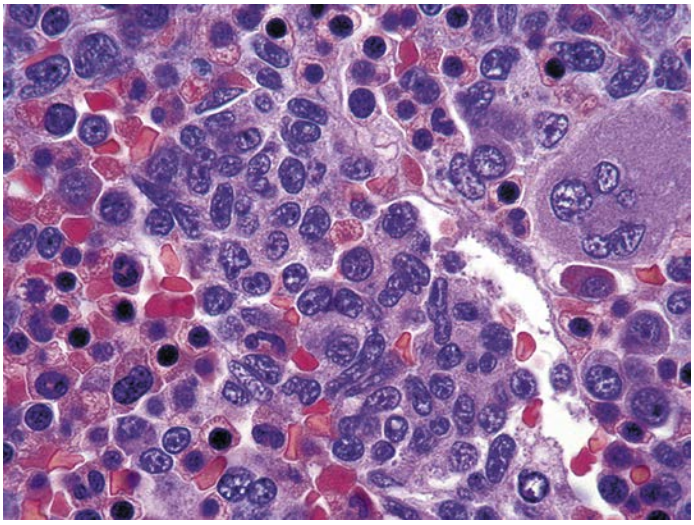

Figure 34.74 Hepatosplenic T-cell lymphoma showing intrasinusoidal involvement of the bone marrow (×500).

Mycosis Fungoides and Sézary Syndrome

Mycosis fungoides (MF) occurs twice as frequently in men as in women. It usually affects individuals in their middle to late years. The disorder first appears as an eczematoid, psoriasiform, or nonspecific exfoliative dermatitis. The lesions tend to form plaques and then tumors that often ulcerate. Some patients develop generalized erythroderma.

Biopsies of the skin reveal band-like lymphocytic infiltrates in the dermis (see Fig. 34.71), often with admixed histiocytes and occasional eosinophils (LeBoit, 2011). T cells with irregular nuclei (Fig. 34.76) show single-cell infiltration of the epidermis and often form clusters known as Pautrier abscesses (Fig. 34.77). These are usually accompanied by parakeratosis and acanthosis, typically with minimal or no spongiosis, and elongation of rete pegs. The nuclei of at least a portion of neoplastic cells typically have a cerebriform appearance. The extent of the cutaneous infiltrate is not always directly correlated with severity of disease. Communication with the dermatologist or other treating physician is important, and even subtle changes in a clinically suspicious patient should be taken seriously. Diagnostic features and pitfalls have been reviewed by an international consensus conference (Song, 2013).

Phenotype is usually mature T cell with CD8 expression and lack of CD7, but this is not usually conclusive. *TCR* genes are clonally rearranged, and PCR analysis of formalin-fixed biopsy tissue should be attempted in suspicious cases.

In advanced stages of the disease, neoplastic cells infiltrate the lymph nodes, liver, spleen, and other organs. Early nodal involvement (category I) shows dermatopathic changes with no atypical cerebriform lymphocytes. Category II shows dermatopathic changes with scattered atypical cerebriform lymphocytes. Category III shows partial nodal effacement, and category IV shows diffuse involvement.

Rare atypical mononuclear cells with cerebriform nuclei (Sézary cells) may be present in the peripheral blood (Fig. 34.78). Lymphocytosis with these cells (especially in the erythremic patient) is called *Sézary syndrome*.

The disorder may follow a prolonged chronic course. However, following lymph node infiltration, the disease becomes more progressive. Death, occurs within 2 years, usually due to infection.

Therapy is topical in early cases. More advanced disease has been treated with psoralen and ultraviolet A light therapy (PUVA), retinoids, α-interferon, and, more recently, alemtuzumab or vorinostat.

Primary Cutaneous CD30-Positive T-Cell Lymphoproliferative Disorders

This category in the WHO classification includes primary cutaneous ALK negative, lymphomatoid papulosis, and borderline lesions (Querfeld, 2010; Quintanilla-Martinez, 2013a; Swerdlow, 2017). These disorders share the features of dermal infiltrates of polymorphic lymphoid cells, including variable proportions of anaplastic or Reed-Sternberg–like cells with expression of CD30, and a typically relapsing/remitting clinical course.

Cutaneous ALCL resembles systemic ALCL (Fig. 34.79), except that it is indolent and does not exhibit detectable ALK expression or genetic translocations. Lymphomatoid papulosis has been considered a variant of pityriasis lichenoides et varioliformis acuta (PLEVA), with an inverted vase-like lymphoid infiltrate containing variable numbers of

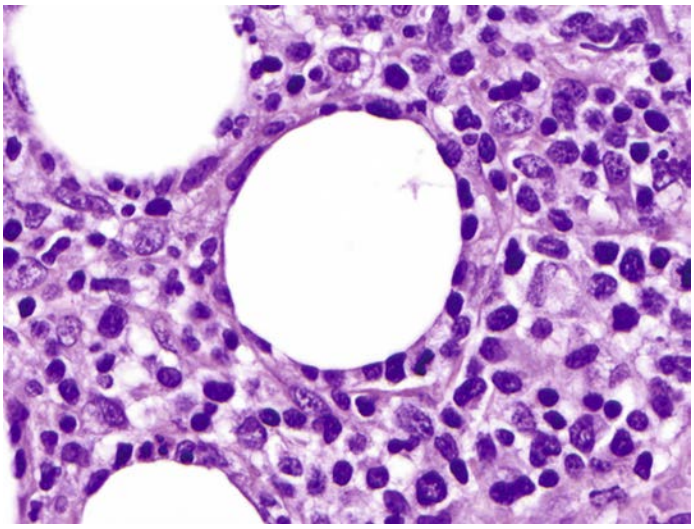

Figure 34.75 Subcutaneous panniculitis-like T-cell lymphoma (×500).

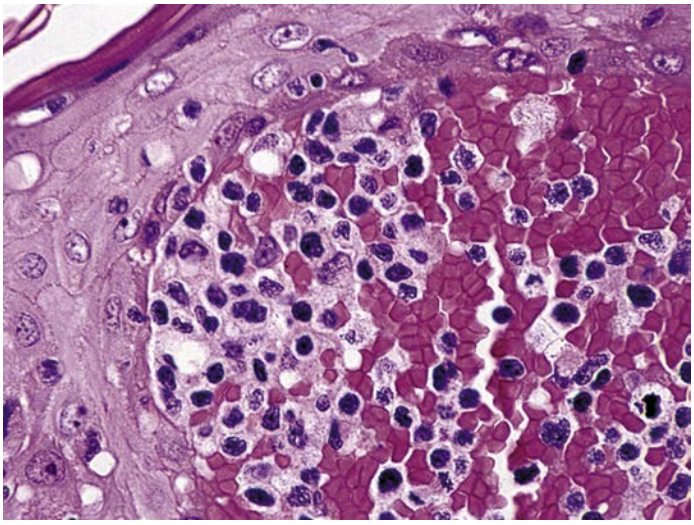

Figure 34.77 Neoplastic lymphocytes with convoluted nuclei in mycosis fungoides (×1000).

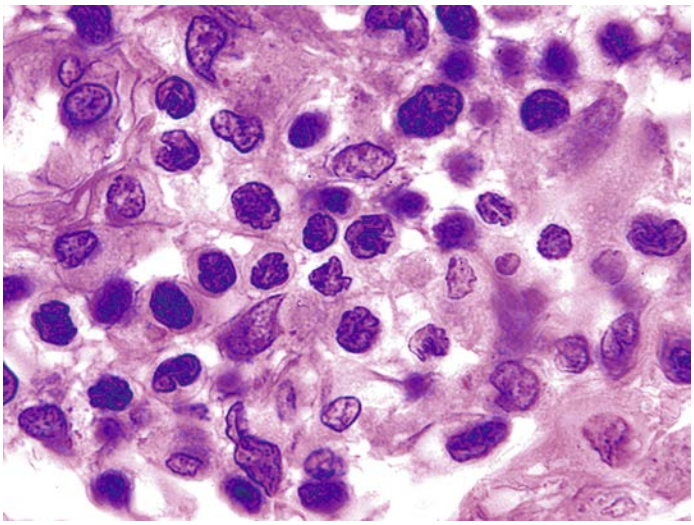

Figure 34.76 Cutaneous T-cell lymphoma, showing a large Pautrier microabscess (×20).

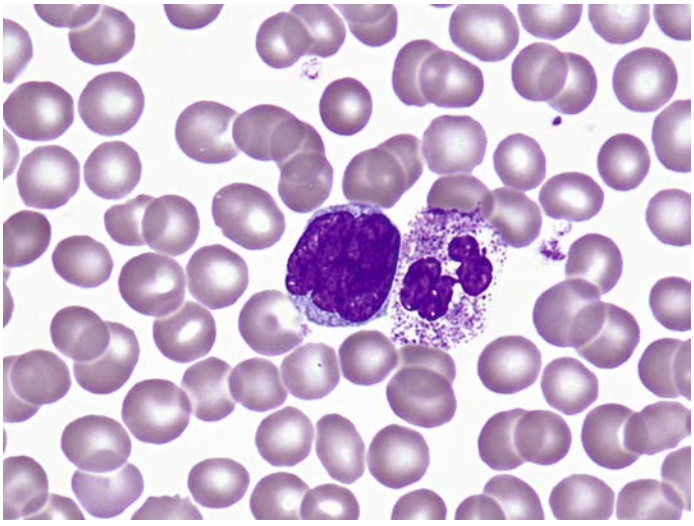

Figure 34.78 Sézary cell in the blood, along with a neutrophil (×1000).

CD30-positive large cells. It has been associated with HL in a number of instances.

Both disorders share the phenotype of CD4-positive mature T cells with variable loss of pan-T-cell antigens, expression of cytotoxic molecules, and strong CD30 expression. ALK is negative, and *TCR* genes are clonally rearranged. *IRF4* translocations detectable by FISH are highly associated with cutaneous ALCL and closely related mucosal ALCL (Wada et al., 2011).

Primary Cutaneous γδ T-Cell Lymphoma

Primary cutaneous γδ T cell lymphoma is a rare lymphoma of adults consisting of a heterogeneous pattern of presentation (dermal, epidermal, and/or subcutaneous) in the skin of adults comprising γδ T cells. These express CD3, CD2, and CD56, often dually negative for CD4 and CD8 or CD8 positive, with lack of CD5 and βF1. They express TCR γ receptor, and TCR γ is clonally rearranged. Histologically, they may mimic SPTCL or MF.

Primary cutaneous CD8-positive aggressive epidermotropic cytotoxic T cell lymphoma is another rare cutaneous T-cell lymphoma of cytotoxic T cells. Cells are small-medium or medium-large and often pleomorphic or blast-like. They express CD3, βF1, CD8, and granzymes B and TIA-1, with variable CD2 and CD7, but negative CD4 and CD5. These often resemble MF in their epidermotropism. The disease is aggressive.

Primary cutaneous CD4-positive small-medium T-cell lymphoproliferative disorder is characterized by pleomorphic CD4-positive T cells, without clinical patches or plaques (as seen in MF). It lacks epidermotropism and is difficult to separate from reactive hyperplasia or from early MF. It has an indolent course (Lan et al., 2014).

Angioimmunoblastic T-Cell Lymphoma

This disorder has been termed *angioimmunoblastic lymphadenopathy with dysproteinemia* (*AILD*) and abnormal immune response. It is a clonal T-cell lymphoma that presents with constitutional symptoms and polyclonal hypergammaglobulinemia. Although once thought to be initially a reactive process with a spectrum of progression to lymphoma, it is now believed to be neoplastic from the onset.

Histology shows paracortical lymph node hyperplasia with depletion of lymphocytes, increased plasma cells, and prominent high endothelial postcapillary venules with PAS-positive hyalinization and "burned-out" residual follicles (Fig. 34.80). Clusters of lymphocytes with small nuclei but moderately abundant clear cytoplasm are usually present and increase in prominence with progression. The tumor is derived from follicular T-helper cells (THCs). The immunophenotype is mature T cell with CD4 predominance but often abundant reactive CD8 cells, coexpression of CD10, BCL6, ICOS, CXCL13, and PD-1, polyclonal plasma cells and B-immunoblasts, and prominent dendritic cells near vessels detected by CD21/CD23 (Miyoshi et al., 2012). CD20 is occasionally expressed, and secondary clonal B-cell proliferations occur that are usually associated with EBV (Jaffe et al., 2013).

TCR genes are usually rearranged and *IgH* genes are also rearranged in a minority of cases, at least some of which are associated with EBV and/or immunosuppression. Trisomy 3 or 5 or an additional X chromosome have each been described. The disease is aggressive, and infectious complications are common (Swerdlow, 2017).

Peripheral T-Cell Lymphoma, NOS

Peripheral T-cell lymphoma (PTCL), NOS, is characteristically diverse and may consist of sheets of large cells (Fig. 34.81), paracortical lymph

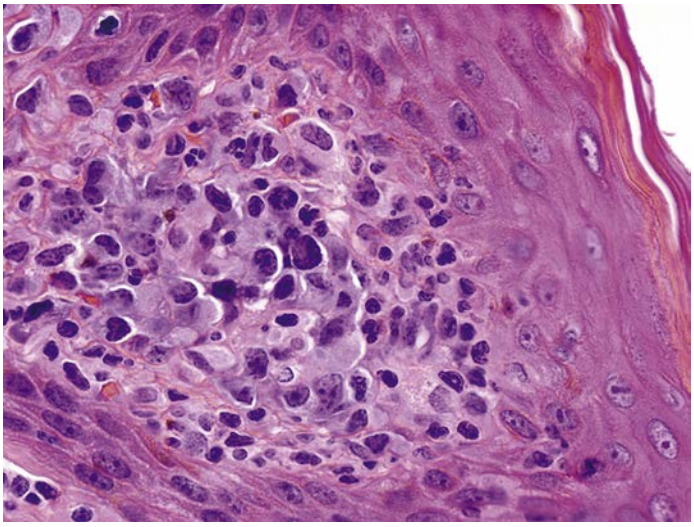

Figure 34.79 Cutaneous anaplastic large-cell lymphoma (×1000).

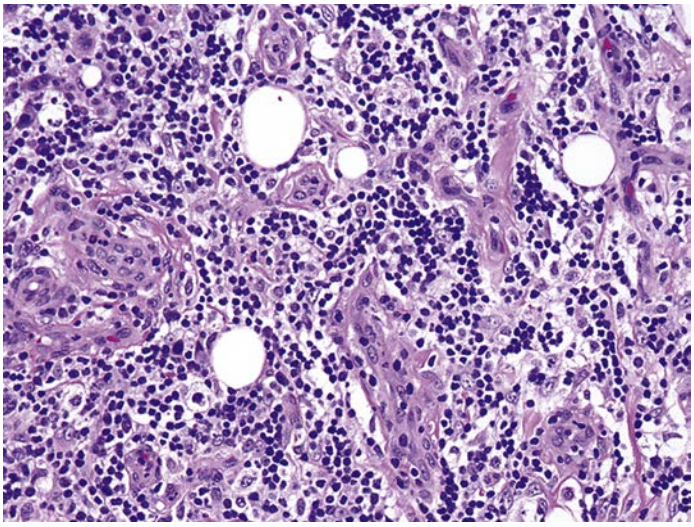

Figure 34.80 Angioimmunoblastic T-cell lymphoma showing arborizing vessels and lymphoid infiltrate infiltrating fat. In other areas of this case, plasma cells and immunoblasts are present. Clear cells are also frequently present (×200).

node expansion by mixed small and large cells, clear cells, predominantly small cells, and cases with striking pleomorphism resembling ALCL or HL. Abnormal patterns of T-antigen expression are helpful for diagnosis. Pan-T-cell antigens (CD3, CD2, CD5, CD7) are usually present in some combination, but one or more are often aberrantly not expressed. CD4+ cases are more frequent than CD8+, but both double-positive and double-negative cases may occur (Swerdlow, 2017). In paraffin sections, CD3, CD45RO, and CD43 are helpful if positive, but the latter two are also present in myeloid tumors and some B-cell lymphomas. CD68 is rarely expressed.

The T-zone variant of PTCL, NOS, shows paracortical expansion with preserved GCC. The cytomorphology is variable, with small and medium-sized cells, lymphocytes, plasma cells, endothelial hyperplasia, and, sometimes, clusters of clear cells and/or cells resembling those in HL.

The lymphoepithelioid variant, formerly known as *Lennert lymphoma*, exhibits clusters of epithelioid histiocytes.

These tumors are typically aggressive and often belie their sometimes bland or reactive appearance. Clonal rearrangement of *TCR* genes is essential for confident diagnosis.

Anaplastic Large Cell Lymphoma, ALK-Positive

ALCL was first recognized relatively recently as NHL reactive with the Hodgkin-associated antibody Ki-1 (anti-CD30) (Stein, 1985). ALK+ ALCL is most common in adolescents and young adults and accounts for about 10% to 15% of pediatric lymphomas.

ALK+ ALCL usually shows diffuse infiltrates or aggregates of large, sometimes pleomorphic cells with abundant cytoplasm and indented or horseshoe-shaped nuclei and sometimes wreath-like multilobulated nuclei (Fig. 34.82). Lymph node sinus and superficial paracortical involvement are common, cohesive sheets of tumor cells often simulate carcinoma, and some cases show a polymorphic Hodgkin-like pattern. True Reed-Sternberg cells are not seen. Histologic variants include monomorphic, small cell, and lymphohistiocytic types, but these also express ALK and show similar phenotype otherwise.

ALK+ ALCL is usually associated with chromosomal abnormalities involving chromosome region 2p23, such as t(2;5)(p23;q35) in which the gene for a tyrosine kinase anaplastic lymphoma kinase (ALK) is fused to that of the nucleolar shuttle protein nucleophosmin (NPM), with a resultant NPM-ALK fusion protein, with both nuclear and cytoplasmic expression (Morris et al., 1995). Variant translocations involving ALK also occur, usually with ALK expression in only the nucleus or cytoplasm by IHC.

Essentially all exhibit CD30. Slightly more than half show peripheral T-cell phenotype by IHC, but with variable expression of CD3, CD5, CD4, CD43, and CD45RO. CD3 seems to be most often negative. There is also variable expression of CD45, CD25, and EMA. CD68 or CD15 is only occasionally expressed. T-cell surface marker-negative cases usually show TCR rearrangements.

CD56, TIA-1, and myeloid markers CD13 and CD33 are often positive (Bovino & Allan, 2008). Signal transducer and activator of transcription 3 (*STAT3*) is overexpressed, with activation of anti-apoptotic pathways, increased expression of BCL2, BCL-XL and survivin. *JUNB* amplification/

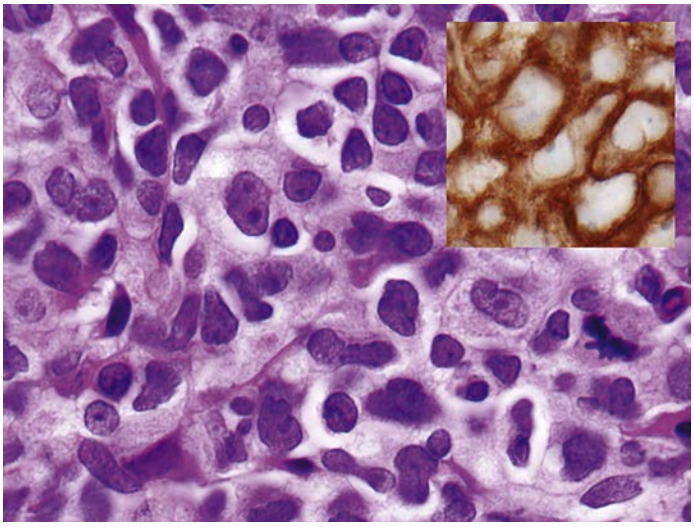

Figure 34.81 Peripheral T-cell lymphoma, NOS; CD3 expression is seen in inset (×1000).

overexpression is related to CD30 expression (Amin & Lai, 2007; Atsaves et al., 2014; Eyre et al., 2014).

The majority exhibit t(2;5)(p23;q35), but variants include t(1;2)(q25;p23) involving *TPM3*, which encodes a tropomyosin; inv(2)(p23;q35), involving *ATIC*; and t(2;3)(p23;q35), involving *TFG* (*TRAK* fused gene). These all show cytoplasmic without nuclear ALK. Other partner genes include *TPM4*, *CLTC*, *MSN*, *RNF213*, and *MYH9*. Those with t(2;17)(p23;q23), ***CLTC-ALK*** are diffuse large B-cell lymphomas (CD20-negative, CD79a+) with IgH rearrangement and, rarely, also TCR rearrangement. They show granular cytoplasmic staining with ALK.

Anaplastic Large-Cell Lymphoma, ALK-Negative

Lymphomas with similar histology and immunophenotype to ALK+ ALCL occur primarily in adults and are clinically varied. These lack ALK translocations. However, 30% show translocations involving ***DUSP22***, possibly associated with improved prognosis, and some (8%) with translocations involving TP63 and poor prognosis (Parrilla Castellar et al., 2014). A variety of "secondary" ALCLs (including progressions of other lymphomas, posttransplant tumors, and EBV- and HTLV-1–associated lymphomas) also express CD30.

Breast Implant–Associated Anaplastic Large-Cell Lymphoma

Breast implant–associated ALCL is a provisional entity in the most recent revised WHO classification with morphologic and immunophenotypic features similar to that of ALK-negative ALCL. It is a very rare entity and

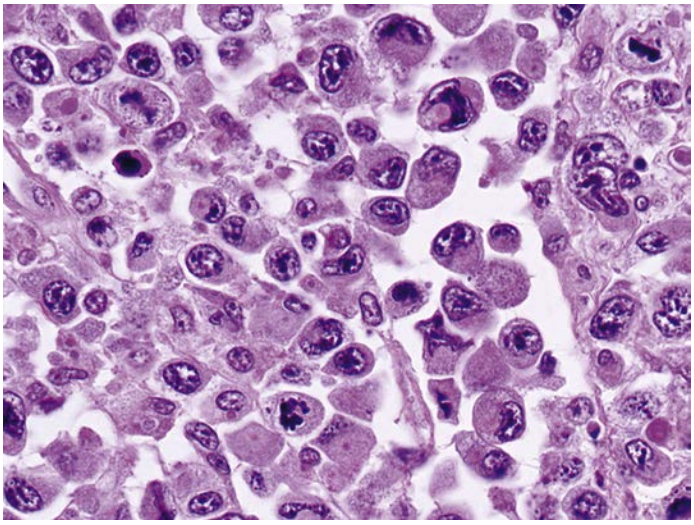

Figure 34.82 Anaplastic large-cell lymphoma in an adolescent (×500).

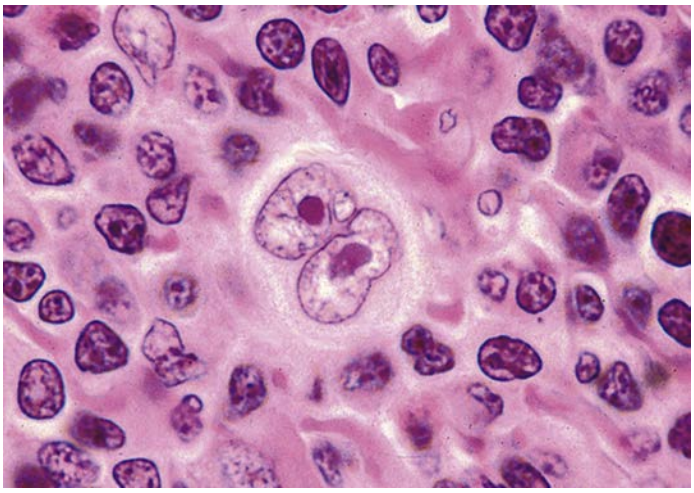

Figure 34.83 A Reed-Sternberg cell in a case of mixed-cellularity Hodgkin lymphoma (×1000).

usually occurs many years after implant placement with frequent clinical history of implant rupture. This disease can present as a localized collection of fluid around the implant (seroma) or as a discrete mass arising from the pericapsular fibrous tissue. Immunophenotypically, the neoplastic cells are positive for CD30, variably positive for one or more T-cell markers, and negative for ALK. The prognosis is excellent and most patients present with early-stage disease (Swerdlow, 2017).

HODGKIN LYMPHOMA

The nomenclature of HL, also called Hodgkin disease, is little changed from that of the Rye Conference (Lukes, 1966). The hallmark of HL is the Hodgkin Reed-Sternberg (HRS vs. RS) cell, which is a large binucleated, multinucleated, or mononuclear (Hodgkin) cell, with each nucleus bearing a very large inclusion-like nucleolus (Fig. 34.83). These neoplastic cells appear in an immunoproliferative background containing variable numbers of lymphocytes, histiocytes, eosinophils, and plasma cells. Degenerating "mummified" neoplastic cells are also often present.

Classical Hodgkin Lymphoma

Mixed cellularity, nodular sclerosis, lymphocyte-depleted, and lymphocyte-rich classical subtypes have similar biology, and a common neoplastic cell referred to as the Hodgkin Reed-Sternberg (HRS) cell. They are all referred to as "classical" HL (King et al., 2014; Swerdlow, 2017; Venkataraman et al., 2014).

The most common phenotype of HRS cells in classical HL is expression of CD30, CD15, PAX5, MUM1, and fascin with absence of CD45 and T-cell markers. B-cell–associated markers CD20 and/or CD79 are expressed in a minority of cases (<30%) and are usually focal and weak. Occasional cases show strong CD20 expression. B-cell transcription factors Oct2 and Bob.1 are absent, as is immunoglobulin J chain. Light-chain immunoglobulin antibodies may show generalized cytoplasmic labeling. Standard Ig and *TCR* gene rearrangement studies are negative in classical HL, but sequencing of amplified single-cell *IgH* genes suggests that most cases of HL are derived from clonal B lymphocytes. EBV is associated with a substantial portion of cases of classical HL.

HL may occur from early childhood to old age. Increased frequency is noted between 15 and 35 years and after age 50 years. Males predominate, especially in childhood; disease in females younger than age 30 years is usually nodular sclerosis in type (Table 34.8).

Nodular Sclerosis

Nodular sclerosis (NS) is characterized by broad bands of collagen separating nodules of lymphoid tissue and the presence of **lacunar variants** of HRS cells with pale cytoplasm and variable nucleoli (Figs. 34.84 and 34.35). Classic HRS cells are variable in number. Fibrosis may be inconspicuous in early lesions, but neoplastic cell clustering is usually present.

NS HL is graded on the basis of the number of neoplastic cells. When sheets of neoplastic cells are present in 25% or more of nodules, the tumor is designated grade 2. This is frequently associated with necrosis and has been termed *syncytial variant*. The NS variety of HL is common, often presenting as a mediastinal mass in a young woman.

Mixed Cellularity

Mixed cellularity shows a diffuse polymorphic infiltrate of lymphocytes, plasma cells, eosinophils, histiocytes, and Reed-Sternberg cells, which sometimes are numerous (Fig. 34.86). Necrosis and disorderly fibrosis may be present. This subtype is less common in young people than is NS, and it is the most frequent subtype with EBV involvement.

Lymphocyte Depletion

This type is uncommon, often presents at older age, and may be associated with diffuse fibrosis. Neoplastic cells predominate and lymphocytes are relatively diminished compared with other forms of HL (Fig. 34.87). It is sometimes associated with an acute febrile illness accompanied by pancytopenia and lymphocytopenia. BM involvement is common, but lymphocytosis and thrombocytosis, often seen in other types of HL, are usually absent.

Normocytic anemia is seen in about 50% of HL cases. Leukocyte and platelet counts are variable, and eosinophilia may be present. Blood and marrow findings and many of the histologic features appear to be manifestations of host responses to the disease. Immunologic studies in HL have shown that cell-mediated immunity is defective when extensive disease is present.

Nodular Lymphocyte–Predominant HL

The histology of NLPHL consists of effacement of lymph node architecture by a nodular infiltrate of small B cells with an associated follicular dendritic network and clustered or scattered large cells referred to as *L&H cells*, after the original Lukes and Butler terminology of lymphocytic and histiocytic HL. Nodularity may be vague. L&H cells are variable in cytology from case to case, although they are usually more uniform within a case. The appearance most often described exhibits large nuclei with vesicular chromatin, moderately prominent nucleoli, and convoluted nuclei resembling popcorn ("popcorn cells"). Cytoplasm is moderate in amount and clear, retracted, or slightly eosinophilic. Probably more often, the neoplastic cells show round to oval nuclei with distinct eosinophilic or basophilic nucleoli, but less prominent than in HRS cells (Fig. 34.89). With experience, these cells become distinctive. Occasional HRS cells may be seen but are not always present and rarely predominate. Their phenotype, however, is different from that of classic HRS cells. L&H cells are usually loosely aggregated in the centers of nodules but are scattered elsewhere. Six immunoarchitectural patterns have been recognized, based on the predominance of B and T cells in the background and the proportion of diffuse and nodular areas in the involved tissue.

The phenotype of L&H cells is mature B cell, expressing CD45, CD20, CD22, CD79a, BCL-6, BOB.1, Oct2, CD75, and usually J-chain (Swerdlow, 2017). CD30 is absent or weak, and EMA is frequently expressed. The nodules are composed mostly of B cells but with abundant admixed CD3 and CD3/CD57-positive T cells, which tend to form rosettes around L&H cells. These are not always present, but are diagnostically helpful when they are. Nodules contain a follicular dendritic network, which may be illuminated by CD21, CD35, or CD23 antibodies. Cytoplasmic Ig is present but does not appear clonal, even though B cells have been proven to be monoclonal by single-cell PCR.

TABLE 34.8
Key Features of Hodgkin Lymphomas

Lymphoma	Demographics, Clinical Presentation	Morphology	Cell Surface Markers	Prognosis
Nodular, lymphocyte predominant (NLPHL)	M > F, 30–50 years, with peripheral lymphadenopathy	Mononuclear cells with convoluted nuclei (popcorn or L&H cells) loosely aggregated in nodules of small B cells	CD45, CD20, bcl-6, J-chain, Oct-2, BOB.1, EBV absent in LP cells	Excellent for stages I, II
Nodular sclerosis	M = F, <30 years with mediastinal mass, occasional spleen or lung involvement; 40% have B symptoms; most patients present with stage II disease	Broad bands of collagen, nodules of lymphoid tissue with aggregates of HRS cells and lacunar cells, multinucleated variants	CD15, CD30, CD45-EBV in 1%–40%	Good with systemic therapy
Mixed cellularity	M > F; median age, 38 years; peripheral lymphadenopathy common, spleen, BM; B symptoms common; patients often stage III or IV	Classic HRS cells in mixture of lymphocytes, plasma cells, eosinophils, histiocytes	CD15, CD30, CD45-EBV in 75%	Good with systemic therapy
Lymphocyte depletion	M > F; median age, 30–37 years; B symptoms, advanced stage common; associated with HIV	Classic HRS cells common with paucity of background lymphocytes; pleomorphic HRS cells mimic sarcoma	CD15, CD30, CD45-EBV pos in HIV-affected patients	Associated with advanced stage
Lymphocyte-rich classical	M > F, older age; peripheral lymphadenopathy; B symptoms rare; most patients with stage I or II disease	Scattered classic HRS cells among numerous small lymphocytes; nodular growth pattern	CD15, CD30; Oct2 and BOB.1 vary; J-chain absent; EBV in 40%–75%	Good, similar to NLPHL

BM, Bone marrow; *EBV,* Epstein-Barr virus; *F,* female; *HIV,* human immunodeficiency virus; *HRS,* Hodgkin Reed-Sternberg; *L&H,* lymphocytic and histiocytic; *LP,* lymphoplasmacytic; *M,* male; *NLPHL,* nodular lymphocyte-predominant Hodgkin lymphoma.

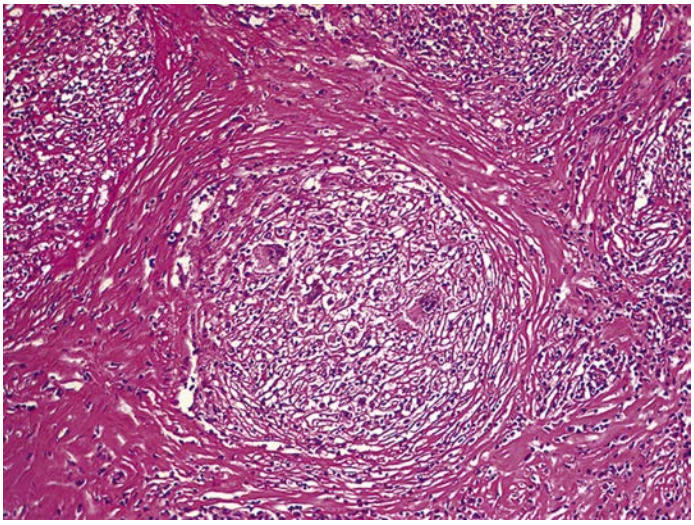

Figure 34.84 Dense fibrosis in a case of nodular sclerosis Hodgkin lymphoma (×200).

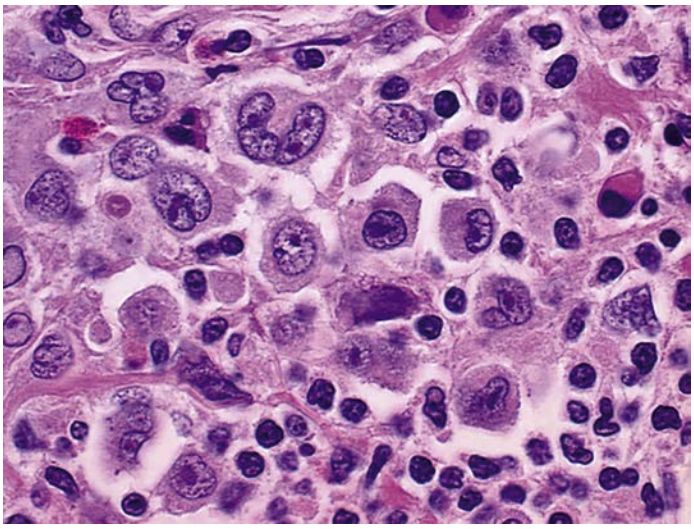

Figure 34.85 A cluster of Hodgkin Reed-Sternberg cells in a nodule of nodular sclerosis Hodgkin lymphoma (×500).

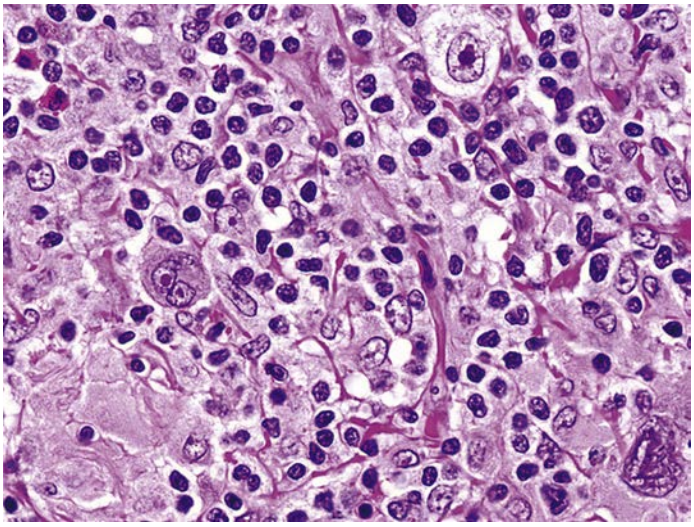

Figure 34.86 Scattered Hodgkin Reed-Sternberg cells in mixed-cellularity Hodgkin lymphoma (×500).

IgH is clonally rearranged by sensitive assays in the research setting, but this usually is not detectable in routine clinical laboratory settings. L&H cells are of GC or post-GC derivation with somatic mutations of *Ig* genes, which are ongoing in about half of studied cases (Braeuninger, 1997).

Histologic variants have been described, including those with a diffuse T-cell rich pattern and with increased L&H cells outside of B-cell nodules, with more advanced stage and greater risk of progression or relapse (Hartmann et al., 2013). Male gender and low albumin may also increase risk (Fanale, 2013). Cases of NLPHL are also noted with involvement by EBV, with atypical features including CD30, weak PAX5 and pleomorphic cells that mimic classical HL (Huppmann et al., 2014).

Progressive transformation of lymph node germinal centers (PTGC) has been described as a precursor lesion to NLPHL, but no relationship has been proven. Most cases of PTGC do not lead to lymphoma.

Nodular Lymphocyte-Rich Classical HL

Nodular lymphocyte-rich classical Hodgkin lymphoma (NLRCHL) is a type of HL that morphologically and clinically resembles NLPHL but shows immunophenotypic characteristics of classical Hodgkin lymphoma (CHL). Typically, germinal centers are preserved and HRS cells are found in the mantle zones. It usually presents in peripheral lymph nodes with early-stage

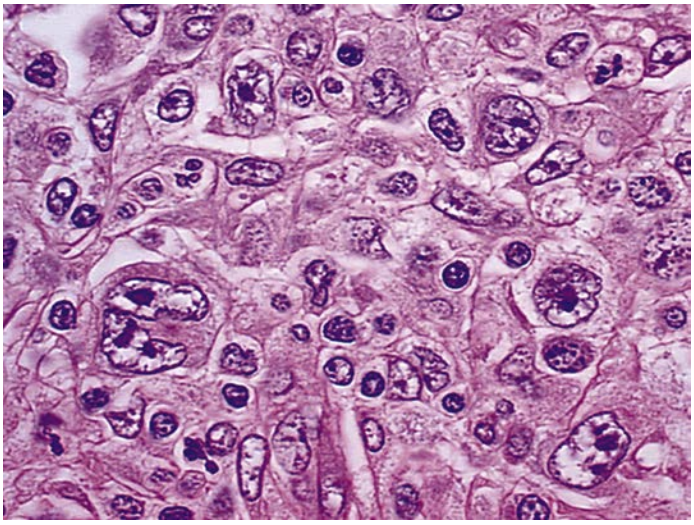

Figure 34.87 Lymphocyte-depleted Hodgkin lymphoma shows predominance of neoplastic cells with few lymphocytes (×500).

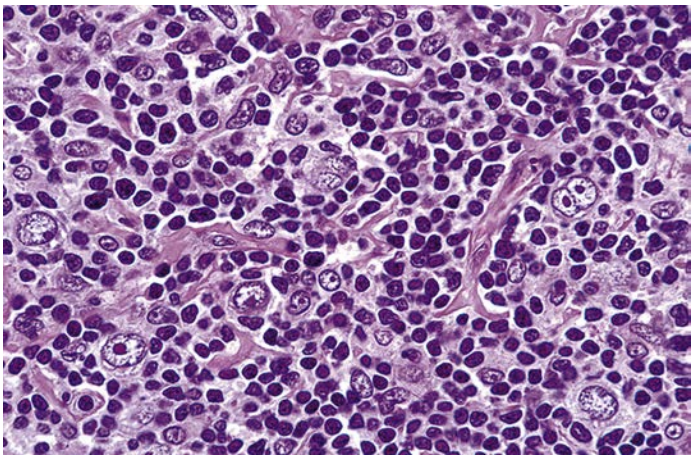

Figure 34.88 Lymphocyte-predominant Hodgkin lymphoma, with lymphocyic and histiocytic (L&H) cells showing round rather than popcorn nuclei (×500).

disease. The HRS cells in this type express CD30 and uniformly lack immunoglobulin J-chain that is present in NLPHL (Anagnostopoulos, 2000). Recent studies show overlap between NLRCHL and NLPHL in expression of B-cell factors bcl-6, Oct-2, and Bob.1, which are variable in NLRCHL but nearly constant in NLPHL. CD15 and MUM-1 are more frequent in NLRCHL, and Pax-5 is expressed in most cases of both types (Nam-Cha, 2009). A large clinical study has shown that patients with NLRCHL are older than those with other CHL and that response and outcome are excellent, resembling NLPHL (Shimabukuro-Vornhagen, 2005).

IMMUNODEFICIENCY-ASSOCIATED LYMPHOPROLIFERATIVE DISORDERS

Lymphomas and uncontrolled polyclonal lymphoid proliferations occur with increased frequency in patients with immune dysfunction (Swerdlow, 2017). These dysfunctional states fall into three main categories: primary (congenital) immunodeficiency states, HIV infection, and iatrogenic immunodeficiency, particularly due to posttransplant immunosuppression but also due to prolonged immunosuppressive therapy for other reasons.

Most of these are B-cell lymphoproliferative disorders associated with infection or reactivation of EBV or other virus and include large B-cell lymphoma and variants, BL, and polymorphic B-cell hyperplasia. Hodgkin and peripheral T-cell lymphomas occur rarely. See Box 34.14 for a summary of lymphoid diseases associated with EBV.

Lymphoproliferative Diseases Associated with Primary Immune Disorders (PIDs)

Primary immunodeficiencies are rare disorders and include Wiskott-Aldrich syndrome (WAS), ataxia-telangiectasia (AT), common variable immunodeficiency syndrome (CVID), severe combined immunodeficiency (SCID), X-linked immunoproliferative disorder (XLP), Nijmegan breakage syndrome (NBS), hyper-IgM syndrome, and autoimmune lymphoproliferative disorder (ALPS) (Chadburn, 2013). There are now hundreds of different genetic PIDs recognized, diagnosed in adults as well as in children. With genomic techniques, the list is likely to continue to expand (Chou et al., 2012; O'Gorman, 2008; Verma et al., 2013). Cytopenias are frequent, often due to autoimmune phenomena (Seidel, 2014).

ALPS involves inherited mutations of the FAS gene, which blocks apoptosis. This involves different mutations of varying effect, may be more common than previously thought and shows an adult onset in some cases. Clinically, it shows lymphadenopathy and presence of CD4/CD8 double-negative T cells. Hyper-IgM syndrome results from mutations in CD40 ligand with inhibition of T-/B-cell interaction and B-cell maturation. AT and NBS are abnormalities of DNA repair. WAS is a syndrome of thrombocytopenia, skin rash, and recurrent infections that is fatal but curable by allogeneic bone marrow transplantation.

Fatal EBV infectious mononucleosis is a common occurrence in XLP and SCID. Large B-cell lymphomas are the most common tumors in most primary immunodeficiencies, and lymphomatoid granulomatosis is increased in WAS.

BOX 34.14

Lymphoid Diseases Associated With EBV

- Mononucleosis-type illness
- Hodgkin lymphoma: MC > LR > NS; LD seen in HIV patients
- Immunodeficiency-associated lymphoproliferative disorders
- Posttransplant lymphoproliferative disorders
- Some DLBCL cases (associated w/inflammations, NOS)
- Lymphomatoid granulosis
- Primary effusion lymphoma
- EBV+ lymphoproliferative disorders of childhood
- Burkitt lymphoma (endemic and HIV associated)
- Extranodal NK-/T-cell lymphoma, nasal type
- Angioimmunoblastic lymphoma
- Plasmablastic lymphoma

DLBCL, Diffuse large B-cell lymphoma; *EBV,* Epstein-Barr virus; *HIV,* human immunodeficiency virus; *LD,* lymphocyte depletion; *LR,* lymphocyte-rich classical; *MC,* mixed cellularity; *NS,* nodular sclerosis.

HIV-Associated Lymphomas

HIV-associated lymphomas include Burkitt, DLBCL (CG, ABC, or primary CNS types) plasmablastic lymphoma (usually in the oral cavity) and primary effusion lymphoma (PEL). Other types, including classical HL, are "rare" but occur at higher frequency in HIV patients than in the general population (Little & Dunleavy, 2013). The incidence of HIV-associated lymphomas has dropped substantially in developed nations since the introduction of combination antiretroviral therapy (cART), and varies inversely with the CD4 count. Lymphoma is particularly frequent when CD4 cells are less than 200/μL. Of HIV-related lymphomas, 40% are also EBV associated. Primary effusion lymphomas in HIV are associated with KHSV/HHV-8 infection and multicentric Castleman disease (Gloghini et al., 2013).

Post-transplant Lymphoproliferative Disorders

PTLDs comprise a unique spectrum of lymphoproliferative disorders occurring due to therapeutic immunosuppression associated with organ transplantation (Swerdlow, 2017). A majority, but not all, are EBV associated (Parker et al., 2010). In many cases, the tumors regress when immunosuppressive therapy is reduced, but this is unpredictable.

Plasmacytic hyperplasia (PH) is composed of numerous plasma cells and scattered immunoblasts. Infectious mononucleosis–like PTLD shows paracortical expansion of lymph nodes with increased immunoblasts. Both are early or low-grade lesions with a slow progression.

Polymorphic PTLD shows increased immunoblasts and plasma cells in a lymphoid background. Monomorphic PTLD is essentially diffuse lymphoma, usually large B cell or, less often, Burkitt. A Hodgkin-like PTLD is likely to be a large B-cell lymphoma with Hodgkin-like features, previously called *polymorphic immunoblastic* in the Working Formulation (Fig. 34.89). Monomorphic T-cell lymphomas also occur rarely.

A spectrum of disorders similar to PTLD also may occur with chronic immunosuppression for other reasons, such as the use of methotrexate in the treatment of rheumatoid arthritis.

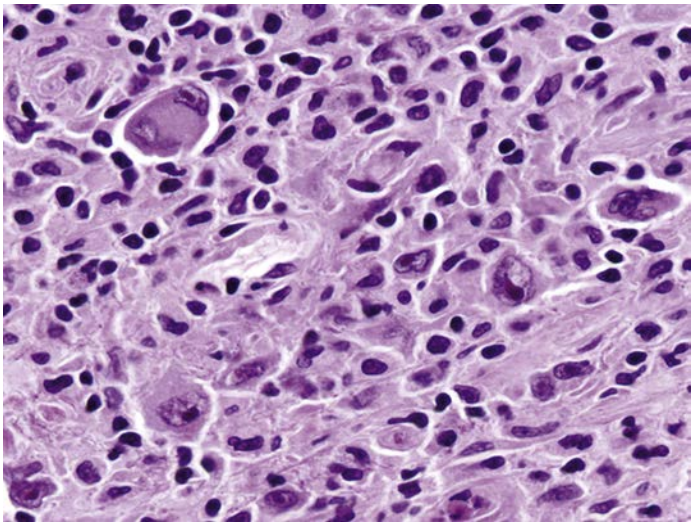

Figure 34.89 Large B-cell lymphoma (anaplastic subtype) arising in polymorphic posttransplant lymphoproliferative disorder, in the gastrointestinal tract (×500).

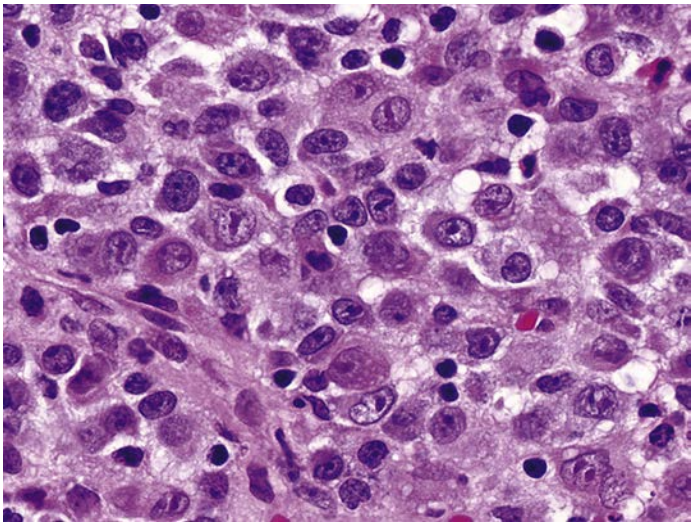

Figure 34.90 Histiocytic sarcoma in a child. This case showed expression of monocytic markers and enzymes, lack of lymphoid markers, and lack of lymphoid gene rearrangements (×500).

HISTIOCYTIC AND DENDRITIC CELL NEOPLASMS

These are rare disorders that affect lymph nodes and soft tissues, and occasionally the BM. **Histiocytic sarcoma**, also known as *true histiocytic lymphoma*, is a malignant tumor of noncirculating cells of monocyte macrophage lineage (Swerdlow, 2017). The differential diagnosis includes monocytic leukemia and large B-cell or peripheral T-cell lymphoma. It resembles a large-cell lymphoma or histiocytic sarcoma of monocytic lineage (Fig. 34.90). Tumor cells show nuclear features of malignancy. These label with CD68, CD163 lysozyme, α_1-antitrypsin, and antichymotrypsin. Others label with other monocyte macrophage markers (e.g., CD64, CD14). Some hemophagocytosis may be seen.

Hemophagocytic Syndromes, or Hemophagocytic Lymphohistiocytosis (HLH)

These present with hepatosplenomegaly, fever and other constitutional symptoms, cytopenias, and infiltrates of macrophages in involved organs, including bone marrow and sometimes lymph nodes. Hemophagocytosis may include red blood cells (Fig. 34.91) or may be limited to platelets and leukocytes. It is often difficult to identify, or not seen at all, in a bone marrow sample. Diagnostic criteria include cytopenias affecting at least 2 lineages in the peripheral blood, hypofibrinogenemia, strikingly elevated ferritin levels, and hypertriglyceridemia (Faitelson & Grunebaum, 2014; Rosado & Kim, 2013). Acquired HLH is usually associated with viral infection related to neoplasms or to primary immunodeficiencies. Familial hemophagocytic syndromes also occur and are associated with perforin and other gene mutations. The cause of acquired HLH is often cryptic, but the disorder frequently follows an aggressive course. Approximately 60% of patients succumb within 2 months, but some patients respond to therapy that often includes etoposide.

Langerhans Histiocytosis

Langerhans cell histiocytosis (LCH) is a neoplastic proliferation of Langerhans cells, which are dendritic cells normally found primarily in the skin (Jaffe, 1999; Swerdlow, 2017). It presents in a variety of ways, including unifocal disease, usually in the bone, and occasionally in the lymph node, skin, or lung, of an adolescent or young adult. These have been termed *eosinophilic granuloma*.

Multifocal unisystem disease usually involves bone in children with frequent spread to adjacent soft tissues, and is also known as *Hand-Schüller-Christian disease*. Skull involvement may lead to diabetes insipidus, tooth loss, or exophthalmos. Multiple lung lesions may be seen in adults.

Multifocal multisystem disease, known as *Letterer-Siwe disease*, occurs in infants. It is an aggressive disease with fever, skin rash, hepatosplenomegaly, lymphadenopathy, bone involvement, and pancytopenia.

Histologically, all forms of LCH consist of infiltrates of Langerhans cells. They are dendritic cells that resemble benign histiocytes but have a coffee bean–shaped nucleus with a linear central groove (Fig. 34.92). Variable numbers of eosinophils and lymphocytes are usually present. The infiltrates form nodules in bone, involve the upper dermis of the skin, and may involve lymph node sinuses and splenic red pulp. Giant cells are sometimes present but differ from multinucleated histiocytes (as in juvenile xanthogranuloma) by the presence of the characteristic nuclei.

Immunophenotyping shows reactivity for CD1a, langerin, and S-100 protein and may be weakly reactive with CD45 and CD68, but is negative for T and B cell–specific antibodies and follicular dendritic markers CD21 and CD35. Electron microscopy remains useful in some cases because of characteristic Birbeck granules, which are pentalaminar racket-shaped structures pathognomonic of Langerhans cells.

Outcome is largely dependent on extent of organ involvement, with localized disease showing a high rate of event-free survival and extensive disease showing only a variable response to chemotherapy. Pulmonary disease in adults may remit spontaneously on cessation of smoking.

A cytologically malignant form of LCH has been termed *Langerhans cell sarcoma* (Zwerdling, 2014). Patients usually present with multiorgan disease, a high mitotic rate, and aggressive behavior.

Interdigitating Dendritic Cell Sarcoma/Tumor

Interdigitating dendritic cell sarcoma/tumor (IDCS) is a rare tumor of lymph node paracortical interdigitating dendritic cells (Swerdlow, 2017). It has the gross and microscopic appearance of a sarcoma and is tan in color, with a firm lobulated appearance, sometimes with hemorrhage or necrosis and microscopic fascicles, whorls, and/or a storiform pattern. Lymphocytes are scattered throughout, and plump epithelioid cells may be present. Atypia is variable.

Immunophenotyping is essential to diagnosis. The tumor cells are positive for S-100, vimentin, and fascin, with variable weak positivity for CD45 and monocyte markers CD68 and lysozyme. CD1a, CD21, and CD35 are negative. Other myeloid B- and T-cell markers, EMA, and CD30 are also negative. Background lymphocytes are reactive T cells. Prognosis is variable.

Follicular Dendritic Cell Sarcoma/Tumor

This is another rare dendritic cell tumor derived from follicular dendritic cells, which are phenotypically different from IDCS. Involvement is usually cervical lymph nodes, with axillary, mediastinal, mesenteric, and retroperitoneal node involvement also described. Microscopically, nodes show fascicles, a storiform pattern, and/or complete whorls.

The immunophenotype shows positivity for CD21, CD23, clusterin, vimentin, fascin, and CD35, with variable S-100 and CD68, negative CD1a, and occasional CD45 and CD20. Other myeloid T- and B-cell markers, cytokeratins, and HMB-45 are negative. CD117 is also negative.

These tumors are indolent, with frequently good response to simple resection.

Indeterminate Dendritic Cell Tumor

These are dendritic cell sarcomas that do not fall into the previous specific categories. The neoplastic cells express CD1a and S-100 without Birbeck granules. They are negative for langerin, CD30, CD163, CD21, CD23, and CD35

Figure 34.91 **A**, Histiocytic hyperplasia occurring in infection-associated hemophagocytic syndrome. This macrophage contains platelets as well as erythrocytes (×1000). Compare with **B**, a histiocyte containing cell debris in a patient with human immunodeficiency virus (×1000). **C**, An abnormal macrophage in Gaucher disease (×1000). **D**, An abnormal macrophage in Niemann-Pick disease (×1000).

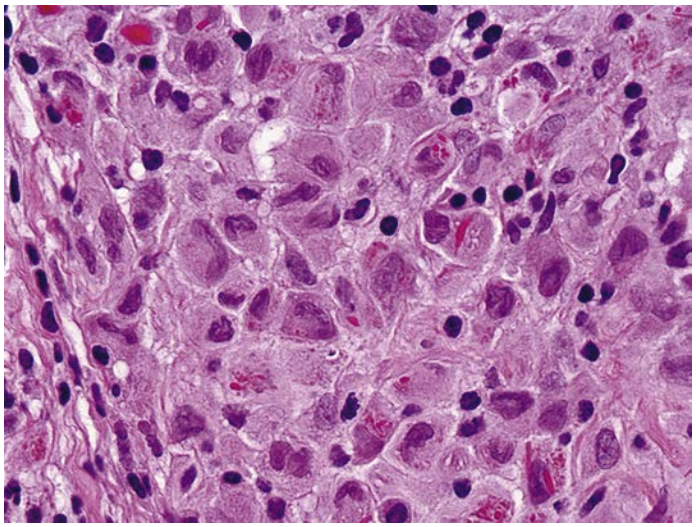

Figure 34.92 Langerhans cell histiocytosis, showing typical nuclear folding and grooves (×500).

SELECTED REFERENCES

Greer JP, Arber DA, Appelbaum FR, et al.: *Wintrobe's clinical hematology*, ed 14., Philadelphia, 2019, Wolters Kluwer, pp 227–250.

This provides an excellent review of clinical correlates of hematopathology/hematology, including laboratory aspects.

Hernandez AM: Peripheral blood manifestations of lymphoma and solid tumors, *Clin Lab Med* 22:215–253, 2002.

This article describes the correlation of findings identified on peripheral blood films in patients with various types of lymphoid leukemia and lymphoma, including morphology of various lymphoma cells in the circulating blood during disease.

Jaffe ES, Arber DA, Campo E, et al.: *Hematopathology*, Philadelphia, 2017, Elsevier.

This is a comprehensive, authoritative, and up-to-date review of hematopathology, incorporating the WHO classification.

Kroft SH: Infectious diseases manifested in the peripheral blood, *Clin Lab Med* 22:253–277, 2002.

A review of both nonspecific hematopoietic changes in the peripheral blood during infection and findings for the few diseases in which peripheral blood film review plays a primary diagnostic role.

Swerdlow SH, Campo E, Harris NL, et al.: *WHO classification of tumours of haematopoietic and lymphoid tissues*, Revised 4th ed., Lyon, France, 2017, IARC.

This provides a comprehensive and uniform classification of hematopoietic neoplasms. It was commissioned by the WHO through the major organizations of hematopathology, with clinical input from cooperative groups and cancer centers, and is intended to provide standard diagnostic criteria for worldwide use. Last updated in 2017.

Wegman-Ostrosky T, Savage SA: The genomics of inherited bone marrow failure: from mechanism to the clinic, *Br J Haematol* 177(4):526–542, 2017.

Excellent review of recent advances in the genomics of bone marrow failure, including congenital neutropenias.

Access the complete reference list online at Elsevier eBooks for Practicing Clinicians.

REFERENCES

Abdel-Wahab O, Levine RL: Mutations in epigenetic modifiers in the pathogenesis and therapy of acute myeloid leukemia, *Blood 2*; 121(18):3563–3572, 2013.

Akasheh N, Walsh MT, Costello RW: Eosinophil peroxidase induces expression of cholinergic genes via cell surface neural interactions, *Mol Immunol* 62(1):37–45, 2014.

Akin C: Valent P: diagnostic criteria and classification of mastocytosis in 2014, *Immunol Allergy Clin North Am* 34(2):207–218, 2014.

Alapat D, Coviello-Malle J, Owens R, Qu P, Barlogie B, Shaughnessy JD, et al.: Diagnostic usefulness and prognostic impact of CD200 expression in lymphoid malignancies and plasma cell myeloma, *Am J Clin Pathol* 137(1):93–100, 2012.

Alder A: Uber konstitutionell bedingte Granulations-veranderungen den Leukocyten, *Archives Klinische Medizinn* 138:372–378, 1939.

Alizon M, Sonigo P, Barre-Sinoussi F, Chermann JC, Tiollais P, Montagnier L, et al: Molecular cloning of lymphadenopathy-associated virus, Nature 312(5996):757–760, 1984 Dec 20-1985 Jan 2.

Amin HM, Lai R: Pathobiology of ALK+ anaplastic large-cell lymphoma, *Blood* 110(7):2259–2267, 2007.

Anagnostopoulos I, Hansmann ML, Franssila K, Harris M, Harris NL, Jaffe ES, et al.: European Task Force on Lymphoma project on lymphocyte predominance Hodgkin disease: histologic and immunohistologic analysis of submitted cases reveals 2 types of Hodgkin disease with a nodular growth pattern and abundant lymphocytes, *Blood* 96(5):1889–1899, 2000.

Auerbach AD: Fanconi anemia and its diagnosis, *Mutat Res* 668(1–2):4–10, 2009.

Baliakas P, Strefford JC, Bikos V, Parry M, Stamatopoulos K, Oscier D: Splenic marginal-zone lymphoma: ontogeny and genetics, *Leuk Lymphoma* 19:1–10, 2014.

Barre-Sinoussi F, Chermann JC, Rey F, Nugeyre MT, Chamaret S, Gruest J, et al.: Isolation of a T-lymphotropic retrovirus from a patient at risk for acquired immune deficiency syndrome (AIDS), *Science* 220(4599):868–871, 1983.

Bene MC, Porwit A: Acute leukemias of ambiguous lineage, *Semin Diagn Pathol* 29(1):12–18, 2012.

Bennett JM, Catovsky D, Daniel MT, Flandrin G, Galton DA, Gralnick HR, et al.: Criteria for the diagnosis of acute leukemia of megakaryocyte lineage (M7). A report of the French-American-British Cooperative Group, *Ann Intern Med* 103(3):460–462, 1985.

Bennett JM, Catovsky D, Daniel MT, Flandrin G, Galton DA, Gralnick HR, et al.: Proposals for the classification of the myelodysplastic syndromes, *Br J Haematol* 51(2):189–199, 1982.

Bennett JM, Catovsky D, Daniel MT, Flandrin G, Galton DA, Gralnick HR, et al.: Proposals for the classification of the acute leukaemias. French-American-British (FAB) co-operative group, *Br J Haematol* 33(4):451–458, 1976.

Berard CW, Hutchison RE: The problem of classifying lymphomas: an orderly prescription for progress, *Ann Oncol* 8(Suppl 2):3–9, 1997.

Bianchi G, Anderson KC, Harris NL, Sohani AR: The heavy chain diseases: clinical and pathologic features, *Oncology (Williston Park)* 28(1):45–53, 2014.

Bjorkholm M, Derolf AR, Hultcrantz M, Kristinsson SY, Ekstrand C, Goldin LR, et al.: Treatment-related risk factors for transformation to acute myeloid leukemia and myelodysplastic syndromes in myeloproliferative neoplasms, *J Clin Oncol* 29(17):2410–2415, 2011.

Boeckh M: Complications, diagnosis, management, and prevention of CMV infections: current and future, *Hematology Am Soc Hematol Educ Program*305–309, 2011. 2011.

Borges AH, Dubrow R, Silverberg MJ: Factors contributing to risk for cancer among HIV-infected individuals, and evidence that earlier combination antiretroviral therapy will alter this risk, *Curr Opin HIV AIDS* 9(1):34–40, 2014.

Braeuninger A, Kuppers R, Strickler JG, Wacker HH, Rajewsky K, Hansmann ML: Hodgkin and Reed-Sternberg cells in lymphocyte predominant Hodgkin disease represent clonal populations of germinal center-derived tumor B cells, *Proc Natl Acad Sci U S A* 94(17):9337–9342, 1997.

Brito-Babapulle F: The eosinophilias, including the idiopathic hypereosinophilic syndrome, *Br J Haematol* 121(2):203–223, 2003.

Brunning R: Morphologic alterations in nucleated blood and marrow cells in genetic disorders, *Hum Pathol* 1:99, 1970.

Burkitt D: A sarcoma involving the jaws in African children, *Br J Surg* 46(197):218–223, 1958.

Cagnetta A, Adamia S, Acharya C, Patrone F, Miglino M, Nencioni A, et al.: Role of genotype-based approach in the clinical management of adult acute myeloid leukemia with normal cytogenetics, *Leuk Res* 38(6):649–659, 2014.

Cancer Genome Atlas Research Network: Genomic and epigenomic landscapes of adult de novo acute myeloid leukemia, *N Engl J Med* 368(22):2059–2074, 2013.

Carbonetti NH: Pertussis leukocytosis: mechanisms, clinical relevance and treatment, *Pathog Dis* 74(7), 2016.

Carlsson G, Melin M, Dahl N, Ramme KG, Nordenskjold M, Palmblad J, et al.: Kostmann syndrome or infantile genetic agranulocytosis, part two: understanding the underlying genetic defects in severe congenital neutropenia, *Acta Paediatr* 96(6):813–819, 2007.

Cazzola M, Della Porta MG, Malcovati L: The genetic basis of myelodysplasia and its clinical relevance, *Blood* 122(25):4021–4034, 2013.

Cazzola M, Kralovics R: From Janus kinase 2 to calreticulin: the clinically relevant genomic landscape of myeloproliferative neoplasms, *Blood* 123(24):3714–3719, 2014.

Cerchietti L, Leonard JP: Targeting the epigenome and other new strategies in diffuse large B-cell lymphoma: beyond R-CHOP, *Hematology Am Soc Hematol Educ Program* 2013:591–595, 2013.

Chadburn A: Immunodeficiency-associated lymphoid proliferations (ALPS, HIV, and KSHV/HHV8), *Semin Diagn Pathol* 30(2):113–129, 2013.

Chalayer E, Ffrench M, Cathebras P: Bone marrow fibrosis as a feature of systemic lupus erythematosus: a case report and literature review, *SpringerPlus* 3:349–1801, 2014. –3-349. eCollection 2014.

Cheah CY, Burbury K, Apperley JF, Huguet F, Pitini V, Gardembas M, et al.: Patients with myeloid malignancies bearing *PDGFRB* fusion genes achieve durable long-term remissions with imatinib, *Blood* 123(23):3574–3577, 2014.

Chen Y, Kantarjian H, Pierce S, Faderl S, O'Brien S, Qiao W, et al.: Prognostic significance of 11q23 aberrations in adult acute myeloid leukemia and the role of allogeneic stem cell transplantation, *Leukemia* 27(4):836–842, 2013.

Chikatsu N, Kojima H, Suzukawa K, Shinagawa A, Nagasawa T, Ozawa H, et al.: ALK+, CD30-, CD20- large B-cell lymphoma containing anaplastic lymphoma kinase (ALK) fused to clathrin heavy chain gene (CLTC), *Mod Pathol* 16(8):828–832, 2003.

Chou J, Ohsumi TK, Geha RS: Use of whole exome and genome sequencing in the identification of genetic causes of primary immunodeficiencies, *Curr Opin Allergy Clin Immunol* 12(6):623–628, 2012.

Christensen RD, Calhoun DA: Congenital neutropenia, *Clin Perinatol* 31(1):29–38, 2004.

Clark TA: Changing pertussis epidemiology: everything old is new again, *J Infect Dis* 209(7):978–981, 2014.

Colby TV: Current histological diagnosis of lymphomatoid granulomatosis, *Mod Pathol Suppl* 1:S39–42, 2012.

Colella R, Hollensead SC: Understanding and recognizing the Pelger-Huet anomaly, *Am J Clin Pathol* 137(3):358–366, 2012.

Csernus B, Timar B, Fulop Z, Bognar A, Szepesi A, Laszlo T, et al.: Mutational analysis of IgVH and BCL-6 genes suggests thymic B-cells origin of mediastinal (thymic) B-cell lymphoma, *Leuk Lymphoma* 45(10):2105–2110, 2004.

Dainiak N: Hematologic consequences of exposure to ionizing radiation, *Exp Hematol* 30(6):513–528, 2002.

Dale DC: Cyclic and chronic neutropenia: an update on diagnosis and treatment, *Clin Adv Hematol Oncol* 9(11):868–869, 2011.

Davey FR, Huntington S: Age-related variation in lymphocyte subpopulations, *Gerontology* 23(5):381–389, 1977.

De Paepe P, Baens M, van Krieken H, Verhasselt B, Stul M, Simons A, et al.: ALK activation by the CLTC-ALK fusion is a recurrent event in large B-cell lymphoma, *Blood* 102(7):2638–2641, 2003.

Dearden C: B- and T-cell prolymphocytic leukemia: antibody approaches, *Hematology Am Soc Hematol Educ Program*645–651, 2012. 2012.

Dinauer MC: Inflammatory consequences of inherited disorders affecting neutrophil function, *Blood* 133(20):2130–2139, 2019.

Dojcinov SD, Venkataraman G, Pittaluga S, Wlodarska I, Schrager JA, Raffeld M, et al.: Age-related EBV-associated lymphoproliferative disorders in the Western population: a spectrum of reactive lymphoid hyperplasia and lymphoma, *Blood* 117(18):4726–4735, 2011.

Dotta L, Badolato R: Primary immunodeficiencies appearing as combined lymphopenia, neutropenia, and monocytopenia, *Immunol Lett* 161(2):222–225, 2014.

Dotta L, Tassone L, Badolato R: Clinical and genetic features of warts, hypogammaglobulinemia, infections and myelokathexis (WHIM) syndrome, *Curr Mol Med* 11(4):317–325, 2011.

Druker BJ, Talpaz M, Resta DJ, Peng B, Buchdunger E, Ford JM, et al.: Efficacy and safety of a specific inhibitor of the *BCR-ABL1* tyrosine kinase in chronic myeloid leukemia, *N Engl J Med* 344(14):1031–1037, 2001.

Duarte-Davidson R, Courage C, Rushton L, Levy L: Benzene in the environment: an assessment of the potential risks to the health of the population, *Occup Environ Med* 58(1):2–13, 2001.

Elliott MA, Tefferi A: Chronic neutrophilic leukemia 2014: update on diagnosis, molecular genetics, and management, *Am J Hematol* 89(6):651–658, 2014.

Eyre TA, Khan D, Hall GW, Collins GP: Anaplastic lymphoma kinase-positive anaplastic large cell lymphoma: current and future perspectives in adult and paediatric disease, *Eur J Haematol*, 2014 Apr 26.

Faitelson Y, Grunebaum E: Hemophagocytic lymphohistiocytosis and primary immune deficiency disorders, *Clin Immunol* 155(1):118–125, 2014.

Falini B, Martelli MP, Bolli N, Sportoletti P, Liso A, Tiacci E, et al.: Acute myeloid leukemia with mutated nucleophosmin (NPM1): is it a distinct entity? *Blood* 117(4):1109–1120, 2011.

Fanale M: A novel prognostic scoring system for NLPHL, *Blood* 122(26):4154–4155, 2013.

Fernandez de Larrea C, Kyle RA, Durie BG, Ludwig H, Usmani S, Vesole DH, et al.: Plasma cell leukemia: consensus statement on diagnostic requirements, response criteria and treatment recommendations by the International Myeloma Working Group, *Leukemia* 27(4):780–791, 2013.

Ferry JA: Burkitt's lymphoma: clinicopathologic features and differential diagnosis, *Oncol* 11(4):375–383, 2006.

Flatley E, Chen AI, Zhao X, Jaffe ES, Dunlap JB, Pittaluga S, et al.: Aberrations of *MYC* are a common event in B-cell prolymphocytic leukemia, *Am J Clin Pathol* 142(3):347–354, 2014.

Foran JM: New prognostic markers in acute myeloid leukemia: perspective from the clinic, *Hematology Am Soc Hematol Educ Program* 47–55, 2010.

Franklin EC: gamma- and mu-Heavy chain diseases and related disorders, *J Clin Pathol Suppl* 6:65–71, 1975.

Furuta GT, Atkins FD, Lee NA, Lee JJ: Changing roles of eosinophils in health and disease, *Ann Allergy Asthma Immunol* 113(1):3–8, 2014.

Gaidano G, Foa R, Dalla-Favera R: Molecular pathogenesis of chronic lymphocytic leukemia, *J Clin Invest* 122(10):3432–3438, 2012.

Galton DA, Goldman JM, Wiltshaw E, Catovsky D, Henry K, Goldenberg GJ: Prolymphocytic leukaemia, *Br J Haematol* 27(1):7–23, 1974.

Garg H, Mohl J, Joshi A: HIV-1 induced bystander apoptosis, *Viruses* 4(11):3020–3043, 2012.

Gascoyne RD, Lamant L, Martin-Subero JI, Lestou VS, Harris NL, Muller-Hermelink HK, et al.: ALK-positive diffuse large B-cell lymphoma is associated with Clathrin-ALK rearrangements: report of 6 cases, *Blood* 102(7):2568–2573, 2003.

Gaulard P, de Leval L: Pathology of peripheral T-cell lymphomas: where do we stand? *Semin Hematol* 51(1):5–16, 2014.

Gessain A, Rua R, Betsem E, Turpin J, Mahieux R: HTLV-3/4 and simian foamy retroviruses in humans: discovery, epidemiology, cross-species transmission and molecular virology, *Virology* 435(1):187–199, 2013.

Gloghini A, Dolcetti R, Carbone A: Lymphomas occurring specifically in HIV-infected patients: from pathogenesis to pathology, *Semin Cancer Biol* 23(6):457–467, 2013.

Go RS, Wester SM: Immunophenotypic and molecular features, clinical outcomes, treatments, and prognostic factors associated with subcutaneous panniculitis-like T-cell lymphoma: a systematic analysis of 156 patients reported in the literature, *Cancer* 101(6):1404–1413, 2004.

Gombart AF, Shiohara M, Kwok SH, Agematsu K, Komiyama A, Koeffler HP: Neutrophil-specific granule deficiency: homozygous recessive inheritance of a frameshift mutation in the gene encoding transcription factor CCAAT/enhancer binding protein—epsilon, *Blood* 97(9):2561–2567, 2001.

Gotlib J: World Health Organization-defined eosinophilic disorders: 2014 update on diagnosis, risk stratification, and management, *Am J Hematol* 89(3):325–337, 2014.

Gotlib J, Maxson JE, George TI, Tyner JW: The new genetics of chronic neutrophilic leukemia and atypical CML: implications for diagnosis and treatment, *Blood* 122(10):1707–1711, 2013.

Granger JM, Kontoyiannis DP: Etiology and outcome of extreme leukocytosis in 758 nonhematologic cancer patients: a retrospective, single-institution study, *Cancer* 115(17):3919–3923, 2009.

Gulino AV, Moratto D, Sozzani S, Cavadini P, Otero K, Tassone L, et al.: Altered leukocyte response to CXCL12 in patients with warts hypogammaglobulinemia, infections, myelokathexis (WHIM) syndrome, *Blood* 104(2):444–452, 2004.

Gulley ML, Tang W: Laboratory assays for Epstein-Barr virus-related disease, *J Mol Diagn* 10(4):279–292, 2008.

Gupta M, Ashok Kumar J, Sitaram U, Neeraj S, Nancy A, Balasubramanian P, et al.: The t(6;9)(p22;q34) in myeloid neoplasms: a retrospective study of 16 cases, *Cancer Genet Cytogenet* 203(2):297–302, 2010.

Hamadeh F, MacNamara SP, Aguilera NS, Swerdlow SH, Cook JR: MYD88 L265P mutation analysis helps define nodal lymphoplasmacytic lymphoma, *Mod Pathol*, 2014 Sep 12.

Harris NL, Jaffe ES, Diebold J, Flandrin G, Muller-Hermelink HK, Vardiman J: Lymphoma classification—from controversy to consensus: the R.E.A.L. and WHO Classification of lymphoid neoplasms, *Ann Oncol* 11(Suppl 1):3–10, 2000.

Harris NL, Jaffe ES, Stein H, Banks PM, Chan JK, Cleary ML, et al.: A revised European-American classification of lymphoid neoplasms: a proposal from the International Lymphoma Study Group, *Blood* 84(5):1361–1392, 1994.

Hartmann S, Eichenauer DA, Plutschow A, Mottok A, Bob R, Koch K, et al.: The prognostic impact of variant histology in nodular lymphocyte-predominant Hodgkin lymphoma: a report from the German Hodgkin Study Group (GHSG), *Blood* 122(26):4246–4252, 2013. quiz 4292.

Hauck F, Klein C: Pathogenic mechanisms and clinical implications of congenital neutropenia syndromes, *Curr Opin Allergy Clin Immunol* 13(6):596–606, 2013.

Helbig G: Advances in the diagnosis and treatment of eosinophilia, *Curr Opin Hematol* 21(1):3–7, 2014.

Hernandez AM: Peripheral blood manifestations of lymphoma and solid tumors, *Clin Lab Med* 22(1):215–252, 2002.

Himmelmann A, Gautschi O, Nawrath M, Bolliger U, Fehr J, Stahel RA: Persistent polyclonal B-cell lymphocytosis is an expansion of functional IgD(+)CD27(+) memory B cells, *Br J Haematol* 114(2):400–405, 2001.

Holland SM: Chronic granulomatous disease, *Hematol Oncol Clin North Am* 27(1):89–99, 2013. viii.

Hong M, Ko YH, Yoo KH, Koo HH, Kim SJ, Kim WS, et al.: EBV-positive T/NK-cell lymphoproliferative disease of childhood, *Korean J Pathol* 47(2):137–147, 2013.

Hsu AP, Sampaio EP, Khan J, Calvo KR, Lemieux JE, Patel SY, et al: Mutations in *GATA2* are associated with the autosomal dominant and sporadic monocytopenia and mycobacterial infection (MonoMAC) syndrome, Blood 2011, 118(10):2653–2655, 2013.

Huang ME, Ye YC, Chen SR, Chai JR, Lu JX, Zhoa L, et al.: Use of all-trans retinoic acid in the treatment of acute promyelocytic leukemia, *Blood* 72(2):567–572, 1988.

Hudnall SD, Molina CP: Marked increase in L-selectin-negative T cells in neonatal pertussis. The lymphocytosis explained? *Am J Clin Pathol* 114(1):35–40, 2000.

Huppmann AR, Nicolae A, Slack GW, Pittaluga S, Davies-Hill T, Ferry JA, et al.: EBV may be expressed in the LP cells of nodular lymphocyte-predominant Hodgkin lymphoma (NLPHL) in both children and adults, *Am J Surg Pathol* 38(3):316–324, 2014.

Isaacson PG: Update on MALT lymphomas, *Best Pract Res Clin Haematol* 18(1):57–68, 2005.

Ishitsuka K, Tamura K: Human T-cell leukaemia virus type I and adult T-cell leukaemia-lymphoma, *Lancet Oncol* 15(11):e517–e526, 2014.

Itzykson R, Kosmider O, Renneville A, Gelsi-Boyer V, Meggendorfer M, Morabito M, et al.: Prognostic score including gene mutations in chronic myelomonocytic leukemia, *J Clin Oncol* 31(19):2428–2436, 2013.

Itzykson R, Kosmider O, Renneville A, Morabito M, Preudhomme C, Berthon C, et al.: Clonal architecture of chronic myelomonocytic leukemias, *Blood* 121(12):2186–2198, 2013.

Jabbour E, Kantarjian H: Chronic myeloid leukemia: 2014 update on diagnosis, monitoring, and management, *Am J Hematol* 89(5):547–556, 2014.

Jaffe ES, Nicolae A, Pittaluga S: Peripheral T-cell and NK-cell lymphomas in the WHO classification: pearls and pitfalls, *Mod Pathol Suppl* 1:S71–87, 2013.

Jaffe R: The histiocytoses, *Clin Lab Med* 19(1):135–155, 1999.

Jardin F: Next generation sequencing and the management of diffuse large B-cell lymphoma: from whole exome analysis to targeted therapy, *Discov Med* 18(97):51–65, 2014.

Kalyanaraman VS, Sarngadharan MG, Robert-Guroff M, Miyoshi I, Golde D, Gallo RC: A new subtype of human T-cell leukemia virus (HTLV-II) associated with a T-cell variant of hairy cell leukemia, *Science* 218(4572):571–573, 1982.

Kang J, Coles M, Cado D, Raulet DH: The developmental fate of T cells is critically influenced by TCRgammadelta expression, *Immunity* 8(4):427–438, 1998.

Katzenstein AL, Doxtader E, Narendra S: Lymphomatoid granulomatosis: insights gained over 4 decades, *Am J Surg Pathol* 34(12):e35–48, 2010.

King RL, Howard MT, Bagg A: Hodgkin lymphoma: pathology, pathogenesis, and a plethora of potential prognostic predictors, *Adv Anat Pathol* 21(1):12–25, 2014.

Klein E, Kis LL, Klein G: Epstein-Barr virus infection in humans: from harmless to life endangering virus-lymphocyte interactions, *Oncogene* 26(9):1297–1305, 2007.

Kraut EH: Clinical manifestations and infectious complications of hairy-cell leukaemia, *Best Pract Res Clin Haematol* 16(1):33–40, 2003.

Krauth MT, Alpermann T, Bacher U, Eder C, Dicker F, Ulke M, et al.: WT1 mutations are secondary events in AML, show varying frequencies and impact on prognosis between genetic subgroups, *Leukemia*, 2014 Aug 11.

Kreslavsky T, Gleimer M, Garbe AI, von Boehmer H: Alphabeta versus gammadelta fate choice: counting the T-cell lineages at the branch point, *Immunol Rev* 238(1):169–181, 2010.

Kroft SH: Infectious diseases manifested in the peripheral blood, *Clin Lab Med* 22(1):253–277, 2002.

Kupfer GM: Fanconi anemia: a signal transduction and DNA repair pathway, *Yale J Biol Med* 86(4):491–497, 2013.

Lagergren J: The white blood cell count and the erythrocyte sedimentation rate in pertussis, *Acta Paediatr* 52:405–409, 1963.

Lairmore MD, Haines R, Anupam R: Mechanisms of human T-lymphotropic virus type 1 transmission and disease, *Curr Opin Virol* 2(4):474–481, 2012.

Lan TT, Brown NA, Hristov AC: Controversies and considerations in the diagnosis of primary cutaneous CD4(+) small/medium T-cell lymphoma, *Arch Pathol Lab Med* 138(10):1307–1318, 2014.

Landgren O: Monoclonal gammopathy of undetermined significance and smoldering multiple myeloma: biological insights and early treatment strategies, *Hematology Am Soc Hematol Educ Program* 478–487, 2013.

Landgren O, Morgan GJ: Biologic frontiers in multiple myeloma: from biomarker identification to clinical practice, *Clin Cancer Res* 20(4):804–813, 2014.

Levine RL: Mechanisms of mutations in myeloproliferative neoplasms, *Best Pract Res Clin Haematol* 22(4):489–494, 2009.

Levine RL, Gilliland DG: Myeloproliferative disorders, *Blood* 112(6):2190–2198, 2008.

Liersch R, Muller-Tidow C, Berdel WE, Krug U: Prognostic factors for acute myeloid leukaemia in adults—biological significance and clinical use, *Br J Haematol* 165(1):17–38, 2014.

Liew PX, Kubes P: The Neutrophil's role during health and disease, *Physiol Rev* 99(2):1223–1248, 2019.

Lin CC, Hou HA, Chou WC, Kuo YY, Wu SJ, Liu CY, et al.: SF3B1 mutations in patients with myelodysplastic syndromes: the mutation is stable during disease evolution, *Am J Hematol* 89(8):E109–E115, 2014.

Little RF, Dunleavy K: Update on the treatment of HIV-associated hematologic malignancies, *Hematology Am Soc Hematol Educ Program* 382–388, 2013. 2013.

Liu X, Loughran Jr TP: The spectrum of large granular lymphocyte leukemia and Felty's syndrome, *Curr Opin Hematol* 18(4):254–259, 2011.

Lugthart S, Groschel S, Beverloo HB, Kayser S, Valk PJ, van Zelderen-Bhola SL, et al.: Clinical, molecular, and prognostic significance of WHO type inv(3)(q21q26.2)/t(3;3)(q21;q26.2) and various other 3q abnormalities in acute myeloid leukemia, *J Clin Oncol* 28(24):3890–3898, 2010.

Lukes RJ, Butler JJ: The pathology and nomenclature of Hodgkin's disease, *Cancer Res* 26(6):1063–1083, 1966.

Malcovati L, Cazzola M: Refractory anemia with ring sideroblasts, *Best Pract Res Clin Haematol* 26(4):377–385, 2013.

Maldonado JE, Hanlon DG: Monocytosis: a current Appraisal, *Mayo Clin Proc* 40:248–259, 1965.

Marins LR, Anizelli LB, Romanowski MD, Sarquis AL: How does preeclampsia affect neonates? Highlights in the disease's immunity, *J Matern Fetal Neonatal Med* 32(7):1205–1212, 2019.

Martinez-Aviles L, Besses C, Alvarez-Larran A, Torres E, Serrano S, Bellosillo B: TET2, ASXL1, IDH1, IDH2, and c-CBL genes in JAK2- and MPL-negative myeloproliferative neoplasms, *Ann Hematol* 91(4):533–541, 2012.

Maxson JE, Gotlib J, Pollyea DA, Fleischman AG, Agarwal A, Eide CA, et al.: Oncogenic CSF3R mutations in chronic neutrophilic leukemia and atypical CML, *N Engl J Med* 368(19):1781–1790, 2013.

Michiels JJ, Berneman Z, Schroyens W, De Raeve H: Changing concepts of diagnostic criteria of myeloproliferative disorders and the molecular Etiology and classification of myeloproliferative neoplasms: from Dameshek 1950 to Vainchenker 2005 and beyond, *Acta Haematol* 133(1):36–51, 2014.

Michiels JJ, Kutti J, Stark P, Bazzan M, Gugliotta L, Marchioli R, et al.: Diagnosis, pathogenesis and treatment of the myeloproliferative disorders essential thrombocythemia, polycythemia vera and essential megakaryocytic granulocytic metaplasia and myelofibrosis, *Neth J Med* 54(2):46–62, 1999.

Micol JB, Duployez N, Boissel N, Petit A, Geffroy S, Nibourel O, et al.: Frequent ASXL2 mutations in acute myeloid leukemia patients with t(8;21)/*RUNX1-RUNX1T1* chromosomal translocations, *Blood* 124(9):1445–1449, 2014.

Miyoshi H, Sato K, Niino D, Arakawa F, Kimura Y, Kiyasu J, et al.: Clinicopathologic analysis of peripheral T-cell lymphoma, follicular variant, and comparison with angioimmunoblastic T-cell lymphoma: bcl-6 expression might affect progression between these disorders, *Am J Clin Pathol* 137(6):879–889, 2012.

Montgomery ND, Dunphy CH, Mooberry M, Laramore A, Foster MC, Park SI, et al.: Diagnostic complexities of eosinophilia, *Arch Pathol Lab Med* 137(2):259–269, 2013.

Morris SW, Kirstein MN, Valentine MB, Dittmer K, Shapiro DN, Look AT, et al.: Fusion of a kinase gene, ALK, to a nucleolar protein gene, NPM, in non-Hodgkin's lymphoma, *Science* 267(5196):316–317, 1995.

Morscio J, Dierickx D, Nijs J, Verhoef G, Bittoun E, Vanoeteren X, et al.: Clinicopathologic comparison of plasmablastic lymphoma in HIV-positive, immunocompetent, and posttransplant patients: single-center series of 25 cases and meta-analysis of 277 reported cases, *Am J Surg Pathol* 38(7):875–886, 2014.

Nam-Cha SH, Montes-Moreno S, Salcedo MT, Sanjuan J, Garcia JF, Piris MA: Lymphocyte-rich classical Hodgkin's lymphoma: distinctive tumor and microenvironment markers, *Mod Pathol* 22(8):1006–1015, 2009.

Nauseef WM: Diagnostic assays for myeloperoxidase and myeloperoxidase deficiency, *Methods Mol Biol* 1124:537–546, 2014.

Nyamweya S, Hegedus A, Jaye A, Rowland-Jones S, Flanagan KL, Macallan DC: Comparing HIV-1 and HIV-2 infection: lessons for viral immunopathogenesis, *Rev Med Virol* 23(4):221–240, 2013.

O'Gorman MR: Recent developments related to the laboratory diagnosis of primary immunodeficiency diseases, *Curr Opin Pediatr* 20(6):688–697, 2008.

Ok CY, Papathomas TG, Medeiros LJ, Young KH: EBV-positive diffuse large B-cell lymphoma of the elderly, *Blood* 122(3):328–340, 2013.

Okosun J, Bodor C, Wang J, Araf S, Yang CY, Pan C, et al.: Integrated genomic analysis identifies recurrent mutations and evolution patterns driving the initiation and progression of follicular lymphoma, *Nat Genet* 46(2):176–181, 2014.

Papaemmanuil E, Gerstung M, Malcovati L, Tauro S, Gundem G, Van Loo P, et al.: Clinical and biological implications of driver mutations in myelodysplastic syndromes, *Blood* 122(22):3616–3627, 2013. quiz 3699.

Park SI, Rogers BB: Monocytopenia as a diagnostic clue to pediatric B-lymphoblastic leukemia with rare circulating blasts, *Pediatr Dev Pathol*, 2013 Jul 1.

Parker A, Bowles K, Bradley JA, Emery V, Featherstone C, Gupte G, et al.: Diagnosis of post-transplant lymphoproliferative disorder in solid organ transplant recipients - BCSH and BTS Guidelines, *Br J Haematol* 149(5):675–692, 2010.

Parrilla Castellar ER, Jaffe ES, Said JW, Swerdlow SH, Ketterling RP, Knudson RA, et al.: ALK-negative anaplastic large cell lymphoma is a genetically heterogeneous disease with widely disparate clinical outcomes, *Blood* 124(9):1473–1480, 2014.

Parry M, Rose-Zerilli MJ, Gibson J, Ennis S, Walewska R, Forster J, et al.: Whole exome sequencing identifies novel recurrently mutated genes in patients with splenic marginal zone lymphoma, *PloS One* 8(12):e83244, 2013.

Paschka P, Du J, Schlenk RF, Gaidzik VI, Bullinger L, Corbacioglu A, et al.: Secondary genetic lesions in acute myeloid leukemia with inv(16) or t(16;16): a study of the German-Austrian AML Study Group (AMLSG), *Blood* 121(1):170–177, 2013.

Pasquet M, Bellanne-Chantelot C, Tavitian S, Prade N, Beaupain B, Larochelle O, et al.: High frequency of *GATA2* mutations in patients with mild chronic neutropenia evolving to MonoMac syndrome, myelodysplasia, and acute myeloid leukemia, *Blood* 121(5):822–829, 2013.

Patel SS, Aasen GA, Dolan MM, Linden MA, McKenna RW, Rudrapatna VK, et al.: Early diagnosis of intravascular large B-cell lymphoma: clues from routine blood smear morphologic findings, *Lab Med* 45(3):248–252, 2014.

Patkar N, Subramanian PG, Deshpande P, Ghodke K, Tembhare P, Mascarenhas R, et al.: MYD88 mutant lymphoplasmacytic lymphoma/Waldenstrom macroglobulinemia has distinct clinical and pathological features as compared to its mutation negative counterpart, *Leuk Lymphoma* 4:1–6, 2014.

Patte C, Auperin A, Michon J, Behrendt H, Leverger G, Frappaz D, et al.: The Societe Francaise d'Oncologie Pediatrique LMB89 protocol: highly effective multiagent chemotherapy tailored to the tumor burden and initial response in 561 unselected children with B-cell lymphomas and L3 leukemia, *Blood* 97(11):3370–3379, 2001.

Pecci A, Klersy C, Gresele P, Lee KJ, De Rocco D, Bozzi V, et al.: MYH9-related disease: a novel prognostic model to predict the clinical evolution of the disease based on genotype-phenotype correlations, *Hum Mutat* 35(2):236–247, 2014.

Petri B, Sanz MJ: Neutrophil chemotaxis, *Cell Tissue Res* 371(3):425–436, 2018.

Piazza R, Valletta S, Winkelmann N, Redaelli S, Spinelli R, Pirola A, et al.: Recurrent SETBP1 mutations in atypical chronic myeloid leukemia, *Nat Genet* 45(1):18–24, 2013.

Pick AM, Nystrom KK: Nonchemotherapy drug-induced neutropenia and agranulocytosis: could medications be the Culprit? *J Pharm Pract*, 2014 Aug 14.

Plo I, Zhang Y, Le Couedic JP, Nakatake M, Boulet JM, Itaya M, et al.: An activating mutation in the CSF3R gene induces a hereditary chronic neutrophilia, *J Exp Med* 206(8):1701–1707, 2009.

Poiesz BJ, Ruscetti FW, Gazdar AF, Bunn PA, Minna JD, Gallo RC: Detection and isolation of type C retrovirus particles from fresh and cultured lymphocytes of a patient with cutaneous T-cell lymphoma, *Proc Natl Acad Sci U S A* 77(12):7415–7419, 1980.

Pui CH, Carroll WL, Meshinchi S, Arceci RJ: Biology, risk stratification, and therapy of pediatric acute leukemias: an update, *J Clin Oncol* 29(5):551–565, 2011.

Pui CH, Evans WE: A 50-year journey to cure childhood acute lymphoblastic leukemia, *Semin Hematol* 50(3):185–196, 2013.

Put N, Van Roosbroeck K, Konings P, Meeus P, Brusselmans C, Rack K, et al.: Chronic lymphocytic leukemia and prolymphocytic leukemia with *MYC* translocations: a subgroup with an aggressive disease course, *Ann Hematol* 91(6):863–873, 2012.

Qayyum S, Choi JK: Adult T-cell leukemia/lymphoma, *Arch Pathol Lab Med* 138(2):282–286, 2014.

Queiros AC, Villamor N, Clot G, Martinez-Trillos A, Kulis M, Navarro A, et al.: A B-cell epigenetic signature defines three biologic subgroups of chronic lymphocytic leukemia with clinical impact, *Leukemia*, 2014 Aug 25.

Querfeld C, Khan I, Mahon B, Nelson BP, Rosen ST, Evens AM: Primary cutaneous and systemic anaplastic large cell lymphoma: clinicopathologic aspects and therapeutic options, *Oncology (Williston Park)* 24(7):574–587, 2010.

Quintanilla-Martinez L, Jansen PM, Kinney MC, Swerdlow SH, Willemze R: Nonmycosis fungoides cutaneous T-cell lymphomas: report of the 2011 Society for Hematopathology/European Association for Haematopathology workshop, *Am J Clin Pathol* 139(4):491–514, 2013a.

Quintanilla-Martinez L, Ridaura C, Nagl F, Saez-de-Ocariz M, Duran-McKinster C, Ruiz-Maldonado R, et al.: Hydroa vacciniforme-like lymphoma: a chronic EBV+ lymphoproliferative disorder with risk to develop a systemic lymphoma, *Blood* 122(18):3101–3110, 2013b.

Rampal R, Al-Shahrour F, Abdel-Wahab O, Patel JP, Brunel JP, Mermel CH, et al.: Integrated genomic analysis illustrates the central role of JAK-STAT pathway activation in myeloproliferative neoplasm pathogenesis, *Blood* 123(22):e123–e133, 2014.

Reilly WA: The granules in the leukocytes in gargoylism, *American journal of diseases of children* 62:482, 1941.

Reinherz EL, Kung PC, Goldstein G, Levey RH, Schlossman SF: Discrete stages of human intrathymic differentiation: analysis of normal thymocytes and leukemic lymphoblasts of T-cell lineage, *Proc Natl Acad Sci U S A* 77(3):1588–1592, 1980.

Remington JS, Thulliez P, Montoya JG: Recent developments for diagnosis of toxoplasmosis, *J Clin Microbiol* 42(3):941–945, 2004.

Rice KL, Lin X, Wolniak K, Ebert BL, Berkofsky-Fessler W, Buzzai M, et al.: Analysis of genomic aberrations and gene expression profiling identifies novel lesions and pathways in myeloproliferative neoplasms, *Blood Cancer J* 1(11):e40, 2011.

Rizzieri DA, Johnson JL, Byrd JC, Lozanski G, Blum KA, Powell BL, et al.: Improved efficacy using rituximab and brief duration, high intensity chemotherapy with filgrastim support for Burkitt or aggressive lymphomas: cancer and Leukemia Group B study 10 002, *Br J Haematol* 165(1):102–111, 2014.

Rodriguez-Pinilla SM, Barrionuevo C, Garcia J, de los Angeles M, Pajares R, Casavilca S, et al.: Epstein-Barr virus-positive systemic NK/T-cell lymphomas in children: report of six cases, *Histopathology* 59(6):1183–1193, 2011.

Rodriguez-Vicente AE, Diaz MG, Hernandez-Rivas JM: Chronic lymphocytic leukemia: a clinical and molecular heterogenous disease, *Cancer Genet* 206(3):49–62, 2013.

Rosado FG, Kim AS: Hemophagocytic lymphohistiocytosis: an update on diagnosis and pathogenesis, *Am J Clin Pathol* 139(6):713–727, 2013.

Roy A, Roberts I, Norton A, Vyas P: Acute megakaryoblastic leukaemia (AMKL) and transient myeloproliferative disorder (TMD) in Down syndrome: a multi-step model of myeloid leukaemogenesis, *Br J Haematol* 147(1):3–12, 2009.

Sandes AF, de Lourdes Chauffaille M, Oliveira CR, Maekawa Y, Tamashiro N, Takao TT, et al.: CD200 has an important role in the differential diagnosis of mature B-cell neoplasms by multiparameter flow cytometry, *Cytometry B Clin Cytom*, 2013 Aug 29.

Saposnik B, Binard S, Fenneteau O, Nurden A, Nurden P, Hurtaud-Roux MF, et al.: Mutation spectrum and genotype-phenotype correlations in a large French cohort of *MYH9*-Related Disorders, *Mol Genet Genomic Med* 2(4):297–312, 2014.

Savage KJ, Monti S, Kutok JL, Cattoretti G, Neuberg D, De Leval L, et al.: The molecular signature of mediastinal large B-cell lymphoma differs from that of other diffuse large B-cell lymphomas and shares features with classical Hodgkin lymphoma, *Blood* 102(12):3871–3879, 2003.

Schmitz R, Ceribelli M, Pittaluga S, Wright G, Staudt LM: Oncogenic mechanisms in Burkitt lymphoma, *Cold Spring Harb Perspect Med* 4(2):10, 2014. 1101/cshperspect.a014282.

Seidel MG: Autoimmune and other cytopenias in primary immunodeficiencies: pathomechanisms, novel differential diagnoses, and treatment, *Blood* 124(15):2337–2344, 2014.

Setoodeh R, Schwartz S, Papenhausen P, Zhang L, Sagatys EM, Moscinski LC, et al.: Double-hit mantle cell lymphoma with *MYC* gene rearrangement or amplification: a report of four cases and review of the literature, *Int J Clin Exp Pathol* 6(2):155–167, 2013.

Shah S, Wu E, Rao VK, Tarrant TK: Autoimmune lymphoproliferative syndrome: an update and review of the literature, *Curr Allergy Asthma Rep* 14(9):462-014–0462-4, 2014.

Shimabukuro-Vornhagen A, Haverkamp H, Engert A, Balleisen L, Majunke P, Heil G, et al.: Lymphocyte-rich classical Hodgkin's lymphoma: clinical presentation and treatment outcome in 100 patients treated within German Hodgkin's Study Group trials, *J Clin Oncol* 23(24):5739–5745, 2005.

Song SX, Willemze R, Swerdlow SH, Kinney MC, Said JW: Mycosis fungoides: report of the 2011 Society for hematopathology/European association for Haematopathology workshop, *Am J Clin Pathol* 139(4):466–490, 2013.

Soverini S, Branford S, Nicolini FE, Talpaz M, Deininger MW, Martinelli G, et al.: Implications of *BCR-ABL1* kinase domain-mediated resistance in chronic myeloid leukemia, *Leuk Res* 38(1):10–20, 2014.

Starr-Spires LD, Collman RG: HIV-1 entry and entry inhibitors as therapeutic agents, *Clin Lab Med* 22(3):681–701, 2002.

Stein H, Mason DY, Gerdes J, O'Connor N, Wainscoat J, Pallesen G, et al.: The expression of the Hodgkin's disease associated antigen Ki-1 in reactive and neoplastic lymphoid tissue: evidence that Reed-Sternberg cells and histiocytic malignancies are derived from activated lymphoid cells, *Blood* 66(4):848–858, 1985.

Swerdlow S, Campo E, Harris N, editors: *WHO classification of tumours of haematopoietic and lymphoid tissues*, Revised 4th ed., Lyon, France, 2017, IARC.

Swerdlow SH, Jaffe ES, Brousset P, Chan JK, de Leval L, Gaulard P, et al.: Cytotoxic T-cell and NK-cell lymphomas: current Questions and Controversies, *Am J Surg Pathol* 38(10):e60–71, 2014.

Tarlock K, Alonzo TA, Moraleda PP, Gerbing RB, Raimondi SC, Hirsch BA, et al.: Acute myeloid leukaemia (AML) with t(6;9)(p23;q34) is associated with poor outcome in childhood AML regardless of FLT3-ITD status: a report from the Children's Oncology Group, *Br J Haematol* 166(2):254–259, 2014.

Tefferi A, Barbui T: Personalized management of essential thrombocythemia-application of recent evidence to clinical practice, *Leukemia* 27(8):1617–1620, 2013.

Tefferi A, Pardanani A, Lim KH, Abdel-Wahab O, Lasho TL, Patel J, et al.: TET2 mutations and their clinical correlates in polycythemia vera, essential thrombocythemia and myelofibrosis, *Leukemia* 23(5):905–911, 2009.

Tefferi A, Thiele J, Vannucchi AM, Barbui T: An overview on CALR and CSF3R mutations and a proposal for revision of WHO diagnostic criteria for myeloproliferative neoplasms, *Leukemia* 28(7):1407–1413, 2014.

Tembhare P, Yuan CM, Xi L, Morris JC, Liewehr D, Venzon D, et al.: Flow cytometric immunophenotypic assessment of T-cell clonality by Vbeta repertoire analysis: detection of T-cell clonality at diagnosis and monitoring of minimal residual disease following therapy, *Am J Clin Pathol* 135(6):890–900, 2011.

Tesfa D, Keisu M, Palmblad J: Idiosyncratic drug-induced agranulocytosis: possible mechanisms and management, *Am J Hematol* 84(7):428–434, 2009.

Tiacci E, Trifonov V, Schiavoni G, Holmes A, Kern W, Martelli MP, et al.: BRAF mutations in hairy-cell leukemia, *N Engl J Med* 364(24):2305–2315, 2011.

Tobinai K, Takahashi T, Akinaga S: Targeting chemokine receptor CCR4 in adult T-cell leukemia-lymphoma and other T-cell lymphomas, *Curr Hematol Malig Rep* 7(3):235–240, 2012.

Torres E, Rivera R, Cardona N, Sanchez V, Lora F, Gomez-Marin JE: Evaluation of IgG anti-toxoplasma avidity and polymerase chain reaction in the postnatal diagnosis of congenital toxoplasmosis, *Pediatr Infect Dis J* 32(6):693–695, 2013.

Tousseyn T, De Wolf-Peeters C: T cell/histiocyte-rich large B-cell lymphoma: an update on its biology and classification, *Virchows Arch* 459(6):557–563, 2011.

Treon SP, Cao Y, Xu L, Yang G, Liu X, Hunter ZR: Somatic mutations in MYD88 and CXCR4 are determinants of clinical presentation and overall survival in Waldenstrom macroglobulinemia, *Blood* 123(18):2791–2796, 2014.
Troussard X, Cornet E, Lesesve JF, Kourel C, Mossafa H: Polyclonal B-cell lymphocytosis with binucleated lymphocytes (PPBL), *OncoTargets Ther* 1:59–66, 2008.
Valent P, Klion AD, Horny HP, Roufosse F, Gotlib J, Weller PF, et al.: Contemporary consensus proposal on criteria and classification of eosinophilic disorders and related syndromes, *J Allergy Clin Immunol* 130(3):607–612, 2012. e9.
Valent P, Sotlar K, Sperr WR, Escribano L, Yavuz S, Reiter A, et al.: Refined diagnostic criteria and classification of mast cell leukemia (MCL) and myelomastocytic leukemia (MML): a consensus proposal, *Ann Oncol* 25(9):1691–1700, 2014.
Valera A, Colomo L, Martinez A, de Jong D, Balague O, Matheu G, et al.: ALK-positive large B-cell lymphomas express a terminal B-cell differentiation program and activated STAT3 but lack *MYC* rearrangements, *Mod Pathol* 26(10):1329–1337, 2013.
van de Vijver E, van den Berg TK, Kuijpers TW: Leukocyte adhesion deficiencies, *Hematol Oncol Clin North Am* 27(1):101–116, 2013. viii.
Varettoni M, Arcaini L, Zibellini S, Boveri E, Rattotti S, Riboni R, et al.: Prevalence and clinical significance of the MYD88 (L265P) somatic mutation in Waldenstrom's macroglobulinemia and related lymphoid neoplasms, *Blood* 121(13):2522–2528, 2013.
Venkataraman G, Mirza MK, Eichenauer DA, Diehl V: Current status of prognostication in classical Hodgkin lymphoma, *Br J Haematol* 165(3):287–299, 2014.
Verma N, Thaventhiran A, Gathmann B, ESID Registry Working Party, Thaventhiran J, Grimbacher B: Therapeutic management of primary immunodeficiency in older patients, *Drugs Aging* 30(7):503–512, 2013.
Vincent Rajkumar S: Multiple myeloma: 2014 Update on diagnosis, risk-stratification, and management, *Am J Hematol* 89(10):999–1009, 2014.
Voehringer D: Regulation of type 2 immunity by basophils, *Adv Exp Med Biol* 785:37–41, 2013.
Vose JM: Mantle cell lymphoma: 2013 Update on diagnosis, risk-stratification, and clinical management, *Am J Hematol* 88(12):1082–1088, 2013.
Vouloumanou EK, Rafailidis PI, Falagas ME: Current diagnosis and management of infectious mononucleosis, *Curr Opin Hematol* 19(1):14–20, 2012.
Wada DA, Law ME, Hsi ED, Dicaudo DJ, Ma L, Lim MS, et al.: Specificity of IRF4 translocations for primary cutaneous anaplastic large cell lymphoma: a multicenter study of 204 skin biopsies, *Mod Pathol* 24(4):596–605, 2011.
Wang RC, Chang ST, Hsieh YC, Huang WT, Hsu JD, Tseng CE, et al.: Spectrum of Epstein-Barr virus-associated T-cell lymphoproliferative disorder in adolescents and young adults in Taiwan, *Int J Clin Exp Pathol* 7(5):2430–2437, 2014.
Wegman-Ostrosky T, Savage SA: The genomics of inherited bone marrow failure: from mechanism to the clinic, *Br J Haematol* 177(4):526–542, 2017.
Welte K, Zeidler C: Severe congenital neutropenia, *Hematol Oncol Clin North Am* 23(2):307–320, 2009.
Wichmann C, Quagliano-Lo Coco I, Yildiz O, Chen-Wichmann L, Weber H, Syzonenko T, et al.: Activating c-KIT mutations confer oncogenic cooperativity and rescue *RUNX1/ETO*-induced DNA damage and apoptosis in human primary CD34+ hematopoietic progenitors, *Leukemia*, 2014 Jun 4.
Yoshie O, Matsushima K: CCR4 and its ligands: from bench to bedside, *Int Immunol*, 2014 Aug 2.
Zambello R, Teramo A, Barila G, Gattazzo C, Semenzato G: Activating KIRs in chronic lymphoproliferative disorder of NK cells: Protection from viruses and disease induction? *Front Immunol* 5:72, 2014.
Zhang D, Loughran Jr TP: Large granular lymphocytic leukemia: molecular pathogenesis, clinical manifestations, and treatment, *Hematology Am Soc Hematol Educ Program* 652–659, 2012. 2012.
Zhang J, Ding L, Holmfeldt L, Wu G, Heatley SL, Payne-Turner D, et al.: The genetic basis of early T-cell precursor acute lymphoblastic leukaemia, *Nature* 481(7380):157–163, 2012.
Zhou Y, Barlogie B, Shaughnessy Jr JD: The molecular characterization and clinical management of multiple myeloma in the post-genome era, *Leukemia* 23(11):1941–1956, 2009.
Zhou Y, You MJ, Young KH, Lin P, Lu G, Medeiros LJ, et al.: Advances in the molecular pathobiology of B-lymphoblastic leukemia, *Hum Pathol* 43(9):1347–1362, 2012.
Zwerdling T, Won E, Shane L, Javahara R, Jaffe R: Langerhans cell sarcoma: case report and review of world literature, *J Pediatr Hematol Oncol* 36(6):419–425, 2014.

CHAPTER 35

THE FLOW CYTOMETRIC EVALUATION OF HEMATOPOIETIC NEOPLASIA

Brent L. Wood, Sindhu Cherian, Michael J. Borowitz

TECHNICAL CONSIDERATIONS, 689
Instrumentation, 689
Reagents, 690
Panel Design, 691
Specimen Handling and Sample Preparation, 692
Data Acquisition, 692
INTERPRETIVE CONSIDERATIONS, 693
Normal Patterns of Antigen Expression, 693
Abnormal Patterns of Antigenic Expression in Hematopoietic Neoplasia, 693
SUMMARY, 705
SELECTED REFERENCES, 707

KEY POINTS

- Flow cytometry is a powerful, rapid, and cost-effective technique for the identification and monitoring of hematopoietic neoplasms.
- Successful implementation of flow cytometry requires careful attention to details of instrument and reagent performance.
- Normal hematopoietic cells are characterized by a reproducible gain and loss of antigen expression with maturation.
- Hematopoietic neoplasms show deviation from the normal patterns of antigen expression, allowing for their diagnosis and classification.
- The flow cytometric detection of residual disease following therapy allows for the monitoring of therapeutic response.

The diagnosis, classification, and post-therapeutic monitoring of hematopoietic neoplasms have greatly benefited from the widespread application of immunophenotypic studies over the past 2 decades. The subdivision of hematopoietic neoplasms by their correspondence to normal hematopoietic lineages and stages of differentiation is a basic tenet of current classification systems (e.g., the World Health Organization [WHO] classification) (Swerdlow et al., 2017). This information is largely provided by immunophenotyping and has resulted in the incorporation of immunophenotypic data into the definition of many hematopoietic neoplasms to the extent that certain diagnoses cannot be confidently made without immunophenotypic studies.

Flow cytometry is a rapid, convenient, and widely available technique for generating immunophenotypic data. The ability to perform multiparametric analysis on an individual cellular basis is a unique feature of the technique that offers distinct advantages over competing immunophenotypic methods, such as immunohistochemistry. Guidelines on the use of flow cytometry for the immunophenotyping of leukemic cells in the clinical laboratory have been published (Clinical and Laboratory Standards Institute, 2007), and National Institutes of Health–sponsored consensus conferences on the flow cytometric analysis of leukemia and lymphoma were convened in 1995 (U.S.-Canadian Consensus, 1997) and 2006 (Davis et al., 2007; Wood, 2007) to attempt standardization of clinical practice. Despite these efforts, considerable heterogeneity exists in the clinical application of this technique to the evaluation of leukemia and lymphoma. This lack of standardization represents a significant challenge to the ability to consistently provide high-quality results. Efforts to improve standardization in flow cytometry in a variety of disease entities and clinical settings are ongoing and have resulted in publication of several consensus guidelines (Borowitz et al., 2010; Arroz et al., 2016). Such efforts attempt to improve the quality of flow cytometric data generation and interpretation.

Medical indications for performing flow cytometry in the setting of hematopoietic neoplasms can be divided into four primary categories:

1. The diagnosis and classification of hematopoietic neoplasms. The ability to accurately identify abnormal subpopulations of cells, assign lineage, and determine maturational stage adds improved reproducibility to the diagnosis of hematopoietic neoplasms, particularly for chronic lymphoproliferative disorders and acute leukemias. Flow cytometry is widely used for these purposes.
2. Detection of antigens used as therapeutic targets. A variety of immunologic reagents are now available for therapeutic use that specifically target antigens expressed by hematopoietic neoplasms (e.g., CD19, CD20, CD22, CD25, CD33, CD52). Confirmation of expression of the antigen of interest by the tumor is often a necessary prerequisite for use of these expensive therapies.
3. Detection of residual neoplastic cells following therapy. The ability of flow cytometry to routinely identify and quantitate the presence of abnormal hematopoietic cells with a sensitivity of 0.01% or better is increasingly being used as a surrogate measure of response to therapy and impending relapse in a variety of hematopoietic neoplasms (Campana, 2003; Borowitz et al., 2008; Buccisano et al., 2012; Paiva et al., 2015; Rawstron, 2015; Chen, 2015; Araki, 2016; Kwok, 2016; Munshi, 2017).
4. Assessment of specific antigenic phenotypes associated with prognosis. This is perhaps the most controversial of the listed indications and is theoretical in many disease entities. However, the expression of specific molecules on the neoplastic population has been associated with clinical outcome in some settings. As examples, CD56 in cases of acute promyelocytic leukemia (Montesinos, 2011), CD20 in adult acute lymphoblastic leukemia (ALL) (Maury, 2010; Thomas, 2009), and CD49d in chronic lymphocytic leukemia (CLL) (Bulian, 2014) have all been reported to be adverse prognostic factors. As will be discussed later, in some settings the prognostic impact conferred by flow cytometry can be accounted for by genetic signature. Thus, care must be taken in interpreting results on individual patients when the entire genetic context is not known.

TECHNICAL CONSIDERATIONS

Several technical considerations critical for producing high-quality flow cytometric data are discussed in this section. Readers interested in a more in-depth discussion of validation of various pre- and postanalytical variables applicable in flow cytometry are referred to the "Practice Guidelines from the ICSH and ICCS" for the "validation of cell-based fluorescence assays" (Barnett et al., 2013; Davis et al., 2013; Tanqri et al., 2013; Wood et al., 2013).

INSTRUMENTATION

The basic principle of flow cytometry relies on the injection of a monodisperse suspension of particles (cells) into the center of a flowing stream of fluid (sheath) that then passes through a small quartz capillary tube at a constant velocity (Shapiro, 2003). The sheath fluid serves to maintain the particles in the center of the flowing stream, where they may be illuminated by one or more focused light sources, typically lasers. The light scattered by the particles is collected by detectors positioned at a variety of angles around the capillary to obtain information about the cross-sectional area and, hence, size (low-angle or forward scatter) or complexity/granularity (high-angle or side scatter) of each individual particle as it transits the capillary. In addition, if fluorescent molecules or fluorochromes are attached to the particles, they may be excited by the incident light, giving rise to fluorescent emission that can be collected with the use of additional detectors and optical filters

(Fig. 35.1). The net result is a multiparametric analysis of each individual particle with the number of parameters evaluated dependent on the number of fluorescent molecules used and the complexity of instrument design. Modern clinical instrumentation is capable of assessing 10 and sometimes more simultaneous fluorochromes (Wood, 2006).

Optimization and standardization of instrument performance are critical for the success of any flow cytometric study, but are of particular importance in the analysis of hematopoietic neoplasms because of the wide range of signal intensities that must be detected. The preferred approach is to define a set of instrument conditions that allow for optimal instrument performance and perform daily quality control of the instrument to consistently achieve that level of performance. Adherence to a consistent and fixed level of instrument performance greatly simplifies quality control and provides reproducible data for interpretation. Daily assessment of the fluorescence intensity and coefficient of variation, using particles that have stable, moderately bright fluorescence and assessment of instrument noise using nonfluorescent particles, is the cornerstone of instrument quality control.

The operator has control over relatively few instrument variables on a flow cytometer, principally detection threshold, detector gain, rate of sample flow and, for some multilaser instruments, laser delay time. The detection threshold or discriminator is associated with a single parameter and is the value that must be achieved for the system to recognize that a particle has passed through the capillary to initiate signal processing. Typically, forward scatter is used to identify particles that have a size greater than some desired value (e.g., cells equal to or larger than lymphocytes). Of particular importance is the gain or voltage supplied to each detector—commonly, a photomultiplier tube—as this has a direct impact on the ability to separate signals of interest from background instrument noise (signal-to-noise ratio). The voltage applied to each detector should be adjusted to optimize the signal-to-noise ratio and allow detection of the weakest required signals for each detector. This often results in positioning of negative cellular populations in such a way that they completely occupy the lowest decade of a logarithmic scale. Finally, for instruments having multiple lasers that intersect the capillary stream at different points (spatially separated lasers), a parameter must be supplied to allow synchronization of signal processing to account for the different times at which a single particle encounters each laser as it transits through the capillary. This laser delay time should be adjusted to maximize signal intensity for each laser. It should be noted that the laser delay time is highly dependent on the transit time of the particle through the capillary; thus, it requires a stable fluidic system to maintain consistency.

The rate at which the sample is introduced or aspirated through the system can be controlled by the operator but is limited by two factors: the rate at which the instrument electronics can process signals that are generated and sample concentration. If particles pass through the instrument more rapidly than they can be processed by the electronics, the data for a subset of the particles will be lost and another subset will show unusual and undesirable artifacts, typically variable loss of signal intensity over a wide range. It is critically important to select a sample aspiration rate and concentration appropriate to the instrument to be used. One additional phenomenon related to sample concentration is termed *coincidence*, the simultaneous presence of more than one particle in the laser, resulting in a single recorded event that has composite characteristics of the particles involved. Coincidence can represent a significant problem for rare event detection and can be minimized using methods for doublet discrimination during analysis—techniques beyond the scope of this chapter (Wood, 2006).

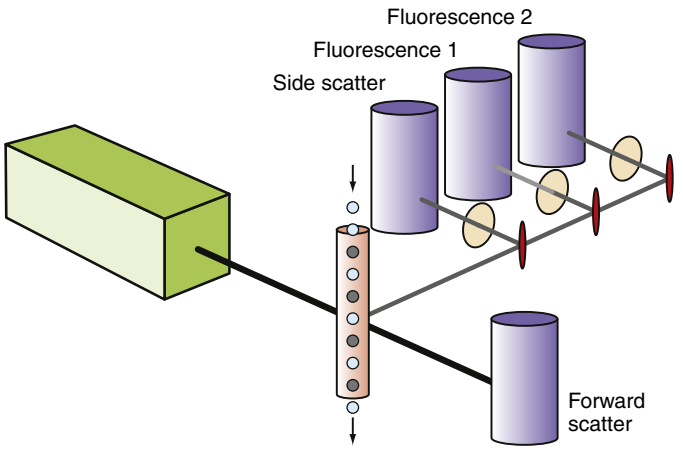

Figure 35.1 Schematic of a flow cytometer. A flowing stream of particles *(center)* is illuminated by a laser *(left)* and the resulting low angle (forward scatter) or right angle (side scatter) light scatter is collected by appropriately positioned detectors. In addition, fluorescent molecules attached to the particles may be excited by the laser light and the resulting emission routed through a series of optical mirrors and filters to the appropriate detectors (fluorescence 1 and fluorescence 2).

REAGENTS

The identification of cellular characteristics beyond those provided by light scatter measurements commonly utilizes fluorochromes that directly interact with cellular structures such as DNA or that indirectly interact through conjugation to antibodies. Each fluorochrome has a unique excitation and emission spectrum that partly determines the performance characteristics of the reagent and dictates which fluorochromes may be used simultaneously (Fig. 35.2). In an effort to increase the number of usable simultaneous fluorochromes possible from a single excitation source,

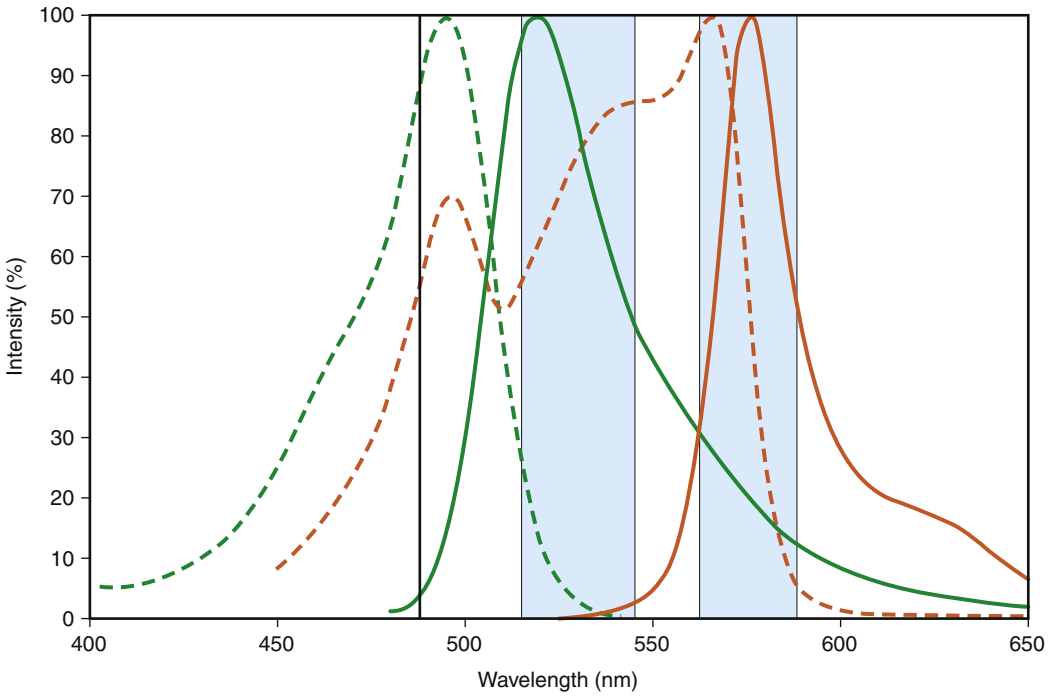

Figure 35.2 Fluorochrome emission spectra. Each fluorescent molecule possesses a characteristic absorption *(dotted line)* and emission spectrum *(solid line)* whose wavelength maxima are spectrally separated; the degree of separation is termed the *Stokes shift*. Although a small amount of fluorescein emission occurs at the same wavelength as phycoerythrin, the fluorescence emission of fluorescein *(green)* can be separated from that of phycoerythrin *(orange)* using appropriate optical filters *(shaded areas)*. The 488-nm laser commonly used to excite each of these fluorochromes is indicated by a black vertical line.

tandem fluorochromes have been devised (e.g., PE-Cy5) that rely on excitation of a primary fluorochrome that transfers its energy to a secondary fluorochrome (Cy5), providing the predominant fluorochrome emission at a longer wavelength. Tandem fluorochromes are required for high-level multicolor flow cytometry, but they have more complex emission spectra as well as decreased fluorochrome stability under some circumstances. The other important fluorochrome characteristic, the intensity of emission, is related to the efficiency of excitation by the light sources utilized and the quantum efficiency of the fluorochrome itself (Fig. 35.3). Emission intensity directly correlates with detection sensitivity and is a key consideration in the design of reagent panels, as discussed later.

The use of multiple simultaneous fluorochromes (i.e., multicolor flow cytometry) is required for the analysis of leukemia and lymphoma. Although three was noted to be the minimum number recommended under early consensus guidelines (U.S.-Canadian Consensus, 1997), the use of more simultaneous fluorochromes is typical in most modern clinical flow cytometry laboratories. The use of six or greater simultaneous fluorochromes is now common, with 10 or more being utilized in some clinical laboratory settings. The benefits of increased numbers of simultaneous fluorochromes is most pronounced in situations in which the abnormal population is small, the background is heterogeneous, and/or the abnormal population does not have uniform immunophenotypic characteristics. In addition, using more fluorochromes makes it possible to extract more information from limited samples. Because most fluorochromes have overlapping emission spectra, determination of the fluorescence due to a specific fluorochrome in a single detector requires subtraction of the portion of the signals contributed by each of the other fluorochromes in the sample, a process termed *compensation*. The appropriate amount of each signal to subtract (i.e., compensation coefficient) may be represented by an n-by-n matrix, where n is the number of fluorochromes. Consequently, as the number of fluorochromes increases, the number of compensation coefficients that must be determined increases geometrically, and software rapidly becomes required to perform this process correctly. To determine the compensation coefficients, a series of samples singly labeled with each fluorochrome are evaluated, with the positive population as bright as the brightest signal one plans to evaluate. Because the spectral characteristics of the tandem fluorochromes can vary significantly between lots and manufacturers, separate compensation controls are often required for each lot and conjugate of these reagents. Software, either on the instrument or on offline computers, is used to analyze the resulting data and to calculate compensation coefficients.

Although the process of determining and correctly applying compensation has been simplified using software, the use of multiple fluorochromes can result in significant display artifacts that are reflected in compromised low-level detection sensitivity (Roederer, 2001). This is a particular problem when one attempts to detect low-level signals in the presence of brightly overlapping fluorochrome emissions. Understanding the impact of compensation-related effects represents a major challenge in interpretation of multicolor flow cytometry. The implications of overlapping fluorochrome emission have direct consequences for panel design and data interpretation (Fig. 35.4). When compensation settings are not appropriate for the reagents used, artifacts arise that can lead to both the misattribution of low-level positivity and an inability to recognize the presence of subpopulations (Fig. 35.5). The use of software compensation provides a nondestructive method for data collection and allows the adjustment of compensation settings following acquisition, thereby supplying a way to correct for inadvertent compensation errors.

Antibodies are an integral part of the immunophenotypic evaluation of leukemia and lymphoma. It is important to determine the correct amount of each antibody to use by evaluating a series of samples labeled with different concentrations of antibodies (i.e., titering) (Stewart & Mayers, 2000). The object of titering is to maximize the signal-to-noise ratio by providing as bright a signal as possible on positive populations while maintaining a low level of background nonspecific binding. For high-specificity antibodies used for cell surface labeling, one should be able to achieve saturation, a consistent intensity on positive populations at higher antibody concentrations, without significant increases in background on negative populations. The inability to do so indicates a poor-quality antibody. For intracellular labeling, saturation typically is not achieved because of relatively high levels of nonspecific antibody binding by intracellular constituents, generally a linear function of antibody concentration, and optimization of signal-to-noise by titering becomes critical for adequate reagent performance.

PANEL DESIGN

The pairing of reagents with appropriate fluorochromes is a key factor in ensuring appropriate signal intensity and detection sensitivity. The following four steps can aid in the construction of appropriate reagent panels:

1. Determine the purpose for each potential combination of reagents. Each reagent combination should have a clearly defined objective or should not be further pursued.
2. Select a group of cellular targets. The selected group of targets or antigens should be able to successfully address the purpose of the reagent combination and should be relatively independent of fluorochrome or availability of commercial conjugates. The reagent combination should be the minimum needed to answer the question being asked. Antibodies are commonly combined in a variety of ways for use in the identification of abnormal hematopoietic populations, but these generally fall into one of the categories outlined in Table 35.1.
3. Assign a fluorochrome to each target. The basic principle is that highly expressed antigens should be coupled with dim fluorochromes, and dimly expressed antigens should be coupled with bright fluorochromes. This principle provides reasonable signal intensities and avoids compensation problems due to excessively bright fluorescence. A second principle involves selecting fluorochrome combinations to avoid compensation problems. Three general classes of these problems include: (1) spillover from one fluorochrome into an adjacent fluorochrome detected at a higher wavelength; (2) cross-laser excitation, most commonly from direct excitation by the red laser of the cyanine dyes used in tandem conjugates (e.g., PE-Cy5 emitting as APC); and (3) tandem fluorochromes having variable emission of the parent fluorochrome (e.g., APC-Cy7 emitting as APC). For a more in-depth discussion of such considerations, the reader is referred to Wood, 2006.
4. Test reagent combinations. The reagent combination must be empirically tested to ensure that signal intensities are as expected, that low-level sensitivity is appropriate where important, and that unexpected interactions between reagents do not occur. A sample prepared with all reagents of interest should be compared with the same sample prepared with a series of preparations, each lacking one of the component reagents (fluorescence-minus-one controls), as well as with a second series containing each single reagent independently (single-stained controls). Unexpected changes in intensity of one or more reagents indicate potential problems with the reagent combination.

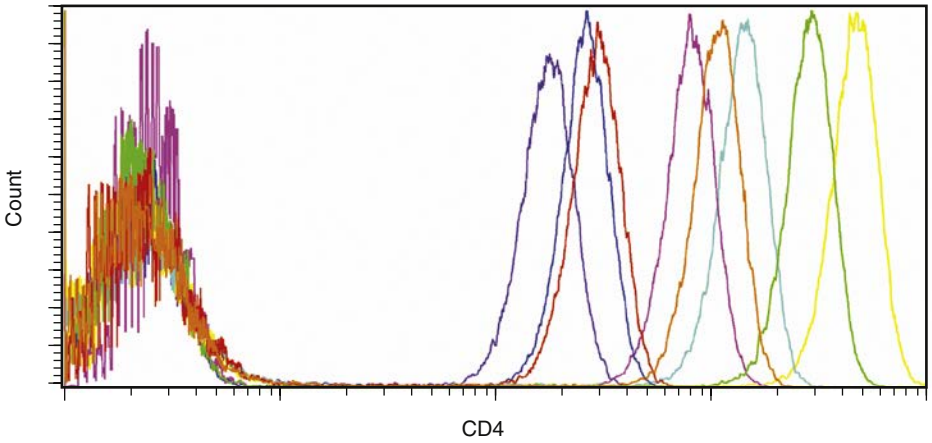

Figure 35.3 Comparison of fluorochrome emission intensity. Fluorochromes are characterized by differences in relative intensity of emission that are important to take into account to achieve optimal sensitivity. The relative fluorescence intensity for CD4 expression on lymphocytes is pictured for fluorescein (FITC) *(blue)*, phycoerythrin (PE) *(green)*, PE-Texas-Red *(orange)*, PE-Cy5 *(yellow)*, PerCP-Cy5.5 *(red)*, PE-Cy7 *(light blue)*, allophycocyanin (APC) *(magenta)*, and APC-Cy7 *(purple)*. The actual intensities observed are dependent on the clone of antibody used, the ratio of fluorochrome to protein in the antibody conjugate, the method of specimen preparation used, the instrument performance characteristics, and the method of instrument setup.

SPECIMEN HANDLING AND SAMPLE PREPARATION

Any specimen from which a single cell suspension can be generated is suitable for flow cytometric immunophenotyping, including peripheral blood, bone marrow, and lymph node, to name a few. Blood and bone marrow may be anticoagulated with ethylenediaminetetraacetic acid (EDTA), heparin, or acid citrate dextrose. Tissue specimens are best transported and stored in tissue culture media, such as RPMI 1640, and a single-cell suspension is generated by mechanical disaggregation using scalpel and forceps, needle and syringe, or wire screen mesh (Braylan & Benson, 1989), followed by filtration through fine-gauge wire mesh to remove aggregates. Specimens of all types are commonly stored at room temperature before preparation, although refrigeration will retard degradation when preparation must be delayed.

Analysis of white blood cells in peripheral blood or bone marrow requires erythrocyte removal for efficient evaluation. Density-gradient centrifugation (e.g., Ficoll-Hypaque) was historically used for this purpose, but it leads to selective loss of cellular subpopulations and gives relatively poor recovery on bone marrow specimens. Erythrocyte lysis using ammonium chloride or a variety of commercial preparations has become the standard technique for sample preparation in clinical laboratories (Carter et al., 1992). Currently recommended methods involve the addition of antibodies to an aliquot of blood or marrow, followed by erythrocyte lysis and washing with a buffered salt solution such as phosphate-buffered saline to remove cell debris, the lysing reagent, and unbound antibody. Inclusion of a small amount of formaldehyde (0.25%–0.50%) with the lysing reagent or following washing is a convenient way to stabilize both the specimen and antibody binding. When analysis of light chain expression on B cells is required, plasma immunoglobulin (Ig) must be removed by repeated washing before antibody addition. Once prepared, samples should be acquired on the instrument as soon as reasonably possible to avoid sample and fluorochrome degradation, although fixation and refrigerated storage will delay degradation.

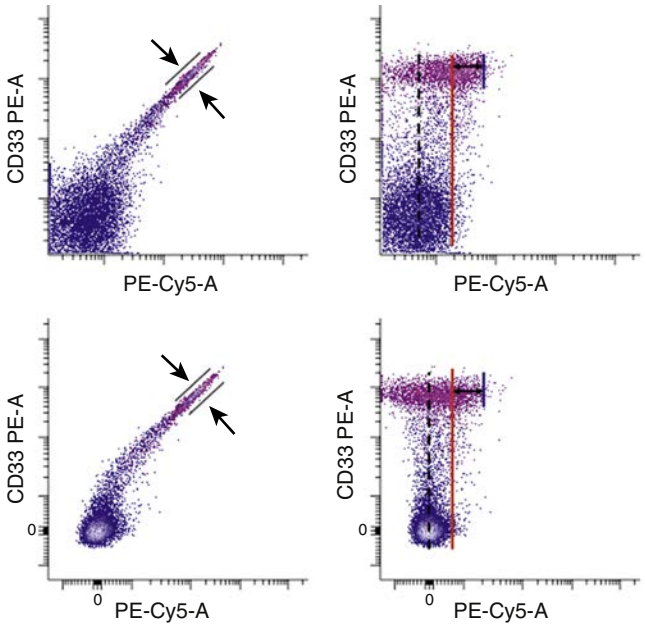

Figure 35.4 Compensation. Dot plots show monocytes *(pink)* and lymphocytes *(blue)* singly stained with CD33-PE represented on both a logarithmic scale *(top)* and a biexponential scale *(bottom)*. In the logarithmic function, values are undefined at zero; thus, dot plots are unable to display zero or negative values. The biexponential function merges a logarithmic region for higher values with a linear region near zero. Thus, it is able to display both zero and negative values, resulting in a symmetric distribution of data around zero following compensation. The fluorescence emission of CD33-PE appears in both phycoerythrin (PE) and PE-Cy5 detectors as PE emits in both regions of the spectrum examined by these detectors. Note that no PE-Cy5 conjugated antibody is used in this experiment. Without compensation applied *(left)*, monocytic cells expressing abundant CD33 show bright signals for both PE and PE-Cy5 with the width of the population *(black arrows)* due to measurement errors inherent in the method. Once compensation is correctly applied *(right)*, the centers *(represented by the dashed line)* of the Pe-Cy5 emission for both CD33-positive and CD33-negative populations is the same. In the logarithmic display, both negative and positive populations have the same low level of PE-Cy5 emission, with a similar number of events either to the left of the dashed line or lying on the vertical axis as are to the right of the dashed line in the logarithmic display. The ability to visualize negative values is one reason that a biexponential display is preferred in some situations. The PE-positive population also shows a higher level of apparent PE-Cy5 background fluorescence *(short blue line)* than the PE-negative population *(red line)* in both displays, the difference between the two represented by *double-headed black arrows*. The practical result is that the sensitivity for the detection of low-level PE-Cy5 is compromised in the presence of bright PE fluorescence. For example, if a PE-Cy5 conjugated antibody had been used in this experiment, CD33-positive cells might have been erroneously interpreted as positive for dim PE-Cy5.

DATA ACQUISITION

As the prepared sample is evaluated on the flow cytometer, it is important to collect enough events to allow detection of the population of interest. For populations that represent a large percentage of the total, relatively few events need to be acquired, but infrequent populations require the acquisition of larger numbers of events. Because in the evaluation of hematopoietic neoplasms one rarely knows what the likely population frequency will be for a given sample, it is most convenient to acquire a fixed number of total events that ensures the desired minimum level of sensitivity. For example, if a sensitivity of 0.1% is desired and 50 events are determined to be adequate for confident population identification, then 50,000 total white blood cell events will need to be acquired. The acquisition of fewer events will compromise the ability to detect low-frequency populations—an important consideration when evaluating for residual disease following therapy and in other situations in which the population of interest is present at low levels.

Instrument carryover between samples becomes a significant concern when evaluating for the presence of small abnormal populations. Most modern commercial instruments have a manufacturer's specification for carryover of roughly 0.1%. Although low in the diagnostic setting, this level may be considered relatively high when one is looking for infrequent populations, as in the setting of low-level residual disease detection. To minimize carryover, a small amount of water or sheath fluid should be run between each aliquot of sample acquired until background returns to an acceptably low level. Failure to do so will result in the sporadic appearance of populations having unexpected immunophenotypes that can be mistaken for neoplastic disease.

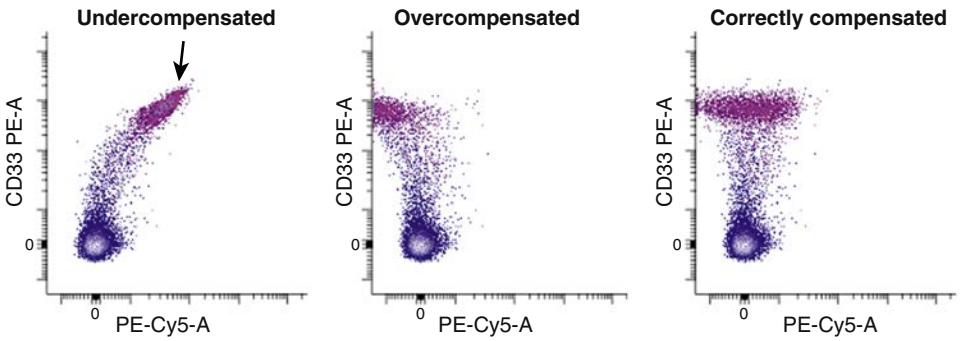

Figure 35.5 Inappropriate compensation. The fluorescence emission of monocytes *(pink)* singly labeled with CD33-PE shows minimal apparent PE-Cy5 fluorescence when 22% of the PE signal is subtracted from the PE-Cy5 signal (i.e., appropriate compensation or spillover correction, *right*). Note the symmetric distribution of events of about zero for PE-Cy5 when the data are correctly compensated. If the degree of spillover correction is decreased to 15% *(left, undercompensated)*, the CD33-positive population appears to express dim PE-Cy5 and could be misinterpreted as positive. Note the lack of symmetry for PE-Cy5 with increasing PE fluorescence and the pointed end of the positive population *(arrow)* as a clue to inaccurate compensation. If the compensation is increased to 26% *(middle, overcompensated)*, the CD33-positive population has a median PE-Cy5 fluorescence lower than the CD33-negative population, providing a clue that the parameter is overcompensated. If one were using a logarithmic scale, the CD33-positive population would be compressed on the *x*-axis and, depending on the degree of overcompensation, might appear not to exist.

INTERPRETIVE CONSIDERATIONS

The identification of hematopoietic neoplasia by immunophenotyping relies on the principle that neoplastic cells express patterns of antigen expression that are distinctly different from those of their normal counterparts. Antigen expression in normal cells is a tightly regulated process, resulting in a characteristic pattern of antigen acquisition and loss with maturation that is cell-lineage specific. Neoplastic cells commonly show nonrandom alterations in antigen expression that include the following:

1. Gain of antigens not normally expressed by cell type or lineage
2. Abnormally increased or decreased levels of expression of antigens normally expressed by a cell type or lineage, including the complete loss of normal antigens in some instances
3. Asynchronous antigen expression (i.e., expression of antigens normally expressed by cell type or lineage but at an inappropriate time during maturation)
4. Abnormally homogeneous expression of one or more antigens by a population that normally exhibits heterogeneous expression of that antigen

The consequence is that the immunophenotypic identification of hematopoietic neoplasia rests on a thorough knowledge of the normal patterns of antigens expressed by hematopoietic cells at different stages of maturation.

TABLE 35.1

Reagent Panel Design Strategies for the Detection of Hematopoietic Neoplasms

Principle	Example Implementation
At least one reagent for positive and specific population identification	Lineage-associated antigens for specific cell lineage (e.g., CD19 for B cells or CD3 for T cells)
Multiple antigens of same lineage and maturational stage to identify aberrant expression levels	Use of CD2, CD3, CD4, CD5, CD7, or CD8 simultaneously to evaluate mature T cells
Multiple antigens of same lineage but different maturational stages to identify normal maturation and distinguish asynchronous antigen expression	Use of CD13 and CD16 simultaneously to demonstrate neutrophilic maturation
Separation of different cell lineages	Use of CD11b and CD15 simultaneously to separate monocytic and neutrophilic maturation
Demonstration of clonality	Use of κ and λ in combination with a B-cell lineage reagent (e.g., CD19)
Identification of frankly aberrant antigen expression	Use of T-cell or NK cell–associated antigens such as CD7 or CD56 in combination with CD34 to demonstrate aberrant nonlineage antigen expression on a myeloid blast

NK, Natural killer.

NORMAL PATTERNS OF ANTIGEN EXPRESSION

All hematopoietic cells arise from the hematopoietic stem cell, a quiescent cell population that possesses long-term regenerative potential and is present at a low frequency in the bone marrow. The stem cell population in humans can be identified if a sufficient number of cells is evaluated that show expression of bright CD34 and CD133, intermediate CD45, dim to absent CD38, variable CD90, and dim CD123, CD117, HLA-DR, CD13, and CD33. Maturation toward lineage-committed progenitors is accompanied by a slight decrease in CD34 and CD45, loss of CD133 and CD90, and an increase in CD38 and HLA-DR. Further maturation along each lineage occurs in the bone marrow until mature, functional—albeit naïve—progeny are released into the peripheral blood. The one exception is T cells, whose earliest precursors migrate to the thymus, where maturation to functional forms occurs. The patterns of antigenic change with maturation for B-cell, T-cell, neutrophilic, monocytic, and erythroid lineages have been elucidated by multiple investigators (Loken et al., 1987, 1988; Inghirami et al., 1990; Terstappen et al., 1990a; Terstappen et al., 1990b; Terstappen & Loken, 1990; Terstappen et al., 1992b; Harada et al., 1993; Hoffkes et al., 1996; Ginaldi et al., 1996b; Almasri et al., 1998; Lucio et al., 1999; McClanahan et al., 1999; Wood, 2004). A summary of each lineage is presented in Figures 35.6 to 35.10.

ABNORMAL PATTERNS OF ANTIGENIC EXPRESSION IN HEMATOPOIETIC NEOPLASIA

Most hematopoietic neoplasms have abnormal immunophenotypes that are characteristic enough to allow their detection, even at relatively low levels of involvement. In some cases, the immunophenotype is characteristic enough to allow classification using immunophenotypic data alone. However, each group has sufficient variability that correct diagnosis relies on recognition of the overall immunophenotypic pattern, and not on the expression of individual antigens or the rigid application of immunophenotypic profiles. The following discussion emphasizes general immunophenotypic principles useful for the diagnosis and classification of hematopoietic neoplasia. A complete discussion of the antigenic abnormalities seen in each subtype of disease is beyond the scope of this chapter. The reader is referred to other references for more detailed discussion of immunophenotype in various hematopoietic neoplasms (Craig & Foon, 2008; Cherian and Wood, 2011).

Acute Leukemia

Diagnosis and Classification

Flow cytometry plays a critical role in establishing a diagnosis of acute leukemia. In the great majority of cases, flow cytometry is initially utilized to confirm that a suspected population of blasts or blast equivalents identified by morphology is truly a progenitor population on the basis of immunophenotype (some caveats to this general principle are listed later). Additionally, with flow cytometry, one can assign lineage to that progenitor population, thereby facilitating classification of the acute leukemia. Finally, with flow cytometry, one can determine how different the neoplastic progenitor population is from normal background progenitors, a feature useful in following patients post-therapy for residual disease.

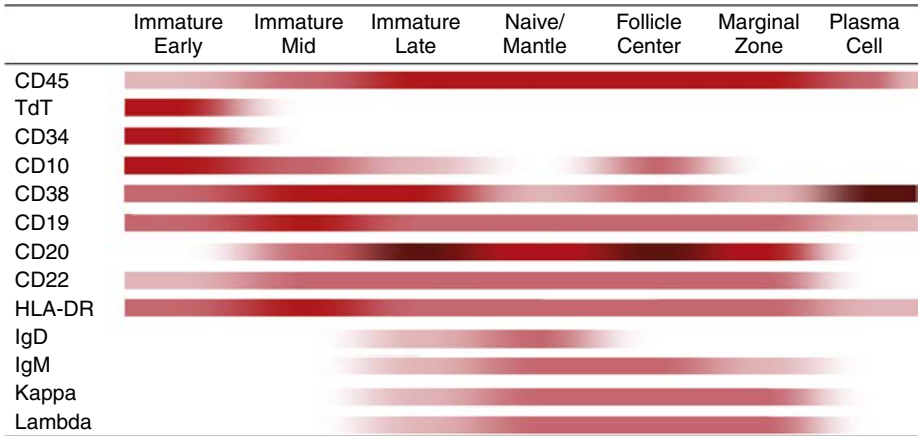

Figure 35.6 B-cell differentiation. The intensity of antigen expression throughout B-cell maturation is depicted for antigens commonly used in the clinical laboratory. Normal mature B cells express κ or λ light chains, never both. Darker colors represent higher levels of antigen expression.

By flow cytometry, progenitor populations can usually be identified using a combination of CD45 versus side scatter characteristics and expression of markers of immaturity that may include CD34, CD117, CD133, CD99, and terminal deoxynucleotidyl transferase (TdT). Though the immunophenotype will indicate immaturity in the majority of cases of acute leukemia, a leukemic population may show an immunophenotype suggesting maturation in rare situations (e.g., B lymphoid blasts may occasionally express surface light chain, and blast equivalents in some monocytic leukemias may be difficult to separate from mature monocytes by immunophenotype alone).

White blood cells express CD45 at distinct levels of intensity characteristic of both lineage and stage of differentiation that, when used in conjunction with orthogonal light scatter (side scatter), allow delineation of the basic white blood cell populations (Borowitz et al., 1993; Stelzer et al., 1993) (Fig. 35.11). CD45 versus side scatter gating is particularly useful for the identification of progenitors, which express intermediate CD45 and low side scatter. CD45 versus side scatter analysis has become standard practice in the clinical laboratory for this purpose. However, CD45 versus side scatter gating should not be used in isolation for progenitor identification, as not all populations of blast equivalents fall in the CD45 versus side scatter defined blast gate. For instance, the abnormal promyelocytes found in acute promyelocytic leukemia and immature monocytic cells that characterize acute leukemia with monocytic differentiation are often excluded from a standard CD45 versus side scatter defined blast gate. Further confounding analysis in some cases is the fact that some populations that are not blasts or blast equivalents can occupy the CD45 versus side scatter defined blast gate. Specifically, basophils, plasmacytoid dendritic cells, and hypogranular neutrophils, populations that can be increased in myeloid neoplasms, will be found within the CD45 versus side scatter defined blast gate (Harrington et al., 2012).

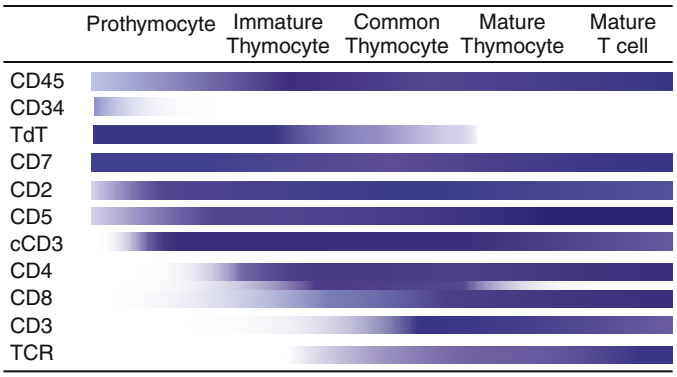

Figure 35.7 T-cell differentiation. The intensity of antigen expression throughout T-cell maturation is depicted for antigens commonly used in the clinical laboratory. T-cell maturation occurs largely in the thymus; most maturational stages will not be seen outside of that organ. At the common thymocyte stage, immature T cells express both CD4 and CD8, with subsequent stages showing expression of one or the other, but not both. Darker colors represent higher levels of antigen expression.

Using current (2017) WHO criteria, most acute leukemias show ≥20% blasts in the peripheral blood and/or bone marrow (Swerdlow et al., 2017). Although flow cytometry is an excellent tool for identifying and characterizing expanded populations of progenitors, two issues suggest caution when utilizing flow cytometric blast percentages to make an initial diagnosis of acute leukemia. First, the blast percentage obtained from bone marrow specimens is often inaccurate because of a combination of peripheral blood dilution (leading to an artifactual decrease) and compromise of nucleated erythroid precursors during specimen processing using lysing reagents (leading to an artifactual increase). Second, progenitors identified by immunophenotyping do not always directly correspond to blasts as identified by morphology. This is true because leukemic populations, similar to normal populations, consist of a maturational continuum, and there is no perfect concordance between specific antigenic changes and the arbitrary morphologic changes that distinguish blasts from more differentiated cells. For these reasons, flow cytometric "blast counts" should not replace morphologic counts when applying the WHO 2017 criteria to establish a diagnosis of acute leukemia. However, if one takes into consideration the limitations noted earlier, the diagnosis of acute leukemia can generally be correctly suggested by flow cytometry.

In addition to facilitating the diagnosis of acute leukemia, flow cytometry can be extremely useful in excluding a diagnosis of acute leukemia when the marrow is populated by an expanded proliferation of cells that mimics acute leukemia. A common situation in which this can occur is the presence of increased normal B-cell precursors (hematogones), which may be seen in a variety of reactive settings. Although hematogones may resemble primitive lymphoblasts morphologically, properly interpreted multiparameter flow cytometry can distinguish these normal immature precursors (hematogones) from acute leukemia (Lucio et al., 1999; Weir et al., 1999; McKenna et al., 2001). Additionally, some nonhematolymphoid tumors—such as small cell carcinoma or pediatric small round cell tumors—can resemble leukemic blasts on smears but are readily distinguished from leukemic blasts by flow cytometry, where they appear as CD45-negative cells lacking specific markers of B-cell, T-cell, or myeloid lineage, often with higher side scatter than might be expected for a cell with so little cytoplasm (Chang et al., 2003).

The major role for flow cytometry in acute leukemia is classification. Classification is largely a matter of lineage assignment and correlation with normal maturational stage. The determination of lineage in particular is a decision of major therapeutic importance, with the primary distinction being whether the leukemia is of myeloid or lymphoid lineage. The immunophenotypic characteristics of acute myeloid leukemia (AML) (Terstappen et al., 1992a; Reading et al., 1993; Bradstock et al., 1994; Macedo, 1995a, 1995b; Khalidi et al., 1999; Weir & Borowitz, 2001; Orfao et al., 2004) and acute lymphoblastic leukemia (Farahat et al., 1995; Khalidi et al., 1998; Weir et al., 1999) and their similarities to normal populations have been well described in numerous publications. In general, it is the overall pattern of antigen expression rather than expression of any single antigen that allows determination of lineage. This is due in part to the lack of lineage specificity of many antigens commonly used for immunophenotyping. As a rule, the more closely an antigen is expressed to the level commonly seen in cells of that lineage, the

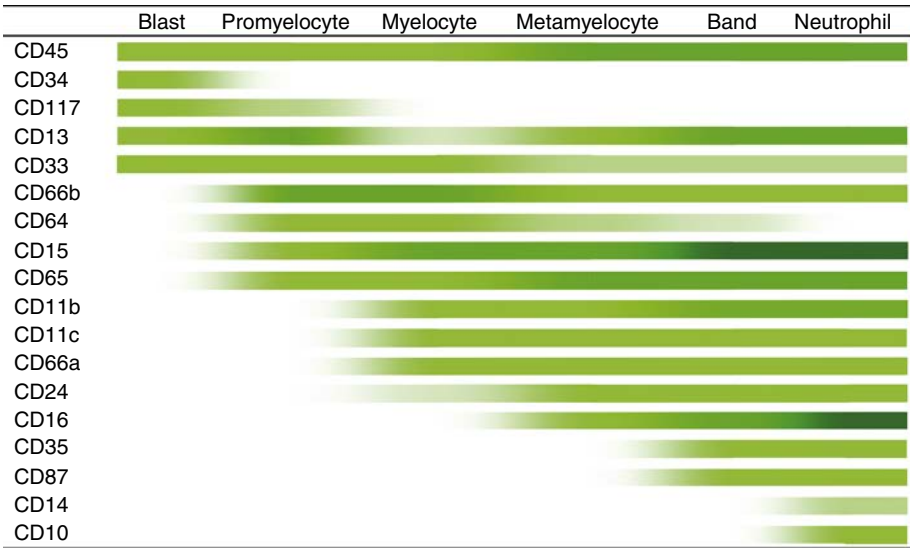

Figure 35.8 Neutrophil differentiation. The intensity of antigen expression throughout neutrophil maturation is depicted for antigens commonly used in the clinical laboratory. Darker colors represent higher levels of antigen expression.

more likely it accurately reflects lineage differentiation. For example, dim expression of the B-cell antigen CD19 has relatively poor lineage specificity, as it may be seen in acute myeloid leukemia, but brighter and more uniform CD19 expression at the level seen on normal B cells is more typical of B lymphoblastic leukemia. A subset of cytoplasmic antigens includes the most lineage-restricted antigens currently known, which may be used to arbitrate lineage assignment in cases in which the surface immunophenotype is unclear. Table 35.2 lists antigens commonly used for lineage assignment. In rare cases, the leukemic cells may show differentiation along more than one lineage (Hanson et al., 1993; Bene et al., 1995; Matutes et al., 1997; Porwit & Bene 2015; Charles & Boyer 2017; Swerdlow et al., 2017), most commonly either myeloid and B cell or myeloid and T cell. If a single blast population shows such differentiation, it is commonly termed *biphenotypic acute leukemia*. If two abnormal blast populations are present, each having a distinct and different lineage, this is termed *bilineal acute leukemia*. Both biphenotypic acute leukemia and bilineal acute leukemia are considered mixed-phenotype acute leukemia (MPAL) using 2017 WHO criteria. Examples of immunophenotypic patterns seen in acute leukemia are provided in Figures 35.12 to 35.15. A diagnostic algorithm for evaluating acute leukemia by flow cytometry is shown in Fig. 35.16.

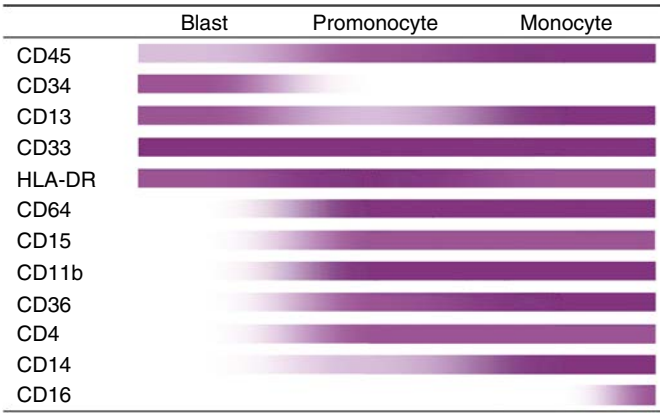

Figure 35.9 Monocyte differentiation. The intensity of antigen expression throughout monocyte maturation is depicted for antigens commonly used in the clinical laboratory. Darker colors represent higher levels of antigen expression.

Prognostic Factors

Several reports have discussed the prognostic significance of particular surface markers in both acute lymphoid and myeloid leukemia (Di Bona 2002; Schabath et al., 2003; Webber et al., 2008; Thomas, 2009; Maury, 2010; Montesinos et al., 2011). Additionally, the presence of recurrent cytogenetic or molecular abnormalities in acute leukemia is well recognized as an important prognostic variable that has therapeutic implications and is an integral part of the WHO classification of acute leukemia (Swerdlow et al., 2017). In many cases, the underlying cytogenetic or molecular genetic abnormality is associated with characteristic immunophenotypic features that aid in suggesting an appropriate classification (Porwit-MacDonald et al., 1996; Orfao et al., 1999; Hrusak & Porwit-MacDonald, 2002). For instance, AML with t(8;21) is associated with an improved prognosis as compared with AML with a normal karyotype. This subtype of AML typically shows coexpression of B-cell markers such as CD19 with variable expression of CD56 in a subset of cases. CD56 expression in AML with t(8;21) (Baer et al., 1997) has been associated with an adverse prognosis within that cytogenetically defined leukemia. However, it has been suggested that this prognostic disadvantage may be secondary to the association of *cKIT*-activating mutations and CD56 expression in t(8;21) AML (De et al., 2007). As our understanding of the complex genetic landscape underlying acute leukemia grows, it will be important to determine whether observations of immunophenotypic associations with prognosis have genetic underpinnings and retain independent prognostic significance once genetic data is accounted for. A summary of phenotypic features associated with cytogenetic or molecular abnormalities is provided in Table 35.3.

Therapeutic Targets

CD33 is one example of a therapeutic target that can be interrogated by flow cytometry and is the target of anti-CD33 (gemtuzumab ozogamicin). CD33 is expressed in the great majority of cases of AML, though intensity of expression is variable across cases and ranges from dim to bright. The level of CD33 expression pretreatment has been demonstrated to correlate with response to anti-CD33 therapy (Walter et al., 2007; Pollard et al., 2016).

In B lymphoblastic leukemia (B-ALL), therapeutic trials have been described using monoclonal antibodies (anti-CD20, rituximab), immunotoxins (anti-CD22, inotuzumab), bispecific T cell engaging small molecules (BiTE) (anti-CD19, blinatumomab), or T cells expressing chimeric antigen receptors (CAR T cell) with targets including CD19 and CD22, among others. Flow cytometry can be used to determine the suitability of different targeted therapies in B-ALL. When following patients who have received such therapies for residual disease, it is critical to recognize potential implications that such therapies may have for population identification.

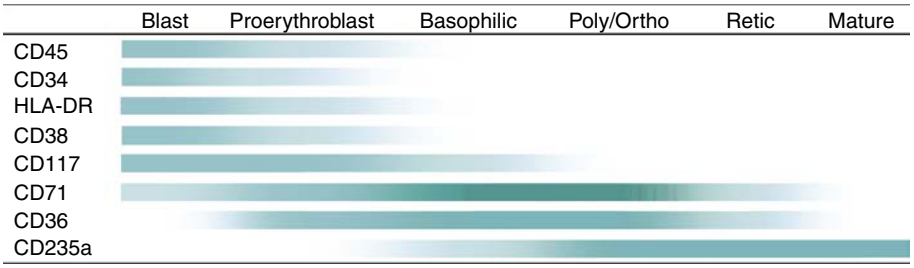

Figure 35.10 Erythroid differentiation. The intensity of antigen expression throughout erythrocyte maturation is depicted for antigens commonly used in the clinical laboratory. Darker colors represent higher levels of antigen expression.

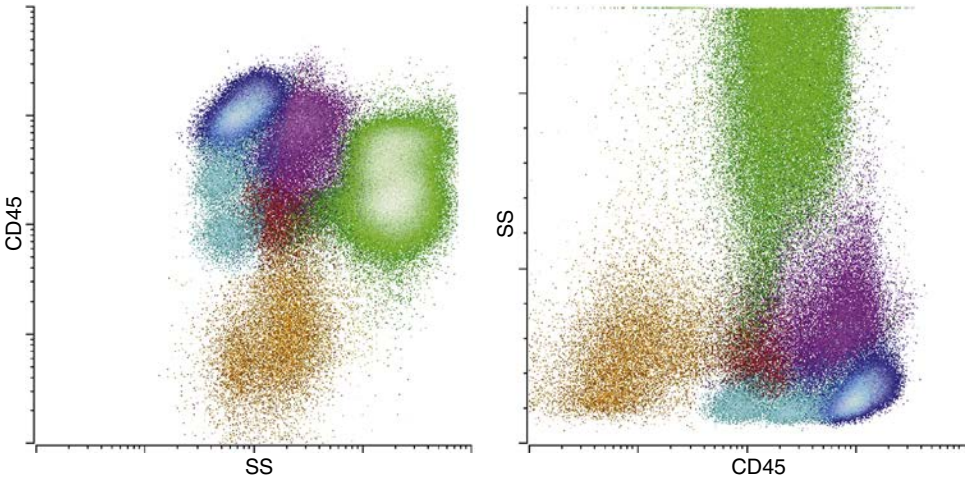

Figure 35.11 CD45 versus side scatter. The display of CD45 versus side scatter is increasingly used in the clinical laboratory as a starting point for the identification of white blood cell populations. Data are commonly displayed with side scatter on a logarithmic *(left)* or linear *(right)* scale. Major white cell populations colored are lymphocytes *(blue)*, B cells *(light blue)*, monocytes *(purple)*, maturing neutrophils *(green)*, blasts *(red)*, basophils *(dark purple)*, and maturing erythrocytes *(orange)*.

TABLE 35.2
Antigens Used for Lineage Assignment in Acute Leukemia

	AML	ALL–B Cell	ALL–T Cell
Definitive	Cytoplasmic MPO	None	Cytoplasmic CD3 Surface CD3 T-cell receptor
Strongly associated	CD117	Cytoplasmic CD79a Cytoplasmic CD22 CD19 CD10—bright	CD7—bright
Moderately associated	CD13 CD33	TdT—bright	CD5 CD2

ALL, Acute lymphoblastic leukemia; *AML,* acute myeloid leukemia; *MPO,* myeloperoxidase.
Using 2017 WHO criteria (Swerdlow et al., 2017), a diagnosis of mixed-phenotype acute leukemia (MPAL) may be made if there are (1) two separate blast populations of a different lineage, or (2) a single-blast population expressing antigens of more than one lineage. In this second scenario, lineage is strictly defined as follows:
1. Myeloid: MPO or evidence of monocytic differentiation
2. T cell: Cytoplasmic CD3 at the level of a mature T cell on at least a subset of blasts
3. B cell: Strong CD19 and one additional B-cell marker or weak CD19 and two additional B-cell markers (can include CD22, CD79a, CD10)
Notes:
These strict criteria for lineage assignment need not be met to assign lineage outside the setting of MPAL and only need to be met in the setting of scenario 2, above.
Dim MPO in a case of a single-blast population that otherwise has typical features of B-ALL is not sufficient to establish a diagnosis of MPAL.

For instance, CD19 is typically an excellent gating reagent for detection of B-ALL at diagnosis and follow-up since this marker is expressed on both normal B cell precursors and on the vast majority of B-ALL. The utility of CD19 as a gating reagent for B-ALL in the residual disease setting breaks down post anti-CD19 CAR T cell or BiTE therapy because patients who have received such therapies may relapse with either CD19-positive or CD19-negative disease (Ruella & Maus, 2016). In the setting of a CD19-negative relapse, CD19 would no longer be adequate for blast identification, and alternative gating strategies must be utilized (Cherian 2018).

Residual Disease Monitoring in Acute Leukemia

Many of the large number of antibodies that can be used to help classify acute leukemia are not, in and of themselves, essential for determination of lineage. However, a larger panel of antibodies, properly selected, can be very useful in identifying specific differences between the leukemic population and background normal elements, thereby enhancing the ability to use flow cytometry to detect small abnormal populations. Thus, the purpose of flow cytometric immunophenotyping in acute leukemia at diagnosis goes beyond simple assignment of lineage and extends to the description of a "leukemia-associated immunophenotype" characteristic of that leukemia which distinguishes the neoplastic population from normal regenerating progenitors. Knowledge of this abnormal immunophenotype that characterizes the leukemic cells is useful in assessing follow-up samples for residual disease (Campana, 2003). An important caveat is that immunophenotypic changes between diagnostic samples and persistent or recurrent disease are frequently observed in both ALL (Borowitz et al., 2005; Galpa et al., 2008; Roshal et al., 2010) and AML (Baer et al., 2001; Voskova et al., 2004). Accordingly, it is necessary that one monitor more than one antigenic pattern and not expect exactly the same immunophenotype seen at diagnosis to persist after therapy. Because of the potential for changes in the neoplastic immunophenotype post-therapy and at relapse, a thorough

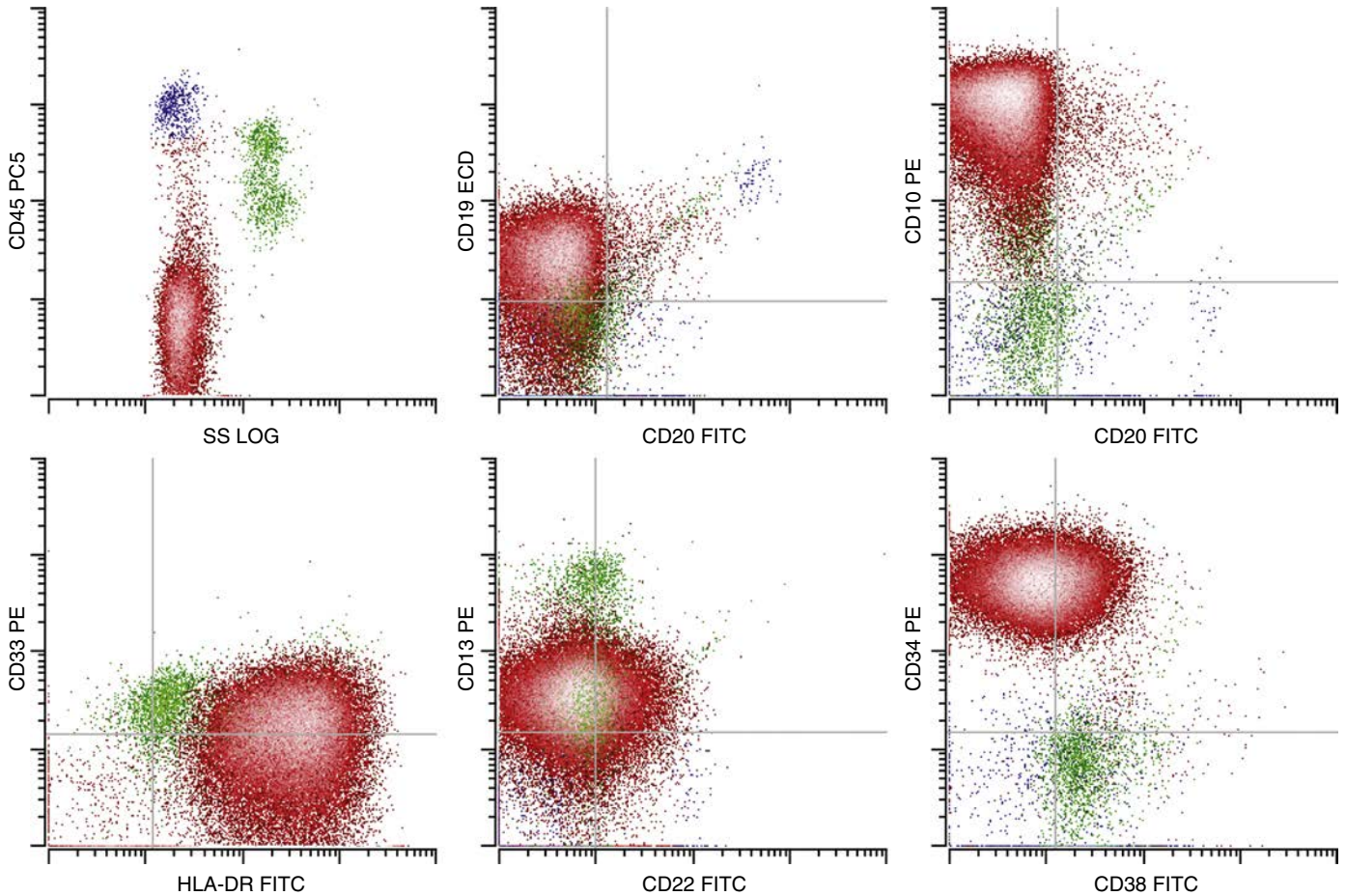

Figure 35.12 B lymphoblastic leukemia/lymphoma. The neoplastic cell population *(red)* in comparison with normal immature B cells shows abnormal expression of B cell–associated antigens CD19 (dim), CD22 (very dim), and CD10 (bright), along with aberrant expression of CD45 (absent), CD34 (bright), and CD38 (dim). In addition, the low-level expression of myeloid-associated antigens CD13 and CD33 is seen—a feature frequently observed in this neoplasm and not suggesting myeloid differentiation by itself. The cells have low side scatter, as is typical of lymphoid blasts.

understanding of the immunophenotypic patterns accompanying normal background hematopoiesis at baseline and in states of marrow regeneration is a prerequisite for evaluation of residual acute leukemia post-therapy. Pairing knowledge of the diagnostic leukemia-associated immunophenotype with an understanding of normal immunophenotypic patterns (so that one can identify a blast population that is "different from normal") provides a robust and powerful tool for identifying residual disease post-therapy.

Minimal/measurable residual disease (MRD) is defined as residual disease present at a level below the limit of morphologic detection. Flow cytometry and molecular methods are both more specific and sensitive for identifying leukemic cells than is morphology. The detection of MRD in acute leukemia has been demonstrated to be correlated with risk for relapse and overall survival for both AML (San Miguel et al., 2001; Feller et al., 2004; Maurillo et al., 2008; Loken et al., 2012; Chen et al., 2015; Araki et al., 2016) and ALL (Coustan-Smith et al., 2000; Dworzak et al., 2002; Borowitz et al., 2008). In several studies, MRD has emerged as the most significant prognostic factor identified in multivariate analysis. An example of MRD detection in ALL is shown in Fig. 35.17. The interested reader is referred to the review by Wood for a more in-depth discussion of MRD detection by flow cytometry (Wood, 2016).

Lymphoma

Diagnosis and Classification

As with leukemia, flow cytometry can contribute both to the diagnosis and classification of mature lymphoid neoplasms. The immunophenotypic diagnosis of lymphoma relies on the identification of an expanded population of abnormal mature lymphocytes. The most common way in which such an expansion is assessed by flow cytometry is through the demonstration of light-chain restriction in B-cell proliferations. As with all neoplastic cells, neoplastic lymphocytes arise from a single precursor that undergoes clonal expansion. However, unlike most cells, each lymphocyte normally expresses one of a series of polymorphic molecules on its surface that provides a unique identity; in the case of B cells, this identifying molecule is immunoglobulin (Ig). Because individual Ig molecules contain one of two forms of light chain—κ or λ—reagents directed against light chains can be used as markers of clonality for B cells (Braylan et al., 1993; Geary et al., 1993; Fukushima et al., 1996).

In the case of T-cell proliferations, the T-cell receptor genetic locus is more complex, but a larger series of reagents directed against the β-chain families of the T-cell receptor can be used to demonstrate clonality for T cells (Lima et al., 2001; Morice et al., 2004; Novikov et al., 2019). The use of reagents directed against killer-inhibitory receptors (KIR antigens) has even been suggested to allow demonstration of natural killer (NK) cell clonality (Morice et al., 2003). The assumption behind all of these assays is that clonality indicates malignancy. It should be emphasized that although clonality is a necessary consequence of neoplasia, clonal expansion is also a normal and necessary component of the immune response following antigenic stimulation; thus, the demonstration of clonality by itself is not sufficient for the diagnosis of lymphoma.

It is increasingly recognized that a subset of otherwise healthy individuals may contain small clonal populations of lymphocytes, best documented in the case of B cells (Rawstron et al., 2002; Chen et al., 2004; Kussick et al., 2004). It is not clear whether these clonal populations represent an early subclinical stage of disease, a precursor population without the full complement of genetic abnormalities required for neoplasia, or an incidental finding of no clinical consequence; however, a subset of individuals with such small clonal populations do appear to develop overt lymphoma over time (Rawstron et al., 2008; Shanafelt & Hanson, 2009; Xochelli et al., 2014; Oishi et al., 2018). The term *monoclonal B-cell lymphocytosis* has been adopted to describe such small populations in the peripheral blood while the phrase *in situ neoplasia* has been adopted for such lymphoid proliferations in the tissues (Nardi et al., 2019). In the peripheral blood, clinical and numeric criteria have been suggested to allow distinction of monoclonal B-cell lymphocytosis from overt lymphoma or leukemia (Shanafelt et al., 2009). Additionally, the size of the population of interest may have implications for the likelihood of progression to a clinically significant lymphoid neoplasm (Strati & Shanafelt, 2015). Given these observations, it is critical that flow cytometric findings indicating a light chain–restricted B-cell

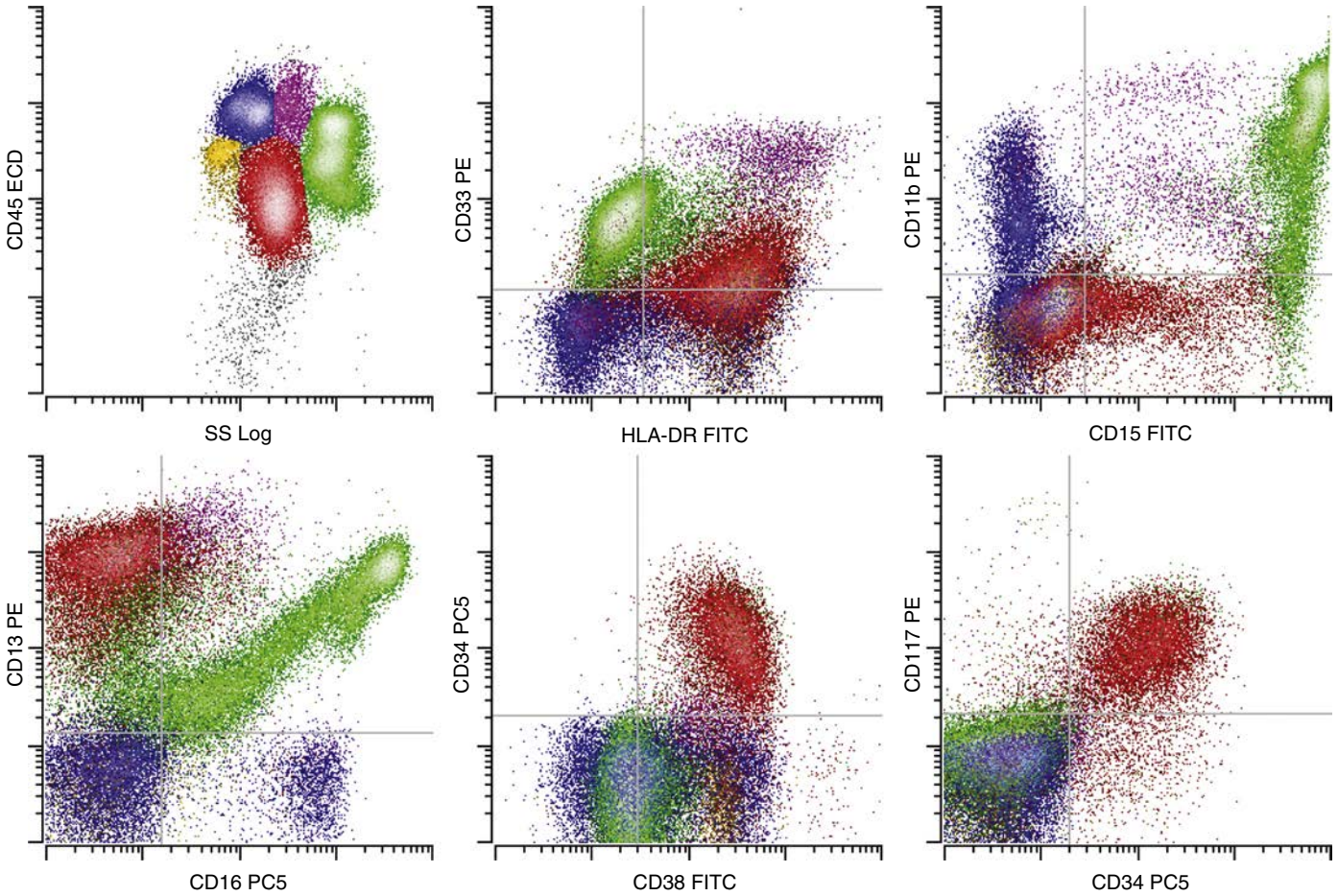

Figure 35.13 Acute myeloid leukemia with differentiation. The neoplastic cell population consists of blasts *(red)* showing abnormal expression of the myeloid-associated antigens CD33 (dim), CD13 (bright), and CD15 (dim partial) in association with immature antigens CD34 and CD117. The blasts do not express the more mature neutrophilic antigens CD11b and CD16, and are typical of the relatively immature forms seen in many cases of acute myeloid leukemia. Background maturing granulocytes *(green)*, monocytes *(purple)*, hematogones *(yellow)*, and lymphocytes *(blue)* are present that are normal and are not part of the leukemic population. All plots show all viable cells.

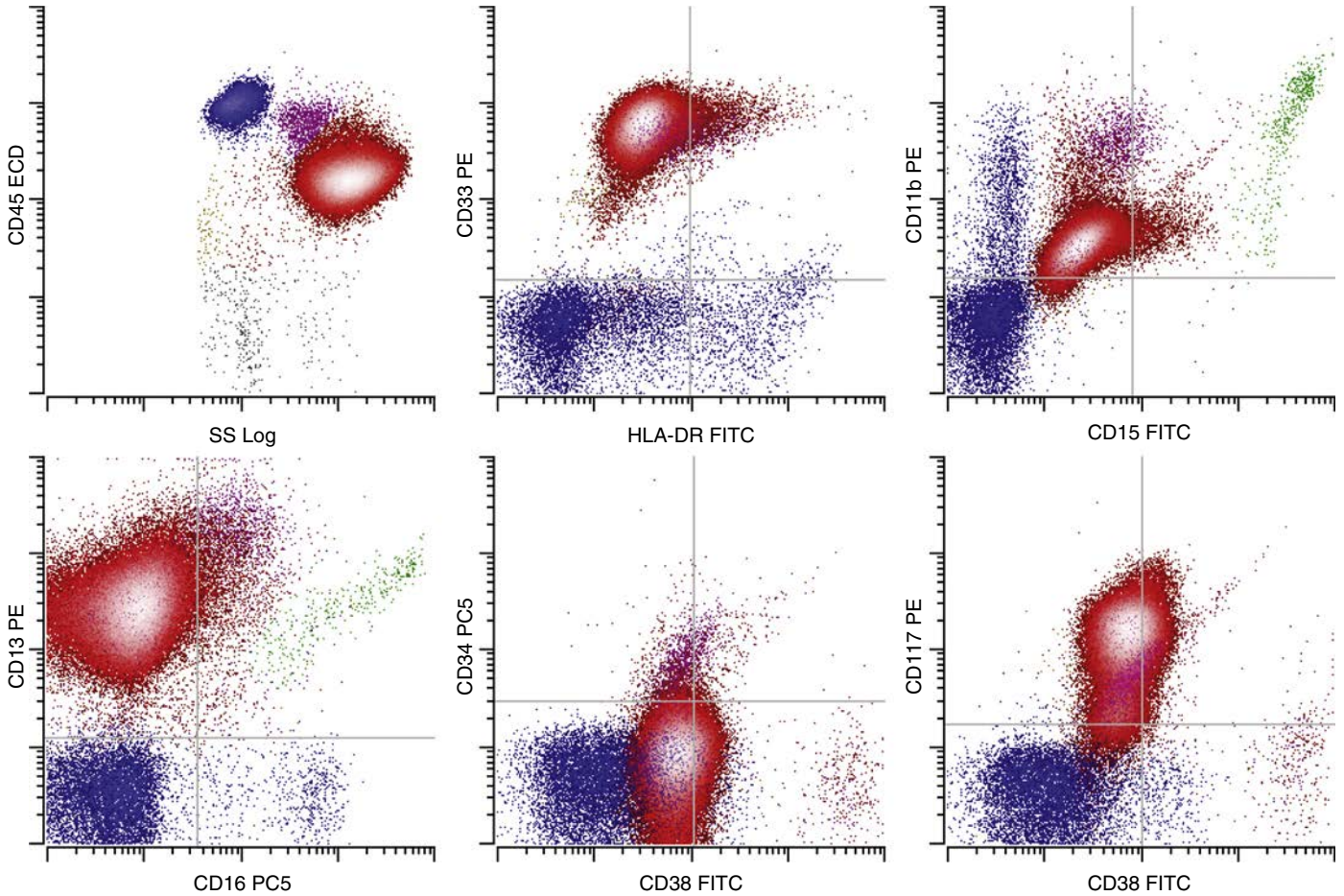

Figure 35.14 Acute promyelocytic leukemia. The neoplastic cell population consists of promyelocytes *(red)* showing abnormal expression of the myeloid-associated antigens CD33 (bright) and CD13 (intermediate), with high side scatter indicating abundant cytoplasmic granularity. The population lacks expression of CD34 and HLA-DR, antigens commonly present on true myeloid blasts, and retains expression of CD117, as is seen on a subset of normal promyelocytes. However, in contrast to normal promyelocytes, abnormal cells lack significant expression of CD15, a characteristic and common abnormality in this neoplasm.

process be put in a morphologic and clinical context before a definitive diagnosis of lymphoma is established.

In addition to light-chain restriction or restricted T-cell receptor β-chain usage, lymphomas, like leukemias, show alterations in antigen expression that deviate from normal maturation. In many cases, these alterations also provide evidence of neoplasia. Moreover, specific alterations are seen in association with different categories of lymphoma, thereby permitting classification as well as diagnosis in many cases. For example, increased expression of the T cell–associated antigen CD5 is seen in CLL or mantle cell lymphoma (Matutes et al., 1994b; Tworek et al., 1998), while expression of the germinal center cell marker CD10 characterizes follicular lymphoma (Mantei & Wood, 2009; Ray et al., 2005). Alteration in the intensity of Ig expression is also a common abnormality in B-cell lymphoma and can be useful in distinguishing normal and neoplastic B cells. With B-cell lymphoma, Ig can be increased, decreased, or even absent (Li et al., 2002). Similarly, T-cell lymphoma often shows alterations in the expression of one or more T-cell antigens (Picker et al., 1987; Ginaldi et al., 1996a). However, special care must be taken in interpreting small populations of phenotypically abnormal T cells, especially in unusual sites, because a large number of reactive conditions can be associated with expansions of populations that are not commonly seen in normal blood or lymph nodes (McClanahan et al., 1999).

An even more powerful method to diagnose lymphoma is to combine the detection of clonality with the ability to identify alterations in antigen intensity through multicolor flow cytometry. For instance, coupling the identification of follicle center B cells using CD19 and CD10 with the detection of κ and λ light chains in a four-color analysis allows one to identify the presence of light-chain restriction specifically within the follicle center B-cell population, greatly increasing both the specificity and the sensitivity of the analysis. Examples of immunophenotypic patterns seen in lymphoma are provided in Figures 35.18 to 35.23. Figure 35.24 provides a diagnostic algorithm for classifying B-cell lymphoma of small to intermediate-sized cells. One important limitation of this type of analysis is that neoplasms containing relatively rare, large abnormal cells (e.g., Hodgkin lymphoma) may be difficult to recognize unless an appropriate antibody combination is used and a sufficiently large number of events are acquired (Fromm et al., 2009). In this regard, the approach is essentially similar to MRD detection. An example of the flow cytometric detection of classical Hodgkin lymphoma is shown in Fig. 35.25.

The classification of lymphoma relies on the recognition of specific patterns of antigenic expression that are similar to some normal maturational stage, yet deviate sufficiently to allow identification of the abnormal population. Among B-cell lymphomas, there are two entities that can be both diagnosed and classified with a high degree of confidence based on immunophenotypic data alone: chronic lymphocytic leukemia/small lymphocytic lymphoma (CLL/SLL) and hairy cell leukemia. CLL/SLL is characterized by the coexpression of CD5 by abnormal B cells; decreased intensity of clonal light-chain expression; decreased expression of a variety of mature B-cell antigens, including CD20, CD22, and CD79b; and presence of the activation antigen CD23 with the membrane glycoprotein CD200 but without significant expression of FMC7, an activation epitope of CD20 (Serke et al., 2001) (see Fig. 35.18). This constellation of immunophenotypic findings is specific for CLL/SLL (Matutes et al., 1994b; Tworek et al., 1998; Palumbo et al., 2009; Alapat et al., 2012) and will allow for a definitive diagnosis if monoclonal B cells with this characteristic immunophenotype account for ≥5000 cells/μL in the peripheral blood. The only other B-cell neoplasm that consistently expresses CD5 is mantle cell lymphoma, a more aggressive lymphoma that is important to distinguish from CLL/SLL. In contrast to CLL/SLL, mantle cell lymphoma shows relatively bright expression of mature B-cell antigens such as CD20 and CD79b, expresses clonal Ig at a relatively normal to high level, and expresses FMC7 without significant CD23 or CD200 (see Fig. 35.19). Although in most cases mantle cell lymphoma can be readily distinguished from CLL/SLL, because some other low-grade lymphoproliferative disorders can occasionally express CD5 and mimic the mantle cell immunophenotype, a definitive diagnosis of mantle cell lymphoma requires documenting a t(11;14) translocation by fluorescent in situ hybridization (FISH) or karyotyping, or demonstrating overexpression of cyclin D1 by

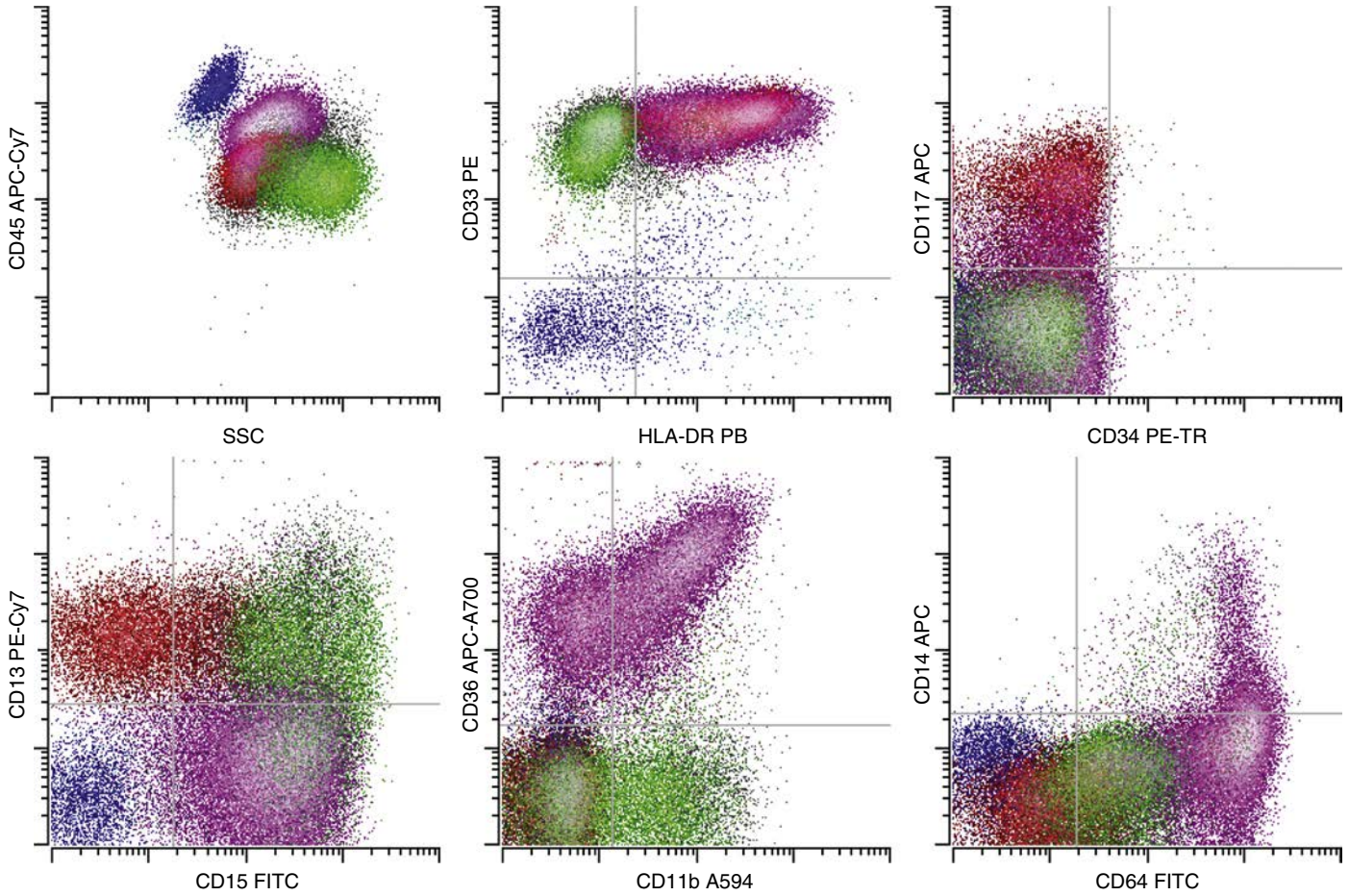

Figure 35.15 Acute myelomonocytic leukemia. The neoplastic cells consist of a relatively small population of blasts *(red)* with a larger population of cells showing monocytic differentiation *(violet)*. The blasts show abnormal expression of CD33 (bright), CD13 (intermediate), HLA-DR (intermediate), and CD117 (intermediate) without CD34. The monocytic differentiation is reflected in the acquisition of early monocyte antigens CD64 (bright) and CD36 (intermediate to bright), along with other more mature myelomonocytic antigens CD15 (intermediate) and CD11b (low to intermediate), without significant acquisition of the mature monocyte antigen CD14 (absent) or marked gain in the expression of CD45, as is seen in mature monocytes. This finding suggests differentiation to the promonocyte stage, a population usually included in morphologic blast counts. In addition, a lesser degree of neutrophilic differentiation *(green)* is present.

immunohistochemistry. These other rare CD5-positive B-cell neoplasms cannot be reliably distinguished by their immunophenotypic criteria; a combination of clinical history, morphology, and cytogenetic abnormalities is often required to reach a correct classification.

Hairy cell leukemia is characterized by increased expression of a variety of B-cell antigens, including CD19, CD20, and CD22; clonal surface light-chain restriction; markedly increased expression of the cell adhesion molecules CD11c and CD103; expression of the α-chain of the interleukin-2 (IL-2) receptor CD25; and expression of the α-chain of the IL-3 receptor CD123 (see Fig. 35.20) (Robbins et al., 1994; Matutes et al., 1994a; Venkataraman et al., 2011). In addition, the cells exhibit a variable degree of increased side scatter secondary to the abundant cytoplasm that they possess, often giving the cells light scatter characteristics similar to those of monocytes, although typically with brighter CD45 expression. This finding, in combination with the monocytopenia that is common in this disorder, is a frequent cause of false-negative results, particularly when one relies on relatively tight gates to identify the lymphocyte population by light scatter parameters alone or with CD45 versus side scatter.

Another immunophenotypic finding that aids in the classification of B-cell lymphoma is expression of CD10, an antigen present on immature B cells and on normal mature B cells as they transit through the follicle center. Among B-cell lymphomas, CD10 is expressed in most cases of follicular lymphoma (Almasri et al., 1998) (see Fig. 35.21), in a significant subset of large B-cell lymphomas, and in Burkitt lymphoma, in each of these cases indicating origin from the follicle center. In follicular lymphoma, the expression of CD10 is often coupled with decreases in CD19 and CD38 intensity (Ray et al., 2005; Yang et al., 2005; Mantei & Wood, 2009) that differ from the normal somewhat higher levels seen in reactive germinal center B cells. Demonstration of *Bcl-2* overexpression by the CD10-positive B-cell population can be useful in confirming neoplasia (Cook et al., 2003), particularly in cases lacking surface light chain expression, and reflects the presence of an underlying t(14;18) characteristic of follicular lymphoma. Although CD10 positivity alone does not allow definitive classification, its presence significantly reduces the possible entities that must be considered, with morphology generally being required to allow definitive classification.

The role of immunophenotyping in the classification of T-cell lymphoma is less well described, although certain associations have been noted that require larger studies for validation. The majority of T-cell lymphomas are composed of T cells that exhibit abnormal patterns of antigenic expression. T-cell lymphomas can express CD4 or CD8 and rarely may be either negative for both CD4 and CD8 or positive for both of these markers.

Among T-cell lymphomas, CD4 expression is most commonly seen. In angioimmunoblastic T-cell lymphoma, abnormal T cells are CD4 positive and commonly show loss or decreased expression of surface CD3 (Serke et al., 2000) with abnormal coexpression of CD10 (Attygalle et al., 2002) (see Fig. 35.23). In mycosis fungoides/Sézary syndrome, abnormal T cells are also typically CD4 positive and can show a variety of immunophenotypic abnormalities, commonly including alterations in the intensity of CD3 and CD4 and decreased expression or loss of CD7 (Bogen et al., 1996; Lima et al., 2003) and CD26 (Kelemen et al., 2008). However, CD7 can be variably decreased on CD4-positive T cells outside the setting of neoplasia. Decreased expression of CD7 is associated with a normal memory immunophenotype, and expanded subpopulations with this immunophenotype may be seen in a variety of reactive conditions, including inflammatory skin lesions (Murphy et al., 2002). Consequently, demonstration of the loss of CD7 by itself does not allow definitive classification or a definitive diagnosis of lymphoma and generally requires the presence of additional antigenic abnormalities to be informative. CD26 loss appears to be more common in Sézary syndrome than in mycosis fungoides; however, similar to CD7, it is not specific for neoplasia (Kelemen et al., 2008). Adult T-cell leukemia/lymphoma characteristically expresses CD4 and shows loss of CD7 and CD26. This entity often shows decreased expression of surface CD3 and is uniformly positive for CD25 (Shao et al., 2010). The immunophenotype is not diagnostic in isolation; confirmation of a suspected diagnosis

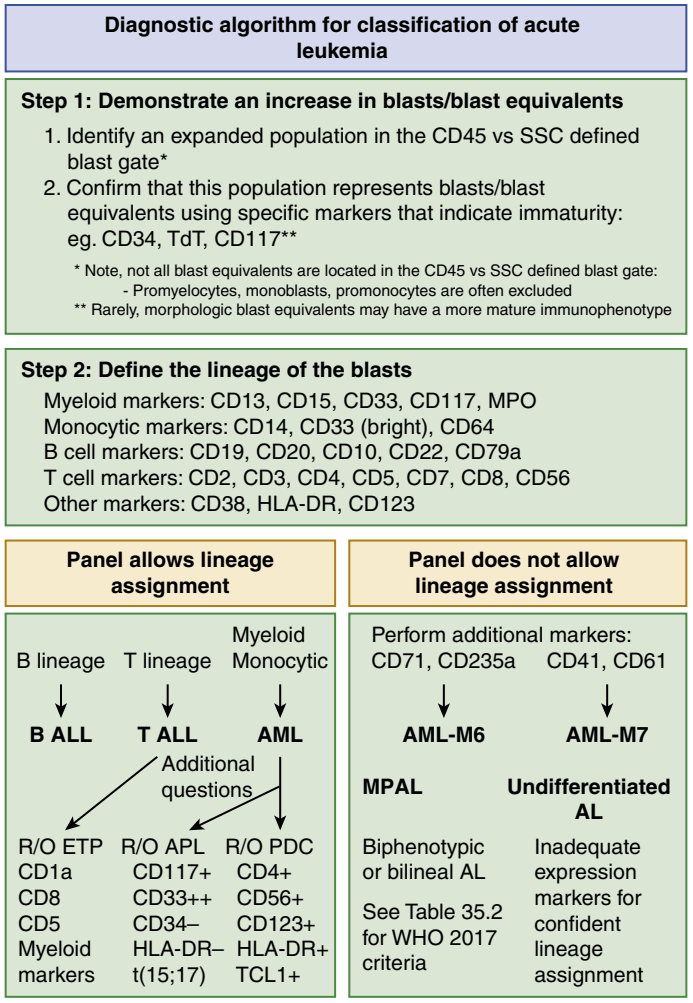

Figure 35.16 This algorithm can assist in diagnosis and classification of acute leukemia. *SSC,* Side scatter; *AL,* acute leukemia; *AML,* acute myeloid leukemia; *ALL,* acute lymphoblastic leukemia; *APL,* acute promyelocytic leukemia; *ETP TALL,* early thymocyte precursor T-cell lymphoblastic leukemia; *PDC,* plasmacytoid dendritic cell neoplasm; *R/O,* rule out.

TABLE 35.3

Association of Immunophenotype with Cytogenetic Abnormalities in Acute Leukemia

	Immunophenotype
Acute Myeloid Leukemia	
t(15;17)	HLA-DR negative, CD15 low to absent,* CD33 bright, CD34 low to absent
t(8;21)	CD34 bright, CD56 positive, CD19 dim
Acute Lymphoblastic Leukemia	
t(12;21) (by FISH)	CD10 positive, CD20 low to negative, CD9 low to negative
KMT2A rearrangement (e.g., t[4;11])	CD10 negative, CD15 positive

*This is a distinguishing feature from normal promyelocytes, which express relatively increased levels of CD15.
FISH, Fluorescent in situ hybridization.

requires demonstration of exposure to HTLV-1, usually via serology studies. T-cell prolymphocytic leukemia is most often CD4 positive and can also coexpress CD8 or express CD8 without CD4 in some cases. Variable loss of pan–T cell antigens may be seen; however, the immunophenotype is not specific, and a suspected diagnosis can be confirmed by genetic testing for a *TCL1* rearrangement (Chen & Cherian, 2013). Anaplastic large cell lymphoma may also be positive for CD4 but is sometimes negative and can infrequently express CD8. Expression of CD30 (often strong) in combination with an aberrant pattern of T-cell antigen expression on a population with forward scatter characteristics of large cells can be useful in the identification of anaplastic large cell lymphoma (Juco et al., 2003; Muzzafar et al., 2009).

CD8 expression is less common in T-cell neoplasms. Large granular lymphoproliferative disorder (large granular lymphocytic leukemia) is generally characterized by clonal expansion of CD8-positive T cells having variably decreased expression of CD5 and/or CD7 and expression of NK cell–associated antigens such as CD57 or CD16 (Richards et al., 1995). However, similar clonal expansions may be seen in a wide variety of reactive conditions—knowledge of the clinical context is required for an understanding of the clinical significance of an expanded large granular lymphocyte population.

When interpreting the significance of T-cell populations, it should be noted that many reactive T-cell subsets can be associated with shifts in antigen expression. For this reason, immunophenotypically "aberrant" T-cell populations should always be interpreted in the context of clinical and morphologic data before making an assessment of neoplasia. Importantly, several lymphoid neoplasms have been associated with characteristic patterns of reactive background T cells, a finding that may provide clues to the diagnosis in some cases. For instance, the distribution of reactive T-cell subsets described in classical Hodgkin lymphoma, nodular lymphocyte-predominant Hodgkin lymphoma, and T cell–rich large B-cell lymphoma are characteristic and differ from the T-cell distribution seen in reactive lymph nodes (Wu et al., 2016). Specifically, classical Hodgkin lymphoma is often associated with an increase in reactive CD4-positive regulatory T cells expressing CD25 (often with bright CD7 and CD45) (Hudnall et al., 2008; Wu et al., 2016), while in lymphocyte-predominant nodular Hodgkin lymphoma, T-cell populations positive for both CD4 and CD8 may be seen (Rahemtulla et al., 2006; Wu et al., 2016).

Therapeutic Targets

The most widely used therapeutic antibody in lymphoid neoplasms is anti-CD20 (rituximab). CD20 is expressed by the great majority of mature B-cell lymphomas; however, determination of CD20 expression is essential to establish the suitability of this therapy. Following therapy, B cells may persist but show loss of CD20 expression. In such cases, assessment of samples using more than one B-cell marker, for instance, a combination of CD19 and CD20, is helpful in demonstrating the presence of residual B cells lacking CD20. CAR T cells directed against CD19 have also been utilized in the treatment of relapsed/refractory mature B-cell neoplasms. Many patients receiving these therapies have also previously been exposed to anti-CD20, leading to loss of CD20 expression. With the addition of anti-CD19 therapy, loss of CD19 may also be seen on the neoplastic cells (Turtle et al., 2016; Turtle et al., 2017), leading to challenges with population identification and the need for alternative markers to identify the abnormal population. Anti-CD52 (alemtuzumab) is occasionally used to treat cases of refractory mature lymphoid neoplasms. Because of the profound immunosuppression associated with this therapy, documentation of CD52 expression is important, although the great majority of lymphomas will express CD52.

Minimal Residual Disease Detection

Detecting low levels of involvement can be important in accurately staging patients with lymphoma (Douglas et al., 1999). This is particularly applicable to studies of bone marrow, in which detection of small populations of light chain–restricted B cells can be seen in cases in which morphology is either negative or equivocal (Duggan et al., 2000; Palacio et al., 2001; Sanchez et al., 2002; Stacchini et al., 2003). Similarly, the peripheral blood may be evaluated for lymphoma to aid in the timing or advisability of stem cell collection; the resulting harvested stem cell product may be tested for the presence of residual lymphoma to minimize the amount of tumor reinfused in patients undergoing bone marrow transplantation. In addition, as in acute leukemia, MRD studies have been used in patients with CLL and have demonstrated an association between the presence of residual disease following therapy and both event-free and overall survival (Rawstron et al., 2001; Moreton et al., 2005; Kwok, 2016). Most successful and sensitive methods for MRD detection in this setting do not rely solely on the demonstration of light chain–restricted B cells by flow cytometry. Although light-chain reagents may sometimes be used, the overall approach is similar to that described earlier for acute leukemia detection in which multiparametric analysis is performed, incorporating many antigens that may be aberrantly expressed in CLL (Rawstron et al., 2013).

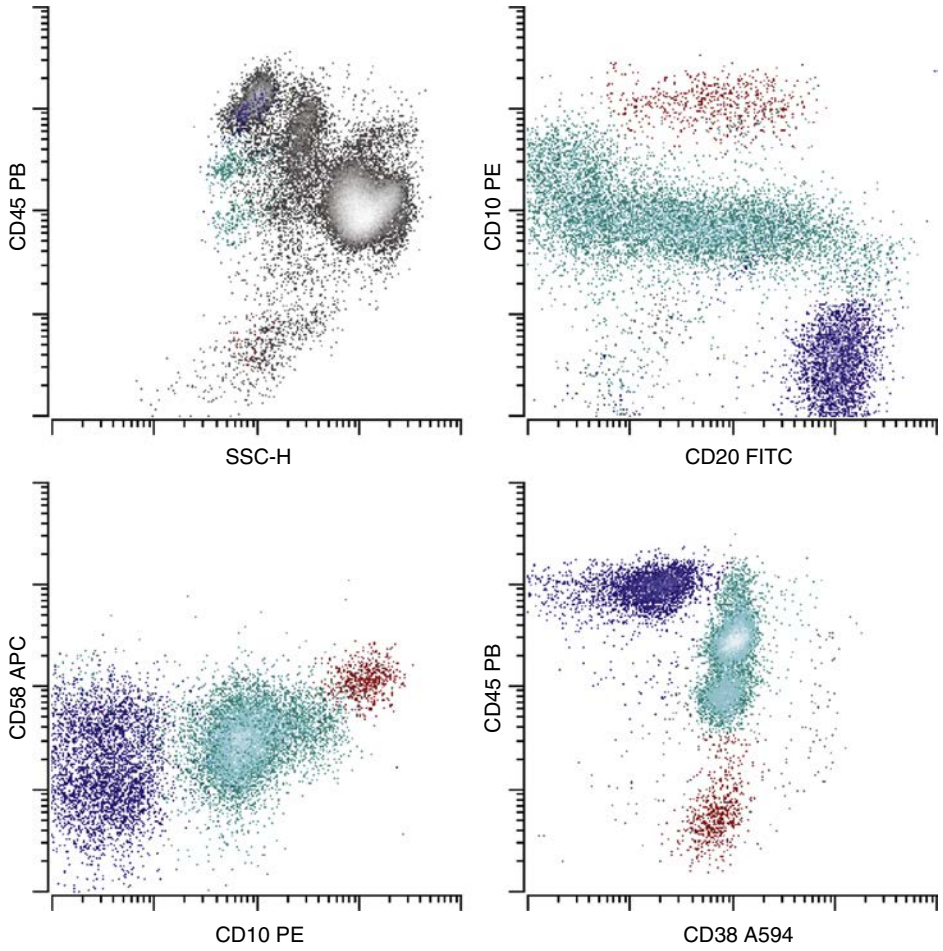

Figure 35.17 Minimal residual disease detection. An abnormal population of immature B cells is identified *(red)* that have abnormally increased expression of CD10 and CD58, abnormally decreased expression of CD45, and normal expression of CD20 and CD38. This composite immunophenotype is different from normal immature B cells *(cyan)* or mature B cells *(dark blue)*, allowing its discrete identification at a level of 0.1% of white cells.

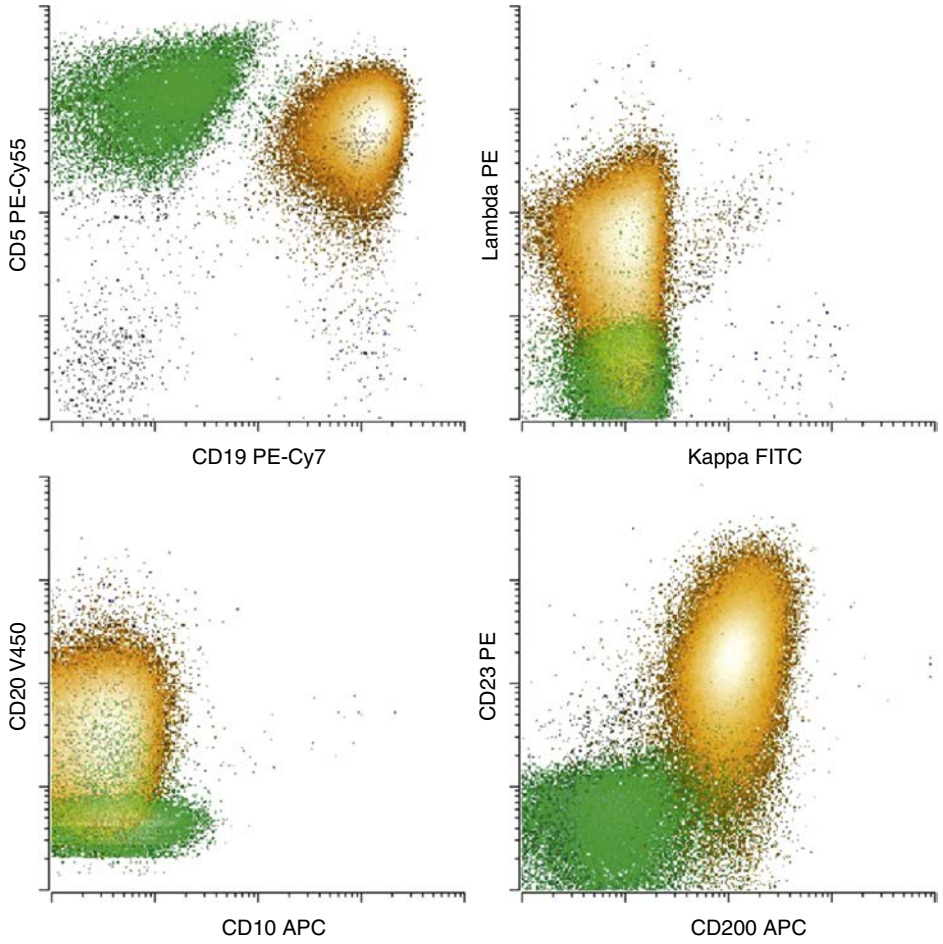

Figure 35.18 Chronic lymphocytic leukemia/small lymphocytic lymphoma (CLL/SLL). The neoplastic B-cell population *(gold)* shows abnormal expression of the B-cell antigens CD19 (intermediate) and CD20 (low) with surface λ light chain expression (low) and coexpression of CD5 and CD23 (intermediate) with CD200. The expression of CD5 with low-level light chain restriction, low-level CD20, and CD23 is characteristic of CLL/SLL. CLL/SLL is typically positive for CD200 without FMC7 (data not shown). The immunophenotype of CLL/SLL should be contrasted with mantle cell lymphoma (see Fig. 35.19). All plots show all lymphoid cells; background reactive T cells are shown in *green*.

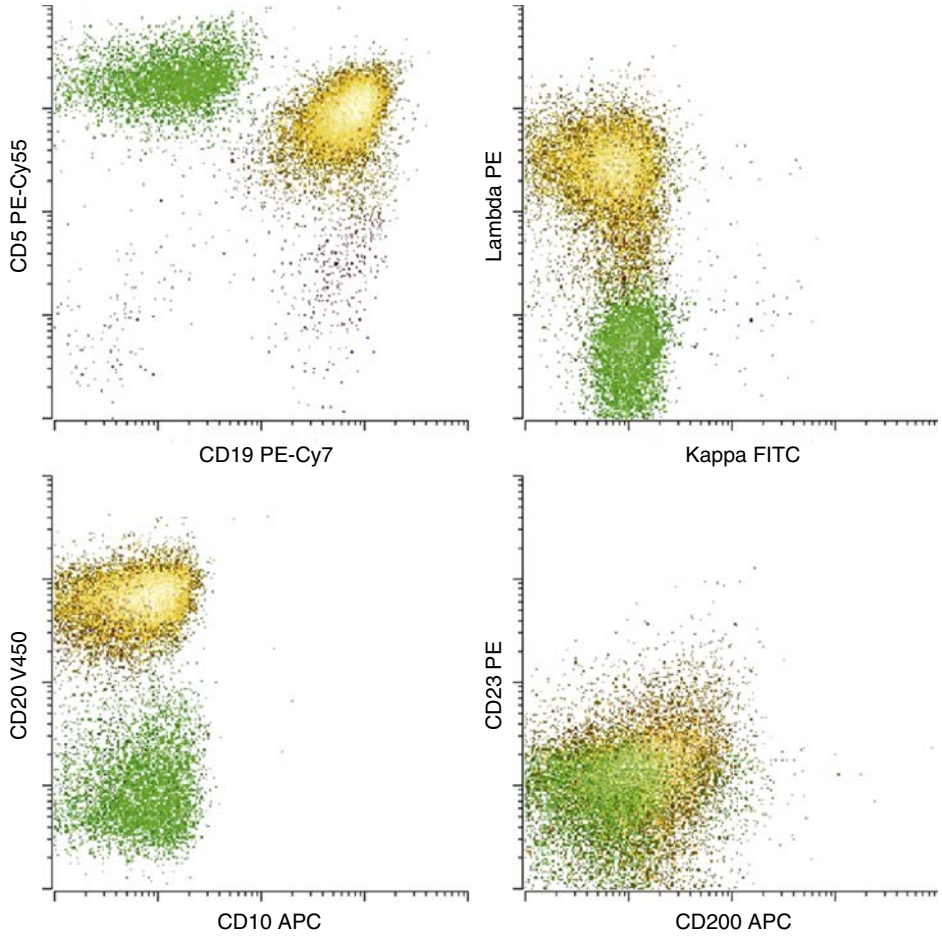

Figure 35.19 Mantle cell lymphoma. The neoplastic B-cell population *(gold)* shows expression of B-cell antigens CD19 (intermediate) and CD20 (intermediate) with κ light chain restriction (bright). CD5 (intermediate) is expressed by the neoplastic B cells, while CD23 and CD200 are very low to absent. Mantle cell lymphoma shows intermediate expression of FMC7 (data not shown). Although both CLL/SLL and mantle cell lymphoma express CD5, the intensity of CD20 and light chain—coupled with the level of expression of CD23, CD200, and FMC7—allow distinction of these B-cell neoplasms in most cases (contrast with Fig. 35.18). Confirmation of a suspected diagnosis of mantle cell lymphoma requires demonstration of t(11;14) by FISH or cyclin D1 overexpression by immunohistochemistry. All plots show all lymphoid cells; background reactive T cells are shown in *green*.

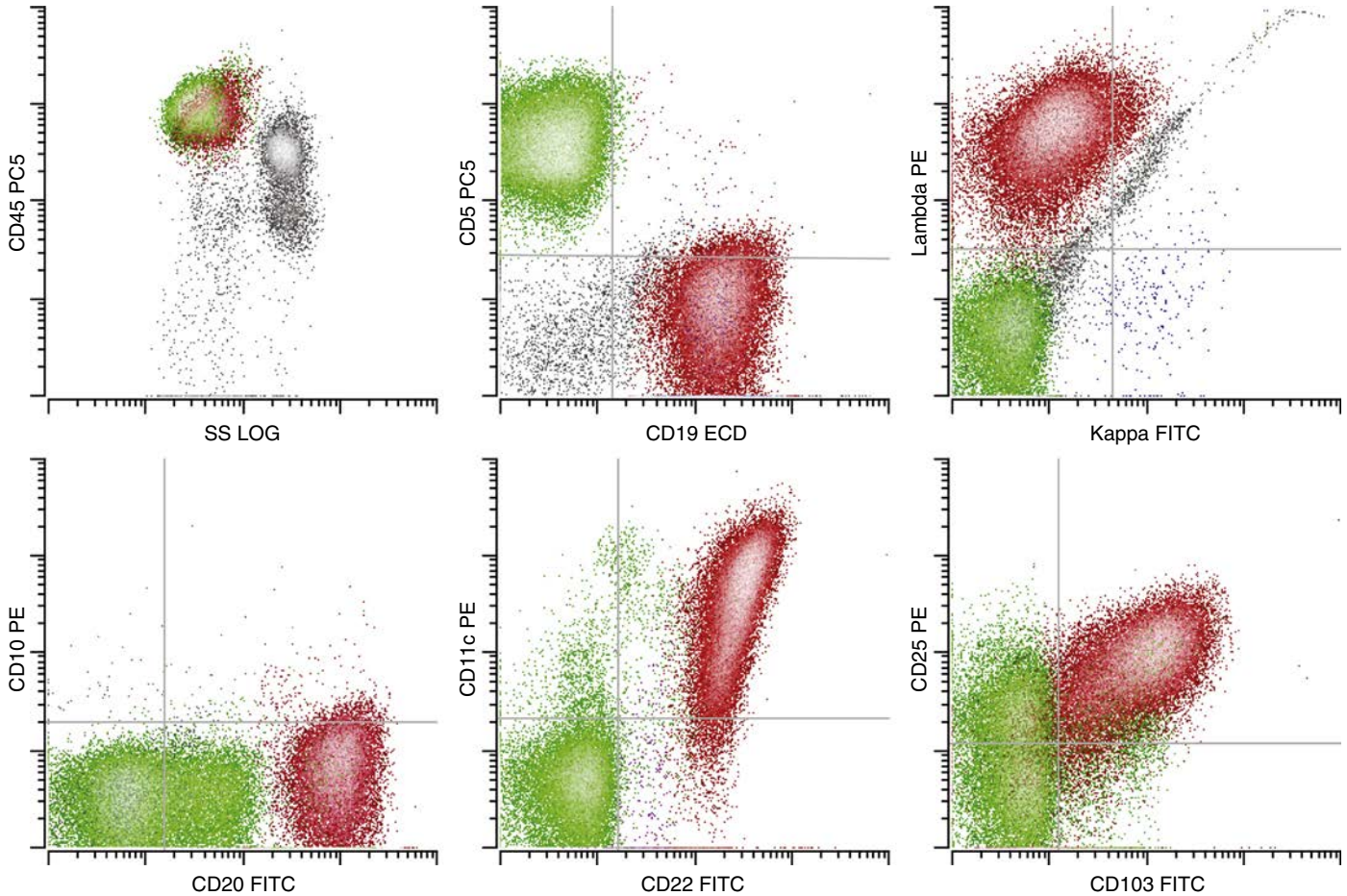

Figure 35.20 Hairy cell leukemia. The neoplastic B-cell population *(red)* shows expression of B-cell antigens CD19 (intermediate), CD20 (bright), CD22 (bright), and surface λ light-chain restriction (intermediate) with aberrant expression of the adhesion molecules CD11c (variably bright), CD103 (intermediate), and CD25 (intermediate). This immunophenotype is diagnostic for hairy cell leukemia. Note the absence of monocytes by CD45 versus side scatter, a characteristic finding in hairy cell leukemia.

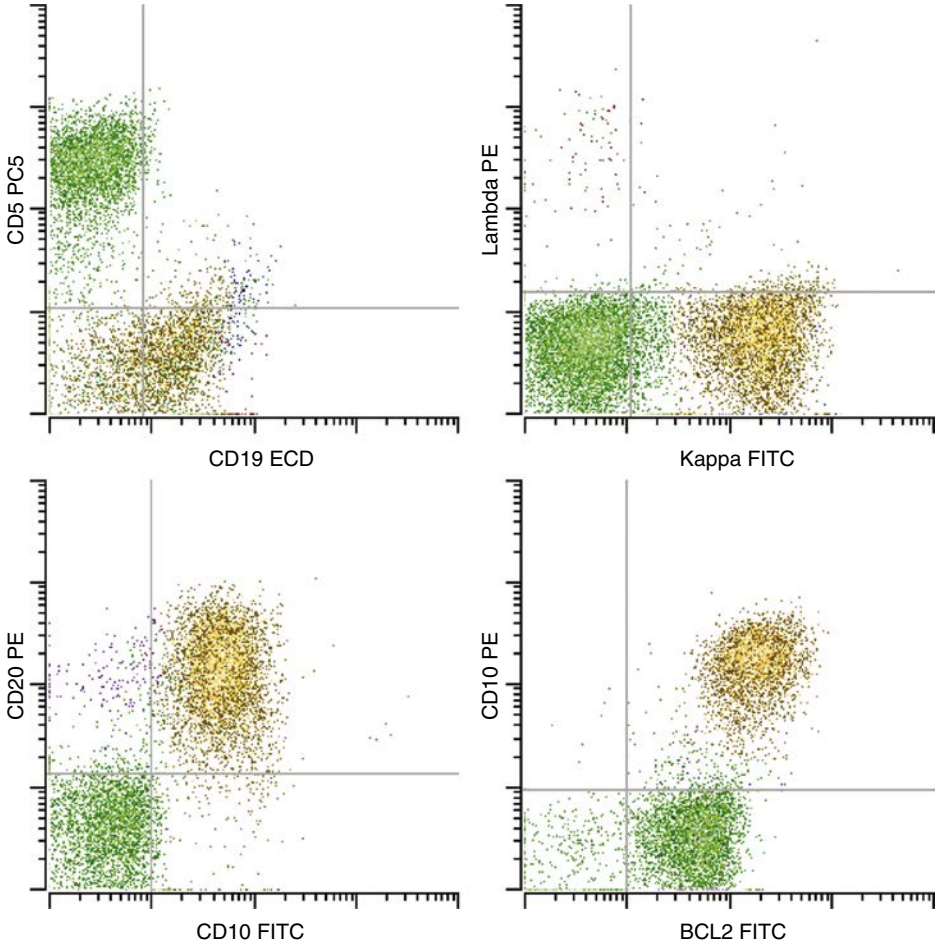

Figure 35.21 Follicular lymphoma. The neoplastic B-cell population *(gold)* shows abnormal expression of the B-cell antigens CD19 (dim), CD20 (intermediate), and surface κ light-chain restriction (intermediate) with coexpression of the follicle center–associated antigen CD10 (intermediate). In addition, the neoplasm shows overexpression of cytoplasmic Bcl-2 due to the presence of the t(14;18) characteristic of follicular lymphoma (i.e., Bcl-2 is expressed at a higher level on the neoplastic population than on the normal background T cells) *(green)*. Overexpression of Bcl-2 by itself is not diagnostic of follicular lymphoma, but its combined expression with CD10 is much more specific, as normal CD10-positive follicular B cells would be expected to be negative. All plots show all lymphoid cells.

Plasma Cell Neoplasms

Plasma cell neoplasms generally are not difficult to identify by flow cytometry (Ruiz-Arguelles, 1994; Ocqueteau, 1998; Paiva et al., 2010; Tembhare et al., 2014), and their immunophenotype at diagnosis (Paiva et al., 2009) and detection following therapy are associated with outcome (Paiva et al., 2008). The expression of bright CD38 and/or CD138 is used to identify the plasma cell population, with common abnormalities being decreased CD45, decreased CD19, decreased or negative CD27, mildly decreased CD38, negative or dim CD81, overexpression of CD200, and/or abnormal coexpression of CD56 and/or CD117 (Flores-Montero et al., 2016) in combination with the identification of cytoplasmic light-chain restriction. Such immunophenotypic abnormalities may be seen in plasma cell neoplasms ranging from monoclonal gammopathy of undetermined significance (MGUS) to smoldering myeloma to multiple myeloma and do not allow confident distinction of these entities, although some studies suggest subtle differences in immunophenotype (Tembhare et al., 2014). Quantitation of the proportion of abnormal plasma cells in clonal plasma cell proliferations appears to have some predictive value. MGUS and smoldering myeloma with a higher proportion of abnormal plasma cells is more likely to progress (Perez-Persona et al., 2010), while persistence of normal background plasma cells has been associated with an improved prognosis in multiple myeloma (Paiva et al., 2009). An example of immunophenotypic abnormalities seen in plasma cell neoplasms is presented in Fig. 35.26. It is important to recognize that flow cytometric analysis typically underestimates the percentage of plasma cells present in a specimen, sometimes dramatically, possibly because of plasma cell aggregation, apoptosis, and peripheral blood dilution. With the development of more sensitive and reproducible flow cytometric methods for abnormal plasma cell detection (Stetler-Stevenson et al., 2016; Arroz et al., 2016; Royston et al., 2016) and the demonstration of prognostic significance of MRD in plasma cell neoplasms (Munshi et al., 2017), the role of flow cytometry for MRD detection in plasma cell neoplasms in clinical practice is growing (Rawstron et al., 2013; Paiva et al., 2015). When considering residual disease monitoring in plasma cell neoplasms, it is important to be aware of potential therapeutic targets that may interfere with residual disease detection. Daratumumab, an anti-CD38 targeting human monoclonal antibody, has shown efficacy in combination with other agents for myeloma (Palumbo et al., 2016; Mateos et al., 2018). The use of this agent in clinical practice is growing and has implications for flow cytometric analysis, as it can lead to loss of detectable surface CD38 expression on all hematopoietic populations, including neoplastic plasma cell populations.

Myelodysplastic Syndromes and Myeloproliferative Disorders

The same principles used to identify other hematopoietic neoplasms can be used to identify the chronic myeloid stem cell neoplasms, for example, the myelodysplastic syndromes and myeloproliferative neoplasms (Elghetany, 1998; Stetler-Stevenson et al., 2001; Wells et al., 2003, Kussick & Wood, 2003a, 2003b; Wood, 2007; Matarraz et al., 2008). Abnormalities in antigen expression can be identified on myeloid blasts, maturing neutrophils, and maturing monocytes. Common abnormalities include (1) alterations in the intensity of expression of antigens, including CD34, CD117, and HLA-DR, and aberrant expression of nonlineage antigens such as CD7 or CD56 on myeloid blasts (Wells et al., 2003; Kussick & Wood, 2003b; Matarraz et al., 2008); (2) abnormal patterns of CD13, CD14, and CD16 expression and decreased side scatter on maturing neutrophils; and (3) aberrant CD56 expression on maturing monocytes (Wells et al., 2003; Kussick & Wood, 2003b). Abnormalities in erythroid maturation have also been described (Della Porta et al., 2006; Westers et al., 2017), although low-grade MDS with abnormalities confined to the erythroid lineage is often difficult to detect. Abnormalities can be demonstrated by flow cytometry when using a comprehensive panel in most chronic myeloid stem cell neoplasms having cytogenetic abnormalities (Kussick et al., 2005). An example of immunophenotypic abnormalities seen in myelodysplasia is presented in Fig. 35.27.

Among myeloproliferative neoplasms, myelofibrosis (primary or secondary) and chronic myeloid leukemia (CML, in particular in cases with disease progression and/or increased blasts) are most likely to show immunophenotypic abnormalities. It should be noted, however, that flow cytometry is not the preferred technique to diagnosis CML and that flow cytometry has a limited role in patients presenting in chronic phase with a granulocytic leukocytosis and no increase in blasts. Uncomplicated essential thrombocythemia and polycythemia vera are unlikely to show abnormalities by flow cytometry, and neither isolated thrombocytosis nor

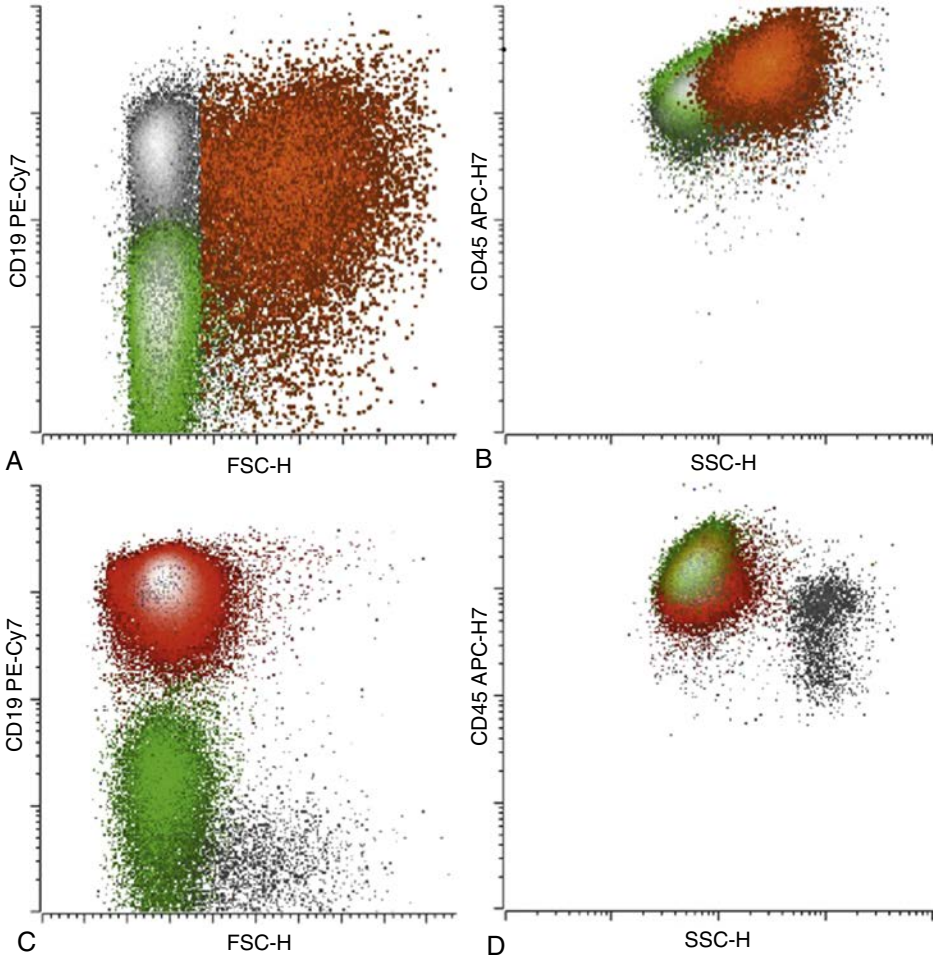

Figure 35.22 Diffuse large B-cell lymphoma. All plots show all viable cells. (A, B) The upper dot plots show an example of diffuse large B-cell lymphoma. The neoplastic cells are colored *orange* and highlighted, while normal T cells are shown in *green* and normal B cells are shown in *gray* (C, D). The lower dot plots show an example of chronic lymphocytic leukemia (CLL) for comparison (neoplastic cells are shown in *red*, while normal background T cells are shown in *green*). The forward and side scatter characteristics of the abnormal cells in the case of diffuse large B-cell lymphoma are increased compared with the background T cells, the background B cells, and the CLL cells. Note that the position of the abnormal large B-cell population (panel B) on a CD45 versus side scatter plot overlaps with the typical CD45 versus side scatter position of monocytes rather than normal lymphocytes. A stringent lymphocyte gating strategy relying on side scatter with either CD45 or forward scatter would exclude the bulk of the abnormal population.

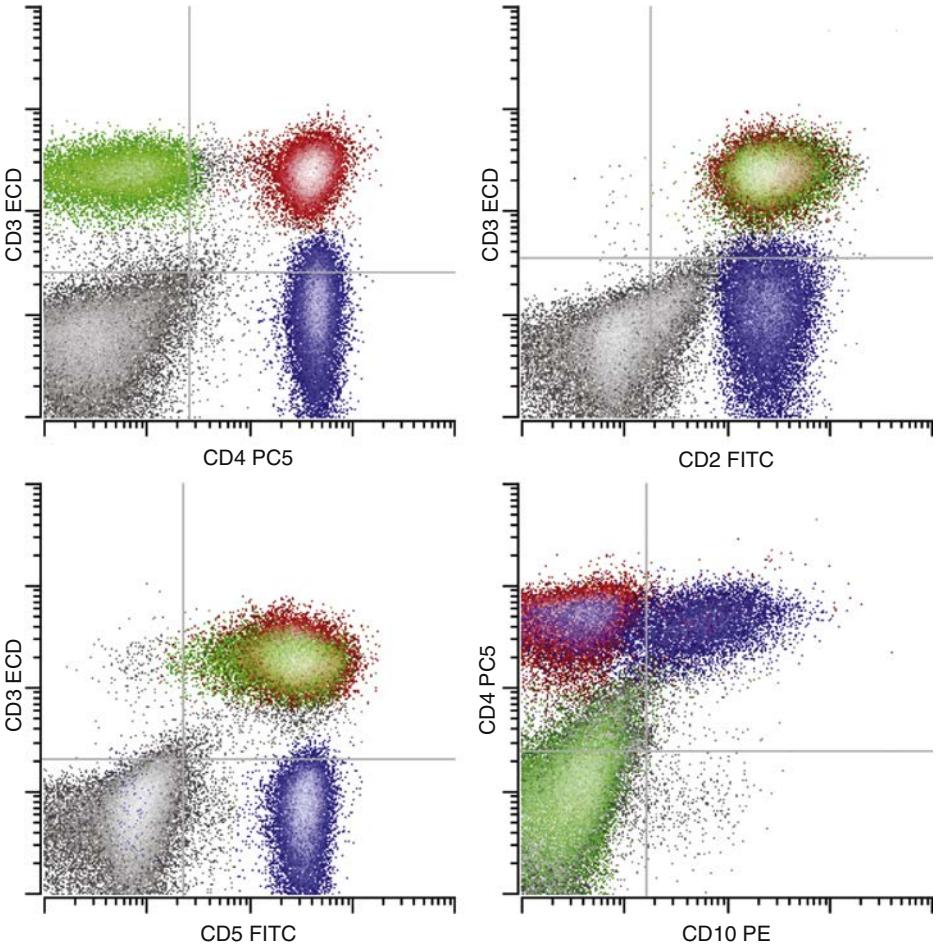

Figure 35.23 Angioimmunoblastic T-cell lymphoma. The neoplastic T-cell population *(blue)* shows expression of the T cell–associated antigens CD2 (intermediate) and CD5 (intermediate), along with the helper T-cell antigen CD4, but without surface CD3. In addition, the neoplastic cells coexpress CD10. The composite immunophenotype is characteristic of that seen in angioimmunoblastic T-cell lymphoma. All plots show all lymphocytes. Normal CD4- and CD8-positive T cells are shown in *red* and *green*, respectively.

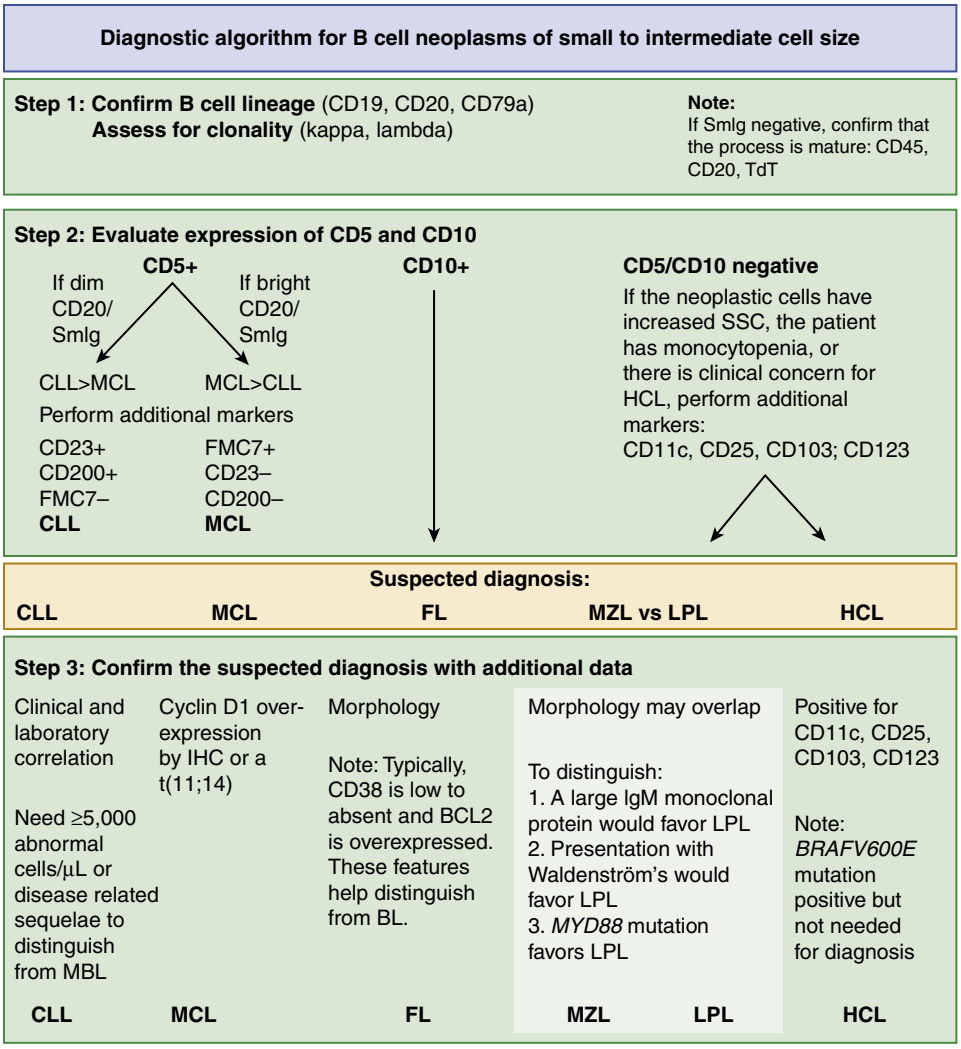

Figure 35.24 This diagnostic algorithm outlines the steps in classification of B-cell lymphomas composed of cells of small to intermediate size. *BL,* Burkitt lymphoma; *CLL,* chronic lymphocytic leukemia; *FL,* follicular lymphoma; *HCL,* hairy cell leukemia; *LPL,* lymphoplasmacytic lymphoma; *MCL,* mantle cell lymphoma; *µMBL,* monoclonal B-cell lymphocytosis; *MZL,* marginal zone lymphoma; *SmIg,* surface immunoglobulin.

erythrocytosis is considered to be an indication for flow cytometry (Davis et al., 2007). Although flow cytometry has been less well studied in the myeloproliferative neoplasms, abnormalities similar to those described in other myeloid neoplasms may be seen on progenitors or maturing myeloid forms and are sometimes present in conjunction with basophilia (Kussick & Wood, 2003a; Ouyang et al., 2015).

Paroxysmal Nocturnal Hemoglobinuria

Certain nonneoplastic hematopoietic disorders can be diagnosed using the same principles used to identify hematopoietic neoplasms. Paroxysmal nocturnal hemoglobinuria (PNH) is an acquired clonal stem cell disorder characterized by the loss of a variety of cell surface proteins on all progeny of a disordered hematopoietic stem cell, including erythrocytes, neutrophils, monocytes, lymphocytes, and platelets. The loss of these proteins is the result of a somatic mutation of a key enzyme required for synthesis of the glycosyl-phosphatidylinositol (GPI) linkage used to attach these proteins to the cell surface. Detection of the loss of GPI-linked proteins is readily accomplished by flow cytometry (Richards et al., 2000, Sutherland et al., 2014), and flow cytometry of the peripheral blood serves as the principal diagnostic method for this disorder. For clinical testing, it is recommended that at least two different cell lineages be evaluated (Borowitz et al., 2010; Fletcher et al., 2014). When considering white blood cells (granulocytes and monocytes), evaluation of at least two GPI-linked reagents, one of which should be the fluorescent derivative of bacterial proaerolysin (FLAER), is recommended (Brodsky et al., 2000; Borowitz et al., 2010). One recent recommendation is to use a four-color combination of FLAER, **CD24**, CD15, and CD45 for high-sensitivity testing of neutrophils; FLAER, **CD14**, CD64, and CD45 for monocytes; and two-color CD235a/**CD59** for red blood cells (Fletcher et al., 2014). In these combinations, FLAER binds the GPI anchor and the antigens listed in bold are GPI-linked, while the remaining reagents are used for population identification. CD157 is another GPI-linked protein that may be used in a single-tube high-sensitivity assay to simultaneously assess for GPI-deficient monocytes and neutrophils (Sutherland et al., 2014). Platelets and lymphocytes are generally not evaluated. An example of PNH is shown in Fig. 35.28.

SUMMARY

Flow cytometry is a powerful, rapid, and cost-effective technique for the identification and monitoring of hematopoietic neoplasms. Successful implementation requires careful attention to instrument and reagent performance, as well as a strong working knowledge of normal patterns of antigenic expression on hematopoietic cells.

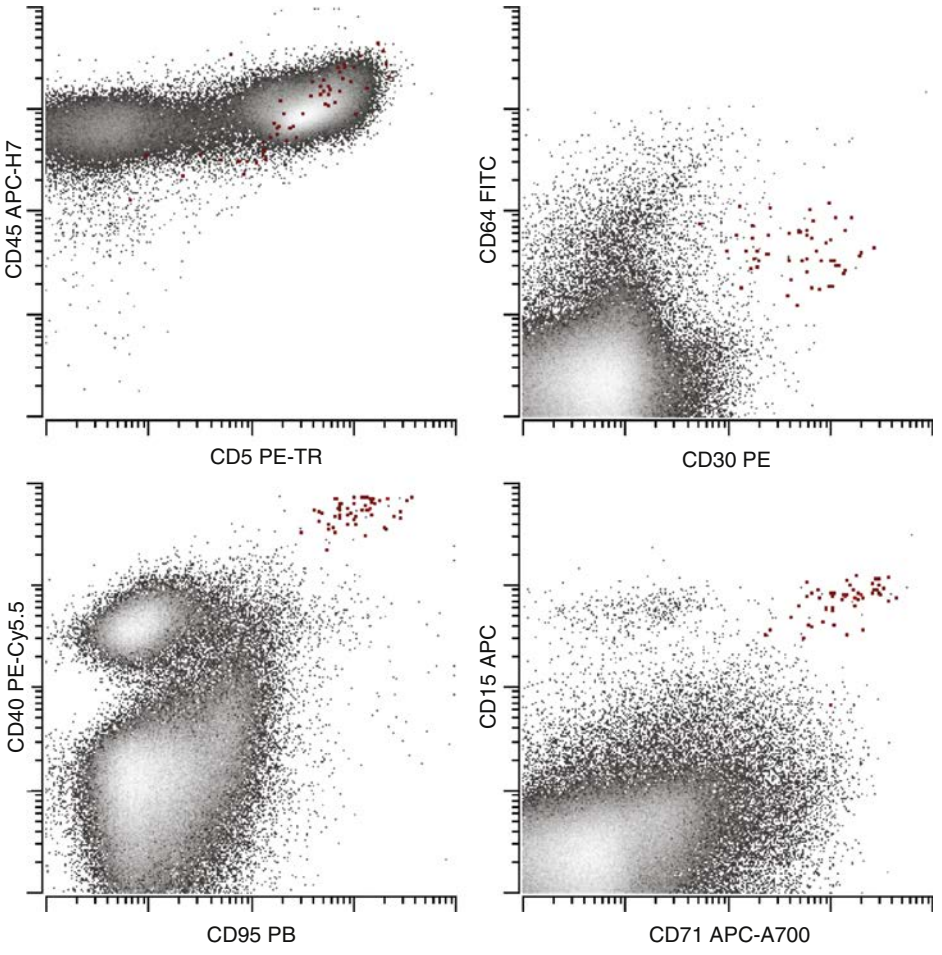

Figure 35.25 Classical Hodgkin lymphoma. A discrete population of cells *(red)* is identified that differs from normal lymphocytes and macrophages, having expression of CD15, CD30, high CD40, high CD71, and high CD95. This immunophenotype is typical for classical Hodgkin lymphoma. Note that these cells commonly show increased autofluorescence that appears as apparent low positivity for FITC-labeled reagents (CD64 in the current example). Also note that Hodgkin cells commonly are rosetted by T cells, giving apparent positivity for CD5 and CD45 *(top left panel)*.

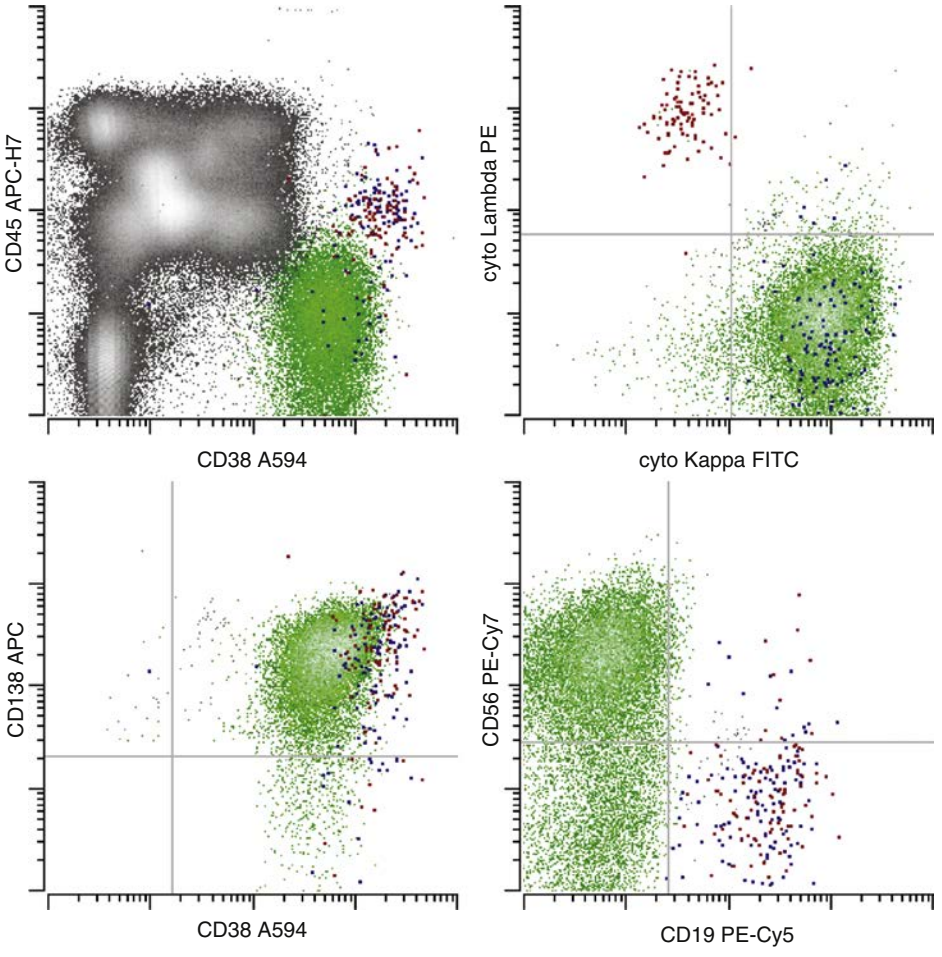

Figure 35.26 Plasma cell neoplasm. The neoplastic plasma cell population *(green)* is identified by the bright expression of CD38 and CD138, but both are slightly decreased in comparison with the few normal polyclonal plasma cells *(emphasized in blue and red)*. Abnormal plasma cells show abnormal expression of CD45 (low to absent) and CD19 (absent), express cytoplasmic κ light chain restriction, and demonstrate aberrant expression of CD56. This immunophenotype is characteristic of that seen in a variety of plasma cell neoplasms, including multiple myeloma, plasmacytoma, and monoclonal gammopathy of uncertain significance (MGUS). Definitive classification requires clinical and laboratory correlation.

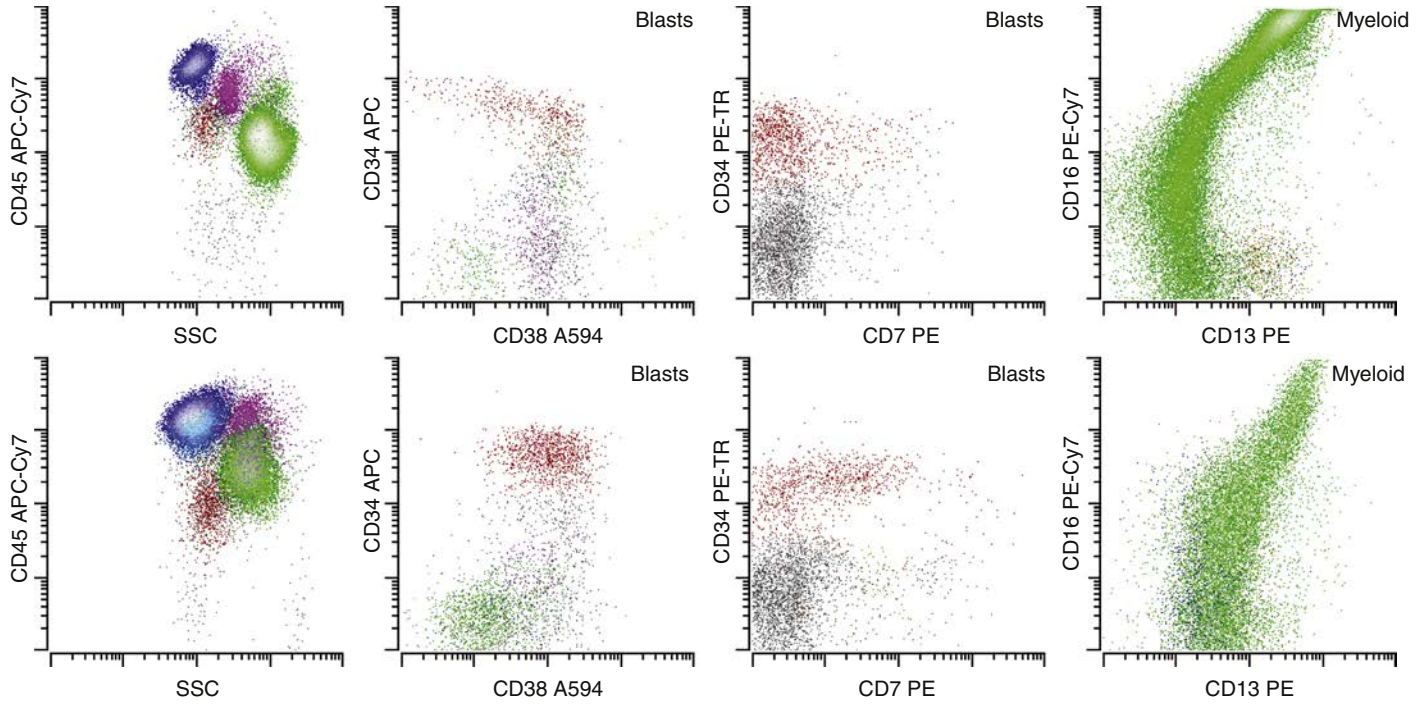

Figure 35.27 Myelodysplasia. A sample from a patient with low-grade myelodysplasia *(lower row)* is compared with normal bone marrow *(upper row)*. Myeloid blasts are shown in *red*, maturing myeloid forms in *green*, monocytes in *purple,* and lymphocytes in *blue*. Abnormalities commonly seen in myelodysplasia include neutrophil hypogranularity as indicated by decreased side scatter *(left),* decreased CD45 expression by the blasts *(left)*, homogeneous expression of markers usually expressed at varying levels on myeloid blasts *(CD38, left center)*, acquisition of lymphoid-associated antigens (CD2, CD5, CD7, and CD56) by myeloid blasts *(right center)*, and abnormal patterns of myelomonocytic maturation, such as abnormal CD13 and CD16 on maturing neutrophilic forms *(right)*. Decreased side scatter is best noted by comparing the relative positions of neutrophils *(green)* and monocytes *(purple)*. It is the combined presence of these abnormalities, rather than a single abnormality, that suggests a myeloid stem cell disorder, such as myelodysplasia.

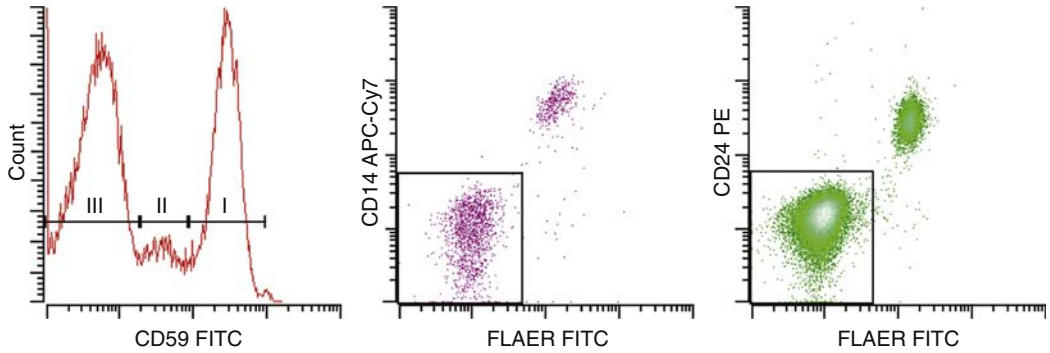

Figure 35.28 Paroxysmal nocturnal hemoglobinuria. Erythrocytes *(left panel)* identified by light scatter properties show differing levels of CD59 expression, corresponding to normal (Type I, 36%), partially deficient (Type II, 9%), and completely deficient (Type III, 54%) forms. A single 6-color tube is used for identification of GPI-deficient monocyte and granulocyte populations: FLAER, CD24, CD14, CD15, CD33, and CD45. Monocytes *(center panel)*—identified by a combination of CD45, CD15 (low), CD33 (high), and side scatter (intermediate)—show a mixture of normal (positive for CD14 and fluorescent aerolysin [FLAER]) and GPI-deficient forms (gated, 81%). Granulocytes *(right panel)*—identified by a combination of CD45, CD15 (high), CD33 (low), and side scatter (high)—show a mixture of normal (positive for CD24 and FLAER) and GPI-deficient forms (gated, 85%). Note the greater percentage of GPI-deficient monocytes and granulocytes compared with GPI-deficient erythrocytes, a common finding in PNH, either because of transfusions or because of the susceptibility of GPI-deficient erythrocytes to complement-mediated lysis.

SELECTED REFERENCES

Cherian S, Wood BL: *Flow cytometry in evaluation of hematopoietic neoplasms: a case-based approach*, Northfield, IL, 2012, CAP Press.

An atlas of clinical neoplastic flow cytometry.

Clinical and Laboratory Standards Institute (CLSI): *Clinical flow cytometric analysis of neoplastic hematolymphoid cells: approved guideline*, 2, Wayne, PA, 2007, Clinical and Laboratory Standards Institute. CLSI Document H43-A2.

A useful reference document related to the clinical performance of flow cytometry for leukemia and lymphoma. An update to a companion document focused on validation of flow cytometry based assays will be available later in 2021 and when published can be referenced as: CLSI. *Validation of assays performed by flow cytometry*, ed 1, Wayne, PA. Clinical Laboratory Standards Institute 2021. CLSI Document H62.

Craig FE, Foon KA: Flow cytometric immunophenotyping for hematopoietic neoplasms, *Blood* 111:3941–3967, 2008.

A comprehensive review of clinical flow cytometry.

Shapiro HM: In *Practical flow cytometry*, 4, New York, 2003, Wiley Liss.

A definitive exposition of technical issues related to flow cytometry.

Swerdlow SH, Campo E, Harris NL, et al.: *World Health Organization classification of tumours of haematopoietic and lymphoid tissues, revised* (vol. 2). Lyon, France, 2017, IARC Press.

A definitive and well-illustrated text expounding the first revision of the most modern and comprehensive classification of human hematopoietic disease achieved through international consensus.

Stewart CC, Mayers GL: Kinetics of antibody binding to cells. In Stewart C, Nicholson JKA, editors: *Immunophenotyping*, 1, New York, 2000, Wiley-Liss, pp 1–22.

The entire volume is an excellent modern general reference on the use of immunophenotyping in a variety of settings.

U.S.-: Canadian consensus recommendations on the immunophenotypic analysis of hematologic neoplasia by cytometry, *Bethesda, MD, November 16-17, 1995, Cytometry* 30:213–274, 1997.

Comprehensive description of consensus guidelines for the practical performance of clinical flow cytometry for the diagnosis of leukemia and lymphoma.

Access the complete reference list online at Elsevier eBooks for Practicing Clinicians.

REFERENCES

Alapat D, Coviello-Malle J, Owens R, et al.: Diagnostic usefulness and prognostic impact of CD200 expression in lymphoid malignancies and plasma cell myeloma, *Am J Clin Pathol* 137:93–100, 2012.

Almasri NM, Iturraspe JA, Braylan RC: CD10 expression in follicular lymphoma and large cell lymphoma is different from that of reactive lymph node follicles, *Arch Pathol Lab Med* 122:539–544, 1998.

Araki D, Wood BL, Othus M, et al.: Allogeneic hematopoietic cell transplantation for acute myeloid leukemia: time to Move toward a minimal residual disease-based definition of complete remission? *J Clin Oncol* 34:329–336, 2016.

Arroz M, Came N, Lin P, et al.: Consensus guidelines on plasma cell myeloma minimal residual disease analysis and reporting, *Cytometry B Clin Cytom* 90:31–39, 2016.

Attygalle A, Al-Jehani R, Diss TC, et al.: Neoplastic T cells in angioimmunoblastic T-cell lymphoma express CD10, *Blood* 99:627–633, 2002.

Baer MR, Stewart CC, Dodge RK, et al.: High frequency of immunophenotype changes in acute myeloid leukemia at relapse: implications for residual disease detection (Cancer and Leukemia Group B Study 8361), *Blood* 97:3574–3580, 2001.

Baer MR, Stewart CC, Lawrence D, et al.: Expression of the neural cell adhesion molecule CD56 is associated with short remission duration and survival in acute myeloid leukemia with, *Blood* 90:1643–1648, 1997. t(8;21)(q22;q22).

Barnett D, Louzao R, Gambell P, et al.: Validation of cell-based fluorescence assays: practice guidelines from the ICSH and ICCS—part IV—postanalytic considerations, *Cytometry B Clin Cytom* 84:309–314, 2013.

Bene MC, Castoldi G, Knapp W, et al.: Proposals for the immunological classification of acute leukemias. European group for the immunological characterization of leukemias (EGIL), *Leukemia* 9:1783–1786, 1995.

Bogen SA, Pelley D, Charif M, et al.: Immunophenotypic identification of Sezary cells in peripheral blood, *Am J Clin Pathol* 106:739–748, 1996.

Borowitz MJ, Craig FE, Digiuseppe JA, et al.: Guidelines for the diagnosis and monitoring of paroxysmal nocturnal hemoglobinuria and related disorders by flow cytometry, *Cytometry B Clin Cytom* 78(4):211–230, 2010.

Borowitz MJ, Devidas M, Hunger SP, et al.: Clinical significance of minimal residual disease in childhood acute lymphoblastic leukemia and its relation to other prognostic factors: a Children's Oncology Group study, *Blood* 111:5477–5485, 2008.

Borowitz MJ, Guenther KL, Shults KE, et al.: Immunophenotyping of acute leukemia by flow cytometric analysis: use of CD45 and right-angle light scatter to gate on leukemic blasts in three-color analysis, *Am J Clin Pathol* 100:534–540, 1993.

Borowitz MJ, Pullen DJ, Winick N, et al.: Comparison of diagnostic and relapse flow cytometry immunophenotypes in childhood acute lymphoblastic leukemia: implications for residual disease detection: a report from the Children's Oncology Group, *Cytometry B Clin Cytom* 68:18–24, 2005.

Bradstock K, Matthews J, Benson E, et al.: Prognostic value of immunophenotyping in acute myeloid leukemia, *Australian Leukaemia Study Group*, *Blood* 84:1220–1225, 1994.

Braylan RC, Benson NA: Flow cytometric analysis of lymphomas, *Arch Pathol Lab Med* 113:627–633, 1989.

Braylan RC, Benson NA, Iturraspe J: Analysis of lymphomas by flow cytometry: current and emerging strategies, *Ann N Y Acad Sci* 677:364–378, 1993.

Brodsky RA, Mukhina GL, Li S, et al.: Improved detection and characterization of paroxysmal nocturnal hemoglobinuria using fluorescent aerolysin, *Am J Clin Pathol* 114:459–466, 2000.

Buccisano F, Maurillo L, Del Principe MI, et al.: Prognostic and therapeutic implications of minimal residual disease detection in acute myeloid leukemia, *Blood* 119(2):332–341, 2012.

Bulian P, Shanafelt TD, Fegan C, et al.: CD49d is the strongest flow cytometry-based predictor of overall survival in chronic lymphocytic leukemia, *J Clin Oncol* 32:897–904, 2014.

Campana D: Determination of minimal residual disease in leukemia patients, *Brit J Haematol* 121:823–838, 2003.

Carter PH, Resto-Ruiz S, Washington GC, et al.: Flow cytometric analysis of whole blood lysis, three anticoagulants, and five cell preparations, *Cytometry* 13:68–74, 1992.

Chang A, Benda PM, Wood BL, et al.: Lineage-specific identification of nonhematopoietic neoplasms by flow cytometry, *Am J Clin Pathol* 119:643–655, 2003.

Charles NJ, Boyer DF: Mixed-phenotype Acute leukemia: diagnostic criteria and Pitfalls, *Arch Pathol Lab Med* 141:1462–1468, 2017.

Chen W, Asplund SL, McKenna RW, et al.: Characterization of incidentally identified minute clonal B-lymphocyte populations in peripheral blood and bone marrow, *Am J Clin Pathol* 122:588–595, 2004.

Chen X, Cherian S: Immunophenotypic characterization of T-cell prolymphocytic leukemia, *Am J Clin Pathol* 140:727–735, 2013.

Chen X, Xie H, Wood BL, et al.: Relation of clinical response and minimal residual disease and their prognostic impact on outcome in acute myeloid leukemia, *J Clin Oncol* 33:1258–1264, 2015.

Cherian S, Miller V, McCullouch V, et al.: A novel flow cytometric assay for detection of residual disease in patients with B-lymphoblastic leukemia/lymphoma post anti-CD19 therapy, *Cytometry B Clin Cytom* 94:112–120, 2018.

Cook JR, Craig FE, Swerdlow SH: bcl-2 expression by multicolor flow cytometric analysis assists in the diagnosis of follicular lymphoma in lymph node and bone marrow, *Am J Clin Pathol* 119:145–151, 2003.

Coustan-Smith E, Sancho J, Hancock ML, et al.: Clinical importance of minimal residual disease in childhood acute lymphoblastic leukemia, *Blood* 96:2691–2696, 2000.

Davis BH, Dasgupta A, Kussick S, et al.: Validation of cell-based fluorescence assays: practice guidelines from the ICSH and ICCS—part II—preanalytical issues, *Cytometry B Clin Cytom* 84:286–290, 2013.

Davis BH, Holden JT, Bene MC, et al.: Bethesda international consensus recommendations on the immunophenotypic analysis of hematolymphoid neoplasia by flow cytometry: medical indications, *Cytometry* 72B:S5–S13, 2006. 2007.

Della Porta MG, Malcovati L, Invernizzi R, et al.: Flow cytometry evaluation of erythroid dysplasia in patients with myelodysplastic syndrome, *Leukemia* 20:549–555, 2006.

Di Bona E, Sartori R, Zambello R, et al.: Prognostic significance of CD56 antigen expression in acute myeloid leukemia, *Haematologica* 87:250–256, 2002.

Douglas VK, Gordon LI, Goolsby CL, et al.: Lymphoid aggregates in bone marrow mimic residual lymphoma after rituximab therapy for non-Hodgkin lymphoma, *Am J Clin Pathol* 112:844–853, 1999.

Duggan PR, Easton D, Luider J, et al.: Bone marrow staging of patients with non-Hodgkin lymphoma by flow cytometry: correlation with morphology, *Cancer* 88:894–899, 2000.

Dworzak MN, Froschl G, Printz D, et al.: Prognostic significance and modalities of flow cytometric minimal residual disease detection in childhood acute lymphoblastic leukemia, *Blood* 99:1952–1958, 2002.

Elghetany MT: Surface marker abnormalities in myelodysplastic syndromes, *Haematologica* 83:1104–1115, 1998.

Farahat N, Lens D, Zomas A, et al.: Quantitative flow cytometry can distinguish between normal and leukaemic B-cell precursors, *Br J Haematol* 91:640–646, 1995.

Feller N, van der Pol MA, van Stijn A, et al.: MRD parameters using immunophenotypic detection methods are highly reliable in predicting survival in acute myeloid leukaemia, *Leukemia* 18:1380–1390, 2004.

Fletcher M, Sutherland R, Whitby L, et al.: Standardizing leucocyte PNH clone detection: an international study, *Cytometry B Clin Cytom* 86B:311–318, 2014.

Flores-Montero J, de Tute R, Paiva B, et al.: Immunophenotype of normal vs. myeloma plasma cells: toward antibody panel specifications for MRD detection in multiple myeloma, *Cytometry B Clin Cytom* 90:61–72, 2016.

Fromm JR, Thomas A, Wood BL: Flow cytometry can diagnose classical Hodgkin lymphoma with high sensitivity and specificity, *Am J Clin Pathol* 131:322–332, 2009.

Fukushima PI, Nguyen PK, O'Grady P, et al.: Flow cytometric analysis of kappa and lambda light chain expression in evaluation of specimens for B-cell neoplasia, *Cytometry* 26:243–252, 1996.

Galpa G, Basso G, Aliprandi S, et al.: Prednisone induces immunophenotypic modulation of CD10 and CD34 in nonapoptotic B-cell acute lymphoblastic leukemia cells, *Cytometry B Clin Cytom* 74:150–155, 2008.

Geary WA, Frierson HF, Innes DJ, et al.: Quantitative criteria for clonality in the diagnosis of B-cell non-Hodgkin's lymphoma by flow cytometry, *Mod Pathol* 6:155–161, 1993.

Ginaldi L, Farahat N, Matutes E, et al.: Differential expression of T cell antigens in normal peripheral blood lymphocytes: a quantitative analysis by flow cytometry, *J Clin Pathol* 49:539–544, 1996a.

Ginaldi L, Matutes E, Farahat N, et al.: Differential expression of CD3 and CD7 in T-cell malignancies: a quantitative study by flow cytometry, *Br J Haematol* 93:921–927, 1996b.

Harrington AM, Olteanu H, Kroft SH: A dissection of the CD45/side scatter "blast gate, *Am J Clin Pathol* 137:800–804, 2012.

Hanson CA, Abaza M, Sheldon S, et al.: Biphenotypic leukaemia: immunophenotypic and cytogenetic analysis, *Br J Haematol* 84:49–60, 1993.

Harada H, Kawano MM, Huang N, et al.: Phenotypic difference of normal plasma cells from mature myeloma cells, *Blood* 81:2658–2663, 1993.

Hoffkes HG, Schmidtke G, Uppenkamp M, et al.: Multiparametric immunophenotyping of B cells in peripheral blood of healthy adults by flow cytometry, *Clin Diagn Lab Immunol* 3:30–36, 1996.

Hrusak O, Porwit-MacDonald A: Antigen expression patterns reflecting genotype of acute leukemias, *Leukemia* 16:1233–1258, 2002.

Hudnall S, Betancourt E, Barnhart E, Patel J: Comparative flow immunophenotypic features of the inflammatory infiltrates of Hodgkin lymphoma and lymphoid hyperplasia, *Cytometry B Clin Cytom* 74(1):108, 2008.

Inghirami G, Zhu BY, Chess L, et al.: Flow cytometric and immunohistochemical characterization of the gamma/delta T-lymphocyte population in normal human lymphoid tissue and peripheral blood, *Am J Pathol* 136:357–367, 1990.

Juco J, Holden JT, Mann KP, et al.: Immunophenotypic analysis of anaplastic large cell lymphoma by flow cytometry, *Am J Clin Pathol* 19:205–212, 2003.

Kelemen K, Guitart J, Kuzel TM, et al.: The usefulness of CD26 in flow cytometric analysis of peripheral blood in Sezary syndrome, *Am J Clin Pathol* 129:146–156, 2008.

Khalidi HS, Chang KL, Medeiros LJ, et al.: Acute lymphoblastic leukemia: survey of immunophenotype, French-American-British classification, frequency of myeloid antigen expression, and karyotypic abnormalities in 210 pediatric and adult cases, *Am J Clin Pathol* 111:467–476, 1999.

Khalidi HS, Medeiros LJ, Chang KL, et al.: The immunophenotype of adult acute myeloid leukemia: high frequency of lymphoid antigen expression and comparison of immunophenotype, French-American-British classification, and karyotypic abnormalities, *Am J Clin Pathol* 109:211–220, 1998.

Kussick SJ, Kalnoski M, Braziel RM, et al.: Prominent clonal B-cell populations identified by flow cytometry in histologically reactive lymphoid proliferations, *Am J Clin Pathol* 121:464–472, 2004.

Kussick SJ, Wood BL: Four-color flow cytometry identifies virtually all cytogenetically abnormal bone marrow samples in the workup of non-CML myeloproliferative disorders, *Am J Clin Pathol* 120:854–865, 2003a.

Kussick SJ, Wood BL: 4 color flow cytometry to identify abnormal myeloid populations, *Arch Pathol Lab Med* 127:1140–1147, 2003b.

Kussick SJ, Fromm JR, Rossini A, et al.: Four-color flow cytometry shows strong concordance with bone marrow morphology and cytogenetics in the evaluation for myelodysplasia, *Am J Clin Pathol* 124:170–181, 2005.

Kwok M, Rawstron AC, Varghese A, Evans PA, O'Connor SJ, Doughty C, Newton DJ, Moreton P, Hillmen P: Minimal residual disease is an independent predictor for 10-year survival in CLL, *Blood* 128:2770–2773, 2016.

Li S, Eshleman JR, Borowitz MJ: Lack of surface immunoglobulin light chain expression by flow cytometric immunophenotyping can help diagnose peripheral B-cell lymphoma, *Am J Clin Pathol* 118:229–234, 2002.

Lima M, Almeida J, dos Anjos Teixeira M, et al.: Utility of flow cytometry immunophenotyping and DNA ploidy studies for diagnosis and characterization of blood involvement in CD4+ Sezary's syndrome, *Haematologica* 88:874–887, 2003.

Lima M, Almeida J, Santos AH, et al.: Immunophenotypic analysis of the TCR-Vbeta repertoire in 98 persistent expansions of CD3(+)/TCR-alphabeta(+) large granular

lymphocytes: utility in assessing clonality and insights into the pathogenesis of the disease, *Am J Pathol* 159:1861–1868, 2001.
Loken MR, Alonzo TA, Pardo L, et al.: Residual disease detected by multidimensional flow cytometry signifies high relapse risk in patients with de novo acute myeloid leukemia: a report from Children's Oncology Group, *Blood* 120:1581–1588, 2012.
Loken MR, Shah VO, Dattilio KL, et al.: Flow cytometric analysis of human bone marrow. II. Normal B lymphocyte development, *Blood* 70:1316–1324, 1987.
Loken MR, Shah VO, Hollander Z, et al.: Flow cytometric analysis of normal B lymphoid development, *Pathol Immunopathol Res* 7:357–370, 1988.
Lucio P, Parreira A, van den Beemd MW, et al.: Flow cytometric analysis of normal B cell differentiation: a frame of reference for the detection of minimal residual disease in precursor-B-ALL, *Leukemia* 13:419–427, 1999.
Macedo A, Orfao A, Gonzalez M, et al.: Immunological detection of blast cell subpopulations in acute myeloblastic leukemia at diagnosis: implications for minimal residual disease studies, *Leukemia* 9:993–998, 1995a.
Macedo A, Orfao A, Vidriales MB, et al.: Characterization of aberrant phenotypes in acute myeloblastic leukemia, *Ann Hematol* 70:189–194, 1995b.
Mantei K, Wood BL: Flow cytometric evaluation of CD38 expression assists in distinguishing follicular hyperplasia from follicular lymphoma, *Cytometry* 76B:315–320, 2009.
Matarraz S, Lopez A, Barrena S, et al.: The immunophenotype of different immature, myeloid, and B cell lineage-committed CD34+ hematopoietic cells allows discrimination between normal/reactive and myelodysplastic syndrome precursors, *Leukemia* 22:1175–1183, 2008.
Mateos MV, Dimopoulos MA, Cavo M, et al.: Daratumumab plus Bortezomib, Melphalan, and Prednisone for Untreated myeloma, *N Engl J Med* 378:518–528, 2018.
Matutes E, Morilla R, Farahat N, et al.: Definition of acute biphenotypic leukemia, *Haematologica* 82:64–66, 1997.
Matutes E, Morilla R, Owusu-Ankomah K, et al.: The immunophenotype of hairy cell leukemia (HCL): proposal for a scoring system to distinguish HCL from B-cell disorders with hairy or villous lymphocytes, *Leuk Lymphoma* 14(Suppl 1):57–61, 1994a.
Matutes E, Owusu-Ankomah K, Morilla R, et al.: Immunological profile of B-cell disorders and proposal of a scoring system for the diagnosis of CLL, *Leukemia* 8:1640–1645, 1994b.
Maurillo L, Buccisano F, Del Principe MI, et al.: Toward optimization of postremission therapy for residual disease-positive patient with acute myeloid leukemia, *J Clin Oncol* 26:4944–4951, 2008.
Maury S, Huguet F, Leguay T, et al.: Group for Research on Adult Acute Lymphoblastic Leukemia: adverse prognostic significance of CD20 expression in adults with Philadelphia chromosome-negative B-cell precursor acute lymphoblastic leukemia, *Haematologica* 95:324–328, 2010.
McClanahan J, Fukushima PI, Stetler-Stevenson M: Increased peripheral blood gamma delta T-cells in patients with lymphoid neoplasia: a diagnostic dilemma in flow cytometry, *Cytometry* 38:280–285, 1999.
McKenna RW, Washington LT, Aquino DB, et al.: Immunophenotypic analysis of hematogones (B-lymphocyte precursors) in 662 consecutive bone marrow specimens by 4-color flow cytometry, *Blood* 98:2498–2507, 2001.
Montesinos P, Rayon C, Vellenga E, et al.: Pethema, Groups H: clinical significance of CD56 expression in patients with acute promyelocytic leukemia treated with all-trans retinoic acid and anthracycline-based regimens, *Blood* 117:1799–1805, 2011.
Moreton P, Kennedy B, Lucas G, et al.: Eradication of minimal residual disease in B-cell chronic lymphocytic leukemia after alemtuzumab therapy is associated with prolonged survival, *J Clin Oncol* 23:1–9, 2005.
Morice WG, Kimlinger T, Katzmann JA, et al.: Flow cytometric assessment of TCR-Vbeta expression in the evaluation of peripheral blood involvement by T-cell lymphoproliferative disorders: a comparison with conventional T-cell immunophenotyping and molecular genetic techniques, *Am J Clin Pathol* 121:373–383, 2004.
Morice WG, Kurtin PJ, Leibson PJ, et al.: Demonstration of aberrant T-cell and natural killer-cell antigen expression in all cases of granular lymphocytic leukaemia, *Br J Haematol* 120:1026–1036, 2003.
Munshi NC, Avet-Loiseau H, Rawstron AC, et al.: Association of minimal residual disease with Superior survival outcomes in patients with multiple myeloma: a Meta-analysis, *JAMA Oncol* 3:28–35, 2017.
Murphy M, Fullen D, Carlson JA: Low CD7 expression in benign and malignant cutaneous lymphocytic infiltrates: experience with an antibody reactive with paraffin-embedded tissue, *Am J Dermatopathol* 24:6–16, 2002.
Muzzafar T, Wei EX, Lin P, et al.: Flow cytometric immunophenotyping of anaplastic large cell lymphoma, *Arch Pathol Lab Med* 133:49–56, 2009.
Nardi V, Kuo FC, Hasserjian RP: Premalignant clonal hematopoietic proliferations: 2017 Society for Hematopathology/European association for Haematopathology Workshop report, *Am J Clin Pathol* 152:347–358, 2019.
Novikov ND, Griffin GK, Dudley G, et al.: Utility of a simple and robust flow cytometry assay for rapid clonality testing in mature peripheral T-cell lymphomas, *Am J Clin Pathol* 151:494–503, 2019.
Ocqueteau M, Orfao A, Almeida J, et al.: Immunophenotypic characterization of plasma cells from monoclonal gammopathy of undetermined significance patients: implications for the differential diagnosis between MGUS and multiple myeloma, *Am J Pathol* 152:1655–1665, 1998.
Oishi N, Montes-Moreno S, Feldman AL: In situ neoplasia in lymph node pathology, *Semin Diagn Pathol* 35:76–83, 2018.
Ouyang J, Zheng W, Shen Q, et al.: Flow cytometry immunophenotypic analysis of Philadelphia-negative myeloproliferative neoplasms: correlation with histopathologic features, *Cytometry B Clin Cytom* 88:236–243, 2015.
Orfao A, Chillon MC, Bortoluci AM, et al.: The flow cytometric pattern of CD34, CD15, and CD13 expression in acute myeloblastic leukemia is highly characteristic of the presence of PML-RAR alpha gene rearrangements, *Haematologica* 84:405–412, 1999.
Orfao A, Ortuno F, de Santiago M, et al.: Immunophenotyping of acute leukemias and myelodysplastic syndromes, *Cytometry* 58A:62–71, 2004.
Paiva B, Vidriales MB, Cervero J, et al.: Multiparameter flow cytometric remission is the most relevant prognostic factor for multiple myeloma patients undergoing autologous stem cell transplantation, *Blood* 112:4017–4023, 2008.
Paiva B, Vidriales MB, Mateo G, et al.: The persistence of immunophenotypically normal residual bone marrow plasma cells at diagnosis identifies a good prognostic subgroup of symptomatic multiple myeloma patients, *Blood* 114:4369–4372, 2009.
Paiva B, Almeida J, Perez-Andres M, et al.: Utility of flow cytometry immunophenotyping in multiple myeloma and other clonal plasma cell–related disorders, *Cytometry B Clin Cytom* 78:239–252, 2010.
Paiva B, Chandia M, Puig N, et al.: The prognostic value of multiparameter flow cytometry minimal residual disease assessment in relapse multiple myeloma, *Haematologica* 100:e53–e55, 2015.
Palacio C, Acebedo G, Navarrete M, et al.: Flow cytometry in the bone marrow evaluation of follicular and diffuse large B-cell lymphomas, *Haematologica* 86:934–940, 2001.
Palumbo GA, Parrinello N, Fargione G, et al.: CD200 expression may help in differential diagnosis between mantle cell lymphoma and B-cell chronic lymphocytic leukemia, *Leuk Res* 33:1212–1216, 2009.
Palumbo A, Chanan-Khan A, Weisel K, et al.: Daratumumab, Bortezomib, and Dexamethasone for multiple myeloma, *N Engl J Med* 375:754–766, 2016.
Perez-Persona E, Mateo G, Garcia-Sanz R, et al.: Risk of progression in smouldering myeloma and monoclonal gammopathies of unknown significance: comparative analysis of the evolution of the monoclonal component and multiparameter flow cytometry of bone marrow plasma cells, *Br J Haematol* 148:110–114, 2010.
Picker LJ, Weiss LM, Medeiros LJ, et al.: Immunophenotypic criteria for the diagnosis of non-Hodgkin's lymphoma, *Am J Pathol* 128:181–201, 1987.
Pollard JA, Loken M, Gerbing RB, et al.: CD33 expression and its association with gemtuzumab ozogamicin response: results from the Randomized phase III Children's Oncology group trial AAML0531, *J Clin Oncol* 34:747–755, 2016.
Porwit-MacDonald A, Janossy G, Ivory K, et al.: Leukemia-associated changes identified by quantitative flow cytometry. IV. CD34 overexpression in acute myelogenous leukemia M2 with t(8;21), *Blood* 87:1162–1169, 1996.
Porwit A, Bene MC: Acute leukemias of ambiguous origin, *Am J Clin Pathol* 144:361–376, 2015.
Rahemtullah A, Reichard K, Preffer F, et al.: A double-positive CD4+CD8+ T-cell population is commonly found in nodular lymphocyte predominant Hodgkin lymphoma, *Am J Clin Pathol* 126:805–814, 2006.
Rawstron AC, Kennedy B, Evans PA, et al.: Quantitation of minimal disease levels in chronic lymphocytic leukemia using a sensitive flow cytometric assay improves the prediction of outcome and can be used to optimize therapy, *Blood* 98:29–35, 2001.
Rawstron AC, Green MJ, Kuzmicki A, et al.: Monoclonal B lymphocytes with the characteristics of "indolent" chronic lymphocytic leukemia are present in 3.5% of adults with normal blood counts, *Blood* 100:635–639, 2002.
Rawstron AC, Bennett FL, O'Connor SJ, et al.: Monoclonal B-cell lymphocytosis and chronic lymphocytic leukemia, *N Engl J Med* 359:575–583, 2008.
Rawstron AC, Child JA, de Tute RM, et al.: Minimal residual disease assessed by multiparameter flow cytometry in multiple myeloma: impact on outcome in the Medical Research Council Myeloma IX Study, *J Clin Pathol* 31:2540–2547, 2013.
Rawstron AC, Bottcher S, Letestu R, et al.: European Research Initiative in CLL: Improving efficiency and sensitivity: European Research Initiative in CLL (ERIC) update on the international harmonised approach for flow cytometric residual disease monitoring in CLL, *Leukemia* 27:142–149, 2013.
Rawstron AC, Gregory WM, de Tute RM, et al.: Minimal residual disease in myeloma by flow cytometry: independent prediction of survival benefit per log reduction, *Blood* 125:1932–1935, 2015.
Ray S, Craig FE, Swerdlow SH: Abnormal patterns of antigenic expression in follicular lymphoma: a flow cytometric study, *Am J Clin Pathol* 124:576–583, 2005.
Reading CL, Estey EH, Huh YO, et al.: Expression of unusual immunophenotype combinations in acute myelogenous leukemia, *Blood* 81:3083–3090, 1993.
Richards SJ, Rawstron AC, Hillmen P: Application of flow cytometry to the diagnosis of paroxysmal nocturnal hemoglobinuria, *Cytometry* 42:223–233, 2000.
Richards SJ, Short M, Scott CS: Clonal CD3+CD8+ large granular lymphocyte (LGL)/NK-associated (NKa) expansions: primary malignancies or secondary reactive phenomena? *Leuk Lymphoma* 17:303–311, 1995.
Robbins BA, Ellison DJ, Spinosa JC, et al.: Diagnostic application of two-color flow cytometry in 161 cases of hairy cell leukemia, *Blood* 82:1277–1287, 1994.
Roederer M: Spectral compensation for flow cytometry: visualization artifacts, limitations, and caveats, *Cytometry* 45:194–205, 2001.
Roshal M, Fromm JR, Winter S, et al.: Immaturity associated antigens are lost during induction for T cell lymphoblastic leukemia: implications for minimal residual disease detection, *Cytometry B Clin Cytom* 78:139–146, 2010.
Royston DJ, Gao Q, Nguyen N, et al.: Single-tube 10-fluorochrome analysis for efficient flow cytometric evaluation of minimal residual disease in plasma cell myeloma, *Am J Clin Pathol* 146:41–49, 2016.
Ruella M, Maus MV: Catch me if you can: leukemia Escape after CD19-directed T cell Immunotherapies, *Comput Struct Biotechnol J* 14:357–362, 2016.
Ruiz-Arguelles GJ, San Miguel JF: Cell surface markers in multiple myeloma, *Mayo Clin Proc* 69:684–690, 1994.
Sanchez ML, Almeida J, Vidriales MB, et al.: Incidence of phenotypic aberrations in a series of 467 patients with B chronic lymphoproliferative disorders: basis for the design of specific four-color stainings to be used for minimal residual disease investigation, *Leukemia* 16:1460–1469, 2002.
San Miguel JF, Vidriales MB, Lopez-Berges C, et al.: Early immunophenotypical evaluation of minimal residual disease in acute myeloid leukemia identifies different patient risk groups and may contribute to postinduction treatment stratification, *Blood* 98:1746–1751, 2001.
Schabath R, Ratei R, Ludwig WD: The prognostic significance of antigen expression in leukaemia, *Best Pract Res Clin Haematol* 16:613–628, 2003.
Serke S, Schwaner I, Yordanova M, et al.: Monoclonal antibody FMC7 detects a conformational epitope on the CD20 molecule: evidence from phenotyping after rituxan therapy and transfectant cell analyses, *Cytometry* 46:98–104, 2001.

Serke S, van Lessen A, Hummel M, et al.: Circulating CD4+ T lymphocytes with intracellular but no surface CD3 antigen in five of seven patients consecutively diagnosed with angioimmunoblastic T-cell lymphoma, *Cytometry* 42:180–187, 2000.

Shanafelt T, Hanson CA: Monoclonal B-cell lymphocytosis: definitions and natural history, *Leuk Lymphoma* 50:493–497, 2009.

Shanafelt TD, Kay NE, Jenkins G, et al.: B-cell count and survival: differentiating chronic lymphocytic leukemia from monoclonal B-cell lymphocytosis based on clinical outcome, *Blood* 113:4188–4196, 2009.

Shao H, Yuan CM, Xi L, et al.: Minimal residual disease detection by flow cytometry in adult T-cell leukemia/lymphoma, *Am J Clin Pathol* 133:592–601, 2010.

Stacchini A, Demurtas A, Godio L, et al.: Flow cytometry in the bone marrow staging of mature B-cell neoplasms, *Cytometry B Clin Cytom* 54:10–18, 2003.

Stelzer GT, Shults KE, Loken MR: CD45 gating for routine flow cytometric analysis of human bone marrow specimens, *Ann N Y Acad Sci* 677:265–280, 1993.

Stetler-Stevenson M, Arthur DC, Jabbour N, et al.: Diagnostic utility of flow cytometric immunophenotyping in myelodysplastic syndrome, *Blood* 98:979–987, 2001.

Stetler-Stevenson M, Paiva B, Stoolman L, et al.: Consensus guidelines for myeloma minimal residual disease sample staining and data acquisition, *Cytometry B Clin Cytom* 90:26–30, 2016.

Strati P, Shanafelt TD: Monoclonal B-cell lymphocytosis and early-stage chronic lymphocytic leukemia: diagnosis, natural history, and risk stratification, *Blood* 126:454–462, 2015.

Sutherland DR, Action E, Keeney M, et al.: Use of CD157 in FLAER-based assays for high sensitivity PNH granulocyte and PNH monocyte detection, *Cytometry B Clin Cytom* 86:44–55, 2014.

Tanqri S, Vall H, Kaplan D, et al.: Validation of cell-based fluorescence assays: practice guidelines from the ICSH and ICCS—part III—analytical issues, *Cytometry B Clin Cytom* 84:291–308, 2013.

Tembhare PR, Yuan CY, Venzon D, et al.: Flow cytometric differentiation of abnormal and normal plasma cells in the bone marrow in patients with multiple myeloma and its precursor diseases, *Leuk Res* 38:371–376, 2014.

Terstappen LW, Hollander Z, Meiners H, et al.: Quantitative comparison of myeloid antigens on five lineages of mature peripheral blood cells, *J Leukoc Biol* 48:138–148, 1990a.

Terstappen LW, Huang S, Picker LJ: Flow cytometric assessment of human T-cell differentiation in thymus and bone marrow, *Blood* 79:666–677, 1992a.

Terstappen LW, Johnsen S, Segers-Nolten IM, et al.: Identification and characterization of plasma cells in normal human bone marrow by high-resolution flow cytometry, *Blood* 76:1739–1747, 1990b.

Terstappen LW, Loken MR: Myeloid cell differentiation in normal bone marrow and acute myeloid leukemia assessed by multi-dimensional flow cytometry, *Anal Cell Pathol* 2:229–240, 1990.

Terstappen LW, Safford M, Konemann S, et al.: Flow cytometric characterization of acute myeloid leukemia. Part II. Phenotypic heterogeneity at diagnosis, *Leukemia* 6:70–80, 1992b.

Turtle CJ, Hanafi LA, Berger C, et al.: Immunotherapy of non-Hodgkin's lymphoma with a defined ratio of CD8+ and CD4+ CD19-specific chimeric antigen receptor-modified T cells, *Sci Transl Med* 8:355ra116, 2016.

Turtle CJ, Hay KA, Hanafi LA, et al.: Durable molecular Remissions in chronic lymphocytic leukemia treated with CD19-specific chimeric antigen receptor-modified T cells after Failure of Ibrutinib, *J Clin Oncol* 35:3010–3020, 2017.

Thomas DA, O'Brien S, Jorgensen JL, al at: Prognostic significance of CD20 expression in adults with de novo precursor B-lineage acute lymphoblastic leukemia, *Blood* 113:6330–6337, 2009.

Tworek JA, Singleton TP, Schnitzer B, et al.: Flow cytometric and immunohistochemical analysis of small lymphocytic lymphoma, mantle cell lymphoma, and plasmacytoid small lymphocytic lymphoma, *Am J Clin Pathol* 110:582–589, 1998.

Venkataraman G, Aguhar C, Kreitman RJ, et al.: Characteristic CD103 and CD123 expression pattern defines hairy cell leukemia: usefulness of CD123 and CD103 in the diagnosis of mature B-cell lymphoproliferative disorders, *Am J Clin Pathol* 136:625–630, 2011.

Voskova D, Schoch C, Schnittger S, et al.: Stability of leukemia-associated aberrant immunophenotypes in patients with acute myeloid leukemia between diagnosis and relapse: comparison with cytomorphologic, cytogenetic, and molecular genetic findings, *Cytometry B Clin Cytom* 62:25–38, 2004.

Walter RB, Gooley TA, van der Velden VH, et al.: CD33 expression and P-glycoprotein-mediated drug efflux inversely correlate and predict clinical outcome in patients with acute myeloid leukemia treated with gemtuzumab ozogamicin monotherapy, *Blood* 109:4168–4170, 2007.

Webber BA, Cushing MM, Li S: Prognostic significance of flow cytometric immunophenotyping in acute myeloid leukemia, *Int J Clin Exper Pathol* 1:124–133, 2008.

Weir EG, Borowitz MJ: Flow cytometry in the diagnosis of acute leukemia, *Semin Hematol* 38:124–138, 2001.

Weir EG, Cowan K, LeBeau P, et al.: A limited antibody panel can distinguish B-precursor acute lymphoblastic leukemia from normal B precursors with four color flow cytometry: implications for residual disease detection, *Leukemia* 13:558–567, 1999.

Wells DA, Benesch M, Loken MR, et al.: Myeloid and monocytic dyspoiesis as determined flow cytometric scoring in myelodysplastic syndrome correlates with the IPSS and with outcome after hematopoietic stem cell transplantation, *Blood* 102:394–403, 2003.

Westers TM, Cremers EM, Oelschlaegel U, Group IMW, et al.: Immunophenotypic analysis of erythroid dysplasia in myelodysplastic syndromes. A report from the IMDSFlow working group, *Haematologica* 102:308–319, 2017.

Wood BL: Multicolor immunophenotyping: human immune system hematopoiesis, *Methods Cell Biol* 75:559–576, 2004.

Wood BL: 9 and 10 color flow cytometry in the clinical laboratory, *Arch Pathol Lab Med* 130:680–690, 2006.

Wood BL: Myeloid neoplasms: myelodysplasia, myeloproliferative disorders, and acute myeloid leukemia, *Clin Lab Med* 27:551–575, 2007.

Wood BL, Arroz M, Barnett D, et al.: Bethesda international consensus recommendations on the immunophenotypic analysis of hematolymphoid neoplasia by flow cytometry: optimal reagents and reporting for the flow cytometric diagnosis of hematopoietic neoplasia, *Cytometry* 72B:S14–S22, 2006. 2007.

Wood B, Jevremovic D, Bene MC, et al.: Validation of cell-based fluorescence assays: practice guidelines from the ICSH and ICCS—part V—assay performance criteria, *Cytometry B Clin Cytom* 84:315–323, 2013.

Wood BL: Principles of minimal residual disease detection for hematopoietic neoplasms by flow cytometry, *Cytometry B Clin Cytom* 90:47–53, 2016.

Wu D, Thomas A, Fromm JR: Reactive T cells by flow cytometry distinguish Hodgkin lymphomas from T cell/histiocyte-rich large B cell lymphoma, *Cytometry B Clin Cytom* 90:424–432, 2016.

Yang W, Agrawal N, Patel J, et al.: Diminished expression of CD19 in B-cell lymphomas, *Cytometry B Clin Cytom* 63:28–35, 2005.

Xochelli A, Kalpadakis C, Gardiner A, et al.: Clonal B-cell lymphocytosis exhibiting immunophenotypic features consistent with a marginal-zone origin: is this a distinct entity? *Blood* 123:1199–1206, 2014.

CHAPTER 36

IMMUNOHEMATOLOGY

Laura Lee Cooling, Theresa Downs

BASIC IMMUNOHEMATOLOGIC CONCEPTS, 708
Blood Group Antigens, 709
Blood Group Alloantibodies and Autoantibodies, 710
The Complement System and Blood Banking, 710

ERYTHROCYTE ANTIGENS AND ANTIBODIES, 711
ABO and H Blood Group Systems (ISBT No. 001 and 018), 711
MNS Blood Group System (ISBT NO. 002), 714
P1PK, GLOB, and FORS Blood Group Systems (ISBT Nos. 003, 028, and 031, Respectively), 716
RH and RHAG Blood Group Systems (ISBT No. 004 and 030), 718
Lutheran Blood Group System (ISBT NO. 005), 723
Kell and KX Blood Group Systems (ISBT NO. 006 AND 019), 725
Lewis Blood Group System (ISBT NO. 007), 727
Duffy Blood Group System (ISBT NO. 008), 728
Kidd Blood Group System (ISBT NO. 009), 730
Diego Blood Group System (ISBT NO. 010), 731
YT Blood Group System (ISBT NO. 011), 732
XG Blood Group System (ISBT NO. 012), 733
Scianna Blood Group System (ISBT NO. 013), 733
Dombrock Blood Group System (ISBT NO. 014), 734
Colton Blood Group System (ISBT NO. 015), 735
LW Blood Group System (ISBT NO. 016), 735
Chido/Rodgers Blood Group System (ISBT NO. 017), 736
Gerbich Blood Group System (ISBT NO. 020), 736
Cromer Blood Group System (ISBT NO. 021), 737
Knops Blood Group System (ISBT 022), 738
Indian Blood Group System (ISBT NO. 023), 739
OK Blood Group System (ISBT NO. 024), 740
RAPH Blood Group System (ISBT NO. 025), 740
JMH Blood Group System (ISBT NO. 026), 740
I Blood Group System (ISBT NO. 027), 741
GIL Blood Group System (ISBT NO. 029), 742
JR Blood Group System (ISBT NO. 032), 742
LAN Blood Group System (ISBT NO. 033), 742
VEL Blood Group System (ISBT NO. 034), 743
CD59 Blood Group System (ISBT NO. 035), 743
Augustine Blood Group System (ISBT 036), 743
KANNO Blood Group System (ISBT 037), 744
SID Blood Group System (ISBT 038), 744
SD^A Antibodies, 744
Possible New Blood Group: Choline Transporter-Like Protein 2 (CTL2/SLC44A2), 744

IMMUNOHEMATOLOGY TESTS AND PROCEDURES, 744
Basic Principles—Hemagglutination, 744
The Antihuman Globulin Test, 746
Compatibility Testing, 748
Antibody Detection, 751
Special Antibody Identification Techniques, 756
Investigation of Autoimmune Hemolytic Anemia, 760

POSITIVE DIRECT ANTIGLOBULIN TESTS AND HEMOLYTIC ANEMIA INDUCED BY MEDICATION, 763
Stimulation of Red Cell Autoantibody Production, 763

GRANULOCYTE SEROLOGY, 763
Human Neutrophil antigens, 763
Granulocyte Antibody Testing, 766
Monoclonal Antibody-Immobilized Granulocyte Antigen (Maiga) Assay, 766

PLATELET SEROLOGY, 767
Human Platelet Alloantigens, 767

SELECTED REFERENCES, 770

KEY POINTS

- Blood group antigens play a variety of physiologic roles as membrane structures involved in maintaining erythrocyte cytoskeleton integrity, as well as in membrane transport, cell signaling, and immune complement regulation, and as receptors/modulators of disease.
- The ABO histo-blood group antigens are widely expressed throughout the body and are the single most important blood group for selection and transfusion of blood products, as well as a major consideration in solid-organ and bone marrow transplantation.
- The recipient immune response to exposure to foreign red cell antigens through transfusion or pregnancy may include antibody production and complement activation, resulting in hemolysis (e.g., transfusion reaction, hemolytic disease of the fetus and newborn).
- Pretransfusion and perinatal blood testing is performed to prevent transfusion reactions and hemolytic disease of the fetus and newborn. This must include the key serologic evaluations of ABO and Rh antigen typing, antibody detection/identification, and crossmatching.
- Antihuman globulin reagents, as used in direct or indirect testing, are integral to virtually all red cell antibody detection and identification techniques.
- Patients with complex serologic problems, such as antibodies to high-frequency antigens and autoantibodies, may require utilization of a variety of special immunohematologic studies (enzymes, adsorption, elution) to identify compatible blood for transfusion.

BASIC IMMUNOHEMATOLOGIC CONCEPTS

The term *immunohematology* refers to the serologic, genetic, biochemical, and molecular study of antigens associated with membrane structures on the cellular constituents of blood as well as the immunologic properties and reactions of blood components and constituents. Fundamental discoveries in the area of immunohematology have played an integral role in the development of transfusion medicine, which includes the transfusion of blood, its components, and its derivatives (see Chapter 37). In this integrated relationship, immunohematologists perform and interpret a wide variety of serologic and molecular assays to aid in the diagnosis, prevention, and management of immunization associated with transfusion, pregnancy, and organ transplantation. Over the years, research in the field of immunohematology has contributed significantly to the fundamental understanding of human genetics and immunology, with broad applications to membrane physiology and function, epidemiology, anthropology, and forensic science.

BLOOD GROUP ANTIGENS

The term *blood group* refers not only to genetically encoded erythrocyte antigens but also to the immunologic diversity expressed by other blood constituents, including leukocytes, platelets, and plasma. Most blood group genes, with few exceptions, are located on the autosomal chromosomes and are inherited following Mendelian rules of inheritance. A majority of blood group alleles demonstrate codominance as well, meaning that genetic heterozygotes at a particular locus will express both gene products.

Many membrane-associated structures on blood cells may be defined as antigens because they have the capability of reacting with a complementary antibody or cell receptor. A majority of these antigens are also immunogens in that they are able to elicit an antibody-mediated immunologic response in a responsive host. Each antigen may have a variety of different epitopes or specific antigenic determinants. Epitopes are discrete, immunologically active regions of the antigen whose molecular configuration can interact with specific lymphocyte membrane receptors or secreted complementary antibody. Clinically, about a dozen antigen systems are significant and are commonly encountered on the transfusion service. In general, these antigens demonstrate polymorphic epitopes with varied distribution in the population, often along racial or ethnic lines. Patients who lack certain antigens may form antibodies when exposed to them; these antibodies may be detected on routine testing in the blood bank.

Immunogenicity

The ability of an antigen to elicit an immune response is known as its *immunogenicity*. The immunogenicity of an antigen is determined not only by certain innate characteristics of the antigen itself but also by the host's genetically determined immune responsiveness. Characteristics of antigens that determine their immunogenicity include degree of foreignness; molecular size and configuration, which may change with temperature, pH, and ionic environment; and antigenic complexity, as measured by the number of available epitopes or antigenic determinants.

Blood group antigens vary greatly in their ability to elicit an immune response. The A, B, and RhD antigens are certainly the most immunogenic. Thus, all blood transfused must be matched for these antigens between the blood donor and the recipient. Approximately 50% to 75% of D-negative individuals would produce anti-D if transfused with only one unit of D-positive blood. After the D antigen, K is the next most immunogenic, followed by Fy^a and common Rh antigens, based on the frequency with which their corresponding antibodies are encountered. Using the same criteria, other common blood group antigens—such as Fy^b, Jk^a, Jk^b, and s—are much less immunogenic. The relative immunogenicities of some clinically important red cell antigens are listed in Table 36.1.

TABLE 36.1
Relative Immunogenicity of Selected Clinically Important Blood Group Antigens*

Antigen	Relative Potency	Antigen	Relative Potency
D	0.70	K	0.10
C	0.041	E	0.0338
k	0.030	e	0.0112
Fy^a	0.0046	C	0.0022
Jk^a	0.0014	S	0.0008
Jk^b	0.0006	s	0.0006

*These figures represent the approximate percentage of persons negative for a specific antigen who, if transfused with one unit of corresponding antigen-positive blood, would develop antibodies to that specific antigen. When the relative potency (frequency) of K antigen is 0.1, as estimated by Kornstad and Heisto (Kornstad L, Heisto H: The frequency of formation of Kell antibodies in recipients of Kell-positive blood. In: Proceedings of the 6th Congress of the European Society of Haematology, Copenhagen, Denmark, August 1958, pp 754–758), the relative potency of other blood groups can be estimated as shown by Klein and Anstee (Klein HG, Anstee DJ: *Mollison's blood transfusion in clinical medicine*, ed 11, Oxford, 2006, Blackwell Scientific Publications).

Chemical Characteristics

The chemical composition, complexity, and molecular size of an antigen determine most of its physical and biological properties, including immunogenicity. As a general rule, pure polysaccharides are not immunogenic except in certain species, such as humans and mice (Virella & Bierer, 2001). Pure lipid and nucleic acids are not immunogenic but can be antigenic because they can serve as haptens. Haptens are well-defined chemical groupings that are too small to be immunogenic by themselves but can induce an antibody response when attached to a carrier protein.

Although pure protein may be immunogenic, the most potent immunogens are usually complex macromolecular glycoproteins and lipoproteins. Thus, it is not surprising that red blood cell (RBC) antigens are glycoproteins, lipoproteins, and glycolipids. Experiments with peptide chain polymers have shown that aromatic amino acids, such as tyrosine and phenylalanine, can contribute significantly to overall immunogenicity (Virella & Bierer, 2001). In glycoproteins, immunogenicity may also be influenced by the extent of branching in the polysaccharide side chains. Whereas the immunogenicity of an antigen relates to the total complex molecular structure, the areas where antigen combines with specific antibody (i.e., the epitopes) are usually limited to one or a few simple structures (terminal sugars, amino acids) exposed on the exterior, mobile surface of the molecule. These are often referred to as *immunodominant structures* because they determine the specificity and optimal binding energy of antigen–antibody interactions.

Antigen Density

The number of antigenic sites on a foreign substance, whether a complex molecule or a cell, will contribute to the strength of an immunologic response. Studies of blood group antigens have demonstrated that antigen density contributes to the efficiency of antibody binding and the extent of complement activation, thus determining the likelihood of RBC hemolysis.

Various techniques have been used over the years to determine the number of copies of specific blood group antigens on the RBC membrane. Historically, radioimmunoassay, enzyme-linked immunosorbent assay (ELISA), electron microscopy using ferritin-labeled anti-immunoglobulin, and flow cytometry have been used to indirectly calculate the number of antigen sites on RBC membranes. Table 36.2 lists the estimated densities of common RBC antigens.

TABLE 36.2
Number of Membrane Sites for Selected Native Erythrocyte Antigens Estimated by Radioimmunoassay*

Antigen	Phenotype	Number of Antigenic Sites	Antigen	Phenotype	Number of Antigenic Sites
A	A_1 adult	$810–1170 \times 10^3$	D	DCce	$9.9–14.6 \times 10^3$
	Newborn	$250–370 \times 10^3$		Dce	$12–20 \times 10^3$
	A_2 adult	$240–290 \times 10^3$		DcEe	$14–16.6 \times 10^3$
	Newborn	140×10^3		DCe	$14.5–19.3 \times 10^3$
	A_1B adult	$460–850 \times 10^3$		DcE	$15.5–33.3 \times 10^3$
	Newborn	220×10^3		DCcEe	$23–21 \times 10^3$
	A_2B adult	140×10^3		D– –	$110–202 \times 10^3$
B	B adult	750×10^3		Weak D (D^u)	$0.8–3 \times 10^3$
	A_1B adult	430×10^3	c	c+C–	$70–85 \times 10^3$
I	I+	500×10^3		c+C+	$37–53 \times 10^3$
K	K+k–	6.1×10^3	e	e+E–	$18.2–24.4 \times 10^3$
	K+k+	3.5×10^3		e+E+	$13.4–14.5 \times 10^3$
			E	e–E+	$0.45-25.6 \times 10^3$

*Figures taken from Klein HG, Anstee DJ: *Mollison's Blood Transfusion in Clinical Medicine*, ed 11, Oxford, 2006, Blackwell Scientific Publications.

BLOOD GROUP ALLOANTIBODIES AND AUTOANTIBODIES

A majority of clinically significant blood group antibodies are immunoglobulin G (IgG) or IgM, although occasionally an IgA antibody is encountered. Blood group antibodies are usually classified as (1) an *alloantibody*, which reacts with a foreign antigen not present on the patient's own erythrocytes, or (2) an *autoantibody*, which reacts with an antigen on the patient's own cells. RBC autoantibodies are discussed later in this chapter.

Some alloantibodies to erythrocyte antigens are called *naturally occurring*—that is, the antigenic stimulus is unknown. Naturally occurring antibodies may appear regularly in the serum of persons who lack the corresponding antigen, such as in the ABO blood group system. Other naturally occurring antibodies are produced only in a small subset of individuals.

Most blood group alloantibodies are produced as the result of immunization to foreign erythrocyte antigens by exposure through transfusion of blood components or through pregnancy. Alloantibodies to RBCs frequently require the selection of specific antigen-negative components for transfusion. Identification of alloantibodies and selection of compatible blood components remain the most important functions of a transfusion medicine service.

THE COMPLEMENT SYSTEM AND BLOOD BANKING

Complement plays a key role in the pathophysiology of hemolysis through its involvement in the sensitization and destruction of transfused RBCs by alloantibody or the destruction of autologous RBCs by autoantibody. Complement is also important in immunohematologic testing.

Role of Complement in Erythrocyte Destruction

Antibody binding to RBC antigens is the most common reason for complement activation on the RBC membrane in vivo. Complement may also be activated on RBCs via a carrier–hapten antibody complex such as penicillin-coated RBCs and antipenicillin antibodies. Complement components may also be attached to the membrane via a nonspecific mechanism induced by certain drugs or when erythrocytes are innocent bystanders in another immune reaction.

RBC–antibody complexes usually activate complement by the classical pathway. However, the mode of destruction and the extent of RBC hemolysis depend primarily on the class of Ig involved and the activity of an individual's reticuloendothelial (RE) system.

Intravascular Hemolysis

Intravascular RBC hemolysis is usually caused by antibodies directed against the ABO antigens. Rarely, other IgM blood group antibodies, as well as some complement-fixing IgG antibodies (e.g., anti-Kidd antibodies), can induce intravascular hemolysis. Intravascular lysis occurs when large amounts of complement are rapidly activated, resulting in complete activation of the complement cascade with assembly of the terminal membrane attack complex (C5b6789). This complex polymerizes to form pores in the RBC membrane so that extracellular fluid enters the cell, causing it to swell and burst by osmotic lysis.

Extravascular Hemolysis

IgG antibodies cause the majority of extravascular hemolysis via the RE system, which removes complement-coated RBCs. When IgG antibodies bind RBCs and activate complement, complement regulatory proteins generally stop the activation process at the C3/C4 level. RBC-bound C3b is degraded to iC3b, which is enzymatically inactive, by factor I and factor H. iC3b is further degraded to C3c and C3dg by factor I and CR1, a cofactor and C3b/C4b receptor (Freedman & Semple, 1994) (Fig. 36.1). Decay accelerating factor (DAF) participates by inhibiting C3 convertase (C4b2b) formation and by promoting C3 convertase degradation. On RBCs, CR1 and DAF carry the Knops and Cromer blood group antigens, respectively.

Initially, C3b/iC3b-coated RBCs are rapidly sequestered in the liver by monocytes and macrophages, which have receptors for C3b (Table 36.3). Although phagocytic cells also have receptors for C4b, the role, if any, of C4b in immune hemolysis of erythrocytes is not defined (Freedman & Semple, 1994). A portion of the RBCs sequestered in the liver are immobilized and destroyed by phagocytosis with a half-life of about 2 minutes (Klein & Anstee, 2006). However, within 15 to 20 minutes, destruction slows and many of the cells escape extravascular destruction through the action of the complement regulatory protein, factor I, as previously described. C3dg, the iC3b fragment produced by factor I cleavage, remains attached to RBCs but has no enzymatic or opsonic properties. As a result, sequestered C3dg-coated RBCs are released back into the circulation and survive normally (see Fig. 36.1). In the circulation, C3dg is cleaved, leaving C3d attached to the RBC membrane.

In the absence of complement activation, IgG-coated RBCs are removed by phagocytic cells via Fcγ receptors. Although phagocytosis is not complement dependent, Mollison (1989) demonstrated that RBCs

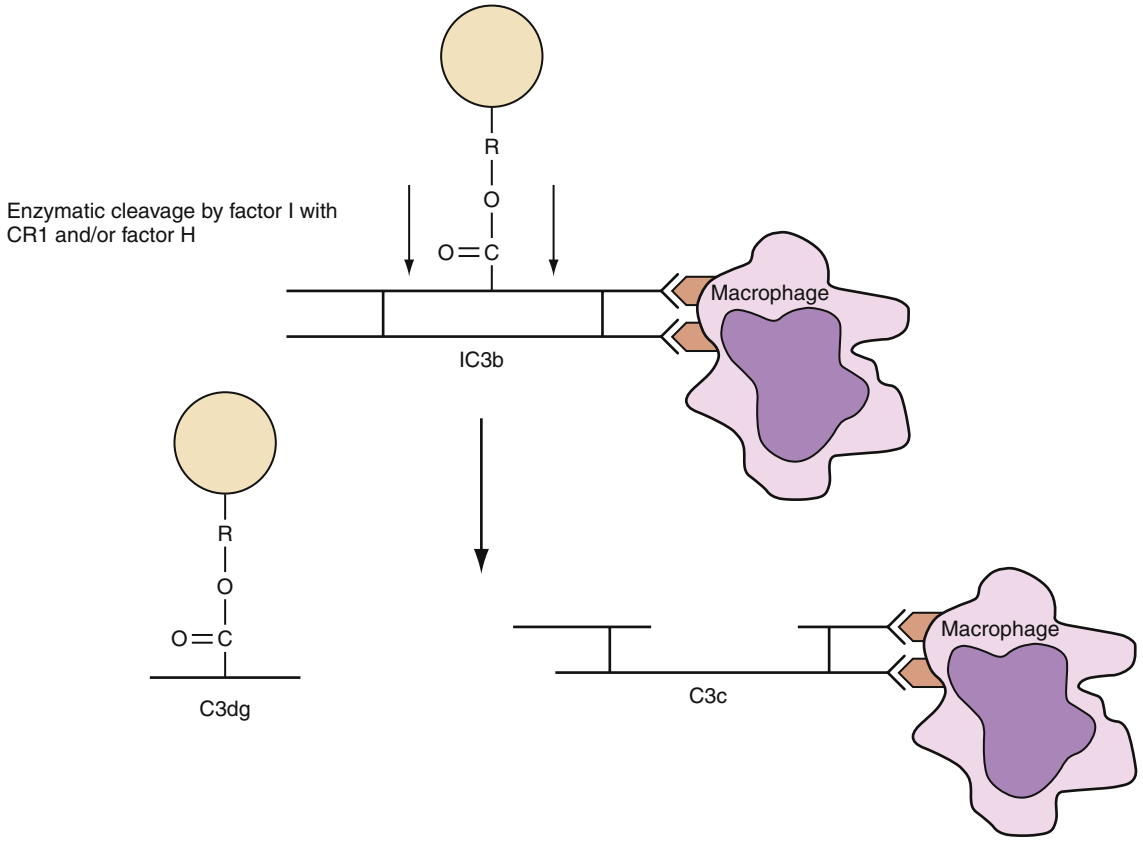

Figure 36.1 Action of factor I in the release of C3b-coated erythrocytes from reticuloendothelial system sequestration.

TABLE 36.3

Complement Receptors on Human Cells

Receptor	Ligand	Distribution
CR1 (CD35)	C3b, C4b	Erythrocytes, neutrophils, monocytes, macrophages, B lymphocytes, follicular dendritic cells
CR2 (CD21)	C3d, C3dg, iC3b	B cells
CR3 (CD11b/CD18)*	iC3b	Monocytes, macrophages, neutrophils, natural killer cells
CR4 (CD11c/CD18)*	iC3b	

*Members of the integrin receptor family.

coated with both IgG and complement tend to show accelerated removal by the liver, whereas RBCs coated only with IgG tend to be destroyed more slowly in the spleen, displaying a linear pattern of removal with a minimum half-life of 20 minutes. Theoretically, RBCs coated only with IgG antibody could also be the targets of antibody-dependent cellular cytotoxicity mechanisms (Klein & Anstee, 2006) because natural killer (NK) cells possess Fcγ receptors.

ERYTHROCYTE ANTIGENS AND ANTIBODIES

ABO AND H BLOOD GROUP SYSTEMS (ISBT NO. 001 AND 018)

More than 700 erythrocyte antigens have been reported in the literature and have been organized into 35 blood group systems by the International Society of Blood Transfusion (ISBT) (Table 36.4). Many described erythrocyte antigens are high-frequency or public antigens expressed by most donors (>90%–99%), whereas others are extremely rare (private antigens). In the following section, we review the more common RBC antigens and antibodies encountered on the transfusion service. Table 36.5 summarizes several commonly encountered RBC alloantibodies according to their Ig class, serologic phase of detection, clinical significance, and statistics on finding compatible blood.

Originally discovered in 1900, the ABO blood group system is the single most important blood group for the selection and transfusion of blood. As histo-blood group antigens, ABO epitopes are found on many tissues and body fluids, including RBCs, platelets, and endothelial cells (Issitt & Anstee, 1998). Because they are so widely expressed, ABO antigens are a major consideration in solid organ and bone marrow transplantation (Rowley et al., 2011).

The ABO blood group system consists of two antigens—A and B—and four phenotypes—groups A, B, AB, and O. A and B are autosomal-codominant antigens (ISBT No. 001) and are expressed on group A, B, and AB red cells, respectively. In contrast, the group O phenotype is an autosomal-recessive phenotype, reflecting the absence of a functional ABO gene. Group O individuals express the H antigen (ISBT No. 018), the biosynthetic precursor of both A and B antigens (Fig. 36.2). Group O is the most frequent ABO phenotype in most populations tested, particularly among Native Americans. Expression of ABO antigens on RBCs is usually accompanied by the presence of naturally occurring antibodies against the missing antithetical antigen(s). Table 36.6 shows the serologic reactions and frequencies of the four major ABO phenotypes.

Null and Weak Phenotypes

The ABO system also contains several phenotypes associated with weakened, anomalous, or complete absence of ABO antigen expression. The most common ABO subtypes encountered in the blood bank are A_1 and A_2. A_1 red cells are distinguished from A_2 (and other weak A subtypes) by agglutination with the lectin *Dolichos biflorus*. Comparison of A_1, A_2, and other weak A subtypes indicates both quantitative and qualitative differences in A antigen expression (Issitt & Anstee, 1998; Swensson et al., 2005). A_2 is the most commonly encountered weak subtype in whites, accounting for nearly 20% of all group A donors. The ABO system contains additional weak A and weak B phenotypes, including several that can cause ABO discrepancies during routine testing (Fung, 2017).

Anomalous ABO expression can be inherited (*cis*-AB, B[A]) or acquired (acquired B). In the *cis*-AB phenotype, A and B antigens are synthesized by the same enzyme and are inherited as a single autosomal-dominant allele. Likewise, the B(A) phenotype, an autosomal-dominant phenotype characterized by trace A antigen expression on group B RBCs, is due to synthesis of A antigen by the *B*-gene enzyme. The acquired B phenotype, on the other hand, is an acquired enzymatic modification of group A_1 red cells in vivo. The acquired B phenotype usually occurs in the setting of bacterial infection or cancer and reflects enzymatic deacetylation of group A antigen to form a B-like antigen on RBCs. The *cis*-AB, B(A), and acquired B phenotypes are usually detected because of discrepancies in ABO typing (Issitt & Anstee, 1998; Fung, 2017).

Bombay and para-Bombay are two rare null phenotypes characterized by an absence of all ABH antigens on RBCs. In the classic Bombay phenotype (O_h), neither AB nor H antigens are present on RBCs or in secretions. Para-Bombay also shows few or no ABH antigens on RBCs, sometimes accompanied by normal expression of ABH antigens in secretions and body fluids.

Biochemistry

The ABO antigens are carbohydrate antigens and, therefore, represent a post-translation modification of glycoproteins and glycolipids. On RBC glycoproteins and polylactosaminylceramides, ABO antigens are usually expressed on type 2 chain oligosaccharides, characterized by repeating lactosaminyl ($Gal\beta1–4GlcNAc\beta1–3)_n$ motifs (see Fig. 36.2). On glycosphingolipids, ABO antigens can be expressed on multiple (types 1, 2, 3, and 4 chain) oligosaccharide precursors. ABH antigens expressed on RBC glycoproteins and most glycosphingolipids (type 2, 3, and 4 chain) are of RBC origin. In contrast, type 1 chain ABO antigens are synthesized by gastrointestinal mucosa, secreted into plasma, and passively adsorbed onto red cell membranes. Synthesis of type 1 chain ABO antigens is linked to the Lewis blood group system.

The first step in the synthesis of ABH antigens is the synthesis of the H or group O antigen, the immediate biosynthetic precursor of both A and B antigens. The H antigen is formed by the addition of fucose (Fuc), in an α1–2 linkage, to a terminal galactose. This reaction is catalyzed by two different enzymes, depending on whether the fucose is being added to a type 1 or type 2 chain oligosaccharide acceptor. Fucosyltransferase type 1 (*FUT1*), the product of the H or *FUT1* gene, catalyzes the formation of type 2 chain H antigen. In contrast, fucosyltransferase type 2 (*FUT2*), the product of the *Secretor* gene, catalyzes the transfer of fucose to type 1 chain precursors to form type 1 chain H or Le^d antigen (Lowe, 1994). Inactivating mutations in *FUT1* are responsible for the Bombay and para-Bombay phenotypes (Kelly et al., 1994). Bombay and para-Bombay nonsecretors also have inactivating mutations in *FUT2* (Reid & Lomas-Francis, 2012).

Once H antigen is formed, it can serve as a substrate for *A* gene and *B* gene glycosyltransferases. The A antigen is formed by *A* gene (*ABO*A*) glycosyltransferase, which adds an *N*-acetylgalactosamine (GalNAc), in an α1–3 linkage, to the subterminal galactose of H antigen. Likewise, the B antigen is formed by the addition of an α1–3 galactose (Gal) to the same galactose by the *B* gene (*ABO*B*) glycosyltransferase. Biochemically, the A and B antigens are very similar, differing only by the presence of an *N*-acetyl group. It is fascinating that such a minor chemical modification should have such profound immunologic consequences. Removal of the *N*-acetyl group on A antigen by circulating deacetylase enzymes is responsible for the acquired B phenotype (Issitt & Anstee, 1998).

Molecular Biology

FUT1 (*H* gene) and *FUT2* (*Se* gene) are located together on chromosome 19q13.3 and reflect a gene duplication (Lowe, 1994). FUT1 is a 365 amino acid, type II transmembrane glycoprotein, composed of a large, 240 amino acid, carboxy-terminal catalytic domain, which is anchored within the Golgi lumen by a short transmembrane and a cytosolic domain. *FUT1* messenger ribonucleic acid (mRNA) is widely expressed in most tissues, with the exception of salivary and parotid glands (Yamamoto et al., 2003). The last is the basis for testing saliva to determine ABH secretor status. The ISBT currently lists more than 40 mutant *FUT1* alleles, including 19 null alleles and 23 weak alleles (Reid & Lomas-Francis, 2012).

The *ABO* gene locus is located on chromosome 9q34 and encodes the A and B glycosyltransferases (Yamamoto, 1995). The gene is large, spanning 19.5 kb, and contains seven exons, although exons 6 and 7 encode the majority of the active enzyme (66%). The product of the *ABO* gene is a 41-kD, 354 amino acid type II transmembrane glycoprotein. Comparison of A and B enzymes shows nearly 98% identity, differing by four key amino acids at residues 176, 235, 266, and 268 (Table 36.7). Amino acids 235, 266, and 268 are critical in determining A versus B enzyme activity: The polymorphism at 176 is not biologically active. Because both A and B recognize the type 2 chain acceptor, any differences in amino acids 235, 266, and 268 dictate whether the enzyme will recognize UDP-GalNAc or UDP-Gal nucleotide sugar donor. Crystallography data indicate that the amino acids associated with *ABO*A* gene product are smaller and able to accommodate the larger UDP-GalNAc donor. To date, more than 200 ABO alleles have been identified.

TABLE 36.4

Terminology for Blood Group System Genes and Gene Products

TRADITIONAL NOMENCLATURE		ISBT NOMENCLATURE		ISGN NOMENCLATURE		
Name	**Symbol**	**Symbol**	**Number**	**Gene**	**Chromosome**	**Gene Product Name**
ABO	ABO	ABO	001	*ABO*	9q34.1	α1,3 *N*-acetyl-galactosaminyltransferase (A antigen)
						α1,3-galactosyltransferase (B antigen)
MNS	MNS	MNS	002	*GYPA*	4q28.2	Glycophorin A (CD235 A)
				GYPB		Glycophorin B (CD235B)
				GYPE		Glycophorin E (CD235E)
P1	P1	P1PK	003	*A4GALT1*	22q13	α1,4-galactosyltransferase
Rh	Rh	RHD	004	*RHD*	1p36.1	RhD protein (CD240)
		RHCE		*RHCE*		RhCE protein
Lutheran	Lu	LU	005	*LU*	19q13.3	Lutheran glycoprotein, B-CAM
Kell	K	KEL	006	*KEL*	7q34	Kell glycoprotein
Lewis	Le	LE	007	*FUT3*	19p13.3	α-3/4-fucosyltransferase
Duffy	Fy	FY	008	*DARC*	1q23	Duffy-associated receptor cytokine glycoprotein
Kidd	Jk	JK	009	*SLC14A1*	18q12	Urea transporter (HUT11)
Diego	Di	DI	010	*SLC4A1*	17q21.3	Anion exchanger 1 (AE1, Band 3)
Yt	Yt	YT	011	*ACHE*	7q22	Acetylcholinesterase
Xg	Xg	XG	012	*XG*	Xp22.3	Xg glycoprotein (CD99)
Scianna	Sc	SC	013	*ERMAP*	1p34	Human erythroid membrane–associated protein
Dombrock	Do	DO	014	*ART4*	12p13.2	ADP-ribosyltransferase (CD297)
Colton	Co	CO	015	*AQPI*	7p14	Aquaporin-1 (CHIP)
Landsteiner-Wiener	LW	LW	016	*LW*	19p13.3	ICAM (CD242)
Chido/Rodgers	Ch/Rg	CH/RG	017	*C4A, C4B*	6p21.3	C4A, C4B complement glycoproteins
Hh	Hh	H	018	*FUT1*	19q13.3	α1,2-fucosyltransferase
Kx	Kx	XK	019	*XK*	Xp21.1	Kx glycoprotein
Gerbich	Ge	GE	020	*GYPC*	2q14	Glycophorin C and glycophorin D (CD236)
Cromer	Cromer	CROM	021	*DAF*	1q32	Decay-accelerating factor (CD55)
Knops	Kn	KN	022	*CR1*	1q32	Complement receptor 1 (CD35)
Indian	In	IN	023	*CD44*	11p13	CD44
Ok	Ok	OK	024	*CD147*	19p13.3	CD147Basigin
Raph	Raph	RAPH	025	*CD151*	11p15.5	Tetraspanin (CD151)
John Milton Hagen	JMH	JMH	026	*SEMA7A*	15q24.3	Semaphorin (CD108)
I	I	I	027	*GCNT2*	6p24.2	β1,6 *N*-acetylglucosaminyltransferase
Globoside	P(Gb4)	GLOB	028	*B3GALNT1*	3q26	β1,3 *N*-acetylgalactosaminyltransferase
GIL	Gill	GIL	029	*AQP3*	9p13	Aquaglyceroporin
RHAG	RHAg	RHAG	030	*RhAG*	6p21-qter	Rh-associated glycoprotein (CD241)
Forssman	Fors	FORS	031	*GBGT1*	9q34.13	α1,3 *N*-acetylgalactosaminyltransferase
Jr	Jr	JR	032	*ABCG2*	4q22	ATP-binding cassette, G family
Lan	Lan	LAN	033	*ABCB6*	2q36	ATP-binding cassette, B family
Vel	Vel	VEL	034	*SMIM1*	1p36.32	Small integral membrane protein 1
CD59	CD59	CD59	035	*CD59*	11p13	Membrane inhibitor of reactive lysis
Augustine	Ata	AUG	036	*SLC29A1*	6p21.1	Nucleoside transporter ENT1
KANNO		KANNO	037	*PRNP*	20p13	Prion protein
SID		SID	038	*B4GALNT2*	17q21	B1,4 N-acetylgalactosaminyltransferase

Data from Daniels G: *Human blood groups*, ed 3, Oxford, 2013, Blackwell Science; Daniels G, Fletcher A, Garratty G, et al: Blood group terminology 2004: From the International Society of Blood Transfusion Committee on Terminology for Red Cell Surface Antigens, *Vox Sang* 87:304–316, 2004; Reid RE, Lomas-Francis C: *The blood group antigen facts book*, ed 3, San Diego, 2012, Academic Press; and the International Society of Blood Transfusion.
ADP, Adenosine diphosphate; *CHIP,* channel-forming integral protein; *ICAM,* intercellular adhesion molecule; *ISBT,* International Society of Blood Transfusion; *ISGN,* International Society for Gene Nomenclature.

The cloning and sequencing of the *ABO* gene locus have also uncovered the molecular basis of group O and weak ABO subtypes. Group O is an autosomal-recessive phenotype due to homozygosity for amorph *ABO* alleles (*ABO*O*). There are many *ABO*O* alleles described to date; however, most ABO alleles can be classified as either O^1 or O^2. Alleles belonging to the O^1 family (*ABO*O1*) share a nucleotide deletion and frameshift (G251D, fs88stop) and account for 95% of all ABO*O alleles. O^2 alleles (*ABO*O2*; *O03*) carry a G802>A, leading to Gly268Arg in the translated protein (see Table 36.7). O^2 and related alleles (Aw08) have been linked to ABO typing discrepancies by an absence of anti-A and/or anti-B in these individuals (Wagner et al., 2005). It has been suggested that the absence of anti-A or anti-B is the result of weak residual enzyme activity (Seltsam et al., 2005). However, this has not been confirmed (Yazer et al., 2008).

Weak ABO subtypes are the result of mutations at the *ABO* gene locus. Most mutations are located within exon 7, which encodes the catalytic domain of the molecule. The majority of described mutations are single-nucleotide polymorphisms (SNPs), although nonsense, frameshift, and translation-initiator mutations are known (Yamamoto, 1995; Seltsam et al., 2006; Reid & Lomas-Francis, 2012). A2, the most common weak A subtype, is the result of a single-nucleotide deletion (nucleotide 1060) and frameshift, resulting in the loss of a stop codon and synthesis of a longer A enzyme with

TABLE 36.5

Serologic Characteristics and Clinical Significance of Red Cell Alloantibodies

		MOST COMMON PHASE OF REACTIVITY			CLINICAL SIGNIFICANCE		APPROXIMATE % OF COMPATIBLE DONORS	
Antibody	**Usual Ig Class**	**Sal**	**Alb**	**AGT**	**HTR**	**HDFN**	**White**	**Black**
D	IgG	Few	X	X	Yes	Yes	15	8
C	IgG		X	X	Yes	Yes	30	68
E	IgG	Few	X	X	Yes	Yes	70	98
c	IgG		X	X	Yes	Yes	20	1
e	IgG		X	X	Yes	Yes	2	2
Cw	IgG/IgM	Some	X	X	Yes	Yes	98	100
K	IgG	Rare		X	Yes	Yes	91	97
k	IgGX				Yes	Yes	0.2	0.1
Kp^a	IgG	Rare		X	Yes	Yes	98	99.9
Kp^b	IgG		X		Yes	Yes	<0.1	0.1
Js^a	IgG		X		Yes	Yes	>99.9	81
Js^b	IgG		X		Yes	Yes	<0.1	1
Fy^a	IgG		X		Yes	Yes	34	90
Fy^b	IgG		X		Yes	Yes	17	77
Jk^a	IgG		X		Yes	Yes	23	9
Jk^b	IgG		X		Yes	Yes	28	5
M*	IgM	X			Few	Yes	22	30
N	IgM	X			Rare	Rare	28	26
S	IgG/IgM		Some	X	Yes	Yes	45	69
s	IgG			X	Yes	Yes	11	3
U	IgG			X	Yes	Yes	0	1
Lu^a†	IgM	X			?	Yes	92	96
Lu^b†	IgG		X		Yes	Mild	<0.1	<0.1
P1‡	IgM	X	Some		Rare	No	21	6
P	IgM	X	Some	Some	Probable	Yes	<0.1	0.1
PP_1P^k†	IgG/IgM	X	Some	Some	Probable	Yes	<0.1	0.1
Le^a‡	IgM	X	Some		Yes	No	78	77
Le^b‡	IgM	X			Yes	No	28	45
I	IgM	X	Few		Rare	No	<0.1	<0.1
i	IgM	X	Few		?	No	<0.1	<0.1

AGT, Antihuman globulin test*; Alb,* albumin; *HDFN,* hemolytic disease of the fetus and newborn; *HTR,* hemolytic transfusion reaction; *Sal,* saline.
*Most examples of anti-M also have a small but significant IgG component.
†Exhibits characteristic mixed-field agglutination pattern.
‡May occasionally show in vitro hemolysis.

decreased enzyme activity. The *cis*-AB and B(A) phenotypes are the consequence of hybrid alleles, with characteristics of both A_1 and *B* gene consensus alleles. *cis*-AB and B(A) individuals can synthesize both A and B antigens (see Table 36.7) (Yamamoto, 1995; Reid & Lomas-Francis, 2012).

ABO Antibodies

Antibodies against ABO antigens are the most important antibodies in transfusion medicine. The practicing pathologist should note that the routine antibody screen does not test for ABO antibodies. All reagent cells in the antibody screen are group O. Patients demonstrate anti-A or anti-B on reverse typing (see later discussion). A valid ABO type requires agreement between the forward and reverse types.

In general, ABO antibodies are naturally occurring. It is believed that the immune stimulus for the formation of ABO antibodies may be exposure to ABH-like substances found in nature, particularly on the bacterial polysaccharides (Cooling, 2015). It is interesting that ABO titers have progressively decreased over the past 2 decades with increasing consumption of pasteurized, commercially packaged foods that are relatively sterile (Mazda et al., 2007). This trend may be reversed with increasing use of probiotic nutritional supplements that contain live bacteria. The latter have been shown to stimulate ABO antibodies, with marked increases in ABO titers within several months (Daniel-Johnson et al., 2009).

ABO antibodies are weak or absent in the sera of newborns until 3 to 6 months of age. Adult levels of ABO antibodies are reached by 5 to 10 years of age and decrease only slightly with advancing age (Auf der Maur et al., 1993). Anti-A,B is found exclusively in group O individuals and appears to recognize an epitope common to both A and B antigens. Before the development of anti-A and anti-B monoclonal antibody typing reagents, anti-A,B was useful in identifying weak and B subgroups. Anti-A,B is still used for typing donor units and cord samples (see ABO Grouping section).

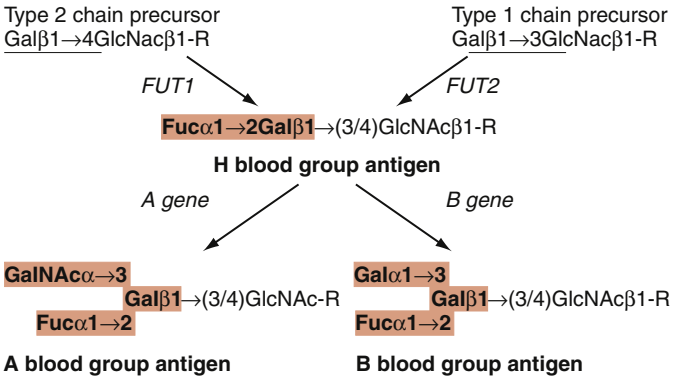

Figure 36.2 Synthesis of type 1 and type 2 chain H and AB antigens. Type 1 chain and type 2 chain precursors *(underlined)* are fucosylated by *FUT1* and *FUT2* fucosyltransferases to form H antigen. H antigen then serves as a substrate for *A* and *B* glycosyltransferases. The terminal carbohydrate epitopes denoting blood group H, A, and B antigens are highlighted in *amber. Fuc,* Fucose; *Gal,* galactose; *GalNAc, N*-acetylgalactosamine; *R,* other oligosaccharide.

In general, ABO antibodies are detected as room temperature, saline agglutinins with optimal reactivity at 4°C (see Table 36.5). Most naturally occurring ABO antibodies are of IgM isotype, although IgA and IgG antibodies with ABO specificity are also present (Rieben et al., 1991). ABO IgG antibodies, reactive at 37°C, can also occur following immune stimulation by transfusion or pregnancy. These antibodies generally are of higher titer and are less readily neutralized by soluble blood group substances. ABO antibodies can fix complement and can cause hemolysis in vivo and in vitro.

TABLE 36.6
Routine ABO Grouping Results and Phenotype Frequencies

CELLS AGAINST KNOWN ANTISERA		SERUM AGAINST RED CELLS OF KNOWN PHENOTYPE				FREQUENCIES IN U.S. POPULATION, %			
Anti-A	**Anti-B**	**A**	**B**	**O**	**Interpretation**	**White**	**Black**	**Native American**	**Asian**
–	–	+	+	–	O	45	49	79	40
+	–	–	+	–	A	40	27	16	28
–	+	+	–	–	B	11	20	4	27
+	+	–	–	–	AB	4	4	<1	5
–	–	+	+	+	Bombay	rare	rare	rare	rare

Composite figures calculated from Mourant AE, Kopec AC, Domaniewska-Sobczak K: The distribution of the human blood groups and other biochemical polymorphisms, ed 2, Oxford, 1976, Oxford University Press.

TABLE 36.7
Key Amino Acids in Distinguishing A, B, and Hybrid Glycosyltransferases*

	AMINO ACID NUMBER OF A/B GLYCOSYLTRANSFERASE					
ABO Allele	**176**	**234**	**235**	**266**	**268**	**Gene Type†**
ABO*A.01	Arg	Pro	Gly	Leu	Gly	AAAA
ABO*B.01	Gly	Pro	Ser	Met	Ala	BBBB
ABO*cisAB.01	Arg	Pro	Gly	Leu	**Ala**	AAAB
ABO*cisAB.04	**Gly**	Pro	Gly	**Met**	Gly	AABA
ABO*cisAB.02	**Gly**	Pro	**Ser**	Leu	Ala	BBAB
ABO*BA.03	**Gly**	Pro	Gly	**Met**	**Ala**	BABB
ABO*BA.02	**Gly**	**Ala**	**Ser**	**Met**	**Ala**	BBBB
ABO*O.02	Arg	Pro	Gly	Leu	**Arg‡**	AAAX

*Data from Reid RE, Lomas-Francis C: *The blood group antigen facts book*, ed 3, San Diego, 2012, Academic Press; and Daniels G: *Human blood groups*, ed 3, Oxford, 2013, Blackwell Science. Amino acids that differ from the *ABO*A.01* (A_1 type) consensus allele are highlighted in bold.
†Gene type refers to amino acid positions 176, 235, 266, and 268. These four positions differ between A (AAAA) and B alleles. Amino acids at 235, 266, and 268 strongly influence substrate specificity. Hybrid glycosyltransferases have amino acids matching both A and B consensus alleles at these positions.
‡*ABO*O.02* allele (historically O^2, *O03*), associated with a group O phenotype, possesses an inactivating missense mutation at amino acid 268.

Clinically, ABO antibodies are a cause of hemolytic transfusion reactions (HTRs) and hemolytic disease of the fetus and newborn (HDFN). ABO antibodies are also a cause of acute rejection in solid-organ transplantation. As a result, solid-organ transplants should be ABO compatible with the recipient's sera. Rare exceptions to the latter are heart transplantation in children younger than 6 to 8 months of age who have not yet developed ABO antibodies (West & Platt, 2010) and transplantation of A_2 organs, which have very weak ABO expression on epithelium and vascular endothelium (Hurst et al., 2010). In ABO-incompatible bone marrow transplantation, ABO antibodies can result in hemolysis and a delay in erythroid and megakaryocyte engraftment (Rowley et al., 2011; Cooling & Gorlin, 2012). For additional information on ABO-incompatible marrow and organ transplants, see the section on Antibody Titers.

Less Common ABO Antibodies

Anti-A_1. Anti-A_1 is a naturally occurring antibody found in the sera of some A_2, A_2B, and other weak A subtypes. Anti-A_1 hemagglutinates A_1 RBCs but not A_2 and other weak A phenotypes. Although uncommon, anti-A_1 has been implicated in transfusion reactions and solid-organ rejection.

Anti-H. Anti-H is usually a benign, naturally occurring antibody in the sera of A_1 and A_1B nonsecretors. Anti-H reacts most strongly with group O erythrocytes, followed by A_2, B, A_2B, A_1, and A_1B (see Table 36.41). Because H antigen is present to some degree on all RBCs, anti-H is an autoantibody in most individuals. In contrast, alloanti-H is a clinically significant alloantibody in Bombay (O_h) and para-Bombay individuals. These individuals require transfusion of rare O_h red cells.

Biological Role

The biological role of ABH antigens is still not known. Multiple studies have linked specific ABO types with a higher incidence of many diseases, including autoimmune, neoplastic, and infectious disorders. A and B antigen expression may stabilize the clustering and spatial organization of sialoglycoproteins (Cohen et al., 2009). Depression of A and B antigen expression can occur in malignancy and is often associated with increased metastatic potential. Groups A, B, and AB individuals also have a twofold higher risk of thrombotic events, including venous thrombosis and pulmonary embolism (Franchini & Mannucci, 2014). This may correlate to ABO differences in circulating von Willebrand factor (vWF), low-density lipoprotein (LDL), cholesterol, and P- and E-selectin. *Plasmodium falciparum* has been shown to bind A and B antigens with rosette formation, a possible risk factor in cerebral malaria (Cooling, 2015). Group O is a receptor for many gastrointestinal pathogens, including norovirus, rotavirus, *Helicobacter pylori*, *Campylobacter jejuni*, and *Vibrio cholerae* El Tor (Cooling, 2015). Group O may be protective against some infections due to anti-A and anti-B, including some enveloped viruses (human immunodeficiency virus [HIV], severe acute respiratory syndrome–associated coronavirus [SARS-CoV]), schistosomiasis, *E. coli*, and other gram-negative organisms (Cooling, 2015).

MNS BLOOD GROUP SYSTEM (ISBT NO. 002)

Discovered in 1927, the MNSs blood group was the second blood group system identified after ABO. Today, the MNSs blood group system consists of 49 antigens, although only four (M/N and S/s) are commonly encountered in the clinical setting (Reid, 2009). As shown in Table 36.8, the M and N antigens are fairly evenly distributed in both blacks and whites, with approximately 25% of donors homozygous for M or N antigen. In contrast, the S antigen is nearly twice as frequent in whites (57%) as in blacks (30%). In a minority (<1%) of blacks, an S–s– or null phenotype can be observed. As with Rh antigens, the MNSs blood group antigens are expressed only on RBCs. Approximately 1 million M/N and 170,000 to 250,000 S/s epitopes are present per RBC.

Null Phenotypes

Three major null phenotypes are present in the MNSs system: U–, M^k, and En (a–). The U– phenotype is the most common and is observed exclusively in blacks. In S–s–U– individuals, complete loss or a recombination of glycophorin B occurs, leading to altered expression of S/s and U antigens. Recombinant glycophorin B, such as the Henshaw phenotype, can react weakly with some examples of human anti-U and are known as U variants (S–s–U^{var}). The En (a–) phenotype is the result of recombination between glycophorin *A* and *B* genes to form a Lepore-type A-B hybrid (exons A1-B2-B5) lacking most of glycophorin A (GYPA). The M^kM^k phenotype lacks all MNSs antigens, including En(a), as the result of recombination and deletion of glycophorins A and B (GYPA and GYPB). Loss of GYPA can coincide with loss of Wr^b expression, an antigen on Band 3. It is believed that Wr^b requires an electrostatic interaction between a glutamic acid (Glu658) on Band 3 and the ENEP antigen on glycophorin A (Poole et al., 1999).

Biochemistry

The M/N antigens reside on GYPA (CD235A), a major RBC membrane glycoprotein. In the membrane, GYPA is present as a dimer, usually in association with Band 3, the erythrocyte anion exchanger (Burton & Bruce, 2011). Following cleavage of a 19 amino acid leader sequence, the mature GYPA is a 31-kD, 131 amino acid, type 1 glycoprotein composed of a large 72 amino acid extracellular domain, a transmembrane domain, and a short cytoplasmic tail (Fig. 36.3). The molecule is heavily glycosylated, possessing 15 *O*-linked and one *N*-linked carbohydrate side chain. The *O*-linked glycans consist predominantly of a disialotetrasaccharide linked to a serine or threonine residue. Because of the large number of sialylated *O*-linked glycans on GYPA, nearly 60% and 50% of the total molecular weight is

TABLE 36.8
Phenotypes of the MNSs System

GLYCOPHORIN A ANTIGENS			GLYCOPHORIN B ANTIGENS					PHENOTYPE FREQUENCIES, %	
M	**N**	**En (a)**	**"N"**	**S**	**s**	**U**	**Phenotype**	**Caucasian**	**Black**
+	0	+					M+N–	28	26
+	+	+					M+N+	50	44
0	+	+					M–N+	22	30
			+	+	0	+	S+s–U+	11	3
			+	+	+	+	S+s+U+	44	28
			+	0	+	+	S–s+U+	45	69
Null Phenotypes									
0	0	0	+	+/0	+/0	+	En (a–)	Rare	Rare
0	0	0	0	0	0	0	M^kM^k	Rare	Rare
			0	0	0	0	S–s–U–	Rare	<1
			0	0	0	wk+	S–s–U^{var} (23% Henshaw+)	Rare	<1

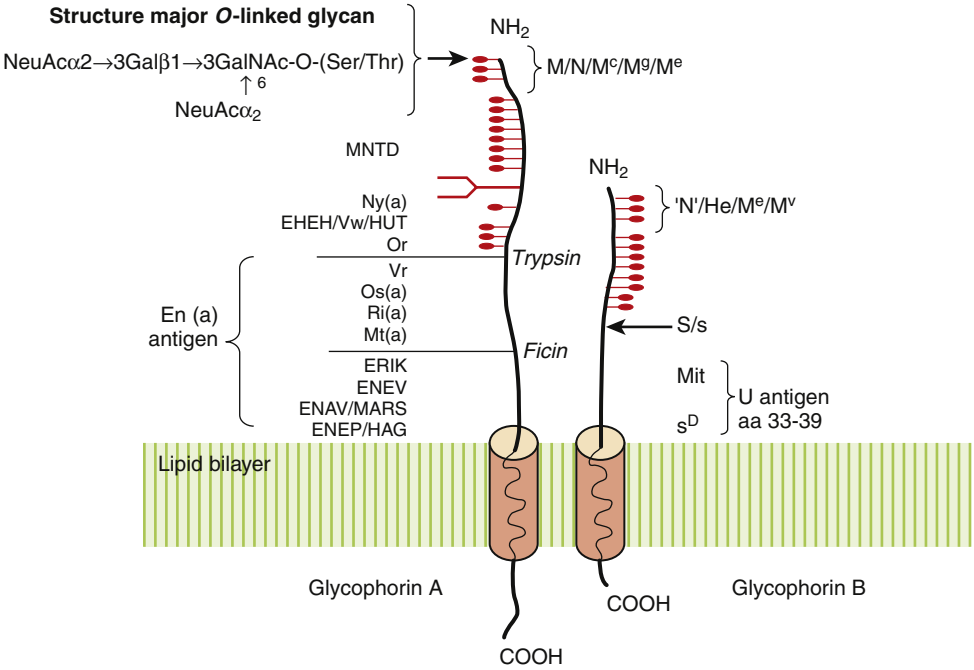

Figure 36.3 Glycophorin A (GYPA) and B (GYPB). GYPA and GYPB possess 11 to 15 *O*-linked glycans (●—), consisting predominantly of a disialotetrasaccharide (78%), along the amino-terminal half of the extracellular domain. GYPA also possesses a single biantennary *N*-glycan, indicated by a *branched structure*. The single transmembrane domain for both molecules is indicated by a *solid amber cylinder*. The allelic antigens, M and N, reside at the extreme amino-terminus of GYPA and differ by only two amino acids at residues 1 and 5. The N antigen is also present at the amino-terminus of GYPB and is designated "N" antigen. The S/s antigens are located at amino acid 29 of GYPB. The locations of high- and low-incidence antigens are shown. The En (a) and U antigens involve large stretches of protein near the lipid bilayer and are missing in deletion and recombinant glycophorins.

carbohydrate and sialic acid, respectively. Not surprisingly, GYPA is the major sialomucin on RBCs and contributes significantly to the overall negative charge or ζ potential (Huang & Blumenfeld, 1995). The M and N antigens reside on the extreme amino-terminus of GYPA.

The S/s and U antigens reside on GYPB(CD235B), a related RBC glycoprotein (see Fig. 36.3). Like GYPA, GYPB undergoes posttranslational processing, resulting in a 20-kD, 72 amino acid glycoprotein composed of a large extracellular *N*-terminal domain containing 11 *O*-linked glycans. Although GYPB shares considerable homology with GYPA at the amino-terminus, GYPB is smaller, lacking both an *N*-glycan and a cytoplasmic tail. In the membrane, GYPB appears to be closely associated with Diego at the AE1-ankyrin and junctional complexes, often as a heterodimer with GYPA (Burton & Bruce, 2011). The S/s epitope (Met48Thr) is located at amino acid 29 in the mature protein (Reid & Lomas-Francis, 2012).

Molecular Biology

The genes for GYPA (*GYPA*) and GYPB (*GYPB*) reside on chromosome 4q28-q31 as part of a 330-kb gene cluster encoding *GYPA*, *GYPB*, and glycophorin E (*GYPE*) (5′-A-B-E-3′). Studies indicate that *GYPB* and *GYPE* arose from GYPA by gene duplication and nonhomologous recombination. Similar to many erythroid-specific genes, the promoter region contains consensus sequences for Sp1 and GATA-1, an erythroid transcription regulatory binding factor (Rahuel et al., 1994). The greater stability of *GYPA* mRNA (>24 hours) over *GYPB* mRNA (<17 hours) may explain the four- to fivefold greater numbers of GYPA on RBCs (Rahuel et al., 1994).

There are nearly 20 allelic GYPA variants reported to date that are responsible for several high- and low-incidence antigens. The biochemical nature of the MNSs antigens has long been known. The M and N antigens lie at the extreme amino-terminus of GYPA (amino acids 1–5) and include both protein and carbohydrate as part of the immune epitope. It is amino acid differences at positions 20 and 25 (1 and 5 in the mature protein), however, that define the M/N antigens (Table 36.9). Further investigation of these amino acid differences revealed that the amino terminal amino acid (Ser for M and Leu for N) are the antigenic determinants (Pedersen et al., 1990) It is not surprising that several low-incidence M and N antigen variants are the result of different amino acid substitutions (M^g, M^c) and/or altered expression of *O*-linked glycans (M_1, Tm, Can). In addition to GYPA, the N antigen is expressed on the extreme amino-terminus of GYPB. The latter is referred to as the "N" antigen to distinguish it from N antigen on GYPA (Issitt & Anstee, 1998).

Twelve *GYPB* alleles are recognized, responsible for S/s, Mv+, Mit+, S^D+, He, and U^{var} phenotypes. Unlike the complexity of the M/N antigens, the S/s antigen is a single amino acid polymorphism on GYPB (Met29Thr on mature protein). The U antigen is a high-incidence antigen (amino acids 33–39 on mature GYPB). Loss of S, s, and U antigens can be observed with M^k and some recombinant *GYPB* alleles such as Henshaw. It is estimated that 90% of Henshaw+ RBCs are U– or U^{var} and account for 23% of all S–s–U– patients.

Over 20 deletion and recombinant *GYPA* and *GYPB* alleles are known. Recombination and gene conversion are responsible for several rare MNS antigens that were historically part of the Miltenberger system. These include misalignments with single crossovers leading to A-B Lepore-type (e.g., Hil) and B-A anti-Lepore (Dantu) variants as well as double crossover events, in which segments of one glycophorin are inserted

TABLE 36.9
MNSs Blood Group Alleles

ISBT No.	Antigen	Glycophorin	Allele	Amino Acid Change*
MNS1	M	GYPA	*GYPA*01*	Ser^{20}-Ser-Thr-Thr-Gly^{24}*
MNS2	N	GYPA	*GYPA*02*	Leu^{20}-Ser-Thr-Thr-Glu^{24}*
MNS8	Mc	GYPA	*GYPA*08*	Ser^{20}-Ser-Thr-Thr-Glu^{24}
MNS11	Mg	GYPA	*GYPA*11*	Ser^{20}-Ser-Thr-Asn^{23}-Gly
MNS30	"N"	GYPB	*GYPB*01*	Leu^{20}-Ser-Thr-Thr-Glu^{24}
MNS6	He	GYPB	*GYPB*06*	Trp^{20}-Ser-Thr-Ser^{23}-Gly^{24}
MNS3	S	GYPB	*GYPB*03*	Met48*
MNS4	s	GYPB	*GYPB*04*	Thr48*
Null phenotypes				
MNS: -1, -2	M-N-	No GYPA	*GYPA*01N*	Δ *GYPA* Exons 2–7
	En (a–)			Δ *GYPB* Exon 1
MNS: -3, -4, -5	S-s-U-	No GYPB	*GYPB*01N*	Δ *GYPB* Exons 2–5
MNS: -1, -2, -3, -4, -5	M-N-	No GYPA	*GYP*01N*	Δ *GYPA* Exons 2–7
MkMk	S-s-U-	No GYPB		Δ *GYPB* Exons 1–5

*The first 19 amino acids are cleaved, with the mature glycophorins A and B starting at amino acid 20. M/N antigens reside along the first 5 amino acids on the mature GYPA protein (aa1 to aa5). Likewise, the S/s polymorphism resides at amino acid 29 on the mature GYPB protein. Allele nomenclature per ISBT.

into the other to form B-A-B and A-B-A hybrids (Reid, 2009; Reid & Lomas-Francis, 2012). Deletion mutants include En(a–), a GYPA null (*GYPA*01N*) and GYPB (U-) null phenotypes (*GYPB*01N*). The M^k allele (*GYP*01N*) is characterized by a large deletion of GYPA and GYPB due to recombination between *GYPA* and *GYPE*. Mutant GYP molecules are frequently accompanied by loss of high-frequency MNS antigens and can display unusual resistance or sensitivity to enzyme treatment (Reid, 2009). GP.Mur, which is present in 2% to 10% of Southeast Asians, is associated with increased AE1/Band 3 (Diego) expression, decreased Rh, and the alloantibody anti-Mi^a (Hsu et al., 2009, 2017).

MNSs Antibodies

Anti-M and Anti-N

Antibodies against M and N antigens are naturally occurring antibodies of IgM isotype, usually detected as room temperature saline agglutinins (see Table 36.5). Anti-M and anti-N may show dosage, reacting more weakly with heterozygous (M/N) cells than with homozygous (M/M or N/N) cells. Because the M and N antigens reside on GYPA, the reactivity of anti-M and anti-N is destroyed by pretreatment of RBCs with proteolytic enzymes or neuraminidase. Some examples of anti-M and anti-N can be enhanced by acidification of serum to pH 6.5, use of an albumin diluent, or preincubation of RBCs in a glucose-containing solution.

Clinically, anti-M is a commonly encountered antibody in the blood bank. In contrast, anti-N is distinctly uncommon despite the fact that 25% of patients are negative for N antigen (M homozygous). The rarity of anti-N is due to the presence of "N" antigen on GYPB. When observed, anti-N is usually an autoantibody, reacting with both N and "N" antigens. An auto-anti-N (anti-N_f) was reported in hemodialysis patients in the past, caused by the use of formaldehyde to sterilize membranes. Formaldehyde reacted with the terminal leucine on N and "N" antigens, creating a neoantigen (Issitt & Anstee, 1998). In general, anti-M and anti-N are clinically insignificant antibodies and only rarely cause hemolytic transfusion reactions or HDFN. In contrast, potent hemolytic alloanti-N is observed in patients lacking GYPB (M+N–S–s– phenotype). In these patients, severe hemolytic transfusion reactions and HDFN can occur after transfusion of N+ RBCs.

Anti-S, -s, and -U

Unlike anti-M and anti-N, antibodies against S, s, and U antigens are always clinically significant (see Table 36.5). All are antibodies of IgG isotype, reactive at 37°C, arising from immune stimulation. Some examples of anti-S and anti-s show dosage. Enzymatic modification of RBCs with proteases, but not neuraminidase, can decrease the reactivity of some anti-S and anti-s. The reactivity of anti-U is resistant to proteolytic digestion. Anti-S, -s, and -U are causes of hemolytic transfusion reactions and HDFN.

Biological Role

Despite the prevalence of GYPA and GYPB on RBCs, their biological role is still unknown—their absence is not associated with any known hematologic or pathologic sequelae. Because they are rich in *O*-glycans and sialic acid, GYPA and GYPB contribute significantly to the ζ potential of red cells, decreasing homotypic and heterotypic red cell adhesion. GYPA also facilitates transport and expression of Band 3 (AE1/Diego), a critical protein in gas exchange. Increased Band 3 expression and osmotic resistance can be observed with Miltenberger type III red cells, a GYP B-A-B hybrid (Hsu et al., 2009). Finally, GYPA and GYPB play a role in *Plasmodium falciparum* infections. *P. falciparum* can adhere to RBCs via sialic acid, which is highly expressed on glycophorins. Glycophorin-deficient phenotypes, such as En (a–) and U-, are relatively resistant to *P. falciparum* in vitro. Similar results can be obtained after neuraminidase treatment of RBCs (Cooling, 2015). Recently, *P. falciparum* P_fEBA-175 erythrocyte binding protein was shown to recognize GYPA O-glycans at Ser 66, Ser69, and Thr72 (Salinas et al., 2014). Selective pressure by *P. falciparum* may account for some hybrid glycophorins such as GP.Dantu, which lacks critical O-glycans and is protective against severe malaria. In addition, the malarial invasin protein MSP also appears to bind GYPA, in association with Band 3, along the En(a) epitope (aa 31-72) (Jaskiewicz et al., 2019). GYPA is also a receptor for Babesia, another intraerythrocytic parasite (Cooling, 2015).

P1PK, GLOB, AND FORS BLOOD GROUP SYSTEMS (ISBT NOS. 003, 028, AND 031, RESPECTIVELY)

Historically, the P blood group system consisted of three antigens; P_1, P^k, and P. With the cloning of the glycosyltransferases necessary for their synthesis, the "P group" is now classified into three separate blood group systems containing six antigens. The antigens are assigned based on the last glycosyltransferase necessary for their synthesis. The P1PK system (ISBT 003) encompasses P^k (P1PK3), P_1 (P1PK1), and NOR (P1PK4) antigens, which all share a terminal α1,4-Gal. GLOB (ISBT 028) contains P (GLOB1) and PX2 (GLOB4) antigens, which share a terminal β1,3-GalNAc. FORS (ISBT 031) contains a single antigen, Forssman, present on rare Apae RBCs. The LKE or Luke antigen is still classified under GLOB collection 209. Related antigens include globo-ABH (type 4 chain ABH) and galactosylgloboside (Gb5). Globo-A is a characteristic feature of A_1 RBCs and may account for antigenic differences between A_1 and A_2 RBCs.

Similar to the Lewis system (see later discussion), the P blood group antigens are glycosphingolipids, consisting of an antigenically active carbohydrate moiety covalently linked to a ceramide lipid tail. P^k and P antigens are high-frequency antigens on most donor RBCs (>99.9%). RBCs are particularly rich in P antigen, which makes up nearly 6% of the total RBC lipid (Van Deenen et al., 1974). P^k and P antigens are also expressed on nonerythroid cells, including lymphocytes, platelets, plasma, kidney, lung, heart, endothelium, placenta, uroepithelium, fibroblasts, and synovium. In contrast, the P_1 antigen is uniquely expressed on RBCs. Approximately 79% of white and 94% of black donors express P_1 on their RBCs (Table 36.10). P_1 strength is variable between individuals and can be lost with in vitro storage.

Null/Weak Phenotypes

Several P blood group phenotypes have been described (see Table 36.10). The P_1 and P_2 phenotypes account for more than 99% of donors. Both possess P^k and P antigens and differ only in expression of the P_1 antigen. Three autosomal-recessive null phenotypes have been identified, as well as weak variants (Kundu et al., 1978, 1980; Issitt & Anstee, 1998). The molecular basis for the null phenotypes has been elucidated (Steffensen et al., 2000; Reid & Lomas-Francis, 2012). An association between the P^k variant and Luke (LKE)-negative phenotype has been noted in some donors (Cooling & Kelly, 2001; Cooling et al., 2003a). Because they lack P antigen, p and P^k individuals are resistant to parvovirus B19 (Brown et al., 1994).

Biochemistry

Synthesis of the P^k, P, and P_1 antigens proceeds from the stepwise addition of sugars to lactosylceramide, a ceramide dihexose (CDH) (Fig. 36.4). The first step is the synthesis of the P^k antigen, the ultimate precursor of all globo-type glycosphingolipids. To make P^k antigen, Gb_3 synthase

TABLE 36.10
P Blood Group System

RBC Phenotype	RBC Antigens	Possible Antibodies	MOLECULAR BASIS		FREQUENCIES, %	
			A4GalT1	B3GALNT1	White	Black
P_1	P^k, P, P_1	None	Normal	Normal	79	94
P_2	P^k, P	Anti-P_1	Alternate start codon, intron 1 SNPs*	Normal	21	6
Null Phenotypes						
$P_1{}^k$	↑P^k, P_1	Anti-P	Normal	Null allele†	Rare	Rare
$P_2{}^k$	↑P^k	Anti-P, anti-P_1	Alternate start codon, intron 1 SNPs*	Null allele†	Rare	Rare
p	None	Anti-P^kPP_1 (Tj^a)	Null allele‡	Normal	Rare	Rare
Weak Phenotypes						
Variant P^k	↑P^k, ↓P	Anti-P	Unknown	Unknown	Rare	Rare
Weak P	↓P^k, ↓P	None	Unknown	Unknown	Rare	Rare

RBC, Red blood cell; *SNP,* single-nucleotide polymorphism.
*Recent studies suggest that P_1 is transcribed by an alternate *A4GALT1* transcript and/or regulated by polymorphisms in intron 1 (Thuresson B, Westman JS, Olsson ML: Identification of a novel *A4GALT1* exon reveals the genetic basis of the P1/P2 histo-blood groups, *Blood* 117:678–687, 2011; Lai YJ, Wu WY, Yang CM, et al.: A systematic study of single-nucleotide polymorphisms in the *A4GALT1* gene suggests a molecular basis for the P_1/P_2 blood groups, *Transfusion* 54:3222–3231, 2014).
†Multiple inactivating mutations have been identified in the *B3GALNT1* open reading frame associated with the P^k phenotype.
‡Multiple inactivating mutations have been identified in the *A4GALT1* open reading frame associated with the p phenotype (Steffensen R, Carlier K, Wiels J, et al.: Cloning and expression of the histo-blood group P^k UDP-galactose: Galβ1-4Glcβ1-1Cer α1,4 galactosyltransferase, *J Biol Chem* 275:16723–16729, 2000).

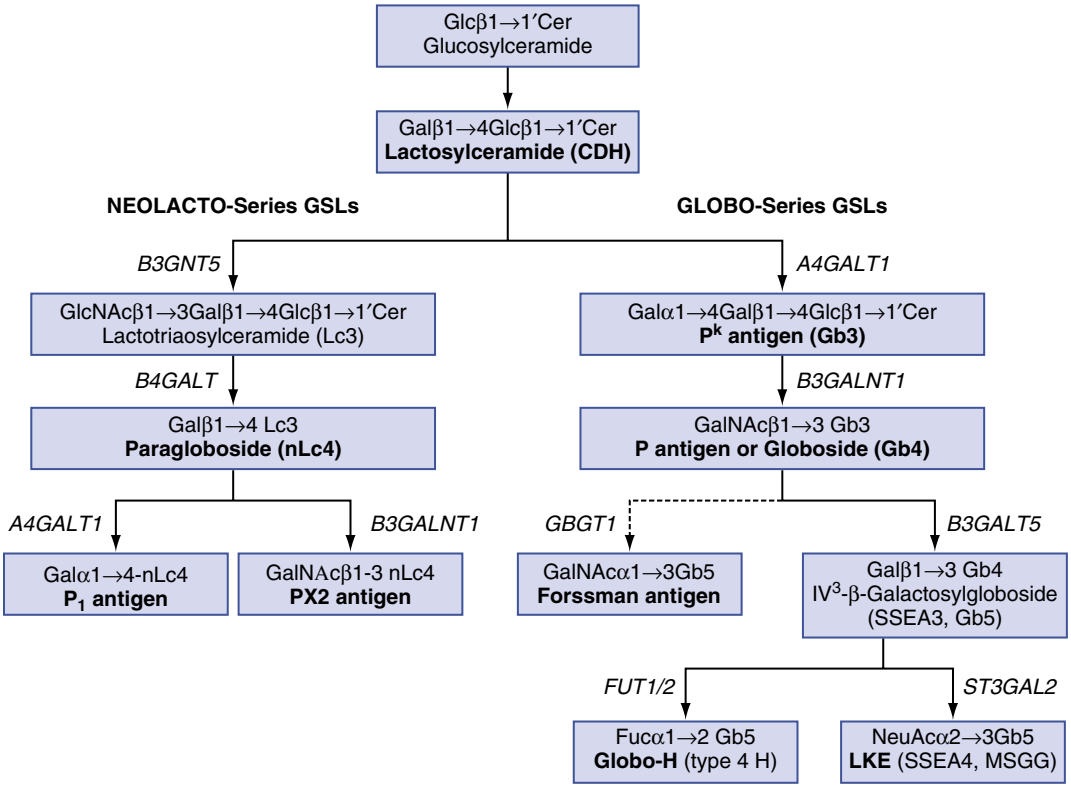

Figure 36.4 Synthesis of P blood group antigens. *Cer,* Ceramide; *Gal,* galactose; *GalNAc, N*-acetylgalactosamine; *Glc,* glucose; *GlcNAc, N*-acetylglucosamine; *NeuAc,* acetylneuraminic acid; *SSEA,* stage-specific embryonic antigen.

(α4GalT1) adds a galactose, in an α1–4 linkage, to CDH. The P^k antigen can then serve as a substrate for Gb_4 synthase (β3GalNAcT1). In some cells, including RBCs, the P antigen is further elongated to form additional globo-family antigens, such as Luke (LKE), Forssman, NOR, and type 4 chain ABH antigens (globo-ABH).

Unlike P^k and P antigens, the P_1 antigen is not a globo-glycosphingolipid but is a member of the neolacto-family (type 2 chain glycosphingolipids). In P_1 individuals, a terminal α1,4 galactose is added to paragloboside to form P_1. Although red cells are rich in type 2 chain glycoproteins, P_1 antigen is only weakly expressed on glycoproteins (Stenfelt et al., 2019). PX2 (GLOB4) is a related neolacto-GSL formed by the action of β3GalNAcT1. PX2 is expressed by rare p cells and can react with alloanti-P.

Molecular Biology

The genes responsible for P^k, P_1, and P have been cloned. As noted, P^k, P_1, and NOR antigens are synthesized by α4GalT1, an α1,4 galactosyltransferase (Steffensen et al., 2000; Iwamura et al., 2003). The *α4GalT1* gene resides on chromosome 22q13 and is organized into three exons, of which only one (exon 3) encodes the enzyme. The α4GalT1 enzyme is a 353 amino acid type II glycoprotein containing two *N*-glycosylation sites and five cysteine residues. Similar to many metal-dependent galactosyltransferases, it possesses a DXD motif or a UDP-Gal binding site. A point mutation (C631>G), leading to a Q211E in the mature enzyme, is responsible for the NOR phenotype (Kaczmarek et al., 2014). The p phenotype is the result of null *A4GALT1* alleles *(A4GALT*01N*), leading to a loss of all globo-GSL synthesis. To date, 37 null alleles are reported due to either missense or frameshift mutations (Kaczmarek et al., 2014).

The molecular basis for the P_1 and P_2 phenotypes remains under investigation. It was originally reported that P_2 was a consequence of a mutation in the *A4GALT1* promoter leading to decreased transcription (Iwamura et al., 2003); however, subsequent studies questioned these findings (Tilley et al., 2006). A later study identified a minor *A4GALT1* mRNA arising from an alternate exon and transcription start site. The minor transcript included

an additional 28 amino acid peptide and contained a single SNP linked to lower *A4GALT1* transcription and P_2 phenotype (Thuresson et al., 2011). This study has now been challenged by a third group. Lai and colleagues (2014) identified 11 SNPs within intron 1, including 8 that showed a linkage with the P_1/P_2 phenotypes. One SNP (G3084>T; rs5751348) was associated with P_2 and lower *A4GALT1* transcription. It was hypothesized that intron 1 contains transcription factor binding sites that regulate P^k and P_1 synthesis. Transcription sites for both KLF1 and RUNX1 were identified within intron 1; however, only RUNX1 was shown to bind and effect *A4GALT1* expression (Westman et al., 2018). Likewise, no significant decrease in A4GALT1 mRNA was observed in a KLF1-null individual (Magor et al., 2015).

This has been somewhat challenged by Kaczmarek and colleagues, who carefully examined P_1 expression by serology, flow cytometry, and genotype (Kaczmarek et al., 2018). They were able to show dosage effect in P_1 expression by genotype, with rs5751348 showing the strongest association. However, the amount of P_1 antigen on red cells genotyping as either P^1P^1 or P^1P^2 was highly variable between individuals, with significant overlap between both groups. As a consequence, no single SNP can "universally predict the [P_1] phenotype" since P_1 expression may be affected by other factors, including transcription factors, paragloboside synthesis, and competing glycolipid pathways (Kaczmarek et al., 2018).

Globoside or P antigen, a β1,3 *N*-acetylgalactosaminyltransferase, is the product of *B3GALNT1* (β3GalT3 in original literature; Okajima et al., 2000). The gene resides on chromosome 3q25 and contains six exons, although only exon 6 encodes the enzyme. A member of the β1,3 galactosyltransferase family, β3GalNAcT1 possesses seven conserved domains common to most β1,3 galactosyltransferases, as well as a DXD motif. The gene is ubiquitously expressed in most tissues. Thirteen null alleles have been reported associated with the P^k phenotype. In mice, the absence of *β3GALNT1* is lethal (Vollrath et al., 2001).

Forssman antigen is the product of *GBGT1*, an α1,3 galactosaminyltransferase related to the ABO gene (Yamamoto et al., 2012). Forssman antigen is expressed on many animal species but is typically absent from humans and old-world apes. In humans, *GBGT1* is located on 9q24 as a pseudogene. *GBGT1* mRNA can be identified in tissues; however, Forssman antigen is not expressed due to two inactivating mutations (Gly230Ser, Gln296Arg) in the translated enzyme. Forssman expression can be observed in the rare weak Apae phenotype. Apae individuals possess an Arg296Gln mutation that restores partial enzyme activity (Yamamoto et al., 2012). Forssman antigen can react with human polyclonal anti-A due to the terminal α1,3-GalNAc epitope.

P Blood Group Antibodies

Anti-P_1

Clinically, the most common antibody observed is anti-P_1, which is detected in one-quarter to two-thirds of P_2 donors (Issitt & Anstee, 1998). Anti-P_1 is a naturally occurring antibody of IgM isotype and is often detected as a weak, room temperature agglutinin. Rare examples of anti-P_1 are reactive at 37°C or show in vitro hemolysis. Because P_1 expression varies in strength among individuals, anti-P_1 may not react with all P_1-positive cells tested. Anti-P_1 can bind complement and may be detected in the indirect antiglobulin test (IAT) if polyspecific antihuman globulin (AHG) is used. Antibody reactivity can be eliminated by prewarming sera or by adding soluble P1 substance from hydatid cyst fluid, earthworms, and bird eggs. Anti-P_1 titers are often elevated in patients with hydatid cyst disease or fascioliasis (liver fluke) and in bird fanciers (Issitt & Anstee, 1998; Cooling, 2015). Some examples of anti-P_1 have I blood group specificity (anti-IP_1).

In general, anti-P_1 is not clinically significant, and its presence rarely requires transfusion of antigen-negative blood. The exception is seen in patients with an anti-P_1 showing in vitro hemolysis. Because of the risk of immediate and delayed hemolytic transfusion reactions, these patients should receive P_1-negative (P_2), crossmatch-compatible units. Anti-P_1 is not a cause of HDFN.

Alloanti-PP_1P^k

Anti-PP_1P^k (historically known as *anti-Tj*[a]) is a separable mixture of anti-P, anti-P_1, and anti-P^k in the sera of p individuals. These antibodies are naturally occurring and may be IgM only or IgM plus IgG (IgG3). Because anti-PP_1P^k antibodies are potent hemolysins, patients can be transfused only with p RBCs. In women, alloanti-PP_1P^k and alloanti-P are associated with HDFN and spontaneous abortion. Early and frequent plasmapheresis has been used with therapeutic success in alloimmunized pregnant women of the p and P^k phenotypes (Kaczmarek et al., 2014).

Alloanti-P

Anti-P is also a naturally occurring IgM alloantibody in the serum of P^k (and p) individuals. It is a potent hemolysin and can cause in vivo hemolysis following transfusion of P-positive (P_1 and P_2) RBCs. Some alloanti-P can react with PX2 present on p red cells with hemolysis. Alloanti-P is a cause of HDFN and is associated with spontaneous abortions.

Auto-Anti-P (Donath-Landsteiner)

An autoantibody with anti-P specificity is seen in patients with paroxysmal cold hemoglobinuria (PCH), a clinical syndrome that may occur in children following viral infection (Cooling, 2017). In PCH, autoanti-P is an IgG, biphasic hemolysin capable of binding RBCs at colder temperatures, followed by intravascular hemolysis at body temperature. This characteristic can be demonstrated in vitro in the Donath-Landsteiner test. See a full description in later sections on immunohematologic methods.

Biological Role

Unlike many antigens, the physiologic role of the P blood group antigens is not known. As GSLs, they are frequently organized into glycolipid-enriched microdomain (GEM) or lipid rafts in the outer cell membrane. GEMs can function as a glycosynapse as well as an organizing platform for glycoproteins, cell adhesion, and cell signaling (Cooling, 2015). Not surprisingly, globo-GSLs demonstrate differential expression during embryogenesis, cellular differentiation, and neoplastic transformation (Jacewicz et al., 1995; Cooling et al., 2003b). In mice, P and extended globo-GSLs are necessary for embryonic development (Vollrath et al., 2001). The P^k antigen is a marker of apoptosis in germinal center B cells, Burkitt lymphoma, and lymphoblastic leukemia (Mangeney et al., 1991). LKE is a marker of embryonic and mesenchymal stem cells (Gang et al., 2007) and is implicated in adhesion, cell signaling, and metastasis in renal cell and breast carcinoma (Satoh et al., 1996; Steelant et al., 2002).

Several P blood group antigens are receptors for microbial pathogens. The P blood group antigen is the receptor for parvovirus B19, a single-stranded deoxyribonucleic acid (DNA) virus associated with multiple clinical sequelae, including aplastic crises (Brown et al., 1994; Cooling, 2015). P^k can bind HIV and may confer resistance to HIV infection (Lund et al., 2009). P, P^k, and LKE blood group antigens on uroepithelium are cell receptors for P-fimbriae, a bacterial adhesin and colonization factor expressed on uropathogenic *Escherichia coli* strains. The P antigen was recently found to bind the LPS receptor TLR4-MD2 complex, acting as an antagonist to LPS and blunting inflammation (Kondo et al., 2013).

The P_1 and P^k antigens are receptors for Shiga toxins, produced by *Shigella dysenteriae* and enterohemorrhagic *E. coli* (EHEC) strains (Cooling, 2015). In addition to gastroenteritis, EHEC infection is the most common cause of community-acquired hemolytic-uremic syndrome, probably reflecting toxin binding to P^k antigen on glomerular vascular endothelium and platelets (Mayer et al., 2012). The P^k antigen also serves as a receptor for *Streptococcus suis* (Cooling, 2015).

RH AND RHAG BLOOD GROUP SYSTEMS (ISBT NO. 004 AND 030)

The first and most clinically important characterization of the Rh system antigens came when Landsteiner and Wiener (1940) published studies of animal experiments involving the immunization of guinea pigs and rabbits with rhesus monkey RBCs. The resulting antiserum agglutinated 85% of human RBCs, and the antigen defined was called the *Rh (rhesus) factor*. This anti-Rh was later reported to have the same specificity as antibodies studied earlier by Levine and Stetson (1939) that were responsible for HDFN. It is interesting to note that the anti-Rh developed by Landsteiner and Wiener was later shown to recognize a different blood group antigen, named *LW* for its discoverers.

Today, the Rh system is probably the most complex red cell antigen system in humans, encompassing over 62 antigens, many phenotypic variants, and complex serologic relationships. Hence, the following review is basic and highlights the most current information. For a detailed historical review of the Rh system, readers should consult Issitt and Anstee (1998) and Daniels (2013).

Theories of Rh Inheritance and Classification System

Using five basic antisera—anti-D, anti-C, anti-E, anti-c, and anti-e—Wiener identified five different factors or antigens (Table 36.11) that, from population and family studies, appeared to be inherited as two complexes of up to three factors each. Eight possible combinations of three-factor complexes were identified if one included "d" as designating the lack of D, because no anti-d had ever been demonstrated. Wiener proposed a single-locus inheritance system with eight alternative common alleles coding for two Rh agglutinogens, capable of expressing up to three different antigenic

TABLE 36.11

Comparison of Wiener, Fisher-Race, and Rosenfield Nomenclatures for Antigens of the Rh Blood Group System

Wiener	Fisher-Race	Rosenfield
Rho	D	RH1
rh′	C	RH2
rh″	E	RH3
hr′	c	RH4
hr″	e	RH5

TABLE 36.12

Wiener and Fisher-Race Nomenclatures for the Rh Haplotypes and Their Population Frequencies*

		FREQUENCIES IN U.S. POPULATION			
Wiener	Fisher-Race†	White	Black	Native American	Asian
R0	Dce	0.04	0.44	0.02	0.03
R_1	DCe	0.42	0.17	0.44	0.70
R_2	DcE	0.14	0.11	0.34	0.21
Rz	DCE	0.00	0.00	0.06	0.01
r	Ce	0.37	0.26	0.11	0.03
r′	Ce	0.02	0.02	0.02	0.02
r″	cE	0.01	0.00	0.01	0.00
r^y	CE	0.00	0.00	0.00	0.00

*Composite figures calculated from Mourant AE, Kopec AC, Domaniewska-Sobczak K: *The distribution of the human blood groups and other biochemical polymorphisms*, ed 2, Oxford, 1976, Oxford University Press.
†In historical Fisher-Race nomenclature, RhD negative was designated as "d." At this time, RhD-negative phenotypes using Fisher-Race denote only the RHCE antigens present on red cells.

determinants. Wiener's nomenclature for the eight different genes and allelic frequencies is provided in Tables 36.12 and 36.13.

Fisher and Race later proposed a different inheritance theory and nomenclature system based on genetic evidence of the antithetical or allelic nature of the C/c and E/e antigens (Race, 1948). These investigators proposed a system of three closely linked loci or subloci on each chromosome, which were inherited as a block of genes (haplotype). They also introduced the DCE nomenclature to name the alleles, including the use of "d" to designate the lack of D locus (see Table 36.11). Rosenfeld proposed a numeric system of naming the antigens in 1962, because the increasing number of Rh antigens rendered an alphabetic notation impractical (Table 36.14). It was also appreciated that this nomenclature contained no inferences as to the genetic inheritance of the antigens. The Rh numbering system only weakly applies to naming Rh alleles, which assigns the allele based on gene (*RHD* or *RHCE*). For Rh antigens on RHCE protein, allelic variants are further classified based on expression of both C/c and E/e antigens: *RHCE*01*=ce; *RHCE*02*=Ce; *RHCE*03*=cE; *RHCE*04*=CE.

Biochemistry

Tremendous progress has been made in deciphering the biochemistry and molecular biology of the Rh blood group system. It is now clear that the Rh complex consists of three integral membrane proteins: RhD, RhCE, and Rh-associated glycoprotein (RhAg). RhD and RhCE are highly homologous proteins, differing by approximately 30 amino acids. Both are 30-kD, 417 amino acid multipass proteins containing 12 transmembrane domains, six extracellular loops, and a cytoplasmic amino- and carboxy-terminus (Fig. 36.5). Both proteins possess two to three molecules of palmitate (C16 fatty acid) covalently linked to transmembrane cysteine residues. Palmitoylation of Rh proteins may help maintain the phospholipid asymmetry of the RBC membrane (Avent, 1999).

RhAg is a 45- to 70-kD multipass glycoprotein, evolutionarily related to RhD and RhCcEe glycoproteins. RhAg is a 409 amino acid glycoprotein with 12 transmembrane domains and a single large *N*-linked carbohydrate side chain on the first extracellular loop. Overall, approximately 170,000 molecules each of Rh and RhAg proteins are present per RBC. RhD, RhCE, and RhAg are erythroid-specific proteins (Avent, 1999).

In the RBC membrane, RhD, RhCE, and RhAg proteins exist as a trimer, composed of three molecules of Rh (RhD and RhCE) and RhAg (Eyers et al., 1994). The importance of RhAg for the expression and correct assembly of Rh proteins cannot be understated. In the absence of functional RhAg protein, neither RhD nor RhCE proteins will be expressed

TABLE 36.13

Frequencies of Common Rh Phenotypes*

REACTION WITH ANTI-†					PHENOTYPE		GENOTYPE		FREQUENCIES, n (%)‡			
D	C	c	E	e	Rh	DCE	Rh	DCE	White	Black	Native American	Asian
+	+	+	+	+	Rh_1Rh_2	DCcEe	R^1R^2	DCe/DcE	0.1176 (89)	0.0374 (100)	0.2992 (89)	0.294 (97)
							R^1r''	DCe/cE	0.0084 (6)		0.0088 (3)	
							$r'R^2$	Ce/DcE	0.0056 (5)		0.0135 (4)	0.0084 (2.8)
							rR^z	ce/DCE			0.0132 (4)	0.0006 (0.2)
+	+	+	–	+	Rh_1rh	DCce	R^1R^0	DCe/Dce	0.0168 (5)	0.1495 (63)	0.0176 (15)	0.042 (50)
							R^1r	DCe/ce	0.3108 (95)	0.0884 (37)	0.0968 (85)	0.042 (50)
+	–	+	+	+	Rh_2rh	DcEe	R^2R^0	DcE/Dce	0.0112 (10)	0.0968 (63)	0.0136 (15)	0.0126 (50)
							R^2r	DcE/ce	0.1035 (90)	0.0572 (37)	0.0748 (85)	0.0126 (50)
+	+	–	–	+	Rh_1Rh_1	DCe	R^1R^1	DCe/DCe	0.176 (91)	0.029 (81)	0.194 (92)	0.490 (93)
							R^1r'	DCe/Ce	0.017 (9)	0.007 (19)	0.017 (8)	0.028 (7)
+	+	–	+	+	Rh_1Rhz	DCEe	R^1R^z	DCe/DCE		0.053 (100)		
+	–	+	+	–	Rh_2Rh_2	DcE	R^2R^2	DcE/DcE	0.02 (88)	0.012 (100)	0.116 (94)	0.044 (100)
							R^2r''	DcE/cE	0.003 (12)		0.007 (6)	
+	+	+	+	–	Rh_2Rhz	DCcE	R^2R^z	DcE/DCE			0.041 (100)	
+	–	+	–	+	Rh_0Rh_0	Dce	R^0R^0	Dce/Dce	0.0016 (5)	0.1936 (46)	0.0004 (8)	0.0009 (33)
							R^0r	Dce/ce	0.0296 (95)	0.2286 (54)	0.0044 (92)	0.0018 (67)
–	–	+	–	+	rhrh	ce	rr	ce/ce	0.1369 (100)	0.0676 (100)	0.0121 (100)	0.0009 (100)
–	+	+	–	+	rh′rh	Cce	rr′	ce/Ce	0.0055 (100)	0.0014 (100)	0.0044 (100)	0.0012 (100)
–	–	+	+	+	rh″rh	cEe	rr″	ce/cE	0.0028 (100)		0.0022 (100)	

*Estimated from haplotype frequencies (p, q from Table 36.12), using p2 for homozygotes and 2pq for heterozygotes.
†+, Positive; –, negative.
‡%, Percentage of genotypes within a given phenotype.

TABLE 36.14

Molecular Basis for RH and RHAG Antigens

ISBT	Name	Frequency, %	RH Protein (D or CE)	Molecular Basis (Protein or Gene Exon)	Comments
RH (ISBT 004)					
RH1	D	85–92	D	RHD, loops 3, 4, 6	
RH2	C	68% whites 27% blacks	CE	Ser103 + Cys16	Antithetical RH4
RH3	E	22–29	CE	Pro226	Antithetical RH5
RH4	C	80	CE	Pro103	Antithetical RH2
RH5	E	80	CE	Ala226 Dependence on Arg229	Antithetical RH3
RH6	F	65	CE	Pro103 + Ala226 Dependence on Arg229	Compound antigen
RH7	Ce	27–28	CE	Ser103 + Ala226	Compound antigen
RH8	C^w	1–2	CE	Gln41>Arg	Antithetical RH51
RH9	C^x	<0.01	CE	Ala36>Thr	Antithetical RH51
RH10	V	30% blacks	CE	Leu235>Val, +Gly336	Often with RH20
RH11	E^w	<0.01	CE	Met167>Lys	E variant type I
RH12	G	84–92	D, CE	Ser103	Anti-C+D
RH17	Hr_0	100	CE	RHCE loops 3,4,6	
RH18	Hr	100	CE	Met238	
RH19	hr^S	98	CE	Ala226, Met238	
RH20	VS	40% blacks	CE	Leu226>Val	Often with RH10
RH21	C^G	68	CE	Ser103	
RH22	CE	1	CE	Ser103 + Pro226	Compound antigen
RH23	D^w	<0.01	Partial D	Gln233, RHD loop 3,6	
RH26	c-like	80	CE	Gly96 + Pro103	Related RH55
RH27	cE	22–28	CE	Pro103 + Pro226	Compound antigen
RH28	hr^H	<0.01	?	Unknown	
RH29	Total Rh	100	CE + D	RHD + RHCE	Made by Rh_{null}
RH30	Go^a	2% blacks	Partial D	On DIV^a	
RH31	hr^B	98	CE	Unknown	Missing on R2R2
RH32	RN	<1% blacks	Partial D	Exons D4–CE5	Antithetical RH46
RH33	Har	<0.01	Partial D	Exons CE4–D5	R_0^{Har}
RH34	Hr^B	100	D + CE	Cys336	
RH35	1114(CeMA)	<0.01	CE	Unclear; CeMA is JAL+	Weak C,e
RH36	Be^a	<0.1	CE	Pro221>Arg	Weak c,e,f
RH37	Evans	<0.01	D–CE hybrid	Exons D6–CE7	
RH39	C-like	100	?	Unknown	On C– and C+ RBCs
RH40	Tar	<0.01	D	Leu100>Pro	
RH41	Ce-like	70	CE	Exon 2, Ala226	
RH42	Ce^S	2% blacks	Partial D	Leu245>Val	Associated $dCce^S$
RH43	Crawford	0.7% D– blacks	CE	Gln223Glu, VS+	ce^S variant; VS+, V+
RH44	Nou	100	?	Unknown	
RH45	Riv	<0.01	Partial D	On DIVa	
RH46	Sec	100	CE	CE exon 4	Antithetical RH32
RH47	Dav	100	CE	Exon 7	
RH48	JAL	<0.01	CE	Arg114Trp or Glu	Antithetical RH57
RH49	STEM	0.4% Indians	CE	W16C,M238V, L278V	
RH50	FPTT	<0.01	Partial D	Exons CE4–D5	
RH51	MAR	>99	CE	Ala36, Gln41	Antithetical RH8,9
RH52	BARC	<0.01	Partial D	Exons CE6–D7	
RH53	JAHK	<0.01	CE	Exon D2 (Ser103), no Cys16	
RH54	DAK	<0.01	Partial D	Unknown	
RH55	LOCR	<0.01	CE	Gly95>Ser	Weak c, e, f; Rh26±
RH56	CeNR	<0.01	CE–D hybrid	Complex epitope	D– –; RH32+
RH57	CEST	>99	CE	Arg114	Antithetical RH48 (Jal)
RH58	CELO	<0.01	CE	Trp16,Gln233,Leu245	Antithetical RH43
RH59	CEAG	<0.01	CE	Ala85	RH31(-), partial e
RH60	PARG	<0.01	CE	Met167Ile	Ce allele
RH61	CEVF	>99%	CE	Trp16Cys,Val233Phe	Absent on ceMO
RH62	CEWA	>99%	CE	Leu38Phe	
RHAG (ISBT 030)					

Continued

TABLE 36.14 —cont'd

Molecular Basis for RH and RHAG Antigens

ISBT	Name	Frequency, %	RH Protein (D or CE)	Molecular Basis (Protein or Gene Exon)	Comments
RHAG1	Duclos	>99	RhAg	Gln106>Glu	
RHAG2	Ol[a]	<0.01	RhAg	Ser227>Leu	Weak Rh expression
RHAG3	DSLK	>99	RhAg	Lys164>Gln	
RHAG4	RHAG4	<0.01	RhAg	Val270Ile	

From Wagner FF, Flegel WA: Review: The molecular basis of the Rh blood group phenotypes, *Immunohematology* 20:23–36, 2004; Reid RE, Lomas-Francis C: *The blood group antigen facts book*, ed 3, San Diego, 2012, Academic Press; and Westhoff CM, Storry JR, Walker P, et al.: A new hybrid *RHCE* gene (CeNR) is responsible for expression of a novel antigen, *Transfusion* 44:1047–1051, 2004.
ISBT, International Society of Blood Transfusion.

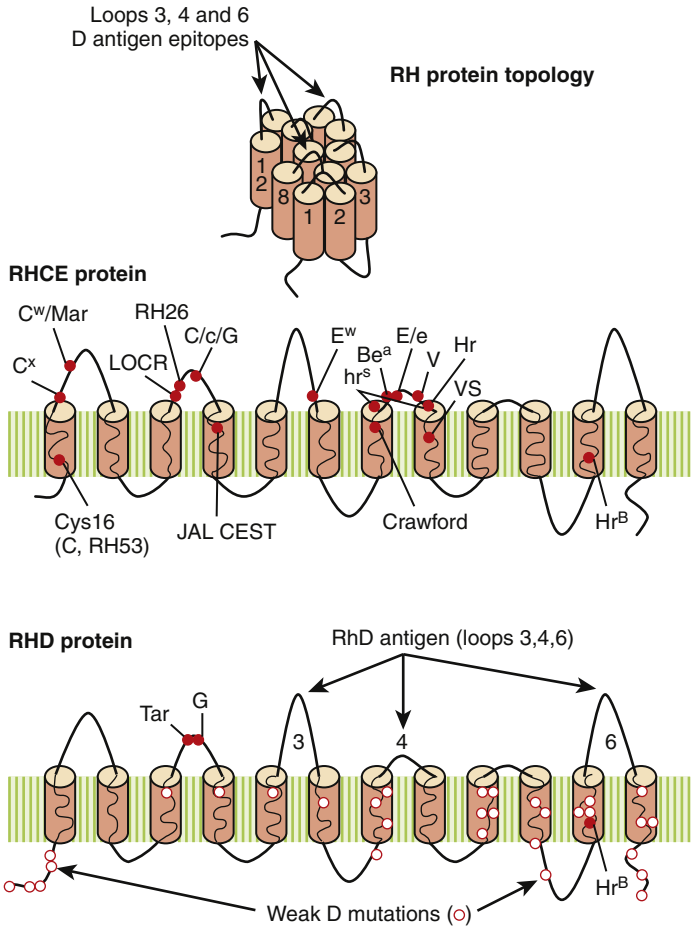

Figure 36.5 RH proteins. Both RHD and RHCE proteins are multipass proteins with 12 transmembrane domains, indicated by *solid amber cylinders*. The location of Rh antigens denoted by single–amino acid polymorphisms is denoted by *red circles*. The RhD epitope is a complex antigen involving structures on the third, fourth, and sixth extracellular loops. Missense mutations in RHD, leading to weak D expression, are indicated by *open circles* (o).

(Rh_{null} and Rh_{mod} phenotypes). In addition to RhAg, Rh proteins may be topologically associated with CD47 (Lutheran), ICAM4 (LW), DARC (Duffy), Band 3 (Diego), and GYPB. At least two non-Rh antigens, Fy5 and U, may require noncovalent interactions between Rh, DARC glycoprotein (Fy5), and GYPB (U), respectively (Ridgwell et al., 1994). Rh is associated with the Band 3-ankyrin metabolon.

Molecular Biology

The genes for RhD (*RHD*) and RhCE (*RHCE*) proteins span 65 kb on chromosome 1p34-36.1 and share nearly 92% sequence identity. The two genes are separated by only 30 kb and have opposite orientations, facing each other at their 3′ ends (Fig. 36.6). The *RHD* gene is also flanked by two homologous sequences known as rhesus boxes. The *RHAG* gene (*RHAG*) resides on chromosome 6p11.1 and shares 36% homology with the *RHD* and *RHCE* genes. All three genes possess 10 exons and at least one GATA-1 consensus sequence in the promoter region (Cherif-Zahar et al., 1994; Iwamoto et al., 1998). It is believed that *RHAG* and *RH* genes arose by gene duplication 250 to 350 million years ago. A second gene duplication 8 to 11 million years ago resulted in the ce and D alleles (cDe or R_0 haplotype). The remaining RHCe alleles are believed to be the product of point mutations, recombination, and gene conversion of the *RHD* and *RHCE* genes (Avent, 1999).

D Antigen

The cloning of *RHD* and *RHCE* genes opened the door to understanding the complex immunology of many Rh antigens and phenotypes. The D antigen, the most immunogenic of all of the Rh antigens, resides on the RHD protein. Current evidence suggests that D is a highly complex antigen, depending on both specific amino acids and the tertiary structure of the RHD protein itself. At least nine "D-specific" amino acids (Met169, Met170, Ile172, Phe223, Ala226, Glu233, Asp350, Ala353, and Gly354) have been identified as functional D epitopes. The nine amino acids lie along the third, fourth, and sixth external loops of the RHD protein, creating six distinct D-epitope clusters or footprints (see Fig. 36.5). Expanded studies have identified 30 distinct D epitopes on RhD (Daniels, 2013).

Weak D Variants

Approximately 1% of D-positive individuals type as weak D (historically known as D^u), characterized by weak or absent RBC agglutination by anti-D at immediate spin during routine serologic testing. In weak D individuals, the D antigen usually requires enhancement with AHG owing to a quantitative decrease in RhD protein. In these individuals, the number of RhD molecules is decreased 40- to 100-fold, ranging from 66 to 5200 molecules per red cell (Reid & Lomas-Francis, 2012). A weak D phenotype can occur with many partial D phenotypes, Ce *in trans* with suppression of *RHD*, in the Rh_{mod} phenotype, and via autosomal-recessive inheritance of two weak *RHD* alleles. To date, 147 weak D types are recognized. Some authors now refer to "weak D" as variant D alleles since the phenotype can arise from diverse genetic backgrounds (Daniels, 2013).

Many of the weak D alleles encode intact RhD with missense mutations along the transmembrane and cytoplasmic domains that may interfere with trafficking, assembly, or membrane stability (see Fig. 36.5) (Wagner et al., 1999). Weak D types 1, 2, and 3 belong to this category of weak D alleles and account for >90% of weak D alleles in whites. In general, these weak D genotypes are not at risk for making alloanti-D (Sandler, 2017; Daniels, 2013). In contrast, the common weak D variant alleles observed in blacks (type 4, DAR) are at potential risk for making anti-D following transfusion of Rh-positive red cells. The most common weak D allele in Asian countries is DEL (D_{el}), which results in extremely weak D expression that can be detected only by adsorption and elution due to unstable splicesite variants (Chen, 2016). As a result, D_{el} individuals can type as Rh negative even in the presence of AHG enhancement. Despite extremely low aberrant D expression, D_{el} individuals are not at risk for HDFN or anti-D if exposed to Rh-positive blood. D_{el} red cells can induce anti-D in Rh-negative recipients (Sandler, 2017).

Partial D Antigens

Partial D antigens are RHD proteins with missing D epitopes. Although they type as D-positive, persons with partial D antigens can make alloanti-D antibodies reactive with allogeneic, but not autologous, RBCs. The alloanti-D produced by these individuals recognizes D-specific epitopes missing on their own RBCs (see Fig. 36.6). Partial D can result from missense mutations (ex. DAR) or, more commonly, from genetic recombination of *RHD* and *RHCE* genes (Avent, 1999). Partial D phenotypes arising from genetic recombination are frequently associated with the generation of new low-incidence antigens on both RhD and

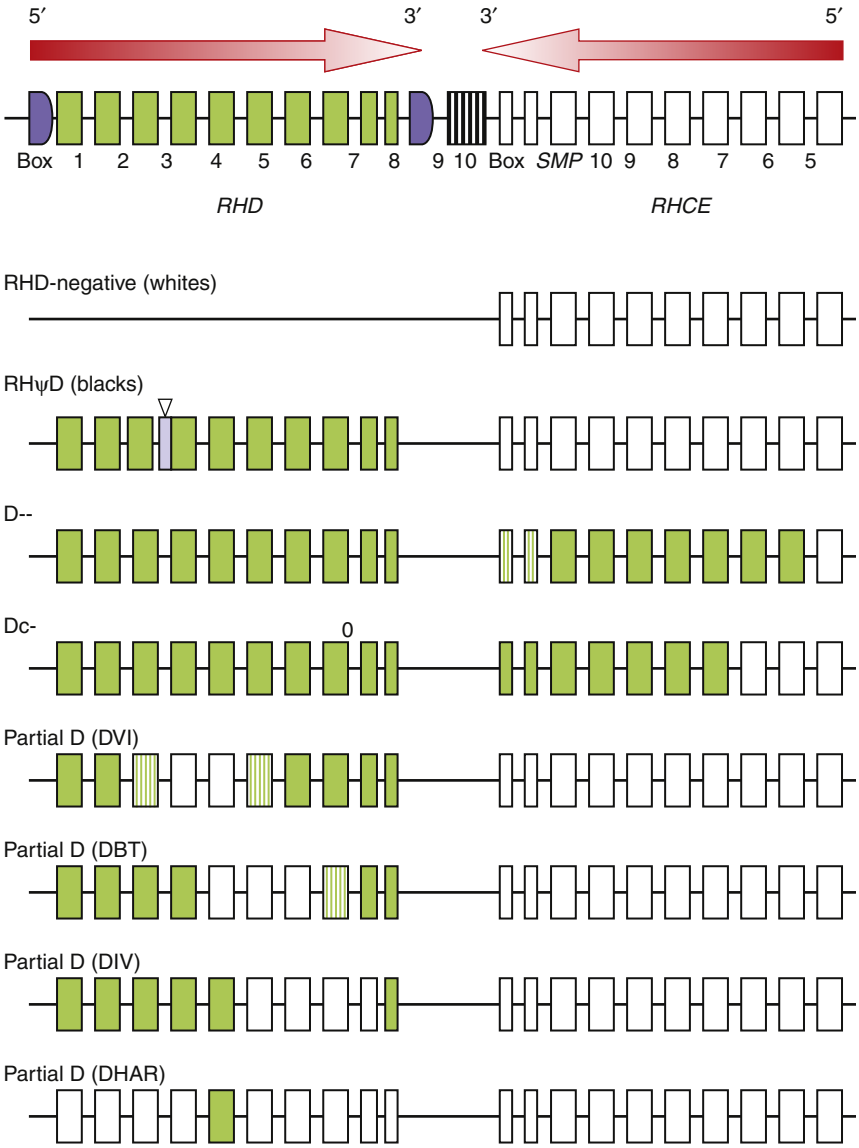

Figure 36.6 The *Rh* gene cluster. *RHD* and *RHCE* genes are closely situated and face each other at their 3′ ends. The *RHD* gene is also flanked by Rh boxes. *SMP* is an unrelated gene. RHD-negative phenotype can result from deletion of the *RHD* gene or, in blacks, a 37–base pair (bp) insertion leading to a frameshift (pseudogene). Also shown are examples of partial D and CE phenotypes that are the result of recombination between *RHD* and *RHCE* genes.

RhCE proteins (see Table 36.14). Studies of African Americans have shown that 29% carry altered *RHD* alleles and 6% possess partial D alleles (Chou, 2018).

Rh-Negative Phenotype

Rh-negative (D–) occurs in approximately 15% of white donors, almost always in association with a ce/ce or rr phenotype. In most whites, D– reflects a deletion of the entire *RHD* gene (see Fig. 36.6). In blacks, D– can result from gene deletion or from inheritance of an *RHD* pseudogene. Nearly 60% of D-negative black people inherit a mutant RHD allele (RHψD) containing a 37–base pair (bp) internal duplication, frameshift, and premature stop codon (Avent, 1999). *RHD* genes containing nonsense mutations and nucleotide deletions have also been reported in some D-negative Japanese and white donors (Daniels, 2013; Reid & Lomas-Francis, 2012).

C/c, E/e, and Compound Rh Antigens

In contrast to the complexity of the D antigen epitope, the C/c and E/e antigens are single–amino acid polymorphisms on the RhCE protein (see Fig. 36.5). Three additional amino acid polymorphisms (Cys16Trp, Ile60Leu, and Ser68Asn) may help stabilize the C and c antigens. Arg229 appears critical to e and f expression (Chen et al., 2004). Because C/c and E/e epitopes are present on the same protein, alloantibodies dependent on the expression of both C/c and E/e antigens can occur. Four alloantibodies with "compound" Rh specificity have been described: anti-ce (f or RH6), anti-Ce (RH7), anti-cE (RH27), and anti-CE (RH22). These antibodies react only with RBCs carrying the appropriately paired antigens, in *cis*, on the same RhCE protein (see Table 36.14). The RHCE protein is home to several additional high- and low-incidence antigens.

G Antigen

The G antigen (RH12) is a high-frequency antigen present on virtually all D-positive and C-positive RBCs. G has been identified as Ser103, a C-type antigen, on RHD and RHCE proteins (see Fig. 36.5). It is not surprising that anti-G alloantibodies have both anti-C and anti-D specificity (anti-C + D) and are frequently accompanied by anti-C (anti-G + anti-C) (Shirey et al., 1997).

Weak and Deletion C/c and E/e Phenotypes

Similar to D, phenotypes with weakened or absent C/c and E/e are known. *RHCE* alleles with point mutations, deletions, and recombinations can lead to weakened CcEe expression. African ethnic groups, in particular, have a high incidence of altered *RHCE* alleles (53%) (Chou et al., 2018). Studies have reported partial C phenotype in 21% to 25% of sickle cell patients (Noizat-Pirenne et al., 2009, Chou et al., 2018). Likewise, point mutations and rearrangements resulting in weakened c and e expression are common among African Americans (18% to 19%) (Reid & Lomas-Francis, 2012; Vege et al., 2009; Chou et al., 2018). Like partial D, patients with altered *RHCE* alleles can make alloantibodies against C, c, and e antigens (Ong et al., 2009; Pham et al., 2009). In one study, 23% of autoantibodies were actually Rh alloantibodies in patients homozygous for altered *RHCE* alleles (Chou et al., 2018).

The deletion phenotypes D••, D— (↑D+, C–c–E–c–), DC–, and Dc– are the result of genetic recombination between *RHCE* and *RHD* genes to yield RHCE-D-CE hybrids (see Fig. 36.6). As a consequence, total ablation of Ee and/or Cc epitopes occurs, with many recombinants expressing new low-frequency Rh antigens (see Table 36.14). Furthermore, many recombinants (e.g., D••, D—) demonstrate exalted D antigen expression on serologic testing owing to a double dose of some D epitopes on both RHD and mutant RHCE-D-CE proteins. For a detailed summary, the reader is referred to Reid and Lomas-Francis (2004).

RHAG Alloantigens

RHAG is a separate blood group system with three antigens: Ol^a, Duclos, and DSLK (Tilley et al., 2010; Reid & Lomas-Francis, 2012). All three are the result of an amino acid polymorphism in the RhAg protein. Both Duclos and DSLK are associated with weak U expression, suggesting an interaction between RhAg and GYPB.

Rh_{null} Phenotype

Rh_{null} erythrocytes lack all Rh antigens as a result of an apparent absence of RhD and RhCE proteins. In addition, Rh_{null} erythrocytes lack the high-frequency antigens Fy5 and LW and may have markedly decreased expression of S/s and U antigens. The absence of these non-Rh antigens reflects the complex topologic association of Duffy, LW, and GYPB proteins with Rh proteins on RBC membranes.

Extremely rare (<1 in 6 million), Rh_{null} cells have abnormalities in RBC morphology (spherocytes, stomatocytes), water content, cell volume, cation fluxes, carbon dioxide (CO_2) permeability, and phospholipid asymmetry (Issitt & Anstee, 1998; Endeward et al., 2006). Rh_{null} cells show increased osmotic fragility and a shortened circulating half-life, often accompanied by a mild hemolytic anemia (Rh deficiency syndrome). Because Rh_{null} individuals can become sensitized to multiple Rh antigens, including high-frequency antigens, transfusion support can be quite difficult. Some alloimmunized Rh_{null} individuals can produce anti-RH29, which reacts with all RBCs except Rh_{null}.

The Rh_{null} phenotype can arise from two distinct genetic backgrounds: regulator and amorph. The Rh_{null}-amorph type is the result of nonsense mutations in the *RHCE* gene in D-negative people. Because of the absence of RhD and RhCE proteins, Rh_{null}-amorph RBCs have reduced (but not absent) expression of RhAg protein (Daniels, 2013). The Rh_{null} regulator type arises from mutations in *RHAG* (Reid & Lomas-Francis, 2012). To date, there are 17 *RHAG* alleles associated with Rh_{null}-regulator phenotype (*RHAG*01N*).

Rh_{mod} Phenotype

Mutations in *RHAG* are also observed in the Rh_{mod} phenotype. Rh_{mod} RBCs have markedly decreased Rh and RhAg expression, detectable only by careful adsorption and elution studies. Similar to Rh_{null} individuals, persons with Rh_{mod} may have laboratory evidence of Rh deficiency syndrome with a mild hemolytic anemia. Most (82%) Rh_{mod} alleles (*RHAG*01M*) possess missense mutations (Daniels, 2013).

Rh Antibodies

Antibodies against Rh antigens are routinely encountered in the blood bank (see Table 36.5). D is the most immunogenic Rh antigen, followed by c, E, C, and e (Harmening, 2012). In general, antibodies against Rh antigens are the result of immune stimulation by transfusion or pregnancy. Exceptions include some examples of anti-C^w and anti-E, which can be naturally occurring. Most antibodies against Rh antigens are of IgG isotype (IgG_1 and IgG_3), although rare examples of IgM and IgA are known. Anti-Rh antibodies are reactive at 37°C and are usually detected in the AHG phase of testing. The reactivity of anti-Rh antibodies can be enhanced with enzyme-treated RBCs. The gel method is extremely sensitive for the detection of Rh antibodies (Weisbach et al., 2006).

Clinically, antibodies against Rh are associated with hemolytic transfusion reactions. However, because Rh antibodies do not fix complement, incompatible RBCs are almost always cleared through extravascular destruction. To prevent sensitization to the D antigen, Rh-negative patients should be transfused with Rh-negative RBCs. This is particularly true for young girls and women of childbearing age. For transfusion in alloimmunized patients, RBC units should be negative for the Rh antigen of interest and crossmatch compatible with the recipient's serum through the AHG phase of testing.

Selection of units matched for D, C/c, and E/e antigens to prevent Rh alloimmunization is now standard practice for sickle cell anemia and other hemoglobinopathy patients. Historically, alloimmunization rates in sickle cell patients were as high as 50%, with most patients making at least one anti-Rh antibody (Aygun et al., 2002). Even with extended Rh matching, alloimmunization remains a significant issue in this population due to variant *RHD* and *RHCE* alleles, leading to efforts to provide genotyped units to at-risk patients (Chou et al., 2018; Dezan et al., 2017). Another example in which extended Rh matching is performed is R_1R_1 (DCe/DCe) patients who have developed anti-E alloantibodies. Because these patients are at increased risk of delayed hemolytic transfusion reactions because of the subsequent development of anti-c, many blood bankers advocate transfusing only R_1R_1 units to R_1R_1 patients (Shirey et al., 1994).

Rh Antibodies in Hemolytic Disease of the Fetus and Newborn

Antibodies against Rh antigens are also a major cause of HDFN. All Rh-negative women should receive Rh immunoglobulin (IgG anti-D, RhIG) prophylactically in midpregnancy, following an invasive procedure (i.e., amniocentesis), and immediately after delivery to prevent alloimmunization. Rh immunoglobulin prophylaxis is also recommended in women with partial D and some weak D phenotypes because these women can be at risk for D alloimmunization (Ansart-Pirenne et al., 2004). Proposed algorithms have recommended *RHD* genotyping for women with discrepant or weak agglutination (1+–2+) by serology using commercial anti-D typing reagents. Women with weak D types 1, 2, or 3 are not at risk for alloimmunization and are not candidates for RhIG prophylaxis. Women with partial D or other weak D genotypes should receive RhIG (Sandler et al., 2017).

RhIG may also be given following transfusion of RhD+ platelet concentrates or after accidental transfusion of RhD+ RBCs. In the latter, RhIG is given after two-volume RBC exchange with RhD-negative RBCs (Nester et al., 2004). Administration of one vial of RhIG is recommended for every 30 mL whole blood or 15 mL packed RBCs transfused (Fung, 2017). RhIG should be given within 72 hours of exposure to prevent active immunization. RhIG is not given to Rh-negative women who are already immunized to D antigen (i.e., have anti-D).

It is also recommended to give RhIG to Rh-negative women with anti-G alloantibodies. As stated earlier, anti-G behaves as an anti-C + anti-D because of recognition of a Ser103 or C-type antigen on both RhD and RhCE proteins. In general, HDFN secondary to anti-G or anti-C + anti-G is mild when compared with HDFN due to anti-D. However, because these women may still become immunized to D-specific epitopes on the RhD protein, many blood bankers advocate giving RhIG to Rh-negative women with anti-G antibodies (Shirey et al., 1997). Separation of anti-G from a true anti-C + anti-D is very laborious, requiring sequential adsorption and elution (Yesus & Akhter, 1985). One clue suggesting the presence of anti-G is an anti-C titer at least fourfold higher than anti-D (Shirey et al., 1997). It is not necessary, however, to separate anti-G from anti-C + anti-D for routine transfusion. With very rare exceptions, RBCs negative for D and C antigens are also negative for G antigen.

Biological Role

The specific physiologic function of the Rh proteins is still unclear; however, there is a strong belief that Rh proteins may constitute a membrane transporter. The Rh proteins are homologous with ammonium transporters of the Mep/Amt family. In addition, Rh-like homologues have been discovered in invertebrate life forms such as the nematode worm *Caenorhabditis elegans* and a marine sponge, *Geodia cydonium* (Avent, 1999). Evidence suggests that RhAG is capable of facilitating NH_4 and CO_2 transport (Daniels, 2013).

LUTHERAN BLOOD GROUP SYSTEM (ISBT NO. 005)

The Lutheran (Lu) blood group system contains 22 antigens, including four pairs of allelic antigens and 14 high-incidence antigens (Storry et al., 2019). Lutheran is a minor constituent of RBC membranes, averaging only 2000 to 5000 molecules per cell, and can vary in strength between donors (Issitt & Anstee, 1998). Even within a single individual, considerable heterogeneity in Lutheran expression is seen, with only 40% to 50% of red cells positive for Lutheran antigens by flow cytometry (El Nemer et al., 1998). Lutheran appears on red cells at the orthochromatic erythroblast stage, concurrent with binding of red cells to laminin (Daniels, 2009). Lutheran antigens are ubiquitously expressed on human tissues. In addition to RBCs, Lutheran glycoprotein is expressed by the colon, small intestine, ovary, testis, prostate, thymus, spleen, pancreas, kidney, skeletal muscle, liver, lung, placenta, brain, heart, and bone marrow (Rahuel et al., 1996).

Null/Weak Phenotypes

A Lu(a–b–) phenotype can occur in three settings with distinct patterns of inheritance: autosomal recessive, autosomal dominant (*In[Lu]*), and X-linked recessive (Table 36.15). The autosomal-recessive phenotype is a true null phenotype, characterized by complete absence of all Lutheran antigens on RBCs. As a consequence, these individuals can make an alloantibody to Lutheran glycoprotein (anti-Lu3) that reacts with all Lu-positive RBCs. The Lu_{null} phenotype is extremely rare and is not associated with altered expression of other red cell antigens.

TABLE 36.15

Phenotypes of the Lutheran System

REACTIONS WITH ANTI-				FREQUENCY IN U.S. POPULATION, %		
Lu^a	**Lu^b**	**Lu-3**	**PHENOTYPE**	**White**	**Black**	**Comments**
+	0	+	Lu (a+b–)	0.1	0.1	
+	+	+	Lu (a+b+)	7	5	
0	+	+	Lu (a–b+)	93	95	
Null Phenotypes (Lu$_{null}$)						
0	0	0	Lu (a–b–)	Very rare	Very rare	Autosomal recessive Normal CD44, i/I, CD75 Make an anti-Lu-3
0/W*	0/w*	w*	Lu (a–b–)	Very rare	Very rare	In (Lu), autosomal dominant ↓CD44, I/i; ↑CD75 *ELKF* mutation
0/W*	0/w*	w*	Lu (a–b–)	Very rare	Very rare	X-linked recessive, GATA1 mutation nl CD44, i, P1

*Weak Lu antigens detected only by adsorption and elution techniques.

The autosomal-dominant and X-linked–recessive forms are characterized by very weak Lutheran expression, often detected only after adsorption and elution. *In(Lu)* is an autosomal-dominant Lu$_{mod}$ phenotype with an incidence of 0.02% to 0.12% (Daniels, 2009). In addition to Lutheran antigens, *In(Lu)* red cells can show weakened expression of P$_1$, i, Indian/CD44, Knops/CD35, OK/CD147, LW, and Colton antigens and enhanced expression of CDw75 (Daniels, 2009; Fraser et al., 2019; Keller et al., 2018). The X-linked Lu$_{mod}$ phenotype has weakened Lutheran; enhanced i and CDw75; and normal P$_1$, i, and CD44 expression. Because both *In(Lu)* and X-linked–recessive Lu$_{mod}$ phenotypes express some Lutheran antigen on RBCs and other tissues, neither is associated with the development of anti-Lu3. *In(Lu)* RBCs can display subtle abnormalities, including increased poikilocytosis and increased hemolysis, during in vitro storage (Ballas et al., 1992). Cases of congenital dyserythropoietic anemia (CDA) have also been linked to the *In(Lu)* phenotype (Keller et al., 2018; Magor et al., 2015).

Biochemistry

The Lutheran antigens reside on two isomeric, type 1 glycoproteins: Lu-glycoprotein (85 kD) and epithelial cancer antigen (B-CAM, 78 kD) (Daniels, 2009). The 85-kD glycoprotein is the predominant isoform found on RBCs and normal tissues. Members of the Ig superfamily, the 78- and 85-kD glycoproteins share a common large (518 amino acid) extracellular domain with five Ig regions and five potential *N*-glycosylation sites (Fig. 36.7). Three Ig domains are of the constant-region-2 (C2) type, whereas the remaining two are variable-region (V) domains. A laminin binding site resides in a flexible hinge region between C2 and V domains.

The 7-kD difference between the 78-kD and 85-kD isoforms reflects the length of the COOH-terminal cytoplasmic tail. In addition to its longer length, the cytoplasmic domain of the 85-kD isoform possesses an SH3 motif, a potential binding site for Src protein. The cytoplasmic domain also interacts with spectrin, a cytoskeletal protein (Kroviarski et al., 2004). Because it is a highly folded protein, stabilized by disulfide bonds, Lutheran is destroyed by sulfhydryl-reducing agents and many proteases.

Molecular Biology

The gene for Lutheran (*LU*) resides on chromosome 19q13.2-13.3. It is a 12.5-kb gene containing 15 exons: alternate splicing of exon 13 is responsible for the 78-kD minor isoform (Rahuel et al., 1996; El Nemer et al., 1997). Although no TATA or CAAT boxes are present in the 5′ flanking or promoter region of the gene, it does possess consensus sequences for several *cis*-regulatory elements, including the ubiquitous Sp1, AP2, EGR-1, EKLF, Ets, and GATA-1, an erythroid transcription binding protein (El Nemer et al., 1997; Singleton et al., 2008).

The molecular basis for most Lutheran antigens is now known (see Fig. 36.7). Lu^b is the consensus allele (*LU*02*). Most Lu antigens are the result of SNPs, including Lu^a (His77, *LU*01*) and Lu^b (Arg77) (Daniels, 2009). The autosomal-recessive, true Lu$_{null}$ phenotype arises from inheritance of two silent amorph *LU* alleles due to nonsense mutations and deletions (Daniels, 2009; Reid & Lomas-Francis, 2012). The molecular basis for the autosomal-dominant *In(Lu)* phenotype was finally identified in 2008. Most *In(Lu)* individuals are heterozygous for a mutant *EKLF* gene, an erythroid transcription factor active in late erythroid differentiation (Singleton et al., 2008). The *In(Lu)* phenotype, therefore, is the result of reduced transcriptional activation and expression of LU glycoprotein. Reduced EKLF activity likely accounts for decreased expression of other blood group antigens. KLF1 mutations are also linked to hereditary persistence of fetal hemoglobin and congenital dyserythropoietic anemia (Keller et al., 2018). Over 60 KLF1 allelic variants have been described with variable effects on red cell phenotype (Keller et al., 2018; Fraser et al., 2019). The basis for the

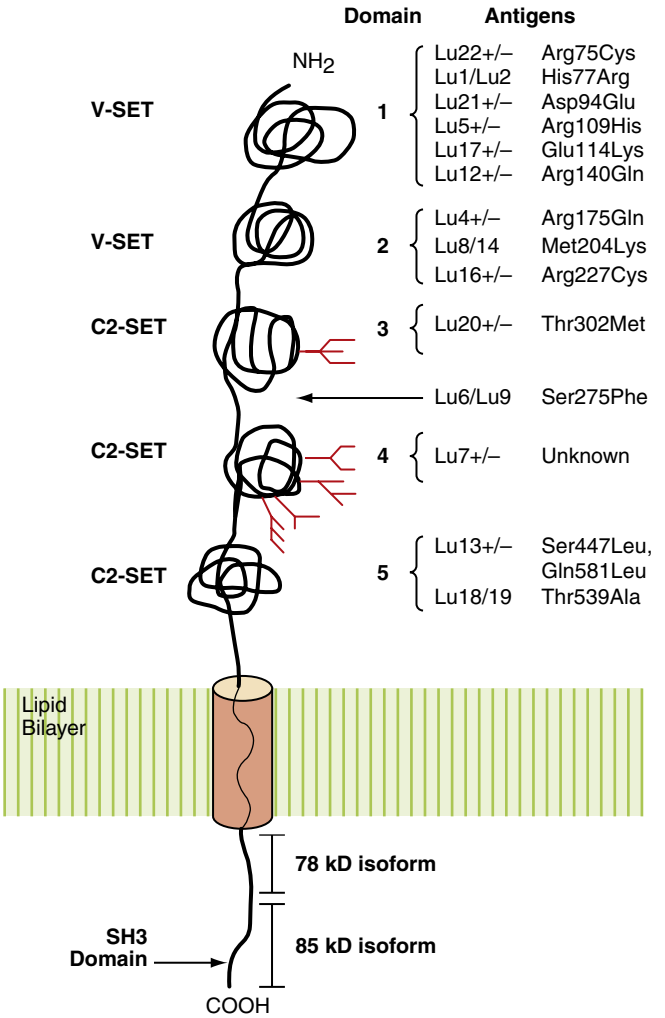

Figure 36.7 Lutheran glycoprotein. The Lutheran antigens reside on one of five immunoglobulin domains (V, C2-like). The transmembrane domain is indicated by a *solid amber cylinder*. The length of the cytoplasmic domain can vary from 19 amino acids (78-kD isoform) to 59 amino acids (85-kD isoform). The latter also possesses a consensus-binding motif for Src protein (SH3 domain).

X-linked recessive In(Lu) phenotype has been identified as mutations in the transcription factor GATA1, which resides on the X chromosome.

Lutheran Antibodies

In general, Lutheran antibodies are not clinically significant and are only rarely associated with HDFN and hemolytic transfusion reactions. Anti-Lu^a is the most common Lutheran alloantibody encountered in the blood bank and is often an IgM, room temperature agglutinin. Because not all RBCs express detectable Lu antigens (El Nemer et al., 1998), anti-Lu^a can display mixed-field agglutination. Antibodies against Lu^b and other Lutheran antigens are most often of IgG isotype, reacting best in the IAT. Reactivity of anti-Lu^a, Lu^b, and other Lutheran antibodies can be inhibited by pretreatment of RBCs with chymotrypsin, trypsin, 2-aminoethylisothiouronium bromide (AET), and dithiothreitol (DTT).

Biological Role

Biologically, Lutheran is a high-affinity receptor for laminin, a basement membrane protein involved in cell differentiation, adhesion, migration, and proliferation. Overexpression of LU glycoprotein in ovarian carcinoma and other cancers is hypothesized to facilitate tumor cell adhesion and metastasis (Rahuel et al., 1996). In sickle cell patients, increased Lutheran expression on reticulocytes and sickle cells may contribute to the pathophysiology of vaso-occlusive crises. Patients with sickle cell disease have indirect evidence of chronic vascular injury with shedding of microvascular endothelial cells and exposure of vascular basement membrane (Solovey et al., 1997). In these patients, increased exposure of laminin on the thrombotic subendothelium, coupled with increased expression of laminin receptor on reticulocytes and sickle cells, may promote red cell adhesion and circulatory stasis (El Nemer et al., 1998; Parsons et al., 2001). Likewise, LU glycoprotein may contribute to thrombosis in polycythemia vera. The *JAK2* mutation was shown to increase phosphorylation of LU glycoprotein and red cell adhesion (Daniels, 2009). In normal erythropoiesis, LU may play a role in migration of maturing erythroid cells out of the marrow (Daniels, 2009).

KELL AND KX BLOOD GROUP SYSTEMS (ISBT NO. 006 AND 019)

First identified in 1945, the Kell (KEL) blood group system currently consists of 39 high- and low-frequency antigens (Tables 36.16 and 36.17). Sixteen Kell antigens belong to 8 sets of allelic antigens, whereas the remainder are predominantly high-incidence antigens (>99% of the population). Many low-incidence Kell antigens (K, Js^a, Ul^a, Kp^a, Kp^c) show distinct racial differences. The Kell antigen is found on RBCs, erythroid and megakaryocyte progenitors, skeletal muscle, and testis. RBCs express approximately 2000 to 6000 copies of Kell protein per cell (Reid & Lomas-Francis, 2012).

Null and Weak Phenotypes

K_0K_0 is an autosomal-recessive, null phenotype that completely lacks all Kell antigens (see Table 36.22). As a consequence, these individuals can

TABLE 36.16
Kell and XK Blood Group Antigens*

ANTIGEN (HIGH FREQUENCY)			Amino Acid Change		ANTIGEN (LOW FREQUENCY)	
ISBT	**Name**	**Percent Donors**	**(High→Low Frequency)**	**Percent Donors**	**Name**	**ISBT**
KEL2	K	99.8	Thr193Met	9	K	KEL1
			Thr193Ser	Rare		
			Ala423Val	Unknown		Weak KEL2
KEL4	Kp^b	99.9	Arg281Trp	2	Kp^a	KEL3
			Arg281Gln	<0.1	Kp^c	KEL21
KEL7	Js^b	>99.9	Leu597Pro	<1% whites 19.5% blacks	Js^a	KEL6
KEL5	Ku	>99.9	Heterogeneous	0.8	K_0	K_{null}
			Heterogeneous	Rare	K_{mod}	
KEL20	Km	>99.9	unknown			
XK1	Kx	>99.9	Mutation XK protein	Rare	McLeod	

ISBT, International Society of Blood Transfusion.
*As referenced in Daniels G: *Human blood groups*, ed 3, Oxford, 2013, Blackwell Science; Daniels G, Flegel WA, Fletcher A, et al.: International Society of Blood Transfusion Committee on Terminology for Red Cell Surface Antigens: Cape Town report, *Vox Sang* 92:250–253, 2007; Daniels G, Fletcher A, Garratty G, et al.: Blood group terminology 2004: From the International Society of Blood Transfusion Committee on Terminology for Red Cell Surface Antigens, *Vox Sang* 87:304–316, 2004; and Reid RE, Lomas-Francis C: *The blood group antigen facts book*, ed 3, San Diego, 2012, Academic Press.

TABLE 36.17
Phenotype Frequencies in the Kell System

REACTIONS WITH ANTI-										FREQUENCY IN U.S. POPULATION, %	
K	**k**	**Kp^a**	**Kp^b**	**Js^a**	**Js^b**	**Ku**	**Km**	**Kx**	**Phenotype**	**White**	**Black**
+	0					++	++	w	K+k–	0.2	Rare
+	+					++	++	w	K+k+	8.8	2
0	+					++	++	w	K–k+	91	98
		+	0			++	++	w	Kp(a+b–)	Rare	0
		+	+			++	++	w	Kp(a+b+)	2.3	Rare
		0	+			++	++	w	Kp(a–b+)	97.7	100
				+	0	++	++	w	Js(a+b–)	0	1
				+	+	++	++	w	Js(a+b+)	Rare	19
				0	+	++	++	w	Js(a–b+)	100	80
Null Phenotypes											
0	0	0	0	0	0	0	0	++	K_0	Exceedingly rare	
0/w	0/w	0/w	0/w	0/w	0/w	w	w	++	K_{mod}	Rare	
0/w	0/w	0/w	0/w	0/w	0/w	0/w	0	0	McLeod	Rare	

++, Strong reactivity; *w,* weak reactivity.

make an alloantibody to the Kell glycoprotein (anti-Ku). Unlike McLeod RBCs (see later discussion), K_0K_0 RBCs have enhanced expression of Kx antigen, present on the XK protein. Unlike Rh_{null} red cells, K_0K_0 red cells have no decrease in CO_2 permeability (Endeward et al., 2006). A K_0K_0 RBC can be produced in the laboratory by treating Kell-positive RBCs with sulfhydryl-reducing agents.

Kell antigens are significantly depressed/absent on McLeod RBCs, an X-linked recessive phenotype characterized by the absence of XK protein on RBCs (Kx antigen, XK1; ISBT 019), acanthocytes, and neuromuscular disorders. Because McLeod individuals lack XK and Kell proteins, these individuals can make alloantibodies directed against both proteins. As a consequence, McLeod individuals are incompatible with both Kell-positive and K_0K_0 RBCs. Depressed Kell expression is also observed on K_{mod} and Gerbich-negative RBCs, two autosomal-recessive phenotypes. As with the K_0K_0 phenotype, some $Kell_{mod}$ individuals have increased Kx (KEL15) expression and can develop an anti-KEL5 (anti-Ku) following RBC transfusion. Transient depression and masking of Kell antigens have been reported in septic patients and in autoimmune hemolytic anemia due to anti-Kell autoantibodies (Judd et al., 1981; Issitt & Anstee, 1998; Bosco et al., 2009). Kell antigens are also depressed (up to 80%) in alleles bearing KEL3 in *cis* (e.g., KKp^a, KEL*1,3; kKp^a, KEL*2,3) (Poole et al., 2006; Kormoczi et al., 2009).

Biochemistry

The Kell antigens (ISBT No. 006) reside on a 93-kD, 732 amino acid glycoprotein (CD238) possessing a short 47 amino acid amino-terminal cytosolic domain, a single transmembrane domain, and a large 665 amino acid extracellular domain that includes the carboxy-terminus and 4-5 *N*-linked glycans (Fig. 36.8). In the KEL1 phenotype, a Thr183>Met substitution voids a glycosylation site, resulting in only four *N*-linked glycans (Lee, 1997).

Overall, the molecule has a complex, folded tertiary structure due to the formation of multiple disulfide bonds by the 15 cysteine residues present in the extracellular domain of the molecule (Lee, 1997). Because of its highly folded nature, the Kell glycoprotein is fairly resistant to proteolytic digestion but is exquisitely sensitive to sulfhydryl-reducing agents such as DTT, AET, 2-mercaptoethanol (2-ME), and ZZAP, a combination of DTT and cysteine-activated papain.

In the RBC membrane, the Kell glycoprotein is covalently linked to the XK protein (ISBT No. 019), a 444 amino acid, nonglycosylated, multipass protein containing 10 transmembrane domains. Encoded by a gene on chromosome Xp21, the XK protein is hypothesized to be a membrane transport protein. On RBCs, the XK protein is covalently linked to the Kell protein through a disulfide bond at C347 on the fifth extracellular loop of XK protein and C72 of Kell. In the absence of XK protein (McLeod phenotype), Kell expression is decreased on RBCs, suggesting that XK protein may help transport Kell. Transfection studies in COS cells, however, show normal transport and folding of the Kell protein in the absence of XK protein (Russo et al., 1998). Nor is expression of XK dependent on Kell expression. The XK protein is expressed on several nonerythroid tissues, including liver, skeletal muscle, heart, brain, and pancreas (Ho et al., 1994).

Molecular Biology

Cloned in 1991, the Kell gene (*KEL*) contains 19 exons spanning 21.5 kb on chromosome 7q34 near the cystic fibrosis gene. The promoter region and exon 1 contain several consensus-binding sequences for GATA-1, an erythroid transcription regulatory binding factor. Kell is a member of the M13 neprilysin family of zinc-neutral endopeptidases and shares homology with common acute lymphocytic leukemia antigen (CALLA, CD10), endothelin-converting enzyme-1 (ECE-1), neutral endopeptidase 24.11 (NEP-24.11), and PEX. The region of greatest homology lies in the carboxy-terminal half of the molecule (amino acids 550–652) and is sometimes referred to as the *NECK domain* (N-24.11, EC-1, K family). This relatively conserved region shares 34% to 36% homology with the carboxy-terminal catalytic domains of NEP-24.11 and ECE-1, as well as a pentameric zinc-binding motif (HELLH), a common feature of zinc-dependent metalloproteinases (Lee, 1997).

With cloning of the Kell gene, the molecular and biochemical basis of several Kell antigens became possible. As shown in Table 36.16, all Kell alloantigens identified and sequenced are single–amino acid polymorphisms in the translated Kell protein, generally in the amino half of the molecule (Lee, 1997). The consensus allele *KEL*02* encodes 20 high-frequency antigens, including k, Kp^b, and Js^b (Reid & Lomas-Francis, 2012).

Several individuals with absent or depressed Kell expression have also been studied. K_0K_0 phenotype arises from homozygosity for a silent *KEL* amorph gene. Thirty K^0 alleles (*KEL*02N*) are recognized, including

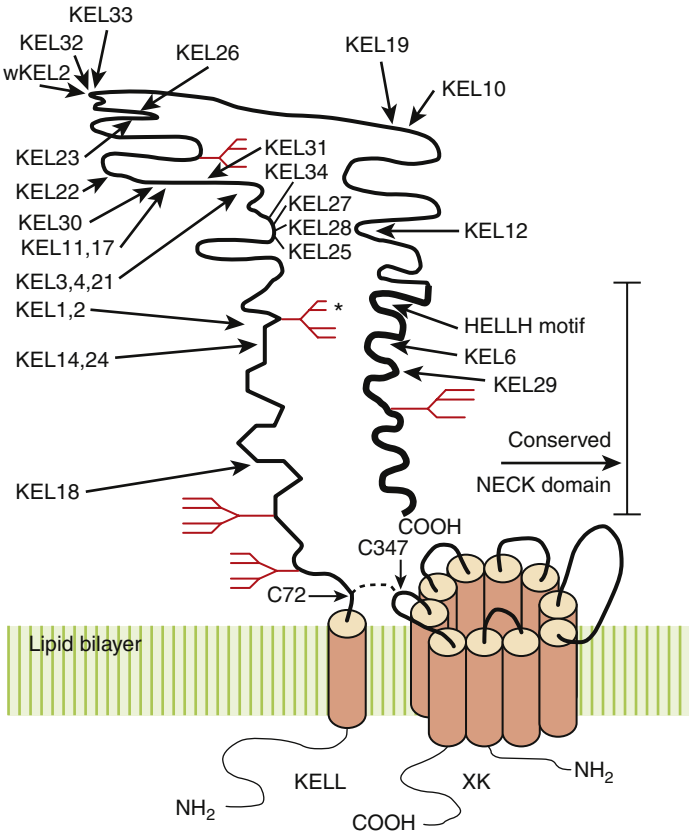

Figure 36.8 Diagram of KELL and XK protein. KELL is covalently linked to the XK protein by a disulfide bond (- - - -) through Cys72 of Kell and Cys347 of XK. The sites of different Kell antigens are indicated by *solid lines*. The *highlighted area* at the carboxy-terminus of KELL represents the domain sharing the most homology to other NECK family proteins (NEP-24.11, ECE-1, PEX). The zinc-binding motif (HELLH) is a consensus sequence shared by zinc-dependent metalloproteinases. The transmembrane domains of KELL and XK protein are indicated by *solid amber cylinders*. The *N*-glycosylation sites are indicated by *branched structures*. The *N*-glycosylation site marked by an *asterisk* is not present in individuals of the KEL1-positive phenotype.

splice-site mutations and premature stop codons (Reid & Lomas-Francis, 2012). K_{mod} is the result of missense mutations and may occur on either K1 or k background. Twelve K_{mod} alleles (*KEL*02M*) are recognized by the ISBT. Several mutations have been identified in the *XK* protein on Xp21, responsible for the McLeod phenotype (Russo et al., 2002). At present, 39 mutant *XK* alleles (*XK*01N*) have been described, including deletion mutants, splice site, and nonsense mutations. The molecular basis for decreased Kell antigen expression with Gerbich-negative phenotypes is unknown. It is speculated that Kell and glycophorin C (Gerbich) may be near neighbors on the RBC membrane.

Kell Antibodies

Alloantibodies against antigens in the Kell blood group system are clinically significant (see Table 36.5). They can be associated with both immediate and delayed hemolytic transfusion reactions. Anti-Kell antibodies are also associated with HDFN. HDFN secondary to maternal anti-Kell antibodies is often characterized by reticulocytopenia, with little or no bilirubinemia. It is now known that maternal anti-Kell (anti-KEL1 or K1) directly suppresses erythroid progenitors, leading to a severe reticulocytopenic anemia in the fetus (Vaughan et al., 1998) with up to 30% of affected infants presenting with fetal hydrops (Van den Akker et al., 2008). Anti-K1 is present in approximately 1% of pregnancies, with HDFN affecting 40% of K1-positive infants (Finning et al., 2007). Several centers now routinely screen and refer prenatal patients with Kell antibodies, with improved perinatal outcomes (Kamphuis et al., 2008). Reports have also described neonatal thrombocytopenia due to suppression of marrow megakaryocytes (Wagner et al., 2000). In general, thrombocytopenia is mild, with only 2% of infants having platelet counts of less than 100×10^9/L (Van den Akker et al., 2008). Similar to RHD, fetal genotyping can be performed on maternal plasma (Finning et al., 2007).

The most commonly encountered antibody against the Kell blood group system is anti-K1, which is second only to RhD in immunogenicity. Antibodies against Kell antigens are of IgG isotype, arising from immune stimulation via transfusion or pregnancy. There are rare reports of naturally

TABLE 36.18

The Lewis Blood Group System

Phenotype	FREQUENCIES IN U.S. ADULTS, %		POSSIBLE GENOTYPE		ABH AND LEWIS SUBSTANCES IN SALIVA AND PLASMA		
	White	Black	Le Gene	Se Gene	Group O	Group A	Group B
Le (a+b–)	22	23	*Le/Le* or *Le/le*	*se/se*	Le^a	Le^a	Le^a
Le (a–b+)	72	55	*Le/Le* or *Le/le*	*Se/Se* or *Se/se*	Type 1H	Type 1H, A	Type 1H, B
					Le^a, Le^b	Le^a, Le^b, ALe^b	Le^a, Le^b, BLe^b
Le (a–b–)	6	22	*le/le*	*Se/se*	Type 1H	Type 1H, A	Type 1H, B
			le/le	*se/se*	Type 1 chain precursor (Le^c)	Type 1 chain precursor (Le^c)	Type 1 chain precursor (Le^c)

occurring anti-K1 antibodies following severe bacterial infections and may be the result of cross-reactive antibodies against bacterial neprilysin homologues (Cooling, 2015), although examples of naturally occurring anti-Kell alloantibodies are known (Judd et al., 1981). Because Kell antigens are sensitive to sulfhydryl-reducing agents, the activity of anti-Kell antibodies can be eliminated by pretreatment of RBCs with AET, DTT, 2-ME, or ZZAP.

Biological Role

Kell cleaves endothelin-3, a vasoactive peptide that functions in endothelial cell migration, neovascularization, axonal growth, and neural crest development. In a murine $Kell_{null}$ model, absence of Kell led to only subtle effects, including decreased blood pressure, blunting endothelin-3 activation of Ca^{++}-dependent K^+ channels, decreased microvascular formation, and mild changes in motor function (Zhu et al., 2009). Because endothelin-3 is also cleaved by ECE-1, a related endothelin-converting enzyme, Kell may have only a minor physiologic role in endothelin-3 homeostasis. The ability of anti-Kell to suppress fetal erythropoiesis also suggests a possible role for Kell during erythroid differentiation and maturation (Vaughan et al., 1998). However, only minor differences in mean corpuscular volume, mean corpuscular hemoglobin, hemoglobin, and reticulocyte counts were observed in $Kell_{null}$ mice (Zhu et al., 2009).

In contrast to Kell, the absence of XK protein is strongly associated with several abnormal clinical and laboratory findings. McLeod RBCs have shortened survival, decreased permeability to water, and abnormal morphology (acanthocytes). The McLeod syndrome, characterized by both hematologic and neuromuscular abnormalities, typically presents with areflexia, dystonia, and choreiform movements late in life. Late-onset muscular dystrophy and cardiomyopathy can also be seen. Both hematologic and neuromuscular defects in McLeod patients are believed to result from the absence of XK protein on red cells, brain, heart, and skeletal muscle (Ho et al., 1994). It is interesting that the Huntington disease gene, another neurodegenerative disorder, is located near the *XK* gene on the X chromosome (Issitt & Anstee, 1998). In fact, modern historians have hypothesized that a K1+ McLeod phenotype might explain Henry VIII's physical and psychological decline late in life, as well as his wives' high miscarriage rate (Whitley & Kramer, 2010).

The McLeod phenotype can also be associated with chronic granulomatous disease (CGD), a functional 0p defect resulting in severe, recurrent, life-threatening bacterial infections. In two thirds of patients, CGD results from a deletion or mutation of the cytochrome *b* gene *(CYBB)* on the X chromosome. Because of the proximity of the *CYBB* and *XK* genes on the X chromosome, approximately 7% of patients with X-linked CGD also express a McLeod phenotype (Curnutte & Bemiller, 1995).

LEWIS BLOOD GROUP SYSTEM (ISBT NO. 007)

The Lewis blood group system is unusual in that the Lewis antigens are not of erythroid origin. It primarily consists of two antigens: $Lewis^a$ (Le^a, LE1) and $Lewis^b$ (Le^b, LE2). Four additional antigens (Le^{ab}, Le^{bH}, ALe^b, BLe^b) reflect the influence of ABO on Lewis synthesis and antigenicity. On RBCs, the Lewis antigens reside on glycosphingolipids, composed of a Lewis-active carbohydrate head group linked to a ceramide (*N*-acyl sphingosine) lipid tail. Lewis antigens are synthesized in the gastrointestinal tract and passively adsorbed onto RBCs from a soluble pool of secreted Lewis substance in plasma (Hauser, 1995). Tissues and fluids expressing Lewis include plasma, saliva, RBCs, platelets, lymphocytes, endothelium, uroepithelium, and bowel mucosa. In some tissues, Lewis antigens are expressed on glycosphingolipids, glycoproteins, and mucins (Cooling, 2015).

Three Lewis phenotypes are observed in adults: Le (a+b–), Le (a–b+), and Le (a–b–). The Le (a+b+) is only rarely observed, usually on RBCs of very young children and some individuals of Polynesian, Japanese, or Taiwanese ancestry (Issitt & Anstee, 1998). As shown in Table 36.18, the Le (a–b–) phenotype is five times more common in blacks than in whites. The Le (a–b–) phenotype is also increased in neonates owing to developmentally delayed expression of the *Lewis* and *Secretor* genes. By 5 years of age, most children will express adult levels of Lewis antigens on their RBCs. The amount of Lewis antigen on RBCs is also influenced by ABO type. Le (a–b+) RBCs from group O donors appear to have more Le^b than A_1 and B cells. As will be discussed later, group A_1 and B donors can convert Le^b to ALe^b and BLe^b, respectively (Issitt & Anstee, 1998).

Biochemistry

Although biosynthetically related to each other, the Le^a and Le^b antigens are not allelic antigens. They represent the complex interaction of two distinct glycosyltransferases: fucosyltransferase type II (FUT2) and fucosyltransferase type III (FUT3). FUT3 is the product of the Lewis gene (*Le/FUT3*) and is an α1–3/4 fucosyltransferase. FUT2, the product of the *Secretor* gene (*Se*), is an α1–2 fucosyltransferase related to the *H* gene, FUT1. How *Le*, *Se*, and *ABO* genes interact to yield the different combinations of RBC and plasma phenotypes is shown in Table 36.18 and Figure 36.9.

The precursor molecule for Lewis and related antigens is a type 1 chain precursor, historically known as the Le^c antigen. In Le (a+b–) donors, FUT3 or Lewis adds an α1–4 linked fucose to Le^c to form the Le^a antigen. Because these donors lack the *Se/FUT2* gene (*se/se*), no type 1 chain H (Le^d) is made. As a result, only Le^a antigen is present in plasma, saliva, and RBCs. The Le (a–b+) red cell phenotype results from the inheritance of both *Le* and *Se* genes. FUT3 still converts a small amount of type 1 chain precursor to Le^a antigen. However, most Le^c substance is converted to type 1 chain H or Le^d by FUT2 (see Fig. 36.9). FUT3 subsequently adds a second fucose to form Le^b antigen (Lowe, 1994). In group A and B persons, type 1 chain H is further modified by the A/B glycosyltransferase to form type 1 chain A and B antigens. Similar to type 1 chain H and Le^c antigens, these molecules can serve as substrates for FUT3 to form ALe^b and BLe^b (see Fig. 36.9). In group A_1 donors, ALe^b is the major Le^b antigen found in plasma (Lindstrom et al., 1992).

The Le (a–b–) red cell phenotype occurs in individuals who lack the *Le/FUT3* gene. Individuals who are negative for both *Le* and *Se* alleles (*le/le*, *se/se*) are unable to synthesize Le^a antigen or type 1 chain H antigens. As a result, only type 1 chain precursor or Le^c antigen is present in secretions and plasma. In contrast, individuals who inherit at least one Se allele can express type 1 chain glycolipids with ABH activity.

Molecular Biology

The *FUT3* or *Lewis* gene resides on chromosome 19p13.3 near two other α1–3 fucosyltransferase genes: *FUT5* and *FUT6*. All three α1–3 fucosyltransferases are highly homologous, consistent with gene duplication (Weston et al., 1992). The gene encodes a 361 amino acid type II glycoprotein with both α1→4 (Le^a) and α1→3 (LeX) fucosyltransferase activity. *FUT3* is highly expressed in colon, stomach, small intestine, lung, and kidney, with weaker expression in salivary gland, bladder, uterus, and liver. *FUT6* is coexpressed with *FUT3* in most tissues (Cameron et al., 1995).

The Le (a–b–) or null phenotype arises from inactivating mutations in *FUT3*. More than 37 *FUT3* null alleles have been reported, with most (89%) possessing at least two mutations (Blood Group Antigen Gene Database, 2015). Many alleles show distinct geographic and ethnic distributions. In whites, Le (a–b–) is most commonly associated with alleles containing mutations at Trp68Arg and Thr105Met ($le^{202,314}$). In contrast, *FUT3* null alleles common in Asia include le^{59}, $le^{59,508}$, and $le^{59,1067}$ (Cooling, 2015). The Lewis weak (Le^w) phenotype, often characterized by a Le (a–b–) RBC

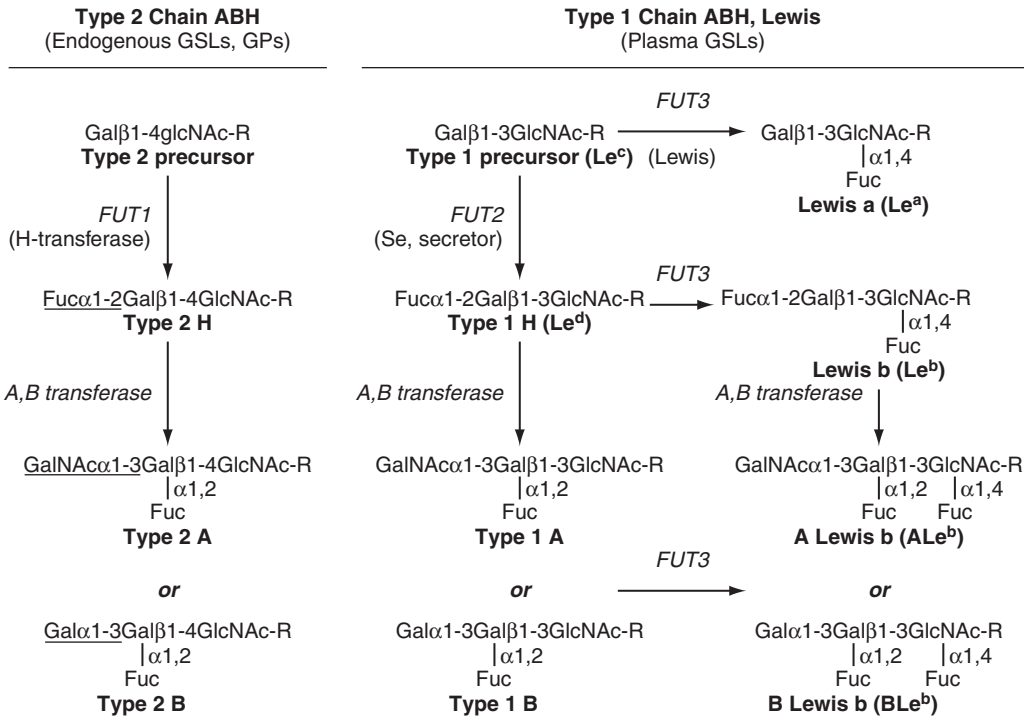

Figure 36.9 Synthesis of Lewis and type 1 chain ABH antigens. *Fuc,* Fucose; *Gal,* galactose; *GalNAc, N*-acetylgalactosamine; *Glc,* glucose; *GlcNAc, N*-acetylglucosamine; *Le,* Lewis; *R,* ceramide.

phenotype and the presence of Lewis-active substance in saliva, is due to a single missense mutation in the transmembrane domain (T59>G). The latter has decreased Golgi retention and reduced activity with glycolipid substrates, leading to discrepant Lewis expression on red cells, saliva, and gastrointestinal tissues (Mollicone et al., 1994; Nishara et al., 1999). Le^w and a Le (a–b–) RBC phenotype can also be a consequence of gene dosage: *Le/le* heterozygous individuals show 50% decreased FUT3 activity in saliva and tissues (Cooling, 2015).

The *FUT2* (*Se*) gene resides on chromosome 19q13.3 as part of a 100-kb gene cluster that includes the *H* gene (*FUT1*) and *Sec1*, an inactive *FUT2*-like pseudogene (Kelly et al., 1995). Multiple null alleles have been reported, with distinct geographic and ethnic distributions. Most null alleles are the result of nonsense mutations (Reid & Lomas-Francis, 2012). There are also examples of recombination among *FUT1*, *FUT2*, and *Sec1* (Koda et al., 1996; Soejima et al., 2008). Weak *FUT2* alleles are known and common in Asia (Reid & Lomas-Francis, 2012; Cooling, 2015). The most common partial secretor phenotype has been linked to an Ile129>Phe mutation and is associated with a Le (a+b+) phenotype (Yu et al., 1995).

Lewis Antibodies

Similar to ABO, antibodies against Le^a and Le^b antigens are naturally occurring IgM antibodies (see Table 36.5), but unlike ABO antibodies, anti-Lewis antibodies are seldom clinically significant. Most examples are detected as room temperature agglutinins; however, some examples are reactive in the IAT. Although uncommon, some examples demonstrate in vitro hemolysis. Because Le^a and Le^b are glycosphingolipids, antibody reactivity can be enhanced by pretreatment of RBCs with enzymes. Antibody reactivity is neutralized by the addition of commercially available soluble Lewis substance or plasma containing the soluble Lewis antigen of interest. Anti-Le^b can be observed in individuals of Le (a+b–) or Le (a–b–) phenotype, whereas anti-Le^a is observed only in Le (a–b–) individuals. Anti-Le^a is not observed in the Le (a–b+) phenotype because these individuals synthesize a small amount of Le^a. It is interesting to note that some Le (a–b+) women can transiently become phenotypically Le (b–), with the development of anti-Le^b, during pregnancy. Some examples of anti-Le^b can demonstrate ABH specificity (anti-LebH, anti-ALe^b, anti-BLe^b), reacting more strongly with Le^b-positive RBCs of specific ABO types.

They are not associated with HDFN and are only rarely associated with hemolytic transfusion reactions. It is speculated that they could play a role in renal graft rejection in black Le (a–b–) individuals (Spitalnik et al., 1984). For transfusion, patients with anti-Lewis antibodies reactive only at room temperature may be safely transfused with crossmatch–compatible RBCs. In contrast, rare examples of anti-Le^a or anti-Le^b that are hemolytic in vitro should receive antigen-negative, crossmatch-compatible RBCs. If antigen-negative blood is not available, infusion of plasma containing the soluble Lewis antigen of interest may be helpful in neutralizing or inhibiting circulating antibody before RBC transfusion (Klein & Anstee, 2006).

Biological Role

The Lewis blood group antigens play an important role in disease. Le (a–b–) is linked to a twofold increased risk of atherosclerotic disease and coronary death, with the strongest association observed in Le (a–b–) individuals carrying the le^{59} allele (Ellison et al., 1999; Djousse et al., 2007). Aberrant expression of sialyl-Le^a occurs in many gastrointestinal and uroepithelial cell cancers and may contribute to tumor metastasis. Sialyl-Le^a is a ligand for the endothelial adhesion molecule E-selectin and may mediate tumor cell–endothelium interactions (Takada et al., 1993). Sialyl-Le^a is also the epitope for the tumor marker CA 19-9, a useful serologic marker for monitoring patients with gastrointestinal and other malignancies.

Secretor status is a host susceptibility factor in several infectious diseases. *Helicobacter pylori*, a causative agent of gastritis and ulcers, binds H, Le^b, and Le^y antigens via BabA recognition of a terminal Fucα1–2Gal epitope (Boren et al., 1993; Cooling, 2015). The latter might explain the increased incidence of ulcers and stomach cancer among blood group O secretors (Yamaoka, 2008). A Lewis null and/or nonsecretor phenotype has also been linked with a higher incidence of recurrent *Candida* vaginitis and urinary tract infection (Cooling, 2015). Le^b and type 1 H antigen are also receptors for most norovirus and rotavirus strains. Several epidemiologic studies have shown that nonsecretors have inherent resistance against infection (Cooling, 2015). In contrast, nonsecretors were recently identified as a risk factor for necrotizing enterocolitis and sepsis in premature infants (Morrow et al., 2011).

DUFFY BLOOD GROUP SYSTEM (ISBT NO. 008)

The Duffy (FY) blood group system was discovered in 1951 and contains five antigens: Fy^a, Fy^b, Fy3, Fy5, and Fy6. Fy^a and Fy^b are autosomal-codominant antigens, whereas Fy3, Fy5, and Fy6 are high-incidence antigens present on all RBCs except the Duffy null phenotype. The Fy4 antigen, originally described on Fy (a–b–) RBCs, is now thought to be a distinct, unrelated antigen and is no longer included in the FY system.

Fy^a and Fy^b antigens are common in whites, whereas the Duffy null or Fy (a–b–) phenotype is the predominant phenotype in blacks (Table 36.19). Fy^x is generally characterized by extremely weak Fy^b expression. In addition to RBCs, the Duffy antigens are expressed on cerebellar Purkinje cells and postcapillary venule endothelial cells. Duffy antigens have also been reported on endothelial cells of renal glomeruli, vasa recta, thyroid, and pulmonary capillaries, as well as on alveolar type 1 squamous cells and epithelial cells of renal collecting tubules (Chaudhuri et al., 1997; Hadley & Peiper, 1997). RBCs possess approximately 12,000 to 14,000 copies of the Duffy glycoprotein per cell (Reid & Lomas-Francis, 2012).

TABLE 36.19

Phenotype Frequencies in the Duffy System

REACTIONS WITH ANTI-				WHITES		BLACKS	
Fy^a	**Fy^b**	**Fy3**	**RBC Phenotype**	**Frequency***	**Genotypes†**	**Frequency***	**Genotypes†**
+	–	+	Fy (a+b–)	17	*FY*A/FY*A*	9	*FY*A/FY*A* *FY*A/FY*B^{ES}*
+	+	+	Fy (a+b+)	49	*FY*A/FY*B*	1	*FY*A/FY*B*
–	+	+	Fy (a–b+)	34	*FY*B/FY*B*	22	*FY*B/FY*B* FY*B/FY*B^{ES}
–	–	–	Fy (a–b–)	Very rare	*FY*amorph*	68	*FY*B^{ES}/FY*B^{ES}*
+/–	w	w	Fy (a+b^w) Fy (a–b^w)	<0.1%	*FY*A/FY*X* *FY*X/FY*X*	Very rare	*FY*A/FY*X* *FY*X/FY*B^{ES}*

++, Strong reactivity; *w,* weak reactivity.
*Frequency (%) U.S. population.
†*FY*A* (*FY*01*), Fy^a allele; *FY*B* (*FY*02*), Fy^b allele; *FY*B^{ES},* FY*B allele carrying a GATA-1 promoter mutation; *FY*X, FY*B* gene containing missense with weak Fy^b expression; *FY*amorph* (*FY*N*), silent *FY* gene containing disruptive mutations (deletion, frameshift, nonsense). See accompanying text.

Biochemistry

The Duffy glycoprotein was recently renamed ACKR1 (atypical chemokine receptor 1) from its previous designation as DARC (Duffy antigen receptor for chemokines) (Fig. 36.10). ACKR1 is a 336 to 338 amino acid, integral membrane glycoprotein, containing a 62 amino acid extracellular amino-terminus, seven transmembrane domains, and an intracellular carboxy-terminus rich in serine and threonine residues. The amino-terminal domain possesses three *N*-glycans (Czerwinski et al., 2007) and is linked to the third extracellular loop by a disulfide bond to form a hepatohelical structure. A second disulfide bond exists between the first and second extracellular loops. DARC exists as a homodimer or as a hetero-oligomer with CCR5, a β-chemokine receptor that plays a role in HIV internalization (Chakera et al., 2008).

The Fy^a, Fy^b, and Fy6 antigens reside on the amino-terminal domain of ACKR1 and are sensitive to proteolytic cleavage. The negatively charged amino-terminal domain is the binding site for *P. vivax* PvDBP ligand. Site-directed mutagenesis has confirmed that amino acids 19 to 26, the Fy6 epitope, are critical for *P. vivax* binding (Tournamille et al., 2005). The high-incidence antigen Fy3 is believed to reside on the third extracellular loop (Hadley & Peiper, 1997; Wasniowska et al., 2004).

Molecular Biology

Located on chromosome 1q22-23, the Duffy gene (*ACKR1*, *DARC*, *FY*) is a 1014-bp gene containing two exons, a small upstream exon encoding the first seven amino acids, and a second exon encoding the rest of the molecule (Hadley & Peiper, 1997). There are two known ACKR1 mRNA transcripts, which give rise to a 336 (isoform B, predominant protein) and 338 amino-acid protein (isoform A, minor), respectively (Hoher et al., 2018). The promoter region for the major protein contains consensus sequences for multiple *cis*-regulatory elements, including AP-1, Sp1, and GATA-1, an erythroid transcription activator-binding protein that controls transcription of DARC in erythroid cells (Iwamoto et al., 1996). Phylogenetic studies indicate that *FY*B* (*FY*02*) is the ancestral gene of human and nonhuman primates (Li et al., 1997). Genetic studies have identified four predominant Duffy alleles—*FY*A (FY*01)*, *FY*B (FY*02)*, *FY*B^{ES}* (*FY*02N.01*), and *FY*X (FY*02W)*—responsible for the Fy^a, Fy^b, Fy_{null}, and Fy^x phenotypes, respectively (see Table 36.19). The codominant alleles, *FY*A* and *FY*B*, differ by a single amino acid (Gly42Asp). The Fy^x phenotype *(FY*X)*, characterized by extremely weak Fy^b expression (10% normal), arises from an R89C substitution in the first cytoplasmic loop, leading to protein instability (Yazdanbakhsh et al., 2000; Reid & Lomas-Francis, 2012). Although rare, *FY*A* alleles bearing the R89C and weak Fy^a expression have been identified. To date, 7 *ACKR1* alleles with weak Fy^a or Fy^b expression have been identified, with the highest frequency among European whites (Hoher et al., 2018).

Three distinct mechanisms are responsible for the Fy_{null} or Fy (a–b–) serologic phenotype. In whites, the *FY* gene is disrupted (*FY*amorph*, *FY*02N.02*), leading to complete absence of DARC on all tissues (Reid et al., 2014). As a result, these individuals can make alloantibodies to all Duffy antigens, including high-incidence antigens (Fy3, Fy5). In contrast, black Fy (a–b–) individuals are homozygous for *FY*B^{ES}* (*FY*02N.01*), an *FY*B* variant that possesses a point mutation in the *FY* gene promoter (–67T>C) that abrogates the consensus binding site for GATA-1. As a result, there is a selective loss of *FY* transcription in RBCs; however, FY transcription is retained in endothelial and epithelial cells, which utilize other promoter enhancer elements. Because Fy^b is expressed on nonerythroid cells, black Fy (a–b–) individuals do not make anti-Fy^b and only rarely make anti-Fy3. In Asian and Oceania populations, GATA mutations can occur on an *FY*A* background (*FY*01N*) with selective loss of Fy^a on red cells (Hoher et al., 2018; Cooling, 2015). Finally, there is increasing recognition that some individuals, particularly donors, who historically typed as Fy (a–b–) by serology are actually Fy (a–b^{+w}) on genotyping (*FY*B^{ES}/FY*X*).

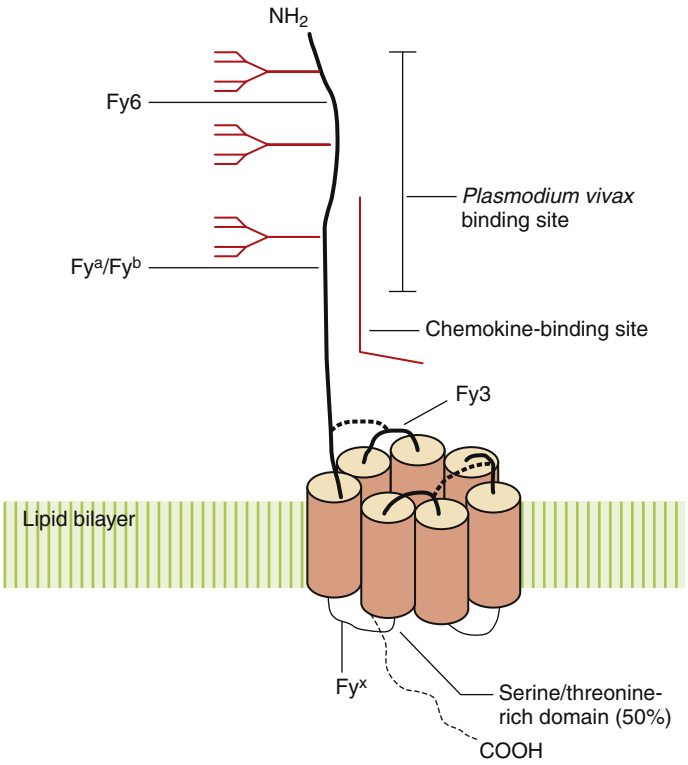

Figure 36.10 Duffy glycoprotein or Duffy antigen receptor for chemokine molecule (DARC). DARC contains a 62 amino acid, extracellular amino-terminal domain and seven transmembrane domains, indicated by *solid amber cylinders*. A disulfide bond exists between the amino-terminal domain and the third extracellular loop. A second disulfide bond exists between the first and second extracellular loops. Three *N*-glycosylation sites are indicated by branched structures. The sites of the Fy3, Fy6, and Fy^a/Fy^b antigens are shown where indicated. The binding site for *Plasmodium vivax* exists between amino acids 8 and 44 and includes the Fy6 and Fy^a/Fy^b antigens. The chemokine-binding site lies in a cleft between the amino-terminal domain and the third extracellular loop. The mutation leading to the Fy^x phenotype, characterized by weak Fy^b expression, is present in the first cytoplasmic loop.

Duffy Antibodies

Antibodies against Fy^a, Fy^b, and other Duffy antigens are clinically significant. They are associated with HDFN and both immediate and delayed hemolytic transfusion reactions. They are usually of IgG isotype, reactive at 37° C, and are detected only in the IAT. Antibodies against Fy^a, Fy^b, and Fy6 antigens, which reside on the long amino-terminal domain of DARC,

TABLE 36.20
Phenotypes of the Kidd System

REACTIONS WITH ANTI-				FREQUENCY (%) U.S. POPULATION		
Jk^a	**Jk^b**	**Jk3**	**Phenotype**	**White**	**Black**	**Comments**
+	0	+	Jk (a+b–)	28	57	Autosomal codominant
+	+	+	Jk (a+b+)	49	34	Sensitive 2M urea
0	+	+	Jk (a–b+)	23	9	
Null Phenotypes (Jk$_{null}$)						
0	0	0	Jk (a–b–)	Very rare	Very rare	Autosomal recessive Resistant 2M urea
0/w*	0/w*	w*	Jk (a–b–)	—	—	*In (Jk)*, autosomal dominant Rare, Japanese only Partially resistant 2M urea

*Weak Jk antigens detected only by adsorption and elution techniques.

can be inhibited by prior protease digestion of RBCs. In contrast, Fy5 and Fy3 antigens are relatively resistant to protease digestion. Antibodies against Duffy antigens can demonstrate dosage.

Clinically, anti-Fy^a is the most common alloantibody encountered and can be observed in Fy (a–) individuals of all races. Anti-Fy^b is relatively uncommon and is observed primarily in nonblacks. Alloantibodies against the high-incidence antigens Fy3 and Fy5 are relatively rare, occurring predominantly in white, Fy$_{null}$ individuals. Anti-Fy3 behaves like an anti-Fy^{a+b}, reacting with all Duffy-positive RBCs. Occasionally, potent anti-Fy3 can be produced by sickle cell, Fy (a–b–) patients despite the expression of Fy^b on nonerythroid tissues (Castilho et al., 2009). Anti-Fy5 also reacts like an anti-Fy^{a+b} but requires the presence of Rh antigens for reactivity. Anti-Fy6 has not been observed clinically but is the epitope for an anti-Duffy monoclonal antibody that blocks *P. vivax* binding (Tournamille et al., 2005).

Biological Role

ACKR1 is a chemokine-binding protein, capable of binding several inflammatory chemokines from the C-X-C and C-C families (Gardner et al., 2004), including interleukin-8, RANTES (regulated upon activation, normal T cell–expressed and presumably secreted), and monocyte chemotactic protein-1 (see Fig. 36.10). Because ACKR1 lacks a DRY motif, it does not transmit an intracellular signal upon binding chemokines. Atypical chemokine receptors are considered negative chemokine regulators, acting as chemokine scavengers and transporters. ACKR1 on red cells likely functions as a "chemokine sink" to control blood chemokine concentrations whereas ACKR1 on endothelial cells helps facilitate leukocyte recruitment and neutrophil diapedesis (Girbl et al., 2018).

In humans, the Fy$_{null}$ phenotype (*FY*02N*) is associated with benign ethnic neutropenia, characterized by low neutrophil counts in people of African ancestry (Reich et al., 2009). In both humans and mice, the absence of ACKR1 on nucleated marrow red cells alters hematopoietic stem cells, leading to generation of a distinct neutrophil population with increased CD16, CD45 and CCR2 (Duchene et al., 2017). As a result, neutrophils are primed to exit the vascular system into tissues, leading to neutropenia. It is hypothesized that the enhanced migration of neutrophils into tissues could represent a selective advantage against bacterial infection. Interestingly, studies in chemotherapy patients have shown that Fy^a-positive individuals were at increased risk for hospitalization secondary to febrile neutropenia (Glisovic et al., 2018).

The Fy$_{null}$ phenotype has also been linked to renal disease, reduced graft survival following renal transplantation, and insulin resistance. In patients with sickle cell disease, the Fy$_{null}$ phenotype is associated with increased chronic organ damage and proteinuria (Afenyi-Annan et al., 2008). In ACKR1-null mice, there is a rise in inflammatory cytokines and insulin resistance, suggesting an increased risk for obesity-related illnesses (Benson et al., 2018). The role of ACKR1 in renal transplantation is mixed, with some studies showing an increase in rejection and chronic lesions (Lerut et al., 2007; Horne et al., 2009).

ACKR1 is also the receptor for *P. vivax*, which binds ACKR1 via PvDBP protein at the Fy6 epitope. Fy$_{null}$ individuals are resistant to most *P. vivax* strains, providing a selective advantage to populations living in malaria-endemic areas (Howes et al., 2011). Fy^a may also be protective against *P. vivax* and may account for the high incidence of Fy^a in Asia. Fy^a is a less efficient receptor, binding 40% to 50% less PvDBP than Fy^b. In the Amazon, the Fy(a+b–) phenotype is associated with a 250% lower risk of *P. vivax* infection (King et al., 2011). Finally, the Fy$_{null}$ phenotype (*FY*02N/FY*02N*) may play a role in HIV susceptibility. However, there are conflicting reports regarding the latter (Cooling, 2015).

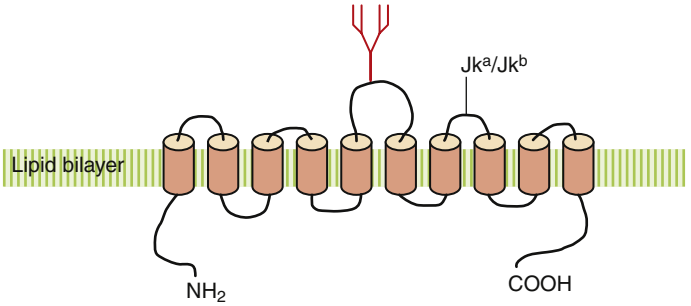

Figure 36.11 The Kidd/urea transporter glycoprotein. The site of Jk^a/Jk^b polymorphism at residue 280 is indicated. The *N*-glycosylation site is indicated by a *branched structure* on the third extracellular loop. The 10 transmembrane domains are represented by *amber cylinders*.

KIDD BLOOD GROUP SYSTEM (ISBT NO. 009)

The Kidd (JK) blood group system is strongly associated with delayed hemolytic transfusion reactions and with intravascular hemolysis (recall that most hemolysis with non-ABO antibodies is extravascular). It consists primarily of two allelic antigens: Jk^a (*JK*01*) and Jk^b (*JK*02*). Inheritance is autosomal codominant with three predominant phenotypes (Table 36.20). A fourth phenotype, Jk$_{null}$ or Jk (a–b–), is very rare, except among Polynesians (≤1%) and Finns. Weak or altered Jk expression due to novel *JK* alleles is also known (Whorley et al., 2009). In addition to RBCs, Kidd antigens are expressed along descending vasa recta endothelial cells of the renal medulla. Evidence suggests low-level, constitutive expression of Kidd on heart, skeletal muscle, colon, small intestine, thymus, brain, pancreas, spleen, prostate, bladder, and liver (Olives et al., 1996). More than 14,000 Kidd epitopes are present per human RBC (Lucien et al., 2002).

Null Phenotypes

Jk$_{null}$ is autosomal recessive, reflecting homozygosity for amorph JK^{null} alleles (see Table 36.20). *In(Jk)* is a second Jk (a–b–) phenotype that is characterized by very weak Kidd expression. Similar to *In(Lu)*, the *In(Jk)* phenotype is autosomal dominant owing to a suppressor gene at a distant, unrelated locus. It is interesting to note that Jk$_{null}$ RBCs are resistant to lysis by 2M urea, a lytic agent used by some automated hematology analyzers. *In(Jk)* RBCs have intermediate resistance to urea (Issitt & Anstee, 1998). No change in gas permeability is seen with Jk$_{null}$ cells (Endeward et al., 2006).

Biochemistry

Apparent resistance to urea by Jk$_{null}$ RBCs became clear with cloning and isolation of the human erythroid urea transporter (UT-B). The latter is a 43- to 45-kD multipass glycoprotein, which shares 60% homology with the vasopressin-sensitive urea transporter of rabbits (UT2) and humans (HUT2, UT-A) (Lucien et al., 1998). The molecule is a 391 amino acid protein with 10 transmembrane domains and a cytosolic amino- and carboxy-terminus (Fig. 36.11). A single *N*-glycan is present on the third extracellular loop (Asn222) and expresses ABO antigens (Lucien et al., 2002).

The Jk^a/Jk^b antigens reside on the fourth extracellular loop at amino acid 280. The third extracellular loop may play a key role in urea transport.

Molecular Biology

The Kidd glycoprotein is encoded by a 30-kb gene (*JK*, *SLC14A1*, *UT-B*) on chromosome 18q12-21. This is the same location as the human *HUT2/UT-A* urea transporter (61% homology), suggesting that the two genes arose by gene duplication. The *JK* gene is organized over 11 exons, although only exons 4 to 11 encode the mature protein (Lucien et al., 1998). Similar to many blood group genes, the promoter region contains a GATA-1 consensus sequence, as well as other *cis*-regulatory elements (AP-2, AP-3, NF-ATp, Sp1, Ets-1). A single-bp transition (G823A) is the molecular basis of the Jk^a/Jk^b polymorphism, resulting in an Asp280 (Jk^a, *JK*01*) or Asn280 (Jk^b, *JK*02*) (Lucien et al., 2002). Seven alleles containing missense mutations are responsible for weak Jk^a (*JK*01W*) and Jk^b (*JK*02W*) expression and can lead to discrepancies in Jk phenotyping by serologic testing. One Jk^a weak allele (*JK*01W.01*; Glu44Lys) is extremely common among some Asian populations (38%–40%) (Wu et al., 2019). To date, 24 Jk^{null} alleles (*JK*0N*) are recognized by ISBT. The etiology of the *In(Jk)* phenotype is unknown.

Kidd Antibodies

Clinically, anti-Jk or Kidd antibodies are a common cause of hemolytic transfusion reactions, accounting for nearly one-quarter of all delayed hemolytic transfusion reactions and 75% of those with true hemolytic sequelae (Ness et al., 1990). They are usually of IgG1 or IgG3 isotype and are capable of activating complement (see Table 36.5). Antibody reactivity can be enhanced with enzyme-treated RBCs and by the presence of complement. Anti-Jk is not enhanced by polybrene. An anti-Jk3, which reacts with all RBCs except Jk_{null}, is observed in Jk_{null} individuals (see Table 36.20). Anti-Jk3 is reported to react with some $Jk(a+^w)$ phenotypes (Whorley et al., 2009). $Jk(a+^w)$ and $Jk(b+^w)$ can also give discordant typing with commercial typing reagents (Whorley et al., 2009; Wu et al., 2019).

Anti-Jk antibodies can be difficult to detect or identify in the blood bank. Anti-Jk antibodies are often of low titer with weak avidity and can display dosage in vitro. Furthermore, anti-Jk antibodies are frequently transient, disappearing rapidly after immune stimulation. As a consequence, patients previously sensitized to Kidd antigens may be negative for anti-Jk antibodies in later blood samples. Following transfusion of crossmatch-compatible, Jk-positive RBCs, sensitized patients can mount a brisk anamnestic antibody response with rapid and extensive in vivo hemolysis as RBCs are cleared by extravascular and intravascular hemolysis. Although uncommon, anti-Jk can cause mild HDFN.

Biological Role

Biologically, JK/UT-B functions in the facilitated transport of urea. In the kidney, transport of urea by JK/UT-B on vasa recta endothelial cells is thought to help stabilize osmotic gradients in the renal medulla during the concentration of urine. On RBCs, JK/UT-B may help preserve the osmotic stability of RBCs as they pass through the kidney. Although Jk_{null} individuals exhibit a slightly decreased capacity to concentrate urine, the absence of JK/UT-B is not associated with a clinical syndrome. It is likely that other mechanisms exist to compensate or reduplicate the function of JK/UT-B on tissues (Lucien et al., 1998). Because Jk antigens are strongly expressed by the kidney, there is some suggestion that they could act as alloantigens in renal transplant patients (Lerut et al., 2007). Four case reports describe the concurrent allograft rejection with new Jk alloantibodies several years after transplantation and transfusion exposure (Rourk & Squires, 2012).

DIEGO BLOOD GROUP SYSTEM (ISBT NO. 010)

The Diego blood group system (DI) consists of 22 antigens, including five sets of allelic antigens: Di^a/Di^b (DI1/DI2), Wr^a/Wr^b (DI3/DI4), Hg(a+)/Mo(a+) (DI12/DI11), Wu/DISK (DI9/DI22), and Sw(a)/SW1 (DI14/DI22). Most antigens (20/22) are rare, low-incidence antigens present on less than 1% of donors. In general, there are no apparent racial differences except Di^a, which is rare in all populations except those of Mongolian ancestry. This includes Asian and Northern India populations due to Mongolian military expansion in ancient times (Petit, 2019). Likewise, Asian populations of Mongolian descent who migrated to the Americas approximately 15,000 years ago are responsible for the high prevalence of Di^a among several native South American Indian peoples, where the frequency of Di^a can reach 50% (Reid & Lomas-Francis, 2012; Begat, 2014). Interestingly, Di^a is not present in circumpolar North American native populations (Eskimo-Aleut), who arose from later Asian migrations (Begat, 2014). In addition to RBCs, Diego antigens are expressed by the human kidney along the collecting ducts (Tanner, 1993). One million copies of Diego glycoprotein (AE1) are present per RBC.

Biochemistry

The Diego blood group system resides on Band 3, also known as AE1. AE1 is a 100-kD, 991 amino acid glycoprotein containing two functionally distinct domains: a large 40-kD amino-terminal cytoplasmic domain and a transmembrane domain comprising the carboxy-terminal half of the molecule (Fig. 36.12). On RBCs, AE1 is an oligomer, usually existing as a dimer or tetramer through the formation of intramolecular disulfide bonds. The carboxy-terminal is associated with carbonic anhydrase, whereas the amino-terminal cytoplasmic domain binds several key cytoskeletal proteins (Band 4.1, Band 4.2, and ankyrin) and glycolytic enzymes: glutaraldehyde-3-phosphate dehydrogenase, aldolase, and phosphofructokinase. Binding of hemochromes or denatured hemoglobin to the extreme amino-terminus of AE1 is believed to play a role in Heinz body formation. AE1 is a critical element in both ankyrin and junctional complexes that provide vertical and lateral stability to the membrane, respectively (Burton & Bruce, 2011).

The remainder of AE1 is membrane associated, containing 12 to 14 transmembrane domains, which constitute the carboxy-terminal half of the molecule. Whereas the amino-terminal domain is involved in membrane stability, the carboxy-terminal domain functions as an anion transporter, facilitating movement of Cl^- and HCO_3^- anions across the cell membrane (Tanner, 1993). Crystal structures of AE1 dimers show that the transmembrane domain is arranged into two distinct subdomains responsible for anion transport and dimerization, respectively (Fici, 2017). It is believed that anions diffuse along a pathway between the two subdomains, followed by anion binding to the transport domain, which transports the anion across the membrane in an "elevator-like" process.

AE1 is closely associated with several membrane proteins important to red cell function that is often referred to as a *Band 3 metabolon* or *macrocomplex* (Burton & Bruce, 2011). Other proteins physically associated with AE1 include Rh complex, glycophorins, aquaporin, glucose transporter, CD47, and carbonic anhydrase. The extracellular domain is also the site of all the Diego antigens described to date. There is a single *N*-glycosylation site, which displays a massive, highly branched, polylactosaminoglycan with both ABO and I blood group activity (Cooling, 2010). It is estimated that nearly half of all ABO epitopes on RBCs are associated with AE1.

Molecular Biology

AE1 is the product of a 20-exon, 17-kb gene (*SLC4A1*) on chromosome 17q21-q22. Di(b+) is considered the reference allele (DI*02). Every Diego antigen identified to date is the result of an amino acid polymorphism in the translated protein (see Table 36.26 and Fig. 36.12). The Diego system also contains two examples of allelic, low-incidence antigens: Mo^a/Hg^a and Jn^a/KREP. In each case, two distinct amino acid substitutions at the same amino acid residue lead to different alloantigens. A similar example exists in the Kell system (Kp^a, Kp^b, and Kp^c).

The most interesting Diego antigen, however, is Wr^b. As stated earlier, AE1 is topically associated with GYPA in the RBC membrane. RBCs lacking GYPA (En [a–] phenotype) are phenotypically Wr (a–b–), implying that Wr^b is on GYPA. Available evidence now suggests that Wr^b is formed by an electrostatic interaction between GYPA and the Wr^b antigen (Glu658) (Poole et al., 1999). Which specific amino acid on GYPA is critical to Wr^b formation is still a matter of debate. However, clearly, part of the Wr^b epitope involves amino acids on GYPA.

Diego Antibodies

Antibodies against Diego blood group antigens can be immune stimulated or naturally occurring. Antibodies against Di^a, Di^b, Wr^b, and ELO are usually immune stimulated. These antibodies are of IgG isotype and are detected in the AHG phase of testing. Anti-Di^a, Di^b, and Wr^b can be associated with decreased red cell survival, hemolytic transfusion reactions, and HDFN. Anti-Wr^b is also associated with autoimmune hemolytic anemia (Issitt & Anstee, 1998).

In contrast, antibodies against the majority of other Diego antigens are usually naturally occurring, room temperature saline agglutinins. Anti-Wr^a is particularly common, occurring in 1 in 100 donors. Antibodies against Wd^a and WARR are also fairly common, with anti-WARR reported in 13% to 18% of donors (Issitt & Anstee, 1998).

Biological Role

Functionally, AE1 plays a critical role in gas transport and acid-base equilibrium. To facilitate the removal of CO_2, RBCs hydrate CO_2 via carbonic

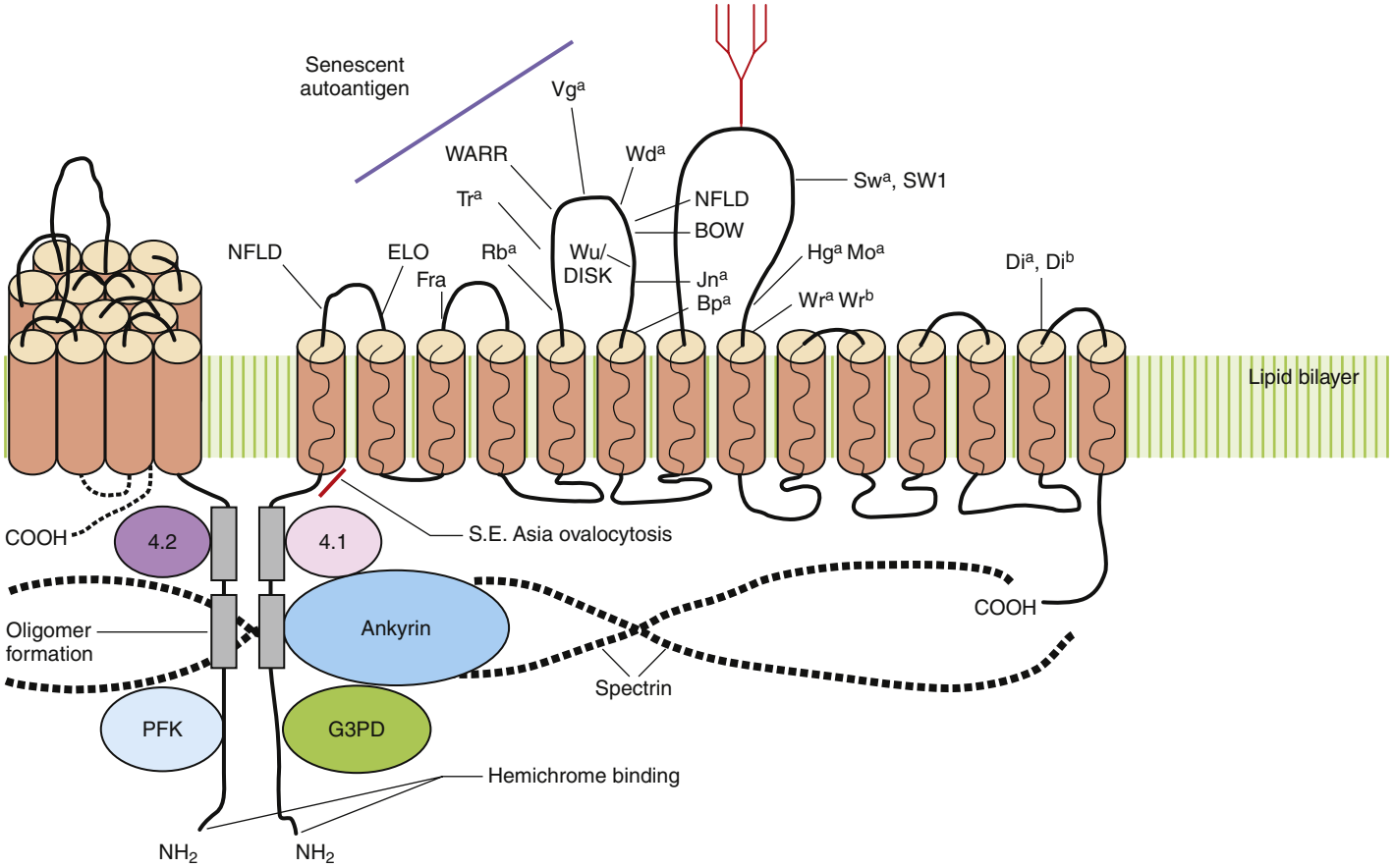

Figure 36.12 Structure of anion exchange protein AE1 (Band 3). AE1 is a multipass glycoprotein with 14 transmembrane domains, indicated by *solid amber cylinders*. The Diego blood group antigens reside along the extracellular loops and are indicated by *solid lines*. The AE1 senescent autoantigen is on the third extracellular loop between Rb^a and Vg^a antigens. The massive *N*-glycan is shown by a branched structure on the fourth extracellular loop. The large cytoplasmic domain has binding sites for cytoskeletal proteins 4.2, 4.1, and ankyrin, as well as the glycolytic enzymes phosphofructokinase (PFK) and glutaraldehyde-3-phosphate dehydrogenase (G3PD). In the red cell membrane, AE1 exists as oligomers (dimers, tetramers) linked by interchain disulfide bonds along the amino-terminal cytoplasmic domain *(solid rectangles)*. An 8 amino acid deletion at the boundary of the amino-terminal cytoplasmic domain and the first transmembrane domain is responsible for Southeast Asia ovalocytosis (SAO).

anhydrase to form bicarbonate ion (HCO_3^-), which is readily soluble in plasma. As the level of intracellular HCO_3^- rises, RBCs exchange HCO_3^- ions for Cl^- in plasma (the Cl^- shift, or Hamburger shift). This process is mediated by AE1 as RBCs pass through capillaries and small capillary venules. Because of the high copy number of AE1 on the RBC membrane, anion exchange is 90% complete within 0.4 to 0.5 second. An increase in HCO_3^- capacity and osmotic resistance is observed with Miltenberger III red cells owing to significantly higher AE1 expression (Hsu et al., 2009). In the kidney, AE1 is expressed along the basolateral membrane of type A intercalated cells of renal collecting ducts, where it functions in acid secretion and bicarbonate readsorption (Tanner, 1993). Given the physiologic importance of AE1, it is not surprising that Diego null phenotype is considered embryonic lethal.

AE1 also plays a role in the RBC cytoskeleton, impacting membrane stability and red cell circulation (see Fig. 36.12). Not surprisingly, mutations in AE1 are associated with red cell abnormalities. Southeast Asia ovalocytosis (SAO) is due to a 27 bp deletion (SLC4A1Δ27) in the amino-cytoplasmic domain and is common in malaria-endemic areas of the Pacific. Affected individuals are heterozygous for the mutation and have an apparent increased resistance to severe malaria (Cooling, 2015). The mutation affects AE1 oligomerization, membrane diffusion, and rigidity, suggesting that SAO red cells may be more susceptible to splenic clearance. AE1 is a target of senescent autoantibodies (Kay, 1994). In addition, red cell damage is often accompanied by AE1 clustering, facilitating removal of red cells damaged by malaria, cold storage, or other insults (Badior & Casey, 2018; Cooling, 2015; Mourao et al., 2018).

Finally, AE1 was recently identified as a receptor for *Bartonella*, the cause of Oroya fever, trench fever, bacillary angiomatosis and "cat scratch" disease (Cooling, 2015). Unlike malaria, *Bartonella* does not impact red cell survival or function, leading to prolonged and chronic bacteremia. There is no correlation between *Bartonella* and Di^a phenotype, despite the high incidence of both in some areas of South America.

YT BLOOD GROUP SYSTEM (ISBT NO. 011)

The YT blood group, historically known as Cartwright, was discovered in 1956 and consists of five antigens, including two autosomal-codominant antigens (Yt^a, Yt^b). Yt^a (Yt1) is a high-incidence antigen expressed by 99.8% of white donors. The incidence of Yt^b (Yt2) varies by race, ranging from 0% in Japanese to 24% to 26% in the Middle East (Issitt & Anstee, 1998). Three additional high incidence antigens have been identified: YTEG (Yt3), YTLI (Yt4), and YT0T (Yt5) (Storry et al., 2019). Yt antigens are missing on PNH III RBCs, which are devoid of all glycosylphosphatidylinositol (GPI)-linked glycoproteins. In addition to RBCs, Cartwright antigens are expressed on neural synapses and neuromuscular junctions (Masson et al., 1994). A total of 7000 to 10,000 molecules of Yt glycoprotein are present per RBC.

Biochemistry

The Cartwright antigens are located on acetylcholinesterase (AChE), a β-carboxyesterase responsible for degradation of the neurotransmitter acetylcholine. Several different molecular forms of AChE have been isolated, including large heteromeric forms composed of several catalytic subunits covalently linked to collagen. On RBCs, AChE is expressed as a palmitoylated, GPI-linked glycoprotein (Fig. 36.13) (Li et al., 1991). Human erythrocyte AChE is unique in the palmitoylation or covalent linkage of a palmitic fatty acid to the inositol ring, which renders the molecule resistant to phospholipase C. In RBC membranes, AChE usually exists as a 160-kD dimer and possesses both *N*- and *O*-linked glycans.

Molecular Biology

The gene for AChE possesses four exons, spanning 4.5 to 4.7 kb, on chromosome 7q22. Alternate splicing of exon 3 is responsible for the GPI-linked form of AChE observed in RBCs (Li et al., 1991). The Yt^a and Yt^b antigens represent a single–amino acid polymorphism at residue 322, where His322 is Yt^a (*YT*01*) and Asn322 is Yt^b (*YT*02*) (Bartels et al., 1993). The Yt^a/Yt^b polymorphism is not located near the catalytic site of

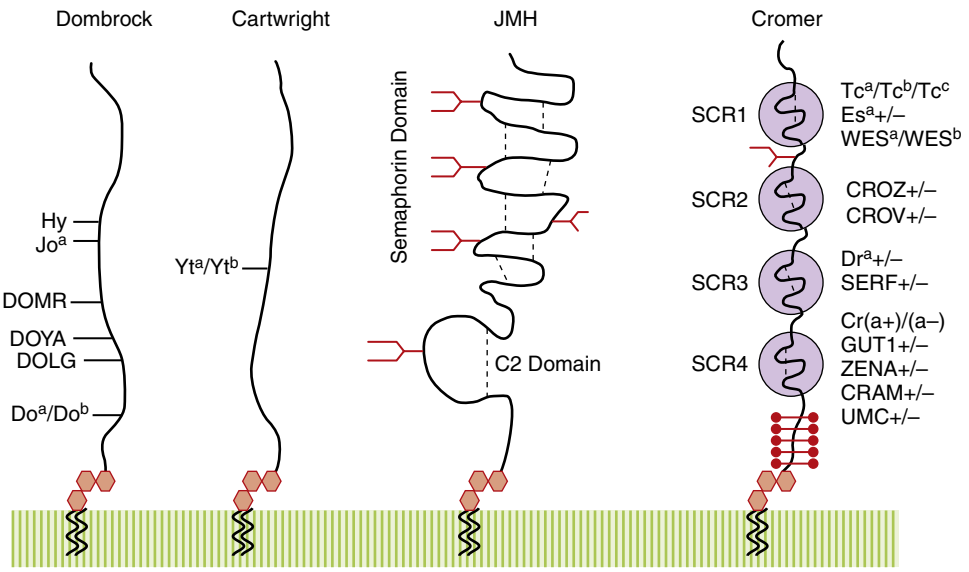

Figure 36.13 Blood group antigens on glycophosphoinositol-linked glycoproteins.

the enzyme and has no effect on enzyme activity (Masson et al., 1994). Missense mutations are responsible for the loss of high-incidence antigens YTEG (*YT*03*, Gly89Glu), YTLI (*YT*04*, Gly57Arg) and YTOT (*YT*05*, Arg34Gln) (Storry et al., 2019).

Cartwright Antibodies

In general, anti-Yt^a and anti-Yt^b are usually clinically benign, although shortened red cell survival and even delayed hemolytic transfusion reactions have been reported. Neither antibody is associated with HDFN (Issitt & Anstee, 1998). Anti-Yt^a and anti-Yt^b are of IgG isotype, arising from immune stimulation, and are usually detected in the IAT. Despite the high incidence of Yt^a in the general population, anti-Yt^a is more common than anti-Yt^b, suggesting that Yt^a is the more immunogenic antigen. Anti-Yt^a is also more likely to cause a positive monocyte-monolayer assay with decreased red cell survival (Arndt & Garratty, 2004). Antibodies against Yt can be inhibited by soluble recombinant AChE protein (Storry et al., 2019).

Biological Role

AChE is a critical enzyme required for the rapid degradation of acetylcholine on postsynaptic membranes of nerves and muscles. The role of AChE in RBCs is unknown.

XG BLOOD GROUP SYSTEM (ISBT NO. 012)

The Xg blood group system contains a single antigen, Xg^a. As a result, only two phenotypes are known: Xg^a-positive and Xg^a-negative. Because the Xg^a antigen is encoded by a gene on the X chromosome, the incidence of the Xg^a-positive phenotype is higher among women. Among whites, approximately 89% of women and 66% of men are Xg^a positive. Similar results have been found in other ethnic populations (Johnson, 2011). Xg appears to be specific for RBCs. Approximately 9000 molecules of Xg^a are present per RBC (Reid & Lomas-Francis, 2012).

Biochemistry and Molecular Biology

The Xg^a antigen is located on a 24- to 29-kD, 180 amino acid glycoprotein named XG protein. A type 1 glycoprotein, XG protein possesses a large 117 amino acid, amino-terminal extracellular domain; a single transmembrane domain; and a short, carboxy-terminal cytoplasmic tail. Of 11 potential *O*-glycosylation sites, only 3 appear to be glycosylated. The protein is encoded by a 2.4-kb gene (*XG*) located on the X chromosome at the pseudoautosomal boundary/X-specific boundary (pAB1X). A mutation located 3.7 kb upstream of the XG transcription start site was identified as the basis for Xg(a–) phenotype in both men and women. The mutation (rs31103G>C) disrupted binding of the erythroid transcription factor GATA1 (Moller et al., 2018).

In the RBC membrane, the XG protein is associated with a second 32 kD sialoglycoprotein, MIC2 or CD99, possibly as a heterodimer. Evidence suggesting a near-neighbor relationship of the XG and MIC2 proteins includes MIC2 inhibition of anti-Xg^a antibodies and coimmunoprecipitation of MIC2 by anti-Xg^a. In women, Xg(a–) is always associated with low CD99 expression. Conversely, CD99 is elevated in Xg(a–) men (Johnson, 2011).

TABLE 36.21
Scianna Blood Group Antigens

Antigen (High Frequency)	Percent Donors	Amino Acid Change (High→Low Frequency)	Percent Donors	Antigen (Low Frequency)
Sc1	99	Gly57Arg	0.7	Sc2
Sc3	100	307delGA	Rare	SC_{null}
		Arg332stop		
		Pro60Ala	Rare	(Rd) Sc4
Sc5 (STAR)	100	Glu47Lys		
Sc6 (SCER)	100	Arg81Gln		
Sc7 (SCAN)	100	Gly35Ser		

From Reid RE, Lomas-Francis C: *The blood group antigen facts book*, ed 3, San Diego, 2012, Academic Press.

Xg^a Antibodies

Anti-Xg^a is not associated with hemolytic transfusion reactions or HDFN (Johnson, 2011). Anti-Xg^a may be immune stimulated or naturally occurring. Most examples are of IgG isotype, including some capable of activating complement. Because of differences in Xg^a-positive phenotype between men and women, most examples (>85%) of anti-Xg^a are observed in men.

SCIANNA BLOOD GROUP SYSTEM (ISBT NO. 013)

The Scianna (Sc) blood group system contains seven antigens. Sc1 and Sc2 are antithetical antigens, with most individuals typing as Sc:1,–2. Sc2 and Sc4/Rd are low-incidence antigens, whereas Sc3, Sc5, Sc6, and Sc7 are high-incidence antigens (Table 36.21) (Brunker et al., 2011). Sc3 is a high-incidence antigen present on all RBCs except Sc_{null} (Sc: –1, –2, –3). Sc–1,2 is more common among oceanic populations of the Pacific Ocean, whereas Sc4 is found most often in Slavic and Ashkenazi Jews. Scianna appears to be specific for RBCs and erythropoietic tissues.

Biochemistry

Scianna antigens reside on erythrocyte membrane-associated protein (ERMAP), a 60- to 68-kD, 446 amino acid glycoprotein. Similar to Lutheran, Ok, and LW proteins, ERMAP is a member of the Ig superfamily. The molecule is a type 1 single-pass transmembrane protein possessing a single IgV domain and a large cytoplasmic domain that is likely involved in signal transduction. The latter possesses both SH3 and B30.2 domains as well as multiple phosphorylation sequences for protein kinase C, tyrosine kinase, and casein kinase II. The molecule possesses 11 cysteine residues and is sensitive to sulfhydryl-reducing agents.

Molecular Biology

The *ERMAP* gene resides on chromosome 1p34 and consists of 11 exons spanning 19 kb. Like many blood group antigens, ERMAP is regulated

TABLE 36.22
Phenotypes of the Dombrock System

REACTIONS WITH ANTI-DOMBROCK ANTIBODIES										FREQUENCY (%) U.S. POPULATION	
Do^a	Do^b	Gy^a	Jo^a	Hy	D06	D07	Phenotype	ISBT	Amino Acid Change	White	Black
+	0	+	+	+	+	+	Do (a+b–)	DO1	Asn265	18	11
+	+	+	+	+	+	+	Do (a+b+)			49	44
0	+	+	+	+	+	+	Do (a–b+)	DO2	Asp265	33	45
Null/Weak Phenotypes											
0	0	0	0	0	0	0	Gy(a–) or Do_{null}†	DO3	Loss exon 2*	Rare	Rare
0	w	w	0/w	0	w	+	Hy(–)	DO4	Gly108Val	Rare	Rare
w	0/w	+	0	w	w	0/w	Jo(a–)	DO5	Thr117Ile	Rare	Rare
0	0	w	w	w	0	?	DOYA(–)	DO6	Tyr183Asp	Rare	Rare
0	+	0	w	w	?	0	DOMR(–)	DO7	Ala144Glu	Rare	Rare
+	0	+	+	+	?	?	DOLG(–)	DO8	Leu225Gln	Rare	Rare
+	0	+	+	+	+	?	DOLC(–)	DO9	Thr189Met	Rare	Rare
+	0	+	+	+	+	+	DODE(–)	DO10	Asp135Glu	Rare	Rare

ISBT, International Society of Blood Transfusion.
*Loss of exon 2 has been associated with splice-site, frameshift, and nonsense mutations (Reid RE, Lomas-Francis C: *The Blood Group Antigen Facts Book*, ed 3, San Diego, 2012, Academic Press).
†Also associated with PNH III red blood cells (RBCs), which lack all glycophosphoinositol (GPI)-linked glycoproteins, including Dombrock, Cartwright, Cromer, JMH, and CD59 antigens.

by the transcription factor KLF1 (Magor et al., 2015). Most Sc antigens are the result of an SNP and amino acid polymorphism (see Table 36.21). Four Sc-null alleles (*SC*O1N*) are known, all containing the same nonsense mutation (R332Stop) (Brunker & Flegel, 2019). An additional amino acid polymorphism (His26>Tyr) has been identified in the leader sequence, which is not expressed on the mature red cell protein (Brunker & Flegel, 2011). Approximately 25% of whites are positive for the His26>Tyr polymorphism.

Scianna Antibodies

Anti-Scianna antibodies are rare and generally benign. They are usually of IgG isotype, with some examples binding complement. Most examples are immune stimulated; however, naturally occurring anti-Sc2 antibodies are known. The antigens are relatively resistant to enzymes but can be weakened with DTT and AET. In general, they are not a cause of transfusion reactions although one case of AHTR due to anti-Sc2 was recently reported (Brunker & Flegel, 2019). Both anti-Sc2 and anti-Sc4 (Rd), have been associated with HDFN. Autoantibodies against Sc1 and Sc3 antigens have been associated with warm autoimmune hemolytic anemia (Brunker & Flegel, 2011). Anti-Scianna antibodies can be neutralized with soluble recombinant ERMAP protein (Seltsam et al., 2009).

Biological Role

The biological role of ERMAP is unknown, although its structure suggests that it may play a role in RBC adhesion and signaling. The IgV domain possesses a C1q recognition sequence that may mediate adhesion between marrow macrophages and erythroblasts in erythroid islands. Because ERMAP shares homology with the B7 family of proteins (CD80, CD86) and neural autoantigens, it is speculated that ERMAP could be involved in immune recognition and autoimmune anemia (Brunker & Flegel, 2011).

DOMBROCK BLOOD GROUP SYSTEM (ISBT NO. 014)

The Dombrock blood group system contains ten antigens. Do^a (DO1) and Do^b (DO2) are autosomal-codominant antigens expressed by 67% and 82% of white donors, respectively (Table 36.22). The remaining Dombrock antigens are all high-incidence antigens found on virtually all donors. In addition to RBCs, Dombrock mRNA has been identified in fetal liver and spleen (Gubin et al., 2000).

Null/Weak Phenotypes

The Do_{null} or Gy(a–) phenotype is a rare, autosomal-recessive phenotype (see Table 36.22). An acquired Do_{null} phenotype can be observed in paroxysmal nocturnal hemoglobinuria type III (PNH-III). A hematopoietic stem cell disorder, PNH III is characterized by chronic hemolysis due to an absence of all GPI-linked glycoproteins, including Cromer, Dombrock, and Cartwright antigens.

Loss of one high-incidence Dombrock antigen is often accompanied by weakened expression of other Dombrock antigens (see Table 36.22). This is due to the heterogeneity of Dombrock alleles, which carry different combinations of Dombrock antigens (Reid, 2005; Baleotti et al., 2006). Hy(–) and DOMR(–) individuals typically have weakened Do^b and Gy^a and weak/absent Jo^a expression, whereas Jo(a–) is often associated with weak Do^a, Hy, and Gy expression (Reid, 2005; Costa et al., 2009). The one example of DOYA(–) types is Co(a–b–), with weakened expression of Gy, Hy, and Jo^a (Reid & Lomas-Francis, 2012).

Biochemistry

Dombrock antigens reside on an adenosine diphosphate (ADP)-ribosyltransferase (CD297), which catalyzes the transfer of ADP-ribose from nicotinamide adenine dinucleotide (NAD) to a protein acceptor. The cloned molecule is a 47- to 58-kD, 314 amino acid glycoprotein that is anchored into the RBC membrane via a GPI glycolipid tail (GPI-linked; see Fig. 36.13). The molecule has five potential *N*-glycosylation sites, two myristoylation sites, and five cysteine residues (Gubin et al., 2000; Daniels, 2013). As a consequence, Dombrock can be destroyed by disulfide-reducing agents and phosphatidylinositol phospholipase C, which cleaves GPI-linked proteins (Gubin et al., 2000).

Molecular Biology

The gene for Dombrock (*ART4*) spans 14 kb on chromosome 12p13.2-12.1. The gene consists of three exons, although exon 2 encodes more than 70% of the translated protein and includes all seven Dombrock antigens. Do^a, Do^b, Jo^a, Hy, DOYA, and DOMR are the result of a single–amino acid polymorphism (see Table 36.22). The Do_{null} or Gy(a–) phenotype is the result of mutations that abolish exon 2 (Reid, 2005).

Dombrock Antibodies

Anti-Dombrock antibodies can be clinically significant, although many examples are benign. They are commonly found in mixtures of alloantibodies and can be difficult to identify. Anti-Dombrock antibodies are capable of causing shortened RBC survival and acute and delayed hemolytic transfusion reactions. Transfusion reactions and accelerated clearance due to anti-Dombrock antibodies can be missed in routine testing, with implicated units often testing as crossmatch-compatible, even in a full IAT crossmatch. Moreover, a posttransfusion direct antiglobulin test and eluate can be negative, with no observable rise in antibody titer with time (Reid, 2005; Baumgarten et al., 2006). More than 50% of anti-Dombrock give positive reactions in the monocyte monolayer assay, which can be used to predict clinical significance (Arndt & Garratty, 2004). Anti-Dombrock is not associated with HDFN.

Antibodies against Dombrock antigens are usually of IgG isotype, arising from immune stimulation by transfusion or pregnancy. Antibody reactivity can be enhanced by the use of papain- or ficin-treated RBCs. Conversely, antibody reactivity is reduced or abolished by the treatment of red cells with sulfhydryl-reducing agents (DTT, AET), trypsin, chymotrypsin, and pronase. Anti-Dombrock can deteriorate with in vitro storage,

complicating pretransfusion testing (Baumgarten et al., 2006). In addition, Dombrock titers may decrease over time in vivo, falling below the level of detection (Reid, 2005).

Biological Role

Although Dombrock is an ADP-ribosyltransferase, no enzyme activity has been reported on RBC membranes (Reid, 2005). No known clinical syndrome is associated with a Do_{null} phenotype. It has been hypothesized that Dombrock may play a role in clearing circulating NAD+ and/or post-translational modification of proteins (Reid, 2005). Dombrock may also contribute to integrin-mediated cell adhesion via an RGD motif at the Do^b antigen; the RGD motif is abolished in the Do^a phenotype.

COLTON BLOOD GROUP SYSTEM (ISBT NO. 015)

The Colton blood group system was initially identified in 1967. It consists of two autosomal-codominant antigens, Co^a and Co^b, and a third high-incidence antigen ("TOR") (Arnaud et al., 2008). Co^a is a high-incidence antigen present on 99.7% of donors. Co^b is expressed by less than 11% of donors, with only 0.3% being Co (a–b+). Although very rare, a Co (a–b–) or null phenotype is reported. Colton antigens are expressed on RBCs, renal proximal tubules, the thin descending limb of Henle, renal vasa recta endothelium, choroid plexus, ciliary body, microvessels, gallbladder, placenta, and some epithelial cells. More than 120,000 to 160,000 molecules of Colton glycoprotein are present per RBC.

Biochemistry

The Colton blood group antigens reside on aquaporin 1 (AQP-1) or channel-forming integral protein, a water-selective membrane channel (Fig. 36.14). Cloned in 1991, AQP-1 is a 269 amino acid multipass integral membrane protein containing six transmembrane domains. Crystallographic studies suggest that the first intracellular and third extracellular loops fold back into the plasma membrane, overlapping at two Asp-Pro-Ala (NPA) sequences to form a water channel. A single *N*-glycosylation site (Asn42), capable of expressing ABH antigens, is found in the first extracellular loop near the Co^a/Co^b and TOR epitopes (residues 45 and 47). The latter is variably glycosylated in vivo, leading to a spectrum of AQP-1 glycoforms, ranging from 40 to 60 kD (Agre et al., 1994). In RBC membranes, AQP-1 exists as a homotetramer, a square array of AQP-1 monomers, which may help stabilize the structure and functional integrity of individual monomers (Knepper, 1994). AQP-1 colocalizes with AE1-ankyrin metabolon complex (Burton & Bruce, 2011).

Molecular Biology

AQP-1 is a 17-kb gene on chromosome 7p14. The gene has four exons and both TATA and Sp1 consensus sequences in the promoter region (Moon et al., 1993). The Co^a and Co^b antigens are the result of an A314T polymorphism, leading to Ala45 (Co^a; *CO*01*) or Val45 (Co^b; *CO*02*) (Smith et al., 1994). A third polymorphism (Gln47>Arg) just distal to the Co^a/Co^b polymorphism was identified in an alloimmunized Turkish patient (TOR) with an apparent anti-Co3 (Arnaud et al., 2008). Six CO-null alleles are described as well as a Co-3 weak allele (Co_{mod}; Pro38>Leu). An acquired Co_{null} phenotype is also reported in rare patients with monosomy 7 and congenital dyserythropoietic anemia (Agre et al., 1994).

Colton Antibodies

Anti-Colton antibodies can be clinically significant: They can be associated with shortened RBC survival, hemolytic transfusion reactions, and HDFN (see Table 36.5). Antibodies to Co^a and Co^b are usually of the IgG isotype, resulting from immune stimulation by transfusion or pregnancy. Some examples of anti-Co^a and anti-Co^b are reported to bind complement. Anti-Colton antibodies are detectable in the AHG phase of testing and are enhanced with protease-treated RBCs. Rare Co_{null} and "TOR-negative" individuals can make an anti-Co3 (anti-Co^{a+b}), an alloantibody that reacts with both Co (a+b–) and Co (a–b+) RBCs (Reid & Lomas-Francis, 2012; Arnaud et al., 2008).

Biological Role

Biologically, AQP-1 is a major molecular water channel on RBCs that facilitates the concentration of urine in kidney (Verkman, 2009). Co_{null} red cells also have decreased CO_2 permeability (Endeward et al., 2006). Despite its importance in water regulation, Colton-null individuals show few or no adverse clinical effects. Co_{null} RBCs appear morphologically normal in appearance and number, although mild decreases in RBC life span are reported (Mathai et al., 1996). The absence of any clinically significant hematologic sequelae in Co_{null} individuals is most likely due to the presence of a second aquaporin, AQP-3. A glycerol and, perhaps, urea transporter, AQP-3 (GIL blood group) is moderately permeable to water and appears to account for the residual water permeability on Co_{null} RBCs (Roudier et al., 1998; Verkman, 2009).

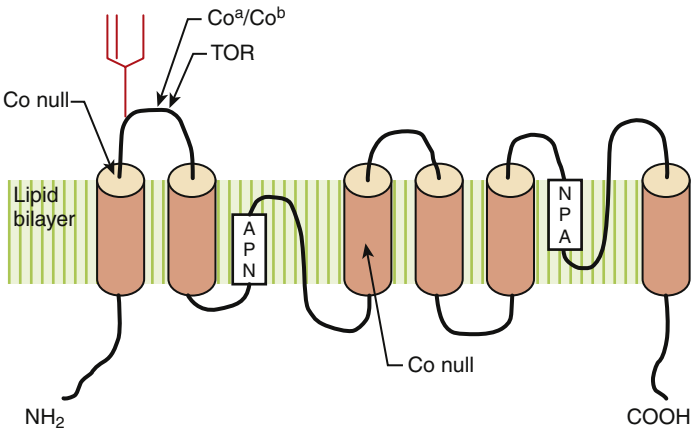

Figure 36.14 Structure of aquaporin-1 (AQP-1, channel-forming integral protein [CHIP]). AQP-1 is a multipass protein containing six transmembrane domains, indicated by *solid amber cylinders*. The first cytoplasmic and third extracellular loops fold back into the lipid bilayer, overlapping at two Asp-Pro-Ala (NPA) motifs, to form a water channel. The *N*-glycosylation site is indicated by a *branched structure* on the first extracellular loop. The Co^a/Co^b polymorphism at amino acid 45 is indicated by a *solid line*. TOR is a rare antigen adjacent to the Co^a/Co^b polymorphism at amino acid 47. The sites of two mutations leading to a Colton null phenotype are also shown.

LW BLOOD GROUP SYSTEM (ISBT NO. 016)

Named in honor of its discoverers, the LW, or Landsteiner-Wiener, blood group system is most important for its role in the history of the Rh blood group system. Landsteiner and Wiener originally developed antibodies against the LW antigens by immunizing rabbits with rhesus monkey red cells. The resulting "anti-Rh" antibodies were initially believed to recognize the RhD antigen. However, later investigators proved that the antibodies developed by Landsteiner and Wiener recognized a non-Rh (LW) antigen.

The LW blood group system consists of two allelic antigens: LW^a and LW^b. LW^a is a high-frequency antigen (99% of white donors). Expression of LW antigen is dependent on RhD protein expression, with the highest expression observed on RhD-positive red cells and weaker expression on RhD-negative cells. LW antigens are absent from Rh_{null} erythrocytes. An LW (a–b–) or null phenotype can also be seen in very rare individuals who are homozygous for a silent LW allele. The LW antigen is expressed on RBCs and placenta. Approximately 3600 to 5000 molecules of LW glycoprotein are present per RBC (Reid & Lomas-Francis, 2012).

Biochemistry

The LW antigens reside on intracellular adhesion molecule type 4 (ICAM-4, CD242), a 40- to 47-kD type 1 glycoprotein. The protein undergoes processing with cleavage of a 30 amino acid leader sequence, resulting in a mature 241 amino acid protein. A member of the Ig superfamily, ICAM consists of two extracellular C2-like domains: a single transmembrane domain and a short cytoplasmic tail. Four *N*-glycosylation sites are present, along with evidence of *O*-glycosylation, which may influence adhesion (Toivanen et al., 2008). Although several amino acids are critical for ICAM-4/integrin binding, the first C2 or Ig domain is most critical (Toivanen et al., 2008). The molecule has three disulfide bonds and is sensitive to reducing agents such as DTT (Reid & Lomas-Francis, 2012).

Molecular Biology

The *ICAM4* gene resides on chromosome 19p13. Seven ICAM alleles have been identified, although only two have been associated with alloantibody formation (Srivastava et al., 2014). The LW^a and LW^b antigens arise from an SNP (A308G), leading to Gln100 (LW^a, *LW*05*) or Arg100 (LW^b, *LW*07*). The *LW*05* allele is the ancestral allele and has even been identified in Neanderthal specimens. Of two LW_{null} individuals studied, one possessed a 10-bp deletion in the coding sequence (Reid & Lomas-Francis, 2012). LW is depressed on *In(Lu)* red cells and in congenital dyserythropoietic anemia type IV, which are associated with mutations in the transcription factor KLF1 (Magor et al., 2015; Fraser et al., 2019).

TABLE 36.23
Chido/Rodgers Blood Group Antigens

Chido (Ch) Antigens		Name	Frequency*	Amino Acid	Frequency*	Name	Rodger (Rg) Antigens
CH/RG†	CH/RGI	Ch1	96%	Argl19>Leu	98%	Rgl	CH/RG11 } CH/RG12
	CH/RG6	Ch3	93%	Ala118>Val	95%	Rg2	CH/RG13 } CH/RG12
		Ch6	96%	Conformational epitope Serl157>Asn	95%	Rg3	
CH/RG7†		WH	Rare	Conformational epitope (Ch6+Rg1) His1106>Asp Lle1105>Leu			
CH/RG2†	CH/RG4	Ch4	96%	Ser1120>Lys Leu1101 Pro			
		Ch2	91%	Conformational epitope (Ch4+Ch5)			
	CH/RG5	Ch5	94%	Gly1054>Asp			

*Calculated from Giles CM: Three Chido determinants detected on the B5Rg+ allotype of human C4: Their expression in Ch-typed donors and families, *Hum Immunol* 18:111–112, 1987 and Issitt PD, Anstee DJ: *Applied Blood Group Serology*, ed 4, Durham, NC, 1998, Montgomery Scientific Publications.
†Conformational epitopes I require the presence of two Ch/Rg antigenic determinants.

LW Antibodies

Clinically benign, anti-LW antibodies are rarely a cause of hemolytic transfusion reactions or HDFN. They usually are of IgG isotype and are detected in the IAT. Antibody activity can be reduced by ethylenediaminetetraacetic acid (EDTA) and pretreatment of RBCs with sulfhydryl-reducing agents (DTT, AET). In addition to anti-LW^a and anti-LW^b, LW_{null} individuals can make an anti-LW^{ab}, which reacts with both LW (a+b–) and LW (a–b+) erythrocytes.

Biological Role

ICAM4/LW glycoprotein is a potential counterreceptor for the β2-integrin protein Mac1 (CD11b/CD18), LFA-1 (CD11a/CD18), and platelet GPIIb/IIIa. It is hypothesized that the LW glycoprotein may participate in adhesive interactions during early erythroid development. Mice lacking ICAM-4 have a decrease in erythroblastic islands in their marrow, although peripheral red cell mass is normal (Toivanen et al., 2008). The addition of soluble ICAM4 to erythroid cultures hastened maturation and enucleation, further supporting a potential role in erythroid development (Choi et al., 2013). LW expression is elevated in sickle cell patients and may be involved in microvascular occlusion (Reid & Lomas-Francis, 2012). LW glycoprotein may also be involved in red cell senescence by binding to CD11/CD18 integrin on splenic macrophages (Toivanen et al., 2008).

CHIDO/RODGERS BLOOD GROUP SYSTEM (ISBT NO. 017)

The Chido/Rodgers (Ch/Rg) blood group system contains 10 antigens, including two pairs of antithetical antigens and three conformational antigens. The latter require coexpression of two spatially distinct Ch/Rg antigens that together generate a third conformational antigen (Table 36.23). Most Ch/Rg antigens are high-incidence antigens (>90%). Similar to Lewis blood group antigens, Ch/Rg antigens are of plasma origin and are passively adsorbed onto RBC membranes. Ch/Rg antigens are weakly expressed on cord RBCs and some GYPA-deficient RBCs (Issitt & Anstee, 1998).

Biochemistry/Molecular Biology

Ch/Rg antigens are antigenic determinants on the C4d fragment of the C4 complement molecule. C4 is the product of two highly homologous genes (99% identity), *C4A* and *C4B*, on chromosome 6p21.3 near the HLA locus. At present, more than 50 C4 alleles have been identified, including null alleles, making the genetics of this system difficult. Each gene spans approximately 22 kb and is organized into 41 exons. Four amino acids in exon 26 are responsible for distinguishing C4A from C4B. Most Ch/Rg antigens are determined by amino acid polymorphisms encoded in exons 25 and 28 (Giles et al., 1988). In general, Chido antigens are on C4B, and Rodgers antigens are on C4A, although examples of C4B-expressing Rodgers antigens (and vice versa) are known (Giles, 1987; Giles et al., 1988). On protein electrophoresis, C4A migrates faster than C4B.

Chido/Rodgers Antibodies

Antibodies against Ch/Rg antigens do not cause hemolytic transfusion reactions or HDFN. Rare reports have described anaphylaxis following transfusion of plasma and platelets (Westhoff et al., 1992). Anti-Ch/Rg antibodies are of IgG isotype and are usually detected with AHG. Antibody reactivity can be enhanced by incubating RBCs in a low–ionic sucrose solution. Antibody reactivity can be inhibited by plasma or by treatment of RBCs with proteases (Reid & Lomas-Francis, 2012).

Biological Role

C4 deficiency is associated with autoimmune disorders and susceptibility to bacterial meningitis. Specific C4 allotypes have been linked to several autoimmune disorders, including rheumatoid arthritis and Graves disease.

GERBICH BLOOD GROUP SYSTEM (ISBT NO. 020)

The Gerbich (Ge) blood group system contains 11 antigens: 6 high-frequency (>99%; Table 36.24) and 5 low-frequency antigens. The Gerbich glycoproteins (GPC/D; Fig. 36.15) are on fetal and adult RBCs, platelets, and kidney, and fetal liver. Between 180,000 and 250,000 molecules of Gerbich are present per RBC (Reid & Lomas-Francis, 2012).

Null/Weak Phenotypes

Three autosomal-recessive phenotypes are associated with the loss of high-incidence Gerbich antigens: Yus (Ge-2,3,4), Gerbich (Ge-2,-3,4), and Leach (Ge-2,-3,-4). The Gerbich phenotype (GYPCΔex3) is common in New Guinea, a holoendemic area for malaria. All three null phenotypes are associated with ovalocytosis. Gerbich antigens are also decreased in patients with hereditary elliptocytosis due to mutations in actin and other cytoskeletal proteins (An & Mohandas, 2008).

Biochemistry

Gerbich antigens are expressed on two biosynthetically related type 1 glycoproteins: glycophorin C (GYPC; see Fig. 36.15) and glycophorin D (GYPD). GYPC is a 40-kD, 128 amino acid glycoprotein bearing one *N*-linked and 12 *O*-linked glycans. GYPD is a 107 amino acid variant, lacking 21 amino acids at the amino-terminus (Reid & Lomas-Francis, 2012). GYPC and GYPD are members of the RBC junctional complex, which is responsible for maintaining the lateral stability of the membrane (Burton & Bruce, 2011; An & Mohandas, 2008). The cytoplasmic domain interacts with AE1 and several cytoskeletal proteins, including spectrin, protein 4.1, and p55. Defects in junctional complex proteins can lead to ovalocytosis.

Molecular Biology

GYPC and GYPD are the products of a single gene, *GYPC*, on chromosome 2q14-121. The gene spans 13.5 kb and is organized into four exons. Exons 1 to 3 encode the extracellular domain; exon 4 is responsible for the transmembrane domain and the cytoplasmic tail. The promoter region contains classical CCAC and TATA sequences as well as transcription factor binding sites for Sp1, GATA-1, and NF-E6. GYPD is the product of leaky translation at a downstream, alternative AUG residue (Met22). The formation of an upstream start codon with synthesis of GYPC is relatively new and is limited to humans (Wilder et al., 2009).

As shown in Table 36.24, the high-frequency antigens Ge2 and Ge4 are the NH_2-termini of GYPD and GYPC, respectively. Ge3 is encoded

TABLE 36.24
Gerbich Blood Group Antigens

HIGH FREQUENCY						LOW FREQUENCY	
ISBT	Name	Frequency	GP*	Amino Acid Change (High→Low)	Frequency	Name	ISBT
GE2	Ge2	>99%	GYPD	aa 1-19			
GE3	Ge3	>99%	GYPC	aa 43-50			
			GYPD	aa 22-29			
GE4	Ge4	>99%	GYPC	N-terminus			
	Wb(–)	>99%	GYPC	Ser8Asn, loss of *N*-glycan	Rare	Webb	GE5
			GYPC+D	Duplication of exon 3	2% blacks 1.5% Finnish	Ls[a]	GE6
	An(a–)	>99%	GYPC	Ser23Ala	0.01%	An[a]	GE7
			GYPD	Ser2Ala			
	Dh(a–)	>99%	GYPC	Leu14Ala	<0.01%	Dh[a]	GE8
			GYPC	Thr32Asn Thr11Asn	Very rare	GEIS	GE9
			GYPD				
GE10	GEPL	>99%	GYPC	Pro45Leu Pro24Leu	Rare	GEPL(–)	
			GYPD				
GE11	GEAT	>99%	GYPC	Asp19Val	Rare	GEAT(–)	
GE12	GETI	>99%	GYPC	Thr27Ile Thr6Ile	Rare	GETI (–)	
			GYPD				
Gerbich Null Phenotypes†							
			GYPC	Deletion exon 2	Rare	Yus	(Ge–2, 3, 4)
			GYPC	Deletion exon 3	10% to 50% Melanesians	Gerbich	(Ge–2, –3, 4)
			GYPC	Deletion exons 3+4	Rare	Leach	(Ge–2, –3, –4)

ISBT, International Society of Blood Transfusion.
*Glycophorin C (GYPC) or glycophorin D (GYPD).
†Yus and Gerbich phenotypes are the result of mutant GPC alleles. No GPD is found in Yus, Gerbich, or Leach phenotypes.

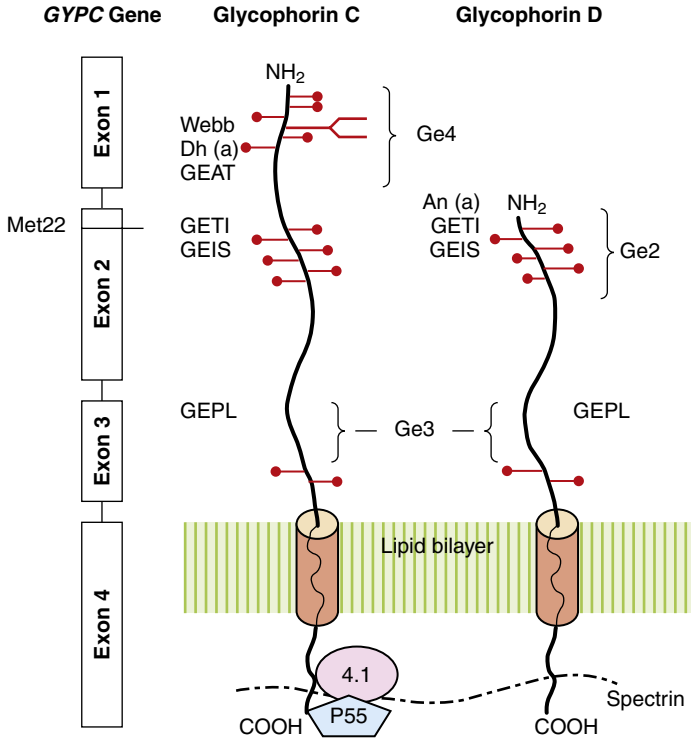

Figure 36.15 Gerbich antigens on glycophorin C (GYPC) and glycophorin D (GYPD). *O*-linked (●—) and *N*-linked glycans are shown. Also shown is the relationship of the *GYPC* gene to both proteins. GYPD is the result of alternative translation at Met22 in exon 2. Deletions of different exons are responsible for the three Gerbich null phenotypes. GYPC and GYPD may interact with spectrin, protein 4.1, and p55 of the cytoskeleton.

by exon 3 and is shared by both molecules. With the exception of Ls[a], low-frequency Ge antigens are the result of single–amino acid polymorphisms. The Leach phenotype results from deletion of exons 3 and 4. As a result, no GYPC or GYPD protein is expressed (see Fig. 36.15). The Yus and Gerbich phenotypes (GYPCΔex3) are deletion mutants characterized by variant GYPC synthesis and complete loss of GYPD synthesis. As a result, Yus and Gerbich can express high-incidence antigens present on GYPC (Ge3, Ge4) but not on GYPD (Ge2). Recent studies show that there is a region of gene duplication between exon 2 and 3 that is susceptible to nonhomologous recombination events with exon deletion (Gourri et al., 2017). Gerbich-negative red cells also show altered glycosylation, with expression of an immature, high-mannose *N*-glycan and decrease in sialylated *O*-glycans (Mayer et al., 2006).

Gerbich Antibodies

Anti-Gerbich antibodies are usually, but not always, clinically significant. Reports have described shortened RBC survival and delayed hemolysis following transfusion of Gerbich-incompatible RBCs. Gerbich antibodies can also inhibit growth and induce apoptosis in early erythroid precursors (Gourri et al., 2017). One report described late-onset, severe HDFN with reticulocytosis, likely due to both extravascular hemolysis and impaired erythropoiesis (Gourri et al., 2017) Autoantibodies against Gerbich antigens have been associated with severe autoimmune hemolytic anemia (Reid & Lomas-Francis, 2012).

Anti-Gerbich antibodies can be of IgM or IgG isotype. Most are immune stimulated, although naturally occurring anti-Ge are known. They may be detected at room temperature and are enhanced by AHG. Gerbich antigens are resistant to chymotrypsin but are sensitive to other proteases (trypsin, pronase).

Biological Role

GYPC and GYPD, in conjunction with AE1, help anchor the membrane to the underlying cytoskeleton. GYPC is also a receptor *P. falciparum* EBA140/BAEBL protein, a sialic acid-dependent invasion protein that recognizes the *N*-glycan on GYPC. Gerbich-negative RBCs (GYPCΔex3) show increased resistance to *P. falciparum* infection in vitro. It is hypothesized that the high incidence of Gerbich-negative RBCs is a selective advantage against severe malaria, although this has not yet been demonstrated (Cooling, 2015). Because they are rich in sialic acid, GYPC and GYPD can also bind influenza virus.

CROMER BLOOD GROUP SYSTEM (ISBT NO. 021)

The Cromer system (CR/CROM) contains 19 antigens, including 6 antithetical antigens, 13 high-incidence antigens, and over 20 possible

TABLE 36.25
Cromer Blood Group Antigens

HIGH-FREQUENCY ANTIGENS			Amino Acid Change (High→Low)	LOW-FREQUENCY ANTIGENS		
ISBT	Name	Frequency		Frequency	Name	ISBT
CROM1	Cr^a	>99%	Ala227Pro	Rare		
CROM2	Tc^a	>99%	Arg52Leu	6% blacks 0% Caucasians	Tc^b	CROM3
			Arg52Pro	Rare	Tc^c	CROM4
CROM5	Dr^a	>99%	Ser199Leu	Rare	Dr(a–)	
CROM6	Es^a	>99%	Ile80Asn	Rare		
CROM7	IFC	>99%	Heterogeneous	Rare	Inab	
CROM9	Wes^b	>99%	Leu8Arg	2% blacks <0.5% whites	Wes^a*	CROM8
			Leu82Pro	Rare	CROK	CROM19
CROM10	UMC	>99%	Thr250Met	Rare		
CROM11	GUT1	>99%	Arg240His	15% Mapuche Indians		
CROM12	SERF	>99%	Pro216Leu	1% Thai		
CROM13	ZENA	>99%	His242Gln			
CROM14	CROV	>99%	Glu156Lys			
CROM15	CRAM	>99%	Gln247Arg			
CROM16	CROZ	>99%	Arg130His	Rare		
CROM17	CRUE	>99%	Leu217Trp	Rare		
CROM18	CRAG	>99%	Asp58Gly	Rare		

ISBT, International Society of Blood Transfusion.
*Because of their proximity, Wes^a weakens Es^a expression.

phenotypes (Table 36.25; see Fig. 36.13). Cromer antigens are present on DAF (CD55), which is widely expressed on tissues and in secretions. DAF has been identified on all hematopoietic cells, vascular endothelium, gastrointestinal and genitourinary epithelium, brain, and body fluids (Storry & Reid, 2002). Cromer is expressed on cord RBCs and placental trophoblasts.

Null/Weak Phenotypes

Inab or Cromer null phenotype is a rare autosomal-recessive phenotype characterized by complete absence of all Cromer antigens but normal expression of CD59 and other GPI-linked glycoproteins. Many individuals with the Inab phenotype suffer from chronic gastrointestinal disorders, particularly a chronic protein-losing gastroenteropathy. CD55/Cromer is also missing on PNH III RBCs, which lack all GPI-linked glycoproteins. Weak Cromer expression (40% normal) is observed in the Dr(a–) phenotype. A mild decrease in CD55 expression is also reported in patients with chronic kidney disease with anemia (Al-Faris et al., 2017).

Biochemistry

CD55/DAF is a highly glycosylated, 319 amino acid, 70-kD GPI-linked glycoprotein (see Fig. 36.13). Like glycophorin A and B, the DAF protein possesses a 34 leader sequence that is cleaved from the mature protein. The extracellular domain consists of four short consensus repeat (SCR) domains capable of binding complement components (C3b/C4b), followed by a 70 amino acid, rigid stalk-region rich in *O*-linked glycans (50% serine/threonine) that may protect the molecule from proteolysis. Each SCR domain contains four highly conserved cysteine residues, resulting in two intrachain disulfide bonds per SCR. As a consequence, DAF is sensitive to sulfhydryl-reducing agents. The molecule contains a single *N*-glycosylation site near SCR1 (Medof et al., 1987). SCR2 and SCR3 are the binding sites for the C3 convertase complexes C3bBb or C4b2a (Lublin, 2005). All four SCR domains are home to Cromer antigens.

Molecular Biology

The *DAF* gene spans 40 kb on chromosome 1q32 and is organized into 11 exons. Cr^a is the reference allele (*CROM*01*). Most Cromer antigens reflect single–amino acid polymorphisms (see Table 36.25; see Fig. 36.13) (Hue-Roye et al., 2007; Daniels, 2013; Storry et al., 2019). The 6 antithetical antigens represent heterogeneity at two amino acid positions (Tc^a/Tc^b/Tc^c, Arg52Pro/Leu and Wes^a/Wes^b/CROK, Arg82Leu/Pro). Because the 34 aa leader sequence is now included in assigning aa positions, the location of all Cromer antigens has changed from reports in the older literature.

Four Cromer null alleles (*CROM*01N*) containing either nonsense or frameshift mutation have been identified for the Inab phenotype. An additional three CD55 null alleles (frameshift, missense) were recently identified in kindreds with CHAPLE syndrome (hyperactivation of complement, angiopathic thrombosis and protein-losing enteropathy) (Ozen et al., 2017).

The Dr(a–) phenotype is the consequence of an SNP (596C>T) that leads to both an Ser199Leu polymorphism and an alternative splice site. In Dr(a–) individuals, two mRNA species are observed, encoding a truncated mutated protein arising from alternate splicing (major transcript) and the full DAF bearing the Leu165 polymorphism (minor transcript). Dr(a–) RBCs have weakened expression of DAF and all Cromer antigens (Storry & Reid, 2002).

Cromer Antibodies

The clinical significance of anti-Cromer antibodies is variable. In some individuals, anti-Cromer antibodies are associated with decreased RBC survival and hemolytic transfusion reactions. Cromer antibodies do not cause HDFN owing to adsorption of antibodies by DAF on trophoblast epithelium (Storry & Reid, 2002; Lublin, 2005). In several cases, a transient loss of anti-Cromer antibodies was noted in the second and third trimesters, with reappearance of the antibody following delivery (Hue-Roye et al., 2007).

Anti-Cromer antibodies are usually of IgG isotype, arising from immune stimulation. They are detected in the IAT and can give weak, variable results (historically, high-titer, low-avidity [HTLA] antibodies). Anti-Cromer can be inhibited by plasma, urine, and platelet concentrates. Antibody reactivity is highly sensitive to pretreatment of RBCs with chymotrypsin and pronase, but not with other proteases. Cromer antigens are weakened, but not destroyed, by AET and DTT.

Biological Role

CD55/DAF protects cells from complement by promoting the decay of two C3 convertases: C4b2a and C3bBb. In murine models of induced autoimmune disease, CD55 knockout mice demonstrate increased disease severity (Lublin, 2005). CD55 is a critical receptor for *P. falciparum*: Inab red cells are resistant to malarial invasion (Egan et al., 2015). CD55 variants bearing different Cromer antigens, however, do not influence *P. falciparum* severity (Schuldt et al., 2017). CD55 is also a receptor for intestinal *E. coli* strains bearing Afa/Dr adhesins, which recognize SCR3. CD55 is an alternate ligand for *H. pylori* and is upregulated in chronic infections. CD55 is also a receptor for several viruses, including hantavirus, coxsackie virus, enterovirus ENV70, and multiple echovirus strains (Cooling, 2015).

KNOPS BLOOD GROUP SYSTEM (ISBT 022)

The Knops (KN) blood group (Table 36.26) contains 10 allelic antigens, including 7 antithetical antigens. Several Knops antigens (Kn^b, Mc^b, Sl^a,

TABLE 36.26

Knops Blood Group Antigens

HIGH FREQUENCY			Amino Acid Change		LOW FREQUENCY	
ISBT	Name	Frequency	(High→Low)	Frequency	Name	ISBT
KN1	Kn^a	99%	Val1561Met	4% whites	Kn^b	KN2
KN3	Mc^a	99%	Lys1590Glu	45% blacks	Mc^b	KN6
KN4	Sl1 (Sla)	98% whites 52% blacks	Arg1601Gly	Blacks only	Sl2 (Vil)	KN7
	Sl4*	100% blacks 96% whites	Ser1610Thr	4% whites	Sl5*	
KN8	Sl3†		Arg1601+Ser1610			
KN9	KCAM	80% to 98% whites	Ile1615Val	70% to 80% West Africans, Afro-Brazilians	KDAS	KN10‡
KN5	Yk^a	92% whites 98% blacks	Unknown			

ISBT, International Society of Blood Transfusion.
*Sl4 and Sl5 are theoretical antigens not formally added to the Knops family at this time.
†Sl3 is a conformational antigen that requires the presence of both Sl1 (Arg1601) and "Sl4" (Ser1610).
‡KDAS, the allelic antigen to KCAM, is still pending final ISBT designation.

KCAM) are racially segregated. Knops antigens are present on adult and cord RBCs, neutrophils, B lymphocytes, and dendritic cells (Reid & Lomas-Francis, 2012). Knops can vary in strength between individuals (200–1200 molecules/RBC), with approximately 1% of donors showing extremely weak Knops expression (50–150 molecules/RBC, Helgeson phenotype). Knops/CR1 can be decreased in the setting of infection and autoimmune disorders due to high levels of circulating immune complexes (Moulds, 2010).

Biochemistry

Knops resides on complement receptor 1 (CR1, CD35), a 220-kD glycoprotein (Moulds, 2010). The extracellular domain consists of 30 SCRs, arranged into four long homologous regions (LHRA-Ds), each containing 7 SCRs. Each LHRA-C contains a complement-binding domain that is capable of binding C4b, C3b, and C5a, as well as malaria (Cooling, 2015) The Knops antigens reside in SCR25 and SCR26 in LHRD. LHRD is also a receptor for mannose-binding lectin. The molecule also possesses six to eight *N*-glycosylation sites.

Molecular Biology

The *CR1* gene resides on chromosome 1q32. Four CR1 isoforms (CR*1–4) are possible, but CR1*1 is the most common (Moulds, 2010). Variation in CR1 strength and copy number is a genetically determined trait and may have arisen due to selective pressure by malaria. To date, all Knops antigens arise from amino acid polymorphisms (Table 36.26; Covas et al., 2007; Moulds, 2010; Scharberg et al., 2019). SL3 is a conformation antigen that requires S11 and S14 coexpression.

Knops Antibodies

Knops antibodies are clinically insignificant. Knops-incompatible RBCs have normal survival following transfusion. Knops antibodies are of IgG isotype, arising from immune stimulation, and are usually detected only with AHG. Historically classified as an HTLA antibody, Knops antibodies are notoriously difficult to work with because of their low avidity, biological variation in Knops expression, antigen degradation, and the common presence of additional alloantibody specificities. Knops antigens are resistant to proteases but are weakened by sulfhydryl-reducing agents (AET, DTT). Autoantibodies to denatured, soluble CR1 are common in lupus, cirrhosis, and HIV infection (Sadallah et al., 2003).

Biological Role

A complement regulatory protein, CR1 can bind C3b/C4b immune complexes, promoting their degradation to iC3b and iC4b by factor 1. CR1 also binds C5a and can accelerate the decay of C3 and C5 convertases. CR1 also enhances phagocytosis of C3b/C4b-coated particles. The latter may promote bacterial adhesion and/or intracellular uptake by *Leishmania* and *S. pneumoniae* (Li et al., 2010; Cooling, 2015). It is hypothesized that CR1 may play a role in *Mycobacterium* infections, possibly via LHRD and mannose-binding lectin (Cooling, 2015).

CR1 is a receptor for the *P. falciparum* invasion protein PfRH4. PfRH4 recognizes the C3b/C4b binding site in LHRA (SCR1-3) (Tham et al., 2010). Several genomic studies have confirmed that low CR1 expression is protective against malaria (Cooling, 2015). CR1 can also bind some PfEMP variants. PfEMP is a malarial protein expressed on infected RBCs and is responsible for RBC rosetting. Some older studies have reported associations between malarial risk and select Knops antigens (Kn^b, McC^b, Sl2), but these have not been observed in recent genomic studies (Cooling, 2015). Furthermore, in vitro studies using CR1 constructs bearing specific combinations of McC and Sl antigens found no difference in PfRH4 binding (Tetteh-Quarcoo et al., 2012).

INDIAN BLOOD GROUP SYSTEM (ISBT NO. 023)

The Indian (IN) blood group contains two autosomal-codominant antigens: In^a (IN1) and In^b (IN2). In^b is a high-frequency allele (99% white), whereas In^a is relatively rare except among Indian (4%) and Arab populations (11%–12%). Five additional high-incidence antigens are known: IN3, IN4, IN5, IN6, and AnWj. Rare IN3- and IN4- have been identified only in Moroccans and Pakistanis, respectively (Poole et al., 2007). IN(-5) and IN(-6) were identified in Asian populations (Storry et al., 2019). Indian antigens are carried by the CD44 glycoprotein and are widely expressed on all hematopoietic cells, epithelial cells, and neural tissue. Approximately 6000 to 10,000 CD44 molecules are present per RBCs (Byrne & Byrne, 2004; Reid & Lomas-Francis, 2012).

Null/Weak Phenotypes

Indian antigens, including AnWj, are depressed on *In(Lu)* RBCs. They are transiently depressed on cord RBCs during pregnancy and autoimmune hemolytic anemia as a result of autoanti-AnWj (Daniels, 2013).

Biochemistry

Indian antigens are present on CD44, a ubiquitous glycoprotein on many cell membranes. CD44 is heterogeneous between tissues owing to tissue-specific differences in mRNA processing and glycosylation. In RBCs, CD44 is an 80- to 85-kD, 341 amino acid type 1 glycoprotein bearing a large, heavily glycosylated extracellular domain containing six cysteine residues, six *N*-glycans, three chondroitin sulfate glycans, and several *O*-linked glycans. The globular head domain is the binding site for hyaluronic acid. The carboxy-terminal cytoplasmic domain interacts with the cytoskeleton (Band 4.1, ankyrin, ezrin, moesin, radixin) and intracellular signaling molecules (Src, Lck, Fyn, protein kinase C) (Ponta et al., 2003).

Molecular Biology

CD44 resides on chromosome 11p13. The gene spans 50 kb and contains 20 exons, which are able to generate an array of splice-form variants. In RBCs, CD44 is encoded by exons 1 through 5, 16, 17, 18, and 20. A single–amino acid polymorphism is responsible for the In^a (*IN*01*, P46) and In^b (*IN*02*, R46) antigens. Missense mutations are responsible for the loss of high-incidence antigens IN3 (H85Q), IN4 (T163R), IN5 (R150H), and IN6 (H92Q) (Poole et al., 2007; Storry et al., 2019).

The basis of the AnWj antigen is unknown but is believed to reside along the O-linked stalk of the molecule, proximal to the lipid bilayer.

AnWj is absent or weak on fetal red cells but is expressed within several weeks after birth, suggesting that it may be related to glycosylation analogous to Lewis and I antigens. A rare autosomal-recessive, AnWj-negative phenotype has been described in Middle Eastern populations linked to a mutation in the transcription cofactor SMYD1 (Vahalom et al., 2018). It is hypothesized that SMYD1 plays an indirect role in AnWj, possibly by regulating expression of a glycosyltransferase or other enzyme necessary for AnWj expression.

Indian Antibodies

Antibodies against both Indian and AnWj antigens can be clinically significant, with shortened RBC survival and transfusion reactions. They are not associated with HDFN. Autoimmune anemia due to autoanti-AnWj has been reported. Anti-Indian antibodies are usually of IgG isotype, arising from immune stimulation. They can present as saline agglutinins and are enhanced by AHG. With the exception of AnWj, Indian antigens are destroyed by proteases and AET. Anti-Indian antibodies are also inhibited by plasma, which contains soluble CD44. Patients with anti-AnWj have been successfully transfused with *In(Lu)* red cells, which has suppressed AnWj expression (Fraser et al., 2019).

Biological Role

CD44 is a major adhesion molecule on leukocytes. CD44 binds a spectrum of extracellular matrix proteins, including collagen, fibronectin, laminin, and hyaluron. In bone marrow, CD44 may participate in the adhesion of erythroid progenitors to stromal fibroblasts. In leukocytes, CD44 may facilitate white blood cell (WBC)–endothelial adhesion, helping to localize WBCs to sites of inflammation. CD44 has been implicated in tumor metastasis, wound remodeling, and embryonic differentiation. CD44 is a receptor for invasive *S. pyogenes* via the hyaluronic acid–binding domain, leading to disruption of the cytoskeleton and tissue penetration (Cooling, 2015). Similarly, CD44 plays a critical role in *Shigella* and *Listeria* invasion. The AnWj antigen is believed to be a receptor for *H. influenzae* type b.

OK BLOOD GROUP SYSTEM (ISBT NO. 024)

The OK system resides on CD147 or Basigin and contains three high-frequency antigens: Ok^a, OKGV, and OKVM. CD147 is widely expressed on epithelium, blood cells, retina, and neural cells (Muramatsu, 2012). There are approximately 3000 molecules of CD147 per RBC. CD147 is highest on red cells but decreases with red cell age.

Biochemistry and Molecular Biology

Ok^a resides on CD147, a 35- to 68-kD, 251 amino acid *N*-linked glycoprotein. A member of the Ig superfamily, CD147 possesses IgC2 and IgV domains. In the membrane, CD147 is present as a homodimer, often in complex with other proteins, including CD44 (Indian), β1-integrins, caveolin, and monocarboxylic acid transporters (Muramatsu, 2012).

The gene for CD147 resides on chromosome 19p13.2-pter and shows a high degree of conservation in primates. The Ok(a–) phenotype arises from a E92K polymorphism (Daniels, 2013). Single–amino acid polymorphisms are also responsible for the OKVM- (Val60Met) and OKGV-negative phenotypes (Gly59Val) (Reid & Lomas-Francis, 2012). Four additional amino acid polymorphisms are known but have not been implicated in alloantibody formation to date (Wanaguru et al., 2013).

CD147 Antibodies

Anti-Ok^a is rare and has been described only in Japan. Anti-Ok^a is of IgG isotype, arising from immune stimulation, and is associated with shortened RBC survival following transfusion of Ok^a-incompatible RBCs. It is not associated with HDFN. The Ok^a antigen is resistant to enzymes, sialidases, and sulfhydryl-reducing agents. Three monoclonal antibodies against Ok^a were developed by the New York Blood Center (Tian & Halverson, 2009).

Biological Role

On WBCs, CD147 is a leukocyte activation–associated protein and may participate in cell adhesion, tumorigenesis, and wound healing via stimulation of enzymes required for remodeling of the extracellular matrix (Muramatsu, 2012). CD147 also plays a role in red cell trafficking and splenic recirculation; its loss with aging is associated with splenic clearance of senescent red cells (Coste et al., 2001; Khandelwal & Saxena, 2006). More important, CD147 is the receptor for PfRH5, a malarial adhesion protein absolutely essential for *P. falciparum* infection and may underlie *P. falciparum*'s tropism for humans (Wanaguru et al., 2013). CD147 is also a receptor for cyclophilin A and B. Cyclophilins are incorporated into several viral proteins and facilitate infection by HIV, SARS-coronavirus, and measles (Cooling, 2015).

RAPH BLOOD GROUP SYSTEM (ISBT NO. 025)

The RAPH blood group system contains a single antigen, RAPH or MER2, located on CD151 or tetraspanin (TM4). CD151 is widely expressed on epithelium, fibroblasts, endothelium, muscle, renal glomeruli and tubules, CD34 cells, early erythroid precursors, megakaryocytes, and platelets. CD151 is strongly expressed in early erythroblasts but is progressively lost with increasing maturation. As a result, MER2 expression is variable among adult donors, with 92% typing MER2-positive and 8% typing MER2-negative. MER2-negative donors strongly express CD151 on other cell lines, such as platelets and lymphocytes.

Null Phenotypes

A MER2-negative, autosomal-recessive phenotype was identified in three individuals of Indian ancestry (Crew et al., 2004). All three individuals had nephrotic syndrome with end-stage renal disease and neurosensory deafness. In addition, two individuals had severe pretibial epidermolysis bullosa, bilateral lacrimal duct stenosis, and nail dystrophy. CD151-null has also been linked to Kindler syndrome, a subtype of epidermolysis bullosa, that is also characterized by widespread blistering, nail dystrophy, and nephropathy (Vahidnezhad et al., 2018).

Biochemistry

CD151 or tetraspanin is a 253 amino acid, 28- to 32-kD multipass protein with four transmembrane domains, four cysteine residues, two extracellular loops, and a single *N*-glycosylation site. The second large extracellular loop contains a QRD motif for integrin binding (aa 194) and is the site of polymorphisms associated with alloantibody formation (Crew et al., 2008). In the cell membrane, tetraspanins are associated with integrins (α3β1, α6β1, α7β1) and are implicated in cell adhesion, tumor metastasis, and signaling (Kumari et al., 2015).

Molecular Biology

CD151 (TSPAN24) is located on chromosome 11p15 and consists of eight exons: Exons 2 through 8 encode the translated protein. The MER2 null phenotype with renal disease has been linked to a nucleotide insertion (exon 5, G383) and a frameshift mutation, leading to a 140 amino acid, nonfunctional protein (Crew et al., 2004). In addition, two SNPs (R171C, R178H) have been identified in three individuals with MER2 alloantibodies (Crew et al., 2004, 2008).

MER2 Antibodies

Six examples of anti-MER2 are known in patients of Indian, Turkish, and Pakistani origin (Crew et al., 2004, 2008). All were of IgG isotype, arising from transfusion and pregnancy. Reactivity is sensitive to disulfide-reducing agents and most proteases except papain (Crew et al., 2004). No reports have described HDFN due to anti-MER2. MER2 can cause hemolytic transfusion reactions in some patients. A monocyte-monolayer assay may be helpful in determining the clinical significance of anti-MER2 antibodies (Crew et al., 2008).

Biological Role

The occurrence of renal disease and neurosensory deafness in all three patients with frameshift mutations suggests that CD151 is critical for basement membrane assembly in the kidney and inner ear. The clustering of tetraspanin (CD151) and β1 integrins, which are important in laminin adhesin, also supports a role for CD151 in basement membrane function and assembly (Crew et al., 2004). RAPH is a receptor for HPV, CMV, and HCV and facilitates *Neisseria meningitidis* adhesion (Cooling, 2015).

JMH BLOOD GROUP SYSTEM (ISBT NO. 026)

The JMH (John Milton Hagen) system contains six high-incidence antigens and can vary in strength among individuals. In addition to RBCs, JMH is found on lymphocytes, activated macrophages, thymus, brain, respiratory epithelium, placenta, testes, and spleen (Reid & Lomas-Francis, 2012).

Variant and Null Phenotypes

JMH weak, JMH variant, and JMH negative have been described (Seltsam et al., 2007). An acquired JMH weak to negative phenotype can occur in the elderly, accompanied by the occurrence of JMH autoantibodies. Five distinct autosomal-recessive JMH variants have been described as the

result of single missense mutations. At least one example of an autosomal-dominant JMH-negative phenotype has been described.

Biochemistry

JMH is carried on CD108 (SEMA7A), a semaphorin family glycoprotein (see Fig. 36.13). The protein is a 666 amino acid protein composed of a large 500 amino acid SEMA domain, a C2-type Ig domain, and five *N*-glycosylation and six myristoylation sites. The molecule contains an RGD sequence essential for promoting axonal growth (Seltsam et al., 2007). The molecule is anchored into the cell membrane by a GPI tail (GPI-linked) and is absent on PNH III RBCs. The molecule contains 19 cysteine residues and is sensitive to sulfhydryl-reducing agents.

Molecular Biology

SEMA7A resides on chromosome 15q24.1 and consists of 14 exons ranging from 42 to 362 bp in size (Seltsam et al., 2007). JMH variants are the result of missense mutations at two mutational hotspots in propeller 3 (R203W [*JMH*01.-02*], R203H [*JMH*01.-03*]) and propeller 7 domains (R460H, R461C). All four mutations may lead to conformational changes based on molecular modeling. An additional missense mutation has been identified in four Native Americans (R347L; St-Louis et al., 2009).

No mutations were identified among JMH-weak and JMH-negative samples. It is interesting to note that *SEMA7A* mRNA can be identified in reticulocytes from JMH-negative individuals, suggesting that the absence of JMH on red cells is posttranscriptional. The absence of JMH on red cells was not due to PNH or related defects in GPI biosynthesis: CD55 and CD59 expression on JMH-negative red cells was normal (Seltsam et al., 2007).

JMH Antibodies

Anti-JMH antibodies do not cause hemolytic transfusion reactions or HDFN, although shortened RBC survival has been documented in some patients. The latter may reflect true alloantibodies in JMH-variant individuals. The antibodies are of IgG isotype and can be naturally occurring. The JMH antigen is sensitive to proteases and DTT. An assay for detection of anti-JMH antibodies was recently developed for gel using immobilized recombinant SEMA7A on polystyrene beads (Seltsam et al., 2008).

Biological Role

Semaphorin proteins are implicated in cell signaling. In hematopoietic cells, SEMA7A can modulate cellular immunity via effects on T cells, monocytes, and NK cells. SEMA7A inhibits NK cell proliferation (Figueiredo et al., 2009) and is a negative regulator of T-cell activation. Conversely, SEMA7A stimulates chemotaxis, secretion of inflammatory cytokines, and dendritic cell maturation in monocytes (Ji & Ivashkiv, 2009). SEMA7 was recently identified as a possible receptor for the *P. falciparum* invasin protein MTRAP, which is expressed by merozoites (Bartholdson et al., 2012).

I BLOOD GROUP SYSTEM (ISBT NO. 027)

The I blood group system contains two biosynthetically related antigens: I and i. The system was named "I" for "individuality" after an extensive search of 22,000 individuals identified only five I– adult donors (Cooling, 2010). The biosynthetic precursor to I antigen, i antigen, is strongly expressed on cord cells because of developmental delays in the enzyme responsible for I antigen synthesis. By 3 months of age, there is a perceptible decrease in i antigen, accompanied by increased I antigen, with an adult I+i– phenotype by 18 to 24 months of age (Marsh, 1961). Increases in I antigen are accompanied by parallel increases in A and B antigens (Cooling, 2010). Both I and i antigens are ubiquitously expressed on glycolipids and glycoproteins on red cells and other tissues.

Null Phenotype

The i_{adult} phenotype is a rare autosomal-recessive phenotype found in fewer than 1 out of 10,000 donors. In Asia, the i_{adult} phenotype can be associated with congenital cataracts (Inaba et al., 2003; Yu et al., 2003). Elevated i antigen is observed on cord RBCs due to delays in I-gene expression. Increased i antigen can be expressed on reticulocytes and in megaloblastic anemia, leukemia, and chronic hemolytic states as a sign of stressed erythropoiesis (Cooling, 2010). Elevated i antigen is observed in HEMPAS (hereditary erythroblastic multinuclearity with positive acidified-serum test), a congenital dyserythropoietic anemia associated with chronic hemolysis, binucleated erythroblasts, and altered red cell glycosylation (Denecke & Marquardt, 2009). The molecular basis of HEMPAS was identified as altered Golgi trafficking due to mutations in SEC23B, a COPII protein (Schwarz et al., 2009).

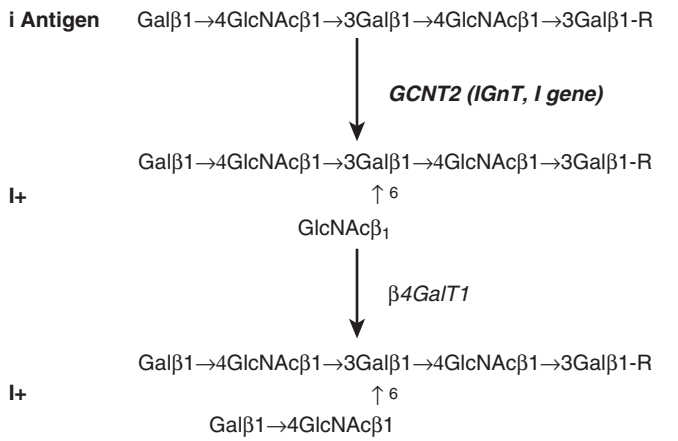

Figure 36.16 Structure of the I and i antigens. The I antigen is composed of two successive lactosaminyl subunits. I antigen requires the action of GCNT2, a 1-6-*N*-acetylglucosaminyltransferase. *Gal,* Galactose; *GlcNAc, N*-acetylgalactosamine; *R,* other oligosaccharide.

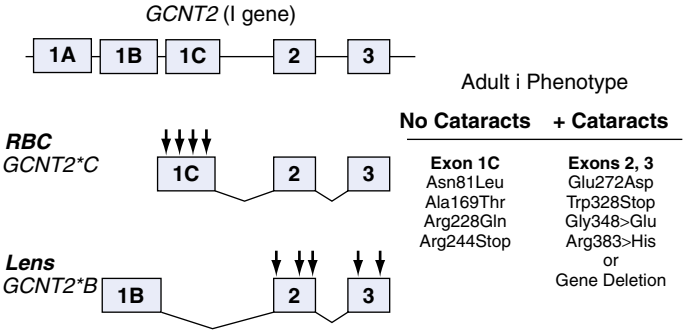

Figure 36.17 The *I* gene, showing three different exons 1. In human red blood cells (RBCs) and lens, a different *GCNT2* mRNA is translated based on which exon 1 is utilized. Mutations in the *GCNT2* gene can result in an i_{adult} phenotype and cataracts. In Europeans, mutations usually are seen only in exon 1C and affect I antigen synthesis in RBCs. In Asia, i_{adult} phenotype involves gene deletion or mutations in exons 2 and 3. As a result, loss of GCNT2 activity is seen in all tissues.

Biochemistry

Type 2 chain oligosaccharides, both i and I antigens, terminate in a Galβ1→4GlcNAc or lactosaminyl epitope, differing only in complexity and multivalency. As shown in Figure 36.16, the i antigen is a linear oligosaccharide containing at least two successive lactosamine epitopes. The I antigen is derived from i antigen by the action of a β1–6 *N*-acetylglucosaminyltransferase, a first step in the synthesis of large branched multivalent complex polylactosamines (see Fig. 36.16). Both i and I can be further modified by other glycosyltransferases to yield ABH, LeX, and related antigens (Cooling, 2010).

Molecular Biology

The I antigen, a β1–6 glucosaminyltransferase, is the product of the *GCNT2* or *IGnT* gene. The gene spans approximately 100 kb in an Alu-rich region on chromosome 6p24. The gene contains five exons, including three tissue-specific exons 1 (Fig. 36.17). As a consequence, three different *GCNT2* splice-forms are possible, depending on which exon 1 is utilized (Inaba et al., 2003). *GCNT2*A* is ubiquitously expressed, whereas *GCNT2*B* is primarily expressed in human lens epithelia, fetal brain, and cerebellum (Yu et al., 2003). *GCNT2*C*, composed of exons E1C, E2, and E3, is the predominant transcript in erythroblasts and reticulocytes. In hematopoietic stem cells, erythroid differentiation is accompanied by transcriptional upregulation of *GCNT2*C* (Twu et al., 2007). The promoter for *GCNT2*C* contains transcription factor binding sites for Sp1, Oct-2, and C/EBPα. C/EBPα phosphorylation and binding is critical for transcriptional activation (Twu et al., 2007). In other tissues, *GCNT2* expression is also regulated by changes in methylation and microRNAs (Cooling, 2019).

The translated GCNT2 protein consists of 402 amino acids with five *N*-glycosylation sites and 9 conserved cysteine residues. Unlike most galactosyl- and glucosaminyltransferases, GCNT2 does not contain a DXD motif. The enzyme is likely highly folded, based on crystallography data from C2GnT, a closely related β1,6 glucosaminyltransferase

(Pak et al., 2006; Cooling, 2010). Sequence differences in exon 1, which encodes 77% of the translated enzyme, may account for the enhanced enzyme activity observed with the GCNT2*C isoform (Yu et al., 2003). Oligosaccharide analysis and enzyme studies indicate that the minimum acceptor for enzyme activity is a tetrasaccharide composed of two lactosamine motifs (Cooling, 2010).

Both the i_{adult} phenotype and congenital cataracts have been linked to mutations in *GCNT2*. In i_{adult} individuals without cataracts, missense mutations have been found in exon E1C, leading to an isolated loss of GCNT2*C activity in RBCs (Inaba et al., 2003; Cooling, 2010). In contrast, i_{adult} with cataracts is the result of mutations in exon E2 or E3 or a major deletion of the *GCNT2* gene. As a result, GCNT2 activity is lost in all tissues, including RBC and lens (Yu et al., 2003; Cooling, 2010). Loss of GCNT2*B activity in the lens is believed to underlie the formation of cataracts in humans; however, a direct causal link has yet to be established. No increase in cataracts was observed in a *GCNT2*-knockout mouse model (Chen et al., 2005).

Anti-I and Anti-i Antibodies

Anti-I and anti-i are antibodies of IgM isotype, reactive at room temperature (see Table 36.5). Autoantibodies to I are relatively common and are usually low-titered cold agglutinins. Some anti-I can have IH specificity, reacting stronger with group O and A_2 RBCs (refer to Table 36.41). Although generally benign, hemolysis secondary to high-titered anti-I is observed in cold autoimmune hemolytic anemia (CAIHA). CAIHA can occur in the setting of malignancy and occasionally infection (e.g., *Mycoplasma pneumoniae*). These antibodies display high thermal amplitude, often agglutinating RBCs at temperatures of 30°C to 34°C. In contrast, alloanti-I is relatively rare and is found as a naturally occurring antibody in i_{adult} individuals. Anti-i is also uncommon but has been reported in CAIHA, infectious mononucleosis, choriocarcinomatosis, and alcoholic cirrhosis.

Biological Role

Despite the common occurrence of major maternal-fetal ABO incompatibility, severe HDFN due to ABO incompatibility is rare (0.04%). It is hypothesized that the developmental delay in I antigen synthesis may play a protective role against HDFN-ABO by minimizing the number of ABH antigens expressed on fetal red cells (Cooling, 2010). This is supported by parallel increases in I and ABH during the first 2 years of life. Additional evidence comes from extended studies of the *N*-glycan on Band 3, which accounts for 50% of the ABH antigen on red cells. Adult red cells had a fourfold increase in ABH expression on Band 3 owing to chain extension and branching (Cooling, 2010).

Ii are oncofetal antigens and can show variable expression with malignancy (Cooling, 2019). *GCNT2* is overexpressed in metastatic breast cancer and prostate and colon cancer. The i antigen is a marker of human mesenchymal stem cells and metastatic melanoma. I antigen also plays a role in the immune response. I antigen is expressed by germinal center B cells but not naïve or memory B cells, which express i antigen. Galactin-9 binding to i-glycans on B cells interferes with CD45-CD22 interaction and BCR signaling (Cooling, 2019). I antigen on NK cells appears to enhance NK cell activity against leukemia cells (Cooling, 2019).

GIL BLOOD GROUP SYSTEM (ISBT NO. 029)

The GIL blood group system contains one high-incidence antigen: GIL (100% donors). The GIL protein is highly expressed on RBCs, kidney, small intestine, stomach, colon, spleen, eye, and respiratory tract (Reid & Lomas-Francis, 2012).

Biochemistry

GIL is carried by aquaglyceroporin (AQP-3), a member of the major intrinsic protein family of water channels. Similar to Colton (AQP1), AQP3 is a 46-kD, 292 amino acid multipass protein containing six transmembrane domains and a single *N*-glycosylation site. The molecule is present in the cell membrane as dimers, trimers, and tetramers (Daniels, 2013).

Molecular Biology

The *AQP3* gene spans 6 kb on chromosome 9p13 and is organized into six exons. The one example of a GIL-negative phenotype is the result of splice site and frameshift mutations, resulting in a truncated 218 amino acid protein. In general, AQP3 is highly conserved; no missense mutations in the translated protein were identified in a recent study of European and African individuals. Two SNPs were identified in the promoter region (A-14G, C-46A); however, neither polymorphism had an impact on AQP3 mRNA levels (Bahamontes-Rosa et al., 2008).

GIL Antibodies

Anti-GIL is associated with hemolytic transfusion reactions. No reports have described clinical HDFN due to anti-GIL despite a positive DAT. Anti-GIL is usually of IgG isotype, reactive at 37°C, and enhanced with AHG. The antigen is resistant to proteases, sialidases, and DTT.

Biological Role

AQP3/Gil is a membrane channel capable of transporting urea and glycerol. On red cells, AQP3 may play a role in malaria infection. AQP3 was shown to be internalized during *P. falciparum* infection as part of the parasitophorous vacuole (Bietz et al., 2009). Because AQP3 protects against hydroxyl radicals and osmotic stress, internalization and loss of AQP3 from the red cell extracellular membrane could accelerate red cell damage (Bahamontes-Rosa et al., 2008).

AQP is present on immature dendritic cells and is implicated in the uptake of soluble antigen by micropinocytosis. AQP3 is highly expressed in epidermis and cutaneous T cells, where it plays a role in skin differentiation, hydration, and inflammation (Boury-Jamot et al., 2009).

JR BLOOD GROUP SYSTEM (ISBT NO. 032)

JR contains a single high-prevalence RBC antigen (Jr^a) present on ABCG2 (ATP-binding cassette, subfamily G, member 2) (Zelinski et al., 2012). Jr/ABCG2 is widely expressed, including cord and mature RBC, stem cells, placenta, cerebral endothelium, lung, renal proximal tubules, liver, breast, and intestinal epithelium (Castilho & Reid, 2013). ABCG2 is a membrane transporter implicated in folate, porphyrin, urate transport, multidrug resistance, and removal of toxic metabolites. Unlike Lan (ABCB6), ABCG2 does not influence porphyria severity (Fukuda et al., 2016).

Biochemistry

ABCG2 is a 655 amino acid, 72-kDa glycoprotein. Like Diego/AE1, ABCG2 has two functional domains: a membrane transporter domain consisting of six transmembrane domains and a long intracellular amino-terminal signaling domain containing three nucleotide-binding motifs. Similar to other RBC transporters (AE1, Colton, GIL), ABCG2 probably exists as dimers and tetramers in the RBC membrane. ABCG2 has a single *N*-glycan site on the third extracellular loop.

Molecular Biology

The *ABCG2* gene is located on chromosome 4q22 and is organized over 16 exons. The gene is highly polymorphic, with nearly 1300 SNPs reported (Castilho & Reid, 2013). The Jr(a–) phenotype is an autosomal-recessive phenotype due to *ABCG2*-null alleles. Twenty-four null (*ABCG2*01N*) and presumed $Jr(a^w)$ alleles (*ABCG2*01W*) are described. The $Jr(a^{+w})$ phenotype is a consequence of heterozygous inheritance of a null and weak allele ($Jr(a^{+w}/–)$. Most Jr(a) weak alleles contain an amino acid polymorphism in the third extracellular loop (Castilho & Reid, 2013).

Jr Antibodies

The Jr(a–) phenotype is rare, with the highest incidence in Japan (0.03%–0.12%) (Castilho & Reid, 2013). Anti-Jr^a is generally of IgG isotype and arises as a result of immune stimulation by transfusion or pregnancy. Antibody reactivity can be enhanced by enzyme treatment. Anti-Jr^a can cause shortened RBC survival and delayed hemolytic transfusion reactions. Anti-Jr^a is associated with mild to severe HDFN, presumably due to suppression of erythropoiesis (Castilho & Reid, 2013).

LAN BLOOD GROUP SYSTEM (ISBT NO. 033)

Lan is a high-incidence antigen expressed on ABCB6 (ATP-binding cassette, family B, member 6) (Helias et al., 2012). The system contains a single antigen: Lan. ABCB6 is expressed on RBCs, including early precursors, fetal liver, heart, megakaryocytes, and skeletal muscle. ABCB6 is located primarily in the plasma and mitochondrial outer membranes.

Biochemistry

ABCB6, like ABCG2/Jr, is a large (842 amino acid) multipass glycoprotein that is present as homodimers in the cell membrane. It is predicted to possess 11 transmembrane domains and a long carboxy-terminal cytoplasmic nucleotide binding domain (NBD). The NBD is the site of ATP binding and hydrolysis, a necessary step in the transport of porphyrin and other substrates (Boswell-Casteel et al., 2018)

Molecular Biology

The gene resides on chromosome 2q36 and is organized over 19 exons. Twenty null alleles have been described to date due to frameshift, nonsense, deletion, and splice site mutations (Reid et al., 2014). An additional four alleles are associated with weak Lan expression. At least nine SNPs have been linked to hereditary disorders associated with abnormal pigmentation, ocular coloboma, and pseudohyperkalemia (Boswell-Casteel et al., 2018).

Lan Antibodies

Anti-Lan are generally of IgG isotype arising from immune stimulation. Anti-Lan can be enhanced by enzyme-treated RBCs. Anti-Lan are a cause of hemolytic transfusion reactions and HDFN (Reid et al., 2014).

Biological Role

ABCB6 is involved in porphyrin transport and is a genetic modifier in hereditary porphyria. Porphyria patients heterozygous for ABCB6 null alleles have substantially more severe disease. In animal studies, loss of ABCB6 led to a 75% decrease in coporphyrin III transport. Unlike ABCG2/Jr, ABCB6 can transport a range of heme-related molecules (Fukuda et al., 2016).

ABCB6 has also been identified as an early receptor for *P. falciparum*: Lan-negative cells, but not Jr-negative cells, are resistant to infection (Egan et al., 2018). In cancer, ABCB6 may interfere with chemotherapy by exporting drug from cells as well as upregulating catalase activity to neutralize inflammatory cell-generated oxygen radicals (Boswell-Casteel et al., 2018). Finally, ABCB6 missense mutations have been associated with ocular coloboma, dyskerchromostosis universalis hereditaria, porphyria, and familial pseudohyperkalemia, characterized by stomatosis at cold temperatures (Fukuda et al., 2016; Boswell-Casteel et al., 2018).

VEL BLOOD GROUP SYSTEM (ISBT NO. 034)

The Vel blood group system contains a single high-incidence antigen (*VEL*01*). Vel resides on SMIM1 or small integral membrane protein 1. SMIM1 is highly expressed on erythroblasts and red cells but not other hematopoietic cells and may be an erythroid-specific protein. In zebra fish, *smim1* expression is associated with erythropoiesis, with reduced erythrocyte production in smim1-knockdown zebra fish (Cvejic et al., 2013). Likewise, there is a correlation between *SMIM1* mRNA and mean hemoglobin content in human RBCs. It is hypothesized that SMIM1 plays a role in the formation and hemoglobinization of RBCs (Cvejic et al., 2013).

Biochemistry

SMIM1 is a small 78 amino acid, 18-kDa glycoprotein containing 3 cysteine residues and a GG transmembrane motif (Ballif et al., 2013; Storry et al., 2013). Current evidence suggests that SMIM1 is a type I transmembrane protein with a 50 amino acid extracellular domain (Storry et al., 2013). Although SMIM1 contains several potential glycosylation sites, there is no evidence that the molecule is glycosylated (Storry & Peyrard, 2017). SMIM1 likely is present as a homodimer in the membrane (Ballif et al., 2013).

Molecular Biology

SMIM1 gene resides on chromosome 1p36 near the *RHD* gene (Ballif et al., 2013; Storry et al., 2013). The gene contains four exons and several GATA1 sites in the promoter region (Cvejic et al., 2013). Most Vel(–) individuals possess a 17-nt deletion in the transmembrane region (Ballif et al., 2013; Cvejic et al., 2013; Storry et al., 2013). Vel-weak individuals tend to be heterozygous for the common *SMIM1*-null allele. There is also evidence of a modifier allele regulating *SMIM1* expression. Genome-wide association studies have found an SNP located in intron 2 (rs1175550G) associated with increased *SMIM1* mRNA levels, likely through binding of TAL1 transcription factor (Cvejic et al., 2013; Storry & Peyrard, 2017). Some heterozygous Vel-weak individuals (SMIM1–/+) also carried a Met51Arg missense mutation. It is unknown whether this polymorphism impacts membrane expression or alters an immune epitope (Cvejic et al., 2013). It is unknown why Vel-negative red cells react weakly with the samples of anti-ABTI, a separate blood group series (Storry & Peyrard, 2017).

Vel Antibodies

The Vel-negative phenotype occurs in 0.0002% to 0.0006% of donors (Ballif et al., 2013), with rates as high as 1/5000 to 1/1200 among Europeans (Storry & Peyrard, 2017). Anti-Vel are usually a mixture of IgM and IgG, with a broad thermal amplitude and ability to fix complement. As such, Vel antibodies are highly significant, capable of causing acute and delayed HTR, as well as HDFN. Anti-Vel was historically considered a high-titer, low-avidity antibody and can be missed in routine testing. Rare Vel-negative units are required for transfusion support for Vel-negative individuals. Autoanti-Vel have rarely been described and vary in clinical significance with regard to transfusion.

CD59 BLOOD GROUP SYSTEM (ISBT NO. 035)

CD59 (membrane inhibitor of reactive lysis, membrane attack complex inhibitory factor) is a high-incidence antigen on RBCs, white cells, placenta, seminal fluid, and other tissues (Kimberely et al., 2007). It plays a critical role in protecting cells from complement-mediated lysis through inhibition of the terminal C5b-C9 membrane attack complex. CD59 is also implicated in T-cell activation, LPS binding, apoptosis, and reproduction.

Biochemistry and Molecular Biology

Like CD55 (DAF, Cromer blood group), CD59 is a GPI-linked glycoprotein and is missing on PNH-red cells. CD59 is a globular glycoprotein with one *N*-glycan, several *O*-glycans, and several sulfhydryl bonds, and it is sensitive to DTT (Weinstock et al., 2015). The gene for CD59 spans over 20 kb on chromosome 11p13 and contains a GC-rich promoter and four exons. Exons 2 through 4 encode the translated protein. Three CD59 null alleles are reported to date (CD59*01N). CD59-null individuals were severely ill with neuropathy, strokes, a mild Coombs-negative hemolytic anemia, and early death (Weinstock et al., 2015).

CD59 Antibodies

There are three known cases of inherited CD59 deficiency, including one patient with an alloanti-CD59 (Weinstock et al., 2015). Alloanti-CD59 is an IgG, enhanced by enzymes and inhibited by soluble CD59. It is presumed that the antibody is clinically significant.

AUGUSTINE BLOOD GROUP SYSTEM (ISBT 036)

The Augustine (AUG) blood group resides on the nucleoside transporter ENT1 and contains two high-incidence antigens: AUG1 (At^a) and AUG2 (Daniels et al., 2015). AUG:-1 phenotype has been described only in blacks. AUG:-1,-2 is an autosomal-recessive, ENT1-null phenotype. Augustine/ENT1 is widely expressed on human tissue, with the highest expression on gastrointestinal tissues, ovary, heart, and adrenal (Boswell-Casteel & Hays, 2017).

Biochemistry

ENT1 is a 456 aa glycoprotein with 11 transmembrane domains, one N-glycan (N48), a cytoplasmic N-terminal domain and external C-terminus that directs protein trafficking, folding and orientation in the membrane (Boswell-Casteel & Hays, 2017). Eight transmembrane domains create a pore that facilitates the transport of nucleotides (purine, pyrimidines) and their cytotoxic analogs (antivirals, cancer reagents) across the membrane.

Molecular Biology

ENT1/AUG is the product of the SLC29A1 gene on chromosome 6p21.1 (Daniels et al., 2015). SLC29A1 contains 13 exons with several tissue-specific alternate promoters. The AUG:-1 phenotype is due to an SNP (Glu391Lys) in the fifth extracellular loop (Daniels et al., 2015). The 391Lys allele is present in 1% to 2.2% of blacks but absent in whites and Asians. The ENT1-null, AUG:-1,-2 phenotype in one French family is the result of a splice mutation in intron 6 (Daniels et al., 2015).

AUG Antibodies

Antibodies to AUG1 and AUG2 are of IgG isotype and immune stimulated. Like most multipass proteins, AUG antigens are resistant to enzyme and disulfide reducing agents (Daniels, 2016). Anti-AUG will react with cord cells. Anti-AUG are clinically significant, capable of causing acute and delayed HTR. Anti-AUG can cause mild HDFN.

Biological Role

ENT1 is a nucleoside transporter for purines, pyrimidines, and therapeutic analogs. In pancreatic cancer, high ENT1 levels are associated with improved survival following treatment with gemcitabine (Boswell-Casteel & Hays, 2017). ENT1 function is inhibited by calcium-channel blockers and ethanol, with ENT1 polymorphisms linked to alcohol's physiologic effects and withdrawal. Both ENT1-null mice and humans have evidence for abnormal bony calcification in tissues and the spine (Daniels et al., 2015; Boswell-Casteel & Hays, 2017).

KANNO BLOOD GROUP SYSTEM (ISBT 037)

The KANNO blood group system was identified in 2019 and is located on the prion protein (PrP^C) classically associated with Creutzfeldt-Jakob disease (CJD) (Omae et al., 2019). In addition to the brain, PrP^C is widely expressed on neural synapses, neuroendocrine cells, and hematopoietic tissues, including spleen, lymph nodes, tonsils, stem cells, dendritic cells, leukocytes, platelets, and red cells (Bernadi & Bruni, 2019). PrP^C expression on red cells is quite low (290 molecules per cell) and is readily detected only by the anti-PrP^C antibody 6H4 (Panigaj et al., 2011).

The system contains a single high-incidence antigen, Kanno. An autosomal-recessive, Kanno-negative phenotype is reported among Asians, particularly among Japanese (Omae et al., 2019; Kawabata et al., 2014).

Biochemistry

The PrP^C protein is a 208 aa GPI-linked glycoprotein located in lipid rafts. The translated protein is 253 aa long due to two signaling domains, which are removed prior to the addition of the GPI-tail. The mature PrPC has two glycosylation sites, resulting in 3 different glycoforms of the molecule. Structurally, PrPC has two distinct domains: an N-terminal "disordered" domain and a globular domain (Pastore & Zagari, 2007). The N-terminal domain is known to bind divalent metals, particularly copper, via the octapeptide (PHGGSWGQ) repeat region. The folded globular domain is composed of 3 α-helical regions and contains a disulfide bond. The globular domain is the location for most pathogenic mutations associated with misfolding with generation of the pathogenic PrP^{SC} form of the molecule (Bernardi & Bruni, 2019).

Molecular Biology

The PrP gene (PRNP) is a 16 kb gene, containing two exons, located on the short arm of chromosome 20 (20p13). The Kanno-negative phenotype is due to a single SNP (Glu219Lys) in the globular domain (Omae et al., 2019). The 219Lys allele ranges from 2.5% to 7.0% in Asian populations. Lys219 has been shown to be a dominant-negative mutation that is protective against prion formation (PrP^{SC}) in animal and humans (Perrier et al., 2002; Hizume et al., 2009). In Japan, 14% of the general population are heterozygous for Glu219Lys alleles compared with only 0.7% of patients with sporadic CJD (0.7%, $p < 0.001$) (Nozaki et al., 2010).

KANNO Antibodies

Anti-KANNO is of IgG isotype, with most known cases stimulated by pregnancy (Kawabata et al., 2014). The antibody reacts weakly in IAT (w+ to 2+) and is nonreactive with enzyme-treated red cells. Cases have been misidentified as anti-JMH; however, anti-KANNO is not sensitive to DTT. Anti-KANNO is not clinically significant: there have been no cases of HDFN or hemolysis following transfusion of KANNO-positive red cells (Kawabata et al., 2014).

Biological Role

Prion protein has been implicated in cell signaling, memory, and neuroprotection (Bernadi & Bruni, 2019). The N-terminal domain, which binds copper, plays a role in metal ion homeostasis and oxidative cell damage. Misfolding of PrP due to mutations or reduction of the disulfide bond underlies the formation of pathogenic prion particles (PrP^{SC}) and transmissible spongiform encephalopathies. Several *PRNP* mutations are associated with CJD, vCJD, fatal familial insomnia, and Gerstmann-Straussler-Scheinker disease (Bernardi & Bruni, 2019). As noted, the KANNO-negative 219Lys allele is a dominant-negative mutant that appears protective against prion-related disease.

SID BLOOD GROUP SYSTEM (ISBT 038)

The Sd^a (SID) antigen was initially described in the 1960s. However, it was designated as a blood group system in late 2019. Sd^a is a high-frequency red cell antigen in whites, with 91% expressing Sd^a on red cells and another 5% expressing Sd^a only in secretions. Sd^a-null individuals, who lack Sd^a on red cells and in secretions, are approximately ≤2% of the population. Sd^a expression is not related to the Lewis system.

Sd^a is expressed on human and animal tissues (Dall'Ollio et al., 2014). In humans, Sd^a is reported on red cells, colon, salivary gland, kidney, urine, saliva, feces, and milk. On kidneys, Sd^a is located along the distal convoluted tubules and collecting ducts, consistent with the distribution of Tamm-Horsfall protein. Tamm-Horsfall protein is the major Sd^a determinant in urine.

Biochemistry and Molecular Biology

Like ABO, the minimum Sd^a antigen is a terminal trisaccharide expressed on glycoproteins (e.g., Tamm-Horsfall protein) and, likely, glycolipids. Sd^a resembles the ganglioside GM2 (GalNAcβ1→4(NeuAcα2→6)Gal-R) although GM2 is not Sd^a active. Sd^a-reactive determinants have been identified on N-linked and O-linked glycoproteins in animals and humans (Dall'Ollio et al., 2014). The rare CAD polyagglutinable phenotype strongly reacts with anti-Sd^a due to the addition of a β→4GalNAc to the O-linked tetrasaccharide on glycophorins (see MNS, Gerbich blood groups section) (Issitt & Petz, 1998). CAD red cells also express Sd^a on type 2 chain glycolipids.

It has long been surmised that the glycosyltransferase *B4GALNT2*, which transfers N-acetylgalactosyltransferase β1-4 to a sialylated acceptor, was likely responsible for Sd^a synthesis (Dall'Ollio et al., 2014). In 2019, mutations in *B4GALNT2* were identified in five Sd(a-) individuals, which is the catalyst for designating Sd^a as a blood group system (Stenflet et al., 2019). Identified mutations included missense mutations (Arg523Trp; Gln436Arg) and a splice mutation. Most Sd(a-) were compound heterozygotes. No mutations were identified in one Sd(a-) individual, possibly due to mutations in regulatory regions.

SD^A ANTIBODIES

Sd^a antibodies are uncommon, naturally occurring antibodies found in ≤2% of whites (Issitt & Anstee, 1998). The antibodies appear to be a mixture of IgM and IgG and are reactive at room temperature, with weaker reactivity at 37°C and the IAT. Reactivity is variable due to biological variation in Sd^a expression on red cells. Sd^a is absent on cord cells. Anti-Sd^a are inhibited by urine, particularly urine from guinea pigs, which is rich in Tamm-Horsfall protein. Sd^a antibodies are not clinically significant.

Biological Role

Sd^a is another xenoantigen that complicates pig-to-human xenotransplantation (Byrne et al., 2018). Sd^a is downregulated in human colon cancer. In pigs, Sd^a is a marker of primordial germ cells (Dall'Ollio et al., 2014).

POSSIBLE NEW BLOOD GROUP: CHOLINE TRANSPORTER-LIKE PROTEIN 2 (CTL2/SLC44A2)

CTL2/SLCAA42 is a choline transporter widely expressed on human tissues, including neutrophils, lymphocytes, and platelets (Flesch & Reil, 2018). The human neutrophil antigen HNA3 is located on CTL2: Alloantibodies to HNA3a have been associated with several cases of transfusion-related acute lung injury (TRALI). In 2019, two red cell alloantibodies were shown to recognize high-incidence antigens on CTL2 (Pro398) in two separate probands (Pro398Ser; Pro398Thr) (Vrignaud et al., 2019). CTL2 is under consideration as another new blood group system pending identification of CTL2 on human red cells.

IMMUNOHEMATOLOGY TESTS AND PROCEDURES

BASIC PRINCIPLES—HEMAGGLUTINATION

Specific hemagglutination is the single most important in vitro immunologic reaction in blood banking because it is the endpoint of almost all test systems designed to detect RBC antigens and antibodies. The hemagglutination process occurs in two stages. The first stage, often referred to as *RBC sensitization*, is simply the combination of paratope and epitope in a reversible reaction that follows the law of mass action and has an associated equilibrium constant. Antigen and antibody are held together by noncovalent attractions. In stage two, multiple RBCs with bound antibody form a stable latticework through antigen-antibody bridges formed between adjacent cells. This latticework is the basis of all visible agglutination reactions.

Formation of the latticework during the second stage of hemagglutination is naturally impeded by the fact that RBCs in solution normally repel one another. This is due to the net negative charge of the RBC membrane created by sialic acid. If RBCs are suspended in an ionic medium such as normal saline, cations arrange themselves around each cell to form an ionic cloud. Cations closest to the cell membrane are firmly bound and move with the RBC, whereas the outer cations move freely. The difference in charge at the surface between the inner and outer cation layers, called the *surface of shear*, creates an electrical potential named the *ζ potential* (Fig. 36.18). The ζ (zeta) potential keeps RBCs in solution about 25 nm apart (Harmening, 2012). Another factor that may be important in keeping RBCs apart is the water of hydration. Proponents of this theory suggest that the hydrophilic polar heads of lipid molecules making up the outer cell membrane bilayer attract water molecules. The water thus creates a surface tension that helps to keep the cells apart.

One situation whereby the natural influence of the ζ potential to keep RBCs apart is circumvented is the phenomenon of rouleaux formation or

"pseudoagglutination." Patients with multiple myeloma, Waldenström macroglobulinemia, and hyperviscosity syndromes have high concentrations of abnormal serum proteins that change the net surface charge on the RBC membrane. The cells thus cluster in clumps that resemble macroscopic hemagglutination. Plasma expanders, such as dextran and hydroxyethyl starch, as well as some intravenous x-ray contrast materials, can also cause rouleaux formation. Rouleaux can be differentiated from true agglutination by direct microscopy (1) by the classical "stacked-coin" formation in rouleaux and (2) by the loss of rouleaux after washing and resuspension in saline. Nonspecific agglutination can also be seen in cord blood samples contaminated with Wharton jelly. The presence of hyaluronic acid and albumin in cord blood is responsible for this problem.

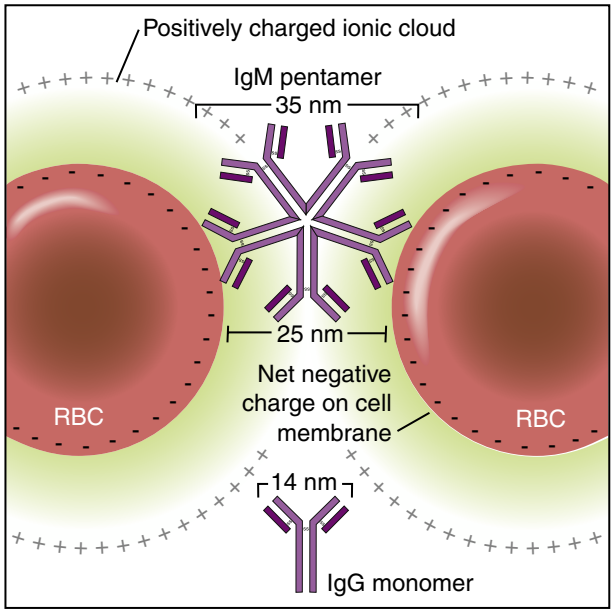

Figure 36.18 Erythrocytes are kept apart in an ionic medium by the ζ potential, which, in turn, influences the agglutinating capacity of immunoglobulin (Ig) G and IgM.

Factors Affecting Specific Hemagglutination

The extent of RBC sensitization and the facilitation of second-stage latticework formation are influenced first by inherent characteristics of the specific antigens and antibodies involved. In most immunohematology procedures, IgM antibodies can facilitate the second stage of hemagglutination because of their large diameter (35 nm) and multivalency, which allows them to span the distance between two adjacent RBCs in solution (see Fig. 36.18). Because of their innate agglutinating ability, IgM antibodies are frequently referred to as *direct agglutinins*. Most IgG antibodies, on the other hand, are considerably smaller (14 nm) and are unable to induce visible agglutination without the assistance of secondary enhancing reagents. Thus, IgG antibodies are commonly referred to as *indirect agglutinins*.

The density and accessibility of specific antigens on the RBC membrane are also critical in second-stage latticework formation. This can be illustrated by comparing the ABO and Rh antigens. Approximately 1 million ABO antigens are present per RBC, displayed on large *N*-glycans of extramembranous glycoproteins. Because of their high density and easy accessibility, ABO antibodies can readily bind exposed ABO antigens and agglutinate RBCs. In contrast, only 10,000 to 30,000 Rh antigens are readily accessible per RBC and, as multipass integral membrane proteins, are considered intramembranous. As a consequence, Rh antigens are less easily agglutinated by Rh antisera. In another example of the influence of antigen density, RBCs that are homozygous for a particular blood group gene will often give stronger reactions than heterozygous cells. This is because homozygotes express twice as many copies, or a double dose, of antigen per cell. In immunohematologic testing, this phenomenon is frequently referred to as *dosage*.

Secondary to inherent antigen and antibody characteristics, the first and second stages of the hemagglutination reaction may also be influenced by manipulating various physical and/or chemical parameters of the reaction environment. An outline of how these various parameters may be controlled is shown in Table 36.27.

TABLE 36.27
Factors Affecting the Hemagglutination Reaction

Reaction Parameter	Effect	Manipulation
Temperature	Influences the equilibrium constant and/or reaction rate, depending on the class of antibody involved.	Decreasing the temperature to 24°C or even to 4°C enhances the reaction of IgM antibodies. Prewarming or maintaining a reaction temperature of 37°C provides the optimum temperature for detection of IgG antibodies, while preventing most IgM antibodies from reacting.
Incubation time	Different Ag/Ab reactions reach equilibrium over different time periods.	Increasing the time of incubation in a given test system may enhance the detection of a weakly reactive antibody.
pH	At a pH range of 6.5 to 7.5, chemical groups on Ag and Ab are oppositely charged, providing optimal ionic forces of attraction for most blood group antibodies.	Changing the pH affects the equilibrium constant for selected antibodies that may react preferentially in a more acidic environment (e.g., anti-M, anti-Pr).
Ionic strength	In an isotonic saline medium, sodium cations and chloride anions cluster around erythrocyte Ag and blood group Ab, respectively, acting to neutralize Ag/Ab-attractive forces.	Addition of LISS reduces the shielding effect on oppositely charged Ab and Ag, thus, increasing the rate of reaction and the equilibrium constant for red cell sensitization.
Antibody concentration	Can affect first- and second-stage agglutination by influencing the number of antibody molecules attached to each erythrocyte.	Increasing the serum-to-cell concentration increases the rate and/or affects the equilibrium constant of red cell sensitization by IgG antibodies. May help to induce second-stage agglutination by IgM antibodies. Addition of PEG, a large space-occupying molecule, effectively increases the relative concentrations of ag and ab respective to the volume of the reaction, greatly increasing the rate of reaction; is used only in AHG testing to detect IgG antibodies.
ζ Potential	Causes red cells to repel one another in solution; if the ζ potential can be reduced or the red cells brought together by physical means, second-stage agglutination of sensitized red cells can be facilitated.	Centrifugation—forcing cells closer together facilitates latticework formation. Enzymes—cleave sialic acid residues to lower the ζ potential and improve accessibility of certain blood group antigens. Albumin—reduces ζ potential and/or water of hydration to allow red cells to approach one another more closely. Polybrene/protamine—provides an excess of cations that neutralize the repulsive force between red cells, producing both nonspecific aggregation and antibody-mediated latticework formation. The final addition of sodium citrate disperses nonspecific aggregates, while specific ag/ab agglutinates remain.

ab, Antibody; *ag,* antigen; *AHG,* antihuman globulin; *LISS,* low–ionic strength saline; *PEG,* polyethylene glycol.

Grading of Hemagglutination Reactions

Hemagglutination in blood bank testing is observed and graded according to the strength of the reaction. Currently, three methods are available for evaluating visual hemagglutination reactions: tube testing, column agglutination (gel technology), solid-phase and/or microtiter plate technology. In test tube reactions, reagents and patient sample are added to a test tube and centrifuged, creating a cell button at the bottom of the test tube. The cell button is gently dislodged while observing for macroscopic agglutination. Column agglutination or gel technology utilizes a dextran acrylamide gel microtube prepared by the manufacturer. The gel traps agglutinates at the top of the chamber if hemagglutination has occurred, while unagglutinated cells pass through the gel layer and form a pellet at the bottom of the microtube. Microtiter plate technology uses serologic techniques in micro well plates instead of test tubes. In solid-phase technology, a microplate is the vessel for the reaction. Reagent or reagent cells (as a monolayer of cells or cell stroma) coat the well, to which patient sample is added. Following incubation and washing, indicator cells are added. When hemagglutination occurs, there is a diffuse adherence of RBC to the well. If no reaction occurs, the RBCs settle to the bottom of the well.

Automated testing systems use column agglutination and solid-phase and microtiter-plate technologies to process samples for ABO, Rh, crossmatch, DAT, and so on. Depending on the instrument, some or all of the testing processes are controlled by the system's computer. Parameters set in the software may determine reaction or require a human interface to review the reaction.

TABLE 36.28

Grading and Scoring of Hemagglutination

Grade	Appearance	Score
H	Hemolysis—presence of free hemoglobin in the serum	10
4+	One solid aggregate	10
3+	Several medium to large aggregates	8
2+	Many small to medium aggregates with a clear background	5
1+	Many small aggregates with a turbid background	3
+ or w	Few small aggregates with many unagglutinated cells	2
$\pm^m$ or $+^m$	Aggregates visible only under microscopic magnification	1
0	Negative—absence of aggregates; all cells unagglutinated	0
mf	Mixed-field agglutination—presence of minor population of agglutinated cells superimposed on a negative background	NA
R	Rouleaux—nonspecific aggregation appearing like a stack of coins; disappears with addition of saline	NA

NA, Not applicable.

Tube Reactions

Hemolysis is considered the strongest positive reaction that can occur and indicates the presence of a potent, complement-fixing antibody. After recipient serum and reagent RBCs are incubated and centrifuged at 37°C, the serum should first be examined for hemolysis before the cell button is resuspended. When reading for agglutination, the tube should be shaken, using a gentle wrist action, until all cells are dislodged. This is most easily accomplished by gently holding the test tube at the top in a vertical fashion and using the wrist to gently dislodge the cell button, while watching closely for agglutinates. As the cell button begins to resuspend, tip the tube gently to observe for agglutinates. Proper illumination with a concave mirror is an invaluable aid for macroscopic reading. By placing the tube about 2.5 inches above a 3-inch concave mirror, aggregates can be differentiated easily from the free cells by looking at the mirror, not at the tube.

Table 36.28 lists two protocols for evaluating the strength of agglutination using numeric grading and/or scoring. Figure 36.19 shows the appearance of different agglutination grades. Although the agglutination grade gives an approximate idea regarding the potency or strength of a particular antibody, the scoring method is much more useful in semiquantitative procedures, particularly when used in conjunction with titration to compare the relative antibody strengths of two different sera.

Unlike tube testing, microcolumn gel technology and solid-phase red cell adherence reactions are fixed after the centrifugation phase. The card or well is ready to read without the need to dislodge the cell button. (See Figs. 36.22 and 36.23 for examples of reactions in gel and solid phase.)

THE ANTIHUMAN GLOBULIN TEST

Many IgG antibodies are not able to directly produce detectable hemagglutination, even after centrifugation and the use of enhancement media and techniques such as polyethylene glycol, low–ionic strength saline (LISS), albumin, or enzymes. To visualize reactions by these antibodies, AHG reagents, which contain specific antibodies to human Igs or complement components, must be utilized. The antibodies in AHG sera act as bridges between RBCs already sensitized with antibody or complement to produce the characteristic latticework of second-stage hemagglutination (Fig. 36.20). This is the basis of the AHG test.

The AHG test is also called the *Coombs test* in honor of one of the investigators who first developed the test for laboratory use (Coombs et al., 1945), although the principle was actually described much earlier (in 1908) by Moreschi (Harmening, 2012). When the test is used to detect antibodies or complement bound to RBCs in vivo, it is called the *direct antiglobulin test* (*DAT*). When the test is used to detect the reaction of antibody and RBCs in vitro after an appropriate incubation phase, it is

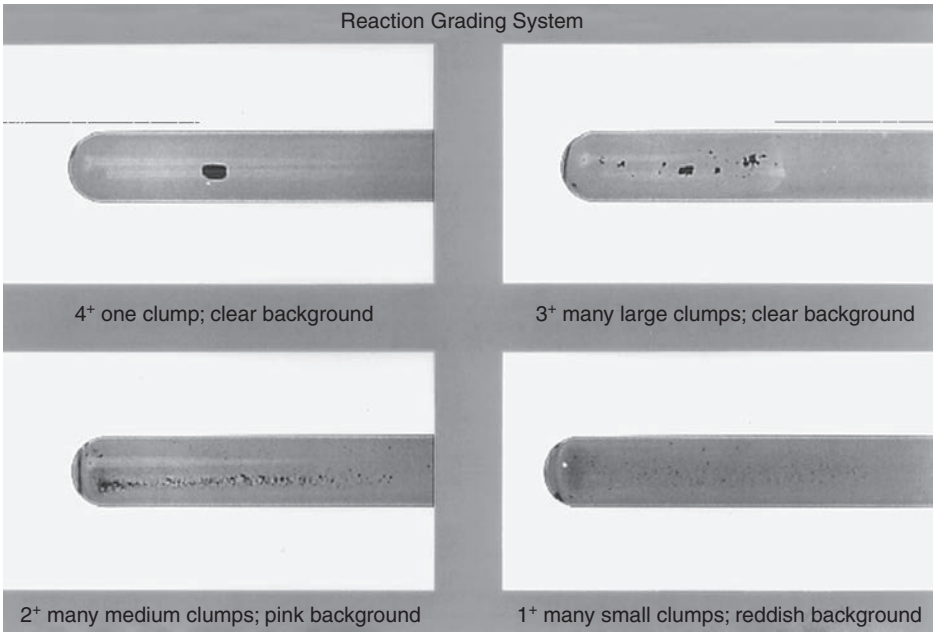

Figure 36.19 Agglutination grading system showing macroscopic hemagglutination reactions.

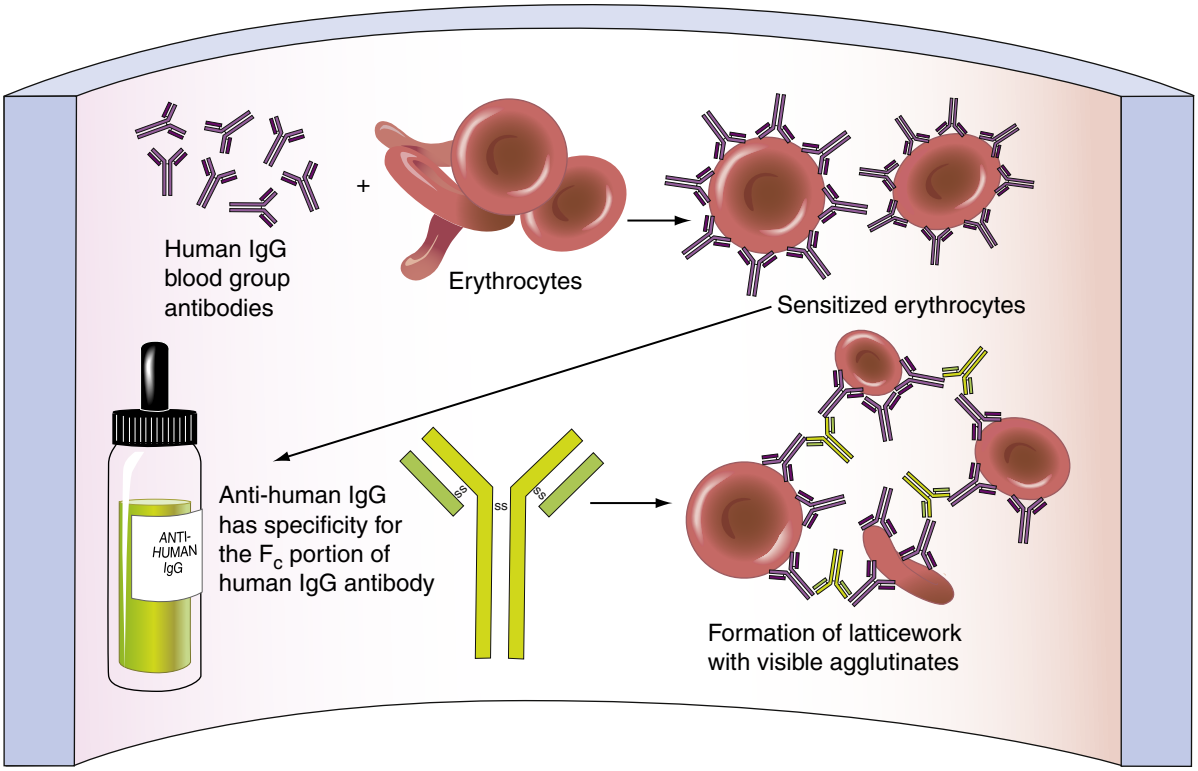

Figure 36.20 Antihuman globulin antibodies form a bridge between adjacent erythrocytes sensitized with human immunoglobulin (Ig)G or complement components.

called the *indirect antiglobulin test* (*IAT*). The red cell antibody screen is an example of an IAT.

Antihuman Globulin Reagents and Procedures

Various preparations of AHG sera are available for blood bank testing, depending on the application (direct or indirect) and whether one wishes to detect RBC sensitization by IgG, complement, or both.

Polyspecific Reagents

Polyclonal, polyspecific AHG reagents are produced by hyperimmunizing animals, usually rabbits, with purified Ig or complement to produce high-titered, high-avidity IgG antibodies. For a given batch of reagent, animal sera are harvested, pooled, adsorbed to remove heterophil agglutinins, and then titrated to ascertain the dilution necessary for optimal reactivity in routine use. Conventional polyspecific (also called *broad-spectrum*) AHG contains polyclonal IgG antibodies to the spectrum of human IgG subclasses and the C3 complement cleavage products C3b and C3d. Some anti-C4b and anti-C4d activity may also be present. However, most manufacturers adsorb out anti-C4 activity from their polyspecific AHG reagents because it has been shown that in vitro complement activation by clinically insignificant cold agglutinins results in much more C4d than C3d binding (Klein & Anstee, 2006). Excluding anti-C4 activity thus reduces the number of false-positives in both DAT and IAT testing using polyspecific reagents. Because immunization against IgG will also produce anti–light chain antibodies in a polyclonal response, one should remember that polyclonal antiglobulin sera may cross-react with IgA or IgM light chains unless the manufacturer specifies that the anti-IgG component is heavy-chain specific.

At present, the most commonly used polyspecific AHG reagents consist of rabbit polyclonal anti-IgG blended with murine monoclonal antibodies to C3b and C3d complement components. AHG composed exclusively from a blend of murine monoclonal antibodies to IgG, C3b, and C3d is available. The activity of anti-IgG and anticomplement in polyspecific antisera, whether polyclonal or monoclonal, will vary somewhat among different manufacturers and among lots produced by the same manufacturer. However, all AHG sera must contain levels of anti-IgG and anti-C3d activity that meet or exceed the reference standards of the U.S. Food and Drug Administration (FDA; 21CFR660.50; Code of Federal Regulations, 2016).

Monospecific Reagents

Commercially available FDA-licensed monospecific reagents include anti-IgG, anti-C3b+C3d, and anti-C3d. Monospecific anti-IgG or anticomplement may also be polyclonal or monoclonal in origin. For monoclonal anti-IgG, manufacturers must blend monoclonals against a variety of IgG epitopes or select a clone with specificity for an epitope common to all variants of IgG to ensure that the spectrum of human IgG subclasses will react with their reagent. With polyclonal monospecific anti-IgG, again, one should keep in mind that it may contain anti–light chain activity unless the manufacturer labels it as heavy-chain specific. Production of murine monoclonal blends of monospecific anticomplement has allowed manufacturers to develop reagents containing quantities of purified anti-C3b and anti-C3d of known potency that are less likely to give false-positive results by other anticomplement activities found in polyclonal reagents (Harmening, 2012).

Choosing Which AHG Reagent to Use

The DAT is an important diagnostic serologic technique used for the detection of antibody binding to RBC membranes in vivo. Laboratory indications include testing cord cells for HDFN, investigation in HTR, and in AIHA studies. The reason for the testing will indicate the type of reagent that should be used. Polyspecific AHG reagents containing both anti-IgG and anticomplement activity are typically used for initial DAT evaluation. This is especially important when the DAT is being performed to aid in the diagnosis of CAIHA and some forms of drug-induced hemolytic anemia in which complement may be the only evidence of immune-mediated hemolysis. Circulating red cells that have been involved in complement activation will have mostly C3d on their surface as the result of complement regulatory protein degradation of C3b (see Fig. 36.1). Therefore, polyspecific AHG sera used in DATs must contain anti-C3d reactivity and usually contain some anti-C3b reactivity as well. One notable exception to the use of polyspecific AHG for DATs is cord blood. Because *only* IgG can cross the placenta, the DAT may be performed with an anti-IgG reagent only (see Prenatal and Postnatal Testing section).

A positive DAT with all reagents tested (polyspecific, IgG, C3) may indicate spontaneous agglutination or autoagglutination. Cells already heavily coated with IgG can agglutinate upon centrifugation in the absence of AHG reagent. IgM cold autoagglutinins that were not dissociated during the washing procedure can also cause autoagglutination. All positive DATs should be evaluated with an inert control such as saline or 6% albumin before positive test reactions are concluded.

The IAT is used for detection of in vitro antibody binding to RBCs, regardless of the antibody's ability to fix complement. Laboratory indications include antibody detection (crossmatch and antibody screening), antibody identification, antibody titration, and RBC phenotyping. It is unclear whether polyspecific AHG, which contains anticomplement reactivity, improves serum antibody detection by the IAT. Rare reports have described antibodies that were detected only by their ability to bind

complement in vitro and would have been missed with the use of monospecific anti-IgG reagents (Fung, 2017; Harmening, 2012). In addition, polyspecific AHG can yield stronger reactions in the IAT than monospecific anti-IgG alone (Wright & Issitt, 1979). A major disadvantage of polyspecific AHG is unwanted detection of complement activation by clinically insignificant cold-reactive autoagglutinins or alloantibodies. As a result, many laboratories choose to use monospecific anti-IgG in antibody detection and identification tests and in crossmatch procedures.

Table 36.29 compares various applications for DAT and IAT techniques. Antiglobulin testing may be performed using test tubes, microtiter plates, or gel microtube techniques (see later section on Compatibility Testing). These procedures may be semiautomated or fully automated, particularly in facilities that perform large-volume testing, such as blood collection centers. Unless otherwise specified, procedures referred to in this chapter employ tube testing. *The AABB Technical Manual* (Fung, 2017), *Judd's Methods in Immunohematology* (Judd et al., 2008), and *Immunohematology Methods* (Mallory, 1993) are excellent general references for most common procedures as well as more specialized techniques.

Quality Control of the Antihuman Globulin Test

To standardize antiglobulin sera and to confirm true-negative antiglobulin reactions, two types of quality control RBCs are normally used: those coated with IgG and those coated with C3b and/or C3d. To sensitize RBCs with IgG, Rh antibodies are usually used. RBCs coated with C3b are prepared by incubation of whole blood in LISS or with human anti-Le^a or anti-I. C3d-coated RBCs are prepared by incubating C3b-coated cells with fresh serum or trypsin to split C3b→C3d. IgG or complement-coated control cells should give a 1+ to 2+ reaction (see Fig. 36.19) when tested with anti-IgG or anti-C3b+C3d.

Quality control cells for the antiglobulin test are referred to as *check cells* or *Coombs control cells*. In a true-negative test, free active antiglobulin reagent should remain. Control cells, sensitized with IgG and/or C3, are added to all negative tests and centrifuged. Hemagglutination of check cells confirms both the presence and reactivity of the AHG reagent, thus validating a negative test result. If the control cells fail to agglutinate in any tube, the tests must be repeated because they are invalid and may have yielded false-negative results. False-negative tests can occur for a variety of reasons and are listed in Table 36.30.

Sensitivity of the Antihuman Globulin Test

Although the antiglobulin test is extremely sensitive, a negative test does not exclude the possible presence of antibodies on RBCs. It is estimated that 200 to 500 IgG or C3 molecules bound per cell are required for detection by antiglobulin antibodies (Issitt & Anstee, 1998). A negative reaction can occur with small quantities of bound IgG and C3. In addition, AHG sera may possess greater activity against some subclasses of IgG than against others. Consequently, certain AHG sera may produce negative results with RBCs coated by a particular IgG subclass.

COMPATIBILITY TESTING

The term *compatibility testing* has historically been used synonymously with the serologic crossmatch test. In its broader context, however, compatibility testing is an entire quality process composed of many procedures designed to provide the safest blood product possible for the recipient of a transfusion. These procedures include proper record keeping, accurate donor and recipient identification, and actual serologic testing of the recipient specimen before transfusion. Under certain conditions, an electronic crossmatch may be performed instead of a serologic crossmatch. Outlined in the following sections and in Table 36.31 are the steps in compatibility testing required by the AABB Standards for Blood Banks and Transfusion Services (Gammon, 2020), referred to henceforth as the AABB Standards.

Specimen Requirements

Recipient Sample Identification

A physician order is required before blood is drawn for a type and screen. The order may be verbal (followed by a written order), on paper, or electronic. Proper identification of patient blood samples and donor units is absolutely essential in blood banking. Recipient blood specimens must be labeled by the phlebotomist at the bedside directly from information on the patient's wristband. If the patient's wristband is not attached for any reason, signed confirmation of the patient's identity by nursing staff should be obtained before the blood is drawn. The recipient's blood specimen label should be legible and should include at least the patient's full name, hospital identification number, and specimen collection date, and it should be securely attached to the specimen tube when it is accepted by blood bank personnel. Unlabeled or improperly labeled blood specimens are unacceptable under any circumstances. During testing, all test tubes or other types of aliquot or reaction containers must be accurately identified directly from the label on the recipient sample.

Each pretransfusion blood sample should be accompanied by an appropriate order or requisition, containing at least the patient's full name and hospital identification number. The signature or initials of the

TABLE 36.29
Applications for Direct and Indirect Antiglobulin Techniques

	Applications	Purpose	What Is Detected
Direct antiglobulin test (DAT)	Investigation of HTR	To detect circulating donor red cells that are sensitized with recipient antibody. A positive DAT is the first immunohematologic evidence of a hemolytic reaction after transfusion.	DAT positive owing to IgG and/or C3d depending on the antibodies responsible.
	Diagnosis of HDFN	To detect maternal antibodies that have crossed the placenta to sensitize fetal red cells.	DAT almost always positive as a result of IgG; occasionally C3d if ABO antibodies involved.
	Diagnosis of AIHA	To detect autoantibody sensitizing a patient's own red cells.	Warm autoantibodies: DAT almost always positive owing to IgG. Cold autoantibodies: DAT may be due to C3d only.
	Investigation of drug-induced hemolysis	To detect antidrug/red cell antibodies and/or subsequent activation of the complement system.	DAT may be positive owing to IgG, C3d, or both, depending on the mechanism involved (see under Investigation of Autoimmune Hemolytic Anemia section).
			Indirect antiglobulin test
	Antibody detection (or antibody screen)	To detect clinically significant IgG alloantibodies in the recipient.	Recipient IgG antibodies bound to reagent screening cells.*
	Antibody identification	To specifically identify those antibodies detected by reagent screening cells or by donor red cells.	Recipient IgG antibodies bound to reagent cells from a panel of 10–12 donors.*
	Crossmatching	To detect antibodies that may have been missed by the antibody screen because of absence of the corresponding antigen or presence of a dosing antibody.	Recipient IgG antibodies bound to donor red cells.*
	Red cell antigen typing	To type patient or donor red cells for antigens that can be detected by IgG antisera reactive only by the AGT. A common example of this would be the weak D test.	Specific binding of reagent IgG antibodies to red cells positive for the corresponding antigen.

AGT, Antihuman globulin test; *AIHA,* autoimmune hemolytic anemia; *HDFN,* hemolytic disease of the fetus and newborn; *HTR,* hemolytic transfusion reaction; *Ig,* immunoglobulin.
*If complement is fixed in vitro, it may be detected if polyspecific antiglobulin is used.

TABLE 36.30

Basic Procedures for Direct and Indirect Antiglobulin Testing by Tube Method

Procedure		REASONS FOR INVALID REACTIONS IN ANTIGLOBULIN TESTING	
		False-Positive	**False-Negative**
Direct antiglobulin test (DAT)	1. Prepare a 3%–5% suspension in normal saline of the red cells to be tested. 2. Add 1 drop of red cell suspension to a tube and wash 3–4 times with saline. 3. Blot the tube after the last wash. 4. Add 2 drops of polyspecific AHG (anti-IgG + anticomplement). 5. Centrifuge and examine for agglutination.* 6. Add check cells to all negative tubes (see Quality Control of the Antihuman Globulin Test section). Note: For DAT, blood samples should be collected in EDTA to prevent fixation of complement in vitro by clinically insignificant cold autoagglutinins.	• Overcentrifugation • Direct agglutination by strong cold agglutinins • Overincubation with enzyme-treated cells • Improper use of PEG or polycation enhancement reagents • Inadequate resuspension of cell button • Rouleaux formation‡ • Dirty glassware • Small fibrin clots may trap cells and mimic agglutination • Cells with a positive DAT will yield false-positive results in any indirect antiglobulin test	• AHG reagent failure† • Failure to add AHG reagents† • Improper or inadequate washing† • Delayed washing (elution of weakly attached antibody) • Serum/cell ratio too low • Failure to add test serum or enhancement reagents • Undercentrifugation • Resuspension of cell button too vigorous
Indirect antiglobulin test (IAT)	1. Add 2–3 drops of patient serum or the recommended number of drops of commercially prepared antisera to each tube. 2. Place 1 drop of the 3%–5% red cell suspension to be tested in a tube (e.g., donor cells, reagent screening cells). 3. Add recommended number of drops of enhancement media (e.g., LISS, PEG) if indicated. 4. Incubate at 37°C for the time period indicated for the assay being performed (15–60 minutes). 5. If indicated in the procedure, centrifuge and examine the serum for hemolysis and the cells for agglutination. 6. Whether step 5 is performed or not, continue by washing the tube(s) 3–4 times with normal saline. 7. Blot tubes dry after the last wash. 8. Add 2 drops of antiglobulin sera (polyspecific or monospecific anti-IgG) to all tubes. 9. Centrifuge and examine for agglutination.* Add check cells to all negative tubes.		

AHG, Antihuman globulin; *EDTA,* ethylenediaminetetraacetic acid; *Ig,* immunoglobulin; *LISS,* low–ionic strength saline; *PEG,* polyethylene glycol.
*Protocol may include optional microscopic examination to confirm macroscopically negative tests.
†Will be detected by the use of Coombs control cells.
‡Rouleaux will cause false-positive results in indirect tests read after 37°C incubation.

phlebotomist should be on the requisition because the test requisition is a permanent record of that particular specimen collection. With increasing use of electronic order entry, a computer-based system may record the physician order and capture the person performing the phlebotomy. The phlebotomist, however, should still sign the specimen for verification and matching against the electronic record. Upon specimen receipt, the label on the tube is compared with the information on the requisition (paper or electronic) for any discrepancies. If there is any doubt as to the proper identity of the sample, another sample must be obtained.

Type of Sample

Although serum has traditionally been the preferred specimen for compatibility testing, plasma is increasingly used owing to newer testing technologies (e.g., gel test). If serum is used, blood samples should be collected in siliconized plain tubes without serum separator gel. Other test methods, such as gel column agglutination, microtiter plates, and automated testing systems, may require a specific type of sample per manufacturer instructions.

Problems with plasma in conventional antiglobulin techniques are primarily technical. Plasma can be associated with small fibrin clots that can trap RBCs and resemble agglutination. Fibrin may also trap serum and cause neutralization of AHG reagent if not removed before washing. Finally, plasma can enhance rouleaux formation if fibrinogen levels are particularly high.

Appearance

Most blood bank laboratories have policies in place to reject grossly hemolyzed recipient blood samples as unacceptable for pretransfusion testing unless there is no other choice. Using serum that is already hemolyzed may mask antibody-induced hemolysis that would ordinarily be detectable in antibody screening tests. Lipemia may rarely cause difficulty in evaluating agglutination results, although lipemia is not usually a cause for rejection of a pretransfusion sample. Automated instruments may have additional specifications regarding sample appearance. For example, a grossly hemolyzed, icteric or lipemic sample can give false-positive readings or a contrast interference error with an automated gel technology instrument.

Age of Sample

According to AABB Standards, a pretransfusion specimen for testing and red cell transfusion is valid for 72 hours. After 72 hours, a new sample must be drawn. Requiring a new pretransfusion sample every 72 hours on previously transfused or pregnant individuals ensures that the sample being tested is fairly representative of the patient's current immune status.

In elective surgery patients, some facilities will extend the age of a preoperative sample up to 1 month provided that the patient (1) has a negative antibody screen, (2) has no history of clinically significant antibodies, (3) is not pregnant, and (4) has not been transfused within the preceding 3 months. Patients failing to meet these criteria are required to have a sample drawn within 72 hours of planned surgery (Banderanko, 2014).

Sample Storage

AABB Standards require that all pretransfusion samples be stored at 1°C to 6°C for at least 7 days posttransfusion, along with at least one representative segment from each of the donor units transfused to the recipient. The purpose of this is to ensure that repeat or additional testing of the donor or patient may be performed later if the patient experiences a delayed hemolytic reaction or other adverse effect of transfusion.

Documentation and Record Keeping

General Considerations

All blood banks must have a manual or computerized system of record keeping that contains the results or outcomes of all tests and activities carried out in the blood bank. Records must be complete and retrievable within a reasonable time frame. Transfer or dissemination of information from any patient records must conform to requirements of the institution's

TABLE 36.31
Required Steps in Pretransfusion Compatibility Testing*

Physician (or other authorized health professional) order	Written (paper or electronic) order for type and screen test • Type and screen • Crossmatch red blood cells • Special requests, such as irradiation, cytomegalovirus (CMV)-negative, antigen-matched, etc. • Oral orders may be accepted if followed by the written request.
Phlebotomy/recipient identification	Phlebotomist must positively identify the recipient and the recipient's blood sample. • Transfusion request and labeled patient blood sample must contain at least two pieces of independent identifying information for that patient (e.g., name, hospital number, date of birth). • Mechanism to identify the date of sample and the phlebotomist (paper or electronic) • Transfusion service will ensure that identifying information on the requisition and sample label are in agreement.
Recipient testing	Perform ABO and Rh typing on recipient's blood specimen—red cell and serum or plasma testing are required. Review previous records for comparison with current typing results. • Clinically significant antibodies • Significant adverse events to transfusion • Special transfusion requirements • Previous ABO group and Rh type • Difficulty in blood typing • Test recipient's serum or plasma to detect clinically significant antibodies • Method must include 37°C incubation with conversion to antihuman globulin using reagent red cells that are not pooled.
Donor testing	Confirm ABO and Rh types on donor red cell units as required. • Confirmation testing for ABO group required on all units (serum testing not required). • Confirmation of Rh type required only on those units labeled as Rh negative (weak D testing is not required).
Crossmatch	Select ABO- and Rh-compatible red cell components for transfusion. Perform serologic or electronic crossmatch of red cell components. • Full antiglobulin crossmatch required if current antibody screen is positive or the patient has a known history of clinically significant antibodies.
Labeling	Label all red cell products or other components with the recipient's identifying information. • Label must contain at least two independent patient identifiers, donor unit number, and compatibility test results, if performed.

*Requirements paraphrased from Fung (2017). See AABB Standards (Gammon, 2020) for specific wording.

confidentiality policies in accordance with federal and state laws and regulations. Records must be preserved for different periods of time, depending on federal, state, and accrediting agency requirements.

Documentation of the entire compatibility testing process must include records of patient identification, order entry, individual special transfusion needs, date and time of testing, results of patient testing, identity of the technologist who performed the testing, and blood component issues. A computerized system is ideal for capturing this information and enables rapid and easy retrieval of these data for a given patient, including records of ABO and Rh type, antibody problems, transfusion history, and requirements for special types of blood products. From a more global perspective, computerized retrieval of data for groups of patients also greatly enhances the monitoring of blood product utilization within the facility, including blood ordering and transfusion practices of physicians.

Results and interpretations of all patient testing should be documented on appropriate manual worksheets or entered into the computer immediately upon observation of the results. In a manual record-keeping system, all forms should be filled out with ink, not pencil. If results must be changed on manual worksheets, original results must not be obliterated. A single line should be placed through them, and the new results dated and initialed by the technologist making the change. A continuously updated list of initials used by all personnel working in the blood bank on all shifts must be part of the permanent blood bank records. Changes to computerized results must also be completely documented as part of the computerized result record with ability to track both original and corrected data (Fung, 2017).

Check of Previous Records

Manual or computerized records must be checked for previous results on a given patient when a new sample is received. ABO and Rh tests on the current specimen should be checked against previous results, if available, to help verify that the specimen was collected from the correct individual. Information on any unexpected antibodies identified previously is also extremely important because the titer of an antibody may fall to levels that cannot be detected by antibody screening procedures. If a clinically significant antibody was previously identified, the patient must receive RBCs negative for the corresponding antigen (antigen-negative) even if current antibody screening tests are negative. Previous difficulties in blood typing, significant adverse events to transfusions, and special requirements for blood products should also be reviewed and documented before type and screen testing and crossmatching tests are completed (Gammon, 2020).

ABO Grouping

Antisera and reagent RBCs for ABO grouping are standardized and readily available commercially. Most blood bank laboratories use monoclonal reagent antisera derived from antibodies produced by hybridoma cell lines. ABO grouping consists of two parts, commonly referred to as *red cell grouping* (forward type) and *serum grouping* (back type). In forward grouping, a 3% to 5% RBC suspension is tested with commercially prepared anti-A and anti-B to test for antigens on the RBC membrane. In reverse grouping, patient or donor serum is tested against reagent cells of known A_1 and B phenotype to test for the expected ABO antibodies in the patient's serum (see Table 36.6). ABO grouping is carried out at room temperature, with only an immediate-spin centrifugation step required to promote a macroscopic agglutination reaction. The manufacturer's directions must be followed for all commercial reagents.

ABO Grouping of Donors

The collecting facility is required to perform a forward and reverse ABO type on all donors. The transfusion service or other laboratory responsible for compatibility testing must confirm the ABO group of all units of RBCs or whole blood received. RBC forward grouping is performed from an integral segment attached to each donor unit. For units labeled as group O, anti-A,B alone may be used for donor confirmatory testing because only group O RBCs will fail to hemagglutinate with anti-A,B.

ABO Grouping of Recipients

Every pretransfusion patient blood specimen must also be tested for ABO group. Both cell and serum groupings are required for initial ABO testing of all patient samples. The results of RBC and serum testing should agree with each other (see Table 36.6) before any results are reported and blood is transfused.

Some blood banks routinely include the use of anti-A,B in the RBC grouping procedure, although this reagent does not usually yield any additional useful information except for the detection of A_x or B_x weak subgroups. Anti-A,B is used as a convenient reagent in repeat testing to confirm initial typing of a group O patient. Anti-A,B may be used for confirmatory typing with neonate and infant samples, especially when the infant has been transfused with group O RBCs. Infant red cells may show weaker reactions on forward typing owing to the decreased number of ABO antigens on infant red cells (see ABO and I Blood Group sections).

AABB Standards require two determinations of the recipient's ABO group prior to transfusion (Gammon, 2020). The first determination is on the current tested sample. The second determination should be done using one of the following methods:

- Comparison with previous historical records
- Testing a second sample collected at a different time from the first sample, including a new verification of patient identification
- Retesting the same sample if the patient identification process was verified using a validated electronic identification system

ABO Grouping Discrepancies

Interpretation of ABO blood grouping results is generally straightforward. In the event that the results of RBC and serum grouping do not

TABLE 36.32

Some Causes of ABO Grouping Discrepancies

	Problems with Red Cell Testing	Problems with Serum Testing
Unexpected positive reactions	Acquired B antigen associated with colon and gastric cancers, intestinal obstructions	Rouleaux-forming proteins present (e.g., plasma expanders, monoclonal gammaglobulins)
	Cord cells contaminated with Wharton jelly	Room temperature alloantibody present (e.g., anti-M, N, P1)
	Autoagglutination caused by cold autoantibodies	Room temperature alloantibody in immunoglobulin (Ig) M phase (e.g., anti-c)
	Cells heavily coated with warm autoantibody	Cold autoagglutinin present (e.g., anti-I, IH)
	Polyagglutination	Passively acquired ABO antibodies, (e.g., incompatible plasma transfusion)
	Acriflavine antibody (against dye used in anti-B)	Passenger lymphocyte-derived antibody associated with minor incompatible bone marrow or solid-organ transplant
	Genetic chimerism*	Subgroup of A with anti-A1 in serum
	Bone marrow transplants*	*Cis*-AB with weak anti-B in serum
	Administration of red cells outside ABO group*	
	B(A) phenomenon	
	Fetomaternal hemorrhage*	
Unexpected negative reactions	A or B subgroups	Age of patient (elderly, newborn)
	Antigen depression due to leukemia or other disease state	Hypogammaglobulinemia or agammaglobulinemia
	High levels of soluble blood group substances	Immunosuppression
	Massive transfusion with compatible red cells outside of ABO group	Bone marrow transplants
	Bone marrow transplants	ABO subgroups
		Long-term parenteral nutrition

*Look for mixed-field appearance of reactions with reagent antisera.

agree, testing is repeated to rule out any clerical or technical error. If results still disagree, an ABO discrepancy is present owing to problems with the patient's serum or cells that must be resolved before an ABO type can be confirmed. Table 36.32 lists some of the many reasons for ABO discrepancies. Several references are available that provide a complete description of these problems and the protocols for resolution (Harmening, 2012; Fung, 2017).

If a blood transfusion is needed emergently and an ABO discrepancy occurs that cannot be resolved in a timely manner, group O packed RBCs, AB plasma components, or both may be given. However, it is important to be certain that a sufficient pretransfusion blood specimen is obtained from the patient so that the workup may be continued. In some cases, it may be necessary to send a pretransfusion specimen to a reference laboratory for further evaluation.

Rh Typing

Several types of antisera are available for detection of the RhD antigen. Today, the most commonly utilized anti-D typing reagents in tube testing are monoclonal blends from several different clones. Some reagents also contain a blend of IgM and IgG anti-D to allow for immediate spin testing and indirect antiglobulin testing for weak D with the same reagent. Manufacturers may offer a control reagent as well to be used with the anti-D reagent. The anti-D used for column agglutination testing is a monoclonal IgM. It is crucial to understand the different anti-D reagents in order to select the appropriate reagent for the facility, patient population, and laboratory use. The manufacturer's instructions detail the specifics of their reagent, uses, and contraindications.

Direct typing for the D antigen is carried out at room temperature by the immediate spin technique after mixing one drop of saline-suspended 3% to 5% RBCs and one drop of commercial anti-D. If weak D testing is necessary, RBCs are tested by IAT with an IgG anti-D. A parallel test with a negative diluent control is always included for the weak D test.

Rh Typing of Donors

As required by the AABB Standards, all whole-blood donor units are tested by the collecting facility for the D antigen by direct agglutination methods. All donor units testing as Rh negative by direct agglutination are tested for a weak D phenotype by the IAT. If routine D testing or weak D testing is positive, the unit is labeled Rh positive. The transfusion service must reconfirm the D type of all RBC units labeled Rh negative by testing red cells from an integral attached segment by a direct anti-D agglutination method. Repeat testing of donor units by the transfusion service for weak D is not required by the AABB Standards.

Rh Typing of Recipients

Every pretransfusion recipient blood specimen must be tested for the D antigen by direct typing. Indirect testing for weak D in recipients is not necessary: Patients who fail to agglutinate after direct agglutination are typed as Rh negative. Some blood banks do perform weak D testing for prenatal specimens; however, more recent data show that many individuals typing as weak D possess a partial D phenotype and are at risk for RhD alloimmunization. Erythrocyte typing for the C, c, E, and e antigens of the Rh system is not performed routinely but may be done to determine the most probable Rh genotype in the evaluation of antibody problems, in parentage studies, and in patients with long-term transfusion requirements.

Rh Grouping Discrepancies

Interpretation of Rh blood grouping results is generally straightforward. Different methodologies and reagents may yield discrepant results; thus, the manufacturer's instructions for use should be reviewed when interpreting. At issue is identifying the patient as Weak D versus Partial D since Partial D patients are at risk of making Anti-D. Policies should be in place for investigation when there is a discrepancy. Until the discrepancy can be resolved, RhD-negative red cells should be issued (Gammon, 2020).

ANTIBODY DETECTION

All specimens submitted for pretransfusion testing must be screened for clinically significant antibodies in the recipient serum (antibody screen). Because clinically significant antibodies typically react at body temperature, most laboratories omit room temperature incubation entirely. AABB Standards require that the method used incorporate incubation at physiologic or body temperature (37°C) followed by conversion to the IAT. If a method other than the IAT is used, it must have documented and validated equivalent sensitivity in its ability to detect clinically significant antibodies (Fung, 2017). A variety of antibody screening protocols utilizing different technologies are in use today.

Reagent Red Blood Cells

Reagent RBCs or screening cells used for the detection and identification of antibodies in a patient's serum are usually obtained from commercial manufacturers. AABB Standards require that antibody detection in recipients be performed using reagent cells that are not pooled. Typically, antibody screening cells consist of two to three group O reagent cells selected from different donors of known phenotype. Sets of cells are prepared so that all antigens to the most commonly encountered blood group antibodies are represented and must include C, c, D, E, e, Fy^a, Fy^b, Jk^a, Jk^b, K, k, Le^a, Le^b, P_1, M, N, S, and s antigens. An *antigram* that lists the blood group antigenic makeup of each cell (Fig. 36.21) accompanies each lot of screening RBCs. When possible, cells that are homozygous for selected antigens are used, which increases the likelihood of detecting weak or dose-dependent antibodies. A three-cell screening panel ensures homozygosity for more antigens—such as Jk^a, Jk^b, Fy^a, Fy^b, S, and s—against which the corresponding antibodies are likely to exhibit dosage, but the additional cell adds expense to pretransfusion testing. Several studies (Cordle et al., 1990; Judd, 2002)

Screening Cell Master List

		Rh								Kell				Duffy		Kidd		Sex linked	Lewis		MNSs				P	Lutheran	
Vial	Donor	D	C	E	c	e	f	C^w	V	K	k	Kp^a	Js^a	Fy^a	Fy^b	Jk^a	Jk^b	Xg^a	Le^a	Le^b	S	s	M	N	P1	Lu^a	Lu^b
I	R1R1	+	+	0	0	+	0	0	0	+	+	0	0	0	+	+	0	+	0	+	+	+	+	0	+	0	+
II	R2R2	+	0	+	+	0	0	0	0	0	+	0	0	+	0	0	+	+	+	0	0	+	0	+	+	0	+

Figure 36.21 The "antigram" accompanying each lot of reagent screening red blood cells.

have shown that using three red blood samples for antibody detection rarely reveals a clinically significant antibody not detected by a two-cell screening procedure.

Antibody Detection Protocols

Tube Tests

In conventional test tube methods, one volume 3% to 5% screening reagent cells and two volumes patient serum (giving an average volume/volume ratio of serum to cells of approximately 50:1) are incubated at 37°C with an enhancement medium for the time specified by the manufacturer and are centrifuged and examined for hemolysis or agglutination. The screening cells are then washed three to four times with saline, and AHG reagent is added for final detection of IgG alloantibodies.

Because different blood group antibodies commonly show characteristic reaction patterns by the IAT technique (see Table 36.5), close examination at different phases of testing in this conventional protocol may yield helpful information in evaluating cases in which the screen is positive:

- Direct agglutination of the cells in albumin or LISS after 37°C incubation frequently indicates the presence of an Rh antibody.
- IgM antibodies possessing a wide thermal range, such as anti-I, anti-P_1, and Lewis antibodies, may show reactions in albumin or LISS. However, these reactions generally become much weaker after conversion to the IAT.
- With rare exceptions, in vitro hemolysis of reagent cells after 37°C indicates the presence of Lewis, Kidd, Ii, P, PP_1P^k, or Vel antibodies.
- The vast majority of IgG antibodies, with the exception of Rh, will not be detected until after washing and conversion to the IAT.
- Reactions of different screening cells in multiple phases or with varying strengths usually indicate that more than one antibody is present.

Column Agglutination Technologies

Column agglutination is an alternative method for alloantibody detection used by many transfusion services. This technology utilizes the differential migration of RBC agglutinates through a small microtube containing a dextran acrylamide size exclusion gel column (Lapierre et al., 1990). A plastic card with six to eight microtubes per card can be used to perform antibody screening or identification, crossmatching, and DAT testing. Gel cards for ABO/Rh typing are also available.

For testing, precisely measured volumes of screening reagent RBCs (0.8% suspension in LISS) and plasma are incubated at 37°C in the reaction chamber above the column matrix. Following incubation, the plastic cards are centrifuged under carefully controlled conditions. IgG-coated RBCs agglutinate as they come into contact with the AHG reagent in the matrix and are trapped. Reaction strength and size determine the migration of the agglutinates, ranging from the largest (4+) agglutinates at the top to migration of weaker, smaller agglutinates farther into the gel column (Fig. 36.22). Unagglutinated RBCs pass easily through the column and are found as a pellet at the bottom. Because the plasma or serum remains in the reaction chamber above the matrix, repeated washing steps and addition of control cells to check the activity of the AHG reagent are unnecessary. The endpoint hemagglutination reactions are very stable, allowing the cards to be kept for supervisory review of questionable reactions. The cards can be photocopied or digitally photographed and downloaded as permanent laboratory data. Dual populations of cells produce a striking picture with two distinct populations: unagglutinated cells at the bottom of the tube and agglutinated cells at the top of the well.

Column agglutination or gel technology has equivalent sensitivity to standard LISS tube testing for antibody detection and is particularly sensitive for detection of anti-Rh antibodies (Weisbach et al., 2006). Gel testing can offer several advantages over conventional tube procedures. It is more standardized than conventional tube testing, with a reliable, stable agglutination endpoint, making it an attractive method

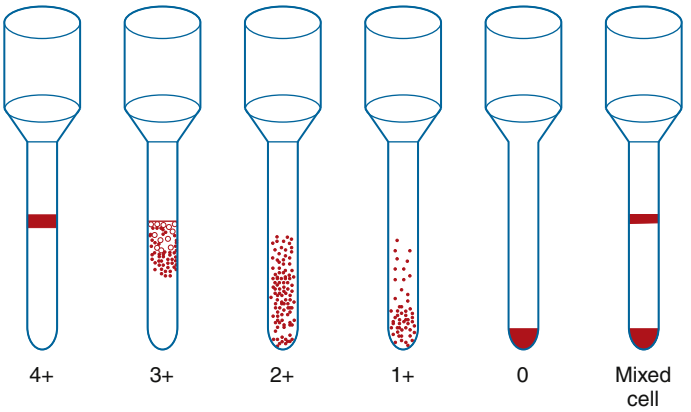

Figure 36.22 Appearance of reaction patterns and grading for gel or column agglutination technology.

for small facilities with cross-trained generalists. It is also less sensitive to clinically insignificant cold antibodies, eliminating unnecessary antibody workups. Additional time savings are achieved through the elimination of repetitive washing steps and manual macroscopic and/or microscopic readings. Finally, testing can be automated, permitting high-throughput testing, electronic interpretation and validation, and digital documentation of results.

Solid-Phase Adherence Tests

Another alternative to tube tests for alloantibody detection is indirect solid-phase adherence test systems. In this application, reagent RBCs are bound to the bottom of microplate wells. Serum and an enhancement reagent are added and incubated at 37°C, allowing the alloantibody to bind to the solid phase. After washing to remove unbound serum globulins, indicator RBCs coated with antihuman IgG are added and the plates are centrifuged. If a reaction has occurred between the reagent cells and the serum alloantibody, the antiglobulin-coated indicator cells will bind and cover the bottom surface of the well, whereas a discrete button in the bottom of the well indicates a negative reaction (Fig. 36.23). Wells may be read manually or with an automated reading device. As with column agglutination, positive reactions are very stable. Thus, the plate may be covered, stored at 2°C to 8°C, and read up to 2 days later.

Direct solid-phase test systems are also available for applications such as ABO and Rh typing of red cells. For these tests, microplate wells are coated with the appropriate antibodies. Test cells are added and incubated; the plates are then centrifuged. For positive reactions, the RBCs adhere to the entire bottom surface of the antibody-coated well; negative reactions result in a tightly packed cell button in the bottom of the well. Instrumentation is available for automated and semiautomated testing using solid-phase technology.

Molecular Methods

In general, molecular testing is not part of a routine pretransfusion test. When a patient exhibits a difficult antibody identification picture, molecular methods may be used to resolve the discrepancy or assist with resolving tube typing discrepancies.

Antibody Identification

When red cell alloantibodies are detected in the serum of a prospective blood recipient, as indicated by a positive antibody screen, the antibody must be identified so that antigen-negative blood can be provided for transfusion, if required. Antibody identification is accomplished by first testing an extended panel of reagent RBCs of known phenotype against the recipient's serum by the IAT technique. An autocontrol is always included as part of the testing to

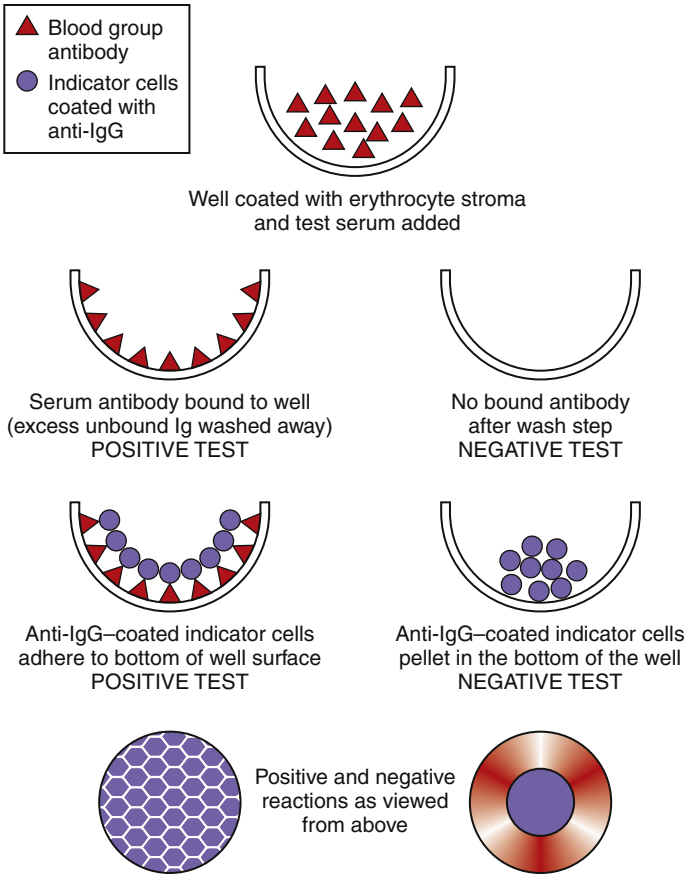

Figure 36.23 Principle of solid-phase adherence technology with appearance of positive and negative reactions.

TABLE 36.33
Simple Panel Example

Cells in A Panel	KNOWN ANTIGENIC COMPOSITION					TEST SERUM	
	D	C	c	E	e	Y	Z
No. 1	+	+	+	0	0	+	0
No. 2	+	+	0	+	+	+	+
No. 3	+	0	+	0	+	+	0
No. 4	0	0	+	0	+	0	0
No. 5	0	0	+	0	+	0	0
No. 6	0	+	0	+	+	0	+

help differentiate whether autoantibody, alloantibody, or both are present. The immunohematologist then compares the pattern of positive and negative serum reactions against the antigen phenotype pattern on the printed worksheet that accompanies each panel to find a match.

Interpreting the Results of Antibody Identification

Table 36.33 is a simple example of an antibody panel. Serum Y reacts with cell numbers 1 through 3, which are positive for the D antigen, but it does not react with cell numbers 4 through 6, which are negative for the D antigen. The pattern of positive and negative serum reactions matches the phenotype pattern for the D antigen; therefore, serum Y appears to contain anti-D. Similarly, the pattern of reactivity for serum Z matches the phenotype pattern for the E antigen; thus, serum Z appears to contain anti-E. Before such identification can be conclusively stated, one must be sure that enough cells of differing antigenic composition are tested to definitively identify a single antibody or combination of antibodies in a given serum.

Fisher's exact method has traditionally been used to statistically calculate the probability that a single antibody has been correctly identified within a confidence interval of 95% (i.e., the probability that the same results would be obtained by random chance because of a different antibody is 1 in 20). This method compares the numbers of positive and negative results against the number of cells tested that express or lack the corresponding antigen and against the total number of cells tested (Race & Sanger, 1975).

TABLE 36.34
Probability Values Based on Fisher's Exact Method

Total Number of Cells Tested	Antigen-Positive Cells That React with Antibody	Antigen-Negative Cells That Do Not React with Antibody	p Value
5	3	2	0.100
6	4	2	0.067
6	3	3	0.050
7	5	2	0.048
	4	3	0.029
8	6	2	0.036
8	5	3	0.018
8	4	4	0.014
9	7	2	0.028
9	6	3	0.012
10	8	2	0.022
10	7	3	0.008
10	6	4	0.005
10	5	5	0.004

Table 36.34 lists the probability values calculated by Fisher's exact method that are achieved with differing combinations of positive and negative cells in the total number tested. It can be seen that a p value of 0.05 can be achieved with a minimum of six cells, with three cells being positive for an antigen reacting with the antibody, and three cells negative for the antigen failing to react with the antibody. Most manufacturers supply reagent cell panels with 10 or 11 cells, with at least one of the combinations of positive and negative cells from Table 36.34, for most of the antigens to which unexpected antibodies are commonly encountered. Consequently, most simple antibody identifications are valid at a p value considerably less than 0.05, except in cases in which there are antibodies to low- or high-frequency antigens, or in which multiple antibodies are present in the same serum. In these situations, additional cells from other panels may have to be tested to achieve identification within the 95% confidence interval.

Figure 36.24 shows the results of a panel tested against patient serum with a conventional tube antiglobulin testing method, examined for agglutination after the 37°C incubation phase, and, finally, after the addition of AHG. In a quick overview of the panel results, an immunohematologist will notice at once that there is agglutination with different cells after centrifugation in both phases of the test, indicating the probable presence of multiple antibodies.

Following is an outline of the strategy used in evaluating antibody identification results:

1. The autocontrol is negative, indicating that the serum reactivity is most probably due to alloantibodies. However, if the autocontrol is positive, it is important that DAT testing be performed to confirm or rule out prior in vivo sensitization of the patient's cells. The DAT should be examined closely for the appearance of mixed-field agglutination. In recently transfused patients, attachment of alloantibody to a minor population of transfused donor RBCs causes classic mixed-field agglutination and is frequently the first sign of a developing immune response that may result in a delayed HTR. In a massively transfused patient, only a small percentage of cells may be DAT positive.
2. The first step that is performed by many immunohematologists in evaluating antibody identification results is to rule out those antibodies of which the serum has failed to react with a cell known to carry the corresponding antigen. Although not required, whenever possible it is best to rule out antibodies based on lack of reactivity with cells demonstrating the homozygous form of an antigen so as not to erroneously rule out weakly reactive antibodies that show dosage. Using the homozygous "rule of thumb" for ruling out antibodies, cell numbers 3, 5, 6, and 7 are not reactive with the serum and may be used to rule out anti-D, anti-C, anti-c, anti-e, anti-M, anti-N, anti-s, anti-P_1, anti-Lu^b, anti-k, anti-Fy^b, anti-Jk^a, and anti-Jk^b. Expression of the antigens f, V, Le^a, Le^b, and Xg^a cannot be characterized as homozygous owing to the mechanisms of their inheritance, but because at least one of these four cells is positive for these antigens and the serum did not react with them, the corresponding antibodies may be eliminated from consideration.

Name *John Doe*

Hospital number *0001234.56*

		Rh								MNSs				P	Lewis		Lutheran		Kell*				Duffy		Kidd			Vial			
Rh phenotype		D	C	E	c	e	f	C^w	V	M	N	S	s	P_1	Le^a	Le^b	Lu^a	Lu^b	K	k	Kp^a	Js^a	Fy^a	Fy^b	Jk^a	Jk^b	Xg^a		37C	AHG	CC
1	rr	0	0	0	+	+	+	0	0	+	0	+	0	+	+	0	0	+	0	+	0	0	+	+	+	0	+	1	0	1	
2	rr	0	0	0	+	+	+	0	0	+	+	0	+	+	0	+	0	+	+	+	0	0	0	+	0	+	+	2	0	3	
3	r′r	0	0	0	+	+	+	0	0	+	0	+	+	+	0	+	0	+	0	+	0	0	0	+	0	+	0	3	0	0	2
4	r″r	0	0	+	+	+	+	0	0	+	+	+	+	0	0	+	+	+	0	+	0	0	0	+	0	+	0	4	1	2	
5	rr	0	0	0	+	+	+	0	0	0	+	+	+	+	0	+	0	+	0	+	0	0	0	+	0	+	+	5	0	0	2
6	R_or	+	0	0	+	+	+	0	+	+	+	0	+	+	0	0	0	+	0	+	0	0	0	0	+	0	0	6	0	0	2
7	R_1R_1	+	+	0	0	+	+	0	0	+	0	+	+	0	+	0	0	+	0	+	0	0	0	+	+	+	0	7	0	0	2
8	R_1R_1	+	+	0	0	+	+	0	0	+	+	+	+	+	0	+	0	+	+	+	0	0	+	0	0	+	+	8	0	3	
9	$R_1R_1^w$	+	+	0	0	+	+	+	0	+	+	0	+	+	0	+	0	+	0	+	0	0	+	+	+	+	+	9	0	1	
10	R_2R_2	+	0	+	+	0	+	0	0	+	+	0	+	+	+	0	0	+	0	+	0	+	0	0	+	+	+	10	1	2	
11	rr	0	0	0	+	+	+	0	0	0	+	0	+	+	0	+	+	+	0	+	+	0	+	+	+	0	0	11	0	1	
																												Auto	0	0	2

Figure 36.24 A typical panel worksheet showing an example of antibody identification results. *AHG,* Antihuman globulin; *CC,* Coombs control cells. *Unless otherwise specified, it is understood that all cells are positive for the high-frequency antigens Kp^b and Js^b.

3. Because of reactions seen in different phases and demonstrating different agglutination strengths, at least two antibodies are likely present in the serum:
   - Cell numbers 4 and 10 show direct agglutination in the 37°C phase, followed by stronger agglutination in the AHG phase, which is very typical of Rh system antibodies. These are the only two cells on the panel positive for the E antigen, which has not been ruled out. Thus, it is likely that anti-E is one of the antibodies involved.
   - Cell numbers 2 and 8 show very strong agglutination in the AHG phase only. Upon examining the antigens across the top of the panel that have not been ruled out, one sees that the phenotype of the panel cells for the K antigen fits the serum reactivity of these two cells. Thus, it is likely that anti-K is a second antibody involved.
   - The remaining serum reactions with cell numbers 1, 9, and 11 cannot be explained by anti-E or anti-K but may be explained by anti-Fy^a, because all three of these cells are positive for the Fy^a antigen, and Fy^a has not been ruled out.
4. Anti-S should be ruled out by testing another cell positive in the homozygous state for S antigen that at the same time is negative for Fy^a, K, and E antigens.
5. Antibodies to low-frequency antigens such as C^w, Lu^a, Kp^a, and Js^a may be ruled out by testing appropriate cells if available. When antibodies to low-frequency antigens are not ruled out, an antiglobulin crossmatch is used to detect any potential incompatibility between donor cells and the theoretical presence of one or more of these antibodies in the patient's serum.
6. Ruling out of additional antibodies may sometimes be accomplished by typing the patient's cells for selected antigens. This is particularly helpful when a patient's serum contains multiple antibodies and the reagent cell resources available to the blood bank are limited. If one of the antibodies that must be ruled out in a mixture of antibodies is anti-Jk^b, for example, the patient's cells may be typed for the Jk^b antigen with specific antisera. If the patient expresses the Jk^b antigen, then the presence of an alloantibody to Jk^b can be conclusively eliminated.
7. On the panel in Figure 36.24, there are at least three cells negative for all three antigens—Fy^a, K, and E—that do not react with the serum. However, to conclusively identify all three antibodies within the 95% confidence interval, three separate cells must be positive only for Fy^a antigen, three positive only for K antigen, and three positive only for E antigen that do react with the serum. Thus, anti-Fy^a can be identified with confidence. However, two more cells positive for K antigen and one more cell positive for E antigen must be tested with the serum to conclusively identify the presence of anti-K and anti-E.
8. If antibody identification is being performed for the first time on a particular patient, it is common practice to type patient RBCs for the antigens to which the individual has developed antibodies as a confirmation of the antibody identification. The patient's RBCs should lack the antigens corresponding to the antibodies present.

Crossmatching

For many years, a major serologic crossmatch was required before the transfusion of whole blood or packed RBCs. This protocol required a 37°C incubation, followed by conversion to the IAT. In 1984, this requirement was eliminated by the AABB Standards as long as (1) the current antibody screen on the patient is completely negative, and (2) there is no past history of clinically significant antibodies. For patients who meet these criteria, an abbreviated procedure designed to detect ABO incompatibility may be used. This may consist of an immediate spin crossmatch or an electronic crossmatch.

Immediate Spin Serologic Crossmatch

The serologic test to detect ABO incompatibility commonly consists of an immediate spin protocol employing a 3% to 5% saline suspension of donor RBCs prepared from an integral segment taken from the selected donor unit. Cells usually are washed once to remove any anticoagulant or plasma protein that could interfere with the testing. A drop of donor cell suspension is mixed with recipient serum, centrifuged immediately, and examined for hemolysis and/or agglutination. This procedure has come to be known as the *abbreviated or immediate-spin crossmatch*.

Use of the immediate-spin crossmatch procedure in clinical settings has shown it to be a safe and cost-effective alternative to the antiglobulin crossmatch (Judd et al., 1988; Cordle et al., 1990; Shulman, 1990), although reports indicate that this technique may fail to detect ABO incompatibility when recipient ABO antibodies are of low titer or when donor cells belong to a weak ABO subgroup (Berry-Dortch et al., 1985; Shulman et al., 1987). Rare false-negative results can occur as the result of a prozone effect in group O/group A major incompatibility, particularly if a delay in centrifugation occurs (Judd et al., 1988). The prozone/delay apparently allows for the fixation of C1 complement on RBC membranes, which sterically hinders hemagglutination. Suspension of donor cells in EDTA-saline eliminates this problem by chelating calcium necessary for formation of the C1 complement complex. In addition to false negatives, the immediate-spin crossmatch can cause false-positive results due to rouleaux, cold-reactive antibodies, and fibrin—all of which may cause delays in issuing the blood for transfusion. In a multicenter study involving 1.3 million immediate-spin crossmatches, the observed risk of acute hemolytic reaction using the immediate-spin crossmatch technique was 0.0004% (Shulman, 1990).

Electronic Crossmatch

In 1994, Butch and colleagues first reported on a proposed standard operating procedure that would replace the immediate-spin serologic crossmatch with a computer electronic crossmatch, or EXM. Similar to the immediate-spin crossmatch, the electronic crossmatch may be used only for patients who have no currently detected clinically significant antibodies or any history of alloantibodies. The EXM reduces human error by assigning final verification of ABO compatibility between donor and recipient by the laboratory computer system (Judd, 1991). In addition, it eliminates time-consuming investigation of false-positive serologic reactions.

The EXM is permissible provided that specific testing criteria are met and extensive validation of the blood bank information system has been performed to meet current AABB Standards and FDA requirements as outlined in a 1997 FDA internal document (Judd, 2002). Critical elements required in computer validation for the EXM (Judd, 1998) include updated hardware, instrumentation interfaces, historical record checks, reaction interpretation algorithms, prevention functions and warnings for ABO assignment/release, and personnel competency assessment. Because the safety of this procedure will be only as good as the electronic information that is entered and stored in the system, maximal use of bar codes to identify both donors and patients should be implemented. After extensive experience with electronic crossmatching at the University of Michigan, Judd (1998) recommended that bar-coded patient identification be mandatory both at the time of sample collection and prior to transfusion and that pretransfusion specimen labels be generated at the bedside from the bar code on the patient identification wristband. Box 36.1 summarizes the AABB Standards requirements.

Antiglobulin Crossmatch

If the pretransfusion antibody screen detects a clinically significant antibody or a check of patient records indicates that such antibodies have been detected previously, an antiglobulin crossmatch must be performed. In the antiglobulin crossmatch, compatibility between recipient serum and donor red cells is tested by the antiglobulin method that is routinely used by the laboratory. Red cell units chosen for transfusion should lack the antigen of interest (antigen-negative) by phenotyping units with commercially available antisera. When commercially available antisera is not available, donor genotyping may be approved for use by the medical director.

Some blood bank laboratories still choose to perform a full antiglobulin crossmatch for all transfusions, regardless of history and pretransfusion testing results. For patients with a negative antibody screen, the full crossmatch may *rarely* detect alloantibodies to low-frequency antigens not present on the screening cells (e.g., Kp^a, Wr^a). In addition, antibody detection tests could theoretically fail because of the presence of an antibody displaying dosage, deterioration of antigen from the reagent cells during storage, or technical error. Despite these concerns, the actual incidence of missing a clinically significant antibody with an abbreviated crossmatch is very low: less than 0.05% (Mintz et al., 1982; Cordle et al., 1990).

Compatibility Testing in Emergencies

In urgent situations, blood may have to be released for transfusion before the completion of compatibility tests or even before a patient blood specimen is available. If the ABO and Rh types of the patient are not known, group O–packed RBCs are released. Practice varies when selecting the Rh of emergency blood components. Some facilities use Rh-negative only for females under 50 years of age, whereas others may start with Rh-negative and switch to Rh-positive after 4 (or more) units. If a blood specimen is available and there is time to perform ABO and Rh typing, type-specific blood may be released. All units must be conspicuously labeled to indicate that they are uncrossmatched and that the patient's serum has not been screened for unexpected antibodies. In these situations, the patient's physician must sign a release form stating that the clinical situation warrants the release of uncrossmatched blood. In such cases, the antibody screen is promptly completed, and crossmatches are performed according to the laboratory's protocol. In the event of a positive screen or incompatible crossmatch, the physician should be notified immediately of any antibodies or incompatibility detected.

Massive transfusion occurs when the number of emergently transfused RBCs equals or exceeds the patient's blood volume in a relatively short time frame (<24 hours). Under these circumstances, many blood banks initiate a massive transfusion policy that permits switching to an immediate-spin or electronic crossmatch, even in a patient with known RBC alloantibodies. In these instances, serum antibody is typically diluted and undetectable in vitro owing to the large volume of donor blood and fluids transfused. Most protocols for massive transfusion return to use of the routine crossmatch procedure within 24 hours of the time the patient is stabilized. Transfusion of antigen-positive units could result in an increase in antibody titer and lead to a delayed HTR in patients with alloantibodies. Communication with the patient's physician is critical in such cases to monitor the patient for hemolysis.

BOX 36.1

Requirements for Implementation of the Electronic Crossmatch*

- Computer system has been validated onsite to ensure that only ABO-compatible whole blood or red blood cell components are selected for transfusion.
- There have been at least two determinations of the recipient's ABO group, one of which is from the current sample and the second by one of the following methods:
  - Testing a second current sample
  - Comparison with previous records
  - Retesting the same sample
- The system contains the following data items:
  - Donation identification number
  - Component name
  - ABO/Rh type of component
  - Confirmed unit ABO group
  - Two unique identifiers for recipient
  - Recipient's ABO group/Rh type
  - Recipient's current antibody screen results†
  - Interpretation of compatibility
- A method exists to verify the correct entry of data prior to the release of components.
- The software contains logic to warn user of discrepancies between donor ABO group and Rh type on the unit label and those determined by blood group confirmatory tests, and to ABO incompatibility between the recipient and donor unit.

* Requirements paraphrased from *Standards for Blood Banks and Transfusion Services,* 32th edition (Gammon, 2020).

† The electronic crossmatch can be used only if current antibody detection tests on the recipient are negative and there is no known history of clinically significant blood group antibodies.

Preoperative Crossmatch Protocols

Most transfusion services have adopted a type and screen–only protocol for elective surgical procedures that do not routinely require transfusion. Blood orders for elective surgical procedures requiring transfusion are set at a level that reflects actual usage patterns for a given operative procedure at a particular institution. The type and screen–only protocol, when used in conjunction with preoperative blood ordering guidelines (maximum surgical blood order schedule [MSBOS]); (Friedman et al., 1976; Henry et al., 1977; Banderanko, 2014), allows for much more efficient blood inventory management and reduction in the crossmatch/transfusion (C/T) ratio. The MSBOS should undergo periodic review and revision, using electronic data from the laboratory information system (LIS) and electronic medical record (EMR), as new surgical procedures are adopted and techniques are refined (Frank et al., 2013).

The preoperative type and screen protocol requires no further serologic work as long as the patient's antibody screen is negative and there is no known history of clinically significant antibodies. If a patient unexpectedly requires transfusion during surgery, ABO- and Rh-compatible units are selected, and an immediate-spin crossmatch or EXM may be performed. If no ABO incompatibility is detected, the blood can be safely released to the operating room with a minimal turnaround time. If the preoperative antibody screen is positive or if previous records indicate a known clinically significant antibody, standard operating procedures should specify a minimum number of antigen-negative units that would be held by the blood bank for use by the patient during surgery. These units must be crossmatched with the patient's serum using a full antiglobulin crossmatch procedure prior to transfusion.

Prenatal, Postnatal, and Infant Testing

All women should be screened as soon as possible for red cell alloantibodies and the potential for HDFN. The initial test is generally a blood type and antibody screen. If clinically significant antibodies are detected, the pregnancy is monitored with titration studies and other clinical diagnostic tests at specific intervals. Note that RhD-negative women who have received Rh immunoglobulin prophylaxis can have a weak anti-D on testing. In addition, Rh immunoglobulin can cross the placenta and cause a positive antibody screen in fetal and cord samples.

At birth, cord samples may be typed for ABO, RhD, and DAT, if indicated: A type and screen is not routinely performed because cord samples are frequently contaminated with maternal blood. Because only IgG antibodies cross the placenta, the DAT can be tested with anti-IgG only. A comparison should be made between mother and infant blood type to evaluate the potential for ABO HDFN. If the mother has clinically significant antibodies, the cord should have a DAT and be phenotyped for the corresponding antigens of interest. An antibody identification should be performed using maternal or cord sample, although maternal blood is often used owing to insufficient serum/plasma in cord samples. If the cord

DAT is positive and the mother does not have clinically significant antibodies, the laboratory should decide whether an eluate procedure should be routinely performed. The cord sample may be used for antibody identification and for eluates if needed.

In RhD-negative women, special precautions and testing are taken both prepartum and postpartum in an effort to prevent RhD alloimmunization (see Rh System). Prepartum, the father may be typed for RhD to determine the risk for HDFN. Alternatively, the fetus may be genotyped to determine RhD status (Finning et al., 2007). Unless the fetus or the father is confirmed as RhD negative, the mother must receive prophylactic Rh immunoglobulin at 28 weeks and after invasive procedures. Prophylactic Rh immunoglobulin is frequently given if trauma or bleeding occurs during the pregnancy. Once delivery has occurred, a fetal RhD type is performed on cord blood to determine the need for additional Rh immune prophylaxis. If the infant is RhD negative or if the mother has become sensitized, Rh immunoglobulin is not given. However, if the infant is RhD positive and the mother is not sensitized, the mother should receive additional Rh immunoglobulin. To determine how much Rh immunoglobulin should be administered postpartum, the mother should be screened for a possible maternal fetal bleed.

The most common screening test for a possible fetal bleed in an RhD-negative mother is the rosette test, which can detect approximately 10 mL of fetal cells in the mother's circulation (Bayliss et al., 1991). To perform the test, maternal blood is incubated with anti-D, which will bind circulating RhD-positive fetal red cells but not maternal RhD-negative red cells. After incubation and washing, indicator red cells are added. The sample is centrifuged and then examined under a microscope. If fetal red cells are present, indicator red cells will bind to anti-D on fetal red cells, forming a rosette. If no fetal red cells are present, the mixture will be smooth and without rosettes.

If the fetal bleed screen is positive, additional studies are necessary to quantitate the extent of the bleed. The Kleihauer-Betke test and flow cytometry are two methods used to calculate the quantity of fetal red cells in maternal circulation. The Kleihauer-Betke test is based on the resistance of fetal hemoglobin to acid, which looks bright pink in a sea of adult red cell ghosts on a peripheral blood smear. The percentage of fetal red cells present is manually determined and then multiplied by the maternal blood volume to determine the volume (mL) of fetal blood present (Fung, 2017). Flow cytometric methods are less labor intensive and are used to calculate the percentage of RhD-positive fetal cells by immunofluorescence (Radel et al., 2008). Once the size of the bleed is determined, the mother should receive sufficient Rh immunoglobulin to neutralize all circulating fetal red cells. Calculations to determine the size of the fetal bleed and the number of Rh vials required are available in the *AABB Technical Manual* (Fung, 2017). In general, one vial of Rh immunoglobulin will suppress immunization of 15 mL of RhD-positive red cells.

SPECIAL ANTIBODY IDENTIFICATION TECHNIQUES

Patients who have undergone repeated transfusions may respond by forming multiple unexpected blood group antibodies. Autoantibodies and alloantibodies to high-frequency antigens will react with all cells tested, including all RBCs used for antibody identification, making it extremely difficult to detect other underlying alloantibodies. When complicated problems such as these are encountered, special techniques are required to resolve the problem and find compatible units for transfusion. Special techniques used in antibody identification frequently involve (1) an attempt to eliminate selected antibody reactivity that is interfering with identification of other specificities in the same serum or (2) an effort to enhance or more clearly characterize the reactivity of an antibody that thus far has escaped definitive identification. Some of these techniques are outlined later in this chapter as well as in Tables 36.35 and 36.36. The reader is also referred to the *AABB Technical Manual* (Fung, 2017), *Applied Blood Group Serology* (Issitt & Anstee, 1998), *Judd's Methods in Immunohematology* (Judd et al., 2008), and *Immunohematology Methods* (Mallory, 1993) as excellent references for most common procedures in addition to more specialized techniques.

Serum Procedures to Eliminate Antibody Reactivity

Hemagglutination Inhibition

Hemagglutination inhibition is used to neutralize selected blood group antibodies with their corresponding antigen found in soluble form in human saliva, serum, or other body fluids, as well as in substances in nature (Table 36.37). Reagents for antibody neutralization have been synthesized using modern molecular techniques (Seltsam et al., 2009). The identity of a suspected antibody is confirmed if it no longer agglutinates antigen-positive reagent cells after addition of soluble antigen. Hemagglutination inhibition may be particularly useful when working with a serum specimen containing multiple specificities. The principle of hemagglutination inhibition is also used to determine the secretor status of individuals with weak ABO subgroups. Care must be taken in interpreting results because weak reactions may be diluted by the inhibition substance. A control set of tubes containing an inert substance (typically saline) should be used in parallel to verify that a negative reaction was the result of inhibition and not of sample dilution.

TABLE 36.35

Special Techniques in Antibody Identification: Serum Procedures*

	Procedure	Application/Effect
Hemagglutination inhibition	Inhibit antibody reactivity by mixing serum with a specific soluble antigen source in parallel with a dilution control; retest against known antigen-positive cells.	Confirm specificity by neutralizing the following antibodies: anti-P1, anti-Le^a and Le^b, anti-Sd^a, anti-ABH, anti-I, anti-Ch/Rg. May also allow for easier identification of other antibodies in a mixture.
Serum adsorption	Adsorb serum antibodies with autologous cells, selected allogeneic cells, or rabbit erythrocyte stroma (REST) at appropriate temperature for reactivity of antibody	Physically removes broadly reactive autoantibodies or alloantibodies from serum by reacting with absorbing cells to allow for detection of underlying IgG antibodies—particularly useful in cases of WAIHA. May be combined with elution in complicated cases involving identification of multiple antibodies.
Sulfhydryl reagents	Pretreat serum with sulfhydryl reagents such as 2-mercaptoethanol (2-ME) or dithiothreitol (DTT)	Destroys pentameric structure of agglutinating IgM antibodies, effectively bypassing cold-reactive autoantibodies and alloantibodies to allow for detection of underlying IgG alloantibodies.
Titration	Prepare serial twofold dilutions of serum and test against antigen-positive indicator cell.	Aids in identification of HTLA antibodies (titer of 1 : 64 or greater). Used to measure increase in production of IgG antibodies during pregnancy. ABO-incompatible organ transplantation May rarely be useful in identifying alloantibodies of a higher titer present with a warm autoantibody.
Prewarming	Keep all test components (test tubes, cells, serum, saline) at 37°C prior to testing; use monospecific anti-IgG AHG reagents.	Bypasses reactivity of cold autoagglutinins or alloagglutinins of limited titer and thermal amplitude—prevents direct agglutination of test cells and/or in vitro complement activation in antibody detection and identification tests.
Saline replacement	For tests in which patient or test red cells are suspended in serum and are suspected to have formed rouleaux, the serum is removed and replaced with equal volume of saline.	Useful in obtaining valid results in ABO serum grouping or evaluating the presence of apparent agglutination when examining screening cells after 37°C incubation and centrifugation. Pseudoagglutination due to rouleaux will be dispersed by removal of the offending proteins and addition of a high–ionic strength medium

AHG, Antihuman globulin; *HTLA,* high-titer, low-avidity; *Ig,* immunoglobulin; *WAIHA,* warm autoimmune hemolytic anemia.
*See also Table 36.30 for effects of antibody concentration, pH, incubation time, etc.

TABLE 36.36
Special Antibody Identification Techniques: Red Cell Procedures

	Procedure	Application/Effect
Enzyme treatment	Two-stage procedure (preferred): • Incubate test red cells with enzyme solution at 37°C. • Wash cells thoroughly to remove enzyme completely and retest cells with serum being investigated.	• Eliminates some antibody reactivity by destroying corresponding antigen structures—MNS, Duffy, Ch/Rg; may be easier to pick out different specificities in a serum containing multiple antibodies. • Enhances sensitization, agglutination, and/or hemolysis by other antibodies—Rh, Kidd, many IgM blood group antibodies; may allow for easier identification of weakly reactive antibodies.
AET/DTT	Pretreat test red cells with AET or DTT; wash away reagent and retest cells with serum being investigated.	Effectively creates Kell "null" cells for use in identifying alloantibodies in a mixture containing antibody to a high-frequency antigen in the Kell system.
Elution	Remove and recover antibody from red cells by techniques such as glycine acid, organic solvents.	Concentrates antibody that was coating red cells into a solution suitable for further identification procedures. Used in investigating positive DAT in cases of HDFN, HTR, autoimmune hemolytic anemia.
Chloroquine diphosphate	• Washed packed red cells are incubated in a 1 : 4 ratio with chloroquine at room temperature. • Reagent is removed by multiple saline washes.	Dissociates IgG from patient red cells with a positive DAT so that they may be typed with blood grouping reagents that require an indirect antiglobulin technique. Only anti-IgG should be used as the AHG reagent, as complement proteins are not dissociated with chloroquine.
ZZAP	For adsorption purposes, aliquots of washed, packed red cells are incubated with ZZAP at 37°C. Cells are then washed with large volumes of saline to remove ZZAP. The combination of DTT and enzymes destroys coating of IgG autoantibodies.	• Removal of autoantibodies from patient cells provides free antigen sites for adsorption of autoantibody from the serum. • ZZAP also can be used to destroy Kell, Cartwright, Gerbich, and Dombrock system antigens.
Dispersal of IgM-mediated autoagglutination	Incubate cell suspension with sulfhydryl reagents or wash cells multiple times with 37°C saline.	Dissociation of cold autoagglutination permits valid ABO red cell typing and may aid in evaluating DAT results.
Lectin typing	Reagents commonly derived from plant seeds are used to test for the presence or absence of a specific blood group antigen on the red cell membrane—used in place of an antibody reagent.	Useful in typing for specific antigens such as A_1, H, and N and in classifying different polyagglutinable red cell conditions.
Cell separation techniques	• Washed cells from the patient are centrifuged in microhematocrit tubes and the top 5 mm containing the lightest cells is harvested. • Differential agglutination may be performed based on known differences in antigen phenotype between donor and recipient	Useful in the following: • Phenotyping of autologous cells in recently transfused individuals • Evaluating whether a DHTR may be evolving in a patient with autoimmune hemolytic anemia • Estimating survival of transfused cells

AET, 2-Aminoethylisothiouronium bromide; *AHG,* antihuman globulin; *DAT,* direct antiglobulin test; *DHTR,* delayed hemolytic transfusion reaction; *DTT,* dithiothreitol; *HDFN,* hemolytic disease of the fetus and newborn; *HTR,* hemolytic transfusion reaction; *Ig,* immunoglobulin; *ZZAP,* combination of DTT and cysteine-activated papain.

TABLE 36.37
Sources of Soluble Antigens for Hemagglutination Inhibition

Soluble Substance	Source
ABH	Secretor saliva
Le^a, Le^b	Secretor saliva
P1	Hydatid cyst fluid or pigeon eggs
Sd^a	Human or guinea pig urine
Ch, Rg	Plasma from Ch/Rg (+) individuals
I	Human milk

Antibody Adsorption

Adsorption is a process used to physically remove antibodies from sera. The adsorption procedure may be performed using washed and/or enzyme-treated autologous RBCs, phenotypically matched allogeneic cells, cells selected to be positive for a specific combination of blood group antigens, or RBC stroma. The incubation temperature and times used in the adsorption process depend on the Ig class and the thermal range of the antibodies being adsorbed. In general, using a low antibody/cell ratio will increase adsorption efficiency.

Adsorption using allogeneic cells is helpful in separating multiple alloantibodies in a complex mixture (differential adsorption) or in eliminating the reactivity of an alloantibody to a high-frequency antigen. In patients with autoantibodies, adsorption with autologous RBCs, phenotypically matched cells, and rabbit erythrocyte stroma (REST) is often used to selectively remove warm- and cold-reactive autoantibodies, respectively. Removal of autoantibodies is necessary to identify any potential underlying alloantibodies that the patient may have (see later discussion in Investigation of Autoimmune Hemolytic Anemia section; Fig. 36.25).

It is crucial to verify transfusion information before performing an adsorption because recently transfused individuals will have multiple red cell populations. In these patients, circulating donor cells could adsorb an alloantibody of interest. If the patient's phenotype is available, testing can be performed with allogeneic phenotype-matched red cells. If the phenotype is not known, three separate adsorptions with R_1R_1, R_2R_2, and rr cells can be performed and tested and the results compared.

Thiol Reagents

Sulfhydryl compounds such as 2-ME or DTT cleave disulfide bonds. These compounds are frequently used to inactivate the agglutinating capacity of IgM antibodies by cleaving intersubunit disulfide bonds as well as bonds linking IgM subunits to the J-chain (Klein & Anstee, 2006), thus destroying the pentameric structure of the IgM molecule. These reagents are useful in investigating the presence of clinically significant IgG alloantibodies in a serum that contains broadly agglutinating IgM cold autoantibodies. They can also be used to dissociate autoagglutination caused by cold antibodies that may interfere with ABO/Rh typing and DAT testing. In prenatal studies, sulfhydryl reagents are frequently utilized to evaluate a serum containing an antibody such as anti-M that commonly has both IgM and IgG components. By destroying the agglutinating anti-M, the serum can be tested for IgG anti-M that is capable of crossing the placenta to cause a mild HDFN.

Serum Antibody Titration

Serum titration is a method used to semiquantitatively determine the amount of antibody present in a given serum/plasma. Serial twofold dilutions of serum are prepared and then tested with RBCs possessing the corresponding antigen. Each dilution is read for macroscopic agglutination, and the titer of the antibody is expressed as the reciprocal of the highest serum dilution that gives macroscopic agglutination. Titers can be performed by any of the methods used for IATs. Automated instruments may also perform titers, thus, standardizing the process. Titers are performed in obstetric patients, ABO-incompatible solid-organ and bone marrow transplantation, and, occasionally, antibody identification studies.

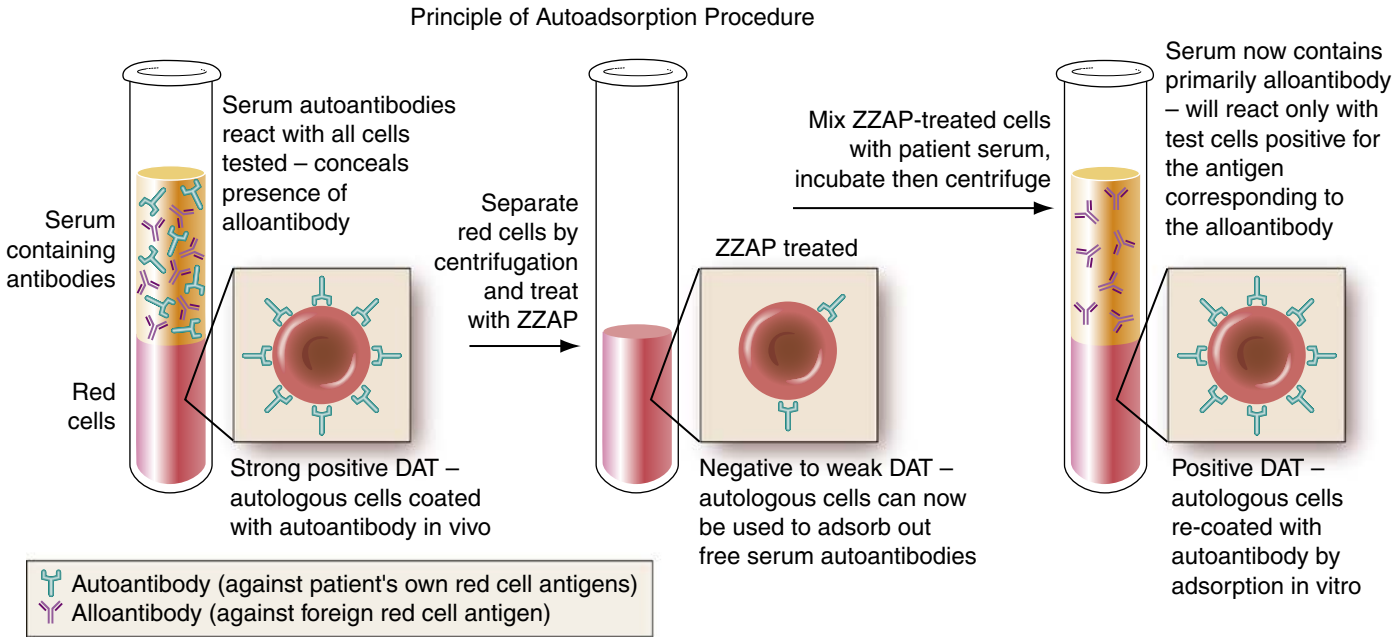

Figure 36.25 Autoadsorption procedure used to evaluate whether underlying alloantibodies are present in a patient with autoimmune hemolytic anemia.

In prenatal studies, clinically significant IgG alloantibodies capable of causing HDFN are titrated periodically in the maternal serum during pregnancy (Judd, 2005). An increasing titer usually indicates that fetal cells possess the corresponding antigen and are stimulating the mother to produce more antibody, providing valuable information to the physician regarding how the pregnancy should be managed. Because of the clinical importance of consistency in prenatal titer reporting, some laboratories require that the initial titer be performed by two technologists for agreement. If a discrepancy exists, a third technologist should perform the titration. The initial sample should be frozen for future studies. When the next titer request is submitted, the initial sample should be tested in parallel with the new sample.

Titers are also performed in the rare setting of major ABO-incompatible solid-organ transplantation, which has risen in popularity with improvements in immunosuppressive therapy. ABO-incompatible heart transplants can be performed in children younger than 6 to 8 months owing to low-titer ABO antibodies in early infancy (West & Platt, 2010). ABO-incompatible living donor kidney transplants, once unthinkable because of the risk of hyperacute rejection, have also been performed in adult patients. To prevent hyperacute rejection, intended recipients undergo an aggressive course of immunosuppression and therapeutic apheresis before and after transplant to reduce ABO titers below a critical threshold (Fehr & Stussi, 2012). Similar to obstetric patients, these patients require a series of ABO titers to monitor treatment efficacy and screen against humoral rejection. Finally, ABO titers may be necessary in ABO-incompatible allogeneic bone marrow transplants. In contrast to peripheral blood stem cells, bone marrow contains significant quantities of red cells that can place the recipient at risk for severe acute HTRs. ABO titers are performed before transplant to assess the risk of hemolysis and the need for pretransplant therapeutic apheresis (Rowley et al., 2011; Cooling & Gorlin, 2012).

Antibody titration can also be used in the presumptive identification of so-called "HTLA" antibodies. These antibodies are often directed against Ch/Rg, JMH, and Knops antigens. HTLA antibodies characteristically give the same weak (+/– or $+/^{-m}$) reactions at multiple serum dilutions, often reacting at dilutions equal to or greater than 1:64. In contrast, other weak alloantibodies will seldom react at dilutions greater than 1:2. If an HTLA antibody is suspected, a titration is performed to demonstrate that the weakly reactive antibody is still reactive at a high dilution, allowing its classification as an HTLA.

It is important to note that both serologic technique and cell selection can affect titer results. For example, if the initial titer was tested against a cell with homozygous antigen expression, all subsequent titers should also be tested with a homozygous cell. Likewise, some laboratories use a tube technique without additives (saline), and others may use a LISS, tube, or gel method—all of which can yield significantly different end titers in parallel testing. Each laboratory should have a policy regarding appropriate cell selection and should perform titers using a technique approved by the laboratory director with proper validation. Titer results and their meaning should be communicated clearly to the physician. Any change in procedure or method *must* be communicated because this can affect titer results and have a direct impact on patient care.

Special Red Cell Procedures for Antibody Identification

Reagent or patient RBCs can be modified in various ways by the immunohematologist to abolish or enhance the reactivity of corresponding antibodies. Patient cells are also subjected to procedures designed to remove antibody that has bound in vivo so that the antibody may be recovered and identified (eluate) and/or may provide RBCs for further testing.

Destruction of Red Cell Antigens

Several reagents are available for treating RBCs, including various proteolytic enzymes (e.g., papain, ficin, trypsin), neuraminidase (removes sialic acid), ZZAP, AET, and DTT. In a serum containing multiple alloantibodies, selective pretreatment of RBCs with enzymes can destroy specific antigens, eliminating specific alloantibody reactivity. Enzymes are also thought to remove the water of hydration and decrease the ζ potential, allowing RBCs to more closely approach one another. As a result, they can enhance the reactivity of a weak, potentially significant antibody and facilitate its identification. Table 36.38 lists antibodies whose reactivity will be enhanced or eliminated by enzyme treatment of test RBCs. Note that AET and DTT can be used to create RBCs negative for all antigens of the Kell blood group system (except Kx); these reagents may also destroy certain antigens reacting with HTLA antibodies.

DTT also denatures CD38, a target of newer immunotherapeutic drugs for multiple myeloma. The drugs daratumumab and isatuximab are anti-CD38 monoclonal antibodies approved for multiple myeloma that can interfere with antibody identification (Chapuy, 2015). Because CD38 is expressed on red cells, patients receiving these drugs can display weak panreactivity during testing, leading to concerns for a high-incidence antibody. Testing with DTT-treated RBCs will resolve anti-CD38 drug reactivity (Baig et al., 2019; Chapuy, 2015). Because DTT denatures the Kell system (except Kx), antibodies to K antigens cannot be determined; generally, K-negative blood is issued to these patients.

Antibody Elution

Elution is the process used to remove antibodies bound to RBCs, as indicated by a positive DAT. Elution is commonly used to concentrate and solubilize antibodies from RBCs for subsequent identification studies. The elution of an antibody with known blood group and/or drug specificity can be diagnostic in the evaluation of acute and delayed hemolytic transfusion reactions, HDFN, autoimmune hemolytic anemia, and immune hemolytic anemia induced by medication.

Elution may be accomplished by a variety of methods that alter or reverse the forces of attraction that hold the antigen and antibody together. Various methods involve adding heat, disrupting antigen structure by exposing the RBC membrane to freezing and thawing, using organic solvents, and

altering the pH to dissociate RBC–antibody complexes. Freeze-thaw and heat elution techniques work well for removal of cold-reactive antibodies, whereas organic solvents and pH alteration are used to remove warm-reactive IgG antibodies. Because organic solvents are carcinogenic, many laboratories have a commercially available acid elution kit.

All methods require numerous washes before elution to remove any serum containing unbound antibody. To ensure the complete removal of serum antibody, the saline from the last wash must be tested against appropriate cells to detect any residual unbound antibody. The last wash control should show an absence of antibody reactivity before the elution procedure is performed. Optimally, eluates should be tested on the same day they are prepared but may be stored at –20°C or lower if there is a delay in testing. Table 36.39 lists some of the common elution methods and their applications. For a more comprehensive listing and specific descriptions of elution procedures, see Mallory (1993) and Judd and colleagues (2008).

Removal of Antibody from Red Cells to Facilitate Antigen Typing

Many antisera used for RBC antigen typing require the IAT technique. As a result, RBC samples with a positive DAT cannot be used for antigen typing because these cells are already coated with IgG antibody and will yield a false-positive result. Most elution methods that remove blood group antibodies from the surface of erythrocytes destroy the cells or the antigens. However, treatment of antibody-coated RBCs with chloroquine diphosphate dissociates antibody while leaving the antigens relatively intact (Edwards et al., 1982). Glycine/EDTA can also be used under carefully controlled conditions to dissociate IgG from RBCs, but overtreatment with this reagent can cause irreversible damage to the RBC membrane. After chloroquine or glycine treatment, RBCs can be antigen typed with AHG-reactive antisera. Note that glycine/EDTA treatment destroys Kell protein. As a result, glycine/EDTA cells cannot be phenotyped for Kell system antigens.

Care should be exercised when interpreting antigen typing results with chloroquine-treated cells. Reports indicate that Rh antigens, and possibly other blood group antigens, can be weakened, resulting in false-negative reactions. Saline-reactive antisera, including monoclonal grouping reagents, should not be used with chloroquine-treated cells (Gamma Biologicals Inc., 2001). For chloroquine or glycine/EDTA, it is prudent to treat known antigen-positive cells in parallel as a control. Only monospecific anti-IgG should be used in the IAT because complement components are not dissociated by chloroquine from DAT-positive RBCs.

TABLE 36.38

Effect on Antigen Expression/Antibody Reactivity by Enzyme* Treatment of Test Cells

Effect	Antigens
Destroyed	Fy^a, Fy^b
	M, N
	HTLA- Ch/Rg, JMH
	Pr
	Xg^a
Variable	Lu^a, Lu^b
	S, s
	Yt^a, Yt^b
Enhanced	ABH
	I/I
	Jk^a, Jk^b
	Le^a, Le^b
	P1
	Rh
	U
	Di^a, Di^b
Usually unaffected	Kell

HTLA, High-titer, low-avidity; *JMH,* John Milton Hagen.
*Using ficin or papain.
Data from Issitt PD, Anstee DJ: *Applied Blood Group Serology*, ed 4, Durham, NC, 1998, Montgomery Scientific Publications; Judd WJ, Johnson S, Storry S: *Judd's Methods in Immunohematology*, ed 3, Durham, NC, 2008, Montgomery Scientific Publications; and Fung M, editor: *Technical Manual*, ed 19, Bethesda, MD, 2017, American Association of Blood Banks.

Red Blood Cell Typing with Lectin Reagents

Lectin typing reagents contain proteins that will recognize specific carbohydrates on the RBC membrane, causing direct hemagglutination. Lectin reagents are usually derived from plant seeds, but these receptor proteins are also found in some invertebrate animals and lower vertebrates. Because the potency of lectin reagents may vary with the preparation, each lot should be standardized before use. Although many lectins have been described, only a few have been found useful in blood banking (Bird, 1988). Sources for selected lectin reagents and their applications are listed in Table 36.40. Procedures for preparation of purified lectins may be found in *Judd's Methods in Immunohematology* (Judd et al., 2008).

Separation of Autologous from Transfused Red Cells

In transfused patients, it may be necessary to separate autologous from transfused cells. Autologous RBCs for antigen typing may be necessary (1) in a transfused patient with multiple alloantibodies, (2) with a warm autoantibody and possible alloantibodies, or (3) with an antibody to a high-incidence antigen. Performing a DAT, and possibly even elution, on separated autologous and/or transfused cells can help determine whether a recently transfused individual with a warm autoimmune hemolytic anemia (WAIHA) is developing a delayed hemolytic transfusion reaction (DHTR) due to new alloantibodies. In rare cases, DAT testing on separated autologous RBCs may be required to differentiate a WAIHA from a DHTR involving a high-incidence antigen. In a final application, one could roughly estimate the proportion of surviving transfused RBCs when a DHTR is suspected.

Two basic techniques for separating autologous from transfused RBCs are differential agglutination and density separation using centrifugation. In the first technique, antibodies are used to agglutinate only one population of cells based on known antigenic differences between recipient and donor. Unagglutinated cells are physically removed from the agglutinates and are sequentially reacted with more antisera until no more agglutinates are formed. In the second technique, washed and packed RBCs are

TABLE 36.39

Antibody Elution Techniques

Method	Principle*	Application
Heat	Addition of heat changes equilibrium constant of antigen–antibody reaction, and antibodies are released.	• Recovery of ABO antibodies in cases of ABO HDFN • Gentle heat elution (at 45°C) may be useful for removing antibody from cells that is causing false-positive direct hemagglutination tests.
Freeze-thaw	Damage to the red cell membrane by hemolysis alters complementary fit between antigen and antibody.	Recovery of ABO antibodies in cases of ABO HDFN
Acid (e.g., digitonin acid, glycine acid/EDTA)	At an acid pH, antigen and antibody become negatively charged and repulse each other.	• Good recovery of most IgG blood group antibodies (may be less sensitive for Kidd) • Glycine/EDTA also used to dissociate antibody but leaves red cells intact for phenotyping
Organic solvents (e.g., chloroform, xylene, ether)	Disrupts lipid bilayer of red cell membrane, altering complementary fit and/or reversing selected attractive forces between antigen and antibody.	High-yield recovery of most IgG blood group antibodies

EDTA, Ethylenediaminetetraacetic acid; *HDFN,* hemolytic disease of the fetus and newborn; *Ig,* immunoglobulin.
*From Issitt PD, Anstee DJ: *Applied Blood Group Serology*, ed 4, Durham, NC, 1998, Montgomery Scientific Publications.

centrifuged in multiple sealed microhematocrit tubes. Transfused cells are older, smaller, and denser than newly formed autologous cells (reticulocytes) and will spin toward the bottom of the tube. After centrifugation, the top 5 mm of each tube is cut away and the cells are harvested from these small segments. These sections will contain the larger and lighter autologous cells. This method will be effective only if the patient is producing normal or high numbers of reticulocytes. When testing separated red cells, nonseparated cells should be tested in parallel as a control. The separated red cells should show clear positives and negatives, and the nonseparated cells should show mixed field agglutination.

Hypotonic cell lysis is a third method that is available for harvesting autologous red cells in patients with sickle cell disease. The method is based on the resistance of hemoglobin S red cells to hypotonic saline. The patient sample is repeatedly washed with 0.3% hypotonic saline to lyse normal donor red cells until gross hemolysis is no longer present. The cells are then washed and resuspended in 0.9% saline for antigen typing. Because sickle cell patients are regularly transfused, this technique is useful for facilities that provide antigen-matched red cells for their sickle cell patients.

Molecular Typing

Because most common blood group antigens are the consequence of SNPs, several commercial and home-brew assays have been developed to genotype donors and patients. The ability to genotype individuals for blood group antigens is extremely useful for multitransfused patients in whom standard serologic typing cannot be performed as a result of circulating donor red cells. Several transfusion services routinely genotype all hemoglobinopathy patients (e.g., sickle cell anemia, β-thalassemia) who have long-term transfusion needs and require antigen-negative units. Genotyping is also useful in patients with multiple alloantibodies or autoantibodies, in whom it can be difficult to exclude an antibody to a high-incidence antigen because of the lack of commercial reagents (e.g., Dombrock). Likewise, serologic phenotyping often cannot be performed in patients with a positive DAT because many reagents require the addition of anti-IgG for typing. Genotyping is commonly used in prenatal testing to identify a fetus at risk for HDFN. Fetal genotyping can often be performed with a maternal blood sample, offering a significant safety advantage over serologic testing, which requires fetal blood sampling (Finning et al., 2007). Finally, large-scale genotyping of donors has the potential to increase the availability of antigen-negative units for patients with clinically significant alloantibodies (Montpetit et al., 2006).

Several methods have been developed for red cell and platelet genotyping, including restriction fragment length polymorphism, allele-specific polymerase chain reaction (PCR), real-time PCR, direct sequencing, and microarray technology (see Chapters 67, 68, 69, and 70). High-throughput screening methods, such as microarray, are amenable to semiautomated processes and permit extended typing for high- and low-incidence antigens. It is important to stress that genotype does not always reflect red cell phenotype because most genotyping methods focus on known common polymorphisms. Unknown polymorphisms may alter protein or gene expression not detected by the primers used. A well-known example is Fy(a–b–) phenotype in blacks, who genotype as $FY^{*}B^{ES}$ but lack Fy expression on red cells because of a promoter mutation. Likewise, many partial RhD and RhCE phenotypes can lead to discrepancies between phenotype and genotype (see Rh section).

INVESTIGATION OF AUTOIMMUNE HEMOLYTIC ANEMIA

Autoantibodies, in general, are produced by an individual's own immune system against self or an antigen that is present in that same individual. Although produced against self-antigens, these antibodies typically react with the same antigen found in other normal individuals. If the antibodies produced are against blood cell constituents, the pathologic result could be hemolytic anemia, thrombocytopenia, or leukopenia. In many cases, these autoantibodies cause no demonstrable clinical symptoms.

The DAT is integral to the diagnosis of autoimmune hemolytic anemia (AIHA) because it can confirm the presence of antibody that has attached to the patient's own red cells in vivo. The DAT can help differentiate AIHA from congenital anemias caused by abnormalities in RBC cytoskeleton, enzymes, or hemoglobin. The DAT may be positive owing to IgG and/or complement components, depending on the class or subclass of autoantibody involved. A positive DAT by itself, however, does not mean that an individual has AIHA. Approximately 8% of hospitalized patients have a positive DAT without any signs of hemolysis (Petz, 1993). In patients with suspected AIHA, the antibody screen may also be positive because of free autoantibody in the serum.

Autoantibodies are categorized as cold (usually IgM) or warm (usually IgG), based on the temperature of in vitro reactivity in the IAT. In some cases, patients may have mixed-type AIHA with both cold and warm reactive autoantibodies. The causative antibodies of these categories of anemias will be described here; additional information regarding the origin and pathophysiology of AIHA is provided in Chapter 33.

Warm Autoimmune Hemolytic Anemia

Individuals with warm reactive autoantibodies account for approximately 70% to 80% of cases of AIHA, having an overall incidence of about 1 in 50,000 to 1 in 80,000 (Issitt & Anstee, 1998). WAIHA may be classified as primary or idiopathic (of unknown origin), or as secondary. Secondary WAIHA is often observed in autoimmune diseases (frequently, systemic lupus erythematosus), in lymphoproliferative disorders, and following viral infections. With the advent of improved diagnostic procedures, the percentage of WAIHA classified as idiopathic has dropped to about 30%

TABLE 36.40
Lectins Useful in Immunohematologic Testing

Lectin	Activity Inhibited by	Serologic Specificity	Application
Ulex europaeus	α-L-Fucose	Anti-H	Secretor status testing, classification of weak A subgroups, investigation of possible Bombay phenotype
Vicia graminea	O-linked N blood group tetrasaccharides (galactose [β1,3] N-acetyl-galactosamine)	Anti-N	Red cell antigen typing
Griffonia simplicifolia I*	α-D-galactose	Anti-B, Tn	• Red cell antigen typing • Investigation of acquired B/polyagglutination
Dolichos biflorus	Terminal α-*N*-acetyl-D-galactosamine	Anti-A, Tn, Cad	Classification of A subgroups, investigation of polyagglutination
Griffonia simplicifolia II*	α- or β-*N*-acetyl-D-glucosamine	Anti-Tk	Confirmation of Tk polyagglutination
Helix pomatia	α-*N*-acetyl-D-galactosamine	Anti-A, Tn, Cad	Gives distinctive mixed-field reaction with VA polyagglutination
Arachis hypogaea	β-D-Galactose	Anti-T, Tk, Th, Tx	Investigation of polyagglutination
Glycine soja (max)	α-*N*-acetyl-D-galactosamine	Anti-T, Tn	
Leonurus cardiaca	α-*N*-acetyl-D-galactosamine	Anti-Cad specific at appropriate dilution	
Salvia sclarea	α-*N*-acetyl-D-galactosamine	Anti-Tn specific	
Salvia horminum	α-*N*-acetyl-D-galactosamine	Anti-Tn, Cad (separable)	
Vicia cretia	Galactose (β1,3) *N*-acetyl-galactosamine	Anti-T, Th	

*Formerly known as *Bandeiraea simplicifolia* I and II.

of cases (Issitt & Anstee, 1998). Patients with warm autoantibodies and a positive DAT will not all present with symptomatic anemia but may exist in a chronic compensated state for some time before progressing to overt clinical anemia.

Serologic Characteristics

Autoantibodies in WAIHA are usually IgG and polyclonal in nature, showing optimal in vitro reactivity at 37°C. A vast majority of warm autoantibodies present in serum and/or recovered in eluates from patients' RBCs can be demonstrated only by the IAT technique. The DAT will be positive in approximately 80% of cases. The DAT profiles in several large studies show that 40% to 50% are due to IgG only, 45% to 60% are caused by IgG and complement, and 0% to 15% are the result of complement only (Issitt & Anstee, 1998). In those instances in which the DAT is negative, the use of more sensitive techniques—such as flow cytometry, enzyme-labeled AHG, and cold wash DAT—can demonstrate low levels of IgG or, less frequently, IgM and IgA on red cells (Englefriet et al., 1992; Judd, 2008).

Ig subclass studies in WAIHA indicate that causative antibodies are predominantly IgG1 and/or IgG3. Despite the ability of these subclasses to activate complement, immune destruction of the patient's autologous cells occurs largely through the spleen and liver via extravascular pathways. Patients whose RBCs are coated with IgG3 antibodies are more likely to show overt anemia, apparently because of the greater capacity of IgG3 for binding to Fc receptors on macrophages (Englefriet et al., 1992). A more recent study shows that the presence of multiple IgG subclasses, rather than a single subclass, has a synergistic effect on the severity of hemolysis (Fabijanska-Mitek et al., 1997).

In general, warm autoantibodies display a broad specificity, reacting with all normal RBCs. Many broadly reactive antibodies can show Rh specificity, as evidenced by weak or absent reactivity to Rh_{null} red cells. On occasion, autoantibodies will demonstrate Rh pseudospecificity, such as anti-e (most frequently), anti-c, and anti-E. Studies with recombinant cell lines show that, in most instances, these antibodies are broadly reacting with the RhCE, RhD, and Band 3 proteins regardless of Rh phenotype (Iwamoto et al., 2001). Notable exceptions to the latter are African Americans with partial RhCE proteins, who serologically type as c- and/or e-positive but can produce true alloanti-c and alloanti-e after immune stimulation (see Rh section). Autoantibodies with apparent specificity for Kell, Kidd, MNSs, ABO, Vel, and LW antigens have also been reported. Relatively few individuals with WAIHA will show a single simple specificity (Issitt & Anstee, 1998).

Serologic Testing Beyond the DAT

Transfusion is usually avoided for as long as possible in patients with WAIHA. If transfusion is necessary, it is important to characterize the autoantibody and exclude the presence of RBC alloantibodies (Eder, 2005). Typical investigation strategies should always include adsorption of the serum followed by antibody detection and identification on the adsorbed serum. Subsequent testing can also be performed on eluted antibody, although it seldom yields further useful information unless the serum is nonreactive.

Autoadsorption. Because a strong, broadly reactive serum autoantibody can mask the presence of significant alloantibodies, adsorption studies should be performed in these patients. Autoadsorption using autologous cells can be performed on patients who have not been recently transfused (within the last 3 months). For patients who have a strong positive DAT, autologous cells should be treated with ZZAP (Branch & Petz, 1982) before adsorption. ZZAP contains DTT, which reduces disulfide bonds in the IgG autoantibodies coating the RBCs. This destabilizes the Ig structure, rendering the autoantibodies susceptible to digestion by cysteine-activated papain, the second component of ZZAP. By stripping bound autoantibody from cells, ZZAP treatment increases the adsorptive capacity of autologous RBCs (see Fig. 36.25). If the serum contains a high concentration of autoantibody, multiple sequential autoadsorptions may be necessary to remove all autoantibody activity. If available in sufficient quantity, autoadsorbed serum may be used to perform crossmatching, particularly if antibody detection studies reveal the presence of underlying alloantibodies.

If the patient has had recent RBC transfusions, and the patient's red cell phenotype is known, adsorption may be performed using allogeneic cells of the same phenotype as the patient. Alternatively, if the patient's RBC phenotype is unknown, differential adsorptions may be performed on three separate aliquots of the patient's serum with different red cell samples of R_1, R_2, and rr phenotypes. One of the red cell samples should lack Jk^a and one should lack Jk^b (Fung, 2017). ZZAP treatment of the adsorbing cells will effectively destroy Fy^a, Fy^b, all Kell system antigens, and the M, N, S, and s antigens, thereby conferring on the adsorbing cell samples the capacity to remove autoantibody activity while preserving potential alloantibodies in the serum. The different aliquots of serum are then tested against cells of known phenotype to detect and/or identify alloantibody specificity.

Elution. In most cases of WAIHA, an eluate of the patient's cells will demonstrate the same broadly reactive antibody seen in serum. In the rare instances in which the serum is only weakly reactive or negative, an eluate may concentrate the warm autoantibody to facilitate identification and evaluation of its spectrum of reactivity. If the eluate is nonreactive with normal reagent RBCs, the presence of drug-induced autoantibodies should be investigated (see later discussion).

Cold Autoimmune Hemolytic Anemia

Cold autoantibodies may be detected in the serum of many normal individuals if tested under the right conditions. However, most of these antibodies are benign cold agglutinins that show optimal reactivity at 4°C and little or no reactivity at 37°C. Cold agglutinins are often a nuisance that can interfere with ABO/Rh typing, antibody detection, and crossmatching when polyspecific AHG is used. Although usually ignored as clinically insignificant, cold agglutinins may become pathologic by virtue of expanded thermal amplitude and a significant increase in titer, frequently in association with certain disease states. DAT, serum titration, and characterization of thermal amplitude are the most important serologic tests in evaluating a possible diagnosis of CAIHA. Table 36.41 outlines some of the serologic differentiating characteristics of various cold agglutinating autoantibodies, both pathologic and benign.

Cold Agglutinin Disease

Cold agglutinin disease (CAD) accounts for about 20% of total cases of AIHA (Issitt & Anstee, 1998). As with WAIHA, CAD may be idiopathic or secondary following infection or malignancy. Recent studies have identified idiopathic or primary CAD as a B-cell clonal disorder histologically distinct from Waldenström macroglobulinemia, mantle zone lymphoma, and other B-cell lymphomas (Berentsen et al., 2019). Primary CAD frequently possesses mutations in either *KMT2D* or *CARD11* genes, with restricted κ light chains (*IGKV3-20 gene*). Heavy-chain restriction (*IGHV4-34*) is common to monoclonal cold agglutinins whereas CAIHA secondary to infection is polyclonal. (Cooling, 2010).

Anti-I is the most frequent autoantibody in idiopathic CAD and *M. pneumoniae* infections. In contrast to the anti-I cold agglutinins found in normal sera (usually less than 1:64 when tested at 4°C), anti-I in CAD is often of very high titer, with ranges of 1:10,000 to 1:1,000,000 (Cooling, 2010, 2019). The antibody also has expanded thermal amplitude, reacting with RBCs at temperatures in the range of 30°C to 34°C in vitro, especially in tests with albumin-suspended RBCs (Issitt & Anstee, 1998). The DAT is typically positive with polyspecific and anti-C3 reagents.

In vivo hemolysis is the result of binding of antibody to a patient's RBCs in the peripheral vessels of the extremities, which are cooler (32°C and lower). As the cells recirculate to the body core and warm to 37°C, complement is activated and cells are destroyed. Hemolysis of cells may occur intravascularly but occurs more commonly via extravascular (C3b) pathways by macrophages in the reticuloendothelial system. Hemolysis may be chronic or episodic depending on the thermal range of the antibody and may be triggered by exposure to cold temperatures.

Because anti-I reacts broadly with virtually all adult RBCs, the antibody can cause great difficulty in compatibility testing. As with warm autoantibodies, one of the primary concerns is to detect and identify any potential underlying IgG alloantibodies. Techniques to circumvent the autoanti-I in serum testing may include prewarming, cold autoadsorption, adsorption with REST, or treatment of the serum with sulfhydryl reagents such as DTT or 2-ME (see Special Antibody Identification Techniques section).

Anti-i and anti-Pr are two additional specificities associated with CAD. Anti-i can be observed in patients with infectious mononucleosis and certain lymphoproliferative disorders. Up to 10% to 20% of patients with infectious mononucleosis will have elevated cold agglutinin titers; however, few will actually develop clinical hemolysis (Eder, 2005; Cooling, 2010). Anti-i is usually an IgM, reacting more strongly with cord cells than with adult cells. Distinguishing anti-i from anti-I may require titrating patient sera with group O adult and cord red cells at 4°C, 24°C, and 37°C (Fung, 2017).

Anti-Pr specificities may initially react similarly to anti-I but may be differentiated by equally strong reactions with cord and adult RBCs (Table 36.42). In addition, anti-Pr is sensitive to trypsin and ficin and is nonreactive with enzyme-treated red cells, unlike anti-I and anti-i, which are enhanced by enzyme treatment. It is believed that anti-Pr recognizes

TABLE 36.41
Differentiating Characteristics of Cold Red Cell Autoagglutinins

Antibody Specificity	Clinical Significance	IAT Antibody Screen*	Ig Class	RELATIVE REACTION STRENGTHS WITH SELECTED RED CELLS AT ROOM TEMPERATURE†				
				O adult	O cord	A_1 adult	A_2 adult	Autologous
I	Acute CAD associated with *Mycoplasma pneumoniae* with antibody titers >1000 at 4°C	Pos	IgM	3+	w+	3+	3+	3+
i	Acute CAD associated with mononucleosis	Pos	IgM	w+	3+	w+	w+	Weaker than O cord
Pr	Rare cause of CAD‡	Pos	Reported cases of IgM, IgA, IgG	3+	3+	3+	3+	3+
P	PCH associated with certain viral infections in children	Neg	IgG§	Negative in routine agglutination tests; autoanti-P is a biphasic hemolysin (Donath-Landsteiner antibody)				
H	Benign except as alloantibody in Bombay phenotype	Weak to neg	IgM	3+	3+	1+	2+	0 to w+
IH	Benign	Weak to neg	IgM	3+	1+	1+	2+	0 to w+

CAD, Cold agglutinin disease; *Ig,* immunoglobulin; *Neg,* negative; *PCH,* paroxysmal cold hemoglobinuria; *Pos,* positive.
*Antigen expression: O adult (I+i– H+s); O cord (I–i+ H+s); A_1 (I+i– H+w); A_2 (I+i– H+).
†Reagent cells showing agglutination in 37°C phase may be much weaker after conversion to indirect antiglobulin test (IAT).
‡May be differentiated from anti-I by enzymes or increasing pH; anti-Pr reactivity is decreased by both techniques.
§Autoanti-P is the only pathologic cold autoantibody known to be routinely of the IgG class to IAT.

TABLE 36.42
Selected Drugs Associated with a Positive DAT and/or Hemolysis Due to Drug-Induced Autoantibodies

Reported Mechanism	Drug
Drug-independent autoantibody induction	Cladribine, fludarabine, levodopa, mefenamic acid, methyldopa, procainamide, checkpoint inhibitors (anti-CTLA4, PD1, PDL-1)
Drug-dependent (reactivity with drug-coated cells)	Aminopyrine, amoxicillin, carbromal, cefamandole, cefazolin, cephalexin, erythromycin, insulin, nafcillin, penicillin, tetracycline, tolbutamide
Drug-dependent (reactivity with uncoated cells)	Acetaminophen, amphotericin B, antazoline, butizide, ceftriaxone, chlorpropamide, diethylstilbestrol, etodolac, 9-hydroxy-methyl-ellipticinium, naproxen, phenacetin, probenecid, propyphenazone, quinine, sodium pentothal, stibophen, sulfamethoxazole, sulfasalazine, trimethoprim
Nonimmunologic protein adsorption	Clavulanate potassium, diglycoaldehyde, sulbactam sodium, suramin, tazobactam sodium
Combination mechanisms	Ampicillin, carbimazole, carboplatin, cefixime, cefotaxime, cefotetan, cefoxitin, ceftazidime, ceftizoxime, cephalothin, chlorinated hydrocarbons, chlorpromazine, cisplatin, cyanidanol, diclofenac, dipyrone, fenoprofen, fluorescein, hydrochlorothiazide, isoniazid, mefloquine, methotrexate, nomifensine, oxaliplatin, piperacillin, quinidine, ranitidine, rifampicin, streptomycin, sulindac, suprofen, teicoplanin, teniposide, ticarcillin, tolmetin, triamterene, zomepirac

DAT, Direct antiglobulin test.
Data from Fung M, editor: *Technical Manual*, ed 19, Bethesda, MD, 2017, American Association of Blood Banks.

O-linked sialic acid residues on glycophorin A and B (Issitt & Anstee, 1998; Cooling, 2010, 2015). Anti-Pr in patients with severe CAD is usually monoclonal and may be IgG, IgM, or IgA (Issitt & Anstee, 1998).

Paroxysmal Cold Hemoglobinuria

PCH is an autoimmune hemolytic syndrome most often seen in children 1 to 3 weeks following an upper respiratory or gastrointestinal infection (Cooling, 2017). Historically, PCH was also seen in syphilitic patients. It can present suddenly with severe hemolysis with an initial hemoglobin of <7 g/dL and reticulocytopenia. In addition to laboratory findings of intravascular hemolysis, PCH patients may have erythrophagocytosis on peripheral blood smear. The latter is highly unusual and should trigger an investigation for possible PCH (Eder, 2005; Cooling, 2017).

Autoanti-P, also known as the Donath-Landsteiner (DL) antibody, is the most common causative antibody in PCH although unusual cases with anti-I, i HI and Pr are known (Cooling, 2017). DL autoantibodies are an IgG, biphasic autohemolysin capable of binding to RBCs at cold temperatures and causing intravascular hemolysis of those cells at body temperature (see Table 36.41). This characteristic can be demonstrated in vitro by the diagnostic DL procedure to aid in the confirmation of PCH. In this test, three sets of tubes containing patient serum and group O cells are incubated—one at 4°C followed by 37°C, one only at 4°C, and one only at 37°C. If the first set shows hemolysis but the other two do not, this indicates the presence of the biphasic hemolysin characteristic of PCH. The DL test requires that a fresh blood sample be used to ensure that an adequate supply of complement is available, because complement is relatively unstable and deteriorates during storage. The sample should be drawn and immediately stored at 37°C until clot formation. It is also important not to draw the blood into an anticoagulant such as EDTA because chelation of calcium ions will prevent complement activation and, thus, in vitro hemolysis.

Because the autoantibody in PCH rarely reacts above 4°C in vitro, routine antibody detection tests are usually negative and crossmatches are compatible. Patient RBCs sensitized by the DL antibody will most commonly give a positive DAT with polyspecific and anti-C3 only. In addition, the DAT is positive only during or immediately after an episode of hemolysis (Eder, 2005). Because the antibody dissociates easily from RBCs during washing, the DAT is usually negative with anti-IgG. IgG may be detected, however, if the cells are washed with cold saline and tested with cold anti-IgG reagent (Fung, 2017).

Because the antibody is biphasic, many clinicians recommend keeping the patient warm and utilizing a blood warmer for transfusion. Although PCH is due to an autoanti-P, it is not necessary to transfuse the patient with rare P-negative red cells. Most patients will have an acceptable transfusion response with routine allogeneic red cells (Eder, 2005; Cooling, 2017).

Mixed-Type AIHA. A "mixed" AIHA occurs in less than 10% of patients and is characterized by the presence of warm and cold autoantibodies (Eder, 2005). The DAT is usually positive with both C3 and IgG, and the patient's serum will react in all phases of testing (at room temperature and at 37°C) in the IAT. The cold-reactive antibody is typically anti-I or anti-i, and the warm-reactive antibody is typically a 37°C reactive IgG autoantibody. To adsorb autoantibody in a mixed AIHA, the sample is sequentially adsorbed at 37°C to adsorb warm-reactive autoantibody followed by incubation in an ice bath for 30 minutes to adsorb cold-reactive antibody. Clinically, mixed AIHA usually is similar to WAIHA, although some patients may have symptoms of both WAIHA and CAD.

POSITIVE DIRECT ANTIGLOBULIN TESTS AND HEMOLYTIC ANEMIA INDUCED BY MEDICATION

At this time, more than 130 drugs have been implicated in drug-induced hemolytic anemia, with an incidence of 1 in 1 to 2 million individuals (Salama, 2009). An even larger number of therapeutic drugs can be associated with a positive DAT (see Table 36.42). It is also well documented that a positive DAT may be produced in patients receiving high-dose intravenous gammaglobulin therapy, owing to passively acquired specific blood group antibodies, as well as nonspecific binding to RBCs by IgG dimers and aggregates in the gammaglobulin preparation (Knezevic-Maramica & Kruskall, 2003). Several theories regarding the immunologic process underlying drug-induced antibodies have been put forth, many of which remain unproven. Moreover, some drugs appear to work by more than one mechanism, further complicating the picture. An example of the latter is the group of cephalosporins, which now account for 93% of drug-induced hemolysis (Garratty, 2004).

Historically, drug-induced hemolytic anemia has been subclassified into four types based on its serologic characteristics. Drug-independent antibodies do not require the addition of drug into the test system for detection, even though the drug is responsible for inducing hemolytic anemia. Drug-dependent antibodies, on the other hand, require the presence of the drug for serologic reactivity. Drug-dependent antibodies can be subclassified into two types, depending on whether antibody reactivity requires drug-coated red cells or simply the presence of drug in serum. Antibody reactivity against drug-coated red cells appears to be directed against the drug itself. Alternatively, reactivity observed after concurrent incubation of red cells, serum, and free drug is believed to reflect immune complex formation between drug and "antidrug" antibody. Finally, nonimmunologic protein adsorption proposes that a change in the red cell membrane causes immunoglobulins and other plasma proteins to be adsorbed nonspecifically to the red cell membrane.

A unifying model has been suggested that may be applicable to many different drugs thought to be operating via the mechanisms mentioned previously (Garratty, 2004). The hypothesis suggests that the immune process is initiated by a primary interaction between RBCs and the drug or its metabolites, even though the drug may be only loosely bound to RBCs in vivo. This provides the composite determinants (or neoantigen) necessary for production of drug-dependent antibodies, as in the drug adsorption and immune complex mechanisms, or of drug-independent autoantibodies that recognize subtle alterations in the RBC membrane.

STIMULATION OF RED CELL AUTOANTIBODY PRODUCTION

Drug-Induced Immune Hemolytic Anemia (DIIHA)

Rarely, individuals develop antibodies after receiving therapeutic drugs. There are at least 130 drugs that have been described in the literature associated with DIIHA. The DAT may be positive with IgG and/or C3. The antibodies are classified into four types: drug-dependent (two subtypes), drug-independent, and nonimmunologic protein adsorption.

Drug-Independent Autoantibodies

Drug-independent autoantibodies can be detected without the presence or addition of the drug to the test system. The best-known example is methyldopa (Aldomet), a hypertensive drug still used in obstetrics. About 20% of hypertensive patients who receive methyldopa for longer than 3 to 6 months will eventually develop a positive DAT, but only 0.8% will develop hemolytic anemia (Petz, 1993). The DAT gradually becomes negative after stopping methyldopa treatment, although it may take months to longer than 2 years. About 10% of patients with Parkinson disease receiving L-dopa, a closely related drug, develop RBC autoantibodies, but these rarely result in overt hemolysis (Petz, 1993).

Checkpoint inhibitors are also associated with autoantibodies and WAIHA due to immune dysregulation (Davis et al., 2019; Cooling et al., 2017). Checkpoint inhibitors are newer antineoplastic agents that enhance the immune system's response to cancer by inhibiting proteins necessary for maintaining self-tolerance (CTLA4-B7, PD-1/PDL-1). Not surprisingly, checkpoint inhibitors are commonly associated with autoimmune side effects, including WAIHA, idiopathic autoimmune thrombocytopenia (ITP), hemophagocytic lymphohistiocytosis, and pure red cell aplasia. WAIHA tends to arise after 2 to 4 drug cycles and is more common with anti-PD1/PDL-1 drugs (Davis et al., 2019). Discontinuing drugs and steroids is effective in the majority of cases.

Serologically, autoantibodies eluted from RBCs or free in the serum are indistinguishable from autoantibodies found in patients with idiopathic WAIHA. The antibodies are usually of the IgG class, with both κ and λ light chains, and many show Rh specificity. Drug-independent antibodies may be found alone as warm autoantibodies (methyldopa, procainamide, and fludarabine) or in combination with drug-dependent antibodies (cefotetan).

Drug-Dependent Autoantibodies (Two Types)

Reactivity with Drug-Coated Cells

About 3% of patients receiving large doses of penicillin intravenously (>10 × 10^6 IU/day) develop a positive DAT, although only a few of these patients will have hemolytic anemia (Salama, 2009). Breakdown products of benzyl penicillin exhibit a high binding affinity for the RBC membrane, which results in the formation of haptenic benzylpenicilloyl determinants. Certain patients can form high-titered antibodies against penicillin metabolites and, to a lesser extent, red cell membrane components. The resulting antibody–drug–RBC complex yields a positive DAT with IgG and sometimes with anti-C3. The DAT becomes negative again within days to several weeks after discontinuing penicillin. Both the patient's serum and eluates prepared from the patient's RBCs usually react only with penicillin-coated RBCs by in vitro testing.

Penicillin antibodies may consist of IgM or IgG. IgM antibodies are very common if a sensitive method is used for detection. Those antibodies associated with immune hemolytic anemia are usually of IgG isotype (Salama, 2009). Hemolysis occurs usually through extravascular destruction mediated by cells of the RE system, although rare cases of complement-mediated intravascular hemolysis have been reported. Several cases of acquired hemolytic anemia have also been reported in association with cephalosporins through a mechanism similar to that of penicillin (Garratty, 2004; Salama, 2009).

Reactivity with Uncoated Cells

A wide variety of drugs may cause hemolytic anemia via the so-called immune complex mechanism (see Table 36.42). In the unifying concept, these drugs loosely bind to the RBC membrane with subsequent formation of antibodies reacting with both drug and membrane components. The cell–drug–antibody complex then may stimulate activation of the complement cascade. Drugs acting by this mechanism most often are associated with episodes of acute intravascular hemolysis with hemoglobinemia and hemoglobinuria that may prove fatal (Petz, 1993). The DAT in these cases is usually positive with anti-C3d only. The antibodies implicated may be IgM or IgG (Fung, 2017). They can be detected only in test systems in which serum/eluate, test cells, and free drug are all present simultaneously. Although the mechanism leading to antibody production may be similar to that of so-called drug adsorption, the drugs in this category are classified separately primarily by the DAT result (C3d+) and characteristic severe intravascular hemolysis.

Nonimmunologic Adsorption of Serum Proteins

Patients taking high-dose cephalothin (6–14 g/day) for prolonged periods have been reported to develop a positive DAT, with a frequency ranging widely from 3% to 81% (Garratty, 2004). Hemolysis is rarely, if ever, associated with the phenomenon (Fung, 2017). It was subsequently shown that RBCs exposed to cephalothin in vitro are able to nonspecifically adsorb plasma and serum proteins (albumin, Igs, complement). In the case of some cephalosporins, a decrease in CD55 and CD58 can be documented (Garratty, 2004). These proteins can be detected by polyspecific AHG sera in the DAT. It has been hypothesized that adsorption occurs because of a change in erythrocyte membrane properties induced by cephalothin and other drugs.

GRANULOCYTE SEROLOGY

HUMAN NEUTROPHIL ANTIGENS

Five human neutrophil antigen (HNA) systems are currently recognized by the International Society for Blood Transfusion (Table 36.43). Antibodies against HNA have been associated with rare cases of neonatal alloimmune neutropenia, autoimmune neutropenia, and transfusion reactions, particularly TRALI. In allogeneic stem cell transplantation, case reports have implicated HNA antibodies in delayed myeloid engraftment (Stroncek et al., 1993; Pocock et al., 2001). HNA antibodies can also lead to positive lymphocyte crossmatches in solid-organ transplantation and may play a role in transplant outcomes (Key et al., 2018).

TABLE 36.43
Human Neutrophil Antigen (HNA) Systems

ISBT System	Historical Names	No. Antigens	Gene Name	Chromosome Location	Gene Product
HNA-1	NA1/2, SH, CD16b, FCRIIIb	4	*FCGR3B*	1q23.3	Low affinity Fcγ receptor, GPI-linked
HNA-2	NB1, CD177, PVR-1	1	*CD177*	19q13.3	Binds proteinase 3 (PR3), GPI-linked
HNA-3	5[b], CTL2	2	*SLC44A2*	19p31.3	Choline transporter
HNA-4	Mart[a], CR3 CD11b/α_M	2	*ITGAM*	16p11.2	CD11b/CD18 β2 integrin
HNA-5	Ond[a], CD11a, $a_L\beta2$, LFA-1	1	*ITGAL*	16p11.2	CD11a/CD18 β2 integrin

GPI, Glycophosphoinositol-linked glycoprotein.

In general, antibodies to HNA antigens are uncommon. In healthy blood donors, HNA-specific alloantibodies can be detected in 0.3% to 2.0% of donors (Toy et al., 2014; Schulz et al., 2014). Individuals with HNA alloantibodies are more likely to be female and demonstrate HLA alloimmunization (Gotschall et al., 2013).

HNA-1 System

HNA-1, historically known as NA (neutrophil antigen 1 and 2), was the first neutrophil alloantigen identified. The system currently possesses four alloantigens: 1a (NA1), 1b (NA2), 1c (SH), and 1d (Bux, 2008; Flesch & Reil, 2018). Both HNA-1a and HNA-1b are common antigens with some variation in relative frequencies between ethnic populations (Table 36.44). HNA-1b is prevalent in both whites (89%) and blacks (78%–84%), with lower expression in Asians (53%), who have higher expression of HNA-1 (90%). HNA-1c can be found in 30% of blacks, 5% of whites, and <1% of Asians. HNA-1 null phenotype is rare in all populations, with the highest incidence in blacks (1%–4%). HNA-1 is also absent in PNHIII. HNA-1 antibodies are detected by most assays except granulocyte agglutination.

HNA-1 is located on the low-affinity Fcγ receptor IIIb (FcγRIIIb; CD16b) and is one of the most prevalent molecules expressed on neutrophils (100,000–200,000 per neutrophil) (Wang & Jonson, 2019). A member of the immunoglobulin superfamily, CD16b is a 233 amino acid, GPI-linked glycoprotein ranging in size from 50 to 80 kDa. The large extracellular domain consists of 2 folded IgG domains and 4 to 6 potential N-glycans. In the resting neutrophil, CD16b is evenly distributed across the membrane. Upon neutrophil activation, however, CD16b localizes to lipid rafts, where it may be associated with FcγRIIa, CD177 (HNA-2), and β2-integrins (HNA-4, HNA-5) (Flesch & Reil, 2018; Wang & Jonson, 2019). FcγRIIIa also exists in soluble form.

The gene for CD16b/FcγRIIIb (*FCGR3B*) is located on chromosome 1q23 within a cluster of five Fc-receptor genes: *FCGR2A*, *FCGR2B*, *FCGR2C*, *FCGR3B* and *FCGR3A* (CD16A). The genes share significant homology and are prone to nonallelic homologous recombination, leading to copy number variation (CNV) (Nagelkerke et al., 2015). Furthermore, the recombination tends to occur at discrete locations, leading to linkage disequilibrium and specific CNV haplotypes involving more than one gene (e.g., *FCGRB3-FCGR2C* haplotype). *FCGRB3* CNV ranges from 0 to 4 copies between individuals. *FCGRB3* mRNA levels correlate with copy number (Recke et al., 2015).

FCGR3B possesses 5 exons although only exons 3 to 5 encode the mature protein (Bertrand et al., 2004). HNA alloantigens (1a–1d) are located within exon 3, which encodes the first IgG domain. As shown in Table 36.45, polymorphisms in two amino acids (Arg36Ser, Asn65Ser) differentiate HNA-1a and HNA-1b. HNA-1c and HNA-1d are antithetical antigens (Ala78Asp) and occur on the background of HNA-1b with an additional change at Asp82Asn. One study has reported higher mRNA levels with HNA-1b/-1c alleles (Recke et al., 2015). An HLA-1 null allele (*FCGR3B*null*) is the result of a premature stop codon (Bertrand et al., 2004). Because it is a GPI-linked glycoprotein, HNA-1 is lacking on PNH cells.

HNA-1 is the most common alloantibody specificity in neonatal alloimmune neutropenia (>70%) and is identified in 30% of patients with autoimmune neutropenia (Conway et al., 1987; Bux et al., 1998). Antibody testing can be particularly challenging for HNA-1. Because HNA-1 is an Fc receptor, nonspecific binding can confuse test results in some assays. To control for nonspecific Fc binding, some laboratories include a monoclonal antibody that interferes with Fc binding (Yasui et al., 2007). *FCGR3B* CNV also impacts the sensitivity of whole cell–based assays, which require use of fresh donated neutrophils from typed donors.

TABLE 36.44
HNA Phenotype Frequencies

HNA Phenotype	Whites	Africans	Asians	Amerindians
HNA-1a+	57–62	46–66	88–91	83–91
HNA-1b+	88–89	78–84	51–54	36–80
HNA-1c+	5	23–38	<1	0–1
HNA-1d+	3	–	–	–
HNA-1null	<1	1–4	<1	<1
HNA-2a+	87–97	98	89–99	–
HNA-2null	3	–	–	–
HNA-3a+	89–97	>99	99	100
HNA-3b+	31–41	13	13–51	0
HNA-4a+	99	–	>99	>99
HNA-4b+	21	–	<1	<1
HNA-5a+	86–92	65	65–94	59–97
HNA-5b+	49	35	31–35	14–41

–, No published data available.
Data from Bux J: Human neutrophil alloantigens, *Vox Sang* 94: 277–285, 2008; Cardone JD, Bordin JO, Chiba AK, et al.: Gene frequencies of the HNA-4a and -5a neutrophil antigens in Brazilian persons and a new polymerase chain reaction-restriction length polymorphism method for HNA-5a genotyping, *Transfusion* 46:1515–1520, 2006; Changsri K, Tobunluepop P, Songthammawat D, et al.: Human neutrophil alloantigen frequencies in Thai blood donors, *Blood Transfus* 12:286–291, 2014; Flesch BK, Reil A: Molecular genetics of the human neutrophil antigens, *Transfus Med Hemother* 45:300–309, 2018; Hajar CGH, Zulkafli Z, Riffin NS, et al.: Human neutrophil antigen frequency data for Malays, Chinese and Indians, *Trans Apher Sci*, 59:102651, 2020; Huvard MJ, Schmid P, Stroncek DF, Flegel WA: Frequencies of SLC44A2 alleles encoding human neutrophil anti-3 variants in the African American population, *Transfusion* 52:1105–1111, 2012; Lopes LB, Baleotti W, Suzuki RB, et al.: HNA-3 gene frequency and a new polymerase chain reaction-restriction fragment length polymorphism method for HNA-3a/b genotyping, *Transfusion* 54:1619–1621, 2014; Portegys J, Rink G, Bloos P, et al.: Towards a regional registry of extended typed blood donors: molecular typing for blood group, platelet and granulocyte antigens, *Transf Med Hemotherapy* 45:331–340, 2018.

Clinically, FcγRIIIb/CD16b captures and clears immune complexes without provoking neutrophil activation (Wang & Jonson, 2019). One hypothesis is that it may act to scavenge immune complexes from binding other Fc-receptors. Whether it plays any role in neutrophil activation is still unclear. There are data to indicate that it participates in intracellular calcium mobilization, cell adhesion, and degranulation although others have attributed the activity to the related receptor RcγRIIIa. A recent study found a correlation between *FCGR3B* copy number and the respiratory burst (Recke et al., 2015). A few studies have examined neutrophil function by HNA allotype. HNA-1b has been associated with increased mRNA levels and respiratory burst (Recke et al., 2015), decreased phagocytosis, and decreased responsiveness to intravenous immunoglobulin (IVIg) in Kawasaki disease (Wang & Jonson, 2019). In general, *FCGR3B* CNV is not associated with autoimmune disease, unlike related *FCGR2/3* genes (Recke et al., 2015; Wang & Jonson, 2019).

HNA-2 System

The HNA-2 system was discovered in 1971 and contains a single high-incidence antigen, HNA-2a (NB1) or CD177 (Flesch & Reil, 2018). HNA-2a is expressed by 87% to 97% of whites, 89% to 99% of Asians, and 98% of blacks (see Table 36.44). HNA-2a is defined by the presence or absence of CD177 on neutrophils. Interestingly, CD177 is expressed on only a subset of neutrophils, which varies significantly between individuals

TABLE 36.45

HNA-1 Antigens and Alleles

Antigen(s)	Allele	Amino Acid Polymorphism				
HNA-1a	*FCGR3B*01*	36Arg	65Asn	78Ala	82Asp	106Val
	*FCGR3B*04*	36Arg	65Asn	78Ala	82Asp	106Ile
HNA-1b	*FCGR3B*05*	36Ser	65Ser	78Ala	82Asp	106Ile
HNA-1b,1c	*FCGR3B*02*	36Ser	65Ser	78Asp	82Asn	106Ile
HNA-1b,1d	*FCGR3B*03*	36Ser	65Ser	78Ala	82Asn	106Ile
HNA-1null	*FCGR3B*null*	Tyr89stop				
HNA-2null	*CD177*	242stop				
HNA-3a	*SLC44A2*01*	151Leu	152Arg			
HNA-3a	*SLC44A2*03*	151Phe	152Arg			
HNA-3b	*SLC44A2*02*	151Leu	152Gln			
HNA-4a	*ITGAM*01*	Arg61				
HNA-4b	*ITGAM*02*	His61				
HNA-5a	*ITGAL*01*	Arg766				
	*ITGAL*02*	Thr766				

Data from Flesch BK, Reil A: Molecular genetics of the human neutrophil antigens, *Transfus Med Hemother* 45:300–309, 2018; and Bertrand G, Duprat E, Lefranc M-P, Marti J, Coste J: Characterization of human FCGR3B*02 (HNA-1b, NA2) cDNAs and IMGT standardized description of FCGR3B alleles, *Tissue Antigens* 64:119–131, 2018.

(1%–99% of neutrophils). In general, women have a higher number of positive neutrophils (49%–59%) than men (43%), suggesting upregulation by estrogen (Stroncek et al., 2004). CD177 can also be found in neutrophil secondary granules with increased expression upon neutrophil activation, infection, and cytokines (G-CSF). CD177 is overexpressed on neutrophils in patients with polycythemia vera as the antigen PRV-1 (Stroncek et al., 2004). In addition to neutrophils, CD177 is expressed only by mature neutrophils and metamyelocytes but not earlier myeloid precursors. CD177 is a GPI-linked glycoprotein and is absent in PNH. CD177 expression can also be lost in CML (Stroncek et al., 2004).

CD177 is transcribed as a 437 amino acid protein, which includes a 21 amino acid signaling domain. The mature protein is a 56- to 64-kD, 416 amino acid GPI-linked glycoprotein with three potential N-glycans. CD177 is located within lipid rafts, possibly in association with CD11b/CD18 (HNA-4) and FcγRIIIb (HNA-1) (Flesch & Reil, 2018). CD177 also binds membrane-associated protein 3 (PR3). This association has led to false positives in testing due to anti-PR3 (ANCA) antibodies (Bayat et al., 2009).

The gene for CD177 is located on chromosome 19q13.31 and is highly polymorphic. An SNP located within the 21 amino acid signaling domain influences the size of the CD177-positive subpopulation (Stroncek et al., 2004). An additional five SNPs may also influence CD177 expression. CD177 expression is also likely regulated by epigenetic factors. Evidence for the latter includes the absence of CD177 in most CML patients. More importantly, in CD177-positive donors, stimulation with G-CSF selectively increases expression only in the CD177-positive neutrophil subpopulation (Stroncek et al., 2004). Recent studies have identified differential methylation and monoallelic silencing among neutrophil subsets (Flesch & Reil, 2018).

The CD177-negative phenotype occurs in 3% of whites, 5% of blacks and 1% to 11% of Asians (Flesch & Reil, 2018). Several CD177 null alleles have been identified that include splice site mutations, frame shift and nonsense mutations. There is some evidence to suggest that gene conversion involving a CD177 pseudogene can also lead to CD177 null. CD177-negative phenotype can also be seen in heterozygous individuals carrying a null and weak allele (Flesch & Reil, 2018). As noted previously, CD177-null is also seen in PNH and CML (Stroncek et al., 2004).

CD177-null individuals are susceptible to producing isoantibodies following transfusion or pregnancy. To date, no alloantibodies directed against CD177 polymorphisms are reported (Flesch & Reil, 2018). Anti-CD177/HNA-2 can be associated with fetal and neonatal alloimmune thrombocytopenia (FNAIT), autoimmune neutropenia, and prolonged neutropenia following allogeneic stem cell transplantation (Stroncek et al., 1993, 2004; Pocock et al., 2001). In bone marrow transplantation, neutropenia is exacerbated by G-CSF administration, which upregulates CD177 on mature neutrophils (Pocock et al., 2001).

HNA-3 System

The HNA-3 system contains two antithetical antigens, HNA-3a and HNA-3b. HNA-3a is a high-incidence antigen found on 95% to 99% of donors (see Table 36.44). The minor HNA-3b allele is more common among whites (0.17–0.21) and Asians (0.25) than blacks (0.07) (Bux, 2008; Xia et al., 2011; Huvard et al., 2012). Alloantibodies against HNA-3 have been linked to TRALI, especially anti-HNA-3a (Gottschall et al., 2013; Schulz et al., 2017). A preliminary report links anti-HNA-3a to adverse outcomes in kidney transplantation (Key et al., 2018). In five female transplant recipients with anti-HNA-3a, three developed either early rejection or glomerulopathy posttransplant.

HNA-3 antigens reside on choline transporter-like protein 2 (CTL2), a 68- to 72-kDa multipass glycoprotein with 10 transmembrane domains and 2 to 3 N-glycans (Flesch & Reil, 2018). CTL2 exists as two protein isoforms (TV1, TV2), which vary by 10 to 12 amino acids at the amino terminus due to alternate exon usage (Flesch et al., 2013). Limited human studies have shown CTL2 transcripts in neutrophils, platelets, microvascular endothelium, liver, lung, brain, inner ear, and colon (Kommareddi et al., 2010; Flesch et al., 2013). The CTL2-TV1 variant displays choline transport properties whereas the CTL2-TV2 isoform expressed by neutrophils does not (Kommareddi et al., 2010).

The CTL2 gene (*SLC44A2*, solute-like carrier 44A2) is located on chromosome 19p13.1. The gene is large, with 22 exons, including two alternate exon 1. The latter account for the TV1 and TV2 protein isoforms (Flesch et al., 2013). The TV2 isoform expressed by neutrophils utilizes the first upstream exon 1. The HNA-3a/b antigens are determined by an SNP (G445A) leading to Arg152 (HNA-3a, *SLC44A2*01*; see Table 36.45) or Gln152 (HNA-3b, *SLC44A2*02*) in the first extracellular loop (Flesch & Reil, 2018). The HNA-3a antigenicity is altered by changes in the adjacent amino acids (151Phe, *SLC44A*03*). Both TV1 and TV2 protein isoforms express HNA-3 antigens.

Clinically, antibodies against HNA-3a have been associated with severe and fatal cases of TRALI. The pathogenicity of HNA-3 antibodies may reflect the expression of CTL2 on both neutrophils and lung endothelium. HNA-3a antibody binding to endothelium and primed neutrophils is reported to induce the reactive oxygen species (ROS) response and increase neutrophil rigidity (Silliman et al., 2007; Berthold et al., 2015). The latter may promote neutrophil accumulation within the pulmonary microvasculature. Finally, it is hypothesized that antibody binding to CTL2-TV1 on lung could also interfere with choline uptake and surfactant production, further exacerbating lung injury and respiratory distress (Flesch et al., 2013). Interestingly, CTL2 is upregulated by glucocorticoids, which is used to stimulate surfactant production and lung maturation in neonates.

Because CTL2 is a multipass protein, testing for HNA-3a antibodies has proved to be more difficult than for other HNA antigens. Glycoprotein capture techniques commonly used to confirm HNA specificity are

unreliable for testing (see Monoclonal Antibody-Immobilized Granulocyte Antigen [MAIGA] Assay section that follows). Newer commercial beads coated with antigen peptides have better performance but still miss 10% to 60% of HNA-3 antibodies (Schulz et al., 2017). Confirmation of HNA-3 antibodies requires whole-cell assays, which preserve CTL2 membrane presentation. In general, granulocyte agglutination is the most sensitive assay for HNA-3 antibodies (Lucas et al., 2002).

HNA-4 System

The HNA-4 system contains two antithetical antigens, HNA-4a and HNA-4b, on glycoprotein CD11b (αM). HNA-4a, or Mart[a], is a high-incidence antigen (90%–100%) in most populations (Cardone et al., 2006). Antibodies to HNA-4a and HNA-b have been associated with neonatal alloimmune neutropenia. Neutropenia appears dependent on the ability of antibodies (alloantibodies or autoantibodies) to interfere with neutrophil adhesion (Flesch & Reil, 2018).

On leukocytes, CD11b is a heterodimer with CD18 (CD11b/CD18; Mac-1, CR3). The CD11b gene (*ITGAM*) is located on chromosome 16p11.2 and encodes a large 11537 amino acid glycoprotein with a 16 amino acid signal peptide and up to 19 N-glycans. The HNA-4a antigen is the result of an SNP (His66Arg, *ITGAM*01*) (Flesch & Reil, 2018).

HNA-5 System

The HNA-5 system possesses a single antigen, HNA-5a, or Ond[a]. Based on allele frequencies, 59% to 88% of individuals are HNA-5a positive (Cardone et al., 2006). HNA-5a resides on CD11a, which is expressed on all leukocytes as a complex with CD18 (CD11a/CD18; LFA-1). The CD11a gene (*ITGAL*) is located on chromosome 16 and encodes a 1170 amino acid glycoprotein that includes a 25 amino acid signal peptide. The mature molecule is an 1145 amino acid, single-pass glycoprotein with 12 N-glycans and 7 disulfide bonds. Alloantibodies against HNA-5a (Arg766) have been associated with neonatal alloimmune thrombocytopenia and, interestingly, prolonged skin graft survival (Flesch & Reil, 2018). To date, no alloantibodies to the antithetical antigen (Thr766) have been reported. Granulocyte agglutination appears to be the most sensitive for detection of HNA-5b antibodies (Bux, 2008).

GRANULOCYTE ANTIBODY TESTING

Granulocyte antibody assays can be broadly categorized as whole-cell assays and antigen-based assays. Whole-cell assays include the granulocyte agglutination test (GAT), granulocyte immunofluorescence test (GIFT), and flow cytometry. HNA antigen assays include monoclonal antibody immobilized granulocyte antigen (MAIGA), an ELISA-based assay, and bead-based flow cytometric assays. It is generally recommended to perform a minimum of two assays when screening for HNA antibodies (Bux, 2008). Granulocyte antibody testing is not available in most hospital laboratories and requires samples to be sent to a blood center specialty reference laboratory for testing.

Whole-Cell Granulocyte Antibody Assays

Whole-cell assays are the oldest methodology and are still incorporated into most testing algorithms. Because granulocytes are susceptible to rapid degradation with storage, whole-cell assays require a fresh sample and testing within 1 day of sample collection (Mutsuhashi et al., 2014). As a consequence, most testing centers request notification to coordinate sample collection and shipping. This is particularly important when evaluating TRALI transfusion reactions, where it may be necessary to crossmatch donor plasma against patient granulocytes.

Whole-cell assays require granulocyte isolation by gradient density centrifugation. Many granulocyte laboratories will use fresh samples drawn from employees with known HNA types. Whole-cell assays are good for screening but are often limited in their ability to identify specific HNA antibody specificities due to binding by non-HNA antibodies, particularly HLA class I antibodies. Because HLA antibodies are not uncommon, all laboratories include parallel testing for HLA antibody(s) as part of the testing algorithm (Bux, 2008). Immune complexes can also lead to false-positive results due to binding to the FcγRII receptor on granulocytes (Bux et al., 2008). Finally, characterizing HNA specificities requires testing against a cell panel of known HNA types. Since cells must be collected fresh from available donors, this can limit the available HNA types for testing. To address the latter, some laboratories have generated HLA-negative, transfected immortalized cell lines expressing a single HNA antigen for testing panels (Yasui et al., 2007, 2008; Simtong et al., 2018).

Granulocyte Agglutination Test

The GAT is a functional assay for neutrophil-binding IgG antibodies (Mutsuhashi et al., 2014). The assay is dependent on IgG binding and activation of neutrophils, with pseudopod formation, neutrophil migration and agglutination. To perform the assay, isolated neutrophils are incubated with patient serum in microtiter wells for 2 to 5 hours. Agglutination is assessed by reading plates with an inverted phase contrast microscope. Results are semiquantitative based on the relative percent of clustered neutrophils: 1+ (25%); 2+ (50%); 3+ (75%) and 4+ (~100%). GAT is the most consistent method for detecting HNA-3 antibodies. HNA-1 antibodies are generally unreactive in the GAT (Lucas et al., 2002).

Granulocyte Immunofluorescence Test

The GIFT has more applications than the GAT assay. The test is an indirect immunofluorescence test and can be used to screen for neutrophil autoantibodies and alloantibodies of IgG or IgM isotype. After brief fixation (<5 minutes, 1% paraformaldehyde), granulocytes are incubated with patient plasma, followed by incubation with a secondary fluorescent-labeled, antihuman (IgG, IgM) and examination under a fluorescent microscope (Mutsuhashi et al., 2014). GIFT can be used for HNA antibody screening or HNA typing. It can also be modified to look for neutrophil-bound antibody on circulating granulocytes in patients with suspected autoimmune neutropenia. Like the GAT, determining specific HNA specificities requires testing against a cell panel of known HNA phenotypes. The GIFT is the most consistent method for detecting HNA-1 antibodies (Lucas et al., 2002).

Flow Cytometry

Flow cytometry has been utilized to evaluate autoimmune neutropenia and to screen for neutrophil alloimmune antibodies. As with the GIFT, flow cytometry can test for neutrophil antibodies of IgG, IgM, and IgA isotypes. One study found that patients with autoimmune neutropenia could be positive for IgG (40%–60% of patients), IgM (42%–69%) and IgA (38%–48%) (Hwang et al., 2011). One caveat with flow cytometric immunofluorescence testing is the need to establish both age- and sex-based normal ranges, especially when evaluating autoimmune neutropenia (Hwang et al., 2011).

MONOCLONAL ANTIBODY-IMMOBILIZED GRANULOCYTE ANTIGEN (MAIGA) ASSAY

The MAIGA assay remains the gold standard test for identification of HNA-specific alloantibodies. Like whole-cell assays, HNA-typed granulocytes or cell lines expressing HNA antigens are necessary to perform the test (Mutsuhashi et al., 2014). Broadly speaking, the MAIGA is essentially an antigen capture immunoassay (see Chapter 45) involving both a murine monoclonal antibody to capture specific granulocyte glycoproteins and a labeled goat antihuman IgG antibody to detect human antibody–glycoprotein complexes. The test is cumbersome and time-consuming, requiring 6 to 8 hours to complete.

In the MAIGA, patient serum is incubated with fixed neutrophils or transfected cell lines in microtiter wells or microcentrifuge tubes (Mutsuhashi et al., 2014; Simtong et al., 2018). After washing, neutrophils are then incubated with a panel of murine monoclonal antibodies directed against specific neutrophil glycoproteins (e.g., anti-CD16b). To release neutrophil proteins, cells are incubated with a mild detergent, sonicated, and centrifuged to produce a supernatant containing solubilized neutrophil glycoprotein-antibody conjugates. The latter is pipetted into individual microtiter wells coated with antimouse immunoglobulin, which will "capture" glycoprotein–monoclonal antibody complexes. To detect the presence of HNA-specific antibody binding, wells are incubated with a goat antihuman IgG antibody labeled with peroxidase or alkaline phosphatase.

Potential issues when testing by MAIGA is the risk of shared epitopes by human and monoclonal antibodies in the assay. Monoclonal antibodies must be evaluated to ensure that antibody binding does not overlap or sterically block critical HNA epitopes (Simtong et al., 2018). To avoid the latter, some laboratories use two or more antibody clones per glycoprotein in their assays (Mutsuhashi et al., 2014; Schulz et al., 2017). In addition, false-positive HNA-2 reactions have been observed with PR3-ANCA antibodies due to PR3-CD177 interaction (Bayat et al., 2009). In older protocols, false positives also occurred due to human antimouse antibodies (HAMAs) if neutrophils were simultaneously coincubated with human serum and murine monoclonal antibodies. Finally, the MAIGA is not reliable for detecting HNA-3 antibodies: HNA-3/CTL2 protein is a multipass protein that is difficult to solubilize and maintain antigen reactivity.

Bead-Based Antibody Capture Assays

The Japanese have developed an extracted antigen antibody capture assay using latex beads (Onodera et al., 2017). In brief, beads are coated with

murine monoclonal antibodies against neutrophil glycoproteins. Neutrophils or transfectant cell lines are incubated with human sera as before, solubilized, and resulting supernatant incubated with beads to capture specific neutrophil glycoproteins. Detection of human anti-HNA antibodies is determined by flow cytometry.

A multiparameter fluorescent immunoassay (see Chapter 45) is now available for HNA antibody testing and is used for screening by some blood centers as part of their TRALI-mitigation strategies (Schulz et al., 2017). Similar to commercial assays for HLA antibodies, the test uses fluorescently coded beads coated with recombinant HNA antigen peptides. After incubation with patient sera, HNA antibody binding is detected by fluorochrome-labeled antihuman IgG and flow cytometry. The beads are sensitive for antibodies against HNA-1, -2, -4 and -5 but have mixed results for anti-HNA-3 antibodies. Published reports indicate 90% sensitivity for detecting antibodies to HNA-3a but only 30% sensitivity for anti-HNA-3b antibodies (Schulz et al., 2017). Overall, there is a 5% false-positive rate among healthy blood donors. Donors who screen positive are subsequently tested by GAT and/or GIFT assays. The test is validated only for IgG antibodies.

PLATELET SEROLOGY

HUMAN PLATELET ALLOANTIGENS

The ISBT transfusion currently recognizes 35 human platelet antigen (HPA) systems. Platelet glycoproteins (GP) bearing HPA antigens are listed in Table 36.46 (Li, 2016). The fibrinogen receptor GPIIb/IIIa is home to 27 HPA antigens, with 19 located on GPIIIa. Three HPA systems reside on GPIa (CD49b), which plays a role in collagen adhesion (GP1a/IIb; α2β1). Three HPA antigens are located on the von Willebrand Factor (vWF) receptor GPIb/IX. The structure and role of these glycoproteins in platelet function are covered in Chapter 41.

One HPA antigen system (Gov) is located on CD109, which is expressed on a subset of CD34+ stem cells, T-cells, endothelial cells, and activated platelets (Lin et al., 2002). Although absent on resting platelets, CD109 within α-granules is translocated upon platelet activation, numbering approximately 2000 molecules per platelet. Structurally, CD109 is a large 170-kD GPI-linked glycoprotein and is known to express ABH antigens. Anti-Gov antibodies are implicated in platelet refractoriness and fetal thrombocytopenia (Fung, 2017). Because it is a GPI-linked glycoprotein, Gov antibodies can be difficult to detect by some assays (Porcelijn et al., 2020).

As shown in Table 36.47, nearly all HPA antigens characterized to date are the result of a single amino acid polymorphism. The single exception is HPA-14b, which is the result of a three-nucleotide in-frame deletion with loss of amino acid Lys611 in GPIIIa. Three HPA antigens (HPA-3a, -9b, -13b) are sensitive to changes in glycosylation (Zhang et al., 2019; Wihadmadyatami et al., 2015). Data suggest that antibody binding to HPA-3a and -9b may require involvement of a critical O-glycan (Ser847) on GPIIb (Zhang et al., 2019). In ISBT nomenclature, the more common allele in each system is "a" (e.g., HPA-3a) and the infrequent allele is "b." Six systems (HPA-1, -2, -3, -4, -5, -15) are considered biallelic antigens since alloantibodies to both the major (a allele) and minor (b allele) have been identified. The remainder are rare HPA alleles and were usually identified during the investigation of neonatal thrombocytopenia (see later discussion).

Platelet allo- and autoantibodies cause thrombocytopenia through antibody binding, opsonization, and platelet clearance. In addition, antibodies against platelet integrins (GPIIb/IIIa) have been shown to suppress megakaryocytes with apoptosis (Liu et al., 2015).

HPA and Neonatal Alloimmune Thrombocytopenia

Like HDFN, FNAIT is due to maternal alloantibodies against paternally inherited fetal HPA antigens. FNAIT occurs in 1:350 to 1:1000 live births and may occur during a first pregnancy (Fung, 2017). Severe FNAIT, defined as a platelet count <25,000/μL, occurs in 1:10,000 live births and carries a risk for intracranial hemorrhage (Curtis, 2015). Treatment consists of IVIg and platelet transfusion in severely affected infants. Historically, washed maternal platelets were recommended for transfusion support; however, current practice recommends routine donor-derived platelet transfusions (Bakchoul et al., 2014). The latter provide equivalent clinical efficacy and promote faster clearance of maternal alloantibodies.

HPA-1a (Pl^{A1}) is the most common alloantibody specificity encountered in FNAIT (70%–85%), followed by antibodies against HPA-5b (10%–15%) (Curtis, 2015). HPA-1a alloimmunization is strongly associated with HLA class II DRB:03 (DRw52)—nearly 90% of women with demonstrable anti-HPA-1a antibodies are also HLA DRB:03 positive. In addition, HLA DRB:03 is associated with higher mean HPA-1a antibody. In HPA-negative women with negative serology by conventional testing, there is experimental evidence for low-avidity HPA-1a antibodies by surface plasma resonance. Interestingly, these low-avidity alloantibodies are more likely to occur in HLA DRB:03 negative women. At present, testing for low-avidity HPA antibody is not available outside of the research setting.

In tissue culture, HPA-1a alloantibodies have been shown to suppress megakaryocyte generation and promote apoptosis (Liu et al., 2015). Anti-HPA-1a also promote endothelial apoptosis and impair angiogenesis with intracranial hemorrhage in a murine model (Yougbare et al., 2015). It is not known whether other HPA specificities located on CD61/GPIIIa are proapoptotic, although similar results can be induced with CD61 monoclonal antibodies. Finally, HPA-1a antibodies have altered fucosylation when compared with other IgG antibodies (Curtis, 2015). Specifically, they lack a core α1-6 fucose on an N-glycan (Asn297) at the C_2H-C_3H hinge region of the Fc domain (see Fig. 47.1). IgG antibodies lacking this core fucose enhance platelet phagocytosis.

The laboratory evaluation of FNAIT requires HPA genotyping of mother, father, and infant, if available (Fung, 2017; Curtis, 2015). When possible, maternal serum is crossmatched against paternal platelets since HPA can be due to new low-incidence antigens.

HPA and Posttransfusion Purpura

Posttransfusion purpura (PTP) is a very rare complication of transfusion, with an estimated incidence of 1: 50,000 to 100,000 transfusions (Hawkins et al., 2019). Clinically, PTP is characterized by an abrupt severe thrombocytopenia (<10,000/μL), sometimes accompanied by bleeding, 5 to 10 days after transfusion (Fung, 2017). Most PTP patients are women with a prior history of

TABLE 36.46
Platelet Glycoproteins Expressing HPA Antigens

CD No.	Protein	Gene	Chromosome	No. HPA Antigens	Function
CD41	Glycoprotein IIb	*ITGA2B*	17q21.32	8	Complex IIb/IIIa Fibrinogen receptor
CD42a	Glycoprotein IX	*GP9*	3q21.3	1	Complex Ib/IX vWF receptor
CD42b	Glycoprotein Ibα	*GP1BA*	17p13.2	1	Complex Ib/IX
CD42c	Glycoprotein Ibβ	*GP1BB*	22q11.2	1	Complex Ib/IX
CD49b	Glycoprotein Ia	*ITGA2*	5q11.2	3	Complex Ia/IIa Collagen receptor
CD61	Glycoprotein IIIa	*ITGB3*	17q21.31	19	Complex IIb/IIIa
CD109	CD109	*CD109*	6q13	1	TGF-β regulation
CD36	Glycoprotein IV, GPIIIb	*CD36*	7q11.2	1	Scavenger receptor, LDL, thrombospondin binding

LDL, Low-density lipoprotein; *TGF-β,* transforming growth factor-β; *vWF,* von Willebrand factor.
Data from Portegys J, Rink G, Bloos P, et al.: Towards a regional registry of extended typed blood donors: molecular typing for blood group, platelet and granulocyte antigens, *Transf Med Hemotherapy* 45:331–340, 2018; Ouabdelmoumene Z, EL Housse H, Zarati F, et al.: Frequencies of human platelet antigens (HPA-1, -2, -3, -4, and -5) among the Moroccan blood donors, *Int J Blood Transfus Immunohematol* 8: Article 100038Zo2ZO2018, 2018. www.ijbti.com; Pai S-C, Burnouf T, Chen J-W, Lin L-I: Human platelet antigen alleles in 998 Taiwanese blood donors determined by sequence-specific primer polymerase chain reaction, *Biomed Res Internl* Article 973789, 2013, https://doi.org/10.11555/2013/973789; Li R, Yang L, Zeng J, Ling Z, Liang X: Genetic polymorphism of human platelet antigens -1 to -17w in the multi-ethnic Chinese Guangxi population, *Int J Clin Exp Med* 9:12992–12999, 2016.

pregnancy. However, any patient with prior transfusions is at potential risk. PTP is analogous to DHTRs, in which recent transfusion provokes an amnestic alloantibody response in a previously sensitized patient. PTP can be precipitated by platelet transfusion as well as whole blood, red cells, and plasma, which can contain residual platelets or platelet fragments. Preliminary data suggest that leukoreduction of red cells and whole blood may decrease the risk for PTP by decreasing the number of residual platelets in these products (Fung, 2017).

Historically, most cases of PTP were attributed to anti-HPA-1a (Pl^{A1}). In fact, HPA-1a was initially discovered in three female PTP patients. With modern testing techniques, multiple HPA systems have been associated with PTP although antibodies against HPA-1a (33%), HPA-1b (34%), and HPA-5b (16%) still account for most cases (Hawkins et al., 2019). In addition, nearly 25% of PTP patients may have two or more HPA specificities. The latter should not be surprising since multiple HPA antigens are carried by a handful of platelet glycoproteins, especially GPIIIa/CD61. At least one study has examined coinheritance of multiple HPA antigens in GPIIIa (Pai et al., 2013). There is also a high rate of HLA antibody alloimmunization in PTP patients, which can interfere with platelet screening assays.

One conundrum surrounding PTP is the perplexing clearance of autologous platelets, which should be nonreactive with alloantibody. Older theories proposed binding of soluble platelet alloantigen or immune complexes to autologous platelets, thereby rendering them "antigen positive." The more likely explanation is the formation of platelet auto- and alloantibodies

TABLE 36.47

Human Platelet Antigens (HPA)

HPA Antigen	Historical Names	Platelet Glycoprotein	Molecular	Allele	Frequencies	(%)
				White/ European	*Africa/Middle East*	*Asia*
HPA-1a	PL^{A1}, Zw^a	GPIIIa	Leu33	85–98	70–86	>99
HPA-1b	PL^{A2}, Zw^b	GPIIIa	Pro33	2–15	10–29	<1
HPA-2a	Ko^b	GPIb	Thr145	95–99	71–86	60–97
HPA-2b	Ko^a, Sib^a	GPIb	Met 145	1–5	14–29	3–40
HPA-3a	Bak^a, Lek^a	GPIIb	Ile843	62–86	60–70	56–100
HPA-3b	Bak^b	GPIIb	Ser843	15–38	23–45	0–44
HPA-4a	Pen	GPIIIa	Arg143	>99	99	>99
HPA-4b	Yuk	GPIIIa	Gln143	<1	1	<1
HPA-5a	Br, HC	GP1a	Glu505	85–99	73–88	98–99
HPA-5b	Zav	GP1a	Lys505	1–15	12–27	<1–2
HPA-6b	Ca^a, Tu	GPIIIa	Arg489>Glu	<1	<1	2
HPA-7b	Mo^a	GPIIIa	Pro407>Ala	<1	<1	0
HPA-8b	Sr^a	GPIIIa	Arg636>Cys	<1	<1	0
HPA-9b	Max^a	GPIIb	Val837>Met	<1	<1	0
HPA-10b	La^a	GPIIIa	Arg62>Gln	<1	<1	0
HPA-11b	Gro^a	GPIIIa	Arg633>His	<1	<1	0
HPA-12b	Iy^a	GP1bβ	Gly15>Glu	1	–	0
HPA-13b	Sit^a	GPIIIa	Thr799>Met	<1	—	0
HPA-14b	Oe^a	GPIIIa	Lys611del	1	—	0
HPA-15a	Gov^a	CD109	Ser682	45-74	47–70	54–85
HPA-15b	Gov^b	CD109	Tyr682	23-55	30–53	15–46
HPA-16b	Duv^a	GPIIIa	Thr140>Ile	<1	—	<1
HPA-17b	Va^a	GPIIIa	Thr195>Met	<1	—	0
HPA-18b	Cab^a	GPIa	Glu716>His	<1	—	—
HPA-19b	Sta	GPIIIa	Lys137>Glu	<1	—	—
HPA-20b	Kno	GPIIb	Thr619>Met	<1	—	—
HPA-21b	Nos	GPIIIa	Gln628>Lys	<1	—	—
HPA-22b	Sey	GPIIb	Lys164>Thr	<1	—	—
HPA-23b	Hug	GPIIIa	Arg622>Trp	<1	—	—
HPA-24b	Cab^{a+}	GPIIIa	Ser 472>Asn	<1	—	—
HPA-25b	Swi^a	GPIa	Thr1087>Met	<1	—	—
HPA-26b	Sec^a	GPIIIa	Lys580>Asn	<1	—	—
HPA-27b	$Cab3^{a+}$	GPIIb	Leu841>Met	<1	—	—
HPA-28b	War	GPIIb	Val740>Leu	<1	—	—
HPA-29b	Kha^b	GPIIIa	Thr33>Met	<1	—	—
HPA-30b	Lap^a	GPIIb	Gln806>His	<1	—	—
HPA-31b	$Cab4^{b+}$	GPIX	Pro123>Leu	<1	—	—
HPA-32b	Dom^b	GPIIIa	Asn174>Ser	<1	—	—
HPA-33b	Bla	GPIIIa	Asp458>Gly	<1	—	—
HPA-34b	Bzh^a	GPIIIa	Ar91>Trp	<1	—	—
HPA-35b	Efs^a	GPIIIa	Arg479>His	<1	—	—
CD36 null	Nak^a	CD36	Complex	<0.1	2–8	5–10

—, No published data.

Data from Pai S-C, Burnouf T, Chen J-W, Lin L-I: Human platelet antigen alleles in 998 Taiwanese blood donors determined by sequence-specific primer polymerase chain reaction, *Biomed Res Internl* Article 973789, 2013, https://doi.org/10.11555/2013/973789; Li R, Yang L, Zeng J, Ling Z, Liang X: Genetic polymorphism of human platelet antigens -1 to -17w in the multi-ethnic Chinese Guangxi population, *Int J Clin Exp Med* 9:12992–12999, 2016; Ouabdelmoumene Z, EL Housse H, Zarati F, et al: Frequencies of human platelet antigens (HPA-1, -2, -3, -4, and -5) among the Moroccan blood donors, *Int J Blood Transfus Immunohematol* 8: Article 100038Zo2ZO2018, 2018, www.ijbti.com; Portegys J, Rink G, Bloos P, et al.: Towards a regional registry of extended typed blood donors: molecular typing for blood group, platelet and granulocyte antigens, *Transf Med Hemotherapy* 45:331–340, 2018; Londero D, Miani M, Rinaldi C, Totis V, de Angelis V: Extensive human platelet specific antigens typing of blood donors of different geographical origin to manage platelet transfusion in alloimmunized patients: Experience from a transfusion center in Northeastern Italy, *Int J Blood Transfus Immunohematol* 8:4–11, 2018.

during the early anamnestic response (Hawkins et al., 2019). Supporting evidence includes demonstration of weak pan-reactive platelet autoantibodies in acute-phase samples, which become undetectable with platelet recovery. Furthermore, transfusion of HPA-negative platelets is rarely effective, which is also consistent with platelet autoantibody. The same phenomena can be observed during red cell alloimmunization, with many patients exhibiting transient autoreactivity in the early immune response.

Laboratory confirmation of PTP requires HPA genotyping and testing serum for HPA antibodies (Hawkins et al., 2019). Most laboratories also include HLA antibody screening in their testing algorithms. High-dose IVIg (1–2 g/kg total) is the treatment of choice for PTP, with most patients (90%) showing improvement within 2 to 3 days of treatment (Judd, 2016; Hawkins et al., 2019). It is still common practice to administer steroids to these patients despite clear evidence for clinical effectiveness. Prophylactic platelet transfusion is contraindicated and may delay recovery. Platelets should be transfused only for life-threatening bleeding, although it should be recognized that these patients will demonstrate a poor transfusion response and are at risk for severe febrile transfusion reactions. When possible, washed RBCs should be provided for transfusion.

CD36 Deficiency

CD36 deficiency (Nak^a-) occurs in 3% to 10% of Asians and 4% to 8% of Africans and blacks. In contrast, CD36 deficiency is extremely rare among whites. In Asians and blacks, isoantibodies against CD36 must be considered as a cause of FNAIT, PTP, platelet refractoriness, and TRALI (Lee et al., 1999; Nakajima et al., 2008). In Japan, anti-CD36 is the most common cause of PTP due to the prevalence of CD36 deficiency.

CD36 platelet deficiency has two subtypes based on CD36 expression on monocytes (Rac et al., 2007; Lee et al., 1999). Type 1 CD36 deficiency is a true null phenotype with an absence of CD36 on platelets, monocytes, erythroid precursors, and other tissues. Type II deficiency is characterized by the absence of CD34 on platelets but conserved expression on monocytes. There is also an acquired type II CD36 deficiency in myelodysplastic syndrome (Sandes et al., 2012). In one study, 11% of myelodysplastic patients lacked detectable CD36 on platelets despite elevated CD36 on other blood elements. Acquired type II CD36 deficiency was often accompanied by macrothrombocytopenia and dysplastic megakaryocytes.

CD36 is a 78- to 88-kDa, 472 amino acid glycoprotein consisting of a single large extracellular loop anchored at each end by its intracellular amino- and carboxy-termini (Rac et al., 2007). The extracellular domain possesses up to 10 N-glycans and 3 disulfide bonds and is capable of binding thrombospondin, collagen, long-chain fatty acids, oxidized low-density lipoprotein, and apoptotic cells. Functionally, CD36 is a class B scavenger receptor family and plays a role in lipid metabolism and atherosclerosis. CD36 is expressed on platelets, monocytes, macrophages, endothelium, adipose tissue, liver, heart, skeletal muscle, placenta, and spinal cord. CD36 expression on platelets is highly variable between individuals (0–14,000 molecules per platelet) and does not correlate well with monocyte expression (Ghosh et al., 2011).

The CD36 gene is located on chromosome 7q11.2 and contains 15 exons, although only exons 3 to 14 encode the transcribed protein. CD36 displays tissue-specific mRNA isoforms due to alternate promoter and exon usage. The gene is also highly polymorphic between individuals. Genome-wide association studies have identified several quantitative trait loci (QTL) that influence CD36 expression on platelets and monocytes (Sato et al., 2007; Pietka et al., 2014). Several CD36 null mutations have been identified in type I CD36 deficiency (Rac et al., 2007). In blacks, the most common mutation is T1264>G, which leads to a premature stop codon (Tyr325ter). In Japan, the most common null mutation is Pro90>Ser and may introduce a novel O-glycan site. Some cases of type I CD36 deficiency appear to be compound heterozygotes with inheritance of a null allele and a weak CD36 allele (Worrel et al., 2019).

The genetic basis of type II CD36 deficiency is still not understood and likely reflects multiple inherited QTL. In Asians, an SNP located upstream of exon 3 (-132A>G) was associated with low CD36 expression (Xu et al., 2014). One case of type I CD36 deficiency was attributed to inheritance of Tyr325Ter and -132G (Worrel et al., 2019). A recent study identified two SNPs far upstream of the transcription start site that appear to regulate CD36 platelet expression; deletion of the region encompassing both SNPs increased CD36 mRNA nearly 40-fold (Madan et al., 2019). To date, over 30 QTL have been linked to CD36 expression on platelets (Ghosh et al., 2016; Madan et al., 2019). Many of these same QTL are also associated with lipid profiles, underscoring the role of CD36 in metabolism (Ghosh et al., 2016; Love-Gregory et al., 2011).

Autoimmune Thrombocytopenia

Idiopathic autoimmune thrombocytopenia (ITP) is the result of autoantibodies against platelets. ITP is classified as acute, or chronic if thrombocytopenia persists >12 months (Lambert & Gernsheimer, 2017). Acute ITP is more often observed in children, usually following a viral illness. In acute ITP, thrombocytopenia is abrupt and severe, with onset 1 to 3 weeks after infection and resolution within a few months. In contrast, chronic ITP is more common in adults, particularly women, and can occur in the setting of other autoimmune, infectious (e.g., HIV, *H. pylori*), and malignant disorders. In most patients, there is a gradual development of moderately severe thrombocytopenia. First-line treatment consists of steroids, followed by IVIg, IV anti-D in Rh-positive patients, cytotoxic therapy, or newer thrombopoietin agonists. Prophylactic platelet transfusion is ineffective and contraindicated except to treat active bleeding.

The most common autoantibodies identified in ITP are against the major platelet glycoprotein complexes: GPIIb/IIIa, GPIb/IX and GPIa/IIa (Lambert & Gernsheimer, 2017; Al-Samkari et al., 2020). In a recent retrospective study, auto-GPIIb/IIIa and auto-GPIb/IX were identified in 74% and 64% of positive tests, respectively (Al-Samkari et al., 2020). Furthermore, nearly two-thirds of patients had antibodies against multiple platelet glycoproteins. In practice, ITP is a clinical diagnosis and does not require laboratory demonstration of autoplatelet antibodies. This is due to the poor sensitivity and specificity of indirect serum assays, which require high levels of free autoantibody for detection. Current direct assays, which test platelet eluates against isolated platelet glycoproteins, may have better sensitivity (Al-Samkari et al., 2020). In contrast, measuring autoantibody on intact patient platelets using immunofluorescence or radiolabeling can be technically challenging due to low platelet numbers, high nonspecific binding to platelet Fc receptors, and platelet activation with release of immunoglobulin stored in α-granules.

Drug-Induced Thrombocytopenia

Many drugs have been shown to suppress hematopoiesis with thrombocytopenia. Drug-associated immune thrombocytopenia can also occur. A drug-induced ITP has been described in several cancer patients taking checkpoint inhibitors (anti-CTL4, anti-PD1/PDL-1) (Davis et al., 2019). Stimulation of platelet autoantibodies has also been described for gold and procainamide (Rao, 2014). In these examples, autoantibody binding to platelets does not require the presence of drug (drug independent).

Over 70 drugs have been implicated in cases of drug-dependent thrombocytopenia, in which drug must be present for antibody binding to platelets in vitro (Arnold et al., 2103; Rao, 2014). Heparin-induced thrombocytopenia (HIT) is the most common drug associated with an acquired severe thrombocytopenia due to autoantibody against platelet factor 4 (PF4; see Chapter 43 for mechanism and diagnosis). Three anticoagulants against GPIIb/IIIa (abciximab, tirofiban, eptifibatide) directly interact with platelets to provoke thrombocytopenia (Rao, 2014). Likewise, cancer trials using monoclonal CD47, which is also expressed by platelets, have reported thrombocytopenia (Huang et al., 2017).

Most drug-dependent antibodies appear to noncovalently bind platelets with subsequent autoantibody binding. Drug-dependent antibodies against quinidine and quinine have been shown to bind epitopes on GPIIIa and GPIb/IX (Peterson et al., 2008). Other well-established drug-dependent antibodies include several antibiotics (vancomycin, Bactrim, penicillin, rifampin, ceftriaxone, suramin), ibuprofen, and oxaliplatin (Arnold et al., 2013). Laboratory investigation of drug-dependent antibodies is available in only a few specialty laboratories.

Platelet Antibody Testing

Whole Platelet Assays

Platelet immunofluorescence/flow cytometry is performed to screen for platelet alloantibodies, especially during the workup of FNAIT. In FNAIT, maternal serum is incubated against paternal platelets to screen for maternal-fetal incompatibility (Curtis, 2015). Many reference laboratories also include a flow cytometric screen of patient serum against donor platelets in the evaluation of platelet refractoriness and PTP. The assay is nonspecific and can be positive due to HLA and ABO antibodies. As discussed earlier, flow cytometry to assess platelet-associated IgG in ITP is technically challenging and is not considered necessary for diagnosis.

Antigen Capture Assays

Monoclonal antibody immobilization of platelet antigens (MAIPA) has been a gold standard assay for the identification of platelet alloantibodies and is similar to the MAIGA assay. Commercial microplate assays and bead arrays with bound platelet glycoproteins of known HPA types are available (Porcelijn et al., 2020). The test can be modified in ITP by testing platelet eluates (Al-Samkari et al., 2020).

SELECTED REFERENCES

Daniels G: *Human blood groups*, ed 3, Oxford, 2013, Blackwell Science.

Summarizes each blood group system, including serology, biochemistry, and molecular basis for the major blood group antigen systems.

Friedman BA, Oberman HA, Chadwick AR, et al.: The maximum surgical blood order schedule and surgical blood use in the United States, *Transfusion* 16:380–387, 1976.

The historical standard for the design, use, and implementation of the MSBOS for blood ordering.

Fung M, editor: *Technical manual*, ed 19, Bethesda, MD, 2017, American Association of Blood Banks.

Techniques and policies for the collection, processing, testing, and dispensing of blood components.

Gammon R: *Standards for blood banks and transfusion services (Committee Chair)*, ed 32, Bethesda, MD, 2020, American Association of Blood Banks.

Issitt PD, Anstee DJ: *Applied blood group serology*, ed 4, Durham, NC, 1998, Montgomery Scientific Publications.

A comprehensive text detailing the history, serology, disease associations, and possible biological roles of blood group antigens and antibodies.

Reid RE, Lomas-Francis C: *The blood group antigen facts book*, ed 3, San Diego, 2012, Academic Press.

A succinct listing of the required serologic and molecular testing for each blood group antibody and antigen.

Access the complete reference list online at Elsevier eBooks for Practicing Clinicians.

REFERENCES

Afenyi-Annan A, Kail M, Combs MR, et al.: Lack of Duffy antigen expression is associated with organ damage in patients with sickle cell disease, *Transfusion* 48:917–924, 2008.

Agre P, Smith BL, Baumgarten R, et al.: Human red cell aquaporin CHIP: expression during normal fetal development and in a novel form of congenital dyserythropoietic anemia, *J Clin Invest* 94:1050–1058, 1994.

Al-Faris L, Al-Humood S, Behbehani F, Sallam H: Altered expression pattern of CD55 and CD59 on red blood cells in anemia of chronic disease, *Med Princ Pract* 26:516–522, 2017.

Al-Samkari H, Rosovsky RP, Leaf RSK, et al.: A modern reassessment of glycoprotein-specific direct platelet autoantibody testing in immune thrombocytopenia, *Blood Adv* 4:9–18, 2020.

An X, Mohandas N: Disorders of red cell membrane, *Br J Haematol* 141:367–375, 2008.

Ansart-Pirenne H, Asso-Bonnet M, Le Pennec P-Y, et al.: RhD variants in Caucasians: Consequences for checking clinically relevant alleles, *Transfusion* 44:1282–1286, 2004.

Arnaud L, Helias V, Menanteau C, et al.: A functional allele of aquaporin-1 mimics a Colton-null phenotype [Abstract], *Transfusion* 48S:13A, 2008.

Arndt PA, Garratty G: A retrospective analysis of the value of monocyte monolayer assay results for predicting the clinical significance of blood group alloantibodies, *Transfusion* 44:1273–1281, 2004.

Arnold DM, Kukaswadia S, Nazi I, et al.: A systematic evaluation of laboratory testing for drug-induced immune thrombocytopenia, *J Thromb Haemost* 11:169–176, 2013.

Auf der Maur C, Hodel M, Nydegger UE, et al.: Age dependency of ABO histo-blood group antibodies: Reexamination of an old dogma, *Transfusion* 33:915–918, 1993.

Avent ND: The rhesus blood group system: Insights from recent advances in molecular biology, *Transfus Med Rev* 13:245–266, 1999.

Aygun B, Padmanabhan S, Paley C, Chandrasekaran V: Clinical significance of RBC alloantibodies and autoantibodies in sickle cell patients who received transfusions, *Transfusion* 42:37–43, 2002.

Badior KE, Casey JR: Molecular mechanism for the red blood cell senescence clock, *Internl Union Biochem Mol Biol* 70:32–40, 2018.

Baig NA, Dukek BA, Albo DK, et al.: False positive antineutrophil antibody test due to daratumumab interference can be overcome using blocking antibodies [abstract], *Transfusion* 59:124, 2019.

Bahamontes-Rosa N, Tena-Tomas C, Wolkow J, et al.: Genetic conservation of the GIL blood group determining aquaporin 3 gene in African and Caucasian populations, *Transfusion* 48:1164–1168, 2008.

Bakchoul T, Bassler D, Heckmann M, et al.: Management of infants born with severe neonatal alloimmune thrombocytopenia: the role of platelet transfusion and intravenous immunoglobulin, *Transfusion* 54:640–645, 2014.

Baleotti W, Rios M, Reid ME, et al.: Dombrock gene analysis in Brazilian people reveals novel alleles, *Vox Sang* 91:81–87, 2006.

Ballas SK, Marcolina MJ, Crawford MN: In vitro storage and in vivo survival studies of red cells from persons with the In(Lu) gene, *Transfusion* 32:607–611, 1992.

Ballif BA, Helias V, Peyrard T, et al.: Disruption of SMIM1 causes the Vel- blood type, *EMBO Mol Med* 5:751–761, 2013.

Banderanko N: *Blood transfusion therapy: a physician's handbook*, 11th ed, Bethseda, Md, 2014, American Association of Blood Banks.

Bartels CF, Zelinski T, Lockridge O: Mutation at codon 322 in the human acetylcholinesterase (ACHE) gene accounts for YT blood group polymorphism, *Am J Hum Genet* 52:928–936, 1993.

Bartholdson JS, Bustamante LY, Crosnier C, et al.: Semaphorin-7A is an erythrocyte receptor for P. falciparum merozoite-specific TRAP homolog, *MTRAP, PLoS Pathog* 8:e1003031, 2012, https://doi.org/10.1371/journal.ppat.1003031. 1-13.

Baumgarten R, van Gelder W, van Wintershoven J, et al.: Recurrent acute hemolytic transfusion reactions by antibodies against Do^a antigens, not detected by crossmatching, *Transfusion* 46:244–249, 2006.

Bayat B, Werth S, Sachs UJH, Santoso S: A novel enzyme-linked immunosorbent assay method for the detection of human neutrophil antigen-2a antibodies, *Transfusion* 49:1819–1824, 2009.

Bayliss KM, Kueck BD, Johnson ST, et al.: Detecting fetomaternal hemorrhage: a comparison of five methods, *Transfusion* 31:303–307, 1991.

Begat C, Bailly P, Chiaroni J, Mazieres S: Revisiting the Diego blood group system in Amerindians: evidence for gene-culture comigration, *PloS One* 10(7):e0132211, 2014, https://doi.org/10.1371/journal.pone.0132211.

Benson TW, Weintraub DS, Crowe M, et al.: Deletion of the Duffy antigen receptor for chemokines (DARC) promotes insulin resistance and adipose tissue inflammation during high fat feeding, *Mol Cell Endo* 473:79–88, 2018.

Berentsen S, Roth A, Randen U, Jilma B, Tjonnfjord GE: Cold agglutinin disease: current challenges and future prospects, *J Blood Med* 10:93–103, 2019.

Bernardi L, Bruni AC: Mutations in prion protein gene: pathogenic mechanisms in C-terminal vs. N-terminal domain, a review, *Int J Mol Sci* 20:3606, 2019.

Berthold T, Glaubitz M, Muschter S, et al.: Human neutrophil antigen-3a antibodies induce neutrophil stiffening and conformational activation of CD11b without shedding of L-selectin, *Transfusion* 55:2939–2948, 2015.

Berry-Dortch S, Woodside CH, Boral LI: Limitations of the immediate spin crossmatch when used for detecting ABO incompatibility, *Transfusion* 25:176–178, 1985.

Bertrand G, Duprat E, Lefranc M-P, Marti J, Coste J: Characterization of human FCGR3B*02 (HNA-1b, NA2) cDNAs and IMGT standardized description of FCGR3B alleles, *Tissue Antigens* 64:119–131, 2004.

Bietz S, Montilla I, Kulzer S, et al.: Recruitment of human aquaporin 3 to internal membranes in the *Plasmodium falciparum* infected erythrocyte, *Mol Biochem Parasitol* 167:48–53, 2009.

Bird GWG: Lectins: a hundred years, *Immunohematol* 4:45–48, 1988.

Blood Group: *Blood group Antigen gene mutation Database*, http://www.ncbi.nlm.nih.gov/projects/gv/mhc/xslcgi.cgi:cmd=bgmut, 2015.

Boren T, Falk P, Roth KA, et al.: Attachment of *Helicobacter pylori* to human gastric epithelium mediated by blood group antigens, *Science* 262:1892–1895, 1993.

Bosco A, Xenocostas A, Kinney J, et al.: An autoanti-Kpb immunoglobulin M that simulates antigen suppression, *Transfusion* 49:750–756, 2009.

Boury-Jamot M, Daraspe J, Bonte F, et al.: Skin aquaporins: function in hydration, wound healing, and skin epidermis homeostasis. In Beitz E, editor: *Handbook of experimental pharmacology 2009*, Berlin, Heidelberg, Germany, 2009, Springer-Verlag.

Boswell-Casteel RC, Hays FA: Equilibrative nucleoside transporters-a review, *Nucleos Nucleot Nucleic Acids* 36:7–30, 2017.

Boswell-Casteel RC, Fukuda Y, Schuetz JD: ABCB6, an ABC transporter impacting drug response and disease, *AAPS J* 20:8, 2018. DOI: 10. 10.1208/s12248-017-0165-6.

Branch DR, Petz LD: A new reagent (ZZAP) having multiple applications in immunohematology, *Am J Clin Pathol* 78:161–167, 1982.

Brown KE, Hibbs FR, Gallinella G, et al.: Resistance to parvovirus B19 infection due to a lack of virus receptor (erythrocyte P antigen), *N Engl J Med* 330:1192–1196, 1994.

Brunker PAR, Flegel WA: Scianna: the lucky 13th blood group system, *Immunohematol* 27:41–57, 2011.

Brunker PAR, Flegel WA: An update on the Scianna blood group system, *Immunohematol* 35:48–50, 2019.

Burton MN, Bruce LJ: Modelling the structure of the red cell membrane, *Biochem Cell Biol* 89:200–215, 2011.

Butch SH, Judd WJ, Steiner EA, et al.: Electronic verification of donor-recipient compatibility: the computer crossmatch, *Transfusion* 34:105–109, 1994.

Bux J: Human neutrophil alloantigens, *Vox Sang* 94:277–285, 2008.

Bux J, Behrens G, Jaeger G, Welte K: Diagnosis and clinical course of autoimmune neutropenia in infancy: analysis of 240 cases, *Blood* 91:181–186, 1998.

Byrne G, Ahmad-Villiers S, Du Z, McGregor C: B4GALNT2 and xenotransplantation: a newly appreciated xenogeneic antigen, *Xenotransplantation* 25:e12394, 2018.

Byrne KM, Byrne PC: Review: other blood group systems—Diego, Yt, Xg, Scianna, Dombrock, Colton, Landsteiner-Wiener, and Indian, *Immunohematol* 20:50–58, 2004.

Cameron HS, Szczepaniak D, Weston BW: Expression of human chromosome 19p α (1,3) fucosyltransferase genes in normal tissues, *J Biol Chem* 270:20112–20122, 1995.

Cardone JD, Bordin JO, Chiba AK, et al.: Gene frequencies of the HNA-4a and -5a neutrophil antigens in Brazilian persons and a new polymerase chain reaction-restriction length polymorphism method for HNA-5a genotyping, *Transfusion* 46:1515–1520, 2006.

Castilho L, Credidio CD, Ribeiro K, et al.: Anti-Fy3 in sickle cell disease patients genotyped as FY^{*B-33}/FY^{*B-33} [Abstract], *Transfusion* 49S:35A, 2009.

Castilho L, Reid ME: A review of the JR blood group system, *Immunohematol* 29:63–68, 2013.

Chakera A, Seeber RM, John AE, et al.: The Duffy antigen/receptor for chemokines exists in an oligomeric form in living cells and functionally antagonizes CCR5 signaling through hetero-oligomerization, *Mol Pharmacol* 73:1362–1370, 2008.

Changsri K, Tobunluepop P, Songthammawat D, et al.: Human neutrophil alloantigen frequencies in Thai blood donors, *Blood Transfus* 12:286–291, 2014.

Chaudhuri A, Nielsen S, Elkjaer ML, et al.: Detection of Duffy antigens in the plasma membranes and caveolae of vascular endothelial and epithelial cells of nonerythroid organs, *Blood* 89:701–712, 1997.

Chapuy CI, Nicholson RT, Aguad MD, et al.: Resolving the daratumumab interference with blood compatibility testing, *Transfusion*1545–1554, 2015.

Chen DP, Sun CF, Ning HC, Wang WT, Tseng CP: Comprehensive analysis of RHD splicing transcripts reveals the molecular basis for the weak anti-D reactivity of Del -red blood cells, *Transfus Med* 26(2):123–129, 2016, https://doi.org/10.1111/tme.12270.

Chen GY, Muramatsu H, Kondo M, et al.: Abnormalities caused by carbohydrate alterations in I β1,6-*N*-acetylglucosaminyltransferase-deficient mice, *Mol Cell Biol* 225:7828–7838, 2005.

Chen XY, Peng J, Novaretti M, et al.: Deletion of arginine codon 229 in the *Rhce* gene alters e and f but not c expression, *Transfusion* 44:391–398, 2004.

Cherif-Zahar B, Le Van Kim C, Rouillac C, et al.: Organization of the gene *(RHCE)* encoding the blood group RhCcEe antigens and characterization of the promoter region, *Genomics* 19:68–74, 1994.

Choi HS, Lee EM, Kim HO, Park MI, Baek EJ: Autonomous control of terminal erythropoiesis via physical interactions among erythroid cells, *Stem Cell Res* 10:442–453, 2013.

Chou ST, Evans P, Vege S, et al.: Rh genotype matching for transfusion support in sickle cell disease, *Blood* 132:1198–1207, 2018.

Code of Federal Regulations: *Title 21—Food and drugs*, *Part 660*, *Subpart F—anti-human globulin*, Washington, DC, 2016, U.S. Government Printing Office.

Cohen M, Hurtado-Ziola N, Varki A: ABO blood group glycans modulate sialic acid recognition on erythrocytes, *Blood* 114:3668–3676, 2009.

Conway LT, Clay ME, Kline WE, et al.: Natural history of primary autoimmune neutropenia in infancy, *Pediatrics* 79:728–733, 1987.

Cooling L: Polylactosamines, there's more than meets the "Ii": a review of the Ii system, *Immunohematol* 26:133–155, 2010.

Cooling L: Blood groups in infection and host susceptibility, *Clin Microbiol Rev* 28:1–70, 2015.

Cooling L: Kids, colds, and complement: paroxysmal cold hemoglobinuria, *Transfusion* 57:1332–1335, 2017.

Cooling LLW, Sherbeck J, Mowers JC, Hugan SL: Development of red blood cell autoantibodies following treatment with checkpoint inhibitors: a new class of antineoplastic immunotherapeutic agents associated with immune dysregulation, *Immunohematol* 33:15–21, 2017.

Cooling L: An update on the I blood group system, *Immunohematol* 35:85–90, 2019.

Cooling L, Gorlin JB: Transfusion reactions associated with hematopoietic progenitor cell reinfusion. In Popovsky MA, editor: *Transfusion reactions*, 4th ed, Bethesda, Md, 2012, AABB Press, pp 289–326.

Cooling L, Hwang D, Gu Y: Globoside synthase can regulate P^k and LKE expression on human RBC: evidence for the Pk-variant phenotype among some LKE-weak and LKE-negative donors [Abstract], *Transfusion* 43:SP194, 2003a.

Cooling LL, Kelly K: Inverse expression of P^k and Luke blood group antigens on human RBCs, *Transfusion* 41:898–907, 2001.

Cooling LLW, Zhang D-S, Naides SJ, et al.: Glycosphingolipid expression in acute nonlymphocytic leukemia: common expression of shiga toxin and parvovirus B19 receptors on early myeloblasts, *Blood* 101:711–721, 2003b.

Coombs RRA, Mourant AE, Race RR: A new test for the detection of weak and incomplete Rh agglutinins, *Br J Exp Pathol* 26:255–266, 1945.

Cordle DG, Strauss RG, Snyder EL, et al.: Safety and cost containment data that advocate abbreviated pretransfusion testing, *Am J Clin Pathol* 94:428–431, 1990.

Costa FP, Ferreira EC, Hue-Roye K, et al.: A new antibody in the Dombrock blood group system, anti-DOMR, masquerades as anti-Hy [Abstract], *Transfusion* 49S:48A, 2009.

Coste I, Gauchat J-F, Wilson A, et al.: Unavailability of CD147 leads to selective erythrocyte trapping in the spleen, *Blood* 97:3984–3988, 2001.

Covas DT, de Oliveira FS, Rodrigues ES, et al.: Knops blood group haplotypes among distinct Brazilian populations, *Transfusion* 47:147–153, 2007.

Crew VK, Burton N, Kagan A, et al.: CD151, the first member of the tetraspanin (TM4) superfamily detected on erythrocytes, is essential for the correct assembly of human basement membranes in kidney and skin, *Blood* 104:2217–2223, 2004.

Crew VK, Poole J, Long S, et al.: Two MER2-negative individuals with the same novel *CD151* mutation and evidence for clinical significance of anti-MER2, *Transfusion* 48:1912–1916, 2008.

Curnutte J, Bemiller L: Chronic granulomatous disease with McLeod phenotype: an uncommon occurrence [Abstract], *Transfusion* 35:S239, 1995.

Curtis BR: Recent progress in understanding the pathogenesis of fetal and neonatal alloimmune thrombocytopenia, *Br J Haematol* 171:671–682, 2015.

Cvejic A, Haer-Wigman L, Stephens JC, et al.: *SMIM1* underlies the Vel blood group and influences red blood cell traits, *Nat Genet* 45:542–545, 2013.

Czerwinski M, Kern J, Grodecka M, et al.: Mutational analysis of the *N*-glycosylation sites of Duffy antigen/receptor for chemokines, *Biochem Biophys Res Commun* 356:816–821, 2007.

Dall'Ollio F, Malagolini N, Chiricolo M, Trinchera M, Harduin-Lepers A: The expanding roles of the Sda/Cad carbohydrate antigen and its cognate glycosyltransferase B4GALNT2, *Biochim Biophys Acta* 1840:433–453, 2014.

Daniel-Johnson J, Leitman S, Klein H, et al.: Probiotic-associated high-titer anti-B in a group A platelet donor as a cause of severe hemolytic transfusion reactions, *Transfusion* 49:1845–1849, 2009.

Daniels G: *Lutheran*, *Immunohematology* 25:152–159, 2009.

Daniels G: The Augustine blood group system, 48 years in the making, *Immunohematol* 32:100–103, 2016.

Daniels G, Ballif BA, Helias V, et al.: Lack of nucleoside transporter ENT1 results in the Augustine-null blood type and ectopic mineralization, *Blood* 125:3651–3654, 2015.

Daniels G, Flegel WA, Fletcher A, et al.: International society of blood transfusion Committee on terminology for red cell surface antigens: Cape Town report, *Vox Sang* 92:250–253, 2007.

Daniels G, Fletcher A, Garratty G, et al.: Blood group terminology 2004: from the international society of blood transfusion Committee on terminology for red cell surface antigens, *Vox Sang* 87:304–316, 2004.

Davis EJ, Salem J-E, Young A, et al.: Hematologic complications of immune checkpoint inhibitors, *Oncol* 24:584–588, 2019.

Denecke J, Marquardt T: Congenital dyserythropoietic anemia type II (CDAII/HEMPAS): where are we now? *Biochim Biophys Acta* 1792:915–920, 2009.

Dezan MR, Ribeiro IH, Oliveira VB, et al.: *RHD* and *RHCE* genotyping by next-generation sequencing is an effective strategy to identify molecular variants within sickle cell disease patients, *Blood Cells Mol Dis* 65:8–15, 2017.

Duchene J, Novitzky-Basso I, Thiriot A, et al.: Atypical chemokine receptor 1 on nucleated erythroid cells regulates hematopoiesis, *Nature Immunol* 18:753–761, 2017.

Djousse L, Karamohamed S, Herbert AG, et al.: Fucosyltransferase 3 polymorphism and atherothrombotic disease in the Framingham offspring study, *Am Heart J* 153:636–639, 2007.

Eder AF: Transfusion therapy in autoimmune hemolytic anemia. In Mintz PD, editor: *Transfusion therapy: clinical principles and practice*, 2nd ed, Bethesda, Md, 2005, AABB Press, pp 27–56.

Edwards JM, Moulds JJ, Judd WJ: Chloroquine dissociation of antigen-antibody complexes: a new technique for typing red blood cells with a positive direct antiglobulin test, *Transfusion* 22:59–61, 1982.

Egan ES, Fiang RHY, Moechtar MA, et al.: A forward genetic screen identifies erythrocyte CD55 as essential for Plasmodium falciparum invasion, *Science* 348:711–714, 2015.

Egan ES, Weekes MP, Kanjee U, et al.: Erythrocytes lacking the Langereis blood group protein ABCB6 are resistant to the malarial parasite Plasmodium falciparum, *Commun Biol* 1:45, 2018, https://doi.org/10.1038/s42003-018-0046-2.

El Nemer W, Gane P, Colin Y, et al.: The Lutheran blood group glycoproteins, the erythroid receptors for laminin, are adhesion molecules, *J Biol Chem* 273:16686–16693, 1998.

El Nemer W, Rahuel C, Colin Y, et al.: Organization of the human *LU* gene and molecular basis of the Lu^a/Lu^b blood group polymorphism, *Blood* 89:4608–4616, 1997.

Ellison RC, Zhang Y, Myers RH, et al.: Lewis blood group phenotype as an independent risk factor for coronary heart disease (The NHLBI Family Heart Study), *Am J Cardiol* 83:345–348, 1999.

Endeward V, Cartron J-P, Ripoche P, et al.: Red cell membrane CO_2 permeability in normal human blood and in blood deficient in various blood groups, and effect of DIDS, *Transfus Clin Biol* 13:123–127, 2006.

Englefriet CP, Overbeeke MAM, von dem Borne AEG: Autoimmune hemolytic anemia, *Semin Hematol* 29(3–12), 1992.

Eyers SAC, Ridgwell K, Mawby WJ, et al.: Topology and organization of human Rh (rhesus) blood group related polypeptides, *J Biol Chem* 269:6417–6423, 1994.

Fabijanska-Mitek J, Lopienska H, Zupanska B: Gel test application for IgG subclass detection in auto-immune haemolytic anaemia, *Vox Sang* 72:233–237, 1997.

Fehr T, Stussi G: ABO-incompatible kidney transplantation, *Curr Opin Organ Transplant* 17:376–385, 2012.

Ficici E, Faraldo-Gomez JD, Jennings ML, Forrest LR: Asymmetry of inverted-topology repeats in the AE1 anion exchanger suggests an elevator-like mechanism, *J Gen Physiol* 149:1149–1164, 2017.

Figueiredo C, Zenk J, Blasczyk R, et al.: Blood group protein semaphorin 7A: a new modulator of NK cell function, *Transfusion* 49S:47A, 2009.

Finning K, Martin P, Summers J, et al.: Fetal genotyping for the K (Kell) and Rh C, c, and E blood groups on cell-free fetal DNA in maternal plasma, *Transfusion* 47:2126–2133, 2007.

Flesch BK, Reil A: Molecular genetics of the human neutrophil antigens, *Transfus Med Hemother* 45:300–309, 2018.

Flesch BK, Wesche J, Berthold T, et al.: Expression of the CTL2 transcript variants in human peripheral blood cells and human tissues, *Transfusion* 53:3217–3223, 2013.

Franchini M, Mannucci PM: ABO blood group and thrombotic vascular disease, *Thromb Haemost* 112:1103–1109, 2014.

Frank SM, Rothschild JA, Masear CG, et al.: Optimizing preoperative blood ordering with data acquired from an anesthesia information management system, *Anesthesiology* 118:1286–1297, 2013.

Fraser NS, Knauth CM, Moussa A, et al.: Genetic variants within the erythroid transcription factor, KLF1, and reduction of the expression of Lutheran and other blood group antigens: review of the In(Lu) phenotype, *Transf Med Reviews* 33:111–117, 2019.

Freedman J, Semple JW: Complement in transfusion medicine. In Garraty G, editor: *Immunobiology of transfusion medicine*, New York, 1994, Marcel Dekker, pp 403–434.

Gamma Biologicals, Inc: *Gamma-Quin chloroquine diphosphate solution for removal of red-cell-bound immunoglobulin—directions for use*, Houston, 2001, Gamma Biologicals, Inc.

Fukuda Y, Cheong PL, Lynch J, et al.: The severity of hereditary porphyria is modulated by the porphyrin exporter and Lan antigen ABCB6, *Nature Commun* 7:12353, 2016, https://doi.org/10.1037/ncomms12353.

Gang EJ, Bosnakovski D, Figueiredo CA, et al.: SSEA-4 identifies mesenchymal stem cells from bone marrow, *Blood* 109:1743–1751, 2007.

Gardner L, Patterson AM, Ashton BA, et al.: The human Duffy antigen binds selected inflammatory but not homeostatic chemokines, *Biochem Biophys Res Commun* 321:306–312, 2004.

Garratty G: Review: drug-induced immune hemolytic anemia—the last decade, *Immunohematol* 20:138–146, 2004.

Ghosh A, Murugesan G, Chen K, et al.: Platelet CD36 surface expression levels affect functional responses to oxidized LDL and are associated with inheritance of specific genetic polymorphisms, *Blood* 23:6355–6366, 2011.

Giles CM: Three Chido determinants detected on the B5Rg+ allotype of human C4: their expression in Ch-typed donors and families, *Hum Immunol* 18:111–112, 1987.

Giles CM, Uring-Lambert B, Goetz J, et al.: Antigenic determinants expressed by human C4 allotypes: a study of 325 families provides evidence for the structural antigenic model, *Immunogenetics* 27:442–448, 1988.

Girbl T, Lenn T, Perez L, et al.: Distinct compartmentalization of the chemokines CXCL1 and CXCL2 and the atypical receptor ACKR1 determine discrete stages of neutrophil diapedesis, *Immunity* 49:1062–1076, 2018.

Glisovic SJ, Pastore YD, Gagne V, et al.: Impact of genetic polymorphism determining leukocyte/neutrophil count on chemotherapy toxicity, *Pharmacogenetic J* 18:270–274, 2018.

Gottschall J, Triulzi D, Kakaiya R, et al.: Human neutrophil antibodies in a blood donor population: a lookback study, *Vox sang* 104:166–170, 2013.

Gourri E, Denomme GA, Merki Y, et al.: Genetic background of the rare Yus and Gr-bich blood group phenotypes: homologous regions of the GYPC gene contribute to deletion alleles, *Br J Haemat* 177:630–640, 2017.

Gubin AN, Njoroge JM, Wojda U, et al.: Identification of the Dombrock blood group glycoprotein as a polymorphic member of the ADP-ribosyltransferase gene family, *Blood* 96:2621–2627, 2000.

Hadley TJ, Peiper SC: From malaria to chemokine receptor: the emerging physiologic role of the Duffy blood group antigen, *Blood* 89:3077–3091, 1997.

Hajar CGH, Zulkafli Z, Riffin NS, et al.: *Human neutrophil antigen frequency data for Malays, Chinese and Indians*, Trans Apher Sci, 2020(in press).

Harmening DM, editor: *Modern blood banking and transfusion practices*, 6th ed, Philadelphia, 2012, FA Davis.

Huang Y, Ma Y, Gao P, Yao Z: Targeting CD47: the achievements and concerns of current studies on cancer immunotherapy, *J Thorac Dis* 9:E168–174, 2017.

Hauser R: Le^a and Le^b tissue glycosphingolipids, *Transfusion* 35:577–581, 1995.

Helias V, Saison C, Ballif BA, et al.: ABCB6 is dispensable for erythropoiesis and specifies the new blood group system Langereis, *Nat Genet* 44:170–173, 2012.

Hawkins J, Aster RH, Curtis BR: Post-transfusion purpura: current perspectives, *J Blood Med* 10:405–415, 2019.

Henry JB, Mintz PD, Webb W: Optimal blood ordering for elective surgery, *J Am Med Assoc* 237:451, 1977.

Hizume M, Kobayashi A, Teruya K, et al.: Human prion protein (PrP) 219K is converted to PrP^{SC} but shows heterozygous inhibition in variant creutzfeldt-Jakob disease infection, *J Biol Chem* 284:3603–3609, 2009.

Ho M, Chelly J, Carter N, et al.: Isolation of the gene for McLeod syndrome that encodes a novel membrane transport protein, *Cell* 77:869–880, 1994.

Hoher G, Fiegenbaum M, Almeida S: Molecular basis of the Duffy blood group system, *Blood Transfus* 16:93–100, 2018.

Horne K, Woolley IJ: Shedding light on DARC: the role of the Duffy antigen/receptor for chemokines in inflammation, infection and malignancy, *Inflamm Res* 58:431–435, 2009.

Howes RE, Patil AP, Piel FB, et al.: The global distribution of the Duffy blood group, *Nat Commun* 2:226, 2011, https://doi.org/10.1038/ncomms1265.

Hsu K, Chi N, Gucek M, et al.: Miltenberger blood group antigen type III (Mi.III) enhances the expression of band 3, *Blood* 114:1919–1928, 2009.

Hsu K, Kuo MS, Yao CC, et al.: The MNS glycophorin variant GP.Mur affects differential erythroid expression of Rh/RhAG transcripts, *Vox Sang* 112:671–677, 2017.

Huang CH, Blumenfeld O: MNSs blood groups and major glycophorins. In Carton JP, Rouger P, editors: *Blood cell biochemistry*, vol. 6. New York, 1995, Plenum Press, pp 153–188.

Hue-Roye K, Lomas-Francis C, Balygorod L, et al.: Three new high-prevalence antigens in the Cromer blood group system, *Transfusion* 47:1621–1629, 2007.

Hurst FP, Sajjad I, Elster EA, et al.: Transplantation of A2 kidneys into B and O recipients leads to reduction in waiting time: USRDS experience, *Transplantation* 89:1396–1402, 2010.

Huvard MJ, Schmid P, Stroncek DF, Flegel WA: Frequencies of SLC44A2 alleles encoding human neutrophil anti-3 variants in the African American population, *Transfusion* 52:1105–1111, 2012.

Hwang K, Park C-J, Huh HJ, et al.: Flow cytometric detection of neutrophil-associated immunoglobulin in patients with or without neutropenia and establishment of the reference interval, *Ann Clin Lab Sci* 41:144–149, 2011.

Inaba N, Hiruma T, Togayachi A, et al.: A novel I-branching β1,6-*N*-acetylglucosaminyltransferase involved in human blood group I antigen expression, *Blood* 101:2870–2876, 2003.

Iwamura K, Furukawa K, Uchikawa M, et al.: The blood group P_1 synthase gene is identical to the Gb3/CD77 synthase gene, *J Biol Chem* 278:44429–44438, 2003.

Iwamoto S, Kamesaki T, Oyamada T, et al.: Reactivity of autoantibodies of autoimmune hemolytic anemia with recombinant rhesus blood group antigens and anion transporter band 3, *Am J Hematol* 68:106–114, 2001.

Iwamoto S, Li J, Sugimoto N, et al.: Characterization of the Duffy gene promoter: evidence for tissue-specific abolishment of expression in Fy(a-b-) of black individuals, *Biochem Biophys Res Commun* 222:852–859, 1996.

Iwamoto S, Omi T, Yamasaki M, et al.: Identification of 5′ flanking sequence of *RH50* gene and the core region for erythroid-specific expression, *Biochem Biophys Res Commun* 243:233–240, 1998.

Jacewicz MS, Acheson DWK, Mobassaleh M, et al.: Maturational regulation of globotriaosylceramide, the shiga-like toxin 1 receptor, in cultured human gut epithelial cells, *J Clin Invest* 96:1328–1335, 1995.

Jaskiewicz E, Jodlowska M, Kaczmarek R, Zerka A: Erythrocyte glycophorins as receptors for Plasmodium merozoites, *Parasites Vectors* 12:317, 2019. Doi.org/10.1186/s13071-019-3575-8.

Ji JD, Ivashkiv LB: Roles of semaphorins in the immune and hematopoietic system, *Rheumatol Int* 29:727–734, 2009.

Johnson NC:XG: The forgotten blood group system, *Immunohematol* 27:68–71, 2011.

Judd WJ: Are there better ways than the crossmatch to demonstrate ABO incompatibility? *Transfusion* 31:192–194, 1991.

Judd WJ: Requirements for the electronic crossmatch, *Vox Sang* 74:409–417, 1998.

Judd WJ: Red blood cell immunology and compatibility testing. In Simon TL, Dzik WH, Simon TL, editors: *Rossi's principles of transfusion medicine Philadelphia*, 5th ed, 2016.

Judd WJ: *Guidelines for prenatal and perinatal immunohematology*, Bethseda, Md, 2005, AABB Press.

Judd WJ, Johnson S, Storry S: *Judd's Methods in immunohematology*, 3rd ed, Durham, N.C., 2008, Montgomery Scientific Publications.

Judd WJ, Steiner EA, O'Donnell DB, et al.: Discrepancies in reverse ABO typing due to prozone: how safe is the immediate-spin crossmatch? *Transfusion* 28:334–338, 1988.

Judd WJ, Walter WJ, Steiner EA: Clinical and laboratory findings on two patients with naturally occurring anti-Kell agglutinins, *Transfusion* 21:184–188, 1981.

Kaczmarek R, Buczkowska A, Mikolajewicz H, et al.: P1PK, GLOB, FORS blood group systems and GLOB collection: biochemical and clinical aspects. Do we understand it all yet? *Transfus Med Rev* 28:126–136, 2014.

Kaczmarek R, Symczak-Kulus K, Bereznicka A, et al: Single nucleotide polymorphisms in A4GALT spur extra products of the human Gb3/CD77 synthase and underlie the P1PK blood group system. PloS One 13:e0196627. Doi: org/10.1371/journal.pone.0196627.

Kamphuis MM, Lindenburg I, van Kamp I, et al.: Implementation of routine screening for Kell antibodies: does it improve perinatal survival? *Transfusion* 48:953–957, 2008.

Kawabata K, Uchikawa M, Ohto H, et al.: Anti-KANNO: a novel alloantibody against a red cell antigen of high frequency, *Transf Med Rev* 28:23–28, 2014.

Kay MMB: Cellular and molecular biology of senescent antigen. In Garratty G, editor: *Immunobiology of transfusion medicine*, New York, 1994, Marcel Dekker, pp 173–198.

Keller J, Vege S, Horn T, et al.: Novel mutations in KLF1 encoding the In(Lu) phenotype reflect a diversity of clinical presentations, *Transfusion* 58:196–199, 2018.

Kelly RJ, Ernst LK, Larsen RD, et al.: Molecular basis for H blood group deficiency in Bombay (O_h) and para-Bombay individuals, *Proc Natl Acad Sci U S A* 91:5843–5847, 1994.

Kelly RJ, Rouquier S, Giorgi D, et al.: Sequence and expression of a candidate for the human secretor blood group α (1,2) fucosyltransferase gene *(FUT2)*, *J Biol Chem* 270:4640–4649, 1995.

Key T, Carter V, Godwin P, et al.: Human neutrophil antibodies are associated with severe early rejection in kidney transplant recipients [abstract], *Transplantation* 102:S214, 2018.

Khandelwal S, Saxena RK: Assessment of survival of aging erythrocyte in circulation and attendant changes in size and CD147 expression by a novel two step biotinylation method, *Exp Gerontol* 41:855–861, 2006.

Kimberely FC, Sivasankar B, Morgan BP: Alternative roles for CD59, *Mol Immunol* 44:73–81, 2007.

King LC, Adams JH, Xianli J, et al.: Fy^a/Fy^b antigen polymorphism in human erythrocyte Duffy antigen affects susceptibility to Plasmodium vivax malaria, *Proc Natl Acad Sci U S A* 108:20113–20118, 2011.

Klein HG, Anstee DJ: *Mollison's blood transfusion in clinical medicine*, 11th ed, Oxford, 2006, Blackwell Scientific Publications.

Knepper MA: The aquaporin family of molecular water channels, *Proc Natl Acad Sci U S A* 91:6255–6258, 1994.

Knezevic-Maramica I, Kruskall MS: Intravenous immune globulins: an update for clinicians, *Transfusion* 43:1460–1480, 2003.

Koda Y, Soejima M, Liu Y, et al.: Molecular basis for secretor type α(1,2)-fucosyltransferase gene deficiency in a Japanese population: a fusion gene generated by unequal crossover responsible for the enzyme deficiency, *Am J Hum Genet* 59:343–350, 1996.

Kommareddi PK, Nair TS, Thang LV, et al.: Isoforms, expression, glycosylation, and tissue distribution of CTL2/SLC44A2, *Protein J* 29:417–426, 2010.

Kondo Y, Ideda K, Tokuda N, et al.: TLR4-MD-2 complex is negatively regulated by an endogenous ligand, globotetraosylceramide, *Proc Natl Acad Sci U S A* 110:4714–4719, 2013.

Kormoczi GF, Scharberg EA, Gassner C: A novel KEL*1,3 allele with weak Kell antigen expression confirming the cis-modifier effect of KEL3, *Transfusion* 49:733–739, 2009.

Kornstad L, Heisto H: The frequency of formation of Kell antibodies in recipients of Kell-positive blood. In *Proceedings of the 6th Congress of the European Society of Haematology, Copenhagen, Denmark*, August 1958, pp 754–758.

Kroviarski Y, El Nemer W, Gane P, et al.: Direct interaction between the Lu/B-CAM adhesion glycoproteins and erythroid spectrin, *Br J Haematol* 126:255–264, 2004.

Kumari S, Devi VG, Badana A, et al.: CD151-A striking marker for cancer therapy, *Biomarkers Canc* 7:7–11, 2015.

Kundu SK, Evans A, Rizvi J, et al.: A new P^k phenotype in the P blood group system, *J Immunol* 7:431–439, 1980.

Kundu SK, Steane SM, Bloom JEC, et al.: Abnormal glycolipid composition of erythrocytes with a weak P antigen, *Vox Sang* 35:160–167, 1978.

Lai YJ, Wu WY, Yang CM, et al.: A systematic study of single-nucleotide polymorphisms in the *A4GALT1* gene suggests a molecular basis for the P_1/P_2 blood groups, *Transfusion* 54:3222–3231, 2014.

Lambert MP, Gernsheimer TB: Clinical updates in adult immune thrombocytopenia, *Blood* 129:2829–2835, 2017.

Landsteiner K, Wiener AS: An agglutinable factor in human blood recognized by immune sera for rhesus blood, *Proc Soc Exp Biol Med* 43:223–224, 1940.

Lapierre Y, Rigal D, Adam J, et al.: The gel test: a new way to detect red cell antigen-antibody reactions, *Transfusion* 30:109–113, 1990.

Lee K, Godeau B, Fromont P, et al.: CD36 deficiency is frequent and can cause platelet immunization in Africans, *Transfusion* 39:873–879, 1999.

Lee S: Molecular basis of Kell blood group, *Vox Sang* 73:1–11, 1997.

Lerut E, Van Damme B, Noizat-Pirenne F, et al.: Duffy and Kidd blood group antigens: minor histocompatibility antigens involved in renal allograft rejection? *Transfusion* 47:28–40, 2007.

Levine P, Stetson RE: An unusual case of intragroup agglutination, *J Am Med Assoc* 113:126, 1939.

Li Y, Camp S, Rachinsky TL, et al.: The gene structure of mammalian acetylcholinesterase, *J Biol Chem* 266:23083–23090, 1991.

Li J, Iwamoto S, Sugimoto N, et al.: Dinucleotide repeat in the 3′ flanking region provides a clue to the molecular evolution of the Duffy gene, *Hum Genet* 99:573–577, 1997.

Li J, Wang JP, Ghiran I, et al.: Complement receptor 1 expression on mouse erythrocytes mediates clearance of Streptococcus pneumonia by immune adherence, *Infect Immun* 78:3129–3135, 2010.

Li R, Yang L, Zeng J, Ling Z, Liang X: Genetic polymorphism of human platelet antigens -1 to -17w in the multi-ethnic Chinese Guangxi population, *Int J Clin Exp Med* 9:12992–12999, 2016.

Lin M, Sutherland DR, Horsfall W, et al.: Cell surface antigen CD109 is a novel member of the α2 macroglobulin/C3, C4, C5 family of thioester-containing proteins, *Blood* 99:1683–1691, 2002.

Lindstrom K, Breimer ME, Jovall P-A, et al.: Non-acid glycosphingolipid expression in plasma of an A_1 Le (a-b+) secretor human individual: identification of an ALe^b heptaglycosylceramide as major blood group component, *J Biochem* 111:337–345, 1992.

Liu Z-J, Bussel JB, Lakkaraja M, et al.: Suppression of in vitro megakaryocytopoiesis by maternal sera containing anti-HPA-1a antibodies, *Blood* 126:1234–1236, 2015.

Londero D, Miani M, Rinaldi C, Totis V, de Angelis V: Extensive human platelet specific antigens typing of blood donors of different geographical origin to manage platelet transfusion in alloimmunized patients: experience from a transfusion center in Northeastern Italy, *Int J Blood Transfus Immunohematol* 8:4–11, 2018.

Lopes LB, Baleotti W, Suzuki RB, et al.: HNA-3 gene frequency and a new polymerase chain reaction-restriction fragment length polymorphism method for HNA-3a/b genotyping, *Transfusion* 54, 2014. 1691-1621.

Love-Gregory L, Sherva R, Schappe T, et al.: Common CD36 SNPs reduce protein expression and may contribute to a protective atherogenic profile, *Human Mol Genet* 20:193–201, 2011.

Lowe JB: Carbohydrate-associated blood group antigens: the ABO, H/Se, and Lewis loci. In Garratty G, editor: *Immunobiology of transfusion medicine*, New York, 1994, Marcel Dekker, pp 3–36.

Lublin DM: Review: Cromer and DAF: role in health and disease, *Immunohematol* 21:39–47, 2005.

Lucas G, Rogers S, de Haas M, Porcelijn L, Bus J: Report on the fourth international granulocyte immunology workshop: progress toward quality assessment, *Transfusion* 42:462–468, 2002.

Lucien N, Sidoux-Walter F, Olives B, et al.: Characterization of the gene encoding the human Kidd blood group/urea transporter protein, *J Biol Chem* 273:12973–12980, 1998.

Lucien N, Sidoux-Walter F, Roudier N, et al.: Antigenic and functional properties of the human red blood cell urea transporter hUT-B1, *J Biol Chem* 277:34101–34108, 2002.

Lund N, Olsson ML, Ramkumar S, et al.: The human P(k) histo-blood group antigen provides protection against HIV-1 infection, *Blood* 133:4980–4991, 2009.

Madan N, Ghazi AR, Kong X, et al.: Runctionalization of CD36 cardiovascular disease and expression associated variants by interdisciplinary high throughput analysis, *PLoS Genet* 15:e1008287, 2019, https://doi.org/10.1371/journal.pgen.1008287.

Magor GW, Tallack MR, Gillinder KR, et al.: KLF1-null neonates display hydrops fetalis and a deranged erythroid transcriptome, *Blood* 125:2405–2417, 2015.

Mallory D: In Rockville M, editor: *Immunohematology methods*, 1st ed, The American National Red Cross, 1993.

Mangeney M, Richard Y, Coulaud D, et al.: CD77: an antigen of germinal center B cells entering apoptosis, *Eur J Immunol* 21:1131–1140, 1991.

Marsh WL: Anti-i: a cold antibody defining the Ii relationship in human red cells, *Br J Haematol* 7:200–209, 1961.

Masson P, Froment MT, Sorenson RC, et al.: Mutation His322Asn in human acetylcholinesterase does not alter electrophoretic and catalytic properties of the erythrocyte enzyme, *Blood* 83:3003–3005, 1994.

Mathai JC, Mori S, Smith BL, et al.: Functional analysis of aquaporin-1 deficient red cells, *J Biol Chem* 271:1309–1313, 1996.

Mayer DCG, Jiang L, Achur RN, et al.: The glycophorin C N-linked glycan is a critical component of the ligan for the *Plasmodium falciparum* erythrocyte receptor BAEBL, *Proc Natl Acad Sci Unit States Am* 103:2358–2362, 2006.

Mayer CL, Leibowitz CS, Kurosawa S, et al.: Shiga toxins and the pathophysiology of hemolytic uremic syndrome in humans and animals, *Toxins* 14:1261–1287, 2012.

Mazda T, Yabe R, NaThalang O, et al.: Differences in ABO antibody among blood donors: a comparison between past and present Japanese, Laotian, and Thai populations, *Immunohematol* 23:38–41, 2007.

Medof ME, Lublin DM, Holers VN, et al.: Cloning and characterization of cDNAs encoding the complete sequence of decay-accelerating factor of human complement, *Proc Natl Acad Sci U S A* 84:2007–2011, 1987.

Mintz PD, Haines AL, Sullivan MF: Incompatible crossmatch following nonreactive antibody detection test: frequency and cause, *Transfusion* 22:107–110, 1982.

Moller M, Lee YQ, Vidovic K, et al.: Disruption of a GATA1-binding motif upstream of XG/PBDX abolishes Xg^a expression and resolves the Xg blood group system, *Blood* 132:334–338, 2018.

Mollicone R, Reguigne I, Kelly RJ, et al.: Molecular basis for Lewis α(1,3/4)-fucosyltransferase gene deficiency *(FUT3)* found in Lewis-negative Indonesian pedigrees, *J Biol Chem* 269:20987–20994, 1994.

Mollison PL: Further observations on the patterns of clearance of incompatible red cells, *Transfusion* 39:347–354, 1989.

Montpetit A, Phillips MS, Mongrain I, et al.: High-throughput molecular profiling of blood donors for minor red blood cell and platelet antigens, *Transfusion* 46:841–848, 2006.

Moon C, Preston GM, Griffin CA, et al.: The human aquaporin-CHIP gene, *J Biol Chem* 268:15772–15778, 1993.

Morrow AL, Meinzen-Derr J, Huang P, et al.: Fucosyltransferase 2 non-secretor and low secretor status predicts severe outcomes in premature infants, *J Pediatr* 158:745–751, 2011.

Moulds JM: The Knops blood group system: a review, *Immunohematol* 26:2–7, 2010.

Mourant AE, Kopec AC, Domaniewska-Sobczak K: *The distribution of the human blood groups and other biochemical polymorphisms*, 2nd ed, Oxford, 1976, Oxford University Press.

Mourao LC, de Paula Baptista R, de Almeida ZB, et al.: Anti-band 3 and anti-spectrin antibodies are increased in Plasmodium vivax infection and are associated with anemia, *Sci Rep* 8:8762, 2018, https://doi.org/10.1038/s41598-018-27109-6.

Muramatsu T: Basigin: a multifunctional membrane protein with an emerging role in infections by malaria parasites, *Expert Opin Ther Targets* 16:999–1011, 2012.

Mutsuhashi M, Tsuno NH, Lino J, et al.: Advances in granulocyte test methodologies, *ISBT Sci Ser* 9:246–252, 2014.

Nagelkerge SQ, Tacke CE, Breunis WB, et al.: Nonallelic homologous recombination of the FCGR2/3 locus results in copy number variation and novel chimeric FCGR2 genes with aberrant functional expression, *Gene Immun* 16:422–429, 2015.

Nakajima F, Nishimura M, Hashimoto S, Okazaki H, Tadokoro K: Role of anti-Nak^a antibody, monocytes and platelets in the development of transfusion-related acute lung injury, *Vox Sang* 95:318–323, 2008.

Ness PM, Shirey RS, Thomas SK, et al.: The differentiation of delayed serologic and delayed hemolytic transfusion reactions: incidence, long-term serologic findings, and clinical significance, *Transfusion* 30:688–693, 1990.

Nester TA, Rumsey DM, Howell CC, et al.: Prevention of immunization to D+ red blood cells with red blood cell exchange and intravenous RH immune globulin, *Transfusion* 44:1720–1723, 2004.

Nishara S, Hiraga T, Ikehara Y, et al.: Molecular behavior of mutant enzymes in vivo, *Glycobiology* 9:373–382, 1999.

Noizat-Pirenne F, Meunier-Costes N, Costes B, et al.: Partial RhC antigen in sickle cell disease patients: clinical relevance and prevention [Abstract], *Transfusion* 49S:17A, 2009.

Okajima T, Nakamura Y, Uchikawa M, et al.: Expression cloning of human globoside synthase cDNAs, *J Biol Chem* 275:40498–40503, 2000.

Olives B, Martial S, Mattei M-G, et al.: Molecular characterization of a new urea transporter in the human kidney, *FEBS Lett* 386:156–160, 1996.

Omae Y, Ito S, Takeuchi M, et al.: Integrative genome analysis identified the KANNO blood group antigen as prion protein, *Transfusion* 59:2429–2435, 2019.

Ong J, Walker PS, Schmulbach E, et al.: Alloanti-c in a c-positive, JAL-positive patient, *Vox Sang* 96:240–243, 2009.

Onodera R, Kurita E, Taniguchi K, et al.: Anti-human neutrophil antigen-1, -1b, and -2 antibodies in neonates and children with immune neutropenias analyzed by extracted granulocyte antigen immunofluorescence assay, *Transfusion* 57:2586–2594, 2017.

Ouabdelmoumene Z, EL Housse H, Zarati F, et al.: Frequencies of human platelet antigens (HPA-1, -2, -3, -4, and -5) among the Moroccan blood donors, *Int J Blood Transfus Immunohematol* 8, 2018. Article 100038Zo2ZO2018. www.ijbti.com.

Ozen A, Comrie WA, Ardy RC, et al.: CD55 deficiency, early-onset protein-losing enteropathy, and thrombosis, *N Engl J Med* 377:52–61, 2017.

Nozaki I, Hamaguchi T, Sanjo N, et al.: Prospective 10-year surveillance of human prion disease in Japan, *Brain* 133:3043–3057, 2010.

Pai S-C, Burnouf T, Chen J-W, Lin L-I: Human platelet antigen alleles in 998 Taiwanese blood donors determined by sequence-specific primer polymerase chain reaction, *Biomed Res Internl:*, 2013, https://doi.org/10.11555/2013/973789. Article 973789.

Pak JE, Arnoux P, Zhou S, et al.: X-ray crystal structure of leukocyte type core 2 β1,6-*N*-acetylglucosaminyltransferase: evidence for a convergence of metal ion-independent glycosyltransferase mechanism, *J Biol Chem* 281:26693–26701, 2006.

Panigaj M, Brouckova A, Glierova H, et al.: Underestimation of the expression of cellular prion protein on human red blood cells, *Transfusion* 51:1012–1021, 2011.

Pastore A, Zagari A: A structural overview of the vertebrate prion proteins, *Prion* 1:185–197, 2007.

Parsons SF, Lee G, Spring FA, et al.: Lutheran blood group and its newly characterized mouse homologue specifically bind α5 chain-containing human laminin with high affinity, *Blood* 97:312–320, 2001.

Pedersen JT, Kaplan H, Wedeck L, et al.: Octapeptide segments from the amino terminus of glycophorin A contain the antigenic determinants of the M and N blood groups systems, *J Lab Clin Med* 116:527–534, 1990.

Perrier V, Kaneko K, Safar J, et al.: Dominant-negative inhibition of prion replication in transgenic mice, *Proc Natl Acad Sci Unit States Am* 99:13079–13084, 2002.

Peterson JA, Nelson TN, Kanack AJ, Aster RH: Fine specificity of drug-dependent antibodies reactive with a restricted domain of platelet GPIIIa, *Blood* 111:1234–1239, 2008.

Petit F, Minnai F, Chiaroni J, et al.: The radial expansion of the Diego blood group system polymorphisms in Asia: mark of co-migration with the Mongol conquests, *Eur J Human Gen* 27:125–132, 2019.

Petz LD: Drug-induced autoimmune hemolytic anemia, *Transfus Med Rev* 8:242–254, 1993.

Pham B-N, Peyrard T, Juszczak G, et al.: Alloanti-c (RH4) revealing that the $(C)ce^S$ haplotype encodes a partial c antigen, *Transfusion* 49:1329–1334, 2009.

Pietka TA, Schappe T, Conte C, et al.: Adipose and muscle tissue profile of CD36 transcripts in obese subjects highlight the role of CD36 in fatty acid homeostasis and insulin resistance, *Diabetes Care* 37:1990–1997, 2014.

Ponta H, Sherman L, Herrlich PA: CD44: from adhesion molecules to signaling regulators, *Nat Rev Mol Cell Biol* 4:33–45, 2003.

Poole J, Banks J, Bruce LJ, et al.: Glycophorin A mutation Ala65→Pro gives rise to a novel pair of MNS alleles ENEP (MNS39) and HAG (MNS41) and altered Wr^b expression: direct evidence for GPA/band 3 interaction necessary for normal Wrb expression, *Transfus Med* 9:167–174, 1999.

Poole J, Tilley L, Warke N, et al.: Two missense mutations in the *CD44* gene encode two new antigens of the Indian blood group system, *Transfusion* 47:1306–1311, 2007.

Poole J, Warke N, Hustinx H, et al.: A *KEL* gene encoding serine at position 193 of the Kell glycoprotein results in expression of KEL1 antigen, *Transfusion* 46:1879–1885, 2006.

Pocock CF, Lucas GF, Giles C, et al.: Immune neutropenia associated with anti-human neutrophil antigen-2a (NB1) antibodies following unrelated donor stem cell transplantation for chronic myeloid leukaemia: perpetuation by granulocyte colony-stimulating factor, *Br J Haematol* 113:483–485, 2001.

Porcelijn L, Huiskes E, de Haas M: Progress and development of platelet antibody detection, *Transf Aph Sci*, 2020. https://doi.org/10.1016/j. transci.2019.102705.

Rac ME, Safranow K, Poncyljusz W: Molecular basis of human CD36 gene mutations, *Mol Med* 13:288–296, 2007.

Portegys J, Rink G, Bloos P, et al.: Towards a regional registry of extended typed blood donors: molecular typing for blood group, platelet and granulocyte antigens, *Transf Med Hemotherapy* 45:331–340, 2018.

Race RR: The Rh genotypes and Fisher's theory, *Blood* 3:27–42, 1948.

Race RR, Sanger R: *Blood groups in man*, 6th ed, Oxford, 1975, Blackwell Scientific Publications.

Radel DJ, Penz CS, Dietz AB, et al.: A combined flow cytometry-based method for fetomaternal hemorrhage and maternal D, *Transfusion* 48:1886, 2008. –1891.

Rahuel C, Elouet J-F, Cartron J-P: Post-transcriptional regulation of the cell surface expression of glycophorins A, B, and E, *J Biol Chem* 269:32752–32758, 1994.

Rahuel C, Le Van Kim C, Mattei MG, et al.: A unique gene encodes spliceoforms of the B-cell adhesion molecule cell surface glycoprotein of epithelial cancer and of the Lutheran blood group glycoprotein, *Blood* 88:1865–1872, 1996.

Rao KV: *Drug-induced hematologic disorders. Chapter 24*, McGraw-Hill Education, 2014, pp 359–374. mhpharmacotherapy.com.

Recke A, Vidarsson G, Ludwig RJ, et al.: Allelic and copy-number variations of FcγRs affect granulocyte function and susceptibility for autoimmune blistering diseases, *J Autoimmunity* 61:36–44, 2015.

Reich D, Nalls MA, Kao WHL, et al.: Reduced neutrophil count in people of African descent is due to a regulatory variant in the Duffy antigen receptor for chemokines gene, *PLoS Genet* 5:e1000360, 2009.

Reid ME: The complexities of the Dombrock blood group system revealed, *Transfusion* 45:92S–99S, 2005.

Reid ME: MNS blood group system: a review, *Immunohematol* 25:95–101, 2009.

Reid ME, Hue-Roye K, Huang A, et al.: Alleles of the LAN blood group system: molecular and serologic investigations, *Transfusion* 54:398–404, 2014.

Ridgwell K, Eyers SAC, Mawby W, et al.: Studies on the glycoprotein associated with Rh (rhesus) blood group antigen expression in the human red blood cell membrane, *J Biol Chem* 269:6410–6416, 1994.

Rieben R, Buchs JP, Fluckiger E, et al.: Antibodies to histo-blood group substances A and B: agglutination titers, Ig class, and IgG subclasses in healthy persons of different age categories, *Transfusion* 31:607–615, 1991.

Roudier N, Verbavatz J-M, Maurel C, et al.: Evidence for the presence of aquaporin-3 in human red blood cells, *J Biol Chem* 273:8407–8412, 1998.

Rourk A, Squires JE: Implications of the Kidd blood group system in renal transplantation, *Immunohematol* 28:91–94, 2012.

Rowley SD, Donato ML, Bhattacharyya P: Red blood cell-incompatible allogeneic hematopoietic progenitor cell transplantation, *Bone Marrow Transplant* 46:1167–1185, 2011.

Russo D, Redman C, Lee S: Association of XK and Kell blood group proteins, *J Biol Chem* 273:13950–13956, 1998.

Russo DCW, Lee S, Reid ME, et al.: Point mutations causing the McLeod phenotype, *Transfusion* 42:287–293, 2002.

Sadallah S, Hess C, Trendelenburg M, et al.: Autoantibodies against complement receptor 1 (CD35) in SLE, liver cirrhosis and HIV-infected patients, *Clin Exp Immunol* 131:174–181, 2003.

Sandes AF, Yamamoto M, Matarraz S, et al.: Altered immunophenotypic features of peripheral blood platelets in myelodysplastic syndrome, *Heamatologica* 97:895–902, 2012.

Salama A: Drug-induced immune hemolytic anemia, *Expert Opin Drug Saf* 8:73–79, 2009.

Salinas ND, Paing MM, Tolia NH: Critical glycosylated residues in exon three of erythrocyte glycophorin A engage Plasmodium falciparum EBA-175 and define receptor specificity, *mBio* 5(5), 2014, https://doi.org/10.1128/mBio.01606-14. e01606-e1614. Published 2014 Sep 9.

Sandler SG, Chen LN, Flegel WA: Serological weak D phenotypes: a review and guidance for interpretating the RhD blood type using the RHD genotype, *Br J Haematol* 179:10–19, 2017.

Sato O, Takanashi N, Motojima K: Third promoter and differential regulation of mouse and human fatty acid translocase/CD36 genes, *Mol Cell Biochem* 299:37–43, 2007.

Satoh M, Handa K, Saito S, et al.: Disialosyl galactosylgloboside as an adhesion molecule expressed on renal cell carcinoma and its relationship to metastatic potential, *Cancer Res* 56:1932–1938, 1996.

Scharberg E, Schulz D, Sturtzel A, et al.: A new Knops antigen antithetical to KCAM [abstract], *Transfusion* 59:123–124, 2019.

Schuldt K, Ehmen C, Sievertsen J, et al.: Lack of association of CD55 receptor genetic variants and severe malaria in Ghanaian children, *G3 Genes-Genomes-Genetics* 7:859–864, 2017.

Schulz U, Reil A, Kiefel V, Bux J, Moog R: Evaluation of a new microbeads assay for granulocyte antibody detection, *Transfusion* 57:70–81, 2017.

Schwarz K, Iolascon A, Verissimo F, et al.: Mutations affecting the secretory COPII coat component SEC23B cause congenital dyserythropoietic anemia type II, *Nat Genet* 41:936–940, 2009.

Seltsam A, Agaylan A, Grueger D, et al.: Rapid detection of JMH antibodies with recombinant Sema7A (CD108) protein and the particle gel immunoassay, *Transfusion* 48:1151–1155, 2008.

Seltsam A, Das Gupta C, Bade-Doeding C, et al.: A weak blood group A phenotype caused by a translation-initiator mutation in the ABO gene, *Transfusion* 46:434–440, 2006.

Seltsam A, Das Gupta C, Wagner FF, et al.: Nondeletional *ABO*O* alleles express weak blood group A phenotypes, *Transfusion* 45:359–365, 2005.

Seltsam A, Grueger D, Blasczyk R, et al.: Easy identification of antibodies to high-prevalence Scianna antigens and detection of admixed alloantibodies using soluble recombinant Scianna proteins, *Transfusion* 49:2090–2096, 2009.

Seltsam A, Strigens S, Levene C, et al.: The molecular diversity of Sema7A, the semaphorin that carries JMH blood group antigens, *Transfusion* 47:133–146, 2007.

Simtong P, Romphruk AV, Hofmann C, et al.: Improvement of monoclonal antibody-immobilized granulocyte assay for the detection of anti-HNA-1 alloantibodies, *Transfusion* 58:200–207, 2018.

Shirey RS, Edwards RE, Ness PM: The risk of alloimmunization to c (Rh4) in R_1R_1 patients who present with anti-E, *Transfusion* 34:756–758, 1994.

Shirey RS, Mirabella DC, Lumadue JA, et al.: Differentiation of anti-D, -C, and -G: clinical relevance in alloimmunized pregnancies, *Transfusion* 37:493–496, 1997.

Shulman IA: The risk of an overt hemolytic transfusion reaction following the use of an immediate spin crossmatch, *Arch Pathol Lab Med* 114:412–414, 1990.

Shulman IA, Nelson JM, Lam HT, et al.: Additional limitations of the immediate spin crossmatch to detect ABO incompatibility [Letter], *Am J Clin Pathol* 87:677, 1987.

Silliman CC, Curtis BR, Kopko PM, et al.: Donor antibodies to HNA-3a implicated in TRALI reactions prime neutrophils and cause PMN-mediated damage to human pulmonary microvascular endothelial cells in a two-event in vitro model, *Blood* 109:1752–1755, 2007.

Singleton BK, Burton NM, Green C, et al.: Mutations in *EKLF/KLF1* form the molecular basis of the rare blood group In(Lu) phenotype, *Blood* 112:2081–2088, 2008.

Smith BL, Preston GM, Spring FA, et al.: Human red cell aquaporin CHIP: molecular characterization of ABH and Colton blood group antigens, *J Clin Invest* 94:1043–1049, 1994.

Soejima M, Fujihara J, Takeshita H, et al.: *Sec1-Fut2-Sec1* hybrid allele generated by interlocus gene conversion, *Transfusion* 48:488–492, 2008.

Solovey A, Lin Y, Browne P, et al.: Circulating activated endothelial cells in sickle cell anemia, *N Engl J Med* 337:1584–1590, 1997.

Spitalnik S, Pfaff W, Cowles J, et al.: Correlation of humoral immunity to Lewis blood group antigens with renal transplant rejection, *Transplantation* 37:265–268, 1984.

Srivastava K, Almarry NS, Flegel WA: Genetic variation of the whole ICAM4 gene in Caucasians and African Americans, *Transfsion* 54:2315–2324, 2014.

Steelant WF, Kawakami Y, Ito A, et al.: Monosialosyl-Gb5 organized with cSrc and FAK in GEM of human breast carcinoma MCF-7 cells defines their invasive properties, *FEBS Lett* 531:83–98, 2002.

Steffensen R, Carlier K, Wiels J, et al.: Cloning and expression of the histo-blood group P^k UDP-galactose: Galβ1-4Glcβ1-1Cer α1,4 galactosyltransferase, *J Biol Chem* 275:16723–16729, 2000.

Stenfelt L, Hellberg A, Moller M, et al.: Missense mutations in the C-terminal portion of the *B4GALNT2*-encoded glycosyltransferase underlying the Sd(a-) phenotype, *Biochem Biophys Rep* 19:100659, 2019.

Stenfelt L, Westman JS, Hellberg A, Olsson ML: The P1 histo-blood group antigen is present on human red blood cell glycoproteins, *Transfusion* 59:1108–1117, 2019.

St-Louis M, Laurent J, Perreault J, et al.: A new Sema7A variant in four Native Americans with anti-JMH, *Transfusion* 49S:118A, 2009.

Storry JR, Clausen FB, Castilho L, et al.: International society of blood transfusion working party on red cell immunogenetics and blood group terminology: report of the Dubai, Copenhagen and Toronto meetings, *Vox Sang* 114:95–102, 2019.

Storry JR, Joud M, Kronborg Chrisophersen M, et al.: Homozygosity for a null allele of *SMIM1* defines the Vel-negative blood group phenotype, *Nat Genet* 45:537–541, 2013.

Storry JR, Peyrard T: The Vel blood group system: a review, *Immunohematol* 33:56–59, 2017.

Storry JR, Reid ME: The Cromer blood group system: a review, *Immunohematol* 18:95–103, 2002.

Stroncek DF, Shapiro RS, Filipovich AH, Plachta LB, Clay ME: Prolonged neutropenia resulting from antibodies to neutrophil-specific antigen NB1 following marrow transplantation, *Transfusion* 33:158–163, 1993.

Stroncek DF, Caruccio L, Bettinotti M: CD177: a member of the Ly-6 gene superfamily involved with neutrophil proliferation and polycythemia vera, *J Translational Med* 2(8), 2004.

Swensson L, Rydberg L, Hellberg A, et al.: Novel glycolipid variations revealed by monoclonal antibody immunochemical analysis of weak ABO subgroups of A, *Vox Sang* 89:27–38, 2005.

Takada A, Ohmori K, Yoneda T, et al.: Contribution of carbohydrate antigens sialyl Lewis A and sialyl Lewis X to adhesion of human cancer cells to vascular endothelium, *Cancer Res* 53:354–361, 1993.

Tanner MJA: Molecular and cellular biology of the erythrocyte anion exchanger (AE1), *Semin Hematol* 30:34–57, 1993.

Tetteh-Quarcoo PB, Schmidt CQ, Tham W-H, et al.: Lack of evidence from studies of soluble protein fragments that Dnops blood group polymorphisms in complement receptor type 1 are driven by malaria, *PloS One* 7:e34820, 2012, https://doi.org/10.1037/journal.pone.0034820.

Tham W-H, Wilson DW, Lopaticki S, et al.: Complement receptor 1 is a host erythrocyte receptor for *Plasmodium falciparum* PfRH4 invasion ligand, *Proc Natl Acad Sci U S A* 107:17327–17332, 2010.

Thuresson B, Westman JS, Olsson ML: Identification of a novel *A4GALT1* exon reveals the genetic basis of the P1/P2 histo-blood groups, *Blood* 117:678–687, 2011.

Tian MH, Halverson GR: Characterization of three novel monoclonal anti-Ok^a, *Immunohematol* 25:174–178, 2009.

Tilley L, Green C, Daniels G: Sequence variation in the 5′ untranslated region of the human *A4GALT1* gene is associated with, but does not define, the P1 blood group-group polymorphism, *Vox Sang* 90:198–203, 2006.

Tilley L, Green C, Poole J, et al.: A new blood group system, RHAG: three antigens resulting from amino acid substitutions in the Rh-associated glycoprotein, *Vox Sang* 98:151–159, 2010.

Toivanen A, Ihanus E, Mattila M, et al.: Importance of molecular studies on major blood groups intercellular adhesion molecule-4, a blood group antigen involved in multiple cellular interactions, *Biochim Biophys Acta* 1780:456–466, 2008.

Tournamille C, Filipe A, Badaut C, et al.: Fine mapping of the Duffy antigen binding site for the *Plasmodium vivax* Duffy-binding protein, *Mol Biochem Parasitol* 144:100–103, 2005.

Toy P, Gajic O, Bacchetti P, et al.: Transfusion-related acute lung injury: incidence and risk factors, *Blood* 119:1757–1767, 2012.

Twu Y-C, Chen C-P, Hsieh C-Y, et al.: I branching formation in erythroid differentiation is regulated by transcription factor C/EBPα, *Blood* 110:4526–4534, 2007.

Vahidnezhad H, Youssefian L, Saeidian AH, et al.: Recessive mutation in tetraspanin CD151 causes Kindler syndrome-like epidermolysis bullosa with multi-systematic manifestations including nephropathy, *Matrix Biol* 66:22–23, 2018.

Vahalom V, Pillar N, Zhao Y, et al.: SMYD1 is the underlying gene for the AnWj-negative blood group phenotype, *Eur J Haematol* 1010:496–501, 2018.

Van Deenen LLM, de Grier J: Lipids of the red cell membrane. In Surgenor DM, editor: *The red cell membrane*, 2nd ed, New York, 1974, Academic Press, pp 147–156.

Van den Akker ES, Klumper FJ, Brand A, et al.: Kell alloimmunization in pregnancy: associated with fetal thrombocytopenia? *Vox Sang* 95:66–69, 2008.

Vaughan JI, Manning M, Warwick RM, et al.: Inhibition of erythroid progenitor cells by anti-Kell antibodies in fetal alloimmune anemia, *N Engl J Med* 338:798–803, 1998.

Vege S, Nickle PA, Shirey R, et al.: A novel 245G>C (Al85Gly) change associated with partial Rhe and alloanti-e [Abstract], *Transfusion* 49S, 2009. 15A.

Verkman AS: Knock-out models reveal new aquaporin functions. In Beits E, editor: *Aquaporins, handbook of experimental pharmacology*, Berlin, 2009, Springer-Verlag, pp 359–381.

Virella G, Bierer BE: The induction of an immune response: antigens, lymphocytes, and accessory cells. In Virella G, editor: *Medical immunology*, 5th ed, New York, 2001, Marcel Dekker, pp 51–76.

Vollrath B, Fitzgerald KJ, Leder P: A murine homologue of the Drosophila brainiac gene shows homology to glycosyltransferases and is required for preimplantation development of the mouse, *Mol Cell Biol* 21:5688–5697, 2001.

Vrignaud C, Mikdar M, Koehl B, et al.: Alloantibodies directed to the SLC44A2/CTL2 transporter define two new red cell alloantigens and a novel human blood group system, *Transfusion* 59(S3):18A, 2019.

Wagner T, Bernascher G, Geissler K: Inhibition of megakaryocytopoiesis by Kell-related antibodies [Letter], *N Engl J Med* 343:72, 2000.

Wagner FF, Blasczyk R, Seltsam A: Nondeletional ABO*O alleles frequently cause blood donor typing problems, *Transfusion* 45:1331–1334, 2005.

Wagner FF, Flegel WA: Review: the molecular basis of the Rh blood group phenotypes, *Immunohematol* 20:23–36, 2004.

Wagner FF, Gassner C, Muller TH, et al.: Molecular basis of weak D phenotypes, *Blood* 93:385–393, 1999.

Wanaguru M, Liu W, Hahn BH, et al.: RH5-Basigin interaction plays a major role in the host tropism of *Plasmodium falciparum*, *Proc Natl Acad Sci U S A* 110:20735–20740, 2013.

Wang Y, Jonson F: Expression, role and regulation of neutrophil Fcγ receptors, *Front Immunol* 10:1958, 2019.

Wasniowska K, Lisowska E, Halverson GR, et al.: The Fy^a, Fy6, and Fy3 epitopes of the Duffy blood group system recognized by new monoclonal antibodies: identification of a linear Fy3 epitope, *Br J Haematol* 124:118–122, 2004.

Weinstock C, Anliker M, von Zabern I: CD59: a long-known complement inhibitor has advanced to a blood group system, *Immunohematol* 31:145–151, 2015.

Weisbach V, Kohnhauser T, Zimmermann R, et al.: Comparison of the performance of microtube column systems and solid-phase systems and the tube low-ionic-strength solution additive indirect antiglobulin test in the detection of red cell alloantibodies, *Transfus Med* 16:276–284, 2006.

West LJ, Platt JL: And justice for all: consideration of ABO compatibility in allocation of hearts for infant transplantation, *Circulation* 121:1884–1886, 2010.

Westhoff CM, Sipherd BD, Wylie DE, et al.: Severe anaphylactic reactions following transfusions of platelets to a patient with anti-Ch, *Transfusion* 32:576–579, 1992.

Westhoff CM, Storry JR, Walker P, et al.: A new hybrid *RHCE* gene (CeNR) is responsible for expression of a novel antigen, *Transfusion* 44:1047–1051, 2004.

Westman JS, Stenfelt L, Vidovic K, et al.: Allele-selective RUNX1 binding regulates P1 blood group status by transcriptional control of A4GALT1, *Blood* 131:1611–1616, 2018.

Weston BW, Nair RP, Larsen RD, et al.: Isolation of a novel human α (1,3) fucosyltransferase gene and molecular comparison to the human Lewis blood group α (1,3/4) fucosyltransferase gene, *J Biol Chem* 267:4152–4160, 1992.

Wihadmadyatami H, Heidinger K, Roder L, et al.: Allantibody against new platelet alloantigen (Lap(a)) on glycorprotein IIb is responsible for a case of fetal and neonatal alloimmune thrombocytopenia, *Transfusion* 55:2920–2929, 2015.

Whitley CB, Kramer K: A new explanation for the reproductive woes and midlife decline of Henry VIII, *Hist J* 53:827–848, 2010.

Whorley T, Vege S, Kosanke J, et al.: JK alleles associated with altered Kidd antigen expression [Abstract], *Transfusion* 49S:48A, 2009.

Wilder JA, Hewett EK, Ganser ME: Molecular evolution of GYPC: evidence for recent structural innovation and positive selection in humans, *Mol Biol Evol* 26:2679–2687, 2009.

Worrel H, Betz B, Harmon C, Wilson T, Cooling L: Type 1 CD36 deficiency with aberrant CD36 bone marrow expression and compound heterozygosity for a CD36-null and CD36-weak allele in an African American male [abstract], *Transfusion* 59:129–130, 2019.

Wright MS: Issitt PD: anticomplement and the indirect antiglobulin test, *Transfusion* 19:688–694, 1979.

Wu PC, Chyan T-W, Feng S-H, Chen M-H, Pai S-C: Genotyping and serotyping profiles showed weak Jk^a presentation for previously typed as Jk_{null} donors, *Vox Sang* 114:268–274, 2019.

Xia W, Bayat B, Sachs U, et al.: The frequencies of human neutrophil alloantigens in the Chinese Han population of Guangzhou, *Transfusion* 51:1271–1277, 2011.

Xu X, Liu Y, Hong X, et al.: Variants of CD36 gene and their association with CD36 protein expression in platelets, *Blood Transfus* 12:557–564, 2014.

Yamamoto FI: Molecular genetics of the ABO histo-blood group system, *Vox Sang* 69(1–7), 1995.

Yamamoto M, Cid E, Yamamoto F: Molecular basis of the human Forssman glycolipid antigen negativity, *Sci Rep* 2:975, 2012, https://doi.org/10.1038/srep00975.

Yamamoto M, Yamamoto F, Luong TT, et al.: Expression profiling of 68 glycosyltransferase genes in 27 different human tissues by the systematic multiplex reverse transcription-polymerase chain reaction method revealed clustering of sexually related tissues in hierarchical clustering algorithm analysis, *Electrophoresis* 24:2295–2307, 2003.

Yamaoka Y: Roles of *Helicobacter pylori* BabA in gastroduodenal pathogenesis, *World J Gastroenterol* 14:4265–4272, 2008.

Yasui K, Hirayama F, Matsuyama N, et al.: New cell lines expressing HNA-1c, -4a, -4b, -5a, or -5b for identification of HNA antibodies, *Transfusion* 48:1037–1039, 2008.

Yasui K, Miyazaki T, Matsuyama N, et al.: Establishment of cell lines stably expressing HNA-1a, -1b, and -2a antigen with low background reactivity in flow cytometric analysis, *Transfusion* 47:478–485, 2007.

Yazdanbakhsh K, Rios M, Storry JR, et al.: Molecular mechanisms that lead to reduced expression of Duffy antigens, *Transfusion* 40:310–320, 2000.

Yazer MH, Hult AK, Hellberg A, et al.: Investigation into A antigen expression on O^2 heterozygous group O-labeled red blood cell units, *Transfusion* 48:1650–1657, 2008.

Yesus YW, Akhter JE: Hemolytic disease of the newborn due to anti-C and anti-G masquerading as anti-D, *Am J Clin Pathol* 84:769–772, 1985.

Yougbare I, Lang S, Yang H, et al.: Maternal anti-platelet β3 integrins impair angiogenesis and cause intracranial hemorrhage, *J Clin Invest* 125:1545–1556, 2015.

Yu L-C, Twu Y-C, Cou M-L, et al.: The molecular genetics of the human I locus and molecular background explain the partial association of the adult I phenotype with congenital cataracts, *Blood* 101:2081–2092, 2003.

Yu L-C, Yang Y-H, Broadberry RE, et al.: Correlation of a missense mutation in the human secretor α 1,2-fucosyltransferase gene with the Lewis (a+b+) phenotype: a potential molecular basis for the weak secretor allele (Se^w), *Biochem J* 312:329–332, 1995.

Zelinski T, Coghlan G, Liu X-Q, et al.: *ABCG2* null alleles define the Jr(a-) blood group phenotype, *Nat Genet* 44:131–132, 2012.

Zhang N, Santoso S, Aster R, Curtis BR, Newman PJ: Bioengineered iPSC-derived megakaryocytes for the detection of platelet-specific patient alloantibodies, *Blood* 134:e1–e8, 2019.

Zhu X, Rivera A, Golub MS, et al.: Changes in red cell ion transport, reduced intratumoral neovascularization, and some mild motor function abnormalities accompany targeted disruption of the mouse Kell gene (Kel), *Am J Hematol* 94:492–498, 2009.

CHAPTER 37

TRANSFUSION MEDICINE

Matthew B. Elkins, Robertson D. Davenport, Paul D. Mintz

BACKGROUND, 771
BLOOD COLLECTION, 771
BLOOD COMPONENT MANUFACTURE, 773
Red Blood Cells, 773
Plasma, 774
Cryoprecipitated Antihemophilic Factor, 774
Platelet Concentrates, 774
Leukocyte Components, 774
Leukocyte-Reduced Blood Components, 774
Special Components, 774
Pathogen Reduction, 775
SELECTION OF BLOOD COMPONENTS, 775
Red Blood Cells, 775
Platelets, 776
PRETRANSFUSION TESTING, 776
TRANSFUSION ADMINISTRATION, 777
Blood Component Therapy, 777
Massive Transfusion, 779
Neonatal and Pediatric Transfusion, 780
TRANSFUSION REACTIONS, 781
Febrile Nonhemolytic Reactions, 781
Allergic Reactions, 781
Severe Allergic (Anaphylactic) Reactions, 781
Acute Hemolytic Reactions, 782
Delayed Hemolytic Reactions, 782
Bacterial Contamination of Blood Components, 782
Transfusion-Related Acute Lung Injury, 783
Transfusion-Associated Circulatory Overload, 183
Graft-Versus-Host Disease, 783
Hypotensive Reactions, 784
Nonimmune Hemolysis, 784
Transfusion-Transmitted Disease, 785
CONCLUSION, 786
SELECTED REFERENCES, 786

KEY POINTS

- Criteria for blood donor eligibility are established by the U.S. Food and Drug Administration (FDA) to minimize risks to both the donor and the transfusion recipient.
- Blood components (red blood cells, platelet concentrates, fresh frozen plasma, cryoprecipitate) are manufactured and stored in a manner to minimize functional loss of desired constituents.
- Leukocyte reduction of blood components reduces alloimmunization to human leukocyte antigens, cytomegalovirus transmission, and febrile reactions. Irradiation of blood components can prevent graft-versus-host disease. Pathogen reduction can significantly reduce risks of transfusion-transmitted infections.
- Accurate identification of the pretransfusion blood sample and the intended recipient is the most important step in preventing acute hemolytic transfusion reactions.
- Restrictive red cell transfusion (hemoglobin target 7–8 g/dL) is associated with improved outcomes in some patient populations.
- Platelet transfusion is generally indicated for microvascular bleeding, platelet count <10,000/μL, or platelet count <50,000/μL before an invasive procedure.
- Failure to respond to platelet transfusion may be due to immune causes (human leukocyte antigens or platelet-specific antibodies), nonimmune clinical causes (bleeding, splenomegaly, disseminated intravascular coagulation, medications), or product-specific causes (ABO incompatibility, age of component).
- Plasma transfusion is generally indicated for coagulation factor deficiency, disseminated intravascular coagulation, dilutional coagulopathy, urgent warfarin reversal, and thrombotic thrombocytopenic purpura.
- Potentially severe adverse effects of transfusion include hemolytic reactions, allergic reactions, transfusion-related acute lung injury, bacterial contamination, and graft-versus-host disease.
- Current risks of transfusion-transmitted human immunodeficiency virus or hepatitis are very low, but the risk for other transfusion-transmitted diseases (cytomegalovirus, parvovirus B-19) may be significant in some populations.

BACKGROUND

Transfusion medicine is a multidisciplinary specialty encompassing all aspects of blood donation, blood component preparation, blood cell serology, and blood transfusion therapy. The term *blood banking* has largely been superseded by *transfusion medicine* to emphasize the importance of patient care and clinical outcomes.

Operationally, transfusion medicine is divided between blood centers and transfusion services. Blood centers recruit and collect blood from donors and manufacture and distribute blood components. Transfusion services perform pretransfusion compatibility testing, select and issue blood components for patients, and provide medical support for blood transfusion. Most hospital transfusion services do not collect their own blood, but rather rely on regional blood centers.

Blood centers and transfusion services (collectively known as *blood establishments*) are regulated by the U.S. Food and Drug Administration (FDA). All blood establishments must be registered with the FDA, and blood centers that manufacture blood components must be licensed for distribution in interstate commerce. Criteria for the acceptability of blood donors, performance of pretransfusion testing, manufacture of blood components, donor infectious disease testing, and evaluation and reporting of adverse events associated with transfusion are all defined by the FDA. Blood establishments are subject to periodic unannounced inspections by the FDA. Compliance with federal regulations is an essential aspect of transfusion medicine. In addition, professional organizations such as AABB (formerly known as the American Association of Blood Banks), the College of American Pathologists, and The Joint Commission have put forth accreditation standards for transfusion services and conduct voluntary peer inspections.

BLOOD COLLECTION

Approximately 60% of the adult U.S. population is eligible to donate blood, although only about 4.5% actually do so annually. Approximately 12.5 million units of whole blood and red blood cells (RBCs) are collected annually in the United States (Ellingson et al., 2017). Virtually all donors are voluntary and noncompensated. The average blood donor is a college-educated white male between 30 and 50 years of age, who is married and has above average income. However, donations among women and minority groups are increasing. Although the utilization of blood components has decreased in recent years, tightening of donor eligibility requirements

TABLE 37.1
Requirements of Allogeneic Donor Qualification

Category	Criteria
Age	At least 16 years or minimum age determined by state law
Whole-blood volume collected	Maximum of 10.5 mL/kg
Donation interval	8 weeks after whole-blood donation
	16 weeks after two-unit red cell collection
	4 weeks after infrequent apheresis
	At least 2 days after plasma, platelet, or leukocyte apheresis
Blood pressure	Systolic pressure between 90 mm Hg and 180 mm Hg; diastolic pressure between 50 mm Hg and 100 mm Hg
Pulse	Regular and between 50 and 100 beats per minute
Temperature	≤37.5°C orally
Hemoglobin/hematocrit	Females: ≥12.5 g/dL/38%; males: ≥13.0 g/dL/39%
Drug therapy	Finasteride, isotretinoin—defer 1 month after last dose
	Dutasteride—defer 6 months after last dose
	Acitretin—defer 3 years after last dose
	Etretinate—defer indefinitely
	Bovine insulin manufactured in the United Kingdom—defer indefinitely
	Ingestion of medications that irreversibly inhibit platelet function (aspirin) within 37 hours of donation precludes use of donor as sole source of platelets
General medical history	Free of major organ disease, cancer, abnormal bleeding tendency
	Family history of CJD or recipient of dura mater or human pituitary growth hormone—defer indefinitely
Pregnancy	Defer if pregnant within the past 6 weeks
Recipient of blood transfusion or tissue transplant	Defer for 12 months from time of transfusion/transplant
Vaccinations and immunizations	Recipient of toxoid, synthetic, or killed viral, bacterial, or other vaccine—no deferral
	Recipient of live, attenuated intranasal flu vaccine—no deferral
	Recipient of live attenuated viral or bacterial vaccine—2- or 4-week deferral from the time of vaccination
	Smallpox vaccine—refer to current FDA guidance
	Other vaccines, including unlicensed vaccines—12-month deferral from time of vaccination
Infectious diseases—indefinite deferral	Viral hepatitis after 11th birthday
	Positive test for hepatitis B surface antigen or HBV NAT
	Repeat reactive test for anti-HBc on more than one occasion
	Clinical or laboratory evidence of HCV, HTLV, HIV, ZIKV, or *T. cruzi* infection by current FDA regulations
	Previous donation associated with hepatitis, HIV, or HTLV transmission
	History of babesiosis or Chagas disease
	Stigma of parenteral drug use
	Injection of nonprescribed drugs
	Risk for vCJD according to current FDA guidelines
Infectious diseases—12-month deferral	Mucous membrane exposure to blood
	Nonsterile skin or needle penetration
	Sexual contact with an individual with a confirmed positive test for hepatitis B surface antigen
	Sexual contact with an individual with viral hepatitis
	Sexual contact with an individual with HIV infection or behavioral risk for HIV infection according to current FDA guidance
	Incarceration in a correctional institution for longer than 72 consecutive hours
	History of syphilis or gonorrhea
West Nile virus	Defer according to current FDA guidance
Malaria	Confirmed diagnosis—defer for 3 years after becoming asymptomatic
	Travel to or residence in an endemic area as defined by the CDC—defer according to FDA guidance

CDC, Centers for Disease Control and Prevention; *CJD,* Creutzfeldt-Jakob disease; *FDA,* U.S. Food and Drug Administration; *HBV,* hepatitis B virus; *HCV,* hepatitis C virus; *HIV,* human immunodeficiency virus; *HTLV,* human T-cell lymphotropic virus; *NAT,* nucleic acid test; *vCJD,* variant of Creutzfeldt-Jakob disease.

and decreased donations have resulted in continued challenges in meeting the demand for blood components. Ongoing efforts to recruit additional donors are critical to ensure an adequate blood supply.

Donor criteria are established for the protection of the blood donor and the transfusion recipient. Current (2015) U.S. donor qualification criteria are listed in Table 37.1. Criteria for donor protection include a minimum age of 16 years, a minimum weight of 110 pounds, normal vital signs, a minimum hemoglobin (Hb) concentration, and a specified donation interval. Criteria for the protection of the transfusion recipient include history or risk factors for infectious disease transmission (hepatitis, human immunodeficiency virus [HIV], malaria, and others), risk for bacteremia, presence of certain medications, and history of malignancy. Blood centers are required to maintain a registry of deferred donors; each donor must be checked against this registry before any donation is made. Finally, every donation must be tested for infectious disease markers as defined by FDA regulations. Current (2019) U.S. donor testing requirements are indicated in Box 37.1.

Blood must be collected in a manner that minimizes the risk for bacterial contamination. The skin at the venipuncture site must be prepared with an antibacterial scrub. Whole blood is collected into sterilized bag sets containing anticoagulant and attached satellite bags to facilitate component manufacture in a closed system. The rate of blood flow must be

BOX 37.1

Current U.S. Donor Infectious Disease Testing

Hepatitis B surface antigen (EIA)
Hepatitis B core antibody (EIA)
Hepatitis C virus antibody (EIA)
HIV-1 and HIV-2 antibodies (EIA)*
HTLV-I and HTLV-II antibodies (EIA)
Trypanosoma cruzi antibodies (EIA)
Serologic test for syphilis
Babesia microti antibody (EIA)^
Babesia microti DNA (nucleic acid test)^
Hepatitis C RNA (nucleic acid test)
HIV RNA (nucleic acid test)
West Nile virus DNA (nucleic acid test)
Hepatitis B DNA (nucleic acid test)
Zika virus RNA (nucleic acid test)

DNA, deoxyribonucleic acid; *EIA,* enzyme immunoassay; *HIV,* human immunodeficiency virus; *HTLV,* human T-cell lymphotropic virus; RNA, ribonucleic acid.
*Combined HIV p24 antigen, HIV-1 antibodies, and HIV-2 antibodies acceptable.
^Testing required on donations collected in endemic areas.

sufficient to prevent clot formation during phlebotomy. The volume of blood withdrawn must be less than 10.5 mL/kg of the donor's weight, including samples for testing. Typically, whole blood donations are 450 or 500 mL.

Blood components can also be collected by apheresis. The advantage of apheresis donation is that a greater volume of the desired components may be obtained from a single donation. The most common use of the apheresis donation is the collection of platelets (commonly called *single-donor platelets*). Plasma may also be collected, typically concurrently with platelets. Apheresis donation allows for the collection of two units of RBCs from suitable donors. Leukocytes may also be collected by apheresis. This is most commonly utilized for the collection of hematopoietic progenitor cells for autologous or allogeneic transplantation. Granulocytes or mononuclear cells may be collected by apheresis for special applications.

Autologous donation is the collection of blood from a patient in advance of scheduled surgery for transfusion during or after the procedure to compensate for expected blood loss. Autologous transfusion prevents the transmission of blood-borne pathogens from allogeneic donors, which is desired by some patients. It is not completely free of risk, however, particularly of bacterial contamination. Whether or not autologous transfusion actually decreases the need for allogeneic transfusion or improves patient outcome is controversial. Benefit in reducing allogeneic blood exposure or improving outcome has not been shown in controlled prospective randomized trials. For patients with antibodies to very common RBC antigens, autologous donation may be used to provide compatible blood products if compatible allogeneic components cannot be located. Candidates for autologous donation must not have underlying disease that would put them at risk from this procedure. They must not be significantly anemic, although a lower Hb level of 11.0 g/dL is allowed. They must not be at risk for bacteremia because the most serious adverse consequence of autologous transfusion is bacterial contamination. Patients with heart disease, particularly aortic stenosis, may be unable to tolerate phlebotomy. Pregnancy does not itself constitute a contraindication to autologous donation; however, the value of autologous donation, except in certain high-risk situations such as placenta previa, is minimal. Autologous donations can occur more frequently than allogeneic donations. Typically, two or three units may be collected several weeks before surgery. Optimally, there should be sufficient time from donation to surgery to allow for recovery of a substantial portion of the collected red cell mass. This may require iron supplementation. Erythropoietin stimulation has been used as an adjunct to autologous donation.

Some patients desire to select donors for themselves (directed or designated donation) rather than receiving blood from the community blood supply. This provides some patients with the perception of greater safety, although no evidence suggests that directed donation reduces the risk for transfusion-transmitted disease. Directed donors must meet all criteria for allogeneic blood donation. In addition, directed donors must be compatible with the intended recipient. In certain situations, directed donation is contraindicated. Donation of any plasma-containing blood component from a mother to her child is particularly problematic because the formation of human leukocyte antigens (HLA) antibodies to fetal antigens is common in pregnancy, and transfusion of such antibodies can precipitate transfusion-related acute lung injury (TRALI; see later discussion). Transfusions from close relatives should be avoided in recipients of hematopoietic progenitor cell transplants because of the risk for immunization to HLA and other histocompatibility antigens, which may endanger graft survival. There are rare circumstances under which directed donation may be desirable. These include rare blood group compatibility requirements and limitations of donor exposure for patients with long-term expected transfusion requirements, such as aplastic anemia. In cases of neonatal alloimmune thrombocytopenia, collection of maternal platelets may be the best way of providing compatible antigen-negative platelets. In the past, donor-specific transfusion was utilized in kidney transplantation. However, with current immunosuppressive regimens, donor-specific transfusion for prolonging renal graft survival is not used.

Adverse effects may occur with blood donations. Minor reactions, mostly presyncope, occur during 2.5% of whole blood donations (Eder et al., 2009). Major reactions, including loss of consciousness, nerve or arterial injury, allergic reaction, and citrate reaction, occur during about 0.07% of whole blood and 0.05% of apheresis platelet collections. Up to 36% of donors interviewed 3 weeks after donation report some adverse effect, mostly minor, such as arm bruise or soreness (Newman et al., 2003). More serious adverse effects, such as vasovagal symptoms, were reported in about 5%, and nausea and vomiting in about 1%. Repeat donors are less likely to have reactions than first-time donors. Smaller donors are at greater risk for postdonation syncope. Most syncopal reactions occur shortly after donation. However, delayed reactions can occur, and if the donor is at work or driving, these can be very serious. Some highly apprehensive donors hyperventilate, leading to respiratory alkalosis and tetany. This can usually be managed easily by coaching the donor to breathe slowly and deeply.

Personnel at a collection site should be prepared to treat donor reactions. Vasovagal syncope can usually be managed easily by placing the donor into a supine position and applying a cold compress to the forehead. It is rare that intravenous fluids are required. A physician should be available to donor site personnel for consultation, and emergency medical support should be available, if necessary. Vasovagal reactions may be minimized by prior hydration of the donor ("water loading"), use of caffeine, encouragement of the donor to flex the leg and trunk muscles ("applied muscle tension"), or by psychological support during the donation (Thijsen & Masser, 2017).

BLOOD COMPONENT MANUFACTURE

Whole-blood donations are commonly manufactured into components. This facilitates the treatment of different patients with requirements for RBCs, plasma, or platelets. The goals of component manufacture are to maintain viability and function, and to prevent detrimental changes or contamination of desired constituents.

RED BLOOD CELLS

RBCs are prepared from whole blood by centrifugation and removal of plasma and platelets. RBCs prepared in the preservative solution CPDA-1, supplemented with dextrose and adenine to preserve red cell adenosine triphosphate (ATP) levels, may be stored for up to 35 days at 1°C to 6°C. RBCs may also have an additive solution containing glucose and other substrates added during manufacture. Such additive solutions permit a longer storage period (42 days) and have a lower hematocrit (Hct). During storage, red cells undergo senescence changes similar to aging in vivo such that a portion of transfused red cells are rapidly cleared by the spleen. The maximum allowable storage time for RBCs is defined by the requirement for recovery of 75% of transfused cells 24 hours after transfusion. Leakage of intracellular potassium occurs during red cell storage due to lack of ATP to fuel the potassium pump. The potassium concentration in the supernatant of RBCs can reach levels of 76 mmol/L, which may appear alarmingly high. However, the total amount of potassium in a unit of RBCs at outdate is small compared with daily physiologic requirements, and hyperkalemia following transfusion is rare except in special circumstances (see later discussion). Hypokalemia may also occur secondary to RBC transfusion due to influx of potassium into transfused RBCs. After transfusion, the intracellular ATP levels are restored and the ATPase potassium pump resumes activity. Red cells lose intracellular 2,3-diphosphoglycerate (2,3-DPG) during storage, resulting in a shift of the Hb-oxygen dissociation curve to the left. Thus, shortly after transfusion, stored red cells have relatively high oxygen affinity. Normal levels of 2,3-DPG are restored within 24 hours of transfusion. The shift in oxygen association with storage is rarely clinically significant.

PLASMA

Plasma is separated from whole blood and frozen for extended preservation. In the liquid state at refrigerator temperatures, there is loss of labile clotting factors, particularly factor VIII and factor V. Fresh frozen plasma (FFP) is separated from the RBCs and is frozen at –18°C within 8 hours of collection. Plasma frozen within 24 hours after phlebotomy is manufactured similarly to FFP but may be frozen at any time up to 24 hours after collection. If this plasma is held at 4°C prior to freezing, it is labeled as PF24. If it is held at room temperature prior to freezing, it is labeled as PF24RT24. The coagulation factor content of FP24 or PF24RT24 is essentially equivalent to FFP (Scott et al., 2009). Frozen plasma may be stored for up to 1 year at –18°C or lower. Before transfusion, both FFP and FP24 are thawed at 37°C and must be transfused within 24 hours. Thawed plasma not used within 24 hours may be relabeled as "thawed plasma." Thawed plasma can be kept at refrigerator temperatures for up to 5 days with maintenance of adequate levels of factors V and VIII (Downes et al., 2001; Scott et al., 2009).

CRYOPRECIPITATED ANTIHEMOPHILIC FACTOR

Cryoprecipitated antihemophilic factor (cryoprecipitate or cryo) is the cold insoluble portion of plasma remaining after FFP has been thawed at refrigerator temperatures. It contains approximately 50% of factor VIII and 20% to 40% of the fibrinogen present in the original plasma unit. Cryo also contains von Willebrand factor (vWF) and factor XIII. FDA regulations require that a unit of cryoprecipitate contain at least 80 IU of factor VIII (21CFR640.56), although most blood centers achieve higher levels routinely. A unit of cryoprecipitate contains approximately 250 mg of fibrinogen; however, testing for the fibrinogen content is not required. Cryoprecipitated antihemophilic factor was a major advance in the treatment of hemophilia A before the development of safe purified clotting factor concentrates. Currently, cryo is used mainly as a source of fibrinogen.

PLATELET CONCENTRATES

Platelet concentrates (PCs) are prepared from whole blood by centrifugation of platelet-rich plasma and removal of platelet-poor plasma. PCs must contain at least 5.5×10^{10} platelets per unit. They are stored at room temperature (20°C–24°C) because platelets stored at refrigerator temperature (1°C–6°C) have greatly diminished posttransfusion survival. Current FDA regulations allow PCs to be stored for up to 5 days with continuous gentle agitation to encourage gas exchange. At the end of storage, the pH of the PCs must be 6.0 or higher. PCs typically contain a small number of red cells, which are visibly apparent and can cause alloimmunization to red cell antigens. PCs contain 30 to 50 mL of plasma. It is typically necessary to pool five or more PCs to obtain a therapeutic dose for a typical adult patient (3.0×10^{11} platelets).

PCs that are pooled using an open system must be transfused within 4 hours. PCs can be pooled and leukocyte reduced at the time of manufacture using a system that maintains sterility, often referred to as *prepooled platelets*. Because the integrity of the container is not compromised in this process, prepooled platelets can be stored for up to 5 days.

PCs prepared by apheresis (platelets, pheresis, or single-donor platelets) are stored and handled in the same manner as platelet concentrates prepared from whole blood. Each apheresis platelet unit should contain a minimum of 3.0×10^{11} platelets. It is possible to collect two or more platelet units in a single apheresis session from some donors. One apheresis platelet unit will typically provide a therapeutic dose for an adult patient. Apheresis platelet units are considered leukoreduced in the process of collection due to the apheresis collection selectivity for the platelets. Apheresis platelets can be further processed by removal of plasma and addition of a platelet additive solution (PAS). PAS platelets may pose a lower risk of allergic reactions.

On September 30, 2019, the FDA issued a Final Guidance, "Bacterial Risk Control Strategies for Blood Collection Establishments and Transfusion Services to Enhance the Safety and Availability of Platelets for Transfusion" with recommendations to enable blood banks and transfusion services to comply with 21 CFR 606.145(a): "Blood collection establishments and transfusion services must assure that the risk of bacterial contamination of platelets is adequately controlled using FDA approved or cleared devices or other adequate and appropriate methods found acceptable for this purpose by FDA." The Guidance may be accessed at https://www.fda.gov/regulatory-information/search-fda-guidance-documents/bacterial-risk-control-strategies-blood-collection-establishments-and-transfusion-services-enhance. Several protocols for compliance for both apheresis platelets and whole blood–derived platelets are described. These include options for bacterial culture, pathogen reduction, and rapid testing for bacteria.

LEUKOCYTE COMPONENTS

Granulocytes can be prepared by apheresis. Granulocytes may be stored at room temperature for up to 24 hours. However, after even brief in vitro storage, granulocytes may have reduced ability to circulate and migrate to areas of inflammation (McCullough et al., 1983). It is desirable that they be transfused as soon as possible after collection. Donor stimulation with granulocyte colony-stimulating factor (G-CSF) is usually necessary to obtain a sufficient number of granulocytes for a therapeutic dose for an adult patient (Heuft et al., 2002). Granulocyte units contain a substantial number of RBCs and must be ABO compatible with the recipient.

Mononuclear cells collected by apheresis can be a source of hematopoietic progenitor cells (HPCs) for autologous or allogeneic transplantation. The number of circulating HPCs can be increased by growth factor (G-CSF or granulocyte-macrophage colony-stimulating factor [GM-CSF]) stimulation, recovery from chemotherapy, or the chemokine receptor blocker plerixafor (Cashen, 2009; Nakasone et al., 2009). Autologous HPCs for transplantation in patients with lymphoma or other malignancies may be collected when the bone marrow is recovering from chemotherapy because there are relatively high numbers of circulating stem cells at that time. HPCs may be stored frozen after addition of a cryoprotective agent, such as dimethylsulfoxide (DMSO), for an extended period of time. After thawing at 37°C, HPCs should be transfused as soon as possible. Mononuclear cells can also be used as a source of lymphocytes for induction of graft-versus-tumor effect, known as *donor lymphocyte infusion* (Castagna et al., 2016) or for future manufacturing to produce cellular therapy products.

LEUKOCYTE-REDUCED BLOOD COMPONENTS

Leukocytes present in blood components, particularly RBCs and PCs, may cause adverse effects. Such untoward effects include febrile nonhemolytic transfusion reactions, immunization to leukocyte (particularly HLA) antigens with subsequent refractoriness to platelet transfusions, transmission of leukocyte-associated viruses, and graft-versus-host disease. To minimize most of these adverse impacts, many blood centers and transfusion services have instituted the use of leukocyte-reduced components for all transfusions (universal leukocyte reduction). It must be noted that leukocyte reduction has not been conclusively shown to prevent posttransfusion graft-versus-host disease and is not used for this purpose (Hayashi et al., 1993). To be considered leukocyte reduced, blood components must be prepared by a method known to reduce the total number of residual leukocytes to fewer than 5×10^6 per unit for RBCs and fewer than 8.3×10^5 for whole blood–derived PCs (Levitt, 2014).

Leukocyte reduction is typically accomplished by filtration at the time of component manufacture (prestorage leukocyte reduction) or at the time of transfusion (poststorage leukocyte reduction). Both methods are effective for removing leukocytes. However, prestorage leukocyte reduction has the advantage of preventing accumulation of leukocyte-derived biological response modifiers, particularly cytokines, which may cause adverse reactions (Silliman et al., 2017). In addition, filtration at the time of manufacture allows for better process control. Certain apheresis devices can reliably produce platelet concentrates containing fewer than 1×10^6 leukocytes. Subtle differences have been noted in the distribution of leukocyte subsets between such components and those produced by filtration (Pennington et al., 2001). These differences, however, are unlikely to be clinically significant.

Leukocyte reduction failures may occur during filtration of blood from donors with sickle trait. Such filtration failures may be due to Hb S polymerization in an environment of low oxygen tension and high osmolality (Beard et al., 2004). Clearly, granulocytes and hematopoietic progenitor cells cannot be leukocyte reduced.

SPECIAL COMPONENTS

Cryoprecipitate-reduced plasma (cryopoor plasma) is the supernatant remaining from the production of cryoprecipitate. It is relatively deficient in high molecular weight forms of vWF but retains close to normal levels of the vWF-cleaving metalloprotease ADAMTS 13 (a disintegrin and metalloprotease with eight thrombospondin) (Raife et al., 2006). For these reasons, cryoprecipitate-reduced plasma has been an alternative to FFP for the treatment of patients with thrombotic thrombocytopenic purpura

(TTP). However, at present, no evidence indicates that plasma exchange with cryoprecipitate-reduced plasma results in improved patient outcome.

RBCs can be stored in the frozen state after addition of a cryoprotective agent, such as glycerol. Frozen RBCs can be stored in mechanical freezers or liquid nitrogen for up to 10 years. Frozen units are thawed rapidly at 37°C. The cryoprotective agent must be removed by progressive addition of washing solutions with decreasing osmolality. Failure to properly deglycerolize frozen RBCs can result in hemolysis. Cryopreservation and deglycerolization of sickle trait red cells requires a modified process (Meryman & Hornblower, 1976). After deglycerolization, red cells can be stored for up to 1 day at 1°C to 6°C if processed by an open method or up to 14 days if processed by a closed method. The main use of frozen RBCs is to maintain an inventory of rare antigen-negative units.

RBCs and PCs can be washed to remove plasma proteins and electrolytes. Washing can be accomplished by manual or automated methods. Loss of cells during the washing process can be substantial. In addition, washing of platelets can result in clumping and activation with reduced viability (Pineda et al., 1989). If this is performed using an open process, washed red cells may be stored for 24 hours at refrigerator temperatures, and washed platelets must be transfused within 4 hours of initiation of washing, when prepared using an open system. The main use of washed components is the prevention of severe allergic reactions to plasma components. Washing is not an effective means of leukocyte reduction.

Transfusion-associated graft-versus-host disease (TA-GVHD) can be prevented by irradiation of components containing viable lymphocytes (RBCs, PCs, granulocytes, and nonfrozen plasma). This can be accomplished by exposure to γ-rays or x-rays. The minimum dose should be 25 Gy delivered to the center of the blood container and no less than 15 Gy to the periphery. Irradiation causes chromosomal damage, which prevents replication of transfused lymphocytes in the recipient. However, irradiated cells remain immunogenic. Thus, irradiation is not equivalent to leukocyte reduction. Irradiation also causes damage to red cell membranes, with increased potassium leakage and decreased posttransfusion survival (Hauck-Dlimi et al., 2015). Irradiated red cell units must have their outdate shortened to no more than 28 days from the date of irradiation. Platelets appear to sustain minimal damage from irradiation. Thus, their expiration date need not be altered, although the increment in platelet count may be reduced (Sweeney et al., 1994; Slichter et al., 2005). Clearly, hematopoietic progenitor cells must not be irradiated. Irradiation is not sufficient to prevent transmission of viral infections, including cytomegalovirus (CMV), or bacterial contamination.

PATHOGEN REDUCTION

Although great progress has been made in reducing the risk for transfusion-transmitted diseases, some risk remains. At present, there are multiple diseases that may be transmitted by transfusion for which there are no FDA-approved screening tests (e.g., prions, dengue, malaria). In addition, new transmissible diseases will continue to emerge as a threat to blood safety. For these reasons, strategies to inactivate contaminating microorganisms (pathogen reduction) have been developed. Blood derivatives such as albumin, coagulation factor concentrates, and immunoglobulin (Ig) are commonly treated by a variety of methods, including heat and solvent-detergent, which are highly effective against viruses, including HIV, hepatitis B virus (HBV), and hepatitis C virus (HCV). The solvent-detergent treatment process disrupts the lipid envelope of viruses such as HIV, HBV, and HCV. However, it is ineffective against nonlipid-enveloped viruses. In addition, it destroys cell membranes; thus, it is not applicable to cellular blood components. Solvent-detergent–treated plasma contains predictable levels of all coagulation factors and is effective in the treatment of TTP (Horowitz et al., 1992; Moake et al., 1994). However, it may contain reduced levels of protein S and has been associated with thrombotic complications (Heger et al., 2016).

The FDA has approved a pathogen reduction process for apheresis platelets and plasma (Intercept Blood System, Cerus Corporation, Concord, CA). Another pathogen reduction technology for platelets, plasma, and whole blood, currently not available in the United States but marketed elsewhere, is the Mirasol PRT System (Terumo BCT, Lakewood, CO) (McClaskey et al., 2009, Yonemura et al., 2017). Both treatments are effective against broad ranges of viruses, bacteria, and protozoans, but not against prions since these pathogens do not contain nucleic acids (Lin et al., 2004; Ruane et al., 2004).

Psoralen compounds used in the IBS intercalate between bases of ribonucleic acid (RNA) and deoxyribonucleic acid (DNA) and, when exposed to ultraviolet (UV) light, form covalent cross-links that prevent replication. Intercept-treated platelet concentrate has been shown to be safe and effective in a randomized trial (McCullough et al., 2004). The treatment process does result in a statistically significant, and possibly clinically significant, reduction in posttransfusion platelet recovery. These platelets do, however, retain functional capability after pathogen reduction (Estcourt et al., 2017). Riboflavin, used in the Mirasol PRT system, causes strand cleavage of nucleic acids when activated by UV light. Because these methods require exposure to light, their applicability to RBCs is limited. Both the Intercept and Mirasol processes have been shown to presumably preclude the need for irradiation of blood components to prevent TA-GVHD (Mintz, 2011; Kleinman & Stassinopoulos, 2018).

TABLE 37.2
ABO Compatibility

	RECIPIENT TYPE			
Donor Type	**O**	**A**	**B**	**AB**
O	R P	R	R	R
A	P	R P		R
B			R P	R
AB	P	P	P	R P

P, Plasma-containing components (platelets, fresh frozen plasma) are compatible; *R,* red cells are compatible.

SELECTION OF BLOOD COMPONENTS

Blood components must be serologically compatible with the recipient. ABO compatibility is the primary consideration. Transfused red cells must be compatible with recipient antibodies, and transfused plasma must be compatible with recipient red cells. Therefore, whole blood would ideally be of identical ABO type to the recipient. RBCs contain a limited amount of plasma and need to be compatible, but not necessarily identical, to the ABO type of the recipient. Similarly, plasma and platelet concentrates contain few, if any, red cells. ABO-compatible blood component selection is summarized in Table 37.2 (Busch, 2005). RBCs must also be negative for clinically significant antigens when transfused to alloimmunized recipients. It is highly desirable to transfuse only Rh-negative red cells to Rh-negative recipients because there is approximately a 30% risk for immunization to Rh(D) (Frohn et al., 2003). This is particularly important for women of childbearing potential because of the risk for hemolytic disease of the newborn in subsequent pregnancies.

Special considerations apply to recipients of ABO-incompatible HPC transplants. During the course of transplantation, such individuals will change their blood type. Transfused red cells should be compatible with both donor and recipient isohemagglutinins, and transfused plasma–containing components should be compatible with both donor and recipient red cells. Thus, the optimal choice for such a patient will depend on current and expected future typing results.

RED BLOOD CELLS

The primary consideration in selection of RBCs is serologic compatibility for the prevention of hemolytic transfusion reactions. Because the posttransfusion survival of red cells is inversely related to length of storage, it has historically been desirable to select fresh (typically less than 10 days old) units in situations in which it is particularly important to limit the number of transfusions, such as intrauterine and neonatal transfusion. However, current clinical data show no benefit through this practice (Carson et al., 2016; Shah et al., 2018). For large-volume transfusions of pediatric patients (such as exchange transfusion or cardiac surgery), it may be desirable to select HbS–negative (sickle-negative) units. It is also preferable to select sickle-negative red cells for transfusion to patients with sickle cell disease because the presence of HbS in donor red cells may complicate monitoring of the effectiveness of transfusion therapy. However, it has never been shown that red cell transfusion from asymptomatic sickle trait donors is deleterious. In addition, in some cases, such as rare blood requirements, the use of a sickle trait donor may be the only option. Heavily transfused patients, particularly those with sickle cell disease, are at risk for alloimmunization and hemolytic transfusion reactions (Vichinsky et al., 1990). Such

patients benefit from prophylactic administration of antigen-matched red cells, particularly Rh and Kell antigens (Matteocci & Pierellil, 2013).

Exchange transfusion of the neonate with hemolytic disease of the newborn (HDN) is a special case. In this situation, antigen-negative red cells and plasma (for oncotic pressure and bilirubin-binding capacity) are needed. Red cells must be compatible with the maternal antibodies, including ABO antibodies. Reconstituted whole blood, prepared by combining RBCs and compatible plasma to a desired Hct (typically 50%), is commonly used, although whole blood may be used if available.

PLATELETS

Major ABO compatibility is less of an issue in platelet transfusion than in red cell transfusion. ABO antigens are expressed weakly on platelets. ABO-incompatible platelet transfusions may result in lower post-transfusion survival, although this usually is not clinically significant. Transfusion of isohemagglutinins contained in the plasma of apheresis platelets from donors with high-titer anti-A or anti-B may cause an acute hemolytic reaction (Larsson et al., 2000). Therefore, if non–ABO-identical platelets must be transfused, overriding consideration is typically given to plasma compatibility with the recipient. Some centers will screen apheresis platelets to ensure that high-titer incompatible anti-A or anti-B (e.g., >1 : 200 reactivity at immediate spin) is not transfused. Replacement of the plasma with PAS may be used to decrease the titer of ABO antibodies in platelet units (Weisberg et al., 2018). However, there is no evidence that the ABO titers are predictive of the risk of hemolysis (Karaffin et al., 2012).

Failure to achieve an expected platelet count increment after platelet transfusion on two or more occasions is commonly considered refractoriness (Hess et al., 2016). Platelet refractoriness may be due to immune causes (HLA or platelet-specific antibodies), nonimmune clinical causes (bleeding, splenomegaly, disseminated intravascular coagulation [DIC], medications), product-specific causes (ABO incompatibility; older products give lower increments), or the fact that some donors' platelets store poorly. A poor increment following a single platelet transfusion must not be presumed to be due to alloimmunization. The refractoriness is often multifactorial and changes with the patient's underlying condition and therapy. HLA antibodies are the most common cause of immune-mediated platelet refractoriness. HLA class I antigens are expressed on platelets, and class I antibodies are common in patients who have been previously pregnant or transfused with non–leukocyte-reduced blood components. Leukocyte reduction has been shown to effectively prevent both alloimmunization and platelet refractoriness in previously unexposed patients with leukemia (Trial to Reduce Alloimmunization to Platelets Study Group, 1997). Antibodies to platelet-specific antigens are a relatively rare cause of platelet refractoriness. Several effective strategies are known for selection of platelets for the alloimmunized refractory recipient. The use of crossmatch-compatible platelets is usually the first line (Wang et al., 2018). If the patient's HLA antibody specificities can be defined, it may be possible to select donors whose platelets are negative for the HLA class I antigens correlating to the patient's antibodies (Schmidt et al., 2019). However, owing to constraints of donor availability, finding optimal matches may be very difficult. Even with a large donor base, many "HLA-matched" transfusions are mismatched for at least one antigen (Dahlke & Weiss, 1984).

PRETRANSFUSION TESTING

The most critical step in pretransfusion testing is proper collection and identification of the recipient's blood sample. The most common cause of an acute hemolytic transfusion reaction (AHTR) is misidentification of the sample or patient (Sazama, 1990; Linden et al., 2000). Each transfusion service must develop and implement policies and procedures for patient identification and specimen collection. The pretransfusion samples should be labeled at the time of phlebotomy by comparison with the patient's permanent identifier (typically a wristband). The label should contain at least two unique identifiers, such as patient name and hospital registration number. The date of sample collection and the identity of the phlebotomist must also be documented. In emergency situations when the patient's identity is unknown, a unique identifier must be assigned. This identifier must remain with the patient throughout the course of transfusion even if the patient is subsequently identified. Policies and procedures must be in place for management of patients with confidential or alias names.

Samples for pretransfusion testing should be collected no more than 3 days before transfusion unless it is known that the patient has not been pregnant or transfused within the preceding 3 months. The common practice of patient admission on the same day as elective surgery presents special challenges, as testing may reveal the presence of alloantibodies, preventing provision of compatible blood. In this setting, pretransfusion samples may be collected during a preceding outpatient visit. One option is to require such patients to wear an identification wristband, although many patients find this undesirable. Another alternative is to assign a unique number to the pretransfusion specimen and affix this number to an identification form that the patient must provide on the day of surgery (Butch et al., 1994). Pretransfusion samples must be retained until at least 7 days after each transfusion. Typically, transfusion services retain pretransfusion samples for a fixed time.

Routine pretransfusion recipient testing consists of ABO and Rh(D) typing and screening for unexpected red cell antibodies. If the antibody screen is positive, antibody identification tests should be performed. Results of current testing should be compared with records of the previous testing, if available. Clinically significant red cell antibodies may become undetectable over time but may cause delayed hemolytic reactions owing to an anamnestic response. Therefore, a history of a clinically significant red cell antibody should be honored by providing only antigen-negative red cells for transfusion. Any discrepancy in current testing or disagreement with previous records must be resolved before pretransfusion testing can be concluded.

Some patients present particular challenges in pretransfusion testing. Newborns typically have weak or absent isohemagglutinins. Expected ABO antibodies may not be present until 6 months of age and maternally derived antibodies may persist in the newborn's circulation for weeks after birth. The occurrence of a weakly expressed Rh(D) antigen may complicate pretransfusion testing. Recently transfused patients may show a mixture of circulating red cells if they have not received ABO-identical units. Unexpected red cell antibodies can be acquired passively from transfusion of platelet concentrates or immunoglobulins. Some patients may lack expected isohemagglutinins because of disease or immunosuppressive therapy. Recipients of allogeneic HPC transplants may have complex and variable typing results that necessitate conclusion of a "declared" blood type. In urgent situations in which the blood type cannot be concluded, selection of group O red cells and group AB plasma is usually safe. If antibody identification tests cannot be completed, a medical judgment must be made regarding the urgency of transfusion and the risk for incompatibility. It may be desirable to issue red cells lacking antigen specificities that cannot be excluded, if available.

The final step of pretransfusion compatibility testing is the crossmatch. The purpose of the crossmatch is a final check of ABO compatibility and, to a lesser extent, detection of unidentified antibodies. A major crossmatch is performed between the recipient's serum or plasma and donor red cells. A minor crossmatch, between recipient red cells and donor or plasma, is usually unnecessary. In the absence of unexpected red cell antibodies, a crossmatch can be performed by direct agglutination ("immediate spin") for detection of ABO incompatibility. When unexpected red cell antibodies are present, the crossmatch should be performed by antiglobulin technique. For antibodies judged to be clinically significant, antigen-negative cells are selected for crossmatch. An alternative to ensure ABO compatibility is the so-called *computer crossmatch* or *electronic crossmatch*. This is applicable when at least two determinations of the recipient's ABO group have been made, at least one on a current sample, at least two determinations of the RBC unit have been made, and there are no unexpected antibodies in the patient's current sample (Butch & Oberman, 1997). A validated computer system can then ensure that issued blood components are ABO compatible. The presence of red cell autoantibodies presents a special problem. In this setting, it is essential that alloantibodies be excluded. Typically, the crossmatch will be positive due to the autoantibodies. Many transfusion services have a policy of issuing "least reactive" units, although the value of this policy has been called into question (Petz, 2003).

In urgent situations, emergency release of blood complements before completion of compatibility testing may be indicated. The goals of emergency release are to provide red cells for oxygen-carrying capacity and plasma for coagulation factor content to a rapidly bleeding patient. ABO compatibility is the first priority (see earlier discussion of component selection). The likelihood of a patient having antibodies to other blood group antigens is much lower and many of these antibodies will not cause acute hemolytic reactions of the same severity as ABO antibodies. Therefore, provision for these antibodies is of lower priority. However, when there is a history of prior antibodies, or when antibody identification tests are partially complete, it may be preferable to select antigen-negative RBCs, if available. Finally, documentation of the medical order for emergency release of blood components should be obtained.

TRANSFUSION ADMINISTRATION

The transfusion service is responsible for developing and implementing policies and procedures for the administration of blood components. A physician's order is required to prepare, dispense, and administer blood components. Optimally, venous access should be established before a blood component is issued. The selection of location and type of access depends on the volume, timing, and expected duration of transfusion therapy. Peripheral access with an 18-gauge needle or catheter is typically sufficient. Smaller catheters may be used; however, high-pressure flow through a small lumen may cause hemolysis, though typically not to a clinically significant degree (Frelich & Ellis, 2001). Central venous access is desirable for high-volume administration or long-term therapy.

Before administration of a transfusion, accurate identification of the component and the intended recipient is essential. This process should include at least two unique recipient identifiers, such as name and registration number, and comparison with a permanent identifier, such as a wristband. Additionally, the unit identifier on the blood container should be checked against the associated documentation (transfusion form or attached tag). The ABO and the Rh type on the unit label must agree with the associated documentation, and compatibility with the patient's recorded blood type should be verified. The expiration time and date of the blood component should be verified as acceptable. Many institutions require that two qualified individuals perform the identity check before transfusion. The physician's order and the patient's consent for transfusion should also be verified. Finally, the blood component unit should be inspected before transfusion for signs of contamination, clot formation, or bacterial growth, including particulates, change in color, gas formation, and clumping of cellular elements.

All blood components must be administered through a filter intended to retain clots and particles—typically, 170- to 260-μm pore size. Administration sets should contain a drip chamber, attached compatible intravenous solution, and a means of controlling the flow rate. During surgery, it is routine practice to add a microaggregate filter (typically, 40-μm pore size) through which the blood component flows first. This decreases the metabolic burden placed on the recipient to process aggregates of fibrin and cellular debris that accumulate during storage and helps to preserve the patency of the intravascular line. Care should be taken to avoid admixture of the blood components with incompatible intravenous solutions. Normal saline is the preferred solution for all transfusions. Calcium-containing solutions should be avoided, as these may precipitate clotting by reversing the citrate anticoagulants. RBCs should not be administered with 5% dextrose, hypertonic saline, or hypotonic saline, as this may cause hemolysis. Medications should not be added to blood components. Leukocyte reduction filters may be used for transfusion of RBCs or PCs, if the blood component has not already been prestorage leukocyte reduced, to reduce the incidence of febrile transfusion reactions, HLA alloimmunization, or CMV transmission. The appropriate filter must be selected for the blood component because clogging or filter failure may occur if improperly used.

It may be desirable to administer refrigerated blood components (RBCs or plasma) through a blood-warming device. Transfusion of cold components faster than 100 mL per minute for 30 minutes may increase the risk for cardiac arrest (Boyan & Howland, 1963). Blood-warming devices should have a visible thermometer and an audible alarm to avoid exceeding temperature limits. Blood components should never be warmed with tap water, conventional microwave ovens, or any other nonapproved warming device.

The desirable rate of administration depends on the patient's blood volume, cardiac status, and hemodynamic state. Except for urgent resuscitation, the transfusion should be started slowly (≈2 mL/minute for the first 15 minutes). The patient should be carefully observed for the first 15 minutes of infusion because severe reactions such as hemolysis, anaphylaxis, or sepsis may manifest after a small volume has entered the circulation. Subsequently, the administration rate may be increased. In general, it is desirable to complete a red cell transfusion within 2 hours and a platelet or plasma transfusion as quickly as tolerated by the patient (usually 30–60 minutes). Any transfusion should be completed within 4 hours of initiation. Patients at risk for volume overload may require slower administration. If the total administration time exceeds 4 hours, smaller-volume blood components (e.g., "split units") should be provided. When high flow rates are required, such as in some resuscitation or surgical situations, an FDA-approved pressure infusion device may be used. When such devices are used, care must be taken to avoid mechanical hemolysis or air embolism. During transfusion, the patient's vital signs should be checked at regular intervals; any suspected reaction should prompt interruption of the transfusion and immediate investigation.

BOX 37.2

Red Cell Transfusion Guidelines

Symptomatic anemia in a euvolemic patient
Acute blood loss of >15% of estimated blood volume
Hb <7.0 g/dL in a critically ill patient
Hb <7.0 g/dL in nonexsanguinating upper GI bleeding
Hb <8.0 g/dL in a patient with an acute coronary syndrome
Sickle cell disease
- Acute sequestration: Hb <5.0 g/dL or decrease of 20% from baseline
- Acute chest syndrome: Target Hb = 10 g/dL, HbS fraction <30%
- Stroke prophylaxis: Target HbS fraction <30%
- General anesthesia: Target Hb = 10.0 g/dL, HbS fraction <60%

GI, Gastrointestinal; *Hb,* hemoglobin.

BLOOD COMPONENT THERAPY

All transfusion decisions are clinical judgments that should be made while taking into account clinical and laboratory data. There are no absolute indications, and few absolute contraindications, to blood transfusion. Many institutions have implemented Patient Blood Management (PBM) programs that attempt a holistic approach to patient care through transfusion medicine (Verdecchia et al., 2016; Sadana et al., 2018). PBM includes appropriate use of transfusions but also nontransfusion treatment modalities (such as iron repletion in a patient with iron-deficiency anemia). PBM programs have been shown to lead to improved patient outcomes and decreased patient care cost. PBM programs have become so prevalent that they may now become recognized through a program offered jointly by AABB and The Joint Commission.

Red Cell Transfusion

RBCs provide oxygen-carrying capacity. Red cell transfusion may be used to treat acute or chronic anemia. A patient's ability to tolerate anemia depends on the degree of anemia, physiologic adaptive mechanisms, and cardiac or respiratory disease. Normal physiologic adaptations to anemia include increased cardiac output, redistribution of blood flow, increased oxygen extraction, and increased red cell 2,3-DPG, resulting in rightward shift of the oxygen-Hb dissociation curve. General guidelines for red cell transfusion are summarized in Box 37.2. Symptomatic anemia, regardless of Hb concentration, in a euvolemic patient is an indication for RBC transfusion. Symptoms of anemia include fatigue, tachycardia, tachypnea, dyspnea on exertion, postural hypotension, and impaired mentation. Anemia may precipitate angina in patients with coronary artery disease. Generally, acute blood loss of greater than 15% of a patient's blood volume may be an indication for red cell transfusion. Studies of postsurgical morbidity in patients who refused blood transfusion have indicated that for patients with a preoperative Hb of at least 6 g/dL, without underlying coronary artery disease and sustaining operative blood loss of less than 2 g/dL of Hb, there is little relationship between mortality and degree of preoperative anemia (Carson et al., 1996). Mortality increases with preoperative Hb levels below 6 g/dL (Spence et al., 1990). However, with a Hb loss of 2 to 4 g/dL, perioperative mortality increases with preoperative Hb levels below 10 g/dL. This risk may be magnified by the presence of cardiovascular disease (angina, myocardial infarction, congestive heart failure, or peripheral vascular disease). One study of patients undergoing elective operations demonstrated no mortality despite Hb levels as low as 6 g/dL, provided that the blood loss was less than 500 mL (Carson et al., 1988).

The Transfusion Requirements in Critical Care (TRICC) study was the first large randomized prospective trial comparing restrictive and liberal transfusion strategies (Hebert et al., 1999). The TRICC trial enrolled 838 critically ill patients with Hb levels <9.0 g/dL. Subjects were randomized to receive liberal or restrictive transfusion regimens. The liberal regimen was a transfusion trigger of 10 g/dL with a target of 10 to 12 g/dL. The restrictive regimen was a transfusion trigger of 7.0 g/dL with a target of 7.0 to 9.0 g/dL. The primary result was no statistically significant difference in 30-day mortality, although a trend favoring lower mortality was noted in the restrictive strategy group (18.7% vs. 23.3%; $p = 0.11$). Cardiac events, primarily pulmonary edema and myocardial infarction, occurred more frequently in the liberal than in the restrictive transfusion group (21.0% vs. 13.2%; $p < 0.001$). Subgroup analysis showed lower mortality in the restrictive strategy group among patients with lower disease severity measured by APACHE II scores (8.7% vs. 16.1%; $p = 0.03$) and among patients younger than 55 years of age (5.77% vs. 13.07%; $p = 0.02$). Thus, it appears that many critically ill adult patients can tolerate Hb levels less than 10 g/dL. The findings of the TRICC trial have been verified in numerous other

populations (Carless et al., 2010). At this point, the guideline of restrictive transfusion thresholds being equal to or better than liberal transfusion thresholds should be considered the rule for almost all populations. The one patient population for which an appropriately powered study addressing the question of liberal versus restrictive transfusion has not been done to date is patients with a concurrent or recent cardiac event.

Transfusion of the patient with sickle cell disease (SCD) presents unique challenges. The indications for transfusion are to augment oxygen-carrying capacity in severe anemia and to improve microvascular circulation by decreasing the proportion of sickle red cells. Oxygen delivery in SCD represents a balance between oxygen-carrying capacity and blood viscosity. Optimal oxygen delivery is usually achieved when the posttransfusion Hct is about 30% (Schmalzer et al., 1987). No universally accepted laboratory parameters are available for transfusion in SCD. Hb values less than 5 g/dL and an acute drop of 20% from baseline during an acute illness are generally accepted indications for red cell transfusion. Acute splenic sequestration can produce sudden hypovolemia and cardiovascular collapse, necessitating prompt transfusion. In this setting, the rise in Hb following transfusion may be greater than expected because of release of sequestered red cells. Careful monitoring is essential to avoid overtransfusion (Powell et al., 1992). Acute chest syndrome may be life-threatening. Prompt transfusion (either simple transfusion or exchange transfusion) may prevent progression to respiratory failure (Mallouh & Asha, 1988). Before general anesthesia is administered, transfusion has been used to achieve a Hb of 10 g/dL and a HbS level of less than 60% although there is not conclusive evidence supporting this practice (Estcourt et al., 2016). In uncomplicated pregnancy, prophylactic red cell transfusion is not beneficial. However, transfusion may be indicated in high-risk pregnancy or with a history of previous fetal loss (Seoud et al., 1994). Exchange transfusion with a goal of achieving HbS levels of 30% or less and Hct of 30% is a typical approach used for both acute sickle events and for long-term prevention of sickle events. Long-term transfusion therapy can reduce the risk for stroke in SCD. In children, transfusion with the goal of maintaining HbS levels below 30% can reduce the risk for stroke (Adams et al., 1998). How long a chronic transfusion regimen must be maintained is an open question. Termination, even after several years of therapy, can result in reversion to high risk for stroke (Adams et al., 2004). Iron overload will develop if simple transfusions are performed for chronic management rather than exchange transfusions. Iron chelators are used to slow or prevent iron accumulation and the sequelae of iron overload. Alloimmunization of sickle cell patients is also frequently encountered. The most common antigen groups against which antibodies form are the Rh, Kell, and Kidd groups. Prophylactically matching RBC units for these RBC antigens (either serologically or molecularly) for sickle cell patients appears to decrease this risk of alloimmunization (Fasano et al., 2019).

In autoimmune hemolytic anemia, transfusion may be indicated for symptomatic anemia. Most patients with autoimmune hemolytic anemia tolerate transfusion of incompatible red cells if alloantibodies have been excluded (Salama et al., 1992). Transfused red cells usually are not cleared any more rapidly than the patient's own red cells. It is important to note that a necessary red cell transfusion must never be withheld because of crossmatch incompatibility. It is far more dangerous to not give such a transfusion to a patient with autoimmune hemolytic anemia than it is to provide it.

Transfusion of 1 U of RBCs to a 70-kg patient can usually be expected to raise the Hb by 1 g/dL and the Hct by 3%. However, the expected Hct increase may range from about 2% to 9% depending on the patient's vascular volume (Gorlin & Cable, 2000). Previously, there was a widely publicized guidance that RBC units should be transfused two at a time. However, as with all medical interventions, the ideal treatment is the minimum dosage needed to treat symptoms. For RBC transfusion, that means that for stable patients, RBC units should be transfused 1 U at a time, with evaluation of the patient after transfusion to determine symptom response to the transfusion (or if the patient has achieved a target Hb/Hct, if that was the stimulus for the transfusion) (Berger et al., 2011). If the patient remains symptomatically anemic, then an additional RBC unit should be transfused. If the patient is no longer symptomatic, there is no indication for additional RBC transfusions.

An area of interest and considerable investigation is the effect of the storage age of RBCs on patient outcomes, since potentially damaging substances accumulate in older blood and the red cells undergo multiple changes that may interfere with oxygen delivery. Shah and colleagues reviewed the current body of studies on this topic, finding no benefit for adults with transfusion of "younger" RBC units versus "older" units (Shah et al., 2018). However, clinical trials to date have not used red cells stored for the allowable maximum number of days.

BOX 37.3

Platelet Transfusion Guidelines

Thrombocytopenia due to decreased production
Stable patient: platelet count <10,000/μL
Invasive procedure with low risk for bleeding: platelet count <20,000/μL
Bleeding, invasive procedure with high risk for bleeding, or surgery with high risk for bleeding: platelet count <50,000/μL
Retinal or central nervous system (CNS) bleeding or surgery: platelet count <100,000/μL
Microvascular bleeding due to platelet dysfunction

The current body of literature on this topic for pediatric patients is less robust. However, there are ongoing studies in pediatric patient populations (such as the ABC PICU trial) that will hopefully provide this guidance soon.

The Age of RBCs in Premature Infants (ARIPI) study was the first large randomized controlled trial (RCT) in pediatrics examining the effect of red cell storage on clinical outcomes. A total of 377 neonates in 6 Canadian tertiary neonatal intensive care units weighing <1250 g and requiring an RBC transfusion were randomized to receive leukoreduced RBCs ≤7 days or be treated by the standard practice of transfusing dedicated units (Fergusson et al., 2012). The average age of the RBCs in the fresh group was 5.1 days; the average age in the control group was 14.6 days. The primary outcome was a composite of death, intraventricular hemorrhage, necrotizing enterocolitis, bronchopulmonary dysplasia, and retinopathy of prematurity. There was no difference in the two groups with respect to the primary outcome (52.9% vs. 52.7%). The rates for the individual morbidities and mortality were similar. Subgroup analyses did not show any differences in patients receiving fresher or older RBCs. The authors concluded that, in this trial, the use of fresh RBCs compared with standard blood bank practice did not improve outcomes in premature, very-low-birth-weight infants requiring a transfusion.

Platelet Transfusion

Platelet transfusion is indicated for prevention or treatment of hemorrhage due to thrombocytopenia or platelet dysfunction, as summarized in Box 37.3. The AABB published evidence-based guidelines addressing the indications for platelet transfusion (Kaufman et al., 2015). The guidelines present prophylactic platelet transfusion to reduce the risk for spontaneous bleeding in hospitalized adult patients with therapy-induced hypoproliferative thrombocytopenia and a platelet count ≤10,000/μL as a "strong recommendation." In addition, the guidelines make the following "weak recommendations":

1. Prophylactic platelet transfusion for patients undergoing elective central venous catheter placement with a platelet count below 20,000/μL
2. Prophylactic platelet transfusion for patients undergoing elective diagnostic lumbar puncture with a platelet count below 50,000/μL
3. Prophylactic platelet transfusion for patients undergoing major elective non-neuraxial surgery with a platelet count below 50,000/μL
4. Platelet transfusion for coronary artery bypass graft (CABG) patients with perioperative bleeding and thrombocytopenia or suspected platelet dysfunction

For bleeding patients or those undergoing an invasive procedure with high risk for bleeding, including some endoscopic and surgical procedures, the goal of platelet transfusion therapy is to achieve sustained levels above 50,000/μL (Kumar et al., 2015). This usually ensures hemostasis, although it may take longer than normal to achieve. For this reason, for patients experiencing bleeding in critical spaces, such as the retina or central nervous system, a target of 100,000/μL is the standard of practice, though the need for this level has never been rigorously evaluated. In bleeding associated with platelet dysfunction or thrombocytopenic bleeding associated with coagulopathy, there is no single transfusion threshold; therapy must be guided by the patient's clinical condition. When the platelet dysfunction is due to medications, reversal of that dysfunction may require platelet transfusions depending on the medication used. The PATCH trial was the first well-powered RCT addressing platelet transfusion for reversal of aspirin effect for intracranial bleeding (Baharoglu et al., 2016). Baharoglu et al. showed that platelet transfusions did not lead to improved outcomes and were actually associated with greater morbidity. Cardiopulmonary bypass and other devices may result in a transient acquired platelet dysfunction that may manifest as microvascular bleeding. The platelet count is not usually a useful indicator in such situations. The AABB Guidelines suggest against routine prophylactic platelet transfusion for patients undergoing CABG surgery (Kaufman et al., 2015).

BOX 37.4

Corrected Count Increment

$$\text{CCI} = \frac{\text{Platelet count increment} \times \text{BSA}}{\text{Number of platelets transfused} \times \left(10^{11}\right)}$$

where *BSA* is the body surface area (m^2)

Example

Pretransfusion platelet count = 8000/μL
Posttransfusion platelet count = 36,000/μL
BSA = 1.5 m^2
Platelet dose = 3.0×10^{11}

$$\text{CCI} = \frac{24{,}000 \times 1.5}{3} = 12{,}000$$

The Prophylactic Platelet Dose (PLADO) trial addressed the optimal prophylactic platelet dose in patients with hypoproliferative thrombocytopenia from stem cell transplantation or chemotherapy (Slichter et al., 2010). Subjects were randomized to one of three arms: a low platelet dose of 1.1×10^{11} platelets/m^2 (half the medium dose), a medium dose of $2.2 \times 10^{11}/m^2$, or a high dose of $4.4 \times 10^{11}/m^2$ (twice the medium dose). The primary outcome measure was the percentage of patients in each dose arm who had at least one episode of World Health Organization (WHO) grade 2 or higher bleeding. The incidence of grade 2 bleeding, higher-grade bleeding, and other adverse events was similar among the three groups. The median number of platelets transfused in the low-dose group was significantly lower than in the other groups, but the number of platelet transfusions was higher (five vs. three in each of the other two groups). Bleeding events were more common on days when the platelet count was 5000/μL or lower, regardless of treatment assignment. This trial demonstrated that low-dose prophylactic platelet transfusion is safe in hypoproliferative thrombocytopenia but may not reduce total platelet transfusions.

Platelet transfusion is relatively contraindicated in immune thrombocytopenic purpura. In this setting, posttransfusion platelet survival is extremely brief; platelet transfusion is indicated only if there is severe hemorrhage. Clearly, transfusion in the setting of intravascular platelet consumption should be undertaken with great caution. Platelet transfusion in heparin-induced thrombocytopenia or thrombotic thrombocytopenic purpura may be deleterious, though the evidence for this risk has been mixed (Goel et al., 2015; Swisher et al., 2009; Zhou et al., 2015).

Transfusion of one apheresis platelet unit, or an equivalent pool of whole blood–derived platelet concentrates (typically, 4–6), can be expected to raise the platelet count of a 70-kg adult by 30,000 to 50,000/μL. However, there are many reasons why this increment may not be achieved. Consumption or bleeding, splenomegaly, platelet antibodies, and drugs are all causes of a poor response to platelet transfusion. Drugs that can cause an inadequate platelet increment include antibiotics, heparin, antiplatelet agents (clopidogrel, tirofiban), quinidine, and antithymocyte globulin, along with many others. In assessing platelet transfusion effectiveness, it is useful to take into account dose and body size by calculating the corrected count increment (CCI; Box 37.4).

A CCI >7500 at 1 hour posttransfusion or a CCI >4500 at 24 hours posttransfusion generally indicates a successful transfusion. Obtaining a platelet count within 1 hour of completing the transfusion may be helpful in distinguishing immune from nonimmune causes of platelet refractoriness. Typically, immune refractoriness will result in an inadequate platelet increment when measured less than 1 hour after completion of the transfusion. Typically, nonimmune refractoriness will manifest as an adequate CCI at 1 hour but shortened survival time, so that the platelet count by 24 hours may be back to baseline. It must be appreciated that the CCI does not indicate that an adequate platelet count has been achieved. It indicates only the adequacy of a platelet count increment in relation to the number of platelets transfused.

Plasma Transfusion

Guidelines for plasma transfusion are summarized in Box 37.5. Plasma may be used to replace any plasma protein deficiency. Purified protein concentrates, such as factor VIII, albumin, Prothrombin complex concentrates (PCCs), or immunoglobulin, are preferable for replacement of specific deficiencies because these are highly purified and standardized and carry extremely low risk for infectious disease transmission. Plasma is most commonly used either for replacement of coagulation factor deficiencies when no factor concentrate is available or for replacement of multiple factors. Multifactorial deficiencies are common in liver disease, massive bleeding, multiorgan system failure, and warfarin therapy. The degree to which factor deficiency may contribute to bleeding in such cases is controversial. Standard coagulation tests, such as prothrombin time (PT) and activated partial thromboplastin time (APTT), are commonly used to assess the need for plasma transfusion. However, these tests are poorly predictive of bleeding risk. For nonbleeding patients, there is no change in bleeding risk for patients with a PT or APTT less than 1.8 to 2.0 times the midpoint of the reference range (which will generally equate to an international normalized ratio [INR] less than 1.8–2.0). Thus, no benefit will be gained by plasma transfusion (Holland et al., 2006). For maximal hemostatic effect, plasma should be transfused immediately before an invasive procedure is performed. For the bleeding patient, plasma transfusion may have to be repeated every 3 to 4 hours to maintain adequate coagulation factor levels. In general, a dose of 15 to 30 mL/kg is necessary to achieve a hemostatic effect. Plasma may be used for rapid reversal of warfarin, although 4-factor prothrombin complex concentrate (PCC) provides faster and more complete reversal of coagulopathy (Kinard & Sarode, 2014). Plasma is also a source of ADAMTS 13 (a disintegrin and metalloprotease with eight thrombospondin), the vWF protease that is commonly deficient or inhibited in TTP.

BOX 37.5

Plasma Transfusion Guidelines

- Coagulation factor deficiency, factor concentrate unavailable, and bleeding or prior to surgery
- Dilutional coagulopathy
- Hemorrhage in liver disease
- Disseminated intravascular coagulation (DIC)
- Coumadin reversal
- Thrombotic thrombocytopenic purpura (TTP)
- Acute trauma resuscitation

BOX 37.6

Cryoprecipitate Transfusion Guidelines

- Factor VIII deficiency, factor concentrate unavailable, and bleeding or prior to surgery
- von Willebrand disease, factor concentrate unavailable, and bleeding or prior to surgery
- Hypofibrinogenemia (fibrinogen <100 mg/dL) and bleeding or prior to surgery
- Factor XIII deficiency and bleeding or prior to surgery
- Uremic bleeding (DDAVP preferred)
- Topical fibrin sealant (commercial product preferred)

DDAVP, Desmopressin.

Cryoprecipitate Transfusion

General guidelines for the transfusion of cryoprecipitate (cryo) are summarized in Box 37.6. Cryo can be used for factor VIII or vWF replacement. High purity or recombinant factor concentrates, however, are better alternatives for each. Cryo is a good source of fibrinogen and factor XIII. Most patients with hypofibrinogenemia also have deficiencies of other coagulation factors and are better treated with plasma. Some patients may require additional supplementation of fibrinogen using cryo or fibrinogen concentrate, such as trauma, DIC, or postpartum hemorrhage (Rourke et al., 2012). Direct comparison between cryoprecipitate and fibrinogen concentrate as a source of fibrinogen in bleeding patients shows no consistent difference between the two (Jensen et al., 2016). Some evidence suggests that cryo may be useful in the treatment of uremic bleeding, possibly by providing high-molecular-weight forms of vWF (Triulzi & Blumberg, 1990). Desmopressin (DDAVP) is the preferred therapy for this situation. However, DDAVP may become ineffective after repeated short-term use, at which point cryo transfusion could be initiated. Cryo, when mixed with calcium and thrombin, can also be used to make a topical fibrin sealant for surgery, although more concentrated, virally inactivated commercial products are available. Each unit of cryo contains at least 80 U of factor VIII activity and 150 mg of fibrinogen, although the actual content is variable.

MASSIVE TRANSFUSION

Massive transfusion, usually defined as replacement of 1 blood volume within 24 hours or ongoing blood loss of 150 mL/minute, necessitates

a systematic approach. Large-volume blood loss is often due to trauma but also occurs in gastrointestinal hemorrhage (particularly with chronic liver disease), ruptured aortic aneurysms, obstetric emergencies, and some surgical procedures such as liver transplantation. No single massive transfusion protocol will be optimal for all patients, although establishing an institutional policy is helpful because these cases can become chaotic. Special attention should be paid to patient and sample identification to avoid transfusion errors.

The priorities in transfusion management of massive bleeding are prevention or treatment of hypovolemic shock, maintenance of adequate oxygen-carrying capacity, maintenance of oncotic pressure, correction or prevention of coagulopathy, and avoidance of adverse effects of transfusion. Initial patient evaluation should include pertinent medical history (especially liver, kidney, cardiovascular, and hematologic diseases), history of previous transfusions or pretransfusion testing problems, examination for microvascular bleeding, complete blood count (CBC), and coagulation profile (PT, APTT, fibrinogen, thromboelastography). Note that in hypovolemia, the CBC will underestimate blood loss. A sample for pretransfusion testing should be obtained and processed as soon as possible. Red cell transfusion should be considered if greater than 15% loss of estimated blood volume (about 750–1000 mL in a 70-kg adult) occurs with ongoing bleeding. RBC transfusions should ideally be fully crossmatched if possible. However, transfusion should not be withheld in a patient with severe hemorrhage due to concerns of incompatibility. Transfusion can be started with group O uncrossmatched RBCs. If the patient's Rh type is unknown, Rh(D)-negative RBCs are preferable, especially for females with childbearing potential.

Coagulopathies may occur during massive transfusion as the result of dilution, consumption, and/or dysfunction of the coagulation factor and platelets. During resuscitation with RBCs and crystalloid/colloid fluids, measured factor levels and platelet counts may be higher than would be expected on a purely dilutional basis (Counts et al., 1979; Murray et al., 1995), with considerable variation between patients. Consumptive coagulopathies occur with DIC, burns, brain injury, hyperthermia, and sepsis. These usually manifest by prolonged PT and APTT, lower than expected fibrinogen and platelet counts, and the presence of fibrin degradation products or D-dimers. Platelet or coagulation factor dysfunction can occur in hypothermia, acidosis, liver disease, or renal failure.

Numerous studies in both the military and civilian populations have addressed the ideal protocol for supplementation of plasma and platelets in massive hemorrhage. Such protocols call for transfusion of RBCs, plasma, and platelets in fixed ratios approximating reconstitution of whole blood in the patient. Several retrospective studies in both military and civilian acute trauma resuscitation have suggested that more aggressive plasma transfusion is associated with lower mortality and improved outcomes, particularly in trauma patients (Holcomb et al., 2008; Cotton et al., 2009; Zehtabchi & Nishijima, 2009; Zink et al., 2009; Mitra et al., 2010). However, many confounding factors in these studies make causal inference problematic. Furthermore, there are few large studies focused on application of these protocols in nontrauma patients. Lacking randomized clinical trials, it is not possible to say definitively that a protocol-driven approach is superior to individualized clinical judgment.

In a laboratory-driven approach, plasma, platelets, and cryoprecipitate are given based on laboratory-determined need, while RBCs and crystalloid are given based on perceived blood loss and hypovolemia. Using traditional laboratory testing, plasma is typically given if PT or APTT is greater than 1.5 times the reference range, and platelets are typically given for counts less than 50,000. It may be prudent to reserve platelet transfusion until after surgical control of major bleeding has been attained because it is likely to be ineffective during rapid blood loss. Cryoprecipitate may be given if the fibrinogen is less than 100 mg/dL, but hypofibrinogenemia is due to acute bleeding usually accompanied by deficiency of other factors; thus, plasma is often a better choice in that setting. However, if there is an element of DIC, as is often seen in trauma, then there is often a depletion of fibrinogen beyond that of the other coagulation factors. Supplementation of the fibrinogen using either cryoprecipitate or fibrinogen concentrate is indicated in that setting. Two trials are running at this writing to determine the clinical utility of fibrinogen supplementation in trauma (Marsden et al., 2019). The CRYOSTAT-2 trial will assess whether early administration of high-dose cryoprecipitate, in addition to standard transfusion support, can improve survival from traumatic bleeding. Therapy is best guided by frequent assessment of coagulation parameters. Thromboelastography and thromboelastometry are functional whole-blood clot assay systems that may also be used in massive transfusion to direct administration of plasma, platelets, cryoprecipitate, tranexamic acid, and coagulation factor concentrates (Whiting & DiNardo, 2014). Comparing the protocol with laboratory-driven approaches is still a topic of debate, though most institutions use a blend of both: starting with a protocol approach that is then tailored based on testing as results become available.

Two other blood products are currently used at some institutions for severe hemorrhage (such as trauma): liquid plasma and whole blood (Van et al., 2017). Liquid plasma is plasma from whole-blood donation that is never frozen but is instead stored at 2°C to 6°C for up to 5 days after the whole-blood dating period. Since liquid plasma does not need to be thawed, it is more readily available for transfusion in traumas. The downside of liquid plasma is that the coagulation factors that are labile at 2°C to 6°C will be at lower concentration after 7 days of storage (Backholer et al., 2017). For this reason, liquid plasma is indicated only for use in trauma resuscitation. Whole blood is also used at some centers for initial resuscitation in trauma (Cotton et al., 2013). The idea is that this supplies all the blood elements needed in the appropriate ratio without requiring coordination of multiple separate products. The downside of this approach is the concern for ABO matching of the blood products for the patient. Many trauma patients do not have a known ABO type at the time of initial transfusion. With the use of components, universal products (type O RBCs, type AB plasma, and so on) can be used without concern for adverse events due to incompatibility. There is no universally compatible whole blood. O whole blood, typically selected for low titer of anti-A and anti-B antibodies, is usually used with a limitation of how many whole-blood units will be administered to a patient (usually limited to 1–2 U) to minimize the volume of incompatible plasma if the patient is a non-O type. Further trials are ongoing looking at expanding the use of both liquid plasma and whole blood in this population.

One other change in the provision of blood for trauma patients is the use of type A plasma in massive transfusion for patients without a known blood type (Zielinkski et al., 2014). With the recognition that plasma is required in these patients, the supply of AB plasma is often insufficient to provide the massive amount of plasma these patients may require. Type A plasma is compatible with 84% of the population (40% A, 44% O) and the levels of anti-B present in the A plasma are typically not sufficient to cause clinically significant hemolysis in these patients (particularly as these patients are hemorrhaging and being transfused with type O RBCs and are often being transfused so rapidly and with such high volumes that there may be very few type B or AB RBCs in their circulation). Multiple clinical comparisons have shown that this substitution of A plasma rather than AB plasma is safe and effective in this setting.

Complications of massive transfusion include hypothermia, hypocalcemia, and acid-base disorders. Hypothermia can be avoided with the use of high-flow warming devices. When the transfusion rate exceeds about 100 mL/minute, a clinically significant drop in ionized calcium may occur as the result of accumulation of citrate, and calcium supplementation should be provided (Giancarelli et al., 2015). Liver disease, hypotension, and hypothermia may exacerbate hypocalcemia. Monitoring the corrected QT interval is useful. Measurement of total calcium will not accurately indicate the level of ionized calcium. During rapid transfusion of RBCs, a modest decrease in arterial pH may be seen (Vretzakis et al., 2000); metabolic alkalosis is common after massive transfusion because of metabolism of citrate.

NEONATAL AND PEDIATRIC TRANSFUSION

Neonates receive RBC transfusions because of anemia of prematurity, HDN, or iatrogenic blood loss. The unique physiology of the neonatal period and relative fragility of the developing brain vasculature necessitate some differences from the approach to older children or adults. Guidelines for neonatal transfusion are summarized in Box 37.7. RBC transfusion of 10 to 15 mL/kg will typically increase the Hb by 2 to 3 g/dL; platelet transfusion of 10 mL/kg will typically increase the platelet count by 40,000 to 50,000/μL. For large-volume transfusion, as in exchange transfusion or cardiac surgery, selection of fresh RBCs (typically <10 days old) may be indicated. However, with transfusion of 10 to 15 mL/kg, most infants tolerate transfusion of RBCs stored until outdate without adverse effects (Strauss et al., 1996). For a premature infant with an expected ongoing transfusion requirement, the use of aliquots of a single unit until outdate can significantly reduce donor exposures. Premature and low-birthweight infants are at greater risk for CMV infection and GVHD (see later discussion).

Exchange transfusion of the neonate for hyperbilirubinemia is usually indicated if the total bilirubin is greater than 25 mg/dL. Relating the total bilirubin to hours since birth is predictive of kernicterus risk (Bhutani et al., 1999). A two-blood volume exchange is typically used, which can be expected to reduce the total bilirubin by 25% and the fetal red cell mass by about 70%. Whole blood or RBCs reconstituted with compatible plasma to Hct of 45% can be used.

BOX 37.7

Guidelines for Neonatal Transfusion

RBC Transfusion

Hct <20% with symptomatic anemia
Hct <30% with supplemental O_2 <35% or mechanical ventilation with MAP <6 cm H_2O
Hct <35% with supplemental O_2 >35% or mechanical ventilation with MAP >6 cm H_2O
Hct <45% with cyanotic congenital heart disease or extracorporeal oxygenation

Plasma Transfusion

Coagulation factor deficiency, factor concentrate unavailable, and bleeding or prior to surgery
Disseminated intravascular coagulation (DIC)

Platelet Transfusion

Platelet count <30,000/μL in term infant with platelet production failure
Platelet count <50,000/μL in stable premature infant
Platelet count <100,000/μL in unstable premature infant

Hct, Hematocrit; *MAP,* mean arterial pressure.
Adapted from Roseff SD, Lugan NLC, Manno CS: Guidelines for assessing appropriateness of pediatric transfusion, *Transfusion* 42:1398–1413, 2002.

TRANSFUSION REACTIONS

Transfusion reactions are a diverse group of adverse reactions to transfusion that usually present during or shortly after transfusion. The workup and treatment of a transfusion reaction must be predicated on the clinical picture, especially in atypical cases. If a transfusion reaction occurs while a transfusion is in progress, the transfusion should be stopped immediately, and the intravenous line should be kept open with saline. It is important to recognize that the unit a patient is reacting to is not necessarily the one that is being infused. All suspected transfusion reactions should be reported to the blood bank or transfusion service. Suspected transfusion reactions are underreported in passive surveillance systems (e.g., investigating only when a suspected transfusion reaction is reported to the blood bank) compared with active surveillance systems (Hendrickson et al., 2016). Multiple studies have shown an incidence of ~1% for a transfusion reaction of any type when active surveillance is used compared with a rate of 0.2% when passive surveillance is used (Harvey et al., 2014).

FEBRILE NONHEMOLYTIC REACTIONS

A febrile transfusion reaction is defined as a rise in temperature of 1°C or greater, possibly accompanied by chills or rigors. Symptoms usually occur during the transfusion but may be delayed for up to 1 hour after the procedure has been completed. A patient who is hypothermic at the start of a transfusion and then manifests an expected temperature rise to normal, without symptoms, is not having a febrile reaction. In some patients, it may be impossible to distinguish between a febrile transfusion reaction and disease-related fever.

It is important to rule out a hemolytic transfusion reaction or bacterial contamination of the unit. Antipyretics, such as acetaminophen (325–500 mg) can be administered. Antipyretics are not necessarily required, as the fever of nonhemolytic transfusion reactions is self-limited and usually resolves within 2 to 3 hours. Diphenhydramine (25–50 mg) is commonly administered in this setting but probably has no effect on the course of febrile reactions.

Controversy continues as to whether the transfusion can be restarted after a febrile reaction has been diagnosed and the patient has been treated. The principal argument in favor of restarting the transfusion is the reduction in the number of donor exposures, especially if pooled platelet concentrates are involved (Oberman, 1994). Arguments against restarting the transfusion include the possibility that the patient may have a continued febrile reaction to the unit and, if a hemolytic reaction or bacterial contamination has not been definitely excluded, a severe reaction may ensue (Widmann, 1994). The decision to restart the transfusion should be driven by the clinical condition of the patient, the severity of the febrile reaction symptoms, the rarity of the blood product involved, and the results of transfusion reaction testing.

Premedication with antipyretics is often used to prevent febrile reactions, although studies thus far have failed to show prevention of febrile reactions by premedication with acetaminophen and/or diphenhydramine even in patients with prior febrile reactions (Tobian et al., 2007). Febrile reactions have been attributed to the accumulation of pyrogenic cytokines in units during storage (Muylle et al., 1993). These biological mediators are produced primarily by leukocytes. Filtration at the time of transfusion will not remove pyrogenic cytokines from blood units, although it may remove other cytokines and activated complement components (Snyder et al., 1996). The use of prestorage leukocyte reduction has been shown to reduce the generation of cytokines in stored platelets and red cells and may be more effective than poststorage leukocyte reduction in preventing febrile reactions (Federowicz et al., 1995). Some, but not all, studies have shown a reduction in the incidence of febrile reactions since the introduction of universal leukocyte reduction (Uhlmann et al., 2001; Dzik et al., 2002; Ibojie et al., 2002). However, it is clear that leukocyte reduction does not prevent all febrile reactions. Accumulated cytokines can be removed by plasma reduction or the washing of cellular blood components (Heddle et al., 1994). Plasma removal appears to be equivalent to prestorage leukocyte reduction in prevention of febrile reactions (Heddle et al., 2002). Plasma removal will not prevent all febrile reactions. Febrile reactions to platelet transfusion may be reduced by using platelet concentrates less than 4 days old (Kelley et al., 2000).

ALLERGIC REACTIONS

Mild allergic reactions to transfusion are commonplace. They may occur with any type of blood component, including autologous RBCs (Domen & Hoeltge, 2003). Presenting symptoms may include pruritus, urticaria, erythema, and cutaneous flushing. About 10% of allergic reactions have pulmonary signs and symptoms but not cutaneous involvement. Gastrointestinal involvement may include nausea, vomiting, abdominal pain, and diarrhea.

Should an allergic reaction occur, the transfusion should be discontinued and intravenous access maintained. If there is upper airway involvement, prompt intubation may be necessary. Oxygen should be administered if there is dyspnea or evidence of desaturation. Mild allergic reactions usually will respond to intravenous antihistamines such as diphenhydramine (50–100 mg). More severe reactions may require epinephrine. In mild cutaneous reactions, the transfusion may be restarted after treatment without recurrence or worsening of the symptoms. In more serious reactions, particularly if there is airway involvement, restarting the transfusion is not advisable.

With rare exceptions (e.g., IgA and haptoglobin deficiencies), the specific antigen to which the patient is reacting cannot usually be identified. Premedication with an antihistamine, such as diphenhydramine 25 to 50 mg, administered orally or intravenously, has historically been given to prevent mild allergic reactions, although the evidence showing benefit from premedication has not been shown in recent studies (Tobian et al., 2007). Steroids such as hydrocortisone (100 mg) may help patients who manifest repeated allergic reactions, although the efficacy of steroids has not been proven.

Patients who have had repeated or significant allergic reactions may benefit from PAS platelets or from the concentration of cellular blood components through the removal of most of the plasma or by the washing of red cells and platelets. However, the routine use of washed components for patients with cutaneous allergic reactions is unwarranted.

SEVERE ALLERGIC (ANAPHYLACTIC) REACTIONS

In addition to the signs of typical milder allergic reactions, anaphylactic or anaphylactoid reactions manifest cardiovascular instability, including hypotension, tachycardia, loss of consciousness, cardiac arrhythmia, shock, and cardiac arrest. Respiratory involvement with dyspnea or stridor may be more pronounced than is seen usually in typical allergic reactions.

If an anaphylactic reaction occurs, the transfusion should be discontinued and intravenous access maintained. Supportive care, including intubation, oxygen, intravenous fluids, and placement of the patient in the Trendelenburg position, should be instituted promptly. Epinephrine should be available immediately. For hypotension unresponsive to supportive measures or for significant bronchospasm, subcutaneous epinephrine 0.3 to 0.5 mg (0.3–0.5 mL of a 1:1000 solution) can be given. This dose can be repeated every 20 to 30 minutes for up to three doses. Alternatively, 0.5 mg of epinephrine may be given intravenously (5 mL of a 1:10,000 solution) and repeated every 5 to 10 minutes for refractory hypotension.

An antihistamine such as diphenhydramine 50 to 100 mg can be given intravenously, particularly when there are cutaneous manifestations such as urticaria. Aminophylline (6 mg/kg loading dose) may be useful when there is bronchospasm. Steroids are probably not effective in the acute situation; however, if symptoms persist, a drug such as hydrocortisone (500 mg) may be given.

Patients with IgA deficiency who develop IgE anti-IgA can have anaphylactic reactions (Vyas et al., 1969). Patients who have significant allergic reactions should be evaluated for their quantitative IgA levels. Recent transfusion may elevate serum IgA levels falsely. However, if IgA deficiency has been established, anti-IgA testing should be done, usually by a reference laboratory. IgA-deficient plasma can be obtained from rare donor registries, if necessary. Red cells and platelets can be washed to remove sufficient amounts of IgA to prevent reactions.

Patients with haptoglobin deficiency can have similar anaphylactic transfusion reactions due to IgG or IgE antihaptoglobin (Shimada et al., 2002). Haptoglobin deficiency is rare in North American populations but is more common than IgA deficiency among Japanese patients suffering anaphylactic reactions.

ACUTE HEMOLYTIC REACTIONS

Acute hemolytic transfusion reactions (AHTRs), by definition, present within 24 hours of transfusion. AHTRs are most commonly caused by transfusion of RBC units that are positive for an antigen against which the recipient has formed antibodies. AHTRs may also be seen with transfusion of antibodies (in donor plasma or intravenous immunoglobulin [IVIg]) into recipients whose RBCs bear the antigen recognized by those antibodies. Presenting signs include fever and chills, nausea, vomiting, pain, dyspnea, tachycardia, hypotension, bleeding, and hemoglobinuria. Fever is the most sensitive initial sign of an AHTR. Therefore, any increase in temperature of 1°C or greater should result in a transfusion being stopped and a laboratory evaluation initiated. Renal failure is a later complication. Pain during an AHTR has been reported as localizing to the flanks, back, abdomen, chest, head, and infusion site. A subjective feeling of distress is reported sometimes. Unexpected bleeding may be due to DIC. During surgery, hypotension and excessive bleeding may be the only signs of an AHTR. Both may be attributed to other causes; therefore, physicians must be mindful of the possibility of a hemolytic reaction in this circumstance.

Laboratory findings in AHTRs include hemoglobinemia, hemoglobinuria, elevated lactate dehydrogenase, hyperbilirubinemia, and low haptoglobin. The blood urea nitrogen and creatinine will be elevated if renal injury has occurred. The direct antiglobulin test (DAT) may show positive results with a mixed-field pattern if transfused incompatible red cells are present in the circulation. Red cell antibody identification studies may or may not show positive results depending on the specificity of the antibody involved and the amount of antibody in the serum. ABO incompatibility due to a clerical error is the most common cause of AHTRs.

In the event of an AHTR, the transfusion should be discontinued and intravenous access maintained. The identity of the patient and the unit or units of RBCs should be reconfirmed, and other units of RBCs that have been dispensed for the patient should be located and quarantined. The reaction must be reported to the blood bank promptly. If a misidentification is discovered, another patient (e.g., with a similar name) may also be at risk for receiving incompatible blood.

Treatment of an AHTR must be guided by the clinical response of the patient. Patients who have minimal symptoms may be managed best by careful observation. In severe reactions, early vigorous intervention may be lifesaving. It bears repeating that the severity of AHTRs is related directly to the volume of incompatible blood transfused. Thus, early recognition, discontinuation of the transfusion, and prevention of the transfusion of additional incompatible units are the essential first steps of treatment. Initial attention must be paid to cardiovascular support. If hypotension is present, fluid resuscitation and pressor support may be indicated. Care should be taken to avoid fluid overload, however, especially in patients with impaired cardiac or renal function.

Because renal failure is a significant problem in some patients, attention should be given to prevention. Early treatments of hypotension and DIC are the most important interventions to limit the extent of possible renal impairment. Maintenance of urine output with intravenous fluids and diuretics, mannitol or furosemide, early in the course of the reaction has been used successfully. Hydration with normal saline and 5% dextrose (1:1 ratio) at a rate of 3000 mL/m^2 per day and administration of sodium bicarbonate to maintain the urine pH above 7.0 have been recommended (Nussbaumer et al., 1995). Infusion of an initial dose of 20% mannitol 100 mL/m^2 given over 30 to 60 minutes followed by 30 mL/m^2 per hour for the next 12 hours has also been recommended (Slavc et al., 1992). However, if oliguria in the face of euvolemia is present, fluid loading may be contraindicated.

Since the load of incompatible red cells in the circulation dictates the severity and course of AHTRs, an exchange transfusion with antigen-negative blood may be considered in severe hemolytic transfusion reactions. The decision to perform an exchange transfusion must be guided by the clinical response of the patient to initial treatments. It is not appropriate to expose a patient to the added risk for infectious disease if the hemolytic process is well tolerated. With ABO incompatibility, however, an exchange transfusion may greatly reduce the chance of morbidity or death.

Further transfusion of red cells should be avoided until the cause of the reaction has been established. Foremost, however, no patient should be allowed to exsanguinate for lack of serologically compatible blood. Group O RBCs lacking other known clinically significant antigens to which the patient currently has an antibody should be obtained, if possible. The results of serologic tests performed up to this point must be considered and clinical judgment exercised. Although the focus of attention in most AHTRs is on red cells, care should be taken to avoid the transfusion of plasma or platelets that may aggravate hemolysis, especially when ABO incompatibility is a possible cause. Undue haste in both serologic evaluation and decision making must be avoided because human errors are committed most often under pressure.

DELAYED HEMOLYTIC REACTIONS

By definition, delayed hemolytic transfusion reactions (DHTRs) occur at least 24 hours after transfusion of the offending unit. The time from transfusion to diagnosis of a DHTR is variable. Most patients present within the first 2 weeks after receiving the transfusion. However, clinical DHTR may be recognized more than 6 weeks later. Almost all DHTRs are due to an anamnestic response to a red cell antigen to which the patient has previously made an antibody, the concentration of which was too low to detect in pretransfusion testing. Rarely, a DHTR may be due to primary alloimmunization to a red cell antigen. Typically, hemolysis is extravascular, but intravascular hemolysis may occur also. Fortunately, these reactions tend to be much less severe than AHTRs; accordingly, they may be overlooked. Some patients will present with only unexpected anemia. Other clinical signs include fever or chills, jaundice, pain, or dyspnea. Rarely, renal failure may ensue. In patients with SCD, DHTRs may precipitate a sickle crisis (Mintz & Williams, 1986).

Laboratory findings in DHTRs include anemia, elevated lactate dehydrogenase, hyperbilirubinemia, low haptoglobin, leukocytosis, the presence of a new red cell antibody, and a positive reaction on a DAT. The degree of hyperbilirubinemia will depend on the rate and amount of hemolysis as well as on liver function. Typically, unconjugated bilirubin levels are elevated during active hemolysis. Depressed haptoglobin levels do not necessarily indicate intravascular hemolysis, as they may be seen with extravascular hemolysis as well.

Many patients tolerate DHTRs well and may need only to be followed carefully. Generally, fluid loading and diuresis are not indicated unless there is active intravascular hemolysis. Complications, such as renal failure or sickle crisis, should be treated as such. If there is a large burden of antigen-positive red cells, an exchange transfusion should be considered. In general, transfusion should be avoided until the causative antibody can be identified and antigen-negative units obtained. However, as with AHTRs, a patient should not be allowed to have significant morbidity from anemia for lack of serologically compatible blood. The selection of red cells for transfusion needs to be based on the results of serologic testing and good communication between the medical director of the blood bank and the patient's physician.

Because extravascular hemolysis is similar to autoimmune hemolytic anemia, in which high-dose IVIg infusion may be useful, IVIg may be considered in the treatment of DHTRs also. A single dose of IVIg, 400 mg/kg, infused within 24 hours prior to transfusion, has been used successfully to prevent transfusion reactions in alloimmunized patients for whom compatible blood could not be obtained (Kohan et al., 1994). Five patients so treated had sustained increases in Hct. No transfusion reaction developed in any of the cases.

BACTERIAL CONTAMINATION OF BLOOD COMPONENTS

The clinical presentation of a transfusion reaction caused by bacterially contaminated blood components is usually dramatic. Onset of symptoms in most cases occurs during the transfusion or shortly after it; delayed presentation of more than 1 day has rarely been reported with contaminated platelet transfusions. Fever, chills, hypotension, shock, nausea, and vomiting are the most commonly reported symptoms (Kuehnert et al., 2001; Perez et al., 2001). Dyspnea, pain, and diarrhea also may occur. High fever and hypotension during or shortly after transfusion are particular clues that a contaminated unit may have been transfused.

The clinical complications due to bacterial contamination are significant, often resulting in shock, renal failure, DIC, and death. The mortality rate is high and depends on the type of component involved, the identity and amount of the causative organism, and the clinical condition of the patient. Patient factors associated with clinical reactions include thrombocytopenia and pancytopenia. Risk factors for fatality include contamination by gram-negative rods, greater patient age, smaller volume of component transfused, and younger age of stored platelet concentrate. The latter two factors most likely reflect greater numbers of organisms in the component. The organism involved depends on the type and storage of the blood component. RBCs have been found to contain *Acinetobacter*, *Escherichia*, *Staphylococcus*, *Yersinia*, and *Pseudomonas* species. gram-positive cocci such as *Staphylococcus* and *Streptococcus*, gram-negative rods such as *Acinetobacter*, *Klebsiella*, *Salmonella*, *Escherichia*, and *Serratia*, and gram-positive rods such as *Propionibacterium* have been reported in platelet concentrates (Kuehnert et al., 2001; Andreu et al., 2002). Some transfusion services culture for bacteria all platelet concentrates that have caused a febrile transfusion reaction because, if a red cell concentrate from the same donation exists, it can be withdrawn.

Usually, treatment must be initiated before the causative organism has been identified. If a reaction occurs, the transfusion should be discontinued, the unit with its associated tubing should be removed, and any other blood bags that have been recently transfused should be recovered. Supportive care of circulation and respiration should be initiated as required. Antibiotic therapy initially should include broad-spectrum coverage, such as a β-lactam and an aminoglycoside, until microbiological stains or cultures indicate the causative organism. From the remaining blood component unit, a sample should be taken for Gram stain and culture. Blood cultures from the transfusion recipient should also be collected at the time of reaction to compare with the results of the unit culture.

Septic transfusion reactions are seen more frequently with platelet transfusions, as the platelet units are kept at room temperature, which permits bacterial growth compared with RBC units stored at 4°C. Therefore, AABB standards require that blood banks and transfusion services have methods to detect and limit bacterial contamination of platelets. Methods cleared or approved by the FDA include culture, measurement of oxygen consumption, and rapid qualitative immunoassay (AuBuchon et al., 2002; Ortolano et al., 2003). Measurements of pH or glucose and inspection for "swirling" have been used as indicators of contamination but are not sufficiently sensitive to meet current AABB standards (Wagner & Robinette, 1996). Some studies have found that apheresis platelets have a lower incidence of septic reactions than pooled whole blood–derived platelets (Ness et al., 2001). Because skin flora, if present, enter the collection at venipuncture, diversion of the first 20 mL decreases the risk by 50% (Eder et al., 2009). Most blood centers culture apheresis platelets and prepooled platelets at the time of manufacture. The components then are held for a brief time (typically at least 12 hours) and are released for distribution if the culture is negative. Although this approach is operationally efficient, it is not optimal in that the culture is taken at a time when the bacterial load is low. The residual risk for a septic reaction with culture-negative apheresis platelets is approximately 1:75,000 (Eder et al., 2007). A method cleared or approved by the FDA may be used for detection of bacterial contamination in platelets closer to the time of issue (Platelet PGD Test, Verax Biomedical Incorporated, Worcester, MA; BacTx Rapid Assay System, Immunentics, Boston, MA). This method is based on the immunological detection of lipopolysaccharide (gram negative organisms) and teichoic acid (gram positive organisms) (Vollmer et al., 2010). These tests have been shown to identify bacterially contaminated units that were not identified by initial culture (at a rate of 1:3069 platelet transfusions), though at a cost of a 0.51% false-positive rate (Jacobs et al., 2011). However, the current version of the test has a false-positive rate in leukocyte-reduced apheresis platelets suspended in plasma of 0.1%. The ideal implementation strategy using this testing to maximize the benefit of this testing while minimizing the cost due to false-positive reactions is still to be determined. Pathogen reduction technology appears to significantly reduce, if not eliminate, bacterial contamination, and its use may obviate the need for bacterial detection methods.

TRANSFUSION-RELATED ACUTE LUNG INJURY

TRALI usually presents during or within hours of transfusion. Its symptoms include dyspnea, hypoxemia, tachycardia, fever, hypotension, and cyanosis (Kleinman et al., 2004). Fever and hypotension, when present, are usually moderate and respond quickly to antipyretics and fluids. Characteristically, there is a lack of abnormal breath sounds. A chest x-ray usually shows pulmonary edema, most commonly in a generalized pattern rather than only along the major vasculature, as seen in cardiac failure. By definition, there are no signs of cardiac failure. Patients with hematologic malignancy or cardiac disease appear to be at higher risk for TRALI (Silliman et al., 2003). This may reflect the fact that these patient groups receive a high number of transfusions. Reported mortality is approximately 10% depending on the severity of the lung injury and the underlying clinical status of the patient. A wide range of severity is seen in this transfusion reaction; milder forms may not be readily recognized.

The differential diagnosis includes circulatory overload, bacterial contamination, allergic reactions, acute respiratory distress syndrome (ARDS), pulmonary embolism, and pulmonary hemorrhage. The diagnosis is established by findings of noncardiogenic pulmonary edema. Pulmonary artery wedge pressure is not elevated. An increase in brain natriuretic peptide (BNP) from pre- to posttransfusion is found in circulatory overload but not in TRALI (Zhou et al., 2005; Tobian et al., 2008). Characteristically, TRALI resolves within 48 to 96 hours from outset (Popovsky et al., 1992). Failure of the patient to improve substantially after this time should call the diagnosis into question. Although chest x-ray findings may persist beyond 7 days, no permanent pulmonary sequelae are evident, unlike with ARDS due to many other causes. A decrease in leukocyte or platelet count may be a useful clue in TRALI caused by transfusion of HLA class I antibodies (Cooling et al., 2002).

The treatment of TRALI is supportive. If a transfusion is in progress, it should be discontinued and blood bags from recently transfused units should be recovered. The blood bank should be consulted regarding the evaluation of TRALI. Usually, oxygen is indicated. Severely affected patients may require mechanical ventilation. Corticosteroids appear to be of little, if any, value. Diuresis is not indicated in the absence of signs of fluid overload.

TRALI has been attributed to the presence of antibodies in the plasma of the transfused unit that are directed against HLA or granulocyte antigens present on recipient leukocytes (Kopko et al., 2002). Plasma from multiparous female donors carry the greatest risk for HLA antibodies that may cause TRALI (Triulzi et al., 2009). Based on this risk, mitigation strategies should be targeted at identifying multiparous women with HLA antibodies and decreasing the use of plasma-rich units from these donors. Some TRALI reactions may be due to the presence in the blood product of lipid inflammatory mediators that activate already primed recipient neutrophils (from surgery, trauma, or inflammation) to cause capillary injury and leakage (Silliman et al., 2003).

TRANSFUSION-ASSOCIATED CIRCULATORY OVERLOAD

Circulatory overload is an all-too-common and preventable transfusion reaction. It presents as congestive heart failure during or shortly after transfusion. Signs and symptoms can include dyspnea, orthopnea, cyanosis, tachycardia, elevated blood pressure, pulmonary edema, jugular venous distention, pedal edema, and headache. The differential diagnosis includes TRALI, allergic reactions, and causes of congestive failure not related to transfusion, such as valvular heart disease. Clearly, patients with preexisting heart disease are at risk for circulatory overload with transfusion. The diagnosis of circulatory overload on clinical and radiologic examination may be difficult. Elevation of BNP can be helpful in making the diagnosis (Zhou et al., 2005; Tobian et al., 2008).

Volume overload should be anticipated in at-risk patients and prevented readily. Blood should be transfused slowly. Transfusion should be completed within 4 hours; if longer than 4 hours is required, alternative strategies should be considered. Small volumes can be transfused with adequate time between transfusions to allow for diuresis. To avoid additional donor exposures, a unit can be split using sterile technique and a portion retained in the blood bank for later transfusion. Units can also be concentrated by plasma removal. A diuretic can be administered before or during the transfusion.

GRAFT-VERSUS-HOST DISEASE

Transfusion-associated graft-versus-host disease (TA-GVHD) can occur when viable donor T cells proliferate and are not recognized by the recipient's immune system as foreign but recognize and reject the host as foreign. Patients with marked cellular immunodeficiencies are at risk for TA-GVHD (Box 37.8). These include congenital cellular immunodeficiencies (DiGeorge syndrome, severe combined immunodeficiency syndrome), immaturity of the immune system (intrauterine transfusions, very-low-birthweight infants), disease-associated immunodeficiencies (Hodgkin lymphoma), and therapy-associated cellular immunodeficiencies (hematopoietic progenitor cell transplantation,

BOX 37.8

Indications for Irradiation of Blood Components for Prevention of TA-GVHD

Absolute Indications

Congenital cellular immunodeficiency
Hematopoietic progenitor cell transplantation
Hodgkin lymphoma
Granulocyte transfusions
Intrauterine transfusions (IUTs)
Transfusion to neonates who have received IUT
Transfusions from biological relatives
Chemotherapy with purine analogs (fludarabine)

Probable Indications

Low-birthweight infants (<1200 g)
Hematologic malignancies other than Hodgkin lymphoma
HLA-matched platelet concentrates
High-dose chemotherapy, radiation therapy, and/or aggressive immunotherapy

Controversial Indications

Large-volume or exchange transfusion of infants who did not receive IUT
Aplastic anemia
Absolute lymphopenia (absolute lymphocyte count <500/mL)
Antithymocyte globulin administration

Irradiation Not Indicated

Solid-organ transplantation
HIV infection
Hemophilia
Small-volume transfusions of term infants who did not receive IUT
Older adult patients
Typical dose immunosuppressive therapy (other than purine analogs)
Immunocompetent surgical patients
Pregnancy
Red cell membrane, metabolic, or hemoglobin disorders (e.g., thalassemia, SCD)

HIV, Human immunodeficiency virus; *HLA,* human leukocyte antigen; *SCD,* sickle cell disease; *TA-GVHD,* transfusion-associated graft-versus-host disease.
Adapted from Gorlin JB, Mintz PD: Transfusion-associated graft-vs-host disease. In Mintz PD, editor: *Transfusion Therapy: Clinical Principles and Practice*, ed 3, Bethesda, MD, 2011, AABB Press, p 650.

fludarabine treatment, antithymocyte globulin). Humoral immunodeficiencies, such as common variable immunodeficiency (CVID), are not a risk factor for GVHD. HIV infection, although it may cause marked T-cell dysfunction, does not increase the risk for TA-GVHD. Common immunosuppressive regimens for solid-organ transplantation and typical chemotherapy regimens for solid tumors do not increase the risk for TA-GVHD. However, TA-GVHD has been reported with highly aggressive chemotherapy for neuroblastoma, germ cell tumors, and some other tumors. Patients with normal immunity may be at risk for TA-GVHD if the donor is homozygous for an HLA haplotype and the recipient is heterozygous but shares one haplotype. In this case, recipient lymphocytes are unable to recognize transfused lymphocytes as foreign, but transfused cells see recipient cells as foreign (Fig. 37.1). This is most likely to occur with donations from close (first- or second-degree) relatives but may also occur owing to chance, particularly in populations that are relatively homogeneous (Aoun et al., 2003).

TA-GVHD typically manifests 2 to 50 days after transfusion. Characteristic findings include rash, diarrhea, fever, liver dysfunction, and pancytopenia. Mortality is greater than 90%, with most patients dying of infection. In contrast to the expected GVHD of allogeneic HPC transplantation, the bone marrow in TA-GVHD is of recipient type and is attacked as well as the other organs. Aggressive immunosuppressive treatments have been tried but with rare exceptions have been unsuccessful. Thus, preventive measures are of paramount importance.

The minimum number of viable transfused T cells necessary to cause TA-GVHD has not been established, but it is clear that current leukocyte reduction methods are not sufficient (Hayashi et al., 1993). Exposure to ionizing radiation (γ-rays or x-rays) can cause chromosomal damage and prevent replication of transfused leukocytes. Current FDA guidelines suggest a midplane dose of 25 Gy, with a minimum dose of 15 Gy to any point of the blood container (see the Special Components section earlier in the chapter). A licensed pathogen reduction system may be used as an alternative to irradiation of platelets for the prevention of TA-GVHD (Mintz, 2011).

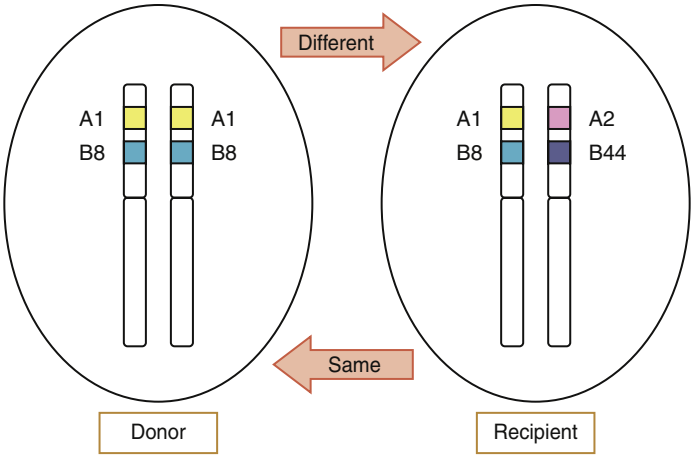

Figure 37.1 Mechanism of TA-GVHD in immunocompetent patients. The donor is homozygous at the HLA class I locus. The recipient is heterozygous and shares one haplotype with the donor. Engrafted donor T cells recognize the recipient as foreign, but the recipient's T cells do not identify donor T cells as foreign. *HLA,* Human leukocyte antigens; *TA-GVHD,* transfusion-associated graft-versus-host disease.

HYPOTENSIVE REACTIONS

Transfusion-associated hypotension is defined as hypotension that occurs during transfusion in the absence of signs or symptoms of other transfusion reactions, such as fever, chills, dyspnea, urticaria, or flushing. The degree of hypotension required for the diagnosis is controversial but could be defined reasonably as a drop of at least 10 mm Hg in systolic or diastolic arterial blood pressure from the pretransfusion baseline. However, if the immediate pretransfusion blood pressure is elevated from the patient's typical blood pressure and the arterial pressure does not fall below the patient's usual blood pressure, this should not be considered a hypotensive reaction. Hypotension begins during the transfusion and resolves quickly when the transfusion is discontinued. If hypotension persists beyond 30 minutes after discontinuation of the transfusion, another diagnosis should be strongly considered. Hypotensive reactions have been associated with red cell and platelet transfusions. Some reactions have been associated with the use of bedside leukocyte reduction filters (Fried et al., 1996; Abe et al., 1997).

If hypotension occurs, the transfusion should be discontinued and intravenous access maintained. The patient should be positioned with head down and feet elevated (Trendelenburg position), and isotonic fluids should be administered. Pressor support is indicated only if the hypotension is severe and refractory to intravenous fluids.

The cause of transfusion-associated hypotension has not been established definitively. However, the condition is most likely due to the release of bradykinin through activation of the contact pathway of coagulation. Some reactions have been associated with angiotensin-converting enzyme (ACE)–inhibitor drugs in the recipient and/or the use of leukocyte-reduction filters. ACE is the major enzyme that breaks down bradykinin in the circulation. Some bedside filters, particularly those with a net-negative surface charge, appear to cause activation of kallikrein and cleavage of high-molecular-weight kininogen, which results in the release of bradykinin (Davenport & Penezina, 1997; Shiba et al., 1997; Mair & Leparc, 1998). However, there is variability because not all such filtered units show activation.

NONIMMUNE HEMOLYSIS

Lysis of red cells can occur as a result of storage, handling, or transfusion conditions. Hyperosmotic or hypo-osmotic fluids mixed with red cells can result in significant lysis. Patients who receive lysed red cells may tolerate them remarkably well. However, transient hemodynamic, pulmonary, and renal impairment may occur, and death due to transfusion of lysed red cells has been reported (Sazama, 1990). The transfusion of autologous blood from a patient with sickle Hb can result in hemolysis and death (DeChristopher & Orlina, 1990). The clinical signs are usually hemoglobinemia and hemoglobinuria. Hyperkalemia may occur, particularly in patients with renal failure. Fever also may occur. Finding lysis of RBCs in the transfused unit and excluding other causes, such as hemolytic transfusion reactions, establishes the diagnosis. All RBC units will show a slight degree in hemolysis with prolonged storage, but this will not result in clinical signs after transfusion. The principal reported complications of nonimmune

TABLE 37.3

Approximate Current Per-Unit Risks for Infectious Disease Transmission in the United States

HIV	1 : 1,860,000
HBV	1 : 765,000 to 1 : 1,006,000
HCV	1 : 1,660,000
HTLV-I/II	1 : 3,390,000
West Nile virus	≈1 : 7,000,000

Data from Stramer SL, Notari EP, Krysztof DE, et al.: Hepatitis B virus testing by minipool nucleic acid testing: does it improve blood safety?, *Transfusion* 53:2449–2458, 2013; Busch MP, Glynn SA, Stramer SL, et al.: A new strategy for estimating risks of transfusion-transmitted viral infections based on rates of detection of recently infected donors, *Transfusion* 45:254–264, 2005; and Zou S, Stramer SL, Dodd RY: Donor testing and risk: current prevalence, incidence, and residual risk of transfusion-transmissible agents in US allogeneic donations, *Transfus Med Rev* 26:119–128, 2012.
HBV, Hepatitis B virus; *HCV,* hepatitis C virus; *HIV,* human immunodeficiency virus; *HTLV,* human T-cell lymphotropic virus.

hemolysis are renal failure and cardiac arrhythmia due to hyperkalemia. Hemolytic transfusion reactions can rarely occur when no red cell antibody is identifiable (Davey et al., 1980). Differentiation of this condition from nonimmune hemolysis may be impossible without careful investigation of the transfusion circumstances.

Should nonimmune hemolysis occur, the transfusion should be discontinued and intravenous access maintained. The blood bag, together with attached tubing and intravenous fluids, should be saved for further investigation. A hemolytic transfusion reaction needs to be ruled out. The serum potassium level should be checked and an electrocardiogram obtained to assess hyperkalemia. Care is supportive. Urine output should be maintained with hydration unless there is a contraindication, such as renal failure.

TRANSFUSION-TRANSMITTED DISEASE

Improvements in donor screening and testing have resulted in dramatic reductions in transfusion-transmitted disease risk over the past 2 decades. For example, the risk for transmitting HIV by blood transfusion in the United States has been reduced from approximately 1 in 100 in certain urban areas in the early 1980s to approximately 1 in 1,860,000 throughout the United States at present (Zou et al., 2012). It is virtually impossible to accurately measure current risk for hepatitis and HIV transmission by epidemiologic methods. Risk estimates for HIV, HBV, and HCV are now based on mathematical models that take into account the probability of marker-negative window-phase donations, viral strains not reliably detected by current assays, persistent antibody-negative carriers, and testing errors (Dodd et al., 2002). Current (2012) risk estimates are summarized in Table 37.3 (Stramer, 2013).

Hepatitis

Historically, HCV has accounted for the majority of cases of posttransfusion hepatitis (PTH). Approximately 10% of chronic HCV is attributable to blood transfusion (Alter et al., 1999). PTH is asymptomatic in the majority of cases. Approximately 75% to 85% of individuals have persistent HCV infection; about 50% of these have evidence of chronic hepatitis. As many as 10% of patients with HCV PTH eventually manifest clinical liver disease (Seeff et al., 1992). Acute PTH due to HBV is typically more severe, with 25% to 30% of individuals having jaundice, with an incubation time of 40 to 60 days (Walsh et al., 1970; Seeff et al., 1975). Less than 10% of infected individuals progress to chronic hepatitis. If acquired before 5 years of age, acute HBV infection is usually less severe, but the risk for chronic hepatitis is much greater. Hepatitis D virus (HDV) requires coinfection with HBV for replication. If acquired simultaneously with HBV, HDV can cause severe hepatitis and liver failure. If acquired during chronic HBV infection (superinfection), HDV significantly increases the risk for severe chronic liver disease. Transfusion-transmitted HDV is rare, and screening methods for HBV are also effective against HDV. Hepatitis A virus and hepatitis E virus have relatively short periods of viremia and do not progress to a chronic carrier state. Transmission of these viruses by transfusion is rare but has occurred (Sherertz et al., 1984; Matsubayashi et al., 2004). Hepatitis G virus (GBV-C) has a prevalence rate of about 1% in asymptomatic blood donors (Roth et al., 1997). Although it is clearly transmissible by transfusion, no causal relationship between GBV-C infection and hepatitis or chronic liver disease has been established (Alter et al., 1997).

Human Immunodeficiency Virus

The clinical manifestations of transfusion-transmitted HIV are similar to those of HIV infection acquired through other routes. An acute viral syndrome occurs in about 60% of cases. Untreated, asymptomatic infection persists for about 10 years before acquired immunodeficiency syndrome (AIDS)-defining illness occurs, although progression tends to be more rapid in older individuals (Blaxhult et al., 1990). The time to AIDS progression for transfusion recipients may be shorter than that for the implicated donor, but this may reflect the effects of age and other cofactors (Busch et al., 1994). Historically, Group O viral isolates were not reliably detected by enzyme immunoassay (EIA) tests. Currently, the prevalence of group O HIV in the United States is low, but it is endemic in some parts of western Africa, and transfusion-transmission by emigrants from such areas has occurred (Pau et al., 1996). Therefore, residence in or emigration from such areas used to be a reason for permanent donor deferral. However, a combined immunoassay for simultaneous detection of HIV p24 antigen and HIV-1 and HIV-2 antibodies that detects group O HIV was approved by the FDA for donor testing (Sickinger et al., 2008). Blood centers that have implemented this test have now discontinued geographic deferral for HIV group O.

Human T-Cell Lymphotropic Virus

Human T-cell lymphotropic virus type I (HTLV-I) is causally associated with adult T-cell lymphoma/leukemia (ATL) and HTLV-associated myelopathy (HAM) (Hall et al., 1996; Manns et al., 1999). Most carriers are asymptomatic. ATL or HAM develops in a small minority of cases after a latent period of many years. HTLV-I is rare in the United States. HTLV-II is prevalent in intravenous drug users in the United States and is also associated with HAM (Murphy et al., 1997).

Cytomegalovirus

CMV is common in the general population. In immunologically competent individuals, it causes minor symptoms but becomes latent in virtually all cases (Larsson et al., 1998). Approximately 50% of blood donors in the United States are CMV seropositive, though there is high regional variation, but the estimated risk for transmission by a seropositive transfusion is about 1% (Preiksaitis et al., 1988). In patients with severe cellular immunodeficiency, CMV can cause pneumonitis, hepatitis, retinitis, and multisystem organ failure. CMV transmission can be minimized by the use of seronegative blood components, although many studies have shown a low rate of CMV infection in such patients. Whether this is due to failure to detect potentially infectious donors or whether viral transmission occurred by other routes is unclear. Several studies, including a prospective randomized trial, have shown that leukocyte-reduced blood components are as effective as seronegative components in reducing the risk for CMV transmission (Bowden et al., 1995). Due to the prevalence of leukoreduction and low risk for CMV transmission causing disease, most blood collection centers do not screen all units for CMV antibodies.

Parvovirus B-19

Parvovirus B-19 is also common in the general population. The incidence of viremia among blood donors is variable, with episodic peaks, but it averages around 1 : 5000 (Hitzler & Runkel, 2002). In most individuals, parvovirus B-19 causes a mild self-limited febrile illness. However, it is trophic for erythrocyte precursors in the bone marrow and can cause red cell aplasia, particularly in the setting of accelerated erythropoiesis. Transfusion-transmitted parvovirus infection has been implicated in causing chronic anemia after bone marrow transplantation and in thalassemia (Zanella et al., 1995; Cohen et al., 1997). Due to the prevalence of seropositivity in the general public, donor centers do not regularly screen for parvovirus antibodies.

West Nile Virus

West Nile virus (WNV) arrived in the United States in 1999. From its initial outbreak in New York, it has spread across the country. Birds are the natural reservoir, with mosquitoes serving as the vector of transmission. Humans are an accidental host, with infection occurring during times of mosquito activity (typically, late summer and fall). Most acute WNV infections are asymptomatic, with a febrile illness occurring in about 1 in 5 infections and neuroinvasive disease in about 1 in 150 infections (Petersen & Marfin, 2002). In 2002, 23 confirmed cases of transfusion-transmitted WNV were reported by the Centers for Disease Control and Prevention (Pealer et al., 2003). In areas of peak WNV activity in 2002, the estimated rate of viremia among blood donors was 1.5 in 1000 (Biggerstaff &

Petersen, 2002). Donor screening for WNV by nucleic acid testing (NAT) was implemented in July 2003 in North America. Subsequently, rare cases of WNV transmission by blood transfusion have been reported, most likely due to the low viral copy number that escaped detection (Macedo de Oliveira & Beecham, 2004).

Zika Virus

Zika virus (ZKV) is transmitted by *Aedes* species mosquitos, by sexual contact with infected individuals, and transplacentally in pregnancy. In 2015 and 2016, large outbreaks of Zika virus occurred, including in Puerto Rico, the U.S. Virgin Islands, and limited local transmission in Florida and Texas. Transfusion-transmitted Zika infection has been documented in Brazil, although to date there have been no confirmed cases in the United States (Magnus, 2018). Current FDA guidance recommends that all donations be tested with a licensed nucleic acid test for Zika virus, or that an FDA-approved pathogen reduction device be used to manufacture platelets or plasma.

Malaria

About 1300 cases of malaria are reported annually in the United States. Transfusion transmission of malaria still occurs rarely (1–2 cases annually). Implicated donors usually have a history of travel to an endemic area (Mungai et al., 2001). At present, donors are screened by a questionnaire detailing travel to endemic areas and symptomatology. Donor centers are not currently performing laboratory testing to identify malaria-contaminated donations.

Babesiosis

Babesia species are endemic in North American mammals and are transmitted by ticks of the genus *Ixodes*. Many cases of babesiosis are asymptomatic or mild. However, it may be more severe in the asplenic or immunosuppressed patient. The parasite is capable of survival in refrigerated red cells and in room-temperature platelet units. Transmission of *Babesia* infection through transfusion is more commonly seen in endemic areas but can be seen in areas remote from these endemic areas due to shipment of blood products around the country (Herwaldt et al., 2011). Serologic and nucleic acid donor screening tests for *B. microti* have been approved by the FDA, although the serologic test is currently not being manufactured. At this time, the FDA requires NAT in high-prevalence areas.

Trypanosoma cruzi

T. cruzi is the cause of Chagas disease and is endemic in parts of Central and South America. There may be more than 300,000 chronic carriers of *T. cruzi* in the United States, largely as the result of immigration (Centers for Disease Control and Prevention, 2015). Rare cases of transfusion-transmitted Chagas disease have been reported in the United States (Nickerson et al., 1989). The risk is dependent on the demographics of the donor population. Seropositivity rates among blood donors have been estimated to be 1:25,000 nationally and as high as 1:2000 in Los Angeles (Leiby et al., 2002; Centers for Disease Control and Prevention, 2006–2007). The majority of reported transfusion-transmitted *T. cruzi* infections have been due to platelet transfusions. However, in contrast to many infectious agents, *T. cruzi* is able to tolerate freeze-thaw cycles. Thus, it may be transmitted in plasma products as well as cellular products. Since the FDA approval of a donor screening EIA test, more than 2000 confirmed positive donors have been detected in the United States (AABB, 2015). In the 4 years following initiation of this testing, no *T. cruzi* transmission via transfusion events has been reported in the United States (FDA Blood Products Advisory Committee, 2011).

Transmissible Spongiform Encephalopathies

Transmissible spongiform encephalopathies (TSEs) are caused by a protein, called a *prion*, that is capable of assuming an abnormal configuration resistant to enzymatic degradation and serves as a template for further abnormal prion deposition. Variant Creutzfeldt-Jakob disease (vCJD) is a human TSE that emerged from an epidemic of bovine spongiform encephalopathy, probably as a result of entry of the pathogenic prion into the human food supply from affected cattle. The transmissibility of vCJD by blood in experimental models suggests a possible risk for transmission by transfusion. The magnitude of such a risk is presently unknown. However, four cases of prion acquisition have been reported in individuals who received transfusions from donors who were themselves diagnosed with vCJD (Chohan et al., 2010). However, it is notable that no cases of transfusion transmission of sporadic or familial CJD have been found to date, despite ongoing surveillance (Crowder et al., 2017). Currently, there is no available serologic test suitable for testing donated units. Thus, donor centers defer at-risk donors based on exposure (vCJD) and family history (familial CJD) risk as determined by a predonation questionnaire.

CONCLUSION

Discovery of the A, B, and O blood groups by Karl Landsteiner in 1900 led to the widespread use of blood transfusion therapy early in the 20th century. This treatment directly afforded a remarkable evolution in surgical, trauma, and medical care. Although remarkable progress has been made in identifying and reducing transfusion-transmitted infection, the incidence of the principal noninfectious risks—TRALI, volume overload, and mistransfusion due to clerical error—has remained stable for many years. Increasing attention has been focused recently on these latter hazards; it is hoped that this will lead to a substantial reduction in their occurrence. Despite the continuing risk for transfusion, a much greater threat is posed by withholding a blood component that is clinically indicated than by transfusing it.

SELECTED REFERENCES

Adams RJ, McKie VC, Hsu L, et al.: Prevention of a first stroke by transfusions in children with sickle cell anemia and abnormal results on transcranial Doppler ultrasonography, *N Engl J Med* 339:5–11, 1998.

This prospective randomized trial showed that chronic transfusion to maintain HbS <30% reduced the risk for stroke in children with sickle cell disease.

Bowden RA, Slichter SJ, Sayers M, et al.: A comparison of filtered leukocyte-reduced and cytomegalovirus (CMV) seronegative blood products for the prevention of transfusion-associated CMV infection after marrow transplant, *Blood* 86:3598–3603, 1995.

This prospective randomized trial demonstrated that leukocyte reduction is equivalent to CMV-seronegative blood components in preventing CMV transmission. However, CMV disease was more common in the group receiving leukocyte-reduced components, which is a point of controversy.

Dzik WH, Anderson JK, O'Neill EM, et al.: A prospective, randomized clinical trial of universal WBC reduction, *Transfusion* 42:1114–1122, 2002.

This prospective randomized trial showed that universal leukocyte reduction was associated with fewer febrile transfusion reactions but not with in-hospital mortality, length of stay, or hospital costs. These latter points are controversial.

Hebert PC, Wells G, Blajchman MA, et al.: A multicenter, randomized, controlled clinical trial of transfusion requirements in critical care, *N Engl J Med* 340:409–417, 1999.

This prospective randomized trial showed that a restrictive strategy of red-cell transfusion is at least as effective as, and possibly superior to, a liberal transfusion strategy in critically ill patients, with the possible exception of patients with acute myocardial infarction and unstable angina.

Heddle NM, Klama L, Singer J, et al.: The role of the plasma from platelet concentrates in transfusion reactions, *N Engl J Med* 331:670–671, 1994.

This prospective randomized trial showed that most febrile reactions to platelet transfusion are due to a constituent in the plasma supernatant, most likely pyrogenic cytokines released during storage.

Kleinman S, Caulfield T, Chan P, et al.: Towards an understanding of transfusion related acute lung injury: statement of a consensus panel, *Transfusion* 44:1774–1789, 2004.

This consensus panel statement summarizes the current understanding of the causes, incidence, outcomes, and strategies for reducing transfusion-related acute lung injury.

Linden JV, Wagner K, Voytovich AE, et al.: Transfusion errors in New York State: an analysis of 10 years' experience, *Transfusion* 40:1207–1213, 2000.

This analysis of transfusion errors reported to the New York State Department of Health showed that transfusion errors are a significant risk. Most errors result from human actions and, thus, may be preventable. A majority of events occur outside the blood bank.

McCullough J, Vesole DH, Benjamin RJ, et al.: Therapeutic efficacy and safety of platelets treated with a photochemical process for pathogen inactivation: the SPRINT trial, *Blood* 104:1534–1541, 2004.

This prospective randomized trial showed that photochemically treated platelets are substantially equivalent to conventional platelets, although posttransfusion platelet count increments and days to next transfusion were decreased compared with conventional platelets.

Petz LD, Garratty G, Calhoun L, et al.: Selecting donors of platelets for refractory patients on the basis of HLA antibody specificity, *Transfusion* 40:1446–1456, 2000.

This retrospective study showed that a strategy of selecting platelet donors based on the recipient's HLA antibody specificities was as effective as HLA matching or crossmatching and allowed for a much larger pool of potential donors.

Rebulla P, Finazzi G, Marangoni F, et al.: The threshold for prophylactic platelet transfusions in adults with acute myeloid leukemia, *N Engl J Med* 337:1870–1875, 1997.

This prospective randomized trial demonstrated that prophylactic platelet transfusion at <10,000/μL is as safe and effective as transfusion at <10,000/μL in acute leukemia and substantially reduces the number of transfusions.

Trial to Reduce Alloimmunization to Platelets Study Group: Leukocyte reduction and ultraviolet B irradiation of platelets to prevent alloimmunization and refractoriness to platelet transfusions, *N Engl J Med* 337:1861–1869, 1997.

This prospective randomized trial demonstrated that reduction of leukocytes by filtration and ultraviolet B irradiation of platelets are equally effective in preventing alloantibody-mediated refractoriness to platelets during chemotherapy for acute myeloid leukemia. Platelets obtained by apheresis from single random donors provided no additional benefit as compared with pooled platelet concentrates from random donors.

Vichinsky EP, Haberkern CM, Neumayr L, et al.: A comparison of conservative and aggressive transfusion regimens in the perioperative management of sickle cell disease, *N Engl J Med* 333:206–213, 1995.

This prospective randomized trial showed that a conservative transfusion strategy (increase the hemoglobin level to 10 g/dL) is as effective as an aggressive transfusion regimen (decrease the HbS level to <30%) in preventing perioperative complications in patients with sickle cell anemia and results in substantially fewer transfusions.

Access the complete reference list online at Elsevier eBooks for Practicing Clinicians.

REFERENCES

AABB: Chagas Biovigilance network. Available at http://www.aabb.org/research/hemovigilance/Pages/chagas.aspx, 2015.

Abe H, Ikebuchi K, Shimbo M, et al.: Hypotensive reactions with a white cell-reduction filter: activation of kallikrein-kinin cascade in a patient (abstract), *Transfusion* 37(Suppl):39S, 1997.

Adams RJ, Brambilla DJ, Granger S, et al.: Stroke and conversion to high risk in children screened with transcranial Doppler ultrasound during the STOP study, *Blood* 103:3689–3694, 2004.

Alter MJ, Kruszon-Moran D, Nainan DV, et al.: The prevalence of hepatitis C virus infection in the United States, 1988 through 1994, *N Engl J Med* 341:556–562, 1999.

Alter HJ, Nakatsuji Y, Melpolder J, et al.: The incidence of transfusion-associated hepatitis G virus infection and its relation to liver disease, *N Engl J Med* 336:747–754, 1997.

American Association of Blood Banks Standards Program Committee: *Standards for blood banks and transfusion services*, ed 31, Bethesda, MD, 2018, AABB.

Andreu G, Morel P, Forestier F, et al.: Hemovigilance network in France: organization and analysis of immediate transfusion incident reports from 1994 to 1998, *Transfusion* 42:1356–1364, 2002.

Aoun E, Shamseddine A, Chehal A, et al.: Transfusion-associated GVHD: 10 years' experience at the American University of Beirut-medical center, *Transfusion* 43:1672–1676, 2003.

AuBuchon JP, Cooper LK, Leach MF, et al.: Experience with universal bacterial culturing to detect contamination of apheresis platelet units in a hospital transfusion service, *Transfusion* 42:855–861, 2002.

Backholer L, Green L, Huish S, et al.: A paired comparison of thawed and liquid plasma, *Transfusion* 57(4):881–889, 2017.

Bacterial risk control strategies for blood collection establishments and transfusion services to Enhance the safety and availability of platelets for transfusion, Draft Guidance for Industry. U.S. Department of Health and Human Services. Food and Drug Administration. Center for Biologics Evaluation and Research, December 2018.
https://www.fda.gov/regulatory-information/search-fda-guidance-documents/bacterial-risk-control-strategies-blood-collections-establishments-and-transfusion-services-enhance.

Baharoglu MI, Cordonnier C, Al-Shahi Salman R, et al.: Platelet transfusion versus standard care after actue stroke due to spontaneous cerebral haemorrhage associated with antiplatelet therapy (PATCH): a randomized, open-label, phase 3 trial, *Lancet* 387(10038):2605–2613, 2016.

Beard MJ, Cardigan R, Seghatchian J, et al.: Variables determining blockage of WBC-depleting filters by Hb sickle cell trait donations, *Transfusion* 44:422–430, 2004.

Berger MD, Gerber B, Arn K, et al.: Significant reduction of red blood cell transfusion requirements by changing from a double-unit to a single-unit transfusion policy in patients receiving intensive chemotherapy or stem cell transplantation, *Haematologica* 97(1):116–122, 2011.

Bhutani VK, Johnson L, Sivieri EM: Predictive ability of a predischarge hour-specific serum bilirubin for subsequent significant hyperbilirubinemia in healthy term and near-term newborns, *Pediatrics* 103:6–14, 1999.

Biggerstaff BJ, Petersen LR: Estimated risk of West Nile virus transmission through blood transfusion during an epidemic in Queens, *Transfusion* 42:1019–1026, 2002. New York City.

Blaxhult A, Granath F, Lidman K, et al.: The influence of age on the latency period to AIDS in people infected by HIV through blood transfusion, *AIDS* 4:125–129, 1990.

Boyan CP, Howland WS: Cardiac arrest and temperature of bank blood, *J Am Med Assoc* 183:58–60, 1963.

Busch MP, Glynn SA, Stramer SL, et al.: A new strategy for estimating risks of transfusion-transmitted viral infections based on rates of detection of recently infected donors, *Transfusion* 45:254–264, 2005.

Busch MP, Operskalski EA, Mosley JW, et al.: Epidemiologic background and long-term course of disease in human immunodeficiency virus type 1-infected blood donors identified before routine laboratory screening, *Transfusion* 34:858–864, 1994.

Butch SH, Oberman HA: The computer or electronic crossmatch, *Transfus Med Rev* 11:256–264, 1997.

Butch SH, Stoe M, Judd WJ: Solving the same-day admission identification problem, *Transfusion* 34(Suppl):93S, 1994.

Carless PA, Henry DA, Carson JL, et al.: Transfusion thresholds and other strategies for guiding allogeneic red blood cell transfusion, *Cochrane Database* 10:1–60, 2010.

Carson JL, Guyatt G, Heddle NM, et al.: Clinical practice guidelines from the AABB: red blood cell transfusion thresholds and storage, *J Am Med Assoc* 316(19):2025–2035, 2016.

Carson JL, Poses RM, Spence RK, et al.: Severity of anaemia and operative mortality and morbidity, *Lancet* 1:727–729, 1988.

Cashen AF: Plerixafor hydrochloride: a novel agent for the mobilization of peripheral blood stem cells, *Drugs Today* 45:497–505, 2009.

Castagna L, Sarina B, Bramanti S, et al.: Donor lymphocyte infusion after allogeneic stem cell transplantation, *Transf Apher Sci* 54:345–355, 2016.

Centers for Disease Control and Prevention (CDC): Blood donor screening for Chagas disease—United States, 2006-2007, *MMWR (Morb Mortal Wkly Rep)* 56:141–143, 2007.

Centers for Disease Control and Prevention: Chagas disease, epidemiology & risk factors. Available at http://www.cdc.gov/parasites/chagas/epi.html, 2015.

Chohan G, Llewelyn C, Mackenzie J, et al.: Variant Creutzfeldt-Jakob disease in a transfusion recipient: coincidence or cause? *Transfusion* 50:1003–1006, 2010.

Cohen BJ, Beard S, Knowles WA, et al.: Chronic anemia due to parvovirus B19 infection in a bone marrow transplant patient after platelet transfusion, *Transfusion* 37:947–952, 1997.

Cooling L, Distenfeld A, Kopko PM, et al.: Transfusion-related acute lung injury, *J Am Med Assoc* 288:315–316, 2002.

Cotton BA, Au BK, Nunez TC, et al.: Predefined massive transfusion protocols are associated with a reduction in organ failure and postinjury complications, *J Trauma* 66:41–48, 2009.

Cotton BA, Podbielski J, Camp E, et al.: A randomized controlled pilot trial of modified whole blood versus component therapy in severely injured patients requiring large volume transfusions, Ann Surg 258(4):527-532.

Counts R, Haisch C, Simon T, et al.: Hemostasis in massively transfused trauma patients, *Ann Surg* 190:91–96, 1979.

Crowder LA, Schonberger LB, Dodd RY, et al.: Creutzfeldt-Jakob disease look-back study: 21 years of surveillance for transfusion transmission risk, *Transfusion* 57(8):1875–1878, 2017.

Dahlke MB, Weiss KL: Platelet transfusion from donors mismatched for crossreactive HLA antigens, *Transfusion* 24:299–302, 1984.

Davenport RD, Penezina OP: Cleavage of high molecular weight kininogen induced by filtration of platelet concentrates, *Transfusion* 37(Suppl):104S, 1997.

Davey RJ, Gustafson M, Holland PV: Accelerated immune red cell destruction in the absence of serologically detectable alloantibodies, *Transfusion* 20:348–353, 1980.

DeChristopher PJ, Orlina AR: *Sudden death associated with autologous transfusion in a surgical patient with hemoglobin SC disease. ISBT and AABB 1990 Joint Congress: book of abstracts*, Bethesda, Md, 1990, American Association of Blood Banks, p 119.

Dente CJ, Shaz BH, Nicholas JM, et al.: Improvements in early mortality and coagulopathy are sustained better in patients with blunt trauma after institution of a massive transfusion protocol in a civilian level I trauma center, *J Trauma* 66:1616–1624, 2009.

Dodd RY, Notari EPIV, Stramer SL: Current prevalence and incidence of infectious disease markers and estimated window-period risk in the American Red Cross blood donor population, *Transfusion* 42:975–979, 2002.

Domen RE, Hoeltge GA: Allergic transfusion reactions: an evaluation of 273 consecutive reactions, *Arch Pathol Lab Med* 127:316–320, 2003.

Downes KA, Wilson E, Yomtovian R, et al.: Serial measurement of clotting factors in thawed plasma stored for 5 days, *Transfusion* 41:570, 2001.

Eder AF, Kennedy JM, Dy BA, et al.: Bacterial screening of apheresis platelets and the residual risk of septic transfusion reactions: the American Red Cross experience (2004-2006), *Transfusion* 47:1134–1142, 2007.

Eder AF, Kennedy JM, Dy BA, et al.: Limiting and detecting bacterial contamination of apheresis platelets: inlet-line diversion and increased culture volume improve component safety, *Transfusion* 49:1554–1563, 2009.

Ellingson KD, Sapiano MRP, Haass KA, et al.: Continued decline in blood collection and transfusion in the United States – 2015, *Transfusion* 57:1588–1598, 2017.

Estcourt LJ, Fortin PM, Trivella M, et al.: Preoperative blood transfusions for sickle cell disease, Cochrane Database of Systemic Reviews 4:1-67

Estcourt LJ, Malouf R, Hopewell S, et al.: Pathogen-reduced platelets for the prevention of bleeding, *Cochrane Database of Systemic Reviews* 7:1–135, 2017.

Fasano RM, Meyer EK, Branscomb J, et al.: Impact of red blood cell antigen matching on alloimmunization and transfusion complications in patients with sickle cell disease: a systemic review, Transfus Med Rev 33(1):12-23

FDA Blood Products Advisory Committee: T. cruzi incidence study in blood donors and its implications for one-time testing of blood donors. Available at https://wayback.archiveit.org/7993/20170111183050/http://www.fda.gov/AdvisoryCommittees/CommitteesMeetingMaterials/BloodVaccinesandOtherBiologics/BloodProductsAdvisoryCommittee/ucm2 88494.htm, August 2, 2011.

Federowicz I, Barrett B, Andersen J, et al.: Characterization of reactions after transfusion of prestorage leukoreduced cellular blood components, *Blood* 86(Suppl):608a, 1995.

Fergusson DA, Hébert P, Hogan DL, et al.: Effect of fresh red blood cell transfusions on clinical outcomes in premature, very low-birth-weight infants: the ARIPI randomized trial, *J Am Med Assoc* 308:1443–1451, 2012.

Frelich R, Ellis MH: The effect of external pressure, catheter gauge, and storage time on hemolysis in RBC transfusion, *Transfusion* 41(6):799–802, 2001.

Fried MR, Eastlund T, Christie B, et al.: Hypotensive reactions to white cell-reduced plasma in a patient undergoing angiotensin-converting enzyme inhibitor therapy, *Transfusion* 36:900–903, 1996.

Frohn C, Dumbgen L, Brand JM, et al.: Probability of anti-D development in D– patients receiving D+ RBCs, *Transfusion* 43:893–898, 2003.

Giancarelli A, Birrer KL, Alban RF, et al.: Hypocalcemia in trauma patients receiving massive transfusion, *J Surg Res* 202:182–187, 2016.

Goel R, Ness PM, Takemoto CM, et al.: Platelet transfusions in platelet consumptive disorders are associated with arterial thrombosis and in-hospital mortality, *Blood* 125(9):1470–1476, 2015.

Gorlin JB, Cable R: What is a unit? *Transfusion* 40:263–265, 2000.

Hall WW, Ishak R, Zhu SW, et al.: Human T lymphotropic virus type II (HTLV-II): epidemiology, molecular properties, and clinical features of infection, *J Acquir Immune Defic Syndr Hum Retrovirol* 13(Suppl 1):S204–S214, 1996.

Harvey AR, Basavaraju SV, Chung K-W, et al.: Transfusion-related adverse reactions reported to the national Healthcare safety network Hemovigilance Module, United States, 2010 to 2012, *Transfusion* 55(4):709–7018, 2014.

Hauck-Dlimi B, Eckstein BR, Strobel J, et al.: Influence of early irradiation on *in vitro* red blood cell (RBC) storage variables of leukoreduced RBCs in additive solution SAG-M, *Vox Sang* 110:362–368, 2015.

Hayashi H, Nishiuchi T, Tamura H, et al.: Transfusion-associated graft-versus-host disease caused by leukocyte-filtered stored blood, *Anesthesiology* 79:1419–1421, 1993.

Heddle NM, Blajchman MA, Meyer RM, et al.: A randomized controlled trial comparing the frequency of acute reactions to plasma-removed platelets and prestorage WBC-reduced platelets, *Transfusion* 42:556–566, 2002.

Heger A, Janisch S, Pock K, et al.: Comparative biochemical studies of fresh frozen plasma and pooled solvent/detergent-treated plasma (OctaplasLG®) with focus on protein S and its impact in different thrombin generation assay set-ups, *Vox Sang* 111:266–273, 2016.

Hendrickson JE, Roubinian NH, Chowdhury D, et al.: Incidence of transfusion reactions: a multicenter study utilizing systemic active surveillance and expert adjudication, *Transfusion* 56:2587–2596, 2016.

Herwaldt BL, Linden JV, Bosserman E, et al.: Transfusion-associated *Babesiosis* in the United States: a description of cases, *Ann Int Med* 155:509–519, 2011.

Heuft HG, Goudeva L, Sel S, et al.: Equivalent mobilization and collection of granulocytes for transfusion after administration of glycosylated G-CSF (3 μg/kg) plus dexamethasone versus glycosylated G-CSF (12 μg/kg) alone, *Transfusion* 42:928–934, 2002.

Hess JR, Trachtenberg FL, Assmann SF, et al.: Clinical and laboratory correlates of platelet alloimmunization and refractoriness in the PLADO trial, *Vox Sang* 111:281–291, 2016.

Hitzler WE, Runkel S: Prevalence of human parvovirus B19 in blood donors as determined by a haemagglutination assay and verified by the polymerase chain reaction, *Vox Sang* 82:18–23, 2002.

Holcomb JB, Wade CE, Michalek JE, et al.: Increased plasma and platelet to red blood cell ratios improves outcome in 466 massively transfused civilian trauma patients, *Ann Surg* 243:447–458, 2008.

Holland LL, Brooks JP: Toward rational fresh frozen plasma transfusion: the effect of plasma transfusion on coagulation test results, *Am J Clin Pathol* 126:133–139, 2006.

Horowitz B, Bonomo R, Prince AM, et al.: Solvent/detergent-treated plasma: a virus-inactivated substitute for fresh frozen plasma, *Blood* 79:826–831, 1992.

Ibojie J, Greiss MA, Urbaniak SJ: Limited efficacy of universal leucodepletion in reducing the incidence of febrile nonhaemolytic reactions in red cell transfusions, *Transfus Med* 12:181–185, 2002.

Jacobs MR, Smith D, Heaton WA, et al.: Detection of bacterial contamination in prestorage culture-negative apheresis platelets on day of issue with the Pan Genera Detection test, *Transfusion* 51:2573–2582, 2011.

Jensen NH, Stenballe J, Afshari A: Comparing efficacy and safety fo fibrinogen concentrate to cryoprecipitate in bleeding patients: a systemic review, *Acta Anaes Scand* 60(8):1033–1042, 2016.

Karafin MS, Blagg L, Tobian AAR, et al.: ABO antibody titers are not predictive of hemolytic reactions due to plasma incompatible platelet transfusions, *Transfusion* 52(10):2087–2093, 2012.

Kaufman R, Djulbegovic B, Gernsheimer T, et al.: Platelet transfusion: a clinical practice guideline, *Ann Intern Med* 162:205–213, 2015.

Kelley DL, Mangini J, Lopez-Plaza I, et al.: The utility of ≤3-day-old whole-blood platelets in reducing the incidence of febrile nonhemolytic transfusion reactions, *Transfusion* 40:439–442, 2000.

Kinard TN, Sarode R: Four factor prothrombin complex concentrate (human): review of the pharmacology and clinical application for vitamin K antagonist reversal, *Expert Rev Cardiovasc Ther* 12:417–427, 2014.

Kleinman S, Stassinopoulos A: Transfusion-associated graft-versus-host disease reexamined: potential for improved prevention using a universally applied intervention, *Transfusion* 58:2545–2563, 2018.

Kohan AI, Niborski RC, Rey JA, et al.: High-dose intravenous immunoglobulin in non-ABO transfusion incompatibility, *Vox Sang* 67:195–198, 1994.

Kopko PM, Marshall CS, MacKenzie MR, et al.: Transfusion-related acute lung injury: report of a clinical look-back investigation, *J Am Med Assoc* 287:1968–1971, 2002.

Kuehnert MJ, Roth VR, Haley NR, et al.: Transfusion-transmitted bacterial infection in the United States, 1998 through 2000, *Transfusion* 41:1493–1499, 2001.

Kumar A, Mhaskar R, Grossman BJ, et al.: Platelet transfusion: a systematic review of the clinical evidence, *Transfusion* 55:1116–1127, 2015. quiz 1115.

Larsson LG, Welsh VJ, Ladd DJ: Acute intravascular hemolysis secondary to out-of-group platelet transfusion, *Transfusion* 40:902–906, 2000.

Larsson S, Soderberg-Naucler C, Wang FZ, et al.: Cytomegalovirus DNA can be detected in peripheral blood mononuclear cells from all seropositive and most seronegative healthy blood donors over time, *Transfusion* 38:271–278, 1998.

Leiby DA, Herron Jr RM, Read EJ, et al.: *Trypanosoma cruzi* in Los Angeles and Miami blood donors: impact of evolving donor demographics on seroprevalence and implications for transfusion transmission, *Transfusion* 42:549–555, 2002.

Lin L, Dikeman R, Molini B, et al.: Photochemical treatment of platelet concentrates with amotosalen and long-wavelength ultraviolet light inactivates a broad spectrum of pathogenic bacteria, *Transfusion* 44:1496–1504, 2004.

Macedo de Oliveira A, Beecham BD: West Nile virus blood transfusion–related infection despite nucleic acid testing, *Transfusion* 44:1695–1699, 2004.

Magnus MM, Esposito DLA, da Costa VA, et al.: Risk of Zika virus transmission by blood donations in Brazil, *Hematol Transfus Cell Ther* 40:250–254, 2018.

Mair B, Leparc GF: Hypotensive reactions associated with platelet transfusions and angiotensin-converting enzyme inhibitors, *Vox Sang* 74:17–30, 1998.

Mallouh AA, Asha M: Beneficial effect of blood transfusion in children with sickle cell chest syndrome, *Am J Dis Child* 142:178–182, 1988.

Manns A, Hisada M, La Grenade L: Human T-lymphotropic virus type I infection, *Lancet* 353:1951–1958, 1999.

Marsden M, Benger J, Brohi K, et al.: CRYOSTAT-2 investigators: coagulopathy, cryoprecipitate and CRYOSTAT-2: realizing the potential of a nationwide trauma system for a national clinical trial, *Br J Anaesth* 122(2):164–169, 2019.

Matsubayashi K, Nagaoka Y, Sakata H, et al.: Transfusion-transmitted hepatitis E caused by apparently indigenous hepatitis E virus strain in Hokkaido, Japan, *Transfusion* 44:934–940, 2004.

Matteocci A, Pierelli L: Red blood cell alloimmunization in sickle cell disease and in thalassaemia: current status, future perspectives and potential role of molecular typing, *Vox Sang* 106:197–208, 2013.

McClaskey J, Xu M, Snyder EL, et al.: Clinical trials for pathogen reduction in transfusion medicine: a review, *Transfus Apheresis Sci* 41:217–225, 2009.

McCullough J, Weiblen BJ, Fine D: Effects of storage of granulocytes on their fate in vivo, *Transfusion* 23:20–24, 1983.

Meryman HT, Hornblower M: Freezing and deglycerolizing sickle-trait red blood cells, *Transfusion* 16:627–632, 1976.

Mintz PD: Cesium cessation? An advantage of pathogen reduction treatments, *Transfusion* 51:1369–1376, 2011.

Mintz PD, Williams ME: Cerebrovascular accident during a delayed hemolytic transfusion reaction in a patient with sickle cell anemia, *Ann Clin Lab Sci* 16:214–218, 1986.

Mitra B, Mori A, Cameron PA, et al.: Fresh frozen plasma (FFP) use during massive blood transfusion in trauma resuscitation, *Injury* 41:35–39, 2010.

Moake J, Chintagumpala M, Turner N, et al.: Solvent/detergent-treated plasma suppresses shear-induced platelet aggregation and prevents episodes of thrombotic thrombocytopenic purpura, *Blood* 84:490–497, 1994.

Mungai M, Tegtmeier G, Chamberland M, et al.: Transfusion-transmitted malaria in the United States from 1963 through 1999, *N Engl J Med* 344:1973–1978, 2001.

Murphy EL, Fridey J, Smith JW, et al.: HTLV-associated myelopathy in a cohort of HTLV-I and HTLV-II-infected blood donors, *Neurology* 48:315–320, 1997.

Murray DH, Pennell BJ, Weinstein SL, et al.: Packed red cells in acute blood loss: dilutional coagulopathy as a cause of surgical bleeding, *Anesth Analg* 80:336–342, 1995.

Muylle L, Joos M, Wouters E, et al.: Increased tumor necrosis factor α (TNF α), interleukin 1, and interleukin 6 (IL-6) levels in the plasma of stored platelet concentrates: relationship between TNF α and IL-6 levels and febrile transfusion reactions, *Transfusion* 33:195–199, 1993.

Nakasone H, Kanda Y, Ueda T, et al.: Retrospective comparison of mobilization methods for autologous stem cell transplantation in multiple myeloma, *Am J Hematol* 84:809–814, 2009.

Ness P, Braine H, King K, et al.: Single-donor platelets reduce the risk of septic platelet transfusion reactions, *Transfusion* 41:857–861, 2001.

Newman BH, Pichette S, Pichette D, et al.: Adverse effects in blood donors after whole-blood donation: a study of 1000 blood donors interviewed 3 weeks after whole-blood donation, *Transfusion* 43:598–603, 2003.

Nickerson P, Orr P, Schroeder ML, et al.: Transfusion-associated *Trypanosoma cruzi* infection in a non-endemic area, *Ann Intern Med* 111:851–853, 1989.

Nussbaumer W, Schwaighofer H, Gratwohl A, et al.: Transfusion of donor-type red cells as a single preparative treatment for bone marrow transplants with major ABO incompatibility, *Transfusion* 35:592–595, 1995.

Oberman HA: Controversies in transfusion medicine: should a febrile transfusion response occasion the return of the blood component to the blood bank? *Transfusion* 34:353–355, 1994.

Ortolano GA, Freundlich LF, Holme S, et al.: Detection of bacteria in WBC-reduced PLT concentrates using percent oxygen as a marker for bacteria growth, *Transfusion* 43:1276–1285, 2003.

Pau CP, Hu DJ, Spruill C, et al.: Surveillance for human immunodeficiency virus type 1 group O infections in the United States, *Transfusion* 36:398–400, 1996.

Pealer LN, Marfin AA, Petersen LR, et al.: Transmission of West Nile virus through blood transfusion in the United States in 2002, *N Engl J Med* 349:1236–1245, 2003.

Pennington J, Garner SF, Sutherland J, et al.: Residual subset population analysis in WBC-reduced blood components using real-time PCR quantitation of specific mRNA, *Transfusion* 41:1591–1600, 2001.

Perez P, Salmi LR, Folléa G, et al.: Determinants of transfusion-associated bacterial contamination: results of the French Bacthem case-control study, *Transfusion* 41:862–872, 2001.

Petersen LR, Marfin AA: West Nile virus: a primer for the clinician, *Ann Intern Med* 137:173–179, 2002.

Pineda AA, Zylstra VW, Clare DE, et al.: Viability and functional integrity of washed platelets, *Transfusion* 29:524–527, 1989.

Popovsky MA, Chaplin Jr HC, Moore SB: Transfusion-related acute lung injury: a neglected, serious complication of hemotherapy, *Transfusion* 32:589–592, 1992.

Powell RW, Levine GL, Yang YM, et al.: Acute splenic sequestration crisis in sickle cell disease: early detection and treatment, *J Pediatr Surg* 27:215–218, 1992.

Preiksaitis JK, Brown L, McKenzie M: The risk of cytomegalovirus infection in seronegative transfusion recipients not receiving exogenous immunosuppression, *J Infect Dis* 157:523–529, 1988.

Raife TJ, Friedman KD, Dwyre DM: The pathogenicity of von Willebrand factor in thrombotic thrombocytopenic purpura: reconsideration of treatment with cryopoor plasma, *Transfusion* 46:74–79, 2006.

Roth WK, Waschk D, Marx S, et al.: Prevalence of hepatitis G virus and its strain variant, the GB agent, in blood donations and their transmission to recipients, *Transfusion* 37:651–656, 1997.

Rourke C, Curry N, Khan S, et al.: Fibrinogen levels during trauma hemorrhage, response to replacement therapy, and association with patient outcomes, *J Thromb Haemost* 10:1342–1351, 2012.

Ruane PH, Edrich R, Gampp D, et al.: Photochemical inactivation of selected viruses and bacteria in platelet concentrates using riboflavin and light, *Transfusion* 44:877–885, 2004.

Sadana S, Pratzer A, Scher LJ, et al.: Promoting high-value practice by reducing unnecessary transfusions with a patient blood management program, *J Am Med Assoc* 178(1):116–122, 2018.

Salama A, Berghofer H, Mueller-Eckhardt C: Red blood cell transfusion in warm-type autoimmune haemolytic anaemia, *Lancet* 340:1515–1517, 1992.

Sazama K: Reports of 355 transfusion-associated deaths: 1976 through 1985, *Transfusion* 30:583–590, 1990.

Schmalzer EA, Lee JO, Brown AK, et al.: Viscosity of mixtures of sickle and normal red cells at varying hematocrit levels: implications for transfusion, *Transfusion* 27:228–233, 1987.

Schmidt AE, Refaai MA, Coppage M: HLA-mediated platelet refractoriness, an ACLPS critical review, *AJCP* 151:353–363, 2019.

Scott E, Puca K, Heraly J, et al.: Evaluation and comparison of coagulation factor activity in fresh-frozen plasma and 24-hour plasma at thaw and after 120 hours of 1 to 6 degrees C storage, *Transfusion* 49:1584–1591, 2009.

Seeff LB, Buskell-Bales Z, Wright EC, et al.: Long-term mortality after transfusion-associated non-A, non-B hepatitis, *N Engl J Med* 327:1906–1911, 1992.

Seeff LB, Wright EC, Zimmerman HJ, et al.: VA cooperative study of post-transfusion hepatitis, 1969-1974: incidence and characteristics of hepatitis and responsible risk factors, *Am J Med Sci* 270:355–362, 1975.

Seoud MA, Cantwell C, Nobles G, et al.: Outcome of pregnancies complicated by sickle cell and sickle-C hemoglobinopathies, *Am J Perinatol* 11:187–191, 1994.

Shah A, Brunskill SJ, Desborough MJR, et al.: Transfusion of red blood cells stored for shorter versus longer duration for all conditions, *Cochrane Database* 12:1–122, 2018.

Sherertz RJ, Russell BA, Reuman PD: Transmission of hepatitis A by transfusion of blood products, *Arch Intern Med* 144:1579–1580, 1984.

Shiba M, Tadokoro K, Sawanobori M, et al.: Activation of the contact system by filtration of platelet concentrates with a negatively charged white cell–removal filter and measurement of venous blood bradykinin level in patients who received filtered platelets, *Transfusion* 37:457–462, 1997.

Shimada E, Tadokoro K, Watanabe Y, et al.: Anaphylactic transfusion reactions in haptoglobin-deficient patients with IgE and IgG haptoglobin antibodies, *Transfusion* 42:766–773, 2002.

Sickinger E, Jonas G, Yem AW, et al.: Performance evaluation of the new fully automated human immunodeficiency virus antigen-antibody combination assay designed for blood screening, *Transfusion* 48:584–593, 2008.

Silliman CC, Boshkov LK, Mehdizadehkashi Z, et al.: Transfusion-related acute lung injury: epidemiology and a prospective analysis of etiologic factors, *Blood* 101:454–462, 2003.

Silliman CC, Burke T, Kelher MR: The accumulation of lipids and proteins durig red blood cell storage: the roles of leukoreduction and experimental filtration, *Blood Transfus* 15:131–136, 2017.

Slavc I, Urban CH, Schwinger W, et al.: ABO-incompatible bone marrow transplantation: prevention of hemolysis by alkaline hydration with mannitol diuresis in conjunction with red cell reduced buffy coat bone marrow, *Wien Klin Wochenschr* 104:93–96, 1992.

Slichter SJ, Davis K, Enright H, et al.: Factors affecting posttransfusion platelet increments, platelet refractoriness, and platelet transfusion intervals in thrombocytopenic patients, *Blood* 105:4106–4114, 2005.

Slichter SJ, Kaufman RM, Assmann SF, et al.: Dose of prophylactic platelets and prevention of hemorrhage, *N Engl J Med* 362:600–613, 2010.

Snyder EL, Mechanic S, Baril E, et al.: Removal of soluble biologic response modifiers (complement and chemokines) by a bedside leukoreduction filter, *Transfusion* 36:707–713, 1996.

Spence RK, Carson JA, Poses R, et al.: Elective surgery without transfusion: influence of preoperative hemoglobin level and blood loss on mortality, *Am J Surg* 159:320–324, 1990.

Stramer SL, Notari EP, Krysztof DE, et al.: Hepatitis B virus testing by minipool nucleic acid testing: does it improve blood safety? *Transfusion* 53:2449–2458, 2013.

Strauss RG, Burmeister LF, Johnson K, et al.: AS-1 red cells for neonatal transfusions: a randomized trial assessing donor exposure and safety, *Transfusion* 36:873–878, 1996.

Sweeney JD, Holme S, Moroff G: Storage of apheresis platelets after gamma radiation, *Transfusion* 34:779–783, 1994.

Swisher KK, Terrell DR, Vesely SK, et al.: Clinical outcomes after platelet transfusions in patients with thrombotic thrombocytopenic purpura, *Transfusion* 49:873–887, 2009.

Thijsen A, Masser B: Vasovagal reactions in blood donors: risks, prevention, and management, *Transfus Med* 29:13–22, 2017.

Tobian AA, King KE, Ness PM: Transfusion premedications: a growing practice not based on evidence, *Transfusion* 47:1089–1096, 2007.

Tobian AA, Sokoll LJ, Tisch DJ, et al.: N-terminal pro-brain natriuretic peptide is a useful diagnostic marker for transfusion-associated circulatory overload, *Transfusion* 48:1143–1150, 2008.

Triulzi DJ, Blumberg N: Variability in response to cryoprecipitate treatment for hemostatic defects in uremia, *Yale J Biol Med* 63:1–7, 1990.

Triulzi DJ, Kleinman S, Kakaiya RM, et al.: The effect of previous pregnancy and transfusion on HLA alloimmunization in blood donors: implications for a transfusion related acute lung injury (TRALI) risk reduction strategy, *Transfusion* 49(9):1825–1835, 2009.

Uhlmann EJ, Isgriggs E, Wallhermfechtel M, et al.: Prestorage universal WBC reduction of RBC units does not affect the incidence of transfusion reactions, *Transfusion* 41:997–1000, 2001.

U.S. Department of Health and Human Services: *The 2011 national blood collection and utilization survey report*, Washington, DC, 2011, DHHS.

Van PY, Holcomb JB, Schreiber MA: Novel concepts for damage control resuscitation in trauma, Curr Opin Crit Care 23(6):498-502.

Verdecchia NM, Wisniewski MK, Waters JH, et al.: Changes in blood product utilization in a seven- hospital system after the implementation of a patient blood management program: a 9-year follow-up, *Transf Med* 21(8):490–499, 2016.

Vollmer T, Hinse D, Kleesiek K, Dreier J The pan genera detection immunoassay: a novel point-of-issue method for detection of bacterial contamination. *J Clin Microbiol* 48:3475–3481, 2010.

Vretzakis F, Papaziogas B, Matsaridou E, et al.: Continuous monitoring of arterial blood gasses and pH during intraoperative rapid blood administration using a Paratrend sensor, *Vox Sang* 78:158–163, 2000.

Vyas GN, Holmadahl L, Perkins HA, et al.: Serologic specificity of human anti-IgA and its significance in transfusion, *Blood* 34:573–581, 1969.

Wagner SJ, Robinette D: Evaluation of swirling, pH, and glucose tests for the detection of bacterial contamination in platelet concentrates, *Transfusion* 36:989–993, 1996.

Walsh JH, Purcell RH, Morrow AG, et al.: Posttransfusion hepatitis after open-heart operations: incidence after the administration of blood from commercial and volunteer donor populations, *J Am Med Assoc* 211:261–265, 1970.

Wang J, Xia W, Deng J, et al.: Analysis of platelet-reactive alloantibodies and evaluation of cross-match-compatible platelets for the management of patients with transfusion refractoriness, *Trans Med* 28:40–46, 2018.

Weisberg SP, Shaz BH, Tumer G, et al.: PAS-C platelets contain less plasma protein, lower anti-A and anti-B titers, and decreased HLA antibody specificities compared to plasma platelets, *Transfusion* 58:891–895, 2018.

Whiting D, DiNardo JA, TEG and ROTEM: Technology and clinical applications, *Am J Hematol* 89:228–232, 2014.

Widmann FK: Controversies in transfusion medicine: should a febrile transfusion response occasion the return of the blood component to the blood bank? *Transfusion* 34:356–358, 1994.

Yonemura S, Doane S, Keil S, et al.: Improving the safety of whole blood-derived transfusion products with a riboflavin-based pathogen reduction technology, *Blood Transfus* 15(4):357–364, 2017.

Zanella A, Rossi F, Cesana C, et al.: Transfusion-transmitted human parvovirus B19 infection in a thalassemic patient, *Transfusion* 35:769–772, 1995.

Zehtabchi S, Nishijima DK: Impact of transfusion of fresh-frozen plasma and packed red blood cells in a 1:1 ratio on survival of emergency department patients with severe trauma, *Acad Emerg Med* 16:371–378, 2009.

Zielinkski MD, Schrager JJ, Johnson P, et al.: Multicenter comparison of emergency release group A versus AB plasma in blunt-injured trauma patients, CTS J 8(1):43-47.

Zink KA, Sambasivan CN, Holcomb JB, et al.: A high ratio of plasma and platelets to packed red blood cells in the first 6 hours of massive transfusion improves outcomes in a large multicenter study, *Am J Surg* 197:565–570, 2009.

Zhou L, Giacherio D, Cooling L, et al.: Use of B-natriuretic peptide (BNP) as a diagnostic marker in the differential diagnosis of transfusion-associated circulatory overload (TACO), *Transfusion* 45:1056–1063, 2005.

Zhou A, Mehta RS, Smith RE: Outcomes of platelet transfusion in patients with thrombotic thrombocytopenic purpura: a retrospective case series study, *Ann Hematol* 94:467–472, 2015.

Zou S, Stramer SL, Dodd RY: Donor testing and risk: current prevalence, incidence, and residual risk of transfusion-transmissible agents in US allogeneic donations, *Transfus Med Rev* 26:119–128, 2012.

CHAPTER 38

HEMAPHERESIS

Margaret A. DiGuardo, Aleh Bobr, Jeffrey L. Winters

INTRODUCTION, 788
Definitions, 788
Basic Principles, 789
DONOR CYTAPHERESIS, 790
Donor Plateletapheresis, 790
Donor Leukocytapheresis, 791
Donor Erythrocytapheresis, 794
Multicomponent Apheresis Donation, 795
Hematopoietic Progenitor Cell Collection by Apheresis, 795
DONOR PLASMAPHERESIS, 798
Plasma Products, 798
Plasma Donor Selection, 799
Plasma Donor Concerns, 799
INDICATIONS FOR THERAPEUTIC HEMAPHERESIS, 799
Therapeutic Cytapheresis, 803
Therapeutic Plasma Exchange, 807
DONOR/PATIENT COMPLICATIONS COMMON TO ALL HEMAPHERESIS PROCEDURES, 811
Electrolyte and Acid-Base Disturbances, 813
Allergic, Anaphylactoid, and Anaphylactic Reactions, 814
Angiotensin-Converting Enzyme Inhibitors, 815
Hypovolemia and Vasovagal Reactions, 815
Hydroxyethyl Starch and Coagulopathy, 816
Hydroxyethyl Starch and Renal Dysfunction, 816
Hydroxyethyl Starch and Other Side Effects, 816
Air Embolus, 816
SUMMARY, 816
SELECTED REFERENCES, 816

KEY POINTS

- Hemapheresis is the process of removing normal or abnormal components from circulating blood.
- Cytapheresis involves the removal of cellular components; plasmapheresis involves the removal of plasma, the liquid component.
- Separation of the blood components is based on size (filtration instruments), density (centrifugation instruments), or a combination of both.
- Donor apheresis maximizes the collection of a scarce resource by allowing donors to donate only what is needed, returning the remaining components back to the donor.
- Donor apheresis is highly regulated. Donor eligibility requirements, frequency of donation, and amount of product allowed to be collected vary according to the components being collected, the instruments being used for the collection, and the frequency of the apheresis donations.
- Hematopoietic progenitor cell–apheresis (HPC-A) collection has advantages over hematopoietic progenitor cell–marrow (HPC-M) harvest, including faster time to engraftment, avoidance of general anesthesia for the donor, quicker donor recovery, decreased expense, and greater donor acceptance.
- There is a dearth of randomized placebo-controlled clinical trials involving apheresis. To address this, the American Society for Apheresis (ASFA) categorizes diseases treated with apheresis according to the strength of the evidence supporting its use.
- Therapeutic cytoreduction for leukocytosis or thrombocytosis is indicated for primary disorders where symptoms of microvascular occlusion or risk factors for complications are present.
- A 1.0 to 1.5 plasma volume plasma exchange will remove 70% of a substance located within the plasma. The treatment of additional plasma volumes results in the removal of a fixed percentage of the remaining substance, leading to diminishing returns in treating greater than 1.5 plasma volumes.
- Therapeutic plasma exchange (TPE) is nonselective, removing pathologic substances as well as beneficial substances such as coagulation factors and protein-bound drugs.
- Complications of donor apheresis are less common than complications seen with whole-blood donation, although the rate of reactions requiring hospitalization has been reported to be greater.
- The most common reactions to donor apheresis, in decreasing frequency, are hematoma/pain; hypocalcemia due to the citrate anticoagulant; vasovagal reactions with syncope; and vasovagal reactions without syncope.
- Complications have been reported to occur in approximately 5% of patients undergoing therapeutic apheresis treatments. If complications due to central venous access placement are included, the complication rate has been reported to be 17%.
- The most common reactions due to therapeutic apheresis procedures, in decreasing frequency, are transfusion reactions from replacement fluids, hypocalcemia due to citrate anticoagulant, hypotension, vasovagal reactions, tachycardia, respiratory distress, tetany/seizure, and rigors/chills.

INTRODUCTION

DEFINITIONS

The word *apheresis* is derived from the Greek word *aphaeresis*, which means "to separate," "to take away by force," or "to remove." The year 2014 marked the 100th anniversary of apheresis, when authors Abel, Rowntree, and Turner first described apheresis procedures involving the separation of canine blood into cellular and plasma components (Abel et al., 1914). Hemapheresis is the process of removing normal (donor) or abnormal (patient) blood constituents from circulating blood. It can be divided into cytapheresis, removal of the cellular component of blood, and plasmapheresis, removal of the plasma fraction. Cytapheresis can be selective, with removal of red blood cells (erythrocytapheresis), platelets (plateletapheresis), or white blood cells (leukocytapheresis). If the red blood cells removed during an erythrocytapheresis are replaced with donor red blood cells in a therapeutic procedure, this is referred to as a *red blood cell exchange*. When a plateletapheresis procedure is performed as a therapeutic procedure, it is referred to as a *thrombocytapheresis*. If, during a plasmapheresis procedure, the removed plasma is replaced by a replacement fluid, the procedure is referred to as a *therapeutic plasma exchange* (*TPE*). Plasmapheresis, in contrast, removes and discards less than 15% of the total plasma volume and does not require replacement fluid. It is important to realize that the terms *plasmapheresis* and *plasma exchange* are not equivalent, even if they are commonly used in this way.

BASIC PRINCIPLES

Apheresis can be performed using either centrifugation or filtration methods. All early apheresis instruments separated whole blood into its components by centrifugation. Centrifugal force is applied to whole blood such that the various components separate according to their specific gravity (density). The most dense component (red blood cells) layers farthest from the axis of rotation and the least dense component (plasma) layers closest to the axis of rotation, with components of intermediate density layering in between (Burgstaler, 2010) (Fig. 38.1). Some mixing does occur at the interfaces of the various layers, resulting in some contamination by components of the adjacent layers. For example, red blood cells are present within the granulocyte layer and vice versa. Depending on whether the whole blood is processed in discrete batches with repetitive cycles or processed continuously, the centrifugation separators are referred to as *intermittent flow* or *continuous flow* centrifuges, respectively (Burgstaler, 2010).

In addition to centrifugation, apheresis can be accomplished by filtration. In this method, components of whole blood are separated based on size rather than density. The whole blood flows over a membrane containing pores of a specific size, which allow only the component of interest to pass through. The remaining elements are then returned to the donor/patient. The separators used in the filtration process may be hollow fiber or flat plate systems, each of which utilize pore size to separate cellular components from plasma (Burgstaler, 2010).

Centrifugation and filtration can also be combined. In these instruments, blood enters a stationary chamber containing a central rotating filter. As the filter rotates, the blood begins to move and separate into layers. The result is that the more dense elements move away from the filter, with the plasma being located directly adjacent to the filter. The plasma can then pass through the filter and be drawn off while the cellular elements are collected from the periphery of the stationary chamber. The advantage of the combination of centrifugation and filtration in this arrangement is that the cellular elements cannot clog the pores of the filter. This means that filters with smaller surface areas than filtration instruments and lower *g* forces than centrifugation instruments can be used (Burgstaler, 2010).

Another basic aspect of apheresis involves determining appropriate volumes to be processed in the various procedures described in this chapter. This is necessary because of the need to limit the amount of blood within the instrument and tubing connected to the donor/patient—the extracorporeal circuit—to avoid hypotension and associated complications. According to Standards for Blood Banks and Transfusion Services, the maximum amount of blood allowed to be out of the donor is 10.5 mL/kg of the donor's weight (Standards Committee of the AABB, 2018). Calculations of blood volume, however, are still necessary to "prescribe" appropriate processing volumes during therapeutic cytapheresis. This is most often accomplished through nomograms or as a calculation performed by the instrument used for the procedure, with input of donor/patient-specific data by the instrument operator, typically height, weight, gender, and hematocrit (Hct). A number of equations and rules are available for this determination (Nadler et al., 1962; Gilcher, 1996). For example, Equations 38.1 and 38.2 can be used to determine blood volume in males and females, respectively (Nadler et al., 1962):

$$\text{Males: BV} = \left(0.3669 \times H^3\right) + (0.03719 \times W) + 0.6041 \qquad \text{(Eq. 38.1)}$$

$$\text{Females: BV} = \left(0.3561 \times H^3\right) + (0.03308 \times W) + 0.1833, \qquad \text{(Eq. 38.2)}$$

where

BV is blood volume in liters
H is height in meters
W is weight in kilograms

Because the blood volume of tissues varies according to the ratio of adipose tissue present, such calculations may overestimate the blood volume in obese patients and underestimate it in muscular patients. These biases are partially corrected for by formulas that cube the height of the patient (Mollison et al., 1998). Alternatively, Gilcher's "rule of fives" can be applied as an estimate of BV in these situations in mL/kg of body weight, as shown in Table 38.1 (Gilcher, 1996):

Additionally, for TPE, the blood volume can be used to further calculate the plasma volume, as given by Equation 38.3 (Buffaloe & Heineken, 1983):

$$\text{PV} = \text{BV}\left[1 - \frac{(0.91)\,(0.96)\,\text{VCH}}{100}\right], \qquad \text{(Eq. 38.3)}$$

where *PV* is plasma volume in liters and *VCH* is venous centrifuge hematocrit.

Finally, the plasma volume can be used to calculate the exchange volume, the volume processed in a TPE procedure, as given by Equation 38.4 (Buffaloe & Heineken, 1983):

$$\text{EV} = \text{PV} \times \text{PVE}, \qquad \text{(Eq. 38.4)}$$

where *EV* is exchange volume in liters and *PVE* is desired number of plasma volumes to exchange. While these equations are representative of an exacting methodology, their use is not always practical in clinical applications. Quite often, the applicable caveats to these are shorthand versions that make assumptions regarding height, weight, and gender:

$$\text{BV} = 70\ \text{mL/kg} \times \text{W} \qquad \text{(Eq. 38.5)}$$

$$\text{PV} = (1 - \text{Hct}) \times \text{BV}. \qquad \text{(Eq. 38.6)}$$

In addition, using the BV, the red cell volume (RV) can be easily estimated with the following equation:

$$\text{RV} = \text{Hct} \times \text{BV} \qquad \text{(Eq. 38.7)}$$

Another basic aspect of hemapheresis that is applicable to all procedures, therapeutic and donor related, is venous access. In donor hemapheresis, peripheral venous access is used—usually, the veins of the antecubital fossa. The use of central venous access in this setting, with the potential for serious complications, would be too risky for the donor. If a donor's peripheral venous access is such that it cannot be used, then another donor should be located. The possible exception to this would be in the setting of allogeneic peripheral hematopoietic progenitor cell harvest, in which an alternative donor may not be available. Obviously, the risks to the donor and the benefits to the recipient must be carefully considered, and the donor must give informed consent before central venous access can be used.

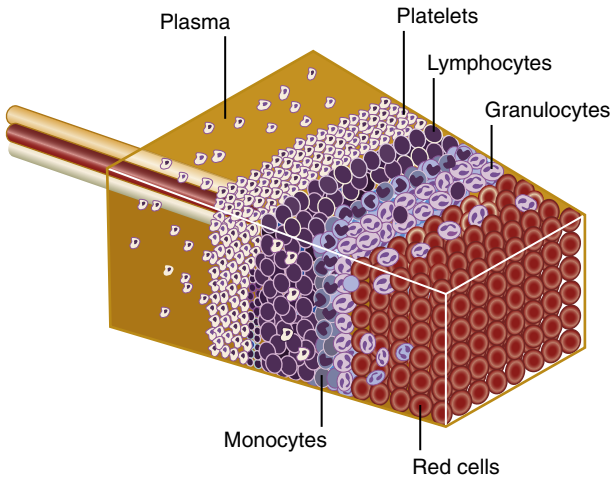

Figure 38.1 Separation of blood components within a centrifugal separation chamber. Blood components placed in a centrifuge are separated based on their density. The densest elements (red blood cells) are farthest from the axis of rotation and the least dense element (plasma) is closest. (Image courtesy of Sergio Torloni, MD.)

TABLE 38.1
Gilcher's Rule of Fives for Estimating Blood Volume per Kilogram of Body Weight

	Obese	Thin	Normal	Muscular
Male	60 mL/kg	65 mL/kg	70 mL/kg	75 mL/kg
Female	55 mL/kg	60 mL/kg	65 mL/kg	70 mL/kg

From Gilcher RO: Apheresis: principles and practice. In Rossi EC, Simon TL, Moss GS, et al., editors: *Principles of Transfusion Medicine*, ed 2, Baltimore, MD, 1996, Williams & Wilkins, pp 537–545.

In the setting of therapeutic hemapheresis procedures, it is often assumed that central access is essential because of damage to peripheral veins from previous medical treatment (e.g., chemotherapy) as well as the need for long-term therapy for some diseases. The Canadian Cooperative Multiple Sclerosis Study Group (Noseworthy et al., 1989) found that among 294 multiple sclerosis patients undergoing weekly TPE procedures for 20 weeks, only 4.4% of patients could not be treated because of poor peripheral venous access. Of those who started the course of therapy, only 5.4% lost peripheral venous access such that the course could not be completed (Noseworthy et al., 1989). In a similar study looking at 46 patients with neurologic diseases requiring hemapheresis, 50% of patients could complete their course of therapy using peripheral access alone. Factors associated with the requirement of central venous access included Guillain-Barré syndrome or hospitalization within a medical intensive care unit (Grishaber et al., 1992). Contrary to popular belief, these authors also found no difference between peripheral venous access and central venous access with regard to the time required to perform the therapeutic procedures (Grishaber et al., 1992). The University of London Hospital performed a single-center 2-year retrospective review of their apheresis practice and found that of 3714 procedures (1061 patients) performed, peripheral access was used in 72%. When looking at purely elective procedures, this number rose to greater than 80% (Putensen et al., 2017). These studies indicate that peripheral venous access, with its lower rate of complications, should be tried initially in therapeutic hemapheresis. Central venous access should be reserved for occasions in which peripheral access fails.

When peripheral venous access is not possible, then both the hemapheresis service and the physician placing the catheter must determine the type of central catheter to be placed. Many routinely used central venous catheters are inadequate for hemapheresis because their walls are too soft and collapse, their length is too long, or their diameter is too small. These characteristics result in pressure alarms from the instruments. The ideal catheters have large diameters and short lengths, creating the lowest possible resistance to blood flow according to Poiseuille's equation:

$$R = \frac{8nL}{\pi r^4}, \qquad \text{(Eq. 38.8)}$$

where:

R is the resistance to flow
n is the viscosity of blood
L is the length of the vessel
r is the radius

A rule of thumb is that if a catheter can be used for dialysis, in which flow rates are greater than those seen in apheresis, it can be used for apheresis.

One last basic principle is the distinction between apheresis and dialysis, as this is often a point of confusion. In dialysis, a highly permeable membrane called the *dialyzer* functions like the kidney by filtering the blood and removing harmful toxins, most often small waste molecules. Dialysis does not remove plasma proteins or clotting factors and does not require volume replacement, therefore potentially being used to significantly decrease a patient's volume status. In contrast, apheresis affects only the intravascular volume and removes either a pathologic cellular or noncellular component by either centrifugation or filtration techniques. If plasma is removed during apheresis, larger proteins, including clotting factors, are also removed. In apheresis procedures in which plasma is removed, a replacement fluid such as albumin or donor plasma is given. The result is that, in contrast to dialysis, apheresis procedures generally do not significantly or intentionally alter a donor's/patient's volume status.

DONOR CYTAPHERESIS

DONOR PLATELETAPHERESIS

Benefits of Apheresis Platelets

The use of apheresis platelets has increased from 25% of platelets transfused in 1987 (Wallace et al., 1993) to 91.1% in 2011 (Whitaker et al., 2011). In part, this is due to the inability to increase platelets derived from whole-blood donations. In addition, there is a perception that apheresis platelets offer advantages over those produced from whole blood. The reported benefits of apheresis platelet products are given in Box 38.1.

An additional advantage of apheresis platelets over pooled nonapheresis products is simplification of inventory management. Pooled products, because they are prepared in an open system, have a 4-hour shelf life after pooling. Apheresis products do not need to be pooled; as a result, they retain their 5-day shelf life. In situations in which platelet products are initially requested but then are not transfused, the use of apheresis products could avoid wastage. The disadvantages of apheresis platelets are the additional expense to obtain them and limited availability in some areas.

BOX 38.1

Reported Benefits of Apheresis Platelet Products

Decreased donor exposure with decreased risk for transfusion-transmitted disease

Decreased donor exposure with delay in alloimmunization to HLA (Sintnicolaas et al., 1981)

Decreased risk of septic platelet transfusion reactions (Ness et al., 2001)

Prestorage leukocyte reduction with delay in alloimmunization to HLA (Trial to Reduce Alloimmunization to Platelets Study Group, 1997), decreased febrile transfusion reactions (Heddle, 1995), and decreased cytomegalovirus infection (Bowden et al, 1995)

HLA, Human leukocyte antigen.

Platelet Product Requirements

Standards for Blood Banks and Transfusion Services require that the minimum number of platelets in an apheresis product should be 3.0×10^{11} in 90% of units tested (Standards Committee of the AABB, 2018). The U.S. Food and Drug Administration (FDA) requires a minimum of 3.0×10^{11} in 75% of units tested (Code of Federal Regulations [CFR], 2014). The result of these requirements, however, is that an apheresis platelet product contains at least as many platelets as a pool of platelets from six whole-blood donations.

Plateletapheresis Donor Selection

The donor requirements for plateletapheresis are the same as those for whole-blood donation (Standards Committee of the AABB, 2018). The FDA has issued additional requirements, as outlined in guidance issued in December 2007, "Guidance for Industry and FDA Review Staff: Collection of Platelets by Automated Methods" (Food and Drug Administration, 2007). FDA guidelines include a proscription on the collection of apheresis platelets from a donor who has ingested aspirin or piroxicam (Feldene) within 2 days of donation. Standards for Blood Banks and Transfusion Services (2014) also require that the use of platelets from a donor taking "medications known to irreversibly inhibit platelet function shall be evaluated." Finally, donors who have taken thienopyridines, such as clopidogrel (Plavix) or ticlopidine (Ticlid), are deferred from apheresis platelet donation for 14 days after the last dose (Food and Drug Administration, 2007).

Additional plateletapheresis-specific requirements include a minimum platelet requirement prior to collection and restrictions on the frequency and number of donations. First, donors must have a platelet count of at least 150,000/μL in order to donate. They can donate as often as twice per week, but there must be a 2-day interval between hemapheresis procedures. A donor cannot donate more than 24 times per year. Finally, if a donor donates multiple plateletapheresis products, such as a double- or triple-platelet product, the donor is deferred from additional hemapheresis donation for 1 week. These concerns will be discussed further later.

According to FDA guidelines, donors must have a precollection minimum platelet count of 150,000/μL to be eligible to donate. This count should be used for current and future eligibility determination and to program the hemapheresis instrument to determine the platelet yield of the collection. The count may be completed before the procedure starts or immediately following the start of the procedure. If the platelet count cannot be obtained before the collection starts or immediately afterward (e.g., collections on a mobile drive), an average of previous measurements from the donor or a default count can be used to program the instrument. In this case, a triple-platelet collection cannot be performed. However, the sample collected must be tested. Finally, the FDA also requires that the hemapheresis device be programmed such that the donor's platelet count will not fall below 100,000/μL (Food and Drug Administration, 2007).

Individuals donating after whole-blood donation, or after an instrument failure resulting in the inability to return the extracorporeal blood volume, must wait 8 weeks before donating by apheresis. Exceptions are if the extracorporeal volume of the instrument is less than 100 mL or if the loss of red blood cells is less than 200 mL. In these cases, the donor is eligible to donate by apheresis after the normal deferral period (Standards Committee of the AABB, 2018). The FDA has provided further guidance on donor eligibility after red blood cell loss, as outlined in Table 38.2.

TABLE 38.2

Donor Eligibility Following Red Blood Cell Loss

Initial Red Blood Cell Loss	Combined Initial Red Blood Cell Loss and Second Red Blood Cell Loss within 8 Weeks	Eligibility
<200 mL	<200 mL	No deferral
<200 mL	>200 mL but ≤300 mL	Defer for 8 weeks from second donation
>200 mL but ≤300 mL	NA	Defer for 8 weeks from first donation
<200 mL	>300 mL	Defer for 16 weeks from second loss
≥300 mL	NA	Defer for 16 weeks from loss

Data from Division of Blood and Blood Products, Center for Biologics Evaluation and Research, 2007.

The FDA has also defined limits on the total amount of plasma that can be removed during an apheresis platelet collection. Donors weighing less than 175 lb can have no more than 500 mL removed; in those weighing greater than or equal to 175 lb., 600 mL can be collected. An exception to these limits exists in that the manufacturer of the plateletapheresis collection device can define a different volume in the labeling of the device (Food and Drug Administration, 2007).

Donor selection for plateletapheresis may be influenced by a number of factors in addition to regulatory considerations. The yield of a plateletapheresis procedure is determined, to a large extent, by the platelet count of the donor, with higher counts associated with a higher yield (Glowitz & Slichter, 1980; Goodnough et al., 1999). Some collection centers will screen whole-blood donors for high normal platelet counts and will recruit these individuals for plateletapheresis to maximize the yield of each collection procedure. Female donors, on average, have higher platelet counts than males (Glowitz & Slichter, 1980; Goodnough et al., 1999), with some evidence also supporting higher platelet yields from female donors (Glowitz & Slichter, 1980). The presence of a higher plasma volume in females enhances the separation and collection of platelets by some instruments and could contribute to the higher yield. The difficulty with female donors is that because of prior pregnancies, they are at increased risk for sensitization against human leukocyte antigen (HLA) and neutrophil antigens. Antibodies to these antigens have been implicated in the development of transfusion-related acute lung injury (TRALI). The AABB issued Association Bulletin #06-07 in November 2006 to address the risk for TRALI. In this bulletin, the AABB requires collection centers to "implement interventions to minimize the preparation of high plasma-volume components from donors known to be leukocyte-alloimmunized or at increased risk of leukocyte alloimmunization" (Strong & Lipton, 2007). Because of this, collection centers have adopted different policies: deferring all females from plateletapheresis donation, deferring females who have been pregnant from plateletapheresis donation, or testing female donors for the presence of HLA and antineutrophil antibodies (Powers et al., 2008). Standard 5.4.1.3 from the AABB currently requires testing for HLA antibodies for all female apheresis platelet donors who have been pregnant (AABB, 2018 5.4.1.3). For a more complete discussion of TRALI, the reader is referred to Chapter 37. Additional donor considerations arise in the selection of platelet products for alloimmunized patients; this is also discussed in greater detail in Chapter 37.

Plateletapheresis Donor Concerns

The typical platelet donor experiences a 20% to 29% drop in platelet count (Szymanski et al., 1973; Heyns et al., 1985), with that among females typically being greater (Rogers et al., 1995; Dettke et al., 1998). However, the fall in platelet count is less than that predicted by the yield from the plateletapheresis procedure due to mobilization of platelets from the spleen (Heyns et al., 1985). The time required for return to baseline following apheresis platelet donation is 4 days in males. For females, a delay in the increase of thrombopoietin levels causes delayed return to normal platelet counts (Dettke et al., 1998). Gender-specific differences in absolute blood volume and absolute mass of circulating platelets may explain the differences in recovery of platelet counts post-plateletapheresis in males versus females (Dettke et al., 1998).

In donors undergoing alternate-day collections, platelet count and apheresis yields have been shown to return to baseline levels by day 10 of collection, with stable counts and yields obtained during subsequent collection procedures (Glowitz & Slichter, 1980). A rebound state characterized by increased platelet yield following repeat procedures has also been seen (Szymanski et al., 1973). In donors with low platelet counts (150,000 to 180,000/mL), employing prolonged collection times to achieve the required platelet yield demonstrated no clinically significant problems in 291 procedures despite postprocedure platelet counts as low as 69,000/mL (Rogers et al., 1995). The results of these studies indicate that, even with repeated plateletapheresis, platelet counts return to normal levels promptly and bleeding complications are uncommon.

Although studies have shown that platelet counts recover quickly following platelet donation, a study suggested that long-term platelet donation could result in baseline platelet count decline (Lazarus et al., 2001). These findings raised concern that frequent apheresis platelet donations could produce thrombocytopenia, prompting the FDA to suggest restrictive policies on donation. Subsequent studies failed to demonstrate declines with long-term donation or with donation of high-yield products such as double- or triple-platelet products (Richa et al., 2008). As a result, the FDA's guidance was less restrictive, allowing for up to 24 procedures as opposed to 24 *components* per rolling 12-month period.

The same does not hold true, however, regarding lymphocyte loss due to plateletapheresis donations. Studies looking at early hemapheresis instruments demonstrated donor lymphocyte losses as great as 5 to 10×10^9 per procedure (Strauss, 1994). Coupled with additional studies that same year demonstrating abnormal cell-mediated immunity with the loss of 1.0 to 1.5×10^{11} lymphocytes within a few weeks (Strauss, 1994), plateletapheresis donations were limited to 24 per year and requirements to warn potential plateletapheresis donors about the possibility of lymphocyte depletion (Food and Drug Administration, 1988). These were also accompanied by additional suggestions from some authors that donors be deferred if their lymphocyte counts fell below 1.2×10^9/L (Strauss, 1994). However, these finding were in contrast to later studies evaluating newer hemapheresis instruments, which showed no differences in lymphocyte counts, lymphocyte subsets, or immunoglobulin (Ig) G levels when nondonors, plateletapheresis donors, and whole-blood donors were compared (Lewis et al., 1999). They reported the loss of lymphocytes over the course of 24 donations using modern hemapheresis equipment to be equivalent to the loss of lymphocytes in a single whole-blood donation (Strauss, 1994). However, an even more recent study evaluating machines that utilize a leukoreduction chamber system (TRIMA Accel) demonstrated CD4+ and CD8+ T-cell lymphopenia in healthy platelet donors undergoing frequent plateletapheresis procedures (Rahmani et al., 2019). More specifically, out of the 60 healthy donors in the cohort, 8 had a CD4+ T-lymphocyte count of <200 cells/μL. It should be noted, however, that these decreased levels did not appear to convey harm to the donors (Rahmani et al., 2019). This group also examined frequent plateletapheresis donors collected on a different device (Fenwal Amicus) and failed to identify lymphopenia, suggesting that their earlier findings may be device specific and related to the leukocyte reduction chamber (Gansner et al., 2019). Thus, while results have been discordant over the years, the most recent studies seem to confirm that lymphocyte depletion in donors can occur and may be device specific. Despite the loss of lymphocytes, there is no evidence to suggest that this loss compromises the integrity of the donor's immune status.

DONOR LEUKOCYTAPHERESIS

Granulocyte Transfusions

Since their first infusion in 1964, granulocytes have been used as an adjunct to antibiotic therapy in neutropenic patients with bacterial and/or fungal infections that are otherwise refractory to treatment. There are no formally established criteria for their use; however, those listed below are typically agreed on as the minimum necessary to proceed (Schiffer, 1990). These include:

1. A proven (by clinical testing) bacterial or fungal infection
2. No response to a trial of appropriate antibiotics/antifungals
3. Absolute neutropenia (<500 cells/μL)
4. A reasonable expectation of patient marrow recovery

Despite the fact that they have been used in practice for over 60 years, the studies regarding their efficacy are mixed, with limited and often weak supporting evidence. This is due, in part, to low numbers as a result of the inherent challenges in obtaining a suitable product, including availability of donors, appropriate and safe mobilization of these donors, and the exquisite timing required. The latter is due to the fact that granulocytes maintain their viability for only a few hours after collection. Logistical preparedness by all teams involved is imperative, requiring a carefully orchestrated schedule and communication plan between the donor/collection center, transportation teams, blood bank staff, clinical staff, and patient such that the infusion can take place within the same day as collection. Combined, these requirements limit the numbers of patients receiving this therapy, which, in turn, leads to challenges in generating a robust study.

This particular obstacle was highlighted in a 2016 Cochrane database systematic review by Stanworth et al. in which 10 randomized controlled trials totaling only 587 participants were eligible for inclusion. This low "n" significantly reduced the power of the study, weakening the overall supporting evidence. Nonetheless, it is a comprehensive overview of all randomized studies from 1975 to 2015 comparing the use of antibiotic monotherapy with a combined regimen of antibiotics plus granulocyte transfusions. It is important to note that an additional 36 studies were examined and excluded either due to lack of randomization (19) or because they examined the use of granulocytes as prophylaxis rather than treatment. With few exceptions, almost all participants had neutropenia secondary to a hematologic malignancy, primarily acute myeloid leukemia (AML). No patients were enrolled with congenital disorders of production or function and the median doses administered ranged from 0.5×10^{10} to 5.5×10^{10}, the latter and largest coming from the RING study (see upcoming discussion). In addition, the definition of neutropenia varied across all trials, with values ranging from 0.1×10^9/L to 1×10^9/L. Finally, the primary outcomes analyzed were clinical response to infection and overall mortality (with a follow-up of 30 days). When assessing all-cause mortality across the studies, six were eligible for analysis, demonstrating varied results and evidence of subgroup differences based on publication date. In the 5 studies (210 participants) published before 2000, it was concluded that there *may* be a reduction in all-cause mortality in the combined therapy cohort when compared with those patients taking antibiotics alone. This is in contrast to the RING study, published after 2000 (Price, 2015) and with 111 participants, which demonstrated no difference in all-cause mortality between the two groups. Furthermore, none of the studies demonstrated a significant difference between treatment groups when examining clinical response to infections. This was also true of clinical reversal in concurrent infections; no difference could be established between the two treatment arms. Given these conflicting results, the authors concluded overall that the use of granulocyte transfusions may not affect the risk of death *or* recovery and that the risk of serious adverse events to the transfusions was largely unknown. In addition, none of the studies provided evidence regarding an effect on quality of life or reduction in days for antibiotic use. The authors further concluded that the supporting evidence for these findings was of either low or very low quality and that the small number of patients included (n = 587) was, in large part, responsible (Estcourt, 2016).

Another group of patients frequently considered for granulocyte transfusions are septic neonates with secondary neutropenia. In this population, indications for granulocyte transfusion include evidence of bacterial sepsis with an absolute neutrophil count below 3000/μL and decreased marrow store of neutrophils, with less than 7% (of nucleated cells) metamyelocytes or more mature forms (Blanchette, 1991; Strauss, 1991). Similar to the adult population, the efficacy of this intervention is not well established. Also similar to the adults, this is due to a lack of adequately powered multicenter trials. A 2011 Cochrane database systematic review looking at "all-cause mortality during initial hospital stay" specifically in the neonatal population concluded that there was inconclusive evidence to "support or refute the routine use of granulocyte transfusions…to reduce neonatal morbidity or mortality" (Pammi, 2011). This conclusion was based on data from 4 trials (n = 79). All were looking at infants with sepsis and neutropenia, but three were comparing antibiotics alone to those on antibiotics plus granulocyte therapy, while one compared granulocyte transfusions to intravenous immunoglobulin therapy. Four additional studies were excluded due to a lack of randomization. The reviewers found no difference in all-cause mortality between patients receiving antibiotics versus antibiotics plus granulocytes. They did observe a reduction in all-cause mortality when comparing granulocyte therapy to intravenous immunoglobulin (IVIg). However, these findings were supported by "borderline statistical significance" (Pammi, 2011).

Granulocyte Donor Selection

As with plateletapheresis, leukocytapheresis donors must fulfill all of the requirements applicable to whole-blood donation. In addition, platelets are removed during the collection, and application of the 150,000/μL platelet count requirement to granulocyte donors may be prudent. Another consideration in selecting donors is the ABO type of both recipient and donor. Significant numbers of red blood cells are present within granulocyte products. Because the red blood cell content is greater than 2 mL, Standards for Blood Banks and Transfusion Services require that the product be crossmatch compatible (Standards Committee of the AABB, 2018).

Also important in donor selection is the cytomegalovirus (CMV) status of the donor and recipient. Granulocyte transfusions have been linked to cases of CMV infection in CMV-seronegative recipients (Winston et al., 1980; Buckner et al., 1983). Therefore, donors for CMV-seronegative patients must also be CMV seronegative. Finally, in alloimmunized patients, it is critical that HLA- or crossmatch-compatible donors be selected. Studies of alloimmunized patients have demonstrated minimal to no recovery, survival, or localization to sites of infection using granulocytes from random donors (Dutcher et al., 1983; McCullough et al., 1986).

Granulocyte Donor Stimulation

The most commonly used method to increase granulocyte yield is to administer steroids to donors 10 to 12 hours before collection. Administration of oral prednisone (MacPherson et al., 1976; Jendiroba et al., 1998) or dexamethasone (Higby et al., 1977) increases granulocyte yield up to twice that of unstimulated donors. In a study of 153 unrelated granulocyte donors who received either prednisolone given intravenously 4 hours before collection or dexamethasone given orally 12 hours before collection, an equal absolute amount of circulating granulocytes was collected in each group (Kolovratova et al., 2012). This suggests that the decision regarding whether to use prednisolone or dexamethasone for granulocyte mobilization should be at the discretion of the physician and donor. The effects of steroids appear to result from mobilization of granulocytes from marrow stores as well as delayed granulocyte apoptosis (Liles et al., 1995). Studies have shown no effect of steroid stimulation on the ability of neutrophils to phagocytose particles or fungi, to kill bacteria, or to undergo chemotaxis when compared with granulocytes from nonstimulated donors (Glasser et al., 1977). In addition, studies have suggested that steroid stimulation has no effect on accumulation of transfused granulocytes at sites of injury (Price & Dale, 1979).

The availability of granulocyte colony stimulating factor (G-CSF) has resulted in the ability to generate even larger granulocyte doses and has led to a resurgence of interest in granulocyte transfusions. Administration of 5 μg/kg of G-CSF every other day resulted in granulocyte collections four to five times those seen in unstimulated donors and greater than those seen with prednisone stimulation (Jendiroba et al., 1998). The use of G-CSF–stimulated granulocyte transfusions has been shown to result in significant and sustained increments in neutrophil counts in patients (Adkins et al., 1997b). The optimum timing for granulocyte collection in G-CSF–stimulated donors is 12 hours after administration of G-CSF (Price, 1998).

As with steroids, concerns have arisen over the function of G-CSF–stimulated granulocytes. Studies have demonstrated normal phagocytosis, chemotaxis, chemiluminescence, and superoxide anion production (Caspar et al., 1993) and normal accumulation at sites of injury (Adkins et al., 1997a). G-CSF has been shown to enhance microbicidal activity (Lieschke & Burgess, 1992) and to inhibit neutrophil apoptosis during storage (Adachi et al., 1994). Concern has also been raised as to whether repeated doses of G-CSF will adversely affect granulocyte function. Again, enhanced phagocytosis and oxidative burst were seen with multiple G-CSF administrations (Joos et al., 2002).

Studies have been performed to evaluate the effect of the combination of steroids and G-CSF (Dale et al., 1998; Liles et al., 1997). Combining 8 mg of dexamethasone with 300 or 600 μg of G-CSF resulted in higher granulocyte yields than either agent alone, leading to a 10-fold increase in neutrophil count at 12 hours. The combination of dexamethasone with 600 μg of G-CSF versus 300 μg of G-CSF resulted in a significantly greater yield (Liles et al., 1997). Granulocyte function with this combined regimen demonstrated no defects (Dale et al., 1998). Subsequent studies comparing 450 μg versus 600 μg doses of G-CSF with 8 mg of dexamethasone found equivalency with regard to both the donor's absolute neutrophil count (ANC) at 12 hours and donor side effects (Liles et al., 2000). Although the study by Liles and colleagues mentioned earlier utilized 450-μg doses of G-CSF in their comparison, vials of G-CSF are currently available only as 480-μg doses. There are no data comparing the efficacy of the currently available 480-μg doses of G-CSF with the 450-μg doses utilized by Liles and colleagues in the study mentioned earlier.

Finally, the route of administration of G-CSF, when given with dexamethasone, also influences granulocyte kinetics. Subcutaneous administration gives a higher sustained ANC compared with IV administration (Stroncek et al., 2002).

Granulocyte Product Requirements

Despite the lack of concrete findings regarding overall efficacy, it is commonly agreed that granulocyte dose is critical for the effectiveness of the therapy. A previous review of the data from the studies prior to 2000, analyzed by quantitative meta-analysis, demonstrated that the dose of neutrophils transfused, as well as the survival rate of the controls, was primarily responsible for the differing success rates reported in the studies and that the highest possible granulocyte doses (>4 × 10^{10} neutrophils) should be used (Vamvakas & Pineda, 1996). This was further substantiated in the RING study in 2015, in which "post hoc secondary analysis suggested that patients receiving higher doses tended to have better outcomes than those receiving lower ones" (Price et al., 2015). This multicenter randomized, open-label, phase 3 trial involved 14 sites with a total of 97 subjects eligible for analysis. There were two treatment arms; patients were randomized to standard antimicrobial therapy or standard antimicrobial therapy plus daily granulocyte transfusions from normal donors stimulated with G-CSF (480 μg) and dexamethasone (8 mg). A dose goal of 40 × 10^9 per transfusion, equivalent to 0.6 × 10^9 granulocytes/kg, was used for all collections. The majority of patients received an average dose of >0.6 × 10^9 granulocytes/kg. However, 30% of patients received lower doses, with some reaching values as low as 0.09 × 10^9 granulocytes/kg. These differences were site specific and not due to any other factors, including mobilization, timing, precounts, or blood processed. Primary outcomes were a measure of clinical success and based on survival for 42 days and clinical response of the infection. In total, 209 of the 316 transfusions studied had available dose per kilogram values. Plotting these in a generalized linear model, in addition to time from collection to administration, the researchers found that each additional 10^9 cells/kg was associated with a 1.75 × 10^9/L ANC increment ($p < 0.001$). Further examination of the relationship between these doses and primary outcome revealed primary success of 59%, 15%, and 37% of high-dose, low-dose, and control patients, respectively. According to the authors, "subjects who received the higher dose fared substantially and significantly better when compared to the low-dose group, both in primary outcome and survival" (Price et al., 2015).

The current adult collection dose requires that 75% of granulocyte components collected have a minimum of 1.0 × 10^{10} granulocytes, while product requirements for neonates shall be defined by the medical director (Standards Committee of the AABB, 2018). Given the data, however, it must be realized that this dose represents a minimum and that higher doses are highly desirable.

Once the appropriate dose has been collected, granulocytes are stored at room temperature (20°C–24°C) without agitation and have an expiration date of 24 hours (Standards Committee of the AABB, 2018). However, neutrophils undergo apoptosis throughout storage, and accumulation of transfused granulocytes at sites of inflammation decreases with increasing time of storage. Therefore, they should be transfused as soon as possible after collection (Price & Dale, 1979). In addition to these requirements, leukocyte reduction filters or microaggregate filters shall not be used (Standards Committee of the AABB, 2018) and irradiation is recommended due to the large number of lymphocytes within the product and compromised immune status of the recipient. Importantly, irradiation will not impair granulocyte function. In addition, a serologic crossmatch is required for any product containing >2 mL of red cells (Standards Committee of the AABB, 2018).

Granulocyte Collection Procedure

Red blood cells and granulocytes have similar densities and sedimentation rates, resulting in poor separation during centrifugation. The addition of sedimenting agents such as hydroxyethyl starch (HES) can improve this separation, thereby enhancing granulocyte collection (Iacone et al., 1981). The mechanism of action of HES is the induction of rouleaux formation among red blood cells. The resulting greater red cell sedimentation rate and greater upward flow of plasma during centrifugation enhances separation (Lee et al., 1995). Different types of HES include the high-molecular-weight hetastarch and the low-molecular-weight pentastarch. While both of these agents have been shown to have equivalent safety profiles (Strauss et al., 1986; Strauss et al., 1987), pentastarch has the benefit of being rapidly excreted with less danger of accumulation. Although the safety profile of pentastarch may be superior, a controlled study has shown greater granulocyte yields with hetastarch (Lee et al., 1995). When used as a volume expander, HES has been found to increase mortality and the requirement for renal replacement therapy in critically ill patients, patients with compromised renal function, septic patients, and patients at risk for bleeding (FDA, 2013) (see discussion under Donor/Patient Complications Common to All Hemapheresis Procedures). However, a retrospective review of 6 academic institutions and 278 procedures by Pagano et al. in 2016 showed that the low doses used during therapeutic leukocytapheresis procedures does not increase renal toxicity (Pagano et al., 2016). Despite these findings, it may still be prudent to evaluate granulocyte donors for the presence of renal disease.

TABLE 38.3

Short-Term Side Effects of Medications Used in Granulocyte Mobilization

Medication	Side Effects
Corticosteroids	Headache
	Flushing
	Insomnia
	Euphoria
	Palpitations
	Epigastric acidity
	Hyperglycemia
G-CSF	Bone pain
	Myalgias
	Arthralgias
	Headache
	Fever
	Chills
	Gastrointestinal discomfort
	Paresthesias
	Chest pain
	Edema
	Fatigue

Data from Volk EE, Domen RE, Smith ML: An examination of ethical issues raised in the pretreatment of normal volunteer granulocyte donors with granulocyte colony-stimulating factor, *Arch Pathol Lab Med* 123:508–513, 1999.
G-CSF, Granulocyte-colony stimulating factor.

Granulocyte Donor Concerns

In addition to granulocytes, platelets and significant numbers of red blood cells are present in the leukocytapheresis product. The donor's hematocrit typically drops by 7% following a granulocyte collection (Hester et al., 1995). This drop is due not only to loss of red blood cells but also to dilutional effects of volume expansion caused by the HES used during the procedure. Platelet count typically drops by 22% after each procedure—an equivalent drop to that seen with plateletapheresis (Hester et al., 1995). Again, a degree of dilutional effect is present. An additional cause for a fall in platelet count is seen in donors stimulated with G-CSF (Bensinger et al., 1993). Healthy donors receiving G-CSF for 10 days typically have a decline in platelet count starting at day 8, with significant differences from baseline at days 10 and 11. The mechanism behind this effect is uncertain and may represent changed platelet distribution, decreased platelet production, or increased intravascular volume (Korbling, 1998). In addition, recovery of platelet count appears to be prolonged, requiring 7 to 10 days among stem cell donors versus 4 to 6 days among platelet donors (Stroncek et al., 1996b).

G-CSF and corticosteroids can cause a number of other side effects (Table 38.3). These side effects are very common, occurring in 90% of allogeneic donors receiving G-CSF for apheresis collection of hematopoietic progenitor cells (HPC-A) (Stroncek et al., 1996a), are usually mild, and are treated symptomatically. For example, bone pain and headache, which tend to be dose related (Stroncek et al., 1996a; Murata et al., 1999), typically respond to mild analgesics. Nausea and vomiting are more common in women, and headache is more common in those younger than 35 years (Murata et al., 1999). More significant but rare side effects of G-CSF include splenic rupture, anaphylaxis, acute iritis, marginal keratitis, gouty arthritis, autoimmune thyroiditis, rheumatoid arthritis exacerbation, thrombosis, erythema multiforme, acute lung injury, and capillary leak syndrome (Korbling, 1998; Volk et al., 1999; Azevedo & Tabak, 2001;

TABLE 38.4

Diseases/Conditions That Are Relative Contraindications to Medications Used for Granulocyte Mobilization

Medication	Condition
Corticosteroids	Hypertension
	Diabetes
	Peptic ulcer disease
G-CSF	Inflammatory conditions
	Gout
	Risk factors for thrombosis

Data from Korbling M: Effects of granulocyte colony-stimulating factor in healthy subjects, *Curr Opin Hematol* 5:209–214, 1998; and Technical Manual Committee, Roback JD, Combs MR, et al., editors: *Technical Manual*, ed 16, Bethesda, MD, 2008, AABB.
G-CSF, Granulocyte-colony stimulating factor.

Arimura et al., 2005; Tigue et al., 2007; Veerappan et al., 2007). These are believed to represent exacerbation of underlying donor/patient illnesses; donors should be evaluated for these when determining suitability (Table 38.4).

Although the short-term effects of G-CSF are predominantly mild, the long-term effects have been a topic for debate. Concerns have been expressed over the possibility of recipients developing hematologic diseases such as myelodysplasia or chronic myelogenous leukemia (Korbling, 1998; Volk et al., 1999). This is due, in part, to studies of normal donors receiving G-CSF, which have demonstrated the following findings: induction of a small population of tetraploid myeloid cells (Kaplinsky et al., 2003), temporary asynchronous allele replication, and persistent aneuploidy up to 265 days following G-CSF administration (Nagler et al., 2004). These findings were similar to those that have been seen in hematologic malignancies. In addition, early reports of leukemic transformation after G-CSF therapy in 10% to 15% of patients with severe congenital neutropenia (SCN) on long-term regimens fueled concerns (Bonilla et al., 1994). This was followed by additional reports of related donors who had developed hematologic malignancies after G-CSF mobilization (Bennett et al., 2006). In response to these collective findings, the World Marrow Donor Association (WMDA) issued a statement affirming that, "in patients with cancer or abnormal blood cells, it [G-CSF] has been shown to stimulate leukemic blood cells. It is unknown whether G-CSF increases or decreases an individual's risk of developing cancer" (Shaw et al., 2015). At the time, it was estimated that to detect a 10-fold increase in the frequency of leukemia above the population background of 0.05%, a study following 2000 stimulated donors for a minimum of 10 years would be needed (Pamphilion et al., 2008).

Two registries had published data that almost met these requirements. The European Bone Marrow Transplant Registry examined unstimulated bone marrow donors and stimulated donors collected by HPC-A between the years 1990 and 2003. Among bone marrow donors, 9 of 28,134 (0.032%) donors developed hematologic malignancies compared with 5 of 16,432 (0.030%) stimulated HPC-A donors (Grupp et al., 2006). The National Marrow Donor Program (NMDP) examined 4015 healthy unrelated allogeneic donors who had donated between 1997 and 2007. Twenty cases of malignancy were identified; this incidence was consistent with the age-adjusted U.S. incidence of cancer in adults. No cases of hematologic malignancy were seen (Confer & Miller, 2007). In 2012, with five additional years of data, a review of the literature including the NMDP data showed "no compelling evidence for an increase in hematological malignancies among healthy donors who receive G-CSF to mobilize cells for donation." These conclusions subsequently prompted the WMDA to issue a revised statement conclusively affirming that there is no increased risk of developing cancer within several years of G-CSF administration (Shaw et al., 2015).

Despite these reassuring findings, donors undergoing G-CSF stimulation should give informed consent before stimulation, and appropriate institutional review should be obtained for use of G-CSF in this non–FDA-approved role.

Long-term steroid treatment is associated with a number of well-known side effects, including the development of posterior subcapsular cataracts (PSCs). Because these complications appear with long-term use, it would seem that short-term steroid stimulation of granulocyte donors should not be associated with them. This may not be the case, however. A single-center double-blind study compared the presence of cataracts in 9 apheresis platelet donors and 11 granulocyte donors matched for age, gender, and number of respective donations (Ghodsi & Strauss, 2001). The frequency of cataracts not associated with steroid administration was equivalent between the two groups, but those associated with steroid administration—PSCs—were more frequent in the granulocyte donors when all eyes were considered (5 of 22 eyes vs. 0 of 18; $p = 0.040$) (Ghodsi & Strauss, 2001). A subsequent multicenter study examined 89 granulocyte donors and 89 control donors (Burch et al., 2005). The granulocyte donors had donated a mean of 13 donations (range, 5 to 39). Six of the granulocyte donors and four of the control donors had evidence of PSC on photographic examination. This was not a statistically significant difference, though only granulocyte donors demonstrated the presence of bilateral PSCs (Burch et al., 2005). This better powered study suggests that cataract formation may not be a concern among granulocyte donors.

BOX 38.2

Advantages and Disadvantages of Double Red Blood Cell Collections

Advantages

- Decreased incidence of donor reactions compared with whole-blood donation (Benjamin et al., 2009)
- Better inventory management of needed blood types (Benjamin et al., 2009)
- Standardized red blood cell dose (Moog, 2013)
- More consistent and controlled component quality (Benjamin et al., 2009)
- Decreased donor exposure if a patient receives both parts of a double red cell collection (Moog, 2013)

Disadvantages

- Stricter donation guidelines for minimum weight, height, hemoglobin, and hematocrit (Benjamin et al., 2009)
- Longer donation interval (Benjamin et al., 2009)
- Potential for citrate toxicity and device-related complications (Benjamin et al., 2009)

DONOR ERYTHROCYTAPHERESIS

Benefits of Erythrocytapheresis

A single unit of red blood cells or the equivalent of 2 units of red blood cells can be collected by apheresis. Advantages and disadvantages of double red blood cell collections are given in Box 38.2.

Erythrocytapheresis Product Requirements

The Standards for Blood Banks and Transfusion Services requires that apheresis red blood cells be collected and prepared by a method that is known to result in a mean hemoglobin >60 g or a packed red cell volume of 180 mL. In addition, at least 95% of the units sampled must have >50 g of hemoglobin or 150 mL packed red cell volume (Standards Committee of the AABB, 2018). If the red blood cell units are leukocyte reduced, then the mean hemoglobin must be >51 g or 153 mL packed red cell volume. Here, at least 95% of tested units must have >42.5 g of hemoglobin or 128 mL packed red blood cell volume (Standards Committee of the AABB, 2018).

The FDA does not define product requirements for red blood cells—single or double—collected by apheresis but instead states that 95% of the products collected must meet "expected or target RBC volume" and "any other target parameters specified in the device's operator manual" (Food and Drug Administration, 2001). The FDA also defines how such validation and testing is to be performed, with the initial validation consisting of testing "100 consecutive RBC units," while subsequent testing must include at least 50 U/month, consisting of both single and double red blood cell products. If a center collects less than 50 U, all units must be tested (Food and Drug Administration, 2001).

Erythrocytapheresis Donor Selection

Allogeneic apheresis red blood cell donors must meet the criteria defined by the FDA and the AABB for whole blood donation. In addition, they are required to meet any other selection criteria defined by the device's operator manual (Food and Drug Administration, 2001).

The FDA and the AABB do not define a minimum hemoglobin/hematocrit for double red cell donation. Instead, it is required that the collection center follow the instrument manufacturer's recommendations (Food and Drug Administration, 2001; Standards Committee of the AABB,

2018). The FDA does, however, require that the hemoglobin/hematocrit be determined by a quantitative method (Food and Drug Administration, 2001). As a result, the copper sulfate method cannot be used to qualify a donor for double red cell donation.

The AABB limits the total volume of red blood cells removed, such that the donor's hematocrit and hemoglobin are not <30% and <10 g/dL, respectively, after volume replacement (Standards Committee of the AABB, 2014). The FDA makes no specific limitations, requiring that the manufacturer's recommendations be followed (Food and Drug Administration, 2001).

The type of product collected determines the donation interval following hemapheresis red blood cell donations. Donors donating a single unit of red blood cells are deferred for 8 weeks. The exception to this would be that, as described in the section on donor plateletapheresis, they could donate platelets or platelets with concurrent plasma as long as the extracorporeal red blood cell volume of the collecting instrument is less than 100 mL (Food and Drug Administration, 2001). Donors donating 2 U of red blood cells are deferred for 16 weeks, and no automated or manual collections are allowed during this time (Food and Drug Administration, 2001).

If a donor experiences an incomplete procedure, that is, the targeted collection is not reached, the FDA defines the length of deferral based on the absolute loss of red blood cells during the initial collection and subsequent collections, as outlined in Table 38.2 (Food and Drug Administration, 2007).

Erythrocytapheresis Donor Concerns

Owing to the removal of 2 U of red blood cells, one of the most frequent concerns is whether reactions are more frequent with double red blood cell collections when compared with whole-blood collections. Benjamin and colleagues compared 4,348,686 whole-blood collections with 206,570 double red cell collections in 26 regional blood centers. They found an age-dependent risk for mild reactions, with donors older than 20 years experiencing more reactions and donors younger than 20 years experiencing fewer reactions when comparing double red cell collections with whole-blood collections (Benjamin et al., 2009). Hematomas and citrate reactions were more common with double red cell collections, while vasovagal-reactions, loss of consciousness, and arterial puncture were more common with whole-blood collections (Benjamin et al., 2009). Most reactions with double red cell collections were citrate related and resolved within 5 to 10 minutes after saline infusion or a decrease in plasma return rate (Moog, 2013). In donors of all ages, fewer major systemic complications were seen with double red cell collections when compared with whole-blood collections (10.2 vs. 14.3 per 10,000 collections; odds ratio, 0.71; confidence interval, 0.32–0.89) (Benjamin et al., 2009). These results suggest that double red cell collections may be most beneficial for younger donors, who are also more likely to experience adverse events with whole-blood collections. The overall lower rate of reactions with double red cell collections despite the removal of a greater red blood cell mass results from the fact that donors are isovolemic at the end of the collection as a result of the infusion of saline. Additionally, with double red cell collections, a specified and controlled absolute red blood cell volume is collected while, with whole-blood collections, the red blood cell volume collected depends on donor hematocrit and blood volume (Moog, 2013).

Another concern with double red blood cell donations is whether donors making such donations are at greater risk of developing iron deficiency than whole-blood donors, particularly for younger donors who have lower iron stores and require more iron during periods of rapid growth (Benjamin et al., 2009). Radtke and colleagues (2004) studied the effect of iron supplementation in double red cell donations and found that, compared with placebo, daily iron supplementation in double red cell donations was associated with higher, more stable ferritin and hemoglobin levels. Further investigation is needed to fully understand the optimal screening for hemoglobin and iron balance in red cell donors.

MULTICOMPONENT APHERESIS DONATION

With current instrumentation, different combinations of blood products can be collected from the same donor. This allows for the optimum utilization of each donor. For example, the maximum amount of plasma would be collected from an AB donor, while that donor's red blood cells, which frequently outdate before they are transfused, would not be collected. An O Rh-negative or Rh-positive donor would provide a double red blood cell collection; plasma, however, which is usually in adequate supply, would not be collected. The various combinations of collections currently available are given in Box 38.3. It should be mentioned that all of the various regulations that apply to individual apheresis collections with regard to donor criteria and donor frequency apply to multiple-component collections. For example, a donor undergoing a double red cell collection with a concurrent plasma collection would have to meet the requirements for a double red cell collection as well as the requirements for frequent or infrequent plasma collection. This would include tracking red blood cell loss (see Table 38.2) and total plasma volume loss (see later discussion of plasma donation).

BOX 38.3

Combinations of Blood Products Available for Multicomponent Collections

- Red blood cell and plasma
- Red blood cell and platelet
- Red blood cell, plasma, and platelet
- Double red blood cell
- Double or triple platelet
- Platelet and single or double plasma
- Double platelet and single plasma
- Double or triple plasma

HEMATOPOIETIC PROGENITOR CELL COLLECTION BY APHERESIS

Benefits of Hematopoietic Progenitor Cell Collection

Hematopoietic progenitor cell collection by apheresis (HPC-A) was developed in the 1980s and has replaced the collection of hematopoietic progenitor cells by bone marrow harvest (HPC-M) for many donors and patients. Donors tolerate hemapheresis better than bone marrow harvest since it is an outpatient procedure and does not require general anesthesia. As a result, HPC-A is less expensive, more convenient, and safer. Also, the donor recovers more quickly from the procedure without the pain and temporary disability that often accompany bone marrow harvest (Winters, 2009; Tanhehco et al., 2013). The use of peripheral blood HPCs in transplantation restores hematopoietic and immune function more rapidly than bone marrow HPCs, with engraftment of white cells and platelets occurring approximately 1 week earlier (Winters, 2009). This means fewer days of immunosuppression and fewer exposures to allogeneic blood products in the recipient (Moog & Muller, 1998; Bensinger et al., 2001). Additionally, in autologous transplantation, collection of peripheral HPCs by hemapheresis can be performed when marrow involvement by malignancy or prior pelvic irradiation is present and would preclude bone marrow harvest (Tanhehco et al., 2013). HPC-A products also confer survival advantage over bone marrow products in allogeneic transplants, when the risk of disease recurrence is high (Bensinger 2012).

Although HPC-A collection provides a number of benefits over bone marrow harvest, it also has disadvantages, including possible adverse effects of mobilization regimens, a greater length of time required for collection, the possibility of a larger volume of component to be transfused at the time of transplantation, and the necessity for central venous access in many cases, along with the accompanying risks and complications (Lee & Klein, 1995). HPC-A products have been associated with the higher rate of chronic graft-versus-host disease (GVHD) (Shinzato et al. 2013, Bensinger 2012) or GVHD more refractory to standard therapy (Flowers et al., 2002). This may result from the larger number of T cells within peripheral blood stem cell products compared with bone marrow. However, in many patients, the more rapid engraftment with peripheral blood HPC transplantation outweighs the possible increased risk of GVHD.

Autologous Versus Allogeneic Hematopoietic Progenitor Cell Harvest

Due to the use of chemotherapy as the original mobilizing agent for HPCs, HPC-A collections were initially limited to autologous transplantation and restricted to patients with Hodgkin lymphoma (HL), non-Hodgkin lymphoma (NHL), and multiple myeloma (MM). The use of HPCs was subsequently expanded to include transplantation for leukemias (Lee & Klein, 1995; Gillespie & Hillyer, 1996; Moog & Muller, 1998). As methods for mobilization that do not depend on chemotherapy have become available, HPC-A collection has expanded to include allogeneic donations as well.

Hematopoietic Progenitor Cell Dose

An important factor in determining the success of HPC transplantation is the dose of HPCs infused. Unfortunately, a method for definitively

TABLE 38.5
Comparison of Methods for Measuring HPCs

	MNC	CFU-GM	CD34+ Cell Count
Minimal dose for engraftment	6.0 to 6.5 × 10^8 MNC/kg	0.5 to 2.0 × 10^5 CFU GM/kg	2.5 × 10^6 CD34+ cells/kg
Correlation with HPC count	Lower	Higher	Higher
Ability to measure	Easy	Challenging	Easy
Turnaround time	Fast (hours)	Slow (2 weeks)	Fast (hours)
Standardization between laboratories	Easy	Challenging	Challenging

CFU-GM, Colony-forming unit granulocyte-macrophage colonies; *MNC*, mononuclear cell count.
Data from Kessinger A, Armitage JO, Smith DM, et al,: High-dose therapy and autologous peripheral blood stem cell transplantation for patients with lymphoma, *Blood* 74:1260–1265, 1989; Kessinger A, Bishop MR, Anderson JR, et al.: Comparison of subcutaneous and intravenous administration of recombinant human granulocyte-macrophage colony-stimulating factor for peripheral blood stem cell mobilization, *J Hematother* 4:81–84, 1995; Bender JG, To LB, Williams S, et al.: Defining a therapeutic dose of peripheral blood stem cells, *J Hematother* 1:329–341, 1992; Lee JH, Klein HG: Collection and use of circulating hematopoietic progenitor cells, *Hematol Oncol Clin North Am* 9:1–22, 1995a; Bensinger W, Appelbaum F, Rowley S, et al: Factors that influence collection and engraftment of autologous peripheral-blood stem cells. J Clin Oncol 13:2547-2555, 1995. and Korbling M, Huh YO, Durett A, et al.: Allogeneic blood stem cell transplantation: peripheralization and yield of donor-derived primitive hematopoietic progenitor cells (CD34+ Thy-1dim) and lymphoid subsets, and possible predictors of engraftment and graft-versus-host disease, *Blood* 86:2842–2848, 1995.

enumerating HPCs is not available. Table 38.5 compares the different methods for estimating HPC dose. It is known that HPCs are found within the mononuclear cell component of blood; as a result, the mononuclear cell count (MNC) can be used as an indicator of when to discontinue HPC collection. Another way of measuring HPC dose is by assessing colony-forming unit granulocyte-macrophage (CFU-GM) colonies grown on soft agar. Finally, a third and most widely used method of determining HPC dose is the measurement of CD34+ cell count within the product. Since HPCs represent a subset of CD34+ cells, the measurement of CD34+ cells gives a better indication of HPC dose than MNC and also correlates with CFU-GM (Lee & Klein, 1995). Although minimal numbers of CD34+ cells/kg are needed for prompt engraftment (see Table 38.5), too many cells have been associated with an increased risk of chronic GVHD in some studies (Zaucha et al., 2001; Heimfeld, 2003). Zaucha and colleagues (2001) found a higher incidence of extensive chronic GVHD in allogeneic transplant patients receiving greater than 8.0 × 10^6 CD34+ cells/kg.

Some authors have suggested that the dose of CD34+ cells needed for engraftment may vary with the number of HPC collection procedures performed (Smolowicz et al., 1999). It is thought that a higher total dose is necessary when CD34+ cells are collected over multiple procedures. This is believed to be due to changes in CD34+ cell subsets seen during the course of multiple collections (Smolowicz et al., 1999).

Hematopoietic Progenitor Cell Mobilization

Early attempts at harvesting hematopoietic progenitor cells from peripheral blood were successful but labor and resource intensive. Peripheral blood contains only 10% of the fraction of CD34+ cells found in bone marrow (Lee & Klein, 1995). This means that when HPCs are collected during steady state (i.e., without mobilization), the number of procedures necessary to achieve a sufficient dose may be large, for example, 12 procedures in one study (Moog & Muller, 1998). The discovery that peripheral HPCs could be mobilized from the bone marrow meant that therapeutic doses of HPCs could be collected by hemapheresis in fewer procedures, making the method more attractive. Chemotherapy, cytokines, or a combination of chemotherapy and cytokines can mobilize HPCs from bone marrow (Lee & Klein, 1995; Gillespie & Hillyer, 1996; Moog & Muller, 1998). The effects of chemotherapy and cytokines on mobilization are independent of one another, with even greater numbers of HPCs collected when chemotherapy and cytokines are used together than when either regimen is used alone. Table 38.6 gives a general comparison of the effectiveness of these three mobilization regimens. The mechanisms of action of the mobilization regimens are summarized in Figure 38.2 and are discussed in more detail later.

The regimen initially used for mobilization was chemotherapy. During the period of rebound hematopoiesis following chemotherapeutic treatment, the number of HPCs present within the peripheral blood increases dramatically (see Table 38.6). This allows for the effective HPC-A collection while decreasing the tumor burden within the patient. The limitation of mobilization with chemotherapy is that it can be applied only to autologous transplants.

Cytokines such as G-CSF dramatically increase the presence of HPCs within the peripheral blood and have the additional benefit of providing minimal short-term toxicity (see Table 38.3). This allows for the mobilization of HPCs in normal donors in preparation for allogeneic transplantation. The mechanism of action of these cytokines is indirect. HPCs in the marrow are bound to stromal cells by adhesion molecules. These molecules include VLA-4 and CXCR4 on the HPCs and VCAM-1 and SDF-1 on the stromal cells. G-CSF increases the number of neutrophils in the marrow, with a subsequent increase in neutrophil-derived proteolytic enzymes, such as elastase and MMP-9. These enzymes cleave VCAM-1 and SDF-1, resulting in the release of HPCs from the stromal cells, allowing them to enter the peripheral circulation (Lapidot & Petit, 2002) (see Fig. 38.2).

TABLE 38.6
Comparison of Different Mobilization Regimens

Regimen	Approximate Day When Peak HPC Concentrations Are Reached	Increase in HPCs Above Steady State
Chemotherapy	Day 14 after completion of chemotherapy	5–15×
Cytokines (G-CSF and GM-CSF)	Day 5 after initiation of cytokine therapy	60×
Chemotherapy and cytokines	Day 5 after initiation of cytokine therapy	1000×

Data from Gillespie TW, Hillyer CD: Peripheral blood progenitor cells for marrow reconstitution: mobilization and collection strategies, *Transfusion* 36:611–624, 1996.
G-CSF, Granulocyte–colony stimulating factor; *GM-CSF,* granulocyte-macrophage colony-stimulating factor; *HPC,* hematopoietic progenitor cell.

In December of 2009, a new medication was approved by the FDA for the mobilization of HPC-A from patients with NHL and MM. This medication, plerixafor, is a CXCR4 inhibitor that was initially investigated as an anti–human immunodeficiency virus (HIV) medication. Plerixafor blocks the interaction between HPCs and stromal cells, resulting in mobilization of HPCs from the marrow (Tanhehco et al., 2013). Currently, plerixafor has been approved for the mobilization of HPC-A from patients who have failed mobilization with G-CSF alone and is given in addition to G-CSF. Plerixafor is not currently approved for use by normal donors or patients with HL, although studies are underway to investigate these possible indications. Plerixafor is also not approved as a mobilizing agent in patients with acute leukemia, as it causes mobilization of leukemic cells in addition to HPCs. However, a recent clinical trial points to a beneficial effect of plerixafor in the treatment of acute leukemia. By disrupting the SDF-1 and CXCR4 interactions, plerixafor causes loss of proliferation and adhesion signals for leukemic cells with loss of protective survival signals and displacement of leukemic cells into the peripheral blood. Here, the leukemic cells are more easily targeted with chemotherapy (Tanhehco et al., 2013; Martinez-Cuadron et al., 2018). Depending on the mobilization agent in use, the composition of the mobilized stem cell product differs and may affect transplant outcomes. Based on microarray analysis, proportionally more B cells, T cells, and mast cell genes are collected with plerixafor compared with more neutrophil and mononuclear phagocytic genes collected with G-CSF (Tanhehco et al., 2013). Furthermore, when plerixafor and

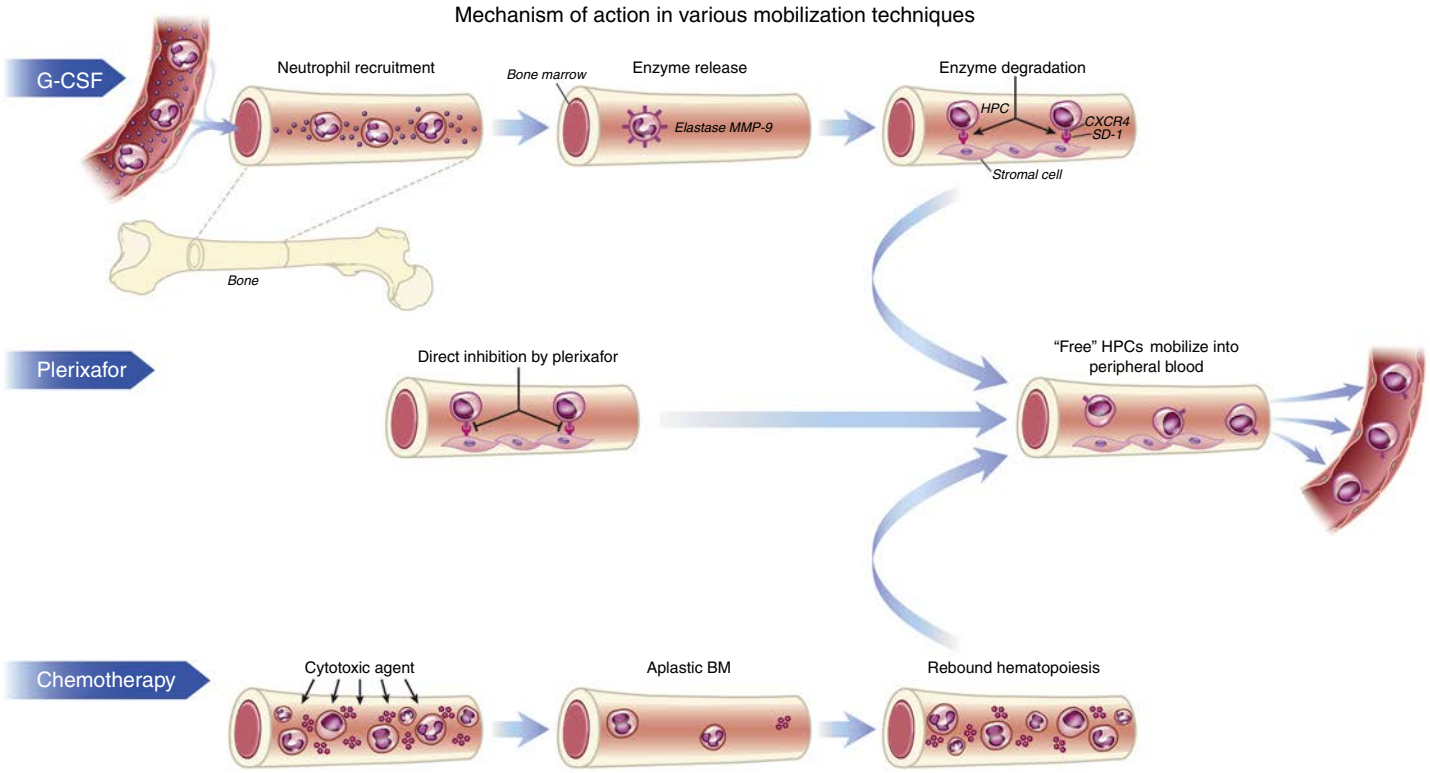

Figure 38.2 Mechanisms of action in various mobilization techniques. G-CSF, Plerixafor, and chemotherapy all have different intrinsic mechanisms of action; however, they share the same common final pathway with release of hematopoietic progenitor cells into the peripheral blood. (Figure illustration created by Paul Honermann, scientific illustrator, Mayo Clinic, Rochester, MN.).

G-CSF are used together, genes are upregulated that were not upregulated from either mobilizing agent alone. The composition of the stem cell product also varies in terms of the mature lymphocyte component, with plerixafor inducing greater numbers of mature lymphocytes. Two retrospective studies showed a strong positive correlation between the absolute lymphocyte count (ALC) in the collected product and the ALC in posttransplant patients with NHL and MM on day 15. Higher ALC in the collected product also correlated with longer posttransplant overall survival and progression-free survival (Tanhehco et al., 2013).

In healthy allogeneic donors, the optimum mobilization regimen appears to be 10 to 16 μg/kg of G-CSF split into two doses and administered subcutaneously (Kroger & Zander, 2002). Twice-daily dosing has been shown to be superior to single dosing, likely due to the relatively short half-life of G-CSF of 3 to 4 hours (Kroger & Zander, 2002). In donors who are poor mobilizers, higher doses of G-CSF can be given. However, when G-CSF doses larger than 10 to 16 μg/kg are used, more adverse donor effects are seen without significant improvement in CD34+ cell yield. In autologous donors, mobilization is complicated by both the underlying disease and previous therapy. For this reason, G-CSF doses >16 μg/kg are needed in autologous HPC collection. If poor mobilization occurs, the patient may need to be remobilized with chemotherapy followed by growth factor, higher doses of growth factor, sequential stimulation with G-CSF, or the use of plerixafor (Kessinger & Sharp, 2003; Pusic & DiPersio, 2008; Cashen, 2009).

In addition to these mobilization regimens, HPCs are mobilized by the collection procedure itself. Studies of the kinetics of HPCs during hemapheresis procedures have shown that larger numbers of HPCs are recovered than would be expected based solely on the number of cells present in the peripheral blood. This means that during the procedure, as HPCs are removed, additional HPCs are released from the marrow (Smolowicz et al., 1999).

Unfortunately, despite attempts to optimize mobilization regimens, not every patient collects a dose of peripheral blood HPCs sufficient for transplantation. Approximately 5% to 10% of patients receiving nonplerixafor mobilization will fail the mobilization attempt. In these cases of previous mobilization failure, when plerixafor is used with G-CSF, success rates of mobilization are greater than 60% (Tanhehco et al., 2013). Factors that have been found to adversely affect HPC harvest are given in Box 38.4. Some of those factors, such as low CD34 count in peripheral blood, can be a trigger for additional mobilization steps, such as administering plerixafor.

BOX 38.4

Factors That Negatively Influence Mobilization for Transplantation

Premobilization Factors

Age >60 years
Progressive disease
Severe bone marrow involvement
Type of disease (Non-Hodgkin lymphoma)
Number of previous chemotherapy or radiation cycles
Type of chemotherapy (methotrexate, lenalidomide)
History of previous failed mobilization

Postmobilization Factors

Low CD34+ cell count on day +4 onward
Low yield with first collection
Low white blood cell count
Platelet nadirs
Neutropenic fever
Need for platelet transfusions
Low peak CD34+ cell counts

Data from Tanhehco YC, Vogl DT, Stadtmauer EA, et al.: The evolving role of plerixafor in hematopoietic progenitor cell mobilization, *Transfusion* 53:2314–2326, 2013.

Although mobilization increases the number of HPCs present in the peripheral blood, it can also have detrimental effects on the donor and HPC product. As discussed in the section on donor concerns in granulocyte collection, G-CSF is associated with minimal short-term side effects and unknown long-term side effects. While these side effects may be unimportant relative to the risks from underlying disease in autologous transplantation, in the setting of allogeneic donation the uncertainty of long-term risks of mobilization must be explained to the donor during the consent process. The delay in platelet recovery seen following G-CSF treatment and granulocyte collection is also seen with HPC harvest (Gillespie & Hillyer, 1996; Stroncek et al., 1996b). In autologous donors, this combined with marrow suppression from recent chemotherapy may result in the need for platelet transfusion. Mobilization is also associated with increased risk of catheter thrombosis (Lee & Klein, 1995). Finally, in addition to mobilizing HPCs, the regimens described previously have been

shown to mobilize tumor cells into the peripheral blood by some (Brugger et al., 1994; Gazitt et al., 1996) but not all authors (Passos-Coelho et al., 1995). The study by Brugger and colleagues (1994) demonstrated mobilization of tumor cells on days 1 through 7 following the start of chemotherapy in patients without bone marrow involvement, and on days 9 through 16 in those with marrow involvement. Mobilization of tumor cells in these latter patients occurred within the time frame of HPC collection. Gazitt and colleagues (1996) found that mobilization of plasma cells in MM patients occurred later—days 5 and 6—than mobilization of stem cells—days 1 through 3. Differences in mobilization of tumor cells versus HPCs have led many to suggest that single collections early in the course of mobilization may be better than multiple collections. It should be realized that although tumor contamination does occur, the effect of this contamination on relapse is uncertain.

Hematopoietic Progenitor Cell Collection Procedure

Timing of the progenitor cell collection procedure will depend on the mobilization protocol used. For chemotherapy mobilization, it is critically important to monitor white blood cell count after initiation of chemotherapy. It was shown that in 1 to 3 days after white blood cell count recovers to more than 0.5×10^9/L, the levels of cytokines and circulating CD34+ cells are the highest (Dreger et al., 1993; Tuchman et al., 2015). That is why the first day of collection depends on the white blood cell count recovery in chemotherapy mobilizing regiment.

Cytokine mobilization usually follows a more predictable schedule, with 4 consecutive days of G-CSF injections, with addition of plerixafor in poor mobilizers (peripheral blood CD34+ count less than 20 cells/μL) on day 4.

Another important variable in collection is the use of apheresis equipment. Currently in the United States, there are two FDA-approved devices for progenitor cell collection: TerumoBCT Spectra Optia (Lakewood, CO) and Fresenius Amicus (Lake Zurich, IL). Characteristics of these devices are given in Table 38.7. Another variable to consider is the whole-blood flow rate during the procedure. It would seem that higher flow rates would result in a higher volume processed and a concurrent larger number of HPCs collected. However, in donors/patients with high white blood cell counts (>35,000/μL), high whole-blood flow rates have been shown to decrease CD34+ cell collection efficiency and result in lower CD34+ cell yields (Burgstaler & Pineda, 2004; Cooling et al., 2010).

Although the whole-blood flow rate can adversely affect collection efficiency, the concept of increasing the amount of blood processed to increase the HPC yield is a valid one. Standard HPC collection involves the processing of approximately 1.5 to 3.0 blood volumes per procedure (Lee & Klein, 1995). Alternatively, large-volume leukocytapheresis (LVL) involves processing more than 5 blood volumes, or more than 15 L (Reik et al., 1997). The benefits of such procedures include the collection of large numbers of HPCs per procedure, with the resulting need for fewer collection procedures and greater mobilization of HPCs during the procedure (Lee & Klein, 1995; Moog & Muller, 1998). In addition, improved yield of HPCs in patients who mobilize poorly has been seen (Smolowicz et al., 1997). Disadvantages of LVL include longer time required to complete the procedure and an increased incidence of citrate reactions (see discussion at the end of the chapter) (Moog & Muller, 1998). In standard leukocytapheresis procedures, thrombosis of central catheters is the most common complication (Goldberg et al., 1995). In LVL, citrate reactions predominate, occurring in 33% of donations (Lin et al., 1995). This is due to the greater amount of citrate anticoagulant that is infused. Some authors have attempted to minimize this by adding heparin to the anticoagulant before the procedure (Reik et al., 1997) and/or providing IV calcium supplementation during the procedure (Bolan et al., 2002; Buchta et al., 2003).

Hematopoietic Progenitor Cell Donor Concerns

Compared with other apheresis procedures, there are several unique considerations for HPC donors. These include the use of mobilizing agents, the need to process large volumes of blood, and the requirement for HLA matching between donor and recipient, which results in pediatric HPC donors who would otherwise be ineligible for other donation procedures (Winters, 2009). In adult HPC donors, the most common reactions are related to the mobilization and include bone pain in approximately 80% of donors and headache in approximately 50%. In general, the frequency of HPC reactions is less in pediatric patients, with a substantial decrease in those reactions caused by mobilization. Compared with approximately 80% of adult patients, mobilization-related reactions occur in only 15% to 17.5% of pediatric patients (Winters, 2009). Common and rare reactions associated with G-CSF are discussed earlier in the section on granulocyte collections.

TABLE 38.7

Comparison of Instrumentation for the Collection of Mononuclear Cells

Variables	TerumoBCT Spectra Optia	Fresenius Amicus
CD 34+ cell collection efficiency	++	++
Degree of automation	+++	+++
Flexibility with manual operation	++	++
Mobility of device	+++	+++
Approval for both therapeutic and donor procedures in the United States	++++	++
Extracorporeal volume	+	+
Platelet loss	+++	+
Time per procedure	++	+++
Sensitivity to high white blood cell count and/or high platelet count	+++	+++

Data from Burgstaler EA: Current instrumentation for apheresis. In McLeod BC, Szczepiorkowski ZM, Weinstein R, et al., editors. *Apheresis: Principles and Practice*, ed 3, Bethesda, MD, 2010, AABB Press, pp 95–130; Reinhardt P, Brauninger S, Bialleck H, et al.: Automatic interface-controlled apheresis collection of stem/progenitor cells: results from an autologous donor validation trial of a novel stem cell apheresis device, *Transfusion* 51:1321–1330, 2011; Brauninger S, Bialleck H, Thorausch K, et al.: Mobilized allogeneic peripheral stem/progenitor cell apheresis with Spectra Optia v.5·0, a novel, automatic interface-controlled apheresis system: Results from the first feasibility trial, *Vox Sang* 101:237–246, 2011; Brauninger S, Bialleck H, Thorausch K, et al.: Allogeneic donor peripheral blood "stem cell" apheresis: Prospective comparison of two apheresis systems, *Transfusion* 52:1137–1145, 2012; Rox JM, Wenzel F, Kobbe G, et al.: Influence of high inlet flow rates on efficacy of stem cell apheresis using the Spectra Optia Apheresis System, *Vox Sang* 101:337, 2011; and Kim SR, Choung HK, Kim DW, et al.: Evaluation of a new cell separator for collection of peripheral blood CD34+ progenitor cells in pediatric patients, *Transfusion* 51:306–312, 2011.

The large volume (20–30 L) of processed blood required for HPC donation may require central venous access, which is associated with a threefold increase in complications, including pneumothorax, hemothorax, thrombosis, bleeding, vascular injury, and infection. Fortunately, the majority of allogeneic adult HPC donations (80%–95%) can be collected using peripheral access (Winters, 2009). For pediatric donors, there is a greater need for central venous access, which is inversely related to age. In one study, donations from children less than 6 years old were collected peripherally only 1% of the time, compared with the 80% of children greater than 13 years of age whose donations were collected peripherally (Winters, 2009). Another effect of the large amount of blood processed in HPC collection is the greater exposure to citrate anticoagulant and therefore greater risk of hypocalcemia, hypomagnesemia, hypokalemia, and metabolic alkalosis. A more detailed discussion of the effects of citrate toxicity is included in the Donor/Patient Complications Common to all Hemapheresis Procedures section later in the chapter.

In addition to common reactions, G-CSF is associated with changes in several hematologic parameters, including a predictable increase in the leukocyte count, an increase in the lymphocyte count, and a decrease in the platelet count. Platelet loss can be significant, ranging from a 15% to 50% decline from preprocedure platelet count depending on the apheresis device used (Burgstaler & Pineda, 2004; Kobbe et al., 1997). In addition, patients undergoing autologous peripheral blood stem cell collections may be thrombocytopenic from the chemotherapy routinely used as part of the mobilization regimen. Bleeding complications in these patients are uncommon (Goldberg et al., 1995). However, patients may require platelet transfusions before or after collections to avoid bleeding complications.

DONOR PLASMAPHERESIS

PLASMA PRODUCTS

Two types of plasma products are collected by donor plasmapheresis: fresh frozen plasma (FFP) and source plasma. Source plasma is plasma that is subsequently used to manufacture derivative products. These derivative

products include albumin, immunoglobulins, coagulation factor concentrates, and laboratory reagents. FFP is the liquid component of whole blood that has been frozen within 6 to 8 hours after collection. The benefit of collecting FFP by plasmapheresis is that 600 to 700 mL of plasma can be collected from a single donor. This can then be divided into multiple units of a volume equivalent to FFP derived from whole-blood donations. Alternatively, the entire volume can be frozen as "jumbo plasma." These large units have the benefit of limiting donor exposure in patients requiring large volumes of FFP, such as in TPE for thrombotic thrombocytopenic purpura (TTP). An additional benefit is that the large volume of collection can maximize the production of frequently used or rare products, such as type AB FFP or IgA-deficient FFP.

PLASMA DONOR SELECTION

The donor criteria for plasmapheresis vary according to the frequency of donation. Donors donating plasma less frequently than every 4 weeks are classified as "infrequent" donors and must fulfill whole-blood donor requirements. In addition, AABB Standards require that donors taking warfarin be deferred from plasma donation for 1 week following their last dose of medication (Standards Committee of the AABB, 2018). This is due to the fact that the plasma of individuals taking this medication will have decreased vitamin K–dependent coagulation factor activity.

A donor donating more frequently than every 4 weeks is classified as a "frequent" donor and must fulfill criteria outlined in the CFR (Standards Committee of the AABB, 2014). These requirements are similar in many ways to those for whole-blood donation, with differences in deferrals for malaria and transfusion-transmitted disease exposure (CFR, 2014). In addition, the CFR requires that frequent plasma donors have a total serum protein of at least 6.0 g/dL; this is determined before each donation. Donors must also have a serum protein electrophoresis or quantitative immunodiffusion performed every 4 months as well as an annual physical examination by a physician (CFR, 2014). Frequent plasma donors are limited to two donations within a 7-day period with at least 2 days between donations (CFR, 2014).

Both frequent and infrequent plasma donors, as well as those donors donating multicomponent collections or plateletapheresis, are limited in the amount of plasma that they can donate within a 12-month period. Donors weighing 110 to 175 lb can donate up to 12 L; those weighing more than 175 lb can donate 14.4 L (FDA, 1995).

PLASMA DONOR CONCERNS

The risks of donor plasmapheresis are those common to any hemapheresis procedure. In addition, concern arises over possible depletion of immunoglobulins or removal of coagulation factors faster than they can be replenished, especially in frequent donors. Studies of long-term donors (Wasi et al., 1991) and donors undergoing frequent donations (Ciszewski et al., 1993) have not supported these concerns.

INDICATIONS FOR THERAPEUTIC HEMAPHERESIS

Therapeutic apheresis procedures, both cytapheresis and TPE, have been used to treat a wide variety of illnesses, often without a clear scientific basis. Although the number of publications related to therapeutic apheresis has been increasing, the percentage of randomized controlled trials has been decreasing. Additionally, many of the available randomized controlled trials lack adequate power to draw definitive conclusions (Crookston et al., 2017). In this way, apheresis has been analogous to the bloodletting of the early 18th century, with which it has frequently been compared. As a result, it is difficult in some cases to determine for which diseases and disorders hemapheresis is truly indicated. To help determine when hemapheresis procedures are indicated, the American Society for Apheresis (ASFA) publishes regularly updated recommendations and guidance on the use of apheresis (Padmanabhan et al., 2019). Diseases are grouped into four indication categories, as given in Table 38.8. Each indication is assigned a grade that indicates the strength of the ASFA recommendation and quality of the evidence supporting the recommendation. These are defined in Table 38.9. Table 38.10 lists diseases that have been categorized by the ASFA in the most recent publication of the categorization.

A discussion of all of the disorders listed in Table 38.10 is beyond the scope of this chapter. The interested reader is referred to three sources: the textbooks *Apheresis: Principles and Practice* (McLeod et al., 2010) and *Therapeutic Apheresis: A Physician's Handbook* (Crookston et al., 2017), both published by the AABB, and the special issue of the *Journal of Clinical Apheresis* entitled "Guidelines on the Use of Therapeutic Apheresis in Clinical Practice—Evidence-Based Approach from the Apheresis Applications Committee of the American Society for Apheresis, The Eighth Special Issue," published by the ASFA (Padmanabhan et al., 2019).

A final consideration is that not every possible disorder that has or could be treated by hemapheresis is included in the resources mentioned here. Similarly, not every potential disorder has been classified by the ASFA. In circumstances in which requests are made to perform therapeutic hemapheresis procedures for category III indications or for those indications that have not been categorized, a physician must determine whether hemapheresis is indicated by evaluating the pathophysiology of the disease process, the evidence that exists in the medical literature, and the risks of the hemapheresis procedure to the patient, including financial risks (Shaz et al., 2014). Hemapheresis procedures should not be attempted solely because "we tried everything else" or "when in doubt, pheresis it out." The interested reader is referred to the article "How we developed and use the ASFA guidelines for therapeutic apheresis procedures" (Shaz et al., 2014) and Chapter 4 of *Principles of Apheresis Technology* entitled "Clinical

TABLE 38.8
ASFA Categorization of Apheresis Indications

Category	Description
I	Disorders for which apheresis is accepted as first-line therapy, either as a primary standalone treatment or in conjunction with other modes of treatment.
II	Disorders for which apheresis is accepted as second-line therapy, either as a standalone treatment or in conjunction with other modes of treatment.
III	Optimum role of apheresis therapy is not established. Decision making should be individualized.
IV	Disorders for which published evidence demonstrates or suggests apheresis to be ineffective or harmful. Institutional review board (IRB) approval is desirable if apheresis is undertaken in these circumstances.

Data from Padmanabhan A, Connelly-Smith L, Aqui N, et al.: Guidelines on the use of therapeutic apheresis in clinical practice: evidence-based approach from the Apheresis Applications Committee of the American Society for Apheresis. The Eighth Special Issue, *J Clin Apheresis* 34:171–354, 2019.
ASFA, American Society for Apheresis.

TABLE 38.9
ASFA Recommendation Grades

Recommendation Grade	Description
1A	Strong recommendation with high-quality evidence. Can apply to most patients in most circumstances without reservation.
1B	Strong recommendation with moderate-quality evidence. Can apply to most patients in most circumstances without reservation.
1C	Strong recommendation with low-quality or very-low-quality evidence. May change when higher-quality evidence becomes available.
2A	Weak recommendation with high-quality evidence. Best action may differ depending on circumstances or patient or societal values.
2B	Weak recommendation with moderate-quality evidence. Best action may differ depending on circumstances or patient or societal values.
2C	Weak recommendation with low-quality or very-low-quality evidence. Other alternatives may be equally reasonable.

Data from Padmanabhan A, Connelly-Smith L, Aqui N, et al.: Guidelines on the use of therapeutic apheresis in clinical practice: evidence-based approach from the Apheresis Applications Committee of the American Society for Apheresis. The Eighth Special Issue, *J Clin Apheresis* 34:171–354, 2019.
ASFA, American Society for Apheresis.

TABLE 38.10

Diseases Treated by Hemapheresis

Disorder	Hemapheresis Procedure	ASFA Category	ASFA Recommendation Grade
ABO-incompatible stem cell transplant			
Major (HPC)-M (marrow)	Therapeutic plasma exchange (TPE)	II	1B
Major HPC-A (apheresis)	TPE	II	2B
Minor HPC-A	Red cell exchange (RCE)	III	2C
Ma0jor or minor with pure red cell aplasia	TPE	III	2C
Acute disseminated encephalomyelitis (ADEM)	TPE	II	2C
Acute inflammatory demyelinating polyneuropathy (Guillain-Barré syndrome)	TPE	I	1A
	Immunoadsorption (IA)	I	1B
Acute liver failure	TPE	III	2B
	TPE-High-volume	I	1A
Age-related macular degeneration (AMD); dry AMD	Double-filtration plasmapheresis (DFPP)	II	2B
Amyloidosis	TPE	IV	2C
Amyotrophic lateral sclerosis (ALS)	TPE	IV	1C
Antineutrophil cytoplasmic antibody (ANCA)-associated rapidly progressive glomerulonephritis (Wegener granulomatosis)			
Dialysis independent	TPE	III	2C
Diffuse alveolar hemorrhage	TPE	I	1C
Dialysis dependent	TPE	I	1A
Anti–basement membrane antibody disease (Goodpasture syndrome)			
Dialysis independent	TPE	I	1B
Diffuse alveolar hemorrhage	TPE	I	1C
Dialysis dependent	TPE	III	2B
Atopic dermatitis, recalcitrant	Extracorporeal photopheresis (ECP)	III	2A
	IA	III	2C
	TPE/DFPP	III	2C
Autoimmune hemolytic anemia			
Warm autoimmune hemolytic anemia	TPE	III	2C
Cold agglutinin disease	TPE	II	2C
Babesiosis, severe	RCE	II	2C
Burn shock resuscitation	TPE	III	2B
Catastrophic antiphospholipid antibody syndrome (CAPS)	TPE	I	2C
Chronic focal encephalitis (Rasmussen encephalitis)	TPE	III	2C
Chronic inflammatory demyelinating polyneuropathy (CIDP)	TPE	I	1B
Coagulation factor inhibitors	TPE	III	2C
Cryoglobulinemia			
Symptomatic/severe	TPE	II	2A
Symptomatic/severe	IA	II	2B
Cutaneous T-cell lymphoma			
Erythrodermic	ECP	I	1B
Nonerythrodermic	ECP	III	2C
Dilated cardiomyopathy (New York Heart Association Functional Class II–IV)	TPE	III	2C
	IA	II	1B
Erythropoietic protoporphyria, liver disease	TPE	III	2C
	RCE	III	2C
Familial hypercholesterolemia			
Homozygotes	Lipid apheresis (LA)	I	1A
Heterozygotes	LA	II	1A
Homozygotes/heterozygotes with small blood volume	TPE	II	1B
Focal segmental glomerulosclerosis			
Recurrent in transplanted kidney	TPE/IA	I	1B
Steroid resistant in native kidney	TPE	III	2C
Recurrent in transplanted kidney/steroid resistant in native kidney	LA	II	2C
Graft-versus-host disease			
Chronic	ECP	II	1B
Acute	ECP	II	1C
Heart transplant			
Prophylaxis of acute cellular rejection (ACR)	ECP	II	2A
Treatment of ACR/recurrent rejection	ECP	II	1B

Continued

TABLE 38.10

Diseases Treated by Hemapheresis—cont'd

Disorder	Hemapheresis Procedure	ASFA Category	ASFA Recommendation Grade
Desensitization, donor-specific human leukocyte antigen (HLA) antibodies	TPE	II	1C
Treatment of antibody-mediated rejection (AMR)	TPE	III	2C
Hemolytic-uremic syndrome (HUS)			
Typical HUS (infection-associated)	See Thrombotic microangiopathy, infection associated		
Atypical HUS	See Thrombotic microangiopathy, complement mediated		
Hemolysis, elevated liver enzymes, and low platelets syndrome (HELLP Syndrome)			
Postpartum	TPE	III	2C
Antepartum	TPE	IV	2C
Hemophagocytic lymphohistiocytosis (HLH), Hemophagocytic syndrome, Macrophage activation syndrome	TPE	III	2C
Heparin-induced thrombocytopenia and thrombosis (HIT/HITT)			
Precardiac bypass	TPE	III	2C
Thrombosis	TPE	III	2C
Hereditary hemochromatosis	Erythrocytapheresis	I	1B
Henoch-Schönlein Purpura (HSP)			
Crescentic	TPE	III	2C
Severe extrarenal disease	TPE	III	2C
Hyperleukocytosis			
Symptomatic	Leukocytapheresis	II	2B
Prophylaxis	Leukocytapheresis	III	2C
Hypertriglyceridemic pancreatitis			
Severe	TPE	III	1C
Prevention of relapse	TPE	III	2C
Hyperviscosity in monoclonal gammopathy			
Symptomatic	TPE	I	1B
Prophylaxis for rituximab	TPE	I	1C
Immunoglobulin (Ig) A nephropathy			
Crescentic	TPE	III	2B
Chronic progressive	TPE	III	2C
Immune thrombocytopenia (ITP)	TPE/IA	III	2C
Inclusion-body myositis	TPE	IV	2C
	Leukocytapheresis	IV	2C
Inflammatory bowel disease	Adsorptive cytapheresis (AC)	III	1B
	ECP	III	2C
Lambert-Eaton myasthenic syndrome	TPE	II	2C
Liver transplant, ABO incompatible			
Desensitization, living donor	TPE	I	1C
Desensitization, deceased donor	TPE	III	2C
Desensitization	ECP	III	2C
Humoral rejection	TPE	III	2C
Acute rejection/immunosuppression withdrawal	ECP	III	2B
Lung allograft rejection			
Bronchiolitis obliterans syndrome	ECP	II	1C
Antibody-mediated rejection/desensitization	TPE	III	2C
Malaria	RCE	III	2B
Multiple sclerosis			
Acute attack/relapse	TPE	II	1A
	IA	II	1B
Chronic progressive	IA	III	2B
	TPE	III	2B
Myasthenia gravis			
Acute treatment	TPE/IA	I	1B
Long-term treatment	TPE/IA	II	2B
Myeloma cast nephropathy	TPE	II	2B
Nephrogenic systemic fibrosis	TPE/ECP	III	2C
Neuromyelitis optica			
Acute	TPE	II	1B
	IA	II	1C
Maintenance	TPE	III	2C

TABLE 38.10
Diseases Treated by Hemapheresis—cont'd

Disorder	Hemapheresis Procedure	ASFA Category	ASFA Recommendation Grade
N-methyl-D-aspartate receptor (NMDAR) antibody encephalitis	TPE/IA	I	1C
Overdose and poisoning			
Mushroom poisoning	TPE	II	2C
Envenomation	TPE	III	2C
Drug overdose/poisoning	TPE	III	2C
Paraneoplastic neurologic syndromes	TPE/IA	III	2C
Paraproteinemic polyneuropathies			
IgG/IgA/IgM	TPE	I	1B
Anti–myelin-associated glycoprotein (MAG) neuropathy	TPE	III	1C
Multiple myeloma	TPE	III	2C
Multifocal motor neuropathy	TPE	IV	1C
Pediatric autoimmune neuropsychiatric disorders associated with streptococcal infections (PANDAS)	TPE	II	1B
Pemphigus vulgaris	TPE	III	2B
	ECP/IA	III	2C
Peripheral vascular disease	LA	II	1B
Phytanic acid storage disease (Refsum disease)	TPE/LA	II	2C
POEMS syndrome	TPE	IV	1C
Polycythemia vera and erythrocytosis			
Polycythemia vera	Erythrocytapheresis	I	1B
Secondary erythrocytosis	Erythrocytapheresis	III	1C
Polymyositis/dermatomyositis	TPE	IV	2A
	Lymphocytapheresis	IV	2A
Posttransfusion purpura (PTP)	TPE	III	2C
Progressive multifocal leukoencephalopathy (PML) associated with natalizumab	TPE	III	1C
Pruritus due to hepatobiliary diseases, treatment resistant	TPE	III	1C
Psoriasis, disseminated pustular	TPE	IV	2C
	AC	III	2C
	ECP	III	2B
Red cell alloimmunization prevention and treatment			
Pregnancy less than 20 weeks	TPE	III	2C
Rh-positive red cell exposure	RCE	III	2C
Renal transplant			
ABO compatible			
Antibody-mediated rejection	TPE/IA	I	1B
Desensitization, living donor with donor-specific human leukocyte antigen (HLA)	TPE/IA	I	1B
Desensitization, deceased donor with high panel reactive alloantibody (PRA)	TPE/IA	III	2C
ABO incompatible			
Desensitization, living donor	TPE/IA	I	1B
Humoral rejection	TPE/IA	II	1B
Rheumatoid arthritis	TPE	IV	1B
Scleroderma (progressive systemic sclerosis)	TPE	III	2C
	ECP	III	2A
Schizophrenia	TPE	IV	1A
Sepsis with multiorgan failure	TPE	III	2B
Sickle cell disease			
Acute			
Stroke	RCE	I	1C
Chest syndrome, severe	RCE	II	1C
Other complications	RCE	III	2C
Nonacute			
Prophylaxis for stroke	RCE	I	1A
Pregnancy	RCE	II	2B
Recurrent vaso-occlusive pain crisis	RCE	II	2B
Preoperative management	RCE	III	2A

Continued

TABLE 38.10
Diseases Treated by Hemapheresis—cont'd

Disorder	Hemapheresis Procedure	ASFA Category	ASFA Recommendation Grade
Steroid-responsive encephalopathy associated with autoimmune thyroiditis (Hashimoto encephalopathy)	TPE	II	2C
Stiff-person syndrome	TPE	III	2C
Sudden sensorineural hearing loss	LA/Rheopheresis/TPE	III	2A
Sydenham chorea, severe	TPE	III	2B
Systemic lupus erythematosus (SLE)			
Severe (e.g., cerebritis, diffuse alveolar hemorrhage)	TPE	II	2C
Nephritis	TPE	IV	1B
Thrombocytosis			
Symptomatic	Thrombocytapheresis	II	2C
Prophylactic or secondary	Thrombocytapheresis	III	2C
Thrombotic microangiopathy, coagulation mediated (THBD, DGKE, and PLG mutations)	TPE	III	2C
Thrombotic microangiopathy, complement mediated (formerly atypical hemolytic uremic syndrome)			
Factor H autoantibody	TPE	I	2C
Complement factor gene mutations	TPE	III	2C
Thrombotic microangiopathy, drug associated			
Gemcitabine	TPE	IV	2C
Quinine	TPE	IV	2C
Ticlopidine	TPE	I	1B
Clopidogrel	TPE	III	2B
Thrombotic microangiopathy, infection associated			
STEC-HUS, severe (Shiga toxin)	TPE	III	2C
pHUS (*Streptococcus pneumoniae*)	TPE	III	2C
Thrombotic microangiopathy, hematopoietic progenitor cell transplant associated, refractory	TPE	III	2C
Thrombotic thrombocytopenic purpura (TTP)	TPE	I	1A
Thyroid storm	TPE	II	2C
Toxic epidermal necrolysis (TEN), refractory	TPE	III	2B
Vasculitis, other			
Hepatitis B polyarteritis nodosa	TPE	II	2C
Idiopathic polyarteritis nodosa	TPE	IV	1B
Behcet disease	AC	II	1C
	TPE	III	2C
Voltage-gated potassium channel (VGKC) antibody–related diseases	TPE/IA	II	1B
Wilson disease with fulminant hepatic failure and hemolysis	TPE	I	1C

Data from Padmanabhan A, Connelly-Smith L, Aqui N, et al.: Guidelines on the use of therapeutic apheresis in clinical practice: evidence-based approach from the Apheresis Applications Committee of the American Society for Apheresis. The Eighth Special Issue, *J Clin Apheresis* 34:171–354, 2019.
ASFA, American Society for Apheresis. See Table 38.8 for explanation of ASFA categories and Table 38.9 for explanation of recommended grades.

Decision Making and the American Society for Apheresis Guidelines" (Winters & Nord, 2017) for a discussion of clinical decision-making in such circumstances.

THERAPEUTIC CYTAPHERESIS

Therapeutic Plateletapheresis

Thrombocytosis

Thrombocytosis is defined as an increase in the number of platelets present in the blood. This can range from mild increases to increases resulting in platelet counts greater than 1,000,000/μL. Thrombocytosis is most often acquired and can be divided into either primary (essential thrombocytosis [ET]) or secondary causes (Table 38.11). Secondary thrombocytosis, also known as *reactive thrombocytosis* (*RT*), accounts for more than 85% of thrombocytosis, even when platelet values are extremely elevated (Sulai & Tefferi, 2012). Correct classification of thrombocytosis is important because thromboembolic complications are rare in RT (unless provoked by underlying malignancy or atherosclerosis) but are more common in ET (Sulai & Tefferi, 2012). In one study, thromboembolic complications occurred in 4% of patients with RT but 56% in ET (Buss et al., 1994).

Both thrombotic and hemorrhagic events may complicate thrombocytosis, with thrombotic events predominating (Sulai & Tefferi, 2012). Hemorrhagic complications include epistaxis, gingival bleeding, and mild gastrointestinal or genitourinary hemorrhage. Arterial thrombotic events are more common than venous events and include both microvascular thrombosis, such as erythromelalgia, and macrovascular thrombosis, such as myocardial infarction. Particularly catastrophic outcomes are seen in patients with occlusion of large abdominal vessels and cerebral sinus thrombosis. Risk factors found to be associated with thrombotic and hemorrhagic complications in primary thrombocytosis are given in Box 38.5.

Because of concern over the occurrence of these complications, studies have focused on efforts to reduce elevated platelet counts. Treatments include medications and therapeutic thrombocytapheresis. The decision to treat and the level of treatment is based on the patient's risk stratification for thrombohemorrhagic events (Tefferi & Barburi, 2017). Low-risk patients may simply be monitored or treated with daily aspirin, while higher-risk patients may be treated with cytoreductive

TABLE 38.11

Diseases Associated with Thrombocytosis

Primary	Essential thrombocythemia
	Agnogenic myeloid metaplasia
	Polycythemia vera
	Chronic myelogenous leukemia
Secondary (reactive)	Splenectomy
	Acute hemorrhage
	Iron deficiency
	Chronic inflammatory diseases
	Solid malignancies
	Rebound after myelosuppression

Reprinted from Buss DH, Cashell AW, O'Connor ML, et al.: Occurrence, etiology, and clinical significance of extreme thrombocytosis: a study of 280 cases, *Am J Med* 96:247–253, 1994, with permission from Excerpta Medica, Inc.

BOX 38.5

Factors Associated with Complications in Primary Thrombocytosis

Thrombosis

Increasing age
Previous thrombotic event
Longer duration of thrombocythemia

Hemorrhage

Platelet count >2,000,000/μL
NSAID ingestion

NSAID, Nonsteroidal anti-inflammatory drug.
Data from Cortelazzo S, Viero P, Finazzi G, et al.: Incidence and risk factors for thrombotic complications in a historical cohort of 100 patients with essential thrombocythemia, *J Clin Oncol* 8:556–562, 1990; Tefferi A, Hoagland HC: Issues in the diagnosis and management of essential thrombocythemia, *Mayo Clin Proc* 69:651–655, 1994.

agents, such as hydroxyurea. Therapeutic thrombocytapheresis is reserved as a temporary treatment for patients symptomatic from their thrombocytosis.

Therapeutic Thrombocytapheresis Indications

The role of hemapheresis in the treatment of thrombocytosis is to intervene when patients become symptomatic and to stabilize their condition until medical management reduces the platelet count. The platelet count itself does not correlate with the risk for thrombosis, even when the count is >1,000,000/μL (Schafer, 1984, 1996; Buss et al., 1994; Tefferi & Hoagland, 1994). Thrombocytapheresis can also be used in the preoperative setting to possibly prevent bleeding and in the treatment of pregnant women (Isbister, 1997). The benefit of thrombocytapheresis in this latter patient group is again uncertain, as there is a lack of correlation between platelet count and pregnancy outcome (Schafer, 1996). It must be stressed that the effects of thrombocytapheresis in thrombocytosis are temporary, lasting hours to days, and medical management must be instituted at the same time.

Thrombocytapheresis procedures in this setting can be performed on any instrument that can collect platelets from donors. Typically, the goal of the procedure is to process 1.0 to 1.5 blood volumes (Baron et al., 1993) or to process for a defined length of time, such as 3 hours (Burgstaler & Pineda, 1994). In a study comparing the ability of the Spectra Optia apheresis system to reduce platelet counts, DiGuardo et al. found that processing for 3 hours resulted in a median reduction in platelet count of 66.8% (DiGuardo et al., 2019). Just as there is no defined level at which thrombosis occurs, no target for platelet reduction has been defined. The patient's symptoms should be treated, with improvement/resolution being the desired endpoint.

Thrombocytapheresis for symptomatic thrombocytosis is a category II indication with a 2C recommendation grade and prophylactic thrombocytapheresis for asymptomatic thrombocytosis is a category III indication with a 2C recommendation grade, according to the ASFA (Padmanabhan et al., 2019).

Therapeutic Leukocytapheresis

Hyperleukocytosis

Hyperleukocytosis is an extreme elevation in white blood cell count. The causes of such elevations include malignant and nonmalignant disease, with the former resulting in the highest counts. This can produce a number of symptoms, including central nervous system leukostasis, characterized by neurologic deficits, and pulmonary leukostasis, characterized by poor oxygenation and chest pain (Isbister, 1997). Traditionally, because white blood cells are more rigid than red blood cells, hyperleukocytosis was thought to result in increased viscosity with changes in blood flow within the microvasculature (Isbister, 1997). Occlusion of the microvasculature would result, in turn, in leukostasis and ischemia. However, this may not represent the entire picture. The white blood cell count does not necessarily correlate with the onset of symptoms. More recent evidence suggests that the interactions of adhesion molecules expressed on the leukemic blasts and endothelial cells may also contribute to vascular occlusion and endothelial injury (Liesveld, 1997; Porcu et al., 2000; Stucki et al., 2001).

In addition to vascular occlusive symptoms of hyperleukocytosis, another potential problem resulting from markedly elevated white blood cell count is tumor lysis syndrome (Isbister, 1997). This most often occurs during the patient's initial chemotherapy and results from the release of massive quantities of intracellular tumor contents, producing damage to the kidneys and/or initiating disseminated intravascular coagulation.

Higher mortality rates occur during the first week of therapy among patients with white blood cell counts greater than 100,000/μL. These deaths were associated with a significantly greater number of central nervous system (CNS) hemorrhages than in those with white blood cell counts <50,000/μL (Dutcher et al., 1987). Similarly, the presence of pulmonary leukostasis is also associated with early mortality (Lester et al., 1985). In one study, average survival of patients with pulmonary leukostasis was 0.2 months versus 15.4 months in those with CNS leukostasis (Lester et al., 1985). As in thrombocytosis, the definitive treatment of these elevated white blood cell counts is to treat the underlying disease, in this case leukemia.

Therapeutic Leukocytapheresis Indications

As in therapeutic thrombocytapheresis, the role of leukocytapheresis in hyperleukocytosis is to decrease the white blood cell count to relieve symptoms and/or prevent tumor lysis syndrome. As with thrombocytapheresis, the indication for treating a patient is the presence of symptoms indicating leukostasis. Additionally, leukocytapheresis can be used to treat pregnant women to prolong pregnancy until the child can be delivered and the mother can be started on chemotherapy. Again, hemapheresis represents an adjunct to therapy and not a primary treatment modality. The definitive therapy is chemotherapy that should be started at the same time or shortly after hemapheresis is initiated, since the reduction in white blood cell counts with leukocytapheresis is temporary. Although hemapheresis can reverse or lessen leukostasis symptoms in some patients, no correlation has been found between the degree of leukoreduction, as an absolute value or as a percentage, and overall survival (Porcu et al., 1997). Overall, multiple studies summarized in meta-analysis show that leukocytapheresis does not improve overall mortality (Oberoi et al., 2014) (Choi et al., 2018). Limited observational studies have suggested that leukocytapheresis may improve 2- to 3-week mortality rates after diagnosis but does not appear to affect the long-term mortality or overall survival rates of these patients (Porcu et al., 1997; Thiébaut et al., 2000; Giles et al., 2001; Tan et al., 2005). All of the studies performed on the role of the leukocytapheresis are retrospective analysis. As such, they represent low-quality evidence; therefore, the role of leukocytapheresis in the treatment of hyperleukocytosis is unclear.

Leukocytapheresis procedures share similarities with granulocyte collections, as previously described. HES can be used to enhance the separation of cellular components during centrifugation, resulting in more efficient white blood cell removal. This is especially important when the cells are more mature granulocytes, as seen in chronic-phase chronic myelogenous leukemia (CML). The total blood volume processed is usually 8 to 10 L or two blood volumes (McLeod et al., 1993). With this strategy, reductions in white blood cell count of 50% to 85% have been reported (Burgstaler & Pineda, 1994). As in therapeutic thrombocytapheresis, no goal has been defined for the reduction in white blood cells, and improvement/resolution of the patient's symptoms is the endpoint. Symptomatic hyperleukocytosis is a category II indication with a 2B recommendation grade for leukocytapheresis. Prophylactic leukocytapheresis for asymptomatic hyperleukocytosis is a category III indication with a 2C recommendation grade according to the ASFA (Padmanabhan et al., 2019).

Red Cell Exchange

Red cell exchange (RCE), or therapeutic erythrocytapheresis, is a form of cytapheresis that removes the patient's red blood cells and replaces them with allogeneic red blood cells. This form of hemapheresis has been used occasionally to treat hyperparasitemia in malaria and other parasitic infections of red blood cells, such as babesiosis (Powell & Grima, 2002). It is most commonly used in the treatment of sickle cell disease (SCD).

Sickle Cell Anemia

SCD is an inherited autosomal-recessive disorder present in 1 in 200 to 500 African American newborns (Wayne et al., 1993). It is also seen in people from sub-Saharan and Western Africa, Arab countries, the Mediterranean basin, and India (Davies & Roberts-Harewood, 1997). SCD results from a mutation that substitutes a valine for a glutamic acid at position six of the β-globin chain of hemoglobin, producing hemoglobin S (Davies & Roberts-Harewood, 1997). This change decreases the solubility of hemoglobin when deoxygenated, causing crystal formation that alters the shape of the red blood cells and damages their membranes. Repeated episodes lead to irreversible sickling of the cells. Even in the absence of sickling, the red blood cells in sickle cell anemia are abnormally "sticky." The combination of this "stickiness" and sickling leads to occlusion of small vessels, endothelial damage, and thrombosis (Wayne et al., 1993; Davies & Roberts-Harewood, 1997).

SCD is characterized by chronic hemolytic anemia and episodes of acute sickling crises. Crises are most often due to vascular occlusion and infarction and include crises of pain, aplasia, splenic sequestration, hemolysis, cerebrovascular accidents, acute chest pain syndrome, and priapism. They are treated by correcting factors that enhance sickling: dehydration, hypoxia, and acidosis. This is done through hydration, alkalinization, and the administration of supplemental oxygen (Wayne et al., 1993; Davies & Roberts-Harewood, 1997). In addition, painful crises are treated by the administration of analgesics and sometimes by red blood cell transfusion.

Red cell transfusion in SCD can be divided into three categories: acute simple transfusion, chronic simple transfusion, and RCE transfusion. Acute simple transfusion consists of the transfusion of red blood cells to increase oxygen-carrying capacity and is indicated for the treatment of symptomatic anemia, splenic sequestration crisis, aplastic crisis, blood loss, accelerated hemolysis, and preoperative preparation (Wayne et al., 1993). Chronic simple transfusion consists of regular transfusions of red blood cells in an attempt to suppress endogenous red cell production with the goal of keeping the percentage of red cells containing hemoglobin S below 30%. This form of therapy is indicated for cerebrovascular disease and debilitating vaso-occlusive symptoms. It can also be used to treat SCD complicated by pulmonary disease, cardiac disease, or high-risk pregnancy, and for preoperative preparation (Wayne et al., 1993).

RCE in SCD is used to remove hemoglobin S–containing red blood cells while replacing them with hemoglobin A–containing red blood cells. The goal of RCE is to leave the patient with a hematocrit of approximately 30% and a "sicklecrit"—the percentage of cells containing hemoglobin S—of less than 30% (Wayne et al., 1993; Davies & Roberts-Harewood, 1997). To do this, the fraction of red cells remaining (FCR) must be calculated based on the patient's current hemoglobin S percentage and the desired hemoglobin S percentage. This can be calculated by Equation 38.9. If the patient's hematocrit is to be increased by the procedure, then the adjusted FCR must be calculated according to Equation 38.10 (COBE BCT, 1997). It should be noted that increasing the hematocrit too much can result in decreased oxygen delivery owing to increased viscosity. This results from the fact that the sickle cells and endothelium of these patients are "stickier" than normal.

$$\text{Desired FCR\%} = (\text{Desired hemoglobin S}/\text{Current hemoglobin S}) \times 100 \quad \text{(Eq. 38.9)}$$

$$\text{Adjusted FCR\%} = \text{Desired FCR\%} \times (\text{Current hematocrit}/\text{Desired hematocrit}) \times 100 \quad \text{(Eq. 38.10)}$$

These values are then entered into the hemapheresis instrument along with other values to determine the volume of red blood cells necessary to perform the procedure. The benefits of RCE over the other strategies of transfusion are given in Box 38.6.

In the sickle cell disease patients with procedure hematocrit of 26 or higher, one can consider modified RCE procedure where isovolemic hemodilution precedes the procedure (Sarode et al., 2011). Use of isovolemic hemodilution allows for effective RCE with 11% fewer RBC units. This approach is especially valuable in the patients undergoing chronic RCE with goals of prevention of SCD complications.

Acute chest syndrome is a crisis characterized by respiratory symptoms, chest and abdominal pain, infiltrates on chest radiograph, and an abnormal chest examination. Its etiology is multifactorial and includes underlying infection. The result is hypoxia leading to occlusion of small vessels in the lung and possible thrombosis of the pulmonary arteries (Davies & Roberts-Harewood, 1997). It occurs in 20% to 50% of sickle cell patients and has a mortality rate of 2% to 14%, with a higher mortality rate in adults. Repeated episodes may progress to chronic pulmonary disease (Wayne et al., 1993). Treatment includes hydration, supplemental oxygen, and antibiotics. RCE is used to remove hemoglobin S–containing cells and has been associated with improvement (Wayne et al., 1993).

Priapism is a painful, sustained erection that results from occlusion of vessels in the corpus cavernosum by sickled cells. It is associated with dehydration and acidosis and is treated with supplemental oxygen, hydration, and analgesics (Wayne et al., 1993). It is seen in 40% of adult males and 6% of preadolescent males with SCD. If prolonged (over 6 hours), priapism is referred to as fulminant priapism and may require surgical intervention or RCE. A significant percentage of patients will suffer from impotence if not treated (Davies & Roberts-Harewood, 1997). Although RCE has been reported as effective in treating priapism, it is not without risks. A syndrome of neurologic events called ASPEN syndrome (association of sickle cell disease, priapism, exchange transfusion, and neurologic events) has been reported to occur in some patients treated with RCE. It consists of neurologic events ranging from headache and seizure activity to obtundation requiring ventilator support. The syndrome is thought to be due to decreased cerebral blood flow from the abrupt elevation in hematocrit and to the release of vasoactive substances from the penile detumescence. Aggressive treatment has been associated with complete neurologic recovery (Siegel et al., 1993). Patients suffering from priapism undergoing RCE should be monitored for symptoms of ASPEN syndrome.

Stroke is a common and devastating symptom of SCD, which occurs in 11% of patients by 20 years of age (Adams et al., 1998). Two studies have addressed the role of chronic red cell transfusion therapy to prevent first stroke in children with SCD, commonly referred to as the STOP trial and the STOP II trial (Adams et al., 1998; Adams & Brambilla, 2005). In the STOP trial, 130 children defined to be at high risk for stroke through transcranial Doppler screening were randomized to receive either standard care or chronic red cell transfusion every 3 to 4 weeks (simple transfusion or RCE). There were 11 stroke events in the standard care group versus only 1 stroke event in the transfusion group (Adams et al., 1998). Due to the evidence that transfusion greatly decreases the risk for first stroke in children, the STOP trial was halted prematurely.

The STOP II trial then investigated how long SCD patients should undergo chronic transfusion therapy. Children with SCD who were at high risk for stroke and had already received red cell transfusions for 30 months or longer with normal Doppler results were randomized to either continue or stop transfusion. The STOP II trial was also halted early given the development of high-risk Doppler results in 14 patients and stroke in 2 patients who stopped transfusions early, compared with no high-risk Doppler results or stroke in the patients who remained on chronic transfusion therapy. The mean number of months between last transfusion and either high-risk Doppler results or stroke was 4.6 months (Adams & Brambilla, 2005). In practice, the risks of chronic transfusion, including iron overload, alloimmunization, and infectious disease transmission must be weighed against the risk for stroke in each SCD patient. In all SCD patients undergoing chronic transfusions, appropriate management may alleviate some of the risks associated with transfusion—for example, decreasing alloimmunization by matching for ABO, C, D, E, and Kell antigens. Additional crises and disorders in SCD patients for which RCE is indicated include cerebrovascular accident, retinal artery vaso-occlusion, hepatic failure, and septic shock. RCE has also been used to decrease the percentage of hemoglobin S at the initiation of chronic simple transfusion therapy, to prevent sickling due to contrast dye during cerebral angiograms, and in preparation for surgery (Wayne et al., 1993). It should be noted that a study has shown

BOX 38.6

Benefits of Red Blood Cell Exchange by Apheresis Compared With Simple or Chronic Transfusion

- Decreased amount of hemoglobin S without increasing hematocrit and, therefore, viscosity
- Use of fewer units of red blood cells to achieve the same percentage of hemoglobin S
- Decreased contribution to iron overload in chronically transfused patients

Reprinted from McLeod BC: Introduction to the third special issue: Clinical applications of therapeutic apheresis, *J Clin Apheresis* 15:1–5, 2000, with permission of Wiley-Liss, Inc., a subsidiary of John Wiley & Sons, Inc.

BOX 38.7

Characteristics Indicating Best Responders to Extracorporeal Photopheresis Among CTCL Patients

Erythrodermic skin stage
WBC count <15,000/mm^3
Disease of short duration
Normal percentage of CD8+ T cells
Immunocompetent patient
Absence of bulky lymph nodes or visceral disease
Presence of Sézary cells in the circulation

CTCL, Cutaneous T-cell lymphoma; *WBC,* white blood cell.
Data from Zic JA: The treatment of cutaneous T-cell lymphoma with photopheresis, *Dermatol Ther* 16:337–346, 2003.

no benefit of RCE versus a conservative transfusion regimen designed to increase hemoglobin to 10 g/dL in preventing complications of surgery (Vichinsky et al., 1995).

Acute stroke in SCD is a category I indication with a 1C recommendation grade for RCE. Acute chest syndrome is a category II indication with 1C recommendation grade for RCE. Other acute complications of SCD are categorized as category III indications for RCE with 2C recommendation. Nonacute indications for RCE in SCD patients according to the ASFA include stroke prophylaxis (category I indication, 1A recommendation grade), vaso-occlusive pain crisis (category II indication, 2B recommendation grade), and, finally, preoperative management (category III indication, 2A recommendation grade) (Padmanabhan et al., 2019).

Other indications for RCE, which are not specific to patients with SCD, include treatment of severe malaria or babesiosis. Severe malaria is a category III indication with a 2B recommendation grade for RCE. Severe babesiosis is a category II indication with a 2C recommendation grade for RCE (Padmanabhan et al., 2019).

Extracorporeal Photopheresis

Extracorporeal photopheresis, also called *extracorporeal photochemotherapy* (*ECP*) or *photopheresis*, is a form of leukocytapheresis. In this procedure, a small percentage of a patient's white blood cells are collected by hemapheresis. These cells are then treated by incubation with a psoralen compound and are exposed to ultraviolet A (UVA) irradiation within the instrument. The treated cells are then reinfused into the patient (Zic et al., 1999). This appears to result in a disease-dependent immunomodulatory effect that may stimulate or suppress an immune response. Currently, this therapy is approved by the FDA only for the treatment of cutaneous T-cell lymphoma (CTCL). In 2006, the Centers for Medicare Services (CMS) expanded their approval of ECP to include not only CTCL but also chronic GVHD and acute cardiac allograft rejection. In 2012, the CMS further expanded its approval to include the treatment of chronic rejection characterized by bronchiolitis obliterans syndrome in patients with lung transplantation. For coverage, however, the CMS requires that the treated patient be enrolled in a research protocol fulfilling certain criteria.

Extracorporeal Photopheresis Indications

Cutaneous T-Cell Lymphoma. The first disease treated by ECP was CTCL, a skin-based T-cell lymphoma characterized by a long premalignant phase (4–10 years) of eczematous skin lesions. The disease progresses through a series of phases characterized by increasing skin involvement until the development of the tumor phase, characterized by cutaneous masses. CTCL may then progress to a leukemic phase known as *Sézary syndrome*, in which malignant clonal CD4+ T cells are found circulating in the blood. Median survival depends on the stage of the disease at diagnosis; 10-year survival ranges from 85% for the initial plaque phase to 20% for the tumor stage (Zic et al., 1999).

In 1987, Edelson reported responses in 64% of 37 CTCL patients treated with ECP (Edelson et al., 1987). Combined analysis of more than 400 patients reported in the literature has found an overall response rate of CTCL to ECP of 55.7%, with 17.6% of patients having a complete response. Response rates vary from 64% for stage IB patients (generalized patches and plaques) to 27.3% for stage IVB patients (visceral involvement) (Zic, 2003). Factors predictive of response to ECP are given in Box 38.7. The median time until clearing of skin lesions in such patients is 11 months; patients who show an early response (clearing in 6–8 months) maintain their response (Zic et al., 1999). ECP has also been associated with longer survival from time of diagnosis (longer than 60 months among ECP-treated patients vs. 31 months for patients receiving chemotherapy) (Christensen & Heald, 1991).

BOX 38.8

Factors Associated With the Development of Chronic Graft-Versus-Host Disease

Increased donor age
Increased recipient age
Human leukocyte antigen disparity
Unrelated donor
Prior acute graft-versus-host disease
Alloimmunized female donor

Data from Foss FM, Gorgun G, Miller KB: Extracorporeal photopheresis in chronic graft-versus-host disease, *Bone Marrow Transplant* 29:719–725, 2002.

The mechanism of action of ECP in CTCL has not been completely elucidated. ECP is known to induce a CD8+ T-cell response to expanded pathologic T-cell clones within the patient (Zic, 2003). It is thought that upon exposure to UVA, 8-methoxypsoralen (8-MOP) exogenously added to the collected buffy coat reacts with cellular constituents, irreversibly binding to DNA, proteins, and lipids. This induces an increase in the number of HLA class I molecules present on the exposed cell and apoptosis of the targeted lymphocytes. It is interesting to note that apoptosis occurs in exposed lymphocytes, including malignant T cells, but not monocytes. Monocytes, as a result of their exposure to subphysiologic temperatures and contact with walls of the tubing during collection and photoactivation, undergo selective gene activation and transcription, allowing them to differentiate into immature dendritic cells (DCs). Newer evidence suggests that platelets are the driving force behind the monocyte-to-DC maturation pathway (Edelson, 2014). First, plasma fibrinogen coats the ECP plastic flow chamber, allowing resting platelets to adhere to the fibrinogen with their αIIbβ3 receptors. The adherent platelets are then activated to express P-selectin, which serves as a receptor for monocyte binding via ligand PSGL-1. Activated monocytes can then bind additional platelet ligands and are induced to mature into DCs. These DCs phagocytose the apoptotic malignant T cells and can present the tumor antigens from these cells within their HLA class I molecules. Upon reinfusion of the UVA-exposed ECP product, these antigen-presenting cells can then activate cytotoxic T cells, resulting in an immune response to the abnormal T cell clones (Zic, 2003). This is associated with a shift in the patient's cytokine profile from that of a Th2 response to a Th1 response (Zic, 2003). The beneficial effects of the procedure do not result from direct cytotoxicity of 8-MOP and UVA on abnormal T cells or tumor cells, as only 10% to 15% of the lymphocyte pool is harvested, and less than 5% of CTCL cells are treated (Christensen & Heald, 1991).

Erythrodermic CTCL is a category I indication with a 1B recommendation grade for ECP according to the ASFA (Padmanabhan et al., 2019). Nonerythrodermic CTCL is a category III indication with a 2C recommendation grade for ECP (Padmanabhan et al., 2019).

Graft-Versus-Host Disease and Solid-Organ Rejection. Chronic graft-versus-host disease (cGVHD) occurs in 27% to 50% of matched related sibling donor transplants and in 42% to 72% of unrelated bone marrow or peripheral blood stem cell transplants (Foss et al., 2002). Factors associated with cGVHD are given in Box 38.8.

A number of studies have reported the use of ECP in cGVHD (Foss et al., 2002). In these studies, patients with cGVHD unresponsive to other therapies have shown improvement in skin, oral, and visceral (hepatic) lesions with the use of ECP. Treatment has been associated with normalization of CD4/CD8 ratios, decreased numbers of natural killer cells, earlier tapering of steroid doses, and maintenance of the response for a median of 12 months. No increase in infection rates or CMV activation was noted in the patients studied (Foss et al., 2002). Those patients who were more likely to respond were those who started therapy within 10 months of transplant.

As with CTCL, the mechanism behind ECP in cGVHD is unclear. It is remarkable that therapy associated with immune activation in one disease (CTCL) is associated with immune suppression in another (cGVHD). Platelet-induced monocyte-to-DC maturation (previously discussed in CTCL) may also be an essential component of ECP's effects in cGVHD. Edelson proposed that it is the level of maturity of DCs that determines whether ECP has an upregulatory or downregulatory effect on T-cell responses (Edelson, 2014). When monocytes are exposed to UVA-activated 8-MOP, exposure is not uniform; rather, it occurs in a Gaussian distribution. Those monocytes that receive higher exposures have truncated maturation and become tolerizing immunosuppressive immature DCs, while those monocytes that receive minimal exposure mature into long-living immunostimulatory DCs. Given that ECP's therapeutic effect

TABLE 38.12

Diseases in Which Extracorporeal Photopheresis Has Been Reported as Effective

Disease Category	Specific Example
Malignancy	Cutaneous T-cell lymphoma (CTCL)
Graft-versus-host disease (GVHD)	Mucocutaneous GVHD
	Hepatic GVHD
Organ rejection	Heart
	Kidney
	Lung
Autoimmune diseases	Systemic lupus erythematosus
	Rheumatoid arthritis
	Juvenile dermatomyositis
	Pemphigus vulgaris
	Epidermolysis bullosa acquisita
	Crohn disease
	Psoriasis
	Scleroderma
Infectious diseases	Chronic Lyme arthritis
	AIDS-related complex (ARC)
Other diseases	Severe atopic dermatitis
	Psoriasis
	Nephrogenic systemic fibrosis

Data from van Iperen HP, Beijersbergen van Henegouwen GM: Clinical and mechanistic aspects of photopheresis, *J Photochem Photobiol B* 39:99–109, 1997; Zic JA, Miller JL, Stricklin GP, et al.: The North American experience with photopheresis, *Ther Apher* 3:50–62, 1999; Mathur K, Morris S, Deighan C: Extracorporeal photopheresis improves nephrogenic fibrosing dermopathy/nephrogenic systemic fibrosis: Three case reports and review of literature, *J Clin Apher* 23:144–150, 2008; and Padmanabhan A, Connelly-Smith L, Aqui N, et al: Guidelines on the use of therapeutic apheresis in clinical practice: evidence-based approach from the Apheresis Applications Committee of the American Society for Apheresis. The Eighth Special Issue, *J Clin Apheresis* 34:171–354, 2019.

occurs much faster with GVHD and organ transplant rejection than with CTCL, the less mature immunosuppressive DCs might dominate early while the fully mature immunostimulatory DCs would dominate later. In cGVHD patients, ECP is also associated with a decrease in antigen recognition and processing by DCs, as well as decreased numbers of DCs. This, in turn, decreases CD8+ T-cell stimulation, with a shift in Th1 response to a Th2 response through inhibition of Th2 cytokine secretion (Foss et al., 2002). The result is decreased alloreactivity by T cells.

Similar to cGVHD, solid-organ rejection is a disorder of alloreactive T cells. ECP has similarly been used to treat rejection in heart, lung, kidney, and liver transplantation. In cardiac transplantation, the use of ECP has been reported to histologically reverse 89% of treated rejection episodes without side effects. Similar rates have been reported with other transplant types (Dall'Amico & Murer, 2002).

Chronic GVHD is a category II indication with a 1B recommendation grade. Acute GVHD is a category II indication with a 1C recommendation grade. Treatment of cellular cardiac allograft rejection is a category II indication with a 1B recommendation grade. Prophylaxis of cardiac allograft rejection is a category II indication with a 2A recommendation grade (Padmanabhan et al., 2019).

Other Diseases. Additional diseases that have been treated with ECP are listed in Table 38.12. Many, but not all, of these diseases have a common thread of T-cell alloreactivity or autoreactivity. Some of these diseases have been assigned categories and recommendation grades by the ASFA (see Table 38.10).

Extracorporeal Photopheresis Procedure

An important aspect of this procedure is the clean separation of whole blood into plasma and buffy coat. The product must allow the transmission of UVA light to photoactivate the 8-MOP. The presence of significant numbers of red blood cells within the leukocytapheresis product will reflect or absorb the UVA irradiation, resulting in failure to photoactivate the product. As a result, it is critical that the hematocrit of the leukocytapheresis product be less than 7% (Zic et al., 1999). Similarly, it is important that excess plasma not be present. Excess plasma will dilute the white blood cells, resulting in fewer passages of each cell through the photoactivation chamber (Zic et al., 1999).

TABLE 38.13

Mechanisms of Action of Therapeutic Plasma Exchange by Disease

Mechanism	Disease
Removal of pathologic antibodies	Multiple myeloma, Goodpasture syndrome, pretransplant desensitization, and so on
Replacement of deficient plasma components	TTP (ADAMTS13 in donor FFP)
Increased sensitivity of lymphocytes and plasma cells to chemotherapy	AIDP, systemic sclerosis, CNS demyelinating disease
Removal of immune complexes with enhanced monocyte/macrophage function	SLE
Removal of proinflammatory cytokines and adhesion molecules	MG, ANCA + vasculitis, TTP, therapy-resistant sepsis
Changes in lymphocyte numbers	AIDP, systemic sclerosis, SLE
Increased T regulatory cells and T suppressor activity	AIDP, CIDP, SLE
Correction of Th1/Th2 ratio favoring Th1 predominance	AIDP, SLE

Data from Reeves HM, Winters JL: The mechanisms of action of plasma exchange, *Br J Haematol* 164:342–351, 2014.
*ADAMTS13, **A** **d**isintegrin **a**nd **m**etalloprotease with eight **t**hrombo**s**pondin; AIDP,* acute inflammatory demyelinating polyneuropathy; *ANCA,* antineutrophil cytoplasmic antibody; *CIDP,* chronic inflammatory demyelinating polyneuropathy; *CNS,* central nervous system; *FFP,* fresh frozen plasma; *MG,* myasthenia gravis; *SLE,* systemic lupus erythematosus; *TTP,* thrombotic thrombocytopenic purpura.

Two complications of this procedure are photosensitivity and possible leukemogenesis. Patients undergoing ECP are sensitive to sunlight (Knobler et al., 1993). They should avoid direct or indirect sunlight exposure for 24 hours following completion of the procedure by covering exposed skin, using sunscreen, and wearing wraparound UV protective eyewear. Another possible complication of ECP could be mutagenesis from DNA damage caused by photoactivation of the 8-MOP. This theoretically could result in the reinfusion of cells with damaged DNA still capable of cell division. These cells could then give rise to hematologic malignancies. Although evidence has not been found to support this concern, it is still a theoretical risk of the procedure (van Iperen et al., 1997).

THERAPEUTIC PLASMA EXCHANGE

Mechanisms of Action of Plasma Exchange

Several different disease-dependent mechanisms of action are responsible for the beneficial effects of TPE. The two most obvious and well-understood mechanisms include removal of disease-causing substances from the blood (i.e., IgM in Waldenström macroglobulinemia) and replacement of deficient substances by utilizing plasma from healthy donors as the replacement fluid (i.e., FFP as a replacement source of ADAMTS13 [a disintegrin and metalloprotease with eight thrombospondin] in TTP). However, more recent studies suggest that the beneficial effects of TPE in many diseases may be more than is explained by simple removal of humoral factors or replacement of deficient molecules and represents alterations in the immune system (Reeves & Winters, 2014). Table 38.13 lists possible mechanisms of action of TPE for different diseases, including many novel mechanisms involving alterations in immune function.

Several more recently investigated mechanisms of action of TPE are briefly discussed later. By removing pathologic antibodies pretransplant in recipients of crossmatch or ABO-incompatible organs, TPE combined with immunosuppression has greatly improved our ability to perform successful incompatible organ transplants. When used to treat autoimmune diseases, such as acute inflammatory demyelinating polyneuropathy (AIDP) or systemic sclerosis, TPE can cause a postprocedure rebound in which the antibody-producing cells have increased sensitivity to immunosuppressant agents. This is thought to be due to the loss of negative feedback on the antibody-producing cells induced by removal of sufficient immunoglobulin during TPE (Reeves & Winters, 2014). In diseases mediated by immune complexes, such as systemic lupus erythematosus (SLE), TPE not only directly removes immune complexes but may indirectly aid in immune complex destruction and clearance through enhanced monocyte function, improved reticuloendothelial function, and upregulation of complement-clearing receptors on red blood cells. Another proposed

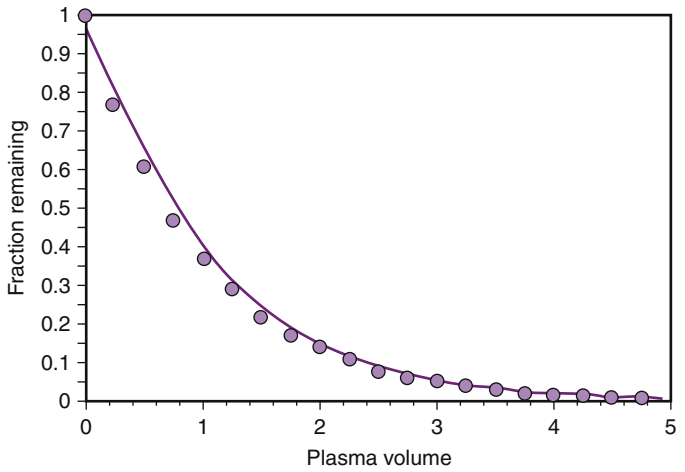

Figure 38.3 Removal of substances during plasma exchange. The removal of substances limited to the intravascular compartment, whether pathologic or normal, can be predicted by an exponential equation (see Eq. 38.11). A fixed percentage of the remaining substance is removed with each blood volume. This means that as the number of blood volumes processed increases, a progressively smaller amount of the substance is removed, resulting in diminishing returns.

mechanism of action of TPE is cytokine removal, although the supporting evidence is mixed, with several studies also indicating cytokine production through contact with the apheresis device (Reeves & Winters, 2014). In patients with autoimmune diseases, alterations in the immune system may explain some of the mechanisms of action for TPE. These changes include decreased B cells, increased T cells, increased T suppressor cell function, and a shift from Th2 to Th1 response. While in some disorders the mechanism of action of TPE may simply involve removal of pathologic immunoglobulin or replacement of deficient protein, in most autoimmune diseases the mechanism involves complex alterations in immune function that are not well understood.

Efficacy of Removal

The goal of TPE is to remove a pathologic substance present within the plasma by removing the patient's plasma and replacing it with a substitution fluid. The removal is nonspecific in that all of the substances present in the plasma, including normal substances, are removed. Removal of a substance can be predicted by Equation 38.11, as shown in Figure 38.3 (Derksen et al., 1984b):

$$Y = Y_0 e^{-x} \qquad \text{(Eq. 38.11)}$$

where

Y is the final concentration of the substance

Y_0 is the initial concentration of the substance

x is the total number of times the patient's volume is exchanged

This model assumes that the intravascular compartment is closed and that exchange between the intravascular and extravascular compartments does not occur. Based on this equation, 30% of the initial quantity of a substance will remain within the patient's plasma after one plasma volume exchange, and 10% will remain after the exchange of two plasma volumes. As more plasma volumes are exchanged, a fixed percentage of the remaining substance is removed (approximately 70%), such that an increasingly smaller total amount is removed. As can be seen in Figure 38.3, the marginal benefit of removing additional plasma volumes declines after 1.5 to 2.0 plasma volumes. Thus, most TPE procedures are limited to 1.0 to 1.5 plasma volume exchanges.

The assumption that no exchange occurs between intravascular and extravascular compartments during the procedure is not valid for all substances. As a result, the amount removed and the concentration in the plasma at the end of the procedure may not match that predicted. For example, IgM is located predominantly within the intravascular space (76%), with negligible influx from the extravascular space (Derksen et al., 1984b). As a result, during TPE, the equation will accurately predict the removal of IgM. IgA, however, is evenly distributed between the intravascular and extravascular spaces and can move between the two compartments. During TPE, as the concentration of IgA within the intravascular space falls, IgA within the extravascular space follows its concentration gradient and moves into the intravascular space. The result is that after the procedure is complete, the plasma concentration of IgA is not as low as predicted. This would lead one to believe that the procedure was not as efficient as expected (Derksen et al., 1984b). If one measures the IgA within the collection bag, one would see that the total amount of IgA removed was greater than predicted and that the procedure was more efficient than expected. Not only was IgA being removed from the intravascular compartment, it was also being removed from the extravascular compartment (Derksen et al., 1984b).

Four patterns of removal in TPE using 5% albumin as the replacement fluid have been identified. In the first pattern, seen with fibrinogen and C3, the concentration decreases to a greater extent than expected. This is due to the combination of removal and consumption of these factors during the procedure. In the second pattern, such as with IgM, cholesterol, and alkaline phosphatase, the change in concentration is what is predicted. These substances are confined to the intravascular space or have little exchange between compartments. In the third pattern, as seen with lactate dehydrogenase (LD) and creatinine phosphokinase (CPK), the concentration is less than predicted owing to movement of these substances between compartments. Finally, in the fourth pattern, concentrations are much greater than predicted or do not change at all, which may be due to rapid equilibration. This pattern is seen with small inorganic and organic molecules such as potassium, bicarbonate, and glucose (Orlin & Berkman, 1980).

The pattern of removal of immunoglobulins during TPE depends on whether normal immunoglobulin or a paraprotein is involved. The removal of normal IgG has been reported to be predictable by Equation 38.11; it behaves as if it is entirely intravascular (Chopek & McCullough, 1980; Orlin & Berkman, 1980). Others, however, have reported behavior similar to that of a substance equilibrating between the two compartments (Derksen et al., 1984b). In the case of paraproteins, the removal of immunoglobulins may appear to be half of what is expected when looking at plasma concentrations (Chopek & McCullough, 1980). This difference is attributed to expansion of the patient's plasma volume due to the presence of the paraprotein (Chopek & McCullough, 1980). In other words, the plasma volume of the patient is greater than what is predicted by standard equations (e.g., Eq. 38.3), such that if these are used to calculate a 1.5 plasma volume exchange, the real volume exchanged will be less.

In addition to the effect on removal of the substance from the plasma, the distribution between the intravascular and extravascular compartments and the ability to move between these compartments will influence the rise in plasma levels of the substance following TPE. The concentrations of substances that diffuse rapidly and have a large extravascular component will rise rapidly. The increase in concentrations of those substances that are predominantly intravascular will depend on the rate of synthesis of the substance. Most substances return to normal levels within 48 to 72 hours. Exceptions to this include fibrinogen, complement, and immunoglobulins, for which mean recoveries at 48 hours were 65%, 65%, and 44% of initial values, respectively. Cholesterol also shows a slow recovery, with 67% to 72% of preapheresis values achieved 1 week after hemapheresis (Orlin & Berkman, 1980).

For the majority of substances removed by TPE, the rate of synthesis does not increase following the procedure (Derksen et al., 1984a). For some substances, especially the immunoglobulins, rebound may occur. Rebound is an increase in concentration after completion of a procedure to a level greater than that seen initially (Derksen et al., 1984a; Dau, 1995). This may result from the removal of inhibitory substances by the procedure or the removal of negative feedback on the responsible cell. As a result, concurrent treatment with cytotoxic agents during the procedure is suggested to prevent rebound (Dau, 1995). In addition, TPE may enhance the efficacy of cytotoxic agents by increasing the metabolic activity of autoreactive immune cells, making them more sensitive to such agents (Dau, 1995). Another point related to this is that TPE will only temporarily decrease the level of a pathologic substance unless additional therapy is instituted to stop its production. This means that, in most cases, TPE should be viewed as an adjunct to other therapies.

Replacement Fluids

In TPE, 1.0 to 1.5 plasma volumes are removed; therefore, this volume must be replaced with another fluid. A number of replacement fluids are available, each of which has advantages and disadvantages. Replacement fluids used in TPE include 5% albumin, FFP, plasma cryoprecipitate reduced (cryopoor plasma), saline, and HES.

Albumin in a concentration of 5% is the most widely used replacement fluid. It is a hyperoncotic fluid for most patients and, therefore, will result in the net flow of fluid from the extravascular space. This can result in a mild dilutional anemia (Chopek & McCullough, 1980). The main advantage of 5% albumin is that it does not transmit viral diseases. Disadvantages are that it is expensive and has at times been in short supply

because of FDA-mandated recalls. Hypotensive reactions due to prekallikrein activation (Alving et al., 1978) and febrile reactions due to pyrogens have been reported (Pool & McLeod, 1995). Both of these reactions are rare. In addition, the albumin may not function comparably to the albumin present in the plasma before exchange. Although exchange with 5% albumin provides physiologic concentrations of the protein, the drug- and metabolite-binding sites of this albumin are occupied by preservatives such as sodium caprylate and may not be available for normal physiologic functions (Koch-Weser & Sellers, 1976). Standard practice is to use a 5% albumin solution for 60% to 70% of the replacement volume. The remaining volume is replaced by crystalloid (normal saline). Of note, to avoid hypotension due to fluid shifts, the crystalloid should be given at the beginning of the procedure and the colloid as the final portion of the replacement.

FFP is used as the primary replacement fluid in treating TTP and may also be used to prevent the dilutional coagulopathy seen with repeated TPE. Advantages of FFP are that it is relatively inexpensive and provides physiologic concentrations of coagulation factors. Disadvantages include the danger of transmission of transfusion-transmitted viral diseases, transfusion reactions, the need to have an ABO-compatible product, and an increase in the frequency of citrate reactions (see discussion at the end of the chapter). This last disadvantage results from the fact that the patient is infused not only with citrate anticoagulant but also with the citrate within the FFP. When used to treat TTP, 60% to 70% of the replaced volume will be FFP, and the remainder will be normal saline. When used to prevent coagulopathy, units of FFP can be given at the end of the procedure, with most of the replacement volume being 5% albumin.

Plasma cryoprecipitate reduced is also used in the treatment of TTP, specifically in those unresponsive to TPE with FFP. The advantages and disadvantages of plasma cryoprecipitate reduced are the same as those for FFP, with the exception that plasma cryoprecipitate reduced does not provide physiologic concentrations of all coagulation factors, lacking fibrinogen and factor VIII.

Saline is used for a portion of most TPE procedures (30%–40%); it is used to prime the instrument and to make the anticoagulant solution. The use of saline for greater volumes is problematic in that it is a crystalloid and not a colloid and can redistribute into the extravascular space, resulting in hypotension and edema following the procedure. The advantages of saline are that it is inexpensive and does not carry the risk for transmitting disease.

The final option is the use of synthetic colloidal fluid, such as HES. HES is derived from plant starches and consists of large starch molecules that can be added to saline to generate a colloidal solution, which will remain in the intravascular space. TPE using HES as the replacement fluid has been described (Burgstaler & Pineda, 1990; Rock et al., 1997). The benefits of HES are that it is inexpensive and does not carry infectious disease transmission risks. The disadvantages include allergic reactions and renal dysfunction (see discussion at the end of this chapter). Also, high-molecular-weight HES hetastarch has a half-life of 25.5 hours; thus, significant amounts can persist after frequent TPE procedures, resulting in volume expansion and alterations in partial thromboplastin time, total protein, albumin, hematocrit, and fibrinogen (Rock et al., 1997). These changes are less frequent with pentastarch, a low-molecular-weight HES, because of its shorter half-life. HES is an alternative replacement solution for those who have reactions to albumin or FFP (Burgstaler & Pineda, 1990). It can also be used in those who require TPE, but whose religious beliefs preclude the use of replacement fluids derived from blood.

Patient Concerns

TPE is a relatively safe procedure but, like any procedure, it can be associated with complications that are significantly higher when FFP is used as the replacement fluid (Basic-Jukic et al., 2005; Shemin et al., 2007) (see the "Donor/Patient Complications Common to All Hemapheresis Procedures" section later in the chapter). Many of the concerns about patients undergoing TPE involve the removal of unintended substances, such as therapeutic drugs and coagulation factors. Despite the fact that TPE has been a treatment modality for a variety of diseases for over 50 years, little information is available regarding its effects on therapeutic drugs. The effects of TPE on a variety of medications are given in Box 38.9. From a practical standpoint, because TPE may remove a portion of a drug dose, drugs that are given once daily should be withheld until after the procedure, if possible. Drugs that are administered more often should also be scheduled so that they are not given directly prior to TPE.

Two of the most important determinants of drug removal by TPE are the percentage of protein-bound drug and the volume of distribution (Vd). A highly protein-bound drug that is predominantly limited to the intravascular compartment (low Vd) should be efficiently removed, while a poorly protein-bound drug that is distributed throughout the body tissues and fat (high Vd) will not be efficiently removed. However, some studies cite the time between drug administration and start of TPE as the most influential determinant on drug removal, surpassing the effects of protein-binding and Vd (Ibrahim & Balogun, 2012). The distribution half-life of the drug determines the time for the drug to be fully distributed in the extravascular space and, thus, determines how much time is needed between the last dose of the drug and the start of TPE. TPE can also indirectly affect drugs. For example, TPE removes circulating anticholinesterase antibodies, thus, prolonging the effects of anticholinesterase medications (Ibrahim & Balogun, 2012). Such agents should be avoided immediately following TPE. It is important to note that serum drug levels do not always correlate with clinical effects. Therefore, even though TPE may decrease drug levels, this decrease does not necessarily alter the biological effect (Ibrahim & Balogun, 2012).

The majority of available research regarding TPE's effect on drug removal has focused on assessing serum drug concentrations. However, this method tends to overestimate drug removal because it fails to include other important determinants, such as redistribution, postprocedure rebound, endogenous drug clearance, and underlying organ dysfunction. Ibrahim and Balogun recommend examining the amount of drug in the waste plasma rather than in the serum for a more accurate estimate of drug removal (Ibrahim & Balogun, 2012). When waste plasma has been examined, most studies found diminished to no effect of TPE on drug removal when compared with studies examining preprocedure and postprocedure serum drug concentrations (Ibrahim & Balogun, 2012).

The often unintentional effect of drug removal seen with TPE is occasionally cited as a desirable effect in certain cases of drug overdose or drug toxicity. For example, reports of TPE to treat overdoses of the highly

BOX 38.9

Effects of Plasma Exchange on Medications as Reported in the Literature

Medications That Do Not Require Dose Supplementation Because of Insignificant Removal, Redistribution from Tissue Stores, or Drug Binding to Red Blood Cells

Acyclovir
Azathioprine
Carbamazepine
Cyclophosphamide
Cyclosporine
Digitoxin
Digoxin
Oxcarbazepine
Phenobarbital
Phenytoin
Prednisolone
Prednisone
Propranolol
Quinine
Tacrolimus
Valproic acid
Vancomycin

Medications That Are Removed and May Require Dose Supplementation

Basiliximab
Ceftazidime
Ceftriaxone
Chloramphenicol
Cisplatin
Diltiazem
Interferon-α
Intravenous immunoglobulin (IVIg)
Palivizumab
Propoxyphene
Propranolol
Rituximab
Tobramycin
Verapamil
Vincristine

Data from Kale-Pradhan PB, Woo MH: A review of the effects of plasmapheresis on drug clearance, *Pharmacotherapy* 17:684–695, 1997; Kintzel PE, Eastlund T, Calis KA: Extracorporeal removal of antimicrobials during plasmapheresis, *J Clin Apher* 18:194–205, 2003; Ibrahim RB, Liu C, Cronin SM, et al.: Drug removal by plasmapheresis: An evidence-based review, *Pharmacotherapy* 27:1529–1549, 2007.

protein bound drug amlodipine have been successful (Ibrahim & Balogun, 2012). TPE has been used to treat amiodarone-induced thyrotoxicosis through transient removal of total and free T4/T3. Other applications of TPE to treat drug toxicity include treating severe rituximab infusion reactions and preventing digoxin toxicity in patients with renal failure (Ibrahim & Balogun, 2012). However, caution is recommended, as much of the available research using TPE to treat overdoses comes from case reports and studies with significant experimental pitfalls.

Following TPE using 5% albumin as a replacement fluid, decreases in the levels and activities of coagulation factors (Flaum et al., 1979; Orlin & Berkman, 1980) and abnormal coagulation tests (Flaum et al., 1979) have been seen. Flaum and colleagues (1979) demonstrated significant decreases in the levels of factors V, VII, VIII, IX, and X, and von Willebrand factor (vWF) activity following TPE. These deficits returned to normal in 24 hours, with the exception of factors VIII and IX and vWF activity, which returned to normal in 4 hours (Flaum et al., 1979). Orlin and Berkman noted reductions in fibrinogen levels to 25% of preapheresis levels, with levels reaching 66% of preapheresis levels at 72 hours (Orlin & Berkman, 1980). These studies indicate that a risk for bleeding exists in hemostatically challenged patients following TPE. In one study of 1727 TPE procedures, the frequency of exit site bleeding was 1.2% (Shemin et al., 2007). In another study reviewing 4857 TPE procedures, the frequency of puncture-site hematoma was 2.4% and the frequency of hemorrhage was 0.06% (Basic-Jukic et al., 2005). Although significant hemorrhage is uncommon, the risk for bleeding is especially relevant for patients undergoing serial procedures on consecutive days. At-risk patients, such as those who have undergone or will undergo surgical procedures or biopsies in proximity to their TPE, may require FFP as a portion of their replacement fluid. This should be given at the end of the procedure to prevent its removal.

In addition to increased risk for bleeding, increased risk for thrombosis is possible. Because of the nonspecific nature of TPE removal, inhibitors of coagulation, such as antithrombin, are also removed during TPE (Ibrahim & Balogun, 2012). This could theoretically lead to thrombosis. In one study of 4857 TPE procedures, the risk for TPE-related clotting was 1.7% (Basic-Jukic et al., 2005).

Finally, platelets are also lost during TPE (Perdue et al., 2001). In a study of 71 patients undergoing TPE with the COBE Spectra, Fresenius AS104 (Fresenius HemoCare, Redmond, WA) or the Haemonetics LN9000 (Haemonetics, Braintree, MA), platelet loss ranged from 0% to 71% (Perdue et al., 2001). Factors found to influence platelet loss included the instrument used, with the Fresenius AS104 having relatively increased loss (18.6% vs. 2.6% and 1.6% for the Haemonetics LN9000 and the COBE Spectra, respectively), and the disease being treated. Patients with hyperviscosity syndrome due to dysproteinemia had the greatest loss, but no bleeding complications occurred (Perdue et al., 2001). Greater platelet loss with the Fresenius AS104 in comparison with the COBE Spectra was felt to be due to differences in *g* force and dwell time between the two instruments (Burgstaler & Pineda, 2001).

Special concerns for bleeding may apply to patients on warfarin undergoing TPE without plasma replacement. Although warfarin and TPE without plasma replacement have known independent effects on coagulation, limited data exist evaluating their combined effect. In one prospective observational study of 8 patients undergoing 121 single-plasma volume TPE procedures with 5% albumin replacement, average preprocedure to postprocedure values showed an increase in international normalized ratio (INR; 2.09 to 4.12) with a decrease in fibrinogen (263 to 105 mg/dL) and factor II (29% to 13%) following TPE (Zantek et al., 2014). Preprocedure coagulation values were predictive of postprocedure values. In addition, the effect of TPE on INR was less pronounced in patients starting with normal or mildly elevated INR values. Only one bleeding complication was reported, consisting of minor catheter site oozing. As previously discussed, the effect of TPE on coagulation parameters is temporary. Although a concern for bleeding exists for patients on warfarin undergoing TPE without plasma replacement, the risk for bleeding must be weighed against the risk of plasma transfusion. More studies are needed to clarify optimal management of patients on anticoagulants scheduled to undergo TPE without plasma replacement.

Procedures for Selective Removal of Plasma Components

As previously discussed, TPE is nonselective. Each TPE removes approximately 150 g of plasma proteins (110 g of albumin and 40 g of globulin) (Randerson et al., 1982; Lysaght & Samtleben, 1985) to eliminate 1 to 2 g of pathologic substance. Repeated TPE can result in bleeding due to loss of coagulation factors and immunodeficiency due to loss of immunoglobulins.

BOX 38.10

Criteria for Use of Low-Density Lipoprotein (LDL) Apheresis in Familial Hypercholesterolemia (FH)

U.S. Food and Drug Administration Criteria

- Functional FH homozygotes with an LDL cholesterol >500 mg/dL
- Functional FH heterozygotes with an LDL cholesterol ≥300 mg/dL who have failed a 6-month trial of maximal drug therapy and an American Heart Association Step II diet
- Functional FH heterozygotes with an LDL cholesterol ≥200 mg/dL and documented coronary artery disease who have failed a 6-month trial of maximal drug therapy and an American Heart Association Step II diet

German Committee of Physicians and Health Insurance Funds

- Homozygotes for FH
- Patients with severe hypercholesterolemia in whom maximal dietary and drug therapies for >1 year have failed to lower cholesterol sufficiently

International Panel on Management of FH

- Homozygotes for FH
- Heterozygotes for FH with symptomatic coronary artery disease in whom LDL cholesterol is >4.2 mmol/L or decreases by <40% despite maximal medical management

Heart—United Kingdom

- Homozygotes for FH in whom LDL cholesterol is reduced by <50% and/or >9 mmol/L with drug therapy
- Homozygotes for FH in whom LDL cholesterol is reduced by <50% and/or >9 mmol/L with drug therapy
- Progressive coronary artery disease, severe hypercholesterolemia, and Lp(a) >60 mg/dL in whom LDL cholesterol remains elevated despite drug therapy.

Data from Thompson GR: HEART-UK LDL Apheresis Working Group. Recommendations for the use of LDL apheresis, *Atherosclerosis* 198:247–255, 2008.
Lp(a), Lipoprotein a.

If other replacement fluids are used, additional risks may be present, including disease transmission and allergic reactions. Because of these disadvantages, a number of procedures have been developed to selectively remove a plasma component, allowing return of the patient's "cleansed" plasma. The benefits of such procedures are that depletion of normal plasma components and the need for substitution fluids are avoided. The drawbacks to such procedures are that they are more expensive to perform than TPE because of the costs of selective removal columns. In addition, although many devices are available worldwide to perform these types of procedures, only two are available in the United States and have been licensed by the FDA.

Selective removal procedures most often involve an initial separation step, in which the cellular elements of whole blood are separated from the plasma. The plasma is then perfused through the selective removal device, where the substance of interest is removed by chemical, physical, or immunologic means. The treated plasma is then recombined with the cellular components and reinfused. The selective removal device may then be regenerated with the bound substance removed and diverted to a waste collection bag. Following this, the selective removal device is used to treat additional plasma. If the device cannot be regenerated, then it is discarded. Examples of selective removal procedures are discussed in the following sections.

Selective Removal of Low-Density Lipoproteins

Lipoprotein apheresis, also called *LDL-apheresis*, is indicated for the treatment of familial hypercholesterolemia (FH) in homozygotes and in heterozygotes unresponsive to drug therapy (Winters, 2012). This disorder results in accelerated atherosclerosis due to the inability of the liver to clear LDL cholesterol from the blood caused by mutations in the hepatic LDL receptor. While TPE has been previously used to treat these patients, TPE results in the nonselective removal of both LDL and the cardioprotective high-density lipoprotein (HDL). In contrast, lipoprotein apheresis selectively removes LDL while maintaining the beneficial effects of retained HDL. Criteria for the treatment of patients with LDL-apheresis vary worldwide and are given in Box 38.10. Comparisons of the life expectancy of patients treated with these techniques and their untreated siblings, as well as series and case reports of treated patients, have been reported. Significant reductions in cholesterol, improvements in xanthomas, disappearance of electrocardiographic (ECG) abnormalities, regression of coronary artery lesions, improvement in exercise tolerance, and prolongation of life span have been seen (Winters, 2013).

Following lipoprotein apheresis, there is a temporary decrease in LDL by 60% to 65%. This is followed by a rapid increase in LDL during the next 48 hours and a continued slower increase in LDL during the next 1 to 2 weeks. Repeated lipoprotein apheresis procedures cause repetitive acute drops in LDL with a decrease in the average LDL over time. The goal of lipoprotein apheresis is to reduce the time-averaged LDL cholesterol by ≥60% of baseline or to reduce the total cholesterol by >50% of baseline (Winters, 2013). Equation 38.12 can be used to calculate the time-averaged LDL cholesterol:

$$\text{Cmean} = \text{Cmin} + K(\text{Cmax} - \text{Cmin}), \qquad \text{(Eq. 38.12)}$$

where

Cmean is the time-averaged cholesterol

Cmin is the cholesterol level immediately after the apheresis procedure

K is the rebound coefficient

Cmax is the cholesterol level immediately prior to the apheresis procedure

A number of methods are available for the selective removal of LDL. These methods include double-filtration plasmapheresis, heparin-induced extracorporeal low-density lipoprotein precipitation (HELP), dextran sulfate absorption, immunoadsorption, direct adsorption of lipoproteins from whole blood, and dextran sulfate whole-blood perfusion. However, only the dextran sulfate system and the HELP system are currently FDA approved for use in the United States.

In the dextran sulfate absorption method (Liposorber, Kaneka, Osaka, Japan), two columns of dextran sulfate are used to continuously remove LDL cholesterol. Plasma is separated from whole blood using a hollow fiber separator and is pumped through the dextran sulfate column. The negatively charged dextran sulfate interacts with the positively charged apolipoprotein B of the LDL cholesterol, resulting in its removal. When the first column becomes saturated, flow is switched to the second column and the first column is regenerated with 4.1% NaCl and then lactated Ringer's solution. Treated plasma is mixed with the cellular elements and returned to the patient. Studies using this system have demonstrated a 53% reduction in cholesterol with one plasma volume exchange (Thompson et al., 1995) as well as a 36% reduction in fibrinogen and a 5% loss of HDL (Schulzeck et al., 1992).

The second method of lipoprotein apheresis approved by the FDA for use in the United States is HELP (B Braun Medical Inc., Bethlehem, PA). With this technique, plasma is separated from whole blood using a hollow fiber separator. A sodium acetate buffer of pH 4.84 containing heparin is added to the plasma to precipitate the LDL. This precipitate is then removed by filtration, with the heparin being adsorbed from the plasma by a diethylaminoethyl cellulose filter. The acetate and extra volume are then removed through bicarbonate dialysis/ultrafiltration. The treated plasma is combined with the cellular elements and returned to the patient (Winters, 2012). Results of treatment in one trial demonstrated reductions in LDL cholesterol of greater than 30%, with reductions in HDL and fibrinogen of 15% and 58%, respectively (Lane et al., 1993). Comparisons of these two FDA-approved systems for lipoprotein apheresis have shown similar reductions in LDL cholesterol, lipoprotein a (Lp(a)), HDL, and other plasma components. Reductions in HDL, fibrinogen, and other plasma components are less than those seen with TPE. These systems have also demonstrated similar reaction rates but differ in terms of cost and simplicity of operation (Winters, 2012).

Some systems, such as the HELP system and secondary filtration, remove additional plasma components such as fibrinogen. Because of the removal of large macromolecules other than LDL, these systems have been used to alter blood flow characteristics in certain disease states. This form of apheresis has been referred to as *rheophoresis*. These devices have been used to treat age-related macular degeneration (Klingel et al., 2003), sudden sensorineural hearing loss (Suckfull et al., 1999; Suckfull, 2002), stroke (Jaeger et al., 1999), and myocardial ischemia (Jaeger et al., 1999). According to the ASFA, homozygous FH is a category I indication for lipoprotein apheresis with a grade 1A recommendation. Heterozygous FH is a category II indication for lipoprotein apheresis with a grade 1A recommendation. TPE is a category II indication with a grade 1B recommendation for FH homozygotes or heterozygotes whose blood volume is too small for them to be treated with a selective removal system (Padmanabhan et al., 2019).

While LDL is the most well-studied risk factor for coronary artery disease, elevated levels of Lp(a) have emerged as having an independent association with cardiovascular disease (Leebmann et al., 2013). Lp(a) is composed of an LDL particle with bound apolipoprotein B and apolipoprotein (a). Patients with elevated Lp(a) have an increased risk for coronary artery disease, cerebrovascular disease, and peripheral artery disease, with Lp(a) contributing to vascular inflammation and atherothrombosis. Two studied variants in the gene encoding Lp(a), *rs10455872* and *rs3798220*, have odds ratios of 1.70 and 1.92, respectively, for coronary artery disease (Leebmann et al., 2013). Four observational studies evaluating the effect of LDL apheresis on patients with isolated Lp(a) elevation or concomitant elevated LDL cholesterol have been performed in Germany and Italy. The cardiovascular event rate decreased in all 4 studies (Thompson & Parhofer, 2019).

According to the ASFA, Lp(a) hyperlipoproteinemia is a category II indication for lipoprotein apheresis with a grade 1B recommendation.

Another emerging indication for LDL apheresis is drug-resistant nephrotic syndrome in the setting of focal segmental glomerulonephritis (FSGS). Several clinical studies performed in Japan have shown improvement of proteinuria and at least partial remission after 2 years in 50% of the patients treated with LDL apheresis (Muso, 2014; Muso et al., 2015). The challenge in interpreting results of these studies is that the ordinary treatment is not standardized and was left to the discretion of each individual provider. The mechanism of LDL apheresis effect on FSGS is unclear. Based on these results, the FDA granted humanitarian use device designation for LDL apheresis equipment in the treatment of drug-resistant FSGS in May of 2017.

Therapeutic Plasma Exchange Indications

TPE is justified if at least one of the following general indications are met: (1) removal of substances too big to be removed by other procedures, (2) removal of substances with a long enough half-life to provide a therapeutic period of decreased serum concentration, and (3) removal of substances that are acutely toxic and resistant to removal by other methods (Basic-Jukic et al., 2005). Selected disorders for which TPE is indicated will be briefly outlined in Table 38.14. A more extensive list of TPE indications can be found in the ASFA guidelines (Padmanabhan, 2019).

DONOR/PATIENT COMPLICATIONS COMMON TO ALL HEMAPHERESIS PROCEDURES

Hemapheresis procedures—both donor and therapeutic—are safe, with minimal risk for complications. Those that do occur are generally traumatic complications associated with venous access or physiologic complications, including citrate-mediated, allergic-type, and volume-related problems. Because citrate-mediated reactions are common and may require the attention of the physician, they are discussed in some detail here. Reaction rates among hemapheresis donors in the American Red Cross system have been found to be 577.5/10,000 donations for platelet donations and 538.3/100,000 donations for double red cell donations. This compares with a reaction rate of 348.9/10,000 donations for whole blood donors (Eder et al., 2008). Reactions requiring outside medical care (i.e., reactions that could not be addressed at the donation site) were 3.2, 2.9, and 2.9/10,000 donations for whole-blood, platelet, and double red cell donations, respectively. There was no statistically significant difference between the frequencies of these more severe reactions, though the types of reactions differed. In whole-blood donors, 46% of those reactions requiring outside medical care were syncopal reactions. In hemapheresis donors, 39% were phlebotomy related, such as large hematomas or nerve injury (Eder et al., 2008). In older studies, the rate of serious reactions—those requiring hospitalization—has been found to be 0.01% (2/19,736 donations) (Despotis et al., 1999), which is 20 times greater than that reported to occur with allogeneic whole-blood donation (1/198,119 donations; 0.0005%) (Popovsky et al., 1995). Therefore, although apheresis donation appears to have a lower reaction rate than whole-blood donation, the risk for serious reactions, although small, is greater.

The most common reactions seen among apheresis donors are due to venipuncture (McLeod et al., 1998; Eder et al., 2008). Table 38.15 lists the adverse effects of apheresis donation reported by McLeod, their frequency, and comparable frequency among whole-blood donors. As with whole-blood donation, first-time donors had reactions more frequently than repeat donors (McLeod et al., 1998; Eder et al., 2008).

Reactions were found to be more frequent among platelet donors than among plasma or granulocyte donors (5.9% and 9.4%, respectively, vs. 12%), which may have been due to a greater number of first-time donors in this group (McLeod et al., 1998). Reactions are also more frequent among platelet donors than double red cell donors (Eder et al., 2008). Despotis and colleagues (1999) found associations between citrate/hypotensive reactions and the associated donor weight, gender, and type of collection instrument used. For venipuncture-related complications, only female

TABLE 38.14

Common Indications for Plasma Exchange

Indications	Pathogenesis	Replacement Fluid	Schedule	Special Considerations
Neurologic disorders				
Acute inflammatory demyelinating polyneuropathy (Guillain-Barré syndrome)	Complement fixing antibodies to peripheral myelin	Albumin	Daily, until clinical improvement with best response if initiated within 7 days of symptoms.	Efficacy of TPE is equivalent to IVIg, though the direct costs of TPE are less than those for IVIg. (Winters, 2011)
Chronic inflammatory demyelinating polyneuropathy	Unclear, but likely at least partially antibody mediated	Albumin	2–3/week until improvement, followed by tapering	Frequent relapses after discontinuation of treatment occur but respond to additional TPE.
Myasthenia gravis	Anti-acetylcholine receptor or muscle-specific kinase (MuSK) antibodies	Albumin	Acute: Daily for 5–6 days; Chronic Weekly/biweekly maintenance	Recommended in severe disease with impaired respiratory function, swallowing or in preparation for thymectomy (Sanders & Scoppetta, 1994, Iwasaki et al., 1993)
Hematologic Disorders				
Thrombotic microangiopathy, Thrombotic thrombocytopenic purpura (TTP)	Antibodies to or congenital deficiency of ADAMTS13 resulting in inability to cleave multimers of von Willebrand factor (vWF)	Plasma	Daily, until platelet count is above 150×10^9 on 2 consecutive days, LD is "near normal" and nonfixed neurologic symptoms have resolved	Important to draw ADAMTS13 level prior to starting first TPE. Presence or absence of schistocytes at discontinuation of TPE does not affect relapse and is not a criterion for discontinuation of therapy (Egan et al., 2004)
Thrombotic microangiopathy (TMA), complement mediated	Factor H autoantibody or mutations in complement or complement regulatory genes	Plasma	Daily, until platelet count is above 150×10^9 on 2 consecutive days, LD is "near normal" and nonfixed neurologic symptoms have resolved	TPE may be used to treat the acute manifestations of the disease. Eculizumab, a chimeric antibody that prevents formation of membrane attacking complex, is used for long-term control and renal protection. If complement-mediated TMA is suspected, the patient should be treated with eculizumab.
Hyperviscosity	Large concentrations of paraprotein increases blood viscosity	Albumin	Daily, until clinical improvement	70% of patients with Waldenström macroglobulinemia (WM) and 5% of multiple myeloma (MM) patients may have hyperviscosity symptoms. Hyperviscosity in MM requires more TPE sessions and may lead to fluid shifts due to extravascular distribution of offending paraprotein, in comparison with intravascular distribution of paraprotein in WM (IgM).
Multiple myeloma with acute renal failure	Renal failure that is caused by filtration of monoclonal free light chains with resulting tubular injury	Albumin	Daily, until free light chain level is reduced to less than 50%	Cast nephropathy is one of many causes of renal failure in MM and is the only one in which there is evidence of response to therapy. As a result, therapy should be guided by the presence of casts on biopsy (Leung et al., 2008), as treatment of simple "acute renal failure in MM" is not responsive to TPE (Clark et al., 2005).
Nephrologic Disorders				
Anti–basement membrane antibody disease (Goodpasture syndrome)	Complement-fixing antibodies to type IV collagen found in renal glomerular and pulmonary alveolar basement membrane	Albumin	Daily or every other day for 7–14 days, until resolution of glomerular or pulmonary injury	The success and the length of the procedure depend on the severity and stage of the disease. If patient is dialysis independent and/or diffuse alveolar hemorrhage is present, the TPE is highly effective. However, if the patient is dialysis dependent at presentation, response is limited (Levy et al., 2001).
Cryoglobulinemia	Presence of immunoglobulins that reversibly precipitate in the cooler temperatures of the extremities	Albumin	Daily, until resolution of symptoms	May present with renal failure and/or cutaneous manifestations. Warming the patient, treatment room, and use of blood warmers on the apheresis device should be considered to prevent precipitation of the protein in the apheresis device (Hillyer & Berkman, 1996).
Focal segmental glomerulosclerosis (FSGS)	Idiopathic, with possible circulating pathologic factor injuring glomeruli	Albumin	Daily or every other day, termination based on clinical scenario	The most effective use of TPE in management of FSGS is treatment of recurrent FSGS in transplanted kidney in hopes of saving the transplant. The treatment of steroid-resistant FSGS in the native kidney is generally not effective, but response may be patient dependent (Padmanabhan et al., 2019).

*ADAMTS13, **A** **d**isintegrin **a**nd **m**etalloprotease with eight **t**hrombo**s**pondin; IVIg,* intravenous immunoglobulin; *LD,* lactate dehydrogenase; *TPE,* therapeutic plasma exchange.

TABLE 38.15

Reaction Rates Among Apheresis and Whole-Blood Donors

Reaction	Apheresis Donations	Whole–Blood Donations
Hematoma or pain	1.15%	9%–16%
Citrate toxicity	0.4%	N/A
Mild vasovagal	0.05%	2%–5%
Vasovagal with syncope	0.08%	0.1%–0.3%

Data from McLeod BC, Price TH, Owen H, et al.: Frequency of immediate adverse effects associated with apheresis donation, *Transfusion* 38:938–943, 1998 (apheresis); and Newman BH: Donor reactions and injuries from whole blood donation, *Transfus Med Rev* 11:64–75, 1997 (whole blood).
N/A, Not available.

TABLE 38.16

Reaction Rates Among Patients Undergoing Therapeutic Apheresis Procedures

Reaction	Frequency
Transfusion reactions	1.6%
Citrate toxicity	1.2%
Hypotension	1.0%
Vasovagal reactions	0.5%
Pallor and diaphoresis	0.5%
Tachycardia	0.4%
Respiratory distress	0.3%
Tetany and seizure	0.2%
Chills or rigors	0.2%

Data from McLeod BC, Sniecinski I, Ciavarella D, et al.: Frequency of immediate adverse effects associated with therapeutic apheresis, *Transfusion* 39:282–288, 1999.

gender was associated as a risk factor (Despotis et al., 1999). The instrument used for collection also influenced reaction rates. McLeod found that the Fenwal CS3000 had fewer reactions than other instruments. This could possibly be due to lower citrate infusion rates with this instrument and the lack of single-needle procedures performed on this instrument. Such single-needle procedures, which alternate between drawing and returning through the single intravenous line, result in larger extracorporeal volumes (McLeod et al., 1998). Despotis and colleagues (1999) noted that the relationship between donor weight and citrate reactions was different when the COBE Spectra and the Fenwal CS3000 were compared. Donors with lower weights had a higher probability of citrate reactions on the Fenwal CS3000, and those with higher weights had a higher probability on the COBE Spectra. The authors of this study believed that this was due to the methods by which these instruments determine the anticoagulant infusion rate (Despotis et al., 1999). Finally, Eder and colleagues (2008) also found a correlation between reactions during both platelet and double red cell donation and age (younger, more reactions) and sex (females, more reactions) (Eder et al., 2008).

Reactions among therapeutic hemapheresis procedures have been reported to occur in 4.75% of procedures (McLeod et al., 1999). The reactions identified and their overall frequencies are given in Table 38.16. The rate of reactions varied with regard to procedure, replacement fluid, and patient. For example, the reaction rate for TPE using albumin was 3.35% as compared with 7.81% for TPE using plasma as the replacement fluid. Leukocytapheresis demonstrated a reaction rate of 5.71%, HPC-A collection had a rate of 1.66%, and no reactions occurred in the 18 patients who underwent therapeutic thrombocytapheresis. Patients with neurologic disorders were more likely than other categories of patients to experience vasovagal reactions (McLeod et al., 1999).

Shemin and colleagues (2007) examined the frequency of complications during the performance of TPE. Of 1727 TPE procedures in 174 patients, 614 procedures (36%) were complicated by a reaction. Most complications were mild, and no deaths occurred. Of the reactions, 0.2% required discontinuation of the procedure and 0.1% required additional medical management beyond that available in the apheresis unit. The most common reactions were fever (7.7%), urticaria (7.4%), and hypocalcemic symptoms (7.3%). Similar to that reported by McLeod, differences were seen based on the replacement fluid used. Urticaria and pruritus were more common with the use of FFP as a replacement fluid; hypotension was more common with the use of albumin and saline (Shemin et al., 2007).

It should be noted that the study by McLeod did not include complications or reactions due to venous access but that the study by Shemin and colleagues did. Studies that included these data have noted higher reaction rates with TPE. For example, Couriel and Weinstein (1994) noted adverse effects in 17% of therapeutic apheresis procedures. These were predominantly mild, consisting of citrate reactions, but 6.15% of procedures were complicated by severe reactions, reactions that were life-threatening, or reactions that resulted in termination of the procedure. All of these reactions were due to central venous access and consisted of a pneumothorax, a hemopneumothorax, catheter-related bacteremia, and a sternocleidomastoid hematoma. The patient with the hemopneumothorax exsanguinated because of the complication (Couriel & Weinstein, 1994). Of the two severe reactions requiring additional medical intervention reported by Shemin and colleagues (2007), one was due to arterial puncture during central line placement. Although only one death due to therapy was reported by Couriel and Weinstein and no deaths attributable to therapeutic hemapheresis were reported in the studies by McLeod and Shemin, additional deaths have been reported by other authors. A majority of such deaths have been ascribed to cardiopulmonary arrest during hemapheresis; additional causes have included anaphylaxis, pulmonary embolus, and vascular perforation due to central venous access. Huestis (1989) estimated a mortality rate for therapeutic hemapheresis of 3 per 10,000 procedures (0.03%), and Mokrzycki and Kaplan (1994) estimated the mortality rate to be 0.05% of procedures, based on a review of the literature available at that time.

As discussed under the description of each procedure, specific complications are associated with specific procedures, such as those due to G-CSF administration in granulocyte harvest. A discussion of complications and risks common to all hemapheresis procedures follows.

ELECTROLYTE AND ACID-BASE DISTURBANCES

Citrate is used as the primary anticoagulant in both donor and therapeutic apheresis procedures because it effectively prevents coagulation while being short acting and easily reversible, unlike heparin. Citrate ions chelate calcium ions, producing a soluble complex that is excreted in the urine. As a result, the chelated calcium ions are unavailable for biological reactions such as those involved in the coagulation cascade. Within the apheresis instrument, plasma citrate concentrations reach 15 to 24 mmol/L, lowering the calcium ion concentration below 0.2 to 0.3 mmol/L, the level necessary for coagulation (Strauss, 1996). Without compensatory mechanisms from the donor/patient, the resulting hypocalcemia would be incompatible with life. Upon return of blood from the apheresis instrument to the donor/patient, the citrate is diluted throughout total extracellular fluid. In addition, the liver, kidneys, and muscles rapidly metabolize citrate, releasing the bound calcium (Strauss, 1996). The body responds to the decrease in ionized calcium by increasing parathyroid hormone levels, resulting in mobilization of calcium from skeletal stores and increased absorption by the kidneys (Silberstein et al., 1986). Finally, calcium bound to albumin is also mobilized and buffers the decline (Bolan et al., 2003a).

In TPE procedures, the volume of plasma removed must be replaced by a similar volume of replacement fluid. When plasma is used as the replacement fluid, additional citrate is infused in the form of the anticoagulant present in this solution, further increasing the risk for citrate toxicity seen in these patients. If albumin is used as the replacement fluid, one would therefore expect less citrate toxicity; however, this is not always the case. Normally, 40% to 55% of serum calcium is bound to albumin, with the unbound portion representing the physiologically active ionized calcium. Albumin preparations are depleted of this calcium and, as a result, bind patient calcium when infused during TPE. This can lead to a drop in ionized calcium with subsequent hypocalcemia. Goss and Weinstein (1999) demonstrated a higher incidence of citrate reactions and greater decreases in ionized calcium levels in neurology patients receiving TPE with 5% albumin as the replacement fluid when compared with those receiving 10% pentastarch as the replacement fluid. A subsequent study demonstrated that the addition of calcium gluconate to the albumin preparation before administration more effectively reduced the incidence of citrate toxicity when compared with IV calcium gluconate or oral calcium carbonate (Weinstein, 1996). The effect was due to the saturation of calcium binding sites on the albumin, thereby maintaining ionized calcium levels in the patient.

Despite compensatory mechanisms, citrate infusion can result in a decrease in ionized calcium levels to the point at which symptoms develop in the donor/patient. These result from a decrease in ionized calcium to

levels at which the excitability of nerve membranes increases, causing spontaneous depolarization (Strauss, 1996). Resulting signs and symptoms of acute citrate toxicity can include perioral paresthesia, acral paresthesia, shivering, lightheadedness, twitching, and tremors. In addition, some patients experience nausea and vomiting. As the ionized calcium levels fall further, these symptoms may progress to carpopedal spasm, tetany, and seizure (Strauss, 1996). Therefore, it is important to elicit the presence of early symptoms from the donor/patient so that interventions can occur before the more severe symptoms manifest. In addition to the symptoms described previously, other reported symptoms include prolongation of the QT interval on electrocardiogram, depressed myocardial contraction, and fatal arrhythmias (Strauss, 1996). Hypotension may also be seen with citrate reactions (Goodnough et al., 1999) and may be due to depressed myocardial function and vascular smooth muscle relaxation (Bunker et al., 1962).

Factors that have been found to influence the rate of citrate reactions in donor and therapeutic apheresis include alkalosis due to hyperventilation (Strauss, 1996), the rate of infusion of the anticoagulant solution (Strauss, 1996), the amount of citrate infused (Strauss, 1996), and the donor's serum albumin level before the start of the procedure (Bolan et al., 2003a). It should be noted that intermittent-flow hemapheresis procedures tend to have a greater frequency of citrate reactions, as the rate of citrate infusion is higher when the separation chamber is emptied than during continuous apheresis procedures. Also, the method by which an instrument calculates the dose of anticoagulant may influence the rate of reactions among certain donor subgroups (Despotis et al., 1999).

The treatment of acute citrate reactions is relatively simple when reactions are identified early. Treatment includes slowing the reinfusion rate to allow for dilution and metabolism of the citrate, increasing the donor/patient blood/citrate ratio to decrease the amount of citrate infused, giving oral calcium in the form of calcium antacids, and giving intravenous calcium (Strauss, 1996). Bolan and colleagues (2003a, 2003b) found that administration of 2 g of oral calcium carbonate was associated with a statistically significant reduction in the severity of paresthesia (Bolan et al., 2003b). Physiologically, this dose was also associated with the greatest improvement in ionized and total calcium levels among the doses examined (Bolan et al., 2003a). However, it did not reduce overall symptom development and it did not affect the occurrence of more severe symptoms (Bolan et al., 2003b).

Administration of intravenous calcium, in the form of calcium gluconate or calcium chloride, is usually not necessary in donor procedures but is common in the setting of therapeutic apheresis procedures. In HPC-A collections, the continuous infusion of calcium gluconate or calcium chloride has been found to prevent hypocalcemic symptom development (Bolan et al., 2002; Buchta et al., 2003), with calcium chloride maintaining higher ionized calcium levels (Buchta et al., 2003). In a study comparing calcium gluconate infused continuously, prophylactically at the start of HPC collection, or at the time of symptom development, continuous infusion maintained higher calcium levels and changes in calcium levels were insignificant with the other two modes of administration (Kishimoto et al., 2002). When administered to treat symptoms, the usual dose is 10 mL of calcium gluconate IV infused over 10 to 15 minutes (Hester et al., 1983). In patients with low ionized calcium levels before the start of the procedure, calcium gluconate can be given prophylactically.

While the acute effects of citrate toxicity are well documented, the long-term effects are still being investigated. Amrein and colleagues (2010) compared 102 frequent plasma/platelet donors to 102 matched controls and found that bone mineral density scores were significantly lower in the apheresis donors than in the control group, with a mean difference up to 3.5%. They hypothesized that citrate exposure in apheresis causes repetitive stress to the donor/patient's calcium homeostasis. Additionally, repeated loss of serum proteins—notably, albumin—may have untoward effects on bone mineral homeostasis. Additional research focused on citrate's effect on bone metabolism is needed to clarify appropriate donation/treatment intervals based on risk/benefit ratios. Magnesium is another physiologically important divalent cation. Similar to calcium, magnesium is bound by citrate. As a result, the infusion of citrate in the setting of plateletapheresis decreases ionized magnesium by 30% (Mercan et al., 1997). Mercan and colleagues (1997) also found that magnesium levels fall more rapidly than calcium levels during citrate infusion and that they recover more slowly. Hypomagnesemia can induce signs and symptoms similar to hypocalcemia, including muscle spasms, muscle weakness, decreased vascular tone, and impaired cardiac contractility. In addition, hypomagnesemia can impair calcium and potassium homeostasis, including inhibition of the release of parathyroid hormone when markedly decreased (Mercan et al., 1997). As a result, patients with low magnesium levels before undergoing apheresis may exhibit signs and symptoms of citrate toxicity due to hypomagnesemia and not hypocalcemia. Patients who cannot rapidly metabolize citrate are at higher risk for symptoms due to hypocalcemia and hypomagnesemia because less of the free active forms of the cations are available (Kamochi et al., 2002). These symptoms may be unresponsive to the administration of calcium supplementation. To avoid hypomagnesemia, it is common at some institutions to measure magnesium levels before initiation and to supplement magnesium before performing procedures if indicated. Reports have described the use of prophylactic magnesium infusions similar to those done with calcium. Haddad and colleagues (2005) investigated prophylactic administration of magnesium to allogeneic HPC-A donors. Supplementation was associated with normal ionized magnesium levels during the procedure, as well as greater parathyroid hormone response and higher blood glucose levels. However, no differences were seen with regard to the symptoms (mild paresthesias, coldness, and nausea) (Haddad et al., 2005).

As described, citrate is rapidly metabolized. This process consumes hydrogen ions; as a result, metabolic alkalosis due to citrate infusion may develop. The risk for this occurrence is greatest in patients with renal disease, who cannot adequately excrete bicarbonate (Kelleher & Schulman, 1987) and in those receiving replacement fluids containing citrate (Kelleher & Schulman, 1987; Dzik & Kirkley, 1988). A study comparing patients with TTP undergoing TPE with FFP replacement versus patients with myasthenia gravis undergoing TPE with albumin demonstrated increased frequency of metabolic alkalosis in the former group (Marques & Huang, 2001). Patients with TTP demonstrated a mean creatinine level of 1.3 mg/dL and mean blood urea nitrogen (BUN) of 24.8 mg/dL (Marques & Huang, 2001). Although the metabolic alkalosis seen in these patients did not reach critical levels (>35 mEq/L HCO_3^-) and resolved following cessation of TPE, it was associated with a critical decline in potassium (<3.0 mEq/L) during the procedures (Mercan et al., 1997). The presence of alkalosis can worsen hypocalcemia (Edmondson et al., 1975) and slow citrate metabolism (Dzik & Kirkley, 1988). Unfortunately, the symptoms of metabolic alkalosis are nonspecific, usually presenting as worsening symptoms of hypocalcemia. Alkalosis resolves with time or dialysis and can be avoided by reducing the amount of citrate infused by adjusting the blood/citrate ratio and/or using replacement fluids that lack citrate (Pearl & Rosenthal, 1985).

Metabolic alkalosis results in a shift in hydrogen ions from intracellular locations (in an attempt to compensate pH) with a concurrent flux of potassium into these cells to maintain electrical neutrality. The result is that significant drops in potassium can occur during large-volume hematopoietic progenitor cell collections in addition to those seen in the TTP patients described previously. Schlenke and colleagues (2000) found an average drop in potassium levels of 11.3% ± 7% in a study of 96 large-volume leukapheresis procedures. Despite this decline, none of the patients in this study experienced symptoms attributable to hypokalemia. Symptoms of hypokalemia include weakness, hypotonia, and cardiac arrhythmia (Schlenke et al., 2000). Treatment of such complications would consist of replacement of the potassium, orally or intravenously. A prudent option would be to prevent the reaction by determining the potassium level before the start of the procedure and supplementing if indicated.

ALLERGIC, ANAPHYLACTOID, AND ANAPHYLACTIC REACTIONS

Allergic, anaphylactoid, and anaphylactic reactions result from the release of vasoactive substances from mast cells and basophils. When the target antigen binds to the IgE molecule, substances including histamine, leukotriene C4, leukotriene D4, prostaglandin D_2, and platelet-activating factor are released. This causes smooth muscle contraction, increased vascular permeability, and vasodilatation, resulting in a variety of symptoms. Mast cells and basophils can also be activated by complement-derived factors such as C3a and C5a, which can be produced by antigen–IgG interactions and other mechanisms (Vamvakas & Pineda, 2001). These types of reactions can range from mild urticarial reactions to life-threatening anaphylactic reactions. Signs and symptoms of these reactions include pruritus, urticaria, erythema, flushing, angioedema, upper and lower airway obstruction, hypotension, shock, nausea, vomiting, and diarrhea (Vamvakas & Pineda, 2001).

Allergic reactions have been reported in both donors and patients undergoing hemapheresis procedures. Among donors, reactions have been reported among platelet, plasma, and granulocyte donors. In platelet and plasma donors, reactions to ethylene oxide gas used to sterilize the tubing sets used for the procedures have been described (Leitman et al., 1986; Muylle et al., 1986). These reactions have occurred predominantly in

donors who had undergone numerous previous procedures. It is thought that during the procedures, ethylene oxide present within the plastic binds to proteins within the plasma. The proteins serve as carrier molecules and the ethylene oxide as a hapten, resulting in an immune response with the generation of IgE antibodies to ethylene oxide. In most of the donors who experienced allergic phenomena, IgE antibodies to ethylene oxide were identified (Leitman et al., 1986). Reactions ranged from urticaria, flushing, and periorbital edema (Leitman et al., 1986) to an anaphylactic reaction consisting of wheezing, flushing, swelling of the lips, and hypotension (Muylle et al., 1986). The overall rate of allergic reaction in one study was 1.0% of platelet donors. The reactions also showed an increased frequency with the Fenwal CS3000 than with the Haemonetics V-50 (Haemonetics, Braintree, MA). This was thought to be due to the fact that at the start of processing with the CS3000, a mixture of saline and anticoagulant that was used to prime the bag was infused into the patient. This was not the case with the V-50. It was postulated that this resulted in a bolus of ethylene oxide that produced the symptoms (Leitman et al., 1986). Of importance is that manufacturers of hemapheresis tubing sets are now utilizing gamma irradiation to sterilize the kits, avoiding donor exposure to ethylene oxide.

Allergic reactions have been reported among granulocyte donors as well. In addition to ethylene oxide reactions, granulocyte donors are exposed to low- or high-molecular-weight HES to enhance red cell sedimentation. Although these substances are poor immunogens and have not been able to induce antibody formation, allergic reactions have occurred in the setting of HES use in hemapheresis (Dutcher et al., 1984) and as a volume expander (Ring & Messmer, 1977). The mechanism behind the production of anaphylactoid reactions with HES is thought to be due to the ability of HES to activate the alternative complement cascade. This would result in the production of C3a and C5a, both of which can cause mast cell and basophil release (Dutcher et al., 1984). Reactions reported to occur with HES include mild urticarial reactions and severe reactions with respiratory and cardiac arrest. The rate of allergic reaction in a study of patients receiving HES for volume expansion was 0.085%, with severe (anaphylactic) reactions occurring in 0.006% (Ring & Messmer, 1977). Reactions have occurred with both high-molecular-weight (hetastarch) (Ring & Messmer, 1977) and low-molecular-weight HES (pentastarch) (Kannan & Milligan, 1999). Because of this risk, Dutcher and colleagues (1984) recommended excluding people with a history of allergies as granulocyte donors.

Among therapeutic hemapheresis patients, reactions to ethylene oxide or HES could occur. In addition, TPE procedures frequently use plasma products as replacement solutions. As a result, patients are also at risk for allergic and anaphylactic reactions due to transfusion reactions. The most common allergic reaction within the setting of plasma product infusion is the urticarial reaction. This reaction occurs in 1% to 3% of plasma infusions and consists of hives scattered over the body. In 1 in 20,000 to 47,000 transfusions, anaphylaxis occurs (Vamvakas & Pineda, 2001). The most common cause of this last reaction is the infusion of plasma containing IgA into an IgA-deficient individual who possesses anti-IgA antibodies (Vamvakas & Pineda, 2001).

The treatment of allergic, anaphylactoid, and anaphylactic reactions depends on their severity. In donor reactions, the procedure should be stopped. Simple reactions such as urticaria can then be treated with oral antihistamines (e.g., diphenhydramine). The same treatment can be provided with therapeutic procedures, although in this case the procedure can be restarted following antihistamine administration. A simple allergic reaction is the only type of reaction in which the procedure can be restarted following treatment. In addition, the patient can be premedicated with antihistamines before subsequent procedures are performed.

Anaphylactic reactions are life-threatening. The procedure, whether donor or therapeutic, must be immediately discontinued. Vascular access should be kept open using saline. For less severe reactions, epinephrine 0.3 to 0.5 mg can be given subcutaneously, with the dose repeated every 20 to 30 minutes for up to three doses. In addition, aminophylline 6 mg/kg can be given for bronchospasm. This loading dose should be followed by an infusion of 0.5 to 1.0 mg/kg/hour. Volume expansion with normal saline or lactated Ringer's solution can be given for hypotension. Oxygen should be given for respiratory distress. For severe reactions, epinephrine 0.5 mg can be given intravenously, with repeated dosing every 5 to 10 minutes. Dopamine can also be given for hypotension unresponsive to volume. The airway must be protected, and endotracheal intubation may be indicated (Vamvakas & Pineda, 2001).

Obviously, the best course of action is to avoid such reactions. Donors who have experienced such reactions should be deferred from future donation. Patients with mild reactions should be premedicated with antihistamines. Those with severe reactions due to IgA should receive IgA-deficient replacement fluids. For most procedures, this could be albumin or saline. For procedures requiring plasma as a replacement fluid, as in TPE for TTP, IgA-deficient plasma products must be used.

ANGIOTENSIN-CONVERTING ENZYME INHIBITORS

The use of angiotensin-converting enzyme (ACE) inhibitors by patients undergoing hemapheresis procedures is associated with reactions similar in many respects to the allergic reactions described previously. These reactions consist of flushing, hypotension, bradycardia, and dyspnea (Strauss, 1996) and have been seen in patients undergoing TPE (Owen & Brecher, 1994), lipoprotein apheresis using dextran sulfate columns (Agishi, 1994), and treatment with staphylococcal A protein columns (Owen & Brecher, 1994). These reactions result from activation of the kinin system and generation of bradykinin when patient plasma comes in contact with the negatively charged plastic of the apheresis set. Normally, bradykinin is rapidly inactivated by kininase I and II. ACE inhibitors, however, block the actions of these enzymes such that high levels accumulate, producing the symptoms described previously (Strauss, 1996). During TPE with albumin, prekallikrein-activating factor present in the albumin can trigger the formation of bradykinin (Owen & Brecher, 1994). Again, the presence of ACE inhibitors prevents degradation of this substance. These reactions can be avoided by withholding ACE inhibitors for 24 to 48 hours before hemapheresis procedures (Owen & Brecher, 1994). Some newer ACE inhibitors have longer half-lives; withholding these drugs for longer periods or switching to ACE inhibitors with shorter half-lives may be necessary.

HYPOVOLEMIA AND VASOVAGAL REACTIONS

Hypotension can be seen during both donor and therapeutic hemapheresis procedures. This can be the result of two different pathophysiologic mechanisms. In hypovolemia, hypotension results from intravascular volume depletion due to too much volume being present within the extracorporeal circuit. Such reactions are characterized by both increased vascular tone and increased cardiac output as the sympathetic nervous system attempts to compensate for the hypovolemia (Strauss, 1996). Increasing both heart rate and contractility produces the increase in cardiac output. These reactions are not common among hemapheresis donors, as Standards for Blood Banks and Transfusion Services limit the amount of volume that that can be present within the extracorporeal circuit to 10.5 mL/kg (Standards Committee of the AABB, 2018), and the donors fulfill health and weight requirements. In therapeutic procedures, the patient has an underlying disease that may make hypovolemia more likely. For example, the presence of hypotension has been found to be more common in patients with neurologic disease (McLeod et al., 1999). Standards for Blood Banks and Transfusion Services do not prescribe limits on extracorporeal volume during therapeutic hemapheresis procedures, although application of the limits used during donor hemapheresis procedures would seem prudent (Strauss, 1996).

The second mechanism causing hypotension during hemapheresis procedures is the vasovagal reaction. In contrast to hypovolemia, in which the body compensates for hypotension by increasing sympathetic tone, during a vasovagal reaction parasympathetic output increases disproportionately, resulting in slowing of the heart rate and decreased vascular tone (Strauss, 1996). Factors that have been associated with such reactions in whole-blood donors include younger age, low weight, first-time donation, and inattentive staff (Newman, 1997). Tomita and colleagues (2002) examined the incidence of vasovagal reactions among apheresis donors and whole-blood donors at the same collection center. They noted that the incidence of these reactions among apheresis donors increased with age, unlike what has been reported with whole-blood donors. The age-related increase in vasovagal reactions was even more common in women and was thought to result from a lower circulating blood volume in these populations (older adults and women), leading to a greater percentage of the donor's blood being within the extracorporeal circuit during collection. It was also noted that the incidence of reactions increased with increasing cycles during a collection, and it was theorized that hypocalcemia was involved in the onset of vasovagal reactions (Tomita et al., 2002).

Hypovolemic and vasovagal reactions are treated similarly. The procedure should be temporarily interrupted, and a fluid bolus should be infused. If the reaction is due to hypovolemia, blood pressure should increase and pulse rate should decrease in response to this intervention. If the reaction is due to a vasovagal reaction, this may not occur. Additional treatments for vasovagal reactions include placing the donor/patient in

the Trendelenburg position (supine position with feet higher than head), applying cold compresses to the forehead and neck, and reassuring the donor/patient (Strauss, 1996).

HYDROXYETHYL STARCH AND COAGULOPATHY

As discussed under the section dealing with TPE, removal of plasma from a patient and replacement of the volume with albumin or some other fluid that does not contain coagulation factors can result in mild temporary abnormalities in coagulation. These changes are usually short-lived, with return of most coagulation factors to normal levels within 24 to 48 hours. The use of HES as volume replacement or as a sedimenting agent is also associated with changes in coagulation factor levels. Both high-molecular-weight HES, such as hetastarch, and low-molecular-weight HES, such as pentastarch, result in prolongation of the partial thromboplastin time (PTT) as well as decreases in fibrinogen levels. This is thought to result from the dilutional effects produced when these substances are infused. High-molecular-weight, but not low-molecular-weight HES is also associated with decreases in factor VIII activity, factor VIII antigen, and vWF antigen, as well as prolongation of bleeding time (Strauss et al., 1988). It is thought that this last effect is a result of the decrease in vWF antigen levels and may represent an acquired von Willebrand disease–like state. The risk of coagulopathy with HES appears to be dose dependent. In the setting of volume expansion in critical care, the maximum dose of HES needed to avoid such complications has been suggested to be 20 mL/kg/24-hour period. Doses up to 3600 mL have been given in this setting without difficulty (Nearman & Herman, 1991). The danger in hemapheresis procedures is that multiple collections or therapeutic procedures may be necessary in a given donor/patient over consecutive days. Because HES, especially high-molecular-weight HES, has a long half-life, this may result in an accumulation of HES over the course of the hemapheresis procedures and the potential danger of coagulopathy.

HYDROXYETHYL STARCH AND RENAL DYSFUNCTION

When used as a volume expander, HES can cause new or worsening renal dysfunction, particularly in critically ill patients. Three randomized controlled trials published in 2012 highlight the increased risk for mortality and renal injury in patients with sepsis and those admitted to the intensive care unit (ICU) (Perner et al., 2012; Guildet et al., 2012; Myburgh et al., 2012). Based on these studies, on June 24, 2013, the FDA added a black box warning to HES (FDA, 2013). HES should be avoided in critically ill patients with sepsis, patients in the ICU, and patients or donors with preexisting renal dysfunction. However, it is important to note that the dose of HES used in apheresis procedures is much smaller than that used for volume expansion (9.8 vs. 70 mL/kg). A multicenter retrospective study examining the use of HES during leukocytapheresis compared outcomes, laboratory values, and the need for renal replacement therapy in patients in whom HES was used as a sedimenting agent and those in whom it was not used. This study found no associated adverse effects with the use of HES (Pagano et al., 2016).

HYDROXYETHYL STARCH AND OTHER SIDE EFFECTS

As has been mentioned, HES has a long half-life. This is dependent on the metabolism of HES by α-amylase and subsequent renal excretion of the breakdown products (Yacobi et al., 1982). Persistent pruritus due to deposition of HES in the skin has been reported as one of the most frequent complications of HES administration. Skin deposits have been detected for up to 4 years following administration (Sirtl et al., 1999; Stander et al., 2001).

In addition to skin deposition, a case report has described marrow and organ failure in a patient undergoing chronic TPE (20 months) with HES used as the replacement fluid. In this patient, foamy macrophages containing HES were found replacing bone marrow as well as infiltrating duodenal mucosa, liver, peritoneum, and dura mater. These cells were also present in ascitic fluid (Auwerda et al., 2002).

AIR EMBOLUS

Air embolus is a rare complication of hemapheresis procedures. It occurs when air enters the venous system through a leak in the hemapheresis instrument or the venous access. Air entering the right ventricle and pulmonary artery produces obstruction to right ventricular output and pulmonary artery vasoconstriction (Montacer-Kuhssari et al., 1994). Symptoms of air embolism include dyspnea, tachypnea, cyanosis, tachycardia, and hypotension. The reason for the rarity of this complication is that all modern hemapheresis instruments possess sensors that can detect air within the extravascular circuit and stop the procedure. Should air embolism occur, however, treatment consists of placing the donor/patient in the Trendelenburg position on the left side. This traps the air in the apex of the right ventricle, away from the pulmonary outflow tract, improving right ventricular outflow. Over time, the air will dissolve.

SUMMARY

In summary, hemapheresis represents a safe and effective technique for the production of needed blood components as well as for the treatment of a variety of diseases. Although hemapheresis is often compared with the 18th-century practice of bloodletting, it shares little with this practice. Hemapheresis is selective in what is removed from the donor/patient and is generally a safe procedure. However, hemapheresis is not without risk and should be applied only to those diseases and disorders for which the possibility of benefit exists and for which evidence in support of this benefit has been shown.

SELECTED REFERENCES

Ibrahim RB, Liu C, Cronin SM, et al.: Drug removal by plasmapheresis: an evidence-based review, *Pharmacotherapy* 27:1529–1549, 2007.

An extensive review of the literature concerning the effects of plasma exchange on drug clearance and metabolism. The article provides suggestions for therapy modification and future research.

Ibrahim RB, Balogun RA: Medications in patients treated with therapeutic plasma exchange: prescription dosage, timing, and drug overdose, *Semin Dial* 25:176–189, 2012.

A review of the published literature of the removal of medications, both overdose and therapeutic concentrations, by plasma exchange. Describes the pharmacokinetic parameters and procedure parameters that determine the degree of removal of a drug.

Linz W, Chibber V, Hofmann J, et al.: *Principles of apheresis technology*, ed 6, Vancouver, BC, Canada, 2017, American Society for Apheresis.

A comprehensive textbook that discusses technical aspects of apheresis technology and instrumentation. It includes a discussion of medical decision making, apheresis patient care, apheresis program management, quality considerations, and ethical considerations. This textbook includes self-study questions for preparation for the American Society for Clinical Pathology Qualification in Apheresis Examination.

McLeod BC, Weinstein R, Winters JL, et al.: *Apheresis: principles and practice*, ed 3, Bethesda, MD, 2010, AABB Press.

A comprehensive textbook that addresses both donor and therapeutic apheresis, including the history of apheresis, currently available instrumentation, and an in-depth discussion of the mechanism of action and the physiology of apheresis.

Padmanabhan A, Connelly-Smith L, Aqui N, et al.: Guidelines on the use of therapeutic apheresis in clinical practice: evidence-based approach from the apheresis applications committee of the American Society for apheresis. The Eighth special issue, *J Clin Apheresis* 34:171–354, 2019.

A comprehensive review of the use of therapeutic apheresis. Includes one-page summaries describing treatment recommendations and technical considerations for more than 50 diseases. Also provides categorization and strength of evidence for the use of apheresis in the diseases discussed.

Shaz BH, Schwartz J, Winters JL: How we developed and use the ASFA guidelines for therapeutic apheresis procedures, *Transfusion* 54:17–25, 2014.

A discussion of the clinical decision-making process to be used when considering performing a therapeutic hemapheresis procedure and how to utilize the ASFA guidelines in this process.

Access the complete reference list online at Elsevier eBooks for Practicing Clinicians.

REFERENCES

AABB [Internet]: Association bulletin. http://www.aabb.org/programs/publications/bulletins/Documents/ab14-07.pdf, 2014 #14-07, Available at.

Abel JJ, Rowntree LC, Turner BB: Plasma removal with return of corpuscles, *J Pharmacol Exper Ther* 5:625–641, 1914.

Adachi S, Kubota M, Lin Y, et al.: In vivo administration of granulocyte colony-stimulating factor promotes neutrophil survival in vitro, *Eur J Haematol* 53:129–134, 1994.

Adams RJ, Brambilla D: Discontinuing prophylactic transfusions used to prevent stroke in sickle cell disease, *N Engl J Med* 353:2769–2778, 2005.

Adams RJ, McKie VC, Hsu L, et al.: Prevention of a first stroke by transfusions in children with sickle cell anemia and abnormal results on transcranial Doppler ultrasonography, *N Engl J Med* 339:5–11, 1998.

Adkins D, Goodgold H, Hendershott L, et al.: Indium-labeled white blood cells apheresed from donors receiving G-CSF localize to sites of inflammation when infused into allogeneic bone marrow transplant recipients, *Bone Marrow Transplant* 19:809–812, 1997a.

Adkins D, Spitzer G, Johnston M, et al.: Transfusions of granulocyte-colony-stimulating factor-mobilized granulocyte components to allogeneic transplant recipients: analysis of kinetics and factors determining posttransfusion neutrophil and platelet counts, *Transfusion* 37:737–748, 1997b.

Agishi T: Anion-blood contact reaction (ABC reaction) in patients treated by LDL apheresis with dextran sulfate-cellulose column while receiving ACE inhibitors, *J Am Med Assoc* 271:195–196, 1994.

Alving BM, Hojima Y, Pisano JJ, et al.: Hypotension associated with prekallikrein activator (Hageman-factor fragments) in plasma protein fraction, *N Engl J Med* 299:66–70, 1978.

Amrein K, Katschnig C, Sipurzynski S, et al.: Apheresis affects bone and mineral metabolism, *Bone* 46:789–795, 2010.

Arimura K, Inoue H, Kukita T, et al.: Acute lung injury in a healthy donor during mobilization of peripheral blood stem cells using granulocyte-colony stimulating factor alone, *Haematologica* 90:e27–e29, 2005.

Auwerda JJ, Wilson JH, Sonneveld P: Foamy macrophage syndrome due to hydroxyethyl starch replacement: a severe side effect in plasmapheresis, *Ann Intern Med* 137:1013–1014, 2002.

Azevedo AM, Tabak DG: Life-threatening capillary leak syndrome after G-CSF mobilization and collection of peripheral blood progenitor cells for allogeneic transplantation, *Bone Marrow Transplant* 28:311–312, 2001.

Baron BW, Mick R, Baron JM: Combined plateletpheresis and cytotoxic chemotherapy for symptomatic thrombocytosis in myeloproliferative disorders, *Cancer* 72:1209–1218, 1993.

Basic-Jukic N, Kes P, Glavas-Boras S, et al.: Complications of therapeutic plasma exchange: experience with 4857 treatments, *Ther Apher Dial* 9:391–395, 2005.

Bender JG, To LB, Williams S, et al.: Defining a therapeutic dose of peripheral blood stem cells, *J Hematother* 1:329–341, 1992.

Benjamin RJ, Dy BA, Kennedy JM, et al.: The relative safety of automated two-unit red blood cell procedures and manual whole-blood collection in young donors, *Transfusion* 49:1874–1883, 2009.

Bennett CL, Evens AM, Andritsos LA, et al.: Haematological malignancies developing in previously healthy individuals who received haematopoietic growth factors: report from the Research on Adverse Drug Events and Reports (RADAR) project, *Br J Haematol* 135:642–650, 2006.

Bensinger W, Appelbaum F, Rowley S, et al: Factors that influence collection and engraftment of autologous peripheral-blood stem cells. *J Clin Oncol* 13:2547–2555, 1995.

Bensinger WI: Allogeneic transplantation: peripheral blood vs. bone marrow, *Curr Opin Oncol* 24:191–196, 2012.

Bensinger WI, Martin PJ, Storer B, et al.: Transplantation of bone marrow as compared with peripheral-blood cells from HLA-identical relatives in patients with hematologic cancers, *N Engl J Med* 344:175–181, 2001.

Bensinger WI, Price TH, Dale DC, et al.: The effects of daily recombinant human granulocyte colony-stimulating factor administration on normal granulocyte donors undergoing leukapheresis, *Blood* 81:1883–1888, 1993.

Blanchette VS, Hume HA, Levy GJ, et al.: Guidelines for auditing pediatric blood transfusion practices, *Am J Dis Child* 145:787–796, 1991.

Bolan CD, Cecco SA, Wesley RA, et al.: Controlled study of citrate effects and response to i.v. calcium administration during allogeneic peripheral blood progenitor cell donation, *Transfusion* 42:935–946, 2002.

Bolan CD, Cecco SA, Yau YY, et al.: Randomized placebo-controlled study of oral calcium carbonate supplementation in plateletpheresis: II. Metabolic effects, *Transfusion* 43:1414–1422, 2003a.

Bolan CD, Wesley RA, Yau YY, et al.: Randomized placebo-controlled study of oral calcium carbonate administration in plateletpheresis: I. Associations with donor symptoms, *Transfusion* 43:1403–1413, 2003b.

Bonilla MA, Dale D, Zeidler C, et al.: Long-term safety of treatment with recombinant human granulocyte colony-stimulating factor (r-metHuG-CSF) in patients with severe congenital neutropenias, *Br J Haematol* 88:723–730, 1994.

Bowden RA, Slichter SJ, Sayers M, et al.: A comparison of filtered leukocyte-reduced and cytomegalovirus (CMV) seronegative blood products for the prevention of transfusion-associated CMV infection after marrow transplant, *Blood* 86:3598–3603, 1995.

Brauninger S, Bialleck H, Thorausch K, et al.: Mobilized allogeneic peripheral stem/progenitor cell apheresis with Spectra Optia v.5·0, a novel, automatic interface-controlled apheresis system: results from the first feasibility trial, *Vox Sang* 101:237–246, 2011.

Brauninger S, Bialleck H, Thorausch K, et al.: Allogeneicdonor peripheral blood "stem cell" apheresis: prospective comparison of two apheresis systems, *Transfusion* 52:1137–1145, 2012.

Brugger W, Bross KJ, Glatt M, et al.: Mobilization of tumor cells and hematopoietic progenitor cells into peripheral blood of patients with solid tumors, *Blood* 83:636–640, 1994.

Buchta C, Macher M, Bieglmayer C, et al.: Reduction of adverse citrate reactions during autologous large-volume PBPC apheresis by continuous infusion of calcium-gluconate, *Transfusion* 43:1615–1621, 2003.

Buckner CD, Clift RA, Thomas ED, et al.: Early infectious complications in allogeneic marrow transplant recipients with acute leukemia: effects of prophylactic measures, *Infection* 11:243–250, 1983.

Buffaloe GW, Heineken FG: Plasma volume nomograms for use in therapeutic plasma exchange, *Transfusion* 23:355–357, 1983.

Bunker JP, Bendixen HH, Murphy AJ: Hemodynamic effects of intravenously administered sodium citrate, *N Engl J Med* 266:372–377, 1962.

Burch JW, Mair DC, Meny GM, et al.: The risk of posterior subcapsular cataracts in granulocyte donors, *Transfusion* 45:1701–1708, 2005.

Burgstaler EA: Current instrumentation for apheresis. In McLeod BC, Szczepiorkowski ZM, Weinstein R, et al.: *Apheresis: principles and practice*, ed 3, Bethesda, Md, 2010, AABB Press, pp 95–130.

Burgstaler EA, Pineda AA: Hydroxyethylstarch as replacement in therapeutic plasma exchange, *Prog Clin Biol Res* 337:395–397, 1990.

Burgstaler EA, Pineda AA: Therapeutic cytapheresis: continuous flow versus intermittent flow apheresis systems, *J Clin Apheresis* 9:205–209, 1994.

Burgstaler EA, Pineda A: Therapeutic plasma exchange: a paired comparison of Fresenius AS104 vs. COBE Spectra, *J Clin Apheresis* 16:61–66, 2001.

Burgstaler EA, Pineda AA, Winters JL: Hematopoietic progenitor cell large volume leukapheresis (LVL) on the Fenwall Amicus blood separator, *J Clin Apheresis* 19:103–111, 2004.

Buss DH, Cashell AW, O'Connor ML, et al.: Occurrence, etiology, and clinical significance of extreme thrombocytosis: a study of 280 cases, *Am J Med* 96:247–253, 1994.

Cashen AF: Plerixafor hydrochloride: a novel agent for the mobilization of peripheral blood stem cells, *Drugs Today* 45:497–505, 2009.

Caspar CB, Seger RA, Burger J, et al.: Effective stimulation of donors for granulocyte transfusions with recombinant methionyl granulocyte colony-stimulating factor, *Blood* 81:2866–2871, 1993.

Choi MH, Choe YH, Park Y, et al.: The effect of therapeutic leukapheresis on early complications and outcomes in patients with acute leukemia and hyperleukocytosis: a propensity score-matched study, *Transfusion* 58:208–216, 2018.

Chopek M, McCullough J: Protein and biochemical changes during plasma exchange. In Berkman EM, Umlas J, editors: *Therapeutic hemapheresis*, Washington, DC, 1980, AABB, pp 13–52.

Christensen I, Heald P: Photopheresis in the 1990s, *J Clin Apheresis* 6:216–220, 1991.

Ciszewski TS, Ralston S, Acteson D, et al.: Protein levels and plasmapheresis intensity, *Transfus Med* 3:59–65, 1993.

Clark WF, Stewart AK, Rock GA, et al.: The Canadian Apheresis Group: plasma exchange when myeloma presents as acute renal failure: a randomized, controlled trial, *Ann Intern Med* 143:777–784, 2005.

COBE BCT: *COBE Spectra red blood cell exchange inservice student workbook*, Lakewood, Colo, 1997, COBE BCT.

Code of Federal Regulations: *: 21 CFR 640*, Washington, DC, April 1, 2014, Government Printing Office.

Confer DL, Miller JP: Long-term safety of filgrastim (rhG-CSF) administration, *Br J Haematol* 137:77–78, 2007.

Cooling L, Hoffman S, Herrst M, et al.: A prospective randomized trial of two popular mononuclear cell collection sets for autologous peripheral blood stem cell collection in multiple myeloma, *Transfusion* 50:100–119, 2010.

Cortelazzo S, Viero P, Finazzi G, et al.: Incidence and risk factors for thrombotic complications in a historical cohort of 100 patients with essential thrombocythemia, *J Clin Oncol* 8:556–562, 1990.

Couriel D, Weinstein R: Complications of therapeutic plasma exchange: a recent assessment, *J Clin Apheresis* 9:1–5, 1994.

Crookston K, Delaney M, De Simone NK, Kim HC, Kiss JE, Linz WJ, Pierce A, Schwartz J, Shaz BH, Szczepiorkowski ZM, Winters JL: *Therapeutic apheresis: a Physician's Handbook*, 5th edition, Bethesda, Maryland, 2017, AABB.

Dale DC, Liles WC, Llewellyn C, et al.: Neutrophil transfusions: kinetics and functions of neutrophils mobilized with granulocyte-colony-stimulating factor and dexamethasone, *Transfusion* 38:713–721, 1998.

Dall'Amico R, Murer L: Extracorporeal photochemotherapy: a new therapeutic approach for allograft rejection, *Transfus Apheresis Sci* 26:197–204, 2002.

Dau PC: Immunologic rebound, *J Clin Apheresis* 10:210–217, 1995.

Davies SC, Roberts-Harewood M: Blood transfusion in sickle cell disease, *Blood Rev* 11:57–71, 1997.

Derksen RH, Schuurman HJ, Gmelig Meyling FH, et al.: Rebound and overshoot after plasma exchange in humans, *J Lab Clin Med* 104:35–43, 1984a.

Derksen RH, Schuurman HJ, Meyling FH, et al.: The efficacy of plasma exchange in the removal of plasma components, *J Lab Clin Med* 104:346–354, 1984b.

Despotis GJ, Goodnough LT, Dynis M, et al.: Adverse events in platelet apheresis donors: a multivariate analysis in a hospital-based program, *Vox Sang* 77:24–32, 1999.

Dettke M, Hlousek M, Kurz M, et al.: Increase in endogenous thrombopoietin in healthy donors after automated plateletpheresis, *Transfusion* 38:449–453, 1998.

DiGuardo M, Burgstaler EA, Winters JL: An institutional review of the Spectra Optia for use in therapeutic plateletapheresis procedures, *J Clin Apheresis* 34:148–149, 2019.

Dreger P, Marquardt P, Haferlach T, et al.: Effective mobilisation of peripheral blood progenitor cells with "Dexa-BEAM" and G-CSF: timing of harvesting and composition of the leukapheresis product, *Br J Cancer* 68:950–957, 1993.

Dutcher JP, Aisner J, Hogge DE, et al.: Donor reaction to hydroxyethyl starch during granulocytapheresis, *Transfusion* 24:66–67, 1984.

Dutcher JP, Schiffer CA, Johnston GS, et al.: Alloimmunization prevents the migration of transfused indium-111-labeled granulocytes to sites of infection, *Blood* 62:354–360, 1983.

Dutcher JP, Schiffer CA, Wiernik PH: Hyperleukocytosis in adult acute nonlymphocytic leukemia: impact on remission rate and duration, and survival, *J Clin Oncol* 5:1364–1372, 1987.

Dzik WH, Kirkley S: Citrate toxicity during massive blood transfusion, *Transfus Med Rev* 2:76–94, 1988.

Edelson RL: Mechanistic insights into extracorporeal photochemotherapy: efficient induction of monocyte-to-dendritic cell maturation, *Transfus Apher Sci* 50:322–329, 2014.

Edelson R, Berger C, Gasparro F, et al.: Treatment of cutaneous T-cell lymphoma by extracorporeal photochemotherapy. Preliminary results, *N Engl J Med* 316:297–303, 1987.

Eder AF, Dy BA, Kennedy JM, et al: The American Red Cross donor hemovigilance program: complications of blood donation reported in 2006, Transfusion 48:1809–1819, 2008.

Edmondson JW, Brashear RE, Li T: Tetany: quantitative interrelationships between calcium and alkalosis, *Am J Physiol* 228:1082–1086, 1975.

Egan JA, Hay SN, Brecher ME: Frequency and significance of schistocytes in TTPHUS patients at the discontinuation of plasma exchange therapy, *J Clin Apher* 19:165–167, 2004.

Estcourt LJ, Stanworth SJ, Hopewell S, et al.: Granulocyte transfusions for treating infections in people with neutropenia or neutrophil dysfunction, *Cochrane Database Syst Rev* 4, 2016. CD005339.

Flaum MA, Cuneo RA, Appelbaum FR, et al.: The hemostatic imbalance of plasma-exchange transfusion, *Blood* 54:694–702, 1979.

Flowers ME, Parker PM, Johnston LJ, et al.: Comparison of chronic graft-versus-host disease after transplantation of peripheral blood stem cells versus bone marrow in allogeneic recipients: long-term follow-up of a randomized trial, *Blood* 100:415–419, 2002.

Food and Drug Administration [Internet]: Place unknown, Publisher unknown, date unknown. Available at: http://www.fda.gov/BiologicsBloodVaccines/SafetyAvailability/ucm358271. updated 2013 Nov 26; cited 2014 Sept 6.

Food and Drug Administration (Division of Blood and Blood Products, Center for Biologics Evaluation and Research): *Guideline for the collection of platelets, pheresis prepared by automated methods*, Bethesda, Md, 1988, FDA.

Food and Drug Administration (Division of Blood and Blood Products, Center for Biologics Evaluation and Research): *Memorandum to registered blood and source plasma establishments. Revision of FDA memorandum of August 27, 1982. Requirements for infrequent plasmapheresis donors*, Bethesda, Md, 1995, FDA.

Food and Drug Administration (Division of Blood and Blood Products, Center for Biologics Evaluation and Research): *Recommendations for collecting red blood cells by automated apheresis methods*, Bethesda, Md, 2001, FDA.

Food and Drug Administration (Division of Blood and Blood Products, Center for Biologics Evaluation and Research): *Guidance for industry and FDA review staff: collection of platelets by automated methods*, Rockville, Md, 2007, FDA.

Foss FM, Gorgun G, Miller KB: Extracorporeal photopheresis in chronic graft-versus-host disease, *Bone Marrow Transplant* 29:719–725, 2002.

Gansner JM, Papari M, Goldstein J, et al.: Severe CD4+ T-cell lymphopenia is not observed in frequent plateletpheresis donors collected on the Fenwal Amicus, *Transfusion* 59:2783–2787, 2019.

Gazitt Y, Tian E, Barlogie B, et al.: Differential mobilization of myeloma cells and normal hematopoietic stem cells in multiple myeloma after treatment with cyclophosphamide and granulocyte-macrophage colony-stimulating factor, *Blood* 87:805–811, 1996.

Ghodsi Z, Strauss RG: Cataracts in neutrophil donors stimulated with adrenal corticosteroids, *Transfusion* 41:1464–1468, 2001.

Gilcher RO: Apheresis: principles and practice. In Rossi EC, Simon TL, Moss GS, et al.: *Principles of transfusion medicine*, ed 2, Baltimore, Md, 1996, Williams & Wilkins, pp 537–545.

Giles FJ, Shen Y, Kantarjian HM, et al.: Leukapheresis reduces early mortality in patients with acute myeloid leukemia with high white cell counts but does not improve long-term survival, *Leuk Lymphoma* 42:67–73, 2001.

Gillespie TW, Hillyer CD: Peripheral blood progenitor cells for marrow reconstitution: mobilization and collection strategies, *Transfusion* 36:611–624, 1996.

Glasser L, Huestis DW, Jones JF: Functional capabilities of steroid-recruited neutrophils harvested for clinical transfusion, *N Engl J Med* 297:1033–1036, 1977.

Glowitz RJ, Slichter SJ: Frequent multiunit plateletpheresis from single donors: effects on donors' blood and the platelet yield, *Transfusion* 20:199–205, 1980.

Goldberg SL, Mangan KF, Klumpp TR, et al.: Complications of peripheral blood stem cell harvesting: review of 554 PBSC leukaphereses, *J Hematother* 4:85–90, 1995.

Goodnough LT, Ali S, Despotis G, et al.: Economic impact of donor platelet count and platelet yield in apheresis products: relevance for emerging issues in platelet transfusion therapy, *Vox Sang* 76:43–49, 1999.

Goss GA, Weinstein R: Pentastarch as partial replacement fluid for therapeutic plasma exchange: effect on plasma proteins, adverse events during treatment, and serum ionized calcium, *J Clin Apheresis* 14:114–121, 1999.

Grishaber JE, Cunningham MC, Rohret PA, et al.: Analysis of venous access for therapeutic plasma exchange in patients with neurological disease, *J Clin Apheresis* 7:119–123, 1992.

Grupp SA, Frangoul H, Wall D, et al.: Use of G-CSF in matched sibling donor pediatric allogeneic transplantation: a consensus statement from the Children's Oncology Group (COG) transplant discipline committee and Pediatric Blood and Marrow Transplant Consortium (PBMTC) executive committee, *Pediatr Blood Cancer* 46:414–421, 2006.

Guildet B, Martinet O, Boulain T, et al.: Assessment of hemodynamic efficacy and safety of 6% hydroxyethyl starch 130/0.4 vs. 0.9% NaCl fluid replacement in patients with severe sepsis: the CRYSTMAS study, *Crit Care* 16:R94, 2012.

Haddad S, Leitman SF, Wesley RA, et al.: Placebo-controlled study of intravenous magnesium supplementation during large-volume leukapheresis in healthy allogeneic donors, *Transfusion* 45:934–944, 2005.

Heddle NM: Febrile nonhemolytic transfusion reactions to platelets, *Curr Opin Hematol* 2:478–483, 1995.

Heimfeld S: Bone marrow transplantation: how important is CD34 cell dose in HLA-identical stem cell transplantation? *Leukemia* 17:856–858, 2003.

Hester JP, Dignani MC, Anaissie EJ, et al.: Collection and transfusion of granulocyte concentrates from donors primed with granulocyte stimulating factor and response of myelosuppressed patients with established infection, *J Clin Apheresis* 10:188–193, 1995.

Hester JP, McCullough J, Mishler JM, et al.: Dosage regimens for citrate anticoagulants, *J Clin Apheresis* 1:149–157, 1983.

Heyns AP, Badenhorst PN, Lotter MG, et al.: Kinetics and mobilization from the spleen of Indium-111-labeled platelets during platelet apheresis, *Transfusion* 25:215–218, 1985.

Higby DJ, Henderson ES, Burnett D, et al.: Filtration leukapheresis: effects of donor stimulation with dexamethasone, *Blood* 50:953–959, 1977.

Hillyer CD, Berkman EM: Plasma exchange in dysproteinemias. In Rossi EC, Simon TL, Moss GS, et al.: *Principles of transfusion medicine*, ed 2, Baltimore, Md, 1996, Williams & Wilkins, pp 569–575.

Huestis DW: Risks and safety practices in hemapheresis procedures, *Arch Pathol Lab Med* 113:273–278, 1989.

Blood 87:3959–3962, 1996.

Iacone A, Di Bartolomeo P, Di Girolamo G, et al.: Hydroxyethyl starch and steroid improved collection of normal granulocytes with continuous flow centrifugation gravity leukapheresis, *Haematologica* 66:645–655, 1981.

Isbister JP: Cytapheresis: the first 25 years, *Ther Apher* 1:17–21, 1997.

Iwasaki Y, Kinoshita M, Ikeda K, et al.: Neuropsychological function before and after plasma exchange in myasthenia gravis, *J Neurol Sci* 114:223–226, 1993.

Jaeger BR, Marx P, Pfefferkorn T, et al.: Heparin-mediated extracorporeal LDL/fibrinogen precipitation—H.E.L.P.—in coronary and cerebral ischemia, *Acta Neurochir Suppl (Wien)* 73:81–84, 1999.

Jendiroba DB, Lichtiger B, Anaissie E, et al.: Evaluation and comparison of three mobilization methods for the collection of granulocytes, *Transfusion* 38:722–728, 1998.

Joos K, Herzog R, Einsele H, et al.: Characterization and functional analysis of granulocyte concentrates collected from donors after repeated G-CSF stimulation, *Transfusion* 42:603–611, 2002.

Kale-Pradhan PB, Woo MH: A review of the effects of plasmapheresis on drug clearance, *Pharmacotherapy* 17:684–695, 1997.

Kamochi M, Aibara K, Nakata K, et al.: Profound ionized hypomagnesemia induced by therapeutic plasma exchange in liver failure patients, *Transfusion* 42:1598–1602, 2002.

Kannan S, Milligan KR: Moderately severe anaphylactoid reaction to pentastarch (200/0.5) in a patient with acute severe asthma, *Intensive Care Med* 25:220–222, 1999.

Kaplinsky C, Trakhtenbrot L, Hardan I, et al.: Tetraploid myeloid cells in donors of peripheral blood stem cells treated with rhG-CSF, *Bone Marrow Transplant* 32:31–34, 2003.

Kelleher SP, Schulman G: Severe metabolic alkalosis complicating regional citrate hemodialysis, *Am J Kidney Dis* 9:235–236, 1987.

Kessinger A, Armitage JO, Smith DM, et al.: High-dose therapy and autologous peripheral blood stem cell transplantation for patients with lymphoma, *Blood* 74:1260–1265, 1989.

Kessinger A, Bishop MR, Anderson JR, et al.: Comparison of subcutaneous and intravenous administration of recombinant human granulocyte-macrophage colony-stimulating factor for peripheral blood stem cell mobilization, *J Hematother* 4:81–84, 1995.

Kessinger A, Sharp JG: The whys and hows of hematopoietic progenitor and stem cell mobilization, *Bone Marrow Transplant* 31:319–329, 2003.

Kim SR, Choung HK, Kim DW, et al.: Evaluation of a new cell separator for collection of peripheral blood CD34+ progenitor cells in pediatric patients, *Transfusion* 51:306–312, 2011.

Kintzel PE, Eastlund T, Calis KA: Extracorporeal removal of antimicrobials during plasmapheresis, *J Clin Apher* 18:194–205, 2003.

Kishimoto M, Ohto H, Shikama Y, et al.: Treatment for the decline of ionized calcium levels during peripheral blood progenitor cell harvesting, *Transfusion* 42:1340–1347, 2002.

Klingel R, Fassbender C, Fassbender T, et al.: Clinical studies to implement rheopheresis for age-related macular degeneration guided by evidence-based-medicine, *Transfus Apheresis Sci* 29:71–84, 2003.

Knobler RM, Trautinger F, Graninger W, et al.: Parenteral administration of 8-methoxypsoralen in photopheresis, *J Am Acad Dermatol* 28:580–584, 1993.

Kobbe G, Soehngen D, Heyll A, et al.: Large volume leukapheresis maximizes the progenitor cell yield for allogeneic peripheral blood progenitor donation, *J Hematother* 6:125–131, 1997.

Koch-Weser J, Sellers EM: Binding of drugs to serum albumin (first of two parts), *N Engl J Med* 294:311–316, 1976.

Kolovratova V, List J, Worel P, et al.: Administration of Prednisolone intravenously or Dexamethason orally in random donors reveals equal results in granulocyte collection: a single centre experience, *Vox Sang* 103:75–78, 2012.

Korbling M: Effects of granulocyte colony-stimulating factor in healthy subjects, *Curr Opin Hematol* 5:209–214, 1998.

Korbling M, Huh YO, Durett A, et al.: Allogeneic blood stem cell transplantation: peripheralization and yield of donor-derived primitive hematopoietic progenitor cells (CD34+ Thy-1dim) and lymphoid subsets, and possible predictors of engraftment and graft-versus-host disease, *Blood* 86:2842–2848, 1995.

Kroger N, Zander AR: Dose and schedule effect of G-GSF for stem cell mobilization in healthy donors for allogeneic transplantation, *Leuk Lymphoma* 43:1391–1394, 2002.

Lane DM, McConathy WJ, Laughlin LO, et al.: Weekly treatment of diet/drug-resistant hypercholesterolemia with the heparin-induced extracorporeal low-density lipoprotein precipitation (HELP) system by selective plasma low-density lipoprotein removal, *Am J Cardiol* 71:816–822, 1993.

Lapidot T, Petit I: Current understanding of stem cell mobilization: the roles of chemokines, proteolytic enzymes, adhesion molecules, cytokines, and stromal cells, *Exp Hematol* 30:973–981, 2002.

Lazarus EF, Browning J, Norman J, et al.: Sustained decreases in platelet count associated with multiple, regular plateletpheresis donations, *Transfusion* 41:756–761, 2001.

Lee JH, Klein HG: Collection and use of circulating hematopoietic progenitor cells, *Hematol Oncol Clin North Am* 9:1–22, 1995.

Lee JH, Leitman SF, Klein HG: A controlled comparison of the efficacy of hetastarch and pentastarch in granulocyte collections by centrifugal leukapheresis, *Blood* 86:4662–4666, 1995.

Leebmann J, Roeseler E, Julius U, et al.: Lipoprotein apheresis in patients with maximally tolerated lipid-lowering therapy, lipoprotein(a)-hyperlipoproteinemia, and pro-

gressive cardiovascular disease: prospective observational multicenter study, *Circulation* 128:2567–2576, 2013.
Leitman SF, Boltansky H, Alter HJ, et al.: Allergic reactions in healthy plateletpheresis donors caused by sensitization to ethylene oxide gas, *N Engl J Med* 315:1192–1196, 1986.
Lester TJ, Johnson JW, Cuttner J: Pulmonary leukostasis as the single worst prognostic factor in patients with acute myelocytic leukemia and hyperleukocytosis, *Am J Med* 79:43–48, 1985.
Leung N, Gertz MA, Zeldenrust SR, et al.: Improvement of cast nephropathy with plasma exchange depends on the diagnosis and on reduction of serum free light chains, *Kid Int* 73:1282–1288, 2008.
Levy JB, Turner AN, Rees AJ, et al.: Long-term outcome of anti-glomerular basement membrane antibody disease treated with plasma exchange and immunosuppression, *Ann Intern Med* 134:1033–1042, 2001.
Lewis SL, Kutvirt SG, Bonner PN, et al.: Effect of long-term platelet donation on lymphocyte subsets and plasma protein concentrations, *Transfus Sci* 18:205–213, 1999.
Lieschke GJ, Burgess AW: Granulocyte colony-stimulating factor and granulocyte-macrophage colony-stimulating factor (2), *N Engl J Med* 327:99–106, 1992.
Liesveld JL: Expression and function of adhesion receptors in acute myelogenous leukemia: parallels with normal erythroid and myeloid progenitors, *Acta Haematol* 97:53–62, 1997.
Liles WC, Dale DC, Klebanoff SJ: Glucocorticoids inhibit apoptosis of human neutrophils, *Blood* 86:3181–3188, 1995.
Liles WC, Huang JE, Llewellyn C, et al.: A comparative trial of granulocyte-colony-stimulating factor and dexamethasone, separately and in combination, for the mobilization of neutrophils in the peripheral blood of normal volunteers, *Transfusion* 37:182–187, 1997.
Liles WC, Rodger E, Dale DC: Combined administration of G-CSF and dexamethasone for the mobilization of granulocytes in normal donors: optimization of dosing, *Transfusion* 40:642–644, 2000.
Lin JS, Burgstaler EA, Pineda AA, et al.: Effects of whole blood flow rates on mononuclear cell yields during peripheral blood stem cell collection using Fenwal CS 3000 Plus, *J Clin Apheresis* 10:7–11, 1995.
Lysaght MJ, Samtleben WS: Closed-loop plasmapheresis. In MacPherson JL, Kasprisin DO, editors: *Therapeutic hemapheresis*, Boca Raton, Fla, 1985, CRC Press, pp 149–168.
MacPherson JL, Nusbacher J, Bennett JM: The acquisition of granulocytes by leukapheresis: a comparison of continuous flow centrifugation and filtration leukapheresis in normal and corticosteroid-stimulated donors, *Transfusion* 16:221–228, 1976.
Marques MB, Huang ST: Patients with thrombotic thrombocytopenic purpura commonly develop metabolic alkalosis during therapeutic plasma exchange, *J Clin Apheresis* 16:120–124, 2001.
Martinez-Cuadron D, Boluda B, Martinez P, et al.: A phase I-II study of plerixafor in combination with fludarabine, idarubicin, cytarabine, and G-CSF (PLERIFLAG regimen) for the treatment of patients with the first early-relapsed or refractory acute myeloid leukemia, *Ann Hematol* 97:763–772, 2018.
Mathur K, Morris S, Deighan C: Extracorporeal photopheresis improves nephrogenic fibrosing dermopathy/nephrogenic systemic fibrosis: three case reports and review of literature, *J Clin Apher* 23:144–150, 2008.
McCullough J, Clay M, Hurd D, et al.: Effect of leukocyte antibodies and HLA matching on the intravascular recovery, survival, and tissue localization of 111-indium granulocytes, *Blood* 67:522–528, 1986.
McLeod BC: Introduction to the third special issue: clinical applications of therapeutic apheresis, *J Clin Apheresis* 15:1–5, 2000.
McLeod BC, Price TH, Owen H, et al.: Frequency of immediate adverse effects associated with apheresis donation, *Transfusion* 38:938–943, 1998.
McLeod BC, Sniecinski I, Ciavarella D, et al.: Frequency of immediate adverse effects associated with therapeutic apheresis, *Transfusion* 39:282–288, 1999.
McLeod BC, Strauss RG, Ciavarella D, et al.: Management of hematological disorders and cancer, *J Clin Apheresis* 8:211–230, 1993.
Mercan D, Bastin G, Lambermont M, et al.: Importance of ionized magnesium measurement for monitoring of citrate-anticoagulated plateletpheresis, *Transfusion* 37:418–422, 1997.
Mokrzycki MH, Kaplan AA: Therapeutic plasma exchange: complications and management, *Am J Kidney Dis* 23:817–827, 1994.
Mollison PL, Engelfriet CP, Contreras M: Appendix 5. In *Blood transfusion in clinical medicine*, ed 10, Malden, Mass, 1998, Blackwell Science, p 561.
Montacer-Kuhssari J, Voller H, Keller F: Pulmonary air embolism, *Intensive Care Med* 20:166–167, 1994.
Moog R: Collection of red blood cell units by apheresis, *Transfus Apher Sci* 48:141–143, 2013.
Moog R, Muller N: Technical aspects and performance in collecting peripheral blood progenitor cells, *Ann Hematol* 77:143–147, 1998.
Murata M, Harada M, Kato S, et al.: Peripheral blood stem cell mobilization and apheresis: analysis of adverse events in 94 normal donors, *Bone Marrow Transplant* 24:1065–1071, 1999.
Muso E: Beneficial effect of LDL-apheresis in refractory nephrotic syndrome, *Clin Exp Nephrol* 18:286–290, 2014.
Muso E, Mune M, Hirano T, et al.: Immediate therapeutic efficacy of low-density lipoprotein apheresis for drug-resistant nephrotic syndrome: evidence from short-term results from the POLARIS study, *Clin Exp Nephrol* 19:379–386, 2015.
Muylle L, Baeten M, Avonts G, et al.: Anaphylactoid reaction in platelet-pheresis donor with IgE antibodies to ethylene oxide, *Lancet* 2:1225, 1986.
Myburgh JA, Finfer S, Bellomo R, et al.: CHEST Investigators. Australian and New Zealand intensive care Society clinical trials group. Hydroxyethyl starch or saline for fluid resuscitation in intensive care, *N Engl J Med* 367:1901–1911, 2012.
Nadler SB, Hidalgo JU, Bloch T: Prediction of blood volume in normal human adults, *Surgery* 5:224, 1962.
Nagler A, Korenstein-Ilan A, Amiel A, et al.: Granulocyte colony-stimulating factor generates epigenetic and genetic alterations in lymphocytes of normal volunteer donors of stem cells, *Exp Hematol* 32:122–130, 2004.
Nearman HS, Herman ML: Toxic effects of colloids in the intensive care unit, *Crit Care Clin* 7:713–723, 1991.
Ness P, Braine H, King K, et al.: Single-donor platelets reduce the risk of septic platelet transfusion reactions, *Transfusion* 41:857–861, 2001.
Newman BH: Donor reactions and injuries from whole blood donation, *Transfus Med Rev* 11:64–75, 1997.
Noseworthy JH, Shumak KH, Vandervoort MK: Long-term use of antecubital veins for plasma exchange. The Canadian Cooperative multiple sclerosis study group, *Transfusion* 29:610–613, 1989.
Oberoi S, Lehrnbecher T, Phillips B, et al.: Leukapheresis and low-dose chemotherapy do not reduce early mortality in acute myeloid leukemia hyperleukocytosis: a systemic review and meta-analysis, *Leuk Res* 38:460–468, 2014.
Orlin JB, Berkman EM: Partial plasma exchange using albumin replacement: removal and recovery of normal plasma constituents, *Blood* 56:1055–1059, 1980.
Owen HG, Brecher ME: Atypical reactions associated with use of angiotensin-converting enzyme inhibitors and apheresis, *Transfusion* 34:891–894, 1994.
Pagano MB, Harmon C, Cooling L, et al.: Use of hydroxyethyl starch in leukocytapheresis procedures does not increase renal toxicity, *Transfusion* 56:2848–2856, 2016.
Pammi M, Brocklehurst P: Granulocyte transfusions for neonates with confirmed or suspected sepsis and neutropenia, *Cochrane Database Syst Rev* 10:CD003956, 2011.
Pamphilion D, Nacheva E, Navarrete C, et al.: The use of granulocyte-colony-stimulating factor in volunteer unrelated hematopoietic stem cell donors, *Transfusion* 48:1495–1501, 2008.
Passos-Coelho JL, Ross AA, Moss TJ, et al.: Absence of breast cancer cells in a single-day peripheral blood progenitor cell collection after priming with cyclophosphamide and granulocyte-macrophage colony-stimulating factor, *Blood* 85:1138–1143, 1995b.
Pearl DG, Rosenthal MH: Metabolic alkalosis due to plasmapheresis, *Am J Med* 79:391–393, 1985.
Perdue JJ, Chandler LK, Vesely SK, et al.: Unintentional platelet removal by plasmapheresis, *J Clin Apheresis* 16:55–60, 2001.
Perner A, Haase N, Guttormsen AB, et al.: Hydroxyethyl starch 130/0.42 versus Ringer's acetate in severe sepsis, *N Engl Med* 367:124–134, 2012.
Pool M, McLeod BC: Pyrogen reactions to human serum albumin during plasma exchange, *J Clin Apheresis* 10:81–84, 1995.
Popovsky MA, Whitaker B, Arnold NL: Severe outcomes of allogeneic and autologous blood donation: frequency and characterization, *Transfusion* 35:734–737, 1995.
Porcu P, Cripe LD, Ng EW, et al.: Hyperleukocytic leukemias and leukostasis: a review of pathophysiology, clinical presentation and management, *Leuk Lymphoma* 39:1–18, 2000.
Porcu P, Danielson CF, Orazi A, et al.: Therapeutic leukapheresis in hyperleucocytic leukaemias: lack of correlation between degree of cytoreduction and early mortality rate, *Br J Haematol* 98:433–436, 1997.
Powell VI, Grima K: Exchange transfusion for malaria and babesia infection, *Transfus Med Rev* 16:239–250, 2002.
Powers A, Stowell CP, Dzik WH, et al.: Testing only donors with a prior history of pregnancy or transfusion is a logical and cost-effective transfusion-related acute lung injury prevention strategy, *Transfusion* 48:2549–2558, 2008.
Price TH, Boeckh M, Harrison RW, et al.: Efficacy of transfusion with granulocytes from G-CSF/dexamethasone-treated donors in neutropenic patients with infection, *Blood* 126:2153–2161, 2015.
Price TH: Granulocyte colony-stimulating factor-mobilized granulocyte concentrate transfusions, *Curr Opin Hematol* 5:391–395, 1998.
Price TH, Dale DC: Blood kinetics and in vivo chemotaxis of transfused neutrophils: effect of collection method, donor corticosteroid treatment, and short-term storage, *Blood* 54:977–986, 1979.
Pusic I, DiPersio JF: The use of growth factors in hematopoietic stem cell transplantation, *Curr Pharm Des* 14:1950–1961, 2008.
Putensen D, Leverett D, Patel B, Rivera J: Is peripheral access for apheresis procedures underutilized in clinical practice? – a single center experience, *J Clin Apheresis* 32:553–559, 2017.
Radtke H, Mayer B, Rocker L, et al.: Iron supplementation and 2-unit red blood cell apheresis: a randomized, double-blind, placebo-controlled study, *Transfus* 44:1463–1467, 2004.
Rahmani M, Fortin BM, Berliner N, et al.: CD4+ T-cell lymphopenia in frequent platelet donors who have ceased platelet donation for at least 1 year, *Transfusion* 59:1644–1647, 2019.
Randerson DH, Blumenstein M, Habersetzer R, et al.: Mass transfer in membrane plasma exchange, *Artif Organs* 6:43–49, 1982.
Reeves HM, Winters JL: The mechanisms of action of plasma exchange, *Br J Haematol* 164:342–351, 2014.
Reik RA, Noto TA, Fernandez HF: Safety of large-volume leukapheresis for collection of peripheral blood progenitor cells, *J Clin Apheresis* 12:10–13, 1997.
Reinhardt P, Brauninger S, Bialleck H, et al.: Automatic interface-controlled apheresis collection of stem/progenitor cells: results from an autologous donor validation trial of a novel stem cell apheresis device, *Transfusion* 51:1321–1330, 2011.
Richa E, Krueger O, Burgstaler EA, et al.: The effect of double- and triple-apheresis platelet product donation on apheresis donor platelet and white blood cell counts, *Transfusion* 48:1325–1332, 2008.
Ring J, Messmer K: Incidence and severity of anaphylactoid reactions to colloid volume substitutes, *Lancet* 1:466–469, 1977.
Rock G, Sutton DM, Freedman J, et al.: Pentastarch instead of albumin as replacement fluid for therapeutic plasma exchange. The Canadian Apheresis Group, *J Clin Apheresis* 12:165–169, 1997.
Rogers RL, Johnson H, Ludwig G, et al.: Efficacy and safety of plateletpheresis by donors with low-normal platelet counts, *J Clin Apheresis* 10:194–197, 1995.
Rox JM, Wenzel F, Kobbe G, et al.: Influence of high inlet flow rates on efficacy of stem cell apheresis using the Spectra Optia Apheresis System, *Vox Sang* 101:337, 2011.
Sanders DB, Scoppetta C: The treatment of patients with myasthenia gravis, *Neurol Clin* 12:343–368, 1994.

Sarode R, Matevosyan K, Rogers ZR, et al.: Advantages of isovolemic hemodilution-red cell exchange therapy to prevent recurrent stroke in sickle cell anemia patients. *J Clin Apher*. 26(4):200–207, 2011.

Schafer AI: Bleeding and thrombosis in the myeloproliferative disorders, *Blood* 64:1–12, 1984.

Schafer AI: Management of thrombocythemia, *Curr Opin Hematol* 3:341–346, 1996.

Schiffer CA: Granulocyte transfusions: an overlooked therapeutic modality, *Transfus Med Rev* 4:2–7, 1990.

Schlenke P, Frohn C, Steinhardt MM, et al.: Clinically relevant hypokalemia, hypocalcemia, and loss of hemoglobin and platelets during stem cell apheresis, *J Clin Apheresis* 15:230–235, 2000.

Schulzeck P, Olbricht CJ, Koch KM: Long-term experience with extracorporeal low-density lipoprotein cholesterol removal by dextran sulfate cellulose adsorption, *Clin Investig* 70:99–104, 1992.

Shaw BE, Confer DL, Hwang W, Pulsipher MA: A review of the genetic and long-term effects of G-CSF injections in healthy donors: a reassuring lack of evidence for the development of haematological malignancies, *Bone Marrow Transplant* 50:334–340, 2015.

Shemin D, Briggs D, Greenan M: Complications of therapeutic plasma exchange: a prospective study of 1,727 procedures, *J Clin Apheresis* 22:270–276, 2007.

Shinzato A, Tabuchi K, Atsuta Y, et al.: PBSCT is associated with poor survival and increased chronic GvHD than BMT in Japanese paediatric patients with acute leukaemia and an HLA-matched sibling donor, *Pediatr Blood Cancer* 60:1513–1519, 2013.

Siegel JF, Rich MA, Brock WA: Association of sickle cell disease, priapism, exchange transfusion and neurological events: ASPEN syndrome, *J Urol* 150:1480–1482, 1993.

Silberstein LE, Naryshkin S, Haddad JJ, et al.: Calcium homeostasis during therapeutic plasma exchange, *Transfusion* 26:151–155, 1986.

Sintnicolaas K, Vriesendorp HM, Sizoo W, et al.: Delayed alloimmunisation by random single donor platelet transfusions: a randomised study to compare single donor and multiple donor platelet transfusions in cancer patients with severe thrombocytopenia, *Lancet* 1:750–754, 1981.

Sirtl C, Laubenthal H, Zumtobel V, et al.: Tissue deposits of hydroxyethyl starch (HES): dose-dependent and time-related, *Br J Anaesth* 82:510–515, 1999.

Smolowicz AG, Villman K, Berlin G, et al.: Kinetics of peripheral blood stem cell harvests during a single apheresis, *Transfusion* 39:403–409, 1999.

Smolowicz AG, Villman K, Tidefelt U: Large-volume apheresis for the harvest of peripheral blood progenitor cells for autologous transplantation, *Transfusion* 37:188–192, 1997.

Standards Committee of the AABB: In Price TH, editor: *Standards for blood banks and transfusion services*, ed 29, Bethesda, Md, 2014, AABB.

Stander S, Szepfalusi Z, Bohle B, et al.: Differential storage of hydroxyethyl starch (HES) in the skin: an immunoelectron-microscopical long-term study, *Cell Tissue Res* 304:261–269, 2001.

Strauss RG: Transfusion therapy in neonates, *Am J Dis Child* 145:904–911, 1991.

Strauss RG: Effects on donors of repeated leukocyte losses during plateletpheresis, *J Clin Apheresis* 9:130–134, 1994.

Strauss RG: Mechanisms of adverse effects during hemapheresis, *J Clin Apheresis* 11:160–164, 1996.

Strauss RG, Hester JP, Vogler WR, et al.: A multicenter trial to document the efficacy and safety of a rapidly excreted analog of hydroxyethyl starch for leukapheresis with a note on steroid stimulation of granulocyte donors, *Transfusion* 26:258–264, 1986.

Strauss RG, Stansfield C, Henriksen RA, et al.: Pentastarch may cause fewer effects on coagulation than hetastarch, *Transfusion* 28:257–260, 1988.

Strauss RG, Villhauer PJ, Imig KM, et al.: Selecting the optimal dose of low-molecular-weight hydroxyethyl starch (pentastarch) for granulocyte collection, *Transfusion* 27:350–352, 1987.

Stroncek DF, Clay ME, Petzoldt ML, et al.: Treatment of normal individuals with granulocyte-colony-stimulating factor: donor experiences and the effects on peripheral blood CD34+ cell counts and on the collection of peripheral blood stem cells, *Transfusion* 36:601–610, 1996a.

Stroncek DF, Clay ME, Smith J, et al.: Changes in blood counts after the administration of granulocyte-colony-stimulating factor and the collection of peripheral blood stem cells from healthy donors, *Transfusion* 36:596–600, 1996b.

Stroncek DF, Matthews CL, Follmann D, et al.: Kinetics of G-CSF-induced granulocyte mobilization in healthy subjects: effects of route of administration and addition of dexamethasone, *Transfusion* 42:597–602, 2002.

Strong MD, Lipton KS: *Transfusion-related acute lung injury*, Bethesda, Md, 2007, AABB. Association Bulletin #06-07.

Stucki A, Rivier AS, Gikic M, et al.: Endothelial cell activation by myeloblasts: molecular mechanisms of leukostasis and leukemic cell dissemination, *Blood* 97:2121–2129, 2001.

Suckfull M: Fibrinogen and LDL apheresis in treatment of sudden hearing loss: a randomised multicentre trial, *Lancet* 360:1811–1817, 2002. https://mail.tnq.co.in/service/home/~/?auth=co&loc=en_US&id=1522&part=2.2.

Suckfull M, Thiery J, Schorn K, et al.: Clinical utility of LDL-apheresis in the treatment of sudden hearing loss: a prospective, randomized study, *Acta Otolaryngol* 119:763–766, 1999.

Sulai NH, Tefferi A: Why does my patient have thrombocytosis? *Hematol Oncol Clin N Am* 26:285–301, 2012.

Szymanski IO, Patti K, Kliman A: Efficacy of the Latham blood processor to perform plateletpheresis, *Transfusion* 13:405–411, 1973.

Tan D, Hwang W, Goh YT: Therapeutic leukapheresis in hyperleukocytic leukaemias—the experience of a tertiary institution in Singapore, *Ann Acad Med Singapore* 34:229–234, 2005.

Tanhehco YC, Vogl DT, Stadtmauer EA, et al.: The evolving role of plerixafor in hematopoietic progenitor cell mobilization, *Transfusion* 53:2314–2326, 2013.

Technical Manual Committee: In Roback JD, Combs MR, et al.: *Technical manual*, ed 16, Bethesda, Md, 2008, AABB.

Tefferi A, Barbui T: Polycythemia vera and essential thrombocytopthemia: 2017 update on diagnosis, risk-stratification, and management, *Am J Hematol* 92:94–108, 2017.

Tefferi A, Hoagland HC: Issues in the diagnosis and management of essential thrombocythemia, *Mayo Clin Proc* 69:651–655, 1994.

Thiébaut A, Thomas X, Belhabri A, et al.: Impact of pre-induction therapy leukapheresis on treatment outcome in adult acute myelogenous leukemia presenting with hyperleukocytosis, *Ann Hematol* 79:501–506, 2000.

Thompson G, Parhofer KG: Current role of lipoprotein apheresis, Curr Atheroscler Rep 21:26, https://doi.org/10.1007/s11883-019-0787-5 2019.

Thompson GR: HEART-UK LDL apheresis Working group. Recommendations for the use of LDL apheresis, *Atherosclerosis* 198:247–255, 2008.

Thompson GR, Maher VM, Matthews S, et al.: Familial Hypercholesterolaemia Regression Study: a randomised trial of low-density-lipoprotein apheresis, *Lancet* 345:811–816, 1995.

Tigue CC, McKoy JM, Evens AM, et al.: Granulocyte-colony stimulating factor administration to healthy individuals and persons with chronic neutropenia or cancer: an overview of safety considerations from the Research on Adverse Drug Events and Reports project, *Bone Marrow Transplant* 40:185–192, 2007.

Tomita T, Takayanagi M, Kiwada K, et al.: Vasovagal reactions in apheresis donors, *Transfusion* 42:1561–1566, 2002.

Trial to Reduce Alloimmunization to Platelets Study Group: Leukocyte reduction and ultraviolet B irradiation of platelets to prevent alloimmunization and refractoriness to platelet transfusions, *N Engl J Med* 337:1861–1869, 1997.

Tuchman SA, Bacon WA, Haung L, et al.: Cyclophosphamide-based hematopoietic stem cell mobilization before autologous stem cell transplantation in newly diagnosed multiple myeloma, *J Clin Apheresis* 30:176–182, 2015.

Vamvakas EC, Pineda AA: Meta-analysis of clinical studies of the efficacy of granulocyte transfusions in the treatment of bacterial sepsis, *J Clin Apheresis* 11:1–9, 1996.

Vamvakas EC, Pineda A: Allergic and anaphylactic reactions. In Popovsky MA, editor: *Transfusion reactions*, ed 2, Bethesda, Md, 2001, AABB Press, pp 83–127.

van Iperen HP, Beijersbergen van Henegouwen GM: Clinical and mechanistic aspects of photopheresis, *J Photochem Photobiol, B* 39:99–109, 1997.

Veerappan R, Morrison M, Williams S, et al.: Splenic rupture in a patient with plasma cell myeloma following G-CSF/GM-CSF administration for stem cell transplantation and review of the literature, *Bone Marrow Transplant* 40:361–364, 2007.

Vichinsky EP, Haberkern CM, Neumayr L, et al.: A comparison of conservative and aggressive transfusion regimens in the perioperative management of sickle cell disease. The Preoperative Transfusion in Sickle Cell Disease Study Group, *N Engl J Med* 333:206–213, 1995.

Volk EE, Domen RE, Smith ML: An examination of ethical issues raised in the pretreatment of normal volunteer granulocyte donors with granulocyte colony-stimulating factor, *Arch Pathol Lab Med* 123:508–513, 1999.

Wallace EL, Surgenor DM, Hao HS, et al: Collection and transfusion of blood and blood components in the United States, 1989, Transfusion 33:139–144, 1993.

Wasi S, Santowski T, Murray SA, et al.: The Canadian Red Cross plasmapheresis donor safety program: changes in plasma proteins after long-term plasmapheresis, *Vox Sang* 60:82–87, 1991.

Wayne AS, Kevy SV, Nathan DG: Transfusion management of sickle cell disease, *Blood* 81:1109–1123, 1993.

Weinstein R: Prevention of citrate reactions during therapeutic plasma exchange by constant infusion of calcium gluconate with the return fluid, *J Clin Apheresis* 11:204–210, 1996.

Whitaker BI, Henry RA, Hinkins S: *The 2011 national blood collection and utilization survey report*, Washington, DC, 2011, Department of Health and Human Services [Internet]. Available at: http://www.hhs.gov/ash/bloodsafety/2011-nbcus.pdf. Cited 2014 Dec 15.

Winston DJ, Ho WG, Young LS, et al.: Prophylactic granulocyte transfusions during human bone marrow transplantation, *Am J Med* 68:893–897, 1980.

Winters JL: Chapter 7—unique considerations for allogeneic peripheral blood hematopoietic progenitor cell (HPC) donors. In Eder A, Goldman M, editors: *Blood donor health and safety*, Bethesda, Md, 2009, AABB Press, pp 123–145.

Winters JL: Low density lipoprotein (LDL) apheresis: principles and indications, *Semin Dial* 25:145–151, 2012.

Winters JL: Randomized controlled trials in therapeutic apheresis, *J Clin Apheresis* 28:48–55, 2013.

Winters JL, Brown D, Hazard E, et al.: Cost-minimization analysis of the direct costs of TPE and IVIg in the treatment of Guillain-Barré syndrome, *BMC Health Serv Res* 11:1472–6963, 2011.

Winters JL, Nord A: Chapter 4 – clinical decision making and the American Society for apheresis guidelines. In Linz W, Chhibber V, Hofmann J, Torloni SA, Vrielink H, Mason H, Quirolo K, Kempin S, editors: *Principles of apheresis technology: technical principles of apheresis medicine*, 6th edition, Vancouver, Canada, 2017, American Society for Apheresis, pp 65–92.

Yacobi A, Stoll RG, Sum CY, et al.: Pharmacokinetics of hydroxyethyl starch in normal subjects, *J Clin Pharmacol* 22:206–212, 1982.

Zantek ND, Morgan S, Zantek PF, et al.: Effect of therapeutic plasma exchange on coagulation parameters in patients on warfarin, *J Clin Apheresis* 29:75–82, 2014.

Zaucha JM, Gooley T, Bensinger WI, et al.: CD34 cell dose in granulocyte colony-stimulating factor-mobilized peripheral blood mononuclear cell grafts affects engraftment kinetics and development of extensive chronic graft-versus-host disease after human leukocyte antigen-identical sibling transplantation, *Blood* 98:3221–3227, 2001.

Zic JA: The treatment of cutaneous T-cell lymphoma with photopheresis, *Dermatol Ther* 16:337–346, 2003.

Zic JA, Miller JL, Stricklin GP, et al.: The North American experience with photopheresis, *Ther Apher* 3:50–62, 1999.

CHAPTER 39

TISSUE BANKING AND PROGENITOR CELLS

Yen-Michael S. Hsu, Matthew B. Elkins

SOURCES OF TISSUE, 817
TISSUE BANK ACTIVITIES, 817
Donor Screening, 818
Cryopreservation, 818
SKIN BANKING, 819
MUSCULOSKELETAL TISSUES, 819
CARDIAC VALVES, 820
CORNEA, 820
REPRODUCTIVE TISSUE, 820
HEMATOPOIETIC PROGENITOR CELL BANKING, 821
HPC Quantification and Potency Evaluation, 821
Sources and Selection of Hematopoietic Grafts, 821
T-Cell Depletion, 823
Cryopreservation of Hematopoietic Grafts, 823
Reinfusion of Progenitor Cell Products, 824
Ex Vivo Manipulation of Hematologic Cells, 824
Use of Dendritic Cells In Cancer Immunotherapy, 824
Adoptive Cell Transfer/Chimeric Antigen Receptors, 824
SELECTED REFERENCES, 825

KEY POINTS

- A wide range of allogeneic tissues are used for transplantation.
- Allograft tissue is screened, tested, and processed to improve its safety.
- Allograft tissue is stored by a variety of methods, including cryopreservation.
- Risks and complications are associated with the use of allograft tissue.
- A wide range of assisted reproductive techniques are available to infertile couples and individuals.
- Hematopoietic progenitor cells can be derived from multiple sources and transplanted in different ways, depending on the needs of the recipient.
- It is important to consider the balance between the graft-versus-host reaction and the graft-versus-leukemia effect.

Throughout the United States, tissue banks routinely provide hundreds of products that not only extend life but also, in many instances, significantly improve the quality of life for the patients they serve. More than 2 million musculoskeletal allografts (American Association of Tissue Banks, 2017) and 85,000 corneas (Eye Bank Association of America, 2018) are transplanted annually in the United States—a number that far exceeds the approximately 30,000 to 40,000 solid-organ transplants per year (Organ Procurement and Transplantation Network [OPTN] and Scientific Registry of Transplant Recipients [SRTR], 2017). Clinical applications of allogeneic and autologous tissue and the types of tissue available have grown exponentially in the last 2 decades. Yet, aside from the patients and physicians served by these tissue banks, many people are unaware of the vast scope of activities in today's health care environment that are under the umbrella of tissue banking. Over the past 30 years, tissue banking in the United States has evolved from a system of incidental hospital bone or sperm banks to a system of regulated, accredited facilities, much like blood banks, providing an expanding variety of high-quality, carefully screened and tested products for use by physicians (Box 39.1).

Many tissue banks provide a wide range of products and services in procurement of skin, bone, and heart valves, along with processing and storage. Other tissue banks focus their services in specialized areas such as reproductive tissue or hematopoietic progenitor cells (HPCs). One bank may recruit donors and procure and process tissue such as skin for burn patients or bone for orthopedic repairs. Another may collect, process, and store HPCs for lifesaving bone marrow transplants. Processing of musculoskeletal tissues and cardiac valves, which requires extensive equipment, personnel, and quality assurance, is performed primarily by a few large tissue banks that subcontract with other tissue banks, which collect, store, and issue these products. In addition, an exponential growth has occurred over the past 2 decades in reproductive banks that provide assistance to infertile couples or individuals.

SOURCES OF TISSUE

Tissues used for transplantation come from two primary sources: living donors and deceased donors. Living donors may be individuals who donate for their own use (autologous HPCs or sperm), as directed donors for a given individual (allogeneic HPCs or sperm donation), or altruistically for unknown recipients (surgical discard bone, sperm donation, allogeneic HPCs). A large majority of bone, skin, and cardiac valves used for transplantation, as well as eye tissue, come from deceased donors. Unlike solid-organ donation, where there is a need for the organs to be obtained while circulation is maintained, deceased donor tissue can be obtained for several hours after death and up to 24 hours later if the body is refrigerated. This substantially increases the number of available tissue donors. Because corneal tissue has minimal contact with the circulatory system, some individuals who would otherwise be excluded as tissue donors may still be eye donors.

Deceased donor tissue is procured primarily from hospital operating rooms or morgues and medical examiners' offices. Harvesting of tissue is performed in a sterile or clean environment using aseptic techniques. Many tissues, such as bone, are then frozen for subsequent processing and refreezing or freeze-drying. Specialized tissues such as cornea are processed immediately and stored for only a short time (48–72 hours) before use. Tissue from living donors is procured in the operating room (surgically salvaged bone or bone marrow) or in specialized clean environments that apheresis centers and sperm banks are equipped to provide. These tissues are collected under sterile conditions, processed immediately, and either used within 24 hours or frozen for subsequent use.

TISSUE BANK ACTIVITIES

The major activities of tissue banks are outlined in Box 39.2. A major impetus for the movement to formal, accredited tissue banks was the concern about transfusion-transmitted disease. As with blood banks and transfusion services (see Chapters 37 and 38), donor recruitment, screening, and testing are critical functions of the tissue bank. Since the early 1990s, cases involving disease transmission documented that careful screening by both review of the medical record and serologic testing, as well as maintenance of detailed records, was critical to safe tissue banking practices and, thus, acceptance of allograft tissue by both the public and health care providers. The Joint Commission (TJC) has standards for tissue banking practices that are targeted primarily at the transplantation facility. These standards focus on the necessity for implantation facilities to keep clear, precise records regarding tissue receipt, storage, and use so that all allogeneic tissues can be traced from donor to recipient. TJC standards also require institutions to establish a mechanism for physicians to report adverse reactions and the originating tissue bank to be notified. Accredited full-service tissue banks, in the same manner as blood banks, investigate suspected reactions or complications extensively. "Look-back" reviews should include reviews of the complications associated with other tissue from the same donor; the current health of the donor, if living; and quarantining of other tissue from the same donor. The American Association of Tissue Banks (AATB) provides strict standards and accreditation for organizations involved in any area of

BOX 39.1

Categories of Transplantable Tissue

Musculoskeletal
Bone
Cartilage
Meniscus
Tendon
Ligament
Fascia

Skin

Cardiovascular
Heart valves
Saphenous vein

Corneal (eye)

Reproductive
Sperm
Ova
Embryo

Hematopoietic
Bone marrow
Peripheral blood progenitor cells
Umbilical cord blood progenitor cells

Other
Ear ossicles
Dura mater
Parathyroids
Pancreatic islet cells

BOX 39.2

Tissue Banking Activities

Donor recruitment
Acquisition of tissues
Processing and storage of tissues
Provision of tissues for transplantation
Public and professional education
Quality assurance and record keeping
Recipient records

tissue banking. Several states also require tissue banks to be licensed, and the U.S. Food and Drug Administration (FDA) regulates the screening, processing, and storage of donor tissue used for transplantation purposes (FDA, 2019).

DONOR SCREENING

Tissue donors are carefully screened to prevent the transmission of bacterial, viral, and/or genetic disease, as well as to ensure the quality of the tissue obtained (Box 39.3). With deceased tissue donors, unlike blood donors, information regarding medical and social history is obtained from the family or close friends as well as from physicians' records.

Reports of tissue transplant complications in the early 1990s focused on the transmission of human immunodeficiency virus (HIV) (Simonds et al., 1992) and hepatitis C virus (HCV) (Conrad et al., 1995). More recently, attention has been focused on testing of tissue donors for additional disease transmission vectors (*Trypanosoma cruzi*, West Nile virus, *Babesia*, chikungunya virus, influenza H1N1, and SARS-CoV-2 virus), as well as for transmission of nonscreened infectious agents such as Creutzfeldt-Jakob disease (Centers for Disease Control and Prevention [CDC], 2003) and others (Kainer et al., 2004). However, isolated cases of transmission of uncommon pathogens by tissue and organ donors will likely continue to occur. The impracticality of screening for all transmissible diseases emphasizes the continued need for careful screening of tissue and organ donors by medical history and family interview as well as by laboratory testing. Asking the right questions in the correct manner is a critical function that needs to be performed by well-trained, experienced individuals who are able to identify possible risks in the donor medical history, in information about possible risk behaviors, or in available laboratory data.

Other parts of the review process are targeted at ensuring the quality of the donated tissue. Musculoskeletal donors need to be carefully screened for any history of trauma that might result in a weakened

BOX 39.3

Comprehensive Donor Testing

Donor Screening
Review of medical history and medical records
Infectious diseases (including history of foreign travel)
Malignant disease
Collagen and immune complex diseases
History of genetic diseases
Trauma
Exposure to drugs, toxic substances, or biological hazards
Physical examination of living donors
Review of autopsy records for deceased donors
Review of social history for risk behaviors

Donor Serologic Testing
Antibody to human immunodeficiency virus (confirmation by nucleic acid testing)
Antibody to human T-cell lymphotropic virus
Antibody to hepatitis C virus (confirmation by nucleic acid testing)
Hepatitis B surface antigen
Antibody to hepatitis B core antigen
Serologic tests for syphilis
Antibody to West Nile virus
Antibody to *Trypanosoma cruzi* (Chagas disease)
Bacteriologic testing of tissue product

structural bone graft. Sperm donations are reviewed not only for genetic disease but also to ensure viable sperm that will have a reasonable chance of resulting in successful fertilization. The use of umbilical cord blood for unrelated allogeneic bone marrow and peripheral blood transplantation requires screening and testing of both the mother and the cord blood. When tissue is procured from living donors, with the exception of HPCs, the tissue is frozen and quarantined for a minimum of 180 days, at the end of which the donor serologic testing is repeated. This prevents the use of tissue from any donor who was in the "window" period for HIV or HCV—that is, those who had been exposed to the virus but did not demonstrate antibody at the time of donation. The addition of nucleic acid testing for HCV and HIV1/2 has also increased the safety of donated allograft tissue by decreasing the time between donor exposure and a positive laboratory test (Ooley et al., 2018). Because of concerns about the sensitivity of testing specimens from deceased donors, tissue banks that process these tissues must utilize test kits that have been approved by the FDA for the testing of deceased donors (Food & Drug Administration, 2019).

CRYOPRESERVATION

Tissues such as HPCs, sperm, and skin and some types of musculoskeletal tissue require the presence of viable cells and have a very short shelf life at refrigerator temperatures, thus requiring cryopreservation. The goal of all cryopreservation techniques is to extend the usable storage period of the material being frozen by reducing the metabolic demand of cells at lower temperatures with no loss of viability due to the freezing or thawing procedures. Cryopreservation of animal sperm has been an established agricultural practice for decades, and human researchers have been able to gain from their experiences. Generally, cryopreservation of human tissues uses cryoprotectant agents such as dimethyl sulfoxide (DMSO) or glycerol, balanced tissue culture media, and some form of protein supplementation, such as autologous plasma, albumin, or other colloidal suspensions. The actual freezing is often performed using a controlled-rate freezer, a mechanical device that controls the rate at which freezing of the tissue takes place, usually −1°C/minute down to temperatures of −80°C. DMSO is the cryoprotective agent of choice for tissues such as skin, HPCs, and other nucleated cell suspensions or tissues; glycerol is generally used for the freezing of sperm. Cryoprotectant agents function by preventing the formation of intracellular ice crystals during freezing and balancing the osmotic pressure and concentration of intracellular versus extracellular water during the thawing process. The formation of extracellular ice crystals or too rapid an increase in extracellular osmotic pressure with resulting dehydration of the cell during thawing can result in damage to the cells leading to loss of viability. Cryoprotectant agents, such as DMSO, work by slowing the rate at which this change occurs (Gorin, 1986). Most tissue banks use liquid nitrogen and controlled-rate freezing processors that are programmed to compensate for the heat released, called the *heat of fusion*, at the change from the liquid state to the frozen state (Gorin, 1986).

Uncompensated, the heat of fusion can result in decreased viability of the cells or frozen tissue.

Once frozen, cryopreserved tissues are stored at varied temperatures from −50°C to −86°C in a mechanical freezer to vapor (−150°C) or liquid (−196°C) phase liquid nitrogen. Expiration dates for cryopreserved tissues are generally 5 years after collection, although these are arbitrary limits, and the actual length of storage possible for many tissues has not been determined. For example, the definitive expiration date for cord blood units is currently unknown due to different processing and storage methods and the effects of long-term storage on unit potency. Therefore, expiration dates are determined based on the cord blood bank's own viability and recovery data. Other tissues that do not require the presence of viable cells, such as structural bone, may be frozen or freeze-dried by a variety of other methods. Some freeze-dried tissues have expiration dates of 5 years, and others may be stored indefinitely.

SKIN BANKING

The most common use of allogeneic skin grafts is as a temporary cover for patients with extensive third-degree burns until autologous or autogeneic skin can be recovered and grafted. Donated skin may be used as full-thickness grafts, split-thickness grafts, or as a decellularized matrix (via high-percentage glycerol storage or lyophilization). Because of the high concentration of histocompatibility antigens and antigen-presenting cells (APCs) in viable cell preparations (full-thickness and split-thickness grafts), all cellular allogeneic skin grafts are eventually rejected (Zhou et al., 2013). When used to cover burns, the grafts are generally replaced periodically until autografting can be performed. Most deceased donor skin provided as an allograft is a split-thickness graft with a thin layer of epidermis without dermis; therefore, ABO matching is not required (Eastlund, 1998). As a temporary graft, however, split-thickness skin grafts provide vital, immediate cover as a barrier against infection plus fluid, electrolyte, and heat loss from extensive burns, allowing for patient stabilization and eventual autografting.

Generally, skin is harvested from deceased donors with uninfected, unblemished skin who have a body surface area of at least 1.75 m^2. The skin is harvested with a dermatome from areas of the back, legs, and upper arms. The skin is generally disinfected before harvest and is soaked in antibiotic-containing tissue culture solution until it is used or frozen.

Skin can be stored at 2°C to 8°C for several days (Kagan et al., 2005) or cryopreserved and stored for several years. Because of today's need for extensive review of the donor's history and laboratory records, skin grafts are more commonly frozen for subsequent use. The most commonly used cryoprotectant is 10% to 15% glycerol (American Association of Tissue Banks, 2002), and the graft is generally incubated for a period of time (20–30 minutes) in the freezing solution to allow the solution to permeate the graft. The skin is then frozen in strips supported by gauze mesh and is frozen flat (Eastlund, 1998). Skin can be frozen with or without controlled-rate freezing and is easily stored at −50°C to −80°C. However, lower temperatures are commonly used for longer storage by many tissue banks (Kearney, 1998). Frozen skin allografts are thawed rapidly at 37°C and are used immediately or washed with physiologic solutions to dilute the cryoprotectant.

The limited supply of cellular human skin allografts has stimulated efforts targeted at other options, including artificial barriers, engineered skin, and xenogeneic substitutions, such as pigskin. Multiple commercial products are currently available that are acellular dermal matrix grafts either made from human or xenogeneic skin or artificial protein matrices. This framework allows for fibroblast infiltration, collagen deposition, and neoepithelization. Because the immunologically active cells are removed, the graft is tolerated (not rejected) significantly longer than traditional human skin allografts. Additional products combine these frameworks with either autologous or allogeneic cultured fibroblasts. Cultures of epithelial cells have been made in order to expand the available supply of autologous skin (Wang et al., 2007). The fibroblasts provide additional tropic factors, resulting in improved healing rates and scar formation, generally with end results similar to allogeneic skin grafts (Shahrokhi et al., 2014). These products have not only been employed as skin graft for burns, but they also have applications in ophthalmic, plastic, ear, nose and throat, and dental surgeries (Shorr et al., 2000). At this point, the currently available commercial products do not provide the complexity and long-term efficacy of autologous skin transplants but can be used for short-term coverage. The products made from allogeneic human tissue require the identical patient consents and tracking required for other human tissue products.

MUSCULOSKELETAL TISSUES

Bone banking began several decades ago, when physicians first stored surgical discard bone, mostly femoral heads from joint replacement surgery, for future use in spinal fusions and other orthopedic procedures. Generally, this involved simple storage of the bone in an unmonitored freezer somewhere in the hospital. Often, no testing or processing of the surgical discard bone was performed, nor were monitoring of storage conditions and tracking of tissue sources or recipients conducted. In some situations, the original donor/patient was not even asked for consent. Today, these practices have been almost eliminated by the use of musculoskeletal tissue from registered, accredited tissue banks. Thus, patients can confidently elect to have a bone allograft as part of a surgical procedure (Tomford, 1993). In addition to autogeneic bone grafts, living donor bone donation is still used as a source of some types of bone. Living donors are now screened and tested and must provide informed consent. In addition, the bone tissue obtained is further processed to reduce the risk of infectious disease transmission, and detailed records of the source donor and recipient are kept for tracking and follow-up purposes.

Surgical discard bone and deceased donor bone are processed in a similar fashion. Extraneous tissue, blood, and marrow elements are removed by high-pressure pulse washing, and the tissue is soaked in antibiotic solutions. Bacteriologic culturing of the tissue is done at collection, during processing, and before freezing. Tissue that requires the presence of viable cells such as cartilage, femoral head, tibia, whole bone, or tendon is usually washed, soaked, and frozen at temperatures between −60°C and −150°C. With other tissues, when viability is not an issue, ethanol soaks may be used to remove lipid content, generally in the preparation of demineralized, lyophilized bone, which also decreases the infectivity of the tissue. Most bone tissue is further sterilized by the use of low-dose irradiation. In addition, lyophilization, which is possible with bone products such as cancellous and cortical bone chips, appears to reduce the immunogenicity and infectivity of these products. The use of ethylene oxide to end-sterilize bone tissue has been generally eliminated, because adverse reactions were reported in multiple recipients (Jackson et al., 1990). The bone tissue is cut and shaped and then preserved by freezing or freeze-drying.

Bone allografts serve mainly as a mechanical support and a framework for the host's bone-forming cells to replace lost tissue. The osteoinductive function of the allograft bone is dependent in part on the presence of certain growth factor glycoproteins (Mohan & Baylink, 1991), but they do not appear to cause any significant allograft reaction on the part of the host. Because bone tissue is processed to remove blood, marrow, and other extraneous tissue, most studies have failed to demonstrate the presence of ABO antigens (Ezra-Cohn & Cook, 1961). The antigenicity of the resulting product is low; thus, histocompatibility or blood-type matching is not required. Because large osteoarticular grafts, such as whole bone-patellar-tendon grafts, are not extensively processed, they may contain residual red blood cells, and instances of immunization to Rh system antigens have been reported (Hill et al., 1974). Many surgeons using these larger grafts will attempt to provide Rh-compatible tissue to Rh-negative females of childbearing age.

In addition to autogeneic bone, allograft bone is used for spinal fusion surgery, replacement of failed prosthetic joints, packing of benign bone cysts, reconstruction of maxillofacial deficits, restoration of alveolar bone in periodontal pockets, and even replacement of resected bone for tumors such as osteosarcoma (Kagan et al., 2005). Tendon and cartilage allografts are used primarily for knee repair surgery. Some patients will be confronted with the option of having autologous tissue recovered from their iliac crest for many elective orthopedic procedures or the option of receiving allograft tissue from a tissue bank. Advantages and disadvantages are associated with each (i.e., autograft vs. allograft). Autografts appear to incorporate quicker, are not immunogenetic, and do not transmit disease. However, they are associated with longer anesthesia time, increased blood loss, and prolonged recovery from the donor site. Because of the wide supply of allografts, an exact fit can usually be made. No donor site recovery is needed, and the surgical procedure is generally shorter. Although the risk of transmitted disease is greatly reduced by today's procedures, it is still present. Allografts also have a poorer capacity for osteoconduction and osteoinduction (Torroni, 2009), which makes them unsatisfactory for larger grafts.

Recent investigation and clinical trials have focused on the use of synthetic scaffolds or cages infused with the patient's own bone marrow stromal cells and various signalling proteins to create a graft that is almost identical to an autologous graft without the necessity of a donor site (Torroni, 2009). Bone morphogenetic proteins and other signaling molecules added to the synthetic scaffolds promote the marrow stromal

cells differentiation into osteoprogenitor cells, eventually resulting in the formation of new bone. Similar strategies are currently being investigated to create engineered tendons and ligaments (Gonzalez-Quevedo et al., 2018).

CARDIAC VALVES

Aortic valve replacement may utilize human heart valves or pig valves. With the use of human valve tissue, anticoagulants are not required and the incidence of thromboembolism or infection is lower. Human valves are ideal for use in children, pregnant women, or patients with a history of bacterial endocarditis. They are, however, utilized less often overall because procedures to place them are more technically difficult. Aortic and pulmonic valves are commonly procured from deceased organ donors when the whole heart is rendered unsuitable for transplantation because of events such as cardiac arrest that do not affect the integrity or function of the aortic or pulmonic valves. Procurement is performed in the operating room. The valves are carefully dissected with a cuff of myocardium, inspected for valve integrity, and frozen by controlled-rate freezing in liquid nitrogen using DMSO as the cryoprotective agent (O'Brien et al., 1988). Although blood group antigens have been demonstrated on the endothelium of cryopreserved hearts, the major mechanical function of these is dependent only on the nonviable connective tissue. After transplantation, host cells eventually replace the donor endothelium. Several studies have documented that neither ABO compatibility (Weipert et al., 1995) nor human leukocyte antigen (HLA) compatibility (Yap et al., 2006) is necessary for long-term function of these allograft valves. However, the use of allograft valves does induce the formation of HLA antibodies, especially in children, and may create difficulty in identifying a compatible donor for those patients later requiring whole-heart transplantation (Hooper et al., 2005). Because thawing of the allograft valves is generally performed by operating room personnel and not by experienced tissue bank technologists, detailed instructions and protocols are necessary to prevent cracking of the valve.

Vein allografts or autografts have also been used for valve replacement, predominantly pulmonic valve rather than aortic due to the pressures involved for valve replacement. Because the role of ABO matching in the long-term function of these tissues has been controversial, ABO-compatible tissue is generally used (Laub et al., 1992).

CORNEA

Corneal transplantation has been regularly performed in the United States since 1961, although the first corneal transplant is recorded to have taken place in 1905. Presently, more than 85,000 corneal transplants are performed each year (Eye Bank Association of America, 2018). There are 86 accredited eye banks in the United States involved in recruitment, screening, procurement, and transplantation of corneal tissue, as well as public and professional education. Loss of vision due to corneal disease can result from infection, trauma, burns, or congenital disease. Long-term (>10 years) success rates for corneal allografts are well above 90%.

Corneal donation is possible from many donors when other tissues are not retrievable because of age, trauma, or disease. Corneal tissue is recovered from donors up to 80 years of age. Generally, eye enucleation is performed in the operating room or morgue from deceased donors within 6 hours of death. Subsequently, the cornea is then removed in a sterile environment in the eye bank and is placed in supplemented sterile tissue culture media. The corneas are stored at 4°C and are transplanted within 48 to 72 hours. This allows for appropriate serologic screening of the donor but ensures maximum viability of the graft.

The corneal graft has long been considered an "immunologically privileged site" (Medawar, 1948). Because the cornea is almost entirely avascular, host APCs and effector lymphocytes do not circulate through the allograft cornea. Thus, histocompatibility and blood group matching are not required. Approximately 10% of all corneal grafts are rejected, most commonly due to vascularization. The presence of cornea vascularization at the time of transplant and prior rejected corneal grafts both increase the likelihood of rejection (Qazi et al., 2013). The use of HLA-matched corneal transplants in an attempt to provide successful grafts for this group of patients has not shown consistent benefit (Bohringer et al., 2018). Artificial corneas generally have worse long-term outcomes and are currently used for patients in whom donor cornea transplantation has failed. The ideal criteria for the selection of transplanting donor versus artificial corneas in these patients has not been determined (Akpek et al., 2014).

REPRODUCTIVE TISSUE

Because of the exponential growth in knowledge of fetal development and reproductive technologies, particularly in vitro fertilization (IVF), approximately 1.7% of births in the United States now occur with assisted reproductive technologies (CDC, 2017). Reproductive banks are currently able to assist more individuals and couples who wish to maintain or achieve fertility. Guidelines and standards for anonymous-donation sperm banking have been established by the American Society for Reproductive Medicine and the American Association of Tissue Banks. Most reproductive banks in the United States today function as for-profit corporations but must still meet these guidelines and standards.

Reproductive banks serve two types of donors: client-directed donors and anonymous bank donors. These include men and women who are about to undergo chemotherapy, radiation therapy, or surgery for malignant diseases that will affect their reproductive ability. Client-directed sperm donations are generally targeted to intimate partners of men who, for a variety of reasons, are concerned about future fertility. Other men will predeposit their sperm before vasectomy as insurance against life changes when they may wish to father additional children. Individuals with low sperm counts may bank their sperm to allow collection of sufficient gametes for fertilization of the intimate partner. Less frequently, males who have occupational exposure (such as nuclear power plant employees) that may lead to infertility or the potential for genetic defects may elect to store their sperm. Sperm collected and stored for intimate partners is tested in the same manner in which anonymous donor collections are screened. Semen from infected donors, which still may be usable by the intimate partner, must be quarantined and stored separately from other client deposits. Directed donations are also made to sperm banks for specific individuals who are not intimate partners.

Collected semen is mixed with a glycerol–egg yolk solution that acts as a cryoprotectant, the egg yolk providing supplemental protein that assists in preserving the sperm during the thawing process. The semen-preservative mixture is aliquoted into straws or vials, precooled to a temperature of 5°C, frozen by controlled-rate freezing with liquid nitrogen, and stored in the liquid phase of liquid nitrogen at −196°C. Cryopreserved sperm can be used for artificial insemination or in vitro fertilization. Client-directed donations are kept indefinitely, and anonymous sperm bank donor samples are usually stored for 5 years. For individuals desiring artificial insemination, these attempts are not always successful; these individuals are counseled to deposit adequate sperm for several reproductive procedures.

Sperm banks also provide sperm from anonymous donors for infertile couples or individuals. Sperm banks maintain libraries of sperm donors so that individuals can select donors with similar physical characteristics, such as hair and eye color, race, and the like. Anonymous sperm donors are rigorously screened, not only to ensure the safety of the recipient and potential offspring but also to provide the highest probability of successful fertilization. Sperm collected from anonymous donors is quarantined for 180 days before issue. During these 180 days, the donor is tested monthly, not only by the standard serologic assays employed for all tissue donors but also for infections such as cytomegalovirus, *Neisseria gonorrhoeae*, and *Chlamydia*. Sperm donors are tested for genetic diseases such as Tay-Sachs disease, cystic fibrosis, sickle cell disease, and thalassemia. Generally, complete genetic karyotyping is performed on anonymous sperm donors. Collections are also examined for sperm number, function, and viability. Not until all of these criteria have been met and reviewed by the medical director of the sperm bank are tissues released for use. Female patients confronted with loss of fertility due to age, disease, or chemotherapy, and who have an intimate partner, are still frequently guided to IVF with cryopreservation of the resulting embryos for later implantation. Many reproductive banks also provide donor ova collection for infertile individuals. These donors are screened in the same manner in which anonymous sperm donors are tested.

Historically, attempts at ova banking (egg banking) had not been as successful as embryo cryopreservation due to unfertilized ova having a very low rate of fertilization when they are subsequently thawed and attempts at IVF are made. Recently, improvements in the cryopreservation strategies, particularly vitrification rather than slow freezing, have increased oocyte survival, fertilization rates, and pregnancy rates (Boldt, 2011). Attempts have also been made at cryopreserving ovarian tissue for future implantation with very limited success in humans. Of continuing concern is an increase in chromosomal abnormalities in both oocyte and ovarian tissue banking. Continuing research is needed in this area to provide women with the opportunity for future fertility with a chosen partner (Porcu et al., 2008).

BOX 39.4

Indications for Hematopoietic Transplantation

Acute myeloid leukemia
Acute lymphoblastic leukemia
Chronic myelogenous leukemia
Multiple myeloma
Non-Hodgkin lymphoma
Myelodysplastic syndromes
Hodgkin disease
Neuroblastoma
Ewing sarcoma
Rhabdomyosarcoma
Aplastic anemia
Sickle cell anemia
Thalassemia
Severe combined immunodeficiency

IVF and embryo banking are offered by many reproductive banks and hospital-based fertility centers. Since the original success attained with IVF as a treatment for tubal obstruction in 1983 (Steptoe & Edwards, 1983), significant advances have been made in this area that improve the success rate of IVF. They include technical innovations in culture media, embryo cryopreservation, and morphologic criteria for selection of the best embryo to transfer (Houghton et al., 2002; Boldt et al., 2003). In addition to its use for women with fallopian disease, the success of intracytoplasmic sperm injection of the oocyte (Palermo et al., 1992) has made IVF the preferred technique for many infertile couples, utilizing either the partner's sperm or donor sperm, as it results in higher fertilization rates as compared with artificial insemination (Boyle et al., 2004). In addition, IVF offers couples with certain genetic diseases, such as hemophilia and cystic fibrosis, the opportunity for preimplantation genetic diagnosis with subsequent selection of embryos in an attempt to reduce the risk of disease transmission to their offspring.

The advent of all of these technologies has raised many ethical and scientific issues related to disposition of unused embryos, preimplantation screening of embryos, multiple gestations, and the possibility of unknown genetic risks to the health of children conceived through IVF (Lucifero et al., 2004). Thus, a multidisciplinary approach to this field is needed to include members of the public as well as scientific and medical professionals (Cetin & Pardi, 2003).

HEMATOPOIETIC PROGENITOR CELL BANKING

Hematopoietic progenitor cell transplantation has been the epitome of personalized and precision medicine practice since 1959, illustrated by the seminal work of syngeneic bone marrow transplants between genetically identical individuals (identical twins) as an attempt to cure hematopoietic malignancies (Thomas et al., 1959). Cells with colony-forming unit (CFU) potential found in the spleen or marrow were able to restore hematopoietic function in lethally irradiated, genetically identical murine models (Lorenz et al., 1951). Restoration of hematopoiesis in the human recipient is dependent on the transplantation of sufficient numbers of pluripotential HPCs that make up about 1% of normal marrow cells and are capable of both self-replication and differentiation into all lineages of blood cells (see Chapter 32). Identification of the HLA system as the major histocompatibility system in humans and the ability of tissue-typing laboratories to identify individuals' HLA types at the allele level allowed bone marrow transplantation to be performed between HLA-matched individuals, generally first-degree relatives, who were not genetically identical. Today, HPC banks exist as highly specialized tissue banks that select, collect, process, store, and distribute HPC products. These are derived from bone marrow, peripheral blood, or umbilical cord blood for patients with a wide variety of diseases; further applications for HPCs are an active area of research (Box 39.4). In 2017, over 23,000 transplantations (8780 cases with allogeneic graft and 14,599 cases with autologous grafts) were performed in the United States (www.CIBMTR.org). Terminology of the various HPC products is listed in Table 39.1. Data from both autologous and allogeneic hematopoietic transplants are now maintained by the Center for International Blood and Marrow Transplant Research (CIBMTR), which is a joint effort of the National Marrow Donor Program (NMDP) and the International Bone Marrow Transplant Registry (IBMTR) in the United States. The CIBMTR has been funded since 2006 by a contract from the U.S. Department of Health and Human Services to gather and maintain data on clinical and research activities in hematopoietic transplantation (www.CIBMTR.org).

TABLE 39.1

Terminology of Hematopoietic Progenitor Cell Products

HPC	Hematopoietic progenitor cells, formerly hematopoietic stem cells
HPC, apheresis	Hematopoietic progenitor cells, apheresis, formerly peripheral blood progenitor cells or hematopoietic stem cells
HPC, marrow	Bone marrow–derived hematopoietic progenitor cells
HPC, umbilical cord blood	Cord blood–derived hematopoietic progenitor cells

HPC QUANTIFICATION AND POTENCY EVALUATION

HPCs are morphologically indistinguishable from other mononuclear cells seen in the marrow or peripheral blood, yet collection of adequate numbers of cells is essential to ensuring marrow engraftment in the recipient. HPC collections have traditionally been targeted at collecting sufficient nucleated cells to ensure a minimum number of progenitor cells. With increasing use of peripheral blood hemapheresis procedures to obtain progenitor cell grafts, it became necessary to develop an assay that could be completed on the same day and used to determine the number of hemapheresis collections required. Quantitation of the number of cells bearing the CD34 antigen by flow cytometry has become the widely accepted method for assessing the adequacy of peripheral blood progenitor cell collections. The CD34 antigen is restricted to primitive cells of all lineages (Berenson et al., 1988). Collection of hemapheresis products using CD34+ cell enumeration as an index of graft efficacy has proved to result in enduring hematopoietic engraftment (Bittencourt et al., 2002). Standardization of the CD34 cell assay and availability of flow cytometric analysis have resulted in the use of CD34+ cell measurements by most programs to determine the number and adequacy of peripheral blood progenitor cell collections (Keeney et al., 2004). Generally, peripheral blood progenitor cell collections containing greater than 3×10^6 CD34+ cells per kilogram of recipient body weight are considered adequate to provide for neutrophil engraftment in 8 to 10 days. Bone marrow grafts could be assayed for progenitor cell activity by the use of colony-forming assays (Iscove et al., 1971). With this technique, a sample of mononuclear cells from the graft is cultured in methylcellulose media supplemented with hematopoietic growth factors and essential amino acids for 10 to 14 days. At the end of this period, the plates are examined for the numbers and types of characteristic CFUs, including burst-forming unit-erythroid (BFU-E), granulocyte-macrophage (CFU-GM), and mixed colonies: granulocyte, erythrocyte, monocyte, and megakaryocyte (CFU-GEMM). Clusters containing more than 50 cells are scored as a colony. Collections containing greater than 1×10^5 CFUs per kilogram of recipient weight are considered adequate. A faster HPC potency assay with a faster turnaround time (1–2 hours) was recently explored. High level of intracellular aldehyde dehydrogenase (ALDH) activity was used to identity human cells with stemness. Thus, a flow cytometry–based assay was developed to evaluate and correlate the ALDH-positive cells with CD34-positive cells and the CFU output in various human HPC grafts (Shoulars et al., 2016). While promising, more validation and prospective clinical investigations on the ALDH biomarker predicting HPC potency are needed to supplement or to even substitute the lengthy CFU assay in a clinical setting.

SOURCES AND SELECTION OF HEMATOPOIETIC GRAFTS

Hematopoietic tissues for transplantation may come from one or more sources (Table 39.2). Individuals who have autologous or autogeneic grafts donate their own cells, which are procured and stored, before receiving high-dose chemotherapy and/or radiation therapy. Following this myeloablative therapy, the patient's own cells are thawed and reinfused. The patient's own HPCs in the transplant will home, engraft (in the marrow stroma), and differentiate into mature blood cells. Patients who are not candidates for autologous transplantation, such as those with acute leukemia, congenital hematologic disease, or an inability to generate an autologous HPC product with adequate cell dose, can be considered for an

TABLE 39.2
Comparison of Hematopoietic Progenitor Cell Sources and Products with Collection and Complications

	Cord Blood (HPC, UCB)	Autologous (HPC, Apheresis + Marrow)	Allogeneic (HPC, Apheresis + Marrow)
Type of donor	Umbilical cord blood	Patient	Related or unrelated matched donor
Product	Cord blood progenitor/stem cells	Bone marrow or peripheral blood progenitor cells	Bone marrow or peripheral blood progenitor cells
Collection	Placenta umbilical cord at birth	Intraoperative marrow or hemapheresis	Intraoperative marrow or hemapheresis
Major complication	Insufficient progenitor cells	Recurrence of original disease	Graft-versus-host disease

HPC (hematopoietic progenitor cell), *apheresis* = PBPCs (peripheral blood hematopoietic progenitor cells); *HPC, marrow* = BMPCs (bone marrow hematopoietic progenitor cells); *HPC, UCB* (umbilical cord blood) = UCBPCs (umbilical cord blood hematopoietic progenitor cells).

allogeneic transplant with acceptable HLA matching. However, with the advent of novel nontransplantation-based therapeutic modalities, allogeneic transplantation should be selectively offered (Deeg et al., 2010). The selection of an allogeneic donor heavily emphasizes the HLA similarity to the recipient, as the degree of dissimilarity between the donor and recipient HLA may lead to graft rejection. Conversely, allogeneic hematopoietic tissue contains viable committed lymphocytes that are capable of recognizing the foreign HLAs of the host and creating a graft-versus-host (GVH) reaction. This immune response of the graft to the host can vary from mild (Grade 1) to severe (Grades 3 and 4). The GVH reaction, particularly Grades 3 and 4, remains one of the most significant morbidity and mortality risks associated with allogeneic hematopoietic cell transplantation. For these reasons, donors are selected who are the best HLA match available (Howard et al., 2015). Donors may be HLA-matched siblings or other family members, or the patient may receive a graft from an unrelated HLA-matched individual identified through one of several worldwide donor registries. These registries, the largest in the United States being the NMDP, recruit healthy individuals who are willing to altruistically donate their bone marrow or peripheral blood hematopoietic progenitor cells (PB-HPCs). Marrow or PB-HPCs from registry donors are harvested at a hospital or blood center; the product is then transported by courier to the transplant center. Anonymity is maintained for both donor and recipient. Because of the need for an almost perfect HLA match, registries must have millions of donors in order to achieve adequate confidence to identify matching donors for a given patient. Despite these resources, ideal HLA-matched HPC donors may not be identified for all patients. One option for these patients is transplantation from a haploidentical donor (Handgretinger & Lang, 2008). As of 2017, over 800 cases of haploidentical transplant grafts are derived from PB-HPC and nearly 400 cases were utilizing BM-HPC grafts (www.CIBMTR.org). The utilization of haploidentical donors increases the pool of potential donors but it also increases the risk of fatal graft failure and GVH reactions due to the presence of bidirectional HLA alloreactivities to donor and recipient T cells. Recent advances suggest improved outcomes in haploidentical transplants with selective T-cell depletion and the posttransplant cyclophosphamide regimen (Busca & Aversa, 2017; Kasamon et al., 2015; Bashey et al., 2017). An additional source of allogeneic HPC source is umbilical cord blood. These cord blood HPC units do not require a high degree of HLA matching and are available immediately because these cord blood units are collected selectively and prospectively by cord blood banks.

Bone Marrow (BM-HPC)

Bone marrow is harvested from the iliac crest of the donor in the operating room under sterile conditions. Donors will elect to have general or spinal anesthesia. The amount of marrow to be collected is dependent on the recipient size. Generally, sufficient marrow is collected to provide at least 2-3 × 10^8 viable nucleated cells per kilogram of recipient body weight. For a 70-kg adult, this will generally require the collection of about 700 mL of marrow. The technique involves the collection of approximately 3 to 5 mL per aspiration into a heparinized syringe. Aspirating too large a volume from one aspiration will result in diluting the marrow content with peripheral blood.

Usually, two providers will harvest marrow at the same time from each side of the donor iliac crest. As it is collected, the aspirated marrow is filtered through large-pore filters to remove bone spicules or clots, and supplemental anticoagulant is added. Because the HPCs are contained within the mononuclear cell fraction, the collected marrow can be further processed to reduce the red blood cell mass (often required for ABO-incompatible transplants) or plasma (volume reduction) while preserving the buffy coat. Generally, allogeneic bone marrow HPC products are collected immediately before transplantation but may be cryopreserved for later infusion.

The bone marrow HPC product was the graft source of choice since the inception of stem cell transplantation. Since the late 1980s, however, the development of less invasive blood harvesting technologies has allowed the use of blood apheresis/separation for component manufacturing. The apheresis machine was later optimized and developed to collect HPCs from the peripheral blood in the late 1990s. According to the NMDP, the rise of peripheral blood HPC practice commenced in 2000 and, by 2003, PB-HPC transplant cases exceeded the BM-HPC. From 2012 to 2016, 23% of allogeneic transplants were obtained from bone marrow.

Peripheral Blood Hematopoietic Progenitor Cells (PB-HPCs)

During the post-chemotherapy period, bona fide HPCs were detected in the peripheral blood (Richman et al., 1976). This discovery has led to the development of technologies that would allow the collection of HPCs from peripheral blood. Further, this approach was incentivized by the need to collect autologous HPC graft material with a mitigated risk of bone marrow tumor cell contamination. Hemapheresis systems were developed that allow the safe collection of adequate numbers of these cells to provide for engraftment of the recipient after chemotherapy (Kessinger et al., 1988). Because of the relative ease of hemapheresis collection over marrow harvest and the increased rate of engraftment, progenitor cells obtained from the peripheral blood are increasingly being used in the allogeneic setting as well. From 2012 to 2016, nearly 99% of autologous hematopoietic transplants derived from PB-HPCs; 68% of allogeneic hematopoietic transplants employ PB-HPCs (www.CIBMTR.org). In most patients undergoing autologous transplantation, large-volume apheresis collection (14–20 L blood volume processed per hemapheresis) is now well established as an efficient means of collecting adequate numbers of HPCs in a reasonable number of procedures to provide for adequate, timely hematopoietic recovery. Offering hemapheresis collection as an option over traditional bone marrow harvest has positively affected the recruitment of volunteer donors for the national marrow donor programs. The instrumentation and procedures used for peripheral blood progenitor cell harvest are described in Chapter 38.

The greatest advantage of peripheral blood progenitor cells over marrow is the time to neutrophil and platelet engraftment. In a randomized controlled clinical trial, neutrophil engraftment among the PB-HPC cohort was 5 days earlier than the BM-HPC cohort. Platelet engraftment was 7 days shorter with the PB-HPC cohort (Gianni et al., 1989). This noted earlier engraftment could be associated with the typically higher CD34+ cell doses collected in PB-HPC when compared with the doses derived from BM-HPC. However, despite differences in engraftment rates, the overall survival in patients receiving either type of HPC products was not significantly different. Interestingly, PB-HPC transplantation was found to result in a significantly higher rate of chronic graft-versus-host disease (GVHD), whereas BM-HPC was associated with significantly more graft failures (Anasetti, 2012). The higher risk of GVHD in allogeneic recipients of PB-HPCs versus marrow (Cutler et al., 2001) has stimulated trials of new technologies to modify these grafts (see T-Cell Depletion section). Collection of HPCs in the nonmobilized patient or donor would require multiple apheresis procedures given that the steady-state CD34+ cell frequency in the nonmobilized peripheral blood and marrow is about 0.1% to 0.2% and 1% to 2% of leukocytes, respectively. Thus, mobilization therapies are required to increase the numbers of circulating HPCs and, thus, improve the efficiency of hemapheresis collection. Richman and colleagues (1976) recognized that although there was a drop in the number of circulating CD34+ cells following chemotherapy, this was followed by a fourfold

to fivefold increase in the percentage of circulating CD34+ cells just as the absolute neutrophil count began to recover, usually around 14 to 21 days following therapy. This increase in circulating CD34+ cells is greatest when utilizing chemotherapeutic agents such as cyclophosphamide and etoposide. If hemapheresis collection is performed in this window, large numbers of HPCs can be recovered with a limited number of procedures, even though the total white cell count may be less than 10,000/μL. Because the period of increased numbers of circulating CD34+ cells is short (2–3 days), close monitoring of the patient's white cell count and peripheral blood CD34+ cell counts and timing of the hemapheresis collection are critical. In addition, some investigators have felt that collecting autologous HPCs in the recovery phase of chemotherapy decreases the likelihood of tumor cells contaminating the apheresis product.

The use of hematopoietic growth factors such as granulocyte-macrophage colony-stimulating factor (GM-CSF or sargramostim) and granulocyte colony-stimulating factor (G-CSF or filgrastim) also results in a significant increase in the numbers of circulating CD34+ cells in peripheral blood (Siena et al., 1989). Doses of 5 to 10 μg/kg of body weight for 4 to 5 days will result in a fivefold to tenfold increase in the number of HPCs in the peripheral blood. The use of G-CSF alone has proved to be more efficient than chemotherapy priming for the collection of CD34+ cells. The combination of chemotherapy priming and the use of growth factors (primarily G-CSF) results in the maximum mobilization of PB-HPCs and the need for the fewest number of hemapheresis procedures to collect a transplant dose of HPCs—a strategy employed by most autogeneic transplant programs. The use of G-CSF in the healthy allogeneic donor to mobilize HPCs has been investigated; aside from mild effects such as bone pain and headache, it is well tolerated (Anderlini et al., 1997). Since 2015, the FDA approved several filgrastim biosimilars (e.g., filgrastim-sndz and filgrastim-aafi), which were defined to demonstrate the same clinical indication, mechanism of action, route of administration, dosage form, and dosage strength as the reference drug. In 2008, the FDA approved the use of plerixafor as an additional mobilization drug for donors who failed the G-CSF–mediated HPC mobilization (Hopman & DiPersio, 2014). This drug blocks the CXCR4-SDF-1 interaction that is required for HPC targeting to the bone marrow niche. This blockage results in increased mobilization of HPCs. Plerixafor is generally well tolerated, with gastrointestinal irritation the most commonly observed side effect. Despite the improvement in the mobilization algorithm, there are still examples of mobilization failure. Currently, there are several novel mobilization drugs in various phases of clinical trials. For example, bortezomib, a proteasome inhibitor that disrupts the very late antigen 4 (VLA-4)/vascular cell adhesion molecule 1 (VCAM-1) pathway, has successfully completed the phase II clinical trial (Niesvizky et al., 2013). Parathyroid hormone (PTH) has also completed the phase I clinical trial (Ballen et al., 2007).

Umbilical Cord Blood

The fact that a large amount of CFU cells or progenitor cells are present in umbilical cord blood has been known for many years, but its clinical efficacy was proven with a full hematopoietic rescue in a Fanconi anemia patient in 1989 (Gluckman et al., 1989). The apparent success of many of these early cord blood transplants led to the organization of several cord blood banks in the United States and Europe in an attempt to provide another source of progenitor cell tissue for patients requiring an allogeneic transplant from an unrelated donor. The Cord Blood Transplantation (COBLT) study, which collected data from 1997 to 2004, established standardized procedures for donor screening, HLA matching, cord blood processing, and storage and data collection. These data clearly established that cord blood transplants in children with a wide range of malignant and nonmalignant conditions could result in a high degree of engraftment and a 2-year event-free survival rate of 55% for children with high-risk malignancies and 78% for children with nonmalignant conditions (Martin et al., 2006; Kurtzberg, 2009). In addition, because the progenitor cells are obtained from cord blood, there appears to be a greater degree of tolerance for some degree of HLA incompatibility between donor and recipient without the appearance of a Grade 3 or 4 GVH reaction. Thus, hematopoietic transplantation might become available for some patients who otherwise have no HLA-matched donor (Barker et al., 2005). More recently, in patients with minimal residual disease, cord blood transplantation has comparable overall survival to HLA-matched unrelated donor transplantation, with less disease relapse risk (Milano et al., 2016).

Umbilical cord progenitor cells are harvested by cannulating the umbilical cord vessels while the placenta is still in utero or, more commonly, following delivery. The number of HPCs recovered is directly proportional to the volume of cord blood collected, which varies with the size of the infant/placenta and with the experience of the individual performing the collection (Wen et al., 2012). Volumes ranging from 40 to 150 mL are common for experienced centers. This results in the harvesting of approximately 4 to 11 × 10^8 nucleated cells. Collections that are not adequate in volume (<40 mL) are usually discarded. Generally, umbilical cord blood collections are not further processed to reduce their volume but are then frozen directly with DMSO and liquid nitrogen storage. Careful screening and testing of the mother are essential to ensure the safety of the cord blood product as well as the absence of genetic disease. In addition to FDA-approved laboratory measurements for serologically transmissible disease and confirmation by NAT on a maternal sample, bacteriologic testing on a sample of the umbilical cord blood unit is completed.

Some collection centers use specially trained staff deployed to the delivery room who are not distracted by the care of the mother and/or the infant. The use of a dedicated staff results in larger volume collections and reduction in the risk of bacterial contamination of the cord blood. Additionally, whether the plasma depletion or red blood cell depletion processing during the manufacturing could improve the graft quality and transplantation outcome remains controversial (Barker et al., 2017; Chow et al., 2007).

From 2012 to 2016, approximately 9% of allogeneic transplants utilized umbilical cord blood–derived HPCs (CIBMTR.org). A logistical advantage of cord blood HPC over both bone marrow and apheresis products is that the cord blood is banked earlier and is more immediately available for use, thus, decreasing time to transplantation.

Although umbilical cord blood banking offers the exciting potential for improved histocompatibility and, thus, availability for more patients, the remaining critical issue is the lack of sufficient total HPCs in most cord blood units to achieve usual engraft times in adults. Low HPC dose is associated with delayed or failed engraftment, which can lead to increased morbidity and mortality. Transplantation of two cord-blood units has extended the use of cord-blood transplantation to adults, but the engraftment remains inferior to that achieved with marrow or peripheral-blood stem cells (De Lima, 2002; Barker et al., 2005; Haspel et al., 2008).

T-CELL DEPLETION

Techniques to reduce the numbers of T lymphocytes in allogeneic hematopoietic grafts aim to reduce the GVHD incidence and severity. Manipulations are done to directly (e.g., pan or subset T-cell negative selection) or to indirectly (e.g., CD34+ HPC positive selection) remove the T-cells. Techniques specifically targeting T-cells have included soybean lectin agglutination, E-rosette formation, combinations of the two, counterflow elutriation, monoclonal antibodies, and the application of monoclonal antibodies in vivo in the recipient posttransplant to reduce donor T-cells. The HPC CD34+ positive selection can be done with commercially available immunomagnetic beads that are cross-linked with a monoclonal antibody (Saad et al., 2017).

The major disadvantage of T-cell depletion is the resultant increase in the incidence of disease relapse. Patients who demonstrate mild GVHD appear to have a lower incidence of relapse of neoplastic disease than do those patients who have no GVHD. The presence of the donor T-cell population is apparently critical to "graft-versus-leukemia effect," with recognition of host antigens by donor T-cells generating an immune response that eliminates residual host tumor cells.

CRYOPRESERVATION OF HEMATOPOIETIC GRAFTS

Because HPC grafts from all autogeneic and many allogeneic collections are cryopreserved and stored before use, the cryopreservation process directly affects the efficacy and quality of HPC transplants. Peripheral blood stem cell products are routinely cryopreserved in a saline solution mixture and supplemented with a protein, usually albumin or autologous plasma, and cryoprotectants such as DMSO without or with 1% dextran-40. The most common protocol involves the use of 10% DMSO as a cryoprotective agent, controlled-rate freezing at -1°C/minute until heat of fusion, then –1°C/minute until –40°C, followed by 10°C/minute until –50°C to –86°C, and, finally, stored in liquid nitrogen in either the vapor or liquid phase (≤ –150°C per FDA requirements). The use of DMSO provides significant improvement in postthaw viability over glycerol. Because toxicities are associated with the postthaw infusion of progenitor cell products containing DMSO, other investigators have looked at using lower concentrations or adding hetastarch or other additives. Attempts to wash products after thawing to reduce the amount of DMSO present resulted in significant loss of progenitor cells. Therefore, strategies using DMSO are now targeted at reducing the volume of the prefreezing product, lowering the amount of

TABLE 39.3
Adverse Reactions Observed in Patients Transfused with Cryopreserved Progenitor Cell Products

Frequency	Contributing Factors
Common	
Chills	Volume of product reinfused
Nausea	Type and amount of cryoprotectant reinfused
Emesis	Volume of incompatible red cells (allogeneic products)
Fever	Bacterial contamination
Headache	
Dyspnea	
Uncommon	
Renal failure	
Cardiac arrest	
Hypotension	
Sepsis	

DMSO necessary, or new additive solutions that allow decreased DMSO concentrations (Clarke et al., 2009; Stylianou et al., 2006).

REINFUSION OF PROGENITOR CELL PRODUCTS

Regardless of the source of the progenitor cell graft, HPCs are infused to the recipient in a manner very similar to that of any blood product transfusion. Pluripotential progenitor cells, with their unique membrane receptors, will home to the marrow space, engraft, and replicate. Products that have been cryopreserved with DMSO in most cases are thawed and immediately reinfused, typically without washing. Some programs do wash HPCs prior to infusion for patients who are at higher risk of toxicity (e.g., neonatal). HPCs collected by hemapheresis that are not further processed may contain large numbers of red blood cells. Cryopreservation in DMSO does not maintain mature red blood cell membrane integrity, and these products will contain a large amount of free hemoglobin when thawed. Recipient reactions to both the free hemoglobin and DMSO vary from mild—characterized by nausea, chills, or headache—to more severe reactions that can include hypotension, vomiting, systemic inflammatory response syndrome, renal failure, cardiac arrest, and neurologic ischemia/toxicity (Stroncek et al., 1991; Hoyt et al., 2000). Such adverse reactions are shown in Table 39.3. Recipients of cryopreserved progenitor cell products are generally premedicated with antihistamines and/or antiemetics. Adequate hydration and the use of diuretics are indicated to decrease renal toxicities associated with free hemoglobin and larger-volume infusions. Because the pluripotential HPCs do not express ABO antigens, they will engraft in the marrow stroma of ABO-incompatible individuals, thus abrogating the need for donors to be ABO compatible. However, if mature ABO-incompatible red blood cells are present in these grafts, RBC reduction during the HPC graft processing or elective washing procedure for thawed HPC grafts is necessary. Close monitoring of acute hemolysis in patients should always be practiced.

EX VIVO MANIPULATION OF HEMATOLOGIC CELLS

Gene therapy offers promise to correct pathogenic mutations and restore the expression of functional proteins for improved cellular function. Conversely, genetic modification engineering can be implemented to manufacture therapeutic cell products with desirable phenotype. As an example, patients with sickle cell disease can experience significant symptomatic improvement if there are 30% or more of red blood cells with normal beta-hemoglobin in circulation. Extending this rationale, researchers could use nonreplicating engineered virus to correct the defective beta-globin in autologous hematopoietic stem/progenitor cells (HSPCs), followed by reinfusion of these genetically modified HSPCs to generate an adequate amount of normal red blood cells (Ribeil et al., 2017). In the area of blood product manufacturing, the modification of human platelet antigen (HPA) gene by the clustered regularly interspaced short palindromic repeats/CRISPER associated protein 9 (CRISPR/Cas9) technology has brought a potential new promise to generate progenitor-derived megakaryocytes that produce specific HPA-negative platelets for patients suffering from thrombocytopenia due to HPA-specific allogeneic antibodies (Zhang et al., 2016).

There are other innovative approaches to manipulating the hematopoietic progenitors. While a cord blood transplant can take longer to engraft compared with bone marrow or PB-HPC products, a CD34-purified HPC graft derived from a haploidentical donor can be coinfused. This has been tested and shown to allow faster engraftment with less GVHD incidence (van Besien et al., 2019). Ex vivo expansion of cord blood units is another highly creative and investigative approach to increasing the transplantable HPC doses. Cord HPCs have been be cocultured with mesenchymal stromal cells, resulting in expansion of both primitive and mature hematopoietic progenitors in unfractionated cord blood. In one study, expanded cord blood transplanted in combination with unmanipulated cord blood significantly improved engraftment as compared with unmanipulated cord blood only. The median time to neutrophil engraftment was 15 days in recipients of expanded cord blood as compared with 24 days in historical controls who received unmanipulated cord blood only ($p < 0.001$). The median time to platelet engraftment was 42 days and 49 days, respectively ($p = 0.03$) (De Lima et al., 2012; Robinson, 2006). Additionally, the use of an aryl hydrocarbon receptor inhibitor, stemregenin-1 (SR-1), to expand cord blood HPC has been tested in a phase I study and showed marked HPC expansion, faster engraftment time, and no graft failure (Wagner et al., 2016).

USE OF DENDRITIC CELLS IN CANCER IMMUNOTHERAPY

Dendritic cells (DCs) are used in cancer immunotherapy in attempts to harness the power and specificity of the patient's own immune system to treat the tumors. The aim of the DC immunotherapy approach is to induce antigen-specific expansion of effector and memory CD8+ T cells that will directly reduce the tumor mass and that can also induce an immunologic memory to control tumor relapse. For an optimally functioning vaccine, the vaccine-elicited CD8+ T cells should meet several criteria. They should be of high avidity, able to recognize peptide-MHC class I complexes on tumor cells, able to express high levels of granzyme and perforin (essential proteins for cytotoxic activity against cancer cells), able to enter a tumor microenvironment, and able to overcome the immunomodulatory mechanisms operational in a tumor cell. DCs initiate an immunologic response by presenting the captured antigen, in the form of peptide–MHC molecule complexes, to naïve immune cells. DCs are at the center of the immune system owing to their ability to control both tolerance and immune responses. These key properties of DCs render them central candidates for antigen delivery and vaccination, including therapeutic vaccination against cancer. There are two approaches used with DCs. In one, a vaccination approach is utilized in which the antigen is provided together with an adjuvant to elicit a therapeutic T-cell response in vivo. Alternately, autologous antigen-specific DCs are isolated and expanded ex vivo and then reinfused into the patient.

DCs are generated ex vivo by culturing HPCs or monocytes with cytokine combinations (Kirkling, 2018; Balan, 2018). These expanded DCs have been tested as therapeutic vaccines for a variety of neoplastic conditions. A consistent conclusion from these studies is that DC-based vaccines are safe and can induce the expansion of circulating CD4+ T cells and CD8+ T cells that are specific for tumor antigens. Improved clinical outcomes have been seen in trials for treatment of mesothelioma (Belderbos et al., 2019), B-cell non-Hodgkin lymphoma (Lin et al., 2014), prostate cancer (Higano et al., 2009; Kantoff et al., 2020), melanoma (Schwartzentruber et al., 2011; Oshita et al., 2012; Gargett et al., 2018), multiple sclerosis (Zubizarreta et al., 2019), liver cancer (Lee et al., 2015), non–small cell lung carcinoma (Lee et al., 2017), and glioblastoma multiforme (Okada et al., 2011; Pellagatta et al., 2018), among others. Sipuleucel-T is an FDA-approved commercial system based on this paradigm for treatment of prostate cancer (Higano et al., 2009; Kantoff et al., 2010).The ex vivo–generated sensitized DCs may be evaluated using assays such as immunophenotyping, MHC-peptide tetramer staining, cytokine flow cytometry, enzyme-linked immunospot, and lymphocyte killing activities (Maecker et al., 2005; Strioga et al., 2013; Tej et al., 2014). However, as modified DC-based products advance through clinical trials, assay standardizations and consensus cell characterizations will be needed to improve product quality and clinical outcomes (De Wolf et al., 2018).

ADOPTIVE CELL TRANSFER/CHIMERIC ANTIGEN RECEPTORS

T cells can be genetically engineered to deliver a direct cytotoxic effect against target-specific cells, such as tumor and viral-infected cells. One of the approaches is through the introduction of genes encoding artificial

T-cell receptors, called *chimeric antigen receptors* (CARs), specific to cancer-associated or viral-associated antigens (June et al., 2018; Johnson et al., 2018). CARs are proteins that allow the engineered T cells to recognize a specific protein (antigen) on tumor cells and simultaneously activate T cells to confer cytotoxicity to the targeted tumor cells. Most CARs are composed of an antigen-binding domain, an extracellular spacer/hinge region, a transmembrane domain, and an intracellular signaling domain resulting in T-cell activation after antigen binding (Curran et al., 2012). The most successful trials were the CAR-T cell against CD19+ B-cell malignancies, such as B acute lymphoblastic leukemia (B-ALL) and diffuse large B-cell lymphoma (DLBCL), which received FDA Breakthrough Designation during the phase II clinical trial. In August and October of 2017, anti-CD19 CAR-Ts against pediatric B-ALL and adult DLBCL, respectively, were approved by the FDA for clinical use. There are still numerous ongoing clinical trials using CARs to treat a wide range of hematologic and nonhematologic malignancies (Beatty, 2018). Targeted T cells, using the CAR mechanism, have been successfully tried in humans to treat multiple myeloma (Raje et al., 2019), chronic lymphocytic leukemia (Geyer et al., 2019), glioblastoma (Goff et al., 2019; O'Rourke et al., 2017), prostate cancer (Junghans et al., 2016), and sarcoma (Ahmed et al., 2015).

Also, T cells can be engineered to combat viral infection and malignancies (Cruz et al., 2013; Rapoport et al., 2015; Ahmed et al., 2017). By means of direct pulsing of viral-specific peptide or gene transduction of MHC-restricted virus-specific T-cell receptor repertoire, T cells were selectively made to provide robust and direct neutralization of infected cells (Barrett et al., 2018, Kaeuferle et al., 2019). Posttransplantation viral reactivation remains a serious threat and is associated with high mortality. The utilization of viral-specific T cells has become a great contender in providing immediate and long-lasting protection for posttransplant patients, rivaling and potentially superior to that of gold standard antiviral drugs. There are currently many clinical trials focusing on treating posttransplantation viremia, such as cytomegalovirus, Epstein-Barr virus, adenovirus, BK virus, human herpesvirus 6, respiratory syncytial virus, and influenza virus (Rooney et al., 2012).

For manufacturing investigative cell therapy products, the general approach is to have the staff from a tissue or cell therapy laboratory isolate cells (e.g., DCs or lymphocytes) by leukapheresis with or without immunomagnetic cell isolation, then purify, test, store, and culture under Current Good Tissue Practice (cGTP)/Current Good Manufacturing Practice (cGMP) conditions. For all cells and tissues that require premarketing evaluation, an FDA Investigational New Drug (IND) application must be filed and approved prior to the commencement of human clinical trials in the United States. Details regarding the manufacturing and handling of these investigative cell products must be described in the Chemistry, Manufacturing, and Control section of the IND application to ensure product safety and quality.

SELECTED REFERENCES

Boyle KE, Vlahos N, Jarow JP: Assisted reproductive technology in the new millennium: Part II, *Urology* 63:217–224, 2004.

This, with part I, is an excellent review of current approaches to infertility.

Cetin I, Pardi G: A multidisciplinary approach to the future of reproduction, *Placenta* 24:s3–s4, 2003.

This is a good review of reproductive options for cancer patients.

Gorin NC: Collection, manipulation and freezing of haematopoietic stem cell. In Gladstone AH, editor: *Clinics in haematology*, London, 1986, WB Saunders, pp 19–48.

A lengthy, comprehensive description of cell freezing physiology and practices.

Kessinger A, Armitage JO, Landmark JD, et al.: Autologous peripheral hematopoietic stem cell transplantation restores hematopoietic function following marrow ablative therapy, *Blood* 71:723, 1988.

Provides the earliest work and later refinements in autologous hematopoietic transplants by one of the first groups to describe this therapy.

Kurtzberg J: Update on umbilical cord blood transplantation, *Curr Opin Pediatr* 21:22–29, 2009.

This is an excellent review of state-of-the-art cord blood transplantation by one of the leading experts in this discipline.

Storb R: Allogeneic hematopoietic stem cell transplantation—yesterday, today, and tomorrow, *Exp Hem* 31:1–10, 2003.

Interesting, nontechnical review by one of the leaders in hematopoietic transplantation.

Access the complete reference list online at Elsevier eBooks for Practicing Clinicians.

REFERENCES

Ahmed N, Brawley VS, Hegde M, et al.: Human epidermal growth factor receptor 2 (HER2)-specific chimeric antigen receptor-modified T cells for the immunotherapy of HER2-positive sarcoma, *J Clin Oncol* 33(15):1688–1696, 2015.

Ahmed N, Brawley V, Hegde, et al.: HER2-specific chimeric antigen receptor-modified virus-specific T cells for progressive glioblastoma: a phase 1 dose-escalation trial, *JAMA Oncol* 3(8):1094–1101, 2017.

Akpek EK, Alkharashi M, Hwang FS, et al.: Artificial corneas versus donor corneas for repeat corneal transplants, *Cochrane Database Syst Rev* 11, 2014.

American Association of Tissue Banks: *2012-2015 American association of tissue banks (AATB) national tissue recovery through utilization Survey report*, *McLean*, VA, 2017, AATB.

Anderlini P, Korbling M, Dale D, et al.: Allogeneic blood stem cell transplantation: consideration for donors, *Blood* 90:903–908, 1997.

Balan S, Arnold-Schrauf C, Abbas A, et al.: Large-scale human dendritic cell differentiation revealing notch-dependent lineage bifurcation and heterogeneity, *Cell Rep* 24(7):1902–1915, 2018.

Barker JN, Weisdorf DJ, DeFor TE, et al.: Transplantation of 2 partially HLA-matched umbilical cord blood units to enhance engraftment in adults with hematologic malignancy, *Blood* 105:1343–1347, 2005.

Barker JN, Kurtzberg J, Ballen K, et al.: Optimal practices in unrelated donor cord blood transplantation for hematologic malignancies, *Biol Blood Marrow Transplant* 23:882–896, 2017.

Barrett AJ, Prockop S, Bollard CM: Virus specific T cells: broadening applicability, *Biol Blood Marrow Transplant* 24(1):13–18, 2018.

Bashey A, Zhang M-J, McCurdy SR, et al.: Mobilized peripheral blood stem cells versus unstimulated bone marrow as a graft source for T-cell-replete haploidentical donor transplantation using post-transplant cyclophosphamide, *J Clin Oncol* 35:3002–3009, 2017.

Beatty GL, O'Hara MH, Lacey SF, et al.: Activity of Mesothelin-specific chimeric antigen receptor T cells against pancreatic carcinoma metastases in a phase 1 trial, *Gastoenterology* 155(1):29–32, 2018.

Belderbos RA, Baas P, Berardi R, et al.: A multicenter, randomized, phase II/III study of dendritic cells loaded with allogeneic tumor cell lysate (MesoPher) in subjects with mesothelioma as maintenance therapy after chemotherapy: DENdritic cell Immunotherapy for Mesothelioma (DENIM) trial, *Transl Lug Cancer Res* 8(3):280–285, 2019.

Berenson RJ, Andrews RG, Bensinger WI, et al.: Antigen CD34+ marrow cells engraft lethally irradiated baboons, *J Clin Invest* 81(3):951–955, 1988.

Besser MJ, Shapira-Frommer R, Treves AJ, et al.: Clinical responses in a phase II study using adoptive transfer of short-term cultured tumor infiltration lymphocytes in metastatic melanoma patients, *Clin Cancer Res* 16(9):2646–2655, 2010.

Bittencourt H, Rocha V, Chevret S, et al.: Association of CD34 cell dose with hematopoietic recovery, infections, and other outcomes after HLA-identical sibling bone marrow transplantation, *Blood* 99(8):2726–2733, 2002.

Bohringer D, Grotejohann B, Ihorst G, et al.: Rejection prophylaxis in corneal transplant – a randomized study of HLA matching (the FANCY study), *Dtsch Arztebl Int* 115:259–265, 2018.

Boldt J: Current results with slow freezing and vitrification of the human oocyte, *Reprod Biomed Online* 23(3):314–322, 2011.

Boldt J, Cline D, McLaughlin D: Human oocyte cryopreservation as an adjunct to IVF-embryo transfer cycles, *Hum Reprod* 18:1250–1255, 2003.

Busca A, Aversa F: In-vivo or e-vivo T cell depletion or both to prevent graft-versus-host disease after hematopoietic stem cell transplantation, *Expert Opin Biol Ther* 17:1401–1415, 2017.

Centers for Disease Control and Prevention (CDC): Update: creutzfeldt-Jakob disease associated with cadaveric dura mater grafts—Japan, 1979–2003, *MMWR (Morb Mortal Wkly Rep)* 52:1179, 2003.

Centers for Disease Control and Prevention (CDC): Assisted reproductive technology, *ART Fertility Clinic Success Rates Report*, 2017.

Chow R, Ndemanee A, Rosenthal J, et al.: Analysis of hematopoietic cell transplants using plasma-depleted cord blood products that are not red blood cell reduced, *Biol Blood Marrow Transplant* 13(11):1346–1357, 2007.

www.CIBMTR.org Center for International Blood and Marrow Transplant Research, accessed August 2019.

Clarke DM, Yadock DJ, Nicoud IB, et al.: Improved post-thaw recovery of peripheral blood stem/progenitor cells using a novel intracellular-like cryopreservation solution, *Cytotherapy* 11(4):472–479, 2009.

Conrad EU, Gretch D, Obermeyer KR, et al.: The transmission of hepatitis C virus by tissue transplantation, *J Bone Joint Surg Am* 77:214–224, 1995.

Cruz CR, Micklethwaite KP, Savoldo B, et al.: Infusion of donor-derived CD19-redirected virus-specific T-cells for B-cell malignancies relapsed after allogeneic stem cell transplant: a phase 1 study, *Blood* 122(17):2965–2973, 2013.

Curran KJ, Pegram HJ, Brentjens RJ: Chimeric antigen receptors for T-cell immunotherapy: current understanding and future directions, *J Gene Med* 14(6):405–415, 2012.

Cutler C, Giri S, Jeyapalan S, et al.: Acute and chronic graft-versus-host disease after allogeneic peripheral blood stem-cell and bone marrow transplantation: a meta-analysis, *J Clin Oncol* 19:3685–3691, 2001.

Deeg HJ, Sandmaier BM: Who is fit for allogeneic transplantation? *Blood* 116(23):4762–4770, 2010.

De Lima M, St John LS, Wieder ED: Double-chimaerism after transplantation of two human leucocyte antigen mismatched, unrelated cord blood units, *Br J Haematol* 119(3):773–776, 2002.

De Lima M, McNiece I, Robinson SN, et al.: Cord-blood engraftment with ex vivo mesenchymal-cell coculture, *N Engl J Med* 367(24):2305–2315, 2012.

Eastlund T: The histo-blood group ABO system and tissue transplantation, *Transfusion* 38:975–988, 1998.

Eye Bank Association of America: Statistical report. 2018 www.restoresight.org, 2018.

Ezra-Cohn HE, Cook SF: Blood typing compact human bone tissue, *Nature* 191:1267–1268, 1961.

Fahner PJ, Mirza MI, van Gulik TM, et al.: Systematic review of preservation methods and clinical outcomes of infrainguinal vascular allografts, *J Vasc Surg* 44:518–524, 2006.

Food & Drug Administration, Tissue & Tissue Products, https://www.fda.gov/vaccines-blood-biologics/tissue-tissue-products, referenced August 2019.

Gargett T, Abbas MN, Rolan P, et al.: Phase I trial of Lipovaxin-MM, a novel dendritic cell-targeted liposomal vaccine for malignant melanoma, *Cancer Immunol Immunother* 67(9):1461–1472, 2018.

Geyer MB, Riviere I, Senechal B, et al.: Safety and tolerability of conditioning chemotherapy followed by CD19-targeted CAR T cells for relapsed/refractory CLL, *JCI Insight* 4:e122627, 2019.

Gianni AM, Bregni M, Siena S, et al.: Rapid and complete hematopoietic reconstitution following combined transplantation of autologous blood and bone marrow cells: a changing role for high-dose chemo-radiotherapy? *Hematol Oncol* 7:139–148, 1989.

Gluckman E, Broxmeyer H, Auerbach A, et al.: Hematopoietic reconstitution in a patient with Fanconi's anemia by means of umbilical-cord blood from an HLA-identical sibling, *N Engl J Med* 321:1174–1178, 1989.

Goff SL, Morgan RA, Yang JC, et al.: Pilot trial of adoptive transfer of chimeric antigen receptor-trasduced T cells targeting EGFRvIII in patients with glioblastoma, *J Immunother* 42(4):126–135, 2019.

Gonzalez-Quevedo D, Martinez-Medina I, Campos A, et al.: Tissue engineering strategies for the treatment of tendon injuries, *Bone Joint Res* 7:318–324, 2018.

Handgretinger R, Lang P: The history and future prospective of haplo-identical stem cell transplantation, *Cytotherapy* 10:443–451, 2008.

Haspel RL, Kao G: Yeap BY, et al: Preinfusion variables predict the predominant unit in the setting of reduced-intensity double cord blood transplantation, *Bone Marrow Transplant* 41:523–529, 2008.

Higano CS, Schellhammer PF, Small EJ, et al.: Integrated data from 2 randomized, double-blind, placebo-controlled, phase 3 trials of active cellular immunotherapy with Sipuleucel-T in advanced prostate cancer, *Cancer* 115:3670–3679, 2009.

Hill Z, Vacl J, Kalasova E, et al.: Haemolytic disease of the newborn due to anti-D antibodies in a Du positive mother, *Vox Sang* 27:92–94, 1974.

Hooper DK, Hawkins JA, Fuller TC, et al.: Panel-reactive antibodies late after allograft implantation in children, *Ann Thorac Surg* 79:641–644, 2005.

Hopman RK, DiPersio JF: Advances in stem cell mobilization, *Blood Rev* 28(1):31–40, 2014.

Houghton FD, Hawkhead JA, Humpherson PG, et al.: Non-invasive amino acid turnover predicts human embryo developmental capacity, *Hum Reprod* 17:999–1005, 2002.

Howard CA, Fernandez-Vina MA, Appelbaum FR, et al.: Recommendations for donor human leukocyte antigen assessment and matching for allogeneic stem cell transplantation: consensus opinion of the Blood and Marrow Transplant Clinical Trials Network (BMT CTN), *Biol Blood Marrow Transplant* 21(1):4–7, 2015.

Hoyt R, Szer J, Grigg A: Neurological events associated with the infusion of cryopreserved bone marrow and/or peripheral blood progenitor cells, *Bone Marrow Transplant* 25:1285–1287, 2000.

Iscove NN, Senn JS, Till JE, et al.: Colony formation by normal and leukemic human marrow cells in culture: effect of conditioned medium from human leukocytes, *Blood* 37:1–5, 1971.

Jackson DW, Windler GE, Simon TM: Intraarticular reaction associated with the use of freeze-dried, ethylene oxide-sterilized bone-patella tendon-bone allografts in the reconstruction of the anterior cruciate ligament, *Am J Sports Med* 18:1–10, 1990.

Johnson LA, Morgan RA, Dudley ME, et al.: Gene therapy with human and mouse T-cell receptors mediates cancer regression and targets normal tissues expressing cognate antigen, *Blood* 114(3):535–546, 2009.

June CH, O'Connor RS, Kawalekar OU, et al.: CAR-T cell immunotherapy for human cancer, *Science* 359(6382):1361–1365, 2018.

Junghans RP, Ma Q, Rathore R, et al.: Phase I trial of anti-PSMA Designer CAR-T cells in prostate cancer: possible role for interacting interleukin 2-T cell Pharmacodynamics as a determinant of clinical response, *Prostate* 76(14):1257–1270, 2016.

Kaeuferle T, Krauss R, Blaeschke F: Strategies of adoptive T-cell transfer to treat refractory viral infections post allogeneic stem cell transplantation, *J Hematol Oncol* 12:13, 2019.

Kagan RJ, Robb EC, Plessinger MS: Human skin banking, *Clin Lab Med* 25:587–605, 2005.

Kainer MA, Linden JV, Whaley DN, et al.: Clostridium infections associated with musculoskeletal-tissue allografts, *N Engl J Med* 350:2564–2571, 2004.

Kalos M, Levine BL, Porter DL, et al.: T cells with chimeric antigen receptors have potent antitumor effects and can establish memory in patients with advanced leukemia, *Sci Transl Med* 3(95), 2011. 95ra73.

Kantoff PW, Higano CS, Shore ND, et al.: IMPACT study investigators. Sipuleucel-T immunotherapy for castration-resistant prostate cancer, *NEJM* 363:411–422, 2010.

Kasamon YL, Bolanos-Meade J, Prince GT, et al.: Outcomes of nonmyeloablative HLA-haploidentical blood or marrow transplantation with high-dose post-transplantation cyclophosphamide in older adults, *J Clin Oncol* 33:3152–3161, 2015.

Kearney JN: Quality issues in skin banking: a review, *Burns* 24:299–305, 1998.

Keeney M, Gratama JW, Sutherland DR: Critical role of flow cytometry in evaluating peripheral blood hematopoietic stem cell grafts, *Cytometry* 58A:72–75, 2004.

Kirkling ME, Cytlak U, Lau CM, et al.: Notch signaling facilitates *in* vitro generation of cross-presenting classical dendritic cells, *Cell Rep* 23(12):3658–3672, 2018.

Laub GW, Muralidharan S, Clancy R: Cryopreserved allograft veins as alternative coronary artery bypass conduits: early phase results, *Ann Thorac Surg* 54:826–831, 1992.

Lee JH, Lee Y, Lee M, et al.: A phase I/IIa study of adjuvant immunotherapy with tuour antigen-pulsed dendritic cells in patients with hepatocellular carcinoma, *Br J Cancer* 113(12):1666–1676, 2015.

Lee JM, Lee MH, Garon E, et al.: Phase I trial of intratumoral injection of *CCL21* gene-modified dendritic cells in lung cancers elicits tumor-specific imune responses and CD8+ T-cell infiltration, *Clin Cancer Res* 23(16):4556–4568, 2017.

Lin Y, Atwell T, Weisbrod A, et al.: Dendritic cell vaccine treatment for B-cell non-Hodgkin lymphoma: clinical trial in progress, *Blood* 124(21):4474, 2014.

Lorenz E, Uphoff D, Reid TR, et al.: Modification of irradiation injury in mice and Guinea pigs by bone marrow injections, *Natl Cancer Inst* 12:197–201, 1951.

Lucifero D, Chaillet JR, Trasler JM: Potential significance of genomic imprinting defects for reproduction and assisted reproductive technology, *Hum Reprod* 10:3–18, 2004.

Maecker HT, Moon J, Bhatia S, et al.: Impact of cryopreservation on tetramer, cytokine flow cytometry, and ELISPOT, *BMC Immunol* 6:17, 2005.

Martin PL, Carter SL, Kernan NA, et al.: Results of the cord blood transplantation study (COBLT): outcomes of unrelated donor umbilical cord blood transplantation in pediatric patients with lysosomal and peroxisomal storage diseases, *Biol Blood Marrow Transplant* 12:184–194, 2006.

Medawar PB: Immunity to homologous grafted skin. III. The fate of skin homografts transplanted to the brain, to subcutaneous tissue and to the anterior chamber of the eye, *Br J Exp Pathol* 29:58–62, 1948.

Milano F, Gooley T, Wood B, et al.: Cord-blood transplantation in patients with minimal residual disease, *N Engl J Med* 375(10):944–953, 2016.

Mohan S, Baylink DJ: Bone growth factors, *Clin Orthop* 263:30–48, 1991.

O'Brien MF, Stafford EG, Gardner MAH: Cryopreserved viable allograft aortic valves. In Yankoh AC, Hetzer R, Miller DC, et al.: *Cardiac valve allografts 1972–1987*, New York, 1988, Springer-Verlag, pp 311–318.

Okada H, Kalinski P, Ueda R, et al.: Induction of CD8+ T-cell responses against novel glioma-associated antigen peptides and clinical activity by vaccinations with α-type 1 polarized dendritic cells and polyinosinic-polycytidylic acid stabilized by lysine and carboxymethylcellulose in patients with recurrent malignant glioma, *J Clin Oncol* 29(3):330–336, 2011.

Ooleey PW: *AABB 31st Edition blood banks/transfusion services standards committee: standards for blood banks and transfusion services*, Bethesda, MD, 2018, AABB, pp 32–33.

Organ Procurement and Transplantation Network (OPTN) and Scientific Registry of Transplant Recipients (SRTR): *OPTN/SRTR 2012 annual data report*, Rockville, MD, 2017, Department of Health and Human Services, Health Resources and Services Administration, Healthcare Systems Bureau, Division of Transplantation.

O'Rourke DM, Nasrallah MP, Desai A, et al.: A single dose of peripherally infused EGFRvIII-directed CAR T cells mediates antigen loss and induces adaptive resistance in patients with recurrent glioblastoma, *Sci Transl Med* 9(399):1–15, 2017.

Oshita C, Takikawa M, Kume A, et al.: Dendritic cell-based vaccination in metastatic melanoma patients: phase II clinical trial, *Oncol Rep* 28(4):1131–1138, 2012.

Palermo GD, Joris H, Devroey P: Pregnancies after intracytoplasmic injection of a single spermatozoan into an oocyte, *Lancet* 340:17–18, 1992.

Pellegatta S, Eoli M, Cuccarini V, et al.: Survival gain in glioblastoma patients treated with dendritic cell immunotherapy is associated with increased NK but not CD8+ T cell activation in the presence of adjuvant temozolomide, *OncoImmunology* 7(4), 2018. e1412901.

Porcu E, Bazzocchi A, Notarangelo L, et al.: Human oocyte cryopreservation in infertility and oncology, *Curr Opin Endocrinol Diabetes Obes* 15:529–535, 2008.

Qazi Y, Hamrah P: Corneal allograft rejection: immunopathogenesis to therapeutics, *J Clin Cell Immunol* Suppl 9, 1-20

Raje N, Berdeja J, Lin Y, et al.: Anti-BCMA CAR T-Cell therapy bb2121 in relapsed or refractory multiple myeloma, *N Engl J Med* 380(18):1726–1737, 2019.

Ramos CA, Rouce R, Robertson CS, et al.: In vivo fate and activity of second- versus third-generation C19-specific CAR-T cells in B cell non-Hodgkin's lymphomas, *Mol Ther* 26(12):2727–2737, 2017.

Rapoport AP, Stadtmauer EA, Binder-Scholl GK, et al.: NY-ESO-1 specific TCR engineered T-cells mediate sustained antigen-specific antitumor effects in myeloma, *Nat Med* 21(8):914–921, 2015.

Ribeil JA, Hacein-Bey-Abina S, Payen E, et al.: Gene therapy in a patient with sickle cell disease, *N Engl J Med* 376(9):848–855, 2017.

Richman CM, Weiner RS, Yankee RA: Increase in circulating stem cells following chemotherapy in man, *Blood* 47:1031–1039, 1976.

Robinson SN, Ng J, Niu T, et al.: Superior ex vivo cord blood expansion following coculture with bone marrow-derived mesenchymal stem cells, *Bone Marrow Transplant* 37(4):359–366, 2006.

Rooney C, Leen A: Moving successful virus-specific T-cell therapy for hematopoietic stem cell recipients to late phase clinical trials, *Mol Ther Mucleic Acids* 13:1–e55, 2012.

Saad A, Lamb LS: Ex vovo T-cell depletion in allogeneic hematopoietic stem cell transplant: past, present and future, *Bone Marrow Transplant* 52(9):1241–1248, 2017.

Schwartzentruber DJ, Lawson DH, Richards JM, et al.: gp100 peptide vaccine and interleukin-2 in patients with advanced melanoma, *NEngl JMed 2* 364(22):2119–2127, 2011.

Shahrokhi S, Arno A, Jeschke MG: The use of dermal substitutes in burn surgery: acute phase, *Wound Repair Regen* 22(1):14–22, 2014.

Shorr N, Perry J, Goldberg RA, et al.: The safety and applications of acellular human dermal allograft in ophthalmic plastic and reconstructive surgery: a preliminary report, *Ophthalm Plast Reconstr Surg* 16:223–230, 2000.

Shoulars K, Noldner P, Troy JD, et al.: Development and validation of a rapid, aldehyde dehydrogenase bright-based cord blood potency assay, *Blood* 127:2346–2354, 2016.

Siena S, Bregni M, Brando B, et al.: Circulation of CD34+ hematopoietic stem cells in the peripheral blood of high-dose cyclophosphamide-treated patients: Enhancement by intravenous recombinant human granulocyte-macrophage colony stimulating factor, *Blood* 74:1905–1914, 1989.

Simonds RJ, Holmberg SD, Hurwitz RL, et al.: Transmission of human immunodeficiency virus type 1 from a seronegative organ and tissue donor, *N Engl J Med* 326:726–732, 1992.

Steptoe P, Edwards R: Pregnancy in an infertile patient after transfer of an embryo fertilized in vitro, *Brit Med J* 286:1351–1352, 1983.

Stroncek DF, Fautsch SK, Lasky LC, et al.: Adverse reactions in patients transfused with cryopreserved marrow, *Transfusion* 31:521–526, 1991.

Stylianou J, Vowels M, Hadfield K: Novel cryoprotectant significantly improves the post-thaw recovery and quality of HSC from CB, *Cytotherapy* 8(1):57–61, 2006.

Tel J, Anguille S, Waterborg CE, et al.: Tumoricidal activity of human dendritic cells, *Trends Immunol* 35(1):39–46, 2014.

Thomas ED, Lochte HL, Cannon JH, et al.: Supralethal whole body irradiation and isologous marrow transplantation in man, *J Clin Invest* 38:1709–1716, 1959.

Tomford WW: *Musculoskeletal tissue banking*, New York, 1993, Raven Press.

Torroni A: Engineered bone grafts and bone flaps for maxillofacial defects: state of the art, *J Oral Maxillofac Surg* 67:1121–1127, 2009.

U.S. Department of Health and Human Services, Food and Drug Administration, Center for Biologics Evaluation and Research: Guidance for industry-current good tissue practice (CGTP) and additional requirements for manufacturers of human cells, tissues, and cellular and tissue-based products (HCT/Ps), http://www.fda.gov/BiologicsBloodVaccines/GuidanceComplianceRegulatoryInformation/Guidances/default.htm, 2011.

U.S. Food and Drug Administration. Current good tissue practice for human cell, tissue and cellular and tissue-based product establishments, inspection and enforcement, final rule. 21 Code of Federal Regulations, part 1271, last updated February 21, 2014.

Wagner Jr JE, Brunstein CG, Boitano AE, et al.: Phase I/II trial of StemRegenin-1 expanded umbilical cord blood hematopoietic stem cells supports testing as a standalone graft, *Cell Stem Cell* 18(1):144–155, 2016.

van Besien K, Artz A, Champlin RE, et al.: Haploidentical vs haplo-cord transplant in adults under 60 years receiving fludarabine and melphalan conditioning, *Blood Adv* 3(12):1858–1867, 2019.

Wang X, Tse-Chao H, Da-Wen S, et al.: Cryopreservation of tissue-engineered dermal replacement in ME_2SO: toxicity study and effects of concentration and cooling rates on cell viability, *Cryobiology* 55:60–65, 2007.

Weipert J, Meisner H, Mendler N: Allograft implantation in pediatric cardiac surgery: surgical experience from 1982–1994, *Ann Thorac Surg* 60(Suppl):S101–S104, 1995.

Wen SH, Zhao WL, Lin PY, et al.: Associations among birth weight, placental weight, gestational period and product quality indicators of umbilical cord blood units, *Transfus Apher Sci* 46(1):39–45, 2012.

De Wolf C, Van De Bovenkamp M, Hoefnagel M: *Regulatory perspective on in vitro potency assays for human dendritic cells used in anti-tumor immunotherapy* 20:1289–1308, 2018.

Yap CH, Skillington PD, Matalanis G, et al.: Anti-HLA antibodies after cryopreserved allograft valve implantation does not predict valve dysfunction at three-year follow-up, *J Heart Valve Dis* 15:540–544, 2006.

Zhang N, Zhi H, Curtis BR, et al.: CRISPR/Cas9-mediated conversion of human platelet alloantigen allotypes, *Blood* 127(6):675–680, 2016.

Zhou J, He W, Luo G, et al.: Fundamental immunology of skin transplantation and key strategies for tolerance induction, *Arch Immunol Ther Exp* 61(5):397–405, 2013.

Zubizarreta I, Florez-Grau, Vila G, et al.: Immune tolerance in multiple sclerosis and neuromyelitis optica with peptide-loaded tolerogenic dendritic cells in a phase 1b trial, *Proc Natl Acad Sci USA* 116(17):8463–8470, 2019.

This page intentionally left blank

PART 5

Hemostasis and Thrombosis

EDITED BY | A. Koneti Rao, Matthew R. Pincus

CHAPTER 40

COAGULATION AND FIBRINOLYSIS

Ravi Sarode, Craig M. Kessler

OVERVIEW OF HEMOSTASIS, 828
PHYSIOLOGIC HEMOSTASIS, 828
Endothelium and Platelets, 828
Coagulation Protein System, 829
The Formation of Fibrin Clot and the Fibrinolytic System, 830
The Anticoagulation Protein Systems, 831
Current Hypothesis For Initiation of The Hemostatic System, 832
CLINICAL HEMOSTASIS, 833
Primary Hemostasis, 833
Secondary Hemostasis, 833
Laboratory Evaluation of Hemostasis, 833
Approach To Patients With Coagulation Disorders, 836
HEREDITARY COAGULATION PROTEIN DEFECTS, 836
Deficiency of Factor VIII (Hemophilia A) Or Factor IX (Hemophilia B), 837
Hereditary Deficiencies of Other Coagulation Factors, 840
ACQUIRED COAGULATION DISORDERS, 843
Disseminated Intravascular Coagulation (DIC), 843
Liver Disease, 844
Vitamin K Deficiency, 844
Massive Transfusion, 845
Acquired Coagulation Factor Deficiencies, 845
SELECTED REFERENCES, 846

KEY POINTS

- Physiologic hemostasis consists of endothelium, platelets, plasma coagulation proteins, natural anticoagulants, and the fibrinolytic system.
- Primary hemostasis involves platelets and von Willebrand factor. Secondary hemostasis is initiated by the tissue factor pathway and then amplified and propagated by the intrinsic pathway to generate thrombin that converts fibrinogen to fibrin.
- Routine coagulation tests (prothrombin time and activated partial thromboplastin time) may help identify a hemostatic defect in a bleeding patient, but mild to moderate abnormalities of these tests do not predict a bleeding tendency in a nonbleeding patient.
- Acquired coagulopathy often reflects multiple coagulation defects rather than specific protein defects.

OVERVIEW OF HEMOSTASIS

Hemostasis is a physiologic response to a vascular injury to limit blood loss. Therefore, it is initiated rapidly, is localized, and is well regulated. Recently, there has been an evolution in our understanding of the physiologic hemostatic system (Fig. 40.1). Initially, the hemostatic system was referred to as the *coagulation cascade* based on the waterfall model of Ratnoff and Davies; MacFarland published simultaneously a sequence of proteolytic reactions beginning with factor XII (FXII; Hageman factor) activation and leading to thrombin formation that proteolyzes fibrinogen to form a clot (MacFarland, 1964; Ratnoff & Davies, 1964). However, the physiologic basis of this pathway was questioned because patients with FXII deficiency did not bleed. Furthermore, in the mid-1970s, the cofactors for FXII activation—prekallikrein and high-molecular-weight kininogen—were identified and their deficiencies also did not cause bleeding (Weuppers & Cochrane, 1972; Colman et al., 1975; Saito et al., 1975). Later, the physiologic role of tissue factor (TF) and FVIIa was recognized along with its regulator tissue factor pathway inhibitor (TFPI) (Osterud & Rappaport, 1977). Thus, the physiologic hemostatic system is a cell-based model in which cellular elements such as endothelium, platelets, neutrophils, monocytes, and macrophages express TF and provide phospholipid (PL) surface for various coagulation proteins for attachment and sequential activation of coagulation factors to generate thrombin at the site of injury. Thrombin converts fibrinogen to a fibrin clot. Natural anticoagulants regulate thrombin generation, and the fibrinolytic system dissolves the clot once it has served its purpose.

PHYSIOLOGIC HEMOSTASIS

The physiologic hemostatic system, a tightly regulated balance between formation and dissolution of hemostatic plugs modulated by a series of enzymes and scaffolding proteins, has two major parts. The first part is its cellular component, which consists mostly of platelets and endothelial cells but also includes neutrophils and monocytes. The second part is a large group of plasma proteins, which participate in clot formation (coagulation), dissolution of clots (fibrinolysis), and the action of naturally occurring serine protease inhibitors (anticoagulation) that terminate the activity of several enzymes of the coagulation and fibrinolytic systems.

ENDOTHELIUM AND PLATELETS

Normal hemostasis involves interplay between the cellular components and proteins involved in clot formation and lysis. Intact endothelium that lines the vascular wall in a physiologic state exerts a hemostatic balance. When vascular integrity is breached, blood coagulation is initiated. Intact endothelial cells secrete an ectonucleotidase, CD39, that degrades adenosine diphosphate (ADP) (Pinsky et al., 2002). Endothelial cells also secrete prostacyclin and nitric oxide (NO), which prevent platelet activation and aggregation, thereby reducing the risk of arterial thrombosis (Hong, 1980; Palmer et al., 1987; Shariat-Madar et al., 2006). Endothelial cells additionally bind plasminogen, tissue plasminogen activator, and single-chain urokinase, all of which contribute to fibrinolysis and maintenance of hemostatic balance (Barnathan et al., 1988; Cesarman et al., 1994). The glycosaminoglycans present on endothelium bind antithrombin (AT), which then neutralizes thrombin and FXa (Marcum et al., 1984). Thrombomodulin on endothelium binds to thrombin; that complex then converts protein C to activated protein C (APC) (Esmon & Owen, 1981).

When a vessel wall is injured, subendothelial collagen is exposed and platelets adhere to the site of injury (Van der Meijden et al., 2009). Von Willebrand factor helps platelets adhere to the injured vessel wall by binding to exposed collagen at the A3 domain and to the platelet receptor GP Ib/IX/V complex (He et al., 2003). This adhesion event activates platelets, initiating a signaling cascade within them (Zaffran et al., 2000). The stimulated platelets release the contents of their granules, recruit additional platelets to aggregate to those already adherent and provide a phospholipid surface for the activation of multiple coagulation factors. Furthermore, in flowing blood, FXII autoactivates if exposed to collagen or in the milieu of activated platelets, leading to the cascade of proteolytic events producing thrombin (Van der Meijden et al., 2009).

Once prothrombin has been activated to thrombin in the intravascular compartment, the resulting thrombin stimulates endothelium to

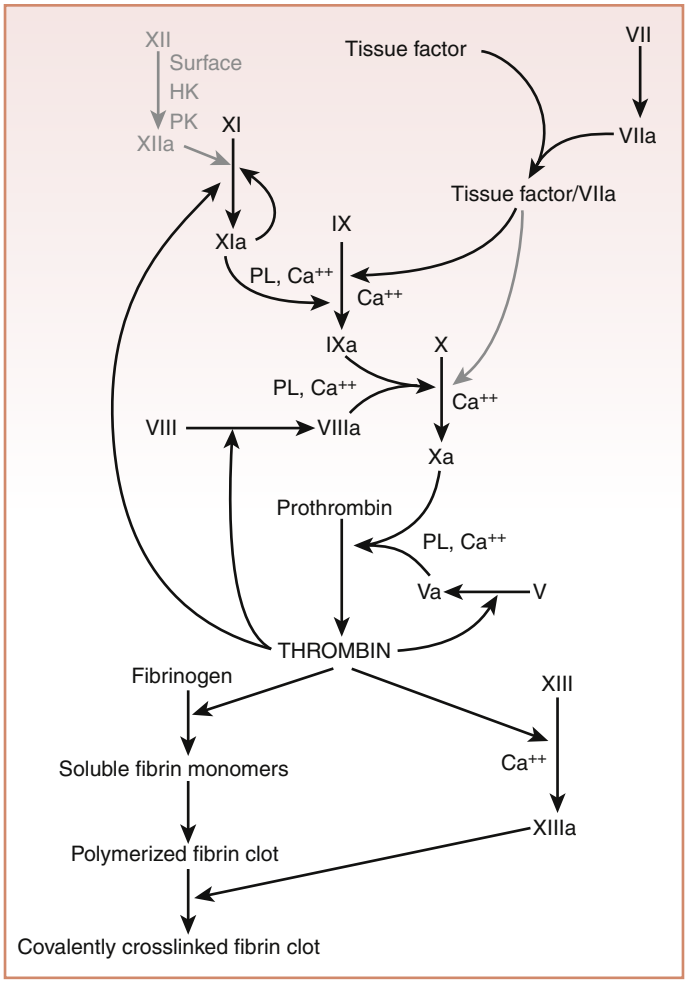

Figure 40.1 Schematic diagram of physiologic blood coagulation. Note that labels for the "contact phase" factors constituting factor XII (FXII), high-molecular-weight kininogen (HK), and prekallikrein (PK) are in *gray*. Although FXI is activated by FXIIa on a surface under artificial in vitro conditions, such as in activated partial thromboplastin time (APTT), this pathway is not believed to contribute to normal physiologic hemostasis. Similarly, whereas tissue factor (TF)/FVIIa can directly activate X to Xa in the in vitro prothrombin time (PT) test under conditions in which supraphysiologic concentrations of TF are employed, this reaction is shown as grayed because it does not contribute significantly to clot formation under normal in vivo physiologic conditions. Normal clotting in vivo is initiated when sufficient TF/FVIIa becomes available to activate FIX to FIXa. Subsequently, FIXa in the presence of FVIIIa activates FX to FXa, which, in turn, activates prothrombin to thrombin in the presence of FVa. Thrombin not only then proceeds to clot fibrinogen and to activate platelets but additionally exerts critically important positive feedback by activating both factor VIII and factor V. Physiologic amplification of thrombin formation is believed to result from thrombin activating FXI to FXIa, thereby providing an additional pathway for the activation of FIX. Phospholipid (PL) protein complexes present on the surface membranes of platelets in vivo. *Ca*++, Calcium ions.

upregulate TF, and TF forms a complex with FVIIa. The complex of FVIIa–TF activates FIX to FIXa, which converts zymogen FX to enzymatically active FXa (see Fig. 40.1). In the presence of FVa from liver or injured endothelium, FXa activates prothrombin (FII) to thrombin (FIIa). Under normal circumstances, the rate-limiting component of prothrombinase complex formation and the ultimate generation of thrombin activity is the concentration of FXa (Rand et al., 1996). Thrombin then proteolyzes fibrinogen to form fibrin. In static in vitro systems, as little as 5 to 10 pM TF is sufficient to induce clot formation, leading to a 1000- to 2000-fold amplification of the process, which increases the concentration of thrombin to 10 to 20 nM, which is sufficient to initiate clot formation (Mann, 2003). In a static model of blood coagulation, the addition of 5 pM TF results in an average clot time of approximately 5 minutes—sufficiently fast for physiologic hemostasis. Thrombin also is a major physiologic activator of platelets together with other agonists, such as collagen, ADP, platelet-activating factor, and epinephrine. Inactivated platelets probably circulate without promoting coagulation. When platelets are activated (see Chapter 41), their membranes become a site for additional thrombin formation. According to a cell-based model of coagulation (Hoffman & Monroe, 2001), activated platelets offer the most important source of negatively charged phospholipids (mainly, phosphatidylserine) and procoagulant membranes (Furie & Furie, 2005) needed for coagulation factor action in the propagation phase. This pathway for thrombin formation conjoins with FXII autoactivation on exposed vessel collagen and downstream elaboration of thrombin as well (Van der Meijden et al., 2009). Critical reactions to form FXa and thrombin are accelerated 300,000-fold on the platelet surface. Platelets control three important phases of coagulation: thrombin generation, fibrin formation, and clot retraction (Heemskerk et al., 2013).

TABLE 40.1
Proteins of the Plasma Coagulation System

Surface-Bound Zymogens	Vitamin K–Dependent Zymogens	Cofactors/Substrates
Factor XII	Factor VII	High-molecular-weight kininogen
Prekallikrein	Factor IX	Factor VIII
Factor XI	Factor X	Factor V
	Factor II	Fibrinogen
	Protein C	Protein S

COAGULATION PROTEIN SYSTEM

Characterization of Coagulation Proteins

The proteins that constitute the coagulation system consist of zymogens and cofactors (Table 40.1). The zymogens (proenzymes) of the coagulation system can be grouped into the phospholipid-bound and the surface-bound categories. Phospholipid-bound zymogens make up the physiologically important hemostatic system. These proteins are vitamin K dependent. Vitamin K is required for an essential γ-carboxylation reaction that takes place on the glutamic acid residue of each of these proteins located in their amino-terminal regions (see Chapter 43, Fig. 43.1). This carboxylation reaction allows these proteins to bind to phospholipid and cell membranes, where they are activated. Without this carboxylation reaction, these proteins do not function normally in the hemostatic system. Proenzymes include FX, FIX (Christmas factor), FVII, and FII (prothrombin). Protein C is a vitamin K–dependent phospholipid-bound zymogen; however, when activated (APC), it functions as an anticoagulant by inactivating FVa and FVIIIa (see Chapter 42). Protein S is another natural anticoagulant that is also vitamin K dependent and acts as a cofactor for APC.

The surface-bound proenzymes are proteins of the plasma kallikrein/kinin system (see Table 40.1). Surface-bound proenzymes include FXII (Hageman factor), prekallikrein (Fletcher factor), and FXI. These protein zymogens are also known as the *contact system* because FXII autoactivates when associated with a negatively charged surface, such as a glass tube and several physiologic substances (Wiggins & Cochrane, 1979; Miller et al., 1980). The autoactivation phenomenon of FXII allows for a common laboratory test, activated partial thromboplastin time (APTT), which is used to assess the integrity of the coagulation system. Although absolutely essential for a normal APTT, the proteins of the plasma kallikrein/kinin system do not have a role in hemostasis. These proteins (FXII, prekallikrein, and high-molecular-weight kininogen) may participate in blood pressure regulation, fibrinolysis, inflammation, angiogenesis, and thrombosis (Schmaier, 2002, 2003, 2004; Shariat-Madar et al., 2006; Maas et al., 2008; LaRusch et al., 2010).

Although deficiencies of FXII, prekallikrein, and high-molecular-weight kininogen are not associated with bleeding, investigations indicate that they may have a role in arterial and venous thrombosis. Recently, activation of the contact factor coagulation pathway has been shown to occur in vivo from negatively charged surfaces such as polyphosphate, extracellular RNA, and collagen. In detail, polyphosphate (PolyP) in humans consists of 60 to 100 phosphate units, and it is released from platelet dense granules upon platelet activation. PolyP has prohemostatic, prothrombotic, and proinflammatory properties. It has been identified as an activator of the contact phase (Wang et al., 2019). It is a potent activator of thrombin and coagulation FXI, and it accelerates FV activation and abolishes the inhibitory effect of TFPI.

TF (47-kDa protein) is an essential cofactor for activated FVIIa. It is found in most tissues and cells. Upregulation of TF results in the formation of complexes with FVII that produce the initiation of hemostatic reactions. FVIII (antihemophilic factor) is a 330-kDa protein. When activated

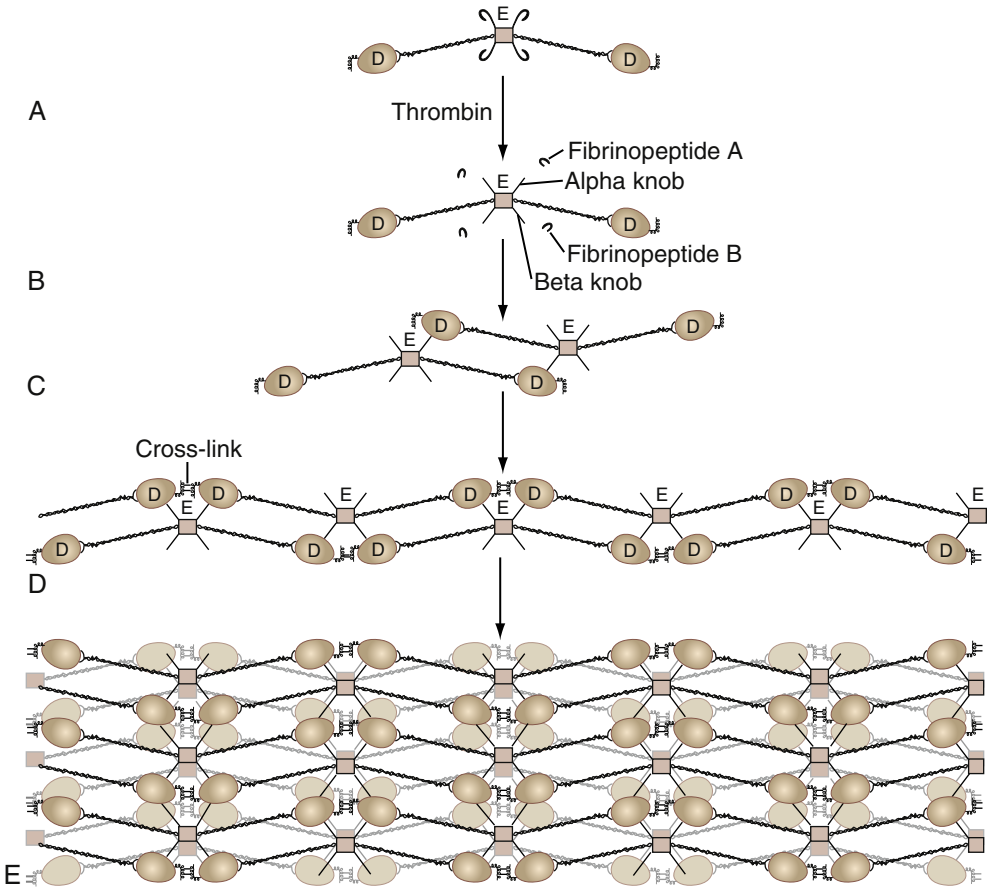

Figure 40.2 Formation of a fibrin clot. A, Schematic of fibrinogen. B, Thrombin proteolyzes fibrinopeptides A and B from fibrinogen to leave soluble fibrin monomer. Soluble fibrin monomer then associates side to side (C) and end to end (not shown, for clarity) to form fibrin polymers. D, Thrombin-activated factor XIII (factor XIIIa) covalently cross-links the fibrin polymers into an increasingly complex structure and an ultimately insoluble clot (E). Note that "E" corresponds to the central domain of the original fibrinogen molecule and "D" to the peripheral domains. (Modified with permission from Doolittle RF: Fibrinogen and fibrin, Sci Am 245:126–135, 1981.)

to FVIIIa, it is a cofactor for FIXa in the activation of FX. Its absence is associated with the most severe clinically recognized bleeding disorder, hemophilia A. FV is also a 330-kDa protein with homology to FVIII. When activated to FVa, it serves as a cofactor for FXa in the activation of FII (prothrombin) to thrombin. Fibrinogen is a 330-kDa protein that not only is the main substrate of thrombin (FIIa) but is also the principal adhesive molecule for platelet aggregation. When fibrinogen is proteolyzed by thrombin, a fibrin monomer is formed. These monomers associate end to end and side to side to form a polymerized fibrin clot. The clot is stabilized by activated FXIII, a tissue transglutaminase that cross-links the strands of associating fibrin (Fig. 40.2).

Physiologic Protein Assemblies

Certain critical protein assemblies in hemostatic reactions accelerate these proteolytic events. The proteins of the coagulation system that are essential for hemostasis or control of bleeding were originally identified by observation of affected patients and, more recently, through mouse knockout studies. Deficiencies in coagulation factors VIII and IX are the most prominent bleeding disorders that occur in patients who survive gestation and birth. Rare patients who have congenital deficiencies of coagulation factors VII, X, V, and II usually do not have severe bleeding states. In contrast, murine models have demonstrated that mouse embryos containing complete genetic knockouts of factor VII, X, V, or II die of massive hemorrhage during gestation or at birth (Cui et al., 1996; Rosen et al., 1997; Sun et al., 1998; Dewerchin et al., 2000). This information suggests that the human patient who has a deficiency of factor VII, X, V, or II may have some factor, albeit less than 1%, to allow for a milder clinical phenotype than that seen in mouse models. Alternatively, other compensatory mechanisms may be operative in the human patient. All of these proteins participate in two critically important assemblies that are essential for normal hemostasis: tenase and prothrombinase complexes.

Extrinsic tenase involves TF and FVIIa complex on the PL surface, converting FX to FXa. The intrinsic tenase complex comprises the assembly of FIXa and FVIIIa on phospholipid surfaces to convert FX to FXa. When all of these components are present, the rate of FX activation by FIXa is increased 1.4×10^8-fold over the rate of FX activation by FIXa alone. The prothrombinase complex comprises the assembly of FXa and FVa on phospholipid membranes or cell membranes in an ordered structure with FII (prothrombin) to accelerate its activation to FIIa (thrombin). When all of these components are present, the rate of FII activation by FXa is increased 1.7×10^8-fold over the rate of FII activation by FXa alone. Because these coagulation reactions occupy critical regulatory points within the physiologic hemostatic system, they are also the target of a number of anticoagulant agents for venous thrombosis that are currently in use, that is, direct FXa and thrombin inhibitors.

THE FORMATION OF FIBRIN CLOT AND THE FIBRINOLYTIC SYSTEM

The six peptide chains of the fibrinogen molecule are organized into a structure described as having a central E domain and two terminal D domains. When thrombin is formed, it cleaves fibrinopeptide A from the Aα chain and fibrinopeptide B from the Bβ chain of fibrinogen in the E domain region (Doolittle, 1981). The remainder of this thrombin-proteolyzed fibrinogen is called a *soluble fibrin monomer*. Soluble fibrin monomers then assemble with an end-to-end and side-to-side association to form a noncovalent fibrin polymer (see Fig. 40.2). Activated FXIII, a transglutaminase, cross-links fibrin monomeric subunits into an insoluble, cross-linked fibrin clot. When insoluble, cross-linked fibrin is made, a new linkage between the D domains of two adjacent fibrin monomers occurs. In the process, a neo-epitope of interaction is formed (see Fig. 40.2).

The fibrinolytic system regulates fibrin clot degradation and clot dissolution. In fibrinolysis, the circulating zymogen plasminogen is converted to its active form plasmin mainly by endogenous tissue plasminogen activator (tPA) (Draxler & Medcalf, 2015). Two other plasminogen activators are single-chain urokinase plasminogen activator (ScuPA) and two-chain urokinase plasminogen activator (TcuPA). These activators are found in the endothelium as well as in neutrophils and monocytes. The natural plasminogen activators tPA, ScuPA, and TcuPA convert zymogen plasminogen to the active enzyme plasmin (Fig. 40.3). tPA is produced constitutively, and ScuPA is increased in inflammatory states. Plasminogen activator inhibitor-1 (PAI-1) is the major inhibitor of tPA and TcuPA. α_2-Antiplasmin, a serine protease inhibitor (serpin), is the most potent and

highly selective inhibitor of plasmin. However, the plasma concentration of α_2-antiplasmin, even if high (approximately 1 mM), is only about half the plasma concentration of plasminogen. The fibrinolytic system is also regulated by thrombin-activatable fibrinolysis inhibitor (TAFI) (Vercauteren et al., 2013). TAFI is a carboxypeptidase able to remove lysine residues from fibrin, such that it indirectly controls plasmin by interfering with the binding of plasminogen and tPA to fibrin.

The binding of both plasminogen and tPA to fibrin can increase plasmin generation by two orders of magnitude. The active plasmin molecule is a potent protease, and it recognizes multiple substrates. Plasmin will degrade soluble fibrinogen to produce fibrinogen degradation products (Fig. 40.4A). Plasmin cleaves fibrinogen into an X fragment of similar molecular mass by eliminating portions of the α-chain (Marder & Budzynski, 1974). Plasmin then cleaves the X fragment asymmetrically between the D and E domains to produce fragment Y. Plasmin further degrades the Y fragment to produce soluble D and E domains that are called *soluble fibrinogen degradation products* or, in the case of fibrin digestion by plasmin, *fibrin degradation products*. Their presence indicates that plasmin has been formed. Plasmin will also degrade insoluble, crossed-linked fibrin (Fig. 40.4B). When it does, it liberates a D-D-dimer domain formed as a result of the neo-epitope between these two domains (see Fig. 40.4B) (Marder et al., 1976). The presence of soluble D-dimer indicates that, first, thrombin has been formed, followed by clotting, then the clot has been cross-linked by FXIIIa, and, finally, plasmin has been formed and has cleaved the insoluble, cross-linked fibrin clot.

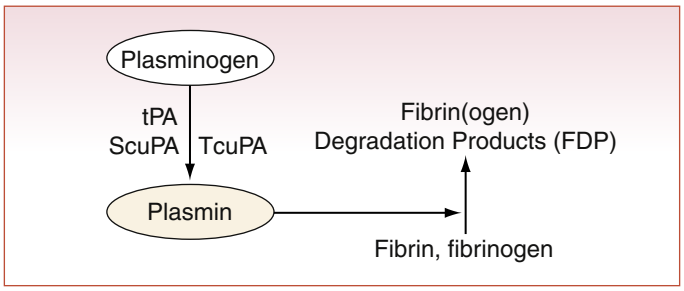

Figure 40.3 Fibrinolysis. Zymogen plasminogen is converted to plasmin by tissue plasminogen activator (tPA), single-chain urokinase plasminogen activator (ScuPA), and two-chain urokinase plasminogen activator (TcuPA). Formed plasmin degrades fibrinogen or fibrin to form fibrinogen or fibrin degradation products, respectively.

THE ANTICOAGULATION PROTEIN SYSTEMS

Coagulation is tightly regulated by natural anticoagulants and the fibrinolytic system to avoid thrombus formation and extension. Three major anticoagulant systems regulate the enzymes of the coagulation protein system to help to inhibit clot formation. These systems are the protein C/protein S system, the plasma serine protease inhibitor system, and TFPI, a Kunitz-type serine protease inhibitor. AT is the main serine protease inhibitor of coagulation enzymes of the plasma serine protease inhibitor system. Each of these systems plays a critical role in the proper regulation of the coagulation system. Moreover, in murine deletion models, complete deficiencies of protein C, protein S, AT, and TFPI are incompatible with the survival of mammalian gestation, delivery, or life ex utero (Huang et al., 1997; Jalbert et al., 1998; Hayashi et al., 2006; Burstyn-Cohen et al., 2009).

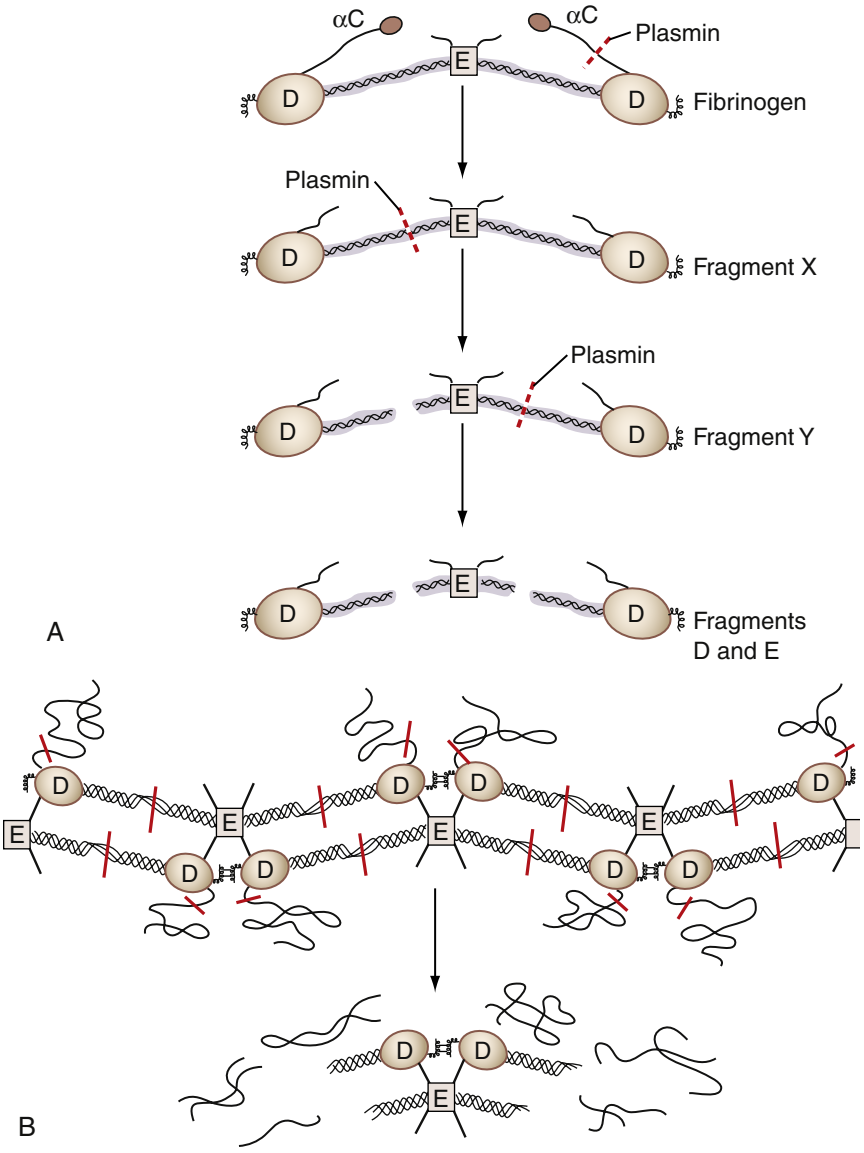

Figure 40.4 A, Plasmin-cleaved soluble fibrinogen or fibrin. When plasmin cleaves fibrinogen, initially small portions from the α-chain (αC) are removed to make Fragment X. Fragment X is then asymmetrically cleaved into Fragment D and Fragment Y. Fragment Y is further cleaved by plasmin into Fragments D and E. (Modified with permission from Greenberg CS, Lai T-S: Fibrin formation and stabilization. In Loscalzo J, Schafer AI, editors: Thrombosis and hemorrhage, ed 3, Philadelphia, 2003, Lippincott Williams & Wilkins, p 83, Fig. 5.3B.) B, Plasmin-cleaved insoluble, cross-linked fibrin. When insoluble, cross-linked fibrin is proteolyzed by plasmin, the neo-epitope between the D-domains is preserved, and the liberated fragment consists of the D-dimer together with an E domain. (Modified with permission from Doolittle RF: Fibrinogen and fibrin, Sci Am 245:126–135, 1981.)

Protein C/Protein S System

When activated, protein C, a 62-kDa vitamin K–dependent protein, is an enzyme that functions as an inhibitor. When free thrombin binds to thrombomodulin on endothelium, this complex then converts protein C to APC. Its activation is increased when protein C binds to the endothelial protein C receptor (EPCR). The complex formed by APC+EPCR needs to dissociate in order to allow binding of APC with protein S to inactivate FVa and FVIIIa (Esmon, 2006). Protein S, a 69-kDa vitamin K–dependent protein, is a cofactor, or receptor, for APC on cell membranes. It allows APC to bind to cell surfaces in such a manner as to orient itself to inactivate FVa and FVIIIa. The enzyme uses this cofactor as a receptor to localize its activity to perform its inhibitory function. Plasma protein S is in equilibrium between the free form (40%) and a bound form (60%) that is complexed to C4b-binding protein; only the free form functions as a cofactor for APC. APC also binds to three receptors on endothelial cells: (1) endothelial cell protein C receptor to activate (2) protease-activated receptor (PAR) 1 and (3) apolipoprotein E receptor 2 (ApoER2) (Esmon, 1999; Coughlin, 2000; Yang et al., 2009). Activation of PAR1 on endothelial cells may contribute to the anticoagulant function of activated protein C by liberating tPA. APC on endothelial cells also has an inflammatory effect via activation of sphingosine-1-phosphate receptor transactivation and activation of ApoER2 (Finigan et al., 2005; Yang et al., 2009). Thus, APC reduces thrombin formation, stimulates fibrinolysis, and initiates inflammation to reduce thrombosis risk.

Antithrombin

This serpin is a 58-kDa protein that inhibits each of the following hemostatic enzymes: IIa, Xa, VIIa, IXa, XIa, kallikrein, and XIIa. It exerts its anticoagulant effect primarily by inhibiting FIIa and FXa (Fig. 40.5). Antithrombin has two functional sites: the heparin-binding site (at the amino terminus of the protein) and the reactive site (Arg329-Ser394). The ability of antithrombin to function as an inhibitor of coagulation protein enzymes is potentiated by endogenous and exogenous heparins. In fact, it is the presence of antithrombin that gives heparin its anticoagulant properties. In the presence of heparins, antithrombin undergoes a conformational change that increases from 1000-fold to 4000-fold its inhibitor effect on FIIa (Perry, 1994). Trace amounts of circulating TF or TF transiently exposed by damaged vessels contribute to FVIIa inactivation by antithrombin (Vatsyayan et al., 2014).

In addition to antithrombin, other serpins regulate the enzymes of the hemostatic and inflammatory systems. Heparin cofactor II is a serpin that specifically inhibits thrombin in the presence of dermatan sulfate. Protein Z inhibitor is a serpin that specifically inhibits factor Xa in the presence of its cofactor protein Z—a vitamin K–dependent protein. C1 inhibitor (C1 esterase inhibitor) is the most potent inhibitor of FXIIa, kallikrein, and FXIa in plasma. Its main function is to regulate the amount of free bradykinin in the intravascular compartment and reduce inflammatory events (Han et al., 2002; Schmaier, 2002; Maas et al., 2008). The absence of C1 inhibitor is the causative factor for types I and II hereditary angioedema, a disorder associated with excessive bradykinin delivered to tissues.

Tissue Factor Pathway Inhibitor

In addition to the serpins, there is the Kunitz-type serine protease inhibitor, TFPI (Crawley & Lane, 2008). TFPI is the most potent inhibitor of the FVIIa–tissue factor complex. Under physiologic conditions, TFPI exerts its inhibitory effects by forming a quaternary complex with FVIIa, TF, and FXa (see Fig. 40.5). It is noteworthy that the murine TFPI knockout is embryonically lethal (Jalbert et al., 1998). TFPI is produced by microvascular endothelium, and it seems mainly associated with glycosaminoglycans on the endothelial wall. Only approximately 20% of TFPI circulates in plasma associated with lipoproteins (Caplice et al., 2001). Another family of Kunitz-type serine protease inhibitors, the amyloid β-protein precursor (AβPP) and related members, is present in platelets and brain and regulates factors XIa, IXa, Xa, VIIa/TF, and plasmin (Van Nostrand et al., 1990; Schmaier et al., 1993, 1995; Mahdi et al., 1995, 2000). This inhibitor does not inhibit thrombin. The exact function of this inhibitor is not completely known, but it is believed to be a cerebral anticoagulant (Del Zoppo, 2009). AβPP and amyloid precursor-like/protein 2 gene–deleted mice survive gestation but have an accelerated rate of thrombosis in a carotid artery thrombosis model (Xu et al., 2009).

Prostacyclins, Nitric Oxide, and Thrombospondin-5

In physiologic conditions, endothelial cells produce vasoactive hormones able to control the primary phase of hemostasis. Endothelial cells express the cyclooxygenase-2 enzyme that produces prostacyclins (PGI_2) from arachidonic acid (Mitchell et al., 2008). PGI_2 is a vasodilator and inhibits platelet aggregation. The actions of prostacyclins are mediated by cell membrane prostacyclin (IP) receptors and intracellular peroxisome proliferator-activated receptors (PPARβ and PPARγ). Endothelial cells also express the NO synthase enzyme (eNOS, NOS3), and they release NO derived from L-arginine. NO is a potent vasodilator that also inhibits platelet adhesion and aggregation. NO activates guanylate cyclase and cGMP. Activated platelets adhering to collagen seem also able to produce NO under shear flow (Cozzi et al., 2015), thus, controlling platelet adhesion and vasoconstriction directly at the sites of vessel damage.

Thrombospondin-5, also known as *cartilage oligomeric matrix protein* (*COMP*), is an extracellular protein able to control vascular tone. COMP is released by a variety of cartilage and muscle tissues and activated platelets. COMP inhibits thrombin and acts as a natural anticoagulant in mice (Liang et al., 2015). It determines a dose-dependent prolongation of thrombin time.

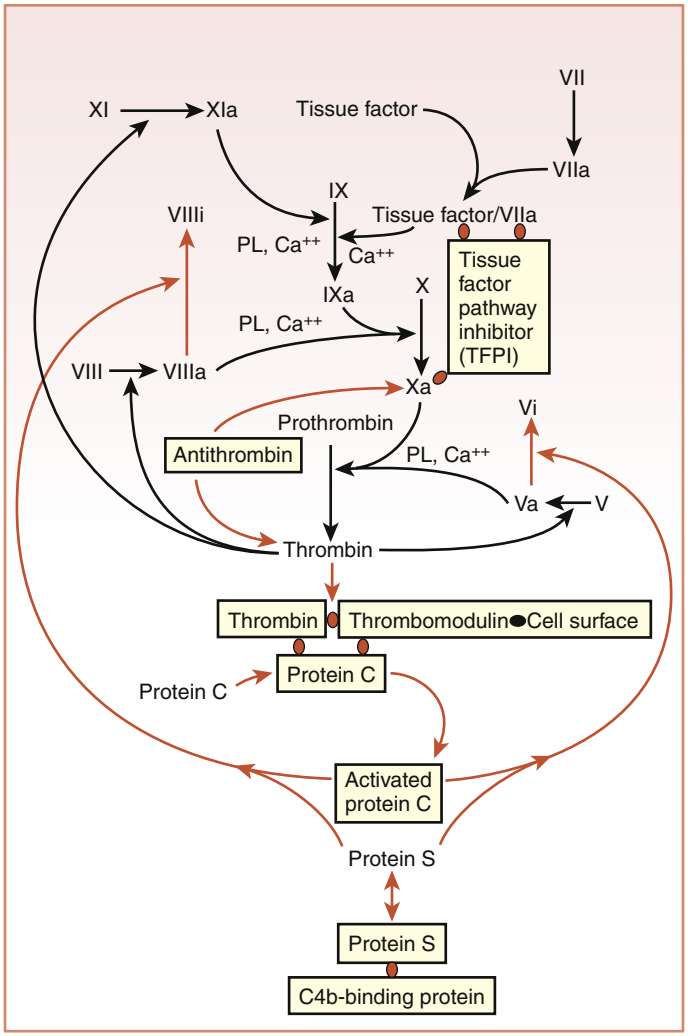

Figure 40.5 Natural inhibitors of coagulation: antithrombin (AT); components of the protein C pathway (thrombomodulin, protein C, protein S); and tissue factor pathway inhibitor (TFPI). Three major anticoagulant systems are recognized. Antithrombin inhibits factor Xa and thrombin to prevent thrombosis. It is important to note that antithrombin inhibits every enzymatic form of blood coagulation serine proteases (factor XIIa, plasma kallikrein, factor XIa, factor IXa, and factor VIIa), even though this is not indicated in the figure for readability purposes. The protein C system requires that this zymogen is activated to activated protein C by thrombin when bound to the endothelial cell membrane protein thrombomodulin. Protein S is a cofactor for activated protein C to inactivate factors Va and VIIIa. C4b-binding protein regulates protein S activity. TFPI makes a quaternary complex with tissue factor/factor VIIa and factor Xa to inhibit both enzymes.

CURRENT HYPOTHESIS FOR INITIATION OF THE HEMOSTATIC SYSTEM

More proteins participate in coagulation reactions in vitro than are critical for hemostatic reactions in vivo. The original coagulation cascade waterfall

hypothesis initiated by FXII has been replaced by one whereby TF and FVIIa are initiators (Gailani & Broze, 1993). TF is ubiquitous throughout the body, although it is rich in the brain, lung, and placenta. Its expression is upregulated after injury. Regulation of the expression of TF is a major control mechanism for the initiation of hemostasis. TF is not fully active on intact cells; it becomes able to activate coagulation when cell membrane properties are modified. This process is called *decryption* of *encrypted* TF and is still not completely understood. Different mechanisms of TF decryption have been proposed: an exposition of phosphatidylserine, dimerization of TF, and oxidation of a specific disulfide bond in TF (Smith et al., 2015). In conditions in which a vessel wall injury is limited to endothelial activation, blood-borne TF has been characterized on microparticles released by leukocytes and involved in the initiation of coagulation (Furie & Furie, 2005). Activated macrophages have been shown to express TF on their cell membrane and microparticles involved in physiologic hemostasis and thrombosis (Rak, 2014). There is a developing notion that endothelial cell TF is the initial nidus that leads to hemostasis and thrombosis (Furie, 2009; Ivanciu et al., 2014).

The FVIIa–TF complex activates FIX, leading, in turn, to FX activation. It must be noted that at the concentrations of factors ordinarily present in the body, FVIIa/TF does not directly activate appreciable amounts of FX because of the presence of TFPI—a point emphasized diagrammatically in Figure 40.1 by the graying of this reaction. Once FX has been activated to FXa, this FXa, in turn, contributes to the activation of thrombin from prothrombin. Thrombin then proteolyzes fibrinogen to form fibrin. Although TF-dependent coagulation reactions are rapidly inhibited by TFPI, if the stimulus for thrombin formation is sufficiently strong, coagulation is maintained through the activation of FXI by thrombin (Meijers et al., 2000). Activation of FXI to FXIa results in increased activation of FIX and eventually increases the formation of thrombin. Further modulation of hemostatic balance in the direction of clot formation is exerted by TAFI (also known as *carboxypeptidase U*). Among its actions, TAFI cleaves C-terminal lysine residues from fibrin, thereby decreasing the binding of plasminogen to the clot and diminishing clot lysis (Leurs et al., 2005).

CLINICAL HEMOSTASIS

PRIMARY HEMOSTASIS

At the site of endothelial cell injury, subendothelial collagen and von Willebrand factor (vWF) are exposed. The disrupted endothelium alters laminar blood flow at the site of injury; thereby, platelets undergo shape change from discoid to spherical and produce pseudopodia that will breach the site of endothelial damage by binding to vWF via GPIb/IX/V receptors. This step is called *platelet adhesion* (attachment of platelets to a nonplatelet surface), which is followed by *secretion*. During secretion, contents of alpha and dense granules from platelets are released along with the generation of thromboxane A2 (TXA2) via the cyclooxygenase-1 (COX-1) pathway. TXA2 causes vasoconstriction and activates platelets via the TXA receptor. During the next step of platelet activation, the signal transduction within platelets leads to a conformational change in GPIIb/IIIa, allowing fibrinogen (acts as a ligand) to bring adjacent platelets together, causing aggregation (attachment of one platelet to another). Activation of platelets leads to exposure of phosphatidylserine (PS) similar to altered endothelium that also exposes PS for secondary hemostasis that begins simultaneously to generate thrombin.

SECONDARY HEMOSTASIS

Secondary hemostasis can be divided into two different phases: (1) the TF pathway (previously called the *extrinsic pathway*), which is the initiator of coagulation; and (2) the intrinsic pathway, which amplifies and propagates thrombin generation. The TF pathway begins with endothelial injury and expression of TF on the cell surface, which binds the small amount of FVIIa present in circulation to form a TF+FVIIa complex. This complex is known as *extrinsic tenase* because this will activate FX to FXa on the cell surface in the presence of Ca^{++}. This FXa along with FVa on the cell surface (PL) and Ca^{++} forms a *prothrombinase complex*, converting prothrombin to thrombin. As soon as a small amount of thrombin is generated by the TF pathway, this thrombin activates the TFPI, which shuts down the TF pathway by inhibiting the TF+FVIIa and FXa complex. The same thrombin also initiates the intrinsic pathway by activating FXI to FXIa and FIX to FIXa on the cell surface (PL) with Ca^{++}. FIXa along with FVIIIa on the cell surface (PL) and Ca^{++} forms the *intrinsic tenase* and converts FX to FXa, which, along with FVa, forms the prothrombinase complex converting prothrombin to thrombin. This intrinsic pathway is the primary pathway of thrombin formation. Thus, the TF pathway is the initiator and the intrinsic pathway is the amplifier and propagator of thrombin, and these two pathways are interrelated. The previous concept of independent extrinsic and intrinsic pathways is not physiologic because if these two were independent pathways producing thrombin, then patients with hemophilia A and B would not have bleeding tendencies. The independence of extrinsic and intrinsic pathways to produce thrombin is "true only in the test tubes" where prothrombin time (PT) and activated partial thromboplastin time (APTT), respectively, assess them. Thrombin is the main enzyme in the coagulation system because it activates FV and FVIII to their activated forms to amplify further thrombin generation and converts fibrinogen to fibrin monomers. It also activates FXIII to FXIIIa to cross-link these fibrin monomers to stabilize the clot.

LABORATORY EVALUATION OF HEMOSTASIS

Laboratory evaluation of primary hemostatic defects presenting as mucocutaneous type bleeding due to platelets and vWF is described in Chapter 41. Patients with bleeding tendency due to secondary hemostasis defects often present with ecchymoses, soft tissue, and joint bleeds. Bleeding tendencies could be congenital or acquired. Therefore, an elaborate personal and family history of bleeding is the prerequisite for appropriate laboratory testing. Most congenital bleeding disorders often are diagnosed early in childhood; however, mild bleeding disorders may not be revealed until later in life when there is a robust hemostatic challenge.

Routine coagulation screening tests are useful to identify a hemostatic defect in a bleeding phenotype. However, performing these tests to assess hemostasis in a nonbleeding patient is not clinically useful—it often may lead to unnecessary expensive further testing and could delay surgeries.

Prothrombin time (PT), APTT, fibrinogen, thrombin time and D-dimers are considered screening coagulation tests along with platelet count for initial evaluation of a bleeding patient. Whole blood is collected in 3.2% sodium citrate (blue top) in a 9:1 ratio (blood:citrate) by a single needlestick without trauma or prolonged stasis and mixed well by gently inverting 3 to 5 times (avoid vigorous mixing that may activate platelets) (Adcock, 1998). The specimen should be transported to the laboratory at room temperature, and the testing should be completed within 4 hours of collection. However, if the testing cannot be performed within 4 hours of collection, then ideally the specimen should be centrifuged immediately to separate plasma from cellular component and frozen at −20°C and then transported on dry ice for testing to the laboratory. The separated plasma ideally should be platelet free (<10 K) before freezing because frozen plasma that is rich in platelets upon thawing will cause disruption of platelets releasing platelet factor 4, which binds to heparin and may give false low anti-FXa activity, or phospholipids released from platelet membranes bind to lupus anticoagulant and may give false-negative results. The specimen should not be held at room temperature for more than 4 hours to avoid loss of FVIII (and, to some extent FV, both being heat-labile factors) to avoid getting spuriously long APTT and low FVIII (and vWF) that might result in a further unnecessary investigation. Improper sample handling is often encountered in office clinics that send out their specimens to remote reference laboratories for coagulation testing. Thus, the preanalytic part of coagulation testing is crucial for accurate diagnosis and management.

Prothrombin Time

PT is a simple test in which the patient plasma is mixed with a PT reagent that contains tissue thromboplastin and CaCl2. Tissue thromboplastin consists of tissue factor and phospholipid. The source of tissue thromboplastin is important because nonhuman sources (e.g., rabbit brains) may have lower sensitivity to various vitamin K–dependent coagulation factors as compared with human sources (e.g., placenta) or recombinant tissue thromboplastin. The international normalized ratio (INR) was developed to harmonize PT results for monitoring vitamin K antagonist (VKA) therapy. The INR is a calculated value obtained by first calculating the prothrombin time ratio (PTR) by dividing the patient PT by the control PT, and then raising this PTR by an international sensitivity index (ISI) [INR = $(PTR)^{ISI}$]. Ideally, the INR should be used only for monitoring VKA therapy. However, due to the inclusion of the INR in the model of end-stage liver disease (MELD) score calculation, it is often also used to assess hemostasis in patients not on VKA for no good

reason other than the convenience. When the INR was used for MELD score calculation, the PT reagents most likely had a higher ISI with less sensitivity for vitamin K–dependent factor deficiencies than most current PT reagents, especially recombinant tissue thromboplastin. With different ISI, the INR can be different; hence, the MELD score can also be significantly different.

Isolated prolonged PT is usually due to an FVII deficiency and may also be prolonged due to mild deficiencies of common pathway FII, FV, and FX depending on the reagent's sensitivity. Recombinant tissue thromboplastin is very sensitive to even mild reduction of FVII (40%–45% activity), which is not clinically relevant since most patients with mild to moderate FVII deficiency are clinically asymptomatic and are often diagnosed when there is an incidental prolonged PT. Hemostatic levels of FVII for major surgery are 10% to 20%; however, even mild prolongation of PT/INR often results in unnecessary plasma transfusion to correct a laboratory value that is not clinically relevant. Because of rebalanced hemostasis in patients with cirrhosis (discussed later), several societies have recommended ignoring PT/INR values obtained preprocedurally in cirrhotics.

Activated Partial Thromboplastin Time

APTT is another routinely performed test to assess clinical hemostasis with poor sensitivity and specificity in a nonbleeding patient. APTT generally assesses coagulation factors in the intrinsic pathway as well as the common pathway. In APTT, a contact activator (e.g., ellagic acid, silica, kaolin) is added to the patient's plasma to initiate the activation of contact factors (prekallikrein, HMWK, and FXII) in the presence of PLs. After incubation for 3 to 5 minutes, the plasma is recalcified and the clotting time is recorded (usual range, 23–35 sec). Unfortunately, APTT reagents are not well standardized; hence, there is significant variation from one reagent to another and when we include coagulation instruments from different companies, the variability in APTT is even more significant. The APTT reagents come with three different quantities of PL with different sensitivities for various needs. APTT-factor sensitive (APTT-FS) has the highest amount of PL, making this reagent very sensitive to detect even slightly lower levels of coagulation factors in the intrinsic pathway. APTT-LA (lupus anticoagulant sensitive) reagent has the smallest amount of PL, making it very sensitive to detect even a weak LA. APTT-FSL (factor and lupus sensitive) has an intermediate amount of PL; hence, it should be used in daily practice because this will detect clinically relevant decreased amounts of coagulation factors and lupus anticoagulant.

Isolated prolonged APTT is a common clinical finding. Further investigation should be dictated by a personal and family history of bleeding if that is the presenting symptom, whereas in a nonbleeding patient it is essential to check previous APTTs. If the previous APTTs were normal, then the current prolongation is due to an acquired defect, most likely lupus anticoagulant. However, if the previous APTTs are also prolonged, then the contact factor deficiency should be considered and investigated because FXII-, HMWK-, and PK-deficient patients do not bleed.

In a bleeding patient, if APTT is prolonged, unfractionated heparin should be excluded. If the previous APTTs were also prolonged, then a congenital bleeding disorder of intrinsic pathway should be considered and investigated by measuring FVIII first (common thing first!) followed by FIX or, rarely, FXI. If the previous APTTs were normal and current presentation includes soft tissue hematomas, easy bruising, and other conditions, with a prolonged APTT, then acquired hemophilia should be considered due to autoantibody against FVIII.

Thrombin Time (TT)

Thrombin time (TT) is usually not a commonly ordered test because of its limited utility in laboratory assessment of most bleeding disorders. In the TT test, bovine thrombin (3–5 U/mL) is added to the patient's plasma and the clotting time recorded. The upper limit of the normal range should be adjusted close to 25 sec to make TT more sensitive to detect dysfibrinogenemia. The most frequent cause of prolonged TT is heparin followed by hypofibrinogenemia and then dysfibrinogenemia. Direct thrombin inhibitors (oral and parenteral) significantly prolong TT.

Fibrinogen Assay

Fibrinogen assay should be measured routinely in a bleeding patient and patients with cirrhosis. The fibrinogen assay is based on TT (Clauss method) in which a standard curve is generated by using known calibrators and bovine thrombin at a very high concentration of 50 U/mL (for TT 3–5 U/mL) so that the clotting time is independent of thrombin concentration. Bovine thrombin is added to the patient's plasma and the clotting time obtained is used to extrapolate fibrinogen value from the standard curve. A very high amount of the direct thrombin inhibitor will give false low fibrinogen levels.

If there is clinical suspicion for hypofibrinogenemia, the direct fibrinogen assay should be performed rather than relying on PT and APTT to be prolonged because, in the majority of patients with mild to moderate hypofibrinogenemia, PT and APTT are likely to be normal. When PT and APTT were performed manually in the past, the endpoint was a solid, firm clot formation on the side of the test tube. However, with automation, the endpoint of PT/APTT is the change in optical density or turbidity due to formation of fibrin strands. Therefore, the endpoint is often sooner than the manual method; hence, automated PT and APTT are usually normal, with mild to moderate hypofibrinogenemia.

D-Dimers

D-Dimers are generated by plasmin that cleaves the cross-linked fibrin clot. Increased D-dimers suggest that a clot is undergoing lysis in the circulation. In the D-dimer assay, a monoclonal antibody against the D-dimer molecule is attached to latex particles that agglutinate in the presence of D-dimers, causing a change in optical density. The optical density is then read off a standard curve to obtain a D-dimer value. In the appropriate clinical setting, it is useful for a diagnosis of disseminated intravascular coagulation (DIC), where it is elevated, and to rule out deep vein thrombosis (DVT) and pulmonary embolism (PE) in patients with low clinical probability, where the D-dimer is not elevated. A large hematoma will also increase D-dimers while undergoing resolution.

APTT Mixing Study

In the past, when there were no specific tests to detect lupus anticoagulant (such as dilute Russell viper venom time, PTT-LA with hexagonal PL neutralization, and silica clotting time), a mixing study involving equal parts of patient plasma and normal pooled plasma (NPP) has been often helpful. A circulating inhibitor was suspected when there was incomplete correction, and a factor deficiency was suspected when there was complete correction of the prolonged APTT. However, it must be emphasized that the routine use of such a mixing study for mildly prolonged APTT can lead to a missed or wrong diagnosis (Yates et al., 2019). This is due to several reasons, including poorly standardized mixing study protocols. Often, these studies are performed without proper controls and there is often a lack of understanding of how many normal plasmas should be used to prepare NPP. Also, performing a mixing study only on immediate mixing and without 2-hour incubation at 37°C leads to missing an autoantibody against FVIII, the cause of acquired hemophilia. Investigation of isolated prolonged APTT should be based on a thorough clinical history of bleeding or no bleeding/clotting. Mildly prolonged APTT due to lupus anticoagulant can be corrected with NPP, resulting in misinterpretation of a factor deficiency and, hence, unnecessary measuring intrinsic pathway factors. The presence of a lupus anticoagulant may influence clot-based assays for intrinsic pathway factor levels, especially FVIII. However, if one looks at factor assay curves, especially FVIII assay, there is an inhibitory pattern observed indicating that there is interference by the lupus anticoagulant. The lupus anticoagulant effect is revealed by the observation that with each subsequent dilution of the patient's plasma during FVIII assay, the FVIII activity increases by >20%. Such patients generally do not have a bleeding tendency and have had normal APTTs in the past.

Acquired hemophilia is not an uncommon clinical condition and generally presents with a prolonged APTT with significant clinical bleeding in the soft tissues. Such a patient with normal APTTs in the past and in the right clinical setting should be tested first for FVIII level, which is often diagnostic of acquired hemophilia. Later, a proper two-step mixing study can be done to identify a time and temperature-dependent inhibitor. In a two-step mixing study, the patient's plasma is first mixed with the NPP and immediately tested for APTT (which often corrects, unless the patient has concomitant LA). The second tube with the patient's plasma and NPP is incubated at 37°C for 2 hours and then tested for APTT, which shows further prolongation as compared with the immediate mix.

A routine mixing study for PT is not warranted because isolated prolonged PT due to autoantibody against FVII is extremely rare. Most of these patients with isolated prolonged PT/INR generally have vitamin K deficiency. Therefore, these patients should be given intravenous vitamin K (10 mg), which is both diagnostic and therapeutic, confirming vitamin K deficiency, especially in sick patients due to poor diet and antibiotic use.

Heparin Monitoring

Therapeutic heparin monitoring is required to avoid over- and under-anticoagulation because of unpredictable pharmacokinetics (PK) and

pharmacodynamics (PD) of unfractionated heparin (UFH). The unpredictable PK and PD are due to the presence of many larger polysaccharide molecules that get attached to the endothelium, platelets, and acute-phase reactant proteins, such as vWF and fibrinogen, causing reduced availability for their action on antithrombin to act as an anticoagulant in the first 24 to 72 hours of therapy in patients with DVT/PE. Therefore, UFH is given as a bolus to saturate these cells and proteins. The continuous intravenous infusion is then monitored every 6 hours until the APTT is within the therapeutic range. The APTT therapeutic range has to be established for each new lot number of APTT reagent in each laboratory, that is, every 6 to 12 months. This therapeutic range is established by measuring APTT and anti-Xa activity simultaneously on 50 patients on stable UFH (but not on VKA) and extrapolating corresponding APTT for anti-Xa activity of 0.3 to 0.7 U/mL from a linear regression curve. However, this therapeutic range is not adjusted for different lots of UFH obtained by the hospital pharmacy!

Heparin resistance is often encountered when APTT is used to monitor UFH therapy in patients with very high levels of FVIII due to an acute-phase effect or those with low AT levels (often acquired and rarely due to congenital deficiency). The very high levels of FVIII can be suspected when the baseline APTT is either at the lower end of the normal range or even shorter than the lower limit of normal. Most clinicians often do not pay attention to this phenomenon, which results in patients getting higher amounts of UFH. This increases anti-Xa activity, which may lead to severe bleeding despite APTT showing resistance. In the case of heparin resistance due to high FVIII, an anti-Xa assay should be used to monitor UFH. However, if anti-Xa activity is also low despite higher UFH, then AT deficiency should be suspected. If the AT activity is <50%, then AT concentrate may be given; that will prolong APTT appropriately as well as improve ant-Xa activity.

Anti-Xa Activity Assay for Heparin Monitoring

This assay provides an accurate measurement of both UFH and low-molecular-weight heparin (LMWH) levels for therapeutic monitoring. There are two types of anti-Xa assays, one with and the other without exogenously added AT to the reagent. The assay without added AT that relies on AT in the patient's plasma is a better assay because it will detect heparin resistance due to AT deficiency by showing lower anti-Xa activity despite adequate UFH dose. UFH/LMWH present in the patient's plasma binds to the patient's own AT and neutralizes the known amount of FXa present in the reagent. The remaining free FXa acts on a chromogenic substrate to generate a color. The higher the amount of heparin in plasma the lower the amount of free FXa and, hence, lighter the color. This intensity of the color is read as an optical density, and the amount of anti-Xa activity is read off of a standard curve generated with commercial calibrators. This assay is quite robust and, currently, liquid reagents with 7 days' stability on board the coagulation instrument have resulted in replacing APTT in monitoring UFH routinely. The heparin assay is known to reduce the number of times that heparin dose has to be adjusted as compared with APTT, thus saving both nursing and pharmacy time. Therefore, it is very cost-effective for the hospitals.

Coagulation Factor Assays

One-stage clot-based assays are the most commonly used methods for coagulation factors. The basic principle is similar for all coagulation factor assays. A standard curve is prepared by making serial dilutions of NPP with the factor-deficient plasma that is to be measured (e.g., FVIII-deficient plasma for FVIII assay) to obtain 100%, 50%, 25%, and 12.5% factor activity. Then, either PT (for FVII, II, V, and X assays) or APTT (for FXII, XI, IX, and VIII assays) are performed and plotted against appropriate dilutions (Figs. 40.6 and 40.7). The patient's plasma is then similarly diluted with that particular factor-deficient plasma, and corresponding PTs or APTTs are measured. The value of factor activity in the patient's plasma is then extrapolated from the standard curve using PT or APTT. The rationale for making serial dilution of patient plasma is mostly to dilute out the effect of lupus anticoagulant interference in the APTT-based assay; with each subsequent dilution of patient plasma, the effect of LA is diluted whereas the factor activity increases. This curve obtained in the presence of LA is known as a *nonparallel curve*. This pattern alerts the laboratory technician to make a further dilution of the patient plasma until the LA effect has disappeared and the correct factor level is obtained. If this step is not performed, then patients with isolated prolonged APTT may have spuriously low FVIII activity, which may lead to misdiagnosis and mismanagement of that patient.

Chromogenic FVIII Assay

There are caveats with the one-stage FVIII assay at present, with many extended half-life (EHL) FVIII concentrates on the market that often show lower than expected recovery in patient plasma. This lower recovery of EHL-FVIII is usually attributed to variable amounts of phospholipid present in various APTT reagents and variable sensitivity of modified FVIII to phospholipids in APTT reagents. Similarly, hemophilia A patients on emicizumab have normal APTT; hence, FVIII levels or FVIII inhibitor titer based on the one-stage APTT cannot be measured. Therefore, the chromogenic FVIII assay is used in such situations. In the chromogenic assay, activated FIX is added to the patient plasma, which then binds to FVIIIa in patient plasma (the bovine thrombin in the reagent converts FVIII to FVIIIa). The FVIIIa and FIXa complex then acts on FX to give FXa, which, in turn, cleaves a chromogenic substrate to generate a color. The amount of color is proportional to FVIII levels and reads off a standard curve. The other advantage of chromogenic FVIII assay is that it is unaffected by the presence of LA.

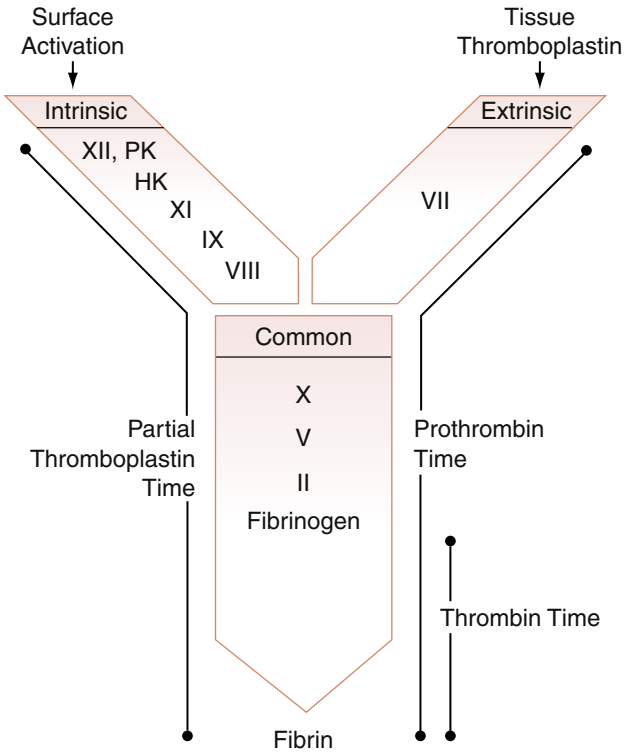

Figure 40.6 Organization of the coagulation system based on current assays. The intrinsic coagulation system consists of the protein factors XII, XI, IX, and VIII and prekallikrein (PK) and high-molecular-weight kininogen (HK). The extrinsic coagulation system consists of tissue factor (tissue thromboplastin) and factor VII. The common pathway of the coagulation system consists of factors X, V, and II, and fibrinogen (I).

Viscoelastic Measurement of Real-Time Clot

PT and APTT are often useful screening tests to assess hemostasis affecting coagulation factors in a bleeding patient. However, they have many limitations in assessing global hemostasis in real time in a bleeding patient who needs blood component therapy. Also, the turnaround time for PT and APTT is not fast enough for surgeons/anesthesiologists to make a timely decision in the operating room (OR).

Thromboelastography (TEG) and rotational thromboelastometry (ROTEM) are two global hemostasis assays with similar principles for viscoelastic measurement of a clot in real time (Agren, 2013). Both use whole blood and should be used to differentiate between coagulopathic and surgical bleeding. They cannot predict a bleeding tendency in a non-bleeding patient. There is a pin in the cup that records the torsion during the rotational movement while a clot is formed and various parameters are reflected on a tracing. In TEG, the pin is fixed and the cup rotates; in ROTEM, the cup is fixed and the pin rotates. The tracing is displayed on a monitor in the OR thus being a point-of-display rather than a point-of-care test because current machines are kept outside the ORs in the United States. The clotting time (CT) in ROTEM or reaction time (R) in TEG reflects the amount of thrombin generated. If CT or R is prolonged, this suggests clotting factor(s) deficiency and plasma transfusion is indicated in a bleeding patient. The maximum clot firmness (MCF) in ROTEM or maximum amplitude (MA) in TEG reflects the strength of the clot provided by both fibrinogen and platelets. The deficiency of either will reduce

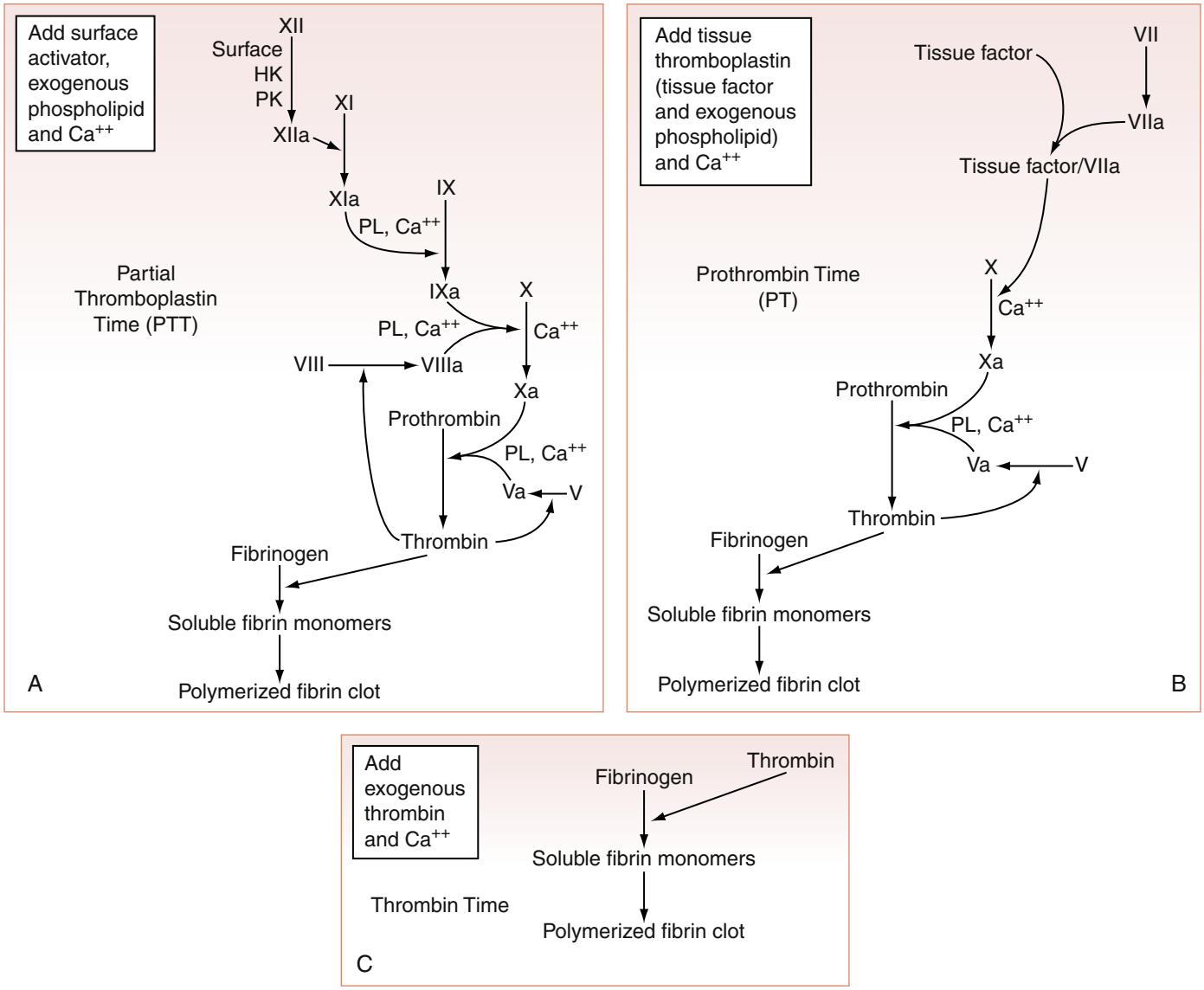

Figure 40.7 Coagulation screening tests. A, Activated partial thromboplastin time (APTT, "PTT" on the figure) requires the presence of every protein except tissue factor and factor VII. B, Prothrombin time (PT) requires tissue factor and factors VII, X, V, and II and fibrinogen. C, In thrombin time (or thrombin clotting time), exogenous thrombin is added to plasma to proteolyze (clot) fibrinogen. The endpoint in each of these tests is the number of seconds until detection of a clot, following addition of the indicated reagents to citrated platelet-free patient plasma. Because virtually all measuring systems employed detect the formation of a polymerized fibrin clot, whether or not any cross-linking of fibrin occurs, none of these tests will provide information with respect to factor XIIIa activity.

these values. In ROTEM, FIBTEM is another test run simultaneously that contains cytochalasin B to block platelet function. MCF in FIBTEM reflects the contribution of only fibrinogen to the clot firmness; if MCF is low, that indicates the need for cryoprecipitate transfusion.

On the other hand, if the MCF is normal in FIBTEM but low in EXTEM, it suggests a platelet defect (either number or function), which indicates the need for platelet transfusion in a bleeding patient. In TEG, if MA is low, then a platelet mapping test can be performed to differentiate between fibrinogen and platelet defect. In ROTEM, if INTEM CT is prolonged (EXTEM CT being normal), it suggests the presence of heparin, which is then confirmed by HEPTEM that contains hepzyme to neutralize heparin and correct prolonged INTEM CT. When EXTEM shows increased clot lysis (>15%), APTEM is performed. APTEM contains aprotinin, which inhibits plasmin and shows correction of lysis parameters. This finding indicates the use of a fibrinolytic agent such as tranexamic acid or Amicar. FXIII deficiency can also affect clot stability and show increased clot lysis.

APPROACH TO PATIENTS WITH COAGULATION DISORDERS

A thorough clinical personal and family history is absolutely essential for appropriate testing and management of patients with a bleeding disorder. A systematic step-by-step approach is often rewarding and cost-effective (Table 40.2). As mentioned before, preanalytic variables should be kept in mind when interpreting unexpected test results and repeating tests to show that reproducibility is a better practice to avoid patient harm. Routine coagulation tests often guide subsequent specific testing in a bleeding patient or patients with a positive history of bleeding. Investigation of incidentally encountered abnormal coagulation tests should be taken up judiciously to both avoid unnecessary testing and health care cost, and patient harm by using blood component (often plasma) to correct an abnormal test result. Access to prior coagulation test results is often useful to differentiate congenital from acquired bleeding disorders because prior tests are likely to be normal in acquired disorder versus mostly abnormal in congenital disorders (Table 40.3).

HEREDITARY COAGULATION PROTEIN DEFECTS

Protein or factor deficiencies can be quantitative or qualitative. In quantitative disorders, the factor level determined by routine clot-based methods (functional activity assays) is similar to that obtained by immunologic (antigen) assays. In qualitative disorders, the functional assay result is decreased, but the antigen level is significantly higher or normal, indicating the presence of a dysfunctional protein or an inhibitor to the function of that protein.

TABLE 40.2
Patterns of Clinical Bleeding in Disorders of Hemostasis

Characteristics	Primary Hemostasis (Platelet/Vascular Problem)	Secondary Hemostasis (Coagulation Factor Problem)
Onset	Spontaneous, immediate after trauma	Delayed after trauma
Sites	Skin, mucous membranes	Deep tissues
Form	Petechiae, ecchymosis	Hematomas
Mucous membrane	Common (nasal, oral, gastrointestinal, genitourinary)	Less common
Other sites	Rare	Joint, muscle, central nervous system, retroperitoneal space
Clinical examples	Thrombocytopenia, platelet defects, von Willebrand disease, scurvy	Factor deficiency, liver disease, acquired inhibitors

TABLE 40.3
Differential Diagnosis of Abnormal Coagulation Screening Tests

Abnormal Activated Partial Thromboplastin Time (APTT) Alone

Associated with bleeding: VIII, IX, and XI defects

Not associated with bleeding: XII, prekallikrein (PK), high-molecular-weight kininogen, lupus anticoagulants

Abnormal Prothrombin Time (PT) Alone

Factor VII defects

Combined Abnormal APTT and PT

Medical conditions: Anticoagulants, disseminated intravascular coagulation (DIC), liver disease, vitamin K deficiency, massive transfusion

Rarely, dysfibrinogenemia; factor X, V, and II defects

TABLE 40.4
Classification of Hemophilia A and B

	CLASSIFICATION		
	Severe	Moderate	Mild
Percentage of patients	50–70	10	30–40
Factor VIII or factor IX activity, %	<1	1–5	6–30
Pattern of bleeding episodes	~2–4 per month	~4–6 per year	Uncommon
Cause(s) of bleeding	Spontaneous	Minor trauma	Major trauma Surgery

DEFICIENCY OF FACTOR VIII (HEMOPHILIA A) OR FACTOR IX (HEMOPHILIA B)

Hemophilia A (FVIII deficiency) is the most common severe congenital bleeding disorder, affecting 1 in 5000 to 10,000 males without ethnic predilection. Hemophilia B (FIX deficiency, Christmas disease) is also a severe congenital bleeding disorder, affecting 1 in 25,000 to 30,000 males. The FVIII and FIX genes are both located on the X chromosome, with the result that hemophilia A and B are X-linked recessive disorders primarily affecting males. Females carrying a hemophilia mutation on one of their two X chromosomes are carriers. Hemophilia A can affect females when carriers have imbalanced lyonization of the normal X chromosome or Turner syndrome (XO), or when they are daughters of an affected male and a carrier female.

Hemophilia is defined as mild, moderate, or severe depending on the baseline factor activity level (Blanchette et al., 2014) (Table 40.4). Factor levels correlate with the degree of bleeding symptoms (Pavlova & Oldenburg, 2013). However, among patients, there is considerable variability in bleeding pattern.

Severe hemophilia A and B usually manifest very early in life, often as cephalohematomas at birth (whether a vaginal or cesarean section delivery), postintramuscular vitamin K hematomas, or prolonged bleeding with newborn heel sticks. The classic presentation of the hemophilias was provided in the Talmud, which emphasized the risk of bleeding associated with circumcision. Surprisingly, it is uncommon to observe bleeding at the umbilical stump in those affected by hemophilia A or B. As the child progresses into toddler age, bleeding predominantly manifests as acute and recurrent hemarthroses, muscle and soft-tissue hematomas, and then gum and dental bleeding associated with loss of deciduous teeth. In childhood through adulthood, the bleeding frequency increases in proportion to activity intensity and trauma. However, even the frequency of spontaneous bleeding increases—for example, hemorrhage unassociated with known trauma. This suggests that even the stress of weight-bearing, normal torque on the joints and supporting structures can precipitate bleeding events. The hinge joints remain the primary sites of hemophilia-related bleeding complications throughout life, such as ankles, knees, and elbows, although even the ball-and-socket joints can bleed occasionally. Repeat hemorrhage into the same joint often leads to restricted range of motion, support muscle atrophy with disability, acute and chronic pain, and structural deterioration. Iron uptake into the joint synovium triggers the local release of proinflammatory and proteolytic cytokines, particularly IL-1 beta and IL-6, which, in turn, induce chondrocyte apoptosis and cartilage damage (Van Vulpen et al., 2015) via impaired scavenging, degradation, and transport of iron from the joint synovium. Life-threatening hemorrhage usually occurs in the brain and paratracheal regions and is typically related to trauma (see Table 40.2). The treatment of severe hemophilia (FVIII or FIX activity <1% of normal) has traditionally required frequent administration of plasma-derived or genetically engineered products containing the specific missing clotting factor, using strategies that reverse active bleeding or prevent spontaneous and minor traumatic hemorrhage (primary or secondary prophylaxis). Newer approaches utilize "disruptive" therapies, which promote thrombin generation and hemostasis by circumventing the need for the deficient clotting factor (Weyland and Pipe, 2019).

Mild hemophilia (FVIII or FIX activity >5% of normal) is rarely symptomatic for spontaneous bleeding. However, it manifests with prolonged bleeding after trauma or major surgery, and patients rarely need factor replacement. Moderate severity hemophilia (FVIII or FIX activity 1% to 5% of normal) is characterized by an intermediate bleeding phenotype.

Hemophilia is suspected based on bleeding symptoms or a family history of hemophilia. About one-third of hemophilia A cases arise from spontaneous mutations. Laboratory evaluation of patients with such a bleeding history should include APTT, PT, and platelet count. Diagnosis is confirmed by an FVIII or FIX assay. Hemophilia can be diagnosed as early as the birth of a male neonate with a positive family history because FVIII and FIX levels can be directly measured in cord blood.

It is important to appreciate that in the coagulation laboratory, measurement of at least two dilutions of patient-citrated plasma should be assayed in duplicate against standard curves for FVIII or FIX coagulant activity in order to fully characterize the severity of disease in those with severe FVIII or FIX deficiency because the dilution curves are not linear at lower values. FVIII levels above 10% are easier to evaluate because the standard curve spans between 10% and 150% FVIII/FIX activity. Variations of the one-stage assay method are the most commonly employed techniques to measure FVIII or FIX activities in plasma.

The type of clotting factor concentrate administered can affect assay of the factor—for example, assay discrepancies of up to 40% are possible during clinical monitoring of recombinant FIX and plasma-derived FIX concentrates (EMA, 2014) and between modified recombinant FVIII (rFVIII) extended half-life products, such as pegylated FVIII and Fc fusion, versus standard (or B-domain deleted) half-life recombinant FVIII concentrates (Nagoya et al., 2019).

Several additional comments regarding hemophilia care are pertinent:

1. Only 25% of the world's hemophilia population receives adequate care, and opportunities are still available to provide enough clotting factor concentrate to prevent joint damage, long-term morbidity from bleeding complications, and death from bleeding.
2. The standard of care for severe hemophilia A and B in the resource-rich world now includes the initiation of primary prophylaxis with the administration of clotting factor replacement therapy either before or shortly after the first bleeding event in childhood. Prophylaxis regi-

mens should be maintained indefinitely, although some young adults can do well off prophylaxis. The target FVIII or FIX trough activity level to maintain should be individualized according to the patient's lifestyle.

3. Primary prophylaxis is not perfect in its ability to prevent joint deterioration, even when the individual has not experienced any clinical hemorrhage. In addition, there are those rare individuals who manifest no joint deterioration despite recurrent bleeding events (Manco-Johnson et al., 2007).
4. All of the currently available clotting factor concentrates for FVIII or FIX replacement are viral safe, without any reported transmission of human immunodeficiency virus, hepatitis C virus, hepatitis B virus, and so on. The viral attenuation processes in the pooled human plasma-derived factor concentrates have rendered these products free from transmitting such lipid-enveloped infectious agents as severe acute respiratory syndrome, West Nile virus, and so forth. However, these products still may potentially transmit non-lipid-coated viruses, such as parvovirus B19, despite ultrafiltration.
5. The most common cause of severe hemophilia A is a partial inversion of the FVIII gene up to and including intron 22, which accounts for up to 40% to 45% of such patients (Naylor et al., 1992; Lakich et al., 1993). These inversions are due to homologous recombination between the region that includes the *F8A* gene in intron 22 and one of the two other homologous regions located more than 400 kb 5′ (telomeric) to the FVIII gene (Lakich et al., 1993; Kaufman et al., 2001). Several types of these inversions have been described (Kaufman et al., 2001). If the intron 22 inversion is not detected, the definition of the responsible mutation is difficult because of the large size of the FVIII gene (approximately 186,000 bp long). In contrast, the FIX gene is one-fifth the size of the FVIII gene, and the mutations responsible for hemophilia B are easier to define by genetic analysis.

More diagnostic testing may be required for patients with mild to moderate deficiency of FVIII for whom a diagnosis of hemophilia A may be less apparent (e.g., a female patient with low FVIII and apparent autosomal inheritance). In patients with von Willebrand disease, a secondary deficiency of FVIII may occur (see Chapter 41) because FVIII is normally bound to vWF in the plasma (Weiss et al., 1977). Further, a unique vWF abnormality has been described in which a missense mutation in vWF impairs its capacity to bind to and promote FVIII secretion into plasma. This abnormality, first described in a French patient from Normandy, has been named von Willebrand disease "Normandy," or type 2N. It should be suspected in a patient with normal vWF antigen and functional studies (see Chapter 41) but reduced FVIII levels, whose inheritance is autosomal recessive rather than sex linked (Schneppenheim et al., 1996).

FIX activity levels during childhood remain at about 75% of adult levels. A 25% increment in FIX expression begins at puberty in both sexes (Andrew et al., 1992). It has been assumed that this is a result of steroid hormone action. It is interesting to note that a rare form of FIX deficiency, hemophilia B Leyden, undergoes postpubertal phenotypic resolution. Patients with this condition present with hemophilia B in early childhood, with FIX activity ranging from less than 1% to 13% of normal. Plasma levels rise to as high as 70% of normal after the onset of puberty with resolution of bleeding complications (Reitsma, 2001). Mutations in hemophilia B Leyden have been identified in the promoter region of the FIX gene, within which a consensus sequence for steroid receptor binding is located (Crossley et al., 1992).

Evaluation of Carriers

Detection of carriers is useful for the prediction of symptoms and prenatal counseling. Carriers are expected to have approximately 50% of normal factor activity, a value generally able to prevent bleeding. However, some hemophilia carriers may experience menorrhagia and other bleeding symptoms, phenotypically like males with mild hemophilia (Arun & Kessler, 2001; Plug et al., 2006). In hemophilia A, if the mutation is known, the potential carrier may be tested for that mutation. Otherwise, the woman should be tested for the common intron 22 inversion or get whole exosome sequencing. A detailed genetic analysis of the woman, the affected male, and intervening family members may define the mutation. These techniques provide an extremely high likelihood of detection of carriers when all family members are available for study. A less optimal, but more readily available and cost-effective approach is the calculation of the ratio of FVIII activity to the level of vWF antigen to predict carrier status. The ratio of FVIII/vWF had a median value of 0.71 (range, 0.18–2.2) in a group of 147 carriers versus a median value of 1.39 (range, 0.58–2.48) in a group of 25 noncarriers. A value of FVIII/vWF:Ag ratio ≤0. 9 was found in only one noncarrier (4%) versus in 113 (76.9%) carriers (Labarque et al., 2017).

Prenatal diagnosis of the hemophilias can be performed at a number of high-risk obstetric centers by chorionic villous sampling at 9 to 14 weeks' gestation or by amniocentesis after the 16th week. If the genetic basis of the disease is known within a family, then mutational analysis or examination for the intron 22 inversion can be performed on the cell samples (Ljung, 1999; Arun & Kessler, 2001). Fetoscopic blood sampling can be performed at 20 weeks' gestation for coagulation factor analysis, although it carries a higher risk and is less precise. However, because fetal deoxyribonucleic acid is detectable in maternal circulation within 10 days of conception, collection of maternal plasma should be sufficient to make a prenatal diagnosis of hemophilia presently, obviating the use of the invasive diagnostic techniques listed earlier. In hemophilia B, 30% to 40% of carriers will be missed by measurement of FIX activity, and mutation analysis is important for defining carrier status (Graham, 1979; Ljung, 1999). Similar to hemophilia A, hemophilia B arises spontaneously in one-third of affected individuals.

Treatment of Hemophilia

The primary principle of hemophilia treatment is to prevent or reverse bleeding episodes, spontaneously occurring, traumatic, or surgically induced. The secondary goals of hemophilia treatment are to avoid the formation of alloantibody inhibitors, which neutralize the coagulation function of exogenously administered replacement products and to improve the convenience of treatment in order to improve adherence to any long-term treatment regimens. Well-conducted prospective clinical trials have indicated that the development of FVIII inhibitors is the most serious complication of FVIII replacement therapy and affects 29% to 45% of previously untreated patients (PUPs) with severe hemophilia A. In contrast, there is a 1.5% to 3% incidence of neutralizing alloantibody inhibitor development in PUPs with severe hemophilia B. They predominate in those individuals with large FIX gene deletions.

The landscape of hemophilia treatment has expanded rapidly over the past few years and bioengineering innovations have yielded modifications of standard recombinant replacement products that extend their circulating half-lives. New technologies have also been applied to develop "disruptive" treatment strategies, which circumvent the need to replace the specific deficient clotting protein by promoting thrombin generation using "mimetic" proteins or by "rebalancing" normal coagulation through interfering with the natural modulators of the coagulation pathways, that is, tissue factor pathway inhibitor, antithrombin, and so on. Lastly, gene therapy is emerging as a potential "cure" for the hemophilias.

All modern replacement products for hemophilia A and B are viral safe and equivalently efficacious in treating and preventing bleeding events. No transmission of blood-borne pathogens (including prion-related disease) has been documented for any of the currently available products. Cryoprecipitate for FVIII replacement or fresh frozen plasma for FIX replacement is no longer considered the standard of care in most of the world.

FVIII replacement concentrates are characterized as plasma-derived (pd) from pooled normal plasma from tens of thousands of donors or as recombinant genetically engineered products. The plasma-derived (pd) products are available as high specific activity, immunoaffinity processed, highly purified FVIII without vWF protein or as low specific activity pd FVIII concentrates containing substantial amounts of vWF protein. Standard recombinant FVIII concentrates are all ultra-purified and very high specific activity products, further defined by the presence or absence of extraneous human or animal proteins in the media bathing the murine-derived cell cultures synthesizing the FVIII or at the end commercial product. They can be full-length native FVIII protein or B-domain deleted truncated FVIII coagulant protein.

The category of EHL rFVIII concentrates is further characterized according to how they are bioengineered to convey longer circulating activity levels. These techniques include pegylation of the B-domain deleted FVIII construct; covalent bonding of the heavy and light chains of FVIII into a single-chain structure; or B-domain deleted rFVIII fused to the IgG-1 Fc-domain. EHL rFVIII products are also distinguished according to whether they are synthesized by murine-derived Chinese hamster ovary or baby hamster kidney cell lines or synthesized in human embryonic kidney cell lines. Replacement FIX concentrates are available as pd, high specific activity, or immunoaffinity or dual affinity chromatographically purified products. They are all nano-filtered and solvent detergent treated to enhance viral safety.

Standard recombinant FIX concentrates are synthesized by Chinese hamster ovary (CHO) cell lines. EHL rFIX concentrates are synthesized in CHO or human embryonic kidney cell lines and are further characterized as pegylated, albumin-fusion, or IgG-1 Fc domain fusion proteins.

Although plasma-derived FVIII and FIX replacement products remain commercially available and are very effective in promoting hemostasis in

individuals with hemophilia A and B, they are believed capable of transmitting nonenveloped viruses such as parvovirus B19 or prions, the agents causing Creutzfeldt-Jakob disease (CJD) and variant CJD (vCJD). These pathogens are not eliminated by current viral inactivation and product purification technologies and are emblematic of the hypothetical potential of these products to transmit yet undiscovered or unrecognized blood-borne infectious agents in the future. Thus, in 2014, the Medical and Scientific Advisory Council of the National Hemophilia Foundation advocated recombinant FVIII and FIX concentrates as the treatment of choice for individuals with hemophilia A and B.

The important Survey of Inhibitors in Plasma-Product Exposed Toddlers (SIPPET) study (Peyvandi et al., 2016) reported a cumulative alloantibody FVIII neutralizing inhibitor incidence of 44.5% (28.4% high titer) in PUPs treated with recombinant FVIII concentrates produced in hamster cell lines and 26.8% (18.6% high titer) with plasma-derived FVIII (pdFVIII) products containing vWF. As a result of these data, many clinicians believe strongly that PUPs with severe hemophilia A should receive plasma-derived products containing vWF to reduce the likelihood of inhibitor development. The caveat here is that the individual PUP's FVIII gene mutation may be critical to determining susceptibility to inhibitor formation (in the SIPPET study, no inhibitors occurred in PUPs with a low genetic risk [non-null mutations] who received pdFVIII versus 31% inhibitor incidence in PUPs with high genetic risk [null mutations] treated with pdFVIII). In contrast, the risk of inhibitor formation in PUPs with either low- or high-risk FVIII gene mutations did not differ when treated with rFVIII (43% and 47%, respectively). Furthermore, the fact that the use of pdFVIII did not eliminate inhibitor formation in PUPs implies that the replacement factor choice is only one of the multiple variables involved in inhibitor formation. A second caveat is that the results from the SIPPET study do not apply to inhibitor formation in previously treated hemophilia A patients in whom rFVIII products have *not* been associated with increased inhibitor incidence. Lastly, SIPPET concerns cannot be extrapolated at this time to the newer generations of EHL FVIII concentrates as these products have not been examined in similar prospective randomized trials.

Replacement clotting factor concentrates are dosed on the basis of weight and desired plasma activity. Plasma with 100% clotting factor activity has 1 U/mL of that clotting factor. By convention, one unit of a coagulation factor is the amount of that factor present in 1 mL of normal pooled human plasma. Each unit of intravenously administered pd or recombinant FVIII/kg ideally raises the plasma FVIII activity by about 2%, and each unit of recombinant FIX/kg raises the plasma FIX activity by about 1%. To raise the FVIII plasma activity of a 70-kg man by 100%, the calculated dose will be as follows:

$$\text{Body weight (kg)} \times 0.5\ \text{IU/kg} \times \text{FVIII activity increase desired (\%)} = \text{Dose required, or } (70\ \text{kg})(0.5)(100) = 3500\ \text{U to be infused.}$$

The mean plasma half-life of standard exogenously administered FVIII to adults with severe hemophilia A is about 8 to 12 hours. EHL recombinant FVIII concentrates have mean circulating half-lives of about 18 to 24 hours (about 1.5 times normal).

To raise the FIX plasma activity of a 70-kg man by 100%, the calculated dose will be as follows (Shapiro et al., 2005):

$$\text{Body weight (kg)} \times \text{desired FIX increase (\%)} \times 1\ \text{IU} = \text{Dose required, or } (70\ \text{kg})(100) = 7000\ \text{U to be infused.}$$

About one-third of FIX-deficient patients have a lower recovery after recombinant FIX infusion, requiring 20% higher dosing. The mean plasma half-life of exogenously administered pd or standard recombinant FIX to adults with severe hemophilia B is about 18 to 24 hours. EHL recombinant FIX concentrates in adults have mean circulating half-lives ranging between 82 to 110 hours (about 5 times normal). The mean circulating half-lives of FVIII or FIX concentrates in young children up to 6 years old are about 15% to 20% lower than in adults due to accelerated plasma clearances. Dosing strategies in young children should take these pharmacokinetic differences into consideration. The very active person with hemophilia may wish to maintain a trough clotting factor activity level of 15% to minimize bleeding events during rigorous athletics or work-related requirements. In contrast, for the sedentary individual, a trough level of 1% may be sufficient.

Complications of Treatment

An important complication of replacement therapy, occurring mainly in patients with severe hemophilia, is the development of alloantibodies (inhibitors) that interfere with the coagulation factor function. Inhibitors occur in 20% to 30% of patients with severe hemophilia A and 3% to 5% with severe hemophilia B. They are quite uncommon in patients with moderate or mild hemophilia, probably because the infused factor is not recognized as a foreign antigen in these individuals (Eckhardt et al., 2013). Inhibitors reduce or abolish/neutralize, depending on their titer or the response to replacement therapy. Periodic inhibitor screening is very important for effective and prompt management of this complication (Soucie et al., 2014).

Characterization of a specific inhibitor requires careful quantitation. In general, lower-titer FVIII inhibitors (<5 Bethesda units [BU]) can still be treated with replacement factor. In contrast, higher-titer inhibitors (>10 BU) typically need the administration of the so-called bypassing agents: recombinant FVIIa, FEIBA (FVIII inhibitor bypassing agent that is an activated prothrombin complex concentrate [PCC]), and recombinant porcine FVIII (Hay et al., 2006). A simple mixing test as described previously for the APTT can underestimate the presence of an inhibitor. Further, as indicated earlier, there is no unanimity on how such mixing assays should be performed. In order to diagnose the presence of a FVIII or FIX inhibitor, a formal FVIII or FIX "Bethesda" inhibitor assay should be performed (Kasper et al., 1975). In the classic Bethesda assay, the patient's plasma is serially diluted with imidazole buffered saline (IBS), then one part patient plasma is mixed with one part normal pooled plasma and incubated for 2 hours at 37°C. The control is a 1:1 mix of normal pooled plasma with IBS. In the Nijmegen modification, the IBS is replaced with FVIII deficient plasma for serial dilution, which makes this method more sensitive to detect low-titer inhibitors (Verbruggen et al., 1995). After incubation, FVIII is measured in patient plasmas and the control plasma, and the percentage of residual FVIII activity is determined. One BU is defined as the amount of inhibitor antibody in patient plasma that inhibits half the FVIII activity in the control plasma (Fig. 40.8). Therefore, patient plasma producing a residual FVIII activity of 50% is considered to contain 1 BU of inhibitor per milliliter. If this same plasma had been diluted tenfold before assaying for the inhibitor, then this result would indicate an inhibitor value of 10 BU/mL.

This assay is sensitive, but at times it is difficult to reproduce. A common observation is that varying dilutions of plasma may yield different estimates of the inhibitor titer. For assigning the level of BUs, the dilution that comes closest to the 50% residual factor is chosen for the calculation of the FVIII inhibitor titer. Values on the standard curve should be read-only at between 25% and 75% residual FVIII activity. If below 25%, higher dilutions of the sample are needed. If residual activity using the 1:1 diluted patient specimen is above 75%, a demonstrable inhibitor may not be present. It is, in fact, important for the laboratory to determine a lower limit of sensitivity of this assay, typically about 0.5 BU. It is additionally of note that a plot made of residual FVIII activity versus increasing volume of original patient plasma in the Bethesda assay may distinguish between an inhibitor capable of reducing FVIII activity into the unmeasurable range (type I inhibitor) and an inhibitor that preserves some degree of residual FVIII activity, even at high inhibitor titer (type II inhibitor), presumably reflecting a target epitope at a less critical region of the FVIII molecule (Gawryl & Hoyer, 1982; Luna-Zaizar et al., 2009).

Treatment of Acute Bleeds Associated With Neutralizing Alloantibody Inhibitors in Hemophilia A and B

The approach to the reversal/treatment of acute hemorrhagic episodes is predicated on circumventing the neutralizing effects of antibodies on exogenous replacement therapies. In the context of low responding inhibitors (≤5 BU and no anamnestic response to reexposure to exogenous FVIII or FIX), high doses of any construct human FVIII or FIX concentrate (200 IU/kg) can be administered to saturate and "overwhelm" the respective inhibitor. The caveat to this approach is that the incremental increase in clotting factor activity (recovery) and the circulating half-life will be blunted by the effects of the inhibitor. Second, for hemophilia B patients, particularly those with large FIX gene deletions, there is a small but significant incidence of developing potentially serious and life-threatening allergic or anaphylactic reactions to FIX and some also develop nephrotic syndrome. In these patients, as well as those with high responding alloantibody inhibitors to FVIII or FIX (>5 BU and anamnestic responses to reexposure to the clotting factor), the treatment of choice for acute bleeds is a "bypassing agent," such as FVIII inhibitor bypass activity (FEIBA) or recombinant FVIIa.

On the other hand, recombinant porcine B-domain deleted FVIII concentrate, synthesized in CHO cells to treat acute bleeding in acquired autoantibody FVIII inhibitor patients, has also been used in phase II clinical

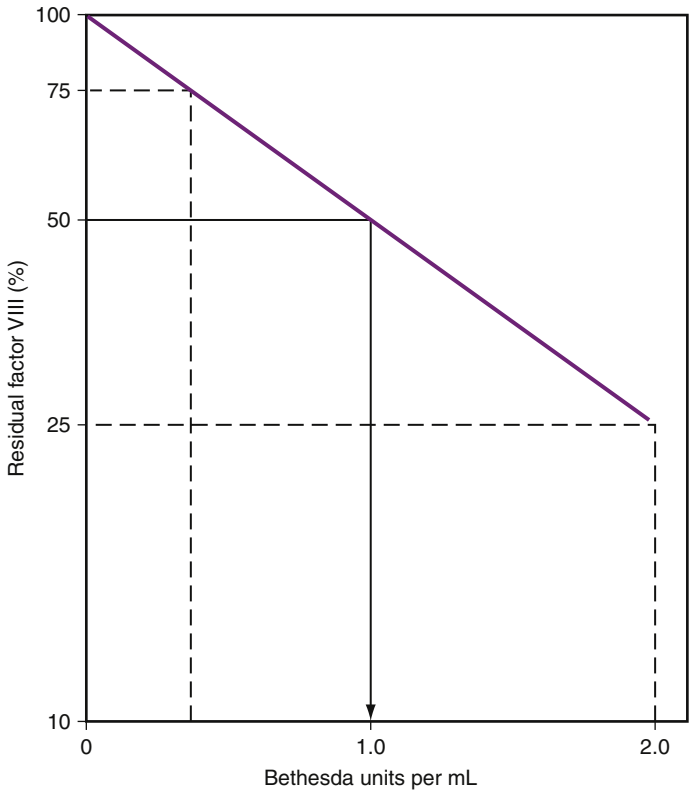

Figure 40.8 Expression of factor VIII inhibitor titer in Bethesda units. In this assay for an inhibitor to factor VIII, the percent of residual factor VIII activity in normal plasma is determined after incubation with patient plasma. By convention, 1 international Bethesda unit of inhibitor is the amount of antibody that destroys 0.5 U factor VIII activity after 2 hours of incubation at 37°C. As shown in the figure, the percent of residual factor VIII activity on a log scale is plotted against Bethesda units/mL in a linear scale. For a sample to be evaluable in this assay, the level of factor VIII activity should fall between 25% and 75%. Patient samples that produce residual factor VIII activity below 25% need to be diluted further so that the 50% residual factor VIII activity point can be found. (Redrawn with permission from Bockenstedt PL: Laboratory methods in hemostasis. In Loscalzo J, Schafer AI, editors: Thrombosis and hemorrhage, ed 3, Philadelphia, 2003, Lippincott Williams & Wilkins, p 370, Fig. 21.7.)

trials to treat bleeding in allo-FVIII antibody inhibitor patients with congenital hemophilia A. The product has demonstrated good efficacy and safety (Mannucci & Franchini, 2017) but has not been licensed by the FDA for use in congenital hemophilia A with inhibitors. Recombinant porcine FVIII was developed on the premise that there is a lower cross-reactivity of porcine FVIII with antihuman FVIII antibodies.

Disruptive Therapies for the Hemophilias

The concept of "rebalancing" the coagulation cascade to generate thrombin and to establish hemostasis without specific replacement of the deficient coagulation factor protein has evolved rapidly and has yielded novel therapeutic strategies for hemophilia A and B with and without alloantibody inhibitors.

Emicizumab-kxwh (Hemlibra, Genentech/Roche) is the first commercially available agent in this category. It is indicated for the prevention of bleeding in any individual (infants and adults, but there are no clinical efficacy or safety data in patients less than 1 year of age) with severe hemophilia A with and without inhibitors (Barg et al., 2019). It has the advantage of being subcutaneously administered in weekly, every other week, or every 4 weeks dosing regimens. Emicizumab is a genetically engineered bispecific IgG antibody that functions as an "FVIII mimetic" by substituting for the severely deficient FVIII and serving as a cofactor to produce the tenase complex in the coagulation cascade. As a substitute for FVIIIa, it bridges FIXa and FX to facilitate hemostasis. This is critical to the ultimate thrombin generation and multiple well-conducted clinical trials have demonstrated impressive reductions in annualized bleeding rates in severe hemophilia A with or without inhibitors (Mahlangu et al., 2018, Oldenburg et al., 2017). The most concerning adverse events within these clinical trials, only in inhibitor patients who received repeated and large amounts of FEIBA for breakthrough bleeds, was the development of thrombotic complications in 5 individuals. A unique feature of these hypercoagulable events is the presence of thrombotic microangiopathic anemia and the unusual location of some of the thrombi.

Laboratory monitoring of emicizumab is not required while on routine prophylactic dosing. In fact, the APTT will be artefactually decreased and the one-stage FVIII activity assay will be misleadingly elevated and will not accurately correlate with the clinical hemostatic status of the patient. Chromogenic FVIII activity assays that use bovine reagents do measure FVIII activity in emicizumab patients who have received an exogenous FVIII replacement. Similar limitations occur with the clot-based Bethesda assay; a bovine-reagent chromogenic-based Bethesda inhibitor assay is available. Emicizumab can be measured in plasma, but this does not provide a reliable "FVIII-equivalence" assay to predict in vivo hemostasis.

Another emerging disruptive therapy for hemophilia A or B with or without inhibitors is fitusiran (Sanofi-Genzyme), which interferes with antithrombin synthesis in the liver and, thus, leads to increased thrombin generation in vivo. Fitusiran binds to and degrades messenger ribonucleic acid for antithrombin and thereby interferes with AT translation by the hepatocyte. This synthetic, double-stranded small interfering ribonucleic acid oligonucleotide is also administered subcutaneously as a weekly or monthly therapeutic; clinical trials have demonstrated reduced annualized bleeding rates in patients with hemophilia A and B, with or without inhibitors (Pasi et al., 2017). In these studies, two severe hemophilia A patients have developed a fatal thrombosis after concurrent repeated administration of high-dose factor VIII concentrate. Theoretical benefits have been speculated for fitusiran to prevent bleeding complications in other rare bleeding disorders, such as severe deficiency of factors V, VII, X, and XI. No clinical trials in these latter coagulopathies have been conducted as yet.

Concizumab (Novo Nordisk) is the third disruptive therapy for hemophilia A and B with and without inhibitors. It is a daily subcutaneously administered high-affinity, anti-TFPI monoclonal antibody, which results in an increased generation of FXa and, ultimately, increased thrombin generation. Clinical trials have demonstrated decreased annualized bleeding rates with few side effects (Shapiro et al., 2019). That being said, the clinical trials with a different anti-TFPI construct (Bayer) were terminated due to thrombotic complications.

Gene Therapy for the Hemophilias

Congenital hemophilia A and B appear to be ideal disorders for gene therapy for the following reasons:(1) FVIII and FIX genes were cloned in the early 1980s, (2) the proteins expressed by the genes (FVIII/FIX) are easily measured in small amounts of plasma, (3) incremental increases in protein expression due to gene therapy could change the phenotypic bleeding profile in a significant manner, (4) hemophilic animal models have been developed to provide proof of principle that gene therapy would be feasible and useful, and (5) individuals with congenital severe hemophilia A and B have been enthusiastic and willing to participate in gene therapy clinical trials with the potential that their bleeding rates and the consequences therefrom could be eliminated or at least ameliorated.

The most successful clinical gene therapy studies currently employ nonintegrating recombinant adenoassociated viral (AAV) vectors to carry the genetic "payload" to the targeted hepatocytes for cellular transduction. Although no long-term immunologic or oncologic toxicities have been observed with either FVIII or FIX gene therapies to date, longitudinal vigilance is indicated. In addition, gene therapy trials have been hampered somewhat by the presence of preexisting neutralizing antibodies to the AAV capsid in potential participants. Also, all of the gene therapy trials have observed some degree of lost transgene expression over time, attributed to either episomal latency within the hepatocyte or by yet to be fully elucidated immunologic mechanisms.

The most successful FIX gene therapy results have been accomplished in trials that incorporate a FIX molecule with a gain-of-function FIX mutation (FIX-Padua) with AAV capsids (Batty & Lillicrap, 2019). Some patients have experienced sustained FIX activity levels in the 30% to 40% range (compared to baseline levels of ≤2%). Gene therapy trials in severe hemophilia A have also achieved clinically significant incremental increases in FVIII levels, frequently in the normal range (≥50% activity). The durability of the response has emerged as an issue to watch over time in these patients (Pasi et al., 2020).

HEREDITARY DEFICIENCIES OF OTHER COAGULATION FACTORS

The other hereditary deficiencies of coagulation factors have an autosomal inheritance (Table 40.5). With the exception of FXI deficiency, these disorders are very rare. However, they have a higher prevalence in areas where consanguineous marriage is practiced (Mannucci et al., 2004). Deficiencies of factors XIII, X, VII, V, and II are defined rare inherited coagulation

TABLE 40.5

Characterization of Coagulation Factors and Their Deficiencies

Factor	Molecular Weight, kDa	Gene Location	Normal Circulating Half-Life	Incidence	Inheritance	Bleeding Severity
Fibrinogen	330	4q31.3-q32.1	2–4 days	1:1 million	Recessive	Mild–severe*
II	72	11p11.2	3–4 days	Very rare	Recessive	Mild–moderate
V	330	1q24.2	36 hours	1:1 million	Recessive	Moderate
V and VIII combined	—	LMAN1:18q21.32 MCFD2:2p21	36 hours for FV; 10–14 hours for FVIII	1:2 million	Recessive	Mild–moderate
VII	50	13q34	3–6 hours	1:500,000	Recessive	Mild–severe
VIII	330	Xq28	10–14 hours	1:10,000	Sex-linked	Mild–severe
IX	56	Xq27	18–24 hours	1:30,000	Sex-linked	Mild–severe
X	58	13q34	40–60 hours	1:500,000	Recessive	Mild–severe
XI	160	4q35.2	40–70 hours	Rare†	Recessive	Mild–moderate
XII	80	5q33-qter	50–70 days	Rare	Recessive	No bleeding
PK	88	4q33-q35	Not known	Very rare	Recessive	No bleeding
HK	120	3q27	9–10 hours	Extremely rare	Recessive	No bleeding
XIII	320	A:6p25.1 B:1q31.3	11–14 days	<1:1 million	Recessive	Moderate–severe

HK, High-molecular-weight kininogen; *PK*, prekallikrein.
*May be associated with thrombosis.
†Rare except in those of Ashkenazi Jewish descent

disorders (RICDs) that represent 2% to 5% of inherited coagulation factor defects in the general population. The most common RICDs include deficiencies of FXI and FVII, followed by FV, FX, fibrinogen, and FXIII (Ruiz-Saez, 2013).

In general, most patients with RICDs have partial defects because they have relatively mild bleeding disorders. Most coagulation-based assays have difficulty detecting these factors once their levels are below 5% to 10%. In vivo, however, the presence of even this small level of coagulation factor can greatly influence bleeding risk. In contrast, findings in knockout mice indicate that a true null of each of these proteins is associated with virtually 100% mortality from hemorrhage before or at the time of birth. With hereditary factor deficiencies, heterozygous-deficient individuals have approximately 50% (most commonly, 30%–60%) of the normal level of the affected factor. The symptoms of these disorders are quite variable. Coagulation factor deficiencies may be suspected on the basis of symptoms, family history, or abnormal screening tests, and the laboratory diagnosis is confirmed by specific factor assays. Once a specific protein deficiency is recognized, clinical history usually distinguishes a congenital from an acquired defect.

Disorders with Prolonged APTT and Normal PT

Factor XI

FXI deficiency is common in Ashkenazi Jews, in whom heterozygote frequency is 8% (Asakai et al., 1991; Emsley et al., 2010). This ethnic population constitutes about 50% of the FXI-deficient patients seen in the United States. Most patients with FXI deficiency rarely have a spontaneous hemorrhage. This notion is further supported by the lack of any spontaneous bleeding reported in a recent trial in which antisense treatment was administered to decrease the activity of FXI to 25% normal in knee replacement surgery with the aim to reduce the incidence of venous thrombosis (Buller et al., 2015). Bleeding typically occurs after trauma or surgery, particularly involving areas of the body with high fibrinolytic activity (mouth, nose, genitourinary tract). Women can experience menorrhagia and postpartum hemorrhage. Bleeding can occur in heterozygotes and does not necessarily correlate with the residual FXI level (Leiba et al., 1965; Bolton-Maggs et al., 1988). However, the bleeding tendency may be modified by additional defects such as hemophilia, von Willebrand disease, and platelet function defects (Brenner et al., 1997). Diagnosis depends on the determination of the FXI activity below the reference range. The most widely used APTT reagents will have prolonged APTT results for patient samples with FXI activity below 20% to 25% and mixed results when levels are 25% to 60%. The lower limit of the normal range is probably between 60% and 70% (Bolton-Maggs et al., 1995). Therefore, a normal APTT does not rule out a mild FXI deficiency. In cases in which the marked elevation of FVIII may be present, APTT can be normalized even when other factors are reduced (Lawrie et al., 1998). Thrombin generation assay performed in specific sample conditions appears to be able to identify the bleeding phenotype of patients with FXI deficiency (Pike et al., 2015). In all patients with FXI deficiency, preoperative management is critical to prevent bleeding complications. Patients with a severe deficiency (FXI <10%–20%) should receive treatment with fresh frozen plasma to raise their FXI levels. Usually, replacement therapy of 20 mL/kg loading dose with a maintenance dose of 5 to 10 mL/kg every 24 hours is sufficient to cover patients with severe FXI deficiency through elective surgery (Kessler et al., 1996). Patients with levels from 20% to 70% may or may not bleed.

The severity of the surgery, the patient's past history of bleeding following prior surgeries, and perhaps the bleeding histories of family members with the same level of FXI activity should be considered when the strategy for bleeding prevention is being formulated. Antifibrinolytic therapy with tranexamic acid or epsilon aminocaproic acid has been a very effective adjunctive therapy when used alone or in combination with replacement therapies. This is particularly useful in the United States, where only fresh frozen plasma or solvent/detergent (S/D) treated, pooled human plasma (Octaplas, Octapharma) is available for FXI replacement therapy.

Pooled human plasma-derived FXI concentrates are available in France and the United Kingdom (LFB Hemoleven and BPL FXI), but neither has been approved by the United States FDA. Rare arterial and venous thrombotic episodes have been reported with both (or that can have a prothrombotic effect) (Bauduer et al., 2015; Ling et al., 2016). Off-label use of lower-dose (15–30 μg/kg) recombinant factor VIIa concentrate (NovoSeven) has also provided effective and safe hemostasis for surgery in severe FXI deficiency. No large clinical trials have utilized this approach (O'Connell et al., 2008, Riddell et al. 2011).

The development of neutralizing antibodies that function as inhibitors to exogenously administered sources of FXI in patients with severe FXI deficiency have been described, although these are rare (Salomon et al., 2003). These patients should be treated with rFVIIa concentrate (Kenet et al., 2009).

FXII, Prekallikrein, and High-Molecular-Weight Kininogen

FXII, prekallikrein, and HMWK deficiencies are associated with prolonged APTT but are not associated with any bleeding risk. FXII deficiency is most common, occurring in all racial and ethnic backgrounds. It is associated with a very long PTT. Prekallikrein deficiency is less common (Girolami et al., 2014) but is seen in the United States in all ethnic groups. It is associated with a slightly prolonged APTT that corrects to normal when sitting on a bench for 1 hour at 37°C. HMWK deficiency is a rare disorder that also is associated with a very long APTT. These protein deficiencies are not associated with bleeding—a point emphasized diagrammatically in Figure 40.1 by the graying of this portion of the coagulation "cascade." Because no replacement therapy for hemostasis is necessary for FXII, PK, or HMWK deficiency, it is important to recognize these defects to prevent unnecessary treatment. Deficiencies of FXII, PK, and HMWK

have been associated with reduced thrombosis risk. Deletions of these proteins in mice are associated with delayed times to thrombosis in arterial thrombosis models (Renne et al., 2005; Stavrou et al., 2015; Merkoulov et al., 2008). When a deficiency in the proteins of the kallikrein/kinin system is suspected, a FXII assay should be performed first because it is the most common.

Disorders with Prolonged APTT and PT

Prolonged PT and APTT most commonly are due to general medical conditions described later in the Acquired Coagulation Disorders section. When hereditary disorders are considered, the following, although much less common, should be considered.

Disorders of Fibrinogen

Hereditary fibrinogen abnormalities include two categories of plasma fibrinogen defects: type I, afibrinogenemia or hypofibrinogenemia, with absent or low plasma fibrinogen antigen levels (quantitative fibrinogen deficiencies); and type II, dysfibrinogenemia or hypodysfibrinogenemia, which determines normal or reduced antigen levels associated with the disproportionately low functional activity (qualitative fibrinogen deficiencies). In the type I disorder, null mutations occur in the FGA, FGB, and FGG fibrinogen encoding genes (de Moerloose et al., 2013).

Fibrinogen deficiencies may prolong the PT and APTT if the plasma concentration of the protein is sufficiently low, usually less than 100 mg/dL. Afibrinogenemia is a bleeding disorder of variable severity (Fried & Kaufman, 1980; Lak et al., 1999). Umbilical stump and mucosal bleeding are the most common symptoms, as is an increased incidence of musculoskeletal and central nervous system bleeding. Patients also exhibit poor wound healing. Hypofibrinogenemia is a decreased level of normal fibrinogen that has a similar but milder pattern of bleeding. Both afibrinogenemia and hypofibrinogenemia are associated with recurrent miscarriage, as well as with antepartum and postpartum hemorrhage (Goodwin, 1989; Kobayashi et al., 2000). Paradoxically, reports have described thrombotic events in patients with afibrinogenemia (Chafa et al., 1995; Lak et al., 1999; Dupuy et al., 2001).

Dysfibrinogenemia is a qualitative fibrinogen deficiency characterized by the production of dysfunctional fibrinogen (Miesbach et al., 2010). Most patients with congenital dysfibrinogenemia are heterozygous because of molecular defects in produced protein, although rare homozygous cases have been reported. Dysfibrinogenemias are most commonly acquired in association with liver disease. Acquired dysfibrinogenemias are mainly due to posttranslational modifications of the fibrinogen protein as a result of synthesis in an abnormal liver. These defects are common in patients with hepatitis B and C. Patients with dysfibrinogenemia are usually asymptomatic or have mild bleeding. In some cases, however, thrombosis has been reported with or without a bleeding history (Hanss & Biot, 2001). The thrombin time and reptilase time, which measure clotting time during the conversion of fibrinogen into fibrin, are often prolonged in dysfibrinogenemia. When thrombin proteolyzes fibrinogen in the thrombin time, fibrinopeptides A and B are released from the Aα and Bβ chains of fibrinogen. Reptilase clots fibrinogen by liberating only fibrinopeptide A (Funk et al., 1971). Proteolysis of fibrinopeptide A from fibrinogen is sufficient to induce clot formation. Fibrinopeptide B liberation increases the rate of association of the fibrin monomers, but not the actual physiologic clot (Martinelli & Scheraga, 1980; Nawarawong et al., 1991). Bleeding risk is associated only with fibrinopeptide A release defects, not with fibrinopeptide B release defects. Therefore, a patient can have long PT and APTT from a fibrinopeptide B release defect and not have any bleeding risk—hence, the reason for using both the thrombin time and reptilase time to assess dysfibrinogenemias. Assays that measure clottable fibrinogen will show lower levels than assays that measure fibrinogen antigen. A normal fibrinogen has a ratio of clottable fibrinogen activity to fibrinogen antigen greater than 95%. Ratios less than this raise the possibility of a dysfibrinogenemia. For many years, cryoprecipitate has served as a good source of fibrinogen when replacement is needed. A number of virally inactivated fibrinogen concentrates are now available for therapeutic administration, both in Europe and North America. Human fibrinogen viral attenuated concentrates (RiaSTAP [CSL Behring] and Fibryga [Octapharma]) are available for the treatment and prevention of acute bleeding episodes in persons with congenital fibrinogen deficiency, including afibrinogenemia and hypofibrinogenemia. Primary prophylaxis is easily achieved with these products; however, thrombotic complications may arise.

These concentrates are not indicated for acquired noncongenital hypofibrinogenemias, including those with dysfibrinogenemia, DIC, massive postpartum hemorrhage, and others.

FII (Prothrombin) Deficiency

Prothrombin deficiency may be the rarest inherited coagulation factor deficiency (1 : 2,000,000) (Bolton-Maggs et al., 2004). A true prothrombin deficiency in mice is incompatible with life after birth (Sun et al., 1998). Hypoprothrombinemia (type I deficiency) manifests as a concomitant reduction in prothrombin activity and antigen levels. Bleeding symptoms include mucosal bleeding, hematomas, and hemarthrosis. Dysprothrombinemia (type II deficiency) presents with reduced activity and normal antigen levels. The clinical presentation of dysprothrombinemia is less predictable—patients may be asymptomatic or may have only mild bleeding manifestations (Bolton-Maggs et al., 2004). Depending on the sensitivity of the reagents, both PT and APTT may be prolonged in prothrombin deficiency. However, a specific FII assay is best if there is clinical suspicion or positive family history in the presence of normal screening tests. A PT reagent-based prothrombin assay with factor-deficient plasma is most convenient. Purified or recombinant factor II is currently not available. Prothrombin complex concentrates are the treatment of choice, although fresh frozen plasma can serve as an alternative source of prothrombin. The half-life of the protein is long (2–4 days); thus, replacement therapy every 3 to 4 days is typically sufficient.

FV Deficiency

Heterozygous FV deficiency is usually asymptomatic. Homozygous FV deficiency is rare (1 : 1,000,000), presenting in children with a mild to severe bleeding phenotype (Girolami et al., 1998; Lak et al., 1999). Individuals with severe factor V deficiency (FV:c <1%) may well have some functional FV considering that 50% of true null mice die at the time of development of the cardiovascular system (days 9 to 11), and the other half die at birth from hemorrhage (Cui et al., 1996). A biological reason for a milder than expected bleeding phenotype in FV-deficient subjects may be related to the presence of residual factor V activity in platelets (Bouchard et al., 2015). The most frequent symptoms are mucosal tract bleeding and bleeding after invasive procedures. FV deficiency is associated with prolongation of both the APTT and PT (but a normal thrombin time), and it is confirmed by a PT reagent-based, single-stage FV assay. Patients with FV deficiency should also have an FVIII assay performed to evaluate for combined deficiency of FV and FVIII (Nichols et al., 1998; Zhang & Ginsburg, 2004). The only suitable replacement product available is fresh frozen plasma (solvent/detergent if available). Human platelets contain 20% of total plasma FV; they can also be a source of this protein in acute bleeding (Tracy et al., 1982). The goal of replacement therapy should be to elevate the FV level to at least 10% to 15% (Peyvandi & Mannucci, 1999). The half-life of FV is quite short (16–36 hours); thus, to achieve the hemostatic level of 20%, daily infusions may be needed. During treatment, secondary volume overload needs to be taken into account and actively treated. Acquired inhibitors to FV are relatively common from the surgical use of topical bovine thrombin to aid incision hemostasis. The bovine thrombin is contaminated with bovine FV; when the patient makes an antibody against bovine FV, that antibody then cross-reacts with human FV, causing the deficiency. Most cases are not severe, but their management can be challenging due to the lack of specific replacement therapy (Ardillon et al., 2014). Acquired FV deficiency is treated with platelet transfusion because FV in platelets is protected from the antibody and FV is delivered to the site of injury by platelets. Plasma infusion is ineffective because the antibody will immediately neutralize the transfused FV.

FX Deficiency

Heterozygous FX deficiency is asymptomatic. Homozygous FX deficiency is a severe bleeding disorder that presents in infancy. The bleeding phenotype correlates well with FX activity levels. Symptoms include umbilical cord bleeding, mucosal bleeding, severe soft-tissue hematomas, and hemarthroses (Peyvandi et al., 1998a). One-stage PT-based FX assays are sufficient for diagnosis, although additional assays are commercially available. Before the diagnosis of an inherited deficiency is made, it is important to rule out a vitamin K deficiency or other acquired causes for the FX deficiency. For example, FX deficiency is the most common factor deficiency associated with primary amyloidosis, occurring in less than 10% of patients and probably due to adsorption of FX onto amyloid fibrils (Uprichard & Perry, 2002). Factor X concentrates are available in some countries in Europe. Bleeding can also be treated with prothrombin complex concentrates, fresh frozen plasma, and recombinant FVIIa (Boggio & Green, 2001). The half-life of factor X (40–60 hours) may require daily treatment or continuous infusion to keep FX levels above 20%.

Combined Deficiency of FV and FVIII

Combined FV and FVIII deficiency is a rare autosomal-recessive disorder that results from a single gene defect rather than from coinheritance

of defects in both FV and FVIII genes. This defect of the endoplasmic reticulum results in impaired transport of both FV and FVIII from the intracellular site of synthesis. Patients typically have FV and FVIII levels between 5% and 30%, their bleeding phenotype is mild to moderate, and it is weakly related to the factor level activity. In two-thirds of patients, this results from the null expression of LMAN1 (previously known as ERGIC-53) (Nichols et al., 1998). LMAN1 shuttles between the endoplasmic reticulum and the Golgi and is believed to facilitate protein trafficking through the secretion pathway (Zhang et al., 2003). Other patients have a mutation of *MCFD2*, which directly interacts with LMAN1 (Zhang et al., 2003). Bleeding manifestations include epistaxis, easy bruising, menorrhagia, and postpartum hemorrhage, as well as bleeding following surgery, dental extraction, and trauma (Seligsohn et al., 1982; Peyvandi et al., 1998b). Testing usually demonstrates disproportionate prolongation of the PTT compared with the PT. Replacement therapy is usually reserved for surgical, traumatic, or gynecologic bleeding (Mumford et al., 2014). It includes both FVIII concentrates and fresh frozen plasma (as a source of FV).

Combined Deficiency of Vitamin K–Dependent Clotting Factors

Vitamin K–dependent clotting factor deficiency affecting multiple vitamin K–dependent coagulation (II, VII, IX, and X) and anticoagulant (protein S and protein C) factors occurs with vitamin K deficiency and hepatic dysfunction. It also results from heritable dysfunction of hepatic enzyme γ-glutamyl carboxylase (type I) or the vitamin K epoxide reductase enzyme complex (type II) (Brenner et al., 1998; Zhang & Ginsburg, 2004). Severely affected individuals may present as neonates with fatal hemorrhages, umbilical stump bleeding, or spontaneous intracranial hemorrhage; in infancy or early childhood with hemarthroses, soft-tissue hematomas, or gastrointestinal hemorrhages; or as adults with easy bruising, mucosal bleeding, and bleeding following surgery. Diagnosis is established by the prolongation of both APTT and PT and associated reductions in levels of vitamin K–dependent clotting factors. These patients may respond to vitamin K (oral or parenteral) supplementation with normalization of APTT, PT, and factor levels, as well as the resolution of bleeding symptoms. This makes the establishment of a diagnosis of an inherited abnormality difficult in that other acquired causes of vitamin K deficiency (hemorrhagic disease of the newborn, liver disease, and prolonged use of broad-spectrum antibiotics) or factitious warfarin administration could manifest similarly. For patients who do not respond fully to vitamin K administration, fresh frozen plasma can be used for acute bleeding or surgery. In addition, prothrombin complex concentrates and combination therapy and vitamin K supplementation may constitute alternative treatment options (Napolitano et al., 2010).

Disorders with Normal APTT and Prolonged PT

FVII Deficiency

FVII deficiency is the most common rare hereditary coagulation factor deficiency (Mariani & Bernardi, 2009). The bleeding manifestations are variable, with epistaxis, mucosal bleeding, and menorrhagia commonly reported (Peyvandi et al., 1997). Severe FVII deficiency is autosomal recessive, often presenting shortly after birth, and may have a dramatic presentation with intracranial hemorrhage in 15% to 60% of cases (Ragni et al., 1981). The diagnosis is suspected with the finding of isolated prolongation of PT. However, FVII, a vitamin K–dependent clotting factor, is low in the newborn period and will also be low in the presence of vitamin K deficiency. Therefore, the reevaluation of infants with mild deficiencies is required after they reach a few months of age or after vitamin K replacement in older patients. Functional FVII activity is measured by a PT-based, FVII-deficient plasma coagulant assay. The use of recombinant human thromboplastin will yield results that are more likely to reflect in vivo FVII levels. Samples for FVII testing should not be stored at 4°C, as this can lead to cold activation of FVII as a result of C1 inhibitor inactivation and FXIIa formation in the tube with FVII activation (Kitchen et al., 1992). Cold activation of FVII results in an overestimation of the actual plasma FVII level. Therapeutic options include recombinant FVIIa (15–20 μg/kg), fresh frozen plasma, or 4-factor prothrombin complex concentrates. For major surgery, plasma FVII levels of at least 20% are sufficient (Bolton-Maggs et al., 2004).

Disorders with Normal APTT and PT

FXIII Deficiency

Factor XIII stabilizes and cross-links fibrin (Hsieh & Nugent, 2008). Factor XIII deficiency can determine delayed bleeding, usually 24 to 36 hours after surgery or trauma; spontaneous bleeding also occurs. Coagulation assays such as PT, PTT, and TT are normal. A reduced plasma factor XIII activity, determined with an immunoassay for factor XIII, leads to the diagnosis. Clot dissolution in 5M urea or monochloroacetic acid is useful for the diagnosis (Lorand et al., 1980), but these assays are not standardized and have low sensitivity. More robust quantitative activity assays are based on cross-linking of glycine–ethyl ester into a specific peptide (Fickenscher et al., 1991), incorporation of an amine substrate into fibrinogen (Kohler et al., 1998), or incorporation of a biotinylated peptide to spermine attached to microtiter plates (Hitomi et al., 2009).

Testing for FXIII deficiency is suggested for individuals with a positive bleeding history, particularly with features such as delayed bleeding, umbilical stump bleeding, or miscarriage, in which the PT and APTT are normal (Anwar & Miloszewski, 1999). Of severely FXIII-deficient patients, 30% die in middle age from spontaneous intracerebral hemorrhage unless they are receiving prophylactic therapy (Lorand et al., 1980). Acquired deficiency of FXIII has been described in a variety of diseases, including Henoch-Schönlein purpura, isoniazid treatment for tuberculosis, various forms of colitis, erosive gastritis, and some forms of leukemia (Board et al., 1993), although FXIII level determination and therapeutic management are controversial. The half-life of FXIII is very long; thus, replacement with cryoprecipitate is usually sufficient for most patients. Plasma-derived and recombinant FXIII concentrates are currently commercially available (Dorey, 2014).

Hereditary Hemorrhagic Disorders of Fibrinolysis

Hereditary bleeding disorders resulting from excessive fibrinolysis are rare. α_2-Antiplasmin deficiency determines enhanced plasmin activity and fibrinolysis (Fay et al., 1992; Aoki et al., 1980). Patients typically present with delayed bleeding. Measurement of α_2-antiplasmin with either immunologic or functional assays leads to the diagnosis. Plasma transfusion and oral fibrinolysis inhibitors can control bleeding episodes and enable surgical procedures.

Acquired α_2-antiplasmin deficiency has been described in amyloidosis, DIC, acute promyelocytic leukemia malignancies, severe liver disease (impaired synthesis), nephrotic syndrome (increased renal excretion), abdominal aortic aneurysm, and following the administration of thrombolytic agents (Okajima et al., 1994). Although not recommended for routine use as a screening test, the whole-blood clot lysis time can be helpful as a first-order test to detect deficiencies of α_2-antiplasmin. In brief, whole blood is allowed to clot; then, the time to clot lysis is recorded. In normal individuals, the presence of α_2-antiplasmin effectively prevents lysis from occurring in this in vitro setting, even 24 hours after initial clot formation. In contrast, in the presence of a severe deficiency of α_2-antiplasmin or in some fibrinolytic states, clot lysis can be observed after several hours. In such instances, follow-up testing specific for the α_2-antiplasmin activity should be employed. Also, a euglobulin lysis time (ELT) can evaluate the global function of the fibrinolytic system. Plasma is admixed with dilute acid to precipitate a plasma fraction relatively rich in plasminogen activator, plasminogen (euglobulin fraction), and fibrinogen but relatively poor in antiplasmins. This euglobulin fraction is then redissolved in the buffer and clotted by recalcification; the time for clot lysis is then measured. Euglobulin clot lysis is normally complete in 2 to 5 hours, but the time may be shortened with increased fibrinolysis associated with the increased plasminogen activator activity. A shortened ELT is an expression of a hyperfibrinolytic state; also, it can be adopted to rule out acquired disorders such as DIC. Plasminogen activator, plasminogen, and plasminogen activator inhibitor may be assayed directly.

ACQUIRED COAGULATION DISORDERS

Acquired bleeding disorders are due to anticoagulation, DIC, liver disease, vitamin K deficiency, massive transfusion, and specific inhibitors of coagulation proteins. The topic of anticoagulation is addressed extensively in Chapter 43. In general, prolongations of PT and APTT arising in a patient should raise the possibility, as discussed in the following sections, of anticoagulants, DIC, liver disease, vitamin K deficiency, and massive transfusion. Only after these clinical states have been excluded should attention be directed to specific protein defects influencing PT and PTT.

DISSEMINATED INTRAVASCULAR COAGULATION (DIC)

DIC is a clinicopathologic syndrome in which activation of the coagulation and fibrinolysis systems results in the simultaneous formation of thrombin and plasmin with the consumption of coagulation factors and inhibitors of

TABLE 40.6

ISTH Diagnostic Scoring System for DIC

Risk assessment: Does the patient have an underlying disorder known to be associated with overt DIC?

- If yes, proceed.
- If not, do not use this algorithm.

Order global coagulation tests (PT, platelet count, fibrinogen, D-dimer)

Score the test results:

- Platelet count (>100 k/μL = 0, <100 k/μL = 1, <50 k/μL = 2)
- Elevated D-dimer (<0.4 μg/mL = 0, 0.4–4.0 μg/mL = 2, >4.0 μg/mL = 3)
- Prolonged PT (<3 sec = 0, >3 sec but <6 sec = 1, >6 sec = 2)
- Fibrinogen level (>100 mg/dL = 0, <100 mg/dL = 1)

Calculate score:

- If ≥5, compatible with overt DIC: Repeat score daily.
- If <5, suggestive (not affirmative) for nonovert DIC: Repeat next 1–2 days.

DIC, Disseminated intravascular coagulation; *ISTH,* International Society on Thrombosis and Haemostasis; *PT,* prothrombin time.
Note that in this example of score implementation, a D-dimer test having an upper normal limit of 0.4 μg/mL was employed. More generally, for the particular analyte employed as an "elevated fibrin marker," no increase = 0, moderate increase = 2, and strong increase = 3.

the system. There are a few scoring systems for DIC diagnosis; however, they often are not used in clinical practice, probably due to poor sensitivity and specificity as well as reproducibility in daily practice (Iba et al., 2019, Yamazaki et al., 2019) (Table 40.6).

These changes result in the clinical features of usually widespread bleeding (especially from puncture sites, wounds, and surgical sites) and laboratory findings of prolonged PT, APTT, decreased fibrinogen, elevated D-dimers, and thrombocytopenia. The peripheral blood smear examination may show microangiopathic hemolytic anemia (MHA) with schistocytes and helmet cells in both acute and chronic DIC. However, the absence of MHA does not exclude DIC. DIC can be an acute, life-threatening, or chronic clinical condition depending on the underlying cause. Identifying DIC and the underlying condition responsible for it are critical to adequate management.

DIC can occur in patients with sepsis, malignancy, obstetric complications, or massive tissue injury (Schmaier, 1991). DIC can also arise during surgery as a result of the release of thromboplastin material. In circulatory arrest operations on the arch of the aorta or the main pulmonary arteries, DIC is a frequent complication related to hypothermia induced in the patient and tissue destruction. Abruptio placentae, placenta previa, amniotic fluid embolism, and HELLP syndrome (hemolysis, elevated liver enzymes, and low platelets) are associated with acute hemorrhagic DIC, whereas the retained dead fetus is associated with a DIC that is not hemorrhagic but rather prothrombotic. DIC with sepsis is most commonly seen with gram-negative infection but can occur with gram-positive infection and in the immunosuppressed patient with fungemia.

This clinical laboratory phenotype of DIC most probably results from a hyperfibrinolytic state and is the form of DIC most commonly recognized. A prothrombotic state as the result of DIC is usually associated with normal PT, normal to shortened APTT due to high FVIII with mildly reduced platelet count and normal or elevated fibrinogen (acute-phase effect, like FVIII). The D-dimers are elevated.

Management of DIC

The treatment of the underlying cause often results in the resolution of DIC. The practice of using plasma, platelets, or cryoprecipitate to correct an abnormal coagulation test parameter in a nonbleeding patient can result in worsening of the clinical condition due to exacerbation of microthromboses as a result of the "adding fuel to the fire" effect. Therefore, in a nonbleeding patient with only laboratory evidence of DIC, a low-dose heparin (3–5 IU/kg/hour) may help to neutralize thrombin and, thus, downregulate the DIC process. This effect is often observed as improved platelet count and fibrinogen value, and gradual improvement of PT and APTT—of course, treatment of the underlying cause is imperative. In a patient with acute DIC and bleeding, again, control of the underlying cause is essential, along with appropriate use of blood components, including plasma to correct coagulopathy, platelet transfusion to maintain platelet count >20 × 10^9/L and cryoprecipitate to maintain fibrinogen >100 mg/dL.

LIVER DISEASE

Hepatocytes synthesize all coagulation factors except for FVIII and vWF. Therefore, both acute and chronic liver diseases affect laboratory coagulation parameters. Chronic liver disease (cirrhosis) is increasing worldwide due to alcohol, hepatitis C, and other causes. Acute fulminant liver disease is often associated with drugs, viral infection, sepsis, and more.

Cirrhosis

Patients with cirrhosis often have prolonged PT and mild to moderate thrombocytopenia. Cirrhotic patients have been shown to have rebalanced hemostasis, in which, despite abnormal coagulation parameters, they have normal hemostasis with no excessive bleeding tendency (Tripodi & Mannucci, 2011). Large epidemiologic studies have demonstrated that cirrhotics have double the incidence of DVT/PE and portal vein thrombosis than the general population (Ambrosino et al., 2017; Mancusio, 2016). Most bleeding in cirrhosis is associated with increased portal pressure causing variceal bleeding—that is, surgical rather than coagulopathic bleeding—that responds to surgical intervention and not to blood component transfusion to correct laboratory values. Blood components increase portal pressure further, leading to worsening of variceal bleeding and harm to the patients.

Rebalanced Primary Hemostasis

Cirrhotics have mild to moderate thrombocytopenia, which is multifactorial, including splenomegaly, decreased thrombopoietin (TPO), bone marrow suppression due to nutritional deficiency, or infection. However, there are extremely high levels of vWF with increasing severity of cirrhosis from Child-Pugh stage A to C with mean vWF being two- to fourfold that of normal (300%–600%). This increased vWF improves the adhesive function of platelets manyfold and, thus, normalizes primary hemostasis. A randomized clinical trial using eltrombopag (a TPO mimetic) was discontinued due to higher portal vein thrombosis in the treatment arm compared with placebo, suggesting that cirrhotics do not need platelet counts >50 K for surgical hemostasis (Afdhal et al., 2012).

Also, platelet transfusions often fail to increase platelet count due to sequestration in the enlarged spleen within minutes of the transfusion. Multiple platelet transfusions are detrimental due to the presence of ~300 cc of plasma in each dose of platelet that further increases portal pressure; the resulting bleeding is often attributed to thrombocytopenia instead.

Rebalanced Secondary Hemostasis

The liver makes both procoagulants and natural anticoagulants. However, routine coagulation tests, PT/INR, and APTT reflect only decreased procoagulants and not the decreased natural anticoagulants (AT, PC, and PS). The cirrhotic plasma in the presence of thrombomodulin generates the same amount of thrombin as normal plasma despite an INR >3, reflecting rebalanced secondary hemostasis (Tripodi et al., 2005). The viscoelastic measurements with TEG/ROTEM often show normal reaction time/clotting time (R/CT) values despite very long PT/INR (De Pietri et al., 2016). TEG/ROTEM should not be used routinely other than for R/CT parameters because both MA and MCF are usually lower than normal due to thrombocytopenia. Primary hemostasis is rebalanced in-vivo and does not reflect in MA/MCF due to absence of endothelium in the system.

Thus, it is futile to attempt correction of mild to moderately prolonged PT/INR (1.5–2.5). If the PT/INR is prolonged >2.5, it could be due to vitamin K deficiency and/or hypo/dysfibrinogenemia, which is observed in up to 30% to 45% of cirrhotics. Many patients with cirrhosis have fibrinogen <100 mg/dL; hence, fibrinogen should be routinely measured if the patient is scheduled for a high-risk procedure or has nonvariceal bleeding. Hypo/dysfibrinogenemia should be treated with cryoprecipitate.

Rebalanced Fibrinolytic System

Plasminogen and α_2-antiplasmin are reduced, but endothelial-derived tPA and PAI-I are increased; therefore, fibrinolysis is also rebalanced. Usually, patients with end-stage cirrhosis may exhibit hyperfibrinolysis with large ecchymoses and severe hypofibrinogenemia. These patients may benefit from antifibrinolytics along with cryoprecipitate.

VITAMIN K DEFICIENCY

Vitamin K, a lipid-soluble vitamin, is provided by dietary intake of leafy green vegetables and by the synthesis of intestinal flora. In clinical practice, vitamin K deficiency is seen most often in acutely ill patients on antibiotics who have subsisted on parenteral nutrition. Not infrequently, intravenous fluids are not supplemented with vitamin K. After

a few weeks of parenteral nutrition and antibiotic treatment, the patient becomes vitamin K deficient, which is reflected in the gradual increase in PT/INR from the normal at baseline. Vitamin K deficiency can also be seen in patients who have an anatomic bypass of the small intestine, malabsorption, biliary tract obstruction, and, rarely, reduced dietary intake. For example, alcoholics are often vitamin K deficient. Warfarin also inhibits the enzymatic pathway necessary for vitamin K utilization (see Fig. 43.1). Vitamin K has a critical role in the γ-carboxylation reaction of several glutamic acid residues within coagulation factors II, VII, IX, and X and proteins C, S, and Z. This γ-carboxylation is critical for the proteins to bind to cells and phospholipids so that they can participate in physiologic coagulation reactions. Thus, patients will have reduced vitamin K–dependent factors II, VII, IX, and X. If antigen levels of these patients are measured, they will frequently be higher. All such clinical scenarios should be treated with 10 mg intravenous vitamin K in 25 to 50 mL of normal saline slowly infused over 15 to 30 minutes. This approach is both diagnostic and therapeutic, avoiding unnecessary investigations of prolonged PT/INR. The intravenous route is preferred for its rapid onset of action, within 2 to 4 hours, as opposed to oral and subcutaneous routes that have unpredictable absorption.

MASSIVE TRANSFUSION

Massive transfusion is defined as the replacement of more than 1.0 blood volume or at least 10 units of packed red blood cells in 24 hours, usually following major trauma. Trauma-induced coagulopathy (TIC) is unique and still not well understood (Cohen et al., 2017). TIC is not merely either dilutional coagulopathy due to infusion of liters of colloids/crystalloids or red cell transfusions during the transfer from the trauma site to the emergency department (ED) of the hospital nor just massive DIC initiated by the tissue factor released after trauma. TIC exists in addition to these and may involve endothelial perturbation affecting thrombomodulin and activated protein C pathway. The coagulopathy is made worse by hypothermia and acidosis. Therefore, recently, the use of liquid plasma and low titer O whole blood at the trauma site is undergoing clinical trials to improve hemostasis and prevent the onset of coagulopathy. Once the coagulopathy sets in, then it is difficult to catch up with when the patient arrives in the ED. Massive transfusion protocols (MTPs) have been developed to manage such patients by transfusing balanced amounts of various blood components. ROTEM is also used as an algorithmic approach to provide goal-directed transfusion therapy because of the real-time tracings displayed in the OR. Plasma transfusion is indicated when EXTEM CT is prolonged, or transfusion of cryoprecipitate if the FIBTEM shows a low value along with low EXTEM MCF, or transfusion of platelets if low EXTEM MCF is associated with normal FIBTEM. In places where ROTEM is unavailable, MTPs consisting of a red cell:plasma:platelet ratio of 1:1:1 or 2:1:1 are used. Although surgical mishap resulting in massive transfusions during nontrauma surgery may occur, coagulopathy in such a patient is more controlled than trauma. Often, goal-directed transfusion therapy with ROTEM guidance is useful in these circumstances. However, postpartum hemorrhage seems to require a trauma level transfusion strategy, especially regarding fibrinogen levels.

ACQUIRED COAGULATION FACTOR DEFICIENCIES

Rarely, spontaneous autoantibody against coagulation protein can be formed and may present with a bleeding tendency (Kruse-Jarres et al., 2017). The most common of these rare acquired bleeding disorders is acquired hemophilia A (AHA) due to an autoantibody formation against FVIII. The inhibitor is an IgG that binds to FVIII and causes its clearance or inhibits its function, resulting in a severe bleeding tendency that, if not diagnosed promptly and treated, can be fatal. AHA is encountered in two peaks—one in young women during the postpartum period and the second in the elderly (6th–8th decades). Some patients may have an underlying autoimmune disorder; otherwise, it is seen as a primary disorder. Both males and females are affected and present with significant soft-tissue hemorrhage (usually in areas with much adipose tissue), hematuria, and, rarely, joint bleed. These patients have a prolonged APTT with normal PT. In the right clinical setting when there is significant bleeding and the patient has previously normal APTT, a stat FVIII level, especially by the chromogenic method, would establish the diagnosis. If there is no access to stat FVIII assay, then a two-step mixing may be performed to show time- and temperature-dependent inhibitor. FVIII levels are often reduced to single digits or in the teens despite a high-titer inhibitor, suggesting that the assay is probably detecting dissociated FVIII from its IgG inhibitor in vitro. Hemorrhage in these patients is treated with a bypassing agent such as FEIBA or rFVIIa. Recently, emicizumab and recombinant porcine FVIII have been other options. AHA generally responds well to immunosuppression therapy with corticosteroids (1 mg/kg), cyclophosphamide, and rituximab (both low, 100-mg weekly × 4 fixed-dose as well as lymphoma dose, 375 mg/m^2 × 4 weeks) (Aggarwal, 2005). The response to therapy can be monitored with improvement in APTT initially and then FVIII levels, and inhibitor titer twice a month.

FX deficiency is rarely encountered in patients with amyloidosis, in whom the amyloid fibrils selectively adsorb FX from the plasma (Chan & Ogunsile, 2017). In such cases, patients present with bleeding tendencies that are associated with prolonged PT and APTT with normal thrombin time. FX is usually moderate to severely deficient (<5% activity). Plasma infusion, plasma exchange, and nonactivated PCC have been often ineffective because, within minutes of infusion, the amyloid fibrils rapidly adsorb out FX. The best option is to use FEIBA to treat bleeding.

Recombinant human thrombin has mostly replaced bovine thrombin in clinical practice. However, rarely upon exposure to bovine thrombin, a patient may make an antibody against either bovine thrombin or bovine FV that is present as a contaminant in bovine thrombin (Gaava et al., 2016). These antibodies may cross-react with human thrombin or human FV, causing prolonged PT and APTT. Thrombin time is also prolonged with an antibody against bovine thrombin but not with an antibody against FV. A mixing study will support a diagnosis of inhibitor due to incomplete to no correction of prolonged PT/APTT/TT. Most of these patients do not bleed; however, if there is bleeding, they should be treated with corticosteroids that often eliminate the inhibitor(s). These inhibitors are often transient following exposure to some antibiotics. In severe bleeding cases, FEIBA or rFVIIa can be used.

Lupus Anticoagulant

This circulating inhibitor was initially identified in patients with systemic lupus erythematosus (SLE); because it prolonged APTT similarly to heparin, it was called *lupus anticoagulant* (LA). It was initially thought to interact with phospholipids in the coagulation cascade during APTT testing in the test tube. It is triply misnomered because most LAs are (1) found in non-SLE patients, (2) are prothrombotic, and (3) interact with PL bound to a protein moiety such as prothrombin or β_2-glycoprotein I. Between 1960 and 1980, there was no specific diagnostic test for LA. Hence, a mixing study was used to differentiate between factor deficiency and LA as a cause of prolonged APTT. Recently, more specific tests—such as the dilute Russell viper venom test (DRVVT), silica clotting time, and PTT-LA—are available to detect LA (see Chapter 42). Hence, they should be used to identify the cause of prolonged APTT in a nonbleeding or thrombotic patient because a weak LA with mildly prolonged APTT will show complete correction on mixing study, leading to unnecessary investigation of factor deficiency in the intrinsic pathway (Pengo, 2009). The sensitivity of each APTT reagent for LA depends on its PL content. Some patients with a strong LA may also have prolonged PT/INR that should be recognized at the beginning of VKA therapy because such patients should be monitored with chromogenic FX rather than INR for proper anticoagulation therapy.

Rarely, patients with a very strong LA may also have an autoantibody against prothrombin, causing very prolonged PT and APTT. These patients with "lupus anticoagulant and hypoprothrombinemia syndrome" generally have severe prothrombin deficiency, and present with significant clinical bleeding rather than clotting despite the presence of LA. Most of these patients are children, who respond well to corticosteroids. The bleeding should be managed with PCC.

SELECTED REFERENCES

Adcock DM, Kressin DC, Marlar RA: Minimum specimen volume requirements for routine coagulation testing: dependence on citrate concentration, *Am J Clin Pathol* 109:595–599, 1998.

A seminal paper that describes the importance of an appropriate volume of blood to anticoagulant ratio to avoid fallacies of testing.

Cohen MJ, Christie SA: Coagulopathy of trauma, *Crit Care Clin* 33(1):101–118, 2017.

An important paper that describes the unique coagulopathy of trauma.

Gailiani D, Broze G: Factor XI activation in a revised model of blood coagulation, *Science* 253:909–912, 1991.

Classic paper that presents for the first time the modern view of assembly and interaction of proteins of the coagulation system.

Iba T, Levy JH, Yamakawa K, et al.: Scientific and Standardization Committee on DIC of the international society on thrombosis and haemostasis, *J Thromb Haemost* 17(8):1265–1268, 2019.

An important paper describing the ISTH recommendations on DIC.

Marder VJ, Budzynski AZ, Barlow GH: Comparison of the physio-chemical properties of fragment D derivatives of fibrinogen and fragment D-D of cross-linked fibrin, *Biochim Biophys Acta* 427:1–14, 1976.

Classic paper describing the D-dimer.

Mahlangu J, Oldenburg J, Paz-Priel I, et al.: Emicizumab prophylaxis in patients who have hemophilia A without inhibitors, *N Engl J Med* 379(9):811–822, 2018.

Article describing an important advancement in the management of hemophila A.

Pengo V, Tripodi A, Reber G, et al.: Update of the guidelines for lupus anticoagulant detection. Subcommittee on lupus anticoagulant/Antiphospholipid antibody of the Scientific and Standardisation Committee of the international society on thrombosis and haemostasis, *J Thromb Haemost* 7:1737, 2009.

An important paper on diagnostic criteria for lupus anticoagulant.

Proctor RR, Rapaport SI: The partial thromboplastin time with kaolin: a simple screening test for first stage plasma clotting factor deficiencies, *Am J Clin Pathol* 36:212–219, 1961.

Description of activated partial thromboplastin time.

Shariat-Madar Z, Mahdi F, Schmaier AH: Identification and characterization of prolylcarboxypeptidase as an endothelial cell prekallikrein activator, *J Biol Chem* 277:17962–17969, 2002.

Paper that identifies a physiologic activator of the plasma kallikrein/kinin system, the so-called contact activation system.

Tripodi A, Mannucci PM: The coagulopathy of chronic liver disease, *N Engl J Med* 365:147–156, 2011.

An excellent paper describing rebalanced hemostasis in cirrhosis.

Yates SG, Fitts E, De Simone N, Sarode R: Prolonged activated partial yhromboplastin time: to mix or not to mix—is that the question? *Transfus Apher Sci* 58(1):39–42, 2019.

An important paper describing fallacies of routine mixing studies for prolonged activated partial thromboplastin time.

Access the complete reference list online at Elsevier eBooks for Practicing Clinicians.

REFERENCES

Adcock DM, Kressin DC, Marlar RA: Minimum specimen volume requirements for routine coagulation testing: dependence on citrate concentration, *Am J Clin Pathol* 109:595–599, 1998.

Afdhal NH, Giannini EG, Tayyab G, et al.: Eltrombopag before procedures in patients with cirrhosis and thrombocytopenia, *N Engl J Med* 23;367(8):716–24, 2012.

Aggarwal A, Grewal R, Green RJ, et al.: Rituximab for autoimmune haemophilia: a proposed treatment algorithm, *Haemophilia* 11:13–19, 2005.

Agren A, Wikman AT, Holmstrom M, et al.: Thromboelastography (TEG(R)) compared to conventional coagulation tests in surgical patients—a laboratory evaluation, *Scand J Clin Lab Invest* 73:214–220, 2013.

Andrew M, Vegh P, Johnston M, et al.: Maturation of the hemostatic system during childhood, *Blood* 80:1998–2005, 1992.

Ambrosino P, Tarantino L, Di Minno G, et al.: The risk of venous thromboembolism in patients with cirrhosis, *A systematic review and meta-analysis Thromb Haemost. 5* 117(1):139–148, 2017.

Anwar R, Miloszewski KJ: Factor XIII deficiency, *Br J Haematol* 107:468–484, 1999.

Aoki N, Sakata Y, Matsuda M, et al.: Fibrinolytic states in a patient with congenital deficiency of alpha 2-plasmin inhibitor, *Blood* 55:483–488, 1980.

Ardillon L, Lefrançois A, Graveleau J, et al.: Management of bleeding in severe factor V deficiency with a factor V inhibitor, *Vox Sang* 107(1):97–99, 2014.

Arun B, Kessler CM: Clinical manifestations and therapy of the hemophilias. In Colman RW, Hirsh J, Marder VJ, et al.: *Hemostasis and thrombosis: basic principles and clinical practice*, 4, Philadelphia, 2001, Lippincott-Raven.

Asakai R, Chung DW, Davie EW, et al.: Factor XI deficiency in Ashkenazi Jews in Israel, *N Engl J Med* 325:153–158, 1991.

Barg AA, Rosenberg N, Budnik I, et al.: Prospective controlled monitoring of Hemlibra prophylaxis initiation in a large Cohort of hemophilia a patients:real-world data, *Blood* 134, 2019.

Barnathan ES, Kuo A, van der Keyl H, et al.: Binding of tissue type plasminogen activator to human endothelial cells: evidence for two distinct binding sites, *J Biol Chem* 263:7792–7799, 1988.

Batty P, Lillicrap D: Advances and challenges for hemophilia gene therapy, *Hum Mol Genet* 28(Issue R1):R95–R101, 2019.

Bauduer F, de Raucourt E, Boyer-Neumann C, et al.: French Postmarketing Study Group. Factor XI replacement for inherited factor XI deficiency in routine clinical practice: results of the HEMOLEVEN prospective 3-year postmarketing study, *Haemophilia* 21(4):481–489, 2015.

Blanchette VS, Key NS, Ljung LR, et al.: Definitions in hemophilia: Communication from the SSC of the ISTH, *J Thromb Haemost* 12(11):1935–1939, 2014.

Board PG, Losowsky MS, Miloszewski KJ, et al.: Inherited and acquired deficiency, *Blood Rev* 7:229–242, 1993.

Bockenstedt PL: Laboratory methods in hemostasis. In Loscalzo J, Schafer AI, editors: *Thrombosis and hemorrhage*, 3, Philadelphia, 2003, Lippincott Williams & Wilkins.

Boggio L, Green D: Recombinant human factor VIIa in the management of amyloid-associated factor X deficiency, *Br J Haematol* 112:1074–1075, 2001.

Bolton-Maggs PH, Patterson DA, Wensley RT, et al.: Definition of the bleeding tendency in factor XI–deficient kindreds—a clinical and laboratory study, *Thromb Haemost* 73:194–202, 1995.

Bolton-Maggs PH, Perry DJ, Chalmers EA, et al.: The rare coagulation disorders—review with guidelines for management from the United Kingdom Haemophilia Centre Doctors' Organisation, *Haemophilia* 10:593–628, 2004.

Bolton-Maggs PH, Young Wan-Yin B, McCraw AH, et al.: Inheritance and bleeding in factor XI deficiency, *Br J Haematol* 69:521–528, 1988.

Bouchard BA, Chapin J, Brummel-Ziedins KE, et al.: Platelets and platelet-derived factor Va confer hemostatic competence in complete factor V deficiency, *Blood* 125(23):3647–3650, 2015.

Brenner B, Laor A, Lupo H, et al.: Bleeding predictors in factor-XI–deficient patients, *Blood Coagul Fibrinolysis* 8:511–515, 1997.

Brenner B, Sanchez-Vega B, Wu SM, et al.: A missense mutation in gamma-glutamyl carboxylase gene causes combined deficiency of all vitamin K–dependent blood coagulation factors, *Blood* 92:4554–4559, 1998.

Büller HR, Bethune C, Bhanot S, et al.: Factor XI antisense oligonucleotide for prevention of venous thrombosis, *N Engl J Med* 372:232–240, 2015.

Burstyn-Cohen T, Heeb MJ, Lemke G: Lack of protein S in mice causes embryonic lethal coagulopathy and vascular dysgenesis, J Clin Invest 119:2942–2953

Caplice NM, Panetta C, Peterson TE, et al.: Lipoprotein (a) binds and inactivates tissue factor pathway inhibitor: a novel link between lipoproteins and thrombosis, *Blood* 98(10):2980–2987, 2001.

Cesarman GM, Guevara CA, Hajjar KA: An endothelial cell receptor for plasminogen/tissue plasminogen activator (t-PA). II. Annexin II–mediated enhancement of t-PA–dependent plasminogen activation, *J Biol Chem* 269:21198–21203, 1994.

Chafa O, Chellali T, Sternberg C, et al.: Severe hypofibrinogenemia associated with bilateral ischemic necrosis of toes and fingers, *Blood Coagul Fibrinolysis* 6:549–552, 1995.

Chan IS, Ogunsile FJ: An acquired factor X inhibitor: the importance of understanding coagulation, *Am J Med* 130(7):e307–e308, 2017.

Colman RW, Bagdasarian A, Talarnos RC, et al.: Williams trait: human kininogen deficiency with diminished levels of plasminogen proactivator and prekallikrein associated with abnormalities of the Hageman factor–dependent pathways, *J Clin Invest* 56:1650–1662, 1975.

Cohen MJ, Christie SA: Coagulopathy of trauma, *Crit Care Clin* 33(1):101–118, 2017.

Coughlin SR: Thrombin signaling and protease-activated receptors, *Nature* 407:258–264, 2000.

Cozzi MR, Guglielmini G, Battiston M, et al.: Visualization of nitric oxide production by individual platelets during adhesion in flowing blood, *Blood* 125(4):697–705, 2015.

Crawley JTB, Lane DA: The haemostatic role of tissue factor pathway inhibitor, *Arterioscler Thromb Vasc Biol* 28:233–242, 2008.

Crossley M, Ludwig M, Stowell KM, et al.: Recovery from hemophilia B Leyden: an androgen-responsive element in the factor IX promoter, *Science* 257:377–379, 1992.

Cui J, O'Shea KS, Purkayastha A, et al.: Fatal haemorrhage and incomplete block to embryogenesis in mice lacking coagulation factor V, *Nature* 384:66–68, 1996.

Del Zoppo GJ: Bleeding in the brain: amyloid-β may keep clots away, *Nat Med* 15:1132–1133, 2009.

de Moerloose P, Casini A, Neerman-Arbez M: Congenital fibrinogen disorders: an update, *Semin Thromb Hemost* 39(6):585–595, 2013.

De Pietri L, Bianchini M, Montalti R, et al.: Thrombelastography-guided blood product use before invasive procedures in cirrhosis with severe coagulopathy: a randomized, *Controlled trial.Hepatology* 63(2):566–73, 2016.

Dewerchin M, Liang Z, Moons L, et al.: Blood coagulation factor X deficiency causes partial embryonic lethality and fatal neonatal bleeding in mice, *Thromb Haemost* 83:185–190, 2000.

Doolittle RF: Fibrinogen and fibrin, *Sci Am* 245:126–135, 1981.

Dorey E: First recombinant factor XIII approved, *Nat Biotechnol* 32(3):210, 2014.

Draxler DF, Medcalf RL: The fibrinolytic system—more than fibrinolysis? *Transfus Med Rev* 29(2):102–109, 2015.

Dupuy E, Soria C, Molho P, et al.: Embolized ischemic lesions of toes in an afibrinogenemic patient: possible relevance to in vivo circulating thrombin, *Thromb Res* 102:211–219, 2001.

Eckhardt CL, van Velzen AS, Peters M, et al.: Factor VIII gene (F8) mutation and risk of inhibitor development in nonsevere hemophilia A, *Blood* 122:1954–1962, 2013.

Emsley J, Mcewan PA, Gailani D: Structure and function of factor XI, *Blood* 115:2569–2577, 2010.

Esmon CT: The endothelial protein C receptor, *Curr Opin Hematol* 13:382, 2006.

Esmon CT: Endothelial protein C receptor, *Thromb Haemost* 82:251–258, 1999.

Esmon CT, Owen WG: Identification of an endothelial cell cofactor for thrombin—Catalytic activation of protein C, *Proc Natl Acad Sci U S A* 78:2249–2252, 1981.

European Medicines Agency (EMA): *Workshop report: Characterisation of new clotting factor concentrates (FVIII, FIX) with respect to potency assays used for labelling and testing of post infusion samples. Human Medicines Development and Evaluation*, 26 June 2014. EMA/135928/2014.

Fay WP, Shapiro AD, Shih JL, et al.: Brief report: complete deficiency of plasminogen-activator inhibitor type 1 due to a frame-shift mutation, *N Engl J Med* 327:1729–1733, 1992.

Fickenscher K, Aab A, Stuber W: A photometric assay for blood coagulation factor XIII, *Thromb Haemost* 65:535–540, 1991.

Finigan JH, Dudek SM, Singleton PA, et al.: Activated protein C mediates novel lung endothelial barrier enhancement: role of sphingosine 1-phosphate receptor transactivation, *J Biol Chem* 280:17286–17293, 2005.

Fried K, Kaufman S: Congenital afibrinogenemia in 10 offspring of uncle–niece marriages, *Clin Genet* 17:223–227, 1980.

Funk C, Gmür J, Herold R, et al.: Reptilase-R—a new reagent in blood coagulation, *Br J Haematol* 21:43–52, 1971.

Furie B: Pathogenesis of thrombosis, *Hematology Am Soc Hematol Educ Program*255–258, 2009.

Furie B, Furie BC: Thrombus formation in vivo, *J Clin Invest* 115:3355–3362, 2005.

Gailani D1, Broze Jr GJ: Factor XI activation in a revised model of blood, *Coagulation* 253(5022):909–912, 1991.

Girolami MT, Hofer CK: Coagulation monitoring: current techniques and clinical use of viscoelastic point-of-care coagulation devices, *Anesth Analg* 106:1366–1375, 2008.

Gawryl MS, Hoyer LW: Inactivation of factor VIII coagulant activity by two different types of human antibodies, *Blood* 60:1103–1109, 1982.

Gavva C, Yates SG, Rambally S: Transfusion management of factor V deficiency: three case reports and review of the literature, *Transfusion* 56(7):1745–1749, 2016.

Girolami A, Simioni P, Scarano L, et al.: Hemorrhagic and thrombotic disorders due to factor V deficiencies and abnormalities: an updated classification, *Blood Rev* 12:5–51, 1998.

Girolami A, Vidal J, Salagh M, et al.: The old and the new in prekallikrein deficiency: Historical context and a family from Argentina with PK deficiency due to a new mutation (Arg541Gln) in exon 14 associated with a common polymorphysm (Asn124Ser) in exon 5, *Semin Thromb Hemost* 40(5):592–599, 2014.

Goodwin TM: Congenital hypofibrinogenemia in pregnancy, *Obstet Gynecol Surv* 44:157–161, 1989.

Graham JB: Genotype assignment (carrier detection) in the haemophilias, *Clin Haematol* 8:115–145, 1979.

Greenberg CS, Lai T-S: Fibrin formation and stabilization. In Loscalzo J, Schafer AI, editors: *Thrombosis and hemorrhage*, 3, Philadelphia, 2003, Lippincott Williams & Wilkins.

Han ED, MacFarlane RC, Mulligan AN, et al.: Increased vascular permeability in C1 inhibitor–deficient mice mediated by the bradykinin type 2 receptor, *J Clin Invest* 109:1057–1063, 2002.

Hanss M, Biot F: A database for human fibrinogen variants, *Ann N Y Acad Sci* 936:89–90, 2001.

Hay CRM, Brown S, Collins PW, et al.: The diagnosis and management of factor VIII and IX inhibitors: a guideline from the United Kingdom Haemophilia Center Doctors Organization, *Br J Haematol* 133:591–605, 2006.

Hayashi M, Matsushita T, Mackman N, et al.: Fatal thrombosis of antithrombin-deficient mice is rescued differently in the heart and liver by intercrossing with low tissue factor mice, *J Thromb Haemost* 4:177–185, 2006.

He L, Pappan LK, Grenache DG, et al.: The contributions of the alpha 2 beta 1 integrin to vascular thrombosis in vivo, *Blood* 102:3652–3657, 2003.

Heemskerk JW, Mattheij NJ, Cosemans JM: Platelet-based coagulation: different populations, different functions, *J Thromb Haemost* 11(1):2–16, 2013.

Hitomi K, Kitamura M, Perez Alea M, et al.: A specific colorimetric assay for measuring transglutaminase 1 and factor XIII activities, *Anal Biochem* 394:281–283, 2009.

Hoffman M, Monroe DM: A cell-based model of hemostasis, *Thromb Haemost* 85(6):958–965, 2001.

Hong SL: Effect of bradykinin and thrombin on prostacyclin synthesis in endothelial cells from calf and pig aorta and human umbilical cord vein, *Thromb Res* 18:787–795, 1980.

Hsieh L, Nugent D: Factor XIII deficiency, *Hemophilia* 14:1190–1200, 2008.

Huang Z-F, Higuchi D, Lasky N, et al.: Tissue factor pathway inhibitor gene disruption produces intrauterine lethality in mice, *Blood* 90:944–951, 1997.

Iba T, Levy JH, Yamakawa K, et al.: Scientific and Standardization Committee on DIC of the international society on thrombosis and haemostasis, *J Thromb Haemost*(8)1265–1268, 2019.

Ivanciu L, Krishnaswamy S, Camire RM: New insights into the spatiotemporal localization of prothrombinase in vivo, *Blood* 124:1705–1714, 2014.

Jalbert LR, Rosen ED, Moons L, et al.: Inactivation of the gene for anticoagulant protein C causes lethal perinatal consumptive coagulopathy in mice, *J Clin Invest* 102:1481–1488, 1998.

Johansson PI, Stissing T, Bochsen L, et al.: Thrombelastography and tromboelastometry in assessing coagulopathy in trauma, *Scand J Trauma Resusc Emerg Med* 17:45, 2009.

Kasper CK, Aledort L, Counts RB, et al.: A more uniform measurement of factor VIII inhibitors, *Thromb Diath Haemorrh* 34:869–872, 1975.

Kaufman RJ, Antonarakis SE, Fay PJ, et al.: Factor VIII and hemophilia A. In Colman RW, Hirsh J, Marder VJ, et al.: *Hemostasis and thrombosis*, 4, Philadelphia, 2001, Lippincott Williams & Wilkins, pp 135–156.

Kenet G, Lubetsky A, Luboshitz J, et al.: Lower doses of rFVIIa therapy are safe and effective for surgical interventions in patients with severe FXI deficiency and inhibitors, *Haemophilia*(5)1065–1073, 2009.

Kessler CM, Hoyer L, Feinstein DI: The hemophilias. In McArthur JR, Schechter GP, editors: *Hematology: the educational program of the American society of Hematology*, Washington, DC, 1996, American Society of Hematology, pp 95–105.

Kitchen S, Malia RG, Preston FE: A comparison of methods for the measurement of activated factor VII, *Thromb Haemost* 68:301–305, 1992.

Kobayashi T, Kanayama N, Tokunaga N, et al.: Prenatal and peripartum management of congenital afibrinogenaemia, *Br J Haematol* 109:364–366, 2000.

Kohler HP, Ariens RA, Whitaker P, et al.: A common coding polymorphism in the FXIII α-subunit gene (FXIIIVal34Leu) affects cross-linking activity, *Thromb Haemost* 80:704, 1998.

Kruse-Jarres R, Kempton CL, Baudo F, et al.: Acquired hemophilia A: updated review of evidence and treatment guidance, *Am J Hematol* 92(7):695–705, 2017.

Labarque V, Perinparajah V, Bouskill V, et al.: Utility of factor VIII and factor VIII to von Willebrand factor ratio in identifying 277 unselected carriers of hemophilia A, *Am J Hematol* 92:E94–E96, 2017.

Lak M, Keihani M, Elahi F, et al.: Bleeding and thrombosis in 55 patients with inherited afibrinogenaemia, *Br J Haematol* 107:204–206, 1999.

Lakich D, Kazazian H, Antonarakis SE, et al.: Inversions disrupting the factor VIII gene are a common cause of severe hemophilia A, *Nat Genet* 5:236–241, 1993.

LaRusch GA, Mahdi F, Shariat-Madar Z, et al.: Factor XII stimulates ERK1/2 and Akt through uPAR, integrins, and the EGFR to initiate angiogenesis, *Blood* 115:5111–5120, 2010.

Lawrie AS, Kitchen S, Purdy G, et al.: Assessment of actin FS and actin FSL sensitivity to specific clotting factor deficiencies, *Clin Lab Haematol* 20:179–186, 1998.

Leiba H, Ramot B, Many A: Heredity and coagulation studies in ten families with factor XI (plasma thromboplastin antecedent) deficiency, *Br J Haematol* 11:654–665, 1965.

Leurs J, Hendriks D, Carboxypeptidase U, TAFIa): A metallocarboxypeptidase with a distinct role in haemostasis and a possible risk factor for thrombotic disease, *Thromb Haemost* 94:471–487, 2005.

Liang Y, Fu Y, Qi R, et al.: Cartilage oligomeric matrix protein is a natural inhibitor of thrombin, *Blood* 126:905–914, 2015.

Ling G, Kagdi H, Subel B, et al.: Safety and efficacy of factor XI (FXI) concentrate use in patients with FXI deficiency: a single-centre experience of 19 years, *Haemophilia* 22(3):411–418, 2016.

Ljung RCR: Prenatal diagnosis of haemophilia, *Haemophilia* 5:84–87, 1999.

Lorand L, Losowsky MS, Miloszewski KJM: Human factor XIII: fibrin-stabilizing factor. In Spaet TH, editor: *Progress in hemostasis and thrombosis*, New York, 1980, Grune and Stratton, pp 245–249.

Luna-Zaizar H, Esparza-Flores MA, Lopez-Guido B, et al.: Kinetics of factor VIII: C inhibitors and treatment response in severe hemophilia patients, *Int J Lab Hematol* 31:673–682, 2009.

Maas C, Govers-Riemslag JW, Bouma B, et al.: Misfolded proteins activate factor XII in humans, leading to kallikrein formation without initiating coagulation, *J Clin Invest* 118:3208–3218, 2008.

MacFarland D: An enzyme cascade in the blood clotting mechanism, and its functions as a biochemical amplifier, *Nature* 202:498–499, 1964.

Mahlangu J, Oldenburg J, Paz-Priel I, et al.: Emicizumab prophylaxis in patients who have hemophilia A without inhibitors, *N Engl J Med* 379(9):811–822, 2018.

Mahdi F, Rehemtulla A, Van Nostrand WE, et al.: Protease nexin-2/amyloid β-protein precursor regulates factor VIIa and the factor VIIa–tissue factor complex, *Thromb Res* 99:267–276, 2000.

Mahdi F, Van Nostrand WE, Schmaier AH: Protease nexin-2/amyloid β-protein precursor inhibits factor Xa in the prothrombinase complex, *J Biol Chem* 270:23468–23474, 1995.

Manco-Johnson MJ, Abshire TC, Shapiro AD, et al.: Prophylaxis versus episodic treatment to prevent joint disease in boys with severe hemophilia, *N Engl J Med* 357:535–544, 2007.

Mann KG: Thrombin formation, *Chest* 124:4S–10S, 2003.

Mancuso A: Management of portal vein thrombosis in cirrhosis: an update, *Eur J Gastroenterol Hepatol* 28(7):739–743, 2016.

Mannucci PM, Duga S, Peyvandi F: Recessively inherited coagulation disorders, *Blood* 104:1243–1252, 2004.

Mannucci PM, Franchini M: Porcine recombinant factor VIII: an additional weapon to handle anti-factor VIII antibodies, *Blood Transfus* 15(4):365–368, 2017.

Marder VJ, Budzynski AZ, Barlow GH: Comparison of the physicochemical properties of fragment D derivatives of fibrinogen and fragment D-D of cross-linked fibrin, *Biochim Biophys Acta* 18;427(1):1–14, 1976.

Marcum JA, McKenney JB, Rosenberg RD: Acceleration of thrombin-antithrombin complex formation in rat hindquarters via heparinlike molecules bound to endothelium, *J Clin Invest* 74:341–350, 1984.

Marder VJ, Budzynski AZ: Degradation products of fibrinogen and cross-linked fibrin-projected clinical applications, *Thromb Diath Haemorrh* 32:49–56, 1974.

Mariani G, Bernardi F: Factor VII deficiency, *Semin Thromb Hemost* 35:400–406, 2009.

Martinelli RA, Scheraga HA: Steady state kinetic study of the bovine thrombin-fibrinogen interaction, *Biochemistry* 19:2343–2350, 1980.

Meijers JCM, Tekelenburg WL, Bouma BN, et al.: High levels of coagulation factor XI as a risk factor for venous thrombosis, *N Engl J Med* 342:696–701, 2000.

Merkoulov S, Komar AA, Schmaier AH, et al.: Deletion of the murine kininogen gene 1 (mKng1) causes loss of plasma kininogen and delays thrombosis, *Blood* 111:1274–1281, 2008.

Miesbach W, Scharrer I, Henschen A, et al.: Inherited dysfibrinogenemia: clinical phenotypes associated with five different fibrinogen structure defects, *Blood Coagul Fibrinolysis* 21:35–40, 2010.

Miller G, Silberberg M, Kaplan AP: Autoactivability of human Hageman factor, *Biochem Biophys Res Commun* 92:803–810, 1980.

Mitchell JA, Ali F, Bailey L, et al.: Role of nitric oxide and prostacyclin as vasoactive hormones released by the endothelium, *Exp Physiol* 93(1):141–147, 2008.

Mumford AD, Ackroyd S, Alikhan R, et al.: Guideline for the diagnosis and management of the rare coagulation disorders: a United Kingdom haemophilia centre Doctors' Organization guideline on behalf of the British Committee for standards in Haematology, *Br J Haematol* 167(3):304–326, 2014.

Nagoya A, Kaneko M, Kazama, et al.: Discrepancies between the one-stage clotting assay and chromogenic assay in patients with hemophilia A receiving standard or extended half-life factor VIII products in clinical settings, *Thromb Res* 185:150–152, 2019.

Napolitano M, Mariani G, Lapecorella M: Hereditary combined deficiency of the vitamin K–dependent clotting factors, *Orphanet J Rare Dis* 5:21, 2010.

Nawarawong W, Wyshock E, Meloni FJ, et al.: The rate of fibrinopeptide B release modulates the rate of clot formation: a study with an acquired inhibitor to fibrinopeptide B release, *Br J Haematol* 79:296–301, 1991.

Naylor JA, Green PM, Rizza CR, et al.: Factor VIII gene explains all cases of haemophilia A, *Lancet* 340:1066–1067, 1992.

Nichols WC, Seligsohn U, Zivelin A, et al.: Mutations in the ER-Golgi intermediate compartment protein ERGIC-53 cause combined deficiency of coagulation factors V and VIII, *Cell* 93:61–70, 1998.

O'Connell NM, Riddell AF, Pascoe G, et al.: Recombinant factor VIIa to prevent surgical bleeding in factor XI deficiency, *Haemophilia* 14(4):775–781, 2008.

Oldenburg J, Mahlangu JN, Kim B, et al.: Emicizumab prophylaxis in hemophilia A with inhibitors, *N Engl J Med* 377(9):809–818, 2017.

Okajima K, Kohno I, Soe G, et al.: Direct evidence for systemic fibrinogenolysis in patients with acquired alpha-2-plasmin inhibitor deficiency, *Am J Hematol* 45:16–24, 1994.

Osterud B, Rappaport SI: Activation of factor IX by the reaction product of tissue factor and factor VII, *Proc Natl Acad Sci U S A* 74:5260–5264, 1977.

Palmer RMJ, Ferrige AG, Moncada S: Nitric oxide release accounts for the biologic activity of endothelium-derived relaxing factor, *Nature* 327:524–526, 1987.

Pavlova A: Oldenburg J: defining severity of hemophilia: more than factor levels, *Semin Thromb Hemost* 39(7):702–710, 2013.

Pasi KJ, Rangarajan S, Georgiev P, et al.: Targeting of antithrombin in hemophilia A or B with RNAi therapy, *N Engl J Med* 377(9):819–828, 2017.

Pasi KJ, Rangarajan S, Mitchell N, et al.: Multiyear follow-up of AAV5-hFVIII-SQ gene therapy for hemophilia A, *N Engl J Med 2* 382(1):29–40, 2020.

Pengo V, Tripodi A, Reber G, et al.: Update of the guidelines for lupus anticoagulant detection. Subcommittee on lupus anticoagulant/Antiphospholipid antibody of the Scientific and Standardisation Committee of the international society on thrombosis and haemostasis, *J Thromb Haemost* 7:1737, 2009.

Perry DJ: Antithrombin and its inherited deficienciestripodi, *Blood Rev* 8(1):37–55, 1994.

Peyvandi F, Mannucci PM: Rare coagulation disorders, *Thromb Haemost* 82:1207–1214, 1999.

Peyvandi F, Mannucci PM, Asti D, et al.: Clinical manifestations in 28 Italian and Iranian patients with severe factor VII deficiency, *Haemophilia* 3:242–246, 1997.

Peyvandi F, Mannucci PM, Lak M, et al.: Congenital factor X deficiency: spectrum of bleeding symptoms in 32 Iranian patients, *Br J Haematol* 102:626–628, 1998a.

Peyvandi F, Tuddenham EG, Akhtari AM, et al.: Bleeding symptoms in 27 Iranian patients with the combined deficiency of factor V and factor VIII, *Br J Haematol* 100:773–776, 1998b.

Peyvandi F, Mannucci PM, Garagiola I, et al.: A randomized trial of factor VIII and neutralizing antibodies in hemophilia A, *N Engl J Med* 374:2054–2064, 2016.

Pike GN, Cumming AM, Hay CR, et al.: Sample conditions determine the ability of thrombin generation parameters to identify bleeding phenotype in FXI deficiency, *Blood* 126(3):397–405, 2015.

Pinsky DJ, Broekman MJ, Peschon JJ, et al.: Elucidation of the thromboregulatory role of CD39/ectoapyrase in the ischemic brain, *J Clin Invest* 109:1031–1040, 2002.

Plug I, Mauser-Bunschoten EP, Bröcker-Vriends AH, et al.: Bleeding in carriers of hemophilia, *Blood* 108:52–56, 2006.

Ragni MV, Lewis JH, Spero JA, et al.: Factor VII deficiency, *Am J Hematol* 10:79–88, 1981.

Rak J: New checkpoint of the coagulant phenotype, *Blood* 124:3511–3513, 2014.

Rand MD, Lock JB, van't Veer C, et al.: Blood clotting in minimally altered whole blood, *Blood* 88:3432–3445, 1996.

Ratnoff OD, Davies E: Waterfall sequence for intrinsic blood coagulation, *Science* 145:1310–1312, 1964.

Reitsma PH: Genetic principles underlying disorders of procoagulation and anticoagulation proteins. In Colman RW, Hirsh J, Marder VJ, et al.: *Hemostasis and thrombosis: basic principles and clinical practice*, 4, Philadelphia, 2001, Lippincott-Raven.

Renne T, Pozgajova M, Gruner S, et al.: Defective thrombus formation in mice lacking coagulation factor XII, *J Exp Med* 202:271–281, 2005.

Riddell A, Abdul-Kadir R, Pollard D, et al.: Monitoring low dose recombinant factor VIIa therapy in patients with severe factor XI deficiency undergoing surgery, *Thromb Haemost* 106(3):521–527, 2011.

Rosen ED, Chan JCY, Idusogie E, et al.: Mice lacking factor VII develop normally but suffer fatal perinatal bleeding, *Nature* 390:290–294, 1997.

Ruiz-Saez A: Occurrence of thrombosis in rare bleeding disorders, *Semin Thromb Hemost* 39:684–692, 2013.

Saito H, Ratnoff OD, Waldmann R, et al.: Fitzgerald trait: deficiency of a hitherto unrecognized agent, Fitzgerald factor, participating in surface mediated reactions of clotting, fibrinolysis, generation of kinins, and the property of diluted plasma enhancing vascular permeability, *J Clin Invest* 55:1082–1089, 1975.

Salomon O, Zivelin A, Livnat T, et al.: Prevalence, causes, and characterization of factor XI inhibitors in patients with inherited factor XI deficiency, *Blood* 101:4783–4788, 2003.

Schmaier AH: Disseminated intravascular coagulation—Pathogenesis and management, *J Intens Care Med* 6:209–228, 1991.

Schmaier AH: The plasma kallikrein/kinin system counterbalances the renin angiotensin system, *J Clin Invest* 109:1007–1009, 2002.

Schmaier AH: The kallikrein/kinin and the renin angiotensin systems have a multilayered interaction, *Am J Physiol Reg Integr Comp Physiol* 285:R1–R13, 2003.

Schmaier AH: The physiologic basis of assembly and activation of the plasma kallikrein/kinin system, *Thromb Haemost* 91:1–3, 2004.

Schmaier AH, Dahl LD, Hasan AAK, et al.: Factor IXa inhibition by protease nexin-2/amyloid β-protein precursor on phospholipid vesicles and cell membranes, *Biochemistry* 34:1171–1178, 1995.

Schmaier AH, Dahl LD, Rozemuller AJM, et al.: Protease nexin-2/amyloid β-protein precursor: a tight-binding inhibitor of coagulation factor IXa, *J Clin Invest* 92:2540–2545, 1993.

Schneppenheim R, Budde U, Krey S, et al.: Results of a screening for von Willebrand disease type 2N in patients with suspected haemophilia A or von Willebrand disease type 1, *Thromb Haemost* 76:598–602, 1996.

Seligsohn U, Zivelin A, Zwang E: Combined factor V and factor VIII deficiency among non-Ashkenazi Jews, *N Engl J Med* 307:1191–1195, 1982.

Shapiro AD, Paola JD, Cohen A, et al.: The safety and efficacy of recombinant human blood coagulation factor IX in previously untreated patients with severe or moderately severe hemophilia B, *Blood* 105:518–525, 2005.

Shapiro AD, Angchaisuksiri P, Astermark J, et al.: Subcutaneous concizumab prophylaxis in hemophilia A and hemophilia A/B with inhibitors: phase 2 trial results, *Blood* 28(22):134, 2019.

Shariat-Madar Z, Mahdi F, Warnock M, et al.: Bradykinin B2 receptor knockout mice are protected from thrombosis by increased nitric oxide and prostacyclin, *Blood* 108:192–199, 2006.

Smith SA, Travers RJ, Morrissey JH: How it all starts: initiation of the clotting cascade, *Crit Rev Biochem Mol Biol 1*– 11, 2015.

Soucie JM, Miller CH, Kelly FM, et al.: Haemophilia Inhibitor Research Study Investigators: a study of prospective surveillance for inhibitors among persons with haemophilia in the United States, *Haemophilia* 20:230–237, 2014.

Stavrou EX, Fang C, Merkulova A, et al.: Reduced thrombosis on *KLKB1*$^{-/-}$ mice is mediated by increased Mas receptor, prostacyclin, Sirt1 and KLF4 and decreased tissue factor, *Blood* 125:710–719, 2015.

Sun WY, Witte DP, Degen JL, et al.: Prothrombin deficiency results in embryonic and neonatal lethality in mice, *Proc Natl Acad Sci U S A* 95:7597–7602, 1998.

Tracy PB, Eide LL, Bowie EJ, et al.: Radioimmunoassay of factor V in human plasma and platelets, *Blood* 60:59–63, 1982.

Tripodi A, Mannucci PM: The coagulopathy of chronic liver disease, *N Engl J Med* 365:147–156, 2011.

Tripodi A, Salerno F, Chantarangkul V, et al.: Evidence of normal thrombin generation in cirrhosis despite abnormal conventional coagulation tests, *Hepatology* 41(3):553–558, 2005.

Uprichard J, Perry DJ: Factor X deficiency, *Blood Rev* 16:97–110, 2002.

Van der Meijden PEJ, Munnix ICA, Auger JM, et al.: Dual role of collagen in factor XII–dependent thrombus formation, *Blood* 114:881–890, 2009.

Van Nostrand WE, Schmaier AH, Farrow JS, et al.: Protease nexin-II (amyloid β-protein precursor): a platelet α-granule protein, *Science* 248:745–748, 1990.

Van Vulpen LF, Schutgens RE, Coeleveld K, et al.: IL-1β, in contrast to TNFα, is pivotal in blood-induced cartilage damage and is a potential target for therapy, *Blood* 126:2239–2246, 2015.

Vatsyayan R, Kothari H, Mackman N, et al.: Inactivation of factor VIIa by antithrombin in vitro, ex vivo and in vivo: role of tissue factor and endothelial cell protein C receptor, *PloS One* 9(8), 2014. e103505.

Verbruggen B, Novakova I, Wessels H, et al.: The Nijmegen modification of the Bethesda assay for FVIII: C inhibitors—improved specificity and reliability, *Thromb Haemost* 73:247–251, 1995.

Vercauteren E, Gils A, Declerck PJ: Thrombin activatable fibrinolysis inhibitor: a putative target to enhance fibrinolysis, *Semin Thromb Hemost* 39(4):365–372, 2013.

Wang Y: Ivanov I, Smith SA,D, Morrissey JH. Polyphosphate, Zn^{2+} and high molecular weight kininogen modulate individual reactions of the contact pathway of blood clotting, *J Thromb Haemost* 17(12):2131–2140, 2019.

Weiss HJ: Sussman II, Hoyer LW: stabilization of factor VIII in plasma by the von Willebrand factor: studies on posttransfusion and dissociated factor VIII and in patients with von Willebrand's disease, *J Clin Invest* 60:390–404, 1977.

Weuppers KD, Cochrane CG: Plasma prekallikrein: Isolation, characterization, and mechanism of action, *J Exp Med* 135:1–20, 1972.

Weyand AC, Pipe SW: New therapies for hemophilia, *Blood* 133:389–398, 2019.

Wiggins RC, Cochrane CC: The autoactivability of human Hageman factor, *J Exp Med* 150:1122–1133, 1979.

Xu F, Previti M, Nieman M, et al.: A βPP/APLP2 family of Kunitz serine protease inhibitors regulate cerebral thrombosis, *J Neurosci* 29:5666–5670, 2009.

Yamazaki R, Nishiyama O, Saeki S, et al.: The utility of the Japanese Association for Acute Medicine DIC scoring system for predicting survival in acute exacerbation of fibrosing idiopathic interstitial pneumonia, *PloS One* 14(8):e0212810, 2019.

Yang XV, Banerjee Y, Fernandez JA, et al.: Activated protein C ligation of ApoER2 (LRP8) causes Dab1-dependent signaling in U937 cells, *Proc Natl Acad Sci U S A* 106:274–279, 2009.

Yates SG, Fitts E, De Simone N, Sarode R: Prolonged activated partial yhromboplastin time: to mix or not to mix – is that the question? *Transfus Apher Sci* 58(1):39–42, 2019 Feb.

Zaffran Y, Meyer SC, Negrescu E, et al.: Signaling across the platelet adhesion receptor glycoprotein Ib-IX induces αIIbβ3 activation in both platelets and a transfected Chinese hamster ovary cell system, *J Biol Chem* 275:16779–16787, 2000.

Zhang B, Cunningham MA, Nichols WC, et al.: Bleeding due to disruption of a cargo-specific ER-to-Golgi transport complex, *Nat Genet* 34:220–225, 2003.

Zhang B, Ginsburg D: Familial multiple coagulation factor deficiencies: new biologic insight from rare genetic bleeding disorders, *J Thromb Haemost* 2:1564–1572, 2004.

CHAPTER 41

PLATELET DISORDERS AND VON WILLEBRAND DISEASE

A. Koneti Rao, Natthapol Songdej, Jorge A. Di Paola

NORMAL PLATELET BIOLOGY, 847
Platelet Structure, 847
Platelet Membrane Glycoproteins and Phospholipids, 848
Role of Platelets in Hemostasis and Platelet-Activation Mechanisms, 848
LABORATORY EVALUATION OF PLATELET DISORDERS, 849
Initial Laboratory Evaluation, 849
Studies of Platelet Function, 849
Platelet Aggregation and Secretion Studies, 849
Evaluation of Platelet Function Using Flow Cytometry, 852
High-Throughput DNA Sequencing for the Diagnosis of Inherited Platelet Disorders, 852
QUANTITATIVE PLATELET DISORDERS, 852
Thrombocytopenia, 852
Thrombocytosis, 856
INHERITED DISORDERS OF PLATELET FUNCTION, 857
Overview, 857
Abnormalities of Glycoprotein Adhesion Receptors, 857
Abnormalities of Platelet Granules, 858
Abnormalities of Platelet Receptors, Signaling Pathways, and Secretion, 860
Defects in Cytoskeletal Proteins, 860
Defects in Cytoskeletal Linking Proteins, 860
Disorders of Platelet Procoagulant Activities: Scott Syndrome, 860
Transcription Factor Mutations and Associated Platelet Dysfunction, 861
Evaluation of Patients with Suspected Inherited Platelet Disorders, 861
Therapy of Inherited Platelet Function Defects, 861
ACQUIRED DISORDERS OF PLATELET FUNCTION, 862
Myeloproliferative Neoplasms, 862
Acute Leukemias and Myelodysplastic Syndromes, 862
Dysproteinemias, 862
Uremia, 862
Acquired Storage Pool Disease, 863
Antiplatelet Antibodies and Platelet Function, 863
Drugs and Food Supplements That Inhibit Platelet Function, 863
VON WILLEBRAND FACTOR, VON WILLEBRAND DISEASE, AND THROMBOTIC THROMBOCYTOPENIC PURPURA, 864
Von Willebrand Factor Biology, 864
Laboratory Tests for Von Willebrand Factor, 865
Von Willebrand Disease, 865
Acquired Von Willebrand Syndrome, 867
Thrombotic Thrombocytopenic Purpura, 867
SELECTED REFERENCES, 868

KEY POINTS

- Platelets are highly complex cells that participate in critical steps central to hemostasis and thrombosis, including adhesion to subendothelium, aggregation, secretion of granule contents, and provision of membrane surface for activation of coagulation factors.
- Abnormalities of either platelet number or platelet function can play an important role in the balance of hemostasis and thrombosis.
- Almost unique to laboratory medicine and pathology, assessment of platelet pathology may be performed in real time on living cells obtained from the patient.
- A number of inherited and acquired disorders, autoimmune processes, and drugs affect platelet counts and platelet function.
- In a large proportion of patients with inherited platelet disorders, the underlying genetic and molecular mechanisms are unknown.
- Von Willebrand factor (vWF) is a multimeric protein synthesized by endothelial cells and megakaryocytes that plays a central role in platelet adhesive interactions.
- Abnormalities related to vWF lead to the bleeding disorder von Willebrand disease and thrombotic thrombocytopenic purpura, associated with vascular occlusions and hemolysis.

NORMAL PLATELET BIOLOGY

PLATELET STRUCTURE

Blood platelets are highly complex, anucleate cells that derive from bone marrow megakaryocytes. Peripheral blood film offers the opportunity for evaluation of platelet numbers, size, distribution, and structure under the light microscope.

Electron microscopy allows more precise characterization of the structural abnormalities (White, 2004), with the opportunity to examine in greater detail specific platelet organelles (Clauser & Cramer-Borde, 2009). An array of 3-dimensional high-resolution structural approaches have emerged and provide novel insights into platelets (Yadav & Storrie, 2017).

Platelet features that may be visualized ultrastructurally are shown in Figure 41.1. The outer surface of the platelet, the *glycocalyx*, is rich in glycoproteins. A submembranous band of *microtubules*, composed of the protein tubulin, provides structural support for the discoid platelet shape. Contractile *microfilaments* composed of actin and myosin may also be seen. An extensive *open canalicular system* within the platelet is in direct communication with the extracellular environment. Often seen in proximity to the open canalicular system is the *dense tubular system*. The dense tubular system also functions as a calcium-sequestering pump, maintaining low levels of cytoplasmic calcium in the resting platelet.

A variety of inclusions are recognized within the platelet cytoplasm, including *mitochondria*, *glycogen*, and *granules*. Lighter staining α-granules, less frequent dense core (or "bull's-eye") granules, lysosomes, and peroxisomes are also seen. Three-dimensional electron microscopic studies have revealed morphologically distinct α-granule subtypes and demonstrated that high spatial segregation of different stored proteins exists within individual α-granules (van Nispen tot Pannerden et al., 2010). The α-granule proteins derive both from endocytic uptake and de novo synthesis by megakaryocytes, and include fibrinogen, platelet-derived growth factor (PDGF), von Willebrand factor (vWF), the factor V binding protein multimerin, β-thromboglobulin (βTG), and the heparin-neutralizing platelet factor (PF) 4. P-selectin, a constituent of the α-granule membrane, translocates to the plasma membrane of the platelet when α-granule contents are released. The dense granules contain a nonmetabolic pool of adenosine diphosphate (ADP) and adenosine triphosphate (ATP), 5-hydroxytryptamine (5-HT, serotonin), calcium, and inorganic polyphosphate (polyP).

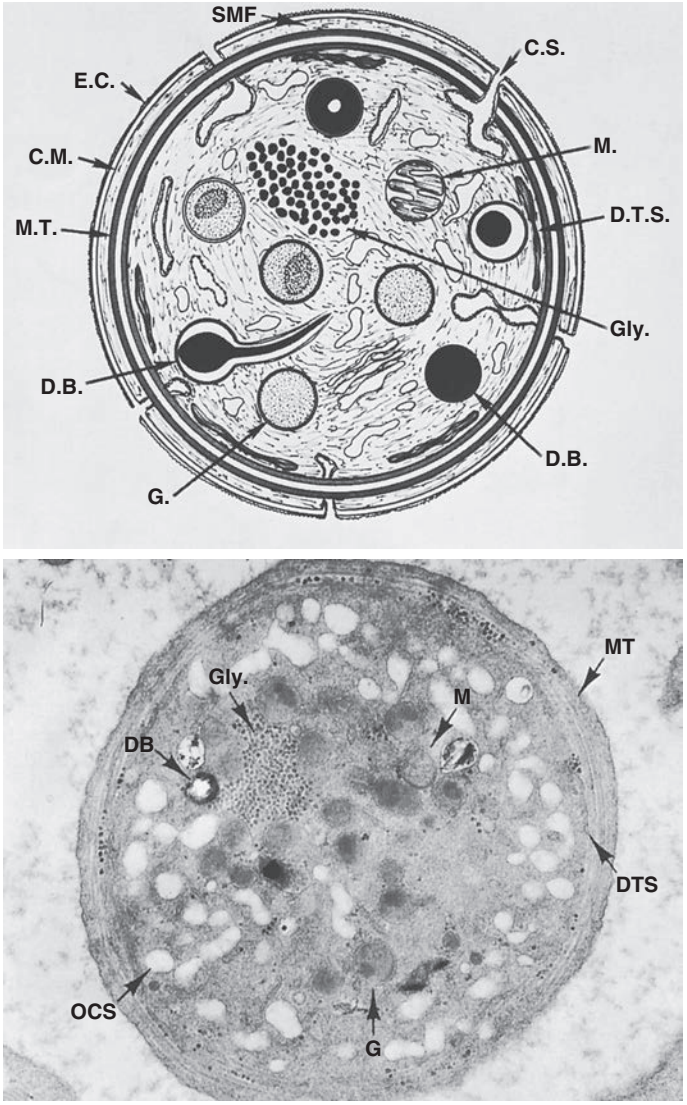

Figure 41.1 Discoid platelets. Shown are ultrastructural features observed in thin sections of discoid platelets cut in the equatorial plane. The peripheral zone includes the exterior coat (EC), the trilaminar unit membrane (CM), and the submembrane area containing specialized filaments (SMFs) that form the wall of the platelet and line channels of the surface-connected canalicular system (also referred to as the *open canalicular system,* or *OCS*). The matrix of the platelet interior is the sol-gel zone containing actin microfilaments, structural filaments, the circumferential band of microtubules (MTs), and glycogen (Gly). Formed elements embedded in the sol-gel zone include mitochondria (M), granules (G), and dense bodies (DBs). Collectively, they constitute the organelle zone. The membrane systems include the OCS and the dense tubular system (DTS), which serve as the platelet sarcoplasmic reticulum. The electron micrograph shows a platelet sectioned in the equatorial plane (30,000×), which reveals most of the structures indicated on the diagram. (With permission from White JG, Bloom AL, Forbes CD, et al., editors: *Hemostasis and thrombosis,* New York, 1994, Churchill Livingstone.)

PLATELET MEMBRANE GLYCOPROTEINS AND PHOSPHOLIPIDS

Historically, analyses of platelet surface glycoproteins in patients with inherited platelet disorders have been key to our current understanding of fundamental aspects of platelet function. Table 41.1 shows the major platelet membrane glycoproteins that function as receptors for adhesive ligands. The GPIIb-IIIa receptor complex (also referred to as *integrin αIIbβ3*), which in its activated form serves as a receptor for fibrinogen, is the most abundant platelet receptor, with ~80,000 to 100,000 copies per platelet. This is followed by the major platelet receptor for vWF, GPIbα, at ~30,000 copies. GPIbα is disulfide linked to GPIbβ and noncovalently linked to GPIX and GPV; together, these glycoproteins make up the GPIb-IX-V complex. The copy number for other platelet surface glycoproteins is lower. GPVI and GPIa-IIa mediate platelet interactions with collagen.

Platelet membranes contain several phospholipids that play a major role in platelet function, including phosphatidylinositol, phosphatidylcholine, phosphatidylserine (PS), and phosphatidylethanolamine. Phosphatidylinositides are the source of signaling molecules inositoltrisphosphate and diacylglycerol, which are produced following platelet activation. Negatively charged PS is expressed in the inner membrane leaflet of the resting platelet; on platelet activation, PS translocates to the outer leaflet, an essential step in the formation of a procoagulant platelet surface that is critical in several blood coagulation mechanisms.

ROLE OF PLATELETS IN HEMOSTASIS AND PLATELET-ACTIVATION MECHANISMS

Following injury to the blood vessel, platelets adhere to exposed subendothelium by a process (*adhesion*) that involves the interaction of a plasma protein, vWF, and a specific glycoprotein complex on the platelet surface, GPIb-IX-V (Fig. 41.2), which binds vWF particularly under conditions of high shear stress. Adhesion is followed by recruitment of additional platelets, which interact with each other to form clumps, a process called *aggregation*. This involves binding of fibrinogen to specific platelet surface receptors—a complex composed of GPIIb-IIIa, which is platelet- and megakaryocyte-specific and binds vWF as well. Resting platelets do not bind fibrinogen. Stimulation of platelets leads to a series of intracellular signaling responses, including binding of the adapter proteins talin and kindlin to the cytoplasmic tails of the GPIIb-IIIa receptor complexes (Smythe et al., 2016). These events produce conformational changes in the GPIIb-IIIa complex that expose binding sites for fibrinogen, a prerequisite for platelet aggregation. Activated platelets release contents of their granules (*secretion* or *release reaction*), such as ADP and serotonin from the dense granules, which cause recruitment of additional platelets. In addition, platelets play a major role in coagulation mechanisms; several key enzymatic reactions occur on the platelet membrane lipoprotein surface (*platelet coagulant activity*).

Platelet Activation and Signaling Events (see Fig. 41.2)

Several physiologic agonists interact with specific receptors on the platelet surface to induce events that culminate in well-recognized responses, including a change in platelet shape from discoid to spherical (shape change), aggregation, secretion, and thromboxane A2 (TXA2) production (Shattil & Newman, 2004; Smythe et al., 2016). These agonists include ADP, collagen, thrombin, TXA2, epinephrine, and platelet-activating factor (PAF), and they induce signaling events in platelets. Platelets possess at least three well-defined purinergic receptors that mediate the responses to ADP: P2Y1, P2Y12, and P2X1 (not shown). The P2Y1 receptor mediates the rise in cytoplasmic Ca^{2+}; the P2Y12 receptor mediates inhibition of adenylyl cyclase to lower cyclic adenosine monophosphate (cAMP) levels in platelets and is the receptor targeted by antiplatelet agents, such as clopidogrel and prasugrel. P2X1 functions as an ion channel to amplify the platelet activation process. Thrombin induces platelet responses through the protease-activated receptors (PARs); human platelets possess PAR1 and PAR4 receptors. GPVI is the principal collagen receptor in platelets and is a member of the immunoglobulin (Ig) receptor superfamily. Ligation of the platelet receptors by agonists such as thrombin, TXA2, and ADP initiates the production of several intracellular messenger molecules, including products of hydrolysis of phosphoinositides (PI) by phospholipase C (diacylglycerol, and inositol 1,4,5-triphosphate [IP3]) and conversion of arachidonic acid to TXA2. These mediators induce or modulate the various platelet responses of Ca^{2+} mobilization, protein phosphorylation, aggregation, secretion, and thromboxane production. The interaction between the platelet surface receptors and the key intracellular enzymes (e.g., phospholipases A2 and C, adenylyl cyclase [not shown]) is mediated by a group of distinct proteins called *G-proteins* that bind and are modulated by GTP. These include rap1A and rap1b (or RIAM) proteins, shown in Fig. 41.2. As in most secretory cells, platelet activation results in a rise in cytoplasmic ionized calcium concentration; IP3 functions as a messenger to mobilize Ca^{2+} from intracellular stores. This increase in cytoplasmic Ca^{2+} levels regulates other events, such as the activation of phospholipase A2, leading to TXA2 production, and phosphorylation by myosin light-chain kinase of myosin light chain, which is involved in shape change and secretion. Diacylglycerol (DAG) activates the protein kinase C (PKC) family of enzymes that phosphorylate several proteins, including pleckstrin. PKC activation is considered to play a major role in platelet responses, including secretion and the activation of GPIIb-IIIa. Platelets possess several families of G-proteins that function as molecular switches in transmitting the signal from the surface receptors to the intracellular effectors. For example, phospholipase C (PLC) activation and calcium mobilization on activation by ADP (P2Y1), TXA2, or thrombin is mediated by Gαq, whereas signaling through the P2Y12 ADP receptor and inhibition of adenylyl cyclase is mediated by Gαi. Another well-recognized response of platelets to activation is synthesis of TXA2. The initial and rate-limiting step in TXA2 production is the mobilization of arachidonic acid (AA) from phospholipids (predominantly phosphatidylcholine) by phospholipase A2. Free AA is converted by

TABLE 41.1

Selective List of Adhesive Platelet Membrane Glycoproteins

	Alternate Designation(s)	Structural Family	Principal Ligand(s)	Major Function
GPIIb-IIIa	CD41-CD61, $\alpha_{IIb}\beta_3$,	Integrin	Fibrinogen, von Willebrand factor (vWF)	Aggregation (platelet-platelet interaction)
GPIb-IX-V	CD42a-d complex	Leucine-rich glycoprotein	vWF, thrombin, P-selectin, coagulation contact factors	Adhesion (platelet-subendothelium interaction)
GPVI		Immunoglobulin receptor superfamily	Collagen	Signaling following platelet-collagen interaction
GPIa-IIa	CD49b-CD29, $\alpha_2\beta_1$	Integrin	Collagen	Adhesion (platelet-collagen interaction)
P-selectin	CD62P, GMP 140, PADGEM	Selectin	P-selectin–glycoprotein ligand-1 (PSGL-1)	Platelet-leukocyte interaction
PECAM-1	CD31	Immunoglobulin receptor superfamily	PECAM-1/PECAM-1 homophilic interactions	Platelet-endothelial cell interaction
GPIV	CD36, GPIIIb	Scavenger receptor family	Thrombospondin, collagen, oxidized low-density lipoproteins	Scavenger, adhesion

cyclooxygenase to prostaglandins (PG) G2 and H2 (not shown), which are converted by thromboxane synthase to TXA2. Binding of fibrinogen to the GPIIb-IIIa complex results in the activation of tyrosine kinases and associated events ("outside-in signaling") (Shattil & Newman, 2004). Numerous other mechanisms and events occur in platelets on activation involving small GTPases, tyrosine kinases, and phosphatases; these are beyond the scope of this chapter. While the agonists mentioned earlier activate platelets to function in hemostasis, there are other agonists—such as prostacyclin (PGI2), produced by endothelial cells—that inhibit platelet responses. PGI2 does this by increasing platelet cAMP levels through activation of adenylyl cyclase.

Platelet Coagulant Activity

Platelets play a vital role in coagulation. Numerous proteins, including coagulation factor V and fibrinogen, are released from α-granules. ADP, ATP, serotonin, and the pro-hemostatic polyphosphates (Smith & Morrissey, 2014) are released from dense granules. Importantly, several of the key enzymatic reactions leading to factor X and prothrombin activation, and to thrombin generation, require the platelet membrane surface to proceed at an optimum rate (Smythe et al., 2016). Platelet activation results in movement or "flip-flop" of PS and other phospholipids from the internal to the external surface of the membrane (Zwaal et al., 2005). This is essential to the role of platelets in blood coagulation mechanisms.

LABORATORY EVALUATION OF PLATELET DISORDERS

INITIAL LABORATORY EVALUATION

The diagnostic process begins with a detailed clinical evaluation followed by laboratory studies (Gresele & Subcommittee on Platelet, 2015; Sivapalaratnam et al., 2017). Platelet disorders may occur in association with other inherited or acquired disorders or syndromes; thus, a detailed clinical evaluation is essential. To better assess the intensity of bleeding symptoms, a number of validated standardized bleeding assessment tools are available (Rodeghiero et al., 2010). This evaluation should also include an assessment of ingestion of medications, herbal supplements, and over-the-counter substances. Many such compounds affect platelet number or function.

The initial laboratory evaluation of platelet disorders includes a complete blood count, including the platelet count. The normal platelet count is 150 to 400 × 10^9/L. In severe thrombocytopenia, below the established linearity of a given automated instrument or in the presence of cellular fragments spuriously affecting the automated count, a manual phase contrast count with a hemocytometer chamber may be required. Many instruments also provide the mean platelet volume (MPV) and a histogram of MPV. Some automated instruments also assess platelet maturity, as reflected by the RNA content of "reticulated platelets"—analogous to reticulocyte measurements in the erythroid series (Hoffmann, 2014; Dusse & Freitas, 2015). Such measurements offer the opportunity to detect a thrombopoietic response from the bone marrow. Evaluation of the peripheral blood film provides valuable information regarding platelet count and size distribution, and on associated changes in other blood cells. A simple diagnostic approach that utilizes immunofluorescence labeling of peripheral blood smears using antibodies specific for proteins known to be affected has been proposed as a diagnostic tool for several inherited platelet disorders (Greinacher et al., 2017).

STUDIES OF PLATELET FUNCTION

No currently available laboratory test faithfully reflects the enormously complex platelet role in hemostasis. Several instruments and approaches have been developed to study platelet function (Harrison & Lordkipanidze, 2013; Gresele et al., 2014; Gresele & Subcommittee on Platelet, 2015; Mumford, Frelinger et al., 2015). A large number of biochemical and functional approaches, many in research laboratories, have been applied as a part of phenotype-driven and candidate gene approaches in unraveling the underlying mechanisms in patients identified (Gresele & Subcommittee on Platelet, 2015). These approaches have taken a major change in direction with the recent application of high-throughput deoxyribonucleic acid (DNA) sequencing methods to define the genetic basis in patients (Lentaigne et al., 2016; Sivapalaratnam et al., 2017; Heremans & Freson 2018; Downes et al., 2019).

Bleeding Time

For many years, the template bleeding time test was used as a "global" test for the adequacy of primary hemostasis. In such testing, a standardized cut was made on the volar surface of the forearm and the duration it took for the bleeding to stop constituted the bleeding time. The bleeding time has a relatively poor predictive value of clinical bleeding (Rodgers & Levin, 1990), carries risk for scarring, and requires considerable technical expertise and time. It has been largely abandoned in most centers.

PFA-100/200 and Cone and Plate Analyzer

In the platelet function analyzer (PFA-100 and PFA-200) (Favaloro & Bonar, 2014; Harrison & Lordkipanidze, 2013), anticoagulated whole blood is flowed under high shear force through a narrow hole punched out of a membrane coated with collagen and either epinephrine or ADP. The time to full occlusion of the channel is recorded as "closure time." This is dependent on plasma vWF, platelet count and function, and hematocrit. Whereas inhibition of the platelet cyclooxygenase by aspirin or other mild to moderate impairments of platelet function prolong closure times with the collagen/epinephrine membranes, only more profound impairment of platelet function or of vWF prolong closure times in the collagen/ADP cartridges. Although abnormal in some platelet disorders, this instrument does not have sufficient sensitivity or specificity to be relied on as a screening tool for platelet disorders (Hayward et al., 2006). Definitive identification of abnormalities of platelets or vWF requires more specific studies.

Several additional ex vivo systems to assess platelet function have been developed in which shear forces play a major role. Notable among these is the development of the Impact-R instrument based on the cone and plate method for generation of shear (Varon et al., 1998). Limitations of this method both in the diagnosis of bleeding disorders (Revel-Vilk et al., 2009) and in monitoring antiplatelet therapy (van Werkum et al., 2010) have been described. Several other methods aiming to detect inherited and acquired disorders relating both to platelets and to vWF have been developed, but their role in clinical practice remains to be defined (Harrison & Lordkipanidze, 2013).

PLATELET AGGREGATION AND SECRETION STUDIES

Platelet function can be evaluated in vitro through study of platelet aggregation and secretion in response to a battery of platelet-stimulating agents

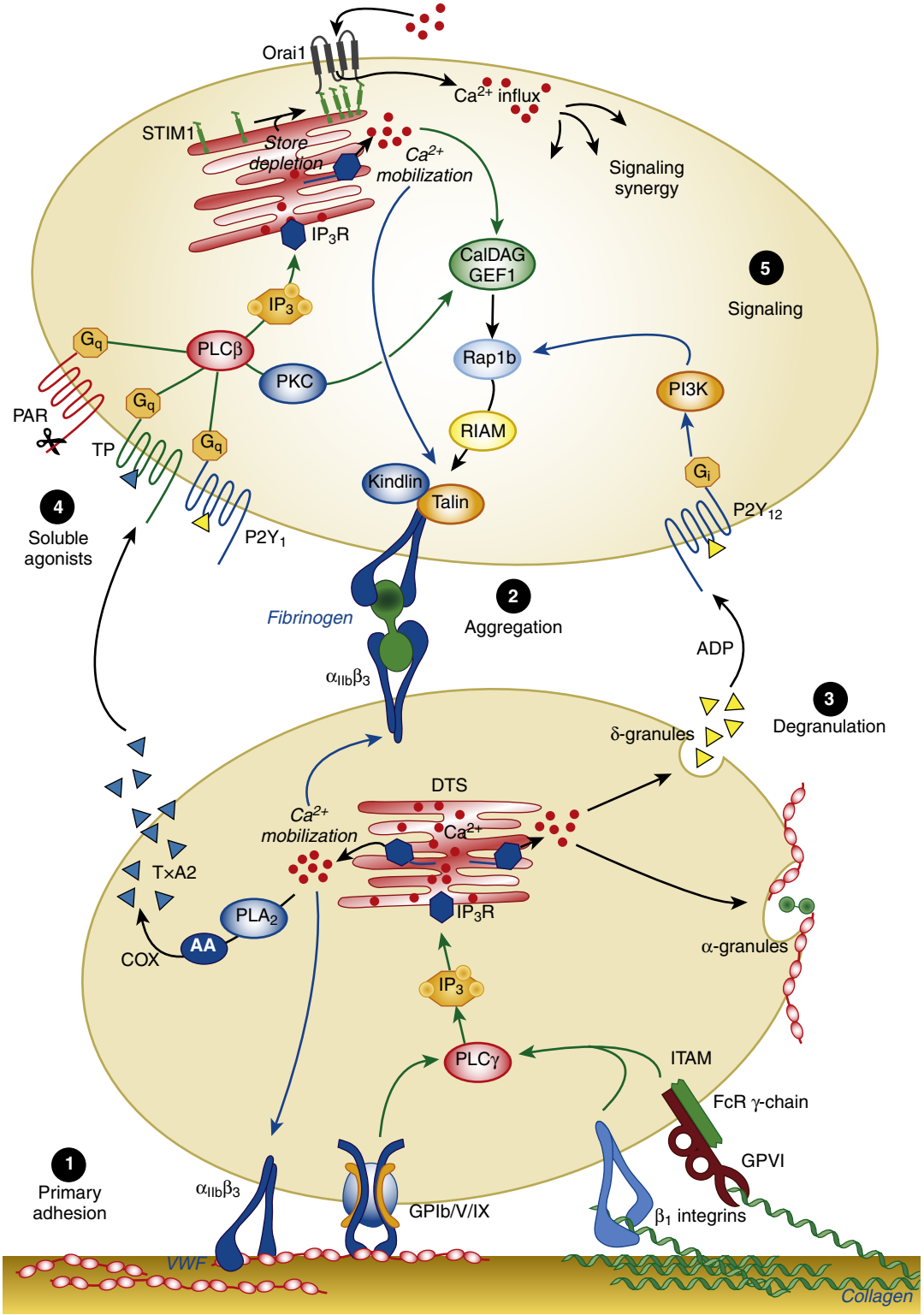

Figure 41.2 Platelet proteins and molecular pathways important for hemostasis. The stages of hemostatic plug formation are broadly divided into platelet adhesion and initial signaling events, platelet aggregation, secretion, soluble agonist receptor activation, and subsequent signaling. *AA,* Arachidonic acid; *AC,* adenylyl cyclase; *Ca^{2+},* calcium; *CalDAG GEF1,* calcium and diacylglycerol-regulated guanine nucleotide exchange factor; *COX,* cyclooxygenase; *DTS,* dense tubular system; *IP3,* inositol (1,4,5)-trisphosphate; *IP3R,* IP3 receptor; *ITAM,* immunoreceptor tyrosine-based activation motif; *PAR,* protease-activated receptor; *PGH_2,* prostaglandin H_2; *PIP2,* phosphatidylinositol (4,5)-bisphosphate; *PI3K,* PI3-kinase; *PKC,* protein kinase C; *PLA_2,* phospholipase A_2; *PLC,* phospholipase C; *RIAM,* Rap1-GTP interacting adapter molecule; *Src,* Src family kinases; *STIM1,* stromal interaction molecule 1; *TP,* thromboxane receptor. GP1b (alpha) is a vital protein that interacts with von Willbrand factor and is involved in platelet-type von Willebrand Disease (vide infra).Talin and kindlin are adapter proteins that bind to the GpIIb/IIIa proteins inducing structural changes that allow for the binding of GpIIb/IIIa to fibrinogen. (For discussion in greater depth of these molecules and their roles in platelet activation, see Wei AH, Schoenwaelder SM, Andrews RK: New insights into the haemostatic function of platelets, *Brit J Haematol* 47:415–430, 2009, from which this figure is reproduced with permission.)

(Cattaneo et al., 2013; Harrison & Lordkipanidze, 2013; Gresele et al., 2014; Mumford et al., 2015). These studies are generally performed using platelet-rich plasma (PRP) harvested from blood collected using sodium citrate as the anticoagulant. Ethylenediaminetetraacetic acid (EDTA), routinely used to collect samples for blood counts, dissociates the platelet GPIIb-IIIa complexes; thus, aggregation studies cannot be performed using such a sample. When citrated PRP is continuously stirred in a platelet aggregometer and a light beam is passed through the suspension; platelet aggregation in response to an added agonist can be monitored by changes in light transmittance. Change in platelet shape from discoid to spheroid is seen as an initial decrease in transmittance, whereas the subsequent formation of platelet clumps allows more light to pass through the suspension to the photodetector and is recorded as an increase in light transmittance (Harrison et al., 2011). Recommendations have been published from the International

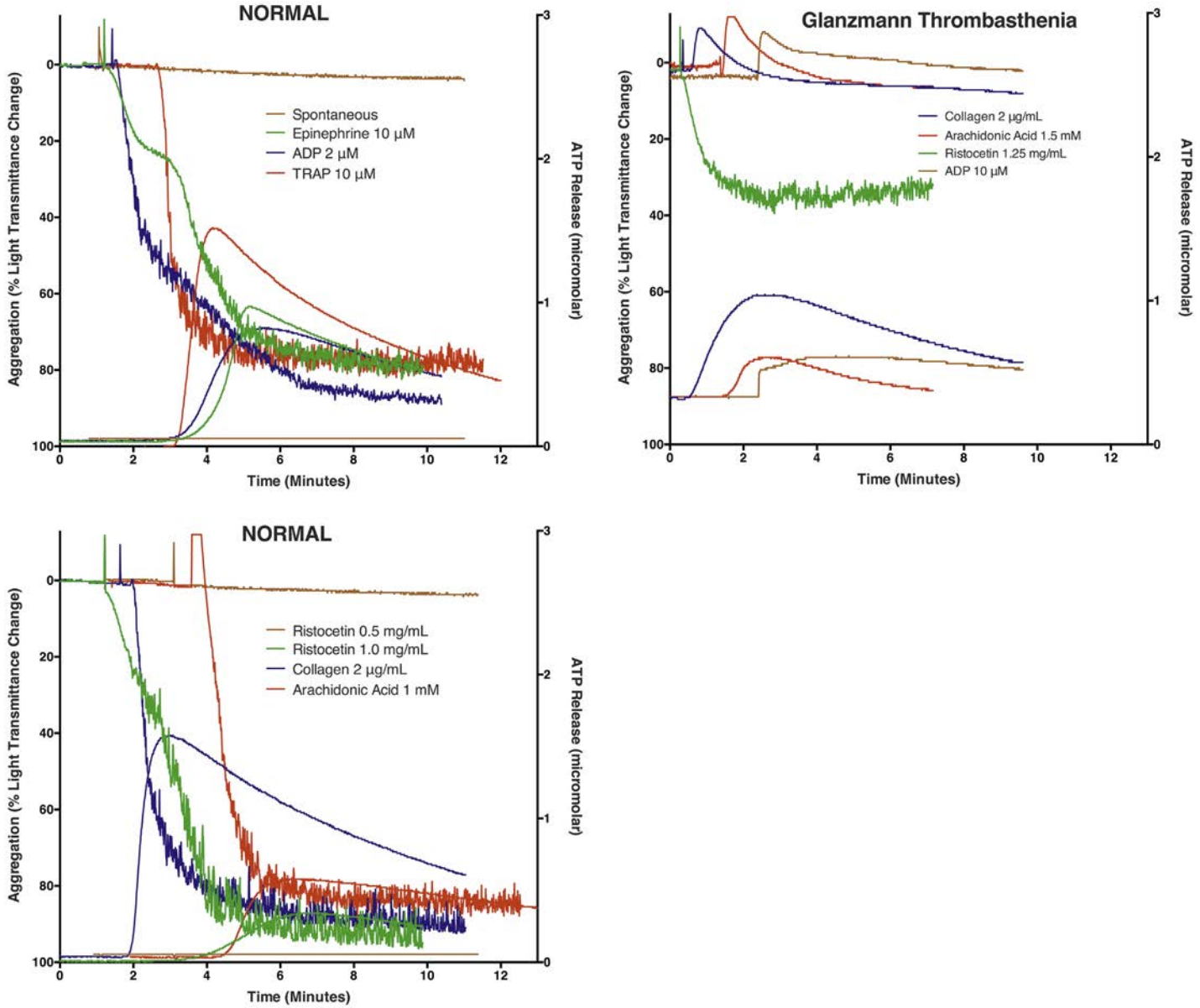

Figure 41.3 Platelet Lumi-Aggregometer tracings in a normal individual *(left panels)* and a patient with Glanzmann thrombasthenia *(right panel).* Following addition of an agonist to stirred platelet-rich plasma, aggregation of platelets leads to increasing light transmittance, registered in the displays as downward-going deflections. Dense granule secretion is simultaneously monitored by the luminescence resulting when ATP released from platelets reacts with luciferin-luciferase reagent present in the cuvette and displays as upward-going deflections. In the Glanzmann thrombasthenia patient, initial platelet shape change (upward deflection of aggregation tracing) is seen, but virtually no aggregation follows due to deficiency of GPIIb-IIIa. Only ristocetin produces aggregation since vWF binding to GPIb-IX-V remains intact. ATP secretion in response to platelet agonists is variable in Glanzmann thrombasthenia patients.

Society on Thrombosis and Haemostasis (ISTH) (Cattaneo et al., 2013) and others (Hayward et al., 2019) for the standardization of light-transmission aggregometry. In instruments equipped with a second channel for monitoring secretion, the release of ATP from platelet-dense granules is simultaneously measured (Fig. 41.3). This is accomplished by adding the firefly luminescence substrate and enzyme, luciferin and luciferase, to the PRP. Released ATP then functions as a cofactor in the light-producing luciferin-luciferase reaction, and light emission is recorded with a second photodetector. Thus, aggregation and secretion can be monitored simultaneously and independently (Pai et al., 2011). In most cases, the release of ATP may be assumed to reflect the release of the other dense granule constituents, which are less easily measured (i.e., ADP, serotonin, calcium, polyphosphates). Direct biochemical measurements of serotonin, ATP, and ADP can also be performed (Holmsen & Dangelmaier, 1989). Platelet-dense granule secretion may be studied in parallel with aggregation by labeling platelets with ^{14}C-serotonin and then measuring the release of radioactivity following platelet activation (Lan & Schmaier, 2005). On platelet activation, contents of the α-granules, dense granules, and the lysosomal granules are released. These can monitored by different methods (Mumford et al., 2015).

Platelets have surface receptors for several agonists (see Fig. 41.2). Frequently employed agonists in the laboratory include collagen, epinephrine, ADP, U46619 (a TXA2 analog), AA, ristocetin, PAR-1 agonist (SFLLRN), and the calcium ionophore A23187. Platelet responses to these stimuli, with the exception of ristocetin, are dependent on active metabolic processes. In contrast, ristocetin-induced clumping of platelets occurs to a large degree even in the presence of metabolic inhibitors and in formalin-fixed platelets; therefore, it is often referred as *agglutination*.

Although of paramount importance in vivo, thrombin is difficult to employ as an agonist with PRP because of interference from fibrin formation. The partially trypsinized γ-thrombin, however, retains platelet-stimulating activity but largely lacks clotting activity and can be useful. Thrombin cleaves the G-protein–coupled transmembrane platelet PAR1 receptor. Thus, thrombin receptor–activating peptide (TRAP), consisting of amino acid sequence SFLLRN, derived from the extracellular "tethered ligand" region of the thrombin receptor, activates platelets and is useful in platelet function testing. Strong agonists such as collagen and thrombin are capable of directly inducing secretion and TXA2 synthesis in addition to inducing aggregation. In contrast, secretion and TXA2 synthesis following platelet stimulation with weaker agonists such as ADP or epinephrine may be considered secondary responses following attainment of a threshold level of aggregation (Cattaneo, 2009). The potential diagnostic yields and limitations of aggregation and secretion studies in patients have been reviewed (Mezzano et al., 2009; Dawood et al., 2012).

Other methods have also been developed to test platelet function (Harrison & Lordkipanidze, 2013). Electrical impedance measurements, as opposed to

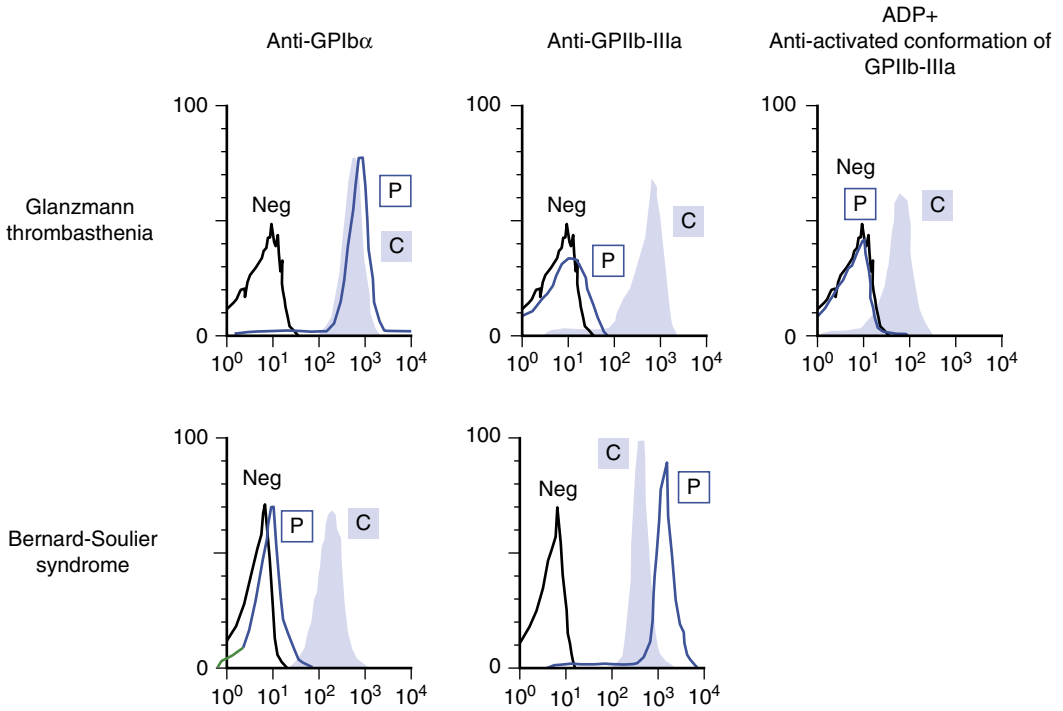

Figure 41.4 Flow cytometric evaluation of platelet membrane glycoprotein (GP) disorders, Glanzmann thrombasthenia, and Bernard-Soulier syndrome. Platelets from healthy controls (C) or from patients (P) were incubated with monoclonal antibodies against GPIbα, GPIIb-IIIa, or a monoclonal antibody (PAC-1) that recognizes only the conformationally altered active form of GPIIb-IIIa that occurs following platelet activation (e.g., in response to ADP). In the patient with Glanzmann thrombasthenia *(upper panel)*, there is virtual absence of GPIIb-IIIa, although GPIbα is present at normal levels. In the patient with Bernard-Soulier syndrome *(lower panel)*, a severe deficiency of GPIbα expression but no decrease in GPIIb-IIIa expression is seen. (Modified with permission from Nurden AT, George JN: Inherited disorders of the platelet membrane: Glanzmann thrombasthenia, Bernard-Soulier syndrome, and other disorders. In Colman RW, editor: *Hemostasis and thrombosis: basic principles and clinical practice,* ed 4, Philadelphia, 2001, Lippincott Williams & Wilkins.)

monitoring light transmission, have been used to study platelet aggregation not only in PRP but also in whole blood (Cardinal & Flower, 1980). The resulting curves of electrical impedance over time share many similarities to those of light transmittance recordings, although there are characteristic differences between these two approaches (Ingerman-Wojenski & Silver, 1984; Joseph et al., 1987). When impedance aggregometry is combined with ATP secretion measurement on whole-blood samples (Ingerman-Wojenski & Silver, 1984), relatively rapid evaluation of platelet function, requiring only a small volume of blood, may be performed (McGlasson & Fritsma, 2009). Additionally, platelet aggregation in whole blood may be monitored optically by means of the coaggregation of fibrinogen-coated beads (*Verify Now*) impregnated with a dye that absorbs light in the infrared region of the electromagnetic spectrum (Harrison & Lordkipanidze, 2013). This approach has been applied for assessing the effect of treatment with platelet inhibitors (GPIIb-IIIa inhibitors, aspirin, and clopidogrel).

The contractile abilities of activated platelets also result in contraction (or "retraction") of formed clots. In the test tube, *clot retraction* may be quantitatively assessed. In thrombocytopenia or Glanzmann thrombasthenia, clot retraction is delayed or incomplete. GPIIb-IIIa (Coller et al., 1983) as well as a number of additional platelet cytoskeletal and contractile proteins (de Witt et al., 2014) are required for effective clot retraction.

EVALUATION OF PLATELET FUNCTION USING FLOW CYTOMETRY

Flow cytometry has proved useful for assessing the expression of specific platelet surface glycoprotein receptors and for assessing platelet activation, including ability of GPIIb-IIIa to undergo conformational change, and expression of markers of platelet secretion (e.g., P-selectin from α-granules; Fig. 41.4) (Krueger et al., 2002). Flow cytometry has been used to assess platelet expression of annexin V, dense granules, and release of microparticles. Due to the small volumes of blood required, flow cytometry can be particularly valuable in diagnostic evaluations of children and neonates. Recently, mass cytometry using multiple metal conjugated antibodies has been applied to document heterogeneity of normal platelets in circulation and novel alterations in platelet glycoproteins in Glanzmann thrombasthenia (Blair et al., 2018).

HIGH-THROUGHPUT DNA SEQUENCING FOR THE DIAGNOSIS OF INHERITED PLATELET DISORDERS

The advent of high-throughput DNA sequencing (HTS) is a major advance in the diagnostic approach to patients with inherited platelet disorders (Lentaigne et al., 2016; Simeoni et al., 2016; Heremans & Freson, 2018; Downes et al., 2019). This has transformed the diagnostic landscape from a phenotype-based, laboratory-based, and candidate-gene approach to one that is genotype based. It has provided new insights into genotype-phenotype correlations, discovery of novel genes causing inherited platelet disorders, and the unraveling of unknown molecular pathways regulating megakaryocyte-platelet biology. The application of HTS to patients by different groups has been based on targeted gene panels and whole-exome sequencing (WES) (Leo et al., 2015; Lentaigne et al., 2016; Simeoni et al., 2016; Bastida et al., 2018; Heremans & Freson, 2018, Downes et al., 2019), with whole-genome sequencing being tested. Overall, these approaches provide a genetic diagnosis in about 40% to 50% of patients with inherited platelet disorders, combining those with defects in platelet number and function (Heremans & Freson, 2018; Downes et al., 2019). However, in a large fraction of such patients, the genetic diagnosis remains elusive despite state-of-the art studies. They may have abnormalities in unknown genes or in noncoding regions of the genome. Moreover, a substantial number of variants detected in known genes remain as variants of unknown significance. The advantages of a genetic diagnosis are clear and include a predictive value beyond bleeding (such as predisposition to leukemia or renal failure). As of now, access to these HTS approaches and the required expertise is limiting.

QUANTITATIVE PLATELET DISORDERS

THROMBOCYTOPENIA

Decreased platelet production and increased platelet destruction (Table 41.2) constitute two of the major causes of thrombocytopenia. Additionally, thrombocytopenia may be seen with splenomegaly of any cause because of increased splenic sequestration of platelets.

Inherited Thrombocytopenias

Inherited thrombocytopenias are being recognized with increasing frequency; several distinct genetic abnormalities have been documented in such patients (Althaus & Greinacher, 2009; Balduini et al., 2013a, 2013b; Kumar & Kahr, 2013; Noris et al., 2014; Almazni et al., 2019) (Fig. 41.5). These patients may present with isolated thrombocytopenia or in conjunction with characteristic syndromes. In some patients, the platelets have defects in function as well. These entities are discussed further in the section on Inherited Disorders of Platelet Function.

TABLE 41.2
Mechanisms of Platelet Destruction

Type of Thrombocytopenia	Specific Example(s)
Immune Mediated	
Autoantibody-mediated platelet destruction by reticuloendothelial system (RES)	Primary immune thrombocytopenic purpura; secondary immune thrombocytopenia associated with lymphoproliferative disease; collagen vascular disease; infections such as infectious mononucleosis; human immunodeficiency virus syndrome
Alloantibody-mediated platelet destruction by RES	Neonatal alloimmune thrombocytopenia; posttransfusion purpura; passive alloimmune thrombocytopenia; alloimmune platelet transfusion refractoriness
Drug-dependent, antibody-mediated platelet destruction by RES	Drug-induced immune thrombocytopenic purpura (e.g., quinine)
Platelet activation by binding of immunoglobulin G (IgG) Fc of drug-dependent IgG to platelet Fcγlla receptors	Heparin-induced thrombocytopenia
Non–Immune Mediated	
Platelet activation by thrombin or proinflammatory cytokines	Disseminated intravascular coagulation; septicemia/systemic inflammatory response syndromes
Platelet destruction via ingestion by macrophages (hemophagocytosis)	Infections; certain malignant lymphoproliferative disorders
Platelet destruction through platelet interactions with altered von Willebrand factor	Thrombotic thrombocytopenic purpura; hemolytic-uremic syndrome; aortic stenosis
Platelet losses on artificial surfaces	Cardiopulmonary bypass surgery; use of intravascular catheters
Decreased platelet survival associated with cardiovascular disease	Inherited and acquired heart disease; cardiomyopathy; pulmonary embolism

Modified with permission from Warkentin TE, Kelton JG: Thrombocytopenia due to platelet destruction and hypersplenism. In Hoffman R, Benz EJ Jr, Shattil SJ, et al., editors: *Hematology: basic principles and practice*. Philadelphia, 2005, Elsevier Churchill Livingstone, pp 2305–2325.

From a mechanistic perspective, inherited thrombocytopenias are associated with mutations in genes with diverse function. However, for some, the specific function in megakaryocytes/platelets is unclear. In the last 2 decades, there has been an explosive increase in our knowledge of gene mutations linked to inherited thrombocytopenias; over 20 genes are implicated (Lentaigne et al., 2016; Simeoni et al., 2016,; Almazni et al., 2019; Downes et al., 2019) (see Fig. 41.5). These genes include transcription factors (*RUNX1*, *FLI1*, *GATA1*, *GFI1b*, *HOXA11*, *ETV6*, *MECOM/EVI1*, *IKZF5*), thrombopoietin receptor c-*MpL*, cytoskeletal proteins and related signaling (*MYH9*, *TUBB1*, *ACTN1*, *FLNA*, *WASP*, *DIAPH1*, *PTPRJ*, *SRC*), surface membrane glycoproteins and related signaling (*GPIBA*, *GPIBB*, *GPIX*, *ITGA2B*, *ITGB3*), proteins involved in vesicle transport (*NBEAL2*), exon-junction complex involved in RNA processing (*RBM8A*), and cAMP-dependent protein kinase (*PRKACG*). Mutations in the *ANKRD26* 5′ untranslated region result in loss of RUNX1 and FLI1 binding, and ANKRD26 silencing (Bluteau et al., 2014; Marquez et al., 2014; Lentaigne et al., 2016; Almazni et al., 2019). The application of high-throughput sequencing permits identification of the gene abnormality in ~50% of patients with inherited thrombocytopenias.

A better understanding of inherited thrombocytopenias is important beyond the predisposition to bleeding, which is variable and often mild. First, many patients are initially recognized in their adulthood (Balduini et al., 2013a). In the absence of a family history, there is the risk for misdiagnosis as immune thrombocytopenia and the potential for unnecessary therapy, such as with steroids or splenectomy. Second, some gene mutations have prognostic implications, such as the predisposition to myeloid or lymphoid malignancies with *RUNX1*, *ANKRD26*, and *ETV6* mutations (Noetzli et al., 2015; Songdej & Rao, 2017); or worsening renal function or hearing loss, as with *MYH9* mutations. Further, there may be therapeutic implications, as in the potential role of eltrombopag in patients with *MYH9* mutations (Balduini et al., 2013a). Moreover, some reports have documented recurrence of leukemia following hematopoietic stem cell transplantation of the patient from an undiagnosed sibling donor with an unrecognized *RUNX1* mutation (Owen et al., 2008; Songdej & Rao, 2017). Lastly, several entities are associated with platelet function abnormalities as well, as in patients with *RUNX1* and other transcription factor mutations (Songdej & Rao, 2017) (see later discussion).

From a clinical perspective, patients with inherited thrombocytopenias may be characterized based on inheritance patterns or platelet size (Table 41.3) or diameter (Balduini et al., 2013a, 2013b; Kumar & Kahr, 2013; Noris et al., 2013, 2014).

Autosomal-Dominant Thrombocytopenias

The best recognized and most common of the inherited thrombocytopenias are the diverse group of autosomal-dominant syndromes, referred to as *MYH9-related disorder* (*MYH9-RD*) (Althaus & Greinacher, 2009; Bury et al., 2019). These include the May-Hegglin anomaly, Fechtner syndrome, Epstein syndrome, and Sebastian syndrome and share features of increased platelet size, cytoplasmic inclusions in leukocytes (Döhle bodies), and premature release of platelets. They arise from mutations in *MYH9* encoding the nonmuscle myosin heavy chain IIA, a contractile cytoskeletal protein. All *MYH9* syndromes have macrothrombocytopenia; other features such as nephritis, sensorineural deafness, and cataracts serve to distinguish them (Althaus & Greinacher, 2009; Bury et al., 2019). In patients having familial platelet disorder with predisposition to acute myeloid leukemia (FPD/AML), autosomal-dominant thrombocytopenia is secondary to mutations in the *RUNX1* gene (Song et al., 1999; Songdej & Rao, 2017). In these patients, platelet size is normal and their function is abnormal (Rao, 2013a, 2013c; Songdej & Rao, 2017) (see later discussion). Patients with platelet-type von Willebrand disease (VWD) are characterized by thrombocytopenia, gain-of-function mutations in *GPIBA*, and enhanced responsiveness to ristocetin on platelet aggregation (Miller, 1996). Other thrombocytopenias inherited in an autosomal-dominant manner include velocardiofacial syndrome and DiGeorge syndrome, which arise due to deletions within chromosome 22q11 and are associated with cardiac abnormalities, parathyroid and thymus insufficiencies, cognitive impairment, and facial dysmorphology (velocardiofacial only); and the Paris-Trousseau/Jacobsen syndrome, which is characterized by psychomotor retardation and facial and cardiac abnormalities, and arises due to deletion of a portion of chromosome 11,11q23-24, which encompasses the transcription factor *FLI1* gene. Platelets in the latter disorder are increased in size and have giant α-granules. A dominant form of macrothrombocytopenia (Mediterranean macrothrombocytopenia, Bolzano variant) has been described in southern Europe; this has been associated with mutations in GPIbα and considered a heterozygous form of Bernard-Soulier syndrome (BSS) (Savoia et al., 2001). Autosomal-dominant BSS resulting from a point mutation in a leucine tandem repeat of GPIbα has been described in the American population (Miller et al., 1992). Autosomal-dominant thrombocytopenias have been reported in association with mutations in the genes encoding cytoskeletal protein β-1 tubulin TUBB1 (*TUBB1*) and α actinin-1 (*ACTN1*), cytochrome c (*CYCS*), *ANKRD26*, and *PRKACG* (Manchev et al., 2014; Balduini et al., 2013a, 2013b; Kumar & Kahr, 2013; Noris et al., 2014). *ANKRD26* mutations are associated with increased risk of hematologic myeloid malignancies (Marquez et al., 2014). Autosomal-dominant inherited macrothrombocytopenia has been linked to *DIAPH1*, which, like MYH9-RD, is associated with hearing loss (Stritt et al., 2016), and to mutations in genes encoding GPIIb *(ITGA2B)* or GPIIIa *(ITGB3)*; these lead to constitutive activation of the GPIIb-IIIa integrin complex (Balduini et al., 2013a, 2013b). Other gene mutations that have been linked to autosomal-dominant inherited thrombocytopenia include *SFLN4*, *TPM4*, and SRC (Almazni et al., 2019). SRC mutations have also been associated with α-granule deficiency and myelofibrosis (MF) (Almazni et al., 2019). Most recently, mutations in another TF, IKZF5, have also been linked to autosomal-dominant thrombocytopenia (Lentaigne et al., 2016).

Autosomal-Recessive Thrombocytopenias

In classical BSS, macrothrombocytopenia results from biallelic mutations involving the GPIb-IX-V complex (see later discussion). Congenital amegakaryocytic thrombocytopenia (CAMT) is an autosomal-recessive disorder associated with mutations in the thrombopoietin receptor *MPL*. It is characterized by severe thrombocytopenia and absence of megakaryocytes in the bone marrow. Other causes of recessive thrombocytopenia include the gray platelet syndrome (see later discussion) linked to mutations in the *NBEAL2* gene, which encodes a BEACH protein involved in vesicular trafficking (Albers et al., 2011; Gunay-Aygun et al., 2011; Kahr

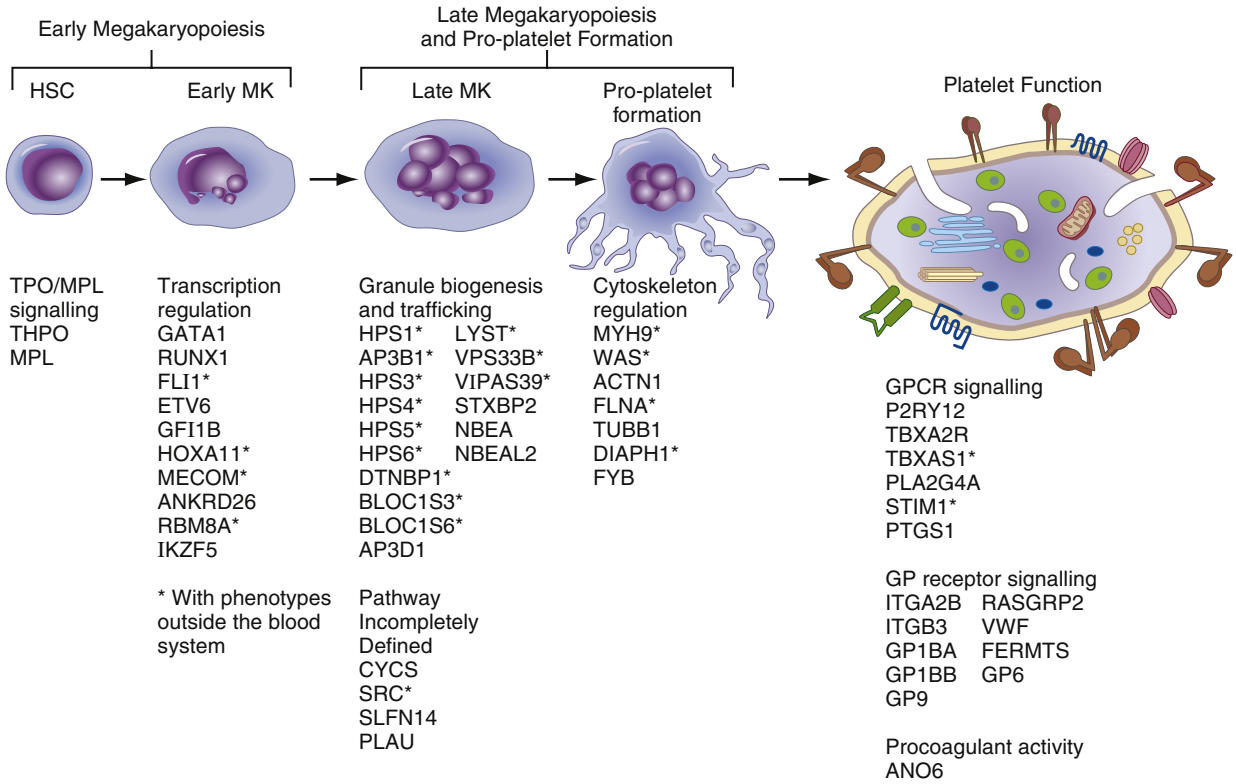

Figure 41.5 Genes underlying inherited disorders of platelet number and function. The figure shows the processes of megakaryopoiesis and platelet formation, selected aspects of platelet function, and the genes underlying the inherited platelet disorders. Each of the genes shown are categorized according to their effect on megakaryocytes and platelet biology. Those shown with asterisks are typically associated with phenotypes outside the blood system. *HSC,* Hematopoietic stem cell. (Adapted with permission from Lentaigne C, Freson K, Laffan MA, et al.: Inherited platelet disorders: toward DNA-based diagnosis, *Blood* 127(23): 2814–2823, 2016.)

TABLE 41.3

Classification of Inherited Thrombocytopenias by Platelet Size

Small Platelets (MPV <7 fL)	Normal-Sized Platelets (MPV 7–11 fL)	Large Platelets (MPV>11 fL)
Wiskott-Aldrich syndrome	Inherited amegakaryocytic thrombocytopenia	*MYH9*-related disorders
X-linked thrombocytopenia	Thrombocytopenia absent radius syndrome	Bernard-Soulier syndrome
FYB-related thrombocytopenia	Radioulnar synostosis with amegakaryocytic thrombocytopenia	*ITGA2B/ITGB3*-related thrombocytopenia
PTPRJ-related thrombocytopenia	*RUNX1* mutations (FPD/AML)	Gray platelet syndrome
	Jacobsen/Paris-Trousseau syndrome	Velocardiofacial syndrome
	ANKRD26-related thrombocytopenia	*GATA1*–related thrombocytopenia
	ETV6-related thrombocytopenia	Type 2B von Willebrand disease/Platelet-type von Willebrand disease
	IKZF5-related thrombocytopenia	*ACTN1*-related thrombocytopenia
	CYCS-related thrombocytopenia	*TUBB1*-related macrothrombocytopenia
		FLNA-related macrothrombocytopenia
		DIAPH1-related macrothrombocytopenia
		PRKACG-related macrothrombocytopenia
		GNE-related macrothrombocytopenia
		SLFN14-related macrothrombocytopenia
		TPM4-related macrothrombocytopenia
		GALE-related macrothrombocytopenia
		Thrombocytopenia associated with sitosterolemia

FPD/AML, Familial platelet disorder with predisposition to acute myeloid leukemia.
Modified with permission from Kumar R, Kahr WHA: Inherited thrombocytopenia: Clinical manifestations, laboratory abnormalities, and molecular defects of a heterogeneous group of conditions. In Rao AK, editor: *Hematology/oncology Clinics of North America: disorders of the platelets* (vol 27), Philadelphia, 2013, Elsevier, pp 465–494.

et al., 2011). Thrombocytopenia with absent radii (TAR) syndrome is associated with skeletal abnormalities and inherited in an autosomal-recessive manner. Other genes that cause an autosomal-recessive thrombocytopenia involve mutations in *FYB*, *GNE*, and *GALE*, each with distinct features or mechanisms. Small platelets are present in patients with *FYB* mutation, *GNE* mutations increase platelet clearance, and mutations in *GALE* have effects on galactose metabolism and glycosylation (Almazni et al., 2019). Recently, biallelic loss-of-function variants in *PTPRJ*, which encodes for a receptor-like protein tyrosine phosphatase, have also been associated with microthrombocytopenia, with spontaneous bleeding and impaired platelet responses to collagen (Marconi et al., 2019).

Sex-Linked Inherited Thrombocytopenias

Patients with Wiskott-Aldrich syndrome (WAS) and the related X-linked thrombocytopenia have mutations in the *WAS* gene (Massaad et al., 2013; Buchbinder et al., 2014). These patients characteristically have small platelets and the thrombocytopenia may occur in the absence of other immunologic features of the syndrome. Mutations in transcription factor GATA1

TABLE 41.4

Immunologic Thrombocytopenic Purpura (ITP)

PROPOSED DEFINITIONS OF DISEASE

Primary ITP

- Primary ITP is an autoimmune disorder characterized by isolated thrombocytopenia (peripheral platelet count <100 × 10^9/L) in the absence of other causes and disorders that may be associated with thrombocytopenia.
- The diagnosis of primary ITP remains one of exclusion; no robust clinical or laboratory parameters are currently available to establish this diagnosis with accuracy.
- The main clinical problem with primary ITP is an increased risk for bleeding, although bleeding symptoms may not always be present.

Secondary ITP: All Forms of Immune-Mediated Thrombocytopenia Except Primary ITP*

- Newly diagnosed ITP: within 3 months from diagnosis
- Persistent ITP: between 3 and 12 months from diagnosis; includes patients not reaching spontaneous remission and not maintaining complete response off therapy
- Chronic ITP: lasting for longer than 12 months
- Severe ITP: presence of bleeding symptoms at presentation sufficient to mandate treatment or occurrence of new bleeding symptoms requiring additional therapeutic intervention with a different platelet-enhancing agent or an increased dose

RECOMMENDATIONS FOR THE DIAGNOSIS OF ITP IN CHILDREN AND ADULTS

Basic Evaluation	Tests of Potential Utility in the Management of an ITP Patient	Tests of Unproven or Uncertain Benefit
Patient history	Glycoprotein-specific antibody	TPO
Family history	Antiphospholipid antibodies (including anticardiolipin and lupus anticoagulant)	Reticulated platelets
Physical examination	Antithyroid antibodies and thyroid function	Platelet-associated IgG
Complete blood count and reticulocyte count	Pregnancy test in women of childbearing potential	Platelet survival study
Peripheral blood film	Antinuclear antibodies	Bleeding time
Quantitative immunoglobulin measurement**	Viral PCR for parvovirus and CMV	Serum complement
Bone marrow examination (in selected patients)		
Blood group (Rh)		
Direct antiglobulin test		
Helicobacter pylori†		
HIV†		
HCV†		

Modified with permission from Rodeghiero F, Stasi R, Gernsheimer T: Standardization of terminology, definitions and outcome criteria in immune thrombocytopenic purpura of adults and children: report from an international working group, *Blood* 113:2386–2393, 2009.
Upper panel: ITP—proposed definitions of disease.

Lower panel: Recommendations for the diagnosis of ITP in children and adults.
CMV, Cytomegalovirus; *HCV,* hepatitis C virus; *HIV,* human immunodeficiency virus; *PaIgG,* platelet-associated immunoglobulin G; *PCR,* polymerase chain reaction; *Rh,* rhesus; *TPO,* thrombopoietin.
Modified with permission from Provan D, Stasi R, Newland AC: International consensus report on the investigation and management of primary immune thrombocytopenia, *Blood* 115:168–186, 2010.
*The acronym ITP should be followed by the name of the associated disease (for thrombocytopenia after exposure to drugs, the term *drug-induced* should be used) in parentheses, for example, "secondary ITP (lupus-associated)," "secondary ITP (HIV-associated)," and "secondary ITP (drug-induced)."
**Quantitative immunoglobulin level measurement should be considered in children with ITP and is recommended in children with persistent or chronic ITP as part of the reassessment evaluation.
†Recommended by the majority of international consensus panel members for adult patients regardless of geographic locale.

are associated with thrombocytopenia, anemia, and alteration in red cell morphology (Songdej & Rao, 2017). Mutations in the *FLNA* gene, which encodes filamin A, are associated with the X-linked dominant syndromes encompassing periventricular nodular heterotopia and otopalatodigital spectrum of disorders (Berrou et al., 2013); they have macrothrombocytopenia. The FLNA mutation has been also identified as a cause of nonsyndromic isolated thrombocytopenia.

Immune Thrombocytopenias

Immune thrombocytopenias (ITPs) are a heterogeneous group of disorders characterized by autoimmune-mediated platelet destruction (Rodeghiero et al., 2009; Provan et al., 2010). These disorders are also associated with impaired platelet production (Rodeghiero et al., 2009). *Primary* ITP is a diagnosis of exclusion, made in the absence of other causes or disorders associated with thrombocytopenia (Table 41.4). *Secondary* ITP (see Table 41.4) consists of all forms of immune-mediated thrombocytopenia except primary ITP. The clinical history is usually helpful in arriving at a tentative diagnosis, in particular in distinguishing between the newly diagnosed, persistent, chronic, and severe forms of secondary ITP, as defined in Table 41.4. A platelet count of <100,000 platelets/μL has been recommended as a threshold for diagnosis of ITP (Rodeghiero et al., 2009). This threshold seeks to avoid overdiagnosis of disease in apparently healthy people with platelet counts of 100 to 150,000/μL and to avoid inclusion of many women with pregnancy-related thrombocytopenia. Several expert panels (Provan et al., 2010; Rodeghiero et al., 2009; Neunert et al., 2011) have addressed critical issues concerning the diagnosis and management of ITP. No single laboratory test for the diagnosis of ITP constitutes a gold standard status. Several laboratory approaches were deemed to be either of "potential utility" or of "unproven or uncertain benefit," as shown in Table 41.4.

Antiplatelet antibodies, many targeted against specific platelet glycoproteins (see later discussion), can be detected only in approximately 60% of patients with ITP, which may be because of unrecognized platelet antigens, limited test sensitivity, or other platelet loss mechanisms (Cines et al., 2009a, 2009b). Of particular interest, antecedent infectious diseases are present in approximately 60% of pediatric ITP patients. Molecular mimicry, in which immune responses initially directed against an infectious organism cross-react with platelet antigens in both children and adults, appears likely in a number of instances, including infection with human immunodeficiency virus and hepatitis C virus (Karpatkin & Nardi, 1992; Karpatkin et al., 1995; Cines et al., 2009a; Stasi et al., 2009; Zhang et al., 2009). There is an association between *Helicobacter pylori* infection and ITP (Semple, 2009; Stasi et al., 2009; Yeh et al., 2010). In addition to the accelerated platelet destruction in ITP, there is also defective platelet production (McMillan, 2007; Cines et al., 2009a, 2009b). The observations that thrombopoietin mimetic agents are effective in increasing the platelet counts in these patients add further support for impaired platelet production in ITP (McMillan, 2007).

In both children and adults, there is insufficient evidence to recommend or suggest the routine use of antiplatelet, antiphospholipid and antinuclear antibodies, thrombopoietin levels, or platelet parameters obtained on automated analyzers in the evaluation of patients with suspected ITP (Neunert et al., 2011; George et al., 1996). A bone marrow examination is not necessary irrespective of age in patients presenting with typical ITP.

General treatment principles in primary ITP include immunosuppression, increasing platelet production, or decreasing platelet clearance, alone or in combination (Cuker & Neunert, 2016; Neunert et al., 2019). First-line treatment includes short-duration corticosteroids and/or intravenous immunoglobulin; second-line therapies include thrombopoietin receptor

agonists, rituximab (a chimeric antibody against CD20 on B cells) and splenectomy. For refractory patients, other treatment strategies may be employed (Cuker & Neunert, 2016; Neunert et al., 2019).

Drug-Induced Immune Thrombocytopenia (DITP)

Thrombocytopenia can be caused by a large number of drugs. DITP may be induced by classic drug-dependent antibodies (e.g., quinine), haptens (e.g., penicillin), fiban-dependent antibodies (e.g., tirofiban, integrilin), monoclonal antibodies (abciximab), autoantibodies (e.g., gold), and immune-complex formation (e.g., heparin, protamine) (Aster et al., 2004; Aster, 2007a; Al-Nouri & George, 2012; Arnold et al., 2013; Chong et al., 2013). Most commonly implicated drugs include quinine, quinidine, trimethoprim-sulfamethoxazole, vancomycin, and piperacillin/tazobactam (Von Drygalski et al., 2007; Arnold et al., 2013, 2015). Recently, oxaliplatin has been implicated to cause thrombocytopenia due to drug-dependent antibodies (Curtis et al., 2018). Other chemotherapy agents implicated in DITP include cyclophosphamide, irinotecan, dactinomycin, fludarabine, and cisplatin. A list of drugs implicated in DITP is provided in several publications (Aster & Bougie, 2007; Al-Nouri & George, 2012; Arnold et al., 2013). Information is available at www.uptodate.com/contents/drug-induced-thrombocytopenia.

The clinical features of DITP include a platelet count less than 20,000/μL and bleeding symptoms that typically begin 5 to 10 days after starting the drug. Interestingly, with GPIIb-IIIa antagonist drugs ("fibans") eptifibatide and tirofiban, acute severe thrombocytopenia may occur, even following the first exposure to the drug (Aster & Bougie, 2007). This acute thrombocytopenia results from preexisting antibodies in the patients binding to novel epitopes exposed in the drug-bound GPIIb-IIIa complex. With abciximab, which is a chimeric human-mouse Fab fragment specific for GPIIIa, preexisting antibodies against murine determinants on the chimeric antibody cause acute thromocytopenia (Aster et al., 2004). The targets of drug-dependent antibodies in patients with DITP due to quinine, sulfonamides, and others are often epitopes on platelet GPIIb-IIIa or GPIb-IX (Ahmadi et al., 2019). In the case of gold and procainamide, autoantibodies are induced that have specificity for platelet GP. Heparins (see later discussion) and protamine (Bakchoul et al., 2013; Cuker & Cines, 2013; Lee et al., 2013) induce thrombocytopenia by formation of immune complexes that bind and activate platelets.

Laboratory assessment for DITP employs normal test platelets as the target for antibody binding in the presence, but not the absence, of added drug. Recommendations regarding such testing and the appropriate controls have been advanced (Arnold et al., 2015). While a positive test generally carries high specificity for DITP, a negative test result does not necessarily exclude DITP due to the low sensitivity that has been observed with such testing (Arnold et al., 2015).

The laboratory approach to heparin-induced thrombocytopenia is discussed in Chapter 43.

BOX 41.1

Reactive Conditions in Which Elevated Platelet Counts May Be Found

Transient Processes

Acute blood loss
Recovery (rebound) from thrombocytopenia
Acute infection or inflammation
Response to exercise

Sustained Processes

Iron deficiency
Hemolytic anemia
Asplenia (e.g., after splenectomy)
Cancer
Chronic inflammatory or infectious diseases
Connective tissue disorders
Temporal arteritis
Inflammatory bowel disease
Tuberculosis
Chronic pneumonitis
Drug reactions
- Vincristine
- All-*trans*-retinoic acid
- Cytokines
- Growth factors

Reprinted with permission from Schafer AI: Thrombocytosis, *N Engl J Med* 350:1211–1219, 2004.

THROMBOCYTOSIS

In most patients, thrombocytosis is acquired. In the rare patients with inherited thrombocytosis, this results from gain-of-function mutations in either thrombopoietin or its receptor (MPL) (Skoda, 2009; Sulai & Tefferi, 2012). Acquired thrombocytosis may be primary, related to autonomous clonal bone marrow disorders, such as the myeloproliferative neoplasms (MPNs) and myelodysplastic syndromes, or reactive and secondary to conditions such as infections, chronic inflammation, malignancy, hemolysis, iron-deficiency anemia, or splenectomy (Box 41.1) (Skoda, 2009; Harrison et al., 2010; Sulai & Tefferi, 2012; Schafer, 2004) (see later discussion). The blood film should be reviewed to confirm the increase in platelets and exclude spurious thrombocytosis due to red cell abnormalities (microspherocytes and fragments). A number of clinical and laboratory findings may provide clues as to whether one is dealing with an autonomous clonal process or a reactive process (Table 41.5). This distinction is important because of the implications regarding the potential for thrombohemorrhagic complications and disease transformation in MPN, and regarding treatment strategies (cytoreduction). The platelet counts do not provide a reliable clue in this distinction. Extreme thrombocytosis (platelet counts greater than 1000 × 10^9/L), may occur in patients with either process; surgical complications and hematologic malignancies were the two dominant causes in one series with a substantial difference in etiology between inpatients and outpatients (Hsieh et al., 2019). Patients with MPN may have abnormalities in platelet and megakaryocyte structure and platelet function (see later discussion). The presence of cytogenetic abnormalities, such as in JAK2V617F and calreticulin, are strongly associated with primary thrombocytosis (Campbell

TABLE 41.5

Clinical Findings That May Distinguish Between Clonal and Secondary (Reactive) Thrombocytosis

Finding	Clonal Thrombocytosis*	Secondary (Reactive) Thrombocytosis
Underlying systemic disease	No	Often clinically apparent
Digital or cerebrovascular ischemia	Characteristic	No
Large-vessel arterial or venous thrombosis	Increased risk	No
Bleeding complications	Increased risk	No
Splenomegaly	Yes, in about 40% of patients	No
Peripheral blood smear	Variable, may include giant platelets	Normal platelets
Platelet function	May be abnormal	Normal
Bone marrow megakaryocytes		
• Number	Increased	Increased
• Morphologic features	Giant, dysplastic forms with increased ploidy; associated with large masses of platelet debris	Normal
Presence of cytogenetic abnormalities (mutations in *JAK2*, *MPL*, *CALR*, *BCR-ABL1*)	Present	Absent

BCR-ABL1, fusion gene formed by translocation between chromosomes 9 and 22; *CALR,* calreticulin; *JAK2,* Janus kinase 2; *MPL,* thrombopoietin receptor gene.
*Clonal thrombocytosis includes essential thrombocythemia and other myeloproliferative disorders.
Modified with permission from Schafer AI: Thrombocytosis, *N Engl J Med* 50:1211–1219, 2004.

BOX 41.2

Inherited Disorders of Platelet Function

I. Abnormalities of glycoprotein adhesion receptors
  A. Integrin $\alpha_{IIb}\beta_3$ (glycoprotein IIb/IIIa; CD41/CD61): Glanzmann thrombasthenia
  B. Glycoproteins Ib (CD42b,c)/IX (CD42a)/V: Bernard-Soulier syndrome
  C. Glycoprotein Ibα (CD42b,c): Platelet-type (pseudo-) von Willebrand disease
  D. Integrin $\alpha_2\beta_1$ (glycoprotein Ia/IIa; VLA-2; CD49b/CD29)
  E. CD36 (glycoprotein IV)
  F. Glycoprotein VI
II. Abnormalities of platelet granules
  A. δ-Storage pool deficiency
  B. Gray platelet syndrome (α-storage pool deficiency)
  C. α,δ-Storage pool deficiency
  D. Quebec platelet disorder
III. Abnormalities of platelet receptors, signaling and secretion
  A. Defects in platelet agonist receptors or agonist-specific signal transduction
  • Adenosine diphosphate (ADP) receptor defects ($P2Y_{12}$, $P2X_1$),
  • Thromboxane A_2 receptor defect
  • Collagen receptor defect
  • Epinephrine receptor defect
  B. Defects in guanosine triphosphate (GTP)–binding proteins
  • Gαq deficiency
  • Gαs hyperfunction and genetic variation in extra-large Gαs
  • Gαi1 deficiency
  • CaLDAG-GEFI deficiency (*RASGRP2*)
  C. Phospholipase C (PLC)-β_2 deficiency and defects in PLC activation
  D. Calcium mobilization
  E. Defects in protein phosphorylation protein kinase C (PKC)-θ deficiency
  F. Defects in arachidonic acid metabolism and thromboxane production
  • Phospholipase A_2 deficiency
  • Cyclooxygenase [prostaglandin H_2 synthase-1 deficiency],
  • Thromboxane synthase deficiency
IV. Abnormalities of platelet coagulant activity (Scott syndrome)
V. Abnormalities of a cytoskeletal structural protein
  • β_1-tubulin
  • Filamin A
VI. Abnormalities in cytoskeletal linking proteins
  A. Wiskott-Aldrich syndrome protein (WASP)
  B. Kindlin-3: Leukocyte adhesion defect (LAD)-III; LAD-1 variant; integrin activation deficiency disease defect (IADD)
VII. Abnormalities of transcription factors leading to functional defects
  A. RUNX1 (familial platelet dysfunction with predisposition to acute myelogenous leukemia)
  B. GATA-1
  C. FLI1 (Paris-Trousseau/Jacobsen syndrome)
  D. GFI1B
  E. ETV6
VIII. Other Disorders
  • Arthrogryposis renal dysfunction-cholestasis syndrome (ARC) (*VPS33B, VPS16B*)

& Green, 2006; Skoda, 2009; Klampfl et al., 2013; Nangalia et al., 2013). Lastly, studies utilizing platelet transcript profiling of patients with thrombocytosis have shown that specific biomarker gene subsets may predict their thrombocytosis class (Gnatenko et al., 2010; Nagalla & Bray, 2010).

Patients with MPN may develop bleeding or thrombotic events. Unless additional associated risk factors, such as malignancy, are present, thrombotic events are unlikely in reactive thrombocytosis (Sulai & Tefferi, 2012). However, in one study (Ho et al., 2012), reactive thrombocytosis occurred in about 10% of patients in the recovery phase after an admission to the intensive care unit and was associated with an increase in venous thromboembolism.

INHERITED DISORDERS OF PLATELET FUNCTION

OVERVIEW

Box 41.2 provides a list of inherited platelet disorders associated with impaired platelet function (Fig. 41.6). Figure 41.5 shows the genes underlying inherited platelet disorders, including those of function and number. Although rare, these disorders provide enormous insights into platelet physiology. In most patients with inherited abnormalities of platelet aggregation and secretion, the underlying molecular-genetic mechanisms remain unknown. Not all disorders resulting in an impaired platelet role in hemostasis are due to a defect in the platelets per se. Examples are patients with VWD and afibrinogenemia, with deficiencies of specific plasma proteins essential for normal platelet function. In VWD, platelet adhesion to subendothelium is abnormal, which is also the case in patients with BSS, in whom platelets are deficient in the GPIb-IX-V complex, the receptor for VWF on platelets (see Fig. 41.6). Binding of fibrinogen to the GPIIb-IIIa complex is a prerequisite for platelet aggregation. Thus, platelet aggregation on activation is impaired in both inherited afibrinogenemia and in Glanzmann thrombasthenia, in which platelets are deficient in platelet membrane GPIIb-IIIa complex. Platelet aggregation and secretion are the end result of numerous processes that follow the initial interaction of an agonist with the platelet (see Figs. 41.2 and 41.6). Thus, abnormalities in many platelet events may lead to a decrease in these responses. Patients with defects in "platelet secretion and signal transduction" are a heterogeneous group considered together for convenience rather than based on an understanding of the molecular abnormality. The common characteristics in these patients are abnormal aggregation responses and an inability to release dense granule contents upon activation of platelet-rich plasma with agonists such as ADP, epinephrine, and collagen (Bennett & Rao, 2013). In aggregation studies, the second wave of aggregation is blunted or absent. The platelet dysfunction in such patients arises from diverse mechanisms. A small proportion of these patients have a deficiency of dense granule stores (storage pool deficiency). In some of the others, impaired platelet function arises due to aberrations in signal transduction events that lead to secretion and aggregation. Another group consists of patients who have an abnormality in platelet interactions with coagulation proteins; the best described is Scott syndrome, characterized by impaired expression of surface PS on activation (Weiss, 1994, 2009; Kodigepalli et al., 2015). Defects related to platelet cytoskeleton or structural proteins may also be associated with platelet dysfunction, as in WAS or in patients with abnormalities related to kindlin-3. Several reports document impaired platelet function associated with mutations in transcription factors (RUNX1, GATA1, FLI1, GFI1b, and others) that regulate gene expression in megakaryocytes and platelets. As a group, they may be more common than appreciated. In addition to the patients described earlier, there are patients who have abnormal platelet function associated with systemic disorders or are syndromic, such as Hermansky-Pudlak syndrome or Chédiak-Higashi syndrome (Westbury et al., 2015; Sivapalaratnam et al., 2017). These and other entities are described in the following sections. The gene symbols, where relevant, are shown in italics.

ABNORMALITIES OF GLYCOPROTEIN ADHESION RECEPTORS

Integrin $\alpha_{IIb}\beta_3$ (Glycoprotein IIb/IIIa; CD41/CD61): Glanzmann Thrombasthenia (*ITGA2B/ITGB3*)

Glanzmann thrombasthenia is a rare autosomal-recessive disorder characterized by markedly impaired platelet aggregation in response to activation with all physiologic agonists, a prolonged bleeding time, and relatively more severe mucocutaneous bleeding manifestations than most inherited platelet function disorders (Nurden et al., 2013; Diz-Kucukkaya & Lopez, 2013; Nurden & Nurden, 2014; Rao & Coller, 2015a). It has been reported in clusters in populations where consanguinity is common. The primary abnormality in thrombasthenia is a quantitative or qualitative defect in the GPIIb-IIIa complex, a heterodimer consisting of GPIIb (*ITGA2B*) and GPIIIa (*ITGB3*) whose synthesis is governed by two distinct genes located on chromosome 17. Thus, thrombasthenia may arise due to a mutation in either gene, leading to decreased platelet surface expression of the complex. Because of this, fibrinogen binding to platelets on activation and aggregation is impaired. Numerous distinct mutations involving *ITGA2B* and *ITGB3* have been described in thrombasthenia (Nurden et al., 2015; Rao & Coller, 2015a) and included in the database for this entity (https://glanzmann.mcw.edu/). Clot retraction, a function of the interaction of GPIIb-IIIa with the platelet cytoskeleton, is also impaired. Investigation of Glanzmann thrombasthenia has advanced the understanding of platelet pathophysiology and development of major antiplatelet agents (Coller & Shattil, 2008).

The diagnostic hallmark of thrombasthenia is absence or marked decrease of platelet aggregation (see Fig. 41.3) in response to virtually all platelet agonists (except ristocetin), with absence of both the primary and secondary wave of aggregation; the shape change response is preserved.

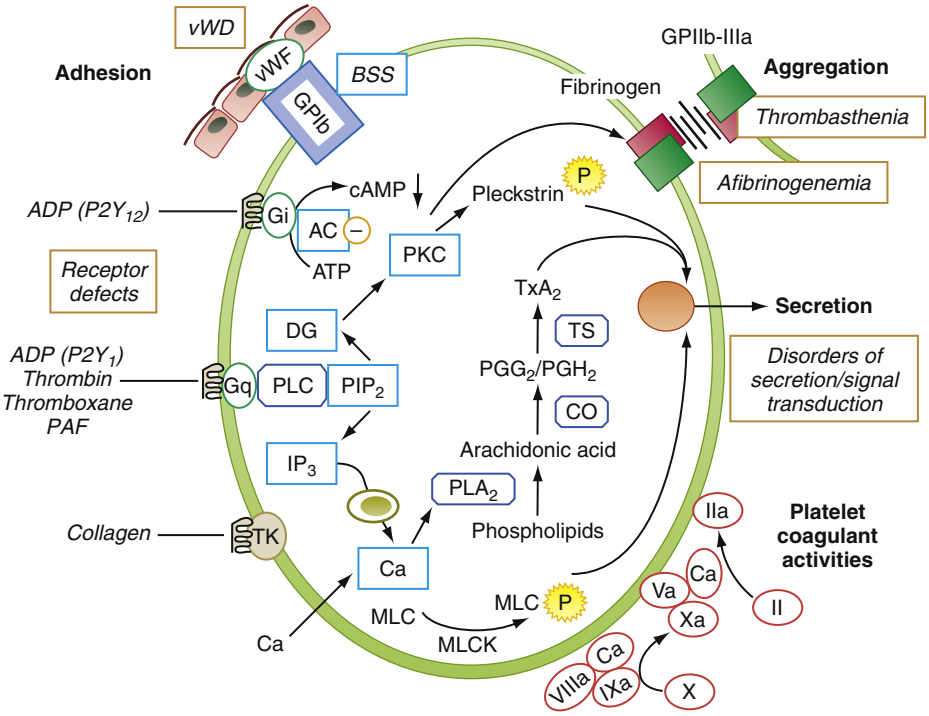

Figure 41.6 A schematic representation of selected platelet responses to activation and inherited disorders of platelet function. *AC,* Adenylyl cyclase; *BSS,* Bernard-Soulier syndrome; *CO,* cyclooxygenase; *DAG,* diacylglycerol; *G,* GTP-binding protein; *IP3,* inositol trisphosphate; *MLC,* myosin light chain; *MLCK,* myosin light-chain kinase; *P2Y1, P2Y12,* G-protein–coupled adenosine diphosphate (ADP) receptors; *PAF,* platelet-activating factor; *PGG2/PGH2,* prostaglandins G2 and H2; arachidonic pathway intermediates; *PIP2,* phosphatidylinositol bisphosphate; *PKC,* protein kinase C; *PLA$_2$,* phospholipase A$_2$; *PLC,* phospholipase C; *TK,* tyrosine kinase; *TS,* thromboxane synthase; *VWD,* von Willebrand disease; *vWF,* von Willebrand factor. The Roman numerals in the circles represent coagulation factors. (Modified with permission from Rao AK: Inherited disorders of platelet function: disorders of signal transduction and secretion, *Am J Med Sci* 316:69–76, 1998.)

Platelet dense granule secretion may be decreased with weak agonists (e.g., ADP) but normal on activation with thrombin. Heterozygotes have approximately half the number of platelet GPIIb-IIIa complexes, the platelet aggregation responses are normal, and these individuals do not have a bleeding disorder.

Because the platelet antigen Pl^{A1} is associated with glycoprotein IIIa, this antigen is typically decreased in patients with Glanzmann thrombasthenia (Kunicki & Aster, 1978; Von dem Borne et al., 1981). The diagnosis of Glanzmann thrombasthenia can be established by demonstrating a marked decrease in platelet GPIIb-IIIa using flow cytometry (Giannini et al., 2008; Miller, 2009), as illustrated in Figure 41.4. Definitive characterization of the mutations in *ITGA2B* and *ITGB3* may be undertaken by molecular techniques (Nurden et al., 2011; Buitrago et al., 2015; Rao & Coller, 2015a). Although inherited afibrinogenemia is also characterized by a similar absence of platelet aggregation, in this disorder prothrombin time (PT), activated partial thromboplastin time (APTT), and thrombin time are markedly prolonged, whereas they are normal in thrombasthenia.

Glycoproteins Ib (CD42b,c)/IX (CD42a)/V: Bernard-Soulier Syndrome (*GP1BA, GP1BB, GP9*)

BSS is a rare autosomal-recessive platelet function disorder resulting from an abnormality in the platelet GPIb-IX-V complex, which consists of four polypeptides and distinct gene products: GPIbα (*GP1BA*), GPIbβ (*GP1BB*), GPIX (*GP9*) and GPV (*GP5*) (Diz-Kucukkaya & Lopez, 2013; Rao & Coller, 2015a; Savoia et al., 2014). This complex mediates the vWF binding to platelets and, thus, plays a major role in platelet adhesion to the subendothelium, especially at higher shear rates. Platelet GPIb-IX-V complexes are markedly reduced in number or functionally abnormal in BSS. Although GPV is also decreased in BSS platelets, it is not required for platelet surface GPIb-IX expression. Bleeding time is markedly prolonged, the platelet counts are moderately decreased, and the platelets are markedly increased in size. In platelet aggregation studies, responses to the commonly used agonists ADP, epinephrine, thrombin, and collagen are normal. Characteristically, aggregation in PRP in response to ristocetin is decreased or absent. These findings in the aggregometer are almost the reciprocal of those in Glanzmann thrombasthenia. Although ristocetin-induced aggregation is impaired in both VWD and BSS, plasma vWF and factor VIII are normal in BSS. Moreover, in BSS, the addition of exogenous vWF (present in plasma cryoprecipitate fractions) does not restore ristocetin-induced agglutination of platelets. Thrombin-induced responses may also be decreased.

Platelets from patients with BSS have a striking decrease in surface membrane glycoprotein Ib (Nurden, 2014a), which can be demonstrated using flow cytometry (see Fig. 41.4). Numerous specific point mutations or deletions in GPIbα, GPIbβ, and GPIX, when present in homozygous or doubly heterozygous fashion, result in the classical BSS phenotype (Savoia et al., 2014). Mutations in *GP1BA* are most common. The variants identified are available in the Leiden Open Variation Databases (LOVD) at http://www.lovd.nl/GP1BA, http://www.lovd.nl/GP1BB, and http://www.lovd.nl/GP9.

Glycoprotein Ibα (CD42b,c): Platelet-type or Pseudo–von Willebrand Disease (*GP1BA*)

This disorder results from dominant gain-of-function variants in GP1BA (Miller et al., 1991) and there is enhanced binding of vWF to platelet GPIbα with subsequent removal of high-molecular-weight forms of vWF in plasma (Weiss et al., 1982). Patients have variable thrombocytopenia, made worse by pregnancy, and variably enlarged platelets (Sanchez-Luceros et al., 2017). The platelets are hyper-responsive to low doses of ristocetin in aggregation studies. Because the abnormality is in platelet GPIbα rather than in vWF, this entity has been called *platelet-type VWD* or *pseudo-VWD*.

Glycoprotein VI (*GP6*)

GPVI receptor on platelets, encoded by GP6, mediates collagen-induced platelet activation. Several families have been described (Jandrot-Perrus et al., 2019) with recessive GP6 variants, in whom the platelets failed to aggregate in response to collagen, collagen-related peptide (CRP), and convulxin while responses to other agonists were normal.

Integrin $\alpha_2\beta_1$ (Glycoprotein Ia/IIa; VLA-2; CD49b/CD29) (*ITGA1/ITGA2*)

α2β1 (GPIa/IIa) also mediates platelet adhesion to collagen and platelet activation under certain conditions. Two patients have been reported with mild bleeding symptoms and decreased levels of platelet α2β1 (Rao & Coller, 2016).

ABNORMALITIES OF PLATELET GRANULES

Patients with deficiencies of dense granule contents or deficiencies in their secretion are characterized by absence of the second wave of aggregation upon stimulation of PRP with ADP or epinephrine. Responses to collagen, thromboxane analog (U46619), and AA may also be impaired. Conceptually, platelet function is abnormal either when the granule contents are diminished (storage pool deficiency [SPD]) or when there is an aberration in the activation mechanisms governing their secretion (see Box 41.2).

Deficiency of Granule Stores

The term *storage pool deficiency* (*SPD*) refers to patients with deficiencies in platelet content of dense granules (δ-SPD), α-granules (α-SPD, gray platelet syndrome) or both types of granule (αδ-SPD) (Gunay-Aygun et al., 2004; Rao, 2013c; Rao & Coller, 2015a; Hayward et al., 2006).

δ-Storage Pool Deficiency

Patients with dense granule SPD (δ-SPD) are a heterogeneous group and have a mild to moderate bleeding diathesis associated with a variably prolonged bleeding time. In platelet studies, the second wave of aggregation in response to ADP and epinephrine is absent or blunted, and the collagen response is markedly impaired. However, both impaired (Weiss & Lages, 1981) and normal (Ingerman et al., 1978) aggregation responses to AA have been noted. The responses to epinephrine may also be variable and normal (Weiss & Lages, 1988). Interestingly, some patients with δ-SPD have had prolonged bleeding times and normal aggregation (Nieuwenhuis et al., 1987; Israels et al., 1990). Thrombin-induced secretion of acid hydrolases is also impaired in SPD platelets; this is corrected by addition of exogenous ADP (Lages et al., 1988).

Normal platelets possess 3 to 8 dense granules per platelet (each 200–300 nm in diameter). Under the electron microscope, dense granules are decreased in SPD platelets (White, 1987). Other methods to demonstrate a decrease in dense granules include fluorescence microscopy after staining platelets with mepacrine (quinacrine); specific staining by uranyl ions (uranaffin reaction) of both the membrane and core of the dense granules; and, more recently, super-resolution microscopy (Knight et al., 2017). Flow cytometry can also be applied to assess the fluorescent staining of dense granules (Linden et al., 2004). By direct biochemical measurements, the total platelet and granule ATP and ADP contents are decreased (Holmsen, 1979) along with other dense granule constituents, calcium, polyphosphate, and serotonin. Incubation of normal platelets with ^{14}C-serotonin results in its incorporation into dense granules and subsequent secretion upon activation. In SPD platelets, the initial rate of uptake of ^{14}C-serotonin is normal, but its retention over 4 to 6 hours is decreased.

Other abnormalities reported in some patients with δ-SPD include decreased synthesis of prostaglandins, TXA2, and malondialdehyde in platelets activated with collagen and epinephrine, but not arachidonate; impaired liberation of AA from membrane phospholipids; alterations in agonist-induced rise in cytoplasmic Ca^{2+} levels; and impaired platelet procoagulant activity (prothrombinase activity) upon activation (Rao & Coller, 2016).

δ-SPD has been reported in association with other syndromic inherited disorders, such as Hermansky-Pudlak syndrome (HPS) (characterized by oculocutaneous albinism and increased reticuloendothelial ceroid), Chédiak-Higashi syndrome, WAS, TAR syndrome, and Griscelli syndrome (Menasche et al., 2000; Gunay-Aygun et al., 2004; Huizing et al., 2008). TAR syndrome is caused by a compound inheritance of a low-frequency regulatory SNP and a rare null mutation in exon-junction complex subunit *RBM8A* (Albers et al., 2012). The simultaneous occurrence of δ-SPD and defects in skin pigment granules, as in HPS, points to the interrelatedness of the two kinds of granules with respect to genetic control, a concept further advanced by animal models (Huizing et al., 2001, 2008; Novak et al., 1984; Menasche et al., 2000; Gunay-Aygun et al., 2004).

Dense granule membranes possess the lysosomal proteins lysosomal-associated membrane protein 2 (LAMP2) and CD63 (granulophysin or LAMP3) (Nishibori et al., 1993; Israels et al., 1996) as well as P-selectin and GPIIb-IIIa. Granulophysin is deficient in HPS platelets (Gerrard et al., 1991). Studies with antigranulophysin antibody demonstrated the presence of the normal number of granules in platelets of two nonalbino SPD patients (McNicol et al., 1994). These patients, therefore, may have the granules but with reduced contents.

A substantial amount of our information in SPD has been obtained from patients with HPS, which is characterized by oculocutaneous albinism, platelet SPD, and lipofuscinosis (Gunay-Aygun et al., 2004; Huizing et al., 2008). There is a large group of HPS patients in northwest Puerto Rico, where HPS occurs in 1 in every 1800 individuals (gene frequency, 1 in 21) (Witkop et al., 1990; Gahl et al., 1998). There are at least 10 known HPS-causing genes leading to various subtypes of human HPS, with most patients being in HPS-1 (*HPS1*) and from Puerto Rico (Gunay-Aygun et al., 2004; Huizing et al., 2008; Cullinane et al., 2011; Sivapalaratnam et al., 2017). There are several mouse models of HPS; some constitute models for the human subtypes (Gunay-Aygun et al., 2004; Huizing et al., 2008). Together, the human disease and mouse models have been an invaluable source of information about vesicle formation and trafficking. The human HPS subtypes are autosomal recessive, and the heterozygotes have no clinical findings. In addition to the albinism, which is variable between the HPS subtypes, most patients have inherited nystagmus and decreased visual acuity. There are two additional manifestations in HPS patients: granulomatous colitis and pulmonary fibrosis (Gahl et al., 1998; Gunay-Aygun et al., 2004). Interestingly, some patients described to have δ-SPD have been subsequently shown to have mutations in transcription factors *RUNX1* (Weiss et al., 1979b; Michaud et al., 2002; Connelly et al., 2014) and GFI1B (Ferreira et al., 2017), indicating the multiple genetic abnormalities associated with δ-SPD.

Chédiak-Higashi syndrome is a rare autosomal-recessive disorder characterized by oculocutaneous albinism, immunodeficiency, neurologic dysfunction, and the presence of giant cytoplasmic inclusions in different cells (Huizing et al., 2001, 2008). Chédiak-Higashi syndrome patients have defective cytotoxic T and natural killer (NK) cell function. It arises from mutations in the lysosomal trafficking regulator (*LYST*) gene on chromosome 1. The protein coded by this gene (CHS1) is a member of the BEACH protein family and is considered to participate in intracellular membrane fusion reactions and vesicle trafficking (Huizing et al., 2001, 2008; Tchernev et al., 2002). These patients may develop hemophagocytic lymphohistiocytosis.

Gray Platelet Syndrome

The term *gray platelet syndrome* (*GPS*) is derived from the gray appearance of platelets with paucity of granules in peripheral blood smears from these patients. Patients with GPS have an isolated deficiency of α-granule contents with normal dense granules. GPS is a heterogeneous disorder (Nurden & Nurden, 2007, 2008). These patients have a lifelong bleeding diathesis, mild thrombocytopenia, and a prolonged bleeding time (Nurden & Nurden, 2008; Pluthero et al., 2018). Under the electron microscope, platelets and megakaryocytes reveal absent or markedly decreased α-granules. The platelets are severely and selectively deficient in α-granule proteins: PF4, β-thromboglobulin, vWF, thrombospondin, fibronectin, factor V, high-molecular-weight kininogen, and PDGF. Platelet aggregation responses have been variable. Responses to ADP and epinephrine were normal in most patients; in some patients, aggregation responses to thrombin, collagen, and ADP have been impaired. Impaired thrombin-induced Ca^{2+} mobilization and an increase in Ca^{2+} transport have also been reported. Plasma PF4 levels are elevated in some patients. There is increased reticulin in the bone marrow from GPS patients, attributed to elevated PDGF levels. Some patients have splenomegaly and myelofibrosis. Studies on megakaryocytes cultured from peripheral blood of three GPS patients show that vWF is synthesized but is secreted into extracellular space instead of normal α-granule packaging (Drouin et al., 2001).

The molecular mechanisms leading to α-granule deficiency are heterogeneous and include failure of α-granule maturation during megakaryocyte differentiation, transport or targeting of proteins to α-granules, and/or synthesis of granule membranes and contents (Nurden & Nurden, 2007; Maynard et al., 2010). Proteomic studies in a GPS patient suggested a failure to incorporate endogenously synthesized megakaryocytic proteins into α-granules (Maynard et al., 2010). Some GPS patients have elevated plasma PF4 (Nurden & Nurden, 2007), suggesting that PF4 synthesis was normal and the primary defect was impaired granule biogenesis with leakage of PF4. Some patients with decreased α-granule contents have a mutation in transcription factor RUNX1 (Michaud et al., 2002; Weiss et al., 1979b), and PF4 is a transcriptional target of RUNX1 (Aneja et al., 2011). This suggests that decreased platelet PF4 in these patients may represent defective PF4 synthesis. X-linked thrombocytopenia GPS has been reported in association with a mutation in *GATA-1* (Tubman, 2007). Most recessive GPS patients identified to date have had recessive mutations in *NBEAL2*, which encodes for a protein linked to vesicle transport (Pluthero et al., 2018). Autosomal-dominant GPS due to mutations in transcription factor gene *GFI1B* has been reported in two kindreds (Stevenson et al., 2013; Monteferrario et al., 2014). Mutations in *VPS33B* and *VPS16B* genes encoding proteins involved in vesicle trafficking have been associated with human α-granule deficiency in arthrogryposis multiplex congenita, renal dysfunction, and cholestasis (ARC) syndrome (Urban & Christensen, 2012; Chen et al., 2017). Thus, multiple mechanisms and inheritance patterns can lead to α-granule deficiency.

Quebec Platelet Syndrome

Quebec platelet syndrome (QPS) is an autosomal-dominant disorder associated with delayed mucocutaneous bleeding and abnormal proteolysis of α-granule proteins due to increased amounts of platelet urokinase-type plasminogen activator (uPA) (Blavignac et al., 2011). These patients are characterized by normal to reduced platelet counts, proteolytic degradation of α-granule proteins, deficiency of the factor V–binding protein multimerin, and defective aggregation selectively with epinephrine. Platelet factor V, but not plasma factor V, is degraded along with other α-granule proteins, including fibrinogen, vWF, thrombospondin, osteonectin, fibronectin, and P-selectin. The increased plasmin activity in QPS megakaryocytes is due to a direct tandem duplication of the uPA gene (*PLAU*) (Paterson et al., 2010; Diamandis, 2008). This increase in intraplatelet generation of plasmin leads to degradation of several α-granule proteins. Patients with QPS suffer from mucocutaneous bleeding following injury that is unresponsive to platelet transfusions but responsive to fibrinolytic inhibitors.

ABNORMALITIES OF PLATELET RECEPTORS, SIGNALING PATHWAYS, AND SECRETION

Signal transduction mechanisms encompass processes that are initiated by the interaction of agonists with specific platelet receptors and include responses such as G-protein activation and activation of effector enzymes such as phospholipase C and phospholipase A2 (see Figs. 41.2 and Fig. 41.4). If the key components in signal transduction are the surface receptors, the G-proteins, and the effectors, evidence now exists for specific platelet abnormalities at each of these levels, although the specific gene involved is unknown in several of such patients.

Defects in Receptors

Patients with defects in platelet-agonist interaction have impaired responses because of an abnormality in the platelet surface receptor for a specific agonist. Such receptor defects have been documented for epinephrine, collagen, ADP, and TXA2 (Rao, 2013c; Rao & Coller, 2015a; Sivapalaratnam et al., 2017). Several patients have been described with a mutation in the TXA2 receptor. Hirata and colleagues described an Arg 60–to–Leu mutation of the human TXA2 receptor in a dominantly inherited bleeding disorder (Hirata et al., 1994). Other mutations (*D304N* and *V2416*) have also been described (Mumford et al., 2010; Flamm et al., 2012). Several patients have been described with a defect in the P2Y12 ADP receptor (Cattaneo et al., 1992, 1997; Nurden et al., 1995; Daly et al., 2009), which is coupled to inhibition of adenylyl cyclase. Because ADP and TXA2 play a synergistic role in platelet responses to several agonists, these patients with receptor defects manifest abnormal responses to multiple agonists. Specific deficiencies in the P2Y1 (Oury et al., 1999) and P2X (Oury et al., 2000) ADP receptors have also been documented but are less well characterized.

A few patients have been described with isolated blunting of platelet responses to collagen associated with deficiencies in platelet GPIa and GPVI (Rao & Coller, 2015a; Nieuwenhuis et al., 1985, 1986; Kehrel et al., 1988; Jandrot-Perrus et al., 2019). Reduced surface expression by flow cytometry of GPIa on the platelets of 18 individuals from 2 unrelated families with an autosomally dominant bleeding disorder has been reported; Western blot analysis also showed mildly reduced GPIa. However, no mutations in either GPIa or GPIIa could be demonstrated (Noris et al., 2006). Abnormalities of GPVI have been associated with increased bleeding tendency in several families and associated with mutations in GPVI (Rao & Coller, 2015a; Jandrot-Perrus et al., 2019). In some of these patients, evidence has been provided for a defect in GPVI signaling. Deficiency of platelet GPVI in some patients has been attributed to anti-GPVI antibody-mediated loss of this GP (Boylan et al., 2004).

Defects in G-Proteins and Their Activation

G-proteins are a heterogeneous group of proteins that link surface receptors and intracellular effector enzymes; defects in G-protein activation can impair signal transduction. Patients with deficiencies in the level of Gαq (Gabbeta et al., 1997) and Gαi1 (Patel et al., 2003) have been described. A patient with Gαq deficiency had a mild bleeding disorder, abnormal aggregation and secretion responses to a number of agonists, and diminished GTPase activity (a reflection of G-protein α-subunit function) on activation. Additionally, impaired platelet responses have been reported in association with Gαs hyperfunction (which leads to increased cAMP levels) and alterations in the Gαs gene (*GNAS1*) (Freson et al., 2001b). Several families have been described with decreased platelet aggregation, impaired aIIbB3 activation (decreased PAC-1 or fibrinogen binding) in response to multiple agonists and a mutation in RAS guanyl-releasing protein-2 (*RASGRP2*), the gene encoding for the protein calcium and DAG-regulated guanine exchange factor-1 (CalDAG-GEF1) (Canault et al., 2014; Palma-Barqueros et al., 2019).

Defects in Phospholipase C Activation, Calcium Mobilization, and Protein Phosphorylation

Platelet signal transduction is also impaired by defects in phospholipase C activation, calcium mobilization, and protein phosphorylation. Some patients have been identified with a relatively mild bleeding diathesis and impaired dense granule secretion, although their platelets have normal granule stores and, in general, synthesize substantial amounts of TXA2. On laboratory testing, these patients have abnormal aggregation and secretion, particularly in response to weaker agonists (ADP, epinephrine, PAF). The response to relatively stronger agonists such as arachidonate and high concentrations of collagen may be normal. Such patients appear to be more common than those with SPD or defects in TXA2 synthesis. Defects in early platelet activation events, including Ca^{2+} mobilization, phosphatidylinositol hydrolysis, and phosphorylation of pleckstrin (a protein phosphorylated by protein kinase C) have been described (Rao, 2013c; Rao & Coller, 2015a). Specific deficiencies at the level of phospholipase C-β2 (Lee et al., 1996; Yang et al., 1996) and protein kinase C-θ (Sun et al., 2004) have been documented. Activation of GPIIb-IIIa and platelet fibrinogen-binding is a prerequisite for aggregation and is a signal-transduction–dependent process. Defects in GPIIb-IIIa activation due to upstream signal-transduction defects have been noted in some patients (Gabbeta et al., 1996). In some of these patients, the mutation has been in a transcription factor, *RUNX1* (Songdej & Rao, 2017). In many of these patients, the causative gene abnormality is not established.

Abnormalities in Arachidonic Acid Metabolism and Thromboxane Synthesis

A major platelet response to activation is liberation of AA from phospholipids and its subsequent conversion to TXA2, which plays a synergistic role in the response to several agonists. Patients have been described with impaired liberation of AA from membrane phospholipids related to an abnormality in phospholipase A2, group IVA (encoded by *PLA2G4A*) (Adler et al., 2008), as well as with inherited deficiencies of cyclooxygenase and thromboxane synthase (Genevieve et al., 2008; Rao, 2013c; Rao & Coller, 2015a; Chan et al., 2020). These lead to diminished TXA2 production on platelet stimulation. Mutations in thromboxane synthase (encoded by *TXBSA1*) have been associated with increased bone density disorder and impaired response upon activation with AA (Genevieve et al., 2008).

DEFECTS IN CYTOSKELETAL PROTEINS: β1-TUBULIN (TUBB1) AND FILAMIN (FLNA)

Variants in *TUBB1* have been associated with macrothrombocytopenia, rounded platelets with abnormal marginal bands of microtubules, and mild abnormalities of platelet aggregation, secretion, and adhesion to collagen (Kunishima et al., 2009). Filamin A is an actin-binding protein and the predominant platelet filamin. Several syndromic and nonsyndromic patients have been reported with X-linked recessive and dominant variants in *FLNA* associated with macrothrombocytopenia (Kunishima et al., 2010, Berrou et al., 2013). Platelet function abnormalities in these patients include defects in platelet aggregation, secretion, GPVI signaling, and thrombus growth on collagen.

DEFECTS IN CYTOSKELETAL LINKING PROTEINS

Wiskott-Aldrich Syndrome (WAS)

WAS is an X-linked inherited disorder affecting T lymphocytes and platelets, characterized by thrombocytopenia, small platelets, immunodeficiency, and eczema (Remold-O'Donnell et al., 1996; Massaad et al., 2013; Buchbinder et al., 2014). Bleeding manifestations are variable and driven by the thrombocytopenia. WAS arises from mutations in the gene coding for the WAS protein (WAS), a multidomain protein that relays signals from the cell surface to the actin cytoskeleton and regulates its reorganization. Platelet abnormalities include decreased survival, dense granule SPD, and deficiencies of platelet GPIb, GPIIb-IIIa, and GPIa. Platelet aggregation responses have been variable, from decreased to enhanced (Buchbinder et al., 2014; Rao & Coller, 2015a).

Kindlin-3 Deficiency–Leukocyte Adhesion Deficiency (*FERMT3*)

Mutations in another cytoskeletal linking protein, kindlin-3, encoded by the *FERMTS3* gene, is associated with markedly abnormal aggregation responses to multiple agonists resembling Glanzmann thrombasthenia and features of leukocyte adhesion–deficiency (LAD) disorder (Pasvolsky et al., 2007; Moser et al., 2008; Malinin et al., 2009). This disorder, called LAD-III, is characterized by a hemorrhagic diathesis in combination with a variable predisposition to infections and inflammation without pus formation, and poor wound healing. Kindlin-3 binds to the cytoplasmic domain of the integrin β3 subunit of αIIbβ3. Platelet aggregation studies demonstrate defects similar to those observed in GT, with the absence of both the primary and secondary waves of aggregation (Pasvolsky et al., 2007; Moser et al., 2008; Malinin et al., 2009).

DISORDERS OF PLATELET PROCOAGULANT ACTIVITIES: SCOTT SYNDROME (ANO6)

Platelet activation results in redistribution of PS to the outer surface; this is important in the expression of platelet procoagulant activities (PCAs). Several specific key enzymatic coagulation reactions occur on the platelet surface. A few patients have been described in whom the platelet contribution

to blood coagulation is impaired, but aggregation and secretion responses are normal; this entity has been named the *Scott syndrome* (Weiss, 1994, 2009). Defects in PCA may also be secondary to abnormalities in platelet aggregation, such as in patients with SPD and thrombasthenia. Patients with Scott syndrome have a bleeding disorder; the bleeding time, platelet aggregation responses, and coagulation tests (PT and PTT) have been normal. In the original patient described by Weiss, platelet factor Xa binding sites as well as the platelet binding of factors IXa and VIIIa were diminished, associated with a decreased surface expression of PS following platelet activation (Weiss, 1994). In patients with Scott syndrome, the serum PT, which reflects the consumption of prothrombin and completeness of clotting of whole blood, is abnormally short, indicating incomplete coagulation (Weiss et al., 1979a). More specific assays of "platelet factor 3," the phenomenologic designation of the platelet contribution to accelerating clot formation, are also abnormal. Recessive mutations in phospholipid scramblase, TMEM16F (transmembrane protein 16F) encoded by *ANO6* have been identified in patients with Scott syndrome (Suzuki et al., 2010; Castoldi et al., 2011; Boisseau et al., 2018).

TRANSCRIPTION FACTOR MUTATIONS AND ASSOCIATED PLATELET DYSFUNCTION

Transcription factors regulate the cellular expression of genes, often in a combinatorial manner. Each transcription factor regulates multiple genes. Mutations in transcription factors RUNX1, FLI1, GATA-1, and GFI1B have been linked to inherited platelet dysfunction and thrombocytopenia (Songdej & Rao, 2017). These mutations may be more common in patients with inherited platelet function abnormalities than generally considered (Rao, 2013a; Stockley et al., 2013).

RUNX1 *(RUNX1)* Mutations (Familial Platelet Disorder with Predisposition to Acute Myelogenous Leukemia)

An association between inherited platelet function abnormalities, thrombocytopenia, and a predisposition to AML has been reported in several families and linked to autosomal-dominant mutations in *RUNX1* (Song et al., 1999; Sun et al., 2004; Songdej & Rao, 2017) (see Chapter 80 for a discussion of RUNX1 in AML). Megakaryopoiesis is impaired and numerous platelet abnormalities are reported, including impaired aggregation and secretion, α- and δ-granule deficiency, abnormal GPIIb-IIIa activation, decreased platelet myosin light-chain and pleckstrin phosphorylation, selective decrease in platelet protein kinase C-θ and 12-lipoxygenase, and decreased platelet thrombopoietin receptors (Mpl) (Song et al., 1999; Sun et al., 2004; Songdej & Rao, 2017). Platelet expression of numerous RUNX1-regulated genes is decreased, including *MYL9*, *PRKQ*, *ALOX-12*, *PF4*, *RAB1B*, *PCTP*, and *MPL*—each involved in distinct aspects of platelet-megakaryocyte biology (Songdej & Rao, 2017).

GATA-1 (*GATA1*) Mutations

GATA-1 mutations have been associated with an X-linked syndrome consisting of dyserythropoiesis, anemia, thrombocytopenia, and large platelets (Freson et al., 2017). Platelet abnormalities reported include impaired responses to collagen, ADP, and ristocetin, decreased platelet GPIbβ, GαS protein and mRNA, and α-granules (Drachman, 2004; Tubman et al., 2007; Freson et al., 2017).

FLI1 (*FLI1*) Mutations

FLI1, a member of the E-twenty-six (ETS) family of TFs, regulates expression of several megakaryocytic genes, including *ITGA2B*, *GP1BA*, *GP9*, and *c-MPL* (Kumar & Kahr, 2013). Distal deletion of chromosome 11, which includes the *FLI1* locus (11q23.3-24), is associated with a rare autosomal-dominant disorder, Jacobsen syndrome, and its accompanying platelet disorder, Paris-Trousseau syndrome (Favier et al., 2003; Raslova et al., 2004). The clinical features of Jacobsen syndrome include mental retardation, abnormal craniofacial appearance, and abnormalities in multiple organ systems (Kumar & Kahr, 2013). *FLI1* variants are associated with macrothrombocytopenia with giant α-granules in a subpopulation of circulating platelets (1%–5%), bone marrow dysmegakaryopoiesis, impaired platelet aggregation with ADP, collagen, thrombin-receptor activating peptide, decreased dense granules, impaired mepacrine handling and CD63, and decreased thrombin-induced platelet release of α-granule contents (Stevenson et al., 2015, Saultier et al., 2017; Stockley et al., 2013).

GFI1B (*GFI1B*) Mutations

Mutations in *GFI1B* are associated with an autosomal-dominant platelet disorder characterized by dysmegakaryopoiesis, macrothrombocytopenia, α-granule deficiency, and variable bleeding tendency. In one study, a mutation was identified in GFI1B in a family with a bleeding disorder originally described in 1976 (Ardlie et al., 1976; Stevenson et al., 2013; Monteferrario et al., 2014). The family had red cell anisopoikilocytosis, impaired platelet aggregation responses, and decreased platelet P-selectin, fibrinogen, glycoprotein Ibα, and glycoprotein IIIa (Stevenson et al., 2013). A second study uncovered a truncating mutation in *GFI1B* in a family originally reported in 1968 and subsequently diagnosed with GPS (Kurstjens et al., 1968; Monteferrario et al., 2014). These subjects also had bone marrow MF and emperipolesis. Other findings in these patients include expression of CD34 in platelets (Rabbolini et al., 2017).

EVALUATION OF PATIENTS WITH SUSPECTED INHERITED PLATELET DISORDERS

A carefully conducted history, including the family history, and physical examination is important. A platelet count may help determine whether the bleeding tendency is explicable by thrombocytopenia alone. In some patients, bleeding diathesis results from a combination of mild thrombocytopenia and platelet dysfunction. A prolonged PFA-100 closure time may suggest a platelet defect. However, it may be normal in patients with platelet function defects. Because VWD appears to be more prevalent than inherited platelet defects, a simultaneous evaluation of plasma factor VIII and vWF is indicated (see later discussion).

Bleeding manifestations in patients with inherited platelet function defects are highly variable. In patients suspected to have a platelet function defect, the next step is to perfrom studies to assess platelet aggregation and secretion responses in vitro. Platelet studies are usually performed using PRP harvested from anticoagulated blood, and responses are monitored to various agonists. The patterns of responses observed may often provide clues to the nature of the underlying platelet defect, although specific techniques, largely available in research laboratories, are required to delineate the precise platelet mechanisms that are altered. In studies performed using light transmission aggregometry, patients with classical Glanzmann thrombasthenia are characterized by the absence of both the primary and secondary waves of aggregation in response to commonly used agonists, except ristocetin (see Fig. 41.4). Impaired or absent response to ristocetin but with normal aggregation response to other agonists suggests VWD or BSS. In the latter disorder, the platelet counts are decreased and the platelet size is increased. Although these findings may occur in some variants of VWD (e.g., type 2B), plasma levels of vWF and factor VIII, as well as the multimeric pattern of vWF, are normal in BSS. However, abnormalities are observed in vWF (see later discussion). Patients with impaired granule secretion or diminished dense granule contents generally show a decreased or absent second wave of aggregation in response to ADP and epinephrine, and blunted responses to other agonists (collagen, U46619), associated with a decreased release of dense granule contents. In addition to assessing the aggregation responses, the simultaneous assessment of release/secretion of dense granule ATP/ADP provides important information on the nature of the platelet defect (Gresele & Subcommittee on Platelet, 2015). As indicated earlier, application of new generation sequencing represents a major advance in the diagnostic evaluation of patients with platelet disorders (Lentaigne et al., 2016; Sivapalaratnam et al., 2017; Downes et al., 2019) and will likely become a part of the early evaluation of inherited platelet disorders. As of now, the relative prevalence of the various inherited platelet function disorders remains unknown; studies with DNA sequencing will provide new insights on this.

THERAPY OF INHERITED PLATELET FUNCTION DEFECTS

Platelet transfusions and 1-desamino-8D-arginine vasopressin (DDAVP) administration have been the mainstays of therapy for patients with inherited platelet defects. Because of highly variable bleeding manifestations, therapeutic approaches need to be individualized. Platelet transfusions come with potential risks associated with blood products, including alloimmunization. Patients with Glanzmann thrombasthenia and BSS may develop antibodies against the missing platelet glycoproteins, which may compromise the efficacy of subsequent platelet transfusions. An alternative to platelet transfusions is intravenous administration of DDAVP, which was shown to shorten the bleeding time in a substantial number of patients with platelet function defects (Rao et al., 1995; Mannucci, 1998). This response appears to be dependent on the abnormalities leading to the platelet dysfunction. Most patients with Glanzmann thrombasthenia have not responded to DDAVP infusion with a shortening of the bleeding time. Responses in patients with disorders of platelet secretion, signal transduction, or storage pool deficiency have been variable, with a

shortening of bleeding time in some patients. DDAVP administration induces a rise in plasma vWF, factor VIII, and tissue plasminogen activator. DDAVP does not correct abnormal in vitro platelet aggregation or secretion responses in patients with platelet defects (Rao et al., 1995). Recombinant factor VIIa has developed into an important agent for the management of bleeding events in patients with Glanzmann thrombasthenia, particularly those with antibodies against platelet GP and some other inherited defects (Poon & d'Oiron, 2000; Almeida et al., 2003). Additional approaches that have been utilized to improve hemostasis in patients with inherited platelet defects include the administration of antifibrinolytic agents such as ε-aminocaproic acid or tranexamic acid and a short (3- to 4-day) course of prednisone (20–50 mg) (Mielke et al., 1981). Allogeneic bone marrow transplantation has been successfully performed with complete correction in patients with thrombasthenia (Flood et al., 2005; Fujimoto et al., 2005).

ACQUIRED DISORDERS OF PLATELET FUNCTION

Alterations in platelet function occur in many acquired disorders of diverse etiologies (Rao, 2013a; Rao & Bennett, 2013; Brennan et al., 2019). The specific biochemical and pathophysiologic aberrations leading to platelet dysfunction are poorly understood in most of them. In some, such as the MPNs, there is production of intrinsically abnormal platelets by the bone marrow. In others, the dysfunction results from interaction of platelets with exogenous factors, such as pharmacologic agents, artificial surfaces (cardiopulmonary bypass), compounds that accumulate in plasma due to renal failure, and antibodies. In these disorders, the bleeding is usually mucocutaneous and variable. The platelet dysfunction is identified by an abnormal bleeding time, prolonged PFA-100 closure time, and abnormal platelet aggregation studies. The correlation between the abnormalities in these studies and clinical bleeding is weak.

MYELOPROLIFERATIVE NEOPLASMS

Bleeding tendency, thromboembolic complications, and qualitative platelet defects are all recognized in MPNs, which include essential thrombocythemia (ET), polycythemia vera (PV), chronic idiopathic MF, and chronic myelogenous leukemia (Pearson, 2002; Kessler, 2004; Papadakis et al., 2010; Spivak 2017) (see Chapter 34). Thrombotic events are more frequent than hemorrhagic events in PV and ET. Platelet abnormalities reflect their development from an abnormal clone of cells, but some alterations may be secondary to enhanced platelet activation in vivo. Increased blood viscosity (as in PV), increased platelet counts, and endothelial and leukocyte dysfunction also contribute to hemorrhagic events. Bleeding is usually mucocutaneous and may manifest after surgery or trauma. Thrombosis can involve arteries, veins, and the microvasculature and may occur in unusual locations, such as abdominal wall vessels or the hepatic, portal, and mesenteric circulations. Indeed, MPNs account for a substantial proportion of patients with Budd-Chiari syndrome or portal vein thrombosis. Erythromelalgia, characterized by redness and burning pain in the extremities, is strongly associated with ET and PV and is thought to be due primarily to arteriolar platelet thrombi (van Genderen et al., 1995; Michiels et al., 2006). Predictors for arterial thrombosis are age older than 60 years, a history of thrombosis, cardiovascular risk factors, leukocytosis, and the presence of the *JAK2* V617F mutation.

Several studies have examined platelet function and morphology in patients with MPN (Schafer, 1984; Landolfi et al., 1997; Rao, 2013b; Rao & Bennett, 2013). Under the electron microscope, platelet findings include reduction in dense and α-granules, alterations in the open canalicular and dense tubular systems, and a reduction of mitochondria (Maldonado et al., 1974). Bleeding time is prolonged in a minority (≈17%) of MPN patients (Schafer, 1984). Platelet aggregation responses are highly variable in MPN patients and often vary in the same patient over time. Decreased platelet responses to ADP, epinephrine, and collagen are more common, although some patients may demonstrate spontaneous or enhanced responses to agonists (Schafer, 1984; Papadakis et al., 2010). Aggregation is impaired in response to epinephrine more frequently than with other agonists; however, a diminished response to epinephrine is not pathognomonic of an MPN. It has been attributed to a decrease in the number of platelet α_2-adrenergic receptors. Decreases in platelet surface GPIIb-IIIa complexes, GPIb-IX, and GPIa-IIa have been documented in MPN, as well as impaired signal transduction–dependent activation of GPIIb-IIIa. Platelet GPIV (CD36), a membrane GP related to platelet-collagen and platelet-thrombospondin interactions, and platelet receptors for the Fc portion of IgG have been noted to be increased in MPN patients.

Abnormalities in platelet arachidonic acid pathways with reduced formation of lipoxygenase products and enhanced TXA2 production has been reported in MPN patients (Schafer, 1982). Other abnormalities reported include defects in platelet signaling mechanisms, including in calcium mobilization and protein phosphorylation; decreased PGD2-induced activation of adenylyl cyclase and reduction in platelet PGD2 receptors, indicating an impairment in platelet inhibitory mechanisms; and reduced expression of the thrombopoietin receptor (MpL) in PV and idiopathic myelofibrosis but not ET or chronic myelogenous leukemia (Rao, 2013b; Rao & Bennett, 2013). Recent studies provide evidence for a major role of megakaryocytes in the pathogenesis of myelofibrosis in MPN (Psaila et al., 2020). Abnormalities in plasma vWF and acquired VWD may occur in MPN patients and contribute to the hemostatic defect (see the Acquired von Willebrand Syndrome section later in the chapter) (Budde & van Genderen, 1997; Elliott & Tefferi, 2005). A major advance in understanding the pathogenesis of MPN is the identification of gain-of-function mutations in the *JAK2* or *MPL* genes in approximately 95% of patients with PV and approximately 50% to 60% of patients with ET and MF (Spivak, 2017).

ACUTE LEUKEMIAS AND MYELODYSPLASTIC SYNDROMES

The major cause of bleeding in these conditions is thrombocytopenia. However, these disorders may be associated with platelet dysfunction (Rao, 2013b; Rao & Bennett, 2013; Brennan et al., 2019). Acquired platelet defects associated with clinical bleeding are more common in acute myelogenous leukemia but have been reported in acute lymphoblastic and myelomonoblastic leukemias, hairy cell leukemia, and myelodysplastic syndromes. Reduced aggregation responses to ADP, epinephrine, and collagen have been reported along with diminished nucleotide secretion, TXA2 production, and platelet PDGF and β-thromboglobulin. Acquired forms of VWD and a Bernard-Soulier–like platelet defect have been described in hairy cell leukemia and myelodysplastic syndromes. In acute leukemias and myelodysplastic syndromes, platelets may be morphologically abnormal, and ultrastructural studies have shown decreased microtubules, reduced number and abnormal sizes of dense granules, and excessive membranous systems. The megakaryocytes exhibit dysplasia.

DYSPROTEINEMIAS

Excessive clinical bleeding may occur in these patients and has been attributed to multiple mechanisms, including platelet dysfunction due to coating of platelets by the paraprotein, specific coagulation abnormalities, hyperviscosity, and amyloid deposition in blood vessels (Rao, 2013b; Rao & Bennett, 2013).

UREMIA

The hemostatic defect in uremia has been attributed to platelet dysfunction and impaired platelet–vessel wall interaction as the major mechanisms (Gangji et al., 2006; Sohal et al., 2006; Pavord & Myers, 2011; Rao, 2013b; Rao & Bennett, 2013). Circulating reticulated platelets are increased in patients on dialysis, indicating accelerated platelet turnover. The bleeding times are prolonged in uremia and typically shortened following red cell transfusions or treatment with erythropoietin (Livio et al., 1982; Moia et al., 1987), indicating that anemia also contributes to the hemostatic defect. Multiple platelet abnormalities are recognized in uremia (Boccardo et al., 2004). Platelet adhesion to the subendothelium, an early step in hemostasis, involves the interaction with vWF. Adhesion of platelets from uremic whole blood perfused over de-endothelialized rabbit aorta has been reported to be impaired (Castillo et al., 1986). Most studies have found normal or increased plasma vWF antigen levels and activity (ristocetin cofactor), although in some, vWF activity was consistently lower than the antigen level. The multimeric structure of vWF was normal. Many studies have shown impaired platelet aggregation responses to several agonists in uremia, sometimes with conflicting results. Plasma PF4 and β-thromboglobulin are elevated in uremia and increase further with hemodialysis, reflecting reduced renal clearance and platelet activation by membrane dialyzers. Several studies have shown reductions in products of arachidonic acid metabolism (PGG2/PGH2, TXA2) in uremic platelets. Other platelet defects described in uremia include increased platelet cAMP levels and adenylyl cyclase (which inhibit platelet responses), and decreased agonist-induced Ca^{2+} mobilization, clot retraction, and platelet procoagulant activity.

The pathogenesis of the hemostatic defect in uremia is linked to accumulation of dialyzable and nondialyzable molecules in the uremic plasma. One

such compound, guanidinosuccinic acid, accumulates in uremic plasma, inhibits platelets in vitro, and stimulates generation of nitric oxide, which inhibits platelet adhesion and platelet responses by increasing cGMP levels (Boccardo et al., 2004; Sohal et al., 2006). Exposure of human endothelial cells to uremic plasma leads to enhanced nitric oxide production. Enhanced prostacyclin-like activity has been observed in uremic plasma (Remuzzi et al., 1978). Aggressive dialysis is an important component of the overall management and corrects the bleeding diathesis in some patients but is only partially effective in others (Gangji et al., 2006; Galbusera et al., 2009). Elevation of the hematocrit with packed red blood cell transfusions or recombinant erythropoietin shortens the bleeding time and corrects mild bleeding in uremic patients.

ACQUIRED STORAGE POOL DISEASE

Several patients have been reported in whom the dense granule SPD appears to be acquired (Rao, 2013b; Rao & Bennett, 2013). In general, this defect probably reflects in vivo release of platelet contents due to activation or production of abnormal platelets. Acquired SPD has been observed in patients with antiplatelet antibodies, systemic lupus erythematosus, chronic ITP, disseminated intravascular coagulation (DIC), hemolytic-uremic syndrome, renal transplant rejection, multiple inherited cavernous hemangioma, MPN, acute and chronic leukemias, severe valvular heart disease, in patients undergoing CPB, and in platelet concentrates stored for transfusion.

ANTIPLATELET ANTIBODIES AND PLATELET FUNCTION

Binding of an antibody to platelets may induce several effects, including accelerated destruction, platelet activation, cell lysis, aggregation, secretion of granule contents, and PS exposure. Platelet-antibody interaction may lead to impaired function, both as a consequence of activation and due to antibody binding to specific glycoproteins. Patients with ITP have decreased platelet survival and may have impaired platelet function and abnormally prolonged bleeding times even at adequate counts. Antibodies may induce platelet dysfunction by multiple mechanisms. In many patients, the antibodies are directed against specific platelet surface membrane glycoproteins GPIb-IX-V, GPIIb-IIIa, GPIa-IIa, GPVI, and glycosphingolipids (Cines et al., 2009a, 2009b). In one report, the anti-GPVI antibody induced clearance of the GPVI/FcRγ complex from the platelet surface (Boylan et al., 2004).

DRUGS AND FOOD SUPPLEMENTS THAT INHIBIT PLATELET FUNCTION

Many drugs affect platelet function (Box 41.3) (Rao & Bennett, 2013; Brennan et al., 2019). For several, the effects on platelets have been studied in vitro; the relevance of such findings to the drug levels achieved in clinical practice is not well established, however. The clinical impact of these effects is often unclear. Moreover, the impact of concomitant administration of multiple drugs, each with a mild effect on platelet function, is unknown, although this is clinically relevant. Because of their widespread use, aspirin and nonsteroidal antiinflammatory agents are an important cause of platelet inhibition in clinical practice. Aspirin ingestion results in inhibition of platelet aggregation and secretion upon stimulation with ADP, epinephrine, and low concentrations of collagen. Aspirin irreversibly acetylates and inactivates the platelet cyclooxygenase and inhibits synthesis of endoperoxides (PGG2 and PGH2) and TXA2. It is recommended that aspirin be discontinued 5 to 7 days prior to platelet aggregation studies. Several other nonsteroidal antiinflammatory drugs also impair platelet function by inhibiting the cyclooxygenase enzyme and may prolong bleeding time. Compared with aspirin, the inhibition of cyclooxygenase by these agents is generally short-lived and reversible.

Ticlopidine, clopidogrel, and prasugrel are orally administered thienopyridine derivatives that inhibit platelet function by inhibiting ADP binding to the platelet P2Y12 receptor. While these three are prodrugs that are metabolized to active compounds in vivo, ticagrelor is a direct-acting P2Y12 antagonist. All of them prolong the bleeding time and inhibit platelet aggregation responses to several agonists, to various extents depending on agonist concentrations. GPIIb-IIIa receptor antagonists are a class of compounds that inhibit fibrinogen binding and platelet aggregation. These include a monoclonal antibody against the GPIIb-IIIa receptor (abciximab), a synthetic peptide containing the KGD sequence (eptifibatide), and a peptidomimetic (tirofiban). They are potent inhibitors of aggregation (both primary and secondary) in response to all the usual agonists except ristocetin; all prolong bleeding time and are far more potent as platelet inhibitors than aspirin. Immune-mediated thrombocytopenia is a potential complication of the GPIIb-IIIa antagonists (Aster & Bougie, 2007) (see Chapter 43). Cilostazol and dipyridamole increase cAMP levels and interfere with platelet function. Vorapaxar inhibits the thrombin (PAR-1) receptor on platelets. More recently, tyrosine kinase inhibitors ibrutinib and acalabrutinib have been shown to inhibit platelet function.

BOX 41.3

Drugs That Affect Platelet Function

Cyclooxygenase Inhibitors

Aspirin
Nonsteroidal anti-inflammatory agents
- Indomethacin, phenylbutazone, ibuprofen, sulfinpyrazone, sulindac, meclofenamic acid, and others

Adenosine Diphosphate (ADP) Receptor Antagonists

Ticlopidine, clopidogrel, prasugrel, ticagrelor

Thrombin PAR-1 Receptor Antagonist (Vorapaxar)

Glycoprotein (GP)IIb-IIa Receptor Antagonists
c7E3 (abciximab), tirofiban, eptifibatide

Drugs That Increase Platelet Cyclic Adenosine Monophosphate (cAMP) or Cyclic Guanosine Monophosphate (cGMP)

Adenylate cyclase activators
- Prostaglandins I_2, D_2, E_1, and analogs

Phosphodiesterase inhibitors
- Dipyridamole
- Cilostazol
- Anagrelide
- Milrinone
- Methylxanthines (caffeine, theophylline, aminophylline)

Nitric Oxide and Nitric Oxide Donors

Antimicrobials
Penicillins
Cephalosporins
Nitrofurantoin
Hydroxychloroquine
Miconazole

Cardiovascular Drugs

β-Adrenergic blockers (propranolol)
Vasodilators (nitroprusside, nitroglycerin)
Diuretics (furosemide)
Calcium channel blockers
Quinidine
Angiotensin-converting enzyme inhibitors

Anticoagulants

Heparin

Thrombolytic Agents

Streptokinase, tissue plasminogen activator, urokinase

Psychotropics and Anesthetics

Tricyclic antidepressants
- Imipramine, amitriptyline, nortriptyline

Phenothiazines
- Chlorpromazine, promethazine, trifluoperazine

Selective serotonin reuptake inhibitors
- Fluoxetine, sertraline, paroxetine, and others

Local anesthetics
General anesthesia (halothane)

Chemotherapeutic Agents

Mithramycin
Carmustine
Daunorubicin
Tyrosine kinase inhibitors

Miscellaneous Agents

Dextrans and hydroxyethyl starch
Lipid-lowering agents (clofibrate, halofenate)
ε-Aminocaproic acid
Antihistaminics
Ethanol
Vitamin E
Radiographic contrast agents
Food items (omega-3 fatty acids, vitamin E, onions, garlic, ginger, cumin, turmeric, cloves, black tree fungus, *Gingko biloba*, ginseng)

Modified with permission from Rao AK: Acquired disorders of platelet function. In Colman RW, editor: *Hemostasis and thrombosis: basic principles and clinical practice*, Philadelphia, 2006, Lippincott Williams & Wilkins.

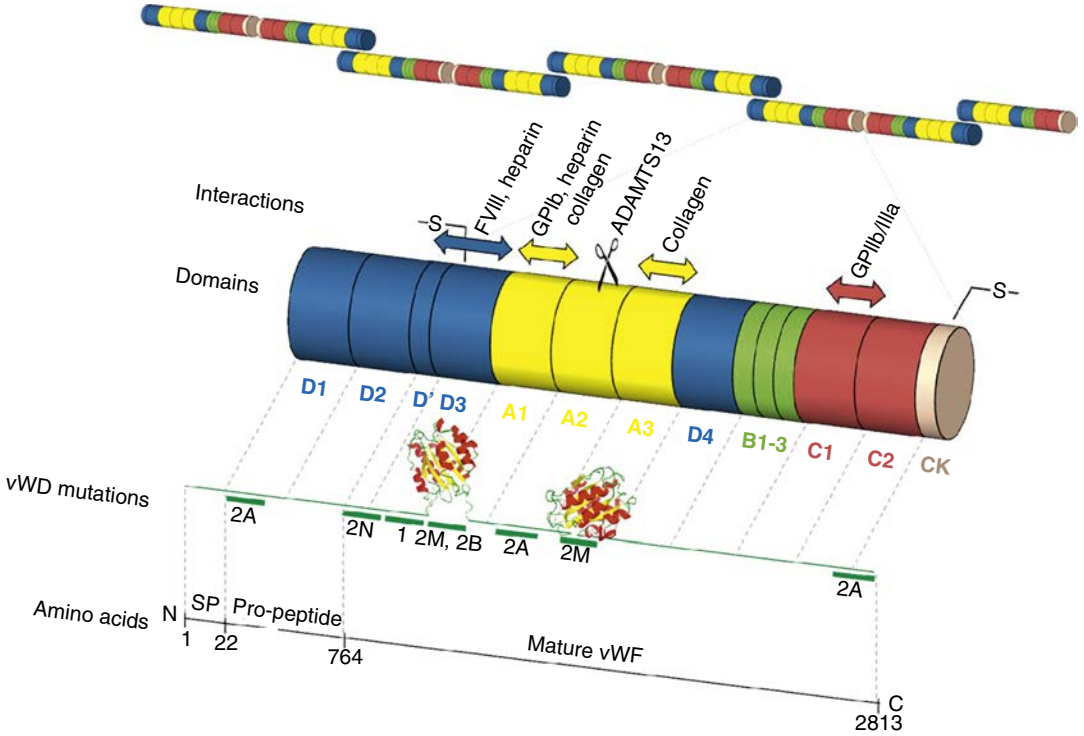

Figure 41.7 Schematic representation of von Willebrand factor (vWF). vWF is synthesized as a pre-pro-vWF molecule that comprises a 22-residue signal peptide, a 741-residue propeptide, and the 2050-residue mature subunit. After removal of the signal peptide (SP), pro-vWF subunits associate in the endoplasmic reticulum in "tail-to-tail" dimers by the formation of disulfide bonds, after which dimers further multimerize by forming "head-to-head" disulfide bonds between the amino-terminal regions. The propeptide and the mature subunit form pro-vWF (2791 residues) consisting of four types of repeated domains as indicated. Crystal structures within the A1 and A3 domains are depicted. The main binding sites that are important for the hemostatic function of vWF are indicated, together with the ADAMTS13 cleavage site. Major regions in which mutations have been found that are associated with VWD types 1 and 2 are also shown. (Reprinted with permission from De Meyer SF, Deckmyn H, Vanhoorelbeke K: von Willebrand factor to the rescue, *Blood* 113:5049–5057, 2009.)

The antibody caplacizumab, used in the treatment of thrombotic thrombocytopenic purpura (TTP), binds to the A1 domain of vWF to inhibit vWF interaction with GP1bα. These therapeutic agents inhibit platelet function and are associated with increased bleeding.

Selective serotonin reuptake inhibitors (SSRIs) inhibit platelet function. These include fluoxetine, sertraline, paroxetine, fluvoxamine, citalopram, and escitalopram. Serotonin in plasma is taken up by platelets, incorporated into dense granules, and secreted on platelet activation. SSRIs inhibit serotonin uptake, and inhibit platelet aggregation and secretion responses upon activation. In epidemiologic studies, patients on SSRIs have had increased gastrointestinal bleeding and increased bleeding with surgery (Movig et al., 2003; McCloskey et al., 2008; Brennan et al., 2019).

β-Lactam antibiotics, including penicillins and cephalosporins, inhibit platelet aggregation responses and may contribute to a bleeding diathesis at high doses (Rao, 2013b; Rao & Bennett, 2013). These include carbenicillin, penicillin G, ticarcillin, ampicillin, nafcillin, azlocillin, cloxacillin, mezlocillin, oxacillin, piperacillin, and apalcillin. Platelet inhibition appears to be dose dependent, taking about 2 to 3 days to manifest and 3 to 10 days to abate after drug discontinuation. Cephalosporins may also impair platelet function. The general context in which bleeding events are encountered in patients on antibiotics prevents identification of the precise role played by antimicrobials because of the presence of concomitant factors (thrombocytopenia, DIC, infection, vitamin K deficiency).

A host of other medications (see Box 41.3) (Rao, 2013b; Rao & Bennett, 2013; Brennan et al., 2019) and agents, including food substances, inhibit platelet responses but the clinical significance for many is unclear (Rao, 2013b; Rao & Bennett, 2013). These include herbal medicines, such as gingko (*Gingko biloba*), and food supplements, such as garlic (*Allium sativum*), fish oil and alcohol. Their role and interaction with pharmaceutical drugs needs to be considered in the evaluation of patients with unexplained bleeding.

VON WILLEBRAND FACTOR, VON WILLEBRAND DISEASE, AND THROMBOTIC THROMBOCYTOPENIC PURPURA

VON WILLEBRAND FACTOR BIOLOGY

Von Willebrand factor (vWF) plays key roles both in primary hemostasis and in secondary hemostasis. In the latter role, vWF serves as a carrier protein for factor VIII; in the absence of vWF, plasma factor VIII is rapidly cleared from the circulation (see Chapter 40). In primary hemostasis, vWF mediates platelet adhesion to exposed collagen at sites of vascular injury. Plasma vWF derives from secretion by endothelial cells. This secretion has a major constitutive component, but there is an additional releasable pool of vWF that is stored in the endothelial Weibel-Palade bodies. Megakaryocytes also synthesize vWF, which is stored in the platelet α-granules and released upon platelet activation. Although such released vWF may not raise the plasma vWF appreciably, a local increase of vWF at sites of injury may be significant.

The *VWF* gene is located on chromosome 12 and is 178 kB long with 52 exons. There is a partial, but nonfunctional, duplication of the *VWF* gene on chromosome 22 (*VWF* pseudogene). Following cleavage of an N-terminal propeptide fragment, the mature 2050 amino acid vWF protein is composed of a series of functional domains and subdomains (Springer, 2014; Lenting et al., 2015). The *VWF* gene and its resulting gene products are shown schematically in Figure 41.7. The individual VWF monomeric units are bound together by multiple disulfide bonds, occurring both near the N-termini and C-termini (Tsai, 2003). The resulting multimers may achieve molecular weights exceeding 20 MDa. The higher-molecular-weight multimers are subsequently lost when vWF released into the circulating plasma comes in contact with and activates the metalloproteinase ADAMTS13 (a disintegrin and metalloprotease with eight thrombospondin motifs) (Muia et al., 2014). ADAMTS13 cleaves between Tyr842 and Met843 within the A2 domain of vWF multimeric subunits. Following initial proteolysis, the ADAMTS13 proteolysis of potential sites within vWF comes to a halt, presumably due to steric hindrance of the ADAMTS13 penetrating deeper into the vWF multimeric structure. Deficiency of ADAMTS13, either due to a congenital abnormality or to the formation of autoantibodies against the enzyme, results in "unusually large" vWF multimers circulating in the plasma. These forms are capable of spontaneously aggregating platelets as well as forming large strands anchored to endothelial P-selectin that can result in RBC fragmentation—two characteristic attributes of TTP.

At sites of vessel injury, vWF binds to exposed subendothelial collagen. The bound vWF and the GPIbα on the platelet surface interact, effectively tethering the platelet to the injury site. This ligand-receptor interaction produces an outside-to-inside signaling across the platelet

TABLE 41.6

Laboratory Patterns of Different Types of von Willebrand Disease

	vWF:Ag	vWF:RCo	vWF:RCo/ vWF:Ag	FVIII:C	Multimeric Pattern	Platelet Count	Specialized Testing
Quantitative Disorders of vWF							
Type 1	↓	↓	≥0.6	Normal to ↓	Normal	Normal	
Type 1C	↓	↓	≥0.6	Normal to ↓	Normal	Normal	Increased ratio of vWFpp/ vWF:Ag
Low vWF levels	↓	↓	≥0.6	Normal to ↓	Normal	Normal	
Type 3	↓↓↓	↓↓↓	≥0.6	↓↓↓	Absent	Normal	
Qualitative Disorders of vWF							
Type 2A	↓	↓↓	≤0.6	Normal to ↓	Loss of HMW-vWF	Normal	
Type 2B	↓	↓↓	≤0.6	Normal to ↓	Loss of HMW-vWF	↓↓	LD-RIPA enhanced with patient-derived plasma (vWF)
Platelet-type vWD	↓	↓↓	≤0.6	Normal	Loss of HMW-vWF	↓↓	LD-RIPA enhanced with patient-derived platelets
Type 2M	↓	↓↓	≤0.6	Normal to ↓	Normal	Normal	
Type 2N	Normal to ↓	Normal to ↓	≥0.6	↓↓	Normal	Normal	Decreased vWF:FVIII-binding capacity

Modified with permission from Ng C, Motto DG, Di Paola J: Diagnostic approach to von Willebrand disease, *Blood* 125:2029–2037, 2015.

membrane, leading to platelet activation. One component of this platelet activation consists of a subsequent inside-to-outside signaling event within GPIIb-IIIa that allows it to bind fibrinogen. In the laboratory, vWF may be assayed antigenically, functionally, and even structurally. While the vWF antigen (vWF:Ag) was formerly quantified by a variety of gel electrophoretic approaches, it may now be measured with high precision by rapid methods such as the enzyme-linked immunosorbent assay (ELISA) or immunoturbidometric procedures.

LABORATORY TESTS FOR VON WILLEBRAND FACTOR

vWF is capable of binding to a number of different molecules (see Fig. 41.6). The functional tests currently employed in the evaluation of patients assess vWF binding to platelets, collagen, and factor VIII. vWF binds to the GPIbα chain of the platelet GPIb-IX-V complex. This receptor was discovered by Brinkhous and Read in 1978 to possess the unusual, but certainly convenient, property of retaining reactivity with its ligand vWF even in formalin-fixed, lyophilized platelets in an aqueous suspension (Brinkhous & Read, 1978). The antibiotic ristocetin enhances the binding of vWF to platelet GPIbα. The "ristocetin cofactor" assay of vWF reactivity with platelets has served as the primary measure of vWF functional activity for many years. When formalin-fixed platelets are incubated under stirring conditions with ristocetin and plasma, the rate and extent of platelet aggregation is a function of the amount of plasma vWF. This test may be performed either manually in a standard platelet aggregometer or by a variety of automated approaches. It is the higher-molecular-weight multimers that are most active in binding to platelets so that ristocetin cofactor activity is diminished when there is a deficiency in the higher-molecular-weight multimers, even if the total amount of vWF is normal because of relative abundance of lower-molecular-weight multimers.

Ristocetin cofactor activity assays using platelets have suffered a relatively high coefficient of variation (i.e., low precision) compared with other tests performed in the coagulation laboratory (Kitchen et al., 2006; Ng et al., 2015). Thus, alternative approaches to quantify vWF-platelet interaction have been pursued with relative success. Most notable is the replacement of platelets (whether fresh or formalinized) by recombinant GPIbα in functional ELISA assays of vWF "ristocetin cofactor" activity (vWF:GPIbR) (Federici et al., 2004; Hui et al., 2007; Flood et al., 2009; Bodó et al., 2015). An interesting modification of such assays employs GPIbα with a gain-of-function mutation such as those seen in platelet-type VWD (see later discussion), and does not require the addition of ristocetin for vWF binding (Bodó et al., 2015). This approach may be particularly useful in individuals possessing phenotypically normal variations in vWF who would otherwise be classified as a type 2M VWD (see later discussion) solely because their variant form of vWF lacks the ability to bind ristocetin (Flood et al., 2009). However, the new ELISA-based functional assays in some instances provide discordant results both with each other and with traditional ristocetin cofactor assays, potentially leading to differences in VWD subtyping (Timm et al., 2015).

Functional ELISA tests have also been developed for quantitation of vWF collagen binding activity (vWF:CBA). Typically, wells are coated with type 3 or a mixture of types 1 and 3 collagen, patient plasma incubated in the wells, and bound vWF subsequently quantitated by means of conjugated anti-vWF antibody. vWF:CBA is strongly dependent on the binding of high-molecular-weight vWF multimers. vWF also binds to type 4 and type 6 collagen; some mutations within the vWF A1 domain appear to alter binding to these collagens (Flood et al., 2015). Assays for vWF binding to types 4 and 6 collagen are not presently in clinical use.

Evaluation of the ability of a patient's plasma vWF to bind factor VIII (also referred to as vWF:FVIIIB) has progressed from a laborious multiday procedure to a same-day standardized ELISA procedure, now available commercially in some countries (see the Type 2N (Normandy) section later in the chapter) (Veyradier et al., 2011; Lillicrap, 2013a).

Multimeric analysis of plasma vWF has made substantial contributions to defining the various phenotypes of VWD. At low resolution, multimeric analysis determines the relative distribution of vWF by molecular weight range (see Fig. 41.7). At higher resolution, abnormal patterns of the multimers within a narrow size range may additionally be resolved. It should be noted that platelet α-granules contain megakaryocyte-synthesized vWF that, like the endothelial vWF, contained in Weibel-Palade bodies has not been exposed to ADAMTS13. vWF isolated from endothelial cells or platelets, accordingly, contains higher multimers than plasma vWF.

VON WILLEBRAND DISEASE

The term *von Willebrand disease* encompasses a broad array of quantitative and qualitative inherited abnormalities of vWF (Table 41.6). Overall, the prevalence of VWD associated with significant bleeding has been estimated to be 1:10,000 (Ng et al., 2015), although higher estimates have been reported in population-based studies (Federici et al., 2014).

Type 1 VWD: Partial Quantitative Abnormality

In type 1 VWD, vWF molecules are present in decreased amounts in plasma but are qualitatively normal. The entire size spectrum of vWF multimers is present, albeit in decreased amounts (Fig. 41.8). Type 1 is the most commonly diagnosed VWD subtype, estimated at 75% of all cases (Lillicrap, 2013b). vWF gene mutations have been detected in approximately two-thirds of cases when Type 1 VWD is defined by levels as low as <30 IU/dL. In addition to the *vWF* gene itself, studies are also being undertaken to detect mutations at alternative genetic loci that contribute to vWF synthesis, secretion, and clearance (Lillicrap, 2013b). In type 1 VWD, there is roughly a commensurate decrease in vWF, whether measured antigenically or with respect to its various functions—i.e., interacting with platelets (vWF:RCo activity), with collagen (vWF:CBA activity), or in its chaperone role for circulating factor VIII. In normal plasma, the ratio of vWF functional activity to that of vWF:Ag is expected to be ≥0.6 (Ng et al., 2015a). Flood and colleagues have reported that using a cutoff of 0.6 for the ratio of vWF:CBA/vWF:Ag, sensitivity of these assays with

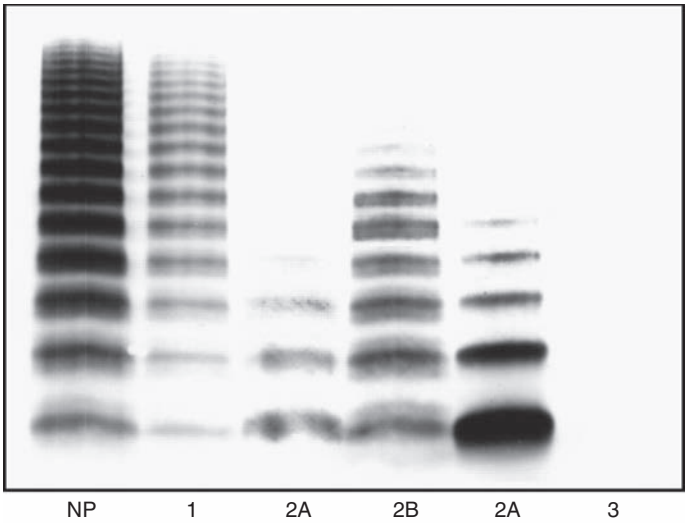

Figure 41.8 Multimeric patterns in selected variants of Von Willebrand disease (VWD). Plasma samples were analyzed for von Willebrand factor (vWF) by sodium dodecyl sulfate (SDS)-agarose gel electrophoresis and Western blotting. Patterns are shown for pooled normal plasma (NP) and patients with the indicated types of VWD. Note that in the VWD 2A and 2B there is relative loss of higher-molecular-weight multimers, although to varying extents. Of note, the extent of multimer loss is variable in each subtype, and the differences in extent of multimer loss between the 2A and 2B subtypes do not distinguish these subtypes in diagnostic studies. Functional studies such as platelet aggregation in response to ristocetin are required to distinguish between the decrease-of-function 2A subtype and the increase-of-function 2B subtype (see text). (Adapted with permission from Sadler JE: New concepts in von Willebrand disease, Annu Rev Med 56:173–191, 2005; and Sadler JE: von Willebrand disease. In Bloom AL, Forbes CD, Thomas DP, Tuddenham EGD, editors: *Hemostasis and thrombosis,* New York, 1994, Churchill Livingstone, pp 843–857.)

respect to vWF multimer abnormalities was 100% for healthy controls, 99% for type 1 VWD patients, and 100% for patients with type 2A and type 2B VWD (see later discussion) (Flood et al., 2013; Sharma & Haberichter, 2019).

Multigenic factors influence the level of circulating vWF, which adds complexity to efforts to diagnose type 1 VWD (Sanders et al., 2015). Not only the *vWF* gene is involved, but likely also genes encoding intracellular transporter proteins, ABO genes affecting posttranslational modifications of the vWF molecule, genes affecting vWF proteolysis and clearance, and still other genetic factors influence the quantity and functionality of vWF. The ABO antigenic system exerts a particularly strong effect on plasma vWF levels, which are approximately 25% lower in type O individuals than in those whose blood group is non–blood group O (Franchini et al., 2014). In some instances, this could make the difference between being considered normal or deficient in vWF level. Differences in vWF clearance between blood group O and non–blood group O individuals appear related to their blood group status but not to the actual ABH antigenic loading on vWF molecules (Groeneveld et al., 2015). While ABO status appears to affect vWF clearance rates, the underlying mechanism for this variability still remains unclear. A recent analysis evaluating clinical bleeding, laboratory measures of vWF, and vWF sequencing concluded that treatment considerations should be based solely upon baseline vWF level and not modified because of ABO blood group status (Gill et al., 2014).

Because of the relatively high prevalence both of mild bleeding symptoms and levels of <50 IU/dL (the traditional cutoff for abnormal levels in most laboratories) of vWF in the general population, it may be erroneous to conclude that simply demonstrating a mild to moderate decrease in plasma vWF level is actually the *cause* of an individual patient's increased bleeding tendency (Sadler, 2003a). Interestingly, in a recent report, Gill et al. studied almost 1400 individuals undergoing tonsillectomy and showed that vWF levels did not correlate with postsurgical bleeding (Gill et al., 2020). Therefore, for the patients that bleed, it is important to consider other etiologies for hemostatic abnormality as well, such as a platelet defect. The approach to patients with mild deficiencies of vWF continues to be debated (Gudmundsdottir et al., 2007; Onundarson et al., 2008). It has been proposed that, unless more diagnostic family or personal information is available, an individual with a vWF level of 30 to 50 U/dL may better be considered to have a "low vWF level" rather than "type 1 VWD" (Nichols et al., 2009; Sadler, 2009) (see Table 41.6). Independently of these definitions, if an individual has low vWF levels associated with mucocutaneous bleeding, diagnostic approach and treatment are similar to those used for VWD type 1.

A subset of type 1 patients has been designated type 1C, where the "C" serves to indicate abnormally increased clearance of vWF from the circulation (Haberichter et al., 2006). The laboratory identification of these patients has been facilitated by measurement of plasma level of mature vWF protein in relation to that of the vWF propeptide (vWFpp). Cleavage and release of vWFpp from the immature vWF molecule after residue 763 releases the 2050-residue mature subunit of vWF (see Fig. 41.7) occurs at equimolar concentrations. However, they have disparate half-lives in plasma (12 hours for vWF vs. 2 hours for vWFpp), making the vWFpp/vWF an attractive and reliable measure of vWF clearance. The finding of an increased vWFpp/vWF:Ag ratio in the context of a reduced vWF antigen has shown success in identifying the type 1C subtype (Haberichter et al., 2006, 2008). This diagnosis has therapeutic implications as patients with type 1C are not suitable for DDAVP treatment.

Type 3 VWD: Severe Quantitative Abnormality

In type 3 VWD, there is a severe, if not in fact total, absence of *VWF* gene product. Whereas type 1 VWD is generally expressed in autosomal-dominant fashion, type 3 is autosomal recessive, with neither parent typically showing symptomatic disease. Since vWF serves as a carrier molecule for factor VIII, protecting it from proteolysis, type 3 patients not only suffer the consequences of the dysfunctional interaction of vWF and platelets but also significantly low factor VIII levels (typically <10%) (James & Lillicrap, 2012). These patients can have severe bleeding in joints and muscles due to their low factor VIII levels.

Qualitative Abnormalities: Type 2A, Type 2B, Type 2M, and Type 2N VWD

Patients with type 2 VWD subtypes have a qualitative abnormality of this complex protein. These patients are divided into the following subtypes.

Type 2A

In type 2A VWD, there is a lack of higher-molecular-weight multimers (HMWMs) in plasma (see Fig. 41.8), with corresponding loss of vWF functionality. Type 2A is caused by *vWF* mutations that prevent proper multimerization or by mutations that increase the susceptibility of fully formed vWF to proteolysis by ADAMTS13. The interaction of plasma vWF with platelets is impaired due to the lack of HMWMs so that both measurement of plasma vWF:RCo and ristocetin-induced aggregation of the patient's PRP are decreased. The ratios of vWF:RCo/vWF:Ag and of vWF:CBA/vWF:Ag are generally <0.6.

Type 2B

In type 2B VWD, point mutations within the vWF molecule confer a gain-of-function capability with respect to its ability to bind the platelet GPIb. This enhanced binding of the abnormal type 2B vWF molecules to circulating platelets leads to a depletion of HMWMs in plasma (see Fig. 41.8) and often to a mild to moderate thrombocytopenia. This increase of function can be demonstrated by the ability of low ristocetin concentrations of ~0.3 to 0.5 mg/mL to aggregate the PRP of such patients, which does not occur with intact vWF. As in the case of type 2A, the ratios of vWF:RCo/vWF:Ag and of vWF:CBA/vWF:Ag are typically <0.6.

Type 2M

Patients with type 2M VWD have a decrease-of-function phenotype resembling type 2A, yet their vWF contains the normal full complement of molecular weight components in multimeric analysis as the molecular defect is due to loss of function mutations in the vWF platelet binding site. The original patients fitting this subtype had missense mutations that led to loss of interaction with the platelet GPIb-IX-V complex. Such patients usually have a decreased ratio of vWF:RCo/vWF:Ag, yet may retain a normal vWF:CBA/vWF:Ag ratio as their HMWMs are intact. More recently, however, the 2M subtype has been considered also to include several missense mutations leading to selective decrease in collagen binding, in which case the only phenotypic test that may be abnormal is the vWF:CBA ratio (Lillicrap, 2013a, 2013b).

Type 2N (Normandy)

These patients have point mutations within the vWF molecule that specifically impair its ability to bind factor VIII. They may show quite normal levels of vWF antigen and even ristocetin cofactor activity but will have abnormally low plasma factor VIII as unbound factor VIII is highly susceptible to degradation. Since the *vWF* gene is transmitted autosomally, type 2N VWD should be suspected when there appears to be an autosomal inheritance pattern of factor VIII deficiency, and males and females can be affected. Definitive diagnosis is made by demonstrating impaired binding

of normal factor VIII to the patient vWF, such as by the ELISA test, and by molecular diagnostic methods (James & Lillicrap, 2012). Evaluation of a commercial ELISA procedure in the French population reported that it detected all patients with type 2N VWD (vWF : FVIIIB values <15%), as well as all heterozygous carriers of a known 2N mutation (values between 30% and 65%) and that no hemophilia A patients or carriers or normal subjects exhibited a markedly decreased vWF : FVIIIB level (Veyradier et al., 2011). These authors went on to estimate that type 2N VWD might actually account for around 10% of patients with decreased FVIII : C together with an FVIII : C/vWF : Ag ratio lower than 0.6 (Veyradier et al., 2011). The great majority of mutations resulting in a type 2N VWD phenotype are clustered within the FVIII-binding D′/D3 region of vWF (see Fig. 41.7), and genotypic/phenotypic associations have emerged from DNA sequence analyses. For example, the R816W and T791M mutations result in FVIII levels <10% with poor DDAVP responsiveness, while the R854Q mutation is associated with FVIII levels of around 25% and a greater likelihood of responsiveness to DDAVP (Lillicrap, 2013a).

Platelet-Type VWD

In the autosomal-dominant bleeding disorder termed *platelet-type VWD* (Miller & Castella, 1982; Weiss et al., 1982) the genetic defect is not in *vWF*; rather, it is a gain-of-function defect in *GP1BA*, which encodes for platelet GPIbα. This results in enhanced binding of normal vWF to platelets and in its clearance from plasma. Additionally, the heightened binding in vivo of vWF to the mutant GPIbα may induce a conformational change in vWF and enhanced proteolysis by ADAMTS13 (Nishio et al., 2004). Laboratory assessment of plasma vWF and enhanced responsiveness of patient PRP to low concentrations of ristocetin in this entity are indistinguishable from type 2B VWD. Genetic analysis of *GP1BA* and of *vWF* provides the definitive distinction between platelet-type VWD and type 2B VWD. Several point mutations in a conformationally sensitive portion of the GPIbα (Miller et al., 1991; Russell & Roth, 1993; Woods et al., 2014), as well as a 9–amino acid deletion in an unexpectedly distant region of the glycoprotein Ib α chain (Othman et al., 2005), have been reported in this rare disorder.

ACQUIRED VON WILLEBRAND SYNDROME

The term *acquired von Willebrand syndrome* (AVWS) describes patients with recent onset, yet no prior personal or family history, of an increased bleeding tendency whose laboratory studies show abnormalities similar to those seen in inherited VWD (Tiede et al., 2011). This is a heterogeneous group with a varied set of disease associations. In most patients, a quantitative or qualitative loss of vWF activity is due to one of the following three pathophysiologic mechanisms (Federici et al., 2013): (1) loss of HMWMs due to elongation of vWF in abnormal flow conditions with subsequent excessive cleavage by ADAMTS13, as seen in aortic stenosis or with cardiac-assist devices (Bortot et al., 2019); (2) development of a neutralizing or nonneutralizing autoantibody that binds to the patient's vWF, leading to its removal from the circulation; or (3) adsorption of vWF to circulating cells, most often lymphoproliferative or other malignant cell clones. Decreased vWF synthesis has also been invoked in patients with hypothyroidism (Levesque et al., 1993) and those receiving valproate (Kreuz et al., 1990). Additionally, increased proteolytic degradation of vWF by plasmin or other proteases may occur (Federici et al., 2013).

Analysis of the patient's plasma provides a picture similar to that of inherited VWD, particularly type 2 variants with the loss of the highest multimers. In AVWS associated with pathophysiologically high shear, such as in aortic stenosis (Sadler, 2003b; Vincentelli et al., 2003), angiodysplasias (Veyradier et al., 2001), or following placement of cardiac-assist devices, the largest vWF multimers are missing. The most common bleeding events are gastrointestinal, and, in fact, the association of aortic stenosis with gastrointestinal bleeding preceded our understanding of the role of vWF in its pathophysiology (Heyde, 1958). Dramatic correction of bleeding following surgical repair of aortic stenosis was a landmark finding (Vincentelli et al., 2003). In a study of 31 patients with advanced heart failure who had received continuous-flow left ventricular–assist devices, the mean levels of vWF : RCo activity and vWF : Ag were 102% and 204%, respectively, yet with decreased or absent HMWMs in all patients (Uriel et al., 2010). Six of these patients received heart transplants, following which the vWF multimeric patterns returned to normal.

Abnormalities in plasma vWF also occur in MPN patients, which may contribute to the hemostatic defect. Plasma vWF, particularly the large vWF multimers, are decreased inversely related to the platelet counts, and have improved following cytoreduction (Budde & van Genderen, 1997). These changes in plasma vWF occur in patients with reactive thrombocytosis as well. It has been postulated that enhanced vWF proteolysis by ADAMTS13 may be occurring, possibly because of platelet-induced conformational effects on plasma vWF (Elliott & Tefferi, 2005).

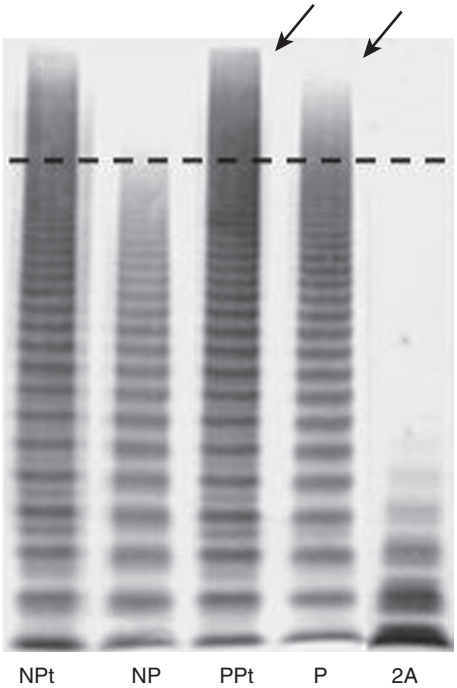

Figure 41.9 Ultra-large von Willebrand factor (vWF) multimers in platelets and plasma from a healthy normal subject and a patient with thrombotic thrombocytopenic purpura (TTP). vWF within normal platelets (NPt) and normal endothelial cells *(not shown)* comprises a very large range of multimer sizes. Once released into the circulation from cellular stores (predominantly endothelial), the vWF undergoes limited proteolysis by ADAMTS13. The resulting upper extent of vWF multimer size observed in normal plasma (NP) is indicated by the *dashed line*. In TTP, in which there is a characteristic deficiency of ADAMTS13, patient plasma (P) retains the full distribution of vWF multimers, including the ultra-large forms, present in the patient platelets (PPt) or endothelial cells *(not shown)*. (Modified with permission from Perez-Rodriguez A, Loures E, Rodriguez-Trillo A: Inherited ADAMTS13 deficiency (Upshaw-Schulman syndrome): a short review, *Thromb Res* 134:1171–1175, 2014.)

Defining the etiology of AVWS may be difficult in some patients, especially in those without obvious cardiovascular causes. In contrast to the laboratory's ability to identify autoantibodies to clotting factors such as factor VIII (see Chapter 40), mixing studies in AVWS based on vWF functional activity rarely identify neutralizing autoantibodies directed against vWF. Efforts to develop novel assays capable of detecting such antibodies are ongoing (Franchi et al., 2014).

THROMBOTIC THROMBOCYTOPENIC PURPURA

Thrombotic microangiopathies (TMAs) comprise a syndrome of disorders of diverse etiologies that produce characteristic vascular pathologic abnormalities (George & Nester, 2014). In recent years, our understanding has greatly increased with respect to the role of vWF in TMAs. TTP may be either congenital (Upshaw-Schulman syndrome) (Kremer Hovinga & George, 2019) or acquired, the pathophysiologies of which have recently been extensively reviewed (Zheng, 2015). Neurologic abnormalities or other signs of organ injury (renal, cardiac) are characteristically seen. Notably, in the congenital forms, severe acute kidney injury is rare (George, 2019). Laboratory studies in the congenital and/or acquired forms reveal thrombocytopenia together with a microangiopathic hemolytic anemia. In 1998, two independent groups (Furlan et al., 1998; Tsai & Lian, 1998) demonstrated that the pathogenesis of TTP was related to deficient activity of the plasma metalloproteinase ADAMTS13, which normally cleaves the higher-molecular-weight vWF molecules (so-called "unusually large" vWF multimers) that have been released into the circulation from endothelial cells. The enzyme deficiency results in the persistence in the plasma of these highly reactive forms of vWF (Fig. 41.9) (Perez-Rodriguez et al., 2014) capable of binding both to endothelial cells and to platelets, producing a pathologic meshwork of platelet-rich thrombi in the microcirculation (Moake et al., 1986; Tsai & Lian, 1998; Padilla et al., 2004; Chauhan et al., 2007; Perez-Rodriguez et al., 2014; Zheng, 2015).

TABLE 41.7
Etiology, Epidemiology, and Pathogenesis of TTP, HUS, and ADAMTS13-Related Parameters

	Inherited TTP	Acquired TTP	HUS
Etiology	ADAMTS13 mutation	Antibody to ADAMTS13, endothelial cell activation	*Escherichia coli* or other microorganisms
Epidemiology	5–10 cases per year per million	≤1 case per year per million	1–5 cases per year per million, mainly in children
Pathogenesis	Defective cleavage of vWF multimers, massive secretion of ultra-large vWF multimers, increased platelet deposition under shear condition, occlusion of blood vessels in microcirculation		Intoxication with Shiga-like toxin, damage of endothelial cells, enterohemorrhagic colitis, renal disorder
ADAMTS13 antigen	Very low or absent	Low or variable	Normal or moderately decreased
ADAMTS13 activity	≤5%–10%	≤5%–10% or variable	30%–100%
Inhibitor against ADAMTS13	No	Mostly yes	No

Congenital TTP exhibits distinctive features and requires lifelong followup along with, in most cases, plasma therapy for enzyme replacement. Investigators studying a series of 73 patients from the United Kingdom (Alwan et al., 2019) reported headaches, lethargy, and abdominal pain as the most common symptoms of congenital TTP even in the absence of typical laboratory features of the disease. However, those symptoms responded very well to prophylactic therapy with plasma. The location of mutations in the *ADAMTS13* gene was significantly associated with age of presentation, with mutations located in the regions of the gene before the spacer domain presenting at an earlier age when compared with post spacer mutations (Alwan et al., 2019). In the etiologically distinct TMA termed *Shiga toxin–related hemolytic uremic syndrome* (HUS), plasma ADAMTS13 levels are not decreased to the low levels associated with TTP (Furlan et al., 1998; George & Nester, 2014). Nevertheless, in the typical forms of *E. coli*– or *Shigella* toxin–associated diarrheal HUS, long vWF strings have been observed to bind both to endothelial cells and to platelets, and the possibility raised that the toxin may interfere with ADAMTS13 binding to the vWF strings (Moake, 2009). Atypical HUS (aHUS) is a rare complement-mediated thrombotic microangiopathy that has a similar clinical presentation to HUS and TTP. It almost invariably presents with renal failure but approximately 20% of patients have extrarenal manifestations—mostly CNS changes, including altered mental status, seizures, and focal deficits. Additional symptoms are diarrhea and respiratory and cardiovascular abnormalities. Over the last decade, several mutations in the genes that encode for complement proteins have been associated with aHUS. Unhinged complement activation likely leads to endothelial cell damage and TMA. Interestingly, ADAMTS13 levels are usually normal or slightly decreased, indicating that although clinically difficult to differentiate from TTP, the pathophysiology is unique to this disease (Zhang et al., 2017; Berger, 2019).

Characteristic clinical and laboratory aspects of TTP and HUS are summarized in Table 41.7 (Shenkman & Einav, 2014).

ADAMTS13 testing has increasingly been found to be helpful both for the purpose of prognostication and for guidance in treatment, such as the decision to institute rituximab anti-B lymphocyte immunotherapy (Coppo et al., 2010; Hovinga et al., 2010; Zheng, 2010). An ADAMTS13 level below 10%, with or without a demonstrable anti-ADAMTS13 antibody, in a patient having both thrombocytopenia and microangiopathic hemolytic anemia provides strong support for a diagnosis of TTP (Sayani & Abrams, 2015). However, there are limits for both the specificity and the sensitivity of ADAMTS13 testing with respect to TTP diagnosis. For ADAMTS13 levels in the range of 10% to 40%, in addition to TTP, other conditions such as connective tissue disorders (see later discussion), uremia, inflammation, and pregnancy may need to be considered as well. Moreover, neither a normal level of ADAMTS13 nor the absence of demonstrable neutralizing antibodies excludes this diagnosis (George et al., 2004; Peyvandi et al., 2004). One study of acquired TTP reported a positive predictive value of 91% and negative predictive value of 100% using a 20% activity level cutoff for ADAMTS13 activity (Barrows & Teruya, 2014). Reduced ADAMTS13 levels have been reported in a number of disease states, including systemic connective tissue disorders (Mannucci et al., 2003), ITP, and DIC (Moore et al., 2001), although the mechanisms for this observed reduction are not well understood.

The original ADAMTS13 assays involved a number of steps, including reacting the patient's plasma with a protease-free vWF substrate previously denatured with guanidine or urea, performing gel electrophoresis on the degraded vWF, immunoblotting, and then demonstrating an abnormal persistence of the higher-molecular-weight vWF multimers. There have been efforts to simplify the ADAMTS13 assays. An early modification of this method was in the final step, in which a vWF collagen-binding assay was substituted for vWF multimeric analysis (Gerritsen et al., 1999). Subsequently, efforts were directed toward the development of simplified assays employing synthetic peptides that recapitulated the critical residues of vWF required for proteolysis by ADAMTS13 (Kokame et al., 2004; Whitelock et al., 2004). Such assays, whether based on chromogenic or fluorescence resonance energy transfer changes following proteolytic cleavage, offer the advantage of ease of performance and rapid turnaround times. Variation in results among the available ADAMTS13 assays, however, can be significant (Mackie et al., 2013). Additionally, these same assay formats can be used to assess plasma inhibitory activity directed against ADAMTS13, with results expressed in Bethesda-style units similar to what is done for factor VIII antibodies (Muia et al., 2013) (see Chapter 40). Although the treatment of acquired TTP continues to involve plasma exchange and immunosuppression (Mazepa et al., 2019), emergent therapies—such as caplacizumab, a bispecific antibody that blocks the interaction of the A1 domain of vWF, and GP1bα—are being investigated (Peyvandi et al., 2016; Scully et al., 2019). Results of the HERCULES study, in which patients received caplacizumab or placebo during plasma exchange, showed that patients receiving caplacizumab had faster normalization of the platelet count, decreased thromboembolic events, and decreased recurrences with an overall lower incidence of a composite of TTP-related deaths (Scully et al., 2019).

ACKNOWLEDGMENT

The authors thank Dr. Jonathan Miller for his contributions as an author of this chapter in the prior editions of this textbook.

SELECTED REFERENCES

Arnold DM, Curtis BR, Bakchoul T: Recommendations for standardization of laboratory testing for drug-induced immune thrombocytopenia: communication from the SSC of the ISTH, *J Thromb Haemost* 13:676–678, 2015.
A consensus report on drug-induced immune thrombocytopenias.

Aster RH, Bougie DW: Drug-induced thrombocytopenia, *N Engl J Med* 357:580–587, 2007.
A review of mechanisms of drug-induced thrombocytopenias.

Cattaneo M, Cerletti C, Harrison P: Recommendations for the standardization of light transmission aggregometry: a consensus of the working party from the platelet Physiology Subcommittee of SSC/ISTH, *J Thrombos Haemost*, 2013. https://doi.org/10.1111/jth.12231.
A consensus report on platelet aggregation testing.

Kumar R, Kahr WHA: Inherited thrombocytopenia: clinical manifestations, laboratory abnormalities, and molecular defects of a heterogeneous group of conditions. In Rao AK, editor: *Hematology/oncology Clinics of North America: disorders of the platelets*, vol. 27. Philadelphia, 2013, Elsevier, pp 465–494.
A review of diagnostic approaches to inherited thrombocytopenias.

Kremer Hovinga JA, George JN: Hereditary thrombotic thrombocytopenic purpura, *N Engl J Med* 381(17):1653–1662, 2019.
A review of mechanisms of hereditary thrombotic thrombocytopenic purpura.

Lentaigne C, Freson K, Laffan MA, et al.: Inherited platelet disorders: toward DNA-based diagnosis, *Blood* 127(23):2814–2823, 2016.
A review of application of high-throughput DNA sequencing to inherited platelet disorders.

Neunert C, Terrell DR, Arnold DM, et al.: American Society of Hematology 2019 guidelines for immune thrombocytopenia, *Blood Adv* 3(23):3829–3866, 2019.

A review of recent guidelines for immune thrombocytopenias.
Ng C, Motto DG, Di Paola J: Diagnostic approach to von Willebrand disease, *Blood* 125:2029–2037, 2015.
A review of the laboratory diagnostic approach to Von Willebrand disease.
Provan D, Stasi R, Newland AC: International consensus report on the investigation and management of primary immune thrombocytopenia, *Blood* 115:168–186, 2010.
A consensus report on immune thrombocytopenia.
Rao AK, Bennett JS: Acquired disorders of platelet function. In Marder VJ, Aird WC, Bennett JS, editors: *Hemostasis and thrombosis: basic principles and clinical practice*, ed 6, Philadelphia, 2013, Lippincott Williams & Wilkins, pp 820–828.
A review of acquired platelet function disorders.
Rao AK, Coller BS: Hereditary qualitative platelet disorders. In Kaushansky K, Lichtman M, Prchal JT, et al.: *Williams hematology*, ed 9, New York, 2016, McGraw-Hill, pp 2039–2072.
A review of inherited platelet function disorders.
Sivapalaratnam S, Collins J, Gomez K: Diagnosis of inherited bleeding disorders in the genomic era, *Br J Haematol* 179(3):363–376, 2017.
A review of inherited platelet function disorders.

Access the complete reference list online at Elsevier eBooks for Practicing Clinicians.

REFERENCES

Adler DH, Cogan JD, Phillips JA: Inherited human cPLA(2alpha)deficiency is associated with impaired eicosanoid biosynthesis, small intestinal ulceration, and platelet dysfunction, *J Clin Invest* 118:2121–2131, 2008.

Ahmadi Z, Perdomo J, Wong R, Chong BH: Drug-induced immune thrombocytopenia: mapping of the drug binding site to the membrane-proximal region of platelet GPIX, *Platelets* 30(2):251–255, 2019.

Albers CA, Cvejic A, Favier R: Exome sequencing identifies NBEAL2 as the causative gene for gray platelet syndrome, *Nat Genet* 43:735–737, 2011.

Albers CA, Paul DS, Schulze H, Freson K, Stephens JC, Smethurst PA, et al.: Compound inheritance of a low-frequency regulatory SNP and a rare null mutation in exon-junction complex subunit RBM8A causes TAR syndrome, *Nat Genet* 44(4):435–439, S431–432, 2012.

Almazni I, Stapley R, Morgan NV: Inherited thrombocytopenia: update on genes and genetic variants which may be associated with bleeding, *Front Cardiovasc Med* 6:80, 2019.

Almeida AM, Khair K, Hann I: The use of recombinant factor VIIa in children with inherited platelet function disorders, *Br J Haematol* 121:477–481, 2003.

Al-Nouri ZL, George JN: Drug-induced thrombocytopenia: an updated systematic review, 2012, *Drug Saf* 35:693–694, 2012.

Althaus K, Greinacher A: MYH9-related platelet disorders, *Semin Thromb Hemost* 35:189–203, 2009.

Alwan F, Vendramin C, Liesner R, Clark A, Lester W, Dutt T, et al.: Characterization and treatment of congenital thrombotic thrombocytopenic purpura, *Blood* 133(15):1644–1651, 2019.

Aneja K, Jalagadugula G, Mao G: Mechanism of platelet factor 4 (PF4) deficiency with RUNX1 haplodeficiency: RUNX1 is a transcriptional regulator of *PF4*, *J Thromb Haemost* 9:383–391, 2011.

Ardlie NG, Coupland WW, Schoefl GI: Hereditary thrombocytopathy: a familial bleeding disorder due to impaired platelet coagulant activity, *Aust N Z J Med* 6:37–45, 1976.

Arnold DM, Curtis BR, Bakchoul T: Recommendations for standardization of laboratory testing for drug-induced immune thrombocytopenia: communication from the SSC of the ISTH, *J Thromb Haemost* 13:676–678, 2015.

Arnold DM, Nazi I, Warkentin TE: Approach to the diagnosis and management of drug-induced immune thrombocytopenia, *Transfus Med Rev* 27:137–145, 2013.

Aster RH, Bougie DW: Drug-induced immune thrombocytopenia, *N Engl J Med* 357:580–587, 2007.

Aster RH, Curtis BR, Bougie DW: Thrombocytopenia resulting from sensitivity to GPIIb-IIIa inhibitors, *Semin Thromb Hemost* 30:569–577, 2004.

Bakchoul T, Zollner H, Amiral J: Anti-protamine-heparin antibodies: incidence, clinical relevance, and pathogenesis, *Blood* 121:2821–2827, 2013.

Balduini CL, Pecci A, Noris P: Diagnosis and management of inherited thrombocytopenias, *Semin Thromb Hemost* 39:161–171, 2013a.

Balduini CL, Savoia A, Seri M: Inherited thrombocytopenias frequently diagnosed in adults, *J Thromb Haemost* 11:1006–1019, 2013b.

Barrows BD, Teruya J: Use of the ADAMTS13 activity assay improved the accuracy and efficiency of the diagnosis and treatment of suspected acquired thrombotic thrombocytopenic purpura, *Arch Pathol Lab Med* 138:546–549, 2014.

Bastida JM, Lozano ML, Benito R, Janusz K, Palma-Barqueros V, Del Rey M, et al.: Introducing high-throughput sequencing into mainstream genetic diagnosis practice in inherited platelet disorders, *Haematologica* 103(1):148–162, 2018.

Bennett JS, Rao AK: Hereditary disorders of platelet function. In Marder VJ, Aird WC, Bennett JS, editors: *Hemostasis and thrombosis: basic principles and clinical practice*, ed 6, Philadelphia, 2013, Lippincott, pp 805–819.

Berger BE: Atypical hemolytic uremic syndrome: a syndrome in need of clarity, *Clin Kidney J* 12(3):338–347, 2019.

Berrou E, Adam F, Lebret M, Fergelot P, Kauskot A, Coupry I, et al.: Heterogeneity of platelet functional alterations in patients with filamin A mutations, *Arterioscler Thromb Vasc Biol* 33(1):e11–18, 2013.

Blair TA, Michelson AD, Frelinger 3rd AL: Mass cytometry reveals distinct platelet subtypes in healthy subjects and novel alterations in surface glycoproteins in Glanzmann thrombasthenia, *Sci Rep* 8(1):10300, 2018.

Blavignac J, Bunimov N, Rivard GE: Quebec platelet disorder: update on pathogenesis, diagnosis, and treatment, *Semin Thromb Hemost* 37:713–720, 2011.

Bluteau D, Balduini A, Balayn N: Thrombocytopenia-associated mutations in the ANKRD26 regulatory region induce MAPK hyperactivation, *J Clin Invest* 124:580–591, 2014.

Boccardo P, Remuzzi G, Galbusera M: Platelet dysfunction in renal failure, *Semin Thromb Hemost* 30:579–589, 2004.

Bodó I, Eikenboom J, Montgomery R, et al.: Platelet-dependent von Willebrand factor activity. Nomenclature and methodology: communication from the SSC of the ISTH, *J Thromb Haemost* 13(7):1345–1350, 2015.

Boisseau P, Bene MC, Besnard T, Pachchek S, Giraud M, Talarmain P, et al.: A new mutation of ANO6 in two familial cases of Scott syndrome, *Br J Haematol* 180(5):750–752, 2018.

Bortot M, Ashworth K, Sharifi A, et al.: Turbulent flow Promotes cleavage of VWF (von Willebrand factor) by ADAMTS13 (A disintegrin and metalloproteinase with a thrombospondin type-1 motif, member 13), *Arterioscler Thromb Vasc Biol* 39(9):1831–1842, 2019.

Boylan B, Chen H, Rathore V: Anti-GPVI-associated ITP: an acquired platelet disorder caused by autoantibody-mediated clearance of the GPVI/FcRgamma-chain complex from the human platelet surface, *Blood* 104:1350–1355, 2004.

Brennan Y, Levade M, Ward CM: Acquired platelet function disorders, *Thromb Res*, 2019.

Brinkhous KM, Read MS: Preservation of platelet receptors for platelet aggregating factor/von Willebrand Factor by air drying, freezing, or lyophilization: new stable platelet preparations for von Willebrand Factor assays, *Thromb Res* 13:591–597, 1978.

Buchbinder D, Nugent DJ, Fillipovich AH: Wiskott-Aldrich syndrome: diagnosis, current management, and emerging treatments, *Appl Clin Genet* 7:55–66, 2014.

Budde U, van Genderen PJ: Acquired von Willebrand disease in patients with high platelet counts, *Semin Thromb Hemost* 23:425–431, 1997.

Buitrago L, Rendon A, Liang Y: αIIbβ3 variants defined by next-generation sequencing: Predicting variants likely to cause Glanzmann thrombasthenia, *Proc Natl Acad Sci U S A* 112:E1898–E1907, 2015.

Bury L, Megy K, Stephens JC, Grassi L, Greene D, Gleadall N, et al.: Next-generation sequencing for the diagnosis of MYH9-RD: Predicting pathogenic variants, *Hum Mutat*, 2019.

Campbell PJ, Green AR: The myeloproliferative disorders, *N Engl J Med* 355:2452–2466, 2006.

Canault M, Ghalloussi D, Grosdidier C: Human CalDAG-GEFI gene (RASGRP2) mutation affects platelet function and causes severe bleeding, *J Exp Med* 211:1349–1362, 2014.

Cardinal DC, Flower RJ: The electronic aggregometer: a novel device for assessing platelet behavior in blood, *J Pharmacol Methods* 3:135–158, 1980.

Castillo R, Lozano T, Escolar G: Defective platelet adhesion on vessel subendothelium in uremic patients, *Blood* 68:337–342, 1986.

Castoldi E, Collins PW, Williamson PL: Compound heterozygosity for 2 novel TMEM16F mutations in a patient with Scott syndrome, *Blood* 117:4399–4400, 2011.

Cattaneo M, Cerletti C, Harrison P: Recommendations for the standardization of light transmission aggregometry: a consensus of the working party from the platelet Physiology Subcommittee of SSC/ISTH, *J Thromb Haemost*, 2013, https://doi.org/10.1111/jth.12231.

Cattaneo M, Lecchi A, Randi AM: Identification of a new inherited defect of platelet function characterized by severe impairment of platelet responses to adenosine diphosphate, *Blood* 80:2787–2796, 1992.

Cattaneo M, Lombardi R, Zighetti ML: Deficiency of (^{33})P-2MeS-ADP binding sites on platelets with secretion defect, normal granule stores and normal thromboxane A_2 production, *Thromb Haemost* 77:986–990, 1997.

Cattaneo M: Light transmission aggregometry and ATP release for the diagnostic assessment of platelet function, *Semin Thromb Hemost* 35:158–167, 2009.

Cattaneo M, Cerletti C, Harrison P, Hayward CP, Kenny D, Nugent D, et al.: Recommendations for the standardization of light transmission aggregometry: a consensus of the working party from the platelet Physiology Subcommittee of SSC/ISTH, *J Thromb Haemost* 11:1183–1189, 2013.

Chan MV, Hayman MA, Sivapalaratnam S, et al.: Identification of a homozygous recessive variant in PTGS1 resulting in a congenital aspirin-like defect in platelet function. Haematologica. 2020;105 (Epub ahead of print).

Chauhan AK, Goerge T, Schneider SW: Formation of platelet strings and microthrombi in the presence of ADAMTS-13 inhibitor does not require P-selectin or beta(3) integrin, *J Thromb Haemost* 5:583–589, 2007.

Chen CH, Lo RW, Urban D, Pluthero FG, Kahr WH: alpha-granule biogenesis: from disease to discovery, *Platelets* 28(2):147–154, 2017.

Chong BH, Choi PY, Khachigian L: Drug-induced immune thrombocytopenia, *Hematol Oncol Clin North Am* 27:521–540, 2013.

Cines DB, Bussel JB, Liebman HA: The ITP syndrome: pathogenic and clinical diversity, *Blood* 113:6511–6521, 2009a.

Cines DB, Liebman H, Stasi R: Pathobiology of secondary immune thrombocytopenia, *Semin Hematol* 46:S2–S14, 2009b.

Clauser S, Cramer-Borde E: Role of platelet electron microscopy in the diagnosis of platelet disorders, *Semin Thromb Hemost* 35:213–223, 2009.

Coller BS, Peerschke EI, Scudder LE: A murine monoclonal antibody that completely blocks the binding of fibrinogen to platelets produces a thrombasthenic-like state in normal platelets and binds to glycoproteins IIb and/or IIIa, *J Clin Invest* 72:325–338, 1983.

Coller BS, Shattil SJ: The GPIIb/IIIa (integrin alpha IIb beta 3) odyssey: a technology-driven saga of a receptor with twists, turns, and even a bend, *Blood* 112:3011–3025, 2008.

Connelly JP, Kwon EM, Gao Y: Targeted correction of RUNX1 mutation in FPD patient-specific induced pluripotent stem cells rescues megakaryopoietic defects, *Blood* 124:1926–1930, 2014.

Coppo P, Schwarzinger M, Buffet M: Predictive features of severe acquired ADAMTS13 deficiency in idiopathic thrombotic microangiopathies: the French TMA Reference Center experience, *PloS One* 5, 2010. e10208.

Cuker A, Cines DB: Protamine-induced thrombocytopenia? *Blood* 121:2818–2819, 2013.

Cuker A, Neunert CE: How I treat refractory immune thrombocytopenia, *Blood* 128(12):1547–1554, 2016.

Cullinane AR, Curry JA, Carmona-Rivera C: A BLOC-1 mutation screen reveals that PLDN is mutated in Hermansky-Pudlak syndrome type 9, *Am J Hum Genet* 88:778–787, 2011.

Curtis BR, Podoltsev HN, Lacy J, Curtis S, Samuel MS, Zutavern K, et al.: Patients treated with oxaliplatin are at risk for thrombocytopenia caused by multiple drug-dependent antibodies, *Blood* 131(13):1486–1489, 2018.

Daly ME, Dawood BB, Lester WA: Identification and characterization of a novel P2Y 12 variant in a patient diagnosed with type 1 von Willebrand disease in the European MCMDM-1VWD study, *Blood* 113:4110–4113, 2009.

Dawood BB, Lowe GC, Lordkipanidze M: Evaluation of participants with suspected heritable platelet function disorders including recommendation and validation of a streamlined agonist panel, *Blood* 120:5041–5049, 2012.

de Witt SM, Verdoold R, Cosemans JM, et al.: Insights into platelet-based control of coagulation, *Thromb Res* 133(Suppl 2):S139–S148, 2014.

Diamandis M, Paterson AD, Rommens JM: Quebec platelet disorder is linked to the urokinase plasminogen activator gene (PLAU) and increases expression of the linked allele in megakaryocytes, *Blood* 113:1543–1546, 2008.

Diz-Kucukkaya R, Lopez JA: Inherited disorders of platelets: membrane glycoprotein disorders, *Hematol Oncol Clin North Am* 27:613–627, 2013.

Downes K, Megy K, Duarte D, Vries M, Gebhart J, Hofer S, et al.: Diagnostic high-throughput sequencing of 2,396 patients with bleeding, thrombotic and platelet disorders, *Blood*, 2019.

Drachman JG: Inherited thrombocytopenia: when a low platelet count does not mean ITP, *Blood* 103:390–398, 2004.

Drouin A, Favier R, Masse JM: Newly recognized cellular abnormalities in the gray platelet syndrome, *Blood* 98:1382–1391, 2001.

Dusse LMS, Freitas LG: Clinical applicability of reticulated platelets, *Clin Chim Acta* 439:143–147, 2015.

Elliott MA, Tefferi A: Thrombosis and haemorrhage in polycythaemia vera and essential thrombocythaemia, *Br J Haematol* 128:275–290, 2005.

Favaloro EJ, Bonar R: External quality assessment/proficiency testing and internal quality control for the PFA-100 and PFA-200: an update, *Semin Thromb Hemost* 40:239–253, 2014.

Favier R, Jondeau K, Boutard P: Paris-Trousseau syndrome: clinical, hematological, molecular data of ten new cases, *Thromb Haemost* 90:893–897, 2003.

Federici AB, Bucciarelli P, Castaman G: The bleeding score predicts clinical outcomes and replacement therapy in adults with von Willebrand disease, *Blood* 123:4037–4044, 2014.

Federici AB, Budde U, Castaman G: Current diagnostic and therapeutic approaches to patients with acquired von Willebrand syndrome: a 2013 update, *Semin Thromb Hemost* 39:191–201, 2013.

Federici AB, Canciani MT, Forza I: A sensitive ristocetin co-factor activity assay with recombinant glycoprotein Ib alpha for the diagnosis of patients with low von Willebrand factor levels, *Haematologica* 89:77–85, 2004.

Ferreira CR, Chen D, Abraham SM, Adams DR, Simon KL, Malicdan MC, et al.: Combined alpha-delta platelet storage pool deficiency is associated with mutations in GFI1B, *Mol Genet Metab* 120(3):288–294, 2017.

Flamm MH, Colace TV, Chatterjee MS: Multiscale prediction of patient-specific platelet function under flow, *Blood* 120:190–198, 2012.

Flood VH, Friedman KD, Gill JC: Limitations of the ristocetin cofactor assay in measurement of von Willebrand factor function, *J Thromb Haemost* 7:1832–1839, 2009.

Flood VH, Gill JC, Friedman KD: Collagen binding provides a sensitive screen for variant von Willebrand disease, *Clin Chem* 59:684–691, 2013.

Flood VH, Johnson FL, Boshkov LK: Sustained engraftment post bone marrow transplant despite anti-platelet antibodies in Glanzmann thrombasthenia, *Pediatr Blood Cancer* 45:971–975, 2005.

Flood VH, Schlauderaff AC, Haberichter SL: Crucial role for the VWF A1 domain in binding to type IV collagen, *Blood* 125:2297–2304, 2015.

Franchi F, Biguzzi E, Stufano F: A two-step approach (Enzyme-linked immunosorbent assay and confirmation assay) to detect antibodies against von Willebrand factor in patients with Acquired von Willebrand Syndrome, *Thromb Res* 134:1316–1322, 2014.

Franchini M, Crestani S, Frattini F: ABO blood group and von Willebrand factor: biological implications, *Clin Chem Lab Med* 52:1273–1276, 2014.

Freson K, Hoylaerts MF, Jaeken J: Genetic variation of the extra-large stimulatory G protein alpha-subunit leads to Gs hyperfunction in platelets and is a risk factor for bleeding, *Thromb Haemost* 86:733–738, 2001b.

Freson K, Wijgaerts A, Van Geet C: GATA1 gene variants associated with thrombocytopenia and anemia, *Platelets* 28(7):731–734, 2017.

Fujimoto TT, Kishimoto M, Ide K: Glanzmann thrombasthenia with acute myeloid leukemia successfully treated by bone marrow transplantation, *Int J Hematol* 81:77–80, 2005.

Furlan M, Robles R, Galbusera M: von Willebrand factor-cleaving protease in thrombotic thrombocytopenic purpura and the hemolytic-uremic syndrome, *N Engl J Med* 339:1578–1584, 1998.

Gabbeta J, Yang X, Kowalska MA: Platelet signal transduction defect with G alpha subunit dysfunction and diminished G alpha(q) in a patient with abnormal platelet responses, *Proc Natl Acad Sci U S A* 94:8750–8755, 1997.

Gabbeta J, Yang X, Sun L: Abnormal inside-out signal transduction-dependent activation of glycoprotein IIb-IIIa in a patient with impaired pleckstrin phosphorylation, *Blood* 87:1368–1376, 1996.

Gahl WA, Brantly M, Kaiser-Kupfer MI: Genetic defects and clinical characteristics of patients with a form of oculocutaneous albinism (Hermansky-Pudlak syndrome), *N Engl J Med* 338:1258–1264, 1998.

Galbusera M, Remuzzi G, Boccardo P: Treatment of bleeding in dialysis patients, *Semin Dial* 22:279–286, 2009.

Gangji AS, Sohal AS, Treleaven D: Bleeding in patients with renal insufficiency: a practical guide to clinical management, *Thromb Res* 118:423–428, 2006.

Genevieve D, Isidor PB, Bellais S, Serre V, Djouadi F, Picard C, et al.: Thromboxane synthase mutations in an increased bone density disorder (Ghosal syndrome), *Nat Genet* 40(3):284–286, 2008.

George JN, Nester CM: Syndromes of thrombotic microangiopathy, *N Engl J Med* 371:654–666, 2014.

George JN, Vesely SK, Terrell DR: The Oklahoma thrombotic thrombocytopenic purpura-hemolytic uremic syndrome (TTP-HUS) Registry: a community perspective of patients with clinically diagnosed TTP-HUS, *Semin Hematol* 41:60–67, 2004.

George JN, Woolf SH, Raskob GE: Idiopathic thrombocytopenic purpura: a practice guideline developed by explicit methods for the American Society of Hematology, *Blood* 88:3–40, 1996.

George JN: "Congenital TTP: toward a turning point," Blood 133 (15): 1615–1617.

Gerrard JM, Lint D, Sims PJ: Identification of a platelet dense granule membrane protein that is deficient in a patient with the Hermansky-Pudlak syndrome, *Blood* 77:101–112, 1991.

Gerritsen HE, Turecek PL, Schwarz HP: Assay of von Willebrand factor (vWF)-cleaving protease based on decreased collagen binding affinity of degraded vWF: a tool for the diagnosis of thrombotic thrombocytopenic purpura (TTP), *Thromb Haemost* 82:1386–1389, 1999.

Giannini S, Mezzasoma AM, Guglielmini G: A new case of acquired Glanzmann's thrombasthenia: diagnostic value of flow cytometry, *Cytometry B Clin Cytom* 74:194–199, 2008.

Gill JC, Flood VH, Christopherson PA, et al.: The management of bleeding risk in Von Willebrand disease: should blood group O make a difference? *Blood* 124:2829, 2014.

Gill JC, Conley SF, Johnson VP, Christopherson PA, Haberichter SL, Diaz CD, et al.: Low VWF levels in children and lack of association with bleeding in children undergoing tonsillectomy, *Blood Adv* 4(1):100–105, 2020.

Gnatenko DV, Zhu W, Xu X: Class prediction models of thrombocytosis using genetic biomarkers, *Blood* 115:7–14, 2010.

Greinacher A, Pecci A, Kunishima S, Althaus K, Nurden P, Balduini CL, et al.: Diagnosis of inherited platelet disorders on a blood smear: a tool to facilitate worldwide diagnosis of platelet disorders, *J Thromb Haemost* 15(7):1511–1521, 2017.

Gresele P: Subcommittee on Platelet, P: "Diagnosis of inherited platelet function disorders: guidance from the SSC of the ISTH, *J Thromb Haemost* 13(2):314–322, 2015.

Gresele P, Harrison P, Bury L, Falcinelli E, Gachet C, Hayward CP, et al.: Diagnosis of suspected inherited platelet function disorders: results of a worldwide survey, *J Thromb Haemost* 12(9):1562–1569, 2014.

Groeneveld DJ, van Bekkum T, Cheung KL: No evidence for a direct effect of von Willebrand factor's ABH blood group antigens on von Willebrand factor clearance, *J Thromb Haemost* 13:592–600, 2015.

Gudmundsdottir BR, Marder VJ, Onundarson PT: Risk of excessive bleeding associated with marginally low von Willebrand factor and mild platelet dysfunction, *J Thromb Haemost* 5:274–281, 2007.

Gunay-Aygun M, Falik-Zaccai TC, Vilboux T: NBEAL2 is mutated in gray platelet syndrome and is required for biogenesis of platelet alpha-granules, *Nat Genet* 43:732–734, 2011.

Gunay-Aygun M, Huizing M, Gahl WA: Molecular defects that affect platelet dense granules, *Semin Thromb Hemost* 30:537–547, 2004.

Haberichter SL, Balistreri M, Christopherson P: Assay of the von Willebrand factor (VWF) propeptide to identify patients with type 1 von Willebrand disease with decreased VWF survival, *Blood* 108:3344–3351, 2006.

Haberichter SL, Castarnan G, Budde U: Identification of type 1 von Willebrand disease patients with reduced von Willebrand factor survival by assay of the VWF propeptide in the European study: molecular and Clinical Markers for the Diagnosis and Management of Type 1 VWD (MCMDM-1VWD), *Blood* 111:4979–4985, 2008.

Harrison CN, Bareford D, Butt N: Guideline for investigation and management of adults and children presenting with a thrombocytosis, *Br J Haematol* 149:352–375, 2010.

Harrison P, Lordkipanidze M: Clinical tests of platelet function. In Michelson AD, editor: *Platelets*, ed 3, San Diego, 2013, Elsevier, pp 519–545.

Harrison P, Mackie I, Mumford A: Guidelines for the laboratory investigation of heritable disorders of platelet function, *Br J Haematol* 155:30–44, 2011.

Harrison P, Lordkipanidze M: Testing platelet function, *Hematol Oncol Clin North Am* 27(3):411–441, 2013.

Hayward CPM, Moffat KA, Brunet J, Carlino SA, Plumhoff E, Meijer P, et al.: Update on diagnostic testing for platelet function disorders: what is practical and useful? *Int J Lab Hematol* 41(Suppl 1):26–32, 2019.

Hayward CP, Rao AK, Cattaneo M: Congenital platelet disorders: overview of their mechanisms, diagnostic evaluation and treatment, *Haemophilia* 12(Suppl 3):128–136, 2006.

Heremans J, Freson K: High-throughput sequencing for diagnosing platelet disorders: lessons learned from exploring the causes of bleeding disorders, *Int J Lab Hematol* 40(Suppl 1):89–96, 2018.

Heyde EC: Gastrointestinal bleeding in aortic stenosis, *N Engl J Med* 259:196, 1958.

Hirata T, Kakizuka A, Ushikubi F: Arg60 to Leu mutation of the human thromboxane A2 receptor in a dominantly inherited bleeding disorder, *J Clin Invest* 94:1662–1667, 1994.

Ho KM, Yip CB, Duff O: Reactive thrombocytosis and risk of subsequent venous thromboembolism: a cohort study, *J Thromb Haemost* 10:1768–1774, 2012.

Hoffmann JJ: Reticulated platelets: analytical aspects and clinical utility, *Clin Chem Lab Med* 52:1107–1117, 2014.

Holmsen H, Dangelmaier CA: Measurement of secretion of serotonin, *Methods Enzymol* 169:205–211, 1989.

Holmsen H: Secretable storage pools in platelets, *Annu Rev Med* 30:119–134, 1979.

Hovinga JAK, Vesely SK, Terrell DR: Survival and relapse in patients with thrombotic thrombocytopenic purpura, *Blood* 115:1500–1511, 2010.

Hsieh RW, Ravindran A, Hook CC, Begna KH, Ashrani AA, Pruthi RK, et al.: Etiologies of Extreme thrombocytosis: a Contemporary series, *Mayo Clin Proc* 94(8):1542–1550, 2019.

Hui SKR, Biswas TK, Miller JL: Development of a functional ELISA for von Willebrand factor activity using the extracellular domain of human platelet glycoprotein Ib alpha secreted from Chinese hamster ovary cells, *Am J Clin Pathol* 128:60, 2007.

Huizing M, Anikster Y, Gahl WA: Hermansky-Pudlak syndrome and Chediak-Higashi syndrome: disorders of vesicle formation and trafficking, *Thromb Haemost* 86:233–245, 2001.

Huizing M, Helip-Wooley A, Westbroek W: Disorders of lysosome-related organelle biogenesis: clinical and molecular genetics, *Annu Rev Genomics Hum Genet* 9:359–386, 2008.

Ingerman CM, Smith JB, Shapiro S: Hereditary abnormality of platelet aggregation attributable to nucleotide storage pool deficiency, *Blood* 52:332–344, 1978.

Ingerman-Wojenski CM, Silver MJ: A quick method for screening platelet dysfunctions using the whole blood lumi-aggregometer, *Thromb Haemost* 51:154–156, 1984.

Israels SJ, McMillan EM, Robertson C: The lysosomal granule membrane protein, LAMP-2, is also present in platelet dense granule membranes, *Thromb Haemost* 75:623–629, 1996.

Israels SJ, McNicol A, Robertson C: Platelet storage pool deficiency: diagnosis in patients with prolonged bleeding times and normal platelet aggregation, *Br J Haematol* 75:118–121, 1990.

James PD: Lillicrap D: von Willebrand disease: clinical and laboratory lessons learned from the large von Willebrand disease studies, *Am J Hematol* 87(Suppl 1):S4–S11, 2012.

Jandrot-Perrus M, Hermans C, Mezzano D: Platelet glycoprotein VI genetic quantitative and qualitative defects, *Platelets* 30(6):708–713, 2019.

Joseph R, Welch KMA, D'Andrea G: Epinephrine does not induce platelet aggregation in citrated whole blood, *Thromb Res* 45:871–872, 1987.

Kahr WH, Hinckley J, Li L: Mutations in NBEAL2, encoding a BEACH protein, cause gray platelet syndrome, *Nat Genet* 43:738–740, 2011.

Karpatkin S, Nardi M: Autoimmune anti-HIV-1gp120 antibody with antiidiotype-like activity in sera and immune complexes of HIV-1-related immunologic thrombocytopenia, *J Clin Invest* 89:356–364, 1992.

Karpatkin S, Nardi MA, Hymes KB: Sequestration of anti-platelet GPIIIa antibody in rheumatoid factor immune complexes of human immunodeficiency virus 1 thrombocytopenic patients, *Proc Natl Acad Sci U S A* 92:2263–2267, 1995.

Kehrel B, Balleisen L, Kokott R: Deficiency of intact thrombospondin and membrane glycoprotein Ia in platelets with defective collagen-induced aggregation and spontaneous loss of disorder, *Blood* 71:1074–1078, 1988.

Kessler CM: Propensity for hemorrhage and thrombosis in chronic myeloproliferative disorders, *Semin Hematol* 41:10–14, 2004.

Kitchen S, Jennings I, Woods TAL: Laboratory tests for measurement of von Willebrand factor show poor agreement among different centers: results from the United Kingdom National External Quality Assessment Scheme for Blood Coagulation, *Semin Thromb Hemost* 32:492–498, 2006.

Klampfl T, Gisslinger H, Harutyunyan AS: Somatic mutations of calreticulin in myeloproliferative neoplasms, *N Engl J Med* 369:2379–2390, 2013.

Knight AE, Gomez K, Cutler DF: Super-resolution microscopy in the diagnosis of platelet granule disorders, *Expert Rev Hematol* 10(5):375–381, 2017.

Kodigepalli KM, Bowers K, Sharp A: Roles and regulation of phospholipid scramblases, *FEBS Lett* 589(3–14), 2015.

Kokame K, Matsumoto M, Fujimura Y: VWF73, a region from D1596 to R1668 of von Willebrand factor, provides a minimal substrate for ADAMTS-13, *Blood* 103:607–612, 2004.

Kremer Hovinga JA, George JN: Hereditary thrombotic thrombocytopenic purpura, *N Engl J Med* 381(17):1653–1662, 2019.

Kreuz W, Linde R, Funk M: Induction of von Willebrand disease type I by valproic acid, *Lancet* 335:1350–1351, 1990.

Krueger LA, Barnard MR, Frelinger 3rd AL, Furman MI, Michelson AD: Immunophenotypic analysis of platelets, *Curr Protoc Cytom Chapter 6: Unit 6 10*, 2002.

Kumar R, Kahr WHA: Inherited thrombocytopenia: clinical manifestations, laboratory abnormalities, and molecular defects of a heterogeneous group of conditions. In Rao AK, editor: *Hematology/Oncology Clinics of North America: disorders of the platelets*, vol. 27. Philadelphia, 2013, Elsevier, pp 465–494.

Kunicki TJ, Aster RH: Deletion of the platelet-specific alloantigen Pl^{A1} from platelets in Glanzmann's thrombasthenia, *J Clin Invest* 61:1225–1231, 1978.

Kunishima S, Kobayashi R, Itoh TJ, Hamaguchi M, Saito H: Mutation of the beta1-tubulin gene associated with congenital macrothrombocytopenia affecting microtubule assembly, *Blood* 113(2):458–461, 2009.

Kunishima S, Ito-Yamamura Y, Hayakawa A, Yamamoto T, Saito H, FLNA p: V528M substitution is neither associated with bilateral periventricular nodular heterotopia nor with macrothrombocytopenia, *J Hum Genet* 55(12):844–846, 2010.

Kurstjens R, Bolt C, Vossen M: Familial thrombopathic thrombocytopenia, *Br J Haematol* 15:305–317, 1968.

Lages B, Dangelmaier CA, Holmsen H: Specific correction of impaired acid hydrolase secretion in storage pool-deficient platelets by adenosine diphosphate, *J Clin Invest* 81:1865–1872, 1988.

Lan Z, Schmaier AH: Platelet aggregation testing in platelet-rich plasma—Description of procedures with the aim to develop standards in the field, *Am J Clin Pathol* 123:172–183, 2005.

Landolfi R, Marchioli R, Patrono C: Mechanisms of bleeding and thrombosis in myeloproliferative disorders, *Thromb Haemost* 78:617–621, 1997.

Lee GM, Welsby IJ, Phillips-Bute B: High incidence of antibodies to protamine and protamine/heparin complexes in patients undergoing cardiopulmonary bypass, *Blood* 121:2828–2835, 2013.

Lee SB, Rao AK, Lee KH: Decreased expression of phospholipase C-beta 2 isozyme in human platelets with impaired function, *Blood* 88:1684–1691, 1996.

Lentaigne C, Freson K, Laffan MA, Turro E, Ouwehand WH: Inherited platelet disorders - towards DNA—based diagnosis, *Blood*, 2016.

Lentaigne C, Freson K, Laffan MA, Turro E, Ouwehand WH, Consortium B-B: The ThromboGenomics C: "Inherited platelet disorders: toward DNA-based diagnosis, *Blood* 127(23):2814–2823, 2016.

Lenting PJ, Christophe OD, Denis CV: Von Willebrand factor biosynthesis, secretion and clearance: connecting the far ends, *Blood* 125:2019–2028, 2015.

Leo VC, Morgan NV, Bem D, Jones ML, Lowe GC, Lordkipanidze M, et al.: Use of next-generation sequencing and candidate gene analysis to identify underlying defects in patients with inherited platelet function disorders, *J Thromb Haemost* 13(4):643–650, 2015.

Levesque H, Borg JY, Cailleux N: Acquired von Willebrand's syndrome associated with decrease of plasminogen activator and its inhibitor during hypothyroidism, *Eur J Med* 2:287–288, 1993.

Lillicrap D: Translational medicine advances in von Willebrand disease, *J Thromb Haemost* 11(Suppl 1):75–83, 2013a.

Lillicrap D, von Willebrand disease: Advances in pathogenetic understanding, diagnosis, and therapy, *Hematology Am Soc Hematol Educ Program* 2013:254–260, 2013b.

Linden MD, Frelinger III AL, Barnard MR: Application of flow cytometry to platelet disorders, *Semin Thromb Hemost* 30:501–511, 2004.

Livio M, Gotti E, Marchesi D: Uraemic bleeding: role of anemia and beneficial effect of red cell transfusions, *Lancet* II:1013–1015, 1982.

Mackie I, Langley K, Chitolie A: Discrepancies between ADAMTS13 activity assays in patients with thrombotic microangiopathies, *Thromb Haemost* 109:488–496, 2013.

Maldonado JE, Pintado T, Pierre RV: Dysplastic platelets and circulating megakaryocytes in chronic myeloproliferative diseases. I. The platelets: ultrastructure and peroxidase reaction, *Blood* 43:797–809, 1974.

Malinin NL, Zhang L, Choi J: A point mutation in KINDLIN3 ablates activation of three integrin subfamilies in humans, *Nat Med* 15:313–318, 2009.

Manchev VT, Hilpert M, Berrou E: A new form of macrothrombocytopenia induced by a germ-line mutation in the PRKACG gene, *Blood* 124:2554–2563, 2014.

Manchev VT, Hilpert M, Berrou E, Elaib Z, Aouba A, Boukour S, et al.: A new form of macrothrombocytopenia induced by a germ-line mutation in the PRKACG gene, *Blood* 124(16):2554–2563, 2014.

Mannucci PM, Vanoli M, Forza I: Von Willebrand factor cleaving protease (ADAMTS-13) in 123 patients with connective tissue diseases (systemic lupus erythematosus and systemic sclerosis), *Haematologica* 88:914–918, 2003.

Mannucci PM: Hemostatic drugs, *N Engl J Med* 339:245–253, 1998.

Marconi C, Di Buduo CA, LeVine K, Barozzi S, Faleschini M, Bozzi V, et al.: Loss-of-function mutations in PTPRJ cause a new form of inherited thrombocytopenia, *Blood* 133(12):1346–1357, 2019.

Marquez R, Hantel A, Lorenz R: A new family with a germline ANKRD26 mutation and predisposition to myeloid malignancies, *Leuk Lymphoma* 55:2945–2946, 2014.

Massaad MJ, Ramesh N, Geha RS: Wiskott-Aldrich syndrome: a comprehensive review, *Ann N Y Acad Sci* 1285:26–43, 2013.

Maynard DM, Heijnen HF, Gahl WA: The alpha granule proteome: novel proteins in normal and ghost granules in gray platelet syndrome, *J Thromb Haemost* 8:1786–1796, 2010.

Mazepa MA, Masias C, Chaturvedi S: How targeted therapy disrupts the treatment paradigm for acquired TTP: the risks, benefits, and unknowns, *Blood* 134(5):415–420, 2019.

McCloskey DJ, Postolache TT, Vittone BJ: Selective serotonin reuptake inhibitors: measurement of effect on platelet function, *Transl Res* 151:168–172, 2008.

McGlasson DL, Fritsma GA: Whole blood aggregometry for diagnostic platelet function testing, *Semin Thromb Hemost* 35:168–180, 2009.

McMillan R: The pathogenesis of chronic immune thrombocytopenic purpura, *Semin Hematol* 44:S3–S11, 2007.

McNicol A, Israels SJ, Robertson C: The empty sack syndrome: a platelet storage pool deficiency associated with empty dense granules, *Br J Haematol* 86:574–582, 1994.

Menasche G, Pastural E, Feldmann J: Mutations in RAB27A cause Griscelli syndrome associated with haemophagocytic syndrome, *Nat Genet* 25:173–176, 2000.

Mezzano D, Quiroga T, Pereira J: The level of laboratory testing required for diagnosis or exclusion of a platelet function disorder using platelet aggregation and secretion assays, *Semin Thromb Hemost* 35:242–254, 2009.

Michaud J, Wu F, Osato M: In vitro analyses of known and novel RUNX1/AML1 mutations in dominant familial platelet disorder with predisposition to acute myelogenous leukemia: implications for mechanisms of pathogenesis, *Blood* 99:1364–1372, 2002.

Michiels JJ, Berneman Z, Van Bockstaele D: Clinical and laboratory features, pathobiology of platelet-mediated thrombosis and bleeding complications, and the molecular etiology of essential thrombocythemia and polycythemia vera: therapeutic implications, *Semin Thromb Hemost* 32:174–207, 2006.

Mielke Jr CH, Levine PH, Zucker S: Preoperative prednisone therapy in platelet function disorders, *Thromb Res* 21:655–662, 1981.

Miller JL, Castella A: Platelet-type von Willebrand's disease: characterization of a new bleeding disorder, *Blood* 60:790–794, 1982.

Miller JL, Cunningham D, Lyle VA: Mutation in the gene encoding platelet glycoprotein Iba in platelet-type von Willebrand disease, *Proc Natl Acad Sci U S A* 88:4761–4765, 1991.

Miller JL, Lyle VA, Cunningham D: Mutation of leucine-57 to phenylalanine in a platelet glycoprotein Ib alpha leucine tandem repeat occurring in patients with an autosomal dominant variant of Bernard-Soulier disease, *Blood* 79:439–446, 1992.

Miller JL: Glycoprotein analysis for the diagnostic evaluation of platelet disorders, *Semin Thromb Hemost* 35:224–232, 2009.

Miller JL: Platelet-type von Willebrand disease, *Thromb Haemost* 75:865–869, 1996.

Miller JL, Cunningham D, Lyle VA, Finch CN: Mutation in the gene encoding the alpha chain of platelet glycoprotein Ib in platelet-type von Willebrand disease, *Proc Natl Acad Sci U S A* 88(11):4761–4765, 1991.

Moake J: Thrombotic thrombocytopenia purpura (TTP) and other thrombotic microangiopathies, *Best Pract Res Clin Haematol* 22:567–576, 2009.

Moake JL, Turner NA, Stathopoulos NA: Involvement of large plasma von Willebrand factor (vWF) multimers and unusually large vWF forms derived from endothelial cells in shear stress-induced platelet aggregation, *J Clin Invest* 78:1456–1461, 1986.

Moia M, Mannucci PM, Vizzotto L: Improvement in the haemostatic defect of uraemia after treatment with recombinant human erythropoietin, *Lancet* 8570:1227–1229, 1987.

Monteferrario D, Bolar NA, Marneth AE: A dominant-negative GFI1B mutation in the gray platelet syndrome, *N Engl J Med* 370:245–253, 2014.

Moore JC, Hayward CP, Warkentin TE: Decreased von Willebrand factor protease activity associated with thrombocytopenic disorders, *Blood* 98:1842–1846, 2001.

Moser M, Nieswandt B, Ussar S: Kindlin-3 is essential for integrin activation and platelet aggregation, *Nat Med* 14:325–330, 2008.

Movig KL, Janssen MW, de Waal Malefijt J: Relationship of serotonergic antidepressants and need for blood transfusion in orthopedic surgical patients, *Arch Intern Med* 163:2354–2358, 2003.

Muia J, Gao W, Haberichter SL: An optimized fluorogenic ADAMTS13 assay with increased sensitivity for the investigation of patients with thrombotic thrombocytopenic purpura, *J Thromb Haemost* 11:1511–1518, 2013.

Muia J, Zhu J, Gupta G: Allosteric activation of ADAMTS13 by von Willebrand factor, *Proc Natl Acad Sci U S A* 111:18584–18589, 2014.

Mumford AD, Dawood BB, Daly ME: A novel thromboxane A2 receptor D304N variant that abrogates ligand binding in a patient with a bleeding diathesis, *Blood* 115:363–369, 2010.

Mumford AD, Frelinger 3rd AL, Gachet C, Gresele P, Noris P, Harrison P, et al.: A review of platelet secretion assays for the diagnosis of inherited platelet secretion disorders, *Thromb Haemost* 114(1):14–25, 2015.

Nagalla S, Bray PF: Platelet RNA chips dip into thrombocytosis, *Blood* 115:2–3, 2010.

Nangalia J, Massie CE, Baxter EJ: Somatic CALR mutations in myeloproliferative neoplasms with nonmutated JAK2, *N Engl J Med* 369:2391–2405, 2013.

Neunert C, Lim W, Crowther M: The American Society of Hematology 2011 evidence-based practice guideline for immune thrombocytopenia, *Blood* 117:4190–4207, 2011.

Neunert C, Terrell DR, Arnold DM, Buchanan G, Cines DB, Cooper N, et al.: American Society of Hematology 2019 guidelines for immune thrombocytopenia, *Blood Adv* 3(23):3829–3866, 2019.

Ng C, Motto DG, Di Paola J: Diagnostic approach to von Willebrand disease, *Blood* 125:2029–2037, 2015.

Nichols WL, Rick ME, Ortel TL: Clinical and laboratory diagnosis of von Willebrand disease: a synopsis of the 2008 NHLBI/NIH guidelines, *Am J Hematol* 84:366–370, 2009.

Nieuwenhuis HK, Akkerman JW, Houdijk WP: Human blood platelets showing no response to collagen fail to express surface glycoprotein Ia, *Nature* 318:470–472, 1985.

Nieuwenhuis HK, Akkerman J-WN, Sixma JJ: Patients with a prolonged bleeding time and normal aggregation tests may have storage pool deficiency: studies on one hundred six patients, *Blood* 70:620–623, 1987.

Nieuwenhuis HK, Sakariassen KS, Houdijk PM: Deficiency of platelet membrane glycoprotein Ia associated with a decreased platelet adhesion to subendothelium: a defect in platelet spreading, *Blood* 68:692–695, 1986.

Nishibori M, Cham B, McNicol A: The protein CD63 is in platelet dense granules, is deficient in a patient with Hermansky-Pudlak syndrome, and appears identical to granulophysin, *J Clin Invest* 91:1775–1782, 1993.

Nishio K, Anderson PJ, Zheng XL: Binding of platelet glycoprotein Ib alpha to von Willebrand factor domain A1 stimulates the cleavage of the adjacent domain A2 by ADAMTS13, *Proc Natl Acad Sci U S A* 101:10578–10583, 2004.

Noetzli L, Lo RW, Lee-Sherick AB, Callaghan M, Noris P, Savoia A, et al.: Germline mutations in ETV6 are associated with thrombocytopenia, red cell macrocytosis and predisposition to lymphoblastic leukemia, *Nat Genet* 47(5):535–538, 2015.

Noris P, Biino G, Pecci A: Platelet diameters in inherited thrombocytopenias: analysis of 376 patients with all known disorders, *Blood* 124:e4–e10, 2014.

Noris P, Guidetti GF, Conti V: Autosomal dominant thrombocytopenias with reduced expression of glycoprotein Ia, *Thromb Haemost* 95:483–489, 2006.

Noris P, Klersy C, Gresele P: Platelet size for distinguishing between inherited thrombocytopenias and immune thrombocytopenia: a multicentric, real life study, *Br J Haematol* 162:112–119, 2013.

Novak EK, Swank RT, Hui SW: Platelet storage pool deficiency in mouse pigment mutations associated with seven distinct genetic loci, *Blood* 63:536–544, 1984.

Nurden AT, Fiore M, Nurden P: Glanzmann thrombasthenia: a review of ITGA2B and ITGB3 defects with emphasis on variants, phenotypic variability, and mouse models, *Blood* 118:5996–6005, 2011.

Nurden AT, George JN: Inherited abnormalities of the platelet membrane. In Colman RW, Hirsh J, Marder VJ, editors: *Hemostasis and thrombosis: basic principles and practice*, Philadelphia, 2001, Lippincott, pp 921–943.

Nurden AT, Nurden P, Bermejo E: Phenotypic heterogeneity in the Gray platelet syndrome extends to the expression of TREM family member, TLT-1, *Thromb Haemost* 100:45–51, 2008.

Nurden AT, Nurden P: Inherited platelet disorders and understanding of platelet function, *Br J Haematol* 165:165–178, 2014.

Nurden AT, Nurden P: The gray platelet syndrome: clinical spectrum of the disease, *Blood Rev* 21:21–36, 2007.

Nurden AT: Platelet membrane glycoproteins: a historical review, *Semin Thromb Hemost* 40:577–584, 2014a.

Nurden P, Savi P, Heilmann E: An inherited bleeding disorder linked to a defective interaction between ADP and its receptor on platelets. Its influence on glycoprotein IIb-IIIa complex function, *J Clin Invest* 95:1612–1622, 1995.

Nurden AT, Pillois X, Wilcox DA: Glanzmann thrombasthenia: state of the art and future directions, *Semin Thromb Hemost* 39(6):642–655, 2013.

Nurden AT, Pillois X, Fiore M, Alessi MC, Bonduel M, Dreyfus M, et al.: Expanding the mutation spectrum affecting alphaIIbbeta3 integrin in Glanzmann thrombasthenia: screening of the ITGA2B and ITGB3 genes in a large international cohort, *Hum Mutat* 36(5):548–561, 2015.

Onundarson PT, Gudmundsdottir BR, Marder VJ: On the significance of marginally low von Willebrand factor, *Thromb Haemost* 100:1213–1214, 2008.

Othman M, Notley C, Lavender FL: Identification and functional characterization of a novel 27-bp deletion in the macroglycopeptide-coding region of the *GPIBA* gene resulting in platelet-type von Willebrand disease, *Blood* 105:4330–4336, 2005.

Oury C, Lenaerts T, Peerlinck K: Inherited deficiency of the phospholipase C coupled platelet P2Y1 receptor leads to a mild bleeding disorder, *Thromb Haemost*(Suppl)20–21, 1999.

Oury C, Toth-Zsamboki E, Van Geet C: A natural dominant negative P2X1 receptor due to deletion of a single amino acid residue, *J Biol Chem* 275:22611–22614, 2000.

Owen CJ, Toze CL, Koochin A: Five new pedigrees with inherited RUNX1 mutations causing familial platelet disorder with propensity to myeloid malignancy (FPD/AML), *Blood* 112:4639–4645, 2008.

Padilla A, Moake JL, Bernardo A: P-selectin anchors newly released ultralarge von Willebrand factor multimers to the endothelial cell surface, *Blood* 103:2150–2156, 2004.

Pai M, Wang G, Moffat KA: Diagnostic usefulness of a lumi-aggregometer adenosine triphosphate release assay for the assessment of platelet function disorders, *Am J Clin Pathol* 136:350–358, 2011.

Palma-Barqueros V, Ruiz-Pividal J, Bohdan N, Vicente V, Bastida JM, Lozano M, et al.: RASGRP2 gene variations associated with platelet dysfunction and bleeding, *Platelets* 30(4):535–539, 2019.

Papadakis E, Hoffman R, Brenner B: Thrombohemorrhagic complications of myeloproliferative disorders, *Blood Rev* 24:227–232, 2010.

Pasvolsky R, Feigelson SW, Kilic SS: A LAD-III syndrome is associated with defective expression of the Rap-1 activator CalDAG-GEFI in lymphocytes, neutrophils, and platelets, *J Exp Med* 204:1571–1582, 2007.

Patel YM, Patel K, Rahman S: Evidence for a role for Galphai1 in mediating weak agonist-induced platelet aggregation in human platelets: reduced Galphai1 expression and defective Gi signaling in the platelets of a patient with a chronic bleeding disorder, *Blood* 101:4828–4835, 2003.

Paterson AD, Rommens JM, Bharaj B, Blavignac J, Wong I, Diamandis M, et al.: Persons with Quebec platelet disorder have a tandem duplication of PLAU, the urokinase plasminogen activator gene, *Blood* 115(6):1264–1266, 2010.

Pavord S, Myers B: Bleeding and thrombotic complications of kidney disease, *Blood Rev* 25:271–278, 2011.

Pearson TC: The risk of thrombosis in essential thrombocythemia and polycythemia vera, *Semin Oncol* 29:16–21, 2002.

Perez-Rodriguez A, Loures E, Rodriguez-Trillo A: Inherited ADAMTS13 deficiency (Upshaw-Schulman syndrome): a short review, *Thromb Res* 134:1171–1175, 2014.

Peyvandi F, Ferrari S, Lavoretano S: von Willebrand factor cleaving protease (ADAMTS-13) and ADAMTS-13 neutralizing autoantibodies in 100 patients with thrombotic thrombocytopenic purpura, *Br J Haematol* 127:433–439, 2004.

Peyvandi F, Scully M, Kremer Hovinga JA, Cataland S, Knobl P, Wu H, Artoni A, et al.: Caplacizumab for acquired thrombotic thrombocytopenic purpura, *N Engl J Med* 374(6):511–522, 2016.

Pluthero FG, Di Paola J, Carcao MD, Kahr WHA: NBEAL2 mutations and bleeding in patients with gray platelet syndrome, *Platelets* 29(6):632–635, 2018.

Poon MC, d'Oiron R: Recombinant activated factor VII (NovoSeven) treatment of platelet-related bleeding disorders. International Registry on recombinant factor VIIa and inherited platelet disorders group, *Blood Coagul Fibrinolysis* 11(Suppl 1):55–68, 2000.

Provan D, Stasi R, Newland AC: International consensus report on the investigation and management of primary immune thrombocytopenia, *Blood* 115:168–186, 2010.

Psaila, B, Wang, G, Rodriguez-Meira, et al. Single-cell analyses reveal megakaryocyte-biased hematopoiesis in myelofibrosis and identify mutant clone-specific targets. Molecular Cell, 78:477–492, 2020.

Rabbolini DJ, Morel-Kopp MC, Chen Q, Gabrielli S, Dunlop LC, Chew LP, et al.: Thrombocytopenia and CD34 expression is decoupled from alpha-granule deficiency with mutation of the first growth factor-independent 1B zinc finger, *J Thromb Haemost* 15(11):2245–2258, 2017.

Rao AK, Bennett JS: Acquired disorders of platelet function. In ed 6, Marder VJ, Aird WC, Bennett JS, editors: *Hemostasis and thrombosis: basic principles and clinical practice*Philadelphia, 2013, Lippincott, pp 820–828.

Rao AK, Coller BS: Hereditary qualitative platelet disorders. In Kaushansky K, Lichtman M, Kipps T, editors: *Williams hematology*, New York, 2015a, McGraw-Hill.

Rao AK, Ghosh S, Sun L: Effect of mechanism of platelet dysfunction on response to DDAVP in patients with inherited platelet function defects. A double-blind placebo-controlled trial, *Thromb Haemost* 74:1071–1078, 1995.

Rao AK: Acquired disorders of platelet function. In Michelson AD, editor: *Platelets*, Amsterdam, 2013b, Academic Press, pp 1049–1073.

Rao AK: Inherited platelet function disorders: overview and disorders of granules, secretion, and signal transduction, *Hematol Oncol Clin North Am* 27:585–611, 2013c.

Rao AK: Spotlight on FLI1, RUNX1, and platelet dysfunction, *Blood* 122:4004–4006, 2013a.

Rao AK, Coller BS: *Hereditary qualitative platelet disorders*, New York, 2016, McGraw Hill.

Raslova H, Komura E, Le Couedic JP: FLI1 monoallelic expression combined with its hemizygous loss underlies Paris-Trousseau/Jacobsen thrombopenia, *J Clin Invest* 114:77–84, 2004.

Remold-O'Donnell E, Rosen FS, Kenney DM: Defects in Wiskott-Aldrich syndrome blood cells, *Blood* 87:2621–2631, 1996.

Remuzzi GD, Marchesi M, Livio AE: Altered platelet and vascular prostaglandin-generation in patients with chronic renal failure and prolonged bleeding times, *Thromb Res* 13:1007–1115, 1978.

Revel-Vilk S, Varon D, Shai E: Evaluation of children with a suspected bleeding disorder applying the Impact-R [Cone and Plate(let) Analyzer], *J Thromb Haemost* 7:1990–1996, 2009.

Rodeghiero F, Stasi R, Gernsheimer T: Standardization of terminology, definitions and outcome criteria in immune thrombocytopenic purpura of adults and children: report from an international working group, *Blood* 113:2386–2393, 2009.

Rodeghiero F, Tosetto A, Abshire T, Arnold DM, Coller B, James P, et al.: ISTH/SSC bleeding assessment tool: a standardized questionnaire and a proposal for a new bleeding score for inherited bleeding disorders, *J Thromb Haemost* 8(9):2063–2065, 2010.

Rodgers RPC, Levin J: A critical reappraisal of the bleeding time, *Semin Thromb Hemost* 16(1–20), 1990.

Russell SD, Roth GJ: Pseudo-von Willebrand disease: a mutation in the platelet glycoprotein Iba gene associated with a hyperactive surface receptor, *Blood* 81:1787–1791, 1993.

Sadler JE: Aortic stenosis, von Willebrand factor, and bleeding, *N Engl J Med* 349:323–325, 2003b.

Sadler JE: Low von Willebrand factor: sometimes a risk factor and sometimes a disease, *Hematology Am Soc Hematol Educ Program*106–112, 2009. 2009.

Sadler JE: Von Willebrand disease type 1: a diagnosis in search of a disease, *Blood* 101:2089–2093, 2003a.

Sanchez-Luceros A, Woods AI, Bermejo E, Shukla S, Acharya S, et al.: PT-VWD posing diagnostic and therapeutic challenges - small case series, *Platelets* 28(5):484–490, 2017.

Sanders YV, van der Bom JG, Isaacs A, et al.: CLEC4M and STXBP5 gene variation contribute to von Willebrand factor level variation in von Willebrand disease, *J Thromb Haemost* 13:956–966, 2015.

Saultier P, Vidal L, Canault M, Bernot D, Falaise C, Pouymayou C, et al.: Macrothrombocytopenia and dense granule deficiency associated with FLI1 variants: ultrastructural and pathogenic features, *Haematologica* 102(6):1006–1016, 2017.

Savoia A, Balduini CL, Savino M: Autosomal dominant macrothrombocytopenia in Italy is most frequently a type of heterozygous Bernard-Soulier syndrome, *Blood* 97:1330–1335, 2001.

Savoia A, Kunishima S, De Rocco D, Zieger B, Rand ML, Pujol-Moix N, et al.: Spectrum of the mutations in Bernard-Soulier syndrome, *Hum Mutat* 35(9):1033–1045, 2014.

Sayani FA, Abrams CS: How I treat refractory thrombotic thrombocytopenic purpura, *Blood* 125:3860–3867, 2015.

Schafer AI: Bleeding and thrombosis in the myeloproliferative disorders, *Blood* 64:1–12, 1984.

Schafer AI: Deficiency of platelet lipoxygenase activity in myeloproliferative disorders, *N Engl J Med* 306:381–386, 1982.

Schafer AI: Thrombocytosis, *N Engl J Med* 350:1211–1219, 2004.

Scully M, Cataland SR, Peyvandi F, Coppo P, Knobl P, Kremer Hovinga JA, et al.: Caplacizumab treatment for acquired thrombotic thrombocytopenic purpura, *N Engl J Med* 380(4):335–346, 2019.

Semple JW: Infections, antigen-presenting cells, T cells, and immune tolerance: their role in the pathogenesis of immune thrombocytopenia, *Hematol Oncol Clin North Am* 23:1177–1192, 2009.

Sharma R, Haberichter SL: New advances in the diagnosis of von Willebrand disease, *Hematology Am Soc Hematol Educ Program 2019* (1):596–600, 2019.

Shattil SJ, Newman PJ: Integrins: dynamic scaffolds for adhesion and signaling in platelets, *Blood* 104:1606–1615, 2004.

Shenkman B, Einav Y: Thrombotic thrombocytopenic purpura and other thrombotic microangiopathic hemolytic anemias: diagnosis and classification, *Autoimmun Rev* 13:584–586, 2014.

Simeoni I, Stephens JC, Hu F, Deevi SV, Megy K, Bariana TK, et al.: A high-throughput sequencing test for diagnosing inherited bleeding, thrombotic, and platelet disorders, *Blood* 127(23):2791–2803, 2016.

Sivapalaratnam S, Collins J, Gomez K: Diagnosis of inherited bleeding disorders in the genomic era, *Br J Haematol* 179(3):363–376, 2017.

Skoda RC: Thrombocytosis, *Hematology Am Soc Hematol Educ Program* 2009:159–167, 2009.

Smith SA, Morrissey JH: Polyphosphate: a new player in the field of hemostasis, *Curr Opin Hematol* 21:388–394, 2014.

Smythe MA, Whiteheart SW, Italiano JE, Bray P, Coller BS: *Platelet, morphology, biochemistry and function*, New York, 2016, McGraw Hill.

Sohal AS, Gangji AS, Crowther MA: Uremic bleeding: pathophysiology and clinical risk factors, *Thromb Res* 118:417–422, 2006.

Song WJ, Sullivan MG, Legare RD: Haploinsufficiency of CBFA2 causes familial thrombocytopenia with propensity to develop acute myelogenous leukaemia, *Nat Genet* 23:166–175, 1999.

Songdej N, Rao AK: Hematopoietic transcription factor mutations: important players in inherited platelet defects, *Blood* 129(21):2873–2881, 2017.

Spivak JL: Myeloproliferative neoplasms, *N Engl J Med* 376(22):2168–2181, 2017.

Springer TA: von Willebrand factor, Jedi knight of the bloodstream, *Blood* 124:1412–1425, 2014.

Stasi R, Willis F, Shannon MS: Infectious causes of chronic immune thrombocytopenia, *Hematol Oncol Clin North Am* 23:1275–1297, 2009.

Stevenson WS, Morel-Kopp MC, Chen Q: GFI1B mutation causes a bleeding disorder with abnormal platelet function, *J Thromb Haemost* 11:2039–2047, 2013.

Stevenson WS, Rabbolini DJ, Beutler L, Chen Q, Gabrielli S, Mackay JP, et al.: Paris-Trousseau thrombocytopenia is phenocopied by the autosomal recessive inheritance of a DNA-binding domain mutation in FLI1, *Blood* 126(17):2027–2030, 2015.

Stockley J, Morgan NV, Bem D, et al.: Enrichment of FLI1 and RUNX1 mutations in families with excessive bleeding and platelet dense granule secretion defects, *Blood* 122:4090–4093, 2013.

Stritt S, Nurden P, Turro E, Greene D, Jansen SB, Westbury SK, et al.: A gain-of-function variant in DIAPH1 causes dominant macrothrombocytopenia and hearing loss, *Blood* 127(23):2903–2914, 2016.

Sulai NH, Tefferi A: Why does my patient have thrombocytosis?, *Hematol Oncol Clin North Am* 26:285–301, viii, 2012.

Sun L, Mao G, Rao AK: Association of CBFA2 mutation with decreased platelet PKC-θ and impaired receptor-mediated activation of GPIIb-IIIa and pleckstrin phosphorylation: proteins regulated by CBFA2 play a role in GPIIb-IIIa activation, *Blood* 103:948–954, 2004.

Suzuki J, Umeda M, Sims PJ: Calcium-dependent phospholipid scrambling by TMEM16F, *Nature* 468:834–838, 2010.

Tchernev VT, Mansfield TA, Giot L: The Chediak-Higashi protein interacts with SNARE complex and signal transduction proteins, *Mol Med* 8:56–64, 2002.

Tiede A, Rand JH, Budde U: How I treat the acquired von Willebrand syndrome, *Blood* 117:6777–6785, 2011.

Timm A, Hillarp A, Philips M: Comparison of automated von Willebrand factor activity assays, *Thromb Res* 135:684–691, 2015.

Tsai HM, Lian EC: Antibodies to von Willebrand factor-cleaving protease in acute thrombotic thrombocytopenic purpura, *N Engl J Med* 339:1585–1594, 1998.

Tsai HM: Shear stress and von Willebrand factor in health and disease, *Semin Thromb Hemost* 29:479–488, 2003.

Tubman VN, Levine JE, Campagna DR: X-linked gray platelet syndrome due to a GATA1 Arg216Gln mutation, *Blood* 109:3297–3299, 2007.

Urban D, Li L, Christensen H, et al.: The VPS33B binding protein VPS16B is required in megakaryocyte and platelet α-granule biogenesis, *Blood* 120:5032–5040, 2012.

Uriel N, Pak SW, Jorde UP: Acquired von Willebrand syndrome after continuous-flow mechanical device support contributes to a high prevalence of bleeding during long-term support and at the time of transplantation, *J Am Coll Cardiol* 56:1207–1213, 2010.

van Genderen PJ, Michiels JJ, van Strik R: Platelet consumption in thrombocythemia complicated by erythromelalgia: reversal by aspirin, *Thromb Haemost* 73:210–214, 1995.

van Nispen tot Pannerden H, de Haas F, Geerts W: The platelet interior revisited: electron tomography reveals tubular alpha-granule subtypes, *Blood* 116:1147–1156, 2010.

van Werkum JW, Bouman HJ, Breet NJ: The Cone-and-Plate(let) analyzer is not suitable to monitor clopidogrel therapy: a comparison with the flowcytometric VASP assay and optical aggregometry, *Thromb Res* 126:44–49, 2010.

Varon D, Lashevski I, Brenner B: Cone and plate(let) analyzer: monitoring glycoprotein IIb/IIIa antagonists and von Willebrand disease replacement therapy by testing platelet deposition under flow conditions, *Am Heart J* 135:S187–S193, 1998.

Veyradier A, Balian A, Wolf M: Abnormal von Willebrand factor in bleeding angiodysplasias of the digestive tract, *Gastroenterology* 120:346–353, 2001.

Veyradier A, Caron C, Ternisien C: Validation of the first commercial ELISA for type 2N von Willebrand's disease diagnosis, *Haemophilia* 17:944–951, 2011.

Vincentelli A, Susen S, Le Tourneau T: Acquired von Willebrand syndrome in aortic stenosis, *N Engl J Med* 349:343–349, 2003.

Von dem Borne AEG, van Leeuwen EF, von Reisz LE: Neonatal alloimmune thrombocytopenia: detection and characterization of the responsible antibodies by the platelet immunofluorescence test, *Blood* 57:649–656, 1981.

Von Drygalski A, Curtis BR, Bougie DW: Vancomycin-induced immune thrombocytopenia, *N Engl J Med* 356:904–910, 2007.

Weiss HJ, Lages B: Platelet malondialdehyde production and aggregation responses induced by arachidonate, prostaglandin-G_2, collagen, and epinephrine in 12 patients with storage pool deficiency, *Blood* 58:27–33, 1981.

Weiss HJ, Lages B: The response of platelets to epinephrine in storage pool deficiency—evidence pertaining to the role of adenosine diphosphate in mediating primary and secondary aggregation, *Blood* 72:1717–1725, 1988.

Weiss HJ, Meyer D, Rabinowitz R: Pseudo von Willebrand's disease: an intrinsic platelet defect with aggregation by unmodified human factor VIII/von Willebrand factor and enhanced adsorption of its high-molecular-weight multimers, *N Engl J Med* 306:326–362, 1982.

Weiss HJ, Vicic WJ, Lages BA: Isolated deficiency of platelet procoagulant activity, *Am J Med* 67:206–213, 1979a.

Weiss HJ, Witte LD, Kaplan KL: Heterogeneity in storage pool deficiency: studies on granule-bound substances in 18 patients including variants deficient in alpha-granules, platelet factor 4, beta-thromboglobulin, and platelet-derived growth factor, *Blood* 54:1296–1319, 1979b.

Weiss HJ: Impaired platelet procoagulant mechanisms in patients with bleeding disorders, *Semin Thromb Hemost* 35:233–241, 2009.

Weiss HJ: Scott syndrome: a disorder of platelet coagulant activity, *Semin Hematol* 31:312–319, 1994.

Weiss HJ, Meyer D, Rabinowitz R, Pietu G, Girma JP, Vicic WJ, et al.: Pseudo-von Willebrand's disease. An intrinsic platelet defect with aggregation by unmodified human factor VIII/von Willebrand factor and enhanced adsorption of its high-molecular-weight multimers, *N Engl J Med* 306(6):326–333, 1982.

Westbury SK, Turro E, Greene D, Lentaigne C, Kelly AM, Bariana TK, et al.: Human phenotype ontology annotation and cluster analysis to unravel genetic defects in 707 cases with unexplained bleeding and platelet disorders, *Genome Med* 7(1):36, 2015.

White JG: Electron microscopy methods for studying platelet structure and function, *Methods Mol Biol* 272:47–63, 2004.

White JG: Inherited abnormalities of the platelet membrane and secretory granules, *Hum Pathol* 18(2):123–139, 1987.

Whitelock JL, Nolasco L, Bernardo A: ADAMTS-13 activity in plasma is rapidly measured by a new ELISA method that uses recombinant VWF-A2 domain as substrate, *J Thromb Haemost* 2:485–491, 2004.

Witkop CJ, Babcock MN, Rao GHR: Albinism and Hermansky-Pudlak syndrome in Puerto Rico, *Bol Asoc Med P R* 82:333–339, 1990.

Woods AI, Sanchez-Luceros A, Bermejo E: Identification of p.W246L as a novel mutation in the GP1BA gene responsible for platelet-type von Willebrand disease, *Semin Thromb Hemost* 40:151–160, 2014.

Yadav S, Storrie B: The cellular basis of platelet secretion: emerging structure/function relationships, *Platelets* 28(2):108–118, 2017.

Yang X, Sun L, Ghosh S: Human platelet signaling defect characterized by impaired production of 1,4,5 inositoltrisphosphate and phosphatic acid, and diminished pleckstrin phosphorylation. Evidence for defective phospholipase C activation, *Blood* 88:1676–1683, 1996.

Yeh JJ, Tsai S, Wu DC: P-selectin-dependent platelet aggregation and apoptosis may explain the decrease in platelet count during Helicobacter pylori infection, *Blood* 115:4247–4253, 2010.

Zhang W, Nardi MA, Borkowsky W: Role of molecular mimicry of hepatitis C virus protein with platelet GPIIIa in hepatitis C-related immunologic thrombocytopenia, *Blood* 113:4086–4093, 2009.

Zhang K, Lu Y, Harley KT, Tran MH: Atypical hemolytic uremic syndrome: a brief review, *Hematol Rep* 9(2):7053, 2017.

Zheng XL: ADAMTS13 and von Willebrand factor in thrombotic thrombocytopenic purpura, *Annu Rev Med* 66:211–225, 2015.

Zheng XL: ADAMTS13 testing: why bother? *Blood* 115:1475–1476, 2010.

Zwaal RF, Comfurius P, Bevers EM: Surface exposure of phosphatidylserine in pathological cells, *Cell Mol Life Sci* 62:971–988, 2005.

CHAPTER 42

LABORATORY APPROACH TO THROMBOTIC RISK

Robert A. DeSimone, Jacob H. Rand

ENDOGENOUS ANTICOAGULANT MECHANISMS, 870
Overview, 870
Tissue Factor Pathway Inhibitor, 870
Antithrombin, 870
The Protein C–Protein S System, 871
Fibrinolytic System, 871
Annexins A2 and A5, 871
PROTHROMBOTIC STATES, 872
Overview, 872
Tissue Factor Pathway Inhibitor Deficiency, 872
Antithrombin Deficiency, 873
Abnormalities of the Protein C–Protein S System, 873
Hypofibrinolysis, 874
Elevation of Coagulation Factor Levels, 875
Dysfibrinogenemia, 875
Antiphospholipid Syndrome and Lupus Anticoagulants, 875
Other Prothrombotic Abnormalities and Novel Genetic Variants, 876
APPROPRIATE LABORATORY UTILIZATION, 877
SELECTED REFERENCES, 878

KEY POINTS

- Several regulatory mechanisms have evolved to limit the extent of clot formation after coagulation is triggered. Under normal conditions, these allow hemostasis to be achieved while preventing the growth of a hemostatic plug into an intravascular thrombus. Among these regulatory systems are the antithrombin mechanism, the protein C–protein S system, the fibrinolytic system, and the tissue factor pathway inhibitor mechanism.
- Deficiencies of the major regulatory proteins (antithrombin, protein C, and protein S) increase the risk for venous thrombosis. Increased levels of procoagulant factors and variants of the genes for coagulation factors V and prothrombin—specifically, factor V_{Leiden} and prothrombin g20210a—also increase the risk for venous thrombosis.
- The factor V_{Leiden} variant results in resistance to activated protein C (APC) by reducing the susceptibility of factor Va to proteolysis by APC. The prothrombin G20210A variant is associated with increased levels of prothrombin due to a promoter polymorphism, a base pair substitution at 20210.
- Inherited or acquired dysfibrinogenemias and defective fibrinolysis may also increase the risk of venous thrombosis.
- The autoimmune disorder antiphospholipid syndrome (APS) increases the risk of both venous and arterial thrombosis, thrombotic microangiopathy, and pregnancy complications attributable to a reduction in placental perfusion. APS is detected with immunoassays for antiphospholipid antibodies and coagulation assays, known as lupus anticoagulants, that report inhibition of phospholipid-dependent coagulation reactions in vitro but not in vivo. There is accumulating evidence for the role of complement in APS, particularly for the catastrophic form of the disorder.
- When evaluating a patient for thrombotic risk, it is important to decide whether diagnostic testing is appropriate, to understand the clinical significance of the assays, and to appropriately plan the timing of testing. Recent thrombotic events, anticoagulant therapy, normal pregnancy, and acute-phase reactions can all affect the levels of these endogenous anticoagulant factors.

Following vascular injury, hemostatic regulatory mechanisms limit the amount, location, and duration of clot formation to effectively seal blood vessels at sites of injury while preventing the initiation of hemostasis from extending into occlusive thrombosis. Dysfunction in these regulatory systems may lead to the pathologic condition of excessive clot formation (thrombosis). Both genetic and acquired deficiencies and abnormalities of such regulatory factors are capable of increasing the risk for thromboembolism. This chapter discusses a number of factors that influence the balance toward bleeding or toward thrombosis, as well as the role of the laboratory in identifying abnormalities associated with these factors.

ENDOGENOUS ANTICOAGULANT MECHANISMS

OVERVIEW

The endogenous anticoagulants play a key role in maintaining a balance between an adequate hemostatic response to injury that would result in bleeding and an excessive response that would lead to thrombosis and tissue damage. (For a schematic overview of physiologic anticoagulant pathways, see Fig. 40.5 in Chapter 40.) An inhibitory mechanism has been identified for virtually each step of the coagulation system, as follows.

1. Tissue factor (TF), a major initiator of coagulation, is inhibited by the protein tissue factor pathway inhibitor (TFPI, or TFPI-1).
2. The phospholipid membrane surface that is required for the assembly of coagulation enzyme-substrate complexes becomes shielded by the binding of annexin A5 and its subsequent two-dimensional crystallization.
3. The catalytic sites of the activated coagulation enzymes are neutralized by the serpin antithrombin.
4. The prothrombotic enzymatic specificities of thrombin—that is, cleavage of fibrinogen, activation of factors V, VIII, XI, and XIII, and activation of platelets—are lost when it binds to thrombomodulin and it develops specificity for activating protein C.
5. Following their activation by thrombin, factors Va and VIIIa are proteolyzed by activated protein C, which was itself activated by thrombin bound to thrombomodulin.
6. Formed fibrin is degraded by the fibrinolytic system.

TISSUE FACTOR PATHWAY INHIBITOR

Coagulation is triggered by the exposure of circulating blood to membrane-bound tissue factor (TF), which, in turn, complexes with factor VII/VIIa to initiate coagulation. The protein named *tissue factor pathway inhibitor* (*TFPI*, or *TFPI-1*; Fig. 42.1) limits the activity of the TF-VII/VIIa complex (Smithies & Weaver, 2004; Crawley & Lane, 2008; Maroney et al., 2013). This is accomplished through its two reactive binding sites: one for factor Xa that had just been activated by the tissue factor–factor VIIa complex and a second binding site for the tissue factor–factor VIIa complex itself (Esmon, 2003). Thereby TFPI "jams up" the tissue factor–factor VIIa enzymatic machinery. However, this inhibition occurs only after the coagulation process has begun to generate an initial quantity of factor Xa. TFPI provides a negative feedback mechanism for dampening the coagulation process.

ANTITHROMBIN

Antithrombin (previously known as *antithrombin III*) is a circulating plasma serine protease inhibitor (serpin) that neutralizes thrombin and factor Xa and, to a lesser extent, the other serine proteases—that is, factors IXa, XIa, XIIa, and VIIa (Stassen et al., 2004). The activity of antithrombin is markedly enhanced by the glycosaminoglycans on the endothelial cell surface, which include heparan sulfate, dermatan sulfate, and small amounts of

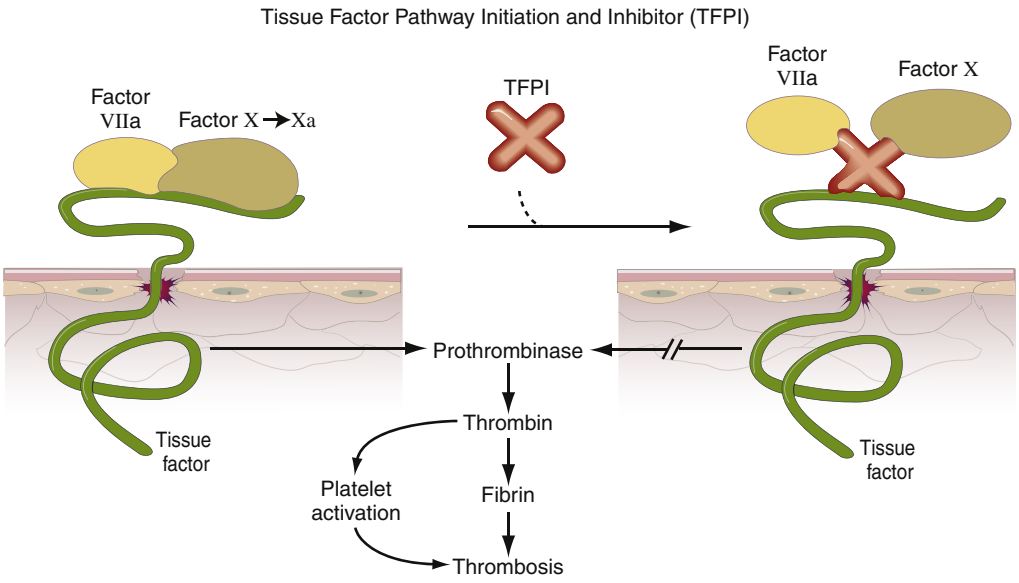

Figure 42.1 Tissue factor pathway initiation and inhibitor mechanisms. *TFPI,* Tissue factor pathway inhibitor.

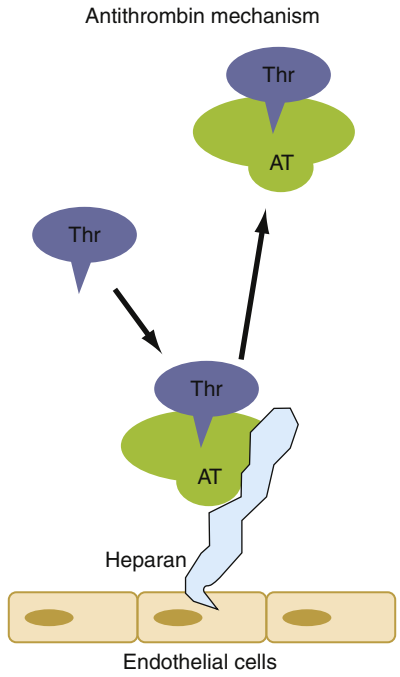

Figure 42.2 Antithrombin inhibitor mechanisms. *AT,* Antithrombin (formally termed *antithrombin III*); *Heparan,* heparan sulfate (a glycosaminoglycan); *Thr,* thrombin (or another coagulation enzyme, such as factor X).

heparin (Fig. 42.2). The vascular endothelial surface is effectively coated with antithrombin bound to the glycosaminoglycans, which gives this surface significant capacity to inactivate circulating thrombin. A similar cofactor effect is accomplished pharmacologically by heparin anticoagulant therapy (discussed in Chapter 43).

THE PROTEIN C–PROTEIN S SYSTEM

The Protein C–Protein S system is a multipronged mechanism that includes a major anticoagulant component (Fig. 42.3) along with an indirect fibrinolytic component (Esmon, 2009). Protein C, a key player in this system, is a vitamin K–dependent proenzyme that binds to the endothelial cell protein C receptor (EPCR) (Stearns-Kurosawa et al., 1996). The system is initiated when circulating thrombin binds to the endothelial cell transmembrane glycoprotein thrombomodulin (TM; see Fig. 42.3). This TM-bound thrombin undergoes a change in its specificity that converts it from a potent procoagulant enzyme to one that activates protein C bound to the EPCR, thereby releasing an activation peptide (Esmon, 2004). This process generates activated protein C (APC), an active serine protease with anticoagulant properties. A second vitamin K–dependent inhibitory plasma protein, protein S (see Fig. 42.3), serves as a critical cofactor for the enzymatic activity of APC. Protein S is a nonenzymatic cofactor molecule that binds in reversible equilibrium to C4BP (Rigby & Grant, 2004). Only the unbound and free form of protein S possesses APC cofactor activity. The complexes of APC and protein S inactivate factor Va and factor VIIIa, thereby significantly diminishing additional thrombin formation and, consequently, the rate of fibrin formation (Esmon, 2003). Again, similar to the TFPI system, inhibition of coagulation occurs after its activation—that is, thrombin exhibits anticoagulant properties only after there has been sufficient thrombin to initiate hemostasis. Significant evidence has accumulated to support the idea that the protein C system may have additional important defense properties, including anti-inflammatory activity and cytoprotective effects, including an ability to ameliorate chronic graft versus host disease via PAR-1 dependent biased signaling on T cells (Sinha, 2019; Castellino & Ploplis, 2009; Esmon, 2003).

FIBRINOLYTIC SYSTEM

The fibrinolytic system is discussed in Chapter 40. In addition to proteolysis of factors Va and VIIIa, the protein C system also appears to exert significant, although indirect, fibrinolytic activity. This appears to involve the thrombin-activated fibrinolytic inhibitor (TAFI) (Van de Wouwer et al., 2004) along with plasminogen activator inhibitor-1 (PAI-1) (Madden et al., 1991; Meltzer et al., 2010). TAFI is a plasma carboxypeptidase that is rapidly activated by the thrombin–thrombomodulin complex (Van de Wouwer et al., 2004). The active form of the carboxypeptidase cleaves C-terminal lysine residues from fibrin that has already undergone proteolytic cleavage by plasmin. Loss of these residues impairs the efficient binding of plasminogen-activating proteins to fibrin, thereby downregulating the fibrinolytic process. APC, via inactivation of factor Va, causes a decrease in thrombin generation, thus also slowing TAFI activation. PAI-1 is inhibited by APC, thereby increasing overall fibrinolytic activity (Madden et al., 1991).

ANNEXINS A2 AND A5

The annexins are a family of potent phospholipid-binding proteins present throughout the animal and plant kingdoms that share 4 to 8 homologous annexin binding sites for the phospholipids. Several annexins have been identified in humans, of which annexin A2 and annexin A5 display thromboregulatory roles. Annexin A2 (previously known as *annexin II*) binds to the membrane surfaces of vascular endothelial cells as tetrameric complexes consisting of two annexin A2 molecules bound to two S-100 protein molecules (Liu et al., 2015). These tetramers then bind tissue plasminogen activator (tPA) and plasminogen to promote the formation of plasmin. Transgenic annexin A2–null mice have significantly reduced fibrinolysis.

Annexin A5 (previously known as *annexin V*) has potent anticoagulant properties that result from its rapidly assembling two-dimensional crystals over membranes that express anionic phospholipids, thereby shielding the membrane from availability for the binding and assembly of coagulation factor complexes. The protein is highly expressed by vascular endothelial cells and placental trophoblasts, where it is ideally positioned to promote the maintenance of blood fluidity. Transgenic annexin A5–null mice have significantly reduced litter sizes and fetal weights, which are a consequence of placental thrombosis (Ueki et al., 2012).

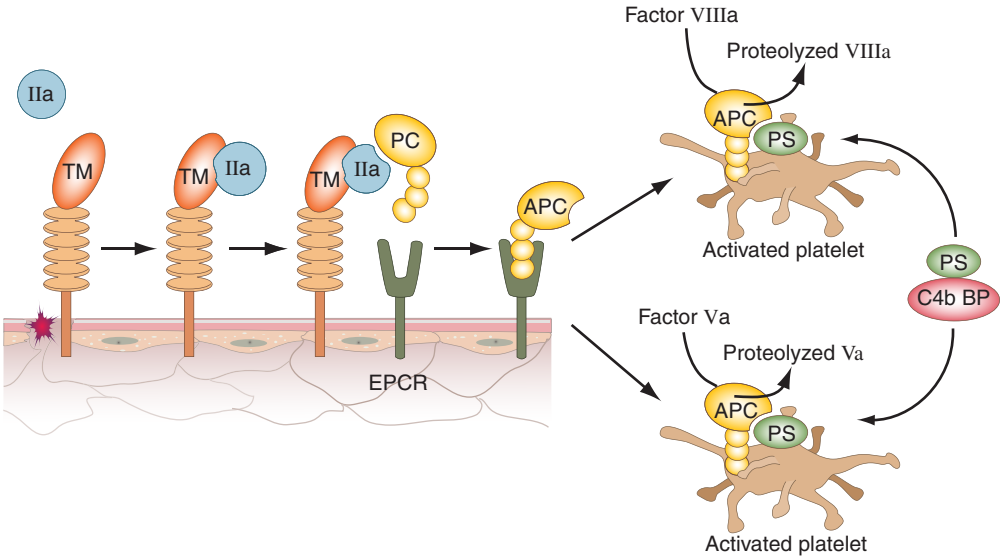

Figure 42.3 Protein C pathway. *APC,* Activated protein C; *C4bBP,* complement factor 4b-binding protein; *EPCR,* endothelial cell protein C receptor; *IIa,* thrombin; *PC,* protein C; *PS,* protein S; *TM,* thrombomodulin.

TABLE 42.1
Prevalence and Estimated Increased Thrombotic Risk of Thrombophilic Factors

Risk Factors for Thrombosis	Prevalence in General Population, %	Prevalence in Thrombophilic Population, %	Estimated Thrombotic Risk, Fold
Decreased antithrombin	0.02–0.17**	1–3**	10–20**
Decreased protein C	0.14–0.50**	3–5**	10**
Decreased protein S	0.03–0.13**	1–5**	10**
Factor V_{Leiden} (heterozygous)	1–5*,**	10–50**	5**
Factor V_{Leiden} (homozygous)	<0.01%	2–4	10–15
Prothrombin G20210A	2–5*,**	6–18*	3
Elevated factor VIII	11**	25**	2.0–4.5
Elevated fibrinogen	5–12	20–30	2–3
Dysfibrinogenemia	<0.1	<1	Variable
Thrombomodulin mutations	<0.01	0.2–0.8	2–4
Elevated homocysteine	5**	10**	3**
Lupus anticoagulant	1–5	10–30	2–10
Oral contraceptives	N/A	N/A2-3	
Pregnancy	N/A	N/A	4–8

N/A, Not applicable.
*Factor V_{Leiden} and prothrombin 20210 prevalence for heterozygosity in general white population; however, both very low (<0.1%) in African and East Asian populations.
**De Stefano et al., 1996; Rosendaal, 1999.
Data also from Abdollahi M, Cushman M, Rosendaal FR, et al.: Obesity: Risk of venous thrombosis and the interaction with coagulation factor levels and oral contraceptive use, *Thromb Haemost* 89:493–498, 2003; Bauer KA, Rosendaal FR, Heit JA: Hypercoagulability: Too many tests, too much conflicting data, *Hematology Am Soc Hematol Educ Program* 2002;353–368, 2002; Franco RF, Rosendaal FR: Genetic risk factors of venous thrombosis, *Hum Genet* 109:369–384, 2001; Goldhaber SZ, Grodstein F, Stampfer MJ, et al.: A prospective study of risk factors for pulmonary embolism in women, *JAMA* 277:642–645, 1997; Grady D, Wenger NK, Herrington D, et al.: Postmenopausal hormone therapy increases risk for venous thromboembolic disease. The heart and estrogen/progestin replacement study, *Ann Intern Med* 132:689–696, 2000; Heit JA, Silverstein MD, Mohr DN, et al.: Risk factors for deep vein thrombosis and pulmonary embolism: A population-based case-control study, *Arch Intern Med* 160:809–815, 2000; Kim V, Spandorfer J: Epidemiology of venous thromboembolic disease, *Emerg Med Clin North Am* 19:839–859, 2001; and Overby DW, Kohn GP, Cahan MA, et al: Prevalence of thrombophilias in patients presenting for bariatric surgery, *Obes Surg* 19:1278–1286, 2009.

PROTHROMBOTIC STATES

OVERVIEW

An increase in procoagulant factors or a decrease in regulatory factors can tip the balance to excessive fibrin production, resulting in thrombus formation. These imbalances can be caused by genetic or acquired factors or by a combination of the two (Tables 42.1 and 42.2). A complete assessment of the recognized and established risk factors must be made to determine the overall risk potential for an individual (see Table 42.2). The following factors are the major known components involved in increased risk for thrombus development (see Table 42.1 for a summary of prevalence and relative risk).

TISSUE FACTOR PATHWAY INHIBITOR DEFICIENCY

Transgenic mice lacking the K1 domain of TFPI succumb to embryonic lethality from an apparent consumptive coagulopathy (Huang et al., 1997). Mice heterozygous for this TFPI mutation appear to exhibit normal growth and development, reproductive capability, and survival, but do exhibit a mild prothrombotic state in an experimental vein injury model (Maroney et al., 2008). Complete absence of TFPI has not been described in humans, suggesting that, as with the mouse model, it may produce embryonic lethality. Partial TFPI deficiency might be a weak prothrombotic risk factor in humans because patients with plasma TFPI levels below 10% of the normal reference range were found to have a slightly increased risk for venous thrombosis (Dahm et al., 2003) and an increased risk for the development of coronary artery disease (Morange et al., 2004). Also, oral estrogen therapy reduces total plasma TFPI concentration and activity in humans by about 25% (Harris et al., 1999) and may be a contributing factor to estrogen-associated thrombosis.

Interestingly, anti-TFPI activity has been demonstrated in patients in antiphospholipid syndrome (APS; described later) and is thought to contribute to the increased risk of thrombosis in patients with that disorder (Adams et al., 2001; Müller-Calleja et al., 2019). In addition, the inhibition of TFPI by monoclonal antibodies to augment coagulation is currently being investigated as a hemophilia therapy in Phase 2 studies (Chowdary, 2018).

TABLE 42.2

Estimated Thrombotic Risk for Cooperativeness of Multiple Factors

Risk Factor 1	Risk Factor 2	Combined Risk (Fold Greater)
Protein C	Factor V_{Leiden} (heterozygous)	25–45
Protein S	Factor V_{Leiden} (heterozygous)	25–50
Factor V_{Leiden} (heterozygous)	Elevated factor VIII	12–20
Factor V_{Leiden} (heterozygous)	Oral contraceptives	8–20
Factor V_{Leiden} (heterozygous)	Pregnancy	25–40

ANTITHROMBIN DEFICIENCY

Both hereditary and acquired deficiencies of antithrombin have been identified (Egeberg, 1965; Bloemenkamp et al., 2003; Patnaik & Moll, 2008). Genetic deficiency of antithrombin is a rare disorder affecting approximately 1 in 10,000 individuals in the general population, and about 1% of patients with familial venous thrombosis are diagnosed for this deficiency (Adcock et al., 1997). Antithrombin deficiency is an autosomal trait, having an apparent dominant expression and high penetrance, with a large number of genetic mutations having been identified (Adcock et al., 1997; Lane et al., 1997). Heterozygous individuals have plasma antithrombin levels around 50% of normal and develop thrombosis; this is in contrast to heterozygous carriers for the genes for coagulation factor deficiencies, who are typically asymptomatic. Both type I (decreased activity with concomitant decreased antigen) and type II (decreased activity with normal levels of antigen) antithrombin mutations have been described in antithrombin-deficient individuals (Lane et al., 1997). Except for unique type II mutations in the heparin-binding region, where patients typically manifest venous thrombosis, homozygous antithrombin deficiency is incompatible with life (Kuhle et al., 2001). The most common clinical presentation of antithrombin deficiency is deep venous thrombosis in the lower extremities and pulmonary embolus. Thrombi may also occur in the retinal, mesenteric, and splenic veins (Bloemenkamp et al., 2003). Acquired deficiencies of antithrombin occur in disseminated intravascular coagulation (DIC) (Asakura et al., 2001), liver disease, nephrotic syndrome, the acute period following venous thrombosis, during extracorporeal membrane oxygenation, asparaginase chemotherapy, and during heparin therapy (Marlar & Mastovich, 1990). In some cases, acquired defects can cause plasma levels to drop to 30% to 50% of normal and may be mistaken for genetic deficiencies. Antithrombin levels are initially decreased in the newborn period, reaching adult levels by 6 months (Streif et al., 1999).

Both antithrombin activity and antigen levels in plasma can be determined by using commercially available assays. Antithrombin activity is determined by inhibition of thrombin or factor Xa, which is currently best measured using a chromogenic assay. Antithrombin antigen assays are performed by enzyme-linked immunosorbent assay (ELISA), immunoturbidimetry, or by nephelometry. Laboratories performing a single assay should rely on an activity assay so as not to miss a type II deficiency, in which the antigen level is normal.

There is no significant difference in clinical presentation between type I and II antithrombin deficiencies. Type II antithrombin deficiency has been further subclassified into reactive site defects (type II RS) with mutations near the thrombin binding site at the carboxyterminal end of antithrombin, heparin binding site defects (type II HBS), and pleotrophic effect mutations (type II PE) that produce conformational changes in antithrombin that can result in multiple defects. However, the type of antithrombin deficiency is unlikely to impact upon clinical management. Still, knowledge of the type may provide prognostic information regarding the risk of thrombosis. For example, type II HBS is the most common type and has been associated with lower penetrance for thrombosis. A high risk of venous thromboembolic disease is seen in patients with type I antithrombin deficiency and in patients with type II specifically with defects affecting the thrombin binding domain. It is important to know that in contrast to reference ranges for coagulation factors, the reference ranges for both antithrombin activity and antigen are fairly narrow, usually around 80% to 120% of normal (Adcock et al., 1997; Kuhle et al., 2001) and should be calibrated against the International Reference Standard.

ABNORMALITIES OF THE PROTEIN C–PROTEIN S SYSTEM

Protein C Deficiency

Both genetic and acquired deficiencies of protein C can increase the risk for thrombosis. The clinical presentation of severe protein C deficiency includes venous thromboembolism, neonatal purpura, warfarin-induced skin necrosis (Moll, 2004; Tai et al., 2004; Goldenberg & Manco-Johnson, 2008), and fetal loss. As with other enzyme deficiencies, two subtypes, types I and II, have been described. Type I is characterized by a decrease in synthesis of a fully functional protein (antigen = activity), while mutations associated with type II protein C deficiency translate into a dysfunctional protein (antigen > activity) (Marlar & Mastovich, 1990; Marlar et al., 1990; Lane et al., 1996). In addition to hereditary deficiency, a number of conditions can give rise to acquired protein C deficiency, including liver disease, severe infection (including meningococcemia), septic shock, and DIC.

Protein C function can be assayed using clotting activity, where the endpoint is fibrin formation, or chromogenic activity (hydrolysis of activated protein C–specific chromogenic substrate) assays; antigen levels are measurable with several types of immunoassays. A key requirement for these clotting assays is the in vitro activation of protein C by Agkistrodon contortix (southern copperhead) snake venom (Protac), which substitutes for the in vivo activator, thrombin-thrombomodulin. The clotting method is typically a two-stage phospholipid assay based on either the activated partial thromboplastin time (APTT) or thromboplastin (PT)-based coagulation assays. In the first stage, the patient's plasma is incubated with the Protac to completely activate protein C, a step that is not calcium dependent. The second stage consists of the addition of an activator (aPTT, PT, or Russell viper venom reagent) to initiate the clotting process. The time until detection of the fibrin clot or hydrolysis of the substrate is proportional to the plasma protein C activity. The clot-based assays provide some advantages in that there is increased sensitivity for detecting both type I and type II protein C deficiencies, as well as increased sensitivity for most coagulation instruments regardless of fibrin clot detection methods. On the negative side, however, clot-based assays may underestimate protein C, particularly under conditions in which there is a deficiency of other factors involved in measuring protein C activity, such as low protein S, heterozygosity or homozygosity for factor V_{Leiden}, warfarin antagonism, or vitamin K deficiency. In addition, an underestimation can occur in situations in which there is increased factor VIII activation. Similarly, conditions that prolong the clotting time may result in overestimation of protein C activity; examples include the presence of heparin in the patient's plasma, direct thrombin and Xa inhibitors, specific factor inhibitors, or the presence of a lupus anticoagulant.

The commercially available assays for measuring protein C antigen use a variety of combinations of capture and detection protein C antibodies. These assays exhibit variable degrees of recognition for uncarboxylated protein C and protein C/inhibitor complexes. All of the immunoassays cross-react with protein C type II mutations and should not be used for screening purposes, but they can help in distinguishing between types I and II in patients with low protein C activity. Type I heterozygous protein C deficiency is the more common of the two and reflects structurally normal protein C. Homozygous type I protein C deficiency reflects a complete absence of the protein and manifests as neonatal purpura fulminans. Chromogenic functional assays are not subject to quantitative or qualitative variations in protein C, coagulation factors, anticoagulants, or inhibitors; thus, they are more precise than clot-based methods.

Protein S Deficiency

Both genetic and acquired deficiencies of protein S are associated with increased risk of thrombosis. As discussed earlier, protein S together with APC binds to the phospholipid membranes, enhancing the enzymatic inactivation of factors Va and VIIIa (Hackeng et al., 1994; van Wijnen et al., 1996). Protein S circulates in both free and bound forms with about 40% of the protein S free in plasma, whereas the remaining 60% is bound to the complement system protein, C4b-binding protein (C4bBP) (Nelson & Long, 1992). Several different pathologic and physiologic conditions can alter the ratio of free and bound protein S, thereby effectively modulating the protein C inhibitory pathway (Mackie et al., 2001). Protein S levels characteristically decrease during pregnancy, with values averaging only 60% of those of non-pregnant controls from the 10th week of pregnancy onward (Cerneca et al., 1997; ten Kate & van der Meer, 2008). Of note, C4bBP is an acute-phase reactant and protein S activity may be decreased in inflammatory conditions (D'Angelo et al., 1988) due to an increase in the bound fraction. Acquired causes of protein S deficiency include oral hormonal contraceptive use, DIC, vitamin K deficiency, acute

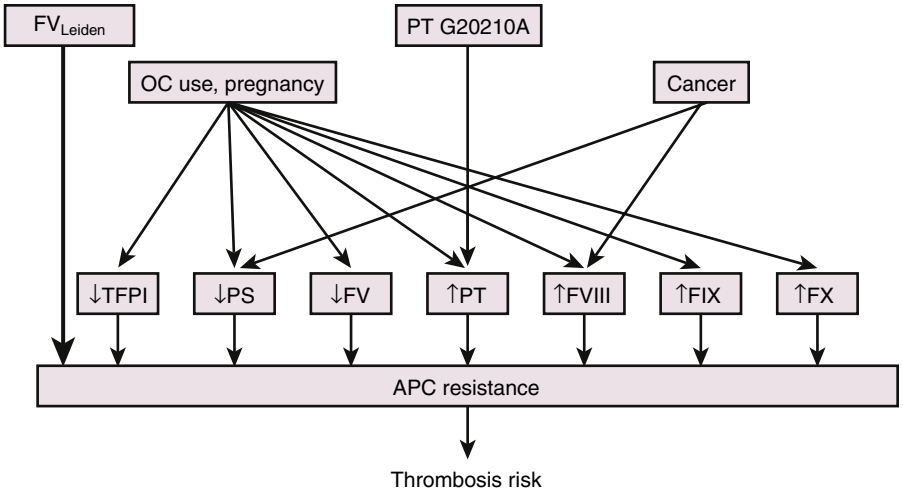

Figure 42.4 Activated protein C (APC) resistance as a complex phenotype. FV, factor V; PT, prothrombin; OC, oral contraception; TFPI, tissue factor pathway inhibitor; PS, protein S; PT, prothrombin time, FVIII, factor VIII; FIX, factor IX; FX, factor X. Redrawn with permission from Castoldi E, Rosing J: APC resistance: Biological basis and acquired influences, *J Thromb Haemost* 8:445–453, 2010.

thromboembolism, nephrotic syndrome, human immunodeficiency virus (HIV) infection, liver disease, and L-asparaginase chemotherapy.

Mutations of the autosomal gene encoding protein S are expressed with variable penetrance (Rezende et al., 2004). As with antithrombin and protein C, the classical quantitative type I deficiency (decreased protein S activity with concomitant decreased total antigen) and a qualitative type II deficiency (decreased protein S activity with normal levels of free and total antigen) have been reported. A third type of mutation, type III deficiency, is characterized by total protein S antigen measurements within the normal range and selectively reduced concentrations of free protein S and functional activity because of increased binding to C4bBP. Some studies have suggested that type III individuals might not have increased risk for thrombosis (Brouwer et al., 2005; Libourel et al., 2005). Patients with homozygous protein S deficiency with severely decreased protein S activity (<1%) present with similar clinical manifestations to homozygous protein C deficiency (Brouwer et al., 2005), that is, neonatal purpura fulminans.

Plasma protein S levels may be measured with protein S clotting activity assays as well as with antigenic assays for free protein S and total protein S antigen. Definitive diagnosis of protein S deficiency can be difficult owing to the complexity of protein S interaction with C4bBP (Nelson and Long, 1992; Goodwin et al., 2002; Persson et al., 2003; ten Kate & van der Meer, 2008). The functional assay methods are based on the activity of protein S to serve as a cofactor for the anticoagulant effects of APC (Wolf et al., 1989; Preda et al., 1990). A major disadvantage of functional protein S assays is poor specificity (false-positive results for protein S deficiency). However, some of the assays are not specific for protein S because they are also affected by defective activated protein C resistance (APC-R) due to factor V_{Leiden} variant (see later discussion). Screening of the plasma samples for APC-R prior to the performance of the functional protein S assays may provide a way to address this issue. The early methods for determining free protein S antigen concentrations, in which bound protein S complexes were precipitated using polyethylene glycol (PEG), have been replaced by immunoassays that use antibodies with specificities for free and total protein S (Goodwin et al., 2002; Persson et al., 2003; ten Kate & van der Meer, 2008). Reaching a definitive diagnosis of congenital deficiency of protein S can be challenging given the complexity of the interaction of protein S with C4bBP (an acute-phase reactant), the acquired conditions (which can change the equilibrium of free and bound forms), and the presence of vitamin K antagonists (Simmonds et al., 1998; Mackie et al., 2001; Goodwin et al., 2002; Rezende et al., 2004; ten Kate & van der Meer, 2008). Reference intervals for both antigen and activity typically range between ~60% to ~150%. Special reference ranges for women who may be on oral contraceptives or pregnant are typically not provided. However, these situations should be taken into account when interpreting results that are below the standard reference ranges for these patient populations.

Activated Protein C Resistance and Factor V_{Leiden} Variant

APC-R is detected when the addition of exogenous APC to plasma does not result in the expected anticoagulant effect, as manifested by appropriate prolongation of clotting time tests, such as the APTT (Dahlback, 1999; Castoldi & Rosing, 2010). APC-R is most often attributable to factor V_{Leiden} variant, which is considered one of the most common genetic risk factors for venous thrombosis, with a prevalence in individuals with European ancestry of about 4% (Ridker et al., 1995; Heijmans et al., 1998). The polymorphism, an arginine residue substituted with a glutamine residue (R506Q), eliminates one of the two cleavage sites in factor Va (Aparicio & Dahlback, 1996). Factor V_{Leiden} increases the relative risk of thrombosis about 4- to 5-fold in the heterozygous condition and 10- to 15-fold in the homozygous individual (Simone et al., 2013; Castoldi & Rosing, 2010). The presence of factor V_{Leiden}, even in heterozygotes, will reduce the APC-mediated prolongation of coagulation and thereby produce a reduction of the ratio of clotting times of APC-treated plasma compared with plasma that was not treated with APC.

There are several variations of these assays, with factor V–deficient plasma frequently included to increase specificity for abnormalities attributable to a genetic abnormality of the patient's own factor V. As mentioned, a pair of clotting tests are performed, with and without the addition of APC. If the ratio of clotting time with added APC divided by clotting time in the absence of added APC is sufficiently high (in most assays >1.8 or 2.0), then APC-R or factor V_{Leiden} is highly likely to be excluded. Lower ratios, in contrast, suggest that the sample is APC resistant and that the patient may have factor V_{Leiden} (or another factor V variant, or possibly acquired APC resistance), which should be confirmed by direct DNA-based genotyping (Castoldi & Rosing, 2010). Also of potential clinical importance, however, are those cases of acquired APC-R not associated with a genetic abnormality of the patient's factor V molecule. As shown in Figure 42.4, several abnormalities may affect regulation of the coagulation pathways and may additionally exert a prothrombotic influence by virtue of increasing APC-R (Cumming et al., 1995; Graf et al., 2003; Castoldi & Rosing, 2010). Such forms of APC-R are better detected with assays that include factor V–deficient plasma.

HYPOFIBRINOLYSIS

Thrombosis can result from reduced fibrinolysis in the setting of underexpression of plasminogen or its activators or by overexpression of inhibitors of fibrinolysis. Consensus has been difficult to achieve with respect to assessment through system-based assays, specific component functional assays, or molecular studies with respect to the individual patient. Laboratory diagnosis of hypofibrinolytic defects is challenging because plasma levels of fibrinolysis inhibitors (such as PAI-1) vary widely in normal individuals and because levels of plasminogen activators are normally very low.

Euglobulin clot lysis time, developed in 1950, provides a measure of some aspects of the fibrinolytic system (Sartori et al., 2003). The persistence of this assay reflects the pressing need for an updated and more precise global indicator of abnormal fibrinolysis. This assay involves the selective precipitation of the "euglobulin" fraction of the plasma sample, which includes fibrinogen, plasminogen activator, and plasminogen; the euglobulin fraction is then re-dissolved, clotted with thrombin, and the time to clot lysis is measured. An abnormal rate of euglobulin clot lysis may lead to more detailed testing of the fibrinolytic system, such as specific assays for plasminogen activator, plasminogen, and other proteins upregulating or downregulating fibrinolysis. Individuals with the longest clot lysis times (fourth quartile) have been reported to have a twofold increased risk of thrombosis relative to individuals with the shortest clot lysis times (first quartile) (Meltzer et al., 2009).

Assessment of the mechanical properties of clots throughout the period of their formation and observing subsequent lysis with viscoelastic tests such as rotational thromboelastometry (ROTEM) or thromboelastography (TEG) represents a potentially different approach to detecting hypofibrinolysis (Kamada et al., 2001; Salooja & Perry, 2001; Vig et al., 2001; Meltzer et al., 2009; Kuiper et al., 2016). These instruments measure clot rigidity or strength during the clot formation and breakdown process (Kamada et al., 2001; Salooja & Perry, 2001; Vig et al., 2001; Meltzer et al., 2009; Kupesiz et al., 2010). Accordingly, they may offer the potential for real-time assessment of the fibrinolytic state, which could be of particular benefit in conjunction with the monitoring of antifibrinolytic therapy (Kupesiz et al., 2010). Viscoelastic tests may be helpful in diagnosing hyperfibrinolysis and guiding antifibrinolytic therapy in patients who are experiencing active bleeding but are believed to be less useful in patients who are not symptomatic at the time of testing.

ELEVATION OF COAGULATION FACTOR LEVELS

Prothrombin G20210A Variant and Elevation of Prothrombin

This polymorphism in the prothrombin gene at base pair number 20210 is a guanine-to-adenine substitution in the 3′-untranslated region of the gene (Colucci et al., 2004). Heterozygosity for this polymorphism has been associated with an approximately twofold increased risk for venous thrombosis (Simone et al., 2013) and is the second most common inherited thrombophilia in individuals with European ancestry following the factor V_{Leiden} variant. Heterozygous individuals characteristically have levels of plasma prothrombin approximately 15% to 30% higher than those in individuals lacking this polymorphism, although even these higher levels usually fall within the established reference interval for prothrombin activity of most laboratories. Accordingly, molecular diagnostic procedures are required for the diagnosis of prothrombin G20210A (Poort et al., 1996; Gruenewald et al., 2000). Heterozygosity for prothrombin G20210A is a relatively common genetic risk factor for venous thrombosis in populations of European descent (about 3%), with lower prevalence in non-European populations (De Stefano et al., 1996; Rosendaal, 1999). Homozygous individuals are relatively rare and have been reported to display striking phenotypic heterogeneity, with approximately 40% appearing to be asymptomatic for thromboembolic events (Bosler et al., 2006).

Elevation of Other Coagulation Factors

Elevations of several other coagulation factors have also been reported to impart an increased risk of thrombosis. As levels of factors VII, VIII, IX, XI, or fibrinogen are elevated, the relative risks for developing thrombosis are proportionately increased (1.5- to 6.0-fold) (Kannel et al., 1987; O'Donnell et al., 1997; Kyrle et al., 2000; Meijers et al., 2000). The most studied of these reported risk factors is factor VIII. Factor VIII is regulated by genetic mechanisms and physiologic mechanisms that increase the release of stored factor VIII in times of stress and exercise. Some familial elevation of factor VIII has been reported, but transiently high levels can be seen in patients with a concomitant increase in plasma von Willebrand factor level and in patients with stress due to a variety of clinical conditions (Vormittag et al., 2009). There is a stratified increase of risk, with patients having factor VIII levels of 120% to 150% reported to have a 1.5-fold to 2.0-fold greater risk of venous thrombosis; levels of 300% to 400% have a 3- to 6-fold increased relative risk of venous thrombosis.

More recently, thrombophilia was reported associated with factor IX-Padua, a variant with a substitution of leucine for arginine at position 338 (R338L). Although the quantitative level of factor IX protein in the patient's plasma was normal, the clotting factor activity of factor IX was eightfold greater than normal, leading to more efficient generation of thrombin (Simioni et al., 2009). The gain-of-function mutation of factor IX-Padua has been exploited in gene therapy trials for patients with hemophilia B (George et al., 2017).

DYSFIBRINOGENEMIA

There are few published reports of abnormalities associated with increased risk of thrombosis due to dysfunctional fibrinogen molecules (Haverkate & Samama, 1995; de Moerloose et al., 2010). A recent study that evaluated 101 patients with congenital dysfibrinogenemia concluded that these patients and their relatives are not only at a higher risk for major bleeding, including postpartum hemorrhage, but also at higher risk for thrombotic events (Casini et al., 2015). The frequency of recognized cases of dysfibrinogenemia among individuals with familial thrombosis is about 0.8%. In addition, patients with congenital afibrinogenemia have been recognized to experience both arterial and venous thrombosis (Nagler et al., 2016). The assays commonly employed to assess fibrinogen are functional assays assessing clot formation and antigenic assays. As discussed in Chapter 40, an imbalance in the ratio of such assays provides an indication of a decrease-of-function dysfibrinogenemia. Subtleties in the ability of fibrinogen—and, perhaps more important, of the resulting fibrin—to bind proteins having an influence on the balance of hemostasis and thrombosis (e.g., tissue plasminogen activator) are not detected by such assays. Accordingly, it is possible that the frequency by which dysfibrinogenemias underlie thrombotic events may become better understood in future studies with larger data sets.

BOX 42.1

Sydney Investigational Criteria for Diagnosis of Antiphospholipid Syndrome

Clinical

Vascular thrombosis (one or more episodes of arterial, venous, or small vessel thrombosis). For histopathologic diagnosis, there should not be evidence of inflammation in the vessel wall.

Pregnancy morbidities attributable to placental insufficiency, including three or more otherwise unexplained recurrent spontaneous miscarriages before 10 weeks' gestation. Also, one or more fetal losses after the 10th week of gestation, stillbirth, episode of preeclampsia, preterm labor, placental abruption, intrauterine growth restriction or oligohydramnios that are otherwise unexplained.

Laboratory

aCL or anti-β2GPI IgG and/or IgM antibody present in medium or high titer on two or more occasions, at least 12 weeks apart, measured by standard ELISAs.

Lupus anticoagulant in plasma, on two or more occasions, at least 12 weeks apart detected according to the guidelines of the International Society of Thrombosis and Haemostasis Scientific Standardization Committee on Lupus Anticoagulants and Phospholipid-Dependent Antibodies.

"Definite APS" is considered to be present if at least one of the clinical criteria and one of the laboratory criteria are met.

aCL, Anticardiolipin; *β2GPI,* β2-glycoprotein I; *ELISA,* enzyme-linked immunosorbent assay; *Ig,* immunoglobulin.
Source: Miyakis S, Lockshin MD, Atsumi T, et al.: International consensus statement on an update of the classification criteria for definite antiphospholipid syndrome (APS), *J Thromb Haemost* 4:295–306, 2006.

ANTIPHOSPHOLIPID SYNDROME AND LUPUS ANTICOAGULANTS

APS is an autoimmune disorder characterized by the concurrence of clinical events—vascular thrombosis and/or pregnancy complications—with laboratory markers, described later. An international consensus statement has provided diagnostic criteria for "definite APS" that are currently in use (Miyakis et al., 2006), listed in Box 42.1.

A brief review of the history of this disorder will explain the confusing terminologies and the relative absence of mechanistic testing. The initial recognition of this condition can be traced to astute clinical observations over 6 decades ago that began linking 2 anomalous laboratory findings—the biological false-positive syphilis test and a coagulation inhibitor—to the clinical manifestations of thrombosis and pregnancy complications. The serologic test for syphilis, in which the primary antigen test is cardiolipin (diphosphatidyl glycerol) was evolved into a quantitative immunoassay for antibodies against cardiolipin (Harris et al., 1983). Detection of the coagulation "anticoagulants" are both misnomers that were based on the early misconceptions that (1) phospholipids are the major antigenic targets of this autoimmune disorder and (2) that the distinctive coagulation abnormalities in this disorder were limited to patients with systemic lupus erythematosus (SLE). Both of these were incorrect. While the phospholipid cardiolipin is the primary target in syphilis, the actual targets in APS are serum and plasma proteins that bind phospholipid. This phenomenon, named *lupus anticoagulant* (*LA*), was first identified in landmark initial studies done in patients from a lupus clinic. However, it came to be understood that although many patients with SLE have this inhibitor of phospholipid-dependent coagulation reactions, the majority of patients with the lupus anticoagulant do not have SLE. The laboratory diagnosis of APS continues to be made through improvements on these same assay principles. Widely accepted assays that report on disease mechanisms need to await the further elucidation of the pathogenic basis of this disorder (Giannakopoulis, 2007, 2009).

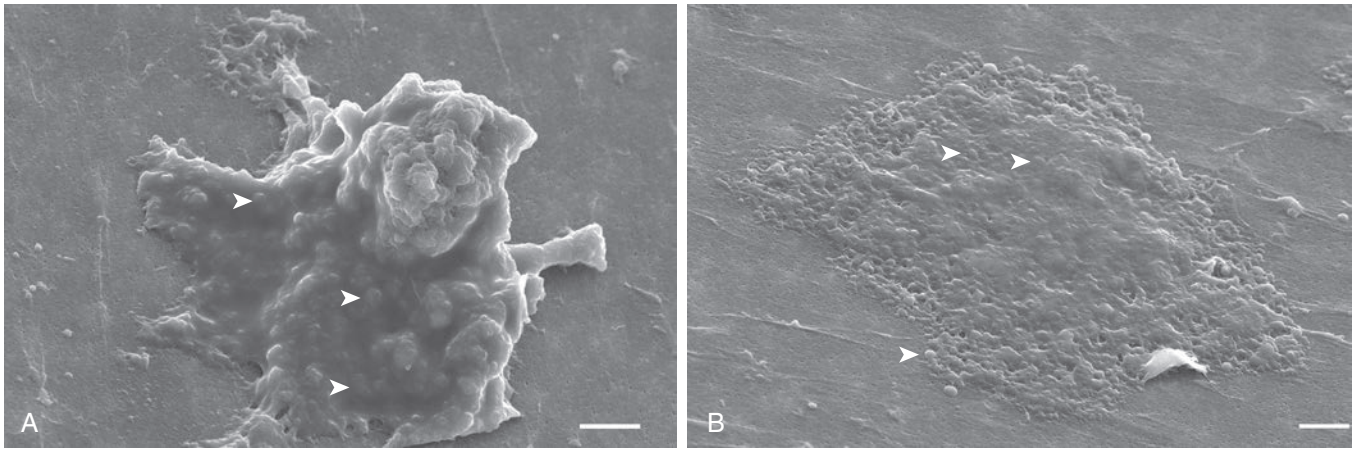

Figure 42.5 The interaction of human APS plasma with phospholipid vesicles results in complex multilayered individual structures composed of phospholipid vesicles *(arrowheads for representative examples)* with vertical dimensions, aggregated by proteinaceous materials (A), whereas similar interactions of control plasma with lipid vesicles results in mostly flattened mat-like structures with little vertical dimension (B). (Reproduced with permission from Taatjes DJ, Bouffard N, von Turkovich M, et al.: Visualization of macro-immune complexes in the antiphospholipid syndrome by multi-modal microscopy imaging, *Micron* 100:23–29, 2017.)

The serum protein β2GPI, a member of the complement control family, is a major antigenic target in this disorder. APS antibodies may recognize any of the protein's 5 homologous domains. However, antidomain I immunoglobulin G (IgG) antibodies that recognize an epitope in the region of witG40-R43 within the amino-terminal domain appear to be associated with an increased risk of thrombosis, although inconsistencies among these assays have been reported (Yin et al., 2018). Partly because of these discrepancies, immunoassays for antidomain I antibodies have not yet been included in the diagnostic criteria. Interestingly, APS patients can also exhibit autoantibodies against other PL-associated proteins, including, but not limited to, prothrombin, protein C, protein S, TFPI, annexin A2, and others. The potential clinical significances of these are not yet clear and assays for these antibodies have not been included in the formal consensus diagnostic criteria for APS.

The LA phenomenon is due to autoantibody-protein complexes that block the ability of the PL membrane to serve as a platform for the assembly of coagulation protein complexes. The LA has classically been referred to as "paradoxical" because it is "anticoagulant in vitro and procoagulant in vivo." This discrepancy may be explained by scanning electron microscopic imaging studies of the interaction of PL vesicles with plasmas from APS patients. Such studies demonstrate the formation of macro-immune complexes on phospholipid membranes (Fig. 42.5) that block the availability of membrane surfaces from serving as platforms for the assembly of coagulation enzyme-substrate complexes (Taatjes et al., 2017) in laboratory conditions in which the concentration of phospholipids can be limited. The prothrombotic effects of these antibodies may be attributable to the mechanisms described later and the ability of these macro-immune complexes to activate complement (Rand et al., 2017).

The presence of a persistently positive LA together with high titers of anti-β2GPI have been shown to correlate with increased risk for thrombosis (de Laat et al., 2009). The combination of anti-β2GPI, aCL antibodies, and LA test positivity has the highest association with recurrent venous thromboembolism (Pengo et al., 2006; Pengo et al., 2011). A positive LA test alone has also been demonstrated to be a significant risk factor for adverse pregnancy outcomes (Lockshin et al., 2012).

Proposed thrombogenic mechanisms for APS antibodies have included interference with annexin A5 anticoagulant activity, interference with annexin A2 fibrinolytic activity, antibody binding to TFPI, downregulation of TM, interference with protein S, increased platelet activation, and endothelial perturbation. There has been increased recognition of a potential role for complement activation in the APS disease process and a role for germline variants of complement regulatory genes in increasing the risk of thromboembolism, particularly the catastrophic form of APS (Chaturvedi et al., 2020).

Recommendations for standardizing LA assays have been proposed through the Scientific Standardization Committee of the International Society on Thrombosis and Haemostasis related to the diagnosis of APS (Pengo et al., 2010b), listed in Box 42.2.

Most clinical laboratories employ APTT and dilute Russell viper venom time (dRVVT) to detect LA. In the dRVVT test, the coagulation cascade is initiated at a later step than in APTT, with direct factor X activation by the venom in PL-dependent fashion and likely with a lower concentration of PL. The various APTT reagents have different sensitivities to LAs. The clotting time of plasma from LA patients is prolonged in these assays. When mixed with equal parts of normal pooled plasma, the plasma from LA patients will prolong the clotting time of the mixture beyond the clotting time of the normal control plasma itself. Whereas specific coagulation factor inhibitors, such as those directed against factor VIII, are typically time- and temperature-dependent (see Chapter 40), LAs more commonly are immediate acting even at room temperature. It is important to note that LAs may artifactually interfere with quantitative measurement of coagulation factors assayed in an APTT-based system, leading to misdiagnosis of factor deficiencies. A telltale pattern that should itself arouse suspicion of an LA is a persisting increase in apparent factor activity, with increasing dilutions of patient plasma used in the assay. Such apparent increases in factor activity, also known as *nonparallelism* or *crossing lines*, result from decreased interference by progressive dilutions of LA. Preincubation of LA plasma with an excess quantity of PL will neutralize the LA and result in significant shortening of a subsequently performed clotting time compared with plasmas that do not have the excess PL added. Sources of neutralizing PL that have been used for this purpose include purified PLs, purified hexagonal phase PLs, and complex PLs derived from frozen and thawed washed platelets (platelet neutralization procedure [PNP]) (Favaloro & Wong, 2008, 2009). International consensus statements on investigational criteria for APS (Miyakis et al., 2006; Favaloro & Wong, 2009) combine the clinical criteria of vascular thrombosis and pregnancy complications with laboratory criteria. These laboratory criteria include a positive LA, aCL antibodies of IgG or IgM of greater than 40 IU, and medium- or high-titer IgG or IgM anti-β2GPI antibodies. To establish the diagnosis, the tests should be abnormal when repeated at least 12 weeks apart before a diagnosis of aPL antibodies is made.

The clinical course of high-risk patients found to have positive tests for APS reveals an increase in first thrombotic events (Pengo et al., 2011) and increased risk for recurrent thrombosis (Pengo et al., 2010b). Important considerations in laboratory testing include (1) processing to ensure that the specimen is platelet poor; (2) choosing two tests, such as the dRVVT or a silica-activated APTT with low PL content; (3) eliminating the influence of anticoagulants in mixing studies; (4) correcting prolonged clotting time in the presence of excess PL; and (5) ensuring that specific comments on the laboratory's reference ranges and interpretations accompany the LA profile and the aCL antibodies and β2GPI antibody assays (Ledford-Kraemer, 2008; Pengo et al., 2009; Pengo et al., 2010a). It is important for clinical laboratories to be aware that the currently available direct-acting oral anticoagulants may cause false-positive LA tests (Favaloro & Lippi, 2017; Cohen et al., 2018) and that several neutralizing approaches have recently been suggested to address this (Cox-Morton et al., 2019; Favresse et al., 2018).

OTHER PROTHROMBOTIC ABNORMALITIES AND NOVEL GENETIC VARIANTS

Several acquired conditions have been associated with increased risk of venous thrombosis. The relative risk for many of these has been determined and appears to combine with genetic causes to increase the overall

BOX 42.2

Laboratory Detection of Lupus Anticoagulants (LAs)

A. Blood collection
   1. Blood should be collected before the start of any anticoagulant drug regimen or a sufficient period after its discontinuation.
   2. Fresh venous blood in 0.109 M sodium citrate (ratio 9 : 1)
   3. Double centrifugation removes residual platelets.
   4. Quickly frozen plasma required if LA assays are postponed.
   5. Frozen plasma must be thawed at 37°C.

B. Initial testing
   1. Use two separate screening tests based on different principles, each with a *low level of phospholipid* (*PL*):
      a. Dilute Russell viper venom time (dRVVT)
      b. LA-sensitive activated partial thromboplastin time (APTT; preferably with silica activator)
   2. Exclude the presence of heparin, LMW heparin, direct thrombin inhibitors, or factor Xa inhibitors.
      a. Indirect (heparin) and direct thrombin inhibitors should be suspected from prolongation of the thrombin time.
   3. Results of screening tests are potentially suggestive of LA when their clotting times are longer than the local cutoff value*

C. Mixing studies for prolonged LA-sensitive APTT or dRVVT
   1. Pooled normal plasma (PNP) for mixing studies should ideally be prepared in-house. Alternatively, adequate commercial frozen or lyophilized PNP can be used.
   2. Plasma with prolonged screening values should be mixed as 1 part patient plasma with 1 part PNP and reassayed without incubation (i.e., <30 minutes after mixing).
   3. Results of mixing tests are suggestive of LA when their clotting times are longer than the local cutoff value.†

D. Confirmatory tests for prolonged APTT or dRVVT
   1. Confirmatory tests are performed by increasing the PL concentration beyond that used in the screening tests.
   2. Bilayer or hexagonal (II) phase PL should be used to increase the concentration of PL.‡
   3. Results are confirmatory of LA if the % correction is above the local cutoff value.

E. A report with an explanation of the results should be given.§

APTT, Activated partial thromboplastin time; *LMW,* low molecular weight.
Additional ISTH subcommittee explanations and qualifications are reported in detail in the original source of this table (Pengo et al., 2009).
Adapted from Pengo V, Tripodi A, Reber G, et al.: Update of the guidelines for lupus anticoagulant detection. Subcommittee on Lupus Anticoagulant/Antiphospholipid Antibody of the Scientific and Standardisation Committee of the International Society on Thrombosis and Haemostasis, *J Thromb Haemost* 7:1737–1740, 2009.

* The cutoff value is the 99th percentile of the distribution of clotting times performed on plasmas from healthy donors. Testing described should be performed with the *local* reagent/instrument combination on plasmas from at least 40 adult healthy donors younger than 50 years of age. Cutoff values established elsewhere should not be substituted, even if they refer to the same method and instrument.

† In the case of mixing studies, the cutoff value would be the 99th percentile of the distribution of clotting times when plasmas from healthy donors are mixed in equal parts with PNP. Alternatively, the distribution may be of a derived "index of circulating anticoagulant" = [(b – c)/a] × 100, where a, b, and c are the clotting times of the patient plasma, mixture, and PNP, respectively.

‡ In the case of confirmatory testing, a distribution of values for "% correction" = [(screen – confirm)/screen] × 100, based on testing of plasmas from healthy donors at low (screen) and high (confirm) PL concentrations is obtained first. A patient result above the cutoff value assigned to this distribution (e.g., above the 99th percentile) would then be considered as a positive confirmatory test. Note that the clotting time of the confirmatory test in LA-positive samples is not always shortened to within the normal range of controls. Accordingly, to avoid false-negative results, confirmatory tests are recommended to be performed in all normal controls. These results should be used to establish the cutoff value.

§ International Society on Thrombosis and Haemostasis (ISTH) guidelines further state, "Results should be expressed as ratio of patient-to-PNP for all procedures (screening, mixing, and confirm)."

risk for thrombosis. Common conditions that have a strong association with venous thrombosis include trauma, surgery and the postoperative state, pregnancy, immobility, obesity and diet, smoking, and previous thrombosis. Additionally, malignancy, chronic DIC, oral contraceptive use and hormone replacement therapy, heparin-induced thrombocytopenia, thrombotic thrombocytopenic purpura, nephrotic syndrome, essential thrombocythemia, polycythemia vera, and inflammatory conditions have all been associated with increased risk of venous thrombosis. Hepatic insufficiency, a condition that has long been associated with bleeding complications, has more recently been associated with thrombotic complications (Tripodi & Mannucci, 2011).

Perturbations, genetic or acquired, in the clearance of the amino acid homocysteine can lead to elevated levels of the amino acid in blood and to an associated increased risk of thrombosis. The most devastating of these is the cystathione-β-synthetase gene, which, in the homozygous state, leads to severe thrombosis and atherosclerosis (Mudd et al., 1985). Acquired causes, mostly associated with diet and vitamin intake, also are significant factors raising homocysteine levels in plasma. The associated risk for thrombosis with elevated homocysteine levels may correlate with the degree of elevation in homocysteine. Two common polymorphisms associated with the homocysteine-metabolizing enzyme methylenetetrahydrofolate reductase (MTHFR) had previously been thought to be associated with increased risk of thrombosis. However, this hypothesis has not been sustained. More recent studies have failed to establish MTHFR as an independent risk factor for thrombosis in adults (Tosetto et al., 1997; Franco et al., 1999), although a possible relationship with childhood stroke remains less clear (Prengler et al., 2001). Accordingly, it is currently not recommended to evaluate MTHFR polymorphisms as a cause of venous thrombosis in adults (Legnani et al., 1997; Franco et al., 1999).

Still, hyperhomocysteinemia has been reported to be a risk factor for the development of pulmonary embolisms and DVT (den Heijer et al., 1996, 1998; Ray, 1998). Meta-analysis of case-controlled studies have reported an odds ratio of 2.5 to 2.95 for venous thromboembolic disease in patients with elevated homocysteine concentration—that is, homocysteine concentrations greater than two standard deviations above the mean of the control group (den Heijer et al., 1998; Ray, 1998). Interestingly, some studies had suggested that the risk of thrombosis increases 10- to 50-fold in patients who have both hyperhomocysteinemia and an inherited thrombophilia (e.g., factor V_{Leiden}) (Ridker et al., 1997; Margaglione et al., 1998). However, other studies failed to confirm these findings (De Stefano et al., 2000). At this time, both the American College of Medical Genetics and Genomics and the American College of Obstetricians and Gynecologists recommend against the evaluation of MTHFR polymorphisms as part of the routine evaluation of thrombophilia. Plasma levels of homocysteine may nevertheless be included as part of an investigation for possible thrombophilia.

With the fast pace of advances in molecular genetic testing and the forthcoming anticipated economies of scale, there will likely be an increasing role for high-throughput testing for the diagnosis of thrombotic and hemostatic abnormalities (Downes et al., 2019). Although these approaches are eagerly awaited owing to the possibility of improved diagnosis and the uncovering of new mutations and variants, they might also bring new problems. For example, it would not be surprising if this technology also brings to light new "variants of unknown significance."

APPROPRIATE LABORATORY UTILIZATION

The laboratory evaluation of thrombophilia is complex, including the appropriate tests to order, on whom to perform them, and the appropriate timing for testing (Foy & Moll, 2009). Among the major issues are (1) there is currently no global test to grade the thrombotic risk status of an individual, thus, a series of individual tests must be ordered for assessment of risk; and (2) there is a broad range of thrombotic risk among the various thrombophilias—ranging from a very high risk associated with hereditary antithrombin deficiency to a much lower risk associated with the prothrombin G20210A variant. Several questions must be considered when evaluating patients for testing: Does the patient (and family) history justify an evaluation? Are the tests to be ordered appropriate for addressing major accepted risk factors? Is the timing appropriate to provide proper evaluation? Are there underlying therapeutic, pathologic, or physiologic conditions that interfere with interpretation of results?

Most experts agree that the following clinical situations warrant testing for the major inherited thrombophilias (including levels of protein S, protein C, and antithrombin and the factor V_{Leiden} and prothrombin gene variants) and APS: (1) patients with venous thromboembolism who have at least one first-degree relative with documented venous thromboembolism before the age of 45 years (APS testing not necessary); (2) young patients (<45 years old) who experienced venous thromboembolism; (3) patients with recurrent venous thromboembolism; and (4) patients with venous thromboembolism in multiple sites that are in atypical areas. In addition, patients experiencing warfarin-induced skin necrosis should be tested for protein C deficiency and patients with arterial thrombosis should be evaluated for APS.

Evaluations should generally be limited to situations in which it is determined that the results may impact on future treatment and at a time when the patient is asymptomatic, at least several months after the acute thrombotic event, and off anticoagulant therapy. Unfortunately, during

the immediate postthrombotic period before anticoagulation, plasma factors are consumed, inviting the potential for erroneous diagnoses. Heparin significantly decreases antithrombin levels, increases protein S levels, and may mask LAs (unless a heparin-neutralizing molecule such as protamine or polybrene, or the enzyme heparinase, is included in the assay). Warfarin decreases protein C and protein S levels. Direct oral anticoagulants—such as dabigatran, rivaroxaban, and apixaban—may falsely increase levels of detected protein C, protein S, and antithrombin in clot-based assays, and may also lead to the false-positive detection of LAs. Only genetic risk markers can be evaluated at any time by molecular diagnostic techniques. Attempts have been made to circumvent the test abnormalities produced by oral anticoagulation by using ratios of protein C or protein S to one or another of the vitamin K–dependent coagulation factors. However, the variability of such ratios is considerable, inviting the opportunity for misdiagnosis. An erroneous diagnosis can be made when plasma factor levels decrease during a variety of acquired conditions such as pregnancy, hormone therapy, and after surgery.

It is of critical importance to educate referring physicians on the appropriateness and inappropriateness of testing for hypercoagulable risk and to communicate these laboratory results to physicians and patients in a manner that accurately reflects the patient's risk for thrombosis. Decisions such as whether to prescribe oral contraceptives, how to manage pregnancies, and whether to recommend long-term anticoagulant therapy are often not straightforward. In the case of inherited disorders, genetic counselors may be a helpful resource for consultation. In all such instances, knowledge not only of available testing but also of limits in interpretation of these tests will contribute greatly to reaching the most appropriate clinical decisions.

ACKNOWLEDGMENT

The authors thank Drs. Richard Marlar, Louis Fink, Jonathan Miller, and John Mitsios for their contributions as authors of this chapter in the prior editions of this textbook.

SELECTED REFERENCES

Casini A, Blondon M, Lebreton A, et al.: Natural history of patients with congenital dysfibrinogenemia, *Blood* 125:553–561, 2015.
An article that looks at patients with congenital dysfibrinogenemia.

Castellino FJ, Ploplis VA: The protein C pathway and pathologic processes, *J Thromb Haemost* 7:140–145, 2009.
Review of the protein C pathway and the disease pathogenesis.

Esmon CT: Basic mechanisms and pathogenesis of venous thrombosis, *Blood Rev* 23:225–229, 2009.
Review on the pathogenesis of venous thrombosis.

Giannakopoulos B, Passam F, Ioannou Y, et al.: How we diagnose the antiphospholipid syndrome, *Blood* 113:985–994, 2009.
Review of the antiphospholipid syndrome.

Pengo V, Tripodi A, Reber G, et al.: Subcommittee on lupus anticoagulant/antiphospholipid antibody of the Scientific and Standardisation Committee of the international Society on thrombosis and haemostasis. Update of the guidelines for lupus anticoagulant detection, *J Thromb Haemost* 7:1737–1740, 2009.
Consensus group report on standardization of lupus anticoagulant testing.

Poort SR, Rosendaal FR, Reitsma PH, et al.: A common genetic variation in the 3′-untranslated region of the prothrombin gene is associated with elevated plasma prothrombin levels and an increase in venous thrombosis, *Blood* 88:3698–3703, 1996.
Classic paper describing prothrombin gene variant associated with elevated thrombotic risk.

ten Kate MK, van der Meer J: Protein S deficiency: a clinical perspective, *Haemophilia* 14:1222–1228, 2008.
A review that describes protein S deficiency.

Access the complete reference list online at Elsevier eBooks for Practicing Clinicians.

REFERENCES

Adams MJ, Donohoe S, Mackie IJ, Machin SJ: Anti-tissue factor pathway inhibitor activity in patients with primary antiphospholipid syndrome. Br J Haematol 114:375–379.

Adcock DM, Fink L, Marlar RA: A laboratory approach to the evaluation of hereditary hypercoagulability, *Am J Clin Pathol* 108:434–449, 1997.

Asakura H, Ontachi Y, Mizutani T, et al.: Decreased plasma activity of antithrombin or protein C is not due to consumption coagulopathy in septic patients with disseminated intravascular coagulation, *Eur J Haematol* 67:170–175, 2001.

Aparicio C, Dahlbäck B, Molecular mechanisms of activated protein C resistance. Properties of factor V isolated from an individual with homozygosity for the Arg506 to Gln mutation in the factor V gene, Biochem J 313(Pt 2):467-472, 1996.

Bloemenkamp KW, Helmerhorst FM, Rosendaal FR, et al.: Thrombophilias and gynaecology, *Best Pract Res Clin Obstet Gynaecol* 17:509–528, 2003.

Bosler D, Mattson J, Crisnan D: Phenotypic heterogeneity in patients with homozygous prothrombin 20210AA genotype. A paper from the 2005 William Beaumont Hospital Symposium on molecular Pathology, *J Mol Diagn* 8:420–425, 2006.

Brouwer JL, Veeger NJ, van der Schaaf W, et al.: Difference in absolute risk of venous and arterial thrombosis between familial protein S deficiency type I and type III. Results from a family cohort study to assess the clinical impact of a laboratory test-based classification, *Br J Haematol* 128:703–710, 2005.

Castoldi E, Rosing J: APC resistance: biological basis and acquired influences, *J Thromb Haemost* 8:445–453, 2010.

Cerneca F, Ricci G, Simeone R, et al.: Coagulation and fibrinolysis changes in normal pregnancy. Increased levels of procoagulants and reduced levels of inhibitors during pregnancy induce a hypercoagulable state, combined with a reactive fibrinolysis, *Eur J Obstet Gynecol Reprod Biol* 73:31–36, 1997.

Chaturvedi S, Braunstein EM, Yuan X, et al.: Complement activity and complement regulatory gene mutations are associated with thrombosis in APS and CAPS, *Blood* 135:239–251, 2020.

Chowdary P: Inhibition of tissue factor pathway inhibitor (TFPI) as a treatment for Haemophilia: Rationale with Focus on Concizumab, *Drugs* 78:881–890, 2018.

Cohen H, Efthymiou M, Isenberg DA: Use of direct oral anticoagulants in antiphospholipid syndrome, *J Throm Haemost* 16:1028–1039, 2018.

Colucci M, Binetti BM, Tripodi A, et al.: Hyperprothrombinemia associated with prothrombin G20210A mutation inhibits plasma fibrinolysis through a TAFI-mediated mechanism, *Blood* 103:2157–2161, 2004.

Cox-Morton S, MacDonald S, Thomas W: A diagnostic solution for haemostasis laboratories for patients taking direct oral anticoagulants using DOAC-Remove, Br J Haematol [Epub ahead of print].

Crawley JT, Lane DA: The haemostatic role of tissue factor pathway inhibitor, *Arterioscler Thromb Vasc Biol* 28:233–242, 2008.

Cumming AM, Tait RC, Fildes S, et al.: Development of resistance to activated protein C during pregnancy, *Br J Haematol* 90:725–727, 1995.

Dahlback B: Activated protein C resistance and thrombosis: molecular mechanisms of hypercoagulable state due to FVR506Q mutation, *Semin Thromb Hemost* 25:273–289, 1999.

Dahm A, Van Hylckama Vlieg A, Bendz B, et al.: Low levels of tissue factor pathway inhibitor (TFPI) increase the risk of venous thrombosis, *Blood* 101:4387–4392, 2003.

de Laat B, Pengo V, Pabinger I, et al.: The association between circulating antibodies against domain I of beta2-glycoprotein I and thrombosis: an international multicenter study, *J Thromb Haemost* 7:1767–1773, 2009.

de Moerloose P, Boehlen F, Neerman-Arbez M: Fibrinogen and the risk of thrombosis, *Semin Thromb Hemost* 36:7–17, 2010.

D'Angelo A, Vigano-D'Angelo S, Esmon CT: Comp PC: acquired deficiencies of protein S. Protein S activity during oral anticoagulation, in liver disease, and in disseminated intravascular coagulation, *J Clin Invest* 81:1445, 1988.

De Stefano V, Casorelli I, Rossi E, et al.: Interaction between hyperhomocysteinemia and inherited thrombophilic factors in venous thromboembolism, *Semin Thromb Hemost* 26:305–311, 2000.

De Stefano V, Finazzi G, Mannucci PM: Inherited thrombophilia: pathogenesis, clinical syndromes, and management, *Blood* 87:3531–3544, 1996.

den Heijer M, Koster T, Blom HJ, et al.: Hyperhomocysteinemia as a risk factor for deep-vein thrombosis, *N Engl J Med* 334:759–762, 1996.

den Heijer M, Rosendaal FR, Blom HJ, et al.: Hyperhomocysteinemia and venous thrombosis: a meta-analysis, *Thromb Haemost* 80:874–877, 1998.

Downes K, Megy K, Duarte D, et al.: Diagnostic high-throughput sequencing of 2396 patients with bleeding, *Thrombotic, and Platelet Disorders* 134:2082–2091, 2019.

Egeberg O: Inherited antithrombin deficiency causing thrombophilia, *Thromb Diath Haemorrh* 13:516–530, 1965.

Esmon CT: The protein C pathway, *Chest* 124:26S–32S, 2003.

Esmon CT: Structure and functions of the endothelial cell protein C receptor, *Crit Care Med* 32:S298–S301, 2004.

Favaloro EJ, Wong RC: Antiphospholipid antibodies and the antiphospholipid syndrome II: Limitations, standardization, and clinical utility of laboratory testing, *Semin Thromb Hemost* 34:309–312, 2008.

Favaloro EJ, Wong RC: Current clinical and laboratory practice for the investigation of the antiphospholipid syndrome: findings from the 2008 Australasian antiphospholipid antibody survey, *Pathology* 41:666–675, 2009.

Favaloro EJ, Lippi G: Interference of direct oral anticoagulants in haemostasis assays: high potential for diagnostic false positives and false negatives, *Blood Transfus* 15:491–494, 2017.

Favresse J, Lardinois B, Sabor L, et al.: Evaluation of DOAC-Stop® procedure to overcome the effect of DOACs on several thrombophilia screening tests, *TH Open* 2:e202–e209, 2018.

Foy P, Moll S, Thrombophilia: 2009 update, *Curr Treat Options Cardiovasc Med* 11:114–128, 2009.

Franco RF, Morelli V, Lourenco D, et al.: A second mutation in the methylenetetrahydrofolate reductase gene and the risk of venous thrombotic disease, *Br J Haematol* 105:556–559, 1999.

George LA, Sulivan SK, Giermasz A, et al.: Hemophilia B gene therapy with a high-specific-activity factor IX variant, *N Engl J Med* 377:2215–2227, 2017.

Giannakopoulos B, Passam F, Rahgozar S, et al.: Current concepts on the pathogenesis of the antiphospholipid syndrome, *Blood* 109:422–430, 2007.

Goldenberg NA: Manco-johnson MJ: protein C deficiency, *Haemophilia* 14:1214–1221, 2008.

Goodwin AJ, Rosendaal FR, Kottke-Marchant K, et al.: A review of the technical, diagnostic, and epidemiologic considerations for protein S assays, *Arch Pathol Lab Med* 126:1349–1366, 2002.

Graf LL, Welsh CH, Qamar Z, et al.: Activated protein C resistance assay detects thrombotic risk factors other than factor V Leiden, *Am J Clin Pathol* 119:52–60, 2003.

Gruenewald M, Germowitz A, Beneke H, et al.: Coagulation factor II activity determination is not useful as a screening tool for the G20210A prothrombin gene allele, *Thromb Haemost* 84:141–142, 2000.

Hackeng TM, van't Veer C, Meijers JC, et al.: Human protein S inhibits prothrombinase complex activity on endothelial cells and platelets via direct interactions with factors Va and Xa, *J Biol Chem* 269:21051–21058, 1994.

Harris EN, Gharavi AE, Boey ML, et al.: Anticardiolipin antibodies: detection by radioimmunoassay and association with thrombosis in systemic lupus erythematosus, *Lancet* 2:1211–1214, 1983.

Harris GM, Stendt CL, Vollenhoven BJ, et al.: Decreased plasma tissue factor pathway inhibitor in women taking combined oral contraceptives, *Am J Hematol* 60:175–180, 1999.

Haverkate F, Samama M: Familial dysfibrinogenemia and thrombophilia. Report on a study of the SSC Subcommittee on Fibrinogen, *Thromb Haemost* 73:151–161, 1995.

Heijmans BT, Westendorp RG, Knook DL, et al.: The risk of mortality and the factor V Leiden mutation in a population-based cohort, *Thromb Haemost* 80:607–609, 1998.

Huang ZF, Higuchi D, Lasky N, et al.: Tissue factor pathway inhibitor gene disruption produces intrauterine lethality in mice, *Blood* 90:944–951, 1997.

Kamada Y, Yamakage M, Niiya T, et al.: Celite-activated viscometer Sonoclot can measure the suppressive effect of tranexamic acid on hyperfibrinolysis in cardiac surgery, *J Anesth* 15:17–21, 2001.

Kannel WB, Wolf PA, Castelli WP, et al.: Fibrinogen and risk of cardiovascular disease. The Framingham Study, *J Am Med Assoc* 258:1183–1186, 1987.

Kuhle S, Lane DA, Jochmanns K, et al.: Homozygous antithrombin deficiency type II (99 Leu to Phe mutation) and childhood thromboembolism, *Thromb Haemost* 86:1007–1011, 2001.

Kuiper G, Kleinegris MF, van Oerle R, et al.: Validation of a modified thromboelastometry approach to detect changes in fibrinolytic activity, *Throm J* 14:1–13, 2016.

Kupesiz A, Rajpurkar M, Warrier I, et al.: Tissue plasminogen activator induced fibrinolysis: standardization of method using thromboelastography, *Blood Coagul Fibrinolysis* 21:320–324, 2010.

Kyrle PA, Minar E, Hirschl M, et al.: High plasma levels of factor VIII and the risk of recurrent venous thromboembolism, *N Engl J Med* 343:457–462, 2000.

Lane DA, Bayston T, Olds RJ, Antithrombin mutation database: 2nd (1997) update, et al.: For the plasma coagulation inhibitors subcommittee of the Scientific and standardization Committee of the international Society on thrombosis and haemostasis, *Thromb Haemost* 77:197–211, 1997.

Lane DA, Mannucci PM, Bauer KA, et al.: Inherited thrombophilia: Part 1, *Thromb Haemost* 76:651–662, 1996.

Ledford-Kraemer MR: Laboratory testing for lupus anticoagulants: Pre-examination variables, mixing studies, and diagnostic criteria, *Semin Thromb Hemost* 34:380–388, 2008.

Legnani C, Palareti G, Grauso F, et al.: Hyperhomocyst(e)inemia and a common methylenetetrahydrofolate reductase mutation (Ala223Val MTHFR) in patients with inherited thrombophilic coagulation defects, *Arterioscler Thromb Vasc Biol* 17:2924–2929, 1997.

Libourel EJ, Bank I, Veeger NJ, et al.: Protein S type III deficiency is no risk factor for venous and arterial thromboembolism in 168 thrombophilic families: a retrospective study, *Blood Coagul Fibrinolysis* 16:135–140, 2005.

Liu Y, Myrvang HK, Dekker LV: Annexin A2 complexes with S100 proteins: structure, function, and pharmacological manipulation, *Br J Pharmacol* 172:1664–1676, 2015.

Lockshin MD, Kim M, Laskin CA: Prediction of adverse pregnancy outcome by the presence of lupus anticoagulant, but not anticardiolipin antibody, in patients with antiphospholipid antibodies, *Arthritis Rheum* 64:2311–2318, 2012.

Mackie IJ, Piegsa K, Furs SA, et al.: Protein S levels are lower in women receiving desogestrel-containing combined oral contraceptives (COCs) than in women receiving levonorgestrel-containing COCs at steady state and on cross-over, *Br J Haematol* 113:898–904, 2001.

Madden RM, Levin EG, Marlar RA: Thrombin and the thrombin-thrombomodulin complex interaction with plasminogen activator inhibitor type-1, *Blood Coagul Fibrinolysis* 2:471–476, 1991.

Margaglione M, D'Andrea G, d'Addedda M, et al.: The methylenetetrahydrofolate reductase TT677 genotype is associated with venous thrombosis independently of the coexistence of the FV Leiden and the prothrombin A20210 mutation, *Thromb Haemost* 79:907–911, 1998.

Marlar RA, Adcock DM, Madden RM: Hereditary dysfunctional protein C molecules (type II): assay characterization and proposed classification, *Thromb Haemost* 63:375–379, 1990.

Marlar RA, Mastovich S: Hereditary protein C deficiency: a review of the genetics, clinical presentation, diagnosis and treatment, *Blood Coagul Fibrinolysis* 1:319–330, 1990.

Maroney SA, Cooley BC, Sood R, et al.: Combined tissue factor pathway inhibitor and thrombomodulin deficiency produces an augmented hypercoagulable state with tissue-specific fibrin deposition, *J Thromb Haemost* 6:111–117, 2008.

Maroney SA, Ellery PE, Wood JP, et al.: Comparison of the inhibitory activities of human tissue factor pathway inhibitor (TFPI)alpha and TFPIbeta, *J Thromb Haemost* 11:911–918, 2013.

Meijers JC, Tekelenburg WL, Bouma BN, et al.: High levels of coagulation factor XI as a risk factor for venous thrombosis, *N Engl J Med* 342:696–701, 2000.

Meltzer ME, Doggen CJ, de Groot PG, et al.: The impact of the fibrinolytic system on the risk of venous and arterial thrombosis, *Semin Thromb Hemost* 35:468–477, 2009.

Meltzer ME, Lisman T, de Groot PG, et al.: Venous thrombosis risk associated with plasma hypofibrinolysis is explained by elevated plasma levels of TAFI and PAI-1, *Blood* 116:113–121, 2010.

Miyakis S, Lockshin MD, Atsumi T, et al.: International consensus statement on an update of the classification criteria for definite antiphospholipid syndrome (APS), *J Thromb Haemost* 4:295–306, 2006.

Moll S: Warfarin-induced skin necrosis, *Br J Haematol* 126:628, 2004.

Morange PE, Simon C, Alessi MC, et al.: Endothelial cell markers and the risk of coronary heart disease: the Prospective Epidemiological Study of Myocardial Infarction (PRIME) study, *Circulation* 109:1343–1348, 2004.

Mudd SH, Skovby F, Levy HL, et al.: The natural history of homocysteinuria due to cystathionine beta-synthase deficiency, *Am J Hum Genet* 37:1–31, 1985.

Müller-Calleja N, Hollerbach A, Ritter S, et al.: Tissue factor pathway inhibitor primes monocytes for antiphospholipid antibody-induced thrombosis, *Blood* 134:1119–1131, 2019.

Nelson RM, Long GL: Binding of protein S to C4b-binding protein. Mutagenesis of protein S, *J Biol Chem* 267:8140–8145, 1992.

Nagler M, Kremer Hovinga JA, Alberio L, et al.: Thromboembolism in patients with congenital afibrinogenemia. Long-term observational data and systematic review, *Thromb Haemost* 116:722–732, 2016.

Patnaik MM: Moll S: inherited antithrombin deficiency: a review, *Haemophilia* 14:1229–1239, 2008.

Pengo V, Banzato A, Bison E, et al.: Antiphospholipid syndrome: critical analysis of the diagnostic path, *Lupus* 19:428–431, 2010a.

Pengo V, Ruffatti A, Iliceto S: The diagnosis of the antiphospholipid syndrome, *Pathophysiol Haemost Thromb* 35:175–180, 2006.

Pengo V, Ruffatti A, Legnani C, et al.: Clinical course of high-risk patients diagnosed with antiphospholipid syndrome, *J Thromb Haemost* 8:237–242, 2010b.

Pengo V, Ruffatti A, Legnani C, et al.: Incidence of first thromboembolic event in asymptomatic carriers of high-risk antiphospholipid antibody profile: a multicenter prospective study, *Blood* 118:4714–4718, 2011.

Persson KE, Dahlback B, Hillarp A: Diagnosing protein S deficiency: Analytical considerations, *Clin Lab* 49:103–110, 2003.

Preda L, Tripodi A, Valsecchi C, et al.: A prothrombin time-based functional assay of protein S, *Thromb Res* 60:19–32, 1990.

Prengler M, Sturt N, Krywawych S, et al.: Homozygous thermolabile variant of the methylenetetrahydrofolate reductase gene: a potential risk factor for hyperhomocysteinaemia, CVD, and stroke in childhood, *Dev Med Child Neurol* 43:220–225, 2001.

Rand JH, Wu XX, Wolgast LR, et al.: A novel 2-stage approach that detects complement activation in patients with antiphospholipid antibody syndrome, *Thromb Res* 156:119–125, 2017.

Ray JG: Meta-analysis of hyperhomocysteinemia as a risk factor for venous thromboembolic disease, *Arch Intern Med* 158:2101–2106, 1998.

Rezende SM, Simmonds RE, Lane DA: Coagulation, inflammation, and apoptosis: different roles for protein S and the protein S-C4b binding protein complex, *Blood* 103:1192–1201, 2004.

Ridker PM, Hennekens CH, Selhub J, et al.: Interrelation of hyperhomocyst(e)inemia, factor V Leiden, and risk of future venous thromboembolism, *Circulation* 95:1777–1782, 1997.

Ridker PM, Miletich JP, Stampfer MJ, et al.: Factor V Leiden and risks of recurrent idiopathic venous thromboembolism, *Circulation* 92:2800–2802, 1995.

Rigby AC, Grant MA: Protein S: a conduit between anticoagulation and inflammation, *Crit Care Med* 32:S336–S341, 2004.

Rosendaal FR: Venous thrombosis: a multicausal disease, *Lancet* 353:1167–1173, 1999.

Salooja N, Perry DJ: *Thrombelastography*, *Blood Coagul Fibrinolysis* 12:327–337, 2001.

Sartori MT, Saggiorato G, Spiezia L, et al.: Influence of the Alu-repeat I/D polymorphism in t-PA gene intron 8 on the stimulated t-PA release after venous occlusion, *Clin Appl Thromb Hemost* 9:63–69, 2003.

Simioni P, Tormene D, Tognin G, et al.: X-linked thrombophilia with a mutant factor IX (factor IX Padua), *N Engl J Med* 361:1671–1675, 2009.

Simmonds RE, Ireland H, Lane DA, et al.: Clarification of the risk for venous thrombosis associated with hereditary protein S deficiency by investigation of a large kindred with a characterized gene defect, *Ann Intern Med* 128:8–14, 1998.

Simone B, De Stefano V, Leoncini E, al at: Risk of venous thromboembolism associated with single and combined effects of Factor V Leiden, Prothrombin 20210A and Methylenetethraydrofolate reductase C677T: a meta-analysis involving over 11,000 cases and 21,000 controls, *Eur J Epidemiol* 28:621–647, 2013.

Sinha RK, Flynn R, Zaiken M, et al.: Activated protein C ameliorates chronic graft-versus-host disease by PAR1-dependent biased cell signaling on T cells, *Blood* 134:776–781, 2019.

Smithies MN, Weaver CB: Role of the tissue factor pathway in the pathogenesis and management of multiple organ failure, *Blood Coagul Fibrinolysis* 15:S11–S20, 2004.

Stassen JM, Arnout J, Deckmyn H: The hemostatic system, *Curr Med Chem* 11:2245–2260, 2004.

Stearns-Kurosawa DJ, Kurosawa S, Mollica JS, et al.: The endothelial cell protein C receptor augments protein C activation by the thrombin-thrombomodulin complex, *Proc Natl Acad Sci U S A* 93:10212–10216, 1996.

Streif W, Mitchell LG, Andrew M: Antithrombotic therapy in children, *Curr Opin Pediatr* 11:56–64, 1999.

Taatjes DJ, Bouffard N, von Turkovich M, et al: Visualization of macro-immune complexes in the antiophospholipid syndrome by multi-modal microscopy imaging, Micron 100:23–29.

Tai CY, Ierardi R, Alexander JB: A case of warfarin skin necrosis despite enoxaparin anticoagulation in a patient with protein S deficiency, *Ann Vasc Surg* 18:237–242, 2004.

Tosetto A, Missiaglia E, Frezzato M, et al.: The VITA project: C677T mutation in the methylene-tetrahydrofolate reductase gene and risk of venous thromboembolism, *Br J Haematol* 97:804–806, 1997.

Tripodi A, Mannucci PM: The coagulopathy of chronic liver disease, *N Engl J Med* 364:147–156, 2011.

Ueki H, Mizushina T, Laoharatchatathanin T, et al.: Loss of maternal annexin A5 increases the likelihood of placental platelet thrombosis and foetal loss, *Sci Rep* 2:827, 2012.

Van de Wouwer M, Collen D, Conway EM: Thrombomodulin-protein C-EPCR system: Integrated to regulate coagulation and inflammation, *Arterioscler Thromb Vasc Biol* 24:1374–1383, 2004.

van Wijnen M, Stam JG, van't Veer C, et al.: The interaction of protein S with the phospholipid surface is essential for the activated protein C-independent activity of protein S, *Thromb Haemost* 76:397–403, 1996.

Vig S, Chitolie A, Bevan DH, et al.: Thromboelastography: a reliable test? *Blood Coagul Fibrinolysis* 12:555–561, 2001.

Vormittag R, Simanek R, Ay C, et al.: High factor VIII levels independently predict venous thromboembolism in cancer patients: the cancer and thrombosis study, *Arterioscler Thromb Vasc Biol* 29:2176–2181, 2009.

Wolf M, Boyer-Neumann C, Martinoli JL, et al.: A new functional assay for human protein S activity using activated factor V as substrate, *Thromb Haemost* 62:1144–1145, 1989.

Yin D, de Laat B, Devreese KMJ, Kelchtermans H: The clinical value of assays detecting antibodies against domain I of β2-glycoprotein I in the antiphospholipid syndrome, *Autoimmun Rev* 17:1210–1218, 2018.

CHAPTER 43

ANTITHROMBOTIC THERAPY

Grace Ming Lee, Thomas L. Ortel

VITAMIN K ANTAGONISTS, 879
Brodifacoum and Long-Acting Anticoagulant Rodenticides, 882
ANTITHROMBIN-DEPENDENT PARENTERAL ANTICOAGULANTS, 882
Unfractionated Heparin, 882
Low-Molecular-Weight Heparin, 883
Fondaparinux, 883
Heparin-Induced Thrombocytopenia, 883
TARGET-SPECIFIC ANTICOAGULANTS, 885
Parenteral Agents, 885
Oral Agents, 885
Reversal Agents for Oral Target-Specific Anticoagulants, 887
ANTIPLATELET THERAPY, 888
Aspirin, 888
P2Y12 Inhibitors, 889
Glycoprotein IIb/IIIa Inhibitors, 890
SELECTED REFERENCES, 891

KEY POINTS

- Warfarin has historically been the most commonly used oral anticoagulant. It is a vitamin K antagonist and blocks γ-carboxylation of a series of glutamic acid residues during the synthesis of factors II, VII, IX, and X, and proteins C and S. The resulting decreased functionality of the coagulation factors leads to prolongation of prothrombin time (PT), which is monitored as the international normalized ratio, and partial thromboplastin time.
- Heparin binds to antithrombin and increases its ability to inhibit thrombin, factor Xa, and, to a lesser extent, other serine protease coagulation factors. Thus, heparin is considered to be an "indirect" thrombin inhibitor. The anticoagulant effect of heparin is commonly monitored by prolongation of partial thromboplastin time, with actual quantitation of heparin anticoagulant activity being assayed as anti–factor Xa activity. Where necessary to monitor low-molecular-weight heparin or fondaparinux, this is done by measuring its anti–factor Xa activity.
- Heparin-induced thrombocytopenia (HIT) is a complication of heparin therapy in which antibodies develop against complexes of heparin and platelet factor 4 (PF4). The antibody/PF4/heparin complexes bind to platelets through the Fcγ receptor and cause platelet activation, leading to arterial and/or venous thrombosis. Both immunologic and functional assays are employed in the evaluation of possible HIT.
- Target-specific oral anticoagulants directly inhibit either thrombin or factor Xa. These anticoagulant agents do not typically need to be monitored, but they have variable effects on the PT and activated partial thromboplastin time (APTT). The oral thrombin inhibitor dabigatran etexilate can be assayed by a dilute thrombin time or an ecarin clot time, and the factor Xa inhibitors rivaroxaban, apixaban, and edoxaban can be assayed by anti–factor Xa assays.
- Antiplatelet therapy is used primarily for the prevention of recurrent stroke or myocardial infarction. The laboratory can monitor the resulting reactivity of platelets from treated patients and, in some instances, can detect apparent resistance to aspirin or other therapeutic agents.

Antithrombotic therapy, which includes therapies targeting platelets as well as the coagulation system, is used to prevent and treat thromboembolic disease. Antiplatelet agents are most frequently used to prevent stroke and myocardial infarction, but they are also used in patients with peripheral arterial disease and may have a modest benefit in preventing recurrent venous thromboembolism (VTE). Anticoagulant agents are most frequently used to prevent and treat VTE, to prevent stroke and peripheral arterial embolism in patients with atrial fibrillation, and to prevent thromboembolic complications in patients with prosthetic heart valves. The clinical laboratory plays a critical role in the evaluation and management of patients on these therapies.

VITAMIN K ANTAGONISTS

Warfarin is the most commonly prescribed of the oral vitamin K antagonists. It is a racemic mixture of the stereoisomers S-warfarin and R-warfarin, with S-warfarin being the more potent in producing an anticoagulant effect. Warfarin inhibits vitamin K reductase (vitamin K 2,3-epoxide reductase [VKOR]) and blocks regeneration of the active form of vitamin K, which is necessary for γ-carboxylation of specific glutamate residues within the amino-terminal Gla domains of factors II, VII, IX, and X and proteins C and S (Fig. 43.1). With the decreasing extent of γ-carboxylation of glutamic acid within these domains, the affected proteins are unable to bind into the highly ordered protein/Ca^{++}/phospholipid membrane complexes that are essential for normal hemostatic activity (Ageno et al., 2012). Consequently, those laboratory tests that are dependent on the proper function of these factors become more abnormal with increasing antagonism of vitamin K.

The degree of anticoagulation with warfarin is typically assessed by measuring prothrombin time (PT), although activated partial thromboplastin time (APTT) is also typically prolonged. Thrombin time (TT) is unaffected by warfarin therapy, because fibrinogen synthesis is not vitamin K dependent. Prolongation of PT is determined by decreases in the activity of three of the vitamin K–dependent coagulation factors—specifically, factors VII, X, and II. Initial prolongation of PT will primarily be due to the effect on factor VII, which has the shortest half-life (4–6 hours). Therapeutic efficacy depends on decreased levels of factors X and II, however, which have longer half-lives (24–48 hours and 48–72 hours, respectively). The different half-lives of the vitamin K–dependent factors is why 4 to 6 days of therapy with warfarin is generally recommended before assuming that laboratory monitoring actually reflects a steady-state level of anticoagulation. For clinical situations that require a more rapid onset of effective anticoagulation (e.g., treatment of acute VTE), heparin or low-molecular-weight heparin (LMWH) is administered concomitantly with warfarin until steady-state efficacy of the warfarin is confirmed by laboratory testing. Because warfarin also interferes with the γ-carboxylation of proteins C and S, which are part of the natural anticoagulant system, there are certain clinical settings where initiation of warfarin can be associated with a paradoxical prothrombotic state, such as in patients with protein C deficiency (McGehee et al., 1984), protein S deficiency (Berkompas, 1991), or acute heparin-induced thrombocytopenia (HIT) (Warkentin et al., 1997).

PT is performed by adding a source of phospholipid and tissue factor (referred to as *thromboplastin*), and calcium, to citrated plasma. The time to clot formation is then measured by mechanical or optical methods. Individual thromboplastin reagents can vary substantially in their sensitivity to the decreased levels of the vitamin K–dependent factors, however. This variable sensitivity is also affected by the instrument system used to measure PT (D'Angelo et al., 1989). To correct for these differences, the international normalized ratio (INR) was developed in order to improve standardization of PT reporting worldwide (Kirkwood, 1983). To calculate an INR, the logarithms of PT results obtained on normal individuals and patients on warfarin using a primary international reference thromboplastin are plotted against the logarithms of PT results obtained using the testing laboratory's thromboplastin reagent (Fig. 43.2). The resulting slope of this plot is the international sensitivity index (ISI) for that particular thromboplastin reagent and instrumentation combination (Kitchen & Preston, 1999; Adcock & Johnston, 2002; Poller, 2004; Van den Besselaar et al., 2004; Favaloro & Adcock, 2008). The PT ratio is determined by dividing the patient PT result by the geometric mean normal PT for the local laboratory (determined by using a population of normal individuals with the same reagent/instrumentation). This PT ratio is then raised to the power of the ISI to determine the INR according to the following equation:

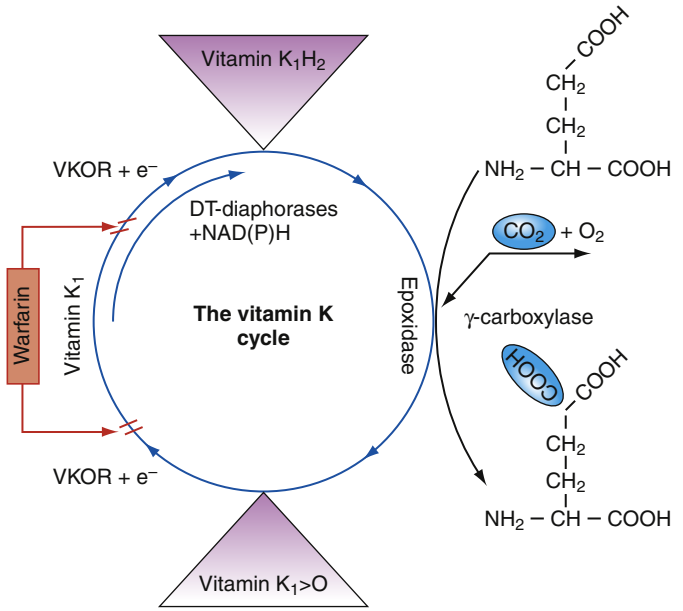

Figure 43.1 The vitamin K–dependent γ-carboxylation system. The γ-carboxylase converts vitamin K–dependent proteins to γ-carboxyglutamic acid (Gla) containing proteins by adding carbon dioxide (CO_2) to glutamic acid (Glu) residues in newly synthesized proteins. The γ-carboxylase requires reduced vitamin K_1 (vitamin K_1H_2) as a cofactor for this posttranslational modification reaction. Concomitant with γ-carboxylation, vitamin K_1H_2 is converted to vitamin K_1 2,3-epoxide (vitamin K_1>O). The epoxide is reduced by the warfarin-sensitive enzyme vitamin K_1 2,3-epoxide reductase (VKOR) to the vitamin K_1H_2 cofactor. This cyclic interconversion of vitamin K metabolites constitutes the vitamin K cycle. At high tissue concentrations, vitamin K_1 quinone (vitamin K_1) can be reduced to vitamin K_1H_2 by the alternative pathway of the cycle. This pathway is catalyzed by NAD(P)H dehydrogenases (DT-diaphorases), which are not inhibited by warfarin. (From Wallin R, Hutson SM: Warfarin and the vitamin K-dependent gamma-carboxylation system, *Trends Mol Med* 10:299–302, 2004.)

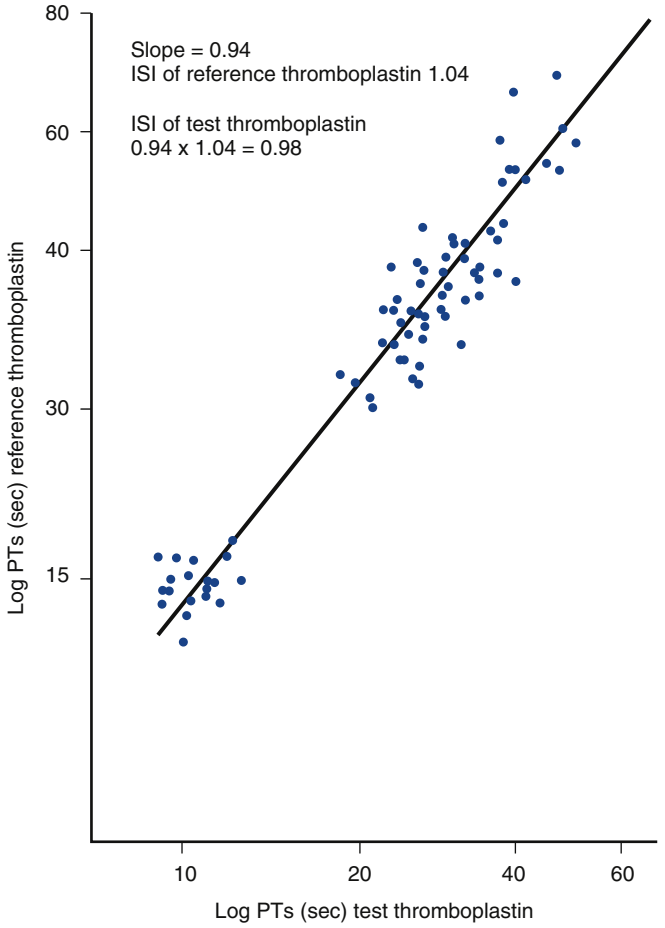

Figure 43.2 An example of a thromboplastin calibration using the World Health Organization (WHO) international sensitivity index (ISI) model. Prothrombin times were performed on a series of normal subjects and patients on stable warfarin anticoagulation with a reference thromboplastin (*y*-axis) and a test thromboplastin (*x*-axis) under calibration. (From Kitchen S, Preston FE: Standardization of prothrombin time for laboratory control of oral anticoagulant therapy, *Semin Thromb Hemost* 25:17–25, 1999.)

$$\text{INR} = (\text{patient PT in seconds} / \text{mean normal PT in seconds})^{\text{ISI}}.$$

The INR seeks to represent the PT ratio that would be obtained if the international reference thromboplastin had actually been used to test the patient. Although the concept of generating the INR sounds straightforward, actually obtaining an accurate INR result can be difficult in practice (Cunningham et al., 1994; Favaloro et al., 2010).

Because of the importance of accurate monitoring of anticoagulant therapy with the vitamin K antagonists, several additional points regarding the ISI and the INR need to be taken into consideration. First, the ISI must be correctly specified not only for each type of PT reagent but also for each new *lot* of thromboplastin in addition to specifying the coagulation instrument model being used in a given laboratory. Second, in plasma samples from patients being treated with warfarin and a second anticoagulant (e.g., heparin in the acute management of VTE), the prolonged PT will reflect the combined effect of both anticoagulant agents. Heparin can either be removed or neutralized to more specifically assess the anticoagulant contribution of the warfarin alone, as described later. An analogous strategy does not exist for the removal or neutralization of the parenteral direct thrombin inhibitors argatroban and bivalirudin, which are used in the treatment of patients with HIT (see later discussion). Transitioning the patient to warfarin can be difficult because of the effect that the parenteral direct thrombin inhibitors have on PT and the INR (Hursting et al., 1999; Kelton et al., 2013). Third, although most lupus anticoagulants exert a more pronounced effect on APTT than on PT, the presence of a lupus anticoagulant in some patients may render the PT inaccurate as a means of monitoring warfarin therapy. This may depend on the reagents used (Moll & Ortel, 1997). In such instances, a direct chromogenic assay for factor X (rather than a clotting assay) may aid in monitoring of anticoagulant intensity (Rosborough & Shepherd, 2004). Finally, thromboplastins are prepared from a variety of sources, spanning recombinant human tissue factor and nonhuman-derived materials. In some cases, thromboplastin originating from a nonhuman source may contribute to an abnormally prolonged PT (and, thus, an increased INR) that would not have been obtained had a human thromboplastin been used instead. This phenomenon has been reported in patients with factor VII Padua, who have a nonpathogenic polymorphism in their factor VII molecule that supports normal hemostatic interactions with human tissue factor but diminished interaction with tissue factor of various animal origins, notably rabbit (Pollak et al., 2006; Kirkel et al., 2010).

The plasma half-life of warfarin is 20 to 60 hours, with a mean of 40 hours. The maximum effect of a dose lasts for up to 48 hours after administration. S-warfarin is metabolized by CYP2C9, and R-warfarin is metabolized by the CYP1A2 and CYP3A4 enzymes. Genetic polymorphisms in CYP2C9 lead to an alteration in the pharmacokinetics of warfarin (Aithal et al., 1999; Taube et al., 2000). In addition, mutations in genes encoding for VKORC1, which generates the reduced form of vitamin K necessary for γ-carboxylation, have been identified to lead to variable sensitivity to inhibition by warfarin, affecting pharmacokinetics and dosing (Rieder et al., 2005). Specific allelic combinations of CYP2C9 and VKORC1 are associated with a wide range of warfarin sensitivities (Table 43.1). Allelic frequencies and their relationships to race and therapeutic warfarin dose are shown in Table 43.2. Although observational studies suggested potential benefits from genotype-guided dosing of vitamin K antagonists (Epstein et al., 2010; Anderson et al., 2012), three large prospective randomized clinical trials demonstrated that pharmacogenetic-based dosing resulted in either no (Kimmel et al., 2013; Verhoef et al., 2013) or minimal (Pirmohamed et al., 2013) improvement in the time that the INR was in the therapeutic range for the first 4 to 12 weeks of therapy. Whether CYP2C9 or VKORC1 genotype data will be beneficial in other aspects of warfarin management needs to be determined.

True genetic resistance to warfarin therapy, characterized by exceptionally high doses of warfarin (e.g., >100 mg/day) to achieve a target therapeutic range, is uncommon (O'Reilly et al., 1964). In instances in which inappropriate responses to warfarin are marked and persistent, the metabolites can be measured using high-performance liquid chromatography (Lombardi et al., 2003). These measurements can also be used to confirm medication compliance. More commonly, drugs that affect S-warfarin metabolism may markedly alter the potency of warfarin treatment (Box 43.1). Some drugs or herbal medications induce CYP2C9 and

TABLE 43.1

Phenotype Characteristics of Warfarin Metabolism Genotype Combinations*

Warfarin Sensitivity	GENOTYPE COMBINATION VKORC1	CYP2C9	Prevalence N (%)	Clinical Considerations
Very high	A/A	*1/*3, *2/*2, *2/*3, *3/*3	23 (2.6%)	May need a lower dose and more frequent INR monitoring
	G/A	*3/*3		
High	A/A	*1/*2	36 (4.0%)	Lower dose and frequent INR monitoring
	G/A	*2/*3		
	G/G	*3/*3		
Moderate	A/A	*1/*1	238 (26.6%)	Lower dose and frequent INR monitoring
	G/A	*1/*2, *1/*3, *2/*2		
	G/G	*2/*3		
Mild	G/G	*1/*2, *1/*3, *2/*2	109 (12.2%)	Frequent INR monitoring
Normal	G/A	*1/*1	262 (29.2%)	Standard INR monitoring
Less than normal	G/G	*1/*1	228 (25.4%)	May require higher dose to maintain optimal INR

INR, International normalized ratio.
*Genotype is defined by the combination of measured allelic variations in CYP2C9 and VKORC1. Phenotype is the expected warfarin sensitivity based on the genotype.
From Epstein RS, Moyer TP, et al.: Warfarin genotyping reduces hospitalization rates results from the MM-WES (Medco-Mayo Warfarin Effectiveness study), *J Am Coll Cardiol 55*(25):2804–2812, 2010.

TABLE 43.2

Allele Frequencies in Derivation Cohort (N = 1015) and Relationship to Race and Therapeutic Warfarin Dose*

SNP Alleles	Gene Location	White (N = 838)	African American (N = 153)	Other or Mixed Race (N = 24)	Univariate Association with Dose in Total Population, Per Allele (95% CI)
CYP2C9*2 (C > T)	3608C > T	13.1%	5.2%	10.4%	–17% (–22% to –12%)
CYP2C9*3 (A > C)	42614A > C	6.0%	1.0%	4.2%	–30% (–36% to –24%)
CYP2C9*5 (C > G)	42619C > G	0%	1.3%	2.1%	NS
VKORC1 861 C > A	–4451C > A	36.0%	8.8%	26.1%	14% (9% to 18%)
VKORC1 3673 G > A	–1639G > A	36.6%	9.5%	41.7%	–29% (–31% to 26%)
VKORC1 5808 T > G	IVS1 + 324T > G	25.1%	4.6%	8.3%	25% (29% to 22%)
VKORC1 6853 G > C	IVS2 + 124G > C	37.2%	24.3%	41.7%	–37% (–42% to –32%)
VKORC1 9041 G > A	626 G > A	39.4%	51.3%	41.7%	18% (14% to 23%)
F2 Thr165Met	494 C > T	13.3%	1.3%	30.0%	–5.8% (–11.4% to 0.0%)

CI, Confidence interval; *NS,* not significant; *SNP,* single-nucleotide polymorphism.
*Frequency values are reported for the variant allele at each SNP. CYP2C9 gene locations are taken from http://www.cypalleles.ki.se/cyp2c9.htm.
From Gage BF, Eby C, et al: Use of pharmacogenetic and clinical factors to predict the therapeutic dose of warfarin, *Clin Pharmacol Ther 84*(3):326–331, 2008.

BOX 43.1

Drug and Supplement Interactions with Warfarin

Increased clearance of warfarin (decreased INR)

Barbiturates
Rifampin
Hyperforin (present in St. John's wort)

Decreased clearance of warfarin (increased INR)

Amiodarone
Fluconazole
Miconazole
Phenylbutazone
Sulfamethoxazole

INR, International normalized ratio.

cause warfarin to be metabolized faster, necessitating an increased dose to achieve the same anticoagulant effect. Other drugs interfere with the metabolism of warfarin and, thus, enhance the anticoagulant effect. In fact, several hundred compounds are known to alter the metabolism of warfarin (Ansell et al., 2008). Antibiotics may interfere with the metabolism of warfarin or they may suppress the gut flora, which supplies a significant amount of vitamin K in humans. Rifampin, for example, may dramatically increase the metabolism of warfarin, thereby necessitating very high doses of warfarin to achieve anticoagulation (Krajewski, 2010). Foods, particularly green leafy vegetables rich in vitamin K, may make anticoagulation with warfarin more difficult. Different warfarin products may vary in potency so that switching to, or between, different generic formulations may require more frequent monitoring and dosage adjustments (Bongiorno & Nutescu, 2004).

Warfarin is considered an agent with a narrow therapeutic index; a target INR has been established for most clinical indications in which it is used. For patients with atrial fibrillation and for the prevention and treatment of VTE, a target INR of 2.5 (range, 2–3) is recommended (Kearon et al., 2012; You et al., 2012). For patients with mechanical aortic valves (bileaflet and newer-generation tilting disk), the recommended target INR is also 2.5 (range, 2–3). The recommended target INR for patients with mechanical mitral valves and patients with older mechanical aortic valves (e.g., the caged-ball valve) is higher, at 3.0 (range, 2.5–3.5) (Whitlock et al., 2012). The INR is regularly monitored to keep patients on warfarin therapy within the target range to prevent thrombotic complications but minimize the risk for potential hemorrhagic complications. The most important factor influencing the risk of bleeding is the intensity of anticoagulant therapy, represented by the target INR (Ageno et al., 2012). Other variables include a prior history of bleeding, advanced age, serious comorbid conditions such as renal insufficiency or liver disease, and the use of concomitant therapies, particularly antiplatelet agents (Ageno et al., 2012).

Efforts to improve the control of warfarin therapy have led to several advances, including the formation of anticoagulation clinics dedicated to the management of warfarin therapy and the development of point-of-care monitors that use capillary blood obtained by a fingerstick to provide immediate feedback with the INR result. These monitors measure a thromboplastin-mediated clotting time using a capillary whole-blood

or nonanticoagulated venous whole-blood sample, converting the result to a PT and/or an INR (Leaning & Ansell, 1996). Results obtained with different point-of-care PT instruments and laboratory-based instruments may not be comparable (Nutescu, 2004). Indeed, even the patient specimen itself will vary, as the point-of-care monitor will use whole blood as opposed to the clinical laboratory, which will routinely use a citrated plasma sample. Quality assurance and quality control plans should be in place to oversee point-of-care INR testing (Van Cott, 2009). In general, markedly out-of-range INR measurements obtained with a point-of-care monitor should be confirmed by analyzing a sample of citrated plasma in the clinical laboratory (Sunderji et al., 2005).

BRODIFACOUM AND LONG-ACTING ANTICOAGULANT RODENTICIDES

Brodifacoum is a long-acting vitamin K antagonist, with a prolonged terminal half-life of 16 to 36 days (Arepally & Ortel, 2019). Brodifacoum belongs to a class of long-acting anticoagulant rodenticides (LAARs) that were originally developed in the 1970s to overcome warfarin resistance in rodent populations (King & Tran, 2015). Poisoning by LAARs has historically occurred after accidental/intentional ingestion or after occupational exposure (King & Tran, 2015). In 2018, a multistate outbreak of LAAR poisoning was reported in >300 patients due to brodifacoum-tainted synthetic cannabinoids (Kelkar et al., 2018). Clinically, affected patients present with a bleeding diathesis, most commonly with gross hematuria, oral mucosal bleeding, epistaxis, and gastrointestinal bleeding, although deaths have been reported (Arepally & Ortel, 2019). On laboratory testing, patients have a prolonged INR (mean INR = 15) and select deficiency of vitamin K–dependent proteins (factors X, VII, IX, and II). Patients can undergo confirmatory anticoagulant testing, usually by quantifying LAAR levels using high-performance liquid chromatography, where brodifacoum and/or additional vitamin K antagonists will be detected (examples include difenacoum, bromadiolone, warfarin, and chlorophacinone). Initial management of brodifacoum and LAAR toxicity is focused on controlling bleeding and correcting the coagulopathy. All patients should receive oral vitamin K_1. If the patient is actively bleeding and rapid correction of INR is required, intravenous vitamin K_1 should be administered as well. For patients with major bleeding, 4-factor prothrombin complex concentrate or fresh frozen plasma should be considered as first-line therapy. There is no consensus on vitamin K_1 dosing; however, patients should receive at least twice-daily dosing titrated to clinical signs of bleeding and laboratory test results (King & Tran, 2015). Once bleeding has resolved and the PT/INR have significantly shortened, the patient can be transitioned to oral vitamin K_1 (Schulman & Furie, 2015). Because brodifacoum is fat soluble and has a high volume of distribution, prolonged maintenance treatment with vitamin K_1 is necessary. Again, there is no consensus on duration of therapy; however, in a review of LAAR poisoning, median duration of vitamin K_1 treatment was 140 days, up to 730 days (King & Tran, 2015). During this time, monitoring of PT/INR is considered sufficient, as serum brodifacoum levels do not necessarily correlate with tissue levels (Schulman & Furie, 2015). Vitamin K_1 can be discontinued when it is no longer needed to maintain a normal PT/INR (Schulman & Furie, 2015).

ANTITHROMBIN-DEPENDENT PARENTERAL ANTICOAGULANTS

UNFRACTIONATED HEPARIN

Heparin is a natural polymer of sulfated glycosaminoglycans with a wide range of molecular weights that is prepared from porcine intestinal mucosa. Heparin is cleared through a combination of a rapid saturable mechanism and a much slower first-order mechanism, resulting in a nonlinear response to an increasing dose. The apparent biological half-life of heparin increases from approximately 30 minutes after an IV bolus of 25 U/kg to approximately 60 minutes after a bolus of 100 U/kg (Garcia et al., 2012). Heparin exerts its anticoagulant effect by binding to the plasma protein antithrombin, a circulating natural anticoagulant. The antithrombotic effect is derived from the accelerated inhibition of the serine proteinase coagulation factors, with the most critical inhibition being that of thrombin (factor IIa) and factor Xa (Fig. 43.3). Additional effects of heparin include the release of tissue factor pathway inhibitor (TFPI), an increase in tissue plasminogen activator and thereby fibrinolysis, and impairment of platelet function (Salzman et al., 1980). Unfractionated heparin (UFH) can be given subcutaneously or intravenously, with a rapid onset of action (Garcia et al., 2012), and may be used prophylactically or therapeutically for the treatment of venous as well as arterial thromboembolism. The rapid

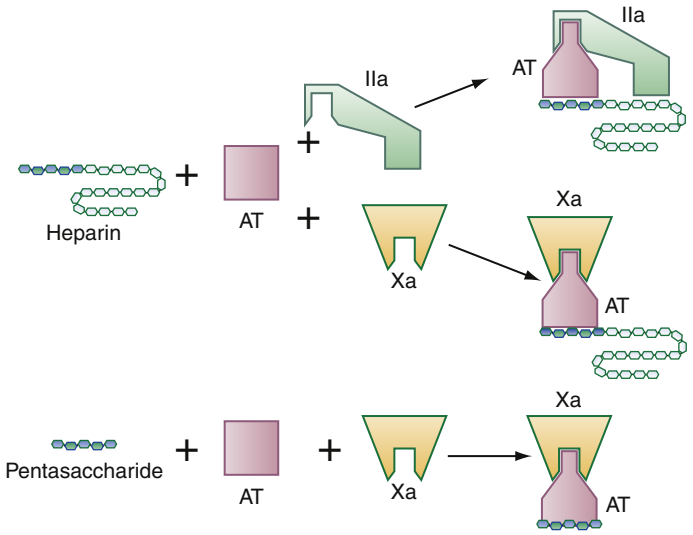

Figure 43.3 Hypothetical mechanisms for heparin/heparan sulfate regulation of protein–protein interactions. Binding of a specific pentasaccharide sequence of heparin present in unfractionated heparin (UFH) and low-molecular-weight heparin (LMWH) or in isolated form (fondaparinux) to antithrombin (AT) produces a conformational change in AT sufficient for inhibition of the serine protease factor Xa. Effective inhibition of thrombin (factor IIa) also requires direct interaction with a region of the heparin molecule distinct from the pentasaccharide sequence, necessitating a longer glycosaminoglycan sequence. Such thrombin-binding regions are characteristically more available in UFH than in the LMWH products. (Modified from Nugent MA: Heparin sequencing brings structure to the function of complex oligosaccharides, *Proc Natl Acad Sci U S A* 97:10301–10303, 2000.)

anticoagulant effect of heparin is particularly important in the acute management of patients with VTE, because inadequate anticoagulation early in treatment can lead to an increased risk for subsequent thrombotic complications (Kearon et al., 2012).

A variety of laboratory methods can be used to measure UFH. These include APTT, TT, anti–factor Xa activity, activated clotting time (ACT), and protamine reversal. For patients receiving heparin for the treatment of VTE, as well as for most other nonsurgical indications for therapy with UFH, APTT is the most commonly used assay. In contrast to warfarin monitoring, for which the international community has established the INR to minimize performance variations in reagent/instrument combinations, comparable standardization has not been developed for APTT when used for monitoring heparin. Historically, many clinicians targeted a 1.5- to 2.5-fold increase in APTT over an individual patient's baseline APTT, or the midpoint of the laboratory's normal reference interval for APTT, for the treatment of patients with VTE. This target was based on a study from the 1970s reporting that maintaining APTT in this range was associated with a reduced risk of recurrent VTE (Basu et al., 1972). However, subsequent studies demonstrated that APTT results could vary markedly for samples containing the same amount of UFH depending on the reagent and the laboratory instrumentation (Shapiro et al., 1977; Kitchen et al., 1996). For example, with heparin levels of 0.3 to 0.7 U/mL, determined by an anti–factor Xa assay standardized with UFH, APTT ratios have been reported to range from 1.6 to 2.7 to 3.7 to 6.2 times the control value (Garcia et al., 2012). Consequently, the therapeutic APTT range at an individual institution needs to be determined based on the responsiveness of the reagent and the instrumentation in use (Garcia et al., 2012).

Establishing a therapeutic APTT range for heparin therapy requires performing a linear regression analysis of the APTT plotted against anti–factor Xa heparin levels for patients undergoing therapeutic heparin anticoagulation. An example of such an analysis is shown in Figure 43.4. This relationship must be reevaluated each time a change in reagent lot (or instrumentation) occurs for either of these tests. Furthermore, it is recommended that the relationship between the APTT and anti–factor Xa levels should be determined using plasma samples obtained from patients actually undergoing heparin therapy and not by using normal plasma samples spiked with exogenous heparin (Olson et al., 1998). This approach would incorporate the heterogeneity encountered with individual patient samples, which exhibit variability in the levels of factor VIII, fibrinogen, antithrombin, and the contact factors (factor XII, high-molecular-weight kininogen, and prekallikrein), as well as the possible presence of a lupus anticoagulant.

In addition to the heterogeneity encountered in different patient samples, there is also variability observed among the different anti–factor Xa

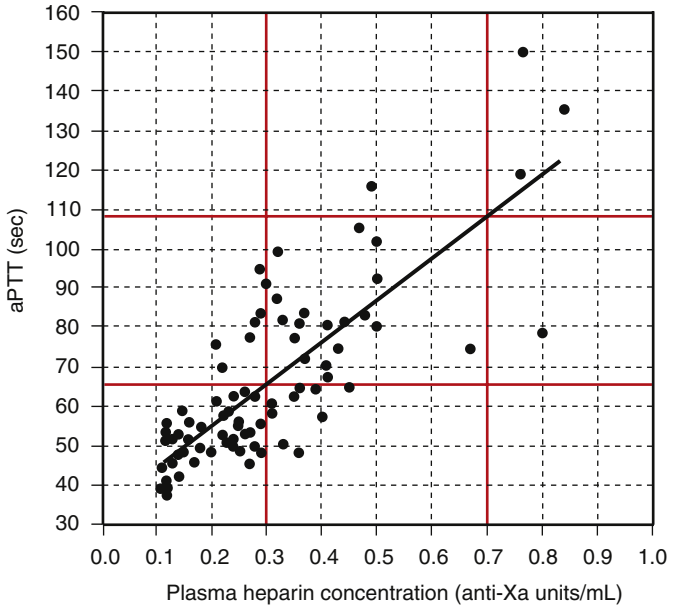

Figure 43.4 Linear regression analysis of relationship between activated partial thromboplastin time (APTT) and anti–factor Xa (Xa) heparin level performed on plasma samples from patients undergoing heparin therapy. With this particular reagent/instrument combination, the regression analysis yields an APTT range of 66 to 108 seconds that would correspond to an anti–factor Xa range of 0.3 to 0.7 U/mL.

assays performed with the various available reagent/instrument combinations. One contributor to such variability is whether the particular assay system includes the addition of exogenous antithrombin (Lehman et al., 2006). Providing an excess of antithrombin may produce a higher heparin level for the patient who is deficient in endogenous antithrombin. In a sense, this yields the more accurate measurement of the amount of heparin present in the circulation. Viewed from a different perspective, however, the more appropriate measurement to guide dosing may be the one that reflects the actual inhibitory ability of infused heparin—that is, the method that remains dependent on the patient's own antithrombin level. Regardless of the approach taken, using the anti–factor Xa assay to define specific APTT ranges did not improve interlaboratory assessment of 44 inpatients receiving heparin therapy in a cross-validation study (Cuker et al., 2009). Although debate continues regarding the optimal approach to monitoring heparin therapy, it is generally recommended that for patients who have a prolonged baseline APTT before initiation of heparin therapy, an alternative method such as the anti–factor Xa assay should be employed.

Heparin is also used extensively to prevent clot formation during cardiac bypass surgery as well as during a number of interventional vascular procedures. In these settings, the concentration of heparin (e.g., 2–4 anti–factor Xa U/mL) is typically higher than that used in the treatment of VTE. At these levels of UFH, the APTT is prolonged into a range where it does not perform optimally. ACT, which uses glass beads, kaolin, or diatomaceous earth to activate whole-blood samples obtained from the patient, is frequently used to guide heparin therapy during such procedures. As for all of the coagulation assays used to monitor an anticoagulant effect, the importance of establishing local reference intervals using normal controls for ACT testing cannot be overemphasized. It is vital to obtain a baseline ACT value before heparin therapy is instituted and to realize that for occasional patients with a markedly prolonged baseline ACT (such as one who may have a lupus anticoagulant or a severe contact factor deficiency), an alternative approach to monitoring should be considered—typically, an anti–factor Xa heparin assay.

Heparin Resistance

Heparin resistance refers to a clinical situation in which a patient appears to require unusually high doses of heparin in order to achieve a target APTT (e.g., >35,000 U/day in a patient receiving heparin for the treatment of venous thromboembolism) (Garcia et al., 2012). Heparin resistance is also occasionally encountered during cardiac bypass procedures, defined as an inability to achieve a target ACT prior to or during the procedure (Finley & Greenberg, 2013). Causes of heparin resistance include massive thrombosis with release of heparin-binding proteins (e.g., platelet factor 4, fibronectin); elevated factor VIII levels (often evidenced by short APTT prior to starting UFH); treatment with nitroglycerin; severe obesity; antithrombin deficiency (<30% activity); HIT; and cancer (Edson et al., 1967; Bharadwaj et al., 2003; Francis & Groce, 2004). In some instances of apparent heparin resistance as measured by APTT, such as in the case of elevated factor VIII levels, simply changing to anti–factor Xa assays will provide a more accurate measure of the circulating heparin level (Garcia et al., 2012). As noted earlier, whether a measured heparin level within the target range represents an accurate anticoagulant effect in a patient with a subtherapeutic APTT remains unclear. Race has also been shown to be a variable, contributing to differences in sensitivity to the anticoagulant effect of heparin (Shimada et al., 2010).

LOW-MOLECULAR-WEIGHT HEPARIN

LMWHs are derived from UFH by chemical or enzymatic depolymerization, resulting in shorter fragments that exhibit reduced binding to proteins and cells and a more predictable pharmacokinetic profile (Garcia et al., 2012). The elimination half-life of LMWHs is dose independent and approximately 3 to 6 hours following a subcutaneous injection (Garcia et al., 2012). The LMWHs have a mean molecular weight of approximately 4000 to 5000, which corresponds to about 15 saccharide units. This chain length is sufficient to promote the inactivation of factor Xa by antithrombin, but it is insufficient to promote the inactivation of thrombin by antithrombin, which requires a slightly longer chain length (Gray et al., 2008). Consequently, the LMWHs primarily inhibit factor Xa, with less inhibitory activity directed against thrombin. Anti–factor Xa assays, rather than the APTT, should be used when measurement of an LMWH is needed (Boneu & de Moerloose, 2001). Monitoring plasma levels of LMWH is typically not required, but it may be helpful in certain patient populations, including children and newborns, pregnant women, morbidly obese patients, and patients with renal failure (because these agents are primarily cleared by the kidney). When monitoring is performed, blood should be drawn approximately 4 hours after the last administered dose because this is when the peak level is anticipated to occur (Bounameaux & de Moerloose, 2004; Harenberg, 2004). Target peak anti–factor Xa levels for selected LMWHs are provided in Table 43.3. In some situations, measurement of the anti–factor Xa level at a trough (i.e., immediately prior to a dose) may be useful in determining whether the drug is accumulating in an individual patient, but levels at this time point have not been established.

FONDAPARINUX

Fondaparinux is a small synthetic pentasaccharide that represents the minimal glycosaminoglycan sequence needed for binding to antithrombin. This binding is sufficient to enhance the reactive site of antithrombin binding to factor Xa, neutralizing the enzyme (see Fig. 43.3). Fondaparinux exhibits essentially no antithrombin activity because of its short length. It has a longer half-life than heparin or LMWH (terminal half-life of 17 hours in young subjects, and 21 hours in older individuals) and can be given subcutaneously once daily; dose is based on weight and does not ordinarily require measurement of blood levels (Garcia et al., 2012). It will cause a modest prolongation of PT as well as APTT, but this is typically only by a few seconds at most (Smogorzewska et al., 2006). If necessary, the level can be measured by an anti–factor Xa assay. However, this should be done with fondaparinux as the agent used to generate the standard curves (Smogorzewska et al., 2006). Fondaparinux is cleared by the kidneys; thus, the dose must be reduced in patients with compromised renal function (Nagler et al., 2012).

HEPARIN-INDUCED THROMBOCYTOPENIA

Thrombocytopenia arising in the setting of heparin therapy is not infrequent. A transient mild drop in platelet count early after the initiation of heparin therapy is common and reflects a nonimmune process. This drop is not associated with any clinical manifestations and characteristically resolves with continued administration of UFH. In contrast, a platelet count drop that begins within 5 to 10 days of starting heparin therapy is consistent with an immune-mediated disorder referred to as *heparin-induced thrombocytopenia* (HIT) (Arepally & Ortel, 2010; Greinacher, 2015). Paradoxically, the dropping platelet count in HIT is associated with an increased risk for venous and/or arterial thromboembolism, which is referred to as *heparin-induced thrombocytopenia and thrombosis* (*HITT*). HIT is mediated by antibodies that bind macromolecular complexes formed by platelet factor 4 (PF4), a protein found in platelet α-granules and free in plasma, in complex with heparin (Greinacher et al., 1994). When multiple immunoglobulin G (IgG) molecules bind to the resultant PF4/heparin complexes, the Fc regions of these antibodies can bind to the FcγRIIA receptors on platelet surfaces, causing platelet activation and release of

highly procoagulant microparticles (Arepally & Ortel, 2010). The relationship between the amount of released PF4 and circulating platelets and monocytes contributes to the development of the syndrome (Fig. 43.5). Rarely, antibodies to other chemokines that have shared sequence structures with PF4 (the CXC family of chemokines), such as interleukin-8 (IL-8) and neutrophil-activating protein-2, may also cause HIT (Amiral et al., 1996). The development of this immune response is associated with substantial morbidity and mortality, necessitating early diagnosis and initiation of appropriate therapeutic measures, described later.

A presumptive diagnosis of HIT is made on clinical grounds, particularly in cases in which the time course and extent of the drop in platelet count fit together convincingly with the patient's history of heparin therapy. Treatment decisions will frequently need to be made prior to obtaining the results of confirmatory laboratory testing (Linkins et al., 2012). Several algorithmic approaches have been developed that attempt to assess the pretest likelihood of true HIT in the individual patient, most notably the 4T system (Table 43.4). Patients with a low 4T score have a very low probability of having HIT (0%–3%), and testing for antibodies to PF4/heparin in this situation is generally not indicated (Arepally & Ortel, 2010). This is important, because the frequency of positive laboratory results can be quite high in certain patient populations, even though the syndrome itself is relatively infrequent (e.g., following cardiac bypass surgery; medical or surgical intensive care unit [ICU] patients) (Arepally & Ortel, 2006). Although a low 4T score is a very robust means to exclude a diagnosis of HIT, an intermediate or high 4T score is less useful for the identification of patients who do have HIT. In a systematic review and meta-analysis, the positive predictive value of the 4T score for patients with intermediate or high 4T scores was 0.14 (0.09–0.24) and 0.64 (0.40–0.82), respectively (Cuker et al., 2014). To improve on this modest positive predictive value, a clinical scoring system called the HIT Expert Probability (HEP) score, was developed based on broad expert opinion (Cuker et al., 2010). This scoring system encompasses 8 clinical domains, many of which are further itemized, with each clinical feature assigned a score ranging from –3 (strongly argues against a diagnosis of HIT) to +3 (strongly supports a diagnosis of HIT). In a prospective study, the HEP score exhibited similar diagnostic accuracy as the 4T score—sensitivity 95.3% (confidence interval [CI]: 84.2–99.4) and specificity 35.7% (CI: 29.8–42.0) (Pishko et al., 2018). The HEP score also demonstrated a significantly higher area under the curve (AUC) when applied to patients in the ICU and utilized by trainees and more inexperienced clinicians when compared with the 4T score (AUC in the ICU = 0.86 and AUC among trainees = 0.80). This suggests some unique settings in which this scoring system might be superior to the 4T score.

A clinical diagnosis of HIT needs to be confirmed with a laboratory test demonstrating heparin-dependent antibodies. Immunoassays detect antibodies that bind to PF4/heparin complexes, whereas functional assays detect antibodies capable of activating platelets. A test that has perfect sensitivity and specificity and could be performed rapidly in a cost-effective fashion would be ideal. Many laboratories use a testing strategy in which the initial (and, in most cases, the only) test is a readily performed PF4–enzyme-linked immunosorbent assay (ELISA) that has high sensitivity but lower specificity. Sensitivity has been reported to be as high as 98.1% for the polyspecific ELISA (detects IgG, IgM, and IgA isotypes), but specificity is lower—only 89.4% in one analysis (Cuker & Ortel, 2009). Several strategies have been studied in an effort to improve the diagnostic specificity of the ELISA assay. Higher absorbance values in the ELISA are associated with an improved ability to identify patients more likely to have HIT and a thromboembolic complication (Zwicker et al., 2004) and are more likely to be associated with a positive functional assay (Warkentin et al., 2008). The ability to block antibody binding with excess heparin added to the patient plasma sample has also been shown to improve the specificity of the assay (Whitlatch et al., 2010; McFarland et al., 2012), although this approach appears to be most beneficial in patients with weakly positive ELISA results (Althaus et al., 2011). The IgG-specific ELISA has also been shown to improve assay specificity (McFarland et al., 2012), although with a slight loss in sensitivity (Cuker & Ortel, 2009). Anti-PF4/heparin antibodies of the IgM and IgA classes appear to have only a minor role in the development of HIT (Greinacher et al., 2007), although rare cases have been reported.

Once a positive ELISA test has been obtained, a functional test can be helpful to provide further laboratory support for the presence or absence of HIT. Functional tests typically are much more demanding to perform but provide higher specificity in addition to high sensitivity. In North America, the gold standard of functional testing for HIT has been the serotonin release assay (SRA), in which washed platelets that have taken up exogenous ^{14}C-labeled serotonin are challenged with patient plasma in the presence of different heparin concentrations, and the amount of released serotonin is measured as the endpoint. Although relatively few laboratories in North America offer this test, it is available through

TABLE 43.3

Target Peak Anti–Factor Xa Results for Therapeutic Low-Molecular-Weight Heparins and Fondaparinux

Agent and Frequency of Administration	Target Range* (Anti–Factor Xa units/mL, Except Where Indicated)
Enoxaparin, twice daily	0.6–1.0
Enoxaparin, once daily	>2.0
Dalteparin, once daily	1.05
Tinzaparin, once daily	0.85
Nadroparin, twice daily	0.6–1.0
Nadroparin, once daily	1.3
Fondaparinux, once daily	1.20–1.26 mg/L†

*Measured 4 hours after drug administration.
†Measured 3 hours after drug administration.
Adapted from Garcia DA, Baglin TP, et al.: Parenteral anticoagulants: Antithrombotic Therapy and Prevention of Thrombosis, 9th ed: American College of Chest Physicians Evidence-Based Clinical Practice Guidelines, Chest 141(2 Suppl): e24S–e43S, 2012.

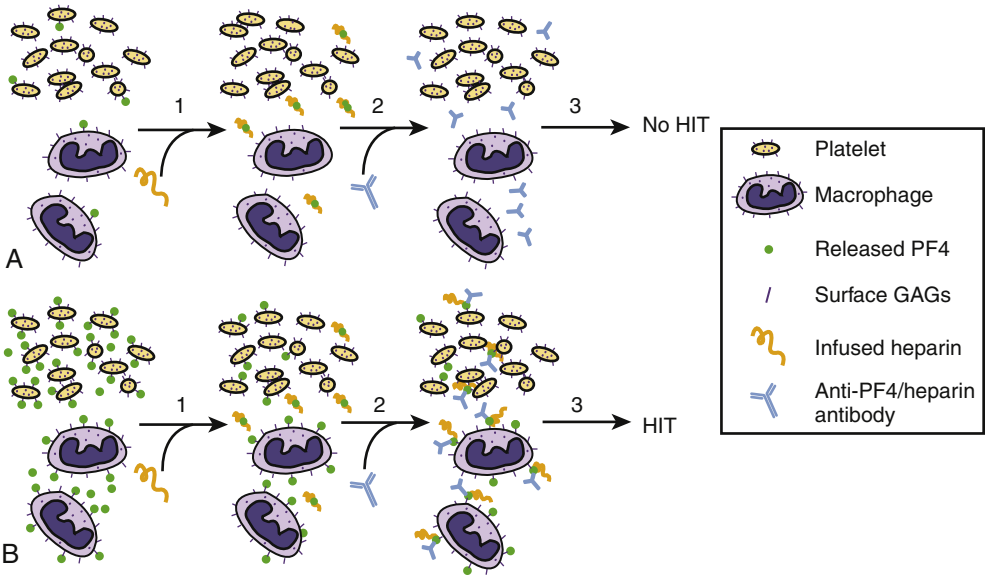

Figure 43.5 Mechanistic basis of heparin-induced thrombocytopenia (HIT). **A,** Platelets and monocytes from a patient with little released platelet factor 4 (PF4) on the left. Following heparinization (1), the small amount of surface-bound PF4 becomes complexed to the higher-affinity circulating heparin and induces anti–PF4/heparin antibody production (2). Because there are not many surface PF4/GAG complexes for the antibodies to bind, they largely remain unattached to cells and do not activate the platelets or the monocytes (3). The patient does not develop HIT. **B,** Same as (A), but with a great deal of released PF4 bound to the GAGs on the surface of both platelets and monocytes. After heparinization (1), some PF4/surface GAG complexes remain. Circulating free PF4/heparin induces antibody production (2), and because there remain antigenic targets on platelets and monocytes, the antibodies bind to these cells and activate them (3), resulting in both thrombocytopenia and the prothrombotic state seen in HIT. (Modified from Kowalska MA, Rauova L, Poncz M: Role of the platelet chemokine platelet factor 4 [PF4] in hemostasis and thrombosis, *Thromb Res* 125:292–296, 2010.)

several reference laboratory services. Alternative functional assays include a heparin-induced platelet activation assay that has a comparable sensitivity and specificity as the serotonin-release assay (Eichler et al., 1999) and flow cytometric methods that detect the formation of platelet microparticles (Mullier et al., 2010) or expression of phosphatidylserine on platelet surfaces using a fluorescein-labeled annexin A5 (Poley & Mempel, 2001). As well, the PF4-dependent P-selectin expression assay (PEA) is a flow-based assay that detects functional, platelet-activating anti-PF4/heparin antibodies (Padmanabhan et al., 2016). This assay uses washed platelets and measures P-selectin expression on platelets treated with PF4 alone and with PF4 plus high-dose UFH (125 U/mL). Results are expressed as "percent activation" in relation to platelets that have been treated with thrombin receptor-activating peptide to induce maximum P-selectin expression. In a study comparing the diagnostic performance of the SRA against the PEA, the PEA had higher diagnostic accuracy (AUC for PEA 0.92 vs. SRA 0.82, $p = 0.02$) and sensitivity than the SRA (sensitivity for PEA 96% vs. SRA 54%). Specificity was comparable (specificity for PEA 85% vs. SRA 92%).

Irrespective of which functional assay is chosen, important considerations for all of these assays include appropriate use of positive and negative control samples (Warkentin et al., 2011a) as well as selection of appropriate platelet donors for these assays. Ultimately, regardless of the laboratory strategy used to optimize sensitivity and specificity, the most important variable to improve diagnostic specificity is careful assessment of the clinical likelihood of HIT prior to requesting laboratory testing. A diagnostic strategy that combines the 4T scoring system with laboratory testing is shown in Figure 43.6.

The complex relationship between the clinical syndrome of HIT and the presence of anti-PF4/heparin antibodies detected by a functional assay or by ELISA is shown in Figure 43.7. Patients receiving treatment with LMWH can also develop HIT, although less frequently than patients being treated with UFH. Anti-PF4/heparin antibodies that develop in a patient receiving UFH will cross-react with LMWHs; thus, these agents should not be administered to a patient with known HIT. Fondaparinux is the least immunogenic of the glycosaminoglycans and does not appear to cross-react with circulating anti-PF4/heparin antibodies in vivo. Further, fondaparinux has been safely used as an anticoagulant in patients with HIT (Warkentin et al., 2011b; Kang et al., 2015). Several patients with what appears to be fondaparinux-induced thrombocytopenia have been described (Warkentin et al., 2007), but this event is extremely rare.

The laboratory sometimes will be called upon to perform testing for HIT on individuals who have been positive for HIT at some time in the past but are currently not thrombocytopenic. Given variability among patients in the rate of disappearance of detectable antibodies together with variability in the manifestation of an anamnestic response upon reexposure to heparin, testing may be required before reexposure to heparin is considered as well as subsequent to the initiation of such therapy if instituted. Although it has been demonstrated that HIT-associated antibodies frequently do not recur if the patient is rechallenged with heparin more than 6 months following loss of detectable antibody (Warkentin & Sheppard, 2014), close laboratory monitoring of such rechallenged patients is critical. In the event that an anamnestic response does develop, the reemergence of antibody can be dramatic, necessitating rapid detection of falling platelet counts as well as repeat testing for anti-PF4/heparin antibodies.

TARGET-SPECIFIC ANTICOAGULANTS

PARENTERAL AGENTS

Parenteral direct thrombin inhibitors are primarily used for the management of patients with HIT. Lepirudin, a recombinant form of the leech protein hirudin, was approved by the U.S. Food and Drug Administration (FDA) in the United States in 1998 for the treatment of patients with HIT, but production was halted in Europe in 2011 and North America in 2012 for business reasons (Kelton et al., 2013). Argatroban, a short-acting reversible direct thrombin inhibitor (half-life, 40–50 minutes), is approved in the United States for the treatment of HIT (Kelton et al., 2013). A therapeutic target of 1.5 to 3.0 times the baseline APTT has been suggested as the effective anticoagulant range of argatroban (Kelton et al., 2013). Argatroban is metabolized in the liver and can be used in patients with impaired renal function, but it should be used with caution in patients with significant hepatic insufficiency (e.g., if the baseline PT is prolonged). Bivalirudin, a hirudin-analog that binds to both the active and fibrin-binding sites of circulating and clot-bound thrombin (half-life, 24 minutes), is approved for use in the United States for percutaneous coronary intervention in patients who have or are at risk for HIT. When used in patients with HIT, the bivalirudin dose is adjusted to achieve a target APTT similar to the strategy with argatroban. In addition to prolonging the APTT, each of these agents also has an effect on PT, most notably argatroban. TT will be markedly prolonged with each of these agents, but a dilute TT (1 : 4 dilution of patient plasma with normal plasma) can be used to monitor these agents (Love et al., 2007).

ORAL AGENTS

Dabigatran etexilate, an oral prodrug of the direct thrombin inhibitor dabigatran, was approved by the FDA for the prevention of thromboembolic complications in patients with atrial fibrillation and for the treatment of patients with VTE. Rivaroxaban, apixaban, and edoxaban are three factor Xa–specific inhibitors that are also approved for the treatment of patients with atrial fibrillation and VTE. Rivaroxaban and apixaban have also received approval for thromboprophylaxis following major orthopedic surgery. Unlike the oral vitamin K antagonists, these agents are administered in fixed doses and do not require routine laboratory monitoring (Connolly et al., 2009; Granger et al., 2011; Patel et al., 2011). Measurement of anticoagulant activity may be desirable in selected clinical settings, however, including hemorrhage, prior to surgical procedures, recurrent thromboembolism, and in certain high-risk populations, including those at the extremes of body weight, the elderly, and those with renal insufficiency. The characteristics of these target-specific oral anticoagulants are summarized in Table 43.5.

Target-specific oral anticoagulants differ in their effects on the commonly used screening hemostasis tests, and different test reagents exhibit variable sensitivities to the individual drugs. Individual laboratories should perform dose-response studies using calibration standards to determine the sensitivity of their particular reagents to these agents. In addition,

TABLE 43.4

Pretest Scoring System for Heparin-Induced Thrombocytopenia: the 4T's Score*

Clinical Feature	2	1	0
Thrombocytopenia	>50% fall and platelet nadir 20–100 × 10^9 L^{-1}	30%–50% fall or platelet nadir 10–19 × 10^9 L^{-1}	Fall <30% or platelet nadir <10 × 10^9 L^{-1}
Timing of fall in platelet count or other sequelae	Clear onset between days 5 and 10; or ≤1 day (if heparin exposure within past 30 days)	Consistent with days 5–10 fall, but not clear (e.g., missing platelet counts); or onset after day 10; or fall ≤1 day (prior heparin exposure 30–100 days ago)	Fall in platelet count <4 days without recent heparin exposure
Thrombosis or other sequelae (e.g., skin lesions)	New thrombosis; skin necrosis; postheparin bolus acute systemic reaction	Progressive or recurrent thrombosis; erythematous skin lesions; suspected thrombosis not yet proven	None
Other cause for thrombocytopenia not evident	None apparent	Possible	Definite

*MA score (2, 1, or 0) is assigned for each clinical feature. Cumulative scores are then used to assign pretest probability scores of high (6–8 points), intermediate (4–5 points), or low (≤3 points) likelihood of disease. Clinical laboratory testing is typically not necessary for a 4T score of 3 points or less.
Adapted from Lo GK, Juhl D, et al.: Evaluation of pretest clinical score (4 T's) for the diagnosis of heparin-induced thrombocytopenia in two clinical settings, *J Thromb Haemost* 4(4):759–765, 2006.

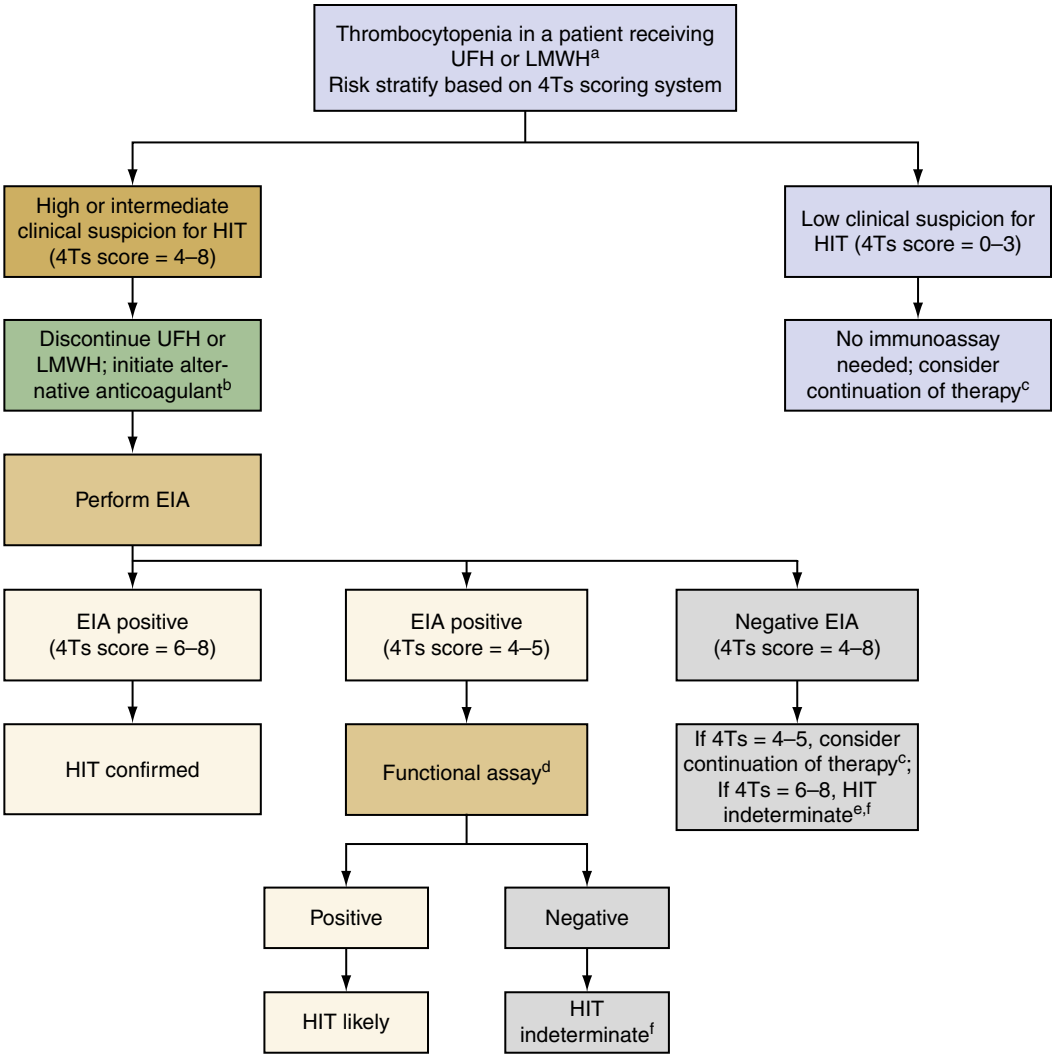

Figure 43.6 Diagnostic algorithm for heparin-induced thrombocytopenia (HIT). *UFH,* Unfractionated heparin; *LMWH,* low-molecular-weight heparin; *EIA,* enzyme-linked immunoassay. [a]Thrombocytopenia can be absolute (<150,000/μL) or relative (>30% decrease in platelet counts from the highest platelet count prior to initiation of heparin therapy). [b]Decision to initiate alternative anticoagulant therapy should be guided by assessment of patient's bleeding risk and comorbidities. [c]Decision to continue UFH or LMWH should be individualized. [d]Functional assay recommended, if clinically available. [e]Antibodies with non-PF4/heparin specificity may be causative of disease. [f]Decision to continue alternative anticoagulant therapy should be individualized. (Illustration from Arepally GM, Ortel TL: Heparin-induced thrombocytopenia, *Annu Rev Med* 61:77–90, 2010.)

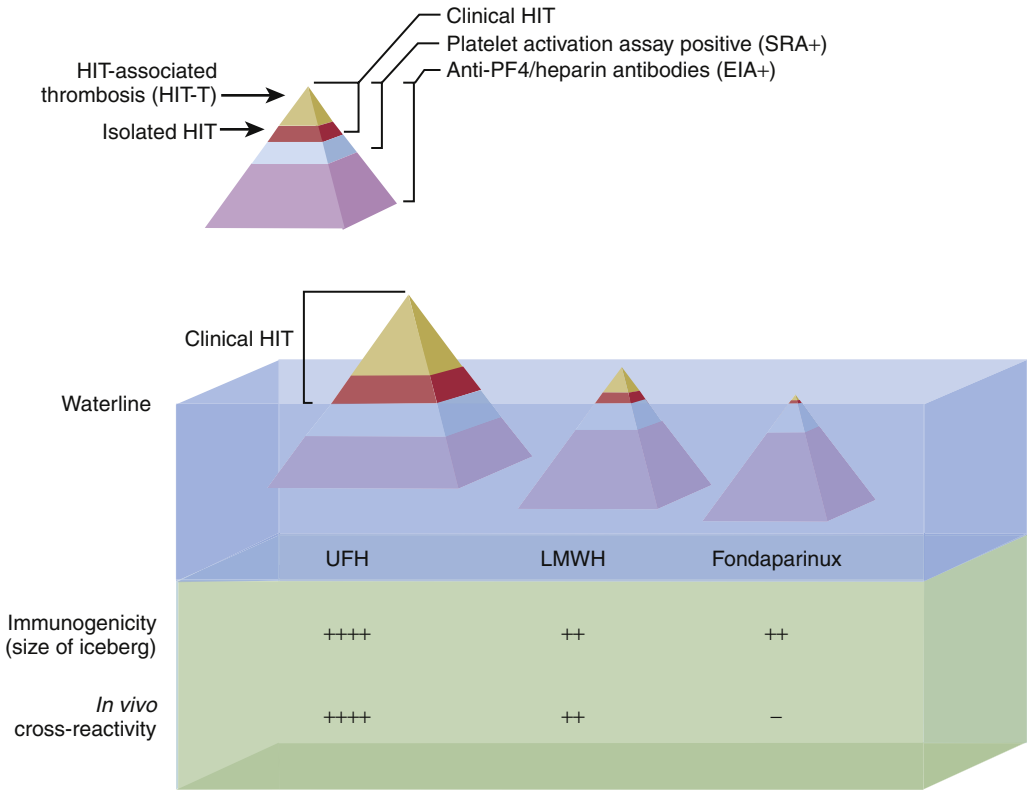

Figure 43.7 The relationship between the clinical manifestations of HIT (with or without thrombosis), the type of heparin administered, and the antibodies that cause HIT. This can be conceptualized as an "iceberg." The visible component of the iceberg (the portion above the waterline) represents clinically evident features of HIT, such as thrombocytopenia and/or thrombosis. The mass of the iceberg corresponds to the entire spectrum of anti–platelet factor 4 (PF4)/heparin antibodies generated. Some of these antibodies will be biologically active (platelet activating), and others will be non-platelet-activating, which may make them unlikely to cause clinical consequences. The type of heparin given to the patient determines the overall size of the iceberg, with unfractionated heparin (UFH) being the largest (most immunogenic), and low-molecular-weight heparin (LMWH) and fondaparinux having lesser immunogenicity. Also illustrated in this figure is in vivo cross-reactivity. UFH forms antigens that are readily recognized by HIT antibodies. In contrast, fondaparinux forms poorly recognized antigens. LMWH is intermediate. (Illustration by Chen AY, from Kelton JG, Warkentin TE: Heparin-induced thrombocytopenia: A historical perspective, *Blood* 112:2607–2616, 2008.)

TABLE 43.5

Oral Target-Specific Oral Anticoagulants

	Dabigatran Etexilate	Rivaroxaban	Apixaban	Edoxaban
Target	Thrombin	Factor Xa	Factor Xa	Factor Xa
Bioavailability	6.5%	80%	~66%	~50%
Time-to-peak effect	2 hr	2–3 hr	1–2 hr	1–2 hr
Half-life	12–14 hr	7–13 hr	8–13 hr	5–11 hr
Elimination	80% renal, 20% hepatobiliary	67% renal (30% inactive), 33% hepatobiliary	25% renal, 75% hepatobiliary	35% renal, 65% hepatobiliary
Interactions	Potent P-gp inhibitors/inducers	Strong dual CYP 3A4 and P-gp inhibitors/inducers	Strong dual CYP 3A4 and P-gp inhibitors/inducers	P-gp
Antidote	Yes (idarucizumab)	Yes (andexanet alfa)	Yes (andexanet alfa)	No

gp, Glycoprotein.

Data from Yeh CH, Fredenburgh JC, et al.: Oral direct factor Xa inhibitors, *Circ Res* 111(8):1069–1078, 2012; Bauer KA: Pros and cons of new oral anticoagulants, *Hematology Am Soc Hematol Educ Program* 2013:464–470, 2013; Graff J, Harder S: Anticoagulant therapy with the oral direct factor Xa inhibitors rivaroxaban, apixaban and edoxaban and the thrombin inhibitor dabigatran etexilate in patients with hepatic impairment, *Clin Pharmacokinet* 52(4):243–254, 2013.

given the relatively short half-life of these drugs, interpretation of the data obtained from an individual patient needs to be considered in the context of when the most recent dose was administered. Given the unique characteristics of each agent, we will review them separately.

Dabigatran etexilate. Dabigatran has relatively little effect on the PT/INR at clinically relevant plasma concentrations, with only modest increases observed at the higher concentrations (Lindahl et al., 2011). However, considerable variability in sensitivity exists between the different thromboplastin reagents (Cuker et al., 2014). In addition, two studies have found that PT/INR results are more prolonged when performed using a point-of-care INR meter compared with results obtained using a laboratory, plasma-based PT (Van Ryn et al., 2012; Hawes et al., 2013). APTT is more sensitive to dabigatran than PT, but the response is curvilinear and exhibits a varying relationship between drug level and anticoagulant effect (Van Ryn et al., 2010; Lindahl et al., 2011). TT is exquisitely sensitive to the presence of dabigatran, and a normal TT can be used to effectively exclude the presence of drug anticoagulant effect. A modification of this assay, which dilutes the patient sample, has been developed as an assay that can be used to assess the anticoagulant effect of dabigatran (Van Ryn et al., 2010). The ecarin clotting time has also been shown to provide a linear response to dabigatran over a broad range (Hawes et al., 2013), but it is limited by lack of standardization, variable sensitivity of different lots of ecarin, and limited availability (Cuker et al., 2014). The importance of considering the time elapsed between when the last dose of dabigatran was taken and when the blood sample for testing was obtained is shown in Figure 43.8.

Dabigatran also has an effect on several other coagulation assays that might be obtained in these patients. ACT is prolonged with higher concentrations of dabigatran, but this test is relatively insensitive at concentrations that would be encountered in patients taking approved therapeutic doses of the drug (Douxfils et al., 2012; Hawes et al., 2013). Thromboelastography has been reported to display a prolonged R-value in the presence of therapeutic levels of dabigatran (Davis et al., 2012), but the sensitivity of this assay to lower concentrations has not been determined. Fibrinogen levels can be significantly underestimated at higher concentrations of dabigatran with assays that use a lower amount of thrombin (Lindahl et al., 2011).

Rivaroxaban. Rivaroxaban prolongs PT in a concentration-dependent, linear fashion, but assay sensitivity varies considerably among thromboplastin reagents (Cuker et al., 2014). At peak levels, most PT values are prolonged regardless of the reagent (Francart et al., 2014). At trough levels, however, PT is relatively insensitive (Francart et al., 2014). APTT is also prolonged in a dose-dependent manner, but the relationship between rivaroxaban concentration and APTT prolongation is nonlinear (Cuker et al., 2014). As with PT, considerable variability exists between reagents. Neither TT nor ecarin clot time is affected by rivaroxaban, because it has no inhibitory activity against thrombin. Several studies have demonstrated that a linear, concentration-dependent relationship can be obtained between rivaroxaban concentration and anti–factor Xa activity over a wide range of concentrations (Asmis et al., 2012; Billoir et al., 2018). Standard curves for the anti–factor Xa assays should be generated with rivaroxaban calibrators and controls. Excellent correlation between rivaroxaban concentration and anti–factor Xa activity was demonstrated in a study using a rivaroxaban-calibrated anti–factor Xa assay (Billoir et al., 2018).

Apixaban. Apixaban prolongs PT in a concentration-dependent manner, but PT is relatively insensitive to the presence of apixaban at therapeutic concentrations (Douxfils et al., 2013). APTT is also prolonged in a concentration-dependent manner, but the response reaches a plateau at higher concentrations (Douxfils et al., 2013). As with rivaroxaban, there is no effect on TT or ecarin clotting time, and there is a linear, concentration-dependent response in an anti–factor Xa assay (Barrett et al., 2010; Douxfils et al., 2013). Again, the anti–factor Xa assay should be specifically calibrated to apixaban (Billoir et al., 2018).

Edoxaban. Edoxaban prolongs PT in a dose-dependent, linear fashion, but there is variability in the magnitude of PT prolongation with different thromboplastin reagents (Morishima & Kamisato, 2015) and there is insufficient sensitivity at low drug levels (Cuker & Husseinzadeh, 2015). Edoxaban also prolongs APTT, although it is relatively insensitive to on-therapy levels of the drug (Cuker & Husseinzadeh, 2015). Anti–factor Xa activity correlates linearly with edoxaban over a broad range of concentrations, from typical trough to peak levels (Cuker & Husseinzadeh, 2015).

Although the target-specific oral anticoagulants have different effects on the individual coagulation assays, which vary depending on the individual reagents and instruments being used, there are certain approaches that can be suggested when the laboratory is asked to evaluate a particular patient sample. Important information that would help with interpretation of the data includes the specific drug administered, the time since the last dose, and clinical objectives for which the data are needed. A suggested approach is provided in Table 43.6.

REVERSAL AGENTS FOR ORAL TARGET-SPECIFIC ANTICOAGULANTS

Idarucizumab. Idarucizumab is a humanized monoclonal Fab fragment that binds specifically to dabigatran with an affinity that is ~350 times greater than thrombin (Das & Liu, 2015). Idarucizumab is indicated for dabigatran reversal in patients with life-threatening bleeding or in patients who require emergency surgery or an urgent procedure. It is administered at an initial dose of 5 g (given as 2 separate 2.5-g doses, no more than 15 minutes apart). In the Phase III study of 503 patients, this initial 5-g dose resulted in 100% reversal of anticoagulation within 4 hours as determined by the diluted TT or the ecarin clotting time (Pollack et al., 2017). In this study, 23% of patients developed recurrent bleeding after 12 hours, which was associated with increased levels of unbound dabigatran and subsequent reelevation of coagulation parameters. These patients required a second 5-g dose of idarucizumab. Reelevation of coagulation parameters was hypothesized to be due to the short half-life of idarucizumab (~45 minutes) and the reequilibration of unbound dabigatran from the extravascular to the intravascular space (Pollack et al., 2017). In this Phase III study, thrombosis rates at 90 days ranged from 6.3% to 7.4%, possibly due to patients' underlying thrombotic state along with low rates of reinitiation of anticoagulation (Pollack et al., 2017).

Andexanet alfa. Andexanet alfa is a recombinant, catalytically inactivate decoy of factor Xa. As a decoy molecule, andexanet alfa has been modified so that it is unable to cleave and activate prothrombin or assemble into the prothrombinase complex. Instead, the modified protein binds and sequesters factor Xa inhibitors (Das & Liu, 2015). Additionally, andexanet alfa is able to bind and inhibit TFPI, thus increasing tissue factor-mediated thrombin generation (Siegal et al., 2017). Andexanet alfa is approved for the reversal of apixaban and rivaroxaban in patients with life-threatening bleeding. Andexanet alfa is administered as a bolus (400 or 800 mg) followed by an infusion for up to 120 minutes (4 or 8 mg/minute). Dose is

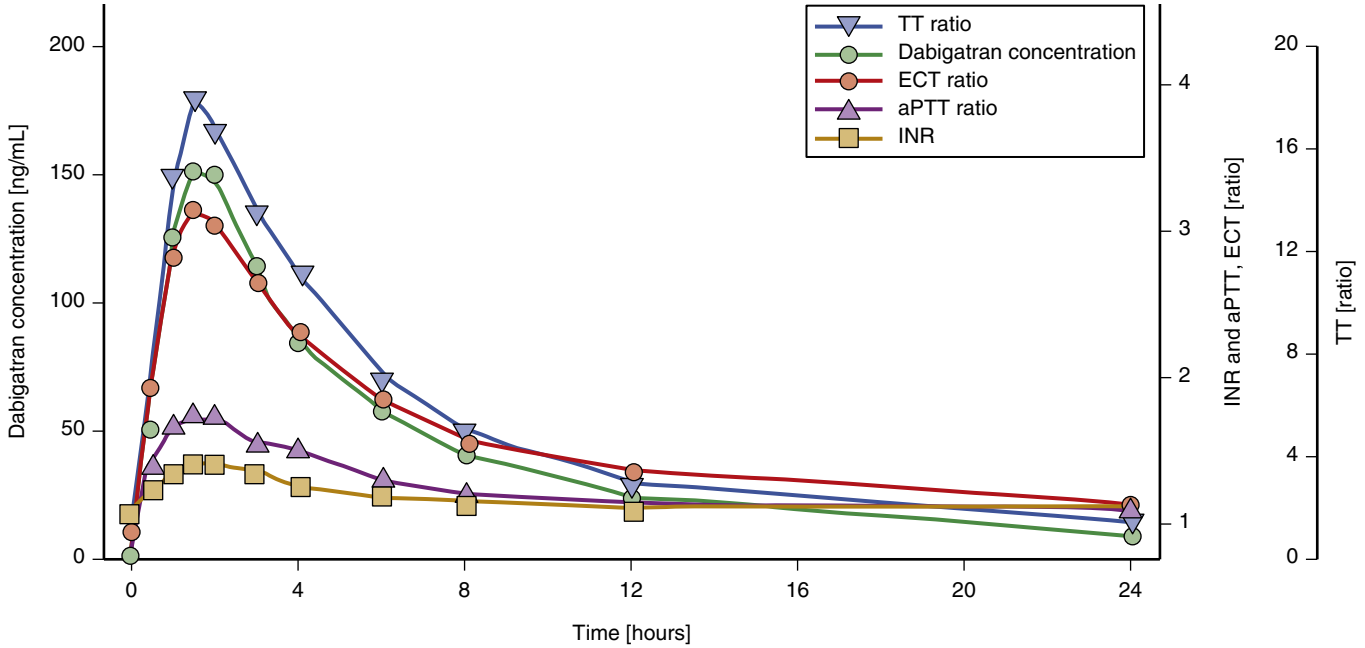

Figure 43.8 Effect of time following a single dose of dabigatran on coagulation test results. Geometric means of activated partial thromboplastin times (APTTs), international normalized ratios (INRs), thrombin time (TT) results, ecarin clotting time results, and plasma concentrations of dabigatran are graphed against time following a single oral dose of 200 mg dabigatran etexilate (N = 6). The APTT, thrombin time, and ecarin clotting time results are depicted as a ratio compared to the baseline value. (Illustration from van Ryn J, et al.: Dabigatran etexilate—a novel, reversible, oral direct thrombin inhibitor: Interpretation of coagulation assays and reversal of anticoagulant activity, *Thromb Haemost* 103:1116–1127, 2010.)

TABLE 43.6

Suggested Approach to Laboratory Assessment of the Target-Specific Oral Anticoagulants

	DETERMINE PRESENCE OF DRUG *BELOW* REPORTED ON-THERAPY DRUG LEVELS		ESTIMATE DRUG LEVELS WITHIN ON-THERAPY RANGE		ESTIMATE DRUG LEVELS *ABOVE* REPORTED ON-THERAPY DRUG LEVELS	
Drug	**Suggested Tests**	**Interpretation**	**Suggested Tests**	**Interpretation**	**Suggested Tests**	**Interpretation**
Dabigatran	TCT	Normal TCT likely excludes clinically relevant drug levels	Dilute TCT, ECT	May help to assess compliance	Dilute TCT, ECT	Provides best approach to quantitate excess drug levels
Rivaroxaban, apixaban, and edoxaban	Anti–factor Xa	Normal anti–factor Xa likely excludes clinically relevant drug levels	Anti–factor Xa	May help to assess compliance	Anti–factor Xa	Provides best approach to quantitate excess drug levels

ECT, Ecarin clotting time; *TCT,* thrombin clotting time.
Adapted from Cuker A, Siegal DM, et al.: Laboratory measurement of the anticoagulant activity of the non-vitamin K oral anticoagulants, *J Am Coll Cardiol* 64(11): 1128–1139, 2014.

determined by the specific factor Xa inhibitor taken, the dose of the factor Xa inhibitor, and the time of the last dose (Portola Pharmaceuticals, Inc., 2018). In a recent single-arm study, median reduction of anti–factor Xa activity levels at the end of the bolus was 92% for patients receiving either apixaban or rivaroxaban. At 12 hours, 82% of participants had achieved excellent or good clinical hemostatic efficacy (Connolly et al., 2019). In this study, anti–factor Xa levels did rise slightly at 4, 8, and 12 hours. However, once administered, anti–factor Xa activity levels are not routinely monitored, as levels do not correlate with hemostatic efficacy and are unlikely to predict clinical response (Connolly et al., 2019). In this single-arm study, thrombotic events occurred in 10%. Additionally, during the 30-day follow-up period, 14% of patients died (Connolly et al., 2019). Many of these events occurred in patients who were delayed or unable to resume anticoagulation. Currently, the package insert for andexanet alfa contains a boxed warning for thromboembolic risk, ischemic risk, cardiac arrest, and sudden death (Portola Pharmaceuticals, Inc., 2018).

ANTIPLATELET THERAPY

Several classes of compounds are currently used to diminish or block platelet activity (Michelson, 2010). These include the cyclooxygenase inhibitor aspirin, adenosine diphosphate (ADP) receptor antagonists, the phosphodiesterase inhibitor dipyridamole, and platelet surface glycoprotein (GP) IIb/IIIa receptor antagonists. In contrast to treatment with warfarin or heparin, antiplatelet therapy traditionally has not been as closely monitored in the clinical laboratory. Increasingly, however, the laboratory, including point-of-care strategies, is coming to play a greater role. Questions that can potentially be answered by laboratory testing include the following: (1) whether a patient's platelets are resistant to inhibition by a particular agent; (2) what dose of agent is required to achieve a desired intensity of inhibition; (3) when, following termination of therapy, platelet function has returned to an adequate level to withstand significant hemostatic challenges such as surgery; and (4) whether thrombocytopenia observed following antiplatelet therapy may reasonably be attributed to the specific therapy itself.

ASPIRIN

No currently used drug has a longer and more eventful history than aspirin (Rosendaal & Reitsma, 2014). Aspirin is rapidly absorbed but has a short half-life (~15–20 minutes) due to hepatic clearance. It irreversibly acetylates cyclooxygenase-1 and -2. In the case of the anucleate platelet, this effectively means that recovery from aspirin inhibition occurs only as platelets newly released from megakaryocytes enter the circulation. Although human platelets circulate in the blood for an average of 10 days, substantial normalization of platelet functional responsiveness occurs within 5 to 7 days following termination of aspirin therapy. This phenomenon may be due to the ability of thromboxane A2, the active product from the platelet cyclooxygenase pathway, released by newly released platelets unaffected by aspirin, to stimulate nearby platelets whose cyclooxygenase has been

TABLE 43.7
P2Y12 ADP Receptor Antagonists

Name	Mechanism of Action	Time to Maximum Level	Elimination Half-Life	Notes
Clopidogrel	Irreversible inhibition	1 hour for circulating drug; 3–7 days for maximal antiplatelet effect	8 hours for circulating drug	More rapid inhibition of platelet function can be achieved with a loading dose; antiplatelet effect lasts up to 10 days.
Prasugrel	Irreversible inhibition	30 minutes	7 hours	Antiplatelet effect lasts 5–7 days.
Ticagrelor	Reversible inhibition	1.5 hours	7 hours	Residual antiplatelet effect decreased to 30% after ~2.5 days.

Data from Eikelboom JW, Hirsh J, et al.: Antiplatelet drugs: Antithrombotic Therapy and Prevention of Thrombosis, 9th ed: American College of Chest Physicians Evidence-Based Clinical Practice Guidelines, *Chest* 141(2 Suppl):e89S–e119S, 2012; Ortel TL: Perioperative management of patients on chronic antithrombotic therapy, *Blood* 120(24):4699–4705, 2012.

acetylated by aspirin. However, individual patient responses to therapeutic aspirin administration vary (Sanderson et al., 2005). Because relative resistance to the platelet inhibitory effects of aspirin may imply the need for additional or alternative antiplatelet treatment in some clinical settings, the laboratory may play a useful role in measuring such resistance.

Two main approaches have been used to assess platelet resistance to aspirin. First, because platelets are the principal cell type to produce thromboxane, assay of this substance provides a measure of the activity of platelet cyclooxygenase. Thromboxane A2 undergoes conversion to thromboxane B2 and, hence, to the more stable 11-dehydro-thromboxane B2. Measurement of this metabolite has been used as an indirect measure of platelet cyclooxygenase activity (Catella et al., 1986). Assay of urinary 11-dehydro-thromboxane B2 has been employed for this purpose (Eikelboom et al., 2002).

A second approach that more directly assesses actual platelet function is the measurement of platelet aggregation following stimulation of platelets in vitro by an agonist entirely dependent on an intact cyclooxygenase pathway. Arachidonic acid is typically employed as an agonist using platelet-rich plasma and light transmittance aggregometry. Of great importance for the validation of such functional assays, however, is rigorous standardization of the testing procedure and inclusion of appropriate controls. Alternative methods have been developed to provide comparable information directly on anticoagulated whole blood. For example, the VerifyNow (Accumetrics, San Diego, CA) instrument permits optical platelet aggregation studies to be performed using whole blood. In this approach, fibrinogen-coated plastic beads impregnated with an infrared dye are added to citrated whole blood. Following the addition of arachidonic acid, the fibrinogen-coated beads coaggregate with the platelets, presumably through fibrinogen binding to the stimulated platelets through the conformationally active forms of platelet surface GPIIb/IIIa. Whereas erythrocytes had previously precluded optical aggregometry with whole blood, the introduction of infrared techniques has permitted rapid quantitation of platelet aggregation (as increasing infrared light transmittance) and of its inhibition by aspirin or other antiplatelet agents (Smith et al., 1999; Wang et al., 2003).

In addition to aggregometry, other methods may be employed to detect activation of platelets by agonists, and, consequently, inhibition of that activation by antiplatelet therapies. Flow cytometry may be used for this purpose through the detection of markers of platelet activation. Translocation of P-selectin from the intracellular α-granule of the resting platelet to the extracellular membrane following sufficient platelet stimulation provides one such marker, although the relatively small number of P-selectin molecules detectable even on the fully activated platelet limits the dynamic range of this marker (Michelson et al., 2001). Antibodies sensitive to conformational change in the GPIIb/IIIa molecule associated with platelet activation (e.g., PAC-1) potentially offer a greater dynamic signal range, extending from resting to fully activated platelets (Michelson, 2009).

P2Y12 INHIBITORS

Several drugs that interfere with ADP signaling through the P2Y12 receptor are available (Table 43.7). Clopidogrel and prasugrel are thienopyridines that are metabolized by the cytochrome P450 system in the liver to active agents that irreversibly inhibit platelet function. In contrast, ticagrelor is a direct-acting, reversible P2Y12 antagonist that exhibits a rapid onset and offset of antiplatelet effect (Michelson, 2010). Efforts to detect residual ADP purinergic P2Y12 receptors on the platelet surface following treatment by P2Y12 receptor antagonists have been difficult. The reasons for this are severalfold. First, the presence on the platelet surface of the additional P2Y1 class of ADP receptors that remains responsive to ADP

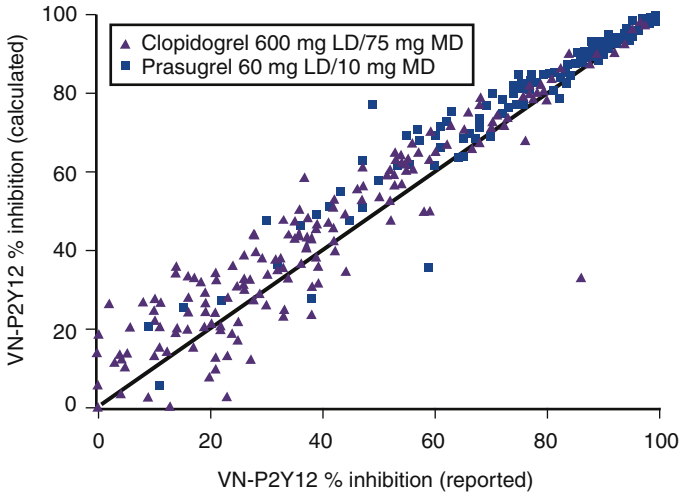

Figure 43.9 Association of "percent inhibition" reported by VerifyNow P2Y12 (*x*-axis) based solely on posttreatment measurement and calculated percent inhibition (*y*-axis) based on decrease in PRU (P2Y12 reaction units) posttreatment compared with pretreatment baseline PRU. Correlation coefficient (r) was calculated using Lin's concordance method. ■, Prasugrel; ▲, clopidogrel; filled line, unity line. (From Varenhorst C, James S, Erlinge D, et al.: Assessment of P2Y(12) inhibition with the point-of-care device VerifyNow P2Y12 in patients treated with prasugrel or clopidogrel coadministered with aspirin, *Am Heart J* 157:562.e1–9, 2009.)

following P2Y12 receptor antagonism complicates interpretation of residual responsiveness to ADP challenge in treated patients. Second, analysis of P2Y12 receptor antagonist therapy is almost universally undertaken in the setting of patients who are taking aspirin as well as a P2Y12 antagonist. Third, it has become increasingly common for patients to be started on combined P2Y12 receptor antagonist and aspirin therapy very early in the course of their evaluation for possible acute coronary syndrome or other potentially catastrophic thrombotic disorders. Accordingly, there is no opportunity in such instances to establish a baseline platelet function study that might be used to assess reduction in responsiveness following initiation of P2Y12 receptor antagonist therapy. Rather than identifying a true reduction in responsiveness that can reliably be attributed to antiplatelet therapy, the laboratory will be able to provide only a snapshot of platelet responsiveness for the patient already under treatment.

Through comparison of response to ADP by patients' platelets versus their responsiveness to other platelet agonists, derived estimates of the inhibition attributable to P2Y12 receptor antagonism have been proposed. As recently demonstrated, for levels of derived percent inhibition greater than approximately 20%, the correspondence of these values to true percent reduction of posttreatment responses compared with pretreatment responses using the VerifyNow whole-blood device appears reasonably good (Fig. 43.9) (Varenhorst et al., 2009). In addition to whole-blood aggregation, assessments of responsiveness to ADP receptor antagonists may be made by traditional light transmittance aggregometry of patient platelet-rich plasma, arguably a gold standard for assessment of platelet function. Flow cytometric approaches have also been introduced that assess the phosphorylation of intracellular vasodilator-stimulated phosphoprotein—the degree of which reflects with some measure of specificity the downstream signaling following the binding of ADP to platelet P2Y12 receptors (Harrison, 2012).

Efforts to sort out the relative merits of these different methods have been described in a number of publications (Alstrom et al., 2009; Gremmel

et al., 2009; Varenhorst et al., 2009; Bidet et al., 2010; Bouman et al., 2010; Cuisset et al., 2010). Nevertheless, caution is still in order with respect to how much reliance can be placed on current assays of platelet function to guide therapy (Chan et al., 2014). At the conclusion of a double-blind study assessing four different methodologic approaches in 116 patients with coronary artery disease, Lordkipanidze and colleagues (2008) remarked, "The assessment of platelet function inhibition by clopidogrel is highly test-specific. Decision to increase clopidogrel dosage may vary on the basis of the assay used, thus highlighting the need for unambiguous guidelines with respect to assay selection, as platelet function assays are not interchangeable. At present, platelet function testing evaluating clopidogrel efficacy cannot be recommended in routine clinical practice." Similarly, based on a study of 1069 patients on clopidogrel undergoing elective coronary stent implantation, caution was expressed by the authors, who concluded, "None of the tests provided accurate prognostic information to identify low-risk patients at higher risk of bleeding following stent implantation" (Breet et al., 2010). These conclusions were confirmed by the GRAVITAS investigators (Price et al., 2011), who found that using a high-dose clopidogrel regimen in patients with high on-treatment platelet reactivity defined by the VerifyNow assay did not reduce the incidence of death from cardiovascular causes, nonfatal myocardial infarction, or stent thrombosis compared with a standard-dose regimen of clopidogrel. Accordingly, it appears fair to say that the clinical usefulness of platelet function testing related to P2Y12 receptor inhibition to date has been modest at best.

Analogous to the use of pharmacogenetics to guide oral anticoagulant therapy with warfarin (reviewed earlier), significant effort has been devoted to developing a role for assessing genotypic variations affecting the metabolism of P2Y12 inhibitors. In particular, clopidogrel is a prodrug that acquires its ability to antagonize P2Y12 receptors only after it has been transformed in vivo to active metabolite. Cytochrome (CYP) 2C19 plays an important role in the in vivo bioactivation of clopidogrel (Kazui et al., 2010), and certain polymorphisms have been found to be associated with a lower clopidogrel responsiveness (Hulot et al., 2006; Brandt et al., 2007) and a higher risk of adverse cardiac events (Sibbing et al., 2009; Simon et al., 2009). The potential significance of this was spotlighted by a warning label mandated for Plavix (clopidogrel) by the FDA in March 2010, accompanied by the following announcement on the FDA website (http://www.fda.gov/Drugs/DrugSafety/PostmarketDrugSafetyInformationforPatientsandProviders/ucm203888.htm):

> The liver enzyme CYP2C19 is primarily responsible for the formation of the active metabolite of Plavix. Pharmacokinetic and antiplatelet tests of the active metabolite of Plavix show that the drug levels and antiplatelet effects differ depending on the genotype of the CYP2C19 enzyme. The following represent the different alleles of CYP2C19 that make up a patient's genotype:
> - The CYP2C19*1 allele has fully functional metabolism of Plavix.
> - The CYP2C19*2 and *3 alleles have no functional metabolism of Plavix. These two alleles account for most of the reduced function alleles in patients of Caucasian (85%) and Asian (99%) descent classified as poor metabolizers.
> - The CYP2C19*4, *5, *6, *7, and *8 and other alleles may be associated with absent or reduced metabolism of Plavix but are less frequent than the CYP2C19*2 and *3 alleles.
> - A patient with two loss-of-function alleles (as defined above) will have poor metabolizer status.

Shortly after the appearance of this boxed warning, the American College of Cardiology Foundation (ACCF) and the American Heart Association (AHA) published a consensus document providing guidance on this issue (Holmes et al., 2010). These groups recommended that "adherence to existing ACCF/AHA guidelines for the use of antiplatelet therapy should remain the foundation for therapy" and "the evidence base is insufficient to recommend either routine genetic or platelet function testing at the present time" (Holmes et al., 2010). It was also noted that there was no information that routine testing improved the outcome in subgroups of patients with specific genotypes. Nevertheless, the extent to which genotyping of individual patients actually contributes to their clinical management continues to be a subject of investigation (Shuldiner et al., 2009; Sibbing et al., 2010; Tresukosol et al., 2014).

Currently, there are no approved reversal agents for the P2Y12 inhibitors. However, promising results were recently seen in a Phase I study evaluating PB2452, a neutralizing monoclonal antibody fragment that binds ticagrelor and its active metabolites (Bhatt et al., 2019). In this study, healthy volunteers were pretreated with ticagrelor and then randomized to placebo or PB2452 at varying doses. PB2452 was administered as an intravenous bolus followed by a prolonged infusion (up to 16 hours). Using light transmission aggregometry, VerifyNow, and a vasodilator-stimulated phosphoprotein phosphorylation immunoassay, evidence of ticagrelor reversal and restoration of platelet function was seen within 5 minutes, was maximal at 30 minutes, and was sustained for more than 20 hours in a dose-dependent manner when compared with placebo. Adverse events were mostly limited to localized issues at the infusion site, such as bruising and extravasation (Bhatt et al., 2019).

GLYCOPROTEIN IIB/IIIA INHIBITORS

Therapeutic agents that interfere with the platelet surface receptor GPIIb/IIIa include abciximab, eptifibatide, and tirofiban (Eikelboom et al., 2012). These agents are primarily used in the acute setting and, generally, laboratory assessment of residual platelet function is not necessary. In those situations in which this might be needed, platelet aggregation studies using whole blood as well as platelet-rich plasma have proven helpful in defined clinical settings such as percutaneous transluminal coronary angioplasty (PTCA) for assessing the degree of residual platelet reactivity following inhibition of platelets by abciximab, eptifibatide, and other antagonists of the platelet GPIIb/IIIa complex (Hezard et al., 2000; Matzdorff et al., 2001). Flow cytometric approaches have also been used to monitor residual functionality of the GPIIb/IIIa complex following treatment of patients with GPIIb/IIIa inhibitors (Hezard et al., 2000; Matzdorff et al., 2001) as well as to quantify platelet microparticles as an indicator of platelet activation (Craft et al., 2004).

Following the introduction of GPIIb/IIIa antagonists in PTCA and other invasive procedures, recognition that thrombocytopenia can complicate administration of this drug has been increasing (Abrams & Cines, 2004; Aster et al., 2009). In some instances, this fall in the platelet count appears to be due to an immediate interaction between drug and platelet, possibly caused by preformed drug-dependent antibodies (Aster et al., 2004). This thrombocytopenia with all of the currently available agents is driven by naturally occurring antibodies and may occur in patients not previously exposed to the drug. In other instances, the time course of the thrombocytopenia suggests the development of antibodies to the drug itself or to a neo-epitope formed by binding of the drug to its platelet target (Curtis et al., 2002, 2004; Nurden et al., 2004). Although definitively establishing such a drug-dependent cause by laboratory methods is difficult and at times may simply prove elusive, available methods currently employed for evaluation of such acquired thrombocytopenia include flow cytometry, monoclonal antibody-specific immobilization of platelet antigens, and related techniques.

ACKNOWLEDGMENT

We gratefully acknowledge the contribution of Louis M. Fink, Richard A. Marlar, and Jonathan L. Miller, who authored this chapter in previous editions.

SELECTED REFERENCES

Ageno W, Gallus AS, et al.: Oral anticoagulant therapy: antithrombotic therapy and prevention of thrombosis, 9th ed: American College of chest Physicians evidence-based clinical practice guidelines, *Chest* 141(2 Suppl):e44S–e88S, 2012.

Excellent comprehensive review of oral anticoagulant therapy.

Review on the diagnosis and management of heparin-induced thrombocytopenia.

Aster RH, Curtis BR, et al.: Thrombocytopenia resulting from sensitivity to GPIIb-IIIa inhibitors, *Semin Thromb Hemost* 30(5):569–577, 2004.

Important review of thrombocytopenia secondary to antiplatelet therapy.

Chan NC, Eikelboom JW, et al.: Role of phenotypic and genetic testing in managing clopidogrel therapy, *Blood* 124(5):689–699, 2014.

Excellent review on the role of laboratory testing in managing therapy with clopidogrel.

Cuker A, Siegal DM, et al.: Laboratory measurement of the anticoagulant activity of the non-vitamin K oral anticoagulants, *J Am Coll Cardiol* 64(11):1128–1139, 2014.

Reviews the role of the laboratory in evaluating the target-specific oral anticoagulants.

Garcia DA, Baglin TP, et al.: Parenteral anticoagulants: antithrombotic therapy and prevention of thrombosis, 9th ed: American College of chest Physicians evidence-based clinical practice guidelines, *Chest* 141(2 Suppl):e24S–e43S, 2012.

Summarizes the characteristic properties of heparin, low-molecular-weight heparin, fondaparinux, and the parenteral direct thrombin inhibitors.

Greinacher A: Heparin-induced thrombocytopenia, *N Engl J Med* 373:252–261, 2015.

Review of the diagnosis and management of heparin-induced thrombocytopenia.

Holmes Jr DR, Dehmer GJ, et al.: ACCF/AHA clopidogrel clinical alert: approaches to the FDA "boxed warning": a report of the American College of Cardiology foundation Task Force on clinical expert consensus documents and the American heart association, *Circulation* 122(5):537–557, 2010.

Response to the FDA boxed warning concerning clopidogrel.

Kelton JG, Arnold DM, et al.: Nonheparin anticoagulants for heparin-induced thrombocytopenia, *N Engl J Med* 368(8):737–744, 2013.

Summarizes the properties and use of the parenteral direct thrombin inhibitors.

Kimmel SE, French B, et al.: A pharmacogenetic versus a clinical algorithm for warfarin dosing, *N Engl J Med* 369(24):2283–2293, 2013.

Randomized trial investigating the utility of pharmacogenetic data in the initial management of warfarin therapy.

Access the complete reference list online at Elsevier eBooks for Practicing Clinicians.

REFERENCES

Abrams CS, Cines DB: Thrombocytopenia after treatment with platelet glycoprotein IIb/IIIa inhibitors, *Curr Hematol Rep* 3(2):143–147, 2004.

Adcock DM, Johnston M: Evaluation of frozen plasma calibrants for enhanced standardization of the international normalized ratio (INR): a multi-center study, *Thromb Haemost* 87(1):74–79, 2002.

Ageno W, Gallus AS, et al.: Oral anticoagulant therapy: antithrombotic therapy and prevention of thrombosis, 9th ed: American College of chest Physicians evidence-based clinical practice guidelines, *Chest* 141(2 Suppl):e44S–e88S, 2012.

Aithal GP, Day CP, et al.: Association of polymorphisms in the cytochrome P450 CYP2C9 with warfarin dose requirement and risk of bleeding complications, *Lancet* 353(9154):717–719, 1999.

Alstrom U, Granath F, et al.: Platelet inhibition assessed with VerifyNow, flow cytometry and PlateletMapping in patients undergoing heart surgery, *Thromb Res* 124(5):572–577, 2009.

Althaus K, Strobel U, et al.: Combined use of the high heparin step and optical density to optimize diagnostic sensitivity and specificity of an anti-PF4/heparin enzyme-immunoassay, *Thromb Res* 128(3):256–260, 2011.

Amiral J, Marfaing-Koka A, et al.: Presence of autoantibodies to interleukin-8 or neutrophil-activating peptide-2 in patients with heparin-associated thrombocytopenia, *Blood* 88(2):410–416, 1996.

Anderson JL, Horne BD, et al.: A randomized and clinical effectiveness trial comparing two pharmacogenetic algorithms and standard care for individualizing warfarin dosing (CoumaGen-II), *Circulation* 125(16):1997–2005, 2012.

Ansell J, Hirsh J, et al.: Pharmacology and management of the vitamin K antagonists: American College of chest Physicians evidence-based clinical practice guidelines (8th edition), *Chest* 133(6 Suppl):160S–198S, 2008.

Arepally GM, Ortel TL: Bad weed: synthetic cannabinoid-associated coagulopathy, *Blood* 133(9):902–905, 2019.

Arepally GM, Ortel TL: Clinical practice: heparin-induced thrombocytopenia, *N Engl J Med* 355(8):809–817, 2006.

Arepally GM, Ortel TL: Heparin-induced thrombocytopenia, *Annu Rev Med* 61:77–90, 2010.

Asmis LM, Alberio L, et al.: Rivaroxaban: quantification by anti-FXa assay and influence on coagulation tests—a study in 9 Swiss laboratories, *Thromb Res* 129(4):492–498, 2012.

Aster RH, Curtis BR, et al.: Drug-induced immune thrombocytopenia: pathogenesis, diagnosis, and management, *J Thromb Haemost* 7(6):911–918, 2009.

Barrett YC, Wang Z, et al.: Clinical laboratory measurement of direct factor Xa inhibitors: anti-Xa assay is preferable to prothrombin time assay, *Thromb Haemost* 104(6):1263–1271, 2010.

Basu D, Gallus A, et al.: A prospective study of the value of monitoring heparin treatment with the activated partial thromboplastin time, *N Engl J Med* 287(7):324–327, 1972.

Bauer KA: Pros and cons of new oral anticoagulants, *Hematology Am Soc Hematol Educ Program 2013*464–470, 2013.

Berkompas DC: Coumadin skin necrosis in a patient with a free protein S deficiency: case report and literature review, *Indiana Med* 84(11):788–791, 1991.

Bharadwaj J, Jayaraman C, et al.: Heparin resistance, *Lab Hematol* 9(3):125–131, 2003.

Bhatt DL, Pollack CV, et al.: *Antibody-based ticagrelor reversal agent in healthy volunteers* 380(19):1825–1833, 2019.

Bidet A, Jais C, et al.: VerifyNow and VASP phosphorylation assays give similar results for patients receiving clopidogrel, but they do not always correlate with platelet aggregation, *Platelets* 21(2):94–100, 2010.

Billoir P, Barbay V, et al.: Anti-Xa oral anticoagulant plasma concentration assay in real life: rivaroxaban and apixaban quantification in emergency with LMWH calibrator, *Ann Pharmacother* 53(4):341–347, 2018.

Boneu B, de Moerloose P: How and when to monitor a patient treated with low molecular weight heparin, *Semin Thromb Hemost* 27(5):519–522, 2001.

Bongiorno RA, Nutescu EA: Generic warfarin: implications for clinical practice and perceptions of anticoagulation providers, *Semin Thromb Hemost* 30(6):619–626, 2004.

Bouman HJ, Parlak E, et al.: Which platelet function test is suitable to monitor clopidogrel responsiveness? A pharmacokinetic analysis on the active metabolite of clopidogrel, *J Thromb Haemost* 8(3):482–488, 2010.

Bounameaux H, de Moerloose P: Is laboratory monitoring of low-molecular-weight heparin therapy necessary? No, *J Thromb Haemost* 2(4):551–554, 2004.

Brandt JT, Close SL, et al.: Common polymorphisms of CYP2C19 and CYP2C9 affect the pharmacokinetic and pharmacodynamic response to clopidogrel but not prasugrel, *J Thromb Haemost* 5(12):2429–2436, 2007.

Breet NJ, van Werkum JW, et al.: Comparison of platelet function tests in predicting clinical outcome in patients undergoing coronary stent implantation, *J Am Med Assoc* 303(8):754–762, 2010.

Catella F, Healy D, et al.: 11-Dehydrothromboxane B2: a quantitative index of thromboxane A2 formation in the human circulation, *Proc Natl Acad Sci U S A* 83(16):5861–5865, 1986.

Connolly SJ, Crowther M, et al.: Full study of andexanet alfa for bleeding associated with factor Xa inhibitors, *N Engl J Med* 380(14):1326–1335, 2019.

Connolly SJ, Ezekowitz MD, et al.: Dabigatran versus warfarin in patients with atrial fibrillation, *N Engl J Med* 361(12):1139–1151, 2009.

Craft JA, Masci PP, et al.: Increased platelet-derived microparticles in the coronary circulation of percutaneous transluminal coronary angioplasty patients, *Blood Coagul Fibrinolysis* 15(6):475–482, 2004.

Cuisset T, Frere C, et al.: Clopidogrel response: Head-to-head comparison of different platelet assays to identify clopidogrel non responder patients after coronary stenting, *Arch Cardiovasc Dis* 103(1):39–45, 2010.

Cuker A, Arepally G, et al.: The HIT expert probability (HEP) score: a novel pretest probability model for heparin-induced thrombocytopenia based on broad expert opinion, *J Thromb Haemost* 8:2642–2650, 2010.

Cuker A, Husseinzadeh H: Laboratory measurement of the anticoagulant activity of edoxaban: a systematic review, *J Thromb Thrombolysis* 39:288–294, 2015.

Cuker A, Ortel TL: ASH evidence-based guidelines: is the IgG-specific anti-PF4/heparin ELISA superior to the polyspecific ELISA in the laboratory diagnosis of HIT? *Hematology Am Soc Hematol Educ Program*250–252, 2009.

Cuker A, Ptashkin B, et al.: Interlaboratory agreement in the monitoring of unfractionated heparin using the anti-factor Xa-correlated activated partial thromboplastin time, *J Thromb Haemost* 7(1):80–86, 2009.

Cunningham MT, Johnson GF, et al.: The reliability of manufacturer-determined, instrument-specific international sensitivity index values for calculating the international normalized ratio, *Am J Clin Pathol* 102(1):128–133, 1994.

Curtis BR, Divgi A, et al.: Delayed thrombocytopenia after treatment with abciximab: a distinct clinical entity associated with the immune response to the drug, *J Thromb Haemost* 2(6):985–992, 2004.

Curtis BR, Swyers J, et al.: Thrombocytopenia after second exposure to abciximab is caused by antibodies that recognize abciximab-coated platelets, *Blood* 99(6):2054–2059, 2002.

D'Angelo A, Seveso MP, D'Angelo SV, et al.: Comparison of two automated coagulometers and the manual tilt-tube method for the determination of prothrombin time, *Am J Clin Pathol* 92(3):321–328, 1989.

Das A, Liu D: Novel antidotes for target specific oral anticoagulants, *Exp Hematol Oncol* 4:25, 2015.

Davis PK, Musunuru H, et al.: The ex vivo reversibility of dabigatran-induced whole-blood coagulopathy as monitored by thromboelastography: Mechanistic implications for clinical medicine, *Thromb Haemost* 108(3):586–588, 2012.

Douxfils J, Chatelain C, et al.: Impact of apixaban on routine and specific coagulation assays: a practical laboratory guide, *Thromb Haemost* 110(2):283–294, 2013.

Douxfils J, Mullier F, et al.: Impact of dabigatran on a large panel of routine or specific coagulation assays. Laboratory recommendations for monitoring of dabigatran etexilate, *Thromb Haemost* 107(5):985–997, 2012.

Edson JR, Krivit W, et al.: Kaolin partial thromboplastin time: high levels of procoagulants producing short clotting times or masking deficiencies of other procoagulants or low concentrations of anticoagulants, *J Lab Clin Med* 70(3):463–470, 1967.

Eichler P, Budde U, et al.: First workshop for detection of heparin-induced antibodies: validation of the heparin-induced platelet-activation test (HIPA) in comparison with a PF4/heparin ELISA, *Thromb Haemost* 81(4):625–629, 1999.

Eikelboom JW, Hirsh J, et al.: Aspirin-resistant thromboxane biosynthesis and the risk of myocardial infarction, stroke, or cardiovascular death in patients at high risk for cardiovascular events, *Circulation* 105(14):1650–1655, 2002.

Eikelboom JW, Hirsh J, et al.: Antiplatelet drugs: antithrombotic therapy and prevention of thrombosis, 9th ed: American College of chest Physicians evidence-based clinical practice guidelines, *Chest* 141(2 Suppl):e89S–e119S, 2012.

Epstein RS, Moyer TP, et al.: Warfarin genotyping reduces hospitalization rates results from the MM-WES (Medco-Mayo Warfarin Effectiveness study), *J Am Coll Cardiol* 55(25):2804–2812, 2010.

Favaloro EJ, Adcock DM: Standardization of the INR: how good is your laboratory's INR and can it be improved? *Semin Thromb Hemost* 34(7):593–603, 2008.

Favaloro EJ, McVicker W, et al.: Improving the harmonisation of the international normalized ratio (INR): time to think outside the box? *Clin Chem Lab Med* 48(8):1079–1090, 2010.

Finley A, Greenberg C: Review article: heparin sensitivity and resistance: management during cardiopulmonary bypass, *Anesth Analg* 116(6):1210–1222, 2013.

Francart SJ, Hawes EM, et al.: Performance of coagulation tests in patients on therapeutic doses of rivaroxaban. A cross-sectional pharmacodynamic study based on peak and trough plasma levels, *Thromb Haemost* 111(6):1133–1140, 2014.

Francis JL, Groce 3rd JB: Challenges in variation and responsiveness of unfractionated heparin, *Pharmacotherapy* 24(8 Pt 2):108S–119S, 2004.

Gage BF, Eby C, et al.: Use of pharmacogenetic and clinical factors to predict the therapeutic dose of warfarin, *Clin Pharmacol Ther* 84(3):326–331, 2008.

Graff J, Harder S: Anticoagulant therapy with the oral direct factor Xa inhibitors rivaroxaban, apixaban and edoxaban and the thrombin inhibitor dabigatran etexilate in patients with hepatic impairment, *Clin Pharmacokinet* 52(4):243–254, 2013.

Granger CB, Alexander JH, et al.: Apixaban versus warfarin in patients with atrial fibrillation, *N Engl J Med* 365(11):981–992, 2011.

Gray E, Mulloy B, et al.: Heparin and low-molecular-weight heparin, *Thromb Haemost* 99(5):807–818, 2008.

Greinacher A, Juhl D, et al.: Heparin-induced thrombocytopenia: a prospective study on the incidence, platelet-activating capacity and clinical significance of antiplatelet factor 4/heparin antibodies of the IgG, IgM, and IgA classes, *J Thromb Haemost* 5(8):1666–1673, 2007.

Greinacher A, Potzsch B, et al.: Heparin-associated thrombocytopenia: Isolation of the antibody and characterization of a multimolecular PF4-heparin complex as the major antigen, *Thromb Haemost* 71(2):247–251, 1994.

Gremmel T, Steiner S, et al.: Comparison of methods to evaluate clopidogrel-mediated platelet inhibition after percutaneous intervention with stent implantation, *Thromb Haemost* 101(2):333–339, 2009.

Harenberg J: Is laboratory monitoring of low-molecular-weight heparin therapy necessary? Yes, *J Thromb Haemost* 2(4):547–550, 2004.

Harrison P: Advances in the monitoring of P2Y12 therapy, *Platelets* 23(7):510–525, 2012.

Hawes EM, Deal AM, et al.: Performance of coagulation tests in patients on therapeutic doses of dabigatran: a cross-sectional pharmacodynamic study based on peak and trough plasma levels, *J Thromb Haemost* 11(8):1493–1502, 2013.

Hezard N, Metz D, et al.: Use of the PFA-100 apparatus to assess platelet function in patients undergoing PTCA during and after infusion of c7E3 Fab in the presence of other antiplatelet agents, *Thromb Haemost* 83(4):540–544, 2000.

Hulot JS, Bura A, et al.: Cytochrome P450 2C19 loss-of-function polymorphism is a major determinant of clopidogrel responsiveness in healthy subjects, *Blood* 108(7):2244–2247, 2006.

Hursting MJ, Zehnder JL, et al.: The International Normalized Ratio during concurrent warfarin and argatroban anticoagulation: Differential contributions of each agent and effects of the choice of thromboplastin used, *Clin Chem* 45(3):409–412, 1999.

Kang M, Alahmadi M, et al.: Fondaparinux for the treatment of suspected heparin-induced thrombocytopenia: a propensity score-matched study, *Blood* 125(6):924–929, 2015.

Kazui M, Nishiya Y, et al.: Identification of the human cytochrome P450 enzymes involved in the two oxidative steps in the bioactivation of clopidogrel to its pharmacologically active metabolite, *Drug Metab Dispos* 38(1):92–99, 2010.

Kearon C, Akl EA, et al.: Antithrombotic therapy for VTE disease: antithrombotic therapy and prevention of thrombosis, 9th ed: American College of chest Physicians evidence-based clinical practice guidelines, *Chest* 141(2 Suppl):e419S–e494S, 2012.

Kelkar AH, Smith NA, et al.: An outbreak of synthetic cannabinoid-associated coagulopathy in Illinois, *N Engl J Med* 379(13):1216–1223, 2018.

King N, Tran MH: Long-acting anticoagulant rodenticide (superwarfarin) poisoning: a review of its historical development, epidemiology, and clinical management, *Trans Med Rev* 20:250–258, 2015.

Kirkel D, Lin TW, et al.: Asymptomatic factor VII deficiency: gene analysis and structure-function relationships, *Blood Coagul Fibrinolysis* 21(1):91–94, 2010.

Kirkwood TB: Calibration of reference thromboplastins and standardisation of the prothrombin time ratio, *Thromb Haemost* 49(3):238–244, 1983.

Kitchen S, Jennings I, et al.: Wide variability in the sensitivity of APTT reagents for monitoring of heparin dosage, *J Clin Pathol* 49(1):10–14, 1996.

Kitchen S, Preston FE: Standardization of prothrombin time for laboratory control of oral anticoagulant therapy, *Semin Thromb Hemost* 25(1):17–25, 1999.

Krajewski KC: Inability to achieve a therapeutic INR value while on concurrent warfarin and rifampin, *J Clin Pharmacol* 50(6):710–713, 2010.

Leaning KE, Ansell JE: Advances in the monitoring of oral anticoagulation: point-of-care testing, patient self-monitoring, and patient self-management, *J Thromb Thrombolysis* 3(4):377–383, 1996.

Lehman CM, Rettmann JA, et al.: Comparative performance of three anti-factor Xa heparin assays in patients in a medical intensive care unit receiving intravenous, unfractionated heparin, *Am J Clin Pathol* 126(3):416–421, 2006.

Lindahl TL, Baghaei F, et al.: Effects of the oral, direct thrombin inhibitor dabigatran on five common coagulation assays, *Thromb Haemost* 105(2):371–378, 2011.

Linkins LA, Dans AL, et al.: Treatment and prevention of heparin-induced thrombocytopenia: antithrombotic therapy and prevention of thrombosis, 9th ed: American College of chest Physicians evidence-based clinical practice guidelines, *Chest* 141 (2 Suppl):e495S–e530S, 2012.

Lo GK, Juhl D, et al.: Evaluation of pretest clinical score (4 T's) for the diagnosis of heparin-induced thrombocytopenia in two clinical settings, *J Thromb Haemost* 4(4):759–765, 2006.

Lombardi R, Chantarangkul V, et al.: Measurement of warfarin in plasma by high performance liquid chromatography (HPLC) and its correlation with the international normalized ratio, *Thromb Res* 111(4–5):281–284, 2003.

Lordkipanidze M, Pharand C, et al.: Comparison of four tests to assess inhibition of platelet function by clopidogrel in stable coronary artery disease patients, *Eur Heart J* 29(23):2877–2885, 2008.

Love JE, Ferrell C, et al.: Monitoring direct thrombin inhibitors with a plasma diluted thrombin time, *Thromb Haemost* 98(1):234–242, 2007.

Matzdorff AC, Kuhnel G, et al.: Comparison of GP IIB/IIIA inhibitors and their activity as measured by aggregometry, flow cytometry, single platelet counting, and the rapid platelet function analyzer, *J Thromb Thrombolysis* 12(2):129–139, 2001.

McFarland J, Lochowicz A, et al.: Improving the specificity of the PF4 ELISA in diagnosing heparin-induced thrombocytopenia, *Am J Hematol* 87(8):776–781, 2012.

McGehee WG, Klotz TA, et al.: Coumarin necrosis associated with hereditary protein C deficiency, *Ann Intern Med* 101(1):59–60, 1984.

Michelson AD: Methods for the measurement of platelet function, *Am J Cardiol* 103(Suppl):20A–26A, 2009.

Michelson AD: Antiplatelet therapies for the treatment of cardiovascular disease, *Nat Rev Drug Discov* 9(2):154–169, 2010.

Michelson AD, Barnard MR, et al.: Circulating monocyte-platelet aggregates are a more sensitive marker of in vivo platelet activation than platelet surface p-selectin. Studies in baboons, human coronary intervention, and human acute myocardial infarction, *Circulation* 104:1533–1537, 2001.

Moll S, Ortel TL: Monitoring warfarin therapy in patients with lupus anticoagulants, *Ann Intern Med* 127(3):177–185, 1997.

Morishima Y, Kamisato C: Laboratory measurements of the oral direct factor Xa inhibitor edoxaban. Comparison of prothrombin time, activated partial thromboplastin time, and thrombin generation assay, *Am J Clin Pathol* 143:241–247, 2015.

Mullier F, Bailly N, et al.: Contribution of platelet microparticles generation assay to the diagnosis of type II heparin-induced thrombocytopenia, *Thromb Haemost* 103(6):1277–1281, 2010.

Nagler M, Haslauer M, et al.: Fondaparinux—data on efficacy and safety in special situations, *Thromb Res* 129(4):407–417, 2012.

Nurden P, Clofent-Sanchez G, et al.: Delayed immunologic thrombocytopenia induced by abciximab, *Thromb Haemost* 92(4):820–828, 2004.

Nutescu EA: Point of care monitors for oral anticoagulant therapy, *Semin Thromb Hemost* 30(6):697–702, 2004.

Olson JD, Arkin CF, et al.: College of American Pathologists Conference I on laboratory monitoring of anticoagulant therapy: laboratory monitoring of unfractionated heparin therapy, *Arch Pathol Lab Med* 122(9):782–798, 1998.

O'Reilly RA, Aggeler PM, et al.: Hereditary transmission of exceptional resistance to coumarin anticoagulant drugs. The first reported kindred, *N Engl J Med* 271:809–815, 1964.

Ortel TL: Perioperative management of patients on chronic antithrombotic therapy, *Blood* 120(24):4699–4705, 2012.

Padmanabhan A, Jones CG, et al.: A novel PF4-dependent platelet activation assay identifies patients likely to have heparin-induced thrombocytopenia/thrombosis, *Chest* 150(3):506–515, 2016.

Patel MR, Mahaffey KW, et al.: Rivaroxaban versus warfarin in nonvalvular atrial fibrillation, *N Engl J Med* 365(10):883–891, 2011.

Pirmohamed M, Burnside G, et al.: A randomized trial of genotype-guided dosing of warfarin, *N Engl J Med* 369(24):2294–2303, 2013.

Pishko AM, Fardin S, et al.: Prospective comparison of the HEP score and 4Ts score for the diagnosis of heparin-induced thrombocytopenia, *Blood Adv* 2(22):3155–3162, 2018.

Poley S, Mempel W: Laboratory diagnosis of heparin-induced thrombocytopenia: advantages of a functional flow cytometric test in comparison to the heparin-induced platelet-activation test, *Eur J Haematol* 66(4):253–262, 2001.

Pollack CH, Reilly PA, et al.: Idarucizumab for dabigatran reversal – full cohort analysis, *N Engl J Med* 377(5):431–441, 2017.

Pollak ES, Russell TT, et al.: Asymptomatic factor VII deficiency in African Americans, *Am J Clin Pathol* 126(1):128–132, 2006.

Poller L: International normalized ratios (INR): the first 20 years, *J Thromb Haemost* 2(6):849–860, 2004.

Portola Pharmaceuticals: Inc. *Andexxa ® (coagulation factor Xa (recombinant), inactivated-zhzo) [package insert]*, South San Francisco, CA: Portola Pharmaceuticals, Inc; 2018.

Price MJ, Berger PB, et al.: Standard- vs high-dose clopidogrel based on platelet function testing after percutaneous coronary intervention. The GRAVITAS randomized trial, *J Am Med Assoc* 305(11):1097–1105, 2011.

Rieder MJ, Reiner AP, et al.: Effect of VKORC1 haplotypes on transcriptional regulation and warfarin dose, *N Engl J Med* 352(22):2285–2293, 2005.

Rosborough TK, Shepherd MF: Unreliability of international normalized ratio for monitoring warfarin therapy in patients with lupus anticoagulant, *Pharmacotherapy* 24(7):838–842, 2004.

Rosendaal FR, Reitsma PH: 5000 years old and still going strong, *J Thromb Haemost* 12(11):1763, 2014.

Salzman EW, Rosenberg RD, et al.: Effect of heparin and heparin fractions on platelet aggregation, *J Clin Invest* 65(1):64–73, 1980.

Sanderson S, Emery J, et al.: Narrative review: aspirin resistance and its clinical implications, *Ann Intern Med* 142(5):370–380, 2005.

Schulman S, Furie B: How I treat poisoning with vitamin K antagonists, *Blood* 125(3):438–442, 2015.

Shapiro GA, Huntzinger SW, et al.: Variation among commercial activated partial thromboplastin time reagents in response to heparin, *Am J Clin Pathol* 67(5):477–480, 1977.

Shimada YJ, Nakra NC, et al.: Relation of race (Asian, African-American, European-American, and Hispanic) to activated clotting time after weight-adjusted bolus of heparin during percutaneous coronary intervention, *Am J Cardiol* 105(5):629–632, 2010.

Shuldiner AR, O'Connell JR, et al.: Association of cytochrome P450 2C19 genotype with the antiplatelet effect and clinical efficacy of clopidogrel therapy, *J Am Med Assoc* 302(8):849–857, 2009.

Sibbing D, Braun S, et al.: Platelet reactivity after clopidogrel treatment assessed with point-of-care analysis and early drug-eluting stent thrombosis, *J Am Coll Cardiol* 53(10):849–856, 2009.

Sibbing D, Koch W, et al.: Cytochrome 2C19*17 allelic variant, platelet aggregation, bleeding events, and stent thrombosis in clopidogrel-treated patients with coronary stent placement, *Circulation* 121(4):512–518, 2010.

Siegal D, Lu G, et al.: Safety, pharmacokinetics, and reversal of apixaban anticoagulation with andexanet alfa, *Blood Adv* 1(21):1827–1838, 2017.

Simon T, Verstuyft C, et al.: Genetic determinants of response to clopidogrel and cardiovascular events, *N Engl J Med* 360(4):363–375, 2009.

Smith JW, Steinhubl SR, et al.: Rapid platelet-function assay: an automated and quantitative cartridge-based method, *Circulation* 99(5):620–625, 1999.

Smogorzewska A, Brandt JT, et al.: Effect of fondaparinux on coagulation assays: results of College of American Pathologists proficiency testing, *Arch Pathol Lab Med* 130(11):1605–1611, 2006.

Sunderji R, Gin K, et al.: Clinical impact of point-of-care vs laboratory measurement of anticoagulation, *Am J Clin Pathol* 123(2):184–188, 2005.

Taube J, Halsall D, et al.: Influence of cytochrome P-450 CYP2C9 polymorphisms on warfarin sensitivity and risk of over-anticoagulation in patients on long-term treatment, *Blood* 96(5):1816–1819, 2000.

Tresukosol D, Suktitipat B, et al.: Effects of cytochrome P450 2C19 and paraoxonase 1 polymorphisms on antiplatelet response to clopidogrel therapy in patients with coronary artery disease, *PloS One* 9(10), 2014. e110188.

Van Cott EM: Point-of-care testing in coagulation, *Clin Lab Med* 29(3):543–553, 2009.

Van den Besselaar AM, Barrowcliffe TW, et al.: Guidelines on preparation, certification, and use of certified plasmas for ISI calibration and INR determination, *J Thromb Haemost* 2(11):1946–1953, 2004.

Van Ryn J, Baruch L, et al.: Interpretation of point-of-care INR results in patients treated with dabigatran, *Am J Med* 125(4):417–420, 2012.

Van Ryn J, Stangier J, et al.: Dabigatran etexilate—a novel, reversible, oral direct thrombin inhibitor: interpretation of coagulation assays and reversal of anticoagulant activity, *Thromb Haemost* 103(6):1116–1127, 2010.

Varenhorst C, James S, et al.: Assessment of P2Y(12) inhibition with the point-of-care device VerifyNow P2Y12 in patients treated with prasugrel or clopidogrel coadministered with aspirin, *Am Heart J* 157(3):562.e1–562.e9, 2009.

Verhoef TI, Ragia G, et al.: A randomized trial of genotype-guided dosing of acenocoumarol and phenprocoumon, *N Engl J Med* 369(24):2304–2312, 2013.

Wang JC, Aucoin-Barry D, et al.: Incidence of aspirin nonresponsiveness using the Ultegra rapid platelet function assay-ASA, *Am J Cardiol* 92(12):1492–1494, 2003.

Warkentin TE, Elavathil LJ, et al.: The pathogenesis of venous limb gangrene associated with heparin-induced thrombocytopenia, *Ann Intern Med* 127(9):804–812, 1997.

Warkentin TE, Greinacher A, et al.: Laboratory testing for heparin-induced thrombocytopenia: a conceptual framework and implications for diagnosis, *J Thromb Haemost* 9(12):2498–2500, 2011a.

Warkentin TE, Maurer BT, et al: Heparin-induced thrombocytopenia associated with fondaparinux, N Engl J Med 356(25):2653–2655; discussion 2653-2655, 2007.

Warkentin TE, Pai M, et al.: Fondaparinux treatment of acute heparin-induced thrombocytopenia confirmed by the serotonin-release assay: a 30-month, 16-patient case series, *J Thromb Haemost* 9(12):2389–2396, 2011b.

Warkentin TE, Sheppard JI: Serological investigation of patients with a previous history of heparin-induced thrombocytopenia who are reexposed to heparin, *Blood* 123(16):2485–2493, 2014.

Warkentin TE, Sheppard JI, et al.: Quantitative interpretation of optical density measurements using PF4-dependent enzyme-immunoassays, *J Thromb Haemost* 6(8):1304–1312, 2008.

Whitlatch NL, Kong DF, et al.: Validation of the high-dose heparin confirmatory step for the diagnosis of heparin-induced thrombocytopenia, *Blood* 116(10):1761–1766, 2010.

Whitlock RP, Sun JC, et al.: Antithrombotic and thrombolytic therapy for valvular disease: antithrombotic therapy and prevention of thrombosis, 9th ed: American College of chest Physicians evidence-based clinical practice guidelines, *Chest* 141 (2 Suppl):e576S–e600S, 2012.

Yeh CH, Fredenburgh JC, et al.: Oral direct factor Xa inhibitors, *Circ Res* 111(8):1069–1078, 2012.

You JJ, Singer DE, et al.: Antithrombotic therapy for atrial fibrillation: antithrombotic therapy and prevention of thrombosis, 9th ed: American College of chest Physicians evidence-based clinical practice guidelines, *Chest* 141(2 Suppl):e531S–e575S, 2012.

Zwicker JI, Uhl L, et al.: Thrombosis and ELISA optical density values in hospitalized patients with heparin-induced thrombocytopenia, *J Thromb Haemost* 2(12): 2133–2137, 2004.

This page intentionally left blank

PART 6

Immunology and Immunopathology

EDITED BY H. Davis Massey, Richard A. McPherson

CHAPTER 44

OVERVIEW OF THE IMMUNE SYSTEM AND IMMUNOLOGIC DISORDERS

Richard A. McPherson, H. Davis Massey

LYMPHOID CELLS, 894
T Lymphocytes, 894
B Lymphocytes, 895
Antigen-Presenting Cells, 895
Natural Killer Cells, 895
NONLYMPHOID CELLS, 896
Neutrophils and Eosinophils, 896
Basophils and Mast Cells, 896
HUMORAL FACTORS, 896
Immunoglobulins, 896
Complement, 896
Cytokines, 896
HISTOCOMPATIBILITY ANTIGENS, 896
MECHANISMS OF IMMUNOLOGIC INJURY, 896
LABORATORY APPLICATIONS OF IMMUNOLOGIC ASSESSMENT, 897
THERAPEUTICS IN IMMUNOLOGY, 898
SELECTED REFERENCES, 900

KEY POINTS

- The immune system consists of cellular and humoral components that defend the body against invading microorganisms. Deficiency of individual factors of the immune system can leave an individual susceptible to different infections.
- The lymphoid cells of the immune system are composed of T cells that act directly against foreign antigens and B cells that differentiate into immunoglobulin (Ig)-secreting plasma cells capable of synthesizing immunoglobulins that combine with foreign antigens. Antigen-presenting cells are crucial for cell-to-cell communication during the direction of an immune response.
- The mechanisms by which lymphocytes differentiate into T cells and B cells involve rearrangement of genes for the T-cell antigen receptor and of genes for immunoglobulins, respectively.
- Lymphocytes from patient specimens are characterized by detection of surface proteins, termed cluster of differentiation, or CD markers, which designate their subset and function.
- Additional cellular elements are natural killer lymphocytes plus neutrophils, eosinophils, and the effectors of IgE-mediated hypersensitivity—basophils and mast cells.
- In addition to immunoglobulins or antibodies, humoral elements include a cascading series of enzyme activation in the complement system that results in enzymatic destruction of foreign cells and recruitment of inflammatory cells by cytokine actions.
- Histocompatibility antigens play a major role in antigen presentation to T cells and form the immunologic identity of an individual, which is important in rejection of organ transplants.
- Immunologic injury can occur as the result of excessive response to specific antigenic exposures, as in an allergic response, or as a result of circulating immune complexes.
- Autoimmune disease results when the mechanisms for maintaining immunologic tolerance to self-(auto)antigens fail, resulting in the formation of various autoantibodies plus activation of the cellular immune system against the patient's own tissues.
- Laboratory measurements of the immune system involve relatively simple techniques for counting lymphocytes and their subsets as well as for quantifying overall concentrations of immunoglobulins and complement proteins. More complex methods—such as detection of gene rearrangements, autoantibody characterization, and allergen reactivity with IgE—are useful for diagnosing various disorders of the immune system.
- Therapeutic approaches to disorders of the immune system include stimulation or replacement of deficient components and reduction or removal of other factors that are abnormal or are present in excess.

The immune system is structured to recognize, respond to, and destroy a wide variety of invading organisms such as bacteria, viruses, fungi, and parasites that otherwise would be capable of promoting infection that is harmful to the body. Discovery of components of the immune system has very often followed investigation of serious infections and the specific reactions that the body uses to combat pathogenic organisms. In general, this immunologic function can be summarized as searching for foreign (or nonself) antigens that do not belong in the body and then destroying them. In this process, the immune system also maintains surveillance over the appearance of new or foreign antigens on tumor cells and attempts to destroy them while leaving unharmed the normal (or self) antigens on healthy cells. Disease states may arise as a result of various aspects of immunologic function going awry, as in hypersensitivity reactions, autoimmune disease, and various immunodeficiency disorders. When functioning properly, the immune system is responsible for rejection of allogeneic organ/tissue transplants and graft-versus-host disease; the quest for tolerance in transplantation continues. This overview highlights components of the immune system and their functions along with some of the significant clinical disorders of immunity.

LYMPHOID CELLS

The lymphoid cells of the body reside in the lymph nodes, the spleen, the mucosal surfaces, and the circulation. They derive from multipotential hematopoietic stem cells, with their production moving progressively from the yolk sac in the embryo to the liver in the fetus, and, finally, to the bone marrow in the infant through adult ages (Weissman, 1994). The various lymphoid cells are conveniently identified by the presence of unique protein markers on their surfaces that endow those cells with particular functions.

T LYMPHOCYTES

T lymphocytes undergo differentiation in the thymus. After originating in the bone marrow, prothymocytes pass from the cortex to the medulla of the thymus, during which time they undergo maturation. This involves a selection process such that self-reactive thymocytes are eliminated, while thymocytes that can recognize antigens through interactions with molecules of the major histocompatibility complex (MHC) are retained (Nossal, 1994; von Boehmer, 1994). During maturation, they undergo genetic programming in which the gene for the T-cell antigen receptor (TCR) is rearranged to produce protein receptors that are invariant in their antigen specificity for the life span of that T lymphocyte as well as for all its descendant cells. T lymphocytes account for about 60% to 70% of all lymphocytes in the blood. They are also found in paracortical areas of lymph nodes and within periarteriolar lymphoid sheaths in the spleen.

A majority (>95%) of T lymphocytes have antigen receptors made of α- and β-subunits linked with disulfide bonds to form a molecular heterodimer

that resides on the outer membrane of the cell in association with the CD3 molecular complex (CD3 is a pan–T-cell marker). The α- and β-subunit TCR proteins have variable, joining, and constant regions (α also contains a diversity region), with corresponding encoding regions in the *TCR* gene that undergo rearrangement, resulting in high specificity binding for a particular antigen. The CD3 proteins assist transduction of the signal to the interior of the cell when an antigen binds to the TCR on the lymphocyte surface (Janeway & Bottomly, 1994; Weiss & Littman, 1994). A small percentage of T lymphocytes have a TCR composed of γ- and δ-subunits that similarly interact with CD3. These cells are generally found at mucosal surfaces of the gastrointestinal and respiratory tracts. T cell proliferations may be characterized as neoplastic (clonal) or benign (polyclonal) according to whether their DNA shows predominantly a single form of *TCR* gene rearrangement or a complete spectrum of such rearrangements, as normally occurs in a heterogeneous lymphocyte population.

Examination of T lymphocytes by flow cytometry focuses on a variety of surface markers. CD4 is found on about 60% of $CD3^+$ cells; these are helper/inducer T cells that direct the functions of other cells of the immune system by secreting cytokines that stimulate various functions. Two distinct subpopulations of $CD4^+$ helper cells have been identified: Th1 cells, which secrete interleukin (IL)-2 and interferon (IFN)-γ; and Th2 cells, which secrete IL-4 and IL-5. Th1 cells facilitate macrophage activation, delayed-type hypersensitivity, and the production of antibodies with opsonizing action. Th2 cells direct synthesis of other antibodies, such as IgE, and activate eosinophils. The marker CD8 is found on about 30% of T cells (thus, the normal ratio of $CD4^+$ to $CD8^+$ cells in the blood is typically 2:1). These $CD8^+$ T cells exhibit cytotoxicity and suppressor activity in the immune response.

The mechanism of antigen recognition is different between $CD4^+$ and $CD8^+$ subsets of T lymphocytes. CD4 molecules bind to the MHC class II molecules on antigen-presenting cells, whereas CD8 molecules interact with MHC class I molecules. Accordingly, $CD4^+$ T cells recognize antigens only in the context of MHC class II antigens, and $CD8^+$ T cells recognize them only through MHC class I antigens. A subset of T helper cells termed, *T regulatory (Treg) cells*, are important for immune tolerance and prevention of autoimmune disorders (see Chapter 53). Treg cells have surface markers for CD4 and CD25 (IL-2 receptor); thus, they are driven by IL-2. The transcription factor FOXP3 plays a role in Treg function, and mutation in the *foxp3* gene results in dysregulation of immune tolerance and progression to autoimmune diseases.

B LYMPHOCYTES

B lymphocytes make up roughly 10% to 20% of peripheral lymphocytes in the blood. They also are found in the bone marrow, lymph nodes, spleen, and other lymphoid tissues. In the spleen and lymph nodes, they aggregate into lymphoid follicles. Differentiation of B lymphocytes occurs in the bone marrow, where both positive selection and negative selection take place, as well as at peripheral locations. Antigenic stimulation of B cells leads to the formation of plasma cells that secrete immunoglobulins—the basis of specificity in humoral immunity. The B-cell antigen receptor complex uses surface IgM as the antigen-binding component. The antigen specificity of immunoglobulins derives from a rearrangement process in which both heavy- and light-chain genes are realigned. The heavy-chain gene has variable, diversity, joining, and constant regions, whereas the light-chain gene has variable, joining, and constant regions. Maturation of an antibody response entails switching from IgM to another heavy-chain type (usually IgG) as the result of further gene rearrangement, although the light-chain type remains fixed (Corcoran, 2005).

B cells have on their surfaces receptors for complement—CD21, which is also the receptor for Epstein-Barr virus (EBV), thus making these cells susceptible to EBV infection, and for the Fc region of immunoglobulins they have CD19 and CD20, which are frequently used for immunologic identification of B cells.

ANTIGEN-PRESENTING CELLS

Macrophages function as mononuclear phagocytes in inflammation. They also process ingested antigens and present them to immune effector cells in association with MHC molecules on their membranes (Fig. 44.1). T cells are not activated by soluble antigens; thus, presentation of antigens in this manner is necessary for T-cell stimulation and induction of cell-mediated immunity (Germain, 1994; Trombetta & Mellman, 2005). Macrophages also secrete cytokines such as IL-1 for modulation of inflammatory processes. Macrophages can directly lyse tumor cells in their role of immunosurveillance and are effector cells for some types of cell-mediated immunity (e.g., delayed hypersensitivity).

Dendritic cells (found in lymphoid tissues and in interstitial regions of other organs) and Langerhans cells (found in the epidermis) have extensive dendritic cytoplasmic processes that are rich in MHC class II molecules. Consequently, they are very efficient at presenting antigens (although they probably are not phagocytic) and are considered to be extremely important in that task within the entire immune system (Park & Chio, 2005).

NATURAL KILLER CELLS

Natural killer (NK) cells constitute 10% to 15% of lymphocytes in the peripheral blood. They are neither T cells nor B cells and were formerly called *null cells*. NK cells have the function of lysing other cells without

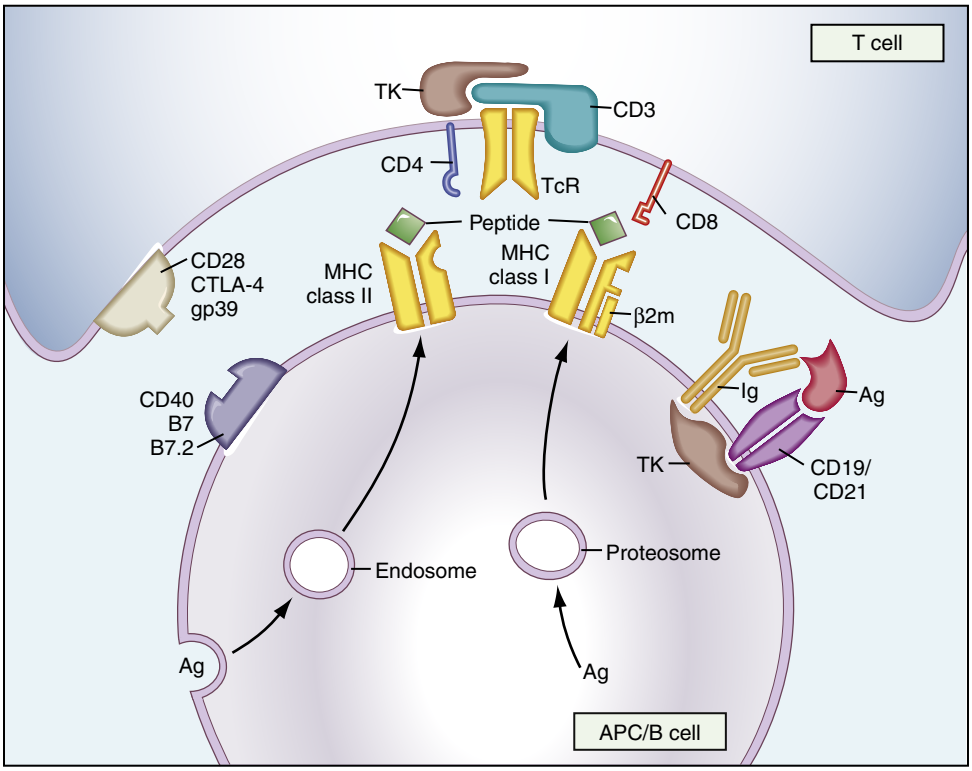

Figure 44.1 Cellular interactions in the immune system. Antigen-presenting cells (APCs) process external or internal antigens (Ag) and present antigen peptide fragments, in association with a major histocompatibility complex (MHC) molecule, to T cells. On the T cell, a specific antigen receptor (TcR), along with the coreceptor CD4 or CD8 molecule, recognizes the antigen–MHC complex. Cellular activation proceeds through the CD3 complex and activation of tyrosine kinases (TKs). The B-cell receptor is composed of membrane-bound immunoglobulin (Ig) complexed to associated membrane proteins, and the CD19/21 coreceptor. On antigen recognition, cellular TKs are also activated. Costimulatory activation of T cells or B cells is provided by cellular receptors binding their ligands (the ligand B7 or B7.2 for T-cell costimulation through CD28 and CTLA-4 molecules, and the gp39 ligand for the B cell CD40 molecule). (Redrawn with permission from Paul W, Seder R: Lymphocytic responses and cytokines, *Cell* 76:229, 1994; and Weiss A, Littman D: Signal transduction by lymphocyte antigen receptors, *Cell* 76:263, 1994.)

prior sensitization. They can attack tumor cells, cells infected with viruses, and others as well. Consequently, they form the initial defense against aberrant cells. NK cells are characterized by the surface markers CD16 and CD56, which are commonly used for their identification. CD16 is the Fc receptor for IgG; hence, NK cells are able to lyse selectively those cells that are coated with antibodies (antibody-dependent cell-mediated cytotoxicity, which is important in some hypersensitivity reactions). NK cells also secrete cytokines such as IFN-γ. It is interesting to note that NK cells are recognizable on examination of standard stained blood smears as large granular lymphocytes (Kronenberg, 2005).

NONLYMPHOID CELLS

These cells are not genetically programmed to recognize specific antigens or to interact with lymphoid cells in the induction of an immune response. Instead, they are effectors of immune reactions that are triggered by various factors.

NEUTROPHILS AND EOSINOPHILS

Neutrophils are drawn to regions of inflammation by chemoattractants such as IL-8. They then release from their granules toxic substances and enzymes that digest cellular structures indiscriminately. Neutrophils also ingest cellular debris, as do eosinophils, and remove it from tissue sites.

BASOPHILS AND MAST CELLS

Basophils (and their counterparts in tissues, the mast cells) have on their surfaces high-affinity Fc receptors that bind circulating IgE. Uptake of IgE onto the membranes of basophils apparently is not antigen dependent; instead, it is driven by mass action between the amount of total IgE and the available basophils. When the antigen (or allergen) comes into contact with basophil surface-bound IgE that recognizes it, those basophils become activated and release substances such as histamine, which mediate some hypersensitivity reactions. Thus, basophil specificity is directed by the particular IgE that is bound to its surface from the blood; theoretically, a basophil could have multiple different IgE molecules on its surface and, thus, could react with many different allergens.

HUMORAL FACTORS

IMMUNOGLOBULINS

Antibody molecules can be bound to B-cell surfaces for stimulation of further immunoglobulin secretion. They also circulate in the blood and appear at mucosal surfaces of the respiratory and gastrointestinal tracts, where they are likely to come into contact with potentially pathogenic microorganisms. The major immunoglobulins in the blood are IgM, IgG, and IgA. These antibodies presumably arise following exposure to a multitude of foreign antigens and may remain for years with continued secretion to replace molecules that are lost through normal clearance of proteins from the circulation. At mucosal surfaces, the primary type of antibody is dimeric IgA, which is secreted at that site (Fagarasan, 2004) (see Chapter 47). The other immunoglobulins are IgD (which resides on B-cell surfaces, where it may be involved in immune signal transduction but does not achieve substantial concentrations as free molecules in the blood) and IgE (which functions by binding to surfaces of basophils and stimulates the release of vasoactive substances from those cells in the presence of specific allergens).

Immunoglobulins in the blood function by attaching to antigens on the surfaces of foreign cells, bacteria, viruses, and the like, and by facilitating their destruction through nonspecific effectors such as complement and NK cell activation. Disease monitoring by immunoglobulin testing includes qualitative analysis for clonal versus polyclonal detection (e.g., for diagnosis of multiple myeloma) and quantitative analyses both for overall concentrations of IgM, IgG, and IgA (to detect possible selective or combined deficiencies or overproduction of immunoglobulin classes) and for titers of specific antibodies against individual antigens (e.g., isohemagglutinins, *Pneumococcus*, *Haemophilus*, tetanus, and diphtheria).

COMPLEMENT

This set of interacting proteins has the role of enzymatically destroying targets (e.g., cells, bacteria) to which they have been directed by antibodies or through other means (see Chapter 48). Measurements of complement components have two major uses in clinical diagnosis: to detect congenital deficiencies (which are relatively rare) that may predispose to certain disorders such as infection or progression to autoimmune disease, and to detect acquired complement level reductions that reflect current activity of systemic autoimmune diseases such as systemic lupus erythematosus (Wen et al., 2004).

CYTOKINES

These soluble substances are the means by which cellular immune responses are regulated. They are short-acting mediators that are elaborated by some cells and diffuse to other cells, where they act (Leonard, 2003). Many cytokines are pleiotropic in that they can act on different cell types. They can act in an endocrine manner by stimulating cells at a distance, they can act on cells in their immediate vicinity (paracrine), and they can stimulate the same cells that secreted them (autocrine). The specific actions of cytokines include hematopoiesis through colony-stimulating factors that induce granulocyte and macrophage production, natural immune responses (through IL-1, tumor necrosis factor [TNF]-α, interferons, and IL-8), stimulation of lymphocyte growth and activation (through IL-2 and others), and activation of nonspecific inflammatory cells (see Chapter 49). Cytokines are still being discovered as more details emerge regarding cell-to-cell communication.

Clinical use of cytokines includes both suppression of the immune response in allogeneic organ transplantation by drugs such as cyclosporine, which blocks production of IL-2, and enhancement of the immune response in therapies against cancer or infection. These latter treatments are largely experimental, although it has been shown that pretreatment with antibodies against TNF-α can prevent deleterious Jarisch-Herxheimer reactions resulting from antibiotic treatment of *Borrelia recurrentis* infection in sheep (Fekade et al., 1996). This model very probably presages a host of new therapies by which immune responses will be selectively enhanced or suppressed according to particular clinical needs.

HISTOCOMPATIBILITY ANTIGENS

The MHC (also called the *human leukocyte antigen [HLA] complex*) is encoded on human chromosome 6 and includes class I molecules (HLA A, B, and C), class II molecules (HLA DP, DQ, and DR), and the intervening class III molecules of some complement components and TNF-α and TNF-β (see Chapter 50). The functions of class I and class II antigens have already been discussed briefly in terms of how they participate in antigen presentation to T cells. These antigens were discovered and their highly polymorphic natures were described in studies of immune tolerance and rejection of transplanted allogeneic organs. Consequently, one of the most important clinical uses of HLA typing involves matching potential organ or tissue donors with recipients who are in need of a transplant. Another significant clinical application is seen in the typing of affected patients and their family members to establish their risk for developing some diseases that are associated with particular HLA types (e.g., ankylosing spondylitis with HLA B27; see Chapter 51). Still another use of HLA typing involves providing matched platelets for patients who have become refractory to platelet transfusions as the result of HLA antibody formation after exposure to multiple donors (e.g., following transfusion support for chemotherapy or hematopoietic progenitor cell transplantation; see Chapter 38).

MECHANISMS OF IMMUNOLOGIC INJURY

Immunologic responses can cause injury to normal tissues and to invading organisms that may have triggered a response. These injurious responses are conveniently classified into four types of hypersensitivity. Type I is anaphylactic or allergic in nature; it is mediated by IgE bound to the surface of basophils and mast cells. When specific antigens (or allergens) bind to surface IgE, the basophils are stimulated to release histamine and other vasoactive substances that are the immediate mediators of allergic reactions (Kemp & Lockey, 2002). Clinical strategies for treatment of asthma and allergies have addressed different aspects of this sequence of events, from counteracting the effects or release of histamine back to desensitization. Successful use of a recombinant humanized monoclonal antibody against IgE to treat such individuals has been demonstrated (Milgrom et al., 1999). In the future, this therapy could be based in part on measurement of IgE concentrations in serum.

Type II occurs when antibodies bind to antigens on the surfaces of cells; damage may occur as the result of binding and activation of complement (e.g., immune hemolysis), antibody-dependent cell-mediated cytotoxicity (e.g., lysis of tumor cells or parasites), or antibody-mediated interference with cellular functions (e.g., autoantibodies against acetylcholine receptors in myasthenia gravis).

BOX 44.1

Domains of Immunology Testing

Cellular Immunity

- Complete blood count and differential
- Lymphocyte enumeration (CD2, CD3, CD4, CD8, CD19, CD20, CD56) for T cells, B cells, NK cells
- HIV antibodies/viral load/genotype
- Skin testing for anergy
- Lymphocyte function/activation
- Neutrophil activation (oxidative burst)
- Lymphocyte adhesion defect (CD11a, CD11b, CD11c, CD18)

Humoral Immunity

- Quantitative immunoglobulins (IgG, IgA, IgM)
- IgG subclasses
- Immunoglobulin function/stimulation (protein antigens: tetanus, diphtheria; carbohydrate antigens: *Pneumococcus*, *Haemophilus*); ABO blood group isohemagglutinins

Complement

- C3, C4 for consumption
- Screening for deficiency: CH50
- Confirming deficiency: C1–C9
- C4d deposition
- Circulating immune complexes

Cytokines

- Interleukins
- Interferons
- Tumor necrosis factors

Human Leukocyte Antigens (HLAs)

- HLA antibodies for matching organs and bone marrow in allogeneic transplants
- Identity testing
- HLA genotyping (high-resolution)
- HLA typing for disease association (HLA-B27)

Autoimmune Diseases

- Systemic rheumatic diseases: Antinuclear antibodies; anti-dsDNA, anti-Sm, anti-RNP, anti-SSA, anti-SSB, anti-Scl70, anticardiolipin, anti-CCP
- Organ-specific diseases: Antithyroid, anti–parietal cell, antiendomysial, antiadrenal, antiskin, antimitochondria, anti–smooth muscle
- Vasculitis: Cryoglobulins (RF), c-ANCA, p-ANCA

Allergy/Hypersensitivity/Asthma

- Total IgE
- Allergen-specific IgE: Foods, pollens, animals, insects, mold
- Skin tests for allergy

c-ANCA, Classical antineutrophil cytoplasmic antibodies; *HIV,* human immunodeficiency virus; *NK,* natural killer; *p-ANCA,* protoplasmic-staining antineutrophil cytoplasmic antibodies; *RF,* rheumatoid factor.

Type III results from immune complex formation between exogenous antigens such as bacteria or viruses and antibodies, or between endogenous autoantigens and autoantibodies. Typical tissue damage occurs in organs that contain numerous small blood vessels wherein circulating immune complexes deposit, or in places where endogenous antigens naturally occur.

Type IV is cell-mediated or delayed hypersensitivity, which depends on functioning $CD4^+$ T cells or other cytotoxicity from $CD8^+$ T cells. Type IV is the basis of the immune reaction to viruses, fungi, protozoa, and parasites, as well as to intracellular microbes such as mycobacteria. Patients with acquired immunodeficiency syndrome are susceptible to infection with these and other opportunistic agents when they lose $CD4^+$ T cells.

LABORATORY APPLICATIONS OF IMMUNOLOGIC ASSESSMENT

Examinations of the immune system for evaluation of potential deficiencies or disorders are listed in Box 44.1.

Cellular immunity has several levels of investigation, beginning with leukocyte count and differential commonly available on automated hematology analyzers as part of the complete blood cell count. Deficiencies of neutrophils often occur with chemotherapy for malignancy, whereas elevation of neutrophils is a sign of acute infection, particularly with bacteria. Rare individuals may have normal numbers of neutrophils but may be susceptible to infection owing to defects of function (e.g., chronic granulomatous disease) that can be assessed by neutrophil activation (by oxidative burst) in response to stimuli or by bacterial killing assays.

Different populations of lymphocytes are enumerated by flow cytometric techniques that quantitate cells according to the expression of surface protein markers specific for T cells (CD2, CD3), subsets of T cells (CD4, CD8), B cells (CD19, CD20), monocytes (CD14), and NK cells (CD16, CD56). Because the most common cause of lymphocyte disorder today is infection with the human immunodeficiency virus (HIV), the most frequently monitored lymphocyte surface markers are CD4 and CD8 for the effects of HIV infection and prediction of susceptibility to opportunistic infection. HIV infection is usually diagnosed by detection of anti-HIV antibodies confirmed by Western blot. Monitoring of HIV infection also includes quantitative viral loads by molecular diagnostic methods such as reverse transcriptase polymerase chain reaction, and use of antiretroviral drugs is guided by HIV genotyping (and, on rare occasions, by phenotype testing of drug resistance). Lymphocyte function is not often measured directly, but this can be done by stimulation assays that look at lymphocyte proliferation (e.g., by incorporation of tritiated thymidine into DNA) or by cell cycle analysis performed with flow cytometry after stimulation. Of course, skin testing is a direct reflection of T-cell response to antigens in vivo.

Humoral immunity is often assessed by quantitative immunoglobulin measurements of total IgG, IgA, and IgM; deficiency of one or more immunoglobulin classes can lead to increased susceptibility to infection. Measurement of IgG subclasses can also be useful in this type of evaluation. Serum protein electrophoresis and immunofixation electrophoresis provide additional information regarding the clonality of immunoglobulins. A monoclonal band of immunoglobulins indicates a clonal population of B cells or plasma cells that have escaped regulation and might result in a plasma cell dyscrasia such as multiple myeloma. In contrast, a polyclonal distribution of immunoglobulins is generally taken to indicate a reactive process of an otherwise normal immune system.

Direct measurement of immunoglobulin function is done by evaluating the titers of antibodies against specific antigens. The presence of isohemagglutinins against ABO blood group antigens is conveniently examined to detect anti-A and anti-B antibodies in persons who lack those blood groups. Common immunizations result in the presence of detectable antibodies against the protein antigens of diphtheria and the tetanus toxoid, and against the carbohydrate antigens of *Pneumococcus* and *Haemophilus*. Measurements of antibodies against these antigens are standard procedures for evaluation of immunodeficiencies. If they are lacking, reimmunization can be done to elicit evidence of an immune response.

Longitudinal profiling of **transcriptomics** plus other omics of genome, metabolism, and autoantibodies has been accomplished as proof of principle in a single individual over 14 months (Chen et al., 2012). Although this methodology is currently very costly, it points the way to future examinations to study disease states, particularly in the evaluation of inflammatory states and whether their etiologies can be established as anti-infectious, autoimmune, anti-tumor, or other condition. This approach possibly may serve as a guide to early and specific therapy.

A novel approach to cancer diagnosis has emerged in which antibodies to tumors are detected according to their pattern of binding, in a microarray, to thousands of random sequence peptides representing essentially all possible epitopes (Stafford et al., 2014). The **immunosignature** of the peptides to which patient serum antibodies bind has allowed the successful classification of cancers in patients with over 98% accuracy. This system has the promise to provide comprehensive analysis of the immune response for the early diagnosis of malignancies and, potentially, any disease condition in which antibodies are produced, including infectious diseases (Richer et al., 2015).

The **complement system** is most frequently examined by measurement of C3 and C4 components to look for depressions that suggest consumption through activation. Although circulating immune complexes (CICs) are the presumptive cause of decreased C3 and C4 concentrations, CICs are rarely measured directly. However, deposition of CICs in tissues can be detected by immunofluorescent staining for immunoglobulin and C3 or C4d. Hereditary deficiencies of individual complement components are screened for by the CH50 test, which traditionally used antibody-coated horse erythrocytes in a hemolysis assay (now often replaced by an equivalent assay using liposomes in place of erythrocytes) and then are confirmed with specific immunoassays for deficiencies of individual complement proteins.

Determinations of **cytokine** concentrations are usually considered investigational procedures without definitive application despite the understanding we have of the roles they play in pathophysiology. Some of the potential candidates for future monitoring are the interleukins IL-1β,

IL-2, IL-2 receptor, IL-4, IL-5, IL-6, IL-8, IL-10, IL-12, and IL-13. These factors can be elaborated as locally acting messengers in many different inflammatory processes; thus, they lack specificity for distinguishing different etiologies such as infection versus autoimmunity. They act at sites of tissue injury or inflammation; thus, they do not reach easily measured concentrations in blood. Perhaps by looking at concentrations of multiple factors simultaneously both in blood and at the tissue level, interpretation will be feasible using patterns related to specific stimuli and physiologic insults. Other substances that fall into this category of immunomodulating agents include TNF-α and IFN-α, -β, and -γ. A recent clinical application utilizes the quantitation of IFN-γ released by lymphocytes in a peripheral blood specimen after in vitro stimulation with mycobacterial antigens to determine previous exposure status of a patient to that organism.

HLA testing and cross-matching between donors and recipients form the basis of solid-organ and bone marrow transplantation. Traditional serologic testing for antigens and antibodies has now been expanded with high-resolution HLA genotyping. HLA typing has also been used for matching platelet transfusions in select refractory patients. HLA typing has been used for identity testing, and some antigenic types (e.g., HLA-B27) are recognized to be associated with specific autoimmune disorders.

Applications of testing to **autoimmune diseases** are multiple. Systemic rheumatic diseases such as lupus erythematosus, rheumatoid arthritis, and scleroderma are commonly diagnosed with a battery of autoantibody assays, including the antinuclear antibody plus individual antibodies such as anti-DNA, anti-Sm, anti-RNP, anti-SS-A, anti-SS-B, Scl-70, anticardiolipin, rheumatoid factor, and anti–cyclic citrullinated peptide. Organ-specific autoimmune diseases are characterized by tissue or organelle reactive autoantibodies such as antithyroid, anti–parietal cell, antiskin, antiendomysial (antitissue transglutaminase), antimitochondrial, anti–smooth muscle, antiadrenal, and so forth. Antibodies important in vasculitis include cryoglobulins and classical antineutrophil cytoplasmic antibodies/protoplasmic-staining antineutrophil cytoplasmic antibodies. Although some autoantibodies are etiologic and serial measurements of their titers are important for monitoring disease progress, other antibodies are nonetiologic and, thus, are most useful for diagnosis alone.

For decades, the automated methods for measuring autoantibodies and other serologies have largely been based on enzyme-linked immunosorbent assay (ELISA) technologies (see Chapter 45). Newer methods have been developed in which antigens are coated on small beads using combinations of two colored dyes to identify the antigen. The beads are then allowed to bind immunoglobulin, which is detected by fluorescent-labeled anti-Ig. This configuration allows multiplexing of different assays in the same reaction mixture, resulting in labor saving and faster turnaround times. Many of these bead assays are likely to yield results somewhat different from ELISAs because they detect relatively high-avidity antibodies but not the low-avidity antibodies that can be detected by ELISA. This feature is particularly important for quantitating anti-dsDNA antibodies and is likely to cause some initial confusion among clinicians as immunoassays are converted to the new platform. On the positive side, high-avidity anti-dsDNA antibody measurement by bead immunoassay correlates well with the Farr assay, which also detects high-avidity antibodies that are recognized to have clinical significance (Venner et al., 2013).

Immunoassays for syphilis also have gone through changes in which the order of testing has been reversed so that the treponemal-specific assay for antibody against treponemal protein is done first. Positive specimens then are tested with the rapid plasma reagin (RPR) as a confirmatory test (Binnicker et al., 2012). This reversal in test order is due to the ability to automate immunoassays for antibodies against proteins, but not against cardiolipin, in the RPR. Discrepant results from these two assays should be evaluated by a third assay that relies on a different principle.

Allergies, hypersensitivities, and asthma have common pathways in which allergens are recognized by specific IgE that is bound to the surfaces of basophils and mast cells, thereby liberating histamine and creating allergic symptoms. Diagnostic evaluation of allergies includes measurements of total IgE plus allergen-specific IgE to determine which allergens are significant for particular patients. Typical allergens for this testing include foods, pollens, molds, animal dander, and insects. Skin testing in vivo with these allergens is complementary because a positive response depends on the presence of reactive IgE plus competent T cells with CD4.

Evaluation for possible immunodeficiency is usually initiated when a young child presents with numerous and often life-threatening infections. However, for children born with **severe combined immunodeficiency (SCID)**, waiting for repeat infections before initiating a diagnostic workup may allow fatal infections to develop in the first few months of life. Accordingly, many states have now implemented SCID screening of newborns using heel-stick blood samples that are already collected for other neonatal congenital disease testing (see Chapter 52). SCID screening is based on quantitation of the T-cell receptor excision circles (TRECs) of DNA that are normally present in mature lymphocytes (Puck, 2012). This approach can lead to early diagnosis and curative hematopoietic stem cell transplant prior to a first major infection in affected children.

BOX 44.2

Therapeutic Targets in the Immune System

Cellular Immunity
- Glucocorticoids
- Anti–T cell drugs (e.g., calcineurin inhibitors)
- Anti-CD20 (e.g., rituximab)
- Antilymphocyte globulin
- Photopheresis
- Interleukin-2
- Antiretroviral drugs

Humoral Immunity
- Intravenous immunoglobulins (pooled)
- Plasma exchange (to remove harmful antibodies, cryoglobulins)
- Humanized monoclonal/chimeric antibodies for target antigen neutralization (e.g., anti-CD20)

Complement
- Plasmapheresis to remove complement-activating immune complexes
- Eculizumab to inhibit terminal complement activity

Cytokines
- Interferons
- Anti–tumor necrosis factor-α
- Granulocyte–colony stimulating factor (G-CSF)

Human Leukocyte Antigens
- Organ transplant rejection: plasmapheresis
- Graft-versus-host disease: photopheresis

Autoimmune Diseases

Suppression of cellular or humoral immunity by:
- Glucocorticoids
- Alkylating agents (e.g., cyclophosphamide)
- Antimetabolites (e.g., methotrexate, azathioprine)
- Nonsteroidal antiinflammatory drugs
- Anti–T cell drugs

Allergy/Hypersensitivity/Asthma
- Antihistamines
- Glucocorticoids
- Allergen desensitization injections
- Leukotriene antagonists
- β-Adrenergic agonists
- Anti-IgE monoclonal antibody
- Anti-IL-5 monoclonal antibody (suppresses eosinophils)
- Antiinflammatory monoclonal antibodies against interleukins
- Enhanced T-cell antitumor activity
  - Inhibitors of PD-1 pathway
  - Chimeric antigen receptor T-cell therapy

THERAPEUTICS IN IMMUNOLOGY

Therapeutic targets in the immune system are important to consider because of the need to measure the effects of such treatments to make adjustments and guide clinical management (Box 44.2). One of the most common abnormalities of cellular immunity today is HIV infection, for which antiretroviral drugs are essential with monitoring that includes viral load measurements and genotyping to predict response to specific drugs.

Cellular immunity is the target of several different drugs that act against T cells. Thus, these drugs are often used to suppress immune responses against allogeneic solid-organ transplants and graft-versus-host disease (GVHD) from allogeneic bone marrow transplants. They include the cyclophilin-binding drugs cyclosporine and tacrolimus, which inhibit calcineurin, and the immunosuppressants sirolimus and mycophenolate, both of which block activation of T cells and B cells. Therapeutic drug monitoring of blood concentrations of these immunosuppressants is useful to achieve therapeutic effect (usually as a synergistic action of agents from different drug

classes) while avoiding drug toxicities. Polyclonal antilymphocyte globulin is used to reduce the circulating numbers of T cells in an effort to block transplant rejection. Also used is monoclonal anti-CD3 antibody, which binds to that molecule on T cells to reduce their numbers. Experimental anti–IL-2 receptor (CD25) antibody has also been used to block organ transplant rejection. Extracorporeal photopheresis has been successfully applied in the treatment of GVHD and even for cellular rejection of transplanted solid organs, beyond its well-established role in controlling cutaneous T-cell lymphoma.

Humoral immunity can be enhanced by passive intravenous infusion of immunoglobulin (IVIg) fractions pooled from multiple individuals who can be expected to contain antibodies against a multitude of infectious agents; high-titer immunoglobulins against specific microorganisms are also available (e.g., against hepatitis B virus). IVIg is also used to modulate some autoimmune disorders such as myasthenia gravis, possibly by interfering with the attachment of harmful autoantibodies to tissue sites. Alternatively, harmful antibodies can be removed by plasma exchange using apheresis, in which plasma proteins are replaced by another protein solution such as 5% albumin.

Monoclonal antibodies designed to interact with very specific antigens on cell surfaces or in the blood are now in use for several clinical applications (Griggs & Zinkewich-Peotti, 2009). Because of the potential side effects of stimulating immune or even allergic responses, these large-molecule drugs have been reconfigured to appear as naturally occurring proteins by humanizing them with constant regions derived from human immunoglobulin genes. An example of such a chimeric antibody is anti-CD20, which has application in treating B-cell lymphomas as well as in modulating the synthesis of some autoantibodies.

Complement consumption through CICs can be addressed therapeutically by plasmapheresis to remove those CICs (usually in the form of cryoglobulins) and, thus, lower the harmful deposition burden in tissues such as the renal glomeruli or other vessels. Eculizumab is a therapeutic preparation of a humanized monoclonal antibody that is a terminal complement inhibitor, specifically acting against complement protein C5. It is used for treatment of paroxysmal nocturnal hemoglobinuria (Hillmen et al., 2006) and of atypical hemolytic uremic syndrome (Noris et al., 2010). It is also being evaluated for use in other conditions in which complement activation plays a key role.

Cytokines in regular clinical use include IFN-α for combating infection with hepatitis B virus or hepatitis C virus and IFN-γ for stimulating immune responsiveness. TNF-α can be neutralized in the circulation by specific therapeutic antibodies or a modified receptor molecule to decrease undesired inflammatory responses in conditions such as rheumatoid arthritis and Crohn disease. Granulocyte–colony stimulating factor is used regularly in clinical practice to rescue patients who have developed leukopenia after chemotherapy and to mobilize hematopoietic stem cells for collection from peripheral blood to prepare for transplantation. Administration of IL-2 does succeed in raising CD4 counts, but this approach has not yet been found to improve outcome in HIV infection (INSIGHT-ESPRIT Study Group, 2009). It is likely that other stimulators or inhibitors of cytokines will come into clinical practice in the future.

HLA mismatches in allogeneic transplanted organs are typically dealt with by administration of immunosuppressant drugs but can also be treated with extracorporeal photopheresis to diminish cellular immune rejection as well as with plasmapheresis to remove HLA antibodies that the host might have previously formed or later formed in response to the transplanted organ.

Autoimmune diseases have been treated with different groups of drugs to reduce the inflammatory response, such as corticosteroids, alkylating agents (e.g., cyclophosphamide), antimetabolites (e.g., methotrexate, azathioprine), nonsteroidal antiinflammatory drugs, and even some of the immunosuppressants normally used to reduce T-cell activity in preventing organ transplant rejection. A new medication under trial for systemic lupus erythematosus is a monoclonal antibody against B lymphocyte stimulator, which is a member of the TNF family that acts to stimulate B-cell proliferation and immunoglobulin secretion (Cancro et al., 2009). Other future therapies of autoimmune disorders will likely involve stimulation or suppression of specific sites in the immune response by specific monoclonal antibodies; bone marrow transplantation has also been successful in some cases.

Allergies and hypersensitivities are often treated long term by desensitization methods in which allergens are used to stimulate IgG that competes with IgE to neutralize those allergens that are known to cause problems in individual patients. Medications that are commonly used to control symptoms acutely and chronically are antihistamines, corticosteroids, leukotriene antagonists, and adrenergic agonists.

Asthma treatments have been expanded with new biological drugs that interfere with mechanisms of allergy. The anti-IgE monoclonal antibody omalizumab reduces IgE concentrations in the circulation, leading to attenuation of severe asthma (Buhl, 2005). The monoclonal antibodies mepolizumab and reslizumab bind and neutralize IL-5, which is a signal for production of eosinophils. The resulting reduction of circulating eosinophils is also useful for treating severe asthma. Another biological employed in asthma is benralizumab, which is directed against the alpha chain of the IL-5 receptor on eosinophils. This monoclonal antibody binds to the IL-5 receptor on eosinophils, thereby blocking attachment of IL-5, suppressing eosinophil recruitment, and probably hastening the clearance of eosinophils by cellular mechanisms (Thompson et al., 2017).

Biological drugs are those that derive from living cells such as **monoclonal antibodies**, which are designed to have high specificity of action. Clinical application of monoclonal antibody therapy has seen explosive growth in recent years. Technologies have matured, allowing standardized production of humanized monoclonal antibodies, thus preventing host antibody formation against the therapeutic antibody. This results in extended action of these biological drugs. Targets of therapeutic monoclonal antibodies have expanded from initial uses of neutralizing TNF-α to a series of other critical factors in the inflammatory response. Examples are those directed against IL-17A, IL-23, and IL-4 receptor α (blocks binding of IL-4 to its receptor on cell membranes).

Biosimilar drugs are those developed to act against the same targets as initially patented biological drugs. Because biosimilars derive from biosynthesis (i.e., formation of a new monoclonal antibody), they can have some variation in specificity and action compared with the original biological drug. Various monoclonal antibodies that block inflammation have been used for treatment of rheumatoid arthritis, eczema, psoriasis, ankylosing spondylitis, and inflammatory bowel disease. These drugs are currently very expensive and should be expected to remain so while they stay under patent protection.

Nonbiological drugs derive from chemical syntheses and should be expected to have more uniformity and standardized action. An example of a nonbiological drug used for immune downregulation is crisaborole, which inhibits phosphodiesterase 4B, thereby diminishing inflammation. It is used for treatment of atopic dermatitis (Deleanu & Nedelea, 2019).

These drugs target the immune system itself to achieve some level of immunosuppression directed against conditions of the immune system, such as autoimmune disorders, rejection of transplanted organs, and GVHD. In contrast, using the immune system as a tool to treat other diseases is now emerging as effective therapy for some malignancies. A sophisticated approach for enhancing natural T-cell antitumor activity is use of immune checkpoint inhibitors. **Programmed cell death protein 1 (PD-1) and its ligand (PD-L1)** on cell surfaces interact with the immune system to suppress killing of normal host cells during an immune response and to prevent autoimmune diseases (LaFleur et al., 2018). Unfortunately, this suppressive process can also protect tumor cells from an immune response, especially if PD-1 is overexpressed. Inhibitory monoclonal antibodies against PD-1 (e.g., pembrolizumab, nivolumab, and cemiplimab) or PD-L1 (atezolizumab, avelumab, and durvalumab) block inhibitory immune checkpoints, allowing T cells to attack tumor cells. Monoclonal antibody (ipilimumab) against cytotoxic T-lymphocyte-associated protein 4 (CTLA-4, which downregulates the immune response) also allows T cells to attack tumors. Assays for expression of PD-1 on tumor biopsies predicts effectiveness of these monoclonal antibodies. This therapeutic approach has achieved great success in cases of melanoma and some other malignancies, with great promise for broader use (Bhandaru & Rotte, 2019).

Another advanced immunotherapy against tumors is **chimeric antigen receptor T-cell (CAR T-cell) therapy** (Feins et al., 2019). In this process of adoptive immunotherapy, autologous T cells are collected from peripheral blood mononuclear cells, genetically engineered to produce a receptor for tumor antigen in a chimeric protein with the T-cell receptor, expanded to large numbers in cell culture, and then infused into the patient. The CAR T-cells then accumulate at the tumor, where binding to tumor antigen stimulates these reengineered T cells to proliferate and destroy tumor cells. This innovative therapy has been used as a last ditch effort in lymphoma of adults and in leukemia of children, but only in small numbers owing to its complexity and extreme expense. However, future developments in biomanufacturing could well make CAR T-cell therapy more widely used in early phases of treatment.

SELECTED REFERENCES

Feins S, Kong W, Williams E, et al.: An introduction to chimeric antigen receptor (CAR) T-cell immunotherapy for human cancer, *Am J Hematol* 94:S3–S9, 2019.

This critical review presents the strategy and initial clinical trials for CAR T-cell therapeutics.

Kemp SF, Lockey RF: Anaphylaxis: a review of causes and mechanisms, *J Allergy Clin Immunol* 110:341–348, 2002.

An excellent review article covering the immunopathology, pathophysiology, and many causative agents of anaphylaxis, as well as its clinical management.

Kronenberg M: Toward an understanding of NKT cell biology: progress and paradoxes, *Annu Rev Immunol* 26:877–900, 2005.

This comprehensive review discusses the present state of knowledge of natural killer T cells.

LaFleur MW, Muroyama Y, Drake CG, et al.: Inhibitors of the PD-1 pathway in tumor therapy, *J Immunol* 200:375–383, 2018.

This review discusses the PD-1 pathway and its inhibitors and their expanding role in cancer immunotherapy.

Park C, Chio YS: How do follicular dendritic cells interact intimately with B cells in the germinal center? *Immunology* 114:2–10, 2005.

In this review, the function and interaction of follicular dendritic cells with B cells are nicely presented, along with good illustrations.

Puck JM: Laboratory technology for population-based screening for severe combined immunodeficiency in neonates: the winner is T-cell receptor excision circles, *J Allergy Clin Immunol* 129:607–616, 2012.

This article describes the molecular basis for measurement of T-cell receptor excision circles that is now used in screening for severe combined immunodeficiency in heel-stick blood samples from neonates.

Trombetta ES, Mellman I: Cell biology of antigen processing in vitro and in vivo, *Annu Rev Immunol* 23:975–1028, 2005.

This extensive review covers in detail the properties of antigen-presenting cells, as well as regulation, processing, and transport of antigen.

Wen L, Atkinson JP, Giclas PC: Clinical and laboratory evaluation of complement deficiency, *J Allergy Clin Immunol* 113:585–593, 2004.

This article presents a brief description of the three complement pathways, an organ system review of the effect of complement deficiencies, and a diagnostic screening approach for complement-deficient states.

Access the complete reference list online at Elsevier eBooks for Practicing Clinicians.

REFERENCES

Bhandaru M, Rotte A: Monoclonal antibodies for the treatment of melanoma: present and future strategies, *Methods Mol Biol* 1904:83–108, 2019.

Binnicker MJ, Jespersen DJ, Rollins LO: Direct comparison of the traditional and reverse syphilis screening algorithms in a population with a low prevalence of syphilis, *J Clin Microbiol* 50:148–150, 2012.

Buhl R: Anti-IgE antibodies for the treatment of asthma, *Curr Opin Pulm Med* 11:27–34, 2005.

Cancro MP, D'Cruz DP, Khamashta MA: The role of B lymphocyte stimulator (BLyS) in systemic lupus erythematosus, *J Clin Invest* 119:1066–1073, 2009.

Chen R, Mias GI, Li-Pook-Than J, et al.: Personal omics profiling reveals dynamic molecular and medical phenotypes, *Cell* 148:1293–1307, 2012.

Corcoran AE: Immunoglobulin locus silencing and allelic exclusion, *Semin Immunol* 17:141–154, 2005.

Deleanu D, Nedelea I: Biological therapies for atopic dermatitis: an update, *Exp Ther Med* 17:1061–1067, 2019.

Fagarasan S: Regulation of IgA synthesis at mucosal surfaces, *Curr Opin Immunol* 16:277–283, 2004.

Fekade D, Knox K, Hussein K, et al.: Prevention of Jarisch-Herxheimer reactions by treatment with antibodies against tumor necrosis factor α, *N Engl J Med* 335:311–315, 1996.

Germain R: MHC-dependent antigen processing and peptide presentation: providing ligands for T lymphocyte activation, *Cell* 76:287–299, 1994.

Griggs J, Zinkewich-Peotti K: The state of the art: immune-mediated mechanisms of monoclonal antibodies in cancer therapy, *Br J Cancer* 101:1807–1812, 2009.

Hillmen P, Young NS, Schubert J, et al.: The complement inhibitor eculizumab in paroxysmal nocturnal hemoglobinuria, *N Engl J Med* 355(12):1233–1243, 2006.

Janeway C, Bottomly K: Signals and signs for lymphocytic responses, *Cell* 76:275–285, 1994.

Leonard WJ: Type 1 cytokines and interferons and their receptors. In Paul WE, editor: *Fundamental immunology*, ed 5, Philadelphia, 2003, Lippincott, p 701.

Milgrom H, Fick RB, Su JQ, et al.: Treatment of allergic asthma with monoclonal anti-IgE antibody, *N Engl J Med* 341:1966–1973, 1999.

Noris M, Caprioli J, Bresin E, et al.: Relative role of genetic complement abnormalities in sporadic and familial aHUS and their impact on clinical phenotype, *Clin J Am Soc Nephrol* 5:1844–1859, 2010.

Nossal G: Negative selection of lymphocytes, *Cell* 76:229–239, 1994.

Paul W, Seder R: Lymphocyte responses and cytokines, *Cell* 76:241–245, 1994.

Richer J, Johnston SA, Stafford P: Epitope identification from fixed-complexity random-sequence peptide microarrays, *Mol Cell Proteomics* 14:136–147, 2015.

Stafford P, Cichacz Z, Woodbury NW, et al.: Immunosignature system for diagnosis of cancer, *Proc Natl Acad Sci U S A* 111:E3072–E3080, 2014.

The INSIGHT-ESPRIT Study Group and SILCAAT Scientific Committee: Interleukin-2 therapy in patients with HIV infection, *N Engl J Med* 361:1548–1559, 2009.

Thompson K, Lee J, Morrow LE, et al.: Two new medications for severe eosinophilic asthma, *US Pharm* 42(Specialty & Oncology suppl):16–19, 2017.

Venner AA, Ibanez D, Gladman DD, et al.: Comparison of three anti-dsDNA assays: performance and correlation with systemic lupus erythematosus disease activity, *Clin Biochem* 46:317–320, 2013.

Von Boehmer H: Positive selection of lymphocytes, *Cell* 76:219–228, 1994.

Weiss A, Littman D: Signal transduction by lymphocyte antigen receptors, *Cell* 76:263–274, 1994.

Weissman I: Developmental switches in the immune system, *Cell* 76:207–218, 1994.

CHAPTER 45

IMMUNOASSAYS AND IMMUNOCHEMISTRY

Katsumi Aoyagi, Yoshihiro Ashihara, Yasushi Kasahara

IMMUNOASSAYS AND IMMUNOCHEMISTRY, 901
General Characteristics of Antigen–Antibody Reaction, 901
Characteristics of Antigens, 902
Characteristics of Antibodies, 902
Kinetics of Antigen–Antibody Reaction, 902
OVERVIEW OF GENERAL PRINCIPLES OF IMMUNOASSAYS, 903
Classes of Immunoassays, 903
Conjugation Chemistry, 903
Characteristics of the Solid Phase, 904
PRECIPITIN AND NEPHELOMETRIC IMMUNOASSAYS, 904
Background and Principles of Precipitin Reaction, 904
Nephelometric Immunoassays, 904
PARTICLE IMMUNOASSAY, 905
Principle of Particle Agglutination, 905
Summary, 907
RADIOIMMUNOASSAY, 909
Background, 909
Assay Principles and Methods, 909
Summary, 911
ENZYME IMMUNOASSAY, 911
Background and Classification, 911
Heterogeneous Enzyme Immunoassays, 911
Chemiluminescent Enzyme Immunoassay, 912
Homogeneous Enzyme Immunoassays, 914
Summary, 916
FLUORESCENT IMMUNOASSAY, 917
Background and Classification, 917
Heterogeneous Fluorescent Immunoassay, 917
Homogeneous Fluorescent Immunoassay, 918
CHEMILUMINESCENT IMMUNOASSAY, 919
Background, 919
Chemiluminescent Immunoassay Using Acridinium Esters as Labels, 919
Electrochemiluminescent Immunoassay, 919
INSTRUMENT AUTOMATION AND MODULATION OF ASSAY SYSTEMS, 919
Homogeneous Assay Systems, 919
Heterogeneous Immunoassay Systems, 919
Practical Flow of the Immunoassay in the Analytic System, 920
Instrumentation and Key Points for Heterogeneous Immunoassay, 920
High-Throughput Fully Automated Heterogeneous Immunoassay Systems, 920
Remote Maintenance, 921
RAPID AND SIMPLE TEST DEVICES FOR POINT-OF-CARE TESTING, 921
Background, 921
Immunochromatographic Devices, 921
Magnetic Biosensor Assay, 922
Summary, 923
NONCOMPETITIVE IMMUNOASSAY FOR SMALL MOLECULES, 923
Background, 923
Anti-Idiotype Antibody-Based Immunoassay, 923
Open-Sandwich Immunoassay, 923
Antimetatype Antibody–Based Immunoassay, 923
SENSITIVE IMMUNOASSAY FOR TOTAL ANTIGEN INCLUDING COMPLEX USING SPECIMEN-PRETREATMENT METHOD, 925
Background, 925
Highly Sensitive Immunoassay for Viral Antigen Using Specimen-Pretreatment Method, 925
Sensitive Immunoassay for Host Antigen Without The Influence of Auto-Antibody Using Specimen-Pretreatment Method, 925
Summary, 926
SIMULTANEOUS MULTIPLE IMMUNOASSAYS, 926
Background, 926
Microspot Assay, 926
Multianalyte Microarray Immunoassay, 926
Flow Cytometric Immunoassay, 926
Microchannel Assay Using Compact Discs, 927
Summary, 927
SINGLE-MOLECULE DETECTION, 927
Background, 927
Single-Molecule ELISA, 927
Single-Fluorescent Immunoassay, 927
Summary, 928
SELECTED REFERENCES, 928

KEY POINTS

- Antigens can have a wide variety of types of chemical composition such as proteins, carbohydrates, and lipids. They can range in size from very small molecules, such as hormones, to very large ones on viral or bacterial particles.
- Antibodies can be polyclonal as in an immune response with somewhat broad specificity. Monoclonal antibodies are developed from cloned hybridomas; thus, they have very high specificity for antigens.
- Immunoassays are based on interactions of antigens and antibodies that are described mathematically with standard kinetic equations of immunochemistry.
- Laboratory immunoassays have evolved from simple immunoprecipitation and nephelometry through the more sensitive radioimmunoassays, enzyme immunoassays, fluorescent immunoassays, and chemiluminescent immunoassays.
- Instrumentation for modern immunoassays relies on highly precise and accurate specimen delivery as well as very sensitive detection techniques to avoid spectrophotometric interferences.
- High-throughput instrumentation allows for rapid and low-cost operations in measurement of multiple analytes by immunoassay.
- New portable testing with single-sample devices also exploits immunoassays to achieve rapid results at point-of-care settings.
- Highly sensitive immunoassays have the capacity to detect even single molecules, which promises sophisticated monitoring of diseases, such as cancer recurrence.

IMMUNOASSAYS AND IMMUNOCHEMISTRY

GENERAL CHARACTERISTICS OF ANTIGEN–ANTIBODY REACTION

Biological ligands based on the affinity between molecules, such as enzyme and substrate, hormone and receptor, and antigen and antibody, play an important role in living organisms. Specific recognition characteristics of immunoassays (antigen–antibody [Ag–Ab] reactions) have become widely

used as analytic tools, adding to the wide range of methods available in clinical laboratory testing.

Immunoassays can be used for the detection of antigens or antibodies. For antigen detection, the corresponding specific antibody should be prepared as one of the reagents. The reverse is true for antibody detection. The sensitivity of immunoassays has been enhanced through the development of new types of signal detection systems and solid-phase technology. Immunoassays have been optimized to detect less than 0.1 pg/mL of antigen present in blood. They can be applied to the detection of haptens as small molecules; proteins and protein complexes as macromolecules; and any antibody to allergens, infectious agents, and autologous antigens.

CHARACTERISTICS OF ANTIGENS

An *antigen* can be defined as any substance that can represent antigenic sites (epitopes) to produce corresponding antibodies, from small molecules such as haptens and hormones to macromolecules such as proteins, glycoproteins, glycolipids, and other natural products. Artificial chemical compounds can also be antigens acting as haptens. Antigens should have at least one epitope. Epitopes that can be recognized by antibodies include amino acid sequences of peptides in proteins and high-dimensional protein structures, such as neoantigenic sites.

CHARACTERISTICS OF ANTIBODIES

Immunoglobulin, an important plasma protein, refers to antibodies in the context of the biological functions of immunoglobulin specific to antigens. Antibodies, therefore, are produced in response to antigenic stimulation. Antibodies are formed of both functional and heterogeneous molecules that bind antigens via the antigen-combining site. Five classes (isotypes) of immunoglobulin have been identified: IgG, IgM, IgA, IgD, and IgE. IgG is further divided into four subclasses, and both IgA and IgM have two subgroups. All known antibody molecules have a heavy chain with a κ or a λ light chain. The molecular structure of antibodies is composed of variable regions and constant regions. The hypervariable domain (epitope-binding spot) can be assembled to interact with a wide variety of epitopes (antigen determinants). In laboratory medicine, two categories of antibodies can be distinguished: antibodies as reactants and antibodies as analytes. Antibodies as analytes are often classified by IgG, IgM, and IgA subtypes. Antibodies as reactants are prepared from antiserum obtained through animal immunization with purified antigen.

Polyclonal Antibodies

A polyclonal antibody can be obtained through immunization with an antigen, which presents various epitopes. In other words, the antibody generated is specific against each epitope. The avidity of a polyclonal antibody to a complex antigen is usually stronger than a single monoclonal antibody. Carrier proteins may be needed for the immunization of smaller molecules, such as haptens or hormones.

Monoclonal Antibodies

Monoclonal antibodies (Koehler & Milstein, 1975) have been developed using the biotechnologies somatic cell fusion, selection of the resulting hybridoma, and limiting dilution to ensure that the clone is derived from a single cell. They are defined as uniform homogeneous antibodies directed to specific epitopes. An established cell line allows the secretion of all reactive immunoglobulin specific to single epitopes. Monoclonal antibodies have made it possible to analyze molecules on an epitope-to-epitope basis because of their narrow specificity. Yet, monoclonal antibodies, in contrast to polyclonal antibodies, do not have the ability to recognize the entire molecule. For monoclonal antibodies, different antigens with a common epitope appear to be the same antigen. CA 19-9 antibody (Magnani et al., 1983) as a tumor marker can detect different sizes and shapes of molecules that have common carbohydrate epitopes. Monoclonal antibodies enable identification of isoenzymes, subtypes, and isotypes of protein, and conformational changes in molecules because they can discern the slightest differences in molecules.

Monoclonal antibodies may be cross-reactive with different antigens. This cross-reactivity can be explained by the probable existence of the same amino acid sequences, carbohydrates, or lipids on different molecules. Monoclonal antibody technology has allowed the development of extremely useful and nearly ideal immunoassay systems for clinical laboratory testing.

The production methods and applications of monoclonal antibodies have been extensively reviewed (Nakamura, 1983; Zola, 1987). Advantages of monoclonal antibodies are as follows:

Monoclonal antibodies provide a well-defined reagent.
Monoclonal antibody production can yield an unlimited quantity of homogeneous reagent with highly consistent affinity and specificity.
Monoclonal antibodies can be prepared through immunization with a nonpurified antigen.
Monoclonal antibodies have certain limitations in their use, as follows:
- Insufficient reactivity is seen in precipitation or agglutination because network formation in the immunocomplex is weak or does not occur when single monoclonal antibodies are used.
- Antigens with multiple heterogeneous epitopes are more difficult to characterize immunochemically with a single monoclonal antibody.

Antibody Production by Recombinant Technology

Skerra and Pluckthun (1988) developed an expression system for the Fv fragment of variable domains of an antibody specific to phosphoryl choline using recombinant technology in *Escherichia coli*. This technology makes it possible to produce chimeric antibody fused to an enzyme.

The technology called *phage display* has emerged for the production of antibodies (Winter et al., 1994). In this method, antibody fragments of predetermined binding specificity are constructed from a repertoire of antibody variable (*V*) genes, thereby eliminating the need for immunization and hybridoma technology. The *V* genes can be assembled in vitro. The phage selected from the repertoire by binding to antigen and antibody fragments is expressed in infected bacteria. Furthermore, the binding affinity of the antibodies is improved through a mutation/maturation process.

Seo et al. indicated an ex vivo method for rapid generation of monoclonal antibodies on the basis of the finding that gene conversion in DT40 cells was enhanced by treatment of the cells with a histone deacetylase inhibitor, trichostatin A (Seo et al., 2006). This treatment involves a diversified library of DT40 cells (ADLib), in which each cell has different surface IgM specificity. Antigen-specific DT40 cells are selected from ADLib using antigen-conjugated magnetic beads; their specificity can be examined by various immunologic assays, using culture supernatant containing secreted IgM. The antibody from selected cells is expressed in mammalian cells as a recombinant antibody.

These technologies to develop monoclonal antibodies without immunization for animal and hybridoma technology will allow the use of specific antibodies with high avidity or affinity by improving the selection process or maturation technology.

KINETICS OF ANTIGEN–ANTIBODY REACTION

Certain aspects of equilibrium or the law of mass action in chemistry can be applied to the Ag–Ab reaction. The kinetics of the reversible Ag–Ab reaction is as follows (Steward, 1986):

$$\mathrm{Ag} + \mathrm{Ab} \underset{K_2}{\overset{K_1}{\leftrightarrow}} \mathrm{AgAb} \qquad \text{(Eq. 45.1)}$$

where
Ag = free antigen
Ab = free antibody sites
AgAb = antigen–antibody complex concentration
K_1 and K_2 = association and dissociation rate constants, respectively

The rate of formation of the Ag–Ab complex is represented as follows:

$$d\,[\mathrm{AgAb}]/dt = K_1\,[\mathrm{Ag}]\,[\mathrm{Ab}] - K_2\,[\mathrm{AgAb}] \qquad \text{(Eq. 45.2)}$$

and at equilibrium, the net rate is zero. Therefore,

$$K_1/K_2 = [\mathrm{AgAb}]\,/\,[\mathrm{Ag}]\,[\mathrm{Ab}] = K_a \qquad \text{(Eq. 45.3)}$$

(association equilibrium constant or affinity constant).

K_a is the parameter limited to site-to-site reactions, although antigens and antibodies often have multiple binding sites on the molecule. The apparent association constant for multiple antigen and antibody reactions may be referred to as *avidity* instead of *affinity*. The K_a value may be obtained from the following equations and experimental data:

$$[\mathrm{Ab}] = [\mathrm{Ab}]_t - [\mathrm{AgAb}] \qquad \text{(Eq. 45.4)}$$

where
[*Ab*] = antibody concentration at equilibrium
$[Ab]_t$ = total original antibody concentration

$$K_a = B/\left([\mathrm{Ab}]_t - B\right) F \qquad \text{(Eq. 45.5)}$$

where
F = free antigen or analyte
B = bound antigen or analyte

A Scatchard plot is produced when the amount of antigen bound (*B*) is plotted on the *x*-axis and the bound over free (*B/F*) ratio of analytes is

plotted on the *y*-axis. The two parameters that can be determined from the Scatchard plot are the dissociation or affinity constant from the slope of the line and the concentration of antibody-binding sites from the X-intercept (Scatchard, 1949).

OVERVIEW OF GENERAL PRINCIPLES OF IMMUNOASSAYS

CLASSES OF IMMUNOASSAYS

A brief classification and a list of features of various immunoassays appear in Table 45.1. Precipitation immunoassays provide the simplest method for antigens and antibodies to react with each other without involving the detection of any labels. The resulting Ag–Ab complex in the gel or liquid phase may be observed qualitatively as a precipitant by the naked eye and quantitatively with a detector.

The particle agglutination immunoassay (Kasahara, 1992b) uses inert particles as labels as opposed to direct precipitation of the Ag–Ab complexes. Antigens or antibodies attached to particles such as erythrocytes, latex, or metal sol react with the analyte in the specimen. As a result of this immune reaction, large particles show significant agglutination patterns that may be seen by the naked eye. Yalow and Berson (1959) reported on the development of a radioimmunoassay (RIA) using radioisotopes as labels. This breakthrough allowed for the quantitative detection of a trace level of analytes and contributed to the advancement of basic research and clinical medicine. Insulin, for example, was quantified by RIA, which subsequently replaced the insulin bioassay. RIA may be formatted in a solid-phase procedure for easy separation of bound and free labels. Since the development of RIAs, the search for alternative labels to hazardous radioisotopes has intensified, with the aim of developing nonisotopic immunoassays using enzymes, fluorescent labels, and other reporter groups.

The enzyme immunoassay (EIA), using enzymes as labels, was developed in the early 1970s (Engvall & Perlman, 1971; Van Weeman & Schuurs, 1971) and rapidly gained wide popularity. Enzymes can amplify signals, depending on the turnover of enzyme catalytic activity. Efforts to improve substrates and to increase sensitivity have led to the introduction of chromophore, fluorophore, and later chemiluminescent compounds. Depending on the substrate chosen, the assay method can be defined as a fluorescent enzyme immunoassay or as a chemiluminescent enzyme immunoassay (Thorpe et al., 1984).

Fluorescent immunoassays (FIAs) use fluorophores as labels. Fluorophores require optimal wavelength light energy for their excitation to produce detectable emission light. FIA sensitivity is likely to decrease because of the nonspecific background fluorescence present in biological specimens. Fluorophores that have a delayed fluorescence emission time of 100 ns (nanoseconds) are suitable for application on time-resolved FIA. The introduction of a new class of fluorescent compounds has resulted in improvements in FIA, such as the elimination of background noise. Sophisticated instrumentation has been introduced that can detect low concentrations (10^{-15} M) of analytes using FIAs.

Chemiluminescent immunoassays use chemiluminescent compounds as labels. Chemiluminescent compounds include chemically synthesized molecules as well as natural products such as aequorin. Unlike fluorophores, most chemiluminescent compounds require chemical rather than light energy to generate emission light. The reduction–oxidation reaction is a process common to all chemiluminescent assays. Signal amplification is not expected of chemiluminescent labels because chemiluminescent molecules generate just one photon through molecular decomposition. A series of new and innovative compounds for electrochemiluminescence have proved suitable for application on immunoassays. Metal chelate with tribiphenyls emits light through a continuous reduction–oxidation reaction on the surface of electrodes (Blackburn et al., 1991).

In the various types of assays mentioned earlier, the main factors affecting assay sensitivity are the association constant (affinity or avidity) of the reactant, the signal intensity of the labels, and the signal/noise ratio of the detection signal reduced by background from the signals themselves or by a nonspecific reaction.

Iodine-125 (^{125}I) requires about 7 million molecules to generate 1 photon/second, based on half-life calculations of radioisotopes (Bounaud et al., 1987). Chemiluminescent substrates to enzymes can increase events by an order of magnitude six times greater than that of iodine-125. This is attributable to the catalytic amplification capacity of enzymes.

CONJUGATION CHEMISTRY

Depending on the assay chosen, the method of conjugation that couples one molecule to others, enzymes (or cofactors) to antigens (or antibodies), or antigens (or antibodies) to solid phase may vary. The coupling reaction applied should be performed under conditions that avoid the reduction of any of the biological activities of the protein. In the glutaraldehyde method (Avrameas et al., 1978), glutaraldehyde, along with two (or possibly more) aldehyde groups as coupling reagents, has been used for conjugation of protein amino groups. This method is based on mixed reactions, including aldol condensation at high pH (the pKa of the NH residue is 8.6 to 10.8). With this method, shown in Figure 45.1, the resulting conjugate has different forms because of the existence of multiple active sites for coupling. The periodate oxidation method (Nakane & Pierce, 1966) for the conjugation of antibodies uses horseradish peroxidase, which contains carbohydrates in its molecules. The methods mentioned earlier are not suitable for regulation of site-specific reactions, such as when configurational stereospecificity of conjugates is required.

As shown in Figure 45.2, new coupling methods (Kato et al., 1975; Kitagawa et al., 1978) have been developed using a sophisticated coupling reagent, M-maleimidobenzyl-*N*-hydroxysuccinimide ester (MBS). The MBS is a bivalent reagent consisting of an activated ester and maleimide, and it can react with an NH_2 group and an SH group, respectively. The carboxy group can also be used as a specific site for conjugating with α- or

TABLE 45.1
Classification of Various Immunoassays and Their Characteristics

	Labels (Reporter Groups)	B/F Separation*	Signal Detection	Sensitivity
Precipitation immunoassays	Not required	Not required	Naked eye, turbidity, nephelometry	~10 μg/mL[1]
Particle immunoassays	Blood cells, artificial particles (gelatin, particles, latex, etc.)	Not required	Naked eye, pattern analyzer, spectrophotometry, particle counting	~5 ng/mL[2]
Radioimmunoassays	Radioisotopes (^{125}I, ^{3}H)	Required	Photon counting	~5 pg/mL
Enzyme immunoassays	Enzymes	Required	Spectrophotometry, fluorometry photon counting (CL-EIA)	~5 pg/mL ~0.1 pg/mL[3]
Fluorescence immunoassays	Fluorophores	Required	Photon counting	~5 pg/mL[4]
Chemiluminescence immunoassays	Chemiluminescent compounds	Required	Photon counting	~5 pg/mL[4]
Electrochemiluminescence immunoassays		Required		

Data from Ritchie R: *Automated immunoanalysis, Part I and Part II*, New York, 1978, Marcel Dekker; Haux P, Dybois H, McGovern M, et al.: Evaluation of the TIna-quant ferritin assay on the Boehringer Mannheim/Hitachi 704 System, *Clin Chem* 34:1174, 1988, abstract; Isomura M, Ueno M, Shimada K, et al.: Highly sensitive chemiluminescent enzyme immunoassay with gelatin-coated ferrite solid phase, *Clin Chem* 40:1830, 1994; and Sgoutas DS, Barton EG, Hammarstrom M, et al.: Four sensitive thyrotropin assays critically evaluated and compared, *Clin Chem* 25:1785–1789, 1989.
B/F, Bound over free.
*Washing step for separation of bound labels in immunocomplex from free labels. Homogeneous assays included are not required for B/F separation.

ε-NH_2 residues of proteins using *N*-hydroxysuccinimide (NHS) as the coupling reagent. The NHS coupling reagent extends to conjugate protein or the carboxyl group introduced on the solid phase.

CHARACTERISTICS OF THE SOLID PHASE

All heterogeneous immunoassays using conjugate with labels, including radioisotopes, require at least one separation step to distinguish the reacted immunocomplex (bound) from unreacted materials (free). Immobilization of antigens or antibodies for solid phase is performed by covalent binding or physical adsorption through noncovalent interactions. Gel particles made of agarose, polyacrylamide, and plastic beads, or titer plates composed of polystyrene, have been used as the solid phase, as well as particles coated with iron oxide that can be separated by a magnetic field.

The inner wall of a tube or a microtiter well is commonly used as a solid phase. With these relatively large solid phases, shaking of the reaction mixture may be needed to shorten the time required for the immune reaction to take place. The prozone phenomenon, or hook effect, caused by high concentrations of the analyte is likely to be observed in a one-step immunoassay when limited quantities of solid-phase antibody or labeled antibody are employed. Microtiter or strip-type plates may cause an "edge effect." This effect can be explained by the different kinetics of the immune reaction or enzyme activity with variations in temperature. A difference in temperature may be present between the wells located at the edge of the microtiter plate and the center of the plate. A difference of about 2°C may be observed with an infrared thermometer between the edge and the center of wells at ambient temperature. The size and shape of the solid phase are critical factors affecting the immunoreaction kinetics and the capturing capacity of solid-phase antibody or antigen. Small spherical magnetic particles or latex particles with 3000 Å diameters provide a larger total surface area for immunoabsorbency than is usually obtained with other solid phases. The larger total surface area helps shorten the immunologic reaction time (Nishizono et al., 1991).

The particles used for the particle agglutination assay are listed in Table 45.2. The phenomenon of particle agglutination (direct agglutination) caused by an immune reaction was first observed in tests after incubation of bacterial pathogens with infected patient serum. Agglutination of erythrocytes after incubation with serum led to the discovery of ABO blood types. Particle immunoassays are based on the agglutination principle and use the reactant of an antibody or an antigen attached to the inert particle as a label, as opposed to direct precipitation of an Ag–Ab immunocomplex. As a label, the particle can significantly increase the immunoassay sensitivity regardless of whether the resulting agglutination is detected by the naked eye or with spectrophotometric instruments for quantification.

Erythrocytes, gelatin particles, liposomes, metal sols, and various kinds of latex particles, including latex modified with iron oxide or dyes, are all suitable solid phases. The diameter of these particles used for agglutination reactions varies from 0.01 to 7 μm. No single theory can explain the kinetics of agglutination (Kasahara, 1992a) because of the wide variety of particle sizes used as labels. Brownian motion is not significant at room temperature for dispersed particles larger than 3 to 5 μm. However, the theory of potential energy of interaction between particles, or the theory of colloidal coagulation reaction, can apply to small particles, such as latex microparticles. The IgM antibody, being multivalent, is estimated to be 750 times more efficient than the bivalent IgG antibody in an agglutination reaction. The distance between particles in flocculation should be less than or equal to 120 Å because of the molecular length of the antibody. In summary, important factors to consider in an immune reaction are the surface properties of particles, such as charge and hydrophobicity, and the stability of dispersion.

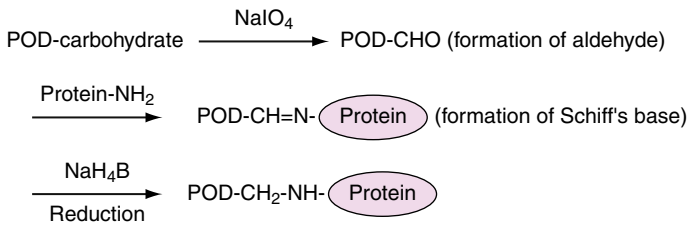

Figure 45.1 Coupling scheme for conjugation of protein with horseradish peroxidase (POD) based on the Nakane method.

PRECIPITIN AND NEPHELOMETRIC IMMUNOASSAYS

BACKGROUND AND PRINCIPLES OF PRECIPITIN REACTION

The precipitate that forms when large complexes of antigen and antibody combine to form an insoluble lattice has been widely used to identify and quantify immunoprecipitin reactions. The modes of application of precipitin techniques have the advantages of sensitivity, specificity, and simplicity. The sensitivity limitation of these assays is a major consideration. Even under the best conditions of enhanced sensitivity afforded by newer light-scattering techniques, the lower limit of sensitivity of immunoprecipitin assays remains in the range of 0.1 to 0.5 mg/dL. This lower limit of sensitivity appears to be sufficient for the quantification of many major serum proteins. The precipitin reaction forms the basis for many quantitative and qualitative immunochemical techniques now used in the clinical laboratory (Kabat, 1961).

Factors affecting the precipitin reaction were extensively investigated by Heidelberg in 1935, who found that the relative proportions of reactants; conditions of temperature, pH, and ionic strength of the medium; and antibody characteristics of avidity and affinity were all important in the formation of the immune precipitate (Heidelberg & Kendall, 1935). On the pattern of precipitin formation, it can be noted that there is a point at which precipitation is maximum or optimal, which is designated as *the point of equivalence*. Continued addition of antigen once the point of equivalence has been reached produces a solubilizing effect on the precipitate. The dynamic range suitable for the determination of analytes should be up to the zone of equivalence. Optimization of the antibody concentration as a reactant is necessary in addition to optimization of buffer solutions. Typical precipitant reaction methods are as follows:

1. Qualitative Precipitant Assay Methods
   - Single immunodiffusion (Williams & Chase, 1970)
   - Double immunodiffusion (Garvey et al., 1977)
   - Double immunodiffusion in two dimensions (Williams & Chase, 1970)
   - Electroimmunodiffusion reaction (Ritzmann & Daniels, 1975)
   - Immunoelectrophoresis (Rose, 1973)
2. Semiquantitative Precipitant Assay Methods
   - Single radial immunodiffusion (Fahey & McKelvey, 1965; Mancini et al., 1965)
   - Single-dimension electroimmunodiffusion ("rocket" electrophoresis) (Axelsen, 1975)

NEPHELOMETRIC IMMUNOASSAYS

A number of techniques for immunoprecipitin analysis have been developed that use light-scattering devices (Ritchie, 1978). The occurrence of immune complex formation has been related to the amount of such light scattering and has been used as a basis for antigen quantitation. Sophisticated instruments have been designed to rapidly measure light scattering. Measurements of scattered light are generally referred to as *turbidimetry* or *nephelometry*.

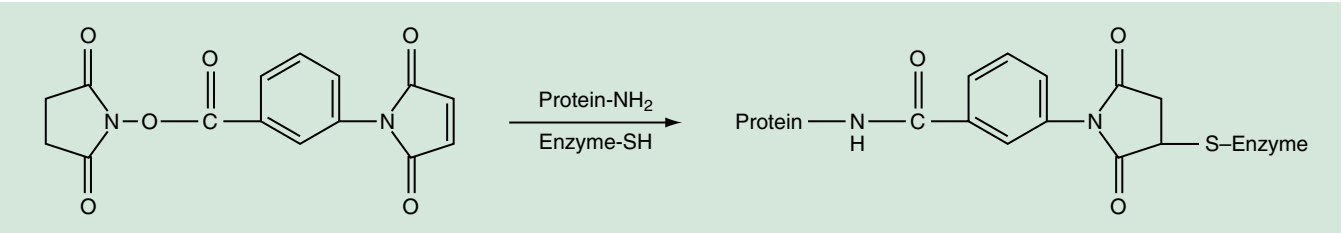

Figure 45.2 Preparation of enzyme–protein conjugate using hetero-bifunctional coupling reagent.

PARTICLE IMMUNOASSAY

PRINCIPLE OF PARTICLE AGGLUTINATION

The agglutination reaction may be used to detect antibodies in specimens with specific antigens sensitized to a particle (passive or direct agglutination; Fig. 45.3B). Reverse agglutination using a corresponding antibody sensitized to particles can be employed to detect soluble antigens in the specimen (Fig. 45.3A). A hapten unit single-binding site (for drugs, hormones, or small particles) does not form a cross-linking structure; thus, it cannot become agglutinated unless it is immobilized on the solid phase. As shown in Figure 45.4, when a particle or carrier immobilized with a hapten is used as a reactant, an agglutination inhibition reaction occurs that allows detection of the hapten. This assay is based on a competitive-type principle in which agglutination of hapten particles with a limited amount of antibody, whether free or sensitized on particles, is inhibited by the hapten present in the specimen. Also, labeled particles can react with reactants fixed on the solid phase of the membrane. After immunoreaction, particles within the immunocomplex can be developed to show color on part of the membrane. This type of assay has been popular as a simple device for the qualitative detection of human chorionic gonadotropin (hCG) and other analytes.

Hemagglutination

Hemagglutination tests (Boyden, 1951) are simple to perform and do not require special equipment. For this reason, both advanced and developing countries have adopted a variety of hemagglutination tests. A popular worldwide hemagglutination test is used for the detection of antibody

TABLE 45.2
Particles Used as Labels for Particle Agglutination Immunoassay

	Assay Method	Supply
Human erythrocyte	Direct hemagglutination (Landsteiner)	ABO blood type
	Erythrocyte antibody hemagglutination: titer plate/slide	Human immunodeficiency virus antibody
Avian erythrocyte	Direct hemagglutination	Human influenza virus (HIV) antibody
Fixed animal erythrocyte	Passive hemagglutination: titer plate	*Treponema pallidum* antibody
	Reverse passive hemagglutination: titer plate	Hepatitis B surface antigen (HBsAg)
Latex	Reverse passive agglutination: slide	Chorionic gonadotropin
	Reverse passive agglutination: turbidimetry	Immunoglobulin (Ig) E
	Reverse passive agglutination	Ferritin
Latex (color)	Immunochromatography	Human chorionic gonadotropin (hCG)
Microcapsule	Passive agglutination: titer plate	*T. pallidum* antibody
Gelatin particle	Passive agglutination: titer plate	HIV, *T. pallidum* antibody
	Reverse passive agglutination: charge-coupled device (CCD) camera	Human hemoglobin (hHb)
Polypeptide particle	Passive and reverse agglutination	*T. pallidum* antibody, HBs antibody
Silicate particle	Passive agglutination: titer plate/CCD camera	*T. pallidum* antibody
Gold particle	Reverse agglutination enhancement photometry	Total estrogen
Metal sols	Reverse agglutination	hCG, hHb

From Nakamura RM, Kasahara Y: Heterogeneous enzyme immunoassays. In Nakamura RM, Kasahara Y, Rechnitz GA, editors: *Immunochemical assays and biosensor technology for the 1990s*, Washington, DC, 1992, American Society for Microbiology. Reproduced with permission.

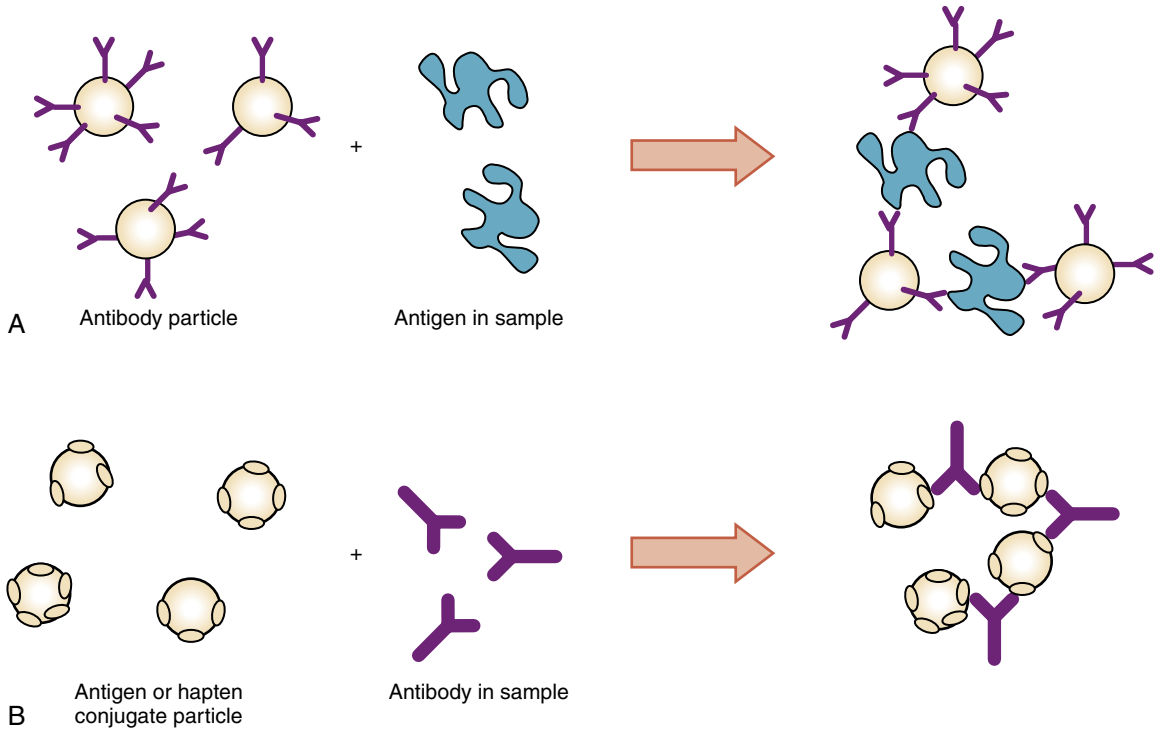

Figure 45.3 Principles of passive particle agglutination immunoassay for detection of antigen with multiple **A,** epitopes or **B,** antibodies. (*From Nakamura RM, Kasahara Y, Rechnitz GA, editors:* Immunochemical assays and biosensor technology for the 1990s, *Washington, DC, 1992, American Society for Microbiology.*)

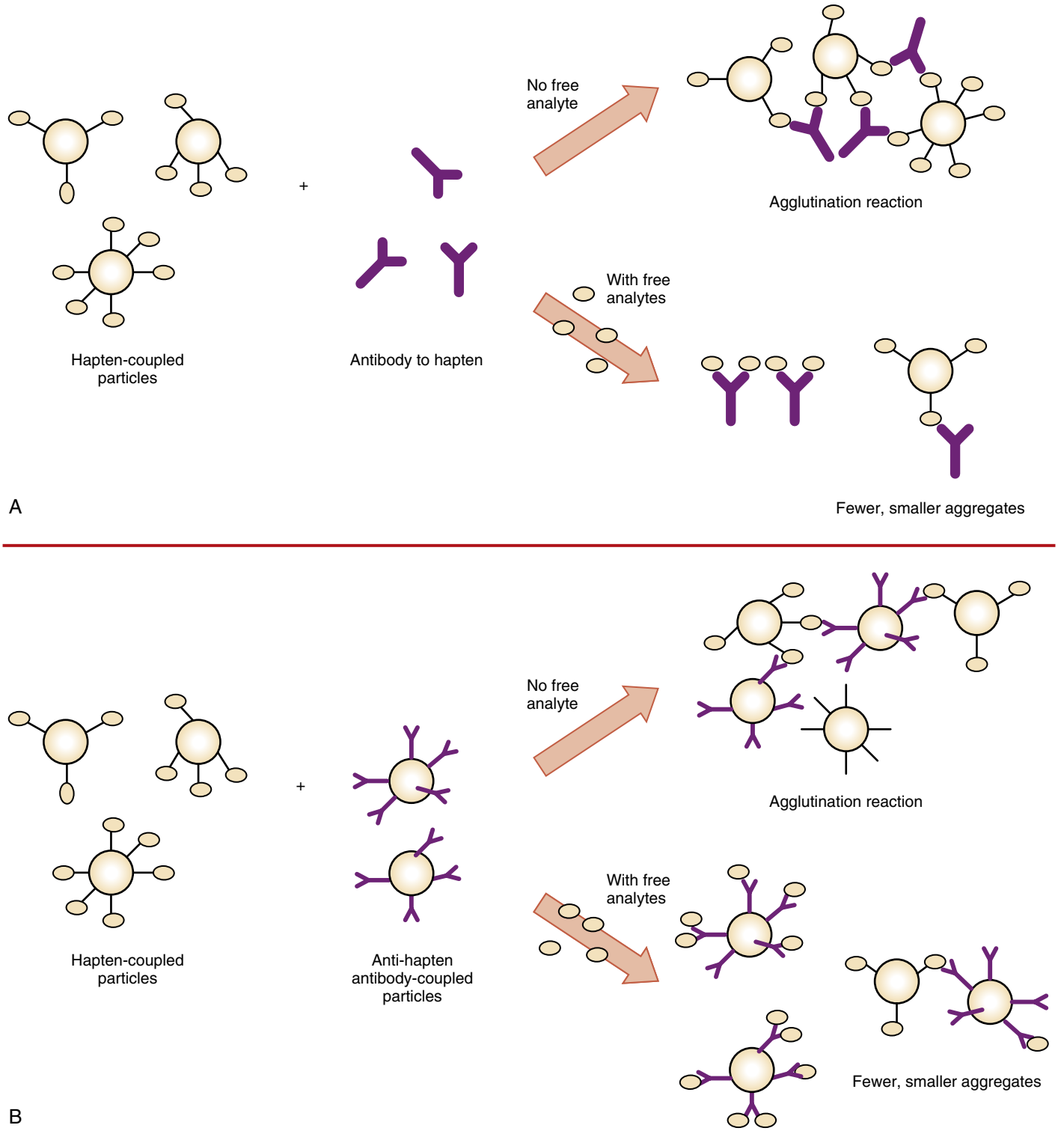

Figure 45.4 Principles of particle inhibition immunoassay for detection of antigen with single epitope (hapten), using antigen particle with (**A**) free or (**B**) fixed antibody. *(With permission from Nakamura RM, Kasahara Y, Rechnitz GA, editors:* Immunochemical assays and biosensor technology for the 1990s*, Washington, DC, 1992, American Society for Microbiology.)*

to *Treponema pallidum*, marketed as SERODIA-TP, by Fujirebio, Inc. (Tokyo, Japan). In the United States, the hemagglutination test for *T. pallidum* was approved in 1981 by the Centers for Disease Control and Prevention. It was also recommended by the World Health Organization because of its superiority over other tests in terms of specificity and sensitivity (Kasahara, 1992b).

In the *T. pallidum* agglutination test, the reagent consists of sensitized and unsensitized sheep red cells as well as a serum diluent solution for the reconstitution of lyophilized sensitized cells as a positive control. Both qualitative and semiquantitative tests can be carried out using the following serum dilution protocol and a titer plate as a reaction container as follows: using a 25-μL pipette dropper, place 4 drops 100 μL of serum diluent in well 1 (Fig. 45.5) and 1 drop in wells 2 to 4 for the qualitative assay (wells 2–8 are used for the quantitative assay). The resulting agglutination patterns are shown in Figure 45.6. Negative patterns, indicating that immunoreaction has not taken place, show condensed flocculation particles with a cross-packing structure at the bottom of the microtiter well. On the other hand, positive patterns, indicating that immunoreaction has occurred, show an expanded agglutination pattern of particles. Agglutinated particles cannot be sedimented any further to obtain condensation as negative patterns because their global shape is lost on account of the agglutination of particles. In the first and second rows, serum and unsensitized cells (negative control) were used, respectively. Specimens 1 and 2 show negative results.

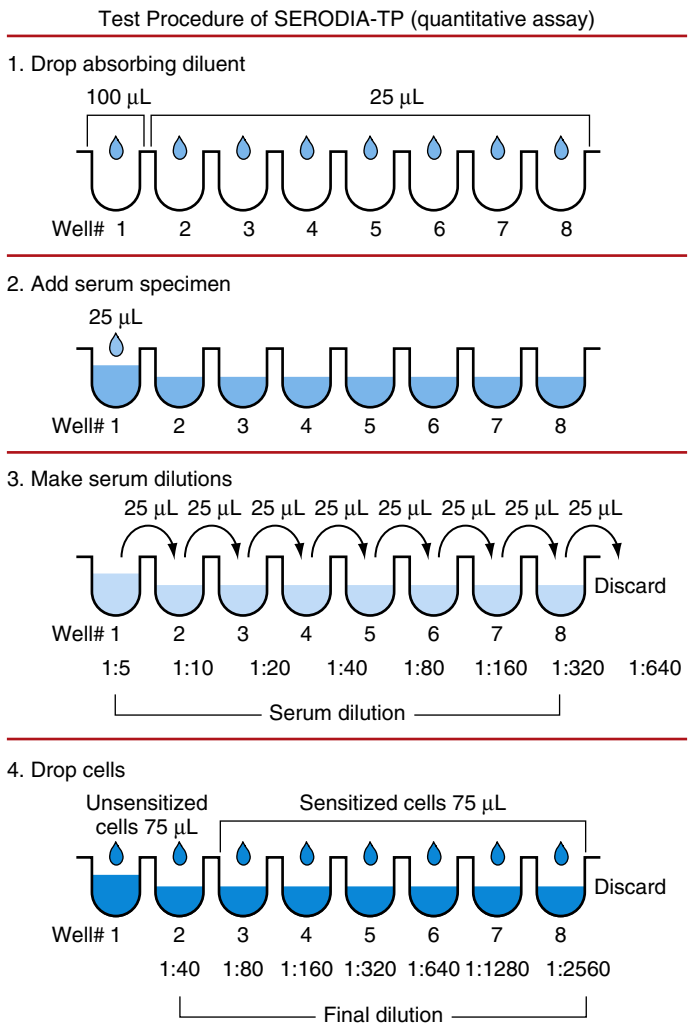

Figure 45.5 Hemagglutination assay for detection of *Treponema pallidum* antigen (Serodia-TP, Fujirebio, Inc., Tokyo, Japan) based on semiquantitative test protocols. (*With permission from Nakamura RM, Kasahara Y, Rechnitz GA, editors:* Immunochemical assays and biosensor technology for the 1990s*, Washington, DC, 1992, American Society for Microbiology.*)

Specimens 3 to 8 show negative or positive results, depending on the specimen dilution. A positive result is observed for specimens 7 and 8 up to 1:2560 (rows 3–8).

Hemagglutination kits are now available for the detection of antibodies to hepatitis type B virus (HBV), hepatitis type C (HCV), human immunodeficiency virus (HIV1/2), thyroglobulin, thyroid microsome, and other substances. Reverse hemagglutination tests are used for the detection of HBV surface antigen, α-fetoprotein (AFP), human hemoglobin in stool specimens, and so forth. The sensitivity of hemagglutination tests is approximately 50 ng/mL for antigen (analyte) detection. Kemp and colleagues (1988) developed a hemagglutination assay that uses a mouse monoclonal antibody specific to the surface antigen of human erythrocytes. The antibody can recognize an epitope common to different types of red cells or to abnormal cells, such as those found in sickle cell anemia. As shown schematically in Figure 45.7, blood cells in the specimens are used as solid-phase particles; the resulting agglutination can be observed by the naked eye. Bivalent antibodies are conjugated chemically; thus, one antibody specifically reacts with the surface epitopes of the blood cell and the other is specific to the target antigen or analyte. The assay is applied for the detection of antibody to HIV and for the detection of various antigens. Unlike conventional agglutination formats, the separation of plasma or serum is not required. This assay is simple, saves time, and offers safety advantages because it eliminates the need for serum separation for hazardous HIV- or HBV-positive specimens.

Gelatin Particle Agglutination

The development of a special gelatin particle with a highly hydrophilic surface that is able to prevent nonspecific binding of materials present in a specimen has provided an alternative to erythrocytes (Ikeda, 1984). This particle is made by phase separation and three-dimensional cross-linkage at 40°C and optimum pH. The resulting particle is fixed with formaldehyde or glutaraldehyde, and its diameter is about 3 µm. The physical properties of gelatin particles in comparison with those of erythrocytes are shown in Figure 45.8. A gelatin particle has no antigenicity; therefore, it is free from problems associated with heterophilic antibodies when erythrocytes are used as particles. This type of artificial particle requires much less serum dilution to avoid nonspecific binding and guarantees a more sensitive detection than with blood cells. Other synthetic particles (Hirayama et al., 1991) made from block copolymer composed of L-glutamic acid and derivatives have been developed by Hirayama and colleagues (1991) as alternatives to gel particles. These synthetic particles can be stained with dye of any color because the particles themselves are colorless, as are gelatin particles. The gelatin particle agglutination test was initially applied to the detection of antibodies to human T-cell lymphotropic virus, which was first discovered as a retrovirus in humans. This agglutination test (Ikeda, 1984) soon became very popular for blood screening for HIV, HBV, and HCV because of its high sensitivity and specificity, its simplicity, and the fact that strict temperature control is not required to perform the tests. Gelatin particle agglutination can replace any assay based on hemagglutination with the exception of assays that use RBCs in specimens as particles.

Latex Agglutination

Latex agglutination (Galvin, 1984), using latex as particles, has been employed for the detection of various analytes, such as hCG for qualitative pregnancy tests, and for the quantitative detection of other plasma proteins with or without instrumentation. The format of this qualitative assay is simple. For example, one might have to mix only a couple of drops of latex sensitized with reactant and specimen using a stick on a black slide. Two to three minutes later, phase inversion agglutination resulting from the immune reaction can be observed by the naked eye. Latex agglutination was adapted for quantitative assays using light detection methods based on turbidimetry (light absorption) or nephelometry (light scattering). With these techniques, latex agglutination achieves an enhanced sensitivity of subnanograms per milliliter, while the sensitivity of the assay measuring intact precipitation of the Ag–Ab complex remains below 0.5 µg/mL.

Latex Turbidimetric Assay

Light adsorption (light loss by scattering on the surface of a particle) is proportional to the diameter of the particle and depends on the wavelength of light used. Most latex reagents commercially available use latex with a diameter of less than 1 µm and are applied in automated chemistry analyzers using photometric measuring principles. To further improve sensitivity, efforts were made to upgrade reagents and instrumentation and to optimize particle size, selection of appropriate wavelength, and improvements in computer software for integration of data. Automated systems now use latex particles that can perform about 200 tests per hour at a subnanogram-per-milliliter sensitivity.

Particle-Counting Immunoassay

The particle-counting immunoassay (PACIA) (Masson & Holy, 1986) uses optical cell counting to assess the decrease in the number of unagglutinated particles after an immune reaction. In the PACIA format, the rate assay—that is, the rate of decrease in the number of unagglutinated particles—or the endpoint of the assay reaction can be measured. The endpoint assay can be used to obtain a sensitivity at the nanogram-per-milliliter level. However, a longer incubation time is required for an endpoint immunologic reaction.

Other Particle Immunoassays

Quasielastic scattering immunoassays were developed using a measurement of the change in response to particle size distribution (Yarmush et al., 1987). This technique uses a laser light beam to measure the reduction in the mean diffusion coefficient of particles as a result of immune reaction. Other methods measure the change in angular anisotropy of scattered light with the increasing average size of the particle. Particles with diameters about equal to the size of a wavelength achieve a size-dependent angular variation of scattered light.

SUMMARY

Indirect hemagglutination and gelatin particle agglutination tests using microtiter plates are popular procedures for qualitative and semiquantitative

determination of various analytes. These tests do not require additional instrumentation or strict temperature control. Most important, they guarantee a sensitivity equal to or greater than conventional enzyme immunoassays when applied to antibody detection of infectious agents. Latex as a solid phase provides great kinetic advantages, such as a shorter immune reaction time. For this reason, it was possible to adapt latex for use in existing or sophisticated instruments by applying different principles, resulting in an assay sensitivity of about three orders of magnitude greater than standard immunoprecipitation assays. Latex is susceptible to interferences from unknown factors present in specimens. To eliminate this problem,

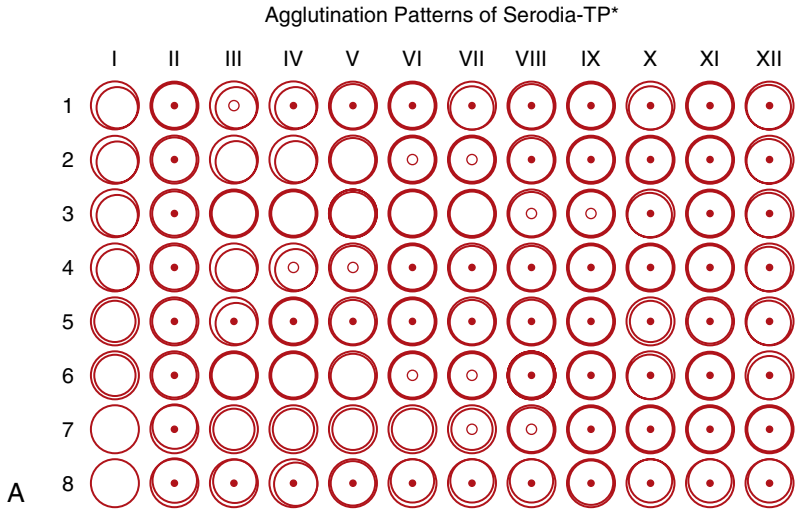

Row no.	I	II	III	IV	V	VI	VII	VIII	IX	X	XI	XII	
Type of cells added		Unsensitized cells	Sensitized cells										Result
Final dilution of serum specimen		1:40	1:80	1:160	1:320	1:640	1:1280	1:2560	1:5120	1:10240	1:20480	Medium control	Titer
Serum specimen													
No. 1	–	–		–	–	–	–	–	–	–	–	–	Inconclusive
No. 2	–	–	++	++	+	+	–	–	–	–	–	–	1:640
No. 3	–	–	++	++	++	++	++	+	–	–	–	–	1:2560
No. 4	–	–	+	+	–	–	–	–	–	–	–	–	1:160
No. 5	–	–	–	–	–	–	–	–	–	–	–	–	Negative
No. 6	–	–	++	++	++	+	–	–	–	–	–	–	1:640
No. 7	–	–	++	++	++	++	+	–	–	–	–	–	1:1280
No. 8	–	–	–	–	–	–	–	–	–	–	–	–	Negative

*Trademark for agglutination test for *T. pallidum* antibody, Fujirebio, Inc., Tokyo, Japan

B

Figure 45.6 Hemagglutination patterns for detection of (**A**) anti–*Treponema pallidum* antibody, and (**B**) interpretation as positive or negative at final serum dilution. (*From Nakamura RM, Kasahara Y, Rechnitz GA, editors:* Immunochemical assays and biosensor technology for the 1990s, *Washington, DC, 1992, American Society for Microbiology.*)

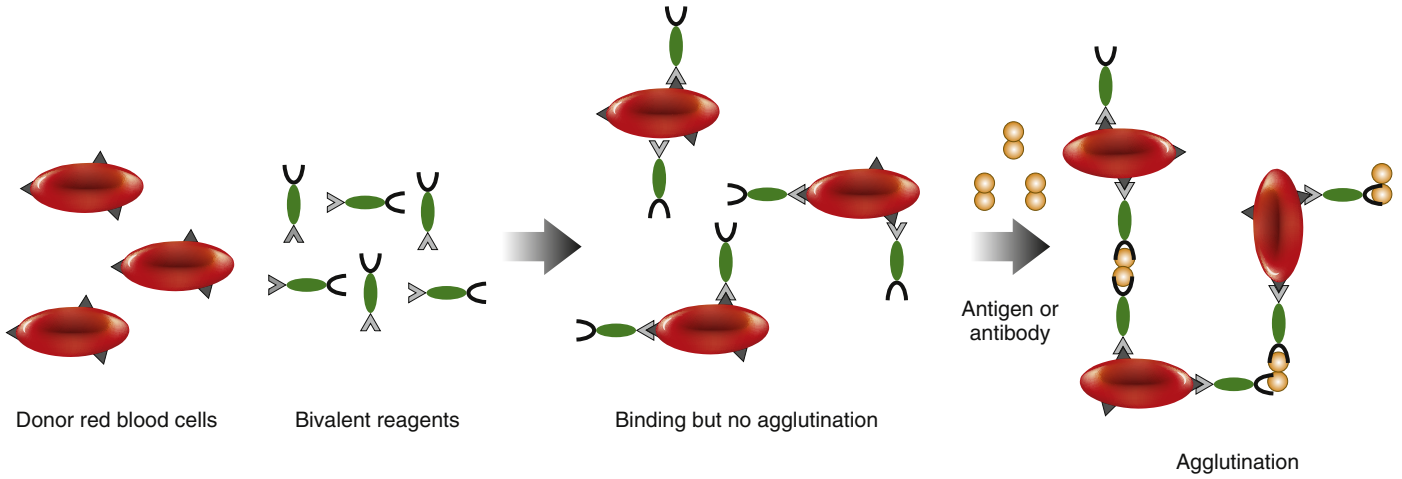

Figure 45.7 Schematic presentation of an assay based on autologous erythrocyte agglutination, using erythrocytes in the specimen as particles. (*With permission from Nakamura RM, Kasahara Y, Rechnitz GA, editors:* Immunochemical assays and biosensor technology for the 1990s, *Washington, DC, 1992, American Society for Microbiology.*)

various absorbents have to be used in both the reagent and the incubation medium. The great advantage of particle immunoassay is its simplicity because it does not require separation of bound and free reactants.

RADIOIMMUNOASSAY

BACKGROUND

Since RIA technology using radioisotopes as labels was first developed by Yalow and Berson (1959), it has been improved dramatically in sensitivity and precision. Numerous variations in the method have been introduced into the clinical laboratory. Two main RIA techniques, competitive and noncompetitive heterogeneous formats, require washing steps to separate bound and free labels (conjugates). The competitive assay follows the law of mass action, which specifies the reaction between analytes and binding proteins, receptors, and antibody. The key factor in assay optimization is the binding affinity of the antibody. The Scatchard plot of the ratio of bound to free antibody to analyte concentration is commonly used to evaluate antibody performance. Figure 45.9 shows the Scatchard plot for cyclosporine determination. As described earlier in the Kinetics of Antigen–Antibody Reaction section, from the following equation:

$$B/F = K_a([Ab]_t - B) \qquad \text{(Eq. 45.6)}$$

the *y*-axis is the *B/F* ratio that is proportional to free [*Ab*] from $[Ab]_t - B$, equal to free [*Ag*]. Therefore, K_a represents the slope of the plot. In Figure 45.9, the affinity constant K_a is 8.1×10^9 L/M for the antibody specific to cyclosporine. Radioactive emissions, such as γ-rays of iodine-125 labels, can be measured in terms of counts per minute (CPM) using a γ-scintillation counter. Typical radioisotopes used as labels and their properties are shown in Table 45.3. The choice of label affects the assay protocol considerably. For example, the most popular label, iodine-125, requires a rather short time for signal counting but has a limited shelf life because of its short half-life. On the other hand, the tritium (^3H) label requires a longer time for counting, thereby increasing the total assay time. Most RIAs now use iodine-125 as labels to expedite the conjugation process and to retain the biological activity of the reactants. A commonly used method for conjugation of iodine-125 with proteins is the chloramine-T method (Hunter & Greenwood, 1962). Tyrosine, in particular, has greater reactivity with iodate because of its hydroxy group at the para-position on the aromatic ring. The signal can be measured in terms of CPM as γ-ray emissions. Unlike enzymes, isotopes as labels with a small Stokes radius are not likely to disrupt antigenic activity because of the lack of steric hindrance when isotopes are conjugated with small antigens (haptens).

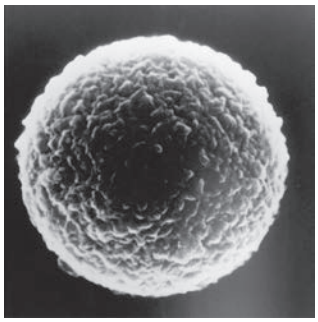

Physical properties	Carrier: Gelatin particles	Carrier: Sheep erythrocytes
Diameter, µm	2 to 6	6
Specific gravity	1.05 to 1.10	1.10
Electrophoretic mobility; µm/s/V/cm	–0.75 to –1.85	–1.15

Figure 45.8 Electron micrograph (×25,000) and physical properties of gelatin particles in comparison with sheep erythrocytes. (*With permission from Nakamura RM, Kasahara Y, Rechnitz GA, editors:* Immunochemical assays and biosensor technology for the 1990s, *Washington, DC, 1992, American Society for Microbiology, p 139.*)

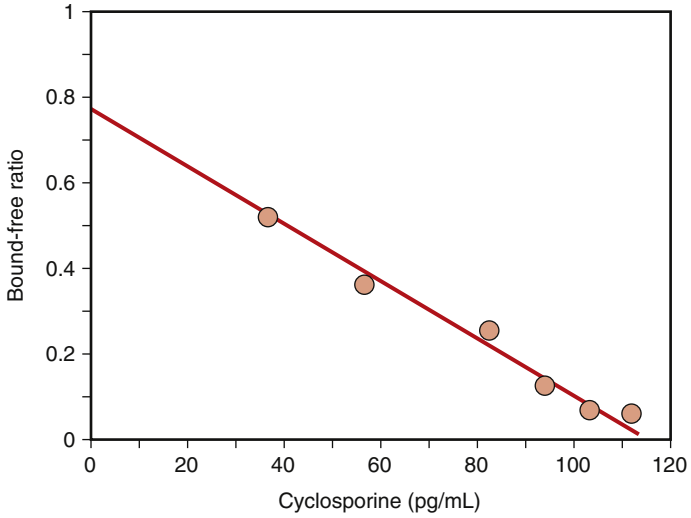

Figure 45.9 Scatchard plot of cyclosporine antibody binding characteristics ($K_a = 8.1 \times 10^9$ L/M).

ASSAY PRINCIPLES AND METHODS

Various methods (antigen excess) based on the competitive binding reaction (Ekins, 1960) to antibodies between labeled antigens and nonlabeled antigens (analytes present in the specimen) have been developed for a wide variety of analytes. A conventional competitive method is shown in Figure 45.10. At first, known amounts of labeled antigen and antigen in the specimen are mixed and reacted competitively with a constant amount of antibody coated on a solid phase, such as sepharose beads or the inner wall of plastic tubes. After the immune reaction reaches its equilibrium, the mixture is washed to remove unreacted conjugates and antigens, and the immune complex trapped on the solid phase is separated. The washing step is referred to as B/F separation. Applying the competitive principle, the plot of antigen-bound percentage against logarithmic concentration of analyte provides the standard curve shown in Figure 45.10. The CPM plot on the standard curve gives the concentration of analytes.

A second antibody method is shown in Figure 45.11. The first antibody specific to a particular antigen (analyte) reacts competitively with both the conjugate and the antigen. Then, the immune complex is captured by the second antibody specific to the first antibody, on the solid phase. When the second antibody is coated on a fine solid phase, the immune complex on the second reaction can be separated as a precipitant from the unreacted molecules. For antibody determination, labeled antibody and antibody in the specimen react competitively with the antigen (analyte) fixed on the solid phase. The steeper slope of the standard curve provides more precise data. Competitive methods require lesser amounts of antibody or antigen (analyte) than the sandwich-type assays described later. Noncompetitive assays, originally demonstrated by Miles and Hales (1968), have recently gained greater popularity.

Immunoradiometric assays and sandwich assays (Fig. 45.12) have alternative relationships between analyte and antibody. The classical competitive assay achieves an immunologic response with a minimum amount of antibody; the sandwich assay uses a large amount of antibody on the solid phase. Monoclonal antibody technology has made it possible to manufacture large quantities of specific antibodies at moderate costs, thereby allowing the sandwich assay to be exploited. The sandwich assay, which uses excess antibody, is more sensitive than the competitive assay. When background noise is completely omitted, the ultimate theoretical sensitivity of the sandwich assay is one molecule of analyte, which is possible when the amount of antibody used in the assay system approaches infinity. As shown in Figure 45.12, the antibody on the solid phase first captures the antigen (analyte) in the specimen. Following B/F separation, the conjugate reacts with the antigen (analyte) fixed on the solid phase. The signal can then be

TABLE 45.3
Properties of Radioisotopes Used as Labels for Radioimmunoassays

Isotope	Half-Life	Type of Decay	Specific Activity (mCi/mmol)
^{125}I	60 days	γ	2200
^{131}I	8.1 days	β^-, γ	16,100
^3H	12.3 years	β^-	29
^{14}C	5760 years	β^-	6062
^{32}P	14.3 days	β^-	9120

counted after the elimination of free conjugates through a washing step. This assay requires antigens with more than two antigenic sites. When two different antibodies (i.e., a solid-phase antibody specific to one antigenic site and a conjugate antibody specific to another antigenic site) are used, the assay protocol can be simplified by performing a one-step sandwich. Thus, the solid phase can mix together with the antigen in the specimen and conjugate simultaneously. Interference does not occur because the antibodies on both the solid phase and conjugate are capable of recognizing different antigenic sites. In this assay, the signal generated is proportional to the analyte concentration present in the specimen, as in the two-step sandwich assay. This assay method can be applied to antibody detection with an assay format using antigen as the solid phase or labeled antigen. For a two-step format, antigen as the solid phase or labeled antibody specific to the target antibody can be used. Using the sandwich format, assay

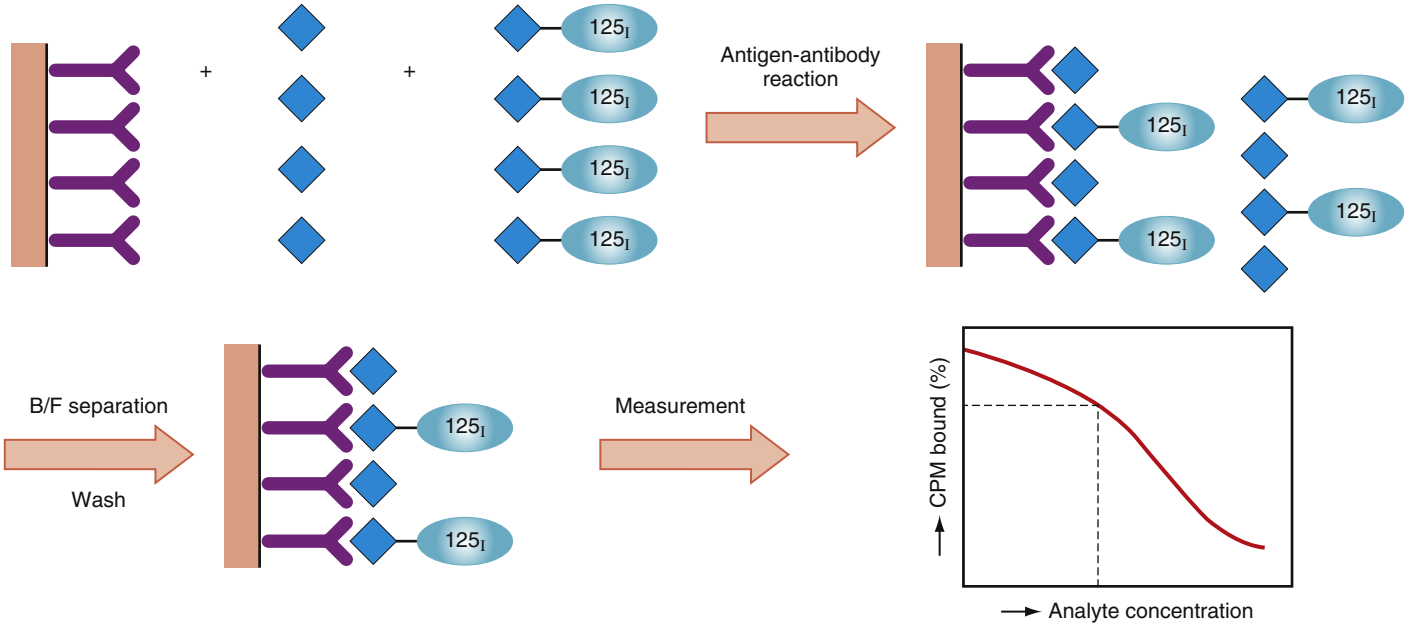

Figure 45.10 Assay principle of competitive radioimmunoassay (RIA) using first antibody as solid phase.

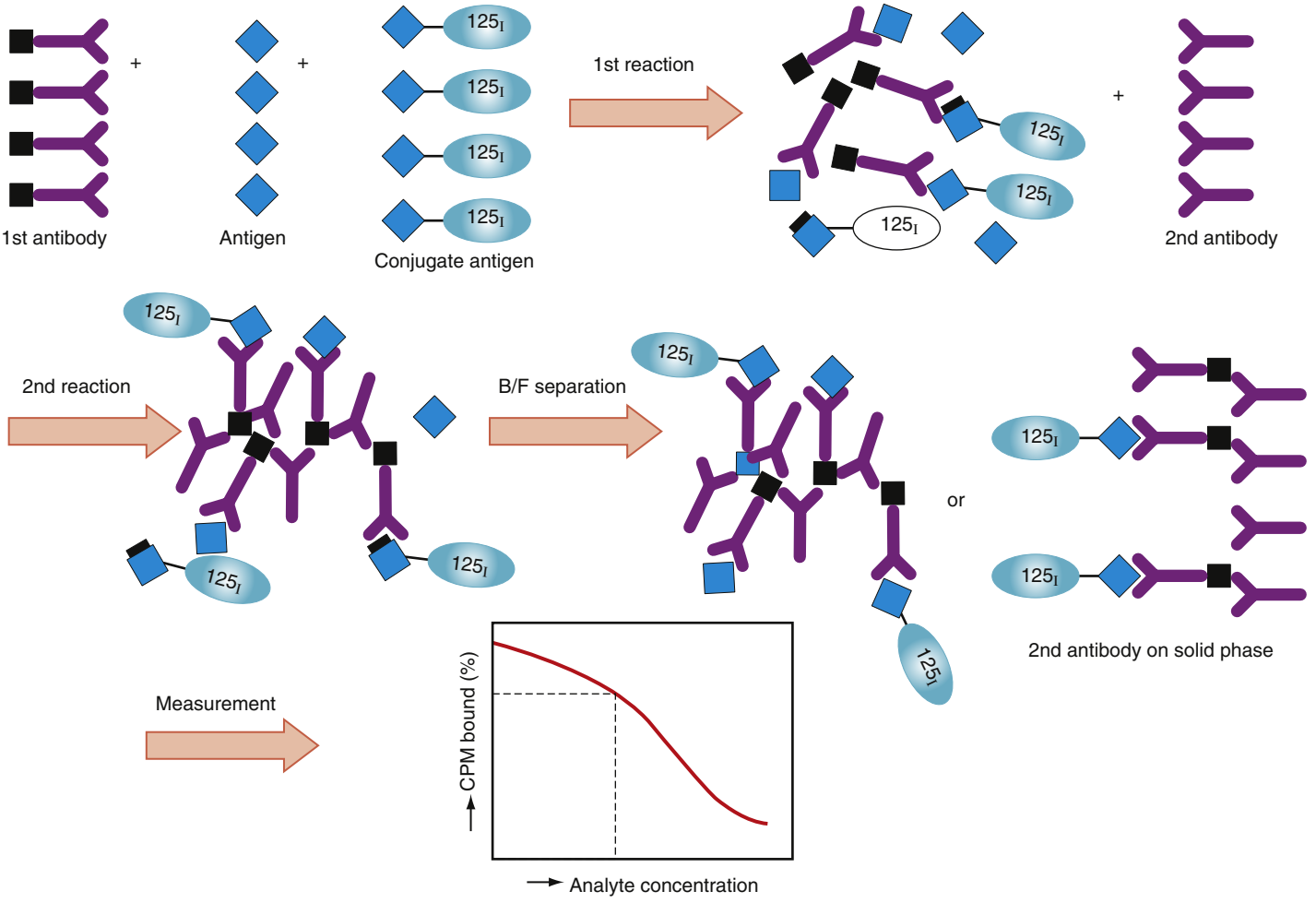

Figure 45.11 Assay principle of competitive radioimmunoassay (RIA) method using second antibody for B/F (bound/free) separation.

sensitivity (Rodriguez-Espinosa et al., 1987) is high. An example is seen when an immunoradiometric assay is used for determination of the peptide hormone thyroid-stimulating hormone (TSH). The level of assay sensitivity is below 0.07 μU/mL of TSH as compared with about 0.7 μU/mL with conventional competitive antigen-labeled assay.

SUMMARY

Compared with other immunoassays, RIAs are advantageous for a number of reasons, including precision and high sensitivity, ease of isotope conjugation, signal detection without optimization, and stability against interference from the assay environment, among others. Disadvantages of RIAs are the short shelf-life of the reagents and the need to protect against hazardous radioactivity. Furthermore, as discussed later, RIAs may not be applied to homogeneous immunoassays because signals from isotopes cannot modulate Ag–Ab reactions.

ENZYME IMMUNOASSAY

BACKGROUND AND CLASSIFICATION

Quantitative immunoassays using enzymes as labels were developed as alternatives to radioisotopes (Avrameas & Guilbert, 1971; Engvall & Perlman, 1971; Van Weeman & Schuurs, 1971). The most widely used are the enzyme-linked immunosorbent assay (ELISA), the EIA, and the enzyme-multiplied immunoassay technique (EMIT), which is a registered trade name of SYVA Co. (Dade Behring Inc., Cupertino, CA) (Rubenstein et al., 1972). Essentially, heterogeneous EIAs are similar to RIAs, except that they use enzymes as labels. Enzymes make it possible to develop homogeneous EIAs, eliminating the otherwise necessary washing steps for B/F separation. Table 45.4 compares the features of heterogeneous and homogeneous EIAs versus RIAs. Improvements in EIAs have provided many innovative formats with different degrees of speed, sensitivity, simplicity, and precision. Advantages and disadvantages of EIAs are listed in Box 45.1 (Nakamura & Kasahara, 1992).

HETEROGENEOUS ENZYME IMMUNOASSAYS

The assay principle of heterogeneous EIAs is similar to that of RIAs, except that enzyme activity, not radioactivity, is measured. EIAs require a secondary process to obtain signals through the catalytic reaction of enzymes. Microtiter plate wells, plastic beads, plastic tubes, magnetic particles, and latex with filters, among others, can be used as the solid phase for the separation of bound and free conjugates. The use of small magnetic particles and latex allows shortening of the immunoreaction time, thereby reducing the total assay time. The development of substrates to be cleaved by enzymes was marked by the introduction of colorimetric and fluorometric substrates, and later chemiluminescent substrates, which increased the signal sensitivity. The enzymes commonly used in various heterogeneous EIAs are horseradish peroxidase, alkaline phosphatase, β-galactosidase, glucose oxidase, urease, and catalase. The most widely used enzymes and their characteristics are listed in Table 45.5. Assay sensitivity using enzymes may be determined by the turnover rate of each enzyme and by selection of signal measurement in which chemiluminometry is the most sensitive method.

The assay format of heterogeneous EIAs, similar to RIAs, can be divided into competitive and noncompetitive assays (Fig. 45.13). Competitive assays (analyte excess) use antigen–enzyme conjugates (Fig. 45.13A). Noncompetitive assays (reactant excess) include two-site immunometric sandwich assays (Fig. 45.13B1) and indirect assays to measure antibodies (Fig. 45.13B2). Immunometric sandwich assays have gained much popularity for the determination of antigens such as tumor markers, plasma

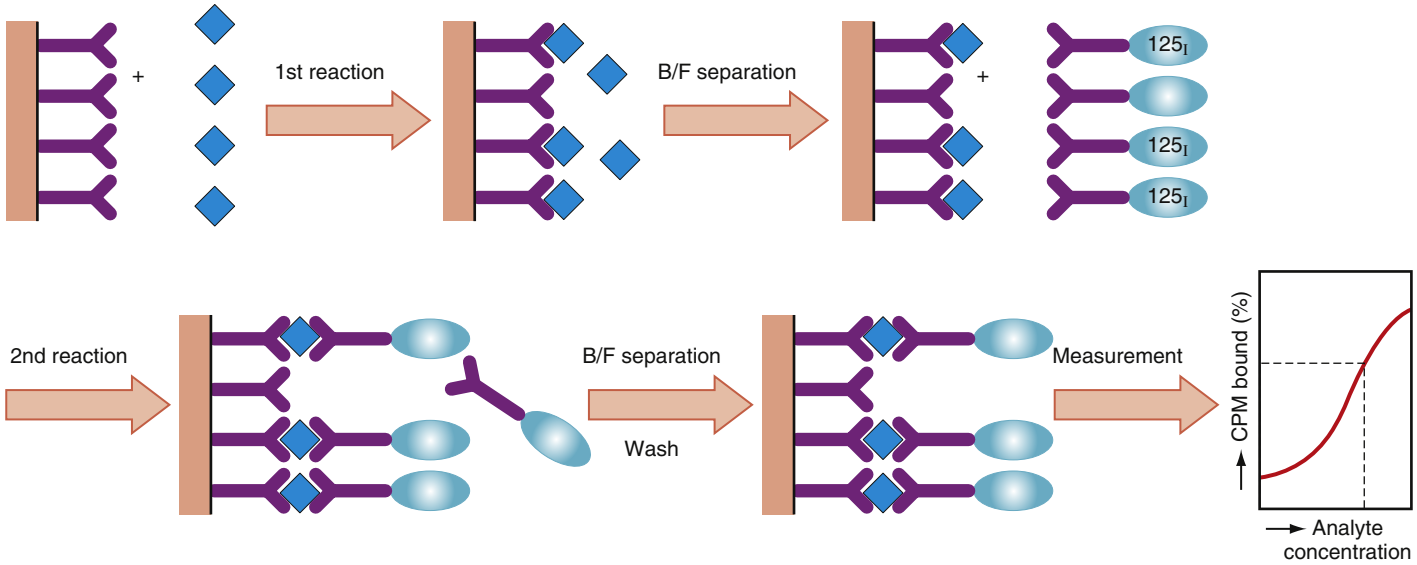

Figure 45.12 Assay principle of sandwich radioimmunoassay (RIA) method using solid phase, also referred to as immunoradiometric assay. *B/F,* Bound/free.

TABLE 45.4
Comparison of Radioimmunoassay, Heterogeneous Enzyme Immunoassay, and Homogeneous Enzyme Immunoassay

Assay	Immunologic Reaction Steps	Enzyme Reaction Steps	Signal Detection Steps
Radioimmunoassay Sample + (labeled analyte or Ab) – ^{125}I	Immunoreaction with washing steps for separation	Not required	Radioactive decay (γ-ray)
Heterogeneous enzyme immunoassay Sample + (labeled analyte or Ab) – enzyme	Immunoreaction with washing steps for separation	Enzyme reaction with additional reagent	Optical density Fluorescence Luminescence
Homogeneous enzyme immunoassay Sample + (labeled analyte or Ab) – enzyme or cofactors	Immunoreaction and/or systemic reaction is carried out in one solution, which includes reagent for signal development of enzyme.	Immunoreaction and/or systemic reaction is carried out in one solution, which includes reagent for signal development of enzyme.	Optical density Fluorescence Luminescence

Ab, Antibody.

proteins, and infectious agents. Indirect assays for antibody measurement (Fig. 45.13B2) have been adopted for the detection of antibodies to infectious agents (e.g., HIV, HBV, HCV) and to autoantibodies.

Heterogeneous EIA (see Fig. 45.13) consists of the following steps:

1. The solid phase with the attached reactants is mixed with analyte, regardless of whether the assay is based on the competitive or noncompetitive format.
2. Following the addition of conjugate and incubation, washing steps are performed with a buffer solution containing a detergent, one or two steps after the immune reaction. The immune reaction should reach certain yields to obtain a stable and precise assay.
3. The solid phase, with the immunocomplex containing enzyme-labeled antigen or antibody, is incubated at constant temperature with the enzyme–substrate solution.
4. The enzyme reaction is stopped (stopping is not needed in rate assay), and the substrate reaction product is measured with various detectors, depending on the substrate used.

Colorimetric Enzyme Immunoassay

In this assay, enzyme reaction is performed by using chromogenic substrates to develop a color by prime catalytic reaction—for example, horseradish peroxidase, catalyzing ABTS (diammonium salt of 2,2′-azino-di[{3-ethyl-benzothiazoline-6-sulfonate}]) with H_2O_2 to form a green color, and alkaline phosphatase specific to the *p*-nitrophenylphosphate to form a yellow color. Both enzymes are the most commonly used types of colorimetric enzyme immunoassays. A spectrophotometer is used to measure the optical density of the resulting chromogen. Many instruments are available for the measurement of optical density in tubes or microtiter plates, ranging from a fully automated system that performs sample pipetting and data printout to simpler manual devices. When the EIA reaction is performed on nitrocellulose membrane (Western blotting method) or other membranes, substrates that generate insoluble dyes are utilized. An hCG pregnancy test with an immunoassay format that is sold as an over-the-counter test commonly uses benzidine derivatives to react with peroxidase or indoxyl phosphate derivatives to react with alkaline phosphatase to generate insoluble dyes. The dye accumulating on the solid phase through enzyme reaction can be read by the naked eye. Theoretically, the measurement of optical density is limited to a range of 0 to 2.0. Therefore, the determination of optical density for analytes that require determination of a wide dynamic range can be problematic, even when an excess amount of conjugate and a solid phase with sufficient capturing capacity are used with a sandwich-type assay.

Efforts to improve EIAs, the milestone of nonisotopic immunoassays, have brought to light several disadvantages of RIAs, such as hazardous isotopic waste, radiolysis of labeled analytes, and the short half-life of iodine-125. Ishikawa and Kohno (1989) developed an ultrasensitive EIA capable of detecting 3 fmol of specific IgG antibody. However, to achieve this level of sensitivity, several tedious steps are required, such as immunocomplex transfer from a first solid phase to another solid phase to reduce background signals.

Fluorescent Enzyme Immunoassay

Fluorescent EIAs are identical to other EIAs, except that they use fluorescent substrates. In the fluorescent EIA, a fluorophore is generated by an enzyme reaction. Following excitation of the fluorophore at its optimal light excitation wavelength, light at a characteristic wavelength is emitted. Instruments such as a fluorometer require both a supplier of the excitation light source and a photomultiplier tube as a detector of the emission fluorescence. Substances that emit fluorescent light may be present in the specimen. These substances may increase the background signal, which may interfere with the assay's sensitivity. Thus, close attention should be paid to the selection of substrates for EIAs to avoid interfering factors. Compared with colorimetric EIAs, fluorescent assays generate a signal intensity that is at least one order of magnitude greater.

BOX 45.1

Advantages and Disadvantages of Enzyme Immunoassay

A. Advantages
   1. Sensitive assays can be developed by the amplification effect of enzymes.
   2. Reagents are relatively cheap and can have a long shelf life.
   3. Multiple simultaneous assays can be developed.
   4. A wide variety of assay configurations can be developed.
   5. Equipment can be inexpensive and is widely available.
   6. No radiation hazards occur during labeling or disposal of wastes.
B. Disadvantages
   1. Measurement of enzyme activity can be more complex than measurement of the activity of some types of radioisotopes.
   2. Enzyme activity may be affected by plasma constituents.
   3. Homogeneous assays at the present time have the sensitivity of 10^{-9} M and are not as sensitive as radioimmunoassays.
   4. Homogeneous EIAs for large protein molecules have been developed but require complex immunochemical reagents.

EIA, Enzyme immunoassay.
From Nakamura RM, Kasahara Y: Heterogeneous enzyme immunoassays. In Nakamura RM, Kasahara Y, Rechnitz GA, editors: *Immunochemical assays and biosensor technology for the 1990s*, Washington, DC, 1992, American Society for Microbiology. Reproduced with permission.

CHEMILUMINESCENT ENZYME IMMUNOASSAY

Chemiluminescent enzyme immunoassays (CL-EIAs) use chemiluminescent substrates that react with various enzymes employed as labels. The chemiluminescent enzymatic reaction generates light, similar to bioluminescence, which involves the use of natural substrates such as luciferin–adenosine triphosphate. Over the past 20 years, much attention has been paid to the application of chemiluminescence in immunoassays, and a variety of systems consisting of substrates and enzymes have been developed. Current systems using luminol derivatives to peroxidase with an enhancer or dioxetane derivatives to alkaline phosphatase achieve highly sensitive immunoassays. These assays are effective tools in practical diagnosis. The enzymatic oxidation reaction of luminol analogs has long been used for CL-EIA. Use of peroxidase with H_2O_2 is a common method that is interchangeable with an alternative coupling enzyme producing H_2O_2, such as glucose oxidase or uricase. The discovery of enhancers by Thorpe and colleagues (1985) for luminol-based chemiluminescence remarkably improved the assay's sensitivity. Enhancers include phenol derivatives and aromatic compounds. For example, luminol-peroxidase with *p*-iodophenol as an enhancer achieves a light emission increase of up to 2800-fold in the optimized reaction mixture. This assay is able to detect TSH at 0.04 μU/mL when serum is used as the specimen. However, oxidative reactions,

TABLE 45.5

Characteristics of Typical Enzymes Used as Labels for Enzyme Immunoassay

Enzyme Characteristic	Peroxidase (EC1.11.1.7)	β-Galactosidase (EC3.2.1.23)	Alkaline Phosphatase (EC3.1.3.1)
Source	Horseradish	*Escherichia coli*	Bovine intestine
Molecular weight, daltons	40,000	530,000	100,000
Specific activity	250 U/mg	600 U/mg	2500–5000 U/mg
Turnover rate*	10,000	318,000	250,000
Measurement of enzyme	Colorimetry, fluorometry, luminometry	Colorimetry, fluorometry, luminometry	Colorimetry, fluorometry, luminometry
Highly sensitive measurement	Luminometry	Fluorometry	Luminometry
Method for enzyme labeling	Periodate oxidation (Nakane method)	Dimaleimide method, cross-linking reagent†	Glutaraldehyde method, cross-linking reagent†

*Number of substrate molecules produced by a molecule of enzyme for 1-minute reaction; molecule number/minute.
†The reagent contains chemically reactive groups, such as maleimide and succinimide.

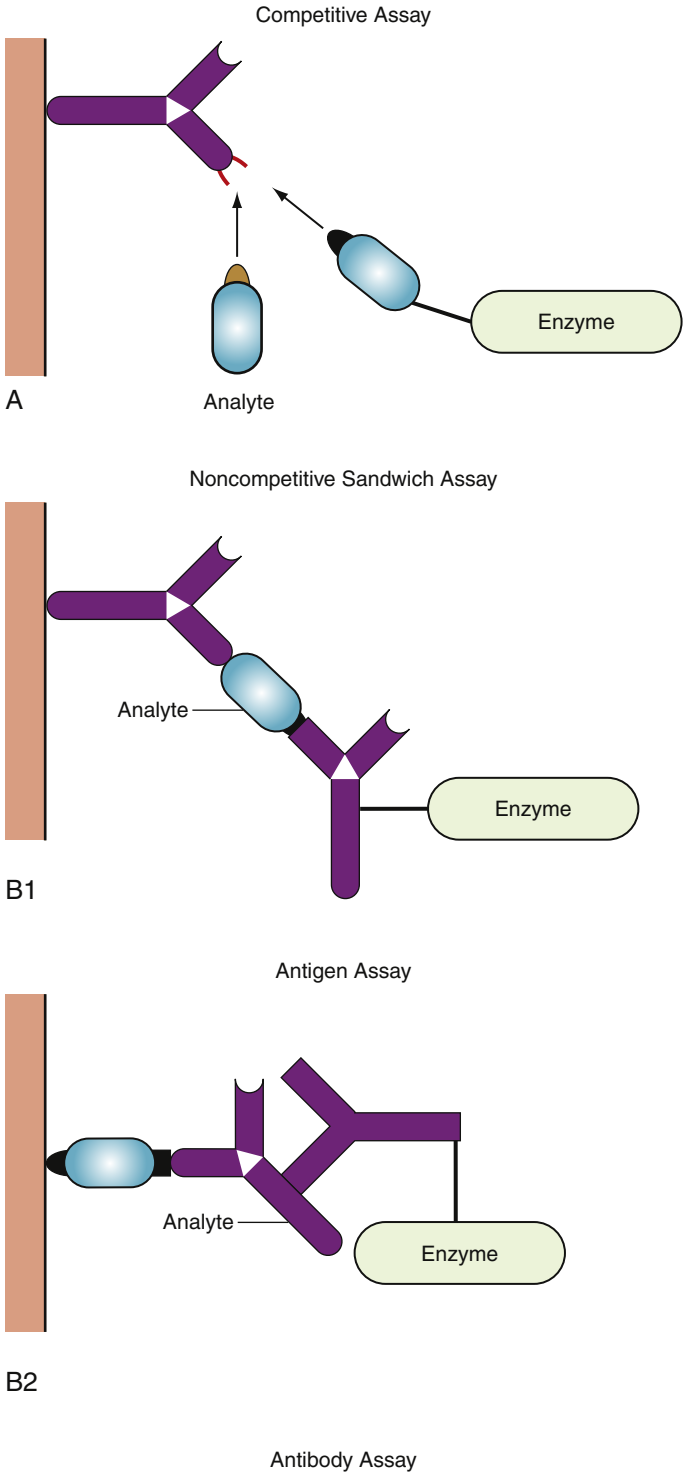

Figure 45.13 Assay principles of heterogeneous enzyme immunoassay (EIA) using solid phase. **A,** Competitive assay. **B1** and **B2,** Noncompetitive sandwich assay.

such as those for luminol, are likely to be interfered with by multiple factors that cause increased nonspecific background signals (noise).

Bronstein and colleagues (1989a) developed a chemiluminescent substrate for alkaline phosphatase that differs considerably from other compounds. This new substrate is known as AMPPD (disodium 3-(4-methylspiro [1,2-dioxetane-3,2′-tricyclo-[3.3.1.1]decan]-4-yl) phenyl phosphate), an adamantyl dioxetane derivative. It requires no additional molecules for the emission of chemiluminescent light, unlike luminol, which needs oxidative compounds from outside the luminol molecules. AMPPD is a novel molecule that is a complete substrate because it is composed of the adamantyl group as a stabilizer of the entire molecule, the dioxetane bond as an energy source, and phosphoryl ester as a cleavage site of the enzyme, along with a phenyl group for chemiluminescence—all assembled within one molecule. The structure of the molecule and the reaction process for light generation are shown in Figure 45.14. Cleavage of the phosphoester bond of AMPPD by alkaline phosphatase triggers chemically initiated electron exchange luminescence by releasing electron-rich dioxetane. A chemiluminescent signal with a maximum wavelength of 477 nm can be detected within a couple of minutes to a few hours depending on the substrate concentration. The alkaline phosphatase with AMPPD assay system has a sensitivity of less than 10^{-20} mol (Bronstein et al., 1989b, 1991; Kricka, 1991).

CL-EIA uses AMPPD as a substrate to react with alkaline phosphatase, which is used as the enzyme label. CL-EIA can be performed on a fully automated instrument. This novel substrate made it possible to develop an extremely sensitive CL-EIA system. Ferrite particles 0.3—a few μm in diameter as the solid phase—shorten immunoreaction time to within 30 minutes and provide a larger surface area for the immunoabsorbent. The relationship between the chemiluminescent signal and the concentration of analytes is linear up to about seven orders of dynamic range. The sensitivity of CL-EIA (Nishizono et al., 1991) was 10-fold greater than that of conventional RIAs when AFP was assayed; AFP was detected at a level of 30 pg/mL, with an assay time of 30 minutes. Thus, the new CL-EIA systems are a definite improvement over RIAs in terms of sensitivity, time efficiency, and procedural simplicity, and they are increasing in popularity.

Hashida and colleagues (1995) reported that a highly sensitive CL-EIA using immune complex transfer (ICT) technique, which could markedly reduce the nonspecific signals by transfer of the immune complexes from the first solid phase to the second one, has been developed to increase the sensitivity of immunoassay to detect HIV1 p24 antigen. The antigen was reacted simultaneously with 2,4-dinitrophenyl–biotinyl–bovine serum albumin–anti-p24 Fab conjugate and anti-p24 Fab–b-D-galactosidase conjugate. The complex that was formed, comprising the three components, was trapped onto polystyrene beads coated with affinity-purified (anti-2,4-dinitrophenyl group) IgG. The polystyrene beads were washed to eliminate excess anti-p24 Fab–b-D-galactosidase conjugate. Then, the complex was eluted from the polystyrene beads with excess ε*N*-2,4-dinitrophenyl–L-lysine and was transferred onto polystyrene beads coated with streptavidin to eliminate nonspecifically bound anti-p24 Fab–b-D-galactosidase conjugate more completely. The b-D-galactosidase activity bound to the latter beads was assayed by fluorometry. The detection limit of p24 per assay was 0.1 amol (2.4 fg) and was 30-fold less than that by the conventional EIAs. After that, a semiautomated CL-EIA using the ICT method for the detection of hepatitis B surface antigen (HbsAg) was developed and was demonstrated to be as sensitive as HBV DNA PCR (Takeda et al., 2013). The cutoff value (0.5 mIU/mL) was 8.0 standard deviations above the mean of the HBsAg-negative specimens. The CL-EIA using the ICT method may be useful not only for an earlier detection of HBV reactivation but also for the monitoring of hepatitis B patients.

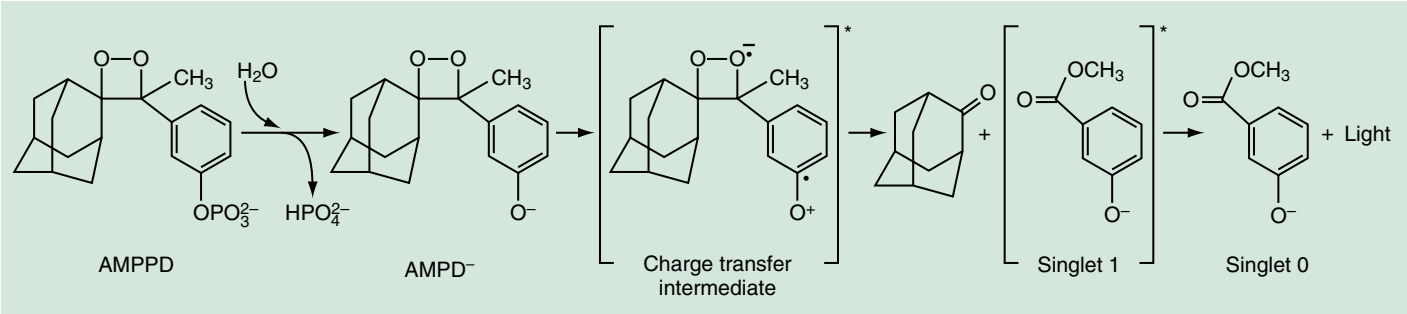

Figure 45.14 Adamantyl 1,2-dioxetane phenyl phosphate (AMPPD): a chemiluminescent substrate for alkaline phosphatase (ALP) detection. Hydrolytic phosphate cleavage by ALP triggers chemically initiated electron exchange luminescence (CIEEL) decomposition of AMPPD by releasing the electron-rich dioxetane phenolate ($AMPD^-$). Charge transfer from the phenolate to the dioxetane ring takes place, forming the charge transfer (CT) intermediate and subsequent breakdown of the cyclic peroxide. Release of energy occurs with light emission.

HOMOGENEOUS ENZYME IMMUNOASSAYS

Background

Two options are available to eliminate tedious assay procedures. One is to design fully automated instruments to access heterogeneous types of reagents. The other is to develop innovative reagents that do not require complicated washing steps, such as those needed for heterogeneous EIAs. Enzymes and their cofactors are advantageous labels in homogeneous EIAs because enzyme activity can be modulated easily by changing factors in the microenvironment of the Ag–Ab reaction. This is not the case when radioisotope decay is used as the signal. At present, homogeneous EIAs are generally less sensitive than their heterogeneous counterparts. Conventional heterogeneous EIAs have equal sensitivity to RIAs in many applications, whereas homogeneous EIAs (Nakamura & Robbins, 1988) remain one or two orders of magnitude less sensitive than RIAs. Homogeneous EIAs may require complex immunochemical reagents, but the assay systems are rapid and simple and are adaptable to conventional instruments. Various types of homogeneous EIAs are available. In each of these assays, the Ag–Ab interaction modulates the activity of the enzyme or enzyme label in the presence of the substrate. Modulation of the enzyme activity reflects the degree of the immunochemical reaction. Table 45.6 lists the characteristics of typical homogeneous EIAs. Homogeneous EIAs can be classified as competitive and noncompetitive binding assays. Competitive assays usually consist of enzyme-labeled antigens. However, the antigen (analyte) may be conjugated to the substrate or to a prosthetic group of the enzyme in other assay formats. In contrast, noncompetitive binding assays use a conjugate of antibody labeled with enzyme. Among the various methods reported, five homogeneous EIAs deserve our attention.

Enzyme-Multiplied Immunoassay Technique

EMIT, the first homogeneous EIA, was developed by Rubenstein and Schneider (1972). The EMIT system is illustrated in Figure 45.15. In EMIT, the conjugation of enzymes to haptens does not disrupt enzyme activity. However, the binding of hapten-specific antibodies to haptens results in inhibition of enzyme activity. Free haptens in the standard or sample relieve this inhibition by competing for antibodies. Thus, in the presence of antibodies, enzyme activity is proportional to the concentration of free haptens. As a general rule, the antibody inhibits the enzyme by inducing or preventing conformational changes necessary for enzyme activity (Rowley et al., 1975). The exception to this inhibition mechanism is the EMIT thyroxine assay, which uses malate dehydrogenase. In this assay, the thyroxine-malate dehydrogenase conjugate is enzymatically inactive, but it becomes activated when it is bound by thyroxine antibody (Ullman et al., 1979). It is believed that conjugated thyroxine inhibits the enzyme by binding to the active site, increasing the "apparent" K_m of the substrate. The antibody reactivates the enzyme by "pulling" the thyroxine out of the active site. In the EMIT assay system, malate dehydrogenase and glucose-6-phosphate dehydrogenase have been found to be most useful because they are less likely to be affected by serum constituents. These assays generally measure drugs at a concentration of milligrams per liter. However, the digoxin assay has a much lower limit of sensitivity in the range of 0.8 to 2.0 μg/L.

Substrate-Labeled Fluorescent Immunoassay

The substrate-labeled fluorescent immunoassay (SLFIA) (Burd et al., 1977) uses a characteristic fluorogenic substrate, umbelliferyl β-galactoside, attached to the antigen (analyte) as a conjugate. Umbelliferone is the fluorescent product produced when the substrate is cleaved with the enzyme β-galactosidase, which cannot cleave the substrate–antigen complex when it is reacted with the specific antibody. The free antigen (analyte) in the specimen solution competes with the antigen conjugated with the substrate to form the immunocomplex (Fig. 45.16). The antigen concentration in the sample is proportional to the fluorescent intensity of the cleaved fluorescent product. SLFIA can be used to assay drugs and haptens as well as protein ligands such as IgG and IgM. A disadvantage of this method is that the amplification properties of the enzyme are not utilized; thus, the assay system has limited sensitivity in the range of 10^{-9} to 10^{-10} molar concentration of the analyte.

Apoenzyme Reactivation Immunoassay

The apoenzyme reactivation immunoassay (ARIS) is a homogeneous assay developed by Morris and colleagues (1981) using the prosthetic group consisting of flavin adenine dinucleotide (FAD)-conjugated antigen (analyte) and glucose oxidase apoenzyme. As shown in Figure 45.17, the antigen (analyte) and a constant amount of analyte–FAD conjugate compete for a limited amount of specific antibody. At equilibrium, the level of free conjugate is proportional to the amount of antigen (analyte) in the specimen. The apoenzyme combines with the free but not with the antibody-bound form of conjugate to reactivate glucose oxidase activity in proportion to the amount of free conjugate in the mixture. Active enzyme is generated in the procedure, and an amplification mechanism is built into this assay. ARIS has been used to assay for theophylline and IgG (Morris et al., 1981; Morris, 1985). This FAD-labeled conjugate assay is readily adapted to the measurement of high-molecular-weight proteins (e.g., thyroid binding globulin) (Schroeder et al., 1985) as well as other haptens, such as phenytoin and hormones.

Enzyme Inhibitory Homogeneous Immunoassay

The enzyme inhibitory homogeneous immunoassay (EIHIA), developed by Ashihara and colleagues (1988), consists of antibody conjugated with enzyme and insoluble substrate. This assay is most suitable for the determination of large antigens (analytes). The EIHIA can be made to be homogeneous because the immunocomplex of conjugate with large antigen blocks the enzyme reaction with the solid substrate (Fig. 45.18). α-Amylase has been used as a labeled enzyme for the determination of ferritin and AFP. The immunoreaction of analyte with enzyme-labeled antibody can reach a

TABLE 45.6

Classification and Characteristics of Typical Homogeneous Enzyme Immunoassays*

Name and Assay Type	Conjugate	Manner of Modulation
Competitive		
EMIT	Antigen with lysozyme, G6PD*	Steric hindrance
SLFIA	Antigen with substrate	Steric hindrance
ARIS	Antigen with prosthetic group	Steric hindrance
Enzyme-channeling immunoassay	Antigen with G6PDH* and hexokinase*	Enhancement by proximity
Biotin-enzyme avidin immunoassay	Antigen with avidin	Steric hindrance
CEDIA	Antigen with fragments of subunit	Steric hindrance
Noncompetitive		
Hybrid antibody immunoassay	Hybrid antibodies specific to antigen and to inhibitor	Steric hindrance
Proximal linkage immunoassay	Antibody with G6PD* and hexokinase*	Substrate cascade by proximity
EIHIA	Antibody with amylase*	Steric hindrance
Enzyme enhancement immunoassay	Antibody with β-galactosidase* and succinyl antibody	Charge effect
AEST	Antibody with peroxidase	Stabilization

From Kasahara Y: Principles and applications of particle immunoassay. In Nakamura RM, Kasahara Y, Rechnitz GA, editors: *Immunochemical assays and biosensor technology for the 1990s,* Washington, DC, 1992, American Society for Microbiology. Reproduced with permission.
AEST, associated enzyme sensitive technique; *ARIS,* apoenzyme reactivation immunoassay; *CEDIA,* cloned enzyme donor immunoassay; *EIHIA,* enzyme inhibitory homogeneous immunoassay; *EMIT,* enzyme-multiplied immunoassay technique; *G6PD,* glucose-6-phosphate dehydrogenase; *SLFIA,* substrate-labeled fluorescent immunoassay.
*Enzyme discussed in detail in the text.

plateau within 10 minutes; thus, EIHIA based on a noncompetitive binding assay requires less incubation time to achieve a sensitive detection level. Using this method, the measuring range of ferritin in serum is 10 to 800 ng/mL; for AFP, it is 5 to 200 ng/mL. Dextranase has been used as an alternative enzyme (Nishizono et al., 1988). EIHIA has also been applied to a simple dry-film format (Ashihara et al., 1991). The dry film consists of three major layers, each containing a developing zone for immunologic and enzymatic reaction, a barrier zone, and a color-developing zone. An inhibitor specific to human amylase present in serum is used to prevent serum background. The assay for serum C-reactive protein is completed in only 6 minutes by simply placing the specimen on the slide using dry chemistry instrumentation. Nevertheless, the sensitivity of the system remains inadequate for application to analytes such as tumor markers.

Cloned Enzyme Donor Immunoassay

The cloned enzyme donor immunoassay was first achieved through the application of recombinant deoxyribonucleic acid (DNA) technology to homogeneous immunoassays by Henderson and colleagues (1986).

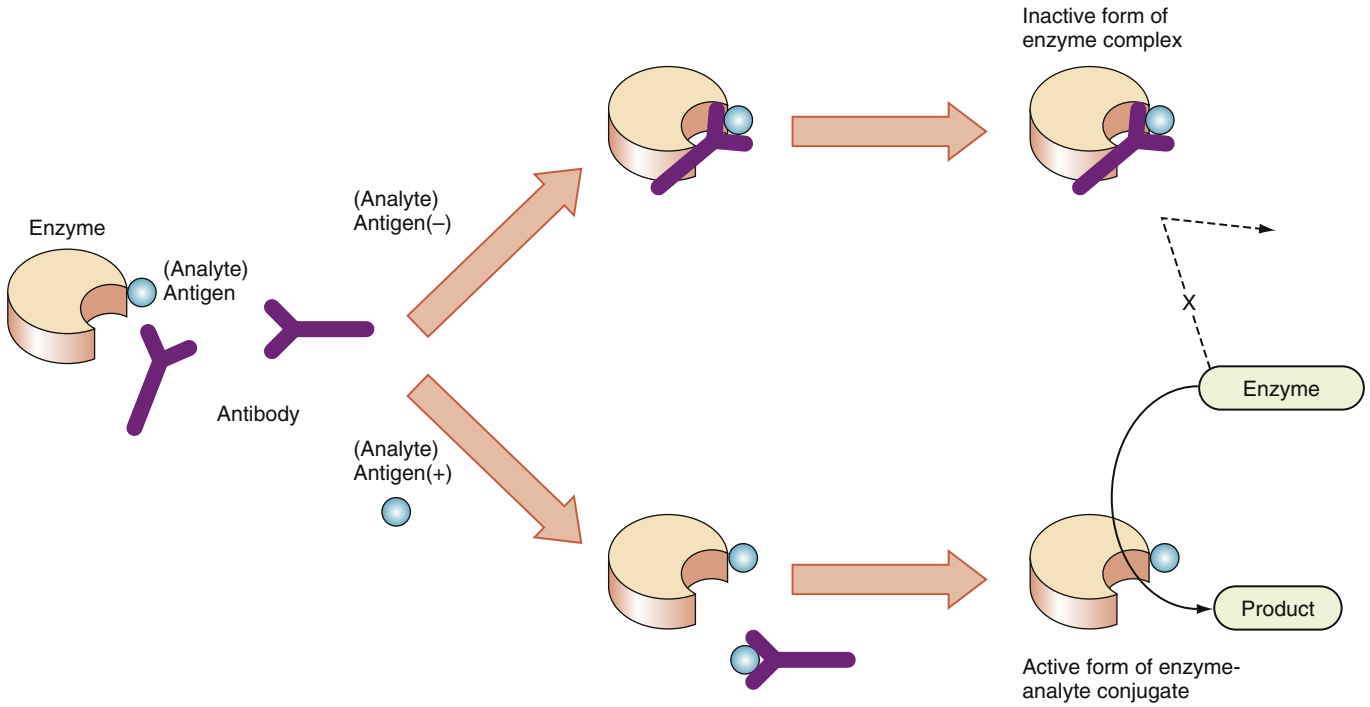

Figure 45.15 Enzyme-multiplied immunoassay technique (EMIT) system diagram. The activity of an enzyme as a label is inhibited by the binding of antibody to antigen (analyte) conjugated with enzyme. The analyte is usually a hapten. Glucose-6-phosphate dehydrogenase (G6PD) and lysozyme are usually used as enzymes. In the assay, enzyme activity is proportional to the concentration of the analyte. (*With permission from Nakamura RM, Kasahara Y, Rechnitz GA, editors:* Immunochemical assays and biosensor technology for the 1990s, *Washington, DC, 1992, American Society for Microbiology.*)

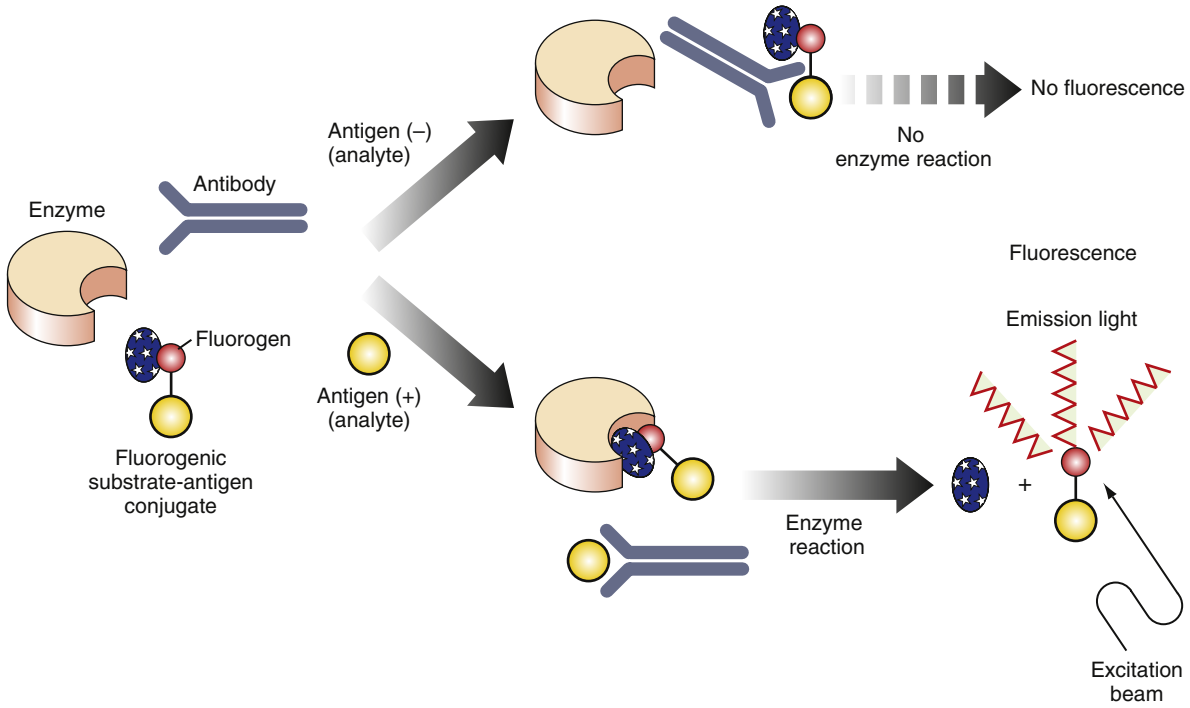

Figure 45.16 Substrate-labeled fluorescent immunoassay (SLFIA). The substrate β-galactosylumbeliferone is conjugated with the antigen (analyte) and forms a nonfluorescent substrate. The substrate can be cleaved by the enzyme β-galactosidase to form a fluorescent product. However, when the substrate–antigen conjugate is allowed to react with specific antibody to the antigen, no cleavage of the substrate complex with the β-galactosidase enzyme occurs. In this assay, the concentration of the antigen (analyte) is directly proportional to the fluorescent intensity measured. (*With permission from Nakamura RM, Kasahara Y, Rechnitz GA, editors:* Immunochemical assays and biosensor technology for the 1990s, *Washington, DC, 1992, American Society for Microbiology.*)

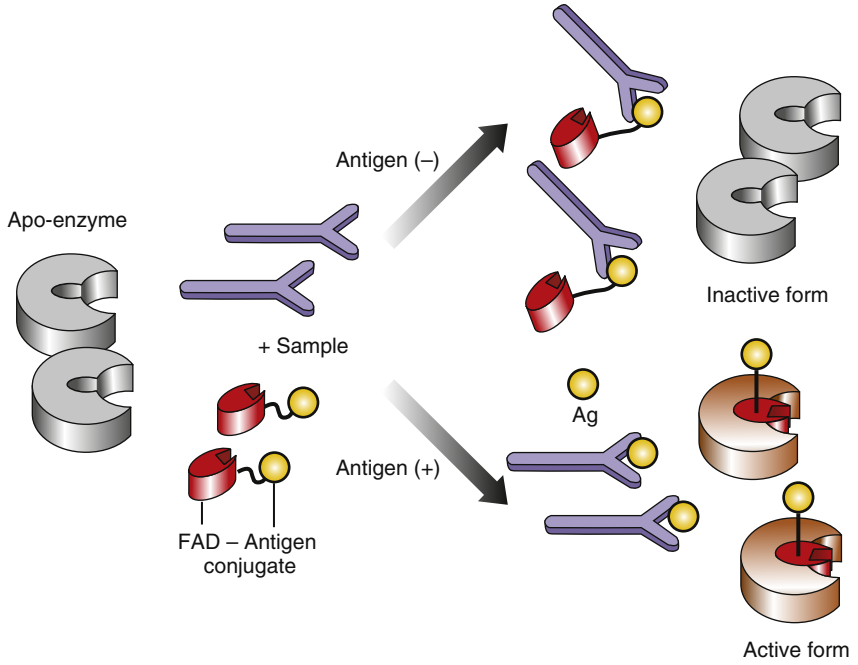

Figure 45.17 Apoenzyme reactivation immunoassay (ARIS). Flavin adenine dinucleotide (FAD) attached to the antigen is used. The apoenzyme is apoglucose oxidase, which requires FAD cofactor for activity. In the assay, the concentration of antigen (analyte) is proportional to the enzyme activity generated. (*With permission from Nakamura RM, Kasahara Y, Rechnitz GA, editors: Immunochemical assays and biosensor technology for the 1990s, Washington, DC, 1992, American Society for Microbiology.*)

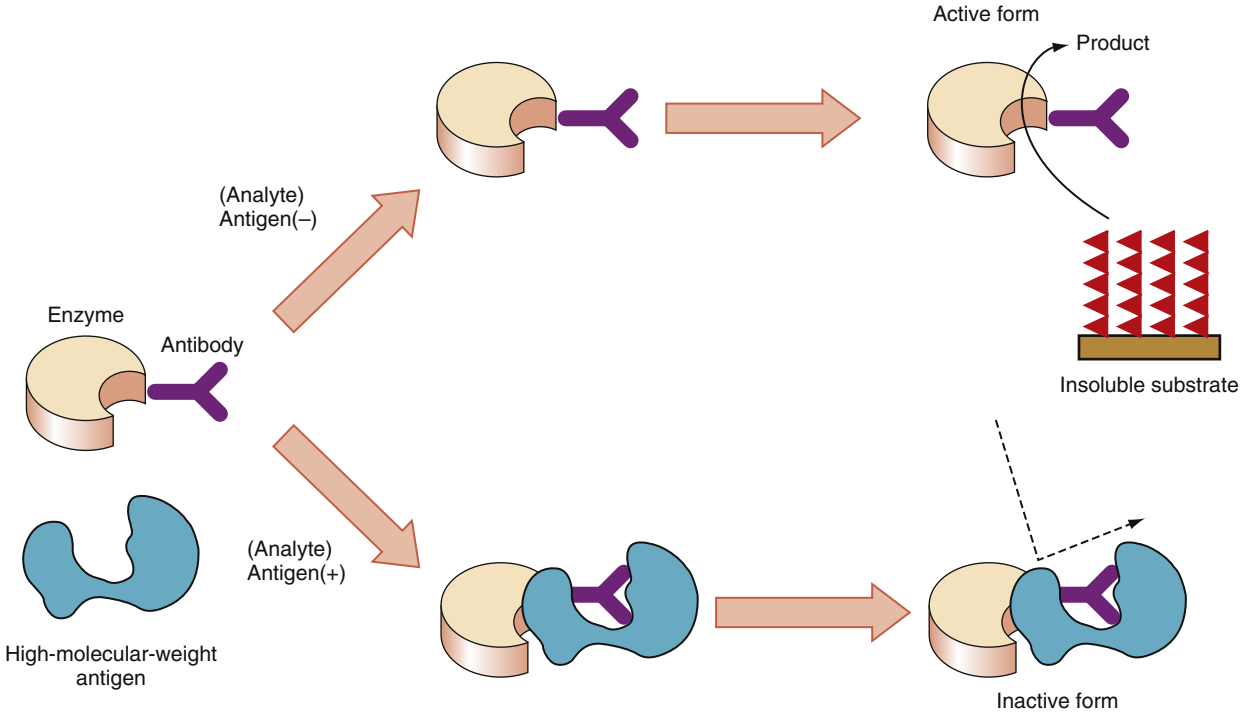

Figure 45.18 Enzyme inhibitory homogeneous immunoassay (EIHIA). The enzyme α-amylase from *Bacillus subtilis* or dextranase from *Chaetomium gracile* is conjugated to the specific antibody to the high-molecular-weight antigen. The high-molecular-weight antigen can be ferritin or α-fetoprotein. The α-amylase enzyme is inactive when the enzyme antibody conjugate reacts with specific antibody. The active enzyme form can react with the starch-insoluble substrate. The antigen concentration is directly proportional to the enzyme activity of the assay reaction. (*With permission from Nakamura RM, Kasahara Y, Rechnitz GA, editors:* Immunochemical assays and biosensor technology for the 1990s, *Washington, DC, 1992, American Society for Microbiology.*)

Microgenics Corp. (Concord, CA) was able to engineer β-galactosidase protein into a large polypeptide (an enzyme acceptor [EA]) and a small polypeptide (an enzyme donor [ED]). EAs and EDs assemble to form enzymatically active tetramers. In the assay (Fig. 45.19), a hapten antigen (analyte) is attached to an ED, and an analyte-specific antibody is used to inhibit spontaneous assembly of the active enzyme. The antigens (analytes) in patient serum compete with the analytes in the analyte–ED conjugate for antibody, modulating the amount of active β-galactosidase formed. The signal generated by enzyme substrates is directly proportional to the analyte concentration in the patient serum. The test for digoxin is a colorimetric assay that requires no serum pretreatment or predilution. The assay system is suitable for use with automated chemistry analyzers.

SUMMARY

EIAs can be applied to all Ag–Ab systems, including those involving serum protein, hormones, drugs, and other antigens and the antibodies directed against pathogens. Heterogeneous EIAs using chromogenic substrates can have a sensitivity comparable with that of RIAs, and they have gained wide acceptance for application in various immunoassays. Heterogeneous EIAs using sophisticated substrates that generate chemiluminescent light and small particles as the solid phase are sensitive enough to detect less than 1 pg/mL of analytes. Thus, their sensitivity is much higher than that of RIAs. In addition, the assay manipulation is greatly simplified by fully automated instruments. Compared

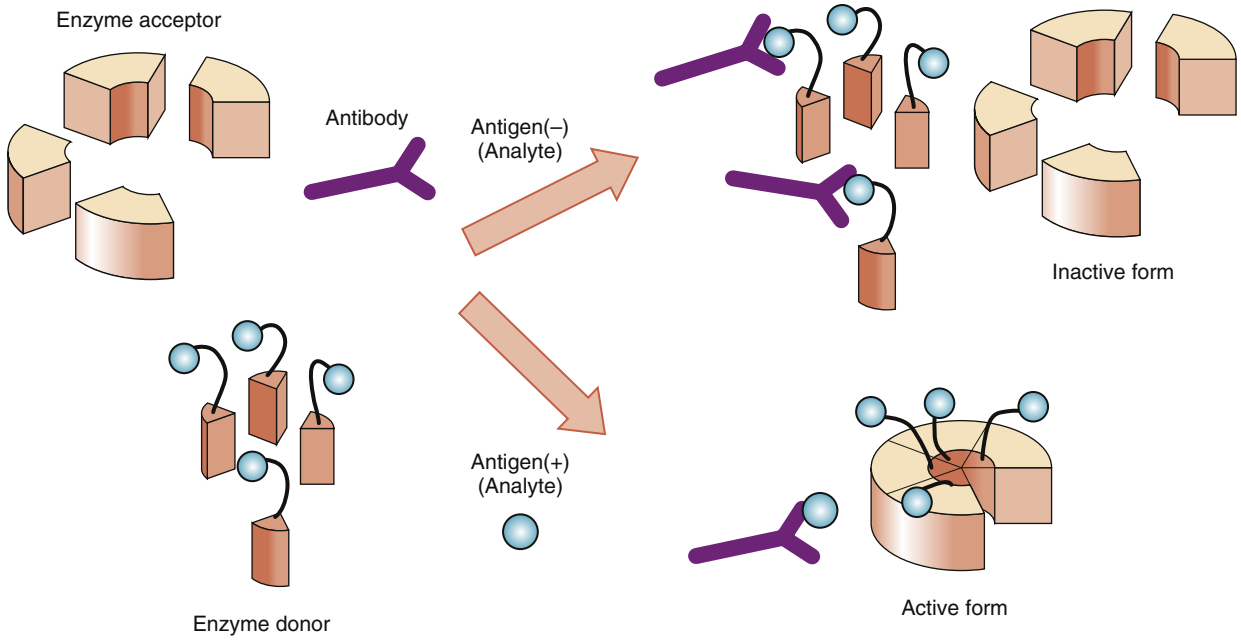

Figure 45.19 Cloned enzyme donor immunoassay (CEDIA). Enzyme acceptors associate with enzyme donors to form an active β-galactosidase tetramer. The antibody inhibits the association of enzyme acceptor with enzyme donor–antigen conjugate. (*With permission from Nakamura RM, Kasahara Y, Rechnitz GA, editors:* Immunochemical assay and biosensor technology for the 1990s*, Washington, DC, 1992, American Society for Microbiology.*)

with heterogeneous EIAs, homogeneous EIAs have certain limitations in sensitivity, dynamic range, and large analyte application. Also, high background signals (noise) and relatively low assay signals are inevitable because of elimination of the washing steps for the separation of bound and free conjugates. Homogeneous EIAs are advantageous because they are based on a simple assay format and can be adapted to existing automatic instrumentation. At this time, heterogeneous EIAs with fully automated instruments remain the best choice in terms of sensitivity and simplicity, as well as for safety reasons, because they do not require the use of radioisotopes.

FLUORESCENT IMMUNOASSAY

BACKGROUND AND CLASSIFICATION

Coons and colleagues (1941) first introduced the use of fluorescent compounds as immunochemical labels to detect antigens in tissue sections. Immunofluorescence assays on tissue sections are currently very well established in the pathology laboratory. Over the past several years, many FIA procedures have been developed to detect the concentrations of drugs, hormones, and a wide variety of proteins and polypeptides (Nakamura & Kasahara, 1992). In the initial stages of development, analytic FIAs were hindered by a decrease in sensitivity caused by background fluorescence of biological samples. Gradually, the sensitivity of fluorometric methods improved, and detection of analytes at concentrations of 10^{-15} M became possible. Further advancements were achieved through improvements in instrumentation and the introduction of unique substrates with various immunochemical and enzymatic reactions.

Selection of the fluorochrome label is important. The label should be stable and should demonstrate high molar extinction coefficiency and quantum yield. It should also emit at appropriate wavelengths without interference with ligand–antibody reactions. When most fluorophores or fluorescent molecules are irradiated with light at appropriate wavelengths, an electron in the ground state is transited into the excited state of the molecule. As the electron returns to the ground state, physical energy is released in the form of a photon of lower energy (longer wavelength) than the exciting light. The fluorescence spectrum reveals a wavelength of maximal emission characteristic of a particular fluorescent compound. One of the typical labels, fluorescein isothiocyanate (FITC), has a less than 1-nanosecond time interval between excitation and emission, whereas other compounds (e.g., europium) exhibit delayed fluorescence with an interval of several hundred nanoseconds. The various FIAs may be classified as heterogeneous and homogeneous, ligand or antibody labeled, competitive or noncompetitive, and solid or nonsolid phase. The most common methods are discussed here.

HETEROGENEOUS FLUORESCENT IMMUNOASSAY

Heterogeneous FIA procedures include a washing step to separate bound from free fluorescent labels. The assay procedure is similar to that of heterogeneous EIAs and RIAs. Most commercially available assays use a solid-phase antigen or antibody system. The assay can be competitive or noncompetitive—a property shared by RIAs and EIAs.

Fluoroimmunometric Method

With the fluoroimmunometric method, the analyte reacts with excess labeled antibodies in the solution. Residual labeled antibodies bind to excess solid-phase bound antigens. The solid-phase matrix is washed, and fluorescence intensity is inversely related to the analyte concentration. This method can be adapted to the assay of haptens and complex proteins. Solid-phase FIA procedures were developed for the serologic assay of antibodies to rubella, toxoplasmosis, viral antigens, and antinuclear antibodies. Heterogeneous FIA methods for antigen determination were developed for serum proteins and hormones, including immunoglobulins, cortisol, progesterone, and thyroxine. The major advantage of heterogeneous FIAs is the significant reduction in interference by naturally fluorescent substances in patient samples, caused by the physical removal of interference factors during the separation step.

Radial Partition Immunofluorometric Assay

In radial partition immunoassays, radial chromatography is used and the assay is carried out on glass-fiber filter papers (Giegel et al., 1982). This procedure has been automated for the assay of hCG and several other analytes in serum (Rogers et al., 1986).

Time-Resolved Fluoroimmunoassay

This method uses special instrumentation and fluorescent labels to increase assay sensitivity. It involves the use of fluorescent labels exhibiting delayed fluorescence with a time period of 100 ns or longer between excitation and emission. Because most substances responsible for background fluorescence have a short decay period, measurement of the delayed fluorescence signal will significantly reduce the effects of background fluorescence. This is accomplished with the time-resolved fluorometer, a special instrument that produces a fast light pulse that excites the fluorophore. Fluorescence is measured a little while after excitation. Thus, the effect of nonspecific background, which generally decays in less than 10 nanoseconds, can be removed (Halonen et al., 1973; Soini & Kojola, 1983). Fluorophores exhibiting delayed fluorescence that have been used in these assays (Soini & Hemmila, 1979) include the following:

- Pyrene derivatives with a decay time of almost 100 ns
- Rare earth metal chelate labels with a very long decay time of almost 50 to 100 μs. These include europium (Eu^{3+}), samarium (Sm^{3+}), and terbium (Tb^{3+}).

- Time-resolved fluoroimmunoassays have been developed to measure many analytes, including hCG, IgG, cortisol, insulin, and others.

HOMOGENEOUS FLUORESCENT IMMUNOASSAY

By definition, these immunoassays are performed on homogeneous specimen samples. They do not require the separation of bound from free conjugates and usually are not sensitive to background interference in the samples. Homogeneous FIAs also have the advantage of being quick to perform. However, when compared with heterogeneous assays, they show certain disadvantages. Homogeneous FIAs have a limited sensitivity near 10^{-10} m/L with standard instrumentation. Labeled impurities in the sample may increase background interference. The assays require relatively pure labeled antigen or specific antibody, as well as special instrumentation, to achieve higher sensitivity.

Fluorescence Polarization Assay

A polarizing lens or prism can resolve light into rays in a single plane. When viewed at the right angle of an excitation beam of vertically polarized light, fluorescent compounds in solutions emit partially polarized fluorescence. The fluorescence polarization principle was first applied to immunoassay procedures by Dandliker and colleagues (Dandliker & de Saussure, 1970; Dandliker et al., 1973). Polarized light transmitted through the sample can excite the fluorescent label regardless of binding to antibody. However, as shown in Figure 45.20, random thermal motion causes small molecules labeled with a hapten to tumble freely in solution, losing their polarized orientation. When the labeled antigen is bound to antibody with a molecular mass greater than 160 kDa, the molecular motion is slowed enough to increase the polarized signal.

Studies using labeled antibody or antibody fragments showed no change in polarization upon mixing antigen and labeled antibody, even though immune reaction had occurred. This method is most useful for the measurement of small antigens and haptens (Jolley, 1981). Abbott Laboratories has adapted this approach for the assay of many therapeutic and abused drugs on the TDx (Abbott Diagnostics, Abbott Park, IL). They developed a next-generation analyzer, the IMx, to measure molecules with large masses, such as tumor markers, hormones, and infection-related antigens or antibodies (Fiore et al., 1988). They combined two assay principles: fluorescence polarization and microparticle EIA. The demand for random-access capabilities led Abbott to develop a fully automated, high-throughput random-access analyzer named the AXSYM. This system is being used in clinical laboratories (Smith et al., 1993).

Fluorescence Excitation Transfer Immunoassay

The fluorescence excitation transfer immunoassay (FETI) method (Ullman et al., 1976) uses two labels: fluorescein as the donor fluorescent label and rhodamine as the acceptor or quencher. FITC has a maximum emission of 525 nm, and tetraethylrhodamine has a strong absorption peak at 525 nm. Therefore, when FITC-labeled antigen and rhodamine-labeled antibody bind, quenching of FITC fluorescence occurs. This phenomenon involves an energy transfer from an electronically excited fluorescent dye to an acceptor dye. The rate of energy transfer is inversely proportional to the sixth power of the distance between donor and acceptor molecules. For adequate reduction of fluorescence with quenching, the donor–acceptor distance between labels should be about 50 to 70 Å. This method is useful for the assay of antigen with multivalent antigenic determinants. Separate portions of specific antibody are labeled with fluorescein and rhodamine. The mixture of differently labeled fluorescein-tagged antibody and rhodamine-labeled antibody reduces the intensity of the fluorescein label by adjusting the ratio and amount of donor and acceptor molecules so that they can react in close proximity to permit energy transfer. These problems have been overcome using new fluorescent compounds. The FETI method has been improved with the use of a fluorescence marker such as europium (III) (Eu[III]) trisbipyridine cryptate as a donor, and a fluorophore such as allopycocyanin as an acceptor (Alpha et al., 1987; Mathis, 1995). These transient compounds reveal a large Stokes shift in which the excited europium at 337 nm transfers energy through an acceptor molecule at an excitation of 620 nm and eventually emits fluorescent light at 665 nm, as in the time-resolved mode. Mathis (1993) developed the fluorescence resonance energy transfer using cryptate-chelating rare metal and applied it to the detection of AFP and carcinoembryonic antigen (CEA) in serum. CIS Bio International (Ceze, France) developed an automated homogeneous immunoassay system, KRYPTOR, for the detection of cancer markers such as CEA, CA 19-9, CA 125, and AFP, using the time-resolved amplified cryptate emission. The sensitivity for AFP was 0.25 ng/mL for 9 minutes' incubation.

Fluorescent Protection Immunoassay

In this assay (Nargessi et al., 1979), the protein antigen is labeled with fluorescein and then is reacted with specific antibody to the antigen. The antigen-specific antibody will sterically inhibit the reaction of a second antibody specific to fluorescein, which functions to quench the fluorescence of fluorescein when it binds to the fluorophore. The ability of the specific antifluorescein antibody to interact with fluorescein coupled to the surface of the antigen will decrease. The procedure may be used to

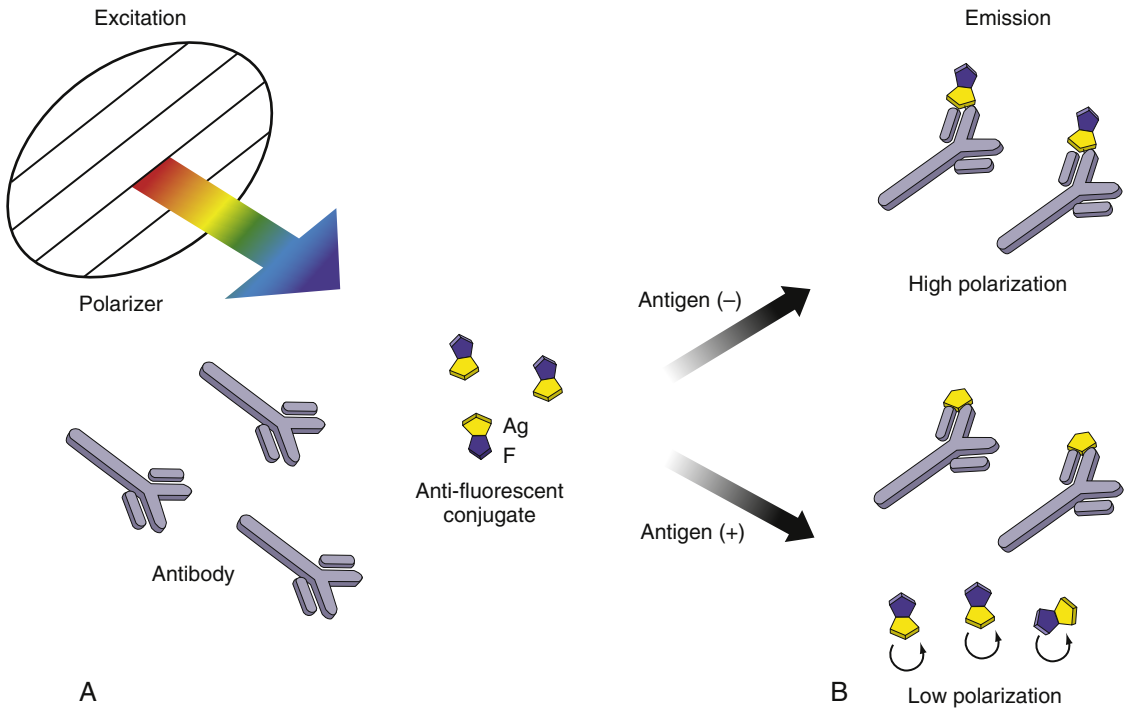

Figure 45.20 Assay principle of fluorescence polarization immunoassay (FPIA). **A,** A polarized beam can excite both an unbound conjugate and the conjugate bound to antibody (Ab) existing at the same angle as the irradiating beam. The conjugate consists of hapten (H) with a fluorescent molecule (F). **B,** Orientation of the molecules at the time of fluorescence emission. Small hapten conjugates free of antibody can quickly change their orientation and emit fluorescence at different angles that is not detected. However, the conjugate bound to the antibody still remains at the same angle because of its very slow movement, and it emits fluorescence that is detected.

assay for antibody concentration or for antigen (analyte) concentration in a homogeneous system.

CHEMILUMINESCENT IMMUNOASSAY

BACKGROUND

Chemiluminescent immunoassays (CLIAs) use chemiluminescence-generating molecules as labels, such as luminol derivatives, acridinium esters, or nitrophenyl oxalate derivatives and ruthenium tri-bipridyl [$Ru(bpy)_3^{2+}$] with tripropylamine for electrochemiluminescence. Basically, the assay method does not differ from that of heterogeneous immunoassays, RIAs, and FIAs. Light generation of luminol derivatives requires OH^-/H_2O_2 as a chemical trigger or H_2O_2 with peroxidase as an enhanced chemiluminescent trigger. Acridinium esters chemically triggered with OH^-/H_2O_2 display a relatively high chemiluminescent quantum yield for light emission compared with luminol. Other chemiluminescent molecules include aequorin, a natural compound (Actor et al., 1998). Labels of chemiluminescent compounds produce light electrochemically on the surface of electrodes and can be applied to homogeneous assay formats. Both CLIAs using acridinium esters and electro-CLIAs are applicable for practical diagnostic testing. Their characteristics are described in the following section.

CHEMILUMINESCENT IMMUNOASSAY USING ACRIDINIUM ESTERS AS LABELS

In this method (Weeks et al., 1983), acridinium esters (Fig. 45.21) are directly conjugated with protein molecules. Acridinium esters can oxidatively react with H_2O_2 under alkaline conditions to produce high-energy intermediates that decompose to the excited fragment, generating light. The light emission of acridinium esters is extremely fast, within 5 to 10 seconds after initiation of the oxidation reaction. *Flash-type chemiluminescence*, as this process is called, has a much steeper spectrum of light emission to reactive time than glow-type chemiluminescence triggered by enzymes. The sensitivity of this assay is higher than that of RIA, and testing is less time consuming. The solubility of acridinium esters and the stability of conjugates with proteins in storage have been improved through modification of the molecule and conjugation chemistry. This technology is likely to bring improvements in the assay of haptens such as hormones.

ELECTROCHEMILUMINESCENT IMMUNOASSAY

Electrochemiluminescent immunoassay (ECLIA) uses electrochemical compounds that generate light electrochemically, linked with the cycle reaction of the oxidative reduction. With optimization of reaction solutions, selection of appropriate conjugation method, and development of suitable compounds such as $Ru(bpy)_3^{2+}$ and tetrapentylammonium (TPA), it became possible to apply electrochemiluminescent technology to immunoassays (Blackburn et al., 1991). $Ru(bpy)_3^{2+}$ has a reaction site for the conjugation of analytes using activation reagent such as NHS. $Ru(bpy)_3^{2+}$, thus conjugated with antibodies, can be applied to sandwich-type assays for large molecules. The conjugate generates light on the surface of gold electrodes. $Ru(bpy)_3^{2+}$ on solid phase and TPA are oxidized on the surface of electrodes to form $Ru(bpy)_3^{2+}$ and TPA^+, respectively. TPA^+ spontaneously loses electrons. $Ru(bpy)_3^{3+}$ can generate emission light at 620 nm when it returns to $Ru(bpy)_3^{2+}$ as a ground state through reduction with TPA. The efficiency of light generation (quantum yield) depends on the proximity between the electrode and the conjugate and, thereby, on the diffusion mobility of the conjugate. Free conjugates can generate more light than conjugates fixed on the solid phase as a result of immune reaction. This allows easy access to the homogeneous assay format, but relatively high background noise interferes with assay sensitivity, as it does in other homogeneous assays. The assay protocol for the determination of analytes is as follows: magnetic microparticles coated with antibody as the solid phase and sample mix together for immune reaction. After washing for bound and free conjugates by magnetic separation according to the assay format, the solid-phase suspension is introduced into the detector with the electrode to measure chemiluminescence. The detection limit of ECLIAs has been reported as 0.2 to 0.4 ng/mL for CEA and 0.4 ng/mL for AFP. This assay does not require complicated instruments. A further advantage is that ECLIAs require less time for signal detection, similar to FIAs and other CLIAs.

INSTRUMENT AUTOMATION AND MODULATION OF ASSAY SYSTEMS

HOMOGENEOUS ASSAY SYSTEMS

Although many homogeneous immunoassays have been developed for manual protocol as described in this chapter, most have not yet been automated. For the EMIT method, fully automated generic chemistry analyzers can be adapted to use these (Boyd et al., 1985). A few instruments are available for homogeneous FIAs, and these assay systems are not interchangeable. The BRAHMS KRYPTOR system, which is the newest, has been developed with special features, including the use of a time-resolved fluorescence detector. It uses a two-wavelength method for internal standard correction of fluorescence intensity at 620 nm and 665 nm, making it possible to increase the sensitivity of the detection limit.

HETEROGENEOUS IMMUNOASSAY SYSTEMS

Until the early 1980s, most heterogeneous labeled immunoassays were manually performed. Then, Boehringer Mannheim (which merged with Roche Diagnostics in 1998) developed a fully automated random-access analyzer, the ES-600, based on colorimetric enzyme immunoassays, using horseradish peroxidase as the enzyme (Wu et al., 1987). From the late 1980s onward, many companies endeavored to develop fully automated EIA systems, which were high-throughput, sensitive, randomly accessible systems. Antigens associated with early onset of infectious disease, cytokines, growth factors, and hormones such as calcitonin exist at extremely low concentrations in serum, requiring a highly sensitive detection method for measuring these analytes (Nishizono et al., 1991; Isomura et al., 1994, 1999). Among the various methods, CLIAs and their enzymes are the most sensitive assay systems capable of detecting analytes present at very low concentrations.

The fully automated instruments currently available are also capable of using fluorescent enzyme immunoassays. These assay systems are classified into several groups based on the generation and detection of signals and the type of solid phase. With respect to the detection signal, the AIA2000, 360 (Tosoh, Tokyo, Japan) and the AxSYM (Abbott, Abbott Park, IL) employ a fluorescent method of the EIA that uses alkaline phosphatase and a specific substrate, 4-methylumbelliferylphosphate. Three types of systems are available for CL-EIAs. Lumipulse (Fujirebio, Tokyo, Japan), Access (Beckman Coulter, Brea, CA), and Immulite (Siemens Healthcare, Erlangen, Germany) have used a stable chemiluminescent substrate, phenyl phosphoryl adamantyl dioxetane, for alkaline phosphatase (Babson et al., 1991; Nishizono et al., 1991; Patterson et al., 1994). Acridinium ester as a chemiluminescent label was applied to the ADVIA Centaur XP (Siemens Healthcare, Erlangen, Germany) and Architect i2000 (Abbott Diagnostics, Lake Forest, IL), and later to the Centaur (Siemens Healthcare, Erlangen, Germany). In the Cobas e411 (Roche Diagnostics, Basel, Switzerland), $Ru(bpy)_3^{2+}$ is used as an electrochemiluminescent label (Erler, 1998).

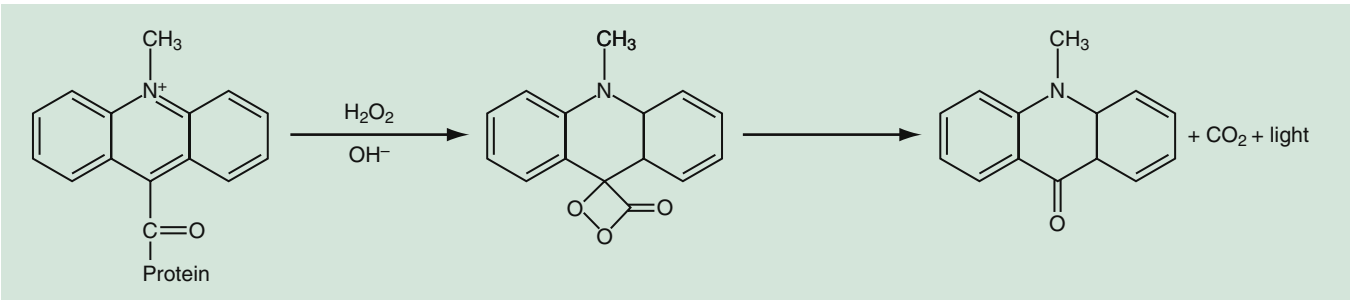

Figure 45.21 Chemiluminescent immunoassay mechanism with acridinium ester based on oxidative decomposition.

PRACTICAL FLOW OF THE IMMUNOASSAY IN THE ANALYTIC SYSTEM

The market demands that instrumentation be able to perform a large number of tests with random-access capability. To meet these criteria, it is necessary to improve reagents and avoid tediousness in performing heterogeneous immunoassays. To simplify the system for application in a fully automated assay system, individual cartridges of prepackaged reagents or predispensed reaction cuvette reagents were designed. A generic system for heterogeneous labeled immunoassays is depicted schematically in Figure 45.22. The operator selects the desired test items by means of a computer program and loads reagent cartridges or bottles for each test. For a particular analyte, the cartridges and the reaction cuvette are fed automatically into the instrument. Samples are transported to the appropriate position for dispensing. The assay is designed to use reaction trays or carousels that automate mixing and separation steps that depend on performance through first and second immune reactions and the signal generation reaction. All steps of the assay are carried out sequentially on the reaction line, and the signals generated are measured by a detector. Test results are printed out within 20 to 40 minutes and are sent automatically online to the host computer. The system can carry out about 60 to 200 tests per hour, processing 10 to 20 analytes in each sample specimen by the random-access manner.

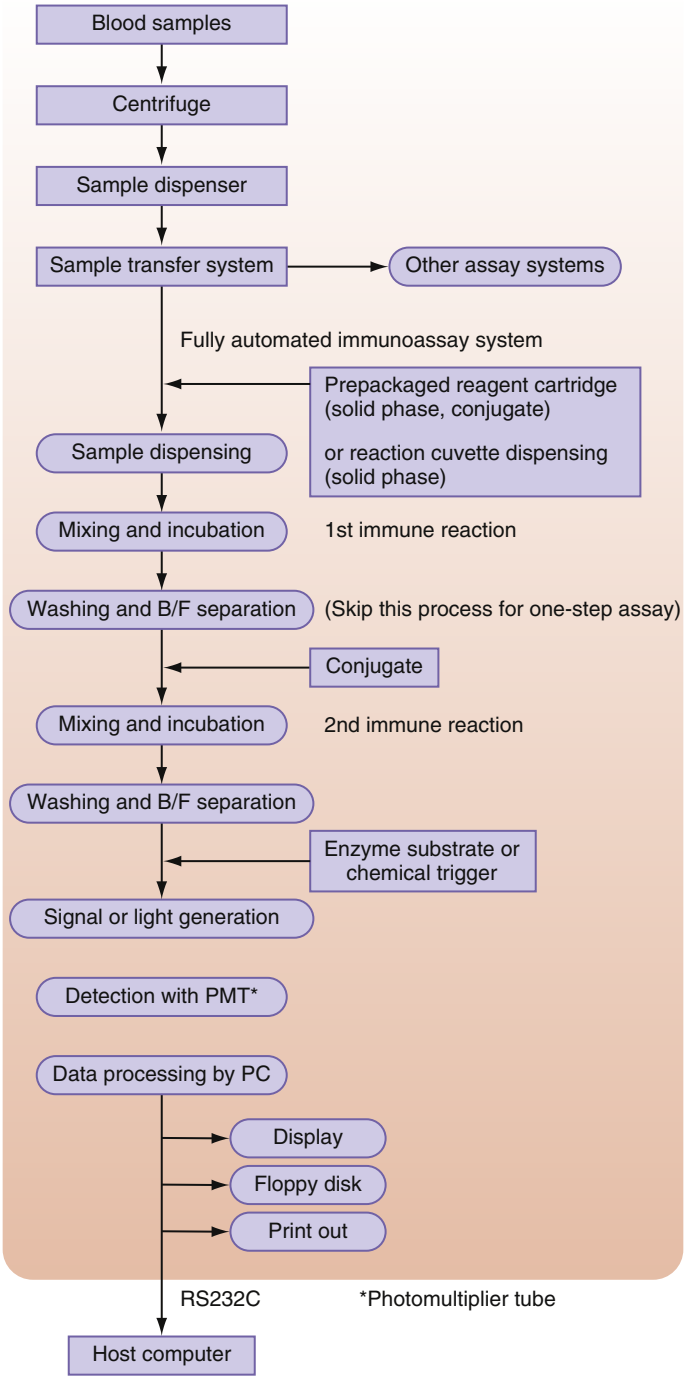

Figure 45.22 Brief diagram of fully automated immunoassay system in clinical laboratory automation. *B/F,* Bound over free; *PC,* personal computer.

INSTRUMENTATION AND KEY POINTS FOR HETEROGENEOUS IMMUNOASSAY

Although the assay principle is similar in many instruments, big differences among instruments may be noted with respect to sampling format, heating control, B/F separation, carryover, waste flow, and so forth. Thus, we should pay attention to how well the instrument performs after implementation.

Reaction Cuvette

In an immunoassay system, the design of cuvette features is very important to obtain reproducible data. Manufacturers use certain types of cuvettes to achieve easy access and rapid handling of reagents. An all-in-one type of cuvette containing the reagents and the reaction cell has been introduced in the Lumipulse system. The Immulite system utilizes a unique reaction cell for B/F separation. The AxSYM (Abbott, Abbott Park, IL) uses another unique reaction vessel consisting of a reagent, an incubation well, and a sample well within a cuvette for B/F separation. The system combines the content of this assay cuvette into a matrix cell. The latter can be used to capture the solid latex phase followed by B/F separation and the second immune reaction of the labeled antibody and the solid phase.

Sampling and Fluid Delivery Type

In general, fluid delivery is selected from two different types: a disposable chip or a fixed-probe nozzle. Cross-contamination of samples should be avoided in all assay systems. The disposable chip can completely prevent cross-contamination. In the case of the fixed-probe system, even though the original sample is divided into several small aliquots, cross-contamination still occurs. Therefore, the disposable chip system is the best way to avoid cross-contamination and to minimize biohazardous waste. On the other hand, the running cost of using chips for the assay is higher than that of the probe assay. Environmental effects of the disposable chips must be considered.

Carryover

Carryover from an extremely high concentration of analyte in one sample to the next sample sometimes causes misjudgment in clinical diagnosis. A disposable plastic tube is the simplest way to prevent this problem. On the other hand, the fixed-probe nozzle has several cost advantages, as mentioned earlier. Thus, most of the technologies concerned with sample engineering have focused on minimizing sample carryover through washing and tip maintenance steps. Now, several fixed-probe tips have made it possible to limit carryover to less than the order of 10^{-7}. Even with such low carryover, some samples still create problems (e.g., an HBsAg strong positive sample followed by a negative). In this case, a software system can be used to check the subsequent result by automatically retesting weakly positive values following strong positive results.

Bound/Fixed Separation and Washing Systems

In a heterogeneous immunoassay, the bound conjugate has to be separated from the free label. This B/F separation depends on the characteristics of the solid phase. The IMx and AxSYM systems use latex microparticles as the solid phase and employ a porous membrane to entrap the latex for separation of particles of the solid phase from particles of the liquid phase. The Diagnostics Product Corporation has developed a unique cell for B/F separation systems in which the reaction solution spins out from an inner cell to an outer waste cell, while the bound phase stays in a solid-phase bead (¼-inch bead). Advantages of this format are the avoidance of cross-contamination or carryover from one reaction mixture to the next and the fact that no excess washing process is required. All other systems use magnetic particles and magnetic beads, for which easy and rapid separation can be achieved by applying a magnetic field.

HIGH-THROUGHPUT FULLY AUTOMATED HETEROGENEOUS IMMUNOASSAY SYSTEMS

Table 45.7 compares several of the commercial high-throughput immunoassay systems that have been introduced in the past few years. It shows the instrument specifications of each analyzer. By reducing the incubation and reaction times, a rapid result can be obtained in 10 to 25 minutes.

Thus, a high-throughput machine performing approximately 200 tests/hour is possible. Furthermore, several manufacturers have demonstrated a new system concept that aligns the different analytic systems needed in a clinical laboratory. Many clinical laboratories have introduced an automated sample transporting line, which is connected to different analytic instruments controlled independently. However, several analyzers are not amenable to this approach because the speed of the instrument throughput or cycle time cannot be harmonized easily. To solve these problems, ARCHITECT (Abbott, Abbott Park, IL) is an example of a new machine concept in which one system computer can control several immunoassay analyzers connected to one chemistry analyzer called a *modular system*. Several other combinations still under development are based on this concept, which will make it possible to simplify the clinical laboratory and to lower total assay cost.

REMOTE MAINTENANCE

The daily maintenance of immunoassay analyzers has traditionally been a manual task assigned to laboratory technicians. However, certain system abnormalities are difficult to identify, especially with the sampling unit, reaction units, signal detection unit, and data storage. Progress in software development and information systems has made it possible to ensure high-quality system performance (Truchaud et al., 1997). Using a remote tracking system via the Internet, system conditions can be collected for data reliability analysis and troubleshooting. IVD systems make it possible for users to monitor system reliability in terms of data reproducibility, system performance, and quality control by using specifically assigned control values supplied by IVD system suppliers or third parties. Remote maintenance allows users to prevent daily glitches that would otherwise affect hospital management. Remote maintenance makes it possible to do the following:

1. Monitor daily performance
2. Detect parts abnormalities and conduct replacement
3. Minimize downtime
4. Improve mean time between failures
5. Detect data abnormalities
6. Provide system improvement information

A number of versatile software programs supplied by third parties can be used for remote maintenance. Under a customer agreement, IVD system manufacturers provide versatile software to ensure the system's safe management for security, including software validation compliance and personal information.

RAPID AND SIMPLE TEST DEVICES FOR POINT-OF-CARE TESTING

BACKGROUND

A strong demand for a home test (e.g., hCG for pregnancy diagnosis) has simplified the immunoassay format—the test must be simple, rapid, and reproducible. With these goals in mind, many hCG tests have been developed and have resulted in the first-generation test format with a flow-through enzyme immunoassay.

IMMUNOCHROMATOGRAPHIC DEVICES

To eliminate stepwise reagent additions in these two formats, further improvement has been accomplished with the use of immunochromatographic techniques that ensure a simpler and quicker immunoassay. Immunochromatography consists of simultaneous B/F separation and signal generation followed by lateral flow on porous materials such as a nitrocellulose membrane or a glass-fiber sheet. Through the capillary action of the membrane, the analyte in the sample can migrate from the proximal end to the distal end, where an absorbent pad is set to maintain a constant capillary flow rate. The sample loading zone, labeling zone, and detection zone are set between the two ends. The immunochromatographic method is classified into several formats (Figure 45.23). The proximal end is employed as the sample loading port connected to a pad containing labeled antigen or antibody, under which a nitrocellulose membrane is in contact with the pad, which serves as a fixed detection zone. The distal end of the membrane is attached to the absorbent pad as a source of capillary force. The sample, loaded by means of a dropper, reconstitutes the antibody or antigen labeled with colloidal gold or colored latex, which forms an immunocomplex with the analyte being detected, and the complex migrates to the detection zone. The antibody or antigen immobilized in the detection

TABLE 45.7
High-Throughput Fully Automated Heterogeneous Immunoassay Systems

	AIA-CL2400, Tosoh	ADVIA Centaur XP, Siemens	Alinity i, Abbott	Lumipulse L2400 Fujirebio	Cobas e801, Roche
Package of reagent	Freeze-drying in portion package	Reagent pack (solution)	Solution in bottle	Solution in bottle	Reagent pack (solution)
Reaction cuvette	Reagent cup	Disposable cuvette	Disposable cuvette	Disposable cuvette	Disposable cuvette
Reaction principle	Chemiluminescent enzyme immunoassay	Chemiluminescent immunoassay	Chemiluminescent immunoassay	Chemiluminescent enzyme immunoassay	Electrochemiluminescent immunoassay
Labeled substance	Alkaline phosphatase	Acridinium ester	Acridinium ester	Alkaline phosphatase	Ruthenium
Enzyme substrate	DIFURAT	None	None	Adamantyl 1,2-dioxetane phenyl phosphate	None
Detector signal	Chemiluminescence	Chemiluminescence	Chemiluminescence	Chemiluminescence	Electrochemiluminescence
Assay format	S-1, S-2, competitive	S-1, S-2, competitive	S-1, S-2, competitive	S-1, S-2, competitive; delayed S-1	S-1, S-2, competitive; delayed backtitration
Pretreatment	Yes	Yes	Yes	Yes	Yes
Reaction flow	Turntable	Turntable	Turntable	Turntable	Turntable
Cycle time, seconds	15	15	18	15	42
Reaction time, minutes	8, 9, 18, or 19	18	8, 22	20	9, 18, or 27
Reaction temperature	37°C	37°C	37°C	37°C	37°C
Maximum analyte number	40	30	47	24	48
Throughput, tests/hour	240	240	200	240	300
Solid phase	Magnetic bead	Magnetic particle	Magnetic particle	Magnetic particle	Magnetic particle
First result time, minutes	~18	18	15/29	24	9
B/F separation	Magnetic field	Magnetic field	Magnetic field	Magnetic field	Magnetic field
Sampling method	Disposable chip	Disposable chip	Fixed probe	Disposable chip	Disposable chip
Sample auto dilution	Yes	Yes	Yes	Yes	Yes

B/F, Bound over free.

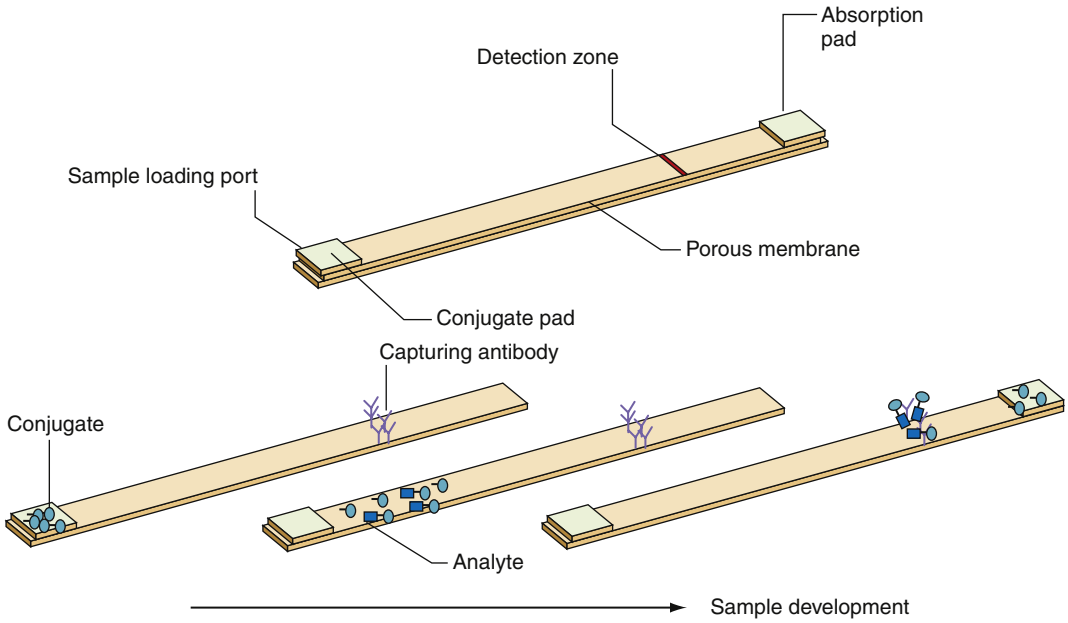

Figure 45.23 Typical immunochromatographic test strip by sample loading. Assay flows are illustrated in the lower part of the figure. In general, the proximal end of the lateral flow serves as the sample loading portion consisting of a pad containing antibody or antigen labeled with colored latex or colloidal gold. Analyte in the sample forms a complex with the conjugate and migrates to the detection zone, thereby immobilizing the capturing antibody to form a positive colored line. Excess amounts of conjugate and sample migrate to the distal end of the strip.

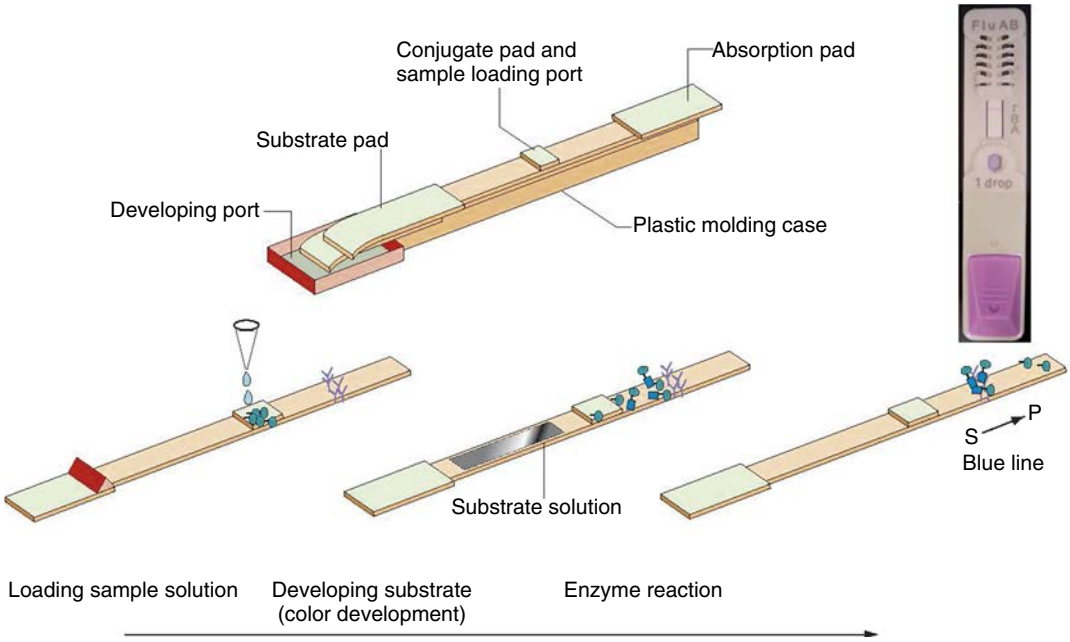

Figure 45.24 Immunochromatographic device using enzyme immunoassay (EIA). A sensitive amplification method is applied for immunochromatography using an enzyme. The sample is applied to the sample loading portion at the center of the strip. With this method, a developing solution is employed as the mobile phase and can serve as a washing buffer. The photograph at right shows the plastic molded housing and assay results for *Treponema pallidum* (TP) antibody.

zone can capture the complex and form a positive red or blue line. Excess labeling substance migrates to the absorbent pad. The mobile phase for sample migration is the sample itself. Therefore, samples strongly colored owing to the presence of a high concentration of bilirubin or hemoglobin may interfere with judgment in reading the results with the naked eye. In this format, the signal to be read is produced directly in the detection zone as a concentrated zone of colored particles.

Yamauchi and colleagues (1997) established a novel platform format in which EIA can be performed automatically, including a washing procedure and enzyme-labeled conjugate. The device is depicted schematically in Figure 45.24. In this format, the positioning of each of the zones is completely different from that of other immunochromatography formats mentioned previously. The proximal end has a developer solution, which makes it possible to carry out the washing process to take place spontaneously with capillary force. The sample is applied to a pad that is set in the center portion of the device and that contains the labeled conjugate in dry form. The distal end connects to an absorbent pad. Two drops of sample are dropped on the sample pad to react with the conjugate following reconstitution of the dried alkaline phosphatase–labeled conjugate. The reaction mixture containing the immunocomplex formed between the analyte and the labeled conjugate can spread to both ends. Once the reservoir of developing solution is ruptured, the dried substrate is reconstituted to become the soluble enzyme substrate in the detection zone. At this time, fluidic flow is directed toward the distal end. Serum components and excess nonreacted conjugate can be washed away to the absorbent. If the sample contains analyte, then the immobilized antibody captures the complex in the detection zone to form a colored line. This method has a number of advantages over other immunochromatographic devices developed by the sample. With such devices, hemolytic serum or lipemic serum may interfere with assay judgment by the naked eye, owing to high background color. However, with this new device, which is equipped with a connected reservoir, interference by colored components does not occur. This device has been useful in detecting HBsAg, anti-HBs antibody (Yamauchi et al., 1997), and antibody to *T. pallidum* (Hasegawa et al., 1995). Most of its components, such as the membrane, absorbent pad, and sample compartment, have built-in molded plastic housing.

MAGNETIC BIOSENSOR ASSAY

Bruls and colleagues (2009) developed a magnetic actuated immunosensor using magnetic nanoparticles as both coated solid phase with ligand, such as antibodies or antigens and signal. Ten microliters of blood sample are injected into the inlet of the cartridge and mixed with beads coated with antibody; the beads are then actuated by magnetic fields using a handheld instrument. The bead-captured antigens are then separated on the active

device wall whose surface is coated with second capturing antibodies by a magnetic field. Then, the second magnetic fields are set on the opposite side of the wall. Unbound beads migrate to the opposite wall without any washing step. The signals on the active wall are detected by counting nanoparticles with a combination of an LED and photodetector, using the Fourier-transformed infrared principle. Magnetic particles on the surface are cut off from the LED beam. Reduced beams correspond to magnetic particles. This method can detect pico molar levels of intact PTC with less than 10 minutes incubation. Recent data show that TnI in blood have been detected at levels of subpico molar at 5 minutes' incubation.

SUMMARY

Rapid and simple immunoassay devices can be classified into three major types: flow-through, dipping, and immunochromatography, along with combination formats of these three types. Several immunochromatographic formats are summarized in Table 45.8. Most immunochromatographic devices employ direct-labeled conjugate, colloidal metal, or colored latex. These types of formats are actually well suited for direct migration of the immunocomplex, along with migration of the sample solution. However, many of these devices require a large volume of sample, in the range of 100 to 200 μL. On the other hand, the EIA-type device allows the assay to be carried out using a smaller amount of sample—25 μL—but a developer is required. The current stream of rapid tests for point-of-care testing (POCT) is strongly oriented toward devices using immunochromatography because, unlike other immunoassay devices, special skills are not required to perform the test correctly. One simply needs to follow the manufacturer's directions for genetic testing and a certain number of protein assays could be shifted to nucleic acid assays, even in the field of POCT, particularly for the diagnosis of infectious diseases.

NONCOMPETITIVE IMMUNOASSAY FOR SMALL MOLECULES

BACKGROUND

Haptens such as hormones, vitamins, drugs, or toxins play a wide variety of roles in biology; thus, their accurate measurement is essential in biomedical fields. Haptens have mainly been measured using competitive immunoassays because, in general, their limited molecular size impedes the simultaneous binding of two antibodies to one hapten molecule for sandwich immunoassays, already mentioned in the Assay Principles and Methods section. Several methodologies have been developed for smaller haptens, including the idiometric assay using anti-idiotype antibodies (Barnard & Kohen, 1990; Kobayashi et al., 2000); open-sandwich immunoassay (Lim et al., 2007); and antimetatype antibody–based immunoassay (Towbin et al., 1995; Voss, 1996). The general assay principle for each of these methods is shown in Figures 45.25 and 45.26.

ANTI-IDIOTYPE ANTIBODY-BASED IMMUNOASSAY

The idiometric assay needs two main types of anti-idiotype antibodies. The alpha-type recognizes an epitope within the variable region of the primary antihapten antibody, but it can bind to the primary antihapten antibody in the presence or absence of the hapten analyte at the binding site. On the other hand, the beta-type antibody competes with the hapten at the binding site. Briefly, after the hapten in samples reacts with primary antihapten antibody on the solid phase, the beta-type antibody reacts with the binding sites of the primary antihapten antibody that are not occupied by haptens. Then, the labeled alpha-type antibody results in the binding of the primary antihapten antibody with hapten. Kobayashi and colleagues (2000) applied it to detect UDCA 7-NAG and 11-deoxycortisol (Kobayashi et al., 2003). It was reported that an idiometric assay for cortisol was threefold more sensitive than a competitive assay and could determine normal urinary cortisol levels (Niwa et al., 2009).

OPEN-SANDWICH IMMUNOASSAY

The open-sandwich immunoassay is based on the association of separated VH and VL chains from the variable domain of antibodies by the presence of antigen (Ihara et al., 2009; Islam et al., 2011). As shown in Figure 45.25B, the VL fragment on the solid phase was incubated with the labeled VH fragment and antigen in sample. This assay was also developed to detect hapten molecules in the homogeneous assays without the washing step.

ANTIMETATYPE ANTIBODY–BASED IMMUNOASSAY

The antimetatype antibody–based immunoassay is the only nonconventional sandwich immunoassay that enables the simultaneous recognition of a hapten by two antibodies. Generating an antimetatype antibody is a key benefit of developing sensitive and specific immunoassays for hapten. Few studies have so far confirmed that antimetatype antibodies for haptens such as digoxin and angiotensin II can be established by classical immunization procedures (Towbin et al., 1995). The development of antimetatype antibodies by classical immunization procedures suitable for wide application is highly improbable because the hapten-antibody immunocomplex structure is very difficult to maintain.

TABLE 45.8
Simple and Rapid Immunoassay Device Specifications

Assay Principle	Kit Name (Analyte)	Sample Specimens	Sample Volume, μL	Mobile Phase	Reaction Time, min	Sensitivity	Housing	Manufacturer
Immunochromatographic Format								
One step (all in one)	Biocard Troponin I test	Serum	150–200	Serum	15	0.1 ng/mL	MP	ANIBIOTECH OY
	QuickVue hCG	Urine	3 drops (75)	Urine	3	25 mIU/mL	MP	QUIDEL
	Cardiac TROP T sensitive	Blood	150	Plasma	5–20	0.1 ng/mL	MP	Roche Diagnostics
	Determine HBsAg 2	Whole blood/plasma/serum	50	Plasma/serum	15–30	0.1 IU/mL	TS	Abbott
	Alere Triage Cardiac Panel	Whole blood/plasma	250	Plasma	20	CK-MB: 1 ng/mL Myoglobin: 5 ng/mL Troponin I: 0.05 ng/mL	MP	QUIDEL
	Espline Flu AB	Nasal passage	20 (1 drop)	Developer	15	1.1×10^4 pfu/mL (A/New Caledonia/20/99)	MP	Fujirebio Inc.
	OraQuick ADVANCE Rapid HIV-1/2 Antibody Test	Oral fluid, plasma, blood	—	Developer	20–40	—	MP	OraSure Technologies, Inc.
	ImmunoCard ST HpSA	Stool	100	Developer	10	64 ng/mL	MP	Meridian Bioscience, Inc.

MP, Molded plastic housing; *TS,* test strip.

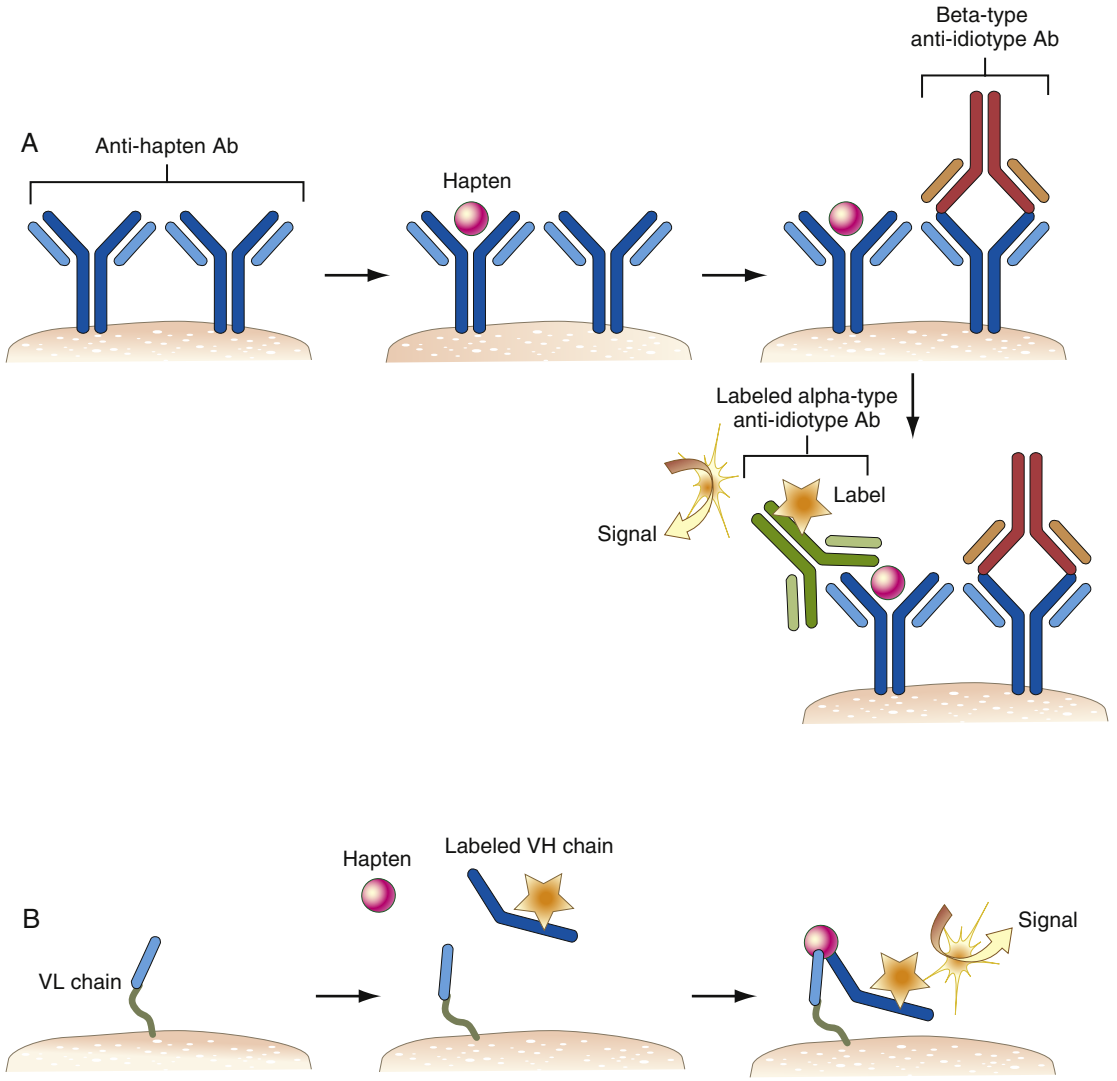

Figure 45.25 Assay principle of two kinds of hapten immunoassays. **A,** Idiometric assay using anti-idiotype antibodies. **B,** Open sandwich immunoassay.

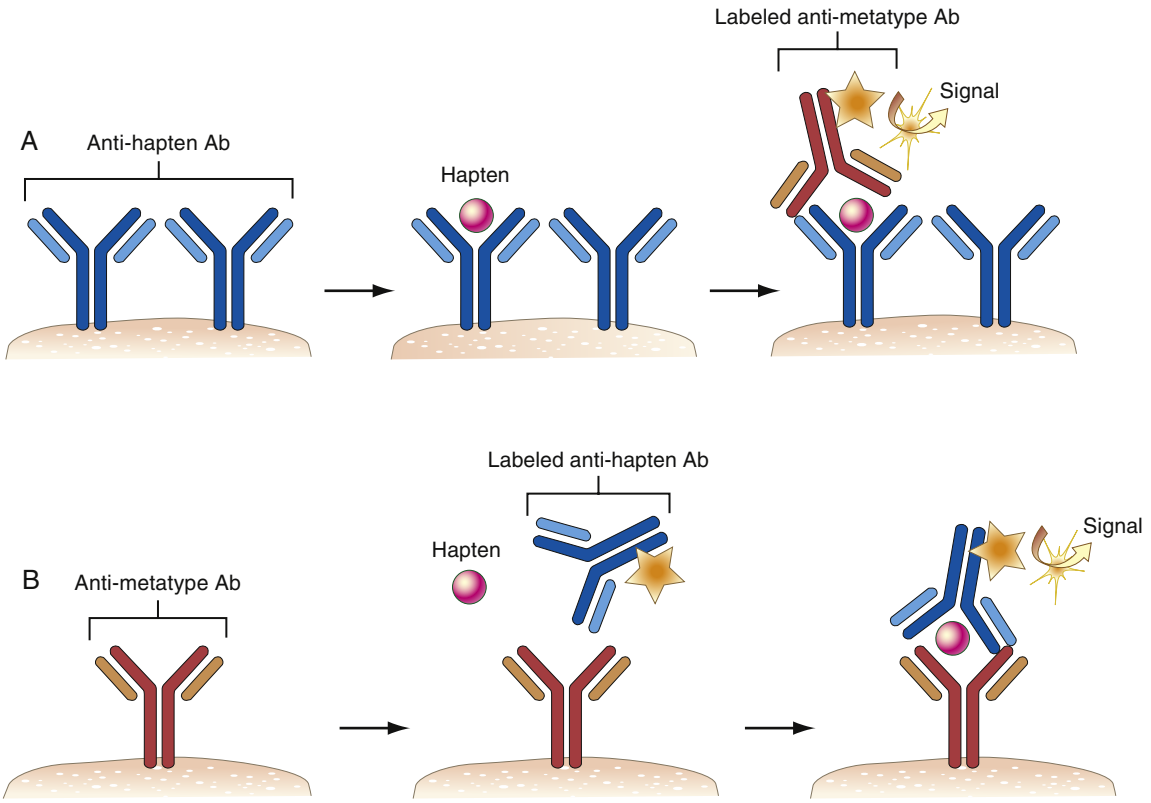

Figure 45.26 Hapten immunoassay procedure using antimetatype antibody. **A,** Combination of antihapten antibody for the solid phase and labeled antimetatype antibody for the conjugate. **B,** Combination of antimetatype antibody for the solid phase and labeled antihapten antibody for the conjugate.

A recent report describes the development of a novel and widely applicable sandwich assay for haptens based on antimetatype antibodies (Omi et al., 2015). Omi and colleagues employed an ex vivo antibody development system (Autonomously Diversifying Library system) generated from chicken DT40 B-lymphocyte line (Seo et al., 2005, 2006). In this system, antimetatype antibodies recognizing hapten-primary antibody immunocomplexes were selected from artificial antibody libraries using a magnetic beads–based affinity isolation method; this led to the successful development of sandwich assays for two haptens: estradiol and 25-OH vitamin D. A sandwich assay reagent for 25-OH vitamin D allowing for equal detection of 25-OH vitamin D_2 and 25-OH vitamin D_3 on an automated immunoassay instrument was further developed commercially as the first sandwich-type immunoassay reagent with antimetatype antibody. In addition, this sandwich assay for 25-OH vitamin D proved sensitive and specific enough for routine diagnostic use and showed high correlation with isotope dilution tandem mass spectrometry (ID-MS/MS) analysis. Yoshimi and colleagues also could successfully develop antimetatype antibody to the complex of aldosterone and anti- aldosterone mouse monoclonal antibody, they reported a sandwich assay for aldosterone using the combination of mouse monoclonal antibody to aldosterone and enzyme labeled antimetatype antibody, showing a high correlation with liquid chromatography/tandem mass spectrometry (LC/MS/MS) (Yoshimi et al., AACC presentation, 2019). Therefore, this method provides a simple, practical approach for the routine assay of haptens, a development that is expected to facilitate major advances in analytic and clinical chemistry.

SENSITIVE IMMUNOASSAY FOR TOTAL ANTIGEN INCLUDING COMPLEX USING SPECIMEN-PRETREATMENT METHOD

BACKGROUND

In vital fluid specimens, there are various complexes, such as those of the target antigen and antibody, and the specific binding of proteins to receptors. In addition, there are instances in which target antigens exist in virus particles. Sensitive immunoassays for target antigens in the various complexes found in vital fluids have been reported that use a simple specimen-pretreatment method to extract the target antigen effectively. The combination of immunoassay with an effective specimen-pretreatment process has been introduced as the immunoassay for total antigen including complex via pretreatment (iTACT) method. This method has a significant potential to demonstrate new clinical utility, especially in infectious disease and autoimmune disease.

HIGHLY SENSITIVE IMMUNOASSAY FOR VIRAL ANTIGEN USING SPECIMEN-PRETREATMENT METHOD

The sensitive immunoassay for viral antigen has several merits when compared with nucleic acid amplification detection systems. Immunoassay can generally detect quantities with lower variance, it is not expensive, and it has less contamination risk.

However, in general, the viral antigens lie on the surface or capsid of the virus particle, and antibodies to the viral antigens are produced in the blood. Immunoassays must overcome these obstructing factors for a quantitative approach to the viral antigen. New highly sensitive immunoassays for viral antigens, in the presence or absence of antiviral antigen antibody, have been described using a simple specimen-pretreatment method for clinical application (Aoyagi et al., 1999, 2001; Kimura et al., 2002).

HCV core antigen exists as a capsid protein inside of HCV particles and is a suitable candidate for the detection of the HCV protein (Fig. 45.27). In the blood of HCV-infected patients, there are numerous anti-HCV core antibodies that inhibit the detection of the core antigen. Therefore, destruction of the complex containing the HCV particles and inactivation of the anti-HCV core antibody present in the blood by the specimen-pretreatment process is required. Aoyagi and colleagues (1999, 2001) developed a simple specimen-pretreatment method using a higher concentration of detergent or denaturant, such as sodium dodecyl sulfate. They then demonstrated that this simple pretreatment method allowed for the highly sensitive detection of the viral antigen using monoclonal antibodies recognizing the denatured antigen. The limitation of detection was 0.06 pg of recombinant HCV core antigen/mL.

This specimen-pretreatment method was also applied to the detection of HBV core antigen or HBV core–related antigen, thereby highlighting new clinical utilities (Kimura et al., 2003; Rokuhara et al., 2003; Tanaka et al., 2008). Specifically, the HBV core–related antigen assay can detect HBV core antigen, p22 core-related antigen, and HBV envelope antigen simultaneously using monoclonal antibodies that recognize these denatured antigens by specimen-pretreatment methods (Kimura et al., 2002). This assay reflects the HBV load in the liver and is useful for monitoring HBV patients undergoing various drug therapies. In addition, conventional HBsAg assays are used as a clinical marker of HBV infection. However, they have so far failed to accurately detect HBsAg in blood because of interference by patient-derived antibodies against HBsAg. A novel sensitive HBsAg assay has been developed using a simple pretreatment process involving acidic treatment, including a higher concentration of detergent to dissociate the HBsAg molecule from HBsAg–anti-HBsAg complexes (Matsumoto et al., 2017). This has been termed the *immunoassay for total antigen including complex via pretreatment (iTACT)–HBsAg*. The iTACT- HBsAg appears to detect total HBsAg with high sensitivity, even in the presence of HBsAb, and may be useful in identifying subclinical or occult HBV carriers.

SENSITIVE IMMUNOASSAY FOR HOST ANTIGEN WITHOUT THE INFLUENCE OF AUTO-ANTIBODY USING SPECIMEN-PRETREATMENT METHOD

In immunoassays for host antigen such as thyroglobulin or insulin, and so on, there are known interferences by endogenous autoantibodies to host antigen. As an application of the iTACT method for host antigen,

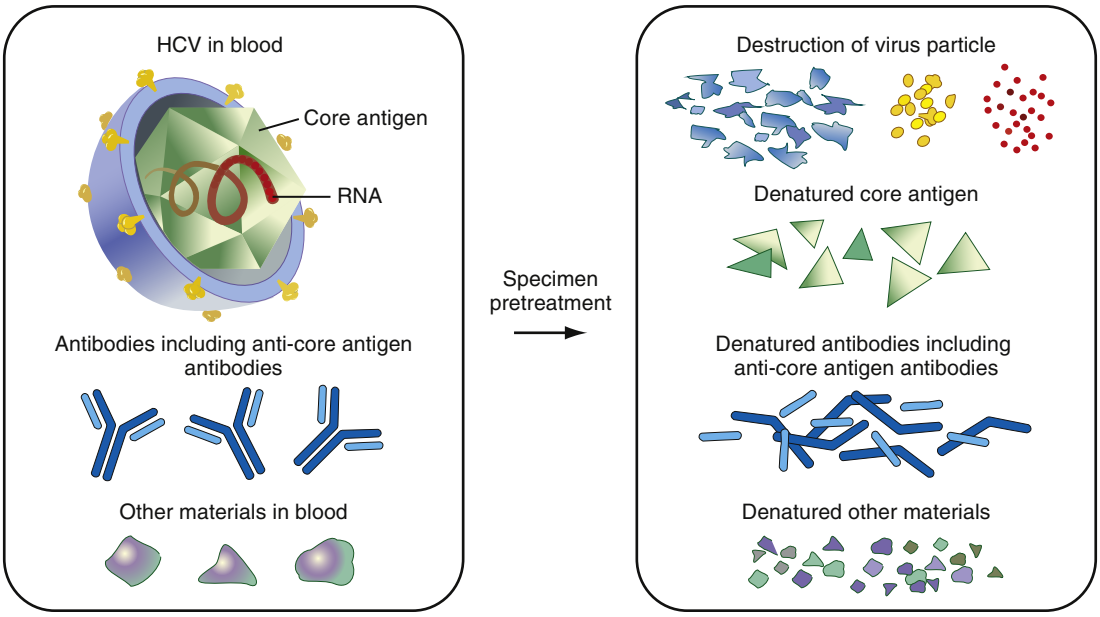

Figure 45.27 Effect of the specimen-pretreatment method for the detection of hepatitis C virus core antigen.

Kitamura and colleagues reported the development of a novel immunoassay for thyroglobulin without the interference of the autoantibody to thyroglobulin by introducing an automated specimen-pretreatment process (Kitamura et al., 2019). By this automated pretreatment process, autoantibody to thyroglobulin in specimen was inactivated, and simultaneously, thyroglobulin was freed from the complex with autoantibody to thyroglobulin. In the correlation study using autoantibody-positive samples, there were many discrepant samples showing higher measured values using the iTACT-thyroglobulin assay compared with the conventional assay, which produced negative or lower measured values. The automated immunoassay system for iTACT-thyroglobulin appears to be less subject to interferences by autoantibody and would be able to provide an accurate thyroglobulin concentration. The highly sensitive detection of free-formed antigens by dissociation from most associating materials through the specimen-pretreatment process will be applied to other target antigens.

SUMMARY

There are many specific interference substances, such as antiviral antibodies or autoantibodies, against host antigens in sensitive immunoassays for antigen detection. By introducing a simple specimen-pretreatment process, various specific interference substances can be inactivated and the target antigen can be released from the complex. The combination of immunoassay and pretreatment process can cover the many disadvantages of conventional immunoassay compared with nucleic acid amplification testing or LC-MS/MS analysis, and can be applied to other target antigens with the potential for new clinical utility.

SIMULTANEOUS MULTIPLE IMMUNOASSAYS

BACKGROUND

Recent immunoassay advancements have led to the development of novel technological concepts that allow simultaneous multiple detection as a way to reduce reagent cost. This means that anywhere from 5 to 100 analytes can be detected simultaneously in an individual sample. These technologies are classified into two broad categories in terms of the type of solid phase used. The first, microsectioning technology, is adapted to immunoassays using a microchip as the solid phase; the second uses microparticles as the solid phase. In the second, two technologies have been applied to the recognition of individual assay analyte parameters. One is direct recognition of the solid phase using fluorolabeled latex; the other involves the use of particles of different sizes. In the latter case, limited recognition is possible because the resolution is dependent on particle size. Miniaturized technologies such as these are considered highly advantageous for minimizing the cost of reagents, saving energy, and protecting the environment because of the small mass of reagent and sample volumes required.

MICROSPOT ASSAY

The microchip solid surface is fractionated into small areas using microdotting technology. A total of 100 to 200 reaction sites are produced in a 3-mm-diameter area of a polystyrene flat plate (Ekins, 1998). In each site, a spotting area 80 μm in diameter receives a volume of less than 1 nL of solution ink-jetted automatically. With this method, the ambient assay theory established by Ekins has been applied, and the sensitivity and detection limit depend on the antibody occupancy but not on the surface area on the solid phase. The detection limit for TSH was found to be 0.01 mIU/L in an 18-hour assay using this ambient analyte assay method. Therefore, it is evident that a highly sensitive assay can be achieved even on the microspot area. Boehringer Mannheim, which later merged with Roche Diagnostics, applied an avidin-coated solid phase uniformly to the surface area and then ink-jetted biotin-binding antibody or antigen on the spot. Multiple parameters—including HIV antibody, HBsAg, anti–hepatitis C antigens, and rubella—can be detected simultaneously on the microchip made of polystyrene. The assay format is a three-step fluorescent immunoassay. Finally, a confocal laser scanner detects the fluorescent signal on the chip. This chip assay is also available for the application of DNA detection.

MULTIANALYTE MICROARRAY IMMUNOASSAY

Silzel and colleagues (1998) developed an analyte mass assay that measures total analyte mass within a sample. Therefore, the basic concept of this method is different from that of the ambient assay, which measures analyte concentration. A polystyrene film was used as the solid phase. An 80-pL droplet was ink-jetted onto the film, and DBCY5 was adopted as the labeling marker because of the long Stokes shift from the excitation wavelength at 670 nm to the emission wavelength at 710 nm, with near-infrared fluorescence emission. The detection apparatus used in this method consists of a microscope attached to a Pelitier-cooled charge-coupled device camera and a GaAlAs diode laser. In this format, 10^5 molecules of DBCY5 per 80 pL area could be detected in calibration solutions. The IgG subclass was applied to the present system for multiparameter detection. Four parameters—IgG1, 2, 3, and 4—were detected, and the sensitivity was shown to be comparable with that of ELISA, although a much smaller amount of antibody (100 times less) sufficed to cover the surface area as compared with an ELISA plate.

Protein chips microfabricated with highly dense spotting sites having 1250 reaction sites per 1 × 2 cm have been developed by Zyomyx (Hayward, CA) The protein chip is composed of silicon-based substrate as a solid phase and six lanes with a 5 × 50 array/lane (Peluso et al., 2003). Isomura employed the chip and applied a simultaneous fluorescent sandwich immunoassay for some target proteins (e.g., AFP, interleukin [IL]-6, Erk-2, c-Jun, Grb2, c-Src, H-Ras) (Isomura & Okamura, 2003). As shown in Figure 45.28, reaction sites are microfabricated to a pillar structure and then are coated with titanium oxide. The surface is coated with poly L-lysine polymer linking with polyethylene glycol-biotin. After binding of streptavidin to biotin, the solid streptavidin can bind to biotinylated antibodies. The assay can be performed in a flow device. The detection limit for IL-6 was found to be 5 to 50,000 ng/L in a 3-hour assay with the use of this protein biochip assay method.

Efforts to find better diagnostic markers are ongoing. The proteomics assay based on matrix-assisted laser desorption/ionization is expected to serve as a tool for the discovery of new markers. Advancements in glycomics (Finkelstein, 2007), the systematic study of the structure and physiologic function of carbohydrates, should lead to the development of new markers as well. The combination of these with existing markers will be evaluated for the enhancement of multiple marker assays.

FLOW CYTOMETRIC IMMUNOASSAY

Luminex (Austin, TX) has developed a simultaneous multiparameter fluorescent immunoassay using flow cytometric technology in which two types of fluorophores for recognition of the analyte serve to mark the latex particles used as solid phase (Fulton et al., 1997; Oliver et al., 1998). Two different types of fluorophores and fluorescence intensities mark the analyte mapping of each particle. More than 60 analytes can be detected simultaneously in principle. The assay procedure is as follows. The sample is mixed with antibody labeled with R-phycoerythrin, and a second antibody is immobilized on latex as the solid phase. The mixture is incubated for 10 to 30 minutes and then is injected into the flow system. A total of 1000 particles are separated, as in flow cytometry, and both an enhanced fluorescence signal from the excited R-phycoerythrin as a result of the labeling and two fluorescence signals on the particle are detected simultaneously by laser scanner. Carson and Vignali (1999) applied this approach to the simultaneous detection of 15 cytokines, such as IL-1, IL-2, IL-4, and IL-6. Simultaneous detection was less sensitive than the assay of individual cytokines. However, it is still a sensitive assay compared with conventional ELISA: sensitivity was 100 pg/mL for IL-2, 10 pg/mL for IL-4, 100 pg/mL for granulocyte-macrophage colony-stimulating factor, and 200 pg/mL for interferon-γ.

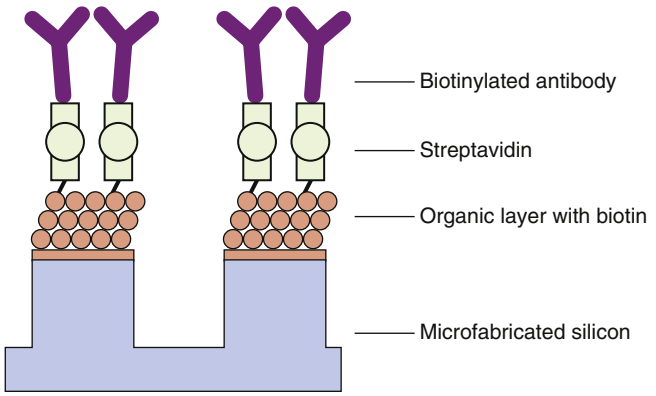

Figure 45.28 Protein biochip using fluorescence immunoassay (FIA). Sandwich FIA is applied for multiple detections using microfabricated silicon as a solid substrate. The surfaces of more than 1000 pillars are coated with an organic polymer layer containing biotin. Streptavidin that is bound to biotin then binds to biotinylated antibody specific to analyte and reacts with antigen in the sample. The silicon device containing different antibodies specific to different antigens is set in a molded plastic device.

From the point of view of clinical application, simultaneous multiple assays may not appear as attractive as might have been expected. In some cases, the sensitivity and specificity of this technique need to be assessed more carefully. However, simultaneous multiple assays based on miniaturization technology should be the ultimate goal for laboratory diagnostics given the advantages they offer in terms of cost containment, reduction of burden on patients from phlebotomy, and clinical utility.

The logistic regression model, using multiple markers, has improved the sensitivity and accuracy of diagnostic immunology but has met with only limited success. Recent advancements in laboratory pharmacogenomic testing for selection of the appropriate therapeutic drug in the right dosage for the right patient require further statistical calculation to obtain additional valuable test results. Pharmacogenomic testing is useful for protein assay as well. The Multivariate Index Assay by Vermillion Inc. (Fremont, CA), which was approved by the FDA in 2009, is a multiple-protein assay that comprises five conventional biomarker assays developed with certain types of algorithms. Several genetic testing methods based on algorithms have been approved by the FDA for laboratory testing, but not as kits. Genetic testing for multiple markers, as well as protein or carbohydrate testing, is likely to provide reliable options for diagnostics and for selection of therapeutic drugs.

MICROCHANNEL ASSAY USING COMPACT DISCS

Gyros AB (Uppsala, Sweden) developed a simultaneous microfluidic fluorescent immunoassay using a compact disc (CD) as microlaboratory technology in which the microfluidic flow can be obtained by centrifugal force (Poulsen et al., 2004). On the CD, 104 assays can be performed simultaneously by fluorescent column immunoassay. The solid phase consists of plastic microparticles bound to streptavidin. Specific antibody binding with biotin is applied to the column. A total of 100 nL of sample can be automatically metered by separation of the hydrophobic breaking valve in which the wall has been coated with hydrophobic polymer. The valve can open by centrifugal force; several types of break settings in the channel of the CD make it possible to perform a rapid and simple assay by changing the rpm to control reactions. This assay has been applied to the detection of human IgG, with a sensitivity of 1 ng/mL.

Samsung (Seoul, Korea) commercialized a unique compact disc–type POCT system that consists of multi-analyte tests and a small fully automated immunochemistry analyzer, LABGEO^{IB10}. Whole-blood samples (500 μL) are pipetted onto and spun down the disc of a handheld instrument, triggering a centrifugal force that separates plasma and blood cells. After a period of 20 minutes, the signal for D-dimer can be detected (Song et al., 2014). Three analytes can be tested simultaneously as multiple assays, including troponin I, N-terminal–pro hormone B-type natriuretic peptide (NT-proBNP), MB fraction of creatine phosphokinase (CK-MB), and myoglobin as cardiac markers (Belenky et al., 2013). Assay performance for troponin-I shows 50 to 30,000 ng/L of measurable range and 9.2% to 12.6% of whole assay coefficient of variation (CV).

SUMMARY

Remarkable technological advancements have been made in the development of microchannel assays in the past 10 to 15 years. Recent progress made in assay miniaturization has made it possible to overcome several difficulties with microfluidic movement of sample and reagent and sample evaporation using capillary flow, small vacuum pumps, and capillary electrophoresis in combination with a handheld instrument. Moreover, the value of multiplexed protein measurement is being established in applications such as comprehensive proteomic surveys, studies of protein networks and pathways, validation of genomic discoveries, and clinical biomarker development (Kingsmore, 2006).

SINGLE-MOLECULE DETECTION

BACKGROUND

Current various immunoassay systems have made it possible to produce high sensitivity at atto-molar levels in 10 to 40 minutes of reaction time in clinical laboratories. However, it is still difficult to detect clinical markers in very low concentrations of less than atto-molar levels. Due to recent advances in highly sensitive measurement technology, we may soon be able to determine the distribution values of tumor necrosis factor-α (TNF-α) and interleukins in normal subjects, which is very difficult to define in blood, and detect various viral antigen levels equivalent to nucleic acid amplification technology.

SINGLE-MOLECULE ELISA

Rissin and colleagues (2010) developed a single-molecule ELISA for serum protein detection at subfemtomolar concentrations. This differs from conventional ELISA; it is defined as *digital ELISA* (*D-ELISA*), in which a single bead as solid phase can be set in each well in the plate. In D-ELISA, femtoliter well arrays are used as reaction vessels to obtain a single signal; in conventional ELISA, 96 well plates are used as direct solid-phase binding capture antibodies. In femtoliter well arrays, each of the wells can accommodate a single bead. Magnetic particles with a 2.7-μm diameter as solid phase are used in D-ELISA. The procedure is almost identical to that of conventional ELISA—namely, 100 μL of sample is incubated with 200,000 beads for 2 hours at 23°C. Then, B/F separation using conventional magnet equipment is performed by a washing procedure. β-Galactosidase–labeled second-captured antibodies are added and incubated in wells for 45 minutes and the second B/F step is performed. After reaction with streptavidin-enzyme, D-ELISA requires one additional step: concentrated beads in 10-μL buffer are transferred into femtoliter well arrays and reacted with fluorescent substrate. Signals in each well are detected using an image CCD camera (558 nm excitation, 577 emission). TNF-α and PSA were measured in this platform and showed extremely high sensitivity for PSA, limit of detection (LOD) of 200 aM in whole serum; for TNF-α, it was 600 aM in whole serum. Moreover, Rissin and colleagues (2011) reported a method for combining the detection of single molecules (digital) and an ensemble of molecules (analog) for use in high-sensitivity ELISAs with broad dynamic range. The combined digital and analog PSA assay provided linear response over approximately 4 logs of concentration ([PSA] from 8 fg/mL–100 pg/mL or 250 aM–3.3 pM). This approach extends the dynamic range of ELISA from picomolar levels down to subfemtomolar levels in a single measurement.

Kim and colleagues reported a novel device employing one million femtoliter droplets immobilized on a substrate for the quantitative detection of extremely low concentrations of biomolecules in a sample (Kim et al., 2012). Surface-modified polystyrene beads carrying either zero or a single biomolecule-reporter enzyme complex are efficiently isolated into femtoliter droplets formed on hydrophilic-in-hydrophobic surfaces. Using a conventional micropipette, this is achieved by sequential injection first with an aqueous solution containing beads, and then with fluorinated oil. The concentration of target biomolecules is estimated from the ratio of the number of signal-emitting droplets to the total number of trapped beads. The performance of the digital counting device was demonstrated by detecting a streptavidin-β-galactosidase conjugate with an LOD of 10 zM. When combined with bead-based D-ELISA, the LOD for the detection of PSA reached 2 aM.

SINGLE-FLUORESCENT IMMUNOASSAY

Singulex (Alameda, CA) developed the Erenna Immunoassay System on the basis of the fluorescent immunoassay. In this system, single molecules of fluorescence can be detected by releasing a fluorescent conjugate from the immune complex consisting of solid-phase antibodies, antigens, and fluorescent-labeled antibodies (Todd et al., 2007). The immunoassay platform itself is a conventional fluorescent immunoassay that uses magnetic particles as solid phase and fluorescent dye–labeled antibodies. The fluorescent dye released by elution buffer is loaded into the capillary flow cell, and the fluorescent signal as a single molecule is detected by a confocal microscope. The immunoassay reaction lasts 1 to 2 hours. By releasing fluorescent antibodies from the magnetic particles, the nonspecific binding signal coming from the fluorescent conjugate on the particles could be minimized, resulting in extremely sensitive detection. In the case of cTnI, the frequency distribution in 100 normal subjects' plasma samples appears from 0.3 to 9.0 ng/L. LOD and 10% CV were 0.2 ng/L and between 0.78 and 1.6 ng/L, respectively.

Recently, the biophotonics analysis platform based on antiresonant reflecting optical waveguides was reported (Yin et al., 2007). Orthogonally intersecting liquid-core and solid-core antiresonant reflecting optical waveguides allow for planar fluorescence excitation and detection of single biomolecules in flow. The silicon-based chip can be integrated with advanced sample preparation steps on dedicated microfluidic chips, enabling full sample-to-answer analysis of molecular biomarkers on a chip-based system.

In addition, both nucleic acid detection with fluorescent complementary nucleic acid probe and protein detection on the fluorescent immunoassay have been demonstrated using a planar multimode interference waveguide platform. In application, zika virus nucleic acid and NS1 antigen complexes can be excited and detected simultaneously on-chip with high specificity and sensitivity (Stambaugh et al., 2018).

SUMMARY

Various single-molecule detection immunoassays make it possible to demonstrate reference values of various cytokines or cTnI in serum or plasma and possible to detect low levels of cancer markers for relapse monitoring. These single-molecule detection platforms have great potential to diagnose various diseases in the early phase or develop a new high-sensitivity marker as a fully automated immunoassay analyzer or portable immunoassay device.

SELECTED REFERENCES

Aoyagi K, Ohue C, Iida K, et al.: Development of a simple and highly sensitive enzyme immunoassay for hepatitis C virus core antigen, *J Clin Microbiol* 37:1802–1808, 1999.

A new highly sensitive immunoassay for antigens in viral particles in the presence or absence of antiviral antigen antibodies is described using a simple pretreatment method for clinical application. This specimen-pretreatment method can be also applied to the more precise measurement of other viral antigens and can lead to new clinical utilities in various infectious diseases.

Ekins R: Ligand assays: from electrophoresis to miniaturized microarrays, *Clin Chem* 44:2015–2030, 1998.

A new sensitive immunoassay in a miniaturized microarray format is described in this report. This method can be applied to immunoassays and to DNA/RNA analysis and may well revolutionize the diagnostic and pharmaceutical fields as the DNA chip and the protein chip have done.

Kasahara Y: Homogeneous enzyme immunoassays. In Nakamura RM, Kasahara Y, Rechnitz GA, editors: *Immunochemical assays and biosensor technology for the 1990s*, Washington, DC, 1992a, American Society for Microbiology, pp 169–182.

I*n this review, Kasahara describes the historical progression of immunoassay development and reviews homogeneous enzyme immunoassays. It also addresses test sensitivity and procedure simplification and their applicability to small haptens and large proteins.*

Kasahara Y, Ashihara Y: Simple devices and their possible application in clinical laboratory downsizing, *Clin Chim Acta* 267:87–102, 1997.

Immunochromatographic assays are powerful tools for point-of-care testing and near-patient testing. This report describes immunochromatographic assays in a simplified immunoassay format for point-of-care testing and near-patient testing and discusses laboratory downsizing and laboratory automation, with specific reference to the situation in Japan.

Kricka LJ: Chemiluminescent and bioluminescent techniques, *Clin Chem* 37:1472–1481, 1991.

In this excellent review, Kricka describes the characteristics and mechanisms of light emission from most of the chemiluminescent and bioluminescent molecules employed as detection signals in immunoassays and nucleic acid detection.

Nakamura RM, Kasahara Y: Heterogeneous enzyme immunoassays. In Nakamura RM, Kasahara Y, Rechnitz GA, editors: *Immunochemical assays and biosensor technology for the 1990s*, Washington, DC, 1992, American Society for Microbiology, pp 149–167.

In this reference, assay principles and assay performance are discussed, and practical application of heterogeneous enzyme immunoassays is described. This review will help the general reader gain an understanding of nonisotopic immunoassays and will assist the researcher in developing enzyme immunoassays.

Access the complete reference list online at Elsevier eBooks for Practicing Clinicians.

REFERENCES

Actor JK, Kuffner T, Dezzutti CS, et al.: A flash-type bioluminescent immunoassay that is more sensitive than radioimaging: quantitative detection of cytokine cDNA in activated and resting human cells, *J Immunol Methods* 211:65–77, 1998.

Alpha B, Lehn JM, Mathis G: Energy transfer luminescence of Eu(III) and Tb(III) cryptases of macrobicyclic polypyridine ligands, *Angew Chem Int Ed Engl* 26:266–267, 1987.

Aoyagi K, Iida K, Ohue C, et al.: Performance of a conventional enzyme immunoassay for hepatitis C virus core antigen in the early phases of hepatitis C infection, *Clin Lab* 47:119–127, 2001.

Ashihara Y, Hiraoka T, Makino Y, et al.: Immunoassay for determining low- and high-MR antigens with a dry multilayer film, *Clin Chem* 37:1525–1526, 1991.

Ashihara Y, Nishizono I, Miyagawa E, et al.: Homogeneous enzyme immunoassay for high molecular weight antigen (I), *J Clin Lab Anal* 2:138–142, 1988.

Avrameas S, Guilbert B: Dosage enzymoimmunologique de proteines a l'aide d'immunoabsorbants et d'antigenes marques aux enzymes, *C R Acad Sci* 273:205–207, 1971.

Avrameas S, Ternynck T, Guesdon JL: Coupling of enzymes to antibodies and antigens, *Scand J Immunol* 7(Suppl):7–23, 1978.

Axelsen NH: Quantitative immunoelectrophoresis: new developments and applications, *Scand J Immunol*(Suppl 2)1–230, 1975.

Babson AL, Olson DR, Palmieri T, et al.: The IMMULITE assay tube: a new approach to heterogeneous ligand assay, *Clin Chem* 37:1521–1522, 1991.

Barnard G, Kohen F: Idiometric assay: noncompetitive immunoassay for small molecules typified by the measurement of estradiol in serum, *Clin Chem* 36:1945–1950, 1990.

Belenky A, Brennan E: *Samsung point of care systems—cardiac/acute care biomarkers—LABGEO^{IB} clinical chemistry analytes—LABGEO^{PT}.* XVII Forum—National Days of Laboratory Medicine of Russia, 2013. http://www.mma-expo.ru/lab/2013/visitors/presentations/5-1%20-%20Belenky%20Alexander%20-%20Samsung%20POINT%20OF%20CARE%20Systems.pdf.

Blackburn GF, Shah HP, Kenten JH, et al.: Electrochemiluminescence detection for development of immunoassay and DNA probe assays for clinical diagnostics, *Clin Chem* 37:1534–1539, 1991.

Bounaud MP, Bounara JY, Bouin-Pineau MH, et al.: Chemiluminescence immunoassay of thyrotropin with acridinium-ester-labeled antibody evaluated and compared with two other immunoassays, *Clin Chem* 33:2096–2100, 1987.

Boyd JC, Savory MG, Margrey M, et al.: Adaptation of EMIT drug assays to a random-access automated clinical analyzer, *Ann Clin Lab Sci* 15:39–44, 1985.

Boyden SV: The absorption of protein on erythrocytes treated with tannic acid and subsequent hemagglutination by antiprotein sera, *J Exp Med* 93:107–120, 1951.

Bronstein I, Edwards B, Voyta JC: 1,2-Dioxetanes: novel chemiluminescent enzyme substrates—applications to immunoassays, *J Biolumin Chemilumin* 4:99–111, 1989a.

Bronstein I, Juo RR, Voyta JC: Novel chemiluminescent adamantyl 1,2-dioxetane enzyme substrate. In Stanley P, Kricka LJ, editors: *Bioluminescence and chemiluminescence*, Chichester, UK, 1991, John Wiley & Sons, pp 74–82.

Bronstein I, Voyta J, Thorpe G, et al.: Chemiluminescent assay of alkaline phosphatase applied in an ultra-sensitive enzyme immunoassay of thyrotropin, *Clin Chem* 35:1441–1446, 1989b.

Bruls DM, Evers TH, Kahlman JA, et al.: Rapid integrated biosensor for multiplexed immunoassays based on actuated magnetic nanoparticles, *Lab Chip* 9:3504–3510, 2009.

Burd JF, Wong RC, Feeney JE, et al.: Homogeneous reactant-labeled fluorescent immunoassay for therapeutic drugs exemplified by gentamicin determination in human serum, *Clin Chem* 23:1402–1408, 1977.

Carson RT, Vignali DA: Simultaneous quantitation of 15 cytokines using a multiplexed flow cytometry assay, *J Immunol Methods* 227:41–52, 1999.

Coons AH, Creech JH, Jones RN: Immunologic properties of an antibody containing a fluorescent group, *Prop Soc Exp Biol Med* 47:200, 1941.

Dandliker WB, de Saussure VA: Fluorescence polarization in immunochemistry, *Immunochemistry* 7:799–828, 1970.

Dandliker WB, Kelly RJ, Dandliker J, et al.: Fluorescence polarization immunoassay: theory and experimental method, *Immunochemistry* 10:219–227, 1973.

Ekins RP: The estimation of thyroxine in human plasma by an electrophoretic technique, *Clin Chem Acta* 5:453–459, 1960.

Engvall E, Perlman P: Enzyme-linked immunosorbent assay (ELISA): quantitative assay of immunoglobulin G, *Immunochemistry* 8:871–874, 1971.

Erler K: Elecsys immunoassay systems using electrochemiluminescence detection, *Wien Klin Wochenschr Suppl* 3:5–10, 1998.

Fahey JL, McKelvey EM: Quantification determination of serum immunoglobulins in antibody-agar plates, *J Immunol* 94:84–90, 1965.

Finkelstein J: Glycochemistry and glycobiology, *Nature* 446:999–1051, 2007.

Fiore M, Mitchell J, Doan T, et al.: The Abbott IMx automated benchtop immunochemistry analyzer system, *Clin Chem* 34:1726–1732, 1988.

Fulton RJ, McDade RL, Smith PL, et al.: Advanced multiplexed analysis with the FlowMetrix system, *Clin Chem* 43:1749–1756, 1997.

Galvin JP: Particle enhanced immunoassays—a review, diagnostic immunology. In Rippey JH, Nakamura RM, editors: *Technology assessment*, *Skokie*, *Ill*, 1984, College of American Pathologists, pp 18–30.

Garvey JS, Cremer NE, Sussdorf DH: Methods in immunology. ed 3 *Reading*, Mass, 1977, WA Benjamin, , pp 273–327.

Giegel JL, Brotherton MM, Cronen P, et al.: Radial partition immunoassay, *Clin Chem* 28:1894–1898, 1982.

Halonen P, Meurman O, Lovgren T, et al.: Detection of viral antigens by time resolved fluoroimmunoassay. In Bachman PA, editor: *Current topics in microbiology and immunology*, New York, 1973, Springer-Verlag, pp 133–146.

Hasegawa A, Andoh A, Ashihara Y: *Simple and rapid detection of antibodies to HIV-1/2 using immunochromatography.* Presented at: IUVDT World STD/AIDS Congress 1995; March 19–23, 1995; Singapore, p. 145. Abstract.

Hashida S, Hashinaka K, Nishikata I, et al.: Measurement of human immunodeficiency virus type 1 p24 in serum by an ultrasensitive enzyme immunoassay, the two-site immune complex transfer enzyme immunoassay, *J Clin Microbiol* 33:298–303, 1995.

Haux P, Dybois H, McGovern M, et al.: Evaluation of the TIna-quant ferritin assay on the Boehringer Mannheim/Hitachi 704 system, *Clin Chem* 34:1174 Abstract, 1988.

Heidelberg M, Kendall FE: The precipitin reaction between type III pneumococcus polysaccharide and homologous antibody, *J Exp Med* 61:563–591, 1935.

Henderson DR, Freidman SB, Harris JD, et al.: CEDIA, a new homogeneous immunoassay system, *Clin Chem* 32:1637–1641, 1986.

Hirayama C, Ihara H, Shibata M, et al.: Polypeptide artificial carrier particles for use in passive agglutination immunoassay, *Polymer J* 23:161, 1991.

Hunter WH, Greenwood FC: Preparation of iodine-131 labeled human growth hormone of high specific activity, *Nature* 194:495–496, 1962.

Ihara M, Suzuki T, Kobayashi N, et al.: Open-sandwich enzyme immunoassay for one-step noncompetitive detection of corticosteroid 11-deoxycortisol, *Anal Chem* 81:8298–8304, 2009.

Ikeda M: New agglutination test for serum antibodies to adult T-cell leukemia virus, *Gann* 75:845–848, 1984.

Ishikawa E, Kohno T: Development and applications of sensitive enzyme immunoassay for antibodies, *J Clin Lab Anal* 3:252–265, 1989.

Islam KN, Ihara M, Dong J, et al.: Direct construction of an open-sandwich enzyme immunoassay for one-step noncompetitive detection of thyroid hormone T4, *Anal Chem* 83:1008–1014, 2011.

Isomura M, Honda N, Kawada A, et al.: Development of a highly sensitive enzyme immunoassay for human calcitonin using solid phase coupled with multiple antibodies, *Ann Clin Biochem* 36:629–635, 1999.

Isomura M, Okamura C: Microfabricated protein biochip for multiple fluorescent sandwich immunoassay, *Clin Chem* 49:A13, 2003.

Isomura M, Ueno M, Shimada K, et al.: Highly sensitive chemiluminescent enzyme immunoassay with gelatin-coated ferrite solid phase, *Clin Chem* 40:1830, 1994.

Jolley ME: Fluorescence polarization immunoassay for the determination of therapeutic drug levels in human plasma, *J Anal Toxicol* 5:236–240, 1981.

Kabat EA: *Kabat and Meyer's experimental immunochemistry*, ed 2 *Springfield*, *Ill*, 1961, Charles C Thomas.

Kasahara Y: Principles and applications of particle immunoassay. In Nakamura RM, Kasahara Y, Rechnitz GA, editors: *Immunochemical assays and biosensor technology for the 1990s*, Washington, DC, 1992b, American Society for Microbiology, pp 127–147.

Kato K, Hamaguchi Y, Fukui H, et al.: Enzyme-linked immunoassay—a simple method for synthesis of the rabbit antibody-β-d-galactosidase complex and its general applicability, *J Biochem* 78:423–425, 1975.

Kemp BE, Rylatt DB, Bundesen PG, et al.: Autologous red cell agglutination assay for HIV-I antibodies: simplified test with whole blood, *Science* 241:1352–1354, 1988.

Kim SH, Iwai S, Araki S, et al.: Large-scale femtoliter droplet array for digital counting of single biomolecules, *Lab Chip* 12:4986–4991, 2012.

Kimura T, Rokuhara A, Sakamoto Y, et al.: Sensitive enzyme immunoassay for hepatitis B virus core-related antigens and their correlation to virus load, *J Clin Microbiol* 40:439–445, 2002.

Kimura T, Rokuhara A, Matsumoto A, et al.: New enzyme immunoassay for detection of hepatitis B virus core antigen (HBcAg) and relation between levels of HBcAg and HBV DNA, *J Clin Microbiol* 41:1901–1906, 2003.

Kingsmore SF: Multiplexed protein measurement: technologies and applications of protein and antibody arrays, Nat Rev Drug Discov 5:310-320, 2006.

Kitagawa T, Fujitake T, Taniyama H, et al.: Enzyme immunoassay of viomycin, new cross-linking reagent for enzyme-labelling and a preparation method for antiserum of viomycin, *J Biochem* 83:1493–1501, 1978.

Kobayashi N, Oiwa H, Kubota K, et al.: Monoclonal antibodies generated against an affinity-labeled immune complex of an anti-bile acid metabolite antibody: an approach to noncompetitive hapten immunoassays based on anti-idiotype or anti-metatype antibodies, *J Immunol Methods* 245:95–108, 2000.

Kobayashi N, Shibusawa K, Kubota K, et al.: Monoclonal anti-idiotype antibodies recognizing the variable region of a high-affinity antibody against 11-deoxycortisol. Production, characterization and application to a sensitive noncompetitive immunoassay, *J Immunol Methods* 274:63–75, 2003.

Koehler G, Milstein C: Continuous cultures of fused cells secreting antibody of predefined specificity, *Nature* 256:495, 1975.

Lim SL, Ichinose H, Shinoda T, et al.: Noncompetitive detection of low molecular weight peptides by open sandwich immunoassay, *Anal Chem* 79:6193–6200, 2007.

Magnani JL, Steplewski Z, Koprowski H: Identification of the gastrointestinal and pancreatic cancer-associated antigen detected by monoclonal antibody 19-9 in the sera of patients as a mucin, *Cancer Res* 43:5489–5492, 1983.

Mancini G, Carbonara AO, Hereman JF: Immunochemical quantitation of antigens by single radial immunodiffusion, *Immunochemistry* 2:235, 1965.

Masson PL, Holy HW: Immunoassay by particle counting. In Rose NR, Friedman H, Fahey JL, editors: *Manual of clinical laboratory immunology*, ed 3, Washington, DC, 1986, American Society for Microbiology, pp 43–48.

Mathis G: Rare earth cryptates and homogeneous fluoroimmunoassays with human sera, *Clin Chem* 39:1953–1959, 1993.

Mathis G: Probing molecular interactions with homogeneous techniques based on rare earth cryptates and fluorescence energy transfer, *Clin Chem* 41:1391–1397, 1995.

Matsumoto A, Imaizumi M, Tanaka Y, et al.: Novel and highly sensitive immunoassay for total hepatitis B surface antigen, including that complexed with hepatitis B surface antibody, *J Gastroenterol* 52:376–384, 2017.

Miles LEM, Hales CM: Labelled antibodies and immunological assay systems, *Nature* 219:186–189, 1968.

Morris DL: Effect of antibodies to glucose oxidase in the apoenzyme reactivation immunoassay system, *Anal Biochem* 151:235–241, 1985.

Morris DL, Ellis PB, Carrico FJ, et al.: Flavin adenine dinucleotide as label in homogeneous colorimetric immunoassays, *Anal Chem* 53:658–665, 1981.

Nakamura RM: Monoclonal antibodies: methods and clinical applications, *Clin Physiol Biochem* 1:160–172, 1983.

Nakamura RM, Kasahara Y: Fluorescence immunoassays. In Nakamura RM, Kasahara Y, Rechnitz GA, editors: *Immunochemical assays and biosensor technology for the 1990s*, Washington, DC, 1992, American Society for Microbiology, pp 205–227.

Nakamura RM, Robbins BA: Current status of homogeneous enzyme immunoassays, *J Clin Lab Anal* 2:51, 1988.

Nakane PK, Pierce GB: Enzyme-labeled antibodies: preparation and application for localization of antigens, *J Histochem Cytochem* 14:929–931, 1966.

Nargessi RD, Landon J, Smith DS: Use of antibodies against the label in non-separation non-isotopic immunoassay; "indirect quenching" fluoroimmunoassay of protein, *J Immunol Methods* 26:307–313, 1979.

Nishizono I, Ashihara Y, Tsuchiya H, et al.: Homogeneous enzyme immunoassay for high molecular weight antigens (II), *J Clin Lab Anal* 2:143–147, 1988.

Nishizono I, Iida S, Suzuki N, et al.: Rapid and sensitive chemiluminescent enzyme immunoassay for measuring tumor markers, *Clin Chem* 37:1639–1644, 1991.

Niwa T, Kobayashi T, Sun P, et al.: An enzyme-linked immunometric assay for cortisol based on idiotype-anti-idiotype reactions, Analytica Chimica Acta 638:94-100, 2009.

Oliver KG, Kettman JR, Fulton RJ: Multiplexed analysis of human cytokines by use of the FlowMetrix system, *Clin Chem* 44:2057–2060, 1998.

Omi K, Ando T, Sakyu T, et al.: A novel noncompetitive immunoassay detection system for haptens based on anti-metatype antibodies, *Clin Chem* 61:627–635, 2015.

Patterson W, Werness P, Payne WJ, et al.: Random and continuous-access immunoassays with chemiluminescent detection by Access automated analyzer, *Clin Chem* 40:2042–2045, 1994.

Peluso P, Wilson D, Do D, et al.: Optimizing antibody immobilization strategies for the construction of protein microarrays, *Anal Biochem* 312:113–124, 2003.

Poulsen E, Sandegren F: *CD microlaboratories—a fully automated solution for fast and flexible IgG quantification in biopharmaceutical process development*. IBC Antibody Therapeutics, November 30–December 2, 2004. Available online at www.gyos.com/tech-presentation.html.

Rissin DM, Kan CW, Campbell TG, et al.: Single-molecule enzyme-linked immunosorbent assay detects serum proteins at subfemtomolar concentrations, *Nat Biotechnol* 28:595–599, 2010.

Ritchie R: *Automated immunoanalysis, part I and part II*, New York, 1978, Marcel Decker.

Ritzmann SE, Daniels JC, editors: *Serum protein abnormalities—diagnostic and clinical aspects*, Boston, 1975, Little, Brown and Co.

Rodriguez-Espinosa J, Mora-Brugues J, Ordonez-Llanos J, et al.: Technical and clinical performances of six sensitive immunoradiometric assays of thyrotropin in serum, *Clin Chem* 33:1439–1445, 1987.

Rogers LC, Kahn SE, Oeser TH, et al.: The stratus immunofluorometric assay system evaluated for quantifying human chorionic gonadotropin in serum, *Clin Chem* 32:1402, 1986.

Rokuhara A, Tanaka E, Matsumoto A, et al.: Clinical evaluation of a new enzyme immunoassay for hepatitis B virus core-related antigen; a marker distinct from viral DNA for monitoring lamivudine treatment, *J Viral Hepat* 10:324–330, 2003.

Rose NR, Bigazzi PE, editors: *Methods in immunodiagnosis*, New York, 1973, John Wiley and Sons, pp 1–30.

Rowley GL, Rubenstein JE, Huisjen J, et al.: Mechanism by which antibodies inhibit hapten-malate dehydrogenase conjugates, *J Biol Chem* 250:3759–3766, 1975.

Rubenstein KE, Schneider RS, Ullman EF: Homogeneous enzyme immunoassay: a new immunological technique, *Biochim Biophys Res Commun* 47:846–851, 1972.

Scatchard G: The attractions of proteins for small molecules and ions, *Ann N Y Acad Sci U S A* 51:660–672, 1949.

Schroeder HR, Dean CL, Johnson PK, et al.: Coupling aminohexyl-FAD to proteins with dimethyladipimidate, *Clin Chem* 31:1432–1437, 1985.

Seo H, Hashimoto S, Tsuchiya K, et al.: An ex vivo method for rapid generation of monoclonal antibodies (ADLib system), *Nat Protoc* 1:1502–1506, 2006.

Seo H, Masuoka M, Murofushi H, et al.: Rapid generation of specific antibodies by enhanced homologous recombination, *Nat Biotechnol* 23:731–735, 2005.

Sgoutas DS, Barton EG, Hammarstrom M, et al.: Four sensitive thyrotropin assays critically evaluated and compared, *Clin Chem* 25:1785–1789, 1989.

Silzel JW, Cercek B, Dodson C, et al.: Mass-sensing, multianalyte microarray immunoassay with imaging detection, *Clin Chem* 44:2036–2043, 1998.

Skerra A, Pluckthun A: Assembly of a functional immunoglobulin Fv fragment in *Escherichia coli*, *Science* 240:1038–1041, 1988.

Smith J, Osikowicz G: Abbott AxSYM random and continuous access immunoassay system for improved workflow in the clinical laboratory, *Clin Chem* 39:2063–2069, 1993.

Soini E, Hemmila I: Fluoroimmunoassay: present status and key problems, *Clin Chem* 25:353–361, 1979.

Soini E, Kojola H: Time resolved fluorometer for lanthanide chelates: a new generation of nonisotopic immunoassays, *Clin Chem* 29:65–68, 1983.

Song J, Kweon TD, Song Y, et al.: Analytical and clinical performance of a new point of care LABGEOIB D-dimer test for diagnosis of venous thromboembolism, *Ann Clin Lab Sci* 44:254–261, 2014.

Stambaugh A, Parks JW, Stott MA, et al.: Optofluidic detection of Zika nucleic acid and protein biomarkers using multimode interference multiplexing, *Biomed Optic Express* 9:3725–3730, 2018.

Steward MW: Overview: introduction to methods used to study the affinity and kinetics of antibody-antigen reactions. In Weir M, editor: *Handbook of experimental immunology, vol I, Immunochemistry, ed 4*, London, UK, 1986, Blackwell Scientific Publications, p 25.

Takeda K, Maruki M, Yamagaito T, et al.: Highly sensitive detection of hepatitis B virus surface antigen by use of a semiautomated immune complex transfer chemiluminescence enzyme immunoassay, *J Clin Microbiol* 51:2238–2244, 2013.

Tanaka E, Matsumoto A, Yoshizawa K, et al.: Hepatitis B core-related antigen assay is useful for monitoring the antiviral effects of nucleoside analogue therapy intervirology, *Intervirology* 51:3–6, 2008.

Thorpe GH, Haggart R, Kricka LJ, et al.: Enhanced luminescent enzyme immunoassays for rubella antibody, immunoglobulin E and digoxin, *Biochem Biophys Res Commun* 119:481–487, 1984.

Thorpe GH, Kricka LJ, Moseley SB, et al.: Phenols as enhancers of the chemiluminescent horseradish peroxidase-luminol-hydrogen peroxide reaction: application in luminescence-monitored enzyme immunoassays, *Clin Chem* 31:1335–1341, 1985.

Towbin H, Motz J, Oroszlan P, et al.: Sandwich immunoassay for the hapten angiotensin II. A novel assay principle based on antibodies against immune complexes, *J Immunol Methods* 181:167–176, 1995.

Todd J, Freese B, Lu A, et al.: Ultrasensitive flow-based immunoassays using single-molecule counting, *Clin Chem* 53:1990–1995, 2007.

Truchaud A, Neel TL, Brochard H, et al.: New tools for laboratory design and management, *Clin Chem* 43:1709–1715, 1997.

Ullman EF, Schwartzberg M, Rubenstein KD: Fluorescent excitation transfer assay: a general method for determination of antigen, *J Biol Chem* 251:4172–4178, 1976.

Ullman EF, Yoshida RA, Blakemore J, et al.: Mechanism of inhibition of malate dehydrogenase by thyroxine derivatives and reactivation by antibodies: homogeneous enzyme immunoassay for thyroxine, *Biochim Biophys Acta* 567:66–74, 1979.

Van Weeman BD, Schuurs AH: Immunoassay using antigen enzyme conjugates, *FEBS Lett* 15:232, 1971.

Voss Jr EW: Perturbation of antibody bound bifluorescent-ligand probe by polyclonal anti-metatype antibodies interacting with epitopes proximal to the liganded antibody active site, *Mol Immunol* 33:79–88, 1996.

Weeks I, Beheshti I, McCapra F, et al.: Acridinium esters as high specific activity labels in an immunoassay, *Clin Chem* 29:1474–1479, 1983.

Williams CA, Chase MW: *Methods in immunology and immunochemistry*, vol. III. New York, 1970, Academic Press.

Winter G, Griffiths AD, Hawkins RE, et al.: Making antibodies by phage display technology, *Annu Rev Immunol* 12:433–455, 1994.

Wu AH, Wong SS, Waldron C, et al.: Automated quantification of choriogonadotropin: Analytical correlation between serum and urine with creatinine correction, *Clin Chem* 33:1424–1426, 1987.

Yalow RS, Berson SA: Assay of plasma insulin in human subjects by immunological methods, *Nature* 184:1648–1649, 1959.

Yamauchi S, Fujiwara Y, Hasegawa A, et al.: Simple devices for sensitive and rapid detection of HBs-Ag and HBs-Ab by immunochromatography using enzyme, *Clin Chem* 43:S242, 1997.

Yarmush DM, Morel G, Yarmush ML: A new technique for mapping epitope specificities of monoclonal antibodies using quasi-elastic light scattering spectroscopy, *J Biochem Biophys Methods* 14:279–289, 1987.

Yin D, Lunt EJ, Rudenko MI, et al.: Planar optofluidic chip for single particle detection, manipulation, and analysis, *Lab Chip* 7:1171–1175, 2007.

Zola H: *Monoclonal antibodies: a manual of techniques*, Boca Raton, Fla, 1987, CRC Press.

CHAPTER 46

LABORATORY EVALUATION OF THE CELLULAR IMMUNE SYSTEM

Roger S. Riley, Ronald Mageau, Jonathan Ben-Ezra

GENERAL PRINCIPLES OF CELLULAR IMMUNOLOGY, 930
Lymphocyte Activation and Proliferation, 930
Unraveling the Biochemical Pathways of Lymphocyte Activation, 931
Antigen-Induced Activation of T Lymphocytes, 931
T-Cell Recognition, Activation, and Signal Transduction, 931
Signal Transduction Following Antigen-Specific Stimulation, 931
T-Cell Responses, 932
B-Cell Responses in Cellular Immunity, 933

FLOW AND IMAGE CYTOMETRY IN EVALUATION OF CELLULAR IMMUNITY, 933
The Flow Cytometer and Other Tools, 934

GATING AND DATA ANALYSIS, 936
Immunophenotypic Analysis, 936
DNA Analysis, 937
DNA Studies of Interest in Cellular Immunology, 939
Quantitative Flow Cytometry, 939

CLINICAL SIGNIFICANCE OF CELLULAR IMMUNE TESTING, 939

CLINICAL INTERPRETATION OF CELLULAR IMMUNE TESTING, 939
Age and the Immune Response, 940
Malnutrition and the Immune Response, 940
Cancer and the Immune Response, 940

METHODOLOGIC APPROACH TO CELLULAR IMMUNE TESTING, 940
Stages of Study: The Screening Stage, 941
Stages of Study: The Confirming Stage, 941
Stages of Study: Analytic Immune Studies, 942

LABORATORY EVALUATION OF LYMPHOCYTE FUNCTION, 943
Lymphocyte Transformation Assays, 943
Cytotoxicity Assays, 944

LABORATORY EVALUATION OF GRANULOCYTE AND MONOCYTE FUNCTION, 946
Assays of Neutrophilic Activation, 946
Assays of Phagocytosis and Endocytosis, 947
Assays of Enzymatic Activity and Intracellular Killing, 948
Assays of Opsonization, 949
Assays of Membrane Permeability, 949

QUALITY CONTROL AND QUALITY ASSURANCE IN THE CELLULAR LABORATORY, 949

SELECTED REFERENCES, 950

KEY POINTS

- Humoral immune tests assess production of specific antibody responses to past or recent infections, and cellular immune assays measure current immune responses.
- The immune system changes with age and nutritional status. Differences in immune responses of test subjects associated with immaturity, immunosenescence, or malnutrition should be taken into account when evaluating the results of specific tests.
- Primary immunodeficiency may be associated with an increased incidence of malignancy. Malignancy, chemotherapy, and radiotherapy can significantly suppress the immune response and alter cellular immunoassay results.
- Evaluation of the cellular immune response is undertaken in a graduated sequence of stages that may include both in vitro and in vivo testing to identify areas of immunodeficiency.
- Measurement of lymphocyte activation may be accomplished in vitro by flow cytometry using activation-specific fluorescent-labeled monoclonal antibodies and vital dyes. The usefulness of this approach has increased significantly with the development of fluorochromes with different excitation spectra.

The understanding of the immune system is greatly enhanced by the detection of specific abnormalities in patients with suspected immunodeficiency. These advances have come from studies of immune cell differentiation and function, experimental gene deletion, and detailed analysis of human immunodeficiency syndromes. New experimental approaches have helped to elucidate the mechanisms and functional basis of immune dysregulation in patients with primary (congenital) genetic mutations of the immune system or secondary (acquired) infections. Because some immunodeficiencies cannot be accurately diagnosed by the combination of clinical symptoms and appropriate immune function assays, genetic information is becoming an increasingly important component of diagnostic testing and interpretation. The mission of the clinical immunology laboratory is to translate new research leads into highly standardized and clinically relevant tests for the individual patient.

Studies of the human cellular immune system have principally focused on three areas: (1) primary immunodeficiency, which reveals the impact of congenital immune defects on host defense; (2) acquired immunodeficiency, such as human immunodeficiency virus (HIV) infection, in which infection damages the immune system directly; and (3) autoimmune diseases, in which the effect of excessive or inappropriate immune activity is evident. In addition, cellular immune defects in patients with diseases with immune dysfunctional features—such as chronic infection, cancer, malnutrition, or traumatic injury—provide crucial insight into immune-mediated host defense.

The general concept of **immunity** is often equated with humoral immunity because antibodies to infectious agents introduced by natural infection or by immunization have been studied for more than a century. Cellular immunology, as currently practiced in the clinical and research laboratory, is a relatively new science (Good, 2002; Kaufmann, 2019; Moulin, 1989; Silverstein, 1979; Hamilton, 2006). The modern science of cellular immunology developed during the 1980s through a series of independent events and major research discoveries, including the use of monoclonal antibodies to identify immune cells, the development of analytic and sorting capabilities of the flow cytometer, the discovery of cytokine regulation of immune response, the birth of molecular immunology, and, above all, the tremendous need to understand and control the emerging HIV epidemic (Herzenberg, 2004). The appearance of HIV occurred virtually in parallel with the potential to identify $CD4^+$ T cells. The first analyses of cellular immune functional deficiency in the acquired immunodeficiency syndrome (AIDS) were based on analysis of lymphocyte proliferative response (Masur et al., 1981; Siegal et al., 1981) and have since evolved into a range of functional approaches, with the ultimate goal of developing a vaccine against the HIV virus (Butler et al., 2019; Cossarizza et al., 2013; Mittag & Tarnok, 2011; Perfetto et al., 2004; Virgo & Gibbs, 2012). During the past decade, further developments in cellular immunology, genetics, and other sciences resulted in the emerging field of cellular immunotherapy, also

called adoptive cell therapy, in which engineered immune effector cells are used in the treatment of cancer, autoimmune diseases, viral infection, and other diseases. Immunotherapy using chimeric antigen receptor T cells (CAR-T cells) is currently the most promising form of cellular immunotherapy (Paucek et al., 2019; Sermer & Brentjens, 2019).

In contrast to humoral immunity, cellular immune function is both fundamentally complex and difficult to measure. Basic humoral immune tests measure the specific antibody product of a past response to a specific virus or microbe; by contrast, most cellular immunoassays measure current responses. Because a majority of peripheral blood lymphocytes are resting cells, the cellular immune reaction must be re-created or generated freshly within the test system. The system must be capable of triggering the response, supporting the reaction by providing all needed elements available in vivo, and having a measurable endpoint.

This chapter presents current cellular immunologic tests in light of future trends. Cellular immune assessment is moving away from single assays and single-number fixed endpoints toward an integrated analysis of cell function at several levels that reflect cellular interactions as a dynamic process.

GENERAL PRINCIPLES OF CELLULAR IMMUNOLOGY

Two main immune cell types are known: (1) T lymphocytes (T cells), and (2) B lymphocytes (B cells) (Bodduluru et al., 2015; Chaplin, 2010; Germain, 2019; Janeway et al., 2004; LeBien & Tedder, 2008; Marshall et al., 2018; Masopust & Schenkel, 2013). T lymphocytes are defined by expression of the T-lymphocyte receptor, which binds to antigen and CD3, a surface determinant associated with the T-cell receptor that is essential for activation. T lymphocytes have different, clonally variable receptors for a large range of antigens, require thymic maturation for normal function, and mediate cellular immunity (Kumar et al., 2018). B lymphocytes are identified by surface immunoglobulin (detected by monoclonal antibodies such as CD19 or CD20) and, upon appropriate activation, develop into plasma cells secreting specific antibody and, thus, mediating humoral immunity (Cyster & Allen, 2019; Tarlinton, 2019). Loss of the normal thymus will compromise T-lymphocyte function and affect T-dependent B-lymphocyte activation. Failure at the bone marrow level can affect both T-lymphocyte and B-lymphocyte immune responses, although specific linkages may be involved.

The distinction between a specific and nonspecific immune response is a fundamental necessity because the system must be able to distinguish between self and nonself (LeGuern, 2003; Smith, 2004). In general, self-recognition is accomplished by incorporating the molecular major histocompatibility complex (MHC) self-antigen system into the antigen recognition phase. Antigen must be processed and presented in the context of self-MHC to be recognized and to lead to response and development of immune memory. The antigen-processing function is carried out by antigen-presenting cells (APCs); the best studied is the monocyte. This response triggers lymphocyte activation and proliferation, which may include production of effector cells and triggering of B lymphocytes to produce antibody. This type of immunity, often termed *adaptive immunity*, is retained as "memory" and typically is elicited following immunization or natural infection (Germain, 2019; LeGuern, 2003; Marshall et al., 2018; Smith, 2004). Lack of expression of MHC class II antigen can be detected on lymphocytes by flow cytometry using monoclonal antibodies against human leukocyte antigen (HLA)-DR or HLA-DQ and is a hallmark of MHC class II deficiency.

A second fundamental type of immunity can be described as innate immunity. This type of immunity is an ancient host response to infectious agents or self cells with absent or altered self-recognition molecules. It is encoded within the genome, does not have memory, and is not improved by repeated contact (Brubaker et al., 2015; Gasteiger et al., 2017; Janeway & Medzhitov, 2002). The innate immune system consists of (1) external barriers (i.e., skin, mucosal surfaces) to prevent microorganisms from entering the body; and (2) a programmed, coordinated series of events to destroy microorganisms that penetrate the external barriers or molecules that arise within the host from disease processes. These events include both chemically mediated (cytokines, complement, interferon) and cellular components (phagocytes, natural killer [NK] cells). The modern era of discovery about innate immunity began in 1989, when the late Charles Janeway, an immunologist at Yale University, predicted that sentinel cells (i.e., macrophages, dendritic cells) have nonclonal, germline pattern recognition receptors (PRRs) that directly recognize some invariant molecular signatures of microbes (pathogen-associated molecular patterns [PAMPs]) not found in the host (Janeway & Medzhitov, 2002). Lipopolysaccharide, a lipoglycan component of the Gram-negative bacteria cell wall, is the best characterized PAMP. Additional PAMPs include other lipoglycans, such as peptidoglycans and 1,3-β-glucans proteins such as bacterial flagellin, and microbial nucleic acids (Mogensen, 2009). More recently, it was found that certain substances released from host tumor cells or dead or dying cells resulting from hypoxia, infection, or other disease processes also activate PRRs. These host molecules have been termed *damage-associated molecular patterns*, or DAMPs (Herwald & Egesten, 2016; Schaefer, 2014). In 1997, studies of *Drosophila melanogaster* (fruit fly) identified the Toll-like receptor (TLR) as the major effector of the innate immune response in the fly, which has no adaptive immune system. Since that time, multiple TLRs have been found in humans, largely on dendritic cell, macrophage and neutrophil membranes, as well as on epithelial cells lining the respiratory and gastrointestinal systems. TLRs can be thought of as a primitive, highly conserved alarm system that recognizes bacterial pathogens and stimulates the expression of molecules that initiate the local inflammatory response and phagocytosis (Beutler, 2009; Kumar et al., 2009). TLRs are highly conserved molecules characterized by an extracellular domain of leucine-rich repeats and an intracellular signaling domain with homology to that of the interleukin (IL)-1 and IL-18 receptor family. TLR signaling initiates the transcriptional expression of genes that constitute a core inflammatory response, including proinflammatory cytokines such as IL-1α, IL-β, tumor necrosis factor (TNF)-α, and IL-6, as well as numerous chemokines and cell surface receptors that regulate T- and B-cell immune responses (Iwasaki & Medzhitov, 2010; Kawai & Akira, 2010; Vijay, 2018).

Subsequent to the discovery of the TLRs, a large number of other PRRs have been characterized on the cell surface, cytoplasm, and nucleus of mammalian cells. These include C-type lectin receptors, NOD-like receptors (NLRs), RIG-I-Like receptors (intracellular retinoic acid-inducible gene-I-like receptors [RLRs]), leucine-rich repeats (LRLs), and cytosolic DNA sensors (CDS) (Amarante-Mendes et al., 2018). The cascade of transcriptional changes and posttranslational modifications results from the binding of a ligand to a PRR lead to the secretion of cytokines and chemokines, the recruitment of phagocytic cells, the induction of antimicrobial peptides, pyroptotic cell death, and many other changes that constitute the innate immune response. The inflammasome, restriction factors, the proteasome, C-reactive protein, the endosomal/phagocytic system, and transcription factors such as NFκB play an essential role in this response (Krakauer, 2019).

Unlike phagocytic cells, NK cells are not functionally developed at birth, probably because the key cytokine, interferon (IFN)-γ, which is needed for development and maturation of this system, is also downregulated at birth. The NK cell, once called the *K cell*, *null cell*, or *third population*, has neither surface immunoglobulin nor a rearranged T-cell receptor (Bonavida et al., 2009). The NK system is constitutively active and does not have to be primed by antigen to kill (Hamerman et al., 2005; Yokoyama et al., 2004). NK cells make up a diverse population that has eluded conventional classification by cell lineage analysis. However, CD56 is currently considered the most definitive immunophenotypic marker for the NK cell (Trinchieri, 1995). NK cells have been best known as cells that can kill nonspecifically (naturally) virus-infected cells and bacteria and can prevent tumor cell metastasis. However, NK cells also regulate T- and B-cell functions as well as hematopoiesis (Poli et al., 2018). These functions of NK cells are probably dependent on their ability to produce lymphokines, particularly IFN-γ. NK cells are important for antigen-independent activation of phagocytic cells early in infection and for favoring the development of antigen-specific T-helper type 1 (Th1) cells. When armed with specific antibody, however, these cells can kill specifically.

LYMPHOCYTE ACTIVATION AND PROLIFERATION

Although the immune system is classically divided into humoral and cellular components, this separation is in no way absolute in that considerable interdependence is seen between B and T cells. The most commonly measured functional cellular immune parameter is lymphocyte proliferation (Perfetto et al., 2002). Measurement of lymphocyte activation/proliferation has evolved substantially since the late 1950s and early 1960s, when cell division was determined by counting the number of lymphocytes that had transformed into blasts. The latter method was later replaced by the quantitation of incorporated radiolabeled nucleic acid precursors (tritiated thymidine) into newly synthesized deoxyribonucleic acid (DNA). Although this "bulk assay" remains the most commonly used laboratory procedure for measuring cellular proliferation, new reagents and new procedures have recently become available to assess lymphocyte activation and proliferation. These include commercially available cell surface proliferation

markers, the ability to measure the percentages of cells in specific phases of the cell cycle, the quantitation of cell-associated and secreted cytokines/cytokine receptors, and the ability to assess the number of cell divisions in lymphocytes labeled with tracking dyes. In this section, we review the molecular events involved in T-lymphocyte activation and proliferation plus review some of the new methods that have been developed to assess the functions of the cellular immune system.

UNRAVELING THE BIOCHEMICAL PATHWAYS OF LYMPHOCYTE ACTIVATION

Specific interaction of mitogen or antigen/MHC with the appropriate lymphocyte receptors leads to a cascade of cellular processes that include changes in membrane transport, rearrangement of the cytoskeletal system (polarizing the lymphocyte toward the APC), and activation of several signaling pathways (Almeida et al., 2016; Cantrell, 2015; Harding & Neefjes, 2005; Heinzel et al., 2018). These changes ultimately lead to a number of outcomes, including T-cell differentiation, cytokine secretion, proliferation, anergy, or apoptosis. Ongoing investigations are unraveling the complex molecular and biochemical pathways that drive the activated T cell down these pathways. Specific abnormalities in these pathways are constantly being discovered, which underlie many of the primary immunodeficiency diseases. Unfortunately, abnormalities in a bulk proliferation assay indicate only that there is limited or no cell division and provide no information regarding the underlying abnormality in lymphocyte activation. Therefore, more sophisticated assays are required to investigate underlying T-cell abnormalities.

ANTIGEN-INDUCED ACTIVATION OF T LYMPHOCYTES

Antigen/MHC-induced activation of T lymphocytes involves a series of complex and defined events that differ slightly between the activation of a naïve T cell versus the activation of a memory T cell. Antigen is processed by B cells or monocytes, leading to the assembly of immunogenic peptides into class I or class II products of MHC genes (van der Merwe & Davis, 2003). The peptide–MHC complex is presented to T cells bearing the appropriate T-cell receptor (Chakraborty & Weiss, 2014). In addition, the APC expresses a series of adhesion and costimulatory molecules that interact with appropriate ligand/counter-receptors on the T-cell surface. Ligation of the T-cell receptor alone is not sufficient for activation of the T cell, which has led to the development of the two-signal model for T-cell activation (Bretscher, 2004; Bretscher, 2019). The first signal delivered via the T-cell antigen receptor (TCR)/CD4/CD8 modulates transition of the T cell from the early stages of activation (i.e., G_0 to G_1). Signal two is delivered via the costimulatory pathways, most notably CD28, and to lesser extents, LFA-3, CD2, CD5, and CD7, and leads to the induction of IL-2 and other cytokine genes required for T-cell proliferation and differentiation to effector cells.

T-CELL RECOGNITION, ACTIVATION, AND SIGNAL TRANSDUCTION

Lymphocytes are unique in that they express surface receptors able to identify virtually any molecule or foreign substance (antigen). Structural diversity within these receptors is created by the differential rearrangement of T-cell receptor genes. In general, only a limited number of circulating lymphocytes are able to recognize any single antigen. When a lymphocyte recognizes a foreign antigen in vivo, cells proliferate rapidly in a clonal manner to generate a large number of both effector and memory cells (Cantrell, 2015).

The TCR complex is composed of both a heterodimeric antigen recognition structure (i.e., the TCR) and a noncovalently bound transducing complex referred to as CD3 (Chakraborty & Weiss, 2014; Dong et al., 2019; Malissen, 2003). The TCR cannot be expressed on the cell surface without CD3 and has no inherent signaling capabilities of its own. The antigen recognition structure is composed of structurally divergent α and β chains (or, less frequently, γ and δ chains), and the CD3-transducing complex is composed of five invariant polypeptide chains: α, β, ε, η, and a ζ chain dimer. Each of the CD3 proteins contains a motif called the *immune tyrosine activation motif* (*ITAM*), which binds the SH2 domains of protein tyrosine kinases. The ζ chain (which exists as a ζ homodimer, a ζ with an η, or a ζ with an Fc ε RI γ chain) contains three ITAMs and is the most significant component of the TCR complex involved in signal transduction from the TCR (Alarcon et al. 2003; Weiss & Littman, 1994). Originally described by Reth, these motifs play an essential role in early events following T-cell activation (Chakraborty & Weiss, 2014; Irving & Weiss, 1991; Reth, 1989). CD4 and CD8 molecules on the surfaces of T cells are also noncovalently attached to the TCR complex. They bind to HLA class II and class I molecules, respectively, on the APC and are also involved in transduction of activation signals (Fig. 46.1). Processed antigen is presented to T cells in the context of the MHC antigens. In general, $CD4^+$ T cells respond to exogenously processed antigens presented in the context of MHC class II, and $CD8^+$ T cells respond to endogenously processed antigens presented in the context of MHC class I. CD4 and CD8 are also associated with tyrosine kinases involved in the early events following T-cell activation. In addition to these interactions and the costimulatory molecular interactions, another group of molecules present (adhesion molecules) on both the APC and the responding T cell bind to each other and serve to increase the avidity of the binding.

Costimulatory molecules identified on APCs include B7 (CD80) (Linsley et al., 1991), B7.2 (Azuma et al., 1993), and heat-stable antigen (HSA) (Liu et al., 1992), among others (Foletta et al., 1998; Wingren et al., 1995). On T cells, CD28 is the primary costimulatory molecule and binds B7; CTLA-4, on the other hand, binds both B7 and B7.2 and is involved in downmodulating T-cell activation (Linsley et al., 1991). The receptor on T cells for HSA has not been identified. Antigen presentation in the presence of reagents that block the costimulatory molecules leads to anergic response (tolerance) on subsequent exposure to that specific antigen but does not affect the responses to other antigens (Tan et al., 1993). The ability to make nonimmunogenic transplantable tumors immunogenic by transfecting them with the *B7* gene (Baskar et al., 1993; Chen et al., 1992; Janeway & Bottomly, 1994; Townsend & Allison, 1993) suggests that costimulatory molecules play an important role in T-cell activation in vivo.

SIGNAL TRANSDUCTION FOLLOWING ANTIGEN-SPECIFIC STIMULATION

The presentation of antigen to T cells leads to aggregation of the TCR–CD3 complexes and activation of protein tyrosine kinases (PTKs). The TCR itself has a small cytoplasmic tail with no known transducing activity. It is the associated ζ chains of the CD3 complex that contain the ITAMs and that have been shown to coprecipitate PTK activity. Two well-known classes of cytoplasmic PTK families are involved in the very early events following T-cell receptor aggregation: Src and Syk/ZAP-70. Signaling cascades downstream from the TCR–CD3 complex and the CD28 costimulatory pathway are fairly well understood (Foletta et al., 1998; Samelson, 2002). Activation of TCR-associated tyrosine kinases ZAP70, $p59^{fyn}$, and $p56^{lck}$ leads to activation of three pathways: $p21^{ras}$, calcium/calcineurin, and protein kinase C (PKC). These pathways are discussed further in Chapters 24 (Fig. 24.15) and 77 (Fig. 77.1). Activation of $p21^{ras}$ activates mitogen-activated protein kinases, which, in turn, phosphorylate several transcription factors, thereby regulating gene expression. Activation of the PTKs also activates phospholipase C, which hydrolyzes phosphatidyl inositol and leads to generation of the second messengers diacyl glycerol (DAG) and inositol triphosphate (IP_3). DAG activates PKC, and IP_3 leads to rapid and sustained increases in cytoplasmic calcium. The increase in free calcium activates the calmodulin-dependent phosphatase calcineurin. These events also lead to the induction of DNA-binding proteins and the transcription of numerous genes, including IL-2 and the IL-2 receptor required for T-cell proliferation.

Understanding the pathways leading to T-cell activation has led to the discovery of molecular defects in several acquired immunodeficiency diseases and may ultimately help provide therapeutic strategies to correct these deficiencies (Milner & Holland, 2013; Ochs & Hagin, 2014; Rosen, 2000). For example, mutations in the PTK ZAP-70 have been reported and are associated with the autosomal form of severe combined immunodeficiency (SCID) syndrome in humans (Elder, 1998). Mutations in the common γ chain of the interleukin receptors IL-2, IL-4, IL-7, IL-9, and IL-15 lead to transduction abnormalities and are associated with the X-linked form of SCID (Noguchi et al., 1993). It is interesting to note that another form of autosomally inherited SCID is associated with mutations in the downstream Janus family protein tyrosine Jak3, the only signaling molecule associated with the common γ chain (Pesu et al., 2005). As an increasing number of the underlying abnormalities leading to T-cell immunodeficiency are discovered, including at least 10 different molecular defects for SCID alone (Fischer et al., 2005; Sponzilli & Notarangelo, 2011), it has been proposed that these disorders be classified using a comprehensive system that would identify the disorders according to abnormalities in differentiation, maturation, and function (Gelfand, 1993). These designations would begin to focus on the actual physiologic or biochemical defect and may ultimately provide new options for therapy, including gene therapy (Booth et al., 2011; Buckley, 2004; Conley, 2005; Ochs & Hagin, 2014).

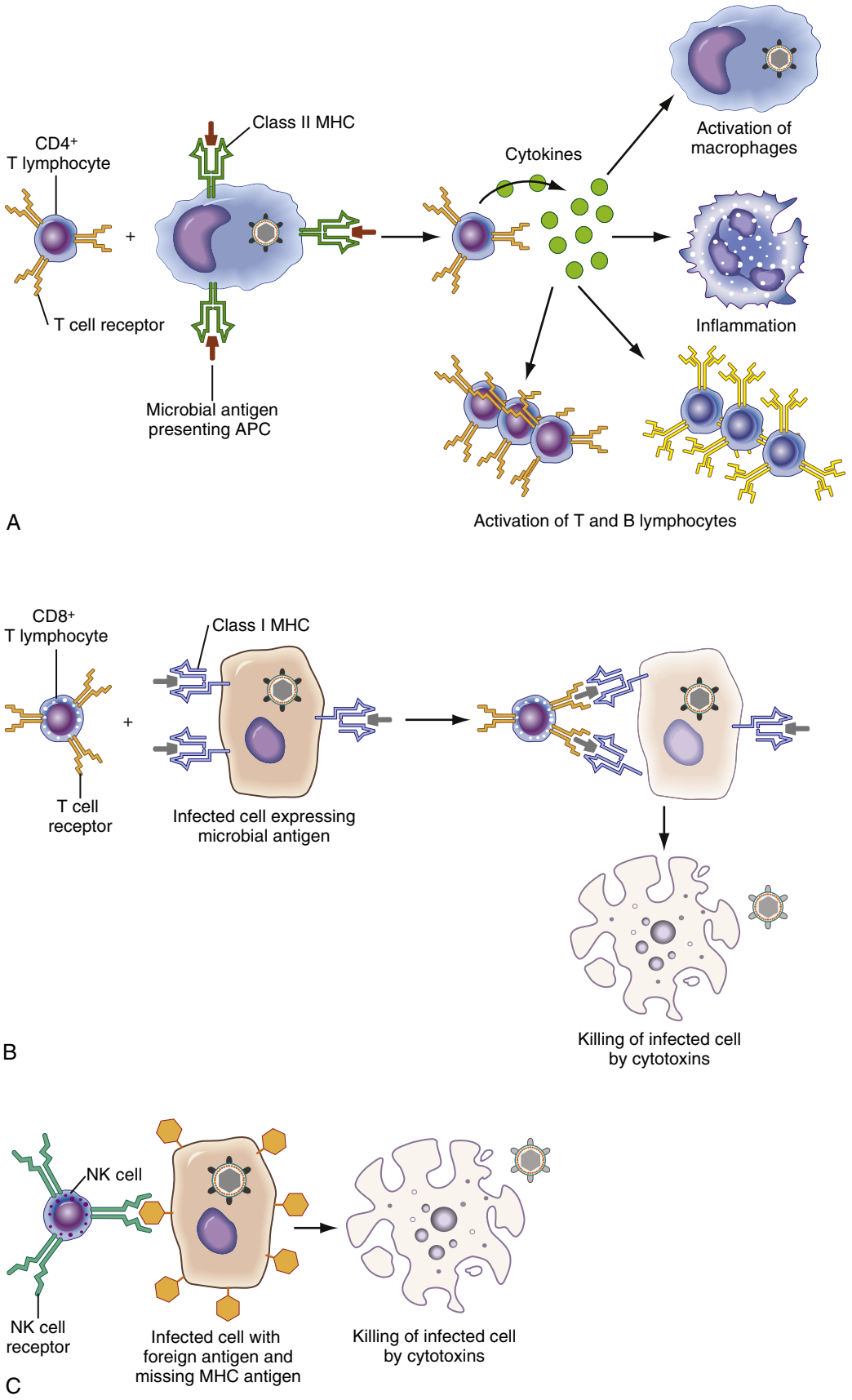

Figure 46.1 A schematic illustration of immune cell function. **A,** Function of helper T lymphocytes. Helper T cells are activated by contact with an antigen-processing cell (APC) that has ingested and processed a foreign or altered self substance and displays processed antigen fragments bound to a class II self–major histocompatibility complex (MHC) receptor. Simultaneous binding of the T-cell receptor complex (TCR) in conjunction with a CD4 coreceptor activates the T cell primarily through a complex signaling mechanism involving the SRC kinase family. The activated T cell coordinates the immune response by secreting cytokines that have a multitude of effects, including recruitment and activation of macrophages, activation of the inflammatory system, and activation of cytotoxic T lymphocytes and other helper T lymphocytes. **B,** Function of cytotoxic T lymphocytes. Cytotoxic, CD8-positive cells are activated primarily by contact with infected, damaged, dysplastic, or neoplastic self-cells expressing processed microbial or abnormal self-antigens bound to the class I MHC. Activation of the cell occurs via the TCR in conjunction with the CD8 coreceptor that is specific for the class I MHC. The target cell is killed by the release of cytotoxic chemicals, including perforin, granzymes, and granulysin. **C,** Function of natural killer (NK) cells. NK cells are activated by cytokines or interferons and directly recognize "missing-self" virally infected or tumor cells that have only low levels of MHC I self-antigen. Unlike cytotoxic T cells, prior sensitization is not required. Killing of the target cell occurs via the release of cytotoxic chemicals, similar to cytotoxic T lymphocytes. (Diagrams courtesy Dr. Peter Ping, Motifolio, Inc., Ellicott City, MD.)

T-CELL RESPONSES

Recently, the designation of T-cell type I versus type II cytokine responses has been preferred for those T-cell responses that lead to cytokine secretion patterns known to be involved in cellular immunity versus cytokine secretion patterns observed in humoral immunity, respectively. Type I responses are characterized by the secretion of cytokines known to enhance inflammation (proinflammatory) and induce activation and proliferation of T cells and monocytes, namely, IL-2, IFN-γ, and IL-12. Type II responses are characterized by the secretion of cytokines that suppress inflammation (anti-inflammatory) and stimulate B cells to divide and differentiate into immunoglobulin-secreting cells (i.e., IL-4, IL-5, IL-10, and IL-13).

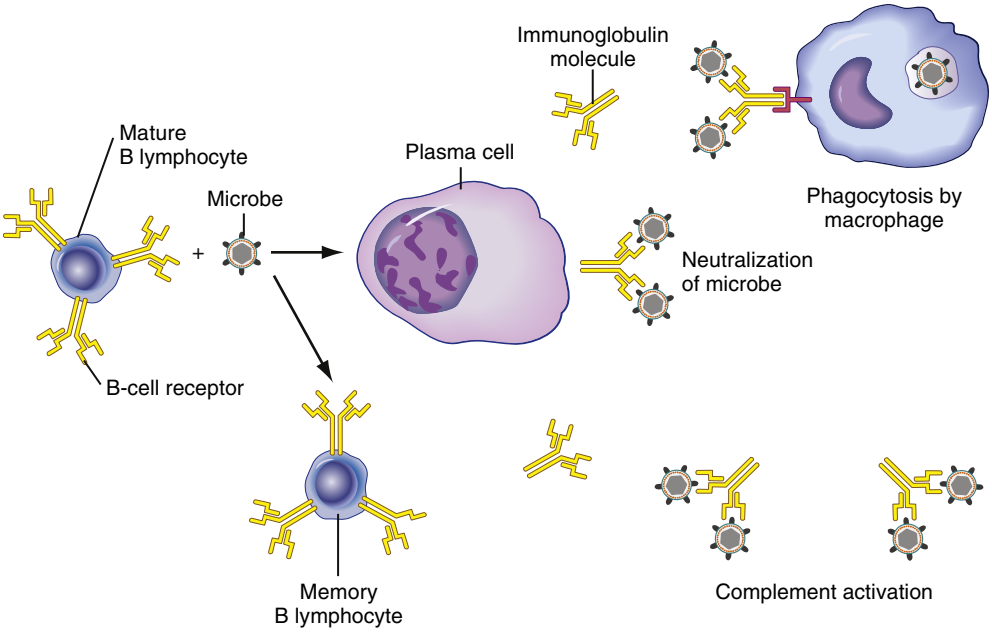

Figure 46.2 Function of B lymphocytes. Each B lymphocyte has a unique variable domain in its surface immunoglobulin molecules (B-cell receptor) that permits it to recognize a specific antigen. An encounter with this specific antigen, in conjunction with a cytokine signal from a T helper cell, results in activation of the B cell. An activated B cell can differentiate into an antibody-producing plasma cell or a memory T cell. In the lymph node, the activated B cell may also undergo a germinal center reaction, resulting in hypermutation of the variable region of the immunoglobulin gene. (Diagram courtesy Dr. Peter Ping, Motifolio, Ellicott City, MD.)

Evidence suggests that secretion of type I cytokines regulates the secretion of type II cytokines and vice versa (Paul, 1993). For example, in the presence of IL-4 both in vivo (Chatelain et al., 1992) and in vitro (Seder et al., 1993; Seder et al., 1992), T cells will not develop into IFN-γ–secreting cells (i.e., this environment favors the development of a humoral immune response). It has been suggested that the relative amounts of IL-4 and IL-12 that are present during stimulation of naïve T cells will shift the response one way or the other (Paul & Seder, 1994).

Several factors are involved in regulating the type of T-cell response that ensues following antigenic stimulation. In addition to the cytokine environment, evidence suggests that the dose of antigen influences the type of response (Bretscher, 1992; Madrenas et al., 1995). The predominant response that develops following T-cell activation has significant clinical implications. It has been postulated that the development of a type I response to HIV infection may lead to protective immunity (Clerici & Shearer, 1994). Clearly, a type II response is not protective, as most infected persons seroconvert and eventually succumb to profound immunosuppression. Clerici and Shearer (1993, 1994) argue that repeated exposure to low-dose HIV-1 may lead to protective type I cellular immunity. Results reported by this group indicate that between 39% and 75% of peripheral blood mononuclear cells of HIV-1–seronegative and polymerase chain reaction–negative high-risk individuals (i.e., men who have sex with men, intravenous drug users, and infants born to HIV-1–positive mothers) secreted IL-2 in response to the env protein in vitro. These scientists propose that seronegative high-risk individuals develop protective cell-mediated immunity as a result of low-dose immunization or infection.

B-CELL RESPONSES IN CELLULAR IMMUNITY

Antibody-producing B cells govern the humoral immune response to contain and eliminate primarily extracellular pathogens and, to a lesser extent, intracellular threats. Initiation of B-cell activation involves initial antigen binding and requires costimulatory signals. These signals, in some cases—as in nonpeptide antigens, for example—may be delivered by the antigen itself, by TLRs, by surface immunoglobulin cross-linking, or by other mechanisms (Mond et al., 1995). Alternatively, the Th2 subset of $CD4^+$ helper T cells provides important costimulatory triggers to activate B cells in response to peptide antigens (Fig. 46.2).

Surface immunoglobulin on naïve B cells binds antigen and transmits intracellular signals. It also delivers antigen into the cell, where it is processed into peptide fragments and then distributed and bound to MHC class II surface receptors. Epitopes of these fragments are recognized by specific Th2 class helper T cells primed by related antigen exposure, and costimulatory signals are transmitted between CD40-ligand (CD154) on T cells and CD40 receptor molecules on B cells (Jones & Janeway, 1981). These interactions generate T-cell cytoskeletal changes and subsequent release of cytokines, including IL-4, which binds to B cells to favor cell cycle progression and, hence, clonal expansion, and also promotes isotype switching to immunoglobulin (Ig) G1 and IgE. These engaged T cells also release transforming growth factor (TGF)-β, which has been shown to induce isotype switching to IgG2B and IgA, along with IL-5 and IL-6, which promote B-cell differentiation into plasma cells (Isakson et al., 1982). These cellular interactions occur in the T cell/B cell zone borders of primary lymphoid organs. Differentiation into effectors/plasma cells with antibody secretion appears to be sentinel for the primary/early focus of humoral immune response. Some activated B cells migrate into germinal centers and undergo further enhancement—including affinity maturation, IgH variable gene alteration, and isotype switching—to provide what is thought of as a more durable, prolonged response. A subset of memory cells is also produced that provide low-level surveillance with an associated rapid amnestic response upon antigen reexposure.

FLOW AND IMAGE CYTOMETRY IN EVALUATION OF CELLULAR IMMUNITY

Since its development 3 decades ago, laser-based single-cell analysis (flow and image cytometry) has become an essential tool for the medical research laboratory and the standard of laboratory clinical practice in the study of the cellular immune response (Adan et al., 2017; Aebisher et al., 2017; Gascue et al., 2018; Herzenberg, 2004; McKinnon, 2018; Pierzchalski et al., 2011; Virgo & Gibbs, 2012; Galkowski, 2017). Measures of immune competence and immune modulation of specific surface markers and receptors, characterization of lineage by the immunophenotyping of hematolymphoid neoplasms, detection of minimal residual disease, monitoring patients receiving organ transplantation, and immunotherapy are analyses that are commonly performed in many laboratories, as detailed by many authors (Campbell & Fraser, 2018; Jaye et al., 2012; Mittag & Tarnok, 2011; Vajpayee & Mohan, 2011; Virgo & Gibbs, 2012). Classification of cell types by these means enables the definition of biological and effector functions on a molecular basis and allows these measures to be related to disease process and definition. These are but a few of the applications that are possible when laser-based technologies are applied.

Two major technologies are used. The first is termed *flow-through*, in which the particles that are being counted and their physical and chemical characteristics are measured by particles passing in a fluid stream in a single-cell suspension (Givan, 2004; Keren, 1989; Stewart & Stewart, 2004). In the second, known as *static analysis*, the particles are stationary and the stage or the laser moves as in image analysis (Cossarizza & Radbruch, 2013). Image analysis technology is slowly making its mark in the laboratory in the evaluation of touch preparations or cytospins, chromosome preparations, and tissue sections for certain applications, such as DNA and fluorescent in situ hybridization (FISH). Advances in recent years in the availability of fluorescent probes for use in FISH and chromosome painting will make these analyses more relevant and useful tools in the clinical laboratory (Stewart et al., 2002; Weinberg, 1993). As with many techniques, including cell cycle analysis in DNA, each of the new markers and new techniques must be defined, evaluated, and correlated with

patient outcomes before agreeing on absolute clinical utility. There is great interest in instrumentation that combines the strengths of flow cytometry and the static advantages of image analysis. These instruments, known as scanning laser cytometers, use the traditional flow cytometry measures of forward scatter, side scatter, and fluorescence on cells in suspension or fixed onto a glass slide. Experience with these systems will reveal whether this approach offers measurement advantages not available with the current flow cytometric and image system configurations (Mach et al., 2010; McGrath et al., 2011; Pozarowski et al., 2013; Yan et al., 2018). Scanning image cytometers and image analysis are beyond the scope of this chapter.

Combined advances in electronic pulse processing, optics, and data storage, along with advances in computer technology and software, have allowed flow cytometry technology to become a routine tool in the clinical and research laboratory. Furthermore, the wide availability of workshop-clustered monoclonal antibodies now numbering 371 (Engel, 2015), labeled in multicolor, directly conjugated, and in premixed formats, has allowed the simultaneous detection of multiple surface antigens, as well as cytoplasmic and nuclear constituents. The ability to perform multiparameter analysis is the greatest strength of flow cytometry (Mittag & Tarnok, 2011; Pierzchalski et al., 2011). Measurement of both phenotypic and intracellular markers is now done routinely in many laboratories. The major manufacturers have turned the art of flow cytometry into a routine laboratory measurement—a "black box" science—much to the dismay of many (Chapman, 2000). As described, this black box approach phenomenon is largely the result of the use of flow cytometry in the phenotyping of T-cell subsets in monitoring patients with HIV (Cossarizza et al., 2013; Mandy, 2004). Before the onset of the HIV epidemic, flow cytometry was used in the clinical laboratory primarily for the characterization of leukemias and other hematologic malignancies, and for DNA analysis of tumors for synthesis phase (S phase) and DNA index (DI). Although flow cytometry technology may be trending more toward a black box application, the HIV epidemic brought the power of the flow cytometer to a much larger number of institutions and laboratories. This has allowed the technology to become an integral part of many diagnoses and to be used as an important adjunct in the treatment of patients (Woo et al., 2014). Despite its simplification, many issues with regard to U.S. Food and Drug Administration (FDA) regulation, proficiency testing, data management, and reproducibility of data remain. Although all current flow cytometers can adequately perform routine immunophenotyping and other assays, most laboratory problems are related to the nonavailability of standard quality control reagents and calibrators, and the lack of reliable, rapid methods for data transfer and storage that are compatible with laboratory information systems. More important for clinicians is an understanding of the technology, along with its strengths and pitfalls, and how it can be used for quality control and quality assurance, specimen preparation, and data interpretation. Some of these issues are discussed later, although it is not the purview of this chapter to describe all nuances of flow cytometric analysis.

THE FLOW CYTOMETER AND OTHER TOOLS

See Chapter 35 for a complete description of flow cytometry.

The Light Source and Signal Processing

Today's clinical flow cytometer is rarely used for cell separation (i.e., cell sorting). This property continues to be associated with research instruments in the highly specialized laboratory. Most multifaceted clinical flow cytometers incorporate 1 to 3 lasers with 4 or more photomultiplier tubes to perform 5- to 10-color immunophenotypic analysis (Fig. 46.3) (Shapiro, 2004; Zucker & Fisher, 2013). The most advanced research flow cytometers on the market currently have 5 or 6 diode or solid-state lasers, including ultraviolet (355 nm), near-UV (372 nm), violet (405 nm), blue (488 nm), green (532 nm), olive (552), yellow-green (561 nm), and red (633 nm) and infrared (805 nm), with up to 64 fluorescence detectors and the ability to resolve up to 40 colors. Commercial manufacturers of flow cytometers and cell sorters include ACEA Biosciences, Inc. (San Diego, CA), Apogee Flow Systems (Hertfordshire, UK), Becton Dickinson (San Jose, CA), Beckman Coulter (Fullerton, CA), Bio-Rad Laboratories (Hercules, CA), CompuCyte Corp. (Westwood, MA), Cytek (Fremont, CA), MilliporeSigma (Billerica, MA), Fluid Imaging Technologies, Inc. (Yarmouth, ME), Luminex Corporation (Austin, TX), Miltenyi Biotec (Bergisch Gladbach, Germany), ORFLO Technologies, LLC (Ketchum, ID), Sony Biotechnology, Inc. (Champlain, IL), Stratedigm Corporation (San Jose, CA), Sysmex Partec GmbH (Munster, Germany), ThermoFisher Scientific (Waltham, MA), and Union Biometrica, Inc. (Holliston, MA). Analytic software is provided by the instrument manufacturers, as well as by several independent software companies, including Applied Cytometry (Sheffield, UK), CyFlo Ltd. (Turku, Finland), Cytognos S.L. (Santa Marta de Tormes, Spain), De Novo Software (Los Angeles, CA), eBioscience, Inc. (San Diego, CA), Tree Star, Inc. (Ashland, OR), Verity Software House (Topsham, ME), and Walter and Eliza Hall Institute of Medical Research (Melbourne, Australia).

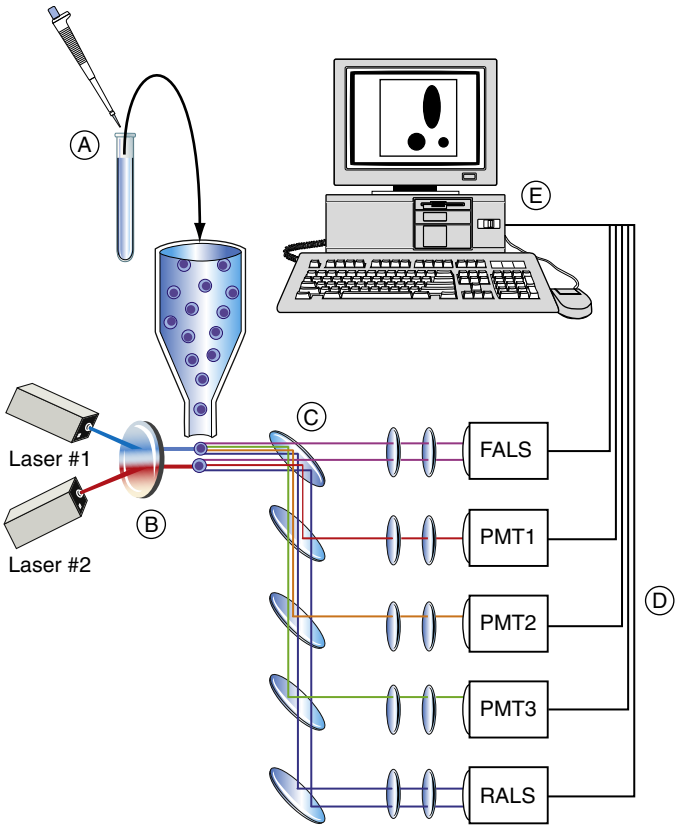

Figure 46.3 Structural components and function of the flow cytometer. **A,** Fluorochrome-labeled monoclonal antibody solutions are added to a cell suspension from peripheral blood, bone marrow aspirate, or a lymph node. The tubes are incubated at room temperature for a short period of time. **B,** Labeled cell suspensions are passed through the flow cell of a flow cytometer. Many flow cytometers are automated, but some models require the operator to process the tubes individually. More than 10,000 cells from each tube are typically analyzed to produce statistically valid information. **C,** Each cell passes individually through the highly focused laser beam of the flow cytometer, a process termed *single-cell analysis*. The fluorochrome of each labeled monoclonal antibody attached to the cell is excited by the laser light and emits light of a certain wavelength. The cells also scatter light at multiple angles. Photodetectors placed at forward and right angles to the axis of the laser beam collect the emitted or scattered light (photomultiplier tubes, PMT). Forward-angle light-scatter signals (FALS) and right-angle scatter signals (RALS), and as many as five fluorochrome signals, can be detected from each cell (multiparametric analysis). **D,** The signals from each photodiode are digitized and passed to a computer for storage, display, and analysis. Typically, all data recorded from each cell are stored for possible later recall for further analysis (list mode data storage). **E,** A variety of histograms for visual display can be generated automatically or at the discretion of the operator. List mode data can also be transferred to a separate computer for analysis. Presently, most commercial flow cytometers utilize a standardized file format for list mode storage, and a variety of computer programs are commercially available for data analysis and display.

The Flow Cell and Fluidics

Two common flow cells are used in the clinical laboratory, but because most clinical instruments are used in the measurement of CD4 cells in the monitoring of HIV disease, a closed system is used as a biohazard precaution (Bogh & Duling, 1993; Chapman, 2000; McCoy, 2002). The first, known as a *stream-in-air* or *flow-in-air flow cell*, allows the optical measurement point to be directly on the sample stream. This type of flow cell minimizes the distance between the flow chamber and the sample injector tip, thus minimizing carryover between specimens and the sample wash time necessary between samples. This chamber allows greater sample flow rate variability than a closed system. Other advantages of the stream-in-air tips are important in cell sorting and are not considered here. With the closed system, often referred to as a *quartz tip flow cell*, the focal point is within the chamber. Disadvantages of these quartz systems include the thickness of the quartz and, thus, the diffraction of the laser beam or the scattering of the signal. Additionally, the relatively large cross-section (200 μm^2) makes the flow rate more difficult to control. The success of these quartz flow cells in the

TABLE 46.1

Representative Fluorochromes Used in Flow Cytometric Analysis

Fluorochrome	Ex, nm	Em, nm	Excitation laser lines, nm	Comment
Hoechst 33342	343	461	355	Nucleic acid probe, AT selective
DAPI	359	461	355	Nucleic acid probe, AT selective
Pacific Blue	410	455	360, 405, 407	
Pacific Orange	400	551	360, 405, 407	
CFSE		517	488	
Fluorescein isothiocyanate (FITC)	493	525	488	pH sensitive
Alexa Fluor 488	495	519	488	Good photostability
Acridine Orange (AO)	510	530	488	Nucleic acid probe
R-Phycoerythrin (PE)	496, 565	575	488, 532, 561	High quantum yield, poor photostability
PE/Texas Red (Red 613)	496, 565	613	488, 532, 561	
Propidium iodide (PI)	305, 540	620	325, 360, 488	Nucleic acid probe, DNA intercalating, used as viability dye
Thiazole orange (TO)	510	530	488	Nucleic acid probe
7-Amino actinomycin D (7-ADD)	546	647	488	Nucleic acid probe, GC selective, used as viability dye
PE/Cy5 conjugates	496, 565	670	488	Tandem dyes, Cychrome, R670, Tri-Color, Quantum Red
Peridinin chlorophyll protein (PerCP)	482	675	488	
PerCP/Cy 5.5	482	690	488	Tandem dye
PE/Cy 5.5	496, 565	695	488	Tandem dye
PE/Cy 7	496, 565	774	488	Tandem dye
Texas Red	589	615	595, 633	Sulfonyl chloride
Allophycocyanin (APC)	645	660	595, 633, 635, 647	
Alexa Fluor 647	650	668	595, 633, 635, 647	
APC/Cy7 (PharRed)	650, 755	785	595, 633, 635, 647	

CFSE, Carboxyfluorescein diacetate succinimidyl ester; *Em (nm),* Emission wavelength in nanometers; *Ex (nm),* excitation wavelength in nanometers.

clinical system depends on illumination and collection optics. Flow cytometric manufacturers have made many advances in these systems regarding both safety and maximum sensitivity with the provision of low-power, laser-based systems currently using diode or solid-state lasers (Austin Suthanthiraraj & Graves, 2013; Piyasena & Graves, 2014; Sack & Tarnok, 2013).

Many terms are used in the definition of flow cytometry systems, which include *flow rate*, *sheath pressure*, *core size*, *resulting particle velocity*, *resulting coefficients of variation* (*CVs*), and so forth. However, the most important factor for a laboratory worker to understand is that in DNA analysis, the cells are analyzed at a slow flow rate to increase the time a particle spends in the beam, allowing greater sensitivity and better CVs. In immunophenotyping, sensitivity typically is not an issue, and the particle flow rate can be increased. Most clinical systems were developed with compromises to accommodate the most common application of immunophenotypic analysis (Baumgarth & Roederer, 2000). Research flow cytometers offer much greater flexibility and operator control over sample flow rate, differential pressure, and time.

Colors and More Colors: Applications of Fluorochromes

Fluorescent probes (fluorochromes) are sensitive and versatile compounds that have been extensively utilized in the biological sciences since their introduction by Weber and Lawrence in the early 1950s. There are many techniques for their measurement, and some fluorescent probes can be coupled to other excited states or chemical species by energy transfer or chemical reactions. Information derived from fluorochromes includes the intensity and/or polarization of the emitted light, the fluorescence emission and excitation spectrum, the time dependence of the emitted light, and energy transfer between fluorescent probes.

Fluorochromes are most commonly used clinically for the detection and quantitation of cell surface and intracellular antigens (Table 46.1). However, fluorescence emission can also reveal much information about the cellular environment since the chemical and biological properties of a fluorochrome are not only influenced by their chemical composition but also by the physical and chemical environment of the fluorochrome, along with a variety of other factors.

There are no perfect fluorochromes. However, the properties of an "ideal" fluorochrome include a large extinction coefficient in the excitation wavelength, a high quantum yield, an optimal excitation wavelength that avoids autofluorescence from naturally occurring compounds, photostability, biological inertness, minimal "quenching," and minimal pH sensitivity.

The influence of their chemical structure on the properties of chromophores has led to studies of many organic compounds as fluorochromes and even to the synthesis of specific fluorochromes for some applications. The existing biological dyes and even dyes utilized in the textile or other industries have been targets of these investigations. Although most commonly used as labels for monoclonal antibodies in the clinical laboratory, chromophores are also useful in research studies for the quantitation of cellular properties or biological activities, since they can be affected by the intracellular environment or act as substrates in intracellular biochemical reactions. The utilization of a compound as a fluorogenic substrate requires that it undergo a change in fluorescent properties with a change in the biological property or substance being studied. The present fluorochromes used in clinical applications can be classified as single, tandem, and protein.

Single Fluorescent Dyes

Single fluorescent dyes are chemical substances with fluorescence properties that can be complexed to CD antigens and other biological molecules. Fluorescein isothiocyanate (FITC) was the first fluorescent dye, synthesized by Robert Seiwald and Joseph Burckhalter in 1958. FITC is a derivative of fluorescein, with an isothiocyanate reactive group (–N = C = S), replacing a hydrogen atom. FITC is reactive toward nucleophiles, including amine and sulfhydryl groups on proteins, and has achieved wide-ranging applications in the biological and medical sciences, including flow cytometry. FITC has peak excitation and emission wavelengths of approximately 495 nm and 519 nm, giving the emission a green color. Although FITC has a tendency toward photobleaching or losing its fluorescent properties when continually exposed to light, modern fluorescein derivatives, including Alexa 488 and DyLight 488, have greater photostability and higher fluorescence intensity.

Phycoerythrin (PE) and allophycocyanin (APC) are members of the phycobiliprotein family present in organisms such as algae and cyanobacteria, where they are a component of the photosynthetic system. Structurally, phycobiliproteins consist of a protein complex covalently bound to photosynthetic pigments termed *phycobilins*. PE is maximally excited at 565 nm and emits light in the yellow-orange region of the visible spectrum (573 nm). PE is among the brightest fluorophores available for flow cytometry. APC is maximally excited at 652 nm and emits red light at 658 nm. APC has a lower extinction coefficient and quantum yield and is not as bright as PE. Other single dyes include Alexa Fluor 405, Pacific Blue, Texas Red, and PerCP.

Tandem Dyes

A tandem dye consists of covalently attached fluorescent molecules. One of these molecules, the donor, is a protein-based (i.e., PE, APC) or synthetic dye with a large extinction coefficient, while the acceptor fluorochrome is a smaller synthetic dye, such as Cy5, Cy5.5, Cy7, Alexa Fluor 647, and Alexa Fluor 705. The acceptor fluorochrome is activated by energy received from the donor, a process termed *Förster resonance energy transfer* (*FRET*). The use of multiple different tandem dyes in combination with single fluorochromes permit many labeled monoclonal antibodies to be analyzed with a single laser wavelength. Most tandem dyes are designed for multicolor flow cytometry using the 488-nm and 640-nm lasers available in nearly all clinical flow cytometers. Peridinin chlorophyll protein (PerCP)-Cy5.5 and PE-Texas Red are common tandem dyes that use the 488-nm wavelength.

Fluorescent Proteins

Fluorescent proteins, including green fluorescent protein (GFP), mCherry, and yellow fluorescent protein, enter cells without permeabilization of the cell membrane, and are used to study intracellular substances.

The use of multicolor fluorescence has allowed the concept of multiparameter analysis to become a reality in most laboratories (Fig. 46.4). For example, parameters can evaluate (1) different functional subsets of a particular cell population using an intracellular fluorescent probe; (2) use of multiple colors to identify small clusters of otherwise unidentifiable events (as in detection of minimal residual disease [MRD]); (3) the activation status of cells at a particular disease stage (e.g., use of HLA-DR and CD38 on CD4 and CD8s in HIV staging using an anchor gate approach); and (4) cell surface expression and the DI or S phase of a particular cell population, as in defining the CD19 S phase in acute leukemia. Obviously, the possible combinations are nearly infinite and their sophistication is enhanced by the specific dyes and DNA/ribonucleic acid (RNA) probes that are now available. A discussion of some of these approaches and techniques follows.

GATING AND DATA ANALYSIS

IMMUNOPHENOTYPIC ANALYSIS

Analysis of cell populations with the flow cytometer uses a combination of parameters that, when applied, define a specific cell population. Flow cytometry uses parameters similar to those that have been used for many years in hematology, including size (forward light scatter), cytoplasmic granularity (side scatter), and affinities for specific dyes, and combines them with the immunologic tools already mentioned. These include multiple fluorescent dyes bound to antibodies or probes, DNA measurements as obtained using propidium iodide (PI) or 4′6-diamidino-2-phenylindole, and other nuclear markers. The key is the simultaneous detection of these parameters with today's analytic systems. For many years, the clinical laboratory flow cytometer could use only three simultaneous measurements. Staining of cell populations was limited by the unavailability of directly conjugated monoclonal antibodies, necessitating the use of a secondary goat anti-mouse (GAM) reagent or the use of biotin-labeled antibodies. Definitions of positive and negative populations in high-background cases made it necessary to use a subtraction channel-by-channel algorithm to differentiate positive from negative (Bagwell, 1993). In cases in which the cell population had a defined boundary between negative and positive, a cursor was set so that no more than 2% of the events considered negative fell to the right of the cursor, thereby defining the positive events when a matched isotypic control was used. Although this approach seemed reasonable at the time (Lewis, 1993) and worked well with bright cell clusters, it has become cumbersome when identifying leukemic cells or performing analyses of cell activation markers. However, hematopoietic neoplasms are particularly problematic because each neoplastic clone has its own "relative" fluorescent intensity, and isotype controls may have little relevance. Applying hard and fast rules to cursor settings led to the underestimation of positive clusters. The failure of this approach is especially dramatic in the analysis of monoclonality by κ and λ light chain expression where small, but significant, differences were often lost.

Use of isotype controls in certain situations has been challenged on many fronts, both from technical aberrations associated with their use and from added costs to the laboratory. New software algorithms have the capability of making intensity measurements and defining clusters based on population means intensities, including relative fluorescent intensities, as well as actual molecules of equivalent soluble fluorochrome quantitation (see later discussion). Clearly, the need to remember what we are measuring and an understanding of the biology of the population of interest need to be considered in designing an analysis protocol. Fortunately, some sophisticated software approaches and better reagents have allowed us to use multiparameter gating to define populations, rather than trying to make estimates of fluorescence expression using cursor values. Many investigators have used the multiparameter approach in defining cluster and other populations of interest (Baumgarth & Roederer, 2000; Kraan et al., 2003; Loken et al., 1990; Stewart & Stewart, 2004). These approaches take many forms, a few of which are reviewed here.

With the arrival of multicolor fluorescence came the need to analyze the numbers of cells expressing one or more colors at the same time in a particular cell population defined by forward angle light scatter (FALS) and SSC regions (Loken et al., 1977; Loken et al., 1976). When this method was first developed, scientists were thinking basically about the mathematics and the accounting of all cells and the numbers of these cells expressing one or more colors. A binary approach to this analysis was developed, known as Prism (Coulter, Hialeah, FL). These analysis regions were hard-gated and were set into the instrument by the operator and could not be redefined at a later time using list mode analysis. This approach was later modified to allow some regating; other manufacturers, as well as third-party software applications, made this Prism binary approach work on a

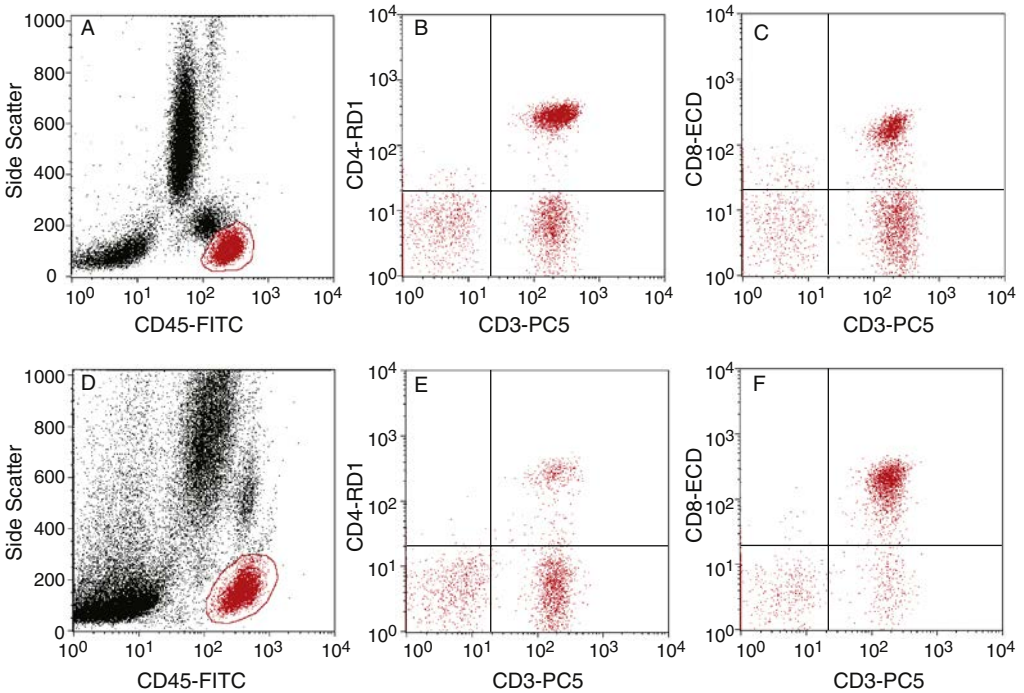

Figure 46.4 Flow cytometric immunophenotypic lymphocyte subset analysis. Use of four-color flow cytometry for the performance of peripheral blood lymphocyte subset enumeration. **A,** A dot-plot histogram of CD45 fluorescence intensity (CD45-FITC) versus side scatter (SS) as a gating strategy to discriminate lymphocytes (gated area) from other peripheral blood cells in a normal control individual. **B** and **C,** Dot-plot histograms of $CD3^+CD4^+$ and $CD3^+CD8^+$ cell populations. **D** through **F,** Corresponding histograms from a human immunodeficiency virus (HIV)-infected individual, demonstrating a marked decrease in $CD4^+$ lymphocytes and the corresponding relative increase in $CD8^+$ lymphocytes. Directly conjugated monoclonal antibodies were conjugated with fluorescein isothiocyanate (FITC), phycoerythrin (PE), energy-coupled dye (ECD), or a PE-Cy5 tandem (PC5).

postanalysis basis. Loken then defined bone marrow populations using CD45 versus SSC gating—a unique approach to defining the heterogeneous populations found in bone marrow (Loken et al., 1990; Stelzer et al., 1993). This approach became particularly relevant with the discovery that the vast majority of acute leukemia blast cells, both of lymphoid and myeloid origin, show downregulated CD45 expression, permitting the use of CD45 fluorescence intensity and light scatter to separate acute leukemia populations from lymphocytes, monocytes, and maturing myeloid cells (Borowitz, 1992; Posekany et al., 1991). Loken further promoted the use of CD45 and CD14 dual-parameter analysis gated on the lymphocyte region of FALS versus SSC for peripheral blood. Many agencies embraced this approach for HIV flow cytometry panels to minimize the effects of contaminating monocytes in the lymphocyte population because they might interfere with a true CD4 lymphocyte count, as monocytes have CD4 receptors on their surface (Passlick et al., 1989). Agencies that promoted this type of analysis included the Centers for Disease Control and Prevention (CDC, 1992), the National Institute of Allergy and Infectious Disease, Division of AIDS (DAIDS) (Calvelli et al., 1993), the National Committee for Clinical Laboratory Standards (NCCLS) (NCCLS, 1992), and the College of American Pathologists (CAP).

Unfortunately, even though this approach solved a lot of problems, it did not ensure that each tube in the panel had the same contents as the tubes containing CD45 and CD14. Thus, the required purity correction might be overestimated, leading to incorrect values for CD4. These issues were reviewed during a conference held by the CDC a year after the HIV guidelines for the performance of CD4 counts were published (Stelzer et al., 1993). Other analyses of this approach have been performed by the AIDS Clinical Trial Group (ACTG) Flow Advisory Committee in the DAIDS Proficiency CD4/CD8 program (Kagan et al., 1993) and by CAP in its proficiency testing program (Homburger et al., 1993).

A new approach to gating was evaluated in HIV panels that followed from Loken's original approach to a bone marrow definition of clusters (Loken et al., 1990). The use of CD45 as a gating parameter has simplified the analysis of bone marrow, leukemias, and HIV panels. In bone marrow and leukemia workups, CD45 is usually set as the third or fourth color and is paired with forward light scatter or side scatter. This allows the definition of a blast (potentially malignant) population. The blast population is then defined using a panel of monoclonals and the three available color parameters. In the HIV, one-tube, four-color method, CD45 allows the definition of a large lymphocyte-gated region, which is secondarily gated for CD45. This can also be done without the use of light scatter parameters, as previously described, or with the use of a two-tube, three-color panel. Newer analytic reagent products from some manufacturers include precounted beads in the monoclonal antibody–containing tube, thus permitting an absolute lymphocyte count, known as a *flow differential*, to be performed at the same time as the lymphocyte subset enumeration (van de Geijn et al., 2011). This removes the requirement of needing a hematology counter when performing T-cell enumerations and avoids the problems of white cell deterioration with shipping and the performance of an accurate differential to get accurate T-cell numbers. These methods are just becoming incorporated into ACTG HIV trial work and that of other laboratories. Recently, there has been great interest in simplified, inexpensive flow cytometric instruments and protocols for the evaluation of HIV diagnosis and monitoring in resource-limited regions of the world or at the bedside (Givens et al., 2017; Koyalta et al., 2013; Pattanapanyasat, 2012). The advent of effective antiretroviral treatment, instrumentation for near-patient CD4 T-cell counting, and changes in the World Health Organization–recommended protocols for HIV monitoring may decrease the need for lymphocyte enumeration by the clinical laboratory (Kestens & Mandy, 2017).

Another gating strategy is the use of a multicolor definition of a particular subset of interest. This approach, commonly referred to now as an *anchor gate*, uses the particular properties of some cells to investigate another set of parameters. When applied specifically to T lymphocytes, it is referred to as a *T gate* (Mandy et al., 1992). An anchor gate (Paxton et al., 1995) is especially useful when looking at activation markers, as in the HIV subsets of CD3/CD8 expressing CD38 and HLA-DR, or when looking at the expression of CD45Ra and CD45Ro against CD3/CD4 or CD3/CD8. The advantage of this method is that it is intuitive, and each color acts as a quality control check for the other subset. Furthermore, one has the choice to define the expression of biologically relevant markers in relation to functional or biologically relevant populations. This approach lends itself well to quantitative fluorescence. Although the concept of quantitative fluorescence is not new, the techniques used to measure fluorescence equivalents or fluorescence thresholds or other similar designations are new. Quantitative fluorescence measurements will be described after DNA gating and analysis.

Another approach to anchor gating involves CD34 harvesting, which uses CD34 and CD45 staining with or without 7-amino-actinomycin D (7-AAD) as a viability assessment in the identification and enumeration of CD34 progenitor cells. With these methods, beads can also be used to obtain the number of cells recovered. These methods have great utility in bone marrow transplantation protocols in which progenitor cells are harvested from cord blood, bone marrow, or peripheral blood (e.g., the International Society for Hematotherapy and Graft Engineering) and reinfused. This approach has become the standard for most laboratories performing transplants. A commercial system called ProCount (Becton Dickinson) uses a similar approach and reagents to automate the process (Pranke et al., 2006). Complex immunophenotypic analysis with six or more monoclonal antibodies is becoming more common in clinical and research laboratories for the detection of (1) minor lymphocyte subpopulations of clinical relevance in patients with autoimmune and immunodeficiency diseases; (2) small, immunologically aberrant subpopulations; and (3) MRD in patients with hematologic malignancy.

DNA ANALYSIS

General Aspects

Conceptually, DNA analysis should be less complex than immunophenotyping analysis. However, a review of the literature and its prognostic capabilities, as well as performance by laboratories on proficiency tests, indicates otherwise (Darzynkiewicz et al., 2017; Tirindelli Danesi et al., 1997). Because publication of several thousand reports in the 1980s and the early 1990s yielded conflicting findings regarding the diagnostic and prognostic significance of ploidy and S phase activity in various human tumors, a DNA consensus conference was held and the proceedings published in *Cytometry* (Shankey et al., 1993). This report was a historical review of major tumor types (in fresh, frozen, and paraffin samples) and the clinical value of the performance of ploidy by DI and the value of the S phase. These parameters were analyzed in terms of their effectiveness as prognostic markers. The 1994 CAP Conference looked at the previous markers and some additional potential tumor surrogates. In each case, the DI and the S phase were less predictable as prognostic markers than was hoped. This was largely attributed to the variability in technical performance and analysis of these assays (both instrument and sample preparation) and the inherent risk of tumor heterogeneity and, therefore, of appropriate sampling of the tumor. Specific recommendations were made with each tumor type for appropriate quality control measures that should be taken and for proper deconvolution of the histograms. Since that time, the routine utilization of DNA analysis in the clinical laboratory has considerably declined. Because of the high degree of variability and lack of prognostic significance, it was suggested by some that clinical DNA measurements be performed only by expert laboratories or be completely eliminated (ASCO, 1996). The FDA to date has not cleared any methods and still considers this a research test. However, several groups have made significant inroads into solving some of the issues associated with DNA analysis (Fig. 46.5) (Corver & ter Haar, 2011; Krueger & Wilson, 2011; Shankey & Rabinovitch, 2002). The future of this technique in clinical medicine is discussed later in the chapter.

Sample Preparation

DNA preparative methods are reasonably simple and inexpensive to perform. Many references for the original methods exist, as do many modifications. The most common methods are those used on fresh and frozen tissues and developed by Krishan, Vindelov, Crissman, Steinkamp, and others (Rabinovitch, 1993; Vindelov & Christensen, 1994) and those used on paraffin blocks (Hedley et al., 1983). In each case, whether the cells are enucleated or the cell membrane is preserved, the DNA dye PI is used most commonly in the majority of clinical laboratories and has already been described. PI staining is straightforward as long as timing, saturation, and removal of RNA parameters are followed. Measures of gross karyotypic abnormalities are made by comparing the peak (fluorescence intensity, PI uptake) of the tumor versus a diploid calibrator. Factors affecting this measurement include the CVs of the peaks for both the calibrator and the suspected tumor, the G_2/G_1 ratio, the linearity of the instrument, and linearity as measured by the deconvolution software package and the percent of tumor present (sampling) in the sample (Shankey & Rabinovitch, 2002). It is common to find laboratories reporting out a diploid tumor result on a sample containing "no" tumor. Tumors with near diploid values need stringent rules of interpretation, as does the definition of tetraploidy. Additional problems are associated with the definitions of aggregates, doublets, and debris; the treatment of sliced and cut nuclei; and the S phase population. The descriptive and semiquantitative acronym BAD is used by software analysis packages to model the effects of background, aggregates, and doublets (Rabinovitch, 1993, 1994). The impact of this parameter on the analysis is controversial.

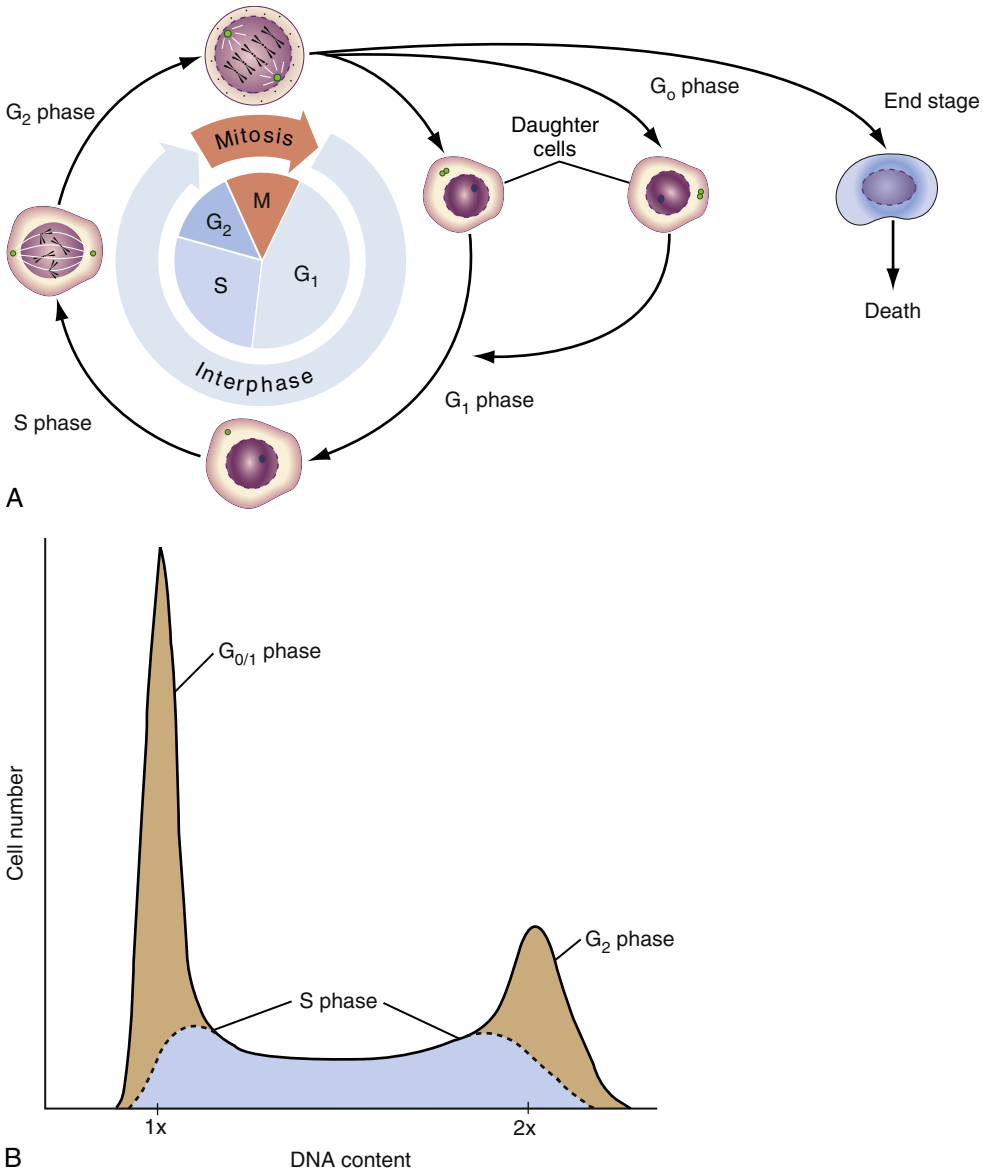

Figure 46.5 The cell cycle. **A,** Schematic illustration of the cell cycle of an asynchronous cell population. Most cells are in the resting (G_0) or early proliferative (G_1) stage of the cell cycle and have diploid (2N or 2C) DNA content. Cells that are actively synthesizing DNA (S phase) have increased DNA content (2N–4N). Cells in the second gap (G_2) phase or undergoing mitosis (M) contain precisely twice the diploid amount of DNA (4N or 4C). **B,** Flow cytometric DNA histogram of a normal proliferating cell population stained with propidium iodide. Cells in the $G_0/_1$, S, and G_2M phases of the cell cycle can be differentiated by this technique. Resolution of DNA analysis depends on the fluorochrome utilized for staining DNA, resolution of the instrument, and other factors. Mathematical modeling is required for analysis of cell cycle data because of "overlap" of the S phase curve into the $G_0/_1$ and G_2M regions. (Reprinted with permission from Riley RS, Mahin EJ, Ross W: *Clinical applications of flow cytometry*. New York, 1993, Igaku-Shoin Medical Publishers.)

The resulting S phase and DI measurements based on a single-parameter mode of analysis (PI only) are subject to these deconvolution algorithms, leading to great interlaboratory variability (Coon et al., 1994). These deconvolution algorithms for DNA have been studied extensively; however, many models used for analysis need further study. The DNA consensus document makes specific recommendations applicable to certain tumor types and suggests that laboratories perform their analyses accordingly. Even with these guidelines, a level of ambiguity remains in the interpretation and performance of the clinical laboratory, which contributes to the discordance of results in comparative studies and in proficiency tests (Coon et al., 1988; Coon et al., 1994; Wheeless et al., 1991). Difficulty in achieving consensus makes interpretation of results more difficult for the novice laboratory as well as for clinicians who are trying to compare their laboratory results with recent literature on the treatment of their patients. This is especially true in the classification of S-phase values. S-phase measures are subject to the effects of debris and aggregate modeling as described by Rabinovitch and others (Bagwell, 1993; Rabinovitch, 1994; Shankey et al., 1993). Furthermore, it is critical that decisions made with regard to which mathematical model is used for a particular tumor be kept constant, and that the list mode data be retained without modeling in case further analysis is necessary.

Other approaches using DNA and RNA probes, such as thymidine derivatives, bromodeoxyuridine and acridine orange (RNA), are used to improve the quality of the models in the estimation of proliferative and kinetic properties of a specific tumor. It is important to remember that proliferation measures are not the same as measures of S-phase quantitation, which provide a static model or a picture in time of all cells being analyzed. Integration of the area for the number of cells between 2C and 4C in a DNA histogram is not capable of giving any information on cells "stuck" in S_0 (cells actually stop DNA synthesis) nor is it capable of measuring the number of infiltrating normal cells that also might be proliferating. The S-phase value may often be higher than the actual proliferative capacity owing to artifacts of tumor heterogeneity. The single-parameter histogram yields reasonable results when dealing with an asynchronous, relatively homogeneous cell population. Pulse labeling is most commonly used in larger academic settings and to measure the effectiveness of radiation and chemotherapy by obtaining true measures of G_0/G_1 cells and G_2 + M compartments, which are not possible to attain using single-parameter measures of S phase.

Other approaches using nuclear and cytoplasmic probes as well as surface markers can be used to separate a population of interest from a mixture of cell types (Darzynkiewicz, 2010). This type of multiparameter analysis is especially useful in the measure of S phase in hematologic malignancy. Specific blast populations can be identified by FITC fluorescence and FALS; those events can be analyzed for DNA content and S phase using PI. Staining methods are altered to preserve cell surface properties or nuclear properties (Bauer & Jacobberger, 1994; Carothers, 1994; Clevenger & Shankey, 1993; Ramaekers & Hopman, 1993). These methods usually involve staining the surface marker of interest (e.g., KI-67, cyclin B1, cytokeratin, CD10) with the monoclonal antibody, fixing it in an alcohol (or commercial fixation and permeabilization reagent), then treating it with a detergent to allow penetration of PI or another nuclear dye. Staining methods are selectively modified to preserve membrane and nuclear properties specific to the probe of interest (Bauer & Jacobberger, 1994).

Cell fixation with zinc salts has recently been reported as a more optimal technique to permit simultaneous multiparametric analysis of cell surface and intracellular proteins, DNA content, and other measurements, while permitting long-term storage of the labeled cells (Christensen et al., 2011; Jensen et al., 2010).

DNA STUDIES OF INTEREST IN CELLULAR IMMUNOLOGY

There has been an explosion of literature on apoptosis (i.e., programmed cell death) and its relevance to traditional DNA parameters and other phenotypic considerations. It is not within the scope of this chapter to handle this topic. Although many studies are ongoing, apoptotic measurements are still not part of the routine clinical laboratory (Telford et al., 2011).

As mentioned earlier, clinical laboratory DNA analysis has come under much scrutiny; these studies are no longer being reimbursed in most regions.

QUANTITATIVE FLOW CYTOMETRY

The definition of cell types in immunologic terms, such as effector cells, implies the property of these cells to regulate, up or down, specific molecular functions through surface receptors. Known as immunologic phenotypes (Poncelet et al., 1993), these cells need other measurable properties to define their biological roles in maturation and disease processes. One of the observed phenomena is the differential expression of cell surface antigens (CDs) in relative terms and in absolute quantitative terms. Before the availability of absolute measures, descriptive terms such as *bright* or *dim*, *bimodal*, and so forth, were used in the literature to describe a visual phenomenon of antigen-density differences. Although descriptive, these terms are difficult to define and standardize between laboratories and patients. They also lack precision in defining an event and cannot be objectively used to monitor patients' treatment or cell definition (cell type) by measures of CD expression and overlapping expression. Evidence suggests that quantitative differences in antigen expression in chronic lymphocytic leukemia and other leukemias may be important in determining the prognosis (Poncelet & Carayon, 1985). These measures are also used in the definition of MRD and in the investigation of a viral effect or activation in HIV disease (Poncelet et al., 1991). The percent of a specific cell present often does not give the true clinical picture. This is particularly true in leukopenic cases and when the blast population represents a relatively small percentage of total cells present.

Quantitative flow cytometry is defined as the quantitation of fluorescence intensity (FI) as determined by the antibody-binding capacity of a given fluorochrome antibody conjugate. It is an indirect measure of the amount of cell surface antigen present per individual cell (Marti et al., 2003; Stelzer et al., 1997; Wang et al., 2011). Investigators have described the use of polystyrene beads or cell lines coated with saturating amounts of antibody to determine the absolute numbers of receptors or antigenic sites per cell, also referred to as *antigen density* (Poncelet et al., 1993). ABC units are defined as a measure of relative antibody-binding capacity. This method does not need to match the fluorescein/protein ratio, as both the cells and the standards are being stained with the same antibody. Use of FI measurements should give the user a means to avoid this situation. More information can be obtained by referring to the 1997 U.S./Canadian consensus document that reviews the necessary parameters for standardization (Stelzer et al., 1997).

Although early in its development, quantitative phenotypes will help us define cluster analysis software programs for cell quantification and identification by establishing mean channel FI as a means of separating cells of different functional phenotypes.

CLINICAL SIGNIFICANCE OF CELLULAR IMMUNE TESTING

The decision to test the immune response is usually made in the context of the patient's clinical presentation, as described in Box 46.1. The most common reasons for the initiation of a clinical laboratory request include increased or unexplained susceptibility to infection, increased severity of common infections, or an unusual reaction to immunization. Unusual infections, especially those caused by opportunistic agents or severe infections that are unresponsive to treatment, and certain allergic or atopic states may also prompt immune testing. In recent years, potential HIV infection has replaced possible primary immunodeficiency as the leading presumptive diagnosis. Because few, if any, cellular immune tests are totally and specifically diagnostic, and because they may be expensive and time-consuming, the request for laboratory evaluation should be approached with caution and a clear understanding of how the result will lead to improved management of the patient. Under these circumstances, the responsibility of the clinical immunology laboratory is to establish a sufficient range of tests to enable judicious testing for determination of the nature and extent of the immune alteration as well as interpretation of the results in the context of the current clinical presentation and past medical history.

BOX 46.1

Presentation of Possible Immunodeficiency

- Frequent bacterial infection
- Unusually severe systemic reaction to a virus
- Development of infection with an unusual organism, such as fungus or protozoa
- Systemic reaction following live virus vaccination
- Family history of recurrent infections
- Exposure to the human immunodeficiency virus

The principal task of the clinical immunologist, aided by the laboratory, is often to distinguish the features of primary immunodeficiency or suspected acquired immunodeficiency due to HIV infection from immune changes associated with other clinical conditions that may produce immune changes that could appear phenotypically identical to primary immunodeficiency (Tebo et al., 2014). In this regard, immune changes may accompany many clinical entities, such as malignancy; traumatic injury, such as burns or accidents resulting in major blood loss or organ damage; hematologic disease, such as Fanconi anemia, hemophilia, and immune thrombocytopenia; lymphoproliferative disorders. such as histiocytosis; the hemoglobinopathies. such as sickle cell anemia and thalassemia; and a fairly wide range of chromosomal abnormalities. such as DiGeorge syndrome, Down syndrome, Bloom syndrome, William congenital dyskeratosis, epidermolysis bullosa, and Duncan syndrome (X-linked lymphoproliferative disorder). Autoimmune diseases—such as rheumatic disease, mixed connective tissue disease, type 1 diabetes mellitus, systemic lupus erythematosus, amyotrophic lateral sclerosis, multiple sclerosis, and myasthenia gravis—may be associated with cellular immune changes and are discussed elsewhere in this textbook.

Primary immunodeficiency disorders nearly always present in the context of infection or hematologic change. Laboratory evaluation of these disorders requires a stepwise approach to minimize blood drawing and to logically choose among available tests for the purpose of differential diagnosis. Some presumptive diagnoses may appear to be too frequently suspected, for example, Wiskott-Aldrich syndrome, although this does need to be ruled out in cases of unexplained thrombocytopenia. However, Wiskott-Aldrich syndrome may be missed if response to mitogens alone rather than to antigens as well is not tested, and the immune defect may become more marked with time so that follow-up testing may be needed.

HIV infection can be readily diagnosed by direct testing, but the clinical immunology laboratory is sometimes used as a proving ground before the patient or guardian is approached for informed consent for HIV testing. This is based on the observation that an inverted CD4/CD8 ratio is virtually always found among HIV-positive adults. Thus, as a result of the current AIDS epidemic, the inverted CD4/CD8 ratio has become identified as a marker of HIV infection. However, a number of diseases other than HIV involve the immune system and can produce an inverted CD4/CD8 ratio or extremely low CD4 cell numbers. These include, but are not limited to, DiGeorge syndrome, benign thymoma, the early phase of hepatitis C virus infection, Kawasaki disease, protein-calorie malnutrition, and malignancy.

CLINICAL INTERPRETATION OF CELLULAR IMMUNE TESTING

The clinician or laboratorian interpreting cellular immune function assays is often confronted by the issue of how to evaluate the potential clinical significance of an impaired in vitro immune response. Studies of even relatively well-defined disorders have shown that very significant differences in clinical symptoms may occur. However, newer testing strategies can be helpful in subclassifying patients by the level and extent of the defect.

For example, the DiGeorge syndrome (22q11.2 deletion syndrome) (DiGeorge, 1974) is classically a triad of thymic and parathyroid aplasia and conotruncal defects. Patients with the DiGeorge syndrome show marked differences in severity of infection in spite of relatively similar

findings of reduced numbers of mature T lymphocytes and a poor response to mitogens. Initially, a very high degree of fatality was associated with this syndrome. Improved surgical and anesthesia methods have led to a significant decrease in the incidence of severe infection, although some infants still develop intractable and ultimately fatal infection (Bastian et al., 1989). Recently, it has been possible to use more exact lymphocyte phenotype analysis to determine the severity of the immune defect and to more accurately predict clinical outcome. Using longitudinal testing over several months and a multiple parametric approach, it now seems that severity may be predictable from consistently low $CD4^+$ T-cell numbers, an inverted CD4/CD8 ratio, and reduced lymphokine IL-2 production (Cunningham-Rundles et al., 1994). Investigation into the significance of monosomic deletions of chromosome 22q11.2, which are the leading causes of DiGeorge syndrome, velocardiofacial syndrome, and conotruncal anomaly face syndrome, illustrates the importance of new genetic information. Although only DiGeorge syndrome was originally described as an immunodeficiency disorder, new studies looking at the frequency of immunodeficiency in the other clinical syndromes associated with the chromosome 22q11.2 microdeletion have shown that more than 75% of patients have evidence of immunocompromise, the severity of which does not correlate with any particular phenotypic feature (Sullivan et al., 1998).

T-cell function may be as important, or more important, in HIV infection than the loss of $CD4^+$ T cells or the rate of loss. In some viral-associated illnesses, considerable uncertainty exists as to how close the association is between an immune deficit detected ex vivo and the patient's in vivo immune function (Landay et al., 1991; Lloyd et al., 1992). In other diseases, immune abnormalities have been identified as disease markers, but there is no clear understanding of cause and effect. An example is seen in some forms of chronic fatigue syndrome associated with altered orthostatic response (Rowe et al., 1999) and increased plasma levels of TNF-α (Moss et al., 1999).

AGE AND THE IMMUNE RESPONSE

Current studies demonstrate that the immune system changes as part of the aging process (Weiskopf, 2009; Fulop et al., 2014; Montecino-Rodriguez et al., 2013; Nikolich-Zugich, 2012; Weiskopf et al., 2009). Although considerable variation in this is seen, and much is a consequence of altered nutritional status (Afacan et al., 2012; Maijo et al., 2014; Monk et al., 2011), it is essential that the clinical laboratory provide relevant laboratory values for age-matched controls.

The study of pediatric patients presents particular issues for the laboratory diagnosis of immunodeficiency. Development of the immune system in the child is not complete at birth; in addition, children have not been exposed to a wide variety of abnormal environmental agents and may have vulnerability to infection (Rytter et al., 2014; Ygberg & Nilsson, 2012). Congenital viral exposure or prematurity alone may be associated with immune abnormalities. Key differences in the pediatric immune response include marked lymphocytosis and deficit in endogenous antibodies at birth, elevated B cells that show a deficient response to polysaccharide antigen, increased $CD4^+/CD8^+$ T-cell ratio, few NK cells, decreased cytokine production, and oligoclonal T-cell expansions (Marodi, 2006; Philbin & Levy, 2009; Wedderburn et al., 2001). These differences are reflected in marked differences in the normal range of lymphocyte subsets and must be taken into account during evaluation of results (Bonilla & Oettgen, 1997; Denny et al., 1992; Shearer et al., 2003; Tosato et al., 2015). Also, marked differences in response to various activators have been noted as compared with adults. The neonatal response of premature infants to certain microbial activators may be stronger than that of adults or full-term infants because of rapid changes in immune regulation (Cunningham-Rundles & Nessin, 2000; Veber et al., 1991), or because of fundamental differences in perinatal programming (Prescott et al., 1998). The immune system of elderly individuals also shows changes in comparison with that of younger adults. In particular, cumulative alterations in critical B- and T-cell subpopulations, altered cell signaling and cytokine production, and other changes may contribute to the increased incidence of autoimmune disease and cancer in this group (Alvarez-Rodriguez et al., 2012; Hakim et al., 2004; Montecino-Rodriguez et al., 2013). The deterioration of immune responses with increasing age has been designated *immunosenescence* (Malaguarnera et al., 2001). Zinc deficiency appears to be one of many factors that may lead to immunosenescence (Maywald & Rink, 2015).

MALNUTRITION AND THE IMMUNE RESPONSE

Although it is generally believed that malnutrition is relatively rare in developed countries, growing evidence suggests that malnutrition is fairly common, especially in certain age groups (Pennington, 1996). Malnutrition is associated with immunodeficiency and causes significant vulnerability to infection (Cunningham-Rundles & Cervia, 1996; Keusch, 2003). For example, zinc deficiency can present as a profound immunodeficiency that may be related to the primary lack of zinc uptake at the gastrointestinal tract, to acrodermatitis enteropathica, or to lack of adequate zinc in the diet (Moynahan, 1974; Prasad, 2009; Tuerk & Fazel, 2009). Persons with hypogammaglobulinemia and associated malabsorption affecting zinc levels may show poor proliferative response in vitro and infections that resolve with zinc repletion (Cunningham-Rundles et al., 1981). This is associated with the fact that zinc is required for the biological activity of thymic hormone, is needed for the production of functionally mature T cells and for activation of T cells, and may play a role in intercellular signaling within the immune system (Cunningham-Rundles & Lin, 1998; Haase et al., 2008; Hirano et al., 2008; Prasad, 1998). Increasing evidence suggests that micronutrient imbalance will alter immune response through specific effects on the immune response (Amati et al., 2003; Savino & Dardenne, 2010; Tilg & Moschen, 2013). In many clinical settings, malnutrition may be a complicating factor. The interaction of infection with altered metabolism secondary to the acute phase response can cause temporal shifts in trace elements, leading to transient suppression of the immune response. Physical stress may have a similar effect and may lead to enhanced vulnerability to infection in the context of immunosuppression (Cunningham-Rundles, 1999). This is a two-way process. Growth failure may be the first sign of HIV infection in an HIV-positive child (Peters et al., 1998). For this and other reasons, immune evaluation should be an ongoing process in the context of continuing treatment or other testing.

CANCER AND THE IMMUNE RESPONSE

Primary immunodeficiency is associated with an increased incidence of cancer (Cunningham-Rundles et al. 1987), and it is increasingly clear that tumors develop in association with infection by HIV and other viruses and bacteria (Aoki & Tosato, 2004; Engels et al., 2008; Grivennikov et al., 2010). In the patient with cancer, generalized immunodeficiency or reduction in response to antigenic challenge may appear in association with the development of primary malignancy, may occur during metastasis, or may be caused by the side effects of therapeutic intervention. Reduced immune response to nonspecific activators studied ex vivo in proliferation assays does correlate with stage of disease and has prognostic significance for survival (Heimdal et al., 1999). An inverted CD4/CD8 ratio and increased suppressor cell activity are often observed in untreated cancer patients, and changes in cytokine production have been observed (Livingston et al., 1987; Smyth et al., 2004). Experimental studies have shown that tumors may be surprisingly immunogenic but may drive the immune response toward a nonprotective response (Loose & Van de Wiele, 2009).

The development of new immunotherapeutic approaches is increasing, suggesting that response to tumor-specific antigens will be used more in the future (Schultes & Nicodemus, 2004; Steinman & Mellman, 2004; Waller, 2004). Immune response assays may also be used to track and evaluate response to treatments such as IL-2 (Lissoni et al., 1999) and cancer vaccines (Yannelli & Wroblewski, 2004). In many patients, chemotherapy will produce transient suppression of immune response that resolves within a short time, and radiation may have longer-term effects (Katz & Fauci, 1993). Assessment of immune response in the cancer patient requires highly selective and discriminating use of tests and activators, which reflect relevant processes as well as specificity of response.

METHODOLOGIC APPROACH TO CELLULAR IMMUNE TESTING

Human studies have been based on observation of peripheral blood immune cells because the peripheral compartment is most accessible and readily measured, but this approach may not reflect regional events. Knowledge of the differences between systemic and mucosal immune response may ultimately explain many current paradoxes that arise when immune response measured in vitro or ex vivo is compared with host defense in vivo (Xu-Amano et al., 1993). Systemic cellular immune function appears to be regulated through functionally distinct T-helper–type cytokine patterns ("the cytokine network"), such that when Th1 cytokines, IL-2, and IFN-γ are produced, cellular immune host defense is favored. When Th2 cytokines, IL-4, IL-5, IL-6, and IL-10 are produced, B lymphocyte response is induced (Balkwill & Burke, 1989; Muller, 2006; Seillet et al., 2014; Yamamura et al., 1991).

In contrast to systemic immunity, the primary activity of the mucosal immune response is to protect the mucosa by blocking microbial, toxin,

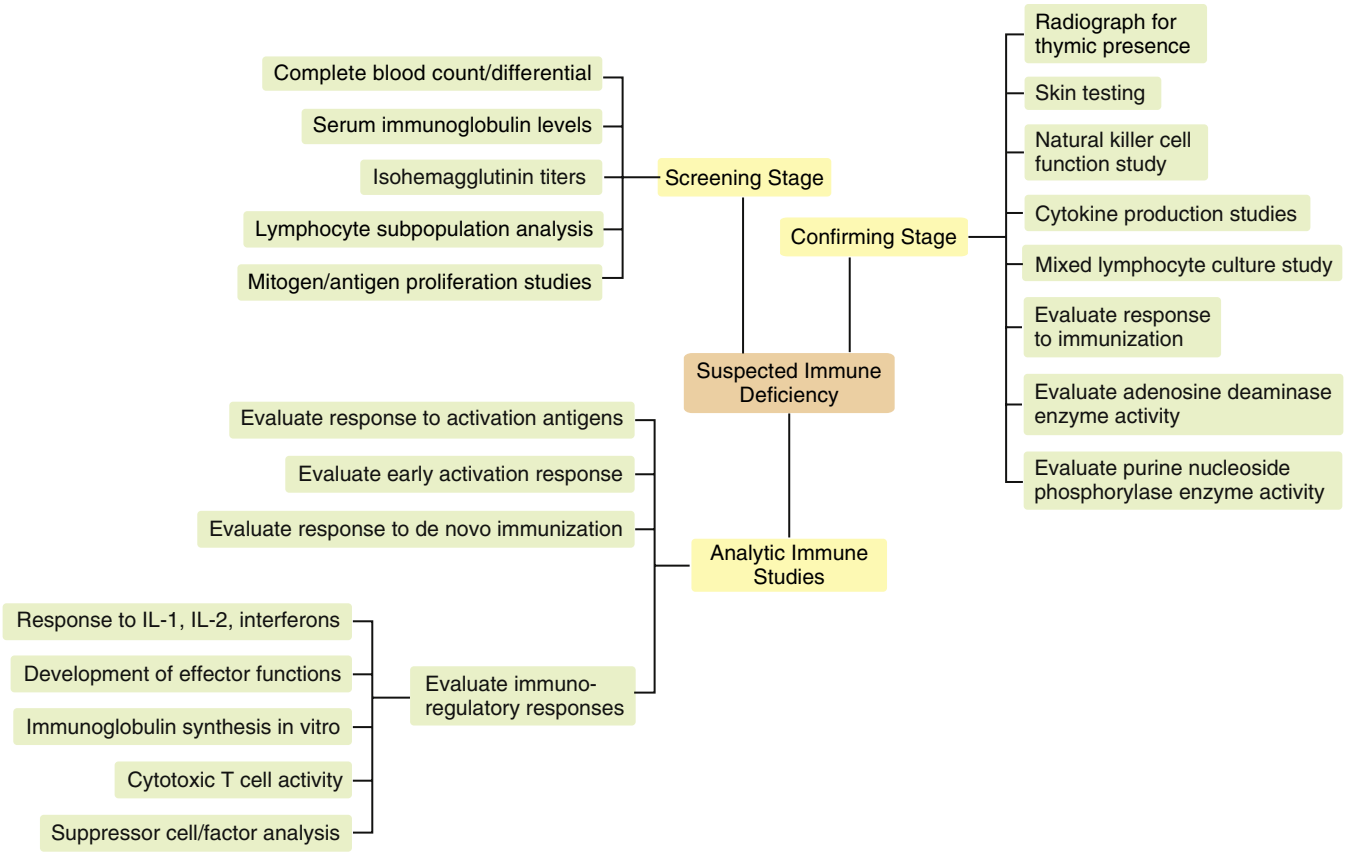

Figure 46.6 The three phases of the clinical evaluation of a suspected deficiency of cellular immunity.

and antigen entry through secretion and transport of IgA to the lumen of the gut—a process mediated by the innate immune system and a special type of memory T lymphocyte with reduced proliferative capacity capable of providing B-cell help (Cheroutre, 2004; McDermott & Huffnagle, 2014; Nochi & Kiyono, 2006). Both lamina propria T lymphocytes and intraepithelial T lymphocytes develop in relative independence of the thymus and function differently from peripheral blood T cells in using the CD2 signal transduction pathway rather than the T-cell receptor/CD3 pathway.

At present, tests of mucosal immunity usually are not performed in the clinical immunology laboratory, and, with rare exceptions, the immune cells under study are from the peripheral blood compartment. For this reason, use of in vivo skin testing and examination of humoral immune response to previously encountered vaccines are useful to the cellular immunologist, as these provide other means of assessment. In all cases, the use of a stepwise approach and repeated testing is highly informative.

STAGES OF STUDY: THE SCREENING STAGE

Evaluation of immune function in a patient with a possible immunodeficiency is normally achieved in stages (Fig. 46.6). The first stage is a screening analysis of possible areas of deficiency in correlation with the medical history, family history, and physical examination findings (Box 46.2). A complete blood count and leukocyte differential count must be obtained in all patients, and the peripheral blood film reviewed. Other critical assays include serum immunoglobulin levels (IgG, IgA, IgM, IgD, IgE), complement levels, and isohemagglutinin titers (Cassimos et al., 2009). These screening studies should be accompanied by appropriate flow cytometric analysis of lymphocyte subpopulations. In children, studies must include the use of a B-cell marker to assess possible B-cell shifts, which may occur transiently in the neonate and may be reflected in low T-cell populations (Allsopp, 1998). The use of an NK cell marker is also strongly recommended in young children older than 3 months of age, because NK cell levels in this population may be reduced or absent at birth (Zola et al., 1983).

Although there is frequently a limitation on the quantity of blood to be drawn for such studies, it is essential that the first evaluation be performed on blood specimens obtained at the same time. Functional studies need to be performed on fresh anticoagulated blood whenever possible (or blood stored at room temperature in the dark for less than 24 hours) before mononuclear cells are isolated. When blood is being sent by air or transport to a distant laboratory, it is extremely important to include a control specimen drawn in parallel from a healthy person to serve as an internal standard for the shipping process. The type of tube chosen to draw the blood is important. The use of lithium heparin– or ethylenediaminetetraacetic acid–containing tubes is not recommended for any lymphocyte functional studies. Sodium heparin (preservative free) or acid citrate dextrose tubes must be used. Blood collected in heparinized tubes can also be used for flow cytometric analysis, although the timing of specimen preparation and analysis is critical (Nicholson & Green, 1993; NCCLS, 1992).

The question of when the blood should be drawn is important. In general, most data have been obtained from blood drawn in the morning, and circadian effects may influence results. When this cannot be done, it is helpful to continue to maintain uniformity of drawing time for an individual patient. This is most critical when measuring absolute numbers of T lymphocyte subsets in the monitoring of HIV disease or as part of a clinical trial (Malone et al., 1990).

The screening stage also includes a panel approach to assess mitogenic and antigenic proliferative response. The proliferative response of lymphocytes to a range of activators continues to be one of the most sensitive tools to assess normal function. When this includes an appropriate T-cell and B-cell activator, it can be useful in defining the areas of defect. Although this is not always done, the use of multiple concentrations of each activator is strongly recommended.

STAGES OF STUDY: THE CONFIRMING STAGE

General Aspects

Once the screening of the individual has been achieved and evidence of a potential immunodeficiency has been observed, initial findings should be confirmed by repeated tests. Minimally, a positive and a negative (normal range and abnormal range) test should be carried out. Additional tests sometimes may be added to the panel; this may provide the beginning phase of analytic studies.

It is important to make appropriate arrangements to draw blood when the patient is in the most clinically stable state. Double baseline studies are recommended before intervention is undertaken, which can encompass the confirming phase. In some cases of apparent immunodeficiency, sequestration of immune cells is reflected in low percentages of T lymphocytes in the peripheral compartment. The confirmation stage should also include a careful reevaluation of the patient's medical history and family history. Studies that may be used at this confirming stage are shown in Box 46.3.

BOX 46.2

Basic Screening Immunology Studies

- Complete blood count with leukocyte differential count
- Isohemagglutinin titers
- Lymphocyte subpopulation analysis (numbers and percentages of T and B cells) by flow cytometry
- Lymphocyte activation in vitro to mitogens and microbial activators
- Serum immunoglobulins, including immunoglobulin subclasses if evidence of clinical infection with encapsulated bacteria. In some cases, immunoglobulin levels are normal but heterogeneous nonbinding antibodies are produced. Thus, additional studies are needed.

BOX 46.3

Confirming and First-Stage Analytic Studies

- Radiograph for thymic shadow
- Skin test
- Natural killer cell activity (if child is 6 months or older)
- Cytokine production in response to activation T-helper 1, T-helper 2 (interleukin [IL]-2, interferon [IFN]-γ, IL-4, and so on)
- Mixed lymphocyte culture reaction with patient as stimulator and patient as responder

Response to immunization

- Test for presence of age-appropriate specific antibodies
- Naturally occurring antibody response to isohemagglutinins (anti-A and anti-B blood group substances) if patient has A, B, or O blood type
- Test for adenosine deaminase and purine nucleoside phosphorylase enzyme deficiency

BOX 46.4

Causes of Skin Test Anergy

- Lack of appropriate antigenic history when panel does not include ubiquitous activators
- Primary immunodeficiency
- Viral infection
- Malnutrition
- Granulomatous disease
- Neoplasia

BOX 46.5

Analytic and Immunoregulatory Studies

Development of activation antigens during response to stimulation, such as Tac antigen, transferrin receptor, upregulation for MHC class II on T cells, soluble receptors, and so on
Early activation response (e.g., calcium channels)
Immunoregulation
- Response to IL-1, IL-2, interferons
- Development of effector functions
- Immunoglobulin synthesis in vitro
- Cytotoxic T-cell activity
- Suppressor cell/factor analysis

Gene activation, cell cycle analysis
Response to immunization: de novo immunization

IL, Interleukin; *MHC,* major histocompatibility complex.

BOX 46.6

Immunophenotyping Lymphocyte Subpopulations

Basic peripheral blood panel (whole blood, lysed red blood cells*)
- CD45/CD14
- Isotype mouse immunoglobulin controls
- CD3/CD19
- CD3/CD4
- CD3/CD8
- CD3/CD56 and 16

Isolated mononuclear cells, activation panel†
- CD45/CD14

Isotype mouse immunoglobulin controls
- CD3/CD25 (IL-2R)
- CD3/HLA-DR

HLA, Human leukocyte antigen; *IL,* interleukin.
* If low CD3, then repeat and add CD2. Further, monoclonals against T-cell receptor paired with CD3 may be added. Monocyte markers also may be evaluated. These may be performed using three- or four-color reagents using CD45 gating.
† After 2 days of culture, remove cells and wash before staining with monoclonal antibodies listed; analyze control cells containing no activator, then analyze activated cells. Activators may include mitogen, IL-2, and/or interferon-.

Thymic Presence

The roentgenogram for thymic shadow may be inadequate because the thymus is highly prone to stress depletion and is no longer visible (Dooley & Liston, 2012; Gui et al., 2012; Rezzani et al., 2014; Simanovsky et al., 2012). Although it is difficult to determine with accuracy, the actual size of the thymus assessed by magnetic resonance imaging has been found to correlate with $CD4^+$ T-lymphocyte number in HIV infection (Vigano et al., 1999). Recent studies suggest that the human thymus can be thought of as a chimeric organ that comprises both central and peripheral lymphoid tissues. These studies also have shown that thymic involution is an integral part of immunosenescence, mediated by a complex process involving multiple molecular mediators, including cytokines and steroid hormones (Dooley & Liston, 2012; Haynes et al., 2000). As described in the subsequent specific section on flow cytometric evaluation of T-lymphocyte subsets, expression of normal maturation antigens acquired during thymic development will suffice to identify the presence of a working thymus.

Skin Testing

The use of a skin test panel can be important at this point. This approach to cellular immune assessment originally served as the departure point for the development of the cellular immune functional tests because it measures delayed-type hypersensitivity directly in vivo. Experience with the delayed-type hypersensitivity skin test has shown good overall correlation between lack of reactivity, termed *anergy*, and immunodeficiency (Deodhar, 1983; Maas et al., 1998), but it has not been useful as an analytic tool to dissect out the reason for lack of response. In addition, the skin test is not very quantifiable. Use of the purified protein derivative skin test to assess the possible presence of *Mycobacterium tuberculosis* is an exception, although anergic individuals do not respond. In addition, false positives are seen in persons who have been vaccinated with bacille Calmette-Guérin (Huebner et al., 1993). The relative effectiveness of a standardized *Candida albicans* skin test product in children has been reported (Ohri et al., 2004).

Reasons for lack of skin test response are shown in Box 46.4. Some studies have been based on a de novo immunization skin test using dinitrofluorobenzene. Although this once was used rather extensively, the approach is no longer considered useful because of ambiguities in the underlying mechanism of reaction. The introduction of the "skin window" test may ultimately provide a more quantitative and informative measure of in vivo immune response because the reaction can be used to test autologous tumor response (Black et al., 1988). However, despite some reservations, the importance of the skin test as a convincing demonstration that immune defects noted in vitro may have prognostic significance in vivo should not be underestimated.

STAGES OF STUDY: ANALYTIC IMMUNE STUDIES

A basic outline of analytic studies is provided in Box 46.5. Although a complete description of these approaches is beyond the scope of this discussion, these studies generally attempt to identify the underlying mechanism of immune defect by proceeding through a series of steps. Although there are different possible ways of doing this, one good way is to assess the general level of defect by following the general plan of assessing the presence of cell types and the relative proportions of all in light of areas of diminished general function and then to perform studies of effector function.

If cell populations have been determined to be essentially intact in the absence of activation, the issue of intrinsic failure may be studied by many different approaches, including the use of expanded lymphocyte surface marker analysis, framework determinants to the TCR, and activation antigens, such as CD25, CD38, and HLA-DR (Box 46.6). Absence of MHC class II upregulation in response to IFN-γ is one example. Although cell populations may express a reference normal differentiation antigen, they may also coexpress others inappropriately, which may be a key to functional abnormality. For example, $CD8^+$ T cells coexpressing CD38 are not functionally the same as CD8 cells that do not express this marker and are expanded in HIV disease (Giorgi & Detels, 1989). Absence of expression of certain molecules, such as CD28, is another important indicator. In some primary immunodeficiency syndromes, upregulation of the IL-2 receptor

in response to IL-2 may be abnormal. Receptors may not be translocated normally or receptors may be shed prematurely (Cunningham-Rundles et al., 1990).

Development of the immune response may be kinetically abnormal because of delayed secondary recruitment during the amplification phase. This should be tested by doing time course studies. In some cases, cytokines may not be made or may be functionally altered. Effector functions may be missing or impaired. Evaluation of this may require a detailed approach. Attempts to restore response by addition of cytokine may be useful, although this may circumvent the lesion through compensation rather than fill in the actual deficiency. New testing strategies may utilize whole blood rather than isolated mononuclear cells (Bocchieri et al., 1995). This system provides an excellent ex vivo mirror of immune response, because the actual relationships among cells are not altered. Furthermore, this system can be used to measure cytokine production (Petrovsky & Harrison, 1995; Suni et al., 1998).

The cellular immunology laboratory is advised to choose basic analytic studies that are normally done on a routine basis so that a basis for comparison is available. Establishment of laboratory normal ranges and maintenance of reagent quality control, especially for certain variable elements, are essential for the accuracy and sensitivity of these tests.

LABORATORY EVALUATION OF LYMPHOCYTE FUNCTION

Developmental defects, inherited genetic abnormalities, and acquired infections cause profound immunodeficiency states. Additionally, severe burns, trauma, and therapeutic intervention may lead to immunodeficiency. Bulk assays can be used to ascertain whether an individual has a decreased T-cell proliferative response and have been available for some time, but they are limited both by poor reproducibility and by the limited information garnered from bulk assays. Recent technological developments have allowed for the production of a variety of reagents that can be used to assess multiple activities along the pathway of T-cell activation. These reagents include monoclonal antibodies specific for T-cell activation markers, reagents, and systems for the detection of intracellular cytokines, and tracking dyes and nonradioactive DNA precursors developed to assess lymphocyte proliferation.

LYMPHOCYTE TRANSFORMATION ASSAYS

Principles of Lymphocyte Transformation

The most common in vivo procedure used to assess cellular immunity is a simple skin test. A positive skin test for the detection of a delayed-type hypersensitivity response implies intact cellular immunity as well as intact monocyte chemotaxis (Ananworanich & Shearer, 2002; Borut et al., 1980). Although skin testing is easily performed, negative results are difficult to interpret, especially in young children, and skin testing is not as sensitive as in vitro lymphocyte stimulation assays (Borut et al., 1980). Other in vivo correlates of cell-mediated immunity include contact sensitivity, granuloma formation, and allograft rejection. The recent development of transdermal methods for antigen delivery may augment skin antigen testing and vaccine delivery (Kasempimolporn et al., 2019; Lee et al., 2013).

Mitogen-Induced Blastogenesis

The measurement of lymphocyte proliferation in response to stimulation by various antigens or mitogens is a standard method for testing the functional capacity of lymphocytes, as well as the immunomodulatory activity of biological or chemical molecules. In the past, laboratories assessed the proliferative capacity of lymphocytes by measuring the rate of incorporation of radiolabeled DNA nucleosides (tritiated thymidine) following prolonged incubation of peripheral blood mononuclear cell cultures with mitogens (3–4 days) or antigens (5–10 days) (Maluish & Strong, 1986). In general, only a limited number of T cells respond to any one antigen in vitro; therefore, cells must be cultured from 5 to 10 days to detect a response. In vitro lymphocyte transformation in response to a mitogen was first reported by Nowell (1960). Mitogens and IL-2 in general are the most potent stimuli, as they induce the rapid proliferation of the largest proportion of lymphocytes. For this reason, proliferation can be detected in 3 to 4 days, providing an effective screening tool. Of the mitogens, phytohemagglutinin (PHA) and concanavalin A (Con A), ionomycin calcium salt, and magnetic beads coated with anti-CD3/CD28 monoclonal antibodies induce T-cell blastogenesis, and pokeweed mitogen and staphylococcal protein A trigger B-cell activation. The cellular signaling pathways of mitogen-induced B-cell activation have recently been described (Nikitin et al., 2014).

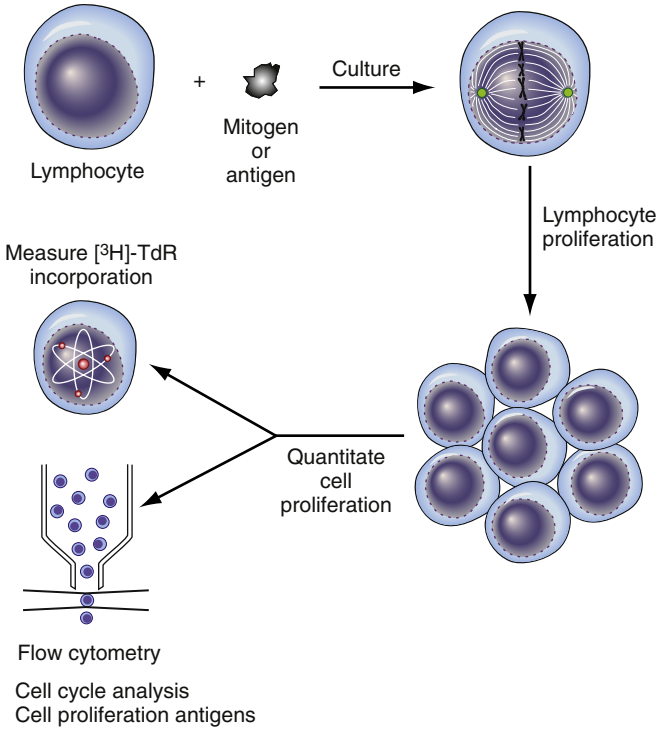

Figure 46.7 Principle of lymphocyte stimulation assay. Lymphocytes are cultured with antigen or mitogen. If stimulation occurs, a proliferative reaction takes place, with the formation of daughter cells. The amount of proliferation can be determined from tritiated thymidine (^{3}H-TdR) incorporation, by flow cytometric cell cycle kinetic analysis, or by measuring a cell proliferation antigen such as Ki-67. (Reprinted with permission from Riley RS, Mahin EJ, Ross W: *Clinical applications of flow cytometry*. New York, 1993, Igaku-Shoin Medical Publishers.)

In the standard mitogen-induced blastogenesis procedure, lymphocytes are isolated with Ficoll-Hypaque density gradient centrifugation and cultured for several days with a mitogen or specific soluble antigen in media enriched with human AB serum. Tritiated thymidine is added to the culture media, and the plates are incubated for an additional 4 to 24 hours. The cells are isolated (harvested) from the plates using a special device (cell harvester) and are transferred to disks of filter paper (Fig. 46.7). These disks are placed in scintillation fluid, and radioactive emissions are measured in a liquid scintillation counter. The mitogen-induced blastogenesis technique is classified as a **bulk assay method** because the response of the entire cell population is measured.

Several controls are necessary in bulk assays of lymphocyte proliferation because the assays may be influenced by the number of cultured cells, incubation time and temperature, mitogen concentration, and various inhibitory factors that may be present. The results are expressed as a stimulation index, which is the ratio of radioisotope incorporation into the test versus control cells. The relative proliferation index is the ratio of the δ counts per minute (cpm) of the test subject (cpm of stimulated cells minus unstimulated control cells) to the δ cpm of a panel of normal individuals tested simultaneously.

Bulk assays, in addition to their inherent technical problems, provide no information on the specific cell subsets that are responding. Cram and coworkers were among the first to resolve this problem through analysis of blastogenesis at the single-cell level by flow cytometry (Cram et al., 1976). Since that time, flow cytometry with its inherent multiparameter potential has become the instrument of choice for analysis of lymphocyte transformation and other aspects of the cellular immune response. Comprehensive reviews of flow cytometry and methods used to assess lymphocyte activation and proliferation have been published by Maluish and Perfetto (Maluish & Strong, 1986; Perfetto et al., 2002).

Precise measurement of the proportion of lymphocytes in the various phases of the cell cycle (i.e., cell cycle analysis) is critical for flow cytometric studies of blastogenesis and lymphocyte proliferation. In general, two distinct approaches are used in cell cycle analysis. In the past, the preferred approach was to measure the level of FI (fluorescence intensity) emitted by DNA staining dyes. The most commonly used dye was PI, a phenanthridinium-based compound that intercalates stoichiometrically into DNA (i.e., the amount or intensity of fluorescence is proportional to the amount of DNA in a cell). Using complex mathematical modeling, the percentages of cells

in the G_0/G_1, S, and G_2 phases can be determined from the distribution of the FI. Most peripheral blood lymphocytes are in the resting phase of the cell cycle, with fewer than 5% of cells in the S phase. Many fluorescent dyes with different DNA binding affinities and spectral properties have also been used, including ethidium bromide, DAPI, Hoechst 33258, and Hoechst 33342. Bromodeoxyuridine (5-bromo-2-deoxyuridine [BrdU]) is another substance used to measure the proliferation of lymphocytes and other cells. BrdU is a synthetic analog of thymidine that is incorporated into the DNA of replicating cells while substituting for thymidine. Fluorochrome-labeled antibodies specific for BrdU are used to measure BrdU incorporation and cell proliferation. The quantitation of cell cycle–related nuclear proliferation antigens is another approach for the measurement of cell cycling and proliferation in lymphocyte and other cell populations. Ki-67 antigen is a nuclear protein expressed by proliferating cells in all phases of the cell cycle, but not by resting cells (Sawhney & Hall, 1992). Labeled monoclonal antibodies specific for Ki-67 can be measured by flow cytometric or immunohistochemical techniques to obtain the **Ki-67 proliferation index.**

The use of dyes that stably integrate into the membranes of live lymphocytes or other cells is a more recently described means of measuring lymphocyte proliferation. After washing away excess dye, the lymphocytes are stimulated to divide. With each successive division, the amount of dye per cell is halved. The fluorescence emitted from the cells after culture can be modeled, and the number of cell divisions can be estimated. This method has been standardized into cell proliferation kits that include both the software required for analyses and the tracking dye (Sigma Immunochemicals, St. Louis, MO). The evaluation of multiple dyes by many investigators has revealed PKH26, PKH67, carboxyfluorescein diacetate succinimidyl ester (CFSE), and the far-red dye CellVue Claret as most suitable for their ability to quantify lymphocyte proliferation (Begum et al., 2013; Gil et al., 2009; Tario et al., 2007; Tario et al., 2012; Tario et al., 2011; Tosevski & Mair, 2014; Zolnierowicz et al., 2013). This assay may provide the most accurate assessment of cell proliferative response in in vitro culture systems, with the substantial advantage over standard bulk assays of allowing the measurement of specific lymphocyte subsets. CFSE indices appear to correlate more closely with TdR assays than measurement of $CD69^+$ cells (Angulo & Fulcher, 1998).

Many laboratories have replaced the tritiated thymidine incorporation assays with a combination of cell surface marker induction assays, metabolic assays, and measurement of the percentage of cells at various phases of the cell cycle following activation (Cost et al., 1993). The flow cytometer has been used for most recent studies of lymphocyte proliferation, but the application of other instrumentation, such as the automated cell counter, has been described (Gibson et al., 2016).

The recently developed ability to measure the production of cell-associated cytokines at the single-cell level also has significant potential as a clinical tool for evaluation of the cellular immune response (Freer, 2014; Nomura et al., 2008; Suni & Maino, 2011). Cytokine flow cytometry (intracellular cytokine detection) is performed by stimulating target cells for 4 to 6 hours in the presence of membrane transport blocking reagents (brefeldin A or monensin) to prevent the secretion of cytokines. Cells are then labeled with subset-specific monoclonal antibodies, fixed, permeabilized, and labeled with fluorescently tagged monoclonal antibodies specific for the cytokine of interest (Freer & Rindi, 2013; Qiu et al., 2014; Ghanekar, 2006). The assay has been developed with the presence of costimulatory antibodies for the sensitive detection of antigen responses in whole-blood cultures after relatively short incubation periods (Suni et al., 1998). Special attention is being focused on the development of antibodies that recognize the nascent forms of the cytokines (within the Golgi) and optimization of the timing of culture to detect maximal cytokine response (Mascher et al., 1999). Clinical studies have begun to demonstrate the potential utility of this technique. For example, patients suffering very severe burns who show a shift to a Th2 cytokine response may be at increased risk for the development of multiple-organ dysfunction syndrome (Zedler et al., 1999), and clinically active multiple sclerosis patients may show increased production of IL-10 (Inoges et al., 1999). Expansion of this technique to incorporate the ability to simultaneously measure proliferation and specific cytokine synthesis at the single-cell level has been reported but has not yet been evaluated in a clinical setting (Mehta & Maino, 1997). A version of this technique, the cytometric bead array (CBA) assay, uses multiple fluorescent particles of varying FI, each covalently coupled to a monoclonal antibody specific for a specific cytokine or other analyte (Morgan et al., 2004; Tarnok et al., 2003; Varro et al., 2007). Commercial CBA reagents, controls, and software are available for the simultaneous analysis of up to 30 proteins, including cytokines, chemokines, growth factors, immunoglobulins, and phosphorylated cell signaling proteins. In comparison to ELISA, CBA assays provide more rapid results with a higher dynamic range and lower sample requirements (Elshal & McCoy, 2006). The versatility of flow cytometric bead assays has been demonstrated by many other investigators. For example, Qi and coworkers developed a method for enzyme-free signal amplification on magnetic beads, combining the click chemistry–mediated ligation chain reaction in combination with the hybridization chain reaction using fluorophore-tagged hairpin probes (Qi et al., 2017). Flow cytometric analysis of the beads permitted analysis of microRNA at the femtomolar (fM) level.

Clearly, new assays are being developed that measure different events involved in T-cell activation. Methods and reagents are available to measure the earliest phosphorylation/dephosphorylation events through signal transduction, gene transcription, and cell division. As these methods are adapted for routine clinical use, we will have a veritable armamentarium of methods to assess many of the processes involved in lymphocyte activation and proliferation. Although many of these new technologies are still within the domain of research laboratories, the methods are constantly being simplified and adapted for use and evaluation in clinical laboratories.

Mixed Lymphocyte Culture

The mixed lymphocyte culture (MLC) assay is a special type of lymphocyte stimulation assay based on the ability of histoincompatible lymphocytes from one individual to stimulate the lymphocytes of another individual (mixed lymphocyte reaction) (Bach & Segall, 1974; Dupont et al., 1976; Mickelson & Hansen, 1990). Although complex in origin, the D locus of the HLA system is the major determinant of the MLC phenomenon. When two cells share common D loci, they are not able to stimulate each other, but when the D loci are different, the cells are stimulated. The MLC is unilateral (one way) when one group of cells is made incapable of responding (by treatment with radiation or mithramycin); it is bidirectional (two way) when no radiation or mithramycin is utilized. In the one-way MLC, untreated cells are termed the *responder population*, and treated cells are the *stimulator population* (Fig. 46.8).

Numerous factors must be considered in performance and interpretation of the MLC assay. Because the reaction is complex, lack of stimulation between two cell types cannot be considered as conclusive evidence of histocompatibility at the HLA-D locus. Other minor histocompatibility loci may also be involved as well as some non-HLA loci. In addition, specific and nonspecific serum factors can inhibit the assay, and lymphocytes from diseased individuals may not perform well. Numerous controls (including autologous controls) must be included, and the assay must be performed as expected for the results to be accepted as valid. The principal clinical use of the MLC assay is to assist in the selection of a compatible donor for a bone marrow transplant because the MLC is a predictor of host response to a transplanted organ. To prevent graft rejection or graft-versus-host disease, donor and recipient cells must be mutually nonstimulatory (El-Agroudy et al., 2004).

Flow cytometric quantitation of the cells or supernatant from the mixed lymphocyte reaction (MLR) has been reported. In the method reported by Cram and Kanda, nuclear DNA content during lymphocyte blastogenesis was determined with a DNA-specific fluorochrome (PI) (Cram et al., 1976; Kanda et al., 1985). With this technique, the proliferative index (percentages of cells in the S phase and G_2M phase of the cell cycle) is a direct measurement of de novo DNA synthesis. A good correlation ($r = 0.9493$) was observed between the flow cytometric measurement of the mixed lymphocyte reaction and the results using a traditional MLC with ^{3}H-thymidine incorporation. Other investigators have utilized BrdU, Ki-67, or CFSE for the flow cytometric quantitation of T-cell proliferation in the MLR (Bontadini et al., 1990; Marin et al., 2003; Palutke et al., 1987; Palutke et al., 1989; Onoe, 2003;Tanaka, 2005). Multiparametric analysis has also been used to measure nuclear DNA content in conjunction with T-cell subsets, activation antigens, apoptosis, cytokine secretion, dendritic cell maturation, and other parameters during the MLR (Fan et al., 2018; Lavergne & del Llano, 1990; Nguyen et al., 2003; Suresh et al., 2005; Uchida et al., 1987, 1988; Williams et al., 1984).

The MLC has also proven of great value when combined with other techniques in numerous basic and clinically related research studies of the immune system. For example, in recent studies, Fischbacher and coworkers (2015) studied T-cell activity following stem cell transplantation for acute myeloid leukemia by measuring cytokine concentrations in the supernatants of mixed-lymphocyte-culture reactions, while Oldhafer et al. (2019) used a mixed lymphocyte-hepatocyte culture to study the response of human hepatocytes to immunosuppressive agents.

CYTOTOXICITY ASSAYS

Cell death (cytotoxicity) is the endpoint commonly used in functional assays of the cellular immune system. In these assays, cell cytotoxicity may occur as the result of complement activity (complement-mediated cytotoxicity)

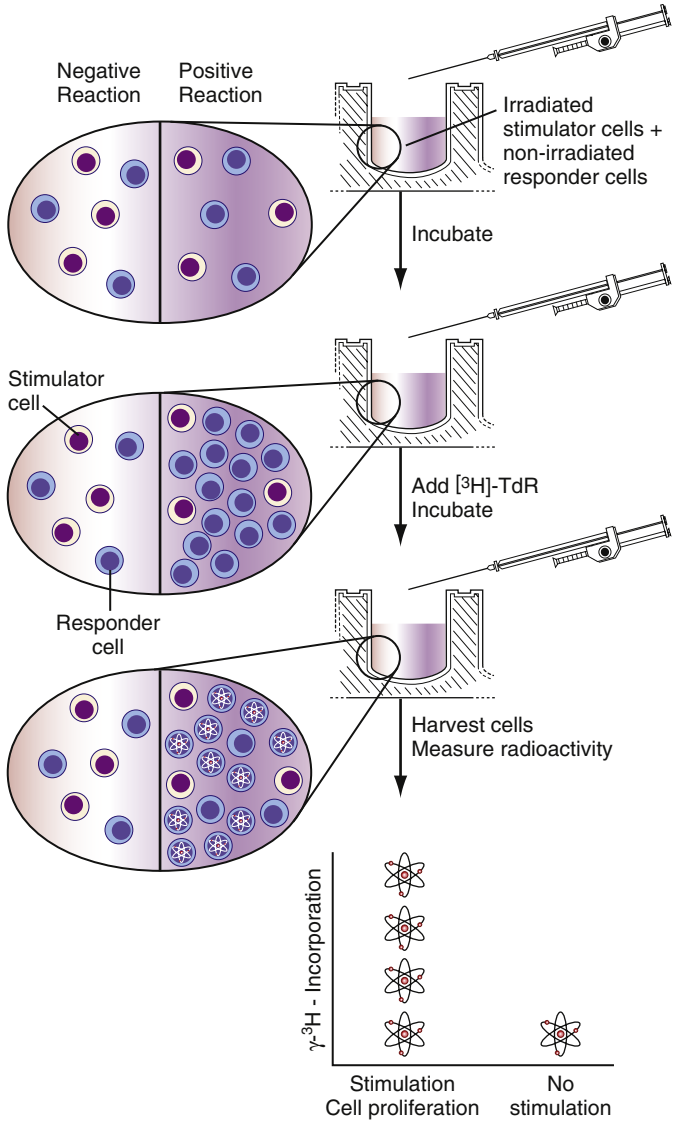

Figure 46.8 The one-way mixed lymphocyte culture assay (MLC). Irradiated stimulator cells, which are incapable of cell division, are mixed with nonirradiated responder cells, which can proliferate and divide. After incubation under cell culture conditions for approximately 1 week, responder cells proliferate in the presence of a disparity in the human leukocyte antigen (HLA)-D locus *(right side of diagram)*, but no proliferation occurs if the responder and stimulator cells are HLA-D compatible *(left side of diagram)*. Tritiated thymidine is added to the reaction mixture, and the degree of proliferation is determined by liquid scintillation counting. (Reprinted with permission from Riley RS: Basic principles of immunodiagnosis. In McClatchey KD, editor: *Clinical laboratory medicine*, Baltimore, 1994, Williams & Wilkins.)

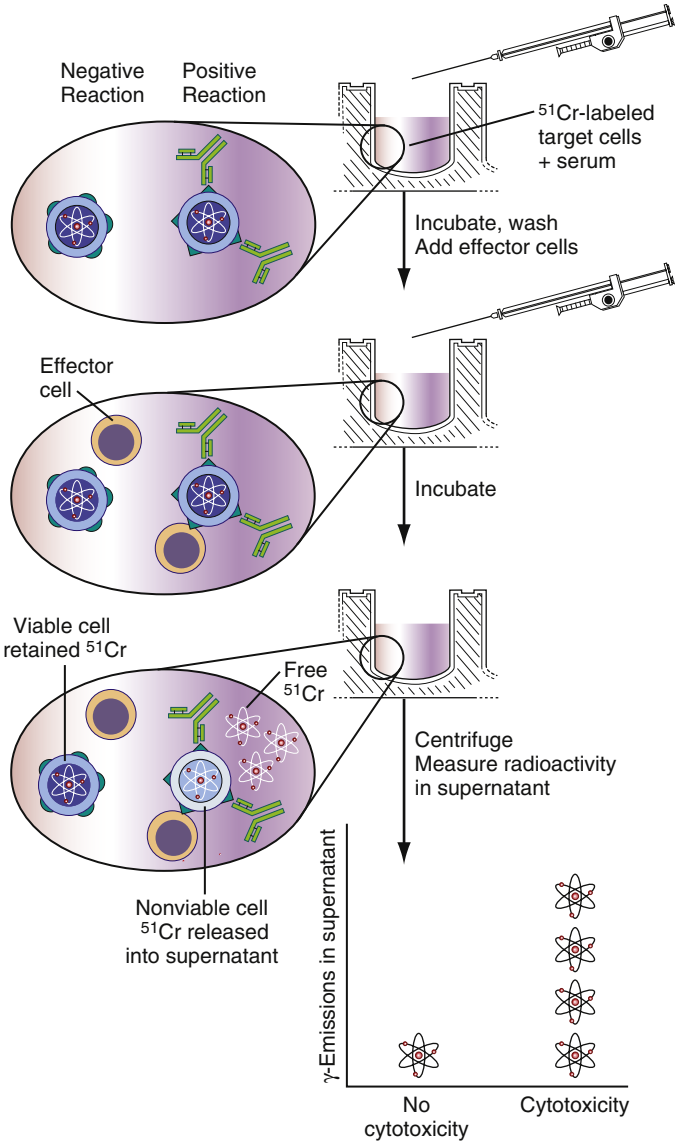

Figure 46.9 Principle of the antibody-dependent cell-mediated cytotoxicity (ADCC) assay. This assay is performed with mononuclear cells from a kidney organ donor or from several unrelated individuals (panel cells), which are stimulated with phytohemagglutinin (PHA) and labeled with ^{51}Cr. Following incubation with eluate from another nephrectomy specimen or from normal human serum, labeled cells are washed and incubated with effector cells from a normal unrelated individual. Radioactivity (γ-emissions) in the cells at the end of the experiment represents unlysed cells. The results are expressed as % cytotoxicity. (Reprinted with permission from Riley RS: Basic principles of immunodiagnosis. In McClatchey KD, editor: *Clinical laboratory medicine*, Baltimore, 1994, Williams & Wilkins.)

or may be due to the direct effect of one cell on another (cell-mediated cytotoxicity). Conventionally, target cell lysis is determined by the release of a substance such as ^{51}chromium (^{51}Cr) from the target cell upon death, or by the incorporation of a vital dye such as eosin or trypan blue. A variation of these assays, the microlymphocytotoxicity assay, is widely used in the clinical histocompatibility laboratory for human organ transplantation. However, the accuracy and reproducibility of these assays are often compromised by the length and technical complexity of the assays, technical problems such as poor uptake or nonspecific release of the marker, or the need for subjective interpretation of the results. The advent of new markers, in combination with the quantitative and multiparametric abilities of the flow cytometer, has made cytotoxicity assays much more practical for biomedical research studies. Other than in histocompatibility testing, these assays have not achieved widespread utilization in patient care.

Cytotoxic T-Cell (CTL) Assays

Cytotoxic T cells (CTLs, T killer cells, cytolytic T cells, CD8$^+$ T cells, killer T cells) constitute a subset of T cells important in the host defense against altered class I MHC-positive self cells, especially cells infected with a virus or other pathogen. CTLs recognize altered target cells by the presence of peptide fragments produced by processing of the foreign antigen and presented by the class I MHC receptor to the T-cell antigen receptor. Recognition of an MHC complex on a target cell by a CTL induces cell death by apoptosis by the granule-exocytosis pathway (granule endocytosis) or the FAS-FAS ligand pathway (Barry & Bleackley, 2002; Lieberman, 2003).

Transfused ^{51}Cr-labeled cells, especially red blood cells, have been used since the early 1950s to study cellular in vivo distribution and kinetics. In the early to mid-1960s, Goodman (1961), Sanderson (1964), and Wigzell (1965) independently described the use of ^{51}Cr-labeled mouse tumor of lymph node cells to study antibody-dependent complement-mediated cytotoxicity. Since that time, the **chromium release assay** has become the standard technique for the measurement of complement- or cell-mediated cytotoxicity. In the chromium release assay for cytotoxic T-cell activity, the binding of CTLs to infected ^{51}Cr-labeled target cells with virus peptide on syngeneic class I MHC induces apoptosis with the proportional release of ^{51}Cr into the supernatant (Fig. 46.9) (Burleson et al., 2018; Levin et al., 1978; van der Haar Avila et al., 2019). Alternatives for the chromium release assay were developed because of its disadvantages, including its relatively limited sensitivity and use of a radioisotope. The most widely employed alternative techniques include flow cytometry, imaging cytometry, chemiluminescence, and variations of the enzyme-linked immunosorbent assay (ELISA) (Fassy et al., 2017; La Muraglia et al., 2015; Rossignol et al., 2017).

Measurement of antibody- or cell-mediated cytotoxicity by flow cytometry is based on the discrimination of viable and nonviable cells with fluorescent dyes (Alheim, 2013; Liu et al., 2004; Lorenzo-Herrero et al., 2019; Popescu et al., 2014; van der Haar Avila et al., 2019). In addition to relatively high sensitivity, flow cytometry permits multiparametric analysis, with simultaneous detection of up to 12 or more markers at the single-cell level. The permeability of the cell membrane is the most widely used parameter of cell viability measured by flow cytometry. Damaged or nonviable cells have altered membrane permeability, and many leak some intracellular substances into the supernatant while losing the ability to prevent other dyes from penetrating the cell membrane. PI and 7-AAD were the first fluorescent dyes to be used for flow cytometric measurements of cell viability because they are excluded by live cells but rapidly penetrate cells with damaged membranes. Fluorescein diacetate, carboxyfluorescein diacetate (CFDA), and calcein are lipid-soluble, nonfluorescent probes that are metabolized by cytoplasmic esterases to produce a charged, fluorescent product that is retained within the cell if the cell membrane is intact (Fassy et al., 2017; Talbot et al., 1987; Zarcone et al., 1986). Other dyes used for viability determination include PKH-1 (Slezak & Horan, 1989), hydroxystilbamidine methanesulfonate (Fluoro-Gold [FG]) (Barber et al., 1999), SYTO13 (Shenkin, 2007), Cell Tracker Orange (Kim et al., 2007), and calcofluor white M2R (Berglund et al., 1987). In many cases, the simultaneous use of two or more markers permits the most accurate measurement of cytotoxicity. One example is the use of PKH-1 in conjunction with PI. PKH-1 is a fluorochrome that emits light in the green region of the spectrum, binds avidly to the cytoplasmic membrane, and is not transferred to other cells. In one application, PKH-1 is used to label the target cells, while a second fluorochrome with a red emission signal (PI) is used to detect nonviable cells (Slezak & Horan, 1989). This combination of markers allows statistically valid quantitation of both dead and live effectors and targets, permitting the simultaneous determination of percent target lysis, effector-to-target ratio, viability of the effector cells at the termination of the assay, and viable effector-to-target cell ratios.

The enzyme-linked immunospot (ELISPOT) assay is a very sensitive, extremely versatile adaptation of the sandwich ELISA (Kalyuzhny, 2005; Sedgwick, 2005). Originally described by Czerkinsky and coworkers in 1983 to detect individual B cells secreting antigen-specific antibodies, the ELISPOT was rapidly adapted to detect T-cell cytokine excretion (Arvilommi, 1996; Czerkinsky et al., 1983; Schmittel et al., 2000; Stott, 2000). Because the ELISPOT assay can reproducibly detect the proportion of antigen-specific or cytokine-secreting cells at a sensitivity of 1/100,000 to 1/1,000,000, it has achieved widespread use in research involving cancer, infectious disease, immune disease, and solid-organ transplantation (Augustine & Hricik, 2012; Caspell & Lehmann, 2018; Hwai et al., 2018; Lehmann & Zhang, 2012; Pike et al., 2016; Slota et al., 2011). Clinically, the ELISPOT is used in immune monitoring and the detection of latent tuberculosis and CMV infection (Achkar et al., 2011; Chanouzas et al., 2018; Favi et al., 2017; Rego et al., 2018). The ELISPOT utilizes polyvinylidene fluoride (PVDF)-backed microplates coated with a monoclonal or polyclonal capture antibody specific for the desired analyte, usually IFN-γ (Kalyuzhny, 2005; Weiss, 2012). A cell suspension and appropriate antigens or mitogens are added to the microplates, and they are incubated in a humidified carbon dioxide (CO_2) incubator at 37°C for a specified time. The plates are washed to remove cells and debris, a biotinylated polyclonal antibody specific for the analyte is added, the plates are washed a second time to remove unbound antibody, and avidin-horseradish peroxidase and a precipitating substrate is added to develop the assay. Colored spots on the plate represent individual analyte-producing cells (Fig. 46.10). The spots can be manually or automatically detected and counted (Neubauer et al., 2018; Zadorozhny & Martynov, 2018). A variation of this assay using fluorochrome-labeled antibodies (Fluorospot assay) permits the simultaneous detection of two or three cytokines (Ahlborg & Axelsson, 2012; Gazagne et al., 2005; Janetzki et al., 2014; Rebhahn et al., 2008). A variation of the ELISPOT for the detection of granzyme B, rather than IFN-γ, has shown better correlation with the chromium release assay for the measurement of cytotoxic T cell activity (Ranieri et al., 2014; Salk et al., 2013; Shete et al., 2017).

Natural Killer Cell–Mediated Cytotoxicity

NK cells are critical members of the innate immune system characterized by their capability to lyse target cells without prior sensitization, termed *spontaneous cell-mediated cytotoxicity* (Bodduluru et al., 2015; Cruz-Munoz et al., 2019; Mace & Orange, 2019; Moretta et al., 2014; Poli et al., 2018; Sinkovics, 2005). NK cells play an essential role in immunoregulation and immunosurveillance, particularly against viruses and tumors (Falco et al., 2019; Vitale et al., 2019). They are functionally and immunophenotypically heterogeneous but have traditionally been divided into two distinct groups defined by the surface density of CD16 and CD56 (i.e., CD56bright/CD16dim, CD16bright/CD56dim) (Bryceson et al., 2010; Lanier, 2014; Milush et al., 2009; Morice, 2007; Poli et al., 2009; Wilk & Blish, 2018). Release of ^{51}Cr from labeled target cells is the standard method for the characterization of NK cells (Friberg et al., 1996). The chronic myeloid leukemia cell line K562 has been used as the standard target in these assays. A variety of other techniques are under evaluation because the ^{51}Cr-release technique has many disadvantages, including the use of radioisotopes, low sensitivity, and the spontaneous release of ^{51}Cr. These methods include the incorporation of radioactive nucleotides during cell proliferation, dye exclusion, target cell enzyme release, image analysis, and flow cytometry (Fassy et al., 2017). Flow cytometric analysis has been performed using a wide variety of markers to differentiate live and dead target cells, including CFDA, PI, Hoechst 33342, fluorochrome octadecylamine-fluorescein isothiocyanate (F-18), usually in combination with multiparametric analysis of cell surface makers, degranulation, cytokine production, and other parameters (Bryceson et al., 2010; Lee et al., 2014; Mhatre et al., 2014; Ortaldo et al., 2014; Scherbakova et al., 2013; Li, 2018; Wong, 2019).

Microlymphocytotoxicity Assay

The dye exclusion lymphocytotoxicity assay is the standard technique for the detection of an antibody–antigen interaction on a cell surface. The lymphocytotoxicity assay was introduced by Terasaki and McClelland in 1964 and was later accepted as the National Institutes of Health standard procedure for histocompatibility testing (Terasaki & McClelland, 1964). In the histocompatibility laboratory, variations of the lymphocytotoxicity assay are used for HLA typing, detection of anti-HLA antibodies, and crossmatch testing (Bilgen et al., 2019; Duquesnoy & Marrari, 2003; Fidler, 2012).

In the lymphocytotoxicity procedure, viable cells (usually lymphocytes) are incubated with serum-containing antisera. If a cell surface antigen is present that is recognized by antibodies in the sera, an antigen–antibody complex will form on the surface. These complexes are detected by the sequential addition of rabbit complement and a vital dye, such as eosin, to the reaction mixture. The occurrence of complement fixation on the cell membrane leads to activation of the terminal complement components, and eventually to cell lysis and death. Dead cells are detected and counted by phase microscopy after differential uptake of the eosin dye and fixation with formalin. Antibody-bound lymphocytes will die, take up the eosin dye, and give a positive reaction. Unbound lymphocytes will remain viable, exclude the eosin dye, and give a negative reaction (dye exclusion; Fig. 46.11).

LABORATORY EVALUATION OF GRANULOCYTE AND MONOCYTE FUNCTION

Monocytes and granulocytes are extremely important in the early inflammatory response. Abnormalities in their functions lead to profound deficiencies in cellular immunity (Boyette et al., 2017; Ley et al., 2018; Liew & Kubes, 2019). The activity of neutrophils and macrophages is complex and involves activation of the cell, margination and passage through the vessel wall (diapedesis), movement toward an inflammatory stimulus (chemotaxis, chemokinesis), opsonization, engulfment of the offending agent (phagocytosis), and intracellular killing via the generation of toxic oxygen radicals (Hidalgo et al., 2019; Roberts & Hallett, 2019; Zarbock & Ley, 2009). Until the modern era of flow cytometry, laboratory analysis of these nonspecific immune parameters was difficult to measure, with available assays being subjective and lacking standardized methods and quality control. In contrast to the subjective assays, many flow cytometric studies are rapid, reproducible, and statistically valid. In addition, the multiparametric capabilities of the flow cytometer permit the simultaneous determination of several cell functions as well as an assessment of the interrelationship between cell function and other parameters (Elloumi & Holland, 2014; O'Gorman et al., 2011). Flow cytometric assays have been described for the measurement of phagocytosis of microorganisms, degranulation and enzymatic activity, intracellular killing and degradation of microorganisms, exocytosis, opsonization, oxidative metabolism, membrane potential, phagosomal pH, calcium mobilization, F-actin assembly, cell volume, apoptosis, receptor expression, adhesion and aggregation, and other parameters (Elbim & Lizard, 2009; Nordenfelt, 2014; Sharma et al., 2014; van Eeden et al., 1999; Zarbock & Ley, 2009).

ASSAYS OF NEUTROPHILIC ACTIVATION

Neutrophil activation results when stimulatory substances (e.g., chemotactic factors, immune complexes, opsonized particles) bind to surface

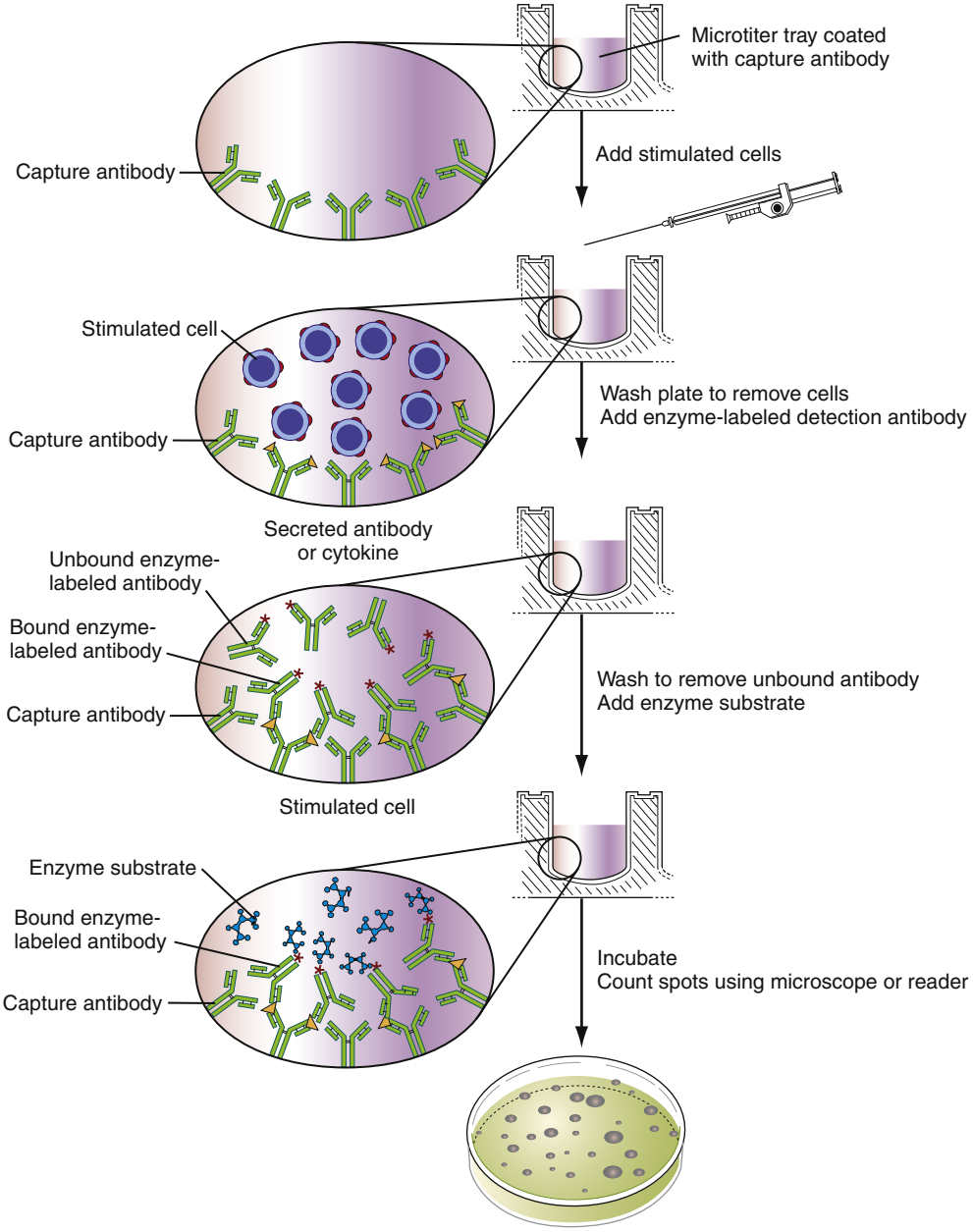

Figure 46.10 Principle of the enzyme-linked immunosorbent spot (ELISPOT) assay. ELISPOT assays bear many similarities to conventional sandwich enzyme-linked immunosorbent assays. A polyvinylidene difluoride (PVDF)–backed microplate is immobilized with an antibody specific for the analyte under evaluation. Immune cells are stimulated with an appropriate antigen or mitogen and then are pipetted into the wells of the microplate. The microplate is incubated in a humidified carbon dioxide (CO_2) chamber at 37°C for a specified period of time during which stimulated immune products, such as cytokines and antibodies, are secreted. The secreted analyte binds to the immobilized antibody on the microplate. The microplate is washed to remove cells and unbound substances, and a biotinylated polyclonal antibody specific for the chosen analyte is added. Unbound biotinylated antibody is removed by washing, and streptavidin conjugated with alkaline-phosphatase conjugate is added. Following another wash to remove unbound enzyme, the reaction is completed by the addition of the enzyme substrate solution (BCIP/NBT). Dark, blue-black precipitate spots mark the original locations of analyte-secreting cells. The spots can be counted manually under a stereomicroscope, or automatically with a commercial automated ELISPOT reader system.

receptors to initiate metabolic and structural changes in the cell that result in locomotion, degranulation, phagocytosis, the oxidative burst, and other processes. Early studies of neutrophil activation utilized 7-nitrobenz-2-oxa-1,3-diazole-phallacidin, a fluorescent derivative of an acidic phallotoxin isolated from mushrooms of the *Amanita* genus, to measure changes in the equilibrium of F-actin that occur during cell activation (Belloc et al., 1990; Packman & Lichtman, 1990). However, the flow cytometric detection of neutrophil activation antigens—especially CD11b, CD13, and CD64—has become the standard technique for studies of neutrophil activation, usually performed in conjunction with other measurements of intracellular neutrophil function, such as the oxidative burst and measurement of the production and release of neutrophil secretion products such as myeloperoxidase, neutrophil elastase, and lactoferrin (Alvarez-Larran et al., 2005; Grey et al., 2011).

ASSAYS OF PHAGOCYTOSIS AND ENDOCYTOSIS

Conventional analysis of phagocytosis uses particles that are visible within the cell and can be counted after ingestion or an ingestible substance that can be extracted from the cell and measured. Live or heat-killed *Candida albicans* or staphylococci fulfill the first criterion and permit a simple, convenient means of measuring phagocytosis. Target cells (i.e., neutrophils and monocytes) are incubated with yeast particles in fresh serum, Giemsa-stained cell preparations are made, and 200 cells are examined and counted for the presence of ingested microorganisms (Lehrer, 1970; Lehrer & Cline, 1969). The results are expressed as the percentage of target cells showing phagocytosis and the number of particles per phagocytic neutrophil. Oil droplets containing dissolved oil red O stain and coated with *Escherichia coli* liposaccharide and C3 complement have also been used for the measurement of phagocytosis.

Flow cytometric assays of phagocytosis are quantitative and more accurate than subjective studies using visual counting of phagocytosed microorganisms. Different investigators have used a variety of labeled targets to study phagocytosis by both neutrophils and monocytes. Labeled targets have included fluorescent beads coated with opsonins (Bassøe & Bjerknes, 1985; Bassøe et al., 1983; Bjerknes, 1984; Bjerknes, 1989; Bjerknes & Bassøe, 1984; Dunn & Tyrer, 1981; Ogle et al., 1988; Steinkamp et al., 1982), fluorescein-labeled *C. albicans* (Busetto et al., 2004), FITC-labeled zymosan particles (Nuutila & Lilius, 2005), fluorescein-labeled *Staphylococcus aureus* (Carvalho et al., 2009), fluorescein-labeled *E. coli* (Cacciapuoti et al., 2007; Danikas et al., 2008; Hirt et al., 1994), enhanced green fluorescent protein (EGFP)–expressing *E. coli* (Bicker et al., 2008; Gille et al., 2006), bis-carboxyethyl-carboxyfluorescein pentaacetoxymethylester-labeled *C. albicans* (Pattanapanyasat et al., 2007), and Oregon Green (Nordenfelt, 2014). For example, green fluorescent microspheres coated with C3b, iC3b, IgG, mixtures of these substances, bovine serum albumin, or human F(ab′)2 are utilized in the technique developed by Ogle and collaborators (1988). In this assay, neutrophils are incubated with coated

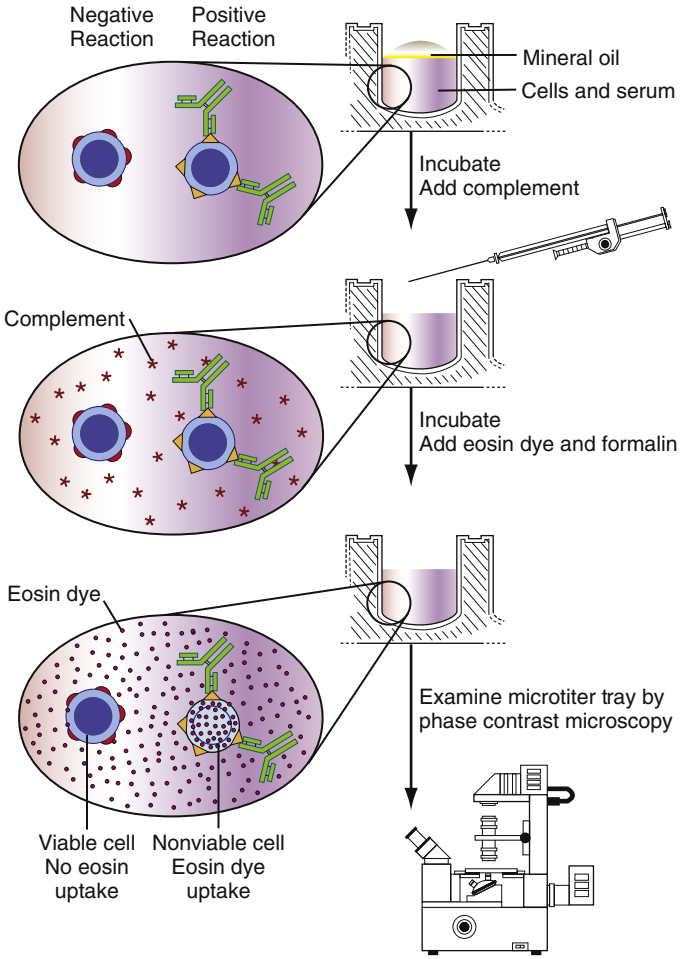

Figure 46.11 Principle of microlymphocytotoxicity by dye exclusion. Cells and serum are incubated together in the wells of a microtiter tray. Mineral oil at the top of the wells prevents fluid evaporation. Complement is added, and a second incubation is performed. The cells are washed, eosin is added, and the cells are fixed with formalin. Cells that fixed antibody and were killed through the action of complement take up eosin and appear dark and nonrefractive under a phase-contrast microscope. In contrast, living cells are refractive and are easily identified by phase-contrast microscopy. Variations of the microlymphocytotoxicity assay are used for human leukocyte antigen (HLA) typing, HLA crossmatch, and detection of anti-HLA antibodies. (Reprinted with permission from Riley RS, Mahin EJ, Ross W: *Clinical applications of flow cytometry*, New York, 1993, Igaku-Shoin Medical Publishers.)

microspheres alone or in the presence of cytochalasin D to inhibit phagocytosis. Externally bound microspheres are then stained with a red-labeled antibody against the immobilized ligand(s), and flow cytometric analysis is performed. The ratio of red-to-green fluorescence in the cytochalasin D–inhibited mixtures is used to correct the uninhibited mixtures for externally bound, nonphagocytosed particles. Net phagocytosis is thus represented by the corrected green fluorescence. The specificity of this technique was confirmed with the use of fluid phase C3b and iC3b and monoclonal antibodies to the receptors. The recent development of more sophisticated multiparametric assays, such as mass cytometry, which combines flow cytometry with mass spectrometry, has permitted researchers to measure phagocytic activity simultaneously with cell signaling, transcriptional events, and the quantitation of multiple proteins (Schulz et al., 2019).

Receptor-mediated endocytosis is a common method for the cellular uptake of viruses, hormones, proteins, toxins, and other ligands (Schmid, 2019). Endocytosis is a complex process that involves capping, internalization of the ligand, intracellular movement, and entry of the ligand into a subcellular compartment. Fluorescent dyes were first used to study endocytosis by Ohkuma and Poole (1978), who studied intralysosomal pH in living cells using a fluorometer and FITC-dextran. Subsequent investigators have used flow cytometry and fluorescent-labeled ligands or liposomes to follow the internalization of various ligands, while others have utilized changes in pH sensitivity to study internalization and/or intracellular movement (Becker et al., 1997; Elguindi et al., 1985; Finney & Sklar, 1983; Metezeau et al., 1982; Murphy et al., 1984; Murphy et al., 1984; Ruud et al., 1989; Truneh et al., 1983; van Deurs et al., 1984). A different technique was utilized by Wang Yang et al. (1988), who utilized

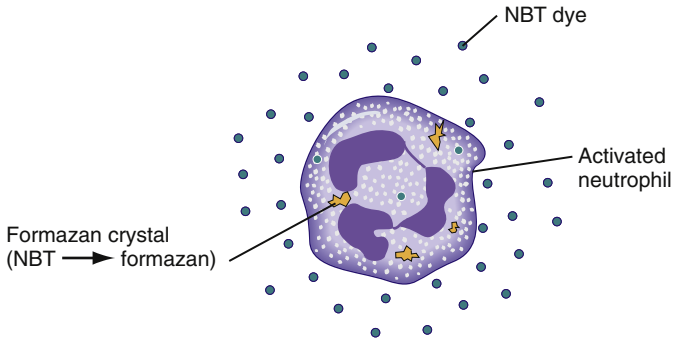

Figure 46.12 Principle of the nitroblue tetrazolium (NBT) reduction assay. Neutrophils are incubated with NBT. Enzymatic activity in the activated neutrophil converts NBT into an insoluble brownish-black precipitate (formazan), which is visible under the microscope. The proportion of neutrophils with intracytoplasmic precipitated material is determined. (Reprinted with permission from Riley RS: Basic principles of immunodiagnosis. In McClatchey KD, editor: *Clinical laboratory medicine*, Baltimore, 1994, Williams & Wilkins.)

flow cytometric pulse profiles to study capping and endocytosis by mouse B lymphocytes and BCL_1 cells. In this assay, the cells were stained with FITC-labeled anti-immunoglobulin and were permitted to undergo changes in a temperature-controlled flow cytometer sample compartment. Cap formation resulted in decreases in area values from pH-dependent quenching as the internalized antibody entered the acidic subcellular compartments. Fattorossi et al. (1989) described a related procedure utilizing FITC-conjugated, heat-killed *C. albicans* (F-Ca) opsonized with purified antibodies or normal human serum. Neutrophils were first incubated with the labeled, opsonized *Candida* particles and subsequently with ethidium bromide. Although ethidium bromide does not penetrate intact cell membranes, it binds to membrane-bound particles and causes a shift from green to red fluorescence through resonance energy transfer. Because internalized particles retain green fluorescence, the number of internalized or surface-bound particles can be ascertained by contour plot analysis. Fluoresceinated derivatives of α-fetoprotein and transferrin were used by Torres et al. (1990) to study the endocytosis of these substances, and Fibach et al. (1988) studied the uptake of a fluorescent fatty acid derivative [12-(1-pyrene) dodecanoic acid] by a variety of peripheral blood cells. Flow cytometry and electron microscopy were used by Kershaw et al. (2009) to study the endocytosis and intracellular trafficking of chemokine CCR5, while Clark and coworkers (2019) used z-stack confocal microscopy and flow cytometry to study marker expression during the endocytosis and processing of *Aspergillus fumigatus* conidia by the BEAS-2B cell line derived from respiratory epithelial cells.

ASSAYS OF ENZYMATIC ACTIVITY AND INTRACELLULAR KILLING

Intracellular killing of microorganisms is mediated by complex enzymatic mechanisms. Oxygen-dependent mechanisms of cell killing are the most important, although oxygen-independent mechanisms have also been described. The increase in oxidative metabolism during phagocytosis is referred to as the *oxidative burst* (Thomas, 2017). During this process, the key event is the activation of a membrane-bound pyridine nucleotide-dependent oxidase (NADPH oxidase), which reduces oxygen to O_{2-} (superoxide anion) and oxidizes NAD(P)H to $NAD(P)^+$ (Buvelot et al., 2019). Subsequently, hydrogen peroxide (H_2O_2), hydroxyl radical (OH), and singlet oxygen are generated. All of these compounds are directly toxic to the cell, with the H_2O_{2-} halide-myeloperoxidase system being the most important mechanism of bacterial killing. In the presence of H_2O_2 and halide ions (I^-, Cl^-), myeloperoxidase catalyzes direct halogenation of the bacterial cell wall and causes damage to the cell wall by converting amino acids into aldehydes.

In the clinical laboratory, the nitroblue tetrazolium (NBT) reduction assay is the conventional method for determination of the oxidative capacity of the neutrophil. NBT is a yellow dye in its oxidized state, but when reduced, it forms formazan, a crystalline substance that has a deep blue color (Fig. 46.12) (Urban & Jarstrand, 1979). NBT can be attached to latex particles or microorganisms to permit phagocytosis or it can be ingested in soluble form by neutrophils that have been stimulated by endotoxin or other means. If the normal oxidizing environment in the phagolysosome is present, the resultant blue particles can be detected microscopically or the formazan can be extracted and measured spectrophotometrically. Approximately 10% of normal unstimulated neutrophils ingest and reduce NBT, but this is increased to 80% with stimulated neutrophils.

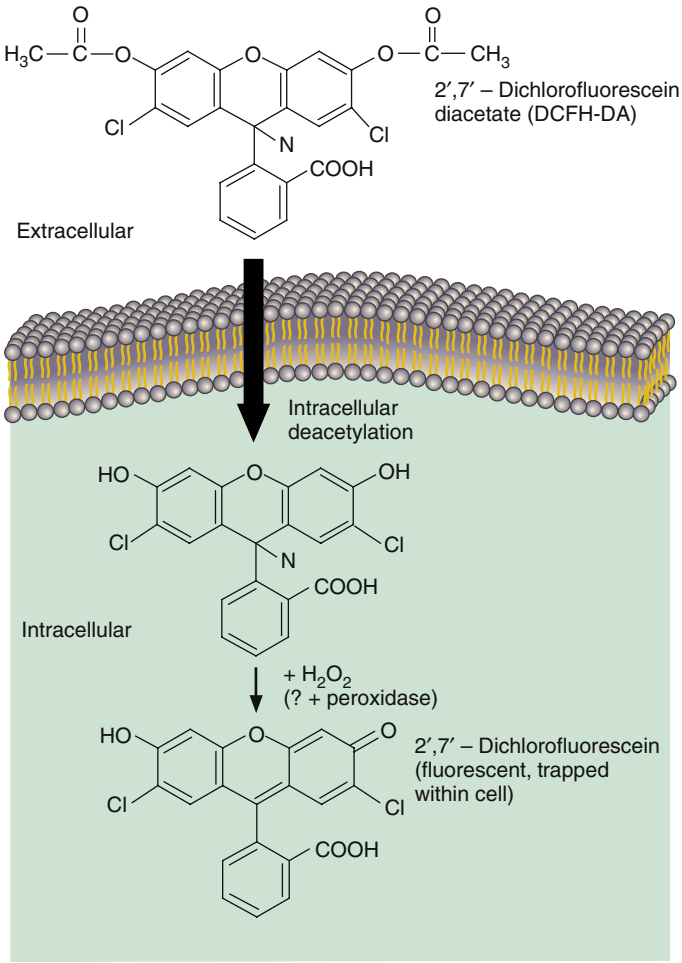

Figure 46.13 Flow cytometric analysis of the oxidative burst of polymorphonuclear leukocytes. In this assay, dichlorofluorescein-diacetate (DCFH-DA) is taken up by the cell and is trapped by deacetylation, with the formation of 2′,7′-dichlorofluorescein. During the oxidative burst, nonfluorescent 2′,7′-dichlorofluorescein is converted into the fluorescent product dichlorofluorescein. The fluorescent intensity in the green region of the spectrum is proportional to the oxidative capacity of the cell. (Reprinted with permission from Bass DA, Parce JW, Dechatelet LR, et al.: Flow cytometric studies of oxidative product formation by neutrophils: a graded response to membrane stimulation. *J Immunol* 130:1910–1917, 1983.)

A flow cytometric variation of the NBT assay has been described. With this technique, neutrophils are incubated for a short time with FITC-labeled Con A, rendering the cell membrane fluorescent (Fattorossi et al., 1990). The cells are then incubated with NBT and an agent to trigger respiratory activity, such as phorbol myristate acetate. The formazan that is subsequently produced has a distinct fluorescent peak at 520 nm that corresponds with the peak emission of fluorescein, and fluorescence quenching of surface fluorescence by formazan is proportional to the intensity of the respiratory burst. In addition, simultaneous changes in cell size and forward light scatter occur.

Bass et al. (1983) described one of the first non–NBT-based flow cytometric–based assays to measure neutrophil oxidative metabolism and oxidative burst at the single-cell level. This technique uses the fluorogenic substrate dichlorofluorescein-diacetate (DCFH-DA) to quantitate H_2O_2 production during the oxidative burst (Bass et al., 1983). DCFH-DA is a small, nonpolar substance that is actively taken up by the cell and deacetylated by intracellular esterases into a nonfluorescent compound (2′,7′-dichlorofluorescein [DCFH]), which is trapped within the cell. In the presence of H_2O_2 and peroxidase, DCFH is oxidized into dichlorofluorescein, which is highly fluorescent in the green region of the spectrum (Fig. 46.13) (Bass et al., 1983). Other fluorochromes that have been used to directly measure the oxidative burst include dihydrorhodamine 123, dihydrotetramethylrosamine, 4-carboxydihydrotetramethylrosamine succinimidyl ester, and hydroethidine (Chen & Junger, 2012; Elbim & Lizard, 2009; Model et al., 1997; Smith & Weidemann, 1993; Walrand et al., 2003).

Flow cytometric measurements of the oxidative burst have been combined with the quantitation of other metabolic or antigenic changes in the phagocytic cell to fully utilize the multiparametric power of the flow cytometer. In particular, several investigators have described flow cytometric techniques for the simultaneous measurement of phagocytosis and intracellular killing. In one of the earliest studies, phagocytic activity was determined by the internalization of viable, FITC-labeled *C. albicans* (Bjerknes, 1984). At selected intervals, fungi were extracted from the cells, and the fraction of killed fungi was measured by the uptake of PI. Later variations of this technique were developed to simultaneously measure phagocytosis and the oxidative burst (Carvalho et al., 2009; Fine et al., 2017; Lehmann et al., 1998; McCloskey & Salo, 2000; Meaney et al., 2016; O'Gorman, 2018; Prodan et al., 1995; Trinkle et al., 1987).

A technique for the assessment of surface antigen expression, phagocytosis, and cell proliferation in human bone marrow cells was described by Lund-Johansen et al. (1990). With this technique, incubation of leukocytes with ethidium monoazide-labeled *C. albicans*, followed by staining with an FITC-labeled monoclonal antibody, permitted correlation of surface antigen expression with phagocytic capacity. After incubation with the labeled *C. albicans*, aliquots of the cells were fixed and stained with PI for cell cycle analysis. Haynes et al. (1990) reported a novel method to measure protein digestion within the phagocytic vacuole based on the fluorescent quenching that occurs when rhodamine is attached to albumin at a high molar ratio. In the phagocytic vacuole, digestion of albumin releases free rhodamine and restores fluorescence. This method was affected less by vacuole pH than fluorescein-based methods and measured digestion even in the presence of abnormal phagocytosis.

ASSAYS OF OPSONIZATION

Phagocytosis of microorganisms and other foreign bodies is greatly enhanced by the presence of certain chemical substances (opsonins) on the surface of the foreign body. In patients with certain immunoglobulin and complement deficiencies, increased susceptibility to infection results in part from decreased opsonization. Opsonins in the serum can be detected by incubating the serum with normal neutrophils and yeast particles, and by visually quantitating phagocytosis of yeast particles by normal neutrophils. In addition, flow cytometric methods have been used for the measurement of serum opsonin function (Bassøe & Bjerknes, 1984; Sjursen et al., 1987; Sjursen et al., 1989; Sjursen et al., 1987). In this assay, live FITC-labeled *Neisseria meningitidis* organisms were preopsonized by incubation with serum for 7.5 minutes and then were incubated with human polymorphonuclear neutrophilic leukocytes (PMNLs) for 5 minutes at a bacteria-to-PMNL ratio of 20:1. Results were expressed in the number of bacteria incubated per phagocyte. High-throughput flow cytometry was recently used by Teo et al. (2015) to quantitate opsonic antibodies against erythrocytes infected with *Plasmodium falciparum* parasites.

ASSAYS OF MEMBRANE PERMEABILITY

Fluorescein diacetate has been extensively utilized to monitor changes in membrane permeability. In this regard, fluorescein diacetate is enzymatically hydrolyzed within the cell, with the production of fluorescein. Free fluorescein is released into the extracellular environment across the cell membrane through a process that follows energy-dependent, first-order kinetics and that is dependent on membrane integrity and permeability. The efflux of fluorescein is inhibited by metabolic poisons and glucose depletion, and has been used to study the effects of a variety of agents on the cell membrane (Prosperi et al., 1985, 1986). Prosperi (1990) showed that the fluorescein efflux is also related to the ionic gradient (membrane potential) of the cell.

QUALITY CONTROL AND QUALITY ASSURANCE IN THE CELLULAR LABORATORY

Throughout this chapter, we have tried to point out areas where the clinician and laboratory staff must pay particular attention to the methods used and the interpretations made in evaluation of the cellular response. Quality assurance and quality control parameters are not well defined in this area of the laboratory, and few absolute standards exist as compared with chemistry analytes or humoral antibody measures. The success of the cellular laboratory rests in its approach to the problem and the longitudinal assessment of the condition being diagnosed. It was clearly pointed out that baseline studies need to be repeated if the original evaluation is performed at a time of immunologic stress.

Basic parameters of diurnal variations in lymphocyte subsets are obvious but are often forgotten or overlooked. Malone (1990) pointed out that

variability in CD4 measures of absolute counts is 50% owing to biology, with the other 50% related to other technical issues (Malone et al., 1990). Factors affecting the longitudinal evaluation of CD4 absolute counts in a clinical trial setting have been reviewed by Fei et al. (1993). Furthermore, Fahey et al. (1990) reviewed the prognostic value of both humoral and cellular assays in HIV. With other clinical cellular assays, variability is inherent in the assay owing to lack of standard formats and methods as well as reagents. Furthermore, instrument calibration and sensitivity are not well monitored. Cytotoxic T lymphocyte assays are particularly difficult to standardize. Historic assays such as mitogen proliferation are also fraught with variability between laboratories. Therefore, laboratories that offer these immunologic tests must have an extensive database by which they can interpret an individual patient's result. Cellular laboratories must establish normal ranges for their assays and must be aware that adult normal ranges are not applicable to pediatric assays. This is particularly problematic because pediatric normal ranges are difficult to determine owing to lack of available subjects in the first year of life, and correct interpretation of laboratory results depends on these normal values. Data between laboratories should be compared carefully.

When available, a cellular immunology laboratory must use available standards in the performance of flow cytometry and DNA analysis, and should be aware of state and federal regulations with regard to the laboratory, including the Human Health and Services Clinical Laboratory Improvement Act of 1988. Furthermore, laboratory staff should participate in proficiency testing, when available, and should be involved in continuing education seminars, including competency evaluations for all personnel involved in testing. All assays performed in the laboratory must include a normal control and, when possible, in-process controls to establish the validity of the assay. Shipped samples must be carefully monitored for exposure to heat and cold and time since patient procurement. A clinical history should accompany the samples for particular studies being ordered so that the laboratory director can take the correct approach to testing.

A consensus document with recommendations on the immunophenotypic analysis of hematologic neoplasia by flow cytometry has been published (Braylan et al., 1997). This document was painstakingly developed by concerned providers in the medical community to cover laboratory procedures, selection of antibodies for identification of neoplasms, data analysis and interpretation, medical reporting, and indications in the absence of standardized kits and other devices. The FDA has put into effect the Analyte Specific Regulation (ASR) (Analyte Specific Regulation, 1997), which moves reagents such as monoclonals from research use status to ASRs (Analyte Specific Regulation, Nov. 21, 1997). This rule does not allow manufacturers to tell laboratory users how to use their reagents. They cannot specify intended use. The ASR rule does provide for stable, well-defined reagents manufactured under good manufacturing practices. All laboratories using these reagents as a "home brew test" must perform their own clinical trial and validation studies and must use a disclaimer in the final report. The consensus document allows a laboratory to perform its assays in a consistent manner and in keeping with the definition of clinical significance used across a large number of laboratories and institutions. The document is not a standard but is consistent with other published standards from the NCCLS that are already in use.

The cellular laboratory is faced with a more difficult job of interpretation because the data are not easily standardized. Furthermore, quality assurance of the sample and the evaluation being performed depends on careful documentation of biological and logical parameters that may influence the results. The future of tests used in evaluation of the cellular component of the immune response resides in the development of new methods that may lend themselves to better standardization.

SELECTED REFERENCES

Adan A, Alizada G, Kiraz Y, Baran Y, Nalbant A: Flow cytometry: basic principles and applications, *Crit Rev Biotechnol* 37(2):163–176, 2017.
A concise review of the technologic aspects and biomedical applications of flow cytometry.

Allsopp CE, Nicholls SJ, Langhorne J: A flow cytometric method to assess antigen-specific proliferative responses of different subpopulations of fresh and cryopreserved human peripheral blood mononuclear cells, *J Immunol Methods* 214:175–186, 1998.
The authors of this paper describe a useful approach to analyzing lymphocyte proliferative responses to antigen that makes use of a stable membrane-bound dye in combination with surface monoclonal antibody labels to identify subpopulations without the need for presorting.

Ananworanich J, Shearer WT: Delayed-type hypersensitivity skin testing. In Rose NR, Hamilton RG, Detrick B, editors: *Manual of clinical laboratory immunology*, ed 6, Washington, DC, 2002, ASM Press, pp 212–219.
This paper provides a practical and comprehensive review of skin testing for evaluation of the cellular immune response.

Balkwill FR, Burke F: The cytokine network, *Immunol Today* 10:299–304, 1989.
A concise review of cytokines and cytokine function.

Barry M, Bleackley RC: Cytotoxic T lymphocytes: all roads lead to death, *Nat Rev Immunol* 2:401–409, 2002.
This paper provides a thorough review of cytotoxic T-cell function.

Baumgarth N, Roederer M: A practical approach to multicolor flow cytometry for immunophenotyping, *J Immunol Methods* 243:77–97, 2000.
This article describes basic multicolor flow cytometry, technical problems that may be expected, and artifacts frequently encountered, offering suggestions for handling them.

Beutler BA: TLRs and innate immunity, *Blood* 113:1399–1407, 2009.
This article is a succinct, up-to-date review of innate immunity and the role of Toll-like receptors.

Bjerknes R, Bassøe C-F, Sjursen H, Laerum OD, Solberg CO: Flow cytometry for the study of phagocyte functions, *Rev Infect Dis* 11:16–33, 1989.
The authors present a comprehensive review of the evaluation of phagocytic cell function by flow cytometry.

Bryceson YT, Fauriat C, Nunes JM, et al.: Functional analysis of human NK cells by flow cytometry, *Methods Mol Biol* 612:335–352, 2010.
This article is a current, thorough review of NK cell function analysis by flow cytometry.

Chaplin DD: Overview of the immune response, *J Allergy Clin Immunol* 125:S3–23, 2010.
This article provides a concise, well-written, up-to-date summary of the immune system.

Cossarizza A, De Biasi S, Gibellini L, et al.: Cytometry, immunology, and HIV infection: three decades of strong interactions, *Cytometry* 83:680–691, 2013.
Aa review of the research and clinical applications of flow cytometry in HIV infection, emphasizing the integration of basic discoveries in diagnosis, treatment, and monitoring.

Elbim C, Lizard G: Flow cytometric investigation of neutrophil oxidative burst and apoptosis in physiological and pathological situations, *Cytometry* 75:475–481, 2009.
An excellent review of fluorescent probes and flow cytometric techniques for evaluation of neutrophil function, with an emphasis on primary immuno deficiency disease.

Falco M, Pende D, Munari E, Vacca P, Mingari MC, Moretta L: Natural killer cells: from surface receptors to the cure of high-risk leukemia (Ceppellini Lecture), *HLA* 93(4):185–194, 2019.
A review of past and recent discoveries regarding NK cell function and the application of these discoveries to stem cell transplantation and other therapies.

Galkowski D, Ratajczak MZ, Kocki J, Darzynkiewicz Z: Of cytometry, stem cells and fountain of youth, *Stem Cell Rev Rep* 13(4):465–481, 2017.
A review ot the biology and biomedical applications of stem cells.

Gasteiger G, D'Osualdo A, Schubert DA, Weber A, Bruscia EM, Hartl D: Cellular innate immunity: an old game with new players, *J Innate Immun* 9(2):111–125, 2017.
A review of recent discoveries regarding innate immune cells and their potential biomedical applications.

Ghanekar SA, Maecker HT, Maino VC: Monitoring of immune response using cytokine flow cytometry. In Detrick B, Hamilton RJ, Folds JD, editors: *Manual of molecular and clinical laboratory immunology*, ed 7, Washington, DC, 2006, ASM Press, pp 353–360.
A practical, useful review on cytokine flow cytometry.

Good RA: Cellular immunology in a historical perspective, *Immunol Rev* 185:136–158, 2002.
A classic review of historical developments in cellular immunology, written by a pioneer in the field.

Herzenberg LA, Herzenberg LA: Genetics, FACS, immunology, and redox: a tale of two lives intertwined, *Annu Rev Immunol* 22:1–31, 2004.
An historical account of the development of the flow cytometer from the inventors.

Janeway Jr CA, Medzhitov R: Innate immune recognition, *Annu Rev Immunol* 20:197–216, 2002.
A classic review of the innate immune system from the immunologists who discovered the system.

Kalyuzhny AE: ELISPOT assay on membrane microplates, *Methods Mol Biol* 536:355–365, 2009.
A detailed review of the ELISPOT assay.

Kaufmann SHE: Immunology's coming of age, *Front Immunol* 10:684, 2019.
A concise review of the history of immunology and its impact on modern bioscience and medicine.

Keren DF: Surface marker assays in immunodeficiency diseases. In Keren DF, editor: *Flow cytometry in clinical diagnosis*, Chicago, 1989, ASCP Press, pp 213–247.
A comprehensive review of the flow cytometric diagnosis of immunodeficiency diseases by a major leader in the field.

Kumar BV, Connors TJ, Farber DL: Human T cell development, localization, and function throughout life, *Immunity* 48(2):202–213, 2018.
A concise review of T-cell development, function, and the biomedical applications of T-cell modulation.

Ley K, Hoffman HM, Kubes P, et al.: Neutrophils: new insights and open questions, *Sci Immunol 3(30)*, 2018.
An excellent review of neutrophil development, function, and pathology.

Liew PX, Kubes P: The neutrophil's role during health and disease, *Physiol Rev* 99(2):1223–1248, 2019.
A detailed review of neutrophil function.

Malaguarnera L, Ferlito L, Imbesi RM, et al.: Immunosenescence: a review, *Arch Gerontol Geriatr* 32:1–14, 2001.
This review provides a good summary of age-related changes that occur in both arms of the immune system.

Maluish AE, Strong DM: Lymphocyte proliferation. In Rose NR, Friedman H, Fahey JL, editors: *Manual of clinical laboratory immunology*, Washington, DC, 1986, American Society for Microbiology, pp 274–281.
An excellent summary of laboratory techniques for the measurement of lymphocyte proliferation.

Mandy FF: Twenty-five years of clinical flow cytometry: AIDS accelerated global instrument distribution, *Cytometry* 58:55–56, 2004.

An article highlighting the role of HIV evaluation in development of the flow cytometer.
Marshall JS, Warrington R, Watson W, Kim HL: An introduction to immunology and immunopathology, *Allergy Asthma Clin Immunol* 14(Suppl 2):49, 2018.
This is a concise, well-written review of innate and adaptive immunity.
McCoy JP: Jr: basic principles of flow cytometry, *Hematol Oncol Clin North Am* 16:229–243, 2002.
An excellent summary of flow cytometric analysis, emphasizing instrument operation and function.
Morice WG: The immunophenotypic attributes of NK cells and NK-cell lineage lymphoproliferative disorders, *Am J Clin Pathol* 127:881–886, 2007.
An excellent review of NK cells and NK cell function.
Nomura L, Maino VC, Maecker HT: Standardization and optimization of multiparameter intracellular cytokine staining, *Cytometry* 73:984–991, 2008.
An important article on the standardization of flow cytometric analysis for cytokine analysis.
Ochs HD, Hagin D: Primary immunodeficiency disorders: general classification, new molecular insights, and practical approach to diagnosis and treatment, *Ann Allergy Asthma Immunol* 112:489–495, 2014.
A comprehensive review of the primary immunodeficiency diseases, emphasizing early diagnosis and the significance of new molecular discoveries and techniques.
Paucek RD, Baltimore D, Li G: The cellular immunotherapy revolution: arming the immune system for precision therapy, *Trends Immunol* 40(4):292–309, 2019.
An excellent review of the role of immunotherapy in personalized medicine, with a focus on T-cell–based immunotherapy.
Perfetto SP, Chattopadhyay PK, Roederer M: Seventeen-colour flow cytometry: unravelling the immune system, *Nat Rev Immunol* 4:648–655, 2004.
This paper describes a powerful form of flow cytometry capable of simultaneously examining several physical parameters and 17 fluorescent colors.
Perfetto SP, Currier J, Birx DL: T-lymphocyte activation and cell signaling. In Rose NR, Hamilton RG, Detrick B, editors: *Manual of clinical laboratory immunology*, ed 6, Washington, DC, 2002, ASM Press, pp 224–237.
This paper provides a comprehensive review of the theoretical and practical aspects of T-cell function and evaluation.
Sedgwick JD: ELISPOT assay: a personal retrospective, *Methods Mol Biol* 302:3–14, 2005.
A historical account of the development of the ELISPOT assay.
Sinkovics JG, Horvath JC: Human natural killer cells: a comprehensive review, *Int J Oncol* 27:5–47, 2005.
A thorough, comprehensive review of the NK cell.
Stewart CC, Goolsby C, Shackney SE: Emerging technology and future developments in flow cytometry, *Hematol Oncol Clin North Am* 16:477–495, 2002.
A review of emerging applications and the future role of the flow cytometer in the medical sciences, from a leader in the field.
Tebo AE, Detrick B, Hamilton RG, et al.: Clinical laboratory immunology: an indispensable player in laboratory medicine, *Am J Clin Pathol* 142:437–444, 2014.
A review of the increasing importance, but declining emphasis, of clinical laboratory immunology in medical education.
Vijay K: Toll-like receptors in immunity and inflammatory diseases: past, present, and future, *Int Immunopharmacol* 59:391–412, 2018.
A review of the history, biology, and function of Toll-like receptors and their current and future biomedical applications.
Virgo PF, Gibbs GJ: Flow cytometry in clinical pathology, *Ann Clin Biochem* 49:17–28, 2012.
A comprehensive review of the principles, technological aspects, and applications of flow cytometry in clinical hematology and immunology.
Woo J, Baumann A, Arguello V: Recent advancements of flow cytometry: new applications in hematology and oncology, *Expert Rev Mol Diagn* 14:67–81, 2014.
A comprehensive review of the applications of flow cytometry in clinical hematology and immunology, with an emphasis on new discoveries and technology.

Access the complete reference list online at Elsevier eBooks for Practicing Clinicians.

REFERENCES

Achkar JM, Lawn SD, Moosa MY, Wright CA, Kasprowicz VO: Adjunctive tests for diagnosis of tuberculosis: serology, ELISPOT for site-specific lymphocytes, urinary lipoarabinomannan, string test, and fine needle aspiration, *J Infect Dis* 4(204 Suppl) :S1130–1141, 2011, https://doi.org/10.1093/infdis/jir450.

Adan A, Alizada G, Kiraz Y, Baran Y, Nalbant A: Flow cytometry: basic principles and applications, *Crit Rev Biotechnol* 37(2):163–176, 2017, https://doi.org/10.3109/07388551.2015.1128876.

Aebisher D, Bartusik D, Tabarkiewicz J: Laser flow cytometry as a tool for the advancement of clinical medicine, *Biomed Pharmacother* 85:434–443, 2017, https://doi.org/10.1016/j.biopha.2016.11.048.

Afacan NJ, Fjell CD, Hancock RE: A systems biology approach to nutritional immunology - focus on innate immunity, *Mol Aspects Med* 33(1):14–25, 2012, https://doi.org/10.1016/j.mam.2011.10.013.

Ahlborg N, Axelsson B: Dual- and triple-color fluorospot, *Methods Mol Biol* 792:77–85, 2012, https://doi.org/10.1007/978-1-61779-325-7_6.

Alarcon B, Gil D, Delgado P, Schamel WW: Initiation of TCR signaling: regulation within CD3 dimers, *Immunol Rev* 191:38–46, 2003.

Alheim M: Flow cytometry-based cytotoxicity and antibody binding assay, *Curr Protoc Cytom 66*, Unit 6 34. 2013, https://doi.org/10.1002/0471142956.cy0634s66.

Almeida L, Lochner M, Berod L, Sparwasser T: Metabolic pathways in T cell activation and lineage differentiation, *Semin Immunol* 28(5):514–524, 2016, https://doi.org/10.1016/j.smim.2016.10.009.

Alvarez-Larran A, Toll T, Rives S, Estella J: Assessment of neutrophil activation in whole blood by flow cytometry, *Clin Lab Haematol* 27(1):41–46, 2005.

Alvarez-Rodriguez L, Lopez-Hoyos M, Munoz-Cacho P, Martinez-Taboada VM: Aging is associated with circulating cytokine dysregulation, *Cell Immunol* 273(2):124–132, 2012, https://doi.org/10.1016/j.cellimm.2012.01.001.

Amarante-Mendes GP, Adjemian S, Branco LM, Zanetti LC, Weinlich R, Bortoluci KR: Pattern recognition receptors and the host cell death molecular Machinery, *Front Immunol* 9:2379, 2018, https://doi.org/10.3389/fimmu.2018.02379.

Amati L, Cirimele D, Pugliese V, Covelli V, Resta F, Jirillo E: Nutrition and immunity: laboratory and clinical aspects, *Curr Pharm Des* 9(24):1924–1931, 2003.

Analyte Specific Regulation MD: Classification/reclassification; restricted devices; analyte specific reagents, *Fed. Reg*, 1997. 66243–62260.

Ananworanich J, Shearer WT: Delayed-type hypersensitivity skin testing. In Rose NR, Hamilton RG, Detrick B, editors: *Manual of clinical laboratory immunology*, 6th ed, Washington, DC, 2002, ASM Press, pp 212–219.

Angulo R, Fulcher DA: Measurement of Candida-specific blastogenesis: comparison of carboxyfluorescein succinimidyl ester labelling of T cells, thymidine incorporation, and CD69 expression, *Cytometry* 34(3):143–151, 1998.

Aoki Y, Tosato G: Neoplastic conditions in the context of HIV-1 infection, *Curr HIV Res* 2(4):343–349, 2004.

Arvilommi H: ELISPOT for detecting antibody-secreting cells in response to infections and vaccination, *APMIS* 104(6):401–410, 1996.

ASCO: Clinical practice guidelines for the use of tumor markers in breast and colorectal cancer. Adopted May 17, 1996, by American Society of Clinical Oncology, *J Clin Oncol* 14:2843–2877, 1996.

Augustine JJ, Hricik DE: T-cell immune monitoring by the ELISPOT assay for interferon gamma, *Clin Chim Acta* 413(17–18):1359–1363, 2012, https://doi.org/10.1016/j.cca.2012.03.006.

Austin Suthanthiraraj PP: Graves SW: Fluidics, *Curr Protoc Cytom*, Chapter 1, Unit 1 2. 2013, https://doi.org/10.1002/0471142956.cy0102s65.

Azuma M, Ito D, Yagita H, Okumura K, Phillips JH, Lanier LL, Somoza C: B70 antigen is a second ligand for CTLA-4 and CD28, *Nature* 366(6450):76–79, 1993.

Bach F, Segall M: Pooled stimulating cells as a "standard stimulator" in mixed lymphocyte culture, *Transplantation* 22:117–135, 1974.

Bagwell CB: Theoretical aspects of flow cytometry data analysis. In Bauer D, Duque RE, Shankey TV, editors: *Clinical flow cytometry: Principles and applications*, Baltimore, 1993, Williams & Wilkins, pp 41–61.

Balkwill FR, Burke F: The cytokine network, *Immunol Today* 10(9):299–304, 1989.

Barber L, Prince HM, Rossi R, Bertoncello I: Fluoro-Gold: an alternative viability stain for multicolor flow cytometric analysis, *Cytometry* 36(4):349–354, 1999.

Barry M, Bleackley RC: Cytotoxic T lymphocytes: all roads lead to death, *Nat Rev Immunol* 2(6):401–409, 2002.

Baskar S, Ostrand-Rosenberg S, Nabavi N, Nadler LM, Freeman GJ, Glimcher LH: Constitutive expression of B7 restores immunogenicity of tumor cells expressing truncated major histocompatibility complex class II molecules, *Proc Natl Acad Sci U S A* 90(12):5687–5690, 1993.

Bass DA, Parce JW, Dechatelet LR, Szejda P, Seeds MC, Thomas M: Flow cytometric studies of oxidative product formation by neutrophils: a graded response to membrane stimulation, *J Immunol* 130(4):1910–1917, 1983.

Bassøe CF, Bjerknes R: Phagocytosis by human leukocytes, phagosomal pH, and degradation of seven species of bacteria measured by flow cytometry, *J Med Microbiol* 19:115–125, 1985.

Bassøe CF, Laerum OD, Glette J, Hopen G, Haneberg B, Solberg CO: Simultaneous measurement of phagocytosis and phagosomal pH by flow cytometry: role of polymorphonuclear neutrophilic leukocyte granules in phagosome acidification, *Cytometry* 4:254–262, 1983.

Bassøe CF, Bjerknes R: The effect of serum opsonins on the phagocytosis of Staphylococcus aureus and zymosan particles, measured by flow cytometry. Acta Pathologica, Microbiologica, Et Immunologica Scandinavica Section C, *Immunology* 92(1):51–58, 1984.

Bastian J, Law S, Vogler L, Lawton A, et al.: Prediction of persistent immunodeficiency in the DiGeorge anomaly, *J Pediatr* 115(3):391–396, 1989.

Bauer KD, Jacobberger JW: Analysis of intracellular proteins, *Methods Cell Biol* 41:351–376, 1994.

Baumgarth N, Roederer M: A practical approach to multicolor flow cytometry for immunophenotyping, *J Immunol Methods* 243(1–2):77–97, 2000.

Becker D, Kuhn U, Lempertz U, Enk A, Saloga J, Knop J: Flow-cytometric screening for the modulation of receptor-mediated endocytosis in human dendritic cells: implications for the development of an in vitro technique for predictive testing of contact sensitizers, *J Immunol Methods* 203(2):171–180, 1997.

Begum J, Day W, Henderson C, Purewal S, Cerveira J, Summers H, ET AL: A method for evaluating the use of fluorescent dyes to track proliferation in cell lines by dye dilution, *Cytometry* 83(12):1085–1095, 2013, https://doi.org/10.1002/cyto.a.22403.

Belloc F, Vincendeau P, Freyburger G, Dumain P, Boisseau MR: Flow cytometric study of the activation of polymorphonuclear cells, *J Leukoc Biol* 48(4):353–358, 1990.

Berglund DL, Taffs RE, Robertson NP: A rapid analytical technique for flow cytometric analysis of cell viability using calcofluor white M2R, *Cytometry* 8(4):421–426, 1987.

Beutler BA: TLRs and innate immunity, *Blood* 113(7):1399–1407, 2009.

Bicker H, Hoflich C, Wolk K, Vogt K, Volk HD, Sabat R: A simple assay to measure phagocytosis of live bacteria, *Clin Chem* 54(5):911–915, 2008.

Bilgen T, Canbakan M, Sahin G, Titiz MI: Comparison of cytotoxic flow cytometric cross match with complement dependent lymphocytotoxicity and flow cytometric cross match in renal transplant patients, *Transplant Proc* 51(4):1021–1023, 2019, https://doi.org/10.1016/j.transproceed.2019.01.099.

Bjerknes R: Flow cytometric assay for combined measurement of phagocytosis and intracellular killing of Candida albicans, *J Immunol Methods* 72:229–241, 1984.

Bjerknes R, Bassøe CF: Phagocyte C3-mediated attachment and internalization: flow cytometric studies using a fluorescent quenching technique, *Blut* 49:315–323, 1984.

Black MM, Zachrau RE, Hankey BF, Wesley M: Skin window reactivity to autologous breast cancer. An index of prognostically significant cell-mediated immunity, *Cancer* 62(1):72–83, 1988.

Bocchieri MH, Talle MA, Maltese LM, Ragucci IR, Hwang CC, Goldstein G: Whole blood culture for measuring mitogen induced T cell proliferation provides superior correlations with disease state and T cell phenotype in asymptomatic HIV-infected subjects, *J Immunol Methods* 181(2):233–243, 1995.

Bodduluru LN, Kasala ER, Madhana RM, Sriram CS: Natural killer cells: the journey from puzzles in biology to treatment of cancer, *Cancer Lett* 357(2):454–467, 2015, https://doi.org/10.1016/j.canlet.2014.12.020.

Bogh LD, Duling TA: Flow cytometry instrumentation in research and clinical laboratories, *Clin Lab Sci* 6(3):167–173, 1993.

Bonavida B: NK cell phenotypic and functional heterogeneities and molecular mechanisms of cytotoxicity, *Crit Rev Oncog* 19(1–2):21–45, 2014.

Bonilla FA, Oettgen HC: Normal ranges for lymphocyte subsets in children, *J Pediatr* 130(3):347–349, 1997.

Bontadini A, Conte R, Dinota A, Belletti D, Tassi C, Tazzari PL, Gobbi M: Mixed lymphocyte reactions evaluated by means of bromodeoxyuridine incorporation, *Haematologica* 75(1):7–11, 1990.

Booth C, Gaspar HB, Thrasher AJ: Gene therapy for primary immunodeficiency, *Curr Opin Pediatr* 23(6):659–666, 2011, https://doi.org/10.1097/MOP.0b013e32834cd67a.

Borowitz MJ: Acute lymphoblastic leukemia. In Knowles DM, editor: *Neoplastic Hematopathology*, Baltimore, 1992, Williams & Wilkins, pp 1295–1314.

Borut TC, Ank BJ, Gard SE, Stiehm ER: Tetanus toxoid skin test in children: correlation with in vitro lymphocyte stimulation and monocyte chemotaxis, *J Pediatr* 97(4):567–573, 1980.

Boyette LB, Macedo C, Hadi K, Elinoff BD, Walters JT, Ramaswami B, ET AL: Phenotype, function, and differentiation potential of human monocyte subsets, *PLoS One 12(4)*e0176460, 2017, https://doi.org/10.1371/journal.pone.0176460.

Braylan RC, Atwater SK, Diamond L, Hassett JM, Johnson M, Kidd PG, et al.: U.S.-Canadian Consensus recommendations on the immunophenotypic analysis of hematologic neoplasia by flow cytometry: data reporting, *Cytometry* 30(5):245–248, 1997.

Bretscher P: The two-signal model of lymphocyte activation twenty-one years later, *Immunol Today* 13(2):74–76, 1992.

Bretsche P: Living with the ups and downs of the two signal model, *Immunol Cell Biol* 82(2):141–148, 2004.

Bretscher PA: The history of the two-signal model of lymphocyte activation: a personal perspective, *Scand J Immunol* 89(6):e12762, 2019, https://doi.org/10.1111/sji.12762.

Brubaker SW, Bonham KS, Zanoni I, Kagan JC: Innate immune pattern recognition: a cell biological perspective, *Annu Rev Immunol* 33:257–290, 2015, https://doi.org/10.1146/annurev-immunol-032414-112240.

Bryceson YT, Fauriat C, Nunes JM, Wood SM, Bjorkstrom NK, Long EO, Ljunggren HG: Functional analysis of human NK cells by flow cytometry, *Methods Mol Biol* 612:335–352, 2010.

Buckley RH: Molecular defects in human severe combined immunodeficiency and approaches to immune reconstitution, *Annu Rev Immunol* 22:625–655, 2004.

Burleson GR, Burleson FG, Dietert RR: Evaluation of cell-mediated immune function using the cytotoxic T-lymphocyte assay, *Methods Mol Biol* 1803:199–208, 2018, https://doi.org/10.1007/978-1-4939-8549-4_13.

Busetto S, Trevisan E, Patriarca P, Menegazzi R: A single-step, sensitive flow cytofluorometric assay for the simultaneous assessment of membrane-bound and ingested Candida albicans in phagocytosing neutrophils, *Cytometry* 58(2):201–206, 2004.

Butler AL, Fischinger S, Alter G: The Antibodiome-mapping the humoral immune response to HIV, *Curr HIV AIDS Rep* 16(2):169–179, 2019, https://doi.org/10.1007/s11904-019-00432-x.

Buvelot H, Jaquet V, Krause KH: Mammalian NADPH oxidases, *Methods Mol Biol* 1982:17–36, 2019, https://doi.org/10.1007/978-1-4939-9424-3_2.

Cacciapuoti C, Terrazzano G, Barone L, Sica M, Becchimanzi C, Rotoli B, et al.: Glycosyl-phosphatidyl-inositol-defective granulocytes from paroxysmal nocturnal haemoglobinuria patients show increased bacterial ingestion but reduced respiratory burst induction, *Am J Hematol* 82(2):98–107, 2007.

Calvelli T, Denny TN, Paxton H, Gelman R, Kagan J: Guideline for flow cytometric immunophenotyping: a report from the National Institute of Allergy and infectious diseases, division of AIDS, *Cytometry* 14(7):702–715, 1993.

Campbell JDM, Fraser AR: Flow cytometric assays for identity, safety and potency of cellular therapies, *Cytometry B Clin Cytom* 94(5):569–579, 2018, https://doi.org/10.1002/cyto.b.21735.

Cantrell D: Signaling in lymphocyte activation, *Cold Spring Harb Perspect Biol* 7(6), 2015, https://doi.org/10.1101/cshperspect.a018788.

Carothers AD: Counting, measuring, and mapping in FISH-labelled cells: sample size considerations and implications for automation, *Cytometry* 16(4):298–304, 1994.

Carvalho RP, Mesquita JS, Bonomo A, Elsas PX, Colombo AP: Relationship of neutrophil phagocytosis and oxidative burst with the subgingival microbiota of generalized aggressive periodontitis, *Oral Microbiol Immunol* 24(2):124–132, 2009.

Caspell R, Lehmann PV: Detecting all immunoglobulin classes and subclasses in a Multiplex 7 color ImmunoSpot((R)) assay, *Methods Mol Biol* 1808:85–94, 2018, https://doi.org/10.1007/978-1-4939-8567-8_8.

Cassimos DC, Liatsis M, Stogiannidou A, Kanariou MG: Children with frequent infections: a proposal for a stepwise assessment and investigation of the immune system, *Pediatr Allergy Immunol*, 2009.

Centers for Disease Control C: Guidelines for the performance of CD4+ T-cell determinations in persons with human immunodeficiency virus infection, *MMWR Morb Mortal Wkly Rep* 41:1–17, 1992.

Chakraborty AK, Weiss A: Insights into the initiation of TCR signaling, *Nat Immunol* 15(9):798–807, 2014, https://doi.org/10.1038/ni.2940.

Chanouzas D, Small A, Borrows R, Ball S: Assessment of the T-SPOT.CMV interferon-gamma release assay in renal transplant recipients: a single center cohort study, *PloS One* 13(3):e0193968, 2018, https://doi.org/10.1371/journal.pone.0193968.

Chaplin DD: Overview of the immune response, *J Allergy Clin Immunol* 125(2 Suppl 2):S3–S23, 2010.

Chapman GV: Instrumentation for flow cytometry, *J Immunol Methods* 243(1–2):3–12, 2000.

Chatelain R, Varkila K, Coffman RL: IL-4 induces a Th2 response in Leishmania major-infected mice, *J Immunol* 148(4):1182–1187, 1992.

Chen L, Ashe S, Brady WA, Hellstrom I, Hellstrom KE, Ledbetter JA, et al.: Costimulation of antitumor immunity by the B7 counterreceptor for the T lymphocyte molecules CD28 and CTLA-4, *Cell* 71(7):1093–1102, 1992.

Chen Y, Junger WG: Measurement of oxidative burst in neutrophils, *Methods Mol Biol* 844:115–124, 2012, https://doi.org/10.1007/978-1-61779-527-5_8.

Cheroutre H: Starting at the beginning: new perspectives on the biology of mucosal T cells, *Annu Rev Immunol* 22:217–246, 2004.

Christensen R, Owens DM, Thomsen A, Pedersen S, Jensen UB: Zinc fixation for flow cytometry analysis of intracellular and surface epitopes, DNA content, and cell proliferation, *Curr Protoc Cytom Chapter 7, Unit 7 40*, 2011, https://doi.org/10.1002/0471142956.cy0740s57.

Clark HR, Powell AB, Simmons KA, Ayubi T, Kale SD: Endocytic markers associated with the internalization and processing of Aspergillus fumigatus conidia by BEAS-2B cells, *mSphere* 4(1), 2019, https://doi.org/10.1128/mSphere.00663-18.

Clerici M, Shearer GM: A TH1—>TH2 switch is a critical step in the etiology of HIV infection, *Immunol Today* 14(3):107–111, 1993.

Clerici M, Shearer GM: The Th1-Th2 hypothesis of HIV infection: new insights, *Immunol Today* 15(12):575–581, 1994.

Clevenger CV, Shankey TV: Cytochemistry II: immunofluorescence measurement of intracellular antigens. In R D, Bauer KD, Shankey TV, editors: *Clinical flow cytometry: Principles and applications*, Baltimore, 1993, Williams & Wilkins, pp 157–175.

Conley ME: Molecular basis of immunodeficiency, *Immunol Rev* 203:5–9, 2005.

Coon JS, Deitch AD, de Vere White RW, Koss LG, Melamed MR, Reeder JE, et al.: Interinstitutional variability in DNA flow cytometric analysis of tumors. The National cancer Institute's flow cytometry network experience, *Cancer* 61(1):126–130, 1988.

Coon JS, Paxton H, Lucy L, Homburger H: Interlaboratory variation in DNA flow cytometry. Results of the College of American Pathologists' Survey, *Arch Pathol Lab Med* 118(7):681–685, 1994.

Cooper MA, Colonna M, Yokoyama WM: Hidden talents of natural killers: NK cells in innate and adaptive immunity, *EMBO Rep* 10(10):1103–1110, 2009.

Corver WE, ter Haar NT: High-resolution multiparameter DNA flow cytometry for the detection and sorting of tumor and stromal subpopulations from paraffin-embedded tissues, *Curr Protoc Cytom Chapter 7, Unit 7 37*, 2011, https://doi.org/10.1002/0471142956.cy0737s55.

Cossarizza A, De Biasi S, Gibellini L, Bianchini E, Bartolomeo R, Nasi M, et al.: Cytometry, immunology, and HIV infection: three decades of strong interactions, *Cytometry* 83(8):680–691, 2013, https://doi.org/10.1002/cyto.a.22318.

Cossarizza A, Radbruch A: Cytometry for immunology: a stable and happy marriage, *Cytometry* 83(8):673–675, 2013, https://doi.org/10.1002/cyto.a.22336.

Cost KM, Fineman D, Steger S: A flow cytometry-based screening assay for lymphocyte proliferation, *Clin. Immunol Newslett* 13:82–85, 1993.

Cram LS, Gomez ER, Thoen CO, Forslund JC, Jett JH: Flow microfluorometric quantitation of the blastogenic response of lymphocytes, *J Histochem Cytochem* 24:383–387, 1976.

Cruz-Munoz ME, Valenzuela-Vazquez L, Sanchez-Herrera J: Santa-Olalla Tapia J: from the "missing self" hypothesis to adaptive NK cells: insights of NK cell-mediated effector functions in immune surveillance, *J Leukoc Biol* 105(5):955–971, 2019, https://doi.org/10.1002/JLB.MR0618-224RR.

Cunningham-Rundles C, Cunningham-Rundles S, Iwata T, Incefy G, Garofalo JA, Menendez-Botet C, et al.: Zinc deficiency, depressed thymic hormones, and T lymphocyte dysfunction in patients with hypogammaglobulinemia, *Clin Immunol Immunopathol* 21(3):387–396, 1981.

Cunningham-Rundles C, Siegal FP, Cunningham-Rundles S, Lieberman P: Incidence of cancer in 98 patients with common varied immunodeficiency, *J Clin Immunol* 7(4):294–299, 1987.

Cunningham-Rundles S: *Issues in assessment of human immune function.In Military strategies for Sustainment of nutrition and immune function in the field. In pp. 235–248*, Institute of Medicine National Academy Press, 1999.

Cunningham-Rundles S, Cervia JS, Malnutrition, Defense H: In Walker WA, Watkins JB, editors: *Pediatrics: basic science and clinical application*, 2nd ed, New York, 1996, Marcel Dekker, pp 295–307.

Cunningham-Rundles S, Harbison M, Guirguis S, Valacer D, Chretien PB: New perspectives on use of thymic factors in immune deficiency, *Ann N Y Acad Sci* 730:71–83, 1994.

Cunningham-Rundles S, Lin DH: Nutrition and the immune system of the gut, *Nutrition* 14(7–8):573–579, 1998.

Cunningham-Rundles S, Nessin M: Bacterial infections in the immunologically compromised host. In Nataro JP, Blaser MJ, Cunningham-Rundles S, editors: *Persistent bacterial infections*, Washington, DC, 2000, American Society of Microbiology Press, pp 145–164.

Cunningham-Rundles S, Yeger-Arbitman R, Nachman SA, Kaul S, Fotino M: New variant of MHC class II deficiency with interleukin-2 abnormality, *Clin Immunol Immunopathol* 56(1):116–123, 1990.

Cyster JG, Allen CDC: B cell responses: cell interaction dynamics and decisions, *Cell* 177(3):524–540, 2019, https://doi.org/10.1016/j.cell.2019.03.016.

Czerkinsky CC, Nilsson LA, Nygren H, Ouchterlony O, Tarkowski A: A solid-phase enzyme-linked immunospot (ELISPOT) assay for enumeration of specific antibody-secreting cells, *J Immunol Methods* 65(1–2):109–121, 1983.

Danikas DD, Karakantza M, Theodorou GL, Sakellaropoulos GC, Gogos CA: Prognostic value of phagocytic activity of neutrophils and monocytes in sepsis. Correlation to CD64 and CD14 antigen expression, *Clin Exp Immunol* 154(1):87–97, 2008.

Darzynkiewicz Z: Cytometry of the cell cycle: in search for perfect methodology for DNA content analysis in tissue specimens, *Cell Cycle* 9(17):3395–3396, 2010, https://doi.org/10.4161/cc.9.17.13015.

Darzynkiewicz Z, Huang X, Zhao H: Analysis of cellular DNA content by flow cytometry, *Curr Protoc Immunol* 119:5 7 1–5 7 20, 2017, https://doi.org/10.1002/cpim.36.

Denny T, Yogev R, Gelman R, Skuza C, Oleske J, Chadwick E, et al.: Lymphocyte subsets in healthy children during the first 5 years of life, *Jama* 267(11):1484–1488, 1992.

Deodhar SD: Basics in practical applications and standardization of techniques of cellular immunology, *Lab Res Methods Biol Med* 8:71–78, 1983.

DiGeorge AM: Congenital absence of the thymus and its immunologic consequences: Concurrence with congenital hypothyroidism. In B. D, editor: *Birth Defects Immunologic Deficiency Disease in Man*, Vol. 4(1), pp. 116. White Plains, NY: The National Foundation-March of Dimes, 1974.

Dong ZL, Lin J, Zhang B, Zhu Y, Li N, et al.: Structural basis of assembly of the human T cell receptor-CD3 complex, *Nature* 573(7775):546–552, 2019, https://doi.org/10.1038/s41586-019-1537-0.

Dooley J, Liston A: Molecular control over thymic involution: from cytokines and microRNA to aging and adipose tissue, *Eur J Immunol* 42(5):1073–1079, 2012, https://doi.org/10.1002/eji.201142305.

Dunn PA, Tyrer HW: Quantitation of neutrophil phagocytosis, using fluorescent latex beads. Correlation of microscopy and flow cytometry, *J Lab Clin Med* 98(3):374–381, 1981.

Dupont B, Hansen JA, Yunis EJ: Human mixed lymphocyte culture reactions: genetics, specificity, and biological implications, *Adv Immunol* 23:107–202, 1976.

Duquesnoy RJ, Marrari M: Multilaboratory evaluation of serum analysis for HLA antibody and crossmatch reactivity by lymphocytotoxicity methods, *Arch Pathol Lab Med* 127(2):149–156, 2003, https://doi.org/10.1043/0003-9985(2003)127<149:MEOSAF>2.0.CO;2.

El-Agroudy AE, Ismail AM, El-Chenawy FA, Shehab El-Din AB, Ghoneim MA: Pre-transplant mixed lymphocyte culture still has an impact on graft survival, *Am J Nephrol* 24(3):296–300, 2004.

Elbim C, Lizard G: Flow cytometric investigation of neutrophil oxidative burst and apoptosis in physiological and pathological situations, *Cytometry* 75(6):475–481, 2009.

Elder ME: ZAP-70 and defects of T-cell receptor signaling, *Semin Hematol* 35(4):310–320, 1998.

Elguindi I, Redziniak G, Metezeau P, Meybeck A, Goldberg ME: Modulation of membrane receptor endocytosis by chemical effectors of membrane fluidity, *Biol Cell* 54(3):199–205, 1985.

Elloumi HZ, Holland SM: Diagnostic assays for chronic granulomatous disease and other neutrophil disorders, *Methods Mol Biol* 1124:517–535, 2014, https://doi.org/10.1007/978-1-62703-845-4_31.

Elshal MF, McCoy JP: Multiplex bead array assays: performance evaluation and comparison of sensitivity to ELISA, *Methods* 38(4):317–323, 2006, https://doi.org/10.1016/j.ymeth.2005.11.010.

Engels EA, Biggar RJ, Hall HI, Cross H, Crutchfield A, Finch JL, et al.: Cancer risk in people infected with human immunodeficiency virus in the United States, *Int J Cancer* 123(1):187–194, 2008.

Fahey JL, Taylor JM, Detels R, Hofmann B, Melmed R, Nishanian P, Giorgi JV: The prognostic value of cellular and serologic markers in infection with human immunodeficiency virus type 1, *N Engl J Med* 322(3):166–172, 1990.

Falco M, Pende D, Munari E, Vacca P, Mingari MC, Moretta L: Natural killer cells: from surface receptors to the cure of high-risk leukemia (Ceppellini Lecture), *HLA* 93(4):185–194, 2019, https://doi.org/10.1111/tan.13509.

Fan Y, Naglich JG, Koenitzer JD, Ribeiro H, Lippy J, Blum J, et al.: Miniaturized high-throughput multiparameter flow cytometry assays measuring in vitro human dendritic cell maturation and T-cell activation in mixed lymphocyte reactions, *SLAS Discov* 23(7):742–750, 2018, https://doi.org/10.1177/2472555218775409.

Fassy J, Tsalkitzi K, Goncalves-Maia M, Braud VM: A Real-time cytotoxicity assay as an alternative to the standard chromium-51 release assay for measurement of human NK and T cell cytotoxic activity, *Curr Protoc Immunol* 118:7 42 41–47 42 12, 2017, https://doi.org/10.1002/cpim.28.

Fattorossi A, Nisini R, Le Moli S, De Petrillo G, D'Amelio R: Flow cytometric evaluation of nitro blue tetrazolium (NBT) reduction in human polymorphonuclear leukocytes, *Cytometry* 11(8):907–912, 1990.

Fattorossi A, Nisini R, Pizzolo JG, D'Amelio R: New, simple flow cytometry technique to discriminate between internalized and membrane-bound particles in phagocytosis, *Cytometry* 10(3):320–325, 1989.

Favi E, Santangelo R, Iesari S, Morandi M, Marcovecchio GE, Trecarichi EM, et al.: Enzyme-linked immunospot assay as a complementary method to assess and monitor Cytomegalovirus infection in kidney transplant recipients on Pre-emptive Antiviral therapy: a single-center experience, *Transplant Proc* 49(8):1766–1772, 2017, https://doi.org/10.1016/j.transproceed.2017.07.001.

Fei DT, Paxton H, Chen AB: Difficulties in precise quantitation of CD4+ T lymphocytes for clinical trials: a review, *Biologicals* 21(3):221–231, 1993.

Fibach E, Giloh H, Rachmilewitz EA, Gatt S: Flow cytofluorometric analysis of the uptake of the fluorescent fatty acid pyrene-dodecanoic acid by human peripheral blood cells, *Cytometry* 9(6):525–528, 1988.

Fidler SJ: Crossmatching by complement-dependent lymphocytotoxicity, *Methods Mol Biol* 882:359–377, 2012, https://doi.org/10.1007/978-1-61779-842-9_21.

Fine N, Barzilay O, Glogauer M: Analysis of human and mouse neutrophil phagocytosis by flow cytometry, *Methods Mol Biol* 1519:17–24, 2017, https://doi.org/10.1007/978-1-4939-6581-6_2.

Finney DA, Sklar LA: Ligand/receptor internalization: a kinetic, flow cytometric analysis of the internalization of N-formyl peptides by human neutrophils, *Cytometry* 4(1):54–60, 1983.

Fischbacher D, Merle M, Liepert A, Grabrucker C, Kroell T, Kremser A, et al.: Cytokine release patterns in mixed lymphocyte culture (MLC) of T-cells with dendritic cells (DC) generated from AML blasts contribute to predict anti-Leukaemic T-cell reactions and patients' response to immunotherapy, *Cell Commun Adhes* 22(2–6):49–65, 2015, https://doi.org/10.1080/15419061.2016.1223634.

Fischer A, Le Deist F, Hacein-Bey-Abina S, Andre-Schmutz I, Basile Gde S, de Villartay JP, Cavazzana-Calvo M: Severe combined immunodeficiency. A model disease for molecular immunology and therapy, *Immunol Rev* 203:98–109, 2005.

Foletta VC, Segal DH, Cohen DR: Transcriptional regulation in the immune system: all roads lead to AP-1, *J Leukoc Biol* 63(2):139–152, 1998.

Freer G: Intracellular staining and detection of cytokines by fluorescence-activated flow cytometry, *Methods Mol Biol* 1172:221–234, 2014, https://doi.org/10.1007/978-1-4939-0928-5_20.

Freer G, Rindi L: Intracellular cytokine detection by fluorescence-activated flow cytometry: basic principles and recent advances, *Methods* 61(1):30–38, 2013, https://doi.org/10.1016/j.ymeth.2013.03.035.

Friberg DD, Bryant JL, Whiteside TL: Measurements of natural killer (NK) activity and NK-cell quantification, *Methods* 9(2):316–326, 1996.

Fulop T, Le Page A, Fortin C, Witkowski JM, Dupuis G, Larbi A: Cellular signaling in the aging immune system, *Curr Opin Immunol* 29:105–111, 2014, https://doi.org/10.1016/j.coi.2014.05.007.

Gascue A, Merino J, Paiva B: Flow cytometry, *Hematol Oncol Clin North Am* 32(5):765–775, 2018, https://doi.org/10.1016/j.hoc.2018.05.004.

Gasteiger G, D'Osualdo A, Schubert DA, Weber A, Bruscia EM, Hartl D: Cellular innate immunity: an old Game with new players, *J Innate Immun* 9(2):111–125, 2017, https://doi.org/10.1159/000453397.

Gazagne A, Malkusch W, Vingert B, Fridman WH, Tartour E: Fluorospot assay: methodological analysis, *Methods Mol Biol* 302:289–296, 2005, https://doi.org/10.1385/1-59259-903-6:289.

Gelfand EW: Abnormalities of signal transduction and T cell immunodeficiency. In Gupta S, Griscelli C, editors: *New concepts in immunodeficiency disease*, New York, 1993, John Wiley & Sons, pp 231–248.

Germain RN: The cellular determinants of adaptive immunity, *N Engl J Med* 381(11):1083–1085, 2019, https://doi.org/10.1056/NEJMcibr1909387.

Gibson JN, Beesetty P, Sulentic C, Kozak JA: Rapid quantification of mitogen-induced blastogenesis in T lymphocytes for identifying immunomodulatory drugs, *J Vis Exp (118)*, 2016, https://doi.org/10.3791/55212.

Gil L, Alonso R, Lopez C, Blanco A, Romero Y, Guillen G, Hermida L: A CFSE-based assay of proliferative response of lymphocytes to stimulation with dengue viruses, *Acta Virol* 53(3):147–152, 2009.

Gille C, Spring B, Tewes L, Poets CF, Orlikowsky T: A new method to quantify phagocytosis and intracellular degradation using green fluorescent protein-labeled Escherichia coli: comparison of cord blood macrophages and peripheral blood macrophages of healthy adults, *Cytometry* 69(3):152–154, 2006.

Giorgi JV, Detels R: T-cell subset alterations in HIV-infected homosexual men: NIAID Multicenter AIDS cohort study, *Clin Immunol Immunopathol* 52(1):10–18, 1989.

Givan AL: Flow cytometry: an introduction, *Methods Mol Biol* 263:1–32, 2004.

Givens M, Weaver A, Bickman S, Logan C, et al.: Near patient CD4 count in a hospitalized HIV patient population, *Cytometry B Clin Cytom* 92(6):451–455, 2017, https://doi.org/10.1002/cyto.b.21248.

Good RA: Cellular immunology in a historical perspective, *Immunol Rev* 185:136–158, 2002.

Goodman HS: A general method for the quantitation of immune cyotysis, *Nature* 190:269–270, 1961.

Grey D, Sack U, Scholz M, Knaack H, et al.: Increased CD64 expression on polymorphonuclear neutrophils indicates infectious complications following solid organ transplantation, *Cytometry* 79(6):446–460, 2011, https://doi.org/10.1002/cyto.a.21049.

Grivennikov SI, Greten FR, Karin M: Immunity, inflammation, and cancer, *Cell* 140(6):883–899, 2010, https://doi.org/10.1016/j.cell.2010.01.025.

Gui J, Mustachio LM, Su DM, Craig RW, Size T, Thymic A-related: Involution: early programming, Sexual Dimorphism, progenitors and stroma, *Aging Dis* 3(3):280–290, 2012.

Haase H, Ober-Blobaum JL, Engelhardt G, Hebel S, Heit A, Heine H, Rink L: Zinc signals are essential for lipopolysaccharide-induced signal transduction in monocytes, *J Immunol* 181(9):6491–6502, 2008.

Hakim FT, Flomerfelt FA, Boyiadzis M, Gress RE: Aging, immunity and cancer, *Curr Opin Immunol* 16(2):151–156, 2004.

Hamerman JA, Ogasawara K, Lanier LL: NK cells in innate immunity, *Curr Opin Immunol* 17(1):29–35, 2005.

Harding CV, Neefjes J: Antigen processing and recognition, *Curr Opin Immunol* 17(1):55–57, 2005.

Haynes AP, Fletcher J, Garnett M, Robins A: A novel flow cytometric method for measuring protein digestion within the phagocytic vacuole of polymorphonuclear neutrophils, *J Immunol Methods* 135(1–2):155–161, 1990.

Haynes BF, Sempowski GD, Wells AF, Hale LP: The human thymus during aging, *Immunol Res* 22(2–3):253–261, 2000.

Hedley DW, Friedlander ML, Taylor IW, Rugg CA, Musgrove EA: Method for analysis of cellular DNA content of paraffin-embedded pathological material using flow cytometry, *J Histochem Cytochem* 31(11):1333–1335, 1983.

Heimdal JH, Aarstad HJ, Klementsen B, Olofsson J: Peripheral blood mononuclear cell (PBMC) responsiveness in patients with head and neck cancer in relation to tumour stage and prognosis, *Acta Otolaryngol* 119(2):281–284, 1999.

Heinzel S, Marchingo JM, Horton MB, Hodgkin PD: The regulation of lymphocyte activation and proliferation, *Curr Opin Immunol* 51:32–38, 2018, https://doi.org/10.1016/j.coi.2018.01.002.

Herwald H, Egesten A: On PAMPs and DAMPs, *J Innate Immun* 8(5):427–428, 2016, https://doi.org/10.1159/000448437.

Herzenberg LA: Genetics, FACS, immunology, and redox: a tale of two lives intertwined, *Annu Rev Immunol* 22:1–31, 2004.

Hidalgo A, Chilvers ER, Summers C, Koenderman L: The neutrophil life cycle, *Trends Immunol* 40(7):584–597, 2019, https://doi.org/10.1016/j.it.2019.04.013.

Hirano T, Murakami M, Fukada T, Nishida K, Yamasaki S, Suzuki T: Roles of zinc and zinc signaling in immunity: zinc as an intracellular signaling molecule, *Adv Immunol* 97:149–176, 2008.

Hirt W, Nebe T, Birr C: [Phagotest and Bursttest (Phagoburst), test kits for study of phagocyte functions], *Wien Klin Wochenschr* 106(8):250–252, 1994.

Homburger HA, Rosenstock W, Paxton H, Paton ML, Landay AL: Assessment of interlaboratory variability of immunophenotyping. Results of the College of American Pathologists flow cytometry Survey, *Ann N Y Acad Sci* 677:43–49, 1993.

Huebner RE, Schein MF, Bass Jr JB: The tuberculin skin test, *Clin Infect Dis* 17(6):968–975, 1993.

Hwai H, Chen YY, Tzeng SJ: B-cell ELISpot assay to quantify antigen-specific antibody-secreting cells in human peripheral blood mononuclear cells, *Methods Mol Biol* 1808:133–141, 2018, https://doi.org/10.1007/978-1-4939-8567-8_11.

Inoges S, Merino J, Bandres E, De Castro P, Subira ML, Sanchez-Ibarrola A: Cytokine flow cytometry differentiates the clinical status of multiple sclerosis (MS) patients, *Clin Exp Immunol* 115(3):521–525, 1999.

Irving BA, Weiss A: The cytoplasmic domain of the T cell receptor zeta chain is sufficient to couple to receptor-associated signal transduction pathways, *Cell* 64(5):891–901, 1991.

Isakson PC, Pure E, Vitetta ES, Krammer PH: T cell-derived B cell differentiation factor(s). Effect on the isotype switch of murine B cells, *J Exp Med* 155(3):734–748, 1982.

Iwasaki A, Medzhitov R: Regulation of adaptive immunity by the innate immune system, *Science* 327(5963):291–295, 2010.

Janetzki S, Rueger M, Dillenbeck T: Stepping up ELISpot: Multi-level analysis in FluoroSpot assays, *Cells* 3(4):1102–1115, 2014, https://doi.org/10.3390/cells3041102.

Janeway Jr CA, Bottomly K: Signals and signs for lymphocyte responses, *Cell* 76(2):275–285, 1994.

Janeway Jr CA, Medzhitov R: Innate immune recognition, *Annu Rev Immunol* 20:197–216, 2002.

Janeway Jr CA, Travers P, Walport M, Shlomchik MJ: *Immunobiology*, 6th ed., Garland Publishing, 2004.

Jaye DL, Bray RA, Gebel HM, Harris WA, Waller EK: Translational applications of flow cytometry in clinical practice, *J Immunol* 188(10):4715–4719, 2012, https://doi.org/10.4049/jimmunol.1290017.

Jensen UB, Owens DM, Pedersen S, Christensen R: Zinc fixation preserves flow cytometry scatter and fluorescence parameters and allows simultaneous analysis of DNA content and synthesis, and intracellular and surface epitopes, *Cytometry* 77(8):798–804, 2010, https://doi.org/10.1002/cyto.a.20914.

Jones B, Janeway Jr CA: Cooperative interaction of B lymphocytes with antigen-specific helper T lymphocytes is MHC restricted, *Nature* 292(5823):547–549, 1981.

Kagan J, Gelman R, Waxdal M: Kidd, P: NIAID Division of AIDS flow cytometry quality assessment program, *Ann N Y Acad Sci* 677:50–52, 1993.

Kalyuzhny AE: Chemistry and biology of the ELISPOT assay, *Methods Mol Biol* 302:15–31, 2005.

Kanda H, Matsuura T, Akiyama T, Kurita T: A flow-cytometric DNA analysis in mixed lymphocyte reaction, *Transplant Proc* 17(5):2157–2158, 1985.

Kasempimolporn S, Areekul P, Thaveekarn W, Sutthisri R, Boonchang S, Sawangvaree A, Sitprija V: Application of transdermal patches with new skin test reagents for detection of latent tuberculosis, *J Med Microbiol* 68(9):1314–1319, 2019, https://doi.org/10.1099/jmm.0.001037.

Katz P, Fauci AS: Immunosuppressives and immunoadjuvants. In Samter M, Talmage DW, Frank MM, editors: *Immunological diseases*, 4th ed, Boston, 1993, Little, Brown & Co, pp 675–698.

Kaufmann SHE: Immunology's coming of age, *Front Immunol* 10:684, 2019, https://doi.org/10.3389/fimmu.2019.00684.

Kawai T, Akira S: The role of pattern-recognition receptors in innate immunity: update on Toll-like receptors, *Nat Immunol* 11(5):373–384, 2010.

Keren DF: Surface marker assays in immunodeficiency diseases. In Keren DF, editor: *Flow cytometry in clinical diagnosis*, Chicago, 1989, ASCP Press, pp 213–247.

Kershaw T, Wavre-Shapton ST, Signoret N, Marsh M: Analysis of chemokine receptor endocytosis and intracellular trafficking, *Methods Enzymol* 460:357–377, 2009.

Kestens L, Mandy F: Thirty-five years of CD4 T-cell counting in HIV infection: from flow cytometry in the lab to point-of-care testing in the field, *Cytometry B Clin Cytom* 92(6):437–444, 2017, https://doi.org/10.1002/cyto.b.21400.

Keusch GT: The history of nutrition: malnutrition, infection and immunity, *J Nutr* 133(1):336S–340S, 2003.

Kim GG, Donnenberg VS, Donnenberg AD, Gooding W, Whiteside TL: A novel multiparametric flow cytometry-based cytotoxicity assay simultaneously immunophenotypes effector cells: comparisons to a 4 h 51Cr-release assay, *J Immunol Methods* 325(1–2):51–66, 2007.

Koyalta D, Jenabian MA, Nadjiouroum N, Djouater B, Djemadji-Oudjeil N, Ndjoyi-Mbiguino A, Belec L: Single-platform, volumetric, CD45-assisted pan-leucogating flow cytometry for CD4 T lymphocytes monitoring of HIV infection according to the WHO recommendations for resource-constrained settings, *BMC Res Notes* 6:169, 2013, https://doi.org/10.1186/1756-0500-6-169.

Kraan J, Gratama JW, Keeney M, D'Hautcourt JL: Setting up and calibration of a flow cytometer for multicolor immunophenotyping, *J Biol Regul Homeost Agents* 17(3):223–233, 2003.

Krakauer T, Inflammasomes, Autophagy, Death C: The Trinity of innate host defense against intracellular bacteria, *Mediators Inflamm* 2019:2471215, 2019, https://doi.org/10.1155/2019/2471215.

Krueger SA, Wilson GD: Flow cytometric DNA analysis of human cancers and cell lines, *Methods Mol Biol* 731:359–370, 2011, https://doi.org/10.1007/978-1-61779-080-5_29.

Kumar BV, Connors TJ, Farber DL: Human T cell development, localization, and function throughout life, *Immunity* 48(2):202–213, 2018, https://doi.org/10.1016/j.immuni.2018.01.007.

Kumar H, Kawai T, Akira S: Toll-like receptors and innate immunity, *Biochem Biophys Res Commun* 388(4):621–625, 2009.

La Muraglia 2nd GM, O'Neil MJ, Madariaga ML, Michel SG, et al.: A novel approach to measuring cell-mediated lympholysis using quantitative flow and imaging cytometry, *J Immunol Methods* 427:85–93, 2015, https://doi.org/10.1016/j.jim.2015.10.005.

Landay AL, Jessop C, Lennette ET, Levy JA: Chronic fatigue syndrome: clinical condition associated with immune activation, *Lancet* 338(8769):707–712, 1991.

Lanier LL: Of snowflakes and natural killer cell subsets, *Nat Biotechnol* 32(2):140–142, 2014, https://doi.org/10.1038/nbt.2810.

Lavergne JA, del Llano AM: Assessment of cellular activation by flow cytometric methods, *Pathobiology* 58:107–117, 1990.

LeBien TW, Tedder TF: B lymphocytes: how they develop and function, *Blood* 112(5):1570–1580, 2008, https://doi.org/10.1182/blood-2008-02-078071.

Lee MY, Shin MC, Yang VC: Transcutaneous antigen delivery system, *BMB Rep* 46(1):17–24, 2013, https://doi.org/10.5483/bmbrep.2013.46.1.001.

Lee SB, Cha J, Kim IK, Yoon JC, Lee HJ, Park SW, et al.: A high-throughput assay of NK cell activity in whole blood and its clinical application, *Biochem Biophys Res Commun* 445(3):584–590, 2014, https://doi.org/10.1016/j.bbrc.2014.02.040.

LeGuern C: Regulation of T-cell functions by MHC class II self-presentation, *Trends Immunol* 24(12):633–638, 2003.

Lehmann AK, Halstensen A, Bassoe CF: Flow cytometric quantitation of human opsonin-dependent phagocytosis and oxidative burst responses to meningococcal antigens, *Cytometry* 33(4):406–413, 1998.

Lehmann PV, Zhang W: Unique strengths of ELISPOT for T cell diagnostics, *Methods Mol Biol* 792:3–23, 2012, https://doi.org/10.1007/978-1-61779-325-7_1.

Lehrer RI: Measurement of candidacidal activity of specific leukocyte types in mixed cell populations. I. Normal, myeloperoxidase-deficient, and chronic granulomatous disease neutrophils, *Infect, Immunol* 1970:42–47, 1970.

Lehrer RI, Cline MJ: Interaction of Candida albicans with human leukocytes and serum, *J Bacteriol* 98:996–1004, 1969.

Levin AC, Massey RJ, Deinhardt F: Spontaneous human mononuclear cell cytotoxicity to cultured tumor cells: reproducibility of serial measurements with the use of a chromium-51-release microcytotoxicity assay, *J Natl Cancer Inst* 60(6):1283–1294, 1978.

Lewis DE, Cytochemistry I: Cell surface immunofluorescence. In Bauer KD, Duque RE, Shankey TV, editors: *Clinical flow cytometry: principles and applications*, Baltimore, 1993, Williams & Wilkins, pp 143–156.

Ley K, Hoffman HM, Kubes P, Cassatella MA, Zychlinsky A, Hedrick CC, Catz SD: Neutrophils: new insights and open questions, *Sci Immunol* 3(30), 2018, https://doi.org/10.1126/sciimmunol.aat4579.

Lieberman J: The ABCs of granule-mediated cytotoxicity: new weapons in the arsenal, *Nat Rev Immunol* 3(5):361–370, 2003.

Liew PX, Kubes P: The neutrophil's role during health and disease, *Physiol Rev* 99(2):1223–1248, 2019, https://doi.org/10.1152/physrev.00012.2018.

Linsley PS, Brady W, Grosmaire L, Aruffo A, Damle NK, Ledbetter JA: Binding of the B cell activation antigen B7 to CD28 costimulates T cell proliferation and interleukin 2 mRNA accumulation, *J Exp Med* 173(3):721–730, 1991.

Linsley PS, Brady W, Urnes M, Grosmaire LS, Damle NK, Ledbetter JA: CTLA-4 is a second receptor for the B cell activation antigen B7, *J Exp Med* 174(3):561–569, 1991.

Lissoni P, Brivio F, Viviani S, Fumagalli L: Which immunological parameters are clinically essential to monitor IL-2 cancer immunotherapy? *J Biol Regul Homeost Agents* 13(2):110–114, 1999.

Liu L, Packard BZ, Brown MJ, Komoriya A, Feinberg MB: Assessment of lymphocyte-mediated cytotoxicity using flow cytometry, *Methods Mol Biol* 263:125–140, 2004, https://doi.org/10.1385/1-59259-773-4:125.

Liu Y, Jones B, Aruffo A, Sullivan KM, Linsley PS, Janeway C: Heat-stable antigen is a costimulatory molecule for CD4 T cell growth, A, Jr *J Exp Med* 175(2):437–445, 1992.

Livingston PO, Cunningham-Rundles S, Marfleet G, Gnecco C, Wong GY, Schiffman G, et al.: Inhibition of suppressor-cell activity by cyclophosphamide in patients with malignant melanoma, *J Biol Response Mod* 6(4):392–403, 1987.

Lloyd A, Hickie I, Hickie C, Dwyer J, Wakefield D: Cell-mediated immunity in patients with chronic fatigue syndrome, healthy control subjects and patients with major depression, *Clin Exp Immunol* 87(1):76–79, 1992.

Loken MR, Brosnan JM, Bach BA, Ault KA: Establishing optimal lymphocyte gates for immunophenotyping by flow cytometry, *Cytometry* 11(4):453–459, 1990.

Loken MR, Parks DR, Herzenberg LA: Two-color immunofluorescence using a fluorescence-activated cell sorter, *J Histochem Cytochem* 25(7):899–907, 1977.

Loken MR, Sweet RG, Herzenberg LA: Cell discrimination by multiangle light scattering, *J Histochem Cytochem* 24(1):284–291, 1976.

Loose D, Van de Wiele C: The immune system and cancer, *Cancer Biother Radiopharm* 24(3):369–376, 2009.

Lorenzo-Herrero S, Sordo-Bahamonde C, Gonzalez S, Lopez-Soto A: A flow cytometric NK cell-mediated cytotoxicity assay to evaluate Anticancer immune responses in vitro, *Methods Mol Biol* 1884:131–139, 2019, https://doi.org/10.1007/978-1-4939-8885-3_8.

Lund-Johansen F, Bjerknes R, Laerum OD: Flow cytometric assay for the measurement of human bone marrow phenotype, function and cell cycle, *Cytometry* 11(5):610–616, 1990.

Maas JJ, Roos MT, Keet IP, Mensen EA, Krol A, Veenstra J, et al.: In vivo delayed-type hypersensitivity skin test anergy in human immunodeficiency virus type 1 infection is associated with T cell nonresponsiveness in vitro, *J Infect Dis* 178(4):1024–1029, 1998.

Mace EM, Orange JS: Emerging insights into human health and NK cell biology from the study of NK cell deficiencies, *Immunol Rev* 287(1):202–225, 2019, https://doi.org/10.1111/imr.12725.

Mach WJ, Thimmesch AR, Orr JA, Slusser JG, Pierce JD: Flow cytometry and laser scanning cytometry, a comparison of techniques, *J Clin Monit Comput* 24(4):251–259, 2010, https://doi.org/10.1007/s10877-010-9242-4.

Madrenas J, Wange RL, Wang JL, Isakov N, Samelson LE, Germain RN: Zeta phosphorylation without ZAP-70 activation induced by TCR antagonists or partial agonists, *Science* 267(5197):515–518, 1995.

Maijo M, Clements SJ, Ivory K, Nicoletti C, Carding SR: Nutrition, diet and immunosenescence, *Mech Ageing Dev* 136–137:116–128, 2014, https://doi.org/10.1016/j.mad.2013.12.003.

Malaguarnera L, Ferlito L, Imbesi RM, Gulizia GS, Di Mauro S, Maugeri D, et al.: Immunosenescence: a review, *Arch Gerontol Geriatr* 32(1):1–14, 2001.

Malissen B: An evolutionary and structural perspective on T cell antigen receptor function, *Immunol Rev* 191:7–27, 2003.

Malone JL, Simms TE, Gray GC, Wagner KF, Burge JR, Burke DS: Sources of variability in repeated T-helper lymphocyte counts from human immunodeficiency virus type 1-infected patients: total lymphocyte count fluctuations and diurnal cycle are important, *J Acquir Immune Defic Syndr* 3(2):144–151, 1990.

Maluish AE, Strong DM: Lymphocyte proliferation. In Rose NR, Friedman H, Fahey JL, editors: *Manual of clinical laboratory immunology*, Washington, D.C, 1986, American society for Microbiology, pp 274–281.

Mandy FF: Twenty-five years of clinical flow cytometry: AIDS accelerated global instrument distribution, *Cytometry* 58(1):55–56, 2004.

Mandy FF, Bergeron M, Recktenwald D, Izaguirre CA: A simultaneous three-color T cell subsets analysis with single laser flow cytometers using T cell gating protocol. Comparison with conventional two-color immunophenotyping method, *J Immunol Methods* 156(2):151–162, 1992.

Marin L, Minguela A, Torio A, Moya-Quiles MR, Muro M, Montes-Ares O, et al.: Flow cytometric quantification of apoptosis and proliferation in mixed lymphocyte culture, *Cytometry* 51(2):107–118, 2003, https://doi.org/10.1002/cyto.a.10007.

Marodi L: Innate cellular immune responses in newborns, *Clin Immunol* 118(2–3):137–144, 2006, https://doi.org/10.1016/j.clim.2005.10.012.

Marshall JS, Warrington R, Watson W, Kim HL: An introduction to immunology and immunopathology, *Allergy Asthma Clin Immunol* 14(Suppl 2):49, 2018, https://doi.org/10.1186/s13223-018-0278-1.

Marti GE, Vogt Jr RF, Stetler-Stevenson M: Clinical quantitative flow cytometry: "Identifying the optimal methods for clinical quantitative flow cytometry, *Cytometry B Clin Cytom* 55(1):59, 2003.

Mascher B, Schlenke P, Seyfarth M: Expression and kinetics of cytokines determined by intracellular staining using flow cytometry, *J Immunol Methods* 223:115–121, 1999.

Masopust D, Schenkel JM: The integration of T cell migration, differentiation and function, *Nat Rev Immunol* 13(5):309–320, 2013, https://doi.org/10.1038/nri3442.

Masur H, Michelis MA, Greene JB, Onorato I, et al.: An outbreak of community-acquired Pneumocystis carinii pneumonia: initial manifestation of cellular immune dysfunction, *N Engl J Med* 305(24):1431–1438, 1981.

Maywald M, Rink L: Zinc homeostasis and immunosenescence, *J Trace Elem Med Biol* 29:24–30, 2015, https://doi.org/10.1016/j.jtemb.2014.06.003.

McCloskey PS, Salo RJ: Flow cytometric analysis of group B streptococci phagocytosis and oxidative burst in human neutrophils and monocytes, *FEMS Immunol Med Microbiol* 27(1):59–65, 2000.

McCoy JP: Jr: basic principles of flow cytometry, *Hematol Oncol Clin North Am* 16(2):229–243, 2002.

McDermott AJ, Huffnagle GB: The microbiome and regulation of mucosal immunity, *Immunology* 142(1):24–31, 2014, https://doi.org/10.1111/imm.12231.

McGrath MA, Morton AM, Harnett MM: Laser scanning cytometry: capturing the immune system in situ, *Methods Cell Biol* 102:231–260, 2011, https://doi.org/10.1016/B978-0-12-374912-3.00009-2.

McKinnon KM: Flow cytometry: an overview, *Curr Protoc Immunol* 120:5 1 1–5 1 11, 2018, https://doi.org/10.1002/cpim.40.

Meaney MP, Nieman DC, Henson DA, Jiang Q, Wang FZ: Measuring granulocyte and monocyte phagocytosis and oxidative burst activity in human blood, *J Vis Exp* 115, 2016, https://doi.org/10.3791/54264.

Mehta BA, Maino VC: Simultaneous detection of DNA synthesis and cytokine production in staphylococcal enterotoxin B activated CD4+ T lymphocytes by flow cytometry, *J Immunol Methods* 208(1):49–59, 1997.

Metezeau P, Djavadi-Ohaniance L, Goldberg ME: The kinetics and homogeneity of endocytosis of a receptor-bound ligand in a heterogeneous cell population studied by flow cytofluorometry, *J Histochem Cytochem* 30(4):359–363, 1982.

Mhatre S, Madkaikar M, Ghosh K, Desai M, Pujari V, Gupta M: Rapid flow cytometry based cytotoxicity assay for evaluation of NK cell function, *Indian J Exp Biol* 52(10):983–988, 2014.

Mickelson EM, Hansen JA: The mixed lymphocyte culture (MLC) test. In Zachary AA, Teresi GA, editors: *ASHI laboratory manual*, 2nd ed, New York, 1990, American Society For Histocompatibility And Immunogenetics, pp 339–356.

Milner JD, Holland SM: The cup runneth over: lessons from the ever-expanding pool of primary immunodeficiency diseases, *Nat Rev Immunol* 13(9):635–648, 2013, https://doi.org/10.1038/nri3493.

Milush JM, Long BR, Snyder-Cappione JE, Cappione 3rd AJ, York VA, Ndhlovu LC, et al.: Functionally distinct subsets of human NK cells and monocyte/DC-like cells identified by coexpression of CD56, CD7, and CD4, *Blood* 114(23):4823–4831, 2009.

Mittag A, Tarnok A: Recent advances in cytometry applications: preclinical, clinical, and cell biology, *Methods Cell Biol* 103:1–20, 2011, https://doi.org/10.1016/B978-0-12-385493-3.00001-2.

Model MA, KuKuruga MA, Todd 3rd RF: A sensitive flow cytometric method for measuring the oxidative burst, *J Immunol Methods* 202(2):105–111, 1997.

Mogensen TH: Pathogen recognition and inflammatory signaling in innate immune defenses, *Clin Microbiol Rev* 22(2):240–273, 2009, https://doi.org/10.1128/CMR.00046-08. Table of Contents.

Mond JJ, Lees A, Snapper CM: T cell-independent antigens type 2, *Annu Rev Immunol* 13:655–692, 1995.

Monk JM, Hou TY, Chapkin RS: Recent advances in the field of nutritional immunology, *Expert Rev Clin Immunol* 7(6):747–749, 2011, https://doi.org/10.1586/eci.11.69.

Montecino-Rodriguez E, Berent-Maoz B, Dorshkind K: Causes, consequences, and reversal of immune system aging, *J Clin Invest* 123(3):958–965, 2013, https://doi.org/10.1172/JCI64096.

Moretta L, Montaldo E, Vacca P, Del Zotto G, Moretta F, Merli P, et al.: Human natural killer cells: origin, receptors, function, and clinical applications, *Int Arch Allergy Immunol* 164(4):253–264, 2014, https://doi.org/10.1159/000365632.

Morgan E, Varro R, Sepulveda H, Ember JA, Apgar J, Wilson J, et al.: Cytometric bead array: a multiplexed assay platform with applications in various areas of biology, *Clin Immunol* 110(3):252–266, 2004, https://doi.org/10.1016/j.clim.2003.11.017.

Morice WG: The immunophenotypic attributes of NK cells and NK-cell lineage lymphoproliferative disorders, *Am J Clin Pathol* 127(6):881–886, 2007.

Moss RB, Mercandetti A, Vojdani A: TNF-alpha and chronic fatigue syndrome, *J Clin Immunol* 19(5):314–316, 1999.

Moulin AM: Immunology old and new: the beginning and the end. In Paulin MH, editor: *Essays on the history of immunology*, Toronto, 1989, Wall and Thompson, pp 292–298.

Moynahan EJ: Letter: acrodermatitis enteropathica: a lethal inherited human zinc-deficiency disorder, *Lancet* 2(7877):399–400, 1974.

Muller W: Dissecting the cytokine network, *Cell Immunol* 244(2):162–164, 2006, https://doi.org/10.1016/j.cellimm.2007.01.008.

Murphy RF, Bisaccia E, Cantor CR, Berger C, Edelson RL: Internalization and acidification of insulin by activated human lymphocytes, *J Cell Physiol* 121(2):351–356, 1984.

Murphy RF, Tse DB, Cantor CR, Pernis B: Acidification of internalized class I major histocompatibility complex antigen by T lymphoblasts, *Cell Immunol* 88(2):336–342, 1984.

Neubauer JC, Sebastien I, Germann A, von Briesen H, Zimmermann H: Towards a full automation of the ELISpot assay for Safe and Parallelized Immunomonitoring, *Methods Mol Biol* 1808:237–247, 2018, https://doi.org/10.1007/978-1-4939-8567-8_20.

Nguyen XD, Eichler H, Dugrillon A, Piechaczek C, Braun M, Kluter H: Flow cytometric analysis of T cell proliferation in a mixed lymphocyte reaction with dendritic cells, *J Immunol Methods* 275(1–2):57–68, 2003.

Nicholson JKA, Green TA: Collaborating Laboratories: selection of anticoagulants for lymphocyte immunophenotyping: effect of specimen age on results, *J Immunol Methods* 165:31–35, 1993.

Nikitin PA, Price AM, McFadden K, Yan CM, Luftig MA: Mitogen-induced B-cell proliferation activates Chk2-dependent G1/S cell cycle arrest, *PloS One* 9(1):e87299, 2014, https://doi.org/10.1371/journal.pone.0087299.

Nikolich-Zugich J: The aging immune system: challenges for the 21st century, *Semin Immunol* 24(5):301–302, 2012, https://doi.org/10.1016/j.smim.2012.09.001.

Nochi T, Kiyono H: Innate immunity in the mucosal immune system, *Curr Pharm Des* 12(32):4203–4213, 2006.

Noguchi M, Yi H, Rosenblatt HM, Filipovich AH, et al.: Interleukin-2 receptor gamma chain mutation results in X-linked severe combined immunodeficiency in humans, *Cell* 73(1):147–157, 1993.

Nomura L, Maino VC, Maecker HT: Standardization and optimization of multiparameter intracellular cytokine staining, *Cytometry* 73(11):984–991, 2008.

Nordenfelt P: Quantitative assessment of neutrophil phagocytosis using flow cytometry, *Methods Mol Biol* 1124:279–289, 2014, https://doi.org/10.1007/978-1-62703-845-4_18.

Nowell PC: Phytohemagglutinin: an initiator of mitosis in cultures of normal human leukocytes, *Cancer Res* 20:462–466, 1960.

Nuutila J, Lilius EM: Flow cytometric quantitative determination of ingestion by phagocytes needs the distinguishing of overlapping populations of binding and ingesting cells, *Cytometry* 65(2):93–102, 2005.

O'Gorman MR, Zollett J, Bensen N: Flow cytometry assays in primary immunodeficiency diseases, *Methods Mol Biol* 699:317–335, 2011, https://doi.org/10.1007/978-1-61737-950-5_15.

O'Gorman MRG: Flow cytometry assays in primary immunodeficiency diseases, *Methods Mol Biol* 1678:321–345, 2018, https://doi.org/10.1007/978-1-4939-7346-0_14.

Ochs HD, Hagin D: Primary immunodeficiency disorders: general classification, new molecular insights, and practical approach to diagnosis and treatment, *Ann Allergy Asthma Immunol* 112(6):489–495, 2014, https://doi.org/10.1016/j.anai.2014.04.007.

Ogle JD, Noel JG, Sramkoski RM, Ogle CK, Alexander JW: Phagocytosis of opsonized fluorescent microspheres by human neutrophils. A two-color flow cytometric method for the determination of attachment and ingestion, *J Immunol Meth* 115(1):17–29, 1988.

Ohkuma S, Poole B: Fluorescence probe measurement of the intralysosomal pH in living cells and the perturbation of pH by various agents, *Proc. Natl. Acad. Sci. U.S.A* 75:3327–3331, 1978.

Ohri LK, Manley JM, Chatterjee A, Cornish NE: Pediatric case series evaluating a standardized Candida albicans skin test product, *Ann Pharmacother* 38(6):973–977, 2004.

Oldhafer F, Wittauer EM, Falk CS, DeTemple DE, Beetz O, Timrott K, et al.: Alloresponses of mixed lymphocyte hepatocyte culture to immunosuppressive drugs as an in-vitro model of hepatocyte transplantation, *Ann Transplant* 24:472–480, 2019, https://doi.org/10.12659/AOT.915982.

Ortaldo JR, Wiltrout RH, Reynolds CW: Natural killer activity: early days, advances, and seminal observations, *Crit Rev Oncog* 19(1–2):1–13, 2014.

Packman CH, Lichtman MA: Activation of neutrophils: measurement of actin conformational changes by flow cytometry, *Blood Cell* 16(1):193–205, 1990.

Palutke M, KuKuruga D, Tabaczka P: A flow cytometric method for measuring lymphocyte proliferation directly from tissue culture plates using Ki-67 and propidium iodide, *J. Immunol Meth* 105(1):97–105, 1987.

Palutke M, Tabaczka PM, Kukuruga DL, Kantor NL: A method for measuring lymphocyte proliferation in mixed lymphocyte cultures using a nuclear proliferation antigen, Ki-67, and flow cytometry, *Am J Clin Pathol* 91(4):417–421, 1989.

Passlick B, Flieger D, Ziegler-Heitbrock HW: Identification and characterization of a novel monocyte subpopulation in human peripheral blood, *Blood* 74(7):2527–2534, 1989.

Pattanapanyasat K: Immune status monitoring of HIV/AIDS patients in resource-limited settings: a review with an emphasis on CD4+ T-lymphocyte determination, *Asian Pac J Allergy Immunol* 30(1):11–25, 2012.

Pattanapanyasat K, Sukapirom K, Tachavanich K, Kaewmoon S: Flow cytometric quantitation of opsonophagocytosis and intracellular killing of Candida albicans using a whole blood microassay, *Cytometry* 71(12):1027–1033, 2007.

Paucek RD, Baltimore D, Li G: The cellular immunotherapy revolution: arming the immune system for precision therapy, *Trends Immunol* 40(4):292–309, 2019, https://doi.org/10.1016/j.it.2019.02.002.

Paul WE: *Fundamental immunology New York*, Bauer Press, 1993.

Paul WE, Seder RA: Lymphocyte responses and cytokines, *Cell* 76(2):241–251, 1994.

Paxton H, Pins M, Denton G, McGonigle AD, Meisner PS, Phair JP: Comparison of CD4 cell count by a simple enzyme-linked immunosorbent assay using the TRAx CD4 test kit and by flow cytometry and hematology, *Clin Diagn Lab Immunol* 2(1):104–114, 1995.

Pennington JA: Intakes of minerals from diets and foods: is there a need for concern? *J Nutr* 126(9 Suppl):2304S–2308S, 1996.

Perfetto SP, Chattopadhyay PK, Roederer M: Seventeen-colour flow cytometry: unravelling the immune system, *Nat Rev Immunol* 4(8):648–655, 2004.

Perfetto SP, Currier J, Birx DL: T-lymphocyte activation and cell signaling. In Rose NR, Hamilton RG, Detrick B, editors: *Manual of clinical laboratory immunology*, 6th ed, Washington, DC, 2002, ASM Press, pp 224–237.

Pesu M, Candotti F, Husa M, Hofmann SR, Notarangelo LD, O'Shea JJ: Jak3, severe combined immunodeficiency, and a new class of immunosuppressive drugs, *Immunol Rev* 203:127–142, 2005.

Peters VB, Rosh JR, Mugrditchian L, Birnbaum AH, Benkov KJ, Hodes DS, LeLeiko NS: Growth failure as the first expression of malnutrition in children with human immunodeficiency virus infection, *Mt Sinai J Med* 65(1):1–4, 1998.

Petrovsky N, Harrison LC: Cytokine-based human whole blood assay for the detection of antigen-reactive T cells, *J Immunol Methods* 186(1):37–46, 1995.

Philbin VJ, Levy O: Developmental biology of the innate immune response: implications for neonatal and infant vaccine development, *Pediatr Res* 65(5 Pt 2):98R–105R, 2009, https://doi.org/10.1203/PDR.0b013e31819f195d.

Pierzchalski A, Mittag A, Tarnok A, Introduction A: Recent advances in cytometry instrumentation, probes, and methods–review, *Methods Cell Biol* 102:1–21, 2011, https://doi.org/10.1016/B978-0-12-374912-3.00001-8.

Pike KA, Hui C, Krawczyk CM: Detecting secreted analytes from immune cells: an overview of technologies, *Methods Mol Biol* 1458:111–124, 2016, https://doi.org/10.1007/978-1-4939-3801-8_9.

Piyasena ME, Graves SW: The intersection of flow cytometry with microfluidics and microfabrication, *Lab Chip* 14(6):1044–1059, 2014, https://doi.org/10.1039/c3lc51152a.

Poli A, Michel T, Patil N, Zimmer J: Revisiting the functional impact of NK cells, *Trends Immunol* 39(6):460–472, 2018, https://doi.org/10.1016/j.it.2018.01.011.

Poli A, Michel T, Theresine M, Andres E, Hentges F, Zimmer J: CD56bright natural killer (NK) cells: an important NK cell subset, *Immunology* 126(4):458–465, 2009.

Poncelet P, Carayon P: Cytofluorometric quantification of cell-surface antigens by indirect immunofluorescence using monoclonal antibodies, *J Immunol Methods* 85(1):65–74, 1985.

Poncelet P, George F, Lavabre-Bertrand T: Immunological detection of membrane bound antigens and receptors, *Cells Tissues Methods Immunol Anal* 3:389–417, 1993.

Poncelet P, Poinas G, Corbeau P, Devaux C, Tubiana N, Muloko N, et al.: Surface CD4 density remains constant on lymphocytes of HIV-infected patients in the progression of disease, *Res Immunol* 142(4):291–298, 1991.

Popescu I, Pipeling M, Akulian J, McDyer J: Phenotypic and functional characterization of cytotoxic T lymphocytes by flow cytometry, *Methods Mol Biol* 1186:21–47, 2014, https://doi.org/10.1007/978-1-4939-1158-5_3.

Posekany KJ, Riley RS, Gagnon GA, Holbrook CT: Bimodal CD45 fluorescence distribution in precursor B-cell acute lymphoblastic leukemia, *Am J Clin Pathol* 96:423–424, 1991.

Pozarowski P, Holden E, Darzynkiewicz Z: Laser scanning cytometry: principles and applications-an update, *Methods Mol Biol* 931:187–212, 2013, https://doi.org/10.1007/978-1-62703-056-4_11.

Pranke P, Hendrikx J, Alespeiti G, Nardi N, Rubinstein P, Visser J: Comparative quantification of umbilical cord blood CD34+ and CD34+ bright cells using the ProCount-BD and ISHAGE protocols, *Braz J Med Biol Res* 39(7):901–906, 2006.

Prasad AS: Zinc and immunity, *Mol Cell Biochem* 188(1–2):63–69, 1998.

Prasad AS: Zinc: role in immunity, oxidative stress and chronic inflammation, *Curr Opin Clin Nutr Metab Care* 12(6):646–652, 2009.

Prescott SL, Macaubas C, Holt BJ, Smallacombe TB, Loh R, Sly PD, Holt PG: Transplacental priming of the human immune system to environmental allergens: universal skewing of initial T cell responses toward the Th2 cytokine profile, *J Immunol* 160(10):4730–4737, 1998.

Prodan M, Tulissi P, Perticarari S, Presani G, Franzin F, Pussini E, Pozzato G: Flow cytometric assay for the evaluation of phagocytosis and oxidative burst of polymorphonuclear leukocytes and monocytes in myelodysplastic disorders, *Haematologica* 80(3):212–218, 1995.

Prosperi E: Intracellular turnover of fluorescein diacetate. Influence of membrane ionic gradients on fluorescein efflux, *Histochem J* 22(4):227–233, 1990.

Prosperi E, Croce AC, Bottiroli G, Supino R: Influence of daunorubicin on membrane permeability properties: detection by means of intracellular accumulation and efflux of fluorescein, *Chem Biol Interact* 54(3):271–280, 1985.

Prosperi E, Croce AC, Bottiroli G, Supino R: Flow cytometric analysis of membrane permeability properties influencing intracellular accumulation and efflux of fluorescein, *Cytometry* 7(1):70–75, 1986.

Qi Y, Qiu L, Fan W, Liu C, Li Z: An enzyme-free flow cytometric bead assay for the sensitive detection of microRNAs based on click nucleic acid ligation-mediated signal amplification, *Analyst* 142(16):2967–2973, 2017, https://doi.org/10.1039/c7an00989e.

Qiu JG, Mei XL, Chen ZS, Shi Z: Cytokine detection by flow cytometry, *Methods Mol Biol* 1172:235–242, 2014, https://doi.org/10.1007/978-1-4939-0928-5_21.

Rabinovitch PS: Practical considerations for DNA content and cell cycle analysis. In Bauer KD, Duque RE, Shankey TV, editors: *Clinical flow cytometry: Principles and applications*, Baltimore, 1993, Williams & Wilkins, pp 143–156.

Rabinovitch PS: DNA content histogram and cell-cycle analysis, *Methods Cell Biol* 41:263–296, 1994.

Ramaekers FC, Hopman AH: Detection of genetic aberrations in bladder cancer using in situ hybridization, *Ann N Y Acad Sci* 677:199–213, 1993.

Ranieri E, Popescu I, Gigante M: CTL ELISPOT assay, *Methods Mol Biol* 1186:75–86, 2014, https://doi.org/10.1007/978-1-4939-1158-5_6.

Rebhahn JA, Bishop C, Divekar AA, Jiminez-Garcia K, et al.: Automated analysis of two- and three-color fluorescent Elispot (Fluorospot) assays for cytokine secretion, *Comput Methods Programs Biomed* 92(1):54–65, 2008, https://doi.org/10.1016/j.cmpb.2008.06.002.

Rego K, Pereira K, MacDougall J, Cruikshank W: Utility of the T-SPOT((R)).TB test's borderline category to increase test resolution for results around the cut-off point, *Tuberculosis* 108:178–185, 2018, https://doi.org/10.1016/j.tube.2017.12.005.

Reth M: Antigen receptor tail clue, *Nature* 338(6214):383–384, 1989.

Rezzani R, Nardo L, Favero G, Peroni M, Rodella LF: Thymus and aging: morphological, radiological, and functional overview, *Age (Dordr)* 36(1):313–351, 2014, https://doi.org/10.1007/s11357-013-9564-5.

Roberts RE, Hallett MB: Neutrophil cell shape change: mechanism and Signalling during cell Spreading and phagocytosis, *Int J Mol Sci* 20(6), 2019, https://doi.org/10.3390/ijms20061383.

Rosen FS: A brief history of immunodeficiency disease, *Immunol Rev* 178:8–12, 2000.

Rossignol A, Bonnaudet V, Clemenceau B, Vie H, Bretaudeau L: A high-performance, non-radioactive potency assay for measuring cytotoxicity: a full substitute of the chromium-release assay targeting the regulatory-compliance objective, *mAbs* 9(3):521–535, 2017, https://doi.org/10.1080/19420862.2017.1286435.

Rowe PC, Barron DF, Calkins H, Maumenee IH, Tong PY, Geraghty MT: Orthostatic intolerance and chronic fatigue syndrome associated with Ehlers-Danlos syndrome, *J Pediatr* 135(4):494–499, 1999.

Ruud E, Michaelsen T, Kindberg GM, Berg T, Funderud S, Godal T: Heterogeneity of degradation of B-cell endocytosed monoclonal antibodies reacting with different sIgM epitopes, *Scandinavian J Immunol* 29(3):299–308, 1989.

Rytter MJ, Kolte L, Briend A, Friis H, Christensen VB: The immune system in children with malnutrition–a systematic review, *PloS One* 9(8):e105017, 2014, https://doi.org/10.1371/journal.pone.0105017.

Sack U, Tarnok A: Harmonization of cytometry instrumentation and technologies, *Cytometry* 83(12):1055–1056, 2013, https://doi.org/10.1002/cyto.a.22415.

Salk HM, Haralambieva IH, Ovsyannikova IG, Goergen KM, Poland GA: Granzyme B ELISPOT assay to measure influenza-specific cellular immunity, *J Immunol Methods*. 398-399, 44–50, 2013, https://doi.org/10.1016/j.jim.2013.09.007.

Samelson LE: Signal transduction mediated by the T cell antigen receptor: the role of adapter proteins, *Annu Rev Immunol* 20:371–394, 2002.

Sanderson AR: Cytotoxic reactions of mouse Iso-Antisera: Preliminary considerations, *Br J Exp Pathol* 45:398–408, 1964.

Savino W, Dardenne M: Nutritional imbalances and infections affect the thymus: consequences on T-cell-mediated immune responses, *Proc Nutr Soc* 69(4):636–643, 2010, https://doi.org/10.1017/S0029665110002545.

Sawhney N, Hall PA: Ki67–structure, function, and new antibodies, *J Pathol* 168(2):161–162, 1992.

Schaefer L: Complexity of danger: the diverse nature of damage-associated molecular patterns, *J Biol Chem* 289(51):35237–35245, 2014, https://doi.org/10.1074/jbc.R114.619304.

Scherbakova A, Lust H, Everaus H, Aints A: A mathematical model of natural killer cell activity, *Cytometry* 83(6):585–591, 2013, https://doi.org/10.1002/cyto.a.22283.

Schmid SL: A nostalgic look back 40 years after the discovery of receptor-mediated endocytosis, *Mol Biol Cell* 30(1):1–3, 2019, https://doi.org/10.1091/mbc.E18-06-0409.

Schmittel A, Keilholz U, Thiel E, Scheibenbogen C: Quantification of tumor-specific T lymphocytes with the ELISPOT assay, *J Immunother* 23(3):289–295, 2000.

Schultes BC, Nicodemus CF: Using antibodies in tumour immunotherapy, *Expert Opin Biol Ther* 4(8):1265–1284, 2004.

Schulz D, Severin Y, Zanotelli VRT, Bodenmiller B: In-depth characterization of monocyte-derived macrophages using a mass cytometry-based phagocytosis assay, *Sci Rep* 9(1):1925, 2019, https://doi.org/10.1038/s41598-018-38127-9.

Seder RA, Gazzinelli R, Sher A, Paul WE: Interleukin 12 acts directly on CD4+ T cells to enhance priming for interferon gamma production and diminishes interleukin 4 inhibition of such priming, *Proc Natl Acad Sci U S A* 90(21):10188–10192, 1993.

Seder RA, Paul WE, Davis MM: Fazekas de St Groth B: the presence of interleukin 4 during in vitro priming determines the lymphokine-producing potential of CD4+ T cells from T cell receptor transgenic mice, *J Exp Med* 176(4):1091–1098, 1992.

Seillet C, Belz GT, Mielke LA: Complexity of cytokine network regulation of innate lymphoid cells in protective immunity, *Cytokine* 70(1):1–10, 2014, https://doi.org/10.1016/j.cyto.2014.06.002.

Sermer D, Brentjens R: CAR T-cell therapy: full speed ahead, *Hematol Oncol* 37(Suppl 1):95–100, 2019, https://doi.org/10.1002/hon.2591.

Shankey TV, Rabinovitch PS: DNA content flow cytometry. In Rose NR, Hamilton RG, Detrick B, editors: *Manual of clinical laboratory immunology*, 6th ed, Washington, DC, 2002, ASM Press, pp 171–184.

Shankey TV, Rabinovitch PS, Bagwell B, Bauer KD, Duque RE, Hedley DW, et al.: Guidelines for implementation of clinical DNA cytometry. International Society for analytical Cytology, *Cytometry* 14(5):472–477, 1993.

Shapiro HM: Lasers for flow cytometry, *Curr Protoc Cytom Chapter 1, Unit 1 9*, 2004, https://doi.org/10.1002/0471142956.cy0109s27.

Sharma L, Wu W, Dholakiya SL, Gorasiya S, et al.: Assessment of phagocytic activity of cultured macrophages using fluorescence microscopy and flow cytometry, *Methods Mol Biol* 1172:137–145, 2014, https://doi.org/10.1007/978-1-4939-0928-5_12.

Shearer WT, Rosenblatt HM, Gelman RS, Oyomopito R, et al.: Lymphocyte subsets in healthy children from birth through 18 years of age: the Pediatric AIDS Clinical Trials Group P1009 study, *J Allergy Clin Immunol* 112(5):973–980, 2003, https://doi.org/10.1016/j.jaci.2003.07.003.

Shete A, Suryawanshi P, Chavan C, Kulkarni A, et al.: Development of IFN-gamma secretory ELISPOT based assay for screening of ADCC responses, *J Immunol Methods* 441:49–55, 2017, https://doi.org/10.1016/j.jim.2016.12.001.

Siegal FP, Lopez C, Hammer GS, Brown AE, et al.: Severe acquired immunodeficiency in male homosexuals, manifested by chronic perianal ulcerative herpes simplex lesions, *N Engl J Med* 305(24):1439–1444, 1981.

Silverstein AM: History of immunology. Cellular versus humoral immunity: determinants and consequences of an epic 19th century battle, *Cell Immunol* 48(1):208–221, 1979.

Simanovsky N, Hiller N, Loubashevsky N, Rozovsky K: Normal CT characteristics of the thymus in adults, *Eur J Radiol* 81(11):3581–3586, 2012, https://doi.org/10.1016/j.ejrad.2011.12.015.

Sjursen H, Bjerknes R, Halstensen A, Naess A, et al.: *Serum opsonins to group B meningococci*, *Acta Pathologica Microbiologica*, *et Immunologica Scandinavica section*, 1987.

Sjursen H, Bjerknes R, Halstensen A, Naess A, Sarnes S, et al.: Flow cytometric assay for the measurement of serum opsonins to Neisseria meningitidis serogroup B, serotype 15, *J Immunol Methods* 116(2):235–243, 1989.

Sjursen H, Bjerknes R, Halstensen A, Solberg CO: Serum opsonins to group B meningococci in patients and vaccinated volunteers [abstract no. 204], *Cytometry* 8(suppl 1):38, 1987.

Slezak SE, Horan PK: Cell-mediated cytotoxicity. A highly sensitive and informative flow cytometric assay, *J Immunol Methods* 117(2):205–214, 1989.

Slota M, Lim JB, Dang Y, Disis ML: ELISpot for measuring human immune responses to vaccines, *Expert Rev Vaccines* 10(3):299–306, 2011, https://doi.org/10.1586/erv.10.169.

Smith JA, Weidemann MJ: Further characterization of the neutrophil oxidative burst by flow cytometry, *J Immunol Methods* 162(2):261–268, 1993.

Smith KA: The quantal theory of how the immune system discriminates between "self and non-self", *Med. Immunol* 3(3):1–22, 2004.

Smyth MJ, Cretney E, Kershaw MH, Hayakawa Y: Cytokines in cancer immunity and immunotherapy, *Immunol Rev* 202:275–293, 2004.

Sponzilli I, Notarangelo LD: Severe combined immunodeficiency (SCID): from molecular basis to clinical management, *Acta Biomed* 82(1):5–13, 2011.

Standards NCfCL: *Clinical applications of flow cytometry: quality assurance and immunophenotyping of peripheral blood lymphocytes. NCCLS Document H42-T*, Villanova, PA, 1992, National Committee for Clinical Laboratory Standards, ISBN: 1-56238-155-5.

Steinkamp JA, Wilson JS, Saunders GC, Stewart CC: Phagocytosis: flow cytometric quantitation with fluorescent microspheres, *Science* 215:64–66, 1982.

Steinman RM, Mellman I: Immunotherapy: bewitched, bothered, and bewildered no more, *Science* 305(5681):197–200, 2004.

Stelzer GT, Marti G, Hurley A, McCoy Jr P, Lovett EJ, Schwartz A: U.S.-Canadian Consensus recommendations on the immunophenotypic analysis of hematologic neoplasia by flow cytometry: standardization and validation of laboratory procedures, *Cytometry* 30(5):214–230, 1997.

Stelzer GT, Shults KE, Loken MR: CD45 gating for routine flow cytometric analysis of human bone marrow specimens, *Ann N Y Acad Sci* 677:265–280, 1993.

Stewart CC, Goolsby C, Shackney SE: Emerging technology and future developments in flow cytometry, *Hematol Oncol Clin North Am* 16(2):477–495, 2002. vii-viii.

Stewart CC, Stewart SJ: Multiparameter data acquisition and analysis of leukocytes, *Methods Mol Biol* 263:45–66, 2004.

Stott DI: Immunoblotting, dot-blotting, and ELISPOT assays: methods and applications, *J Immunoassay* 21(2–3):273–296, 2000.

Sullivan KE, Jawad AF, Randall P, Driscoll DA, Emanuel BS, McDonald-McGinn, et al.: Lack of correlation between impaired T cell production, immunodeficiency, and other phenotypic features in chromosome 22q11.2 deletion syndromes, *Clin Immunol Immunopathol* 86(2):141–146, 1998.

Suni MA, Maino VC: Flow cytometric analysis of cell signaling proteins, *Methods Mol Biol* 717:155–169, 2011, https://doi.org/10.1007/978-1-61779-024-9_9.

Suni MA, Picker LJ, Maino VC: Detection of antigen-specific T cell cytokine expression in whole blood by flow cytometry, *J Immunol Methods* 212(1):89–98, 1998.

Suresh V, Carey BS, Shaw S, Tse WY, Cartwright N, Akoh J, et al.: A retrospective study of the prognostic impact of cytokine secretion in mixed lymphocyte culture on long-term graft function following allogeneic renal transplantation, *Transpl Int* 18(9):1067–1071, 2005, https://doi.org/10.1111/j.1432-2277.2005.00172.x.

Talbot D, Shenton BK, Givan AL, Proud G, Taylor RM: A rapid, objective method for the detection of lymphocytotoxic antibodies using flow cytometry, *Clin Genet* 31(1):25–34, 1987.

Tan P, Anasetti C, Hansen JA, Melrose J, Brunvand M, Bradshaw J, et al.: Induction of alloantigen-specific hyporesponsiveness in human T lymphocytes by blocking interaction of CD28 with its natural ligand B7/BB1, *J Exp Med* 177(1):165–173, 1993.

Tario Jr JD, Gray BD, Wallace SS, Muirhead KA, Ohlsson-Wilhelm BM, Wallace PK: Novel lipophilic tracking dyes for monitoring cell proliferation, *Immunol Invest* 36(5–6):861–885, 2007, https://doi.org/10.1080/08820130701712933.

Tario Jr JD, Humphrey K, Bantly AD, Muirhead KA, Moore JS, Wallace PK: Optimized staining and proliferation modeling methods for cell division monitoring using cell tracking dyes, *J Vis Exp* 70:e4287, 2012, https://doi.org/10.3791/4287.

Tario Jr JD, Muirhead KA, Pan D, Munson ME, Wallace PK: Tracking immune cell proliferation and cytotoxic potential using flow cytometry, *Methods Mol Biol* 699:119–164, 2011, https://doi.org/10.1007/978-1-61737-950-5_7.

Tarlinton D: B cells still front and centre in immunology, *Nat Rev Immunol* 19(2):85–86, 2019, https://doi.org/10.1038/s41577-018-0107-2.

Tarnok A, Hambsch J, Chen R, Varro R: Cytometric bead array to measure six cytokines in twenty-five microliters of serum, *Clin Chem* 49(6 Pt 1):1000–1002, 2003.

Tebo AE, Detrick B, Hamilton RG, Khanolkar A, O'Gorman MR, Schmitz JL, Abraham RS: Clinical laboratory immunology: an indispensable player in laboratory medicine, *Am J Clin Pathol* 142(4):437–444, 2014, https://doi.org/10.1309/AJCPX25MFWNEYRIG.

Telford WG, Komoriya A, Packard BZ, Bagwell CB: Multiparametric analysis of apoptosis by flow cytometry, *Methods Mol Biol* 699:203–227, 2011, https://doi.org/10.1007/978-1-61737-950-5_10.

Teo A, Hasang W, Boeuf P, Rogerson S: A Robust phagocytosis assay to evaluate the opsonic activity of antibodies against Plasmodium falciparum-infected erythrocytes, *Methods Mol Biol* 1325:145–152, 2015, https://doi.org/10.1007/978-1-4939-2815-6_12.

Terasaki PI, McClelland JD: Microdroplet assay of human serum cytotoxins, *Nature* 204:998–1004, 1964.

Thomas DC: The phagocyte respiratory burst: historical perspectives and recent advances, *Immunol Lett* 192:88–96, 2017, https://doi.org/10.1016/j.imlet.2017.08.016.

Tilg H, Moschen AR: Malnutrition and microbiota–a new relationship? *Nat Rev Gastroenterol Hepatol* 10(5):261–262, 2013, https://doi.org/10.1038/nrgastro.2013.48.

Tirindelli Danesi D, Spano M, Altavista P, Pantarotto M, Filippini C, Mazzini G, et al.: Quality control study of the Italian Group of Cytometry on flow cytometry DNA content measurements: II. Factors affecting inter- and intralaboratory variability, *Cytometry* 30(2):85–97, 1997.

Torres JM, Esteban C, Aguilar J, Mishal Z, Uriel J: Quantification of alpha-fetoprotein and transferrin endocytosis by lymphoid cells using flow cytometry, *J Immunol Methods* 134(2):163–170, 1990.

Tosato F, Bucciol G, Pantano G, Putti MC, Sanzari MC, Basso G, Plebani M: Lymphocytes subsets reference values in childhood, *Cytometry* 87(1):81–85, 2015, https://doi.org/10.1002/cyto.a.22520.

Tosevski V, Mair F: Tracking cells and monitoring proliferation, *Methods Mol Biol* 1193:51–54, 2014, https://doi.org/10.1007/978-1-4939-1212-4_6.

Townsend SE, Allison JP: Tumor rejection after direct costimulation of CD8+ T cells by B7-transfected melanoma cells, *Science* 259(5093):368–370, 1993.

Trinchieri G: Natural killer cells wear different hats: effector cells of innate resistance and regulatory cells of adaptive immunity and of hematopoiesis, *Semin Immunol* 7(2):83–88, 1995.

Trinkle LS, Wellhausen SR, McLeish KR: A simultaneous flow cytometric measurement of neutrophil phagocytosis and oxidative burst in whole blood, *Diagn Clin Immunol* 5(2):62–68, 1987.

Truneh A, Machy P, Barbet J, Mishal Z, Lemonnier FA, Leserman LD: Endocytosis of HLA and H-2 molecules on transformed murine cells measured by fluorescence dequenching of liposome-encapsulated carboxyfluorescein, *EMBO J* 2(12):2285–2291, 1983.

Tuerk MJ, Fazel N: Zinc deficiency, *Curr Opin Gastroenterol* 25(2):136–143, 2009.

Uchida A, Moore M, Klein E: Autologous mixed lymphocyte-tumor reaction and autologous mixed lymphocyte reaction. I. Proliferation of two distinct T-cell subsets, *Int J Cancer* 40(2):165–170, 1987.

Uchida A, Moore M, Klein E: Autologous mixed lymphocyte-tumor reaction and autologous mixed lymphocyte reaction. II. Generation of specific and non-specific killer T cells capable of lysing autologous tumor, *Int J Cancer* 41(5):651–656, 1988.

Urban T, Jarstrand C: Nitroblue tetrazolium (NBT) reduction by bacteria. Some properties of the reaction and its possible use, *Acta Pathol Microbiol Scand B* 87(4):227–233, 1979.

Vajpayee M, Mohan T: Current practices in laboratory monitoring of HIV infection, *Indian J Med Res* 134(6):801–822, 2011, https://doi.org/10.4103/0971-5916.92627.

van de Geijn GJ, van Rees V, van Pul-Bom N, Birnie E, Janssen H, Pegels H, et al.: Leukoflow: multiparameter extended white blood cell differentiation for routine analysis by flow cytometry, *Cytometry* 79(9):694–706, 2011, https://doi.org/10.1002/cyto.a.21105.

van der Haar Avila I, Marmol P, Cany J, Kiessling R: Pico de Coana Y: evaluating antibody-dependent cell-mediated cytotoxicity by flow cytometry, *Methods Mol Biol* 1913:181–194, 2019, https://doi.org/10.1007/978-1-4939-8979-9_13.

van der Haar Avila I, Marmol P, Kiessling R: Pico de Coana Y: evaluating antibody-dependent cell-mediated cytotoxicity by chromium release assay, *Methods Mol Biol* 1913:167–179, 2019, https://doi.org/10.1007/978-1-4939-8979-9_12.

van der Merwe PA, Davis SJ: Molecular interactions mediating T cell antigen recognition, *Annu Rev Immunol* 21:659–684, 2003.

van Deurs B, R:opke C, Thorball N: Kinetics of pinocytosis studied by flow cytometry, *Eur J Cell Biol* 34(1):96–102, 1984.

van Eeden SF, Klut ME, Walker BA, Hogg JC: The use of flow cytometry to measure neutrophil function, *J Immunol Methods* 232(1–2):23–43, 1999.

Varro R, Chen R, Sepulveda H, Apgar J: Bead-based multianalyte flow immunoassays: the cytometric bead array system, *Methods Mol Biol* 378:125–152, 2007, https://doi.org/10.1007/978-1-59745-323-3_9.

Veber MB, Cunningham-Rundles S, Schulman M, Mandel F, Auld PA: Acute shift in immune response to microbial activators in very-low-birth-weight infants, *Clin Exp Immunol* 83(3):391–395, 1991.

Vigano A, Vella S, Principi N, Bricalli D, Sala N, Salvaggio A, et al.: Thymus volume correlates with the progression of vertical HIV infection, *Aids* 13(5):F29–F34, 1999.

Vijay K: Toll-like receptors in immunity and inflammatory diseases: past, present, and future, *Int Immunopharmacol* 59:391–412, 2018, https://doi.org/10.1016/j.intimp.2018.03.002.

Vindelov LL, Christensen IJ: Detergent and proteolytic enzyme-based techniques for nuclear isolation and DNA content analysis, *Methods Cell Biol* 41:219–229, 1994.

Virgo PF, Gibbs GJ: Flow cytometry in clinical pathology, *Ann Clin Biochem* 49(Pt 1):17–28, 2012, https://doi.org/10.1258/acb.2011.011128.

Vitale M, Cantoni C, Della Chiesa M, Ferlazzo G, Carlomagno S, Pende D, et al.: An historical overview: the discovery of how NK cells can kill Enemies, Recruit defense Troops, and more, *Front Immunol* 10:1415, 2019, https://doi.org/10.3389/fimmu.2019.01415.

Waller EK: Cellular immunotherapy and cancer, *Semin Oncol* 31(2 Suppl 4):87–90, 2004.

Walrand S, Valeix S, Rodriguez C, Ligot P, Chassagne J, Vasson MP: Flow cytometry study of polymorphonuclear neutrophil oxidative burst: a comparison of three fluorescent probes, *Clin Chim Acta* 331(1–2):103–110, 2003.

Wang L, Gaigalas AK, Yan M: Quantitative fluorescence measurements with multicolor flow cytometry, *Methods Mol Biol* 699:53–65, 2011, https://doi.org/10.1007/978-1-61737-950-5_3.

Wang Yang MC, Harvey NE, Cuchens MA: Buttke TM: pulse profile analyses of endocytosis in capped B lymphocytes and BCL1 cells, *Cytometry* 9(2):131–137, 1988.

Wedderburn LR, Patel A, Varsani H, Woo P: The developing human immune system: T-cell receptor repertoire of children and young adults shows a wide discrepancy in the frequency of persistent oligoclonal T-cell expansions, *Immunology* 102(3):301–309, 2001.

Weinberg DS: Relative applicability of image analysis and flow cytometry in clinical medicine. In Bauer KD, Duque RE, Shankey TV, editors: *Clinical flow cytometry: principles and applications*, Baltimore, 1993, Williams & Wilkins, pp 359–371.

Weiskopf D, Weinberger B, Grubeck-Loebenstein B: The aging of the immune system, *Transpl Int* 22(11):1041–1050, 2009.

Weiss A, Littman DR: Signal transduction by lymphocyte antigen receptors, *Cell* 76(2):263–274, 1994.

Weiss AJ: Overview of membranes and membrane plates used in research and diagnostic ELISPOT assays, *Methods Mol Biol* 792:243–256, 2012, https://doi.org/10.1007/978-1-61779-325-7_19.

Wheeless LL, Coon JS, Cox C, Deitch AD, deVere White RW, Fradet Y, et al.: Precision of DNA flow cytometry in inter-institutional analyses, *Cytometry* 12(5):405–412, 1991.

Wigzell H: Quantitative Titrations of mouse H-2 antibodies using Cr-51-Labelled target cells, *Transplantation* 3:423–431, 1965.

Wilk AJ, Blish CA: Diversification of human NK cells: lessons from deep profiling, *J Leukoc Biol* 103(4):629–641, 2018, https://doi.org/10.1002/JLB.6RI0917-390R.

Williams JM, Loertscher R, Cotner T, Reddish M, Shapiro HM, Carpenter CB, et al.: Dual parameter flow cytometric analysis of DNA content, activation antigen expression, and T cell subset proliferation in the human mixed lymphocyte reaction, *J Immunol* 132(5):2330–2337, 1984.

Wingren AG, Parra E, Varga M, Kalland T, Sjogren HO, Hedlund G, Dohlsten M: T cell activation pathways: B7, LFA-3, and ICAM-1 shape unique T cell profiles, *Crit Rev Immunol* 15(3–4):235–253, 1995.

Woo J, Baumann A, Arguello V: Recent advancements of flow cytometry: new applications in hematology and oncology, *Expert Rev Mol Diagn* 14(1):67–81, 2014, https://doi.org/10.1586/14737159.2014.862153.

Xu-Amano J, Kiyono H, Jackson RJ, Staats HF, et al.: Helper T cell subsets for immunoglobulin A responses: oral immunization with tetanus toxoid and cholera toxin as adjuvant selectively induces Th2 cells in mucosa associated tissues, *J Exp Med* 178(4):1309–1320, 1993.

Yamamura M, Uyemura K, Deans RJ, Weinberg K, Rea TH, Bloom BR, Modlin RL: Defining protective responses to pathogens: cytokine profiles in leprosy lesions, *Science* 254(5029):277–279, 1991.

Yan W, Wu J, Wong KKY, Tsia KK: A high-throughput all-optical laser-scanning imaging flow cytometer with biomolecular specificity and subcellular resolution, *J Biophotonics* 11(2), 2018, https://doi.org/10.1002/jbio.201700178.

Yannelli JR, Wroblewski JM: On the road to a tumor cell vaccine: 20 years of cellular immunotherapy, *Vaccine* 23(1):97–113, 2004.

Ygberg S, Nilsson A: The developing immune system - from foetus to toddler, *Acta Paediatr* 101(2):120–127, 2012, https://doi.org/10.1111/j.1651-2227.2011.02494.x.

Yokoyama WM, Kim S, French AR: The dynamic life of natural killer cells, *Annu Rev Immunol* 22:405–429, 2004.

Zadorozhny SS, Martynov NN: Automatic search of spots and color classification in ELISPOT assay, *Methods Mol Biol* 1808:43–50, 2018, https://doi.org/10.1007/978-1-4939-8567-8_4.

Zarbock A, Ley K: Neutrophil adhesion and activation under flow, *Microcirculation* 16(1):31–42, 2009.

Zarcone D, Tilden AB, Cloud G, Friedman HM, Landay A, Grossi CE: Flow cytometry evaluation of cell-mediated cytotoxicity, *J Immunol Methods* 94(1–2):247–255, 1986.

Zedler S, Bone RC, Baue AE, von Donnersmarck GH, Faist E: T-cell reactivity and its predictive role in immunosuppression after burns, *Crit Care Med* 27(1):66–72, 1999.

Zola H, Moore HA, Bradley J, Need JA, Beverley PC: Lymphocyte sub-populations in human cord blood: analysis with monoclonal antibodies, *J Reprod Immunol* 5(5):311–317, 1983.

Zolnierowicz J, Ambrozek-Latecka M, Kawiak J, Wasilewska D, Hoser G: Monitoring cell proliferation in vitro with different cellular fluorescent dyes, *Folia Histochem Cytobiol* 51(3):193–200, 2013, https://doi.org/10.5603/FHC.2013.0027.

Zucker RM, Fisher NC: Evaluation and purchase of an analytical flow cytometer: some of the numerous factors to consider, *Curr Protoc Cytom Chapter 1, Unit1 28*, 2013, https://doi.org/10.1002/0471142956.cy0128s63.

CHAPTER 47

LABORATORY EVALUATION OF IMMUNOGLOBULIN FUNCTION AND HUMORAL IMMUNITY

Richard A. McPherson, Roger S. Riley, H. Davis Massey

STRUCTURAL PROPERTIES OF ANTIBODIES, 952
Antibody Molecules, 952
Antibody–Antigen Interaction, 953
THE GENETIC BASIS OF ANTIBODY DIVERSITY, 955
GENERAL PROPERTIES OF IMMUNOGLOBULINS, 956
Immunoglobulin M, 956
Immunoglobulin G, 956
Immunoglobulin A, 956
Immunoglobulin D, 959
Immunoglobulin E, 959
Summary, 959
CLINICAL SIGNIFICANCE OF IMMUNOGLOBULINS, 959
Disease Pathogenesis, 959
Disease Diagnosis, 961
Disease Prevention and Therapy, 967
SELECTED REFERENCES, 967

KEY POINTS

- Five different classes of antibody are known—immunoglobulin (Ig) M, IgG, IgA, IgD, and IgE—each with a distinct heavy chain.
- Two different light-chain types have been identified: κ and λ.
- Antigens react with antibodies at the Fab region, which contains variable regions of both heavy and light chains.
- The Fc region on the heavy chains determines what other proteins will bind to the antibody (e.g., complement).
- IgG is prevalent in blood and tissue fluids; IgM is found mainly in the blood; secretory IgA is found primarily on epithelial surfaces; IgD is bound mostly to B cells; and IgE is bound largely to basophils and mast cells.
- Polyclonal increases in immunoglobulins occur as part of the immune response and may be found in chronic disease.
- Monoclonal increases in immunoglobulins suggest a plasma cell dyscrasia.
- Diagnosis of disorders of immunoglobulins is aided by their quantitative measurement, in addition to qualitative measures of their clonality by immunofixation electrophoresis and by determination of free light-chain concentrations.
- Cryoglobulins can arise as excess monoclonal immunoglobulin (type I), which causes hyperviscosity, or as an IgM autoantibody against IgG (types II and III), which forms circulating immune complexes and causes vasculitis.
- Oligoclonal bands of immunoglobulin in cerebrospinal fluid suggest autoimmune disorders, such as demyelinating disease or infection.
- Antibodies are the effector molecules of humoral (B cell–mediated) immunity. They are immunoglobulins that react specifically and bind with the antigens that stimulated their production. By mass, immunoglobulins make up about 20% of plasma proteins in healthy individuals. Antibody activity is associated with the slowest migrating proteins on electrophoresis: the γ-globulins. The focus of this chapter is to discuss the general structural and functional properties of immunoglobulins, their laboratory evaluation, and their clinical significance.

STRUCTURAL PROPERTIES OF ANTIBODIES

ANTIBODY MOLECULES

The molecular structure of antibodies has been well elucidated (Padlan, 1991; Poljak, 1991; Tedford & Stimson, 1991). An immunoglobulin (Ig) molecule is a Y-shaped glycoprotein. It has two identical antigen-binding sites at the tips of the Y (Fab region) and binding sites for complement components and/or various cell surface receptors on the tail of the Y (Fc region). Each immunoglobulin molecule is composed of two identical heavy (H) chains and two identical light (L) chains. These polypeptide chains are held together by noncovalent interactions that are stabilized by disulfide bonds. Parts of both the H and L chains form the antigen-binding sites. Each immunoglobulin L and H chain consists of a variable region of about 110 amino acid residues at its amino-terminal end (the tips of the Y), which forms the antigen-binding site, linked to a constant region. The H chain constant region is three or four times larger than that of the L chain. Each chain is composed of repeating, similarly folded domains: An L chain has one variable region (VL) and one constant region (CL) domain, whereas an H chain has one variable region (VH) and three or four constant region (CH) domains (Fig. 47.1). The amino acid sequence variation in the variable regions of both L and H chains is, for the most part, confined to three small hypervariable regions that come together at the amino-terminal end of the molecule to form the antigen-binding site. Each antigen-binding site is only large enough to bind an antigenic determinant the size of five or six sugar residues.

Five different heavy-chain isotypes (γ, α, μ, δ, ε) and two light-chain isotypes (κ and λ) have been identified, with some of the isotypes having further subtypes. For example, γ has subtypes γ1, γ2, γ3, and γ4. The isotypes are formed as a result of variations in the constant regions of the heavy and light chains. These isotypic designations are the basis for the nomenclature of antibodies. Because the heavy chain alone determines effector functions, immunoglobulins are conveniently referred to by their heavy-chain isotype (class) using an English letter terminology (IgG, IgA, IgM, IgD, and IgE).

Antibodies have two identical antigen-binding sites. An antigen-binding site is made up of amino acids from one H chain class and one L chain class. Thus, the four-chain Y monomer molecules (see Fig. 47.1) possess two identical antigen-combining sites and are said to be **bivalent**. Such antibody molecules can cross-link antigen molecules into a large lattice if the antigen molecules each have three or more antigenic determinants. Once the lattice reaches a certain size, it precipitates out of solution (Davies & Metzer, 1983). This cross-linking is physiologically important because it enhances the engulfment of antigen, such as that expressed by bacteria and by phagocytic leukocytes. It is also involved in activation of the complement system. In addition, cross-linking may be required for the triggering of antibody-producing cells (B lymphocytes) by antigen. The efficiency of antigen-binding and cross-linking reactions by antibodies is greatly increased by a flexible hinge region, where the arms of the Y join the tail, allowing the distance between the two antigen-binding sites to vary.

Multivalence affects the avidity with which an antibody can bind certain types of antigens. A particulate antigen (such as a bacterium or virus) has repeating antigenic determinants on its surface. An antibody molecule may interact with a single particle in such a manner that both of its antigen-combining sites are bound to antigenic determinants on that particle rather than to antigenic determinants on two adjacent particles. When this type of binding occurs, the effective energy of interaction or avidity is greatly increased compared with that associated with monovalent attachments to two particles. This mechanism has been shown to be physiologically important in the neutralization of viruses by antibodies of relatively low binding affinity.

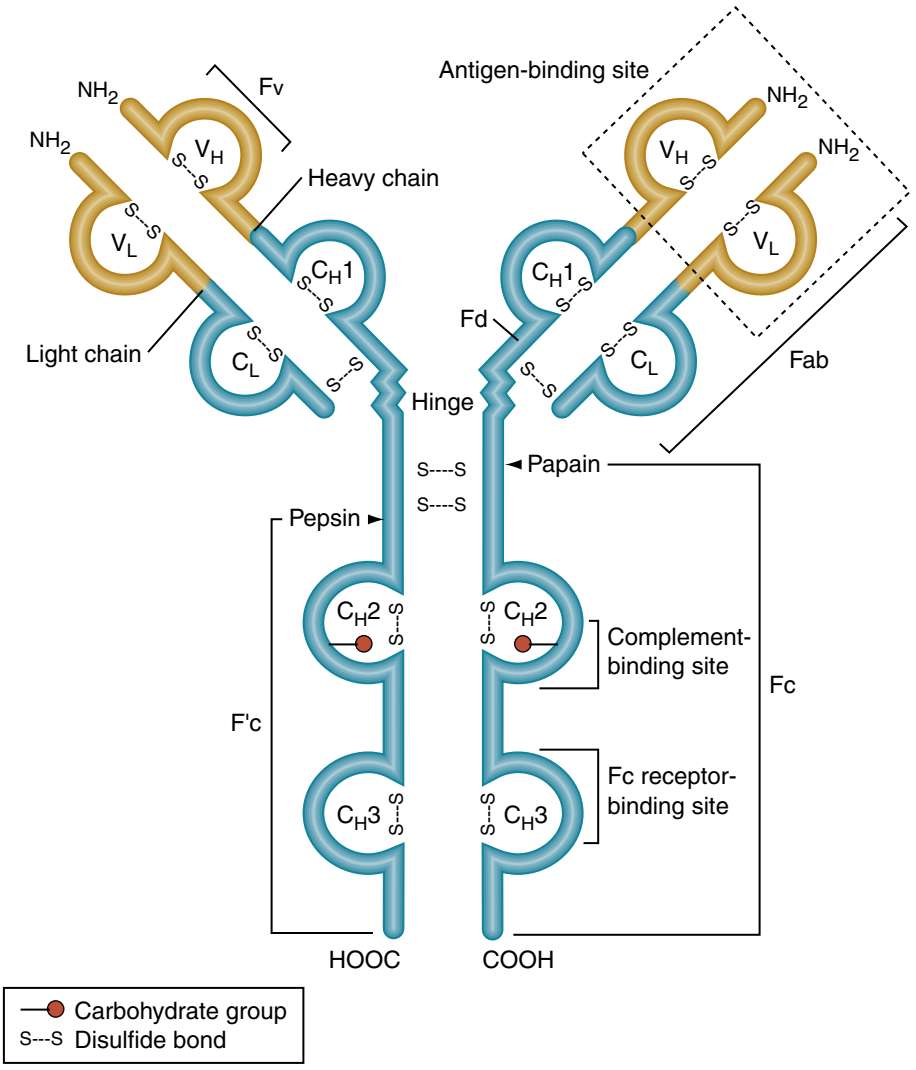

Figure 47.1 Schematic representation of immunoglobulin G molecule. The relative positions of the interchain disulfide bonds and the intrachain disulfide bonds that form the loop regions are shown. Each of the loops delineates the domain of the light and heavy chain labeled accordingly. Probable sites of enzymatic cleavage in the "hinge" region by papain or pepsin are indicated. The papain fragments are designated Fab and Fc. The pepsin fragments are Fc′ and Fab′2 (2 Fab fragments disulfide-linked). Digestion of Fab with pepsin under proper conditions yields the fragment Fv (VH and VL noncovalently associated). The part of the heavy chain that contributes to the Fab fragment is designated Fd.

The protective effect of immunoglobulins is not due simply to their ability to bind antigen. They engage in a variety of biological activities mediated by the tail of the Y, the Fc region of the molecule. This part of the antibody molecule determines what will happen to the antigen once it is bound. Immunoglobulins with the same antigen-binding capacity can have a variety of different Fc regions and, therefore, different functional properties, such as activating the complement system and attaching to Fc receptors on macrophages, thereby aiding phagocytosis of antigens.

Because of its exposed location and loosely folded structure, the **hinge region** is readily attacked by various proteolytic enzymes. As the name suggests, the hinge region confers a certain amount of flexibility on the molecule, allowing it to assume the Y-shaped structure. This permits an antibody to become attached to a single particle (e.g., a bacterium) through both of its antigen-combining sites or to stretch out to its full length to join two particles. The unique properties conferred by the hinge region on Ig molecules are related to its rich content of proline and hydrophilic amino acid residues. The inter–H chain disulfide bonds of IgG, IgA, and IgD molecules are located in the hinge region (see Fig. 47.1).

The proteolytic enzymes papain and pepsin cleave antibody molecules into different characteristic fragments that lead to an understanding of the structure–function relationship of the protein. Papain cleavage produces two separate and identical Fab (fragment antigen-binding) fragments, each with one antigen-binding site, and one Fc fragment (so-called because in nonhuman primates, it readily crystallizes). On the other hand, pepsin cleavage produces one F(ab′)2 fragment, so-called because it consists of two covalently linked F(ab′) fragments (each slightly larger than a Fab fragment). The rest of the molecule is broken down into smaller fragments of various sizes (see Fig. 47.1). Because F(ab′)2 fragments are bivalent, they can still cross-link antigens and form precipitates. This is not true of the univalent Fab fragments. Neither of these fragments (subunits of antibodies) has the other biological properties of intact antibody molecules because they lack the tail (the Fc region) that mediates these properties. However, monovalent Fab is the form of postimmunization monospecific, affinity-purified ovine antibody that is used therapeutically in patients for such applications as removing toxic levels of digoxin (Digibind) or neutralizing crotalid snake venoms (CroFab).

Each B-cell clone makes antibody molecules with a unique antigen-binding site. Initially, the molecules are inserted into the plasma membrane, where they serve as cell surface receptors for antigen. When antigen binds to the membrane-bound antibodies, B cells are activated to multiply, differentiate to a plasma cell, and synthesize a large amount of soluble antibody with the same antigen-binding site, which is secreted into the blood. Humoral antibodies defend humans and animals against infection by inactivating viruses and bacterial toxins via VH/VL domains and by recruiting complement and various cells to kill and ingest invading microorganisms via CL domains in the Fc region of the molecule. The biological properties of the various immunoglobulin domains are summarized in Table 47.1.

ANTIBODY–ANTIGEN INTERACTION

The binding of an antigen to antibody is reversible. The affinity and the number of binding sites contribute to the strength of an antibody–antigen interaction. This reversible binding is a result of many relatively weak noncovalent forces, including hydrophobic and hydrogen bonds, van der

TABLE 47.1
Biological Properties of Immunoglobulin Domains

Domain	Known or Probable Function
CH3	1 Cytotrophic reactions involving: a. Macrophages and monocytes b. Heterologous mast cells c. Cytotoxic killer (K) cells d. B cells 2. Noncovalent assembly of heavy and light chains
CH2	1. Binding of complement (C1q) 2. Control of catabolic rate
CH1/CL	1. Noncovalent assembly of heavy and light chains 2. Covalent assembly of heavy and light chains 3. Spacers between interdomain interactions involving antigen binding and effector functions VH/VL1.
	1. Antigen binding 2. Noncovalent bonding of heavy and light chains

Used with permission from Dorrington KJ, Painter RH: Biological activities of the constant region of immunoglobulin G. In Mandel TE et al., editors: *Progress in immunology III,* Canberra, 1977, Australian Academy of Science.

Waals forces, and ionic interactions. These weak forces are effective only when the antigen molecule is close enough to allow some of its atoms to fit into complementary recesses (regions) on the antibody surface. The complementary regions of a four-chain antibody unit are its two identical antigen-binding sites, whereas the corresponding region on the antigen is an antigenic determinant. Most antigenic macromolecules have many different antigenic determinants; if two or more of them are identical, the antigen is said to be *multivalent*.

The **affinity** of an antibody molecule reflects the tightness of fit of an antigenic determinant to a single antigen-binding site, and it is independent of the number of antigenic sites. However, the total **avidity** of an antibody for a multivalent antigen, such as a polymer with repeating subunits, is defined as the total binding strength of all of its binding sites together. A typical IgG molecule binds at least 10,000 times more strongly to a multivalent antigen if both antigen-binding sites are engaged than if only one site is involved.

For the same reason, if the affinity of the antigen-binding sites in an IgG and an IgM molecule is the same, the IgM molecule (because it is a pentamer and thus has 10 binding sites) will have much greater avidity for a multivalent antigen than an IgG molecule (which has two binding sites). This difference in avidity is important in view of the fact that antibodies produced early in an immune response usually have much lower affinities than those produced later. The increase in the average affinity of antibodies produced as time passes after immunization is called *affinity maturation*. This occurs because the antibody response to an antigen is heterogeneous—that is, antibodies with different antigen-combining sites are elicited against the antigen by the responding clones of B lymphocytes. Because of its high total avidity, IgM (the major Ig class produced early in immune responses) can function even when each of its binding sites has only low affinity.

Avidity of an antibody can be assessed by introducing a chaotropic agent such as urea into the assay mixture to break apart low-energy molecular interactions. Under these conditions, high-avidity antibodies remain bound to their antigens, whereas those of low avidity dissociate from their antigens and are not detected. Measurement of IgG antibody avidity is applied clinically for differentiating recent infections from previous infections in cases in which the IgM response is prolonged and, therefore, not useful for this purpose. As an example, West Nile virus infection shows low-avidity IgG antibodies in recent infections (2–43 days after onset of symptoms) but high-avidity IgG antibodies at 6 months or more after onset (Levett et al., 2005). Similar use of antibody avidity measurements to distinguish recent/acute from longer-term/chronic infections has been applied to the human immunodeficiency virus (HIV) (Keating et al., 2012); hepatitis C virus (Kanno & Kazuyama, 2002); toxoplasmosis (Rodrigues et al., 2015); human cytomegalovirus (De Paschale et al., 2014); measles, mumps, and rubella (Kontio et al., 2012); and other infectious agents.

The size of the antigen–antibody complex is determined by the valence of the antigen and the relative concentrations of the antigen and antibody. The antigen–antibody precipitation reaction is based on cross-linking of multivalent antigens by bivalent antibodies. If only one species of antibody (a monoclonal response) is present, molecules with only one antigenic determinant cannot be cross-linked. If an antigen is bivalent, it can form small cyclic complexes or linear chains with antibody, whereas an antigen with three or more antigenic determinants can form large three-dimensional lattices that readily precipitate. However, most antisera elicited against an antigen contain a variety of different antibodies (a polyclonal response) that react with different determinants on the antigen and can cooperate in cross-linking the antigen. By contrast, homogeneous (monoclonal) antibodies can precipitate molecules only if they contain repeating identical antigenic determinants.

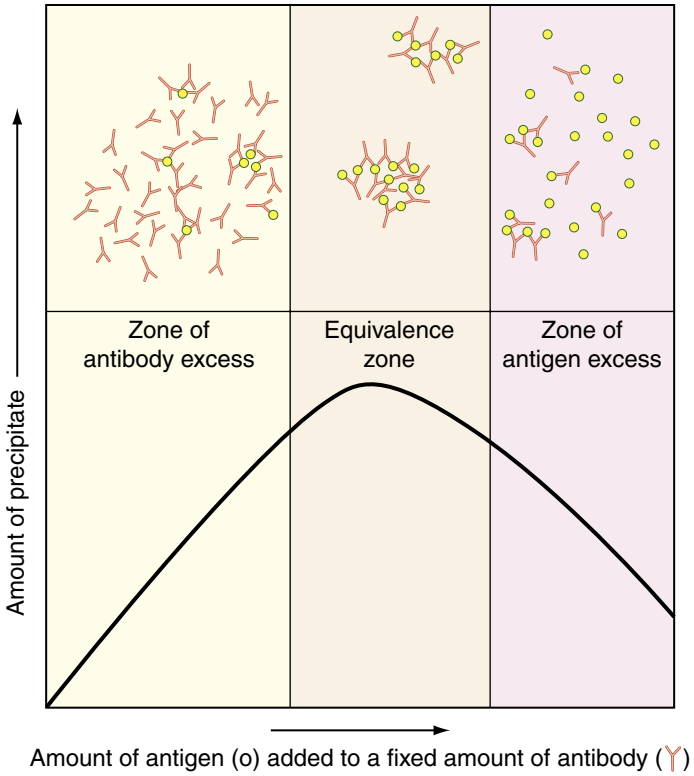

Figure 47.2 Antibody and antigen concentrations influence the size of antigen–antibody complexes formed. The largest complexes are formed when both molecules are present at approximately the same molar concentration (zone of equivalence), whereas the smallest complexes are formed when the antigen is present in great excess. Note that the small complexes formed in antigen excess have only a few antibody molecules per complex. For this reason, they are inefficiently cleared from the extracellular fluids by macrophages.

Given valence conditions that allow the formation of large aggregates, the size of the antigen–antibody complexes that form depends critically on the relative molar concentrations of the two reactants. If an excess of antigen or antibody is present, large complexes are unlikely to form (Fig. 47.2). This property is crucial to understanding seemingly paradoxical reactions in some immunoassays that depend on antigen–antibody complex formation. For example, a vast excess of antigen can completely saturate all antibody-binding sites, leading to a negative signal (i.e., no agglutination). This phenomenon is sometimes referred to as the *prozone effect*. The prozone effect remains a potential problem for modern assay systems, including syphilis testing, in which extremely high-titer antibodies can be missed unless the specimen is tested at dilutions (Smith & Holman, 2004) and even in immunofixation electrophoresis (see later discussion, Fig. 47.6E).

The prozone effect, or **hook effect**, occurs in many different immunoassays, particularly those based on sandwich formation involving a capture antibody (usually solid phase) that binds antigen plus a second reporter antibody (typically labeled with an enzyme, fluorescent or chemiluminescent dye, or radioactivity) also directed against the antigen. When antigen is present in excess, it can saturate both capture and reporter antibodies, thereby preventing sandwich formation. This situation is analogous in part to the right side of Figure 47.2, where signal strength diminishes at high antigen concentration. Assay results can be inappropriately low or even nonreactive with exceedingly high antigen concentrations. As the specimen is further diluted and reassayed, the measured value paradoxically increases

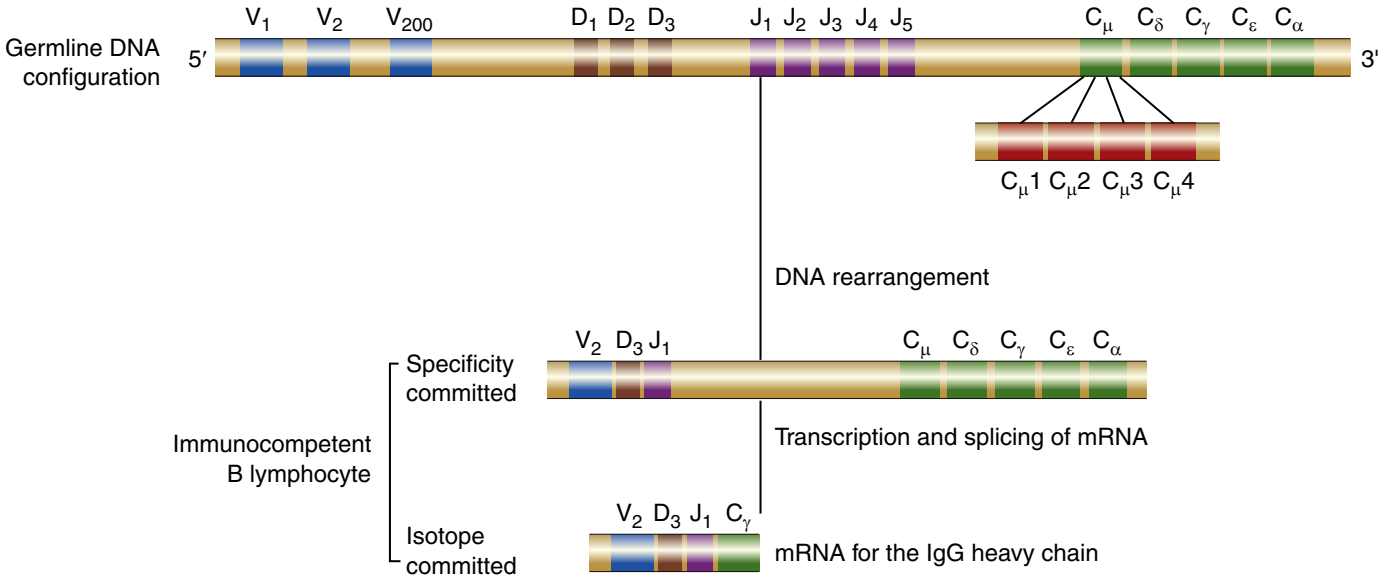

Figure 47.3 Organization and rearrangement of heavy chain immunoglobulin (Ig) genes (exons) on the mouse 12 chromosome. Each VH gene also has a leader sequence, which is not shown. The constant region genes are identified by the heavy-chain isotype, and more than one gene exists for the Cγ and Cα isotypes. Unlike Cγ and Cα genes, CH genes are composed of multiple exons, as illustrated for the Cμ gene (Cμ1–Cμ4 domains). The switch sites are located at the 5′ end of each of the CH genes and are not shown. The *solid line* represents the intervening sequences (introns) between genes or gene segments. Each heavy chain is encoded by four distinct gene segments: V, D, J, and C. (Redrawn with permission from Marcu KB: Immunoglobulin heavy-chain constant region genes, *Cell* 29:719, 1982. Copyright © by Cell Press.)

as antigen concentration falls back into the assay range. This manifestation of the prozone is termed the *hook effect* after the shape of the dose-response curve, which is directly proportional to antigen concentration in most specimens but reverses and falls off at much higher antigen concentrations. The hook effect occurs in immunoassays in which the antigen concentration can vary over several orders of magnitude. The assay may be configured to measure antigens over only two or three orders of magnitude, but when antigen concentration ranges over 4, 5, or more orders of magnitude, the hook effect will likely occur, giving rise to falsely low results. Immunoassays in which the hook effect can be prominent include those for human chorionic gonadotropin, IgA (especially in IgA myeloma), and immunoglobulin light chains.

The size and composition of antibody–antigen complexes are not only important in influencing precipitation reactions in vitro, but they are crucial in determining the fate of the complexes in the body. Complexes formed at equivalence or in antibody excess have multiple protruding Fc regions and, therefore, bind strongly to Fc receptors in macrophages, which ingest and degrade them. Small complexes, formed in antigen excess, have only one Fc region per complex. Therefore, they bind poorly to Fc receptors on macrophages and are less efficiently destroyed. Instead, they may be deposited in small blood vessels in the skin, kidneys, joints, and brain, where they may activate the complement system, causing inflammation and the destruction of tissue.

Although it appears that antigen–antibody complexes have a rigid "lock-and-key" appearance, antibodies are dynamic entities that undergo structural fluctuations (Karplus & McCammon, 1983; Wilson et al., 1991). Conformational changes may even be required for binding. These adjustments include side chain shifts of up to 20 to 30 nm, aromatic ring rotations, conformational changes, and even small rotations between VH and VL domains (Bhat et al., 1990; Standfield et al., 1990; Herron et al., 1991).

THE GENETIC BASIS OF ANTIBODY DIVERSITY

It is estimated that a human is able to make at least 10^6 to 10^9 different antibody molecules. Special genetic mechanisms have evolved to produce the very large number of immunoglobulin molecules that develop in response to antigen stimulation without the need for an excessive number of genes (Max, 2003).

Immunoglobulin molecules are produced by three separate gene pools encoding the κ, λ, and H chains, respectively. The gene pools for light and heavy chains reside on different chromosomes. In each pool, separate gene segments that encode for different parts of the variable regions of light and heavy chains can be brought together by site-specific recombination events during B cell differentiation. The light chain gene pools contain one or more constant (C) genes and sets of variable (V) and joining (J) gene segments. The H chain gene pool contains a set of C genes and sets of V, diversity (D), and J gene segments. To make an antibody molecule, a VL gene segment is recombined with a JL gene segment to produce a V gene for the light chain, and a VH gene segment is recombined with D and JH segments to produce a V gene for the heavy chain (Fig. 47.3). Each of the assembled gene segments is then cotranscribed with the appropriate constant region sequence to produce a messenger RNA molecule that encodes for the complete polypeptide chain. By variously combining inherited gene segments encoding for VL and VH regions, vertebrates can make thousands of different light chains and thousands of different H chains that can associate to form millions of different antibody molecules.

The baseline repertoire of antibody molecules can be expanded still further by somatic hypermutation, which seems to be activated by exposure to antigen. Thus, the selective role of antigen in the presence of somatic mutation appears to lead to fine-tuning of the immune response and to a virtually unlimited diversity of antibody molecules. Somatic point mutations in immunoglobulin genes occur in B cells (not germ cells) during the lifetime of the animal or of humans (Tonegawa, 1983). The somatic hypermutations are largely confined to the H chain and L chain variable region genes and the introns immediately surrounding them. It is estimated that close to one mutation will occur in the H or L chain V region of an individual cell with each cell division. This not only increases antibody diversity but may cause a change in the affinity with which the antibody binds its ligand. Those emerging B cells that can bind the antigen more avidly have an advantage over other B cells that do not bind the antigen as avidly. As the concentration of antigen falls, those B cells that have more avid receptors dominate the population of responding cells. This results in greater affinity of the antibodies being produced on rechallenge than in the initial response. Thus, this process of somatic hypermutation can result in the presence in immunized individuals of high-affinity antibodies that are much more effective on a weight basis.

All B cells initially make IgM antibodies. Some later switch to make antibodies of other classes (isotypes: IgG, IgA, etc.) that have the same antigen-binding site (idiotype) as the original IgM antibodies (**allelic exclusion**; Table 47.2). Such class switching in combination with allelic exclusion allows the same antigen-binding sites (same VH and light chain) to be distributed among antibodies with many different biological properties (secondary effector functions) (Corcoran, 2005).

Thus, the gene organization mechanism permits the assembly of immunoglobulin molecules with a variety of specificities. Antibody

TABLE 47.2
Summary of Immunoglobulin Variants

Type of Variation	Distribution	Variant	Location	Examples
Isotypic	All variants present in serum of a normal individual	Classes	C_H	IgM, IgE
		Subclasses	C_H	IgA1, IgA2
		Types	C_L	κ, λ
		Subtypes	C_L	λOz+, λOz–
		Subgroups	V_L, V_H	$V_{\kappa I}$, $V_{\kappa II}$, V_{HI}, V_{HII}
Allotypic	Allelic forms not present in all individuals	Allotypes	Mainly C_H/C_L Occasionally V_H/V_L	Gm group (human γ chain; e.g., IgG1, G1m3, G1m17) b_4, b_5, b_6, b_9 (rabbit light chain)
Idiotypic	Antigenic individuality specific to each immunoglobulin molecule	Idiotypes	V_H/V_L	Determinant identified by antibody specific to an individual immunoglobulin

Modified with permission from Sell S: *Immunology, immunopathology, and immunity,* ed 4. New York, 1987, Elsevier Science.

diversity depends on the presence of multiple gene segments, their rearrangement into different sequences, the combination of different light and heavy chains in the assembly of immunoglobulin molecules, and somatic mutations.

GENERAL PROPERTIES OF IMMUNOGLOBULINS

The various classes of human immunoglobulins and their properties (Spiegelberg, 1974; Kolar & Capra, 2003) are summarized in Tables 47.3 and 47.4.

IMMUNOGLOBULIN M

This glycoprotein is the major class of antibody secreted into the blood in the early stages of a **primary** antibody response. Normally, the secreted form of IgM is a pentamer composed of five four-chain units, a macroglobulin with a 19S sedimentation rate, and a molecular weight of 900 kDa. However, in human autoimmune disorders, such as systemic lupus erythematosus (SLE), the monomeric 7S form may be detected in appreciable amounts in serum. Selective IgM deficiency is a rare disorder associated with the absence of IgM and normal levels of other immunoglobulin classes. The cause of this disorder is unknown.

Because pentameric IgM has a total of 10 antigen-binding sites, it is more efficient than 7S monomeric IgM or IgG molecules in cross-linking antigen and in activating the complement system when bound to antigen. Thus, this high efficiency in binding and activating complement, coupled with its early appearance during the course of infection, makes IgM a particularly potent agent in combating microbial invasions.

Each IgM pentamer contains one copy of another polypeptide chain, called a *J (joining) chain*, which has a molecular weight of 15 kDa. This accessory polypeptide is produced by IgM-secreting cells. It is an acidic glycoprotein with a high content of cysteine residues and, thus, is disulfide linked between two adjacent IgM monomeric Fc regions at the carboxy-terminal end. Presumably, oligomerization is initiated at this site.

IgM is also the first class of antibody to be produced by developing B cells. The immediate precursors of B cells, called pre-B cells, make μ chains but not light chains, which accumulate in the cells. Pre-B cells then begin to synthesize light chains, which combine with μ chains to form four-chain monomer IgM molecules. The two μ-chain and two light-chain component is inserted into the plasma membrane, where it functions as a receptor for antigen. At this point, the cells have become B lymphocytes and can respond to antigen.

Perhaps because of its large size, secreted pentamer IgM is not found to any significant extent in tissue spaces; it is confined to the blood circulation and does not cross the placenta. IgM is a minor component of secretory immunoglobulins at mucosal surfaces and in breast milk.

IgM is phylogenetically the most primitive of the immunoglobulins, and most variants of the genes from the μ chain appear to have evolved into heavy chain genes for the other immunoglobulin classes. Additional physical and biological properties of IgM, as well as the other classes of immunoglobulin, are given in Tables 47.3 and 47.4.

IMMUNOGLOBULIN G

IgG is the best-studied isotype at both structural and functional levels (Burton, 1985). Antibodies of this class constitute the major immunoglobulin in the blood. They are copiously produced during the **secondary** immune response. The Fc region of IgG molecules binds to specific receptors on phagocytic cells, such as macrophages and polymorphonuclear leukocytes, thereby increasing the efficiency with which the phagocytic cells can ingest and destroy infecting microorganisms that have become coated with IgG antibodies in response to infection. These receptors on antibodies attached to target cells also guide natural killer (NK) lymphocytes to destroy them through the process of antibody-dependent cell-mediated cytotoxicity (ADCC). The best-known function of IgG is complement activation via the classical cascade. The Fc region of IgG can bind to and thereby activate the first component of the complement system, which unleashes a biochemical attack that kills the microorganisms. At least two molecules of IgG are required for complement activation compared with one molecule of IgM, which has five Fc regions.

IgG molecules are the only antibodies that can pass from mother to fetus. Cells of the placenta that are in contact with maternal blood have receptors that bind the Fc region of IgG molecules and mediate their passage to the fetus. The antibodies first are ingested by receptor-mediated endocytosis and then are transported across the cell and released by exocytosis into the fetal blood. Other classes of antibodies do not bind to these receptors and, therefore, cannot pass across the placenta. The ability of IgG to cross the placenta provides a major line of defense against infection for the first weeks of an infant's life. Normally, the human fetus begins to receive significant quantities of maternal IgG transplacentally at around 12 weeks' gestation. The quantity increases steadily until, at birth, cord serum contains a concentration of IgG comparable with that of maternal serum. Barring any immunologic disorders, adult levels of IgG are reached by the seventh year of life and remain relatively constant thereafter.

IgG antibodies have a high diffusion coefficient, which enables them to diffuse into the extravascular body spaces more readily than other Ig classes. IgG, being the predominant immunoglobulin in these spaces, carries the major burden of neutralizing bacterial toxins and of binding microorganisms to enhance their phagocytosis. Furthermore, only IgG antibodies coating target cells, such as tumor cells, can sensitize them for extracellular killing by ADCC; the NK cells responsible for ADCC also possess Fc receptors for IgG.

There are four subclasses of human IgG. These four subclasses reflect the existence of four antigenetically distinct H chains (γ1–γ4), which are similar but not identical in amino acid sequence and general properties. For example, IgG1 is the dominant subclass in adult humans. IgG3 is the most effective binder of complement, followed by IgG1 and IgG2. IgG4 in most cases fails completely to bind complement by the classical pathway. All subclasses except IgG2 have been demonstrated to cross the placenta. A summary of the physical and biological properties of IgG is given in Tables 47.3 and 47.4 and for the subclasses in Table 47.5.

IMMUNOGLOBULIN A

Antibodies of this class constitute the major class of antibody in secretions (milk, saliva, tears, and respiratory and intestinal secretions). It

TABLE 47.3

Physical Properties of Human Immunoglobulins

WHO Designation	IgM	IgG	IgA	IgD	IgE
Heavy chains	μ	γ	α	δ	ε
Heavy chain subclasses	μ_1, μ_2	γ_1, γ_2, γ_3, γ_4	α_1, α_2	—	—
Light chains	κ or λ	κ or λ	κ or λ	κ or λ	κ or λ
Molecular formula	IgM(κ) $(2\mu 2\kappa)_5$ IgM(λ) $(2\mu 2\lambda)_5$	IgG(κ) 2γ2κ IgG(λ) 2γ2λ	IgA(κ) $(2\alpha 2\kappa)_{1\text{-}3}$ IgA(λ) $(1\alpha 2\lambda)_{1\text{-}3}$ IgA(κ) $(2\alpha 2\kappa)_2$S† IgA(λ) $(2\alpha 2\lambda)_2$S	IgD(κ) 2δ2κ IgD(λ) 2δ2λ	IgE(κ) 2ε3κ IgE(λ) 2ε2λ
Number of four-chain units per molecule	5	1	1–3	1	1
Heavy-chain molecular weight, kDa	70	50–60	55	62	70
Light-chain molecular weight, kDa	23	23	23	23	23
Sedimentation coefficient, S20W	18.0–19.0	6.7–7.0	6.6–14.0	6.9–7.0	7.9–8.0
Molecular weight, kDa	900	143–160	159–447	177–185	187–200
Electrophoretic mobility	γ1–β1	γ2–α1	γ2–β2	γ1	γ1
Carbohydrate content, %	7–14	2.2–3	7.5–9.0	12–13	11–12
Heavy-chain allotypes	—	Gm	Am	—	—
Light-chain allotypes	Km(κ)*	Km(κ)*	Km(κ)*	Km(κ)*	Km(κ)
Valency for antigen binding	5 (10)	2	2.4 (? polymeric forms)	2	2
Number of domains on the heavy chains	5	4	4	4	5

WHO, World Health Organization.
*Formerly designated Inv marker.
†Dimer in external secretions carries secretory component -S.

TABLE 47.4

Properties of Human Immunoglobulins

	IgM	IgG	IgA	IgD	IgE
Physiologic					
Normal adult serum concentration, mg/mL	1.2–4.0	8.0–16.0	0.4–2.2	0.03	17–450 ng/mL
International units/mL	69–322	92–207	54–268	—	<100
Percentage total immunoglobulin	13	80	6	1	0.002
Intravascular distribution, %	41	48	76	75	51
Synthetic rate, mg/kg/day	2.2	35	24	0.4	0.003
Catabolic rate in serum, % per day (or half-life, days)	10.6 (5–6)	6 (18–23)	24 (5–6.5)	37 (2.8)	90
Biological					
Agglutinating capacity	+4	±	+2	–	–
Complement-fixing capacity via classical pathway	+4	+	–	–	–
Homologous anaphylactic hypersensitivity	–	–	–	–	+4
Heterologous guinea pig anaphylaxis	–	+	–	–	–
Fixation to homologous mast cells and basophils	–	±	–	–	+4
Cytophilic binding to macrophages	–	+	±	–	–
Placental transport to fetus	–	+	–	–	–
Rheumatoid factor–binding activity	–	+	–	–	–
Present in external secretions	±	+	+4	–	+2
Other Characteristic Properties					
IgM—Produced early in immune response, first effective defense against bacteremia					
IgG—Combats microorganisms and their toxins in extravascular fluids					
IgA—Defends external body surfaces					
IgD—Present on lymphocyte surface of immunocompetent cells, important for B-cell activation and/or immunoregulation					

exists as a four-chain monomer (like IgG) or as a dimer of two such monomer units. IgA molecules in secretions are dimers that carry a single J chain, similar to the one associated with pentameric IgM, and an additional glycopolypeptide chain of 70 kDa called *secretory component* (SC). IgA dimers pick up SC from the surface of the epithelial cells lining the intestine, the bronchi, or the milk, salivary, or tear ducts. SC is synthesized by the epithelial cells and is initially exposed on the nonluminal (external) surface of these cells, where it serves as a receptor for binding dimer IgA. The resulting dimer IgA–receptor complexes are ingested by receptor-mediated endocytosis and are transferred across the epithelial cell cytoplasm in the form of a membrane vesicle, which fuses with the plasma membrane on the luminal side of the epithelial cell. The extramembrane portion of the IgA receptor is then enzymatically cleaved and released as part of the secretory IgA molecule ($[\alpha_2,L_2,]_2 - J\alpha$) into the lumen. The amino-terminus of the dimer IgA receptor remaining attached to dimer IgA is the SC (Fig. 47.4). Thus, the fully assembled dimeric secretory IgA molecule is the synthetic product of two distinct types of cells: plasma cells and epithelial cells. In addition to

TABLE 47.5

Properties of Human Immunoglobulin G Subclasses

	IgG1	IgG2	IgG3	IgG4
Physiologic				
Percentage distribution of total normal serum IgG	66 ± 8	23 ± 8	7.3 ± 3.8	4.2 ± 2.6
Synthetic rate, mg/kg/day in serum	25	?	3.4	?
Fraction catabolic rate, % per day (half-life, day)	8 (23)	6.9 (23)	16.8 (7)	6.9 (23)
Ratio of κ/λ	1.4–2.4	1.0–1.1	1.1–1.3	5.0–7.0
Allotypic markers (Gm types)	a, z, f, x	n	bo, bi, bz, g, st, etc.	?
Biological				
Complement-fixing capacity via classical pathway	+2	±	+3	–
Heterologous skin-binding capacity	+	–	+	+
Placental transport to fetus	+	±	+	+
Macrophage receptor	+	–	+	–
Reaction with protein A	+	+	–	+
Dominant Antibody Activities				
Antitetanus toxoid	+2	+	+	±
Antidiphtheria toxoid	+2	+	+	±
Antithyroglobulin	+2	+	+	±
Anti-DNA	+2	+2	±	±
Anti-Rh	+2	–	–	±
Anti–factor VIII	–	–	–	+
Antidextran	–	+	–	–
Antilevan	–	+	–	–
Antiteichoic acid	–	+	–	–
Number of inter–heavy chain disulfide bonds in hinge region	2	4	5	2
Position of light–heavy chain disulfide bond on the heavy chain	N214	N131	N131	N131

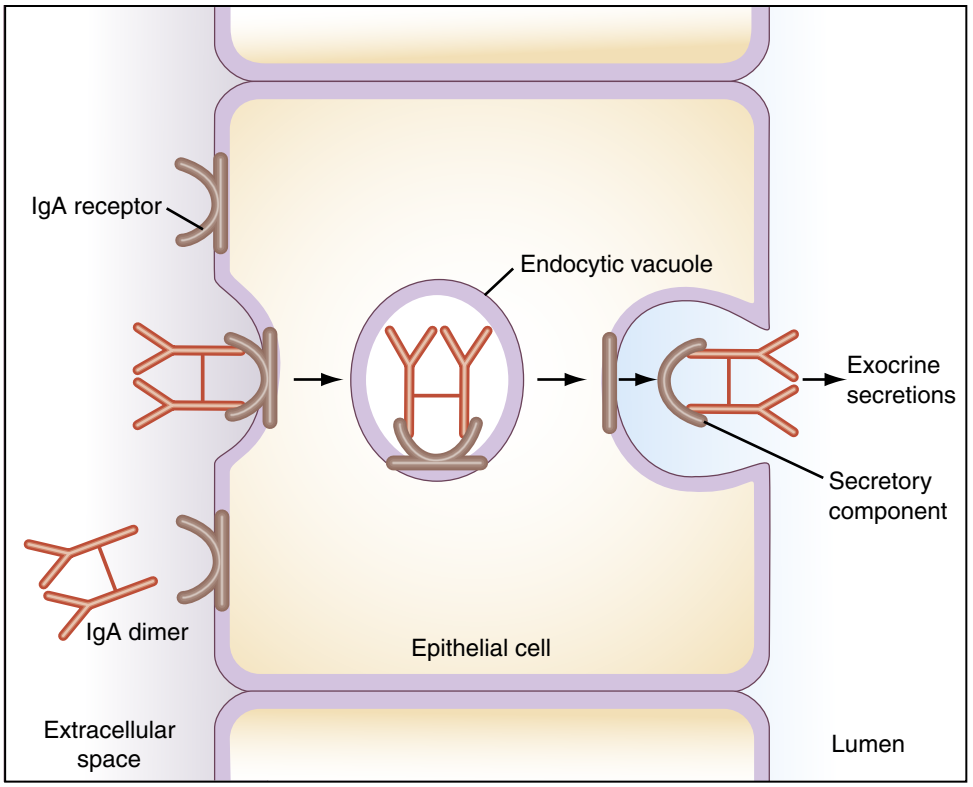

Figure 47.4 The mechanism by which the secretory component mediates the transport of a dimeric immunoglobulin (Ig) A molecule across an epithelial cell. The entire complex is transported from the extracellular fluid into the lumen of the epithelial tube. The secretory component is synthesized by the epithelial cell as a transmembrane glycoprotein and serves as a receptor on its basolateral surface for binding the IgA dimer. The receptor–IgA complex enters the cell in an endocytotic vesicle, which crosses the cell and is exocytosed at the apical surface. Cleavage of the receptor frees the dimer IgA for discharge at the exterior surface (lumen side). The portion of the receptor that remains attached to the IgA dimer is called the *secretory component*. This transport mechanism is responsible for depositing IgA in various exocrine secretions (e.g., saliva, milk, bile, tears, sweat), as well as in the mucous layer that protects the inner lining of the nasopharyngeal passages, intestine, and genitourinary tract.

this transport role, SC may protect the dimer IgA molecules from being digested by proteolytic enzymes in secretions.

In humans, it has been possible to classify IgA antibodies into two subclasses—IgA1 and IgA2—based on differences in antigenic structure and variation in the arrangement of interchain disulfide bridges. Whereas IgA2 is a minor component of serum IgA, this subclass is the dominant form in secretions. Furthermore, secretory IgA reaches adult levels sooner than serum IgA. The IgA system in the intestinal tract of humans, for example, may be fully developed by 2 years of age, whereas serum IgA levels do not normally reach adult concentrations until 12 years of age.

Because of its presence near external membranes, secretory IgA constitutes a first line of defense against microorganisms in the external environment. It has been postulated that IgA inhibits the adherence of microorganisms to the surface of mucosal cells, thereby preventing their entry into body tissues. One property of secretory IgA that is important in this respect is its multivalence, which is associated with high avidity of binding to antigens, which may be especially relevant in the neutralization of viruses. Antiviral activity by IgA antibodies has been demonstrated in individuals given either of the polio vaccines. Secretory IgA may also combine with certain antigens in food, preventing their absorption into the bloodstream and, thus, reducing the incidence of allergic reactions. For example, IgA immunodeficiencies can lead to increased levels and incidence of humoral antibodies directed against antigens derived from food and intestinal organisms.

IgA possesses the following effective properties: it fixes complement through the alternative pathway; through a specific Fc receptor on macrophages, it can serve as an opsonin for phagocytosis; and it can induce eosinophil degranulation through a specific receptor, which has implicated IgA in antiparasitic responses. The physical and biological properties of IgA are listed in Tables 47.3 and 47.4.

IMMUNOGLOBULIN D

Although only a minor component of the serum, IgD is a major membrane immunoglobulin found on the surface of a high proportion of B lymphocytes, especially in newborns. During the course of B-cell differentiation, these cells synthesize and display IgD molecules as well as IgM molecules. Whereas this appears to contradict the "one-cell-one-immunoglobulin" rule, the antigen-binding sites (idiotype) of the two types of molecules and their light chains are identical. Only their CH regions differ. The membrane-bound IgD may serve as one of the receptors with which B cells bind antigen and are stimulated to undergo clonal proliferation. Some evidence suggests that IgM-bearing B cells can respond to certain T-independent antigens and that the acquisition of IgD is needed for B cells (IgM- and IgD-bearing) to respond to the T-cell help required for T-dependent antigen responsiveness.

Furthermore, if IgD molecules are selectively removed from IgM- and IgD-bearing B cells by taking advantage of the much greater sensitivity of the δ chain to papain, these cells are rendered susceptible to becoming tolerant. The precise role played by surface IgD in an immune response remains unknown, but the generally held view is that it turns on, turns off, or modulates (controls) B-cell division or differentiation.

IgD usually is detected in serum at about 6 months of age, and its concentration throughout life is always very low. In disease states, however, IgD concentration can vary greatly. In chronic infection, IgD serum levels increase, as do those of the other immunoglobulins. To date, no specific increase in IgD has been associated with a particular disease. Patients with allergies and autoimmune diseases do not show an abnormal IgD concentration. IgD is usually absent in hypogammaglobulinemic individuals.

To date, IgD has not been assigned a specific biological role as a humoral antibody. IgD activity against a number of antigens has been reported on occasion. Surface IgD, which has proteins similar to those of surface IgM, is a marker for mature B cells and its role as a receptor is generally accepted, even though the nature and purpose of the signal it transmits remains controversial (Carsetti et al., 1993; Roes & Rajewski, 1993). IgD does not bind complement, does not cross the placenta, and does not bind to cells through its Fc region. The secreted form of IgD, as well as that of the other immunoglobulins, lacks the carboxy-terminal transmembrane peptide that anchors it to the surface of B cells. Tables 47.3 and 47.4 list additional properties of IgD.

IMMUNOGLOBULIN E

Of the various classes of immunoglobulin, IgE is present at the lowest serum concentration (see Table 47.4). It has the ability to attach to human skin (homocytotropic antibody) and to initiate aspects of the allergic reaction (reaginic antibody). The biological activity of IgE is accounted for by its property of binding through the Fc region to basophils and to their tissue equivalent: mast cells. IgE may also be important in the humoral immune response to parasitic disease because it is often found at high levels in the serum of patients with helminthic infection. IgE may play a part in allowing white blood cells (WBCs), antibodies, and complement components to enter sites of inflammation, leading to an immediate hypersensitivity reaction. IgE antibodies provide a striking example of the **bifunctional** nature of antibody molecules. The Fc portion of the molecule binds to the target cells, whereas the Fab portion binds the allergen (see Chapter 56 for the role of IgE in allergic diseases and related assays).

As with IgA, IgE is produced mainly in the linings of the respiratory and intestinal tracts and is part of the external secretory system of antibody. A deficiency of IgE has been inconsistently associated with deficiency of IgA in individuals with impaired immunity, who present with undue susceptibility to infection. IgE does not cross the placenta, and IgE–antigen complexes do not bind complement by the classical pathway (see Table 47.4).

SUMMARY

Five different classes of antibody (IgM, IgG, IgA, IgD, and IgE), four subclasses of IgG antibody (IgG1, IgG2, IgG3, and IgG4), and two subclasses of IgA antibody (IgA1 and IgA2) are present in humans. Each of these antibody isotypes possesses a distinct H chain (μ, γ, α, δ, ε, γ1, γ2, γ3, and γ4, and α1, α2, respectively). The H chains contain the Fc region of the antibody, which determines what other proteins will bind to the antibody and, therefore, the biological properties of the class and subclass. Either type of L chain (κ or λ) can be associated with any class of H chain.

Structural differences among the five classes of immunoglobulins correspond to functional differences in their sites of production and action, their relative levels of production in primary and secondary immune responses, and their roles as physiologic effectors. For example, IgG is prevalent in both blood and tissue fluids, whereas IgM is chiefly confined to the blood, and secretory IgA is found primarily on epithelial surfaces. IgD and IgE are principally bound to cells, IgD to B cells, and IgE to basophils and mast cells.

CLINICAL SIGNIFICANCE OF IMMUNOGLOBULINS

Immunoglobulins play important roles in disease pathogenesis, diagnosis, prevention, and therapy.

DISEASE PATHOGENESIS

Monoclonal hyperimmunoglobulinemia is a prominent feature of multiple myeloma and Waldenström macroglobulinemia. Antibodies against native antigens may result in autoimmune disease, as discussed in Chapters 53 and 55. Hypoglobulinemia or agammaglobulinemia is often the prime characteristic of some immunodeficiency disorders (see Chapter 52). Polyclonal hypergammaglobulinemia can result from chronic inflammation or other disorders, such as cirrhosis of the liver due to excess pan–B cell stimulation.

Hyperimmunoglobulinemia

Serum Immunoglobulin Levels

Valid interpretation of serum immunoglobulin levels requires recognition of biological variations that exist throughout the life span of individuals. The most important of these variables are age, sex, and race. In neonates, levels of circulating immunoglobulins are much lower than at all other ages, because essentially all immunoglobulins at that stage were passively transferred from mother to fetus in utero. Immunoglobulin levels rise through childhood to more stable concentrations in mature adults. Normal IgG, IgA, and IgM concentrations at any particular age can vary as much as tenfold from lower to upper limits of the reference ranges. A very large study of immunoglobulin concentrations in a northern New England (99% white) population of 115,017 serum samples demonstrated the expected rise from infancy, more stable values after adolescence, and then in older individuals further slight increase in IgA, nearly stable IgG, and slight reduction in IgM (Ritchie et al., 1998). Little difference was noted between males and females in terms of IgA and IgG median levels, whereas males exhibited lower IgM than females at all ages except the very young. That study might be considered definitive for age and gender

TABLE 47.6

Polyclonal Hyperimmunoglobulinemias: Some Associated Disease States

Condition	Immunoglobulin (Ig) Classes
Immunodeficiency Diseases	
Hyperimmunoglobulin E and recurrent infections	IgE
Wiskott-Aldrich syndrome	IgA, IgE
"Dysgammaglobulinemia type I"	IgM
Hyperimmunoglobulin A and recurrent infections	IgA
Acquired immunodeficiency syndrome (AIDS)	All classes
Infections	
Congenital infections (syphilis, toxoplasmosis, rubella, cytomegalovirus)	IgM
Infectious mononucleosis	IgM or all
Trypanosomiasis	IgM or all
Intestinal parasitism	All classes
Several helminthic infections	IgE
Visceral larva migrans	All classes
Chronic granulomatous disease of childhood	All classes
Leprosy	All classes
Chronic infection in general	All classes, with a preference for IgG
Liver Diseases	
Chronic active hepatitis	IgG predominates
Acute hepatitis	IgG predominates
Biliary cirrhosis	IgM predominates
Lupoid hepatitis	All classes
Pulmonary Disorders	
Pulmonary hypersensitivity syndrome	All classes
Sarcoidosis	All classes
Berylliosis	All classes
Autoimmune Disorders	
Systemic lupus erythematosus	All classes
Rheumatoid arthritis	IgA or all
Many autoimmune states, such as thyroiditis	All classes
Scleroderma	All classes
Cold agglutinin disease	IgM
Anaphylactoid purpura	IgA
Miscellaneous	
Down syndrome	All classes
Amyloidosis	All classes
Narcotic addiction	IgM
Renal tubular disease	All classes

through the sheer number of subjects, although the population was not racially diverse.

A smaller but still reasonably large group of healthy white subjects (3213) from a single community (Tecumseh, Michigan) showed that mean concentrations of IgG and IgA increased with age, with slight but significant differences between the sexes. Females had higher serum levels of IgG and lower levels of IgA. Although these sex differences for IgG and IgA are statistically significant, their biological meaning is not apparent. IgM levels in these subjects remained relatively constant with age. However, females had higher mean levels of IgM (1.06 mg/mL) than males (0.77 mg/mL) (Cassidy et al., 1974).

Several studies have reported that immunoglobulin levels are higher in persons with darker-pigmented skin. A study of a healthy biracial population in Evans County, Georgia, demonstrated that black people had higher levels of the three major immunoglobulins (IgM, IgG, and IgA) when compared with white people (Lichtman et al., 1967). The most prominent difference was seen in IgG. No urban–rural difference in immunoglobulin levels was noted in this study. White subjects in Rochester, New York, had serum levels of IgM and IgG that were similar to those of white subjects in rural Georgia. A triracial study in Durban, Natal, South Africa, showed that Bantu male adults had significantly higher levels of IgM (32% more), IgG (40% more), and IgA (32% more) in their sera than comparable white male adults in this community who were born in the same year and had the same ABO blood group. Healthy Asiatic male adults had about 20% more IgG, 23% more IgA, and 7% more IgM than comparable white male adults. A study of subjects in the Washington, D.C., metropolitan area revealed that black people had significantly higher IgG levels than white people but similar IgA and IgM levels (Tollerud et al., 1995). Control groups used in these studies were matched for age, sex, and race as well as for several environmental factors. Increases in gammaglobulin often are first noted after serum protein electrophoresis, measurement of total protein, or measurements of albumin and γ-globulin fractions.

BOX 47.1

Selected Conditions Associated with Monoclonal Immunoglobulins

- Multiple myeloma
- Waldenström macroglobulinemia
- Chronic lymphocytic leukemia
- Other leukemias
- Lymphomas
- "Benign" monoclonal gammopathy (MGUS, monoclonal gammopathy of uncertain significance)
- Systemic capillary leak syndrome
- Amyloidosis
- Chronic liver disease, such as chronic active hepatitis, primary biliary cirrhosis
- Autoimmune disorders, including rheumatoid arthritis, systemic lupus erythematosus, thyroiditis, pernicious anemia, polyarteritis nodosa, Sjögren syndrome
- Gaucher disease
- Malignancies of various types
- Hereditary spherocytosis
- HIV infection, including AIDS

AIDS, Acquired immunodeficiency syndrome; *HIV,* human immunodeficiency virus.

Increases in immunoglobulins are referred to as *monoclonal* or *polyclonal*. Monoclonal immunoglobulins from any one individual are structurally identical and are believed to result from the clonal expansion of a single immunoglobulin-producing lymphoid cell; thus, they are specific for a particular antigen. Polyclonal immunoglobulins in the same individual are structurally different from one another in one or more important ways: by class, as polyclonal IgG, IgA, or IgM; by light chain; or by antigen specificity. Polyclonal immunoglobulins arise from the expansion of several to many different immunoglobulin-producing lymphoid cells.

Polyclonal Immunoglobulins

Polyclonal increases in immunoglobulins have been associated with many disease states (Table 47.6) (Cushman & Grieco, 1973; Buckley, 1977). Serum protein electrophoresis is often sufficient to establish this condition. Immunoelectrophoresis, immunofixation, and determination of individual immunoglobulins or immunoglobulin light chains may be helpful at times to confirm a polyclonal distribution or an increased concentration in one or more immunoglobulin classes. Increases in serum immunoglobulins may result from decreased catabolism and increased synthesis. The control mechanisms for these events are not well understood. The implications of elevated immunoglobulins are unknown. Most immunoglobulins appear not to be directed toward a definable specific antigenic determinant or set of specific antigenic determinants. It should also be noted that most autoantibodies are not monoclonal but rather are polyclonal. In general, persistent polyclonal increases in gammaglobulin are thought to be related to antigenic stimulation of a chronic nature or loss of immunoglobulin regulation.

Monoclonal Immunoglobulins

Monoclonal immunoglobulins or fragments of immunoglobulins have been associated with a number of disease conditions (Box 47.1) (Wells & Fudenberg, 1974; Benbassat et al., 1976; Atkinson et al., 1977; Schaefer et al., 1978; Kelly et al., 1985). These immunoglobulins have also been referred to as *immunoglobulins with restricted heterogeneity*. Protein electrophoresis of serum and urine (Fig. 47.5) is commonly used to screen for monoclonal gammopathy.

Figure 47.5 Serum protein electrophoresis performed in agarose gel. This gel demonstrates the variation in electrophoretic migration of monoclonal bands as typically encountered in diagnosing and monitoring patients with plasma cell disorders, such as multiple myeloma. This routine analysis of serum specimens from two controls and 28 patients included 14 individuals with monoclonal bands.

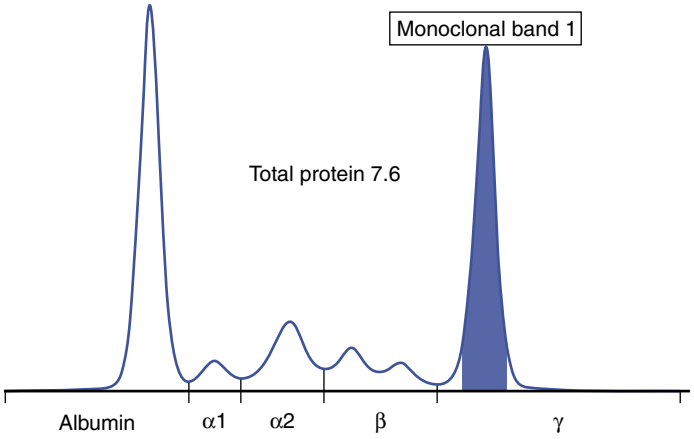

Fractions	%	Ref. %	g/dL	Ref. g/dL
Albumin	**38.1**<	59.1 - 73.2	2.9	3.5 - 5.6
Alpha 1	**4.0**>	1.6 - 3.2	0.3	0.1 - 0.3
Alpha 2	**12.1**>	6.8 - 11.2	0.9	0.2 - 1.0
Beta	**10.5**	7.5 - 13.1	0.8	0.5 - 1.1
Gamma	**35.3**>	7.5 - 16.9	2.7	0.5 - 1.5

Monoclonal band	%	g/dL
Monoclonal band 1	32.3	2.5

Figure 47.6 Quantitation of monoclonal band (MCB) concentration from densitometric tracing of serum protein electrophoresis. The MCB demarcated as the solid section constituted 32.3% of the area under the entire tracing for all serum fractions. Multiplying 32.3% × total protein of 7.6 g/dL yields the concentration of MCB as 2.5 g/dL.

The incidence of monoclonal immunoglobulins (M components, M proteins) in unselected population studies is estimated to be 0.9% (Bachman, 1965; Axelsson & Hellen, 1968; Cohen, 1985). Of course, a much higher percentage of positive results is found in clinical laboratories where the sera to be tested are preselected. Multiple myeloma, Waldenström macroglobulinemia, and B-cell neoplasms are some of the diseases that are associated with elevated levels of monoclonal immunoglobulins. It was earlier believed that monoclonal gammopathies were rare in cases of chronic lymphocytic leukemia or well-differentiated lymphocytic lymphoma. It has now been shown that when high-resolution electrophoresis and immunofixation are combined to study samples from these patients, most are found to have a monoclonal gammopathy (Keren et al., 1988). Monoclonal gammopathies have also been demonstrated in patients with Burkitt lymphoma and B-cell acute lymphocytic leukemia.

Although the antigen-combining specificities of monoclonal gammopathies generally are not known, some result in paraproteinemic neuropathies. This clinical syndrome is generally due to the interaction of an IgM paraprotein with myelin-associated glycoprotein (MAG), gangliosides (e.g., GM1 in motor neuropathy, GD1b in sensory neuropathy), or other glycosphingolipids (Ropper & Gorson, 1998).

The term *monoclonal gammopathy of undetermined significance* (MGUS) was coined by Kyle to categorize individuals in whom a monoclonal component is demonstrated in the serum but who lack other key features for diagnosing a malignant condition (Kyle, 1982). As many as 3% of individuals over the age of 70 years have an MGUS (Kyle & Rajkumar, 2003). Subjects with MGUS may have as many as 10% plasma cells in the bone marrow. This is considerably less than the bone marrow plasmacytosis associated with multiple myeloma. About 20% of individuals with MGUS will develop a malignant B-cell lymphoproliferative disorder—most commonly multiple myeloma—over a 10-year period. Some of the other cases develop into chronic lymphocytic leukemia, amyloidosis, well-differentiated lymphocytic lymphoma, and other B-cell proliferative diseases. Subjects with MGUS have quantities of M component ranging from 300 mg/dL to greater than 3000 mg/dL and usually do not have Bence Jones protein in the urine. It is recommended that such patients be followed with serum protein electrophoresis every 6 to 12 months to determine whether the process is progressing or regressing.

The risk of progression with MGUS is about 1% per year even after 25 years of a stable condition (Kyle & Rajkumar, 2003). A 31-year follow-up study of MGUS in New Zealand showed progression to hematologic malignancy in 64% of 11 patients originally detected by screening 2192 subjects in a town in 1967 (Colls, 1999).

A special consideration is MGUS that is observed in organ transplant patients who have received immunosuppressive drugs that alter T lymphocyte functions, including the modulation of B cell responsiveness. These monoclonal gammopathies may be transient in up to 75% of cases (Radl et al., 1985). They may occur in both monoclonal and oligoclonal forms (Stanko et al., 1989), and they may coincide with infections of cytomegalovirus or Epstein-Barr virus (Drouet et al., 1999). Their progression is likely stimulated by high circulating levels of interleukin-6 (Nickerson et al., 1994).

Cryoglobulins

Cryoglobulins are immunoglobulins that precipitate upon storage at refrigerated temperatures (4°C), and as a group are associated with hematologic, autoimmune, and chronic infections, such as hepatitis C virus. Type I cryoglobulins consist of a single monoclonal immunoglobulin that precipitates in the cold without binding other proteins. This type of molecule is typically IgM encountered in Waldenström macroglobulinemia, where it can produce a hyperviscosity syndrome due to very thick consistency of the circulating blood that can be exacerbated by cold ambient temperatures encountered by the patient.

Type II cryoglobulins are distinctly different from type I. The abnormality in type II is a monoclonal IgM autoantibody that is directed at the Fc region of normal polyclonal IgG (Cacoub et al., 2002). This autoantibody is the same as rheumatoid factor. It is also referred to as *mixed cryoglobulin*, containing both IgM and IgG. It is commonly encountered in rheumatoid arthritis and in chronic hepatitis C virus infection for unknown reasons. The presence of IgM anti-IgG leads to formation of circulating immune complexes (CICs), with IgG normally occurring in the blood. These CICs then deposit in small blood vessels, causing vasculitis, glomerulonephritis, arthritis, and so forth.

Type III cryoglobulins have been described as a variant of type II in which the IgM autoantibody against IgG is polyclonal. Type III can be found in chronic infections and inflammatory states. Many such cases in the past could have been confused with type II because of methods that would not permit sensitive typing of the light chains in a minor band of IgM in the presence of large amounts of IgG, because both light-chain types would appear in the cryoprecipitate.

DISEASE DIAGNOSIS

Laboratory evaluation of immunoglobulin levels and functions may be helpful in the diagnosis and management of disease. Complement fixation tests, hemagglutination assays, and other immunoassays can detect an increased or changing titer of antibodies against specific antigens, such as those present on microorganisms.

Requests to examine sera for the presence of a monoclonal protein usually are generated by a physician who recognizes that a patient has clinical symptoms and signs of such a disorder or by laboratory examination of a serum protein electrophoresis that suggests a monoclonal protein (Fig. 47.6). Many times, the physician's suspicion of a plasma cell

dyscrasia is triggered by findings of anemia (with one or more cytopenias), elevated total serum protein with elevated globulins, and proteinuria; other findings may include hyperuricemia, hypercalcemia, elevated alkaline phosphatase, bone pain, or lytic lesions of bone on x-ray. If indeed an M component is present in a serum protein electrophoresis, quantitative measurement of immunoglobulins by radial immunodiffusion, nephelometry, or another suitable technique can identify the specific immunoglobulin if only one of the three major classes is increased. Of course, this neither determines the light chain of a monoclonal immunoglobulin nor detects light-chain myelomas. Biclonal gammopathies may be confusing.

Quantitative immunoglobulins are useful in monitoring the course of the disease and its treatment and may be helpful in separating a benign from a malignant condition. Monoclonal IgG levels of 2 g/100 mL or IgA levels of 1 g/100 mL (Isobe & Osserman, 1971) or greater suggest a malignant condition. In many malignant immunocytopathies, the concentration of nonmonoclonal immunoglobulins is reduced. Thus, a deficiency of polyclonal immunoglobulins is suggestive of malignancy. Paradoxically, patients with a malignant immunocytopathy are immunodeficient even though they possess large quantities of a "nonsense" immunoglobulin produced by a poorly controlled clone of lymphoid cells.

Immunofixation

Confirmation of heavy-chain and light-chain types of a monoclonal band today is done almost exclusively by immunofixation electrophoresis (IFE). Immunoelectrophoresis (IEP) was an older procedure in which patient and normal serum specimens were electrophoresed in adjacent lanes, followed by diffusion of individual antisera against light and heavy chains from a trough cut into the agarose support medium. After overnight incubation, the pattern of precipitin arcs formed by the antisera with their target immunoglobulins was interpreted as monoclonal or polyclonal distribution. Readers are referred to earlier editions of this book for more information about IEP and pictures of the gels, which are no longer commonly used in modern clinical laboratories. IFE has virtually replaced IEP in the clinical laboratory because of its speed, sensitivity, and ease of interpretation. IFE has greater sensitivity for detecting small monoclonal bands in the presence of polyclonal immunoglobulins. IFE also has the advantage of a more rapid readout because diffusion through gel is not required. Replicate samples of patient serum are subjected to electrophoresis through high-resolution gel before monospecific antisera are applied directly to the separated serum proteins. The gel is washed, and the protein–antibody conjugates are stained and read directly (Fig. 47.7). One lane is treated with a precipitating reagent that fixes all proteins in the same pattern as the serum protein electrophoresis. Maintaining all serum proteins in register with the immunofixed immunoglobulins adds to the ease of confirming and identifying monoclonal paraproteins.

Occasionally, the concentration of the monoclonal protein in a patient's serum is so high that it exceeds the capacity of the reagent antibodies to form precipitating complexes by IFE. This phenomenon corresponds to the zone of antigen excess depicted in Figure 47.2. The result is a halo of precipitated complexes (where the concentrations are nearer to equivalence) with a clear central zone of antigen excess (see Fig. 47.7E). Although this result appears atypical, it is straightforward to interpret and to confirm by repeating the IFE with a greater dilution of patient serum (Keren, 1999).

Either technique may be applied to other body fluids, most commonly urine. Monoclonal light chains in the urine (Bence Jones protein) may be detected in more than half of patients with multiple myeloma (Isobe & Osserman, 1971; Wells & Fudenberg, 1974). Polyclonal light chains may be detected in patients with other disorders, usually as part of complete immunoglobulin molecules. The original method to detect Bence Jones protein was based on precipitation in urine heated to 40°C to 60°C and then redissolution when further heated to 100°C. IFE of urine is more specific and more sensitive than the older Bence Jones assay. IFE may be performed on urine samples with sufficient protein or subsequent to concentration by lyophilization or by selective membranes (Minicon, Millipore Corporation, Billerica, MA).

Immunoglobulins at very high concentrations can significantly increase the viscosity of blood, leading to problems with organ perfusion. Measurements of the viscosity of serum have been done to assess this effect, but they are rarely used today because other methods for quantifying immunoglobulin concentrations, such as nephelometry, are widely practiced. Furthermore, serum viscosity by itself is a poor indicator of whole-blood viscosity with cellular elements present, which is really the crucial factor clinically in the patient.

Immunoglobulin Free Light-Chain Analysis

The synthesis of immunoglobulin heavy chains and light chains is regulated differently by virtue of their genes being on different chromosomes (heavy-chain genes on chromosome 14; κ light-chain genes on chromosome 2; λ light-chain genes on chromosome 22). Light chains are normally synthesized in slight excess and are cleared from the circulation in a few hours; thus, they do not accumulate in the blood. However, in some monoclonal plasma cell disorders, light-chain synthesis can greatly exceed heavy-chain production, with the resultant release of variable quantities of free light chains (FLC). Because of the relatively rapid renal clearance of small light chains compared with that of an intact immunoglobulin, measurement of FLCs in serum or urine has been used to assess plasma cell mass and growth in monoclonal disorders. Although the concentration of the intact immunoglobulin of an M spike has long been used in monitoring myelomas, this new and more rapidly responsive marker of light-chain release has recently been introduced for clinical use.

Reagent anti–light chain antibodies used for IFE react with κ or λ light chains both as part of intact immunoglobulins and as FLCs. The principle of specifically measuring FLCs is to use reagent antibodies that react with epitopes on the light chains that are normally hidden by association with heavy chains. Consequently, the FLC assay gives quantitative information that is complementary to results of quantitative immunoglobulin measurement as well as protein electrophoresis (PEL) and IFE. One operational advantage of FLC analysis is its automation (Jaskowski et al., 2006).

Analysis of FLCs entails measurement of both κ and λ light chains in serum and/or urine. Results are abnormal if the κ or λ value is very high and the other is low. To accentuate differences, the ratio of κ to λ measurements is calculated (rFLC). If rFLC is abnormally high, the interpretation is that of plasma cell proliferation with a κ light-chain type (i.e., a high κ value in the numerator). If rFLC is below the normal cutoff value, the interpretation is that of proliferation with a λ light chain type (i.e., high λ value in the denominator). Use of rFLC also allows application to patients who have renal disease and do not clear light chains from plasma normally and, thus, might have elevations of both κ and λ light chains.

Consensus guidelines for use of serum FLC analysis have been developed by the International Myeloma Working Group (Dispenzieri et al., 2009). They include the following:

1. Serum screening for plasma cell disorders. The serum FLC assay combined with serum PEL and IFE is sufficient to screen for pathologic monoclonal plasmaproliferative disorders, except for AL amyloidosis (light-chain amyloidosis), for which the additional test of 24-hour urine IFE is essential. This recommendation allows the FLC assay to replace the 24-hour urine IFE for all plasma cell disorders but AL. Avoiding 24-hour collections of urine is considered positively by many physicians and patients.
2. Serum FLC (sFLC) assay for prognosis. This assay should be performed at the time of diagnosis for MGUS, smoldering or active multiple myeloma, solitary plasmacytoma, and AL amyloidosis. The baseline values of FLC predict progression of these disorders and, thus, can help to frame therapy or at least to make recommendations for frequency of monitoring and helping patients to understand the risks of their disease.
3. FLC assay for quantitative monitoring of response. The only recommended indications for routine serial use of the FLC assay are seen in oligosecretory multiple myeloma and in AL amyloidosis. Other potential conditions for which data were not sufficient to recommend use include light-chain myeloma and measurable intact immunoglobulin disease. Also recommended is use in patients who have achieved a complete response to determine whether it is a stringent complete response.

An update to the IMWG guidelines added the use of sFLC as a biomarker of malignancy with a threshold level of ≥100 mg/L to diagnose multiple myeloma in patients without other indications (Rajkumar et al., 2014). A further update recommends use of sFLC for assessing response in multiple myeloma only when the M component is not practicably measurable in serum (<10 g/L or in urine (<200 mg/24 hours) (Kumar et al., 2016).

Much more clinical outcome information needs to be accrued before it can be recommended that FLC assays should be used routinely for both diagnosis and monitoring of virtually any plasma cell disorder. However, they have achieved wide use in the diagnosis and monitoring of various plasma cell disorders, including multiple myeloma and amyloid light-chain amyloidosis. This includes a role in predicting progression of plasma cell dyscrasias to overt multiple myeloma, and the prognosis for AL amyloidosis at time of diagnosis (Tosi et al., 2013).

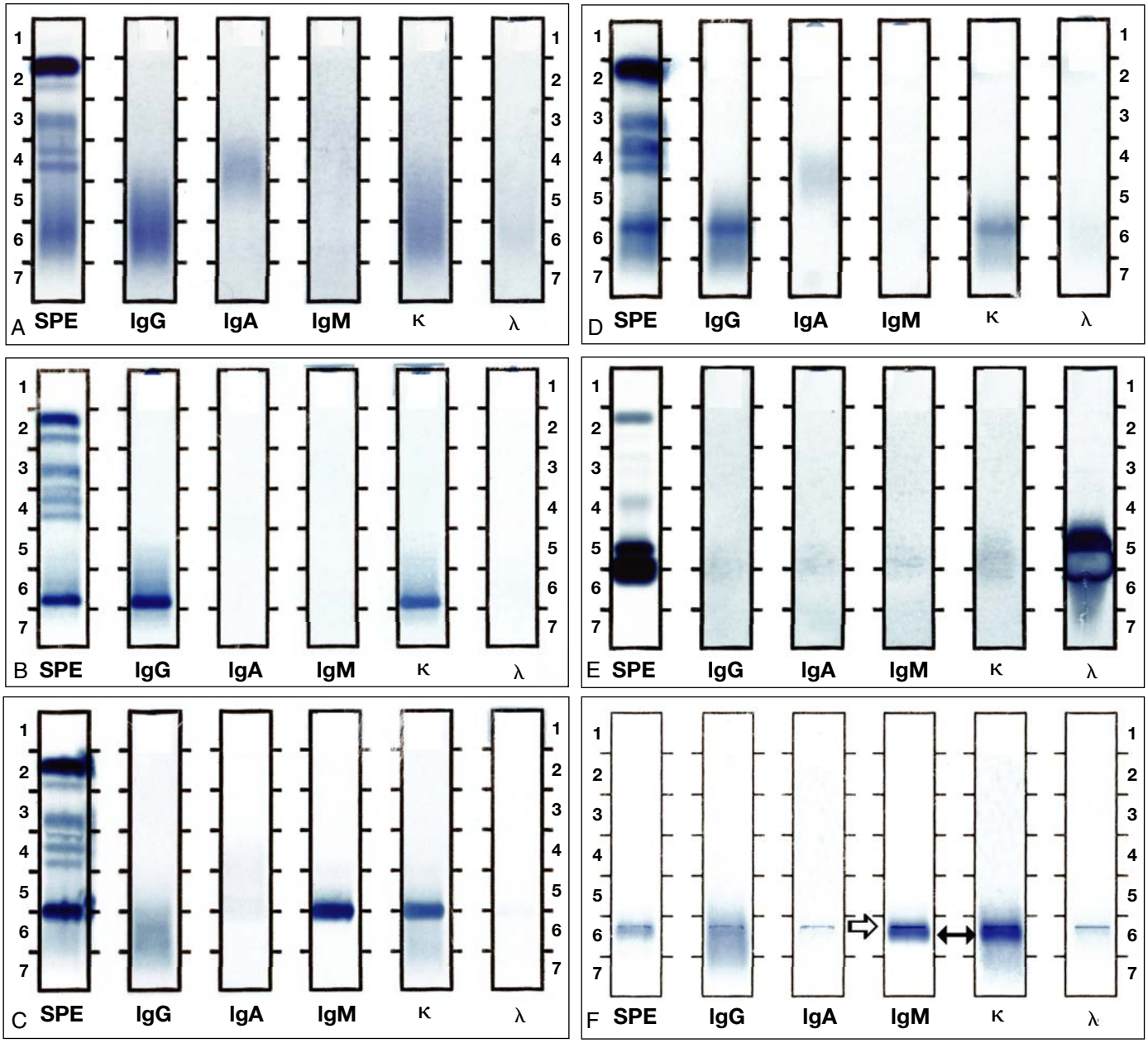

Figure 47.7 Monoclonal immunoglobulins (Ig) demonstrated by serum immunofixation. Replicate samples of patient serum were subjected to electrophoresis through agarose at pH 8.6. The separated proteins were allowed to react with monospecific antisera, and the gels were washed, fixed, and stained. **A,** Normal polyclonal pattern of immunoglobulins. **B,** Monoclonal IgG-κ immunoglobulin (M protein) in serum with loss of most normal polyclonal immunoglobulins. **C,** Monoclonal IgM-κ immunoglobulin in serum. **D,** Minor band of IgG-κ immunoglobulin in serum, along with normal-appearing immunoglobulins—possible monoclonal gammopathy of undetermined significance (MGUS). **E,** Two bands of λ light chains in urine. The lower band demonstrates antigen excess with artifactual clearing in its central region surrounded by a ring of immunofixed protein. The upper smaller band sometimes results from dimerization of free light chains through disulfide bonds. **F,** Type II mixed cryoglobulin precipitated from serum containing monoclonal IgM-κ *(solid arrow)* and polyclonal IgG. Some undissolved cryoglobulin *(open arrow)* remained at the application point of each lane. *IgA,* Sample reacted with anti-IgA (α-heavy chain specific); *IgG,* sample reacted with anti-IgG (γ-heavy chain specific); *κ,* sample reacted with anti-κ; *λ,* sample reacted with anti-λ; *IgM,* sample reacted with anti-IgM (μ-heavy chain specific); *SPE,* all proteins in sample precipitated with acid reagent (serum protein electrophoresis).

A major problem still facing use of FLC assays is the lack of a universal assay standard that leads to excess assay imprecision. Other technical problems include polymerization with overestimation of true concentration and nonlinearity upon serial dilutions (Udd et al., 2017).

Heavy–Light Chain Immunoassay

Heavy–light chain (HLC) immunoassays are designed to quantitate monoclonal immunoglobulin bands by measuring the amount of unique epitopes created where constant regions of heavy-chain molecules attach to constant regions of light-chain molecules (Bradwell et al., 2009). There are six possible combinations routinely measured—IgGκ, IgGλ, IgMκ, IgMλ, IgAκ, and IgAλ—with ratios calculated for IgGκ/IgGλ, IgMκ/IgMλ, and IgAκ/IgAλ. If a ratio falls outside the reference range, the HLC immunoassay is interpreted as "possible monoclonal band" and quantitation is performed. This technique does not directly visualize a monoclonal band but rather infers it from the calculated ratio. A recent study performed a head-to-head comparison of HLC and serum protein electrophoresis (SPEP) quantitations of monoclonal bands in the serum of 518 patients with multiple myeloma of IgG and IgA types (Katzmann et al., 2015). The intention was to provide better quantitation of monoclonal bands when they overlap with other normal serum proteins that normally migrate in the beta region of the SPEP (e.g., transferrin, β-lipoprotein, and C3 component of complement). The results showed that the HLC immunoassay held no significant advantage over SPEP in measuring IgG monoclonal bands—all of which in this study migrated in the gamma region and, thus, had no interferences. Of the 30 IgA bands in the study, all migrated in the beta region, but 7 cases were missed by SPEP, although successfully detected by HLC. This slight advantage of HLC over SPEP suggests that HLC could best be used for patients who have IgA bands migrating in the beta region (Calderon, 2015). However, a large band of IgA should be readily measurable by SPEP

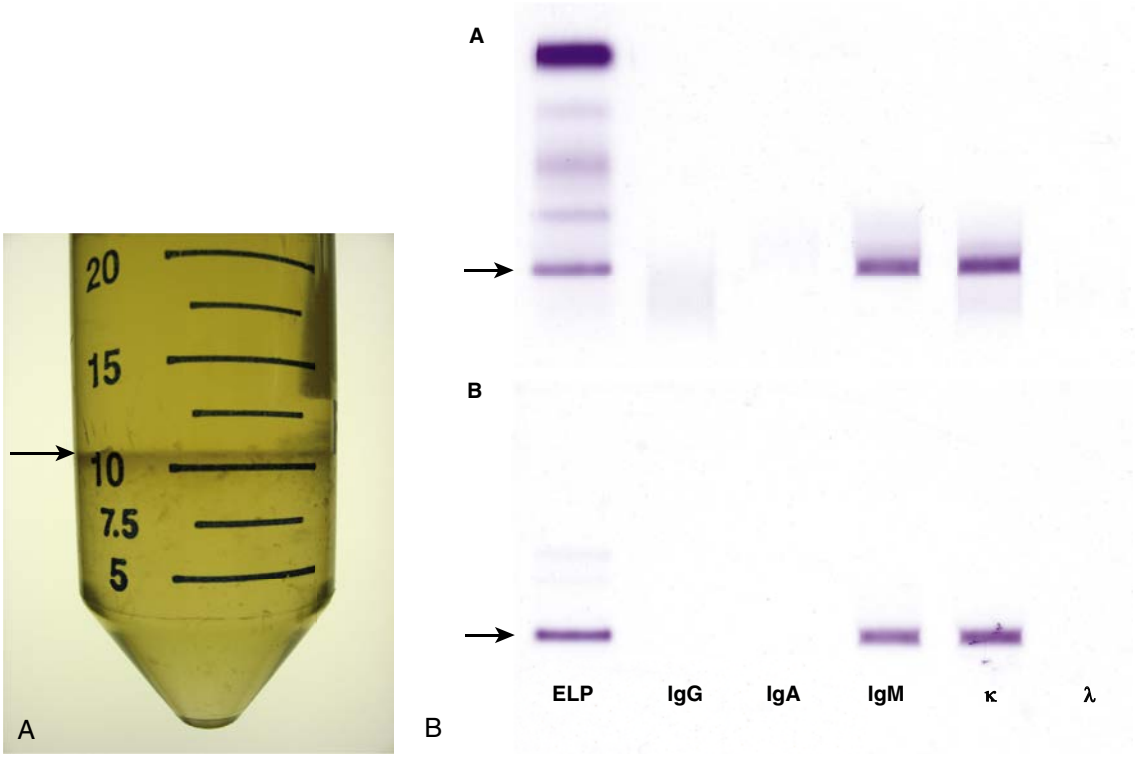

Figure 47.8 **A,** Type I cryoglobulin in the plasma of a patient undergoing plasmapheresis for hyperviscosity syndrome due to monoclonal immunoglobulin (Ig) M-κ. Plasma removed during plasma exchange was stored at 4°C in a 50-mL tube. The cryoglobulins that precipitated in the cold occupied approximately 20% of this patient's plasma volume. The *arrow* indicates the top of the cryoglobulin that settled in the tube. **B,** IFE demonstrating IgM-κ monoclonal band in whole serum *(upper panel)* that formed a type I cryoglobulin in the cryoprecipitate *(lower panel)*. Results in **A** and **B** are from different patients.

regardless of its migration and, thus, should not require HLC assay. In addition, in monitoring low levels of the paraprotein after chemotherapy or bone marrow transplantation, normal polyclonal immunoglobulins of the same HLC combination as the paraprotein will also reappear with reconstitution of normal plasma cells. They, in principle, should react in the HLC as the paraprotein would, thereby leading to a falsely elevated estimate.

A study of M-proteins in the α_2-β region (which is generally considered the most difficult region for SPEP to quantitate owing to overlapping normal serum proteins) in 166 clinical samples and 27 external quality assessment samples showed slightly higher sensitivity of IFE over HLC. However, the use of HLC allowed good M-protein quantitation in that electrophoretic region (Jacobs et al., 2018).

Still another comparison study of 463 newly diagnosed patients with M proteins compared SPEP/IFE and HLC (Michallet et al., 2018). Patients who subsequently had very good partial response showed poor concordance between these methods versus those with partial or complete response, suggesting a possible prognostic role for HLC. Proponents of HLC have reasoned that abnormal HLC ratios are due both to elevation of the clonal protein and to suppression of the nonclonal immunoglobulins. These factors could reflect both disease progression and inhibition of polyclonal immunoglobulins, thus, leading to more powerful prognosis. Cases of light chain myeloma and oligosecretory disease were not studied by HLC and presumably would not be successfully assessed by this method.

Cryoglobulin Testing

Accurate laboratory test results for cryoglobulins are especially sensitive to improper preanalytic handling. Clinicians must be aware of specimen temperature requirements when ordering these studies to avoid false-negative results (Shihabi, 2006; Chan et al., 2008). Testing for cryoglobulins in serum begins with a period of incubation in the cold (4°C) to detect turbidity or precipitate after 24 or 72 hours compared with an aliquot of the patient's serum kept at 37°C as a control for other precipitating substances not related to cold phenomena. Any cryoprecipitate is sedimented by centrifugation, washed briefly with cold saline to remove other serum proteins, and then redissolved (and dissociated) in warm saline for electrophoresis and immunofixation to identify immunoglobulin components (i.e., heavy and light chains).

Type I cryoglobulins typically form a relatively large volume of cryoprecipitate (e.g., up to 10% or even 20% of the serum volume—sometimes referred to as the "cryocrit"; Fig. 47.8A). Upon IFE, type I cryoglobulins exhibit a single heavy chain and a single light chain type, often monoclonal IgM (Fig. 47.8B). The whole serum not treated with cryoprecipitation usually demonstrates a large amount of the same monoclonal band. The concentration of the band should fall after successful plasma exchange.

Type II cryoglobulins typically show only a small amount of cryoprecipitate that is less than 1% of the serum volume. Thus, quantitating the percentage of cryocrit is not analytically valid for serial measurements to monitor a patient's progress. IFE shows a monoclonal band of IgM plus polyclonal IgG (see Fig. 47.7F). This pattern is observed frequently because of its association with chronic hepatitis C.

IFE findings in type III cryoglobulin would be similar to those in type II with a relatively small amount of cryoprecipitate that demonstrates both polyclonal IgM and polyclonal IgG.

A recent review and update emphasizes present lack of standardization for measurement of cryoglobulins (Kolopp-Sard & Miossec, 2018).

Oligoclonal Immunoglobulin Bands in Cerebrospinal Fluid

Evaluation of intrathecal synthesis of immunoglobulin is aided by high-resolution electrophoresis of cerebrospinal fluid (CSF) protein that spreads out the γ region to display individual bands of different immunoglobulin clones. The interpretation of CSF protein electrophoresis requires simultaneous electrophoresis of the patient's serum to ensure that findings in the CSF are unique and do not reflect just the passive transfer of clonal immunoglobulins from the blood. Oligoclonal bands as a marker of synthesis of immunoglobulins in the central nervous system suggest the possibility of an autoimmune process, such as a demyelinating disease. Another possibility is an immunologic response to central nervous system infection; thus, the interpretation of oligoclonal bands in CSF must be made in the context of other diagnostic findings, such as cell counts, viral serologies, bacterial cultures, syphilis testing, nucleic acid amplification tests for viruses, and so forth.

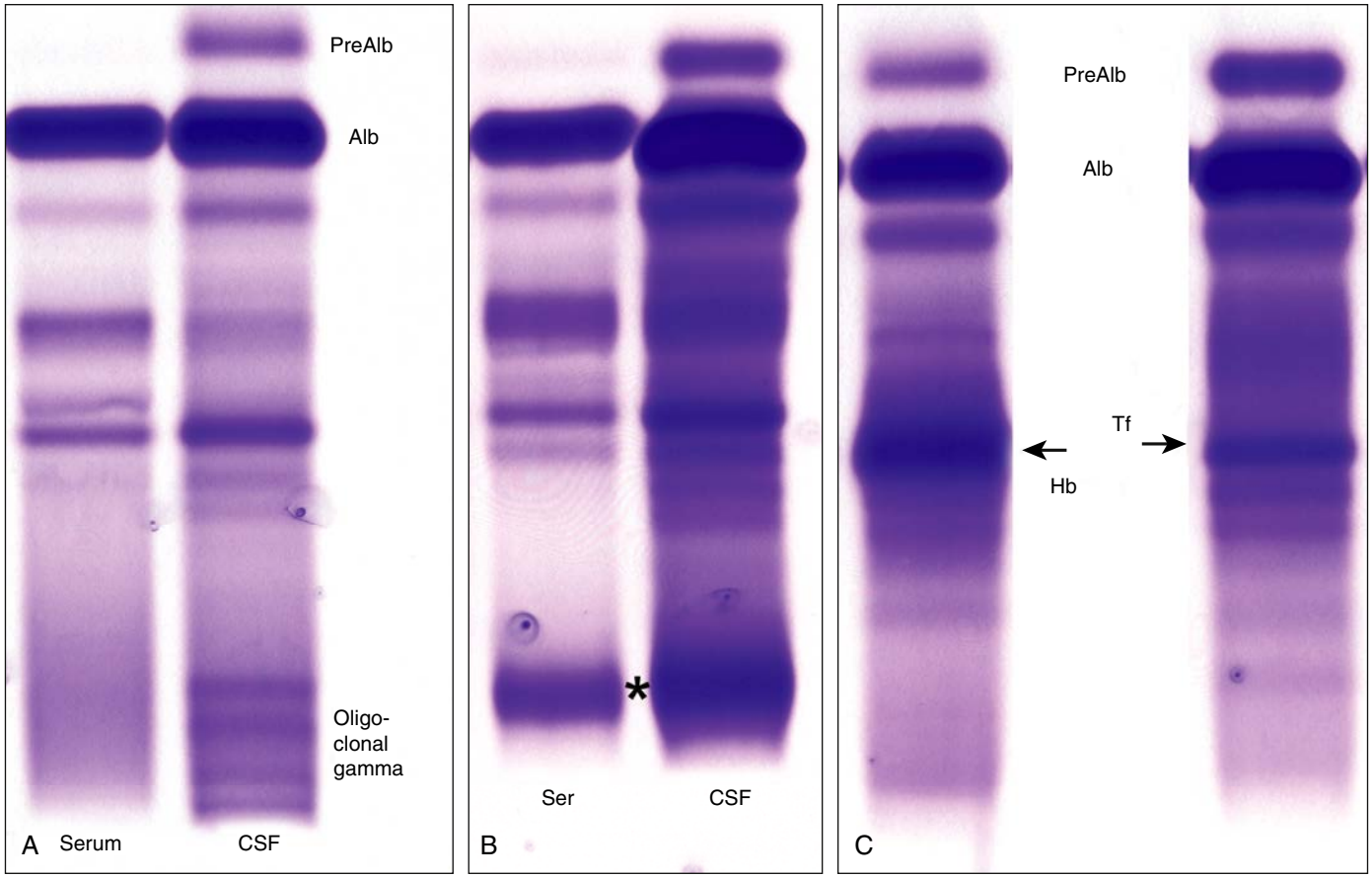

Figure 47.9 Protein electrophoretic patterns in serum and cerebrospinal fluid (CSF). **A,** Serum and CSF from the same patient showing positive oligoclonal bands in the γ region of the CSF but not in the patient's serum. **B,** Monoclonal band of immunoglobulin in both serum and CSF interpreted as negative for oligoclonal bands in CSF. **C,** Artifact of hemoglobin (Hb) in CSF *(left lane)* adjacent to the position of transferrin (Tf) *(right lane).*

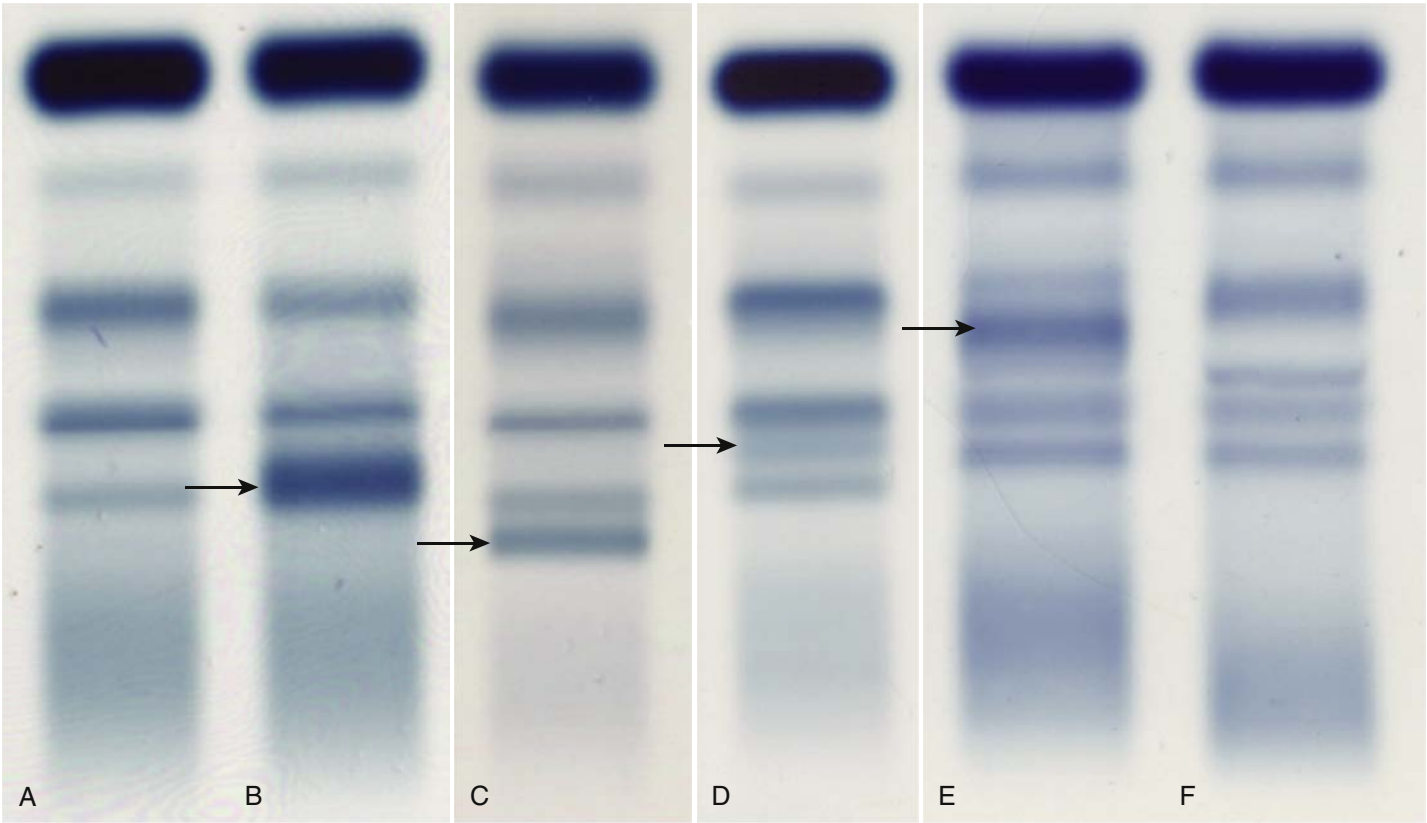

Figure 47.10 Low-intensity bands of monoclonal and other proteins migrating about the β region. **A,** Normal serum protein electrophoresis pattern. **B,** Minor band of immunoglobulin (Ig) A-κ *(arrow)* overlapping C3. **C,** Fibrinogen *(arrow)*, not to be confused with a monoclonal band. **D,** Minor band of IgA-κ *(arrow)* migrating between transferrin and C3. **E,** Hemolysed specimen with a minor band of hemoglobin-haptoglobin *(arrow)*. **F,** Redraw of serum without hemolysis from same patient as in **E**. **E** and **F** were electrophoresed on a different gel system from **A** through **D**; relative mobilities of normal serum proteins can vary in different systems.

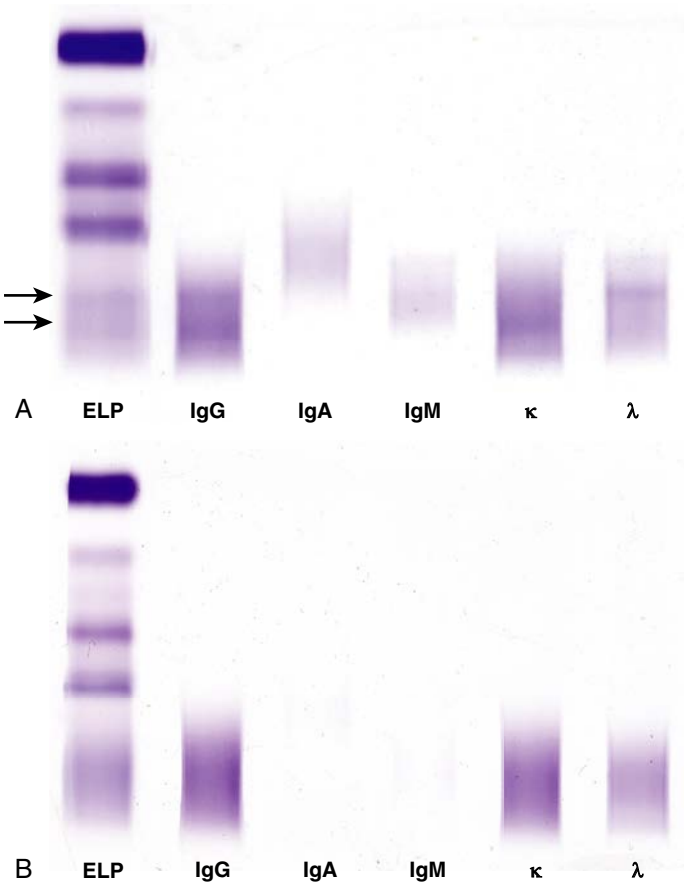

Figure 47.11 **A,** Oligoclonal bands of IgG-κ and IgG-λ in a patient who received autologous hematopoietic stem cell transplant 2 years earlier for IgG-λ multiple myeloma. Note minor bands of both IgG-κ and IgG-λ. **B,** IFE showing intense staining for polyclonal IgG (κ and λ) with faint amounts of IgA and IgM in a patient who received an autologous hematopoietic stem cell transplant 3 months earlier for IgG-κ multiple myeloma (this band now absent). The polyclonal IgG in this serum is due to intravenous infusions of gamma globulins. *IgA,* Sample reacted with anti-IgA (α-heavy chain specific); *IgG,* sample reacted with anti-IgG (γ-heavy chain specific); *κ,* sample reacted with anti-κ; *λ,* sample reacted with anti-λ; *IgM,* sample reacted with anti-IgM (μ-heavy chain specific); *ELP,* all proteins in sample precipitated with acid reagent (serum protein electrophoresis).

The protein electrophoretic pattern of CSF and serum from a patient with multiple sclerosis is shown in Figure 47.9A. The CSF was concentrated, and the serum was diluted to achieve comparable amounts of stainable protein in each application. CSF has a relatively higher concentration of prealbumin than does serum. Albumin is the predominant band in both fluids. The other significant band in CSF is transferrin because of its small molecular size that permits ultrafiltration from blood into CSF. The higher molecular weight proteins in serum (α2 plus β-lipoprotein) are absent from CSF. C3 is also identifiable in CSF, along with a band of asialotransferrin in the β2 region. After all these landmark proteins of CSF are recognized, oligoclonal bands should be evaluated in the γ region, which normally has only a small quantity of polyclonal immunoglobulins. The oligoclonal bands in Figure 47.9A are discrete and clearly separate from one another.

Examination of serum and CSF sometimes shows a clonal band of immunoglobulin present in both (Fig. 47.9B). However, this finding is not indicative of intrathecal synthesis and, thus, is not a positive result for oligoclonal bands. Presumably, it represents clonal proliferation of plasma cells in the body with passive movement of the monoclonal antibody from blood into CSF.

Another distortion of the electrophoretic pattern occurs with release of hemoglobin (Hb) into the CSF, resulting in a major band in the β region close to transferrin (Fig. 47.9C). This band of Hb should not be confused with clonal immunoglobulin in CSF. Confirmation that this band is Hb depends on visual examination of the CSF for blood or hemolysis (red color). A band of red Hb can also be seen in the β region before staining of the electrophoretic gel.

A consensus statement on analysis of CSF was commissioned from experts in multiple sclerosis by the Consortium of Multiple Sclerosis Clinics (Freedman et al., 2005). That group recommended qualitative assessment of CSF for IgG using IFE on unconcentrated CSF compared directly with a serum specimen from the same patient. Interpretation of the pattern should consist of one of the following:

Type 1: No bands in CSF and serum

Type 2: Oligoclonal bands in CSF, not in serum; indicates intrathecal IgG synthesis

Type 3: Oligoclonal bands in CSF plus other oligoclonal bands in CSF and serum; indicates intrathecal IgG synthesis

Type 4: Identical oligoclonal bands in CSF and serum; indicates systemic immune reaction with passive transfer to CSF; no intrathecal IgG synthesis

Type 5: Monoclonal band in CSF and serum; paraprotein; no intrathecal IgG synthesis

Problems in Detecting Monoclonal Bands

Clearly demarcated monoclonal bands are straightforward to identify when they are at high concentration and migrate separately from other serum proteins, particularly when the γ fraction is clear of normal polyclonal immunoglobulins owing to replacement of normal plasma cells with the malignant clone. Several examples of clear-cut monoclonal bands are presented in Figure 47.5. The area under the tracing for such bands can be readily integrated to calculate concentration of a monoclonal protein for monitoring in serial specimens.

Sometimes the monoclonal bands are much less pronounced and may be difficult to distinguish within a background of normal proteins. Figure 47.7D shows such a minor band of IgM-κ that can still be readily identified by IFE. However, when small monoclonal proteins migrate in the β or even α2 region, they can escape detection because of overlap with normal proteins such as transferrin or C3 (Fig. 47.10B). A monoclonal band migrating between normal serum proteins may also be mistakenly disregarded (Fig. 47.10D); thus, it is very important to interpret such electrophoreses with a firm expectation of where normal bands migrate and what their intensities should be.

False-positive interpretations of monoclonal bands can occur owing to the presence of fibrinogen from an unclotted specimen (Fig. 47.10C) or when hemolysis occurs as the result of improper specimen collection (Figs. 47.10E and 47.10F). Confirmation that a small band is a monoclonal paraprotein is typically done with IFE.

Treatment of multiple myeloma with the therapeutic monoclonal antibodies (t-mAb) daratumumab (anti-CD38) and elotuzumab (anti-signaling lymphocytic activation molecule F7 [anti-SLAMF7]) results in low-level but distinct M spikes from the t-mAb itself by SPEP and IFE (Murata et al., 2018). Both of these interfering M spikes are IgG1κ and might be falsely interpreted as M spikes made by the patient. While these two t-mAbs usually migrate separately from a patient's own endogenous M spike, occasionally they do comigrate on electrophoresis (Tang et al., 2018). One method for mitigating the influence of the t-mAb has used a mouse anti-t-mAb to alter its migration (Axel et al., 2014).

In addition to electrophoretic and immunologic measurements of immunoglobulins, FLC, and HLC, matrix-assisted laser desorption ionization-time of flight (MALDI-TOF) (see Chapter 5) has been proposed for detecting monoclonal bands by looking for presence of overexpressed clones (Willrich et al., 2018). With the advantage of very fast analysis time (<1 minute per sample), this method might gain in popularity. Presently, however, sample preparation time is very long and impractical for large-scale use.

Oligoclonal Immunoglobulin Bands in Serum

In contrast to monoclonal immunoglobulin bands that derive from clonal plasma cell disorders such as multiple myeloma, oligoclonal banding patterns occasionally appear in the serum of patients who do not have plasma cell disorders. Oligoclonal patterns may show multiple and distinct bands on SPEP that are revealed on IFE to consist of immunoglobulins with both κ light chains and λ light chains in the same specimen, thereby ruling out the possibility of deriving from the same parent clone. They are usually IgG but can also be IgA or IgM, even in the same patient. These likely represent an immune response against an infection or other antigens. They have been observed in immunosuppressed solid-organ transplant patients with cytomegalovirus infections (Myara et al., 1991; Pham et al., 1998; Cakalaroski et al., 2000) in some patients with HIV infection (in which case these bands are directed against HIV proteins) (Amadori et al., 1990; Konstantinopoulos et al., 2007), and in patients after chemotherapy or bone marrow transplant for multiple myeloma (in which case the antibodies

react with tumor antigens on plasma cells; Fig. 47.11A) (Mark et al., 2008; Rahiff et al., 2012). For interpretation of oligoclonal banding patterns in serum, it is appropriate to determine the clinical context. Such bands might appear prior to a diagnosis of HIV and, if so, should lead to a consideration of that diagnosis. They can also have positive prognostic significance in multiple myeloma patients as an antitumor response.

Patients whose multiple myeloma has been successfully treated should show clearance of their monoclonal immunoglobulin bands and can appear to have severe hypogammaglobulinemia. These patients often receive immunoglobulin infusions to guard against infections prior to reconstitution of their own immune systems. The IFE of such a patient might show no monoclonal band but rather polyclonal IgG from infusions that contain no IgA or IgM (Fig. 47.11B).

DISEASE PREVENTION AND THERAPY

Passive immunization is the administration of preformed antibodies obtained from another individual of the same species (homologous γ-globulins) or a different species (heterologous γ-globulins); it results in immediate protection against infection. The immunity is short-lived and decays as the antibodies are used and catabolized. Passive protection in neonatal life is based on transfer of maternal antibodies across the placenta or through colostrum (Pennington, 1991).

Pooled human γ-globulin is useful for temporary protection against several viral and bacterial infections (Berkman et al., 1990; Hammarström & Smith, 1990; Desai, 1991). Depending on the dose used and the time of administration, the disease may be modified to a mild form or entirely prevented. The effect is more complete and more predictable if one uses hyperimmune preparations made from the plasma of individuals who are convalescing from the disease in question or who have recently been immunized against it. Such preparations contain a higher concentration of specific antibodies. Antibodies may also be produced in animals, such as horses; in the past, these antibodies found widespread use. However, prior sensitization to foreign proteins may lead to clinical reactions such as anaphylaxis, serum sickness, pyrexia, and local Arthus reactions.

Monoclonal antibodies have revolutionized many areas of medicine, including research, diagnostics, and therapy. Murine, human, and humanized monoclonal antibodies have been developed (Lefrano & Lefrano, 1990; Morrison, 1992; Mountain & Adair, 1992; Ward, 1992; Shin et al., 1993). Many monoclonal antibodies, often replacing polyclonal antisera, are used for diagnostic purposes (see Chapter 44). Perhaps the most important therapeutic applications of monoclonal antibodies are seen in the fields of transplantation and oncology (Stevenson et al., 1990; Vitetta et al., 1993; Neame et al., 1994). OKT3, a murine monoclonal antibody against the CD3 receptor on lymphocytes, is often used as an antirejection therapy to block the activity of cytotoxic T lymphocytes in renal transplant recipients (Ortho Multicenter Transplant Study Group, 1985). Many potential clinical applications of monoclonal antibodies are being evaluated.

Since their development over 40 years ago, monoclonal antibodies have opened an entirely new avenue of therapeutics in the treatment of disease. Monoclonal antibodies raised against disease-associated antigens are used today to bring about remissions in cancers and ease or eliminate the complications of autoimmune disease, infectious disease and cardiovascular disease. However, modifications to monoclonal antibodies—known as *humanization*—must be made to allow these proteins produced in nonhuman systems to survive under the human immune system's surveillance and to avoid inducing an immune response after therapeutic administration. The most frequently used means of humanization makes use of recombinant DNA technology to graft the complementarity determining region (CDR), which confers antigen binding specificity, of a nonhuman monoclonal antibody into the CDR site of an acceptor human antibody scaffold or framework. However, because a CDR engrafted into the human acceptor scaffold is still nonhuman, it has the potential to trigger antidrug antibody responses. Therefore, once the desired monoclonal antibody has been developed in a nonhuman system, the DNA encoding it (and, therefore, its CDR) is determined and isolated and sequenced. The DNA sequence is inserted into the DNA encoding a human antibody; that DNA is then grafted into cell lines to produce humanized antibodies at large scale. Additional approaches to humanization include removing nonhuman antigens from the surface of the antibodies and replacing them with common human antigens. This process is known as *resurfacing*.

Though expression systems for producing humanized monoclonal antibodies include bacterial, yeast, insect, and plant systems, it is mammalian systems that are preferred. Mammalian cell lines have the advantage of producing properly folded and posttranslationally modified antibodies. The Chinese hamster ovary and human embryonic kidney (HEK) cell lines are most frequently chosen to produce humanized monoclonal antibodies. Commercially available humanized antibodies may differ in the engineering approach used to humanize them, in their affinity for targets, and in their immunogenicity in the human immune system after administration. The differences in affinity can be quite significant after humanization, but this disadvantage may be offset by the longer bioavailability of the humanized forms. The therapeutic humanized monoclonal antibodies may be whole antibody, Fab fragments linked by disulphide bonds, Fv fragments (V domains only), and single-chain antibodies (scFvs with V domains linked by peptides); multiple antibody fragments having different specificities may be fused to create diabodies, triabodies, tetrabodies with 2, 3, and 4 specificities. Though many fully humanized antibodies do not elicit an immune response, some humanized antibodies may do so. Nonetheless, humanization has been shown to reduce immunogenicity (as well as affinity) by virtue of decreasing the nonhuman epitopes on nonhuman-derived antibodies. Therapeutic drug monitoring (TDM) to determine serum antibody concentrations in order to optimize dosing and avoid toxicity is standard for many therapeutic regimens. TDM is not beneficial clinically for drugs that have high intersubject variability or do not have a small therapeutic window, as is the case with monoclonal antibodies. For most therapeutic monoclonal antibodies, there is no maximum tolerated dose, and toxicity is not usually not an issue. Nonetheless, monoclonal drugs are expensive and avoiding unnecessarily high serum concentrations through TDM would help to contain the cost of therapy (Oude Munnink et al., 2016).

A recent example is the use of a monoclonal antibody against tumor necrosis factor-α to prevent Jarisch-Herxheimer reactions resulting from antibiotic treatment of *Borrelia* infection in sheep (Fekade et al., 1996). Anticytokine and antineutrophil adhesion molecule monoclonal antibodies may be effective in conditions associated with acute inflammation and cytokine release, such as acid aspiration, ischemia, or reperfusion injury (myocardial infarction, hemorrhagic shock, aortic aneurysm repair). Antibodies inhibiting neutrophil adhesion may be effective in asthma, pulmonary fibrosis, meningitis, and cerebral malaria; a monoclonal antibody directed against a component of the complement cascade suggested the possibility of eventual therapeutic regulation of specific arms of the inflammatory response (DiLillo et al., 2006). It seems reasonable to expect that a multitude of therapeutic applications will become available in the future, in which monoclonal antibodies will be designed to modulate the actions of one or more naturally occurring mediators of inflammation, infection, or malignant proliferation.

SELECTED REFERENCES

Cacoub P, Costedoat-Chalumeau N, Lidove O, et al.: Cryoglobulinemia vasculitis, *Curr Opin Rheumatol* 14:29, 2002.

This review presents an update on clinical findings in cryoglobulins, with emphasis on patients with hepatitis C.

Chan AO, Lau JS, Chan CH, et al.: Cryoglobulinemia: clinical and laboratory perspectives, *Hong Kong Med J* 14:55, 2008.

A good review of cryoglobulin testing, with case studies.

Colls BM: Monoclonal gammopathy of undetermined significance (MGUS)—31 year follow-up of a community study, *Aust N Z J Med* 29:500, 1999.

This clinical series demonstrates the long-term significance of MGUS.

Dispenzieri A, Kyle R, Merlini G, et al.: International Myeloma Working Group guidelines for serum-free light chain analysis in multiple myeloma and related disorders, *Leukemia* 23:215, 2009.

This article provides official recommendations from the International Myeloma Working Group for clinical use of serum-free light chain testing based on a comprehensive review of the literature.

Fekade D, Knox K, Hussein K, et al.: Prevention of Jarisch-Herxheimer reactions by treatment with antibodies against tumor necrosis factor α, *N Engl J Med* 335:311, 1996.

This is an early clinical trial that showed how inflammatory reactions can be modulated by therapeutic antibodies.

Freedman MS, Thompson EJ, Deisenhammer F, et al.: Recommended standard of cerebrospinal fluid analysis in the diagnosis of multiple sclerosis, *Arch Neurol* 62:865, 2005.

This article is a consensus statement commissioned by the Consortium of Multiple Sclerosis Clinics that establishes the "minimum standard" for evaluation of CSF in patients suspected of having multiple sclerosis.

Keren DF: Procedures for the evaluation of monoclonal immunoglobulins, *Arch Pathol Lab Med* 123:126, 1999.
This review of laboratory procedures provides insight into modern measurements of monoclonal gammopathies.

Kolopp-Sarda M-N, Miossec P: Cryoglobulins: an update on detection, mechanisms and clinical contribution, *Autoimmunity Rev* 17:457–464, 2018.
Comprehensive review of laboratory and clinical aspects of detecting cryoglobulins and monitoring their outcomes.

Kyle RA, Rajkumar SV: Monoclonal gammopathies of undetermined significance: a review, *Immunol Rev* 194:112, 2003.
This is an updated and comprehensive assessment of patients with MGUS.

Ritchie RF, Palomaki GE, Neveux LM, et al.: Reference distributions for immunoglobulins A, G, and M: a practical, simple, and clinically relevant approach in a large cohort, *J Clin Lab Anal* 12:363, 1998.
This article presents reference ranges for immunoglobulins in a very large population by age and gender.

Smith GS, Holman RP: The prozone phenomenon with syphilis and HIV-1 coinfection, *South Med J* 97:379, 2004.
This recent case report reinforces the continuing need for vigilance in antigen–antibody–based testing to avoid missing extremely high values of immune antibody caused by the prozone effect.

Access the complete reference list online at Elsevier eBooks for Practicing Clinicians.

REFERENCES

Amadori A, Gallo P, Zamarchi R, et al.: IgG oligoclonal bands in sera of HIV-1 infected patients are mainly directed against HIV-1 determinants, *AIDS Res Hum Retroviruses* 6:581–586, 1990.

Atkinson JP, Waldmann TA, Stein SF, et al.: Systemic capillary leak syndrome and monoclonal IgG gammopathy, *Medicine* 56(225), 1977.

Axel AE, McCudden CR, Xie H, et al.: Development of clinical assay to mitigate daratumumab, an IgG1κ monoclonal antibody, interference with serum immunofixation (IFE) and clinical assessment of M-protein response in multiple myeloma, *Cancer Res* 74(19Suppl), 2014. Abstract nr 2563, 2014.

Axelsson N, Hellen J: Frequency of M components in 6995 sera from an adult population, *Br J Haematol* 15:417, 1968.

Bachman R: The diagnostic significance of the serum concentration of pathological proteins, *Acta Med Scand* 178:801, 1965.

Benbassat J, Fluman N, Zlotnick A: Monoclonal immunoglobulin disorders: a report of 154 cases, *Am J Med Sci* 27:325, 1976.

Berkman SA, Lee ML, Gale RP: Clinical uses of intravenous immunoglobulins, *Ann Intern Med* 112:278, 1990.

Bhat TN, Bentley GA, Fischmann TO, et al.: Small rearrangements in structures of Fv and Fab fragments of antibody D1.3 upon antigen binding, *Nature* 347:483, 1990.

Bradwell AR, Harding SJ, Fourrier NJ, et al.: Assessment of monoclonal gammopathies by nephelometric measurement of individual immunoglobulin kappa/lambda ratios, *Clin Chem* 55:1646–1655, 2009.

Buckley RH: Serum immunoglobulin concentrations in health and in primary immunodeficiency diseases. In Altmann PL, Katz DD, editors: *Human health and disease*, Bethesda, Md, 1977, Federation of American Societies for Experimental Biology, pp 58–60.

Burton DR: Immunoglobulin G: functional sites, *Mol Immunol* 22:161, 1985.

Cakalaroski K, Ivanovski N, Popov S, et al.: Mono- and oligoclonal immunoglobulin anomalies in kidney transplant patients, *Ann Urol* 34:340–344, 2000.

Calderon B: Heavy/light chain assay for monitoring IgA multiple myeloma: Digging out the IgA from the β-region, *Clin Chem* 61:317–318, 2015.

Carsetti R, Kohler G, Lamers MC: A role for immunoglobulin D: interference with tolerance induction, *Eur J Immunol* 23:168, 1993.

Cassidy JT, Nordby GL, Dodge HJ: Biologic variation of human serum immunoglobulin concentrations: sex-age specific effects, *J Chronic Dis* 27:507, 1974.

Cohen HJ: Multiple myeloma in the elderly, *Clin Geriatr Med* 1:827, 1985.

Corcoran AE: Immunoglobulin locus silencing and allelic exclusion, *Semin Immunol* 17:141, 2005.

Cushman P, Grieco MH: Hyperimmunoglobulinemia associated with narcotic addiction, *Am J Med* 54:320, 1973.

Davies DR, Metzer H: Structural basis of antibody function, *Annu Rev Immunol* 1:87, 1983.

De Paschale M, Ceriani C, Cerulli T, et al.: Antenatal screening for toxoplasmosis gondii, cytomegalovirus, rubella and Treponema pallidum infections in northern Benin, *Trop Med Int Health* 19:743–746, 2014.

Desai RG: Recent advances in intravenous immunoglobulin therapy—Concluding remarks: Current trends and future directions, *Cancer* 68:1460, 1991.

DiLillo DJ, Pawluczkowycz AW, Peng W, et al.: Selective and efficient inhibition of the alternative pathway of complement by a mAb that recognizes C3b/iC3b, *Mol Immunol* 43:1010, 2006.

Drouet E, Chapuis-Cellier C, Bosshard S, et al.: Oligo-monoclonal immunoglobulins frequently develop during concurrent cytomegalovirus (CMV) and Epstein-Barr virus (EBV) infections in patients after renal transplantation, *Clin Exp Immunol* 118:465, 1999.

Hammarström L, Smith CI: New and old aspects of immunoglobulin application: the use of intravenous IgG as prophylaxis and for treatment of infections, *Infection* 18:314, 1990.

Herron JN, He XM, Ballard DW: An antibody to single-stranded DNA: comparison of the three-dimensional structures of the unliganded Fab and a deoxynucleotide–Fab complex, *Proteins* 11:159, 1991.

Isobe T, Osserman EF: Pathologic conditions associated with plasma cell dyscrasias: a study of 806 cases, *Ann N Y Acad Sci* 190:507, 1971.

Jacobs JFM, Haagen I-A, Lodder A, et al.: Analytical validation of the Hevylite assays for M-protein quantification, *Clin Chem Lab Med* 56:1169–1175, 2018.

Jaskowski TD, Litwin CM, Hill HR: Detection of kappa and lambda light chain monoclonal proteins in human serum: automated immunoassay versus immunofixation electrophoresis, *Clin Vaccine Immunol* 13:277, 2006.

Kanno A, Kazuyama Y: Immunoglobulin G antibody avidity assay for serodiagnosis of hepatitis C virus infection, *J Med Virol* 68:229–233, 2002.

Karplus M, McCammon JA: Dynamics of proteins: elements and function, *Annu Rev Biochem* 53:263, 1983.

Katzmann JA, Willrich MAV, Kohlhage MC: Monitoring IgA multiple myeloma: immunoglobulin heavy/light chain assays, *Clin Chem* 61:360–367, 2015.

Keating SM, Hanson D, Lebedeva M, et al.: Lower-sensitivity and avidity modifications of the Vitros anti-HIV 1+2 assay for detection of recent HIV infections and incidence estimation, *J Clin Microbiol* 50:3968–3976, 2012.

Kelly RH, Tardy TJ, Shah PM: Benign monoclonal gammopathy: a reassessment of the problem, *Immunol Invest* 14:193, 1985.

Keren DF, Warren JS, Lowe JB: Strategy to diagnose monoclonal gammopathies in serum: high-resolution electrophoresis, immunofixation, and kappa/lambda quantification, *Clin Chem* 34:2196, 1988.

Kolar G: Capra JD: immunoglobulins: structure and function. In Paul WE, editor: *Fundamental immunology*, Philadelphia, 2003, Lippincott Williams & Wilkins, p 47.

Konstantinopoulos PA, Desube BJ, Pantanowitz L, et al.: Protein electrophoresis and immunoglobulin analysis in HIV-infected patients, *Am J Clin Pathol* 128:596–603, 2007.

Kontio M, Jokinen S, Paunio M, et al.: Waning antibody levels and avidity: implications for MMR vaccine-induced protection, *J Infect Dis* 206:1542–1548, 2012.

Kumar S, Paiva B, Anderson KC, et al.: International Myeloma Working Group consensus criteria for response and minimal residual disease assessment in multiple myeloma, *Lancet Oncol* 17:e328–e346, 2016.

Kyle RA: Monoclonal gammopathy of undetermined significance (MGUS): a review, *Clin Haematol* 11:123, 1982.

Lefrano G, Lefrano MP: Antibody engineering and perspectives in therapy, *Biochemie* 72:639, 1990.

Levett PN, Sonnenberg K, Sidaway F, et al.: Use of immunoglobulin G avidity assays for differentiation of primary from previous infections with West Nile virus, *J Clin Microbiol* 43:5873–5875, 2005.

Lichtman MA, Vaughan JH, Hames CG: The distribution of serum immunoglobulins, anti-γ-G globulins and antinuclear antibodies in White and Negro subjects in Evans County, Georgia, *Arthritis Rheum* 10:204, 1967.

Mark T, Jayabalan D, Coleman M, et al.: Atypical serum immunofixation patterns frequently emerge in immunomodulatory therapy and are associated with a high degree of response in multiple myeloma, *Br J Haematol* 143:654–660, 2008.

Max EE: Immunoglobulins: molecular genetics. In Paul WE, editor: *Fundamental immunology*, Philadelphia, 2003, Lippincott Williams & Wilkins, p 107.

Michallet M, Chapuis-Cellier C, Dejoie T, et al.: Heavy+light chain monitoring correlates with clinical outcome in multiple myeloma patients, *Leukemia* 32:376–382, 2018.

Morrison SL: In vitro antibodies: Strategies for production and application, *Annu Rev Immunol* 10:239, 1992.

Mountain A, Adair JR: Engineering antibodies for therapy, *Biotechnol Genet Eng Rev* 10(1), 1992.

Murata K, McCash SI, Carroll B, et al.: Treatment of multiple myeloma with monoclonal antibodies and the dilemma of false positive M-spikes in peripheral blood, *Clin Biochem* 51:66–71, 2018.

Myara I, Wuenum G, Storogenko M, et al.: Monoclonal and oligoclonal gammopathies in heart-transplant recipients, *Clin Chem* 37:1334–1337, 1991.

Neame PB, Soamboonsrup P, Quigley JG, et al.: The use of monoclonal antibodies and immune markers in the diagnosis, prognosis, and therapy of acute leukemia, *Transfus Med Rev* 8(59), 1994.

Nickerson PW, Rush DN, Jeffery JR, et al.: High serum levels of interleukin-6 in renal transplant recipients with monoclonal gammopathies, *Transplantation* 58:382, 1994.

Ortho Multicenter Transplant Study Group: A randomized clinical trial of OKT3 monoclonal antibody for acute rejection of cadaveric renal transplants, *N Engl J Med* 313:337, 1985.

Oude Munnink TH, Henstra MJ, Segerink LI, et al.: Therapeutic drug monitoring of monoclonal antibodies in inflammatory and malignant disease: Translating TNF-α experience to oncology, *Clin Pharmacol Ther* 99:419–431, 2016.

Padlan EA: Anatomy of the antibody molecule, *Mol Immunol* 31:169, 1991.

Pham H, Lemoine A, Salvucci M, et al.: Occurrence of gammopathies and lymphoproliferative disorders in liver transplant recipients randomized to tacrolimus (FK506)- or cyclosporine-based immunosuppression, *Liver Transpl Surg* 4:146–151, 1998.

Pennington JE: Immunoglobulin therapy in infectious disease, *Cleve Clin J Med* 58:309, 1991.

Poljak RJ: Structure of antibodies and their complexes with antigens, *Mol Immunol* 28:1341, 1991.

Radl J, Valentijn RM, Haaijman JJ, et al.: Monoclonal gammopathies in patients undergoing immunosuppressive treatment after renal transplantation, *Clin Immunol Immunopathol* 37:98, 1985.

Rahiff J, Trusch M, Haag F, et al.: Antigen-specificity of oligoclonal abnormal protein bands in multiple myeloma after allogeneic stem cell transplantation, *Cancer Immunol Immunother* 61:1639–1651, 2012.

Rajkumar SV, Dimopoulos MA, Palumbo A, et al.: International Myeloma Working Group updated criteria for the diagnosis of multiple myeloma, *Lancet Oncol* 15:e538–e548, 2014.

Rodrigues JP, Frei F, Naavarro IT, et al.: Seroepidemiological analysis of toxoplasmosis in college students, *J Venom Anim Toxins Incl Trop Dis* 21(1):1, 2015, https://doi.org/10.1186/1678-9199-21-1.eCollection2015.

Roes J, Rajewski K: Immunoglobulin D (IgD)-deficient mice reveal an auxiliary receptor function for IgD in antigen-mediated recruitment of B-cells, *J Exp Med* 177:45, 1993.

Ropper AH, Gorson KC: Neuropathies associated with paraproteinemia, *N Engl J Med* 338:1601, 1998.

Schaefer AI, Miller JB, Lester EP, et al.: Monoclonal gammopathy in hereditary spherocytosis: a possible pathogenetic relation, *Ann Intern Med* 88:45, 1978.

Shihabi ZK: Cryoglobulins: an important but neglected clinical test, *Ann Clin Lab Sci* 36:395, 2006.

Shin SU, Wright A, Morrison SL: Hybrid antibodies, *Int Rev Immunol* 10:177, 1993.

Spiegelberg HL: Biological activities of immunoglobulins of different classes and subclasses, *Adv Immunol* 19:259, 1974.

Standfield RL, Fieser TM, Lerner RA, et al.: Crystal structures of an antibody to a peptide and its complex with peptide antigen at 2.8Å, *Science* 248:712, 1990.

Stanko CK, Jeffery JR, Rush DN: Monoclonal and multiclonal gammopathies after renal transplantation, *Transplant Proc* 21:3330, 1989.

Stevenson FK, George AJ, Glennie MJ: Anti-idiotypic therapy of leukemias and lymphomas, *Chem Immunol* 48:126, 1990.

Tang F, Malek E, Math S, et al.: Interference of therapeutic monoclonal antibodies with routine serum protein electrophoresis and immunofixation in patients with myeloma, *Am J Clin Pathol* 150:121–E129, 2018.

Tedford MC, Stimson WH: Molecular recognition in antibodies and its application, *Experientia* 47:1129, 1991.

Tollerud DJ, Brown LM, Blattner WA, et al.: Racial differences in serum immunoglobulin levels: relationship to cigarette smoking, T-cell subsets, and soluble interleukin-2 receptors, *J Clin Lab Anal* 9:37, 1995.

Tonegawa S: Somatic generation of antibody-diversity, *Nature* 302:575, 1983.

Tosi P, Tomassetti S, Merli A, et al.: Serum free light-chain assay for the detection and monitoring of multiple myeloma and related conditions, *Ther Adv Hematol* 4:37–41, 2013.
Udd KA, Spektor TM, Berenson JR: Monitoring multiple myeloma, *Clin Adv Hematol Oncol* 15:951–961, 2017.
Vitetta ES, Thorpe PE, Uhr JW: Immunotoxins: Magic bullets or misguided missiles? *Trends Pharmacol Sci* 14:148, 1993.
Ward ES: Antibody engineering: the use of *Escherichia coli* as an expression host, *FASEB J* 6:2122, 1992.
Wells JV, Fudenberg HH: Paraproteinemias, *Dis Mon* 1:45, 1974.
Willrich MAV, Murray DL, Kyle RA: Laboratory testing for monoclonal gammopathies: focus on monoclonal gammopathy of undetermined significance and smoldering multiple myeloma, *Clin Biochem* 51:38–47, 2018.
Wilson IA, Stanfield RL, Rini JM, et al.: Structural aspects of antibodies and antibody—antigen complexes, *Ciba Found Symp* 159(13), 1991.

CHAPTER 48

MEDIATORS OF INFLAMMATION: COMPLEMENT

Katie V. Bean, H. Davis Massey, Gaurav Gupta

STRUCTURE AND FUNCTION OF THE COMPLEMENT SYSTEM, 969
Nomenclature, 969
C3: Central Molecule of Complement Activation Pathways, 970
The Classical Pathway, 971
The Alternative Pathway, 971
The Mannan-Binding Lectin Pathway, 972
Terminal Complement Components, 972
Anaphylatoxins, 972
Regulation of Complement Activation, 973
Complement Receptors, 974
Complement Biosynthesis, 974
Complement Genetics, 974
Complement and Acquired Immunity, 975

GENETIC COMPLEMENT DEFICIENCIES, 976

ASSESSMENT OF COMPLEMENT ACTIVITY IN DISEASE, 977

COMPLEMENT IN DISEASE STATES, 978
Rheumatologic Diseases, 978
Hereditary Angioedema, 979
Infectious Diseases, 979
Thrombotic Microangiopathies, 979
Renal Diseases, 979
Ophthalmologic Diseases, 979
Dermatologic Diseases, 979
Hematologic Diseases, 979
Neurologic Diseases, 980
Cardiovascular Diseases, 980
Biocompatibility, 980
Organ Transplantation, 980

CLINICALLY USEFUL COMPLEMENT INHIBITORS, 981

ASSAYS OF COMPLEMENT, 981
General Principles, 981
Functional Evaluation of the Classical Pathway, 982
Functional Evaluation of the Alternative Pathway, 982
Functional Assay of C1-Inhibitor and Factor H, 982
Complement Levels by Antigenic Assays, 982

KININS AND THE KININ-GENERATING SYSTEM, 983

PERSPECTIVES, 983

SELECTED REFERENCES, 983

KEY POINTS

- The complement system is a group of circulating proteins that promote inflammation and host defense.
- Unregulated tissue damage is a possible complication of complement activation; a large variety of circulating and membrane-bound proteins exist to regulate complement activity.
- Complement component C3 is the central convergence point for all complement activation pathways.
- It is frequently necessary to measure serum complement levels to track disease activity. However, it is important to recognize that serum complement measurements are snapshots of a dynamic process involving variable rates of complement consumption and production.
- Methods are available that allow accurate determination of serum levels of complement components.
- Functional complement assays are sensitive and precise tools that provide information about the activity and integrity of a complement component or pathway.
- The simplest functional assay of the classical pathway (CH50) measures total hemolytic complement activity.

STRUCTURE AND FUNCTION OF THE COMPLEMENT SYSTEM

The complement system comprises a group of greater than 30 circulating or membrane-bound regulatory glycoproteins that control parts of the innate immune system. Like other parts of the immune system, it protects the host against pathogens as well as facilitating clearance of apoptotic cells, counterbalancing the response of the immune system. There are a number of regulatory glycoproteins, either circulating or membrane-bound, that work to create the balance needed for an appropriate response. As will be demonstrated in this chapter, aberrant action of the complement system can lead to the damage of a large variety of organ systems, the severity of which can be catastrophic.

The existence of a group of host defense proteins that would later become the complement system was theorized in the late 19th century. Eventually, with improved lab testing, the many variable glycoproteins were identified and the complement system was further elucidated. Despite their relatively recent discovery, the proteins involved in the complement system are much older than the adaptive immune response. Even very primitive organisms have components of complement similar to the alternative and mannose binding lectin (MBL) pathways, which do not rely on immunoglobulin for activation. Immunoglobulin is utilized for activation in the classical pathway and provides more targeted, specific host defense. Further information on discovery of the complement system is available elsewhere (Frank, 1998).

The purpose of the complement system is to identify foreign cells or microbes and destroy them, which can be accomplished through several different methods. These include direct cell lysis via the membrane attack complex, phagocytosis via C3b opsonization, and inflammation wherein phagocytes, chemotactically attracted to an inflamed site by complement components C5a or C3a, ingest and destroy microbes.

NOMENCLATURE

There are three complement pathways in humans: the classical pathway, alternative pathway, and mannose-binding lectin pathway (MBL pathway). Figure 48.1 demonstrates the reaction sequence. The nomenclature for the proteins of the complement system has been set forth by the World Health Organization (World Health Organization, 1968; IUIS-WHO, 1981). The original naming convention from 1968 indicates that in the future there might be typical biochemical scientific naming given to these enzymes and that the current system could be viewed as a placeholder until this occurs. However, this has not happened yet, and the current naming system remains in place. The classical pathway has nine proteins, which are identified by the uppercase letter C. These are named in order of appearance in the complement cascade, though a notable exception is C4, which acts before C2. Proteins that act solely in the alternative pathway are termed *factors* and have a corresponding uppercase letter to identify them, such as factor B and factor D. In the complement cascade, there are several proteins that require cleavage before they can become active enzymes. The term for this precursor inert enzyme is *zymogen*. There are multiple reactions that result in cleavage of complement proteins, at

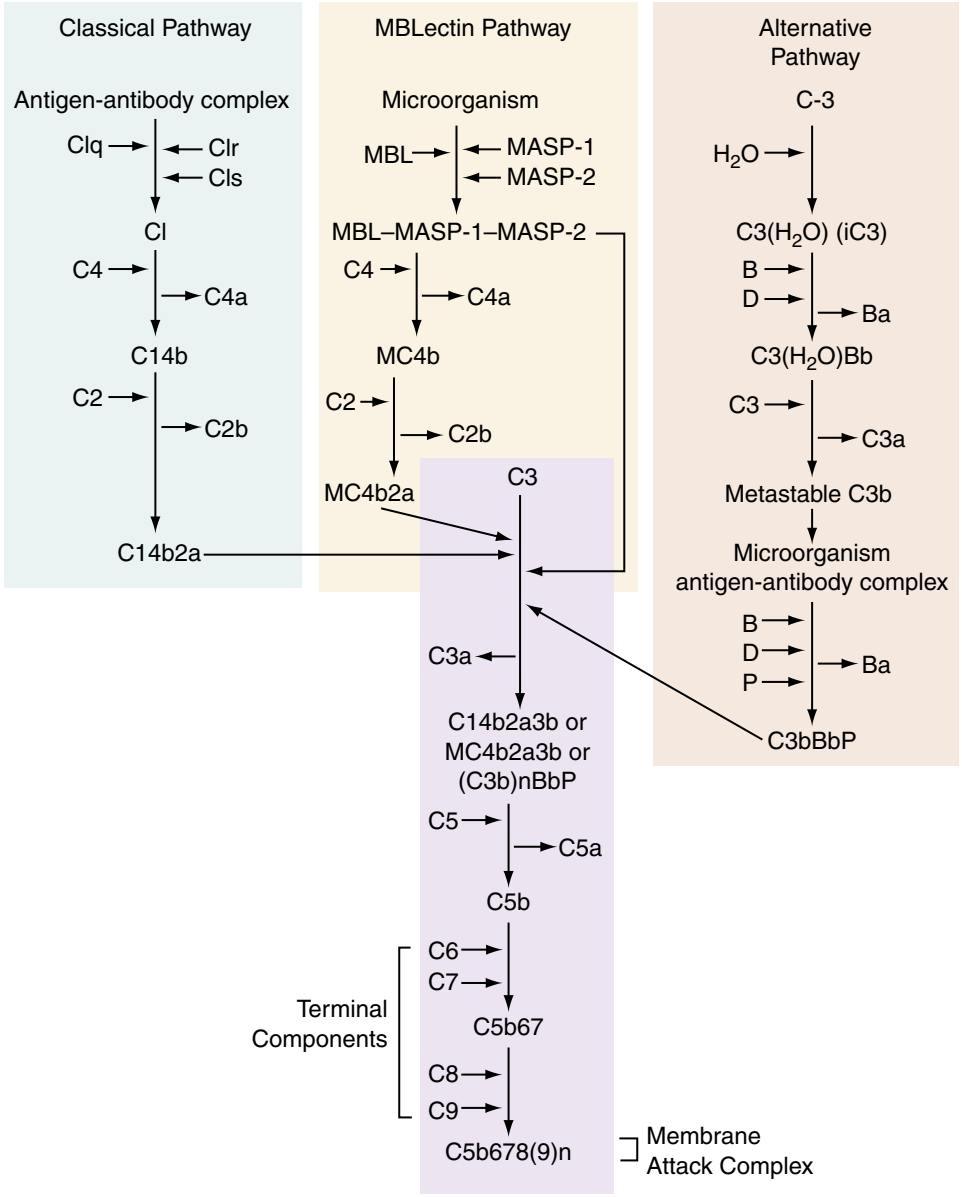

Figure 48.1 The three complement pathways (classical, MBLectin, and alternative) convene to create a convertase that will split C3. In the classical pathway, the immune complex will bind and trigger C1, then C4, and, finally, C2. In the MBLectin pathway, there is interaction between MBL with a carbohydrate group on a microorganism which will promote creation of the complex (MBL-MASP 1-MASP 2, denoted as "M" in the figure). This will complex with and activate C4 and C2. Within the alternative pathway, C3 has a thioester bond that is hydrolyzed, which prompts a conformational change. Thus, causing it to bind factor B (B), this will be cleaved by factor D (D), which will then form a convertase that is fortified by properdin (P). The C3 cleavage product, C3b, also has a thioester bond that is cleaved and able to activate the alternative complement pathway. The C3b convertase will continue to bind and activate later complement components until the activation pathway is at an end. *MASP,* MBL-associated serine proteases; *MBL,* mannose binding lectin

which point the remnants are renamed to include a lowercase letter. For example, after cleavage of C4, the two fragments become C4a and C4b. The suffix "a" denotes the smaller fragment of the pair and "b" is assigned to the larger piece. The exception to this is C2, whose larger split product is termed *C2a*, and the smaller one *C2b*. If the original cleavage product is broken down further, the new suffix will be lowercase letters in alphabetic order, for example, C3c and C3d. Proteins that have become inactive will be renamed with a lowercase *i* attached as a prefix to the beginning of the compound. (e.g., iC3b). The polypeptide chains of native complement proteins are labeled with Greek lowercase letters (α, β, γ). There is an exception to this rule in the case of C1, which should be thought of as a group of three molecules named *C1q*, *C1r*, and *C1s*. In the case of C1q, the polypeptide chains are designated A, B, and C.

If a component—whether it be single or a multicomponent complex—has enzymatic activity, there is a bar over the named compound(s). Abbreviations are used for proteins of the MB Lectin pathway (e.g., MBL for mannan-binding lectin, MASP for MBL-associated serine protease). Multiple soluble regulatory proteins exist throughout the complement cascade and are designated by a letter or illustrative title, for example, C4-binding protein. The regulatory proteins that are membrane bound have a different nomenclature, which includes a CD number and descriptive title (e.g., CD46 is membrane cofactor protein). Complement receptors are denoted by two different naming systems: the first is the abbreviation CR with a number designation added as a suffix (for complement receptors 1–4); the second applies to the remaining complement receptors, for which the component's name has an uppercase letter *R* added as a postfix.

C3: CENTRAL MOLECULE OF COMPLEMENT ACTIVATION PATHWAYS

The protein known as C3 is the central convergence point for the three complement activation pathways (the MBL pathway, alternative pathway, and classical pathway), which all proceed to lysis, phagocytosis, or regulation of the inflammatory response farther down the cascade.

The C3 molecule itself is a two-chain peptide made in many cells, but mainly in hepatocytes. It begins as a single-chain molecule, pro-C3, and is then released into the circulation, where it will bind to the surface of a target. Intrachain disulfide bonds stabilize the α and β chains, while an interchain disulfide bond stabilizes the α and β connections (Fig. 48.2). The α chain has a thioester in the middle that undergoes hydrolysis as water seeps into the molecule, resulting in cleavage of the α and β chain, which continuously activates the alternative complement pathway at a low level. The C3 molecule can also be cleaved via C3 convertase, resulting in the 9-kDa C3a fragment being freed from the larger C3b. The two fragments go on to perform separate functions: C3b coating target proteins to flag them for destruction and C3a to act as an anaphylatoxin signaling other cells and promoting inflammation (Wen et al., 2004). Once the C3 molecule is cleaved, C3b can interact with C3b receptors, which native C3 is unable to do, such as CR1 (C3b/C4b, CD35). The C3b fragment will covalently bind to the surface of its target, for example, a microorganism. The bound target can then interact with the C3b receptors expressed on immunocytes, such as the phagocytes, B lymphocytes, and certain T lymphocytes.

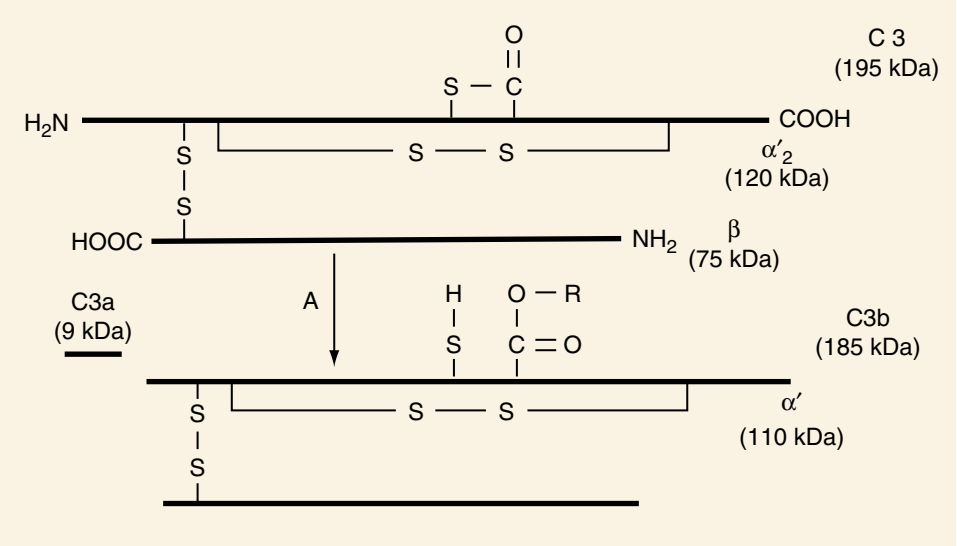

Figure 48.2 C3 cleavage by C3 convertase. The approximate molecular weight of each chain or fragment is given in kilodaltons (C3 convertase is represented by A).

THE CLASSICAL PATHWAY

This was the first of the three complement pathways to be discovered around 1900; thus, it was given the name *classical*. Despite its name, the classical pathway is the newest pathway in terms of an evolutionary perspective. It triggers complement activation via interaction with antibody-sensitized cells. It is made up of nine numbered proteins. More detailed information on this pathway can be found in other sources (Fries & Frank, 1987; Volanakis, 1998).

Classical pathway activation most often occurs after interaction between an antigen and antibody, more specifically a C1-binding antibody. Immunoglobulin (Ig) M and IgG, with the exception of IgG4, are able to activate the classical pathway in humans. The initial protein in the classical pathway sequence is C1 (made of three molecules—*C1q*, *C1r*, and *C1s*). While antibody is the most common way to activate this pathway, there are other molecules that can interact with C1q directly and trigger the cascade. Examples of these molecules include C-reactive protein, serum amyloid P component, β-amyloid, and a number of microorganisms, such as gram-negative bacteria, viruses, mycoplasmas, protozoa, and intracellular components such as deoxyribonucleic acid (DNA), cytoskeletal filaments (Gewurz et al., 1993), and apoptotic cells (Korb & Ahearn, 1997).

Certain infectious agents have been known to usurp the purpose of complement and use it to invade the host. This is the case in prion disease, which might use complement components such as C3 and C1q via the classical pathway to help facilitate its targeting lymphoid follicles (Mabbott, 2004). In an experimental murine model, it was shown that deficiency in C3 and C1q actually leads to a delay in disease development after peripheral inoculation, potentially providing some degree of protection (Mabbott, 2001).

C1 is the first protein in the classical pathway cascade that becomes activated by binding to an immunoglobulin already bound to its target. The C1 protein is 740 kDa, made up of one C1q molecule bound together with two C1r and two C1s chains stabilized by the presence of calcium ions and has been previously described as having a "bouquet of flowers" appearance. When it binds to immunoglobulin, C1q undergoes a conformational change that leads to autoactivation of the two C1r chains. Next, activated C1s2 will proteolytically cleave C4. C4 is cleaved into C4a and C4b, with C4b adhering to the activator surface or becoming hydrolyzed and remaining unbound in the fluid phase. The bound C4b molecules will group around the antigen-antibody-C1 site, which can attract multiple C4b molecules. The smaller product, C4a, is unbound in the fluid phase and acts as an anaphylatoxin (further discussed in the section on anaphylatoxins).

C4b in conjunction with C1s2 will then proteolytically cleave C2 in the company of magnesium ions into C2a and C2b. C2a is the larger of the two fragments and will remain bound to C4b, while C2b is released in the fluid phase. The C4b2a molecular complex is the C3 convertase for the classical pathway, which is chemically unstable and has a short half-life, as the C2a molecule may dissociate from the compound in an inactive form. The classical pathway C3 convertase (C4b2a complex) is necessary for binding C3 and continued cleavage through the complement pathway (see Fig 48.2). C2a, while complexed as part of C4b2a, will bind and cleave C3 into a larger C3b piece and C3a, with C3a remaining unbound in the fluid phase and acting as an anaphylatoxin. C3b will bind to the activator surface, forming C4b2a3b, which is the C5 convertase of the classical pathway and which prompts deposition of the remaining complement proteins on the surface of the target. It is again C2a that will leave C5 in the later steps.

Both IgM and IgG are able to activate the classical complement pathway though they are unequal in their capabilities to do so. A single IgM antibody, which has multiple antigen binding sites, once bound to antigen will undergo a conformational change that reveals a C1q binding site. Once IgM is bound to C1q, this interaction will trigger classical pathway complement activation.

On the other hand, IgG activation of the classical complement pathway relies on a continually exposed C1q binding site. However, it binds with a low affinity to C1q, thus mandating multiple IgG molecules in proximity to each other to prompt activation (Diebolder, 2014). Eventually, with enough IgG antibodies, it can create a C1-binding site. Not only does IgG–antigen complex activate the classical pathway but it can also prompt the alternative pathway, which will be discussed further in the next section (Moore, 1981).

The fact that congregated immunoglobulin binds C1q makes C1q a useful target when testing for soluble immune complexes in serum. Radiolabeled C1 is introduced into a patient's serum or plasma sample. Using one of several separation techniques, unbound C1q can be separated from bound C1q. The part that is bound indicates the presence of immune complexes in the sample (Zubler & Lambert, 1976). Alternatively, the enzyme-linked immunosorbent assay (ELISA) technique may be employed to detect and measure soluble immune complexes by identifying C1q- or C3-bound immune complexes (Stanilova & Slavov, 2001). C1q deposition in tissues can be directly observed in biopsy samples by immunofluorescent labeling of anti-C1q antibodies.

THE ALTERNATIVE PATHWAY

In the mid-1950s, another complement pathway was proposed by Pillemer and colleagues, although its validity would not be established until nearly 2 decades later. From an evolutionary standpoint, this pathway predates the classical pathway and is on the frontier of immunologic defense (Pangburn & Müller-Eberhard, 1984). The alternative pathway functions with low-level constant activity by way of a "tick over" mechanism, an unprompted hydrolysis of C3 to C3(H_2O). This reaction occurs at anywhere from 0.2% to 0.4% of the plasma pool per hour (Pangburn et al., 1981). After the addition of a water molecule, the thioester domain undergoes a structural transformation so that factor B can bind in a magnesium-dependent fashion. The C3(H_2O)–factor B complex can then be bound by factor D, leading to the formation of the initiation C3 convertase, C3(H_2O)Bb. The complex C3(H_2O)Bb will go on to cleave C3 into the anaphylatoxin C3a and the opsonin C3b. The initiation C3 convertase is an unstable structure that can be stabilized by the protein properdin, which will bind it and prolong its half-life from 1 to 18 minutes (Fearon & Austen, 1975). Once cleavage occurs, the serine protease factor D will revert back to an inactive form (Volanakis & Narayana, 1996). In this way, the cycle will continue and generate more C3b.

C3b is a rapidly decaying molecule that requires its target to be close by. The carbonyl group of its thioester will intermingle with a hydroxyl or amide group on a protein or carbohydrate on the exterior of its target (Law et al., 1979).

The spontaneous hydrolysis of C3 may be accelerated after interaction with C3 and multiple activating surfaces—for example, gas bubbles, lipid surfaces, protein complexes, and biomaterial surfaces (Nilsson & Nilsson Ekdahl, 2012).

Additional C3b will start to adhere to the target surface, which leads to the creation of C5 convertase (C3b2BbP) (Kinoshita et al., 1988). This triggers the final common pathway of the complement cascade.

THE MANNAN-BINDING LECTIN PATHWAY

The third pathway for complement activation is the mannose-binding lectin or mannose-binding protein, known as the MBL pathway. This pathway uses its namesake protein to activate the cascade; the binding lectin has a typical serum concentration of 1.5 μg/mL. It is produced by the liver and belongs to a group of molecules called *collectins* (Epstein et al., 1996; Turner, 1996). Other notable members of the collectin family include lung surfactant proteins A and D (SP-A, SP-D), bovine conglutinin, bovine CL-43, and ficolins (Epstein et al., 1996; Thiel, 2007). Lectins are found in a variety of organisms, including all mammals and some birds. MBL and ficolins are described as complement-activating soluble pattern recognition molecules, meaning that they recognize pathogen-associated molecular patterns (PAMPs) on the exterior of microbes. After they bind with their specified PAMPs, they undergo a structural change so that they can then interact with a group of three associated proteins that will trigger the complement cascade. These proteins are the MBL-associated serine proteases (MASP-1, MASP-2, MASP-3) (Thiel, 2007).

MBL is similar in configuration to C1q from the classical pathway and will recognize specific pathogenic carbohydrates. Fortunately, it does not recognize native self-carbohydrates, for example, galactose and sialic acid (Epstein et al., 1996). MBL has been reported to interact with a wide variety of microbes, including gram-negative bacteria, acapsular gram-positive bacteria, viruses, yeasts, mycobacteria, parasites, and protozoa (Epstein et al., 1996).

After MBL has interacted with a target carbohydrate group and interfaced with MASP, the complement cascade is triggered when MASP-2 cleaves C4, creating the classical pathway C3 convertase C4b2a (Vorup-Jensen et al., 1998). The serine protease MASP-1 can cleave C3 (Matsushita et al., 1998), which infers that this mechanism can directly activate the alternative pathway (Schweinle et al., 1989).

After creation of the classical pathway's C3 convertase (C4b2a), the complement cascade is triggered in the same way as the classical pathway; the alternative pathway might participate as well (Suankratay et al., 1998).

In addition to activating complement, MBL has a number of other functions. It is thought that it might facilitate riddance of targeted microbes by interacting with a specific receptor on phagocytes (Tenner et al., 1995; Hansen & Holmskov, 1998). In addition, MBL has been thought to modulate the adaptive immune system and temper the body's inflammatory and allergic responses (van de Wetering et al., 2004; Thiel 2007).

Pathologically, there are specific immune complexes that have been known to prompt activation of the MBL pathway. In certain patients, such as those with rheumatoid arthritis (RA), the terminal galactose on some IgG molecules may be absent (named *IgG-G0*), which allows it to interact with MBL and activate the classical pathway (Malhotra et al., 1995). The MBL pathway regulation might be influenced by C1 inhibitor (Matsushita & Fujita, 1996) and α_2-macroglobulin (Terai et al., 1995).

TERMINAL COMPLEMENT COMPONENTS

The three complement pathways are triggered in different ways. However, after C3 activation, all follow a final common pathway that ends with creation of the membrane attack complex (MAC). As previously discussed, the C5 convertase is assembled in the complement pathways, which can then cleave C5 into fragments C5a and C5b. C5b is the larger molecule, which can recruit the remaining proteins of the MAC, C6, C7, C8, and C9. Their combining forms the MAC ring.

More specifically, the C5b molecule will bind to a cell membrane and then combine with C6, forming the C5b-6 complex. This will then interact with C7, which is in the fluid phase. The C5b-7 complex is amphiphilic, which allows it to insert into the cell membrane's lipid bilayer (Podack et al., 1979). Despite this penetration of the lipid bilayer, it is insufficient for cell lysis. Next, the C8 protein will interact with the C5b-7 complex via direct contact with C5b. With the addition of C8, the newly formed C5b-8 complex can further perforate the lipid bilayer so that a more efficient pore is created, which leads to erythrocyte lysis (Ramm et al., 1982). After the formation of C5b-C8, the final component of the MAC, C9, can adhere by interfacing with the α chain of C8, creating the fully functional MAC (Plumb & Sodetz, 1998). Notably, multiple C9 proteins will gather and polymerize to create a channel within the cell membrane. This hollow, cylindrical channel can be observed under electron microscopy (Podack & Tschopp, 1984). Once the MAC is formed, it interrupts the crucial lipid bilayer and its hydrophilic center allows ions to move freely (Bhakdi & Tranum-Jensen, 1991; Tegla et al., 2011). The subsequent influx of calcium ions (Ca^{2+}) shuts down mitochondrial activity, causing apoptosis (Tegla et al., 2011).

The number of C9 proteins recruited to the MAC complex varies and the number of C9 molecules will dictate the size of the pore created. As few as one or two C9 proteins are required to result in apoptosis of a nucleated cell. However, with the addition of more C9 molecules, the efficiency of cell death induced by the MAC increases.

The MAC is able to lyse gram-negative bacteria, viruses, and erythrocytes. Many nucleated cells are able to defend against a MAC-mediated attack by means of membrane-associated regulatory molecules, which inhibit formation of a MAC (see the section Regulation of Complement Activation). Metabolically active cells are able to expel the MAC from the cell surface via lipid turnover during cell membrane repair (Mold, 1998). Despite these protective mechanisms, nucleated cells are still susceptible to the MAC if the number of MACs overwhelm the cell's available defense (Koski et al., 1983; Tegla et al., 2011). The half-life of the MAC in nucleated cells is estimated at 1 to 3 minutes. In nonnucleated erythrocytes, however, the MAC can remain for up to 72 hours (Tegla et al., 2011).

The MAC can also have an activating effect on some nucleated nontarget cells, such as neutrophils and macrophages, among others. This can lead to the proliferation of neutrophils and macrophages and the creation of reactive oxygen species by them, discharge of eicosanoids from phagocytic cells, initiation of procoagulant activity in endothelial cells and platelets, induction of proinflammatory activity in endothelial cells and smooth muscle cells, production of growth factor (PDGF, bFGF-1, IGF-1), interruption of caspase-reliant apoptosis, and triggering of signal transduction pathways (Niculescu et al., 1993, 1999; Benzaquen et al., 1994; Sims & Wiedmer, 1995; Kilgore et al., 1996; Tedesco et al., 1997; Mold, 1998; Tegla et al., 2011).

ANAPHYLATOXINS

As previously mentioned, there are small, active protein by-products called *anaphylatoxins* that are created through cleavage of complement proteins as part of the activation cascade. Some of these protein fragments are not part of the convertases but have alternative essential functions. The protein fragments C3a, C4a, and C5a are the anaphylatoxins. Their various activities include opsonization, phagocytosis, and immunomodulation, and they assist in the promotion of inflammatory reactions.

The C3a, C4a, and C5a anaphylatoxins are about 10 kDa in size. They are unequal in terms of potency, as follows: C5a > C3a > C4a. However, these characteristics are specific to different tissues. For example, C5a seems to influence many cell types, while C3a seems to be more specific at directing eosinophils to allergic sites (DiScipio et al., 1999). Activity of the anaphylatoxins can be modified into desarginine through cleavage of their carboxy-terminal arginine residues by carboxylpeptidases in the serum, reducing their activity. Several review articles further discuss specifics of anaphylatoxin structure and function (Ember et al., 1998; Bosmann & Ward, 2012; Zhou, 2012).

There are specified receptors on cells that anaphylatoxins will bind. The C3a receptor (C3aR) and C5aR are members of the seven-transmembrane G protein coupled receptor (GPCR) family, which activate the MAPK signaling pathway that mediates the majority of activity related to anaphylatoxins. The receptor C5L2, another member of the GPCR group, is known to bind both C5a and C5a desArg; however, its role remains unclear. For years, it was unclear what the C4a receptor was; it now appears that C4 binds to protease-activated receptor 1 (PAR1) and PAR4, both members of GPCR family. This mediates its effect on endothelial cells, increasing their permeability (HongBin et al., 2017). Further information on complement receptors and their mediated effects is discussed in the section on complement receptors.

Anaphylatoxins work to promote inflammation and generally exert their effects on smooth muscle cells, mast cells, and peripheral circulating leukocytes. The anaphylatoxins lead to neutrophil accumulation, smooth muscle contraction, increase blood vessel porousness, stimulate mucus production from goblet cells, and in nonhuman macrophages promote thromboxane generation (Marom et al., 1985). Additionally, anaphylatoxins induce mast cell and basophil degranulation, which releases vasoactive substances such as histamine and serotonin, leading to vasodilation, thus increasing blood flow to areas of inflammation.

TABLE 48.1

Complement Regulatory Proteins

Protein	Molecular Weight, kDa	Target	Mechanism of Action
Fluid Phases			
C1 inhibitor	105	C1	Dissociates the C1 complex by binding to C1r and C1s
Factor H	150	C3b	Cofactor for C3b inactivation by factor I
C4-binding protein	550	C4	Cofactor for C4b inactivation by factor I
S protein (vitronectin)	84	C5b-7	Inhibits insertion of the MAC into cell membranes
Clusterin	70	C5b-7	Inhibits insertion of the MAC into cell membranes
Factor J	20	C1, C3, B	Inhibits C1 complex formation, inhibits cleavage of C3 by Bb
Cell-Associated			
CR1	190*	C3b, C4b	Dissociation of C3/C5 convertases, cofactor for C3b and C4b inactivation by factor I
DAF (CD55)	70	C3bBb, C4b2a	Dissociation of C3/C5 convertases
MCP (CD46)	45–70	C3b (C4b)	Cofactor for C3b inactivation by factor I
CD59 (protectin)	18–20	C8, C9	Inhibition of formation of the MAC
HRF	65	C8, C9	Inhibition of formation of the MAC

CR1, Complement receptor type 1; *DAF,* decay-accelerating factor; *HRF,* homologous restriction factor; *MAC,* membrane attack complex; *MCP,* membrane cofactor protein.
*Most common isoform of CR1.

C5a works to activate the immune system and mediate inflammation in a variety of ways. It binds to neutrophils, increasing their adhesion and aggregation, induces an oxidative reaction, and prompts the release of lysosomal enzymes. It also promotes movement of monocytes/macrophages and neutrophils toward areas of complement activity in tissue. Generation of C5a during complement activation can vasodilate vessels in the surrounding tissue, promote aggregation of neutrophils to endothelium near the areas of inflammation, and act as a chemotactic to draw phagocytes to the area of complement activation. The C5a-induced neutrophil aggregation can be so profound that it can cause a pulmonary embolus made of the neutrophils. Lung inflammation due to immune complex formation is also thought to be mediated by C5a (Ward, 1997). An experimental rat sepsis model showed that C5a, when produced in large quantities, might obstruct the bactericidal properties of neutrophils. This could contribute to the high mortality rates seen in patients suffering from sepsis (Czermak et al., 1999).

The anaphylatoxins C3a and C5a are able to provide interaction between the innate and adaptive immune systems via their ability to affect the activity of T helper 1 (Th1), Th2, Th17, and T regulatory (Treg) T cells (Zhou, 2012). The evaluation of anaphylatoxin interaction with the adaptive immune system relies on investigational animal models. The effect in these animal models is complicated and variable. Some of these issues include variation in the disease models used, the murine genetics, and interference by interaction with alternative receptors, such as Toll-like receptors. An asthma model demonstrated that C3a could worsen lung injury by exacerbating Th2 immunity. Alternatively, C5a repressed Th2 reaction and seemed to be protective. The theory is that the anaphylatoxins will influence dendritic cells or macrophage cytokine- and antigen-presenting cell activity, which leads to mediation of the T-cell reaction. Notably, within human myeloid cell subpopulations, there is variation in the C3aR and C5aR manifestation, which may explain the differential effects of C3a and C5a on cytokine activation and T-cell reaction.

REGULATION OF COMPLEMENT ACTIVATION

The complement system is a crucial part of the immune system, However, without appropriate regulation, there can be disastrous damage to the host tissues. The mechanisms used to control the complement system in general work in the following ways: avoid far reaching inflammation beyond the targeted site, limit overactivation, and prevent damage to host cells during the immune response. Multiple proteins, which can be either membrane-bound or fluid-phase, work to achieve the aforementioned goals at various steps throughout the complement cascade (Table 48.1).

Fluid-Phase Regulators

Regulation begins early in the classical pathway at the level of C1 and is performed by C1-inhibitor (C1-Inh). C1-Inh hinders autoactivation of C1 in the fluid phase and by weak promoters of the classical pathway. However, it does not prevent the activation that occurs due to immune complexes (Doekes et al., 1983). Some evidence suggests that the C1-Inh is able to displace the $C1qr_2s_2$ compound from an immunoglobulin if the binding affinity is low (Chen et al., 1998). Not only is C1-Inh involved in the classical pathway, but it also works in the MBL pathway by inactivating MASP (Matsushita & Fujita, 1996).

Factor I (previously known as *C3b/C4b inactivator*) works to regulate C4b (Fries & Frank, 1987). It acts to split the C4b α chain into the fragments C4c and C4d. To achieve proteolytic cleavage, the association of C4-binding protein (C4BP) is needed. C4BP is a 570-kDa protein that is able to bind C4b in the fluid phase or in a particle bound state. It is also able to dislodge C2a from the C3 convertase C4b2a in the classical pathway (Gigli et al., 1979).

As the central convergence point of the complement pathway, regulation of the C3 molecule is crucial. Factor I will quickly inactivate unbound C3b via cleavage of three peptide bonds on the α chain and C3 (H_2O) (Davis & Harrison, 1982). This cleavage results in iC3b, which is inert and unable to engage with C5 or factor B. In order to accomplish this regulation, factor I requires a cofactor, factor H, which is a 150-kDa protein. It will work with factor I to cleave C3b both in the fluid phase and membrane bound state (Ollert et al., 1995). It also acts to accelerate decay of the alternative pathway C3 convertase. After the transformation to iC3b, which is bound to the target surface, it is able to bind with complement receptor type 3 (CR3), a receptor on phagocytic cells, and can be phagocytosed.

Additional regulation takes place with the terminal complement components, which prohibit MAC insertion into the cell membrane. S protein (not to be confused with protein S), alternatively known as *vitronectin*, binds the C5b-7 complex, thereby inhibiting its penetration of the cell membrane (Podack et al., 1977) and preventing C9 polymerization (Johnson et al., 1994). S protein also binds the sC5b-9 complex via C5b and C8 (Su, 1996) and inhibits complement activation via binding to the C1q receptor (Lim et al., 1996). Even in experimental models, the complete role of S protein in controlling activation of complement is unclear. However, it has been shown in rabbit models that S protein will bind with sC5b-9 when complement is active. This compound can inhibit the C9-mediated lysis of sensitized sheep red blood cells with attached complement components 1 through 7 (Peake, et al., 1996).

Another regulator in the fluid phase is clusterin (*Sp-40* or *apolipoprotein J*), which targets members of the MAC. Specifically, it inhibits the C5b-7 complex from inserting into the cell membrane (Choi et al., 1989). It also works by targeting the MAC at C9 (Berge et al., 1997).

Cell-Associated Regulatory Proteins

In addition to fluid-phase regulators of complement, there are also cell-associated regulatory proteins that often act as complement receptors. CR1 works in this fashion by binding either C4b or C3b and then as a cofactor with factor I to mediate their cleavage. Membrane cofactor protein (MCP or CD46) is found on most cells, though not erythrocytes, and also works as a cofactor in factor I–mediated cleavage of C4b to C4c/C4d fragments and C3b to iC3b (Seya et al., 1986; Seya & Atkinson, 1989).

Decay-accelerating factor (DAF; CD55) is another receptor that works to inhibit complement. DAF does this by increasing the rate of degeneration of C3 convertase and C5 convertase. DAF is present on all circulating cells, all endothelial cells, and many epithelial cells (Morgan & Meri, 1994).

TABLE 48.2
Cell Receptors for Complement Protein Fragments

Receptor	Molecular Weight, kDa	Ligand	Physiologic Role
CR1	190 (most common isoform)	C3b, C4b, iC3b	Phagocytosis, immune complex clearance
CR2	140	C3d, C3dg, iC3b	B-cell activation
CR3	165 (α chain) 95 (β chain)	iC3b, C3d, C3b	Phagocytosis, cellular adhesion
CR4	150 (α chain) 95 (β chain)	iC3b, C3b	Cellular adhesion
C1qRp*	126	C1q, MBL, SP-A	Phagocytosis
C3aR	48	C3a	Chemotaxis, degranulation of serosal-type mast cells, increase in vascular permeability
C5aR	43	C5a, C5a desArg	Chemotaxis, degranulation of serosal-type mast cells, cellular adhesion, increase in vascular permeability

CR1, Complement receptor type 1; *C1qRp,* receptor for the collagenous region of C1q; *CR2,* complement receptor type 2; *CR3,* complement receptor type 3; *C3aR,* C3a receptor; *CR4,* complement receptor type 4; *C5a desArg,* C5a lacking the terminal arginine residue following inactivation by carboxypeptidase-N; *C5aR,* C5a receptor; *MBL,* mannan-binding lectin; *SP-A,* surfactant protein A.
*Other C1q receptors have also been described.

Other regulators of the components of the MAC are homologous restriction factor (HRF), also known as *C8-binding protein*, and CD59, also known as *protectin*, *HRF-20*, *membrane inhibitor of reactive lysis*, and *P-18*. HRF works to bind C8, thus preventing C9 polymerization. It is present on erythrocytes, platelets, both T and B lymphocytes, neutrophils, and monocytes (Morgan & Meri, 1994). CD59 is expressed on all circulating cells, endothelial cells, epithelial cells, spermatozoa, and glomerular podocytes (Morgan & Meri, 1994). It is also found on some cells of the central nervous system (Morgan & Gasque, 1996). It acts to inhibit MAC formation by binding C8 at the β chain and the b domain of C9 (Chang et al., 1994).

Patients with paroxysmal nocturnal hemoglobinuria (PNH) lack DAF, HRF, and CD59 on their cells due to an abnormal glycosyl phosphatidylinositol connection (Volanakis, 1988) (see section on hematologic disorders for further information).

COMPLEMENT RECEPTORS

Complement receptors bind the complement proteins and mediate their effects as well as having other cellular functions (Table 48.2). Their presence has been described on multiple cell types.

Complement receptor type 1 (CR1, CD35, C3b/4b receptor) is one of the best studied complement receptors, made up of a single-chain glycoprotein. It is present on erythrocytes, mononuclear phagocytes, eosinophils, B lymphocytes, certain T lymphocytes, follicular dendritic cells, glomerular podocytes (Ahearn & Rosengard, 1998), and astrocytes (Morgan & Gasque, 1996). CR1 binds C3b, C4b, iC3b to some degree, and C1q (Klickstein et al., 1997). It acts as a cofactor for factor I in its cleavage of C3b, iC3b, and C4b and accelerates the decay of C3 convertase and C5 convertase. Another critical action of CR1 is its role in phagocytosing opsonized target particles. CR1 expressed on erythrocytes works to transport tagged immune complexes to the liver and spleen, where they can be phagocytosed and thus avoid deposition into tissue (Birmingham, 1995). There is some thought that aberrant expression of erythrocyte CR1 is at play in some chronic infections (Teixeira et al., 2001).

Complement receptor 2 (CR2; CD21) is present on B cells, follicular dendritic cells, select T cells, thymocytes (Ahearn & Rosengard, 1998), and astrocytes (Morgan & Gasque, 1996). This receptor interacts with C3d and iC3b while bound to antigen to perform its major function, which is to mediate a B-cell response in the presence of antigens (Carroll, 1998). It also aids in factor I cleavage of iC3b attached to an antigen (Mitomo et al., 1987). Interestingly, CR2 is the receptor on B cells that Epstein-Barr virus interacts with to cause infectious mononucleosis (Fingeroth et al., 1984).

Complement receptor 3 (CR3; Mac-1, CD11b/CD18) belongs to the β2 leukocyte integrin group of adhesion molecules (Gonzalez-Amaro, 1998). It is present on a variety of cells, including, mononuclear phagocytes, granulocytes, natural killer (NK) cells (Ahearn & Rosengard, 1998), and microglial cells (Morgan & Gasque, 1996). The CR3 will bind iC3b, C3b, and C3d (Brown, 1991). CR3 works to promote phagocytosis. It is also a participant in the congregation of monocytes and neutrophils to endothelial cells through contact with its ligand, intercellular adhesion molecule type 1 (ICAM-1). This action, in turn, promotes phagocytic cells to gather where endothelial cells are activated at places of tissue damage.

Complement receptor type 4 (CR4; CD11c/CD18) is a member of the same family as CR3. This receptor is present on myeloid cells, platelets, dendritic cells, NK cells, activated B cells, certain activated T cells (Ahearn & Rosengard, 1998), and microglial cells (Morgan & Gasque, 1996). It will bind both iC3b and C3b, but it binds the latter to a lesser extent (Brown, 1991). CR4 remains a bit mysterious, as we do not yet understand its full function. However, it is able to bind fibrinogen and serves to increase neutrophil aggregation during inflammation (Vorup-Jensen et al., 2005).

The receptor for the anaphylatoxin C5a (C5aR) is present on many cell types, including neutrophils, monocytes, basophils, eosinophils, platelets, mast cells, lung vascular smooth muscle cells, liver parenchymal cells, lung and umbilical vascular endothelial cells, bronchial and alveolar epithelial cells, astrocytes, microglial cells (Ember et al., 1998), and human T cells (Nataf et al., 1999). The interaction of C5a to its receptor will prompt multiple proinflammatory processes, such as mast cell degranulation, chemotaxis of inflammatory cells, oxygen radical production, neutrophil and eosinophil fabrication of leukotrienes and prostaglandins, and induction of cytokines, antibodies, and acute-phase proteins (Ember et al., 1998).

COMPLEMENT BIOSYNTHESIS

The majority (approximately 90%) of complement plasma proteins are produced in the liver. Additionally, many are acute-phase reactants, meaning that during an inflammatory event the liver will increase their production. Notable exceptions to hepatically produced complement proteins include C1q, factor D, properdin, and C7 (Morgan & Gasque, 1997). The C1q protein is synthesized by epithelial cells, monocytes/macrophages, and fibroblasts. Adipocytes are the primary site for the synthesis of factor D. Properdin is primarily made by cells of the immune system, including monocytes, macrophages, lymphocytes, and granulocytes. C7 is synthesized in monocytes and macrophages, and, interestingly, is stored in neutrophils.

While the liver is mainly responsible for production of complement components, cells such as monocytes, macrophages, astrocytes, and cells located within synovial tissue are able to create all the proteins within the classical and alternative pathways. It is thought that this keeps inflammation localized to specific tissues.

The catalyst for complement protein production by any complement-producing cell is usually spurred on by proinflammatory proteins, such as interleukin-1α, interleukin-6, or interferon-γ. Further information about complement protein synthesis can be found elsewhere (Colten & Garnier, 1998).

COMPLEMENT GENETICS

Many of the complement proteins have an autosomal-codominant inheritance pattern. The specific genes that encode complement proteins, complement receptors, and regulatory proteins have been identified along with their chromosome location (Table 48.3). Many of the complement-coding genes have genetic linkage, meaning that they are inherited together. Members of the linkage group include major histocompatibility complex (MHC) class III genes (C2, factor B, and C4), genes that encode regulators of complement activation (C4-binding protein, CR1, CR2, DAF, MCP, and factor H), and genes that encode members of the MAC (C6, C7, and

TABLE 48.3

Complement Proteins in Human Plasma

Protein	Molecular Weight, kDa	Chromosomal Location	Concentration, mg/mL
Common to All Pathways			
C3	185	19p13.3-p13.2	1200–1300
Classical Pathway			
C1q	460	1p34.1-36.3	150
C1r	85	12p13	50
C1s	85	12p13	50
C4	205	6p21.3	30–600
C2	102	6p21.3	20
Alternative Pathway			
Factor B	93	6p21.3	200
Factor D	24	Unknown	2
Properdin	55 (monomer)	Xp11.4-p11.2	25
MBLectin Pathway			
MBL	200–400	10q11.2-q21	0.002–10
MASP-1	93	3q27-28	1.5–13
MASP-2	76	1p36.3-36.2	Unknown
Membrane Attack Complex			
C5	190	9q33	80
C6	110	5p13	45
C7	100	5p13	90
C8	150	1p32 (α, β chains), 9q22.3-q32 (γ chain)	55
C9	70	5p13	60
Control Proteins			
C1-Inh	105	11q11-q13.1	240
C4bp	550	1q32	250
Factor I	88	4q25	35
Factor H	150	1q32	300-450
S protein	84	17q11	500
Clusterin	70	Unknown	50
Factor J	20	Unknown	~5.4

MASP, MBL-associated serine proteases; *MBL,* mannan-binding lectin.

C9) (Schneider & Würzner, 1999). There is structural similarity between members in the three aforementioned groups, which indicates that some of the proteins may have evolved from a few select ancient genes. Most complement-related proteins demonstrate genetic polymorphism, meaning that there is more than one allele for a specific gene. For example, C4 has more than 35 known alleles. Complement proteins are susceptible to aberrant genetic mutations such as other genes, including point mutations, nucleic acid insertion, or nucleic acid deletion. Such errors often result in complement deficiency (Schneider & Rittner, 1997). Analysis of both phenotype and genotype are used to evaluate complement polymorphisms. Further information on this is discussed in Chapter 50. Additional resources are also available (Mauff & Würzner, 1996; Schneider & Rittner, 1997).

COMPLEMENT AND ACQUIRED IMMUNITY

The complement system helps to evoke and form antibody responses from the acquired immune system (Carroll, 2004). This reliance on the complement system to help mold the acquired immune system has been demonstrated through multiple studies. The results of one study disclosed that animals with temporary C3 depletion had decreased antibody responses when provoked by antigens (Pepys, 1974). Other studies have established that genetically absent C2, C3, and C4 in animals (Ochs et al., 1983; Böttger et al., 1985; O'Neil et al., 1988) and humans who were lacking C2, C3, C4, or CR3 (Ochs et al., 1986) all had diminished antibody responses.

Trials using murine models with genetically absent C3, C4, CR1, or CR2 have helped advance the understanding of the interplay between the complement system and development of the acquired immune system. It is thought that complement can influence antibody response to antigens in multiple ways. For example, the threshold to activate B cells is reduced, leading to increased antibody production when CR2 is present and bound with B-cell antigen receptors. Remember that C3d is also in a complex with CR2 and the B-cell antigen receptor. It is thought that complement will assist snaring antigen-antibody complexes by follicular dendritic cells. This helps to form lymphoid germinal centers, which is where B cells obtain memory phenotype.

Deficiency in parts of the classical pathway, CR1 or CR2, may cause the immune system to have a poor response to antigen exposure or, worse, the immune system will not have a secondary response at all. The complement system is important in the creation of B cells displaying CD5, which give rise to *natural* antibodies (Carroll, 1998). Natural antibodies are involved in complement activation and appropriate B-cell reaction to antigenic challenge (Boes et al., 1998; Lutz, 1999).

As previously discussed, self-tolerance is important to prevent damage to host tissues. There are several complement players (C4, CR1, and CR2) that are crucial to maintain B-cell tolerance to native antigens (Prodeus et al., 1998). Complement helps to enhance the acquired immune system's response to antigen due to interaction with antigen-presenting cells (APCs). This is particularly true for C3. As discussed earlier, C3 is cleaved into smaller protein fragments that can bind to antigen. This C3 by-product–antigen complex will increase the sensitivity of APCs (such as B cells, and other APCs that display CR1 and CR2) to the antigen, which will then boost T-cell exposure to the antigen by APCs and, thus, increase the T-cell reaction (Boackle et al., 1998; Kerekes et al., 1998). It is thought that complement can directly affect the T cell–mediated immune response via contact with complement receptors, which are sometimes expressed on select T cells (Kemper & Atkinson, 2007). Complement can also work in an inverse way, causing decreased function of the immune system. For example, there is reduction in Toll-like receptor–induced inflammatory signaling when there is cross-linking of C5a, C3b, and C1q receptors on macrophages and dendritic cells (Cummings et al., 2007). While complement was previously viewed as being part of the innate immune system, it is apparent that there is overlap and that complement can amplify or inhibit the acquired immune system.

GENETIC COMPLEMENT DEFICIENCIES

Genetic complement deficiency is estimated to be the cause of about 6% of primary immunodeficiency, though this estimate varies based on region (Notarangelo et al., 2004). Absolute complement deficiency is thought to be present in about 0.03% of the population worldwide (Wen et al., 2004). Interestingly, inherited deficiency in the MBL complement pathway is much more common. It is estimated that about 5% of the population will have one of three genetic mutations that can lead to MBL deficiency (Sumiya & Summerfield, 1997).

Identification and study of these complement deficiencies is important to improve understanding of the complement system in both health and illness. Furthermore, if a lack of complement can be linked to a specific genetic mutation, then further information about inheritance patterns and screening for potentially affected individuals could be performed. That being said, genetic analysis is not habitually performed as part of the initial work for suspected complement deficiencies due to cost and poor ease of use (Mollnes et al., 2007). In general, genetic deficiency of a complement component often occurs through simple Mendelian inheritance principles. Typically, the absence of a complement component is inherited as an autosomal-recessive trait, though there are some exceptions. Patients who have a heterozygous genotype often have about half or less the expected normal complement levels. Homozygous patients will have very low or undetectable activity of the specific deficient complement component. There are known deficiencies to every protein associated with complement activation (Table 48.4).

There are multiple examples of certain complement deficiencies associated with particular disease states. Deficiency in the MBL pathway, which has autosomal-codominant inheritance, is correlated with multiple disease states. One such example is the increased risk of upper respiratory tract infection in MBL pathway–deficient children between 6 to 18 months old (Turner, 1996). Another study suggested that anomalous MBL genes were

TABLE 48.4
Inherited Deficiencies in Complement and Complement-Related Proteins

Protein	Pattern of Inheritance	Major Clinical Correlate(s)*
Common to All Pathways		
C3	Autosomal recessive	Recurrent pyogenic infections, glomerulonephritis
Classical Pathway		
C1q	Autosomal recessive	Glomerulonephritis, SLE
C1r	Autosomal recessive	Glomerulonephritis, SLE
C1s	Autosomal recessive	Glomerulonephritis, SLE
C4†	Autosomal recessive	SLE, scleroderma, IgA nephropathy, membranous glomerulonephritis
C2†	Autosomal recessive	SLE, DLE, juvenile rheumatoid arthritis, glomerulonephritis
Alternative Pathway		
Factor B	Autosomal recessive	*Neisseria meningitidis* infection
Factor D	Autosomal recessive	Recurrent pyogenic infections
Properdin	X-linked	Recurrent pyogenic infections, fulminant meningococcemia
MBLectin Pathway		
MBL	Autosomal dominant	Recurrent infections
Membrane Attack Complex		
C5	Autosomal recessive	Recurrent disseminated neisserial infections, SLE
C6	Autosomal recessive	Recurrent disseminated neisserial infections
C7	Autosomal recessive	Recurrent disseminated neisserial infections, Raynaud disease
C8 (β or α-γ chains)	Autosomal recessive	Recurrent disseminated neisserial infections
C9	Autosomal recessive	None
Fluid-Phase Control Proteins		
C1-Inh	Autosomal dominant or acquired	Hereditary angioedema, autoimmune diseases‡
C4bp	Autosomal recessive	Angioedema, Behçet-like syndrome
Factor I	Autosomal recessive	Recurrent pyogenic infections
Factor H	Autosomal recessive	Recurrent pyogenic infections, glomerulonephritis, age-related macular degeneration
Cell-Bound Proteins		
CR1	Autosomal recessive§	Association between low erythrocyte expression and SLE
CR3	Autosomal recessive	Leukocyte adhesion deficiency-1 (LAD-1), recurrent pyogenic infections, leukocytosis
DAF/CD59/HRF	Acquired	Paroxysmal nocturnal hemoglobinuria

DAF, Decay-accelerating factor; *DLE,* disseminated lupus erythematosus; *MBL,* mannan-binding lectin; *SLE,* systemic lupus erythematosus.
*Notably, some patients with complement deficiencies, including C2 and members of the MAC, are often clinically well without signs of disease. That being said, a significant group of patients with deficiency in C5 to C9 will be afflicted with autoimmune diseases. Deficiency of C1 to C9 correlates to a CH50 of 0. Deficits in C1, C4, and C2 have been associated with SLE; these patients frequently have negative LE preps. Defects in C3 to C9 have been attributed to low or completely absent bactericidal capabilities. C3 or C5 deficiency has been linked to decreased or absent chemotactic activity and may be the cause of diminished leukocyte responsiveness in the setting of infection.
†Defects in the C4 genes (*C4A* and *C4B*) are termed "q0," indicating quantity of zero. Thus, a deficiency in these genes would be named C4Aq0 or C4Bq0. There is an above expected incidence of autoimmune diseases diagnosed in patients with these genotypes. Patients with heterozygous C2 deficiency have also been found to have higher frequency of autoimmune disease.
‡About 85% of cases are due to silent alleles; the remaining 15% has to do with alleles that encode an acquired aberrant variant C1 inhibitor. Patients with hereditary angioedema will have normal to low C1 levels, normal C3, and a low C4. When the disease is acquired, the C1 and C4 levels will be low and the antigenic C1 inhibitor value is often normal to elevated, while functional C1 inhibitor level will be markedly depressed.
§Homozygous decreased, but not absent, quantitative expression of CR1 on erythrocytes may be related to SLE. There might also be an acquired deficit in the numerical value of CR1 that contributes. Decreased levels of CR3 on leukocytes are able to be measured in both parents in most children with CR3 deficiency.

TABLE 48.5

Major Complement Deficiency Assays Performed on Peripheral Blood

Functional	Immunochemical Single-Protein Quantification	Activation Product	Autoantibody Analysis	Surface Proteins	Genetic Mapping
Total Complement Activity	*Immunoprecipitation*	*ELISA Based on Antibody to Neo-epitopes Found on Activation Products*	*ELISA-Based Assays*	*Flow Cytometric Quantification*	*Detection of Disease-Associated Genetic Variants (Mutations, Polymorphisms)*
a. CH50 and AH50 hemolytic assays	a. RID	a. Split products: C3a, C4a, C5a	Anti-C1q in SLE, anti-C1-Inh in AE, anti–factor H in aHUS, others	CD55/DAF and CD59 in PNH	aHUS (factor H, factor I, factor B, C3)
b. ELISA for CP, AP, MBL (WIELISA)	b. Electroimmunoassay	b. Activated component complexes: C1rs-C1-Inh, others	Functional assays (C3)		MPGN
	c. Nephelometry and turbidimetry	c. Macromolecular complexes	a. C3 nephritic factor in MPGN, type 2		
Single-Component Activity	*Other Methods*				
a. Hemolytic assays using component-deficient sera (e.g., C3, factor H)	a. ELISA				
b. ELISA (e.g., MBL and MASP functional activity with C4 as target)	b. TRIFMA				
c. Chromogenic substrate (C1-Inh)	c. WB				

Modified from Botto M et al.: Complement in human diseases: lessons from complement deficiencies, *Mol Immunol* 46:2774–2783, 2009, Table 1.
AE, Angioedema; *aHUS,* atypical hemolytic-uremic syndrome; *AP,* alternate pathway; *CP,* classical pathway; *ELISA,* enzyme-linked immunosorbent assay; *MASP,* MBL-associated serine proteases; *MBL,* mannan-binding lectin pathway; *MPGN,* membranoproliferative glomerulonephritis; *PNH,* paroxysmal nocturnal hemoglobinuria; *RID,* radial immunodiffusion; *TRIFMA,* time-resolved immunofluorometric assay; *WB,* Western blot; *WIESLA,* three-pathway ELISA (Wieslab, Lund, Sweden).

linked to approximately one-third of meningococcal infections in children (Hibberd et al., 1999). Infusions containing purified MBL have been used to treat patients with MBL deficiencies (Valdimarsson et al., 1998), though its use is not widespread. MBL deficiencies have also been linked to the development of autoimmune disease, for example, systemic lupus erythematosus (SLE) (Turner, 1996), and have been reported to portend an increased risk for recurrent miscarriage (Christiansen et al., 1999).

Interestingly, early classical pathway complement deficiencies are very uncommon, but when present often result in glomerulonephritis and lupus-like disease with dermatologic manifestations (Botto et al., 2009).

Complement is imperative to the removal of antigen–antibody complexes from the serum. It is thought that deficiency in early parts of the complement cascade may lead to impaired clearance. Continued circulation of these immune complexes is thought to lead to their accrual in certain tissues, for example, the kidney, leading to multiple and varied disease states.

Deficiency of factor B, factor D, and properdin (X-linked) of the alternative complement pathway as well as terminal complement components have been ascribed to increased risk of recurring gram-negative cocci infection and septic shock. Hereditary angioedema is due to deficiency in C1-Inh, which can be inherited in an autosomal-dominant pattern or acquired after formation of C1-Inh autoantibodies. Deficiency of C1-Inh leads to recurrent subcutaneous and submucosal edema, which can be serious. Atypical hemolytic uremic syndrome (aHUS) has been described due to factor H deficiency in an 8-month-old child that caused thrombotic microangiopathy and renal failure (Licht et al., 2005).

Frequently used assays to detect complement deficiency are listed in Table 48.5. More information on epidemiology, signs of complement deficiency, and diagnosis can be found elsewhere (Grumach & Kirschfink, 2014).

TABLE 48.6

Complement Deficiency–Related Disease State and Recommended Analysis on Peripheral Blood

Disease	Complement Analysis
Recurrent bacterial infections	CH50, AH50, WIELISA, C3, C3a/C3d, C5–C9 *(Neisseria)*, properdin *(Neisseria)*, MBL *(Neisseria)*
Systemic lupus erythematosus	CH50, C4 (C4A/B), C3a/C3d, anti-C1q autoantibodies
Angioedema	C1 inhibitor antigenic assay, C4, C1q, acquired anti-C1q autoantibody
aHUS	CH50, AH50, C3, C3a/C3d, C3 nephritic factor, factor H, factor B, factor I, anti–factor H antibodies
MPGN	CH50, AH50, C3, C3a/C3d, C3 nephritic factor, factor H, factor I, anti–factor H antibodies
PNH	CD55, CD59 (flow cytometry)

Modified from Botto M et al.: Complement in human diseases: lessons from complement deficiencies, *Mol Immunol* 46:2774–2783, 2009, Table 2.
aHUS, Atypical hemolytic-uremic syndrome; *C3a/C3d,* to exclude excessive complement consumption; *ELISA,* enzyme-linked immunosorbent assay; *MBL,* mannan-binding lectin pathway; *MPGN,* membranoproliferative glomerulonephritis; *PNH,* paroxysmal nocturnal hemoglobinuria; *WIELISA,* three-pathway ELISA (Wieslab, Lund, Sweden).

ASSESSMENT OF COMPLEMENT ACTIVITY IN DISEASE

As previously discussed, complement increases inflammation and is at the root of some autoimmune diseases. Complement activation in autoimmune disease can be initiated by an autoantibody, immune complexes, or by contact with an antigen or other foreign substance. Complement measurement has been used to develop a differential diagnosis and evaluate the activity of certain autoimmune diseases (Table 48.6 lists frequently measured serum complement levels). For example, in active SLE serum, C3 and C4 are depressed, whereas when the disease is quiescent, the C3 and

TABLE 48.7
Complement Activation ELISA Results Using Peripheral Blood in Screening Suspected Complement Deficiencies

IMPAIRED FUNCTION OR DEFICIENCY	ELISA ACTIVITY		
Complement Component	**Classical Pathway**	**Alternative Pathway**	**Lectin Pathway**
C1q, C1r, C1s	Low	Normal	Normal
C4, C2	Low	Normal	Low
MBL, MASP	Normal	Normal	Low
B, D, P	Normal	Low	Normal
C3, C5, C6, C7, C8, C9	Low	Low	Low

Modified from Mollnes TE et al.: Complement analysis in the 21st century, *Mol Immunol* 44:3838–3849, 2007, Table 1.
ELISA, Enzyme-linked immunosorbent assay; *MASP,* MBL-associated serine proteases; *MBL,* mannan-binding lectin pathway.

C4 levels are expected to be normal. Nephelometric assays are often used to assess complement levels, which will be discussed further in the section Assays of Complement later in the chapter.

While complement levels may be helpful in therapy, they should be viewed as a guideline and not dogma. Complement levels can be highly variable depending on the creation and depletion of various complement components. Multiple proteins in the complement cascade act as acute-phase reactants. Thus, their serum levels can rise precipitously during an inflammatory reaction but they may also be low due to catabolism during inflammation, as is the case with autoimmune disease. Therefore, a normal complement level can be attributed to normalcy or due to tissue-damaging inflammation caused by autoimmune disease. Alternatively, a low complement level may also reflect tissue damage. One example of this paradox is in patients with biliary cirrhosis. They often have an elevated catabolism of C3, which may even be a factor in disease development, but frequently have an elevated C3 level. The reason for the high level despite consumption of C3 is that the production of C3 is greater than its destruction.

It is imperative to interpret the complement level in the context of the bodily compartment that the sample was taken from. Complement levels may differ between anatomic locations in disease states. For instance, a patient with RA may have normal or slightly increased levels in the serum, but complement proteins may be very low in the synovial fluid where the tissue is actually being damaged.

In an attempt to elucidate which of the three complement pathways is most active in a disease state, there has been investigation into creating a complement profile. This profile is created by examining multiple complement levels in each of the pathways and deducing which pathway is most likely to be active based on the various levels. It is assumed that a low level of a complement component indicates increased activity in that pathway. For example, a theoretical patient may have decreased C3 and C4 levels with a normal factor B, which would indicate that the classical pathway is primarily active. In another example, if an individual had decreased C3, factor B, and properdin but a normal C4 level, one could suspect that the alternative pathway is most likely active. ELISAs can be used to identify complexes that are created during complement activation. ELISA testing is very sensitive and can determine which pathway is activated in different diseases (Morgan, 1994) (Table 48.7).

On activation, many complement proteins express new antigens (neo-antigens) that are not revealed on the native plasma protein. The neo-antigen present on the MAC, but not present on native terminal components, is perhaps the most interesting. Antibody to this neo-antigen exists and has been used to study serum neo-antigen levels by immunofluorescence and by ELISA (Falk et al., 1983; Sanders et al., 1985). The neo-antigen level is elevated in blood and spinal fluid in many patients with ongoing complement activation (Sanders et al., 1986), and the neo-antigen is present in tissues at sites of terminal complex deposition. For example, it is present in the glomeruli of patients with some forms of glomerulonephritis (Falk et al., 1983) and in lesional skin at sites of active SLE (Biesecker et al., 1982). Unlike C3 deposited in normal skin of patients with SLE and a positive lupus band test, the MAC neo-antigen is found only in lesions.

COMPLEMENT IN DISEASE STATES

Over the last decade, our understanding of the complement system has evolved rapidly, leading to the characterization of diseases fueled by complement dysregulation that are also referred to as "complementopathies" (Baines et al., 2017). These are disorders in which activation of the complement system is a driving factor in disease pathophysiology. Many of these disorders span multiple organ systems and are discussed briefly here.

RHEUMATOLOGIC DISEASES

There are multiple rheumatologic diseases that are due in part to dysfunction of the complement system, such as antiphospholipid syndrome, leukocytoclastic vasculitis, cryoglobulinemia types I, II, and III, neuromyelitis optica, and RA. Defective C1, C2, and C4 are most often associated with autoimmune disease (Wen et al., 2004). The most frequently studied rheumatologic disease that is due to complement dysfunction is SLE (Agnello, 1986; Atkinson, 1986; Liu et al., 2004). It has been cited that patients with SLE have deficiency of C1q, C4, and C2 at rates of 90%, 75%, and 15%, respectively (Pickering et al., 2000). Interestingly, not only is the classical pathway affected but those with MBL pathway deficiency have an increased risk of SLE (Kilpatrick, 2002).

In SLE, there is formation of free and deposited immune complexes that will activate complement, thereby producing the inflammation manifested by SLE. The therapies for SLE try to prevent formation of, or improve clearance of, the inciting autoantibodies. The pathogenesis of SLE is complicated. It is thought that the loss of self-tolerance and autoantibody formation might be related to prolonged exposure to free immune complexes and necrotic cells as a result of impaired complement-mediated clearance, especially in those with complement deficiency (reviewed in Markiewski & Lambris, 2007).

SLE activity is often assessed by a patient's signs and symptoms as well as laboratory complement assessment by measuring C3 and C4, which are usually low in an active disease state. A low C4 level has been thought to be the most accurate sign of active SLE; however, there are patients with active lupus who will have a normal C4 level on serum assay. It has been argued that measurement of unbound sC5b-9 or the MAC neo-antigen would provide a more precise estimation of disease activity (Gawryl et al., 1988). However, this is not used in common practice.

As previously discussed, complement has a crucial part in removing free antigen–antibody complexes from the circulation, especially immune complexes with IgM or IgG. The anaphylatoxin C3b will bind these immune complexes in the setting of complement activation and then begin to bind with cells that express a C3b receptor (CR1), such as erythrocytes. Once bound in the circulation to erythrocytes expressing CR1, the immune complex is no longer able to travel from the plasma to the tissues where it might be deposited. Immune complexes bound to red blood cells instead will travel to the liver where the immune complexes will be removed without affecting the longevity of the erythrocyte (Cornacoff et al., 1983; Birmingham, 1995).

The amount of CR1 expressed per erythrocyte is lower in diseases in which complement is active and immune complexes are formed. This is thought to be due to their removal by the liver (Ross et al., 1985). This reduced CR1 expression is noted not only in SLE but also in patients with chronic cold agglutinin disease, PNH, autoimmune hemolytic anemia, Sjögren syndrome, and mycoplasma pneumonia. Thus, these diseases may have had immune complexes removed as well (Ross et al., 1985; Atkinson, 1986).

As previously discussed, complement proteins are acute-phase reactants. Consequently, if their levels are being assessed to determine disease activity, they may not be depressed due to the increased production seen in acute inflammation. Examples of disease states with normal to high complement levels include juvenile rheumatoid arthritis (JRA), pseudogout, gout, palindromic arthritis, gonococcal arthritis, and Reiter syndrome. However, in rheumatologic conditions—for example, RA—the complement levels may be reduced at areas of active inflammation, such as synovial fluid. The existence of C3 split products, factor B, and decreased total hemolytic complement activity (CH50; see the Assays of Complement section later in this chapter) possibly demonstrates intra-articular

complement activity in patients with diseases such as seronegative RA, SLE, gout, pseudogout, Reiter syndrome, and gonococcal arthritis. These lab abnormalities are not described in patients with degenerative arthritis.

HEREDITARY ANGIOEDEMA

Hereditary angioedema (HAE) is caused by a deficiency in C1-Inh that is manifested by periodic subcutaneous and submucosal, nonpruritic, and nonerythematous edema that can be life-threatening if it involves the laryngeal mucosa. Normally, patients will have resolution of the edema within 48 to 72 hours. HAE may be inherited in an autosomal-dominant manner or can be acquired after formation of autoantibodies to C1-Inh. There are three types of HAE, which are classified depending on the level and activity of C1-Inh. Patients with type I HAE have deficiency of C1-Inh, while those with type II HAE have a functional abnormality of C1-Inh. In type I HAE, the protein and functional levels of C1-Inh will be low (usually regarded as undetectable to less than 30%), while in type II HAE the protein level will be normal to high and the functional level will be low (Wen et al., 2004). There is a heterozygous deficiency of C1-Inh, which also causes the disease. C1-Inh is involved in multiple pathways, including the complement cascade, clotting cascade, and kinin-generation pathway. Thus, it is difficult to discern exactly how an episode of HAE is provoked.

INFECTIOUS DISEASES

Patients with complement deficiencies are at increased risk for certain infections, as discussed earlier. For instance, C3 deficiency or abnormal alternative pathway function increases the risk of gram-negative sepsis. The complement system is also important in the protection against parasitic infections, such as leishmaniasis, trypanosomiasis, giardiasis, and malaria. Both MAC and properdin deficiencies may be at the root of multiple infections by *N. gonorrhoeae* or *N. meningitidis*.

Much research has been done on the infection of a host by human immunodeficiency virus (HIV); it is recognized that HIV is reliant on CR3 located on dendritic cells to gain access to the immune system (Batjay et al., 2004; Stoiber et al., 2005). CR3 may also play a role in infection of cervical epithelial cells by *Neisseria gonorrhoeae* (Edwards et al., 2001).

Multiple reviews are available for further information on the interplay between complement and various bacterial, parasitic, and viral infections (Frank & Fries, 1988; Fishelson, 1994; Moffitt & Frank, 1994; Kozel, 1996; Cooper, 1998).

THROMBOTIC MICROANGIOPATHIES

Thrombotic microangiopathies (TMAs) are a heterogeneous group of disorders presenting with a distinct clinical triad: microangiopathic hemolytic anemia, thrombocytopenia, and organ damage. Two major entities are currently recognized: thrombotic thrombocytopenic purpura (TTP) and hemolytic uremic syndrome (HUS). There are a variety of other conditions that are associated with TMAs, such as drugs, malignancy, infections, scleroderma-associated renal crisis, SLE, malignant hypertension, transplantation, HELLP syndrome (hemolysis, elevated liver enzymes, and low platelets), and disseminated intravascular coagulation (DIC). Complement dysregulation has been implicated in many of these disorders. Among TMAs, atypical HUS (further discussed in the Renal Diseases section that follows) serves as an archetypal disease model of complement dysregulation in which mutations of complement-related proteins represent the first hit of the disease and therapy with complement blockade has proven to be effective (Gavriilaki et al., 2019). In an effort to facilitate early diagnosis and treatment, two recently published consensus documents have changed the terminology of these syndromes from an underlying disease-based model to a pathophysiology-driven model (Loirat et al., 2016; Scully et al., 2017). In addition, these consensus documents provide recommendations with regard to specific tests and management strategies for individual patients.

RENAL DISEASES

Complement appears to play a key role in the glomerular damage found in many of the glomerulonephritides (West, 1998; Thurman, 2015). This is evidenced by the deposition of various complement components near or along the glomerular basement membrane as identified by techniques such as immunofluorescence. An example of this is C3 deposition along the basement membrane. Another example is MAC deposition within the glomerulus in patients affected by SLE. In serum sickness–related kidney injury, there is immune complex–mediated damage to the glomerulus and evidence of alternative and classical pathway activation.

Regarding the exact mechanism of immune complex deposition, there are two potential mechanisms. One is possibly that the antigen-antibody complexes are circulating and then become lodged within the glomerulus while blood is being filtered. After deposition, the complexes then lead to complement activation. Alternatively, there may be antibodies specific to glomerular antigens that can then form immune complexes directly on the glomerular basement membrane and again activate complement (Daha & van Es, 1979).

Immune complex deposition is not the only mechanism of damage in complement-mediated glomerulonephritis—for example, C3 glomerulopathy, specifically dense deposit disease (DDD) or glomerulonephritis with isolated C3 deposits (C3GN). In these diseases, there is an abnormal protein called *C3 nephritic factor* (C3NeF or NFa), which will act to stabilize the C3 convertase of the alternative pathway. Specifically, C3NeF is an autoantibody that will increase the half-life of the alternative pathway C3 convertase by at least 10 times (Daha et al., 1976; Daha & van Es, 1979). This is an evolving area of discovery and there are a number of innate genetic and acquired factors that are involved in the pathogenesis, including defects in properdin. It is not currently standard practice to check C3NeF activity, and the absence of this autoantibody does not rule out the diagnosis (Donadelli et al., 2018). While C3NeF seems to be important, it is not felt to be the sole reason for the nephritis (Thurman & Holers, 2006; Holers, 2008). C3 glomerulopathies are typically characterized by uncontrolled activation of the alternative pathway in the fluid phase (i.e., in the circulation) and/or at tissue surfaces that lack membrane–anchored complement regulators. The glomerular basement membrane is such a sensitive surface that it exclusively depends on attached soluble regulators, such as factor H, for protection. As a consequence, the continuous deposition of C3 and complement debris within the basement membrane that occurs as the result of uncontrolled complement activation leads to glomerular injury (de Vriese et al., 2015).

Alternative pathway dysregulation at the level of the cell membrane with impaired cell surface protection against complement activation leading to renal dysfunction is also seen in aHUS, a variant of hemolytic uremic syndrome without the associated bloody diarrhea. Patients with aHUS often have a defect in alternative pathway proteins such as factor H, factor I, or C3. In some instances, identification of the exact mutation can guide management. For example, patients with factor H mutations are likely to have relapse of aHUS after kidney transplantation and could benefit from liver transplantation as well in order to gain normal factor H levels, thus protecting the renal allograft (Thurman & Holers, 2006; Holers, 2008).

OPHTHALMOLOGIC DISEASES

Complement also plays a role in ophthalmologic disease, specifically age-related macular degeneration (AMD), which is a leading cause of permanent visual impairment in industrialized nations. AMD is typically diagnosed in middle-aged and older individuals. It involves gradual reduction in retinal cells, atrophy of the retina, subretinal bleeding, neovascularization, and the development of retinal lesions called *drusen*. The role of complement in AMD was proposed after C3 and C5a were found within these drusen (Markiewski & Lambris, 2007; Holers, 2008). A polymorphism of factor H portends an increased risk for development of AMD. There may be a role for genetic variants of factor B and C3 as well.

DERMATOLOGIC DISEASES

Multiple dermatologic maladies have been attributed in part to complement-mediated destruction, including bullous pemphigoid, pemphigoid gestationis, cicatricial pemphigoid, epidermolysis bullosa acquisita, dermatitis herpetiformis, and pemphigus vulgaris (Yancey & Lawley, 1998). Serum complement levels are usually normal or slightly elevated in these inflammatory diseases. The role of complement has been further elucidated by use of immunofluorescence analysis of tissue biopsy and blister fluid analysis. Additionally, models to study anti–basement membrane antibody-mediated dermatologic disease were developed by Gammon and colleagues (1984). They were able to conclude that a key factor in development of bullous pemphigoid and epidermolysis bullosa acquisita was C5a, which attracts neutrophils to tissue in these diseases, thus leading to tissue damage.

HEMATOLOGIC DISEASES

Complement is an important contributor in multiple types of autoimmune hemolytic anemias as it opsonizes erythrocytes, thus leading to their removal by the reticuloendothelial system. Interestingly, the complement

levels will often be normal despite its role in these diseases. The complement system is especially involved in the removal of cells covered with IgM cold-reactive autoantibodies that are anti-I specific. Such autoantibodies are referred to as *cold agglutinins*. They may be created de novo or in relation to lymphoproliferative disorders after an infectious illness. The cold agglutinins will bind to erythrocytes most avidly at areas of the body where temperatures are lower than normal core temperature, such as the fingertips, ears, and nose. Once the autoantibody-bearing erythrocytes return to warmer, more proximal circulation, with the increase in temperature the autoantibodies will facilitate cell lysis. While most of the cold agglutinin autoantibodies are IgM mediated, there are some related to IgG, as in the case of paroxysmal cold hemoglobinuria (PCH). This is due to cold-reactive Donath-Landsteiner IgG antibodies, which will act similarly to IgM cold agglutinins and cause lysis upon rewarming.

On the opposite end of the temperature spectrum, there are autoantibodies that will bind more effectively at warmer temperatures and then activate the complement system. These warm antibodies are usually of the IgG subtype. Sometimes, they may be associated with viral infections or lymphoproliferative oncologic maladies. Many of the IgG warm antibodies present in autoimmune hemolytic anemia have Rh antigen and do not activate complement efficiently. Cold agglutinins, anti-A, and anti-B blood group antibodies, on the other hand, are effective activators of complement.

Patients affected by PNH are afflicted by episodic intravascular hemolysis, which is related to alternative pathway activation (Rosse, 1998; Jarva & Meri, 1999). In PNH, the issue is a lack of glycosyl phosphatidylinositol-linked proteins on the patient's erythrocytes due to an X-linked mutation in the phosphatidylinositol glycan A (*PIGA*) gene. The proteins DAF/CD55 and CD59 are encoded by this gene and are integral to complement regulation at the site of the C3 convertase and certain members of the MAC, as previously discussed (see the Regulation of Complement Activation section). Because the *PIGA* gene is abnormal, it implies that cell lines made in the bone marrow, including erythrocytes, are unable to defend themselves from activation of complement on the cells themselves (Holers, 2008). Treatment of PNH is currently aimed at blocking the complement cascade via the monoclonal antibody eculizumab, which acts by binding C5, thus halting the remaining steps of the complement cascade. Additional details about the role of complement and specific therapeutics in hematologic diseases can be found elsewhere (Baines et al., 2017)

NEUROLOGIC DISEASES

Perhaps surprisingly, the nervous system is subject to various diseases as a result of complement dysregulation, despite the blood-brain barrier's presumed ability to effectively prohibit complement from entering the spinal fluid. Multiple diseases have been attributed to complement activation, including multiple sclerosis, myasthenia gravis, neuromyelitis optica, lupus cerebritis, Guillain-Barré syndrome, and Alzheimer disease (Morgan, 1994; Morgan et al., 1997; Shin et al., 1998). Despite the blood-brain barrier, brain tissue samples from patients afflicted by these illnesses have shown complement proteins within the tissue. There is frequently complement activity within the cerebrospinal fluid as well in many of these diseases. It is thought that the inflammation present due to complement activation will lead to a disruption in the blood-brain barrier, which could lead to limited infiltration by complement. That being said, there is also evidence that astrocytes are capable of producing all complement proteins in the setting of an inflammatory milieu (Morgan & Gasque, 1996). Not only are they capable of producing complement proteins, but astrocytes and microglial cells have been shown to display complement receptors under in vitro conditions (Morgan & Gasque, 1997). Hence, despite the presence of the blood-brain barrier, the brain is potentially activating complement from within its own tissue. There are data to implicate complement activity as causing myelin damage; therefore, complement dysregulation may be involved in both central and peripheral nervous system diseases.

Neuromyelitis optica spectrum disorder is a relapsing, autoimmune, inflammatory disorder that typically affects the optic nerves and spinal cord. At least two-thirds of cases are associated with aquaporin-4 antibodies and complement-mediated damage to the central nervous system. In myasthenia gravis, endplate destruction is dependent on complement activation and MAC formation. Complement blockade therapy has been shown to be effective for both disorders (Howard et al., 2017; Pittock et al., 2019).

Complement is also involved in Alzheimer disease and Pick disease, both memory disorders. In Alzheimer disease, for example, there is a protein in amyloid called *β-A4* that will bind C1q and initiate the complement cascade within plaques of the brain. Prion-related diseases may also rely on the complement system to affect the host. It has been demonstrated that in cerebral tissue infected with prion disease, there are active complement components, including C1q and C3b, within the prion-related protein deposits (Kovacs et al., 2004). There is also evidence to suggest that complement may play a role in epilepsy, as evidenced by the increased levels of C1q and C3b in patients with refractory epilepsy (Wyatt et al., 2017). There are also multiple in vitro and murine models that show complement dysregulation as potentially contributing to the development of epilepsy.

CARDIOVASCULAR DISEASES

Complement is known to be important in the ischemia and reperfusion (I/R) injuries seen after a myocardial infarction (Lucchesi & Kilgore, 1997). The presence of both classical and alternative pathway complement components, including the MAC constituents, have been seen in the infarcted myocardium. However, the exact method by which complement may cause an effect on myocardial ischemia and infarction is unknown. Anaphylatoxins could contribute to ongoing inflammation within the myocardium. Experimental animal models using coronary artery obstruction have been used to glean further information (Kilgore et al., 1998). Researchers created rabbit models with genetically deficient C6 and demonstrated that the size of the infarct in these animals was smaller compared with C6-competent rabbits. Notably, the sum of neutrophils present within the affected myocardium was lower in the rabbits with genetically induced C6 deficiency, which demonstrates the importance of terminal complement to promote tissue-damaging inflammation.

Injuries due to I/R are known to cause a great deal of damage within tissues. There is increased evidence that this is attributed in part to complement. Once the flow of blood resumes to the ischemic tissue, there is a surge in blood vessel permeability. Inflammatory cells are drawn to the site of ischemia, where they release cytokines, thus promoting further inflammation. It is thought that innately formed antibodies will bind to antigens on damaged endothelial cells and activate complement system (Markiewski & Lambris, 2007).

Not only has complement been implicated in the severity of I/R injuries related to myocardial ischemia, it has also been associated with the development of atherosclerotic disease (Torzewski et al., 1997). Intimal plaques have been shown to have C5b-9 deposits.

Complement activation has been implicated in the formation of early stages of atherosclerosis development and subsequent progression of the lesions (Niculescu et al., 1987; Seifert et al., 1989). To further support this, rabbits with C6 deficiency have been shown to be less likely to be afflicted by atherosclerotic lesions due to cholesterol than were control rabbits (Schmiedt et al., 1998).

BIOCOMPATIBILITY

Many of the biomaterials implanted in the body activate complement, particularly the alternative complement pathway (Mollnes, 1997). On contact with blood or tissue fluids, these materials may activate complement and produce local inflammation or tissue damage. Materials must be tested for their complement-activating activity before they are widely used.

ORGAN TRANSPLANTATION

The success of organ transplantation has created a major problem—a shortage of human organs to meet the demands of an ever-growing number of patients awaiting such a surgical procedure. Therefore, use of animal donors such as the pig is proposed by many in the field as a logical alternative to human organs. However, vascularized porcine organs are susceptible to an intense rejection reaction termed *hyperacute rejection* when implanted in nonhuman primates or humans (Dalmasso, 1992; Platt, 1998). This reaction is mediated by antibody binding to vascular endothelial cells and complement activation. Complement activation was shown to be crucial in tissue damage in hyperacute rejection of xenografts. Complement activation on xenogeneic endothelial cells leads to their activation (i.e., endothelial cells adopt a procoagulant phenotype), which results in intravascular and interstitial thrombosis and hemorrhage. Such an intense reaction is due to the inability of porcine cell–associated complement regulatory molecules such as DAF, MCP, and CD59 to control human complement activation. Therefore, the success of this promising therapeutic intervention relies on proper control of complement activation.

Complement activation in the donor, the graft and the recipient before, during, and after transplantation is also emerging as a significant contributor to human allograft injury. Ischemia and subsequent reperfusion of the graft triggers complement activation. Following transplantation,

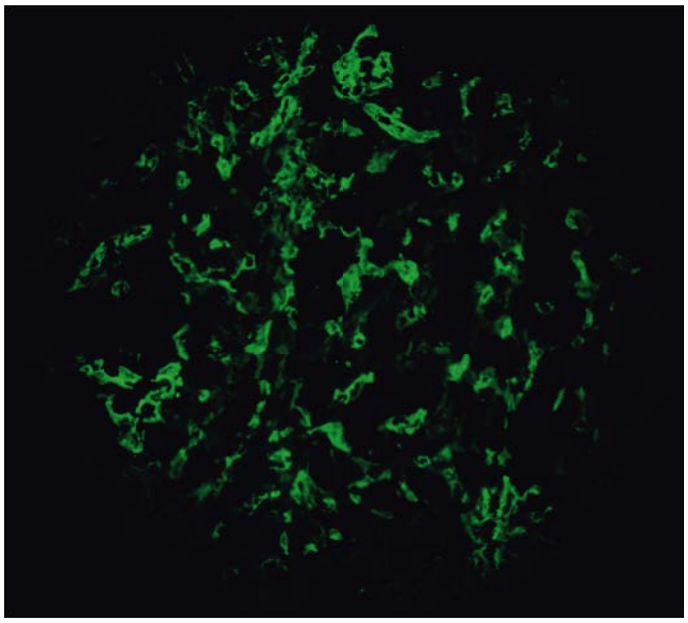

Figure 48.3 Antibodies to C4d with fluorescent labeling are shown staining peritubular capillaries in a transplant kidney biopsy. In the early posttransplant period, this kind of staining pattern is indicative of humoral rejection (40×, fluorescein isothiocyanate).

complement has a role in innate immunologic and inflammatory processes that could further damage the graft. Complement-targeted strategies might have a role in optimizing graft quality as well as in the treatment of antibody-mediated rejection (Baldwin et al., 1995; Biglarnia et al., 2018). Identification of C4d in the peritubular capillaries of renal transplant biopsies by immunofluorescence microscopy is a useful adjunctive study in the recognition of humoral rejection (Fig. 48.3) (Onitsuka et al., 1999).

CLINICALLY USEFUL COMPLEMENT INHIBITORS

Many complement inhibitors have been produced, and still more are in development (Woodruff et al., 2011). To be clinically useful, a complement inhibitor should avoid production of the proinflammatory by-products of complement activation, such as the anaphylatoxins C3a and C5a. Inappropriate activation or inadequate regulation of complement activation is involved in a variety of human diseases. Therefore, the development of agents that selectively block complement activation would be useful in limiting tissue damage. Although eculizumab, a humanized long-acting monoclonal antibody directed against C5 and marketed for the treatment of patients with PNH, is currently the only clinically approved selective complement component blocker, a number of other compounds have now completed clinical trials (Woodruff, 2011; Ricklin & Lambris, 2007). A table listing these pharmacologic agents and their relatively current stage in development has been published (Ricklin et al., 2018). Current strategies used to therapeutically regulate complement may be classed into five major categories: (1) purified plasma protease inhibitors, primarily C1-Inh (currently approved for treatment of hereditary angioedema); (2) soluble complement regulators, such as sCR1, which act to prevent complement attack on host cells; (3) therapeutic antibodies such as eculizumab, intended to selectively block various stages of complement activation; (4) small peptides, nucleotides, and synthetic molecules such as compstatin, which are used to sterically hinder or induce conformational changes in the elements of the complement cascade; and (5) anaphylatoxin receptor inhibitors, intended to reduce the proinflammatory signaling initiated by complement components such as C5a. Because of the critical role of complement in host defense, especially in infection, potential complement inhibitors will have to avoid interfering with intact and properly regulated elements of the system. As mentioned earlier, C1-Inh is absent or reduced in the serum of those with hereditary angioedema and has been administered as a therapeutic concentrate during acute attacks. Because C1-Inh is often reduced in severe inflammatory states as well, concentrates of C1-Inh have been shown to have promising clinical utility in conditions such as septic shock, reperfusion injury, hyperacute transplant rejection, and PNH (Kirschfink & Mollnes, 2001; Davis, 2004).

ASSAYS OF COMPLEMENT

GENERAL PRINCIPLES

Today, there are four main indications for determination of a patient's complement status: (1) complement deficiencies (acquired or inherited); (2) disorders with aberrant complement activation; (3) C1-Inh deficiencies (acquired or inherited); and (4) to monitor patients on complement-regulating drugs. Methods that allow accurate determination of levels of each of the components of the classical, alternative, and MBL pathways, as well as several enzymes and regulators of the complement system, are available. However, many of these assays are not available in routine clinical laboratories and are restricted to research laboratories. We focus our attention here on techniques that do not require a laboratory skilled in complement research for their performance. The reader is referred to other publications for details relative to methods that require more specialized techniques (Whaley, 1985; Harrison & Lachman, 1986; Dodds & Sim, 1997; Giclas, 1997; Würzner et al., 1997; Mollnes et al., 2007).

Available techniques to study complement include quantification of (1) individual components, (2) activation products, (3) function, and (4) autoantibodies to complement proteins. Complement assays can be divided into two types: (1) those that measure complement proteins as antigens in biological fluids and (2) those that measure the functional activity of a given component. Both types of techniques have advantages and disadvantages. Methods used for antigenic (immunochemical) analysis are generally simpler to perform. These antigenic assays are highly specific, require fewer specialized reagents, are cheaper, and are considerably less time-consuming. In these assays, serum or plasma can be used and commonly available methods of freezer storage (–20°C) are sufficient. For these reasons, antigenic assays are easily adaptable to a clinical laboratory.

On the other hand, antigenic assays do not provide information about the activity of a component because they may detect degradation products as well as functionally active components. The presence in serum of small fragments of a protein with antigenic activity may confuse the results. Some antigenic assays use radial immunodiffusion. In these assays, a protein fragment may diffuse more rapidly than the parent molecule, which may result in falsely high levels. As an example, the most commonly employed antigenic assays for C3 measure its major degradation product, C3c, by radial immunodiffusion. For accurate measurements of C3c, the specimen should be thawed at 37°C for a number of days to allow complete conversion of C3 to C3c. In fact, this is not usually done, which can represent a source of error, although the error is small and is not usually of clinical consequence. In general, antigenic assays are not as sensitive as functional assays and may not detect low levels of a component present in certain body fluids. The sensitivity of antigenic assays depends to some degree on the strength of the antibody employed; with the usual assays, as little as 10 μg/mL of protein antigen can be measured.

Kits are available that use inhibition of binding of radiolabeled substrate to detect various complement peptides. Such kits are available for measurement of C3a, C4a, and C5a. The usefulness of these measurements is still being debated. Assays designed to measure the functional activity of the control proteins, factors H and I, in human serum have also been reported but require specialized reagents that may not be commercially available (Gaither et al., 1979). ELISAs have been developed for the measurement of split products of complement proteins or complexes formed following complement activation. These kits measure breakdown products of complement proteins as they are generated after complement activation using specific monoclonal antibodies. Complement activation via the classical pathway can be measured by following the levels of C4d in serum versus those of C4. Also, ELISA of C1r-C1s-C1Inh complexes provides a measure of complement activation via the classical pathway. Activation of the alternative pathway can be measured by ELISA by assessing levels of Bb, C3bBbP, or C3bP complexes in the circulation (Mayes et al., 1984). Measurement of as little as 10 to 20 ng/mL of C3bP in serum has been reported. This assay may also be used to measure surface-bound activation complexes. Activation via either pathway can be monitored by measuring levels of iC3b or sC5b-9, the soluble form of the MAC.

An ELISA test for the measurement of serum or plasma MBL complex activity was developed that eliminates interference by components of the classical pathway (Petersen et al., 2001; Kuipers et al., 2002). In addition, ELISA kits are available that measure the generation of anaphylatoxins in serum/plasma. Because C3a and C5a are rapidly converted to their inactive desArg fragments by carboxypeptidase-N in serum, these assays utilize monoclonal antibodies specific for C3a-desArg and C5a-desArg. Because of their high sensitivity, ELISAs serve as an excellent tool by which to assess complement activation in biological fluids via the classical pathway

TABLE 48.8
CH50 and AH50 Interpretation

Test Result	Interpretation
CH50 very low or 0 (AH50 normal)	Missing C1q, C1r, C1s, C2, or C4
AH50 very low or 0 (CH50 normal)	Missing properdin, or (very rarely) factor B or factor D
CH50 and AH50 very low or 0	Missing C3, C5, C6, C7, C8, or C9
Late components low (especially C3) CH50 and AH50 low	Missing factor H or factor I

Modified from Wen BS, Atkinson J, Giclas PC: Clinical and laboratory evaluation of complement deficiency, *J Allergy Clin Immunol* 113:585–593, 2004.

or the alternative pathway. Seelen and colleagues (2005) describe a simple approach using three ELISAs that is suitable for screening deficiencies of all three pathways and is commercially available (WIELISA, Wieslab, Lund, Sweden). Advantages of this approach include the coverage of all three pathways simultaneously, the ability to detect properdin deficiency in the alternative pathway, and freedom from consideration of the availability of erythrocytes (Mollnes et al., 2007).

FUNCTIONAL EVALUATION OF THE CLASSICAL PATHWAY

Functional complement assays are sensitive and precise tools for providing information about the activity of a complement component. Some of these methods may be used to quantify activity at the molecular level; others can be used to express complement function in arbitrary units. Commercial reagents are available for titrating each component of classical or alternative pathways. Assays that measure the total hemolytic activity in a specimen (CH50) or the functional activity of isolated complement components in general use sheep erythrocytes as targets of complement-mediated lysis. Sheep erythrocytes are more sensitive to antibody- and complement-mediated lysis than erythrocytes from other species. The alternative pathway of complement activation (AH50) is easily measured using rabbit erythrocytes. These cells are particularly sensitive to antibody-independent lysis mediated by human serum. In addition, a functional hemolytic assay using chicken erythrocytes to assess functional MBL levels in serum has been developed, which the authors claim is useful for large-scale testing of patient samples (Petersen et al., 2001; Kuipers et al., 2002). A useful summary of the clinical significance of CH50 and AH50 testing is provided in Table 48.8.

The simplest functional assay of the classical pathway measures total hemolytic complement. Absence of any of the nine components, as occurs in homozygous genetically deficient patients, generally results in a total hemolytic complement titer (CH50) of zero. However, a normal value does not exclude the possibility of reduced levels of individual components in test subjects. When a patient's history and symptoms suggest a possible deficiency, hemolytic or antigenic titrations of individual components may be required. Often, a CH50 titer will be an adequate functional measure of complement activity. In the CH50 assay, commercially available antibodies added to sheep red blood cells react with antigen on red cell surfaces, forming immune complexes. Patient test serum is then added to the mixture as the source of classical pathway complement. Complement in the test serum will bind the immune complex previously formed on the sheep red cells, leading to activation of the classical complement pathway and to red cell lysis. By titrating the addition of patient test serum, it is possible to calculate the complement activity present in the patient sample and to express that activity as the reciprocal of the dilution that causes lysis of 50% of red blood cells in the assay (the CH50). The complement titer is expressed in CH50 units (the reciprocal of the dilution of the complement source that lyses 50% of sensitized sheep erythrocytes).

Serial dilutions of the specimen are prepared and added to antibody-sensitized sheep erythrocytes. In this case, the 50% endpoint is determined by Von Krogh transformation of the data. This empirically derived formula converts the S-shaped dose-response curve to a linear function. Values of $Y/(1 - Y)$ are calculated, in which Y is the fraction of red blood cells lysed in a test dilution. A graph is constructed in which the log of the relative volume of complement is plotted against the log of $Y/(1 - Y)$ values. Usually, a straight line is obtained and the titer is calculated by determining the relative volume of complement at which $Y/(1 - Y) = 1.0$ (or 50% lysis). This value is divided into the reciprocal of original serum dilution (1:60 for human serum) to calculate the concentration of serum complement that lyses 50% of the cells. The complement titer represents the number of 50% hemolytic units present in 1.0 mL of undiluted serum (Mayer, 1961; Rapp & Borsos, 1970). Clinical laboratories may use one of two commercially available variations of this classic test to perform the CH50 assay. One is based on the lysis of liposomes, releasing a marker enzyme; the other is an ELISA that detects the final C9 neo-antigen formed with complete activation of the classical pathway.

FUNCTIONAL EVALUATION OF THE ALTERNATIVE PATHWAY

In this assay, human serum (usually first diluted 1:5) is serially diluted and added to rabbit erythrocytes that are not sensitized with specific antibody, in a buffer that contains magnesium ions and ethylene glycol tetraacetic acid, to chelate calcium ions (calcium ions are required for classical pathway activation, not for alternative pathway activation) (Pangburn, 1988). The alternative pathway titer is designated AH50 and represents the final dilution of human serum in the assay that lyses 50% of the rabbit erythrocytes. A graph similar to that described for total hemolytic complement titration is produced to determine the AH50. Human serum may at times possess "natural" antibody to a carbohydrate widely expressed on cells of species other than humans and nonhuman primates. A high concentration of serum mixed with rabbit erythrocytes may induce agglutination, which can be misleading in interpreting an AH50 titer (Tomlinson & Nussenzweig, 1997). Therefore, it may be useful to absorb the serum with washed, packed rabbit erythrocytes on ice for 15 to 30 minutes to remove a certain proportion of natural antibodies, hence reducing cell agglutination in the assay.

FUNCTIONAL ASSAY OF C1-INHIBITOR AND FACTOR H

Assays for the assessment of C1-Inh function have been developed that are useful in the diagnosis of HAE. One that is in common use is an ELISA-based assay that measures formation of a complex between biotinylated C1s and C1-Inh on an avidin-coated solid phase. A second test makes use of steric hindrance created by the binding of inhibitor to C1r, preventing the subsequent binding of antibody to C1r. During radial immunodiffusion of C1r, unbound and, therefore, active C1r quantities will increase as the amount of C1-Inh present decreases. Factor H functional assays are important for the diagnosis of aHUS, membranoproliferative glomerulonephritis type II (DDD), and AMD. A method described by Sánchez-Corral and colleagues (2004) uses unsensitized sheep red blood cells incubated in serum. With this method, normal serum will provide factor H–conferred protection from hemolysis, whereas factor H–deficient serum will not prevent complement-mediated red cell lysis.

COMPLEMENT LEVELS BY ANTIGENIC ASSAYS

For use in antigenic assays, the specimen (serum or plasma) is stored frozen (–20°C or lower). Bacterial contamination may cause protein denaturation or fragmentation, whereas freezing and thawing do not usually have a major adverse effect on antigenic levels. For certain complement assays, the specimen is diluted in saline to achieve the correct concentration range for accurate measurement.

Antigenic analyses of complement proteins make use of one of several immune precipitin techniques. Single radial immunodiffusion using the method of Fahey or Mancini is commonly used to calculate specific protein quantities. With both methods, antigen is added to wells in a gel that contains antibody, and rings of precipitation are formed. The Fahey method employs antibody that is not in excess. Thus, the diffusion time at which results are read is critical. Diffusion endpoints are not reached, which can lead to inaccurate measurement of antigenic complement levels. The Mancini method uses excess antibody in the gel and is more sensitive and accurate. Most commercial firms preparing immunodiffusion plates use the Mancini method. Radial immunodiffusion kits are available for all components of the classical and alternative pathways. These kits consist of plates coated with a thin layer of 2% agarose-containing monospecific antibody. Protein standard serum (a stabilized pool of normal human serum) is supplied, usually in prediluted solutions. Each standard solution contains a specific amount of the particular protein being measured for use in construction of the reference curve.

Nephelometric methods are also used to measure complement component levels, which in some instances may be comparable with those obtained with radial immunodiffusion (Bossuyt et al., 2002). They are commonly used in hospital laboratories to measure serum C3 and C4.

Ingvarsson and colleagues (2007) described a proteomic approach that uses an antibody-based microarray platform employing recombinant human scFv antibodies, permitting protein expression profiling of serum complement-related proteomes. The microarray data correlated well with conventional clinical laboratory methods when plasma samples from both healthy and complement-deficient individuals were tested. Similarly, Janzi and colleagues (2005) described a reverse array format in which serum samples are themselves spotted to a microarray slide in large sample numbers and are screened for the presence of a single serum protein as proof of the principle that large numbers of serum samples may be simultaneously screened for clinically relevant proteins.

Autoantibodies to Complement Proteins

Autoantibodies directed against a variety of individual complement components, convertases, regulators and receptors have been identified. For several autoantibodies, the functional consequences are well documented and clear associations exist with clinical presentation. Several anticomplement autoantibodies can also be detected in healthy controls, indicating that a second hit is required for such autoantibodies to induce pathology. Some of these well-described antibodies include anti-C1q (associated with SLE), C3NeF (associated with C3 glomerulopathy), and anti–factor H antibody (associated with aHUS). The reader is directed to two excellent reviews on this subject with regard to measurement and clinical relevance of these and other autoantibodies (Dragon-Durey et al., 2013; Ekdahl et al., 2018). Most of the autoantibody testing is performed using ELISAs.

KININS AND THE KININ-GENERATING SYSTEM

The kinin-generating system is another inflammatory response pathway present in plasma that controls the generation of peptides important in the inflammatory response. Briefly, the most important biologically active peptide generated by the system appears to be bradykinin, a nonapeptide with potent activity in many biological systems. It is active in increasing vascular permeability, vasodilation, hypotension, induction of pain, contraction of many types of smooth muscle cells, and activation of the phospholipase A2 system, with activation of cellular arachidonic acid metabolism. Although in many respects it is similar to the complement system, the plasma kinin-generating system is simpler because it is composed of only four plasma proteins. The major proteins of the kinin-generating system as currently understood are Hageman factor, clotting factor XI, prekallikrein, and high-molecular-weight kininogen.

On interacting with negatively charged surfaces—such as those supplied experimentally by glass or naturally by many biologically active materials, such as lipid A of gram-negative bacterial endotoxin—Hageman factor is cleaved and activated. Proteolytic enzymes, including kallikrein, can cleave and activate Hageman factor as well. The cleaved Hageman factor (αHFa) has proteolytic activity, further activating and cleaving additional Hageman factor molecules to generate additional αHFa.

αHFa activates factor XI to factor XIa, resulting in activation of the intrinsic coagulation cascade. αHFa also cleaves the single-chain prekallikrein into a two-chain molecule, kallikrein, with the chains linked by disulfide bonds. Cleaved prekallikrein has proteolytic enzymatic activity located on the lower-molecular-weight chain. Activated kallikrein cleaves high-molecular-weight kininogen at several sites, thereby releasing bradykinin.

Bradykinin has a short half-life mainly caused by the activities of four membrane-bound and/or soluble zinc metallopeptidases: angiotensin 1–converting enzyme, aminopeptidase P, neutral endopeptidase 24.11 (neprilysin), and carboxypeptidases M and N (Moreau et al., 2005). These four act to convert bradykinin to inactive low-molecular-weight peptides lacking known biological activity.

Bradykinin has been postulated to play a role in a variety of diseases. Free bradykinin and lysyl-bradykinin have been found in the nasal fluid of patients with rhinitis. A pathogenic role for bradykinin has also been suggested in diseases ranging from asthma to hereditary or acquired angioedema. Bradykinin is an important mediator of the inflammatory response; when administered locally, it produces the four cardinal signs of inflammation. Development of pharmacologic agents to block or ameliorate the effects of the kinin system has met with limited success but is ongoing (Dietrich, 2009).

PERSPECTIVES

Members of the complement system of proteins play roles in many disease states. In recognition of this, therapies have been designed to directly trigger or block various complement components as part of the treatment of disease. Clinical laboratory detection and measurement of native proteins and the clinically administered therapeutic agent continues to become more commonplace.

SELECTED REFERENCES

Carroll MC: The complement system in regulation of adaptive immunity, *Nat Immunol* 5:981–986, 2004.

This article describes the intricate interaction that exists between complement activation products and T- and B-cell responses. It also covers the nature of the link that exists between innate and adaptive immune responses.

Gonzalez-Amaro R, Diaz-Gonzalez F: Sanchez-Madrid F: adhesion molecules in inflammatory diseases, *Drugs* 56:977–988, 1998.

This article provides an excellent and in-depth review of the process of leukocyte diapedesis. Pharmacologic therapeutic blocking of this process is discussed.

Wen L, Atkinson JP, Giclas PC: Clinical and laboratory evaluation of complement deficiency, *J Allergy Clin Immunol* 113:585–593, 2004.

This article provides a practical clinical approach to complement deficiency testing and an overview of the complement system.

Access the complete reference list online at Elsevier eBooks for Practicing Clinicians.

REFERENCES

Agnello V: Lupus diseases associated with hereditary and acquired deficiencies of complement, *Springer Semin Immunopathol* 9:161–178, 1986.

Ahearn JM: Rosengard AM: complement receptors. In Volanakis JE, Frank MM, editors: *The human complement system in health and disease*, New York, 1998, Marcel Dekker, p 167.

Atkinson JP: Complement activation and complement receptors in systemic lupus erythematosus, *Springer Semin Immunopathol* 9:179–194, 1986.

Baines AC, Brodsky RA: *Complementopathies*, *Blood Rev* 31:213–223, 2017.

Baldwin WM, Pruitt SK, Brauer RB, et al.: Complement in organ transplantation, *Transplantation* 59:797–808, 1995.

Batjay Z, Speth C, Erdei A, et al.: Cutting edge: productive HIV-1 infection of dendritic cells via complement receptor type 3 (CR3, CD11b/CD18), *J Immunol* 173:4775–4778, 2004.

Benzaquen LR, Nicholson-Weller A, Halperin JA: Terminal complement proteins C5b-9 release basic fibroblast growth factor and platelet-derived growth factor from endothelial cells, *J Exp Med* 179:985–992, 1994.

Berge V, Johnson E, Hogasen K: Clusterin and the terminal complement pathway synthesised by human umbilical vein endothelial cells are closely linked when on co-cultured agarose beads, *APMIS* 105:17–24, 1997.

Bhakdi S, Tranum-Jensen J: Complement lysis: a hole is a hole, *Immunol Today* 12:318–320, 1991.

Biesecker G, Lavin L, Ziskind M, et al.: Cutaneous localization of the membrane attack complex in discoid and systemic lupus erythematosus, *N Engl J Med* 306:264–269, 1982.

Biglarnia AR, Huber-Lang M, Mohlin C, Ekdahl KN, Nilsson B: The multifaceted role of complement in kidney transplantation, *Nat Rev Nephrol* 14(12):767–781, 2018.

Birmingham DJ: Erythrocyte complement receptors, *Crit Rev Immunol* 15:133–154, 1995.

Boackle SA, Morris MA, Holers VM, et al.: Complement opsonization is required for presentation of immune complexes by resting peripheral blood B cells, *J Immunol* 161:6537–6543, 1998.

Boes M, Prodeus AP, Schmidt T, et al.: A critical role of natural immunoglobulin M in immediate defense against systemic bacterial infection, *J Exp Med* 188:2381–2386, 1998.

Bosmann M, Ward PA: Role of C3, C5 and anaphylatoxin receptors in acute lung injury and in sepsis, *Adv Exp Med Biol* 946:147–159, 2012.

Bossuyt X, Sneyers L, Marien G, et al.: Novel nephelometric assay for measurement of complement 3d, *Ann Clin Biochem* 39:34–38, 2002.

Böttger EC, Hoffman T, Hadding U, et al.: Influence of genetically inherited complement deficiencies on humoral immune response in Guinea pigs, *J Immunol* 135:4100–4107, 1985.

Botto M, Kirschfink M, Macor P, et al.: Complement in human disease: lessons from complement deficiencies, *Mol Immunol* 46:2774–2783, 2009.

Brown EJ: Complement receptors and phagocytosis, *Curr Opin Immunol* 3:76–82, 1991.

Carroll MC: The role of complement and complement receptors in induction and regulation of immunity, *Annu Rev Immunol* 16:545–568, 1998.

Chang CP, Hüsler T, Zhao J, et al.: Identity of a peptide domain of human C9 that is bound by the cell-surface complement inhibitor, CD59, *J Biol Chem* 269:26424–26430, 1994.

Chen C-H, Lam CK, Boackle RJ: C1 inhibitor removes the entire C1qr2s2 complex from anti-C1Q monoclonal antibodies with low binding affinities, *Immunology* 95:648–652, 1998.

Choi N-H, Mazda T, Tomita M: A serum protein, SP-40, modulates the formation of the membrane attack complex of complement on erythrocytes, *Mol Immunol* 26:835–839, 1989.

Christiansen OB, Kilpatrick DC, Souter V, et al.: Mannan-binding lectin deficiency is associated with unexplained recurrent miscarriage, *Scand J Immunol* 49:193–196, 1999.

Colten HR, Garnier G: Regulation of complement protein gene expression. In Volanakis JE, Frank MM, editors: *The human complement system in health and disease*, New York, 1998, Marcel Dekker, p 217.

Cooper NR: Complement and viruses. In Volanakis JE, Frank MM, editors: *The human complement system in health and disease*, New York, 1998, Marcel Dekker, p 393.

Cornacoff JB, Hebert LA, Smead WL, et al.: Primate erythrocyte-immune complex-clearing mechanism, *J Clin Invest* 71:236–247, 1983.

Cummings KL, Waggoner SN, Tackle R: Role of complement in immune regulation and its exploitation by virus, *Vir Immunol* 20:505–524, 2007.

Czermak BJ, Sarma V, Pierson CL, et al.: Protective effects of C5a blockade in sepsis, *Nat Med* 5:788–792, 1999.

Daha MR, Fearon DT, Austen KF: C3 nephritic factor (C3NeF): stabilization of fluid phase and cell-bound alternative pathway convertase, *J Immunol* 116:1–7, 1976.

Daha MR, van Es LA: Further evidence for the antibody nature of C3 nephritic factor (C3NeF), *J Immunol* 123:755–758, 1979.

Dalmasso AP: The complement system in xenotransplantation, *Immunopharmacology* 24:149–160, 1992.

Davis III AE: Biological effects of C1 inhibitor, *Drug News Perspect* 17:439–446, 2004.

Davis III AE, Harrison RA: Structural characterization of factor I mediated cleavage of the third component of complement, *Biochemistry* 21:5745–5749, 1982.

De Vriese AS, Sethi S, Van Praet J, Nath KA, Fervenza FC: Kidney disease caused by dysregulation of the complement alternative pathway: an Etiologic approach, *J Am Soc Nephrol* 26(12):2917–2929, 2015.

Diebolder CA, Beurskens FJ, et al.: Complement is activated by IgG hexamers assembled at the cell surface, *Science* 343:1260–1263, 2014.

Dietrich W: Aprotinin: 1 year on, *Curr Opin Anaesth* 22:121–127, 2009.

DiScipio RG, Daffern PN, Jagels MA, et al.: A comparison of C3a and C5a-mediated stable adhesion and rolling eosinophils in postcapillary venules and transendothelial migration in vitro and in vivo, *J Immunol* 162:1127–1136, 1999.

Dodds AW, Sim RB, editors: *Complement: a practical approach*, Oxford, 1997, IRL Press.

Doekes G, Es LA, Daha MR: C1 inactivator: its efficiency as a regulator of classical complement pathway activation on soluble IgG aggregates, *Immunology* 49:215–222, 1983.

Donadelli R, Pulieri P, Piras R, et al.: Unraveling the molecular mechanisms underlying complement dysregulation by nephritic factors in C3G and IC-MPGN, *Front Immunol* 9:2329, 2018.

Dragon-Durey MA, Blanc C, Marinozzi MC, van Schaarenburg RA, Trouw LA: Autoantibodies against complement components and functional consequences, *Mol Immunol 15* 56(3):213–221, 2013.

Edwards JL, Brown EJ, Ault KA, et al.: The role of complement receptor 3 (CR3) in *Neisseria gonorrhoeae* infection of human cervical epithelia, *Cell Microbiol* 3:611–622, 2001.

Ekdahl KN, Persson B, Mohlin C, Sandholm K, Skattum L, Nilsson B: Interpretation of Serological complement Biomarkers in disease, *Front Immunol* 24(9):2237, 2018.

Ember JA, Engels MA, Hugli TE: Characterization of complement anaphylatoxins and their biological responses. In Volanakis JE, Frank MM, editors: *The human complement system in health and disease*, New York, 1998, Marcel Dekker, p 241.

Epstein J, Eichbaum Q, Sheriff S, et al.: The collectins in innate immunity, *Curr Opin Immunol* 8:29–35, 1996.

Falk RJ, Dalmasso AP, Kim Y, et al.: Neoantigen of the polymerized ninth component of complement: characterization of a monoclonal antibody and immunohistochemical localization in renal disease, *J Clin Invest* 72:560–573, 1983.

Fearon DT, Austen KF: Properdin: binding to C3b and stabilization of the C3b-dependent C3 convertase, *J Exp Med* 142:856–863, 1975.

Fingeroth JD, Weiss JJ, Tedder TF, et al.: Epstein Barr virus receptor of human B lymphocytes is the C3d receptor CR2, *Proc Natl Acad Sci U S A* 81:4510–4516, 1984.

Fishelson Z: Complement-related proteins in pathogenic organisms, *Springer Semin Immunopathol* 15:345, 1994.

Frank MM: Introduction and historical notes. In Volanakis JE, Frank MM, editors: *The human complement system in health and disease*, New York, 1998, Marcel Dekker, p 1.

Frank MM, Fries LF: The role of complement in defence against bacterial disease, *Bailliere's Clin Immunol Allergy* 2(335), 1988.

Fries LF, Frank MM: Molecular mechanisms of complement action. In Stamatoyannopoulos G, Nienhuis AW, Leder P, et al.: *The molecular basis of blood diseases*, Philadelphia, 1987, Saunders, p 450.

Gaither TA, Hammer CH, Frank MM: Studies of the molecular mechanisms of C3b inactivation and a simplified assay of 1H and the C3b inactivator (C3bINA), *J Immunol* 123:1195, 1979.

Gammon WR, Inman AO, Wheeler Jr CE: Differences in complement-dependent chemotactic activity generated by bullous pemphigoid and epidermolysis bullosa acquisita immune complexes: demonstration by leukocytic attachment and organ culture methods, *J Invest Dermatol* 83:57, 1984.

Gavriilaki E, Anagnostopoulos A, Mastellos DC: Complement in thrombotic microangiopathies: Unraveling Ariadne's Thread into the Labyrinth of complement therapeutics, *Front Immunol* 10:337, 2019.

Gawryl MS, Chudwin DS, Langlois PF, et al.: The terminal complement complex, C5b-9, a marker of disease activity in patients with systemic lupus erythematosus, *Arthritis Rheum* 31:188, 1988.

Gewurz H, Jiang H, Ying S-C, et al.: Nonimmune activation of the classical complement pathway, *Behring Inst Mitt* 93:138, 1993.

Giclas PC: Complement, immune complexes, and cryoglobulin. In Rose NR, Conway de Macario E, Folds JD, et al.: *Manual of clinical laboratory immunology*, 5, Washington, DC, 1997, ASM Press, p 179.

Gigli I, Fujita T, Nussenzweig V: Modulation of the classical pathway C3 convertase by plasma proteins C4b-binding protein and C3b inactivator, *Proc Natl Acad Sci U S A* 76:6596, 1979.

Grumach AS, Kirschfink M: Are Complement Deficiencies Really Rare? Overview on prevalence, clinical importance and modern diagnostic approach, *Molecular Immuno* 61:110–117, 2014.

Hansen S, Holmskov U: Structural aspects of collectins and receptors for collectins, *Immunobiology* 199:165, 1998.

Harrison RA: Lachman PJ: complement technology. In Weir DM, Herzenberg LA, Blackwell C, editors: *Handbook of experimental immunology*, Vol 4. Oxford, 1986, Blackwell Scientific.

Hibberd ML, Sumiya M, Summerfield JA, et al.: Association of variants of the gene for mannose-binding lectin with susceptibility to meningococcal disease, *Lancet* 353:1049, 1999.

Holers VM: The spectrum of complement alternative pathway-mediated diseases, *Immunol Rev* 223:300–316, 2008.

HongBin W, Ricklin D, et al.: C4a activates PAR1 and PAR4, *Proceedings of the National Academy of Sciences Oct* 114(41):10948–10953, 2017.

Howard Jr JF, et al.: REGAIN Study Group. Safety and efficacy of eculizumab in anti-acetylcholine receptor antibody-positive refractory generalised myasthenia gravis (REGAIN): a phase 3, randomised, double-blind, placebo-controlled, multicentre study, *Lancet Neurol16*(12)976–986, 2017.

Ingvarsson J, Larsson A, Sjöholm AG, et al.: Design of recombinant antibody microarrays for serum protein profiling: targeting of complement proteins, *J Proteome Res* 6:3527–3536, 2007.

IUIS-WHO Nomenclature Committee: Nomenclature of the alternative activating pathway of complement, *J Immunol* 127:1261, 1981.

Janzi M, Odling J, Pan-Hammarström Q, et al.: Serum microarrays for large scale screening of protein levels, *Mol Cell Proteomics* 4:1942–1947, 2005.

Jarva H, Meri S: Paroxysmal nocturnal haemoglobinuria: the disease and a hypothesis for a new treatment, *Scand J Immunol* 49:119, 1999.

Johnson E, Berge V, Hogasen K: Formation of the terminal complex on agarose beads: further evidence that vitronectin (complement S-protein) inhibits C9 polymerization, *Scand J Immunol* 39:281, 1994.

Kemper C, Atkinson JP: T-cell regulation: with complements from innate immunity, *Nat Rev Immunol* 7:9–18, 2007.

Kerekes K, Prechl J, Bajtay Z, et al.: A further link between innate and adaptive immunity: C3 deposition on antigen-presenting cells enhances the proliferation of antigen-specific T cells, *Int Immunol* 10:1923, 1998.

Kilgore KS, Flory CM, Miller BF, et al.: The membrane attack complex of complement induces interleukin-8 and monocyte chemoattractant protein-1 secretion from human umbilical vein endothelial cells, *Am J Pathol* 149:953, 1996.

Kilgore KS, Park JL, Tanhehco EJ, et al.: Attenuation of interleukin-8 expression in C6-deficient rabbits after myocardial ischemia/reperfusion, *J Mol Cell Cardiol* 30:75, 1998.

Kilpatrick DC: Mannan-binding lectin: clinical significance and applications, *Biochim Biophys Acta* 1572:401–413, 2002.

Kinoshita T, Takata Y, Kozono H, et al.: C5 convertase of the alternative complement pathway: covalent linkage between two C3b molecules within the trimolecular complex enzyme, *J Immunol* 141:3895, 1988.

Kirschfink M, Mollnes TE: C1-inhibitor: an anti-inflammatory reagent with therapeutic potential, *Expert Opin Pharmacother* 2:1073–1083, 2001.

Klickstein LB, Barbashov SF, Liu T, et al.: Complement receptor type 1 (CR1, CD35) is a receptor for C1q, *Immunity* 7:345, 1997.

Korb LC, Ahearn JM: C1q binds directly and specifically to surface blebs of apoptotic human keratinocytes, *J Immunol* 158:4525, 1997.

Koski CL, Ramm LE, Hammer CH, et al.: Cytolysis of nucleated cells by complement: cell death displays multi-hit characteristics, *Proc Natl Acad Sci U S A* 80:3816, 1983.

Kovacs GG, Gasque P, Strobel T, et al.: Complement activation in human prion disease, *Neurobiol Dis* 15:21–28, 2004.

Kozel TR: Activation of the complement system by pathogenic fungi, *Clin Microbiol Rev* 9:34, 1996.

Kuipers S, Aerts PC, Sjoholm AG, et al.: A hemolytic assay for the estimation of functional mannose-binding lectin levels in human serum, *J Immunol Methods* 268:149–157, 2002.

Law SK, Lichtenberg NA, Levine RP: Evidence for an ester linkage between the labile binding site of C3b and receptive surfaces, *J Immunol* 123:1388, 1979.

Licht C, Weyersberg A, Heinen S, et al.: Successful plasma therapy for atypical hemolytic uremic syndrome caused by factor H deficiency owing to a novel mutation in the complement cofactor protein domain 15, *Am J Kidney Dis* 45:415–421, 2005.

Lim BL, Reid KBM, Ghebrehiwet B, et al.: The binding protein for globular heads of complement C1q, gC1qR: functional expression and characterization as a novel vitronectin binding factor, *J Biol Chem* 271:26739, 1996.

Loirat C, HUS International, et al.: An international consensus approach to the management of atypical hemolytic uremic syndrome in children, *Pediatr Nephrol31*(1)15–39, 2016.

Liu CC, Manzi S, Danchenko N, et al.: New advances in measurement of complement activation: lessons of systemic lupus erythematosus, *Curr Rheumatol Rep* 6:375–381, 2004.

Lucchesi BR, Kilgore KS: Complement inhibitors in myocardial ischemia/reperfusion injury, *Immunopharmacology* 38:27, 1997.

Lutz HU: How pre-existing, germline-derived antibodies and complement may help induce a primary immune response to nonself, *Scand J Immunol* 49:224, 1999.

Mabbott NA: The complement system in prion diseases, *Curr Opin Immunol* 16:587–593, 2004.

Mabbott NA, Bruce NE, et al.: Temporary depletion of complement component C3 or genetic deficiency of C1q significantly delays onset of scrapie, *Nat Med* 7(4):485–487, 2001.

Malhotra R, Wormald MR, Rudd PM, et al.: Glycosylation changes of IgG associated with rheumatoid arthritis can activate complement via the mannose-binding protein, *Nat Med* 1:237, 1995.

Markiewski MM, Lambris JD: The role of complement in inflammatory diseases from behind the scenes into the spotlight, *Am J Pathol* 171:715–727, 2007.

Marom Z, Shelhammer J, Berger M, et al.: Anaphylatoxin C3a enhances mucous glycoprotein release from human airways in vitro, *J Exp Med* 161:657, 1985.

Matsushita M, Endo Y, Fujita T: MASP1 (MBL-associated serine protease 1), *Immunobiology* 199:340, 1998.

Matsushita M, Fujita T: Inhibition of mannose-binding protein-associated serine protease (MASP) by C1 inhibitor (C1 INH), *Mol Immunol* 33:44, 1996.

Mauff G, Würzner R: Complement genetics. In Herzenberg LA, Weir DM, Blackwell C, editors: *Weir's handbook of experimental immunology*, Vol 2. Malden, Mass, 1996, Blackwell Science, p 5.

Mayer MM: Complement and complement fixation. In Kabat EA, Mayer MM, editors: *Experimental immunochemistry*, 2, Springfield, Ill, 1961, Charles C Thomas, p 133.

Mayes JT, Schreiber RD, Cooper NR: Development and application of an enzyme-linked immunoabsorbent assay for the quantification of alternative complement pathway activation in human serum, *J Clin Invest* 73:160, 1984.

Mitomo K, Fujita T, Iida K: Functional and antigenic properties of complement receptor type 2, CR2, *J Exp Med* 165:1424, 1987.

Moffitt MC, Frank MM: Complement resistance in microbes, *Springer Semin Immunopathol* 15:327, 1994.

Mold C: Cellular responses to the membrane attack complex. In Volanakis JE, Frank MM, editors: *The human complement system in health and disease*, New York, 1998, Marcel Dekker, p 309.

Mollnes TE: Biocompatibility: complement as mediator of tissue damage and as indicator of incompatibility, *Exp Clin Immunogenet* 14:24, 1997.

Mollnes TE, Jokiranta TS, Truedsson L, et al.: Complement in the 21st century, *Mol Immunol* 44:3838–3849, 2007.

Moore FD, Fearon DT, Austen KF: IgG on mouse erythrocytes augments activation of the human alternative complement pathway by enhancing deposition of C3b, *J Immunol* 126:1805, 1981.

Moreau ME, Garbacki N, Molinaro G, et al.: The kallikrein-kinin system: current and future pharmacological targets, *J Pharmacol Sci* 99:6–38, 2005.

Morgan BP: Clinical complementology: recent progress and future trends, *Eur J Clin Invest* 24:219, 1994.

Morgan BP, Gasque P: Expression of complement in the brain: role in health and disease, *Immunol Today* 17:461, 1996.

Morgan BP, Gasque P: Extrahepatic complement biosynthesis: where, when and why? *Clin Exp Immunol* 107:1, 1997.

Morgan BP, Gasque P, Singhrao S, et al.: The role of complement in disorders of the nervous system, *Immunopharmacology* 38:43, 1997.

Morgan BP, Meri S: Membrane proteins that protect against complement lysis, *Springer Semin Immunopathol* 15:369, 1994.

Nataf S, Davoust N, Ames RS, et al.: Human T cells express the C5a receptor and are chemoattracted to C5a, *J Immunol* 162:4018, 1999.

Niculescu F, Badea T, Rus H: Sublytic C5b-9 induces proliferation of human aortic smooth muscle cells: role of mitogen activated protein kinase and phosphatidylinositol 3-kinase, *Atherosclerosis* 142:47, 1999.

Niculescu F, Rus H, Shin S, et al.: Generation of diacylglycerol and ceramide during homologous complement activation, *J Immunol* 150:214, 1993.

Niculescu F, Rus HG, Vlaicu R: Immunohistochemical localization of C5b-9, S-protein, C3d and apolipoprotein B in human arterial tissues with atherosclerosis, *Atherosclerosis* 65:1, 1987.

Nilsson B, Nilsson Ekdahl K: The tick-over theory revisited: is C3 a contact-activated protein? *Immunobiology* 217:1106–1110, 2012.

Notarangelo L, Casanova JL, Fischer A, et al.: Primary immunodeficiency diseases: an update, *J Allergy Clin Immunol* 114:677–687, 2004.

Ochs HD, Wedgwood RJ, Frank MM, et al.: The role of complement in the induction of antibody responses, *Clin Exp Immunol* 53:208, 1983.

Ochs HD, Wedgwood RJ, Heller SR, et al.: Complement, membrane glycoproteins, and complement receptors: their role in regulation of the immune response, *Clin Immunol Immunopathol* 40:94, 1986.

Ollert MW, Davis K, Bredehorst R, et al.: Classical complement pathway activation on nucleated cells: role of factor H in the control of deposited C3b, *J Immunol* 155:4955, 1995.

O'Neil KM, Ochs HD, Heller SR, et al.: Role of C3 in humoral immunity: defective antibody production in C3-deficient dogs, *J Immunol* 140:1939, 1988.

Onitsuka S, Yamaguchi Y, Tanabe K, et al.: Peritubular capillary deposition of C4d complement fragment in ABO-incompatible renal transplantation with humoral rejection, *Clin Transplant* 13(Suppl 1):33–37, 1999.

Pangburn MK: Alternative pathway of complement, *Methods Enzymol* 162:639, 1988.

Pangburn MK, Müller-Eberhard HJ: The alternative pathway of complement, *Springer Semin Immunopathol* 7:163, 1984.

Pangburn MK, Schreiber RD, Müller-Eberhard HJ: Formation of the initial C3-convertase of the alternative pathway: acquisition of C3b-like activities by spontaneous hydrolysis of the putative thioester in native C3, *J Exp Med* 154:856, 1981.

Peake PW, Sreenstein JD, Pussell BA, et al.: The behaviour of human vitronectin in vivo: effects of complement activation, conformation and phosphorylation, *Clin Exp Immunol* 106:416, 1996.

Pepys MB: Role of complement in the induction of antibody production in vivo, *J Exp Med* 140:126, 1974.

Petersen SV, Thiel S, Jensen L, et al.: An assay for the mannan-binding lectin pathway of complement activation, *J Immunol Methods* 257:107–116, 2001.

Pickering MC, Botto M, Taylor PR, et al.: Systemic lupus erythematosus, complement deficiency, and apoptosis, *Adv Immunol* 76:227–324, 2000.

Pillemer L, Blum L, Lepow IH, et al.: The properdin system and immunity. I. Demonstration and isolation of a new serum protein, properdin, and its role in immune phenomena, *Science* 120:279, 1954.

Pittock SJet al: Eculizumab in aquaporin-4-positive neuromyelitis optica spectrum disorder, *N Engl J Med 15* 381(7):614–625, 2019.

Platt JL: New directions for organ transplantation, *Nature* 392:11, 1998.

Plumb ME, Sodetz JM: Proteins of the membrane attack complex. In Volanakis JE, Frank MM, editors: *The human complement system in health and disease*, New York, 1998, Marcel Dekker, p 119.

Podack ER, Biesecker G, Müller-Eberhard HJ: Membrane attack complex of complement: generation of high affinity phospholipid binding sites by fusion of five hydrophilic plasma proteins, *Proc Natl Acad Sci U S A* 76:897, 1979.

Podack ER, Kolb WP, Müller-Eberhard HJ: The sC5b-7 complex: formation, isolation, properties and subunit composition, *J Immunol* 119:2024, 1977.

Podack ER: Tschopp J: membrane attack by complement, *Mol Immunol* 21:589, 1984.

Prodeus AP, Goerg S, Shen L-M, et al.: A critical role for complement in maintenance of self-tolerance, *Immunity* 9:721, 1998.

Ramm LE, Whitlow MB, Mayer MM: Size of the transmembrane channels produced by complement proteins C5b-8, *J Immunol* 129:1143, 1982.

Rapp HJ, Borsos T, editors: *Molecular basis of complement action*, New York, 1970, Appleton-Century-Crofts.

Reiter Y, Ciobotariu A, Fischelson Z: Sub-lytic complement attack protects tumor cells from lytic doses of antibody and complement, *Eur J Immunol* 22:1207, 1992.

Ricklin D, Lambris JD: Complement-targeted therapeutics, *Nat Biotechnol* 25:1265–1275, 2007.

Ricklin D, Mastellos DC, Reis ES, Lambris JD: The renaissance of complement therapeutics, *Nat Rev Nephrol14*(1)26–47, 2018.

Ross GD, Yount WJ, Walport MJ, et al.: Disease-associated loss of erythrocyte complement receptors (CR1, C3b receptors) in patients with systemic lupus erythematosus and other diseases involving autoantibodies and/or complement activation, *J Immunol* 135:2005, 1985.

Rosse WF: Paroxysmal nocturnal hemoglobinuria and complement. In Volanakis JE, Frank MM, editors: *The human complement system in health and disease*, New York, 1998, Marcel Dekker, p 481.

Sánchez-Corral P, González-Rubio C, Rodríguez de Córdoba S, et al.: Functional analysis in serum from atypical hemolytic uremic syndrome patients reveals impaired protection of host cells associated with mutations in factor H, *J Mol Immunol* 41:81–84, 2004.

Sanders ME, Koski CL, Robbins D, et al.: Activated terminal complement in cerebrospinal fluid in Guillain-Barré syndrome and multiple sclerosis, *J Immunol* 136:4456, 1986.

Sanders ME, Schmetz MA, Hammer CH, et al.: Quantitation of activation of the human terminal complement pathway by ELISA, *J Immunol Methods* 85:245, 1985.

Schmiedt W, Kinscherf R, Deigner H-P, et al.: Complement C6 deficiency protects against diet-induced atherosclerosis in rabbits, *Arterioscler Thromb Vasc Biol* 18:1790, 1998.

Schneider PM, Rittner C: Complement genetics. In Dodds AW, Sim RB, editors: *Complement: a practical approach*, New York, 1997, Oxford University Press, p 165.

Schneider PM, Würzner R: Complement genetics: biological implications of polymorphism and deficiencies, *Immunol Today* 20:2, 1999.

Schweinle JE, Ezekowitz RAB, Tenner AJ, et al.: Human mannose-binding protein activates the alternative complement pathway and enhances serum bactericidal activity on a mannose-rich isolate of *Salmonella*, *J Clin Invest* 84:1821, 1989.

Scully M, et al.: International Working Group for Thrombotic Thrombocytopenic Purpura. Consensus on the standardization of terminology in thrombotic thrombocytopenic purpura and related thrombotic microangiopathies, *J Thromb Haemost15*(2)312–322, 2017.

Seelen MA, Roos A, Daha MR: Role of complement in innate and autoimmunity, *J Nephrol* 18:642–653, 2005.

Seifert PS, Hugo F, Hansson GK, et al.: Prelesional complement activation in experimental atherosclerosis: terminal C5b-9 complement deposition coincides with cholesterol accumulation in the aortic intima of hypercholesterolemic rabbits, *Lab Invest* 60:747, 1989.

Seya T, Atkinson JP: Functional properties of membrane cofactor protein of complement, *Biochem J* 264:581, 1989.

Seya T, Turner JR, Atkinson JP: Purification and characterization of a membrane protein (gp45–70) that is a cofactor for cleavage of C3b and C4b, *J Exp Med* 163:837, 1986.

Shin ML, Rus H, Niculescu F: Complement system in central nervous system disorders. In Volanakis JE, Frank MM, editors: *The human complement system in health and disease*, New York, 1998, Marcel Dekker, p 499.

Sims PJ, Wiedmer T: Induction of cellular procoagulant activity by the membrane attack complex of complement, *Semin Cell Biol* 6:275, 1995.

Stanilova SA, Slavov ES: Comparative study of circulating immune complexes quantity detection by three assays—CIF-ELISA, C1q-ELISA and anti-C3 ELISA, *J Immunol Methods* 253:13–21, 2001.

Stoiber H, Pruenster M, Ammann CG, et al.: Complement-opsonized HIV: the free rider on its way to infection, *Mol Immunol* 42:153–160, 2005.

Su HR: S-protein/vitronectin interaction with the C5b and the C8 of the complement membrane attack complex, *Int Arch Allergy Immunol* 110:314, 1996.

Suankratay C, Zhang X-H, Zhang Y, et al.: Requirement for the alternative pathway as well as C4 and C2 in complement-dependent hemolysis via the lectin pathway, *J Immunol* 160:3006, 1998.

Sumiya M, Summerfield JA: The role of collectins in host defense, *Semin Liver Dis* 17:311, 1997.

Tedesco F, Pausa M, Nardon E: The cytolytically inactive terminal complement complex activates endothelial cells to express adhesion molecules and tissue factor procoagulant activity, *J Exp Med* 185:1619–1627, 1997.

Tegla CA, Cudrici C, Patel S, et al.: Membrane attack by complement: the assembly and biology of terminal complement complexes, *Immunol Res* 51:45–60, 2011.

Tenner AJ, Robinson SL, Ezekowitz RAB: Mannose binding protein (MBP) enhances mononuclear phagocyte function via a receptor that contains the 126,000 M® component of the C1q receptor, *Immunity* 3:485, 1995.

Terai I, Kobayashi K, Matsushita M, et al.: α 2-Macroglobulin binds to and inhibits mannose-binding protein–associated serine protease, *Int Immunol* 7:1579–1584, 1995.

Teixeira JE, Martinez R, Camara LM, et al.: Expression of complement receptor type 1 (CR1) on erythrocytes of paracoccidiodomycosis patients, *Mycopathology* 152:125–133, 2001.

Thiel S: Complement activating soluble pattern recognition molecules with collagen-like regions, mannan-binding lectin, ficolins and associated proteins, *Mol Immunol* 44:3875–3888, 2007.

Thurman JM, Holers VM: The central role of the alternative complement pathway in human disease, *J Immunol* 176:1305–1310, 2006.

Thurman JM: Complement in kidney disease: core curriculum 2015, *Am J Kidney Dis*65(1):156–168, 2015.

Tomlinson S, Nussenzweig V: Human alternative complement pathway-mediated lysis of rabbit erythrocytes is enhanced by natural anti-gal α 1–3gal antibodies, *J Immunol* 159:5606, 1997.

Torzewski J, Bowyer DE, Waltenberger J, et al.: Processes in atherogenesis: complement activation, *Atherosclerosis* 132:131, 1997.

Turner MW: Mannose-binding lectin: the pluripotent molecule of the innate immune system, *Immunol Today* 17:532, 1996.

Valdimarsson H, Stefansson M, Vikingsdottir T, et al.: Reconstitution of opsonizing activity by infusion of mannan-binding lectin (MBL) to MBL-deficient humans, *Scand J Immunol* 48:116, 1998.

Van de Wetering JK, van Golde LM, Batenburg JJ: Collectins: players of the innate immune system, *Eur J Biochem* 271:1229–1249, 2004.

Volanakis JE: Structure, molecular genetics, and function of complement control proteins: an update, *Year Immunol* 3:275, 1988.

Volanakis JE: Overview of the complement system. In Volanakis JE, Frank MM, editors: *The human complement system in health and disease*, New York, 1998, Marcel Dekker, p 9.

Volanakis JE, Narayana SV: Complement factor D, a novel serine protease, *Protein Sci* 5:553, 1996.

Vorup-Jensen T, Carman CV, Shimaoka M, Schuck P, Svitel J, Springer TA: Exposure of acidic residues as a danger signal for recognition of fibrinogen and other macromolecules by integrin $\alpha X\beta_2$, *Proc Natl Acad Sci USA* 102:1614–1619, 2005.

Vorup-Jensen T, Jensenius JC, Thiel S: MASP-2, the C3 convertase generating protease of the MBLectin complement activating pathway, *Immunobiology* 199:348, 1998.

Ward PA: Recruitment of inflammatory cells into lung: roles of cytokines, adhesion molecules and complement, *J Lab Clin Med* 129:400, 1997.

West C: Complement and glomerular disease. In Volanakis JE, Frank MM, editors: *The human complement system in health and disease*, New York, 1998, Marcel Dekker, p 571.

Whaley K, editor: *Methods in complement for clinical immunologists*, Edinburgh, 1985, Churchill Livingstone.

World Health Organization: Nomenclature of complement, *Bull WHO* 39:934, 1968.

Woodruff TM, Nandakumar KS, Tedesco F: Inhibiting the C5-C5a receptor axis, *Mol Immunol* 48:1631–1642, 2011.

Würzner R, Mollnes TE, Morgan BP: Immunochemical assays for complement components. In Johnstone AP, Turner MW, editors: *Immunochemistry 2: a practical approach*, Oxford, 1997, Oxford University Press, p 197.

Wyatt SK, Witt T, Barbaro N, et al.: Enhanced classical complement pathway activation and altered phagocytosis signaling molecules in human epilepsy, *Exper Neurology* 295:184–193, 2017.

Yancey KB, Lawley TJ: Role of complement in diseased and normal skin. In Volanakis JE, Frank MM, editors: *The human complement system in health and disease*, New York, 1998, Marcel Dekker, p 597.

Zhou W: The new face of anaphylatoxins in immune regulation, *Immunology* 217:225–234, 2012.

Zubler RH, Lambert PH: The 125I-C1q binding test for the detection of soluble immune complexes. In Bloom BR, David JR, editors: *In vitro methods in cell-mediated and tumor immunity*, New York, 1976, Academic Press, p 565.

CHAPTER 49

MEDIATORS OF INFLAMMATION: CYTOKINES AND ADHESION MOLECULES

Stefanie Krick

CYTOKINES, 984
Cytokine Family, 984
Cytokine Receptors, 984
Cytokines in Disease States, 986
Cytokine Assays, 986
Clinically Useful Cytokine-Based Therapeutics, 986

CHEMOKINE AND CHEMOKINE RECEPTOR FAMILY, 988
Clinically Useful Chemokine-Based Therapeutics, 989
Atypical Chemokine Receptors, 990
Chemokine Receptor Homologues, 992

CELL ADHESION MOLECULES, 992
Integrins, 992
Selectins, 993

LEUKOCYTE EXTRAVASATION, 994

PERSPECTIVES, 995

SELECTED REFERENCES, 995

KEY POINTS

- Cytokines are soluble proteins released by cells to facilitate communication and interaction between cells, to modulate the immune response, to direct cell differentiation, and to orchestrate associated inflammatory and reparative activities.
- Adhesion molecules are complex cell surface glycoproteins that mediate cellular interactions, such as cell migration during embryogenesis, wound healing, and the inflammatory response.

CYTOKINES

Cytokines coordinate multiple biological processes, including embryonic development, nonspecific (innate) and specific (adaptive) immune responses, inflammatory responses, hematopoiesis, cellular migration, activation, development and maturation, bone remodeling, regulation of metabolism, disease pathogenesis, and aging. Cytokines can act at the picomolar to femtomolar range and are redundant and pleiotropic with synergistic or antagonistic effects: individual cytokines are able to elicit several distinct types of responses, and multiple cytokines have similar physiologic roles (Moraga et al., 2014). They are released by many cell types and may act in an autocrine, paracrine, or, in some instances, endocrine action (Zhang et al., 2007). The term *cytokine* encompasses lymphokines, monokines, interleukins, colony-stimulating factors (CSFs), interferons (IFNs), the tumor necrosis factor (TNF) family, the chemokine family, and adipokines (adipocytokines).

Cytokines are produced by various cell types, predominantly by T helper cells and macrophages, but also by other immune cells, vascular cells, epithelial cells, and other cell types. Secretion and binding of cytokines to specific cell surface receptors creates a web of communication between cells. Cytokine signals are received at the cell surface not only as single messages but also in complex, subtle synergistic and antagonistic combinations. Target cells display surface cytokine receptors, arrayed as "antennae." Using these receptors, cells sample, process, and respond to combinations of soluble and substrate-bound cytokines in a manner dependent on surface receptor density and state of activation.

CYTOKINE FAMILY

The cytokine family of proteins is remarkably extensive: more than 100 known members have been identified. Consequently, there are a number of overlapping nomenclature and classification systems for cytokines based on biological function, receptor binding properties, originating cell type, and common structural motifs (Brocker et al., 2010). Cytokine families based on cell family and function include the TNF, IL, and IFN families; CSFs, growth factors, and adipokines (Table 49.1). Each member of the TNF family is the product of a separate gene. However, there are considerable overlaps in biological properties of TNF proteins (Dinarello, 2007). The TNF/TNF receptor superfamily mediates cellular differentiation, survival, and death and coordinates organ development (Baud'huin et al., 2013). Within the IL family, subfamilies are the IL-1 family, with members including IL-1α, IL-1β, IL-18, IL-33, IL-36, IL-37, and IL-38; the common γ chain cytokine family including IL-2, IL-4, IL-7, IL-9, IL-15 and IL-21; the IL-6 family, including IL-6, leukemia inhibitory factor, IL-11, oncostatin, ciliary neurotropic factor, and cardiotropin I; and the IL-10 family, including IL-10, IL-19, IL-20, IL-22, IL-23, IL-26, IL-28A and IL-28B and IL-29 (IFN-λ); the IL-12 family (IL-12, IL-23, IL-27 and IL-35); cytokines of the type 2 immune response (IL-5, IL-13, IL-25, IL-31 and TSLP) and the IL-17 family (Akdis et al., 2016). The CSFs are IL-3, granulocyte-CSF (G-CSF), granulocyte-macrophage-CSF (GM-CSF), and macrophage-CSF. Similar to the TNF family, CSFs have overlapping functions, in the case of CSFs, initiation of cell division in responding cells, but are distinct gene products with specific receptors (Metcalf, 2010). Other cytokines, including IL-1β, IL-2, IL-4, IL-6, IL-7, IL-15, fibroblast growth factors (FGFs), transforming growth factors-β (TGFs-β), TGF-α, epidermal growth factor (EGF), platelet-derived growth factor (PDGF), erythropoietin, insulin-like growth factor-1 (IGF-1), IGF-2, TNF-α, IFN-γ, nerve growth factor (NGF), and brain-derived neurotrophic factor (BDNF), also function as growth factors (Akdis et al., 2011). IFN cytokines such as IFN-α and IFN-β promote innate and adaptive immune responses (Ivashkiv & Donlin, 2014). Angiogenic cytokines include vascular endothelial growth factor (VEGF), IL-1, IL-6, and IL-8. Adipokines mediate communication between adipose tissue and other key metabolic organs (liver, muscle, pancreas, and central nervous system) (Cao, 2014). The adipokine family includes all products of cells localized in white adipose tissue. The best characterized of these are leptin (regulates body weight, proinflammatory), adiponectin (anti-inflammatory), resistin (insulin resistance), and secreted frizzled-related protein 5 (Sfrp5; anti-inflammatory, plays role in adipogenesis), as well as vaspin, visfatin, apelin, serum amyloid A, angiotensinogen, omentin, chemerin, zinc-α_2-glycoprotein (ZAG), IL-6, and TNF-α (Ouchi et al., 2011; Leal Vde & Mafra, 2013). The osteoclast-activating cytokine receptor activator of nuclear factor-κB ligand (RANKL) is a member of the TNF superfamily. RANKL binds to its receptor RANK expressed on the membranes of osteoclast progenitors and induces osteoclast differentiation and activation. Binding of RANKL to the decoy receptor osteoprotegerin (OPG) interrupts osteoclastogenesis and prevents excessive bone resorption (Gruber, 2010). The extensive chemokine family is described separately later in this chapter.

CYTOKINE RECEPTORS

Clinically, it may be useful to also group cytokines according to the structural homology of their receptors, as some drugs target cytokine-receptor interactions. Receptor homology partially accounts for the cytokine functional pleiotropy and redundancy described earlier. Cytokine signaling is initiated when cytokines bind the extracellular domains of their transmembrane protein receptors, which leads to activation of cytosolic proteins that are responsible for regulating gene transcription in the nucleus and thereby controlling cell proliferation, differentiation, maturation, and survival (Wang et al., 2009).

There are five major cytokine receptor types (Table 49.2): (1) IL-1 receptors characterized by three immunoglobulin (Ig)-like domains; (2) TNF receptors (TNFRs), whose members share a conserved cysteine-rich common extracellular binding domain; (3) class I cytokine receptors (or

TABLE 49.1

Cytokines by Type and Function

Cytokine Type	Cytokines	Actions
Adipokine (cytokine released from adipocytes)	IL-1α, TNF-α, IL-6, leptin, adiponectin, resistin, others	Proinflammatory, proatherogenic, anti-inflammatory
Angiogenic	VEGF, IL-1, IL-6, IL-8	Neovascularization, prometastatic
Anti-inflammatory	IL-10, IL-13, TGF-β, IL-22, IL-1Ra, IFN-α/β	Upregulate inflammatory genes, depress cytokine-mediated lethality, downregulate autoimmune disease
Chemokine	IL-8, MCP-1, MIP-1α	Increase cell migration and activation
Colony-stimulating	IL-3, IL-7, G-CSF, GM-CSF, M-CSF, erythropoietin	Hematopoiesis, proinflammatory, anti-inflammatory
gp130 signaling pathway	IL-6, IL-11, others	Growth factors, B-cell activation, acute-phase response
Lymphocyte growth	IL-2, IL-4, IL-7, IL-15	Clonal expansion, Th1/Th2/Th17 regulation
Mesenchymal tissue growth	FGF, TGF-β, others	Fibrosis, prometastatic
Nerve growth	NGF, BNDF	Nerve and Schwann cell growth, B-cell activation
Osteoclast-activating	RANKL	Bone resorption, immune stimulation
Proinflammatory	IL-1α, IL-1β, TNF-α, IL-6, IL-12, IL-18, IL-23, MIF, IL-32, IL-33, CD40L	Upregulate inflammatory mediators and innate immune responses
Th1	IFN-γ, IL-12, IL-18	Upregulate Th1 response, clonal expansion of CTL
Th2	IL-4, IL-5, IL-18, IL-25, IL-33	Upregulate Th2 response, increase antibody production
Th17	IL-17, IL-23, IFN-γ	Upregulate Th17 response, autoimmune response
Type I IFN	IFN-α, IFN-β	Antiviral, upregulate MHC class I, antiangiogenic, anti-inflammatory
Type II IFN	IFN-γ	Macrophage activation, upregulate MHC class II

BNDF, Brain-derived neurotrophic factor; *CSF,* colony-stimulating factor; *CTL,* cytotoxic T lymphocyte; *IFN,* interferon; *IL,* interleukin; *MCP-1,* monocyte chemotactic protein-1; *MHC,* major histocompatibility complex; *MIF,* macrophage migration inhibitory factor; *MIP-1α,* macrophage inhibiting protein-1α; *NGF,* nerve growth factor; *RANKL,* receptor activator of NFκB.

TABLE 49.2

Selected Cytokines Grouped by Receptor Class

Receptor Class	Structure and Signaling Pathway	Example Receptors
IL-1; immunoglobulin superfamily	These receptors contain paired antiparallel β sheets forming the sandwich-like structure known as the *Ig-fold* seen in antibodies.	IL-1, IL-18, SCF (*c-kit*), M-CSF
Tumor necrosis factor	These receptors share a cysteine-rich common extracellular domain and activate the NFκB pathway.	TNF-α, TNF-β, NGF, CD40, CD27, CD30, CD120
Type I (hemopoietin receptors)	These transmembrane protein receptors have paired high-affinity α and β chains and share a common extracellular motif (WSXWS); they signal the nucleus through the JAK/STAT, RAS-RAF-MAP kinase, and PI3 pathways.	IL-2, IL-3, IL-4, IL-5, IL-6, IL-7, IL-9, IL-11, IL-12, IL-15, IL-21, GM-CSF, EPO, PRL, GH, G-CSF, LIF
Type II	These transmembrane protein receptors are similar to type I, but lack the WSXWS motif while having conserved cysteine pairs in their extracellular domain. They signal the nucleus through the JAK/STAT, RAS-RAF-MAP kinase, and PI3 pathways.	IFN-α, IFN-γ, IFN-β, IL-10

CSF, Colony-stimulating factor; *IFN,* interferon; *IL,* interleukin; *JAK,* Janus kinase; *STAT,* signal transducers and activation of transcription; *TNF,* tumor necrosis factor.

hematopoietin receptors), which lack intrinsic tyrosine kinase activity; (4) class II cytokine receptors, which also lack intrinsic tyrosine kinase activity; and (5) chemokine receptors (discussed separately later in this chapter).

Class I and class II receptors share a conserved extracellular region, the cytokine receptor homology domain (CHD), but are classified based on the CHD divergence. Class I receptors have two pairs of cysteines linked through a disulfide bond and a C-terminal WSXWS motif, whereas class II receptors also have two pairs of cysteines but lack the WSXWS motif (Puigserver, 2018).

Lacking tyrosine kinase activity, the class I and class II receptors communicate with the Janus kinase (JAK) family of tyrosine kinases and one member of the TYK kinase family. Cytokine-receptor interaction results in the phosphorylation and activation of the appropriate JAK/TYK kinases and phosphorylation of the intracellular domains of the receptors. Phosphorylated tyrosine residues in the receptors bind members of the STAT (signal transducers and activation of transcription) family of cytoplasmic transcription proteins, leading to phosphorylation and dissociation from their receptor complexes. Once dissociated, the STAT proteins dimerize and translocate into the cell nucleus, where they bind DNA recognition sequences and function as transcription factors.

Class I receptors also make use of the RAS-RAF-MAP kinase and PI3 pathways to initiate gene transcription. Subfamilies of the class I receptors include the G-protein gp130, common gamma chain (γ_c, or CD132), and common beta chain (β_c, or CD131) receptors (Wang et al., 2009). Cytokines such as IL-6 and IL-11, which share the G-protein–coupled seven-transmembrane receptors, signal via the gp130 signal-transducing molecule. Cytokines that utilize the γ_c receptors signal via JAK3 kinase. The β_c receptors recognize IL-3, IL-5, and GM-CSF and initiate signaling via JAK2 kinase (Wang et al., 2009). Class II cytokine receptors recognize the IFN cytokines, IL-10, and others. Proinflammatory IFNs signal predominantly through STAT1, whereas the anti-inflammatory cytokine IL-10 signals primarily through STAT3. Therefore, STAT1 and STAT3 play opposing roles in cell survival and proliferation (Regis et al., 2008). The IL-1 receptor family consists of four receptor complexes, two decoy receptors, and two negative regulators. Signaling occurs via the MyD88 adaptor (Garlanda et al., 2013). The TNFR family consists of 29 members including TNFR1, TNFR2, OPG, and RANK (Kumar et al., 2013) and are key regulators of the immune response. Some members of the TNFR family, such as TNFR1, contain a death domain, and ligand binding initiates processes leading to cell death (Kumar et al., 2013).

The IL17 receptor family consists of five subunits, including IL-17RA-D with IL-17RA serving as a co-receptor, which is used by several of the six IL-17 family ligands (IL-17A-F) (Amatya et al., 2017). The IL17R family all have a conserved cytoplasmic domain, which is known as the SEFIR domain and related to the Toll/IL-R′ (TIR) domain. Connection to IκB kinase and stress-activated protein kinases (CIKS), also known as Act1, is a cytosolic adaptor protein, which is required for the activation of IL-17 signaling (Novatchkova et al., 2003; Chang et al., 2006). The cytoplasmic tail of IL17RA also has a distal domain that negatively regulates signaling, whereas the extracellular regions contain two fibronectin III–like domains, which mediate ligand binding and protein–protein interactions (Shen et al., 2009; Maitra et al., 2007). IL-17 has been shown to activate

NF-κb signaling, leading to secretion of proinflammatory cytokines (Yao et al., 1995; Fossiez et al., 1996). Furthermore, IL-17 can regulate tissue-specific genes with diverse physiologic functions, such as occluding in gut epithelia, mucin 1, kallikrein 1, RANKL, and osteoprotegerin (Ramani et al., 2016; Gaffen et al., 2008).

In addition, endocytosis is a key mechanism involved in cytokine receptor signaling. Recent reports have demonstrated that PI3K can control cytokine receptor endocytosis through both kinase activity-dependent and -independent mechanisms (Chen et al., 2017).

In summary, cytokines are produced, released, and recognized by many different cell types. The extent of influence of these soluble proteins can be long range (systemic) when released into the circulation or their action may be highly localized, producing effects only on the cell releasing them or on its neighboring cells, and downstream signaling is dependent on the cytokine receptor class and structure as well as cell and tissue type.

CYTOKINES IN DISEASE STATES

Under homeostatic conditions, proinflammatory cytokine responses necessary for host immune defense are balanced by anti-inflammatory responses to protect the host from injury that results from unregulated inflammation. When the system is continually challenged, as in persistent viral and bacterial infections or immune dysregulation in autoimmune diseases, a chronic proinflammatory response occurs. For example, dysregulation of IL-1 cytokine signaling is associated with inflammatory bowel disease (IBD), rheumatoid arthritis (RA), and psoriasis (Gu et al., 2013). Aberrations in the IL-6/IL-12 cytokines likewise result in IBD and RA, as well as systemic lupus erythematosus (SLE), asthma, and Castleman disease (Brocker et al., 2010; Akdis et al., 2011). Dysregulation of the IFN response is associated with SLE, Sjögren syndrome, systemic sclerosis, myositis, and RA (Ivashkiv & Donlin, 2014). IL-17A has been linked to many autoimmune disorders, including IBD, RA, and multiple sclerosis (MS), as well as certain cancers (Brocker et al., 2010). IL-18 is linked to RA and Crohn disease (CD) (Akdis et al., 2011). IL-5 and IL-13 play a role in allergic asthma. IL-7, IL-9, and other inflammatory cytokines are likewise believed to play causative roles in autoimmune diseases, whereas the anti-inflammatory cytokine IL-10 appears to play a protective role (Akdis et al., 2011). Patients with chronic infections and/or autoimmune diseases also have an increased risk for concomitant osteoporosis, as RANKL expression—and, therefore, bone resorption—is upregulated by proinflammatory cytokines, including IL-1, IL-6, IL-11, and IL-17, and TNF-α (Nakashima & Takayanagi, 2011). Even in acute inflammatory diseases such as sepsis, there is dysregulation of the inflammatory cytokine network, including IL-6, IL-8, and IL-10 (Matsumoto et al., 2018).

Dysfunction of cytokine receptors also contributes to disease pathologies. Mutations that later affect binding/function of the γ_c receptors or their associated JAK3 kinase can significantly limit the activity of the cytokines that signal through this pathway and can lead to severe combined immunodeficiency (SCID) diseases (Wang et al., 2009). Mutations that impact the function of JAK2 kinase are correlated with hematologic malignancies, particularly myeloproliferative neoplasms (Vainchenker et al., 2008). Overexpression or mutations that impact function of receptor tyrosine kinases (RTKs) are linked to cancers, atherosclerosis, bone disorders, and diabetes (Kazi et al., 2014). The IL-20R cytokines, including IL-19, IL-20, and IL-24, all signal through the IL-20RA/IL-20RB receptor complex, which has been suggested to be involved in regulating autoimmune diseases such as RA, IBD, and MS (Chen et al., 2018; Kragstrup et al., 2017; Andoh et al., 2009; Muls et al., 2017).

CYTOKINE ASSAYS

Because of their biological importance, clinical laboratory detection and measurement of cytokines is becoming more common. Bioassays are usually considered to be the gold standard for detecting cytokine activity, but they are often time-consuming, costly, and unmanageable in the hospital laboratory. ELISA kits are widely available for many of the cytokines described earlier; for example, IL-1α, IL-1β, IL-4, IL-5, IL-6, IL-10, IFN-γ, and TNF-α can be measured individually clinically. In addition, panels or multiplex assays can be used to measure sets of cytokines in a single assay, which holds great promise due to low volume requirements and high sensitivity. A study comparing multiple testing sites and four high-sensitivity cytokine multiplex assays, including both Luminex and electrochemiluminescence platforms, suggests that these assays vary in their ability to measure serum and/or plasma cytokines sufficiently reproducible, but may be useful in longitudinal studies looking at trends and not absolute changes in cytokine levels (Crabb Breen et al., 2011).

CLINICALLY USEFUL CYTOKINE-BASED THERAPEUTICS

Because of the profound biological effects of these powerful proteins, attempts at mass-producing and therapeutically administering cytokines are ongoing. Cytokines used therapeutically include G-CSF and GM-CSF, which are used to treat bone marrow suppression associated with radiation, chemotherapy, and transplantation; GM-CSF, used to treat Crohn disease (CD); erythropoietin (EPO), used therapeutically to treat anemia and bone marrow failure; IFN-α, to treat hepatitis B and C; and IFN-β, used to treat MS (Dinarello, 2007). Other promising therapeutic approaches include manipulating cytokine activity through cloning and producing recombinant forms of cytokines or their receptor antagonists; delivering cytokines by gene and antisense nucleotide insertion through viral and nonviral vectors (commonly, adenovirus or retrovirus vectors, or nonviral DNA plasmid vectors); vaccinating patients against their own (autologous) cytokines (Cutler & Brombache, 2005); raising cytokine-blocking monoclonal antibodies; and genetically fusing molecules of interest, such as an enzyme, ligand, peptide, or extracellular domain of a surface receptor, to the Fc portion of human IgG1 or albumin (Table 49.3). This fusion approach has the advantage of conferring increased half-life and stability on the fusion product. In some instances, multiple ligands may be sequentially fused to a single gene to create a trap for the target by trapping or binding two target molecules on a single fusion protein, possibly as a result of the trap's high binding affinities (Huang, 2009).

Unfortunately, many disease states are complex conditions driven by an intricate interplay of numerous cytokines. A single "magic bullet" aimed at an individual cytokine or receptor for treating these conditions is unlikely to arise in the very near future. In addition, some cytokines have both pro- and anti-inflammatory effects; targeting these cytokines can result in significant adverse effects. IFN-γ drives several autoimmune diseases but is essential for defense against multiple intracellular microorganisms. IL-2 is required for generation of cytotoxic T cells and forms the basis for several types of vaccines but also drives graft-versus-host disease and limits the success of bone marrow transplantation (Dinarello, 2007). For conditions in which dysregulation of a single cytokine is largely at fault, the challenge is less daunting. Defects in cytokine-signaling pathways resulting from genetic mutations that inactivate JAK/STAT molecules have provided the impetus for the generation of therapeutics aimed at JAK inhibition. Ruxolitinib, a JAK1 and JAK2 inhibitor, is approved for treatment of polycythemia vera and myelofibrosis. Tofacitinib is approved for treatment of RA. Other individual cytokine-related therapeutic agents have also entered routine medical practice in recent years (see Table 49.3). For example, denosumab, a RANKL-neutralizing antibody, is approved for treatment of osteoporosis, RA, and tumor-related osteolysis. Other examples of cytokine-related therapeutic agents include anakinra, an IL-1 receptor antagonist; aldesleukin, a recombinant IL-2; oprelvekin, a recombinant IL-11; recombinant IFNα-2a (Roferon-A); filgrastim (Neupogen), a recombinant G-CSF; and sargramostim (Leukine), a recombinant GM-CSF. Treatment for many chronic inflammatory diseases involves targeted inhibition of TNF-α. TNF-α inhibitors such as etanercept (Enbrel), a soluble TNF-α receptor, are approved for treatment of psoriasis, psoriatic arthritis, CD, ulcerative colitis, ankylosing spondylitis, and juvenile arthritis. However, further demonstrating the complexity of the cytokine system, MS worsens with TNF-α inhibition (Schett et al., 2013). Many other cytokine- and cytokine receptor–based therapeutic agents are currently being evaluated in clinical trials. For example, adiponectin enhances insulin action and may have anti-atherogenic and anti-inflammatory properties. Therapeutic strategies to increase adiponectin levels and receptor activities are being investigated as treatments for obesity-induced inflammation and insulin resistance (Cao, 2014).

Furthermore, cytokine-based therapies are frequently used in asthma therapy, with some of the results being promising. Cytokine antagonists are monoclonal antibodies that are used only for certain subtypes of asthma otherwise refractory to conventional treatment strategies. Anti-IL-5 therapies include mepolizumab, reslizumab, and benralizumab, which have shown a reduction in asthma exacerbation rate and some improvement in lung function (Ortega et al., 2014; Castro et al., 2015; FitzGerald et al., 2016; Bleeckeret al., 2016). Anti-IL-13 therapies include tralokinumab and lebrikizumab, which have not shown consistent beneficial results (Hanania et al., 2016). Dupilumab is a fully human monoclonal antibody to the IL-4Rα subunit, which is a receptor complex that is activated by both IL-4 and IL-13, and used in asthma, atopic dermatitis and chronic sinusitis (Beck et al., 2014; Thaci et al., 2016; Bachert et al., 2016). Other anti-cytokine targets in asthma therapy are emergent but still require thorough

TABLE 49.3

Selected Engineered Therapeutic Agents

Class	Generic Name	Agent/Action	Therapeutic Indication(s)
Cytokine			
	Aldesleukin (Proleukin)	Recombinant IL-2, binds and activates IL-2R	HIV, RCC, melanoma
	IFNβ-1a (Avonex)	Recombinant IFNβ-1a, anti-inflammatory cytokine	Relapsing MS
	IL-7 (CYT107)	Recombinant IL-7, modulates expansion of $CD4^+$ T cells	HIV, viral hepatitis, cancer
	IFNγ-1b (Actimmune)	Recombinant IFNγ-1b, stimulates immune response	Chronic granulomatous disease, severe malignant osteopetrosis
	IFNα-2a (Roferon-A)	Recombinant IFNα-2a, stimulates immune response	Leukemias, melanoma, lymphoma, sarcomas, viral hepatitis
	IFNα-2b (Intron A)	Recombinant IFNα-2b, stimulates immune response	Leukemias, melanoma, lymphoma, sarcomas, viral hepatitis
	Erythropoietin (Procrit, Epogen, Aranesp)	Recombinant erythropoietin, stimulates production of red blood cells	Anemia due to kidney failure or chemotherapy
	Filgrastim (Neupogen)	Recombinant G-CSF, stimulates production of granulocytes	Chemotherapy-related neutropenia
	Lenograstim (Neutrogin)	Recombinant G-CSF, stimulates production of granulocytes	Chemotherapy-related neutropenia
	Sargramostim (Leukine)	Recombinant GM-CSF, stimulates bone marrow function and modulates hematopoiesis	Bone marrow stem cell transplantation, HIV, myelodysplastic syndrome, aplastic anemia, leukemia
Anticytokine Antibody			
	Adalimumab (Humira)	Recombinant humanized anti–TNF-α IgG1 mAb, binds and inhibits TNF-α	RA, CD, PA, AS
	Infliximab (Remicade)	Chimeric (75% human/25% mouse) IgG1 mAb, binds TNF-α	RA, CD, AS
	Bevacizumab (Avastin)	Recombinant humanized anti–VEGF-A mAb, inhibits angiogenesis	Colorectal and non–small cell carcinoma
	Certolizumab (Cimzia)	Recombinant, humanized antibody to a Fab′ fragment, with specificity for TNF-α conjugated to an approximately 40-kDa polyethylene glycol, binds both soluble and membrane-bound TNF-α, inhibiting TNF-α activity	RA, CD, PA, AS
	Golimumab (Simponi)	Fully human IgG1κ anti-TNFα mAb	RA, arthritis, ALS
	Siltuximab (Sylvant)	Chimeric anti-IL-6 mAb	Multicentric Castleman disease (HIV-negative, HHV-8 negative)
	Denosumab (Xgeva)	RANKL neutralizing antibody	Osteoporosis, RA, tumor-related osteolysis
	Mepolizumab (Nucala), Reslizumab (Cinqair), Benralizumab (Fasenra)	Anti-IL-5 antibodies	Severe allergic asthma
	Tralokinumab, lebrikizumab (TNX-650)	Humanized anti-IL-13 antibodies	Atopic dermatitis, asthma, refractory Hodgkin lymphoma
Small-Molecule Antagonist			
	Thalidomide	VEGF and TNF mRNA inhibitor	ENL, MM, RCC
	AP12009	TGF-β_2–blocking antisense oligonucleotide	High-grade glioma
	Tofacitinib	JAK3 pathway inhibitor	RA
Cytokine Receptor Antagonist			
	Anakinra (Kineret)	Recombinant IL-1Rα antagonist, competitively inhibits binding of IL-1α to its receptor	RA
	Tocilizumab (Actemra)	Recombinant humanized IL-6R mAb, acts as an immunosuppressant	RA
	Daclizumab (Zenapax)	Recombinant humanized IL-2Rα chain mAb, binds IL-2Rα (CD25) on T cells to prevent allograft rejection	Renal transplant
	Oprelvekin (Neumega)	Recombinant IL-11, stimulates stem cell and megakaryocyte progenitor growth	Chemotherapy-related thrombocytopenia
	Trastuzumab (Herceptin)	Recombinant humanized mAb, binds Her2/neu receptor overexpressed on some carcinomas; inhibits angiogenesis	Breast carcinoma
	Basiliximab (Simulect)	Recombinant chimeric mouse-human mAb, IL-2 receptor antagonist, immunosuppressant	Transplantation rejection
	Tocilizumab (Actemra, RoActemra)	Humanized anti-IL-6 receptor mAb that binds soluble and membrane-bound IL-6 receptor, blocks IL-6 proinflammatory responses	RA
	Ustekinumab (Stelara)	Human Anti-IL-12 and IL-23 mAb, blocks IL-12 and IL-23 proinflammatory responses	Plaque psoriasis, PA

Continued

TABLE 49.3
Selected Engineered Therapeutic Agents—cont'd

Class	Generic Name	Agent/Action	Therapeutic Indication(s)
	Dupilumab	Human monoclonal anti-IL-4Rα antibody	Asthma, atopic dermatitis, chronic sinusitis
Fusion Protein			
	Etanercept (Enbrel)	Soluble TNF-αRII fused to human IgG1 Fc fragment; neutralizes membrane-bound and soluble forms of TNF-α	RA, AS, JRA, PA
	NBI-3001	Recombinant IL-4–*Pseudomonas aeruginosa* exotoxin fusion protein	Malignant high-grade gliomas
	Alefacept (Amevive)	LFA-3 fused to Fc domain IgG1, binds CD2 to inhibit T-cell activation	PA
	L19-IL	Recombinant IL-2 fused to human single-chain F_v antibody fragment, L19 binds fibronectin, while IL-2 locally activates natural killer cells and macrophages	Blocks tumor cell proliferation
	Rilonacept (IL-1 Trap)	Dimeric fusion protein of the ligand-binding domains of IL-1 type I receptor and IL-1 receptor accessory protein fused to human IgG_1	Cryopyrin-associated periodic syndrome
Anti–Cell Adhesion Molecule			
	Natalizumab	Recombinant humanized leukocyte α_4/β_1 integrin mAb, blocks attachment of leukocytes to CNS endothelial cells	MS
	Abciximab	Anti-α_{IIb}/β_3, α_v/β_3 chimeric mAb Fab fragment, antithrombotic	Angioplasty procedures
	Efalizumab (Raptiva)	Recombinant humanized anti-α_L/β_2 mAb, binds CD11a to act as an immunosuppressant	Psoriasis
	Vedolizumab (Entyvio)	Humanized anti-$\alpha_4\beta_7$ mAb, inhibits adhesion and migration of leukocytes into the gastrointestinal tract	UC, CD

ALS, Amyotrophic lateral sclerosis; *AS,* ankylosing spondylitis; *CD,* Crohn disease; *COPD,* chronic obstructive pulmonary disease; *CSF,* colony-stimulating factor; *ENL,* erythema nodosum leprosum; *GM,* granulocyte macrophage; *HIV,* human immunodeficiency virus; *IgG,* immunoglobulin G; *IFN,* interferon; *IL,* interleukin; *JRA,* juvenile rheumatoid arthritis; *LFA,* lymphocyte functional antigen; *mAb,* monoclonal antibody; *MM,* multiple myeloma; *MS,* multiple sclerosis; *PA,* psoriatic arthritis; *RA,* rheumatoid arthritis; *RCC,* renal cell carcinoma, *TNF,* tumor necrosis factor; *UC,* ulcerative colitis.

evaluation and safety testing, including agents that target IL-33, IL-6, and IL-17 (Nabe et al., 2014; Chu et al., 2015; Busse et al., 2013).

CHEMOKINE AND CHEMOKINE RECEPTOR FAMILY

Chemokines (or chemotactic cytokines) are a large group of small secreted proteins that belong to the cytokine family. Chemokines are low-molecular-weight molecules ranging from 8 to 14 kD, defined by their primary amino acid sequence and the structure of the cysteine residues within the mature protein (Hughes et al., 2018). They play an essential role in the homeostasis of the immune system with the ability to stimulate leukocyte migration, but they also function in inflammation and angiogenesis by directing the activation and differentiation of leukocytes and endothelial cells, among other cell types (Zlotnik et al., 2006; Viola & Luster, 2008; Zlotnik & Yoshie, 2012; Miyake et al., 2013a; Bachelerie et al., 2014). Enhanced chemokine or chemokine receptor expression has been demonstrated in, and may be associated with, more aggressive forms of cancer (Miyake et al., 2013b). Beginning with the Keystone Symposium on Chemokines and Chemotactic Receptors held in 1999, a new nomenclature was established for chemokines based on the placement of the N-terminal cysteine residues, giving rise to four chemokine subclasses: CC, CXC, (X)C, and CX3C. In CC chemokines, the two cysteines are immediately adjacent, whereas in the CXC subclass, the cysteines are separated by a single amino acid. The single known member of the CX3C subfamily, also known as *fractalkine*, has three amino acids separating the cysteines. The (X)C chemokines lack the initial cysteine (Zlotnik & Yoshie, 2012). The nomenclature can be somewhat confusing since most chemokines have other common names established before the Keystone Symposium. Also, there exists ambiguity between mouse and human chemokines, as some chemokines are found in one species but not the other, and the mouse homologue may even have a different designation than the human chemokine. Table 49.4 gives a summary of the human and mouse chemokines according to their current categorization along with other names by which they are known.

Chemokine receptors are seven-transmembrane proteins belonging to the G-protein–coupled receptor family. In the new nomenclature, they are categorized by the chemokine subclass that they bind (Zlotnik & Yoshie, 2012). They are also divided into two families: conventional chemokine receptors (cCKRs) and atypical chemokine receptors (ACKRs). cCKRs exist as homodimers but can aggregate into oligomers with other receptors or membrane proteins. Atypical chemokine receptors are related to cCKRs but do not share similar transduction pathways and appear to be involved in regulating chemokine localization and distribution, thereby controlling chemokine-cCKR interactions (Hughes, 2018). All chemokine receptors are expressed in varying combinations on leukocytes but are also expressed on nonhematopoietic cells, including cancers and endothelial cells (Bachelerie et al., 2014). Although there may be specificity in interaction between a single chemokine and a single chemokine receptor, chemokine ligands often have the ability to bind to multiple different receptors and a chemokine receptor may bind any of several different chemokines (see Table 49.4). The multiplicity of interactions between chemokine ligands and receptors may provide some redundancy within the system, but it also means that different chemokines binding to the same receptor could have distinct functional outcomes either due to variation in binding avidity or availability of downstream signaling molecules within the cells. Thus, a specific chemokine, such as CCL11 (also known as *eotaxin*), has an agonistic effect when binding to CCR3 or CCR5 but an antagonistic effect when binding to CXCR3 or CCR2. CXCR3 is considered to promote T helper 1 (Th1) polarization among T helper cells, while CCR3 is preferentially expressed by Th2 cells and eosinophils. Thus, CCL11 should reinforce bias toward a Th2 immune response through its simultaneous agonistic effects on CCR3 and antagonistic effects on CXCR3 (Sallusto & Lanzavecchia, 2000). Chemokine binding to receptors involves a two-step process in which the chemokine initially interacts with the extracellular surface or chemokine recognition site 1 (CRS1). This causes a conformational change in the receptor and interaction of the chemokine with the chemokine recognition site 2 (CRS2), which leads to receptor activation (Scholten et al., 2012). Typical G-protein–coupled chemokine receptors activate downstream enzyme pathways, including PI3K; phospholipases Cβ2, Cβ3, A2, and D; mitogen-activated protein kinase (MAPK); and tyrosine kinases, ultimately resulting in actin polymerization, adhesion, and membrane protrusion required in cell mobility (Bachelerie et al., 2014). Besides defining receptors based on the category of chemokine that they bind, chemokine receptors can also be classified by their predominant function as homeostatic (involved in immune system development and leukocyte trafficking to lymphoid tissues), inflammatory (involved in trafficking of leukocytes into tissues at sites of infection or injury), or both (Bachelerie et al., 2014). While chemokine signaling is essential to normal

TABLE 49.4

Human Chemokines, Alternative Names, Receptor Usage, and Predominant Function

Ligand	Other Names	Receptor Antagonist	Function	Receptor(s) Agonist
CCL1	I-309		Th2 responses	CCR8
CCL2	MCP-1		Innate immunity	CCR1, CCR2
CCL3	MIP-1α		T-cell/Mφ trafficking	CCR1, CCR5
CCL3L1	LD78β		Innate immunity	CCR1, CCR3, CCR5
CCL3L3	LD78β		Th1/Th2 response	
CCL4	MIP-1β		T/DC interaction	CCR1, CCR5
CCL4L1	AT744.2		HIV inhibition	
CCL4L2	—		—	
CCL5	RANTES		Innate/adaptive	CCR1, CCR3, CCR5
CCL7	MCP-3	CCR5	Th2	CCR1, CCR2, CCR3
CCL8	MCP-2		Th2	CCR1, CCR2, CCR5
CCL11	Eotaxin	CXCR3, CCR2	Th2	CCR3, CCR5
CCL13	MCP-4		—	CCR2, CCR3
CCL14	HCC-1		—	CCR1, CCR3, CCR5
CCL15	HCC-2 Leurotactin-1		—	CCR1, CCR3
CCL16	HCC-4		DC maturation	CCR1, CCR2, CCR5, CCR8
CCL17	TARC		Th2	CCR4
CCL18	PARC, DC-CK1	CCR3	T/β-cell chemotaxis	
CCL19	MIP-3β		T/DC homeostasis	CCR7
CCL20	MIP-3α		GALT immunity	CCR6
CCL21	6Ckine		T/DC homeostasis	CCR7
CCL22	MDC		Th2	CCR4
CCL23	MPIF-1		—	CCR1
CCL24	Eotaxin-2		Eosinophil trafficking	CCR3
CCL25	TECK		Thymocyte trafficking	CCR9
CCL26	Eotaxin-3	CCR1, CCR2, CCR5	Th2	CCR3, CX3CR1
CCL27	CTACK, ILC		T-cell trafficking to skin	CCR10
CCL28	MEC		T-cell trafficking to mucosa	CCR10, CCR3
XCL1	Lymphotactin SCM-1α		Ag cross-presentation	XCR1
XCL2	SCM-1β		Ag cross-presentation	XCR1
CXCL1	GROα		Neutrophil	CXCR1, CXCR2
CXCL2	GROβ		Neutrophil	CXCR2
CXCL3	GROϒ		Neutrophil	CXCR2
CXCL4	PF4		Procoagulant	CXCR3-B
CXCL4L1	PF4V1		Procoagulant	CXCR3-B
CXCL5	ENA78		Neutrophil	CXCR2
CXCL6	GCP2		Neutrophil	CXCR1, CXCR2
CXCL7	NAP-2		Neutrophil	CXCR2
CXCL8	IL-8		Neutrophil Th1	CXCR1, CXCR2
CXCL9	MIG	CCR3	Th1	CXCR3
CXCL10	IP-10	CCR3	Th1	CXCR3
CXCL11	I-TAC	CCR3, CCR5	Myelopoiesis B lympho-poiesis	CXCR3, CXCR7
CXCL12	SDF-1		Myelopoiesis B lympho-poiesis	CXCR4, CXCR7
CXCL13	BLC, BCA-1		B/T trafficking LN	CXCR5, CXCR3
CXCL14	BRAK		Mφ trafficking	?
CXCL16	SR-PSOX		NKT cell trafficking	CXCR6
CXCL17	DMC		Mφ/DC trafficking	?
CX3CL1	Fractalkine		NK, T, Mφ trafficking	CX3CR1

Data from Koelink PJ, Overbeek SA, Braber S, et al.: Targeting chemokine receptors in chronic inflammatory diseases: an extensive review, *Pharmacol Ther* 133:1–18, 2012; and Zlotnik A, Yoshie O: The chemokine superfamily revisited, *Immunity* 36:705–716, 2012.

immunologic responses and immune system development, prolonged or excessive chemokine signaling can lead to pathogenic inflammation and autoimmunity, and may promote cancer metastases (Oppenheim et al., 2002; Balkwill, 2004).

CLINICALLY USEFUL CHEMOKINE-BASED THERAPEUTICS

Various chemokines and chemokine receptors are implicated in disease that have become targets of potential therapeutic intervention (Bachelerie et al., 2014). CXCR1 and CXCR2 are expressed on neutrophils, specific subpopulations of monocytes, mast cells, basophils, dendritic cells, natural killer (NK) cells, and some T cells, as well as endothelial cells, epithelial cells, neuronal cells, and mesenchymal stem cells. These receptors have been associated with multiple diseases, including psoriasis, chronic obstructive pulmonary disease (COPD), asthma, RA, IBD, and various cancers (Table 49.5) (Mahler et al., 2004; Bachelerie et al., 2014; Garin, 2011). A pilot study using an anti-CXCL8 antibody in COPD patients showed moderate efficacy (Mahler et al., 2004). Anti-CXCL8 used topically has also been shown to improve symptoms in psoriasis patients

TABLE 49.5

Chemokine Receptor Expression Associated with Various Diseases

Disease	Associated Chemokine Receptors
Atherosclerosis	CCR1, CCR2, CCR5, CXCR2, CXCR3, CXCR4, CX3CR1
Multiple sclerosis	CCR1, CCR2, CCR5, CCR7, CXCR3, CXCR6
Rheumatoid arthritis	XCR1, CCR1, CCR2, CCR5, CXCR1, CXCR2, CXCR3, CXCR4
Psoriasis	CCR1, CCR4, CCR5, CCR6, CCR10, CXCR2, CXCR3, CX3CR1
Type I diabetes	CCR4, CXCR3
IBD	CCR4, CCR5, CCR6, CCR10, CXCR1, CXCR2, CXCR3, CX3R1
Chronic hepatitis	CCR5, CXCR3
Lupus	CCR2, CXCR3, CXCR5
Allograft rejection	CCR1, CCR5, CXCR3
COPD	CCR1, CCR2, CCR3, CCR5, CCR10, CXCR1, CXCR2, CXCR3
Asthma	CCR1, CCR2, CCR3, CCR4, CCR5, CCR8, CXCR1, CXCR2, CXCR3, CXCR4
Atopic dermatitis	CCR4, CCR8, CCR10
HIV	CCR1, CCR2, CCR3, CCR5, CXCR4
Cancers	
Melanoma	CCR2, CCR3, CCR7, CCR9, CCR10, CXCR1, CXCR2, CXCR3, CXCR4
Breast	CCR1, CCR2, CCR3, CCR5, CCR6, CCR7, CCR9, CXXR3, CXCR4, CXCR5, CXCR6, CXCR7
Renal	CCR3, CXCR1, CXCR2, CXCR3, CXCR4, CXCR6
Prostate	CCR2, CCR5, CCR9, CXCR1, CXCR2, CXCR4, CXCR6, CXCR7, CX3R1
Head/Neck	CCR7, CXCR4, CXCR5, CXCR6
Lung	CCR1, CCR2, CCR5, CCR7, CXCR1, CXCR2, CXCR3, CXCR4, CXCR5
Gastrointestinal	CCR1, CCR6, CCR7, CXCR1, CXCR2, CXCR3, CXCR4, CXCR5, CXCR6
Pancreas	CCR5, CXCR1, CXCR2, CXCR4, CXCR5, CXCR6
Liver	CCR6, CXCR4, CXCR7
Ovarian	CCR4, CCR9, CXCR2, CXCR4
Lymphoma	CCR3, CCR4, CCR10, CXCR4, CXCR5
Leukemia	CCR3, CCR4, CCR7, CCR10, CXCR2, CXCR3, CXCR4
Myeloma	CCR1, CCR2, CCR5, CXCR4
Brain	CXCR4, CXCR7
Sarcoma	CXCR4

Data from Garin A, Proudfoot AE: Chemokines as targets for therapy, *Exp Cell Res* 317:602–612, 2011; Koelink PJ, Overbeek SA, Braber S, et al.: Targeting chemokine receptors in chronic inflammatory diseases: an extensive review, *Pharmacol Ther* 133:1–18, 2012; Scholten DJ, Canals M, Maussang D, et al.: Pharmacological modulation of chemokine receptor function, *Br J Pharmacol* 165:1617–1643, 2012; and Scholten DJ, Canals M, Maussang D, et al.: Pharmacological modulation of chemokine receptor function, *Br J Pharmacol* 165:1617–1643, 2012.

(Bizzarri et al., 2006). Another CXCR2 antagonist, reparixin, was shown to improve outcomes in islet cell transplant patients. A phase III trial is underway for islet transplantation in Europe and the United States (Bachelerie et al., 2014). CXCR1 blockade may also prove beneficial in selected breast cancer patients (Ginestier et al., 2010). Small-molecule antagonists of CXCR3 have been developed but have primarily been tested in animal models of arthritis, MS, inflammatory pulmonary disease, and cardiac allografts. An anti-CXCR3 antibody has been used in phase II clinical trials, which showed efficacy against RA but was ineffective against ulcerative colitis (Bachelerie et al., 2014). CXCR4 is a coreceptor for human immunodeficiency virus (HIV) and has been implicated in oncogenesis. The U.S. Food and Drug Administration (FDA) has approved the use of AMD3100, also known as *plerixafor*, to be used in combination with GM-CSF in multiple myeloma and non–Hodgkin lymphoma patients undergoing hematopoietic stem cell transplantation (Bachelerie et al., 2014). Among the CCR receptors, CCR1 has been targeted by eight different antagonists because of its association with diverse inflammatory diseases and cancers. However, clinical trials have not yet been very successful. CCR2 is another broadly expressed receptor implicated in a number of diseases. Animal studies show that CCR2 is required for monocyte egress from bone marrow and, in conjunction with CX3CR1, promotes monocyte infiltration of atherosclerotic plaques (Tacke et al., 2007). In addition, mice deficient in CCR2 developed reduced atherosclerotic lesions (Boring et al., 1998). To date, seven CCR2 antagonists have been developed. MLN1202 has been used in phase II clinical trials and has been shown to significantly reduce C-reactive protein (CRP) levels in plasma of individuals at atherosclerotic risk (Gilbert et al., 2011). As CRP is a known biomarker for atherosclerosis, this implies that CCR2 may be proatherogenic in humans as in mice. MLN1202 was also effective in a phase II trial of MS but was ineffective in a phase II trial involving RA (Bachelerie et al., 2014). Phase II clinical trials were performed with other CCR2 antagonists in MS, SLE, neuropathic pain, and type 2 diabetes but are either ongoing or the results have not been reported. CCR4 is expressed at high levels in adult T-cell leukemia/lymphoma cells; an anti-CCR4 (KW-0761) has been developed by Kyowa Hakko Kirin and approved by the Japanese Pharmaceutical and Medical Devices Agency for use in this disease. Evaluation of this antibody in allergic diseases is ongoing by Amgen (Bachelerie et al., 2014). CCR5 is the predominant HIV coreceptor; maraviroc (UK-427,857) by Pfizer has been FDA approved for use in AIDS patients to control virus infection. Multiple other CCR5 antagonists have been developed. A number of these prospective CCR antagonists remain in clinical trials, but several drug development programs were stopped because of unanticipated drug toxicities, such as ventricular arrhythmias/sudden death or liver toxicity. Anti-CCR5 antibodies have been developed and are being tested in HIV-infected patients (Bachelerie et al., 2014). An antagonist for CCR9 was developed by ChemoCentryx and appeared to be initially successful in phase II and phase II/III trials of patients with Crohn disease. However, when further tested in phase III trials by GlaxoSmithKline, the drug apparently proved ineffective and development was halted (Bachelerie et al., 2014). In most cases (Table 49.6), clinical trials using antagonists for specific chemokine receptors have failed to show efficacy, although several trials remain ongoing. As indicated earlier, the involvement of multiple chemokines in inflammatory diseases and redundancy of a chemokine between multiple different receptors may make monotherapy against a specific chemokine receptor ineffective. Therefore, novel therapeutic strategies could include the development of peptibodies, consisting of promiscuous chemokine-binding peptides, selected from phage display libraries and cloned into human mutated immunoglobulin Fc-protein fusions. Previously developed peptibodies (BKT120Fc and BKT130Fc) showed a marked anti-inflammatory response, thereby attenuating disease progression in animal models for autoimmunity and inflammation (Abraham et al., 2017).

ATYPICAL CHEMOKINE RECEPTORS

As mentioned earlier, ACKRs in vertebrates bind chemokines but fail to activate G-coupled proteins and generally function to suppress inflammation (Bachelerie et al., 2014). ACKR1, referred to more commonly in transfusion medicine as the *Duffy antigen*, is a promiscuous receptor, binding up to 20 different members of the CC and CXC chemokine groups. It is expressed on erythrocytes as well as on endothelial cells (in venules and small veins), some neurons, and possibly some epithelial cells, but not on leukocytes (Bachelerie et al., 2014). Although originally believed to remove chemokines from circulation, it is now thought that ACKR1 is important in maintaining blood levels of chemokines, although these may be maintained in an equilibrium state between free and erythrocyte-bound forms. However, heparin or serum serine proteases can displace chemokines bound to ACKR1 (Schnabel et al., 2010), which may make the chemokines available for inflammatory signaling. ACKR2 is a homologue of CCRs that promiscuously binds many CC chemokines. ACKR2 is expressed in skin, gut, lung, placenta, and on some lymphatic endothelial cells and leukocytes. Chemokine binding to ACKR2 results in receptor-ligand internalization and lysosomal degradation of the ligand. ACKR2 may have a protective role in psoriasis and COPD and act as a tumor suppressor gene (Bachelerie et al., 2014). ACKR3 expression is increased in immunopathologic responses and cancers, especially of hematopoietic and mesenchymal origin. ACKR3 primarily binds CXCL12, and CXCL12 has been shown to be important in tumorigenesis, suggesting that this receptor may also promote this process (Balkwill, 2004). ACKR4 primarily binds CCL19, CCL21, and CCL25. Its biological function is less well understood, but its expression correlates with pulmonary sarcoidosis severity

TABLE 49.6

Summary of Clinical Development of Drug Candidates Targeting Chemokine Receptors

Receptor	Company	Compound	Affinity (nM)	Indication(s)	Clinical Phase	Status
CCR1	Schering AG (Berlex)	BX 471	1.0	MS, psoriasis endometriosis	II	No efficacy
CCR1	Millennium	MLN 3701		MS, multiple myeloma	II	No longer reported
CCR1	Millennium	MLN 3897	2.3	RA, multiple myeloma	II	No efficacy in RA
CCR1	Pfizer	CP-481, 715	64	RA	II	No efficacy
CCR1	AstraZeneca	AZD4818	5.0	COPD	II	No efficacy
CCR1	ChemoCentryx/ GlaxoSmithKline	CCX354	1.5	RA	II	Complete
CCR1	Merck	C-4462		RA	II	No efficacy
CCR1	Merck	C-6448		MS	II	No efficacy
CCR2	Millennium	MLN 1202*		RA	II	No efficacy
				Atherosclerosis, MS	II	Complete
				Diabetes, cancer	II	Ongoing
CCR2	Incyte	INCB8696		MS, lupus	I	No longer reported
CCR2	Incyte	INCB3284	3.7	RA, type II diabetes	II	No longer reported
CCR2	ChemoCentryx	CCX915		MS	I	Terminated
CCR2	ChemoCentryx	CCX140	2.3	Diabetic nephropathy	II	Ongoing
CCR2	Merck	MK-0812	5.0	RA, MS	II	No efficacy
CCR2	Pfizer	PF-4136309		Pain	II	No longer reported
CCR2	BMS	BMS-741672		Diabetic neuropathy, pancreatic cancer	II	Complete ongoing
CCR2	Johnson & Johnson	JNJ-17166864	20.0	Allergic rhinitis	II	No efficacy
CCR3	Pharmaxis	ASM8†		Asthma	II	Terminated
CCR3	GlaxoSmithKline	GSK766994	10.0	Asthma and allergic rhinitis	II	No efficacy
CCR3	Dupont	DPC168	2.0	Asthma	I	Development halted
CCR3	BMS	BMS-639623	0.3	Asthma	I	Ongoing
CCR3	Novartis	QAP-642		Allergic rhinitis	I	Development halted
CCR3	AstraZeneca	AZD3778	8.1	Allergic rhinitis	II	No longer reported
CCR4	Amgen	KW-0761*		Oncology	II	Terminated
CCR4	GlaxoSmithKline	GSK2239633	10.0	Asthma	I	Completed
CCR5	Pfizer	UK-427,857 (Maraviroc)	3.0	RA	II	No efficacy
				AIDS	Approved	Registered drug
CCR5	Schering-Plough	SCH-C	2.0	RA	II	No efficacy
				AIDS	I	Development halted
CCR5	Schering-Plough	SCH-D	0.45	AIDS	II	Development halted
CCR5	GlaxoSmithKline	GW2239633	3.0	AIDS	III	Development halted
CCR5	Incyte	INCB9471	3.1	AIDS	II	Development halted
CCR5	Progenics	PRO 140*		AIDS	II	Completed
CCR5	Tobira	TAK652 (cenicriviroc)	3.1**	AIDS, liver cirrhosis, diabetes	II	Completed
CCR5	AstraZeneca	AZD5672	0.26	RA	II	No efficacy
CCR5	Novartis	NIBR-6465	0.8	AIDS, steatohepatitis	I	Ongoing
CCR5	Sangamo	SB-728‡		AIDS	II	Completed
CCR5	HGS	HGS004*		AIDS	I	Withdrawn
CCR9	ChemoCentryx/ GlaxoSmithKline	CCX282/vercirnon	6.0	IBD, Crohn disease	III	Terminated
CXCR1/CXCR2	Schering-Plough	SCH 527123	3.9 0.049	COPD	II	Ongoing
CXCR1/CXCR2	Dompé	Reparixin	1.0 (CXCR1) 100 (CXCR2)	Pancreatic islet transplantation	III	Ongoing
CXCR2	GlaxoSmithKline	SB-656933	5.1	COPD, cystic fibrosis	I	Ongoing
CXCR2	GlaxoSmithKline	GSK-1325756B		COPD?	I	Completed
CXCR2	AstraZeneca	AZD-5069		Bronchiectasis, COPD, asthma	II	Completed
CXCR3	Amgen	AMG487	8.0	Psoriasis	II	No efficacy

Continued

TABLE 49.6

Summary of Clinical Development of Drug Candidates Targeting Chemokine Receptors—cont'd

Receptor	Company	Compound	Affinity (nM)	Indication(s)	Clinical Phase	Status
CXCR4	Genzyme/Sanofi-Aventis	Plerixafor (AMD3100)	74	Stem cell mobilization for transplantation in cancer (MM, non-Hodgkin lymphoma)	Approved	Registered drug
CXCR4	TaiGen	Burixafor		Stem cell transplantation, prostate cancer, lymphoma	II	Completed
CXCR4	Polyphor	POL6326		Stem cell transplantation, pneumonia, cancer	II	Completed
CXCR4	Medarex	MDX-1338*		Lymphoma, kidney cancer	I	Complete
CXCR4	Biokine	BKT140§		Multiple myeloma	I	Completed

IBD, inflammatory bowel disease; *MM,* multiple myeloma; *RA,* rheumatoid arthritis.
*Neutralizing monoclonal antibodies.
†Antisense oligonucleotide.
‡Zinc finger nuclease.
§Peptide.
**Also has potent antagonist activity at CCR2.
From Bachelerie F, International Union of Basic and Clinical Pharmacology, et al.: LIX. Update on the extended family of chemokine receptors and introducing a new nomenclature for atypical chemokine receptors, *Pharmacol Rev* 66:1–79, 2014. Table 3

(Kriegova et al., 2006). Furthermore, ACKRs have been shown to play a crucial role in neuroinflammation, though their role is complex. ACKRs control inflammation, but knockdown of ACKR2 protected in a mouse model for autoimmune encephalomyelitis with impairment of T-cell priming (Salvi et al., 2017).

CHEMOKINE RECEPTOR HOMOLOGUES

Various pathogens also encode chemokine-binding proteins or chemokine receptor homologues usually stolen from host cells (Bachelerie et al., 2014). In many cases, these proteins act as scavengers to suppress host immune responses and allow the microbes to evade the immune system. However, US28 encoded by human cytomegalovirus (HCMV) has biological activity in HCMV-infected cells, as it aids in HIV infection as well as angiogenesis or tumor formation (Maussang et al., 2009). Other herpesvirus family and poxvirus family chemokine receptor homologues induce calcium flux or chemotaxis, and most are promiscuous for multiple CC and CXC chemokines. These chemokine receptor homologues appear to be important in virus replication, although their exact role in this process is not well understood. Besides the chemokine receptor homologues, various parasites and pathogens encode chemokine binding proteins (CKBPs or evasins), which are low-molecular-weight (90–110 amino acid) peptides that bind chemokines with high avidity and inhibit their chemotactic activity (Bachelerie et al., 2014). Viruses (including leporipoxviruses, orthopoxviruses, parapoxviruses, and herpesviruses), ticks (in tick saliva), and nematodes (*S. mansoni*, the causative agent in schistosomiasis) express these molecules (Bachelerie et al., 2014).

CELL ADHESION MOLECULES

The adhesion mechanisms that bind living tissues into complex multicellular organisms involve several classes of proteins, among which are the cell adhesion molecules (CAMs). These complex transmembrane glycoproteins facilitate cell migration during embryogenesis and wound healing, and they govern the leukocyte trafficking and homing critical to immune response (Ley et al., 2007; Gonzalez-Amaro, 1998). Roles for particular CAMs have been identified or postulated in myriad diseases, ranging from IBD to cancer to primary immunodeficiency states. Numerous investigators are seeking to identify and target CAM interaction sites for therapeutic modulation with specific monoclonal antibodies as well as sense/antisense oligonucleotides or other small molecules designed to block gene transcription (Mousa, 2008).

CAMs are conventionally divided into five groups based on structural homology: cadherins, mucins, integrins, selectins, and immunoglobulin superfamily CAMs. Cadherins mediate calcium-dependent cell–cell interactions, and they serve as important components of varied types of cell–cell junctions (e.g., desmosomes). Mucins are heavily glycosylated proteins that may be cell membrane–associated or secreted, and their ligands include selectins. Adenocarcinomas frequently express abnormal quantities or forms of mucins, and serum tumor markers CA19-9 and CA125 represent epitopes on mucins. Immunoglobulin superfamily (IgSF) CAMs have immunoglobulin-like domains and interact with integrins, selectins, and each other. Integrins and selectins are CAMs integral to effective recruitment of leukocytes to sites of inflammation or infection, which warrant more extensive descriptions to follow.

INTEGRINS

The integrin family of adhesion molecules mediates interaction between elements external to the cell (other cells and the extracellular matrix [ECM]) and those within the cell (cytoskeleton, intracytosolic molecules, and nucleus) (Abram & Lowell, 2009). Each integrin is a heterodimer of noncovalently linked α and β subunits (Table 49.7). The major integrins can be divided into subfamilies based on incorporation of particular subunits, patterns of expression, and ligand specificity. The β_1 integrins, also known as the *very late activation antigens (VLAs)*, arise from the association of a β1 chain subunit (CD29) with any of the α chain subunits (CD49a to CD49h). They are expressed on cells requiring firm anchoring to the ECM as well as on circulating leukocytes, platelets, and some tumor cells. The β_2 integrins, expressed mainly by leukocytes and myeloid cells, result from association of the β_2 chain subunit (CD18) with any of several α subunits. The $\alpha L\beta_2$ integrin, also known as LFA-1 (lymphocyte function-associated antigen [CD11a/CD18]), plays a crucial role in leukocyte adhesion to vascular endothelium during transendothelial migration. The ligand for LFA-1 in this process is intercellular adhesion molecule-1 (ICAM-1), which is an IgSF CAM.

The α integrin subunits are 120- to 180-kDa transmembrane proteins with short intracytoplasmic domains, a long extracellular fragment with seven homologous domains, and, in some cases, an "inserted" (I) domain that features a metal ion–dependent adhesion site (MIDAS) and serves as a primary site for ligand binding (Luo et al., 2007). Conformational changes mediate bidirectional signaling via integrins. Inside-out signaling triggered by chemokines or other agonists increases integrin affinity for ligands by shifting the heterodimer from a low-affinity bent configuration to a higher-affinity extended or open configuration. Avidity of integrins for their ligands is a function not only of conformation but also of the distribution of integrins on the cell surface, however, and binding of proteins such as talin and kindlins to the β integrin cytoplasmic tail contributes to clustering of integrins. Integrin activation also may be enhanced by shear forces such as those resulting from leukocyte adhesion to endothelium (Kim et al., 2011).

The intracytoplasmic tails of α and β integrin subunits associate with cytoskeletal components to transduce outside-in signals such as that of $\alpha L\beta_2$(LFA-1)-ICAM-1 binding. In the process of signal transduction, integrins associate and interact with other cell membrane–associated proteins, cytoskeletal components, and noncytoskeletal cytoplasmic components. The integrin-associated protein (IAP or IAP 50) designated CD47, an IgSF member, is one such membrane-associated protein that, mainly through association with β3 integrins, may function as a signal transducer. Other membrane-associated proteins involved in integrin signaling include caveolin-1 and CD9, which are involved in cell membrane caveola formation and platelet aggregation, respectively (Porter & Hogg, 1998).

TABLE 49.7

Selected Integrins Expressed by Leukocytes and/or Platelets

Integrin	Name	Ligands
$\alpha_1\beta_1$	VLA-1, CD49a/CD29	Collagen, LMN
$\alpha_2\beta_1$	VLA-2, GP Ia/IIa, CD49b/CD29	Collagen, LMN
$\alpha_4\beta_1$	VLA-4, CD49d/CD29	VCAM-1, FBN
$\alpha_5\beta_1$	VLA-5, CD49e/CD29	FBN
$\alpha_6\beta_1$	VLA-6, CD49f/CD29	LMN
$\alpha L\beta_2$	LFA-1, CD11a/CD18	ICAM-1, -2, -3
$\alpha M\beta_2$	Mac-1, CR3, CD11b/CD18	ICAM-1, iC3b
$\alpha X\beta_2$	p150,95, CR4, CD11c/CD18	FBGN, iC3b
$\alpha D\beta_2$	—	ICAM-3, VCAM-1
$\alpha IIb\beta_3$	GPIIb/IIIa, CD41/CD61	FBGN, vWF, FBN, VN
$\alpha V\beta_3$	CD51/CD61	VN, FBGN
$\alpha 4\beta_7$	LPAM-1	MAdCAM-1, FBN
$\alpha E\beta_7$	HML-1	E-cadherin

CR, Complement receptor; *FBGN,* fibrinogen; *FBN,* fibronectin; *GP,* glycoprotein; *ICAM,* intercellular adhesion molecule; *LFA,* lymphocyte functional antigen; *LMN,* laminin; *VCAM,* vascular cell adhesion molecule; *VN,* vitronectin; *vWF,* von Willebrand factor.

Modified from Luo BH, Carman CV, Springer TA: Structural basis of integrin regulation and signaling, *Annu Rev Immunol* 25:619–647, 2007.

Cytosolic molecules, including integrin cytoplasmic domain–associated protein (ICAP-1), help orchestrate the complex activity of β_1-integrin–mediated cell migration.

Perhaps the best studied intracytoplasmic associations of integrin molecules are those with the cytoskeleton-associated proteins α-actinin, talin, filamin, vinculin, tensin, and paxillin. These cytoskeleton proteins, through their association with β_1, β_2, and β_3 integrin subunits, bridge integrin and cytoskeleton and direct cell migration, phagocytosis, stress fiber formation at focal contact sites, and intracellular signal transduction. They also link separate cytoskeletal proteins.

The pattern of integrin distribution is wide, especially among those integrins (mostly β_1) involved in anchoring cells to components of the general ECM, such as collagen and laminin. For those integrins mediating attachment to less widely distributed components, tissue distribution likewise is more restricted. Restricted patterns of integrin expression are exploited clinically for classification of hematolymphoid neoplasms; for example, expression of the α subunit of integrin $\alpha X\beta_2$ (CD11c/CD18) is typical of hairy cell leukemia and of acute myeloid leukemias with monocytic features.

Out of 24 integrin heterodimers, 19 have been targeted for drug discovery (Goodman & Picard, 2012; Raab-Westphal, 2017). The four β1-series integrin collagen receptors have been targeted, including αI, a collagen-laminin receptor, to inhibit tumor angiogenesis and inflammation (the anti-$\alpha I\beta_1$ antibody SAN-300 is in phase II trial for RA) (Raab-Westphal et al., 2017). Integrin $\alpha IIb\beta_3$ antagonists, which vary considerably in design, have been used for many years to prevent thrombosis during percutaneous coronary artery procedures. However, αII antagonists have also been studied for multiple sclerosis, idiopathic Parkinson disease, and cancer without much success. Volociximab, a humanized chimeric IgG4 antibody that inhibits the α5β1 integrin, was developed as antiangiogenic therapy for cancer and macular degenerative disease, but development was stopped due to lack of efficacy (Bell-McGuinn et al., 2011; Almokadem et al., 2011).

The pan-αv integrin antibodies abituzumab and intetumumab bind the αv subunit, thereby inhibiting all five αv integrins, and were developed to inhibit tumor angiogenesis and metastasis. Abituzumab showed promising results in progressive castration-resistant prostate cancer by slowing down progression of metastatic disease and is currently investigated in a phase II trial in individuals with systemic sclerosis–associated interstitial lung disease by integrin-inhibitor-mediated TGF-β inhibition (Katsumoto et al., 2011). Intetumumab is another pan-αv integrin inhibitor with a favorable safety profile, used in melanoma and prostate cancer trials (O'Day, 2011; Heidenreich, 2013). Several studies investigating inhibitors for αvβ1, αvβ3, αvβ5, and αvβ8 are targets, which are currently underway (Mas-Maruno et al., 2010; Elez et al., 2015; Reed et al., 2015; Chang et al., 2017).

Over the past decade, β2 integrins, which are restricted to leukocyte lineages, have received more interest. They were used as targets to develop therapeutic strategies and inhibitory antibodies; small-molecule inhibitors have been generated, including lifitegrast, an αLβ2 antagonist, efalizumab, a humanized αLβ2 antibody, odulimomab, a chimeric IgG1 antibody to prevent delayed graft function, and rovelizumab, a humanized anti-αL antibody, initially developed for cerebral ischemia. All of these agents are still in development or have not shown proven success so far in various diseases (Zong et al., 2012; Frampton et al., 2009; Zimmerer et al., 2013; Tredget et al., 2008).

Abciximab is a mouse/human chimeric monoclonal antibody Fab fragment, while eptifibatide (a synthetic cyclic heptapeptide) and tirofiban (a nonpeptide small-molecule inhibitor) are non-mAb drugs. All three block $\alpha IIb\beta_3$(GPIIb/IIIa)-dependent platelet aggregation (Bledzka et al., 2013). Anti-α integrins are also used to prevent leukocyte extravasation into sites involved by inflammatory diseases. α_4 Integrins are the target of the humanized monoclonal antibody natalizumab, which has been used in the treatment of CD and MS. This novel therapy is not without significant risk, however, as several cases of therapy-related opportunistic infection and progressive multifocal leukoencephalopathy (PML) have been reported specifically with natalizumab (Stuve & Bennett, 2007). Vedolizumab, a humanized monoclonal antibody directed against $\alpha_4\beta_7$ integrin, has been approved more recently for use in the treatment of CD and ulcerative colitis, and it has not been associated with PML in clinical trials to date.

Therapeutic interventions based on disruption of integrin ligands are also being investigated; among the approaches being taken is infusion of an antisense oligonucleotide targeting ICAM-1 messenger RNA.

SELECTINS

The selectin family is composed of three homologous proteins that bind to oligosaccharide moieties on glycoprotein ligands (Ley, 2003). Similarities are greatest among the selectins in their extracellular domains, which include a lectin domain, an EGF domain, and varied numbers of consensus repeat (CR) domains. Selectins are distinguished by the cells that express them and by their subcellular localization. L-selectin (CD62L) is expressed by most leukocytes at the tips of microvilli or microfolds, E-selectin (CD62E) is expressed by activated endothelial cells on their plasma membranes, and P-selectin (CD62P) is expressed by platelets and endothelial cells in secretory granules. L-selectin mediates lymphocyte homing or trafficking of T lymphocytes through binding to ligands expressed in high endothelial venules (HEVs). It also contributes to neutrophil rolling on activated endothelium in regions of inflammation. Its ligands include GlyCAM (glycan-bearing cell-adhesion molecule)-1, MAdCAM (mucosal addressin cell-adhesion molecule)-1, and CD34. P-selectin is stored in the α granules and Weibel-Palade bodies of platelets and endothelial cells, respectively, and is expressed on the cell surface after cell activation. Once on the cell surface, P-selectin binds neutrophils, lymphocytes, and monocytes via its ligands, sialyl-Lewis-X-family– and sialyl-Lewis-A-family–type complex carbohydrate groups. E-selectin on the surface of activated endothelial cells recognizes ligands similar to those recognized by P-selectin. It plays a recognition role for homing effector and memory T cells as they localize to sites of inflammation.

The role of selectins is twofold: to mediate cell–cell interaction and to contribute to cell activation by intracytoplasmic signaling. As with integrins, selectins are critical to the initial tethering and rolling of leukocytes along activated endothelium prior to extravasation. Fluid shear stress exerted by flowing blood supports the process, as the "catch bonds" between selectins and their ligands are strengthened, not weakened, by shear forces (Lawrence et al., 1997). After binding a soluble form of the mucin-like glycoprotein GlyCAM-1 (a high endothelial venule product), L-selectin is able to mediate the activation of β_1 integrins and their adhesion to fibronectin. P- and E-selectin may also serve as signal-transducing receptor molecules because a rise in intracellular free Ca^{2+} within leukocytes adhering to endothelial cells is linked to these selectin molecules (Huang et al., 1993). The most frequently used quantitative assays for soluble plasma or serum selectins are sandwich immunoassays (Mousa, 2008). Numerous investigators have been exploring the potential utility of soluble P-selectin levels as a biomarker for diagnosis of deep vein thrombosis. Concentrations of soluble forms of selectins and other CAMs (e.g., ICAM-1) in the plasma may reflect ongoing inflammation; consequently, they have been explored as potential biomarkers of risk for inflammation-associated disease states such as atherosclerosis (Jenny et al., 2006). Recent reports also demonstrated that selectin expression on tumor cells correlates with poor prognosis and enhanced metastasis, thereby making selectins a potential target for controlling tumor immunity (Borsig et al., 2018). Studies assessing potential therapeutic interventions based on disruption of selectin function are ongoing.

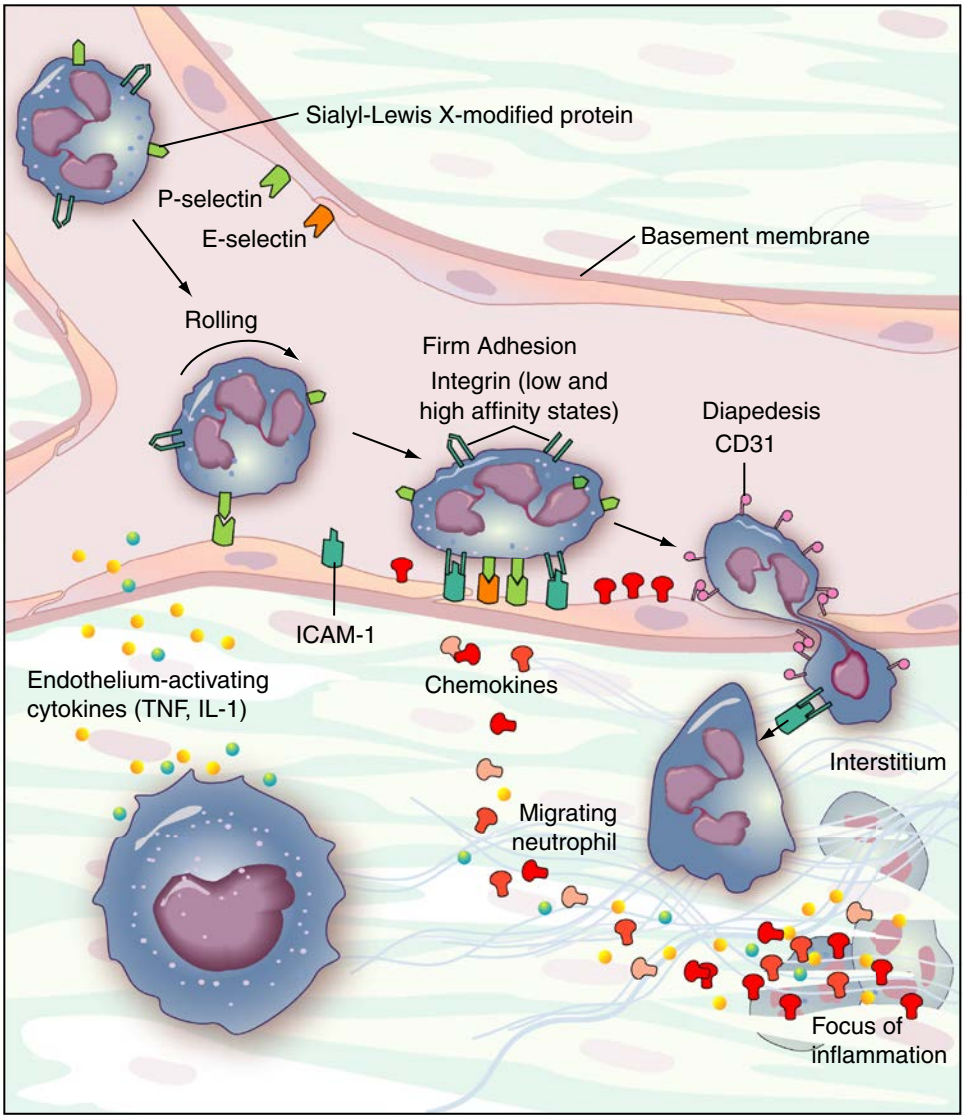

Figure 49.1 Adhesion molecules on the surfaces of leukocytes and activated endothelial cells guide the movement of white blood cells from the bloodstream to foci of tissue inflammation. Direction is provided by a chemotactic gradient. *ICAM,* intercellular adhesion molecule; *IL,* interleukin; *TNF,* tumor necrosis factor.

LEUKOCYTE EXTRAVASATION

Tissue damage or infections initiate host defense mechanisms dependent on the cytokine and cell-adhesion molecule families. Leukocyte mobilization to sites of damage or infection is a crucial step in this process. Selectins initiate the capture and rolling of leukocytes on the endothelial surface. Chemokines on the endothelial surface interact with leukocyte chemokine receptors and trigger the activation of integrins. Leukocyte integrin interaction with cytokine-induced adhesion molecules on the endothelial cell surface is critical to the evolution of inflammatory and immune responses and is required for stable adhesion of leukocytes to the endothelial surface. Subsequent to adhesion and migration, leukocytes transmigrate through the endothelial cell layer either through junctions between cells (paracellular) or through the body of an endothelial cell (transcellular) (Vestweber, 2012). In addition, homing of lymphoid cells to their sites of residence and intravascular spread of metastases involve similar endothelial interactions.

Extravasation of leukocytes occurs during cell homing, as with trafficking of γ/δ T cells to Peyer patches, and as part of the inflammatory/immune response. Both processes involve similar steps and the use of adhesion molecules. In inflammation, the process begins with local release of proinflammatory cytokines such as TNF, IL-1, and IFN-γ, which activate the local endothelium to increase surface expression of adhesion molecules, including members of the immunoglobulin superfamily, vascular cell adhesion molecule (VCAM)-1 and ICAM-1. In addition, endothelial cells release chemotactic agents, including IL-8, forming a surface-bound and soluble chemotactic gradient recognizable by transmigrating inflammatory cells, which localize them to the inflammatory focus.

This process for leukocytes (Fig. 49.1) involves (1) tethering of the passing leukocyte to the endothelial surface mainly by endothelial selectins (E- and P-selectins) and their leukocyte ligand sialyl-Lewis X-modified glycoprotein; and (2) leukocyte rolling in which, through rapid sequential surface expression of mainly leukocyte VLA-4 and $\alpha_4\beta7$ integrin, the shear force provided by the bloodstream rolls leukocytes along the endothelial surface, thereby bringing these integrins into contact with their endothelial ligands, VCAM-1 and MAdCAM-1, respectively. In the case of neutrophils, rolling is mediated by selectins alone. As they roll, leukocyte cell adhesion molecules trigger biochemical events, leading to (3) leukocyte activation and conversion of its integrins to an activated state of increased avidity. This leads to increased leukocyte–endothelial cell adhesion, and eventually to (4) arrest of leukocyte rolling, and (5) leukocyte transmigration of the endothelium with the assistance of the homotypic adhesion molecule CD31 expressed on both leukocytes and the endothelium, while following a chemotactic gradient. Once through the endothelium, integrin-mediated cell migration through the extracellular matrix along a chemotactic gradient completes the leukocyte journey to a focus of inflammation.

Deficiency states for β_2 integrins (leukocyte adhesion deficiency type I) and congenital defects in the expression of selectins and their ligands demonstrate the indispensable role that these receptors play in producing the inflammatory response and in lymphocyte trafficking. In these patients, neutrophils are unable to exit the bloodstream and migrate to sites of inflammation or infection, creating in effect a state of immunosuppression with increased susceptibility to bacterial infection and a paradoxical peripheral neutrophilia (Hanna & Etzioni, 2012). The events surrounding septic shock, thrombosis, reperfusion injury, and metastases also require integrin and selectin activity. This knowledge has led to the therapeutic use of monoclonal antibodies, soluble adhesion molecule ligands, and other interventions, including antisense oligonucleotides, to overcome adhesion molecule–mediated disease (Buckley et al., 1996; Gonzalez-Amaro & Sanchez-Madrid, 1999).

PERSPECTIVES

Dysregulation of cytokine and cell adhesion molecule functions is important in disease states, most notably, autoimmune diseases, and is recognized as a major contributor to many malignancies. Therefore, therapeutic strategies are evolving to enhance or reduce the actions of various cytokines, chemokines, cell-adhesion molecules, and their receptor activities.

SELECTED REFERENCES

Akdis M, Burgler S, Crameri R, et al.: Interleukins, from 1 to 37, and interferon-gamma: receptors, functions, and roles in diseases, *J Allergy Clin Immunol* 127:701–721, 2011. e701–e770.

This article describes a major family of cytokines, the interleukins, their functions, and roles in disease states, and highlights the importance of cytokine networks.

Gonzalez-Amaro R, Diaz-Gonzalez F: Sanchez-Madrid F: adhesion molecules in inflammatory diseases, *Drugs* 56:977–988, 1998.

This article provides an excellent and in-depth review of the process of leukocyte diapedesis. Pharmacologic therapeutic blocking of this process is discussed.

Zlotnik A, Yoshie O: The chemokine superfamily revisited, *Immunity* 36:705–716, 2012.

This article is an overview of the chemokine superfamily of proteins.

Access the complete reference list online at Elsevier eBooks for Practicing Clinicians.

REFERENCES

Abram CL, Lowell CA: The ins and outs of leukocyte integrin signaling, *Annu Rev Immunol* 27:339–362, 2009.

Abraham M, Wald H, Vaizel-Ohayon D, Grabovsky V, Oren Z, Karni A, et al.: Development of novel promiscuous anti-chemokine peptibodies for treating autoimmunity and inflammation, *Front Immunol* 8:1432, 2017.

Akdis M, Burgler S, Crameri R, et al.: Interleukins, from 1 to 37, and interferon-gamma: receptors, functions, and roles in diseases, *J Allergy Clin Immunol* 127:701–721, 2011. e701–e770.

Akdis M, Aab A, Altunbulakli C, Azkur K, Costa RA, Crameri R, et al.: Interleukins (from IL-1 to IL-38), interferons, transforming growth factor beta, and TNF-alpha: receptors, functions, and roles in diseases, *J Allergy Clin Immunol* 138:984–1010, 2016.

Almokadem S, Belani CP: Volociximab in cancer, *Expert Opin Biol Ther* 12:251–257, 2012.

Amatya N, Garg AV, Gaffen S: LIL-17 signaling: the Yin and the Yang, *Trends Immunol* 38:310–322, 2017.

Andoh A, Shioya M, Nishida A, Bamba S, Tsujikawa T, Kim-Mitsuyama S: Expression of IL-24, an activator of the JAK1/STAT3/SOCS3 cascade, is enhanced in inflammatory bowel disease, *J Immunol* 183:687–695, 2009.

Bachelerie F, Ben-Baruch A, Burkhardt AM, et al.: International Union of Basic and Clinical Pharmacology. [corrected]. LIX. Update on the extended family of chemokine receptors and introducing a new nomenclature for atypical chemokine receptors, *Pharmacol Rev* 66:1–79, 2014.

Balkwill F: Cancer and the chemokine network, *Nat Rev Cancer* 4:540–550, 2004.

Bachert C, Mannent L, Naclerio RM, Mullol J, Ferguson BJ, et al.: Effect of Subcutaneous Dupilumab on Nasal Polyp Burden in patients with chronic sinusitis and Nasal Polyposis: a randomized clinical trial, *J Am Med Assoc* 315:469–479, 2016.

Baud'huin M, Duplomb L, Teletchea S, et al.: Osteoprotegerin: multiple partners for multiple functions, *Cytokine Growth Factor Rev* 24:401–409, 2013.

Beck LA, Thaci D, Hamilton JD, Graham NM, Bieber T, Rocklin R, et al.: Dupilumab treatment in adults with moderate-to-severe atopic dermatitis, *N Engl J Med* 371:130–139, 2014.

Bell-McGuinn KM, Matthews CM, Ho SN, Barve M, Gilbert L, Penson R, et al.: A phase II, single-arm study of the anti-alpha5beta1 integrin antibody volociximab as monotherapy in patients with platinum-resistant advanced epithelial ovarian or primary peritoneal cancer, *Gynecol Oncol* 121:273–279, 2011.

Bleecker ER, FitzGerald JM, Chanez P, Papi A, Weinstein SF, Barker P, et al.: Efficacy and safety of benralizumab for patients with severe asthma uncontrolled with high-dosage inhaled corticosteroids and long-acting beta2-agonists (SIROCCO): a randomised, multicentre, placebo-controlled phase 3 trial, *Lancet* 388:2115–2127, 2016.

Bizzarri C, Beccari AR, Bertini R, et al.: ELR+ CXC chemokines and their receptors (CXC chemokine receptor 1 and CXC chemokine receptor 2) as new therapeutic targets, *Pharmacol Ther* 112:139–149, 2006.

Bledzka K, Smyth SS, Plow EF: Integrin αIIbβ3: from discovery to efficacious therapeutic target, *Circ Res* 112:1189–1200, 2013.

Boring L, Gosling J, Cleary M, et al.: Decreased lesion formation in CCR2$^{-/-}$ mice reveals a role for chemokines in the initiation of atherosclerosis, *Nature* 394:894–897, 1998.

Borsig L: Selectins in cancer immunity, *Glycobiology* 28:648–655, 2018.

Brocker C, Thompson D, Matsumoto A, et al.: Evolutionary divergence and functions of the human interleukin (IL) gene family, *Hum Genomics* 5:30–55, 2010.

Breen EC, Reynolds SM, Cox C, Jacobson LP, Magpantay L, Mulder CB, et al.: Multisite comparison of high-sensitivity multiplex cytokine assays, *Clin Vaccine Immunol* 18:1229–1242, 2011.

Buckley TL, Bloemen PG, Henricks PA, et al.: LFA-1 and ICAM-1 are crucial for the induction of hyperreactivity in the mouse airways, *Ann N Y Acad Sci* 796:149–161, 1996.

Busse WW, Holgate S, Kerwin E, Chon Y, Feng J, Lin J, et al.: Randomized, double-blind, placebo-controlled study of brodalumab, a human anti-IL-17 receptor monoclonal antibody, in moderate to severe asthma, *Am J Respir Crit Care Med* 188:1294–1302, 2013.

Cao H: Adipocytokines in obesity and metabolic disease, *J Endocrinol* 220:T47–T59, 2014.

Castro M, Zangrilli J, Wechsler ME, Bateman ED, Brusselle GG, Bardin P, et al.: Reslizumab for inadequately controlled asthma with elevated blood eosinophil counts: results from two multicentre, parallel, double-blind, randomised, placebo-controlled, phase 3 trials, *Lancet Respir Med* 3:355–366, 2015.

Chang SH, Park H, Dong C: Act1 adaptor protein is an immediate and essential signaling component of interleukin-17 receptor, *J Biol Chem* 281:35603–35607, 2006.

Chang Y, Lau WL, Jo H, Tsujino K, Gewin L, Reed NI, et al.: Pharmacologic blockade of alphavbeta1 integrin Ameliorates renal failure and fibrosis in vivo, *J Am Soc Nephrol* 28:1998–2005, 2017.

Chen J, Caspi RR, Chong WP: IL-20 receptor cytokines in autoimmune diseases, *J Leukoc Biol* 104:953–959, 2018.

Chen PH, Yao H, Huang LJ: Cytokine receptor endocytosis: new kinase activity-dependent and -independent roles of PI3K, *Front Endocrinol* 8:78, 2017.

Chu DK, Al-Garawi A, Llop-Guevara A, Pillai RA, Radford K, Shen P: Therapeutic potential of anti-IL-6 therapies for granulocytic airway inflammation in asthma, *Allergy Asthma Clin Immunol* 11:14, 2015.

Cutler A, Brombacher F: Cytokine therapy, *Ann N Y Acad Sci* 1056:16–29, 2005.

Dinarello CA: Historical insights into cytokines, *Eur J Immunol* 37(Suppl 1):S34–S45, 2007.

Elez E, Kocakova I, Hohler T, Martens UM, Bokemeyer C, Van Cutsem E, et al.: Abituzumab combined with cetuximab plus irinotecan versus cetuximab plus irinotecan alone for patients with KRAS wild-type metastatic colorectal cancer: the randomised phase I/II POSEIDON trial, *Ann Oncol* 26:132–140, 2015.

FitzGerald JM, Bleecker ER, Nair P, Korn S, Ohta K, Lommatzsch M, et al.: Benralizumab, an anti-interleukin-5 receptor alpha monoclonal antibody, as add-on treatment for patients with severe, uncontrolled, eosinophilic asthma (CALIMA): a randomised, double-blind, placebo-controlled phase 3 trial, *Lancet* 388:2128–2141, 2016.

Fossiez F, Djossou O, Chomarat P, Flores-Romo L, Ait-Yahia S, Maat C, et al.: T cell interleukin-17 induces stromal cells to produce proinflammatory and hematopoietic cytokines, *J Exp Med* 183:2593–2603, 1996.

Frampton JE, Plosker GL: Efalizumab: a review of its use in the management of chronic moderate-to-severe plaque psoriasis, *Am J Clin Dermatol* 10:51–72, 2009.

Garin A, Proudfoot AE: Chemokines as targets for therapy, *Exp Cell Res* 317:602–612, 2011.

Garlanda C, Dinarello CA, Mantovani A: The interleukin-1 family: back to the future, *Immunity* 39:1003–1018, 2013.

Gilbert J, Lekstrom-Himes J, Donaldson D, et al.: Effect of CC chemokine receptor 2 CCR2 blockade on serum C-reactive protein in individuals at atherosclerotic risk and with a single nucleotide polymorphism of the monocyte chemoattractant protein-1 promoter region, *Am J Cardiol* 107:906–911, 2011.

Ginestier C, Liu S, Diebel ME, et al.: CXCR1 blockade selectively targets human breast cancer stem cells in vitro and in xenografts, *J Clin Invest* 120:485–497, 2010.

Gonzalez-Amaro R: Sanchez-Madrid F: cell adhesion molecules: selectins and integrins, *Crit Rev Immunol* 19:389–429, 1999.

Goodman SL, Picard M: Integrins as therapeutic targets, *Trends Pharmacol Sci* 33:405–412, 2012.

Gruber R: Cell biology of osteoimmunology, *Wien Med Wochenschr* 160:438–445, 2010.

Gu C, Wu L, Li X: IL-17 family: cytokines, receptors and signaling, *Cytokine* 64:477–485, 2013.

Gaffen SL, Hajishengallis G: A new inflammatory cytokine on the block: re-thinking periodontal disease and the Th1/Th2 paradigm in the context of Th17 cells and IL-17, *J Dent Res* 87:817–828, 2008.

Hanna S, Etzioni A: Leukocyte adhesion deficiencies, *Ann N Y Acad Sci* 1250:50–55, 2012.

Huang AJ, Manning JE, Bandak TM, et al.: Endothelial cell cytosolic free calcium regulates neutrophil migration across monolayers of endothelial cells, *J Cell Biol* 120:1371–1380, 1993.

Huang C: Receptor-Fc fusion therapeutics, traps, and MIMETIBODY technology, *Curr Opin Biotechnol* 20:692–699, 2009.

Heidenreich A, Rawal SK, Szkarlat K, Bogdanova N, Dirix L, Stenzl A, et al.: A randomized, double-blind, multicenter, phase 2 study of a human monoclonal antibody to human alphanu integrins (intetumumab) in combination with docetaxel and prednisone for the first-line treatment of patients with metastatic castration-resistant prostate cancer, *Ann Oncol* 24:329–336, 2013.

Hughes CE, Nibbs RJB: A guide to chemokines and their receptors, *FEBS J* 285:2944–2971, 2018.

Ivashkiv LB, Donlin LT: Regulation of type I interferon responses, *Nat Rev Immunol* 14:36–49, 2014.

Jenny NS, Arnold AM, Kuller LH, et al.: Soluble intracellular adhesion molecule-1 is associated with cardiovascular disease risk and mortality in older adults, *J Thromb Haemost* 4:107–113, 2006.

JU K, Kabir NN, Flores-Morales A, et al.: SOCS proteins in regulation of receptor tyrosine kinase signaling, *Cell Mol Life Sci* 71:3297–3310, 2014.

Katsumoto TR, Violette SM, Sheppard D: Blocking TGFbeta via inhibition of the alphavbeta6 integrin: a possible therapy for systemic sclerosis interstitial lung disease, *Int J Rheumatol* 2011:208219, 2011.

Kim C, Ye F, Ginsberg MH: Regulation of integrin activation, *Annu Rev Cell Dev Biol* 27:321–345, 2011.

Koelink PJ, Overbeek SA, Braber S, et al.: Targeting chemokine receptors in chronic inflammatory diseases: an extensive review, *Pharmacol Ther* 133:(1–18), 2012.

Kriegova E, Tsyrulnyk A, Arakelyan A, et al.: Expression of CCX CKR in pulmonary sarcoidosis, *Inflamm Res* 55:441–445, 2006.

Kragstrup TW, Andersen MN, Schiottz-Christensen B, Jurik AG, Hvid M, Deleuran B: Increased interleukin (IL)-20 and IL-24 target osteoblasts and synovial monocytes in spondyloarthritis, *Clin Exp Immunol* 189:342–351, 2017.

Kumar A, Abbas W, Herbein G: TNF and TNF receptor superfamily members in HIV infection: new cellular targets for therapy? *Mediators Inflamm 2013*:484378, 2013.

Lawrence MB, Kansas GS, Kunkel EJ, et al.: Threshold levels of fluid shear promote leukocyte adhesion through selectins (CD62L,P,E), *J Cell Biol* 136:717–727, 1997.

Leal Vde O, Mafra D: Adipokines in obesity, *Clin Chim Acta* 419:87–94, 2013.

Ley K: The role of selectins in inflammation and disease, *Trends Mol Med* 9:263–268, 2003.

Ley K, Laudanna C, Cybulsky MI, et al.: Getting to the site of inflammation: the leukocyte adhesion cascade updated, *Nat Rev Immunol* 7:678–689, 2007.

Luo BH, Carman CV, Springer TA: Structural basis of integrin regulation and signaling, *Annu Rev Immunol* 25:619–647, 2007.

Mahler DA, Huang S, Tabrizi M, et al.: Efficacy and safety of a monoclonal antibody recognizing interleukin-8 in COPD: a pilot study, *Chest* 126:926–934, 2004.

Maitra A, Shen F, Hanel W, et al.: Distinct functional motifs within the IL-17 receptor regular signal transduction and target gene expression. Proc Natl Acad Sci USA 104(18):7056–7511.

Maussang D, Langemeijer E, Fitzsimons CP, et al.: The human cytomegalovirus-encoded chemokine receptor US28 promotes angiogenesis and tumor formation via cyclooxygenase-2, *Cancer Res* 69:2861–2869, 2009.

Mas-Moruno C, Rechenmacher F, Kessler H: Cilengitide: the first anti-angiogenic small molecule drug candidate design, synthesis and clinical evaluation, *Anticancer Agents Med Chem* 10:753–768, 2010.

Matsumoto H, Ogura H, Shimizu K, Ikeda M, Hirose T, Matsuura H, et al.: The clinical importance of a cytokine network in the acute phase of sepsis, *Sci Rep* 8:13995, 2018.

Metcalf D: The colony-stimulating factors and cancer, *Nat Rev Cancer* 10:425–434, 2010.

Miyake M, Goodison S, Urquidi V, et al.: Expression of CXCL1 in human endothelial cells induces angiogenesis through the CXCR2 receptor and the ERK1/2 and EGF pathways, *Lab Invest* 93:768–778, 2013a.

Miyake M, Lawton A, Goodison S, et al.: Chemokine (C-X-C) ligand 1 (CXCL1) protein expression is increased in aggressive bladder cancers, *BMC Canc* 13:322, 2013b.

Moraga I, Spangler J, Mendoza JL, et al.: Multifarious determinants of cytokine receptor signaling specificity, *Adv Immunol* 121:1–39, 2014.

Mousa SA: Cell adhesion molecules: potential therapeutic & diagnostic implications, *Mol Biotechnol* 38:33–40, 2008.

Muls N, Nasr Z, Dang HA, Sindic C, van Pesch V: IL-22, GM-CSF and IL-17 in peripheral CD4+ T cell subpopulations during multiple sclerosis relapses and remission. Impact of corticosteroid therapy, *PloS One* 12, 2017. e0173780.

Nakashima T, Takayanagi H: New regulation mechanisms of osteoclast differentiation, *Ann N Y Acad Sci* 1240:E13–E18, 2011.

Nabe T: Interleukin (IL)-33: new therapeutic target for atopic diseases, *J Pharmacol Sci* 126:85–91, 2014.

Novatchkova M, Leibbrandt A, Werzowa J, Neubuser A, Eisenhaber F: The STIR-domain superfamily in signal transduction, development and immunity, *Trends Biochem Sci* 28:226–229, 2003.

O'Day S, Pavlick A, Loquai C, Lawson D, Gutzmer R, Richards J, et al.: A randomised, phase II study of intetumumab, an anti-alphav-integrin mAb, alone and with dacarbazine in stage IV melanoma, *Br J Cancer* 105:346–352, 2011.

Oppenheim JJ, Yang D, Biragyn A, et al.: Chemokine receptors on dendritic cells promote autoimmune reactions, *Arthritis Res* 4(Suppl 3):S183–S188, 2002.

Ouchi N, Parker JL, Lugus JJ, et al.: Adipokines in inflammation and metabolic disease, *Nat Rev Immunol* 11:85–97, 2011.

Ortega HG, Liu MC, Pavord ID, Brusselle GG, FitzGerald JM, Chetta A, et al.: Mepolizumab treatment in patients with severe eosinophilic asthma, *N Engl J Med* 371:1198–1207, 2014.

Porter JC, Hogg N: Integrins take partners: cross-talk between integrins and other membrane receptors, *Trends Cell Biol* 8:390–396, 1998.

Puigserver: *Chapter 7 signaling transduction and Metabolomics*, 2018.

Regis G, Pensa S, Boselli D, et al.: Ups and downs: the STAT1:STAT3 seesaw of Interferon and gp130 receptor signalling, *Semin Cell Dev Biol* 19:351–359, 2008.

Raab-Westphal S, Marshall JF, Goodman SL: Integrins as therapeutic targets: successes and cancers, *Cancers* 9, 2017.

Ramani K, Garg AV, Jawale CV, Conti HR, Whibley N, Jackson EK, al e: The kallikrein-Kinin system: a novel mediator of IL-17-driven anti-Candida immunity in the Kidney, *PLoS Pathog* 12, e1005952, 2016.

Reed NI, Jo H, Chen C, Tsujino K, Arnold TD, DeGrado WF, et al.: The alphavbeta1 integrin plays a critical in vivo role in tissue fibrosis, *Sci Transl Med* 7:288ra279, 2015.

Sallusto F, Lanzavecchia A: Understanding dendritic cell and T-lymphocyte traffic through the analysis of chemokine receptor expression, *Immunol Rev* 177:134–140, 2000.

Schett G, Elewaut D, McInnes IB, et al.: How cytokine networks fuel inflammation: toward a cytokine-based disease taxonomy, *Nat Med* 19:822–824, 2013.

Schnabel RB, Baumert J, Barbalic M, et al.: Duffy antigen receptor for chemokines (Darc) polymorphism regulates circulating concentrations of monocyte chemoattractant protein-1 and other inflammatory mediators, *Blood* 115:5289–5299, 2010.

Scholten DJ, Canals M, Maussang D, et al.: Pharmacological modulation of chemokine receptor function, *Br J Pharmacol* 165:1617–1643, 2012.

Shen F, Li N, Gade P, et al.: IL-17 receptor signaling inhibits C/EBPbeta by sequential phosphorylation of the regulatory 2 domain. Sci Signal. 2(59):ra8, 2009.

Stuve O, Bennett JL: Pharmacological properties, toxicology and scientific rationale for the use of natalizumab (Tysabri) in inflammatory diseases, *CNS Drug Rev* 13:79–95, 2007.

Salvi V, Sozio F, Sozzani S, Del Prete A: Role of atypical chemokine receptors in Microglial activation and polarization, *Front Aging Neurosci* 9:148, 2017.

Tacke F, Alvarez D, Kaplan TJ, et al.: Monocyte subsets differentially employ CCR2, CCR5, and CX3CR1 to accumulate within atherosclerotic plaques, *J Clin Invest* 117:185–194, 2007.

Tredget EB, Arefanian H, Gill RG, Rajotte RV, Rayat GR: Monotherapy with anti-LFA-1 monoclonal antibody promotes long-term survival of rat islet xenografts, *Cell Transplant* 17:599–608, 2008.

Vainchenker W, Dusa A, Constantinescu SN: JAKs in pathology: role of Janus kinases in hematopoietic malignancies and immunodeficiencies, *Semin Cell Dev Biol* 19:385–393, 2008.

Vestweber D: Novel insights into leukocyte extravasation, *Curr Opin Hematol* 19:212–217, 2012.

Viola A, Luster AD: Chemokines and their receptors: drug targets in immunity and inflammation, *Annu Rev Pharmacol Toxicol* 48:171–197, 2008.

Wang X, Lupardus P, Laporte SL, et al.: Structural biology of shared cytokine receptors, *Annu Rev Immunol* 27:29–60, 2009.

Yao Z, Fanslow WC, Seldin MF, Rousseau AM, Painter SL, Comeau MR, et al.: Herpesvirus Saimiri encodes a new cytokine, IL-17, which binds to a novel cytokine receptor, *Immunity* 3:811–821, 1995.

Zlotnik A, Yoshie O: The chemokine superfamily revisited, *Immunity* 36:705–716, 2012.

Zlotnik A, Yoshie O, Nomiyama H: The chemokine and chemokine receptor superfamilies and their molecular evolution, *Genome Biol* 7:243, 2006.

Zhang JM: An, J: cytokines, inflammation, and pain, *Int Anesthesiol Clin* 45:27–37, 2007.

Zhong M, Gadek TR, Bui M, Shen W, Burnier J, Barr KJ, et al.: Discovery and development of potent LFA-1/ICAM-1 antagonist SAR 1118 as an Ophthalmic Solution for treating Dry Eye, *ACS Med Chem Lett* 3:203–206, 2012.

Zimmerer JM, Horne PH, Fiessinger LA, Fisher MG, Jayashankar K, Garcia SF, et al.: Inhibition of recall responses through complementary therapies targeting CD8+ T-cell- and alloantibody-dependent allocytotoxicity in sensitized transplant recipients, *Cell Transplant* 22:1157–1169, 2013.

CHAPTER 50

HUMAN LEUKOCYTE ANTIGEN: THE MAJOR HISTOCOMPATIBILITY COMPLEX OF HUMANS

Robert Bray, H. Clifford Sullivan, Scott Krummey, Howard M. Gebel

INTRODUCTION, 996

GENETICS OF THE MAJOR HISTOCOMPATIBILITY COMPLEX, 997
Basic Genetics, 997
Composition of the MHC, 998
Localization of MHC Genes, 998
Inheritance, 998
Linkage Disequilibrium, 998
Ethnic Variation, 998

CLASS I MOLECULES—HLA-A, HLA-B, AND HLA-C SUBREGIONS, 998
Structure of Class I Molecules, 999
Organization of Class I Genes, 1001
Regulation of Class I Gene Expression, 1001
Function of Class I Molecules, 1002
Other Class I Genes, 1003

CLASS II MOLECULES—HLA-DR, HLA-DQ, AND HLA-DP SUBREGIONS, 1003
Structure of Class II Molecules, 1003
Organization of Class II Genes, 1004
Linkage Disequilibrium of Genes in The Class II Region, 1004
Regulation of Class II Gene Expression, 1005
Function of Class II Molecules, 1005
Other Class II Genes, 1005

CHARACTERISTICS OF ANTIGENIC FRAGMENTS BOUND BY MHC CLASS I AND CLASS II MOLECULES, 1005

RECOGNITION OF FOREIGN MHC MOLECULES, 1005

MINOR HISTOCOMPATIBILITY MOLECULES, 1006

HLA NOMENCLATURE, 1006
Serologic and Cellular Specificities, 1006
DNA-Based Allele Designations, 1006

TECHNIQUES FOR IDENTIFYING HLA POLYMORPHISM, 1007
DNA-Based Typing of Class I and Class II Alleles, 1007
Serologic Detection of Class I and Class II Molecules, 1009
Cellular Detection of Class II Molecules, 1009

TISSUE/ORGAN TRANSPLANTATION, 1009
Genetic Basis of Transplantation, 1009
Histocompatibility Matching, 1010
Renal Transplantation, 1012
Nonrenal Organ Transplantation, 1012
Allogeneic Hematopoietic Progenitor Cell Transplantation, 1012

SUMMARY, 1013

SELECTED REFERENCES, 1013

KEY POINTS

- The major histocompatibility complex (MHC) is one of the most diverse and polymorphic genetic systems in humans. It consists of human leukocyte antigen (HLA) class I molecules (HLA-A, -B, and -C) and class II molecules (which include HLA-DRB1, -DRB3, -DRB4, -DRB5, -DQA1, -DQB1, -DPA1, and -DPB1). In total, there are over 20,000 unique HLA alleles.
- MHC genes are closely linked and segregate into offspring according to classic Mendelian genetics.
- Characterization of HLA alleles has been facilitated via molecular typing methods, including next generation, whole genome deoxyribonucleic acid (DNA) sequencing.
- The concept of HLA matching varies as a function of the type of transplant. For solid organ transplantation, only HLA-A, -B, and -DR antigens are considered. Hence a "perfect match" for solid organ transplantation would be termed 6 of 6 match or 0-antigen mismatch. For stem cell transplantation, HLA-A, -B, -C, -DRB1, and -DQB1 are considered. However, individual HLA molecules are compared at the allele level. Thus individuals matched for stem cell transplantation would be termed 10 of 10 matched.
- Patients can be sensitized to specific foreign HLA molecules through transfusion, pregnancy, or prior transplantation. Assessment of compatibility between the recipient and the possible donor includes testing for this sensitization.
- The presence of donor-specific HLA antibodies may preclude or compromise a transplant. HLA antibody testing is performed using solid-phase, bead-based assays. Crossmatching may be either a physical test or a virtual assessment of immunologic compatibility.

INTRODUCTION

An individual's survival depends on the ability of the immune system to recognize and respond to a multitude of foreign substances (antigens). Although this defense mechanism is basic to survival, this same defense system can have a negative impact when tissue is transplanted from one individual to another or when dysregulation triggers autoimmune disease. Genes of the MHC encode proteins, HLA class I and class II that are essential for immune recognition (Fig. 50.1). In the human, class I molecules combine with β_2 microglobulin to form a stable heterodimer. Class I molecules include HLA-A, -B, and -C. For class II molecules alpha-beta heterodimers are formed via the combination of the nonpolymorphic DRA1 gene product with an HLA-DRB1 and/or HLA-DRB3, -DRB4, or -DRB5 gene products. HLA-DQA1 combines with HLADQB1, both of which are highly polymorphic, to form a stable DQ molecule. Lastly, HLA-DPA1 combines with HLA-DPB1, again both are highly polymorphic, to form a stable DP molecule. These molecules constitute the classic transplantation antigens. Other molecules encoded within the MHC are the class III molecules. These include the MHC-linked complement components (C2, C4, and Bf), 21-hydroxylase (CYP21), heat-shock protein 70 (HSP70), and tumor necrosis factor (TNF).

During an infection, the invading microorganism may infect or be engulfed by cells and then may be degraded into peptide fragments. Inside the cell (in the endoplasmic reticulum, HLA class I, and class II compartment), nascent HLA class I or class II molecules are loaded with peptide fragments derived from the microorganism. Once these fragments have bound to the HLA molecules and have translocated to the cell surface, receptors on T lymphocytes interact with the peptide/HLA complex (immune synapse), triggering the cellular then humoral immune responses (Fig. 50.2). T-cell–specific surface molecules, CD4

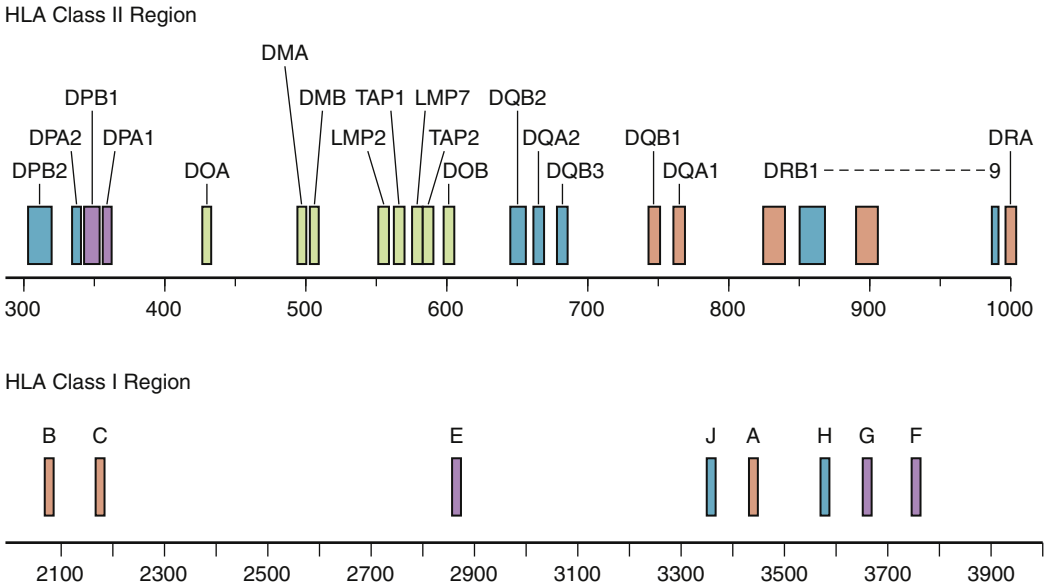

Fig. 50.1 Map of the major histocompatibility complex (MHC) gene on chromosome 6. HLA-DPB2 in the human leukocyte antigen (HLA) class II region is located closest to the centromere. HLA-F is the most telomeric. The region between HLA-DRA and HLA-B is not shown. (Data from Anthony Nolan Research Institute, http://hla.alleles.org/alleles/index.html; Marsh et al., 2002.)

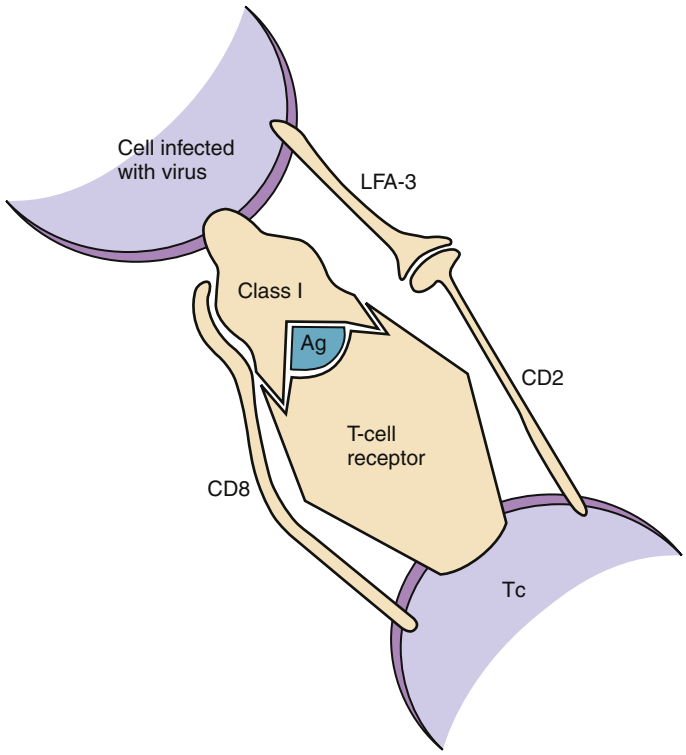

Fig. 50.2 Model of the molecular interactions involved in antigen recognition.

TABLE 50.1
Websites on HLA Transplantation

Address	Information
www.ashi-hla.org	American Society for Histocompatibility and Immunogenetics, HLA typing standards
www.ebi.ac.uk/imgt/hla	HLA sequence database, tools for allele submission and sequence manipulation
www.anthonynolan.org.uk/hig	World Health Organization nomenclature information
www.ihiw18.org	18th International Histocompatibility Workshop
www.bethematch.org	National Marrow Donor Program
www.bloodcell.transplant.hrsa.gov	Bone Marrow and Cord Blood Donation and Transplantation, HRSA
www.wmda.org	Bone Marrow Donors Worldwide
www.ebmt.org	World Marrow Donor Association
www.cibmtr.org	Center for International Blood & Marrow Research
www.ctstransplant.org	Collaborative Transplant Study
www.unos.org	United Network for Organ Sharing
www.optn.transplant.hrsa.gov	Organ Procurement and Transplant Network
www.nhgri.nih.gov	National Human Genome Research Institute
www.srtr.org	Scientific Registry of Transplant Recipients
www.allelefrequencies.net	Allele Frequency Net Database

and CD8, act to strengthen this cellular interaction and to transmit intracellular activation signals. Other cell surface molecules act to increase the affinity of cellular interactions (e.g., CD2 and its ligand, CD58 [LFA-3], or CD11a/CD18 [LFA-1] and its ligand, CD54 [ICAM-1]), and to transmit costimulatory signals (e.g., CD28 and its ligands, CD80/CD86 [B7], or CD40 and its ligand, CD154). The same interactions that occur between T-cell recognition of MHC class I or class II with its associated peptide in response to an invading pathogen also can occur between foreign HLA class I and class II molecules (alloantigens) and in recognition of self-antigens (autoantigens) (see Chapter 51).

The genetics, structure/function, nomenclature, and techniques for detection of human MHC gene products and antibodies against these products are discussed in this chapter. Also discussed is the evolving role of HLA matching for transplantation and the emergence of the virtual crossmatch. In addition to references listed at the end of the chapter, Table 50.1 presents helpful websites that provide both reference material and updates of clinical outcomes.

GENETICS OF THE MAJOR HISTOCOMPATIBILITY COMPLEX

BASIC GENETICS

Mendel's first law, the law of segregation, is based on the principle that hereditary traits are determined by factors that are distributed to progeny. In any one individual, these factors, or *genes* as they are now called, are present on chromosomes (Chapter 70). Each gene may have multiple forms (i.e., alleles). Because humans are diploid, two genes are included per pair of homologous chromosomes. In meiosis, the chromosomes segregate randomly during formation of the gametes (ova or sperm) so that only one of each pair of chromosomes (i.e., a haploid number) is transmitted by any given gamete. The double, or diploid, number of chromosomes is restored when the male and female gamete fuse to form the zygote. Thus, for a trait

determined by one gene, there will always be four possible genetic combinations in the offspring, each with equal probability of occurrence. These laws of segregation and random assortment apply to genes of the MHC system. However, in contrast to other genetic systems, HLA genes are codominant, meaning there is equal expression (with some exceptions) of gene products from both haplotypes. Following are definitions for genetic terms that will be used in this chapter (Crow, 1976; www.nhgri.nih.gov):

Gene: Unit factor of inheritance
Chromosome: Carrier of the unit factors of inheritance
Locus: Position of a gene on a chromosome
Allele: An alternative form of a gene at a single locus
Homozygous: Having identical alleles at a locus, one on each chromosome
Heterozygous: Having different alleles at a locus, one on each chromosome
Codominance: The state in which the allele at each locus expresses its characteristic effect equally in the heterozygote
Genotype: Genetic composition of an organism or individual
Phenotype: Observable characteristics produced by the genes
Polymorphic: Having two or more common distinct genotypes maintained in a population
Homologous chromosomes: The two members of a chromosome pair that have corresponding gene loci, one derived from each parent
Crossing over: Exchange of segments between homologous chromosomes; also termed *recombination.*
Allo-(antigen, graft): Refers to antigenic differences between individuals of a single species
Auto-(antigen, graft): Refers to tissue or antigens of the same individual (i.e., self)

COMPOSITION OF THE MHC

The major histocompatibility gene complex in humans is located on the short arm of chromosome 6 (i.e., 6p21). It spans ~4000 kilobases (kb) and includes 224 identified gene loci, of which 121 are predicted to be expressed (Mungall et al., 2003). Approximately 40% of the expressed genes are estimated to have an immune system function (Aguado et al., 1999). MHC genes are located in six subregions: HLA-A, HLA-C, HLA-B (class I genes) and HLA-DR (DRB1, DRB3,4,5), HLA-DQ (DQA1, DQB1), and HLA-DP (DPB1, DPA1) (class II genes) (see Fig. 50.1). Each subregion encodes a minimum of one cell surface glycoprotein. β_2 microglobulin, encoded on chromosome 15 (15q21.1), contributes to the final tertiary structure of class I molecules. Class II region genes have additional complexities that will be discussed later. With only one exception, DRA1, the MHC gene products are highly polymorphic; that is, each MHC gene has multiple expressed alleles in the human population. Indeed, the MHC genes are the most polymorphic loci known in humans (Parham et al., 1995; https://www.ebi.ac.uk/ipd/imgt/hla/) (Table 50.2). Because MHC genes specify molecules that play an important role in the immune response, diversity is believed to be essential to survival of the species. As the majority of HLA typing methods involve testing at the DNA level, we can now appreciate the enormous diversity that resides within the MHC. As of September 2019, more than 23,000 HLA alleles have been identified that code for more than 16,000 unique proteins (http://hla.alleles.org/nomenclature/stats.html) (Fig. 50.3). Among the MHC genes, the HLA-B locus presents the greatest variability with over 6500 alleles coding for more than 4400 unique proteins. As a result, the HLA B-locus is considered the most polymorphic genetic locus in the entire human genome.

LOCALIZATION OF MHC GENES

The genes of the MHC can be found on the short arm of chromosome 6 (6p). The map order and positioning of the MHC genes were initially determined by meiotic linkage analyses (i.e., studies of crossing over in families) and later by molecular biology techniques, including gene cloning, DNA sequencing, and pulsed field gel electrophoresis. The map order of genes within the MHC is HLA-A, -C, -B, -DR, -DQ, and -DP, with HLA-A being the most distal to the centromere (see Fig. 50.1).

INHERITANCE

The MHC genes are closely linked; that is, they segregate en bloc to the offspring. The complex of linked genes that resides on one pair of homologous chromosomes and that segregates en bloc to the offspring is termed a *haplotype*. Each individual inherits two MHC haplotypes—one from each parent—and thus has two alleles for each of the genes. The inheritance of the MHC genes follows the rules of segregation set down by Mendel, and the alleles at each locus exhibit codominant expression. Within a family, each child inherits one MHC haplotype from the mother and one from the father. By convention, the paternal haplotypes are designated "a" and "b", and the maternal haplotypes "c" and "d". Thus there are four possible MHC genotypes in the offspring: "a/c", "a/d", "b/c", and "b/d" (Fig. 50.4). Because the chance of inheriting a given haplotype is random, the probability of occurrence of any one of the four genotypes is one in four for each offspring. In a family with five children, at least two of the children will be HLA identical assuming no crossover haplotypes have occurred. Although the MHC genes are closely linked, families have been reported in which a crossover has occurred. The frequency of crossing over between two linked genes was thought to be a measure of the distance separating the genes; however, molecular data have suggested the existence of recombination "hot" spots in the intervening DNA that can increase or decrease the likelihood of recombination during meiosis (Cullen et al., 2002).

LINKAGE DISEQUILIBRIUM

The observation that alleles at different genetic loci occur in the population on the same haplotype significantly more frequently than would be expected on the basis of chance alone is called *linkage disequilibrium.* The expected frequency of two alleles (f_1, f_2) is the product of the gene frequency of each allele in that population ($f_{expected} = f_1 \times f_2$). The observed frequency (fo) is determined from family studies within the same population. When the $f_{observed}$ is significantly greater than $f_{expected}$, the two genes are said to be linked. Linkage disequilibrium is a hallmark of the human MHC and extends from HLA-A through HLA-DP. However, the linkage between DQ and DP can vary depending upon the HLA haplotype (Petersdorf et al., 2015). The best known example of linkage disequilibrium is the A1, Cw7, B8, DR17(3), DR52, DQ2 haplotype in Caucasians, which is observed approximately four times more frequently than expected. The significance of linkage disequilibrium as it applies to immune competence and disease is discussed under "Extended Haplotypes" in Chapter 51.

ETHNIC VARIATION

Accumulated data from the study of the world population groups (Dausset & Colombani, 1973; Imanishi et al., 1992; Cadavid & Watkins, 1997; Bugawan et al., 1999) demonstrate that the frequencies of HLA alleles differ significantly among ethnic population groups. MHC haplotypes and linkage disequilibrium of alleles also differ. These observations were taken into account when unrelated allograft hematopoietic progenitor cell donor registries and banks such as the US National Marrow Donor Program (NMDP) were established (Perkins & Hansen, 1994). Both allele and haplotype frequencies dictate the number of volunteers required to find an HLA-matched unrelated donor for any patient. Some patients (e.g., those with rare or unusual HLA alleles or haplotypes) cannot find closely matched unrelated donors from among the more than 36 million volunteers listed in the World Marrow Donor Association registry as of 2019 (www.wmda.org) and more than 20 million in the "Be The Match" registry (Fig. 50.5). Currently, patients are more likely to find a match not only because the number of stem cell donors has increased, but the number of umbilical cord blood units available for transplantation has also increased (Fig. 50.6). It appears that cord blood transplantation may be more tolerant of HLA mismatches; this may be a result of reexposure to noninherited maternal antigens (NIMAs) found in the graft (van Rood et al., 2009) or the immune naivety of cord blood cells. Lastly, the growing success in the use of progenitor cells from partially HLA-mismatched donors may allow transplantation in patients for whom close matches cannot be found (see Chapter 39).

CLASS I MOLECULES—HLA-A, HLA-B, AND HLA-C SUBREGIONS

The HLA-A and -B molecules were the first MHC molecules to be described in humans (Dausset, 1981; van Rood, 1993). Because these molecules were defined by antibody responses to white blood cells (WBCs), they were called **human leukocyte antigens.** Antibodies directed against human WBCs were observed as early as the 1920s, but it was not until the 1950s that a systematic study began. In 1952, Dausset convincingly demonstrated the existence of leukocyte antibodies (leukoagglutinins). Because these leukoagglutinins did not react with leukocytes from the antibody producer but did react with a percentage of leukocytes from red cell group O unrelated individuals, he suggested that leukoagglutinins were alloantibodies. Shortly thereafter, Payne and colleagues (1964) reported that sera from patients who had febrile nonhemolytic blood transfusion reactions

TABLE 50.2

Examples of WHO-Recognized HLA Antigens (Specificities) Defined by Serologic Typing and HLA Alleles Defined by DNA Sequencing[a]

HLA-A Antigens	HLA-A Alleles[b]	HLA-DQ Antigens	HLA-DQB1 Alleles[c]
A1	A*01:01:01:01-01:319	DQ1	
A2	A*02:01:01:01–*02:877	DQ2	DQB1*02:01:01–*02:99
A203	A*02:03	DQ3	
A210	A*02:10	DQ4	DQB1*04:01:01:01–*04:73N
A3	A*03:01:01:01–*03:369	DQ5(1)	DQB1*05:01:01:01–*05:99
A9		DQ6(1)	DQB1*06:01:01:01–*06:99:03
A10		DQ7(3)	
A11	A*11:01:01:01–*11:369	DQ8(3)	DQB1*03:01:01:01–*03:99Q
A19		DQ9(3)	
A23(9)	A*23:01:01:01–*23:96		
A24(9)	A*24:02:01:01–*24:470		
A2403	A*24:03		
A25(10)	A*25:01:01:01–*25:63		
A26(10)	A*26:01:01:01–*26:190		
A28			
A29(19)	A*29:01:01:01–*29:136		
A30(19)	A*30:01:01:01–*30:158N		
A31(19)	A*31:01:02:01–*31.160		
A32(19)	A*32:01:01:01–*32:131		
A33(19)	A*33:01:01:01–*33:191		
A34(10)	A*34:01:01:01–*34:23		
A36	A*36:01		
A43	A*43:01		
A66(10)	A*66:01:01:01–*66:37		
A68(28)	A*38:01:01:01–*68:221		
A69(28)	A*69:01:01:01:–*69:06		
A74(19)	A*74:01:01:01:–*74:36		
A80	A*80:01:01:01–*80:06		

Adapted from IPD-IMGT/HLA website, https://www.ebi.ac.uk/ipd/imgt/hla/.
N, Null or nonexpressed allele.
[a]Each column of the table is independent. Numbers in parentheses indicate the broad serologic specificity. The serologic type may be listed without the broad specificity or molecular equivalents. For example, both A23(9) and A23 are correct designations. A9, A10, and A19 are no longer recognized as a distinct antigens and therefore do not have a molecular equivalents.
[b]HLA-A alleles specify HLA-A antigens. The antigen A1 is specified by either A*01:01 through A*01:319 alleles.
[c]HLA-DQA1 and HLA-DQB1 alleles specify HLA-DQ antigens. The antigen DQ5 (1) is specified by several different DQA1 and DQB1 combinations, including (1) DQA1*01:01 and DQB1*05:01 and (2) DQA1*01:01 and DQB1*05:02 alleles. In the past, serologic split designations were given to specificities that appeared to identify the antigen specified by a single HLA allele (e.g., A2 splits A203, A210; B7 splits B703; B39 splits B3901 and B3902). It is now recognized that other alleles may also encode antigens that carry these serologic specificities, and the WHO Nomenclature Committee has recommended that these splits be discontinued.

frequently contained leukoagglutinins that demonstrated allospecificity. In 1958, Dausset described the first HLA alloantigen MAC (now HLA-A2) and showed it to be genetically inherited.

Originally, leukocyte specificities were thought to be the products of a single locus. A two-locus model, each locus with multiple alleles, was established through HLA studies in families by the identification of recombination events that separated the two allelic series. These two allelic series were called the first, or LA (now HLA-A), and the second, or "four" series (now HLA-B). These names were derived from descriptions of the LA 1, 2, 3 allelic series by Payne in 1967, and of the 4a, 4b allelic series by van Rood in 1969. A third locus was first proposed in 1970; however, it was not confirmed until 1975, when a family with a recombination between HLA-B and the new locus was identified. This third locus was designated HLA-C following the 1975 International Histocompatibility Workshop. Dausset (1981) was awarded the Nobel Prize for Medicine in 1980 for his original work on the human HLA system.

STRUCTURE OF CLASS I MOLECULES

The classical class I molecules, termed *HLA-A*, *HLA-B*, and *HLA-C* in the human, are heterodimers consisting of a transmembrane glycosylated polypeptide (heavy chain, 44-kDa) noncovalently associated with β_2 microglobulin (12-kDa) (Fig. 50.7) (Bjorkman & Parham, 1990). The heavy chain of the class I molecule spans the cell membrane and is oriented with its amino-terminus on the outside of the cell. β_2 microglobulin is associated with the extracellular region of the heavy chain and is necessary for cell surface expression. The extracellular region of the class I heavy chain is divided into three domains designated α1, α2, and α3, each consisting of about 90 amino acid residues. The amino-terminal α_1 domain contains a glycosylation site at the asparagine residue in position 86. The transmembrane segment of approximately 24 amino acids is mostly hydrophobic, whereas the intracellular carboxy-terminal segment of the molecule consists mainly of hydrophilic residues with a cluster of basic residues adjacent to the cytoplasmic surface of the cell membrane.

The polymorphisms of class I molecules (see Table 50.2 and Fig. 50.4) were initially defined by the use of (1) class I–specific antibodies (alloantisera and monoclonal antibodies) that bind to the HLA molecules, (2) cytotoxic T lymphocytes (CTLs) that recognize and kill in response to stimulation by foreign or allogeneic class I molecules in vitro, and (3) isoelectric focusing of isolated class I molecules. More recently, polymerase chain reaction (PCR)–based DNA typing of class I and II alleles and nucleotide sequencing of class I and II alleles represent the primary methods for identifying an individual's HLA repertoire.

Fresh insights into the structure of the HLA molecule came when the three-dimensional structure of the class I molecule was defined using x-ray crystallography (Bjorkman et al., 1987). The structure of the extracellular portion is shown in Figure 50.8. The molecule consists of two pairs of structurally similar domains: α1 has the same tertiary conformation as α_2, and α_3 and β_2 microglobulin have similar tertiary conformations. The α_3 and β_2 microglobulin domains are each composed of two antiparallel β-pleated sheets—one with four strands and one with three strands, connected by a disulfide bond. The α_3 and α_2

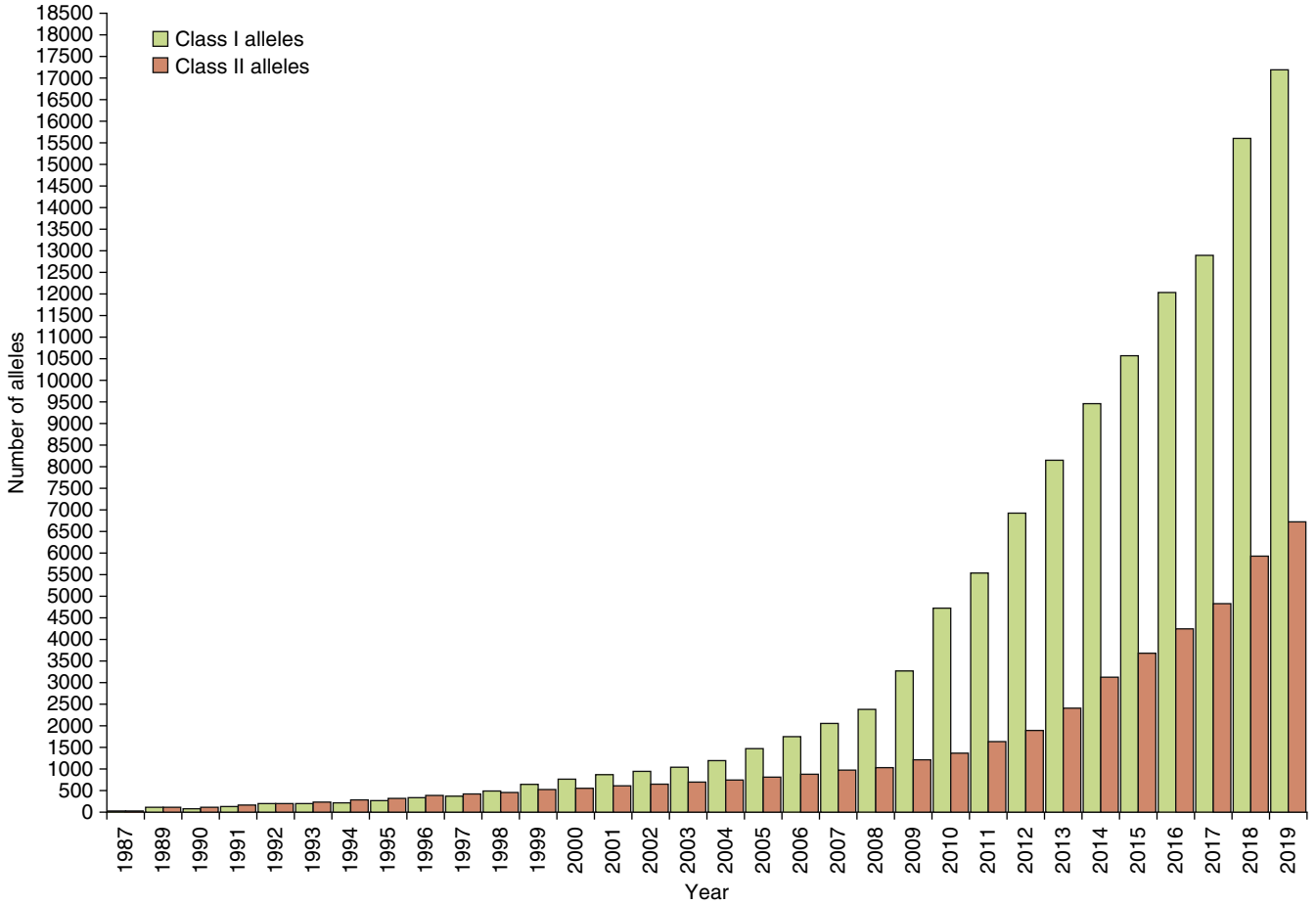

Fig. 50.3 Numbers of class I and class II alleles discovered from 1987 to 2019. The increase in the number of discovered alleles during this period was made possible by the introduction of DNA typing methods; class I alleles include HLA-A, -B, and -Cw; class II alleles include HLA-DRB1, -DQB1, -DQA1, -DPA1, and -DPB1. (Data from Anthony Nolan Research Institute, http://hla.alleles.org/nomenclature/.)

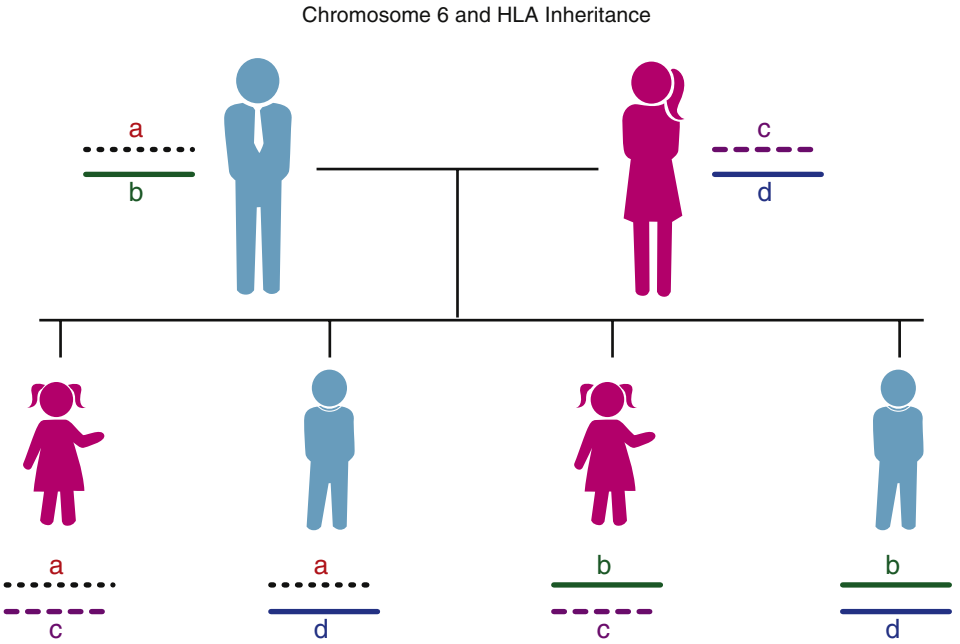

Fig. 50.4 Cartoon depicting inheritance pattern within a family. The "a" and "b" designations indicate the paternal HLA haplotypes, and the "c" and "d" designations the maternal haplotypes. Inheritance patterns follow classic Mendelian genetics. HLA genes are codominantly expressed.

domains interact with one another through these β-pleated sheets, and their structure closely resembles that described for an immunoglobulin constant region domain. The α_1 and α_2 domains are paired to form an eight-strand β-pleated sheet. This sheet is topped by two α-helices forming a groove at the top of the molecule. This groove is the site for binding of antigenic peptide fragments by the class I molecule (see Fig. 50.8). The sides and bottom of the groove are formed by side chains of the amino acids that constitute the helices and β-pleated sheets. Many of the amino acids that line this groove are polymorphic, creating allele-specific differences in antigen-binding specificity among the different class I allelic products (Stern & Wiley, 1994). Other residues in the helical regions of the groove interact with the T-cell receptor during recognition of the class I antigenic fragment complex by a T lymphocyte (see Fig. 50.2).

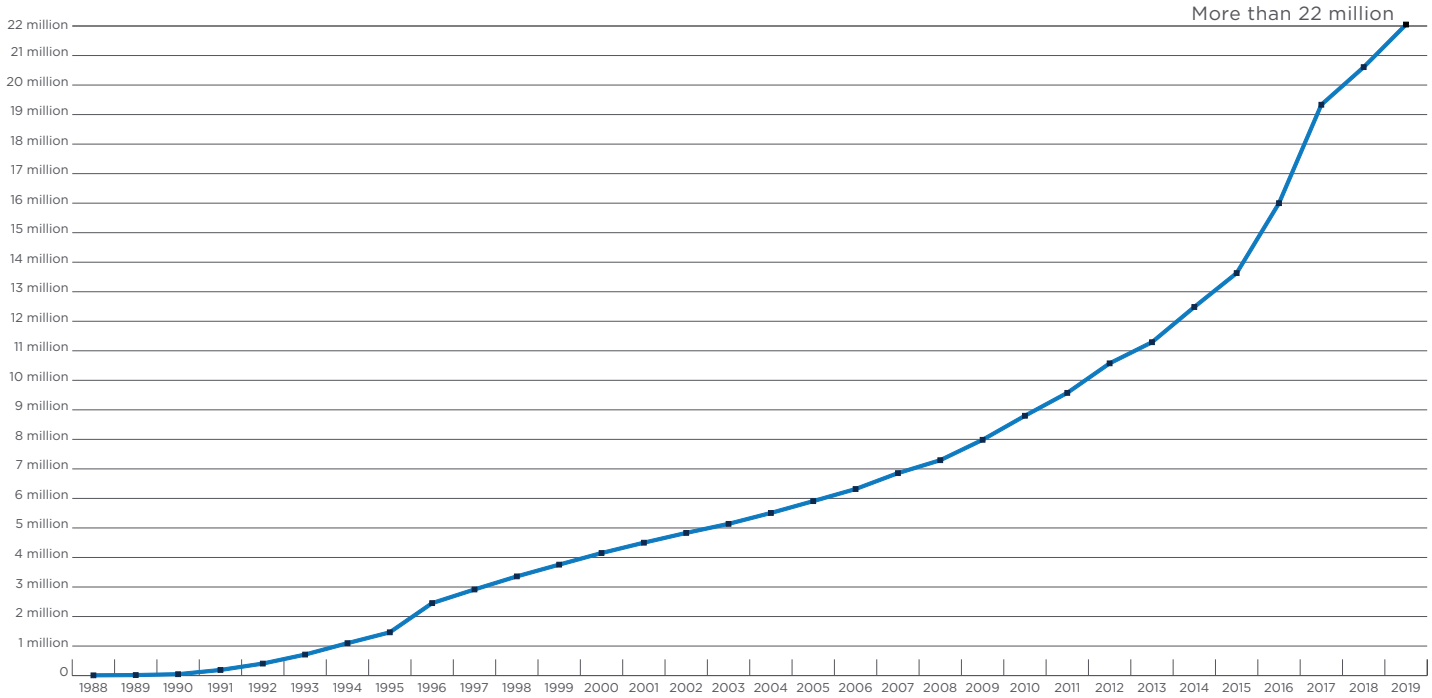

Fig. 50.5 More than 22 million donors for hematopoietic stem cell and bone marrow transplantation were registered by the National Marrow Donor Program in 2019. (Copyright National Marrow Donor Program, 2019.)

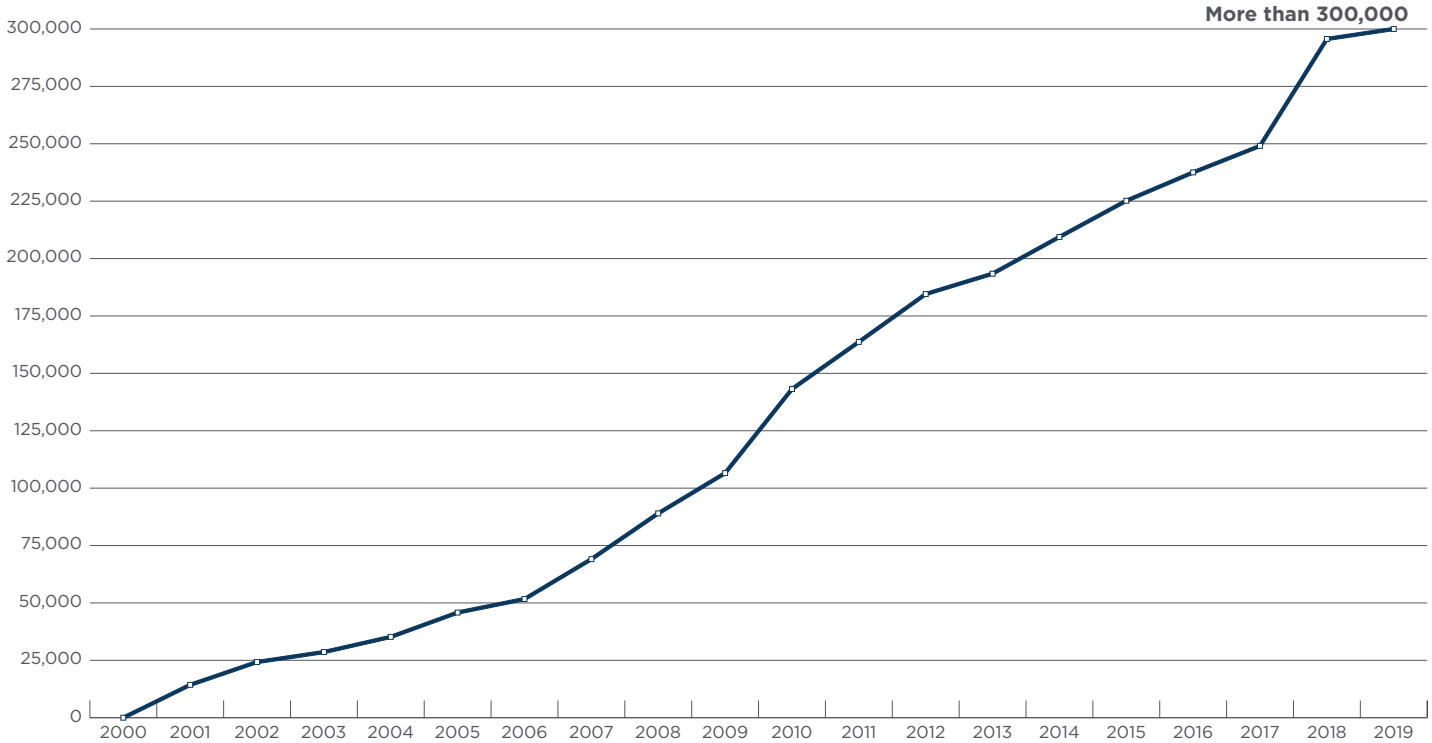

Fig. 50.6 Number of umbilical cord units has increased in the past decade, primarily for the treatment of blood malignancies in pediatric patients. More than one HLA mismatch and more than one cord unit can be used in umbilical cord transplantation. (Copyright National Marrow Donor Program, 2019.)

ORGANIZATION OF CLASS I GENES

The HLA heavy chains are encoded within the MHC on chromosome 6 (see Fig. 50.1) (Shiina et al., 1999) and are highly polymorphic, whereas β_2 microglobulin is encoded on chromosome 15 and is not known to be polymorphic in humans. The typical class I gene is encoded by eight exons. The first exon encodes the 5′ untranslated region and a hydrophobic leader peptide. Exons 2 to 4 encode the three extracellular domains; exon 5 encodes the transmembrane region. The sixth and seventh exons encode the cytoplasmic region, and the eighth exon encodes the 3′ untranslated region, including the poly(A) addition site. Intervening sequences (termed *introns*) between the exons are transcribed into ribonucleic acid (RNA) but are removed during messenger RNA (mRNA) splicing.

REGULATION OF CLASS I GENE EXPRESSION

HLA class I molecules are expressed as transmembrane glycoproteins on the surface of many cell types. However, the level of surface expression can vary extensively (Singer & Maguire, 1990). The resting level of class I molecules is highest on lymphoid cells, with HLA-C expression being ~10 times less than that of HLA-A or -B (Le Bouteiller, 1994). This is a result of inefficient association and a mutated *cis*-regulatory element

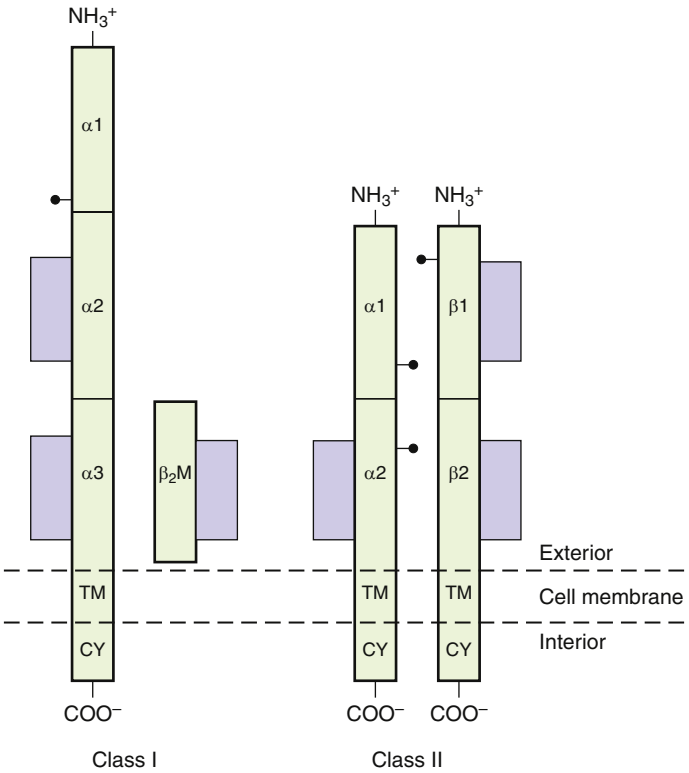

Fig. 50.7 A schematic model of the structure of class I and class II molecules.

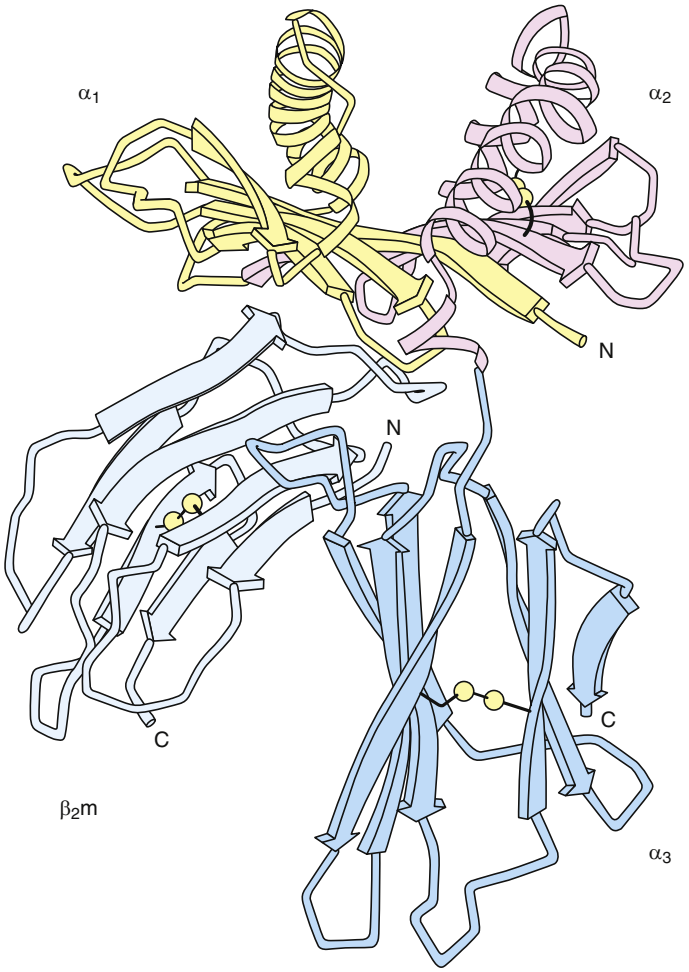

Fig. 50.8 Three-dimensional model of the extracellular portion of a class I molecule. (With permission from Bjorkman PJ, Saper MA, Samraoui B, et al: Structure of the human class I histocompatibility antigen, HLA-A2, Nature 329:506, 1987.)

of transcriptional control found in region I of the HLA-C promoter (enhancer A) that reduces its expression (Neefjes & Ploegh, 1988). Differential expression of HLA molecules appears to reflect the level and antigenic specificity of the allogeneic sensitization seen in patients awaiting kidney transplantation because these patients are subjected to multiple random blood transfusions while on dialysis; additionally, posttransplant, donor-specific antibodies (DSAs) are more prevalent against HLA-A or -B or both HLA-A and -B, and far fewer DSAs are rejected by only HLA-Cw donor-specific antibodies; class I molecules are undetectable on the membranes of certain other cell types such as brain cells, muscle cells, and sperm cells. Sequence elements located upstream of class I genes bind regulatory factors that control the cell surface expression of class I molecules. During an immune response, the cell surface expression of class I genes can be upregulated by binding of cytokine (e.g., interferon-γ and TNF) to upstream regulatory elements. Tumors and certain viruses (e.g., human immunodeficiency virus) can suppress class I expression (Brodsky et al., 1999).

FUNCTION OF CLASS I MOLECULES

The HLA-A, -B, and -C molecules play key roles in an immune response. First, in the adaptive immune response, class I molecules bind peptides derived from proteins degraded or synthesized in the cytosol and display them on the cell surface for interrogation by the antigen receptors on T lymphocytes (see Chapter 46). Presentation of antigen by class I molecules allows T cells to detect and mount a response to foreign material (e.g., a virus, abnormal proteins from a malignant cell). In the cytosol, intracellular antigens (including self-proteins and viral or abnormal proteins) are broken down into peptide fragments (Rock & Goldberg, 1999). These peptide fragments are transported to the endoplasmic reticulum, where they bind to the groove at the top of newly synthesized class I molecules and then are carried to the cell surface (Hansen & Lee, 1997; Pamer & Cresswell, 1998) (see Fig. 50.2). Four genes, located in the class II region of the MHC (Fig. 50.9; see also Fig. 50.1) are involved in this process. Two of these genes (*LMP2* and *LMP7*) encode components of the proteosome complex, a macromolecular structure that degrades proteins within the cytosol (Tanaka et al., 1997). The other two genes (*TAP1* and *TAP2*) encode components of peptide transporters that move peptides from the cytosol into the endoplasmic reticulum (Momburg & Hammerling, 1998). $CD8^+$ CTLs recognize the processed peptide in conjunction with the class I molecule (Jorgensen et al., 1992). In the experimental system used to dissect this mechanism, CTLs were generated by in vitro stimulation with virally infected autologous cells. Recognition and lysis of the target cell were specific for the priming virus strain. Recognition also was affected by allelic polymorphism of class I molecules because only virally infected target cells sharing the appropriate class I allelic product(s) with the responder were lysed (Zinkernagel, 1997a, 1997b). The latter requirement is termed **MHC restriction.** Zinkernagel and his collaborator Doherty were awarded the Nobel Prize for Medicine in 1996 in recognition of the significance of the concept of MHC restriction.

Second, surface expression of class I molecules has a protective function in the innate immune response by preventing target cell lysis effected by natural killer (NK) cells and their killer cell activating and inhibitory receptors (KIR). Unlike CTLs, NK cells do not require activation through the recognition of peptide bound to the class I molecule but can lyse and destroy target cells lacking classical HLA class I molecule expression on the cell surface. Through this innate mechanism, NK cells play an important role in surveillance against viruses and tumor cells that downregulate expression of the class I molecule to avoid recognition by CTLs (Lanier, 1998; Long, 1999).

There are two groups of NK receptors: (1) the C-type lectin receptor CD94/NKG2, whose genes reside on chromosome 12, and (2) the killer cell immunoglobulin-like receptors (KIRs) encoded by genes on chromosome 19. NK cell function appears to be regulated by a balance between positive signaling receptors that initiate and inhibitory receptors that suppress cell activation. Both groups of receptors recognize HLA class I ligands. For example, the KIR2D receptors differentiate between HLA-C ligands based on the presence of specific amino acid residues at codons 77 and 80 (i.e., asn77lys80 vs. ser77asn80). Another NK receptor, KIR3D, recognizes the HLA-Bw4/Bw6 polymorphism. A third NK receptor, CD94/NKG2, recognizes the HLA-E molecule complexed with the HLA leader peptide from some of the allelic products of HLA-A, -B, -C, and -G molecules (Brooks et al., 1999).

NK cells can specifically recognize and lyse allogeneic cells that do not express the specific class I molecules expressed by the effector cell (i.e., "missing self") (Valiante et al., 1997). This could occur even in apparently

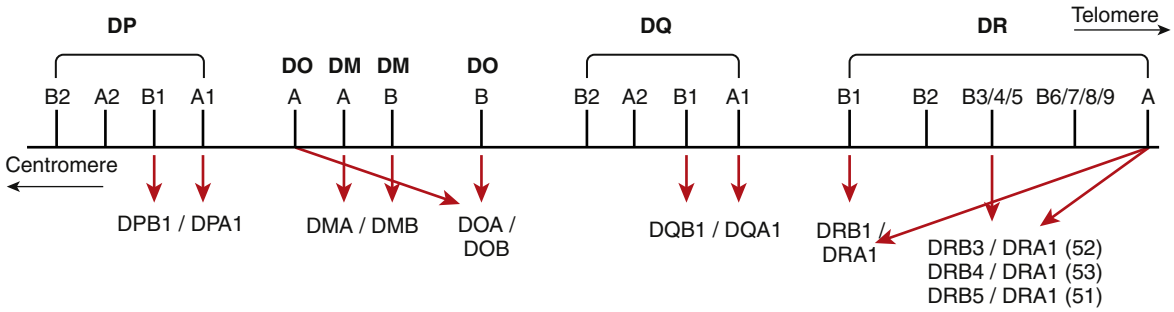

Fig. 50.9 Map of the class II region of the human major histocompatibility complex (MHC). Gene products encoded by each subregion are listed. Not all genes are included.

HLA-matched transplant pairs where one member of the pair is homozygous and the other is heterozygous (e.g., donor: Bw4 and Bw6; recipient: Bw6). Thus Bw4-specific NK cells from the donor might lyse cells without Bw4 from the recipient in a hematopoietic progenitor cell graft. This response may be unidirectional in some settings. In the example, the donor does not lack any HLA molecule present in the recipient; thus the recipient NK cells will not detect any missing self. Because NK cells are relatively radioresistant and make up a subpopulation of about 10% to 15% of peripheral blood lymphocytes, the NK response could be substantial; however, the extent of the role of NK activity in affecting transplant outcome is not known at present (Ruggeri et al., 1999). Since then, based on new knowledge of NK cell function, several donor selection strategies have been used in an attempt to improve the outcome of unrelated donor transplantation (Benjamin et al., 2010). These strategies include (a) the receptor-ligand model, (b) the missing ligand model or donor-recipient KIR ligand mismatch, (c) natural cytotoxicity model, and (d) the KIR gene-gene model or donor selection based on B haplotype content. These strategies have yielded a variety of outcomes that may depend on the type of malignancy; for example, donor selection based on the KIR gene-gene content of donor NK cell receptor has been shown to improve survival in acute myelogenous leukemia (AML) but not acute lymphoblastic leukemia (ALL) (Cooley et al., 2010). Also, haploidentical NK expanded cell transplantation using the KIR-HLA ligand mismatched model was used to successfully treat children with AML using a low-intensity protocol (Rubnitz et al., 2010).

OTHER CLASS I GENES

As many as 20 additional nonclassical or class Ib genes have been identified within the class I region of chromosome 6 by gene cloning (Aguado et al., 1999). Many of these are pseudogenes; however, several encode and express class I–like mRNA and/or molecules HLA-E, -F, and -G. These molecules may be key mediators of both adaptive and innate immune responses (O'Callaghan & Bell, 1998). Their genes are homologous to classical class I genes in structure, and the polypeptides encoded by these loci also associate with β_2 microglobulin. However, just as a high level of allelic polymorphism is a hallmark of the HLA-A, -B, and -C loci, a low level of polymorphism of the HLA-E, -F, and -G loci is a defining feature of these genes. In addition, by comparison with classical class I molecules, the cell surface expression of nonclassical class I molecules is low, and the distribution of these class Ib molecules on specific cell types varies.

HLA-G

HLA-G is expressed principally on extravillous cytotrophoblast cells at the fetal/maternal interface, where it is thought to play a role in maternofetal tolerance (Le Bouteiller & Blaschitz, 1999). HLA-G, as a ligand for at least three NK and other cell inhibitory receptors, protects the invading placental tissue from the cytolytic action of NK cells. Although HLA-G has the capability to bind and present processed antigen (i.e., peptides) to T cells, the diversity of peptides bound by HLA-G appears to be less than the diversity of peptides bound by classical class I molecules. Regulation of expression of HLA-G also differs from that of classical class I genes, as the gene contains no interferon response signal; thus it is not interferon inducible. It has been hypothesized that the soluble forms may act as specific immunosuppressors during pregnancy (Le Bouteiller & Blaschitz, 1999). Recent evidence supports this hypothesis. HLA-G transcripts are present in great numbers in placental extravillous membranes in the first trimester, but at term transcript numbers decline sharply in keeping with the theory that HLA-G provides protection for the allogeneic embryo from maternal NK cell surveillance (Agrawal & Pandey, 2003). This putative role raises the possibility that HLA-G may play a role in tolerance for transplanted tissues. Along these lines, it is interesting to note that liver-kidney transplant recipients with high concentrations of HLA-G in their sera had low numbers of acute rejection episodes and therefore may require less immunosuppressive therapy (Creput et al., 2003).

HLA-E

HLA-E may play a role in protecting a target cell from NK cell–mediated lysis. HLA-E molecules bind a set of almost identical hydrophobic peptides derived from the leader sequences of the classical class I and HLA-G heavy chains. HLA-E displays these bound peptides at the cell surface for recognition by NK cells, providing a check for the integrity of the antigen-presenting pathway (Lee et al., 1998a, 1998b; O'Callaghan & Bell, 1998). Skin grafting in a transgenic mouse model suggests that HLA-E may be recognized as a transplantation antigen (Pacasova et al., 1999). Recent studies suggest that host NK cells may be able to recognize HLA-E on allogeneic cells and possibly tolerate it, even when it is bound to donor peptides. With this finding comes the potential for exploiting this tolerance in pursuit of preventing NK cell–mediated graft rejection and graft-versus-host disease (GVHD) (Matsunami et al., 2002).

HLA-F

The role of HLA-F is unknown. Computer modeling predicts that certain amino acid residues of HLA-F could contribute to a putative peptide-binding groove, consistent with a role in antigen presentation by HLA-F (O'Callaghan & Bell, 1998). To date, HLA-F appears to be normally expressed only on the surfaces of extravillous trophoblasts that have invaded the maternal decidua, and has also been found on the surfaces of lymphoblastic cell lines infected with Epstein-Barr virus (Ishitani et al., 2003).

CLASS II MOLECULES—HLA-DR, HLA-DQ, AND HLA-DP SUBREGIONS

The class II molecules in humans were first recognized by their ability to stimulate allogeneic T cells in the mixed leukocyte culture (MLC). During the 1975 International Histocompatibility Workshop, the MLC was used to define the HLA-D allelic series (Thorsby & Piazza, 1975). Because MLCs required 7 days before results could be obtained, rapid serologic detection of HLA-D was sought. In 1975, it was determined that alloantisera contained antibodies reactive with molecules closely associated with the specificities previously identified as HLA-D by cellular techniques (Dausset, 1981). Following the 1977 International Histocompatibility Workshop, these serologic specificities were termed *DR*, for D-related specificities, because HLA-D and HLA-DR were observed to be associated but not identical to each other. Serologic testing coupled with genetic and immunochemical studies identified additional class II molecules: DR52, DR53, DR51, and DQ. Cellular techniques identified still another class II molecule in the late 1970s (Shaw et al., 1981). This molecule (now termed *HLA-DP*) was initially described as a secondary B-cell antigen (SB) because it was usually weak or undetectable in a primary MLC and required secondary phase stimulation in culture for detection. Subsequently, the DNA coding sequences and locations of these genes within the MHC were further characterized using molecular biology techniques (Beck & Trowsdale, 1999).

STRUCTURE OF CLASS II MOLECULES

The class II HLA-DR, -DQ, and -DP molecules are heterodimers consisting of two noncovalently associated transmembrane glycoproteins: an α chain (33–35 kDa) and a β chain (26–28 kDa) (Gorga, 1992). Both

polypeptide chains span the cell membrane and are oriented with their amino-termini on the outside of the cell. The extracellular regions of the α and β polypeptides are each divided into two domains, designated α_1 and α_2 and β_1 and β_2, and each domain consists of approximately 90 amino acid residues. The α chain has two carbohydrate moieties, one high-mannose and one complex-type glycan, at amino acids 78 and 118, respectively. β chains have one complex-type oligosaccharide at amino acid 19. The amino-terminal α_1 and β_1 domains of α and β chains contain the polymorphic residues, while the membrane proximal α_2 and β_2 domains are highly conserved and are homologous to immunoglobulin constant region domains. A region of approximately 12 amino acids in length connects the second extracellular domain to the hydrophobic transmembrane region (23 amino acids) and a small intracytoplasmic domain (8–15 amino acids).

Based on x-ray crystallography, the class II molecule is similar in structure to the class I molecule (Brown et al., 1993) (see Fig. 50.8). In the class II molecule, the α_1 and β_1 domains of the α and β chains form an eight-stranded β-pleated sheet topped by two α helices to form the antigen-binding groove at the top of the molecule. The α_2 and β_2 domains each form two antiparallel β-pleated sheets that support the groove at the top.

Similar to the class I molecules, the class II molecules are highly polymorphic (see Table 50.2 and Fig. 50.4) (Bodmer et al., 1997, 1999; Marsh et al., 2002). Class II polymorphisms have been defined by (1) class II–specific antibodies (alloantisera and monoclonal antibodies), which bind to class II molecules preferentially recognizing polymorphisms in the α helices; (2) alloproliferative T cells that recognize and proliferate in response to foreign class II molecules in vitro (the MLC); (3) two-dimensional gel electrophoresis of isolated class II molecules; (4) hybridization of restriction endonuclease digests of DNA-encoding class II genes using locus-specific probes (a technique that detects restriction fragment length polymorphism); (5) PCR-based DNA typing of class II alleles; and (6) direct nucleotide sequencing of class II genes. Most of the immunologically relevant class II polymorphism arises from amino acid sequence differences localized in the α_1 and β_1 domains of the two polypeptide chains. Similar to class I, amino acid polymorphisms that lie within the peptide-binding groove of class II influence the peptide-binding specificities for the each of the different class II allelic products. It is important to note here that for HLA-DQ and -DP, the α and β chains are highly polymorphic; in contrast, the α chain that associates with DRB1, DRB3, DRB4, and DRB5 is essentially nonpolymorphic.

ORGANIZATION OF CLASS II GENES

In contrast to the class I molecules, both the α and β chains of class II molecules are encoded within a 1100-kb section of the MHC region (see Figs. 50.1 and 50.9) (Beck & Trowsdale, 1999). The class II region includes three subregions—DR, DQ, and DP—each of which encodes at least one expressed A (encoding an α chain) and B (encoding a β chain) gene. Sequence comparisons suggest that both class I and class II genes arose through a successive series of gene duplications during the evolution of this gene complex. The original duplication in the class II region most likely gave rise to primordial A and B genes. More recent gene duplications generated the DR, DQ, and DP subregions containing multiple genes.

A typical A gene contains five exons encoding (1) the 5′ untranslated region and leader sequence; (2) the α_1 domain; (3) the α_2 domain; (4) the connecting peptide, transmembrane region, cytoplasmic tail, and a portion of the 3′ untranslated region; and (5) the remainder of the 3′ untranslated region, including the poly(A) addition signal. A typical β chain gene is similar to the α chain gene but has an extra exon for the cytoplasmic tail.

DR Subregion

The DR subregion encodes one or two DR molecules, depending on the individual's MHC haplotype (Bodmer et al., 1997, 1999). The subregion contains a single expressed DRA gene that is conserved across different haplotypes differing only in a single amino acid substitution found in the cytoplasmic domain.

The most centromeric DRB gene, *DRB1* (see Fig. 50.9), encodes a highly polymorphic β chain that, when associated with the α chain, exhibits serologic specificities DR1 to DR18. This molecule is the predominant class II molecule on the cell surface, accounting for well over half of total cell surface class II molecules.

The second expressed DRB gene, present only in some class II haplotypes, is located between the DRB1 locus and the DRA locus (see Fig. 50.9). In cells expressing the DR alleles, DRB1*03, *11, *12, *13, and *14 the second DRB gene is termed *DRB3*. (HLA nomenclature is described subsequently.) The *DRB3* gene is polymorphic, although at present the number of identified alleles is approximately 10 times less than the number of DRB1 alleles. The DRB3 product combined with the DRA product forms the DR molecule, which carries DR52 serologic specificity. The allelic subtypes of DRB3 can also be distinguished serologically. In cells expressing DRB1*04, *07, and *09 alleles, the second DRB gene is termed *DRB4*. The DRB4 product combines with the DRA product to form the molecule that carries the serologic specificity DR53. Last, in cells expressing DRB1*15 and *16 alleles, the second DRB gene is termed *DRB5*. This DRB5 product combines with the DRA product to form the DR51 serologic specificity. As with DRB3, DRB5 allelic subtypes can be distinguished serologically. Haplotypes expressing DRB1*01, *08, or *10 alleles do not usually carry a second expressed DRB locus. There are exceptions to these associations. For example, a haplotype carrying DRB1*15 without a DRB5 locus has been described (Wade et al., 1993) as well as a DRB1*08 carrying a DRB3 gene (Smith et al., 1994).

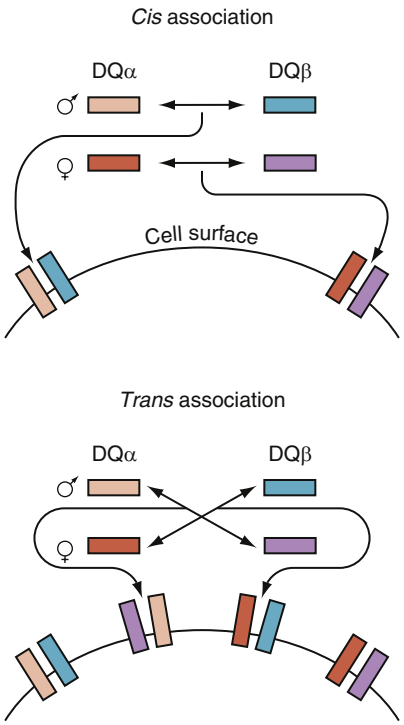

Fig. 50.10 Model of the *cis* and *trans* associations of DQα and DQβ chains.

DQ Subregion

One set of A and B genes, *DQA1* and *DQB1*, encode the DQ heterodimer that carries DQ1 to 9 serologic specificities (see Table 50.2 and Fig. 50.9) (Bodmer et al., 1997, 1999). DQ molecules represent approximately 15% to 20% of the total class II molecules expressed on the cell surface. Both *DQA1* and *DQB1* loci are polymorphic, which creates greater serologic diversity. Additionally, the protein products can associate in *trans* as well as in *cis*, meaning that heterozygotes may potentially express four different DQ molecules on their cell surfaces (Fig. 50.10). Such combinations can create opportunities for unique serologic specificities. As such, patients exposed to DQ molecules can make antibodies that react with the α chain, the β chain, or unique α/β combinations (Tambur et al., 2010). Other DQ-like A and B genes in the DQ subregion such as *DQA2* and *DQB2* are very similar to the *DQA1* and *DQB1* genes; however, no functional protein products are known to be expressed.

DP Subregion

The DP subregion contains two sets of A and B genes (see Fig. 50.9). One set, *DPA1* and *DPB1*, encodes the DP protein product; the other set is made up of pseudogenes. Both *DPA1* and *DPB1* genes are highly polymorphic (Bodmer et al., 1997, 1999). The level of DP expression on the cell surface is very low. DP genes function similar to DQ genes in that *trans* and *cis* associations of A and B gene products can create unique serologic specificities (see Fig. 50.10).

LINKAGE DISEQUILIBRIUM OF GENES IN THE CLASS II REGION

Specific combinations of DRB1/DRB3, DRB1/DRB4, DRB1/DRB5, and DQA1/DQB1 alleles are common. The DQA1/DQB1 combinations found may be controlled in part by the ability of α and β chains to pair

(Kwok et al., 1993). In addition, certain DR and DQ alleles are inherited together more frequently than expected, resulting in linkage disequilibrium in a population. The frequency of these combinations differs strikingly among different ethnic population groups. For example, both the DRB1*11:01, DQB1*05:01 (DR11, DQ5) and DRB1*09:01, DQB1*03:03 (DR9, DQ9[3]) haplotypes frequently are found in populations of direct African heritage, whereas these DR-DQ combinations are rarely found in populations of Caucasian heritage. Crossing over between the DP loci and the DR/DQ loci is common (Petersdorf et al., 2015) Thus less linkage disequilibrium is noted between the DR/DQ and DP alleles. Lists of common DRB1/DQA1/DQB1 haplotypes have been published (Begovich et al., 1992; Imanishi et al., 1992).

REGULATION OF CLASS II GENE EXPRESSION

Class II molecules, HLA-DR, -DQ, and -DP, are constitutively expressed on antigen-presenting cells (APCs) of the immune system, including monocytes, macrophages, dendritic cells, B lymphocytes, and some neoplastic cells. HLA class II expression is highest for HLA-DR, intermediate for HLA-DQ, and lowest for HLA-DP (Glimcher & Kara, 1992; Guardiola & Maffei, 1993); as with class I, differential expression of HLA class II molecules is reflected in the antigenic specificity of allosensitization seen in patients awaiting kidney transplantation. Recent studies have shown that among recipients making donor-specific antibodies posttransplant, HLA-DR– and HLA-DQ–specific antibodies are found more frequently than antibodies against class I. Antibodies against HLA-DP seem to be seen most often among patients who have experienced allograft failure. Whether the presence of DP antibodies was the cause of the rejection or a consequence of rejection and graft damage is not known.

DNA sequences found upstream of the coding sequences in class II genes are critical to expression. Binding of proteins to these regions regulates the expression of class II genes. Alterations in the ability of DNA-binding proteins to interact with the 5′ regulatory DNA sequences eliminating the expression of class II genes lead to an immunodeficiency called the **bare lymphocyte syndrome,** a severe combined immunodeficiency syndrome (Kovats et al., 1994; Mach et al., 1996). Class II genes are inducible by interferon (IFN)–γ in many cell types (Glimcher & Kara, 1992; Mach et al., 1996), and expression may be affected by other cytokines (Guardiola & Maffei, 1993). Expression of class II molecules on APCs, particularly in dendritic cells, may be modulated, following antigen deposition and inflammation. The level of antigenic peptide class II complex expression and the presence of a costimulatory signal on the mature APC may play an important role in transplantation and in autoimmune disease (Nepom & Erlich, 1991; Banchereau & Steinman, 1998).

FUNCTION OF CLASS II MOLECULES

Class II molecules act as antigen presentation molecules in the immune response (see Fig. 50.2), binding antigenic peptide fragments processed from exogenous antigens such as bacteria. The exogenous antigens enter the cell through the endocytic pathway and are degraded into peptide fragments in late endosomes, where they encounter and bind to the newly assembled class II molecules (Watts, 1997). Binding of processed protein peptide fragments to the class II molecule is facilitated by two proteins encoded within the class II region of the MHC: DM and DO (see Fig. 50.9). Peptide binding is affected by polymorphic residues located in the groove of the class II molecule. The complex of antigenic fragment bound to the class II molecule is transported to the cell surface for display to and recognition by circulating T cells.

Antigen receptors on $CD4^+$ T lymphocytes interact with the class II-antigenic fragment complex, triggering activation of the cell (Jorgensen et al., 1992). In the experimental system used to dissect this mechanism, effector T lymphocytes were stimulated in vitro with autologous APCs previously incubated with antigen. As observed for class I, recognition of the antigenic fragment by the effector T cell is influenced by MHC allelic polymorphism. The effector T cell is specific for the priming antigenic peptide in conjunction with the particular class II allelic product that originally presented the antigen (MHC restriction) (Rosenthal & Shevach, 1973).

Each T cell activated by recognition of the complex of antigen fragment bound to class II molecule can perform one or several functions (Paul & Seder, 1994). The $CD4^+$ T cell can help B lymphocytes differentiate to antibody-producing plasma cells, or it can help other T lymphocytes differentiate to either cytotoxic cells or cells with suppressor function. In addition, the T cell itself can function either as a cytotoxic cell, directly killing cells with the appropriate target (i.e., cells expressing class II MHC molecules complexed with the specific antigen), or as a cell with suppressor function, causing a dampening of the immune response. T cells also produce a number of biologically important molecules (such as IFN-γ and many other cytokines) that augment the immune response and increase the expression of MHC molecules on target cells. In addition, T cells produce growth factors such as interleukin (IL)–2. These growth factors affect a wide range of cells from hematopoietic progenitor cells to mature lymphocytes.

OTHER CLASS II GENES

At least four other class II genes—*DOA*, *DOB*, *DMA*, and *DMB*—have been described that express protein products (see Fig. 50.9). The proteins encoded by the *DMA* and *DMB* genes form the DM heterodimer. The proteins encoded by the *DOA* and *DOB* genes form the DO heterodimer. These gene products are not detected on the cell surface but rather are expressed inside the cell, localized to specialized intracellular compartments where newly synthesized class II (DR, DQ, DP) molecules bind their antigenic peptides. The DM molecule regulates peptide binding to HLA-DR, -DQ, and -DP, serving both chaperone-like and editor-like functions (Morris et al., 1994) that favor the presentation of stably bound peptides. The DO molecule negatively regulates the function of DM (van Ham et al., 1997). When DO negatively regulates DM function, cells fail to express antigenic peptides but rather express a processed fragment of the invariant chain (CD79) known as class II invariant chain peptide (CLIP).

CHARACTERISTICS OF ANTIGENIC FRAGMENTS BOUND BY MHC CLASS I AND CLASS II MOLECULES

The function of class I and class II molecules as antigen-binding receptors is similar; however, the peptides they bind have different characteristics (Cresswell, 1994; Engelhard, 1994). Peptides derived from proteins synthesized de novo in the cell (endogenous antigens such as viral antigens) associate with class I molecules in the endoplasmic reticulum. In contrast, peptides from soluble and particulate antigens, taken up by the cell via the endocytic pathway (exogenous antigens) bind with class II molecules in an endosomal compartment. Both class I and class II molecules can alternatively bind self-peptides found in these compartments. Self-peptides result from the normal degradation of cellular proteins. Some of these self-peptides are fragments of histocompatibility molecules themselves. Usually, the self-peptides bound to MHC molecules do not trigger T lymphocytes, as they are molecules to which the immune system of the individual is tolerant. However, these self-peptides may trigger immune responses, initiating a self-destructive process leading to autoimmunity (Nepom & Erlich, 1991) (see Chapters 52, 53, and 55).

Peptide binding to MHC molecules occurs only when the peptide fragment is of a suitable length and contains a particular amino acid sequence or motif that allows it to bind to one or more of the MHC molecules expressed in that individual. Examples of motifs for a peptide that bind to the HLA molecule encoded by A*02:01 are leucine (or methionine or isoleucine) at residue 2 of the peptide, a hydrophilic amino acid at residue 3, and valine (or leucine or isoleucine or alanine) at residue 9. The amino acids that make up the motif are referred to as **anchor** residues of the peptide. Different HLA molecules, either molecules encoded by different alleles at the same locus (HLA-A*02:03, *02:11, or *03:01) or molecules encoded by different loci (B*40:01 or DRB1*04:06), bind peptides with different motifs. The amino acids forming the peptide motif bind to the MHC molecule in pockets found within the antigen-binding groove (Stern & Wiley, 1994). The polymorphic amino acids of the MHC molecules line this groove and thus create differences in peptide-binding specificities for the different MHC molecules.

The peptides bound to class I molecules are 9 to 10 amino acids in length. Both the carboxy- and amino-terminal ends of the peptide are buried in the class I–binding groove, forming a **closed** peptide–MHC complex. The peptides bound to class II molecules vary in length from 12 to 30 amino acids. While maintaining the requirement for specific motif residues nested in the central portion of the peptide, both the carboxy- and amino-terminal ends of the peptide extend outside the class II–binding groove, forming an **open** peptide–MHC complex (Stern & Wiley, 1994).

RECOGNITION OF FOREIGN MHC MOLECULES

Allorecognition involves the recognition by a T lymphocyte of a foreign MHC molecule on a cell from a second (allogeneic) individual. Upon

recognition, the interaction triggers a series of events, resulting in activation of the T cell and initiation of an immune response not unlike the recognition of pathogens. Based on data from models of vascularized organ transplantation, two pathways of allorecognition have been hypothesized (Sayegh & Carpenter, 1996). The direct pathway for allorecognition involves the stimulation of recipient T cells by the donor MHC–peptide complex (i.e., direct recognition of intact foreign MHC molecules). The second route of allorecognition, the indirect pathway, involves stimulation of recipient T cells by self-MHC molecules presenting peptide fragments from donor cells. Indirect presentation occurs when antigen-processing cells of the recipient ingest cellular material from the grafted tissue, degrade the material intracellularly, and display the allogeneic peptide(s) complexed with self-MHC molecules. Peptides derived from polymorphic regions of donor MHC molecules are the major candidates for stimulation of the indirect immune response (Suciu-Foca et al., 1998; Gould & Auchincloss, 1999; Harris et al., 1999).

MINOR HISTOCOMPATIBILITY MOLECULES

Minor histocompatibility antigens (mHAs) can be any polymorphic gene product encoded outside the MHC that differs between donor and recipient and that can stimulate a T-cell response (Goulmy, 1997; Simpson et al., 1998). In other words, mHAs are immunogenic peptides that bind to MHC molecules, which can be recognized by T cells to cause undesirable antidonor responses or GVHD. In the setting of leukemic recipients, mHAs can also produce beneficial graft-versus-leukemia responses. Similar to other protein antigens, the polymorphic protein must be processed into antigenic fragments, and the polymorphic peptide fragment(s) must bind within the groove of MHC molecules. Because of the requirement for antigen presentation by MHC molecules, any polymorphic peptide must carry a motif suitable for MHC-specific binding. Thus not all individuals can present and respond to all mHAs even if there is a difference between donor and recipient. Most mHAs were initially thought to be presented to $CD8^+$ T cells by MHC class I molecules. However, mHAs have been identified that can bind to MHC class II molecules, and mHAs can elicit humoral antibody responses demonstrating that mHAs can elicit dynamic immune responses. In each case, the antidonor response is initiated when the T-cell receptor or B-cell receptor recognizes complexes formed by the polymorphic peptides of the mHAs bound to the MHC molecules expressed on APCs.

The mHAs were originally defined by skin graft rejection and by cytotoxic assays with T-cell clones. These polymorphic peptides have restricted binding to class I MHC molecules, so biochemical definition of the minor histocompatibility antigenic peptide components was accomplished by elution, purification, and sequencing of the mHA peptide bound to a specific MHC molecule (den Haan et al., 1995). As advances in genomic sequencing technology have made large-scale investigation of mHAs more feasible, interest in the potential clinical importance of mHAs in hematopoietic and solid organ transplantation has increased. One recent study showed that the degree of genome-wide mismatch in non-HLA antigens correlated with decreased renal allograft survival, independent of HLA antigen mismatch (Reindl-Schwaighofer et al., 2019). A number of non-HLA antigens have been identified as the targets of donor-directed immune responses. Early studies in this field identified mismatch of the antigen HA-1 as a risk factor for GVHD after bone marrow transplantation in HLA-identical siblings (Goulmy et al., 1996). Currently, over a dozen additional hematopoietic mHAs have been characterized (Oostvogels et al., 2016). Recent studies in renal transplant patients have also identified antigens that can elicit antibody responses, including angiotensin II type I receptor (AT_1), LIMS1, and the endothelial antigens endoglin, Fms-like tyrosine kinase-3 ligand, EGF-like repeats and discoidin I-like domains 3, and intracellular adhesion molecule 4 (Jackson et al., 2015; Dragun et al., 2005; Steers et al., 2019). Future studies will be needed to continue to define the clinical importance of mHAs in transplantation.

HLA NOMENCLATURE

SEROLOGIC AND CELLULAR SPECIFICITIES

HLA terminology is designated by the World Health Organization (WHO) Committee for HLA Nomenclature (see Table 50.2) (Bodmer et al., 1997, 1999). Historically, serologic and cellular defined specificities localized on the HLA protein molecules were assigned according to the results of international workshops during which typing reagents were exchanged among participating laboratories (18th International Histocompatibility Workshop website; see Table 50.1). Assignments included the name of the HLA molecule and a numeric designation based on the order in which the serologically defined specificity was defined. For example, HLA-A1 (or just A1) was the first HLA-A specificity to be assigned, and HLA-A80 was the most recent. Over time, older serologically defined specificities were "split," as the definition became more discriminating. The narrowest definition of the specificity is called the *private* specificity. The broader, shared specificities are called *parent* specificities. For example, B44 and B45 are private specificities of the parent specificity B12. Thus a cell that is either $B44^+$ or $B45^+$ is also considered to be positive for B12. Note here that there is no recognized specificity as B12.

In serologic testing, some alloantisera bind to more than one HLA allelic product—a phenomenon termed *cross-reactivity*. However, this cross-reactivity is a function of shared antigenic determinants (epitopes) across different HLA molecules. This serologic cross-reactivity among allelic products of HLA-A and -B loci has been extensively studied and has been used to cluster molecules within cross-reactive antigen groups (CREGs) (Rodey & Fuller, 1987). Class I molecules within a CREG share one or more epitopes that are not shared by molecules in another CREG. An epitope shared among members of a CREG is called a *public* specificity. Some of the CREG reactivity can be explained by the sharing of amino acid sequences among the HLA molecules in a CREG (Terasaki et al., 1992). However, the various CREG groupings overlap considerably (Ellison et al., 1994). To be able to appropriately name newly discovered HLA alleles, a more logical format for HLA nomenclature assignment was implemented in 2010. This change was defined by the Update to HLA Nomenclature, 2009. The WHO Nomenclature Committee for Factors of the HLA System met during the 15th International Histocompatibility and Immunogenetics Workshop in Buzios, Brazil, in September 2008, and introduced colons into the naming scheme. These colons will allow for the discovery of more than 100 alleles in a given group; the following examples of these changes were listed in the WHO 2008 Workshop Report (http://hla.alleles.org/nomenclature/naming.html).

A*01010101 becomes A*01:01:01:01.
A*02010102L becomes A*02:01:01:02L.
A*260101 becomes A*26:01:01.
A*3301 becomes A*33:01.
B*0808N becomes B*08:08N.
DRB1*01010101 becomes DRB1*01:01:01:01.

For antigen groups that have more than 100 alleles, such as the A*02 and B*15 groups, it will be possible to encode these in a single series. Thus the A*92 and B*95 alleles will now be renamed into the A*02 and B*15 allele series. For example,

A*9201 becomes A*02:101.
A*9202 becomes A*02:102.
A*9203 becomes A*02:103.

The HLA-Bw4 and -Bw6 specificities are broad, public epitopes that reside on the same molecule as the HLA-B locus subtypic specificities, but at a different site. Thus Bw4 and Bw6 are a diallelic system, and all B locus (and some A locus) molecules carry either Bw4 or Bw6 specificities. The region of the HLA molecule carrying the Bw4/Bw6 specificities has been identified in the α1 helix between amino acid residues 77 and 83 (Parham & Lawlor, 1991).

The WHO-designated serologic specificities localized to the class II molecules, HLA-DR and -DQ, have been assigned as described for the class I molecules (Bodmer et al., 1997, 1999) (see Table 50.2). Six HLA-DP types were originally defined by cellular techniques. While class II HLA-DP molecules have not been adequately defined serologically, studies have shown that at least six hypervariable regions may contribute to serologic reactivities (Laux et al., 2003). Twenty-six HLA-D specificities were initially identified by MLC. All HLA-D specificities retain the "w" designation because these specificities are defined functionally by the measurement of stimulation of a responder cell. This stimulation is generated by differences in the DR molecules expressed on a stimulator cell and, to a lesser extent, by additional stimulation by the DQ and DP molecules.

DNA-BASED ALLELE DESIGNATIONS

Nucleotide sequencing has been used to identify the many different alleles encoding the HLA molecules. Currently, a single, serologically defined specificity may reside on 2 to more than 25 different allelic products (see Table 50.2). Each HLA allele is designated by the name of the gene locus followed by an asterisk and a four- to seven-digit number indicating the allele. For example, A*02:01 is an allele of the *HLA-A* gene; B*15:10 is an allele of the *HLA-B* gene; DPB1*01:01 is an allele of the *HLA-DPB1* gene; and DQA1*06:01 is an allele of the *HLA-DQA1* gene.

The first two numbers in the numeric designation of each allele, also called the first field, are frequently based on the serologic type of the resultant molecule and/or the nucleotide sequence similarity to other alleles in the group. For example, the HLA-A molecule expressed by the A*02:01 allele bears the A2 serologic specificity defining the HLA-A2 antigen. However, the HLA-B molecule expressed by the B*15:10 allele does not bear the B15-associated serologic specificity, but rather the B71 serologic specificity defining the B71 antigen. It was designated B*15:10 because of its predicted amino acid sequence similarity to other B15 antigens. Cells expressing DRB1*01:03 were initially serologically typed as DR-blank, DR1, or even DR13. Nucleotide sequencing identified an allele with a similar DNA structure to alleles bearing the DR1 serologic specificity (e.g., DRB1*01:01 and *01:02), and the name of this allele was based on that structural similarity. When a unique serologic specificity was later identified, the DR antigen determined by DRB1*01:03 was given the DR103 serologic designation. The second field of the allele designation refers to the order in which the allele was described. For example, A*02:01 was the first A2 allele to be sequenced, and A*02:03 was the third. As of July 2019, there were 877 unique sequences for the A2 group (see Table 50.2).

Some alleles may differ in the DNA sequence of their coding regions, but their predicted amino acid sequence does not differ (often termed a *silent* or *synonymous* substitution). These combinations of alleles are identified by the third field designation. The first two fields are shared, and the third field is then used to distinguish the unique nucleic acid sequences of the alleles (e.g., B*27:05:01 and B*27:05:02). In addition, two or more alleles may have a fourth field in their name (e.g., DRB4*01:03:01:**01** and DRB4*01:03:01:**02**). The fourth field indicates that the two alleles differ only outside the protein coding region (e.g., introns). In the example listed here, the difference affects the RNA splice site of DRB4*01:03:01:02, resulting in loss of expression of the allele (Sutton et al., 1989). Finally, alleles that are not expressed as proteins at the cell surface may have an **N** added to their names (e.g., A*02:15N, DRB4*01:03:01:02N) to indicate "null." Note that the designation "N" is not required to identify a unique allele but is used for descriptive purposes only. Other designations include **L** (for low expression), **S** (for secreted protein), and **Q** (for questionable surface expression).

New alleles are described in regular reports of the WHO HLA Nomenclature Committee (see Table 50.1) (http://hla.alleles.org/nomenclature/nomenc_reports.html; Bodmer et al., 1999), and the nucleotide sequences of all alleles are deposited in a computerized databank (GenBank, EMBL, IPD-IMGT/HLA databases). Currently, for example, more than 5200 HLA-A alleles have been assigned. New alleles are continually being identified and can be accessed through the website (https://www.ebi.ac.uk/ipd/imgt/hla/).

TECHNIQUES FOR IDENTIFYING HLA POLYMORPHISM

HLA typing or tissue typing is performed in a limited number of laboratories because it uses specialized procedures and reagents. Commercially available kits can be obtained for both DNA-based and serologic testing; however, interpretation of the test results requires considerable experience and knowledge. Histocompatibility laboratories are usually found in medical centers that have organ and/or hematopoietic progenitor cell transplantation programs. HLA testing techniques are discussed in general in this section. For detailed procedures, the reader should refer to the American Society for Histocompatibility and Immunogenetics (ASHI) Laboratory Manual, 4th edition (2001) (see Table 50.1 for the ASHI website). HLA testing laboratories are accredited through ASHI, the European Foundation for Immunogenetics (EFI), and other organizations.

DNA-BASED TYPING OF CLASS I AND CLASS II ALLELES

Although serologic and cellular typing of HLA antigens have been extremely useful, there are a number of technical drawbacks to these techniques. With the advent of rapid and reliable methods for the isolation and characterization of class I and class II genes and the determination of nucleotide sequences of class I and class II alleles, it has become possible to use DNA-based methods for HLA typing. Over the years, various molecular HLA typing methods have been developed (Sequence Based Typing [SBT], Sequence Specific Primers [SSP], real time PCR, Sequence Specific Oligonucleotide Probe Hybridization [SSOPH], and direct sequencing currently referred to as Next Generation Sequence [NGS]) (Madden, 2019), each with its own advantages and disadvantages (see Table 50.2 for summary). DNA-based typing of HLA alleles is a commonly used technique in HLA typing laboratories (Hurley, 1997; Middleton, 1999).

In contrast to other forms of testing, DNA-based typing has five significant advantages as follows:

1. It is specific. The specificity of each DNA typing reagent (i.e., synthetic oligonucleotide primers and probes) is clearly defined and is based on a specific, known nucleotide sequence. Because the oligonucleotides used as DNA typing reagents are synthetic, reagents are not limited and there should be no lot-to-lot variation in specificity.
2. It is flexible. New reagents can be designed as new alleles are discovered and unique nucleotide sequences are identified. Testing can be carried out at several levels of resolution, depending on the typing requirements and the time available for testing.
3. It is more robust than other techniques. DNA typing does not require viable lymphocytes and is not influenced by the health of the patient. Furthermore, DNA-based testing is highly reproducible when standard methods such as SSOP and NGS are used in conjunction with a standard test protocol (Hurley et al., 2000; Profaizer et al., 2016).
4. It can be used for large-scale typing (SSOP, SBT, and NGS). The batching of samples facilitated by automated and computerized methods reduces cost and errors. DNA-based methods are particularly applicable for the HLA typing of large numbers of volunteers for donor registries (Zhou et al., 2015).
5. It can discriminate by detecting the full extent of HLA diversity. HLA alleles can specify HLA proteins that are indistinguishable using serologic typing. For example, an individual carrying the DRB1*04:01 allele would have the same serologic type (DR4) as an individual carrying the DRB1*04:12 allele (DR4). Thus DRB1*04:01 and DRB1*04:12 are "splits" of the broad serologic specificity DR4. These splits, identified by DNA typing, are referred to as "allelic variants." Serologic reagents specific enough to define every split or allele are not available. Currently, 292 alleles of DR4 have been identified with 277 of them resulting in expressed proteins. There are many other examples of splits defined using DNA typing that cannot be identified using serologic methods; some are listed in Table 50.2.

The problems with serologic typing are particularly acute when typing some population groups. For example, populations of direct African origin can express class I and class II antigens that are difficult to identify with currently available serologic reagents (Bozon et al., 1997; Yu et al., 1997; Mytilineos et al., 1998). DNA-based HLA typing has greatly improved the ability to define unique HLA types in these populations and many other populations.

Preparation and Amplification of DNA

Any cell with a nucleus can be used as a source of DNA. Although red blood cells do not contain nuclei, other cells in the blood, such as lymphocytes, are a good source of DNA. Cell lines such as Epstein-Barr virus–transformed B lymphocytes are also a good source of DNA. Because transformed cells can be grown in culture in the laboratory, they provide a renewable supply of DNA and can be used to provide reference DNA for quality control of typing procedures. DNA for HLA typing is usually prepared from whole blood. Many different protocols can be used to isolate DNA from cells, and commercial kits are available for the preparation of DNA. The sensitivity of detection of HLA types is enhanced greatly by the amplification of DNA-encoding HLA genes using the PCR technique (Saiki et al., 1988). A pair of synthetic oligonucleotides (primers) should be complementary to sequences flanking a specific HLA gene and are utilized to generate millions of copies of that gene for use in the HLA typing reaction. Some typing reactions utilize primer sequences that are shared by all alleles at an HLA locus; other typing procedures utilize primer sets that are shared by only a subset of alleles at a locus. Annealing of the primers to sample DNA during the PCR reaction uses reaction conditions that guarantee the primers will bind to perfectly matched sequences (target sequences) and not to sequences of other loci or other alleles that are not matched. By adjusting the temperature of the annealing component of the PCR reaction, the typing laboratory can control the specificity of the amplification.

Sequence-Specific Priming

One method of identification of HLA alleles uses sequence-specific primers (SSPs) in the PCR reaction (Olerup & Zetterquist, 1992; Bunce et al., 1995). These primers anneal to denatured DNA containing the HLA alleles from which the primer sequences were derived. In the subsequent PCR reaction, only these selected alleles are amplified. DNA amplified by the primers is identified by gel electrophoresis or, if the DNA is labeled with a dye during amplification, by fluorescence such as in real-time PCR methods. This procedure is useful for typing a small number of samples

within a short time period; as such, this method is ideal for deceased donor HLA typing, which is time sensitive. Several commercial kits utilizing this method are now available.

Sequence-Specific Oligonucleotide Hybridization

It has been possible to use hybridization of SSOPs to amplified DNA to identify alleles (Gao et al., 1991; Williams et al., 1997; Cao et al., 1999). The use of several different oligonucleotide probes to define a specific HLA allele or the use of sequence-specific priming coupled with hybridization with panels of probes is usually required. A set of oligonucleotides capable of identifying each allele is hybridized to denatured, PCR-amplified DNA, which is attached to a solid support. Hybridization conditions are adjusted so that the probes will anneal to denatured DNA containing the HLA alleles from which the oligonucleotide sequence was derived. The oligonucleotides are labeled with a tag for detection of hybridization. For example, the oligonucleotide might be coupled to an enzyme such as alkaline phosphatase. Following addition of a substrate, alkaline phosphatase cleaves the substrate to yield a colored compound or to produce light (chemiluminescence). After visualization, the pattern of hybridization can be read to determine the alleles present. Figure 50.11 illustrates the approach using an oligonucleotide probe for the DQB1 allele, DQB1*03:02, to identify patients with insulin-dependent diabetes who carry this allele (Todd et al., 1987). The SSOP method is highly accurate, specific, and reliable (Hurley et al., 2000). It is often used in situations in which many samples are typed in large batches. Commercial kits using this method are available.

In a related procedure, called the *reverse format*, the oligonucleotide probes are bound to a solid support (Bugawan et al., 1994). DNA from the samples to be tested is amplified using primers labeled with, for example, biotin. The amplified DNA is then hybridized to the immobilized probes, which contain sequences found in the alleles present in the DNA. After visualization (using an avidin-linked detection system), the pattern of hybridization can be read to determine the alleles present. This procedure is useful for typing both small and large numbers of samples. Commercial kits utilizing this method are available.

Sequence-Based Typing (SBT)

A final method of identification of HLA alleles involves direct determination of the DNA sequences of the HLA alleles carried by an individual (SBT). Alleles may be identified following PCR amplification to separate the alleles based on SSPs or as a mixture of two alleles. Sequencing is labor intensive and highly complex but is used frequently to determine the HLA match at an allele level between hematopoietic progenitor cell transplant patients and their prospective donors (Petersdorf, 1995; Rozemuller & Tilanus, 1996; Scheltinga et al., 1997). Over the years, efforts to develop automated SBT methods have yielded several potentially promising high-throughput approaches, including high-performance liquid chromatography (HPLC) (Etokebe et al., 2003), pyrosequencing (Nordstrom et al., 2000), and reference-strand–mediated conformational analysis (RSCA) (Arguello et al., 1996, 1998). However, none of these SBT methods gained the widespread use compared to Sanger sequencing.

Sanger sequencing generally yields high resolution or second field resolution. Sequencing is preceded by locus-specific PCR amplification to generate sequencing templates. Deoxynucleotidephosphates and DNA polymerase are added to elongation chain products. Extension is terminated by fluorescently labeled dideoxynucleotidephosphates, as they lack the 3′-OH group required for phosphodiester bonds between base pairs. Following multiple rounds of template DNA extension and termination, fragments of varying lengths are produced and can then be separated by size and fluorescence to determine the sequence. Fragments can be run on traditional four-lane sequencing in which amplified PCR products were divided into four separate sequencing reactions and then run on gel electrophoresis. Newer technologies, such as capillary electrophoresis, have allowed for single-lane sequencing, which produces electropherograms as the primary output. A number of commercial Sanger sequencing HLA typing kits have been developed. One well-established limitation of Sanger sequencing is the *cis/trans* ambiguities due to heterozygosity at a given nucleotide position. As a result, there is uncertainty as to which allele, maternal or paternal, each nucleotide pertains. In these circumstances, another method, such as SSP, is needed to resolve the ambiguity (De Santis et al., 2013).

In recent years, NGS has gained traction in clinical HLA laboratories to obtain true allele-level typing providing third and fourth field resolution, thereby increasing the capability of identifying novel alleles (Gandhi et al., 2017). NGS combines clonal sequencing of targeted DNA with high-throughput sequencing. Specifically, HLA genes are amplified, and the resulting amplicons are then fragmented into sequencing appropriate sizes. These fragments are then ligated to adaptor sequences that include a unique index sequence identifying the sample origin of the fragmented DNA. Adaptor ligated DNA, termed *library*, can now be pooled with multiple libraries from different samples, each with their own unique identifying sequences. After the final processing steps (size selection and quantitation), the pooled samples can be loaded onto the sequencer; and the data generated can then be analyzed using specialized software. This method is also referred to as "massively parallel sequencing" since overlapping fragments of DNA are sequenced and their individual sequences aligned to construct a map of the entire full-length gene. There are multiple commercial NGS platforms now available for clinical use, and each has similar protocols and provides comparable results (Profaizer et al., 2016; Erick et al., 2018).

Resolution of DNA-Based Typing

The level of resolution (i.e., the ability to discriminate among alleles) obtained by DNA typing methods is controlled by the choice and number of primers and/or probes used in the assay and the typing method. This choice may depend on the time available for performing the typing, the cost of the typing, the expertise of the laboratory personnel, and the purpose of the typing. Large-scale donor registry typing is usually carried out at low to intermediate resolution, while typing of a potential hematopoietic progenitor cell donor for a specific patient is carried out at high resolution or allele-level resolution.

A multistep approach is often used to identify HLA alleles by DNA-based typing. For this reason, HLA types defined by DNA-based typing may be reported at different levels of resolution. Low-resolution (or generic or serologic) level DNA-based typing produces a result that is similar in appearance and detail to a serologic type. For example, a DNA-defined type, DRB1*11 or DRB1*11:XX, is the approximate equivalent of the serologic type DR11. The "XX" indicates that the allele was not further defined. At this level of resolution, it is not possible to determine which one of the more than 260 DRB1*11 alleles are carried by the individual being tested. Although serologic typing can be as informative as low-resolution typing, results are more reliable with DNA-based testing. Intermediate-resolution–level DNA-based typing may narrow the choices by listing several different possibilities for the type of an individual (e.g., DRB1*11:01 or DRB1*11:04). Finally, high-resolution–level (or allele-level) DNA-based typing identifies the specific allele carried by an individual (e.g.,

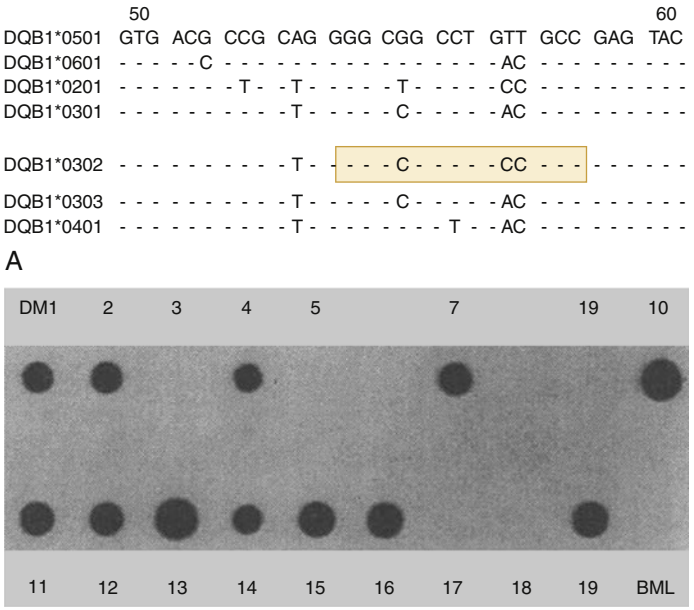

Fig. 50.11 **A** Nucleotide sequence alignments of several DQB1 alleles. The sequences presented cover the codons for amino acids 50 to 60. A dash indicates that the nucleotide is identical to the top sequence. An oligonucleotide that is specific for the DQB1*03:02 sequence is boxed. **B** Oligonucleotide dot blot analysis of 17 insulin-dependent diabetes mellitus patients (DM1 to 19) and one control, *BML*. Amplified DNA containing class II DQB1 sequences for the patients was attached to a membrane and hybridized to the labeled oligonucleotide specific for the DQB1*03:02 sequence (described previously). Positive hybridization signals indicate the patients who carry this DBQ1 gene sequence (patients DM1, 2, 4, 7, 10 to 16, 19). (With permission from Todd JA, Bell J, McDevitt HO: HLA-DQ β gene contributes to susceptibility and resistance to insulin-dependent diabetes mellitus, Nature 329:599, 1987.)

DRB1*11:04). However, this too can be further subdivided. Some alleles differ only by a single nucleotide substitution, which does not change the expressed protein. This difference is represented by the use of a third field designation (e.g., DRB1*11:01:01 differs from DRB1*11:01:02 by a single nucleotide substitution at position 303; this substitution does not change the expressed protein). True allele-level resolution typing can include the noncoding regions (i.e., introns as well as the exons). This is designated by a fourth field (e.g., DRB1*11:01:01:01). Although not significant in determining the protein sequence of the expressed molecule, intronic differences can be used for disease association and anthropologic studies (Kishore & Petrek, 2018).

SEROLOGIC DETECTION OF CLASS I AND CLASS II MOLECULES

Lymphocyte microlymphocytotoxicity testing, which originally was used in the mouse system by Gorer and Amos and later was modified by Terasaki and McClelland for use in the human system, has been used for HLA typing since the 1960s. Serologic testing for HLA-A and -B can be reproducible under controlled, standardized conditions; however, in large-scale testing (e.g., for registries), error rates may increase (Bozon et al., 1997; Yu et al., 1997). The reproducibility for serologically determined HLA-C and class II specificities is much lower, and HLA-DP is not even defined by serology. Though microlymphocytotoxicity serologic assays are still employed in some laboratories, it has been supplanted by DNA-based testing in most typing laboratories. DNA-based testing with its greater resolution is used to determine the HLA type of unrelated individuals and of family members, especially if the segregation of HLA cannot be accurately discriminated by serology (e.g., families where parents are not available, families where parents share an HLA antigen). For example, an offspring inherits DR4 from each parent and so is DR4 antigen homozygous (DR4,DR4). However, high-resolution DNA typing might identify two distinct alleles of the DR4 antigen, DRB1*0401 and DRB1*0403 (DRB1*04 allele heterozygote), providing informative data for haplotype segregation analysis.

Lymphocyte Preparation

Lymphocytes used routinely in HLA serologic typing assays are readily obtained from peripheral whole blood by layering onto a Ficoll-Hypaque gradient to separate the blood cells by density centrifugation. New separation methods isolate lymphocytes by positive or negative selection using monoclonal antibodies adhered to a solid surface. The separated peripheral blood lymphocytes (PBLs) can be used for HLA-A, -B, and -C typing. To test for HLA-DR and -DQ serologic specificities, it is necessary to enrich for B lymphocytes or to use a special two-color fluorescent technique to simultaneously differentiate between unseparated B cells and T cells.

Lymphocyte Microlymphocytotoxicity Assay

The HLA phenotype is determined by testing the unseparated lymphocyte preparation (PBL) or T lymphocytes (for HLA-A, -B, -C) or the enriched B lymphocytes (for HLA-DR, -DQ) against a panel of well-characterized HLA alloantisera. The assay is a two-stage test. During the sensitization stage, the lymphocytes are incubated with the antisera. Prescreened and standardized rabbit serum as a source of complement is added in excess, and the mixture is incubated for an additional period. If the lymphocytes carry a cell surface molecule recognized by complement-fixing antibodies in the alloantiserum, the antibodies bind to the cells and the cells are subsequently lysed following the addition of complement in the second step of the assay. The assay is concluded with the addition of a vital dye (eosin or trypan blue) that identifies dead cells. Reactions are read, and the percentage of dead cells is numerically graded.

HLA Typing Sera Trays

HLA typing reagents are derived from the sera of alloimmunized individuals (multiparous women, transplant recipients, multitransfused patients, and planned immunization of humans). Multiwell plates of human alloantisera (i.e., HLA typing trays) are commercially available. Because of the antigenic complexity of HLA antigens, several antisera should be used to define each specificity. Most laboratories use multiple trays from at least two different vendors or may use locally derived alloantisera. Because most alloantisera are not truly monospecific and many exhibit some cross-reactivity, the reactivity of each antiserum must be thoroughly tested and known to the individual interpreting the results. This requires stringent quality control of each new lot of typing trays with well-characterized reference cells. The titer and the specificity of antibody formed by a sensitized individual may not remain constant over time; therefore supplies of antisera are limited. In an attempt to create a consistent and unlimited supply of reagents, some companies have produced monoclonal antibodies. However, these monoclonal reagents are not available for all HLA specificities.

Cross-Reactivity

HLA alloantisera may react with more than one HLA allelic product. This phenomenon can result from polyspecificity of the antisera and/or from cross-reactivity and is responsible for the complex reactivity patterns of some alloantisera. Poly-specific sera contain two or more HLA-specific antibodies that can be adsorbed to remove one antibody with little effect on the reactivity of the other(s). Cross-reactive antisera contain, most frequently, a single antibody that reacts with an antigenic determinant shared among several different HLA allelic products (i.e., CREG or broad determinants, as previously discussed) (Rodey et al., 1994, 1997). Cross-reactions occur most frequently among allelic products encoded by the same locus (e.g., A2 + A23) but can occur between allelic products encoded by different loci (e.g., A2 + B17).

CELLULAR DETECTION OF CLASS II MOLECULES

The response of one cell in tissue culture to the alloantigens on the surface of a second cell is called the *mixed leukocyte culture* or *mixed lymphocyte reaction* (Hartzman et al., 1971). The MLC is considered an in vitro measure of class II disparity between individuals that recognizes determinants found on class II molecules, which are known collectively as *HLA-D*. The T-cell response is made unidirectional by preventing cells from one of the two individuals from replicating by treating those cells with radiation or mitomycin C prior to addition to the culture. The MLC represents a summation response of a responder cell to differences in the multiple determinants on HLA class II molecules (DR, DQ, and DP) encoded by the irradiated stimulator cell haplotypes. The response to DR molecules appears to predominate.

The use of the MLC as a test to determine histocompatibility has declined significantly because of limitations inherent to the technique and the advent of molecular techniques for HLA typing. The MLC can be influenced by the health of the patient, the type of disease, and the history of prior transfusion (Mickelson et al., 1996). For these reasons, the MLC assay has been replaced by more precise DNA-based typing methods. Currently, in some transplantation centers, the MLC is used to identify renal allograft recipients with specific hyporeactivity to donor HLA molecules following transplantation as a guideline for tapering of immunosuppression (Reinsmoen & Matas, 1993).

Limiting dilution analysis to define the frequency of donor cytotoxic or helper T lymphocytes has been used to predict the extent of allorecognition in hematopoietic progenitor cell transplantation (Madrigal et al., 1997). The correlations of these frequencies with subsequent events such as the extent of GVHD is still controversial.

TISSUE/ORGAN TRANSPLANTATION

Long-term survival of solid organ and hematopoietic progenitor cell grafts represents one of the most challenging goals in medical science. Renal transplantation is the therapy of choice for most patients with end-stage renal disease. Hematopoietic progenitor cell, heart, lung, liver, and pancreas transplantation is gaining wide acceptance as therapeutic procedures with successful outcomes. The primary obstacle to solid organ and to hematopoietic progenitor cell transplantation is immunologically mediated rejection of the foreign tissue. Therefore the success of allografting is dependent on the ability to deter the immune reaction, which may be accomplished by (1) histocompatibility matching between the donor and recipient; (2) immunosuppressive therapy of the recipient (reviewed by Enderby & Keller, 2015); and (3) achieving specific unresponsiveness to donor alloantigen(s) (i.e., tolerance) (Remuzzi et al., 1995).

GENETIC BASIS OF TRANSPLANTATION

The genetic basis of transplantation was first determined in 1916 as a result of tumor transplantation experiments in mice and was subsequently extended to transplants of normal tissue (Snell, 1981). It was demonstrated that skin grafts within inbred strains that were homozygous at histocompatibility loci (i.e., syngeneic grafts) were successful, but grafts between two different inbred strains (allografts) were rejected. Furthermore, allografts from either parent inbred strain (two copies of the same MHC genes; homozygous) to first-generation (F1) hybrids (one copy of each of the two different sets of MHC genes from two homozygous parents) survived in all

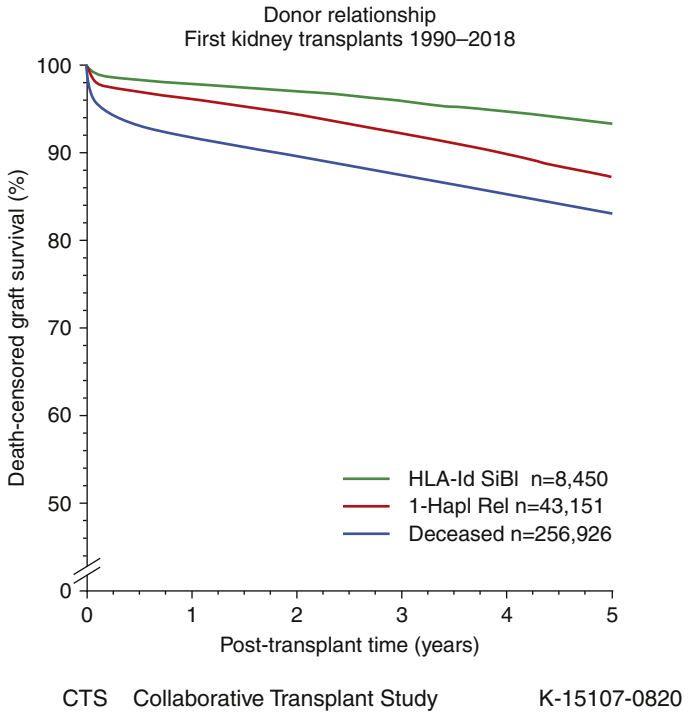

Fig. 50.12 Kaplan-Meier graph of 5-year (first transplant), death-censored, renal graft survival of three categories of histocompatibility matched groups: **HLA-Id Sibl**: human leukocyte antigen HLA-identical siblings; **1-Hapl Rel**: one-haplotype matched, living-related; and **Deceased:** all levels of HLA match for recipients of a deceased donor transplant. Numbers of transplants studied are indicated. (With permission from Collaborative Transplant Study Group, http://www.ctstransplant.org/.)

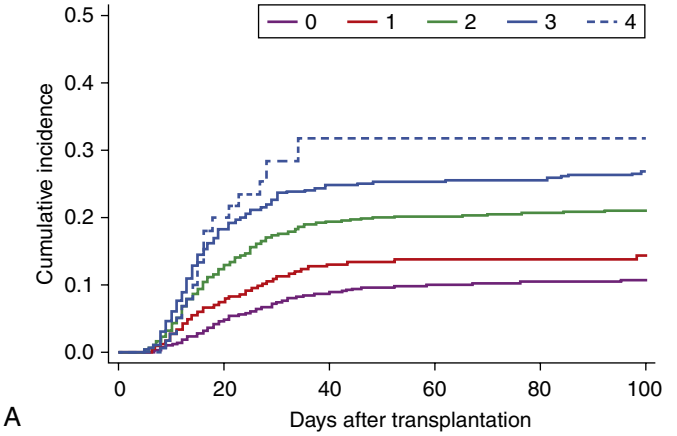

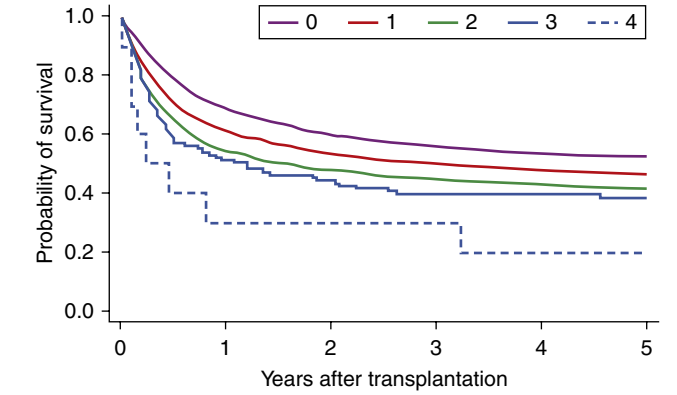

Number at risk

0	4076	2621	2038	1688	1431	1256
1	2352	1335	1046	878	736	623
2	850	443	359	309	268	218
3	130	65	54	47	46	41
4	10	3	3	3	2	2

B

Fig. 50.13 **A** Probability of grades III to IV acute graft-versus-host disease (GVHD). **B** Patient survival. Results are shown for human leukocyte antigen (HLA)-matched (0 mismatches) and 1 to 4 mismatched unrelated donor bone marrow transplants. Mismatches were calculated for HLA-A, -B, -C, -DRB1, and -DQB1 at the allele level. (Data from Morishima et al., 2015.)

animals, whereas grafts from F1 hybrid offspring to either parent (one haplotype mismatch) did not survive. These observations established the laws of transplantation. In 1948, the factors or genes determining the fate of allografts were named *histocompatibility* or *H genes*. Also in 1948, the major histocompatibility locus in the mouse, H-2, was defined by Gorer (Snell, 1981). There are other histocompatibility or H antigens, which are termed *mHags*. Although called minor, mismatching for these antigens can have major effects (Goulmy, 1997; Warren, 2012).

Because convincing evidence already existed in experimental animal models that molecules encoded by the MHC represent the major genetic barrier to successful allografting, HLA typing was used in humans to determine and to optimize compatibility between graft donor and recipient. Initially, the influence of HLA antigens on graft survival was investigated by grafting of nonvascularized skin between family members. As in studies with inbred mice, skin grafts between HLA-identical siblings survived significantly longer than grafts between one-haplotype–matched siblings, parents, or unrelated donors. These observations were extended to renal transplantation during the late 1960s and early 1970s. The most recent data from the International Collaborative Transplant Study (CTS) in Heidelberg and from the United Network for Organ Sharing (UNOS) Registry in the United States (analyzed at the University of California–Los Angeles) confirm the MHC as the major genetic barrier to transplantation for renal grafts (Cecka, 1999; Opelz et al., 1999) (Fig. 50.12); for current updates, see the websites listed in Table 50.1. The data for hematopoietic progenitor cell transplantation also reaffirm the role of the MHC in transplant outcome as measured by both patient survival and GVHD (Hansen et al., 1999; Morishima et al., 2015) (Fig. 50.13).

HISTOCOMPATIBILITY MATCHING

HLA Matching

Although the level of HLA match is an important element in transplant outcome, histocompatibility matching means different things in different settings, and strategies for matching vary. Criteria differ with variables that include the type of graft (e.g., solid vascularized organ vs. hematopoietic progenitor cell), the disease (e.g., chronic myelogenous leukemia vs. aplastic anemia), the age of the patient, and the clinical protocol (e.g., marrow vs. umbilical cord blood; T-cell depletion of marrow vs. non–T-cell depletion) (see Chapter 39).

Matching usually includes evaluation of at least three loci: HLA-A, -B, and -DR. Individuals matched, at whatever resolution, for all three loci are termed *6/6 matches* or *0 mismatches*. Zero mismatches (a term used in solid organ transplantation) may also refer to donor/recipient pairs in which the donor has no detectable HLA differences from the recipient, that is, where the donor is homozygous for the alleles at one or more of the loci (e.g., homozygous donor: A*01:01; B*08:01; DRB1*03:01; heterozygous recipient: A*01:01, A*03:01; B*08:01, B*07:02; DRB1*03:01, DRB1*15:01). Individuals matched for four of six alleles or antigens are termed *4/6 matches*. Apparent differences in the level of match can arise because of the typing method used to assign HLA types (e.g., serologic vs. DNA-based typing). The serologic and DNA nomenclatures, although they are related, can differ. The definition of a match can also vary depending on the typing resolution. A patient and a donor may appear to be matched at the serologic level (e.g., recipient: A2, A26; donor: A2, A26); however, the pair may be mismatched at the level of HLA alleles (e.g., recipient: A*02:01, A*26:01; donor: A*02:05, A*66:01).

Matching for classical HLA molecules at the allele level could optimize outcome for all grafts (both vascular organs and hematopoietic progenitor cells) (Petersdorf et al., 2015; Opelz et al., 1999). However, because of the extremely large number of HLA alleles, allelic-level matching is difficult. Therefore the level of matching that ensures a good outcome for the largest number of patients of all ethnic populations must be considered.

Following hematopoietic progenitor cell transplantation, subtypic determinants or allelic differences initiate important cytotoxic T-cell responses leading to graft rejection and GVHD. Indeed, studies have shown that high-resolution matching for class I and class II alleles of the donor and recipient can improve outcome after unrelated marrow transplantation. Recent data suggest that multiple mismatches are detrimental to outcome; however, the impact of neither single mismatches nor specific loci has not yet been well defined (Petersdorf et al., 2015; Sasazuki et al.,

1998; Hansen et al., 1999). With respect to single-allele mismatches and their impact on transplantation, a report by Flomenberg and colleagues (2004) describes a differential impact of HLA mismatches at specific loci between donor and recipients. This multivariate analysis of more than 1800 donor-recipient pairs showed that single-allele mismatches at HLA-C adversely affected engraftment; mismatches at HLA-A, -B, -C, and -DR were significant in terms of grade III to IV acute GVHD incidence, and that the highest effect on this disease was given by mismatches at HLA-A, whether this was acute or chronic GVHD; mismatches at HLA-A, -B, -C, and -DR showed significant effects on mortality, and again HLA-A mismatches demonstrated the largest impact on survival, perhaps because single-allele mismatches at this locus appeared to induce resistant GVHD. Only a minority of patients awaiting transplantation will receive grafts from fully allele-matched donors (Furst et al., 2013; Gragert et al., 2014). Moreover, the success in finding a compatible donor can be related to the race and ethnicity of the recipient (Gragert et al., 2014). Thus to enable all patients to benefit from lifesaving transplantation, identifying allele mismatches that are well tolerated would allow the selection of mismatched donors to be prioritized according to the biological risk of specific HLA mismatches (Petersdorf, 2015).

Optimal matching for solid organ grafts may differ from matching requirements for hematopoietic progenitor cell transplantation. Recent data suggest that both the HLA loci matched and the level of resolution of HLA testing contribute to renal graft outcome (Zachary & Leffell, 2015). Currently, UNOS facilitates sharing of cadaveric kidneys based on serologic antigenic specificities or their equivalents. Because antigenic matches are infrequently identified, it has been proposed that the HLA class I molecules should be matched for the broader CREG determinants. CREG may define immunodominant determinants recognized in the humoral immune response. Rodey and colleagues (1994) showed that 80% to 90% of the HLA alloantibodies formed by kidney recipients following transplantation are directed to CREG determinants. CREG determinants are shared among different class I HLA molecules and, in contrast to antigenic specificities, have a similar distribution among ethnic population groups. Rare antigenic specificities are included within the CREGs. Because the number of CREGs is less than the number of antigenic specificities, the probability of a CREG-level match is greater than for an antigen or allele-level HLA class I match. Therefore allocation of organs based on CREG matching should result in a higher probability of matched grafts being distributed equitably to recipients of all ethnic populations. CREG matching for the allocation of kidneys has been characterized as immunologically flawed, and its observed positive effect in prolonging graft survival and reducing immunosuppressant requirements has been attributed entirely to the effect of HLA matching (Egfjord et al., 2003). Others cite a positive role for CREG matching in reducing HLA sensitization among minority recipients of renal transplants (Crowe, 2003).

Other strategies focus on matching for biologically relevant fragments of MHC molecules (e.g., molecular matching) (Suciu-Foca et al., 1998; Harris et al., 1999). Recently it has been shown that renal transplants performed across low class II molecular mismatch load have been associated with lower incidences of antibody mediated rejection (Wiebe et al., 2018). Such data suggest that molecular matching assessments may be used as a primary biomarker of alloimmunity (Wiebe et al., 2019). Molecular mismatch information may even be important when considering posttransplant immunosuppression drug levels (Wiebe et al., 2017).

Until recently, direct recognition of alloantigens was thought to be the main pathway for graft rejection responses. However, studies suggest that the indirect response plays a significant role in graft rejection, at least of solid organ grafts (Sayegh & Carpenter, 1996). If the indirect pathway is activated, then the peptide epitopes generated by proteolytic breakdown of the HLA molecule and not the HLA molecule itself would be the immunogenic stimulus. Therefore new innovative strategies can be designed for defining allowable mismatches based on recognition of the peptide fragments. For example, a strategy could consider whether the mismatched donor HLA molecules would be perceived as immunogenic in the recipient (i.e., whether the recipient HLA molecules would bind and present these epitopes). Theoretically, one could identify foreign HLA peptide sequences not presented by specific recipient HLA molecules and thus define allowable mismatches for given HLA molecules. The introduction of solid-based methods (Luminex, enzyme-linked immunosorbent assay [ELISA], and flow cytometry methods) for detecting antibodies to HLA molecules, in which eluted HLA molecules from cells are bound to polystyrene beads (or polystyrene microtiter plates), has allowed the more accurate identification of antibodies generated by patients awaiting transplantation. It is now possible to group HLA molecules based on the immunogenic epitope that is shared among them, thus allowing for better selection of donors for transplantation. The level of sensitization is more accurately interrogated by beads carrying HLA molecules of a single specificity (single-antigen beads), and absorption of alloantisera with these beads elucidates the epitope that the antibody is directed to and can be inferred by testing the unabsorbed and the absorbed serum with a panel of single-antigen beads; reduced panel reactivity in the absorbed serum defines the epitope specificity. Based on these absorption experiments, Marrari and Duquesnoy (2009a, 2009b) and El-Awar and colleagues (2007) have reported several epitopes shared by multiple HLA class I and II molecules. More recently, confirmed epitopes on HLA molecules can be found in the HLA Epitope Registry (http://epregistry.ufpi.br/); see also the Workshop report: a website for the antibody-defined HLA epitope registry (Duquesnoy et al., 2012). Some laboratories are currently using this epitope registry to determine unacceptable antigens in donors based on the patient's immune reactivity assessed using single-antigen Luminex bead methods and the HLAMatchmaker algorithm (Valentini et al., 2007; Duquesnoy, 1999), which can predict some, but not all, of these epitopes. It must be emphasized here that antibody recognition of its cognate antigen is a complex biological interaction. Direct linear protein sequences (eplets) may correlate with an immunologic epitope; however, some epitopes may be created by tertiary and quaternity conformations that may involve distant amino acid sequences. To date, no computer modeling algorithm can reliably predict antibody reactivity in all instances.

HLA-Specific Antibody Detection in Recipient Serum

Patients can be sensitized to specific foreign HLA molecules through transfusion, pregnancy, or prior transplantation. Assessment of compatibility between the recipient and the possible donor includes testing for this sensitization. Recipient serum is tested prior to transplantation on a panel (lymphocytes or immobilized soluble HLA molecules) of known HLA profile to measure panel reactive antibody (PRA). If a solid phase, single antigen bead method is used then a PRA value is calculated based on the specificities identified. This is called a calculated PRA (CPRA). In contrast to cell-based PRA values, CPRA can incorporate both class I and class II specificities. As such, the CPRA provides a superior value for considering the degree of allosensitization. Within UNOS, only CPRA values are allowed and used in organ allocation algorithm. At the time of transplantation, a physical crossmatch may be performed, wherein the recipient's serum is tested with lymphocytes from the prospective donor to identify specific reactivity. Although the techniques used to detect antibody binding may differ among laboratories, the purpose remains the same: to obtain a profile of the immunologic risk factors of a recipient on the waiting list, which will aid the medical team in both pretransplantation and posttransplantation decisions.

Serum Screening and Antibody Identification

Thorough characterization of the antibody profile in patients awaiting transplantation aids in interpretation of the pretransplantation donor-specific crossmatch and in risk stratification. The goals for HLA antibody screening and identification are as follows:

1. To identify the level of HLA allosensitization of the patient. A patient with high CPRA value has a decreased likelihood of finding a crossmatch compatible donor and thus of receiving an unrelated transplant.
2. To identify the HLA specificity of the antibodies that will be used in donor selection.
3. To identify patients with irrelevant antibodies (e.g., immunoglobulin [Ig]M autoantibodies, non-HLA antibodies) so that appropriate techniques may be selected to avoid false-positive readings at the time of the donor-specific crossmatch.

Historically, characterization of HLA-specific antibody present in the recipient serum required testing on a selected panel of well-defined HLA specificities. However, with the advent of solid-phase methods (Luminex and flow cytometry), characterizing HLA antibodies via cell-based methods is only rarely performed. Identification of antibody specificities in patients awaiting transplantation aids in preselecting of compatible donors.

The frequency of screening and the selection of assays used for the screening procedure are decisions based on the immunologic profile of the individual recipient and the practices of the clinical programs. Decreased use of blood transfusions as well as the use of filtered blood products has reduced the need for screening monthly serum samples on all patients (ASHI Standards; see Table 50.1).

Donor-Specific Crossmatch

Physical Crossmatch

The lymphocyte crossmatch tests for the presence of antibodies, if any, in the serum of the potential recipient that react with lymphocytes of the

specific donor. In this physical crossmatch test, lymphocytes are the target cell of choice because they express high levels of most HLA molecules and are easy to isolate. Historically, this test has been the most important contribution of the HLA tissue typing laboratory to clinical renal transplantation. The purpose of the crossmatch is to prevent hyperacute rejection and to detect antibodies that identify immunologic risk factors in patients awaiting transplantation. The occurrence of hyperacute rejection is significantly correlated with a positive direct complement-dependent cytotoxicity (CDC) crossmatch between donor T lymphocytes and recipient serum at the time of transplantation. Reactivity of current valid serum of the recipient to the T lymphocytes of the donor is a contraindication to renal graft transplantation. Detection of donor-reactive antibodies in noncurrent recipient serum samples is not a contraindication but may represent risk for graft loss other than immediate hyperacute rejection (Cardella et al., 1982; Geddes et al., 1999). A donor-specific crossmatch also is used in some centers to predict hematopoietic progenitor cell graft failure (Hansen et al., 1997).

Virtual Crossmatch

Over the past decade, the ability to identify HLA-specific alloantibodies has dramatically improved. So much so that many transplant programs are abandoning the requirement for a pretransplant physical crossmatch in lieu of a virtual crossmatch (VXM). By definition, the VXM is an "assessment of immunologic compatibility based on the patient's alloantibody profile compared to the donor's histocompatibility antigens" (Bray et al., 2014). Virtual crossmatching has become increasingly important for deceased-donor allocation since the implementation of the New Kidney Allocation Scheme, by UNOS, in 2014 (Israni et al., 2014). The new KAS mandated national sharing for candidates with CPRAs of 100% and greater regional sharing for candidates with CPRAs of 99%. As a result, shipping of organs increased. Given the time constraints for deceased-donor allocation, the use of the VXM, for donor acceptance, has increased. Several centers have shown that, when HLA antibody testing is judiciously performed using solid-phase techniques, organs can be safely transplanted into highly sensitized candidates based solely on a VXM. It is anticipated that the use of the VXM will increase.

Antibody-Detection Techniques

Different laboratories may use different combinations of assays to detect HLA antibody. The level of sensitization detected will vary with the assay and the interpretation of the assay.

Direct Complement-Dependent Cytotoxicity

Direct CDC includes all assays that use the addition of complement to detect the direct binding of antibody to lymphocytes. Fixation of complement by the antibody-antigen complexes on the cell surface results in cell death or cytotoxicity. CDC methods include the basic technique (no wash step before addition of complement), the Amos-modified technique (wash step added before addition of complement), and extended-time incubation techniques. The wash step removes serum, which may contain substances that hinder complement activation. The advantages of direct CDC techniques are that they are reproducible and that correlation with the incidence of hyperacute rejection is excellent.

Indirect Crossmatch Techniques

Indirect techniques include the antiglobulin augmented lymphocytotoxicity assay technique (also known as *anti–human globulin cytotoxicity assay*) and flow cytometry. Both use a reagent specific for human immunoglobulin to augment detection of HLA-directed antibody. Indirect techniques detect the presence of antibodies specific for CREGs that frequently go undetected in direct CDC assays. Advantages of the flow cytometry assay include discrimination of the subclass of the cell-bound immunoglobulin (IgG vs. IgM) and characterization of the target cell binding the alloantibody (T lymphocyte vs. B lymphocyte vs. monocyte). An endothelial cell crossmatch has also been developed (Jackson et al., 2013).

RENAL TRANSPLANTATION

Current practice is to select donors for recipients who are ABO and HLA compatible. The original finding that kidney grafts transplanted between HLA-identical siblings survive significantly longer than grafts transplanted between HLA-mismatched siblings or parent-sibling combinations has been consistently confirmed. Figure 50.12 shows a recent analysis of 5-year survival of renal allografts from the international CTS registry among three categories of donors: (1) HLA-identical sibling, ~95% 5-year, death-censored graft survival; (2) one-haplotype living-related, ~88% survival; (3) all cadaver, ~83% survival. The impact of matching for MHC in living-related transplantation is clearly observed by comparing categories 1 and 2.

Although outcome analyses of living-related grafts confirm the role of the MHC as the major genetic barrier to successful graft outcome, demonstration and acceptance of a positive influence of HLA matching in graft outcome for unrelated cadaveric transplantation have been more controversial. However, long-term survival data from collaborative multicenter studies are consistent in showing a highly significant effect of HLA matching on graft survival in cadaveric renal transplantation (Cecka, 1999; Opelz et al., 1999). Moreover, two single-center studies—one from Europe (Oslo) and one from North America (Toronto)—have reported significant improvement in graft survival as a function of HLA match (Geddes et al., 1999; Leivestad et al., 1999).

Graft survival in patients following first kidney transplantations decreases stepwise as the number of mismatches increases from 0 MM to 6 MM (Cecka, 1999; Opelz et al., 1999). However, to ensure equitable sharing of organs for all recipients, including those with rare HLA haplotypes, new algorithms for prioritizing recipients on the waiting list have been adopted by organ-sharing programs (Opelz et al., 1999). The most recent outcome data for both graft and patient survival can be accessed through the CTS website (www.ctstransplant.org).

Matching of the initial graft not only increases survival time for that graft, but it decreases the probability of recipient sensitization and facilitates retransplantation. Accumulation of highly sensitized patients on the waiting list is a significant problem in many centers, as patients wait for long periods of time and may present difficult clinical management problems.

NONRENAL ORGAN TRANSPLANTATION

Survival of heart, liver, lung, and pancreas grafts is good, with between 58% and 67% of first grafts surviving at 5 years. Due to time constraints, HLA matching is not considered in allocation. Additionally, a pretransplant donor crossmatch is not routinely performed unless there is significant HLA sensitization. HLA antibody assessments are recommended to identify the level of sensitization as an immunologic risk factor for the recipient. If feasible, the graft recipients and cadaveric donors of nonrenal vascularized grafts should be typed for HLA to allow for retrospective analyses. Recent international CTS data show no effect of HLA matching on outcomes of liver transplantation; however, the CTS data do show a significant impact of matching for HLA-A, -B, and -DR on outcomes of first heart transplants (Ansari et al., 2014). The acceptable period for cold ischemia preservation may limit the extent of HLA matching possible for heart transplantation.

ALLOGENEIC HEMATOPOIETIC PROGENITOR CELL TRANSPLANTATION

Allogeneic hematopoietic progenitor cell transplantation is performed for hematologic malignancies and disorders, bone marrow failure, certain inherited metabolic disorders such as lipid storage diseases, and congenital immunodeficiency syndrome. From a histocompatibility standpoint, the best donor is either self (autogeneic transplant), if the malignancy is not one that involves the bone marrow or the disease is not genetic, or an identical twin (syngeneic transplant). However, stem cells from an HLA-identical sibling donor are a frequent source. These donor cells usually will be genetically identical to cells of the patient across the entire MHC region. Use of a sibling donor also increases the probability that non-HLA genes that might affect transplantation success and that are not well defined (i.e., minor histocompatibility genes) will be matched (Goulmy, 1997). Haploidentical family members may also be chosen as donors (Aversa et al., 1998), although a greater risk for severe GVHD is associated with mismatched HLA donors. Based on data from the Center for International Bone Marrow Transplant Registry (CIBMTR) (see Table 50.1), more than 9000 allogeneic bone marrow transplants were performed in 2016. Most patients (~70%) do not have an HLA-matched sibling and may be considered for transplantation with cells from an HLA-matched, unrelated donor. To facilitate the search for a matched donor, national registries of unrelated donors have been developed around the world (Hansen, 1996). The NMDP in the United States is such a registry and contains more than 20 million HLA-typed donors (see Fig. 50.5), making it the largest unrelated donor registry in the world (see Table 50.1; www.bethematch.org).

Hematopoietic progenitor cell grafts are among the most difficult of all clinical procedures for several reasons. First, at the time of transplantation, the recipients are nearly totally immunodeficient, either because of inherited deficiency (severe combined immunodeficiency) or because of

pretransplantation conditioning (cytotoxic chemotherapy and irradiation). Conditioning is required to eliminate malignant cells and to prevent the immune system of the recipient from rejecting the donor progenitor cells, which are infused several days after conditioning. The amount of cytotoxic pretreatment is great enough to eliminate circulating leukocytes, nearly eliminate platelets, and abrogate production of new erythrocytes. Thus the recipient is profoundly susceptible to infection and would certainly die if not rescued with infused progenitor cells.

The second risk is the potential for immunologic attack of the recipient by the transplanted allogeneic progenitor cells, resulting in GVHD. GVHD has several forms and can be fatal. In spite of associated difficulties, a number of transplant centers have achieved exceptional success. Recent reports from single institutions and the CIBMTR suggest leukemia-free survival of ~50% at 6 years after unrelated hematopoietic progenitor cell transplantation of patients with acute myelogenous leukemia in early or intermediate stages (see Table 50.1). Survival for adult patients with severe aplastic anemia transplanted with cells from unrelated donors is greater than 60% at 6 years. For patients under 18 years of age, survival is nearly 80% (see Table 50.1; www.bethematch.org, www.cibmtr.org).

In addition to marrow as a source of hematopoietic progenitor cells, collection of hematopoietic progenitor cells from growth factor–mobilized peripheral blood (Anderlini et al., 1997) or umbilical cord blood progenitor cells (Cairo & Wagner, 1997) increases the availability of unrelated donors. New approaches to immunosuppression, including less aggressive conditioning protocols (e.g., "mini-transplants") (Storb et al., 1999), may extend the availability of progenitor cell transplantation as a therapeutic procedure to patients presently excluded by age or by organ dysfunction. Hematopoietic progenitor cell transplantation can also be used to generate immune responses directed at malignant cells. Relapse of disease following transplantation is greater for patients receiving an HLA-matched graft, suggesting that some degree of mismatching may be beneficial in stimulating an immune response against tumor cells (Beatty et al., 1993). As problems surrounding this most difficult procedure are overcome, hematopoietic progenitor cell transplantation may become one of the most widely used methods for the treatment of a variety of diseases (see Chapter 39).

HLA Typing for Hematopoietic Stem Cell Transplantation

Many factors, including histocompatibility, influence the outcome of hematopoietic stem cell transplantation. The pretransplantation workup includes HLA-A, -B, and -DR typing of all available members of the immediate family to identify a matched related donor and to establish inheritance of haplotypes. DNA-based typing for all HLA genes has become standard. As haplotransplants gain popularity (Perales et al., 2018), typing of the extended family may become more prevalent.

The level of HLA typing resolution required for hematopoietic stem cell transplantation differs from that of renal transplantation. Higher-resolution HLA typing is required to match the donor and recipient for stem cell transplantation because stem cell transplantation involves the transfer of an entire immune system to the patient. Current research is focused on defining the loci that must be considered in donor selection, the level of resolution that must be used for matching, and the additive effect of multiple mismatches (Tiercy, 2016; Petersdorf, 2015). The level of matching required may vary for each disease or protocol. Evidence suggests that allele-level matching of unrelated donors and recipients for HLA-A, -B, and -DRB1 is related to improved outcomes. The impact of matching at other HLA loci (e.g., HLA-C, -DQ) may be less than HLA-DP (Petersdorf et al., 2015). Single mismatches may be tolerated; however, multiple mismatches appear to have a negative impact on outcome (Petersdorf, 2015; Hansen et al., 1997; Madrigal et al., 1997; Sasazuki et al., 1998). Furthermore, the positive effect of histocompatibility matching on outcome must be balanced by the positive impact of transplantation early in the course of the disease or other non-HLA factors (Shaw et al., 2018). Data from the CIBMTR and the NMDP have shown that survival following transplantation is reduced as the disease phase advances independent of the degree of HLA match (see data on websites in Table 50.1).

SUMMARY

The HLA class I and class II molecules encoded within the major histocompatibility complex have a significant role in the specificity and character of immune responses. Extensive polymorphism of these molecules provides the diversity needed to ensure survival in an environment of hostile and adaptive pathogens. Unfortunately, this ability of the immune system to distinguish self from non-self extends to the recognition of foreign HLA molecules following tissue transplantation. Definition and characterization of HLA alleles have been combined with clinical protocols to optimize compatibility and to minimize the impact of the immune response on foreign tissue. These advances have contributed to the development of transplantation as a successful treatment modality for many disease entities.

SELECTED REFERENCES

Aguado B, Bahram S, Beck S, et al.: Complete sequence and gene map of a human major histocompatibility complex, *Nature* 401:921, 1999.

Contains the first complete sequence and gene map of an MHC region and represents the collaborative effort of an international group of researchers.

Arguello JR, Little AM, Bohan E, et al.: High resolution HLA class I typing by reference strand mediated conformation analysis (RSCA), *Tissue Antigens* 52:57–66, 1998.

Describes the use of RSCA in separating polymorphic HLA alleles using an automated technology that may provide rapid high-throughput HLA analysis with the additional advantages of time and cost savings.

Etokebe GE, Opsahl M, Tveter AK, et al.: Physical separation of HLA-A alleles by denaturing high-performance liquid chromatography, *Tissue Antigens* 61:443–450, 2003.

Describes the application of HPLC to the task of identifying polymorphic HLA-A alleles in an automated high-throughput setting.

Nordstrom T, Ronaghi M, Forsberg L, et al.: Direct analysis of single-nucleotide polymorphism on double-stranded DNA by pyrosequencing, *Biotechnol Appl Biochem* 31:107–112, 2000.

Describes the technology behind pyrosequencing and its specific application to the tasks of sequencing and verifying the presence of single nucleotide polymorphisms in double-stranded DNA.

Access the complete reference list online at Elsevier eBooks for Practicing Clinicians.

REFERENCES

Agrawal S, Pandey MK: The potential role of HLA-G polymorphism in maternal tolerance to the developing fetus, *J Hematother Stem Cell Res* 12:750–756, 2003.

Aguado B, Bahram S, Beck S, et al.: Complete sequence and gene map of a human major histocompatibility complex, *Nature* 401:921, 1999.

American Society for Histocompatibility and Immunogenetics: *Laboratory manual*, ed 4, Lenexa, Kans, 2001, ASHI.

Anderlini P, Korbling M, Dale D, et al.: Allogeneic blood stem cell transplantation: considerations for donors, *Blood* 90:903, 1997.

Ansari D, Bucin D, Nilsson J: Human leukocyte antigen matching in heart transplantation: systematic review and meta-analysis, *Trans Int* 27:793–804, 2014.

Arguello R, Avakian H, Goldman JM, et al.: A novel method for simultaneous high resolution identification of HLA-A, HLA-B, and HLA-Cw alleles, *Proc Natl Acad Sci U S A* 93:10961, 1996.

Arguello JR, Little AM, Bohan E, et al.: High resolution HLA class I typing by reference strand mediated conformation analysis (RSCA), *Tissue Antigens* 52:57–66, 1998.

Aversa F, Tabilio A, Velardi A, et al.: Treatment of high-risk acute leukemia with T-cell-depleted stem cells from related donors with one fully mismatched HLA haplotype, *N Engl J Med* 339:1186, 1998.

Banchereau J, Steinman RM: Dendritic cells and the control of immunity, *Nature* 392:245, 1998.

Beatty PG, Anasetti C, Hansen JA, et al.: Marrow transplantation from unrelated donors for treatment of hematologic malignancies: effect of mismatching for one HLA locus, *Blood* 81:249, 1993.

Beck S, Trowsdale J: Sequence organization of the Class II region of the human MHC, *Immunol Rev* 167:201, 1999.

Begovich AB, McClure GR, Suraj VC, et al.: Polymorphism, recombination and linkage disequilibrium within the HLA Class II region, *J Immunol* 148:249, 1992.

Benjamin JE, Gill S, Negrin RS: Biology and clinical effects of natural killer cells in allogeneic transplantation, *Curr Opin Oncol* 22:130–137, 2010.

Bjorkman PJ, Parham P: Structure, function and diversity of Class I major histocompatibility complex molecules, *Annu Rev Biochem* 59:253, 1990.

Bjorkman PJ, Saper MA, Samraoui B, et al.: Structure of the human Class I histocompatibility antigen, HLA-A2, *Nature* 329:506, 1987.

Bodmer JG, Marsh SGE, Albert ED, et al.: Nomenclature for factors of the HLA system, 1996, *Tissue Antigens* 49:297, 1997.

Bodmer JG, Marsh SGE, Albert ED, et al.: Nomenclature for factors of the HLA system, 1998, *Tissue Antigens* 53:407, 1999.

Bozon MV, Delgado JC, Selvakumar A, et al.: Error rate for HLA-B antigen assignment by serology: implications for proficiency testing and utilization of DNA-based typing methods, *Tissue Antigens* 50:387, 1997.

Bray RA, et al.: *The acceptability and application of virtual crossmatching in lieu of serologic crossmatching for transplantation. Virtual Crossmatch Working Group Report*, 2014. https://www.cdc.gov/cliac/docs/summary/cliac1114_summary.pdf.

Brodsky FM, Lem L, Solache A, et al.: Human pathogen subversion of antigen presentation, *Immunol Rev* 168:199, 1999.

Brooks AG, Borrego F, Posch PE, et al.: Specific recognition of HLA-E, but not classical, HLA Class I molecules by soluble CD94/NKG2A and NK cells, *J Immunol* 162:305, 1999.

Brown JH, Jardetzky TS, Gorga JC, et al.: Three-dimensional structure of the human Class II histocompatibility antigen HLA-DR1, *Nature* 364:33, 1993.

Bugawan TL, Apple R, Erlich HA: A method for typing polymorphism at the HLA-A locus using PCR amplification and immobilized oligonucleotide probes, *Tissue Antigens* 44(137), 1994.

Bugawan TL, Mack SJ, Stoneking M, et al.: HLA Class I allele distributions in six Pacific/Asian populations: evidence of selection of the HLA-A locus, *Tissue Antigens* 53:311, 1999.

Bunce M, O'Neill CM, Barnardo MC, et al.: Phototyping: comprehensive DNA typing for HLA-A, B, C, DRB1, DRB3, DRB4, DRB5 & DQB1 by PCR with 144 primer mixes utilizing sequence-specific primers (PCR-SSP), *Tissue Antigens* 46:355, 1995.

Cadavid LF, Watkins DI: Heirs of the jaguar and the anaconda: HLA, conquest and disease in the indigenous populations of the Americas, *Tissue Antigens* 50:209, 1997.

Cairo MS, Wagner JE: Placental and/or umbilical cord blood: an alternative source of hematopoietic stem cells for transplantation, *Blood* 90:4665, 1997.

Cao K, Chopek M, Fernandez-Vina MA: High and intermediate resolution DNA typing systems for Class I HLA-A, -B, -C genes by hybridization with sequence specific oligonucleotide probes (SSOP), *Immunogenetics* 1:53, 1999.

Cardella CJ, Falk JA, Nicholson MJ, et al.: Successful renal transplantation in patients with T-cell reactivity to donor, *Lancet* 2:1240, 1982.

Cecka M: The UNOS scientific renal transplant registry. In Cecka M, Terasaki P, editors: *Clinical transplants 1998*, Los Angeles, 1999, UCLA Tissue Typing Laboratory, p 1.

Cooley S, Weisdorf DJ, Guethlein LA, et al.: Donor selection for natural killer cell receptor genes leads to superior survival after unrelated transplantation for acute myelogenous leukemia, *Blood* 116:2411–2419, 2010.

Creput C, Le Friec G, Bahri R, et al.: Detection of HLA-G in serum and graft biopsy associated with fewer acute rejections following combined liver-kidney transplantation: possible implications for monitoring patients, *Hum Immunol* 64:1033–1038, 2003.

Cresswell P: Assembly, transport, and function of MHC Class II molecules, *Annu Rev Immunol* 12:259, 1994.

Crow JF: *Genetics notes*, ed 7, Minneapolis, 1976, Burgess Publishing.

Crowe DO: The effect of cross-reactive epitope group matching on allocation and sensitization, *Clin Transplant* 17(Suppl 9):13–16, 2003.

Cullen M, Perfetto SP, Klitz W, et al.: High-Resolution patterns of meiotic recombination across the human major histocompatibility complex, *Am J Hum Genet* 71(4):759, 2002.

Dausset J: The Nobel Lectures in Immunology. Lecture for the Nobel prize for Physiology or medicine, 1980: the major histocompatibility complex in man, *Science* 213:1469, 1981.

Dausset J, Colombani J, editors: *Histocompatibility testing 1972*, Copenhagen, 1973, Munksgaard.

den Haan JMM, Sherman NE, Blokland E, et al.: Identification of a graft versus host disease-associated human minor histocompatibility antigen, *Science* 268:1476, 1995.

De Santis D, Dinauer D, Duke J, et al.: 16(th) IHIW : review of HLA typing by NGS, *Int J Immunogenet* 40(1):72–76, 2013.

Dragun D, et al.: Antiogensin II type 1-receptor activating antibodies in renal-allograft rejection, *NEJM* 352(6):558–569, 2005.

Duquesnoy RJ, Marrari M: HLAMATCHMAKER: a molecularly based donor selection strategy for highly allosensitized patients, *Hum Immunol* 60:S10, 1999.

Duquesnoy RJ, Marrari M, da M Sousa LCD, et al.: 16th International Histocompatibility Workshop: a website for the antibody-defined HLA epitope registry, *Int J Immunogenetic* 40:1–66, 2012.

Enderby C, Keller CA: An overview of immunosuppression in solid organ transplantation, *Am J Manag Care* 21:S12–S23, 2015.

Egfjord M, Jakobsen BK, Ladefoged J: No impact of cross-reactive group human leucocyte antigen class I matching on long-term kidney graft survival, *Scand J Immunol* 57:362–365, 2003.

El-Awar NR, Akaza T, Terasaki PI, et al.: Human leukocyte antigen I epitopes: update to 103 total epitopes, including C locus, *Transplantation* 84, 2007.

Ellison MD, Bennett LE, Edwards EB, et al.: Multivariate analysis of verified national data to assess the impact of HLA mismatch level on kidney graft survival, *J Am Soc Nephrol* 5:1003, 1994.

Engelhard VH: Structure of peptides associated with Class I and Class II molecules, *Annu Rev Immunol* 12:181, 1994.

Erick C, Castellia b, Michelle AP, et al.: Hla-mapper: an application to optimize the mapping of HLA Sequences produced by massively parallel sequencing procedures, *Hu. Immunol* 79:678–684, 2018.

Etokebe GE, Opsahl M, Tveter AK, et al.: Physical separation of HLA-A alleles by denaturing high-performance liquid chromatography, *Tissue Antigens* 61:443–450, 2003.

Flomenberg N, Baxter-Lowe LA, Confer D, et al.: Impact of HLA class I and class II high-resolution matching on outcomes of unrelated donor bone marrow transplantation: HLA-C mismatching is associated with a strong adverse effect on transplantation outcome, *Blood* 104:1923–1930, 2004.

Furst D, Muller C, Vucinic V, et al.: High-resolution HLa matching in hematopoietic stem cell transplantation: a retrospective collaborative analysis, *Blood* 122(18):3220–3229, 2013.

Gao X, Moraes JR, Miller S, et al.: DNA typing for Class II HLA antigens with allele-specific or group-specific amplification. V. Typing for subsets of HLA-DR1 and DR'Br', *Hum Immunol* 30:147, 1991.

Gragert L, Eapen M, Williams E, et al.: HLA Match likelihoods for hematopoietic stem cell grafts in the U.S. registry, *N Engl J Med* 37(14):339–348, 2014.

Geddes C, Cole E, Wade J, et al.: Factors influencing long-term primary cadaveric kidney transplantation—importance of functional renal mass versus avoidance of acute rejections: the Toronto Hospital experience 1985–1997. In Cecka M, Terasaki P, editors: *Clinical transplants 1998*, Los Angeles, 1999, UCLA Tissue Typing Laboratory, p 195.

Gandhi MJ, Ferriola D, Huang Y, et al.: Targeted next-generation sequencing for human leukocyte antigen typing in a clinical laboratory: metrics of relevance and considerations for its successful implementation, *Arch Pathol Lab Med* 141(6):806–812, 2017.

Glimcher LH, Kara CJ: Sequences and factors: a guide to MHC Class-II transcription, *Annu Rev Immunol* 10(13), 1992.

Gorga JC: Structural analysis of Class II major histocompatibility complex proteins, *Crit Rev Immunol* 11:305, 1992.

Gould DS, Auchincloss H: Direct and indirect recognition: the role of MHC antigens in graft rejection, *Immunol Today* 20:77, 1999.

Goulmy E: Human minor histocompatibility antigens: new concepts for marrow transplantation and adoptive immunotherapy, *Immunol Rev* 157:125, 1997.

Goulmy E, Schipper R, Pool J, et al.: Mismatches of minor histocompatibility antigens between HLA-identical donors and recipients and the development of graft-versus-host disease after bone marrow transplantation, *N Engl J Med* 334:281, 1996.

Guardiola J, Maffei A: Control of MHC Class II gene expression in autoimmune, infectious, and neoplastic diseases, *Crit Rev Immunol* 13:247–268, 1993.

Hansen JA: Development of registries of HLA-typed volunteer marrow donors, *Tissue Antigens* 47:460, 1996.

Hansen JA, Gooley TA, Martin PJ, et al.: Bone marrow transplants from unrelated donors for patients with chronic myeloid leukemia, *N Engl J Med* 338:962, 1998.

Hansen JA, Petersdorf E, Martin PJ, et al.: Hematopoietic stem cell transplants from unrelated donors, *Immunol Rev* 157:141, 1997.

Hansen JA, Yamamoto K, Petersdorf E, et al.: The role of HLA matching in hematopoietic cell transplantation, *Rev Immunogenet* 1:81, 1999.

Hansen TH, Lee DR: Mechanism of Class I assembly with β-2 microglobulin and loading with peptide, *Adv Immunol* 64:105, 1997.

Harris PE, Cortesini R, Suciu-Foca N: Indirect allorecognition in solid organ transplantation, *Rev Immunogenet* 1:19, 1999.

Hartzman RJ, Segall M, Bach ML, et al.: Histocompatibility matching. VI. Miniaturization of the mixed leukocyte culture test: a preliminary report, *Transplantation* 11:268, 1971.

Hurley CK: Acquisition and use of DNA-based HLA typing data in bone marrow registries, *Tissue Antigens* 49:323, 1997.

Hurley CK, Baxter-Lowe LA, Begovich AB, et al.: The extent of HLA Class II allele level disparity in unrelated bone marrow transplantation: analysis of 1,259 National Marrow Donor Program donor-recipient pairs, *Bone Marrow Transplant* 25:385, 2000.

Hurley CK, Tang T, Ng J, et al.: HLA typing by molecular methods. In Rose NR, Conway de Macario E, Folds JD, editors: *Manual of clinical laboratory immunology*, ed 5, Washington, DC, 1997, ASM Press, p 1098.

Imanishi T, Akaza T, Kimura A, et al.: Allele and haplotype frequencies for HLA and complement loci in various ethnic groups. In Tsuji K, Aizawa M, Sasazuki T, editors: *HLA 1991*, vol. 1. New York, 1992, Oxford University Press, p 1065.

Israni AJ, Salkowski N, Gustafson S, et al.: New national allocatin policy for deceased donor kidneys in the United States and possible effects on patient outcomes, *J Am Soc Nephrol* 25:1842–1848, 2014.

Ishitani A, Sageshima N, Lee N, et al.: Protein expression and peptide binding suggest unique and interacting functional roles for HLA-E, F, and G in maternal-placental immune recognition, *J Immunol* 171:1376–1384, 2003.

Jackson AM, Lucas DP, Badders JL: A flow cytometric crossmatch test using endothelial precursor cells isolated from peripheral blood, *Methods Mol Biol* 1034:319–329, 2013.

Jackson AM, Sigdel TK, Delville M, et al.: Endothelial cell antibodies associated with novel targets and increased rejection, *JASN (J Am Soc Nephrol)* 26:1161–1171, 2015.

Jorgensen JL, Reay PA, Ehrich EW, et al.: Molecular components of T-cell recognition, *Annu Rev Immunol* 10:835, 1992.

Kishore A, Petrek M: Next-generation sequencing based HLA typing: Deciphering Immunogenetic Aspects of Sarcoidosis, *Front Genet* 9:1–8, 2018.

Kovats S, Drover S, Marshall WH, et al.: Coordinate defects in human histocompatibility leukocyte antigen Class II expression and antigen presentation in bare lymphocyte syndrome, *J Exp Med* 179:2017, 1994.

Kwok WW, Kovats S, Thurtle P, et al.: HLA-DQ allelic polymorphisms constrain patterns of Class II heterodimer formation, *J Immunol* 150:2263, 1993.

Lanier LL: NK cell receptors, *Annu Rev Immunol* 16:359, 1998.

Laux G, Mansmann U, Deufel A, et al.: A new epitope-based HLA-DPB matching approach for cadaver kidney retransplants, *Transplantation* 75:1527–1532, 2003.

Le Bouteiller P: HLA class I chromosomal region, genes, and products: facts and questions, *Crit Rev Immunol* 14:89–129, 1994.

Le Bouteiller P, Blaschitz A: The functionality of HLA-G is emerging, *Immunol Rev* 167:233, 1999.

Lee N, Goodlett DR, Ishitani A, et al.: HLA-E surface expression depends on binding of TAP-dependent peptides derived from certain HLA Class I signal sequences, *J Immunol* 160:4951, 1998a.

Lee N, Llano M, Carretero M, et al.: HLA-E is a major ligand for the natural killer inhibitory receptor CD94/NKG2A, *Proc Natl Acad Sci U S A* 95:5199, 1998b.

Leivestad T, Reisaeter AV, Brekke IB, et al.: The role of HLA matching in renal transplantation: experience from one center, *Rev Immunogenet* 1:343, 1999.

Long EO: Regulation of immune responses through inhibitory receptors, *Annu Rev Immunol* 17:875, 1999.

Mach B, Steimle B, Martinez-Soria E, et al.: Regulation of MHC Class II genes: lessons from a disease, *Annu Rev Immunol* 14:301, 1996.

Madden K, Chabot-Richards D: HLA testing in the molecular diagnostic Laboratory, *Virchows Arch* 474(2):139–147, 2019.

Madrigal JA, Scott I, Argello R, et al.: Factors influencing the outcome of bone marrow transplants using unrelated donors, *Immunol Rev* 157:153, 1997.

Marrari M, Duquesnoy RJ: Correlations between Terasaki's HLA class II epitopes and HLAMatchmaker-defined eplets on HLA-DR and -DQ antigens, *Tissue Antigens* 74:134–146, 2009a.

Marrari M, Duquesnoy RJ: Correlations between Terasaki's HLA class I epitopes and HLAMatchmaker-defined eplets on HLA-A, -B and -C antigens, *Tissue Antigens* 74:117–133, 2009b.

Marsh SG, Albert ED, Bodmer WF, et al.: Nomenclature for factors of the HLA system, 2002, *Tissue Antigens* 60:407–464, 2002.

Matsunami K, Miyagawa S, Nakai R, et al.: Modulation of the leader peptide sequence of the HLA-E gene up-regulates its expression and down-regulates natural killer cell-mediated swine endothelial cell lysis, *Transplantation* 73:1582–1589, 2002.

Mickelson EM, Longton G, Anasetti C, et al.: Evaluation of the mixed lymphocyte culture (MLC) assay as a method for selecting unrelated donors for marrow transplantation, *Tissue Antigens* 47(27), 1996.

Middleton D: History of DNA typing for human MHC, *Rev Immunogenet* 1:11, 1999.

Momburg F, Hammerling GJ: Generation and TAP-mediated transport of peptides for major histocompatibility complex Class I molecules, *Adv Immunol* 68:191, 1998.

Morishima Y, Kashiwase K, Matsuo K, et al.: Biological significance of HLA locus matching in unrelated donor bone marrow transplantation, *Blood* 125:1189–1197, 2015.

Morris P, Shaman J, Attaya M, et al.: An essential role for HLA-DM in antigen presentation by Class II major histocompatibility molecules, *Nature* 368:551, 1994.

Mungall AJ, Palmer SA, Sims SK, et al.: The DNA sequence and analysis of human chromosome 6, *Nature* 425:805–811, 2003.

Mytilineos J, Lempert M, Scherer S, et al.: Comparison of serological and DNA PCR-SSP typing results for HLA-A and HLA-B in 421 black individuals—a collaborative transplant study report, *Hum Immunol* 59:512, 1998.

Neefjes JJ, Ploegh HL: Allele and locus-specific differences in cell surface expression and the association of HLA class I heavy chain with beta 2-microglobulin: differential effects of inhibition of glycosylation on class I subunit association, *Eur J Immunol* 18:801–810, 1988.

Nepom GT, Erlich H: MHC Class-II molecules and autoimmunity, *Annu Rev Immunol* 9:493, 1991.

Nordstrom T, Ronaghi M, Forsberg L, et al.: Direct analysis of single-nucleotide polymorphism on double-stranded DNA by pyrosequencing, *Biotechnol Appl Biochem* 31(Pt 2):107–112, 2000.

O'Callaghan CA, Bell JI: Structure and function of the human MHC Class Ib molecules HLA-E, HLA-F and HLA-G, *Immunol Rev* 163:129, 1998.

Olerup O, Zetterquist H: HLA-DR typing by PCR amplification with sequence specific primers (PCR-SSP) in 2 hours: an alternative to serological DR typing in clinical practice including donor-recipient matching in cadaveric transplantations, *Tissue Antigens* 39:225, 1992.

Opelz G, Wujciak T, Dohler B, et al.: HLA compatibility and organ transplant survival, *Rev Immunogenet* 1:56, 1999.

Oostvogels R, Lokhorst HM, Mutis T: Minor histocompatibility Ags: identification strategies, clinical results, and translational perspectives, *Bone Marrow Transplant* 51:163–171, 2016.

Pacasova R, Martinozzi S, Bouloues HJ, et al.: Cell surface expression and allogenic function of a human non-classical Class I molecule (HLA-E) in transgenic mice, *J Immunol* 162:5190, 1999.

Pamer E, Cresswell P: Mechanisms of MHC Class I-restricted antigen processing, *Annu Rev Immunol* 16:323, 1998.

Parham P, Adams EJ, Arnett KL: The origins of HLA-A, B, C polymorphism, *Immunol Rev* 143:141, 1995.

Parham P, Lawlor DA: Evolution of Class I major histocompatibility complex genes and molecules in humans and apes, *Hum Immunol* 30:119, 1991.

Paul WE, Seder RA: Lymphocyte responses and cytokines, *Cell* 76:241, 1994.

Payne R, Tripp M, Weigle J, et al.: A new leukocyte isoantigen system in man, *Cold Spring Harb Symp Quant Biol* 29:285, 1964.

Perales MA, Timlinson B, Zhang MJ, et al.: Alternative donor transplantation for acute myeloid leukemia in patients aged >50 years: young HLA-matched unrelated or haploidentical donor? *Haematologica*, May 2019. https://doi.org/10.3324/haematol.2018.215202. [Epub ahead of print].

Perkins HA, Hansen JA: The US national marrow donor program, *Am J Pediatr Hematol Oncol* 16:30, 1994.

Petersdorf EW, Gooley TA, Anasetti C, et al.: Optimizing outcome after unrelated marrow transplantation by comprehensive matching of HLA Class I and II alleles in the donor and recipient, *Blood* 92:3515, 1998.

Petersdorf EW, Longton GM, Anasetti C, et al.: The significance of HLA-DRB1 matching on clinical outcome after HLA-A, B, DR identical unrelated donor marrow transplantation, *Blood* 86:1606, 1995.

Petersdorf EW: HLA mismatching in transplantation, *Blood* 125:1058, 2015a. –1059.

Petersdorf EW, Malkki M, O'hUiqin C, et al.: High HLA-DP expression and graft-versus-host-disease, *N Eng J Med* 373(7):599–609, 2015b.

Profaizer T, Lázár-Molnár E, Close DW, et al.: HLA genotyping in the clinical laboratory: comparison of next-generation sequencing methods, *HLA* 88(1–2):14–24, 2016.

Reindl-Schwaighofer R, Heinzel A, Kainz A, et al.: Contribution of non-HLA incompatibility between donor and recipient to kidney allograft survival: genome-wide analysis in a prospective cohort, *Lancet* 393:910–917, 2019.

Reinsmoen NL, Matas AJ: Evidence that improved late transplant outcome correlates with the development of in vitro donor antigen-specific hyporeactivity, *Transplantation* 55:1017, 1993.

Remuzzi G, Perico N, Carpenter CB, et al.: The thymic way to transplantation tolerance, *J Am Soc Nephrol* 5:1639, 1995.

Rock KL, Goldberg AL: Degradation of cell proteins and the generation of MHC Class I-presented peptides, *Annu Rev Immunol* 17:739, 1999.

Rodey GE, Fuller TC: Public epitopes and the antigenic structure of the HLA molecules, *CRC Crit Rev Immunol* 7:229, 1987.

Rodey GE, Neylan JF, Whelchel JD, et al.: Epitope specificity of HLA Class I alloantibodies. I. Frequency analysis of antibodies to private versus public specificities in potential transplant recipients, *Hum Immunol* 39:272, 1994.

Rodey GE, Revels K, Fuller TC: Epitope specificity of HLA Class I alloantibodies. II. Stability of cross-reactive group antibody patterns over extended time periods, *Transplantation* 63:885, 1997.

Rosenthal AS, Shevach EM: Function of macrophages in antigen recognition by Guinea pig T lymphocytes. I. Requirement for histocompatible macrophages and lymphocytes, *J Exp Med* 138:1194, 1973.

Rozemuller EH, Tilanus MGJ: A computerized method to predict the discriminatory properties for Class II sequencing based typing, *Hum Immunol* 46:27, 1996.

Rubnitz JE, Inaba H, Ribeiro RC, et al.: NKAML: a pilot study to determine the safety and feasibility of haploidentical natural killer cell transplantation in childhood acute myeloid leukemia, *J Clin Oncol* 28:955–959, 2010.

Ruggeri L, Capanni M, Casucci M, et al.: Role of natural killer cell alloreactivity in HLA-mismatched hematopoietic stem cell transplantation, *Blood* 94:333, 1999.

Saiki RK, Gelfand DH, Stoffel S, et al.: Primer-directed enzymatic amplification of DNA with a thermostable DNA polymerase, *Science* 239:487, 1988.

Sasazuki T, Juji T, Morishima Y, et al.: Effect of matching of Class I HLA alleles on clinical outcome after transplantation of hematopoietic stem cells from an unrelated donor, *N Engl J Med* 339:1177, 1998.

Sayegh MH, Carpenter CB: Role of indirect allorecognition in allograft rejection, *Int Rev Immunol* 13:221, 1996.

Scheltinga SA, Johnston-Dow LA, White CB, et al.: A generic sequence-based typing approach for the identification of HLA-A diversity, *Hum Immunol* 57:120, 1997.

Shaw S, Kavathas P, Pollack MS, et al.: Family studies define a new histocompatibility locus, SB, between HLA-DR and GLO, *Nature* 293:745, 1981.

Shaw BE, Logan BR, Spellman SR, et al.: Development of an unrelated donor selection score predicative of survival after HCT: donor age matters most, *Biol Blood Marrow Transplant* 24(5):1049–1056, 2018.

Shiina T, Tamiya G, Oka A, et al.: Genome sequencing analysis of the 1.8Mb entire human MHC Class I region, *Immunol Rev* 167:193, 1999.

Simpson E, Roopenian D, Goulmy E: Much ado about minor histocompatibility antigens, *Immunol Today* 19:108, 1998.

Singer DS, Maguire J: Regulation of the expression of Class I MHC genes, *CRC Crit Rev Immunol* 10:235, 1990.

Smith AG1, Nelson JL, Regen L, Guthrie LA, Donadi E, Mickelson EM, Hansen JA: Six new DR52-associated DRB1 alleles, three of DR8, two of DR11, and one of DR6, reflect a variety of mechanisms which generate polymorphism in the MHC, *Tissue Antigens* 48(2):118–126, 1994.

Snell GD: Studies in histocompatibility, *Science* 213:172, 1981.

Steers NJ, Li Y, Drace Z, et al.: Genomic mismatch at LIMS1 locus and kidney allograft rejection, *NEJM* 380(20):1918–1928, 2019.

Stern LJ, Wiley DC: Antigenic peptide binding by Class I and Class II histocompatibility proteins, *Structure* 2:245, 1994.

Storb R, Yu C, McSweeney P: Mixed chimerism after transplantation of allogeneic hematopoietic cells. In Thomas D, Blume KG, Forman SJ, editors: *Hematopoietic cell transplantation*, ed 2, Oxford, 1999, Blackwell Science, p 287.

Suciu-Foca N, Harris PE, Cortesini R: Intramolecular and intermolecular spreading during the course of organ allograft rejection, *Immunol Rev* 164:241, 1998.

Sutton VR, Kienzle BK, Knowles RW: An altered splice site is found in the DRB4 gene that is not expressed in HLA-DR7, Dw11 individuals, *Immunogenetics* 29:317, 1989.

Tambur AR1, Leventhal JR, Friedewald JJ, et al.: The complexity of human leukocyte antigen (HLA)-DQ antibodies and its effect on virtual crossmatching, *Transplantation 27* 90(10):1117–1124, 2010.

Tanaka K, Tanahashi N, Tsurumni C, et al.: Proteosomes and antigen processing, *Adv Immunol* 64(1), 1997.

Terasaki PI, Takemoto S, Park MS, et al.: HLA epitope matching, *Transfusion* 32:775, 1992.

Thorsby E, Piazza A: Joint report II: typing for HLA-D determinants (LD-1 or MLC). In Kissmeyer-Nielsen F, editor: *Histocompatibility testing*, Copenhagen, 1975, Munksgaard, p 414.

Tiercy JM: How to select the est available related or unrelated donor of hematopoietic stem cells, *Hematologica* 101(6):680–687, 2016.

Todd JA, Bell JI, McDevitt HO: HLA-DQβ gene contributes to susceptibility and resistance to insulin-dependent diabetes mellitus, *Nature* 329:599, 1987.

Valentini RP, Nehlsen-Cannarella SL, Gruber SA, et al.: Intravenous immunoglubulin, HLA allele typing and HLAMatchmaker facilitate successful transplantation in highly sensitized pediatric renal allograft recipients, *Pediatr Transplant* 11:77–81, 2007.

Valiante NM, Uhrber M, Shilling HG, et al.: Functionally and structurally distinct NK cell receptor repertoires in the peripheral blood of two human donors, *Immunity* 7:739, 1997.

van Ham SM, Tjin EPM, Lillemier BF, et al.: HLA-DO is a negative modulator of HLA-DM mediated MHC Class II peptide loading, *Curr Biol* 7:950, 1997.

van Rood JJ: HLA and I, *Annu Rev Immunol* 11(1), 1993.

van Rood JJ, Stevens CE, Smits J, et al.: Reexposure of cord blood to noninherited maternal HLA antigens improves transplant outcome in hematological malignancies, *Proc Natl Acad Sci U S A* 106:19952–19957, 2009.

Wade JA, Hurley CK, Hastings A, et al.: Combinational diversity in DR2 haplotypes, *Tissue Antigens* 41:113, 1993.

Warren EH, Zhang XC, Wenhong SL, et al.: Effect of MHC and non-MHC donor/recipient genetic disparity on the outcome of allogeneic HCT. *Blood* 120:2796-2806, 2012.

Watts C: Capture and processing of exogenous antigens for presentation of MHC molecules, *Annu Rev Immunol* 15:821, 1997.

Wiebe C, Rush DN, Nevins TE, et al.: Class II eplet mismatch modulates tacrolimus trough levels required to prevent donor-specific antibody development, *J Am Soc Neph* 28(11):3353–3362, 2017.

Wiebe C, Kosmoliaptsis PD, et al.: A comparison of HLa molecular mismatch methods to determine HLA immunogenicity, *Transplantation* 102(8):1338–1343, 2018.

Wiebe C, Kosmoliaptsis PD, et al.: HLA-DR/DQ molecular mismatch: a prognostic biomarker for primary alloimmunity, *Am J Transplant* 19(6):1708–1719, 2019.

Williams F, Mallon E, Middleton D: Development of PCR-SSOP for HLA-A typing of bone marrow registry donors, *Tissue Antigens* 49:61, 1997.

Yu N, Ohashi M, Alosco S, et al.: Accurate typing of HLA-A antigens and analysis of serological deficiencies, *Tissue Antigens* 50:380, 1997.

Zachary AA, Leffell MS: *Front Immunol* 7(575):1–14, 2016.

Zhou M, Gao D, Chai X, et al.: Application of high-throughput, high-resolution and cost-effective next generation sequencing-based large-scale HLA typing in donor registry, *Tissue Antigens* 85(1):20–28, 2015.

Zinkernagel RM: Cellular immune recognition and the biological role of major transplantation antigens, *Biosci Rep* 17:91, 1997a.

Zinkernagel RM: The Nobel Lectures in Immunology. The Nobel Prize for Physiology or Medicine, 1996: cellular immune recognition and the biological role of major transplantation antigens, *Scand J Immunol* 46:421, 1997b.

CHAPTER 51

THE MAJOR HISTOCOMPATIBILITY COMPLEX AND DISEASE

Attila Kumánovics, Eszter Lázár-Molnár, Julio C. Delgado

OVERVIEW OF THE HUMAN MAJOR HISTOCOMPATIBILITY COMPLEX DNA SEQUENCE, 1014

GENES IN THE CENTRAL OR CLASS III REGION, 1015

Tumor Necrosis Factor And Lymphotoxin α And β Genes, 1016

Heat-Shock Protein 70 Genes, 1016

C2, C4, And CFB Genes And Typing, 1016

Disease Associations With C2, C4, And CFB Genes, 1017

Complotypes, 1017

EXTENDED HAPLOTYPES, 1017

MHC DISEASE ASSOCIATIONS, 1018

MHC Monogenic Disease Associations, 1019

Polygenic Diseases With MHC Associations, 1020

METHODS OF DETECTING ASSOCIATION OR LINKAGE OF DISEASE WITH GENETIC MARKERS, 1023

Genetic Polymorphism, 1023

Gene And Phenotype Frequencies, 1023

Strength Of Association, 1023

Analysis Of Mode Of Inheritance Based On Sibling Pairs, 1023

Analysis Of Mode Of Inheritance Based On Population Studies, 1023

LOD Score Method, 1023

SUMMARY, 1024

SELECTED REFERENCES, 1024

KEY POINTS

- The major histocompatibility complex (MHC) genomic region contains many genes with immune-related functions, including the human leukocyte antigen (HLA) genes.
- Identification of genes within the MHC has increased the possibility of defining the genetic basis of immunity.
- The clustering of immune-related genes in the MHC region may not be coincidental and may be the result of evolutionary forces joining genes with similar functions.
- The MHC is associated with more diseases than any other region on the human genome.
- Presence of fixed stretches of MHC deoxyribonucleic acid (DNA) (haplotypes) complicates the study of susceptibility genes but also provides the means for their identification.
- Methods are available for detecting associations or linkage between polymorphisms found with the MHC and disease.
- Although MHC class I– and class II–encoded proteins are distinguished by structural and functional similarities shared by the members of each class, class III molecules can be defined only as non-I and non-II because their genes and their products have no common features and are not recognized by T cells.
- Despite convincing genetic association studies showing the importance of the class III region in health and disease, neither the genes responsible for disease nor the underlying mechanism of pathology is known for many of the associated conditions.
- Almost half of the genes within the MHC class III region play roles in the innate immune system, including members of the complement cascade (C4, C2, BF), tumor necrosis factor (TNF, LTA, LTB), and lymphocyte antigen-6 (LY6) families.
- Deficiency of the second component of the complement system is the most common complement protein deficiency state in European populations, but rare in others.
- Complete C4 deficiency is extremely rare. The level of C4 in the serum of patients with C4 null alleles is extremely variable and cannot be used reliably to detect heterozygotes for complete deficiency because there is no correlation between the level of C4 and the number of expressed C4 genes.
- Extended haplotypes are highly characteristic of an ethnic subgroup and have lower frequencies or do not occur at all in other ethnic groups.
- It is critical to know the ethnic distribution of a disease-associated MHC allele to evaluate whether the allele in patients is increased compared with ethnically matched control populations and is in fact truly a marker for the ethnic distribution of the disease.
- A major problem with MHC gene associations is their incomplete penetrance, making ordinary formal segregation and linkage studies difficult to carry out.

Understanding the role of the major histocompatibility complex (MHC) in immune responses and in the pathogenesis of disease requires defining polymorphisms in the class I and class II regions, as well as genes in the central *MHC class III region*. The strong interest in the MHC genomic sequence originates from its established role in regulating inflammation and the innate and adaptive immune responses. Several genes in the MHC play important roles in cellular discrimination of self and nonself that require an essential knowledge of the effects of the MHC system in transplantation medicine and in susceptibility to autoimmunity. Variants of class I and class II genes were described in detail in Chapter 50. In this chapter, we discuss the non–human leukocyte antigen (HLA) region genes, disease associations, and methods for detecting the association of diseases with genetic markers.

OVERVIEW OF THE HUMAN MAJOR HISTOCOMPATIBILITY COMPLEX DNA SEQUENCE

Completion of the MHC deoxyribonucleic acid (DNA) sequence preceded completion of the total human genome sequence by almost 4 years (The MHC Sequencing Consortium, 1999). The rush to complete the entire MHC sequence followed the need to understand the biology and genetics of the mouse MHC (H-2) and HLA regions, which were initially provided by murine inbred experiments and serologic typing (Klein, 1986). Although the MHC was discovered more than 50 years ago, its nature has been resolved only in the last 2 decades, with the advent of DNA cloning and discovery of the structure of class I and class II molecules (Bjorkman et al., 1987; Brown et al., 1993).

The MHC located on the short arm of chromosome 6 spans approximately 4 megabases (Mb) and contains more than 250 identified loci, by far the most gene-dense region of the human genome sequenced to date (Shiina et al., 2009). It encodes the most polymorphic human proteins—the HLA class I and class II molecules, with over 24,000 allelic variants identified so far (Robinson et al., 2015). More than 40% of the total expressed loci in the MHC are associated with immune-related functions. This clustering of immune-related genes in the MHC region may not be

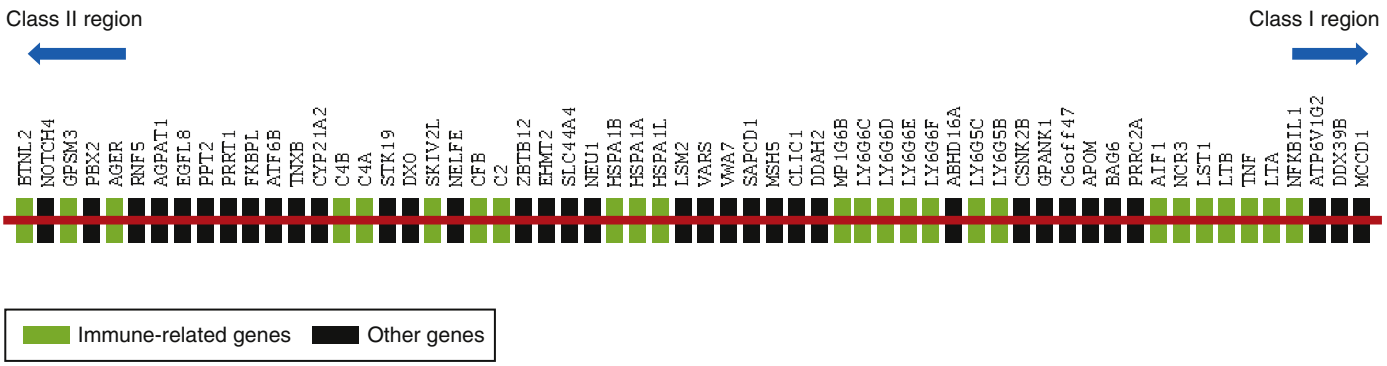

Fig. 51.1 Gene map of the class III region of the major histocompatibility complex. Shown in order but not to scale are 61 genes from centromere to telomere. Genes presenting "immune loci" are marked by green boxes.

coincidental and may be the result of evolutionary forces joining genes with similar functions.

Traditionally, the MHC region has been classified into three regions from telomere to centromere: HLA class I, non-HLA class (MHC class III), and HLA class II. HLA class I and class II gene functions were reviewed in detail in Chapter 50. We will concentrate on the MHC class III region and will later return to HLA class I and class II genes to discuss disease associations.

GENES IN THE CENTRAL OR CLASS III REGION

The human MHC class III, or central MHC region, located between the HLA class I and class II regions, is the most gene-dense region of the human genome. Specifically, the MHC class III region contains 61 protein-coding genes in ~900-kb sequence, with an average gene size of ~8.5 kb (Xie et al., 2003), compared with the entire human genome, which contains, on average, fewer than 11 genes/Mb and has an average gene size of 27 kb (Lander et al., 2001). Although HLA class I– and class II–encoded proteins are distinguished by structural and functional similarities shared by the members of each class, MHC class III molecules can be defined only as non-I and non-II because their genes and their products have no common features and are not recognized by T cells. Figure 51.1 shows a gene map of the MHC class III region.

Despite convincing genetic association studies showing the importance of the MHC class III region in health and disease, neither the genes responsible for disease nor the underlying mechanism of pathology is known for many of the associated conditions. One reason for this is the fact that the functions of nearly half the genes in the MHC class III region are not completely known. A high-throughput yeast two-hybrid system was used to look into the function of several intracellular proteins encoded within the MHC class III region (Lehner et al., 2004). This study revealed that approximately one third of the analyzed proteins encoded within the MHC class III region may have a role in mRNA processing, which again suggests clustering of functionally related genes within this region of the human genome. Specifically, three proteins (STK19, PBX2, and NELFE) of those in the MHC class III region interact with proteins implicated in transcriptional regulation. Four proteins (LSM2, DDX39B, DXO, and SKIV2L) are orthologs of yeast proteins involved in mRNA processing, and another five proteins (PRRC2A, STK19, CLIC1, PBX2, and ABHD16A) interact with proteins previously implicated in RNA processing. Proteins involved in RNA processing are usually categorized as "housekeeping" proteins, but they are often critical for innate immunity against viral RNA. Metabolism of intracellular nucleic acids is also critical for limiting autoimmunity against DNA and RNA. SKIV2L (superkiller viralicidic activity 2-like)–deficient patients have an elevated interferon response (Eckard et al., 2014) and present with trichohepatoenteric syndrome, an inflammatory bowel disease–like intractable diarrhea (Fabre et al., 2012).

The region closer to HLA class II genes contains several genes of known function, including *TNXB* (Morel et al., 1989), which encodes tenascin X, a large extracellular matrix protein expressed in connective tissues, and *NEU1*, which encodes neuraminidase 1, a lysosomal sialidase, and *SLC44A4*, which encodes a choline transporter. Mutations of *TNXB* are a cause of Ehlers-Danlos syndrome (Burch et al., 1997), primary myopathy (Penisson-Besnier et al., 2013), and vesicoureteral reflux (Gbadegesin et al., 2013; Bonten et al., 1996). Mutations of the *NEU1* gene are responsible for congenital sialidosis (Bonten et al., 1996; Canafoglia et al., 2014). Mutations in *SLC44A4* cause autosomal dominant nonsyndromic deafness (Ma et al., 2017).

The region toward the class I genes also contains several genes of known function, including *VARS*, the cytoplasmic valyl-tRNA synthetase, *MSH5*, a homolog of *Escherichia coli* MutS recombinase, and *CSNK2B*, casein kinase type II. Mutations in *VARS* lead to neurodevelopmental encephalopathy and microcephaly (Stephen et al., 2018), mutations in *MSH5* lead to primary ovarian insufficiency (Guo et al., 2017), and pathogenic variants in *CSNK2B* cause intellectual disability and global developmental delay with or without epilepsy (Poirier et al., 2017).

Almost one half of genes within the MHC class III region play roles in the innate immune system, including members of the complement fixation cascade (C4, C2, CFB) and the tumor necrosis factor family (TNF, LTα, LTβ), which will be discussed in greater detail later in this chapter. Other members of the immunoglobulin superfamily are also located within the MHC class III regions: *NCR3* (natural cytotoxicity triggering receptor 3) and the less characterized *LY6G* genes (Loughner et al., 2016). The *NCR3* gene encodes the NKp30 protein responsible for triggering natural killer (NK) cells (Pende et al., 1999). NK cells play a variety of roles in the immune system, including defense against infectious organisms as well as tumors, and have also been implicated in autoimmunity. NKp30 is involved in the killing of cells infected with *Plasmodium falciparum* (Mavoungou et al., 2007) and cytomegalovirus (Arnon et al., 2005), fungi (Li et al., 2013), hematologic and solid tumor cells (Brandt et al., 2009) and contributes to the pathogenesis of primary Sjögren syndrome (Rusakiewicz et al., 2013). Variants in *NCR3* gene contribute to genetic risk of malaria attacks (Delahaye et al., 2007). Increased expression of *NCR3* and the adjacent *LST1* (leukocyte-specific transcript 1) gene has been found in the blood of rheumatoid arthritis patients (Mulcahy et al., 2006); and haplotype-specific variants in these genes alter susceptibility to arthritis in animal models (Yau et al., 2016). *LST1* encodes a palmitoylated transmembrane signaling adaptor and membrane scaffolding protein in myeloid cells (Weidle et al., 2018). Both genes are also significantly upregulated in response to lipopolysaccharide, interferon-γ, and bacterial infection, suggesting a role for these gene products in autoimmune-related inflammation and dendritic cell/NK cell–associated functions. The Ly6 (lymphocyte antigen 6 complex) family of proteins were originally described using antisera to lymphocytes and were used as markers for lymphocyte subset differentiation, but now we know that they belong to a family of 35 genes in humans, 5 of which are located in the MHC class III region. The functions of many Ly6 proteins are still not well understood, but it ranges from neutrophil migration, cell-cell interaction, complement regulation, macrophage activation, to modulation of viral infections (Loughner et al., 2016).

The *NFKBIL1* (NF-κB-inhibitor–like 1) and *BTNL2* (Butyrophilin-like protein 2) genes are also located in the MHC class III region (Albertella & Campbell, 1994; Stammers et al., 2000). Much interest has been focused on the NFKBIL1 (An et al., 2013) and BTNL2 (Swanson et al., 2013) proteins after single mutations in their promoter regions were linked to rheumatoid arthritis (Okamoto et al., 2003) and sarcoidosis (Valentonyte et al., 2005), respectively. BTNL2 may also contribute to the risk of type 1 diabetes (Hippich et al., 2019). *AIF1* (Allograft inflammatory factor-1) encodes a calcium-binding protein highly expressed in monocytes and macrophages and involved in phagocytosis in these cells and in antigen uptake in intestinal M cells, and have also been implicated in rheumatoid arthritis and other inflammatory processes (Kishikawa et al., 2017; Kadoya et al., 2014). Finally, the genes for the microsomal enzyme steroid P450 21-hydroxylase and three members of the major heat-shock protein 70 family are also contained in the MHC class III region and will be discussed later.

TUMOR NECROSIS FACTOR AND LYMPHOTOXIN A AND B GENES

Tumor necrosis factor and lymphotoxin α (LTα) are potent immunomodulatory cytokines produced in response to inflammatory stimuli. TNF and LTα proteins are each encoded by separate genes (*TNF* and *LTA*) and share approximately 34% amino acid identity (Carroll et al., 1987). TNF and LTα are either maintained as cell surface molecules or released from cells. LTα is retained on the cell surface via a transmembrane region. Surface TNF results not from the presence of a transmembrane region, but rather from an association with lymphotoxin β (LTβ) (Browning et al., 1993). LTβ encoded by *LTB* has 21% and 24% amino acid identity with *TNF* and *LTα*, respectively.

To date, several *TNF* promoter polymorphisms have been identified and correlated with susceptibility to various autoimmune and infectious diseases. This work remains controversial both at the genetic level and, more importantly, with regard to functional relevance. As demonstrated for some of the *TNF* promoter polymorphisms, these gene variations may be ethnic-specific markers for other linked and unidentified factors that may have an impact on host immune response in the development of autoimmune diseases and susceptibility or resistance to infectious diseases in a given population (Delgado et al., 2002). Polymorphisms in the *TNF* promoter region have been correlated in large-scale population studies with cerebral malaria (McGuire et al., 1994), rheumatoid arthritis (Criswell et al., 2004), coronary heart disease (Nicaud et al., 2002), type 2 diabetes (Kubaszek et al., 2003), Alzheimer disease (McCusker et al., 2001), ankylosing spondylitis (McGarry et al., 1999), mortality to septic shock (Mira et al., 1999), mucocutaneous leishmaniasis (Cabrera et al., 1995), periodontitis (Ding et al., 2014), immune thrombocytopenia (Hajeer & Hutchinson, 2001; Sarpatwari et al., 2011), inflammatory bowel disease (Zipperlen et al., 2005), and various hematologic and nonhematologic malignancies (He et al., 2014; Ding et al., 2014; Min et al., 2014). Similarly, large-scale analysis has linked both promoter and coding polymorphisms within the *LTA* gene to myocardial infarction (Ozaki et al., 2002), stroke (Wang et al., 2009), sepsis (Tiancha et al., 2011), leprosy (Alcais et al., 2007), autoimmune diseases (Zhang et al., 2015), and hematologic and nonhematologic malignancies (Skibola et al., 2010; Yu et al., 2014).

Anti-TNF therapy is a breakthrough in the management of rheumatoid arthritis, psoriasis, psoriatic arthritis, juvenile arthritis, ankylosing spondylitis, and inflammatory bowel disease (Crohn disease and ulcerative colitis). Genetic variants altering the expression level of TNF can potentially alter the response to anti-TNF therapies as well. Similar to disease association studies, the effect of TNF promoter variants on therapy outcomes and their use in management remains unsettled (Mugnier et al., 2003; Zeng et al., 2013; Murdaca et al., 2014; Song et al., 2015; Liu et al., 2016; Netz et al., 2017).

HEAT-SHOCK PROTEIN 70 GENES

Stress proteins, or heat-shock proteins, are expressed by cells in response to a variety of stress stimuli. This response has been observed in all species examined to date. The family of stress proteins, 70 kDa in size, has a highly conserved amino acid sequence identity as found from primitive eukaryotes to humans. Several studies have identified loci for heat-shock protein 70 (HSP70) on chromosomes 6, 14, and 21 (Hunt & Morimoto, 1985; Sargent et al., 1989). Three genes encoding members of the HSP70 family are located telomeric to the *C2* locus (*HSPA1L*, *HSPA1A*, and *HSPA1B*, formerly known as *HSP70-Hom*, *HSP70-1*, and *HSP70-2*, respectively).

Sequence analysis of *HSPA1A* and *HSPA1B* genes has shown that they are intronless genes that encode an identical protein product of 641 amino acids. *HSPA1L* is also an intronless gene that encodes a protein of 641 amino acids and has 90% sequence identity with *HSPA1A* (Milner & Campbell, 1990). Because of the high degree of sequence similarity between coding regions of the various *HSP70* genes, DNA probes corresponding to coding regions tend to cross-hybridize. However, sufficient sequence differences have been observed between the 5′ and 3′ untranslated regions to design oligonucleotide primers and probes to allow specific amplification and hybridization of the three genes (Milner & Campbell, 1992).

HSP70 plays a critical role in assisting protein folding, disaggregation, and degradation, and therefore it influences all aspects of cell biology. Polymorphisms in the *HSP70* gene cluster have been associated with the magnitude of the heat-shock response (Singh et al., 2006), schizophrenia (Kowalczyk et al., 2014; Pae et al., 2005), leukemia (Ucisik-Akkaya et al., 2010), age-related cataract (Zhang et al., 2013), longevity (Singh et al., 2010), among others. Other polymorphisms in the *HSP70* gene have been correlated to cytokine response in trauma (Schroder et al., 2003), Parkinson disease (Wu et al., 2004), uveitis in patients with sarcoidosis (Spagnolo et al., 2007), and risk for clozapine-induced agranulocytosis in Ashkenazi Jews (Corzo et al., 1995).

C2, C4, AND CFB GENES AND TYPING

The complement C2, C4, and factor B proteins encoded within the MHC class III demonstrate inherited structural variants that can be studied by using techniques that detect differences in net surface charge due to amino acid differences. Two methods are used to separate these proteins: (1) high-voltage agarose gel electrophoresis, which detects variations in mobility due to charge differences between proteins at a given pH, and (2) isoelectric focusing in thin-layer polyacrylamide gels, which shows differences in isoelectric points. Proteins can be visualized by immunofixation electrophoresis using insolubility of antigen-antibody complexes, or by detection of functional hemolytic activity with overlay gels, in which antibody-sensitized sheep erythrocytes are combined with complement-deficient serum (Alper et al., 1983).

At the protein level, C2 shows minor polymorphism by isoelectric focusing. The alleles for C2 are *C* (common), a less common *B* (basic) allele with three rare basic variants, and four rare *A* (acidic) variants (Jahn et al., 1990). The polymorphic site for the *C2*B* allele is carried by the C2a complement fragment. The C2 protein is genetically polymorphic in a wide variety of ethnic groups, although *C2*C* accounts for more than 90% of *C2* genes in most populations (Alper, 1976; Meo et al., 1977). In Caucasian and Asian populations, *C2*B* accounts for 5% to 10% of *C2* genes. A nonexpressed allele (*C2*QO*) is found in 2% of the Caucasian European population (Truedsson et al., 1993a). For C2 typing, proteins are separated by isoelectric focusing in polyacrylamide gels and are visualized by C2-induced hemolysis in overlay gels. Diluted normal human serum can replace C2-deficient serum as a reagent, because C2 is the limiting factor in the classical complement pathway.

Two distinct but closely related loci for the C4 protein (*C4A* and *C4B*), presumably the result of tandem gene duplication, encode for two forms of C4. The genetics of *C4* is extraordinarily complex, not only at the genetic level but also at the protein level. It has been shown that the number of *C4* genes in humans varies from two to four, and in exceptional cases, six (Chung et al., 2002; Wu et al., 2007). The *C4* gene duplication unit includes its neighboring genes *STK19* at the 5′ region and *CYP21* and *TNXB* at the 3′ region (Blanchong et al., 2000). Misalignments (unequal crossing-overs) of heterozygous mono-, bi-, or trimodular chromosomes during meiosis can cause further rearrangements and lead to congenital adrenal hyperplasia and Ehlers-Danlos syndrome by deleting *CYP21* and *TNXB* genes, respectively, in addition to changing the number of *C4* genes. Three quarters of *C4* genes carry endogenous retrovirus sequences that might confer intrinsic protection against exogenous retroviral infection (Schneider et al., 2001). Recent data suggest a negative correlation between the presence of endogenous retrovirus sequences and the level of C4 proteins, as well as a direct relationship between the number of genes and C4 protein levels (Yang et al., 2003).

At the protein level, C4A and C4B differ only by four amino acid residues in the α chain (**PC**PV**LD** and **LS**PV**IH**, encoded by exon 26 of *C4A* and *C4B*, respectively) but these changes lead to altered ligand specificity: C4A preferentially binds to amino groups on immune complexes, whereas C4B preferentially binds to hydroxyl or carbohydrate groups (Yu et al., 1988). C4B is several times more hemolytically active than C4A, but C4A is more active at inhibiting the formation and dissolution of immune complexes than C4B. C4A proteins carry the Rodgers blood group antigenic determinant, whereas C4B carries the Chido determinant. Extensive genetic polymorphism is detectable in C4A and C4B proteins among populations; more than 35 variants have been observed by agarose gel electrophoresis and DNA-based typing methods (Awdeh & Alper 1980; Sim & Cross, 1986; Schneider et al., 1996; Hui et al., 2004). Among the C4A and C4B allotypes, the most common alleles are *C4A*3* and *C4B*1*. *C4A*4*, *C4A*2*, *C4B*2*, and *C4B*5* show a worldwide general distribution. *C4A*6* is also observed in many populations, with the exception of some Mongoloid groups. *C4B*3* is identified mainly in African and Caucasian groups.

C4 typing requires a combination of several techniques (Awdeh & Alper 1980): (1) Immunofixation electrophoresis after treatment with neuraminidase. The patterns produced show three bands for each variant with some overlap occurring between certain variants. Additional treatment of the sample with carboxypeptidase reduces each variant to a single band. (2) Detection of C4A versus C4B by functional hemolytic assay. This method distinguishes C4A and C4B overlapping patterns because C4B variants have 5 to 10 times the hemolytic activity of C4A variants.

(3) Rodgers (C4A) or Chido (C4B) serologic reactivity. The serum is incubated with human anti-Rodgers or human anti-Chido to test for inhibition of agglutination with appropriate positive erythrocytes. Alternatively, C4 variants can be typed for Chido or Rodgers reactivity by immunoblotting. Null alleles of *C4* heterozygotes can be detected in two ways. Electrophoresis of C4 null (*C4A QO* and *C4B QO*) samples demonstrates an absence of bands in homozygotes, but in heterozygotes requires quantification by visual inspection, crossed immunoelectrophoresis, or densitometric scanning of immunofixation patterns. An alternative method is to determine the presence and ratios of the C4A and C4B α chains after sodium dodecyl sulfate polyacrylamide gel electrophoresis of immunoprecipitates. More recently, DNA-based typing methods, including sequence-specific primer (SSP) amplification, restriction fragment length polymorphism analysis, real-time polymerase chain reaction (PCR), and direct DNA sequencing, have been used to complement inconclusive C4A and C4B protein allotyping (Schneider & Mauff, 2003; Wu et al., 2007).

Factor B is synthesized by the *CFB* gene. Human factor B is highly polymorphic, with more than 20 variants identified to date, including several dysfunctional proteins, those present in low concentration, and null alleles. Factor B typing is normally performed by combining agarose electrophoresis and/or isoelectric focusing at the protein level with PCR analysis at the DNA level (Geserick et al., 1998). By using these methods, it is possible to identify two very common alleles, *CFB*F* and *CFB*S*, two less common alleles, *CFB*F1* and *CFB*S1*, and a host of rare alleles. Variants are named for their decimal fraction migration in gel electrophoresis: CFB F to CFB F1 for fast variants, and CFB S to CFB S1 for slow variants. In European Caucasian populations, *CFB*F* has a frequency of 0.2, *CFB*S* of 0.77, *CFB*F1* of 0.01, and *CFB*S1* of 0.01; rare alleles account for only 0.002. *CFB*S* is most common in Caucasian, Mongoloid, and Australoid populations, and *CFB*F* is most common in Negroid populations. *CFB*F1* is observed in African groups, as well as in some Caucasian populations.

DISEASE ASSOCIATIONS WITH C2, C4, AND CFB GENES

Deficiency of the second component of the complement system, C2, has been reported in about 1 in 10,000 Caucasians, and is the most common complement protein deficiency state in that population (Silverstein, 1960; Klemperer et al., 1966). People with complete C2 deficiency are homozygous for null C2 alleles (*C2*Q0* for quantity zero). *C2*Q0* results from a 28-bp gene deletion that generates a frameshift and a stop codon 14 bp distal to the end of exon 6 (Johnson et al., 1992). Rarely, C2 deficiency is the result of missense mutations resulting in impaired C2 secretions that have been termed *C2 deficiency type II* (Wetsel et al., 1996). Although C2 deficiency can lead to disease, most patients (60%) remain asymptomatic. Up to 25% of homozygotes for C2 deficiency have increased susceptibility to bacterial infection due to immunoglobulin deficiency (Densen, 1991; Alper et al., 2003). Between 20% and 40% of reported patients with C2 deficiency have a systemic lupus–like disease (Truedsson et al., 1993b; Sullivan et al., 1994; Jönsson et al., 2007). A polymorphism in the *C2* gene has been correlated with reduced risk for age-related macular degeneration (Gold et al., 2006; Maller et al., 2006).

A high incidence of *C4 null* alleles is seen in the general population. *C4A*Q0* and *C4B*Q0* result from gene deletions, premature stop codons, and other mutations that cause transcription failure (Braun et al., 1990; Barba et al., 1993; Lokki et al., 1999). Thirty-five percent of individuals of all races do not express one *C4A* or *C4B* gene (i.e., carry *C4A*Q0* or *C4B*Q0*), 8% to 10% carry two null alleles, and less than 1% do not express three alleles. Complete C4 deficiency (trans *C4A*Q0*, *C4B*Q0*) haplotypes are extremely rare (Hauptmann et al., 1986). The *C4A*Q0* allele, particularly in homozygous individuals or those with complete C4 deficiency, has been associated with systemic lupus erythematosus (Wilson & Perez, 1988; Huang et al., 1995). This susceptibility is probably related to defective handling of immune complexes (Fielder et al., 1983; Lintner et al., 2016). Children homozygous for *C4B*Q0* have a 3.5-fold greater incidence of bacterial meningitis (Colten & Rosen, 1992). Homozygous C4B deficiency is described in families with non-SLE glomerulonephritis (Ault et al., 1990; Tsuda et al., 2007; Soto et al., 2010), and the *C4B*Q0* allele is thought to increase the risk for Henoch–Schönlein purpura (Stefansson Thors et al., 2005). Increased frequency of the *C4B*Q0* allele has been found in patients with severe coronary artery disease who underwent bypass compared with healthy controls (Szalai et al., 2002).

Absence of homozygous factor B deficiency in humans has led to the notion that the condition might be lethal during embryonic development. Based on inheritance patterns and serum levels, some heterozygotes from *CFB*Q0* have been identified as having reduced protein products (Siemens et al., 1992), and recently compound heterozygous loss-of-function mutations in CFB were identified in a patient with recurrent pneumococcal and meningococcal infections (Slade et al., 2013). The *CFB F* variant has been associated with higher protein concentration but lower hemolytic activity than *CFB S* (Lokki & Koskimies, 1991). Mutations in the *CFB* gene have been associated with age-related macular degeneration (Gold et al., 2006; Maller et al., 2006) and atypical hemolytic-uremic syndrome (Goicoechea de Jorge et al., 2007).

TABLE 51.1

Common Complotypes in Normal Chromosomes of Caucasoid Populations[a]

Complotype	Frequency, %
SC31	0.430
SC01	0.127
FC31	0.096
SC30	0.053
SC42	0.040
SC61	0.034
FC30	0.031
FC01	0.029
SC02	0.029
SC21	0.022
SB42	0.019
SC33	0.014
SC2(1,2)[b]	0.01
3SC32	0.011

[a]Complotypes are given as abbreviated letters and numbers, with four alleles in arbitrary order: *CFB, C2, C4A,* and *C4B*.
[b]*C4B* locus is heteroduplicated.

COMPLOTYPES

The four genes of the complement region occupy approximately 120 kb of genomic DNA (Carroll et al., 1984). The *C2* and *CFB* genes are located in very close proximity, separated by less than 2 kb, but *CFB* and *C4A* are separated by about 30 kb. *C4A* and *C4B* are about 10 kb apart. Alleles of the complement genes occur as a unit at the population level and show striking linkage disequilibrium in haplotypes determined by family studies. That is to say, they occur together as sets on the same chromosome more frequently than expected from the frequencies of their individual alleles and with no well-documented recombinations. For these reasons, haplotypes of the four complement loci have been called *complotypes*, as an abbreviation for "complement haplotypes" (Alper et al., 1983). Although their order from telomere to centromere is *C2*, *CFB*, *C4A*, *C4B* (see Fig. 51.1), the positions of *CFB* and *C2* are transposed for clarity in using variant alleles to designate complotypes. Thus *CFB*S*, *C2*C*, *C4A*QO*, *C4B*1* is a complotype that in abbreviated form is *SC01*. More than a dozen complotypes in Caucasians have frequencies of about 0.01 or higher (Table 51.1). In most populations, the *SC31* complotype is most common. In people of African descent, *FC31* is common, as is *SC42* in East and Southeast Asians.

EXTENDED HAPLOTYPES

Based on the study of the distribution of complotypes in relation to *HLA-B* and *HLA-DR* specificities on normal Caucasian haplotypes determined in family studies, striking linkage disequilibrium involving the whole region became evident. One could easily recognize *HLA-B*, complotype, *DR* allele sets that showed statistically significant three-point linkage disequilibrium (Fig. 51.2) and that define what are regarded as extended haplotypes (Awdeh et al., 1983). A shorthand nomenclature for extended haplotypes has been designed by enclosing *HLA-B*, complotype, and *HLA-DR* variants in brackets. Thus the most common extended haplotype in Caucasians is *[HLA-B8, SC01, DR3]*. Extended haplotypes are highly characteristic of an ethnic subgroup and have lower frequencies or do not occur at all in other ethnic groups (Alper et al., 1982; Fraser et al., 1990).

Initial studies defined extended haplotypes as the genomic interval between *HLA-B* and *DR*. It then became evident that other uncharacterized MHC alleles in the interval were likely to be included. Despite the fact that *HLA-A* alleles have shown limited variation for extended haplotypes,

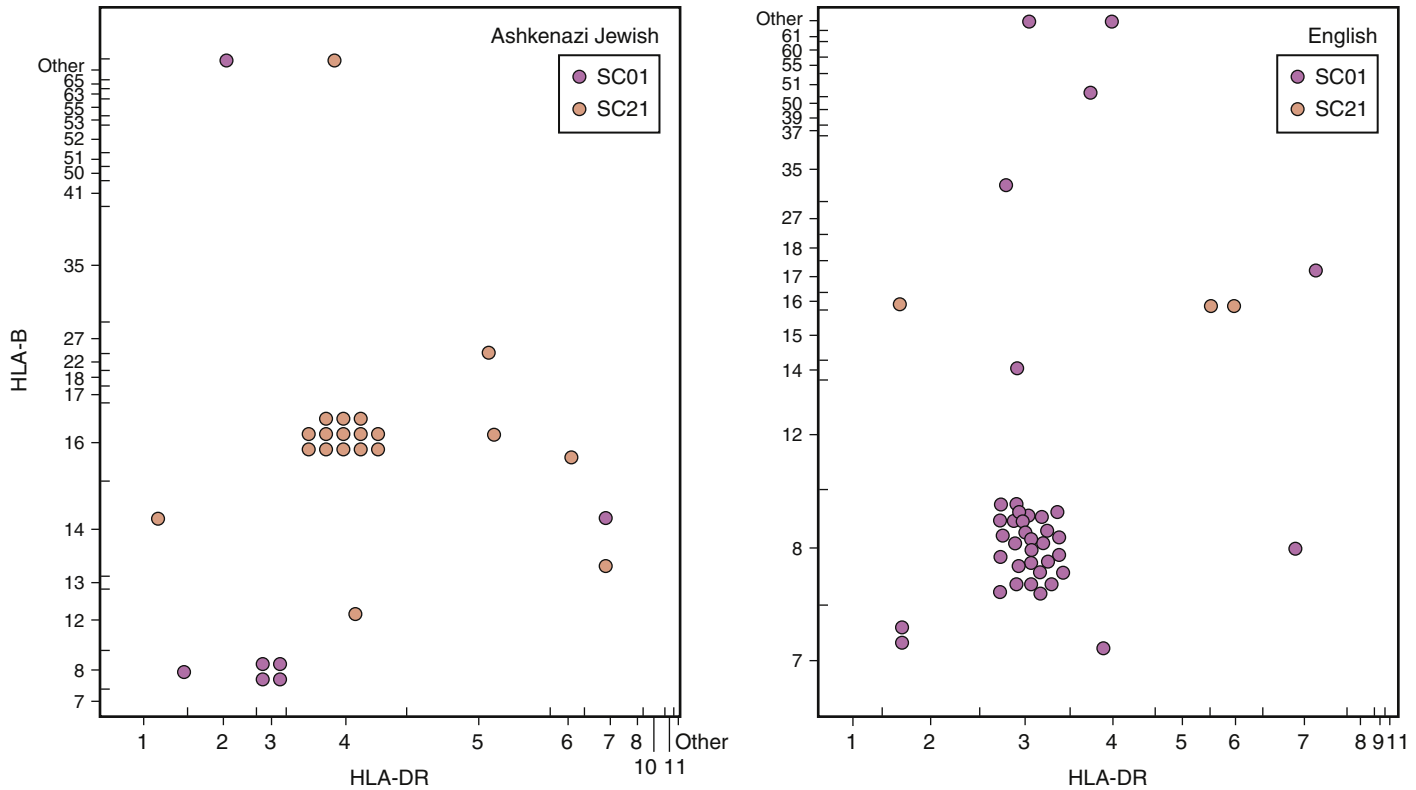

Fig. 51.2 The haplotype distribution of the complotypes (haplotypes of complement alleles) *SC01 (CFB*S, C2*C, C4A*QO, C4B*1)* and *SC21 (CFB*S, C2*C, C4A*A, C4B*1)* in relation to *HLA-B* alleles on the ordinate and *HLA-DR* alleles on the abscissa. Heights and widths representing HLA specificity are proportional to allele frequencies for the respective populations. Clustering represents linkage dysequilibrium and flags the extended haplotypes *[HLA-B16(38), SC21, DR4]* in Ashkenazi Jews *[HLA-B8, SC01, DR3]* and in the English and, to a much lesser extent, among Jews. *HLA,* Human leukocyte antigen. (From Alper CA, Awdeh ZL, Yunis EJ: Conserved, extended MHC haplotypes, Exp Clin Immunogenet 9:58, 1992, Figure 4. Copyright © S. Karger AG, Basel.)

only half such haplotypes show unique and significant *HLA-A* allele associations (Alper et al., 1982). The *HLA-Cw* locus was by far the last to be characterized. Based on genetic distance and previously incomplete typing data of *HLA-B/Cw* pairs, it was evident that conserved haplotypes would also include the HLA-Cw genetic region. Thus, different *HLA-Cw* alleles have been recently associated with different extended haplotypes (Table 51.2) (Clavijo et al., 1998). Furthermore, several *TNF* and *HSP* allele systems and microsatellites have been studied in relation to extended haplotypes (Table 51.3). More recently, models have been created to describe the variable sizes of stretches of conserved DNA in the MHC, using the known frequencies of four different types of small blocks (<0.2 Mb) of relatively conserved DNA sequence: *HLA-Cw/B; TNF;* complotype; and *HLA-DR/DQ* (Yunis et al., 2003). Using HLA allele identification and TNF microsatellites, Yunis and colleagues have shown that some extended haplotypes extend to the *HLA-A* and *HLA-DPB1* loci, which form fixed genetic units of at least 3.2 Mb of DNA. Intermediate fragments of extended haplotypes also exist, which are, nevertheless, larger than any of the four small blocks. This complexity of genetic fixity at various levels should be taken into account in studies of genetic disease association, immune response control, and human diversity.

Extended haplotypes, which account for at least 30% of normal Caucasian haplotypes, have relatively fixed gross structure and DNA sequence and carry very similar (if not identical) alleles even when they are found in apparently unrelated individuals. The frequency of extended haplotypes is more likely to be underestimated than overestimated because haplotypes must be determined from family studies involving thousands of unrelated index cases. The original MHC reference sequence (The MHC Sequencing Consortium, 1999) has been used as the starting point for numerous studies undertaken to ascertain multiple common and rarer extended haplotypes (Walsh et al., 2003; Stewart et al., 2004; Smith et al., 2006; Traherne et al., 2006), and then eight haplotypes have been completely sequenced, and the haplotype *[HLA-A3, B7, DR15]* was designated as the new MHC reference sequence incorporated into the reference human genome assembly (Horton et al., 2008). The advent of next generation (or massively parallel) sequencing technologies enabled the sequencing of individual genomes. However, the current technologies in clinical use struggle with complex portions of the genome, like the MHC. These challenges are now being overcome, and there are novel technologies that can sequence the entire MHC, including some that are capable of phasing the entire diploid MHC, not just the individual HLA genes (Selvaraj et al., 2015; Dapprich et al., 2016; Mostovoy et al., 2016; Zhang et al., 2017). These studies will facilitate the identification of precise disease loci and may help us to better understand events such as recombination and polymorphism.

TABLE 51.2
Common Extended MHC Haplotypes[a]

Extended Haplotype	HLA-Cw Allele	Ethnicity
[HLA-B8, SC01, DR3, DQ2]	0701	Northern Europe
[HLA-B7, SC31, DR2, DQ6]	0702	Northern Europe
[HLA-B44, FC31, DR7, DQ2]	1601	Europe
[HLA-B44, SC30, DR4, DQ7/8]	0501	Europe
[HLA-B57, SC61, DR7, DQ2/3]	0602	Northern Europe
[HLA-B14, SC22, DR1, DQ1]	0802	Northern Europe
[HLA-B35, SC31, DR5, DQ3]	0401	Southern Europe
[HLA-B38, SC21, DR4, DQ8]	1203	Ashkenazi Jews
[HLA-B15, SC33, DR4, DQ8]	0304	Northern Europe
[HLA-B18, F1C30, DR3, DQ2]	0501	Basques, Sardinia, Spain
[HLA-B18, S042, DR2][b]	1203	Northern Europe
[HLA-B42, FC(1,90)0, DR3][c]	1701	African

HLA, Human leukocyte antigen; *MHC,* major histocompatibility complex.
[a]Data from normal Caucasoid population chromosomes from Boston.
[b]Data from patients with C2 deficiency. (Clavijo O, Delgado J, Awdeh ZL, et al: HLA-Cw alleles associated with HLA extended haplotypes and C2 deficiency, Tissue Antigens 52:282–285, 1998.)
[c]Data from chromosomes of normal black population living in Boston. (Clavijo OP, Delgado JC, Yu N, et al: HLA-Cw*1701 is associated with two sub-Saharan African-derived HLA haplotypes: HLA-B*4201, DRB1*03 and HLA-B*4202 without DRB1*03, Tissue Antigens 54:303–306, 1999.)

MHC DISEASE ASSOCIATIONS

The MHC is associated with more diseases than any other region on the human genome. Identification of the key genetic association within the MHC has proven difficult for at least four reasons: (1) MHC has the highest

TABLE 51.3

TNF and *HSP* Gene Polymorphisms in Relation to Common Extended Haplotypes[a]

	COMPLOTYPE				*HSP*				*TNF* MARKERS						
HLA-DR	*C4B*	*C4A*	*CFB*	*C2*	*1B*	*1A*	*e*	*d*	*−308*	*−857*	*−863*	*a*	*b*	*HLA-B*	*HLA-Cw*
3	1	0	S	C	8.5	C	3	1	2	1	1	2	3	8	0701
2	1	3	S	C	9	A	3	3	1	1	1	11	4	7	0702
7	1	3	F	C	9	A	3	3	1	1	1	7, 8	4	44	1601
4	0	3	S	C	9	A	3	3	1	1	1	6, 7	5	44	0501
7	1	6	S	C	9	A	3	4	1	1	1	2	5	57	0602
5	1	3	S	C	9	A	3	3	1	1	1	5	5	35	0401
1	1, 2	2	S	C	9	A	1	4	1	1	2	2	1	14	0802
4	1	2	S	C	9	A	3	3	1	2	1	10	4	38	1203
4	3	3	S	C	9	A	1	4	1	1	2	2	1	62	0304
2	2	4	S	0	9	A	3	3	1	2	1	10	4	18	1203
3	0	3	F1	C	8.5	C	3	4	1	1	1	1	5	18	0501

[a]The numbers or letters under each column refer to a particular allele variant of the complement, heat-shock protein *(HSP)*, tumor necrosis factor *(TNF)* microsatellite, or *TNF* promoter polymorphisms that are associated with the human leukocyte antigen *(HLA)* specificities as noted. See text for explanation. In the case of *TNF-308*, 1 and 2 represent the *−308/G* and *−308/A* variants, respectively. The *TNF-857/C* allele is noted as 1, and the *TNF-857/T* allele as 2. The *TNF-863/C* TNF allele is noted as 1, and the *−863/A* as 2.

Adapted from Clavijo O, Delgado J, Awdeh ZL, et al: HLA-Cw alleles associated with HLA extended haplotypes and C2 deficiency, Tissue Antigens 52:282–285, 1998.

gene density in the genome, (2) and these large numbers of genes are often in strong linkage disequilibrium forming complex haplotype structures, (3) extended haplotypes contain multiple equally plausible candidate loci, and (4) the associated diseases often show non-Mendelian inheritance.

We have reviewed concepts about complotypes and extended haplotypes to enhance our understanding of the relevance of a rather extensive literature on MHC disease associations. Most of the MHC disease associations reported to date are contained within extended haplotypes. It is probably because of this simple fact that so many MHC-allele–associated diseases have been reported, because it is not a single base pair but more than 3 million base pairs of conserved DNA that constitute the marker. For example, complement alleles such as *CFB*F1* and *C4B*3* have been linked to type 1 diabetes, because the extended haplotypes that carry them, *[HLA-B18, F1C30, DR3]* and *[HLA-B62, SC01, DR3]*, are more common in these patients than in the general population. This association means that haplotypes comprising 3 million bases or more in length of conserved genomic DNA carry susceptibility alleles for type 1 diabetes. These 3 million base-long extended haplotypes often contain multiple candidate loci, best illustrated by psoriasis, a chronic inflammatory skin disorder. Psoriasis was associated with *HLA-Cw6* over 30 years ago (Russell et al., 1972), and many studies attempted since to identify the causal gene or genes. Although *HLA-C* itself is the strongest candidate gene, multiple additional HLA class I and class II, and MICA/MICB variants appear to be independently associated with psoriasis (Okada et al., 2014; Gonzalez et al., 1999). Moreover, there are at least four genes (PSORS1C1-3 and CDSN) located next to *HLA-C* that encode skin-expressed genes providing additional candidate genes for this complex skin disease (Kumanovics & Fischer Lindahl, 2004; Zhou et al., 2016). It is also critical to know the ethnic distribution of an associated MHC allele to evaluate whether the allele in patients is increased compared with that in ethnically matched control populations or is in fact truly a marker for the ethnic distribution of the disease (Zhou et al., 2016). Furthermore, it is more difficult to map the genes responsible for disease in Caucasian Americans than in African Americans or Asian Americans because the level of genetic diversity is lower in Caucasians.

Most diseases associated with MHC are autoimmune and do not show clear-cut Mendelian inheritance. Many problems confound attempts to understand the inheritance mechanisms by which these diseases occur, and analysis of MHC markers in patients and their families has clarified the picture only marginally. A major problem with MHC gene associations is their incomplete penetrance, making ordinary formal segregation and linkage studies very difficult (if not impossible) to carry out. This is seen most clearly in monozygotic twins, who presumably have identical genes. If one such twin has one of these diseases (e.g., type 1 diabetes), the other twin does not necessarily have the same disease. For type 1 diabetes, the concordance rate appears to be no higher than 50% (Rubinstein et al., 1977; Barnett et al., 1981). This suggests that penetrance of a disease in a completely susceptible host is incomplete. Although there is excellent reason to consider genes in the MHC as determinants of type 1 diabetes susceptibility, only 15% of MHC-identical siblings of diabetic patients have insulin-dependent diabetes. This difference between 50% and 15% provides evidence for the influence of genes at a second, non–MHC-linked locus (or loci), and suggests the influence of other factors, such as environmental factors, in determining susceptibility.

Incomplete penetrance makes assignment of a specific mode of inheritance difficult and makes the likelihood of finding families with more than one affected member within one or more generations low. Families are frequently used to determine modes of inheritance. Another complicating factor is the inability to determine whether we are studying a group of patients that are homogeneous in terms of genetic determination. About 5% to 6% of random families with a type 1 diabetic proband will have a second affected child. Of these sibling pairs, approximately 60% will be MHC identical, 35% will be haploidentical, and a few percent will share no MHC haplotypes. This pattern suggests recessive inheritance of an MHC-linked susceptibility gene for the disease. At the very least, however, family studies provide highly useful haplotype data and usually allow the assignment of homozygosity for an HLA marker in probands. They have also established that MHC association in most diseases of interest is based on linkage between a susceptibility gene and the MHC.

Yet another unknown is the number of different susceptibility alleles for a disease in any specific population. In this regard, extended haplotypes can be helpful because, if increased in patients, they probably represent a single susceptibility allele that could be anywhere in the region of fixity. However, some patients have only portions of these haplotypes, and this provides little information about the location of specific allele involvement. Furthermore, it appears likely that many MHC-associated diseases are polygenic. Because of this, we will first discuss diseases associated with mutations of a single MHC gene; this will be followed by a discussion of polygenic diseases.

MHC MONOGENIC DISEASE ASSOCIATIONS

Table 51.4 lists MHC monogenic disease associations and their genes. We will discuss the most common diseases. We have already reviewed two of these disorders earlier in the chapter: C2 and C4 protein deficiencies.

Hereditary Hemochromatosis and the *HFE* Gene

As discussed in Chapters 22 and 28, hemochromatosis is an autosomal recessive disease and is the most common hereditary metabolic disease in Caucasians. Hemochromatosis consists of an inherited metabolic defect in iron metabolism, resulting in failure to control iron absorption in the setting of increasing iron stores, leading to tissue iron overload and eventually to organ damage (Adams et al., 2000). The most common manifestations of hemochromatosis are cirrhosis of the liver, hepatocellular carcinoma, diabetes mellitus, and cardiomyopathy. Discovery of the hereditary hemochromatosis *(HH)* gene in the MHC was based on the early finding of increased frequency of the *HLA-A3* allele in HH patients (Simon et al., 1976). After years of effort in the vicinity of the *HLA-A* locus, the *HFE* gene was found several megabase pairs away (Feder et al., 1996). *HFE* encodes a 343–amino acid protein that belongs to a group named MHC class I–related molecules because of their similarities to HLA class I molecules. The HFE protein interacts with the transferrin receptor and modulates enteric absorption of dietary iron (Waheed et al., 1999). At least four

TABLE 51.4
MHC Monogenic Disease Associations

Disease	MHC Gene	OMIM No.[a]
Bare lymphocyte syndrome type 1	*TAP1, TAP2, TAPBP*	604571
C2 deficiency	*C2*	217000
C4 deficiency	*C4A, C4B*	120810
Congenital adrenal hyperplasia	*CYP21A2*	201910
Ehler-Danlos syndrome	*TNXB*	606408
Hereditary hemochromatosis	*HFE*	235200
Hypotrichosis simplex of the scalp	*CDSN*	146520
Sialidosis	*NEU1*	256550

MHC, Major histocompatibility complex.
[a]OMIM number provides disease and gene association information at http://www.ncbi.nlm.nih.gov/omim.

additional iron overload disorders labeled hemochromatosis due to several gene mutations have been identified on the basis of clinical, biochemical, and genetic characteristics.

The *HFE* gene has two common missense mutations: the C282Y mutation, resulting in the substitution of a tyrosine for a cysteine, and the H63D mutation, resulting in the substitution of an aspartate for a histidine. A homozygous C282Y mutation is present 85% of HH patients. The C282Y mutation interferes with protein interaction with β_2-microglobulin, abolishing the cell surface expression of HFE (Waheed et al., 1997; Feder et al., 1997). The H63D variant leads to increased iron tissue release by monocytes and macrophages (Drakesmith et al., 2002). The C282Y mutation has a remarkably high allelic frequency in northern European populations (0.05% to 0.1%) and is rare in non-Caucasian populations. Penetrance of the C282Y homozygous state is as low as 10% or even 1% (Beutler et al., 2002). For this reason, population screening for this mutation is not recommended. The H63D mutation is present at high frequency in control Caucasians (>0.1%) and was also found in non-Caucasian populations. The C282Y mutation has been associated with susceptibility to diabetic retinopathy (Peterlin et al., 2003) and increased risk for Alzheimer disease (Robson et al., 2004).

Congenital Adrenal Hyperplasia Due to 21-Hydroxylase Deficiency

Immediately 3′ to each *C4* locus are two loci for the adrenal steroid enzyme 21 hydroxylase (*CYP21A* and *CYP21A2;* the latter previously known as *CYP21B*) (Carroll et al., 1985; Higashi et al., 1986; White et al., 1986). The two genes are highly homologous, but three mutations cause premature termination of transcription of the *CYP21A* gene, rendering it a pseudogene (White et al., 1988). Congenital adrenal hyperplasia results from a deficiency of enzymes of cortisol and mineralocorticoid biosynthesis. Congenital adrenal hyperplasia is clinically heterogeneous, with four recognized clinical forms: a severe salt-wasting form, a milder late-onset form manifested largely by masculinization in girls, a nonclassic late-onset (also called attenuated and acquired), and a mild cryptic form. All four forms are closely linked to the MHC region and represent the effects of various combinations of alleles. The MHC linkage of this disorder was discovered before any MHC associations were detected and before it was known that the *CYP21* loci were located within the MHC. Subsequently, studies found that 20% or more of European Caucasian patients with the salt-wasting form carried the rare extended haplotype *[HLA-A1, Cw6, B47, FC(91)0, DRB1*07, DRB4*01:01, DQA1*02:01, DQB1*02:01]* (Fleischnick et al., 1983). It has been shown that this haplotype has a deletion of both *C4B* and *CYP21A2*, thus explaining the severity of symptoms and the complete deficiency of the enzyme in homozygotes for this haplotype. Among patients with milder and cryptic disease, a different extended haplotype is common: *[HLA-B65, SC2(1,2), DR1]* (Sinnott et al., 1991). This haplotype is particularly common in southern Europe and has a frequency of over 0.01% among Caucasians living in Boston. In all forms of 21-hydroxylase deficiency, the bulk of MHC haplotypes are not extended, and there is a great variety of complotypes, suggesting that many independent mutations have led to deletion or derangement of the *CYP21A2* gene.

POLYGENIC DISEASES WITH MHC ASSOCIATIONS

Table 51.5 lists some polygenic diseases and their MHC gene associations. This list is not exhaustive, and we will discuss only a few of the diseases in greater detail.

TABLE 51.5
Polygenic Diseases With MHC Associations

Disease	MHC Gene	OMIM No.[a]
Abacavir hypersensitivity	*HLA-B*57:01*	142830
Ankylosing spondylitis	*HLA-B27*	106300
Autoimmune thyroid disease	*HLA-DR3*	608173
Behcet disease	*HLA-B51*	109650
Birdshot chorioretinopathy	*HLA-A29*	605808
Carbamazepine hypersensitivity	*HLA-B*15:02*	608579
Celiac disease	*HLA-DQ2, DQ8*	212750
Multiple sclerosis	*HLA-DR, DQ*	126200
Narcolepsy	*HLA-DQB1*06:02*	161400
Rheumatoid arthritis	*HLA-DR4*	180300
Type 1 diabetes	*HLA-DR, DQ*	222100

MHC, Major histocompatibility complex.
[a]OMIM number provides disease and gene association information at http://www.ncbi.nlm.nih.gov/omim.

Ankylosing Spondylitis

Ankylosing spondylitis (AS) is a common inflammatory rheumatic disease affecting the axial skeleton and causing inflammatory back pain, which can lead to structural and functional impairments and a decreased quality of life (Braun & Sieper, 2007). A strong association has been noted between *HLA-B27* and AS in several populations (Caffrey & James, 1973; Schlosstein et al., 1973). About 90% of Caucasian patients with AS have *HLA-B27*, as compared with 5% to 10% of healthy controls (Rubin et al., 1994), suggesting the involvement of other genetic and environmental factors in disease development. *HLA-B27* shares sequence with proteins from enteric bacteria and peptides that both mimic and bind B27 and may constitute the molecular components of a mechanism for AS (Scofield et al., 1995). Another hypothesis suggests that "auto-display" occurring within or between misfolded B27 molecules provokes an autoimmune attack in AS (Luthra-Guptasarma & Singh, 2004; Sharma et al., 2007). *HLA-B*27* genotyping is frequently performed by flow cytometry. Flow cytometry methods are quick and cost efficient; however, they may show lower sensitivities and specificities compared to molecular typing due to the fact that the monoclonal antibodies used for this assay may not recognize all subgroups of B27 antigens or may cross-react with structurally similar alleles such as the *HLA-B7* family (Levering et al., 2003). Due to such limitations, indeterminate results may be obtained, in which case confirmation by molecular methods is recommended. Although molecular methods are sensitive and specific, interpretation has its own challenges due to the high degree of polymorphism for *HLA-B27*, with over 200 alleles described with diverse ethnic prevalence worldwide (Khan, 2017). In contrast, the number of alleles that are confirmed to be associated with AS is relatively low and includes the most common *HLA-B*27:05* and **27:02* in Caucasians, **27:04* in Asians, and a few others. Other alleles such as *HLA-B*27:06* in Asians and **27:09* among Sardinians were reported to lack association for AS, while the remaining subtypes are either too rare or are too recently described to have been confirmed for AS association. Interestingly, *HLA-B27* has been shown to have a protective role in HCV and HIV infections by being associated with viral clearance and slower onset of AIDS (Neumann-Haefelin, 2013), which may suggest a common ground between more pronounced immune response for effective clearance of some pathogens versus autoimmunity and tissue injury in other circumstances such as through peptide binding and antigen presentation by HLA-B27. For clinical use, *HLA-B27* testing is not diagnostic due to its poor positive predictive value, because among *HLA-B27*–positive individuals in the population at large, only 2% will develop AS and therefore should primarily be used for ruling out disease (Gran & Husby, 1995).

Celiac Disease

Celiac disease (CD), also known as *celiac sprue* and *gluten-sensitive enteropathy*, is a disorder characterized by malabsorption resulting from immune-mediated inflammatory injury to the mucosa of the small intestine after ingestion of wheat gluten in genetically susceptible individuals (Green & Cellier, 2007). Histopathologic findings include villous atrophy, crypt hyperplasia, and increased intraepithelial T lymphocytes. Up to 40% of the genetic risk has been attributed to the HLA region (Bevan et al., 1999; van Heel et al., 2007). Associations of *HLA-DQ2* and *DQ8* with CD represent one of the strongest HLA-disease associations discovered (Sollid

et al., 1989). Of CD patients, 90% to 95% express HLA-DQ2 encoded by *HLA-DQA1*05* allele in combination with *HLA-DQB1*02* allele in *cis* or *trans* arrangement (also referred to as *HLA-DQ2.5*), while the remaining 5% to 10% carry *HLA-DQ8* encoded by the *HLA-DBQ1*03:02* allele, most commonly in combination with *HLA-DQA1*03:01* allele. *HLA-DQ2* or *DQ8* are necessary but not sufficient for the development of CD, which is also reflected by the much higher representation of these alleles in the general population (20% to 30% in Caucasians, 20% in African Americans, 15% to 20% of Hispanics) in contrast to the overall frequency of CD (~1% prevalence worldwide and in the United States) (Gujral et al., 2012; Fasano et al., 2003).

A strong gene dose effect has been observed for *HLA-DQ2.5*, where individuals homozygous for *HLA-DQ2.5* are at higher risk for developing CD compared to heterozygous individuals and show a more severe disease course (Vader et al., 2003). In a large US study cohort involving over 10,000 subjects, 28% with *HLA-DQ2* homozygous haplotype showed positivity for endomysial antibodies (EMA), autoantibodies specific for CD, in contrast to 9% of the *HLA-DQ2* heterozygous group. Similarly, EMA positivity was higher in the *HLA-DQ8* homozygous versus heterozygous individuals. Based on these results, the odds of CD autoantibody positivity among the *HLA-DQ2* and *DQ8* homozygous groups were approximately fourfold higher compared to the heterozygous groups (Pietzak et al., 2009).

HLA-DQ2.5 heterodimers predispose to CD by preferential presentation of highly immunogenic gliadin peptides derived from gluten. These proline- and glutamine-rich peptides that survive gastrointestinal digestion serve as substrates for the enzyme tissue transglutaminase (TTG), undergoing selective deamidation through which they become negatively charged due to the presence of multiple glutamic acid residues. These highly immunogenic, negatively charged peptides bind preferentially to HLA-DQ 2.5 (Fallang et al., 2009) and HLA-DQ8, both of which have positively charged binding grooves (Abadie et al., 2011). Presentation of gliadin peptides to T cells through HLA-DQ2 or DQ8 will result in gluten-specific T-cell activation and clonal expansion into the intestinal mucosa of CD patients, triggering immune effector functions involving cytotoxic CD8+ and NK cells, as well as anti-TTG antibody mediated responses resulting in destruction of mucosal epithelial cells (Di Sabatino & Corazza, 2009). This mucosal damage evolves into villous atrophy characteristic of celiac disease, with significant lymphocytic infiltrates and epithelial hyperplasia.

Another possible explanation for the association of CD with HLA comes from studies showing the binding of atypical invariant chain fragments to HLA-DQ2 (Fallang et al., 2008; Wiesner et al., 2008). Recent crystallographic studies indicate preferential binding of noncanonic CLIP2 to HLA-DQ2.5 over canonic CLIP1 (Nguyen et al., 2017). This results in reduced HLA-DM–mediated exchange of invariant chain variants and other HLA-DQ2 peptides compared with other HLA-DQ molecules, which may provide a basis for the association of *HLA-DQ2* with CD.

HLA-DQ testing should be used to effectively rule out celiac disease in selected clinical situations. Examples of such clinical situations include equivocal small bowel histologic findings in seronegative patients, evaluation of individuals not tested for CD prior to starting a gluten-free diet, and patients with discrepant celiac-specific serology and histology (Rubio-Tapia et al., 2013). HLA testing may be recommended in the presence of strong serologic and clinical evidence when biopsy is not possible or preferred, such as in children and adolescents (Husby et al., 2012). In addition, HLA typing is useful in ruling out individuals who belong to groups at risk for CD, such as first-degree relatives of confirmed CD patients, or conditions known to be associated with CD such as autoimmune diseases (including type I diabetes), liver and thyroid disease, and chromosomal abnormalities (including Williams, Turner, and Down syndromes). Testing negative for both *HLA-DQ* types in these situations makes celiac disease diagnosis very unlikely (negative predictive value >99%), and further workup for CD will not be necessary (Rubio-Tapia et al., 2013). However, HLA DQ testing should not be used routinely in the initial diagnosis of celiac disease as the presence of either *HLA-DQ2* or *DQ8* is not diagnostic due to very low positive predictive value (Rubio-Tapia et al., 2013).

Narcolepsy

Narcolepsy, also known as *cataplexy*, is a sleep disorder characterized by attacks of disabling daytime drowsiness and low alertness. Most patients with narcolepsy carry the specific *HLA-DQB1*06:02* allele (Matsuki et al., 1992; Mignot et al., 1997), which represents one of the strongest HLA-disease associations. However, 15% to 25% of individuals in the general population also carry this risk allele, suggesting that it is necessary but not sufficient for development of the disorder, and additional genetic and environmental factors may be involved (Hor et al., 2010). Patients with narcolepsy have a marked reduction of hypocretin-producing neurons in the hypothalamus compared with normal controls (Matsuki et al., 1992; Blouin et al., 2005). Findings of recent studies are consistent with immunologically mediated destruction of hypocretin-containing cells in patients with narcolepsy (Mignot et al., 2001), implicating T cells targeting self-antigens (Latorre et al., 2018; Pedersen et al., 2019) and antibodies reacting with hypocretin neurons (Cvetkovic-Lopes et al., 2010). Influenza A H1N1A and certain vaccines carrying this strain have been identified as potent environmental triggers in genetically susceptible individuals (Bomfim et al., 2017).

HLA testing in patients with narcolepsy has an excellent negative predictive value (>99%) and is useful in ruling out the disease in patients with unexplained sleepiness (Bassetti et al., 2019). Recent studies indicate a gene dose effect for *HLA-DQB1*06:02* homozygosity doubles the risk of narcolepsy (Tafti et al., 2014). HLA, however, is not only associated with risk for narcolepsy, as several haplotypes containing other alleles in *trans* position are dominantly protective, including *DQB1*06:03*, **06:01* (Hor et al., 2010), *HLA-DQB1*06:09*, and *DQB1*02* alleles (Tafti et al., 2014), and more prevalent in controls compared to narcolepsy.

Behcet Disease

Behcet disease (BD) is a multisystemic disease caused by chronic vasculitis of arteries and veins, characterized by recurrent ulcers, genital ulcers, ocular and skin involvement. Although it shows worldwide distribution, BD clusters in the Mediterranean through Eastern Asia. BD is strongly associated with *HLA-B51*, the predominant split of *HLA-B5* (Ohno et al., 1973; Ohno et al., 1982). Meta-analysis of 4800 cases of various ethnicities and over 16,000 controls indicated that the risk (odds ratio) of *HLA-B51* carriers developing BC is 5.9 (de Menthon et al., 2009). Although no direct evidence is yet available it is hypothesized that *HLA-B51* may bind pathogenic peptides, triggering the development of BD.

Birdshot Chorioretinopathy

Birdshot chorioretinopathy (BCR) is a bilateral, autoimmune uveitis predominantly affecting the posterior segment of the eye with dual, retinal, and choroidal inflammation, named after lesions that show a pattern comparable to that seen in wounds produced by birdshot shotguns (Ryan & Maumenee, 1980). Association of BCR with *HLA-A29* was reported shortly after the disease was originally described (Nussenblatt et al., 1982); it is one of the strongest associations reported, with over 95% of BCR patients expressing *HLA-A*29:02* (Minos et al., 2016). The disease most commonly occurs in Caucasians, where *HLA-A*29:02* is predominantly expressed (up to 7%) over *HLA-A*29:01*, which only rarely has been observed in Caucasian BCR patients. Interestingly, these two alleles differ by only one amino acid not affecting the peptide binding groove. *HLA-A*29:01* is predominantly expressed in Asians, who seem to be exempt from BRC. More recently, *HLA-A*29:10* was also found in a few Caucasian patients (Donvito et al., 2010). Although the disease is primarily diagnosed based on clinical symptoms, the presence of *HLA-A*29:02* is strongly supportive (Herbort et al., 2017). In addition to *HLA-A29*, the development of this rare disease may also involve other genetic or acquired factors not linked to HLA.

Pharmacogenetics of Drug Hypersensitivity

Idiosyncratic adverse reactions to drugs are unpredictable, dose independent, and potentially life-threatening conditions. Clinical data have shown that such reactions involve immune mechanisms, such as T-cell involvement, and develop along a timeline consistent with induction of T-cell–mediated responses. Genetic association studies have identified strong associations with specific HLA alleles.

Abacavir is a reverse transcriptase inhibitor used in combination with other antivirals in the treatment of human immunodeficiency virus infection. A severe hypersensitivity reaction occurs in 5% of abacavir patients, characterized by symptoms such as fever, rash, and acute gastrointestinal and respiratory symptoms, and can lead to potentially life-threatening hypotension if drug therapy is not discontinued (Clay, 2002). Patients with the *HLA-B*57:01* allele are at risk for an abacavir hypersensitivity reaction (Hetherington et al., 2002; Mallal et al., 2002). Abacavir specifically binds to *HLA-B*57:01*, changing the repertoire of self peptides that are presented to T lymphocytes, which activates a T-cell–mediated immune reaction responsible for the manifestations seen in patients with abacavir hypersensitivity (Illing et al., 2012). Up to 6% of Caucasians express the variant allele *HLA-B*57:01*, which places them at high risk of having a hypersensitivity reaction. Although the frequency of the allele is lower, the association of *HLA-B*57:01* with abacavir hypersensitivity has also been found in Hispanics and Africans (Sousa-Pinto et al., 2015). The US Food

and Drug Administration (FDA) recommends screening for the presence of *HLA-B*57:01* allele in all patients before initiating abacavir therapy, which has significantly reduced the incidence of abacavir-induced hypersensitivity (Hughes et al., 2004; Cargnin et al., 2014).

Carbamazepine is an aromatic anticonvulsant drug used primarily in the treatment of epilepsy. It is also used to relieve pain in trigeminal neuralgia and may be used in the treatment of bipolar disorder. Dermatologic reactions, ranging from benign rashes to severe manifestations (including Stevens-Johnson syndrome [SJS] and the more severe toxic epidermal necrolysis [TEN]), have been reported in 5% to 10% patients in association with carbamazepine use. Patients with *HLA-B*15:02* allele are at a high risk for developing severe carbamazepine hypersensitivity reactions such as SJS and TEN, with high mortality rate (Chung et al., 2004; McCormack et al., 2011). The *HLA-B*15:02* allele is predominantly expressed in individuals of Asian descent. Another allele, *HLA-A*31:01*, is more globally expressed and may be a risk factor for carbamazepine-induced hypersensitivity reactions in Caucasians and Asians; however, the association is less consistent (Amstutz et al., 2014). The exact mechanism of how carrying *HLA-B*15:02* or *HLA-A*31:01* results in an increased risk for carbamazepine hypersensitivity is not clear, but a similar mechanism proposed for abacavir hypersensitivity is thought to play a role (Illing et al., 2012).

FDA recommends that patients with ancestry in genetically at-risk populations should be screened for the presence of *HLA-B*15:02* prior to initiating treatment with carbamazepine.

In addition to *HLA-B*15:02*, other members of the HLA-B75 serogroup can also be associated with carbamazepine-induced SJS/TEN, including *HLA B*15:08*, **15:11*, and **15:21* (Jaruthamsophon et al., 2017). In patients who are positive for *HLA-B*15:02* or *HLA-A*31:01*, alternative medication should be used with consideration of cross-reactivity with structurally similar antiepileptic drugs such as oxcarbazepine, lamotrigine, phenytoin, phenobarbital, and primidone (Amstutz et al., 2014).

Allopurinol is a xanthine oxidase inhibitor that decreases the production of uric acid and is widely used for the treatment of gout and hyperuricemia. Patients expressing the *HLA-B*58:01* allele are at risk for developing severe cutaneous adverse reactions (SCAR) when treated with allopurinol. *HLA-B*58:01* allele shows strong association with allopurinol-induced SCAR, including SJS and TEN, which can be life threatening (Yu et al., 2017). Symptoms include rash, fever, eosinophilia, leukocytosis, hepatitis, and progressive kidney failure. The *HLA-B*58:01* allele is commonly found in Asian populations (5.3% in the United States) and at a lower frequency in African Americans (3.8%). The underlying mechanism for allopurinol-induced SCAR is not completely clear, but it involves direct interactions between the allopurine metabolite oxypurinol and *HLA-B*58:01*, resulting in drug-induced changes in self peptide presentation. Drug-specific cytotoxic CD8+ T cells are likely responsible for SJS/TEN, with granulysin being the key mediator of the widespread epidermal necrosis (Stamp et al., 2016). Due to the severity of adverse reactions, guidelines from the Clinical Pharmacogenomics Implementation Consortium recommend testing for the *HLA-B*58:01* allele prior to initiation of the drug (Hershfield et al., 2013).

Rheumatoid Arthritis

Rheumatoid arthritis (RA) is an inflammatory disease, primarily of the joints, with autoimmune features and a complex genetic component. The association between MHC markers and RA is well documented (Nepom & Nepom, 1992; Ollier & Thomson, 1992; Auger et al., 1998; Jawaheer et al., 2001). For most of the populations studied, the primary associated marker is *HLA-DR4* (MacGregor et al., 1995). In Caucasians, for example, the most common RA-associated *DR4* alleles are *DRB1*04:01* and *DRB1*0404*, and in Japanese, Israeli, and Chinese patients it is *DRB1*04:05*. Other *HLA-DR* specificities are also associated with RA: *DR1* has been reported in association with RA in Caucasian, Japanese, Spanish, Greek, and Israeli patients; *DR3* in Kuwaitis; *DR6* in Yakima American Indians; *DR9* in Chileans; and *DR10* in Spanish, Greek, and Israeli patients (Zanelli et al., 2000).

To explain this broad spectrum of different *HLA-DR* associations with RA, it has been proposed that a shared DRB1 peptide epitope is involved in conferring RA susceptibility (Penzotti et al., 1996). The alleles associated with RA share a highly conserved sequence of amino acids in their third hypervariable region (amino acids 67 to 74). Individuals with RA frequently have autoantibodies to citrullinated peptides. Citrullination of self-antigens increases the affinity between these peptides and HLA-DR molecules carrying the shared peptide epitope (Hill et al., 2003; Lundberg et al., 2005). Antibodies to an immunodominant citrullinated alpha-enolase CEP-1 epitope were detected in 43% to 63% of individuals with anticitrullinated protein antibodies, and this subset was preferentially linked to *HLA-DRB1*04* (Mahdi et al., 2009). Thus, if a citrullinated arthritogenic peptide exists, it may bind preferentially to molecules with the RA DRB1 sequence. An alternative explanation may involve molecular mimicry between the shared RA DRB1 and antigenic sequences of a pathogen that can induce RA (Albani et al., 1992). Sequence homology has been found between the shared RA sequence and an HSP from *E. coli* (Auger et al., 1998).

In addition to associations with *DRB1* alleles, at least two additional regions within the MHC have been shown to be linked to and associated with RA susceptibility. One of these regions is located in a 497-kb region in the central portion of the MHC complex, a region that excludes *DRB1*. This region is present on a segment of the highly conserved ancestral conserved haplotype *[HLA-A1, B8, DRB1*03]* (Jawaheer et al., 2002). A second RA susceptibility region has been narrowed to a segment 70 kb telomeric of the *TNFA* gene (Ota et al., 2001).

Juvenile rheumatoid arthritis (JRA), also known as *juvenile idiopathic arthritis*, is the most common type of arthritis in children. RA differs clinically from JRA, and HLA associations with JRA are different as well. Furthermore, other *HLA-DR* associations vary among JRA clinical subsets (Stastny et al., 1993). For example, it has been reported that the frequency of haplotype *HLA-DRB1*08:01*, *DQA1*04:01*, *DQB1*04:02* is increased in the whole pauciarticular group and in patients with the persistent pauciarticular form. The haplotype *HLA-DRB1*13:01*, *DRB3*01:01*, *DQA1*01:03*, *DQB1*06:03* was also associated with patients with persistent pauciarticular JRA (Fernandez-Vina et al., 1994). In keeping with the view that the polyarticular form of JRA is RA occurrence in the young, *DRB1*04:01* shows a strong association.

Type 1 Diabetes

The most studied of all MHC-linked diseases is type 1 diabetes mellitus (Nepom & Erlich, 1991; Thorsby & Ronningen, 1992; Winter et al., 1993; Lernmark, 1999). Type 1 diabetes is a disorder of glucose homeostasis that is characterized by susceptibility to ketoacidosis in the absence of insulin therapy. It is a genetically heterogeneous autoimmune disease affecting about 0.3% of Caucasian populations (Todd, 1990). Alleles of the HLA class II genes *DQ* and *DR* in the MHC region are major determinants of genetic predisposition to type 1 diabetes. Several alleles of these loci are associated with susceptibility to or protection from disease. Striking increases have been noted in the frequency of *HLA-DR3* and *HLA-DR4* among Caucasian patients (Thomson, 1984; Jenkins et al., 1991). Using molecular-based HLA typing analysis, the increase in *DR4* is found primarily in the subset of *DR4* in linkage disequilibrium with *DQB1*03:02* (Kockum et al., 1993). Although the latter gene is now considered a major marker and perhaps a primary determinant of type 1 diabetes susceptibility, it is present in only 70% of Caucasian patients. Even among those who carry it, variability in the relative risk for diabetes is observed: *DRB1*04:01*, *DQB1*03:02* and *DRB1*04:02*, and *DQB1*03:02* are highly associated with the disease, but *DRB1*04:04*, *DQB1*03:02* is less so.

In many Caucasian patient populations with type 1 diabetes, there is an excess of *DR3/DR4* heterozygotes over the number of *DR3* or *DR4* homozygotes predicted by the Hardy-Weinberg equilibrium (Kockum et al., 1999). In addition, the relative risks for some *DR-DQ* genotypes are not simply the sum or product of relative risks for the single haplotype. For example, risk for the *DRB1*03–DQB1*02/DRB1*04:01–DQB1*03:02* genotype is often found to be higher than for the individual *DRB1*03–DQB1*02* and *DRB1*04:01–DQB1*03:02* homozygous genotypes. It has been hypothesized that this synergy occurs through the formation of highly susceptible *trans*-encoded HLA-DQB1 and HLA-DQA1 heterodimers (Nepom et al., 1987; Khalil et al., 1992). The DR-α molecules are not polymorphic, and mixed DR α-β dimers would not result in novel HLA molecules. On the other hand, both the α and β chains of *DQ* are polymorphic, and a DQ α-β dimer composed of transcomplementing chains would be unique to a heterozygous individual and would not be expressed in either parent. In the mouse, such transcomplementation has been demonstrated structurally, and epitopes newly formed in the resulting hybrid molecules allow for an altered functional immune response different from that of either parent (Charron et al., 1984; Long et al., 1984).

The *DRB1*15:01*, *DQB1*06:02* haplotype is negatively associated with type 1 diabetes. Individuals heterozygous for *DRB1*15:01*, *DQB1*06:02* who also carry a susceptibility gene for type 1 diabetes on the other haplotype are not at risk for the disease (Noble et al., 1996). A recently proposed model for type 1 diabetes, which assumes that *DQB1* is a direct determinant of susceptibility, suggests a hierarchy of affinities among different class II molecules that compete for binding to the same type 1 diabetes peptide (Nepom, 1990). Susceptibility occurs if a gene product (e.g., DQB1*03:02) binds and presents the type 1 diabetes peptide. In the

presence of a high-affinity competitor (DRB1*15:01), this event does not occur. Another model proposes that codon 57 of the *DQB*-encoded chain plays a critical role in the pathogenesis of type 1 diabetes. The presence of a nonaspartic acid at position 57 of *DQB1* has been suggested as an important determinant of susceptibility to type 1 diabetes mediated by the *DQB1* genes (Lee et al., 2001; Siebold et al., 2004). The excess presence of valine or serine at this position in diabetic patients carrying the *HLA-DR3* or *DR4* haplotype supports this concept.

METHODS OF DETECTING ASSOCIATION OR LINKAGE OF DISEASE WITH GENETIC MARKERS

GENETIC POLYMORPHISM

Genetic polymorphism is defined as the occurrence of two or more alleles at one gene, each with appreciable frequency in the same population. The frequency has been arbitrarily defined to be higher than 1%. Two groups of genetic polymorphisms are known: balanced (or stable) and transient. A balanced (or stable) polymorphism occurs when two or more alleles are maintained in a population by selection. The heterozygous advantage is the classic example of a balanced polymorphism. A transient polymorphism represents a phase of allelic changes driven by genetic drift or by selection. Polymorphism of a gene can be stable in one population and transient in another, depending on the effect of selection.

GENE AND PHENOTYPE FREQUENCIES

To determine genetic polymorphism, it is necessary to find a representative sample of the population, assess the individuals, count the genes, and estimate the number of genes contained in the entire population. For example, assuming that a population of 100 individuals has been studied for a particular genetic trait or allele at a given gene, we can define the phenotype frequency as the number of individuals carrying the trait or the genetic variant. To calculate the frequency *(f)* of a given allele, divide the number of times that allele occurs (x) by the total occurrences of all alleles of that gene in the population ($x + y + z + \ldots$):

$$f(x) = x / (x + y + z + \ldots) \qquad \text{(Eq. 51.1)}$$

It is possible to calculate the gene frequency (g) without knowing the mode of inheritance by using the following formula:

$$g = 1 - \sqrt{f} \qquad \text{(Eq. 51.2)}$$

STRENGTH OF ASSOCIATION

Several methods have been devised for detecting the degree of association of genetic markers with hypothesized genes for disease susceptibility. One method is to compute the risk for disease among individuals carrying a specific allele of a polymorphic system. In this computation, the relative risk (RR), or odds ratio, calculates the risk for carrying a marker in a population of diseased individuals compared with a control population. This strength of association is the delta of Bergston and Thomson (Svejgaard et al., 1983), which is the same as the etiologic fraction (EF) (Miettinen, 1976). If, in a patient population, "a" individuals carry the specific character but "b" individuals do not, and in the control (normal) population, "c" individuals carry the character, we may write the information conveniently in the 2 × 2 table as follows:

	Character-Positive	**Character-Negative**
Patient	a	b
Control	c	d

The frequency of the character in this patient population (h_p) is:

$$h_p = \frac{a}{a+b} \qquad \text{(Eq. 51.3)}$$

The RR, or odds ratio, is defined as follows:

$$RR = \frac{a \times d}{b \times c} \qquad \text{(Eq. 51.4)}$$

Etiologic fraction is defined as follows:

$$\text{EF} = \frac{\text{RR} - 1}{\text{RR}} \times \frac{a}{a+b} = \frac{\text{RR} - 1}{\text{RR}} \times h_p \qquad \text{(Eq. 51.5)}$$

Similarly, in decreased risk, for which the RR is less than 1, the preventive factor (PF) can be used:

$$\text{PF} = \frac{(1 - \text{RR})\, h_p}{\text{RR}\,(1 - h_p) + h_p} \qquad \text{(Eq. 51.6)}$$

EF and PF fraction can vary between 0 (no association) and 1.0 (maximal association). Apart from providing estimates of having a marker if one already has a disease, these calculations ignore the mode of genetic determination of the disease in question. This is particularly problematic for recessive or more complicated modes, in which both haplotypes are important for determining disease, but heterozygotes and homozygotes for a given marker are given the same weight, that is, both are positive for the marker.

ANALYSIS OF MODE OF INHERITANCE BASED ON SIBLING PAIRS

Analysis of mode of inheritance based on sibling pairs was introduced to help overcome the problems of incomplete penetrance of disease genes and variations in the age of onset (Penrose, 1935). This analysis assumes that if HLA and/or genes closely linked to HLA have no influence on the development of a disease, then the affected sibling pairs will share HLA haplotypes with a normal frequency: 25% will share both haplotypes, 50% will share one haplotype, and 25% will share no haplotypes. Thus observed and expected distributions of haplotype sharing are compared. If susceptibility genes or their closely linked markers are rare and fully penetrant in a purely recessively determined disease, the distributions of two-, one-, and no-haplotype–sharing sibs would be 100, 0, and 0. For dominant determination, the ratios would be 33, 66, and 0. What is observed in diabetes, for example (Rubinstein et al., 1977), is 60, 35, and 5—closer to recessive than dominant predictions. Once the mode of inheritance has been established, disease gene frequency and penetrance can be determined (Thomson & Bodmer, 1977).

ANALYSIS OF MODE OF INHERITANCE BASED ON POPULATION STUDIES

Investigators (Thomson & Bodmer, 1977) have devised a method for analyzing population data for markers closely linked to susceptibility loci for diseases with incomplete penetrance. In essence, this method predicts the proportions of homozygotes, heterozygotes, and noncarriers for the linked marker that are expected in cases of dominant or recessive inheritance. The greatest difference between the two modes of inheritance is observed in the proportions of individuals who are homozygous for the marker. Application of this method to *HLA-B27* and AS led, on statistical grounds, to rejection of a recessive mechanism. Thus it was concluded that susceptibility to AS is inherited as a dominant trait.

The same method of analysis was applied to the distribution of *CFB*F1* among 1107 patients with type 1 diabetes mellitus (Raum et al., 1981). For dominant inheritance, 1.89 homozygotes were predicted; for recessive inheritance, 6.2 homozygotes were predicted. Seven *CFB*F1* homozygotes were found—a result that is consistent only with recessive inheritance. Other modes of inheritance that could be rejected by these observations include simple dominant, epistatic (disease resulting from the presence of nonallelic genes), and overdominant (disease with greater penetrance when two specific alleles are present than when other combinations, including homozygosity for each specific allele, occur). Although a mixed model with different penetrance for homozygotes and heterozygotes could not be completely ruled out, other considerations make such a model unsatisfactory.

LOD SCORE METHOD

The logarithm of the odds (LOD) score is a statistical measure of linkage between a marker locus, such as in the MHC, and a disease susceptibility gene (Sutton, 1980). In the equation for calculating the LOD score, (1) the Z value is the ratio of the maximum likelihood of finding linkage [$P(F_1/\theta)$] to that of no linkage at a particular recombination value of θ, and (2) the $\theta(q)$ value, or recombination frequency, is a measure of the distance from a given locus corresponding to maximum Z value. The LOD score expresses the probability that alleles at two loci will segregate together, in terms of the ratio between the observed and the predicted recombination frequency if they assort independently. Various values of (q) from 0 to 0.5 are substituted into the following equation:

$$P(F_1/\theta) = 1/2\,[\theta^r(1-\theta)^{n-r} + \theta^{n-r}(1-\theta)^r] \qquad \text{(Eq. 51.7)}$$

where n = the number of children in a given family and r = the number of recombinants. The probability of obtaining a pedigree for a given value of θ (recombination frequency from 0 to 0.5), which is expressed as the ratio of $P(F_1/\theta)$ in a family at a given recombination fraction θ (from 0 to 0.5) to $P(F_1/0.5)$ in the same family assuming no recombination, can be expressed as the LOD score (Z). The LOD score is the sum of all z values where Z is

$$z = \log_{10} \frac{P(F_1/\theta)}{P(F_1/0.5)} \qquad \text{(Eq. 51.8)}$$

Values of Z greater than zero favor linkage, and those less than or equal to zero are against linkage. In general, a Z value greater than 3 (for some values of $\theta < 0.5$) means that the odds in favor of linkage are 1000 to 1 (p value = 0.05), as opposed to no linkage or independence. It is easier to calculate linkage for codominant traits (e.g., HLA) than for recessive traits. In studies that examine the linkage of HLA and disease, the parents may have recessive or dominant impenetrant susceptibility genes. Basic problems have been noted in using the LOD score method to detect linkage of partially penetrant genes, apart from impenetrant susceptible siblings. If susceptibility genes are common, as appears to be the case in type 1 diabetes, for example, apparent crossovers or nonidentical siblings could suggest additional susceptibility genes in a parent.

SUMMARY

The MHC comprises many alleles at many loci. The high-resolution typing of class I and class II MHC genes and the identification of genes between and near them have increased the possibility of defining the genetic basis for immune responses and diseases of unknown origin, such as autoimmune diseases in man. The nonrandom association of markers with immune responses or associations with autoimmune diseases due to the presence of fixed stretches of MHC DNA and extended haplotypes and their fragments in the population complicate the study of susceptibility genes but also provide the means for their identification. Even though the human MHC is the most intensively investigated region of the genome, the function of many of the genes within the MHC has not been identified. It is probable that some unknown MHC genes, rather than the one already characterized, are susceptibility genes for some human MHC-associated diseases.

SELECTED REFERENCES

Brown JH, Jardetzky TS, Gorga JC, et al.: Three-dimensional structure of the human class II histocompatibility antigen HLA-DR1, *Nature* 364:33–39, 1993.
This landmark paper shows the first crystal structure of an HLA class II molecule associated with peptide.

Horton R, Gibson R, Coggill P, et al.: Variation analysis and gene annotation of eight MHC haplotypes: the MHC Haplotype Project, *Immunogenetics* 60:1–18, 2008.
This paper reports the sequence and haplotype-specific differences of eight MHC haplotypes to map the genetic variants that confer disease susceptibility.

Illing PT, Vivian JP, Dudek NL, et al.: Immune self-reactivity triggered by drug-modified HLA-peptide repertoire, *Nature* 486:554–558, 2012.
This is the first study to identify the mechanism of an HLA allele-associated adverse drug reaction.

Yunis EJ, Larsen CE, Fernandez-Vina M, et al.: Inheritable variable sizes of DNA stretches in the human MHC: conserved extended haplotypes and their fragments or blocks, *Tissue Antigens* 62:1–20, 2003.
A review of MHC haplotypes and smaller haplotype blocks, and of their allele compositions in the world's populations.

Access the complete reference list online at Elsevier eBooks for Practicing Clinicians.

REFERENCES

Abadie V, Sollid LM, Barreiro LB, Jabri B: Integration of genetic and immunological insights into a model of celiac disease pathogenesis, *Annu Rev Immunol* 29:493–525, 2011.

Adams P, Brissot P, Powell LW: EASL International Consensus conference on haemochromatosis, *J Hepatol* 33:485–504, 2000.

Albani S, Tuckwell JE, Esparza L, et al.: The susceptibility sequence to rheumatoid arthritis is a cross-reactive B cell epitope shared by the Escherichia coli heat shock protein dnaJ and the histocompatibility leukocyte antigen DRB10401 molecule, *J Clin Invest* 89:327–331, 1992.

Albertella MR, Campbell RD: Characterization of a novel gene in the human major histocompatibility complex that encodes a potential new member of the I kappa B family of proteins, *Hum Mol Genet* 3:793–799, 1994.

Alcais A, Alter A, Antoni G, et al.: Stepwise replication identifies a low-producing lymphotoxin-alpha allele as a major risk factor for early-onset leprosy, *Nat Genet* 39:517–522, 2007.

Alper CA: Inherited structural polymorphism in human C2: evidence for genetic linkage between C2 and Bf, *J Exp Med* 144:1111–1115, 1976.

Alper CA, Awdeh ZL, Raum DD, et al.: Extended major histocompatibility complex haplotypes in man: role of alleles analogous to murine t mutants, *Clin Immunol Immunopathol* 24:276–285, 1982.

Alper CA, Raum D, Karp S, et al.: Serum complement "supergenes" of the major histocompatibility complex in man (complotypes), *Vox Sang* 45:62–67, 1983.

Alper CA, Xu J, Cosmopoulos K, et al.: Immunoglobulin deficiencies and susceptibility to infection among homozygotes and heterozygotes for C2 deficiency, *J Clin Immunol* 23:297–305, 2003.

Amstutz U, Shear NH, Rieder MJ, et al.: Recommendations for HLA-B*15:02 and HLA-A*31:01 genetic testing to reduce the risk of carbamazepine-induced hypersensitivity reactions, *Epilepsia* 55:496–506, 2014.

An J, Nakajima T, Shibata H, et al.: A novel link of HLA locus to the regulation of immunity and infection: NFKBIL1 regulates alternative splicing of human immune-related genes and influenza virus M gene, *J Autoimmun* 47:25–33, 2013.

Arnon TI, Achdout H, Levi O, et al.: Inhibition of the NKp30 activating receptor by pp65 of human cytomegalovirus, *Nat Immunol* 6:515–523, 2005.

Auger I, Toussirot E, Roudier J: HLA-DRB1 motifs and heat shock proteins in rheumatoid arthritis, *Int Rev Immunol* 17:263–271, 1998.

Ault BH, Stapleton FB, Rivas ML, et al.: Association of Henoch-Schonlein purpura glomerulonephritis with C4B deficiency, *J Pediatr* 117:753–755, 1990.

Awdeh Z, Alper CA: Inherited structural polymorphism of the fourth component of human complement, *Proc Natl Acad Sci U S A* 77:3576–3580, 1980.

Awdeh ZL, Raum D, Yunis EJ, et al.: Extended HLA/complement allele haplotypes: evidence for T/t-like complex in man, *Proc Natl Acad Sci U S A* 80:259–263, 1983.

Barba G, Rittner C, Schneider PM: Genetic basis of human complement C4A deficiency. Detection of a point mutation leading to nonexpression, *J Clin Invest* 91:1681–1686, 1993.

Barnett AH, Eff C, Leslie RD, et al.: Diabetes in identical twins. A study of 200 pairs, *Diabetologia* 20:87–93, 1981.

Bassetti CLA, Adamantidis A, Burdakov D, et al.: Narcolepsy - clinical spectrum, aetiopathophysiology, diagnosis and treatment, *Nat Rev Neurol*, 2019.

Bevan S, Popat S, Braegger CP, et al.: Contribution of the MHC region to the familial risk of coeliac disease, *J Med Genet* 36:687–690, 1999.

Beutler E, Felitti VJ, Koziol JA, et al.: Penetrance of 845G–> A (C282Y) HFE hereditary haemochromatosis mutation in the USA, *Lancet* 359:211–218, 2002.

Bjorkman PJ, Saper MA, Samraoui B, et al.: Structure of the human class I histocompatibility antigen, HLA-A2, *Nature* 329:506–512, 1987.

Blanchong CA, Zhou B, Rupert KL, et al.: Deficiencies of human complement component C4A and C4B and heterozygosity in length variants of RP-C4-CYP21-TNX (RCCX) modules in caucasians. The load of RCCX genetic diversity on major histocompatibility complex-associated disease, *J Exp Med* 191:2183–2196, 2000.

Blouin AM, Thannickal TC, Worley PF, et al.: Narp immunostaining of human hypocretin (orexin) neurons: loss in narcolepsy, *Neurology* 65:1189–1192, 2005.

Bomfim IL, Lamb F, Fink K, et al.: The immunogenetics of narcolepsy associated with A(H1N1)pdm09 vaccination (Pandemrix) supports a potent gene-environment interaction, *Gene Immun* 18:75–81, 2017.

Bonten E, van der Spoel A, Fornerod M, et al.: Characterization of human lysosomal neuraminidase defines the molecular basis of the metabolic storage disorder sialidosis, *Genes Dev* 10:3156–3169, 1996.

Brandt CS, Baratin M, Yi EC: The B7 family member B7-H6 is a tumor cell ligand for the activating natural killer cell receptor NKp30 in humans, *J Exp Med* 206:1495–1503, 2009.

Braun J, Sieper J: Ankylosing spondylitis, *Lancet* 369:1379–1390, 2007.

Braun L, Schneider PM, Giles CM, et al.: Null alleles of human complement C4. Evidence for pseudogenes at the C4A locus and for gene conversion at the C4B locus, *J Exp Med* 171:129–140, 1990.

Browning JL, Ngam-ek A, Lawton P, et al.: Lymphotoxin beta, a novel member of the TNF family that forms a heteromeric complex with lymphotoxin on the cell surface, *Cell* 72:847–856, 1993.

Burch GH, Gong Y, Liu W, et al.: Tenascin-X deficiency is associated with Ehlers-Danlos syndrome, *Nat Genet* 17:104–108, 1997.

Cabrera M, Shaw MA, Sharples C, et al.: Polymorphism in tumor necrosis factor genes associated with mucocutaneous leishmaniasis, *J Exp Med* 182:1259–1264, 1995.

Caffrey MF, James DC: Human lymphocyte antigen association in ankylosing spondylitis, *Nature* 242:121, 1973.

Canafoglia L, Robbiano A, Pareyson D, et al.: Expanding sialidosis spectrum by genome-wide screening: NEU1 mutations in adult-onset myoclonus, *Neurology* 82:2003–2006, 2014.

Cargnin S, Jommi C, Canonico PL, Genazzani AA, Terrazzino S: Diagnostic accuracy of HLA-B*57:01 screening for the prediction of abacavir hypersensitivity and clinical utility of the test: a meta-analytic review, *Pharmacogenomics* 15:963–976, 2014.

Carroll MC, Campbell RD, Bentley DR, et al.: A molecular map of the human major histocompatibility complex class III region linking complement genes C4, C2 and factor B, *Nature* 307:237–241, 1984.

Carroll MC, Campbell RD, Porter RR: Mapping of steroid 21-hydroxylase genes adjacent to complement component C4 genes in HLA, the major histocompatibility complex in man, *Proc Natl Acad Sci U S A* 82:521–525, 1985.

Carroll MC, Katzman P, Alicot EM, et al.: Linkage map of the human major histocompatibility complex including the tumor necrosis factor genes, *Proc Natl Acad Sci U S A* 84:8535–8539, 1987.

Charron DJ, Lotteau V, Turmel P: Hybrid HLA-DC antigens provide molecular evidence for gene trans-complementation, *Nature* 312:157–159, 1984.

Chung EK, Yang Y, Rennebohm RM, et al.: Genetic sophistication of human complement components C4A and C4B and RP-C4-CYP21-TNX (RCCX) modules in the major histocompatibility complex, *Am J Hum Genet* 71:823–837, 2002.

Chung WH, Hung SI, Hong HS, et al.: Medical genetics: a marker for Stevens-Johnson syndrome, *Nature* 428:486, 2004.

Clavijo O, Delgado J, Awdeh ZL, et al.: HLA-Cw alleles associated with HLA extended haplotypes and C2 deficiency, *Tissue Antigens* 52:282–285, 1998.

Clavijo OP, Delgado JC, Yu N, et al.: HLA-Cw*1701 is associated with two sub-Saharan African-derived HLA haplotypes: HLA-B*4201, DRB1*03 and HLA-B*4202 without DRB1*03, *Tissue Antigens* 54:303–306, 1999.

Clay PG: The abacavir hypersensitivity reaction: a review, *Clin Ther* 24:1502–1514, 2002.

Colten HR, Rosen FS: Complement deficiencies, *Annu Rev Immunol* 10:809–834, 1992.

Corzo D, Yunis JJ, Salazar M, et al.: The major histocompatibility complex region marked by HSP70-1 and HSP70-2 variants is associated with clozapine-induced agranulocytosis in two different ethnic groups, *Blood* 86:3835–3840, 1995.

Criswell LA, Lum RF, Turner KN, et al.: The influence of genetic variation in the HLA-DRB1 and LTA-TNF regions on the response to treatment of early rheumatoid arthritis with methotrexate or etanercept, *Arthritis Rheum* 50:2750–2756, 2004.

Cvetkovic-Lopes V, Bayer L, Dorsaz S, et al.: Elevated Tribbles homolog 2-specific antibody levels in narcolepsy patients, *J Clin Invest* 1(20):713–719, 2010.

Dapprich J, Ferriola D, Mackiewicz K, et al.: The next generation of target capture technologies - large DNA fragment enrichment and sequencing determines regional genomic variation of high complexity, *BMC Genomics* 17:486, 2016.

de Menthon M, Lavalley MP, Maldini C, Guillevin L, Mahr A: HLA-B51/B5 and the risk of Behcet's disease: a systematic review and meta-analysis of case-control genetic association studies, *Arthritis Rheum* 61:1287–1296, 2009.

Delahaye NF, Barbier M, Fumoux F, Rihet P: Association analyses of NCR3 polymorphisms with P. falciparum mild malaria, *Microb Infect* 9:160–166, 2007.

Delgado JC, Baena A, Thim S, et al.: Ethnic-specific genetic associations with pulmonary tuberculosis, *J Infect Dis* 186:1463–1468, 2002.

Densen P: Complement deficiencies and meningococcal disease, *Clin Exp Immunol* 86(Suppl 1):57–62, 1991.

Ding C, Ji X, Chen X, et al.: TNF-alpha gene promoter polymorphisms contribute to periodontitis susceptibility: evidence from 46 studies, *J Clin Periodontol* 41:748–759, 2014.

Di Sabatino A, Corazza GR: Coeliac disease, *Lancet (London, England)* 373:1480–1493, 2009.

Donvito B, Monnet D, Tabary T, et al.: A new HLA extended haplotype containing the A*2910 allele in birdshot retinochoroidopathy: susceptibility narrowed to the HLA molecule itself, *Invest Ophthalmol Vis Sci* 51:2525–2528, 2010.

Drakesmith H, Sweetland E, Schimanski L, et al.: The hemochromatosis protein HFE inhibits iron export from macrophages, *Proc Natl Acad Sci U S A* 99:15602–15607, 2002.

Eckard SC, Rice GI, Fabre A, et al.: The SKIV2L RNA exosome limits activation of the RIG-I-like receptors, *Nat Immunol* 15:839–845, 2014.

Fabre A, Charroux B, Martinez-Vinson C, et al.: SKIV2L mutations cause syndromic diarrhea, or trichohepatoenteric syndrome, *Am J Hum Genet* 90:689–692, 2012.

Fallang LE, Bergseng E, Hotta K, et al.: Differences in the risk of celiac disease associated with HLA-DQ2.5 or HLA-DQ2.2 are related to sustained gluten antigen presentation, *Nat Immunol* 10:1096–1101, 2009.

Fallang LE, Roh S, Holm A, et al.: Complexes of two cohorts of CLIP peptides and HLA-DQ2 of the autoimmune DR3-DQ2 haplotype are poor substrates for HLA-DM, *J Immunol* 181:5451–5461, 2008.

Fasano A, Berti I, Gerarduzzi T, et al.: Prevalence of celiac disease in at-risk and not-at-risk groups in the United States: a large multicenter study, *Arch Intern Med* 163:286–292, 2003.

Feder JN, Gnirke A, Thomas W, et al.: A novel MHC class I-like gene is mutated in patients with hereditary haemochromatosis, *Nat Genet* 13:399–408, 1996.

Feder JN, Tsuchihashi Z, Irrinki A, et al.: The hemochromatosis founder mutation in HLA-H disrupts beta2-microglobulin interaction and cell surface expression, *J Biol Chem* 272:14025–14028, 1997.

Fernandez-Vina M, Fink CW, Stastny P: HLA associations in juvenile arthritis, *Clin Exp Rheumatol* 12:205–214, 1994.

Fielder AH, Walport MJ, Batchelor JR, et al.: Family study of the major histocompatibility complex in patients with systemic lupus erythematosus: importance of null alleles of C4A and C4B in determining disease susceptibility, *Br Med J* 286:425–428, 1983.

Fleischnick E, Awdeh ZL, Raum D, et al.: Extended MHC haplotypes in 21-hydroxylase-deficiency congenital adrenal hyperplasia: shared genotypes in unrelated patients, *Lancet* 1:152–156, 1983.

Fraser PA, Moore B, Stein R, et al.: Complotypes in individuals of African origin: frequencies and possible extended MHC haplotypes, *Immunogenetics* 31:89–93, 1990.

Gbadegesin RA, Brophy PD, Adeyemo A, et al.: TNXB mutations can cause vesicoureteral reflux, *J Am Soc Nephrol* 24:1313–1322, 2013.

Geserick G, Otremba P, Schroder H, et al.: Reference typing report for complement factor B, *Exp Clin Immunogenet* 15:261–263, 1998.

Goicoechea de Jorge E, Harris CL, Esparza-Gordillo J, et al.: Gain-of-function mutations in complement factor B are associated with atypical hemolytic uremic syndrome, *Proc Natl Acad Sci U S A* 104:240–245, 2007.

Gold B, Merriam JE, Zernant J, et al.: Variation in factor B (BF) and complement component 2 (C2) genes is associated with age-related macular degeneration, *Nat Genet* 38:458–462, 2006.

Gonzalez S, Martinez-Borra J, Torre-Alonso JC, et al.: The MICA-A9 triplet repeat polymorphism in the transmembrane region confers additional susceptibility to the development of psoriatic arthritis and is independent of the association of Cw*0602 in psoriasis, *Arthritis Rheum* 42:1010–1016, 1999.

Gran JT, Husby G: HLA-B27 and spondyloarthropathy: value for early diagnosis? *J Med Genet* 32:497–501, 1995.

Green PH, Cellier C: Celiac disease, *N Engl J Med* 357:1731–1743, 2007.

Gujral N, Freeman HJ, Thomson AB: Celiac disease: prevalence, diagnosis, pathogenesis and treatment, *World J Gastroenterol* 18:6036–6059, 2012.

Guo T, Zhao S, Zhao S, et al.: Mutations in MSH5 in primary ovarian insufficiency, *Hum Mol Genet* 26:1452–1457, 2017.

Hajeer AH, Hutchinson IV: Influence of TNFalpha gene polymorphisms on TNFalpha production and disease, *Hum Immunol* 62:1191–1199, 2001.

Hauptmann G, Goetz J, Uring-Lambert B, et al.: Component deficiencies. 2. The fourth component, *Prog Allergy* 39:232–249, 1986.

He YQ, Zhu JH, Huang SY, et al.: The association between the polymorphisms of TNF-α and non-Hodgkin lymphoma: a meta-analysis, *Tumour Biol* 35:12509–12517, 2014.

Herbort Jr CP, Pavesio C, LeHoang P, et al.: Why birdshot retinochoroiditis should rather be called 'HLA-A29 uveitis'? *Br J Ophthalmol* 101:851–855, 2017.

Hershfield MS, Callaghan JT, Tassaneeyakul W, et al.: Clinical Pharmacogenetics Implementation Consortium guidelines for human leukocyte antigen-B genotype and allopurinol dosing, *Clin Pharmacol Ther* 93:153–158, 2013.

Hetherington S, Hughes AR, Mosteller M, et al.: Genetic variations in HLA-B region and hypersensitivity reactions to abacavir, *Lancet* 359:1121–1122, 2002.

Higashi Y, Yoshioka H, Yamane M, et al.: Complete nucleotide sequence of two steroid 21-hydroxylase genes tandemly arranged in human chromosome: a pseudogene and a genuine gene, *Proc Natl Acad Sci U S A* 83:2841–2845, 1986.

Hill JA, Southwood S, Sette A, et al.: Cutting edge: the conversion of arginine to citrulline allows for a high-affinity peptide interaction with the rheumatoid arthritis-associated HLA-DRB1*0401 MHC class II molecule, *J Immunol* 171:538–541, 2003.

Hippich M, Beyerlein A, Hagopian WA, et al.: Genetic contribution to the Divergence in type 1 diabetes risk between children from the general population and children from affected families, *Diabetes* 68:847–857, 2019.

Hor H, Kutalik Z, Dauvilliers Y, et al.: Genome-wide association study identifies new HLA class II haplotypes strongly protective against narcolepsy, *Nat Genet* 42:786–789, 2010.

Huang DF, Siminovitch KA, Liu XY, et al.: Population and family studies of three disease-related polymorphic genes in systemic lupus erythematosus, *J Clin Invest* 95:1766–1772, 1995.

Hughes DA, Vilar FJ, Ward CC, et al.: Cost-effectiveness analysis of HLA B*5701 genotyping in preventing abacavir hypersensitivity, *Pharmacogenetics* 14:335–342, 2004.

Hui J, Oka A, Tomizawa M, et al.: Identification of two new C4 alleles by DNA sequencing and evidence for a historical recombination of serologically defined C4A and C4B alleles, *Tissue Antigens* 63:263–269, 2004.

Hunt C, Morimoto RI: Conserved features of eukaryotic hsp70 genes revealed by comparison with the nucleotide sequence of human hsp70, *Proc Natl Acad Sci U S A* 82:6455–6459, 1985.

Husby S, Koletzko S, Korponay-Szabo IR, et al.: European Society for Pediatric gastroenterology, hepatology, and Nutrition guidelines for the diagnosis of coeliac disease, *J Pediatr Gastroenterol Nutr* 54:136–160, 2012.

Jahn I, Uring-Lambert B, Arnold D, et al.: C2 reference typing report, *Complement Inflamm* 7:175–182, 1990.

Jaruthamsophon K, Tipmanee V, Sangiemchoey A, Sukasem C, Limprasert P: HLA-B*15:21 and carbamazepine-induced Stevens-Johnson syndrome: pooled-data and in silico analysis, *Sci Rep* 7:45553, 2017.

Jawaheer D, Seldin MF, Amos CI, et al.: A genomewide screen in multiplex rheumatoid arthritis families suggests genetic overlap with other autoimmune diseases, *Am J Hum Genet* 68:927–936, 2001.

Jawaheer D, Li W, Graham RR, et al.: Dissecting the genetic complexity of the association between human leukocyte antigens and rheumatoid arthritis, *Am J Hum Genet* 71:585–594, 2002.

Jenkins D, Fletcher J, Penny MA, et al.: DRB genotyping supports recessive inheritance of DR3-associated susceptibility to insulin-dependent diabetes mellitus, *Am J Hum Genet* 49:49–53, 1991.

Johnson CA, Densen P, Hurford Jr RK, et al.: Type I human complement C2 deficiency. A 28-base pair gene deletion causes skipping of exon 6 during RNA splicing, *J Biol Chem* 267:9347–9353, 1992.

Jönsson G, Sjoholm AG, Truedsson L, Bengtsson AA, Braconier JH, Sturfelt G: Rheumatological manifestations, organ damage and autoimmunity in hereditary C2 deficiency, *Rheumatology (Oxford)* 46:1133–1139, 2007.

Kadoya M, Yamamoto A, Hamaguchi M, et al.: Allograft inflammatory factor-1 stimulates chemokine production and induces chemotaxis in human peripheral blood mononuclear cells, *Biochem Biophys Res Commun* 448:287–291, 2014.

Khalil I, Deschamps I, Lepage V, et al.: Dose effect of cis- and trans-encoded HLA-DQ alpha beta heterodimers in IDDM susceptibility, *Diabetes* 41:378–384, 1992.

Khan MA: An Update on the genetic polymorphism of HLA-B*27 with 213 alleles Encompassing 160 subtypes (and still counting), *Curr Rheumatol Rep* 19:9, 2017.

Kishikawa S, Sato S, Kaneto S, et al.: Allograft inflammatory factor 1 is a regulator of transcytosis in M cells, *Nat Commun* 8:14509, 2017.

Klein J: *Natural history of major histocompatibility complex*, New York, 1986, John Wiley & Sons.

Klemperer MR, Woodworth HC, Rosen FS, et al.: Hereditary deficiency of the second component of complement (C'2) in man, *J Clin Invest* 45:880–890, 1966.

Kockum I, Sanjeevi CB, Eastman S, et al.: Complex interaction between HLA DR and DQ in conferring risk for childhood type 1 diabetes, *Eur J Immunogenet* 26:361–372, 1999.

Kockum I, Wassmuth R, Holmberg E, et al.: HLA-DQ primarily confers protection and HLA-DR susceptibility in type I (insulin-dependent) diabetes studied in population-based affected families and controls, *Am J Hum Genet* 53:150–167, 1993.

Kowalczyk M, Owczarek A, Suchanek R, et al.: Heat shock protein 70 gene polymorphisms are associated with paranoid schizophrenia in the Polish population, *Cell Stress Chaperones* 19:205–215, 2014.

Kubaszek A, Pihlajamaki J, Komarovski V, et al.: Promoter polymorphisms of the TNF-alpha (G-308A) and IL-6 (C-174G) genes predict the conversion from impaired glucose tolerance to type 2 diabetes: the Finnish Diabetes Prevention Study, *Diabetes* 52:1872–1876, 2003.

Kumanovics A, Fischer Lindahl K: Good copy, bad copy: choosing animal models for HLA-linked diseases, *Curr Opin Genet Dev* 14:258–263, 2004.

Lander ES, Linton LM, Birren B, et al.: Initial sequencing and analysis of the human genome, *Nature* 409:860–921, 2001.

Latorre D, Kallweit U, Armentani E, et al.: T cells in patients with narcolepsy target self-antigens of hypocretin neurons, *Nature* 562:63–68, 2018.

Lee KH, Wucherpfennig KW, Wiley DC: Structure of a human insulin peptide-HLA-DQ8 complex and susceptibility to type 1 diabetes, *Nat Immunol* 2:501–507, 2001.

Lehner B, Semple JI, Brown SE, et al.: Analysis of a high-throughput yeast two-hybrid system and its use to predict the function of intracellular proteins encoded within the human MHC class III region, *Genomics* 83:153–167, 2004.

Lernmark A: Type 1 diabetes, *Clin Chem* 45:1331–1338, 1999.

Li SS, Kyei SK, Timm-McCann M, et al.: The NK receptor NKp30 mediates direct fungal recognition and killing and is diminished in NK cells from HIV-infected patients, *Cell Host Microbe* 14:387–397, 2013.

Levering WH, Wind H, Sintnicolaas K, Hooijkaas H, Gratama JW: Flow cytometric HLA-B27 screening: cross-reactivity patterns of commercially available anti-HLA-B27 monoclonal antibodies with other HLA-B antigens, *Cytometry B Clin Cytometry* 54:28–38, 2003.

Lintner KE, Wu YL, Yang Y, et al.: Early components of the complement classical activation pathway in human systemic autoimmune diseases, *Front Immunol* 7:36, 2016.

Liu J, Dong Z, Zhu Q, et al.: TNF-alpha promoter polymorphisms predict the response to etanercept more Powerfully than that to infliximab/Adalimumab in Spondyloarthritis, *Sci Rep* 6:32202, 2016.

Lokki ML, Circolo A, Ahokas P, et al.: Deficiency of human complement protein C4 due to identical frameshift mutations in the C4A and C4B genes, *J Immunol* 162:3687–3693, 1999.

Lokki ML, Koskimies SA: Allelic differences in hemolytic activity and protein concentration of BF molecules are found in association with particular HLA haplotypes, *Immunogenetics* 34:242–246, 1991.

Long EO, Gorski J: Mach B: structural relationship of the SB beta-chain gene to HLA-D-region genes and murine I-region genes, *Nature* 310:233–235, 1984.

Loughner CL, Bruford EA, McAndrews MS, Delp EE, Swamynathan S, Swamynathan SK: Organization, evolution and functions of the human and mouse Ly6/uPAR family genes, *Hum Genom* 10:10, 2016.

Lundberg K, Nijenhuis S, Vossenaar ER, et al.: Citrullinated proteins have increased immunogenicity and arthritogenicity and their presence in arthritic joints correlates with disease severity, *Arthritis Res Ther* 7:R458–R467, 2005.

Luthra-Guptasarma M, Singh B: HLA-B27 lacking associated beta2-microglobulin rearranges to auto-display or cross-display residues 169-181: a novel molecular mechanism for spondyloarthropathies, *FEBS Lett* 575:1–8, 2004.

Ma Z, Xia W, Liu F, et al.: SLC44A4 mutation causes autosomal dominant hereditary postlingual non-syndromic mid-frequency hearing loss, *Hum Mol Genet* 26:383–394, 2017.

Mahdi H, Fisher BA, Kallberg H, et al.: Specific interaction between genotype, smoking and autoimmunity to citrullinated alpha-enolase in the etiology of rheumatoid arthritis, *Nat Genet* 41:1319–1324, 2009.

MacGregor A, Ollier W, Thomson W, et al.: HLA-DRB1*0401/0404 genotype and rheumatoid arthritis: increased association in men, young age at onset, and disease severity, *J Rheumatol* 22:1032–1036, 1995.

Mallal S, Nolan D, Witt C, et al.: Association between presence of HLA-B*5701, HLA-DR7, and HLA-DQ3 and hypersensitivity to HIV-1 reverse-transcriptase inhibitor abacavir, *Lancet* 359:727–732, 2002.

Maller J, George S, Purcell S, et al.: Common variation in three genes, including a noncoding variant in CFH, strongly influences risk of age-related macular degeneration, *Nat Genet* 38:1055–1059, 2006.

Mallya M, Campbell RD, Aguado B: Characterization of the five novel Ly-6 superfamily members encoded in the MHC, and detection of cells expressing their potential ligands, *Protein Sci* 15:2244–2256, 2006.

Matsuki K, Grumet FC, Lin X, et al.: DQ (rather than DR) gene marks susceptibility to narcolepsy, *Lancet* 339:1052, 1992.

Mavoungou E, Held J, Mewono L, et al.: A Duffy binding–like domain is involved in the NKp30-mediated recognition of plasmodium falciparum–parasitized erythrocytes by natural killer cells, *J Infect Dis* 195:1521–1531, 2007.

McCormack M, Alfirevic A, Bourgeois S, et al.: HLA-A*3101 and carbamazepine-induced hypersensitivity reactions in Europeans, *N Engl J Med* 364:1134–1143, 2011.

McCusker SM, Curran MD, Dynan KB, et al.: Association between polymorphism in regulatory region of gene encoding tumour necrosis factor alpha and risk of Alzheimer's disease and vascular dementia: a case-control study, *Lancet* 357:436–439, 2001.

McGarry F, Walker R, Sturrock R, et al.: The -308.1 polymorphism in the promoter region of the tumor necrosis factor gene is associated with ankylosing spondylitis independent of HLA-B27, *J Rheumatol* 26:1110–1116, 1999.

McGuire W, Hill AV, Allsopp CE, et al.: Variation in the TNF-alpha promoter region associated with susceptibility to cerebral malaria, *Nature* 371:508–510, 1994.

Meo T, Atkinson JP, Bernoco M, et al.: Structural heterogeneity of C2 Complement protein and its genetic variants in man: a new polymorphism of the HLA region, *Proc Natl Acad Sci U S A* 74:1672–1675, 1977.

Miettinen O: Estimability and estimation in case-referent studies, *Am J Epidemiol* 103:226–235, 1976.

Mignot E, Hayduk R, Black J, et al.: HLA DQB1*0602 is associated with cataplexy in 509 narcoleptic patients, *Sleep* 20:1012–1020, 1997.

Mignot E, Lin L, Rogers W, et al.: Complex HLA-DR and -DQ interactions confer risk of narcolepsy-cataplexy in three ethnic groups, *Am J Hum Genet* 68:686–699, 2001.

Milner CM, Campbell RD: Structure and expression of the three MHC-linked HSP70 genes, *Immunogenetics* 32:242–251, 1990.

Milner CM, Campbell RD: Polymorphic analysis of the three MHC-linked HSP70 genes, *Immunogenetics* 36:357–362, 1992.

Min L, Chen D, Qu L, et al.: Tumor necrosis factor-a polymorphisms and colorectal cancer risk: a meta-analysis, *PloS One* 9:e85187, 2014.

Minos E, Barry RJ, Southworth S, et al.: Birdshot chorioretinopathy: current knowledge and new concepts in pathophysiology, diagnosis, monitoring and treatment, *Orphanet J Rare Dis* 11:61, 2016.

Mira JP, Cariou A, Grall F, et al.: Association of TNF2, a TNF-alpha promoter polymorphism, with septic shock susceptibility and mortality: a multicenter study [see comments], *J Am Med Assoc* 282:561–568, 1999.

Morel Y, Bristow J, Gitelman SE, et al.: Transcript encoded on the opposite strand of the human steroid 21-hydroxylase/complement component C4 gene locus, *Proc Natl Acad Sci U S A* 86:6582–6586, 1989.

Mostovoy Y, Levy-Sakin M, Lam J, et al.: A hybrid approach for de novo human genome sequence assembly and phasing, *Nat Methods* 13:587–590, 2016.

Mugnier B, Balandraud N, Darque A, Roudier C, Roudier J, Reviron D: Polymorphism at position -308 of the tumor necrosis factor alpha gene influences outcome of infliximab therapy in rheumatoid arthritis, *Arthritis Rheum* 48:1849–1852, 2003.

Mulcahy H, O'Rourke KP, Adams C, et al.: LST1 and NCR3 expression in autoimmune inflammation and in response to IFN-gamma, LPS and microbial infection, *Immunogenetics* 57:893–903, 2006.

Murdaca G, Gulli R, Spano F, Mandich P, Puppo F: Pharmacogenetics and future therapeutic scenarios: what affects the prediction of response to treatment with etanercept? *Drug development Research* 75(Suppl 1):S7–s10, 2014.

Nepom BS, Schwarz D, Palmer JP, et al.: Transcomplementation of HLA genes in IDDM. HLA-DQ alpha- and beta-chains produce hybrid molecules in DR3/4 heterozygotes, *Diabetes* 36:114–117, 1987.

Nepom GT: A unified hypothesis for the complex genetics of HLA associations with IDDM, *Diabetes* 39:1153–1157, 1990.

Nepom GT, Erlich H: MHC class-II molecules and autoimmunity, *Annu Rev Immunol* 9:493–525, 1991.

Nepom GT, Nepom BS: Prediction of susceptibility to rheumatoid arthritis by human leukocyte antigen genotyping, *Rheum Dis Clin North Am* 18:785–792, 1992.

Netz U, Carter JV, Eichenberger MR, et al.: Genetic polymorphisms predict response to anti-tumor necrosis factor treatment in Crohn's disease, *World J Gastroenterol* 23:4958–4967, 2017.

Nguyen TB, Jayaraman P, Bergseng E, Madhusudhan MS, Kim CY, Sollid LM: Unraveling the structural basis for the unusually rich association of human leukocyte antigen DQ2.5 with class-II-associated invariant chain peptides, *J Biol Chem* 292:9218–9228, 2017.

Nicaud V, Raoux S, Poirier O, et al.: The TNF alpha/G-308A polymorphism influences insulin sensitivity in offspring of patients with coronary heart disease: the European Atherosclerosis Research Study II, *Atherosclerosis* 161:317–325, 2002.

Noble JA, Valdes AM, Cook M, et al.: The role of HLA class II genes in insulin-dependent diabetes mellitus: molecular analysis of 180 Caucasian, multiplex families, *Am J Hum Genet* 59:1134–1148, 1996.

Nussenblatt RB, Mittal KK, Ryan S, Green WR, Maumenee AE: Birdshot retinochoroidopathy associated with HLA-A29 antigen and immune responsiveness to retinal S-antigen, *Am J Ophthalmol* 94:147–158, 1982.

Ohno S, Aoki K, Sugiura S, Nakayama E, Itakura K, Aizawa M: Letter: HL-A5 and Behcet's disease, *Lancet* 2:1383–1384, 1973.

Ohno S, Ohguchi M, Hirose S, Matsuda H, Wakisaka A, Aizawa M: Close association of HLA-Bw51 with Behcet's disease, *Arch Ophthalmol* 100:1455–1458, 1982.

Okada Y, Han B, Tsoi LC, et al.: Fine mapping major histocompatibility complex associations in psoriasis and its clinical subtypes, *Am J Hum Genet* 95:162–172, 2014.

Okamoto K, Makino S, Yoshikawa Y, et al.: Identification of I kappa BL as the second major histocompatibility complex-linked susceptibility locus for rheumatoid arthritis, *Am J Hum Genet* 72:303–312, 2003.

Ollier W, Thomson W: Population genetics of rheumatoid arthritis, *Rheum Dis Clin North Am* 18:741–759, 1992.

Ota M, Katsuyama Y, Kimura A, et al.: A second susceptibility gene for developing rheumatoid arthritis in the human MHC is localized within a 70-kb interval telomeric of the TNF genes in the HLA class III region, *Genomics* 71:263–270, 2001.

Ozaki K, Ohnishi Y, Iida A, et al.: Functional SNPs in the lymphotoxin-alpha gene that are associated with susceptibility to myocardial infarction, *Nat Genet* 32:650–654, 2002.

Pae CU, Kim TS, Kwon OJ, et al.: Polymorphisms of heat shock protein 70 gene (HSPA1A, HSPA1B and HSPA1L) and schizophrenia, *Neurosci Res* 53:8–13, 2005.

Pedersen NW, Holm A, Kristensen NP, et al.: CD8(+) T cells from patients with narcolepsy and healthy controls recognize hypocretin neuron-specific antigens, *Nat Commun* 10:837, 2019.

Pende D, Parolini S, Pessino A, et al.: Identification and molecular characterization of NKp30, a novel triggering receptor involved in natural cytotoxicity mediated by human natural killer cells, *J Exp Med* 190:1505–1516, 1999.

Penisson-Besnier I, Allamand V, Beurrier P, et al.: Compound heterozygous mutations of the TNXB gene cause primary myopathy, *Neuromuscul Disord* 23:664–669, 2013.

Penrose LS: The detection of autosomal linkage in pairs of brothers and sisters of unspecified parentage, *Ann Eugen* 6:133, 1935.

Penzotti JE, Doherty D, Lybrand TP, et al.: A structural model for TCR recognition of the HLA class II shared epitope sequence implicated in susceptibility to rheumatoid arthritis, *J Autoimmun* 9:287–293, 1996.

Peterlin B, Globocnik Petrovic M, Makuc J, et al.: A hemochromatosis-causing mutation C282Y is a risk factor for proliferative diabetic retinopathy in Caucasians with type 2 diabetes, *J Hum Genet* 48:646–649, 2003.

Pietzak MM, Schofield TC, McGinniss MJ, Nakamura RM: Stratifying risk for celiac disease in a large at-risk United States population by using HLA alleles, *Clinical gastroenterology and hepatology : the official clinical practice, Journal of the American Gastroenterological Association* 7:966–971, 2009.

Poirier K, Hubert L, Viot G, et al.: CSNK2B splice site mutations in patients cause intellectual disability with or without myoclonic epilepsy, *Hum Mutat* 38:932–941, 2017.

Raum D, Awdeh Z, Alper CA: BF types and the mode of inheritance of insulin-dependent diabetes mellitus (IDDM), *Immunogenetics* 12:59–74, 1981.

Robinson J, Halliwell JA, Hayhurst JD, Flicek P, Parham P, Marsh SG: The IPD and IMGT/HLA database: allele variant databases, *Nucleic Acids Res* 43:D423–D431, 2015.

Robson KJ, Lehmann DJ, Wimhurst VL, et al.: Synergy between the C2 allele of transferrin and the C282Y allele of the haemochromatosis gene (HFE) as risk factors for developing Alzheimer's disease, *J Med Genet* 41:261–265, 2004.

Rubin LA, Amos CI, Wade JA, et al.: Investigating the genetic basis for ankylosing spondylitis. Linkage studies with the major histocompatibility complex region, *Arthritis Rheum* 37:1212–1220, 1994.

Rubinstein P, Suciu-Foca N, Nicholson JF: Genetics of juvenile diabetes mellitus. A recessive gene closely linked to HLA D and with 50 per cent penetrance, *N Engl J Med* 297:1036–1040, 1977.

Rubio-Tapia A, Hill ID, Kelly CP, et al.: ACG clinical guidelines: diagnosis and management of celiac disease, *Am J Gastroenterol* 108:656–676, 2013. quiz 677.

Rusakiewicz S, Nocturne G, Lazure T, et al.: NCR3/NKp30 contributes to pathogenesis in primary Sjogren's syndrome, *Sci Transl Med* 5, 2013. 195ra96.

Russell TJ, Schultes LM, Kuban DJ: Histocompatibility (HL-A) antigens associated with psoriasis, *N Engl J Med* 287:738–740, 1972.

Ryan SJ, Maumenee AE: Birdshot retinochoroidopathy, *Am J Ophthalmol* 89:31–45, 1980.

Sargent CA, Dunham I, Trowsdale J, et al.: Human major histocompatibility complex contains genes for the major heat shock protein HSP70, *Proc Natl Acad Sci U S A* 86:1968–1972, 1989.

Sarpatwari A, Bussel JB, Ahmed M, et al.: Single nucleotide polymorphism (SNP) analysis demonstrates a significant association of tumour necrosis factor-alpha (TNFA) with primary immune thrombocytopenia among Caucasian adults, *Hematology* 16:243–248, 2011.

Schlosstein L, Terasaki PI, Bluestone R, Pearson CM: High association of an HL-A antigen, W27, with ankylosing spondylitis, *N Engl J Med* 288:704–706, 1973.

Schneider PM, Mauff G: Complement C4 protein and DNA typing methods, *Methods Mol Biol* 210:269–295, 2003.

Schneider PM, Stradmann-Bellinghausen B, Rittner C: Genetic polymorphism of the fourth component of human complement: population study and proposal for a revised nomenclature based on genomic PCR typing of Rodgers and Chido determinants, *Eur J Immunogenet* 23:335–344, 1996.

Schneider PM, Witzel-Schlomp K, Rittner C, et al.: The endogenous retroviral insertion in the human complement C4 gene modulates the expression of homologous genes by antisense inhibition, *Immunogenetics* 53:1–9, 2001.

Schroder O, Schulte KM, Ostermann P, et al.: Heat shock protein 70 genotypes HSPA1B and HSPA1L influence cytokine concentrations and interfere with outcome after major injury, *Crit Care Med* 31:73–79, 2003.

Scofield RH, Kurien B, Gross T, et al.: HLA-B27 binding of peptide from its own sequence and similar peptides from bacteria: implications for spondyloarthropathies, *Lancet* 345:1542–1544, 1995.

Selvaraj S, Schmitt AD, Dixon JR, Ren B: Complete haplotype phasing of the MHC and KIR loci with targeted HaploSeq, *BMC Genomics* 16:900, 2015.

Sharma R, Vasishta RK, Sen RK, et al.: Refolding of HLA-B27 heavy chains in the absence of beta2m yields stable high molecular weight (HMW) protein forms displaying native-like as well as non-native-like conformational features: implications for autoimmune disease, *i* 1772:1258–1269, 2007.

Shiina T, Hosomichi K, Inoko H, et al.: The HLA genomic loci map: expression, interaction, diversity and disease, *J Hum Genet* 54:15–39, 2009.

Siebold C, Hansen BE, Wyer JR, et al.: Crystal structure of HLA-DQ0602 that protects against type 1 diabetes and confers strong susceptibility to narcolepsy, *Proc Natl Acad Sci Unit States Am* 101:1999–2004, 2004.

Siemens I, Brenden M, Mauff G, et al.: Apparently non-expressed alleles of factor B (BF) code for hypomorphic proteins, *Immunogenetics* 37:24–28, 1992.

Silverstein AM: Essential hypocomplementemia: report of a case, *Blood* 16:1338–1341, 1960.

Sim E, Cross SJ: Phenotyping of human complement component C4, a class-III HLA antigen, *Biochem J* 239:763–767, 1986.

Simon M, Bourel M, Fauchet R, et al.: Association of HLA-A3 and HLA-B14 antigens with idiopathic haemochromatosis, *Gut* 17:332–334, 1976.

Singh R, Kolvraa S, Bross P, et al.: Anti-inflammatory heat shock protein 70 genes are positively associated with human survival, *Curr Pharm Des* 16:796–801, 2010.

Singh R, Kolvraa S, Bross P, et al.: Reduced heat shock response in human mononuclear cells during aging and its association with polymorphisms in HSP70 genes, *Cell Stress Chaperones* 11:208–215, 2006.

Sinnott PJ, Costigan C, Dyer PA, et al.: Extended MHC haplotypes and CYP21/C4 gene organisation in Irish 21-hydroxylase deficiency families, *Hum Genet* 87:361–366, 1991.

Skibola CF, Bracci PM, Nieters A, et al.: Tumor necrosis factor (TNF) and lymphotoxin-alpha (LTA) polymorphisms and risk of non-Hodgkin lymphoma in the Inter-Lymph Consortium, *Am J Epidemiol* 171:267–276, 2010.

Slade C, Bosco J, Unglik G, et al.: Deficiency in complement factor B, *N Engl J Med* 369:1667–1669, 2013.

Smith WP, Vu Q, Li SS, et al.: Toward understanding MHC disease associations: partial resequencing of 46 distinct HLA haplotypes, *Genomics* 87:561–571, 2006.

Song GG, Seo YH, Kim JH, Choi SJ, Ji JD, Lee YH: Association between TNF-alpha (-308 A/G, -238 A/G, -857 C/T) polymorphisms and responsiveness to TNF-alpha blockers in spondyloarthropathy, psoriasis and Crohn's disease: a meta-analysis, *Pharmacogenomics* 16:1427–1437, 2015.

Sollid LM, Markussen G, Ek J, Gjerde H, Vartdal F, Thorsby E: Evidence for a primary association of celiac disease to a particular HLA-DQ alpha/beta heterodimer, *J Exp Med* 169:345–350, 1989.

Soto K, Wu YL, Ortiz A, et al.: Familial C4B deficiency and immune complex glomerulonephritis, *Clin Immunol* 137:166–175, 2010.

Sousa-Pinto B, Pinto-Ramos J, Correia C, et al.: Pharmacogenetics of abacavir hypersensitivity: a systematic review and meta-analysis of the association with HLA-B*57:01, *J Allergy Clin Immunol* 136:1092–1094, 2015. e3.

Spagnolo P, Sato H, Marshall SE, et al.: Association between heat shock protein 70/Hom genetic polymorphisms and uveitis in patients with sarcoidosis, *Invest Ophthalmol Vis Sci* 48:3019–3025, 2007.

Stammers M, Rowen L, Rhodes D, et al.: BTL-II: a polymorphic locus with homology to the butyrophilin gene family, located at the border of the major histocompatibility complex class II and class III regions in human and mouse, *Immunogenetics* 51:373–382, 2000.

Stamp LK, Day RO, Yun J, hypersensitivity A: Investigating the cause and minimizing the risk, *Nat Rev Rheumatol* 12:235–242, 2016.

Stastny P, Fernandez-Vina M, Cerna M, et al.: Sequences of HLA alleles associated with arthritis in adults and children, *J Rheumatol Suppl* 37:5–8, 1993.

Stefansson Thors V, Kolka R, Sigurdardottir SL, et al.: Increased frequency of C4B*Q0 alleles in patients with Henoch-Schonlein purpura, *Scand J Immunol* 61:274–278, 2005.

Stephen J, Nampoothiri S, Banerjee A, et al.: Loss of function mutations in VARS encoding cytoplasmic valyl-tRNA synthetase cause microcephaly, seizures, and progressive cerebral atrophy, *Hum Genet* 137:293–303, 2018.

Stewart CA, Horton R, Allcock RJN, et al.: Complete MHC haplotype sequencing for common disease gene mapping, *Genome Res* 14:1176–1187, 2004.

Sullivan KE, Petri MA, Schmeckpeper BJ, et al.: Prevalence of a mutation causing C2 deficiency in systemic lupus erythematosus, *J Rheumatol* 21:1128–1133, 1994.

Sutton HE: *An introduction to human genetics*, Philadelphia, 1980, Saunders.

Svejgaard A, Platz P, Ryder LP: HLA and disease 1982—a survey, *Immunol Rev* 70:193–218, 1983.

Swanson RM, Gavin MA, Escobar SS, et al.: Butyrophilin-like 2 modulates B7 costimulation to induce Foxp3 expression and regulatory T cell development in mature T cells, *J Immunol* 190:2027–2035, 2013.

Szalai C, Fust G, Duba J, et al.: Association of polymorphisms and allelic combinations in the tumour necrosis factor-alpha-complement MHC region with coronary artery disease, *J Med Genet* 39:46–51, 2002.

Tafti M, Hor H, Dauvilliers Y, et al.: DQB1 locus alone explains most of the risk and protection in narcolepsy with cataplexy in Europe, *Sleep* 37:19–25, 2014.

The MHC sequencing consortium: Complete sequence and gene map of a human major histocompatibility complex. The MHC sequencing consortium, *Nature* 401:921–923, 1999.

Thomson G: HLA DR antigens and susceptibility to insulin-dependent diabetes mellitus, *Am J Hum Genet* 36:1309–1317, 1984.

Thomson G, Bodmer W: The genetic analysis of HLA and disease association. In Dausset J, Svejgaard A, editors: *HLA and disease*, Copenhagen, 1977, Munksgaard.

Thorsby E, Ronningen KS: Role of HLA genes in predisposition to develop insulin-dependent diabetes mellitus, *Ann Med* 24:523–531, 1992.

Tiancha H, Huiqin W, Jiyong J, et al.: Association between lymphotoxin-alpha intron +252 polymorphism and sepsis: a meta-analysis, *Scand J Infect Dis* 43:436–447, 2011.

Todd JA: Genetic control of autoimmunity in type 1 diabetes, *Immunol Today* 11:122–129, 1990.

Traherne JA, Horton R, Roberts AN, et al.: Genetic analysis of completely sequenced disease-associated MHC haplotypes identifies shuffling of segments in recent human history, *PLoS Genet* 2:e9, 2006.

Truedsson L, Alper CA, Awdeh ZL, et al.: Characterization of type I complement C2 deficiency MHC haplotypes. Strong conservation of the complotype/HLA-B-region and absence of disease association due to linked class II genes, *J Immunol* 151:5856–5863, 1993a.

Truedsson L, Sturfelt G, Nived O: Prevalence of the type I complement C2 deficiency gene in Swedish systemic lupus erythematosus patients, *Lupus* 2:325–327, 1993b.

Tsuda T, Moriguchi M, Asanuma Y, et al.: C4B deficiency associated with membranoproliferative glomerulonephritis, *Intern Med* 46:765–770, 2007.

Ucisik-Akkaya E, Davis CF, Gorodezky C, et al.: HLA complex-linked heat shock protein genes and childhood acute lymphoblastic leukemia susceptibility, *Cell Stress Chaperones* 15:475–485, 2010.

Vader W, Stepniak D, Kooy Y, et al.: The HLA-DQ2 gene dose effect in celiac disease is directly related to the magnitude and breadth of gluten-specific T cell responses, *Proc Natl Acad Sci U S A* 100:12390–12395, 2003.

Valentonyte R, Hampe J, Huse K, et al.: Sarcoidosis is associated with a truncating splice site mutation in BTNL2, *Nat Genet* 37:357–364, 2005.

van Heel DA, Franke L, Hunt KA, et al.: A genome-wide association study for celiac disease identifies risk variants in the region harboring IL2 and IL21, *Nat Genet* 39:827–829, 2007.

Waheed A, Parkkila S, Saarnio J, et al.: Association of HFE protein with transferrin receptor in crypt enterocytes of human duodenum, *Proc Natl Acad Sci U S A* 96:1579–1584, 1999.

Waheed A, Parkkila S, Zhou XY, et al.: Hereditary hemochromatosis: effects of C282Y and H63D mutations on association with beta2-microglobulin, intracellular processing, and cell surface expression of the HFE protein in COS-7 cells, *Proc Natl Acad Sci U S A* 94:12384–12389, 1997.

Walsh EC, Mather KA, Schaffner SF, et al.: An integrated haplotype map of the human major histocompatibility complex, *Am J Hum Genet* 73:580–590, 2003.

Wang X, Cheng S, Brophy VH, et al.: A meta-analysis of candidate gene polymorphisms and ischemic stroke in 6 study populations: association of lymphotoxin-alpha in non-hypertensive patients, *Stroke* 40:683–695, 2009.

Weidle UH, Rohwedder I, Birzele F, Weiss EH, Schiller C: LST1: a multifunctional gene encoded in the MHC class III region, *Immunobiology* 223:699–708, 2018.

Wetsel RA, Kulics J, Lokki ML, et al.: Type II human complement C2 deficiency. Allele-specific amino acid substitutions (Ser189 –> Phe; Gly444 –> Arg) cause impaired C2 secretion, *J Biol Chem* 271:5824–5831, 1996.

White PC, New MI, Dupont B: Structure of human steroid 21-hydroxylase genes, *Proc Natl Acad Sci U S A* 83:5111–5115, 1986.

White PC, Vitek A, Dupont B, et al.: Characterization of frequent deletions causing steroid 21-hydroxylase deficiency, *Proc Natl Acad Sci U S A* 85:4436–4440, 1988.

Wiesner M, Stepniak D, de Ru A, et al.: Dominance of an alternative CLIP sequence in the celiac disease associated HLA-DQ2 molecule, *Immunogenetics* 60:551–555, 2008.

Wilson WA, Perez MC: Complete C4B deficiency in black Americans with systemic lupus erythematosus, *J Rheumatol* 15:1855–1858, 1988.

Winter WE, Chihara T, Schatz D: The genetics of autoimmune diabetes. Approaching a solution to the problem, *Am J Dis Child* 147:1282–1290, 1993.

Wu YL, Savelli SL, Yang Y, et al.: Sensitive and specific real-time polymerase chain reaction assays to accurately determine copy number variations (CNVs) of human complement C4A, C4B, C4-long, C4-short, and RCCX modules: elucidation of C4 CNVs in 50 consanguineous subjects with defined HLA genotypes, *J Immunol* 179:3012–3025, 2007.

Wu YR, Wang CK, Chen CM, et al.: Analysis of heat-shock protein 70 gene polymorphisms and the risk of Parkinson's disease, *Hum Genet* 114:236–241, 2004.

Xie T, Rowen L, Aguado B, et al.: Analysis of the gene-dense major histocompatibility complex class III region and its comparison to mouse, *Genome Res* 13:2621–2636, 2003.

Yang Y, Chung EK, Zhou B, et al.: Diversity in intrinsic strengths of the human complement system: serum C4 protein concentrations correlate with C4 gene size and polygenic variations, hemolytic activities, and body mass index, *J Immunol* 171:2734–2745, 2003.

Yau AC, Tuncel J, Haag S, et al.: Conserved 33-kb haplotype in the MHC class III region regulates chronic arthritis, *Proceedings of the National Academy of Sciences of the United States of America* 113:E3716–E3724, 2016.

Yu CY, Belt KT, Giles CM, Campbell RD, Porter RR: Structural basis of the polymorphism of human complement components C4A and C4B: gene size, reactivity and antigenicity, *EMBO J* 5:2873–2881, 1986.

Yu KH, Yu CY, Fang YF: Diagnostic utility of HLA-B*5801 screening in severe allopurinol hypersensitivity syndrome: an updated systematic review and meta-analysis, *International journal of rheumatic diseases* 20:1057–1071, 2017.

Yu X, Huang Y, Li C, et al.: Positive association between lymphotoxin-alpha variation rs909253 and cancer risk: a meta-analysis based on 36 case-control studies, *Tumour Biol* 35:1973–1983, 2014.

Zanelli E, Breedveld FC, de Vries RR: HLA class II association with rheumatoid arthritis: facts and interpretations, *Hum Immunol* 61:1254–1261, 2000.

Zeng Z, Duan Z, Zhang T, et al.: Association between tumor necrosis factor-alpha (TNF-alpha) promoter -308 G/A and response to TNF-alpha blockers in rheumatoid arthritis: a meta-analysis, *Mod Rheumatol* 23:489–495, 2013.

Zhang C, Zhao MQ, Liu J, et al.: Association of lymphotoxin alpha polymorphism with systemic lupus erythematosus and rheumatoid arthritis: a meta-analysis, *International journal of rheumatic diseases* 18:398–407, 2015.

Zhang Y, Gong J, Zhang L, et al.: Genetic polymorphisms of HSP70 in age-related cataract, *Cell Stress Chaperones* 18:703–709, 2013.

Zhang Y, Song J, Day K, Absher D: dCATCH-Seq: improved sequencing of large continuous genomic targets with double-hybridization, *BMC Genomics* 18:811, 2017.

Zhou F, Cao H, Zuo X, et al.: Deep sequencing of the MHC region in the Chinese population contributes to studies of complex disease, *Nat Genet* 48:740–746, 2016.

Zipperlen K, Peddle L, Melay B, et al.: Association of TNF-alpha polymorphisms in Crohn disease, *Hum Immunol* 66:56–59, 2005.

CHAPTER 52

IMMUNODEFICIENCY DISORDERS

Nikita Raje

DIAGNOSTIC CONSIDERATIONS IN IMMUNODEFICIENCY WORKUPS, 1025

EVALUATION OF THE IMMUNE SYSTEM, 1026

Basic Evaluation for Immunodeficiencies, 1026

Adjunctive Tests That are Useful in Immunodeficiency Evaluation, 1028

Intermediate Evaluation for Immunodeficiencies, 1028

Advanced Evaluation for Immunodeficiencies, 1030

NOVEL APPROACHES TO TREATING IMMUNODEFICIENCY DISORDERS, 1034

SUMMARY, 1034

SELECTED REFERENCES, 1034

KEY POINTS

- Primary immunodeficiencies are a group of disorders where the defect lies within the immune system; most of them are caused by single-gene defects.
- Because of the complexity of diagnosing a primary immunodeficiency, the cooperation of the clinician, the research scientist, and the clinical pathologist is required.
- A logical approach to the diagnosis of primary immunodeficiency disorders based on staged diagnostic testing or clinical picture is necessary because of the complex nature of the immune system.
- Preparation for specimen collection, handling, and delivery to a specialty laboratory is required for performing complex immunologic assays.
- As a result of technological advances, molecular genetic testing is increasingly employed in diagnosing primary immunodeficiency disorders and can be paramount in guiding treatment.

Primary immunodeficiency disorders (PIDDs), also known as inborn errors of immunity (IEIs), are a rare group of disorders. As per a 2007 population survey the prevalence of PIDDs in the United States is 1 in 1200 persons (Boyle et al., 2007). The prevalence of PIDD in the United States is estimated at about 38.9 to 50.5 per 100,000 persons with private insurance and 29.1 to 41.1 per 100,000 persons with public insurance between 2001 to 2007 (Kobrynski et al., 2014). The most common immunodeficiency, selective IgA deficiency, has an incidence of 1 in every 1200 healthy blood donors, with IgA levels less than 0.05 mg/dL (Sandler et al., 1994). Whereas data from European countries shows an incidence of IgA deficiency ranging from 1:163 in Spain (Pereira et al., 1997) and 1 in 396 in Finland (Koistinen, 1975), data from other countries shows incidence of 1:651 in Iran, 1:252 in Nigeria, and 1:965 in Brazil (Yazdani et al., 2017). Data from Canada and Australia estimate the incidence of primary immunodeficiency at 2.1 per 100,000 (Baumgart et al., 1997) and 6.8 per 100,000 and 10.6 per 100,000, respectively (Ryser et al., 1988; Stray-Pedersen & Abrahamsen, 1997; Matamoros et al., 2000). Chronic granulomatous disease is found in 1 in 200,000 to 250,000 (Winkelstein et al., 2000). Prevalence is still unknown for some of the newer immunodeficiencies. Overall, the prevalence of PIDD can vary for each type of PIDD affecting various parts of the immune system in various ethnicities.

The immune system is an interlocking group of immune cells, proteins, and immune functions, in which any defect may result in an immunodeficiency. Immune response in humans is of two types: innate and adaptive. The natural physical barriers of the body are the first line of defense against invading microbes and include skin, mucus at exposed mucosal surfaces, and ciliated cells of the respiratory, intestinal, and genital tracts. In addition to physical barriers, immunologic functions of the body exert continual surveillance through acquired and innate modes of action. Innate responses do not require prior antigen exposure and comprise phagocytic cells (macrophages, neutrophils, and monocytes), complement, cytokines, and acute phase reactants (Delves & Roitt, 2000). The adaptive immunologic response is specific, requiring previous antigen exposure for sensitization, and improves with each subsequent challenge from a given antigen. These responses are the result of a proliferation of antigen-specific B and T cells, which are stimulated after cellular receptors bind to antigens. B cells produce antigen-specific antibodies to eliminate extracellular antigens. T cells assist B cells to produce antigen-specific antibodies and also kill cells that are virally infected.

Immunodeficiency disorders can be primary or secondary. Whereas PIDDs are mostly due to single gene defects that directly affect the immune system, secondary immunodeficiencies are due to defects that lie outside the immune system but secondarily affect the immune system. Secondary immunodeficiency disorders can be a result of various causes, including malnutrition, viral infections, hematologic and other types of malignancies, chemotherapy, immunosuppressive medications, and protein losing disorders. On the other hand, most of the primary immunodeficiency disorders are genetic in origin.

The list of IEIs/PIDDs (Tangye et al., 2020) is expanding rapidly. Based on the immune defect, PIDDs are classified in several categories. International Union of Immunological Societies (IUIS) updates the classification every couple of years. The latest classification for 2020 (January) gives 10 categories of PIDDs with a total of 430 disorders, with 65 newly added disorders in the past 2 years. While individual PIDDs are rare disorders, the expanding number of PIDDs makes it important to keep PIDD in the differential diagnosis.

DIAGNOSTIC CONSIDERATIONS IN IMMUNODEFICIENCY WORKUPS

PIDDs are a group of rare disorders that can present with diverse manifestations causing severe morbidity and mortality. Infections are the most common presentation of PIDDs. Malignancy, autoimmunity, autoinflammation, and atopy can be associated with infections or be the sole manifestations of PIDDs. The manifestations can vary in terms of degree of severity, types of symptoms exhibited, or both. These conditions, when unrecognized and left untreated, can result in death from infection or noninfectious complications. Awareness of common clinical presentations can aid physicians in identifying individuals who are more likely to have a primary immune defect. Since PIDDs is a group of rare disorders, identifying children/adults with immunodeficiency presents a significant challenge to physicians. A high index of suspicion for primary immunodeficiencies is recommended for patients with recurrent infections or other features of PIDDs. Most frequently, increased susceptibility to recurrent infection is the first clinical indication of an immune defect. The type of recurrent infection provides insight into the immune defect as noted in Fig. 52.1 and helps guide the clinician in evaluating the patient. Therefore the most critical part of the medical evaluation is obtaining a complete medical history. Clinical signs and symptoms of primary immunodeficiency are presented in Fig. 52.2. Some clues that favor possibility of immunodeficiency include frequent and prolonged infections, opportunistic infections, and failure to thrive (Puck, 1999). Infections with an unusual feature such as the need for an adult to have a myringotomy, severe herpes zoster or herpes zoster appearing in a young child, or serious infection in a sterile organ should be considered a warning sign regardless of frequency. A confirmed report of an immunodeficiency disease occurring in a sibling or first-degree relative should also prompt careful clinical assessment and laboratory investigation, even without a history of severe or unusual infections. In one study of 70 patients with PIDDs, approximately 18.6% had a family history of an immunodeficiency (Kobrynski, 2002). In addition to these warning

signs, the physician should be alerted by noninfectious elements in the history that are unusual, such as a history of autoimmune disease, significant lymphadenopathy, granulomas, malignancy, or intractable diarrhea or very early onset of inflammatory bowel disease in a child. These additional signs and symptoms in conjunction with recurrent infections should prompt evaluation for a possible immune defect.

It is important to consider alternative diagnoses in the evaluation of PIDDs. Various features of infections or other symptoms can provide a clue to differentiate PIDDs from other disorders that mimic PIDDs. It is also important to pay attention to the clinical circumstances and not to dwell exclusively on the number or severity of infectious episodes (Atkinson et al., 2000). For example, when an infectious process involves the same anatomic site repeatedly, the cause is more likely to be structural, not failure of one of the host defenses. Examples include chronic osteomyelitis in one location, recurrent episodes of pneumonia that affect only one lobe of the lung, and recurrent infection of a surgical wound. Additionally, some PIDDs, such as chronic granulomatous disease, may present later in life than expected; however, it is still important to keep these disorders in the differential diagnosis (Lukela et al., 2005).

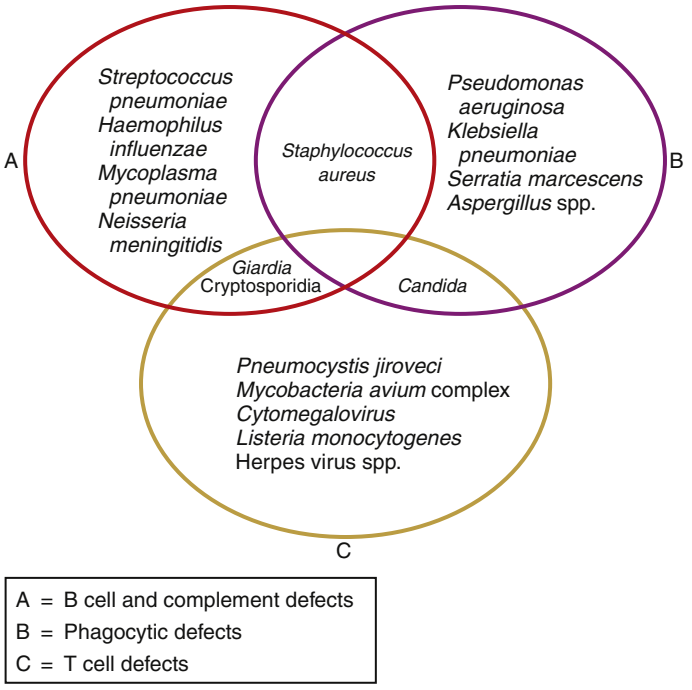

Figure 52.1 Infections associated with cellular immune defects.

EVALUATION OF THE IMMUNE SYSTEM

A careful history and thorough physical examination can guide the testing in patients with suspected immunodeficiency. Based on this information, it may be possible to consider specific category/categories of PIDDs during evaluation. The roles of these host defenses and their correlation with different immunodeficiency disorders are presented in Fig. 52.3.

Based on the previous considerations, when an immune defect is suspected, evaluation of the immune system is best approached in stages, with basic screening tests performed first and more complex testing conducted as indicated. For example, if a patient presents with strong clinical symptoms suggestive of a B- or T-cell disorder but a normal lymphocyte count, further investigation by a lymphocyte enumeration panel is warranted. An overview of this staged approach is given in Fig. 52.4.

BASIC EVALUATION FOR IMMUNODEFICIENCIES

Clinical History and Physical Examination

A thorough clinical history provides the primary clues in diagnosing a PIDD. Part of the first visit should include obtaining all previous medical records, including pathology reports or slides, and results of previous cultures and radiographs. The typical history includes recurrent, persistent infections or infections caused by unusual microbes. The clinician will be guided by the types of infection the patient has acquired. Patients with immunoglobulin deficiencies typically report an increased number of bacterial infections. Repeated viral, fungal, or other opportunistic infections are associated with T-cell immunodeficiencies. Patients with phagocytic defects usually report a history of infections with catalase-positive bacteria such as *Staphylococcus* spp. Complement deficiencies are most frequently associated with infections caused by encapsulated organisms such as *Streptococcus pneumoniae* or *Neisseria* spp. infections (see Fig. 52.1) (Lindegren et al., 2004).

The physical examination in PIDD may reveal findings that are characteristic for that particular PIDD. Patients with PIDD may appear pale, lethargic, and chronically ill. Infants and young children affected with primary immunodeficiency disorders may present with failure to thrive, so monitoring height and weight is important. Small or absent peripheral lymph nodes, tonsils, or adenoids are indicative of X-linked agammaglobulinemia (Lindegren et al., 2004). Hepatomegaly or splenomegaly may suggest presence of lymphoproliferation. In addition to respiratory infection, the infant may experience rhinitis; conjunctivitis; or hematologic, gastrointestinal, and autoimmune disorders (Fleisher, 2003). In contrast, patients with chronic granulomatous disease (CGD) and common

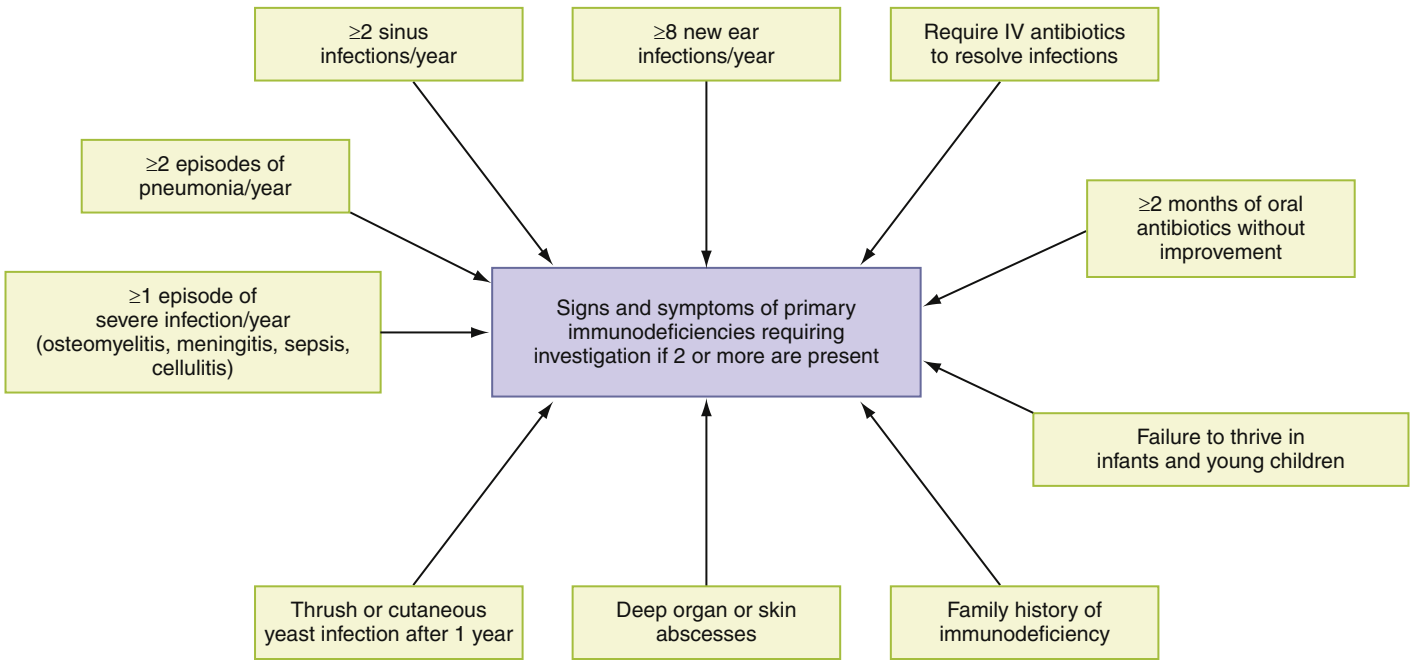

Figure 52.2 Clinical signs and symptoms of primary immunodeficiencies.

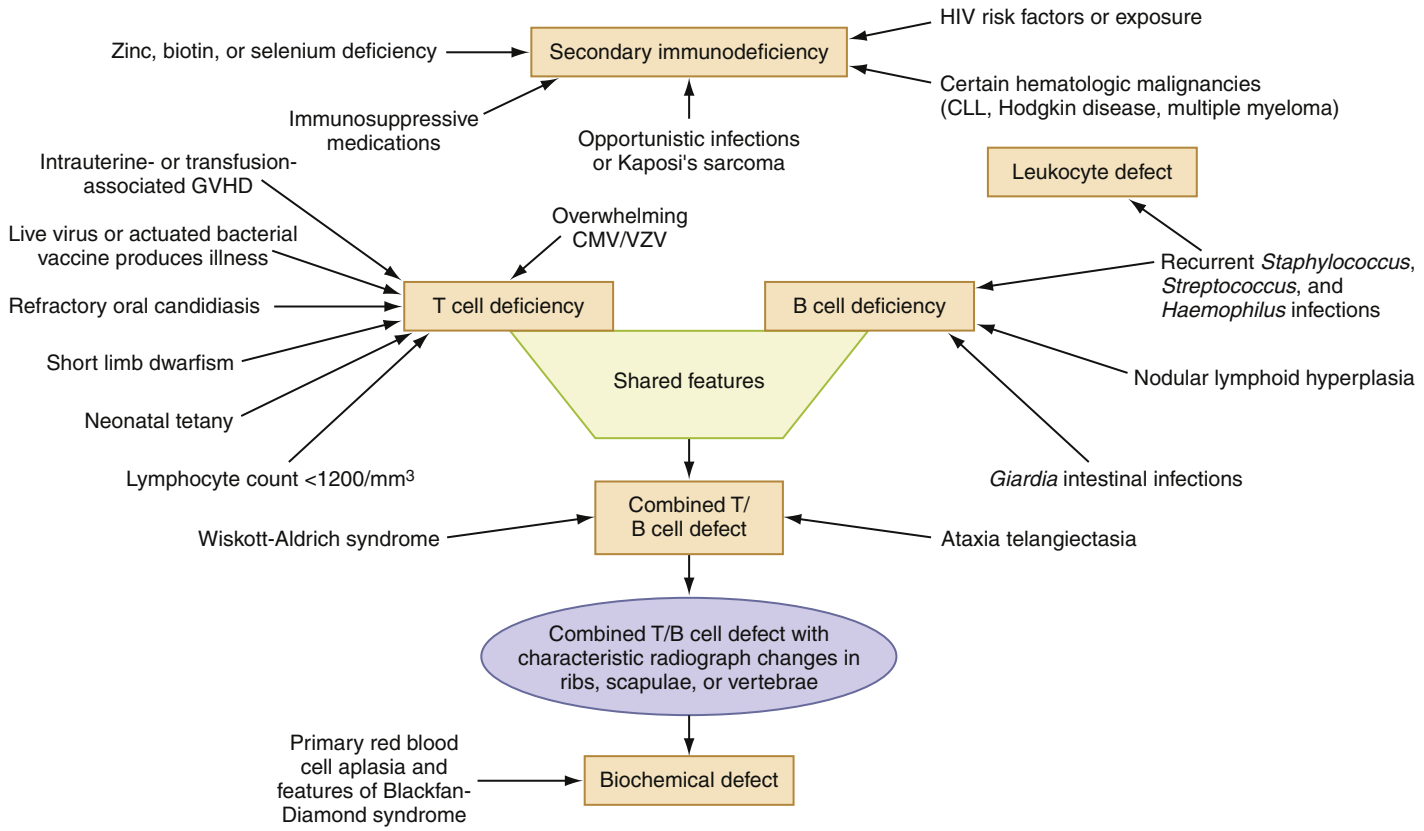

Figure 52.3 Patterns of immunodeficiency disorders. *CLL,* Chronic lymphoid leukemia; *CMV,* cytomegalovirus; *GVHD,* graft-versus-host disease; *HIV,* human immunodeficiency virus; *VZV,* varicella zoster virus.

Basic investigations

- History and physical examination
- Complete blood count and differential
- Quantitative immunoglobulins
- Radiology
- Pulmonary function testing
- Pathology

Secondary investigations

- Antibody titers for vaccines (tetanus, diphtheria, pneumococcus)
- Immunoglobulin subclass analysis
- Lymphocyte enumeration panel
- Complement levels
- T cell functional assessment
- Polymorphonuclear killing assay

Tertiary investigations

- Enzyme assays (adenosine deaminase/purine nucleotide phosphorylase)
- Natural killer cell assays
- Toll like receptor assays
- Advanced phagocyte studies
- Cytokine production and cytokine receptor assays
- Advanced cell surface markers/functional assays
- Antibody production using neoantigens
- Molecular genetics

Figure 52.4 Staged approach for laboratory investigation of primary immunodeficiency.

variable immunodeficiency present with normal or enlarged peripheral lymph nodes (Buckley, 2000). The genetic defect in Wiskott-Aldrich syndrome (WAS) causes immunodeficiency and thrombocytopenia, resulting in the combination of increased bruising, petechiae, and eczematous skin rashes (Zhu et al., 1997). Sparse hair and abnormalities of teeth and nails can be indications of ectodermal dysplasia seen in nuclear factor-kappa B essential modulator (NEMO) deficiency (D'Assante, 2016). Skin rashes such as livedo reticularis, eczematous rash, ichthyosis, and erythroderma can be signs of various PIDDs.

Immune evaluation depends on several factors. Typical basic tests include complete blood count (CBC) with differential and immunoglobulins. However, based on patient's signs and symptoms, initial tests may vary. For example, liver or perianal abscess caused by *Serratia marcescens* is suspicious for CGD, so the testing for CGD can be pursued as an initial test.

Complete Blood Count

The first test performed to examine the immune system is the CBC. A white blood count and differential will provide information on the morphology and number of small lymphocytes (diameter <10 μm). Normal parameters vary, based on the age of the patient, and therefore must be interpreted using age-appropriate reference ranges. Absolute cell counts can provide valuable information. Low absolute neutrophil count can point to immunodeficiencies associated with neutropenia. At a minimum, regardless of age, one expects more than 1500 small lymphocytes per cubic millimeter. Because few (~10%) of the lymphocytes are B lymphocytes, an absolute lymphocyte deficiency primarily reflects T-cell deficiency. Absolute eosinophil count can be elevated in case of Omenn syndrome, autosomal dominant or autosomal recessive hyper-IgE syndrome (HIES), along with various other primary immunodeficiencies (Navabi & Upton, 2016). Absolute monocyte count can be low in GATA2 deficiency (Donadieu et al., 2018). Anemia and thrombocytopenia can be associated with various PIDDs such as autoimmune lymphoproliferative syndrome, common variable immunodeficiency, and chromosome 22q11.2 deletion syndrome. Autoimmune hemolytic anemia can be seen in Wiskott-Aldrich syndrome. Peripheral smear evaluation can provide valuable information. Large vacuoles in neutrophils are seen in Chediak-Higashi syndrome. Small platelets can be seen in Wiskott-Aldrich syndrome. Howell-Jolly bodies can suggest functional asplenia.

Immunoglobulins

Because antibody deficiency diseases are more common than other immune defects, first emphasis should be placed on investigation of immunoglobulins and their production (Stiehm & Conley, 1996; Noroski & Shearer, 1998). Quantitative immunoglobulin assays are readily available in all

commercial and larger hospital laboratories and require only small volumes of serum to perform (Chapters 20 and 47). Because immunoglobulin values increase with age, comparison with age-matched normal ranges is necessary for correct interpretation (Jolliff et al., 1982).

For the first few months of life, IgG is the major immunoglobulin found in infant serum and is maternal in origin. At approximately 3 months of age, dissipation of maternal IgG concentration, combined with a lag in production by the infant, creates a nadir in IgG levels at about 6 months of age. However, primarily IgM and secondarily IgA are synthesized by the infant; thus the absence of these two immunoglobulins may provide clues for a diagnosis of agammaglobulinemia, characterized by pan-hypogammaglobulinemia. The best understood cause of agammaglobulinemia is a defective *BTK* gene (known as X-linked agammaglobulinemia) causing arrest of maturing B cells and absence of mature B cells in circulation. Other autosomal recessive forms of agammaglobulinemia are now known to cause similar pan-hypogammaglobulinemia. Immunoglobulin G levels can be low due to primary immunodeficiency (antibody deficiencies such as XLA or common variable immunodeficiency or part of other combined immunodeficiencies) or secondary causes such as iatrogenic (medications such as corticosteroids, antiepileptics, B-cell–targeted therapy such as rituximab, radiation therapy), acute illness (e.g., sepsis), or protein losing conditions (protein losing enteropathy, protein losing nephropathy). While IgG level is most frequently used, IgG subclasses can be assessed (IgG1, IgG2, IgG3, IgG4) but their use is controversial and minimal. IgG3 has short half-life and can be used before 6 months of age to check if an infant can make antibodies (when the rest of the subclasses are maternal in origin).

Often, IgA is not present in significant amounts until 6 months of age; however, after 4 years of age, IgA levels that remain decreased indicate that this is a permanent defect (Plebani et al., 1986). Selective IgA-deficient patients may be asymptomatic or may have mild symptoms such as increased respiratory or gastrointestinal infection; however, patients may be at risk of developing severe or fatal anaphylactic reactions to plasma in blood products that contain IgA (Lindegren et al., 2004). Such patients, once confirmed for IgA deficiency, would require plasma from other IgA-deficient individuals to avoid future anaphylactic reactions.

Hyper-IgM syndrome is characterized by normal to elevated levels of IgM with markedly low levels of IgA, IgG, and IgE (Levy et al., 1997; Ramesh et al., 1998; Buckley, 2000). Hyper-IgM syndrome is caused by defect in CD40 ligand, CD40, AID, UNG, INO80, and MSH6. In contrast, marked elevations of IgE can be a part of the hyper-IgE syndrome caused by STAT3 loss of function, DOCK8 deficiency, PGM3 defect, TGFBR, ZNF34I, ERBIN deficiency, CARD11 deficiency, interleukin-6 (IL-6) receptor deficiency or IL-6 signal transducer deficiency, and Comel Netherton syndrome (Buckley & Becker, 1978; Tangye et al., 2020) but also are common in immunodysregulation, polyendocrinopathy, enteropathy, immunodysregulation polyendocrinopathy enteropathy X-linked syndrome (IPEX), atypical complete DiGeorge syndrome, Wiskott-Aldrich syndrome, and Omenn syndrome (Ozcan et al., 2008). WAS characteristically shows marked elevation of serum IgA combined with low IgM concentrations (Ochs, 1998). Patients with decreased levels of IgM are often found in the context of generalized immune deficiency/dysregulation and autoimmune diseases. While very low IgM levels have been noted in chromosome 22q11.2 deletion, reduced or lacking IgM+ B cells, or impaired IgG antibody responses against pneumococcus polysaccharides, it may be part of another immunodeficiency disorder (Louis & Gupta, 2014).

A simple way to assess functional antibody levels in children is to check for isohemagglutinins, commonly of the IgM isotype, directed against ABO antigens that the patient lacks (e.g., assessing anti-A antibodies in a patient with the B blood type), because their presence will indicate active functional antibody production (Fleisher, 2003). Isohemagglutinins are naturally occurring antibodies that form at some point after 2 to 3 months of age; however, testing for these antibodies is not valid for children 4 to 6 months of age because of the persistence of maternal immunoglobulin. Additionally, because of relative immaturity, or perhaps inadequate exposure, children with normal immunity may have low concentrations of isohemagglutinins until 5 to 10 years of age (Cooling et al., 2008).

ADJUNCTIVE TESTS THAT ARE USEFUL IN IMMUNODEFICIENCY EVALUATION

Radiologic Imaging

Radiographs, computed tomography (CT), and magnetic resonance imaging (MRI) studies can be helpful as adjunctive tests in assessing or in monitoring complications of immunodeficiencies. Chronic interstitial pneumonia is common in infants, children, and adults with T-cell deficiencies and should be confirmed on chest radiograph. With time, many patients with primary B-cell deficiency (agammaglobulinemia, common variable immunodeficiency) may develop chronic pulmonary fibrosis or bronchiectasis (Sweinberg et al., 1991; Cunningham-Rundles, 1999). Chest CT in a patient who has recurrent respiratory tract infection is the best means of investigating for bronchiectasis; if these changes have developed, further investigation is clearly warranted.

In the past, lateral views of the neck were used to assess pharyngeal lymphoid tissue in children. However, radiographs are not recommended for evaluation of cervical lymphoid tissue because the information they provide is more easily obtained by alternative methods. Frontal views of the chest may reveal an absence of the thymic shadow in infants, but because the thymus can shrink easily because of stress, evaluation of thymic size by this method is not reliable. Bony abnormalities, however, can alert the radiologist to an immunologic problem presenting in childhood. A subset of patients with immunodeficiencies (e.g., cartilage hair hypoplasia) involving abnormalities of T cells, or both T and B cells, have short-limbed dwarfism. These patients show characteristic lesions, usually in the metaphyseal regions of the long bones. Patients with infant-onset adenosine deaminase deficiency show readily identifiable skeletal abnormalities of ribs and hips (Lindegren et al., 2004). Bony abnormalities may be present in patients with HIES; these abnormalities include diffuse osteoporosis, fractures that occur with little trauma, craniosynostosis, and midline bony defects (Grimbacher et al., 1999).

Pulmonary Functions

Immunodeficiency, especially if it has persisted for some time, will often affect the pulmonary system and its function, as previously mentioned. Therefore complete lung volumes, with forced expiratory volumes and diffusing lung capacity for carbon monoxide (DLCO), should be tested even if the chest radiograph is normal. Patients with both T- and B-cell defects are subject to pulmonary infection, often resulting in bronchospasm, restrictive or obstructive disease, or combinations of these abnormalities. Those patients who are both IgA and IgG2 deficient have been shown to have significantly abnormal pulmonary function tests, and a causal relationship may be seen between these deficiencies and deterioration of lung function (Bjorkander et al., 1985).

Pathology

Hair microscopy can reveal pigmentation issues noted in familial hemophagocytic lymphohistiocytosis syndromes such as Chediak-Higashi syndrome, Hermansky-Pudlak syndrome, and Griscelli syndrome. Clumping of hair pigment can also be noted in cartilage hair hypoplasia.

Absence of plasma cells on biopsy of intestine can be noted in antibody deficiencies such as common variable immunodeficiency. Pulmonary alveolar proteinosis can be noted on bronchoalveolar lavage/lung biopsy in cases with GATA 2 deficiency or CSF2RB deficiency. Biopsy of any affected tissue may be helpful.

INTERMEDIATE EVALUATION FOR IMMUNODEFICIENCIES

Specific Antibody Production

Investigation of specific antibody production may require only monitoring of immune response to vaccine antigens and is the most direct method by which to assess B-cell function. This is a useful approach for patients with a history of recurrent bacterial infection and low-normal quantitative immunoglobulin concentrations. Diagnosis of common variable immunodeficiency (CVID) requires meeting criteria. Along with age over 2 years and hypogammaglobulinemia (low IgG level and low IgA and/or IgM), defective specific antibodies define CVID. The definitive method used to assess decreased quantitative immunoglobulins consists of measurement of antigen-specific preimmunization levels and postimmunization antibody levels approximately 4 weeks later. If the child or adult has received the usual immunizations in the past, antibody titers for these vaccine antigens can be measured. The most useful vaccine responses to assess are those associated with the protein antigens of tetanus and diphtheria and with the carbohydrate antigens of *Haemophilus* and *Pneumococcus;* many commercial laboratories have developed sensitive tests such as enzyme-linked immunosorbent assays (ELISAs) that can be used to assess antibody production. Evaluation of immune responses to vaccine must include preimmunization serum antibody concentrations and the patient's age because these factors affect antibody response. The testing laboratory provides guidelines for appropriate antibody responses. A fourfold increase in antibody titer to protein antigens and a twofold increase to polysaccharide antigens have

been used as optimal response by some; but interpretation of polysaccharide response, specifically pneumococcal titers, is more complex. Typically, a titer ≥1.3 μg/mL is considered protective. A protective response to 50% (≤5 years of age) or 70% (>5 years of age) is considered optimal response. At times, measles, mumps, rubella, or varicella antibody titers can be checked. Vaccine titers cannot be interpreted once immunoglobulin infusions are administered. In those cases, either immunoglobulin infusions need to be held for 5 to 6 months prior to evaluation or antibodies to neoantigens are checked in special circumstances as discussed later.

Protein and nonprotein antigens produce different immune responses. Antibody responses to tetanus toxoid and diphtheria toxoid are used in evaluating responses to T-cell–dependent protein antigens. Assessment of B-cell function requires evaluation of responses to carbohydrate antigens, which activate B cells directly (T cell independent). It is important to use carbohydrate antigens that are not conjugated to proteins, such as meningococcal and pneumococcal polysaccharide antigens (Balmer et al., 2003). Children younger than 2 years of age will not respond to unconjugated carbohydrate antigens (Barrett et al., 1984). If severe immunodeficiency is suspected, no live virus vaccines should be administered to the child or any family member until immunodeficiency is ruled out (Go & Ballas, 1996).

IgG Subclasses

IgG consists of four subclasses, IgG1 through IgG4, which are distinguished by both structural and biological differences (Normansell, 1987; Schur, 1987). Although individual roles for each of the IgG subclasses have not been established, antibodies to carbohydrate antigens are concentrated in the IgG2 subclass, and many bacterial cell wall antigens are composed of carbohydrates (Scott et al., 1988). Thus absence of an IgG2 response could result in failure to develop protection against bacterial infection. This relationship is most convincing in the occasional patient with IgA deficiency who also has a deficiency of IgG2 subclass and lacks an antibody response to vaccines for *Pneumococcus*. IgG subclass deficiency has also been implicated as the cause of recurrent infection in patients with normal or near-normal IgG levels (Oxelius, 1979; Wedgwood et al., 1986; Shackelford et al., 1990; Gross et al., 1992; Popa, 1994).

The biological significance of IgG subclass deficiency is not always clear, and some individuals who completely lack genes for IgG2, IgA, and IgE are healthy (Lefranc et al., 1982; Migone et al., 1984). IgG1 is the first type of subclass response to carbohydrate antigens, and conversion to an IgG2 response occurs as the individual matures (Scott et al., 1988). No evidence indicates that those who are restricted to only IgG1 responses are at any disadvantage. Patients with selective IgG3 deficiency were reported to have recurrent upper respiratory tract infections, atopic diseases (allergic rhinitis or asthma), and some patients had impaired responses to various pneumococcal serotypes; such patients often respond to treatment with intravenous immunoglobulin (IVIG) (Abrahamian et al., 2010). To determine the biological significance of IgG subclass deficiency, testing of specific antibody production, usually by administering vaccines such as tetanus, diphtheria, *Haemophilus*, or a pneumococcus, is mandatory. Only patients with a clear antibody deficiency for multiple antigens would be considered to have a significant immune defect.

Lymphocyte Subsets

Stem cells differentiate to develop cells of two lineages: lymphoid and myeloid. Lymphoid cells can further differentiate into T cells, B cells, or natural killer (NK) cells. During the development of various cells, many surface molecules are turned on and off in a regulated manner. These surface molecules are identified by their cluster of differentiation (CD). CD markers help distinguish the stage of maturation and the function of lymphocytes (Buckley, 2000).

Migration of stem cells from the bone marrow to the thymus results in development of T cells (Kruisbeek, 1999). Despite regression of the thymus over time, T-cell development persists throughout life (Jamieson et al., 1999). Unlike antibodies produced by B cells, which recognize antigens in their natural state, T cells recognize peptides along with major histocompatibility complex (MHC) molecules after processing by antigen-presenting cells through CD3, the T-cell receptor (TCR) (Buckley, 2000).

Monoclonal antibodies are useful for detection of CD markers on lymphocytes and enable rapid enumeration of lymphocyte subsets. This can be done by using small volumes of whole blood. The CD designation subdivides T cells (as a group, $CD3^+$) into two major subsets: $CD4^+$ and $CD8^+$ T cells. $CD4^+$ T cells are referred to as "helper" cells and are involved in initiation of immune reactions, cytokine secretion, and augmentation of B-cell responses. $CD8^+$ T cells also release cytokines and are associated with cytolytic (killer) functions. $CD4^+$ and $CD8^+$ markers on T cells serve as signaling molecules and work in conjunction with MHC class I and II antigens to amplify and stabilize engagement of T-cell receptors with antigens. $CD4^+$ cells recognize antigens that are presented in the context of MHC class II antigens, and $CD8^+$ cells recognize antigens presented in context with MHC class I antigens (Buckley, 2000). Immunodeficiency diseases resulting from defective generation of T cells may result in total loss or low numbers of $CD3^+$ T cells, thereby creating similar effects on T-cell subsets, $CD4^+$ and $CD8^+$ cells. For example, chromosome 22q11.2 deletion syndrome or DiGeorge syndrome results in low numbers of $CD3^+$ cells (Hong, 1998). MHC class II deficiency results in a low number of $CD4^+$ cells (Klein et al., 1993), and an abnormality of Zap-70, a signaling molecule integral to the activity of the TCR, leads to reduced numbers of $CD8^+$ T cells (Elder, 1998). If an immune defect is suspected, a panel of T-cell markers is examined by flow cytometry, and the percentage and absolute count of cells in each set are compared with age-appropriate normal ranges (Illoh, 2004).

T regulatory cells (Tregs) are defined as a specialized subset of T helper cells that are able to promote and maintain immune tolerance and subsequently prevent autoimmune diseases. CD4 and CD25 (also known as *IL-2 receptor*) cell surface markers are both used to identify Treg cells. However, a major progress in our understanding of Treg cells came after the recognition of the transcription factor FOXP3, which has been shown to be critical both for the development and function of Treg cells. The induction of genetic mutation in *foxp3* in mice leads to suppression of Treg function and the development of lethal autoimmune disease. In humans, a genetic mutation in *foxp3* will result in the defective development of CD4/CD25 regulatory T cells and manifest clinically by immunodysregulation, polyendocrinopathy, and enteropathy; this is attributed to an X-linked disorder known as IPEX syndrome, first described in 1982, which usually manifests in the first few months of life and results in death within the first 2 years unless treated promptly. Also, IPEX-like syndromes have been described with quantitative or qualitative Treg defects, including CD25, CD122 deficiency, CTLA4 and LRBA defects, STAT3 gain of function (GOF), BACH2, and FERMT1 defects.

In general, Treg cells can be classified into two major types based on the site of their formation: naturally occurring T regulatory cells (nTreg), which are produced in the thymus and are thought to control reactivity toward self-antigens, and adaptive or induced T regulatory cells (iTreg), which are induced in the periphery after encountering an antigen from commensal bacteria or a food antigen in a specific immune microenvironment. It is well established that both types are highly dependent on IL-2 for their proliferation and suppressive function. Tregs have been further characterized into other subsets (Tr1, Th3); are affected by various nutritional (vitamins A and D), cytokine (IL-10), and costimulatory factors (CD80, CD86); and suppress other immune cells by inducing immunologic tolerance. Dysregulation of T regulatory cells can result in autoimmunity, malignancy, and other disease states (Mahdi & Bluth, 2015).

Flow cytometry can be used to quantify B and NK cells as well. Absence of B cells indicates agammaglobulinemia. B cells can be normal in CVID. NK cells can be low in various combined immunodeficiencies such as MCM4 deficiency and X-linked SCID (Tangye et al., 2020).

Flow cytometry can be used to further define subsets of T and B cells as naïve and memory subsets. Age-appropriate ranges should be used to define normal cell counts. Naïve CD4 cells (defined by CD4+ CD62L+ CD45RA+ CCR7+) less than 200 suggests severe T-cell deficiency. Class switched memory B cells are now included as one of the criteria for antibody deficiencies.

T-Cell Functional Assessment

A clinical history of opportunistic infections and a decreased absolute lymphocyte count in a CBC should prompt further investigation of a patient's T-cell function (Fleisher, 2003). Mucocutaneous candidiasis, another indication of defective T-cell function, is characterized by extension of infection from the mucous membranes onto contiguous skin and may involve the fingernails with granulomatous inflammation (Atkinson et al., 2000; Lilic & Gravenor, 2001). Delayed-type hypersensitivity (DTH) skin tests are used as measures of T-cell function because they measure the ability to recall, recognize, and present antigen; mobilize T cells; and generate a specific inflammatory response. Despite a normal absolute lymphocyte count, DTH skin tests should be performed when a T-cell defect is suspected. However, these tests are difficult to interpret in infants because they may not have had sufficient exposure to respond to antigens to mount an immunogenic response, and a reduced or absent response may be normal. Hypersensitivity skin testing should incorporate more than one antigen (Kniker et al., 1985). To ensure proper administration and appropriate interpretation of test results, personnel must be well trained (Fleisher, 2003). The limitation of this test is that the results are not quantitative.

Insight into the capability of T cells can be gained by performing functional assessments of in vitro proliferative responses to different stimuli. Mitogens, antigens, and alloantigens are stimuli that cause proliferation of T cells. Mitogens are usually plant extracts that lack specificity and stimulate both $CD4^+$ and $CD8^+$ T lymphocytes. Typical mitogens used are phytohemagglutinin (PHA), pokeweed mitogen (PWM), and Concanavalin A. Alloantigens on unrelated donor cells also stimulate $CD4^+$ and $CD8^+$ cells in a relatively nonspecific way. Patients with significant T-cell deficiency may still show proliferative responses to these stimulators, indicating the presence of T cells but not their ability to clear infectious agents from the host. Nonetheless, a proliferative response to specific antigens is a good indicator of the host's ability to resist infection (Lane et al., 1985). In the case of specific antigens, tetanus, diphtheria, and *Candida* are commonly used, although sufficient exposure to these antigens is required. Therefore these are not reliable antigens for testing infants during the first year of life. A measure of specific T-cell responses that is useful in infants consists of culturing peripheral blood mononuclear cells with mitogenic concentrations of anti-CD3 monoclonal antibody. This stimulator normally causes proliferation of all $CD3^+$ T cells, and absence of proliferation demonstrates a severe T-cell defect (Hong, 1996).

Polymorphonuclear Killing Assays

Testing neutrophil function requires careful planning because specimens may be transported over long distances to large reference laboratories for testing. Blood collected from a patient should be submitted to the investigating laboratory as soon as possible because neutrophils undergo apoptosis rapidly after collection. If the blood must be stored or transported, it should be collected in a preservative such as ethylenediaminetetraacetic acid (EDTA) or citrate in a polypropylene tube and maintained at room temperature (20° to 25°C). This decreases metabolic activity and minimizes adhesion of cells to the wall of the tube. Even under optimal conditions, cells can be maintained only for approximately 24 to 36 hours (Kuijpers et al., 1999).

Neutropenia or neutrophil dysfunction results in recurrent bacterial or fungal infection in the skin, lymph nodes, liver, lungs, or bones. This most commonly occurs with myelosuppressive therapies used to treat malignant neoplasms. These disorders must be distinguished from CGD, in which phagocytosis is normal, but intracellular killing of infectious organisms is defective, resulting in abscess or granuloma formation in the liver, bones, and lungs (Lekstrom-Himes & Gallin, 2000). CGD inheritance is most commonly X-linked or autosomal recessive owing to mutations involving chromosome locations 16p24, 7q11.23, and 1q25. These changes result in defects in one of the four subunits of nicotinamide adenine dinucleotide phosphate (NADPH) oxidase, the enzyme that catalyzes the formation of hydrogen peroxide. This error causes failure of the metabolic burst in granulocytes following phagocytic ingestion of bacteria (Meischl & Roos, 1998). As a result, molecular oxygen is not reduced to superoxide and other free radicals, such as hydroxyl radical and hydrogen peroxide, which are important components of the intracellular mechanism of bacterial death (Babior, 1978). Therefore CGD is characterized by recurrent infection with catalase-producing organisms, such as *Staphylococcus aureus*, which are capable of destroying the hydrogen peroxide produced by granulocytes. Therefore catalase-positive organisms survive intracellular ingestion, multiply, and cause a granulomatous tissue response that, when excessive, can obstruct the gastrointestinal and genitourinary tracts. Chronic infection with *Serratia* spp., *Klebsiella* spp., *Burkholderia cepacia*, and *Aspergillus* spp. is particularly problematic (Gallin, 1983; Gallin & Malech, 1990). However, patients with CGD do not experience this problem with catalase-negative organisms.

The fundamental biological characteristic of CGD leukocytes is that they will phagocytose bacteria normally but will not kill them. This provides the basis for a bacterial killing assay for CGD. Historically, the nitro blue tetrazolium (NBT) slide test has been the laboratory assay used to screen for CGD and is performed by reference laboratories (Park et al., 1968). In this assay, the patient's neutrophils are incubated with NBT, a pale-yellow dye that is then activated by phorbol-myristate acetate (PMA), a strong, receptor-independent activation stimulus. Functional neutrophils phagocytose, reduce, and precipitate the NBT dye, forming intracellular deposits of black formazan. These deposits are indicative of rapid activation of NADPH-oxidase enzyme, causing reduction of oxygen by NADPH to superoxide that is subsequently catalyzed to hydrogen peroxide by superoxide dismutase (SOD). A technician then microscopically scores neutrophils that contain intracellular black formazan deposits (Kuijpers et al., 1999). However, the NBT slide test has been replaced in most laboratories by a flow cytometry test that detects intracellular oxidation of dichlorofluorescein diacetate or dihydrorhodamine 123 (O'Gorman & Corrochano, 1995). These nonfluorescent dyes, once oxidized, will produce intracellular fluorescent products that are detected by flow cytometry. Flow cytometry is a more objective and reliable method of identifying intracellular products.

The hyper-IgE syndrome is phenotypically similar to CGD, with a classic triad of pneumonia, recurrent cutaneous and pulmonary abscesses, and elevated IgE levels; however, defective polymorphonuclear leukocyte function is not a predominant finding (Buckley & Becker, 1978; Ozcan et al., 2008). In addition, this syndrome includes bone abnormalities, unusual facies, and cutaneous candidiasis. Demonstration of IgE levels greater than 2000 IU/mL (and even as high as 20,000–60,000 IU/mL) with the appropriate clinical manifestations points toward the diagnosis. HIES is actually two distinct entities—autosomal dominant and autosomal recessive—based on inheritance patterns and nonimmunologic features. Each entity is characterized by different genetic mutations. Autosomal dominant HIES (AD-HIES) has been related to dominant-negative mutations of the signal transducer and transcription activator 3 (STAT3), causing impaired signaling of cytokines IL-6 and IL-10; however, signaling for IL-12 and interferon (IFN)-α remains intact. Patients with STAT3 mutations fail to generate helper T cells that secrete IL-17, which is important in providing epithelial and mucosal immunity against fungal and bacterial organisms. It also plays an important role in producing neutrophil chemoattractants. Autosomal recessive HIES (AR-HIES) caused by dedicator of cytokinesis 8 (DOCK8) defect is a distinct disease entity separated from AD-HIES by four major criteria: (1) The inheritance pattern is distinctly different; (2) patients lack connective tissue abnormalities; (3) the incidence of central nervous system complications is higher, and these patients have a higher frequency of varicella-zoster; and (4) herpes simplex virus occurs at a younger age with more complications (Renner et al., 2004).

Complement Evaluation

A number of congenital defects of the complement system have been described, although this is not a frequent cause of primary immunodeficiency disorder. The defects are typically associated with absence of one of the complement molecules or a nonfunctional complement protein, thereby reducing the ability of complement to bind to the surface of invading microorganisms. Individual defects lead to distinct clinical syndromes such as hereditary angioedema or paroxysmal nocturnal hemoglobinuria, a propensity for recurrent bacterial infection, or autoimmune disease (Schneider & Wurzner, 1999). Many of the genetically based deficiencies of the classical activating pathway (C1, C2, C3, C4) and of the terminal components (C5, C6, C7, C8, and C9) can be detected by using antibody-sensitized sheep erythrocytes in a total hemolytic complement assay (CH50). This assay tests for the functional integrity of C1 to C9. Many commercial laboratories perform this assay, but to get accurate results freshly drawn serum or plasma that is then frozen must be used. Therefore logistics must be carefully coordinated if specimens must be sent to a distant location. Deficiencies of alternative pathway component factors D, H, and I and properdin are uncommon but can be detected by a hemolytic assay using unsensitized rabbit erythrocytes as potent activators of the alternative pathway (AH50 assay). If one of these assays is abnormal, identification of individual deficient components rests on specialized functional and immunochemical tests that are specific for each component (see Chapter 48). Patients with alternative pathway defects, such as properdin deficiency, will be predisposed to infection with encapsulated organisms. Atypical hemolytic uremic syndrome can be seen with defect in C3, factor H, or factor I, among other causes.

ADVANCED EVALUATION FOR IMMUNODEFICIENCIES

Enzyme Measurements for Metabolic Defects

Deficiencies of the enzymes adenosine deaminase and purine nucleoside phosphorylase are related to purine metabolism and result in immunodeficiency. Patients with adenosine deaminase deficiency have findings similar to those of severe combined immunodeficiency (SCID) syndrome, a collection of genetic disorders characterized by a severe defect in the function or development of B and T cells. In contrast to SCID, patients deficient in adenosine deaminase have chondro-osseous dysplasia, resulting in skeletal abnormalities, and more severe lymphopenia. Deficient adenosine deaminase is caused by mutation of the gene located on chromosome 20q13.2–q13.11, resulting in toxic accumulation of metabolites that inhibit cell replication and cause apoptosis of lymphocytic cell lines (Buckley, 2000). Lack of adenosine deaminase initially causes loss of T cells ($CD4^+$ T cells in particular) and subsequently B cells, leading to the common form of

severe combined T- and B-cell deficiency (SCID) (Hirschhorn, 1995). As with many primary immune defects first recognized in the severe homozygous form, adenosine deaminase deficiency has been diagnosed as a heterozygous partial deficiency in adults with CD4 lymphopenia and significant T-cell defects (Shovlin et al., 1994).

Purine nucleoside phosphorylase deficiency is characterized by recurrent infection, lymphopenia, neurologic abnormalities, and autoimmune disorders (Myers et al., 2004). This enzyme deficiency causes a decrease in T cells with minimal or no effect on B cells. Purine nucleoside phosphorylase enzymes are usually measured in erythrocyte lysates (Kizaki & Sakurada, 1977), but if blood products have been administered within the previous 3 months the assay may be unreliable. More recently, capillary electrophoresis has been proposed as an alternative inexpensive assay that offers high separation flexibility in diagnosis of errors of metabolism and is capable of determining purine nucleoside phosphorylase or adenosine deaminase enzyme activity and the presence of toxic metabolites (Carlucci et al., 2003).

Natural Killer Cell Assays

Natural killer cells are a subset of lymphocytes that often function with T cells to eradicate intracellular organisms. Complete deficiency of NK cells is rare and is characterized by recurrent herpes infection (Fleisher, 2003). NK cells have the morphology of a large granular lymphocyte and express a unique group of cellular surface markers: CD16, CD56, and CD57 (Trinchieri, 1989). NK cells can be quantified easily by detecting these surface markers using flow cytometry. However, to assess the functional activity of NK cells, chromium release assays, which use chromium-51–loaded K-562 cell lines, have traditionally been performed (Biron et al., 1989). This older assay has limitations in that it is more labor intensive, incorporates radioactive materials, and cannot identify the cellular mechanisms for cell death of the target cells. These disadvantages have driven the development of newer, nonradioactive-based methods, including fluorescent labeling techniques in combination with flow cytometry, to assess NK cell function. Another technique uses a colorimetric substrate to detect granzyme B, the serine protease found in the granules of cytotoxic T lymphocytes and NK cells, and plays a key role in granule-mediated apoptosis by cleaving cellular substrates (Hoppner et al., 2002; Ewen et al., 2003).

Toll-Like Receptor (TLR) Assays

TLR pathways can be defective and lead to innate immune defects. Defects in TLR3 pathway can leave a patient susceptible to herpes simplex encephalitis. Defect in IRAK4 or MyD88 can increase susceptibility to severe bacterial infections. Mononuclear cells produce cytokines in response to TLR-specific ligand stimulation. TLR assay can be used to determine cytokine production using multiplex bead assay in response to ligand stimulation of peripheral blood mononuclear cells.

Additional Phagocyte Analyses

Genetic defects of the innate immune system are related to the formation or function of granules within neutrophils. Myeloperoxidase is the predominant enzyme detected in the primary granules of granulocytes and catalyzes the formation of hypochlorous acid (HOCl), which is capable of killing microorganisms (Kuijpers et al., 1999). However, its absence usually is not associated with clinical symptoms, with the notable exception of patients with diabetes mellitus, who experience increased susceptibility to disseminated candidiasis (Lanza, 1998). Myeloperoxidase deficiency, inherited as an autosomal recessive defect, is one of the most commonly inherited disorders of neutrophils, but its clinical significance is unknown (Lehrer & Cline, 1969; Klebanoff, 1999). Approximately half of affected patients have a deficiency of myeloperoxidase, and the remainder have normal concentrations, along with a structural defect in the enzyme (Nauseef, 1998).

Chédiak-Higashi syndrome and specific granule deficiency are congenital defects resulting in phagocyte granular disorders. Chédiak-Higashi syndrome is an autosomal recessive disorder in which all lysosome-containing cells have giant abnormal granules. In neutrophils, fusion of primary and secondary granules occurs, resulting in delay of fusion with phagosomes and recurrent bacterial infection. Patients with Chédiak-Higashi syndrome have a mild neutropenia, normal immunoglobulin levels, peripheral nerve defects, mild cutaneous and ocular albinism, mild platelet dysfunction, and periodontal disease (Introne et al., 1999).

Neutrophil-specific granule deficiency is a rare disorder characterized by recurrent bacterial infection of the skin and lungs. Patients lack secondary or specific granules of the neutrophils, which play an important role in acute inflammation and do not allow for proper migration of neutrophils. Morphologic examination of stained neutrophils shows characteristic abnormalities in specific granule deficiency (Ganz et al., 1988).

Patients with leukocyte adhesion deficiency (LAD) type 1 (a defect in the integrin CD18, the common β chain of LFA-1, Mac-1, and p150,95 molecules) (Anderson & Springer, 1987) are susceptible to all infections seen in CGD patients, along with otitis media and poor wound healing. Normally, because pathogens cause tissue damage and inflammation, adhesion molecules on vascular endothelium are upregulated and recognized by passing neutrophils bearing the appropriate counterligands, ultimately leading to accumulation of neutrophils at sites of inflammation (see Chapter 49). Patients with LAD lack the adhesion molecules necessary for diapedesis, resulting in tissue neutropenia and therefore more infection (Arnaout & Michishita, 1993). This abnormality starts after birth and is marked by delayed cord separation, chronic skin ulcers, periodontitis, impaired wound healing, and leukocytosis. Deficient leukocytes demonstrate defects of adherence and adhesion-dependent functions such as spreading, phagocytosis, and chemotactic orientation (Anderson & Springer, 1987).

LAD type 2 predominantly affects neutrophils and macrophages, with faulty expression of the selectin ligand sialyl-Lewis X and failure to convert GDP mannose to fucose, resulting in a clinical syndrome similar to LAD type 1. It is also responsible for expression of the rare Bombay blood group (LAD-2) on red blood cells (Etzioni et al., 1993).

Leukocyte mobility is usually evaluated by directed migration through membrane filters or under agarose (Nelson et al., 1975; Cates, 1981). Counting the number of cells at a particular endpoint or "stop filter" microscopically, or radioactive labeling, has the disadvantage of measuring only the fastest cells. This may give an inaccurate assessment of most of the patient's neutrophils. It is actually better to count the number of cells at different points along the filter (Kuijpers et al., 1999). Injections of epinephrine and steroids, which cause polymorphonuclear leukocytes to demarginate and leave the marrow reserves, are used to further assess polymorphonuclear leukocyte mobility. A disorder of actin important in polymorphonuclear leukocyte migration has been described (Southwick et al., 1988).

Adhesion proteins on the surface of neutrophils can be functionally tested with different immobilized ligands bound to a monolayer of endothelial cells attached to a glass slide. They can be measured after pretreatment with chemoattractants. Rolling, attachment, and migration of neutrophils can be monitored over time by a video camera. Phagocytosis can now be assessed by flow cytometry, in which the neutrophils are incubated with fluorescence-labeled microorganisms, the sample is washed to remove labeled undigested microorganisms, and the cells with ingested labeled microorganism are counted (Kuijpers et al., 1999). Much in the same fashion, flow cytometry may be used to assess killing of microbes by employing vital dyes that distinguish live from dead organisms after incubation with neutrophils (Martin & Bhakdi, 1992). Degranulation may be assessed by measuring expression of granule membrane proteins on the neutrophil cell surface by means of flow cytometry (Kuijpers et al., 1999).

Cytokines and Cytokine Receptors

Immune responses are regulated by soluble mediators called *cytokines* that produce a multiplicity of immune events through interactions with appropriate cytokine receptors on tissue and inflammatory cells. Cytokines play an important role as messengers within the immune system and in conjunction with the rest of the body to regulate immune responses (Mire-Sluis & Thorpe, 1998). By studying immunodeficient patients and gene knockout mice, our understanding of the role cytokines play in our host defenses has expanded. Deficiencies in IL-12 and IFN-γ increase susceptibility to *Salmonella* and mycobacterial infections (de Jong et al., 1998). Impaired secretions or responses to IL-12 impair granuloma formation and therefore allow unregulated growth of mycobacterial organisms (Jouanguy et al., 1999). Recent studies show that the pathophysiology of many of these disorders may be the result of defective cytokine signaling, which causes dysfunction or arrested development of B, T, and NK cells (Kelly & Leonard, 2003). Most notably, human X-linked SCID is associated with defects in the interleukin receptor gene *(IL2RG)*, which codes for a common γ chain (γc), a shared component of several cytokine receptors such as IL-4F, IL-7R, IL-9R, and IL-15R. Impaired production of γc leads to cytokine dysfunction and lack of development of affected lymphoid cells (Malek et al., 1999). Additionally, the *JAK3* gene encodes for a tyrosine kinase used in signal transduction through γc-containing cytokine receptors. Defects in this gene have been identified in patients with autosomal recessive SCID. IL-7 is a cytokine with a key role in T-cell development, and a genetic defect in the α subunit of the IL-7 receptor has been identified in patients with a rare disorder of B^+ SCID (Notarangelo et al., 2000). Inflammasome (cytosolic structure of multiple proteins of the innate immune system that activates inflammatory responses) associated autoinflammatory disorders

are associated with defects that lead to overactivation of the IL-1 pathway. IL-1 blockade can be used in the treatment of these disorders. Defect in IL-10 receptor can be a cause of very early onset inflammatory bowel disease (VEOIBD).

Additional Cell Surface Markers/Functional Assays

Advanced flow cytometry assays can be used to detect expression of cell surface or cytoplasmic markers or proteins. Expression of BTK protein in monocytes, FoxP3 on Tregs, DOCK8, WAS protein, SAP, XIAP, CD40 ligand, and CD40 are examples of specialized flow cytometry assays that are available at limited laboratories. Flow cytometry can also be used to check for T cells with α/β TCR vs γ/δ TCR. Flow cytometry can be used to detect excessive double-negative T cells indicating wider double-negative T-cell gap. Increase in α/β DNTs can be an indication for autoimmune lymphoproliferative syndrome (ALPS). Increased soluble IL-2Rα (CD25) can be an indication for chronic T-cell activation and a marker for hemophagocytic lymphohistiocytosis (HLH). CD107a is another maker for chronic T-cell activation/inflammation.

MHC Class I and II Molecules

Congenital mutations affecting MHC class I and class II expression have been described. Class II molecules are found primarily on the antigen-presenting cells, which initiate the acquired immune response. As one might predict, genetic defects of MHC class II (from mutations involving MHC class II gene transcriptional activation) result in a profound immunodeficiency state (Klein et al., 1993) known as *MHC class II deficiency*, according to World Health Organization nomenclature. This is referred to as *bare lymphocyte syndrome type II* and is characterized by lack of expression of MHC II molecules on cellular surfaces. Thymic education and selection of immature T cells are compromised because of loss of antigen processing by MHC class II molecules. Quantities of B and T cells are normal in patients with bare lymphocyte syndrome; however, $CD4^+$ counts are decreased as a result of loss of proper antigen processing. Patients thus are unable to respond to foreign antigens and present with recurrent bacterial, fungal, viral, and protozoal infections. They do not respond to skin testing (type IV DTH), have a decreased ability to respond to mixed lymphocyte reactions, and have pan-hypogammaglobulinemia (Nekrep et al., 2003). An interesting facet of this syndrome is that there is no genetic defect of the MHC class II genes. Instead, a defect occurs in one of the four genes that encode the four regulatory factors essential for surface expression of MHC class II antigens: *CIITA*, *RFXANK*, *RFX5*, and *RFXAP* (Reith & Mach, 2001).

Elimination of foreign antigen can be accomplished by $CD8^+$ T-cell binding to MHC class I antigens expressed on nearly all nucleated cells. It is strange to note that immune defects resulting from MHC class I deficiency, a mutation involving either of the MHC class I cytoplasmic peptide transporters TAP-1 or TAP-2, produce an immune defect characterized by severe lung disease that becomes apparent in later childhood (Donato et al., 1995; de la Salle et al., 1999). This immunodeficiency was previously named *type I bare lymphocyte syndrome* or *human leukocyte antigen (HLA) class I deficiency* and is characterized by a decrease in $CD8^+$ cells and NK cell activity (Yabe et al., 2002). Diagnosis of both defects involves examining expression of these MHC antigens on peripheral blood lymphoid cells by flow cytometry (Illoh, 2004).

Treatment by Targeting Cell Surface Receptors

Recent case reports describe therapies that target cell surface receptors to treat complications associated with primary immunodeficiency disorders. An example is anti-CD20 (rituximab), a monoclonal antibody directed against the CD20 antigen found on B lymphocytes and used to deplete peripheral benign and malignant B lymphocytes. Successful treatment using these monoclonal antibodies has been reported for IgM autoantibody (reactive at 37°C)–mediated autoimmune hemolytic anemia in a child with common variable immunodeficiency, and for lymphoproliferative disorder in a child with WAS caused by depleting peripheral B cells in patients (Sebire et al., 2003; Wakim et al., 2004). IL-1 receptor blockade is used in treatment of autoinflammatory disorders.

Using Novel Immunogens to Assess Antibody Production

Another valuable tool to evaluate specific antibody responses is vaccination with neoantigens such as the bacteriophage ΦX174 and keyhole limpet hemocyanin. These neoantigens may also be used to evaluate patients receiving immunoglobulin replacement therapy because monitoring antibody responses to standard vaccines while receiving passive infusion of pooled immunoglobulins is not possible. Primary and secondary responses may be monitored because the neoantigens provoke a primary IgM response, and then upon reexposure cause a secondary IgG response (Curtis et al., 1970; Ochs & Davis, 1971). Using ΦX174 clearance patterns and isotypes, a patient's response can be measured thereby further defining various degrees and subsets of B-cell deficiency (Ochs & Davis, 1971). Currently this evaluation is available only in some academic institutions using research protocols (Fleisher & Oliveira, 2004). Rabies vaccine and *Salmonella typhi* antibodies are used as neoantigens to evaluate the production of functional antibodies when a patient is on immunoglobulin replacement therapy.

Molecular Genetics

A genetic defect may result in loss of a critical enzyme, may cause developmental arrest in one aspect of the immune system, may cause loss of a structural component, or may create a nonfunctional protein.

A number of the genes involved in the primary immunodeficiency syndromes have now been identified, cloned, and sequenced (Conley, 1992; Puck et al., 1993; Derry et al., 1994; Ramesh et al., 1998; Vihinen et al., 1999; Fischer, 2007; Zhang et al., 2009). In many cases, mouse knockout models have been produced to further study the effects of genes on immune function. In the past, more traditional methods of screening for genetic mutations responsible for immunodeficiencies were used, such as dideoxy fingerprinting and single-strand conformational polymorphism (Sarkar et al., 1992; Sheffield et al., 1993; Puck et al., 1997b). Further advances using fluorescence-based sequencing, which uses fluorescently labeled dideoxynucleotide terminators, allow for simple and sensitive identification of deoxyribonucleic acid (DNA) sequence variations in individuals. Automated multichannel capillary sequences serve as an automated method of rapidly detecting fluorescence-based sequences for multiple patients within hours and make direct sequencing for genetic mutations responsible for immune deficiencies practical (Niemela et al., 2000). Identification of mutated genes facilitates genetic counseling for prenatal diagnosis and aids in the detection of carrier status for defective genes. It also assists in the evaluation of previously undefined immune disorders. An excellent example of how these advanced techniques are enhancing our understanding of primary immunodeficiency disorders is exhibited by hyper-IgM syndrome. Previously, this was categorized as a single disorder, but genetic sequencing has revealed multiple distinct genetic defects affecting B or T cells with variable phenotypes (Durandy et al., 2004).

Analysis of immunodeficiencies with known genetic defects involves testing specific sites on DNA to detect specific mutations. Different methods such as polymerase chain reaction (PCR) may be used to detect the presence or absence of a particular gene, and immunoblotting or flow cytometry can be used to detect protein products and to confirm a diagnosis of primary immunodeficiency when the gene product is absent. High-resolution comparative genomic hybridization arrays or microarrays detect microdeletions associated with complex immunodeficiency syndromes. For example, genomic hybridization arrays and targeted gene sequencing were performed on eight families with variant features of combined immunodeficiency characterized by recurrent sinopulmonary infection, cutaneous viral infection, and elevated serum IgE levels. The analysis revealed novel point mutations in the gene responsible for encoding the dedicator of cytokinesis 8 protein (DOCK8). Homozygous or compound heterozygous deletions in this gene lead to absence of DOCK8 protein in lymphocytes that regulate cytoskeletal rearrangements responsible for cell structure, adhesion, and migration, as well as other functions, resulting in this combined immunodeficiency (Zhang et al., 2009). An example of when it is important to determine the cause of an immunodeficiency is seen in SCID, a heterogeneous group of immunodeficiencies characterized by a number of different molecular defects. Distinguishing between various molecular defects in SCID has implications for treatment, antenatal diagnosis, and carrier testing. It is important to determine whether a patient has X-linked SCID because this may be treated using gene therapy. JAK3-deficient SCID is clinically indistinguishable from X-linked SCID, but gene therapy is not effective (Cavazzana-Calvo et al., 2000). Previously, testing to distinguish between these molecular defects took several weeks to complete because JAK3-deficient SCID is encoded by 23 exons. DNA analysis using single-stranded conformational polymorphism analysis and sequencing of all affected exons was required. More rapid screening methods can now be used to arrive at an expeditious diagnosis, with time-consuming genetic analysis being performed for subsequent confirmation. These protein-based assays employ flow cytometric analysis of γc, immunoblotting for JAK3 and γc, and detection of IL-2–induced tyrosine phosphorylation of JAK3 (Gilmour et al., 2001). However, with defects characterized by nonfunctional protein products, these assays are not useful. Table 52.1 lists some of the identified mutated genes and affected proteins associated with

TABLE 52.1
Gene Mutations, Affected Proteins, and Primary Immunodeficiencies

Disease	Natural Mutant	Protein	Function
Agammaglobulinemia		Btk	Cell activation
APECED		AIRE	Negative selection of T cells
AT		ATM	DNA lesion sensing
Atypical complete DiGeorge syndrome		Base pair deletion on 22a11.2	Oligoclonal T cells
CGD		gp91phox, p22phox, p47phox, p67phox	NADPH oxidase
DC		Dyskerin	Telomere maintenance
FHLH		Munc 13-4	Exocytosis of lytic granules
FHLH		Syntaxin11	Cytotoxicity
Griscelli	Ashen	Rab27a	Exocytosis of lytic granules
HIES AD/AR		STAT3/TYK2	Defective cytokine signaling
HIGM		CD40L	Activation of Ig CSR
HIGM		AID	Ig CSR and SHM
IPEX	Scurfy	FOXP3	Treg function
LAD		β_2 integrin	Adhesion
NBS		Nibrin (NBS1)	DNA repair
Omenn syndrome		RAG, ARTEMIS, IL-7R, RMPR, IL-2Rγ, ZAP70, ADA, DNA ligase IV mutations	Oligoclonal T cells and absence of B cells
	SCID	DNA-PKcs	VDJ (NHEJ)
SCID		Artemis	VDJ (NHEJ)
SCID		Cernunnos, XLF	VDJ (NHEJ)
SCID		γc, JAK3	T (NK) cell development
SCN		HAX-1	Prevention of apoptosis
T-cell deficiency		Orai-1, CRACMI	Ca channel
T-cell deficiency (HLA II expression)		RFXAP, ANK, RFX5, CIITA	HLA class II transcription
Variant combined immunodeficiency		DOCK8	Cytoskeletal arrangements in lymphocytes
WAS		WASP	Cell cytoskeleton, migration
XLP		SAP	Coactivation (SLAM family), NKT
XLP2		XIAP	Control of apoptosis (NKT)
	lpr, gld	fas, fasL	Apoptosis
	Moth-eaten	SHP-1	Phosphatase regulation

AD, Autosomal dominant; *ADA,* adenosine deaminase deficiency; *AID,* activation-induced deaminase; *APECED,* autoimmune polyendocrinopathy candidiasis ectodermal dysplasia; *AR,* autosomal recessive; *AT,* ataxia telangiectasia; *Btk,* Bruton tyrosine kinase; *CGD,* chronic granulomatous disease; *DC,* dyskeratosis congenita; *DNA,* deoxyribonucleic acid; *DNA PKcs,* DNA-dependent protein kinase, catalytic subunit; *DOCK8,* dedicator of cytokinesis 8 protein; *FHLH,* familial hemophagocytic lymphohistiocytosis; *gld,* generalized lymphadenopathy disease; *HIES,* hyper-IgE syndrome; *HIGM,* hyper-IgM syndrome (Ig class switch recombination deficiency [CSR]); *HLA,* human leukocyte antigen; *IPEX,* immunoproliferative enteropathy X-linked syndrome; *LAD,* leukocyte adhesion deficiency; *lpr,* lymphoproliferation; *NADPH,* nicotinamide adenine dinucleotide phosphate; *NBS,* Nijmegen breakage syndrome; *NHEJ,* nonhomologous end-joining; *NK,* natural killer; *SAP,* SLAM-associated protein; *SCID,* severe combined immunodeficiency; *SCN,* severe congenital neutropenia; *SHM,* somatic hypermutations; *Treg,* regulatory T cells; *VDJ,* V(D)J recombination; *WAS,* Wiskott-Aldrich syndrome; *WASP,* Wiskott-Aldrich syndrome protein; *XIAP,* X-linked inhibitor of apoptosis; *XLF,* XRCC4-like factor; *XLP,* X-linked proliferative syndrome; *XLP2,* X-linked proliferative syndrome type 2.

primary immunodeficiencies. Table 52.2 provides a few examples of gene mutations with associated susceptibilities to pathogens.

Next generation sequencing (NGS) has changed the paradigm of molecular testing. Currently, microarray and/or NGS are frequently used for evaluation of PIDDs. NGS is a method used to perform high-throughput parallel sequencing of millions of DNA fragments. NGS can be used to sequence a panel of targeted genes, exome, or genome. Exome and genome sequencing can provide unbiased testing. With these advanced technologies, the number of known genetic defects underlying PIDDs/IEIs is increasing rapidly.

Many of the primary immunodeficiencies are rare disorders that can be difficult to diagnose; in these cases, genetic mutation detection is the most reliable method. These specialized tests are not readily available, and physicians may have difficulty locating laboratories to perform the necessary genetic analyses. Mutation registries and databases are available to provide information about tests for clinical data, immune status, antibody response, cellular function, and enzyme assays. Additionally, some online registries contain information about laboratories that perform these assays, which increases awareness of testing availability and the ability to obtain an exact and prompt diagnosis (Samarghitean et al., 2004).

Prenatal Diagnosis

With advances in technology, the ability to detect prenatally a wider range of immune defects is possible. If the specific mutation is known, or if the inheritance pattern is known to be X linked, analysis of linked polymorphic markers or detection of specific mutations can be performed. Chorionic villous samples, amniocyte DNA prepared directly from fetal cells, or cultured and expanded cell lines can be analyzed (Durandy et al., 1985).

Newborn Screening for Immunodeficiencies

In addition to prenatal testing, newborn blood screening (NBS), traditionally used to screen for genetically inherited metabolic disorders, is now used to screen for inherited immunodeficiencies. In May 2010, SCID screening was added to the recommended uniform newborn screening panel by the Secretary of the US Department of Health and Human Services (Routes et al., 2009). Population-based newborn screening for SCID and related disorders has been instituted in all 50 states. The TREC test has clinical validity, and TRECs are an excellent biomarker of poor T-lymphocyte production in the thymus or increased lymphocyte loss resulting in T-cell lymphopenia (Chan & Puck, 2005). A variety of cases with typical SCID genotypes and other conditions have been detected in a timely manner and referred for appropriate early treatment.

Early detection of primary immunodeficiency is recognized as important for avoiding infectious complications that compromise outcomes. Routine screening of all newborns with the TREC test, implemented as part of an integrated public health program, can achieve presymptomatic diagnosis of SCID and other disorders with T-cell lymphopenia, allowing prompt and effective treatment and leading to a better understanding of the spectrum of these disorders and how to manage them. T-cell development occurs in the thymus, where T-cell antigen receptor (TCR) gene rearrangements involve cutting and splicing of the DNA encoding the alternate variable, diversity, and joining (VDJ) segments to generate a wide

TABLE 52.2
Gene Mutations and Susceptibility to Pathogens

CD40L, CD40	*Pneumocystis jiroveci, Toxoplasma, Cryptosporidium*
IL12p40, IL12Rβ, IFNγR, STAT1	Mycobacteria
IRAK4, MyD88	Encapsulated pathogens
SAP, XIAP	EBV
UNC93B, TLR-3	HSV encephalitis
Complement *C5-C9*	*Neisseria*
EVER 1,2, γc, JAK-3	HPV-epidermodysplasia verruciformis

EVER 1,2, Epidermodysplasia verruciformis 1, 2 genes; *γc,* common cytokine γ chain; *IFNγR,* receptor of the interferon γ receptor; *IL12p40,* p40 subunit of interleukin-12; *IL12Rβ,* β chain of the IL-12 receptor; *IRAK4,* interleukin-1 receptor–associated kinase 4; *JAK-3,* Janus-associated kinase; *MyD88,* Myeloid differentiation primary response protein 88; *SAP,* SLAM-associated protein; *STAT1,* signal transducer and activator of transcription 1; *TLR-3,* Toll-like receptor 3; *UNC93B,* polytopic endoplasmic reticulum CERI-resident membrane protein; *XIAP,* X-linked inhibitor of apoptosis.
Data from Fisher A: Human primary immunodeficiency diseases, *Immunity* 27:835–845, 2007.

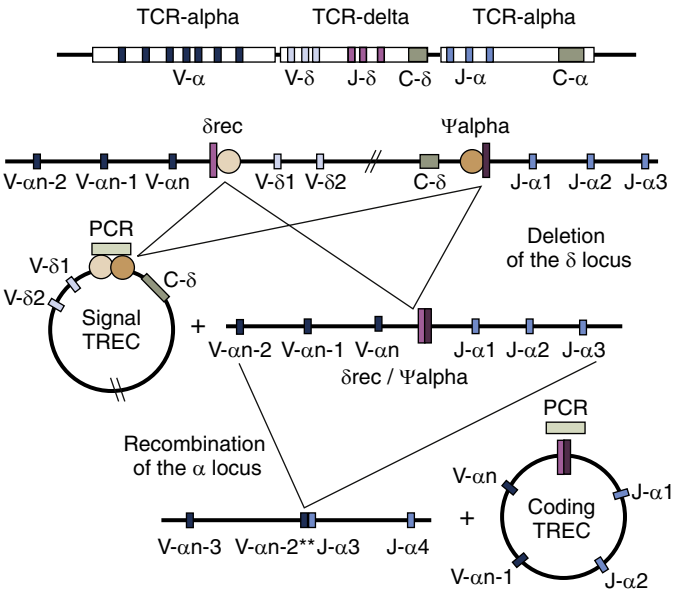

Figure 52.5 T-cell receptor excision circle (TREC) screening. PCR, polymerase chain reaction; TCR, T cell receptor.

repertoire of unique T cells with diverse specificities. Formation of TRECs from excised DNA occurs during the programmed gene rearrangements in the thymus. The excision involves delta-coding segments that are nestled in the T-cell receptor alpha (TRA) locus between the *TRAV* and *TRAJ* genes, which must be removed to allow the generation of the TRA chain. Subsequent ligation of blunt DNA signal ends yields an excised circularized segment of DNA that forms a signal joint (SJ) within the stable circular excision products (termed *TRECs*), which are formed during the process of TRA chain VJ recombination (Serana et al., 2013). The circles are stable, not replicated during mitosis, and therefore become diluted as T cells proliferate. Thus the number of TREC copies per cell population correlates with the production of naïve T cells by the thymus, and a normal TREC number is a biomarker for adequate autologous T-cell production.

TRECs are detected from the dried blood spot collected by the birthing hospital using quantitative RT-PCR (Fig. 52.5). Newborns with screening assays with strong or borderline positive results are referred to coordinating centers within each state for confirmatory follow-up evaluation. The follow-up evaluation consists of CBC with differential and flow cytometry to evaluate T cells (CD3, CD4, CD8, CD45RA, CD45RO), B cells (CD19), and NK cells (CD16, CD56). KRECs (kappa-deleting recombination excision circles) for antibody deficiency and screening for 22q11.2 deletion syndrome is being studied at this time.

NOVEL APPROACHES TO TREATING IMMUNODEFICIENCY DISORDERS

Genetic analysis of primary immunodeficiencies is important not only for diagnosis of the disorder but as a guide for therapy. Understanding the pathophysiology of each immunodeficiency disorder will aid clinicians in providing the missing component and ameliorating symptoms. For example, enzyme replacement therapy has been used in the past to treat enzyme-deficient forms of SCID, such as adenosine deaminase and purine nucleoside phosphorylase SCID; however, this requires prolonged treatment, and results are variable, including decreased thymic output, lymphopenia, and increased viral infection (Gaspar et al., 2006). Direct genetic intervention may become a more suitable treatment as increasing numbers of successful case reports describe using autologous CD34+ hematopoietic stem cells transduced with a retroviral vector containing the normal gene. In children affected with adenosine deaminase deficiency–deficient SCID and SCID-X1, direct genetic intervention is a safe and effective treatment, resulting in reinitiation of thymopoiesis, restoration of cellular immunity, and correction of the metabolic disorder, without enzyme replacement therapy (Gaspar et al., 2006; Aiuti et al., 2009). Targeted therapy based on genetic defect is being increasingly employed. Examples of targeted therapy include use of abatacept in CTLA4 deficiency and JAK inhibitor in case of STAT1 gain of function defect.

Other future strategies may include using chemicals to modify protein glycosylation to prevent protein unfolding and degradation resulting in primary immunodeficiency disorders (Vogt et al., 2007). Although these strategies have been demonstrated only in in vitro models, if the medications can be introduced at nontoxic levels with appropriate bioavailability in humans, clinical application may be practical in the future. Other medications such as gentamicin and ataluren (formerly known as PTC124) prevent premature translation termination at a premature stop codon and may be employed to treat disorders such as muscular dystrophy and cystic fibrosis, characterized by nonsense mutations resulting in absence of a critical protein causing the disorder. Although these treatments are still experimental, the hope of treating primary immunodeficiencies effectively lies in defining the genetic mutation and utilizing mutation-related strategies for treatment (Fischer, 2007).

SUMMARY

Assessment of host defenses is an extraordinarily complex process entailing the cooperation of the clinician, the research scientist, and the clinical pathologist. A logical approach, based on appreciation of the multiple systems involved in host defense and various diagnostic options, can lead to identification of the underlying disorder. The impressive success of modern therapy, incorporating new antimicrobials, recombinant DNA technology, bone marrow transplantation, and gene therapy, allows more precise delineation and characterization of the immunologic deficiency state. This in turn improves recognition and, ultimately, treatment of these patients.

SELECTED REFERENCES

Delves PJ, Roitt IM: The immune system, first of two parts, *N Engl J Med* 343:37–49, 2000.
A general overview of the immune system and the function of innate and acquired responses, as well as the role of B and T cells. This article also provides a glossary of commonly used immunologic terms that clinicians may find useful.

Fleisher TA: Evaluation of suspected immunodeficiency, *MLO Med Lab Obs* 35:10–14, 19; quiz 20–21, 2003.
An overview of the application of laboratory methods to evaluate immune defects; includes a continuing education test.

Kuijpers TW, Weening RS, Roos D: Clinical and laboratory work-up of patients with neutrophil shortage or dysfunction, *J Immunol Methods* 232:211–229, 1999.
This article provides a succinct overview of clinical signs and symptoms exhibited by patients, the physiology of the antimicrobial system of neutrophils, the mechanisms of assay to diagnose these aberrations, and potential treatments for affected patients.

Lekstrom-Himes JA, Gallin JI: Primary immunodeficiency diseases due to defects in phagocytes, *N Engl J Med* 343:1703–1714, 2000.
This review article provides an overview of immunodeficiencies due to phagocytic defects. Also features tables summarizing the syndromes with their corresponding genetic defects, as well as clinical and microscopic photographs to demonstrate the manifestations of the immunodeficiencies.

Lindegren ML, Kobrynski L, Rasmussen SA: Applying public health strategies to primary immunodeficiency diseases: a potential approach to genetic disorders, *MMWR (Morb Mortal Wkly Rep)* 53:1–29, 2004.
Summary of a workshop convened by the CDC to discuss strategies to improve clinical outcomes of patients with primary immunodeficiencies. This summary discusses incidence and birth prevalence of primary immunodeficiency, newborn screening methods, morbidity and mortality data, and information for primary immunodeficiency registries.

Access the complete reference list online at Elsevier eBooks for Practicing Clinicians.

REFERENCES

Abrahamian F, Agrawal S, Gupta S: Immunological and clinical profile of adult patients with selective immunoglobulin subclass deficiency: response to intravenous immunoglobulin therapy, *Clin Exp Immunol* 159:344–350, 2010.

Aiuti A, Cattaneo F, Galimberti S, et al.: Gene therapy for immunodeficiency due to adenosine deaminase deficiency, *N Engl J Med* 360:447–457, 2009.

Anderson DC, Springer TA: Leukocyte adhesion deficiency: an inherited defect in the MAC-1, LFA-1, and p150,95 glycoproteins, *Annu Rev Med* 38(175), 1987.

Arnaout MA, Michishita M: Genetic abnormalities in leukocyte adhesion molecule deficiency. In Gupta S, Griscelli C, editors: *New concepts in immunodeficiency diseases, Chichester*, West Sussex, 1993, John Wiley, pp 191–202.

Atkinson JC, O'Connell A, Aframian D: Oral manifestations of primary immunological diseases, *J Am Dent Assoc* 131:345–356, 2000.

Babior BM: Oxygen-dependent microbial killing by phagocytes: first of two parts, *N Engl J Med* 298:721–725, 1978.

Balmer P, North J, Baxter D, et al.: Measurement and interpretation of pneumococcal IgG levels for clinical management, *Clin Exp Immunol* 133:364–369, 2003.

Barrett DJ, Lee CG, Ammann AJ, et al.: IgG and IgM pneumococcal polysaccharide antibody responses in infants, *Pediatr Res* 18:1067–1071, 1984.

Baumgart KW, Britton WJ, Kemp A, et al.: The spectrum of primary immunodeficiency disorders in Australia, *J Allergy Clin Immunol* 100:415–423, 1997.

Biron CA, Byron KS, Sullivan JL: Severe herpes virus infections in an adolescent without natural killer cells, *N Engl J Med* 320:1731–1735, 1989.

Bjorkander J, Bake B, Oxelius VA, et al.: Impaired lung function in patients with IgA deficiency and low levels of IgG2 or IgG3, *N Engl J Med* 313:720–724, 1985.

Boyle JM, Buckley RH: Population prevalence of diagnosed primary immunodeficiency diseases in the United States, *J Clin Immunol* 27(5):497–502, 2007.

Buckley RH: Primary immunodeficiency diseases due to defects in lymphocytes, *N Engl J Med* 343:1313–1324, 2000.

Buckley RH, Becker WG: Abnormalities in the regulation of human IgE synthesis, *Immunol Rev* 41:288–314, 1978.

Carlucci F, Tabucchi A, Aiuti A, et al.: Capillary electrophoresis in diagnosis and monitoring of adenosine deaminase deficiency, *Clin Chem* 49:1830–1838, 2003.

Cates KL: Defects in neutrophil chemotaxis, *Clin Immunol Allergy* 1:603, 1981.

Cavazzana-Calvo M, Haein-Bey S, de Saint BG, et al.: Gene therapy of human severe combined immunodeficiency (SCID)-X1 disease, *Science* 288:66–72, 2000.

Chan K, Puck JM: Development of population-based newborn screening for severe combined immunodeficiency, *JACI* 115:391–398, 2005.

Conley ME: Molecular approaches to analysis of X-linked immunodeficiencies, *Annu Rev Immunol* 10:215–238, 1992.

Cooling L, et al.: ABO, H and Lewis blood groups and structurally related antigens. In Roback JD, Combs MR, Grossman BJ, editors: *Technical manual*, ed 16, Bethesda Md, 2008, American Association of Blood Banks, pp 361–385.

Cunningham-Rundles C: Common variable immunodeficiency: clinical and immunological features of 248 patients, *J Appl Biomaterials* 92:34–48, 1999.

Curtis JE, Hersh EM, Harris JE, et al.: The human primary immune response to keyhole limpet haemocyanin: interrelationships of delayed hypersensitivity, antibody response and in vitro blast transformation, *Clin Exp Immunol* 6:473–491, 1970.

D'Assante R, Fusco A, Palamaro L, et al.: Unraveling the Link between ectodermal disorders and primary immunodeficiencies, *Int Rev Immunol* 35(1):25–38, 2016, https://doi.org/10.3109/08830185.2015.1010724.

de Jong R, Altare F, Haagen IA, et al.: Severe mycobacterial and salmonella infections in interleukin-12 receptor-deficient patients, *Science* 280:1435–1438, 1998.

de la Salle H, Zimmer J, Fricker D, et al.: HLA class I deficiencies due to mutations in subunit 1 of the peptide transporter TAP-1, *J Clin Invest* 103:R9–R13, 1999.

Derry JM, Ochs HD, Francke U: Isolation of a novel gene mutated in Wiskott-Aldrich syndrome, *Cell* 78:635–644, 1994.

Donadieu J, Lamant M, Fieschi C, et al.: Natural history of GATA2 deficiency in a survey of 79 French and Belgian patients, *Haematologica* 103(8):1278–1287, 2018, https://doi.org/10.3324/haematol.2017.181909.

Donato L, de la Salle H, Hanau D, et al.: Association of HLA class I antigen deficiency related to a TAP2 gene mutation with familial bronchiectasis, *J Pediatr* 127:895–900, 1995.

Durandy A, Dumez Y, Griscelli C: Prenatal diagnosis of severe hereditary immunologic deficiencies, *Arch Fr Pediatr* 42:163–167, 1985.

Durandy A, Revy P, Fischer A: Human models of inherited immunoglobulin class switch recombination and somatic hypermutation defects (hyper-IgM syndromes), *Adv Immunol* 82:295–330, 2004.

Elder ME: ZAP-70 and defects of T cell receptor signaling, *Semin Hematol* 35:310–320, 1998.

Etzioni A, Harlan JM, Pollack S, et al.: Leukocyte adhesion deficiency (LAD). II: a new adhesion defect due to absence of sialyl Lewis X, the ligand for selectins, *Immunodeficiency* 4:307–308, 1993.

Ewen C, Kane KP, Shostak I, et al.: A novel cytotoxicity assay to evaluate antigen-specific CTL responses using a colorimetric substrate for granzyme B, *J Immunol Methods* 279:89–101, 2003.

Fischer A: Human primary immunodeficiency diseases, *Immun Rev* 27:835–845, 2007.

Fleisher RA, Oliveira JB: Functional and molecular evaluation of lymphocytes, *J Allergy Clin Immunol* 114:227–234, 2004.

Gallin JI: Recent advances in chronic granulomatous disease, *Ann Intern Med* 99:657–674, 1983.

Gallin JI, Malech HL: Update on chronic granulomatous diseases of childhood, *J Am Med Assoc* 263:1533–1537, 1990.

Ganz T, Metcalf JA, Gallin JI, et al.: Microbicidal/cytotoxic proteins of neutrophils are deficient in two disorders: Chediak-Higashi syndrome and "specific" granule deficiency, *J Clin Invest* 82:552–556, 1988.

Gaspar HB, Bjorkegren E, Parsley K, et al.: Successful reconstitution of immunity in ADA-SCID by stem cell gene therapy following cessation of PEG-ADA and use of mild preconditioning, *Mol Ther* 14:50513, 2006.

Gilmour KC, Cranston T, Loughlin S, et al.: Rapid protein-based assays for the diagnosis of T-B+ severe combined immunodeficiency, *Br J Haematol* 112:671–676, 2001.

Go E, Ballas Z: Anti-pneumococcal antibody response in normal subjects, *J Allergy Clin Immunol* 98:205–215, 1996.

Grimbacher B, Schaffer AA, Holland SM, et al.: Genetic linkage of hyper-IgE syndrome to chromosome 4, *Am J Hum Genet* 65:735–744, 1999.

Gross S, Blaiss MS, Herrod HG: Role of immunoglobulin subclasses and specific antibody determinations in the evaluation of recurrent infection in children, *J Pediatr* 121:516–522, 1992.

Hirschhorn R: Adenosine deaminase deficiency: molecular basis and recent developments, *Clin Immunol Immunopathol* 76:S219–S226, 1995.

Hong R: Disorders of the T cell system. In Stiehm ER, editor: *Immunologic disorders of infants and children*, ed 4, Philadelphia, 1996, Saunders, pp 339–408.

Hong R: The DiGeorge anomaly (CATCH 22, DiGeorge/velocardiofacial syndrome), *Semin Hematol* 35:282–290, 1998.

Hoppner M, Luhm J, Schlenke P, et al.: A flow-cytometry based cytotoxicity assay using stained effector cells in combination with native target cells, *J Immunol Methods* 267:157–163, 2002.

Illoh O: Current applications of flow cytometry in the diagnosis of primary immunodeficiency diseases, *Arch Pathol Lab Med* 128:23–31, 2004.

Immune Deficiency Foundation: *The clinical presentation of the primary immunodeficiency diseases (physician's primer)*, Towson, Md, 1992, Immune Deficiency Foundation. Available at: www.primaryimmune.org/pubs/book_phys/book_phys.htm.

Introne W, Boissy RR, Gahl WA: Clinical, molecular and cell biological aspects of Chediak-Higashi syndrome, *Mol Genet Metab* 68:283–303, 1999.

Jolliff CR, Cost KM, Stivrins PC, et al.: Reference intervals for serum IgG, IgA, IgM, C3, and C4 as determined by rate nephelometry, *Clin Chem* 28(1):126–128, 1982.

Jamieson BD, Douek DC, Killian S, et al.: Generation of functional thymocytes in the human adult, *Immunity* 10:569–575, 1999.

Jouanguy E, Doffinger R, Dupuis S, et al.: IL-12 and IFN-gamma in host defense against mycobacteria and salmonella in mice and men, *Curr Opin Immunol* 11:3416–3451, 1999.

Kelly J, Leonard WJ: Immune deficiencies due to defects in cytokine signaling, *Curr Allergy Asthma Rep* 5:396–401, 2003.

Kizaki H, Sakurada T: Simple micro-assay methods for enzymes of purine metabolism, *J Lab Clin Med* 89:1135, 1977.

Klebanoff SJ: Myeloperoxidase, *Proc Assoc Am Physicians* 111:383–389, 1999.

Klein C, Lisowska-Grospierre B, LeDeist F, et al.: Major histocompatibility complex class II deficiency: clinical manifestations, immunologic features, and outcome, *J Pediatr* 123:921–928, 1993.

Kniker WT, Lesourd BM, McBryde JL, et al.: Cell-mediated immunity assessed by multitest CMT skin testing in infants and preschool children, *Am J Dis Child* 139:840–845, 1985.

Kobrynski L: Evaluation of a clinical scoring system for the identification of patients with a possible primary immunodeficiency. In *Abstract 379. Presented at: Federation of clinical Immunology Society meeting, June 28-July 1*, 2002. San Francisco.

Koistinen J: Selective IgA deficiency in blood donors, *Vox Sang* 29(3):192–202, 1975.

Kruisbeek AM: Regulation of T cell development by the thymic microenvironment, *Semin Immunol* 11:1–70, 1999.

Lane HC, Depper JM, Greene WC, et al.: Qualitative analysis of immune function in patients with the acquired immunodeficiency syndrome: evidence for a selective defect in soluble antigen recognition, *N Engl J Med* 313:79–84, 1985.

Lanza F: Clinical manifestation of myeloperoxidase deficiency, *J Mol Med* 76:676–681, 1998.

Lefranc M-P, Lefranc G, Rabbitts TH: Inherited deletion of immunoglobulin heavy chain constant region genes in normal human individuals, *Nature* 300:760, 1982.

Lehrer RI, Cline MJ: Leukocyte myeloperoxidase deficiency and disseminated candidiasis: the role of myeloperoxidase in resistance to infection, *J Clin Invest* 48:1478, 1969.

Levy J, Espanol-Boren T, Thomas C: Clinical spectrum of X-linked hyper IgM syndrome, *J Pediatr* 131:47–54, 1997.

Lilic D, Gravenor I: Immunology of chronic mucocutaneous candidiasis, *J Clin Pathol* 54:81–83, 2001.

Louis AG, Gupta S: Primary selective IgM deficiency: an ignored immunodeficiency, *Clin Rev Allergy Immunol* 46:104–111, 2014.

Lukela M, DeGuzman D, Weinberger S, et al.: Unfashionably late, *N Engl J Med* 352:64–69, 2005.

Magen E, Schlesinger M, David M, et al.: Selective IgE deficiency, immune dysregulation, and autoimmunity, *Allergy Asthma Proc* 35:e27–e33, 2014.

Mahdi Z, Bluth MH: T regulatory cells and their role in gastrointestinal autoimmune disease, *Clin Lab Sci* 28(1):56, 2015.

Malek T, Porter B, He Y: Multiple γc-dependent cytokines regulate T cell development, *Immunol Today* 20:71–76, 1999.

Martin E, Bhakdi S: Flowcytometric assay for quantifying opsonophagocytosis and killing of Staphylococcus aureus by peripheral blood leukocytes, *J Clin Microbiol* 30:2246–2255, 1992.

Matamoros Flori N, Mila Llambi J, Espanol Boren T, et al.: Primary immunodeficiency syndrome in Spain: first report of the national registry in children and adults, *Clin Immunol* 20:477–485, 2000.

Meischl C, Roos D: The molecular basis of chronic granulomatous disease, *Springer Semin Immunopathol* 19:417–434, 1998.

Migone N, Oliviero S, De Lange G, et al.: Multiple gene deletions within the human immunoglobulin heavy-chain cluster, *Proc Natl Acad Sci U S A* 81:5811, 1984.

Mire-Sluis AR, Thorpe R, editors: *Cytokines*, San Diego, 1998, Academic Press.

Myers LA, Hershfield MS, Neale WT, et al.: Purine nucleoside phosphorylase deficiency (PNP-def) presenting with lymphopenia and developmental delay: successful correction with umbilical cord blood transplantation, *J Pediatr* 145:710–712, 2004.

Nauseef WM: Insights into myeloperoxidase biosynthesis from its inherited deficiency, *J Mol Med* 76:661–668, 1998.

Navabi B, Upton JE: Primary immunodeficiencies associated with eosinophilia, *Allergy Asthma Clin Immunol* 12:27, 2016, https://doi.org/10.1186/s13223-016-0130-4.

Nekrep N, Fontes JD, Geyer M, et al.: When the lymphocyte loses its clothes, *Immunity* 18:453–457, 2003.

Nelson RD, Quie PG, Simmons RL: Chemotaxis under agarose: a new and simple method for measuring chemotaxis and spontaneous migration of human polymorphonuclear leukocytes and monocytes, *J Imunol* 115:1650, 1975.

Niemela JE, Puck JM, Fisher RE, et al.: Efficient detection of thirty-seven new IL-2RG mutations in human X-linked severe combined immunodeficiency, *Clin Immunol* 95:33–38, 2000.

Normansell DE: Human immunoglobulin subclasses, *Diagn Clin Immunol* 5:115–128, 1987.

Noroski LM, Shearer WT: Screening for primary immunodeficiencies in the clinical immunology laboratory, *Clin Immunol Immunopathol* 86:237–245, 1998.

Notarangelo LD, Giliani S, Mella P, et al.: Combined immunodeficiencies due to defects in signal transduction: defects of the gamma-JAK3 signaling pathway as a model, *Immunobiology* 202:106–119, 2000.

Ochs HD: The Wiskott-Aldrich syndrome, *Semin Hematol* 35:332–345, 1998.

Ochs HD, Davis SD, Wedgwood RJ: Immunologic responses to bacteriophage ΦX174 in immunodeficiency diseases, *J Clin Invest* 50:2559–2568, 1971.

O'Gorman MR, Corrochano V: Rapid whole-blood flow cytometry assay for diagnosis of chronic granulomatous disease, *Clin Diagn Lab Immunol* 2:227–232, 1995.

Oxelius VA: Quantitative and qualitative investigations of serum IgG subclasses in immunodeficiency diseases, *Clin Exp Immunol* 36:112–116, 1979.

Ozcan E, Norarangelo LD, Geha RS: Primary immune deficiencies with aberrant IgE production, *J Allergy Clin Immunol* 12:1054–1062, 2008.

Park BH, Fikrig SM, Smithwick EM: Infection and nitro-blue-tetrazolium reduction by neutrophils: a diagnostic aid, *Lancet* 2:532, 1968.

Pereira LF, Sapiña AM, Arroyo J, Viñuelas J, Bardají RM, Prieto L: Prevalence of selective IgA deficiency in Spain: more than we thought, *Blood* 90(2):893, 1997.

Plebani A, Ugazio AG, Monafo V, et al.: Clinical heterogeneity and reversibility of selective immunoglobulin A deficiency in 80 children, *Lancet* 12:829–831, 1986.

Popa V: Airway obstruction in adults with recurrent respiratory infections and IgG deficiency, *Chest* 105:1066–1072, 1994.

Puck JM: Primary immunodeficiency diseases, *J Am Med Assoc* 278:1835–1841, 1997a.

Puck JM: Genetic aspects of primary immunodeficiencies. In Ochs HD, Smith D, Puck JM, editors: *Primary immunodeficiency diseases: a molecular and genetic approach*, New York, 1999, Oxford University Press.

Puck JM, Deschenes SM, Porter JC, et al.: The interleukin-2 receptor γ chain maps to Xq13.1 and is mutated in X-linked severe combined immunodeficiency, *Hum Mol Genet* 2:1099, 1993.

Puck JM, Middleton L, Pepper AE: Carrier and prenatal diagnosis of X-linked severe combined immunodeficiency: mutation detection methods and utilization, *Hum Genet* 99:628–633, 1997b.

Ramesh N, Seki M, Notarangelo LD, et al.: The hyper IgM (HIM) syndrome, *Springer Semin Immunopathol* 19:383–399, 1998.

Reith W: Mach B: the bare lymphocyte syndrome and the regulation of MHC expression, *Annu Rev Immunol* 19:331–373, 2001.

Renner ED, Puck JM, Holland SM, et al.: Autosomal recessive hyperimmunoglobulin E syndrome: a distinct disease entity, *J Pediatr* 144:93–99, 2004.

Routes JM, Grossman WJ, Verpsky J, et al.: Statewide newborn screening for severe T cell lymphopenia, *J Am Med Assoc* 302:2465–2470, 2009.

Ryser O, Morrell A, Hizid WE: Primary immunodeficiencies in Switzerland: first report of the nation registry in adults and children, *J Clin Immunol* 8:479–485, 1988.

Samarghitean C, Valiaho J, Vihinen M: Online registry of genetic and clinical immunodeficiency diagnostic laboratories, IDdiagnostics, *J Clin Immunol* 24:53–61, 2004.

Sandler SG, Eckrich R, Malamut D, et al.: Hemagglutination assays for the diagnosis and prevention of anaphylactic transfusion reactions, *Blood* 84:2031–2035, 1994.

Sarkar G, Yoon HS, Sommer SS: Dideoxy fingerprinting (ddE): a rapid and efficient screen for the presence of mutations, *Genomics* 13:441–443, 1992.

Schneider PM, Wurzner R: Complement genetics: biological implications of polymorphisms and deficiencies, *Immunol Today* 20:2–5, 1999.

Schur PH: IgG subclasses—a review, *Ann Allergy* 58:89–96, 1987.

Scott MG, Schackelford PG, Briles ED, et al.: Human IgG subclasses and their relation to carbohydrate antigen immunocompetence, *Diagn Clin Immunol* 5:241–248, 1988.

Sebire NJ, Haselden S, Malone M, et al.: Isolated EBV lymphoproliferative disease in a child with Wiskott-Aldrich syndrome manifesting as cutaneous lymphomatoid granulomatosis and responsive to anti-CD20 immunotherapy, *J Clin Pathol* 56:555–557, 2003.

Serana F, Chiarini M, Zanotti C, et al.: Use of V(D)J recombination excision circles to identify T- and B-cell defects and to monitor the treatment in primary and acquired immunodeficiencies, *J Transl Med* 11:119, 2013.

Shackelford PG, Granoff DM, Madassery JV, et al.: Clinical and immunologic characteristics of healthy children with subnormal serum concentrations of IgG2, *Pediatr Res* 27(16), 1990.

Shearer WT, Paul ME, Smith CW, et al.: Laboratory assessment of immune deficiency disorders, *Immunol Allergy Clin North Am* 14:265–299, 1994.

Sheffield VC, Beck JS, Kwitek AE, et al.: The sensitivity of single stand conformation polymorphism analysis for the detection of single base substitutions, *Genomics* 16:325–332, 1993.

Shovlin CL, Simmon HA, Fairbanks LD, et al.: Adult onset immunodeficiency caused by inherited adenosine deaminase deficiency, *J Immunol* 153:2331–2339, 1994.

Smith JK, Krishnaswamy GH, Dykes R, et al.: Clinical manifestations of IgE hypogammaglobulinemia, *Ann Allergy Asthma Immunol* 78:313–318, 1997.

Smith CIE, Ochs HD, Puck JM: Genetically determined immunodeficiency diseases: a perspective. In Ochs HD, Smith CIE, Puck JM, editors: *Primary immunodeficiency diseases: a molecular and genetic approach*, New York, 1999, Oxford University Press.

Southwick FS, Dabiri GA, Stossel TP: Neutrophil actin dysfunction is a genetic disorder associated with partial impairment of neutrophil actin assembly in three family members, *J Clin Invest* 82:1525–1531, 1988.

Stiehm ER, Conley ME: Immunodeficiency disorders: general considerations. In Stiehm ER, editor: *Immunologic disorders of infants and children*, 4th ed, Philadelphia, 1996, Saunders, pp 201–252.

Stray-Pedersen A, Abrahamsen TG, Froland SS: Primary immunodeficiency diseases in Norway, *Clin Immunol* 17:333–339, 1997.

Sweinberg SK, Wodell RA, Grodofsky MP, et al.: Retrospective analysis of the incidence of pulmonary disease in hypogammaglobulinemia, *J Allergy Clin Immunol* 88:96–104, 1991.

Tangye SG, Al-Herz W, Bousfiha A, et al.: Human inborn errors of immunity: 2019 update on the classification from the International union of immunological Societies Expert Committee, *J Clin Immunol*, 2020, https://doi.org/10.1007/s10875-019-00737-x.

Trinchieri G: Biology of natural killer cells, *Adv Immunol* 47:187–376, 1989.

Vihinen M, Kwan SP, Lester T, et al.: Mutations of the human BTK gene coding for bruton tyrosine kinase in X-linked agammaglobulinemia, *Hum Mutat* 13:280–285, 1999.

Vogt G, Vogt B, Chuzhanova N, et al.: Gain-of-glycosylation mutations, *Curr Opin Genet Dev* 17:245–251, 2007.

Wakim M, Shah A, Arndt PA, et al.: Successful anti-CD20 monoclonal antibody treatment of severe autoimmune hemolytic anemia due to warm reactive IgM autoantibody in a child with common variable immunodeficiency, *Am J Hematol* 76:152–155, 2004.

Wedgwood RJ, Ochs HD, Oxelius VA: IgG subclass levels in the serum of patients with primary immunodeficiency, *Monogr Allergy* 20:80, 1986.

Winkelstein JA, Marino MC, Johnston Jr RB, et al.: Chronic granulomatous disease: report on a national registry of 368 patients, *Medicine (Baltim)* 79:155–169, 2000.

Yabe T, Kawamura S, Masako S, et al.: A subject with a novel type I bare lymphocyte syndrome has tapasin deficiency due to deletion of 4 exons by Alu-mediated recombination, *Blood* 100:1496–1498, 2002.

Yazdani R, Azizi G, Abolhassani H, et al.: Selective IgA deficiency: Epidemiology, Pathogenesis, clinical phenotype, diagnosis, Prognosis and management, *Scand J Immunol* 85(1):3–12, 2017, https://doi.org/10.1111/sji.12499.

Zhang Q, Davis JC, Lamborn BS, et al.: Combined immunodeficiency associated with DOCK8 mutations, *N Engl J Med* 361:2046–2055, 2009.

Zhu Q, Watanabe C, Liu T, et al.: Wiskott-Alrich syndrome/X-linked thrombocytopenia: WASP gene mutations, protein expression, and phenotype, *Blood* 90:2680–2689, 1997.

CHAPTER 53

CLINICAL AND LABORATORY EVALUATION OF SYSTEMIC AUTOIMMUNE RHEUMATIC DISEASES

Carlos Alberto von Mühlen, Edward K.L. Chan, Angela Ceribelli, Marvin J. Fritzler

INTRODUCTION AND CLASSIFICATION OF SYSTEMIC AUTOIMMUNE RHEUMATIC DISEASES, 1035

SYSTEMIC LUPUS ERYTHEMATOSUS AND RELATED LUPUS–LIKE DISORDERS, 1036
What Are the Classification Criteria for Systemic Lupus Erythematosus?, 1036
What are "Lupus-Like" Syndromes and Diseases?, 1036
Autoantibody Profile in SLE, 1037
Chronic Discoid Lupus and Other Cutaneous Variants, 1038

SJÖGREN SYNDROME, 1040
Anti-SS-A/ro60 and Anti-SS-B-La Antibodies, 1040
Antimuscarinic Type 3 Receptor Autoantibodies, 1040
Anti-α-Fodrin Antibody, 1041
Antibodies to Nuclear Protein NA14, 1041

SYSTEMIC SCLEROSIS, 1041
Centromere Protein Autoantigens, 1042
Antibodies to Bicaudal D2, 1042
Antibodies to Topoisomerase I (Scl-70), 1042
Antibodies to RNA Polymerases, 1042
Th/To Autoantigens, 1043
Antibodies to Nucleolar Antigen Fibrillarin (U3-snoRNP), 1044
Antibodies to PM/Scl, 1044
Antibodies Targeting the Nucleolar Organizing Region (NOR), 1044
Antibodies to U11/U12 RNA Associated Ribonucleoprotein C3 (RNPC3), 1044
Antieukaryotic Initiation Factor-2B, 1044

RHEUMATOID ARTHRITIS, 1044
Rheumatoid Factor (RF), 1044
Antikeratin Antibody, 1045
Anticitrullinated Peptides (CCP), 1045
Anticarbamylated Protein Antibodies, 1046
Peptidylarginine Deiminase (PAD) Antibodies, 1046
Glycosylated Antibodies, 1046

IDIOPATHIC INFLAMMATORY MYOPATHIES, 1046
Aminoacyl-tRNA Synthetases, 1046
Mi-2/NuRD Complex, 1048
Signal Recognition Particle, 1048
MDA5 (CADM-140), 1048
TIF1-γ/TIF1-α (p155/140), 1048
MJ/NXP2, 1048
Small Ubiquitin-like Modifier Activating Enzyme, 1048
3-Hydroxy-3-Methylglutaryl-Coenzyme A Reductase, 1048
Cytosolic 5′-Nucleotidase 1A, 1048
Myositis-Associated Autoantibodies (MAA), 1049

CONCEPT OF OVERLAP SYNDROMES, 1049
Mixed Connective Tissue Disease (MCTD), 1049

PROFILES OF AUTOANTIBODIES IN VARIOUS SYSTEMIC RHEUMATIC DISEASES, 1049

TECHNIQUES USED TO DETECT AUTOANTIBODIES, 1049
General Considerations, 1049
Indirect Immunofluorescence on HEp2 Cells, 1050
Computer-assisted ANA TIF Technology, 1050
Enzyme-Linked Immunosorbent Assays, 1056
Immunoblotting, 1056
Dot Blots and Line Immunoassays, 1056
Multiplex Bead-Based Assays, 1056
Other Immunoassays, 1057

SELECTED REFERENCES, 1057

KEY POINTS

- Many types of autoantibodies to intracellular antigens are present in the various systemic autoimmune rheumatic diseases. Currently it is considered important not only to detect the presence and quantity of the intracellular autoantibody in the patient but also to identify its antigenic specificity.
- Past studies have shown that distinct diagnostic autoantibody profiles are observed in many of the systemic autoimmune rheumatic diseases. Some of the diseases are characterized by the presence or absence of a specific antibody or by differences in the quantitative level or titer of the autoantibody.
- Much progress has been made in improvement of the sensitivity, specificity, and quality control of the many laboratory assays used for the detection of autoantibodies to intracellular antigens.
- Indirect immunofluorescence microscopy using human cells, like HEp-2 cells, allows the sensitive detection of serum autoantibodies that react very specifically with various cellular proteins and nucleic acids. Antinuclear antibody (ANA) automation is now increasingly employed in immunology laboratories, although identifying only a limited number of patterns.
- Widely used tests for screening of intracellular autoantibodies are immunofluorescence microscopy, immunoenzyme, and multianalyte solid phase immunoassays such as LIA and ALBIA.

INTRODUCTION AND CLASSIFICATION OF SYSTEMIC AUTOIMMUNE RHEUMATIC DISEASES

Many systemic autoimmune rheumatic diseases (SARDs) are characterized by the presence of one or more autoantibodies that may be directed against components of the surface, cytoplasm, nuclear envelope, nucleus, or cell cycle–specific components of the cell. Such autoantibodies, collectively known as anticellular antibodies (previously antinuclear antibodies [ANA]) (Chan, Damoiseaux et al., 2015, 2016), are a hallmark of SARDs (Tan, 1989; von Muhlen & Tan, 1994; Satoh, Vazquez-Del Mercado et al., 2009). Many of the SARDs have a distinctive autoantibody profile with diagnostic and prognostic implications. Moreover, the biochemical and biological functions of many of the target antigens involved in deoxyribonucleic acid (DNA) replication, cell division, splicing of messenger ribonucleic acid (mRNA) precursors, RNA processing, protein quality control, and other fine biologic processes were elucidated by using sera from SARD patients (Tan, 1989; Yao et al., 2013). Classification of the various SARDs has been difficult because of a lack of firm etiologic basis for most of the diseases (Johnson et al., 2007) but recently are being reclassified based on autoantibodies and other molecular markers (Barturen et al., 2018; Fritzler, Martinez-Prat et al., 2018; Lewis et al., 2018; Acosta-Herrera et al., 2019). Our abridged classification of SARDs and related disorders is shown in Box 53.1.

BOX 53.1

Systemic Autoimmune Rheumatic Diseases and Related Disorders

1. Systemic lupus erythematosus (SLE)
   a. Drug-induced lupus erythematosus
2. Sjögren syndrome (primary and secondary)
3. Systemic sclerosis (scleroderma)
   a. Diffuse
   b. Limited/CREST syndrome
   c. Sine scleroderma
4. Rheumatoid arthritis (RA)
   a. Juvenile inflammatory arthritis
   b. Still disease (juvenile and adult)
5. Idiopathic inflammatory myopathies
   a. Dermatomyositis (adult and juvenile; amyopathic form)
   b. Antisynthetase syndrome
   c. Necrotizing myopathies
   d. Inclusion body myositis
6. Overlap syndromes
   a. Mixed connective tissue disease (MCTD)
   b. RA and SLE (lupus)
   c. SLE and scleroderma (lupoderma)
   d. Scleroderma and dermatomyositis (sclerodermatomyositis)
7. Systemic vasculitis
   a. Takayasu arteritis
   b. Giant cell arteritis and polymyalgia rheumatica
   c. Granulomatosis with polyangiitis (Wegener granulomatosis)
   d. Eosinophilic granulomatosis with polyangiitis (Churg-Strauss syndrome)
   e. Polyarteritis nodosa
8. Other syndromes
   a. Undifferentiated connective tissue disease
   b. Behçet disease
   c. Autoimmune syndrome induced by adjuvants (ASIA)[a]

CREST, Calcinosis cutis, Raynaud phenomenon, esophageal dysmotility, sclerodactyly, telangiectasias.
[a]Data from Shoenfeld & Agmon-Levin, 2011; Perricone et al., 2013; Watad et al., 2019.

SYSTEMIC LUPUS ERYTHEMATOSUS AND RELATED LUPUS–LIKE DISORDERS

Systemic lupus erythematosus (SLE) is the prototype SARD and has the following significant features (Cervera et al., 2014; Choi et al., 2016; Dorner & Furie, 2019; Ugarte-Gil et al., 2019):

1. It is a nonorgan-specific autoimmune disease in which the tissue injury is mediated primarily by immune complexes and direct cell-mediated cytotoxicity.
2. It is a multisystem disease that affects persons of all ages and both sexes, although it is most prevalent in women during childbearing years.
3. The disease demonstrates a hyperactive immune system with multiple abnormalities, displaying genetic associations with aberrant immunoregulatory signaling pathways, such as the interferon pathway and toll-like receptors (Kunz, 2013).
4. The typical patient has an average of three different circulating autoantibodies present simultaneously. The prevalence of autoantibodies varies over a wide range, and more than 180 different autoantibody specificities have been identified to date (Yaniv et al., 2015).

WHAT ARE THE CLASSIFICATION CRITERIA FOR SYSTEMIC LUPUS ERYTHEMATOSUS?

In 1971 the American College of Rheumatology (ACR; previously the American Rheumatism Association [ARA]), published preliminary criteria for the classification of systemic lupus erythematosus (SLE) (Cohen & Canoso, 1972; Canoso & Cohen, 1979). Patients were considered to have SLE if four of the criteria were met sequentially or simultaneously during any interval of observation. In 1982 the Subcommittee for SLE Criteria of the ARA published revised criteria that incorporated new immunologic knowledge and improved the disease classification of SLE (Tan et al., 1982). The 1982 revised criteria for classification of SLE included 11 categories, adding (1) abnormal titer of antinuclear antibody by immunofluorescence or an equivalent assay, and (2) antibody to native DNA and/or Sm antigen. In contrast to the 1971 criteria, the 1982 criteria removed Raynaud phenomenon and alopecia because of their lack of sensitivity and specificity.

BOX 53.2

Criteria for Classification of Systemic Lupus Erythematosus[a]

Clinical Criteria

1. Acute cutaneous disease
   - Includes malar rash, photosensitivity, and subacute cutaneous lupus
2. Chronic cutaneous disease
   - Includes discoid rash, panniculitis
3. Oral or nasal ulcers
4. Nonscarring alopecia (in the absence of other causes)
5. Synovitis involving two or more joints
6. Serositis (pleuritis or pericarditis with rub)
7. Renal disorder (persistent proteinuria, cellular casts)
8. Neurologic disorder (seizures, psychosis, peripheral/cranial neuropathy)
9. Hemolytic anemia
10. Leukopenia <4000/mm^3 OR lymphopenia <1000/mm^3 at least once
11. Thrombocytopenia <100,000/mm^3 in the absence of offending drug

Immunologic Criteria

1. ANA+ (anticellular antibodies in HEp-2 cells)
2. Anti-DNA: antibody to native DNA in abnormal titer
3. Anti-Sm: presence of antibody to Sm nuclear antigen
4. Antiphospholipid antibodies (anticardiolipin or anti-β_2 GP I antibodies IgA, IgG, or IgM; or a positive test result for lupus anticoagulant, or a false-positive test for syphilis
5. Low serum complement levels (C3, C4, or CH50)
6. Direct Coombs+ in the absence of hemolytic anemia

[a]The proposed classification is based on 11 criteria. The Systemic Lupus International Collaborating Clinics (SLICC) classification rule is as follows: Classify a patient as having SLE if he or she satisfies four of the clinical and immunologic criteria used in the SLICC classification criteria, including at least one clinical criterion and one immunologic criterion, OR if he or she has biopsy-proven nephritis compatible with SLE in the presence of ANAs or anti-dsDNA antibodies (Tan et al., 1982; Hochberg, 1997; Petri et al., 2012). ANA positivity is a mandatory criteria in the recent EULAR/ACR classification criteria (Aringer et al., 2019).

When the 1982 ARA Criteria for Classification of SLE were compared with the 1971 criteria, there was definite improvement in sensitivity and specificity. The 1982 criteria showed 83% sensitivity and 93% specificity, when evaluated with known SLE and control patients (Tan et al., 1982). In 1997, an update of the criteria was suggested, in which the LE cell test was deleted and anticardiolipin antibodies were added, changes emphasized in the "Guidelines for Referral and Management of SLE in Adults" by the ACR Ad Hoc Committee on SLE Guidelines (1999). The Systemic Lupus International Collaborating Clinics (SLICC) group validated and updated the ACR 1982 SLE criteria (Petri et al., 2012; Ighe et al., 2015; Ines et al., 2015), with resultant improved sensitivity (97% by the updated 2012 SLICC criteria vs. 83% by the 1982 ACR criteria) but lower specificity (84% by SLICC vs. 96% by ACR). The proposal includes at least one clinical and one immunologic criterion satisfied, or biopsy-proven lupus nephritis together with positive ANA or anti-DNA autoantibodies (Box 53.2). More recently, the European League Against Rheumatism (EULAR) and the American College of Rheumatology proposed a new set of SLE criteria where the ANA IFA, or its equivalent, is a mandatory inclusion requirement for SLE classification (Aringer et al., 2019). The new criteria had a sensitivity of 96.1% and specificity of 93.4% in a validation cohort of 1001 patients, representing improvement in relation to the ACR 1982/1997 and SLICC 2012 criteria.

WHAT ARE "LUPUS-LIKE" SYNDROMES AND DISEASES?

There are many diseases and syndromes that share certain clinical features with SLE but have different etiologies and pathogeneses. Diseases in this category include vasculitis, cryoglobulinemia, relapsing polychondritis, lymphoproliferative diseases, rheumatic fever, glomerulonephritis, syphilis, lupoid hepatitis, drug-induced lupus, and occult malignancy (Panush et al., 1993; Panush & Schur, 1997; Rubin, 2015). There is a very broad category of patients who demonstrate fewer than four of the 1982 ARA/ACR classification criteria for SLE (Lom-Orta et al., 1980; Lazaro et al., 1989; Schur, 1993; Rua-Figueroa et al., 2015) but are considered to have "lupus-like" illnesses. These patients have been classified as follows: (1) undifferentiated rheumatic disease; (2) nonrheumatic disease; (3) overlap syndrome; and (4) incomplete, latent, or incipient lupus. If these patients are followed, some are stable with mild symptoms—and up to 75% never fulfill a diagnostic criterion for

specific systemic rheumatic diseases (Mosca et al., 2004) and remain labeled as "undifferentiated connective tissue disease" (UCTD) (Mosca et al., 2014). A few eventually developed definite SLE, while others evolved into other SARD.

AUTOANTIBODY PROFILE IN SLE

The presence of a broad spectrum of autoantibodies is characteristic of SLE, such as antibodies to dsDNA, chromatin or nucleosomes, Sm antigen, U1nRNP, SS-A/Ro60, SS-B/La, C1q, ribosomal RNP, phospholipids and related proteins, and several other nonhistone protein or nonhistone protein-RNA complexes (Gomez-Puerta et al., 2008; Cervera, 2017; Pisetsky, 2017; Sarfaraz et al., 2018).

Anti-dsDNA, anti-Sm, anti-C1q, and antiribosomal P are generally regarded as specific for SLE, but the prevalence of these autoantibodies varies widely depending on demographic variations, cohort composition (inception vs. cross sectional), and diagnostic assays used to detect the autoantibodies. Autoantibodies to dsDNA and chromatin are detectable in up to 90% of individuals with active disease (Mummert et al., 2018), and antibodies to C1q tend to segregate with SLE patients having glomerulonephritis and active disease (Marto et al., 2005; Sinico et al., 2009) (Table 53.1).

Antibodies to Native DNA (Double-Stranded DNA [dsDNA])

Anti-dsDNA antibodies are rather specific for SLE and are observed at a frequency of 75% to 90% in SLE patients with active disease (Pisetsky, 2016; Mummert et al., 2018). Although there have been many reports of antibodies to dsDNA in diseases other than SLE, it is possible that the reactive antibodies to DNA in the other diseases were actually anti–single-stranded (ss)DNA antibodies because the dsDNA antibody tests often use dsDNA preparations contaminated with denatured or ssDNA. Antibodies to dsDNA appear to play a role in the pathogenesis of SLE. In studies of SLE patients, antibody to dsDNA is followed by the appearance of circulating DNA antigen, a sequence of events that results in the formation of immune complexes. Such DNA–anti-DNA immune complexes, mostly containing complement-activating IgG3, have a tropism for basement membranes and are deposited in the kidney glomeruli. This initiates kidney damage through inflammatory pathways that culminate with complement activation and cell lysis (van Bavel et al., 2008; Mortensen & Rekvig, 2009; Radic et al., 2011).

Earlier methods for detection of dsDNA antibodies included insensitive precipitation methods, complement fixation, and passive hemagglutination. Current methods used are indirect immunofluorescence (IFA) on *Crithidia luciliae* substrates, enzyme-linked immunosorbent assay (ELISA), and addressable laser bead immunoassays (Mummert et al., 2018). These can detect anti-dsDNA in 45% to 90% of active untreated SLE patients. Transient increases in anti-DNA antibodies were described in RA patients treated with anti-TNF therapy (Allanore et al., 2004; Bobbio-Pallavicini et al., 2004; Takase et al., 2014). Occasional clinical lupus-like cases may occur in this situation (Swale et al., 2003; Eriksson et al., 2005).

Antibodies to Sm and Nuclear Ribonucleoprotein

Precipitating antibodies to the Sm antigen are considered highly specific markers for SLE (Tan & Kunkel, 1966; von Muhlen & Tan, 1995; Wiik, 2005). Antibodies to both Sm and nuclear ribonucleoproteins (nRNP) are found in SLE patients. Lerner and Steitz (1979) used molecular biology tools to show that Sm and nRNP antigens were macromolecular particles comprised of small nuclear RNAs complexed with a family of well-defined small ribonuclear proteins (snRNP). The particle bound by anti-nRNP is composed of an RNA component designated U1 (U for uridine-rich), complexed to at least seven proteins varying in molecular mass from 12 to 68 kD (Tan, 1989), found at a frequency of 5% to 40% in active SLE (ter Borg et al., 1990).

The Sm antigens consist of several proteins, notated as B/B' (27/28 kD), D1/D2/D3 (14 kD), and E (12 kD) (Tan, 1989), which are components of the Sm core proteins organized as a seven-member ring structure. Purified anti-B/B' antibodies cross-react with the D protein and vice versa. Thus there are at least two epitopes on the B/B' protein recognized by anti-Sm sera. No unique clinical features are apparent in SLE patients with anti-Sm antibodies (Barada et al., 1981), although some authors reported that these autoantibodies are associated with renal disease or disorders of the central nervous system (Yasuma et al., 1990; Ni et al., 2009; Hirohata et al., 2014; Ishizaki et al., 2014). Patients who have antibodies to only U1nRNP have a low frequency of antibodies to dsDNA and a low frequency of clinically apparent renal disease (ter Borg et al., 1990). Anti-Sm and anti-U1nRNP antibodies were historically detected by immunodiffusion, passive hemagglutination, or counterimmunoelectrophoresis. However, the abovementioned methods do not accurately distinguish between antibodies directed against different snRNP. The reactivities with individual RNAs and polypeptides can be best demonstrated by RNA immunoprecipitation (IP) and immunoblotting techniques, respectively. Currently, the most widely used laboratory tests for the detection of anti-Sm and anti-nRNP antibodies are ELISA, dot blot or line immunoassays, and addressable laser bead immunoassays. These tests can differentiate between Sm and nRNP antibodies but do not define the specific antibody epitopes present in patients' sera.

TABLE 53.1

Antigens and Autoantibodies in Systemic Lupus Erythematosus

Antigen	Molecular Structure	Prevalence
Native DNA	Double-strand DNA	55–90%
Denatured DNA	Single-strand DNA	50–90%
Histones	H1, H2A, H2B, H3, H4	50–70%
Nucleosome (chromatin)	DNA-histones complex	50–90%
Sm	Small ribonucleoproteins 29 (B'), 28 (B), 16 (D), and 13(E) kDa, complexed with U1, U2, and U4-U6 snRNAs; spliceosome component	15–30%
Nuclear RNP (U1nRNP)	Proteins 70, 33(A), and 22 (C) kDa, complexed with U1 snRNA; spliceosome component	5–40%
SS-A/Ro	Proteins 60 and 52 kDa, complexed with Y1-Y5 RNAs	24–60%
SS-B/La	Phosphoproteins 48 kDa, complexed with nascent Y1 RNA Pol transcripts	9–35%
Ku	Proteins 86 and 66 kDa, DNA-binding proteins	1–39%
hnRNP protein A1	Nuclear protein 34 kDa	31–37%
PCNA	Protein 36 kDa; auxiliary protein of DNA polymerase	3%
Ribosomal RNP	Phosphoproteins 38, 16, and 15 kDa associated with ribosomes	10–20%
Hsp-90	Heat-shock protein 90 kDa	5–50%
Golgi complex	Golgins, giantin	~1%
HMG-17	Chromatin-associated proteins, 9 to 17 kDa	34–70%
β_2 glycoprotein I	Binds to anionic phospholipids, cardiolipin	25%

Frequencies are mostly related to patients with active disease.
Modified from Nakamura RM, Bylund DJ: Contemporary concepts for the clinical and laboratory evaluation of systemic lupus erythematosus and "lupus-like" syndromes, J Clin Lab Analysis 8:347–359, 1994; Krapf A, von Muhlen CA, Krapf F, et al.: Atlas of immunofluorescent antibodies. Urban & Schwarzenberg, Munich, 1996; Sherer Y, Gorstein A, Fritzler MJ, et al.: Autoantibody explosion in systemic lupus erythematosus: more than 100 different antibodies found in SLE patients, Semi Arthritis Rheumat 34(2):501–537, 2004.

Antibodies to SS-A/Ro and SS-B/La

SLE patients can have antibodies to SS-A/Ro60 alone or they may have both anti-SS-A/Ro60 and anti-SS-B/La. Having anti-SS-A/Ro60 alone was strongly associated with human leukocyte antigen (HLA) DR2 and with being young (<22 years of age at onset). The presence of both anti-SS-A/Ro60 and anti-SS-B/La in SLE was associated with HLA-DR3 and seen in older patients (>50 years of age at disease onset) (Hochberg et al., 1985). A study of 55 patients with SLE showed that patients with anti-SS-A/Ro60 alone had much more serious renal disease (Hochberg et al., 1985). SLE patients with only anti-SS-A/Ro60 also had a higher incidence of concomitant anti-DNA antibodies than those SLE patients with both the anti-SS-A/Ro60 and anti- SS-B/La antibodies (Chan & Tan, 1989). Anti-SS-A/Ro60 autoantibodies have been closely associated with the appearance of nephritis, vasculitis, lymphadenopathy, photosensitivity, and leukopenia in SLE patients. Anti-SS-B/La antibodies, like anti-SS-A/Ro60 antibodies, are antibodies noteworthy for their strong association with Sjögren syndrome, occurring in more than two-thirds of patients with this disorder. The SS-B/La antigen is a cellular protein bound to small cytoplasmic RNA species, forming a small RNP macromolecular complex that may function in processing of RNA polymerase III transcripts (Chan & Tan, 1989).

Attention has been drawn to the differentiation between antibodies to SSA/Ro60 and anti-Ro52/TRIM21 (Schulte-Pelkum et al., 2009). There are different clinical associations for each system, while both anti-SSA/Ro60 and anti-Ro52/TRIM21 are associated with primary Sjögren syndrome and SLE, and anti-Ro52/TRIM21 alone is also associated with scleroderma (Hudson, Pope et al., 2012; Wodkowski et al., 2015) and myositis (Koenig et al., 2007; Mahler, Miller et al., 2014). Masked reactivities in up to 20% of tested sera were reported when both antigens were present in commercial ELISAs, pointing to the fact that each autoantibody should be tested separately.

Clinical Subsets of SLE Associated With Antibodies to SS-A/Ro60

Elevated levels of anti-SS-A/Ro60 autoantibodies are related to several clinical autoimmune disorders, including (1) subacute cutaneous lupus erythematosus; (2) neonatal lupus syndrome with congenital heart block and/or cutaneous lesions; (3) homozygous C2 and C4 deficiency with SLE-like disease; (4) primary Sjögren syndrome vasculitis, rheumatoid factor positivity, and severe systemic symptoms; (5) ANA-negative SLE patients; (6) SLE with interstitial pneumonitis; and (7) serologic features of antiphospholipid syndrome (Bylund & Nakamura, 1991; Robbins et al., 2019).

Anti-Ku Antibodies

The Ku-antigen system consists of a pair of proteins called p70/p80 with DNA helicase activity (Francoeur et al., 1986; Reeves & Sthoeger, 1989; Reeves, 1992). These proteins have a high affinity for DNA and are known to be DNA-binding proteins, interacting covalently with the blunt ends of native DNA or DNA damaged by ionizing radiation (Schild-Poulter et al., 2008). Anti-Ku antibodies were reported in systemic sclerosis and myositis overlap with interstitial lung disease. A multinational cohort of 2140 scleroderma patients found isolated anti-Ku antibodies by line immunoassay in only 1.1% of individuals, with higher frequency of interstitial lung disease (Hoa et al., 2016). Mahler et al. found anti-Ku antibodies by chemiluminescence using full-length recombinant human Ku in 10% of SLE, 4% of systemic sclerosis, and 4% of autoimmune myositis patients (Mahler, Swart et al., 2016). Overlap syndromes were common in those anti-Ku positive individuals: myositis and SLE, scleroderma and SLE, or even mixed connective tissue disease.

Antibodies to Ribosomal P Proteins

The discovery of autoantibodies to ribosomal proteins (anti-Rib-P) dates back more than 50 years when antibodies to ribosomes were identified in SLE sera (Sturgill & Carpenter, 1965). Since then, anti-Rib-P antibodies have been the subject of extensive study and became known as a highly specific biomarker for the diagnosis of SLE. Some studies reported an association with neuropsychiatric SLE (NPSLE) (Bonfa et al., 1987; Mahler, Kessenbrock et al., 2006). The primary targets of anti-Rib-P autoantibodies are three ribosomal phosphoproteins of 38, 19, and 17 kDa (P0, P1, P2) (Elkon et al., 1985). Evidence from in vitro studies and murine models suggests that anti-Rib-P may have a pathogenic role in lupus nephritis and NPSLE. Despite a wealth of evidence, in comparison to other SLE autoantibodies such as anti-Sm and anti-dsDNA, anti-Rib-P has not been included in classification criteria for SLE. A significant challenge is the variability of assays used to detect anti-Rib-P, including the antigens and diagnostic platforms employed (Mahler, Kessenbrock et al., 2004). This may account for the marked discrepancies in frequencies (10–47%) and association with clinical and demographic features reported in SLE cohorts. Although a characteristic pattern by immunofluorescence on HEp-2 cells has been attributed to anti-Rip-P antibodies (www.anapatterns.org), it is not advisable to rely solely on that finding (Mahler, Ngo et al., 2008). Some sera are ANA negative so that novel solid phase commercially available assays, mostly depending on the C22 peptide, are being employed (Mahler, Agmon-Levin et al., 2012).

Proliferating Cell Nuclear Antigen Multiprotein Complex

Antibodies to proliferating cell nuclear antigen (PCNA) proteins are detected in up to 3% of patients with active SLE but show no distinctive clinical associations (Miyachi et al., 1978; Kaneda et al., 2004; Mahler, Miyachi et al., 2012). The PCNA complex has been characterized as cell-cycle related, and PCNA antibodies have been useful probes in the study of DNA replication, cell proliferation, and blast transformation. There are questions about the specificity of anti-PCNA autoantibodies for SLE (Vermeersch et al., 2009).

Antiphospholipid Antibodies in SLE

The antiphospholipid antibody syndrome is characterized by the presence of circulating antibodies to phospholipids and phospholipid-related proteins (anticardiolipin IgG/IgM, anti-β_2 glycoprotein I IgG/IgM, and lupus anticoagulant) and clinical features of arterial and venous thrombosis, thrombocytopenia, hemolytic anemia, miscarriages, central nervous system disease, and several other systemic symptoms (Gomez-Puerta & Cervera, 2014). Antiphospholipid antibodies are found in up to 60% of patients with SLE but also in other disorders such as infectious diseases (Alarcón-Segovia et al., 1989; McNeil et al., 1992). This is a very heterogeneous family of antibodies, functionally and immunochemically (McNeil et al., 1992). Cardiolipin (anionic phospholipid) has been widely used for the detection of antiphospholipid antibodies. Antibodies to anionic phospholipids may be IgG or IgM, whereas antibodies to zwitterionic phospholipids are more frequently IgM.

Antibodies to phospholipids are identified in SLE patients in three ways (Alarcón-Segovia et al., 1992; Cohen et al., 2010): (1) serologically false-positive test for syphilis by a positive Venereal Disease Research Laboratory (VDRL) test; (2) the lupus anticoagulant assay, which is a prolongation of the kaolin partial thromboplastin time (KPTT), which is not corrected by normal plasma; and (3) cardiolipin immunoassay with the use of cardiolipin and/or β_2 glycoprotein I and domain I of β_2 glycoprotein I.

Harris and colleagues (Harris et al., 1983; Pierangeli et al., 2001; Pierangeli & Harris, 2005, 2008) convened international workshops to improve the precision and accuracy of antiphospholipid antibody immunoassays. Reference sera were prepared and standard units (GPL and MPL) were defined. One GPL (MPL) unit is defined as the cardiolipin-binding activity of 1 ug/mL of an affinity-purified standard IgG (IgM) sample (Lakos et al., 2012). However, Lopez et al. (1992) suggested that an IgA-specific assay for antiphospholipid antibody is important in assessing the antiphospholipid syndrome in patients with SLE (Andreoli et al., 2013; Murthy et al., 2013; Despierres et al., 2014; Cousins et al., 2015). A higher prevalence of the IgA isotype was reported as a feature in black patients.

Newly developed assays for domain I of β_2 glycoprotein I autoantibodies increase the specificity of these assays, since it was described that the β_2 glycoprotein is a specific target autoantigen in antiphospholipid antibody syndrome (Obermoser et al., 2004). Furthermore, IgA antibodies targeting β_2 glycoprotein I, or antibodies recognizing a complex of β_2 GP I/oxLDL (oxidized low density lipoprotein), seem to be pathogenic in atherosclerotic vascular disease (Ranzolin et al., 2004; Staub et al., 2006; Matsuura & Lopez, 2008). Domain 4 of the molecule seems to be the target for proatherosclerotic anti-β_2 GP I autoantibodies, and domain 1 was suggested to be involved in the antiphospholipid syndrome as demonstrated in deletion mutants studies (Iverson et al., 2006; Andreoli et al., 2015; Chighizola et al., 2018). Additional antiphospholipids have been identified in recent years, in particular antiprothrombin and antiphosphatidylserine/prothrombin complex antibodies, both associated with increased risk of thrombosis (Sciascia et al., 2014; Chinnaraj et al., 2019).

CHRONIC DISCOID LUPUS AND OTHER CUTANEOUS VARIANTS

A comparatively benign form of lupus may present as "discoid" (i.e., coin or disc shaped) cutaneous lesions without symptoms or findings of

systemic disease. This disorder is called chronic discoid lupus erythematosus (CDLE) (Sontheimer & McCauliffe, 1990). The skin lesions of CDLE are as follows: (1) persistent localized erythema, (2) adherent scales, (3) follicular plugging, (4) telangiectasis, and (5) atrophy (Wallace et al., 1992). Subacute cutaneous lupus erythematosus (SCLE), another skin condition, consists of papulosquamous or nonscarring lesions with a major association to SS-A/Ro60 and Ro52 autoantibodies (McCauliffe et al., 1994). Also, additional variants of CDLE, such as lupus panniculitis (also called lupus profundus) and urticarial lupus, have been described (Sontheimer & McCauliffe, 1990; Al-Attia & Ahmed, 1998).

Unfortunately CDLE is a cutaneous autoimmune disorder that lacks any unifying diagnostic serologic biomarker. It is a mild form of lupus erythematosus that uncommonly progresses to SLE. Otherwise there is considerable overlap between CDLE and SLE, since up to 15% of patients with SLE have cutaneous discoid lesions. About 6% to 12% of patients with SLE had discoid lupus for a varying number of years before the onset of systemic disease (Wallace et al., 1992). Antinuclear antibodies are commonly found, with estimates of prevalence in CDLE from 6% to 50%. The sex ratio of discoid lupus (two females/one male) is much less biased toward females than the systemic form. Figure 53.1 depicts some clinical aspects of cutaneous disease in SLE.

Drug-Induced Lupus Erythematosus and Antihistone Antibodies

Characteristic of drug-induced lupus associated with procainamide, hydralazine, quinidine, isoniazid, and a long list of other drugs and xenobiotics is the presence of histone and/or chromatin autoantibodies (Rubin, 2015; Vaglio et al., 2018). Histones are cationic proteins containing high molar ratios of positively charged amino acids (lysine and arginine), and they are bound to nuclear DNA in eukaryotic cells. The subunit of the histone-DNA complex is called a nucleosome, which has two molecules of each of the "core" histones (H2A, H2B,H3, and H4) and one molecule of H1, along with DNA of about 200 base pairs in length (Burlingame & Rubin, 1990).

In the studies of some drug-induced lupus, the liver enzyme acetyltransferase appears to play a major function (Woosley et al., 1978). Acetyltransferase is an enzyme that acetylates some drugs such as hydralazine and procainamide, playing an important role in detoxification and excretion of the drug. Patients with low levels of acetyltranferase were more prone to develop ANA and clinical symptoms than patients who were treated with hydralazine and had phenotypically high levels of acetyltransferase. Patients with high levels of enzyme and who were rapid acetylators were not protected from the development of ANA. These patients, however, took a longer and larger cumulative dose of hydralazine before developing disease. These findings concerning acetyltransferase phenotypes have been confirmed in patients treated with procainamide (Totoritis et al., 1988). Fifty percent of all patients treated with procainamide developed ANAs after 1 year of treatment (Tan, 1989). The slow acetylators developed ANAs more rapidly than the rapid acetylators (Woosley et al., 1978). All patients on prolonged procainamide treatment developed a positive ANA response irrespective of acetylator phenotype. Some of the drugs (procainamide, hydralazine, quinidine) are no longer widely used and hence the drug-induced lupus syndrome related to these medications has become quite rare.

Drug-induced lupus is typically associated with antibodies to ssDNA, chromatin, and histones, but in SLE, by comparison, in addition to antibodies to histone and chromatin, antibodies to dsDNA, Sm, U1nRNP, and SSA/Ro60 antigens are commonly present. Procainamide was used to treat patients with cardiac arrhythmias, and most patients eventually developed antihistone antibodies, but only 10% to 20% of procainamide-treated patients developed symptomatic autoimmune disease. Patients with symptomatic disease developed a unique type of IgG antihistone antibody, which, rather than reacting with individual histones, shows specific reactivity with

Fig. 53.1 Typical cutaneous lesions in SLE. **A,** Scarring discoid lesions. **B,** Finger vasculitis. **C,** Vasculitis with ulcers. **D,** Lupus panniculitis.

BOX 53.3

Clinical Conditions Associated With Sjögren Syndrome

1. Rheumatoid arthritis
2. Systemic lupus erythematosus
3. Polydermatomyositis
4. Mixed connective tissue disease
5. Primary biliary cholangitis
6. Necrotizing systemic vasculitis
7. Autoimmune thyroiditis
8. Chronic active hepatitis
9. Mixed cryoglobulinemia
10. Hypergammaglobulinemic purpura
11. Systemic sclerosis
12. Ataxia and other nervous system diseases
13. Renal tubular acidosis

the histone H2A–H2B dimer complex. Thus the IgG anti–(H2A-H2B) is a useful diagnostic marker, with high sensitivity and specificity for symptomatic disease, in contrast to the benign form of procainamide-induced autoimmunity, with IgM antibodies to the individual histone.

Antinucleosome Antibodies

Since antihistone antibodies are found in many other conditions, more specific antibodies like antinucleosome (sometimes called antichromatin) autoantibodies have largely replaced assays for antihistones. Synonyms for antinucleosome antibodies are antichromatin, antideoxyribonucleoprotein (DNP), and anti-(H2A-H2B-DNA). Antinucleosome antibodies are found in up to 75% of all patients with SLE, in up to 100% of drug-induced lupus patients, and in 20% to 50% of patients with autoimmune hepatitis type I (lupoid hepatitis). In SLE, antinucleosome antibodies correlate better with kidney disease than anti-dsDNA (Massa et al., 1994; Burlingame & Rubin, 1996; Suer et al., 2004; Duzgun et al., 2007; Stinton et al., 2007; Su et al., 2007; Tikly et al., 2007; Gomez-Puerta et al., 2008; Muller et al., 2008; Sardeto et al., 2012; Mehra & Fritzler, 2014), although emphasis for strong association with active lupus nephritis is being pushed toward the presence of antibodies to the first component of the classical complement cascade: anti-C1q autoantibodies (Tsirogianni et al., 2009). Nevertheless, these autoantibodies have a relatively high specificity for SLE and a clear association of antinucleosome antibodies with lupus disease activity and renal disease in many publications (Su et al., 2007; Gomez-Puerta et al., 2008; Li et al., 2014).

Anti-DFS70 Antibodies

An autoantibody that seems to be protective against SARDs is represented by the dense fine speckled (DFS) nuclear pattern, which can be initially detected by indirect immunofluorescence on HEp-2 cells (Ochs et al., 1994, 2000; Chan et al., 2015; Bentow et al., 2016; Damoiseaux et al., 2019) and then confirmed by a solid phase assay based on the DFS70/LEDGF (lens epithelium-derived growth factor) protein (Singh et al., 2000). In fact, the presence of high titer anti-DFS70 antibodies without other SARD-related autoantibodies is considered useful to aid in the exclusion of ANA-associated rheumatic diseases (Dellavance et al., 2019), and this has also been demonstrated recently by a report confirming that mono-specific anti-DFS70 antibodies might be helpful to discriminate individuals with and without ANA-associated rheumatic diseases (Infantino, Pregnolato et al., 2019).

SJÖGREN SYNDROME

Sjögren syndrome (SjS) is a chronic inflammatory exocrinopathy, an autoimmune disease marked by dryness of the eyes, mouth, and other mucous membranes (Mavragani & Moutsopoulos, 2014). The disease may evolve from exocrine gland involvement to a systemic disorder, as well as to B-cell lymphoproliferative disease. It is much more frequently found in women than men, with an increasing prevalence throughout adult life. Often associated with SjS are other autoimmune diseases, such as RA, SLE, primary biliary cholangitis, and systemic sclerosis (Box 53.3). The affected salivary or lacrimal glands are infiltrated with aggregates of lymphocytes. Extraglandular manifestations include lymphadenopathy, cutaneous vasculitis, interstitial pneumonitis, and peripheral neuropathy.

The disease has been classified as (1) primary SjS, which is not associated with another autoimmune disease, with isolated sicca complex (keratoconjunctivitis sicca and xerostomia) as its hallmark feature; and (2) secondary SjS, in which SARDs or other autoimmune disorders are present. Autoantibodies in SjS are primarily directed to SS-A/Ro and SS-B/La antigens (Tan, 1989), but patients with other autoantibody specificities such as anti-Golgi complex, GW/processing body, or anti-NuMA autoantibodies have been reported (Stinton et al., 2004). The anti-SS-A/Ro and anti-SS-B/La are present in SLE but in lower prevalences than in SjS. Clinical and laboratory characteristics of the disease are seen in Fig. 53.2.

ANTI-SS-A/RO60 AND ANTI-SS-B/LA ANTIBODIES

Anti-SS-A/Ro and anti-SS-B/La are the most clinically important and best characterized autoantibodies in SjS (Chan & Andrade, 1992). The SS-A/Ro autoantigen was first identified as a specific precipitin in the Ouchterlony double-immunodiffusion assay and later shown to be the 60kDa protein (Ro60) existing as ribonucleoprotein complexes with four small hY (human cytoplasmic) RNA molecules (Clark et al., 1969; Alspaugh & Tan, 1975; Wolin & Steitz, 1984). In ANA test performed in clinical laboratories, anti-SS-B/La and anti-SS-A/Ro are often reported as showing nuclear fine speckled pattern. The cellular function for Y RNAs remains unknown but the Ro60 protein is currently postulated to play roles in small RNA regulation and the enhancement of cell survival following exposure to ultraviolet irradiation. Anti-SS-B/La antibodies were first defined by immunodiffusion in association with SS-A/Ro precipitins. SS-B/La is a distinct 48 kDa protein and associates with a variety of small RNAs derived from RNA polymerase III, including Ro hY RNAs, pre-5S RNA, pre-tRNAs, as well as many viral RNAs (Maraia & Bayfield, 2006). The SS-B/La protein has been described to have multiple functions, including as a transcription termination factor for RNA polymerase and a factor in mediating the correct ribosome translational start sites (Meerovitch et al., 1993). Anti-SS-B/La antibodies are almost invariably accompanied by anti-SS-A/Ro antibodies, reflecting the physical association of these molecules in SS-A/Ro and SS-B/La ribonucleoprotein particle complex, but anti-SS-A/Ro antibodies frequently occur in the absence of anti-SS-B/La antibodies.

Many anti-Ro60 positive sera also react with a structurally unrelated 52kDa protein (Ro52, also known as TRIM21) (Chan, 1994; Schulte-Pelkum et al., 2009; Robbins et al., 2019). There has been report of association of Ro60 and Ro52 via direct protein-protein interaction; however, the interaction may be weak or transient and was not observed by other investigators. Ro52/TRIM21 is an E3 ubiquitin ligase. Thus it is possible that Ro60 and/or SS-B/La are substrates for Ro52-mediated ubiquitinylation and somehow they are stabilized during certain disease states and the complexes contribute to the formation of autoantibodies to these components.

The reported prevalence of anti-SS-A/Ro60 and SS-B/La antibodies depends on the method and sensitivity of detection. Overall, anti-SS-A/Ro60 antibodies occur in approximately 60% to 75% of patients with primary SjS and also observed in secondary SS (Table 53.2). Anti-SS-B/La antibodies have been reported to occur in up to 50% of primary SS patients. Locht et al. (2008) reported that among 321 SjS patients, anti-SS-B/La was strongly correlated to organ involvement and cytopenias and thus could serve as a prognostic marker in primary SjS.

By comparison, anti-Ro52/TRIM21 is seen in many SARDs, especially systemic sclerosis where it was reported to be the second most common autoantibody and tended to be associated with interstitial lung disease (Hudson, Pope et al., 2012; Wodkowski et al., 2015). Anti-Ro52/TRIM21 autoantibodies are also comparatively common in autoimmune inflammatory myopathies, especially in antisynthetase syndrome (Mahler, Miller et al., 2014).

ANTIMUSCARINIC TYPE 3 RECEPTOR AUTOANTIBODIES

The defective exocrine secretion in SjS may be associated with the presence of autoantibodies to the muscarinic type 3 receptor (M3R), which were first described as anti-rat parotid gland M3R in sera of primary SjS (Bacman et al., 1996; Yamamoto et al., 1996). Other studies later have also demonstrated that the presence and functional/pathologic roles of anti-M3R autoantibodies in human sera as well as in animal models of SjS (Robinson et al., 1998; Waterman et al., 2000; Cavill et al., 2004; Cha et al., 2006; Kovacs et al., 2008). The functional role of anti-M3R could explain why patients who are free of lymphocytic infiltration in the salivary glands still develop severe dryness.

The controversies regarding anti-M3R autoantibodies lie in their prevalence and specificity. The prevalence of antibodies directed against these receptors ranged from 9% to 90%, depending on the sensitivity of assay systems developed and targeted epitopes on M3R (Gao et al., 2004; Kovacs

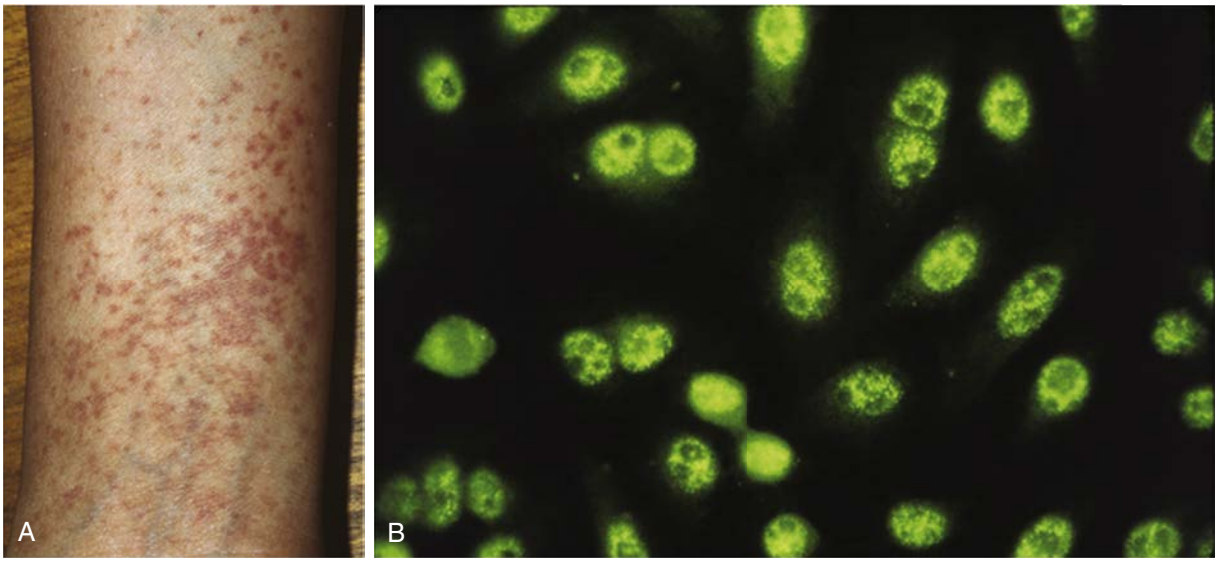

Fig. 53.2 Clinical and laboratory characteristics of Sjögren syndrome. **A,** Hypergammaglobulinemic purpura with photosensitivity (this patient with primary Sjögren syndrome had a total IgG of 12 g/dL at the time this picture was taken), **B,** Fine-speckled nuclear pattern in indirect immunofluorescence assay on HEp-2 cells, characteristic for the presence of anti-SSA/Ro autoantibodies.

TABLE 53.2
Prevalence of Autoantibodies in Primary Sjögren Syndrome (pSjS)

Autoantibodies	Prevalence in pSjS (%)
Anti-SS-A/Ro	60–75
Anti-SS-B/La	25–50
Anti-M3 muscarinic receptor	63
Anti-α-fodrin	40–70
Rheumatoid factor	70
NA14	11–14

Data from Dawson L, Tobin A, Smith P, et al.: Antimuscarinic antibodies in Sjogren's syndrome: where are we, and where are we going? Arthritis Rheum 52(10):2984–2995, 2005; Witte T: Antifodrin antibodies in Sjogren's syndrome: a review, Ann N Y Acad Sci 1051:235–239, 2005; Witte T, Matthias T, Bierwirth J, et al.: Antibodies against alpha-fodrin are associated with sicca syndrome in the general population, Ann N Y Acad Sci 1108:414–417, 2007; von Muhlen CA, Tan EM: Autoantibodies in the diagnosis of systemic rheumatic diseases, Sem Arthritis Rheum 24:323–358, 1995; Dorner T, Egerer K, Feist E, et al.: Rheumatoid factor revisited, Curr Opin Rheumatol 16(3):246–253, 2004; Nozawa K, Ikeda K, Satoh M, et al.: Autoantibody to NA14 is an independent marker primarily for Sjogren's syndrome, Front Biosci (Landmark Ed) 14:3733–3739, 2009; Uomori K, Nozawa K, Ikeda K, et al.: A re-evaluation of anti-NA-14 antibodies in patients with primary Sjogren's syndrome: significant role of interferon-gamma in the production of autoantibodies against NA-14, Autoimmunity 49(5):347–356, 2016.

et al., 2005; Schegg et al., 2008). ELISA (or its variants) has been the most common screening method for this antibody, and linear peptides were not suitable for detection or inhibition studies, indicating that M3R epitope(s) are discontinuous or conformational (Cavill et al., 2002). In fact, the highest prevalence originated from a study utilizing GST-fusion recombinant peptides allowing dimerization of linear peptides, thus maintaining a native tertiary structure found in vivo (Kovacs et al., 2005). More importantly, it is still questionable whether anti-M3R binding is specific to M3R, as indicated by a study where antipeptide M3R (aa208-228) antibodies strongly bind to M1R (Schegg et al., 2008). Nonetheless, full mapping of M3R epitopes, improvement of sensitivity/specificity of assays, proper and well-defined selection of disease and healthy controls, and large patient-oriented studies will allow more consistent findings and thorough information on prevalence and specificity. A current limitation is the lack of a validated commercially available assay for this antibody.

ANTI-α-FODRIN ANTIBODY

α-Fodrin is expressed ubiquitously in nonerythroid tissues and is not uniformly distributed along the cell membrane (Winkelmann & Forget, 1993). α-Fodrin is known to associate with membrane ion channels/pumps such as Na+/K+ ATPase in the salivary gland. In humans it has been reported that anti-α-fodrin antibody is predominantly detected in the sera from SjS patients, suggesting that anti-α-fodrin autoantibody is valuable for the diagnosis of SjS (Watanabe et al., 1999). The frequency of anti-α-fodrin antibodies in SjS varies between 40% and 70% (Witte et al., 2007). Although anti-α-fodrin autoantibodies originally were described as SS-specific autoantibodies, subsequent data have shown that anti-α-fodrin autoantibodies are also present in 10% to 30% of patients with active inflammatory diseases, such as RA or SLE and in 2% of healthy blood donors (Chen et al., 2007; Witte et al., 2007). Although it was concluded that anti-α-fodrin is clearly involved in the pathogenesis of murine models of SjS, there were conflicting data regarding the prevalence and significance of anti-α-fodrin in human SjS (Sordet et al., 2005; Witte, 2005). The frequency of anti-α-fodrin in SjS is lower than previously reported but there are some anti-α-fodrin positive SjS patients who are negative for anti-SS-A/Ro (Ruiz-Tiscar et al., 2005). A meta-analysis of 23 studies reported that anti-α-fodrin showed moderate accuracy for the diagnosis of SS with relative high pooled specificity (83%) but low pooled sensitivity (39%) (Hu et al., 2013). Thus the overall utility of anti-α-fodrin does not add much to the diagnosis of SjS. However, a more recent report in 2016 showed that IgA anti-α-fodrin in combination with rheumatoid factor or ANA greater than 1:320 can be a proxy immunologic test for SjS patients that are negative for anti-SS-A/Ro60 and anti-SS-B/La (Hernandez-Molina et al., 2016).

ANTIBODIES TO NUCLEAR PROTEIN NA14

NA14 was originally identified as a novel 14-kDa nuclear autoantigen recognized by an autoimmune serum from a patient with SjS (Ramos-Morales et al., 1998). More recent reports showed that NA14 protein also localized to centrosomes and play an important role in cell division and proliferation (Pfannenschmid et al., 2003; Errico et al., 2004). Autoantibodies to NA14 were determined in patients with various rheumatic diseases from cohorts in both the United States and Japan (Nozawa et al., 2009). Anti-NA14 were initially observed most frequently in primary SjS (13.6%) and not in secondary SS patients in both patient cohorts from Japan and the United States (Nozawa et al., 2009). A few anti-NA14 positive sera were observed in other SARDs such as SLE, SSc, and PM/DM. However, the specificity for primary SjS was not reproduced in a followup study (Uomori et al., 2016). There was no correlation between anti-NA14 positivity with any clinical activity in this study. In another small-scale study that focused on primary vasculitides, anti-NA14 was reported in SS and RA; in RA, anti-lamin C and anti-NA14 seropositive patients were in a more advanced disease stage than seronegative patients with more frequent extraarticular manifestations (Kubuschok et al., 2016). Future studies will be needed to determine the true specificity of anti-NA14 to SjS and any clinical relevance.

SYSTEMIC SCLEROSIS

Systemic sclerosis (SSc) is a multisystem connective tissue disorder of unknown etiology in which vascular lesions and tissue fibrosis are

prominent features (Denton & Khanna, 2017; Johnson, 2017; Johnson et al., 2018). SSc patients produce autoantibodies directed against nuclear, nucleolar, and mitochondrial and other cytoplasmic antigens (Calise et al., 2018; Ceribelli et al., 2018), which can be predictive (i.e., antedate full features of the disease) as well as diagnostic and prognostic significance (Harris & Rosen, 2003; Mehra et al., 2013). Typically, scleroderma sera have a relatively restricted heterogeneity and limited overlap of autoantibody specificities (Table 53.3).

As captured in the revised classification criteria of SSc (van den Hoogen et al., 2013), SSc can be phenotypically classified into two broad clinical categories: diffuse cutaneous SSc (dcSSc) and limited cutaneous SSc (lcSSc) (Denton & Khanna, 2017). Patients with dcSSc can have rapidly progressive disease affecting the distal and proximal extremities and the trunk and are at greater risk for early visceral involvement. Included in the lcSSc category are patients with the CREST (**C**alcinosis cutis, **R**aynaud phenomenon, **E**sophageal dysmotility, **S**clerodactyly, and **T**elangiectasia) syndrome, a subset that accounts for 20% to 30% of all scleroderma patients (Mehra et al., 2013). Patients with the lcSSc and the CREST variant have cutaneous involvement confined to the distal extremities and face, and they tend to have a better prognosis and clinical course than those with dcSSc (Fig. 53.3).

CENTROMERE PROTEIN AUTOANTIGENS

Autoantibodies to centromere protein (CENP) autoantigens were initially detected by indirect immunofluorescence microscopy using tissue culture cells as substrate where they were localized to the kinetochore region of metaphase chromosomes (Fritzler et al., 1980; Moroi et al., 1980). In immunoblotting studies, the CENP autoantigens consist of three main 19 kDa (CENP-A), 84 kDa (CENP-B), and 120 kDa (CENP-C) components. Autoantibodies to any of the individual CENPs can be found in SSc sera, but anti-CENP-B is most commonly observed (Mahler, You et al., 2011). Autoantibodies to CENPs are the most prevalent in SSc sera, seen in up to 40% of unselected SSc cohorts, although they are seen in up to 85% of the lcSSc or CREST subsets (Steen, 2005; Mahler, You et al., 2011; Mehra et al., 2013). Further, anti-CENP have been shown to predict the onset of SSc, being found in up to 25% of patients with idiopathic Raynaud phenomenon and other individual features of CREST (Rothfield, 1992). In SSc, anti-CENP have been associated with lower overall disease severity; increased chronologic and older age at disease onset; more commonly women; more likely to have lcSSc and lower skin scores; less likely to have finger ulcers, digital tuft resorption, or finger contractures; more likely to have pulmonary hypertension; but less likely to have interstitial lung disease, scleroderma renal crisis, inflammatory arthritis, or inflammatory myositis (Hudson, Mahler et al., 2012).

ANTIBODIES TO BICAUDAL D2

Autoantibodies to the dynein adapter protein bicaudal D2 (BICD2), which shares some sequence identity with CENP-A, were recently reported in 25.7% (116/451) of SSc sera (Fritzler et al., 2018). Of the BICD2 positive sera, 19.0% had single specificity anti-BICD2, and 81.0% had other autoantibodies, notably anti-CENP (83/94; 88.3%). Single specificity anti-BICD2 subjects were more likely to have an inflammatory myopathy (31.8% vs 9.6%, p=.004) and interstitial lung disease (52.4% vs. 29.0%, p=.024). Segatto et al. (2018) also showed worse prognosis and higher rates of disease progression in anti-BICD2 positive scleroderma patients, compared to anticentromere positive or to anti-topo I positive individuals.

ANTIBODIES TO TOPOISOMERASE I (SCL-70)

A second major class of autoantibodies in SSc are directed against the 100 kDa DNA topoisomerase I (topo-I) protein (Mehra et al., 2013). Topo-I was initially reported to be a 70 kDa protein referred to as Scl-70, but this was eventually determined to be a degradation product of the native topo-I (Tan, 1989). By IFA, along with other features, anti-topo-I autoantibodies typically localize in punctate foci in the nucleoplasm and nucleolus of HEp-2 cells (Andrade et al., 2018). In double immunodiffusion studies, autoantibodies to topo-I were detected in 20% of unselected SSc patients (Bernstein et al., 1982) and in 75% of patients with dcSSc (Jarzabek-Chorzelska et al., 1986). More recent studies using solid phase immunoassays have shown that the specificity of anti-topo-I antibodies for SSc is greater than 90% and the frequency ranges from approximately 10% to 40% in adult SSc (Mehra et al., 2013).

In general, anti-topo-I have been associated with a poorer prognosis, increased mortality, pulmonary fibrosis (PF), musculoskeletal and cardiac involvement (Mehra et al., 2013). Analysis of clinical progression in SSc patients with digital ulcers showed that anti-topo-I patients developed Raynaud phenomenon earlier, were younger at the onset of the first digital ulcer, and had double the rate of lung fibrosis as compared with anti-CENP patients (Denton et al., 2012). The clinical utility of serial anti-topo-I measurements is controversial, although they may have value as a biomarker of disease activity, an indicator of the presence of flexion contractures and of renal vascular damage as measured by Doppler ultrasonography, as reviewed in Mehra et al. (2013).

ANTIBODIES TO RNA POLYMERASES

Three RNA polymerases (RNAP: RNAP-I, RNAP-II, RNAP-III) catalyze the transcription of various genes into RNA (Kuwana et al., 1993). The prevalence of anti-RNAP in SSc ranges from 5% to 30% with wide geographic variation (Mehra et al., 2013). Autoantibodies to RNAP-I and RNAP-III (anti-RNAP-I and -III) often coexist in the same SSc patient, a pattern of autoantibody expression that is specific for SSc (Mehra et al., 2013). Although early studies suggested that RNAP autoantibodies might be correlated with a speckled nucleolar pattern of IFA staining, a recent study found that antibodies to RNAP-III were not consistently associated with such an IFA pattern on commercially available HEp-2 cell substrates (Yamasaki et al., 2006). This might be explained when it is appreciated

TABLE 53.3
Autoantigens and Autoantibodies in Systemic Sclerosis

Autoantigen	Molecular Structure	Autoantibody Frequency
Scl-70/topoisomerase I	100 kD native and 70 kD degradation product; DNA topoisomerase I	75% in diffuse scleroderma; 20–59% in all patients; 13% in CREST
Centromere	Proteins 17, 80, and 140 kD, localized at inner and outer kinetochore plates	57–82% in CREST; 8% in diffuse form
RNA Pol I	RNA Pol I complex of subunit proteins, 210-211 kD	4–30% in scleroderma; 13% in diffuse form
RNA Pol II	Transcripts mRNA	4%
RNA Pol III	Transcripts 5S rRNA, tRNA	23% in scleroderma; 45% in diffuse form; 6% in CREST
Fibrillarin	Protein 34 kD, component of U3 RNP particle	6–8%; 5% in diffuse form; 10% in CREST
U1nRNP	Spliceosome complex	2–5% in all patients; 24% in PM/scleroderma overlap
PM-ScL	Complex of 11 proteins, 110-120 kD	4–11%; 24% in PM/scleroderma overlap
Ku	DNA-binding protein	1–14% in scleroderma; 26–55% in PM/scleroderma overlap
Th/To	Protein 40 kD, complexes with 7S and 8S RNAs	1–13% in scleroderma; 1–11% in diffuse form; 8–19% in CREST; up to 3% in PM/scleroderma overlap
NOR-90	Protein 90 kD, human upstream binding factor, localized in nucleolus organizer region	Rare
BICD2	Bicaudal D2 (BICD2), dynein adapter protein, shares some sequence similarity with CENP-A	~27% of SSc, associated with ILD, inflammatory myopathy, worse prognosis and higher rates of disease progression
RNPC3	U11/12 ribonucleoprotein	Associated with gastrointestinal dysfunction, ILD, and malignancy

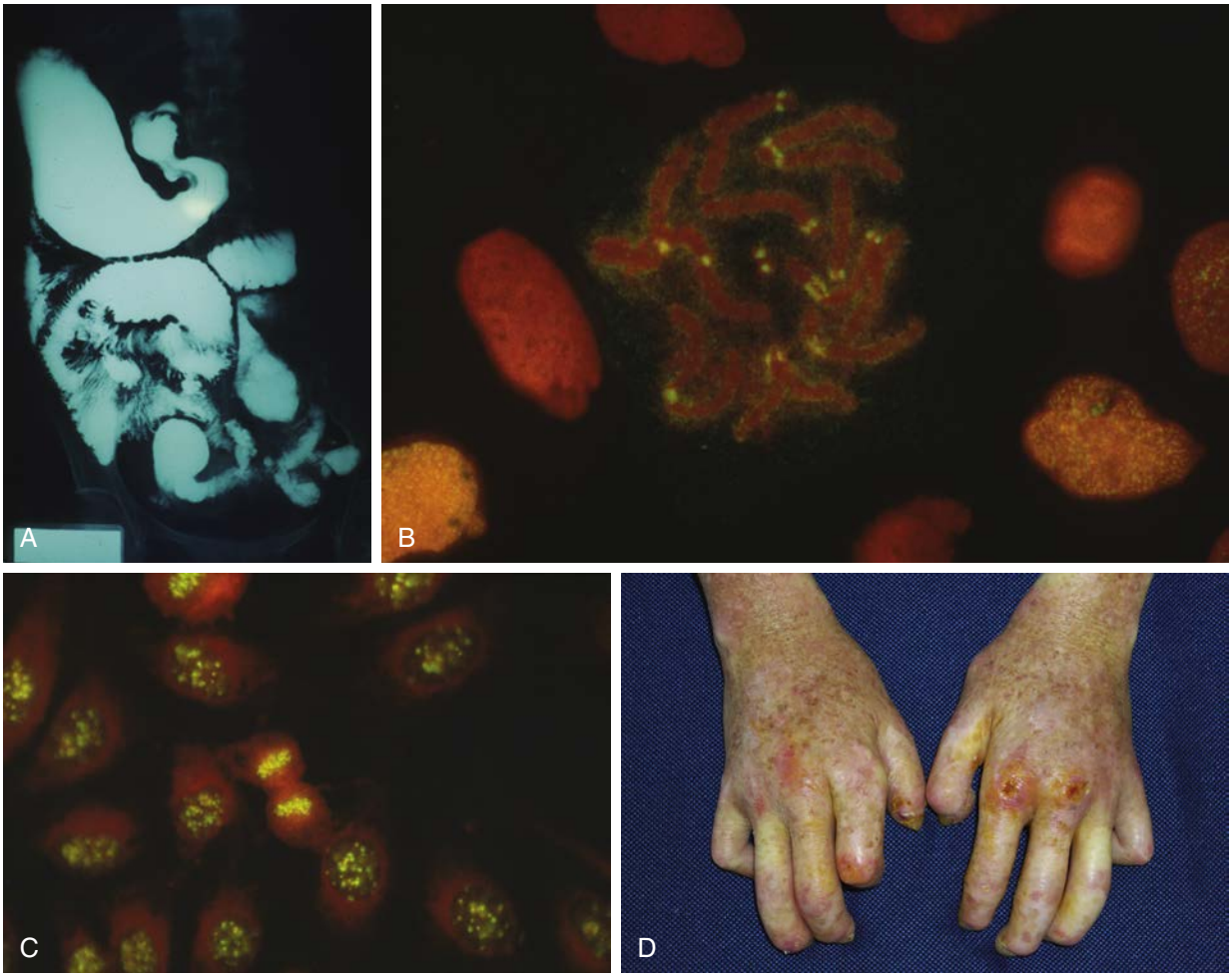

Fig. 53.3 Systemic sclerosis (scleroderma): clinical and laboratory aspects. **A,** Intestinal malabsorption radiologic study showing diffuse dilation and hypoperistaltic waves. **B,** Centromere decoration in rat Indian Muntjac preparation. **C,** Centromere pattern in indirect immunofluorescence assay on HEp-2 cells. **D,** Advanced sclerodactyly.

that anti-RNAP can overlap with a variety of other autoantibodies (Mehra et al., 2013). Thus the IFA pattern is not a sensitive marker for anti-RNAP-III, and more sensitive immunoassays such as ELISA or CIA may be more desirable.

Autoantibodies to RNAP-II in isolation are uncommon and are not entirely specific for SSc because they are also detected in SLE and overlap syndromes (Satoh et al., 1994; Parker et al., 2008). The presence of both anti-RNAP-I and -III is associated with dcSSc (Steen, 2005) and, in some SSc cohorts, a higher risk for renal crisis and the development of malignancy (Mehra et al., 2013; Moinzadeh et al., 2014). However, recent evidence indicates that SSc patients with antibodies to the large subunits of both RNA polymerases-I and -III are protected against cancer (Shah et al., 2019). Despite their reputed association with renal involvement, the survival rate in patients with anti-RNAP is better than in patients with anti-topo-I or anti-U3RNP (fibrillarin) (Steen, 2005). Other than possible renal disease, absolute levels of anti-RNAP at inception or during the disease course do not predict other organ complications or disease outcome, although there was some correlation with the severity of skin involvement (Satoh, Ishikawa et al., 2009). It has also been observed that the expression of RNAP-III is enhanced in tumors from patients with RNAP autoantibodies, suggesting that tumor antigen expression and scleroderma autoantibodies may be associated (Wenzel, 2002; Wooten, 2008; Shah et al., 2010, 2015; Honma et al., 2012).

TH/TO AUTOANTIGENS

The Th/To autoantigen is a multiprotein-RNA complex (human RNase MRP complex) consisting of a catalytic RNA and at least 10 protein components (Mahler, Fritzler et al., 2015). RNase MRP is an endoribonuclease that cleaves various RNAs, including ribosomal, messenger, and mitochondrial RNAs (Van Eenennaam et al., 2002). Almost all protein components of the RNase MRP complex have been identified as autoantibody targets in SARD sera. Rpp25 (ribonuclease P protein subunit p25), a 25 kDa protein subunit of RNase P (Mahler, Gascon et al., 2013) and hPop1 have been described as the primary Th/To autoantigens (Van Eenennaam et al., 2002; Mahler, Fritzler et al., 2015). Recent evidence indicated that autoantibodies to a novel Th/To Rpp38 epitope encompassed by amino acids 229 to 243 were detected in 8/149 (5.4%) limited cutaneous SSc patients but not in any of 159 controls (P=0.003) (Koenig et al., 2019). Although reactivity to the novel antigenic peptide was also correlated with the binding to Rpp25 (rho = 0.44; P <0.0001), subsets of patient sera either reacted strongly with Rpp25 or with the novel Rpp38-derived peptide.

Historically, anti-Th/To antibodies have been detected by IP (Ceribelli et al., 2010), although a commercial line immunoassay (LIA) (Bonroy et al., 2012, Villalta et al., 2012) and an IP real-time PCR assay have become available and were evaluated (Ceribelli, Satoh et al., 2012). A shortcoming of the LIA, which is currently based on the hPop1 autoantigen, is that a number of anti-Th/To antibodies as identified by IP were missed by LIA. While early studies focused on hPop1, it was eventually shown by ELISA, CIA, and other assays that Rpp25 was probably a more important autoantigenic component of the Th/To complex (Van Eenennaam et al., 2002; Mahler, Gascon et al., 2013; Muro et al., 2013; Koenig et al., 2019).

Although described over 20 years ago, the clinical associations of anti-Th/To antibodies are not fully established. They have a prevalence ranging from 1% to 13% in SSc sera and have been associated with lcSSc (Mahler, Fritzler et al., 2015; Nandiwada et al., 2016). In a larger cohort of SSc patients preselected by autoantibody reactivity, anti-Th/To and anti-Rpp25 antibodies were associated with interstitial lung disease and abnormal nailfold capillaroscopy (Mahler, Satoh et al., 2014). In a study of an Italian SSc cohort that used a sensitive IP assay, the prevalence of anti-Th/To was 3.7% and associated with the development of pericarditis and interstitial lung disease, although impairment of pulmonary function was mild and they did not develop pulmonary arterial hypertension (Ceribelli et al., 2010). This same study also reported that anti-Th/To antibodies were present in 57% of antinucleolar antibody-positive SSc patients and were associated with a better prognosis (Ceribelli et al., 2010). It has also been noted that autoantibodies to Rpp25 are the most common autoantibodies in SSc sera that do not have autoantibodies to other targets as

detected by commercially available immunoassays (Mahler, Satoh et al., 2014). In addition to SSc, a few reports have described anti-Th/To antibodies in a sine SSc subset with pulmonary fibrosis (Fischer et al., 2006), rheumatoid arthritis (RA), and interstitial lung disease (Mahler, Fritzler et al., 2015). Inconsistencies in the association of anti-Th/To with other clinical features is hampered by small numbers of anti-Th/To positive patients, differences in the immunoassays employed, differences in ethnicity and environment of the patients, and other recruitment biases (Mahler, Fritzler et al., 2015). Like other SSc-related autoantibodies, in patients with Raynaud phenomenon anti-Th/To antibodies are predictive of emerging SSc (Koenig et al., 2008).

In conclusion, autoantibodies to the Th/To autoantigen are most commonly reactive with Rpp25 and hPop. Although they tend to be associated with a nucleolar ANA IFA pattern on HEp-2 cells, this is not a uniform finding. However, they are important in identifying SSc patients who have been considered to be negative for other SSc-specific or SSc-associated antibodies by widely available commercial assays.

ANTIBODIES TO NUCLEOLAR ANTIGEN FIBRILLARIN (U3-SNORNP)

The fibrillarin terminology is related to the observation that by IFA on HEp-2 cells the autoantigen is localized to the dense fibrillar component of nucleoli. Fibrillarin is the 34 kDa major autoantigen of the small nucleolar anti-U3RNP (snoRNP) macromolecular complex (Smith & Steitz, 1997). While antifibrillarin antibodies are usually considered a highly specific marker for SSc, they are found in less than 10% of SSc cohorts (Mehra et al., 2013). Their detection using advanced diagnostic platforms has been challenging. Other immunoassays that utilized immunoprecipitation of radiolabeled native or recombinant proteins are available in only a few research laboratories. While many studies have indicated that antifibrillarin antibodies are independently expressed with respect to anti-CENP, anti-topo-I, and anti-RNAP (Walker & Fritzler, 2007), when a commercially available LIA was used they were often seen together with other autoantibodies (Mehra et al., 2013). Thus the detection of antifibrillarin antibodies that are based on first identifying the clumpy nucleolar IFA pattern (Reimer et al., 1988) may miss a number of sera that contain these autoantibodies.

Antifibrillarin autoantibodies were more frequently found in black patients than in white or Asian SSc patients (Walker & Fritzler, 2007; Mehra et al., 2013) and have been associated with muscle involvement, more severe disease, a poorer prognosis in black SSc subjects than in white patients (Aggarwal et al., 2009) and an increased risk of pulmonary hypertension (Tormey et al., 2001; Aggarwal et al., 2009). Black SSc patients with antifibrillarin antibodies had a younger age of disease onset and a higher frequency of digital ulcers, pericarditis, and severe lower gastrointestinal involvement (Sharif et al., 2011).

In animal models, the etiology of antifibrillarin antibodies has been linked to mercury, silver, and other heavy metal exposures (Pollard et al., 2010). A study of a small cohort of antifibrillarin positive SSc patients found that they had higher levels of urinary mercury, and in one case the affected SSc patient was a dental hygienist, where exposure to mercury may have been an occupational risk factor (Arnett et al., 2000). In addition, fibrillarin was overexpressed in scleroderma fibroblasts, suggesting an autoantigen source to initiate and maintain a B-cell response (Yang et al., 2003).

ANTIBODIES TO PM/SCL

The PM-Scl autoantigen includes up to 16 proteins of which the 75 and 100 kDa proteins have been identified as the major autoantibody targets (Brouwer et al., 2002; Mahler & Raijmakers, 2007). IFA staining with anti-PM-Scl often, but not invariably, yields a homogenous nucleolar pattern accompanied by fine speckling of the nucleoplasm (Mahler & Raijmakers, 2007). A primary target is an epitope in the PM1-α peptide (Mahler, Raijmakers et al., 2005; Mahler & Fritzler, 2009; D'Aoust et al., 2014). Anti-PM/Scl antibodies are found in 4% to 11% of SSc patients and the 75 kDa protein is the most common target (Raijmakers et al., 2004; Mahler, Raijmakers et al., 2005). Anti-PM/Scl positivity has been associated with an increased risk of pulmonary fibrosis and digital ulceration, although these antibodies may confer relative protection against pulmonary arterial hypertension and lower gastrointestinal involvement (Mahler & Raijmakers, 2007; Hanke et al., 2009). Anti-PM/Scl-75 antibodies were also reported to identify patients with dcSSc and overlap syndromes, whereas anti-PM/Scl-100 antibodies were detected mainly in patients with overlap syndromes (Hanke et al., 2009). Accordingly, anti-PM/Scl antibodies are not particularly specific for SSc: Up to 55% of anti-PM/Scl-positive patients reportedly have isolated polymyositis/dermatomyositis associated with features of SLE and/or SjS (Hanke et al., 2009).

ANTIBODIES TARGETING THE NUCLEOLAR ORGANIZING REGION (NOR)

NOR-90 antibodies recognize the RNA polymerase I transcription factor hUBF (human upstream binding factor) in the fibrillar center of the nucleolus (Chan et al., 1991). NORs are regions where the nucleolus reforms after mitosis along with clusters of ribosomal RNA genes and sites where Scl-70, U3-RNA/fibrillarin, NOR-90, and RNA polymerase I antigens can be detected (Fritzler, von Muhlen et al., 1995; von Muhlen & Tan, 1995; Dagher et al., 2002). Anti-NOR-90 show no specific clinical associations in some series (Wielosz et al., 2014), although they have been associated with lcSSc, mild internal organ involvement, and a favorable prognosis (Dagher et al., 2002). Anti-NOR-90 are not specific for SSc as they are also found in Raynaud disease, malignancies, and other SARDs such as RA, SLE, and SjS (Fujii et al., 1992; Imai et al., 1994; Fritzler, von Muhlen et al., 1995).

ANTIBODIES TO U11/U12 RNA ASSOCIATED RIBONUCLEOPROTEIN C3 (RNPC3)

Autoantibodies to RNPC3 were recently reported in a small cohort of SSc patients more likely to have severe gastrointestinal dysfunction (14% vs 3%; p=0.11) and be male (31% vs. 15%; p=0.04), black (18% vs 6%; p=0.02), have esophageal dysmotility (93% vs 62%; p <0.01), and interstitial lung disease (ILD, 77% vs 35%; p <0.01) (McMahan et al., 2018). In a more recent report, anti-RNPC3 were also shown to be associated with malignancy in 12/318 (3.8%) of SSc. These patients had a short cancer-scleroderma interval (median 0.9 year) and compared to patients with anti-CENP, patients with anti-RNPC3 (OR 4.3; 95% CI 1.10–16.9; p=0.037) and anti-POL III (OR 4.49; 95%CI 1.98–10.2; p <0.001) had a greater than fourfold increased risk of cancer within 2 years of scleroderma onset (Shah et al., 2017). Furthermore, SSc patients with anti-RNPC3 had severe restrictive lung and gastrointestinal disease, Raynaud phenomenon, and myopathy. Studies of anti-RNPC3 have yet to be validated.

ANTIEUKARYOTIC INITIATION FACTOR-2B

Anti-eIF2B antibodies were described for the first time in 2016 in a British cohort (Betteridge, Woodhead et al., 2016), then confirmed in ANA negative (cytoplasmic positive) SSc patients (Pauling et al., 2018). This specificity was detected in 1% to 7% of SSc cases, found to be correlated with diffuse cutaneous manifestations and the presence of interstitial lung disease.

RHEUMATOID ARTHRITIS

RA is a systemic autoimmune disorder characterized by chronic, symmetric, and erosive arthritis of the peripheral joints (Scott et al., 2010). A large percentage of patients have elevated titers of serum rheumatoid factors. There may be associated nonarticular manifestations such as subcutaneous nodules, vasculitis, interstitial fibrosis, and normochromic, normocytic anemia. Sjögren and Felty syndromes may occur in RA. The primary cause of the disease is unknown. RA is associated with several autoantibodies, which can serve as diagnostic and prognostic markers (Aho et al., 1994; Firestein, 2003; Pincus et al., 2014) (Fig. 53.4). These include:

1. Rheumatoid factor (RF): IgA, IgG, IgM
2. Antifillagrin antibodies (also known as anticitrullinated proteins antibodies, ACPA) (Table 53.4):
   a. Antikeratin antibodies (AKA)
   b. Antiperinuclear factor (APF), not commercially available
   c. Antibodies to citrullinated peptides (many times referred to as anti-CCP, anticyclic citrullinated peptide)
   d. Anti-Sa antibodies, targeting citrullinated vimentin (Rodriguez-Mahou et al., 2006)
3. Anticarbamylated proteins antibodies (Shi et al., 2019)
4. Anti-PAD 2/3/4

They all may possibly precede the onset of clinical RA (Klareskog et al., 2004; Bos et al., 2014; Gan et al., 2015; Verheul et al., 2018).

RHEUMATOID FACTOR (RF)

This antibody is directed against the Fc portion of the IgG molecule. Studies of monoclonal and polyclonal RF have shown polyreactive RF with binding specificity for substances other than IgG, such as nuclear

Fig. 53.4 Rheumatoid arthritis (RA). **A,** Subcutaneous nodules in elbow region, common in seropositive RA. **B,** Episcleritis in RA. **C,** Proximal interphalangeal joint synovitis of the third finger in juvenile RA. **D,** Typical hand appearance in adult RA, with intrinsic muscles atrophy and cubital deviation of fingers.

TABLE 53.4
Major Autoantibodies in Rheumatoid Arthritis

	IgM RF	Anti-CCP 1st gen. ELISA	Anti-CCP 2nd gen. ELISA	Anti-Sa	Anti-PAD2/3/4	Anticarbamylated proteins
Year (introduction)	1940	1998	2002	2006	2008	2011
Sensitivity	66–85%	68%	73%	42%	35%	45–67%
Specificity	72%	90–98%	95–98%	92–98%	96%	70–94%

APF, Antiperinuclear factor; *CCP,* cyclic citrullinated peptide; *PAD,* peptidylarginine deiminase; *RF,* rheumatoid factor. See text for references.

components. The polyreactive RF is usually of the IgM class with low affinity, ensuing from an antigen-driven process inside the joints of RA patients (van Esch et al., 2002). RF is not specific for RA and is often seen in cases of chronic infections and other systemic inflammatory conditions. In addition to the common IgM RF, both IgA RF and IgG RF have been detected (Bharadwaj et al., 1999; Dorner et al., 2004). IgA RF has been related to more severe disease with erosions (Houssien et al., 1997). The group of RFs were not proved to be involved in disease pathogenesis (Smolen & Steiner, 1998; Dorner et al., 2004; Liao et al., 2011). The classic Waaler-Rose test (Rose et al., 1948; Waaler, 2007) is not used anymore, as it does not add diagnostic value for RA. Around 15% of RA patients do not show serum autoantibodies, the so-called seronegative RA. This subset of disease may also encompass patients with severe joint and systemic symptoms (Ajeganova & Huizinga, 2015).

ANTIKERATIN ANTIBODY

The antibody reacts against the stratum corneum of rat esophagus (Young et al., 1979). AKA is a fairly specific, but not very sensitive, marker for RA. The occurrence of positive reactions in RA sera is 36% to 59% and 0% to 3% in normal healthy individuals (Aho et al., 1994). Most antikeratin positive sera are also reactive with antiperinuclear factor, suggesting that both antigens share some similarities. Actually, it was demonstrated that AKA reacts with water-soluble acidic-neutral isoforms of filaggrin in the epidermis, and molecular forms of (pro)filaggrin in the rat esophagus epithelium, instead of cytokeratin (Girbal et al., 1993; Simon et al., 1993; Sebbag et al., 2004).

ANTICITRULLINATED PEPTIDES (CCP)

Antibodies to citrullinated peptides constitute early, specific markers for RA (Sebbag et al., 2004; van Venrooij et al., 2006, 2008, 2011; Zendman et al., 2006; Silveira et al., 2007; Wiik et al., 2010). The predictive value of anti-CCP was shown when it was observed that over 50% of ACPA positive individuals will develop RA within 3 years of follow-up (Emery et al., 2017). The unusual amino acid citrulline is generated by action of the enzyme peptidyl arginine deiminase (PAD; mainly isoform 4), which generates a posttranslational modification on peptides containing arginine. It was recently shown that autoantibodies to citrullinated proteins acquire a proinflammatory Fc glycosylation phenotype before onset of RA (Rombouts et al., 2015).

A second generation ELISA is claimed to reach 98% specificity for the diagnosis of RA, with 70% sensitivity, major improvements over the RF test (Lee & Schur, 2003; Sebbag et al., 2004). Furthermore, anti-CCP antibodies can be detected in 50% of patients with early RA, at a time when RF is negative, allowing for improved diagnosis and early specific treatment, with major associations to tobacco smoking and the so-called shared epitope genetic marker (Lee et al., 2007, 2009; Hensvold et al., 2015). Many series in the literature also point to associations with erosive, more severe and progressive disease (Forslind et al., 2004; Kastbom et al., 2004; Sebbag et al., 2004; Soderlin et al., 2004; Alexiou et al., 2008), with increased relapse rates (Haschka et al., 2015) and mortality (Humphreys et al., 2014).

Anti-CCP antibodies are sometimes found in other clinical conditions, such as in viral infections (mainly hepatitis C), Lyme disease, Graves disease, SLE, and SjS (both with associated erosive articular disease) (Payet et al., 2014). Children with juvenile RA generally do not benefit from this laboratory test, as its sensitivity is only 0.2% to 3%. Positive results are seen in the polyarticular, RF positive subset, in children who commonly evolve to the erosive, adult form of RA (Low et al., 2004).

On the other hand, anti-CCP autoantibodies may better discriminate between patients with RA and patients with polyarticular manifestations associated with hepatitis C virus infection (Bombardieri et al., 2004). In 2010 the American College of Rheumatology and the European League Against Rheumatism established new classification criteria for RA (Aletaha et al., 2010), in which ACPA antibodies are an essential serologic component.

ANTICARBAMYLATED PROTEIN ANTIBODIES

Carbamylation is a nonenzymatic process induced by urea or cyanides in tobacco. A homologous citrulline structure, named homocitrulline, is formed from lysine, which could drive autoimmunity in genetically predisposed individuals (Mydel et al., 2010; Feist & Steiner, 2014). Autoantibodies to posttranslationally modified, carbamylated proteins were described in 2011 (Shi et al., 2011), with some important messages: There was no cross-reactivity with citrullinated peptides; patients with anti-CarP antibodies, but ACPA negative, had severe refractory disease; and a novel physiopathogenic process was described for RA (Shi et al., 2014). Prevalence was 16% anti-CarP IgG and 30% anti-CarP IgA positive individuals in ACPA negative patients (Shi et al., 2011). A recent large cohort did not detect association of anti-CarP antibodies with smoking (Jiang et al., 2014). There is limited evidence that anti-CarP may be a biomarker for RA activity and to predict joint damage (Yee et al., 2015). Anti-CarP fetal calf serum and anti-CarP fibrinogen antibodies may precede onset of RA (Gan et al., 2015; Shi et al., 2019). A more recent study reported that the interassay variability of the anti-CarP ELISA ranged from 7% to 11%, and the sensitivity and specificity of anti-CarP was 67% and 86%, respectively (Shi et al., 2019). When evaluated by anti-CCP status, the prevalence of anti-CarP antibodies among anti-CCP positive and negative RA sera was 42% and 16%, respectively. The prevalence of anti-CarP antibodies in comparator diseases and healthy individuals ranged from 6% to 30%.

It has been established that the presence of three biomarkers (ACPA, rheumatoid factor, and anti-carbamylated protein antibodies) are highly discriminatory in correctly identifying RA in a cohort of early arthritis (Fritzler, Martinez-Prat et al., 2018). When comparing the presence of one, two, or three autoantibodies to the patients with zero autoantibodies, the odds ratio (OR) of having the RA diagnosis significantly increases from 3.8 (95% CI 2.9–5.0) for the patients with one autoantibody, to 20.9 (95% CI 12.7–34.3) for the group with two, to 112.2 (95% CI 52.4–240.5) for individuals with three of these autoantibodies (Shi et al., 2015).

PEPTIDYLARGININE DEIMINASE (PAD) ANTIBODIES

Autoantibodies targeting PAD, calcium-dependent enzymes responsible for catalyzing the conversion of arginine to citrulline, were described in 2008 in patients with rheumatoid arthritis (Halvorsen et al., 2008; Harris et al., 2008), even preceding clinical onset (Kolfenbach et al., 2010). Anti-PAD4 antibodies may be a biomarker for more severe disease, with high specificity (96%) but low sensitivity (30–38%) (Umeda et al., 2016; Ren et al., 2017; Reyes-Castillo et al., 2018; Darrah et al., 2019; Martinez-Prat et al., 2019). Anti-PAD3 antibodies correlate with joint erosions in RA patients (Seaman et al., 2016). Anti-PAD2 antibodies seem to be associated with less severe RA disease (Darrah et al., 2018).

GLYCOSYLATED ANTIBODIES

Emerging evidence indicates that glycosylation of antibodies can also provide added value in prediction of RA (Fritzler, Martinez-Prat et al., 2018). Historically, glycosylation of antibodies has been associated with autoimmunity (Biermann et al., 2016). Several studies have demonstrated that the Fc portion of IgG shows different glycosylation patterns in patients with autoimmune diseases when compared to healthy individuals (Seeling et al., 2017), and there is growing evidence that the differences in glycosylation also reflect variations in disease activity (Fritzler, Martinez-Prat et al., 2018). Of potential importance, the ratio between G0/G1 types of glycosylation also changes during the conversion from preclinical to clinical phase. In contrast to the Fc deglycosylation, the Fab regions have increased levels of glycosylation, which alters properties of the antibody in RA compared to healthy individuals. Glycosylation occurs as part of somatic hypermutation of the complementary-determining regions and might have impact on antigen binding characteristics. Recent studies reported that the affinity of ACPA can either increase or decrease based on the glycosylation of their variable domains (Rombouts et al., 2015, 2016; van de Bovenkamp et al., 2018). In addition, the stability of the antibody can increase after Fab glycosylation, which can also lead to the formation of immune complexes. Therefore the glycome status provides valuable evidence in the prediction of RA and related SARDs.

IDIOPATHIC INFLAMMATORY MYOPATHIES

Autoantibodies have shown increasing clinical value as biomarkers in the diagnosis of polymyositis (PM), dermatomyositis (DM), necrotizing myopathies, and inclusion body myositis (IBM), collectively referred to as idiopathic inflammatory myopathies (IIM) (Mahler, Miller et al., 2014; Betteridge & McHugh, 2016; Ceribelli, De Santis et al., 2017; Lundberg et al., 2018; Palterer et al., 2018; Selva-O'Callaghan et al., 2018) (Table 53.5). While progress has been made in updating the Bohan and Peter (1975) classification criteria for IIM, wide international consensus has still to be achieved for new classification criteria (Mahler, Miller et al., 2014). DM is a major clinical subset of IIM, and both the typical DM rash and the presence of perifascicular muscle atrophy have been traditionally regarded as specific findings for this diagnosis (Troyanov et al., 2014). More recently, this classification has been challenged and a new one proposed based on vascular pathology (myovasculopathy), immune myopathy with perimysial pathology as one subset and the second associated with damage to intermediate-size vessels, capillary loss, membrane attack complex deposition on capillaries, and mitochondrial abnormalities (Troyanov et al., 2014). A third subset of DM is the paradoxic adermatopathic DM or possible DM sine dermatitis (Hoogendijk et al., 2004).

Most autoantibodies in IIM sera are directed to intracellular proteins and, based on their disease specificity, can be grouped into myositis specific (MSA) and myositis associated autoantibodies (MAA) (Ghirardello et al., 2013; Mahler, Miller et al., 2014; Satoh et al., 2017). MSA and MAA are increasingly used for the classification, diagnosis, and defining clinical subsets of IIM (Mariampillai et al., 2018). Among the MSA are autoantibodies against a group of proteins known as aminoacyl-tRNA synthetases (ARS) and others directed against signal recognition particle (SRP), 3-hydroxy-3-methylglutaryl coenzyme (HMGCR), chromodomain helicase DNA binding protein 4 (Mi-2), SAE/small ubiquitin-related modifier (SUMO-1), MJ/nuclear matrix protein 2 (NXP2), melanoma differentiation-associated gene 5 (MDA5), clinically amyopathic dermatomyositis p140 (CADM-140), transcription intermediary factor (TIF-1) gamma (p155/140), and cytosolic 5'-nucleotidase 1A (NT5c1A/Mup44) (Satoh et al., 2017).

AMINOACYL-TRNA SYNTHETASES

Autoantibodies to ARS components include those directed to Jo-1 (histidyl), PL-7 (threonyl), PL-12 (alanyl), OJ (isoleucyl), EJ (glycyl), KS (asparaginyl), Zo (phenylalanyl), and Ha (tyrosyl) (Ghirardello et al., 2013; Mahler, Miller et al., 2014). ARS catalyze the ATP-dependent binding of a single amino acid to its specific tRNA during protein translation. Anti-Jo-1 (histidyl tRNA synthetase) is the most prevalent of the ARS autoantibodies, found in 15% to 30% of patients with polymyositis (PM), in 60% to 70% of patients with interstitial lung disease (ILD), but rarely in DM (including juvenile DM) or other SARDs (Mahler & Fritzler, 2010; Ghirardello et al., 2013; Mahler, Miller et al., 2014). An association of anti-Jo-1 autoantibodies with clinical synovitis was described (Klein et al., 2014). The other ARS autoantibodies have a prevalence of less than 5% in IIM.

TABLE 53.5

Autoantigens and Autoantibodies in Idiopathic Inflammatory Myopathies

Autoantigen	Molecular Structure	Antibody Frequency
Jo-1	Histidyl tRNA synthetase protein, 52 kD	23–36% in PM; 60–70% in ILD subset
PL-7	Threonyl tRNA synthetase protein, 80 kD	4% in PM
PL-12	Alanyl tRNA synthetase protein, 110 kD	3% in PM
Zo	Phenylalanyl-tRNA synthetase	<3% in PM
YRS	Tyrosyl-tRNA synthetase	<3% in PM
KS	Asparaginyl-tRNA synthetase	<3% in PM
EJ	Glycyl-tRNA synthetase	<3% in PM
OJ	Isoleucyl-tRNA synthetase	<3% in PM
MDA5/CADM-140	IFN-induced melanoma differentiation-associated gene 5	20–30% in Asian amyopathic DM patients and ILD
Mi-2	Nuclear protein complex, proteins 53 and 61 kD	15–35% in PM; 5–9% in DM
Signal recognition particle (SRP)	54 kD protein complexed with 7 SL RNA	4–8% in PM; does not occur in DM
PM-Scl	Complex of 11 proteins,110–120 kD	8–12% in PM; 25% in PM/scleroderma overlap
U1nRNP	Spliceosome complex	4–17% in PM/DM
SAE	Small ubiquitin-like modifier activating enzyme	4% in myositis patients, 8% in DM
p155/p140 (TIF-1 α/γ)	p155-TIF-1γ (involved in nuclear transcription and cellular differentiation)	21% of myositis patients, 75% in adult DM associated with cancer
HMGCR	200/100 kDa proteins: 3-hydroxy-3-methylglutaryl-coenzyme A reductase	Statin-induced myopathy
MJ/NXP2	Nuclear matrix protein, NXP2/MORC3	25% in juvenile DM
NT5c1A/Mup44	44 kDa human muscle protein	33–80% in inclusion body myositis; specificity >90%

ILD, Interstitial lung disease.

Data from Tan EM, Chan EKL, Sullivan KF, et al.: Antinuclear antibodies (ANAs): diagnostically specific immune markers and clues toward the understanding of systemic autoimmunity, Clin Immunol Immunopathol 47:121–141, 1988; Nakamura RM, Tan EM: Update on autoantibodies to intracellular antigens in systemic rheumatic diseases, Clin Lab Med 12:1–23, 1992; von Muhlen CA, Tan EM: Autoantibodies in the diagnosis of systemic rheumatic diseases, Sem Arthritis Rheum 24:323–358, 1995; Targoff IN: Myositis specific autoantibodies, Curr Rheumatol Rep 8(3):196–203, 2006; Gunawardena H, Betteridge ZE, McHugh NJ: Newly identified autoantibodies: relationship to idiopathic inflammatory myopathy subsets and pathogenesis, Curr Opin Rheumatol 20(6):675–680, 2008; Gunawardena H, Betteridge ZE, McHugh NJ: Myositis-specific autoantibodies: their clinical and pathogenic significance in disease expression, Rheumatology (Oxford) 48(6):607–612, 2009; Larman HB, Salajegheh M, Nazareno R, et al.: Cytosolic 5′-nucleotidase 1A autoimmunity in sporadic inclusion body myositis, Ann Neurol 73(3):408–418, 2013; Mammen AL: Necrotizing myopathies: beyond statins, Curr Opin Rheumatol 26(6):679–683, 2014; Fredi M, Cavazzana I, Franceschini F: The clinico-serological spectrum of overlap myositis, Curr Opin Rheumatol 30(6):637–643, 2018; Amlani A, Choi MY, Tarnopolsky M, et al.: Anti-NT5c1A autoantibodies as biomarkers in inclusion body myositis, Front Immunol 10:745, 2019.

Because the vast majority of studies found anti-ARS autoantibodies only in patients with IIM and not in other SARDs, it was concluded that anti-ARS autoantibodies are myositis specific (Ghirardello et al., 2013; Mehra, Walker et al., 2013). Early on, it was appreciated that anti-ARS were present in the preclinical phase of the disease and predicted clinical outcomes of IIM (Miller et al., 1990). Later it became evident that anti-ARS autoantibodies characterize a distinct IIM clinical phenotype, which is referred to as the **a**nti**s**ynthetase **s**yndrome (aSS) (Mahler, Miller et al., 2014; Pinal-Fernandez et al., 2017). Hence, anti-ARS autoantibodies are the serologic hallmarks of the aSS, which is characterized by inflammatory myopathy and multiple organ involvement, particularly interstitial lung disease. aSS is often accompanied by nonerosive arthritis, Raynaud phenomenon, "mechanic's hands," skin rashes, sicca syndrome, and constitutional symptoms such as fever. Each of the anti-ARS fine specificities are reported to be associated with heterogeneous disease expression and severity (Aggarwal et al., 2014), in which lung and joint involvement is prominent early in the course of the disease. Disease progression and prognosis are predominantly affected by the extent and progression of lung involvement; myositis may only be present as a subclinical feature in a significant number of the non-Jo-1 subsets (Ghirardello et al., 2013). In idiopathic ILD, anti-ARS autoantibodies have been reported in about 7% of patients, thus contributing to the definition of "idiopathic" ILD, but the notion that such autoantibodies have predictive value for immune mediated ILD has yet to be more clearly established (Takato et al., 2013).

There are reports that patients with non-anti-Jo-1 antibodies have different and uncertain clinical outcomes (Kalluri et al., 2009; Burford et al., 2013; Cruellas et al., 2013; Aggarwal et al., 2014). Patients with anti-PL-7 and anti-PL-12 autoantibodies frequently develop ILD (Marie, Josse et al., 2012), gastrointestinal manifestations, and less frequently have myositis compared to anti-Jo-1 positive patients (Hervier et al., 2012). In distinction from inflammatory muscle disease (e.g., myositis), patients with anti-PL-12 autoantibodies have been reported to develop a noninflammatory necrotizing myopathy, and anti-PL-7 autoantibodies were associated with pericarditis (Labirua-Iturburu et al., 2012; Mehndiratta et al., 2012).

Serologically, juvenile IIM (JIIM) tends to be rather different from the adult counterpart (Rider et al., 2013). Like adult IIM, JIIM are also characterized by skeletal muscle weakness, characteristic rashes, and other systemic features. In a large multicenter study, 68% had only one myositis autoantibody and 32% had no identifiable MAA or MSA (Rider et al., 2013). Anti-p155/140 autoantibodies were the most frequent serologic subgroup, present in 32% of patients with juvenile dermatomyositis (JDM) or overlap myositis with juvenile dermatomyositis (JDM), followed by anti-MJ autoantibodies, which were seen in 20% of JIIM patients, primarily in JDM. And unlike adult IIM, other MSAs, including antisynthetase, antisignal recognition particle, and anti-Mi-2, were present in only 10% of JIIM. Hence JIIM is a rather heterogeneous group of illnesses that could be classified on the basis of distinct autoantibody phenotypes that differ from adult IIM.

It has been noted that the majority of IIM patients especially those with the aSS also have anti-Ro52/TRIM21 autoantibodies (Schulte-Pelkum et al., 2009). Patients with both ARS and Ro52/TRIM21 autoantibodies displayed a different clinical phenotype associated with severe myositis and joint impairment. Moreover, the coexistence of anti-Ro52/TRIM21 autoantibodies seems to be associated with an increased risk of cancer (Marie, Hatron et al., 2012) and interstitial lung disease (Hudson, Pope et al., 2012).

Anti-ARS autoantibodies can be identified by several methods. Initially, these autoantibodies were defined by IP in which the anti-ARS was found to co-IP both the synthetase and the isoaccepting tRNA (Targoff et al., 1993). Although many patients have cytoplasmic staining on IFA of HEp-2 cells, with the availability of newer methods for the detection of anti-ARS it is recognized that IFA alone lacks sensitivity, making IFA an unreliable screening test for anti-ARS (Hoffman et al., 2002). Although anti-Jo-1 autoantibodies can be detected by a variety of ELISA methods, addressable laser bead (ALBIA) (Fritzler & Fritzler, 2006), and a chemiluminescent immunoassay (CIA) (Bentow et al., 2013), there is little information about the comparative sensitivity, specificity, and consistency of these assays. Also, autoantibodies to other synthetases are rarely detected by these assays (Ghirardello et al., 2013; Yang et al., 2019), so protein/RNA IP remains the only assay that identifies all the anti-ARS and other MSA and MAA. Line immunoassays (LIA) (Ghirardello et al., 2009, 2010; Ronnelid et al., 2009) became a popular tool to detect many MSA and MAA. Recently, a screening ELISA (research use only) containing Jo-1, PL-7, PL-12, EJ, and KS has been developed for the detection of anti-ARS autoantibodies. Since autoantibodies to ARS are only seen in a minority of patients with IIM, which is by itself a rare condition (Bernatsky et al., 2009), the development and application of immunoassays for the detection of these autoantibodies is a challenge.

MI-2/NURD COMPLEX

Anti-Mi-2 autoantibodies are found in 10% to 30% of IIM patients and are more prevalent in DM than PM (Ghirardello et al., 2013). Variations in prevalence of anti-Mi-2 are attributed to ethnogeographic variables (i.e., it is the most common MSA in Mesoamerican IIM cohorts) (Shamim et al., 2002; Hamaguchi et al., 2011; Ikeda et al., 2011; Zampeli et al., 2019), environmental exposure to ultraviolet light (Love et al., 2009), and immunoassay variables (Ghirardello et al., 2013). In both adult and pediatric IIM, anti-Mi-2 was shown to be associated with characteristic DM cutaneous features such as Gottron sign, heliotrope rash, neck and upper back involvement (aka V and shawl rashes), and cuticular hypertrophy. Of note, these patients do not usually develop lung involvement or arthritis and, accordingly, have a good prognosis (Ghirardello et al., 2013). Anti-Mi-2 antibodies are negatively correlated with malignancy-related myositis (Chinoy et al., 2007; Muro et al., 2012) and have occasionally been reported in amyopathic DM (Ghirardello et al., 2013).

Mi-2 is represented as two closely related molecular species, one called Mi-2α and the other Mi-2β. Anti-Mi-2 autoantibodies bind to a 240 kDa component of a macromolecular enzymatic complex referred to as the Mi-2/nucleosome remodeling and deacetylase (NuRD) complex. This moiety is thought to participate in the regulation of gene expression at the chromatin level via chromatin remodeling ATPase and histone deacetylase (Ghirardello et al., 2013).

SIGNAL RECOGNITION PARTICLE

The prevalence of autoantibodies to a cytoplasmic ribonucleoprotein (RNP) called SRP ranges from 4% to 8% in IIM cohorts (Ghirardello et al., 2013). SRP is a highly conserved cytoplasmic macromolecular RNP complex, consisting of six polypeptides and 7SL RNA in a macromolecular complex. Anti-SRP antibodies selectively IP the 7SL RNA and bind to a 54 kDa protein moiety. It is widely acknowledged that anti-SRP antibodies are highly specific for IIM and thus are thought to be useful in differentiating IIM from genetic or sporadic degenerative myopathies, such as muscular dystrophies (Hengstman, van Brenk et al. 2005). Akin to the ARS described earlier, anti-SRP have been the key autoantibody marker in what is referred to as "anti-SRP syndrome". Characteristics of this syndrome include a severe, rapidly progressing and necrotizing myopathy that is relatively unresponsive to conventional therapies (Hengstman et al., 2006; Ghirardello et al., 2013; Allenbach et al., 2018). Characteristic histopathologic features consist in predominant muscle fiber necrosis and/or regeneration associated with nonspecific myopathic signs and scarce inflammatory cell infiltration (Hengstman et al., 2006; Ghirardello et al., 2013). The clinical course of anti-SRP myopathy appears clinically similar to PM, although patients who did not develop overt myositis after some years of follow-up have been reported (Ghirardello et al., 2013).

MDA5 (CADM-140)

Anti-MDA5 autoantibodies have been primarily reported in 20% to 30% of Asian (Japanese, Korean, Chinese) cohorts (Ghirardello et al., 2013). These autoantibodies were associated with a DM subset characterized by clinically amyopathic DM (CADM) accompanied by acute, rapidly progressive ILD (Sato et al., 2009; Kang et al., 2010; Nakashima et al., 2010; Cao et al., 2012; Gonzalez-Moreno et al., 2018; Sakamoto et al., 2019). In this context it has been suggested that Asian IIM patients that are anti-MDA5 positive are at higher risk of developing rapid progressive ILD than white patients (Ghirardello et al., 2013). Hence anti-MDA5 antibodies seem to be primarily associated with ILD-associated DM and may serve as a prognostic biomarker (Gono et al., 2010; Cao et al., 2012).

The target autoantigen of MDA5 autoantibodies is a cytoplasmic 140 kDa protein initially referred to as clinically amyopathic DM-140 (CADM-140). More recently the target has been more precisely identified as the IFN-induced melanoma differentiation-associated gene 5 (MDA5) (Sato et al., 2009; Nakashima et al., 2010). Curiously, in the context of a possible etiology of this serologic subset of IIM, MDA5 functions as a viral sensor by recognizing cytoplasmic viral RNA and triggers an innate immune response (Yoneyama & Fujita, 2010).

TIF1-Γ/TIF1-α (P155/140)

An autoantibody that bound a 155/140 kDa doublet protein was reported in 20% to 30% of adult and juvenile DM (Targoff et al., 2006; Kaji et al., 2007). More recently, the p155/140 target autoantigen was identified as proteins related to the human transcription intermediary factor 1 (TIF-1) family of proteins that include TIF1-α, TIF1- γ , and TIF1-β (Fujimoto et al., 2012). The main target recognized by anti-p155/140 antibodies is the 155 kDa TIF1-γ autoantigen, while the 140 kDa antigen is the TIF1-α protein (Ghirardello et al., 2013). In addition, some anti-p155/140-positive sera also recognize the TIF1-β protein.

TIF1-γ is the most commonly targeted protein of anti-p155/140 autoantibodies and the most common DM-specific autoantibodies in IIM (Hoshino et al., 2010; Riemekasten et al., 2011; Ghirardello et al., 2013). Clinically they have been associated with life-threatening complications, including malignancy in adult DM (Selva-O'Callaghan et al., 2010; Trallero-Araguas et al., 2012; Ghirardello et al., 2013; Ceribelli, Isailovic et al., 2017; Ogawa-Momohara et al., 2018; Aritomi et al., 2019). A diagnostic algorithm for the diagnosis of occult malignancy in adult DM that includes testing for anti-p155 antibodies has been proposed (Selva-O'Callaghan et al., 2010). Prospective studies and reliable, standardized immunoassays are needed to confirm the predictive value of anti-p155 as a risk factor for cancer-associated DM (Ghirardello et al., 2013; Venalis et al., 2018).

MJ/NXP2

Anti-MJ antibody was initially found in approximately 25% of juvenile DM and associated with calcinosis, severe disease, and muscle contractures (Espada et al., 2009; Gunawardena, Wedderburn et al., 2009; Fredi et al., 2017; Onuora, 2018; Zhong et al., 2019). Anti-MJ autoantibodies bind a nuclear matrix protein, NXP2/MORC3 (Takahashi et al., 2007). The association of anti-MJ autoantibodies and cancer (Ichimura et al., 2012) was not confirmed in other studies (Ceribelli, Fredi et al., 2012), but a more recent report indicated that IgG2 anti-NXP2 antibodies are distinctively associated with cancer in IIM (Aussy et al., 2019).

SMALL UBIQUITIN-LIKE MODIFIER ACTIVATING ENZYME

Autoantibodies to SAE were identified in less than 10% of adult DM patients who presented with severe skin disease and mild myopathic involvement, although over the course of the disease more profound myositis and systemic features became manifest (Betteridge et al., 2007; Tarricone et al., 2012; Fujimoto et al., 2013). The target autoantigen has been identified as the SUMO-1 activating enzyme heterodimer composed of 40 kDa SAE1 and 90 kDa SAE2 subunit. SUMO is localized to the nucleus and is structurally similar to proteins responsible for a posttranslational modification of proteins referred to as sumoylation (Ghirardello et al., 2013).

3-HYDROXY-3-METHYLGLUTARYL-COENZYME A REDUCTASE

One of the more intriguing MSA is directed to 200/100 kDa proteins identified as 3-hydroxy-3-methylglutaryl-coenzyme A reductase, an enzyme inhibited by statins and involved in cholesterol biosynthesis (Mammen et al., 2011; Ghirardello et al., 2013; Albayda & Mammen, 2014; Mohassel & Mammen, 2018). Although anti-HMGCR was initially described as a biomarker of statin-associated necrotizing myopathy (Mammen et al., 2011), subsequent studies have not confirmed a direct or causal association (Mammen, Pak et al., 2012). Nevertheless, a link to patient's statin use is still a relatively common clinical correlation (Mammen, 2014). It has been suggested that immunogenetics play a key role in the B-cell response to HMGCR (Mammen, Gaudet et al., 2012). Clinical parameters include markedly elevated creatine kinase levels, myopathic features on electromyography, and a better prognosis because of a favorable response to immunosuppressive therapy. Anti-HMGCR antibodies are considered highly specific for a necrotizing myopathy. Anti-HMGCR sera are generally negative for all other autoantibodies tested (Ghirardello et al., 2013), although one series from China showed some patients with concomitant anti-MDA5 antibodies (Huang et al., 2018). A number of commercially available immunoassays, including ELISA, CIA, and other solid-phase immunoassays, are increasingly available (Musset et al., 2014).

CYTOSOLIC 5′-NUCLEOTIDASE 1A

Sporadic inclusion body myositis (sIBM) is a subset of IIM characterized by asymmetric muscle involvement, predominantly affecting the long finger flexors, quadriceps muscles, and posterior oropharynx (Amlani et al., 2019). Previous reports have suggested diagnostic criteria for sIBM, although the highest diagnostic sensitivity and specificity requires a combination of

clinical, electrodiagnostic, and pathologic assessment (Schmidt & Dalakas, 2013). Although the precise pathogenesis of sIBM remains unclear and the disease is not responsive to conventional immunosuppression, the immune system is thought to play a significant role in its pathogenesis. A biomarker with high sensitivity and specificity for sIBM was not established until 2011, when Salajegheh et al. (2011) described a serum autoantibody detected by immunoblot of skeletal muscle lysates that targeted a ~44 kDa human **mu**scle **p**rotein (Mup44) in 52% of sIBM serum samples with 100% specificity. Subsequent studies confirmed that anti-Mup44, also known as cytosolic 5′-nucleotidase 1A (NT5c1A), was relatively sensitive (ranging from 33% to 80%) but not specific for sIBM (Amlani et al., 2019). One study indicated that anti-NT5c1A was associated with a six- to ninefold increase in the likelihood of having sIBM as compared to other IIM and proposed possible advantages of avoiding unnecessary steroid treatment and/or invasive muscle biopsies (Larman et al., 2013). In a most recent study using addressable laser bead immunoassay and purified recombinant NT5c1A, anti-NT5c1A autoantibodies had a sensitivity of 48.8% and a specificity of 91.8% for sIBM, establishing a relationship between anti-NT5c1A and higher disease severity (Amlani et al., 2019). IFA on commercial HEp-2 substrates had no utility in screening for anti-NT5c1A antibodies. Hence interpretation of a positive anti-NT5c1A result needs to be taken in the context of clinical and pathologic findings; therefore caution should be taken when applying this biomarker to patients with IIM. The value of anti-NT5c1A autoantibodies will become clearer when validated and reliable immunoassays are developed.

MYOSITIS-ASSOCIATED AUTOANTIBODIES (MAA)

MAAs are not specific for IIM and are commonly found in the setting of overlap syndromes with myositis (Koenig et al., 2007; Vancsa et al., 2010; Cruellas et al., 2013; Ghirardello et al., 2013; Iaccarino et al., 2013). The more common MAA bind to Ro60/SSA, Ro52/TRIM21, 75 and 100 kDa PM/Scl autoantigens, Ku (p70/80) nuclear heterodimer, and components of U1RNP. These autoantibodies are discussed in detail elsewhere in this chapter.

CONCEPT OF OVERLAP SYNDROMES

Overlap syndrome is a term used when patients exhibit symptoms of more than one disease (Maddison, 1991; Kallenberg, 1993; Zimmermann et al., 1998; Pope, 2002; Vancsa et al., 2010; Iaccarino et al., 2013; Fredi et al., 2018). For example, patients who meet the diagnostic criteria for SLE and have typical manifestations suggestive of a second diagnosis, such as RA, have been described (Lazaro et al., 1989). It is uncertain whether overlap syndromes may represent the coexistence of two or more different diseases or the syndrome is a distinct entity.

MIXED CONNECTIVE TISSUE DISEASE (MCTD)

The concept of MCTD was initially proposed by Sharp et al. (1972). The 20 patients described in the initial report had a combination of features usually associated with SLE, systemic sclerosis, and polymyositis. Characteristically, a high titer of autoantibody to a nuclear ribonucleoprotein (U1nRNP) was found in all the patients by hemagglutination (Sharp et al., 1972). The lack of renal and neurologic abnormalities and excellent response of these patients to small doses of oral corticosteroids initially justified the classification apart from SLE and systemic sclerosis. However, the concept of MCTD as a separate group has changed with time. Many feel that MCTD represents an overlap of systemic sclerosis, SLE, and polymyositis: A group of patients originally diagnosed as MCTD was restudied 8 years later and showed a general evolution out of the overlap pattern to one of single disease, and scleroderma was the most prevalent diagnosis (Nimelstein et al., 1980). There appears to be a large overlap that becomes apparent when the abovementioned criteria are applied to a certain population of patients, but recent studies support the existence of MCTD as an individual clinical entity (Flam et al., 2014; Tani et al., 2014).

PROFILES OF AUTOANTIBODIES IN VARIOUS SYSTEMIC RHEUMATIC DISEASES

It has been observed that distinct profiles of ANA are seen in different systemic rheumatic diseases, characteristics of which include the presence or absence of certain antibodies and differences in the mean titers of these antibodies (Nakamura & Tan, 1986; Tan et al., 1988; Bizzaro & Wiik, 2004). Nonetheless, one should be aware of the low positive predictive value of the ANA test in settings with low prevalence of systemic rheumatic diseases and in an aging population (Slater et al., 1996; Satoh, Vazquez-Del Mercado et al., 2009; Abeles & Abeles, 2013; Binder & Ellis, 2013). Some noteworthy features are summarized in Box 53.4.

BOX 53.4

Major Profiles of Autoantibodies in Systemic Autoimmune Rheumatic Diseases

Systemic lupus erythematosus (SLE). Multiple ANAs frequently seen in SLE, often with high levels of anti-dsDNA and antinucleosome antibodies in active disease, together with low complement fractions and high novel biomarker levels such as SIGLEC-1 (Rose et al., 2013). Distinctiveness of anti-Sm, -rRNP, -C1q, -nucleosomes, and -PCNA.

Drug-induced lupus. Restriction of ANAs to antihistone and/or antinucleosome antibodies.

Mixed connective tissue disease (MCTD). Restriction of ANA to U1nRNP (by disease definition).

Sjögren syndrome. Characterized primarily by the presence of antibodies to SS-A/Ro60 and SS-B/La.

Systemic sclerosis. Profile consisting of antibodies to Scl-70/topo I, the centromere/kinetochore antigens, RNA polymerases, and other nucleolar antigens such as fibrillarin and Th/To.

Rheumatoid arthritis (RA). Frequent presence of rheumatoid factor (RF) and anticitrullinated/-carbamylated proteins.

Inflammatory myopathies. Presence of antisynthetase antibodies, Mi-2, PM-Scl, and other myositis-specific autoantibodies.

Undifferentiated connective tissue diseases. Autoantibodies such as anticentromere, anti-CCP, and anti-dsDNA may antedate overt clinical disease by many years.

TECHNIQUES USED TO DETECT AUTOANTIBODIES

GENERAL CONSIDERATIONS

It is important to understand that the sensitivity, specificity, and clinical associations of autoantibody determination vary according to the diagnostic techniques or platforms being used. This variation is further compounded by demographic, geographic, environmental, and genetic factors (Fritzler, 2006; Fritzler & Fritzler, 2009). With the emergence of more sensitive immunoassays, such as ELISA, ALBIA, dot blots and line immunoassays (LIA), chemiluminescence assays (CIA), and particle-based multianalyte technology (PMAT), care must be taken to ensure that cutoffs are based on appropriate population based normal and disease controls (Fritzler, Wiik et al., 2003; Bossuyt et al., 2008). In addition, the source and physicochemical characteristics of the autoantigen (i.e., recombinant vs native, peptides vs full length) used in these newer assays must also be taken into consideration because the use of recombinant antigens and short synthetic peptides may give different results than an assay that detects reactivity to native antigens, such as those represented in indirect immunofluorescence assay (IFA), cell based assays (CBA), immunoblotting, or IP (Okazaki et al., 2006; Kessenbrock et al., 2007).

For the present time, the IFA technique using HEp-2 cells continues to be the preferred screening immunoassay to detect most clinically relevant autoantibodies in SARDs. However, it is important to appreciate that a negative IFA test does not necessarily exclude the presence of a wide spectrum of autoantibodies, including those directed against Ku, Jo-1, SS-A/Ro60, Ro52/TRIM21, SS-B/La, RNA polymerases, PM/Scl, and many of the MSAs. It is also important to understand that the IFA assay can be negative (false negative) even in the face of high titer autoantibodies to native intracellular antigens, like anti-SSA/Ro60 or some rare samples with anti-dsDNA (Mahler, Ngo et al., 2008; Fritzler, 2011). Therefore, in case of high clinical suspicion of SARD and a negative IFA test, the identification of autoantibodies should include specific and sensitive solid phase immunoassays containing an array of relevant autoantigens (Op De Beeck et al., 2012; Bizzaro et al., 2018; Perez et al., 2018; Bossuyt et al., 2019; Giacomelli et al., 2019; Infantino, Tampoia et al., 2019).

There is a common perception that immunoprecipitation is the gold standard for clinical immunoassays, but IP is available in only a few research-based laboratories. In addition, IP has other challenges because many B-cell target autoantigens in SARDs bind to one or more components of heterogeneous macromolecular complexes through a mechanism referred to as intermolecular epitope spreading (Harley & James, 1995;

Deshmukh et al., 2003). Thus any number of protein bands is typically seen in IP assays, but the identity of the actual autoantibody target may require ancillary confirmatory testing. Immunoblotting also has drawbacks because the protocols almost invariably use conditions that denature proteins, and although some protein refolding may occur when they are transferred from polyacrylamide gels to the membranes, conformational epitopes might be underrepresented while cryptic epitopes, otherwise unavailable for binding in other assays (i.e., IFA), may now be exposed and bound to the cognate autoantibody.

In summation, no immunoassay is without limitations, and evaluators of the medical literature need to be aware of various limitations. Accordingly, it is likely not realistic to declare that any one assay is the gold standard by which all other assays must be evaluated. Given the technical complexities of immunoassays used to detect autoantibodies, it is understandable that, despite years of activity, standardization of autoantibody assays, their reporting, and clinical correlations continues to be a major challenge (Kessenbrock et al., 2007; Mahler & Fritzler, 2010; Mahler, 2011; Agmon-Levin et al., 2014). Commonly used methods for autoantibody detection are listed in Table 53.6.

INDIRECT IMMUNOFLUORESCENCE ON HEP2 CELLS

Immunofluorescence microscopy using human cells, such as HEp-2 cells, allows for the sensitive detection of serum antibodies that react very specifically with various cellular proteins and nucleic acids (see Figs. 53.6 to 53.8 later). This technique is nowadays essential in immunology laboratories committed to the routine diagnosis of human autoimmune diseases. Standardization of the indirect immunofluorescence assay (IFA)-ANA, nevertheless, has been difficult. Many factors are involved in the performance of IF-ANA tests. They include (1) substrate and fixative variations, (2) microscopic optics, (3) method and quantitation of results, (4) establishment of reference range, (5) interpretation of results, (6) reference sera, and (7) specificity and avidity of the ANA. The ANA Standardization Committee of the World Health Organization recommends that laboratories should (1) report IF-ANA results at both 1:40 and 1:160 dilutions, and (2) supply information on percentage of normal individuals who are positive at these dilutions in their own experience (Tan et al., 1997).

From a positive immunofluorescence one can associate the specific pattern to the presence of a distinct autoantibody in that particular patient's serum. Since distinct autoantibody patterns occur in distinct diseases, as discussed earlier, the laboratorian offers the clinician the real possibility of narrowing the diagnostic chase. Figures 53.5, 53.6, and 53.7 depict some examples of immunofluorescence patterns as seen in our laboratories. Nomenclature and classification trees for Hep-2 immunofluorescence patterns are shown in Fig. 53.8 with designated anticellular (AC) antibody number. Tables 53.7 and 53.8 also list nuclear and cytoplasmic staining patterns with their associated antigens and diseases. Unabridged information on ANA patterns by indirect immunofluorescence on HEp-2 cells (more recently called anticellular antibodies IFA) and clinical relevance of autoantibodies may be found at www.anapatterns.org (Damoiseaux et al., 2019).

COMPUTER-ASSISTED ANA IFA TECHNOLOGY

Computer-assisted ANA pattern recognition was described almost 2 decades ago (Perner et al., 2002), but integrated hardware and software platforms that provide identification and archiving of IFA patterns obtained on HEp-2 cell substrates have only become available in the last 6 to 7 years (Mahler, Meroni et al., 2014). Features of these automated systems include acquisition, analysis, and storage of digital images of stained HEp-2 cells and local or remote access to the digital images on high-resolution monitors. Difficulties inherent in conventional IFA protocols such as serial dilutions of the test sera, the need for a dark room for fluorescence microscopy, reading and real-time interpreting of the IFA patterns, and manual recording of the results by a technologist make traditional IFA protocols challenging in the setting of modern, high-throughput laboratories (Mahler, Meroni et al., 2014; Roggenbuck et al., 2014). The new automated systems effectively circumvent many of these challenges and create a more continuous workflow and the potential to improve the quality, utility, and standardization of the ANA IFA assay (Mahler, Pierangeli et al., 2014).

At present there are approximately half a dozen automated IFA systems with various user-friendly features (Mahler, Meroni et al., 2014). The systems differ from each other with respect to the use of nuclear counterstains, lack of flexibility in the ANA kit to be used in respective systems (e.g., most systems are restricted to using the manufacturer's slides), throughput, number of patterns that can be identified, and software features (Bonroy et al., 2013; Bossuyt et al., 2013; Maenhout et al., 2014; Mahler, Meroni et al., 2014; Schouwers et al., 2014). These automated systems include a microscope fitted with an automated stage, a digital camera, a light-emitting diode (LED) light source, and software that controls the moving parts and directs image acquisition and storage. All systems perform fluorescent light intensity measurements with assignment of a preliminary categorization of the test sample as positive or negative and staining pattern interpretation. The automated software-based reading is followed by human visual interpretation of the digital images displayed on a high-resolution monitor allowing user confirmation or revision of the preliminary results. By providing high-quality digital images and preliminary classification and pattern interpretation, these automated systems support the operators' decision making and increase the consistency of intertest and interobserver results. The digital images can be stored for training, documentation, follow-up analysis, sequential changes in reactivity, and can be easily transported or can be uploaded into the patients' electronic medical record (EMR) in much the same way as digital images of radiographic and other visually based investigations. Currently available systems are highly reliable in their ability to discriminate positive from negative reactions and estimate fluorescence intensity, but the accuracy and robustness of pattern recognition has yet to reach the accuracy of human interpretation (Foggia et al., 2013; Roggenbuck et al., 2013; Schouwers et al., 2014).

Since the final interpretation is made by the operator, subjectivity is not abolished. Moreover, the characteristics of the HEp-2 substrates, conjugates, and complexity of test sera influence the appearance of certain ANA patterns, and the automated pattern identification of the various systems is based on somewhat different software programming algorithms. Nevertheless, automated systems for ANA HEp-2 analysis are a significant step forward to reduce variability and offer opportunities to increase harmonization of ANA interpretation.

TABLE 53.6

Methods for Detection of Autoantibodies to Nuclear and Intracellular Antigens

Method	Antigen Source	Sensitivity and Use
Immunofluorescence microscopy	Tissue sections; cell lines	Sensitive assay, often used for screening; may be computerized
Double immunodiffusion (Ouchterlony)	Tissue and cell extracts	Requires precipitin reaction, high specificity but not very sensitive
Counterimmunoelectrophoresis	Tissue and cell extracts	Increased sensitivity and speed as compared with immunodiffusion procedure
Immunoblotting, Western blot	Cell extracts	Very sensitive, permits detection of antibodies against soluble and insoluble antigens
Dot blot, linear blot (line immunoassays)	Purified native or recombinant antigens	Qualitative assay, average sensitivity
ELISA	Purified native or recombinant antigens	Very sensitive, quantitative, high throughput, can determine antibody class, low cost
Immunoprecipitation	Radiolabeled native or recombinant proteins	Very sensitive; identity of the actual autoantibody target may require ancillary confirmatory testing
Microsphere multiplexed assay (ALBIA)	Purified native or recombinant antigens	Very sensitive (compares to ELISA), semiquantitative, rapid, expensive proprietary technology
Cell-based assays	Cell line transfected with autoantigen cDNA, followed by IFA	Sensitivity = 45% to >90%; Specificity >95%

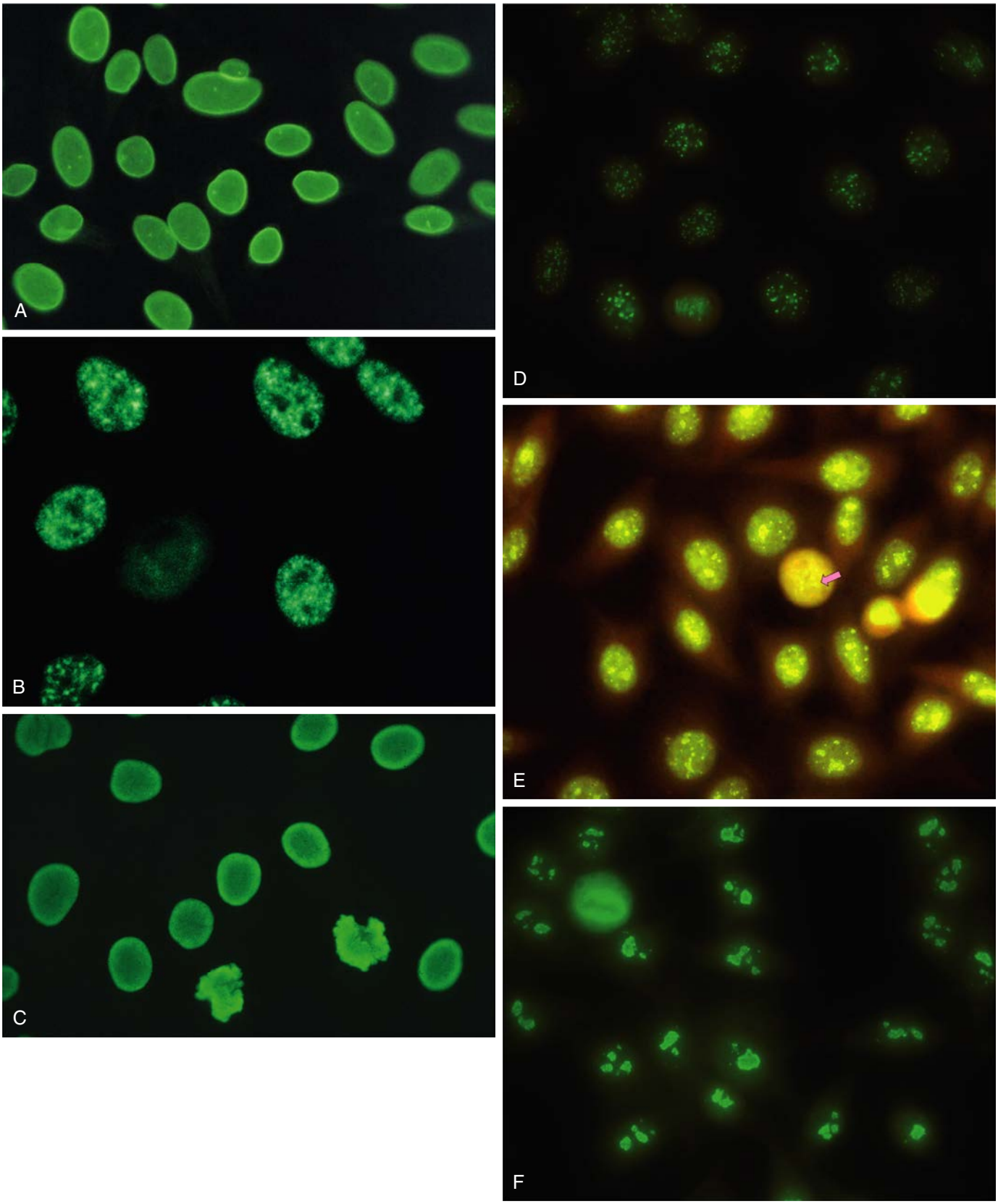

Fig. 53.5 Indirect immunofluorescence with autoantibodies to nuclear and nucleolar antigens in HEp-2 cells, 400×, FITC stain. **A**, Autoantibodies to lamin proteins A, B, and C of the nuclear envelope give a homogeneous nuclear pattern in HEp-2 cells, associated with a continuous nucleoplasmic rim. No rim is seen when the antibodies are specifically directed to histones or dsDNA. Previous reports of a peripheral pattern elicited by anti-dsDNA antibodies were probably due to fixation artifacts. **B**, The speckled nucleoplasmic pattern seen is characteristic of autoantibodies directed to the so-called extractable nuclear antigens, as the anti-U1nRNP shown here. The nucleoli and metaphase cells are negative. **C**, Anti-dsDNA autoantibodies, with homogeneous pattern in interphase as well as in metaphase cells. **D**, From a preparation with anticentromere autoantibodies, typically found in patients with the limited form of scleroderma (CREST syndrome), but also in primary biliary cholangitis. Distinct speckles are seen in the interphase nuclei, one for each chromosome pair, which aggregate in the metaphase plates during cell division. **E**, Autoantibodies to NOR-90 and RNA-polymerase I elicit the same pattern in HEp-2 cells, with nucleolar speckles and dots along some spindles of metaphase cells (arrow). They can be differentiated by other assays, such as immunoblot or immunoprecipitation. **F**, Autoantibodies targeting fibrillarin (U3-nRNP) give a clumpy staining of all nucleoli.

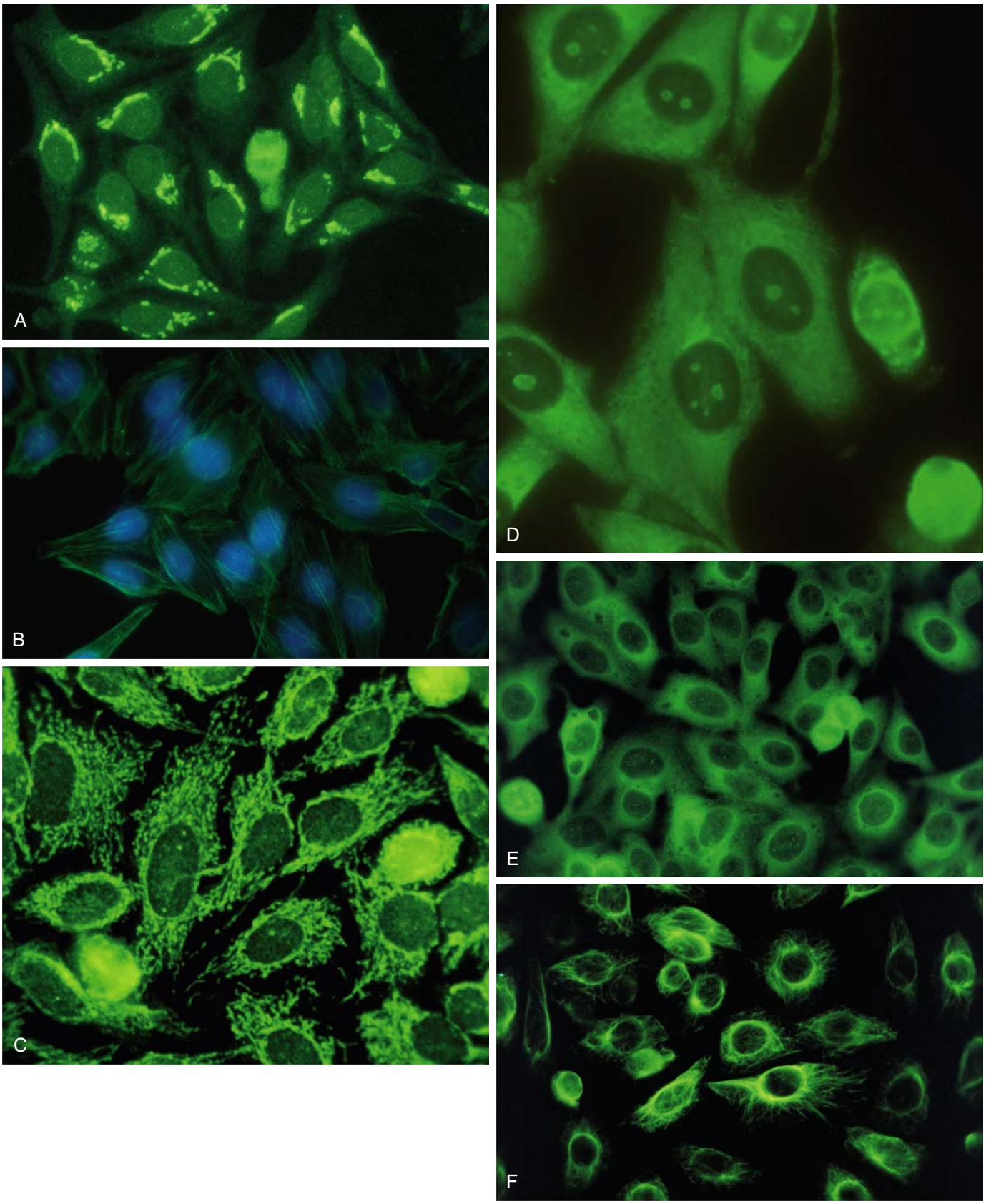

Fig. 53.6 Indirect immunofluorescence of HEp-2 cells with autoantibodies to distinct cytoplasmic antigens, 400x, FITC stain. **A,** The characteristic pattern of autoantibodies to the Golgi complex is seen, with granules arranged in clusters at one pole of the cell and adjacent to the nucleus. **B,** Autoantibodies to nonmuscle myosin decorate the stress fibers of the cytoskeleton (nuclei staining in blue with DAPI). These antibodies are found in patients with myasthenia gravis and chronic liver diseases. **C,** Antimitochondrial autoantibodies display a coarse granular pattern involving the whole cytoplasm, mostly seen in primary biliary cholangitis. **D,** The dense granular, almost homogeneous, cytoplasmic pattern obtained with anti-rRNP antibodies. They target ribosomal phosphoproteins and are clinically associated with central nervous system manifestations in patients with systemic lupus erythematosus. As can be noticed in the picture, not uncommonly such antibodies also stain the nucleoli in a homogeneous pattern, although weakly. **E,** A homogeneous decoration of the cytoplasm conferred by autoantibodies to PL-7 in polymyositis. **F,** Antikeratin antibodies are seen as filamentar staining of cytoskeletal stress fibers and constitute the major specificity found in alcoholic liver disease (69%), also common in rheumatoid arthritis (36% to 59%), psoriasis, and healthy individuals.

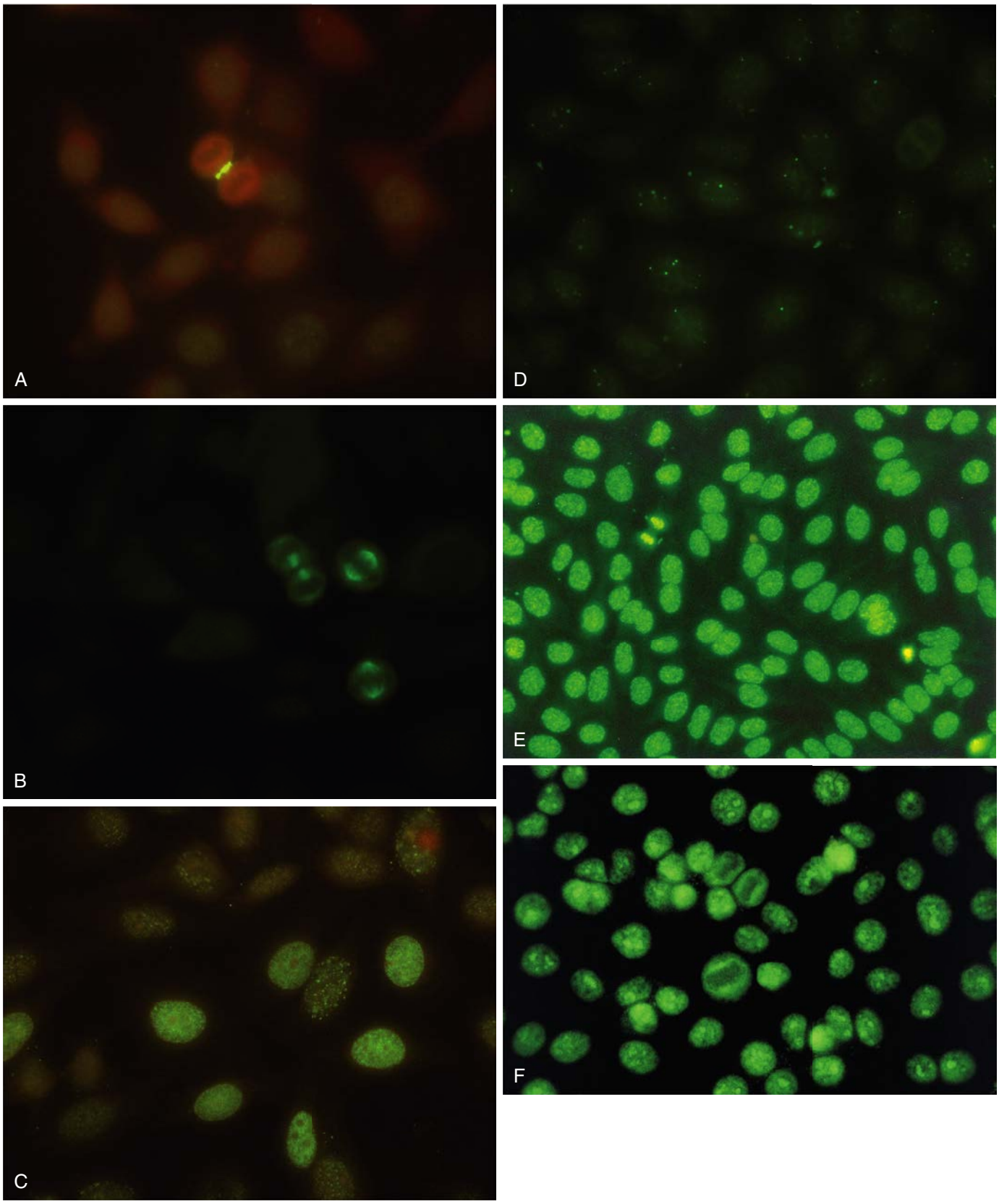

Fig. 53.7 Some other distinct patterns in indirect immunofluorescence of HEp-2 cells, 400x, FITC stain. **A,** Cells at the end of metaphase show antigens condensing in the midbody, also called the intercellular bridge region. The spindle poles of dividing cells can be decorated, as in **B**, with antibodies targeting the mitotic apparatus, such as NuMA (nuclear mitotic-associated protein). **C,** PCNA-autoantibodies give a mosaic of nucleoplasmic patterns, ranging from homogeneous to distinct speckled, according to the phases of cellular division (details in the text). **D,** The pattern obtained with anti-p80-coilin autoantibodies, where one can see from one to eight nucleoplasmic dots. **E,** One of the most common patterns seen in the routine laboratory, dense fine-speckled nuclear in interphase as well as in mitotic cells. This is a nonspecific autoantibody, found in systemic connective tissue diseases, but also in interstitial cystitis, breast cancer, and allergic reactions. **F,** Nuclear and nucleolar stainings are seen with anti-Ku autoantibodies. Chromosomes in mitotic cells are negative (see clinical associations in text).

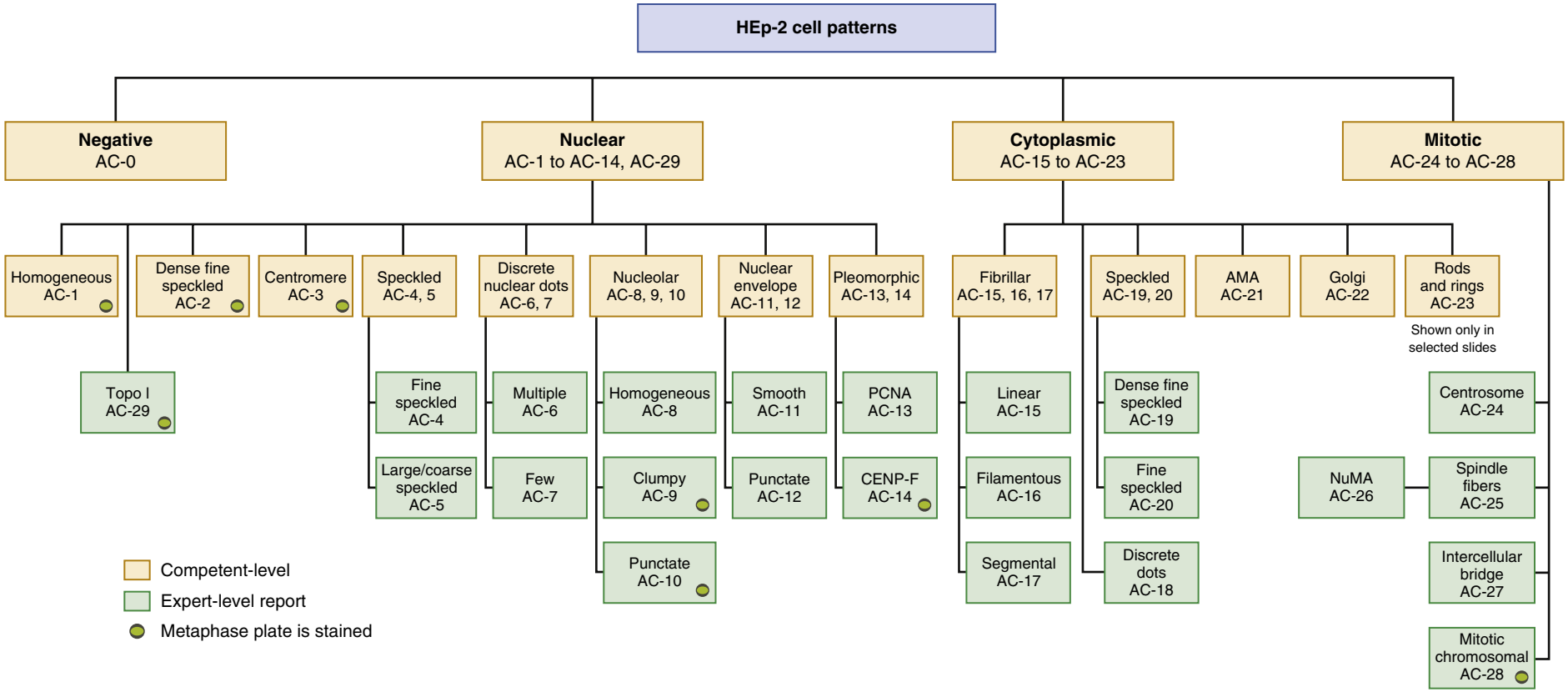

Fig. 53.8 Nomenclature and classification trees for indirect immunofluorescence assay patterns on HEp-2 cells. Each of these patterns has an alphanumeric code for anticell antibody from AC0 through AC29 designating cell organelle that is recognized by each autoantibody.

TABLE 53.7

Synonyms for Nuclear Patterns and Association With Specific Antigens and Diseases

	Synonyms	Antigen Associations	Disease Association
Homogeneous (AC-1)	Diffuse	dsDNA, nucleosomes, histones	SLE, drug-induced lupus, juvenile idiopathic arthritis
Speckled (AC-2,4,5)	Granular	hnRNP, U1RNP, Sm, SS-A/Ro (Ro60), SS-B/La, RNA polymerase III, Mi-2, Ku	MCTD, SLE, SjS, DM, Scl/PM overlap
Dense fine speckled (AC-2)	None	DFS70/LEDGF	Rare in SLE, SjS, Scl
Fine speckled (AC-4)	Fine granular	SS-A/Ro (Ro60), SS-B/La, Mi-2, TIF1γ, TIF1β, Ku, RNA helicase A, replication protein A	SjS, SLE, DM, Scl/PM overlap
Large/coarse speckled (AC-5)	Spliceosome/nuclear matrix	hnRNP, U1RNP, Sm, RNA polymerase III	MCTD, SLE, Scl
Discrete nuclear dots			
Centromere (AC-3)	Kinetochore	CENP-A/B (C)	Limited cutaneous Scl, PBC
Multiple nuclear dots (AC-6)	6-20 nuclear dots, NSpI, PML bodies	Sp100, PML proteins, MJ/NXP-2	PBC, SARD, PM/DM
Few nuclear dots (AC-7)	1 to 6 nuclear dots, Cajal bodies (coiled body)	p80-coilin, SMN	SjS, SLE, Scl, PM, asymptomatic individuals
Nucleolar (AC-8,9,10)			
Homogeneous (AC-8)	None	PM/Scl-75, PM/Scl-100, Th/To, B23/nucleophosmin, nucleolin, No55/SC65	Scl, Scl/PM overlap
Clumpy (AC-9)	None	U3-snoRNP/fibrillarin	Scl
Punctate (AC-10)	Nucleolar speckled	RNA polymerase I, hUBF/NOR-90	Scl, SjS
Nuclear envelope (AC-11,12)			
Smooth nuclear envelope (AC-11)	Nuclear rim, nuclear membrane, membranous	Lamins A,B,C, or lamin-associated proteins	SLE, SjS, seronegative arthritis
Punctate nuclear envelope (AC-12)	Nuclear membrane pores	Nuclear pore complex proteins (i.e. gp210)	PBC
Pleomorphic (AC-13,14)			
PCNA-like (AC-13)	None	PCNA	SLE, other conditions
CENP-F-like (AC-14)	MSA-3, NSp-II	CENP-F	Cancer, other conditions

These disease associations are primarily based on the antigens recognized by antibodies that reveal this particular ANA pattern.
From Chan EKL, Damoiseaux J, Carballo G, et al.: Report of the first international consensus on standardized nomenclature of antinuclear antibody HEp-2 cell patterns (ICAP) 2014-2015, Front Immunol 6, 2015; Damoiseaux J, Andrade LEC, Carballo OG, et al.: Clinical relevance of HEp-2 indirect immunofluorescent patterns: the International Consensus on ANA patterns (ICAP) perspective, Ann Rheum Dis 78(7):879–889, 2019. For further information please refer to www.anapatterns.org.

TABLE 53.8

Synonyms for Cytoplasmic Patterns and Association With Specific Antigens and Diseases

	Synonyms	Antigen Associations	Disease Association
Fibrillar (AC-15,16,17)			
Linear/actin (AC-15)	Actin-like	Actin, nonmuscle myosin	MCTD, chronic active hepatitis, liver cirrhosis, myasthenia gravis, Crohn disease, PBC, long-term hemodialysis, rare in SARD other than MCTD
Filamentous/microtubules (AC-16)	None	Vimentin, cytokeratins	Infectious or inflammatory conditions, long-term hemodialysis, alcoholic liver disease, SARD, psoriasis, healthy controls
Segmental (AC-17)	None	Alpha-actinin, vinculin, tropomyosin	Myasthenia gravis, Crohn disease, ulcerative colitis
Speckled (AC-18 to AC-20)			
Discrete dots (AC-18)	GW body, processing body, lysosome	GW182, Su/Ago2	PBC, SARD, neurologic and autoimmune conditions
Dense fine speckled (AC-19)	Homogeneous	PL-7, PL-12, ribosomal P proteins	Antisynthetase syndrome, PM/DM, SLE, juvenile SLE, neuropsychiatric SLE
Fine speckled (AC-20)	Speckled	Jo-1/histidyl-tRNA synthetase	Antisynthetase syndrome, PM/DM, limited Scl idiopathic pleural effusion
Reticular/AMA (AC-21)	Mitochondria-like	PDC-E2/M2, BCOADC-E2, OGDC-E2, E1α subunit of PDC, E3BP/protein X	Common in PBC, Scl rare in other SARD
Polar/Golgi-like (AC-22)	None	Giantin/macrogolgin, golgin-95/GM130, golgin-160, golgin-97, golgin-245	Rare in SjS, SLE, RA, MCTD, GPA, idiopathic cerebellar ataxia, paraneoplastic cerebellar degeneration, viral infections
Rods and rings (AC-23)	None	IMPDH2, others	HCV patients post-IFN/ribavirin therapy, rare in SLE, Hashimoto, and healthy controls

These disease associations are primarily based on the antigens recognized by antibodies that reveal this particular ANA pattern.
From Chan EKL, Damoiseaux J, Carballo G, et al.: Report of the first international consensus on standardized nomenclature of antinuclear antibody HEp-2 cell patterns (ICAP) 2014-2015, Front Immunol 6, 2015; Damoiseaux J, Andrade LEC, Carballo OG, et al.: Clinical relevance of HEp-2 indirect immunofluorescent patterns: the International Consensus on ANA patterns (ICAP) perspective, Ann Rheum Dis 78(7):879–889, 2019. For further information please refer to www.anapatterns.org.

ENZYME-LINKED IMMUNOSORBENT ASSAYS

An increasing number of enzyme immunoassays have been developed with the use of standard purified and recombinant antigens (Saitta & Keene, 1992). Many of these enzyme immunoassays have proved to be more sensitive than comparable immunodiffusion methods. Thus, because of the high sensitivity of enzyme immunoassays, one needs to determine carefully the reference range of normal patients and the proper cutoff values. Compared with immunodiffusion tests, ELISA tests showed much greater sensitivity but had lower specificity (Nakamura & Tan, 1992). Further, ELISA tests were frequently positive in low titers in sera of patients with rheumatic diseases other than SLE. Increasing sensitivity and decreasing specificity might result in false-positive test results. Furthermore, clinical associations with distinct autoantibodies were mainly determined using ID techniques.

In earlier studies using ELISAs many false-positive reactions were noted. False-positive reactions were caused by poor blocking reagents in the procedure. Also, impure antigen preparations were used. The percentage of clinical laboratories using ELISA increased from 25% to 47% over a 4-year period, from 1989 to 1992, as the technology improved, with pure antigen sources. Homburger et al. (1998) reported a comparison between a commercial ELISA and IF-ANA on HEp-2 cells, concluding that both methods were substantially equivalent for detecting clinically relevant ANA in patients with systemic rheumatic diseases. Reaching an opposite conclusion, Emlen and O'Neill (1997) tested six commercial ELISA kits and concluded for the existence of significant differences in the detection of ANA by immunofluorescence and ELISA. A group of international scientists joined by the World Health Organization reported on the performance of many commercial ELISAs, showing that (1) no single manufacturer was clearly superior to others in terms of their products' overall sensitivity, specificity, and precision; and (2) areas that needed improvement were in kits for the detection of antibodies to dsDNA and to Sm antigens (Tan et al., 1999). Great care should be exercised when selecting ELISA reagents and commercial kits. A good source of quality control data for the best commercial reagents is the periodic review of the College of American Pathologists in Immunology.

New commercial ELISA kits developed for screening purposes claim to detect a variety of autoantibodies in one single assay, but having "total" fractions of cellular antigens in one ELISA well is not technically feasible nowadays. Those assays are not 100% sensitive for the screening of antinuclear antibodies, as they cannot detect certain autoantibodies like antinucleolar specificities, PCNA, or distinct NuMA types. Reported results using those kits, for the moment, should correctly specify to physicians which types of autoantibodies were tested so as not to imply that a particular sample is "negative for all nuclear antibodies." Each ELISA test kit in such a situation should be validated for which antibody specificities it can actually detect (von Muhlen & Nakamura, 2002).

IMMUNOBLOTTING

This very sensitive technique is an important method for characterization of the specific nature of many autoantibodies. One important advantage is that a specific antibody can be identified with the use of crude cell extract antigen preparations (Fig. 53.9). The European Consensus Study observed the following with the immunoblotting test (Nakamura et al., 1994):

1. Antigen preparation is very important in the immunoblotting procedure.
2. Detection of antibodies to nRNP, Sm, and Scl-70 was acceptable. This sensitive method is helpful in the detection of multiple specificities of antibodies in the same specimen.
3. The method requires careful controls to monitor molecular weight bands. For example, histone bands can be confused with a centromeric antigen (CENP-A, 19 kD), and Scl-70 (topoisomerase I) can be confused with other 100 kD bands.
4. Protein degradation can occur in the antigen cell extract used for immunoblotting, especially Scl-70 and centromere antigens.
5. The anti-Sm is distinguished by the presence of anti-D (the D antigen is a 16 kD protein contained in all major nRNP particles).
6. Anti-SS-B/La is readily detected by immunoblotting. Anti–SS-A/Ro is poorly detected by immunoblotting and is insensitive because SS-A/Ro may not demonstrate the proper structure for recognition.

DOT BLOTS AND LINE IMMUNOASSAYS

Line immunoassays are generally considered to be a second-generation dot blot assay (Mahler, Meroni et al., 2014). A broad range of LIAs are commercially available and are most commonly used to confirm autoantibodies

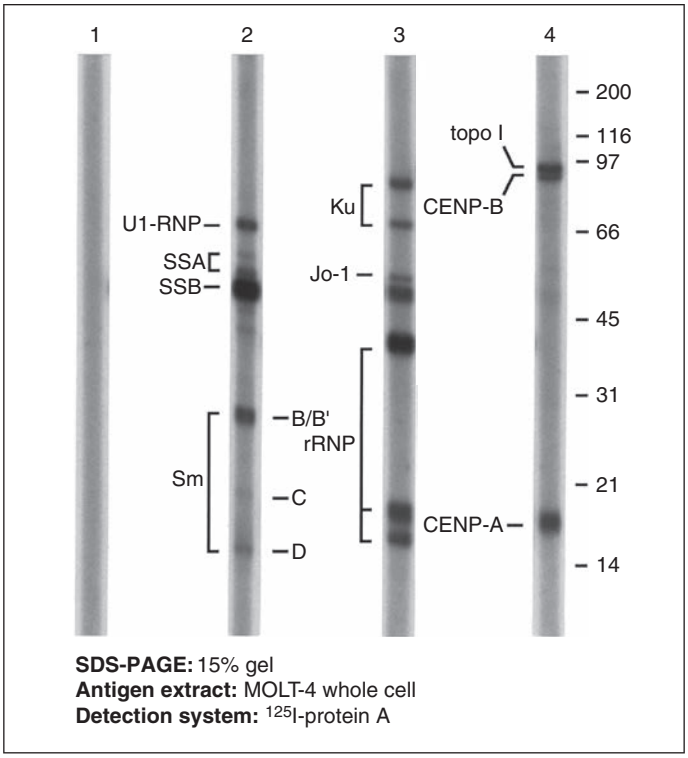

Fig. 53.9 Immunoblotting analysis of common autoantibodies seen in rheumatic diseases. In lane 1, the nitrocellulose strip was probed with a normal human serum (negative control), and no reactivity is seen as expected. The next three lanes show distinct bands obtained by mixing positive control sera containing known specificities. Lane 2 depicts reactivities to the ribonucleoproteins (RNP) SSA (52 and 60 kD), SSB (48 kD), Sm (B/B', 28 kD, D, 14 kD), and U1nRNP (the 70 kD protein) and a faint band around 19 kD, the C antigen. The A protein, with 32 kD, also characteristically recognized by U1nRNP antibodies, is not seen in this experiment. Lane 3 shows the bands obtained by using the human prototype antisera to Jo-1 (52 kD), Ku (two bands around the 70 and 80 kD regions), and ribosomal RNP (15, 18, 37 kD). The small band above the 52 kD antigen is not identified. Lane 4 displays the bands most commonly seen using sera from scleroderma patients (e.g., anti-DNA topoisomerase I [Scl-70, 95 kD]) and anticentromere antibodies (16 kD, CENP-A, 80 kD, CENP-B). On the left, positions in kilodaltons of the broad-range molecular weight standards can be seen. (Used with permission from von Muhlen CA, Tan EM: Autoantibody specificities in autoimmune rheumatic diseases, Rev Br Rheumatol 34:173–194, 1994.)

previously identified by IFA or other screening immunoassays (Pottel et al., 2004; Damoiseaux et al., 2005). Nevertheless, in some laboratories LIAs have also been used as a primary test for disease-specific autoantibodies that are seen in systemic lupus erythematosus, systemic sclerosis, idiopathic inflammatory myopathies, and rheumatoid arthritis as well as paraneoplastic conditions and autoimmune liver diseases (Lopez-Longo et al., 2003; Lee et al., 2012; Mahler, Meroni et al., 2014; Yang et al., 2014). Recent advances in automating the processing of LIAs make them a more appealing platform for high-volume and high-throughput laboratories (Lopez-Longo et al., 2003). As with any immunoassay, LIAs have some drawbacks, including comparative limitations of sensitivity and specificity for certain autoantibodies (Almeida Gonzalez et al., 2010; Lee et al., 2012). The antigen compositions and other features of line immunoassays are reviewed in Mahler, Meroni et al. (2014).

MULTIPLEX BEAD-BASED ASSAYS

Multiplexed immunoassays based on the Luminex technology (Austin, TX) use purified autoantigens individually covalently coupled to distinct laser-reactive addressable laser beads (referred to as ALBIA) (Fritzler, 2006). Those multiplexed assays are being incorporated more and more into the routine work of bigger laboratories. The so-called multiplexed fluorescent microsphere immunoassay uses spectral addresses, allowing for the simultaneous determination of several autoantibodies, all in just one incubation and no wash steps. Martins et al. (2004) demonstrated that results for a proprietary multiplexed assay compared favorably with results from established ELISAs. Agreement, sensitivity, and specificity, respectively, for five nuclear antigens evaluated were as follows: SSA52/SSA60 (99.1, 100.0, and 98.8%), SSB (98.6, 88.9, and 99.5%), Sm (97.6, 95.8, and 97.9%), RNP (97.2, 92.7, and 98.8%), and Scl-70 (93.6, 50.0,

and 99.0%). The multiplexed microsphere-based immunoassay seems to be a sensitive and specific method for the detection and semiquantitation of common antibodies in human sera. Clusters of clinically important autoantibodies, such as those in lupus or in systemic vasculitis, may be rapidly tested in one single batch. This is not to imply that the flow cytometry–based assay may be an alternative to screening autoantibodies with HEp-2 immunofluorescence, as there are clear limitations in identifying important autoantibodies in clinical samples by using the current microsphere technology (Kroshinsky et al., 2009). One recent position paper of the American College of Rheumatology clarifies the state of the art in detecting autoantibodies, aspects well touched in a paper by Meroni and Schur (2010).

Today, several commercial ALBIA kits are available for the detection of autoantibodies to a variety of autoantigens (reviewed in Mahler, Meroni et al., 2014). Similar to LIA, the number of antigens and the antigen composition of these bead-based arrays significantly vary from manufacturer to manufacturer. Although first-generation ALBIAs showed polyreactivity, which was caused by nonspecific binding to the beads, newer ALBIA showed significantly reduced polyreactivity and thus higher specificity (Fritzler, Behmanesh et al., 2006). In one study, when an ALBIA was used for the detection of ANA, 7.4% of healthy donors were positive, the majority of which showed a speckled or a nucleolar staining pattern (Avaniss-Aghajani et al., 2007). Another report using ALBIA showed that the prevalence of ANAs were comparable to expected values of the ANA IFA test while only moderate agreement was found between IFA and ALBIA (Nifli et al., 2006). The majority of ANA IFA positive, multiplex ANA negative sera were also positive by an ANA ELISA utilizing nuclear extracts (Nifli et al., 2006).

While the experience with ALBIA is not nearly as extensive as ELISA, there is evidence indicating that these assays have shortcomings (Shovman, Gilburd et al. 2005, Fritzler and Fritzler 2009, Hanly, Su et al. 2010), especially when comparing the results for specific analytes such as anti-dsDNA. Nevertheless, ALBIA has generally good agreement with several immunoassay platforms (Shovman, Gilburd et al., 2005; Avaniss-Aghajani et al., 2007; Caramaschi et al., 2007; Bardin et al., 2009; Albon et al., 2011). There is general consensus that, because there is considerable variation in the sensitivity of the various commercial diagnostic kits, the identity of the particular assay used to generate the test result should be made available to the clinician (Meroni & Schur, 2010; https://www.rheumatology.org/Practice-Quality/Administrative-Support/Position-Statements). In addition, because of the growing trend of using automated immunoassay systems that provide quantitative results, these laboratories should follow standards of chemistry instrumentation, including a requirement to demonstrate analytic measured ranges and periodic calibrations. Clinical laboratories that adopt multiplexed assays (i.e., ALBIA) must establish reference ranges and cutoff values for each analyte, and the sensitivity and specificity must be established with care as the laboratory findings may present a difficult problem for the clinician who has to interpret the results. A summary of the autoantigen composition of the major ALBIA kits has been recently reviewed (Mahler, Meroni et al., 2014).

An emerging novel, bead-based immunoassay platform is the particle-based multianalyte array technology with advantages of high throughput and real-time antibodies as internal calibrators for each analyte included in the array (Bossuyt et al., 2019; Mahler, Betteridge et al., 2019).

OTHER IMMUNOASSAYS

Double immunodiffusion analysis has been used to determine the specificity of several ANAs. Assay specificity in double immunodiffusion is generally dependent on the quality of control sera used in the procedure, as well as the nature of the antigen preparation. Immunodiffusion tests are not very sensitive, but positive tests have a high degree of specificity. Immunodiffusion commercial kits are available for the detection of antibodies to RNP, Sm, SS-A/Ro, SS-B/La, and Scl-70, as well as other less prevalent markers.

Cell-based assays have become increasingly used for the detection of other autoantibodies, particularly those where conformational epitopes expressed on cell surfaces or in association with other ligands is required for autoantibody binding (Melegari et al., 2012; Behnert et al., 2013; Radzimski et al., 2013; Yeo et al., 2017; Yamashita & Tawara, 2019). The general principle of CBA is to employ a selected cell line and transfect them with the cDNA encoding the autoantigen of interest. When the desired autoantigen target is overexpressed, cells are fixed and then used in a conventional IFA assay. Control cells transfected with an unrelated target can assist in the determination of positive results, an especially important feature in autoimmune sera where reactivity to more than one cellular target may be present.

SELECTED REFERENCES

Damoiseaux J, Andrade LEC, Carballo OG, et al.: Clinical relevance of HEp-2 indirect immunofluorescent patterns: the International Consensus on ANA Patterns (ICAP) perspective, *Ann Rheum Dis* 78(7):879–889, 2019.

Anticellular antibodies (ANA) identified on HEp-2 cells are associated with certain clinical manifestations in different systemic autoimmune rheumatic diseases. This recent paper brings a thorough review on the clinical relevance of ANA patterns and the specific autoantibodies involved in each reactivity. A very important publication for laboratory people and clinicians.

Chan EKL, Damoiseaux J, Carballo G, et al.: Report of the first international consensus on standardized nomenclature of antinuclear antibody HEp-2 cell patterns (ICAP) 2014-2015, *Front Immunol* 6, 2015.

The International Consensus for ANA Patterns (ICAP) brought harmonization to nomenclature of ANA patterns, classifying findings in accordance to the cellular anatomy of each identifiable autoantigen, and spreading knowledge on this important screening test. This was the first publication of this group, with extensive and important contributions offered freely at www.anapatterns.org.

Aringer M, Costenbader K, Daikh D, et al.: 2019. European League against Rheumatism/American College of Rheumatology classification criteria for systemic lupus erythematosus, *Ann Rheum Dis*, 2019.

Latest American College of Rheumatology and European Union League Against Rheumatism joint effort in achieving the most sensitive and specific classification criteria for SLE. Indispensable reference for researchers and physicians interested in lupus.

Fritzler MJ, Martinez-Prat L, Choi MY, et al.: The utilization of autoantibodies in approaches to precision health, *Front Immunol* 9:2682, 2018.

Deep learning and artificial intelligence with their many modifications will form the basis of new strategies for the immunology diagnostics in the near future. Precision medicine, pharmacogenomics, and theranostics are here to stay. The text shows some up-to-date and futuristic insights related to the use of autoantibodies in the clinical laboratory.

Mariampillai K, Granger B, Amelin D, et al.: Development of a new classification system for idiopathic inflammatory myopathies based on clinical manifestations and myositis-specific autoantibodies, *JAMA Neurol* 75(12):1528–1537, 2018.

Evidence-based study to use clinical phenotypes and myositis-specific autoantibodies to achieve a new diagnostic classification of the idiopathic inflammatory myopathies in four subgroups: dermatomyositis, inclusion body myositis, immune-mediated necrotizing myopathy, and antisynthetase syndrome. Formerly known only as polymyositis and dermatomyositis, the spectrum of autoimmune inflammatory myopathies viewed increasing and important expansion in latest years.

Access the complete reference list online at Elsevier eBooks for Practicing Clinicians.

REFERENCES

Acosta-Herrera M, Lopez-Isac E, Martin J: Towards a better classification and novel therapies based on the genetics of systemic sclerosis, *Curr Rheumatol Rep* 21(9):44, 2019.

Aggarwal R, Cassidy E, Fertig N, et al.: Patients with non-Jo-1 anti-tRNA-synthetase autoantibodies have worse survival than Jo-1 positive patients, *Ann Rheum Dis* 73(1):227–232, 2014.

Aggarwal R, Lucas M, Fertig N, et al.: Anti-U3 RNP autoantibodies in systemic sclerosis, *Arthritis Rheum* 60(4):1112–1118, 2009.

Agmon-Levin N, Damoiseaux J, Kallenberg C, et al.: International recommendations for the assessment of autoantibodies to cellular antigens referred to as anti-nuclear antibodies, *Ann Rheum Dis* 73(1):17–23, 2014.

Aho K, Palusuo T, Kurki P: Marker antibodies of rheumatoid arthritis: diagnostic and pathogenetic implications, *Semin Arthritis Rheum* 23(6):379–387, 1994.

Ajeganova S, Huizinga TW: Rheumatoid arthritis: seronegative and seropositive RA: alike but different? *Nat Rev Rheumatol* 11(1):8–9, 2015.

Alarcón-Segovia D, Delezé M, Oria CV, et al.: Antiphospholipid antibodies and the antiphospholipid syndrome in systemic lupus erythematosus: a prospective analysis of 500 consecutive patients, *Medicine* 68:353–365, 1989.

Alarcón-Segovia D, Peréz-Vazquez ME, Villa AR, et al.: Preliminary classification criteria for the antiphospholipid syndrome within systemic lupus erythematosus, *Semin Arthritis Rheum* 21(05):275–286, 1992.

Al-Attia HM, Ahmed YHA: Mucocutaneous disease in Arabs with systemic lupus erythematosus: clinical expression and relevance to autoantibodies, *Lupus* 7(8):535–539, 1998.

Albayda J, Mammen AL: Is statin-induced myositis part of the polymyositis disease spectrum? *Curr Rheumatol Rep* 16(8):433, 2014.

Albon S, Bunn C, Swana G, et al.: Performance of a multiplex assay compared to enzyme and precipitation methods for anti-ENA testing in systemic lupus and systemic sclerosis, *J Immunol Methods* 365(1–2):126–131, 2011.

Aletaha D, Neogi T, Silman AJ, et al.: Rheumatoid arthritis classification criteria: an American College of Rheumatology/European League against Rheumatism collaborative initiative, *Arthritis Rheum* 62(9):2569–2581, 2010. 2010.

Alexiou I, Germenis A, Koutroumpas A, et al.: Anti-cyclic citrullinated peptide-2 (CCP2) autoantibodies and extra-articular manifestations in Greek patients with rheumatoid arthritis, *Clin Rheumatol* 27(4):511–513, 2008.

Allanore Y, Sellam J, Batteux F, et al.: Induction of autoantibodies in refractory rheumatoid arthritis treated by infliximab, *Clin Exp Rheumatol* 22(6):756–758, 2004.

Allenbach Y, Arouche-Delaperche L, Preusse C, et al.: Necrosis in anti-SRP(+) and anti-HMGCR(+)myopathies: role of autoantibodies and complement, *Neurology* 90(6):e507–e517, 2018.

Almeida Gonzalez D, Cabrera de Leon A, Rodriguez Perez Mdel C, et al.: Efficiency of different strategies to detect autoantibodies to extractable nuclear antigens, *J Immunol Methods* 360(1–2):89–95, 2010.

Alspaugh MA, Tan EM: Antibodies to cellular antigens in Sjögren's syndrome, *J Clini Invest* 55:1067–1073, 1975.

Amlani A, Choi MY, Tarnopolsky M, et al.: Anti-NT5c1A autoantibodies as biomarkers in inclusion body myositis, *Front Immunol* 10:745, 2019.

Andrade LEC, Klotz W, Herold M, et al.: International consensus on antinuclear antibody patterns: definition of the AC-29 pattern associated with antibodies to DNA topoisomerase I, *Clin Chem Lab Med* 56(10):1783–1788, 2018.

Andreoli L, Chighizola CB, Nalli C, et al.: Clinical characterization of antiphospholipid syndrome by detection of IgG antibodies against beta2 -glycoprotein i domain 1 and domain 4/5: ratio of anti-domain 1 to anti-domain 4/5 as a useful new biomarker for antiphospholipid syndrome, *Arthritis Rheumatol* 67(8):2196–2204, 2015.

Andreoli L, Fredi M, Nalli C, et al.: Clinical significance of IgA anti-cardiolipin and IgA anti-beta2glycoprotein I antibodies, *Curr Rheumatol Rep* 15(7):343, 2013.

Aringer M, Costenbader K, Daikh D, et al.: *European League against Rheumatism/American College of Rheumatology classification criteria for systemic lupus erythematosus*, Ann Rheum Dis, 2019. 2019.

Aritomi T, Kido T, Nakano K, et al.: Small cell lung cancer patient with anti-transcriptional intermediary factor 1gamma antibody who developed dermatomyositis after Successful Chemoradiotherapy, *Intern Med* 58(3):427–431, 2019.

Arnett FC, Fritzler MJ, Ahn C, et al.: Urinary mercury levels in patients with autoantibodies to U3-RNP (fibrillarin), *J Rheumatol* 27(2):405–410, 2000.

Aussy A, Fréret M, Gallay L, et al.: The IgG2 isotype of anti–transcription intermediary factor 1γ autoantibodies is a biomarker of cancer and mortality in adult dermatomyositis, *Arthritis Rheumatol* 71(8), 2019.

Avaniss-Aghajani E, Berzon S, Sarkissian A: Clinical value of multiplexed bead-based immunoassays for detection of autoantibodies to nuclear antigens, *Clin Vaccine Immunol* 14(5):505–509, 2007.

Bacman S, Sterin-Borda L, Camusso JJ, et al.: Circulating antibodies against rat parotid gland M3 muscarinic receptors in primary Sjogren's syndrome, *Clin Exp Immunol* 104(3):454–459, 1996.

Barada Jr FA, Andrews BS, Davis JS t, et al.: Antibodies to Sm in patients with systemic lupus erythematosus. Correlation of Sm antibody titers with disease activity and other laboratory parameters, *Arthritis Rheum* 24(10):1236–1244, 1981.

Bardin N, Desplat-Jego S, Daniel L, et al.: BioPlex 2200 multiplexed system: simultaneous detection of anti-dsDNA and anti-chromatin antibodies in patients with systemic lupus erythematosus, *Autoimmunity* 42(1):63–68, 2009.

Barturen G, Beretta L, Cervera R, et al.: Moving towards a molecular taxonomy of autoimmune rheumatic diseases, *Nat Rev Rheumatol* 14(2):75–93, 2018.

Behnert A, Fritzler MJ, Teng B, et al.: An anti-phospholipase A2 receptor quantitative immunoassay and epitope analysis in membranous nephropathy reveals different antigenic domains of the receptor, *PloS One* 8(4), 2013. e61669.

Bentow C, Fritzler MJ, Mummert E, et al.: Recognition of the dense fine speckled (DFS) pattern remains challenging: results from an international internet-based survey, *Auto Immun Highlights* 7(1):8, 2016.

Bentow C, Swart A, Wu J, et al.: Clinical performance evaluation of a novel rapid response chemiluminescent immunoassay for the detection of autoantibodies to extractable nuclear antigens, *Clin Chim Acta* 424:141–147, 2013.

Bernatsky S, Joseph L, Pineau CA, et al.: Estimating the prevalence of polymyositis and dermatomyositis from administrative data: age, sex and regional differences, *Ann Rheum Dis* 68(7):1192–1196, 2009.

Bernstein RM, Steigerwald JC, Tan EM: Association of antinuclear and antinucleolar antibodies in progressive systemic sclerosis, *Clin Exp Immunol* 48(1):43–51, 1982.

Betteridge Z, Gunawardena H, North J, et al.: Identification of a novel autoantibody directed against small ubiquitin-like modifier activating enzyme in dermatomyositis, *Arthritis Rheum* 56(9):3132–3137, 2007.

Betteridge Z, McHugh N: Myositis-specific autoantibodies: an important tool to support diagnosis of myositis, *J Intern Med* 280(1):8–23, 2016.

Betteridge ZE, Woodhead F, Lu H, et al.: Brief report: anti-eukaryotic initiation factor 2B autoantibodies are associated with interstitial lung disease in patients with systemic sclerosis, *Arthritis Rheumatol* 68(11):2778–2783, 2016.

Bharadwaj A, Aggarawal A, Misra R: Clinical relevance of IgA rheumatoid factor (RF) in children with juvenile rheumatoid arthritis, *Rheumatol Int* 19(1/2):47–49, 1999.

Biermann MH, Griffante G, Podolska MJ, et al.: Sweet but dangerous - the role of immunoglobulin G glycosylation in autoimmunity and inflammation, *Lupus* 25(8):934–942, 2016.

Bizzaro N, Brusca I, Previtali G, et al.: The association of solid-phase assays to immunofluorescence increases the diagnostic accuracy for ANA screening in patients with autoimmune rheumatic diseases, *Autoimmun Rev* 17(6):541–547, 2018.

Bobbio-Pallavicini F, Alpini C, Caporali R, et al.: Autoantibody profile in rheumatoid arthritis during long-term infliximab treatment, *Arthritis Res Ther* 6(3):R264–272, 2004.

Bohan A, Peter JB: Polymyositis and dermatomyositis (second of two parts), *New Engl J Med* 292:403–407, 1975.

Bombardieri M, Alessandri C, Labbadia G, et al.: Role of anti-cyclic citrullinated peptide antibodies in discriminating patients with rheumatoid arthritis from patients with chronic hepatitis C infection-associated polyarticular involvement, *Arthritis Res Ther* 6(2):R137–141, 2004.

Bonfa E, Golombek SJ, Kaufman LD, et al.: Association between lupus psychosis and anti-ribosomal P protein antibodies, *N Engl J Med* 317:265–271, 1987.

Bonroy C, Van Praet J, Smith V, et al.: Optimization and diagnostic performance of a single multiparameter lineblot in the serological workup of systemic sclerosis, *J Immunol Methods* 379(1–2):53–60, 2012.

Bonroy C, Verfaillie C, Smith V, et al.: Automated indirect immunofluorescence antinuclear antibody analysis is a standardized alternative for visual microscope interpretation, *Clin Chem Lab Med* 51(9):1771–1779, 2013.

Bos WH, van de Stadt LA, Sohrabian A, et al.: Development of anti-citrullinated protein antibody and rheumatoid factor isotypes prior to the onset of rheumatoid arthritis, *Arthritis Res Ther* 16(2):405, 2014.

Bossuyt X, Claessens J, De Langhe E, et al.: Antinuclear antibodies by indirect immunofluorescence and solid phase assays, *Ann Rheum Dis*, 2019.

Bossuyt X, Cooreman S, De Baere H, et al.: Detection of antinuclear antibodies by automated indirect immunofluorescence analysis, *Clin Chim Acta* 415:101–106, 2013.

Bossuyt X, Louche C, Wiik A: Standardisation in clinical laboratory medicine: an ethical reflection, *Ann Rheum Dis* 67(8):1061–1063, 2008.

Brouwer R, Vree Egberts WT, Hengstman GJ, et al.: Autoantibodies directed to novel components of the PM/Scl complex, the human exosome, *Arthritis Res* 4(2):134–138, 2002.

Burford B, Gentry-Maharaj A, Graham R, et al.: Autoantibodies to MUC1 glycopeptides cannot be used as a screening assay for early detection of breast, ovarian, lung or pancreatic cancer, *Br J Cancer* 108(10):2045–2055, 2013.

Burlingame RW, Rubin RL: Autoantibody to the nucleosome subunit (H2A-H2B)-DNA is an early and ubiquitous feature of lupus-like conditions, *Mol Biol Rep* 23(3–4):159–166, 1996.

Burlingame RW, Rubin RL: Subnucleosome structures as substrates in enzyme-linked immunosorbent assays, *J Immunol Meth* 134:187–199, 1990.

Bylund DJ, Nakamura RM: Importance of detection of SS-A/Ro autoantibody in screening immunofluorescence tests for autoantibodies to nuclear antigens, *J Clin Lab Anal* 5(3):212–218, 1991.

Calise SJ, Zheng B, Hasegawa T, et al.: Reference standards for the detection of anti-mitochondrial and anti-rods/rings autoantibodies, *Clin Chem Lab Med* 56(10):1789–1798, 2018.

Canoso JJ, Cohen AS: A review of the use, evaluations, and criticisms of the preliminary criteria for the classification of systemic lupus erythematosus, *Arthritis Rheum* 22(8):917–921, 1979.

Cao H, Pan M, Kang Y, et al.: Clinical manifestations of dermatomyositis and clinically amyopathic dermatomyositis patients with positive expression of anti-melanoma differentiation-associated gene 5 antibody, *Arthritis Care Res* 64(10):1602–1610, 2012.

Caramaschi P, Ruzzenente O, Pieropan S, et al.: Determination of ANA specificity using multiplexed fluorescent microsphere immunoassay in patients with ANA positivity at high titres after infliximab treatment: preliminary results, *Rheumatol Int* 27(7):649–654, 2007.

Cavill D, Waterman SA, Gordon TP: Antibodies raised against the second extracellular loop of the human muscarinic M3 receptor mimic functional autoantibodies in Sjogren's syndrome, *Scand J Immunol* 59(3):261–266, 2004.

Cavill D, Waterman SA, Gordon TP: Failure to detect antibodies to extracellular loop peptides of the muscarinic M3 receptor in primary Sjogren's syndrome, *J Rheumatol* 29(6):1342–1344, 2002.

Ceribelli A, Cavazzana I, Franceschini F, et al.: Anti-Th/To are common antinucleolar autoantibodies in Italian patients with scleroderma, *J Rheumatol* 37(10):2071–2075, 2010.

Ceribelli A, De Santis M, Isailovic N, et al.: The immune response and the pathogenesis of idiopathic inflammatory myositis: a critical review, *Clin Rev Allergy Immunol* 52(1):58–70, 2017.

Ceribelli A, Fredi M, Taraborelli M, et al.: Anti-MJ/NXP-2 autoantibody specificity in a cohort of adult Italian patients with polymyositis/dermatomyositis, *Arthritis Res Ther* 14(2):R97, 2012.

Ceribelli A, Isailovic N, De Santis M, et al.: Myositis-specific autoantibodies and their association with malignancy in Italian patients with polymyositis and dermatomyositis, *Clin Rheumatol* 36(2):469–475, 2017.

Ceribelli A, Isailovic N, De Santis M, et al.: Detection of anti-mitochondrial antibodies by immunoprecipitation in patients with systemic sclerosis, *J Immunol Methods* 452:1–5, 2018.

Ceribelli A, Satoh M, Chan EK: A new immunoprecipitation-real time quantitative PCR assay for anti-Th/To and anti-U3RNP antibody detection in systemic sclerosis, *Arthritis Res Ther* 14(3):R128, 2012.

Cervera R, Doria A, Amoura Z, et al.: Patterns of systemic lupus erythematosus expression in Europe, *Autoimmun Rev* 13(6):621–629, 2014.

Cervera R: Antiphospholipid syndrome, *Thromb Res* 151(Suppl 1):S43–s47, 2017.

Cha S, Singson E, Cornelius J, et al.: Muscarinic acetylcholine type-3 receptor desensitization due to chronic exposure to Sjogren's syndrome-associated autoantibodies, *J Rheumatol* 33(2):296–306, 2006.

Chan EK, Andrade LE: Antinuclear antibodies in Sjogren's syndrome, *Rheum Dis Clin North Am* 18(3):551–570, 1992.

Chan EK, Damoiseaux J, de Melo Cruvinel W, et al.: Report on the second international consensus on ANA pattern (ICAP) workshop in Dresden, *Lupus* 25(8):797–804, 2015. 2016.

Chan EK, Tan EM: Epitopic targets for autoantibodies in systemic lupus erythematosus and Sjogren's syndrom, *Curr Opin Rheumatol* 1(3):376–381, 1989.

Chan EKL BJ: *The SS-A/Ro antigen. Manual of biological markers of disease*. In M. R. van Venrooij WJ, editor: Dordrecht, Netherlands, 1994, Kluwer Academic Publishers, pp 1–18.

Chan EKL, Damoiseaux J, Carballo G, et al.: Report of the first international consensus on standardized nomenclature of antinuclear antibody HEp-2 cell patterns (ICAP) 2014-2015, *Front Immunol* 6, 2015.

Chan EKL, Imai H, Hamel JC, et al.: Human autoantibody to RNA polymerase I transcription factor hUBF: molecular identity of nucleolus organizer region autoantigen NOR-90 and ribosomal RNA transcription upstream binding factor, *J Exp Med* 174:1239–1244, 1991.

Chen Q, Li X, He W, et al.: The epitope study of alpha-fodrin autoantibody in primary Sjogren's syndrome, *Clin Exp Immunol* 149(3):497–503, 2007.

Chighizola CB, Pregnolato F, Andreoli L, et al.: Beyond thrombosis: anti-beta2GPI domain 1 antibodies identify late pregnancy morbidity in anti-phospholipid syndrome, *J Autoimmun* 90:76–83, 2018.

Chinnaraj M, Planer W, Pengo V, et al.: Discovery and characterization of 2 novel subpopulations of aPS/PT antibodies in patients at high risk of thrombosis, *Blood Adv* 3(11):1738–1749, 2019.

Chinoy H, Fertig N, Oddis CV, et al.: The diagnostic utility of myositis autoantibody testing for predicting the risk of cancer-associated myositis, *Ann Rheum Dis* 66(10):1345–1349, 2007.

Choi MY, Barber MR, Barber CE, et al.: Preventing the development of SLE: identifying risk factors and proposing pathways for clinical care, *Lupus* 25(8):838–849, 2016.

Clark G, Reichlin M, Tomasi TB: Characterization of a soluble cytoplasmic antigen reactive with sera from patients with systemic lupus erythematosus, *J Immunol* 102:117–122, 1969.

Cohen AS, Canoso JJ: Criteria for the classification of systemic lupus erythematosus—status 1972, *Arthritis Rheum* 15(5):540–543, 1972.

Cohen D, Berger SP, Steup-Beekman GM, et al.: Diagnosis and management of the antiphospholipid syndrome, *BMJ* 340:c2541, 2010.

Cousins L, Pericleous C, Khamashta M, et al.: Antibodies to domain I of beta-2-glycoprotein I and IgA antiphospholipid antibodies in patients with 'seronegative' antiphospholipid syndrome, *Ann Rheum Dis* 74(1):317–319, 2015.

Cruellas MG, Viana Vdos S, Levy-Neto M, et al.: Myositis-specific and myositis-associated autoantibody profiles and their clinical associations in a large series of patients with polymyositis and dermatomyositis, *Clinics* 68(7):909–914, 2013.

Dagher JH, Scheer U, Voit R, et al.: Autoantibodies to NOR 90/hUBF: longterm clinical and serological followup in a patient with limited systemic sclerosis suggests an antigen driven immune response, *J Rheumatol* 29(7):1543–1547, 2002.

Damoiseaux J, Andrade LEC, Carballo OG, et al.: Clinical relevance of HEp-2 indirect immunofluorescent patterns: the International Consensus on ANA patterns (ICAP) perspective, *Ann Rheum Dis* 78(7):879–889, 2019.

Damoiseaux J, Boesten K, Giesen J: Evaluation of a novel line-blot immunoassay for the detection of antibodies to extractable nuclear antigens, *Ann N Y Acad Sci* 1050:340–347, 2005.

D'Aoust J, Hudson M, Tatibouet S, et al.: Clinical and serologic correlates of anti-PM/Scl antibodies in systemic sclerosis: a multicenter study of 763 patients, *Arthritis Rheumatol* 66(6):1608–1615, 2014.

Darrah E, Giles JT, Davis RL, et al.: Autoantibodies to peptidylarginine deiminase 2 are associated with less severe disease in rheumatoid arthritis, *Front Immunol* 9:2696, 2018.

Darrah E, Martinez-Prat L, Mahler M: Clinical utility of Antipeptidyl arginine deiminase type 4 antibodies, *J Rheumatol* 46(3):329–330, 2019.

Dawson L, Tobin A, Smith P, et al.: Antimuscarinic antibodies in Sjogren's syndrome: where are we, and where are we going? *Arthritis Rheum* 52(10):2984–2995, 2005.

Dellavance A, Baldo DC, Zheng B, et al.: Establishment of an international autoantibody reference standard for human anti-DFS70 antibodies: proof-of-concept study for a novel Megapool strategy by pooling individual specific sera, *Clin Chem Lab Med*, 2019.

Denton CP, Khanna D: Systemic sclerosis, *Lancet* 390(10103):1685–1699, 2017.

Denton CP, Krieg T, Guillevin L, et al.: Demographic, clinical and antibody characteristics of patients with digital ulcers in systemic sclerosis: data from the DUO Registry, *Ann Rheum Dis* 71(5):718–721, 2012.

Deshmukh US, Gaskin F, Lewis JE, et al.: Mechanisms of autoantibody diversification to SLE-related autoantigens, *Ann N Y Acad Sci* 987:91–98, 2003.

Despierres L, Beziane A, Kaplanski G, et al.: Contribution of anti-beta2glycoprotein I IgA antibodies to the diagnosis of anti-phospholipid syndrome: potential interest of target domains to discriminate thrombotic and non-thrombotic patients, *Rheumatology (Oxford)* 53(7):1215–1218, 2014.

Dorner T, Egerer K, Feist E, et al.: Rheumatoid factor revisited, *Curr Opin Rheumatol* 16(3):246–253, 2004.

Dorner T, Furie R: Novel paradigms in systemic lupus erythematosus, *Lancet* 393(10188):2344–2358, 2019.

Duzgun N, Sahin M, Genc Y, et al.: Antinucleosome antibodies and systemic lupus erythematosus, *Ann N Y Acad Sci* 1109:421–428, 2007.

Elkon KB, Parnassa AP, Foster CL: Lupus autoantibodies target ribosomal P proteins, *J Exp Med* 162(2):459–471, 1985.

Emery P, Mankia K, Nam JL: Individuals at risk of rheumatoid arthritis - the evolving story, *Best Pract Res Clin Rheumatol* 31(1):1–2, 2017.

Emlen W, O'Neill L: Clinical significance of antinuclear antibodies: comparison of detection with immunofluorescence and enzyme-linked immunosorbent assays, *Arthritis Rheum* 40(9):1612–1618, 1997.

Eriksson C, Engstrand S, Sundqvist KG, et al.: Autoantibody formation in patients with rheumatoid arthritis treated with anti-TNF alpha, *Ann Rheum Dis* 64(3):403–407, 2005.

Errico A, Claudiani P, D'Addio M, et al.: Spastin interacts with the centrosomal protein NA14, and is enriched in the spindle pole, the midbody and the distal axon, *Hum Mol Genet* 13(18):2121–2132, 2004.

Espada G, Maldonado Cocco JA, Fertig N, et al.: Clinical and serologic characterization of an Argentine pediatric myositis cohort: identification of a novel autoantibody (anti-MJ) to a 142-kDa protein, *J Rheumatol* 36(11):2547–2551, 2009.

Feist E, Steiner G: Rheumatoid arthritis: an antigenic chameleon, *Ann Rheum Dis* 73(10):1753–1754, 2014.

Firestein GS: Evolving concepts of rheumatoid arthritis, *Nature* 423(6937):356–361, 2003.

Fischer A, Pfalzgraf FJ, Feghali-Bostwick CA, et al.: Anti-th/to-positivity in a cohort of patients with idiopathic pulmonary fibrosis, *J Rheumatol* 33(8):1600–1605, 2006.

Flam ST, Gunnarsson R, Garen T, et al.: *The HLA profiles of mixed connective tissue disease differ distinctly from the profiles of clinically related connective tissue diseases*, Oxford, 2014, Rheumatology.

Foggia P, Percannella G, Soda P, et al.: Benchmarking HEp-2 cells classification methods, *IEEE Trans Med Imaging* 32(10):1878–1889, 2013.

Forslind K, Ahlmen M, Eberhardt K, et al.: Prediction of radiological outcome in early rheumatoid arthritis in clinical practice: role of antibodies to citrullinated peptides (anti-CCP), *Ann Rheum Dis* 63(9):1090–1095, 2004.

Francoeur A-M, Peebles CL, Gompper PT, et al.: Identification of Ki (Ku, p70/p80) autoantigens and analysis of anti-Ki autoantibody reactivity, *J Immunol* 136:1648–1653, 1986.

Fredi M, Bartoli F, Cavazzana I, et al.: Calcinosis in poly-dermatomyositis: clinical and laboratory predictors and treatment options, *Clin Exp Rheumatol* 35(2):303–308, 2017.

Fredi M, Cavazzana I, Franceschini F: The clinico-serological spectrum of overlap myositis, *Curr Opin Rheumatol* 30(6):637–643, 2018.

Fritzler M: Autoantibody testing: current challenges and future opportunities. In Conrad K CE, Fritzler MJ, Humbel RL, et al.: *From prediction to Prevention of autoimmune diseases*, Berlin, 2011, Pabst Science Publishers, pp 584–596.

Fritzler MJ, Behmanesh F, Fritzler ML: Analysis of human sera that are polyreactive in an addressable laser bead immunoassay, *Clin Immunol* 120(3):349–356, 2006.

Fritzler MJ, Fritzler ML: Microbead-based technologies in diagnostic autoantibody detection, *Expert Opin Med Diagn* 3(1):81–89, 2009.

Fritzler MJ, Fritzler ML: The emergence of multiplexed technologies as diagnostic platforms in systemic autoimmune diseases, *Curr Med Chem* 13(21):2503–2512, 2006.

Fritzler MJ, Hudson M, Choi MY, et al.: Bicaudal D2 is a novel autoantibody target in systemic sclerosis that shares a key epitope with CENP-A but has a distinct clinical phenotype, *Autoimmun Rev* 17(3):267–275, 2018.

Fritzler MJ, Kinsella TD, Garbutt E: The CREST syndrome: a distinct serologic entity with anticentromere antibodies, *Am J Med* 69:520–526, 1980.

Fritzler MJ, Martinez-Prat L, Choi MY, et al.: The utilization of autoantibodies in approaches to precision health, *Front Immunol* 9:2682, 2018.

Fritzler MJ, von Muhlen CA, Toffoli SM, et al.: Autoantibodies to the nucleolar organizer antigen NOR-90 in children with systemic rheumatic diseases, *J Rheumatol* 22:521–524, 1995.

Fritzler MJ, Wiik A, Fritzler ML, et al.: The use and abuse of commercial kits used to detect autoantibodies, *Arthritis Res Ther* 5(4):192–201, 2003.

Fritzler MJ: Advances and applications of multiplexed diagnostic technologies in autoimmune diseases, *Lupus* 15(7):422–427, 2006.

Fritzler MJ: The antinuclear antibody test: last or lasting gasp? *Arthritis Rheum* 63(1):19–22, 2011.

Fujii T, Mimori T, Hama N, et al.: Detection of anti-NOR-90 in patient sera with anti-nucleolar antibodies using a cDNA that encodes for the NOR-90 autoantigen: correlation of anti-NOR-90 with Sjögren's syndrome (abstract), *Arthritis Rheumat* 35:S72, 1992.

Fujimoto M, Hamaguchi Y, Kaji K, et al.: Myositis-specific anti-155/140 autoantibodies target transcription intermediary factor 1 family proteins, *Arthritis Rheum* 64(2):513–522, 2012.

Fujimoto M, Matsushita T, Hamaguchi Y, et al.: Autoantibodies to small ubiquitin-like modifier activating enzymes in Japanese patients with dermatomyositis: comparison with a UK Caucasian cohort, *Ann Rheum Dis* 72(1):151–153, 2013.

Gan RW, Trouw LA, Shi J, et al.: Anti-carbamylated protein antibodies are present prior to rheumatoid arthritis and are associated with its future diagnosis, *J Rheumatol*, 2015.

Gao J, Cha S, Jonsson R, et al.: Detection of anti-type 3 muscarinic acetylcholine receptor autoantibodies in the sera of Sjogren's syndrome patients by use of a transfected cell line assay, *Arthritis Rheum* 50(8):2615–2621, 2004.

Ghirardello A, Bassi N, Palma L, et al.: Autoantibodies in polymyositis and dermatomyositis, *Curr Rheumatol Rep* 15(6):335, 2013.

Ghirardello A, Bendo R, Rampudda ME, et al.: Commercial blot assays in the diagnosis of systemic rheumatic diseases, *Autoimmun Rev* 8(8):645–649, 2009.

Ghirardello A, Rampudda M, Ekholm L, et al.: Diagnostic performance and validation of autoantibody testing in myositis by a commercial line blot assay, *Rheumatology* 49(12):2370–2374, 2010.

Giacomelli R, Afeltra A, Alunno A, et al.: Guidelines for biomarkers in autoimmune rheumatic diseases - evidence based analysis, *Autoimmun Rev* 18(1):93–106, 2019.

Girbal E, Sebbag M, Gomes-Daudrix V, et al.: Characterisation of the rat oesophagus epithelium antigens defined by the so-called 'antikeratin antibodies', specific for rheumatoid arthritis, *Ann Rheum Dis* 52(10):749–757, 1993.

Gomez-Puerta JA, Burlingame RW, Cervera R: Anti-chromatin (anti-nucleosome) antibodies: diagnostic and clinical value, *Autoimmun Rev* 7(8):606–611, 2008.

Gomez-Puerta JA, Cervera R: Diagnosis and classification of the antiphospholipid syndrome, *J Autoimmun* 48–49:20–25, 2014.

Gono T, Kawaguchi Y, Satoh T, et al.: Clinical manifestation and prognostic factor in anti-melanoma differentiation-associated gene 5 antibody-associated interstitial lung disease as a complication of dermatomyositis, *Rheumatology* 49(9):1713–1719, 2010.

Gonzalez-Moreno J, Raya-Cruz M, Losada-Lopez I, et al.: Rapidly progressive interstitial lung disease due to anti-MDA5 antibodies without skin involvement: a case report and literature review, *Rheumatol Int* 38(7):1293–1296, 2018.

Guidelines: Guidelines for referral and management of systemic lupus erythematosus in adults. American College of Rheumatology Ad Hoc committee on systemic lupus erythematosus guidelines, *Arthritis Rheum* 42(9):1785–1796, 1999.

Gunawardena H, Betteridge ZE, McHugh NJ: Myositis-specific autoantibodies: their clinical and pathogenic significance in disease expression, *Rheumatology* 48(6):607–612, 2009.

Gunawardena H, Betteridge ZE, McHugh NJ: Newly identified autoantibodies: relationship to idiopathic inflammatory myopathy subsets and pathogenesis, *Curr Opin Rheumatol* 20(6):675–680, 2008.

Gunawardena H, Wedderburn LR, Chinoy H, et al.: Autoantibodies to a 140-kd protein in juvenile dermatomyositis are associated with calcinosis, *Arthritis Rheum* 60(6):1807–1814, 2009.

Halvorsen EH, Pollmann S, Gilboe IM, et al.: Serum IgG antibodies to peptidylarginine deiminase 4 in rheumatoid arthritis and associations with disease severity, *Ann Rheum Dis* 67(3):414–417, 2008.

Hamaguchi Y, Kuwana M, Hoshino K, et al.: Clinical correlations with dermatomyositis-specific autoantibodies in adult Japanese patients with dermatomyositis: a multicenter cross-sectional study, *Arch Dermatol* 147(4):391–398, 2011.

Hanke K, Bruckner CS, Dahnrich C, et al.: Antibodies against PM/Scl-75 and PM/Scl-100 are independent markers for different subsets of systemic sclerosis patients, *Arthritis Res Ther* 11(1):R22, 2009.

Hanly JG, Su L, Farewell V, et al.: Comparison between multiplex assays for autoantibody detection in systemic lupus erythematosus, *J Immunol Methods* 358(1–2):75–80, 2010.

Harley JB, James JA: Autoepitopes in lupus, *J Lab Clin Med* 126(6):509–516, 1995.

Harris EN, Gharavi AE, Boey ML, et al.: Anticardiolipin antibodies: detection by radioimmunoassay and association with thrombosis in systemic lupus erythematosus, *Lancet* 2:1211–1214, 1983.

Harris ML, Darrah E, Lam GK, et al.: Association of autoimmunity to peptidyl arginine deiminase type 4 with genotype and disease severity in rheumatoid arthritis, *Arthritis Rheum* 58(7):1958–1967, 2008.

Harris ML, Rosen A: Autoimmunity in scleroderma: the origin, pathogenetic role, and clinical significance of autoantibodies, *Curr Opin Rheumatol* 15(6):778–784, 2003.

Haschka J, Englbrecht M, Hueber AJ, et al.: Relapse rates in patients with rheumatoid arthritis in stable remission tapering or stopping antirheumatic therapy: interim results from the prospective randomised controlled RETRO study, *Ann Rheum Dis*, 2015.

Hengstman GJ, ter Laak HJ, Vree Egberts WT, et al.: Anti-signal recognition particle autoantibodies: marker of a necrotising myopathy, *Ann Rheum Dis* 65(12):1635–1638, 2006.

Hengstman GJ, van Brenk L, Vree Egberts WT, et al.: High specificity of myositis specific autoantibodies for myositis compared with other neuromuscular disorders, *J Neurol* 252(5):534–537, 2005.

Hensvold AH, Magnusson PK, Joshua V, et al.: Environmental and genetic factors in the development of anticitrullinated protein antibodies (ACPAs) and ACPA-positive rheumatoid arthritis: an epidemiological investigation in twins, *Ann Rheum Dis* 74(2):375–380, 2015.

Hernandez-Molina G, Nunez-Alvarez C, Avila-Casado C, et al.: Usefulness of IgA anti-alpha-fodrin antibodies in combination with rheumatoid factor and/or antinuclear antibodies as Substitute immunological criterion in Sjogren syndrome with negative anti-SSA/SSB antibodies, *J Rheumatol* 43(10):1852–1857, 2016.

Hervier B, Devilliers H, Stanciu R, et al.: Hierarchical cluster and survival analyses of antisynthetase syndrome: phenotype and outcome are correlated with anti-tRNA synthetase antibody specificity, *Autoimmun Rev* 12(2):210–217, 2012.

Hirohata S, Sakuma Y, Yanagida T, et al.: Association of cerebrospinal fluid anti-Sm antibodies with acute confusional state in systemic lupus erythematosus, *Arthritis Res Ther* 16(5):450, 2014.

Hoa S, Hudson M, Troyanov Y, et al.: Single-specificity anti-Ku antibodies in an international cohort of 2140 systemic sclerosis subjects: clinical associations, *Medicine* 95(35), 2016. e4713.

Hochberg MC, Boyd RE, Ahearn JM, et al.: Systemic lupus erythematosus: a review of clinico-laboratory features and immunogenetic markers in 150 patients with emphasis on demographic subsets, *Medicine* 64(5):285–295, 1985.

Hochberg MC: Updating the American College of Rheumatology revised criteria for the classification of systemic lupus erythematosus, *Arthritis Rheum* 40(9):1725, 1997.

Hoffman IE, Peene I, Veys EM, et al.: Detection of specific antinuclear reactivities in patients with negative anti-nuclear antibody immunofluorescence screening tests, *Clin Chem* 48(12):2171–2176, 2002.

Homburger HA, Cahen YD, Griffiths J, et al.: Detection of antinuclear antibodies: comparative evaluation of enzyme immunoassay and indirect immunofluorescence methods, *Arch Pathol Lab Med* 122(11):993–999, 1998.

Honma M, Komatsu S, Igawa S, et al.: Rapidly progressive systemic sclerosis associated with breast carcinoma: report of a case with anti-RNA polymerase III antibody, *J Dermatol* 39(6):574–576, 2012.

Hoogendijk JE, Amato AA, Lecky BR, et al.: 119th ENMC international workshop: trial design in adult idiopathic inflammatory myopathies, with the exception of inclusion body myositis, 10-12 October 2003, Naarden, The Netherlands, *Neuromuscul Disord* 14(5):337–345, 2004.

Hoshino K, Muro Y, Sugiura K, et al.: Anti-MDA5 and anti-TIF1-gamma antibodies have clinical significance for patients with dermatomyositis, *Rheumatology* 49(9):1726–1733, 2010.

Houssien DA, Jonsson T, Davies E, et al.: Clinical significance of IgA rheumatoid factor Subclasses in rheumatoid arthritis, *J Rheumatol* 24(11):2119–2122, 1997.

Hu Q, Wang D, Chen W: The accuracy of the anti-alpha-fodrin antibody test for diagnosis of Sjogren's syndrome: a meta-analysis, *Clin Biochem* 46(15):1372–1376, 2013.

Huang L, Wang L, Yang Y, et al.: Coexistence of anti-HMGCR and anti-MDA5 identified by an unlabeled immunoprecipitation assay in a Chinese patient cohort with myositis, *Medicine* 97(47), 2018. e13236.

Hudson M, Mahler M, Pope J, et al.: Clinical correlates of CENP-A and CENP-B antibodies in a large cohort of patients with systemic sclerosis, *J Rheumatol* 39(4):787–794, 2012.

Hudson M, Pope J, Mahler M, et al.: Canadian Scleroderma Research G, et al: clinical significance of antibodies to Ro52/TRIM21 in systemic sclerosis, *Arthritis Res Ther* 14(2):R50, 2012.

Humphreys JH, van Nies J, Chipping J, et al.: Rheumatoid factor and anti-citrullinated protein antibody positivity, but not level, are associated with increased mortality in patients with rheumatoid arthritis: results from two large independent cohorts, *Arthritis Res Ther* 16(6):483, 2014.

Iaccarino L, Gatto M, Bettio S, et al.: Overlap connective tissue disease syndromes, *Autoimmun Rev* 12(3):363–373, 2013.

Ichimura Y, Matsushita T, Hamaguchi Y, et al.: Anti-NXP2 autoantibodies in adult patients with idiopathic inflammatory myopathies: possible association with malignancy, *Ann Rheum Dis* 71(5):710–713, 2012.

Ighe A, Dahlstrom O, Skogh T, et al.: Application of the 2012 systemic lupus international collaborating clinics classification criteria on a Regional Swedish systemic lupus erythematosus register, *Arthritis Res Ther* 17(1):3, 2015.

Ikeda N, Takahashi K, Yamaguchi Y, et al.: Analysis of dermatomyositis-specific autoantibodies and clinical characteristics in Japanese patients, *J Dermatol* 38(10):973–979, 2011.

Imai H, Fritzler MJ, Neri R, et al.: Immunocytochemical characterization of human NOR-90 (upstream binding factor) and associated antigens reactive with autoimmune sera: two MR forms of NOR-90/hUBF autoantigens, *Mol Bio Rep* 19:115–124, 1994.

Ines L, Silva C, Galindo M, et al.: *Classification of systemic lupus erythematosus: systemic lupus international Collaborating Clinics versus American College of Rheumatology criteria*, Hoboken), 2015, Arthritis Care Res.

Infantino M, Pregnolato F, Bentow C, et al.: Only monospecific anti-DFS70 antibodies aid in the exclusion of antinuclear antibody associated rheumatic diseases: an Italian experience, *Clin Chem Lab Med*, 2019.

Infantino M, Tampoia M, Fabris M, et al.: Combining immunofluorescence with immunoblot assay improves the specificity of autoantibody testing for myositis, *Rheumatology* 58(7):1239–1244, 2019.

Ishizaki J, Saito K, Nawata M, et al.: *Low complements and high titre of anti-Sm antibody as predictors of histopathologically proven silent lupus nephritis without abnormal urinalysis in patients with systemic lupus erythematosus*, Rheumatology (Oxford), 2014.

Iverson GM, von Muhlen CA, Staub HL: Patients with atherosclerotic syndrome, negative in anti-cardiolipin assays, make IgA autoantibodies that preferentially target domain 4 of beta2-GPI, *J Autoimmun* 27(4):266–271, 2006.

Jarzabek-Chorzelska M, Blaszczyk M, Jablonska S: Scl-70 antibody - a specific marker of systemic sclerosis, *Br J Dermatol* 115:393–401, 1986.

Jiang X, Trouw LA, van Wesemael TJ, et al.: Anti-CarP antibodies in two large cohorts of patients with rheumatoid arthritis and their relationship to genetic risk factors, cigarette smoking and other autoantibodies, *Ann Rheum Dis* 73(10):1761–1768, 2014.

Johnson SR, Goek ON, Singh-Grewal D, et al.: Classification criteria in rheumatic diseases: a review of methodologic properties, *Arthritis Rheum* 57(7):1119–1133, 2007.

Johnson SR, Soowamber ML, Fransen J, et al.: There is a need for new systemic sclerosis subset criteria. A content analytic approach, *Scand J Rheumatol* 47(1):62–70, 2018.

Johnson SR: Progress in the clinical classification of systemic sclerosis, *Curr Opin Rheumatol* 29(6):568–573, 2017.

Kaji K, Fujimoto M, Hasegawa M, et al.: Identification of a novel autoantibody reactive with 155 and 140 kDa nuclear proteins in patients with dermatomyositis: an association with malignancy, *Rheumatology* 46(1):25–28, 2007.

Kallenberg CGM: Overlapping syndromes, undifferentiated connective tissue disease, and other fibrosing conditions, *Curr Opin Rheumatol* 5:809–815, 1993.

Kalluri M, Sahn SA, Oddis CV, et al.: Clinical profile of anti-PL-12 autoantibody. Cohort study and review of the literature, *Chest* 135(6):1550–1556, 2009.

Kaneda K, Takasaki Y, Takeuchi K, et al.: Autoimmune response to proteins of proliferating cell nuclear antigen multiprotein complexes in patients with connective tissue diseases, *J Rheumatol* 31(11):2142–2150, 2004.

Kang EH, Nakashima R, Mimori T, et al.: Myositis autoantibodies in Korean patients with inflammatory myositis: anti-140-kDa polypeptide antibody is primarily associated with rapidly progressive interstitial lung disease independent of clinically amyopathic dermatomyositis, *BMC Musculoskelet Disord* 11:223, 2010.

Kastbom A, Strandberg G, Lindroos A, et al.: Anti-CCP antibody test predicts the disease course during 3 years in early rheumatoid arthritis (the Swedish TIRA project), *Ann Rheum Dis* 63(9):1085–1089, 2004.

Kessenbrock K, Raijmakers R, Fritzler MJ, et al.: Synthetic peptides: the future of patient management in systemic rheumatic diseases? *Curr Med Chem* 14(26):2831–2838, 2007.

Klareskog L, Alfredsson L, Rantapaa-Dahlqvist S, et al.: What precedes development of rheumatoid arthritis? *Ann Rheum Dis* 63(Suppl 2):ii28–ii31, 2004.

Klein M, Mann H, Plestilova L, et al.: Arthritis in idiopathic inflammatory myopathy: clinical features and autoantibody associations, *J Rheumatol* 41(6):1133–1139, 2014.

Koenig M, Bentow C, Satoh M, et al.: *Autoantibodies to a novel Rpp38 (Th/To) derived B-cell epitope are specific for systemic sclerosis and associate with a distinct clinical phenotype*, Oxford, 2019, Rheumatology.

Koenig M, Fritzler MJ, Targoff IN, et al.: Heterogeneity of autoantibodies in 100 patients with autoimmune myositis: insights into clinical features and outcomes, *Arthritis Res Ther* 9(4):R78, 2007.

Koenig M, Joyal F, Fritzler MJ, et al.: Autoantibodies and microvascular damage are independent predictive factors for the progression of Raynaud's phenomenon to systemic sclerosis: a twenty-year prospective study of 586 patients, with validation of proposed criteria for early systemic sclerosis, *Arthritis Rheum* 58(12):3902–3912, 2008.

Kolfenbach JR, Deane KD, Derber LA, et al.: Autoimmunity to peptidyl arginine deiminase type 4 precedes clinical onset of rheumatoid arthritis, *Arthritis Rheum* 62(9):2633–2639, 2010.

Kovacs L, Feher E, Bodnar I, et al.: Demonstration of autoantibody binding to muscarinic acetylcholine receptors in the salivary gland in primary Sjogren's syndrome, *Clin Immunol* 128(2):269–276, 2008.

Kovacs L, Marczinovits I, Gyorgy A, et al.: Clinical associations of autoantibodies to human muscarinic acetylcholine receptor 3(213-228) in primary Sjogren's syndrome, *Rheumatology* 44(8):1021–1025, 2005.

Krapf A, von Muhlen CA, Krapf F, et al.: *Atlas of immunofluorescent antibodies*, Munich, 1996, Urban & Schwarzenberg.

Kroshinsky D, Stone JH, Bloch DB, et al.: Case records of the Massachusetts General Hospital. Case 5-2009. A 47-year-old woman with a rash and numbness and pain in the legs, *N Engl J Med* 360(7):711–720, 2009.

Kubuschok B, Preuss KD, Baier-Thoenes K, et al.: Autoantibodies against lamin C, NA14 and CK15 in primary vasculitides or autoimmune diseases with secondary vasculitis, *Clin Exp Rheumatol* 34(3 Suppl 97):S60–69, 2016.

Kunz M: Lupus erythematosus. Part I: epidemiology, genetics and immunology, *J Dtsch Dermatol Ges* 11(8):709–719, 2013. quiz 720, 709–720; quiz 721.

Kuwana M, Kaburaki J, Mimori T, et al.: Autoantibody reactive with three classes of RNA polymerases in sera from patients with systemic sclerosis, *J Clini Invest* 91:1399–1404, 1993.

Labirua-Iturburu A, Selva-O'Callaghan A, Vincze M, et al.: Anti-PL-7 (anti-threonyl-tRNA synthetase) antisynthetase syndrome: clinical manifestations in a series of patients from a European multicenter study (EUMYONET) and review of the literature, *Medicine* 91(4):206–211, 2012.

Lakos G, Favaloro EJ, Harris EN, et al.: International consensus guidelines on anticardiolipin and anti-beta2-glycoprotein I testing: report from the 13th International Congress on Antiphospholipid Antibodies, *Arthritis Rheum* 64(1):1–10, 2012.

Larman HB, Salajegheh M, Nazareno R, et al.: Cytosolic 5'-nucleotidase 1A autoimmunity in sporadic inclusion body myositis, *Ann Neurol* 73(3):408–418, 2013.

Lazaro MA, Cocco JAM, Catoggio LJ, et al.: Clinical and serologic characteristics of patients with overlap syndrome: is mixed connective tissue disease a distinct clinical entity? *Medicine* 68:58–65, 1989.

Lee DM, Phillips R, Hagan EM, et al.: Quantifying anti-cyclic citrullinated peptide titres: clinical utility and association with tobacco exposure in patients with rheumatoid arthritis, *Ann Rheum Dis* 68(2):201–208, 2009.

Lee DM, Schur PH: Clinical utility of the anti-CCP assay in patients with rheumatic diseases, *Ann Rheum Dis* 62(9):870–874, 2003.

Lee HS, Irigoyen P, Kern M, et al.: Interaction between smoking, the shared epitope, and anti-cyclic citrullinated peptide: a mixed picture in three large North American rheumatoid arthritis cohorts, *Arthritis Rheum* 56(6):1745–1753, 2007.

Lee SA, Kahng J, Kim Y, et al.: Comparative study of immunofluorescent antinuclear antibody test and line immunoassay detecting 15 specific autoantibodies in patients with systemic rheumatic disease, *J Clin Lab Anal* 26(4):307–314, 2012.

Lerner MR, Steitz JA: Antibodies to small nuclear RNAs complexed with proteins are produced by patients with systemic lupus erythematosus, *Proc Natl Acad Sci U S A* 76(11):5495–5499, 1979.

Lewis MJ, McAndrew MB, Wheeler C, et al.: Autoantibodies targeting TLR and SMAD pathways define new subgroups in systemic lupus erythematosus, *J Autoimmun* 91:1–12, 2018.

Li T, Prokopec SD, Morrison S, et al.: *Anti-nucleosome antibodies outperform traditional biomarkers as longitudinal indicators of disease activity in systemic lupus erythematosus*, Oxford, 2014, Rheumatology.

Liao KP, Weinblatt ME, Solomon DH: The end of rheumatoid factor as we know it? *Arthritis Rheum* 63(5):1170–1172, 2011.

Locht H, Pelck R, Manthorpe R: Diagnostic and prognostic significance of measuring antibodies to alpha-fodrin compared to anti-Ro-52, anti-Ro-60, and anti-La in primary Sjogren's syndrome, *J Rheumatol* 35(5):845–849, 2008.

Lom-Orta H, Alarcon-Segovia D, Diaz-Jouanen E: Systemic lupus erythematosus. Differences between patients who do, and who do not, fulfill classification criteria at the time of diagnosis, *J Rheumatol* 7(6):831–837, 1980.

Lopez LR, Santos ME, Espinoza LR, et al.: Clinical significance of immunoglobulin A versus immunoglobulins G and M anti-cardiolipin antibodies in patients with systemic lupus erythematosus. Correlation with thrombosis, thrombocytopenia, and recurrent abortion, *Am J Clin Pathol* 98(4):449–454, 1992.

Lopez-Longo FJ, Rodriguez-Mahou M, Escalona-Monge M, et al.: Simultaneous identification of various antinuclear antibodies using an automated multiparameter line immunoassay system, *Lupus* 12(8):623–629, 2003.

Love LA, Weinberg CR, McConnaughey DR, et al.: Ultraviolet radiation intensity predicts the relative distribution of dermatomyositis and anti-Mi-2 autoantibodies in women, *Arthritis Rheum* 60(8):2499–2504, 2009.

Low JM, Chauhan AK, Kietz DA, et al.: Determination of anti-cyclic citrullinated peptide antibodies in the sera of patients with juvenile idiopathic arthritis, *J Rheumatol* 31(9):1829–1833, 2004.

Lundberg IE, de Visser M, Werth VP: Classification of myositis, *Nat Rev Rheumatol* 14(5):269–278, 2018.

Maddison PJ: Mixed connective tissue disease, overlap syndromes, and eosinophilic fasciitis, *Ann Rheum Dis* 50:887–893, 1991.

Maenhout TM, Bonroy C, Verfaillie C, et al.: Automated indirect immunofluorescence microscopy enables the implementation of a quantitative internal quality control system for anti-nuclear antibody (ANA) analysis, *Clin Chem Lab Med* 52(7):989–998, 2014.

Mahler M, Agmon-Levin N, van Liempt M, et al.: Multi-center evaluation of autoantibodies to the major ribosomal P C22 epitope, *Rheumatol Int* 32(3):691–698, 2012.

Mahler M, Betteridge Z, Bentow C, et al.: Comparison of three immunoassays for the detection of myositis specific antibodies, *Front Immunol* 10:848, 2019.

Mahler M, Fritzler MJ, Satoh M: Autoantibodies to the mitochondrial RNA processing (MRP) complex also known as Th/To autoantigen, *Autoimmun Rev* 14(3):254–257, 2015.

Mahler M, Fritzler MJ: Epitope specificity and significance in systemic autoimmune diseases, *Ann N Y Acad Sci* 1183:267–287, 2010.

Mahler M, Fritzler MJ: PM1-Alpha ELISA: the assay of choice for the detection of anti-PM/Scl autoantibodies? *Autoimmun Rev* 8(5):373–378, 2009.

Mahler M, Fritzler MJ: Recent advances in peptide Resolved diagnostics of systemic autoimmune diseases. In Conrad K CE, Fritzler MJ, Humbel RL, et al.: *From prediction to Prevention of autoimmune diseases*, Berlin, 2011, Pabst Science Publishers, pp 598–625.

Mahler M, Gascon C, Patel S, et al.: Rpp25 is a major target of autoantibodies to the Th/To complex as measured by a novel chemiluminescent assay, *Arthritis Res Ther* 15(2):R50, 2013.

Mahler M, Kessenbrock K, Raats J, et al.: Technical and clinical evaluation of anti-ribosomal P protein immunoassays, *J Clin Lab Anal* 18(4):215–223, 2004.

Mahler M, Kessenbrock K, Szmyrka M, et al.: International multicenter evaluation of autoantibodies to ribosomal P proteins, *Clin Vaccine Immunol* 13(1):77–83, 2006.

Mahler M, Meroni PL, Bossuyt X, et al.: Current concepts and future directions for the assessment of autoantibodies to cellular antigens referred to as anti-nuclear antibodies, *J Immunol Res* 315179:2014, 2014.

Mahler M, Miller FW, Fritzler MJ: Idiopathic inflammatory myopathies and the anti-synthetase syndrome: a comprehensive review, *Autoimmun Rev* 13(4–5):367–371, 2014.

Mahler M, Miyachi K, Peebles C, et al.: The clinical significance of autoantibodies to the proliferating cell nuclear antigen (PCNA), *Autoimmun Rev* 11(10):771–775, 2012.

Mahler M, Ngo JT, Schulte-Pelkum J, et al.: Limited reliability of the indirect immunofluorescence technique for the detection of anti-Rib-P antibodies, *Arthritis Res Ther* 10(6):R131, 2008.

Mahler M, Pierangeli S, Meroni PL, et al.: Autoantibodies in systemic autoimmune disorders, *J Immunol Res* 263091, 2014. 2014.

Mahler M, Raijmakers R, Dahnrich C, et al.: Clinical evaluation of autoantibodies to a novel PM/Scl peptide antigen, *Arthritis Res Ther* 7(3):R704–713, 2005.

Mahler M, Raijmakers R: Novel aspects of autoantibodies to the PM/Scl complex: clinical, genetic and diagnostic insights, *Autoimmun Rev* 6(7):432–437, 2007.

Mahler M, Satoh M, Hudson M, et al.: Autoantibodies to the Rpp25 component of the Th/To complex are the most common antibodies in patients with systemic sclerosis without antibodies detectable by widely available commercial tests, *J Rheumatol* 41(7):1334–1343, 2014.

Mahler M, Swart A, Wu J, et al.: Clinical and serological associations of autoantibodies to the Ku70/Ku80 heterodimer determined by a novel chemiluminescent immunoassay, *Lupus* 25(8):889–896, 2016.

Mahler M, You D, Baron M, et al.: Anti-centromere antibodies in a large cohort of systemic sclerosis patients: comparison between immunofluorescence, CENP-A and CENP-B ELISA, *Clin Chim Acta* 412(21–22):1937–1943, 2011.

Mammen AL, Chung T, Christopher-Stine L, et al.: Autoantibodies against 3-hydroxy-3-methylglutaryl-coenzyme A reductase in patients with statin-associated autoimmune myopathy, *Arthritis Rheum* 63(3):713–721, 2011.

Mammen AL, Gaudet D, Brisson D, et al.: Increased frequency of DRB1*11:01 in anti-hydroxymethylglutaryl-coenzyme A reductase-associated autoimmune myopathy, *Arthritis Care Res* 64(8):1233–1237, 2012.

Mammen AL, Pak K, Williams EK, et al.: Rarity of anti-3-hydroxy-3-methylglutaryl-coenzyme A reductase antibodies in statin users, including those with self-limited musculoskeletal side effects, *Arthritis Care Res* 64(2):269–272, 2012.

Mammen AL: Necrotizing myopathies: beyond statins, *Curr Opin Rheumatol* 26(6):679–683, 2014.

Maraia RJ, Bayfield MA: The La protein-RNA complex surfaces, *Molecular cell* 21(2):149–152, 2006.

Mariampillai K, Granger B, Amelin D, et al.: Development of a new classification system for idiopathic inflammatory myopathies based on clinical manifestations and myositis-specific autoantibodies, *JAMA Neurol* 75(12):1528–1537, 2018.

Marie I, Hatron PY, Dominique S, et al.: Short-term and long-term outcome of anti-Jo1-positive patients with anti-Ro52 antibody, *Semin Arthritis Rheum* 41(6):890–899, 2012.

Marie I, Josse S, Decaux O, et al.: Comparison of long-term outcome between anti-Jo1- and anti-PL7/PL12 positive patients with antisynthetase syndrome, *Autoimmun Rev* 11(10):739–745, 2012.

Martinez-Prat L, Lucia D, Ibarra C, et al.: Antibodies targeting protein-arginine deiminase 4 (PAD4) demonstrate diagnostic value in rheumatoid arthritis, *Ann Rheum Dis* 78(3):434–436, 2019.

Martins TB, Burlingame R, von Muhlen CA, et al.: Evaluation of multiplexed fluorescent microsphere immunoassay for detection of autoantibodies to nuclear antigens, *Clin Diagn Lab Immunol* 11(6):1054–1059, 2004.

Marto N, Bertolaccini ML, Calabuig E, et al.: Anti-C1q antibodies in nephritis: correlation between titres and renal disease activity and positive predictive value in systemic lupus erythematosus, *Ann Rheum Dis* 64(3):444–448, 2005.

Massa M, de Benedetti F, Pignatti P, Albani S, di Fuccia G, Monestier M, Martini A: Anti-double stranded DNA, anti-histone, and anti-nucleosome IgG reactivities in children with systemic lupus erythematosus, Clini Exp Rheumatol 12: 219–225.

Matsuura E, Lopez LR: Autoimmune-mediated atherothrombosis, *Lupus* 17(10):878–887, 2008.

Mavragani CP, Moutsopoulos HM: Sjogren's syndrome, *Annu Rev Pathol* 9:273–285, 2014.

McCauliffe DP, Yin H, Wang LX, et al.: Autoimmune sera react with multiple epitopes on recombinant 52 and 60 kDa Ro(SSA) proteins, *J Rheumatol* 21(6):1073–1080, 1994.

McMahan ZH, Domsic RT, Zhu L, et al.: *Anti-RNPC3 (U11/U12) antibodies in systemic sclerosis are associated with moderate to severe gastrointestinal dysmotility*, Hoboken), 2018, Arthritis Care Res.

McNeil HP, Hunt JE, Krilis SA: Antiphospholipid antibodies—new insights into their specificity and clinical importance, *Scand J Immunol* 36(5):647–652, 1992.

Meerovitch K, Svitkin YV, Lee HS, et al.: La autoantigen enhances and corrects aberrant translation of poliovirus RNA in reticulocyte lysate, *J Virol* 67(7):3798–3807, 1993.

Mehndiratta P, Mehta S, Manjila SV, et al.: Isolated necrotizing myopathy associated with ANTI-PL12 antibody, *Muscle Nerve* 46(2):282–286, 2012.

Mehra S, Fritzler MJ: The spectrum of anti-chromatin/nucleosome autoantibodies: independent and interdependent biomarkers of disease, *J Immunol Res*368274, 2014. 2014.

Mehra S, Walker J, Patterson K, et al.: Autoantibodies in systemic sclerosis, *Autoimmun Rev* 12(3):340–354, 2013.

Melegari A, Bonaguri C, Russo A, et al.: A comparative study on the reliability of an automated system for the evaluation of cell-based indirect immunofluorescence, *Autoimmun Rev* 11(10):713–716, 2012.

Meroni PL, Schur PH: ANA screening: an old test with new recommendations, *Ann Rheum Dis* 69(8):1420–1422, 2010.

Miller FW, Waite KA, Biswas T, et al.: The role of an autoantigen, histidyl-tRNA synthetase, in the induction and maintenance of autoimmunity, *Proc Natl Acad Sci U S A* 87(24):9933–9937, 1990.

Miyachi K, Fritzler MJ, Tan EM: Autoantibody to a nuclear antigen in proliferating cells, *J Immunol* 121:2228–2234, 1978.

Mohassel P, Mammen AL: Anti-HMGCR myopathy, *J Neuromuscul Dis* 5(1):11–20, 2018.

Moinzadeh P, Fonseca C, Hellmich M, et al.: Association of anti-RNA polymerase III autoantibodies and cancer in scleroderma, *Arthritis Res Ther* 16(1):R53, 2014.

Moroi Y, Peebles C, Fritzler MJ, et al.: Autoantibody to centromere (kinetochore) in scleroderma sera, *Proc Nat Acad Sci U S A* 77:1627–1631, 1980.

Mortensen ES, Rekvig OP: Nephritogenic potential of anti-DNA antibodies against necrotic nucleosomes, *J Am Soc Nephrol* 20(4):696–704, 2009.

Mosca M, Baldini C, Bombardieri S: Undifferentiated connective tissue diseases in 2004, *Clin Exp Rheumatol* 22(3 Suppl 33):S14–18, 2004.

Mosca M, Tani C, Vagnani S, et al.: The diagnosis and classification of undifferentiated connective tissue diseases, *J Autoimmun* 48–49:50–52, 2014.

Muller S, Dieker J, Tincani A, et al.: Pathogenic anti-nucleosome antibodies, *Lupus* 17(5):431–436, 2008.

Mummert E, Fritzler MJ, Sjowall C, et al.: The clinical utility of anti-double-stranded DNA antibodies and the challenges of their determination, *J Immunol Methods* 459:11–19, 2018.

Muro Y, Ishikawa A, Sugiura K, et al.: Clinical features of anti-TIF1-alpha antibody-positive dermatomyositis patients are closely associated with coexistent dermatomyositis-specific autoantibodies and anti-TIF1-gamma or anti-Mi-2 autoantibodies, *Rheumatology* 51(8):1508–1513, 2012.

Muro Y, Sugiura K, Akiyama M: What autoantibody tests should become widely available to help scleroderma diagnosis and management? *Arthritis Res Ther* 15(4):116, 2013.

Murthy V, Willis R, Romay-Penabad Z, et al.: Value of isolated IgA anti-beta2 -glycoprotein I positivity in the diagnosis of the antiphospholipid syndrome, *Arthritis Rheum* 65(12):3186–3193, 2013.

Musset L, Miyara M, Benveniste O, et al.: Analysis of autoantibodies to 3-hydroxy-3-methylglutaryl-coenzyme A reductase using different technologies, *J Immunol Res*405956, 2014. 2014.

Mydel P, Wang Z, Brisslert M, et al.: Carbamylation-dependent activation of T cells: a novel mechanism in the pathogenesis of autoimmune arthritis, *J Immunol* 184(12):6882–6890, 2010.

Nakamura RM, Bylund DJ, Tan EM: Current status of available standards for quality improvement of assays for detection of autoantibodies to nuclear and intracellular antigens, *J Clini Lab Anal* 8:360–368, 1994.

Nakamura RM, Bylund DJ: Contemporary concepts for the clinical and laboratory evaluation of systemic lupus erythematosus and " lupus- like " syndromes, *J Clini Lab Analysis* 8:347–359, 1994.

Nakamura RM, Tan EM: Update on autoantibodies to intracellular antigens in systemic rheumatic diseases, *Clin Lab Med* 12:1–23, 1992.

Nakashima R, Imura Y, Kobayashi S, et al.: The RIG-I-like receptor IFIH1/MDA5 is a dermatomyositis-specific autoantigen identified by the anti-CADM-140 antibody, *Rheumatology* 49(3):433–440, 2010.

Nandiwada SL, Peterson LK, Mayes MD, et al.: Ethnic differences in autoantibody diversity and Hierarchy: more clues from a US cohort of patients with systemic sclerosis, *J Rheumatol* 43(10):1816–1824, 2016.

Ni JD, Yao X, Pan HF, et al.: Clinical and serological correlates of anti-Sm autoantibodies in Chinese patients with systemic lupus erythematosus: 1,584 cases, *Rheumatol Int* 29(11):1323–1326, 2009.

Nifli AP, Notas G, Mamoulaki M, et al.: Comparison of a multiplex, bead-based fluorescent assay and immunofluorescence methods for the detection of ANA and ANCA autoantibodies in human serum, *J Immunol Methods* 311(1–2):189–197, 2006.

Nimelstein SH, Brody S, Mcshane D, et al.: Mixed connective tissue disease: a subsequent evaluation of the original 25 patients, *Medicine* 59(4):239–248, 1980.

Nozawa K, Ikeda K, Satoh M, et al.: Autoantibody to NA14 is an independent marker primarily for Sjogren's syndrome, *Front Biosci (Landmark Ed)* 14:3733–3739, 2009.

Obermoser G, Bitterlich W, Kunz F, et al.: Clinical significance of anticardiolipin and anti-beta2-glycoprotein I antibodies, *Int Arch Allergy Immunol* 135(2):148–153, 2004.

Ochs RL, Muro Y, Si Y, et al.: Autoantibodies to DFS 70 kd/transcription coactivator p75 in atopic dermatitis and other conditions, *J Allergy Clin Immunol* 105(6 Pt 1):1211–1220, 2000.

Ochs RL, Stein Jr TW, Peebles CL, et al.: Autoantibodies in interstitial cystitis, *J Urol* 151:587–592, 1994.

Ogawa-Momohara M, Muro Y, Mitsuma T, et al.: Strong correlation between cancer progression and anti-transcription intermediary factor 1gamma antibodies in dermatomyositis patients, *Clin Exp Rheumatol* 36(6):990–995, 2018.

Okazaki K, Kawa S, Kamisawa T, et al.: Clinical diagnostic criteria of autoimmune pancreatitis: revised proposal, *J Gastroenterol* 41(7):626–631, 2006.

Onuora S: Myositis: anti-NXP2 antibodies associated with severe JDM, *Nat Rev Rheumatol* 14(5):248, 2018.

Op De Beeck K, Vermeersch P, Verschueren P, et al.: Antinuclear antibody detection by automated multiplex immunoassay in untreated patients at the time of diagnosis, *Autoimmun Rev* 12(2):137–143, 2012.

Palterer B, Vitiello G, Carraresi A, et al.: Bench to bedside review of myositis autoantibodies, *Clin Mol Allergy* 16(5), 2018.

Panush RS, Greer JM, Morshedian KK: What is lupus? What is not lupus? *Rheum Dis Clin North Am* 19(1):223–234, 1993.

Panush RS, Schur PH: It is lupus? *Bull Rheum Dis* 46(6):3–8, 1997.

Parker JC, Burlingame RW, Webb TT, et al.: Anti-RNA polymerase III antibodies in patients with systemic sclerosis detected by indirect immunofluorescence and ELISA, *Rheumatology* 47(7):976–979, 2008.

Pauling JD, Salazar G, Lu H, et al.: Presence of anti-eukaryotic initiation factor-2B, anti-RuvBL1/2 and anti-synthetase antibodies in patients with anti-nuclear antibody negative systemic sclerosis, *Rheumatology* 57(4):712–717, 2018.

Payet J, Goulvestre C, Biale L, et al.: Anticyclic citrullinated peptide antibodies in rheumatoid and nonrheumatoid rheumatic disorders: experience with 1162 patients, *J Rheumatol* 41(12):2395–2402, 2014.

Perez D, Gilburd B, Azoulay D, et al.: Antinuclear antibodies: is the indirect immunofluorescence still the gold standard or should be replaced by solid phase assays? *Autoimmun Rev* 17(6):548–552, 2018.

Perner P, Perner H, Muller B: Mining knowledge for HEp-2 cell image classification, *Artif Intell Med* 26(1–2):161–173, 2002.

Perricone C, Colafrancesco S, Mazor RD, et al.: Autoimmune/inflammatory syndrome induced by adjuvants (ASIA) 2013: Unveiling the pathogenic, clinical and diagnostic aspects, *J Autoimmun* 47:1–16, 2013.

Petri M, Orbai AM, Alarcon GS, et al.: Derivation and validation of the Systemic Lupus International Collaborating Clinics classification criteria for systemic lupus erythematosus, *Arthritis Rheum* 64(8):2677–2686, 2012.

Pfannenschmid F, Wimmer VC, Rios RM, et al.: Chlamydomonas DIP13 and human NA14: a new class of proteins associated with microtubule structures is involved in cell division, *J Cell Sci* 116(Pt 8):1449–1462, 2003.

Pierangeli SS, Gharavi AE, Harris EN: Testing for antiphospholipid antibodies: problems and solutions, *Clin Obstet Gynecol* 44(1):48–57, 2001. quiz 58-49.

Pierangeli SS, Harris EN: A protocol for determination of anticardiolipin antibodies by ELISA, *Nat Protoc* 3(5):840–848, 2008.

Pierangeli SS, Harris EN: Clinical laboratory testing for the antiphospholipid syndrome, *Clin Chim Acta* 357(1):17–33, 2005.

Pinal-Fernandez I, Casal-Dominguez M, Huapaya JA, et al.: A longitudinal cohort study of the anti-synthetase syndrome: increased severity of interstitial lung disease in black patients and patients with anti-PL7 and anti-PL12 autoantibodies, *Rheumatology* 56(6):999–1007, 2017.

Pincus T, Gibson KA, Shmerling RH: An evidence-based approach to laboratory tests in usual care of patients with rheumatoid arthritis, *Clin Exp Rheumatol* 32(5 Suppl 85), 2014. S-23–28.

Pisetsky DS: Anti-DNA antibodies—quintessential biomarkers of SLE, *Nat Rev Rheumatol* 12(2):102–110, 2016.

Pisetsky DS: Antinuclear antibody testing - misunderstood or misbegotten? *Nat Rev Rheumatol* 13(8):495–502, 2017.

Pollard KM, Hultman P, Kono DH: Toxicology of autoimmune diseases, *Chem Res Toxicol* 23(3):455–466, 2010.

Pope JE: Scleroderma overlap syndromes, *Curr Opin Rheumatol* 14(6):704–710, 2002.

Pottel H, Wiik A, Locht H, et al.: Clinical optimization and multicenter validation of antigen-specific cut-off values on the INNO-LIA ANA update for the detection of autoantibodies in connective tissue disorders, *Clin Exp Rheumatol* 22(5):579–588, 2004.

Radic M, Herrmann M, van der Vlag J, et al.: Regulatory and pathogenetic mechanisms of autoantibodies in SLE, *Autoimmunity* 44(5):349–356, 2011.

Radzimski C, Probst C, Teegen B, et al.: Development of a recombinant cell-based indirect immunofluorescence assay for the determination of autoantibodies against soluble liver antigen in autoimmune hepatitis, *Clin Dev Immunol*572815, 2013. 2013..

Raijmakers R, Renz M, Wiemann C, et al.: PM-Scl-75 is the main autoantigen in patients with the polymyositis/scleroderma overlap syndrome, *Arthritis Rheum* 50(2):565–569, 2004.

Ramos-Morales F, Infante C, et al.: NA14 is a novel nuclear autoantigen with a coiled-coil domain, *J Biol Chem* 273(3):1634–1639, 1998.

Ranzolin A, Bohn JM, Norman GL, et al.: Anti-beta2-glycoprotein I antibodies as risk factors for acute myocardial infarction, *Arq Bras Cardiol* 83(2):141–144, 2004. 137–140.

Reeves WH, Sthoeger ZM: Molecular cloning of cDNA encoding the p70 (Ku) lupus autoantigen, *J Biol Chem* 264(9):5047–5052, 1989.

Reeves WH: Antibodies to the p70/p80 (Ku) antigens in systemic lupus erythematosus, *Rheum Dis Clin North Am* 18(2):391–414, 1992.

Reimer G, Steen VD, Penning CA, et al.: Correlates between autoantibodies to nucleolar antigens and clinical features in patients with systemic sclerosis (sclerodema), *Arthritis Rheumat* 31:525–532, 1988.

Ren J, Sun L, Zhao J: Meta-analysis: diagnostic accuracy of antibody against peptidylarginine deiminase 4 by ELISA for rheumatoid arthritis, *Clin Rheumatol* 36(11):2431–2438, 2017.

Reyes-Castillo Z, Munoz-Valle JF, Llamas-Covarrubias MA: Clinical and immunological aspects of anti-peptidylarginine deiminase type 4 (anti-PAD4) autoantibodies in rheumatoid arthritis, *Autoimmun Rev* 17(2):94–102, 2018.

Rider LG, Shah M, Mamyrova G, et al.: The myositis autoantibody phenotypes of the juvenile idiopathic inflammatory myopathies, *Medicine* 92(4):223–243, 2013.

Riemekasten G, Philippe A, Nather M, et al.: Involvement of functional autoantibodies against vascular receptors in systemic sclerosis, *Ann Rheum Dis* 70(3):530–536, 2011.

Robbins A, Hentzien M, Toquet S, et al.: Diagnostic utility of separate anti-Ro60 and anti-Ro52/TRIM21 antibody detection in autoimmune diseases, *Front Immunol* 10:444, 2019.

Robinson CP, Brayer J, Yamachika S, et al.: Transfer of human serum IgG to non-obese diabetic Igmu null mice reveals a role for autoantibodies in the loss of secretory function of exocrine tissues in Sjogren's syndrome, *Proc Natl Acad Sci U S A* 95(13):7538–7543, 1998.

Rodriguez-Mahou M, Lopez-Longo FJ, Sanchez-Ramon S, et al.: Association of anti-cyclic citrullinated peptide and anti-Sa/citrullinated vimentin autoantibodies in rheumatoid arthritis, *Arthritis Rheum* 55(4):657–661, 2006.

Roggenbuck D, Hiemann R, Bogdanos D, et al.: Standardization of automated interpretation of immunofluorescence tests, *Clin Chim Acta* 421:168–169, 2013.

Roggenbuck D, Hiemann R, Schierack P, et al.: Digital immunofluorescence enables automated detection of antinuclear antibody endpoint titers avoiding serial dilution, *Clin Chem Lab Med* 52(2):e9–11, 2014.

Rombouts Y, Ewing E, van de Stadt LA, et al.: Anti-citrullinated protein antibodies acquire a pro-inflammatory Fc glycosylation phenotype prior to the onset of rheumatoid arthritis, *Ann Rheum Dis* 74(1):234–241, 2015.

Rombouts Y, Willemze A, van Beers JJ, et al.: Extensive glycosylation of ACPA-IgG variable domains modulates binding to citrullinated antigens in rheumatoid arthritis, *Ann Rheum Dis* 75(3):578–585, 2016.

Ronnelid J, Barbasso Helmers S, Storfors H, et al.: Use of a commercial line blot assay as a screening test for autoantibodies in inflammatory myopathies, *Autoimmun Rev* 9(1):58–61, 2009.

Rose HM, Ragan C, et al.: Differential agglutination of normal and sensitized sheep erythrocytes by sera of patients with rheumatoid arthritis, *Proc Soc Exp Biol Med* 68(1):1–6, 1948.

Rose T, Grutzkau A, Hirseland H, et al.: IFNalpha and its response proteins, IP-10 and SIGLEC-1, are biomarkers of disease activity in systemic lupus erythematosus, *Ann Rheum Dis* 72(10):1639–1645, 2013.

Rothfield NF: Autoantibodies in scleroderma, *Rheum Dis Clin North Am* 18(2):483–498, 1992.

Rua-Figueroa I, Richi P, Lopez-Longo FJ, et al.: Comprehensive Description of clinical characteristics of a large systemic lupus erythematosus cohort from the Spanish Rheumatology Society lupus Registry (RELESSER) with emphasis on complete versus incomplete lupus differences, *Medicine* 94(1):e267, 2015.

Rubin RL: Drug-induced lupus, *Expert Opin Drug Saf* 1–18, 2015.

Ruiz-Tiscar JL, Lopez-Longo FJ, Sanchez-Ramon S, et al.: Prevalence of IgG anti-{alpha}-fodrin antibodies in Sjogren's syndrome, *Ann N Y Acad Sci* 1050:210–216, 2005.

Saitta MR, Keene JD: Molecular biology of nuclear autoantigens, *Rheum Dis Clin North Am* 18(2):283–310, 1992.

Sakamoto N, Ishimoto H, Nakashima S, et al.: Clinical features of anti-MDA5 antibody-positive rapidly progressive interstitial lung disease without signs of dermatomyositis, *Intern Med* 58(6):837–841, 2019.

Salajegheh M, Lam T, Greenberg SA: Autoantibodies against a 43 KDa muscle protein in inclusion body myositis, *PloS One* 6(5), 2011. e20266.

Sardeto GA, Simas LM, Skare TS, et al.: Antinucleosome in systemic lupus erythematosus. A study in a Brazilian population, *Clin Rheumatol* 31(3):553–556, 2012.

Sarfaraz S, Anis S, Ahmed E, et al.: Clinical significance of anti-ribosomal P protein antibodies in patients with lupus nephritis, *Rev Recent Clin Trials* 13(4):281–286, 2018.

Sato S, Hoshino K, Satoh T, et al.: RNA helicase encoded by melanoma differentiation-associated gene 5 is a major autoantigen in patients with clinically amyopathic dermatomyositis: association with rapidly progressive interstitial lung disease, *Arthritis Rheum* 60(7):2193–2200, 2009.

Satoh M, Ajmani AK, Ogasawara T, et al.: Autoantibodies to RNA polymerase II are common in systemic lupus erythematosus and overlap syndrome. Specific recognition of the phosphorylated (IIO) form by a subset of human sera, *J Clin Invest* 94(5):1981–1989, 1994.

Satoh M, Tanaka S, Ceribelli A, et al.: A comprehensive Overview on myositis-specific antibodies: new and old biomarkers in idiopathic inflammatory myopathy, *Clin Rev Allergy Immunol* 52(1):1–19, 2017.

Satoh M, Vazquez-Del Mercado M, Chan EK: Clinical interpretation of antinuclear antibody tests in systemic rheumatic diseases, *Mod Rheumatol* 19(3):219–228, 2009.

Satoh T, Ishikawa O, Ihn H, et al.: Clinical usefulness of anti-RNA polymerase III antibody measurement by enzyme-linked immunosorbent assay, *Rheumatology* 48(12):1570–1574, 2009.

Schegg V, Vogel M, Didichenko S, et al.: Evidence that anti-muscarinic antibodies in Sjogren's syndrome recognise both M3R and M1R, *Biologicals* 36(4):213–222, 2008.

Schild-Poulter C, Su A, Shih A, et al.: Association of autoantibodies with Ku and DNA repair proteins in connective tissue diseases, *Rheumatology* 47(2):165–171, 2008.

Schmidt J, Dalakas MC: Inclusion body myositis: from immunopathology and degenerative mechanisms to treatment perspectives, *Expert Rev Clin Immunol* 9(11):1125–1133, 2013.

Schouwers S, Bonnet M, Verschueren P, et al.: Value-added reporting of antinuclear antibody testing by automated indirect immunofluorescence analysis, *Clin Chem Lab Med* 52(4):547–551, 2014.

Schulte-Pelkum J, Fritzler M, Mahler M: Latest update on the Ro/SS-A autoantibody system, *Autoimmun Rev* 8(7):632–637, 2009.

Schur PH: Clinical features of SLE. In Kelley WN, Harris Jr ED, Ruddy S, et al.: *Textbook of Rheumatology*, Philadelphia, 1993, W.B.Saunders Co., pp 1017–1042.

Sciascia S, Sanna G, Murru V, et al.: Anti-prothrombin (aPT) and anti-phosphatidylserine/prothrombin (aPS/PT) antibodies and the risk of thrombosis in the antiphospholipid syndrome. A systematic review, *Thromb Haemost* 111(2):354–364, 2014.

Scott DL, Wolfe F, Huizinga TW: Rheumatoid arthritis, *Lancet* 376(9746):1094–1108, 2010.

Seaman A, Darrah E, Infantino M, et al.: Anti-peptidyl-arginine deaminase 3 (PAD3) antibodies as a promising marker to measure joint damage in patients with rheumatoid arthritis, *Autoimmun Rev* 15(7):776–780, 2016.

Sebbag M, Chapuy-Regaud S, Auger I, et al.: Clinical and pathophysiological significance of the autoimmune response to citrullinated proteins in rheumatoid arthritis, *Joint Bone Spine* 71(6):493–502, 2004.

Seeling M, Bruckner C, Nimmerjahn F: Differential antibody glycosylation in autoimmunity: sweet biomarker or modulator of disease activity? *Nat Rev Rheumatol* 13(10):621–630, 2017.

Segatto G BC, Montanelli G, Casas S, et al.: Prognostic significance of bicaudal D2 antibodies in Sistemic sclerosis (SSc) patients [abstract], *Arthritis Rheumatol* 70, 2018.

Selva-O'Callaghan A, Pinal-Fernandez I, Trallero-Araguas E, et al.: Classification and management of adul inflammatory myopathies, *Lancet Neurol* 17(9):816–828, 2018.

Selva-O'Callaghan A, Trallero-Araguas E, Grau-Junyent JM, et al.: Malignancy and myositis: novel autoantibodies and new insights, *Curr Opin Rheumatol* 22(6):627–632, 2010.

Shah AA, Hummers LK, Casciola-Rosen L, et al.: Examination of autoantibody status and clinical features associated with cancer risk and cancer-associated scleroderma, *Arthritis Rheumatol* 67(4):1053–1061, 2015.

Shah AA, Laiho M, Rosen A, et al.: Scleroderma patients with antibodies against the large subunits of both RNA polymerases-I and -III are protected against cancer, *Arthritis Rheumatol*, 2019.

Shah AA, Rosen A, Hummers L, et al.: Close temporal relationship between onset of cancer and scleroderma in patients with RNA polymerase I/III antibodies, *Arthritis Rheum* 62(9):2787–2795, 2010.

Shah AA, Xu G, Rosen A, et al.: Brief report: anti-RNPC-3 antibodies as a marker of cancer-associated scleroderma, *Arthritis Rheumatol* 69(6):1306–1312, 2017.

Shamim EA, Rider LG, Pandey JP, et al.: Differences in idiopathic inflammatory myopathy phenotypes and genotypes between Mesoamerican Mestizos and North American Caucasians: ethnogeographic influences in the genetics and clinical expression of myositis, *Arthritis Rheum* 46(7):1885–1893, 2002.

Sharif R, Fritzler MJ, Mayes MD, et al.: Anti-fibrillarin antibody in African American patients with systemic sclerosis: immunogenetics, clinical features, and survival analysis, *J Rheumatol* 38(8):1622–1630, 2011.

Sharp GC, Irvin WS, Tan EM, et al.: Mixed connective tissue disease - an apparently distinct rheumatic disease syndrome associated with a specific antibody to an extractable nuclear antigen (ENA), *Am J Med* 52:148–159, 1972.

Sherer Y, Gorstein A, Fritzler MJ, et al.: Autoantibody explosion in systemic lupus erythematosus: more than 100 different antibodies found in SLE patients, *Semi Arthritis Rheumat* 34(2):501–537, 2004.

Shi J, Knevel R, Suwannalai P, et al.: Autoantibodies recognizing carbamylated proteins are present in sera of patients with rheumatoid arthritis and predict joint damage, *Proc Natl Acad Sci U S A* 108(42):17372–17377, 2011.

Shi J, Milo J, Brady K, et al.: Diagnostic performance of a new anti-carbamylated protein assay in rheumatic diseases, *Scand J Rheumatol* 48(3):249–250, 2019.

Shi J, van Steenbergen HW, van Nies JA, et al.: The specificity of anti-carbamylated protein antibodies for rheumatoid arthritis in a setting of early arthritis, *Arthritis Res Ther* 17:339, 2015.

Shi J, van Veelen PA, Mahler M, et al.: Carbamylation and antibodies against carbamylated proteins in autoimmunity and other pathologies, *Autoimmun Rev* 13(3):225–230, 2014.

Shoenfeld Y, Agmon-Levin N: ASIA' - autoimmune/inflammatory syndrome induced by adjuvants, *J Autoimmun* 36(1):4–8, 2011.

Shovman O, Gilburd B, Barzilai O, et al.: Evaluation of the BioPlex 2200 ANA screen: analysis of 510 healthy subjects: incidence of natural/predictive autoantibodies, *Ann N Y Acad Sci* 1050:380–388, 2005.

Shovman O, Gilburd B, Zandman-Goddard G, et al.: Multiplexed AtheNA multi-lyte immunoassay for ANA screening in autoimmune diseases, *Autoimmunity* 38(1):105–109, 2005.

Silveira IG, Burlingame RW, von Muhlen CA, et al.: Anti-CCP antibodies have more diagnostic impact than rheumatoid factor (RF) in a population tested for RF, *Clin Rheumatol* 26(11):1883–1889, 2007.

Simon M, Girbal E, Sebbag M, et al.: The cytokeratin filament-aggregating protein filaggrin is the target of the so-called "antikeratin antibodies," autoantibodies specific for rheumatoid arthritis, *J Clin Invest* 92(3):1387–1393, 1993.

Singh DP, Ohguro N, Kikuchi T, et al.: Lens epithelium-derived growth factor: effects on growth and survival of lens epithelial cells, keratinocytes, and fibroblasts, *Biochem Biophys Res Commun* 267(1):373–381, 2000.

Sinico A, Rimoldi L, Radice A, et al.: Anti-C1q autoantibodies in lupus nephritis, *Ann N Y Acad Sci* 1173:47–51, 2009.

Smith CM, Steitz JA: Sno storm in the nucleolus: new roles for myriad small RNPs, *Cell* 89(5):669–672, 1997.

Smolen JS, Steiner G: Are autoantibodies active players or epiphenomena? *Curr Opin Rheumatol* 10(3):201–206, 1998.

Soderlin MK, Kastbom A, Kautiainen H, et al.: Antibodies against cyclic citrullinated peptide (CCP) and levels of cartilage oligomeric matrix protein (COMP) in very early arthritis: relation to diagnosis and disease activity, *Scand J Rheumatol* 33(3):185–188, 2004.

Sontheimer RD, McCauliffe DP: Pathogenesis of anti-Ro/SS-A autoantibody- associated Cutaneuos lupus erythematosus, *Immunodermatology* 8(4):751–758, 1990.

Sordet C, Gottenberg JE, Goetz J, et al.: Anti-{alpha}-fodrin autoantibodies are not useful diagnostic markers of primary Sjogren's syndrome, *Ann Rheum Dis* 64(8):1244–1245, 2005.

Staub HL, Franck M, Ranzolin A, et al.: IgA antibodies to beta2-glycoprotein I and atherosclerosis, *Autoimmun Rev* 6(2):104–106, 2006.

Steen VD: Autoantibodies in systemic sclerosis, *Semin Arthritis Rheum* 35(1):35–42, 2005.

Stinton LM, Barr SG, Tibbles LA, et al.: Autoantibodies in lupus nephritis patients requiring renal transplantation, *Lupus* 16(6):394–400, 2007.

Stinton LM, Eystathioy T, Selak S, et al.: Autoantibodies to protein transport and messenger RNA processing pathways: endosomes, lysosomes, Golgi complex, proteasomes, assemblyosomes, exosomes, and GW bodies, *Clin Immunol* 110(1):30–44, 2004.

Sturgill BC, Carpenter RR: Antibody to ribosomes in systemic lupus erythematosus, *Arthritis Rheum* 8:213–218, 1965.

Su Y, Jia RL, Han L, et al.: Role of anti-nucleosome antibody in the diagnosis of systemic lupus erythematosus, *Clin Immunol* 122(1):115–120, 2007.

Suer W, Dahnrich C, Schlumberger W, et al.: Autoantibodies in SLE but not in scleroderma react with protein-stripped nucleosomes, *J Autoimmun* 22(4):325–334, 2004.

Swale VJ, Perrett CM, Denton CP, et al.: Etanercept-induced systemic lupus erythematosus, *Clin Exp Dermatol* 28(6):604–607, 2003.

Takahashi K, Yoshida N, Murakami N, et al.: Dynamic regulation of p53 subnuclear localization and senescence by MORC3, *Mol Biol Cell* 18(5):1701–1709, 2007.

Takase K, Horton SC, Ganesha A, et al.: What is the utility of routine ANA testing in predicting development of biological DMARD-induced lupus and vasculitis in patients with rheumatoid arthritis? Data from a single-centre cohort, *Ann Rheum Dis* 73(9):1695–1699, 2014.

Takato H, Waseda Y, Watanabe S, et al.: Pulmonary manifestations of anti-ARS antibody positive interstitial pneumonia—with or without PM/DM, *Respir Med* 107(1):128–133, 2013.

Tan EM, Chan EKL, Sullivan KF, et al.: Antinuclear antibodies (ANAs): diagnostically specific immune markers and clues toward the understanding of systemic autoimmunity, *Clini Immunol Immunopathol* 47:121–141, 1988.

Tan EM, Cohen AS, Fries JF, et al.: The 1982 revised criteria for the classification of systemic lupus erythematosus, *Arthritis Rheum* 25(11):1271–1277, 1982.

Tan EM, Feltkamp TEW, Smolen JS, et al.: Range of antinuclear antibodies in "healthy" individuals, *Arthritis Rheum* 40(9):1601–1611, 1997.

Tan EM, Kunkel HG: Characteristics of a soluble nuclear antigen precipitating with sera of patients with systemic lupus erythematosus, *J Immunol* 96:464–471, 1966.

Tan EM, Smolen JS, McDougal JS, et al.: A critical evaluation of enzyme immunoassays for detection of antinuclear autoantibodies of defined specificities. I. Precision, sensitivity, and specificity, *Arthritis Rheum* 42(3):455–464, 1999.

Tan EM: Antinuclear antibodies: diagnostic markers for autoimmune diseases and probes for cell biology, *Adv Immunol* 44:93–151, 1989.

Tan EM: Interactions between autoimmunity and molecular and cell biology: bridges between clinical and basic sciences, *J Clini Invest* 84:1–6, 1989.

Tani C, Carli L, Vagnani S, et al.: The diagnosis and classification of mixed connective tissue disease, *J Autoimmun* 48–49:46–49, 2014.

Targoff IN, Mamyrova G, Trieu EP, et al.: A novel autoantibody to a 155-kd protein is associated with dermatomyositis, *Arthritis Rheum* 54(11):3682–3689, 2006.

Targoff IN, Trieu EP, Miller FW: Reaction of anti-OJ autoantibodies with components of the multi-enzyme complex of aminoacyl-tRNA synthetases in addition to isoleucyl-tRNA synthetase, *J Clini Invest* 91:2556–2564, 1993.

Targoff IN: Myositis specific autoantibodies, *Curr Rheumatol Rep* 8(3):196–203, 2006.

Tarricone E, Ghirardello A, Rampudda M, et al.: Anti-SAE antibodies in autoimmune myositis: identification by unlabelled protein immunoprecipitation in an Italian patient cohort, *J Immunol Methods* 384(1–2):128–134, 2012.

ter Borg EJ, Groen H, Horst G, et al.: Clinical associations of antiribonucleoprotein antibodies in patients with systemic lupus erythematosus, *Sem Arthritis Rheum* 20:164–173, 1990.

Tikly M, Gould T, Wadee AA, et al.: Clinical and serological correlates of antinucleosome antibodies in South Africans with systemic lupus erythematosus, *Clin Rheumatol* 26(12):2121–2125, 2007.

Tormey VJ, Bunn CC, Denton CP, et al.: Anti-fibrillarin antibodies in systemic sclerosis, *Rheumatology* 40(10):1157–1162, 2001.

Totoritis MC, Tan EM, McNally EM, et al.: Association of antibody to histone complex H2A-H2B with symptomatic procainamide-induced lupus, *N Engl J Med* 318(22):1431–1436, 1988.

Trallero-Araguas E, Rodrigo-Pendas JA, Selva-O'Callaghan A, et al.: Usefulness of anti-p155 autoantibody for diagnosing cancer-associated dermatomyositis: a systematic review and meta-analysis, *Arthritis Rheum* 64(2):523–532, 2012.

Troyanov Y, Targoff IN, Payette MP, et al.: Redefining dermatomyositis: a description of new diagnostic criteria that differentiate pure dermatomyositis from overlap myositis with dermatomyositis features, *Medicine* vol. 93(24):318–332, 2014.

Tsirogianni A, Pipi E, Soufleros K: Relevance of anti-C1q autoantibodies to lupus nephritis, *Ann N Y Acad Sci* 1173:243–251, 2009.

Ugarte-Gil MF, Gonzalez LA, Alarcon GS: Lupus: the new epidemic, *Lupus*, 2019. 961203319860907.

Umeda N, Matsumoto I, Kawaguchi H, et al.: Prevalence of soluble peptidylarginine deiminase 4 (PAD4) and anti-PAD4 antibodies in autoimmune diseases, *Clin Rheumatol* 35(5):1181–1188, 2016.

Uomori K, Nozawa K, Ikeda K, et al.: A re-evaluation of anti-NA-14 antibodies in patients with primary Sjogren's syndrome: significant role of interferon-gamma in the production of autoantibodies against NA-14, *Autoimmunity* 49(5):347–356, 2016.

Vaglio A, Grayson PC, Fenaroli P, et al.: Drug-induced lupus: traditional and new concepts, *Autoimmun Rev* 17(9):912–918, 2018.

van Bavel CC, Fenton KA, Rekvig OP, et al.: Glomerular targets of nephritogenic autoantibodies in systemic lupus erythematosus, *Arthritis Rheum* 58(7):1892–1899, 2008.

van de Bovenkamp FS, Derksen NIL, Ooijevaar-de Heer P, et al.: Adaptive antibody diversification through N-linked glycosylation of the immunoglobulin variable region, *Proc Natl Acad Sci U S A* 115(8):1901–1906, 2018.

van den Hoogen F, Khanna D, Fransen J, et al.: Classification criteria for systemic sclerosis: an American College of Rheumatology/European League against Rheumatism collaborative initiative, *Arthritis Rheum* 65(11):2737–2747, 2013. 2013.

Van Eenennaam H, Vogelzangs JH, Lugtenberg D, et al.: Identity of the RNase MRP- and RNase P-associated Th/To autoantigen, *Arthritis Rheum* 46(12):3266–3272, 2002.

van Esch WJ, Reparon-Schuijt CC, Hamstra HJ, et al.: Polyreactivity of human IgG Fc-binding phage antibodies constructed from synovial fluid CD38+ B cells of patients with rheumatoid arthritis, *J Autoimmun* 19(4):241–250, 2002.

van Venrooij WJ, van Beers JJ, Pruijn GJ: Anti-CCP antibodies: the past, the present and the future, *Nat Rev Rheumatol* 7(7):391–398, 2011.

van Venrooij WJ, van Beers JJ, Pruijn GJ: Anti-CCP antibody, a marker for the early detection of rheumatoid arthritis, *Ann N Y Acad Sci* 1143:268–285, 2008.

van Venrooij WJ, Zendman AJ, Pruijn GJ: Autoantibodies to citrullinated antigens in (early) rheumatoid arthritis, *Autoimmun Rev* 6(1):37–41, 2006.

Vancsa A, Gergely L, Ponyi A, et al.: Myositis-specific and myositis-associated antibodies in overlap myositis in comparison to primary dermatopolymyositis: relevance for clinical classification: retrospective study of 169 patients, *Joint Bone Spine* 77(2):125–130, 2010.

Venalis P, Selickaja S, Lundberg K, et al.: Association of anti-transcription intermediary factor 1gamma antibodies with paraneoplastic rheumatic syndromes other than dermatomyositis, *Arthritis Care Res* 70(4):648–651, 2018.

Verheul MK, Bohringer S, van Delft MAM, et al.: Triple positivity for anti-citrullinated protein autoantibodies, rheumatoid factor, and anti-carbamylated protein antibodies conferring high specificity for rheumatoid arthritis: implications for very early identification of at-risk individuals, *Arthritis Rheumatol* 70(11):1721–1731, 2018.

Vermeersch P, De Beeck KO, Lauwerys BR, et al.: Antinuclear antibodies directed against proliferating cell nuclear antigen are not specifically associated with systemic lupus erythematosus, *Ann Rheum Dis* 68(11):1791–1793, 2009.

Villalta D, Imbastaro T, Di Giovanni S, et al.: Diagnostic accuracy and predictive value of extended autoantibody profile in systemic sclerosis, *Autoimmun Rev* 12(2):114–120, 2012.

von Muhlen C, Nakamura R: Guidelines for selecting and using laboratory testsfor autoantibodies to nuclear,, nucleolar and other related cytoplasmic antigens. In Nakamura KD, RM, Bylund DJ, editors: *Clinical and laboratory evaluation of human autoimmune diseases*, vol. 1. Chicago, 2002, ASCP Press, p 183.

von Muhlen CA, Tan EM: Autoantibodies in the diagnosis of systemic rheumatic diseases, *Sem Arthritis Rheum* 24:323–358, 1995.

von Muhlen CA, Tan EM: Autoantibody specificities in autoimmune rheumatic diseases, *Rev Br Reumatol* 34:173–194, 1994.

Waaler E: On the occurrence of a factor in human serum activating the specific agglutintion of sheep blood corpuscles, *Apmis* 115(5):422–438, 1939. discussion 439, 2007.

Walker JG, Fritzler MJ: Update on autoantibodies in systemic sclerosis, *Curr Opin Rheumatol* 19(6):580–591, 2007.

Wallace DJ, Pistiner M, Nessim S, et al.: Cutaneous lupus erythematosus without systemic lupus erythematosus: clinical and laboratory features, *Semin Arthritis Rheum* 21(4):221–226, 1992.

Watad A, Bragazzi NL, McGonagle D, et al.: Autoimmune/inflammatory syndrome induced by adjuvants (ASIA) demonstrates distinct autoimmune and autoinflammatory disease associations according to the adjuvant subtype: insights from an analysis of 500 cases, *Clin Immunol* 203:1–8, 2019.

Watanabe T, Tsuchida T, Kanda N, et al.: Anti-alpha-fodrin antibodies in Sjogren syndrome and lupus erythematosus, *Arch Dermatol* 135(5):535–539, 1999.

Waterman SA, Gordon TP, Rischmueller M: Inhibitory effects of muscarinic receptor autoantibodies on parasympathetic neurotransmission in Sjogren's syndrome, *Arthritis Rheum* 43(7):1647–1654, 2000.

Wenzel J: Scleroderma and malignancy. Mechanisms of interrelationship, *Eur J Dermatol* 12(3):296–300, 2002.

Wielosz E, Dryglewska M, Majdan M: Serological profile of patients with systemic sclerosis, *Postepy Hig Med Dosw* 68:987–991, 2014.

Wiik AS, van Venrooij WJ, Pruijn GJ: All you wanted to know about anti-CCP but were afraid to ask, *Autoimmun Rev* 10(2):90–93, 2010.

Wiik AS: Anti-nuclear autoantibodies: clinical utility for diagnosis, prognosis, monitoring, and planning of treatment strategy in systemic immunoinflammatory diseases, *Scand J Rheumatol* 34(4):260–268, 2005.

Winkelmann JC, Forget BG: Erythroid and nonerythroid spectrins, *Blood* 81(12):3173–3185, 1993.

Witte T, Matthias T, Bierwirth J, et al.: Antibodies against alpha-fodrin are associated with sicca syndrome in the general population, *Ann N Y Acad Sci* 1108:414–417, 2007.

Witte T: Antifodrin antibodies in Sjogren's syndrome: a review, *Ann N Y Acad Sci* 1051:235–239, 2005.

Wodkowski M, Hudson M, Proudman S, et al.: Monospecific anti-Ro52/TRIM21 antibodies in a tri-nation cohort of 1574 systemic sclerosis subjects: evidence of an association with interstitial lung disease and worse survival, *Clin Exp Rheumatol* 33(4 Suppl 91):S131–135, 2015.

Wolin SL, Steitz JA: The Ro small cytoplasmic ribonucleoproteins: identification of the antigenic protein and its binding site on the Ro RNAs, *Proc Natl Acad Sci U S A* 81(7):1996–2000, 1984.

Woosley RL, Drayer DE, Reidenberg MM, et al.: Effect of acetylator phenotype on the rate at which procainamide induces antinuclear antibodies and the lupus syndrome, *N Engl J Med* 298(21):1157–1159, 1978.

Wooten M: Systemic sclerosis and malignancy: a review of the literature, *South Med J* 101(1):59–62, 2008.

Yamamoto H, Sims NE, Macauley SP, et al.: Alterations in the secretory response of non-obese diabetic (NOD) mice to muscarinic receptor stimulation, *Clin Immunol Immunopathol* 78(3):245–255, 1996.

Yamasaki Y, Honkanen-Scott M, Hernandez L, et al.: Nucleolar staining cannot be used as a screening test for the scleroderma marker anti-RNA polymerase I/III antibodies, *Arthritis Rheum* 54(9):3051–3056, 2006.

Yamashita S, Tawara N: Determination of cN1A autoantibodies by cell-based immunofluorescence Cytochemistry, *Methods Mol Biol* 1901:89–94, 2019.

Yang JJ, Kim MH, Lee WI, et al.: Relevance of indirect immunofluorescence patterns and autoantibodies identified via line immunoassay in patients with rheumatoid arthritis, *Lab Med* 45(1):25–31, 2014.

Yang JM, Hildebrandt B, Luderschmidt C, et al.: Human scleroderma sera contain autoantibodies to protein components specific to the U3 small nucleolar RNP complex, *Arthritis Rheum* 48(1):210–217, 2003.

Yang Y, Liu Y, Huang L, et al.: Clinical features and cytokine profile in myositis patients with anti-EJ autoantibodies detected by a novel immunoprecipitation assay, *BioMed Res Int* 1856180, 2019. 2019.

Yaniv G, Twig G, Shor DB, et al.: A volcanic explosion of autoantibodies in systemic lupus erythematosus: a diversity of 180 different antibodies found in SLE patients, *Autoimmun Rev* 14(1):75–79, 2015.

Yao B, Li S, Chan EK: Function of GW182 and GW bodies in siRNA and miRNA pathways, *Adv Exp Med Biol* 768:71–96, 2013.

Yasuma M, Takasaki Y, Matsumoto K, et al.: Clinical significance of IgG anti-Sm-specific antibodies in patients with systemic lupus erythematosus, *J Rheumatol* 17:469–475, 1990.

Yee A, Webb T, Seaman A, et al.: Anti-CarP antibodies as promising marker to measure joint damage and disease activity in patients with rheumatoid arthritis, *Immunol Res* 61(1–2):24–30, 2015.

Yeo T, Chen Z, Chai JYH, Tan K, et al.: Detection of LGI1 and CASPR2 antibodies with a commercial cell-based assay in patients with very high VGKC-complex antibody levels, *J Neurol Sci* 378:85–90, 2017.

Yoneyama M, Fujita T: Recognition of viral nucleic acids in innate immunity, *Rev Med Virol* 20(1):4–22, 2010.

Young BJ, Mallya RK, Leslie RD, et al.: Anti-keratin antibodies in rheumatoid arthritis, *Br Med J* 2(6182):97–99, 1979.

Zampeli E, Venetsanopoulou A, Argyropoulou OD, et al.: Myositis autoantibody profiles and their clinical associations in Greek patients with inflammatory myopathies, *Clin Rheumatol* 38(1):125–132, 2019.

Zendman AJ, van Venrooij WJ, Pruijn GJ: Use and significance of anti-CCP autoantibodies in rheumatoid arthritis, *Rheumatology* 45(1):20–25, 2006.

Zhong L, Yu Z, Song H: Association of anti-nuclear matrix protein 2 antibody with complications in patients with idiopathic inflammatory myopathies: a meta-analysis of 20 cohorts, *Clin Immunol* 198:11–18, 2019.

Zimmermann C, Steiner G, Skriner K, et al.: The Concurrence of rheumatoid arthritis and limited systemic sclerosis - clinical and serologic Characteristics of an overlap syndrome, *Arthritis Rheum* 41(11):1938–1945, 1998.

CHAPTER 54

VASCULITIS

Jason Kidd, Eric T. Weimer, J. Charles Jennette

INTRODUCTION, 1058
DIAGNOSTIC CLASSIFICATION OF VASCULITIS, 1058
LARGE VESSEL VASCULITIS, 1059
Takayasu Arteritis, 1060
Giant Cell Arteritis, 1061
MEDIUM VESSEL VASCULITIS, 1062
Polyarteritis Nodosa, 1062
Kawasaki Disease, 1063
SMALL VESSEL VASCULITIS, 1064
ANCA-Associated Small Vessel Vasculitis, 1064
Antiglomerular Basement Membrane Disease, 1068
Cryoglobulinemic Vasculitis, 1069
IgA Vasculitis (Henoch-Schönlein Purpura), 1070
Hypocomplementemic Urticarial Vasculitis, 1071
Rheumatoid Vasculitis, 1072
SUMMARY, 1073
SELECTED REFERENCES, 1073

KEY POINTS

- Vasculitis affects blood vessels of any type in any organ or tissue and causes diverse signs and symptoms of disease that overlap with many other diseases.
- Even if it is not the final diagnosis, vasculitis is often in the differential diagnosis in a patient with evidence of single organ or systemic inflammatory disease.
- Laboratory tests for vasculitis identify a specific etiologic factor or measure perturbations in physiologic molecular and cellular events that result from specific pathogenic events.
- Clinical laboratory tests for the diagnosis of vasculitis include tests that document active inflammation (e.g., C-reactive protein assay), demonstrate injury to a specific organ (e.g., urinalysis), or implicate a specific category of vasculitis (e.g., cryoglobulin assay).
- Vasculitis is categorized into infectious vasculitis that is caused by vessel wall invasion by pathogens and noninfectious vasculitis that is not known to be caused by infection in vessel walls.
- Noninfectious vasculitis is categorized as immune complex–mediated, antineutrophil cytoplasmic autoantibody (ANCA)–mediated, or cell-mediated immune vasculitis.
- Clinical diagnosis of vasculitis is based on both the presence and absence of multiple clinical, pathologic, and laboratory features.
- Accurate and precise diagnosis of a specific category of vasculitis is essential for optimum patient outcome.

INTRODUCTION

Vasculitis is inflammation of blood vessel walls. Blood vessels of any type in any organ or tissue may be affected. Thus the signs and symptoms of disease are extremely diverse and overlap with many other diseases. Consequently, vasculitis often is in the differential diagnosis for both single organ and systemic disease, especially in a patient with evidence of an inflammatory condition. Clinical laboratory tests (i.e., tests for biomarkers) used for the diagnosis of vasculitis fall into three categories: those that document the presence of an inflammatory process (e.g., C-reactive protein [CRP] assay), those that demonstrate injury to a specific organ (e.g., urinalysis), and those that are indicative of a specific category of vasculitis (e.g., cryoglobulin assay, ANCA). This chapter reviews the clinical and pathologic features of the major categories of vasculitis and discusses the role of laboratory testing in the diagnosis and management of these diseases.

DIAGNOSTIC CLASSIFICATION OF VASCULITIS

Laboratory tests for a disease often are based on identification of a specific etiologic factor or measurement of perturbations in physiologic molecular and cellular events that are caused by specific pathogenic events. This approach is difficult to apply to all forms of vasculitis because the etiology and pathogenesis of some forms are unknown. Vasculitis can be categorized into infectious vasculitis that is known to be caused by vessel wall invasion by pathogens that incite the inflammation (Pagnoux et al., 2006), and noninfectious vasculitis that is not known to be caused by infection in vessel walls (Jennette et al., 2013) (Box 54.1). For example, the infectious vasculitis of Rocky Mountain spotted fever (RMSF) is caused by proliferation of *Rickettsia rickettsii* in endothelial cells and smooth muscle cells in small vessels in many tissues (Silverman & Bond, 1984). The immune response to vessel wall rickettsiae causes vascular inflammation resulting in hemorrhage that produces the skin spots typical for RMSF. Bacterial sepsis can cause a small vessel vasculitis that can mimic noninfectious immune-mediated vasculitis (Jain et al., 2007) and must be diagnosed correctly and treated with antimicrobial drugs and not immunosuppression.

Noninfectious vasculitis is caused by inflammation not known to be caused by pathogens in vessel walls. However, it is important to realize that the etiology and pathogenesis of some forms of vasculitides are currently not known, so an infectious etiology cannot be completely ruled out. For example, although the etiology is not known for Kawasaki disease (KD), giant cell arteritis (GCA), and Takayasu arteritis (TA), some theories propose that an unidentified pathogen may be the cause. *Mycobacterium* tuberculosis has been incriminated but not proven to be involved in the pathogenesis of TA and a *Burkholderia* bacterium has been implicated in the pathogenesis of GCA (van Timmeren et al., 2014).

Noninfectious vasculitis can be caused indirectly by an infection that initiates a sequence of pathogenic events that causes vasculitis. For example, cryoglobulinemic vasculitis (CV) can be caused by hepatitis C virus (HCV) infection in the liver, which induces polyclonal, oligoclonal, and monoclonal B-cell proliferations that produce rheumatoid factors (anti-antibodies) that bind to other immunoglobulins to form pathogenic immune complexes (Tedeschi et al., 2007). Laboratory tests for CV comprise identification of the infectious agent (HCV serology) that initiated the autoimmune response, the autoantibodies (rheumatoid factor assay), the pathogenic immune complexes (cryoglobulin assay), secondary disturbances in inflammatory mediators (e.g., hypocomplementemia), and the evidence for end-organ damage (hematuria and proteinuria).

Laboratory testing for RMSF provides a good example of testing strategies for infectious vasculitis. The most direct laboratory test for RMSF is immunohistologic visualization of *R. rickettsii* in vessel walls in a skin biopsy specimen. This test has excellent specificity and 70% sensitivity during the acute phase before antibiotic treatment is started. Serologic testing for antibodies to *R. rickettsii* has poor sensitivity during the first 10 to 12 days but increases to more than 90% after 2 weeks (Nathavitharana & Mitty, 2015). The most definitive serologic finding for RMSF is a rise in titer over several weeks. Analogous testing is applicable to other infectious vasculitis—that is, testing to identify the etiologic infection and testing to demonstrate a specific immune response to the pathogen.

Based on known or putative pathogenic mechanisms, noninfectious vasculitis can be categorized as immune complex–mediated, antineutrophil cytoplasmic autoantibody (ANCA)–mediated, or cell-mediated immune vasculitis (see Box 54.1). Immune complex vasculitis can be caused by antibodies directed against a non–self-antigen (e.g., hepatitis

BOX 54.1

Putative Pathogenic Mechanisms for Vasculitis

Vasculitis Caused by Vessel Wall Infection

Bacterial (e.g., neisserial vasculitis, syphilitic aortitis)
Rickettsial (e.g., Rocky Mountain spotted fever)
Fungal (e.g., cryptococcal vasculitis)
Viral (e.g., cytomegalovirus vasculitis)
Parasitic (e.g., toxoplasmosis vasculitis

Immune Complex–Mediated Vasculitis

Cryoglobulinemic vasculitis
Polyarteritis nodosa
IgA vasculitis (Henoch-Schönlein)
Hypocomplementemic urticarial vasculitis
Lupus vasculitis
Rheumatoid vasculitis
Drug-induced immune complex vasculitis
Cancer-induced (paraneoplastic) immune complex vasculitis
Antiglomerular basement membrane disease

Antineutrophil Cytoplasmic Antibody (ANCA)–Mediated Vasculitis

Microscopic polyangiitis
Granulomatosis with polyangiitis (Wegener)
Eosinophilic granulomatosis with polyangiitis (Churg-Strauss)
Drug-induced ANCA vasculitis

Cell-Mediated Immune Vasculitis

Takayasu arteritis
Giant cell arteritis
Sarcoid vasculitis

BOX 54.2

Names for Vasculitides Adopted by the 2012 International Chapel Hill Consensus Conference on the Nomenclature of Vasculitides

Large Vessel Vasculitis (LVV)

Takayasu arteritis (TA)
Giant cell arteritis (GCA)

Medium Vessel Vasculitis (MVV)

Polyarteritis nodosa (PAN)
Kawasaki disease (KD)

Small Vessel Vasculitis (SVV)

Antineutrophil cytoplasmic antibody (ANCA)–associated vasculitis (AAV)
- Microscopic polyangiitis (MPA)
- Granulomatosis with polyangiitis (Wegener's) (GPA)
- Eosinophilic granulomatosis with polyangiitis (Churg-Strauss) (EGPA)

Immune complex SVV
- Antiglomerular basement membrane (anti-GBM) disease
- Cryoglobulinemic vasculitis (CV)
- IgA vasculitis (Henoch-Schönlein) (IgAV)
- Hypocomplementemic urticarial vasculitis (HUV) (anti-C1q vasculitis)

Variable Vessel Vasculitis (VVV)

Behçet disease (BD)
Cogan syndrome (CS)

Single-Organ Vasculitis (SOV)

Cutaneous leukocytoclastic angiitis
Cutaneous arteritis
Primary central nervous system vasculitis
Isolated aortitis
Others

Vasculitis Associated With Systemic Disease

Lupus vasculitis
Rheumatoid vasculitis
Sarcoid vasculitis
Others

Vasculitis Associated With Probable Etiology

Hepatitis C virus–associated cryoglobulinemic vasculitis
Hepatitis B virus–associated vasculitis
Syphilis-associated aortitis
Drug-associated immune complex vasculitis
Drug-associated ANCA-associated vasculitis
Cancer-associated (paraneoplastic) vasculitis
Others

From Jennette JC, Falk RJ, Bacon PA, et al: 2012 Revised International Chapel Hill Consensus Conference Nomenclature of Vasculitides, *Arthritis Rheum* 65:1–11, 2013.

B immune complex vasculitis caused by antibodies to viral antigens) or autoantibodies directed against an autoantigen (e.g., lupus vasculitis caused by autoantibodies against nuclear antigens). Cell-mediated immunity also can cause vascular inflammation. The pattern of inflammatory injury in GCA and in TA suggests possible cell-mediated immune injury; however, definitive self or non-self targets have not been conclusively identified. In idiopathic vasculitides, another possibility is an autoinflammatory process that is mediated by a disturbance in the regulation of the innate immune response in the absence of a specific antigen target.

The absence of identifiable etiologies or distinctive pathogenic mechanisms in many forms of vasculitis does not allow diagnosis or classification of vasculitides based only on these characteristics. Alternatively, classification and diagnosis is most often based on the presence and absence of multiple clinical, pathologic, and laboratory features. The most widely used approach to categorizing vasculitis is based on the nomenclature of vasculitis proposed by the Chapel Hill Consensus Conferences (CHCC) held in 1994 (Jennette et al., 1994) and modified in 2012 (Jennette et al., 2013). The CHCC nomenclature provides consensus names (Box 54.2; Fig. 54.1) and definitions for many, but not all, forms of systemic and single organ vasculitis. Three major categories are large vessel vasculitis (LVV), medium vessel vasculitis (MVV), and small vessel vasculitis (SVV). This terminology can be misleading if it is taken too literally. In general, LVV more often affects the aorta and its major branches than any other form of vasculitis; MVV is confined to arteries, with a preference for major visceral arteries; and SVV involves not only arteries but also vessels smaller than arteries. Especially with respect to arterial involvement, there is substantial overlap among the categories. For example, although large vessel involvement is the most specific finding, GCA can affect any size artery from the aorta to the smallest arterial vessels, such as those in the uveal tract of the eye (Waldman et al., 2013).

In addition to SVV, MVV, and LVV, the 2012 CHCC also recognized variable vessel vasculitis (VVV), single organ vasculitis (SOV), vasculitis associated with systemic disease, and vasculitis associated with probable etiology (Jennette et al., 2013). VVV is vasculitis with no predominant type of vessel involved that can affect vessels of any size (small, medium, and large) and type (arteries, veins, and capillaries), such as Behçet disease and Cogan syndrome. SOV is vasculitis in arteries or veins of any size in a single organ that has no features that indicate that it is a limited expression of a systemic vasculitis. Some patients originally diagnosed with SOV will develop additional disease manifestations that warrant redefining the case as one of the systemic vasculitides (e.g., cutaneous arteritis later becoming systemic polyarteritis nodosa [PAN]). Vasculitis associated with systemic disease should have a prefix term specifying the systemic disease (e.g., rheumatoid vasculitis, lupus vasculitis). Likewise, vasculitis associated with probable etiology should have a prefix term specifying the association (e.g., hydralazine-associated microscopic polyangiitis [MPA], hepatitis B virus [HBV]–associated vasculitis, HCV-associated CV).

LARGE VESSEL VASCULITIS

CHCC 2012 defines LVV as vasculitis affecting the aorta and its major branches more often than other vasculitides, although any size artery may be affected (Jennette et al., 2013). In fact, in some patients the number of medium and small arteries affected is greater than the number of large arteries affected. For example, in GCA, very few branches of the carotid arteries may be affected, although there is involvement of numerous small arteries extending into the head and neck (Waldman et al., 2013).

The two major variants of LVV are Takayasu arteritis and giant cell arteritis (Table 54.1). Both have similar pathologic features, so they cannot be distinguished based on pathologic features alone (Jennette et al., 2013). Demographic and clinical features are required to make the distinction, especially age. The differential diagnosis for LVV includes syphilitic aortitis, which is an infectious vasculitis caused by tertiary syphilis, and very rarely by secondary syphilis (Dietrich et al., 2014). The resulting aortic inflammation may lead to aneurysms of the aorta that can be life threatening or fatal if not treated appropriately with antibiotics.

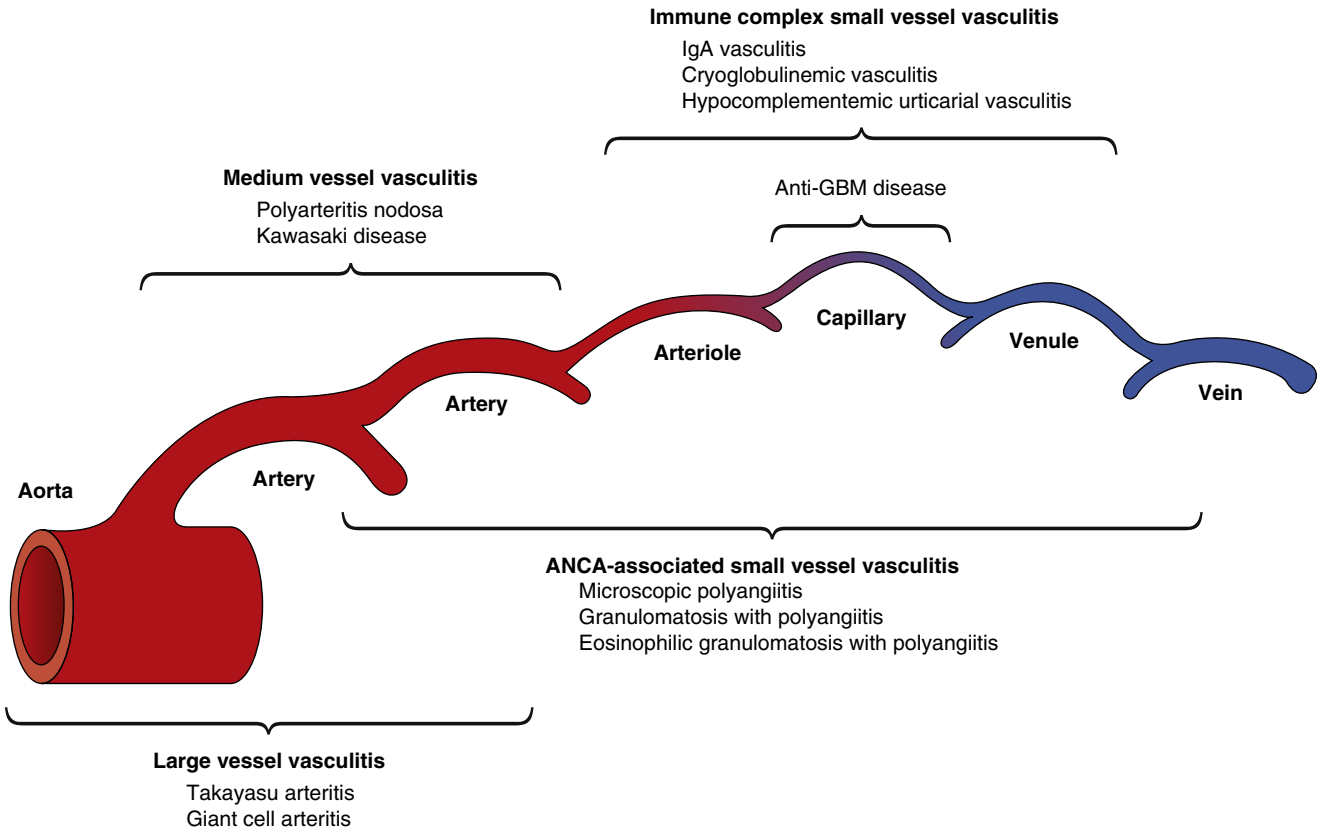

Fig. 54.1 The predominant distribution of vessel involvement by large vessel vasculitis, medium vessel vasculitis, and small vessel vasculitis. Note that all categories of vasculitis can affect all types of arteries. The aorta and the largest arteries are most often affected by large vessel vasculitis. Medium vessel vasculitis most often affects medium arteries, although large and small arteries may be affected. Small vessel vasculitis preferentially affects venules and capillaries, although arteries and veins may be affected. ANCA (antineutrophil cytoplasmic antibody)–associated vasculitis affects the broadest spectrum of vessels, whereas immune complex vasculitis usually is restricted to capillaries or venules or both. (Modified from Jennette JC, Falk RJ, Bacon PA, et al: 2012 Revised International Chapel Hill Consensus Conference Nomenclature of Vasculitides, Arthritis Rheum 65:1–11, 2013, with permission.)

TABLE 54.1

Names and Definitions for Large Vessel Vasculitis Adopted by the 2011-2012 International Chapel Hill Consensus Conference Nomenclature of the Vasculitides

Large vessel vasculitis (LVV)	Vasculitis affecting large arteries more often than other vasculitides. Large arteries are the aorta and its major branches. Any size artery may be affected.
Takayasu arteritis	Arteritis, often granulomatous, predominantly affecting the aorta and/or its major branches. Onset usually in patients younger than 50.
Giant cell arteritis	Arteritis, often granulomatous, usually affecting the aorta and/or its major branches, with a predilection for the branches of the carotid and vertebral arteries. Often involves the temporal artery. Onset usually in patients older than 50 and often associated with polymyalgia rheumatica.

From Jennette JC, Falk RJ, Bacon PA, et al: 2012 Revised International Chapel Hill Consensus Conference Nomenclature of Vasculitides, *Arthritis Rheum* 65:1–11, 2013.

TAKAYASU ARTERITIS

Definition and Epidemiology

Takayasu arteritis is often granulomatous, with a predilection for the aorta and its major branches (Jennette et al., 2013). Onset is usually in patients younger than 50. TA most often affects women between 10 and 40 years of age. TA occurs worldwide with an estimated incidence of 1.2 to 2.6/million per year in the Western countries. TA occurs in all races, but the incidence is higher in Southeast Asia, Central and South America, and Africa (Vaideeswar & Deshpande, 2013).

Pathology

The pathology of TA in the acute active phase is characterized by inflammation of the aorta or larger arteries with a predominance of mononuclear leukocytes often, but not always, accompanied by multinucleated giant cells (Jennette, 2015; Vaideeswar & Deshpande, 2013). Even if disease appears more localized clinically, postmortem pathologic examination usually shows more extensive involvement. Involved vessels may have well-demarcated skip areas resulting in localized narrowing or dilation of lumens. This inflammation can cause arterial stenosis, thrombosis, and aneurysms. There are at least two classification systems based on distribution of vessel involvement (Vaideeswar & Deshpande, 2013). One classifies TA into five types: type I, aortic arch and its branches; type II, descending thoracic and abdominal aorta; type III, aortic arch and thoracoabdominal aorta; type IV, pulmonary artery in addition to the aforementioned types; and type V, coronary artery in addition to the other types (Gulati & Bagga, 2010). Another classifies TA into six types: type I, aortic arch and its branches; type IIa, ascending aorta, arch, and its branches; type IIb, ascending aorta, arch, and its branches, and descending thoracic aorta; type III, thoracic aorta and abdominal aorta; type IV, abdominal aorta; and type V, combination of type IIb and type IV (Hata et al., 1996).

The pathologic differential diagnosis includes syphilitic aortitis that also has inflammatory infiltrates with predominantly mononuclear leukocytes, including plasma cells. The only diagnostic pathologic finding that can identify syphilitic aortitis is immunohistochemical identification of *Treponema pallidum*.

Etiology and Pathogenesis

An autoimmune or infectious etiology that is influenced by genetic and environmental factors and results in cell-mediated immune injury to vessels is incriminated in the pathogenesis of TA; however, specific etiologic factors have not been identified (Vaideeswar & Deshpande, 2013).

Clinical Laboratory Testing

In part because the specific etiology and unique pathogenic mechanisms are not known for TA, no laboratory tests have been identified that are specific for this disease. Erythrocyte sedimentation rate (ESR) and CRP

are the laboratory tests used most often to support a diagnosis of TA and to follow disease activity and response to therapy. The ESR is elevated in 75% to 100% of patients with active disease and tends to return to normal over time. ESR is thought to be a reliable index of inflammatory activity and has been used as a tool to monitor the effectiveness of therapy. Resolution of the disease, both symptomatically and angiographically, has been found to correlate with decline of the ESR, although one surgical series observed that 44% of patients thought to be quiet clinically were not upon arterial biopsy (Langford, 2003).

In a study of TA treatment response, ESR decreased from 55.5 +/– 14.7 mm/h to 21.9 +/– 9.5 mm/h within 3 months (p <0.001) and further to 20.8 +/– 15.2 at 1 year (p = NS). CRP concentrations fell from 4.8 +/– 5.2 mg/dL to 0.5 +/– 0.2 mg/dL at 3 months (p = 0.004) and remained at 0.5 +/– 0.3 mg/dL at 1 year (p = NS) (Valsakumar et al., 2003).

In addition to ESR and CRP, multiple biomarkers have been evaluated as diagnostic and prognostic tests in TA: interleukin 6 (IL-6), serum amyloid A, fibrinogen, complement split fragments, B-cell activating factor (BAFF), IL-12, matrix metalloproteinase 9 (MMP-9), and pentraxin 3 (PTX3) (Chatterjee et al., 2014). None of these have been adopted for widespread use.

Laboratory testing to rule out syphilitic aortitis includes the Venereal Disease Research Laboratory (VDRL) test, *Treponema pallidum* particle agglutination assay (TPPA), and IgG and IgM fluorescent treponemal antibody-absorption (FTA-Abs) (Dietrich et al., 2014). A definitive test is positive immunohistochemical staining for *T. pallidum* organisms in tissue specimens (e.g., a resected aneurysm). A negative test is not as predictive.

Diagnosis, Treatment, and Prognosis

The diagnosis of TA is based primarily on clinical signs and symptoms and on imaging studies to document involved vessels. F-fluorodeoxyglucose (FDG) positron emission tomography (PET) has been shown to differentiate patients with clinically active LVV from control subjects with a sensitivity of 85% and specificity of 83% (Grayson et al., 2018).

The onset of symptoms may be subacute, often delaying diagnosis. Clinically, patients may present with constitutional symptoms, hypertension, and arthralgias. Unlike in GCA, pathologic examination of biopsies or resected vessels is not a routine component of a diagnostic workup for TA. TA has three phases of progression (Vaideeswar & Deshpande, 2013). The first is characterized by low-grade fever, malaise, night sweats, arthralgia, anorexia, and weight loss, with no clinical evidence for large vessel narrowing. The second phase is the vasculitic stage in which the first-phase constitutional symptoms are accompanied by evidence for large vessel inflammation, such as tenderness or pain over vessels (angiodynia). These first two phases may last for several months before signs of more chronic injury appear. The final phase, which may evolve over months or years, has various manifestations of chronic sclerosing vasculopathy affecting the aorta and its major branches, including pulseless disease related to arterial stenosis or occlusion.

In patients with active disease, corticosteroid therapy is the initial treatment of choice. If active disease persists despite corticosteroids, steroid sparing agents can be administered. Methotrexate, cyclophosphamide, mycophenolate mofetil, and azathioprine can be tried; however, most evidence of this is based on case series. In patients with steroid resistant disease, the IL-6 blocker tocilizumab has been used (Salvarini, 2012). Vasodilators, anticoagulants, and nonsteroidal anti-inflammatory agents are often used for symptomatic relief. Surgical intervention may be necessary for symptomatic vascular stenosis or occlusion, usually at a late stage of the disease (Hoffman, 2003).

GIANT CELL ARTERITIS

Definition and Epidemiology

Giant cell arteritis is often granulomatous, with a predilection for the aorta and its major branches (Jennette et al., 2013). In contrast to TA, GCA generally occurs in patients older than 50. GCA is more common in Western countries with the highest incidence and prevalence in whites of Scandinavian descent (González-Gay & Pina, 2015). There is a north-south gradient in the incidence of GCA in Europe, with high rates in Sweden and Norway, which has an incidence of over 20 new cases per 100,000 individuals aged 50 and older per year, and a lower incidence in southern Europe, which has an annual incidence of 10 cases per 100,000 people aged 50 years and older in northwestern Spain (González-Gay & Pina, 2015).

Pathology

The pathology of GCA in the acute active phase is characterized by inflammation of the aorta or large arteries, with a predominance of mononuclear leukocytes often accompanied by multinucleated giant cells (Jennette, 2015) (Fig. 54.2). The chronic inactive phase has nonspecific chronic inflammation and scarring. Although minor focal necrosis may occur, extensive fibrinoid necrosis, especially in arteries, should raise the possibility of another variant of arteritis. The concurrence of another pathologic process that causes chronic inflammation and scarring (e.g., atherosclerosis) complicates the pathologic diagnosis of chronic LVV.

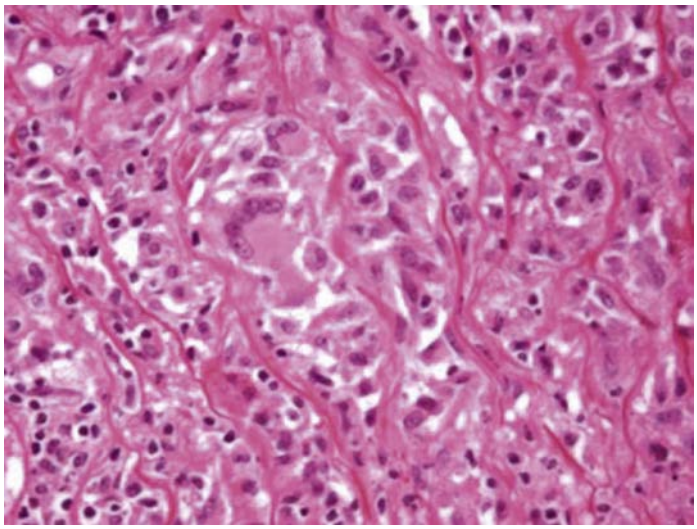

Fig. 54.2 Histopathologic features in the media of the aorta of a patient with giant cell aortitis. Note that the elastic fibers are spread apart by numerous infiltrating mononuclear leukocytes with admixed multinucleated giant cells (H&E stain, ×500).

The most common pathologic pattern in active GCA is transmural inflammation, which is identified in more than 75% of patients, although a minority of specimens will have inflammation confined to the adventitial tissues, including the vasa vasorum (Cavazza et al., 2014). In a study of 274 temporal artery biopsies that had transmural inflammation, most as a result of GCA, 100% had inflammation with predominantly mononuclear leukocytes (lymphocytes, monocytes macrophages, and plasma cells), 75% giant cells, 8% admixed eosinophils, and 2% admixed neutrophils (Cavazza et al., 2014). Although small zones of laminar degeneration (necrosis) may occur in areas of medial inflammation, overt fibrinoid necrosis, especially if accompanied by neutrophils and/or neutrophils with leukocytoclasis, should raise the possibility of a vasculitis other than GCA, such as PAN or ANCA vasculitis (Hamidou et al., 2003; Cavazza et al., 2014).

Etiology and Pathogenesis

Cell-mediated immune mechanisms are incriminated in the pathogenesis of GCA, although the initiating etiologic factors are not known. For example, in GCA, investigations have demonstrated that dendritic cells in vessel walls initiate the recruitment of T cells and macrophages that are the basis for the granulomatous inflammation (Weyand & Goronzy, 2014). Two major immune-response networks have been identified in inflamed arteries: the interleukin-12, type 1 helper T cell (Th1), and interferon-γ axis; and the interleukin-6, type 17 helper T cell (Th17), and interleukin-17 or interleukin-21 axis. Cytokines released by these inflammatory pathways activate leukocytes as well as endothelial cells, vascular smooth muscle cells, and fibroblasts, leading to intimal and medial hyperplasia and fibrosis. Elastolytic and proteolytic enzymes (e.g., matrix metalloproteinases) and growth factors (e.g., vascular endothelial growth factor and platelet derived growth factor) promote both degenerative and proliferative and sclerosing changes that cause pathologic damage in vessel walls (Weyand & Goronzy, 2014). A large-scale genetic analysis comprising 1651 patients with GCA and 15,306 unrelated control subjects from six different European countries of European ancestry identified multiple HLA loci, PTPN22, and other loci that influence Th1, Th17, and Treg cell function as risk factors for GCA (Carmona et al., 2015). The involvement of these genes supports a role for a pathogenic autoimmune response in the pathogenesis of GCA.

Clinical Laboratory Testing

Temporal artery biopsy is the current gold standard for diagnosis of GCA; however, a biopsy that is not diagnostic does not exclude GCA. False-negative results occur in up to 15% of patients and are influenced by the length of the biopsy specimen and the duration of corticosteroid treatment prior to biopsy (Achkar et al., 1994; Poller et al., 2000; Kermani et al., 2013).

Especially in the absence of a tissue diagnosis, laboratory data are very important in reaching an actionable diagnosis of GCA. Laboratory findings that support a diagnosis of GCA are increased ESR and CRP, and thrombocytosis (Kermani et al., 2012; Waldman et al., 2013). An elevated platelet count is an early laboratory marker that can be detected a year before GCA is diagnosed (Lincoff et al., 2000). In a study of patients with GCA confirmed by temporal artery biopsy, elevated CRP and elevated ESR had a sensitivity of 87% and 84%, respectively, and 4% had a normal ESR and CRP (Kermani et al., 2012). American College of Rheumatology (ACR)–European League Against Rheumatism (EULAR) Classification Criteria for GCA (Dasgupta et al., 2012) require, in part, abnormal elevations in CRP, ESR, or both. An additional laboratory criterion is absence of rheumatoid factor or antibodies to cyclic citrullinated peptides.

Diagnosis, Treatment, and Prognosis

The diagnosis of GCA is most accurate when it is based on clinical manifestations, laboratory tests, and confirmation by biopsy of the temporal artery or other affected artery (Waldman et al., 2013; Weyand & Goronzy, 2014). Bilateral temporal artery biopsies increase diagnostic sensitivity (Durling et al., 2014). Corticosteroid therapy should not be discontinued after a negative biopsy result if there is enough evidence to make the diagnosis. GCA with normal ESR and/or normal CRP levels is rare but does occur; thus laboratory testing cannot completely rule out GCA (Kermani et al., 2012).

Imaging studies of large arteries and the aorta (e.g., with PET) are a helpful adjunct to pathology and laboratory testing for making a diagnosis and assessing the status of patients with GCA (Prieto-Gonzalez et al., 2014). One quarter of patients with GCA have involvement of the aorta and its major branches that can be detected with imaging studies (Weyand & Goronzy, 2014). PET also is useful in the early diagnosis of syphilitic aortitis (Treglia et al., 2013).

Most cases of GCA are effectively managed with glucocorticoid monotherapy (Weyand & Goronzy, 2014). Disease flares are common when the glucocorticoids are tapered and often require a short-term increase to induce and maintain remission. Patients with visual impairment or evidence of unstable blood supply to the eyes benefit from high doses of intravenous glucocorticoids. If disease flares, patients may need to be treated with glucocorticoid-sparing agents, including methotrexate or infliximab. An industry sponsored phase II trial examined the use of IL-6 inhibitor tocilizumab as a steroid sparing agent with 85% remission by 12 weeks (Villiger, 2016).

Corticosteroids are the treatment of choice for GCA but may not be sufficiently effective 50% of the time. An immunosuppressive regimen of azathioprine and prednisolone is safe, well tolerated, and effective in ameliorating systemic symptoms and laboratory abnormalities in TA, and it halts the progression in lesions based on angiographic studies, although it does not seem to lead to complete resolution of arterial lesions (Valsakumar et al., 2003). Other agents may be considered, including cyclophosphamide and methotrexate. Patients with underlying diabetes and hypertension are more likely to have a recurrence of disease (Labarca, 2016).

The differential diagnosis for LVV also includes VVV, including Behçet disease and Cogan syndrome, and by infectious vasculitis (e.g., aortitis caused by tertiary syphilis) and lymphoplasmacytic disease (e.g., aortitis as a component of IgG4-related disease) (Miller & Maleszewski, 2011). There is controversy about whether isolated aortitis or isolated giant cell arteritis of a visceral artery is a limited expression of TA or GCA or a distinct form of single organ vasculitis. When single organ LVV is detected, follow-up should include vigilance for additional organ involvement.

MEDIUM VESSEL VASCULITIS

MVV is vasculitis that predominantly affects medium arteries defined as the main visceral arteries and their branches; however, any size artery may be affected (Jennette et al., 2013). The two major categories are polyarteritis nodosa and Kawasaki disease (Table 54.2). Inflammatory aneurysms and stenoses are common. It is important to note that medium arteries also can be affected by large vessel vasculitis and small vessel vasculitis. Thus multiple clinical, laboratory, and pathologic findings must be taken into consideration to make an accurate diagnosis of the disease that is causing arteritis.

TABLE 54.2

Names and Definitions for Medium Vessel Vasculitis Adopted by the 2011-2012 International Chapel Hill Consensus Conference Nomenclature of the Vasculitides

Medium vessel vasculitis (MVV)	Vasculitis predominantly affecting medium arteries defined as the main visceral arteries and their branches. Any size artery may be affected. Inflammatory aneurysms and stenoses are common.
Polyarteritis nodosa	Necrotizing arteritis of medium or small arteries without glomerulonephritis or vasculitis in arterioles, capillaries, or venules, and not associated with ANCA.
Kawasaki disease	Arteritis associated with the mucocutaneous lymph node syndrome and predominantly affecting medium and small arteries. Coronary arteries are often involved. Aorta and large arteries may be involved. Usually occurs in infants and young children.

From Jennette JC, Falk RJ, Bacon PA, et al: 2012 Revised International Chapel Hill Consensus Conference Nomenclature of Vasculitides, *Arthritis Rheum* 65:1–11, 2013.

POLYARTERITIS NODOSA

Definition and Epidemiology

PAN is necrotizing arteritis of medium or small arteries without glomerulonephritis or vasculitis in arterioles, capillaries, or venules, and it is not associated with ANCA (Jennette et al., 2013). PAN is a diagnosis of exclusion that is made after omitting other categories of large, medium, and small vessel vasculitis that can affect medium arteries (Jennette & Falk, 2007). PAN affects patients of all ages, genders, and racial backgrounds, though it is more common in older adults. The annual incidence ranges from 0 to 1.6 cases/million in European countries, and its prevalence is about 31 cases/million (Hernández-Rodríguez et al., 2014). Before vaccination against HBV was available, more than one third of adults with PAN were infected by HBV; however, currently, less than 5% of patients with PAN are infected with HBV in developed countries (Mahr et al., 2004).

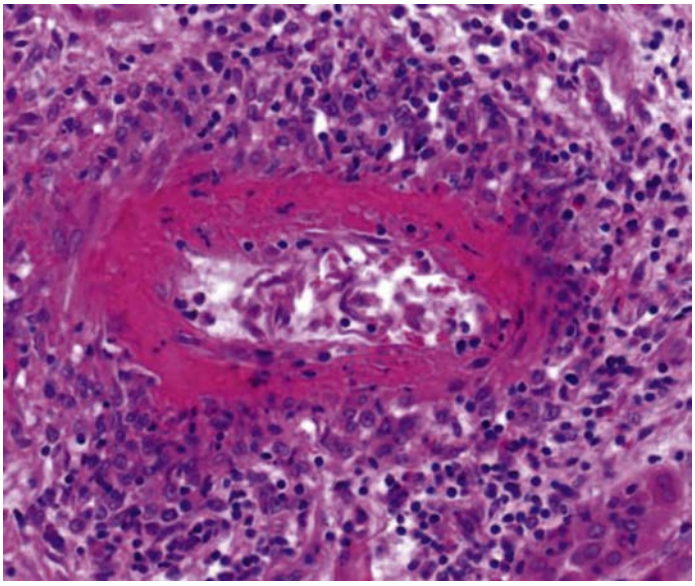

Fig. 54.3 Necrotizing arteritis caused by polyarteritis nodosa. Note the replacement of most of the media by deeply acidophilic fibrinoid necrosis and the perivascular inflammation with a mixture of polymorphonuclear leukocytes and mononuclear leukocytes (H&E stain, ×300).

Pathology

Any type of artery in any organ may be affected; however, main visceral arteries and their initial branches in the parenchyma are the most frequent targets, such as the major mesenteric arteries, renal arteries, hepatic arteries, and coronary arteries. Epineural arteries of peripheral nerves and subcutaneous arteries of the skin are also common targets. When main arteries are involved, nodular inflammatory lesions and pseudoaneurysms can be observed grossly with imaging studies or (less commonly) palpated in the skin. The inflammation has a predilection for arterial branch points. The histopathologic features of PAN (Fig. 54.3) begin as fibrinoid necrosis with intense acute neutrophil-rich inflammation, evolve through chronic inflammation and fibroplasia, and eventually result in fibrosis that may

Fig. 54.4 Cross section of a kidney from a patient with polyarteritis nodosa showing multiple pseudoaneurysms *(black arrow)* and infarcts *(white arrow).*

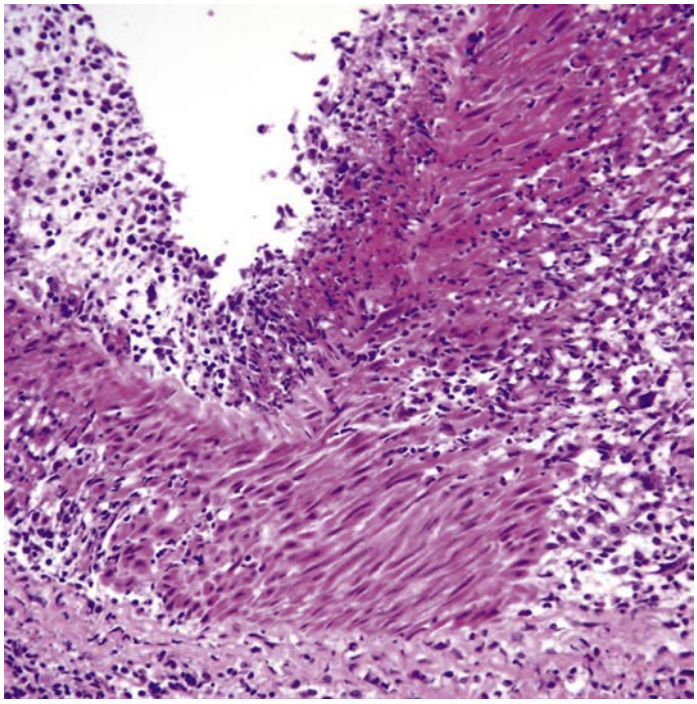

Fig. 54.5 Kawasaki disease arteritis showing segmental transmural necrotizing inflammation with residual areas of intact muscularis adjacent to intense medial inflammation that is continuous with intimal inflammation and adventitial inflammation (H&E stain, ×400).

completely or partially impede blood flow (Jennette & Falk, 2007; Jennette, 2015). Acute occlusion causing infarction may result from thrombosis of arteries at sites of segmental acute inflammation, necrosis, and pseudoaneurysm formation (Fig. 54.4).

Etiology and Pathogenesis

The etiology and pathogenesis of PAN are unknown. A role for infections has been incriminated. During the 1970s, about half of the patients with PAN were infected with HBV, and HBe antigen to anti-HBe antibody seroconversion usually paralleled recovery (Pagnoux et al., 2006). This suggested that PAN was caused by HBV infection. However, the frequency of HBV-associated PAN has declined from 35% in the 1980s to less than 5% in the early 2000s (Mahr et al., 2004). Additional infections that have been incriminated as but not proven to be etiologies for PAN include HCV, human immunodeficiency virus (HIV), cytomegalovirus, and parvovirus B19 (Hernández-Rodríguez et al., 2014). Most cases are idiopathic.

Clinical Laboratory Testing

Laboratory testing in patients with PAN often demonstrates thrombocytosis, low serum albumin, and elevated ESR and CRP. Liver enzymes may be abnormal in patients with viral hepatitis. Testing for HBV, HCV, and HIV in patients with necrotizing arteritis is important because antiviral treatment must be added to immunosuppressive treatment for optimum outcome (Guillevin, 2013). ANCA testing is important to rule out ANCA vasculitis with a component of necrotizing arteritis that is mimicking PAN. Other laboratory abnormalities are dictated by the organ systems that are involved, such as kidneys, pancreas, skeletal muscle, heart, and gastrointestinal tract.

Diagnosis, Treatment, and Prognosis

Clinical manifestations of PAN are protean and depend on the organs affected (Hernández-Rodríguez et al., 2014). Most patients present with constitutional symptoms such as fever, malaise, arthralgias, myalgias, and weight loss. Peripheral neuropathy occurs in approximately 75% of patients, and gastrointestinal involvement occurs in approximately half. The major cutaneous manifestations are inflammatory nodules, infarction, and livedo reticularis. Renal involvement manifests as flank pain and hematuria and, rarely, as retroperitoneal hemorrhage from rupture of an aneurysm. Greater than 2 g/day proteinuria and hematuria with red blood cell casts are not features of PAN and raise the possibility of a small vessel vasculitis such as MPA. Involvement of the gastrointestinal tract, kidneys, heart, and central nervous system is associated with higher mortality. Laboratory abnormalities reveal a prominent acute phase response but are nonspecific. Histologic confirmation of vasculitis in medium-sized arteries is valuable for diagnosis. Positive pathologic findings are more likely if biopsies are obtained from symptomatic organs if feasible. Skin or muscle and nerve are preferred because of higher diagnostic yield and safety. If biopsies are negative or cannot be obtained, visceral angiography may reveal multiple microaneurysms, supporting the diagnosis of PAN.

Current treatment includes high-dose corticosteroids, which are combined with immunosuppressive agents when critical organ involvement or life-threatening complications occur. Intravenous (IV) pulse cyclophosphamide in the remission induction phase, later switched to a safer immunosuppressant for remission maintenance, is a frequently used therapeutic approach (Hernández-Rodríguez et al., 2014). Relapse of disease is common, and studies with steroid-sparing agents are ongoing.

KAWASAKI DISEASE

Definition and Epidemiology

KD is arteritis associated with the mucocutaneous lymph node syndrome and predominantly affects medium and small arteries (Jennette et al., 2013). Coronary arteries are often involved. Aorta and large arteries may be involved. KD usually occurs in infants and young children. Clinical manifestations include persistent fever for 1 week or more, erythematous rash, conjunctivitis, oropharyngeal erythema, and lymphadenopathy. Over 80% of KD cases occur between the ages of 6 months and 4 years. The annual incidence varies from approximately 3 per 100,000 children under 5 years of age in South America to 4 in Australia, 8 in the United Kingdom, 4 to 15 in the United States, 20 to 30 in China, 50 in Taiwan, 90 in Korea, and more than 130 in Japan (Burgner & Harnden, 2005). KD is more common in boys, with a male:female ratio of 1.6:1.

Several epidemiologic observations suggest but do not prove an infectious etiology for KD (Burgner & Harnden, 2005). Geographic clustering of KD cases and epidemics have been reported. The onset of KD has seasonal variations, but the predominant season varies in different countries. In the United Kingdom, Australia, and the United States, KD is most common in the winter and spring; in China, in the spring and summer; and in Korea, during the summer months.

Pathology

Active KD arteritis is characterized by segmental necrotizing arteritis (Fig. 54.5). In the acute phase, in general, KD has more infiltration by monocytes, whereas PAN has more infiltration by neutrophils (Jennette & Falk, 2007). Fibrinoid necrosis occurs with both PAN and KD, but it is less conspicuous in KD. The chronic sclerotic phase is characterized by segmental

transmural chronic inflammation and scarring. Special stains for elastin demonstrate focal disruption of the internal elastica.

The acute lesion of KD is characterized by transmural necrotizing inflammation that is rich in neutrophils and monocytes (Orenstein et al., 2012; Jennette, 2015). Degeneration of artery walls results in aneurysm and pseudoaneurysm formation, with the latter having complete erosion of the necrotizing process into the perivascular tissues. Thrombosis may occur at sites of arteritis, especially sites of aneurysm/pseudoaneurysm formation. Acute arteritis wanes by 2 weeks after fever onset, and it is replaced by varying degrees of subacute and chronic inflammation, including intimal myofibroblast proliferation (Orenstein et al., 2012; Reindel et al., 2014).

Etiology and Pathogenesis

Infection also has been suspected as a cause of KD because concurrent infection with pathogens has been detected by culture, molecular methods, or serologic testing in patients with KD. Although more than 20 different pathogens have been implicated, none have been proven to be a direct cause of KD, and many are infectious diseases commonly found in young children (Burgner & Harnden, 2005; Principi et al., 2013). Mediation by an immune response to a superantigen (possibly of microbial origin) has been studied extensively. KD shares many clinical features with superantigen-mediated diseases (e.g., rash, conjunctivitis, skin sloughing). KD has also been reported in children with toxic shock syndrome, which can be caused by superantigens (Burgner & Harnden, 2005). Despite this, there is no proof that superantigens are involved in the pathogenesis of KD. Multiple inflammatory pathways are upregulated in the inflamed arteries of KD, including a pathway that involves the lymphocyte activation molecule CD84 (Reindel et al., 2014). CD84 was upregulated 16-fold in acute coronary arteritis caused by KD and 32-fold in chronic coronary arteritis caused by KD (5 months to years after onset). CD84 was detected in leukocytes in KD tissues.

Clinical Laboratory Testing

Diagnosis of KD is based primarily on clinical signs and symptoms. Nonspecific laboratory indicators of acute inflammation (i.e., acute phase reactants, including CRP and ESR) are consistently elevated in the acute phase of KD. One study suggests that elevated serum levels of the cardiac natriuretic peptide called N-terminal of the prohormone brain natriuretic peptide (NT-pro-BNP) might be a useful diagnostic tool for KD, especially in patients with cardiac injury and atypical clinical presentations (Cho et al., 2011). The cutoff level of NT-pro-BNP that best distinguished KD from other childhood febrile illnesses was 235.2 pg/mL. The same study concluded that serum levels of high-sensitivity CRP are not useful in distinguishing KD from other childhood febrile illnesses.

Diagnosis, Treatment, and Prognosis

Features of the mucocutaneous lymph node syndrome, especially in a child 5 years of age or younger, are important for diagnosis of KD, but some patients present with other KD manifestations before full-blown mucocutaneous lymph node syndrome, including signs and symptoms of myocardial ischemia caused by coronary arteritis. Although timely treatment with intravenous gamma globulin (IVIG) plus aspirin has profoundly reduced the frequency and severity of coronary arteritis in KD, approximately 10% to 20% of patients develop clinically significant sequelae of coronary arteritis (Orenstein et al., 2012). Myocardial infarction occurs in approximately 2% of KD patients with coronary arteritis (Burgner & Harnden, 2005). Presence of abnormalities on initial echocardiogram may predict resistance to treatment with IVIG (Chbeir et al., 2018). Some patients with disease resistant to IVIG may need to be treated with glucocorticoids. Other agents are currently being studied.

SMALL VESSEL VASCULITIS

SVV is vasculitis predominantly affecting small vessels, defined as small intraparenchymal arteries, arterioles, capillaries, and venules (Jennette et al., 2013). Medium arteries and veins may be affected.

As with other vasculitides, an important diagnostic dichotomy is between infectious SVV and immune-mediated SVV. Viral infection and bacterial infection can mimic immune-mediated SVV, and the diagnostic distinction between these forms of vasculitis is critically important for appropriate treatment with antimicrobial therapy versus immunosuppressive therapy. Detection of the pathogen by culture or by genomic or proteomic assays or serologic detection of an immune response to the pathogen reveals the etiologic infection (Jain et al., 2007; D'Alessandro et al., 2014).

TABLE 54.3

Names and Definitions for ANCA-Associated Small Vessel Vasculitis Adopted by the 2011-2012 International Chapel Hill Consensus Conference Nomenclature of the Vasculitides

ANCA-associated vasculitis (AAV)	Necrotizing vasculitis, with few or no immune deposits, predominantly affecting small vessels (i.e., capillaries, venules, arterioles, and small arteries), associated with MPO-ANCA or PR3-ANCA. Not all patients have ANCA. Add a prefix indicating ANCA reactivity (e.g., PR3-ANCA, MPO-ANCA, ANCA-negative).
Microscopic polyangiitis (MPA)	Necrotizing vasculitis, with few or no immune deposits, predominantly affecting small vessels (i.e., capillaries, venules, or arterioles). Necrotizing arteritis involving small and medium arteries may be present. Necrotizing glomerulonephritis is very common. Pulmonary capillaritis often occurs. Granulomatous inflammation is absent.
Granulomatosis with polyangiitis (Wegener) (GPA)	Necrotizing granulomatous inflammation usually involving the upper and lower respiratory tract, and necrotizing vasculitis affecting predominantly small to medium vessels (e.g., capillaries, venules, arterioles, arteries, and veins). Necrotizing glomerulonephritis is common.
Eosinophilic granulomatosis with polyangiitis (Churg Strauss) (EGPA)	Eosinophil-rich and necrotizing granulomatous inflammation often involving the respiratory tract, and necrotizing vasculitis predominantly affecting small to medium vessels, and associated with asthma and eosinophilia. ANCA is more frequent when glomerulonephritis is present.

From Jennette JC, Falk RJ, Bacon PA, et al: 2012 Revised International Chapel Hill Consensus Conference Nomenclature of Vasculitides, *Arthritis Rheum* 65:1–11, 2013.

Based on immunopathologic features, noninfectious SVV is divided into ANCA-associated vasculitis (AAV) with few or no vessel immune deposits and immune complex SVV with moderate to marked vessel wall deposits of immunoglobulin and/or complement components.

ANCA-ASSOCIATED SMALL VESSEL VASCULITIS

Definition and Epidemiology

AAV is necrotizing vasculitis, with few or no immune deposits, that predominantly affects small vessels (i.e., capillaries, venules, arterioles, and small arteries) and is associated with myeloperoxidase (MPO)–ANCA, or proteinase 3 (PR3)–ANCA (Jennette et al., 2013) (Table 54.3). However, not all patients have MPO-ANCA or PR3-ANCA, at least using current analytic methods. The few or no immune deposits distinguishes ANCA vasculitis from immune complex vasculitis that has moderate to marked vessel wall deposits of immunoglobulin and/or complement components (Jennette et al., 2013). Because of the paucity of immune deposits, ANCA vasculitis is also called pauci-immune vasculitis.

ANCA SVV is classified based on clinicopathologic phenotypes and by the antigen specificity of ANCA. The clinicopathologic variants are MPA, granulomatosis with polyangiitis (GPA) (formerly called Wegener granulomatosis), eosinophilic GPA (EGPA) (formerly called Churg-Strauss syndrome), and renal limited vasculitis (RLV) (Jennette et al., 2013). An additional variant is drug-induced ANCA vasculitis, which may manifest as MPA, GPA, or RLV (Pendergraft & Niles, 2014). An optimum diagnosis should include both the ANCA serology status and the clinicopathologic phenotype (e.g., MPO-ANCA MPA, PR3-ANCA GPA, ANCA-negative EGPA) (Jennette et al., 2013).

MPA is multiorgan pauci-immune small vessel vasculitis with no granulomatous inflammation or asthma. MPA often has necrotizing glomerulonephritis and pulmonary capillaritis. GPA has necrotizing granulomatous inflammation usually involving the upper and lower respiratory tract, as well as vasculitic lesions indistinguishable from those of MPA. EGPA has eosinophil-rich and necrotizing granulomatous inflammation often involving the respiratory tract, as well as asthma and blood eosinophilia. Although there appears to be a prevasculitic phase that is ANCA negative, ANCA-positive EGPA patients typically have

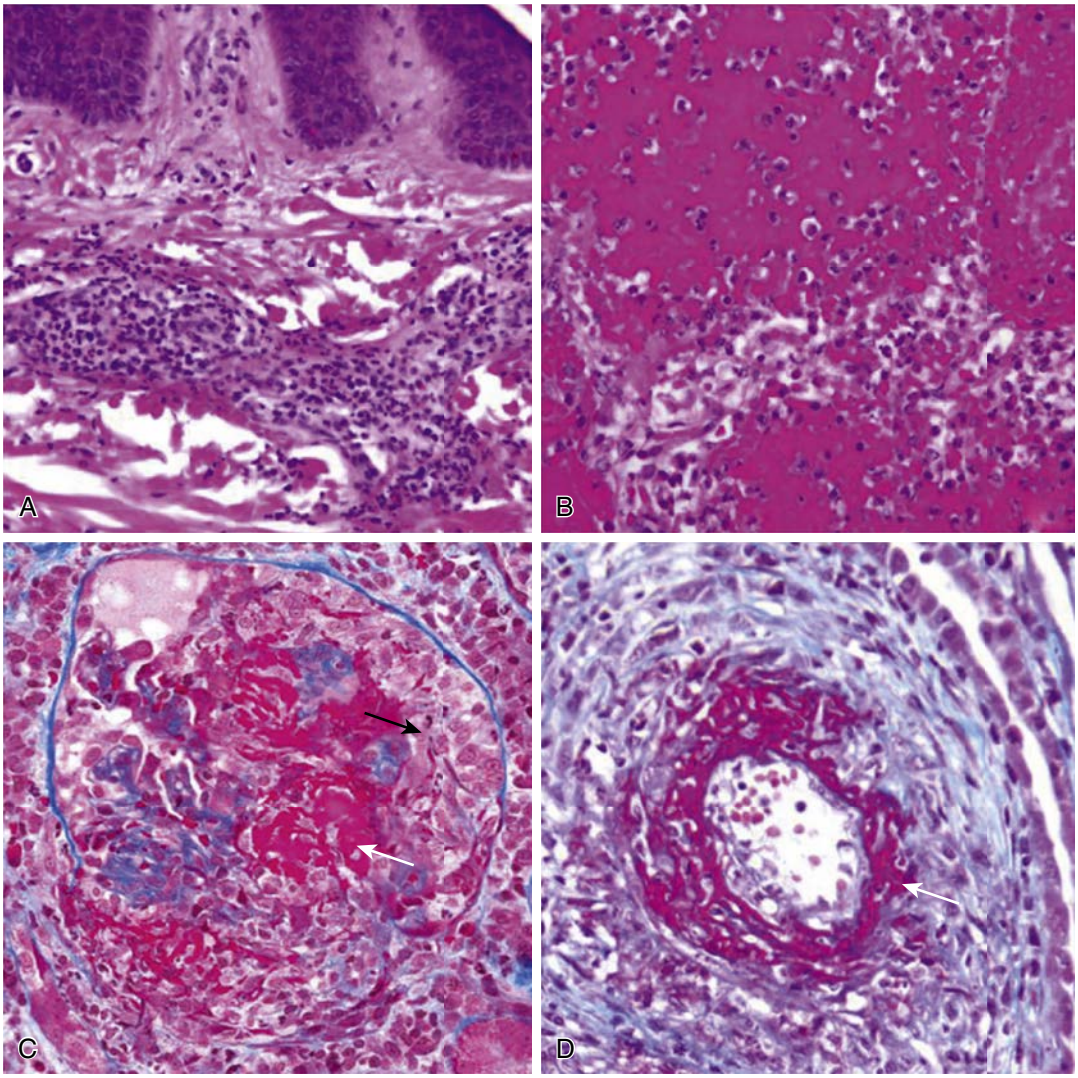

Fig. 54.6 ANCA disease can cause many forms of vascular injury. **A,** Dermal leukocytoclastic angiitis with intense neutrophil-rich infiltrates centered in small dermal vessels (H&E stain, ×400). **B,** Hemorrhagic pulmonary alveolar capillaritis with destruction of alveolar walls by neutrophil-rich inflammation (H&E stain, ×500). **C,** Glomerulonephritis with fibrinoid necrosis of glomerular capillaries *(white arrow)* and adjacent cellular crescent formation *(black arrow)* (Masson trichrome stain, ×500). **D,** Arteritis with extensive irregular fibrinoid necrosis *(white arrow)* (Masson trichrome stain, ×400).

pauci-immune small vessel vasculitis and pauci-immune necrotizing and crescentic glomerulonephritis that is indistinguishable from MPA and GPA. ANCA vasculitis confined to a single organ may occur. One example is ANCA RLV causing pauci-immune necrotizing and crescentic glomerulonephritis.

The incidence of ANCA vasculitis increases with age, with a peak around 60 years old, although children can develop ANCA vasculitis. Gender distribution is about equal, with a possible slight male predominance. The incidence and prevalence of ANCA vasculitis varies among the different clinicopathologic phenotypes and among different geographic locations (Watts et al., 2015). Roughly, the incidence of all forms of ANCA vasculitis is 15 to 20/million, and the prevalence is roughly 50 to 150/million. There is a higher ratio of GPA:MPA in northern Europe (e.g., Germany and Scandinavia) and northern US states (e.g., Montana and Minnesota), and a lower ratio of GPA:MPA in southern Europe (e.g., Greece and Spain) and southern US states (e.g., North Carolina). This is accompanied by the expected differences in ratio of PR3:MPO ANCA specificity in accord with more frequent PR3-ANCA with GPA and more frequent MPO-ANCA with MPA. The precise ratios are not known, but in general there is a reversal of preponderance of MPO-ANCA MPA versus PR3-ANCA GPA from north to south in both Europe and North America. There is a striking preponderance of MPO-ANCA and MPA in Asia. For example, in one study of AAV in Japan, the estimated annual incidence was 15/million adults (>15 years of age) and 45/million older adults (>65 years of age). Ninety-one percent of the patients were MPO-ANCA positive, but none were PR3-ANCA positive, and none had GPA or EGPA (Fujimoto et al., 2006).

Pathology

ANCA vasculitis can affect arteries (usually small arteries), arterioles, capillaries, venules, and veins (usually small veins). In all organs and in all clinicopathologic variants (e.g., MPA, GPA, EGPA), acute ANCA arteritis is characterized by segmental fibrinoid necrosis (Fig. 54.6), and mural and perivascular neutrophil-rich infiltration (Jennette & Falk, 2007; Jennette, 2015). Eosinophils may be numerous, especially in EGPA. Within several days, the neutrophil-rich inflammation is replaced by predominantly mononuclear leukocytes, with numerous monocytes and macrophages and fewer lymphocytes. Within a week, the active inflammatory process wanes and vasculitic lesions develop progressive sclerosis/fibrosis. In a given tissue, such as skin, gut, or kidney, vasculitic lesions of different ages often are observed because persistently active ANCA vasculitis has multiple acute vasculitic lesions developing while prior active lesions are undergoing scarring. Patients in complete remission should have only chronic quiescent lesions. ANCA arteritis is histopathologically indistinguishable from other forms of necrotizing arteritis (e.g., PAN).

When ANCA vasculitis affects venules (e.g., in the dermis), acute lesions have less conspicuous fibrinoid necrosis and more prominent leukocytoclasia (see Fig. 54.6, *A*). This pattern of injury may be called leukocytoclastic angiitis, and it can be caused by other forms of SVV, especially immune complex SVV.

Acute pulmonary alveolar capillaritis is characterized by accumulation of neutrophils in alveolar capillary lumens, destruction of capillary basement membranes (seen with silver stains), and hemorrhage into alveolar air spaces (see Fig. 54.6, *B*).

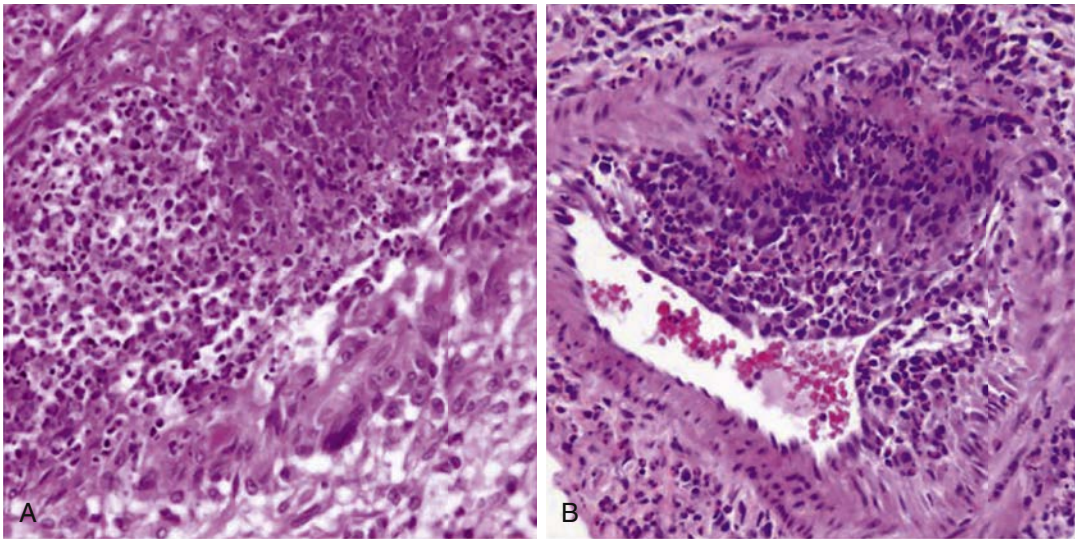

Fig. 54.7 Pulmonary lesions in granulomatosis with polyangiitis (GPA) and eosinophilic GPA (EGPA) include necrotizing granulomatous inflammation and vasculitis. **A,** Necrotizing granulomatous inflammation in a GPA patient showing neutrophil-rich necrotic debris in the upper left with a marginal zone of macrophages, including a giant cell in the lower right (H&E stain, ×500). **B,** Necrotizing arteritis in the lung of a patient with EGPA showing intense eosinophil-rich inflammation (H&E stain, ×400).

The necrotizing glomerulonephritis that often is a component of ANCA vasculitis and that may occur as RLV is characterized by segmental fibrinoid necrosis with adjacent cellular crescent formation in the acute phase (see Fig. 54.6, *C*) and segmental sclerosis with adjacent fibrous crescents in the chronic phase. The pathology of ANCA glomerulonephritis is the same in MPA, GPA, EGPA, and renal limited disease. In addition to necrotizing and crescentic glomerulonephritis, kidney lesions in ANCA disease also include necrotizing arteritis (most often affecting interlobular and arcuate arteries) (see Fig. 54.6, *D*) and leukocytoclastic medullary angiitis affecting the vasa rectae.

Immunohistology demonstrates an absence or paucity of immunoglobulin deposition, which distinguishes ANCA vasculitis from immune complex vasculitis. However, most specimens, including glomeruli affected by ANCA disease, have at least a small amount of immune complex–type staining for immunoglobulins and complement, and a small amount of immune complex–type electron-dense deposits by electron microscopy. ANCA disease also can occur concurrently with anti-GBM disease or immune complex disease, and in this context there is substantial immunostaining for immunoglobulins and complement.

The necrotizing granulomatous inflammation of GPA and EGPA begins as a focus of neutrophil-rich inflammation that may resemble a small abscess. EGPA lesions also contain numerous eosinophils (Jennette, 2011). These lesions may be small and spherical, or they may be large and irregular, creating so-called geographic necrosis. Within days, the focus of acute inflammation is surrounded by a rim of monocytes and macrophages, including multinucleated giant cells (Fig. 54.7, *A*). The central zone of inflammation becomes completely necrotic and evolves from basophilic or eosinophilic cellular fragments (derived primarily from degenerated neutrophils and eosinophils) to amorphous necrotic debris. The adjacent granulomatous inflammation becomes more organized with palisades of elongated macrophages adjacent to the necrosis. Eventually, the central zone forms a cavity or becomes fibrotic. Necrotizing granulomatous inflammation occurs most often in the upper and lower respiratory tract, but occasionally in other tissues such as the nasal tissues, orbit, skin, and kidneys. The differential diagnosis for pulmonary granulomatous inflammation includes mycobacterial and fungal infectious disease. The presence of pulmonary vasculitis along with the granulomatous inflammation is more specific evidence for GPA or EPGA. Numerous eosinophils in the granulomatous inflammation and the vasculitis favor EGPA (see Fig. 54.7, *B*).

Etiology and Pathogenesis

Clinical and experimental observations support a direct role of ANCA in the pathogenesis of vasculitis (Jennette & Falk, 2014; Kallenberg, 2014). Clinical observations that support a pathogenic role include the high frequency of ANCA in the blood, the general correlation of ANCA titers with disease activity (especially if capture assays are used), increased risk for disease when there are higher levels of ANCA antigens on the surface of circulating neutrophils, induction of ANCA, as well as vasculitis by certain drugs (e.g., hydralazine, propylthiouracil, penicillamine, minocycline) and the therapeutic efficacy of apheresis and targeted B-cell therapy (e.g., rituximab).

The best experimental evidence is induction of ANCA-mediated pauci-immune crescentic glomerulonephritis and small vessel vasculitis in experimental animals. The first animal model that was described used IV injection of mouse anti-MPO IgG (derived from immunizing MPO knockout mice with purified mouse MPO) into wild-type mice, resulting in the induction of a pauci-immune glomerulonephritis with segmental fibrinoid necrosis and crescent formation that closely resembled human ANCA glomerulonephritis (Xiao et al., 2002). Some of the mice that received anti-MPO IgG also developed systemic small vessel vasculitis, including alveolar capillaritis and necrotizing arteritis that was histologically indistinguishable from human ANCA disease.

Numerous in vitro and in vivo experiments support the hypothesis that ANCA in the circulation can interact with ANCA antigens (MPO, PR3) on the surface of neutrophils that have been primed by cytokines or complement fragments (e.g., C5a) (Jennette & Falk, 2014). ANCA-activated neutrophils release factors that activate the alternative complement pathway, which in turn recruits more neutrophils and primes and activates neutrophils by engaging the C5a receptors (Xiao et al., 2014). Neutrophils that are activated in the circulation adhere to and penetrate vessel walls and release destructive enzymes and oxygen radicals that cause vascular injury. Hypothetically, primed neutrophils in the extravascular tissues that are activated by ANCA are the cause for the granulomatous inflammation of GPA and EGPA (Jennette & Falk, 2014).

Drugs can induce the development of ANCA, especially MPO-ANCA (Pendergraft & Niles, 2014). Hydralazine, minocycline, propylthiouracil, and levamisole-adulterated cocaine are major causes. A hypothesis has been proposed to explain the induction of ANCA by hydralazine. Patients with ANCA vasculitis have circulating neutrophils that aberrantly transcribe and express neutrophil granule proteins, including the MPO and PR3, because of altered epigenetic regulation of gene expression (McInnis et al., 2015). Hydralazine can function as a nonnucleoside DNA methylation inhibitor, which can reverse epigenetic silencing of PR3 and MPO, resulting in increased expression of both autoantigens and loss of tolerance (Pendergraft & Niles, 2014).

Except for the small minority of cases caused by drugs, the etiology of ANCA disease is not known. Various theories postulate the result of infections (e.g., *Staphylococcus aureus*), environmental exposures (e.g., silica), or dysregulated gene expression (e.g., of PR3 antisense peptides) (Jennette & Falk, 2014; Kallenberg, 2014). One novel theory posits that a protein that is complementary to the autoantigen PR3 triggers the PR3-ANCA autoimmune response through an anti-idiotypic network (Pendergraft et al., 2004). This complementary protein could be an endogenous protein resulting from age-related dysregulation of antisense gene expression or an exogenous protein derived from a pathogen that makes an antisense peptide mimic that is an inhibitor of the antimicrobial function of complementary PR3.

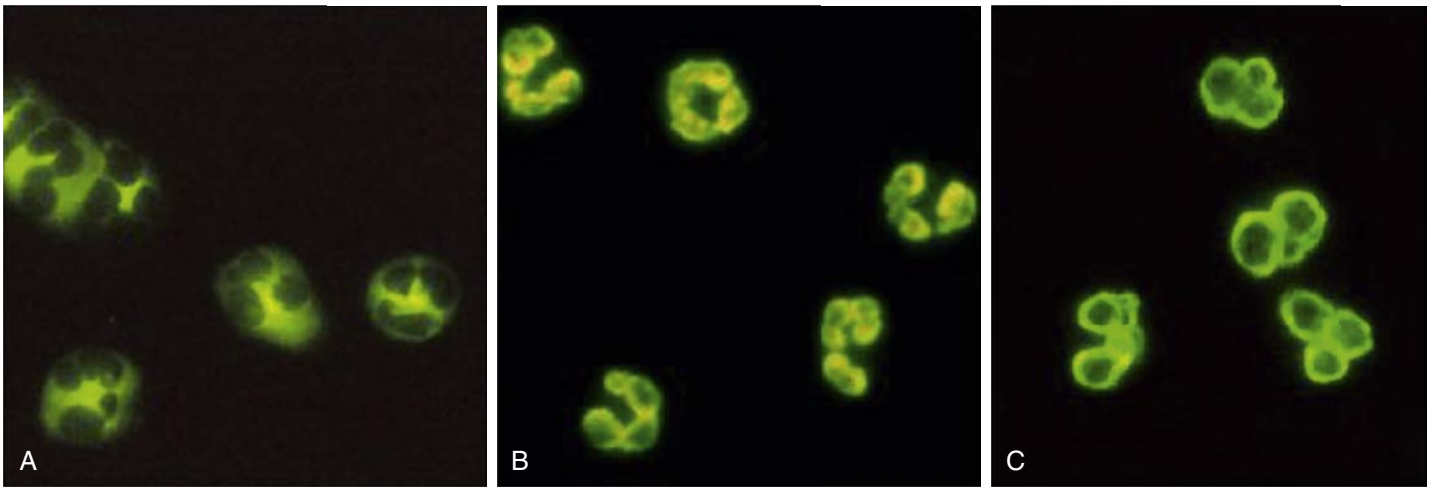

Fig. 54.8 Indirect immunofluorescence (IIF) assay using ethanol-fixed, normal human neutrophils as substrate showing C-ANCA cytoplasmic staining (**A**), P-ANCA perinuclear staining (**B**), and atypical-ANCA showing heaped-up, very perinuclear staining (**C**) (×1000).

Clinical Laboratory Testing

In 1999, an International Consensus Statement on Testing and Reporting of Antineutrophil Cytoplasmic Antibodies recommended that testing in new patients should be by indirect immunofluorescence (IIF) assay and that samples that are positive by IIF should be tested by enzyme-linked immunosorbent assays (ELISAs) for PR3-ANCA and MPO-ANCA (Savige et al., 1999). The recommendation for optimum testing of patients suspected of having ANCA disease was to test by ELISA for PR3-ANCA and MPO-ANCA on all serum samples irrespective of IIF results. An automated ANCA-pattern recognition system (Damoiseaux et al., 2012) and a digital indirect immunofluorescence assay (Sowa et al., 2014) have been evaluated as alternatives to IIF. Pattern recognition systems have had relatively high levels of agreement with manual versus automated interpretation ranging from 74.6% to 89.1% (Melegari et al., 2012; Knutter et al., 2012).

A multicenter European Vasculitis Study Group (EUVAS) study reevaluated the previous 1999 consensus agreement (Damoiseaux et al., 2017). In the updated international consensus statement, 11% to 17% of patients with AAV were negative by IIF and 9% to 16% were negative by immunoassay (Damoiseaux et al., 2018; Bossuyt et al., 2017). Thus no single assay would detect 100% of AAV patients. The updated recommendations were that IIF was no longer needed as the first screening test and adds minimal benefit to antigen-specific assays in the diagnosis of AAV when the pretest probability for the disease is high (Bossuyt et al., 2017). In the revised 2017 recommendations, patients suspected of having AAV should be evaluated by PR3-ANCA and MPO-ANCA immunoassays. If the initial assay is negative, an additional assay may be performed if there is high clinical suspicion or in the event of low antibody levels (Bossuyt et al., 2017). Although immunoassays have become more effective since the 1999 recommendation and despite the updated 2017 recommendation, most laboratories continue to employ both IIF and antigen-specific immunoassays for MPO and PR3 for ANCA testing.

Lastly, another positive development is the production of MPO-ANCA reference material (ERM-DA476/IFCC), released by the Institute for Reference Materials and Measurements. The reference material comes from a single plasmapheresis patient with vasculitis, and currently PR3-ANCA reference materials are being developed. Both of these reference materials should reduce variability between ANCA assays; however, standardization of ANCA assays need to be established.

IIF assay using ethanol-fixed, normal human neutrophils as substrate produces two different staining patterns: cytoplasmic (C-ANCA) (Fig. 54.8, *A*) and perinuclear (P-ANCA) (see Fig. 54.8, *B*) (Savige et al., 2000). The perinuclear staining is an artifact of substrate preparation that results from diffusion of the cationic MPO antigen from the cytoplasm to the nucleus during substrate preparation. This perinuclear relocation does not occur when formalin is used to fix plasma protein in place before preparing neutrophils for IIF. Thus a true P-ANCA will produce cytoplasmic staining on formalin-fixed neutrophils, whereas an antinuclear antibody will stain the nucleus in both ethanol- and formalin-fixed preparations (Falk & Jennette, 1988).

When the antigen specificity is determined by immunoassays, PR3-ANCA typically produces the C-ANCA staining pattern by IIF, and MPO-ANCA typically produces a P-ANCA staining pattern. ANCAs that cause a P-ANCA pattern in IIF assays are not restricted to MPO and include a variety of autoantibodies that occur in inflammatory diseases, including ulcerative colitis, sclerosing cholangitis, autoimmune hepatitis, rheumatoid arthritis, and Felty syndrome (Savige et al., 2000). Positive ANCA IIF results in serum from patients with inflammatory bowel disease, and other nonvasculitic inflammatory diseases may have an atypical pattern that shows more intense and heaped-up perinuclear staining (very perinuclear staining) (see Fig. 54.8, *C*). Antibodies that produce an atypical ANCA IIF pattern usually are not specific for MPO or PR3 (Savige et al., 2000).

Antigen-specific, quantitative immunoassays are the standard of care for diagnosis and some management decisions in patients with ANCA disease. ANCA serotype may be more important than clinicopathologic classification for predicting outcome, including the likelihood of recurrence after induction of remission (Kallenberg, 2014). Detection of ANCA to monitor disease activity and adjust treatment remains controversial; however, epitope-specific assays that can distinguish between pathogenic and nonpathogenic ANCA may change this in the future (Roth et al., 2013).

First-generation ANCA assays were direct noncompetitive ELISA. The second-generation tests (capture ELISA) or third-generation tests (anchor ELISA) are more sensitive and specific for ANCA testing (Cohen Tervaert & Damoiseaux, 2012). Fourth-generation assays may be epitope specific and more effective in guiding therapy (Roth et al., 2013).

Chemiluminescence immunoassays (CIAs) have been used to detect PR3-ANCA and MPO-ANCA with comparable results to direct ELISAs (Mahler et al., 2012). A combination of cell- and microbead-based digital indirect immunofluorescence analysis of ANCA in one reaction environment by the novel multiplexing bead technology for simultaneous screening and confirmatory ANCA testing have been developed (Sowa et al., 2014). Additional testing methodologies include solid-phase bead-based multiplex assays, which can simultaneously detect ANCAs and other autoantibodies (Nifli et al., 2006), and a flow cytometric immunoassay (Trevisin et al., 2008). However, the flow cytometric assays have sensitivity challenges, and the utility for initial screening has not be evaluated. ANCA results by classical testing (IIF and ELISA) compared with multiplex bead analysis were very good ($\kappa = 0.831$) with no significant difference ($p = 0.735$). Automated ANCA titer detection in one dilution demonstrated very good agreement with classical analysis requiring dilution of samples ($\kappa = 0.985$).

Even using current ANCA testing capabilities, patients with clinical features and pathologic findings consistent with ANCA vasculitis can test negative for ANCA. In a study of 539 patients with a clinical diagnosis of ANCA vasculitis, positive ANCA serology was demonstrated in 98% of MPA patients, 96% of GPA patients, 94% of renal-limited pauci-immune crescentic glomerulonephritis patients, and 64% of EGPA patients (Kallenberg, 2014). Of the 364 patients with GPA in this analysis, 12 tested negative for ANCA but 10 had GPA limited to the ear, nose, and throat.

EGPA patients usually have P-ANCA with MPO-ANCA specificity (Sinico et al., 2005). EGPA patients with a positive ANCA have more glomerulonephritis, pulmonary capillaritis, peripheral neuropathy, and biopsy-proven vasculitis, whereas patients with a negative ANCA have more myocarditis (Sablé-Fourtassou et al., 2005; Sinico et al., 2005). All EGPA patients who have biopsy-proven pauci-immune necrotizing and

crescentic glomerulonephritis are ANCA positive (Sinico et al., 2006). It appears that EGPA may have two serologically defined phenotypes: ANCA-positive EGPA with vasculitis and ANCA-negative EGPA without vasculitis.

ANCA specificity correlates with clinical symptoms. Ninety percent of patients with ANCA who have destructive upper respiratory tract disease (e.g., saddle-nose deformity) have PR3-ANCA, whereas most patients with exclusively or predominantly renal involvement have MPO-ANCA (Lionaki et al., 2012). Dual positivity for both MPO-ANCA and PR3-ANCA is rare except in the setting of drug-induced ANCA (Pendergraft & Niles, 2014).

ANCAs are in approximately one third of patients with anti-GBM disease (Jennette, 2003; Rutgers et al., 2005). The dual anti-GBM and ANCA specificity is the result of two different antibody populations rather than one cross-reacting population (Rutgers et al., 2005), and the antigen specificities of anti-GBM antibodies are the same in patients with anti-GBM antibodies only or combined ANCA and anti-GBM antibodies (Hellmark et al., 1997). Compared with patients with anti-GBM alone, patients with both autoantibodies are older, often have features of systemic small vessel vasculitis, and have a better prognosis for renal survival with treatment.

The possibility of drug-induced disease should be considered in patients with ANCA vasculitis. The most common are hydralazine, minocycline, propylthiouracil, and levamisole-adulterated cocaine. If cocaine abuse is a possibility, the urine should be tested for cocaine, and if positive, should be tested for levamisole (Pendergraft & Niles, 2014). Most drug-induced vasculitis is not caused by ANCA. A recent study of 239 patients with all forms of drug-associated cutaneous vasculitis demonstrated that the most common laboratory abnormalities were increased ESR (40%) and cryoglobulins (26%), while leukocytosis and positive ANA were found in less than 25% (Ortiz-Sanjuán et al., 2014). Only rare examples of drug-induced immune complex vasculitis have been described, and most of these have been caused by therapeutic agents that are proteins, such as monoclonal antibodies (Baldo, 2013).

The diagnostic value in patients with vasculitis of ANCA with other specificities has been investigated; however, to date, the only routine testing that has been adopted is for MPO-ANCA and PR3-ANCA. ANCA with specificity for lysosomal membrane protein 2 (LAMP2) has been reported to have high sensitivity and specificity for pauci-immune SVV (Kain et al., 2008); however, not all investigators have confirmed this finding (Roth et al., 2012).

Diagnosis, Treatment, and Prognosis

The diagnosis of ANCA-associated vasculitides as MPA, GPA, or EGPA is based on algorithms that have been derived from the Chapel Hill Consensus Conference definitions (Watts et al., 2007; Abdulkader et al., 2013). The diagnostic evaluation of patients with ANCA disease should include both testing for ANCA specificity (i.e., for PR3-ANCA or MPO-ANCA) and classification as MPA, GPA, EGPA, or RLV. Assessment of the disease stage and severity also is important for tailoring treatment.

Treatment of ANCA disease begins with induction of remission, followed by maintenance of remission (Kallenberg, 2014). In patients with active generalized disease, remission is most often induced with an immunosuppressive agent (e.g., cyclophosphamide or rituximab) and high-dose glucocorticoids. Rituximab has been shown to be noninferior to cyclophosphamide for induction of remission in some patients. Patients presenting with severe kidney failure (i.e., requiring dialysis or an estimated GFR <15) or diffuse alveolar hemorrhage should receive plasma exchange as well as the usual induction therapy. Results from the completed PEXIVAS trial should shed more light on the use of plasma exchange and efficacy of different steroid regimens on induction treatment. Mild localized disease, especially with no renal or pulmonary disease, may be treated with methotrexate and glucocorticoids. When disease is in remission, patients can be treated with Rituxan or azathioprine (Kallenberg, 2014). Once a patient is in remission, glucocorticoids should be tapered within 6 months to reduce the likelihood of infectious complications (McGregor et al., 2012). Other treatment options for refractory disease are IVIG, infliximab, alemtuzumab, and deoxyspergualin (Kallenberg, 2014).

Drug-induced ANCA vasculitis may require not only cessation of the drug and supportive care but also immunosuppression, plasma exchange in severe cases, and dialysis as needed (Pendergraft & Niles, 2014).

ANTIGLOMERULAR BASEMENT MEMBRANE DISEASE

Definition and Epidemiology

Antiglomerular basement membrane (anti-GBM) disease is an autoimmune disease caused by autoantibodies that target the noncollagen domain of the α3 chain of type IV collagen (Cui & Zhao, 2011; Greco et al., 2015). This form of vasculitis can be grouped with immune complex vasculitis because it results from immune complexes forming in situ along capillary basement membranes (Table 54.4). The glomerular capillaries of the kidneys and alveolar capillaries of the lungs contain this autoantigen, and either or both can be injured in anti-GBM disease. When both are involved, the resultant pulmonary-renal syndrome is called Goodpasture syndrome. Most patients with anti-GBM disease have rapidly progressive glomerulonephritis, approximately half have pulmonary disease, and only a few have isolated pulmonary disease.

The incidence of anti-GBM disease is estimated to be 1/million per year (Cui & Zhao, 2011; Greco et al., 2015). It occurs more commonly in whites than blacks. Age distribution is bimodal, with the most common ages being between 20 and 30 years and between 60 and 70 years. The younger patients are predominantly men, and there is a higher frequency of pulmonary disease. The older patients are predominantly women, and there is a lower frequency of pulmonary disease.

TABLE 54.4

Names and Definitions for Immune Complex Small Vessel Vasculitis Adopted by the 2011-2012 International Chapel Hill Consensus Conference Nomenclature of the Vasculitides

Immune complex vasculitis	Vasculitis with moderate to marked vessel wall deposits of immunoglobulin and/or complement components predominantly affecting small vessels (i.e., capillaries, venules, arterioles, and small arteries). Glomerulonephritis is frequent.
Anti-GBM disease	Vasculitis affecting glomerular capillaries, pulmonary capillaries, or both, with basement membrane deposition of anti–basement membrane autoantibodies. Lung involvement causes pulmonary hemorrhage, and renal involvement causes glomerulonephritis with necrosis and crescents.
Cryoglobulinemic vasculitis	Vasculitis with cryoglobulin immune deposits affecting small vessels (predominantly capillaries, venules, or arterioles) and associated with cryoglobulins in serum. Skin, glomeruli, and peripheral nerves are often involved.
IgA vasculitis (Henoch-Schönlein)	Vasculitis, with IgA1-dominant immune deposits affecting small vessels (predominantly capillaries, venules, or arterioles). Often involves skin and gut, and frequently causes arthritis. Glomerulonephritis indistinguishable from IgA nephropathy may occur.
Hypocomplementemic urticarial vasculitis (anti-C1q vasculitis)	Vasculitis accompanied by urticaria and hypocomplementemia affecting small vessels (i.e., capillaries, venules, or arterioles), and associated with anti-C1q antibodies. Glomerulonephritis, arthritis, obstructive pulmonary disease, and ocular inflammation are common.

From Jennette JC, Falk RJ, Bacon PA, et al: 2012 Revised International Chapel Hill Consensus Conference Nomenclature of Vasculitides, *Arthritis Rheum* 65:1–11, 2013.

Pathology

The light microscopic features of anti-GBM glomerulonephritis (GN) are indistinguishable from ANCA glomerulonephritis, although on average the extent of injury is more severe in anti-GBM GN compared to ANCA GN. For example, at the time of biopsy, anti-GBM GN has an average of 77% crescents compared to 49% for ANCA GN (Jennette, 2003). Concurrent anti-GBM plus ANCA GN has an average of 62% crescents. The activity and chronicity of anti-GBM GN lesions tend to be more synchronous than the lesions of ANCA GN. That is, anti-GBM lesions are either mostly acute or mostly chronic, whereas ANCA GN lesions more often have a mixture of acute and chronic lesions. This is in accord with the clinical and serologic observations that anti-GBM disease and anti-GBM seropositivity typically occur as one episode with uncommon relapses, whereas ANCA disease and ANCA seropositivity often are persistent with multiple recurrences even after initial induction of remission.

Anti-GBM pulmonary disease is characterized by extensive hemorrhage into the alveolar air spaces but with less overt influx of neutrophils into alveolar capillaries than is observed with ANCA pulmonary capillaritis. Identification of arteritis in the kidney or lung of a patient with anti-GBM disease is strong evidence for concurrent anti-GBM plus ANCA disease.

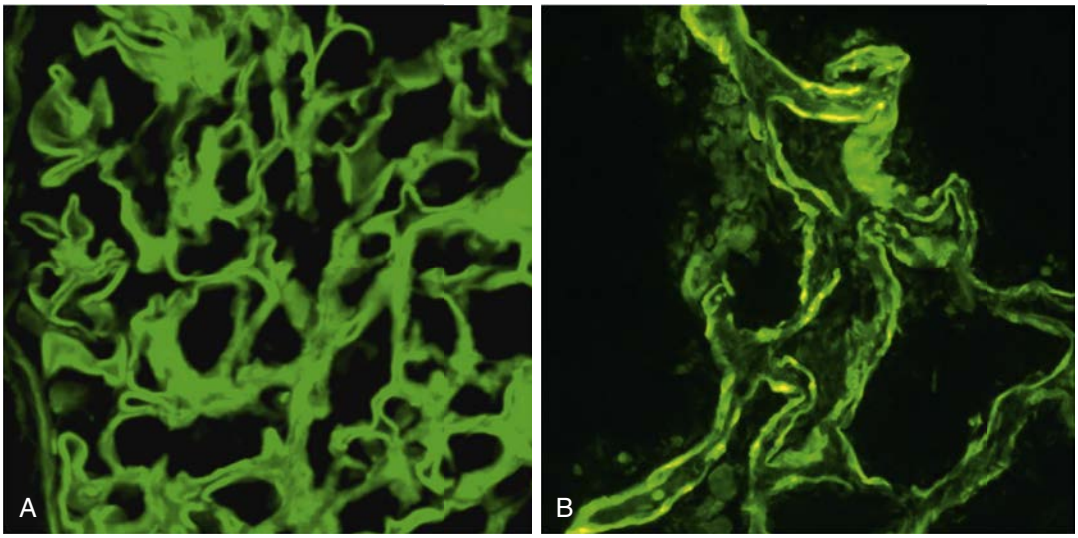

Fig. 54.9 Linear immunofluorescence staining for IgG along glomerular basement membranes (**A**) and pulmonary alveolar capillary basement membranes (**B**); demonstration by direct immunofluorescence microscopy (FITC rabbit antihuman IgG, ×400).

The most definitive pathology finding is demonstration by direct immunofluorescence microscopy of linear staining for IgG along glomerular capillary basement membranes or pulmonary alveolar capillary basement membranes (Fig. 54.9). This usually is accompanied by staining for C3 and other complement components and variable staining for IgM and IgA. This is distinct from the granular staining for immunoglobulin in vessel walls with immune complex vasculitis or the paucity of immunoglobulin staining in vessel walls in ANCA vasculitis (Jennette et al., 2013).

Etiology and Pathogenesis

Both humoral and cellular autoimmune responses have been incriminated in the pathogenesis of anti-GBM disease (Pusey, 2003; Cui & Zhao, 2011). There is compelling evidence that anti-GBM antibodies are pathogenic, which includes (1) the close association of circulating and basement membrane–bound anti-GBM antibodies with disease; (2) relatively good correlation of autoantibody levels with activity of disease; (3) clinical response to therapy that reduces circulating anti-GBM levels, such as apheresis and immunosuppressive therapy; (4) recurrence of disease in kidney transplants in the presence of residual circulating anti-GBM antibodies in the recipient; (5) development of anti-GBM glomerulonephritis in patients with hereditary type IV collagen abnormalities who make nephritogenic autoantibodies directed against donor GBM; and (6) experimental animal studies, including direct transfer of glomerulonephritis to primates by IV injection of human anti-GBM antibodies.

Although anti-GBM antibodies appear to be major pathogenic factors, T cells also play an important role. T-cell help is required for class-switching to produce high-affinity IgG antibodies, and T-cell involvement is indicated by MHC associations.

The etiology of anti-GBM disease is not known. One hypothesis proposes that anti-GBM disease is an autoimmune "conformeropathy" that involves pathogenic conformational changes in the α3 and α5 noncollagen domains of type IV collagen, revealing cryptic epitopes that in turn elicit an autoimmune response (Pedchenko et al., 2010).

Another hypothesis is that autoimmunity to the α3 chain of type IV collagen is triggered by "autoantigen complementarity" that begins with an immune response against a peptide that is antisense or complementary to the autoantigen (Reynolds et al., 2015). Autoantigen complementarity has also been incriminated as a cause for ANCA disease (Pendergraft et al., 2004).

Clinical Laboratory Testing

Anti-GBM assays using ELISAs, chemiluminescence assays (CIAs), dot blots, and Western blots are highly specific (>90%) and sensitive (>95%) for anti-GBM disease (Pusey, 2003). Most commercial assays use bovine or sheep GBM enriched for the noncollagen domain of the α3 chain of type IV collagen (Pusey, 2003). Positive results can be confirmed by Western blotting using collagenase-solubilized human GBM. Indirect immunofluorescence microscopy assays using normal human or primate kidney as substrate were used historically, but they are not sensitive enough for current clinical use.

Rapid screening assays are available for concurrently detecting PR3-ANCA, MPO-ANCA, and anti-GBM antibodies in the same assay for rapid diagnosis of patients with clinical evidence for rapidly progressive glomerulonephritis, hemorrhagic pulmonary capillaritis, or both, using either ELISA (Westman et al., 1997) or dot blot technology (Rutgers et al., 2005). A rapid, random access CIA also has been developed to detect anti-GBM antibodies with 95.6% sensitivity and 99.6% specificity (Mahler et al., 2012).

All patients with anti-GBM disease should be tested for ANCA to rule out concurrent anti-GBM plus ANCA disease, which occurs in approximately one third of patients with anti-GBM disease (Jennette, 2003; Rutgers et al., 2005). The double anti-GBM and ANCA reactivity in assays is the result of two different antibody populations rather than one cross-reacting population (Rutgers et al., 2005).

Diagnosis, Treatment, and Prognosis

Standard treatment is a combined therapy of plasmapheresis, prednisolone, and cyclophosphamide (Pusey, 2003; Cui & Zhao, 2011). Anecdotal reports of success with rituximab therapy have emerged but are not conclusive. The important determinant for the response to therapy and long-term prognosis for anti-GBM disease is early diagnosis to prevent end-stage kidney disease and life-threatening pulmonary hemorrhage. If treatment is started before the serum creatinine is above 5 mg/dL, there is a better chance of renal survival. Even in patients with advanced renal disease, treatment may be beneficial in preventing or ameliorating concurrent pulmonary disease. A recent retrospective analysis of 123 patients with anti-GBM disease classified presentation based on histopathologic classification for ANCA-associated glomerulonephritis and found that patients with sclerotic biopsy samples (>50% globally sclerotic glomeruli) and 100% cellular crescents did not recover from dialysis dependency. Dependency on dialysis at presentation and extent of interstitial infiltration at presentation were also predictors of end-stage kidney disease at follow-up (van Daalen 2018). Renal transplant is usually avoided until circulating anti-GBM autoantibodies can no longer be detected by standard assays.

CRYOGLOBULINEMIC VASCULITIS

Definition and Epidemiology

Cryoglobulinemic vasculitis is vasculitis with cryoglobulin-immune deposits affecting small vessels (predominantly capillaries, venules, or arterioles) and is associated with serum cryoglobulins (Tedeschi et al., 2007; Jennette et al., 2013). Skin, glomeruli, and peripheral nerves are often involved.

Cryoglobulins are immunoglobulins that reversibly precipitate in the cold (Damoiseaux, 2014). Type I cryoglobulins consist of a monoclonal immunoglobulin, generally either IgM or IgG. Type II cryoglobulins contain a monoclonal immunoglobulin with rheumatoid factor (RF) activity and polyclonal immunoglobulins. Most often this is a combination of a monoclonal IgM with polyclonal IgG. Type III cryoglobulins contain polyclonal immunoglobulins, typically IgM and IgG, with RF activity in the IgM fraction. Types II and III are called mixed cryoglobulins.

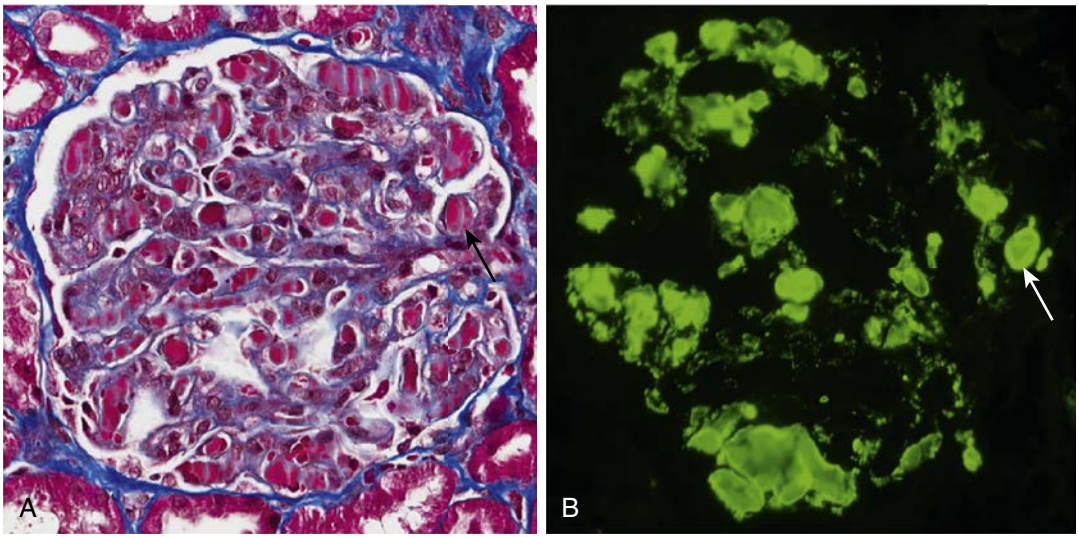

Fig. 54.10 Cryoglobulinemic glomerulonephritis with "hyaline thrombi" seen by light microscopy (**A** Masson trichrome stain, ×500) and by direct immunofluorescence microscopy using FITC-labeled rabbit antihuman C3 (**B** ×500).

Type I cryoglobulins often are associated with B-cell lymphoproliferative diseases, such as Waldenström macroglobulinemia or multiple myeloma. Type II cryoglobulins are often associated with HCV infection, as well as other chronic viral infections and systemic autoimmune diseases. Type III cryoglobulins often are associated with chronic viral infections and systemic autoimmune diseases and may be a transient state between polyclonal hypergammaglobulinemia and type II cryoglobulinemia (Damoiseaux, 2014).

Pathology

CV usually is confined to capillaries (e.g., glomerular capillaries), venules (e.g., dermal venules), and arterioles or very small arteries (e.g., epineural arteries in peripheral nerves). Involvement of medium arteries is extremely rare. The acute inflammation is neutrophil rich with leukocytoclasia. The inflammation may be accompanied by luminal or vessel wall deposits of PAS-positive hyaline material that is a coagulum of cryoglobulins. Cryoglobulinemic glomerulonephritis occurs as a renal-limited process or as a component of systemic CV. Cryoglobulinemic glomerulonephritis usually has a membranoproliferative pattern but may have other patterns of proliferative glomerulonephritis. A useful diagnostic finding is hyaline material in glomerular capillary lumens ("hyaline thrombi") that are composed of cryoglobulins (Fig. 54.10). By immunofluorescence microscopy, these deposits contain the immunoglobulins of the cryoglobulins as well as complement components that have been activated by the cryoglobulin immune complexes (see Fig. 54.10).

Etiology and Pathogenesis

HCV is the main etiologic agent of mixed cryoglobulinemic vasculitis (Cacoub et al., 2014). In some European settings, mixed cryoglobulinemia has been associated with HCV infection in more than 80% of the patients, although only a minority develop signs and symptoms of vasculitis (Pagnoux et al., 2006). Although the association of CV with HCV is approximately 85% in the Mediterranean region, it varies from 30% to 100% in other geographic locations (Damoiseaux, 2014).

Deposition of cryoglobulins in vessel walls incites vasculitis by complement activation. Monoclonal cryoglobulins (type I) are not as effective at activating inflammatory mediator systems as are mixed cryoglobulins (types II and III), which are immune complexes composed of antiantibodies (rheumatoid factors) bound to target antibodies. An important cause for cryoglobulinemia is hepatitis C infection. In HCV-CV, immune complex deposits contain viral proteins (Damoiseaux, 2014).

Clinical Laboratory Testing

Clinical laboratory testing for cryoglobulins is divided into three phases: the preanalytic phase, the analytic phase, and the typing phase (Damoiseaux, 2014). The preanalytic phase entails collecting the sample in prewarmed (37°C) tubes, transporting at 37°C, allowing coagulation of the blood sample at 37°C for at least 1 hour, and centrifugation at 37°C to separate the serum. The analytic phase entails incubating two fractions of the sample at 4°C for 3 to 7 days, visual assessment of precipitation, incubating one fraction at 37°C to assess resolution, and isolating the cryoglobulin from the other fraction for typing. The typing phase includes determining the immunoglobulin composition (e.g., by immunofixation or immunoelectrophoresis) and quantifying the cryoglobulin by assessing cryocrit, total protein content, and/or content of immunoglobulin isotypes (Damoiseaux, 2014).

In addition to a positive cryoglobulin assay, in a patient with clinical evidence for SVV, laboratory detection of low C4, rheumatoid factor, and evidence for HCV infection add additional support for a diagnosis of CV (Lamprecht et al., 2001).

Diagnosis, Treatment, and Prognosis

Detection of mixed cryoglobulins, especially accompanied by low C4, along with purpura, peripheral neuropathy, and/or glomerulonephritis, is strong evidence for CV.

One set of classification criteria for CV requires the detection of cryoglobulins in at least two determinations more than 12 weeks apart (DeVita et al., 2011). In addition to the detection of cryoglobulins, at least two additional patient-reported symptoms, clinical observations, or laboratory findings must be documented to make a diagnosis of CV.

Antiviral therapy with directly acting antivirals (DAAs) is recommended for therapy for HCV and has been associated with high rates of virologic response and clinical response. In patients with severe HCV-CV, an immunosuppressive treatment regimen is often required for the induction phase while awaiting the response to antiviral treatments. Antiviral therapies are often delayed in these patients; however, newer interferon-free antiviral regimens can often suppress HCV viral loads within 2 to 4 weeks, potentially resulting in faster improvement. Apheresis may be beneficial if there is life-threatening disease or rapidly progressive glomerulonephritis.

The 1-year, 3-year, 5-year, and 10-year survival rates for HCV-CV are 95%, 85%, 75%, and 65%, respectively. Mortality is mainly related to infections and end-stage liver disease. Factors associated with a poor prognosis are severe liver fibrosis (HR 5.31), central nervous system involvement (HR 2.74), kidney involvement (HR 1.91), and heart involvement (HR 4.2) (Terrier et al., 2011).

IGA VASCULITIS (HENOCH-SCHÖNLEIN PURPURA)

Definition and Epidemiology

IgA vasculitis (IgAV) (formerly called Henoch-Schönlein purpura) is vasculitis with IgA1-dominant immune deposits affecting small vessels (predominantly capillaries, venules, or arterioles) (Jennette et al., 2013). IgAV often involves the skin and gastrointestinal tract, and it frequently causes arthritis. Glomerulonephritis indistinguishable from IgA nephropathy may occur.

IgAV is most common in children, especially children under age 10 years, which differs from ANCA vasculitis and CV, which are more common in older patients. In fact, IgAV is the most common systemic small vessel vasculitis in children (Chen & Mao, 2015). Depending on ethnic background, 6 to 24/100,000 children younger than 17 years of age will develop IgAV. In Asia, the incidence is as high as approximately 70/100,000

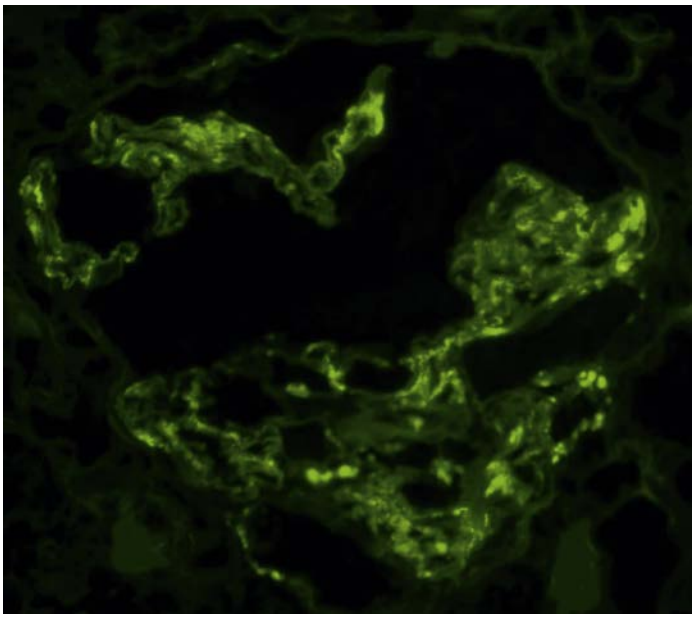

Fig. 54.11 Direct immunofluorescence microscopy of small vessels in the upper dermis of a patient with IgA vasculitis demonstrating coarsely granular deposits of IgA in vessel walls (FITC-labeled rabbit antihuman C3, ×600).

children every year. IgAV is rare in adults, with an annual incidence of 0.1 to 1.8/100,000 individuals (Audemard-Verger et al., 2015). Disease is more frequent in males (male:female ratio of 5:1).

Pathology

The histopathologic features of inflammation in venules, arterioles, and small arteries, caused by IgAV, are indistinguishable from other forms of SVV. In the dermis, this takes the form of a leukocytoclastic angiitis affecting predominantly venules and arterioles. The presence of hyaline aggregates in areas of inflammation or the lumen increases the likelihood of CV. Arteritis affecting arteries in the deep dermis, and especially arteries in the subcutaneous tissue, increases the likelihood of ANCA vasculitis. Numerous eosinophils increase the likelihood of hypersensitivity drug-induced vasculitis or EGPA. However, it is best to correlate the histopathology with immunostaining for IgA, IgG, IgM, C3, and C1q, and with serologic testing for ANCA, cryoglobulins, HCV antigen and antibody, anti-C1q, ANA, C3, and C4 before reaching a diagnosis. Patients with IgAV have immune complex deposits in small dermal vessels that stain brightly by direct immunofluorescence microscopy using antibodies specific for IgA (Fig. 54.11).

The glomerulonephritis of IgAV is indistinguishable from IgA nephropathy (IgAN), although glomerular necrosis and crescents are somewhat more frequent in IgA vasculitis. Because glomerulonephritis is a frequent component of many forms of immune complex SVV, immunopathologic features are very helpful in distinguishing among different forms of SVV (e.g., IgAV with IgA1-dominant glomerular deposits, CV with membranoproliferative lesions and IgG/IgM deposits, anti-GBM disease with necrosis and linear IgG, and ANCA vasculitis with necrosis and a paucity of immunoglobulin deposits in glomeruli).

Etiology and Pathogenesis

Patients with IgAV and IgAN have increased serum levels of IgA1 with abnormal glycosylation of the hinge region (Suzuki et al., 2009, 2011; Mestecky et al., 2013). This abnormality is caused by combined genetic and environmental/infectious influences. There is strong evidence that IgAV and IgAN are caused by vessel wall deposition of aggregates of abnormally glycosylated IgA1 molecules or by deposition of immune complexes composed of IgA1 complexed to anti-IgA1 IgG that recognizes the abnormal hinge region glycosylation (Suzuki et al., 2009, 2011; Mestecky et al., 2013).

Abnormally glycosylated IgA1 molecules also could induce disease through a variety of other mechanisms, such as reduced clearance from the circulation because of lack of Fc receptor engagement by the abnormal IgA, increased self-aggregation of IgA1 in the circulation resulting in deposition in vessel lumens and vessel walls, and increased affinity of the abnormal IgA1 for perivascular and glomerular mesangial matrix.

Vascular deposits containing IgA1 appear to mediate inflammation by activating complement via the lectin pathway and the alternative pathway.

Clinical Laboratory Testing

Abnormally glycosylated IgA1 has been detected in serum using lectin-binding assays and proteomic mass spectroscopy analysis. For example, a lectin that recognizes *N*-acetylgalactosamine was used in an ELISA to measure serum galactose-deficient IgA1 (Moldoveanu et al., 2007). This study concluded that the assay for abnormal IgA1 had diagnostic sensitivity of 76.5%, specificity of 94%, positive predictive value of 88.6%, and negative predictive value of 78.9% for IgAN.

Anti-IgA antibodies with specificity for the IgA1 hinge region have been detected in serum using monoclonal human IgA1 as substrate and by identifying IgA1 in circulating immune complexes. One study concluded that IgA1 glycan-specific IgG antibodies have 88% specificity and 95% sensitivity for IgA nephropathy (Suzuki, 2009). In addition to diagnosis, serologic tests for abnormally glycosylated IgA1 and IgA1 immune complexes may be of value in monitoring disease activity. Serum levels of galactose-deficient IgA1 and IgA1-IgG immune complexes are associated with disease activity of IgA nephropathy (Suzuki et al., 2014).

To date, these research observations on abnormal IgA1 glycosylation and anti-IgA1 antibodies in IgAV and IgAN have not been translated into analytically and clinically validated diagnostic tests, although multiple research laboratories are working on this.

Diagnosis, Treatment, and Prognosis

Until alternative clinical tests are validated, pathologic identification of IgA-dominant immune deposits in vessel walls or glomeruli by direct immunofluorescence microscopy is the gold standard method for confirming a diagnosis of IgAV or IgAN. Immunostaining is required in biopsy specimens because the light microscopic patterns of injury are not as conclusive for distinguishing among the many forms of SVV. For example, a skin biopsy that has leukocytoclastic angiitis by light microscopy could be found by immunofluorescence microscopy to be IgAV with IgA-dominant deposits, CV with IgM and C3 deposits, or ANCA vasculitis with a paucity of immunoglobulin and complement deposits.

The classic triad of symptoms and signs for IgAV are purpura, arthralgias, and abdominal pain. The frequency of renal disease varies from 45% to 85% in different cohorts (Audemard-Verger et al., 2015). The EULAR, the Paediatric Rheumatology International Trials Organisation, and the Paediatric Rheumatology European Society have proposed classification criteria for pediatric patients (Audemard-Verger et al., 2015). Based on these criteria, a patient is classified as IgAV if there are purpura with lower-extremity predominance plus one of the following four criteria: abdominal pain, histopathology demonstrating IgA-dominant deposits in vessels or glomeruli, arthritis or arthralgia, or renal involvement. These criteria have not been adopted for adults and would be problematic in adults because the prevalence of IgAV is much lower than the prevalence of other forms of SVV that cause similar signs and symptoms, especially ANCA disease. For example, a patient who has purpura, arthralgias, and nephritis fulfills the EULAR criteria for IgAV. Such a patient could also have ANCA vasculitis, cryoglobulinemic vasculitis, or other forms of SVV. Especially if applied to adults, the pediatric EULAR criteria should be combined with testing for ANCA, cryoglobulins, HCV infection, and hypocomplementemia.

Because the clinical course of IgAV is relatively benign in most patients, treatment is usually conservative and directed at symptom relief. Patients who develop severe gastrointestinal complications may require steroids or/and immunosuppressive drugs. When kidney disease develops with IgAV, the following Kidney Disease Improving Global Outcome (KDIGO) guidelines can be used (Chen & Mao, 2015). Persistent proteinuria should be treated with angiotensin-converting enzyme inhibitors or angiotensin receptor blockers. If the proteinuria persists and the glomerular filtration rate is greater than 50 mL/min per 1.73 m^2, a 6-month course of corticosteroid therapy should be given. Renal biopsy can be helpful for both diagnosis and prognosis. If severe renal failure and crescentic glomerulonephritis are observed, immunosuppressive therapy similar to that used for other forms of crescentic glomerulonephritis should be provided, including cyclophosphamide.

HYPOCOMPLEMENTEMIC URTICARIAL VASCULITIS

Definition and Epidemiology

Hypocomplementemic urticarial vasculitis (HUV) (anti-C1q vasculitis) is vasculitis accompanied by urticaria and hypocomplementemia affecting small vessels (i.e., capillaries, venules, or arterioles), and it is often

associated with anti-C1q antibodies (Jennette et al., 2013). Glomerulonephritis, arthritis, obstructive pulmonary disease, and ocular inflammation are commonly present in HUV, and HUV has overlapping clinical and laboratory features with systemic lupus erythematosus (SLE), though it also occurs independently of SLE (Venzor et al., 2002; Kallenberg, 2008; Grotz et al., 2009).

HUV is a rare disease. The incidence of all forms of leukocytoclastic vasculitis affecting the skin in a population-based study in Minnesota from 1996 to 2010 identified an incidence rate of 4.5/100,000 person-years (Arora et al., 2014). The cohort included 38 patients with leukocytoclastic vasculitis not otherwise specified (45%), 25 with IgA vasculitis (30%), 10 with urticarial vasculitis (12%), 8 with ANCA vasculitis (10%), and 3 with cryoglobulinemic vasculitis (4%) (Arora et al., 2014). Thus HUV has an incidence of less than 0.5/100,000 person-years in this population.

HUV affects women more frequently than men (ratio 2:1) and has a peak incidence in the fifth decade of life, although HUV has been observed in children (Grotz et al., 2009).

Pathology

The dermal vasculitis in HUV is a leukocytoclastic angiitis that cannot be readily distinguished from other forms of SVV by histology alone. Direct immunofluorescence microscopy demonstrates complement-rich immune complex deposits with prominent C1q in dermal vessels and along the dermal-epidermal junction.

By immunofluorescence microscopy, glomerulonephritis in HUV has extensive capillary wall and mesangial immune complex deposits containing immunoglobulin and complement, including prominent C1q. The most frequent histologic pattern is membranoproliferative glomerulonephritis with thickened capillary walls and endocapillary hypercellularity, although focal or diffuse proliferative glomerulonephritis may also occur. In this respect, HUV glomerulonephritis resembles lupus nephritis, and patients with HUV who also meet clinical criteria for SLE should be considered to have lupus nephritis.

Etiology and Pathogenesis

Experimental studies strongly support a pathogenic role for anti-C1q antibodies in forming pathogenic immune complexes in SLE and HUV, and anti-C1q antibodies may interfere with the clearance of apoptotic cells and enhance induction of autoimmunity (Kallenberg, 2008). The hypocomplementemia appears to be secondary to classical complement pathway activation with reduced C1, C2, C4, and C3 (Kallenberg, 2008). The extensive deposition of immune complexes in the walls of inflamed vessels (e.g., dermal venules and glomerular capillaries) supports an immune complex pathogenesis for the inflammation.

Clinical Laboratory Testing

The typical laboratory test profile is elevated anti-C1q antibodies (essentially 100% sensitive) and hypocomplementemia with low C1q, C3, and C4. In patients who have HUV without overt SLE, ANA often is present without anti–double-stranded DNA. Positive testing for cryoglobulins supports a diagnosis of CV rather than HUV.

C1q has a collagen-like portion attached to globular heads, resembling a bouquet of tulips (Venzor et al., 2002; Kallenberg, 2008). Immune complex Fc regions bind to these globular portions, whereas anti-C1q autoantibodies instead bind to the collagen-like portion. Anti-C1q usually is detected by ELISA using human C1q as the substrate. High ionic strength conditions (0.5–1.0 M NaCl) are used to inhibit binding of immune complexes (Kohro-Kawata et al., 2002). Anti-C1q is detected in a variety of inflammatory diseases, including HUV (100%), rheumatoid vasculitis (77%), Felty syndrome (76%), lupus nephritis (63%), membranoproliferative glomerulonephritis (54%), and SLE without nephritis (33%) (Seelen et al., 2003; Kallenberg, 2008). HUV patients who do not have overt SLE may have low-titer antinuclear antibodies, rheumatoid factor, lupus anticoagulant, and cryoglobulins.

While the presence of anti-C1q antibodies is highly sensitive for HUV (found in 100% of patients), they are neither sensitive nor specific for SLE. Anti-C1q antibodies are more prevalent in SLE patients with lupus nephritis than in patients without nephritis. In a study of 43 patients with SLE, anti-C1q antibodies were identified in 82% of patients with nephritis, compared to only 38% of patients who did not have nephritis (Coremans et al., 1995). In a study of 228 patients with lupus nephritis, the evaluation of anti-C1q, C3, and C4 provided the best prediction of renal flares (Sinico et al., 2009). However, some SLE patients with high titers of anti-C1q antibodies do not develop nephritis.

Diagnosis, Treatment, and Prognosis

HUV is characterized by recurrent episodes of urticaria with underlying leukocytoclastic vasculitis. Skin manifestations include painful, tender, burning, or pruritic urticarial skin lesions that persist for greater than 24 hours, often with central areas of hemorrhage. Once the urticaria resolves, there may be residual purpura. Additional manifestations include angioedema, laryngeal edema, pulmonary involvement, arthritis, arthralgia, glomerulonephritis, and uveitis. Compared to patients with urticaria and vasculitis who do not have hypocomplementemia, HUV patients are more likely to have abdominal pain and chronic obstructive pulmonary disease (COPD) (Mehregan et al., 1992). COPD and acute laryngeal edema are important causes for morbidity and mortality. Around 30% of HUV patients suffer gastrointestinal symptoms: pain, nausea, vomiting, diarrhea, and sometimes ascites in connection with serositis, hepatomegaly, and splenomegaly (Grotz et al., 2009).

The two major diagnostic criteria are chronic urticaria and hypocomplementemia. Minor criteria include anti-C1q antibodies, leukocytoclastic vasculitis, arthralgia and arthritis, uveitis or episcleritis, glomerulonephritis, and abdominal pain (Grotz et al., 2009).

Glucocorticoids are standard therapy for HUV. Depending on clinical severity, additional immunosuppressive agents such as methotrexate, azathioprine, cyclophosphamide, cyclosporine, and mycophenolate mofetil may be added. Apheresis is reserved for very aggressive disease (Grotz et al., 2009).

RHEUMATOID VASCULITIS

Definition and Epidemiology

Rheumatoid vasculitis is an uncommon extraarticular complication of rheumatoid arthritis (RA) and primarily affects small to medium vessels (Ntatsaki et al., 2014; Makol et al., 2015). There has been a decrease in the incidence of rheumatoid vasculitis in the last decade in both Europe and the United States (Ntatsaki et al., 2014). The average annual incidence of rheumatoid vasculitis in the United Kingdom declined from 9.1/million between 1988 and 2002 to 3.9/million between 2001 and 2010 (Ntatsaki et al., 2014). This reduction may be the result of the use of current disease-modifying antirheumatic drugs (DMARDs), including methotrexate.

Pathology

Rheumatoid vasculitis involves small and medium vessels, including medium and small arteries and venules. It is a necrotizing arteritis that is histologically indistinguishable from other forms of necrotizing arteritis, such as PAN and MPA. Its venulitis, especially in the dermis, is histologically indistinguishable from the leukocytoclastic angiitis of ANCA or immune complex disease. In patients with rheumatoid vasculitis, dermal necrotizing venulitis has been identified as the cause of palpable purpura, maculopapular erythema, erythema elevatum diutinum, and hemorrhagic blisters; arteritis has been identified as the cause of subcutaneous nodules, livedo reticularis, and deep ulcers (Chen et al., 2002). Some patients have both patterns of vasculitis.

Etiology and Pathogenesis

There is a strong association between rheumatoid vasculitis and specific HLA genotypes that suggests a role for immune recognition of antigens in its pathogenesis. A role for immune complexes containing autoantibodies has been proposed based on the observed high prevalence and high titer of RF, anticitrullinated peptide antibodies (ACPA), antinuclear antibodies, and circulating or tissue-deposited immune complexes in patients with rheumatoid vasculitis (Makol et al., 2015). However, many RA patients with high titers of RF and ACPA do not develop rheumatoid vasculitis. Immunoglobulin and complement have been detected by immunofluorescence in dermal vessels of patients with dermal rheumatoid vasculitis (Chen et al., 2002).

Clinical Laboratory Testing

Rheumatoid vasculitis should be suspected in a patient with clinical or pathologic evidence for vasculitis who has RF, ACPA, antinuclear antibodies, and circulating or tissue-deposited immune complexes (Makol et al., 2015). Less specific features that are often observed include anemia, leukocytosis, thrombocytosis, elevated ESR, increased CRP, and polyclonal hypergammaglobulinemia. The absence of RF and ACPA has a high negative predictive value for rheumatoid vasculitis (Makol et al., 2015).

In a study of 19 patients with rheumatoid vasculitis, all of the patients were seropositive for RF, no patients were C-ANCA positive, 5 patients were P-ANCA positive by IIF but had negative ELISA for MPO-ANCA, 1 patient with P-ANCA was positive for PR3-ANCA by ELISA, all of the

patients were negative for ANA, and 1 patient was positive for antimitochondrial antibodies (Ntatsaki et al., 2014). Anti-C1q antibody testing is positive in approximately 75% of patients with rheumatoid vasculitis (Seelen et al., 2003; Kallenberg, 2008). This raises the possibility of a relationship with HUV, but anti-C1q positive patients with rheumatoid vasculitis typically do not have other features of HUV, including no hypocomplementemia, or urticarial or immune complex glomerulonephritis.

Diagnosis, Treatment, and Prognosis

The Scott and Bacon diagnostic criteria for rheumatoid vasculitis require the presence of one or more of the following in a patient with RA: mononeuritis multiplex or peripheral neuropathy, peripheral gangrene, biopsy evidence of acute necrotizing arteritis plus systemic illness (e.g., fever and weight loss), deep cutaneous ulcers or extraarticular disease (e.g., pleurisy, pericarditis, scleritis) if associated with typical digital infarcts, or biopsy evidence of vasculitis (Scott & Bacon, 1984).

Hydroxychloroquine and low-dose aspirin are associated with lower odds of developing rheumatoid vasculitis among RA patients, suggesting a possible protective effect (Makol et al., 2015). Among 86 patients treated for rheumatoid vasculitis at Mayo Clinic between 2000 and 2010, 99% received glucocorticoids, 29% received cyclophosphamide, 55% received another disease-modifying antirheumatic drug (methotrexate, azathioprine, mycophenolate mofetil, hydroxychloroquine, minocycline), and 28% received a biologic agent (anti-TNF, rituximab, abatacept, anakinra) (Makol et al., 2014). However, despite aggressive use of cyclophosphamide and biologics, rheumatoid vasculitis remained difficult to treat, with high relapse rates and mortality rates of 12% at 1 year and 60% at 5 years.

SUMMARY

The diagnosis of vasculitis is difficult. Accurate and precise diagnosis requires knowledgeable integration of evidence from the medical history, patient demographics, clinical signs and symptoms, laboratory tests, and pathologic findings. Positive as well as negative laboratory test results are critically important in the diagnostic evaluation of patients with suspected vasculitis, and they are useful for prognostication, predicting and monitoring response to therapy, and predicting or detecting relapse. Over the past 20 years, there has been a valuable increase in the menu of laboratory tests that facilitate the care of patients with vasculitis (e.g., ANCA). More are currently on the verge of entering clinical practice (e.g., IgA1 glycosylation and anti-IgA1 antibody assays), and undoubtedly more will be discovered in the future.

SELECTED REFERENCES

Jennette JC, Falk RJ, Bacon PA, et al.: 2013 Revised international Chapel Hill consensus conference nomenclature of vasculitides, *Arthritis Rheum* 65:1–11, 2013.

This excellent comprehensive review of giant cell arteritis and Takayasu arteritis is by one of the major leaders in the field of large vessel vasculitis. Epidemiology, pathology, putative pathogenesis, and clinical management are reviewed in depth with expert commentary.

Kallenberg CG: Key advances in the clinical approach to ANCA-associated vasculitis, *Nat Rev Rheumatol* 10:484–493, 2014.

This insightful review of ANCA vasculitis covers pathogenesis, clinical presentations, development of diagnostic and classification criteria, and advances in therapy. This expert overview is informed by Professor Kallenberg's participation in many important studies on the pathogenesis and clinical management of ANCA vasculitis.

Makol A, Matteson EL, Warrington KJ: Rheumatoid vasculitis: an update, *Curr Opin Rheumatol* 27:63–70, 2015.

Although rheumatoid vasculitis is a rare extraarticular manifestation of rheumatoid arthritis, it has high morbidity and mortality when it occurs. This timely update presents the clinical manifestations, management, and outcomes of rheumatoid vasculitis in the current era of disease-modifying antirheumatic drugs (DMARDS).

Mestecky J, Raska M, Julian BA, et al.: IgA nephropathy: molecular mechanisms of the disease, *Annu Rev Pathol Mech Dis* 8:217–240, 2013.

This authoritative detailed review describes the discovery of abnormal glycosylation of IgA1 in IgAV and IgAN, which is one of the most impactful advances in the understanding of the pathogenesis of vasculitis that has emerged over the past 10 or more years. This discovery not only has elucidated the pathobiology of these diseases, but it also sets the stage for valuable new clinical laboratory tests.

Pagnoux C, Cohen P, Guillevin L: Vasculitides secondary to infections, *Clin Exp Rheumatol* 24(2 Suppl 41):S71–S81, 2006.

Recognition of infectious vasculitides is critically important because appropriate therapy can be very effective, and failure to make a correct diagnosis can be devastating. These distinguished authors provide an excellent review of the variety of infectious pathogens that can cause vasculitis by multiple pathogenic mechanisms and summarize approaches for diagnosis and treatment.

Pusey CD: Anti-glomerular basement membrane disease, *Kidney Int* 64:1535–1550, 2003.

This article is written by the preeminent physician scientist who has been at the forefront of clinical and basic research on anti-GBM disease. It covers pathobiology and clinical aspects of this aggressive category of immune-mediated vascular injury. This is a rare disease, but it illustrates important concepts of autoimmune vascular inflammation and strategies for their treatment.

Access the complete reference list online at Elsevier eBooks for Practicing Clinicians.

REFERENCES

Abdulkader R, Lane SE, Scott DG, et al.: Classification of vasculitis: EMA classification using CHCC 2012 definitions, *Ann Rheum Dis* 72:1888, 2013.

Achkar AA, Lie JT, Hunder GG, et al.: How does previous corticosteroid treatment affect the biopsy findings in giant cell (temporal) arteritis? *Ann Intern Med* 120:987–992, 1994.

Arora A, Wetter DA, Gonzalez-Santiago TM, et al.: Incidence of leukocytoclastic vasculitis, 1996 to 2010: a population-based study in Olmsted County, *Minnesota*, *Mayo Clin Proc* 89(11):1515–1524, 2014.

Audemard-Verger A, Pillebout E, Guillevin L, et al.: IgA vasculitis (Henoch-Schönlein purpura) in adults: diagnostic and therapeutic aspects, *Autoimmun Rev* 14(7):579–585, 2015.

Baldo BA: Adverse events to monoclonal antibodies used for cancer therapy: focus on hypersensitivity responses, *OncoImmunology* 2(10):e26333, 2013.

Bossuyt X, Cohen Tervaert J-W, Arimura Y, et al.: Position Paper: revised 2017 international consensus on testing of ANCAs in granulomatosis with polyangiitis and microscopic polyangiitis, *Nat Rev Rheumatol* 13(11):683–692, 2017, https://doi.org/10.1038/nrrheum.2017.140.

Burgner D, Harnden A, Kawasaki disease: What is the epidemiology telling us about the etiology? *Int J Infect Dis* 9:185–194, 2005.

Cacoub P, Terrier B, Saadoun D: Hepatitis C virus-induced vasculitis: therapeutic options, *Ann Rheum Dis* 73(1):24–30, 2014.

Carmona FD, Mackie SL, Martín JE, et al.: A large-scale genetic analysis reveals a strong contribution of the HLA class II region to giant cell arteritis susceptibility, *Am J Hum Genet* 96(4):565–580, 2015.

Cavazza A, Muratore F, Boiardi L, et al.: Inflamed temporal artery: histologic findings in 354 biopsies, with clinical correlations, *Am J Surg Pathol* 38:1360–1370, 2014.

Chatterjee S, Flamm SD, Tan CD, et al.: Clinical diagnosis and management of large vessel vasculitis: Takayasu arteritis, *Curr Cardiol Rep* 16(7):499, 2014.

Chbeir D, Gaschignard J, Bonnefoy R, et al.: Kawasaki disease: abnormal initial echocardiogram is associated with resistance to IV Ig and development of coronary artery lesions, *Pediatr Rheumatol Online J* 16(1):48, 2018. Epub 2018 Jul 18.

Chen JY, Mao JH: Henoch-Schönlein purpura nephritis in children: incidence, pathogenesis and management, *World J Pediatr* 11(1):29–34, 2015.

Chen KR, Toyohara A, Suzuki A, et al.: Clinical and histopathological spectrum of cutaneous vasculitis in rheumatoid arthritis, *Br J Dermatol* 147(5):905–913, 2002.

Cho SY, Kim Y, Cha SH, et al.: Adjuvant laboratory marker of Kawasaki disease: NT-pro-BNP or hs-CRP? *Ann Clin Lab Sci* 41:360–363, 2011.

Cohen Tervaert JW, Damoiseaux J: Antineutrophil cytoplasmic autoantibodies: How are they detected and what is their use for diagnosis, classification and follow-up? *Clin Rev Allergy Immunol* 43(3):211–219, 2012.

Coremans IE, Spronk PE, Bootsma H, et al.: Changes in antibodies to C1q predict renal relapses in systemic lupus erythematosus, *Am J Kidney Dis* 26(4):595–601, 1995.

Cui Z, Zhao MH: Advances in human antiglomerular basement membrane disease, *Nat Rev Nephrol* 7(12):697–705, 2011.

D'Alessandro M, Buoncompagni A, Minoia F, et al.: Cytomegalovirus-related necrotising vasculitis mimicking Henoch-Schönlein syndrome, *Clin Exp Rheumatol* 32(3 Suppl 82):S73–S75, 2014.

Damoiseaux J: The diagnosis and classification of the cryoglobulinemic syndrome, *Autoimmun Rev* 13(4–5):359–362, 2014.

Damoiseaux J, Mallet K, Vaessen M, et al.: Automatic reading of ANCA-slides: evaluation of the AKLIDES system, *Clin Dev Immunol*762874, 2012. 2012.

Damoiseaux J, Elena C, Rasmussen N, et al.: Detection of antineutrophil cytoplasmic antibodies (ANCAs): a Multicentre European vasculitis study Group (EUVAS) evaluation of the value of indirect immunofluorescence (IIF) versus antigen-specific immunoassays, *Ann Rheum Dis* 76(4):647–653, 2017, https://doi.org/10.1136/annrheumdis-2016-209507.

Damoiseaux J, Heijnen I, Van Campenhout C, et al.: An international survey on antineutrophil cytoplasmic antibodies (ANCA) testing in Daily clinical practice, *Clin Chem Lab Med* 56(10):1759–1770, 2018, https://doi.org/10.1515/cclm-2017-0306.

Dasgupta B, Cimmino MA, Kremers HM, et al.: Provisional classification criteria for polymyalgia rheumatica: a European League against Rheumatism/American College of Rheumatology collaborative initiative, *Arthritis Rheum* 64:943–954, 2012.

DeVita S, Soldano F, Isola M, et al.: Preliminary classification criteria for the cryoglobulinaemic vasculitis, *Ann Rheum Dis* 70:1183–1190, 2011.

Dietrich A, Gauglitz GG, Pfluger TT, et al.: Syphilitic aortitis in secondary syphilis, *JAMA Dermatol* 150:790–791, 2014.

Durling B, Toren A, Patel V, et al.: Incidence of discordant temporal artery biopsy in the diagnosis of giant cell arteritis, *Can J Ophthalmol* 49:157–161, 2014.

Falk RJ, Jennette JC: Anti-neutrophil cytoplasmic autoantibodies with specificity for myeloperoxidase in patients with systemic vasculitis and idiopathic necrotizing and crescentic glomerulonephritis, *N Engl J Med* 318:1651–1657, 1988.

Fujimoto S, Uezono S, Hisanaga S, et al.: Incidence of ANCA-associated primary renal vasculitis in the Miyazaki Prefecture: the first population-based, retrospective, epidemiologic survey in Japan, *Clin J Am Soc Nephrol* 1(5):1016–1022, 2006.

González-Gay MA, Pina T: Giant cell arteritis and polymyalgia rheumatica: an update, *Curr Rheumatol Rep* 17(2):6, 2015.

Greco A, Rizzo MI, De Virgilio A, et al.: Goodpasture's syndrome: a clinical update, *Autoimmun Rev* 14(3):246–253, 2015.

Grayson PC, Aleshashemi S, Bagheri AA, et al.: F-Fluorodeoxygluocse-Postitron emission tomography as an imaging Biomaker in a prospective, Longitudinal cohort of patients with large vessel vasculitis, *Arthitis Rheumatol* 70(3):439–449, 2018.

Grotz W, Baba HA, Becker JU, et al.: Hypocomplementemic urticarial vasculitis syndrome: an interdisciplinary challenge, *Dtsch Arztebl Int* 106(46):756–763, 2009.

Guillevin L: Infections in vasculitis, *Best Pract Res Clin Rheumatol* 27:19–31, 2013.

Gulati A, Bagga A: Large vessel vasculitides, *Pediatr Nephrol* 25:1037–1048, 2010.

Hamidou MA, Moreau A, Toquet C, et al.: Temporal arteritis associated with systemic necrotizing vasculitis, *J Rheumatol* 30:2165–2169, 2003.

Hata A, Noda M, Moriwaki R, et al.: Angiographic findings in Takayasu arteritis: new classification, *Int J Cardiol* 54:S155–S163, 1996.

Hellmark T, Niles JL, Collins AB, et al.: Comparison of anti-GBM antibodies in sera with or without ANCA, *J Am Soc Nephrol* 8:376, 1997.

Hernández-Rodríguez J, Alba MA, Prieto-González S, et al.: Diagnosis and classification of polyarteritis nodosa, *J Autoimmun* 48–49:84–89, 2014.

Hoffman GS: Large-vessel vasculitis: Unresolved issues, *Arthritis Rheum* 48:2406–2414, 2003.

Jain S, Win HN, Chalam V, et al.: Disseminated gonococcal infection presenting as vasculitis: a case report, *J Clin Pathol* 60:90–91, 2007.

Jennette JC: Rapidly progressive crescentic glomerulonephritis, *Kidney Int* 63:1164, 2003.

Jennette JC: Nomenclature and classification of vasculitis: Lessons learned from granulomatosis with polyangiitis (Wegner's granulomatosis), *Clin Exp Immunol* 164(Suppl 1): 7–10, 2011.

Jennette JC, Falk RJ: Pathologic classification of vasculitis, *Pathol Case Rev* 12:179–185, 2007.

Jennette JC, Falk RJ: Pathogenesis of antineutrophil cytoplasmic autoantibody-mediated disease, *Nature Rev Rheumatol* 10:463–473, 2014.

Jennette JC, Falk RJ, Andrassy K, et al.: Nomenclature of systemic vasculitides: the proposal of an international consensus conference, *Arthritis Rheum* 37:187–192, 1994.

Jennette JC, Falk RJ, Bacon PA, et al.: Revised international Chapel Hill consensus conference nomenclature of vasculitides, *Arthritis Rheum* 65:1–11, 2012. 2013.

Kain R, Exner M, Brandes R, et al.: Molecular mimicry in pauci-immune focal necrotizing glomerulonephritis, *Nat Med* 14(10):1088–1096, 2008.

Kallenberg CG: Anti-C1q autoantibodies, *Autoimmun Rev* 7:612–615, 2008.

Kermani TA, Schmidt J, Crowson CS, et al.: Utility of erythrocyte sedimentation rate and C-reactive protein for the diagnosis of giant cell arteritis, *Semin Arthritis Rheum* 41:866–871, 2012.

Kermani TA, Warrington KJ, Crowson CS, et al.: Large-vessel involvement in giant cell arteritis: a population-based cohort study of the incidence—trends and prognosis, *Ann Rheum Dis* 72:1989–1994, 2013.

Knutter I, Hiemann R, Brumma T, et al.: Automated interpretation of ANCA patterns–a new approach in the serology of ANCA-associated vasculitis, *Arthritis Res Ther* 14(6):R271, 2012.

Kohro-Kawata J, Wener MH, Mannik M: The effect of high salt concentration on detection of serum immune complexes and autoantibodies to C1q in patients with systemic lupus erythematosus, *J Rheumatol* 29:84–89, 2002.

Labarca C, Koster MJ, Crowson CS, et al.: Predictors of relapse and treatment outcomes in biopsy proven giant cell arteritis, *Rheumatology 55* 347(2), 2016.

Lamprecht P, Moosig F, Gause A, et al.: Immunological and clinical follow-up of hepatitis C virus associated cryoglobulinaemic vasculitis, *Ann Rheum Dis* 60:385–390, 2001.

Langford CA: Vasculitis, *J Allergy Clin Immunol* 111:S602–S612, 2003.

Lincoff NS, Erlich PD, Brass LS: Thrombocytosis in temporal arteritis rising platelet counts: a red flag for giant cell arteritis, *J Neuro Ophthalmol* 20:67–72, 2000.

Lionaki S, Blyth ER, Hogan SL, et al.: Classification of antineutrophil cytoplasmic autoantibody vasculitides: the role of antineutrophil cytoplasmic autoantibody specificity for myeloperoxidase or proteinase 3 in disease recognition and prognosis, *Arthritis Rheum* 64:3452–3462, 2012.

Mahler M, Radice A, Sinico RA, et al.: Performance evaluation of a novel chemiluminescence assay for detection of anti-GBM antibodies: an international multicenter study, *Nephrol Dial Transplant* 27(1):243–252, 2012.

Mahr A, Guillevin L, Poissonnet M, et al.: Prevalences of polyarteritis nodosa, microscopic polyangiitis, Wegener's granulomatosis, and Churg-Strauss syndrome in a French urban multiethnic population in 2000: a capture-recapture estimate, *Arthritis Rheum* 51:92–99, 2004.

Makol A, Crowson CS, Wetter DA, et al.: Vasculitis associated with rheumatoid arthritis: a case-control study, *Rheumatology* 53:890–899, 2014.

McGregor JG, Hogan SL, Hu Y, et al.: Glucocorticoids and relapse and infection rates in anti-neutrophil cytoplasmic antibody disease, *Clin J Am Soc Nephrol* 7:240–247, 2012.

McInnis EA, Badhwar AK, Muthigi A, et al.: Dysregulation of autoantigen genes in ANCA-associated vasculitis involves alternative transcripts and new protein synthesis, *J Am Soc Nephrol* 26:390–399, 2015.

Mehregan DR, Hall MJ, Gibson LE: Urticarial vasculitis: a histopathologic and clinical review of 72 cases, *J Am Acad Dermatol* 26:441–448, 1992.

Melegari A, Bonaguri C, Russo A, et al.: A comparative study on the reliability of an automated system for the evaluation of cell-based indirect immunofluorescence, *Autoimmun Rev* 11:713–716, 2012.

Miller DV, Maleszewski JJ: The pathology of large-vessel vasculitides, *Clin Exp Rheumatol* 29(Suppl 64):S92–S98, 2011.

Moldoveanu Z, Wyatt RJ, Lee JY, et al.: Patients with IgA nephropathy have increased serum galactose-deficient IgA1 levels, *Kidney Int* 71:1148–1154, 2007.

Nathavitharana RR, Mitty JA: Diseases from north America: focus on tick-borne infections, *Clin Med* 15:74–77, 2015.

Nifli A-P, George N, Mamoulaki M,et al.: Comparison of a multiplex, bead-based fluorescent assay and immunofluorescence methods for the detection of ANA and ANCA autoantibodies in human serum, *J Immunol Methods* 311(1–2):189–197, 2006, https://doi.org/10.1016/j.jim.2006.02.004.

Ntatsaki E, Mooney J, Scott DG, et al.: Systemic rheumatoid vasculitis in the era of modern immunosuppressive therapy, *Rheumatology* 53:145–152, 2014.

Orenstein JM, Shulman ST, Fox LM, et al.: Three linked vasculopathic processes characterize Kawasaki disease: a light and transmission electron microscopic study, *PloS One* 7(6):e38998, 2012.

Ortiz-Sanjuán F, Blanco R, Hernández JL, et al.: Drug-associated cutaneous vasculitis: study of 239 patients from a single referral center, *J Rheumatol* 41(11):2201–2207, 2014.

Pedchenko V, Bondar O, Fogo AB, et al.: Molecular architecture of the Goodpasture autoantigen in anti-GBM nephritis, *N Engl J Med* 363(4):343–354, 2010.

Pendergraft III WF, Niles JL: Trojan horses: drug culprits associated with antineutrophil cytoplasmic autoantibody (ANCA) vasculitis, *Curr Opin Rheumatol* 26(1):42–49, 2014.

Pendergraft WF, Preston GA, Shah RR, et al.: cPR3105-206, a protein complementary to the autoantigen proteinase 3, triggers autoimmunity, *Nature Med* 10:72–79, 2004.

Poller DN, van Wyk Q, Jeffrey MJ: The importance of skip lesions in temporal arteritis, *J Clin Pathol* 53:137–139, 2000.

Prieto-Gonzalez S, Depetris M, Garcia-Martinez A, et al.: Positron emission tomography assessment of large vessel inflammation in patients with newly diagnosed, biopsy-proven giant cell arteritis: a prospective, case-control study, *Ann Rheum Dis* 73:1388–1392, 2014.

Principi N, Rigante D, Esposito S: The role of infection in Kawasaki syndrome, *J Infect* 67:1–10, 2013.

Reindel R, Bischof J, Kim KY, et al.: CD84 is markedly up-regulated in Kawasaki disease arteriopathy, *Clin Exp Immunol* 177:203–211, 2014.

Reynolds J, Preston GA, Pressler BM, et al.: Autoimmunity to the alpha 3 chain of type IV collagen in glomerulonephritis is triggered by "autoantigen complementarity", *J Autoimmun* 59:8–18, 2015.

Roth AJ, Brown MC, Smith RN, et al.: Anti-LAMP-2 antibodies are not prevalent in patients with antineutrophil cytoplasmic autoantibody glomerulonephritis, *J Am Soc Nephrol* 23:545–555, 2012.

Roth AJ, Ooi J, Hess JJ, et al.: ANCA epitope specificity determines pathogenicity, detectability and clinical predictive value, *J Clin Invest* 123:1773–1783, 2013.

Rutgers A, Slot M, van Paassen P, et al.: Coexistence of anti-glomerular basement membrane antibodies and myeloperoxidase-ANCAs in crescentic glomerulonephritis, *Am J Kidney Dis* 46:253, 2005.

Sablé-Fourtassou R, Cohen P, Mahr A, et al.: Antineutrophil cytoplasmic antibodies and the Churg-Strauss syndrome, *Ann Intern Med* 143:632–638, 2005.

Salvarani C, Magnani L, Catanoso M, et al.: Tocilizumab: a novel therapy for patients with large-vessel vasculitis, *Rheumatology* 51(1):151–156, 2012. Epub 2011 Nov 10.

Savige J, Davies D, Falk RJ, et al.: Antineutrophil cytoplasmic antibodies and associated diseases: a review of the clinical and laboratory features, *Kidney Int* 57:846, 2000.

Savige J, Gillis D, Davies D, et al.: International consensus statement on testing and reporting of antineutrophil cytoplasmic antibodies (ANCA), *Am J Clin Pathol* 111:507–513, 1999.

Scott DG, Bacon PA: Intravenous cyclophosphamide plus methylprednisolone in treatment of systemic rheumatoid vasculitis, *Am J Med* 76:377–384, 1984.

Seelen MA, Trouw LA, Daha MR: Diagnostic and prognostic significance of anti-C1q antibodies in systemic lupus erythematosus, *Curr Opin Nephrol Hypertens* 12:619–624, 2003.

Silverman DJ, Bond SB: Infection of human vascular endothelial cells by Rickettsia rickettsii, *J Infect Dis* 149:201–206, 1984.

Sinico RA, Di Toma L, Maggiore U, et al.: Prevalence and clinical significance of antineutrophil cytoplasmic antibodies in Churg-Strauss syndrome, *Arthritis Rheum* 52:2926–2935, 2005.

Sinico RA, Di Toma L, Maggiore U, et al.: Renal involvement in Churg-Strauss syndrome, *Am J Kidney Dis* 47:770–779, 2006.

Sinico RA, Rimoldi L, Radice A, et al.: Anti-C1q autoantibodies in lupus nephritis, *Ann N Y Acad Sci* 1173:47–51, 2009.

Sowa M, Grossmann K, Knütter I, et al.: Simultaneous automated screening and confirmatory testing for vasculitis-specific ANCA, *PloS One* 9(9):e107743, 2014.

Suzuki H, Fan R, Zhang Z, et al.: Aberrantly glycosylated IgA1 in IgA nephropathy patients is recognized by IgG antibodies with restricted heterogeneity, *J Clin Invest* 119:1668–1677, 2009.

Suzuki H, Kiryluk K, Novak J, et al.: The pathophysiology of IgA nephropathy, *J Am Soc Nephrol* 22:1795–1803, 2011.

Suzuki Y1, Matsuzaki K, Suzuki H, et al.: Serum levels of galactose-deficient immunoglobulin (Ig) A1 and related immune complex are associated with disease activity of IgA nephropathy, *Clin Exp Nephrol* 18(5):770–777, 2014.

Tedeschi A, Baratè C, Minola E, et al.: Cryoglobulinemia, *Blood Rev* 21:183–200, 2007.

Terrier B, Semoun O, Saadoun D, et al.: Prognostic factors in patients with hepatitis C virus infection and systemic vasculitis, *Arthritis Rheum* 63:1748–1757, 2011.

Treglia G, Taralli S, Maggi F, et al.: Usefulness of (18)F-FDG PET/CT in disease extent and treatment response assessment in a patient with syphilitic aortitis, *Clin Nucl Med* 38:e185–e187, 2013.

Trevisin M, Pollock W, Dimech W, Savige J: Evaluation of a multiplex flow cytometric immunoassay to detect PR3- and MPO-ANCA in active and treated vasculitis, and in inflammatory bowel disease (IBD), *J Immunol Methods* 336(2):104–112, 2008, https://doi.org/10.1016/j.jim.2008.03.012.

Van Daalen EE, Jennette JC, McAdoo SP, et al.: Predicting outcome in patients with anti-GBM glomerulonephritis, *Clin J Am Soc Nephrol* 13:63–72, 2018.

Vaideeswar P, Deshpande JR: Pathology of Takayasu arteritis: a brief review, *Ann Pediatr Cardiol* 6(1):52–58, 2013.

Valsakumar AK, Valappil UC, Jorapur V, et al.: Role of immunosuppressive therapy on clinical, immunological, and angiographic outcome in active Takayasu's arteritis, *J Rheumatol* 30:1793–1798, 2003.

van Timmeren MM, Heeringa P, Kallenberg CG: Infectious triggers for vasculitis, *Curr Opin Rheumatol* 26:416–423, 2014.

Venzor J, Lee WL, Huston DP: Urticarial vasculitis, *Clin Rev Allergy Immunol* 23(2):201–216, 2002.

Villiger PM, Adler S, Kuchen S, et al.: Tocilizumab for induction and maintenance of remission in giant cell arteritis: a phase 2, randomised, double-blind, placebo-controlled trial, *Lancet* 387(10031):1921–1927, 2016.

Waldman CW, Waldman SD, Waldman RA: Giant cell arteritis, *Med Clin North Am* 97:329–335, 2013.

Watts R, Lane S, Hanslik T, et al.: Development and validation of a consensus methodology for the classification of the ANCA-associated vasculitides and polyarteritis nodosa for epidemiological studies, *Ann Rheum Dis* 66:222–227, 2007.

Watts RA, Mahr A, Mohammad AJ, et al.: Classification, epidemiology and clinical subgrouping of antineutrophil cytoplasmic antibody (ANCA)-associated vasculitis, *Nephrol Dial Transplant* 30(Suppl 1):i14–i22, 2015.

Westman KW, Bygren PG, Eilert I, et al.: Rapid screening assay for anti-GBM antibody and ANCAs: an important tool for the differential diagnosis of pulmonary renal syndromes, *Nephrol Dial Transplant* 12(9):1863–1868, 1997.

Weyand CM, Goronzy JJ: Giant cell arteritis and polymyalgia rheumatica, *N Engl J Med* 371:50–57, 2014.

Xiao H, Dairaghi DJ, Powers JP, et al.: C5a receptor (CD88) blockade protects against MPO-ANCA glomerulonephritis, *J Am Soc Nephrol* 25:225–231, 2014.

Xiao H, Heeringa P, Hu P, et al.: Antineutrophil cytoplasmic autoantibodies specific for myeloperoxidase cause glomerulonephritis and vasculitis in mice, *J Clin Invest* 110:955–963, 2002.

CHAPTER 55

ORGAN-SPECIFIC AUTOIMMUNE DISEASES

William E. Winter, William L. Clapp, Neil Selwyn Harris, Jaya Ruth Asirvatham, Kimberly Merkel

INTRODUCTION AND OVERVIEW TO THE ORGAN-SPECIFIC AUTOIMMUNE DISEASES, 1074
Definition of Autoimmunity Versus Autoimmune Disease, 1074
Classification of Autoimmune Diseases, 1075
Laboratory Tests for Evaluating Autoimmunity, 1076
Interpretation of Serum Autoantibody Levels in Autoimmune Diseases, 1077
Recent Advances in Diagnostic Technologies, 1078
Autoantibodies as Predictors of Disease, 1078

CUTANEOUS AUTOIMMUNE DISEASES, 1079
Pemphigus, 1079
Pemphigoid, 1081
Linear IgA Dermatosis, 1082
Epidermolysis Bullosa Acquisita, 1082
Dermatitis Herpetiformis, 1082
Vasculitis, 1083
Vitiligo, 1084

GASTROINTESTINAL AND HEPATOBILIARY AUTOIMMUNE DISEASES, 1084
Pernicious Anemia, 1084
Celiac Disease, 1085
Inflammatory Bowel Disease, 1085
Hepatic and Hepatobiliary Autoimmunity, 1086
Autoimmune Pancreatitis, 1089

GLOMERULAR AUTOIMMUNE DISEASES, 1089
Overview, 1089
Glomerulopathies, 1090
Glomerulonephritides, 1093

IMMUNOENDOCRINOPATHIES, 1108
Autoimmune Disorders of Carbohydrate Metabolism, 1108
Autoimmune Thyroid Disease, 1110
Autoimmune Addison Disease, 1111
Autoimmune Disease of the Ovary, 1111
Other Autoimmune Endocrinopathies, 1111

AUTOIMMUNE DISEASES OF THE NEUROMUSCULAR JUNCTION, NERVOUS SYSTEM, AND MUSCLE, 1112
Myasthenia Gravis, 1112
Lambert-Eaton Myasthenic Syndrome, 1112
Multiple Sclerosis, 1112
Paraneoplastic Neurologic Syndromes, 1112
Stiff-Person Syndrome, 1112
Polymyositis, 1113

CONCLUSION, 1113

SELECTED REFERENCES, 1114

KEY POINTS

- Autoimmune disorders frequently affect the skin, gastrointestinal, and hepatobiliary systems; the kidney; the endocrine system; and the nervous system.
- The dominant clinical feature of organ-specific autoimmune disease is chronic inflammation, generally localized in a single organ specific for each individual disease.
- In organ-specific autoimmune diseases, an organ-specific, tissue-specific, or cell-specific autoantigen is targeted. Some autoantigens circulate, some are cell surface molecules, and some are intracellular.
- Clinical recognition of autoimmunity is dependent on the detection of autoantibodies against relevant autoantigens.
- Damage to self can be mediated by humoral and/or cell-mediated autoimmunity, yet the etiology of virtually all organ-specific autoimmune diseases remains elusive.
- Autoimmune diseases occur in a proportion of people that manifest autoimmunity.
- The presence of circulating autoantibodies at significant titers is often useful in establishing the etiology of autoimmune liver disorders.
- An expanding universe of microvolume technologies is speeding the development of autoantibody detection that could support screening programs when clinically indicated.
- The detection of relevant autoantibodies in the setting of clinical disease can confirm an autoimmune etiology for the disease. Likewise, certain autoantibodies in asymptomatic individuals can predict the later development of disease.
- Collectively, organ-specific autoimmune diseases are common and produce significant degrees of morbidity and mortality.

INTRODUCTION AND OVERVIEW TO THE ORGAN-SPECIFIC AUTOIMMUNE DISEASES

DEFINITION OF AUTOIMMUNITY VERSUS AUTOIMMUNE DISEASE

Autoimmunity is aberrant immunity to self (Kamradt & Mitchison, 2001; Lleo et al., 2010). To protect the body from infection and neoplasia (when new antigens may be expressed), the immune system must be able to distinguish self from nonself. The innate immune system uses a large number of nonclonotypic cell surface receptors (such as toll-like receptors and the inflammasome) that seek gross differences between self and nonself to recognize the microbiologic world (Medzhitov & Janeway, 2000; Caso et al., 2018). The adaptive immune system uses clonotypic T-cell receptors for peptide–major histocompatibility complex (MHC) identification, while B cells use clonotypic cell surface antibody (i.e., membrane immunoglobulin) to accomplish this task. The adaptive immune system can recognize very subtle differences between self and nonself that may not be "observed" by the innate immune system receptors.

Normally autoimmunity is prevented by central (thymic) tolerance and peripheral tolerance (Singh & Schwartz, 2006). During T-cell ontogeny in the thymus, at the T-cell receptor double-positive thymocyte stage (i.e., T cells are positive for CD4 and CD8), interaction with class I or class II MHC molecules expressed by epithelial nurse cells "positively" selects such T cells for initial survival. Failure of these double-positive T cells to interact with either class I or class II MHC leads to apoptotic cell death. Once a double-positive T cell is "selected" (aka, "saved"), if it binds extremely tightly to the peptide-MHC complex that positively selected it, the double-positive T cell will undergo apoptosis in a process termed *negative selection*, which is part of central (thymic) tolerance. In general, if developing lymphocytes [either T or B cell (e.g., naïve immature IgM-positive B cells)] strongly signal through their clonotypic antigen receptor, they will be triggered to undergo apoptosis. After *positive selection* via class I MHC, the double-positive T cell (if it survives) is programmed to

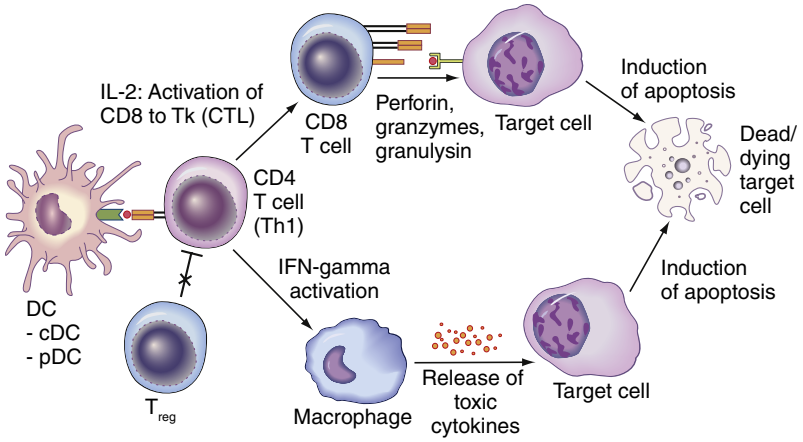

Fig. 55.1 The process of target destruction begins with dendritic cells *(DC)* that present peptides from beta cell autoantigens to CD4 Th1 cells. DCs can be classic (conventional) DCs *(cDCs)* or plasmacytoid DCs *(pDCs)*. Failure to regulate Th1 cells via defective regulatory T-cell (T_{reg}) function could contribute to Th1 cell autoimmunity. Activated autoreactive Th1 cells, in turn, activate CD8 T cells via interleukin-2 and DC upregulation. Activated CD8 T cells are functionally T killer cells (*Tk*; aka, cytotoxic T lymphocytes *[CTL]*). Via cell-cell contact between Th1 cells and macrophages (via CD40L–CD40 interactions *[not shown]*) and interferon-gamma *(IFN-gamma)* secreted by Th1 cells, macrophages are activated. Via both CD8 Tk cells and macrophages, target cells are triggered to undergo apoptosis. In the case of type 1 diabetes, beta cells die.

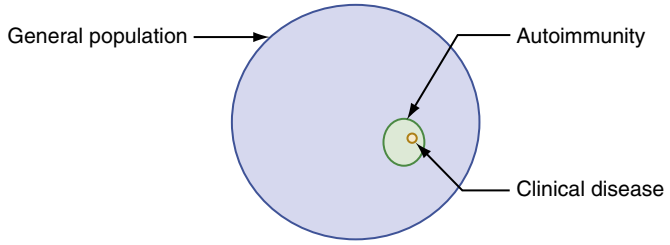

Fig. 55.2 Autoimmunity is defined as laboratory evidence of an auto-("self") reactive state often identified as the detection of a serum autoantibody to self. Of individuals with autoimmunity in the general population, a subset will manifest a clinically evident autoimmune disease.

lose CD4 expression and is destined to become a CD8 T cell. Likewise, after positive selection via class II MHC, the double-positive T cell is programmed to lose CD8 expression and is destined to become a CD4 T cell. Therefore single-positive T cells are found in the thymic medulla. Nonetheless, if these single-positive T cells bind extremely tightly to peptide-MHC complexes presented by medullary thymic epithelial cells (mTEC), dendritic cells, or macrophages, they too will undergo apoptosis as part of central (thymic) tolerance. In this way, CD4 and CD8 T cells exiting the thymus will not display very high levels of affinity for self-peptide plus MHC theoretically preventing (in part) autoimmunity. These CD4 and CD8 T cells constitute the naïve T-cell repertoire that leaves the thymus.

Peripheral tolerance develops when naïve T cells encounter MHC plus antigen-peptide without secondary signals. Such "tolerized" T cells are not able to subsequently respond to antigen, even if the proper secondary signals are then made available. Peripheral tolerance ensures that antigen-presenting cells are activating the naïve T cells in an appropriate immune response: Signal 1 is the T-cell receptor's perception of antigen-peptide presented by MHC (stabilized by MHC-CD4 or MHC-CD8 interactions), whereas signal 2 (a survival signal) is most importantly B7 (from the antigen-presenting cell where B7.1 is CD80 or B7.2 is CD86) engaging CD28 on the T cell. For CD4 T cells, a third set of signals involving cytokines secreted by dendritic cells and natural killer (NK) cells determines whether the newly stimulated CD4 T cell differentiates into a Th1 cell (secreting interleukin 2 [IL-2] and interferon-γ, tumor necrosis factor-α [TNF-α], and granulocyte/monocyte colony-stimulating factor), a Th2 cell (secreting IL-4, IL-5, IL-6, IL-10, IL-13, and eotaxin), a Tfh cell (T follicular helper cell secreting Th1 and/or Th2 cytokines), a Th17 cell (secreting IL-17 and IL-22), or a regulatory T cell (e.g., a CD4+ CD25+ FOXP3+ T cell secreting transforming growth factor-β, IL-4, and IL-10).

Autoimmunity becomes pathologic when clinical disease is manifested (Davidson & Diamond, 2001; Rose, 2016). A normal immune response is directed against "nonself" antigens such as microorganisms that cause infection. Such immune responses are beneficial. In an autoimmune disease, the immune response is directed against "self" antigens that cause injury. When self-antigens are targeted, cellular, tissue, and organ damage can result (Wahren-Herlenius & Dörner, 2013). Most autoimmune diseases involve adaptive humoral (types II and III hypersensitivity reactions) and/or cell-mediated (type IV hypersensitivity reactions) mechanisms (Fig. 55.1) that cause disease.

Autoimmunity is a broader term than *autoimmune disease* (Fig. 55.2). For example, autoantibodies directed against thyroid self-antigens such as thyroperoxidase and thyroglobulin are relatively frequent in the general population (≥5% prevalence in adults) (Stathatos & Daniels, 2012). However, only a subset of individuals with such humoral autoimmunity will manifest clinical autoimmune thyroid disease (AITD). The most common manifestation of AITD is Hashimoto thyroiditis. When agonist autoantibodies against the TSH receptor are produced, Graves disease results.

Defects in innate immunity can also be harmful, causing self-injury (e.g., C1 esterase inhibitor deficiency), paroxysmal nocturnal hemoglobinuria (PNH), various types of atypical hemolytic-uremic syndrome (aHUS) (e.g., inborn errors in C3, CD46, CFB, CFH, CFHR5, CFI, and THBD), and autoinflammatory diseases (e.g., familial Mediterranean fever [FMF], hyperimmunoglobulinemia D with periodic fever syndrome [HIDS], TNF receptor–associated periodic syndrome [TRAPS], Muckle-Wells syndrome [MWS], familial cold autoinflammatory syndrome [FCAS], and chronic infantile neurologic cutaneous articular syndrome [CINCA]) (Park & Atkinson, 2012). While these disorders are fascinating and instructive, we limit our discussion in this chapter to defects involving adaptive immunity causing autoimmune diseases.

An autoimmune disease may be present when one or more of the following findings are associated with the disease: (1) evidence of humoral or cell-mediated autoimmunity (including lymphocytic infiltration of the affected tissue or organ); (2) ability to transfer the disease with antibodies or lymphocytes; (3) beneficial response to immunomodulatory or immunosuppressive therapy; and (4) in the absence of immunosuppression, disease recurrence with organ transplantation. In practical terms, only autoantibody testing is sufficiently robust for routine clinical applications. Therefore most cases of autoimmune disease are substantiated by the finding of autoantibodies that are often directed against the target organ or tissue. However, the detection of autoantibodies, by themselves, indicates a state of "autoimmunity" and not "autoimmune disease." Through the history, physical examination, imaging studies, histologic reports (if a biopsy were performed), and laboratory findings, the physician can judge whether or not disease is present, promoting the diagnosis from "autoimmunity" to a state of "autoimmune disease" (Lyons et al., 2005.; Lleo et al., 2010).

CLASSIFICATION OF AUTOIMMUNE DISEASES

Traditionally autoimmune diseases are classified as "organ specific" or "non-organ specific" (Hayter & Cook, 2012). In an organ-specific autoimmune disease, a single tissue or organ is targeted. In some cases, a single circulating protein or receptor is targeted (e.g., insulin in the autoimmune hypoglycemia syndrome) (Zhang & Zhao, 2014).

One of the best examples of tissue specificity is type 1 diabetes: Within the islets of Langerhans, beta cells are selectively destroyed (Winter et al., 2016; Johnson et al., 2019). Beta cells are the most prevalent of islet cells (~65%); however, there are ample numbers of alpha cells (producing glucagon) and delta cells (producing somatostatin) and lesser numbers of PP cells (pancreatic-polypeptide producing cells). While there is some evidence of impaired alpha cell function early in the course of type 1 diabetes (Ganda et al., 1986), hyperglucagonemia is a pathogenic and well-recognized feature of type 1 diabetes that contributes substantially to hyperglycemia, ketogenesis, and ketosis in diabetic ketoacidosis. Examples of organ-specific autoimmune diseases are listed in Box 55.1. Discoid lupus is not discussed in this chapter because it falls under the heading of lupus (see Chapter 53). Autoimmune hemolytic anemia, autoimmune neutropenia, and immune thrombocytopenic purpura are examined in Chapters 33,

BOX 55.1

Examples of Organ-Specific Autoimmune Diseases

Dermatologic Disorders

Pemphigus vulgaris
Pemphigus foliaceus
Paraneoplastic pemphigus
IgA pemphigus
Bullous pemphigoid
Pemphigoid gestationis
Mucous membrane pemphigoid
Linear IgA dermatosis
Epidermolysis bullosa acquisita
Dermatitis herpetiformis
Cutaneous vasculitis
Autoimmune vitiligo
Autoimmune alopecia

Hepato-Gastrointestinal-Pancreatic Autoimmunity

Pernicious anemia
Celiac disease
Inflammatory bowel disease
Autoimmune hepatitis
Primary biliary cholangitis
Primary sclerosing cholangitis
Autoimmune pancreatitis

Glomerular Autoimmune Diseases (Including Glomerulonephritides)

Membranous nephropathy
IgA nephropathy
Membranoproliferative glomerulonephritis
C3 glomerulopathy
Infection-associated glomerulonephritis
Anti-glomerular basement membrane disease
Pauci-immune glomerulonephritis
Lupus nephritis

Endocrinopathies

Type 1 diabetes mellitus
Acanthosis nigricans with insulin resistance (type B insulin resistance)
Autoimmune hypoglycemia
Insulinomimetic insulin receptor autoantibodies
Chronic lymphocytic (Hashimoto) thyroiditis
Graves disease
Atrophic thyroiditis
Autoimmune Addison disease
Autoimmune disease of the ovary
Autoimmune hypophysitis
Autoimmune diabetes insipidus
Autoimmune hypoparathyroidism due to CaSR agonist autoantibodies
Autoimmune hyperparathyroidism due to CaSR antagonist autoantibodies

Neurologic Disease

Myasthenia gravis
Lambert-Eaton myasthenic syndrome
Multiple sclerosis
Paraneoplastic neurologic syndromes
Stiff-person syndrome
Polymyositis

Hematologic Disorders

Autoimmune hemolytic anemia
Immune thrombocytopenic purpura
Autoimmune neutropenia

34, and 41. Multiple organ-specific autoimmune diseases may also occur concurrently in a single patient (Box 55.2). An example of multiple organ-specific autoimmune diseases coexisting is thyrogastric autoimmunity where autoimmune thyroid disease and pernicious anemia (PA) commonly occur together in families (Cellini et al., 2017). Frequently associated with type 1 diabetes are autoimmune thyroid disease and PA (Kakleas et al., 2015). In hematology, autoimmune hemolytic anemia and immune thrombocytopenic purpura can coexist as Evans syndrome.

Non–organ-specific autoimmune diseases are also termed *systemic* autoimmune diseases because more than one organ and/or tissue is damaged (Wahren-Herlenius & Dörner, 2013). An older term for non–organ-specific autoimmune diseases is *collagen-vascular disease* because many such autoimmune disorders involve joints, connective tissue, and blood vessels (e.g., vasculitis). However, the term is misleading because collagen itself is not usually an autoantigen; therefore *collagen-vascular disease* is not the preferred descriptor. Examples of non–organ-specific autoimmune diseases are listed in Box 55.3.

BOX 55.2

Concurrent (Commonly Coexistent) Organ-Specific Autoimmune Diseases

Autoimmune polyglandular syndrome type I
Autoimmune polyglandular syndrome type II (also known as autoimmune polyendocrinopathy-candidiasis-ectodermal dystrophy [APECED])
Thyrogastric autoimmunity
Type 1 diabetes and autoimmune thyroid disease and/or pernicious anemia
Evans syndrome (autoimmune hemolytic anemia and immune thrombocytopenic purpura)

BOX 55.3

Examples of Non–Organ-Specific Autoimmune Diseases

Systemic lupus erythematosus
Scleroderma
Sjögren syndrome
Rheumatic fever
Rheumatoid arthritis
Goodpasture syndrome
Dermatomyositis
Reactive arthritis (urethritis or cervicitis, arthritis, and conjunctivitis)
Mixed connective tissue disease

LABORATORY TESTS FOR EVALUATING AUTOIMMUNITY

Laboratory tests for evaluating autoimmunity focus on the detection of autoantibodies (Damoiseaux et al., 2015). Tests of T-cell autoreactivity or lymphocyte-proliferation assays are not sufficiently reliable for clinical use. In the setting of clinical disease, the presence of a relevant autoantibody or autoantibodies is highly suggestive that the disease is indeed autoimmune in etiology. For example, goiter and hypothyroidism combined with positivity for thyroperoxidase autoantibodies (TPOA) or thyroglobulin autoantibodies (TGA) establish the diagnosis of Hashimoto thyroiditis.

To detect an autoantibody, the autoantigen must be available in some form whether it is purified (e.g., thyroperoxidase) or not (e.g., thyroid microsomes) (Fenalti & Buckle, 2010). The autoantigen can be present in a tissue section for indirect immunofluorescence (IIF), a cellular fraction, a purified protein or other biomolecule, or a cloned protein or a portion of a protein. Assays for autoantibody detection can be competitive or noncompetitive determinations. As an example of a competitive assay, there is an automated assay for the detection of thyrotropin-binding inhibitory immunoglobulins (TBII). In this assay a labeled monoclonal anti–TSH-receptor antibody competes with the patient's TSH-receptor autoantibodies (TRAbs) for binding to the TSH receptor.

A classic noncompetitive immunoassay method is IIF for islet cell autoantibodies (ICA) (Bottazzo et al., 1974). Patient serum is applied to a cryo-cut section of human blood group O pancreas. After incubation and washing, FITC (fluorescein-isothiocyanate)-labeled goat-antihuman IgG is applied. After washing and the application of glycerol and a coverslip, the slide is examined using an epifluorescence microscope. If the islets fluoresce, the patient's serum contains ICA that bind to islet autoantigens in the tissue that were detected by the FITC-labeled goat-antihuman IgG. ICA testing is illustrated in Fig. 55.3. Cytoplasmic islet autoantigens include glutamic acid decarboxylase (GAD), the insulinoma-2-associated autoantigen, and an asialoglycoconjugate (Nayak et al., 1985).

A wide variety of immunoassay formats are available that often utilize nonradioactive detection of the signal. In addition to IIF, classic first-generation monoplex technologies applied to autoantibody detection include Ouchterlony double immunodiffusion, IIF, agglutination, complement fixation, radioimmunoassay, enzyme-linked immunosorbent assay (ELISA), immunoprecipitation, and Western blotting (aka, immunoblotting). A review by Tozzoli and colleagues (2013) provides a well-organized summary of the second- and third-generation monoplex technologies (e.g., radioimmunoassay-immunoradiometric, radioreceptor, immunoenzymatic, immunoenzymometric, immunoblot and dot, chemiluminescence, and fluorimetric), followed by truly multiplex technologies (e.g., "addressable microbead immunoassays"). Recently immuno-PCR (nucleic acid signal amplification involving an antibody-based assay) has been used to detect autoantibodies (Chang & Wang, 2016).

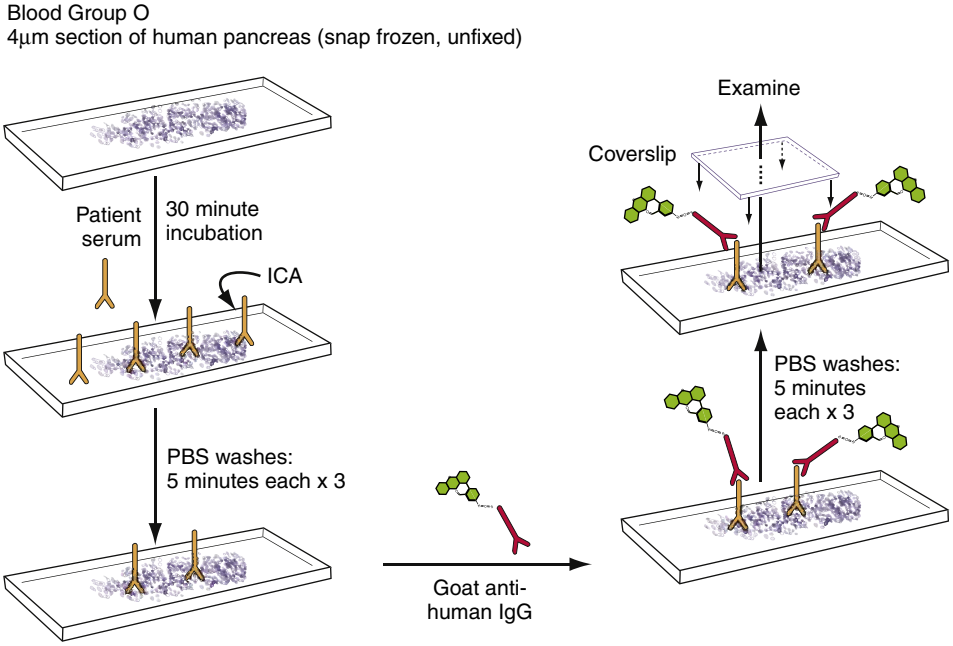

Fig. 55.3 Islet cell cytoplasmic autoantibody *(ICA)* testing is performed by indirect immunofluorescence. Patient serum is applied to a cryo-cut section of snap-frozen human blood group O pancreas. After incubation and washing, FITC (fluorescein-isothiocyanate)-labeled goat-antihuman IgG is applied. After washing and the application of glycerol and a coverslip, the slide is examined using an epifluorescence microscope. If the islets fluoresce, the patient's serum contains ICA that binds to islet autoantigens in the tissue that were detected by the FITC-labeled goat-antihuman IgG. PBS, phosphate-buffered saline.

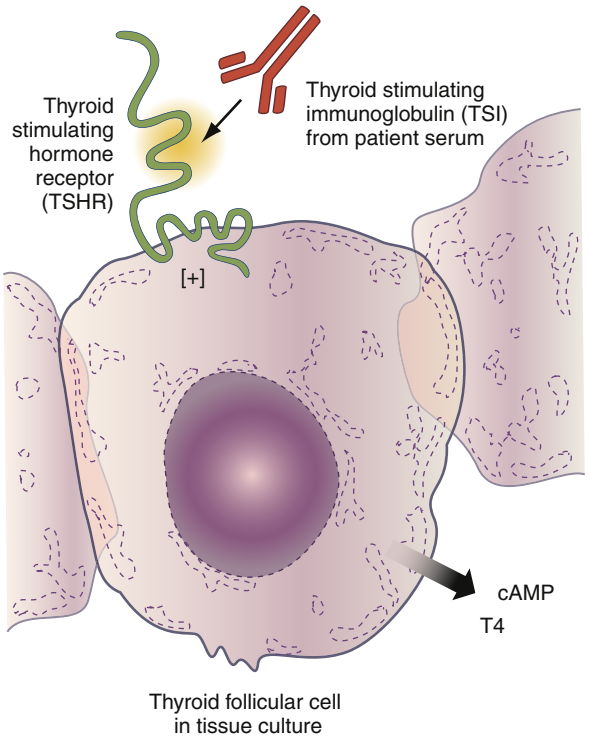

Fig. 55.4 Thyroid-stimulating immunoglobulins (TSIs) are detected by in vitro studies where patient serum is added to thyroid follicular cells. The effect of the TSI is measured by the release of cAMP or T4 from the cell.

Bioassays require living cells such as the detection of thyroid-stimulating immunoglobulins (TSIs) (Gupta, 1992; Winter et al., 2013) (Fig. 55.4). Chemiluminescent, electrochemiluminescent, bead, and flow cytometric technologies are being applied to autoantibody detection. The latest adaptations to autoantibody detection involve matrix and solid-chip technologies theoretically testing for hundreds, if not thousands, of autoantibodies simultaneously.

For many diseases, especially autoimmune blistering diseases of the skin, direct and IIF are key technologies. Biopsy of normal skin adjacent to a skin lesion allows examination of the tissue for in situ autoantibody and/or complement deposition. IIF using patient serum applied to normal tissues can reveal autoantibody reactivity to autoantigens. The salt-split skin (SSS) technique is especially useful in autoimmune diseases affecting the skin.

In the SSS technique, the patient's skin biopsy is initially incubated in the cold in 1 M sodium chloride for 1 day. Using forceps, the epidermis is then gently separated from the dermis. The specimens are next histologically processed using standard methods. For IIF, the SSS can be used as substrate.

INTERPRETATION OF SERUM AUTOANTIBODY LEVELS IN AUTOIMMUNE DISEASES

The two questions that must be answered are "How are positive/negative cutoffs established for autoantibody assays?" and "Does the titer (i.e., concentration) of the autoantibody provide useful clinical information about the natural history, severity, prognosis, or therapy of disease?" Positive/negative cutoffs for autoantibody tests are established using criteria similar to other tests intended to diagnose disease (Tampoia et al., 2012). If the analyte's concentration versus prevalence (frequency) in a population is distributed in a bell-shaped (normal) pattern (e.g., a histogram is developed), a positive (abnormal) test might be defined as the mean concentration of the autoantibody in the healthy population, plus either 2 or 3 standard deviations. If the mean plus 2 standard deviations is chosen as the cutoff, approximately 2.5% of the healthy population will test "positive." A more stringent definition of positivity could employ the mean plus 3 standard deviations as the cutoff, where only approximately 0.15% of the healthy population should test "positive." Furthermore, to ensure fewer "false positives" (at the expense of less sensitivity), some researchers have set autoantibody cutoffs as high as the mean plus 4 or 5 standard deviations. Because sensitivity and specificity are always at odds with one another in choosing a positive/negative cutoff, the best approach to defining a cutoff is to construct a receiver-operator characteristic (ROC) curve (see Chapter 8).

For distributions of results in a healthy population that do not follow a bell-shaped (normal) distribution, a large number of healthy controls need to be tested to define the desired cutoff—that is, the 97.5th percentile (e.g., the upper limit of the central 95% of the distribution) or the 99.85th percentile (e.g., the upper limit of the central 99.7% of the distribution). In such cases, defining the 97.5th percentile in a healthy population likely requires study of 200 or more healthy controls. Defining the 99.85th percentile in a healthy population whose results are not normally distributed is likely beyond the ability (or finances) of any laboratory except, possibly, major reference laboratories.

The answer to the second question—"Does the titer (i.e., concentration) of the autoantibody provide useful clinical information about the natural history, prognosis, severity, or therapy of disease?"—is solely dependent on the specific autoimmune disease and autoantibody under discussion. For example, in Graves disease patients, the titer of TSIs is inversely correlated with the likelihood of remission following pharmacologic antithyroid therapy (e.g., the likelihood of remission following propylthiouracil [PTU] or methimazole [MM] treatment) (Cappelli et al., 2007). Also, the titer of TSIs in maternal Graves disease correlates directly with the likelihood of neonatal Graves disease in the newborn (Barbesino & Tomer, 2013). In nondiabetic individuals with ICA, higher ICA titers

do predict an increased risk for the subsequent development of type 1 diabetes (Orban et al., 2009). This is also true for glutamic acid decarboxylase autoantibody (GADA). In latent autoimmune diabetes of adulthood (LADA—a late-onset form of type 1 diabetes), higher GADA levels predict the need for earlier insulin treatment, which is beneficial (Rosário et al., 2007). Rarely, the autoantibody concentration provides information differentiating two diseases. In typical cases of type 1 diabetes, the GADA titer is only mildly to modestly elevated above the cutoff; however, in type 1 diabetes that is part of stiff-person syndrome, the GADA titer is much higher (Dayalu & Teener, 2012).

As opposed to autoantibody concentrations near the cutoff value, higher concentrations of an autoantibody ensure that the autoantibody is truly present. Also, when studying an antibody that can be induced by an environmental exposure (such as insulin), the assay specificity should be considered. For example, the insulin autoantibody (IAA) assay does not discriminate autoantibodies from antibodies against exogenous insulin (Fineberg et al., 2007). Exogenous-insulin-induced antibodies are typically in much higher concentration than spontaneous IAAs that predict type 1 diabetes. Thus if the patient has been exposed to insulin for more than 14 days with the development of insulin antibodies, IAA should not be determined as an index of islet autoimmunity. Likewise, because therapy-induced insulin antibodies bind insulin and can raise the measured insulin concentration, total insulin measurements in insulin-treated individuals do not reflect the biologically active insulin (Winter et al., 2017). In short, in insulin-treated patients, total insulin measurements do not reflect either the amount of secreted or injected insulin. This becomes an issue in insulin-treated patients who are (1) hyperglycemic and noncompliant with insulin injections suspected or (2) hypoglycemic and excessive insulin administration is suspected. In such cases, C-peptide can be measured to assess endogenous insulin secretion.

As opposed to these examples where the autoantibody concentration influences the prediction, clinical course, or therapy of the disease, in other circumstances the degree of autoantibody positivity appears to be irrelevant. For example, it is highly controversial whether the persistence of GADA after diagnosis relates to beta cell function following the diagnosis of type 1 diabetes (Jaeger et al., 1997). Whereas generalizations are subject to many exceptions, in most autoimmune diseases the detection of an autoantibody is more important than the concentration of the autoantibody when that concentration is above the threshold of positivity. Consistent results require strict attention to the principles of quality assurance and quality control.

RECENT ADVANCES IN DIAGNOSTIC TECHNOLOGIES

To investigate autoimmune diseases, both in the clinical diagnostic setting and for research purposes, the ability to analyze biological samples for a myriad of potential autoantibodies, antigens, and other biomarkers represents a significant advance (Burbelo & O'Hanlon, 2014; Fu et al., 2010; González-Buitrago, 2006). The diagnostics revolution in developing new autoantibody immunoassays also involves the identification of new autoantigens in each of the autoimmune diseases discussed in this chapter. Candidate autoantigens can be identified by Western blotting, two-dimensional electrophoresis, mass spectroscopy, automated immunoprecipitation of cell or tissue extracts with sera from affected individuals, proteomic approaches, and immunoassays (Burbelo & O'Hanlon, 2014).

Traditional noncompetitive or "sandwich" immunoassays detect a single analyte; assays that detect multiple analytes (antigens or antibodies) in a single reaction are termed *multiplex assays* (Fu et al., 2010). Fluorescence is a common label in multiplex assays. Hundreds if not thousands of potential purified autoantigens can be investigated by the application of patient and control sera separately or in competition with one another.

In the *microsphere assay*, antibodies are linked to microspheres. A case in point is the BioPlex 2200 Multiplex Testing System (Krishnan et al., 2018; http://www.bio-rad.com/en-us/category/bioplex-2200-multiplex-testing?ID=a82cd166-67ca-4696-91a8-a98a550936f2). This utilizes the Luminex xMap technology. The 8-μM microspheres are labeled with different fluorophores, and antibodies are coupled to the microspheres. Every antibody to a different antigenic target is covalently attached to a bead with a unique fluorescence emission wavelength.

The beads are first incubated with a serum sample. The beads are washed and are then incubated with biotin-labeled antibodies against all the antigenic targets. After another wash, the beads are incubated with the reporter streptavidin-phycoerythrin conjugate (Krishnan et al., 2018; http://www.bio-rad.com/en-us/category/bioplex-2200-multiplex-testing?ID=a82cd166-67ca-4696-91a8-a98a550936f2). Phycoerythrin is a fluorescent pigment-protein complex. A "sandwich" is generated that is composed of the bead with attached antibody + antigen + biotinylated antigen-specific antibody + streptavidin-phycoerythrin. Analysis is by flow cytometry. The beads are run through a flow cell where analysis is achieved by two lasers: the "classification" laser (635 nm excitation), for identifying the beads, and the "reporter" laser (532 nm excitation), for detecting the target (BioPlex 2200 Multiplex Testing, http://www.bio-rad.com/en-us/category/bioplex-2200-multiplex-testing?ID=a82cd166-67ca-4696-91a8-a98a550936f2). The system detector performs a minimum of 150 measurements per analyte at the rate of 100,000 measurements per minute.

The CytoBead test system (GA Generic Assays GmbH) (Sowa et al., 2014, 2017) uses an IIF reaction on cells in one reaction compartment and multiplex microbead immunoassays in another compartment. For example, the CytoBead ANCA (Sowa et al., 2014) employs ethanol-fixed human neutrophils and in a separate section fluorescent microbeads coated with recombinant antigens PR3 or MPO. The AKLIDES is an automated digital IIF system (Sowa et al., 2014) for standardized immunofluorescence (IF) imaging and data processing. The system uses a sequential, multistage process, including image acquisition by a charge-coupled device (CCD) camera and software-controlled quality control.

The Luciferase Immunoprecipitation System (LIPS) (Burbelo et al., 2011, 2015) is a versatile technique that has been adapted to antibody identification. Antigens are expressed in COS1 cells as recombinant luciferase-antigen fusions. Specifically, the gene encoding luciferase (Ruc), from the coral *Renilla reniformis*, is fused in-frame with a variety of recombinant protein targets (Burbelo et al., 2015). These can be full-length proteins or protein fragments (Burbelo et al., 2015). The latter are reacted with the test sera; if the sera contain antibodies to the antigen, the immunoglobulins will complex with the fusion protein. Protein A/G beads are used to capture IgG molecules that have bound the luciferase-antigen. Addition of a luciferase substrate generates a light signal that permits antibody quantitation.

A completely different technique for analyzing biomarkers is a form of mass spectroscopy called *multiple reaction monitoring* (MRM) (also referred to as *selected reaction monitoring*) (Parker et al., 2014; Gillette & Carr, 2013). This has been adapted to the analysis of proteins in plasma; MRM is especially useful in quantification of specific proteins within highly complex biological mixtures. Unique peptides representing proteins of interest are predefined together with their fragment ions (Gillette & Carr, 2013). Such peptides are termed *proteotypic peptides*. In this procedure, three quadrupole mass spectrometers are linked in tandem. The first quadrupole selects the precursor ion of interest. Fragmentation occurs in the second quadrupole, usually by collision with a neutral gas (Parker et al., 2014; Gillette & Carr, 2013). The third quadrupole then analyzes the fragments. Stable synthetic isotope (^{13}C or ^{15}N)–labeled internal standard peptides are the key to quantification. This is achieved by comparing labeled to unlabeled peak areas. $^{13}C/^{15}N$ standards are otherwise identical to the unlabeled peptide and are distinguishable by m/z only. The overall technique is sometimes referred to as stable isotope dilution (SID) selected reaction monitoring multiple reaction monitoring or SID-MRM-MS analysis (Gillette & Carr, 2013). Each fragment ion from an analyte needs to be sampled for only a few milliseconds to obtain interpretable spectra. More than 100 precursor product ion pairs (referred to as transitions) can thus be recorded per second in MRM (Gillette & Carr, 2013). To apply this technique after extraction, proteins are digested into peptides. Internal standards are then added. In some cases, depletion of abundant proteins using immunoaffinity absorption may be additionally used.

Phage immunoprecipitation sequencing (PhIP seq) uses the T7 bacteriophage, which is designed to express over 400,000 overlapping peptides of all known human protein sequences (Larman et al., 2011). The engineered phage is called a T7 peptidome phage display library (T7-Pep). The T7-Pep library is mixed with patient samples (e.g., cerebrospinal fluid). Autoantibodies present in the biological specimen will bind to the phage-expressed protein. These antibodies and bound phage are captured on a solid phase system. In this way, deoxyribonucleic acid (DNA) from the immunoprecipitated phage can be isolated and sequenced, permitting identification of the antigen to which the autoantibody binds.

AUTOANTIBODIES AS PREDICTORS OF DISEASE

The answer to the question "Can autoantibodies predict disease?" is dependent on the specific disease under review. In the proper circumstances, the detection of an autoantibody can predict the subsequent development of disease (Coco et al., 2006). This is most evident in the current research effort to prevent type 1 diabetes (Sosenko et al., 2015; Jacobsen et al., 2019). In persons with multiple islet autoantibodies (e.g., three or more),

there is conservatively more than a 50% risk of developing type 1 diabetes over the span of 5 to 10 years of follow-up. If there is evidence of beta cell dysfunction with even one islet autoantibody (e.g., ICA), the 10-year risk for type 1 diabetes approaches 100%.

There are many other autoimmune diseases where autoantibody positivity predicts disease (Vojdani, 2008). This has been extensively studied in the organ-specific endocrinopathies of AITD and Addison disease developing in persons with type 1 diabetes who are positive, respectively, for thyroid autoantibodies (e.g., TPOA) or adrenal cytoplasmic autoantibodies (ACA) (Ketchum et al., 1984; Maclaren & Riley, 1985). Likewise, gastric parietal cell autoantibodies (PCA) in persons with type 1 diabetes predict the development of PA (Riley et al., 1982).

If autoantibodies can predict certain diseases, is it prudent that we screen the general population for various organ-specific autoantibodies? The answer to this question is complex. The answer depends on the following factors:

1. Can the disease be prevented, or does early detection of disease only allow earlier treatment of disease?
2. How common is the autoimmune disease?
3. What is the cost of treatment versus the cost of screening?
4. Does screening actually change outcome?
5. What is the morbid burden to the individual and society of delayed diagnosis?

Considering these issues there are few circumstances where screening for autoimmune diseases should be undertaken in the absence of a preexisting autoimmune disease or a family history of autoimmune disease.

In the case of type 1 diabetes, because of the high prevalence of associated AITD, PA, and Addison disease (which if untreated can be rapidly fatal), it is recommended that persons with type 1 diabetes be screened for thyroid autoimmunity with TPOA testing, chronic lymphocytic gastritis (the most common cause of PA) with gastric PCA, and adrenal autoimmunity with adrenocortical cytoplasmic autoantibodies (ACA) or 21-hydroxylase autoantibodies (Maclaren & Riley, 1985). If a person is autoantibody positive, periodic testing would follow: In TPOA-positive individuals, TSH is measured yearly; in PCA-positive individuals, vitamin B_{12} and ferritin are measured yearly; and in ACA-positive individuals, yearly cosyntropin stimulation testing is performed together with supine renin measurements (Haller et al., 2014). The prediction of Addison disease is likely the most important screening to be undertaken because Addisonian crisis can be fatal (Chantzichristos et al., 2019).

Because some autoimmune diseases are strongly familial, it may be beneficial to perform autoantibody screening in first-degree relatives of affected individuals. The best example of this situation is thyrogastric autoimmunity. AITD is strongly familial and is common. Although no single gene causes AITD, it appears to be inherited in a dominant fashion. If the proband has Hashimoto thyroiditis or Graves disease, their first-degree relatives can be screened for TPOA to anticipate AITD. If TPOA were negative, thyroglobulin autoantibodies (TGA) could be sought, but TGA testing is less sensitive that TPOA testing. TPOA-positive or TGA-positive relatives would then have yearly thyroid function testing, including, at a minimum, the measurement of TSH. Gastric autoimmunity (e.g., PCA and PA) is commonly associated with AITD, so PCA testing is worthwhile to pursue. If the person is PCA positive, vitamin B_{12} and ferritin are measured yearly.

CUTANEOUS AUTOIMMUNE DISEASES

As a frequent target of the immune response, the skin presents us with an excellent visual picture of autoimmune disease pathology. Immunobullous disorders, connective tissue disease, vasculitis, and vitiligo each present with characteristic clinical features. However, diagnosis of many of these disorders often relies on utilization of light microscopy and IF testing. Direct immunofluorescence (DIF) and immunoassays are methods used to help establish a diagnosis and are especially critical for classifying the histologically similar autoimmune bullous diseases. Examination of the pattern of immune complex deposition at various locations within the skin may be specific for a particular disorder or may need to be interpreted within the setting of its clinical and histologic findings (Box 55.4). Rapid and definitive differentiation of these autoimmune skin diseases is important as the disorders can differ in their prognosis and treatment decisions.

The autoimmune bullous disorders are a heterogeneous group of mucocutaneous blistering diseases characterized by autoantibodies to specific adhesion proteins of the epidermis and dermoepidermal junction (Table 55.1). Classification of the blister location as intraepidermal or subepidermal divides the immunobullous disorders into the pemphigus and pemphigoid group, respectively. The pemphigus group is associated with antibodies against epidermal desmosomal proteins and intercellular immune deposits between keratinocytes. In pemphigoid, the hemidesmosomal complex and basement membrane zone (BMZ) is targeted. Because there can be considerable overlap in the clinical and histologic features of these blistering disorders, accurate diagnosis of an autoimmune bullous disease requires the detection of tissue-bound and circulating autoantibodies. The detection of circulating autoantibodies can be made by different tests, including IIF, ELISA, immunoblot, and immunoprecipitation. In addition to help with diagnosis, ELISA is also being used to monitor disease activity.

For skin biopsies, site selection and technique are important considerations in the interpretation of histologic and IF results. For blistering disorders, biopsy for DIF should be taken from nonbullous lesional, erythematous skin or uninvolved perilesional skin about 1 cm from a blister (Diercks et al., 2017). Blistered, ulcerated, and uninvolved skin are associated with false-negative results, and it is recommended that biopsies be taken from above the waist if possible (Elston et al., 2016). The DIF specimen should not be placed in formalin. Michel or Zeus medium is recommended for preservation; however, some laboratories may require fresh specimens be received during working hours (Elston et al., 2016). The biopsy for light microscopy should include an intact vesicle or the edge of a larger bulla. That specimen should include both intact and blistered skin.

BOX 55.4

Location of Immunofluorescence Findings in Autoimmune Skin Diseases: Pattern of Deposition

Intraepidermal (Intercellular)

Pemphigus vulgaris
Pemphigus foliaceus
Paraneoplastic pemphigus
IgA pemphigus

Dermal-Epidermal Junction (Basement Membrane Zone)

Bullous pemphigoid
Mucous membrane pemphigoid
Pemphigoid gestationis
Epidermolysis bullosa acquisita
Bullous lupus erythematosus
Linear IgA dermatosis
Lupus erythematosus

Dermal Papillae Disease

Dermatitis herpetiformis

Intravascular

Vasculitis

PEMPHIGUS

Pemphigus describes a rare group of potentially life-threatening, mucocutaneous blistering diseases characterized by the production of antibodies to epidermal adhesion molecules, resulting in loss of cellular cohesion between keratinocytes (acantholysis) and intraepidermal bullae formation (Kershenovich et al., 2014). This intraepidermal acantholysis is considered the histologic hallmark of the pemphigus group and is responsible for the clinical presentation of flaccid blisters and erosions (Schmidt & Zillikens, 2010). Through the direct interference in desmosomal function, pathogenic autoantibodies to desmoglein 3 (Dsg3) and/or Dsg1 on epidermal keratinocytes play an active role in disease activity (Kershenovich et al., 2014). Four major variants have been described in this group and include pemphigus vulgaris (PV), pemphigus foliaceus (PF), paraneoplastic pemphigus (PNP), and IgA pemphigus. Review of their clinical, histopathologic, and immunopathologic findings may provide differentiating features that are helpful in the diagnosis of the pemphigus subtype (Joly & Litrowski, 2011; Kershenovich et al., 2014).

Pemphigus Vulgaris

PV is the most common variant of pemphigus. The mean age of disease onset is between 40 and 60 years of age, with no gender bias (Nancy & Yehuda, 2009; Joly & Litrowski, 2011). Dsg1 and Dsg3 are the target autoantigens for circulating IgG autoantibodies in this disease. Because of differences in the expression of the desmogleins in cutaneous and mucosal epithelium, patients may present with one of two clinical variants. For example, an anti-Dsg3 immune profile will present with mucosal-dominant disease, but the presence of antibodies to both Dsg1 and Dsg3 will result in the mucocutaneous phenotype (Amagai et al., 1999).

TABLE 55.1
Immunopathologic Features and Target Antigens of Autoimmune Bullous Diseases

Diagnosis	Blister Site/Ultra-structural Location	Autoantigen	DIF	IIF
Intraepidermal				
Pemphigus vulgaris	Suprabasal	Dsg 3, Dsg 1	Intercellular IgG and C3	Intercellular IgG (monkey esophagus)
Pemphigus foliaceus	Subcorneal or within granular layer	Dsg 1	Intercellular IgG and C3	Intercellular IgG (guinea pig esophagus or lip)
Paraneoplastic pemphigus	Suprabasal	Dsg 3, Dsg 1, plakin family (desmoplakin 1 and 2, envoplakin, periplakin, BP230, plectin, A2ML1)	Intercellular IgG +/– C3 and at DEJ	Intercellular IgG (rat bladder)
IgA pemphigus	Subcorneal	Desmocollin 1, Dsg 3	Intercellular IgA	Intercellular IgA
Subepidermal				
Bullous pemphigoid	Hemidesmosome	BP180, BP230	Linear IgG and C3 at BMZ	IgG at BMZ SS: epidermal
Pemphigoid gestationis	Hemidesmosome	BP180, BP230	Linear C3 at BMZ	
Mucous membrane pemphigoid	Lamina lucida	BP180, laminin 332, α6β4 integrin, laminin 311, BP230	Linear IgG, C3, and IgA at BMZ	IgG at BMZ SS: epidermal or mixed SS: dermal laminin 332
Epidermolysis bullosa acquisita	Anchoring fibrils	Type VII collagen	Linear IgG and C3 at BMZ, +/– IgA and IgM	IgG at BMZ SS: dermal
Linear IgA dermatosis	Lamina lucida	LAD-1	Linear IgA at BMZ, +/– C3	IgA at BMZ SS: epidermal, dermal, or mixed
Dermatitis herpetiformis	Papillary dermis	Epidermal transglutaminase	Granular IgA at tips of dermal papillae, +/– C3	IgA endomysial antibody (monkey esophagus)

+/–, with or without; *A2ML1,* α2-macroglobulin-like 1; *BP,* bullous pemphigoid; *BMZ,* basement membrane zone; *DEJ,* dermoepidermal junction; *DIF,* direct immunofluorescence; *Dsg,* desmoglein; *IIF,* indirect immunofluorescence; *LAD-1,* linear IgA disease antigen 1; *SS,* salt-split skin.

Patients with PV often present with painful oral mucosal lesions as their first manifestation of disease, and it is the most frequent site of involvement. Skin involvement classically consists of flaccid bullae that rupture easily and multiple painful erosions. Skin lesions may present on any part of the body, but the scalp, head, neck, and flexural surfaces are more favored sites. There is a positive Nikolsky sign in perilesional skin in both PV and pemphigus foliaceus. In the Nikolsky sign, when the skin is slightly rubbed, the top layers of skin slip apart from the lower layers. Of PV cases, 5% to 10% are fatal, and morbidity/mortality is related to the extent of disease and the complications from immunosuppressive treatment (Joly & Litrowski, 2011).

Histologic and Immunologic Features

The intraepidermal acantholysis that characterizes the histology of the pemphigus group of blistering disorders is found in a classic suprabasalar location. Cleavage above the basal layer keratinocytes has been said to resemble a "row of tombstones" sitting on the basement membrane.

DIF evaluation reveals an intercellular pattern of IgG deposition and C3 characteristics of all types of pemphigus, with the exception of IgA pemphigus (Fig. 55.5). Examination of perilesional skin in PV reveals linear and granular staining. This pattern may be described as "chicken wire" because of the hexagonal mesh outline created by the continuous deposition around individual keratinocytes (Fig. 55.6). Increased intensity of the staining pattern may be seen at the level of blister formation within the affected skin (i.e., lower epidermal for PV and superficial layers for pemphigus foliaceus) (Chhabra et al., 2012). The basement membrane zone does not stain in PV patients. Essentially, all patients with PV display IgG staining, whereas complement staining varies between 50% and 100% of cases. IgM or IgA staining is observed in 30% to 50% of cases of pemphigus.

Circulating IgG autoantibodies are detected on the surfaces of the squamous epithelial cells by IIF. For all investigations by IIF, the appropriate choice of tissue substrate is important because different substrates exhibit different autoantigens (Kershenovich et al., 2014). Monkey esophagus is the tissue of choice when testing for PV. On the other hand, guinea pig esophagus is the tissue of choice in cases of pemphigus foliaceus. Reference laboratories offer tests such as "Cutaneous Immunofluorescence Antibodies (IgG), Serum" (see http://www.mayomedicallaboratories.com/test-catalog/Overview/8052).

Reference laboratories provide ELISA-based testing for anti-Dsg1 and anti-Dsg3 autoantibodies. One reference laboratory provides a helpful interpretive summary of skin IF testing (see http://www.mayomedicallaboratories.com/test-catalog/Overview/83680).

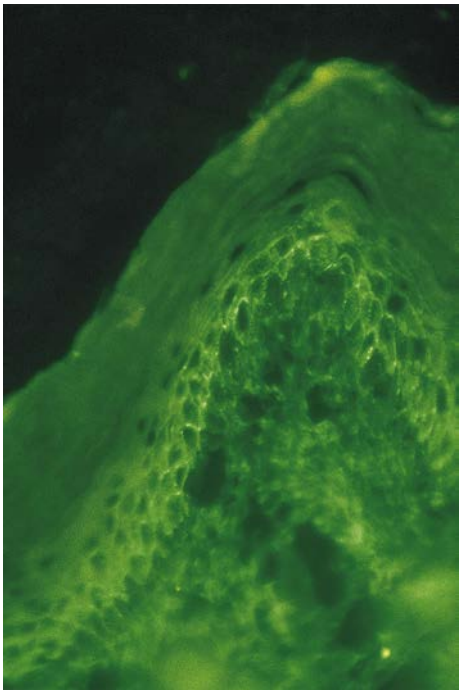

Fig. 55.5 Direct immunofluorescence microscopy of skin lesions in pemphigus shows linear/granular C3 deposition on the cell surfaces (intercellular spaces) of mainly basal keratinocytes without basement membrane zone (BMZ) immunofluorescence (×400).

Pemphigus Foliaceus

PF is characterized clinically by small and superficial flaccid blisters that immediately rupture, evolving into crusted erosions found in a seborrheic

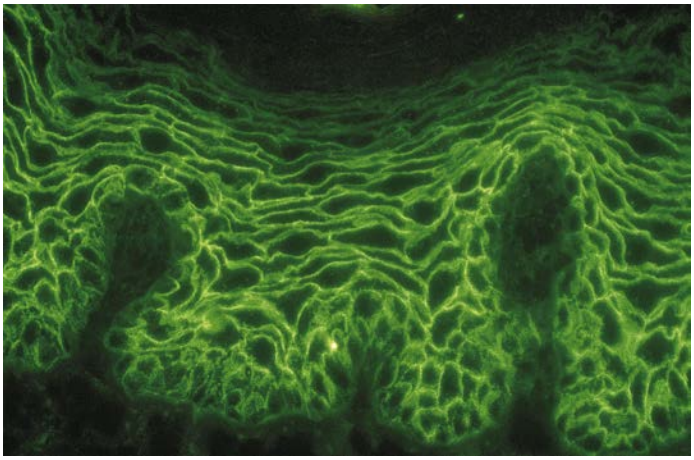

Fig. 55.6 Indirect immunofluorescence microscopy in pemphigus shows linear immunoglobulin (IgG) immunofluorescence on the cell surfaces of epithelial cells (intercellular spaces) using mouse esophagus as tissue substrate (×250).

distribution (upper torso, scalp, and face). In contrast to PV, there is no mucosal involvement. Antibodies to Dsg1 are responsible for the findings in PF. Although PF is considered to have a less severe clinical course, the eruption still requires treatment with prolonged systemic immunosuppressive therapies (Joly & Litrowski, 2011). The serologic hallmark of PF is the demonstration of IgG autoantibodies against Dsg1, and serum levels have been found to correlate with disease severity (Ishii, 2015). Fogo selvagem (endemic pemphigus) and pemphigus erythematosus (Senear-Usher syndrome) are two distinct clinical variants within PF.

Histologic and Immunologic Features

Compared to PV, the epidermal split in foliaceus lesions is found in the most superficial layers of the epidermis. Acantholysis can be found within the granular layer or in a subcorneal location and may result in loss of the stratum corneum. The differences in intraepidermal blister location correlate with the differences in desmoglein expression within the skin between the pemphigus subtypes. Eosinophilic spongiosis has been reported in some cases of PF. *Spongiosis* is the descriptive term for increased intercellular fluid in the epidermis (e.g., intercellular edema) that separates keratinocytes from one another, highlighting their desmosomal connections.

DIF of biopsy tissue will show the same intercellular pattern of fluorescence as described in PV. Guinea pig esophagus is recommended as the most sensitive IIF substrate, and testing should detect circulating IgG autoantibodies to the epithelial cell surface in 90% of specimens (Arbache et al., 2014). In addition, serologic titers reported in PV and PF may correlate with disease activity and treatment response (Mutasim & Adams, 2001).

Paraneoplastic Pemphigus

PNP is a unique form of pemphigus that is characterized by a refractory stomatitis and an association with an underlying malignancy. Non-Hodgkin lymphoma, chronic lymphocytic leukemia, Castleman disease, and thymoma are the most commonly reported neoplasms (Vassileva et al., 2014). In addition to painful mucosal erosions, a polymorphic skin eruption and internal organ involvement are possible (Hertl et al., 2014). The prognosis of the mucocutaneous disease is linked to the presence of the associated neoplasm. In addition to the clinical distinctions from classic pemphigus, the autoantibody profile is more diverse and includes antibodies to the desmogleins and plakin family proteins (i.e., envoplakin, periplakin, plectin, desmoplakin 1 and 2) (Schmidt & Zillikens, 2010).

Histologic and Immunologic Features

The histopathologic features in PNP combine the acantholysis characteristic of pemphigus with changes of interface dermatitis with necrotic keratinocytes. Antibodies in PNP are directed against both desmosomal and hemidesmosomal proteins and explain why DIF shows immunoreactivity within the epidermis and at the BMZ. BMZ deposition of IgG and complement can be found in a linear or granular pattern along the dermoepidermal junction. If the histologic features and DIF findings suggest the diagnosis of PNP, IIF studies should be pursued. IIF testing using rat bladder epithelium is considered the best screening test for PNP (Mutasim & Adams, 2001). Additional laboratory tests such as immunoprecipitation, immunoblotting, and ELISA are helpful in confirming the diagnosis after initial workup.

IgA Pemphigus

The hallmark of IgA pemphigus is the intercellular deposition of IgA as the target antigen is present in desmosomes. Neutrophil infiltration follows the presence of tissue-bound IgA and results in epidermal acantholysis and vesiculation (Zone et al., 2004).

Histologic and Immunologic Features

Subcorneal acantholysis with intraepithelial neutrophilic collections characterize IgA pemphigus histopathology. DIF will show that intercellular IgA deposits are present within the epidermis in a typical pemphigus pattern. Positive IIF for circulating IgA is found in 50% of patients (Mutasim & Adams, 2001).

PEMPHIGOID

The pemphigoid group of autoimmune bullous disorders is characterized by subepidermal blister formation due to the loss of adhesion between the basal layer keratinocytes and the underlying basement membrane. Autoantibodies are directed at one or more structural proteins found in the hemidesmosome, lamina lucida, lamina densa, or anchoring fibrils that make up the BMZ. This group of disorders includes bullous pemphigoid (BP), pemphigoid gestationis (PG), mucous membrane pemphigoid (MMP), and linear IgA dermatosis (LAD).

In addition to the pemphigoid group, epidermolysis bullosa acquisita (EBA) and dermatitis herpetiformis (DH) are other immunobullous disorders that share the histologic hallmark of subepidermal blister formation. Because of clinical and histologic overlap among these disorders, IF studies can play a critical role in the distinction among disorders (see Table 55.1). The SSS technique is an additional test that can be used in the evaluation of the subepidermal blistering disorders to increase the sensitivity of antibody detection and gain further information on the autoantibody binding site (Mutasim & Adams, 2001; Aoki et al., 2010).

Bullous Pemphigoid

BP is the most common type of autoimmune bullous disorder, and it occurs most frequently in the elderly. Clinically, BP patients present with urticarial lesions and tense blisters on the trunk and extremities, with associated pruritus. Mucosal involvement is uncommon and is reported in 10% to 30% of BP patients (Baum et al., 2014). The Nikolsky sign is negative in BP.

In BP, autoantibodies target the two hemidesmosomal proteins: bullous pemphigoid antigen 1 (BPAg1 [BP230]) and bullous pemphigoid antigen 2 (BPAg2 [BP180]). BPAg2, also known as type XVII collagen, is a transmembrane protein that is determined to be the target autoantigen for pathogenic autoantibodies in BP (Vassileva et al., 2014). In it is unclear if autoantibodies to BPAg1, a cytoplasmic plakin family protein, relate to the pathogenesis of BP (Schmidt & Zillikens, 2010). Complement activation is believed to follow autoantibody binding, causing the physical loss of adhesion between the basal cell layer and the basement membrane (Kershenovich et al., 2014).

Histologic and Immunologic Features

A subepidermal blister with a superficial dermal inflammatory infiltrate, including numerous eosinophils, describes the typical histopathologic findings in bullous lesions of BP (Fig. 55.7A). Eosinophilic spongiosis may serve as a clue in early lesions (Baum et al., 2014). Neutrophil predominant and cell-poor variants also exist and may pose a diagnostic challenge.

DIF of perilesional skin reveals linear IgG and/or C3 deposition at the BMZ in BP, PG, and MMP (see Fig. 55.7B). The finding of C3 deposition with a stronger intensity than IgG favors a pemphigoid group disease (Mutasim & Adams, 2001). Complement may sometimes be found as the sole immunoreactant in BP, but more often in PG. IgA and/or IgM staining can also be present but will stain with less intensity. IIF shows circulating IgG anti-BMZ autoantibodies in 75% of patients (Mutasim & Adams, 2001).

Serum IgG autoantibodies to BPAg1 and BPAg2 can be detected using ELISA testing. The sensitivity of ELISA BPAg1 autoantibodies in cases of BP is approximately 60%, and the sensitivity of ELISA BPAg2 autoantibodies for BP is approximately 80% (Roussel et al., 2011).

Pemphigoid Gestationis

PG, previously known as herpes gestationis, is considered to be a form of BP that develops during pregnancy. PG usually develops in the second or third trimester and typically resolves within weeks to months after delivery. Because this is a humoral autoimmune disease, the newborn can be transiently affected through passive maternal transfer of IgG autoantibodies (Mihai & Sitaru, 2007).

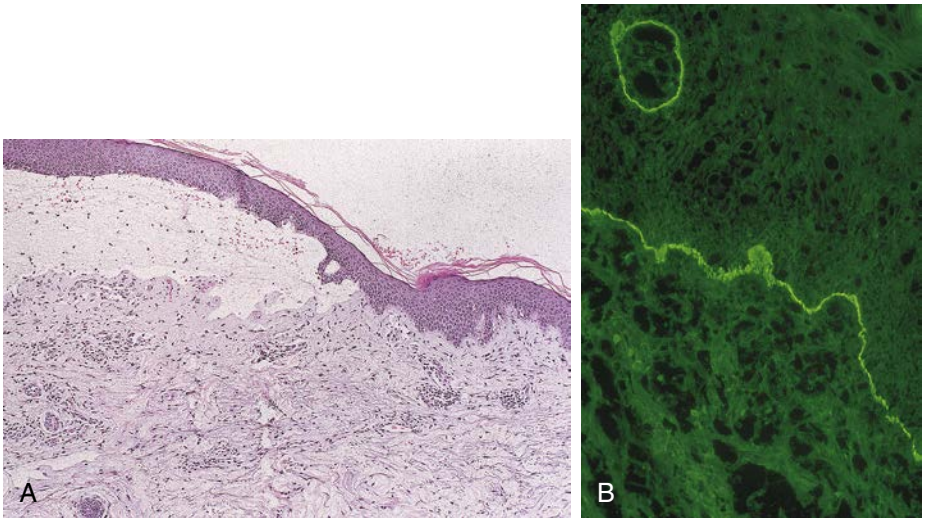

Fig. 55.7 **A** Skin biopsy of pemphigoid reveals a subepidermal split, nonnecrotic epidermis, and variable inflammation, often with prominent eosinophils (H&E, ×100). **B** Direct immunofluorescence microscopy reveals intense linear C3 deposition along the basement membrane zone (BMZ) (×400).

Histologic and Immunologic Features

Linear deposits of C3 are present in 100% of PG patients with IgG deposits found less frequently in 30% to 40% of cases. IIF detects anti-BMZ autoantibodies in only 10% to 20% of patients (Aoki et al., 2010).

Mucous Membrane Pemphigoid

MMP, also known as cicatricial pemphigoid, is a rare, chronic variant of pemphigoid characterized by predominant mucous membrane disease. Erosions, blisters, and scarring may involve oral, conjunctival, nasal, laryngeal, esophageal, and anogenital mucosa. Lesions often heal with scarring, which can interfere with the normal function of the affected area, producing significant morbidity. For example, ocular cicatricial pemphigoid presents with progressive subconjunctival scarring that leads to decreased vision and eventual blindness (Chan, 2012).

Several target autoantigens have been identified with the recognition of a few clinically important variants. MMP with autoantibodies against laminin 332 is clinically indistinguishable from other forms of MMP but is associated with an increased risk of internal malignancy (Vassileva et al., 2014).

Histologic and Immunologic Features

Perilesional skin and mucosal biopsies reveal continuous IgG and C3 deposits, with occasional IgA present along the basement membrane by DIF. IIF studies are usually negative. Because the numerous target autoantigens in MMP vary in their location within the BMZ, the site of autoantibody binding on SSS microscopic exam may be epidermal, dermal, or both. IIF SSS studies do increase the sensitivity of detection and can be positive in approximately 80% of cases of MMP.

LINEAR IgA DERMATOSIS

LAD is a rare subepidermal blistering disease due to IgA autoantibodies directed at autoantigens in the BMZ. Activated complement and neutrophil infiltration result in the disruption of the dermoepidermal attachments and blister formation. The clinical lesions of LAD can be polymorphic, but annular patterns of tense vesicles or blisters are classically described. Most cases of LAD are considered idiopathic, but drug-induced cases are reported. Chronic bullous dermatosis of childhood is considered a childhood form of linear IgA dermatosis.

Histologic and Immunologic Features

The strong presence of IgA linear deposition along the BMZ is characteristic of LAD (Mutasim & Adams, 2001). These features help separate it from the DIF findings in DH. In addition, only LAD shows IgA anti-BMZ autoantibodies by IIF examination (Chhabra et al., 2012).

EPIDERMOLYSIS BULLOSA ACQUISITA

EBA is a rare subepidermal blistering disorder characterized by autoantibodies against type VII collagen, the anchoring fibrils of the BMZ. EBA is a clinically heterogeneous disease and presents with inflammatory and noninflammatory forms. The noninflammatory form manifests as a mechanobullous disorder that is characterized by skin fragility, trauma-induced lesions, and scarring (Vassileva et al., 2014). The inflammatory forms can mimic BP or LAD with a more widespread blistering eruption or present with blisters and scarring of mucous membranes similar to MMP (Mihai & Situra, 2007). EBA has been associated with several systemic diseases, with inflammatory bowel disease (IBD) being most frequent (Vassileva et al., 2014).

Bullous lupus erythematosus is an autoimmune bullous disease that occurs in patients diagnosed with systemic lupus erythematosus (SLE) (Fig. 55.8). It is also due to autoantibodies against type VII collagen. The IF findings can be similar to EBA.

Histologic and Immunologic Features

The presence of multiple types of immunoglobulin at the BMZ is typical of EBA. IgG and C3 are typically present. IgA and IgM are found in 67% and 50% of cases, respectively (Aoki et al., 2010). IIF demonstrates anti-BMZ IgG autoantibodies in a pattern similar to BP. The SSS technique is useful in this situation because it enhances the differentiation of these disorders through the localization of fluorescence. The serum of BP patients shows autoantibody binding to the roof of the blister (epidermal side), and EBA sera will show binding to the blister floor (dermal side). This is based on the localization of the autoantigens responsible for the related disease. The newly developed ELISA for COL7 (type VII collagen) can be used but has a sensitivity of 45% for detection (Koga et al., 2019).

DERMATITIS HERPETIFORMIS

DH is an intensely pruritic and chronic blistering disorder associated with gluten-sensitive enteropathy (e.g., celiac disease). Patients present with papulovesicles and excoriations on the extensor surfaces, typically in a symmetric distribution. The lesions can be found in groups or clusters giving a "herpetiform" appearance—hence the name. Gastrointestinal involvement will manifest as symptoms of malabsorption, but gastrointestinal involvement is present in only approximately 20% of DH patients (Mendes et al., 2013). Symptoms of DH and celiac disease will improve with a gluten-free diet. IgA autoantibodies directed against tissue epidermal transglutaminase (eTG) are thought to play a more central role in the pathogenesis of skin disease in patients with DH (Rose et al., 2009; Ishii, 2015).

Histologic and Immunologic Features

Biopsies should be performed on perilesional normal-appearing skin. Typical histopathologic features include the formation of neutrophilic microabscesses at the tips of dermal papillae and a mixed perivascular inflammatory infiltrate including few eosinophils (Mihai & Situra, 2007) (Fig. 55.9A). As lesions progress, a subepidermal blister may form. The histologic findings of DH may be indistinguishable from linear IgA disease.

The diagnosis of DH requires DIF examination of a skin biopsy, revealing granular IgA deposition in the dermal papilla (Mutasim & Adams, 2001) (see Fig. 55.9B). Other findings may include IgA deposits along the BMZ and the presence of C3 deposits (Arbache et al., 2014). Contrary to the other subepidermal immunobullous disorders, DH patients do not have circulating anti-BMZ autoantibodies. However, serum IgA autoantibodies directed against endomysium, gliadin, tTG (tissue transglutaminase), and eTG can be detected (Mutasim & Adams, 2001; Schmidt &

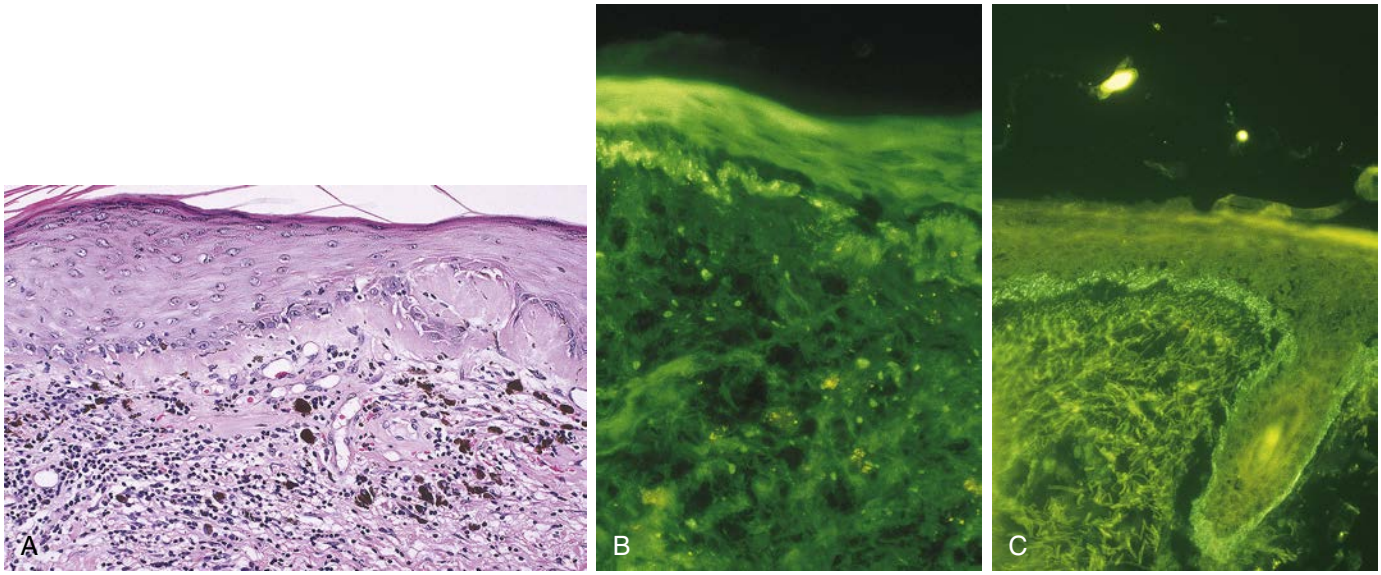

Fig. 55.8 **A,** Skin biopsy of lupus erythematosus reveals epidermal atrophy, vacuolar alternation of basal keratinocytes, marked thickening of the basement membrane zone (BMZ), perivascular and interstitial mainly lymphocytic inflammation, and melanin incontinence (H&E, ×500). **B,** Direct immunofluorescence microscopy reveals continuous granular C3 immunofluorescence along the BMZ (×500). **C,** Direct immunofluorescence microscopy reveals continuous granular C1q along the BMZ (×500).

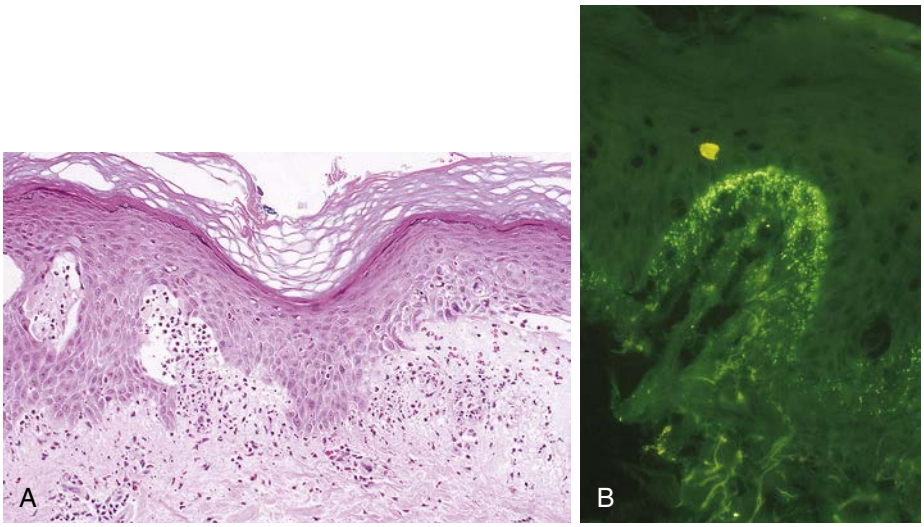

Fig. 55.9 **A,** Skin biopsy of dermatitis herpetiformis reveals a subepidermal split, nonnecrotic epidermis, and neutrophilic microabscesses in the tips of the dermal papillae (H&E, ×200). **B,** Direct immunofluorescence microscopy reveals granular immunoglobulin (Ig) A immunofluorescence in the tips of the dermal papillae and, to a lesser extent, along the basement membrane region (×400).

Zillikens, 2010). IIF can be used to detect antiendomysial autoantibodies when monkey esophagus is used (Arbache et al., 2014) (Fig. 55.10). Presently, ELISA is the preferred method for serologic investigations in DH (Cunha & Barraviera, 2009).

VASCULITIS

Cutaneous vasculitis describes a spectrum of diseases that involve the inflammation and destruction of small or midsize vessels in the skin. It can present as skin-limited disease, but it may also be associated with a larger systemic vasculitis and extracutaneous involvement. Clinically, cutaneous small vessel vasculitis (CSVV) classically presents as palpable purpura of the lower extremities. Clinical findings of nodular erythema, livedo patterns, and ulcers may implicate a midsize vessel vasculitic process such as polyarteritis nodosa (PAN). A mottled purplish discoloration of the skin can be described as "livedo reticularis." While many cases of CSVV are idiopathic, a thorough evaluation for an underlying cause or internal organ involvement should be completed.

Histologic and Immunologic Features

CSVV typically displays a characteristic histologic pattern described as leukocytoclastic vasculitis (LCV). Biopsy shows neutrophils and neutrophilic debris (leukocytoclasia) surrounding the small vessels in the superficial dermis, along with evidence of vessel damage seen as fibrin in vessel walls and extravasated red blood cells. Biopsies should include the subcutis to evaluate the patient for vasculitis involving the larger vessels in the skin.

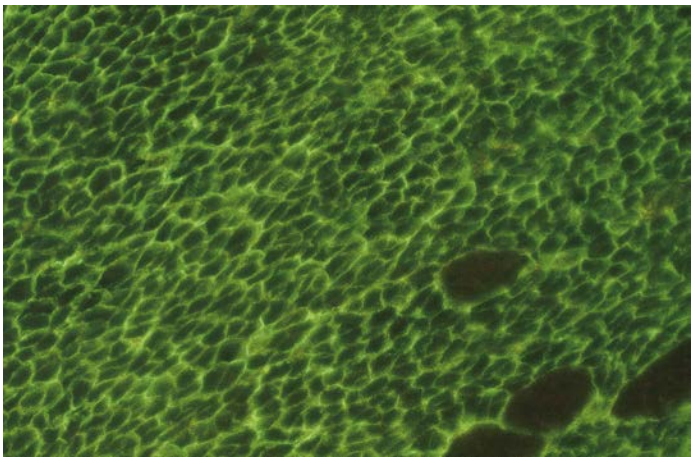

Fig. 55.10 Indirect immunofluorescence microscopy of immunoglobulin (Ig) A endomysial autoantibodies using monkey esophagus as substrate (×400).

Just as in the evaluation of blistering disorders, the timing and location of biopsy impact the diagnostic yield of DIF testing. A biopsy should be performed on a lesion that is less than 24 hours old (Mutasim & Adams, 2001). Deposits of C3, IgM, IgG, and fibrinogen are found within the walls of the postcapillary venules (Aoki et al., 2010). A vasculitis with IgA as

the primary immunoreactant suggests the diagnosis of Henoch-Schönlein purpura (HSP). HSP is a type of CSVV associated with renal and gastrointestinal involvement and is commonly described in children (Mutasim & Adams, 2001). A negative DIF does not exclude a diagnosis of CSVV and should be interpreted together with the clinical and histologic findings.

VITILIGO

Vitiligo is an acquired, chronic depigmenting disorder due to the selective loss of melanocytes in the skin (Ezzedine & Silverberg, 2016). It is the most common pigmentary disorder worldwide with reported prevalence of 0.1% to 4% (Rodriguez-Martin et al., 2012). The cause of melanocyte destruction in vitiligo is thought to be multifactorial and related to both genetic and environmental factors. An autoimmune theory is the leading hypothesis and is supported by its clinical association with other autoimmune disorders (Ezzedine et al., 2015). After innate immune system activation of increased proinflammatory signaling, the adaptive immune system is triggered by activating dendritic cells and melanocyte-specific cytotoxic T cells (Ezzedine et al., 2015; van den Boorn et al., 2009). Several melanocyte antigenic proteins have been identified in vitiligo, including tyrosinase, the rate limiting enzyme in melanin synthesis (Ezzedine et al., 2015). Other theories regarding vitiligo pathophysiology involve oxidative pathways and neural induction (Ezzedine & Silverberg, 2016). Continued research is needed on this subject.

Clinically, vitiligo can be divided into two major forms: segmental vitiligo and vitiligo/nonsegmental vitiligo, which is the most common type (Ezzedine & Silverberg, 2016). Patients present with circumscribed milky-white, or depigmented, macules and patches of the skin and mucous membranes. Vitiligo may be associated with thyroid disease, diabetes, alopecia areata, and PA. Alopecia areata can have an autoimmune basis (Islam et al., 2015). Because of the association with other autoimmune disease, the patient with vitiligo should be evaluated for other signs or symptoms, and additional tests should be performed if indicated (Rodriguez-Martin et al., 2012).

Histologic Features

The diagnosis of vitiligo can generally be made by clinical examination. If biopsy of lesional skin is performed, histologic examination should show an absence of melanocytes and epidermal pigment. Melanocyte presence or absence can be highlighted with the use of immunohistochemical stains. Perilesional skin from an actively spreading vitiligo patch is more likely to show an inflammatory infiltrate of CD4 and CD8 T lymphocytes near the dermoepidermal junction (Ezzedine & Silverberg, 2016).

GASTROINTESTINAL AND HEPATOBILIARY AUTOIMMUNE DISEASES

PERNICIOUS ANEMIA

The term *pernicious anemia* refers specifically to a state of vitamin B_{12} deficiency that results from lack of gastric intrinsic factor (IF), which in turn is a consequence of an autoimmune gastritis (Toh et al., 1998). The autoimmune gastritis affects the body of the stomach with antral sparing and is typically associated with autoantibodies to gastric parietal cells and to IF itself (see later discussion). The parietal cells are the cells that produce acid (HCl) and the vitamin B_{12}-binding protein termed *intrinsic factor*. The latter is a 55 to 60 kDa glycoprotein (15% carbohydrate by weight) (Nicolas & Gueant, 1995). The autoimmune gastritis leads to mucosal atrophy, achlorhydria, and very high serum gastrin concentrations, the latter being an attempted compensation for the inability to secrete gastric acid. The autoimmune gastritis is thought to precede the gastric atrophy by 10 to 20 years (Toh, 2017). PA is typically a disease of middle age or older. While the mean age is 59 to 62 years, it may present in younger individuals. In one study, 10% of patients were between 30 and 40 years of age (Lahner & Annibale, 2009). PA was once thought to be restricted to Northern Europeans but has now been described in many ethnic groups (Toh, 1998). The disorder is initiated by a T-lymphocyte–mediated inflammation of the gastric mucosa.

Gastric acid is also required for the release of vitamin B_{12} from food. Lack of acid leads to food-bound cobalamin malabsorption (Allen, 2009; Carmel, 2000). This condition can be distinguished from PA by absence of antibodies to IF and by normal absorption of free vitamin B_{12} (Allen, 2009). Gastric HCl production is also required for iron absorption and, indeed, iron deficiency anemia is commonly associated with autoimmune gastritis (Toh, 2017). Hershko et al. (2006) showed that among 160 patients with autoimmune gastritis identified by hypergastrinemia and positive antiparietal antibodies, over 50% presented with iron deficiency anemia, while 18% had macrocytic anemia. Compared with those having red cell macrocytosis, patients with iron deficiency anemia were younger and mostly women (Hershko et al., 2006).

To avoid confusion, use of the term "pernicious anemia" should be restricted to the autoimmune gastritis/B_{12} malabsorption syndrome outlined earlier and should not be used interchangeably with any other cause of B_{12} deficiency. Furthermore, not all cases of B_{12} deficiency result in hematologic manifestations; in some instances, neurologic features may predominate or may be the sole clinical manifestation.

Parietal cell autoantibodies (PCA) bind to the H^+/K^+- ATPase on gastric parietal cells (Toh et al., 1998; Bizzaro & Antico, 2014). PCA are more common than IF antibodies but are less specific. PCA are found in 80% to 90% of those with early pernicious anemia. This may fall to 55% in more advanced disease (Bizzaro & Antico, 2014). PCA have been found in about 30% of nonanemic first-degree relatives of those with PA. PCA may be detected in otherwise healthy adults (2.5% of individuals in the fourth decade and 10% of those in the eighth decade) (Toh et al., 1998).

Intrinsic factor binds to vitamin B_{12} and allows specific attachment to a terminal ileal B_{12} receptor called the "cubam" receptor complex (Nielsen et al., 2012). Antibodies to intrinsic factor (IFA) are more specific and are of two major types. These are type I, or blocking, antibodies that prevent the combination of IF and cobalamin and type II, or binding, antibodies that interfere with the attachment of the IF-B_{12} complex to ileal receptor. IFA are found in 40% to 60% of patients with PA. The predominant antibody is type I; about half the positive IFA cases have type II antibodies, and these are rarely present in the absence of type I antibodies (Toh et al., 1998; Bizzaro & Antico, 2014).

PCA can be measured either by IIF staining of rodent or human stomach (Fig. 55.11) or by an ELISA immunoassay. IFAs are typically measured by ELISA.

The anatomic pathology of pernicious anemia is referred to as "autoimmune corpus-restricted atrophic gastritis" (Neumann et al., 2013) or "type A gastritis." Early features include lymphocytic and plasma cell infiltration of the mucosa of the gastric body, which is followed by loss of gastric parietal cells, intestinal metaplasia with the appearance of goblet cells, pancreatic acinar metaplasia, and enterochromaffin-like (ECL) cell hyperplasia, the latter being positive for chromogranin (Neumann et al., 2013). These

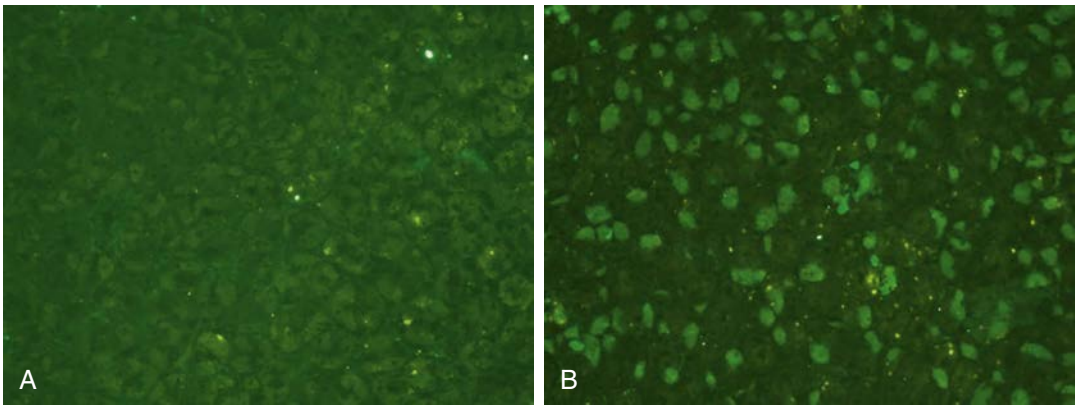

Fig. 55.11 Gastric parietal cell autoantibodies (PCA) can be detected by indirect immunofluorescence: **A,** Negative control. **B,** Positive serum from a patient.

changes are confined to the body of the stomach and are distinct from multifocal atrophic gastritis caused by longstanding *Helicobacter pylori* infection (Neumann et al., 2013). Up to 10% of patients with autoimmune gastritis are predisposed to gastric carcinoid tumors or adenocarcinomas. The relative risk of gastric adenocarcinoma is 6.8 (95% CI 2.6–18.1) (Neumann et al., 2013).

Pernicious anemia may be associated with other autoimmune disorders, including autoimmune thyroid disorders, type I diabetes, Addison disease, and vitiligo. The HLA genotypes HLA-DRB1*03 and DRB1*04 are significantly associated with autoimmune gastritis and PA. These genotypes are also associated with type 1 diabetes and autoimmune thyroid disease (Lahner & Annibale, 2009).

The true prevalence of PA is difficult to determine because disease definitions are not clearly standardized, and estimates vary widely. Studies have placed the prevalence at about 1% to 2% (Carmel, 1996, 2000) and have estimated that PA is responsible for about 30% of all causes of B_{12} deficiency (Dali-Youcef & Andres, 2009).

CELIAC DISEASE

Celiac disease is an immune-mediated small intestinal enteropathy caused by an abnormal immune response to epitopes of wheat gluten in patients who express the HLA-DQ2 or HLA-DQ8 (Di Sabatino et al., 2012). Initially recognized in white populations, celiac disease is increasingly being recognized worldwide. The prevalence in several populations is approximately 1%, with higher rates in countries such as Algeria (5.6%) and Sweden (up to 2.9%) (Leonard et al., 2017; Husby et al., 2019). The prevalence of celiac disease is increased in patients who have an affected first-degree relative and in patients with autoimmune liver disease, type 1 diabetes, autoimmune thyroiditis, or Down syndrome (Fasano & Catassi, 2012; Leonard et al., 2017). The classic symptoms of celiac disease include malabsorption dominated by chronic diarrhea, steatorrhea, and weight loss (Ludvigsson et al., 2014). Patients also present with a diverse range of nonclassic extraintestinal symptoms, including anemia, arthralgia, fatigue, neuropathy, ataxia, depression, short stature, osteoporosis, liver disease, and DH (an extremely pruritic, blistering eruption typically involving the buttocks and the extensor surfaces of the arms and legs that is strongly associated with celiac disease) (Ludvigsson et al., 2014).

Celiac disease is initiated by the ingestion of gliadin, which can be found in foods containing wheat, barley, or rye. Gliadins are rich in glutamine and proline residues that the human intestine cannot fully digest, and, as a result, some intact gliadin peptides cross the intestinal barrier (Guandalini & Assiri, 2014).

Tissue transglutaminases (tTG) are ubiquitous but tightly regulated enzymes that catalyze the posttranslational modification of proteins by the formation of isopeptide bonds (Di Sabatino et al., 2012; Rauharvirta et al., 2016). Through deamidation, tTG converts glutamine residues into negatively charged glutamate residues, which have a much higher affinity for HLA-DQ2 and HLA-DQ8 molecules (Ludvigsson et al., 2014; Tonutti & Bizzaro, 2014). HLA-DQ2 and HLA-DQ8 molecules are expressed on the surface of antigen-presenting cells in the lamina propria and preferentially present gliadin peptides that have undergone deamidation by tTG to lamina propria CD4 T cells (Di Sabatino et al., 2012). Recognition of HLA-bound and tTG-deamidated gliadin peptides by CD4 T cells induces their activation and production of cytokines (Di Sabatino et al., 2012). Some of the cytokines from T follicular helper (Tfh) cells drive the activation and clonal expansion of B cells, with consequent production of IgA antigliadin and anti-tTG autoantibodies. Other cytokines from Th1 cells promote inflammatory processes, leading to the development of the characteristic celiac histology (Di Sabatino et al., 2012).

Serologic tests are fundamental to screening for celiac disease. First-degree family members of patients with celiac disease have up to 25-fold higher frequency of developing celiac disease (Leonard et al., 2017). Most recent guidelines from the US Preventive Services Task Force state that current evidence on the effectiveness of screening asymptomatic populations is scarce and insufficient to recommend for or against screening, and conclude that it is reasonable for clinicians to have a low threshold for testing in high-risk populations (Choung & Murray, 2017). Initial testing involves measuring serum IgA antitissue transglutaminase autoantibodies (anti-tTG) because of their high sensitivity (94%), high specificity (97%), and excellent standardization (Fasano & Catassi, 2012). Baseline IgA should be concomitantly performed to ensure there is no IgA deficiency. In patients with IgA deficiency, the screening test of choice is IgG antideamidated gliadin peptide (DGP), as the sensitivity and specificity of this test approaches that of IgA anti-tTG (Leonard et al., 2017). A presumptive diagnosis of celiac disease can be made when serology is positive and the duodenal biopsy shows characteristic changes. The characteristic histologic findings include increased intraepithelial CD8 T lymphocytes (>25/100 enterocytes), villous blunting, and crypt hyperplasia (Fasano & Catassi, 2012). In cases with discordant results, IgA endomysial autoantibodies (anti-EMA) may be measured as a confirmatory test. This test is nearly 100% specific for active celiac disease but requires fluorescent microscopy and is subject to interobserver variability (Fasano & Catassi, 2012; Tonutti & Bizzaro, 2014). Measurement of IgG tTG and IgA DGP antibodies is not recommended for routine use because of poorer sensitivity and/or specificity (Leonard et al., 2017). Traditional antigliadin antibody tests are no longer recommended due to high rates of false positivity. The sensitivity of serologic testing is significantly reduced in patients on a gluten-free diet; therefore patients should maintain a normal, gluten-containing diet for 1 to 3 months prior to testing (Husby et al., 2019).

The definitive diagnosis of celiac disease requires resolution of symptoms with a gluten-free diet (NIH Consensus, 2004). If the diagnosis is uncertain (persistent symptoms with negative/discordant results or prior gluten-free diet), testing for HLA-DQ2 and HLA-DQ8 may be useful to help classify patients as being at high or low risk for celiac disease. Ninety percent of patients with celiac disease have HLA-DQ2, which is expressed in only a third of the general population. Another 5% of celiac disease patients have HLA-DQ8. The remaining 5% of celiac patients have at least one of the two gene alleles encoding HLA-DQ2 (Fasano & Catassi, 2012). Testing has a high negative predictive value, meaning the disease is very unlikely to develop in patients who are negative for both HLA-DQ2 and HLA-DQ8. Less than 1% of patients with celiac disease are negative for DQ2 and DQ8 (Fasano & Catassi, 2012). A lifelong gluten-free diet is the cornerstone therapy for celiac disease (Fasano & Catassi, 2012).

INFLAMMATORY BOWEL DISEASE

IBD is a heterogeneous disease with an incompletely understood etiopathogenesis. Several immunologic, genetic, and environmental factors have been identified that may contribute to this immunoallergic disorder (Laass et al., 2014). Currently studies are focused on the imbalance between tolerance to the intestinal microbiota and the mucosal immune responses in genetically predisposed individuals (Conrad et al., 2014). First-degree relatives of patients with IBD have a 10- to 15-fold increased risk for IBD (Laass et al., 2014).

Ulcerative colitis (UC) and Crohn disease (CD) are the most frequently diagnosed forms of IBD (Laass et al., 2014). UC is clinically characterized by bloody diarrhea and chronic abdominal pain. CD is characterized by abdominal pain, diarrhea, weight loss, and fever (Laass et al., 2014). Endoscopically, CD is characterized by discontinuous transmural ulcerations with frequent involvement of the ileocecal region (Laass et al., 2014). CD-related lesions can be found throughout the digestive tract, in contrast to UC, in which disease is typically limited to the colon. Histologically, UC is characterized by diffuse mononuclear inflammatory infiltrate of the lamina propria with a basal lymphoplasmacytosis, cryptitis, crypt abscesses, mucosal ulceration, architectural distortion, Paneth cell metaplasia, and pseudopolyp formation. CD is characterized by focal transmural inflammation with scattered lymphoid aggregates; noncaseating, poorly formed granulomas; cryptitis; crypt abscesses; and architectural distortion.

In some patients, a definitive diagnosis of UC or CD cannot be made, and therefore the patient is classified as having "indeterminate colitis." p-ANCA and anti–*Saccharomyces cerevisiae* mannan antibodies (ASCA) are the most extensively studied and used serologic markers associated with IBD (Beniwal & Harrell, 2010).

Atypical p-ANCA is directed against neutrophil granules that stain the rim of the neutrophil nuclei, as well as intranuclear foci (Beniwal & Harrell, 2010). p-ANCA is present in 40% to 80% of UC patients and 5% to 25% of CD patients (Beniwal & Harrell, 2010). ASCA is an antibody against the mannose residues on *S. cerevisiae* cell walls (Lewis, 2011). ASCA is present in 48% to 69% of CD patients and 15% of UC patients (Beniwal & Harrell, 2010). Several IBD-associated antiglycan antibodies have been identified. Glycans are found on the cell walls of bacteria, yeast, fungi, protozoa, and viruses and on the cell surfaces of immune cells and erythrocytes (Beniwal & Harrell, 2010). These are antilaminaribioside carbohydrate antibody (ALCA), antichitobioside carbohydrate antibody (ACCA), antimannobioside carbohydrate antibody (AMCA), and anti-L (anti-laminarin) and anti-C (anti-chitin) (Beniwal & Harrell, 2010).

Additional antibodies have been discovered, including antiflagellin CBir1 (CBir1), anti–*Pseudomonas fluorescens*–associated sequence I2 (anti-I2), and antibodies to the outer-membrane porin C of *Escherichia coli* (anti-OmpC) (Ferrante et al., 2007).

One of the major goals in treating IBD patients is early distinction between UC and CD and prevention of complications such as perforation, fistula formation, and strictures. Some data suggest that the presence of serologic biomarkers such as PR3-ANCA may be able to distinguish between UC and CD, identify patients at increased risk for complications, and predict response to treatment; however, studies in these areas have produced conflicting results (Lewis, 2011; Sura et al., 2014; Horn et al., 2018).

HEPATIC AND HEPATOBILIARY AUTOIMMUNITY

Hepatic Autoantibodies

Antibody testing is the basis of all diagnostic criteria for autoimmune hepatitis (AIH) (Sebode et al., 2017). In 2004, the International Autoimmune Hepatitis Group (IAIHG) Committee for Autoimmune Serology released a consensus statement containing guidelines for autoantibody testing in AIH. One of the recommendations is that initial screening should consist of IIF on fresh, multiorgan rodent sections (liver, kidney, and stomach) to detect smooth muscle autoantibodies (SMA), antinuclear autoantibodies (ANA), anti–LKM-1 autoantibodies (LKM = liver kidney microsomal) , anti–LC-1 autoantibodies (LC = liver cytosol), and antimitochondrial autoantibodies (AMA) (Liberal et al., 2014). IFL using human neoplastic cell lines (HEp2) and automated enzyme immunoassays may be the preferred means of testing in some laboratories (Sebode et al., 2017).

Antinuclear Autoantibodies

The target antigens of ANA are heterogeneous and not well defined. ANA have been shown to be reactive with single- and double-stranded DNA, centromeres, histones, chromatin, and cyclin A. Human epithelial type 2 (HEp2) cells have prominent nuclei, hence nuclear patterns are easier to analyze and additional diagnostic information pointing to variant syndromes may be obtained, therefore IFL is now performed on this cell line in many laboratories (Sebode et al., 2017). A homogeneous staining pattern is the most common pattern in type 1 AIH, and coarse or speckled patterns are less frequently observed. In adults, a clinically significant titer is 1:40 and in children it is 1:20. Titers greater than 1:80, in conjunction with other criteria, are considered diagnostic of autoimmune hepatitis by the International Autoimmune Hepatitis Group (Manns et al., 2010).

ANA have also been found in up to 52% of patients with primary biliary cholangitis (previously called primary biliary cirrhosis [PBC]), where they display a characteristic IFL pattern of multiple nuclear dot or rimlike membranous staining on HEp-2 or HeLa cells (Liberal et al., 2013). ANA are also present in other autoimmune and nonautoimmune conditions, such as viral hepatitis, drug-induced hepatitis, and alcoholic and nonalcoholic fatty liver disease (Liberal et al., 2014).

Anti–Smooth Muscle Autoantibodies

Anti–smooth muscle autoantibodies (SMA) are directed against actin and other constituents of the cytoskeleton, such as tubulin, vimentin, desmin, and skeletin. SMA are found in 50% of patients with AIH and often found with other ANA. Characteristic IFL patterns of SMA can be identified in kidney, stomach, and liver, where they target the artery walls. In the kidney, SMA typically stain the smooth muscle in vessels (V), glomeruli (G), and tubules (T). The TG pattern (tubules and glomeruli) is highly predictive of type-1 AIH (sensitivity 80%, specificity 90%) and the V pattern (vessels) is less specific. In type-1 AIH, SMA are predominantly directed against filamentous actin (F-actin) and the TG pattern is the immunomorphologic expression of this autoreaction (Granito et al., 2006). Anti-F-actin may be analyzed by IFL using fibroblasts and other methods such as ELISA are available, but a gold standard for anti-F-actin has not been established. Seropositivity for anti-F-actin has been associated with earlier onset, greater propensity for liver failure, and relapse after withdrawal of steroid treatment (Himoto & Nishioka, 2013). Note that type 1 AIH and type 2 AIH are differentiated by the autoantibodies that are present (discussed later). In adults with AIH, the SMA titer is usually greater than or equal to 1:80. Pediatric patients may have titers as low as 1:20. SMA are not specific for AIH and have been reported in other types of liver disease (Liberal et al., 2013). Up to 20% of patients with hepatitis C virus–related chronic liver disease are seropositive for SMA, but most lack reactivity against F-actin (Himoto & Nishioka, 2013).

Anti–Liver-Kidney Microsomal Type 1 Autoantibodies

The hallmark autoantibodies of type 2 AIH are anti–liver-kidney microsomal type 1 (anti–LKM-1) autoantibodies. By IFL, anti–LKM-1 stains the hepatocellular cytoplasm and the P3 portion of the proximal renal tubules (pars recta). The IFL patterns of AMA (discussed later) and anti–LKM-1 share some similarities because they will both stain liver and kidney. AMA will stain the liver more faintly and the renal tubules more diffusely, while accentuating the distal tubules. Also, AMA will stain gastric parietal cells, while anti-LKM will not.

Because the molecular targets of anti-LKM and AMA are known, immune-based assays have been developed. The molecular target of anti-LKM-1 is cytochrome P450-2D6 (CYP2D6), and the molecular targets of AMA are enzymes of the 2-oxo-acid dehydrogenase complexes. Anti-LKM-3 is directed against uridine diphosphate glucuronosyl transferases (UGT) and may be rarely identified in type 2 AIH (Philipp et al., 1994). Commercially available ELISAs detect AMA and anti–LKM-1 accurately and can be useful when the IFL pattern is inconclusive.

In adults with AIH, the minimal titer considered relevant is 1:40, and in pediatric patients it is 1:10. The titer is associated with disease activity. Seropositivity for anti-LKM has been associated with younger age at onset, higher levels of liver enzymes, and liver inflammation (Himoto & Nishioka, 2013). Of note, anti-LKM autoantibodies are detected in up to 10% of patients with chronic hepatitis C infection (Liberal et al., 2014).

Antimitochondrial Antibodies

Epitopes recognized by AMA are referred to as M2 antigens and include lipoylated domains of the E2 and E3 binding protein (E3BP) components of the pyruvate dehydrogenase complex (PDC-E2) and the E2 components of the 2-oxo glutarate dehydrogenase (OADC-E2) and branched-chain 2-oxo acid dehydrogenase (BCOADC-E2) complexes (Bowlus & Gershwin, 2014).

AMA can be detected using several methods. IIF was routinely used in the past but lacks specificity and sensitivity. Enzyme-linked immunoassays (EIAs) using recombinant proteins to the three known autoantigens are available. Commercially available EIA tests detect gp210 (nucleoporin 210 kDa, a component of the nuclear pore complex) and Sp100 (SP100 nuclear antigen, a subnuclear organelle and significant component of the promyelocytic leukemia-SP100 nuclear bodies). The titer of AMAs does not correlate with disease severity (Bowlus & Gershwin, 2014).

Anti–Liver Cytosol Type 1 Autoantibodies

Whereas isolated anti–liver cytosol type 1 (anti–LC-1) autoantibodies correlate with type 2 AIH, they are also seen in association with anti–LKM-1 autoantibodies, with other serologic markers of type 1 AIH, and in patients with chronic hepatitis C infection. Anti–LC-1 autoantibodies correlate with disease activity and can be used as a marker of hepatocellular inflammation.

The target of anti–LC-1 autoantibodies is the folate-metabolizing enzyme formimino transferase cyclodeaminase (FTCD), which is present at high concentration in the liver. The IFL pattern is cytoplasmic, with relative sparing of the centrilobular areas. The IFL pattern of anti–LC-1 autoantibodies is obscured when present along with anti–LKM-1 (Liberal et al., 2013).

Other Autoantibodies

Antisoluble Liver Antigen/Liver-Pancreas Autoantibodies. Originally thought to be distinct antibodies, antisoluble liver antigen/liver-pancreas autoantibodies (anti-SLA and anti-LP) are now known to share the same antigenic target, a transfer ribonucleoprotein involved in selenocysteine insertion named SEPSECS (Sep [O-phoshor-serine] tRNA:Sec [selenocysteine] tRNA synthase). Anti-SLA/LP autoantibodies cannot be detected by IFL but are detected by radioimmunoassay, immunoblot, or ELISA. Anti-SLA/LP antibodies have the highest specificity of all autoantibodies for AIH and should be routinely tested, although they are present in only up to 30% of patients. It is controversial if these antibodies characterize a clinically severe subset of AIH (Sebode et al., 2017).

Antineutrophil Cytoplasmic Autoantibodies. Antineutrophil cytoplasmic autoantibodies (ANCA) react to cytoplasmic components of neutrophils displayed as a perinuclear (pANCA) or cytoplasmic (cANCA) pattern. pANCA are frequently detected in type 1 AIH and can be diagnostically helpful when other autoantibodies are absent. The pattern of IFL is atypical in that staining is associated with peripheral nuclear membrane components, hence the name *peripheral antinuclear neutrophil antibody* (pANCA) (Liberal et al., 2014).

Anti–Asialoglycoprotein Receptor Autoantibodies. Anti–asialoglycoprotein receptor (anti-ASGPR) autoantibodies are type II transmembrane glycoproteins also known as hepatic lectins. ASGPR is constitutively expressed on the hepatocellular membrane and is the only liver-specific autoantigen. Anti-ASGPR autoantibodies are present in 88% of AIH patients and can be present in combination with ANA, SMA, and anti–LKM-1. This autoantibody is not specific to AIH as it has also been detected in patients

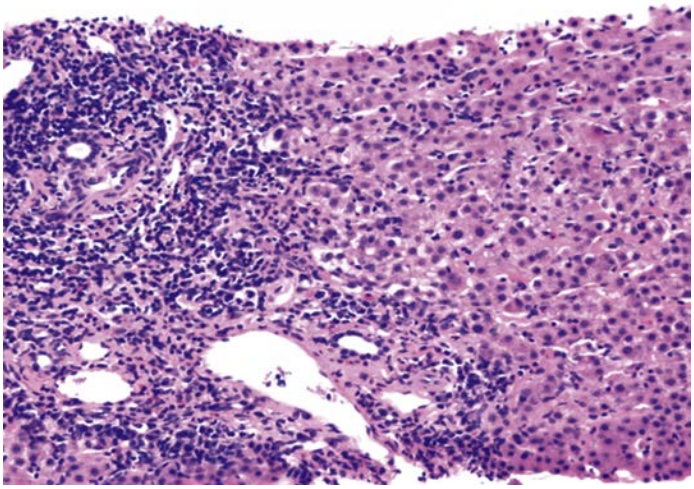

Fig. 55.12 The photomicrograph demonstrates a dense mononuclear infiltrate in the portal tract composed predominantly of lymphocytes, extending out to involve the hepatocytes bordering the portal tract (interface hepatitis) (H&E, ×200). (Image courtesy Dr. Xiuli Liu.)

with viral hepatitis, primary biliary cirrhosis (PBC), and drug-induced hepatitis, but it may have diagnostic value in patients seronegative for conventionally tested antibodies. Titers correlate with inflammatory activity. Detection of anti-ASGPR autoantibodies in clinical practice has limited use due to lack of disease specificity and the difficulty in developing a reliable assay (Liberal et al., 2014).

Autoimmune Hepatitis

AIH is a progressive immune-mediated liver disease characterized by elevated transaminases (e.g., ALT and AST) and immunoglobulins, the presence of characteristic autoantibodies, and histologic evidence of interface hepatitis (Fig. 55.12). An interface hepatitis is characterized by disruption of the parenchymal limiting plate by a dense portal and periportal lymphocyte and plasma cell infiltrate. Women are affected with AIH more frequently than men (sex ratio, 3.6:1), and the disease is seen in all ethnic groups and at all ages (Manns et al., 2010). The clinical presentation is variable but frequently includes progressive fatigue, relapsing jaundice, amenorrhea, weight loss, and occasionally arthralgia. Approximately 25% of patients are asymptomatic and are incidentally diagnosed when liver function tests are found to be abnormal. Rarely, the initial presentation is acute hepatic failure. Ultimately AIH can progress to cirrhosis and hepatocellular carcinoma.

Approximately 40% of AIH patients have a family history of autoimmune disease. Twenty percent have concomitant autoimmune diseases or will develop them during follow-up (Liberal et al, 2014). AIH responds to immunosuppressive treatment. Liver transplantation has also evolved as an effective treatment for the decompensated patient, and the 5-year patient and graft survivals now exceed 80% (Manns et al., 2010).

Diagnosis of AIH requires the presence of characteristic clinical and laboratory features and the exclusion of other conditions that cause chronic hepatitis and cirrhosis. The IAIHG has established inclusion and exclusion criteria for the diagnosis of autoimmune hepatitis (Table 55.2).

Laboratory assessment should include measurements of serum alanine (ALT) or aspartate (AST) aminotransferases, alkaline phosphatase (ALP), albumin, IgG, and bilirubin. Indirect IFL on fresh, multiorgan rodent sections (liver, kidney, and stomach) is pursued to detect SMA, ANA, anti–LKM-1, anti–LC-1, and AMA (Manns et al., 2010). While histology is essential for the diagnosis of AIH, it does not always show typical lesions. Characteristic histologic findings include interface hepatitis with a predominantly lymphoplasmacytic infiltrate, with or without lobular involvement, portal-portal or portal-central bridging necrosis, and frequent liver cell rosettes (Alvarez et al., 1999).

Two types of AIH are recognized according to the serologic profile. Type 1 autoimmune hepatitis is positive for ANA or anti-SMA. Type 2 autoimmune hepatitis is positive for anti–LKM-1 or anti–LC-1. All AIH-2 patients are positive for anti-LKM1 and/or anti-LC1 autoantibodies. Less than one-third are solely positive for anti-LC1 autoantibodies.

In 1993, the International Autoimmune Hepatitis Group proposed diagnostic criteria that were revised in 1999. These 13 criteria were devised primarily through expert consensus and were used to compare studies from different centers. The criteria are complex and include a variety of parameters that contribute questionable diagnostic value. The IAIHG devised a simpler scoring system that was more applicable to routine clinical practice and was based on the data of patients with a well-established diagnosis of AIH (Hennes et al., 2008).

TABLE 55.2

International Autoimmune Hepatitis Group Revised Diagnostic Scoring System

Parameter	Feature	Score
Sex	Female	+2
ALP: AST (or ALT) ratio	>3	–2
	1.5–3	0
	<1.5	+2
Serum globulins or IgG (times above normal)	>2.0	+3
	1.5–2.0	+2
	1.0–1.5	+1
	<1.0	0
ANA, SMA, or anti–LKM-1 titers	>1:80	+3
	1:80	+2
	1:40	+1
	<1:40	0
AMA	Positive	–4
Viral markers of active infection	Positive	–3
	Negative	+3
Hepatotoxic drug history	Yes	–4
	No	+2
Average alcohol intake	<25 g/day	+2
	>60 g/day	–2
Histologic features	Interface hepatitis	+3
	Plasma cells	+1
	Rosettes	+1
	None of the above	–5
	Biliary changes[a]	–3
	Atypical changes[b]	–3
Immune diseases	Thyroiditis, colitis, other	+2
HLA	DR3 or DR4	+1
Seropositivity for other autoantibodies	Anti-SLA/LP, actin, ASGPR, pANNA	+2
Response to therapy	Remission	+2
	Relapse	+3

Adapted from Alvarez F, Berg PA, Bianchi FB, et al: International Autoimmune Hepatitis Group report: review of criteria for diagnosis of autoimmune hepatitis, *J Hepatol* 31(5):929–938, 1999.
Pretreatment score greater than 15: definite AIH; 10 to 15: probable AIH. Posttreatment score greater than 17: definite AIH; 12 to 17: probable AIH. *ALP,* Alkaline phosphatase; *ALT,* alanine aminotransferase; *AMA,* antimitochondrial autoantibodies; *ANA,* antinuclear autoantibodies; *anti–LKM-1,* anti–liver-kidney microsomal type 1 autoantibodies; *ASGPR,* asialoglycoprotein receptor; *AST,* aspartate aminotransferase; *HLA,* human leukocyte antigen; *IgG,* immunoglobulin G; *p-ANNA,* peripheral antinuclear neutrophil antibody; *SLA/LP,* soluble liver antigen/liver pancreas; *SMA,* anti–smooth muscle autoantibodies.
[a]Including granulomatous cholangitis, concentric periductal fibrosis, ductopenia, marginal bile duct proliferation, and cholangiolitis.
[b]Any other prominent feature suggesting a different etiology.

The updated simplified scoring system was proposed for use in clinical practice and is based on just four criteria: autoantibody positivity, elevated IgG levels, histologic findings compatible with AIH, and exclusion of viral hepatitis (Table 55.3) (Hennes et al., 2008). In retrospective studies, the simplified scoring system performed with moderate sensitivity and high specificity in the diagnosis of AIH, in both adults and children, but it has not been validated in prospective studies (Manns et al., 2010, Wobser et al., 2018, Arcos-Machancoses et al., 2018).

Prognostic Relevance of Autoantibodies in Autoimmune Hepatitis

ANA and SMA titers tend to decline or disappear during effective immunosuppressive therapy. Neither the titer at diagnosis nor fluctuations over the course of the disease correlate with disease outcome. Anti-SLA autoantibodies may denote patients with a more severe course of disease and propensity for relapse after steroid withdrawal. Anti–LKM1-autoantibody-positive pediatric patients tend to present at a younger age than ANA/SMA-autoantibody-positive patients. They also have higher bilirubin

TABLE 55.3
Simplified Criteria for the Diagnosis of Autoimmune Hepatitis

Variable	Cutoff	Points
ANA or SMA	≥1:40	1
ANA or SMA	≥1:80	2[a]
Or anti–LKM-1	≥1:40	
Or SLA	Positive	
IgG	>Upper limit of normal	1
	>1.10 times upper limit of normal	2
Liver histology	Compatible with AIH	1
	Typical of AIH	2
Absence of viral hepatitis	Yes	2

Adapted from Hennes EM, Zeniya M, Czaja AJ, et al: Simplified criteria for the diagnosis of autoimmune hepatitis, *Hepatology* 48(1):169–176, 2008.
Score of 6 or higher: probable AIH; 7 or higher: definite AIH. *AIH,* Autoimmune hepatitis; *ANA,* antinuclear autoantibody; *anti-LKM,* anti–liver-kidney microsomal autoantibody type 1; *IgG,* immunoglobulin G; *SLA,* soluble liver antigen; *SMA,* anti–smooth muscle autoantibody.
[a]Addition of points achieved for all autoantibodies cannot exceed a maximum of 2 points.

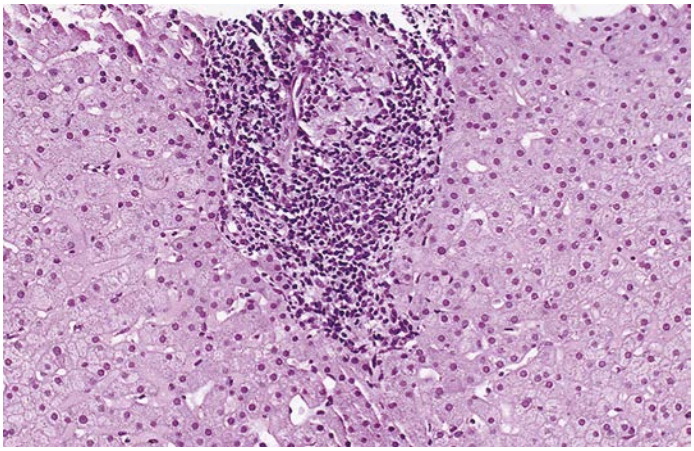

Fig. 55.13 Liver biopsy in primary biliary cirrhosis shows variable portal inflammation with nonsuppurative lymphocytic cholangitis and, in this example, a florid duct lesion with granulomatous inflammation centered on an interlobular bile duct (hematoxylin and eosin [H&E], ×200).

and transaminase levels at diagnosis and more often present in fulminant hepatic failure. AIH-2 patients with anti-LC1 autoantibodies have more severe disease histologically (Liberal et al., 2013).

Primary Biliary Cholangitis (Previously Known as Primary Biliary Cirrhosis; see also Chapter 22)

Primary biliary cholangitis (PBC) is an autoimmune liver disease characterized by immune-mediated destruction of small intrahepatic bile ducts, leading to chronic cholestasis and fibrosis that can eventually result in cirrhosis and liver failure (Fig. 55.13). The name was changed to more accurately reflect the natural history of the disorder (Beuers et al., 2015). This disease typically affects females in their fifth and sixth decades (Bowlus & Gershwin, 2014).

The diagnosis can be established if two of three objective criteria are present: (1) serum AMA at titers greater than or equal to 1:40, (2) unexplained elevated ALP greater than or equal to 1.5 times the upper limit of the reference interval for over 24 weeks, and (3) compatible liver histology. In addition, PBC patients often have elevated transaminases and elevated immunoglobulins, predominantly IgM, which has not been found to bind to the pyruvate dehydrogenase E2 antigen (Bowlus & Gershwin, 2014). Elevated serum lipids may be present in up to 50% of patients, strikingly so in some (Sorokin et al., 2007). If AMA is negative, the diagnosis of PBC is based on characteristic histologic findings and abnormal serum ALP levels. Liver biopsy is not required for the diagnosis of AMA-positive PBC but can be useful for disease staging. In AMA-negative PBC, liver biopsy is required to rule out other conditions, including small-duct primary sclerosing cholangitis (PSC), sarcoidosis, and drug-induced cholestasis.

As discussed in Chapter 22, in a human genome–wide study (GWAS), PBC has a strong association with two single nucleotide polymorphisms (SNPs) in the HLA-2 region, particularly in the gene-encoding interleukin (IL)-12, and a less but significant association with SNPs at the signal transducer and activator of transcription 4 (STAT4) locus and the CTLA4 locus, encoding cytotoxic T lymphocyte–associated protein 4. Histologic findings include nonsuppurative cholangitis and interlobular bile duct injury. The characteristic histologic finding is the "florid duct lesion." This lesion occurs when an interlobular bile duct is destroyed by poorly formed epithelioid granulomas, lymphocytes, and plasma cells. These lesions obstruct bile flow and cause upstream portal tracts to have bile ductular reaction, inflammation, and necrosis, which eventually lead to fibrosis. Ductular reaction describes a rise in ductile number together with increased matrix and neutrophils.

AMA are the serologic hallmark of PBC (present in 95%). AMA-positive and AMA-negative PBC have similar clinical courses, although some data suggest PBC-specific ANA positivity is associated with more severe disease or autoimmune hepatitis overlap (Bowlus & Gershwin, 2014). ANA may be found in up to 70% of patients with PBC. Two IFL patterns are considered specific for PBC: (1) the multiple dots pattern (3-20 variably sized nuclear dots sparing the nucleolus; main target antigen: Sp100) and (2) rimlike/membranous pattern (main target antigen: gp210) (Himoto & Nishioka, 2013). For several decades, the only established treatment for PBC was ursodeoxycholic acid (UDCA). UDCA is well tolerated and has been shown to prevent portal hypertension and esophageal varices, and it delays the time to transplant. In 2016, the US Food and Drug Administration (FDA) approved obeticholic acid (OCA), a farsenoid X receptor (FXR) agonist, as second-line therapy for patients who are intolerant of UDCA or who have a suboptimal response. Bile acids activate FXR to inhibit bile acid synthesis, and OCA is 100 times more potent in this regard (Manne & Kowdley, 2019).

Primary Sclerosing Cholangitis

PSC is a progressive cholestatic liver disease characterized by chronic bile duct destruction and progression to end-stage liver disease (Fig. 55.14). Chronic, progressive injury occurs in small, medium, and large bile ducts with inflammatory and obliterative concentric periductal fibrosis, so-called onion-skinning, leading to biliary strictures. PSC affects both sexes and all age groups, although more than 60% of patients are men. The median age at onset is 30 to 40 years. It has been found that 60% to 80% of northern European cases are associated with IBD, predominantly UC. More than 50% of patients will require liver transplant within 10 to 15 years of diagnosis (Hirschfield et al., 2013). The clinical presentation is variable, with the most common symptoms being fatigue, jaundice, pruritus, and abdominal pain.

A cholestatic profile, with elevated serum ALP between 3 and 10 times the upper limit of the reference interval, is seen in 95% of cases, along with elevated gamma-glutamyl transferase (Yimam & Bowlus, 2014). Serum ALT and AST levels are also typically elevated two to three times higher than the upper limit of the reference interval. Approximately 60% of patients will also have elevated serum IgG levels (Yimam & Bowlus, 2014). In recent years, elevated IgG4 has been found in about 10% of patients. In contrast to IgG4-associated cholangitis, these patients do not respond to corticosteroids and have a more rapidly progressive disease if untreated. Hence all PBC patients should be tested at least once for elevated serum IgG4 (Lindor et al., 2015).

Several autoantibodies are associated with PSC, although none are sufficiently specific or sensitive to be used as a screening test. Perinuclear antineutrophil cytoplasmic autoantibodies (p-ANCA) are seen in 65% to 95% of patients with PSC. Cholangiography is the gold standard for diagnosis of PSC, with the findings of segmental strictures with proximal dilation of the bile ducts creating a "beaded" appearance (Yimam & Bowlus, 2014). Liver biopsy is not necessary when patients have radiographic evidence of PSC, although it can be helpful when small duct PBC is suspected or in excluding other diseases. The histologic findings of PSC are nonspecific and can be normal when only large ducts are involved. The characteristic histologic findings include bile duct proliferation, periductal fibrosis with "onion-skinning" lesions, periductal inflammation, and bile duct obliteration.

Given the heterogeneous nature of PSC, strict diagnostic criteria have not been established. The diagnosis is based on a cholestatic pattern of liver biochemistries (ALP increased proportionately greater than ALT and AST), typical cholangiographic findings, and the absence of a secondary cause of sclerosing cholangitis (Yimam & Bowlus, 2014). Endoscopic therapy of dominant strictures is the mainstay of treatment; there is no established medical treatment for PSC at this time. Liver transplantation is recommended in patients with decompensated cirrhosis, to prolong survival (Lindor et al., 2015).

Overlap Syndrome

Overlap syndrome refers to the simultaneous presence in a single patient of two distinct disease processes. There are two major variants of overlap

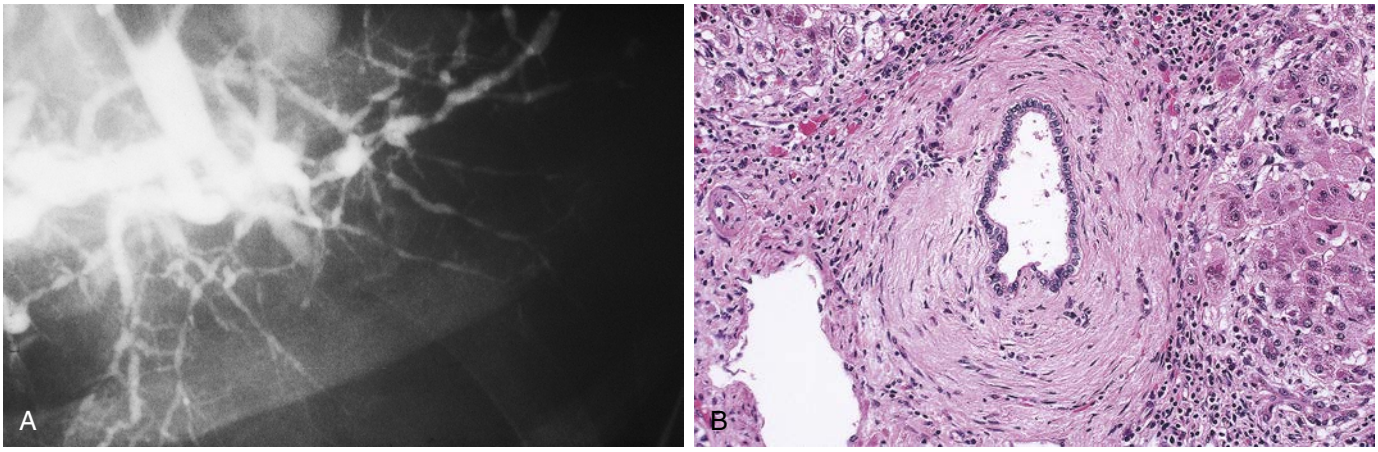

Fig. 55.14 **A** Cholangiogram in primary sclerosing cholangitis reveals the characteristic beading pattern of bile ducts due to multifocal strictures at those sites. **B,** Liver biopsy reveals prominent periductal fibrosis in the characteristic "onion-skin" pattern (H&E, ×500).

syndrome in which the features of AIH are mixed with those of PBC (AIH with features of PBC) or PSC (AIH with features of PSC). In both syndromes, the predominant features are manifestations of autoimmune hepatitis and secondary features of PBC or PSC. Clinical features that should prompt consideration of an overlap syndrome are AMA positivity, ALP levels greater than two times the upper limit of the reference interval, concurrent IBD, and histologic findings of bile duct injury or loss. Uniform diagnostic criteria have not been established for the overlap syndrome. The IAIHG has suggested classifying these patients by their predominant diagnosis and not by the overlapping features (Czaja, 2013a, 2013b).

Autoimmune hepatitis with features of PBC is the only overlap syndrome having proposed diagnostic criteria, known as the Paris criteria. These criteria were created in 1998 and required the presence of at least two of three recognized hallmarks of each disease (Czaja, 2013a, 2013b). Three hallmarks of autoimmune hepatitis are (1) serum ALT greater than five times the upper limit of the reference interval, (2) IgG level greater than twice the upper limit of the reference interval or positive SMA, and (3) histologic features of interface hepatitis. Three hallmarks of PBC are (1) serum ALP levels greater than twice the upper limit of the reference interval or gamma-glutamyl transferase (GGT) levels greater than five times the upper limit of the reference interval, (2) positive AMA, and (3) histologic evidence of florid duct lesions. Recently, a new scoring system for AIH/PBC overlap, with higher sensitivity but lower specificity, has been proposed (Zhang et al., 2018). Ultimately, the diagnosis requires clinical judgment.

Autoimmune hepatitis with features of PSC requires a predominant diagnosis of autoimmune hepatitis, absence of AMA, and cholestatic features, including jaundice, elevated ALP, or histologic findings of bile duct injury or loss. This variant of overlap syndrome typically occurs in the pediatric population and often coexists with IBD (Durazzo et al., 2013). The clinical findings are similar to PSC, with fatigue, jaundice, itching, abdominal pain, and recurrent biliary infections.

AUTOIMMUNE PANCREATITIS

Autoimmune pancreatitis (AIP) is characterized clinically by obstructive jaundice, with or without pancreatic enlargement, and a dramatic response to steroids (Shimosegawa et al., 2011). A rare form of chronic pancreatitis, AIP is now classified into two types. AIP type 1 is seen in older males as part of multiorgan IgG4-related disease with histologic features of lymphoplasmacytic sclerosing pancreatitis (LPSP). The four distinct features of LPSP are dense lymphoplasmacytic infiltrate especially around ducts, storiform fibrosis, obliterative phlebitis, and abundant IgG4-positive plasma cells. Type 2 disease is seen in younger individuals (no gender predilection), not systemic, not IgG4 related, and characterized by another histologic pattern called idiopathic duct-centric pancreatitis (IDCP). A unique feature of IDCP is the granulocyte epithelial lesion (GEL): intraepithelial neutrophils leading to destruction of small and midsize ducts (Shimosegawa et al., 2011). AIP type 2 is more frequently associated with IBD than AIP type 1.

Elevated IgG4 is characteristic but not diagnostic of AIP type 1. AIP patients may display ANA, rheumatoid factor, antilactoferrin, anticarbonic anhydrase II or IV, or hypergammaglobulinemia. However, none of these findings are specific for AIP (O'Reilly et al., 2014).

Diagnostic criteria for AIP vary worldwide. The International Consensus Diagnostic Criteria proposed by the International Association of Pancreatology features a combination of five parameters for the diagnosis of AIP type 1: typical findings on pancreatic parenchymal imaging, serology (serum IgG4 greater than two times above laboratory's upper limit of normal), LPSP histology, other organ involvement, and response to steroid therapy (radiologically demonstrable resolution in about 2 weeks). AIP type 1 can be diagnosed without histology, but AIP type 2 requires histology for definitive diagnosis (Shimosegawa et al., 2011).

The clinical presentation of AIP (obstructive jaundice, pancreatic enlargement) may mimic pancreatic cancer. A pattern of initially elevated serum IgG4 levels with subsequent decline has also been reported. In AIP, CA19-9 levels when elevated drop with treatment, and rising CA19-9 levels should raise suspicion of pancreatic cancer (O'Reilly et al., 2014). A variety of autoantibodies have been described in AIP. Plasminogen-binding protein antibodies have been identified in over 90% of AIP patients in two European series (Smyk et al., 2012); however, another European study did not find a statistically significant difference in serum levels between patients with AIP and pancreatic cancer, in contrast to the former studies (Detlefsen et al., 2018). Autoantibodies to pancreatic secretory trypsin inhibitor have been found in 30% to 40% of AIP patients, respectively, by ELISA and Western blotting (Asada et al., 2006) and antitrypsinogens in 79% by ELISA. Autoantibodies to heat-shock protein 10 (HSP 10) and amylase alpha-2A have also been identified in AIP in 92% and 100% of patients (Endo et al., 2009; Takizawa et al., 2009). A recent study applying an immunoproteomic approach identified 68 distinct autoantigens in AIP, 26 in pancreatic cancer and 21 common to both. The majority were exocrine pancreas autoantigens. Antitransaldolase and antipancreatic lipase may be candidates to distinguish AIP type 1 from type 2 (Felix et al., 2016). However, at the present time, these tests must be considered as research-only tests.

GLOMERULAR AUTOIMMUNE DISEASES

OVERVIEW

Clinical syndromes associated with glomerular disorders include asymptomatic proteinuria, nephrotic syndrome, asymptomatic hematuria, nephritic syndrome, rapidly progressive nephritic syndrome, and chronic renal failure. Nephrosis (i.e., the nephrotic syndrome) is the clinical syndrome characterized by proteinuria (>3.5 g/day), hypoalbuminemia, hyperlipidemia, and edema that sometimes progresses to anasarca (total body edema). Nephritis (i.e., the nephritic syndrome) is characterized by mild proteinuria, hematuria, red cell casts in the urine, mild edema, and hypertension. Overall these findings are the consequence of glomerular injury with damage to the glomerular capillary wall and often the mesangium. Glomerular diseases may be primary, involving the kidney only, or may be secondary, associated with a systemic disorder.

General Mechanisms of Glomerular Injury

Glomerular injury involves the complex interplay of individual genetic factors and environmental associations. Both immune and nonimmune mechanisms of glomerular injury occur. The immune response mechanisms include the innate and adaptive systems. Innate immunity is considered constitutive and ready to react. Components of innate immunity include neutrophils, monocytes, dendritic cells, NK cells, and the complement system. The alternative and lectin pathways of complement activation play a role in innate immune responses. Adaptive immunity is acquired, specific,

TABLE 55.4
Pathologic Features of Immune Glomerular Diseases

Disease	Pathogenesis	LM	IF	EM
Membranous nephropathy	In situ immune complex deposition (PLA_2R is antigen)	Capillary wall thickening	Capillary wall granular IgG and C3	Subepithelial deposits
IgA nephropathy	Abnormal IgA glycosylation	Mesangial hypercellularity	Mesangial dominant IgA (and some C3)	Mesangial deposits
Membranoproliferative glomerulonephritis (MPGN)	Immune complex deposition	Endocapillary hypercellularity, mesangial sclerosis, "double contouring"	Capillary wall IgG (less IgM) and C3	Subendothelial deposits
C3 glomerulonephritis (C3GN)	Dysregulation of alternative pathway of complement	Variable features but often similar to MPGN	Capillary wall dominant C3 (less or no Igs)	Variable but subendothelial deposits
Dense deposit disease (DDD)	Dysregulation of alternative pathway of complement	Variable but often similar to MPGN or mesangial cell hypercellularity	Capillary wall dominant C3 (less or no Igs)	Dense deposits in GBM
Postinfectious glomerulonephritis	Immune complex deposition, planted or circulating antigen	Endocapillary hypercellularity	Capillary wall IgG and C3	Subepithelial "hump"-deposits
Anti-GBM disease	Circulating anti-GBM antibodies (antigen is α3 chain of COL4)	Capillary wall necrosis and crescents	Capillary wall linear IgG and C3	No deposits, GBM ruptures
Pauci-immune glomerulonephritis	ANCAs (antineutrophil cytoplasmic antibodies)	Capillary wall necrosis and crescents	No or sparse Ig/C3 staining	No or sparse deposits
Lupus nephritis (class I–VI)	Immune complex deposition	Variable, class-dependent	"Full-house" staining for all Igs, C3, and C1q	Numerous deposits typically (location is class-dependent)

COL4, Type IV collagen; *EM,* electron microscopy; *IF,* immunofluorescence; *Igs,* immunoglobulins; *LM,* light microscopy.

and characterized by immunologic memory. Adaptive immunity includes humoral responses mediated by B lymphocytes and their antibodies and cellular responses mediated by T lymphocytes. The classical pathway of complement is activated by antibodies.

Potential specific immune mechanisms include (1) circulating antigen-antibody immune complex deposition and complement activation with subsequent inflammation (as seen in cryoglobulinemia); (2) deposition of exogeneous antigens (i.e., "planted" antigens) in the glomeruli to which is bound an antibody or autoantibody again eliciting inflammation (as seen in postinfectious glomerulonephritis); and (3) autoantibodies to intrinsic in situ antigens in the glomeruli again triggering inflammation (as seen in membranous nephropathy [MN]), which in some cases may not be associated with a cellular inflammatory reaction because the immune deposits are separated from the circulation (as seen in MN, where the deposits are on the subepithelial side of the glomerular basement membrane [GBM]).

Approach to the Renal Biopsy

Different glomerular diseases can cause the same clinical syndrome. The light, immunofluorescent, and electron microscopic findings on a renal biopsy establish the specific glomerular disease diagnosis.

The renal biopsy specimen must be carefully handled, divided under a dissecting microscope, and submitted in the appropriate solution (fixative/preservative). Onsite evaluation and specimen division yield higher adequacy rates for the subsequent different microscopy methods (Ferrer et al., 2019; Wooldridge et al., 2019; Sekulic & Crary, 2017). An initial approach is to determine the glomerular cellularity by light microscopy (LM). Proteinuric syndromes are often associated with relatively normocellular glomeruli. These glomerulopathies include minimal change disease, focal segmental glomerulosclerosis (FSGS), and MN. Nephritic syndromes are usually associated with hypercellular glomeruli. These glomerulonephritides include IgA nephropathy, membranoproliferative glomerulonephritis (MPGN), C3 glomerulopathy, postinfectious glomerulonephritis, anti-GBM glomerulonephritis, pauci-immune glomerulonephritis, and lupus nephritis (LN) (at least classes II–IV). In addition to hematoxylin and eosin (H&E)–stained sections, light microscopic evaluation is facilitated by the routine use of PAS, silver, and trichrome stains, which highlight the discrete cellular and extracellular compartments of the renal parenchyma. Immunofluorescence (IF), electron microscopy (EM), and serology are essential to establish the specific diagnosis. Renal pathology is the only area of anatomic pathology where LM, IF, and EM are routinely used to evaluate biopsy specimens.

The type, amount, and location of immune deposits (immunoglobulin/complement components) within glomeruli are determined by IF on frozen sections. When the frozen tissue lacks glomeruli or is not available, IF can be performed on paraffin sections after antigen retrieval (pronase or proteinase K digestion). This method may also detect immune deposits that are masked on frozen sections in some kidney diseases (Nasr et al., 2006, 2018; Messias et al., 2015). The ultrastructural character and exact glomerular location (e.g., subendothelial or subepithelial) of deposits and specific type of cell injury are determined by EM. Studies have shown that EM is essential for a correct diagnosis in 11% to 21% of cases and contributes important data in 20% to 36% of cases (Siegel et al., 1973; Haas, 1997; Kurien et al., 2016). Observations from each form of microscopy, whether LM, IF, or EM, informs the interpretation of the other forms. In brief summary, the findings from LM, IF, and EM are integrated with serologic and other laboratory data and clinical observations to render a glomerular disease diagnosis.

A semiquantitative evaluation of the glomeruli, vasculature, tubules, and interstitium establishes indices of disease activity and chronicity. For example, activity indices include glomerular cellularity and the percentage of glomerular crescents, whereas chronicity indices include the percentages of global glomerulosclerosis and interstitial fibrosis. These are often equally important as the specific disease diagnosis in guiding therapy and predicting prognosis (Sethi et al., 2017). In addition to the pattern and severity of renal injury, there is an increasing emphasis on the renal biopsy providing an etiologic-based diagnosis (Sethi et al., 2016; Sethi & Fervenza, 2019).

The temporal and demographic trends in glomerular disease has been reported in a massive 30-year (1986–2015) single center study of over 21,000 patients (O'Shaughnessy et al., 2017). Among nephrotic subtypes, FSGS was most common, followed in frequency by diabetic glomerulosclerosis, MN, minimal change disease, and MPGN. Notably there was a steady nearly fourfold increase in frequency of diabetic glomerulosclerosis over 30 years. Among nephritis subtypes, LN was most common followed in frequency by IgA nephropathy and ANCA/pauci-immune glomerulonephritis. The following discussion is primarily focused on autoimmune glomerular diseases (Table 55.4).

GLOMERULOPATHIES

Membranous Nephropathy

MN is a common cause of the nephrotic syndrome in adults, especially in the fourth to sixth decades of life. Males are affected more than females. It is a kidney-specific autoimmune disease (Francis et al., 2015; Couser, 2017; Cattran & Brenchley, 2017). MN is also called membranous glomerulonephritis or membranous glomerulopathy. The majority of patients present with the insidious onset of the full nephrotic syndrome. Most cases of MN were previously termed *idiopathic*, but since the discovery of specific autoantigens, these cases are currently termed *primary MN*. *Secondary* forms of MN occur with systemic autoimmune diseases, infections, drugs, and malignancy.

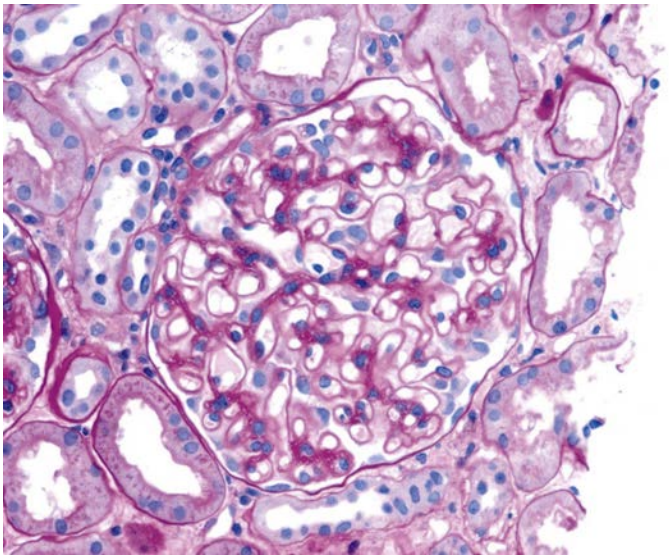

Fig. 55.15 Membranous nephropathy. Early stage showing normocellular glomerulus (PAS, ×400).

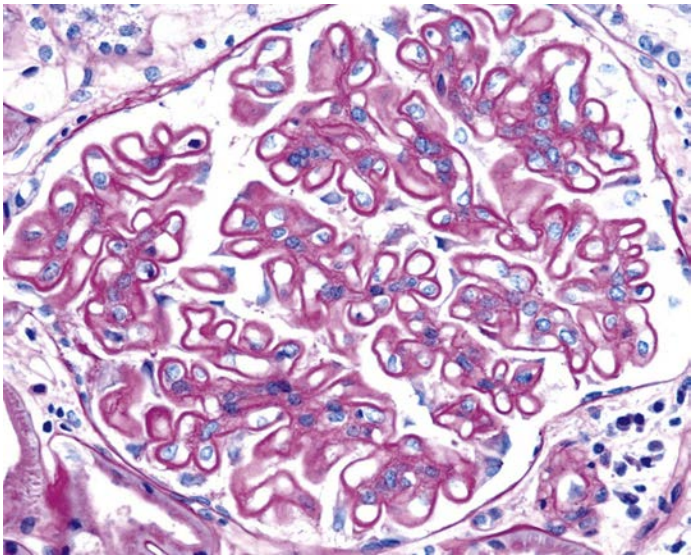

Fig. 55.17 Membranous nephropathy. Thickened and accentuated spherical glomerular capillary loops (PAS, ×400).

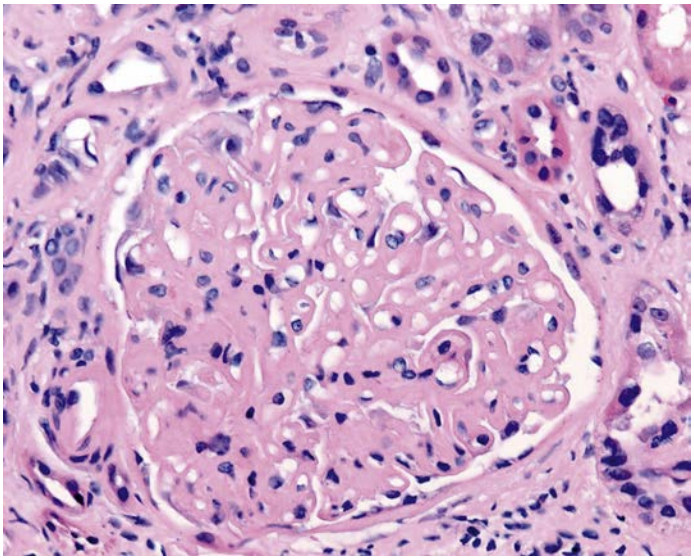

Fig. 55.16 Membranous nephropathy. Later stage with thickened glomerular capillary walls (H&E, ×400).

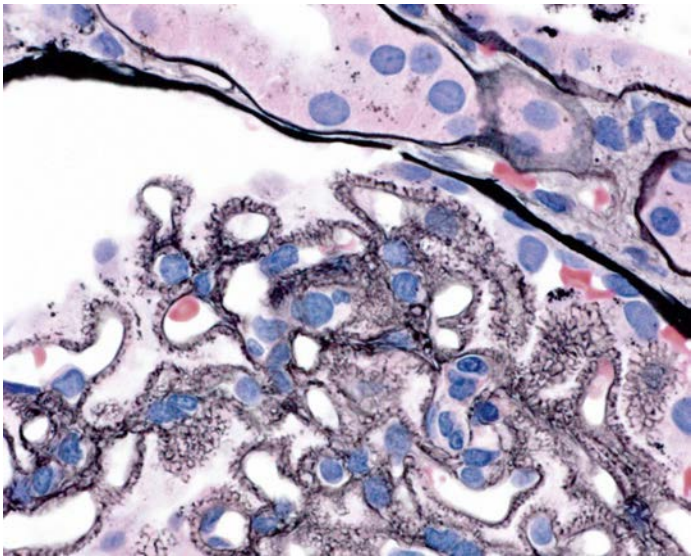

Fig. 55.18 Membranous nephropathy. Glomerular basement membrane (GBM) spikes and vacuolizations. Silver-negative material between spikes and within vacuoles represent immune deposits (Jones stain, ×1000).

MN is characterized by normocellular glomeruli with capillary wall thickening on LM, prominent granular ("lumpy-bumpy") capillary wall staining for IgG and C3 on IF, and subepithelial deposits on EM. Cases of early MN may show no overt changes on LM (Fig. 55.15) and quite subtle staining or segmental glomerular staining on IF. EM readily establishes the diagnosis in such early cases by revealing small subepithelial deposits. The thickened glomerular capillaries often have an accentuated spherical appearance ("cheerios") (Figs. 55.16 and 55.17), and silver stains usually reveal fine "pin-hole" vacuoles and/or spikes of the GBMs (Fig. 55.18). The IF staining is usually diffuse (every glomerulus) and global (entire glomerular tuft) (Fig. 55.19). The granular staining for IgG is usually more intense than for C3. EM demonstrates that over time the subepithelial electron dense deposits are accompanied by remodeling of the GBM (Figs. 55.20 and 55.21). These EM findings occur in stages (Ehrenreich-Churg stages) as follows: stage I: small subepithelial deposits without GBM spikes; stage II: subepithelial deposits with adjacent spikes; stage III: GBM surrounding deposits (intramembranous); and stage IV: distorted, thickened GBMs and electron-lucent areas representing deposit resorption. In addition to the typical morphologic findings, the presence of glomerular hypercellularity, a wider IF spectrum of immunoglobulin and complement staining, and mesangial and/or subendothelial deposits on EM favors a secondary MN. Primary MN may be superimposed on another common glomerular disease such as diabetic glomerulosclerosis.

After many years of investigation, the target autoantigen was identified in podocytes as type-M phospholipase A_2 receptor (PLA_2R) (Beck et al., 2009). Approximately 70% to 80% of patients with idiopathic (primary) MN have circulating anti-PLA_2R autoantibodies measured by ELISA assays (Kanigicherla et al., 2013). Patients with secondary forms of MN (e.g., membranous LN) generally lack these autoantibodies. The autoantibodies appear to be an excellent biomarker of the disease as the levels of anti-PLA_2R antibody correlate with the degree of proteinuria and disease activity (Bech et al., 2014; Hoxha, Harendza et al., 2014; Hoxha, Thiele et al., 2014). Moreover, the antibodies disappear (immunologic remission) before the proteinuria (renal remission) in patients treated with rituximab, an anti-CD20/B-cell monoclonal antibody (Beck et al., 2011). After renal remission, the detection of increasing antibody levels precedes a clinical relapse (Ruggenenti et al., 2015).

Testing for the PLA_2R antigen in renal biopsies has been performed by IF on frozen sections, IF on paraffin sections, and immunohistochemistry (IHC) on paraffin sections (VanBeek & Haas, 2015) (Fig. 55.22).

Detection of enhanced PLA_2R expression in glomeruli by IF or IHC in the renal biopsy correlates with circulating autoantibodies and appears to be more sensitive since some seronegative patients still show glomerular PLA_2R by IHC or IF (Debiec & Ronco, 2011; Hoxha et al., 2012; Ramachandran et al., 2016). In this situation, when the anti-PLA_2R antibodies are not detectable, the kidney may act as a "sink" in absorbing all the circulating anti-PLA_2R antibodies (van de Logt, 2015) Thus PLA_2R

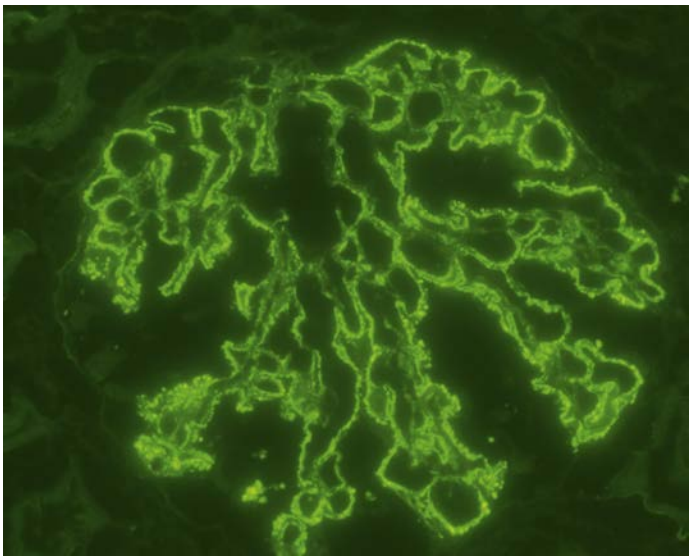

Fig. 55.19 Membranous nephropathy. Granular positivity for IgG along outer aspect of glomerular capillary walls (immunofluorescence, IgG, ×400).

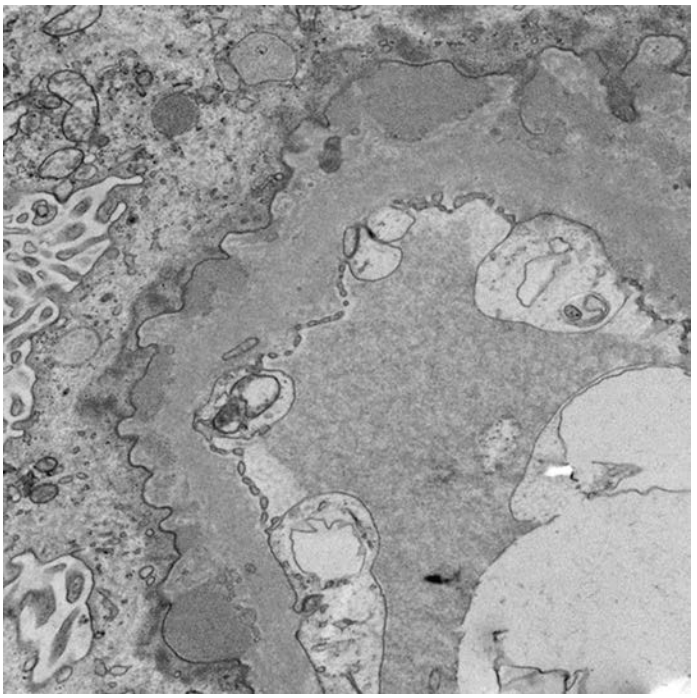

Fig. 55.20 Membranous nephropathy. Glomerular capillary with subepithelial electron-dense deposits with adjacent glomerular basement membrane (GBM) spiking and podocyte foot process effacement (electron microscopy [EM], ×12,000).

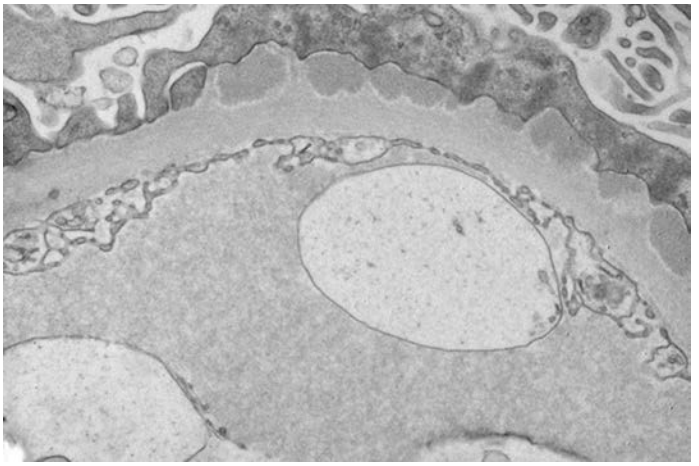

Fig. 55.21 Membranous nephropathy. Subepithelial electron-dense deposits with some intervening glomerular basement membrane (GBM) spikes (EM, ×20,000).

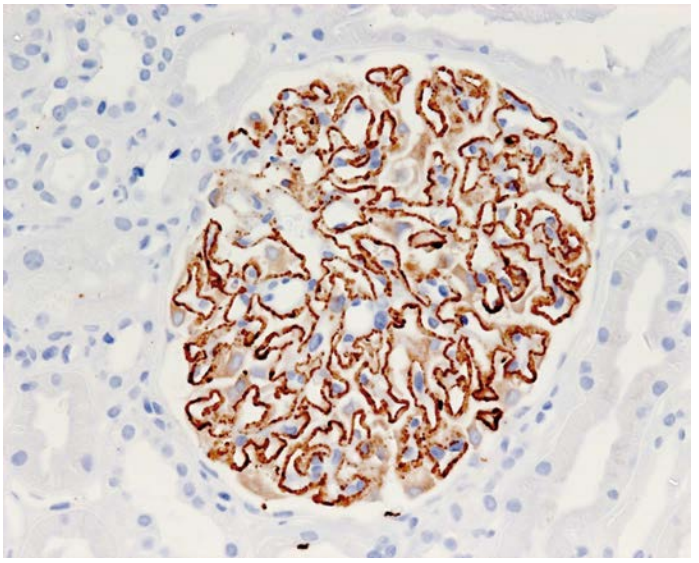

Fig. 55.22 Membranous nephropathy. Glomerular capillary wall granular positive immunoreactivity for PLA_2R (PLA_2R immunohistochemistry [IHC], ×400).

detected by morphologic techniques on a renal biopsy can serve as a footprint of PLA_2R-associated MN (Svobodova et al., 2013). Scenarios exist that account for negative tests for circulating anti-PLA_2R antibodies in patients with MN. In early disease, the antibody levels may be low and not detectable. In immunologic remission, the circulating antibodies are not detected but proteinuria persists because of the lag time between immunologic and renal remission. A primary autoantigen other than PLA_2R, such as THSD7A, is involved or the MN may be a secondary type. Serial, rather than single, measurements of circulating anti-PLA_2R antibodies are recommended in the diagnosis and clinical management of MN.

A serology-based approach, rather than a traditional proteinuria-driven approach, to diagnosis and management of primary MN has naturally emerged (De Vriese et al., 2017). In a large study, a positive serum anti-PLA_2R antibody test (performed by both ELISA and IF) in 60 patients with preserved renal function and no evidence of secondary causes predicted a tissue diagnosis of PLA_2R-associated MN (Bobart et al., 2019). The implication was that in some patients a renal biopsy may not provide information for diagnosis and clinical management. A study of 263 patients revealed 6% of 194 patients with serum positive anti-PLA_2R antibodies had a second relevant diagnosis in addition to MN on renal biopsy (Wiech et al., 2019). Additional renal diseases were found in 10% of 69 patients with MN but serum negative anti-PLA_2R antibodies. These data warrant consideration for individualized management of MN patients.

MN that occurs post renal transplantation is a significant cause of allograft failure but is less understood compared to MN in the native kidney (Leon et al., 2019). MN may be recurrent or a de novo disease. The majority of recurrent MN cases occur within 1 year posttransplant and are associated with anti-PLA_2R antibodies (Kattah et al., 2015). De novo MN typically presents years after transplantation and most cases lack anti-PLA_2R antibodies (Larsen & Walker, 2013). Although de novo MN is often accompanied by antibody-mediated rejection, the exact pathogenesis is unknown.

IF staining for the four subclasses of IgG (IgG1, IgG2, IgG3, and IgG4) has been performed to assist in distinguishing primary MN from secondary forms of MN, including membranous LN (Hemminger et al., 2016). The main IgG subclass found both within the subepithelial deposits of primary MN and the circulating anti-PLA2R antibodies is IgG4 (Beck & Salant, 2014). A caveat is that the IgG1 subclass is often dominant by IF in early stages of idiopathic MN (Huang et al., 2013). In membranous LN, IgG1, IgG2, IgG3 predominate, but IgG4 is still usually present on IF staining. In secondary MN associated with malignancy, IgG1 and IgG2 tend to predominate (Ohtani, 2004). Although IgG subclass staining can be useful in specific cases, the considerable overlap in IF staining limits interpretative specificity.

A genome-wide association study (GWAS) of more than 500 patients with MN revealed significant linkage to the PLA_2R gene on chromosome 2q24 (as well as HLA-DQA1 on 6p21) (Stanescu et al., 2011). Studies in

Chinese patients have reported a strong HLA association with anti-PLA_2R antibody positivity (Le et al., 2017; Cui et al., 2017). Recent molecular studies have focused on the PLA_2R molecule.

It is a 180 kDa membrane receptor with a large extracellular region containing N-terminal cysteine-rich domain (CysR), a fibronectin type II domain (FnII), and eight C-type lectin domains (CTLD1-8) (Beck, 2017). Studies have identified three reactive epitopes targeted by anti-PLA2R antibodies: CysR, CTLD1, and CTLD7 (Kao et al., 2015; Fresquet et al., 2015; Seitz-Polski, 2016). Elegant investigations revealed high anti-PLA_2R antibody activity associated with *intramolecular epitope spreading* beyond the CysR epitope to the CTLD1 and CTLD7 epitopes and active MN disease (Seitz-Polski, 2016). Moreover, anti-PLA_2R antibodies against the CTLD1 and CTLD7 epitopes disappeared with disease remission. Additional studies suggest the presence of PLA_2R epitope spreading at baseline before treatment in MN patients predicts a decreased prospect of clinical remission (Seitz-Polski et al., 2018). Remission in MN patients is often induced by treatment with rituximab, an anti-CD20 antibody. Patients with PLA_2R epitope spreading have high circulating anti-PLA_2R antibody titers. Recent studies suggest higher doses of rituximab are required to induce remission in patients with PLA_2R epitope spreading (Seitz-Polski et al., 2019). Despite these considerable advances, the physiologic role of PLA_2R in normal podocytes remains unknown.

In the fibroinflammatory disorder IgG4-related disease, the most common renal manifestation is a tubulointerstitial nephritis characterized by lymphoplasmacytic infiltrates with IgG4 predominance among plasma cells, tissue eosinophils, and storiform fibrosis, features observed in other involved organs. However, MN has been reported in association with IgG4-related disease (Alexander et al., 2013). In about 50% of these patients, a tubulointerstitial nephritis coexisted with the MN. Although the glomerular immune deposits in this "IgG4-related MN" were primarily IgG4, unlike primary MN, IF staining for PLA_2R was negative. Moreover, circulating anti-PLA2R antibodies have not been detected in IgG4-related disease (Khosroshahi et al., 2012). Thus IgG4-related MN appears to be a secondary form of MN, distinct from primary PLA_2R-associated MN.

Circulating antibodies to a second autoantigen, thrombospondin type-1 domain-containing 7A (THSD7A), have been described in 2% to 5% of adult patients with idiopathic MN (Tomas et al., 2014). Like PLA_2R, THSD7A is an intrinsic human podocyte expressed glycoprotein (Godel et al., 2015). Unlike PLA_2R, THSD7A is expressed on murine podocytes, and injection of human anti-THSD7A antibodies in mice induce a MN (Tomas et al., 2016). Most MN patients with circulating anti-THSD7A antibodies lack antibodies to PLA_2R, but rare cases of dual autoantibody positivity have been reported (Larsen et al., 2016; Wang et al., 2017). IIF and ELISA assays have facilitated the identification of patients with THSD7A-associated MN (Hoxha et al., 2017; Zaghrini et al., 2019). Molecular studies have identified the most amino terminal region of THSD7A as the dominant epitope in THSD7A-associated MN (Seifert et al., 2018). IHC staining of renal biopsies for THSD7A is a sensitive method for diagnosis of THSD7A-associated MN and correlates with the serologic testing for anti-THSD7A antibodies (Hoxha et al., 2016; Larsen et al., 2016; Sharma & Larsen, 2018). There appears to be an association of THSD7A-associated MN with malignancy, and some tumor tissue in these patients has been found to express THSD7A (Hoxha et al., 2016, 2017).

Other forms and potential molecular mechanisms of MN have been reported. An unusual entity, membranous-like glomerulopathy with masked IgG kappa deposits, has been reported predominantly in young women with clinical autoimmune features but generally lacking diagnostic criteria of systemic lupus erythematous (Larsen et al., 2014, 2016). Tissue stains for PLA_2R, and THSD7A were negative. Although the patients had LM and EM findings similar to MN, the presence of mesangial and large humplike subepithelial deposits suggest a possible secondary form of glomerular disease. Immunoglobulin deposits were absent on IF of frozen tissue and they (IgG and kappa light chain) were only revealed by repeat IF on formalin-fixed paraffin-embedded (FFPE) tissue after antigen retrieval (pronase digestion). EM is critical in selecting cases in which IF of pronase digested FFPE may expose immunoglobulin deposition and establish an accurate diagnosis. The nature of this immunoglobulin masking and the molecular etiology of this entity are not clear. A rarely encountered form of glomerular injury is MN with light chain restricted deposits (Rocha & Larsen, 2017). In the majority of patients, a single IgG subclass and kappa light chain restriction were present. Unlike the previous described entity, membranous-like glomerulopathy with masked deposits, MN with light chain restricted deposits included equal numbers of males and females, showed no masking of deposits on IF, and was associated with an increased risk of lymphoproliferative disorders.

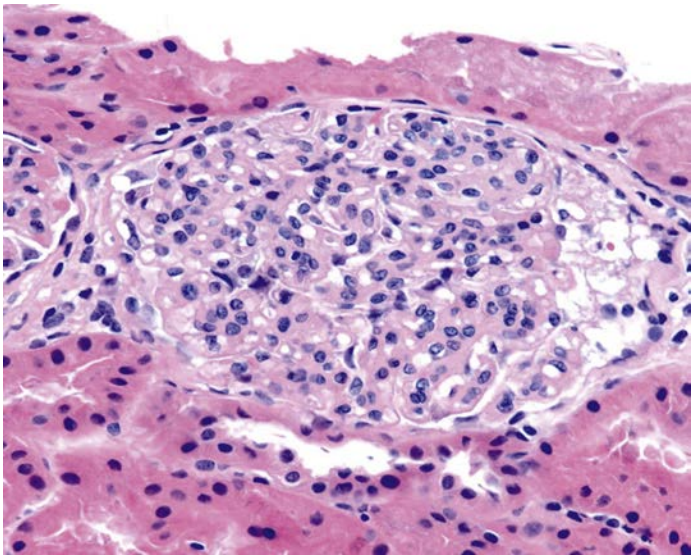

Fig. 55.23 IgA nephropathy. Glomerular hypercellularity (H&E, ×400).

Recent studies using laser microdissection and mass spectrometry have identified the novel proteins exostosin 1 (EXT1) and exostosin 2 (EXT2) in PLA_2R and THSD7A double-negative patients with MN (Sethi et al., 2019). IHC showed granular staining of EXT1 and EXT2 along the GBMs. The majority (80%) of these patients had features of autoimmune disease, including membranous LN (class V). These proteins may be target antigens of secondary autoimmune MN. Membranous nephropathy with crescents has been reported in patients with negative serology for ANCAs and anti-GBM antibodies (Rodriquez et al., 2014). The majority (60%) of these patients were PLA_2R negative. Although rare, a form of early childhood MN (5 months to 2.3 years) due to circulating anti–bovine serum albumin (BSA) has been described (Debiec et al., 2011). In this secondary form of MN, the target is an exogenous antigen, cationic BSA, present in cow milk.

Thus, although MN is now considered a classic autoimmune glomerular disease, it appears to have multiple molecular etiologies.

GLOMERULONEPHRITIDES

IgA Nephropathy

IgA nephropathy (IgAN) is the most common primary glomerulonephritis in the world (Lai et al., 2016; Rodrigues et al., 2017). The incidence of IgAN is highest in Asia (40–50% of primary glomerulonephritis) but it represents 10% to 20% of primary glomerulonephritis in the United States. It occurs in all ages but is most common in the 20s and 30s. IgAN is very uncommon in blacks. The clinical manifestations are broad, but hematuria is the major clinical presentation. Other presentations, usually with accompanying hematuria, include proteinuria, nephrotic syndrome, rapidly progressive nephritic syndrome, and chronic renal failure. IgAN was initially thought to be a benign disease, but studies have indicated 20% to 40% of patients progress to end-stage renal disease (ESRD) over 20 to 30 years. Median life expectancy is reduced by 10 years in patients in the southeastern United States with IgAN (Hastings et al., 2018).

The current diagnosis of IgAN is made by renal biopsy. On LM, the most common finding is mesangial hypercellularity of variable degrees (Figs. 55.23 and 55.24). However, other glomerular patterns of injury may be seen, including endocapillary hypercellularity, membranoproliferative patterns, focal segmental sclerosis (Fig. 55.25), and crescents (Fig. 55.26). IF reveals "dominant" (greater than any other immunoglobulin) glomerular IgA deposition, usually with a mesangial pattern (Fig. 55.27). Deposition of glomerular C3, but not C1q, is common. This finding indicates complement is activated through the alternative or lectin pathways, or both (Maillard et al., 2015). IgAN is essentially an IF diagnosis. EM usually confirms the presence of mesangial (Fig. 55.28) and paramesangial deposits (Fig. 55.29). Peripheral glomerular capillary wall subendothelial deposits are observed in some cases. Separate from primary IgAN, mesangial deposits of IgA may be observed in various system disorders (secondary IgA nephropathy), especially liver disease but also inflammatory bowel disease, infections, and autoimmune disorders (Saha et al., 2018).

The Oxford Classification of IgA nephropathy includes the scoring of histologic variables that are reproducible among pathologists and predictive

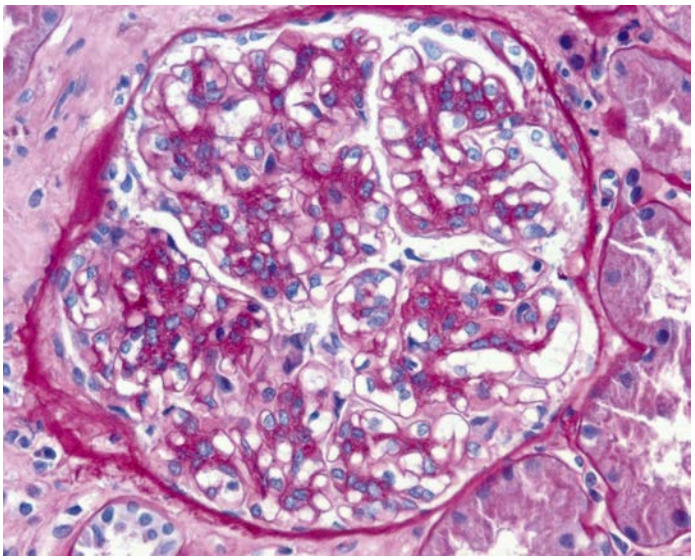

Fig. 55.24 IgA nephropathy. Mesangial hypercellularity and matrix increase (PAS, ×400).

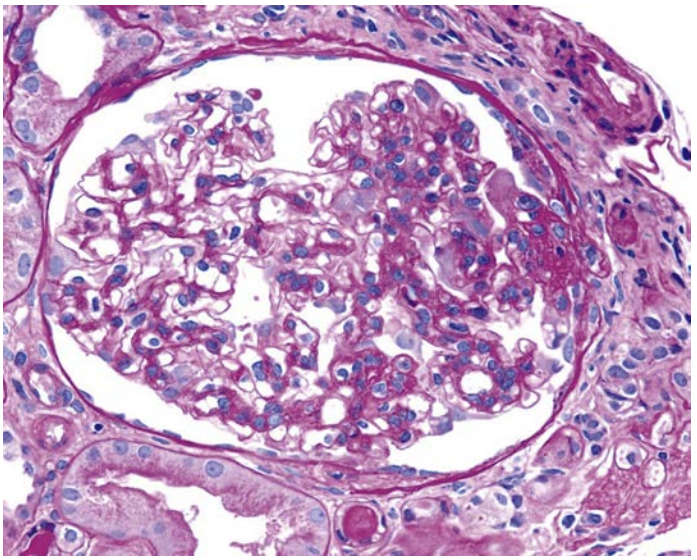

Fig. 55.25 IgA nephropathy with segmental glomerulosclerosis. Mesangial hypercellularity and adhesion to Bowman capsule (PAS, ×400).

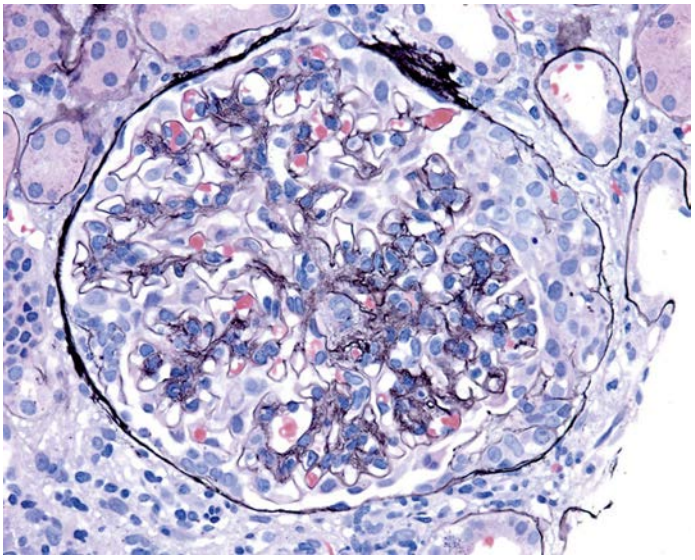

Fig. 55.26 IgA nephropathy with crescent formation. Glomerular hypercellularity with cellular crescent in Bowman space (Jones silver, ×400).

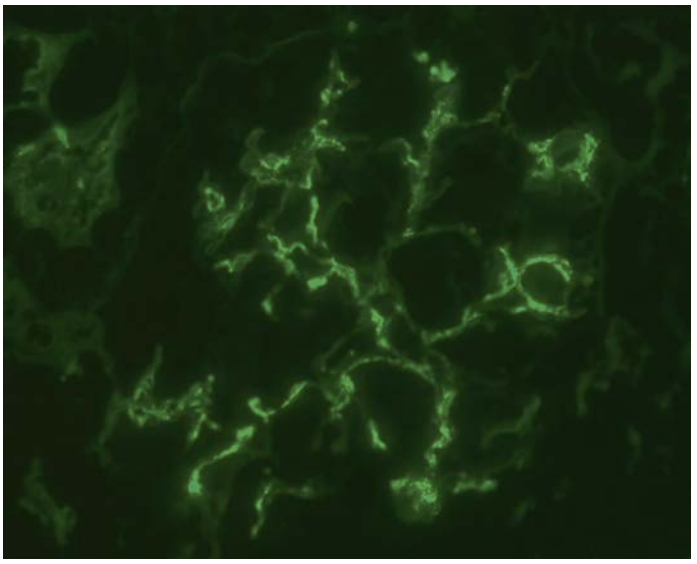

Fig. 55.27 IgA nephropathy. Mesangial (arborizing) staining for IgA (IF], ×400).

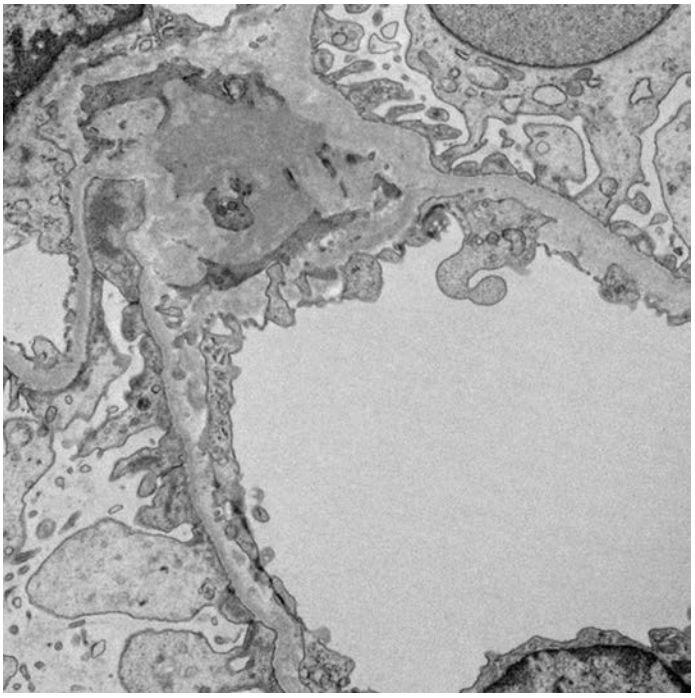

Fig. 55.28 IgA nephropathy. Electron-dense deposits in mesangium (EM, ×12,000).

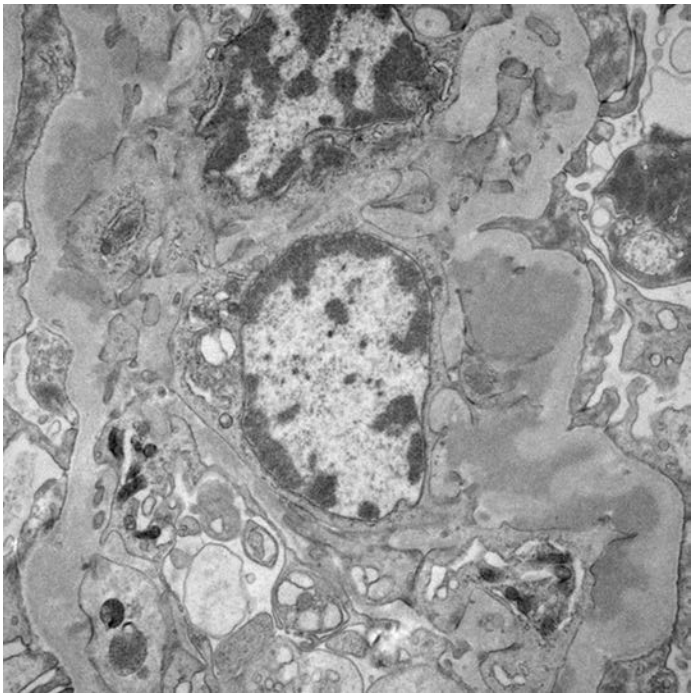

Fig. 55.29 IgA nephropathy. Paramesangial electron-dense deposits (EM, ×15,000).

of renal outcomes (Roberts et al., 2009; Roberts, 2013). Updated histologic features are mesangial hypercellularity (M), endocapillary hypercellularity (E), segmental sclerosis (S), tubular atrophy and interstitial fibrosis (T), and cellular or fibrocellular crescents (C). These lesions are evaluated resulting in the MEST-C score (Trimarchi et al., 2017; Markowitz, 2017). Moreover, it was recommended that the segmental sclerosis (S) score be refined to indicate cases with podocyte hypertrophy and tip lesions, which are associated with proteinuria (Bellur et al., 2017). The cellular or fibrocellular crescent (C) score was added to the original MEST score since subsequent studies indicated the presence of crescents negatively affected renal outcomes (Haas et al., 2017). A number of studies have validated the prognostic value of the Oxford Classification and especially when the MEST score is added to clinical data (Coppo et al., 2014; Barbour et al., 2016). The MEST-C score on renal biopsy maintains predictive value even with long-term observation after the renal biopsy (Coppo et al., 2019).

Human IgA has two subclasses, IgA1 and IgA2, the former representing about 85% of the total circulating IgA. IgAN is considered an autoimmune renal disease with a proposed multihit pathogenesis (Lai et al., 2016; Rodrigues et al., 2017). The *first* and basic hit is aberrant glycosylation of IgA1 leading to elevated levels of circulating IgA1 molecules without galactose in the hinge region. This finding is also found in some relatives of IgAN patients. These abnormal IgA molecules are recognized by IgG (or IgA) autoantibodies *(hit 2)*. The anti-IgA1 autoantibodies are unique and appear to have somatic mutations (Huang et al., 2016). There is formation of circulating nephritogenic galactose-deficient IgA1 immune complexes *(hit 3)*. The immune complexes deposit in the glomeruli and activate mesangial cells leading to cell proliferation and production of extracellular matrix and cytokines *(hit 4)*. This four-hit pathogenic model has recently been supported by studies showing that IgG extracted from IgAN renal biopsy specimens exhibits specific reactivity for galactose-deficient IgA1 (Rizk et al., 2019). Complement activation via the lectin and alternative pathways occurs from the IgA1 circulating immune complexes as well as in the glomeruli (Maillard et al., 2015). It is not clear if primary IgAN can be distinguished from secondary IgAN on the basis of specific immunostaining for galactose-deficient IgA in renal biopsy specimens (Suzuki et al., 2018; Cassol et al., 2019). Additional investigations are required to understand the molecular details of these proposed pathogenic events.

Membranoproliferative Glomerulonephritis

MPGN describes a pattern of glomerular injury that may result from several distinct etiologies of glomerular disease. MPGN may generally be considered a glomerular lesion and not a specific glomerular disease. The clinical presentation is variable but includes proteinuria, nephrotic syndrome, hematuria, nephritic syndrome, and acute kidney injury. The characteristic LM lesion of the MPGN pattern is thickening of the glomerular capillary wall *(membrano)* and glomerular hypercellularity *(proliferative)*. Mesangial hypercellularity and often endocapillary hypercellularity with increased mesangial matrix typically impart a lobular glomerular tuft appearance (Fig. 55.30). Another characteristic lesion is double contours or "tram-tracks" of the GBMs, best observed on silver stains (Fig. 55.31). Immunofluorescence demonstrates primarily glomerular capillary wall granular staining for immunoglobulins (Fig. 55.32). Electron microscopy reveals subendothelial electron-dense deposits, usually some mesangial deposits and mesangial interposition with the formation of new basement membrane material (Figs. 55.33 and 55.34). An older classification included three types (MPGN types I, II, and III), primarily based on EM findings.

However, IF analysis of the composition of glomerular deposits and molecular studies of various MPGN cases have provided insights into the pathogenesis and led to a new classification of these disorders (Sethi & Fervenza, 2012; Cook & Pickering, 2015). Currently there are two main underlying pathogenic pathways that may result in an MPGN pattern by LM. IF findings play a major role in distinguishing between the two pathways: (1) Glomeruli with deposition of predominantly immunoglobulins (IgG and/or IgM) on IF with or without some complement C3 is now termed simply MPGN. These glomerular diseases are also referred to as immune complex-mediated MPGN. (2) Glomeruli with primarily complement deposition (C3) on IF and sparse to absent immunoglobulins are called the C3 glomerulopathies (see later). These glomerular disorders involve dysregulation of the alternative pathway of complement. Other glomerular disorders may exhibit a MPGN pattern on LM but do not appear to involve the discussed two pathogenic pathways. For example, glomeruli with a MPGN pattern, but absent to sparse immunoglobulins and complement components, may be encountered in chronic thrombotic microangiopathies with persistent endothelial injury.

Several variants of immune complex mediated MPGN (MPGN-IC) exist. They include primary (idiopathic) MPGN and secondary forms of

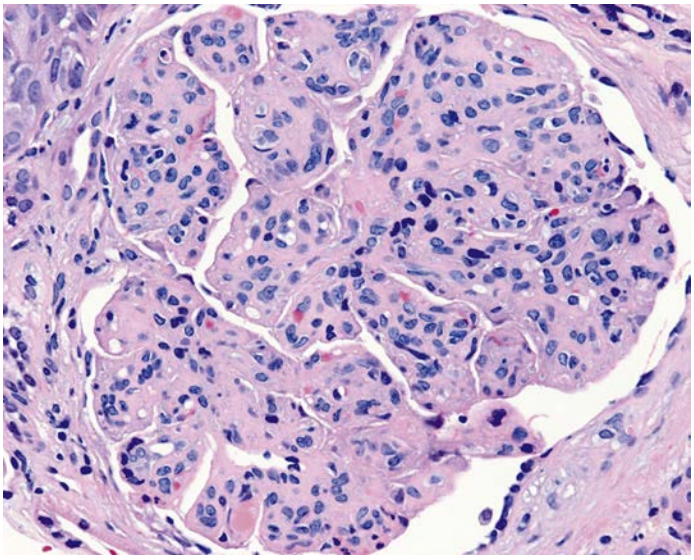

Fig. 55.30 Membranoproliferative glomerulonephritis. Glomerular lobularity with mesangial and endocapillary hypercellularity (H&E, ×400).

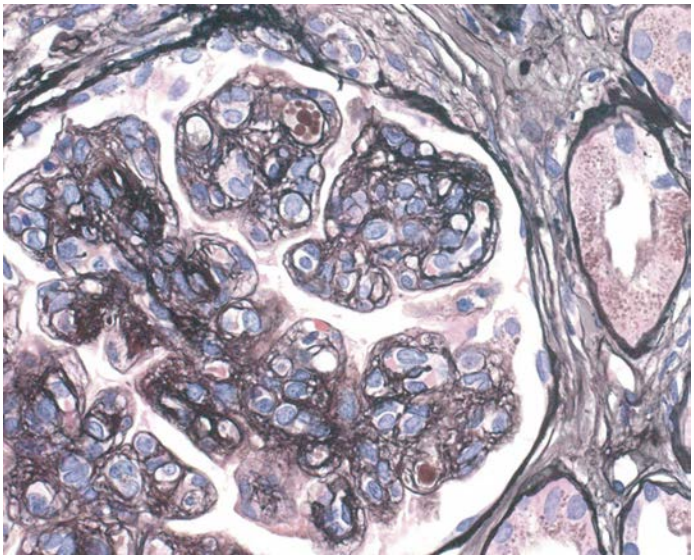

Fig. 55.31 Membranoproliferative glomerulonephritis. Glomerular capillary wall double-contouring due to reduplication of the GBM (Jones silver, ×630).

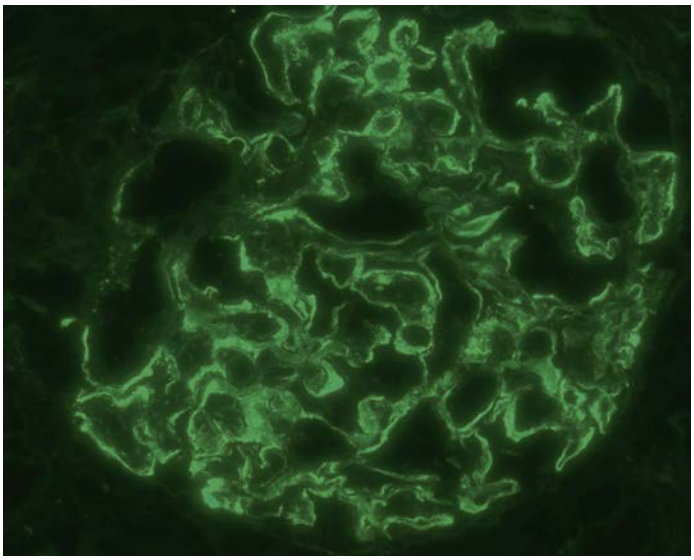

Fig. 55.32 Membranoproliferative glomerulonephritis. Granular staining along capillary walls and mesangium for IgG (IF, ×400).

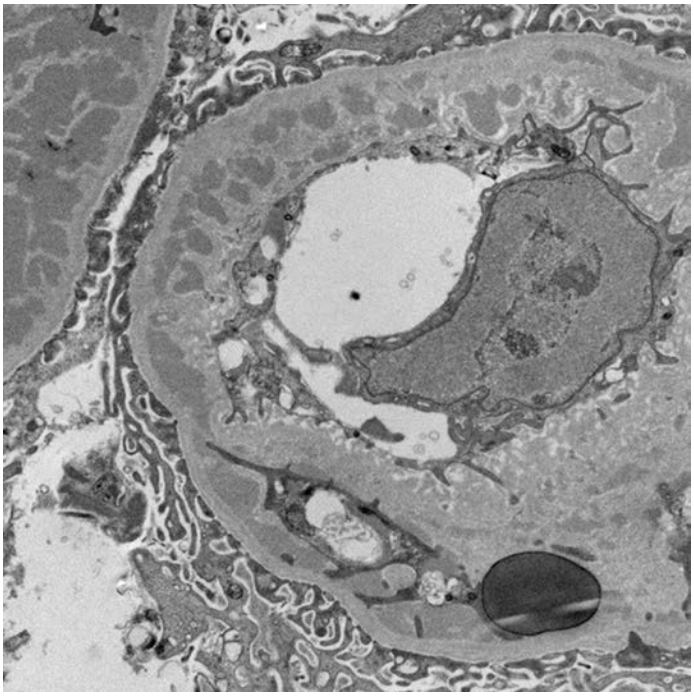

Fig. 55.33 Membranoproliferative glomerulonephritis. Numerous subendothelial electron-dense deposits (EM, ×12,000).

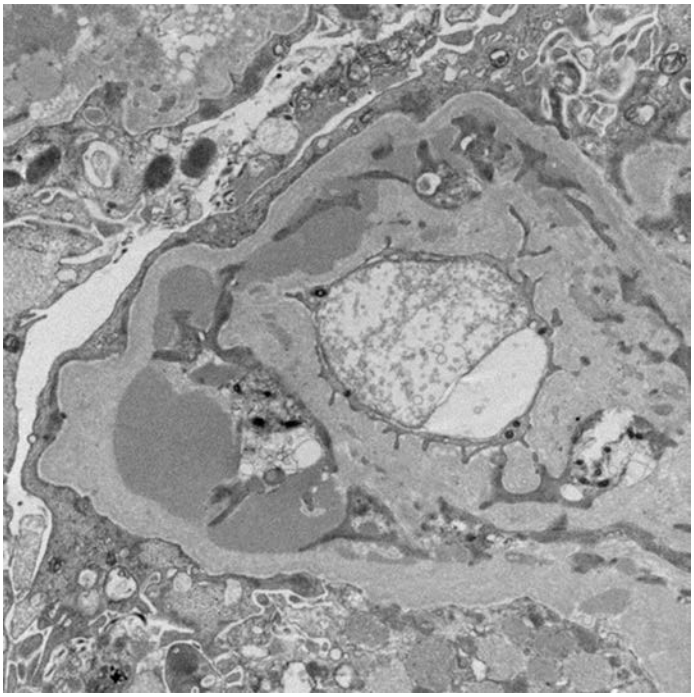

Fig. 55.34 Membranoproliferative glomerulonephritis. Mesangial interposition with prominent subendothelial deposits between outer original glomerular basement membrane (GBM) and new inner GBM (EM, ×12,000).

MPGN-IC associated with infections, autoimmune diseases, neoplasia, and monoclonal gammopathies. The idiopathic forms of MPGN-IC, far less common than the secondary forms, represent a diagnosis of exclusion (Fervenza et al., 2012). Idiopathic MPGN-IC is more common in children and young adults. These patients usually present with severe proteinuria and often hematuria. Persistent decreased serum levels of C3 and C4 are usually present. In MPGN-IC, the formation of antigen-antibody immune complexes would appear to activate the classical pathway of complement. However, abnormalities of the alternative complement pathway, including autoantibodies (C3 nephritic factors, anti-FB, anti-C3b) and mutations (C3 and CFB) have been demonstrated in patients with MPGN-IC as well as in C3 glomerulopathy (Servais et al., 2012; Iatropoulos et al., 2016; Noris et al., 2019).

The secondary forms of MPGN-IC are significantly more common. Hepatitis C is a common cause of MPGN-IC. It may occur with or without cryoglobulinemia. Although MN is the most common glomerular disease associated with hepatitis B infection, MPGN-IC also occurs.

Cryoglobulins have traditionally been classified into three forms. Type I, the rarest type, is composed of a single monoclonal immunoglobulin, usually IgM or IgG, and is usually associated with an underlying lymphoproliferative disease. Types II and III are the mixed cryoglobulins and are more common. Type II is usually characterized by monoclonal IgM complexed with polyclonal IgG. Type III is usually composed of polyclonal IgM with rheumatoid factor activity and polyclonal IgG. By far the most common etiology of both type II and type III cryoglobulinemia is hepatitis C. Serum immunofixation is required for the typing of the cryoglobulins. Typical laboratory results include elevated rheumatoid factor and low C4. Cryoglobulinemic glomerulonephritis (CryoGN) is characterized by MPGN-IC pathologic features with more specific lesions, including glomerular intracapillary "cryoglobulin thrombi" on LM, diffuse glomerular capillary IgM deposition, and subendothelial and luminal deposits with substructure (curved microtubular or annular structures) on EM. Noninfectious forms of mixed CryoGN have been described in association with Sjögren syndrome and lymphoproliferative disorders (Zaidan et al., 2016).

Secondary forms of MPGN-IC occur with autoimmune diseases. Although glomerular involvement in SLE is classified into well-defined lesions (see lupus nephritis), a MPGN-IC pattern may occur as a form of class IV LN. Other autoimmune diseases that may be associated with a MPGN-IC include rheumatoid arthritis, mixed connective tissue disease, and Sjögren syndrome.

Although secondary MPGN-IC may occur with carcinomas, a more common association is with monoclonal gammopathies. The term *monoclonal gammopathy of renal significance* (MGRS) refers to the extremely broad spectrum of distinct renal diseases associated with monoclonal immunoglobulin deposition in the kidney (Sethi et al., 2018; Leung et al., 2019). A MPGN pattern of injury may be seen in these diseases (Sethi et al., 2010). A unique disease is proliferative glomerulonephritis with monoclonal immunoglobulin deposits (PGNMID) (Nasr et al., 2004, 2009). The patients present with severe proteinuria, hematuria, and renal insufficiency. Most patients do not have a detectable circulating monoclonal immunoglobulin, and bone marrow examination is usually negative. MPGN is the most common glomerular pattern on LM but endocapillary hypercellularity and crescents are also seen. By IF, there is only glomerular IgG granular deposition with light chain isotype restriction. Most cases are positive for kappa only, but lambda only staining is noted in 25% of cases. IF staining for IgG subtypes reveals deposition of IgG-3 only in the majority of cases. Granular immune-complex type deposits are observed by EM usually in mesangial and subendothelial regions, with fewer in subepithelial areas. PGNMID has a high recurrence rate in renal allografts (Said et al., 2018). The pathogenesis of PGNMID remains unknown.

C3 Glomerulopathy

C3 glomerulopathies (C3G) are a group of rare glomerular disorders with often a membranoproliferative LM pattern and IF characterized by C3 deposition and little to absent immunoglobulins (Barbour et al., 2016; Smith et al., 2019). C3G is essentially defined by IF, showing "dominant" C3 glomerular deposition greater or equal to 2 orders of magnitude of IF intensity greater than any other immune reactant (Pickering et al., 2013; Hou, 2014). C3G includes two major subgroups: the rare dense deposit disease (DDD, previously known as MPGN type II) and C3 glomerulonephritis (C3GN). Both DDD and C3GN are most common in children and young adults but can affect all ages. They present with hematuria and proteinuria. The serum C3 levels are persistently low. Both disorders tend to progress to end-stage renal failure with a 10-year renal survival less than 50% (Medjeral-Thomas et al., 2014). The LM features are nonspecific and rather heterogenous. The LM glomerular injury patterns include membranoproliferative (most common), endocapillary hypercellularity, mesangial hypercellularity, and crescents. DDD and C3GN are best distinguished on EM: extremely dense osmiophilic sausage-shaped intramembranous deposits in DDD and mesangial and capillary wall (usually subendothelial) deposits in C3GN (Cook & Pickering, 2015). *Osmiophilic* refers to a substance that stains with osmium tetroxide that yields a black color.

It is important to note that some cases of proliferative immune complex glomerulonephritis (e.g., MPGN-IC) may be misdiagnosed as C3GN if the immunoglobulin deposits are masked (Larsen et al., 2015). IF staining on FFPE tissue after pronase digestion appears to be a valuable technique to expose the immune-complex deposits and prevent a misdiagnosis. Also, C4d staining by IF or IHC may be useful in distinguishing an IC-mediated glomerulonephritis, such as MPGN-IC, from a C3 glomerulopathy.

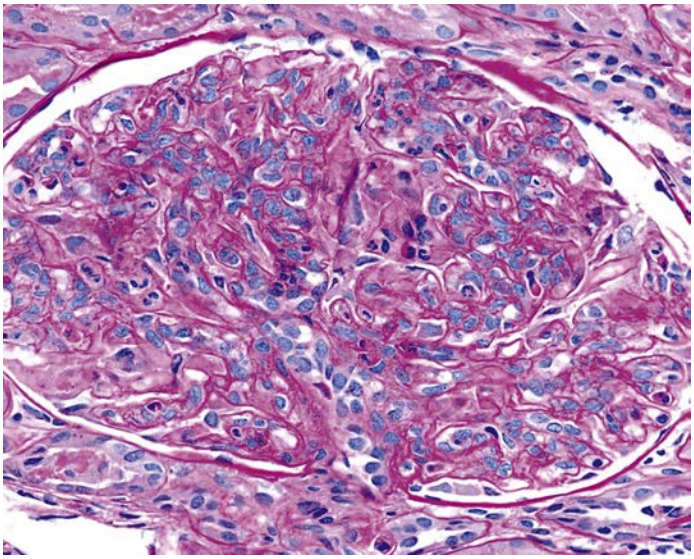

Fig. 55.35 Acute poststreptococcal glomerulonephritis. Endocapillary hypercellularity with infiltration of neutrophils filling capillary lumens (PAS, ×400).

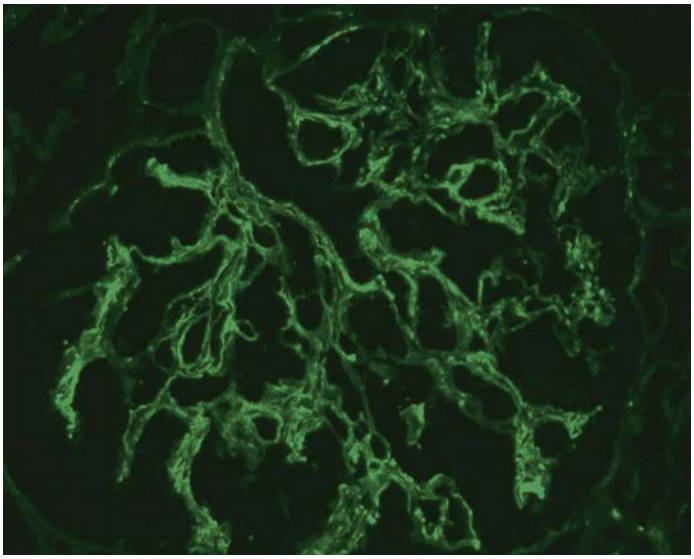

Fig. 55.36 Acute poststreptococcal glomerulonephritis. Capillary wall and mesangial granular staining for C3 (IF, ×400).

Formation of C4d results from activation of the classic and lectin pathways of complement, but not in the alternative pathway. Prominent C4d staining was demonstrated in 90% of cases of IC-mediated glomerulonephritis, and negative/trace C4d staining was shown in 90% of cases of C3 glomerulopathy (Sethi et al., 2015).

Both DDD and C3GN involve dysregulation of the alternative pathway of complement. Laser microdissection and mass spectrometry have identified the glomerular accumulation of alternative pathway proteins, C3 and especially its cleavage product C3dg, and also terminal complement complex proteins (Sethi et al., 2017). Genetic and acquired factors are involved in the pathogenesis (Smith et al., 2019). At least up to 25% of patients with C3G have rare or unique variants in complement genes. Rearrangements in the complement factor H- related factors (regulators of the alternative pathway) lead to abnormal complexes that in turn disrupt complement regulation. Acquired factors include C3 nephritic factors, autoantibodies that target and stabilize C3 convertase, leading to increased consumption of C3 (Smith et al., 2019). C5 nephritic factors (autoantibodies) also occur (Marinozzi, Chauvet et al., 2017). Autoantibodies to factors H and B have also been documented resulting in abnormal activation (Blanc et al., 2015; Marinozzi, Roumenina et al., 2017). The integration of multiple variables, including pathologic and genetic data, has demonstrated overlap between C3G and MPGN-IC and revealed different clusters of complement analysis data may enhance our understanding of disease prognosis (Iatropoulos et al., 2018). DDD and C3GN have a similar rate (40%) of progression to ESRD (Bomback et al., 2018).

Infection-Associated Glomerulonephritis

Infection-associated glomerulonephritis is a broad category of glomerular diseases associated with infections. Although viral infections, including hepatitis C and B (see MPGN), human immunodeficiency virus (HIV), and other infectious agents, may be associated with glomerulonephritis, the following discussion focuses on bacterial infection–associated glomerulonephritis (Nasr et al., 2013). Bacterial infections associated with glomerulonephritis include classic acute poststreptococcal glomerulonephritis (APSGN) and the broad category of infection-related glomerulonephritis (IRGN). APSGN is the model for *postinfectious* glomerulonephritis, in which a latent period (several weeks) typically occurs between a throat or skin infection and the following glomerulonephritis. IRGN is a more appropriate term when the glomerulonephritis develops in the presence of ongoing/persistent infection (Glassock et al., 2015).

The epidemiology of bacterial infection–associated glomerulonephritis in industrialized countries has changed over recent decades. In the United States, most cases are IRGN and associated with nonstreptococcal infection, especially staphylococcal infection. Risk factors include diabetes, alcoholism, malignancy, and intravenous drug use.

APSGN is a well-studied immune-complex-mediated glomerulonephritis (Rodriguez-Iturbe & Hass, 2016). The classic patient is a child, but older patients with debilitating conditions are now more affected in developed countries (Nasr et al., 2008, 2011). However, childhood cases are still reported (Dagan et al., 2016). The typical presentation is an acute nephritic syndrome after a latent period following a throat or skin infection. Serum complement levels, especially C3, are low but they usually return to normal in a month. ASO (antistreptolysin O) and anti-DNAse-B (antideoxyribonuclease-B) antibody titers are typically elevated, especially the latter with skin infections. Pathologic features include glomerular endocapillary hypercellularity, often with prominent neutrophils by LM (Fig. 55.35), granular C3, and often IgG staining in the mesangium and capillary walls by IF (Fig. 55.36) and subepithelial "hump"-like deposits as well as small mesangial and subendothelial deposits by EM (Figs. 55.37 and 55.38). It is noteworthy that some cases only show C3 by IF. The hallmark subepithelial hump deposits often do not typically elicit a GBM remodeling reaction, such as spike formation, and they persist longer in the paramesangial *(notch)* areas. A working model is that streptococcal nephritogenic antigens stimulate immune complex formation in glomeruli. The streptococcal antigens nephritis-associated plasmin receptor (NAPIr) or streptococcal glyceraldehyde-3-phosphate dehydrogenase (GAPDH) and streptococcal pyogenic exotoxin B (SPEB) bind plasmin, localize to the glomeruli in APSGN, and appear to stimulate immune complex formation (Rodriquez-Iturbe & Musser, 2008; Oda et al., 2010).

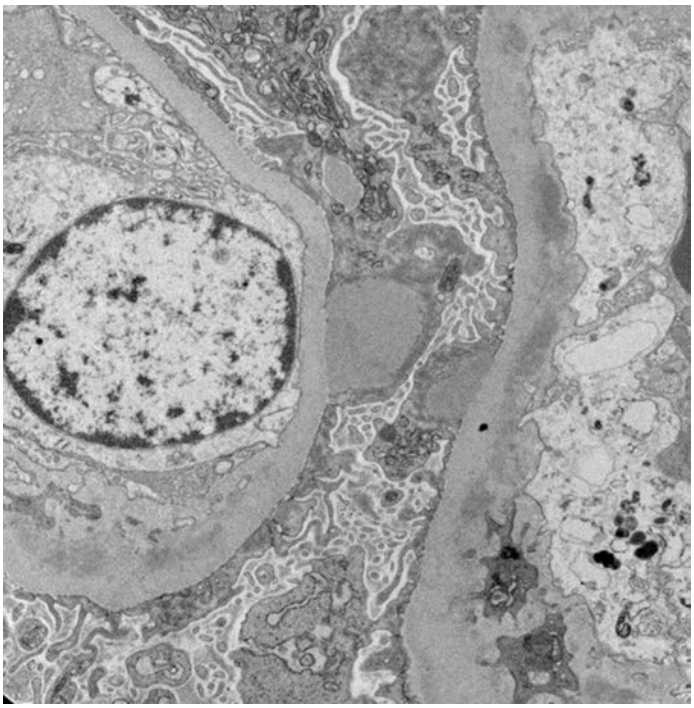

Fig. 55.37 Acute poststreptococcal glomerulonephritis. Prominent subepithelial electron-dense deposits and scattered small subendothelial deposits (EM, ×10,000).

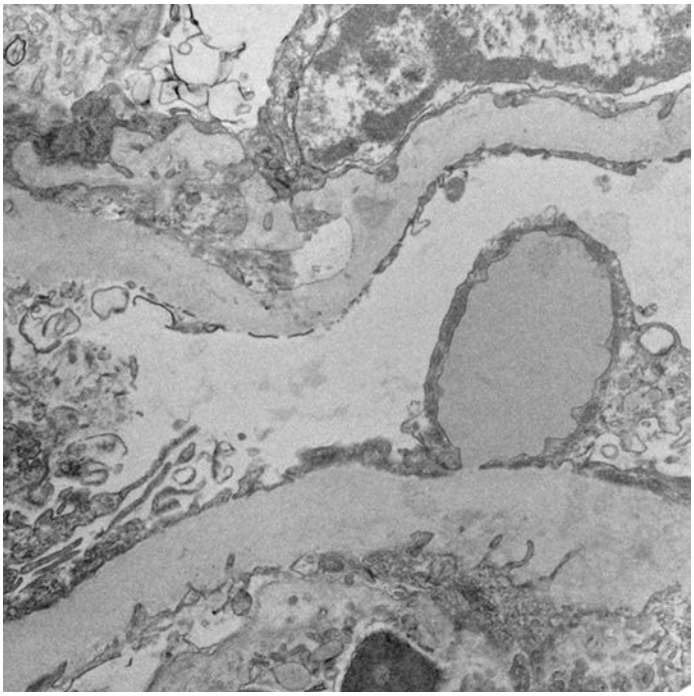

Fig. 55.38 Acute poststreptococcal glomerulonephritis. Large subepithelial humplike deposit (EM, ×15,000).

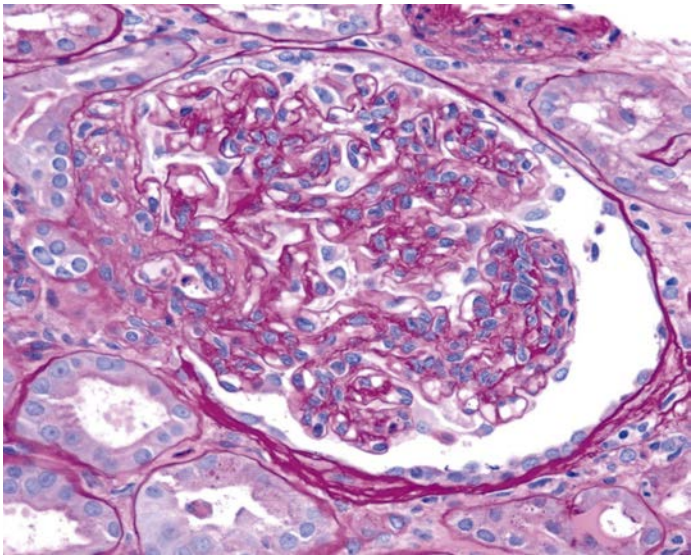

Fig. 55.39 Endocarditis-associated glomerulonephritis. Mesangial and endocapillary hypercellularity with increased mesangial matrix (PAS, ×400).

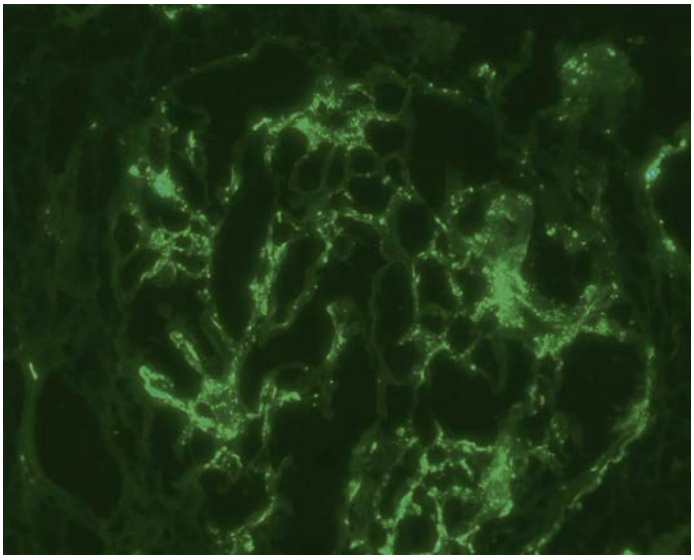

Fig. 55.40 Endocarditis-associated glomerulonephritis. Capillary wall and mesangial granular staining for C3 (IF, ×400).

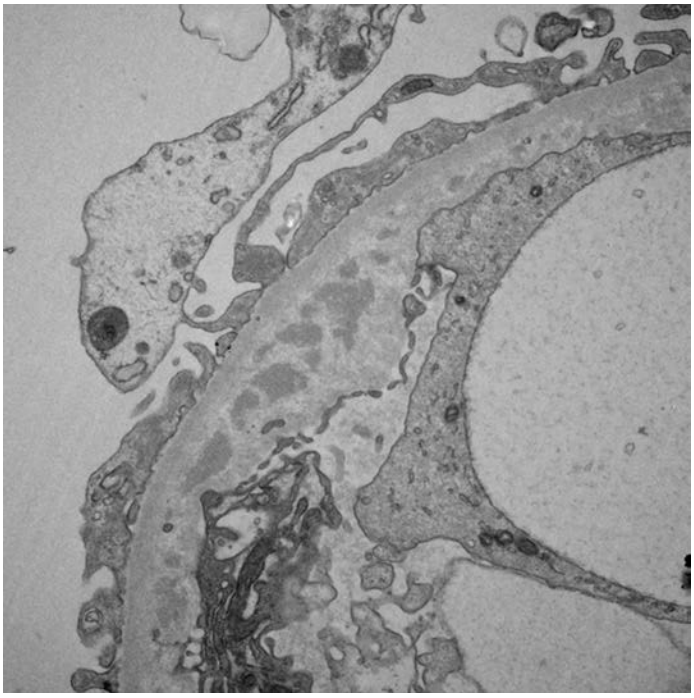

Fig. 55.41 Endocarditis-associated glomerulonephritis. Scattered small subendothelial deposits (EM, ×20,000).

Several bacterial pathogens are implicated in IRGN, but staphylococcus infection-associated glomerulonephritis is most common (Satoskar et al., 2017). Most patients are 50 years or older. Infections include skin (leg ulcers, cellulitis), heart, osteomyelitis, and postsurgical sites. Positive blood cultures are common. Methicillin-resistant *Staphylococcus aureus* (MRSA) is often identified. By LM the findings are similar to APSGN with prominent endocapillary hypercellularity. By IF there is often prominent C3 and weaker IgG staining in the glomeruli. Some cases display significant amounts of glomerular IgA deposition. These cases may be difficult to distinguish from IgA nephropathy (Haas et al., 2008). By EM, mesangial, small subendothelial deposits, and subepithelial humplike deposits are seen. Up to 50% of patients progress to ESRD. Endocarditis-associated glomerulonephritis is a subtype of IRGN that is increasingly recognized (Boils et al., 2015). The most common clinical association is intravenous drug abuse, and *Staphylococcus* is the most common bacteria. Glomerular mesangial and endocapillary hypercellularity are observed (Fig. 55.39). Prominent glomerular C3 deposition is common (Fig. 55.40). Mesangial and subendothelial deposits are observed on EM (Fig. 55.41). In contrast to APSGN, subepithelial humplike deposits are not as common. Glomerular crescents (53%) and ANCA antibody positivity (28%) have been reported.

Anti-Glomerular Basement Membrane Disease

The generic term anti-GBM disease covers the clinical spectrum of disease caused by anti-GBM antibodies: both kidney and lung disease (termed Goodpasture syndrome), kidney-only disease, and rarely lung-only disease (Hudson et al., 2003; Segelmark & Hellmark, 2018; McAdoo & Pusey, 2018). Anti-GBM disease is rare and spatial, and temporal clustering has been shown in some countries (Canney et al., 2016). It has a classic bimodal age distribution: young adults (20–30 years) and older adults (60–70 years) but has been reported in all age groups. Anti-GBM disease typically presents with a rapidly progressive nephritic syndrome with prominent hematuria and red cell casts and often hemoptysis. Renal biopsy typically reveals glomerular capillary fibrinoid necrosis (Fig. 55.42) with cellular crescent formation (Fig. 55.43) and the diagnostic hallmark of linear GBM staining for IgG on IF (Figs. 55.44 and 55.45). EM may show electron-dense fibrin fragments but no electron-dense immune complex deposits (Fig. 55.46).

Circulating autoantibodies bind to the GBM and activate complement leading to recruitment of neutrophils and monocytes with resultant glomerular capillary destruction. The majority of circulating autoantibodies are specific for the C-terminal noncollagenous domain (NC1) of the

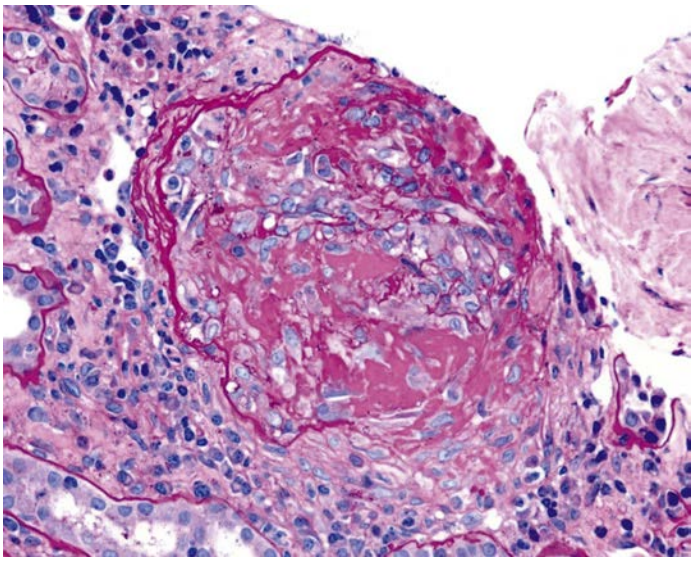

Fig. 55.42 Anti-glomerular basement membrane (GBM) disease. Global glomerular tuft destruction with fibrinoid necrosis (PAS, ×400).

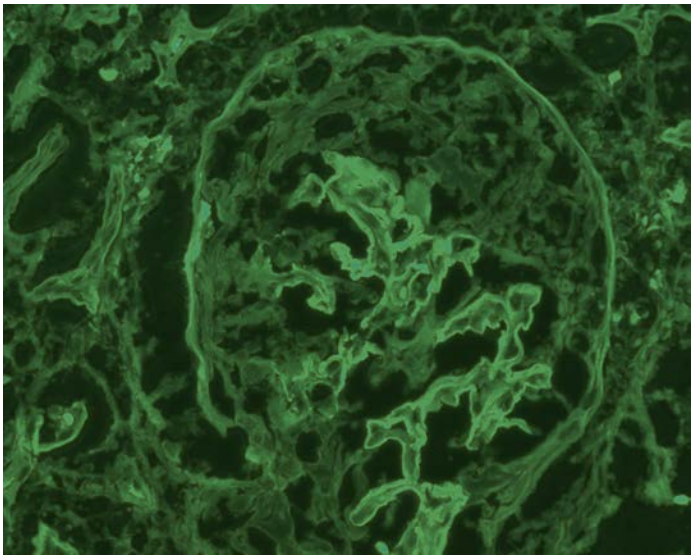

Fig. 55.44 Anti-glomerular basement membrane (GBM) disease. Linear staining for IgG along the glomerular capillary walls. The glomerular tuft is compressed by the crescent (IF, ×400).

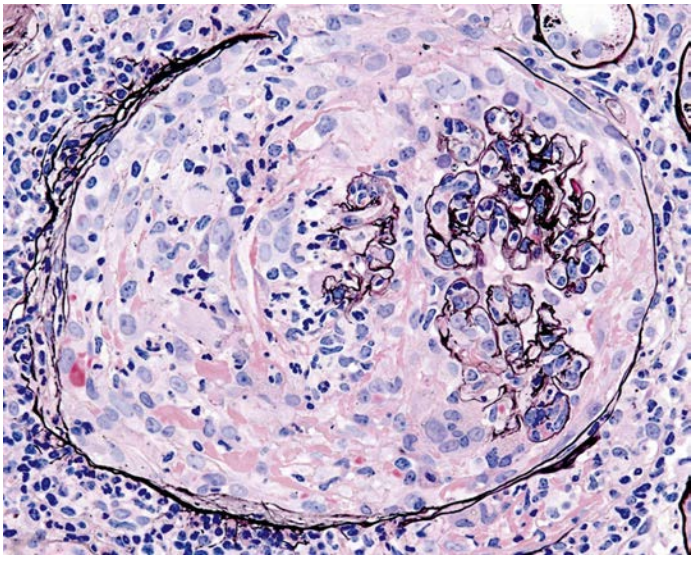

Fig. 55.43 Anti-glomerular basement membrane (GBM) disease. Large cellular crescent with capillary loop destruction and karyorrhectic nuclear debris (Jones silver, ×400).

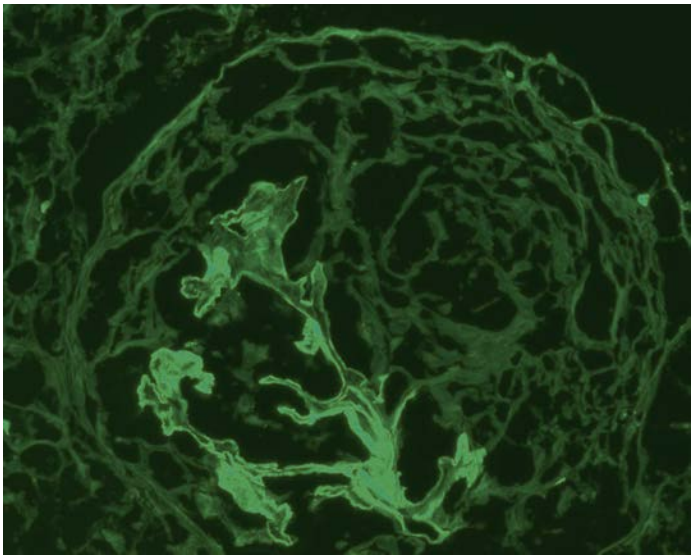

Fig. 55.45 Anti-glomerular basement membrane (GBM) disease. Intense linear staining for IgG along the glomerular capillary walls. The glomerular tuft is partially destroyed and compressed by the crescent (IF, ×400).

α3 chain of type IV collagen (α3[IV] chain) within the GBM (Saus et al., 1988). Circulating autoantibodies to the α5(IV) chain may also be present although they are less abundant. These major epitopes are sequestered within the α345(IV) protomeric hexamer and represent cryptic epitopes. Pathologic insults are believed to cause hexamer dissociation, expose the epitopes, allow binding of the autoantibodies, and initiate the nephritis (Pedchenko et al., 2010). Thus anti-GBM disease has been considered an autoimmune "conformeropathy." Renal survival in recent years has increased with immunosuppression, plasma exchange, and dialysis. Dialysis-dependent patients with 100% cellular crescents or greater than 50% globally sclerotic glomeruli are unlikely to recover and thus intense immunosuppression therapy is not recommended (van Daalen et al., 2018).

Some patients with variable forms of glomerular hypercellularity but few crescents and no pulmonary involvement exhibit linear GBM staining for IgG on IF, but undetectable circulating anti-GBM antibodies (Nasr et al., 2016). Whether the linear IgG deposition along the GBM mediates glomerular disease in these patients is not clear. Another subgroup of anti-GBM disease includes patients that are "double-positive" for both circulating anti-GBM and ANCA antibodies (usually MPO-ANCA). One study of these double-positive patients demonstrated a clinical phenotype that was intermediate between that of classic anti-GBM disease and ANCA-associated glomerular disease (McAdoo et al., 2017).

In Alport syndrome patients that receive a renal transplant, 3% to 5% develop anti-GBM disease because of alloantibodies against collagen IV chains in the allograft kidney that are absent in the patient's native kidney. In contrast to idiopathic anti-GBM disease, in Alport posttransplant anti-GBM disease, the antibodies target α3(IV) and α5(IV) epitopes present on the intact nondissociated α345(IV) hexamer (Olaru et al., 2013).

Pauci-Immune Glomerulonephritis

The characteristic lesion in pauci-immune glomerulonephritis is glomerular capillary necrosis with crescent formation. Early lesions may show only fibrinoid necrosis, which is often segmental (Fig. 55.47). Prominent glomerular cellularity, especially endocapillary hypercellularity, is typically not observed unlike some other forms of immune-complex mediated glomerulonephritis. Cellular crescent formation is characteristic (Figs. 55.48, 55.49, and 55.50). Few to no immune deposits are observed by IF and EM (Fig. 55.51). The paucity of immune deposits distinguishes this glomerular disease from other forms of crescentic glomerulonephritides, such as anti-GBM disease (with linear IgG staining by IF) and immune-complex mediated glomerulonephritis with crescents (with granular immunoglobulin and/or C3 staining by IF).

Pauci-immune glomerulonephritis is the most common cause of crescentic glomerulonephritis and occurs as part of the systemic necrotizing small vessel vasculitides associated with antineutrophil cytoplasmic antibodies. The ANCA-associated vasculitis syndromes include microscopic polyangiitis (MPA), granulomatosis with polyangiitis (GPA; Wegener granulomatosis), and eosinophilic granulomatosis with polyangiitis

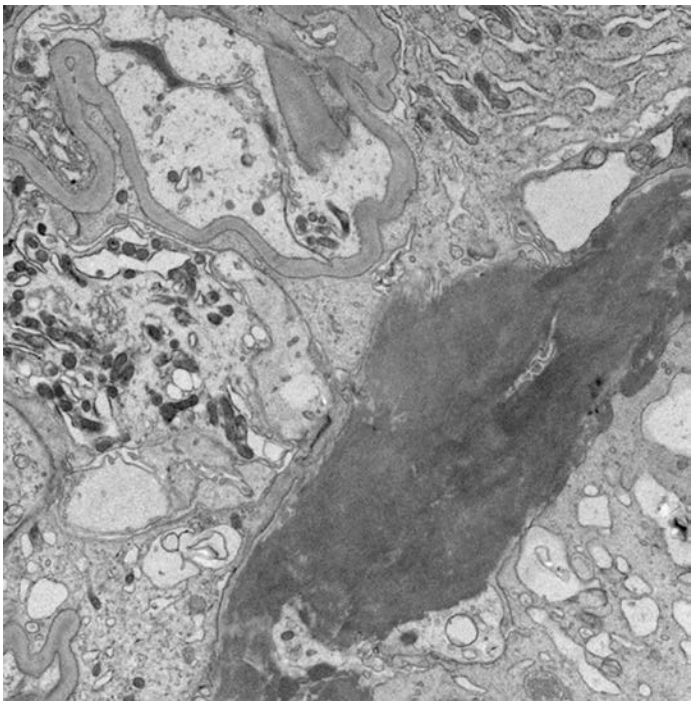

Fig. 55.46 Anti-glomerular basement membrane (GBM) disease. Cellular crescent in Bowman space with electron-dense fibrin aggregate and compressed glomerular capillary loop (EM, ×12,000).

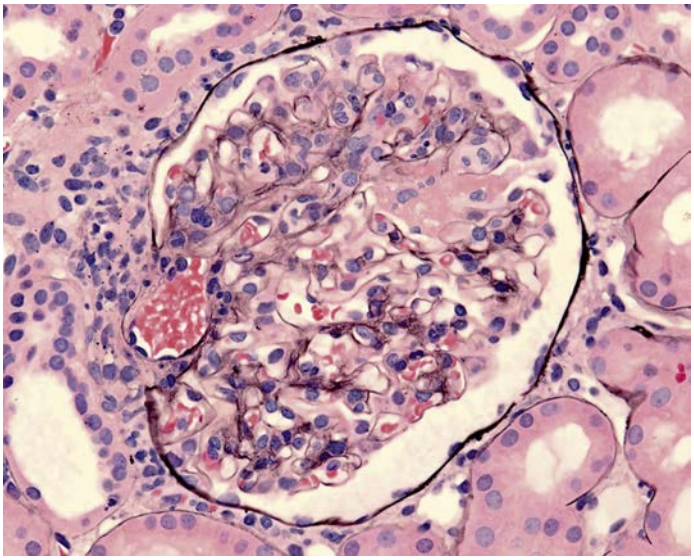

Fig. 55.47 Pauci-immune glomerulonephritis. Glomerulus with segmental small area of fibrinoid necrosis (Jones silver, ×400).

(EGPA; Churg-Strauss syndrome) (Jennette et al., 2013; Jennette & Nachman, 2017). Most patients are over 60 years of age and present with rapidly progressive renal failure, hematuria, and proteinuria. Small vessels, including venules, capillaries, arterioles, and small arteries, are often affected in other sites and organs such as the skin, ear, nose and throat area, and lung. However, kidney involvement usually dominates the clinical features. Necrotizing glomerulonephritis with crescents occurs in all three vasculitis syndromes, and a renal biopsy alone cannot distinguish them. The term *renal limited pauci-immune glomerulonephritis* may be used when only the kidney is involved. Glomerular lesions represent the major finding in the majority of renal biopsies. Vasculitis of the arterioles and small arteries is not observed in most cases but has been reported in about 20% of biopsy cases (Figs. 55.52 and 55.53). Chronic interstitial inflammation is not uncommon. Renal medullary angiitis, a necrotizing leukocytoclastic inflammation of the medullary vasa recta, is a characteristic lesion of ANCA disease (Hendricks et al., 2013) (Figs. 55.54 and 55.55). The finding of renal medullary angiitis in a biopsy not containing cortex and glomeruli should prompt testing for the presence of ANCAs. A histopathologic classification based on the number of normal glomeruli and the

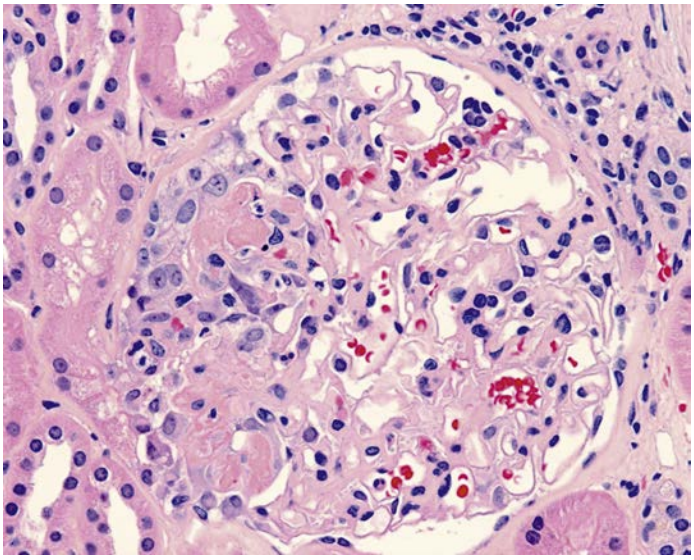

Fig. 55.48 Pauci-immune glomerulonephritis. Glomerulus with segmental fibrinoid necrosis and adjacent cellular crescent (H&E, ×400).

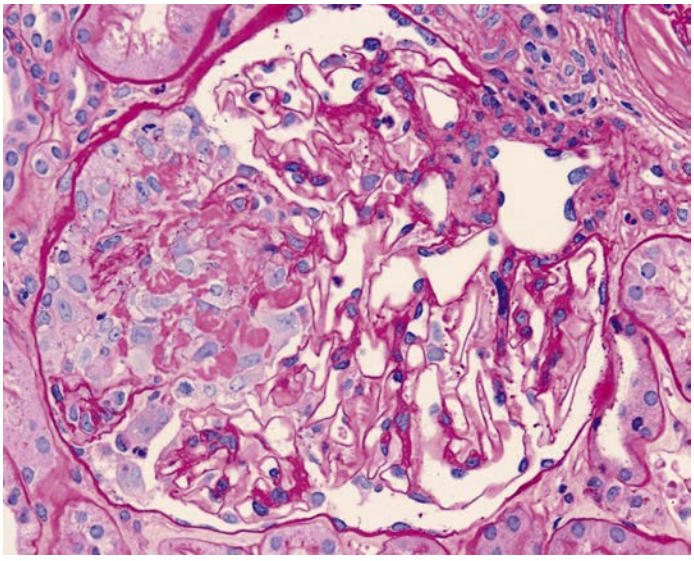

Fig. 55.49 Pauci-immune glomerulonephritis. Glomerulus with segmental fibrinoid necrosis and adjacent cellular crescent (PAS, ×400).

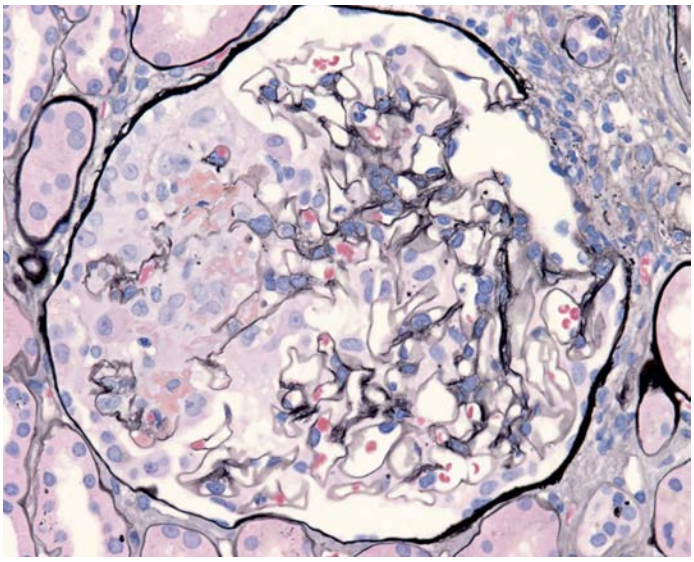

Fig. 55.50 Pauci-immune glomerulonephritis. Glomerulus with segmental fibrinoid necrosis and adjacent cellular crescent. Ruptures of the silver-positive glomerular basement membrane (GBM) are present (Jones silver, ×400).

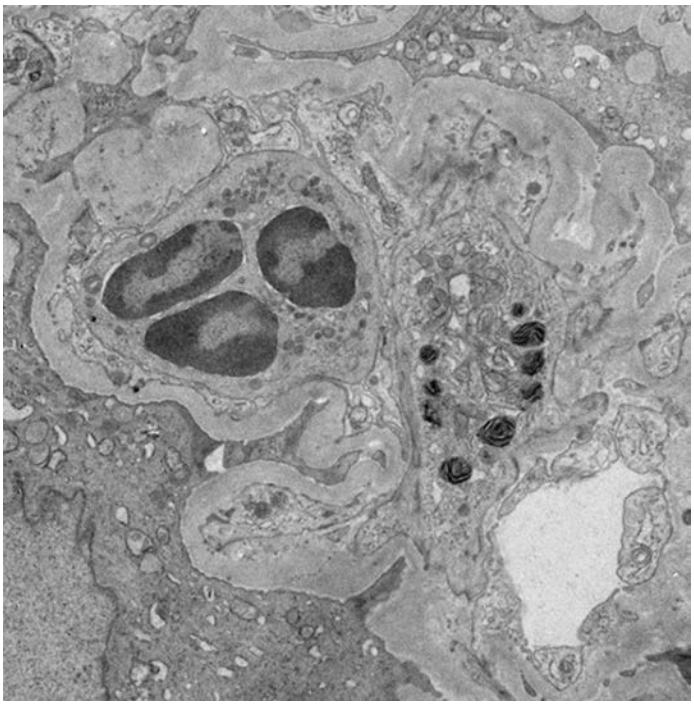

Fig. 55.51 Pauci-immune glomerulonephritis. Glomerulus with capillary loop compression by cellular crescent. No electron-dense deposits are present. A neutrophil is situated in the capillary (EM, ×12,000).

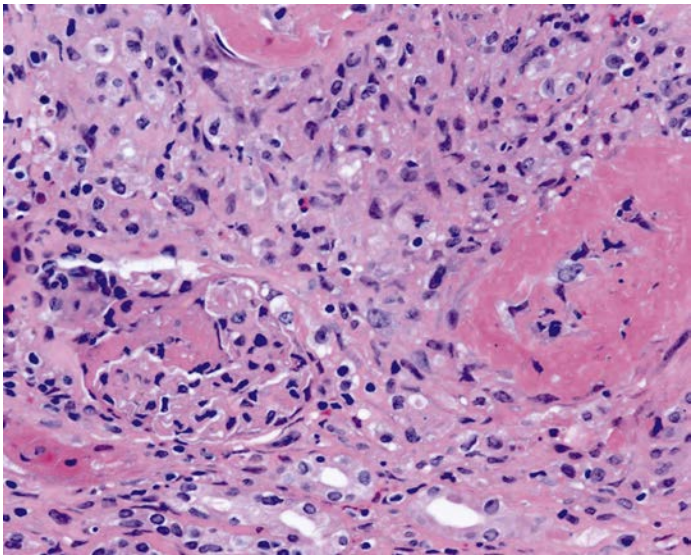

Fig. 55.52 Antineutrophil cytoplasmic autoantibodies (ANCA) small vessel vasculitis. Extensive fibrinoid necrosis of the wall of a small artery *(right).* Glomerulus with segmental fibrinoid necrosis is present *(left)* (H&E, ×200).

degree of glomerular crescents and sclerosis has shown prognostic value (Berden et al., 2010; Bjorneklett et al., 2016). Renal outcomes are best with greater than 50% normal glomeruli, worst with greater than 50% globally sclerotic glomeruli, and intermediate in the crescentic (>50% glomerular crescents) and mixed (<50% normal, crescentic and sclerotic glomeruli) categories. Other studies have emphasized the prognostic value of interstitial fibrosis and tubular atrophy (Berden et al., 2012) and proposed an ANCA-renal risk score based on percentage of normal glomeruli, interstitial fibrosis, and tubular atrophy and estimated glomerular filtration rate (Brix et al., 2018).

Most patients have positive serology for antineutrophil cytoplasmic antibodies. The ANCAs react with the cytoplasmic granules of both neutrophils and monocytes. Using indirect IF, two staining patterns are observed: perinuclear (p-ANCA) and cytoplasmic (c-ANCA). The major p-ANCA specificity is for myeloperoxidase (MPO-ANCA) and the major c-ANCA specificity is for proteinase 3 (PR3-ANCA). Both indirect IF and ELISA assays specific for MPO-ANCA and PR3-ANCA are routinely performed (Bossuyt et al., 2017). There is increasing agreement

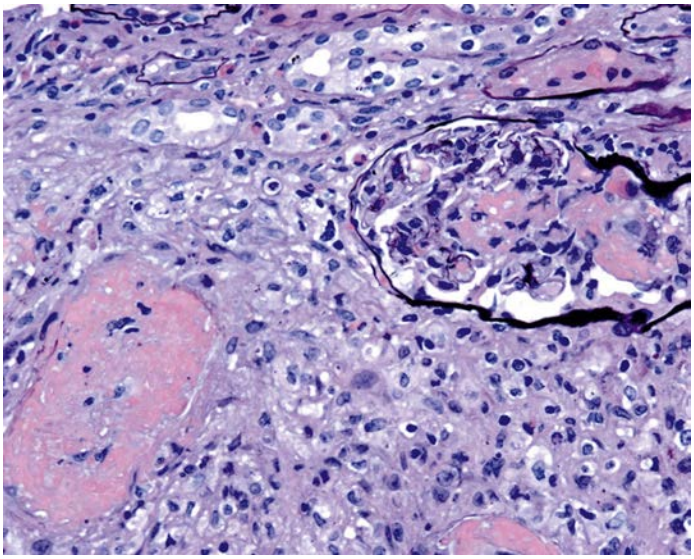

Fig. 55.53 Antineutrophil cytoplasmic autoantibodies (ANCA) small vessel vasculitis. Extensive fibrinoid necrosis of the wall of a small artery *(left)* and segmental fibrinoid necrosis in a glomerulus *(right)* (Jones silver, ×200).

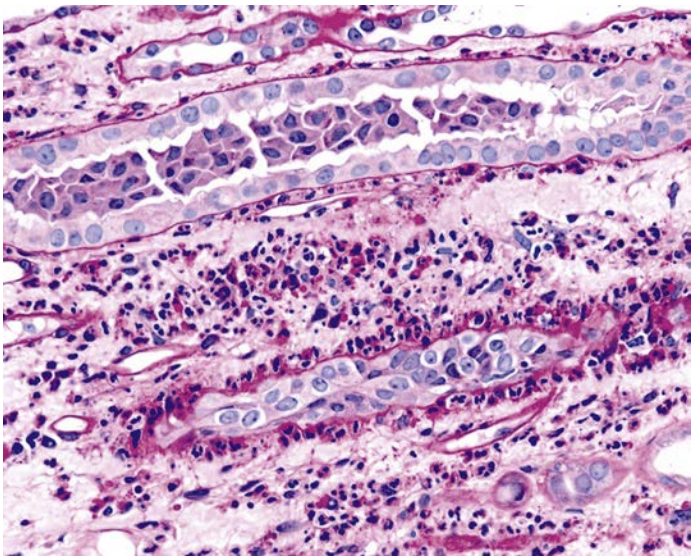

Fig. 55.54 Medullary angiitis. Neutrophil inflammation of the vasa recta and surrounding the medullary tubules (PAS, ×400).

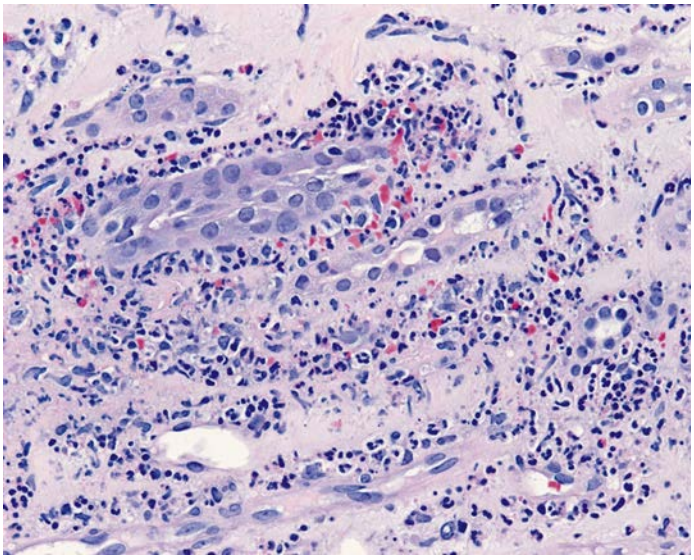

Fig. 55.55 Medullary angiitis. Leukocytoclastic angitis of the vasa recta in the renal medulla with red cell extravasation (H&E, ×400).

that immunoassays (ELISA) are the preferred screening method for the detection of ANCAs. It has been shown that some patients with small vessel vasculitis appear to have MPO-ANCAs that are not detected by conventional assays because of competitive binding of MPO by a fragment of ceruloplasmin (Roth et al., 2013). A trend is to simply use the ANCA serologic types, MPO-ANCA and PR3-ANCA, to characterize and follow patients with ANCA disease (Hilhorst et al., 2015). For example, several studies have indicated ANCA patients with PR3-ANCA positivity have a lower mortality rate but a higher relapse rate than ANCA patients that are MPO-ANCA positive. However, the integration of clinical phenotypes, radiologic information, ANCA serologic typing, and pathologic findings is recommended for accurate diagnosis and management of ANCA disease.

There is compelling evidence from both in vitro studies and in vivo experimental animal studies that ANCAs not only serve as a marker of disease but that they play a direct pathogenic role in the glomerular necrosis and inflammation (Jennette & Falk, 2014). A pathogenic model includes neutrophil priming by cytokines, expression of ANCA autoantigens at the neutrophil surface, interaction with ANCA autoantibodies, activation of complement, neutrophil adherence to vessel endothelium, neutrophil apoptosis and leukocytoclasia, and vessel wall destruction (Jennette & Nachman, 2017). It is not clear how ANCAs are initially generated. However, neutrophil extracellular traps (NETs), a mesh of neutrophil extruded DNA, histones, and granule proteins, appear to provide a platform on which autoantigens and ANCAs accumulate and augment an autoimmune response (Kessenbrock et al., 2009; Nakazawa et al., 2014; Kraaij et al., 2018). Recent studies have focused on the molecular interactions of the autoantigens, PR3 and MPO. For example, PR3-interacting proteins involved in apoptosis, such as annexin-1, are altered in neutrophils from patients with ANCA disease (Everts-Graber et al., 2019).

Exposure to several drugs have been associated with ANCA vasculitis (Pendergraft & Niles, 2014). Propylthiouracil, hydralazine, minocycline, and penicillamine have been reported. Use of cocaine, cut with the anthelminthic agent levamisole, has been associated with ANCA vasculitis characterized by dual positivity for MPO-ANCA and PR3-ANCA (McGrath et al., 2011).

Lupus Nephritis

Systemic lupus erythematosus is the classic autoimmune disease with both acute and chronic clinical manifestations. The American College of Rheumatology (ACR) has included 11 clinical and immunologic criteria (malar rash, discoid rash, photosensitivity, oral ulcers, nonerosive arthritis, pleuritis or pericarditis, renal disorder, neurologic disorder [e.g., seizures or psychosis], hematologic disorder [e.g., pancytopenia], immunologic disorder [including positive anti-double-stranded DNA or positive anti-Sm or positive antiphospholipid antibodies], and positive antinuclear antibody [ANA] test) (Hochenburg, 1997). The presence of four or more of the criteria gives 96% sensitivity and specificity for SLE. A less known classification is one proposed by the Systemic Lupus International Collaborating Clinics (SLICC) group (Petri et al., 2012). It includes 11 clinical criteria, 6 immunologic criteria, and 1 stand-alone criterion (biopsy-proven LN in the presence of ANA or anti-dsDNA antibodies). The SLICC classification requires at least four criteria, including at least one clinical criterion and one immunologic criterion or the standalone renal criterion of biopsy-proven LN. Several studies have indicated the SLICC is more sensitive than the ACR, especially in early SLE disease (Ines et al., 2015; Hartman et al., 2018; Low et al., 2019, Tao et al., 2019). However, the SLICC has been shown to compromise the specificity of diagnosis when the standalone renal criterion (renal biopsy) was applied (Rijnink et al., 2018).

Renal disease in SLE, called lupus nephritis, may involve all parenchymal compartments (glomeruli, vessels, tubules, and interstitium) and produces the greatest risk of morbidity and mortality in lupus patients (Almaani et al., 2017; Yu et al., 2017). LN is most common in black females between 15 and 45 years of age. The clinical findings of LN are diverse and include hematuria (usually microscopic), proteinuria, nephrotic syndrome, urinary red cell casts, renal insufficiency, and tubular defects. The current International Society of Nephrology/Renal Pathology Society (ISN/RPS) classification of lupus nephritis has facilitated communication between pathologists and nephrologists and has provided a standard for clinical-pathologic studies (Weening et al., 2004). It consists of six well-defined classes; however, it relies primarily on LM and focuses on glomerular lesions. Evaluation of extraglomerular pathology, including vascular and tubulointerstitial lesions, may improve the predictive value for renal outcome in LN patients (Wu et al., 2013; Rijnink et al., 2017; Leatherwood et al., 2019). The original ISN/RPS classification has been revisited and revised with proposed additional modifications (Wilhelmus et al., 2015; Bajema et al., 2018).

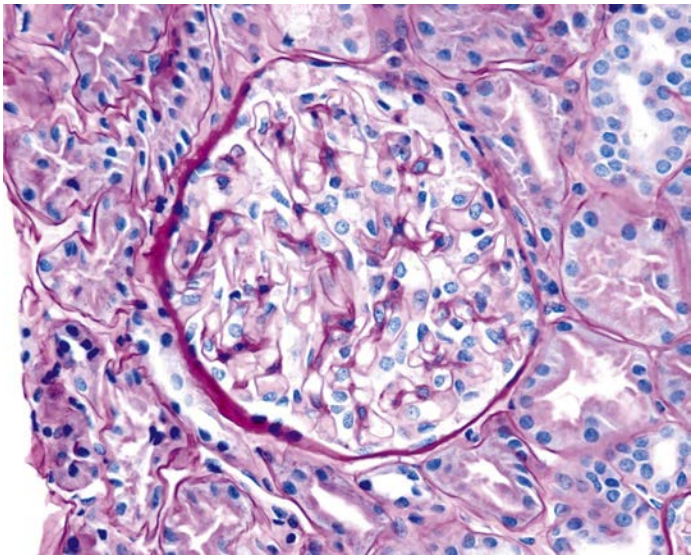

Fig. 55.56 Lupus nephritis class I. The glomerulus is normocellular with patent capillary lumens and no apparent mesangial abnormalities (PAS, ×400).

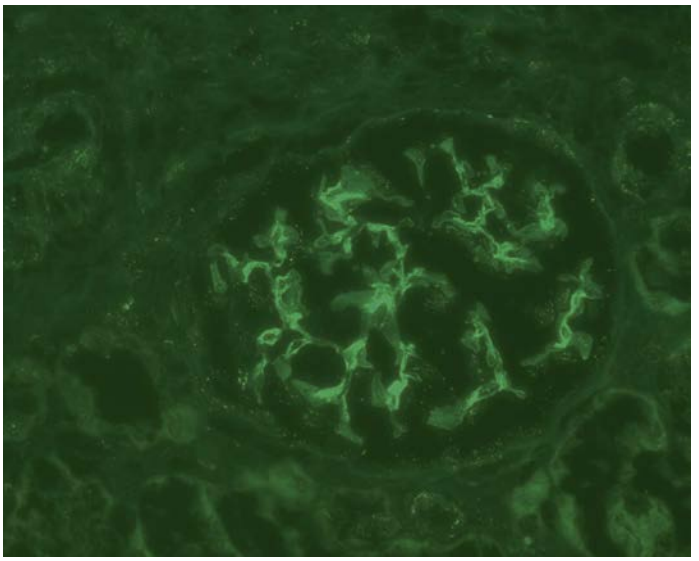

Fig. 55.57 Lupus nephritis class I. Mesangial staining for IgG (IF, ×400).

The six classes of LN are class I, minimal mesangial LN; class II, mesangial proliferative LN; class III, focal LN; class IV, diffuse LN; class V, membranous LN; and class VI, advanced sclerosing LN. The LN classes show various degrees of glomerular hypercellularity on LM and immune deposits detected on IF (typically all immunoglobulin and complement components are present) and EM in all the classes. In renal biopsy specimens, diffuse LN (class IV) is the most commonly encountered class.

Minimal mesangial LN (class I) has normal appearing glomeruli by LM (Fig. 55.56) but mesangial deposits by IF (Fig. 55.57) and EM (Fig. 55.58). Mesangial proliferative LN (class II) shows mesangial hypercellularity by LM (Fig. 55.59) and mesangial deposits by IF (Fig. 55.60) and EM (Fig. 55.61). Focal LN (class III) is characterized by glomerular hypercellularity involving less than 50% of the glomeruli. There is endocapillary hypercellularity, often segmental, with or without necrosis and crescents (Fig. 55.62). Focal mesangial and capillary wall deposits are stained by IF (Fig. 55.63) and mesangial and subendothelial deposits by identified by EM (Fig. 55.64). Diffuse LN (class IV) shows endocapillary hyperplasia in more than 50% of the glomeruli (Fig. 55.65). There is often accompanying karyorrhectic nuclear debris in the inflamed capillaries (Fig. 55.66). Prominent eosinophilic thickening of peripheral glomerular loops, called wire loops, represent large subendothelial deposits (Figs. 55.67, 55.68, and 55.69). Actual capillary intraluminal deposits (called "hyaline thrombi," a misnomer) may be observed (see Fig. 55.69). Intraglomerular accumulation of monocytes is often seen (Fig. 55.70). There is diffuse mesangial and especially capillary wall staining by IF (Figs. 55.71 and 55.72).

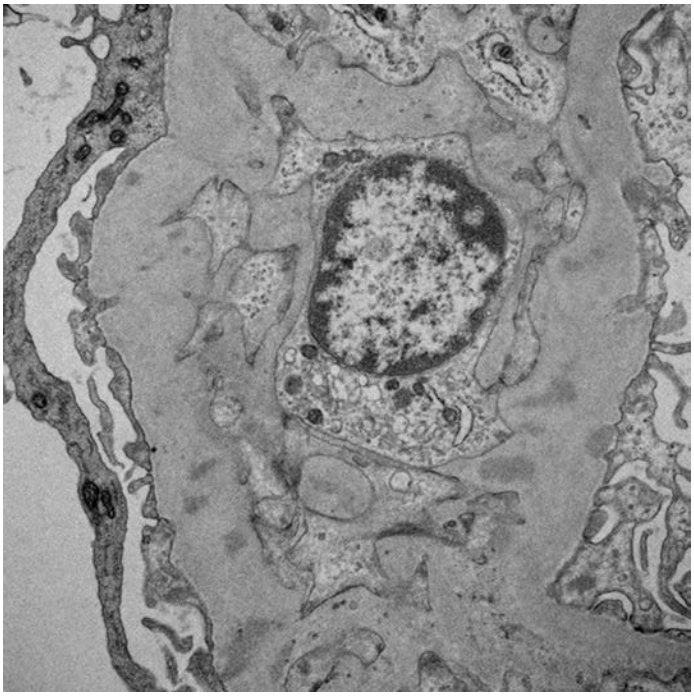

Fig. 55.58 Lupus nephritis class I. Mesangial cell with surrounding small electron-dense deposits (EM, ×15,000).

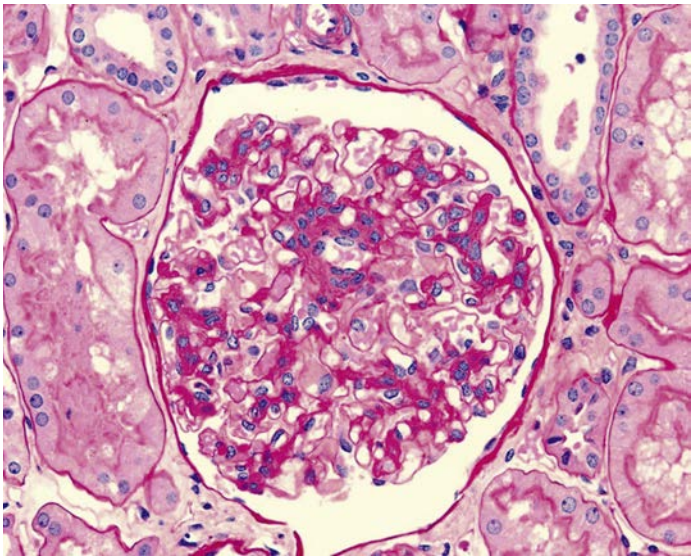

Fig. 55.59 Lupus nephritis class II. Mild mesangial hypercellularity is accompanied by mild mesangial expansion (PAS, ×400).

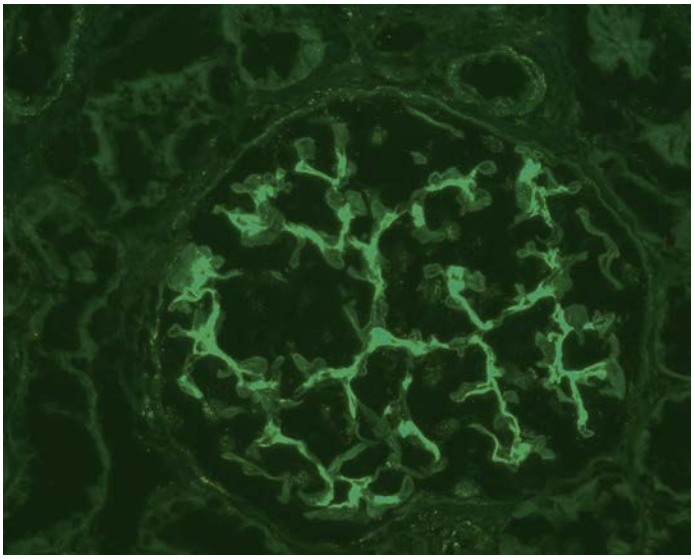

Fig. 55.60 Lupus nephritis class II. Mesangial pattern of IgG deposition (IF, ×400).

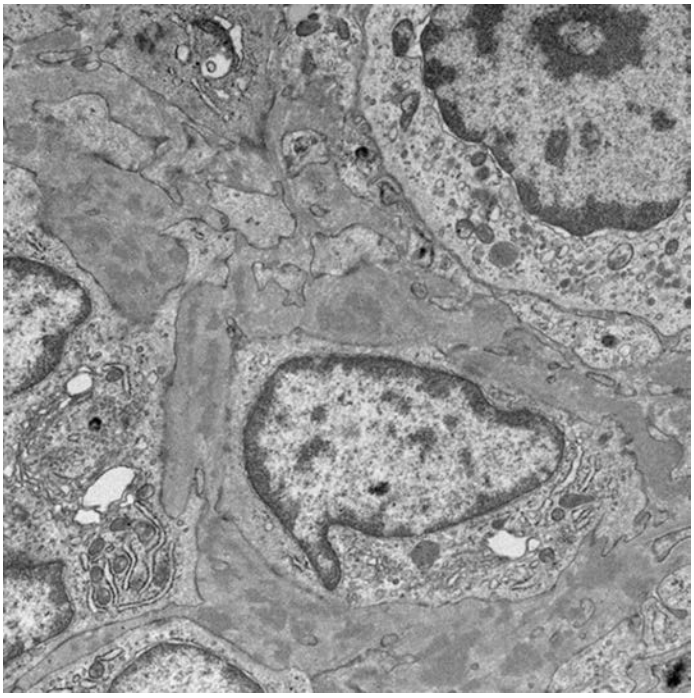

Fig. 55.61 Lupus nephritis class II. Numerous electron-dense deposits within expanded mesangium (EM, ×12,000).

Mesangial and subendothelial deposits are conspicuous by EM (Figs. 55.73 and 55.74). Membranous LN (class V) has a membranous pattern with thickened capillary walls on LM (Fig. 55.75), typically GBM vacuoles and/or spikes on silver stains (Fig. 55.76), diffuse capillary wall staining by IF (Fig. 55.77), and prominent subepithelial deposits by EM (Fig. 55.78). Some cases are mixed with the characteristic lesions of different classes, such as class IV combined with class V (Figs. 55.79 and 55.80). Advanced sclerosing LN (class VI) is defined by greater than 90% global glomerulosclerosis without residual activity.

Mesangial hypercellularity and mesangial immune deposits typify class II LN, but they are present and occur as underlying lesions in classes III, IV, and V. The IF staining in all the LN classes is characteristically full house (or near full house) with staining of all immunoglobulin (IgG, IgM, IgA) and complement (C3, C1q) components. The intense glomerular staining of C1q is a helpful diagnostic finding. The glomerular lesions in classes III and IV are qualitatively similar and differ mainly in the percentage of glomerular involvement. EM is extremely valuable for determination of the precise localization of immune deposits (mesangial, subendothelial, intramembranous, or subepithelial). The electron dense deposits in LN may exhibit a substructure, including tubular or fingerprint forms. A characteristic but not specific ultrastructural finding is tubuloreticular inclusions (TRIs) most commonly present in glomerular endothelial cytoplasm (Fig. 55.81; see Fig. 55.80). TRIs are also found with HIV infection and in other collagen vascular diseases.

In addition to determining the ISN/RPS specific class of LN in a renal biopsy, graded scoring of pathologic lesions is usually performed and incorporated into the NIH activity and chronicity indexes (Austin et al., 1984). The lesions (scored 0–3+) for activity index (total score of 0–24) include endocapillary hypercellularity, neutrophil infiltration, subendothelial hyaline deposits (wire-loop lesions), fibrinoid necrosis/karyorrhexis (x 2 score), cellular crescents (x 2 score), and interstitial inflammation. The lesions (scored 0–3+) for chronicity index (total score of 0–12) include glomerular sclerosis, fibrous crescents, tubular atrophy, and interstitial fibrosis. Although the NIH activity index (AI) and chronicity index (CI) have limitations, they are often used to assess response to therapy and disease progression in individual patients that have follow-up renal biopsies. There is limited data on the value of repeat renal biopsies in LN. However, one study has indicated repeat renal biopsy in LN patients while they are in complete renal remission may guide the immunosuppression therapy and predict disease relapse (De Rosa et al., 2018).

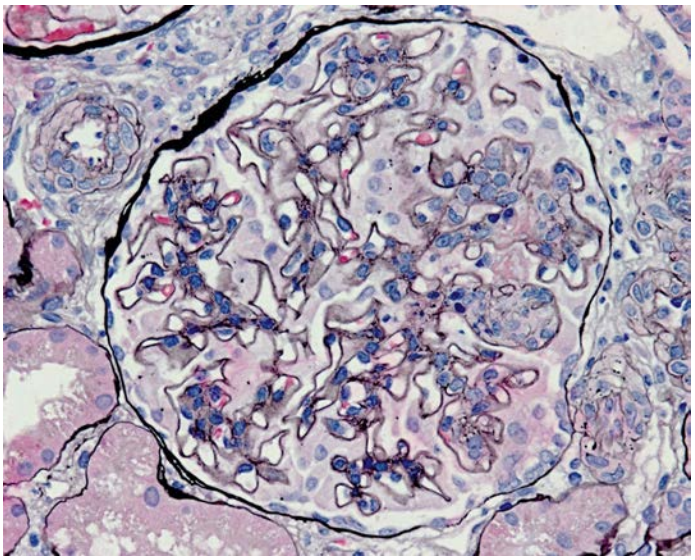

Fig. 55.62 Lupus nephritis class III. Segmental endocapillary hypercellularity with fibrinoid necrosis and karyorrhectic debris (Jones silver, ×400).

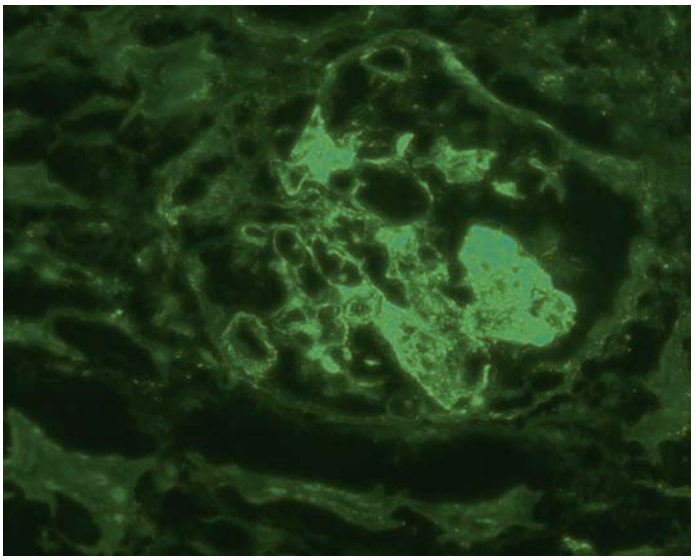

Fig. 55.63 Lupus nephritis class III. Strong staining for IgG in the glomerular mesangium, capillary walls and lumina (IF, ×400).

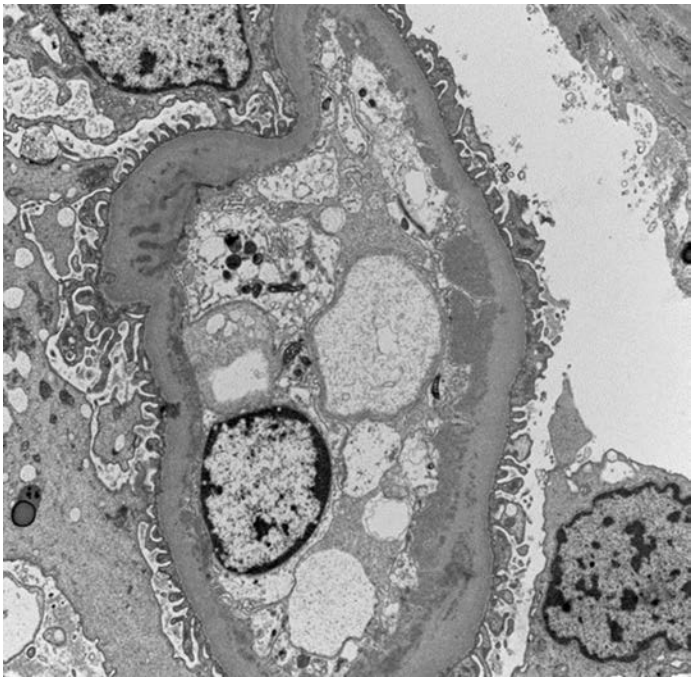

Fig. 55.64 Lupus nephritis class III. Electron-dense subendothelial deposits are present. Podocyte foot processes are intact (EM, ×8000).

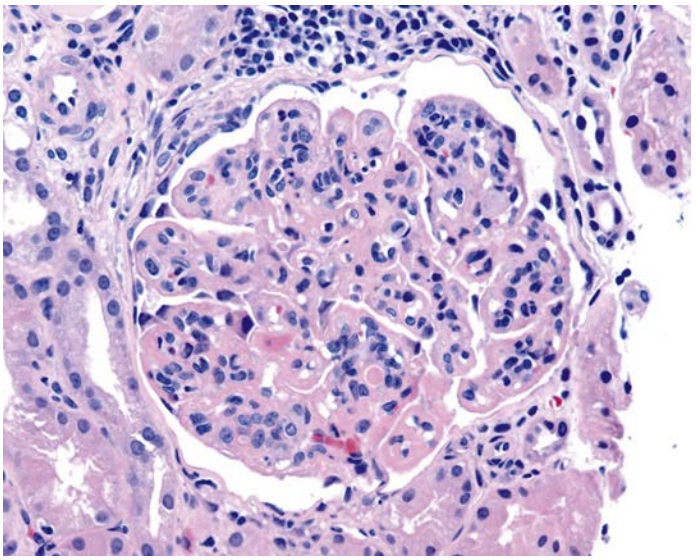

Fig. 55.65 Lupus nephritis class IV. Severe global endocapillary hypercellularity with near occlusion of glomerular capillaries (H&E, ×400).

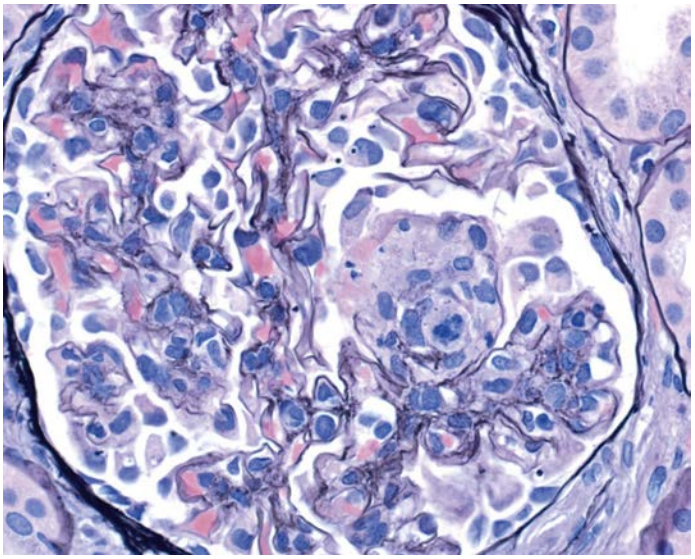

Fig. 55.66 Lupus nephritis class IV. Segmental endocapillary hypercellularity with fibrinoid necrosis, glomerular basement membrane (GBM) ruptures, and karyorrhectic nuclear debris (Jones silver, ×630).

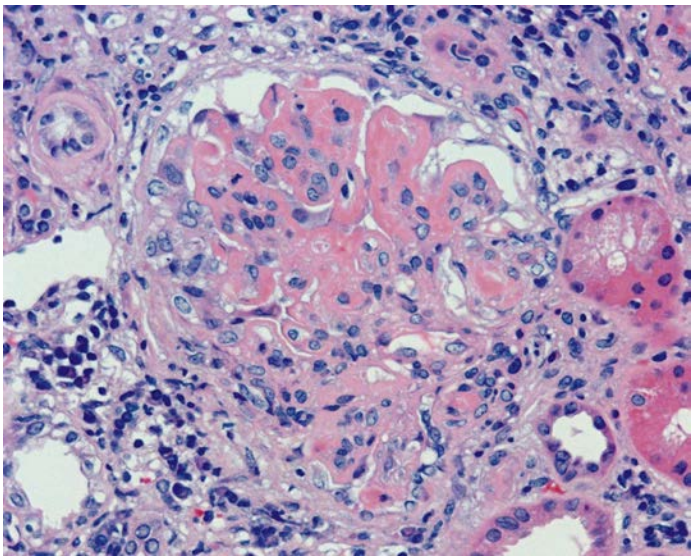

Fig. 55.67 Lupus nephritis class IV. Intense eosinophilic thickening of glomerular capillary walls representing "wire-loop" subendothelial deposits (H&E, ×400).

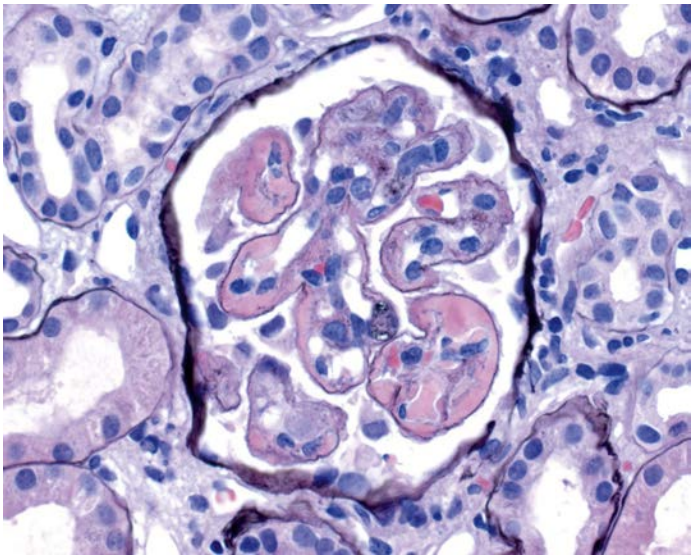

Fig. 55.68 Lupus nephritis class IV. Prominent subendothelial deposits ("wire-loops"). Note the eosinophilic deposits are enclosed by the silver-positive glomerular basement membranes (GBMs) (Jones silver, ×400).

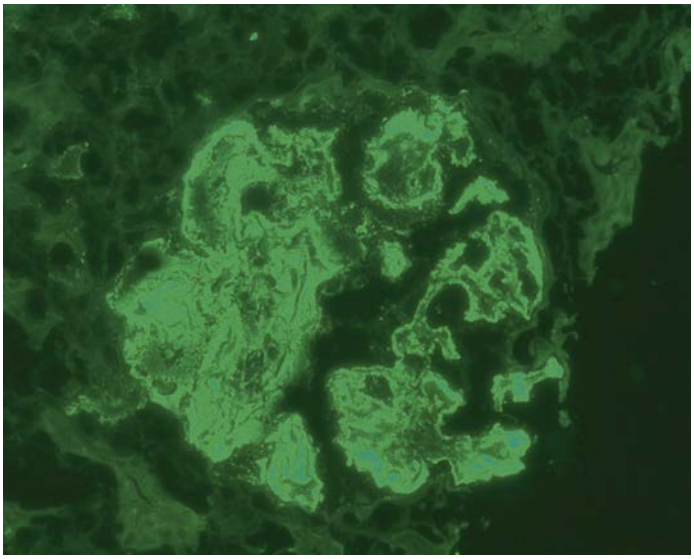

Fig. 55.71 Lupus nephritis class IV. Strong staining for IgG in glomerular mesangium and peripheral capillary loops (IF, ×400).

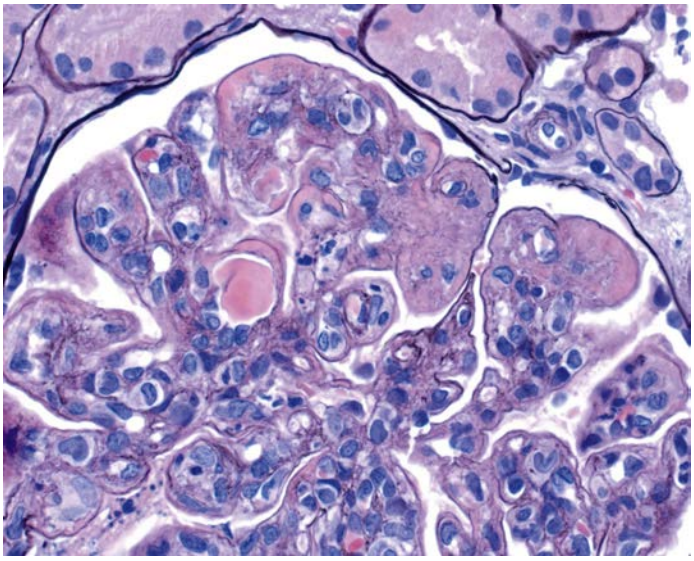

Fig. 55.69 Lupus nephritis class IV. Endocapillary hypercellularity with subendothelial deposits ("wire-loops") and prominent round capillary lumen eosinophilic deposit (so-called "hyaline thrombus") (Jones silver, ×630).

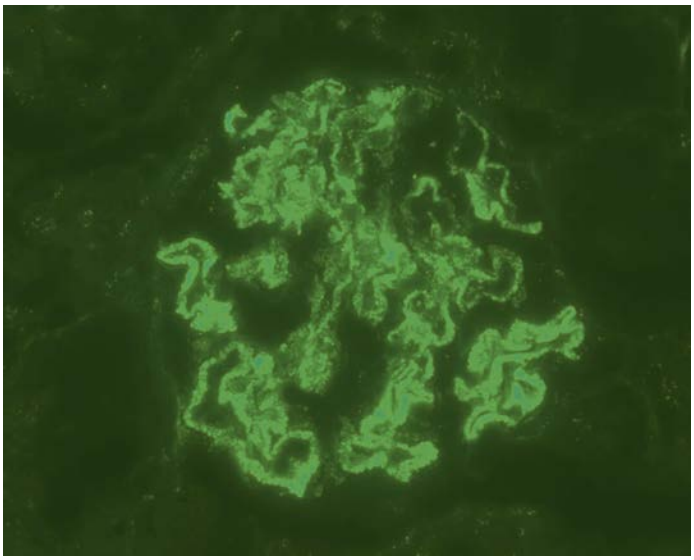

Fig. 55.72 Lupus nephritis class IV. Prominent deposits of C1q in glomerular mesangium and peripheral capillary loops (IF, ×400).

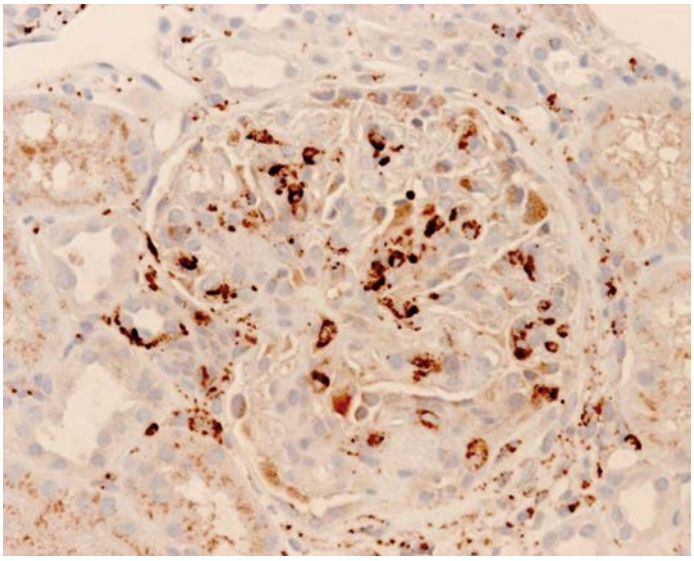

Fig. 55.70 Lupus nephritis class IV. Glomerulus containing prominent numbers of CD68-immunoreactive monocytes (CD68 IHC, ×400).

Some patients with established SLE present with the nephrotic syndrome, and the renal biopsies show normal glomeruli, FSGS, or mesangial proliferation on LM. No endocapillary hypercellularity or crescents are present. IF reveals no deposits or only mesangial deposits. EM reveals prominent podocyte injury characterized by severe foot process effacement and no electron-dense deposits or only mesangial deposits (Kraft et al., 2005; Hu et al., 2016). There is a high disease relapse rate in these patients. The term *lupus podocytopathy* has been proposed for these cases. It is not included in the ISN/RPS classification of LN. The pathologic spectrum in lupus podocytopathy with minimal changelike lesions, FSGS, and apparent class I and II LN suggests different pathogenic mechanisms with the common element of podocyte injury.

Collapsing glomerulopathy (collapsing variant of FSGS) has been described in patients with SLE with or without concurrent lupus nephritis (Salvatore et al., 2012). Collapsing glomerulopathy (CG) appears uncommon in SLE patients but appears similar to idiopathic CG, in that a significant number of patients progress to ESRD. In a study of over 500 renal biopsies from SLE patients, CG was identified in 5% and strongly associated with the presence of apolipoprotein L1 (APOL1) risk alleles (Larsen et al., 2013). Blacks carrying APOL1 risk alleles have an increased risk for FSGS (Kopp et al., 2011).

The complex pathogenesis of LN remains to be fully understood (Hahn, 2019; Fu et al., 2019). Genetic and epigenetic predisposing factors are critically important. Stimulation and interaction of the innate and

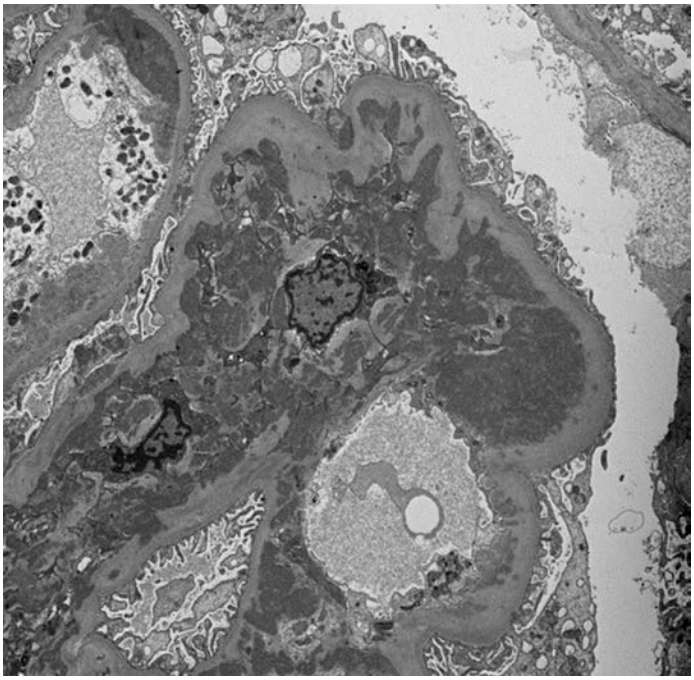

Fig. 55.73 Lupus nephritis class IV. Massive mesangial and subendothelial electron-dense deposits (EM, ×5000).

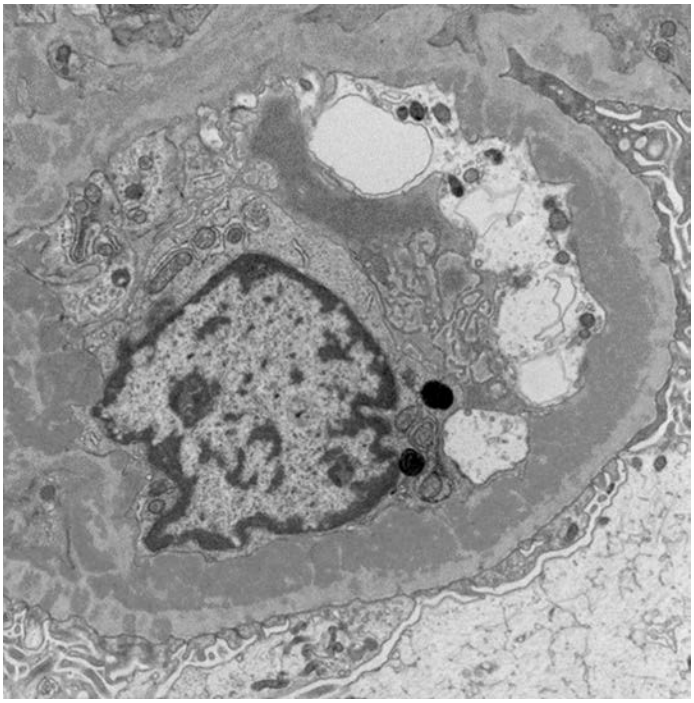

Fig. 55.74 Lupus nephritis class IV. Glomerular loop with a large circumferential subendothelial electron-dense deposit (EM, ×12,000).

adaptive immune responses occurs. B- and T-lymphocyte abnormalities are present. Macrophages and dendritic cells play a role. Underlying metabolic abnormalities of these cells likely play a role (Morel, 2019). Autoantibodies and immune complexes effect tissue damage. Apoptotic pathways and NETs are involved (Mohan & Putterman, 2015).

Most patients have circulating autoantibodies to nuclear antigens (ANAs). Autoantibodies to double-stranded DNA (dsDNA) are most specific, but autoantibodies to histones, ribonucleoproteins (RNP), including the Sm core protein, Rho (SAA) antigen, C1q, and endothelial antigens, are common. The kidney injury in lupus nephritis involves both immune and nonimmune mechanisms (Davidson, 2016; Fu et al., 2019). Glomerular immune deposits and complement activation clearly are involved in LN, but the mechanisms of their deposition are not fully understood. Mediators

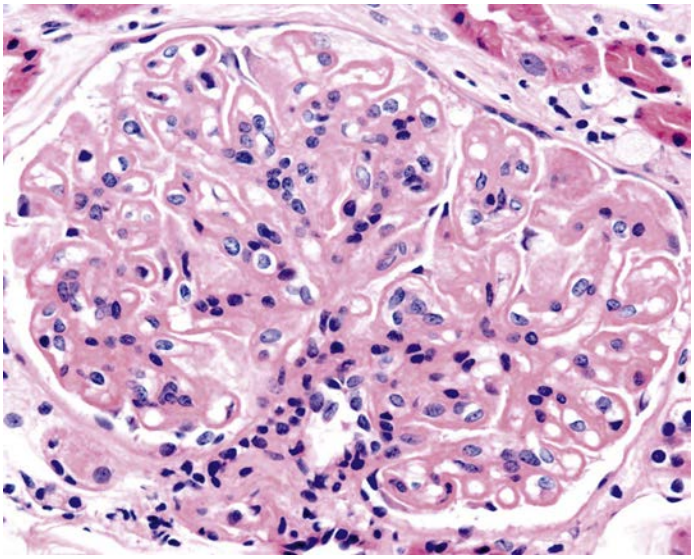

Fig. 55.75 Lupus nephritis class V. Glomerulus with spherical capillary wall thickening and mild mesangial hypercellularity (H&E, ×400).

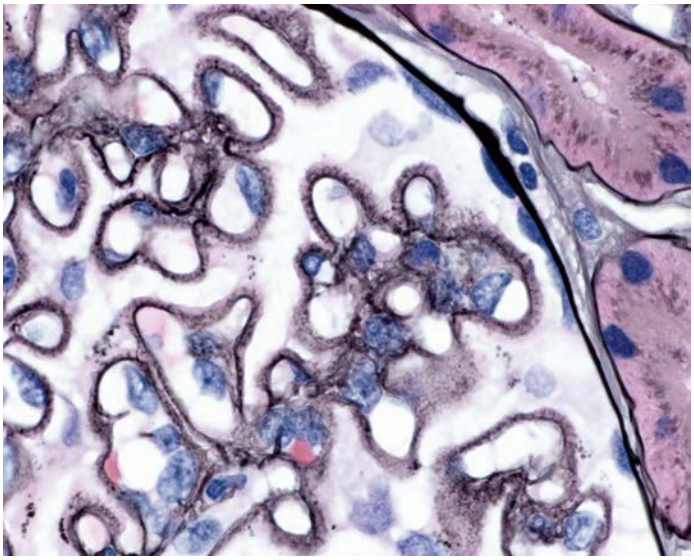

Fig. 55.76 Lupus nephritis class V. Glomerular capillaries with spiking of the glomerular basement membranes (GBMs) (Jones silver, ×630).

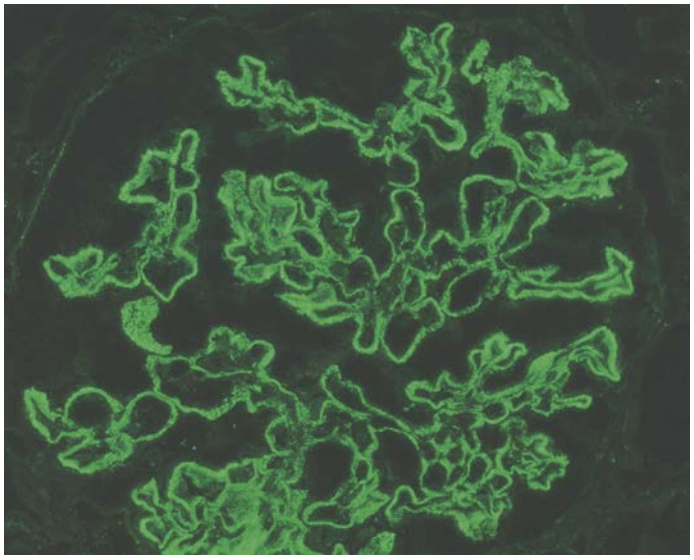

Fig. 55.77 Lupus nephritis class V. Granular (subepithelial) deposits of IgG along the glomerular capillary walls (IF, ×400).

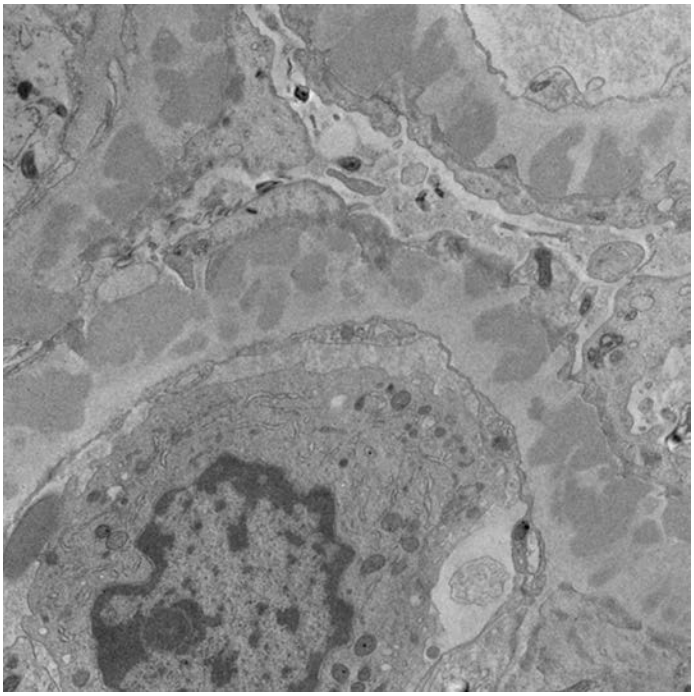

Fig. 55.78 Lupus nephritis class V. Glomerular loops thickened by numerous subepithelial and intramembranous electron dense deposits (EM, ×12,000).

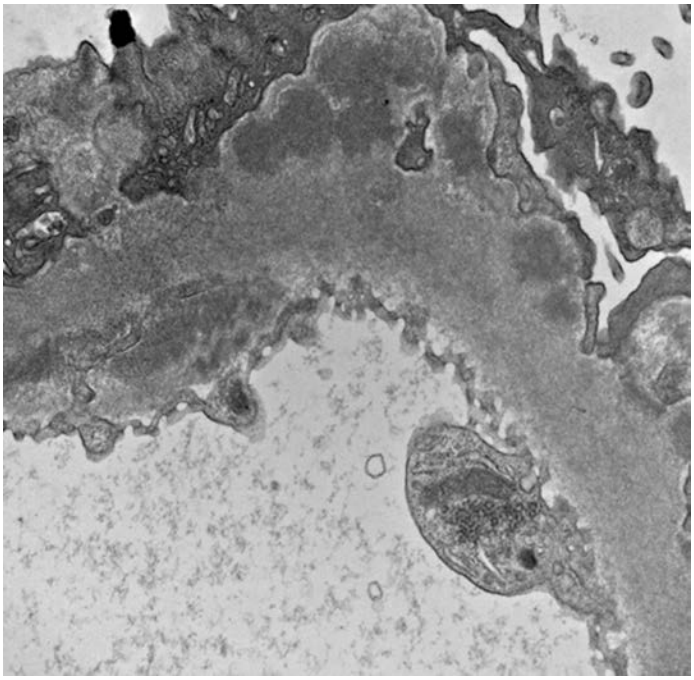

Fig. 55.80 Lupus nephritis combined class IV and V. Subepithelial and subendothelial electron-dense deposits and endothelial tubuloreticular inclusion (TRI) (EM, 25,000).

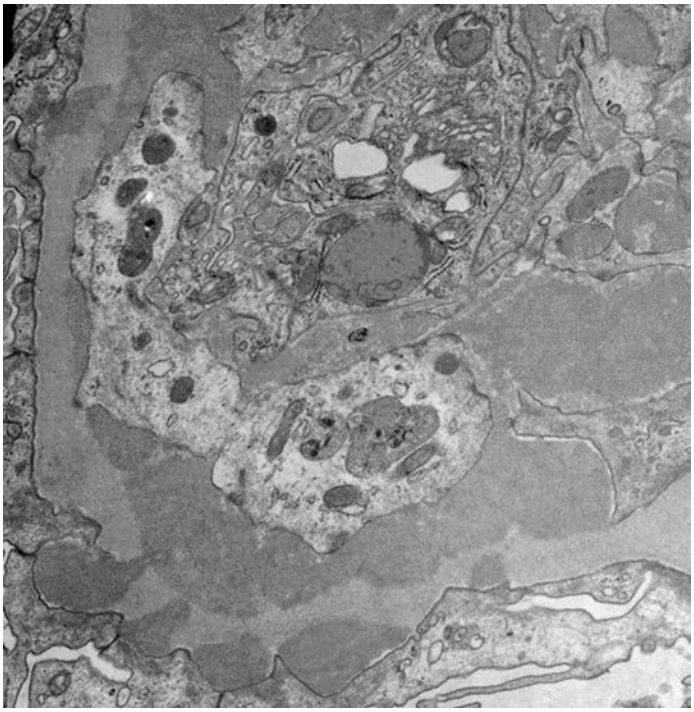

Fig. 55.79 Lupus nephritis combined class IV and V. Large subendothelial and subepithelial electron-dense deposits on both sides of the glomerular basement membrane (GBM) (EM, ×12,000).

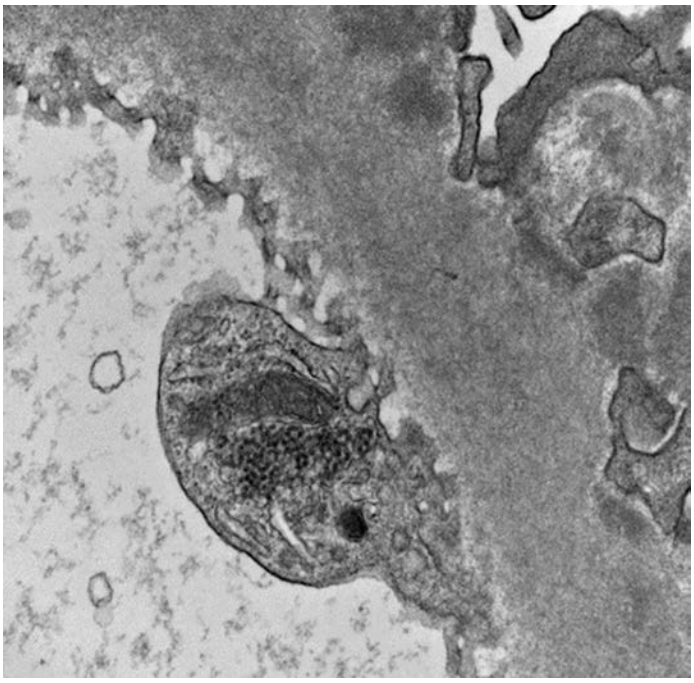

Fig. 55.81 Lupus nephritis combined class IV and V. Tubuloreticular inclusion (TRI) within glomerular endothelial cytoplasm. Higher magnification of Fig. 55.80 (EM ×40,000).

include chemokines, interferons, and interferon regulatory factors (Barnes, 2019; Matta & Barnes, 2019). Neutrophils, T cells, B cells, macrophages, and dendritic cells infiltrate the kidney. Nonimmune mechanisms include disruption of cell-cell interactions, vascular injury and hypoxia, and glomerulosclerosis and interstitial fibrosis.

Newer investigative approaches applied to LN will provide insights into pathogenesis. Studies using single-cell profiling with RNA-seq analysis in renal biopsies of LN revealed multiple populations of T cells, B cells, NK cells, and myeloid cells; prominent interferon responses; and expression of chemokine receptors CXCR4 and CX3CR1 (Arazi et al., 2019; Der et al., 2019). Studies using digital spatial profiling (DSP) for in situ analysis of protein and RNA expression in renal biopsies of LN will also increase our understanding of immune and nonimmune pathogenic mechanisms (Decalf et al., 2019).

IMMUNOENDOCRINOPATHIES

AUTOIMMUNE DISORDERS OF CARBOHYDRATE METABOLISM

Autoimmunity to the islet cells, insulin, or the insulin receptor concern type 1 diabetes mellitus, type B insulin resistance, the insulin autoimmune syndrome, and insulinomimetic autoantibodies. For brevity, autoantibodies to glucagon, the pancreatic islet alpha cells (Winter et al., 1984), and delta cells are not discussed.

Type 1 Diabetes Mellitus

Type 1 diabetes mellitus (T1DM) results from a cell-mediated autoimmune attack on the beta cells that leads to beta cell failure and absolute insulinopenia (Winter et al., 2016; Atkinson, 2012). Insulitis is the descriptive term for the lymphocytic infiltration of the islets that causes beta cell death. However, histologic study of the islets is not used to diagnose T1DM. In addition to cytotoxic CD8 T cells, macrophages also appear to damage beta cells via cytokine release (e.g., TNF-α).

T1DM is a very unusual autoimmune disease based on its early age at onset (an increasing number of children under age 5) and equal prevalence in males and females (with a slight excess of males under age 5). The clinical presentation is that of polyuria, polydipsia, and weight loss. Approximately 30% of children with T1DM present with ketoacidosis. A slower onset form of T1DM in adults is termed *latent autoimmune diabetes of adulthood*, where the patient may first be diagnosed with type 2 diabetes mellitus because of the mild degree of hyperglycemia initially recognized (Leslie et al., 2008; Carlsson, 2019). Heterogeneity within the "T1DM" phenotype is leading investigators to entertain the possibly that T1DM may be more than one disease. A very rare form of type 1 diabetes is the IPEX syndrome. IPEX is characterized by immunodysregulation (I), polyendocrine autoimmune disorders (P), enteropathy (E), and X-linked recessive inheritance (X). Type 1 diabetes is also present in one-third of persons affected with stiff-person syndrome (see later).

TABLE 55.5

Islet Autoantibodies Clinically Useful for the Diagnosis of T1DM

Islet Autoantibody Name	Abbreviation	Common Methods of Detection
Islet cell cytoplasmic autoantibodies	ICA	Indirect immunofluorescence
Insulin autoantibodies	IAA	Immunoprecipitation; ECL
Glutamic acid decarboxylase autoantibodies	GADA	Immunoprecipitation; ELISA; ECL
Insulinoma-2-associated autoantibodies	IA-2A	Immunoprecipitation; ELISA; ECL
Zinc transporter-8 autoantibodies	ZnT8A	ELISA; ECL

ECL, Electrochemiluminescent; *ELISA,* enzyme-linked immunosorbent assay.

T1DM is more common in Europeans and people of European origin than in other ethnicities. Approximately 1 in 100 Finns suffers from type 1 diabetes, whereas type 1 diabetes affects only ~1 in 10,000 persons living in Japan or China. The long-term risks of T1DM relate to the development of macrovascular, microvascular, and neuropathic complications. The present treatment of T1DM requires insulin replacement by subcutaneous injection or continuous subcutaneous infusion. Closed-loop, artificial pancreas systems consisting of an insulin pump and continuous subcutaneous glucose measurement system that are wirelessly linked together and controlled through intelligent and anticipatory programs have been developed (Kovatchev, 2019).

Presently there are five islet autoantibodies that are most useful for the diagnosis of T1DM in a symptomatic patient with hyperglycemia (Table 55.5). None of these autoantibodies are believed to be pathogenic. Applying these five tests in the setting of new-onset T1DM, 95% to 98% or more of patients will be positive for at least one islet autoantibody (Winter & Schatz, 2011).

Islet Cell Cytoplasmic Autoantibodies

Islet cell cytoplasmic autoantibodies (ICA) were first described in 1974 in patients with multigland autoimmunity (Bottazzo et al., 1974). ICA are present in 70% to 80% of new-onset patients with T1DM. The frequency of ICA in the general pediatric population is very low at 1 in 250 (Schatz et al., 1994). Therefore ICA are sensitive and specific for the diagnosis of T1DM in a symptomatic, hyperglycemic patient.

The detection of ICA was described previously. Although IIF is a conceptually simple technology, to perform ICA testing consistently and reliably, persistent and substantial quality assurance and quality control efforts are absolutely necessary. Figure 55.82 illustrates an ICA-positive serum.

Insulin Autoantibodies

Insulin autoantibodies (IAA) were first described in 1983 (Palmer et al., 1983). IAA are present at the time of diagnosis of T1DM in up to 60% of children (Atkinson et al., 1986) but are uncommon in adults. They are present in a few percent of the general population and can be found in other autoimmune diseases such as AITD.

As described, the IAA assay does not distinguish insulin antibodies from insulin autoantibodies; therefore the IAA assay should not be ordered on patients who have been treated with insulin for more than 14 days. IAA are detected by immunoprecipitation of ^{125}I-labeled A-14 monoiodinated insulin (Fig. 55.83). Newer electrochemiluminescent (ECL) assays using insulin or proinsulin as the autoantigen have been developed (Yu et al., 2013).

Glutamic Acid Decarboxylase Autoantibodies

Glutamic acid decarboxylase (GAD) was first identified as the "64K" autoantigen by Baekkeskov et al. (1990). There are two forms of GAD: GAD65 (65 kDa) and GAD67 (67 kDa), which are encoded by separate genes. Autoimmunity to GAD65 is more common than autoimmunity to GAD67, and therefore most immunoprecipitation assays use GAD65 as the autoantigen. ECL and ELISA for GADA have been developed (Miao et al., 2013).

GADA are present at the onset of T1DM in frequencies similar to that of ICA; however, GADA are less specific for the diagnosis of T1DM than ICA because GADA are more common in the general population

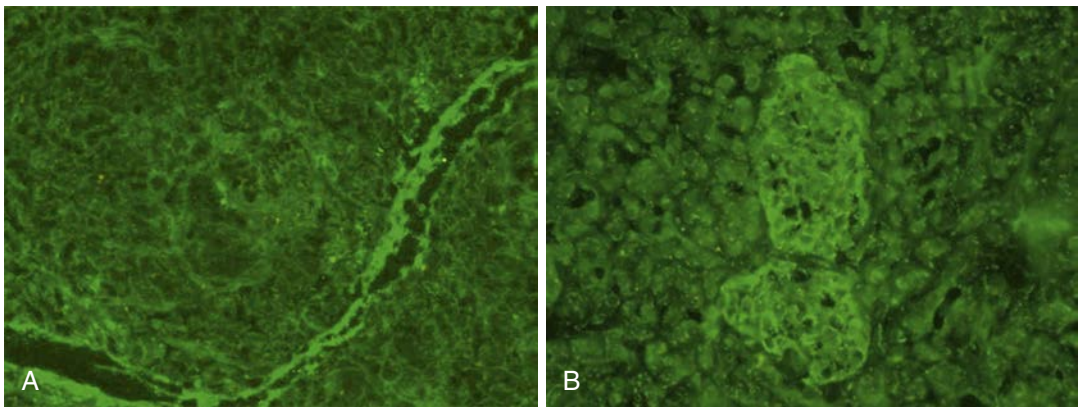

Fig. 55.82 Islet cell cytoplasmic autoantibodies (ICA) can be detected by indirect immunofluorescence. **A,** Negative control. **B,** Positive patient result. Note how all cells of the islet are identified by ICA (e.g., ICA is not beta cell specific). ICA are quantitated in Juvenile Diabetes Foundation (JDF) units that are determined by serial end-point dilution.

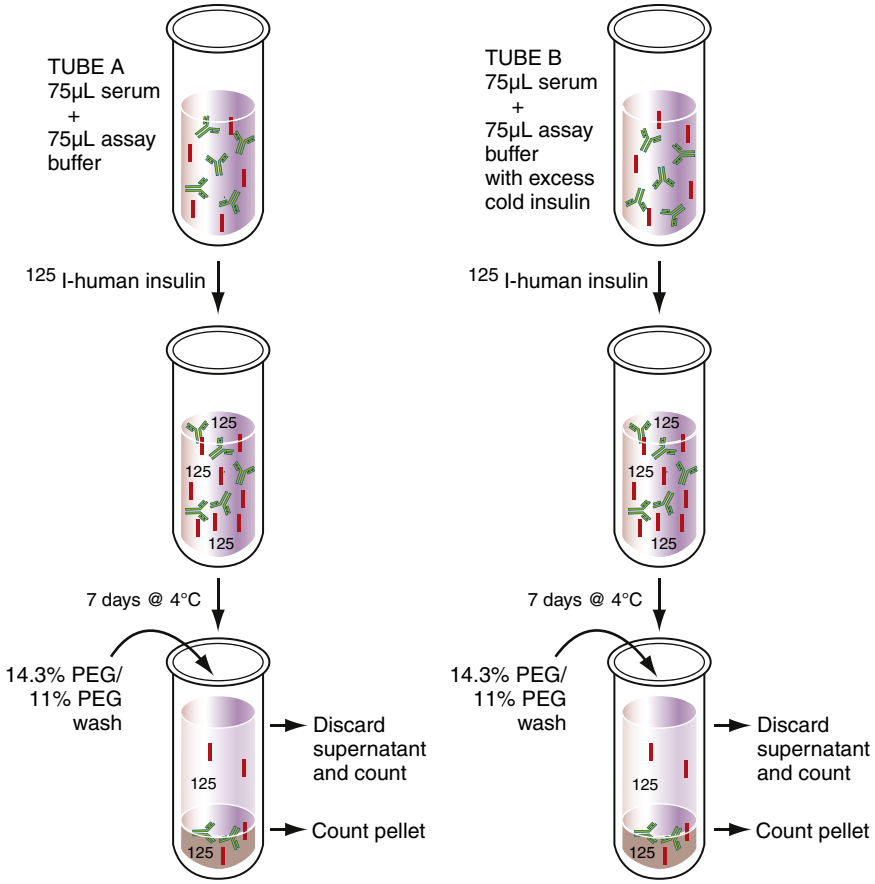

Fig. 55.83 The methodology for the measurement of insulin autoantibodies (IAA) is illustrated. Serum is incubated with A-14 monoiodinated ^{125}I insulin. After incubation at 4°C, the bound tracer is precipitated with two rounds of polyethylene glycol and removed from solution by centrifugation. A parallel set of tubes are run with excess cold insulin to account for nonspecific binding. The pellet is counted in a gamma counter. The concentration of IAA is expressed as the nU/mL of insulin precipitated.

(e.g., a few percent) than ICA (e.g., 1 in 250). Nevertheless, because GADA immunoassays can be automated, if screening for the prediction of T1DM were to be undertaken, GADA testing would be superior to ICA testing.

Insulinoma-2-Associated Autoantibodies

The insulinoma-2-associated autoantigen (IA-2A) is a protein tyrosine phosphatase that was discovered while screening an insulinoma expression library (Lan et al., 1996). IA-2A are less sensitive than ICA or GADA for the detection of islet autoimmunity. At the onset of T1DM, approximately 60% of patients with T1DM will be IA-2A positive. IA-2A is no more specific than GADA and is less specific than ICA. However, like GADA, IA-2A testing can be automated. When the intracellular portion of IA-2 is used for immunoprecipitation testing, the assay is termed the "ICA512" autoantibody. ECL and ELISA testing for IA-2A are available.

Zinc Transporter-8 Autoantibodies

Autoantibodies to the transporter that pumps zinc into insulin secretory granules (the ZnT8 autoantibody) were discovered in 2007 (Wenzlau et al., 2007). The performance of ZnT8A at the time of onset of T1DM is similar to IA-2A. Some T1DM patients who are negative for all other islet autoantibodies are positive for ZnT8A. In the setting of pancreas transplantation for the treatment of T1DM, the appearance of ZnT8A predicts the development of beta cell failure.

ELISA kits are commercially available to conduct ZnT8A testing. In the authors' experience, the commercial ZnT8A ELISA is a robust assay, with a very high ratio of positive signals to cutoff signals. Whereas negative cutoff is less than 15 U/mL, positives are frequently greater than 5000 U/mL (100 times greater than the highest calibrator when the sample is diluted 1 to 100).

In cases where the patient presents with classic symptoms of diabetes, unequivocal hyperglycemia (e.g., random plasma glucose ≥200 mg/dL), and ketonuria or ketonemia, the diagnosis of T1DM is likely, and islet autoantibody testing is not necessary. However, when the diagnosis of T1DM is unclear, such as in obese patients with acute symptoms of diabetes or even ketoacidosis, or lean, young patients with only mild hyperglycemia, islet autoantibody testing may be of value because the presence of islet autoantibodies is pathognomonic of T1DM. Table 55.6 illustrates clinically ambivalent cases where islet autoantibody testing may be instructive in diagnosing T1DM (e.g., positivity for an islet autoantibody indicates the presence of type 1 diabetes).

TABLE 55.6
Clinical Scenarios Where Islet Autoantibody Testing (When Positive) Can Be Diagnostically Helpful

Clinical Findings	Features Favoring T1DM	Features Favoring T2DM
Lean "T2DM" patient with poor glycemic control	Lean favors diagnosis of T1DM	Previous diagnosis of T2DM
Lean prediabetes	Lean favors diagnosis of T1DM	T1DM is usually of acute onset
Lean but not ketotic	Lean favors diagnosis of T1DM	Not ketotic favors diagnosis of T2DM
Ketotic but obese	Ketosis favors diagnosis of T1DM	Obesity favors diagnosis of T2DM

Prediction of T1DM

Presently, various investigators are pursuing studies designed to prevent T1DM or delay its onset (Sherr et al., 2008; Battaglia et al., 2017). Central to these studies is the recognition of prediabetic individuals who are defined by the presence of one or more islet autoantibodies (Wasserfall & Atkinson, 2006). Because of their adaptability to high test volume throughput, IAA, GADA, and IA-2A are often used as initial screening tests. If any of these three tests is positive, ICA and ZnT8A testing can then be carried out. Because prevention therapies are still under investigation, general population screening for islet autoantibodies is not recommended.

Type B Insulin Resistance

In this autoimmune disease, extreme insulin-resistant, nonketotic diabetes results from antagonistic anti-insulin receptor autoantibodies that block (but do not activate) the insulin receptor (Page et al., 2007; Censi et al., 2018). The phenotype of insulin resistance includes dyslipidemia, hypertension, and acanthosis nigricans. Some patients with type b insulin resistance have required insulin doses of more than 10,000 units per day! The diagnosis is established clinically because there are no commercial tests for anti-insulin receptor autoantibodies.

Autoimmune Hypoglycemia

Autoimmune hypoglycemia (also known as the insulin autoimmune syndrome) is not an uncommon cause of hypoglycemia in Japan (Zhang & Zhao, 2014). We have observed at least one case in our institution.

In this disorder, spontaneous autoantibodies arise, directed against circulating insulin (Reis et al., 2018). These IAA can bind insulin excessively, leading to hyperglycemia, or IAA can precipitously release insulin, leading to free insulin excess and hypoglycemia. Autoimmune hypoglycemia has been associated with exposure to sulfur-containing medications such as the thioureas that are used to treat Graves disease. IAA in this disorder are detected using the standard IAA assay that is applicable to T1DM.

Insulinomimetic Insulin Receptor Autoantibodies

Rare cases of hypoglycemia have been described that result from agonist autoantibodies directed against the insulin receptor (i.e., insulinomimetic autoantibodies) (Taylor et al., 1982). There are no commercial tests for such agonist insulin receptor autoantibodies, and the authors are not aware of any investigators that are currently active in this field.

AUTOIMMUNE THYROID DISEASE

The spectrum of AITD spans Hashimoto thyroiditis (HT), causing hypothyroidism to Graves disease (GD), which leads to hyperthyroidism (Orgiazzi, 1999). "Nestled in between" HT and GD is atrophic thyroiditis where antagonistic anti-TSH receptor autoantibodies bind to the TSH receptor blocking and not activating the receptor causing thyroid atrophy and hypothyroidism (Orgiazzi et al., 2003).

HT results from cell-mediated destruction of thyroid hormone-producing thyroid follicular cells. Consequent to a chronic inflammatory cell infiltrate into the thyroid gland, thyromegaly (goiter) can initially result. When sufficient numbers of follicular cells are destroyed, hypothyroidism results. With eventual destruction of the entire gland, goiter dissipates, and the gland may even become fibrotic. Riedel thyroiditis is the rare extension of fibrosis into tissues adjacent to the thyroid gland.

GD results from humoral autoimmunity, where agonist autoantibodies bind to and stimulate the TSH receptor, producing goiter and hyperthyroidism (Menconi et al., 2014). Exophthalmos with proptosis of the eyes is characteristic of GD compared with other causes of hyperthyroidism. Less common in GD is nonpitting myxedema of the lower extremities. If antagonistic autoantibodies are produced against the TSH receptor, the gland atrophies as a consequence of TSH receptor blockade, producing hypothyroidism and atrophic thyroiditis. The prevalence of HT in adults is 5%. The incidence of GD was estimated at 30 cases per 100,000 persons per year in a Minnesota study.

The diagnosis of HT is based on the findings of clinical disease (e.g., goiter and/or hypothyroidism), plus the presence of a thyroid autoantibody—either TPOA or TGA. The diagnosis of GD is based upon the finding of hyperthyroidism and a thyroid autoantibody (TPOA or TGA). Autoantibodies to the TSH receptor (TRAbs: TSH receptor autoantibodies [e.g., TSI or TBII]) support the diagnosis of GD. However, testing for TRAbs is usually not necessary in the classic clinical case of GD when goiter, hyperthyroidism, exophthalmos, and positivity for TPOA or TGA are present. Histology is not used to diagnose either HT or GD.

Thyroperoxidase Autoantibodies

TPOA are directed against thyroperoxidase (TPO). The function of TPO is to organify iodide to iodine to iodinate tyrosine residues that are part of thyroglobulin (Tg). TPO is also responsible for the coupling reaction where monoiodotyrosine (MIT) and diiodotyrosine (DIT) form triiodothyronine (T3) and two DITs form thyroxine (tetraiodothyronine [T4]). Normally, TPO is not accessible to circulating autoantibodies because TPO is attached to the apical surface of thyroid follicular cells interfacing with the colloid in the thyroid follicles that contain Tg. TPOA are detected by immunoassay (Sinclair, 2006). Older technologies used microsomes in agglutination assays or IIF (Fig. 55.84).

Thyroglobulin Autoantibodies

TGA are directed against Tg. Whereas most Tg resides within the colloid of the thyroid follicles, small amounts of iodine-deficient Tg circulate in the plasma.

Neither TPOA nor TGA are believed to be pathogenic in AITD. TGA can interfere in the measurement of Tg, which is relevant when Tg is measured as a tumor marker in cases of differentiated thyroid carcinoma (e.g., papillary thyroid carcinoma and follicular thyroid carcinoma). TGA are also detected by immunoassay. Older technologies involved agglutination assays. Most immunoassay analyzers offer robust, automated measurements of TPOA and TGA.

Thyroid-Stimulating Immunoglobulins

The classic measurement of thyroid-stimulating immunoglobulins (TSI) requires a bioassay where patient serum is added to thyroid slices or cloned thyroid follicular cells (Lytton & Kahaly, 2010). T4 or cyclic AMP (cAMP, the second messenger of the TSH receptor signaling system) are measured in the media as they are released from the TSI-stimulated thyroid follicular cells. Increased T4 or cAMP above the positive cutoff indicate the presence of TSI.

Thyrotropin-Binding Inhibitor Immunoglobulins

TBII were first detected using a radioreceptor assay where ^{125}I-labeled TSH competes with autoantibody in the patient's plasma (or serum) for binding to membrane-bound TSH receptors. Higher concentrations of TBII competed off the ^{125}I-labeled TSH, leading to lower counts in the membrane pellet after washing and centrifugation. An automated, nonradioactive TBII assay was already described.

TBII positivity does not distinguish GD from atrophic thyroiditis. However, whereas GD patients should be TSI positive, patients with atrophic thyroiditis should be TSI negative.

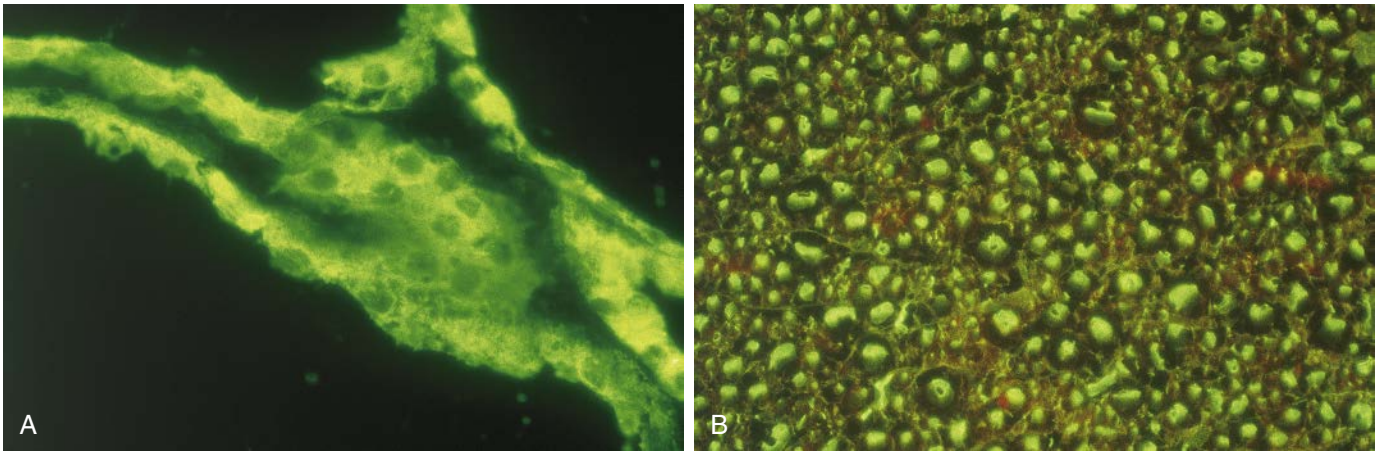

Fig. 55.84 **A,** Indirect immunofluorescence microscopy of thyroid microsomal autoantibodies (TMA) using unfixed monkey thyroid tissue as substrate (×400). **B,** Indirect immunofluorescence microscopy for thyroglobulin autoantibodies (TGA) using methanol-fixed cryostat tissue sections of monkey thyroid gland (×200). The indirect immunofluorescence microscopy technology for the detection of TMA and TGA has been surpassed by various immunoassays with cloned autoantigens.

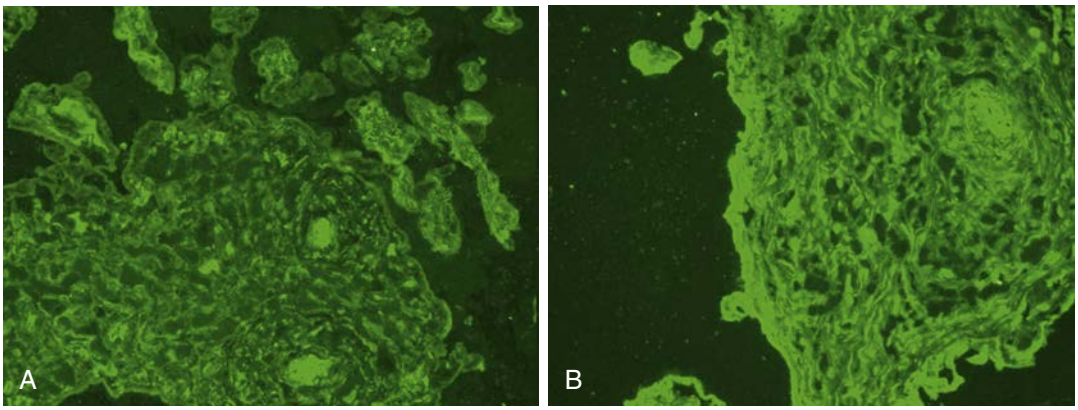

Fig. 55.85 Steroidal cell autoantibodies (SCA) can be detected by indirect immunofluorescence. In this case, the substrate is human placenta. **A,** Negative control. **B,** Positive patient result (note the more intense staining).

There is a relatively new automated immunoassay that claims to measure TSIs via competition between patient sera and a monoclonal anti-TSH receptor antibody. The supposition is that the competing monoclonal anti-TSH receptor autoantibody is a receptor agonist (similar to TSIs in Graves disease). The data supporting this supposition that this is a "TSI" assay and is not really a TBII assay have been questioned.

Treatment of AITD

Treating AITD requires treating the thyroid dysfunction (Gessl et al., 2012). Immunotherapy is not indicated. HT is treated with sodium L-thyroxine (L-T4) replacement. That being said, some patients are reported to require combined L-T4 and L-T3 treatment for the improvement of symptoms although there is controversy about this issue (Hennessey & Espaillat, 2018).

GD is initially treated with antithyroid medications such as propylthiouracil or methimazole that impair thyroid hormone biosynthesis. Because of the potential development of aplastic anemia from propylthiouracil, methimazole is the preferred medication. If the patient does not enter into remission (e.g., hyperthyroidism is persistent off-therapy after 1 or more years of methimazole therapy), treatment options include surgical thyroidectomy or radioactive iodine ablation therapy. While there is no concrete evidence that radioiodine treatment of GD predisposes to thyroid cancer, lifelong surveillance for thyroid neoplasms is justified (Al Eyadeh et al., 2017).

Because of the familial nature of AITD, testing of first-degree relatives for AITD would appear prudent. Likewise, testing for AITD in patients with type 1 diabetes, pernicious anemia, or Addison disease would allow the early detection and treatment of AITD prior to the development of life-threatening crises such as congestive heart failure or coma in HT, or thyroid storm in GD.

AUTOIMMUNE ADDISON DISEASE

Primary adrenal failure causing glucocorticoid (cortisol) and mineralocorticoid (aldosterone) deficiencies is called Addison disease, after the English physician Thomas Addison, who described adrenal insufficiency in 1849. Cortisol deficiency can produce lassitude, fatigue, nausea, gastrointestinal upset, hypovolemia, hypotension, hypoglycemia, and hyponatremia. Aldosterone deficiency can also produce hypovolemia and hypotension with evidence of hyponatremia, hyperkalemia, and acidosis. At times of stress (e.g., serious infection, trauma, or surgery), when the normal physiologic response is to markedly increase cortisol secretion, acute failure to increase cortisol secretion can produce Addisonian crisis. Such Addisonian crisis, if not treated on an emergency basis, can cause death from hypovolemia, hypotension, shock, acidosis, and electrolyte abnormalities (e.g., hyponatremia and hyperkalemia). Addison disease is not a common condition (approximate prevalence in the general population is 1 case in 25,000); however, if not diagnosed and treated appropriately, it can be fatal.

In the preantibiotic era, Addison disease most frequently resulted from infections such as tuberculosis. Presently, in developed countries, Addison disease results most commonly from cell-mediated autoimmune destruction of the adrenal cortex (Brandão Neto & de Carvalho, 2014). Whereas autoimmune Addison disease can exist as an isolated disorder, it may also coexist with other endocrinopathies and related nonendocrine autoimmune diseases (Schatz & Winter, 2002; Bertholf et al., 2012). Autoimmune polyglandular syndrome type I (APS I) is diagnosed when two or more of the following conditions are identified in a patient: hypoparathyroidism, mucocutaneous candidiasis, and adrenal autoantibodies or Addison disease.

Autoimmune polyglandular syndrome type II (APS II) is defined as adrenal autoantibodies or Addison disease plus coexistent AITD and/or type 1 diabetes. APS II is also known as autoimmune polyendocrinopathy-candidiasis-ectodermal dystrophy (APECED). The diagnosis of autoimmune Addison disease is established in patients with endocrinologic confirmation of cortisol and aldosterone deficiency who have evidence of humoral adrenocortical autoimmunity. Histology is not used for diagnosis.

Adrenocortical Autoimmunity

ACA can be detected by IIF using snap-frozen, cryo-cut sections of human adrenal gland. Alternatively, commercial RIA kits are available for the detection of autoantibodies to the cloned enzyme 21-hydroxylase (Betterle et al., 2002). The enzyme 21-hydroxylase catalyzes the conversion of progesterone to desoxycorticosterone (DOC) and 17-hydroprogesterone to 11-desoxycortisol.

Treatment of Autoimmune Addison Disease

The treatment of autoimmune Addison disease involves glucocorticoid and mineralocorticoid replacement. Immunotherapy is not indicated. The presence of ACA or 21-hydroxylase autoantibodies in an asymptomatic patient predicts the development of Addison disease (Naletto et al., 2019). In such cases, yearly serial testing is indicated as described earlier (cosyntropin testing and renin measurements, along with electrolyte measurements). At the earliest confirmation of adrenal hypofunction, glucocorticoid and mineralocorticoid replacement therapy is indicated. If APS I or APS II is present, associated disorders should be sought and treated.

AUTOIMMUNE DISEASE OF THE OVARY

Premature menopause can be caused by autoimmune-mediated ovarian destruction (gonaditis). Autoimmune gonaditis can occur as an isolated condition or it can occur as part of an autoimmune polyglandular syndrome (e.g., APS I or APS II) (Ahonen et al., 1987).

Elder et al. (1981) described steroidal cell autoantibodies in patients with Addison disease (Fig. 55.85). Presently, steroidal cell autoantibodies are sought by IIF using the following tissues as substrate: human testes (i.e., Leydig cell autoantibodies), human placenta (e.g., syncytiotrophoblast autoantibodies), and pregnant-rabbit ovary (e.g., ovarian autoantibodies). Although men can express steroidal cell autoantibodies, men do not appear to suffer from testicular failure. This may be because once spermatogenesis begins during puberty, in otherwise healthy men, it continues throughout life. On the other hand, women are born with all the ova they will ever have. Concerning reproductive problems in women and autoimmunity, AITD is increased in frequency in women with the polycystic ovarian syndrome (Romitti et al., 2018).

OTHER AUTOIMMUNE ENDOCRINOPATHIES

Although lacking diagnostic autoantibodies that are available for clinical use, autoimmune hypophysitis causing hypopituitarism is well recognized in the literature (Chiloiro et al., 2017). The diagnosis requires histologic evidence of a lymphocytic infiltration of the anterior pituitary gland (Chiloiro et al., 2019). Autoimmune hypophysitis can coexist with other autoimmune diseases (Joshi et al., 2018). Similarly, rare cases of diabetes insipidus

have been ascribed to autoimmunity (Hannon et al., 2012). Autoantibodies directed against the parathyroid chief cell calcium sensing receptor (CaSR) that are agonists can induce hypoparathyroidism, whereas antagonists can induce hyperparathyroidism (Thakker, 2004).

AUTOIMMUNE DISEASES OF THE NEUROMUSCULAR JUNCTION, NERVOUS SYSTEM, AND MUSCLE

MYASTHENIA GRAVIS

Myasthenia gravis (MG) is a neuromuscular disorder characterized by muscle weakness that worsens during the day and with activity (Ha & Richman, 2015). Extraocular muscles, facial muscles, and muscles involved in speech, mastication, and swallowing are commonly affected. While it can occur at any age, MG most often affects older men (age ≥60 years) and younger women (age <40 years) and people of all ethnicities.

MG is most commonly caused by autoantibodies directed against the nicotinic acetyl choline (Ach) receptor (AChR) (Oger & Frykman, 2015). AChR autoantibodies (AChRA) are found in 85% to 90% of MG patients. Tests for binding, blocking, and modulating autoantibodies are available. AChRA bind complement. These autoantibodies are measured by RIA. Blocking AChRA interfere with the attachment of ACh to the AChR. Modulating AChRA cause internalization of the AChR, which impairs the muscle's response to acetylcholine. Blocking and modulating AChRA are measured by flow cytometry. If a mother is affected with MG, transplacental transfer of the AChR autoantibodies can cause neonatal MG.

In the 10% to 15% of MG patients lacking AChRA, 30% to 40% will express a muscle-specific kinase (MuSK) autoantibody that is measured by radioimmunoassay RIA. This kinase is necessary for the clustering of AChRs at the neuromuscular junction. Anti-MuSK autoantibodies are usually IgG4 antibodies.

Approximately 5% of patients with MG are negative for both AChRA and anti-MuSK autoantibodies. Autoantibodies to striated muscle autoantigens (striational [striated muscle] antibodies) have been reported in cases of MG and thymoma. These autoantibodies are detected by enzyme immunoassay or IIF, which recognizes autoantibodies against titin, the ryanodine receptor, and the alpha subunit Kv1.4 of the voltage-gated potassium channel (VGKC).

The diagnosis of MG is made on the basis of a compatible clinical history, serologic positivity for an AChRA, an abnormal electrodiagnostic study, and a beneficial response to acetylcholine esterase inhibitors (e.g., the tensilon test) (Berrih-Aknin et al., 2014).

MG symptoms can be treated with drugs that block acetylcholine esterase (e.g., neostigmine) (Díaz-Manera et al., 2012). Further therapy involves immunosuppression with a variety of agents, including glucocorticoids, azathioprine, calcineurin inhibitors, intravenous immunoglobulin, plasmapheresis, and thymectomy (Jordan & Freimer, 2018).

LAMBERT-EATON MYASTHENIC SYNDROME

Another neuromuscular autoimmune disease is Lambert-Eaton myasthenic syndrome (ELMS) (Titulaer et al., 2011). ELMS results from autoantibodies that are directed against presynaptic voltage-gated P/Q calcium channels. With impaired entry of calcium into the presynaptic terminal, acetylcholine-containing vesicles do not bind to the presynaptic membrane, causing deficient acetylcholine release (Pourmand, 2009) and the resulting "channelopathy" (Huang et al., 2019).

Of insidious onset, the clinical features of ELMS can be subtle. The clinical presentation is usually that of proximal muscle weakness that is more severe in the lower extremities than in the upper extremities. Decreased reflexes and autonomic dysfunction are common. The respiratory and bulbar muscles are usually spared. Of tremendous clinical importance is that in approximately 40% of cases there is an underlying malignancy (Schoser et al., 2017). This places the ELMS channelopathy in the category of the paraneoplastic syndromes (Mareska & Gutmann, 2004). Diagnosis of ELMS is confirmed by electrophysiologic testing. Voltage-gated calcium channel (VGCC) autoantibody testing is available. When positive, such autoantibody testing supports the diagnosis of ELMS.

MULTIPLE SCLEROSIS

Multiple sclerosis (MS) is a demyelinating autoimmune disease of the central nervous system and spinal cord that leads to neurologic deficits that vary over time in location, duration, and severity (Frohman et al., 2006). Visual impairment, bowel and bladder incontinence, unsteady gait, and weakness are typical clinical findings in this disorder, which has a waxing-waning course (Harrison, 2014). The onset of disease is usually in the young adult years. There is a female predominance. Demyelination is observed on magnetic resonance imaging (MRI), although the patient's clinical symptomatology may be discordant from the imaging study results.

The diagnosis of MS resides upon compatible history and physical examination findings, an abnormal MRI, and cerebrospinal fluid abnormalities consistent with MS (Karussis, 2014). The cerebrospinal fluid (CSF) in MS usually displays a glucose concentration within the reference interval (approximately two-thirds of plasma glucose), a white blood cell (WBC) count of less than 10 mononuclear cells/uL in 90% of cases (>50 WBC/uL is rare), a protein concentration of less than 60 mg/dL in 90% of cases (if the protein exceeds 100 mg/dL, the diagnosis of MS should be questioned), an increased IgG concentration in 80% of cases, and a myelin basic protein (MBP) concentration of greater than 4 ng/mL in 90% of acute cases. Testing for visual evoked potentials (VEPs), somatosensory evoked potentials (SSEPs), and brainstem auditory evoked potentials (BAEPs) is available to provide neurophysiologic assessment of the patient with MS. Despite its autoimmune etiology there are no clinically useful diagnostic autoantibodies in MS (Schirmer et al., 2014). Biopsy and histology do not play a role in the diagnosis of MS. Immunointerventions are promising therapies (Zhang et al., 2019).

PARANEOPLASTIC NEUROLOGIC SYNDROMES

A panoply of neurologic disorders associated with malignancies have been described (Graus et al., 2010; Tobin & Pittock, 2017). Overall, such disorders are rare (Vernino, 2006). Theoretically a humoral immune response to a cancer can cross-react against neurologic self-antigens, causing autoimmunity and subsequent neurologic disease (Hinton, 1996). In the setting of a recognized malignancy and neuropathy, detection of autoantibodies against a variety of nerve autoantigens can establish an autoimmune basis for the neuropathy (Rosenfeld & Dalmau, 2013; Linnoila & Pittock, 2016).

Immunoblotting, radioimmunoassay (RIA), cytometric bead array (CBA), and IIF are technologies that are commonly employed to detect paraneoplastic autoantibodies in serum, plasma, or CSF. Neuronal nuclear antibodies (ANNA), Purkinje cell antibodies, contactin-associated protein-2 (CASPR2) IgG antibodies, and leucine-rich, glioma-inactivated protein 1 antibodies, among others, can be investigated by IIF. RIA can be used to test for VGKC antibodies. IgG neuronal nuclear antibodies can be detected by immunoblot. These autoantibodies are against antigens that include Hu (neuronal-specific RNA-binding proteins), Ri (ANNA2), and Yo (cerebellar degeneration-related protein 2, 62 kDa).

Extensive panels of autoantibody tests are offered by reference laboratories. For example, Mayo Medical Laboratories offers tests for neuronal nuclear antibodies (antineuronal nuclear antibody-types 1 [ANNA1], 2 [ANNA2], and 3 [ANNA3], and antiglial/neuronal nuclear antibody-type 1 [AGNA-1]); neuronal and muscle cytoplasmic antibodies; Purkinje cell cytoplasmic antibody, types 1 (PCA-1), 2 (PCA-2), and Tr (PCA-Tr); amphiphysin antibody; CRMP-5-IgG; striational (striated muscle) antibodies; cation channel antibodies (N-type and P/Q type calcium channel antibodies, AChR ganglionic neuronal antibody, and neuronal VGKC autoantibody); AChR receptor (muscle) binding antibody; AChR receptor (muscle) modulating antibody; neuromyelitis optica (NMO/aquaporin-4-IgG cell binding assay); CRMP-5-IgG Western blot; amphiphysin Western blot; N-methyl-D-aspartate receptor (NMDA-R) antibody; 2-amino-3-(5-methyl-3-oxo-1,2- oxazol-4-yl) propanoic acid receptor (AMPA-R) antibody; and gamma-amino butyric acid-type B receptor (GABA-B-R) antibody. A comprehensive discussion of all these autoantibodies is beyond the scope of this chapter.

More problematic is the patient without a recognized malignancy who presents with a neuropathy of unknown etiology. In such cases when antineuronal autoantibodies are sought, they are almost always negative, and if positive, antineuronal autoantibodies have a very low positive predictive value for cancer. As counter to these findings, the literature reports that some malignancies are not diagnosed for years after the neurologic presentation. It is likely a low-yield (and expensive) endeavor if a paraneoplastic autoantibody panel is ordered for every patient with an unexplained neuropathy in the absence of a recognized malignancy.

STIFF-PERSON SYNDROME

Stiff-person syndrome (SPS), an acquired autoimmune disease, is characterized by waxing and waning muscle rigidity with spasms that may first affect the axial muscles and progress to involve the proximal limb muscles

(Baizabal-Carvallo & Jankovic, 2014). The usual age of onset of this rare disease is age 30 to 60 years.

These patients with stiffness almost always have high titers of autoantibodies to GAD (e.g., GADA), and type 1 diabetes is observed in approximately one-third of these neurologically affected patients (McKeon & Tracy, 2017). Thyroiditis can occur in SPS patients. Like GADA, ICA are also very common in SPS. GADA are observed in other neurologic diseases, such as cerebellar ataxia, epilepsy, limbic encephalitis, and abnormal eye movement disorders (Alexopoulos & Dalakas, 2013). Amphiphysin autoantibodies detected by immunoblotting are reported in 5% of people with SPS. These later autoantibodies also serve as paraneoplastic autoantibody markers. Of interest, IA-2A are also associated with SPS (Morgenthaler et al, 1997). The GADA assay for SPS is the same GADA assay as that used for type 1 diabetes.

POLYMYOSITIS

Polymyositis is a noninfectious inflammatory myopathy (Sasaki & Kohsaka, 2018). The disorder affects proximal muscles, is symmetric, and is often painful. Weakness can be of chronic onset. Polymyositis most commonly affects older adults. It is often associated with mixed connective tissue disease. The pathogenesis is that of cell-mediated injury of myocytes via the actions of CD8 cytotoxic T cells and macrophages. Jo-1 autoantibodies directed against histidyl tRNA synthetase are characteristic of polymyositis, and such testing is commercially available from reference laboratories (Ghirardello et al., 2013).

CONCLUSION

The diagnosis of an autoimmune disease is best supported by a compatible clinical history and positivity for an organ-specific autoantibody. Indeed, many autoimmune diseases do display organ-specific autoantibodies (e.g., type 1 diabetes, AITD, autoimmune Addison disease, myasthenia gravis, and Lambert-Eaton myasthenic syndrome); however, many autoimmune diseases (e.g., multiple sclerosis) do not manifest such pathognomonic autoantibodies. Autoantibody testing remains the bedrock for the diagnosis of many organ-specific autoimmune diseases. Such markers can also predict the development of disease in asymptomatic but autoantibody-positive individuals. It should be noted that many autoantibodies of potential clinical value are not available outside of research laboratories, limiting their availability. Table 55.7 provides a summary of the clinically important antibodies discussed in this chapter.

TABLE 55.7
Clinically Important Antibodies or Autoantibodies

Disease	Important Autoantibody or Antibody Marker(s)[a,b]
Cutaneous Autoimmune Diseases	
Pemphigus vulgaris	Desmoglein 1 autoantibody
	Desmoglein 3 autoantibody
Pemphigus vulgaris	IIF with anti-IgG; substrate: monkey esophagus
Pemphigus foliaceus	Desmoglein 1 autoantibody
	IIF with anti-IgG; substrate: guinea pig esophagus
Paraneoplastic pemphigus	IgG antibodies to desmogleins and plakin family proteins (i.e., envoplakin, periplakin, plectin, desmoplakin 1 and 2)[c]
	IIF with anti-IgG; substrate: rat bladder
	IIF with anti-C3; substrate: rat bladder
IgA pemphigus	IIF with anti-IgA; substrate: monkey esophagus
Bullous pemphigoid	Bullous pemphigoid antigen 1 (BPAg1 [BP230]) autoantibody
	Bullous pemphigoid antigen 2 (BPAg2 [BP180]) autoantibody
	IIF with anti-IgG; substrate: salt-split human skin
Pemphigoid gestationis	IIF with anti-C3
	IIF with anti-IgG
Mucous membrane pemphigoid	IIF with anti-IgG
Linear IgA dermatosis	IIF with anti-IgA
Epidermolysis bullosa acquisita	IIF with anti-IgG
Dermatitis herpetiformis	IIF with anti-IgA
	IgA autoantibodies to endomysium, gliadin, tTG (tissue transglutaminase) and eTG (epidermal transglutaminase)[c]
Gastrointestinal and Hepatobiliary Autoimmune Diseases	
Pernicious anemia	Gastric parietal cell autoantibody (PCA)
	Intrinsic factor autoantibody
Celiac disease	IgA tissue transglutaminase (tTG) autoantibody
	IgG tissue transglutaminase (tTG) autoantibody
	IgA deamidated gliadin antibody
	IgG deamidated gliadin antibody
	IgA endomysial autoantibody
Inflammatory bowel disease	Perinuclear antineutrophil cytoplasmic autoantibody (p-ANCA)
	IgA IgG anti–*Saccharomyces cerevisiae* mannan antibodies (IgA ASCA)
	IgG anti–*Saccharomyces cerevisiae* mannan antibodies (IgG ASCA)
Autoimmune hepatitis	Smooth muscle autoantibody (SMA)
	Antinuclear autoantibody (ANA)
	Anti–LKM-1 autoantibody (LKM = liver-kidney microsomal)
	Anti–LC-1 autoantibody (LC = liver cytosol)
	Antimitochondrial autoantibody (AMA)
	Antineutrophil cytoplasmic autoantibody (ANCA)
	Antiasialoglycoprotein receptor autoantibodies (anti-ASGPR autoantibodies)[c]
Primary biliary cirrhosis	Antimitochondrial autoantibody (AMA)

TABLE 55.7
Clinically Important Antibodies or Autoantibodies—cont'd

Disease	Important Autoantibody or Antibody Marker(s)[a,b]
Primary sclerosing cholangitis	Perinuclear antineutrophil cytoplasmic autoantibody (p-ANCA)
Autoimmune pancreatitis	No antibodies specific for autoimmune pancreatitis
Glomerular Autoimmune Diseases	
Membranous nephropathy	IgG phospholipase A2 receptor autoantibody (PLA_2RA)
IgA nephropathy	There are no autoantibody tests for IgA nephropathy
Membranoproliferative glomerulonephritis (MPGN)	There are no autoantibody tests for MPGN
C3 glomerulopathy	C3 nephritic factor (C3Nef)
Postinfectious glomerulonephritis	Antistreptolysin O antibody (ASO)
	Anti–deoxyribonuclease-B antibody (anti–DNAse-B)
Anti-glomerular basement membrane glomerulonephritis	Glomerular basement membrane antibodies
Pauci-immune glomerulonephritis	Perinuclear antineutrophil cytoplasmic autoantibody (p-ANCA)
	Cytoplasmic antineutrophil cytoplasmic autoantibody (c-ANCA)
Lupus glomerulonephritis	Anti–ds-DNA autoantibody
	Anti-Sm autoantibody
Immunoendocrinopathies	
Type 1 diabetes	Islet cell cytoplasmic autoantibody (ICA)
	Insulin autoantibody (IAA)
	Glutamic acid decarboxylase autoantibody (GADA)
	Insulinoma-2-associated autoantibodies (IA-2A)
	Zinc transporter-8 autoantibodies (ZnT8A)
Autoimmune thyroid disease	Thyroperoxidase autoantibody (TPOA)
	Thyroglobulin autoantibody (TGA)
	Thyroid stimulating immunoglobulin (TSI)
	Thyrotropin-binding inhibitor immunoglobulin (TBII)
Autoimmune Addison disease	Adrenal cell cytoplasmic autoantibody (ACA)
	21-hydroxylase autoantibody
Ovarian autoimmunity	Steroidal cell autoantibody (SCA)
Autoimmune Diseases of the Neuromuscular Junction, Nervous System, and Muscle	
Myasthenia gravis	Acetyl choline receptor (AChR) autoantibody
	Muscle-specific kinase (MuSK) autoantibody
Lambert-Eaton myasthenic syndrome	Voltage-gated calcium channel (VGCC) autoantibody
Multiple sclerosis	There are no autoantibody tests for multiple sclerosis
Paraneoplastic neurologic syndromes	Too numerous to list; see text
Stiff-person syndrome	Glutamic acid decarboxylase autoantibody (GADA)
Polymyositis	Jo 1 (antihistidyl tRNA synthetase) autoantibody

Anti-C3, Anti-C3 antibody labeled with FITC; *anti-IgA,* anti-IgA antibody labeled with FITC; *anti-IgG,* anti-IgG antibody labeled with FITC; *BMZ,* basement membrane zone; *IIF,* indirect immunofluorescence.
[a]Excludes direct immunofluorescence, which requires biopsy material; not every organ-specific autoimmune disease has a disease-specific autoantibody. Some antibodies are only detected in a subset of affected individuals. Non-disease-specific autoantibodies are listed only when they may be particularly diagnostically helpful.
[b]Regarding IFF, the specific distributions of the antigens are discussed in the text.
[c]Testing may not be available from reference laboratories (e.g., research-only laboratories).

SELECTED REFERENCES

Anhalt GJ, Díaz LA: Pemphigus vulgaris—a model for cutaneous autoimmunity, *J Am Acad Dermatol* 51(1 Suppl):S20–S21, 2004.
Pemphigus vulgaris is an excellent a model of cutaneous autoimmunity.

Atkinson MA: The pathogenesis and natural history of type 1 diabetes, *Cold Spring Harb Perspect Med* 2(11):a007641, 2012.
Among the immunoendocrinopathies, type 1 diabetes mellitus likely displays the highest morbidity and mortality.

Chadban SJ, Atkins RC: *Glomerulonephritis, Lancet* 365(9473):1797–1806, 2005.
The variety of pathologies in the glomerulus and nephron is vast.

Li X, Shen J, Ran Z: Crosstalk between the gut and the liver via susceptibility loci: novel advances in inflammatory bowel disease and autoimmune liver disease, *Clin Immunol* 175:115–123, 2017.
Autoimmunities occur within systems such as concurrent cases of inflammatory bowel disease and autoimmune liver disease.

Selmi C, Barin JG, Rose NR: Current trends in autoimmunity and the nervous system, *J Autoimmun* 75:20–29, 2016.
Autoimmunity is becoming recognized as a cause of a growing number of serious neurologic conditions.

Access the complete reference list online at Elsevier eBooks for Practicing Clinicians.

REFERENCES

Ahonen P, Miettinen A, Perheentupa J: Adrenal and steroidal cell antibodies in patients with autoimmune polyglandular disease type I and risk of adrenocortical and ovarian failure, *J Clin Endocrinol Metab* 64(3):494–500, 1987.

Al Eyadeh AA, Al-Sarihin K, Etewi S, et al.: Thyroid cancer post radioactive iodine treatment for hyperthyroidism - case series and review of the literature, *Endokrynol Pol* 68(5):561–566, 2017.

Alexander MP, Larsen CP, Gibson IW, et al.: Membranous glomerulonephritis is a manifestation of IgG4-related disease, *Kidney Int* 83:455–462, 2013.

Alexopoulos H, Dalakas MC: Immunology of stiff person syndrome and other GAD-associated neurological disorders, *Expert Rev Clin Immunol* 9(11):1043–1053, 2013.

Allen LH: How common is vitamin B-12 deficiency? *American Journal of Clinical Nutrition* 89:693S–696S, 2009.

Almaani S, Meara A, Rovin BH: Update on lupus nephritis, *Clin J Am Soc Nephrol* 12:825–835, 2017.

Alvarez F, Berg PA, Bianchi FB, et al.: International autoimmune hepatitis group report: review of criteria for diagnosis of autoimmune hepatitis, *J Hepatol* 31(5):929–938, 1999.

Amagai M, Tsunoda K, Zillikens D, et al.: The clinical phenotype of pemphigus is defined by the anti-desmoglein autoantibody profile, *J Am Acad Dermatol* 40(2 Pt 1):167–170, 1999.

Aoki V, Sousa Jr JX, Fukumori LM, et al.: Direct and indirect immunofluorescence, *An Bras Dermatol* 85(4):490–500, 2010.

Arazi A, Rao DA, Berthier CC, et al.: The immune cell landscape in kidneys of patients with lupus nephritis, *Nat Immunol* 20:902–914, 2019.

Arbache ST, Nogueira TG, Delgado L, et al.: Immunofluorescence testing in the diagnosis of autoimmune blistering diseases: Overview of 10-year experience, *An Bras Dermatol* 89:885–889, 2014.

Arcos-Machancoses JV, Molera Busoms C, Julio Tatis E, et al.: Accuracy of the 2008 simplified criteria for the diagnosis of autoimmune hepatitis in children, *Pediatr Gastroenterol Hepatol Nutr* 21(2):118–126, 2018.

Asada M, Nishio A, Uchida K, et al.: Identification of a novel autoantibody against pancreatic secretory trypsin inhibitor in patients with autoimmune pancreatitis, *Pancreas* 33(1):20–26, 2006.

Atkinson MA, Maclaren NK, Riley WJ, et al.: Are insulin autoantibodies markers for insulin-dependent diabetes mellitus? *Diabetes* 35(8):894–898, 1986.

Atkinson MA: The pathogenesis and natural history of type 1 diabetes, *Cold Spring Harb Perspect Med 1* 2(11), 2012.

Austin III HA, Muenz LR, Joyce KM, et al.: Diffuse proliferative lupus nephritis: identification of specific pathologic features affecting renal outcome, *Kidney Int* 25:689–695, 1984.

Baekkeskov S, Aanstoot HJ, Christgau S, et al.: Identification of the 64K autoantigen in insulin-dependent diabetes as the GABA-synthesizing enzyme glutamic acid decarboxylase, *Nature* 347(6289):151–156, 1990.

Baizabal-Carvallo JF, Jankovic J: Stiff-person syndrome: insights into a complex autoimmune disorder, *J Neurol Neurosurg Psychiatry*, 2014.

Bajema IM, Wilhelmus S, Alpers CE, et al.: Revision of the International Society of Nephrology/Renal Pathology Society classification for lupus nephritis: clarification of definitions, and modified National Institutes of Health activity and chronicity indices, *Kidney Int* 93:789–796, 2018.

Barbesino G, Tomer Y: Clinical review: clinical utility of TSH receptor antibodies, *J Clin Endocrinol Metab* 98(6):2247–2255, 2013.

Barbour SJ, Espino-Hernandez G, Reich HN, et al.: The MEST score provides earlier risk prediction in IgA nephropathy, *Kidney Int* 89:167–175, 2016.

Barbour TD, Ruserva MM, Pickering MC: Update on C3 glomerulopathy, *Nephrol Dial Transplant* 31:717–725, 2016.

Barnes BJ: Genetic versus non-genetic drivers of SLE: implications of IRF5 dysregulation in both roads leading to SLE, *Curr Rheumatol Rep* 21(1):2, 2009.

Battaglia M, Anderson MS, Buckner JH, et al.: Understanding and preventing type 1 diabetes through the unique working model of TrialNet, *Diabetologia* 60(11):2139–2147, 2017.

Baum S, Sakka N, Artsi O, et al.: Diagnosis and classification of autoimmune blistering diseases, *Autoimmun Rev* 13(4–5):482–489, 2014.

Bech AP, Hofstra JM, Brenchley PE, et al.: Association of anti-PLA(2)R antibodies with outcomes after immunosupression therapy in idiopathic membranous nephropathy, *Clin J Am Soc Nephrol* 9:1386–1392, 2014.

Beck Jr LH, Salant DJ: Membranous nephropathy: from models to man, *J Clin Invest* 124:2307–2314, 2014.

Beck Jr LH, Bonegio RG, Lambeau G, et al.: M-type phospholipase A2 receptor as target antigen in idiopathic membranous nephropathy, *N Eng J Med* 361:11–21, 2009.

Beck Jr LH, Fervenza FC, Beck DM, et al.: Rituximab-induced depletion of anti-PLA2R autoantibodies predicts response in membranous nephropathy, *J Am Soc Nephrol* 22:1543–1550, 2011.

Beck Jr LH: PLA2R and THSD7A: Disparate paths to the same disease, *J Am Soc Nephrol* 28:2579–2589, 2017.

Bellur SS, Lepeytre F, Vorobyeva O, et al.: Evidence from the Oxford classification cohort supports the clinical value of subclassification of focal segmental glomerulosclerosis in IgA nephropathy, *Kidney Int* 91:235–243, 2017.

Beniwal P, Harrell L: The status of diagnostic markers for inflammatory bowel disease, *Curr Gastroenterol Rep* 12:479–484, 2010.

Berden AE, Ferrario F, Hagen EC, et al.: Histopathologic classification of ANCA-associated glomerulonephritis, *J Am Soc Nephrol* 21:1628–1636, 2010.

Berden AE, Jones RB, Erasmus DD, et al.: Tubular lesions predict outcome in antineutrophil cytoplasmic antibody-associated glomerulonephritis after rituximab therapy, *J Am Soc Nephrol* 23:313–321, 2012.

Berrih-Aknin S, Frenkian-Cuvelier M, Eymard B: Diagnostic and clinical classification of autoimmune myasthenia gravis, *J Autoimmun*143–148, 2014. 48–49.

Bertholf RL, Jialal I, Winter WE: The adrenal cortex. In Burtis C, Ashwood E, Bruns D, editors: *Tietz textbook of clinical chemistry and molecular diagnostics*, ed 5, St. Louis, Mo, 2012, Elsevier Saunders, pp 1847–1904.

Betterle C, Dal Pra C, Mantero F, et al.: Autoimmune adrenal insufficiency and autoimmune polyendocrine syndromes: autoantibodies, autoantigens, and their applicability in diagnosis and disease prediction, *Endocr Rev* 23(3):327–364, 2002.

Beuers U, Gershwin ME, Gish RG, et al.: Changing nomenclature for PBC: from 'cirrhosis' to 'cholangitis', *Hepatology* 62(5):1620–1622, 2015.

BioPlex: BioPlex 2200 multiplex testing. Available at: http://www.bio-rad.com/en-us/category/bioplex-2200-multiplex-testing?ID=a82cd166-67ca-4696-91a8-a98a550936f2 Accessed: 2019.

Bizzaro N, Antico A: Diagnosis and classification of pernicious anemia, *Autoimmunity Reviews* 13:565–568, 2014.

Bjorneklett R, Srisandarajah S, Bostad L: Prognostic value of histologic classification of ANCA-associated glomerulonephritis, *Clin J Am Soc Nephrol* 11:2159–2167, 2016.

Blanc C, Togarsimalemath SK, Chauvet S, et al.: Ant-factor H autoantibodies in C3 glomerulopathies and in atypical hemolytic syndrome; one target, two disease, *J Immunol* 194:5129–5138, 2015.

Bobart SA, De Vriese AS, Pawar AS, et al.: Noninvasive diagnosis of primary membranous nephropathy using phospholipase A2 receptor antibodies, *Kidney Int* 95:429–438, 2019.

Boils CL, Nasr SH, Walker PD, et al.: Update on endocarditis-associated glomerulonephritis, *Kidney Int* 87:1241–1249, 2015.

Bomback AS, Santoriello D, Avasare RS, et al.: C3 glomerulonephritis and dense deposit disease share a similar disease course in a large United States cohort of patients with C3 glomerulopathy, *Kidney Int* 93:977–985, 2018.

Bossuyt X, Tervaert J-WC, Arimura Y, et al.: Revised 2017 international consensus on testing of ANCAs in granulomatosis with polyangiitis and microscopic polyangiitis, *Nat Rev Rheumatol* 13:683–692, 2017.

Bottazzo GF, Florin-Christensen A, Doniach D: Islet-cell antibodies in diabetes mellitus with autoimmune polyendocrine deficiencies, *Lancet* 2(7892):1279–1283, 1974.

Bowlus CL, Gershwin ME: The diagnosis of primary biliary cirrhosis, *Autoimmun Rev* 13(4–5):441–444, 2014.

Brandão Neto RA, de Carvalho JF: Diagnosis and classification of Addison's disease (autoimmune adrenalitis), *Autoimmun Rev* 13(4–5):408–411, 2014.

Brix SR, Noriega M, Tennstedt P, et al.: Development and validation of a renal risk score in ANCA-associated glomerulonephritis, *Kidney Int* 94:1177–1188, 2018.

Burbelo PD, Ching KH, Bren KE, et al.: Searching for biomarkers: humoral response profiling with luciferase immunoprecipitation systems, *Expert Review of Proteomics* 8:309–316, 2011.

Burbelo PD, Lebovitz EE, Notkins AL: Luciferase immunoprecipitation systems for measuring antibodies in autoimmune and infectious diseases, *Transl Res* 165:325–335, 2015.

Burbelo PD, O'Hanlon TP: New autoantibody detection technologies yield novel insights into autoimmune disease, *Curr Opin Rheumatol* 26:717–723, 2014.

Canney M, O'Hara PV, McEvoy CM, et al.: Spatial and temporal clustering of anti-glomerular basement membrane disease, *Clin J Am Soc Nephrol* 11:1392–1399, 2016.

Cappelli C, Gandossi E, Castellano M, et al.: Prognostic value of thyrotropin receptor antibodies (TRAb) in Graves' disease: a 120-month prospective study, *Endocr J* 54(5):713–720, 2007.

Carlsson S: Etiology and pathogenesis of latent autoimmune diabetes in adults (LADA) compared to type 2 diabetes, *Front Physiol* 10:320, 2019.

Carmel R: Current concepts in cobalamin deficiency, *Annual Review of Medicine* 51:357–375, 2000.

Carmel R: Prevalence of undiagnosed pernicious anemia in the elderly, *Archives of Internal Medicine* 156:1097–1100, 1996.

Caso F, Costa L, Nucera V, et al.: From autoinflammation to autoimmunity: old and recent findings, *Clin Rheumatol* 37(9):2305–2321, 2018.

Cassol CA, Bott C, Nadasdy GN, et al.: Immunostaining for galactose-deficient immunoglobulin A is not specific for primary immunoglobulin A nephropathy, *Nephrol Dial Transplant*1–7, 2019.

Cattran DC, Brenchley PE: Membranous nephropathy: integrating basic science into improved clinical management, *Kidney Int* 91:566–574, 2017.

Cellini M, Santaguida MG, Virili C, et al.: Hashimoto's thyroiditis and autoimmune gastritis, *Front Endocrinol (Lausanne) 26* 8(92), 2017.

Censi S, Mian C, Betterle C: Insulin autoimmune syndrome: from diagnosis to clinical management, *Ann Transl Med* 6(17):335, 2018.

Chan LS: Ocular and oral mucous membrane pemphigoid (cicatricial pemphigoid), *Clin Dermatol* 30(1):34–37, 2012.

Chang L, Li J, Wang L: Immuno-PCR: an ultrasensitive immunoassay for biomolecular detection, *Anal Chim Acta 3* 910:12–24, 2016.

Chantzichristos D, Persson A, Miftaraj M, et al.: Early clinical Indicators of Addison disease in adults with type 1 diabetes: a Nationwide, observational, cohort study, *J Clin Endocrinol Metab* 104(4):1148–1157, 2019.

Chhabra S, Minz RW, Saikia B: Immunofluorescence in dermatology, *Indian J Dermatol Venereol Leprol*677–691, 2012.

Chiloiro S, Capoluongo ED, Tartaglione T, et al.: The changing clinical spectrum of hypophysitis, *Trends Endocrinol Metab* 30(9):590–602, 2019.

Chiloiro S, Tartaglione T, Angelini F, et al.: An Overview of diagnosis of primary autoimmune hypophysitis in a prospective single-center experience, *Neuroendocrinology* 104(3):280–290, 2017.

Choung RS, Murray JA: The US preventive Services Task Force. Screening for asymptomatic celiac disease: a dearth of evidence, *JAMA* 317(12):1221–1223, 2017.

Coco G, Dal Pra C, Presotto F, et al.: Estimated risk for developing autoimmune Addison's disease in patients with adrenal cortex autoantibodies, *J Clin Endocrinol Metab* 91(5):1637–1645, 2006.

Conrad K, Roggenbuck D, Laass MW: Diagnosis and classification of ulcerative colitis, *Autoimmun Rev* 13:463–466, 2014.

Cook HT, Pickering MC: Histopathology of MPGN and C3 glomerulopathies, *Nat Rev Nephrol* 11:14–22, 2015.

Cook HT, Pickering MC: Histopathology of MPGN and C3 glomerulopathies, *Nat Rev Nephrol* 11:14–22, 2015.

Coppo R, D'Arrigo G, Tripepi G, et al.: Is there long-term value of pathology scoring in immunoglobulin A nephropathy? A validation study of the Oxford classification for IgA nephropathy (VALIGA) update, *Nephrol Dial Transplant*1–8, 2018.

Coppo R, Troyanov S, Bellur S, et al.: Validation of the Oxford classification of IgA nephropathy in cohorts with different presentations and treatments, *Kidney Int* 86:828–836, 2014.

Couser WG: Primary membranous nephropathy, *Clin J Am Soc Nephrol* 12:983–997, 2017.

Cui Z, Xie LJ, Chen FJ, et al.: MHC Class II risk alleles and amino acid residues in idiopathic membranous nephropathy, *J Am Soc Nephrol* 28:1651–1664, 2017.

Cunha PR, Barraviera SR: Autoimmune bullous dermatoses, *An Bras Dermatol* 84(2):111–124, 2009.

Czaja AJ: Diagnosis and management of the overlap syndromes of autoimmune hepatitis, *Can J Gastroenterol* 27(7):417–423, 2013a.

Czaja AJ: The overlap syndromes of autoimmune hepatitis, *Dig Dis Sci* 58:326–343, 2013b.

Dagan R, Cleper R, Davidovits M, et al.: Post-infectious glomerulonephritis in pediatric patients over two decades: severity-associateD features, *Isr Med Assoc J* 18:336–340, 2016.

Dali-Youcef N, Andres E: An update on cobalamin deficiency in adults, *Qjm-an International Journal of Medicine* 102:17–18, 2009.

Damoiseaux J, Andrade LE, Fritzler MJ, et al.: Autoantibodies 2015: from diagnostic biomarkers toward prediction, prognosis and prevention, *Autoimmun Rev*, 2015.

Davidson A, Diamond B: Autoimmune diseases, *N Engl J Med* 345(5):340–350, 2001.

Davidson A: What is damging the kidney in lupus nephritis? *Nat Rev Nephrol* 12:143–153, 2016.

Dayalu P, Teener JW: Stiff Person syndrome and other anti-GAD-associated neurologic disorders, *Semin Neurol* 32(5):544–549, 2012.

De Rosa M, Azzato F, Toblli JE, et al.: A prospective observational cohort study highlights kidney biopsy findings of lupus nephritis patients in remission who flare following withdrawal of maintenance therapy, *Kidney Int* 94:788–794, 2018.

De Vriese AS, Glassock RJ, Nath KA, et al.: A proposal for a serology-based approach to membranous nephropathy, *J Am Soc Nephrol* 28:421–430, 2017.

Debiec H, Lefeu F, Kemper MJ, et al.: Early-childhood membranous nephropathy due to cationic bovine serum albumin, *N Eng J Med* 364:2101–2110, 2011.

Debiec H, Ronco P: PLA2R autoantibodies and PLA2R glomerular deposits in membranous nephropathy, *N Eng J Med* 364:689–690, 2011.

Decalf J, Albert ML, Ziai J: New tools for pathology: a user's review of a highly multiplexed method for *in situ* analysis of protein and RNA expression in tissue, *J Pathol* 247:650–661, 2019.

Der E, Suryawanshi H, Morozov P, et al.: Tubular cell and keratinocyte single-cell transcriptomics applied to lupus nephritis reveal type I IFN and fibrosis relevant pathways, *Nat Immunol* 20:915–927, 2019.

Detlefsen S, de Vos JD, Tanassi JT, et al.: Value of anti-plasminogen binding peptide, anti-carbonic anhydrase II, immunoglobulin G4, and other serological markers for the differentiation of autoimmune pancreatitis and pancreatic cancer, *Medicine (Baltimore)* 97(31):e11641, 2018.

Di Sabatino A, Vanoli A, Giuffrida P, et al.: The function of tissue transglutaminase in celiac disease, *Autoimmun Rev* 11:746–753, 2012.

Díaz-Manera J, Rojas García R, et al.: Treatment strategies for myasthenia gravis: an update, *Expert Opin Pharmacother* 13(13):1873–1883, 2012.

Diercks GF, Pas HH, Jonkman MF: Immunofluorescence of autoimmune bullous diseases, *Surg Pathol Clin* 10(2):505–512, 2017.

Durazzo M, Premoli A, Paschetta E, et al.: Overlap syndromes of autoimmune hepatitis: an open questin, *Dig Dis Sci* 58(2):344–348, 2013.

Elder M, Maclaren N, Riley W: Gonadal autoantibodies in patients with hypogonadism and/or Addison's disease, *J Clin Endocrinol Metab* 52(6):1137–1142, 1981.

Elston DM, Stratman EJ, Miller SJ: Skin biopsy: biopsy issues in specific diseases, *J Am Acad Dermatol* 74:1–16, 2016.

Endo T, Takizawa S, Tanaka S, et al.: Amylase alpha-2A autoantibodies: novel marker of autoimmune pancreatitis and fulminant type 1 diabetes, *Diabetes* 58(3):732–737, 2009.

Everts-Graber J, Martin KR, Thieblemont N, et al.: Proteomic analysis of neutrophils in ANCA-associated vasculitis reveals a dysregulation in proteinase 3-associated proteins such as annexin-A1 involved in apoptotic cell clearance, *Kidney Int* 96:397–408, 2019.

Ezzedine K, Eleftheriadou V, Whitton M, et al.: Vitiligo, *Lancet* 386(9988):74–84, 2015.

Ezzedine K, Silverberg N: A practical approach to the diagnosis and treatment of vitiligo in children, *Pediatrics* 138(1), 2016. pii: e20154126.

Fasano A, Catassi C: Clinical practice. Celiac disease, *N Engl J Med* 367:2419–2426, 2012.

Felix K, Hauck O, Schnolzer M, et al.: Identification of novel serum autoantibodies for differential diagnosis of atuoimmine pancreatitis and pancreatic ductal adenocarcinoma, *Pancreas* 45(9):1309–1319, 2016.

Fenalti G, Buckle AM: Structural biology of the GAD autoantigen, *Autoimmun Rev* 9(3):148–152, 2010.

Ferrante M, Henckaerts L, Joossens M, et al.: New serological markers in inflammatory bowel disease are associated with complicated disease behaviour, *Gut* 56:1394–1403, 2007.

Ferrer G, Andeen NK, Lockridge J, et al.: Kidney biopsy adequacy. A metric based study, *Am J Surg Pathol* 43:84–92, 2019.

Fervenza FC, Sethi S, Glassock RJ: Idiopathic membranoproliferative glomerulonephritis: does it exist? *Nephrol Dial Transplant* 27:4288–4294, 2012.

Fineberg SE, Kawabata TT, Finco-Kent D, et al.: Immunological responses to exogenous insulin, *Endocr Rev* 28(6):625–652, 2007.

Francis JM, Beck LH, Salant DJ: Membranous nephropathy: a journey from bech to bedside, *Am J Kidney Dis* 68:138–147, 2016.

Fresquet M, Jowitt TA, Gummadova J, et al.: Identification of a major epitope recognized by PLA2R autoantibodies in primary membranous nephropathy, *J Am Soc Nephrol* 26:302–313, 2015.

Frohman EM, Racke MK, Raine CS: Multiple sclerosis—the plaque and its pathogenesis, *N Engl J Med* 354(9):942–955, 2006.

Fu Q, Schoenhoff FS, Savage WJ, et al.: Multiplex assays for biomarker research and clinical application: translational science coming of age, *Proteomics Clin Appl* 4:271–284, 2010.

Fu SM, Sung S-SJ, Wang H, et al.: Pathogenesis of lupus nephritis. In Wallace DJ, Hahn BH, editors: *Dubois' lupus erythematosus and related syndromes*, 9TH ed., Edinburgh, 2019, Elsevier, pp 269–293.

Ganda OP, Srikanta S, Gleason RE, et al.: Diminished A-cell secretion in the early phase of type I diabetes mellitus, *Metabolism* 35(11):1074–1077, 1986.

Gessl A, Lemmens-Gruber R, Kautzky-Willer A: Thyroid disorders, *Handb Exp Pharmacol* 214:361–386, 2012.

Ghirardello A, Bassi N, Palma L, et al.: Autoantibodies in polymyositis and dermatomyositis, *Curr Rheumatol Rep* 15(6):335, 2013.

Gillette MA, Carr SA: METHOD OF THE YEAR Quantitative analysis of peptides and proteins in biomedicine by targeted mass spectrometry, *Nature Methods* 10:28–34, 2013.

Glassock RJ, Alvarado A, Prosek J, et al.: Staphylococcus-related glomerulonephritis and poststreptococcal glomerulonephritis: why defining "post" is important in understanding and treating infection-related glomerulonephritis, *Am J Kidney Dis* 65:826–832, 2015.

Godel M, Grahammer F, Huber TB: Thrombospondin type-1 domain-containing 7A in idiopathic membranous nephropathy, *N Eng J Med* 372:1073–1075, 2015.

González-Buitrago JM: Multiplexed testing in the autoimmunity laboratory, *Clin Chem Lab Med* 44:1169–1174, 2006.

Granito A, Muratori L, Muratori P, et al.: Antibodies to filamentous actin (F-actin) in type-1 autoimmune hepatitis, *J Clin Pathol* 59(3):280–284, 2006.

Graus F, Saiz A, Dalmau J: Antibodies and neuronal autoimmune disorders of the CNS, *J Neurol* 257(4):509–517, 2010.

Guandalini S, Assiri A: Celiac disease: a review, *JAMA Pediatr* 168(3):272–278, 2014.

Gupta MK: Thyrotropin receptor antibodies: advances and importance of detection techniques in thyroid diseases, *Clin Biochem* 25(3):193–199, 1992.

Ha JC, Richman DP: Myasthenia gravis and related disorders: pathology and molecular pathogenesis, *Biochim Biophys Acta* 1852(4):651–657, 2015.

Haas M, Racusen LC, Bagnasco SM: IgA-dominant postinfectious glomerulonephritis: a report of 13 cases with common ultrastructural features, *Hum Pathol* 39:1309–1316, 2008.

Haas M, Verhave JC, Liu Z-H, et al.: A multicenter study of the predictive value of crescents in IgA nephropathy, *Kidney Int* 28:691–701, 2017.

Haas M: A reevaluation of routine electron microscopy in the examination of native renal biopsies, *J Am Soc Nephrol* 8:70–76, 1997.

Hahn BH: Overview of lupus pathogenesis. In Wallace DJ, Hahn BH, editors: *Dubois' lupus erythematosus and related syndromes*, 9TH ed., Edinburgh, 2019, Elsevier, pp 44–53.

Haller MJ, Winter WE, Schatz DA: Autoimmune polyglandular syndromes. In Sperling M, editor: *Pediatric endocrinology*, ed 4, Philadelphia, 2014, W.B. Saunders, pp 901–919.

Hannon MJ, Orr C, Moran C, et al.: Anterior hypopituitarism is rare and autoimmune disease is common in adults with idiopathic central diabetes insipidus, *Clin Endocrinol (Oxf)* 76(5):725–728, 2012.

Harrison DM: Multiple sclerosis, *Ann Intern Med* 160(7), 2014. ITC4-2–ITC4-18.

Hartman EAR, van Royen-Kerhof A, Jacobs JWG, et al.: Performance of the 2012 Systemic Lupus International Collaborating Clinics classification criteria in adult and juvenile systemic lupus erythematosus. A systematic review and meta-analysis, *Autoimmunity Rev* 17:316–322, 2018.

Hastings MC, Bursac Z, Julian BA, et al.: Life expectancy for patients from the southeastern United States with IgA nephropathy, *Kidney Int Rep* 3:99–104, 2018.

Hayter SM, Cook MC: Updated assessment of the prevalence, spectrum and case definition of autoimmune disease, *Autoimmun Rev* 11(10):754–765, 2012.

Hemminger J, Nadasdy G, Satoskar A, et al.: IgG subclass staining in routine renal biopsy material, *Am J Surg Pathol* 40:617–626, 2016.

Hendricks AR, Harris AA, Walker PD, et al.: Renal medullary angiitis: a case series from a single insititution, *Hum Pathol* 44:521–525, 2013.

Hennes EM, Zeniya M, Czaja AJ, et al.: Simplified criteria for the diagnosis of autoimmune hepatitis, *Hepatology* 48(1):169–176, 2008.

Hennessey JV, Espaillat R: Current evidence for the treatment of hypothyroidism with levothyroxine/levotriiodothyronine combination therapy versus levothyroxine monotherapy, *Int J Clin Pract* 72(2), 2018.

Hershko C, Ronson A, Souroujon M, et al.: Variable hematologic presentation of autoimmune gastritis: age-related progression from iron deficiency to cobalamin depletion, *Blood* 107:1673–1679, 2006.

Hertl M, Jedlickova H, Karpati S, et al.: S2 guideline for diagnosis and treatment—Guided by the European dermatology Forum (EDF) in cooperation with the European Academy of dermatology and Venereology (EADV), *J Eur Acad Dermatol Venereol* 29(3):405–414, 2015.

Hilhorst M, van Paassen P, Tervaert JWC: Proteinase 3-ANCA vasculitis versus myeloperoxidase-ANCA vasculitis, *J Am Soc Nephrol* 26:2314–2327, 2015.

Himoto T, Nishioka M: Autoantibodies in liver disease: important clues for the diagnosis, disease activity and prognosis, *Autoimmune Highlights* 4:39–53, 2013.

Hinton RC: Paraneoplastic neurologic syndromes, *Hematol Oncol Clin North Am* 10(4):909–925, 1996.

Hirschfield GM, Karlsen TH, Lindor KD, et al.: Primary sclerosing cholangitis, *Lancet* 382(9904):1587–1599, 2013.

Hochenburg MC: Updating the American College of Rheumatology revised criteria for the classification of systemic lupuis erythematosus, *Arthritis Rheum* 40:1725, 1997.

Horn MP, Peter AM, Righini Grunder F, et al.: PR3-ANCA and panel diagnostics in pediatric inflammatory bowel disease to distinguish ulcerative colitis from Crohn's disease, *PLoS One* 13(12):e0208974, 2018.

Hou J, Markowitz GS, Bomback AS, et al.: Toward a working definition of C3 glomerulopathy by immunofluorescence, *Kidney Int* 85:450–456, 2014.

Hoxha E, Beck Jr LH, Wiech T, et al.: An indirect immunofluorescence method facilitates detection of thrombospondin type 1 domain-containing 7A-specific antibodies in membranous nephropathy, *J Am Soc Nephrol* 28:520–531, 2017.

Hoxha E, Harendza S, Pinnschmidt H, et al.: PLA2R antibody levels and clinical outcome in patients with membranous nephropathy and non-nephrotic range proteinuria under treatment with inhibitors of the renin0angiotensin system, *PLos One* 9:e110681, 2014.

Hoxha E, Kneibler U, Stege G, et al.: Enhanced expression of the M-type phospholipase A2 receptor in glomeruli correlates with serum receptor antibodies in primary membrane nephropathy, *Kidney Int* 82:797–804, 2012.

Hoxha E, Thiele I, Zahner G, et al.: Phospholipase A2 receptor autoantibodies and clinical outcomes in patients with primary membranous nephropathy, *J Am Soc Nephrol* 25:1357–1366, 2014.

Hoxha E, Wiech T, Stahl PR, et al.: A mechanism for cancer-associated membranous nephropathy, *N Eng J Med* 374, 2016. 1995–199.

Hu W, Chen Y, Wang S, et al.: Clinical-morphological features and outcomes of lupus podocytopathy, *Clin J Am Soc Nephrol* 11:585–592, 2016.

Huang CC, Lehman A, Albawardi A, et al.: IgG subclass staining in renal biopsies with membranous glomerulonephritis indicates subclass switch during disease progression, *Mod Pathol* 26:799–805, 2013.

Huang K, Luo YB, Yang H: Autoimmune Channelopathies at neuromuscular junction, *Front Neurol* 17(10):516, 2019.

Huang ZQ, Raska M, Stewart TJ, et al.: Somatic mutations modulate autoantibodies against galactose-deficient IgA1 in IgA nephropathy, *J Am Soc Nephrol* 27:3278–3284, 2016.

Hudson BG, Tryggvason K, Sundaramoorthy M, et al.: Alport syndrome, Goodpasture syndrome and type IV collagen, *N Eng J Med* 348:2543–2556, 2003.

Husby S, Murray JA, Katzka DA: AGA Clinical practice update on diagnosis and monitoring of celiac disease- changing utility of serology and histologic measures: expert review, *Gastroenterology* 156:865–889, 2019.

Iatropoulos P, Daina E, Curreri M, et al.: Cluster analysis identifies distinct pathogenetic patterns in C3 glomerulopathies/immune complex- mediated membranoproliferative GN, *J Am Soc Nephrol* 29:283–294, 2018.

Iatropoulos P, Noris M, Mele C, et al.: Complement gene variants determine the risk of immunoglobulin-associated MPGN and C3 glomerulopathy and predict long-term renal outcome, *Mol Immunol* 71:131–142, 2016.

Ines L, Silva C, Galindo M, et al.: Classification of systemic lupus erythematosus: systemic Lupus International Collaborating Clinics versus American College of Rheumatology Criteria. A comparative study of 2,055 patients from a real-life, international systemic lupus erythematosus cohort, *Arthritis Care Res* 67:1180–1185, 2015.

Ishii K: Importance of serological tests in diagnosis of autoimmune blistering diseases, *J Dermatol* 42(1):3–10, 2015.

Islam N, Leung PS, Huntley AC, et al.: The autoimmune basis of alopecia areata: a comprehensive review, *Autoimmun Rev 2015 Feb* 14(2):81–89, 2015.

Jacobsen LM, Larsson HE, Tamura RN, et al.: Predicting progression to type 1 diabetes from ages 3 to 6 in islet autoantibody positive TEDDY children, *Pediatr Diabetes* 20(3):263–270, 2019.

Jaeger C, Allendörfer J, Hatziagelaki E, et al.: Persistent GAD 65 antibodies in long-standing IDDM are not associated with residual beta-cell function, neuropathy or HLA-DR status, *Horm Metab Res* 29(10):510–515, 1997.

Jennette JC, Falk RJ: Pathogenesis of antineutrophil cytoplasmic autoantibody-mediated disease, *Nat Rev Rheumatol* 10:463–473, 2014.

Jennette JC, Falk RJ, Bacon PA, et al.: 2012 Revised international Chapel Hill consensus Conference nomenclature of vasculitides, *Arthritis Rheum* 65(1–11), 2013.

Jennette JC, Nachman PH: ANCA glomerulonephritis and vasculitis, *Clin J Am Soc Nephrol* 12:1680–1691, 2017.

Johnson MB, Cerosaletti K, Flanagan SE, et al.: Genetic mechanisms highlight shared pathways for the pathogenesis of Polygenic type 1 diabetes and Monogenic autoimmune diabetes, *Curr Diab Rep* 19(5):20, 2019.

Joly P, Litrowski N: Pemphigus group (vulgaris, vegetans, foliaceus, herpetiformis, brasiliensis), *Clin Dermatol* 29(4):432–436, 2011.

Jordan A, Freimer M: Recent advances in understanding and managing myasthenia gravis, *F1000Res* 31:7, 2018.

Joshi MN, Whitelaw BC, Carroll PV: MECHANISMS IN ENDOCRINOLOGY: hypophysitis: diagnosis and treatment, *Eur J Endocrinol* 179(3), 2018. R151–R163.

Kakleas K, Soldatou A, Karachaliou F, et al.: Associated autoimmune diseases in children and adolescents with type 1 diabetes mellitus (T1DM), *Autoimmun Rev* 14(9):781–797, 2015.

Kamradt T, Mitchison NA: Tolerance and autoimmunity, *N Engl J Med* 344(9):655–664, 2001.

Kanigicherla D, Gummadova J, McKenzie EA, et al.: Anti-PLA2R antibodies measured by ELISA predict long-term outcome in a prevalent population of patients with idiopathic membranous nephropathy, *Kidney Int* 83:940–948, 2013.

Kao L, Lam V, Waldman M, et al.: Identification of the immunodominant epitope region in phospholipase A2 receptor-mediating autoantibody binding in idiopathic membranous nephropathy, *J Am Soc Nephrol* 26:291–301, 2015.

Karussis D: The diagnosis of multiple sclerosis and the various related demyelinating syndromes: a critical review, *J Autoimmun* 48–49:134–142, 2014.

Kattah A, Ayalon R, Beck Jr LH, et al.: Anti-phospholipase A (2) receptor antibodies in recurrent membranous nepohropathy, *Am J Transplant* 15:1349–1359, 2015.

Kershenovich R, Hodak E, Mimouni D: Diagnosis and classification of pemphigus and bullous pemphigoid, *Autoimmun Rev* 13(4–5):477–481, 2014.

Kessenbrock K, Krumbholz M, Schonermarck U, et al.: Netting neutrophils in autoimmune small-vessel vasculitis, *Nat Med* 15:623–625, 2009.

Ketchum CH, Riley WJ, Maclaren NK: Adrenal dysfunction in asymptomatic patients with adrenocortical autoantibodies, *J Clin Endocrinol Metab* 58(6):1166–1170, 1984.

Khosroshahi A, Ayalon R, Beck Jr LH, et al.: IgG4-related disease is not associated with antibody to the phospholipase A_2 receptor, *Int J Rheumatol* 2012:139409, 2012.

Koga H, Prost-Squarcioni C, Iwata H, et al.: Epidermolysis bullosa acquisita: the 2019 update, *Front Med* 10(5):362, 2019.

Kopp JB, Nelson CW, Sampath K, et al.: *APOL1* genetic variants in focal segmental glomerulosclerosis and HIV-associated nephropathy, *J Am Soc Nephrol* 22:2129–2137, 2011.

Kovatchev B: A Century of diabetes technology: signals, models, and artificial pancreas control, *Trends Endocrinol Metab* 30(7):432–444, 2019.

Kraaij T, Kamerling SWA, van Dam LS, et al.: Excessive neutrophil trap formation in ANCA-associated vasculitis is independent of ANCA, *Kidney Int* 94:139–149, 2018.

Kraft SW, Schwartz MM, Korbet SM, et al.: Glomerular podocytopathy in patients with systemic lupus erythematosus, *J Am Soc Nephrol* 16:175–179, 2005.

Krishnan VV, Selvan SR, Parameswaran N, et al.: Proteomic profiles by multiplex microsphere suspension array, *Journal of Immunological Methods* 461:1–14, 2018.

Kurien AA, Larsen C, Rajapurkar M, et al.: Lack of electron microscopy hinders correct renal biopsy diagnosis: a study from India, *Ultrastruct Pathol* 40:14–17, 2016.

Laass MW, Roggenbuck D, Conrad K: Diagnosis and classification of Crohn's disease, *Autoimmun Rev* 13:467–471, 2014.

Lahner E, Annibale B: Pernicious anemia: new insights from a gastroenterological point of view, *World Journal of Gastroenterology* 15:5121–5128, 2009.

Lai KN, Tang SCW, Schena FP, et al.: IgA nephropathy, *Nat Rev Dis Primers* 2:16001, 2016.

Lan MS, Wasserfall C, Maclaren NK, et al.: IA-2, a transmembrane protein of the protein tyrosine phosphatase family, is a major autoantigen in insulin-dependent diabetes mellitus, *Proc Natl Acad Sci U S A* 93(13):6367–6370, 1996.

Larman HB, Zhao ZM, Laserson U, et al.: Autoantigen discovery with a synthetic human peptidome, *Nature Biotechnology* 29, 2011. 535–U101.

Larsen CP, Ambruzs JM, Bonsib SM, et al.: Membranous-like glomerulopathy with masked IgG kappa deposits, *Kidney Int* 86:154–161, 2014.

Larsen CP, Beggs ML, Saeed M, et al.: Apolipoprotein L1 risks variants associate with systemic lupus erythematosus-associated collapsing glomerulopathy, *J Am Soc Nephrol* 24:722–725, 2013.

Larsen CP, Boils CL, Cossey LN, et al.: Clinicopathologic features of membranous-like glomerulopathy with masked IgG kappa deposits, *Kidney Int Rep* 1:299–305, 2016.

Larsen CP, Cossey LN, Beck LH: THSD7A staining of membranous glomerulopathy in clinical practice reveals cases with dual autoantibody positivity, *Mod Pathol* 29:421–426, 2016.

Larsen CP, Messias NC, Walker PD, et al.: Membranoproliferative glomerulonephritis with masked monotypic immunoglobulin deposits, *Kidney Int* 88:867–873, 2015.

Larsen CP: Walker PD: phospholipase A2 receptor (PLA2R) staining is useful in the determination of de novo vesus recurrent membranous nephropathy, *Transplantation* 95:1259–1262, 2013.

Le WB, Shi JS, Zhang T, et al.: DRB1* 15:01 and HLA-DRB3*02:02 in related membranous nephropathy, *J Am Soc Nephrol* 28:1642–1650, 2017.

Leatherwood C, Speyer CB, Feldman CH, et al.: Clinical characteristics and renal prognosis associated with interstitial fibrosis and tubular atrophy (IFTA) and vascular injury in lupus nephritis biopsies, *Semin Arthritis Rheum*, 2019 (in press).

Leon J, Perez-Saez MJ, Batal I, et al.: Menbranous nephropathy post-transplantation: an update of the pathophysiology and management, *Transplantation*, 2019 (in press).

Leonard MM, Sapone A, Catassi C, et al.: Celiac disease and Nonceliac gluten sensitivity, *JAMA* 318(7):647–656, 2017.

Leslie RD, Kolb H, Schloot NC, et al.: Diabetes classification: Grey zones, sound and smoke: Action LADA 1, *Diabetes Metab Res Rev* 24(7):511–519, 2008.

Leung N, Bridoux F, Batuman V, et al.: The evaluation of monoclonal gammopathy of renal significance: a consensus report of the International Kidney and Monoclonal Gammopathy Research Group, *Nat Rev Nephrol* 15:45–59, 2019.

Lewis JD: The utility of biomarkers in the diagnosis and therapy of inflammatory bowel disease, *Gastroenterology* 140:1817–1826, 2011. e2.

Liberal R, Grant C, Longhi MS, et al.: Diagnostic criteria of autoimmune hepatitis, *Autoimmun Rev* 13(6), 2014.

Liberal R, Mieli-Vergani G, Vergani D: Clinical significance of autoantibodies in autoimmune hepatitis, *J Autoimmun* 46:17–24, 2013.

Lindor KD, Kowdley KV, Harrison ME: Primary sclerosing cholangitis, *Am J Gastroenterol* 110:646–659, 2015.

Linnoila J, Pittock SJ: Autoantibody-associated central nervous system neurologic disorders, *Semin Neurol* 36(4):382–396, 2016.

Lleo A, Invernizzi P, Gao B, et al.: Definition of human autoimmunity—autoantibodies versus autoimmune disease, *Autoimmun Rev* 9(5):A259–266, 2010.

Low ESH, Krishnaswamy G, Thumboo J: Comparing the 1997 update of the 1982 American College of Rheumatology (ACR-97) and the 2012 Performance of the 2012 Systemic Lupus International Collaborating Clinics (SLICC-12) criteria for systemic lupus erythematosus (SLE) classification: which enables earlier classification of SLE in an urban Asian population? *Lupus* 28:11–18, 2019.

Ludvigsson JF, Bai JC, Biagi F, et al.: Diagnosis and management of adult coeliac disease: guidelines from the British Society of Gastroenterology, *Gut* 63(8):1210–1228, 2014.

Lyons R, Narain S, Nichols C, et al.: Effective use of autoantibody tests in the diagnosis of systemic autoimmune disease, *Ann N Y Acad Sci* 1050:217–228, 2005.

Lytton SD, Kahaly GJ: Bioassays for TSH-receptor autoantibodies: an update, *Autoimmun Rev* 10(2):116–122, 2010.

Maclaren NK, Riley WJ: Thyroid, gastric, and adrenal autoimmunities associated with insulin-dependent diabetes mellitus, *Diabetes Care* 8(Suppl 1):34–38, 1985.

Maillard N, Wyatt RJ, Julian BA, et al.: Current understanding of the role of complement in IgA nephropathy, *J Am Soc Nephrol* 26:1503–1512, 2015.

Manne KKV: Obeticholic acid in primary biliary cholangitis: where we stand, *Curr Opin Gastroenterol* 35(3):191–196, 2019.

Manns MP, Czaja AJ, Gorham JD, et al.: Diagnosis and management of autoimmune hepatitis, *Hepatology* 51:2193–2213, 2010.

Mareska M, Gutmann L: Lambert-Eaton myasthenic syndrome, *Semin Neurol* 24(2):149–153, 2004.

Marinozzi M-C, Chauvet S, Le Quintrec M, et al.: C5 nephritic factors drive the biological phenotype of C3 glomeruonephritis, *Kidney Int* 92:1232–1241, 2017.

Marinozzi MC, Roumenina LT, Chauvet S, et al.: Anti-factor B and anti-C3b atotantibodies in C3 glomerulopathy and Ig-associated membranoproliferative GN, *J Am Soc Nephrol* 28:1603–1613, 2017.

Markowitz G: Updated Oxford classification of IgA nephropathy: a new MEST-C score, *Nat Rev Nephrol* 13:385–386, 2017.

Matta B, Barnes BJ: Coordination between innate immune cells, type I IFNs and IRF5 drives SLE pathogenesis, *Cytokine*, 2019 (in press).

McAdoo SP, Pusey CD: Antiglomerular basement membrane disease, *Semin Respir Crit Care Med* 39(4):494–503, 2018.

McAdoo SP, Tanna A, Hruskova Z, et al.: Patients double-seropositive for ANCA and anti-GBM antibodies have varied renal survival, frequency of relapse, and outcomes compared to single-seropositive patients, *Kidney Int* 92:693–702, 2017.

McGrath MM, Isakova T, Rennke HG, et al.: Contaminated cocaine and antineutrophil cytoplasmic antibody-associated disease, *Clin J Am Soc Nephrol* 6:2799–2805, 2011.

McKeon A, Tracy JA: GAD65 neurological autoimmunity, *Muscle Nerve* 56(1):15–27, 2017.

Medjeral-Thomas N, Malik TH, Patel MP: A novle CFHR5 fusion protein causes C3 glomerulopathy in a family without Cypriot ancestry, *Kidney Int* 85:933–937, 2014.

Medzhitov R, Janeway Jr C: Innate immunity, *N Engl J Med* 343(5):338–344, 2000.

Menconi F, Marcocci C, Marinò M: Diagnosis and classification of Graves' disease, *Autoimmun Rev* 13(4–5):398–402, 2014.

Mendes FB, Hissa-Elian A, Abreu MA, et al.: Review: dermatitis herpetiformis, *An Bras Dermatol* 88(4):594–599, 2013.

Messias NC, Walker PD, Larsen CP: Paraffin immunofluorescence in the renal pathology laboratory; more than a salvage technique, *Mod Pathol* 28:854–860, 2015.

Miao D, Guyer KM, Dong F, et al.: GAD65 autoantibodies detected by electrochemiluminescence assay identify high risk for type 1 diabetes, *Diabetes* 62(12):4174–4178, 2013.

Mihai S, Sitaru C: Immunopathology and molecular diagnosis of autoimmune bullous diseases, *J Cell Mol Med* 11(3):462–481, 2007.

Mohan C, Putterman C: Genetic and pathogenesis of systemic lupus erythematosus and lupus nephritis, *Nat Rev Nephrol* 11:329–341, 2015.

Morel L: Immunometabolism. In Wallace DJ, Hahn BH, editors: *Dubois' lupus erythematosus and related syndromes*, 9TH ed., Edinburgh, 2019, Elsevier, pp 153–163.

Morgenthaler NG, Seissler J, Achenbach P, et al.: Antibodies to the tyrosine phosphatase-like protein IA-2 are highly associated with IDDM, but not with autoimmune endocrine diseases or stiff man syndrome, *Autoimmunity* 25(4):203–211, 1997.

Mutasim DF, Adams BB: Immunofluorescence in dermatology, *J Am Acad Dermatol* 45(6):803–822, 2001.

Nakazawa D, Marschner JA, Platen L, et al.: Extracellular traps in kidney disease, *Kidney Int* 94:1087–1098, 2018.

Naletto L, Frigo A, Ceccato F, et al.: The natural history OF autoimmune ADDISON'S disease from the detection OF autoantibodies to development OF the disease: a LONG follow-up study ON 143 patients, *Eur J Endocrinol*, 2019. pii: EJE-18-0313. R3.

Nancy AL, Yehuda S: Prediction and prevention of autoimmune skin disorders, *Arch Dermatol Res* 301(1):57–64, 2009.

Nasr SH, Collins AB, Alexander MP, et al.: The clinicopathologic characteristics and outcome of atypical anti-glomerular basement membrane nephritis, *Kidney Int* 89:897–908, 2016.

Nasr SH, Fidler ME, Said SM: Paraffin immunofluorescence: a valuable ancillary technique in renal pathology, *Kidney Int Rep* 3:1260–1266, 2018.

Nasr SH, Fidler ME, Valeri AM, et al.: Postinfectious glomerulonephritis in the elderly, *J Am Soc Nephrol* 22:187–195, 2011.

Nasr SH, Galgano SJ, Markowitz GS, et al.: Immunofluorescence on pronase-digested paraffin sections: a valuable salvage technique for renal biopsies, *Kidney Int* 70:2148–2151, 2006.

Nasr SH, Markowitz GS, Stokes MB, et al.: Acute postinfectious glomerulonephritis in the modern era: experience with 86 adults and review of the literature, *Medicine* 87:21–32, 2008.

Nasr SH, Markowitz GS, Stokes MB, et al.: Prolferative glomerulonephritis with monoclonal IgG deposits: a distinct entity mimicking immune-complex glomerulonephritis, *Kidney Int* 65:85–96, 2004.

Nasr SH, Radhakrishnan J, D'Agati VD: Bacterial infection-related glomerulonephritis in adults, *Kidney Int* 83:792–803, 2013.

Nasr SH, Satoskar A, Markowitz GS, et al.: Proliferative glomerulonephritis with monoclonal Igg deposits, *J Am Soc Nephrol* 20:2055–2064, 2009.

Nayak RC, Omar MA, Rabizadeh A, et al.: "Cytoplasmic" islet cell antibodies. Evidence that the target antigen is a sialoglycoconjugate, *Diabetes* 34(6):617–619, 1985.

Neumann WL, Coss E, Rugge M, et al.: Autoimmune atrophic gastritis-pathogenesis, pathology and management, *Nature Reviews Gastroenterology & Hepatology* 10:529–541, 2013.

Nicolas JP, Gueant JL: Gastric intrinsic-factor AND its receptor, *Baillieres Clinical Haematology* 8:515–531, 1995.

Nielsen MJ, Rasmussen MR, Andersen CBF, et al.: Vitamin B-12 transport from food to the body's cells-a sophisticated, multistep pathway, *Nature Reviews Gastroenterology & Hepatology* 9:345–354, 2012.

NIH: Consensus development Conference on celiac disease, *NIH Consens State Sci Statements* 21:1–23, 2004.

Noris M, Donadelli R, Remuzzi G: Autoimmune abnormalities of the alternative pathway in membranoproliferative glomerulonephritis and C3 glomerulopathy, *Pediatr Nephrol* 34:1311–1323, 2019.

O'Reilly DA, Malde DJ, Duncan T, et al.: Review of the diagnosis, classification and management of autoimmune pancreatitis, *World J Gastrointest Pathophysiol* 5(2):71–81, 2014.

O'Shaughnessy MM, Hogan SL, Poulton CJ, et al.: Temporal and demographic trends in glomerular disease epidemiology in the southeastern United States, 1986-2015, *Clin J Am Soc Nephrol* 12:614–623, 2017.

Oda T, Yoshizawa N, Yamakami K, et al.: Localization of nephritis-associated plasmin receptor in acute poststreptococcal glomerulonephritis, *Hum Pathol* 41:1276–1285, 2010.

Oger J, Frykman H: An update on laboratory diagnosis in myasthenia gravis, *Clin Chim Acta* 444:126–131, 2015.

Ohtani H, Wakui H, Komatsuda A, et al.: Distribution of glomerular IgG subclass deposits in malignancy-associated membranous nephropathy, *Nephrol Dial Transplant* 19:574–579, 2004.

Olaru F, Luo W, Wang X-P, et al.: Quaternary epitopes of α345 (IV) collagen initiate Alport post-transplant anti-GBM nephritis, *J Am Soc Nephrol* 24:889–895, 2013.

Orban T, Sosenko JM, Cuthbertson D, et al.: Diabetes prevention Trial—type 1 study group. Pancreatic islet autoantibodies as predictors of type 1 diabetes in the diabetes prevention Trial—type 1, *Diabetes Care* 32(12):2269–2274, 2009.

Orgiazzi J: The spectrum of autoimmune thyroid diseases (AITD), *Ann Med Interne (Paris)* 150(4):294–300, 1999.

Orgiazzi J, Madec AM, Ducottet X: The role of stimulating, function-blocking and growth-blocking anti-TSH receptor antibodies (TRAbs) in GD, Hashimoto's disease and in atrophic thyroiditis, *Ann Endocrinol (Paris)* 64(1):31–36, 2003.

Page KA, Dejardin S, Kahn CR, et al.: A patient with type B insulin resistance syndrome, responsive to immune therapy, *Nat Clin Pract Endocrinol Metab* 3(12):835–840, 2007.

Palmer JP, Asplin CM, Clemons P, et al.: Insulin antibodies in insulin-dependent diabetics before insulin treatment, *Science* 222(4630):1337–1339, 1983.

Park HJ, Atkinson JP: Autoimmunity: homeostasis of innate immunity gone awry, *J Clin Immunol* 32(6):1148–1152, 2012.

Parker CE, Domanski D, Percy AJ, et al.: Mass spectrometry in high-throughput clinical biomarker assays: multiple reaction monitoring, *Top Curr Chem* 336:117–137, 2014.

Pedchenko V, Bondar O, Fogo AB, et al.: Molecular architecture of the Goodpasture autoantigen in anti-GBM nephritis, *N Eng J Med* 363:343–354, 2010.

Pendergraft WF, Niles JL: Trojan horses: drug culprits associated with antineutrophil cytoplasmic autoantibody (ANCA) vasculitis, *Curr Opin Rheumatol* 26:42–49, 2014.

Petri M, Orbai A-M, Alarcon GS, et al.: Derivation and validation of the Systemic Lupus International Collaborating Clinics classification criteria for systemic lupus erythematosus, *Arthritis Rheum* 64:2677–2686, 2012.

Philipp T, Durazzo M, Trautwein C, et al.: Recognition of uridine diphosphate glucuronosyl transferases by LKM-3 antibodies in chronic hepatitis D, *Lancet* 344(8922):578–581, 1994.

Pickering MC, D'Agati VD, Nester CM, et al.: C3 glomerulopathy: consensus report, *Kidney Int* 84:1079–1089, 2013.

Pourmand R: Lambert-eaton myasthenic syndrome, *Front Neurol Neurosci* 26:120–125, 2009.

Ramachandran R, Kumar V, Nada R, et al.: Serial monitoring of anti-PLA2R in initial PLA2R-negative patients with primary membranous nephropathy, *Kidney Int* 88:1198–1199, 2015.

Rauharvirta T, Hietikko M, Salmi T, et al.: Transglutaminase 2 and transglutaminase 2 antibodies in celiac disease: a review, *Clinic Rev Allerg Immunol* 57(1):23–38, 2019.

Reis MZR, Fernandes VO, Fontenele EGP, et al.: Insulin autoimmune syndrome in an Occidental woman: a case report and literature review, *Arch Endocrinol Metab* 62(5):566–570, 2018.

Rijnink EC, Teng YKO, Kraaij T, et al.: Validation of the Systemic Lupus International Collaborating Clinics classification criteria in a cohort of patients with full house glomerular deposits, *Kidney Int* 93:214–220, 2018.

Rijnink EC, Teng YKO, Wilhelmus S, et al.: Clinical and histopathologic characteristics associated with renal outcomes in lupus nephritis, *Clin J Am Soc Nephrol* 12:734–743, 2017.

Riley WJ, Toskes PP, Maclaren NK, et al.: Predictive value of gastric parietal cell autoantibodies as a marker for gastric and hematologic abnormalities associated with insulin-dependent diabetes, *Diabetes* 31(12):1051–1055, 1982.

Rizk DV, Saha MK, Hall S, et al.: Glomerular immunodeposits of patients with IgA nephropathy are enriched for IgG autoantibodies specific for galactose-deficient IgA1, *J Am Soc Nephrol*, Aug, 2019 (in press).

Roberts IS, Cook HT, Troyanov S, et al.: The Oxford classification of IgA nephropathy: pathology definitions, correlations and reproducibility, *Kidney Int* 76:546–556, 2009.

Roberts ISD: Oxford classification of immunoglobulin A nephropathy: an update, *Curr Opin Nephrol Hypetens* 22:281–286, 2013.

Rocha AB, Larsen CP: Membranous glomerulopathy with light chain-restricted deposits: a clinicopathological analysis of 28 cases, *Kidney Int Rep* 2:1141–1148, 2017.

Rodrigues JC, Haas M, Reich HN: IgA nephropathy, *Clin J Am Soc Nephrol* 12:677–686, 2017.

Rodriguez EF, Nasr SH, Larsen CP, et al.: Membranous nephropathy with crescents: a series of 19 cases, *Am J Kidney Dis* 64:66–73, 2014.

Rodriguez-Iturbe B, Musser JM: The current state of poststreptococcal glomerulonephritis, *J Am Soc Nephrol* 19:1855–1864, 2008.

Rodriguez-Martin M, Saez M, Merino de Paz N, et al.: When are laboratory tests indicated in patients with vitiligo? *Dermato-Endocrinology* 4(1):58–62, 2012.

Rodriquez-Iturbe B, Haas M: Post-streptococcal glomerulonephritis. In Ferretti JJ, Stevens DL, Fischetti VA, editors: *Streptococcus pyogenes: basic Biology to clinical manifestations*, Oklahoma City, University of Oklahoma Health Sciences Center, 2016, pp 1–24.

Romitti M, Fabris VC, Ziegelmann PK, et al.: Association between PCOS and autoimmune thyroid disease: a systematic review and meta-analysis, *Endocr Connect* 7(11):1158–1167, 2018.

Rosário PW, Reis JS, Fagundes TA, et al.: Latent autoimmune diabetes in adults (LADA): Usefulness of anti-GAD antibody titers and benefit of early insulinization, *Arq Bras Endocrinol Metabol* 51(1):52–58, 2007.

Rose C, Armbruster FP, Ruppert J, et al.: Autoantibodies against epidermal transglutaminase are a sensitive diagnostic marker in patients with dermatitis herpetiformis on a normal or gluten-free diet, *J Am Acad Dermatol* 61(1):39–43, 2009.

Rose NR: Prediction and prevention of autoimmune disease in the 21st Century: a review and Preview, *Am J Epidemiol 1* 183(5):403–406, 2016.

Rosenfeld MR, Dalmau J: Diagnosis and management of paraneoplastic neurologic disorders, *Curr Treat Options Oncol* 14(4):528–538, 2013.

Roth AJ, Ooi JD, Hess JJ, et al.: Epitope specificity determines pathogenicity and detectability in ANCA-associated vasculitis, *J Clin Invest* 123:1773–1783, 2013.

Roussel A, Benichou J, Randriamanantany ZA, et al.: Enzyme-linked immunosorbent assay for the combination of bullous pemphigoid antigens 1 and 2 in the diagnosis of bullous pemphigoid, *Arch Dermatol* 147(3):293–298, 2011.

Ruggenenti P, Debiec H, Ruggerio B, et al.: Ant-phopholipase A2 receptor antibody titer predicts post-rituximab outcome of membranous nephropathy, *J Am Soc Nephrol* 26:2545–2558, 2015.

Saha MK, Julian BA, Novak J, et al.: Secondary IgA nephropathy, *Kidney Int* 94:674–681, 2018.

Said SM, Cosio FG, Valeri AM, et al.: Proliferative glomerulonephritis with monoclonal immunoglobulin G deposits is associated with high rate of early recurrence in the allograft, *Kidney Int* 94:159–169, 2018.

Salvatore SP, Barisoni LMC, Herzenberg AM, et al.: Collapsing glomerulopathy in 19 patients with systemic lupus erythematosus or lupus-like disease, *Clin J Am Soc Nephrol* 7:914–925, 2012.

Sasaki H, Kohsaka H: Current diagnosis and treatment of polymyositis and dermatomyositis, *Mod Rheumatol* 28(6):913–921, 2018.

Satoskar AA, Suleiman S, Ayoub I, et al.: Staphylococcus infection-associated GN-spectrum of IgA staining and prevalence of ANCA in a single- center cohort, *Clin J Am Soc Nephrol* 12:39–49, 2016.

Saus J, Wieslander J, Langeveld JP, et al.: Identification of the Goodpasture antigen as the alpha 3 (IV) chain of collagen IV, *J Biol Chem* 263:13374–13380, 1988.

Schatz D, Krischer J, Horne G, et al.: Islet cell antibodies predict insulin-dependent diabetes in United States school age children as powerfully as in unaffected relatives, *J Clin Invest* 93(6):2403–2407, 1994.

Schatz DA, Winter WE: Autoimmune polyglandular syndrome. II: clinical syndrome and treatment, *Endocrinol Metab Clin North Am* 31(2):339–352, 2002.

Schirmer L, Srivastava R, Hemmer B: To look for a needle in a haystack: the search for autoantibodies in multiple sclerosis, *Mult Scler* 20(3):271–279, 2014.

Schmidt E, Zillikens D: Modern diagnosis of autoimmune blistering skin diseases, *Autoimmun Rev* 10(2):84–89, 2010.

Schoser B, Eymard B, Datt J, et al.: Lambert-Eaton myasthenic syndrome (LEMS): a rare autoimmune presynaptic disorder often associated with cancer, *J Neurol* 264(9):1854–1863, 2017.

Sebode M, Hartl J, Vergani D, et al.: Autoimmune hepatitis: from current knowledge and clinical practice to future research agenda, *Liver Int* 38(1):15–22, 2018.

Segelmark M, Hellmark T: Anti-glomerular basement membrane disease: an update on subgroups, pathogenesis and therapies, *Nephrol Dial Transplant*1–7, 2018.

Seifert L, Hoxha E, Eichhoff AM, et al.: The most terminal region of THSD7A is the predominant target for autoimmunity in THSD7A-associated membranous nephropathy, *J Am Soc Nephrol* 29:1536–1548, 2018.

Seitz-Polski B, Dahan K, Debiec H, et al.: High-dose rituximab and early remission in PLA2R1-related membranous nephropathy, *Clin J Am Soc Nephrol* 14:1173–1182, 2019.

Seitz-Polski B, Debiec H, Rousseau A, et al.: Phospholipase A2 receptor 1 epitope spreading at baseline predicts reduced likelihood of remission of membranous nephropathy, *J Am Soc Nephrol* 29:401–408, 2018.

Seitz-Polski B, Dolla G, Payre C, et al.: Epitope spreading of autoantibody response to PLA2R associates with poor prognosis in membranous nephropathy, *J Am Soc Nephrol* 27:1517–1533, 2016.

Sekulic M, Crary GS: Kidney biopsy yield: an examination of influencing factors, *Am J Surg Pathol* 41:961–972, 2017.

Servais A, Noel L-H, Roumenina LT, et al.: Acquired and genetic complement abnormalities play a critical role in dense deposit disease and other C3 glomerulopathies, *Kidney Int* 82:454–464, 2012.

Sethi S, D'Agati VD, Nast CC, et al.: A proposal for standardized grading of chronic changes in native kidney biopsy specimens, *Kidney Int* 91:787–789, 2017.

Sethi S, Fervenza FC: Membranoproliferative glomerulonephritis: a new look at an old entity, *N Eng J Med* 366:1119–1131, 2012.

Sethi S, Fervenza FC: Standardized classification and reporting of glomerulonephritis, *Nephrol Dial Transplant* 34:193–199, 2019.

Sethi S, Haas M, Markowitz GS, et al.: Mayo Clinic/Renal Pathology Society consensus report on pathologic classification, diagnosis and reporting of GN, *J Am Soc Nephrol* 27:1278–1287, 2016.

Sethi S, Madden BJ, Debiec H, et al.: Exostosin1/exostosin 2-associated membranous nephropathy, *J Am Soc Nephrol* 30:1113–1136, 2019.

Sethi S, Nasr SH, De Vriese AS, et al.: C4d as a diagnostic tool in proliferative GN, *J Am Soc Nephrol* 26:2852–2859, 2015.

Sethi S, Rajkumar SV D, Agati VD: The complexity and heterogeneity of monoclonal immunoglobulin-associated renal diseases, *J Am Soc Nephrol* 29:1810–1823, 2018.

Sethi S, Vrana JA, Fervenza FC, et al.: Characterization of C3 in C3 glomerulopathy, *Nephrol Dial Transplant* 32:459–465, 2017.

Sethi S, Zand L, Leung N, et al.: Membranoproliferative glomerulonephritis secondary to monoclonal gammopathy, *Clin J Am Soc Nephrol* 5:770–782, 2010.

Sharma SG, Larsen CP: Tissue staining for THSD7A in glomeruli correlates with serum antibodies in primary membranous nephropathy: a clinicopathological study, *Mod Pathol* 31:616–622, 2018.

Sherr J, Sosenko J, Skyler JS, et al.: Prevention of type 1 diabetes: the time has come, *Nat Clin Pract Endocrinol Metab* 4(6):334–343, 2008.

Shimosegawa T, Chari ST, Frulloni L, et al.: International Consensus diagnostic criteria for autoimmune pancreatitis: guidelines of the International Association of Pancreatology, *Pancreas* 40(3):352–358, 2011.

Siegel NJ, Spargo BH, Kashgarian M, et al.: An evaluation of routine electron microscopy in the examination of renal biopsies, *Nephron* 10:209–215, 1973.

Sinclair D: Clinical and laboratory aspects of thyroid autoantibodies, *Ann Clin Biochem* 43(Pt 3):173–183, 2006.

Singh NJ, Schwartz RH: Primer: mechanisms of immunologic tolerance, *Nat Clin Pract Rheumatol* 2(1):44–52, 2006.

Smith RJH, Appel GB, Blom AM, et al.: C3 glomerulopathy-understanding a rare complement-driven renal disease, *Nat Rev Nephrol* 15:129–143, 2019.

Smyk DS, Rigopoulou EI, Koutsoumpas AL, et al.: Autoantibodies in autoimmune pancreatitis, *Int J Rheumatol* 2012:940831, 2012.

Sorokin A, Brown JL, Thompson PD: Primary biliary cirrhosis, hyperlipidemia, and atherosclerosis risk: a systematic review, *Atherosclerosis* 194(2):293–299, 2007.

Sosenko JM, Skyler JS, DiMeglio LA, et al.: Type 1 Diabetes TrialNet and Diabetes Prevention Trial–Type 1 Study Groups: a new approach for diagnosing type 1 diabetes in autoantibody-positive individuals based on prediction and natural history, *Diabetes Care* 38(2):271–276, 2015.

Sowa M, Grossmann K, Knutter I, et al.: Simultaneous automated screening and confirmatory testing for vasculitis-specific ANCA, *Plos One* 9(11), 2014.

Sowa M, Hiemann R, Schierack P, et al.: Next-generation autoantibody testing by combination of screening and confirmation-the CytoBeadA (R) technology, *Clinical Reviews in Allergy & Immunology* 53:87–104, 2017.

Stanescu HC, Arcos-Burgos M, Medlar A, et al.: Risk HLA-DQA1 and PLA(2) R1 alleles in idiopathic memnbarbous nephropathy, *N Eng J Med* 364:616–626, 2011.

Stathatos N, Daniels GH: Autoimmune thyroid disease. *Curr Opin Rheumatol* 24(1):70–75, 2012.

Sura SP, Awais A, Cheifetz AS, et al.: Characteristics of inflammatory bowel disease serology in patients with indeterminate colitis, *J Clin Gastroenterology* 48(4):351–355, 2014.

Suzuki H, Yasutake J, Makita Y, et al.: IgA nephropathy and IgA vasculitis with nephritis have a shared feature involving galactose-deficient IgA1-oreiented pathogenesis, *Kidney Int* 93:700–705, 2018.

Svobodova B, Honsova E, Ronco P, et al.: Kidney biopsy is a sensitive tool for retrospective diagnosis of PLA2R-related membranous nephropathy, *Nephrol Dial Transplant* 28:1839–1844, 2013.

Takizawa S, Endo T, Wanjia X, et al.: HSP 10 is a new autoantigen in both autoimmune pancreatitis and fulminant type 1 diabetes, *Biochem Biophys Res Commun* 386(1):192–196, 2009.

Tampoia M, Giavarina D, Di Giorgio C, et al.: Diagnostic accuracy of enzyme-linked immunosorbent assays (ELISA) to detect anti-skin autoantibodies in autoimmune blistering skin diseases: a systematic review and meta-analysis, *Autoimmun Rev* 12(2):121–126, 2012.

Tao JJ, Hiraki LT, Levy DM, et al.: Comparison of sensitivities of American College of Rheumatology and systemic lupus international Collaborating Clinics classification criteria in childhood-onset systemic lupus erythematosus, *J Rheumatol* 46:731–738, 2019.

Taylor SI, Grunberger G, Marcus-Samuels B, et al.: Hypoglycemia associated with antibodies to the insulin receptor, *N Engl J Med* 307(23):1422–1426, 1982.

Thakker RV: Diseases associated with the extracellular calcium-sensing receptor, *Cell Calcium* 35(3):275–282, 2004.

Titulaer MJ, Lang B, Verschuuren JJ: Lambert-Eaton myasthenic syndrome: from clinical characteristics to therapeutic strategies, *Lancet Neurol* 10(12):1098–1107, 2011.

Tobin WO, Pittock SJ: Autoimmune Neurology of the central nervous system, *Continuum (Minneap Minn)* 23:627–653, 2017.

Toh BH, van Driel IR, Gleeson PA: Pernicious anemia, *New England Journal of Medicine* 338, 1998. 995–995.

Toh BH: Pathophysiology and laboratory diagnosis of pernicious anemia, *Immunologic Research* 65:326–330, 2017.

Tomas NM, Beck Jr LH, Meyer-Schwesinger C, et al.: Thrombospondin type-1 domain-containing 7A in idiopathic membranous nephropathy, *N Eng J Med* 371:2277–2287, 2014.

Tomas NM, Hoxha E, Reinicke AT, et al.: Autoantibodies against thrombospondin type 1 domain-containing 7A induce membranous nephropathy, *J Clin Invest* 126:2519–2532, 2016.

Tonutti E, Bizzaro N: Diagnosis and classification of celiac disease and gluten sensitivity, *Autoimmun Rev* 13:472–476, 2014.

Tozzoli R, Bonaguri C, Melegari A, et al.: Current state of diagnostic technologies in the autoimmunology laboratory, *Clin Chem Lab Med* 51(1):129–138, 2013.

Trimarchi H, Barratt J, Cattran DC, et al.: Oxford classification of IgA nephropathy 2016: an update from the IgA nephropathy classification working group, *Kidney Int* 91:1014–1021, 2017.

Van Daalen EE, Jennette JC, McAdoo SP, et al.: Predicting outcome in patients with anti-GBM glomerulonephritis, *Clin J Am Soc Nephrol* 13:63–72, 2018.

Van de Logt AE, Hofstra JM, Wetzels JF: Serum anti-PLA2R antibodies can be initially absent in idiopathic membranous nephropathy; seroconversion after prolonged follow-up, *Kidney Int* 87:1263–1264, 2015.

Van den Boorn JG, Konijnenberg D, Dellemijn TA, et al.: Autoimmune destruction of skin melanocytes by perilesional T cells from vitiligo patients, *J Invest Dermatol* 129:2220–2232, 2009.

VanBeek C, Haas M: Anti-PLA2R-associated membranous nephropathy: a review with emphasis on diagnostic testing methods, *Clin Nephrol* 84:1–9, 2015.

Vassileva S, Drenovska K, Manuelyan K: Autoimmune blistering dermatoses as systemic diseases, *Clin Dermatol* 32(3):364–375, 2014.

Vernino S: Paraneoplastic neurologic syndromes, *Curr Neurol Neurosci Rep* 6(3):193–199, 2006.

Vojdani A: Antibodies as predictors of complex autoimmune diseases, *Int J Immunopathol Pharmacol* 21(2):267–278, 2008.

Wahren-Herlenius M, Dörner T: Immunopathogenic mechanisms of systemic autoimmune disease, *Lancet* 382(9894):819–831, 2013.

Wasserfall CH, Atkinson MA: Autoantibody markers for the diagnosis and prediction of type 1 diabetes, *Autoimmun Rev* 5(6):424–428, 2006.

Weening JJ, D'Agati VD, Schwartz MM, et al.: The classification of glomerulonephritis in systemic lupus erythematosus revisited, *J Am Soc Nephrol* 15:241–250, 2004.

Weich T, Stahl RAK, Hoxha E: Diagnostic role of renal biopsy in PLA2R1-antibody –positive patients with nephrotic syndrome, *Mod Pathol* 32(9):1320–1328, 2019.

Wenzlau JM, Juhl K, Yu L, et al.: The cation efflux transporter ZnT8 (Slc30A8) is a major autoantigen in human type 1 diabetes, *Proc Natl Acad Sci U S A* 104(43):17040–17045, 2007.

Wilhelmus S, Alpers CE, Cook HT, et al.: The revisited classification of GN in SLE at 10 years: time to re-evaluate histopathologic lesions, *J Am Soc Nephrol* 26:2938–2946, 2015.

Winter WE, Jacobsen LM, Pittman D: Insulin, insulin antibodies and insulin autoantibodies, *Medical Laboratory Observer* 49(2):16–19, 2017.

Winter WE, Jialal I, Devaraj S: Thyrotropin receptor antibody assays: clinical utility, *Am J Clin Pathol* 139(2):140–142, 2013.

Winter WE, Schatz DA: Autoimmune markers in diabetes, *Clin Chem* 57(2):168–175, 2011.

Winter WE, Hardt NS, Harris NS: Chapter 30. Carbohydrate disorders. In WA Clarke, editor: *Contemporary practice in clinical chemistry*, Washington, DC, 2016, AACC Press, pp 417–434.

Winter WE, Maclaren NK, Riley WJ, et al.: Pancreatic alpha cell autoantibodies and glucagon response to arginine, *Diabetes* 33(5): 435–437, 1984.

Wobser H, Paur T, Schnoy E, et al.: Suitability of the simplified autoimmune hepatitis score for the diagnosis of autoimmune hepatitis in a German cohort, *United European Gastroenterology J* 6(2):247–254, 2018.

Wooldridge JT, Davis A, Fischer WG, et al.: The impact of renal tissue procurement at bedside on specimen adequacy and best practices, *Am J Clin Pathol* 151:205–208, 2019.

Wu L-H, Yu F, Tan Y, et al.: Inclusion of renal vascular lesions in the 2003 ISN/RPS system for classifying lupus nephritis improves outcome predictions, *Kidney Int* 83:715–723, 2013.

Yimam KK, Bowlus CL: Diagnosis and classification of primary sclerosing cholangitis, *Autoimmun Rev* 13(4–5):445–450, 2014.

Yu F, Haas M, Glassock R, et al.: Redefining lupus nephritis: clinical implications of pathophysiologic subtypes, *Nat Rev Nephrol* 13:483–495, 2017.

Yu L, Dong F, Miao D, et al.: Proinsulin/insulin autoantibodies measured with electrochemiluminescent assay are the earliest indicator of prediabetic islet autoimmunity, *Diabetes Care* 36(8):2266–2270, 2013.

Zaghrini C, Seitz-Polski B, Justino J, et al.: Novel ELISA for thrombospondin type 1 domain-containing 7A autoantibodies in membranous nephropathy, *Kidney Int* 95:666–679, 2019.

Zaidan M, Terrier B, Pozdzik A, et al.: Spectrum and prognosis of noninfectious renal mixed cryoglobulinemuc GN, *J Am Soc Nephrol* 27:1213–1224, 2015.

Zhang W, De D, Mohammed KA, et al.: New scoring classification for primary biliary cholangitis-autoimmune hepatitis overlap, *Hepatol Commun 20* 2(3):245–253, 2018.

Zhang Y, Salter A, Wallström E, et al.: Evolution of clinical trials in multiple sclerosis, *Ther Adv Neurol Disord* 12, 2019. 1756286419826547.

Zhang Y, Zhao T: Hypoglycemic coma due to insulin autoimmune syndrome induced by methimazole: a rare case report, *Exp Ther Med* 8(5):1581–1584, 2014.

Zone JJ, Egan CA, Taylor TB, Meyer LJ: IgA autoimmune disorders: development of a passive transfer mouse model. *J Investig Dermatol Symp Proc* 9(1):47–51, 2004. 1756286419826547.

CHAPTER 56

ALLERGIC DISEASES

Henry A. Homburger, Robert G. Hamilton

OVERVIEW, 1115

PATHOGENESIS OF ALLERGIC DISEASE, 1116

Mechanisms of Immediate Hypersensitivity, 1116

Atopy and the Allergic Phenotype: Genetic Influences and Candidate Genes, 1116

Regulation of Immunoglobulin E Synthesis: Molecular and Cellular Interactions, 1117

Immunoglobulin E: Structural and Functional Characteristics, 1117

Cells and Mediators of Immediate Hypersensitivity Reactions, 1118

LABORATORY TESTING IN THE EVALUATION OF ALLERGIC DISEASES, 1120

The Rationale for Testing, 1120

Allergen Molecules: Protein Component Families, Molecular Structures, and Cross-Reactivity, 1120

In Vivo Test Techniques: Skin Tests and End-Organ Challenge Tests, 1121

Measurement of Total Serum Immunoglobulin E: Analytic Methods and Reference Ranges, 1121

Measurement of Total Serum Immunoglobulin E: Clinical Applications, 1122

Measurement of Allergen-Specific Immunoglobulin E Antibodies: Analytic Methods, 1123

Measurement of Allergen-Specific Immunoglobulin E Antibodies: Clinical Applications, 1123

Future Directions: Component-Resolved Diagnostics and Testing by Microarray Methods, 1127

Tests for Mediators of Immediate Hypersensitivity Reactions, 1128

SELECTED REFERENCES, 1128

KEY POINTS

- The prevalence of allergic disease, particularly food allergy, has increased in recent years throughout the world, especially in developed countries.
- Allergen-specific immunoglobulin E (IgE) antibody is the most important trigger molecule for allergic inflammation.
- Laboratory tests for IgE antibody that support a high likelihood of allergic disease are widely available and clinical practice guidelines advocate their use. A positive IgE antibody test result is an indicator of allergic sensitization and a risk factor that provides support for a clinical history-based diagnosis of allergic disease.
- Treatments for allergic diseases include avoidance, pharmacotherapy, immunotherapy, and therapeutic monoclonal anti-IgE antibody that requires demonstration of a total serum IgE level between 30 and 700 kU/L in serum prior to use.
- Clinical investigations of the natural history of allergic diseases in children have shown a reproducible sequence of sensitization to allergens known as the allergy march that makes it important to establish the diagnosis of allergy at an early age to identify allergen triggers, optimize treatment in order to ameliorate progression of serious diseases such as asthma, and prevent the development of anaphylaxis.
- Tests for total IgE and allergen-specific IgE antibodies are useful in the diagnostic workup of a patient with a high pretest suspicion of having allergic disease.
- Measurement of total serum IgE in children and adults is of limited value in the diagnosis of allergic disease due to the overlap between atopic and nonatopic populations. An elevated total serum IgE level carries a high predictive value for allergic disease, but a normal level does not exclude allergic disease. Measurement of total serum IgE is diagnostically useful in patients suspected of having allergic bronchopulmonary aspergillosis.
- Measurement of allergen-specific IgE antibodies is diagnostically useful and can be recommended in the following clinical situations:
  - (A) Evaluation of children with clinical signs and symptoms of allergy, including eczema, gastrointestinal signs, rhinitis, or wheezing.
  - (B) Evaluation of children and adults suspected of having allergic respiratory disease to establish the diagnosis and to define the specificity of allergen sensitization to pollens, animal proteins, dust mites, fungal antigens, and foods. Results are useful to identify allergen specificities for immunotherapy treatment regimens.
  - (C) Confirmation of sensitization to food allergens and aid in determining the presence of food allergy in children and adults with signs of immediate hypersensitivity following food ingestion.
  - (D) Evaluation of sensitization to insect venom allergens, particularly as an aid in defining venom specificity when skin tests are equivocal or there is sensitization to multiple venoms.
  - (E) Confirmation of the clinical history-based diagnosis of drug hypersensitivity in patients with a clinical history of anaphylactic sensitivity.
  - (F) Confirmation of sensitization to occupational allergens (e.g., natural rubber latex).
- Testing for allergen-specific IgE, IgG, and IgG4 antibodies is not routinely recommended for evaluating the effects of immunotherapy, or for excluding the diagnosis of anaphylactic sensitivity to insect venoms in treated patients.
- Tests for IgE antibodies are indicated only in patients who have had a thorough medical history and physical examination and their history provides suspicion of allergic disease.

OVERVIEW

The prevalence of allergic disease has increased significantly in the United States and throughout the developed world (Devereux, 2014). Longitudinal epidemiologic studies have shown an increased prevalence of sensitization to common allergens and increased prevalences of asthma, atopic dermatitis, food allergy, and allergic rhinitis in children. More than 40% of children age 6 years and older and more than 35% of children age 1 to 5 years have serologic evidence of sensitization to one or more common allergens (Salo, 2014; Visness et al., 2009). Allergic sensitization, which is defined by the presence of immunoglobulin E (IgE) antibodies to one or more allergens, is a significant risk factor for allergic disease. Allergic sensitization is also a distinguishing characteristic of atopy, the inherited tendency to develop allergic diseases.

Estimates of the prevalences of common allergic diseases in the United States vary with disease, patient age, and geographic location. The prevalence of asthma has increased steadily from the 1950s to the present and currently is estimated at between 5% and 10% among adults and children in different states (Centers for Disease Control and Prevention [CDC], 2010). More than 31 million persons in the United States suffer from asthma, with more than 7 million being children (Weiss, 2001, Arroyave, 2013). The prevalence of allergic rhinitis has increased in the United States from about 5% in 1970 to approximately 9% in 2004, thus affecting more than 25 million Americans (National Center for Health Statistics, 2006).

The prevalence of food allergies has also increased. The cumulative prevalence of sensitization to common food allergens in children may be as high as 24% in the United States. In contrast, the cumulative prevalence of food allergies in children is 4% to 8% (see later discussion), and many sensitized children do not display signs and symptoms of systemic

food allergy (Branum, 2009). Given the high overall prevalence of allergic disease in the United States, estimates of the total yearly cost of diagnosing and managing patients with allergic diseases run into the tens of billions of dollars. Simply stated, allergic diseases are a major public health concern.

Recent attempts to explain the increased prevalence of allergic diseases have focused on both genetic and environmental influences. A large number of genes and genetic polymorphisms contribute to the development of allergic diseases (see later discussion), but they fail to account for the risk of developing a particular allergic disease and do not explain the rapid changes in disease prevalences noted previously. Current theories postulate a causative role for environmental influences to account for the increased prevalence of allergic diseases. Several investigators have proposed that diminished exposure to microorganisms during early childhood in developed countries may lead to aberrant development of the adaptive immune system and may predispose to both allergic disease and certain autoimmune diseases (Liu, 2010). This theory, called the *hygiene hypothesis*, postulates that early exposure to bacteria and other microorganisms promotes development of mature antigen-presenting dendritic cells and regulatory T (Treg) cells, whereas diminished exposure leads to high levels of T helper 1 (Th1) and Th2 effector T cells that participate in the pathogenesis of immune-mediated diseases. The proposed mechanism for the beneficial effect of early exposure to microorganisms and environmental antigens includes a role for enhanced release of the anti-inflammatory cytokines interleukin (IL)-10, IL-12, and transforming growth factor-β by dendritic cells, which induces antigen-specific Treg cells (Smits, 2005). This effect may be mediated by interactions between bacterial products (e.g., bacterial endotoxin) and Toll-like receptors (TLR2 and TLR4) on dendritic cells, monocytes, and macrophages of the innate immune system. Longitudinal studies in large cohorts of allergic patients and experimental studies in animal models continue to investigate the epidemiology and biological mechanisms of allergic disease development and to validate the hygiene hypothesis.

The signs and symptoms of allergic diseases can be difficult to distinguish from those of other disorders (Host, 2003). Clinical manifestations of allergy may be relatively mild and self-limited, as in seasonal allergic rhinitis, or they can manifest with severe symptoms that have marked morbidity, such as in allergic asthma. Laboratory tests are useful in the evaluation of patients with allergic disease, but awareness of the basic mechanisms of immediate-type hypersensitivity and knowledge of the empirical relationships between test results and their diagnostic predictive values are required to translate testing results into a clinical diagnosis. This chapter addresses these subjects, beginning with a review of the biological mechanisms of immediate-type hypersensitivity and the "allergic phenotype." It then discusses laboratory tests as they may be applied to the diagnostic evaluation of children and adults with suspected allergic disease based on their clinical history and physical examination.

The distinction between sensitization to an allergen or allergenic component and clinical allergy is a key concept emphasized throughout this chapter. The authors identify the chemical components of common allergens, including species-specific and cross-reactive allergenic components. The minimum number of tests needed to achieve high positive and negative predictive values for allergic disease is overviewed for different clinical conditions. The discussion mentions clinical situations and testing schemes in which laboratory testing is not likely to be cost-effective or may lead to erroneous diagnoses. Recent developments in the laboratory evaluation of allergy include an expanding repertoire of tests for IgE antibodies to putative allergens, including tests for antibodies to highly purified native allergenic proteins and recombinant allergen components. Analytic methods that utilize chip-based microarrays to test for over 100 allergen-specific IgE antibodies simultaneously have proven useful in research studies. These methods lend themselves to interpretive reporting with patient-specific comments that aid in identifying clinically significant patterns of sensitization to allergenic components.

PATHOGENESIS OF ALLERGIC DISEASE

MECHANISMS OF IMMEDIATE HYPERSENSITIVITY

IgE is the principal trigger molecule for allergic inflammation. In the late 1960s, investigators working independently in two laboratories described a new isotype of human immunoglobulin from patients with allergic diseases that was responsible for the skin-sensitizing activity of serum (Ishizaka, 1966; Bennich, 1969). This immunoglobulin, originally called IgND, was later named IgE (Ishizaka, 1967). In the years that followed, investigators have focused on discovering the basic biological mechanisms of immediate hypersensitivity. These include mechanisms that control IgE production by immunocompetent B-lymphocytes and that promote the recruitment of inflammatory cells and release of vasoactive mediators from IgE-sensitized effector cells at sites of allergic inflammation. Recent studies have focused on investigating genetic determinants of the allergic phenotype and on identifying genes responsible for regulating IgE production and for influencing tissue responses to allergic inflammation.

ATOPY AND THE ALLERGIC PHENOTYPE: GENETIC INFLUENCES AND CANDIDATE GENES

The term *atopic* (from the word *atopy*) describes those individuals who are genetically predisposed to produce specific IgE antibodies following exposure to allergens. These individuals are highly likely to develop allergic diseases. Nevertheless, while atopy is characteristic of allergic disease, signs and symptoms of allergic diseases, notably asthma and eczema, may also occur in the absence of atopy. This finding demonstrates that the genetic predisposition to allergic diseases is complex and fails to account entirely for development of clinical allergy. It is useful to consider two principal domains of genetic influence: genes that encode molecules directly involved in immune responses that strongly influence IgE synthesis and determine atopy, and genes that affect other complementary biological functions. These include tissue structure and repair, tissue permeability to allergens, cell migration, and fibrinolysis, which determine the susceptibility of end organs to inflammation and modulate exposure of the immune system to environmental allergens (Holloway, 2010; Holloway, 2014).

Knowledge of genes that predispose to allergic diseases comes from several sources. Population-wide linkage analysis studies have identified the chromosomal locations of candidate genes and positional cloning studies support the relationship of putative allergy genes to known genes for molecules involved in regulating the immune response. Genome-wide association studies examine the relationships between candidate genes for atopy (IgE synthesis) and disease susceptibility in populations with asthma and other common allergic diseases (Holloway, 2010; Holloway, 2014).

Among the various candidate genes, some of the strongest evidence for a role in allergic disease exists for genes encoding molecules that promote IgE synthesis. Included in this group are the following: genes for IL-4, IL-13, IL-4 receptor α chain (IL4R) and signal transducer and activator of transcription 6 (STAT6) (Kabesch, 2006; Holloway, 2007). As described later, the products of these genes collectively influence the development of Th2 cells, and promote the expression and deletional class switching of ε immunoglobulin heavy-chain genes. Class II human leukocyte antigen (HLA) loci and alleles on chromosome 6p strongly influence the immune response and sensitization to specific allergens and allergenic component proteins. For example, responsiveness to the common aeroallergens Derp p and Derp f peptides from dust mites (*Dermatophagoides pteronyssinus* and *Dermatophagoides farinae*) is found in linkage with other loci associated with bronchial hyperresponsiveness in asthmatic individuals (Moffatt, 2010). A similar linkage has been proposed for an atopy gene closely linked to the IgE Fc receptor α-chain locus on chromosome 1q23 (Weidinger, 2008). Studies suggest that additional genes may predispose to allergic disease, including genes for the interleukin 6 receptor (IL6R) and GATA-binding protein 3 involved in the production of Th2 lymphocytes, and genes for TL4R that influence the innate immune response to environmental antigens. Cytokine genes, including the genes for IL-3, IL-5, and IL-33, influence the development, proliferation, and recruitment of allergic effector cells, including mast cells, basophils, and eosinophils.

Other genes influence allergic disease susceptibility by affecting biological functions that facilitate exposure to allergens or determine the response of tissue to inflammation. Mutations in the gene for filaggrin on chromosome 1q21 predispose to atopy and atopic dermatitis (Irvine, 2011). Filaggrin is an important protein component of the cutaneous epidermal barrier. Null mutations in the filaggrin gene may promote allergy development by weakening this barrier (Palmer, 2006). The products of several genes determine the response of tissues to chronic inflammation. *ADAM33* is an exemplary gene. This gene encodes a metalloproteinase that influences airway remodeling and smooth muscle hyperactivity associated with asthma susceptibility and progression (Van Eerdewegh, 2002). Examples of several genes that predispose to atopy and allergic disease are listed Table 56.1. While the genes mentioned earlier influence susceptibility to allergic disease, and mutations and polymorphisms of several candidate genes have been identified, there is no clinical evidence at this time to support routine testing for genetic polymorphisms in the evaluation of patients with allergic disease.

TABLE 56.1
Genes and the Allergic Phenotype

Chromosome	Genetic Locus	Phenotype
6p21-23	HLA D region (HLA-DRB1 and DQB1)	Responder or nonresponder to common allergens
11q12	Fc ε receptor α chain	Enhanced responsiveness to aeroallergens; high total serum immunoglobulin (Ig) E
5q31	Cytokines interleukin (IL)-3, IL-4, IL-5, IL-9, IL-13, and IL-33	High total serum IgE
16	IL-4 receptor	High total serum IgE
20p13	*ADAM33* gene	Enhanced airway responsiveness, airway remodeling
1q21	Filaggrin	Diminished epithelial barrier to allergens

HLA, Human leukocyte antigen.
Note: More than 120 candidate genes have been described to be associated with allergic disease. This table lists a selected sample of genes found in multiple studies. See text for discussion of additional loci and genes.

REGULATION OF IMMUNOGLOBULIN E SYNTHESIS: MOLECULAR AND CELLULAR INTERACTIONS

As noted earlier, class II genes of the HLA D region strongly influence individual responses to exogenous antigens (Pieters, 2000; Wang, 2002). Gene products of the highly polymorphic HLA D region—DR, DQ, and DP molecules expressed on the plasma membranes of antigen-presenting dendritic cells and B cells—bind processed antigen for presentation to immunocompetent T cells, initiating the immune response (Wang, 2002). B cells act as antigen-presenting cells by binding antigen (allergen) through membrane-associated immunoglobulin, that is, IgE-Fc ε RI, (Oettgen, 2014). The cellular and humoral responses that follow antigen presentation are complex and include interactions mediated by cell-to-cell contacts and secretion of stimulatory cytokines. Production of mature IgE antibodies by B cells exemplifies these mechanisms (Fig. 56.1).

All B cells initially produce IgM antibodies. Rearrangement of their V, D, and J exons that encode portions of the Ig variable region create a variable region motif (VDJ) that encodes the antigen binding (Fab) portion of a mature Ig heavy chain. The rearranged VDJ motif determines specificity for antigen and is located upstream from exons that encode the constant regions of the various Ig heavy chains, including the α-, γ-, and ε-exons. Production of mature transcripts for complete Ig molecules that bear these heavy chains requires additional rearrangements at the heavy-chain (IgH) locus. These rearrangements result in a change in expression of heavy-chain constant region domains from μ to another isotype (e.g., γ). This process is referred to as *deletional switch recombination* because endonucleases excise exons encoding domains of the μ-chain in an irreversible process (Coico, 2003; Oettgen, 2014). Two pathways involving rearrangement of Ig heavy-chain genes lead to the production of IgE antibodies: a direct pathway from IgM to IgE and a sequential pathway from IgM to an IgG intermediate to IgE (Wu, 2014).

Synthesis of mature IgE molecules occurs in a series of steps that begins with expression of germline (sterile) transcripts of the ε heavy chain. Germline transcription must occur before deletional switch recombination can proceed. At the molecular level, this process involves interaction with a promoter exon upstream from the four exons that encode domains of the ε heavy chain (see later discussion and Fig. 56.1). The ε-promoter contains binding sites for the transcription factors STAT6 and nuclear factor κB (NF-κB), which drives transcription by activating the promoter. Mutations at binding sites for these transcription factors block isotype switching to IgE. Because germline transcripts are "sterile" and do not encode a functional heavy chain, further metabolism of the germline transcript by endonucleases is required to create a functional heavy chain molecule. Endonucleases excise Cμ and ligate the now adjacent VDJ and Cε sequences. The process of deletional switch recombination involves rearrangement of double-stranded deoxyribonucleic acid (DNA) at specific sites called *S regions* by enzymatically catalyzed breakage, cleavage, and recombination of DNA to create the functional heavy chain.

At the cellular level, IgE synthesis is initiated by cell-to-cell interactions and is driven by soluble cytokine mediators (Oettgen, 2001; Oettgen, 2014). Cytokines produced by T helper/inducer cells of the Th2 phenotype are required for the production of IgE heavy-chain transcripts. The stimulatory cytokines IL-4 and IL-13 provide essential signals for synthesis of IgE. Th2 cells produce several cytokines that act as growth factors for B cells, including IL-4 and IL-13, which have been shown to induce production of germline ε-transcripts in human B cells (Vercelli, 1989; Defrance, 1994). These cytokines exert their effects by interacting with multimeric cell surface receptors composed of α and γ chains. The functional receptors for IL-4 and IL-13 are of 2 types that share a common ligand-binding IL-4R α chain. Type 1 receptors expressed on Th2 cells and mast cells bind only IL-4 and are heterodimers of the IL-4R α chain and γ chain. Type 2 receptors are widely expressed on T cells, bind both IL-4 and IL-13, and are heterodimers of the IL-4R α chain and IL-13R α chain. Binding of IL-4 and IL-13 to these receptors induces a series of phosphorylation reactions, which result in DNA transcription driven by phosphorylated transcription factors. Tyrosine kinases of the Janus family (JAK1, JAK2, and JAK3) are associated with intracellular domains of the IL-4 and IL-13 receptors and catalyze phosphorylation of the receptors, enabling them to bind intracellular transcription factors. The transcription factors, including STAT6 and NF-κB, once phosphorylated, translocate to the nucleus, where they bind to the ε-promoter and induce expression of germline ε-transcripts (Oettgen, 2001; Oettgen, 2014).

Coincident with the interaction of antigen-presenting cells and T cells described earlier, which takes place primarily through the T-cell antigen receptor (TCR) and leads to production of IL-4 and IL-13, a second signal provided by cell-to-cell interaction promotes switch recombination from μ to ε heavy-chain expression (Oettgen, 2014). This signal is provided by the interaction of CD40 (constituitively expressed on B cells) and CD40 ligand (CD154) expressed only on activated T cells. Engagement of the TCR results in upregulation of CD40 ligand on the T-cell surface. CD40 ligand interacts with CD40 on the surface of B cells to catalyze activation of NF-κB, which, in turn, facilitates activation of the ε-promoter through STAT6 and other activation-induced proteins (Oettgen, 2001, 2014). CD40 is a member of the tumor necrosis factor (TNF) receptor superfamily; engagement of CD40 by CD40 ligand antagonizes apoptosis of B cells. Engagement of CD40 by CD40 ligand also upregulates CD80-CD86 expression on B cells, which interacts with CD28 on T cells to strongly amplify cytokine transcription and secretion of IL-4 and IL-13. The importance of CD40 ligand (CD154) to the process of class switching is illustrated by patients with X-linked hyper-IgM syndrome who are deficient in CD40 ligand and are unable to produce IgG, IgA, or IgE antibodies (Korthauer, 1993).

IgE-producing B cells at mucosal sites and in lymph node follicles typically differentiate into short-lived plasmablasts and plasma cells while a small number of long-lived plasma cells persist in bone marrow (Wu, 2014). This finding helps to account for the rapid decline in IgE antibody levels that occur when antigen stimulation is withdrawn. Initial IgE responses to allergen occur primarily at extrafollicular sites where low-affinity antibodies are produced by direct class switching from IgM to IgE. Persistent or recurrent antigenic stimulation promotes development of higher-affinity IgE antibodies by a process of somatic mutation called *affinity maturation*.

IMMUNOGLOBULIN E: STRUCTURAL AND FUNCTIONAL CHARACTERISTICS

The heavy chains of IgE molecules are structurally different from other immunoglobulin isotypes. They confer skin-sensitizing activity by binding to high-affinity Fc ε receptors on tissue mast cells (see later discussion) (Ishizaka, 1966, Bennich, 1969). Immunoglobulin fragments (Fab and Fab′2 fragments) prepared by enzymatic digestion of purified IgE myeloma proteins do not bind to cell surface receptors for IgE and do not mediate skin-sensitizing activity. The unique antigenic determinants of IgE molecules are contained on the Fc ε fragment (Bennich, 1969). While the heavy chains of human IgE molecules resemble other Igs, they differ by having an additional domain, C ε 4, which confers a higher molecular weight. IgE molecules are also more heavily glycosylated than IgG molecules and bind more avidly to lectin proteins. The physicochemical properties and immunologic functions of different regions of the IgE molecule, determined by experiments performed with purified human IgE myeloma proteins and immunoglobulin fragments prepared by enzymatic digestion, are summarized in Table 56.2 (see also Hamilton et al., 2016, CLSI I/LA20 guidance document).

Human IgE protein makes up only approximately 0.0005% of total serum immunoglobulin. The low serum concentration of IgE is partly a function of binding to effector cells but also reflects a high catabolic rate, greater than 70% per day. The half-life of IgE in blood is 1 to 5 days; by comparison, IgG molecules have a serum half-life of approximately 20 days. The half-life of IgE bound to tissue mast cells is much longer, up to

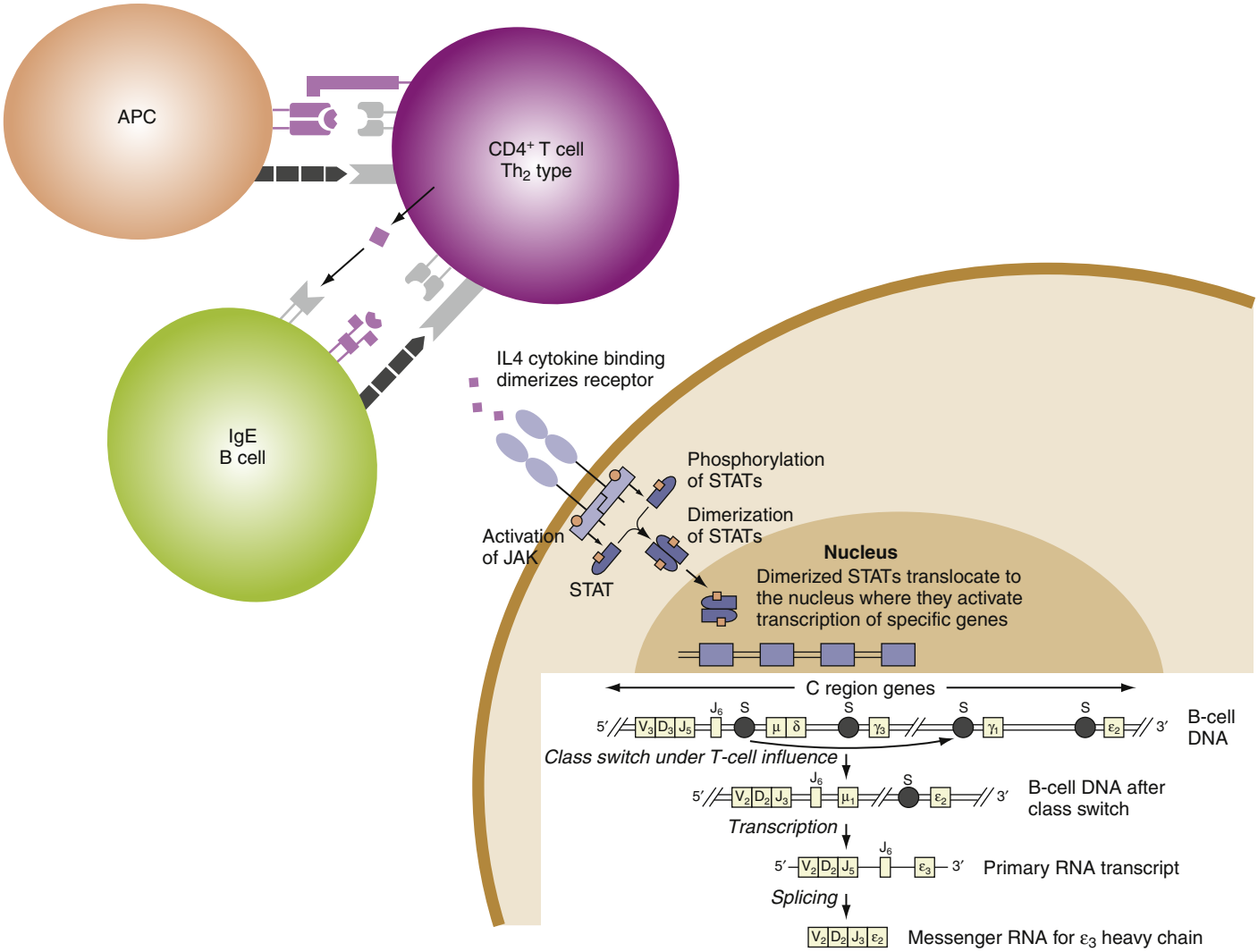

Figure 56.1 Cellular and molecular interactions regulating immunoglobulin (Ig) E synthesis.

TABLE 56.2
Physicochemical Properties of Immunoglobulin E (IgE)

H chain class	ε
Molecular formula	ε_2L_2
Sedimentation coefficient(s)	8
Molecular weight, Da	190,000; H chain molecular weight is 70,000
Carbohydrate, %	18
Complement fixation (classic)	None
Serum half-life, days	1–5
Placental transfer	None
Reaginic activity	4+; Fc-containing fragments inhibit skin-sensitizing activity of native IgE, but Fab-containing fragments do not

Fab, Antigen binding.

several months. Individual IgE molecules have a functional valency of 2, as shown schematically in Figure 56.2.

As noted earlier, human IgE antibodies sensitize mast cells in the skin to release histamine. The skin-sensitizing activity of IgE is heat labile. Heating at 56°C for 2 hours irreversibly modifies the C ε 3 and C ε 4 domains of IgE molecules and abolishes skin-sensitizing activity (Ishizaka, 1967). Reduction and alkylation of inter-ε-chain disulfide bonds also abolishes binding to effector cells. Aggregated human IgE does not fix complement by the classical pathway, and there is no significant placental transfer of human IgE.

CELLS AND MEDIATORS OF IMMEDIATE HYPERSENSITIVITY REACTIONS

Mast cells are the principal effector cells of immediate hypersensitivity reactions. They also promote inflammation, tissue repair, wound healing, and responses to bacterial infection. Other cell types—including eosinophils, basophils, neutrophils, and lymphocytes—also sustain allergic inflammation (Bradding, 2014). Once thought to be closely related cells, mast cells and basophils both stain metachromatically with basic dyes and contain histamine in preformed granules (Galli, 1990). More recent studies have focused on the development of these two cell types from different precursors (Bradding, 2014). Mast cells develop from pluripotent hematopoietic stem cells and bear receptors for stem cell factor. Mast cell precursors originate in the bone marrow as CD34+, tyrosine kinase Kit receptor (CD117) + progenitors. Developing mast cells home to tissues by binding to fibroblasts that contain integrin and vascular cell adhesion molecule 1 (VCAM-1). In peripheral tissues, mast cell precursors under the influence of stem cell factor develop into mature cells.

Two subtypes of human mast cells (described later) require different cytokines for development. Mast cells that predominate at mucosal surfaces require stem cell factor and the T cell cytokines IL-3, IL-4, IL-5, IL-9 and IL-10. Mast cells that develop in submucosal connective tissues require only stem cell factor and develop without additional cytokines from T cells. Unlike mast cells, basophils develop in the bone marrow from granulocyte precursors and enter the circulation as mature cells. Mast cells and basophils both contain histamine in preformed granules, but mast cells typically contain up to 10 times more histamine per cell than basophils.

There are two phenotypically distinct mast cell subtypes, termed *MCt* and *MCtc*. MCt cells contain only tryptase; MCtc cells contain both tryptase and chymase. MCt cells predominate at mucosal surfaces at sites of allergic inflammation, often in proximity to T lymphocytes. MCtc cells

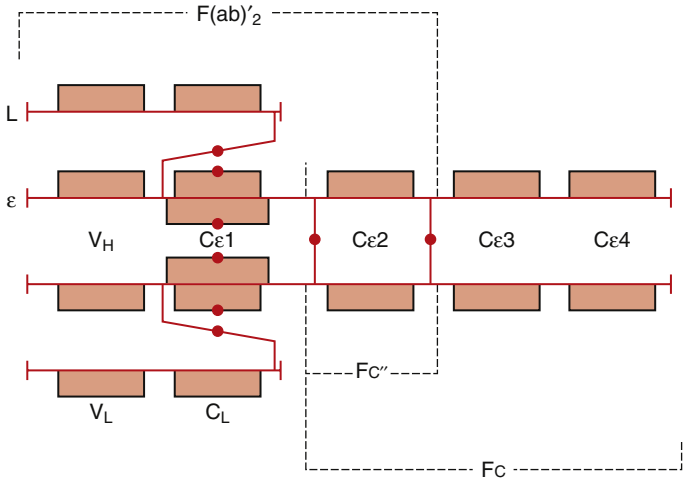

Figure 56.2 Immunoglobulin (Ig) E structure.

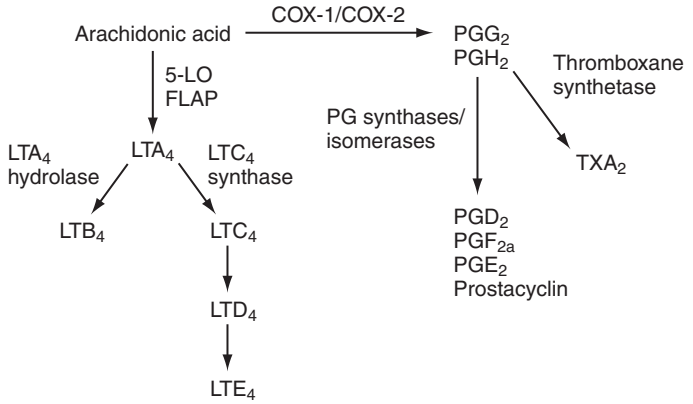

Figure 56.3 Metabolism of arachidonic acid. *COX,* Cyclooxygenase; *FLAP,* 5-lipoxygenase–activating protein; *5-LO,* 5-lipoxygenase; *LT,* leukotriene; *PG,* prostaglandin; *TX,* thromboxane.

are more numerous in submucosal sites and in connective tissues and are not associated with allergic inflammation or T lymphocytic infiltration (Irani, 1986; Bradding, 2014). The two subtypes of mast cells also differ in their cytokine profiles (MCt cells contain little IL-4 but are high in IL-5 content), release of inflammatory mediators (MCt cells release more LCT4 and PGD2 than MCtc cells), and responsiveness to chemoattractants (MCt cells do not respond to C5a). Viewed collectively, mast cells are most numerous in the following tissues: lung (alveolar walls and bronchial epithelium and subepithelium), small intestine (epithelium and subepithelium), nasal mucosa, and skin.

Mast cells release two types of inflammatory mediators: (1) mediators contained in preformed granules and (2) mediators newly synthesized and released in response to signals associated with allergic inflammation. The principal preformed mediators are histamine, tryptase, chondroitin sulfates (proteoglycans), and TNF-α. The newly synthesized inflammatory mediators include cyclooxygenase (prostaglandin) and lipoxygenase (leukotriene) products of arachidonic acid metabolism. In addition to the newly synthesized prostaglandin and leukotriene mediators released within minutes of an allergic trigger, mast cells also synthesize and release several cytokines. Mast cell cytokines released within hours of initiation of inflammation amplify the allergic response (IL-4, IL-5, and IL-13), recruit inflammatory cells (TNF-α) and promote proliferation of fibroblasts and endothelial cells.

The primary mechanism of release of preformed mediators from mast cells involves transmembrane signaling mediated by cell surface (homocytotropic) IgE antibodies bound to high-affinity receptors for IgE (Fc ε RI). Fc ε RI is located diffusely on the plasma membranes of mast cells. Binding of IgE antibodies to Fc ε RI is reversible but of high affinity (Ka = 10^{10} M^{-1}) (Wank, 1983). Although IgE antibodies in blood have a half-life of less than 5 days, the half-life of IgE antibodies bound to Fc ε RI on mast cells is much longer and may persist for months (Oettgen, 2014). Fc ε RIs are saturated at physiologic concentrations of IgE. The number of Fc ε RIs per cell ranges from 40,000 to as many as 500,000. Higher numbers of receptors are induced by culturing cells in the presence of IgE. Cells obtained from atopic individuals typically express higher numbers of Fc ε RI, reflecting upregulation of Fc ε RI by IgE. Pharmacologic treatment with anti-IgE (omalizumab) leads to decreased unbound (free) circulating IgE and downregulated numbers of Fc ε RI on mast cells and basophils (Beck, 2004).

Fc ε RI is a multimetric receptor, composed of α-, β-, and γ-subunits as follows: α1, β1, and γ2. IgE antibodies bind to the α-subunit; the β- and γ-subunits contain intracytoplasmic regions that function in transmembrane signaling (Ravetech, 1991; Metcalfe, 2009). Fc ε RI molecules are mobile within the plasma membranes of sensitized cells, as indicated by capping studies performed with fluorescein-conjugated anti-IgE antibodies. This mobility over short distances is important for the release of mediators from mast cells. Cross-linking (or bridging) of occupied IgE receptors by multivalent antigens or by intact anti-IgE antibodies or their F(ab′)2 fragments triggers release of histamine and other preformed mediators and initiates the synthesis and release of prostaglandin and leukotriene mediators. Univalent allergens, including haptens and Fab fragments of anti-IgE antibodies, do not induce mediator release.

The mechanism of mediator release from sensitized mast cells is exquisitely sensitive; it depends on release of Ca^{++} from intracellular stores in the endoplasmic reticulum and influx of extracellular Ca^{++}. Aggregation of as few as 1000 molecules of IgE per cell can result in release of histamine and other mediators. Transmembrane signaling mediated by Fc ε RI aggregation is a complex process that is dependent on phosphorylation of Fc ε receptor subunit proteins by enzymes of the Src tyrosine kinase family, including LYN and SYK, which produce a series of phosphorylated intermediates, including phospholipase Cγ. Phospholipase Cγ hydrolyzes phosphatidylinositol 4,5-biphosphate (PIP2) to generate inositol 3,4,5-triphosphate (IP3) and diacylglycerol (DAG). IP3 binds to receptors on membranes of the endoplasmic reticulum, resulting in release of stored intracellular Ca^{++}. DAG plus Ca^{++} activates protein kinase enzymes that mediate the influx of additional extracellular Ca^{++} that triggers the release of preformed mediators by a process of exocytosis. Increased intracellular Ca^{++} also promotes activation of cytosolic phospholipase A2, which initiates synthesis of arachidonic acid derived from membrane lipids. Free arachidonic acid is metabolized in mast cells to prostaglandin D_2 by enzymes of the cyclooxygenase (COX) pathway (COX-2, PG synthase, and isomerase), and to the cysteinyl leukotrienes LTB4, LTC4, LTD4, and LTE4 by enzymes of the 5-lipoxygenase pathway (Metcalfe, 2009; Bradding, 2014) (Fig. 56.3).

Histamine is the best-known mediator of allergic inflammation. Injected intradermally, histamine produces a characteristic wheal and flare reaction that results from simultaneous vasoconstriction of postcapillary venules and neurogenic erythema (Petersen, 1997). Histamine in mast cells is contained in preformed granules with approximately 3 to 8 pg of histamine per cell. After release from mast cells, histamine interacts with specific G-protein–coupled receptors, termed *H1* to *H4* (Wess, 1997; Gether, 2000). Engagement of the H1 histamine receptor leads to activation of phospholipase C with subsequent protein kinase C activation and Ca^{++} mobilization that causes the cellular responses associated with acute allergic inflammation. Histamine interacts with different receptors in different tissues. H1 receptors in the airway promote contraction of bronchial smooth muscle, increased mucous production, tissue edema, and increased vascular permeability. H2 receptors in the stomach promote acid secretion. H3 and H4 receptors are found on histaminergic nerves and bone marrow cells, respectively.

Histamine is degraded by two enzymatic pathways, with the major metabolite, *N*-methyl imidazole acetic acid (MIAA) resulting from sequential methylation and deamination of histamine by the enzymes histamine *N*-methyl transferase and monoamine oxidase. Most secreted histamine is excreted in urine as MIAA, with a lesser amount appearing undegraded.

The most abundant preformed proteins in mast cell granules are the neutral proteases, tryptase and chymase. Tryptase is a tetramer comprised of 29 to 40 kDa subunits with a molecular mass of approximately 134 kDa (Schwartz, 1981). Two cDNA subunits of tryptase termed *α* and *β*, cloned from human mast cells, bear approximately 90% sequence homology with one another (Miller, 1990). Most tryptase in human serum occurs in the form of α- and β-monomers. α-Tryptase is currently referred to as *protryptase* and is released constitutively from mast cells. β-Tryptase, currently referred to as *mature tryptase*, is stored in secretory granules as a noncovalent complex with the proteoglycan heparin and is optimally detected in serum within 30 minutes to 4 hours following the initiation of an allergic reaction (Schwartz, 2006). The concentration of protryptase in serum provides an estimate of mast cell mass, while mature tryptase serves as a marker of mast cell activation resulting from allergic inflammation. In addition to

exhibiting enzymatic activity, tryptase promotes growth of fibroblasts and smooth muscle cells, activates mast cells, and promotes release of the chemoattractant IL-8 from epithelial cells (Cairns, 1996).

Newly synthesized prostaglandins and leukotrienes are important proinflammatory allergic mediators. The principal prostaglandin mediator of mast cells is PGD_2 (see Fig. 56.3), which is more potent than histamine on a molar basis. However, it is released in smaller quantities than histamine from activated mast cells (Bradding, 2014). PGD_2 and its metabolite 9α,11βPGF2 promote constriction of airway smooth muscle, peripheral vasodilatation, and inhibition of platelet aggregation.

IgE-mediated mast cell activation also results in synthesis and release of the cysteinyl leukotrienes LTC4, LTD4, and LTE4 (see Fig. 56.3). Eosinophils, basophils, and macrophages also synthesize and release leukotrienes. Production of leukotrienes is upregulated in mast cells exposed to IL-4 (Hsieh, 2001). The cysteinyl leukotrienes are extremely potent bronchoconstrictors, up to 1000 times more potent than histamine, and they promote increased vascular permeability, mucus production, and tissue fibrosis (Bradding, 2014). Leukotrienes play a significant role in allergic inflammation and asthma. Their biological effects are mediated by the cellular receptors CysLT1 and CysLT2, expressed on many different cell types, including bronchial smooth muscle cells, monocytes and macrophages, mast cells, and eosinophils. The role of leukotrienes in asthma is demonstrated by clinical trials showing that the early asthmatic response to allergen is diminished by administration of leukotriene antagonists (Findlay, 1992).

Allergic inflammation often proceeds in two stages: an immediate response to allergen contact that occurs within minutes, followed by a late reaction that occurs up to 24 hours following allergen exposure. This biphasic response occurs commonly in asthma. Both stages of the allergic response depend on the presence and engagement of cell-bound IgE antibodies. The initial response reflects the effects of histamine, prostaglandin, and leukotriene mediators. The late response requires recruitment of additional inflammatory cells, including eosinophils and neutrophils, at sites of allergic inflammation, followed by release of mediators from these activated cells. Release of cytokines and chemoattractants from activated mast cells promotes infiltration and degranulation of leukocytes in the late inflammatory response.

LABORATORY TESTING IN THE EVALUATION OF ALLERGIC DISEASES

THE RATIONALE FOR TESTING

Measurements of total IgE protein (IgE) and allergen-specific IgE antibodies (IgE antibodies) in serum are useful to identify a state of sensitization in allergic (atopic) children and adults. These tests are mainstays in the laboratory evaluation of allergic diseases. First-generation tests for total IgE and allergen-specific IgE antibodies were developed more than 50 years ago, shortly after the discovery of IgE. Most hospital clinical laboratories do not perform a full repertoire of IgE antibody tests on site. Rather, they prefer to send specimens to referral laboratories for analysis of less frequently requested specificities. In recent years, the use of laboratory tests in the evaluation of patients with allergic diseases has increased with changes in the logistics of health care delivery, in particular, the nearly universal adoption of managed care health plans. Other important developments favoring the use of laboratory tests in the practice of clinical allergy include (1) significant improvements in the analytic methods for detecting and quantifying IgE antibodies, including computer-driven automation (autoanalyzers, microarrays); (2) molecular characterization of many species-specific and cross-reactive allergen components with U.S. Food and Drug Administration (FDA) clearance of recombinant allergen proteins for use in diagnostic tests (so-called *component-resolved diagnostics* or *molecular allergy diagnostics*); (3) development of pharmacologic anti-IgE (omalizumab) therapy for the treatment of asthma; and, perhaps most important, (4) expanded empirical knowledge of the natural history of allergic diseases, especially in children (Wahn, 2000; DuToit, 2015; Hamilton, 2016).

Before the era of managed care, it was often possible for patients with symptoms and signs of allergy to see an allergy specialist without prior medical evaluation. This is no longer the case for most patients, who are evaluated initially by primary care physicians. In this paradigm, laboratory tests that suggest a high likelihood of allergic disease or have prognostic significance assume increased importance, since the results may justify referrals to allergy specialists or enable primary care physicians to manage patients within their own practices.

In the field of clinical allergy, tests for total serum IgE and allergen-specific IgE antibodies are ordered principally for diagnosis. In addition, test results may indicate an increased likelihood of persistent allergy and are useful to identify allergen specificities in the planning of immunotherapy treatment regimens in patients with rhinitis or allergic asthma. The results of clinical studies are less clear about the efficacy of laboratory data for evaluating the response to immunotherapy treatment and in monitoring the course of disease. While it is commonplace in clinical studies to monitor the concentrations of IgE antibodies over time in cohorts of patients with particular allergic diseases treated with different therapies or to elucidate the natural history of disease, this practice is not recommended in most clinical situations. It is not clear from clinical studies that repeat testing has value for deciding whether to continue or modify treatment regimens. It is also appropriate to caution against the practice of performing extensive and indiscriminate panels of IgE antibody tests in the evaluation of patients with suspected allergic disease. This practice is not likely to be helpful in diagnosis, may promote misdiagnosis of allergic disease in patients with clinically insignificant sensitization to allergen(s) or result in inappropriate therapy, and is actively discouraged by a consensus recommendation of allergy specialists (Bernstein, 2008; Adkinson & Hamilton, 2015).

ALLERGEN MOLECULES: PROTEIN COMPONENT FAMILIES, MOLECULAR STRUCTURES, AND CROSS-REACTIVITY

Recent studies have identified the common molecular structures and chemical properties of principal protein components that are present in extracts of allergenic substances (Table 56.3) (Kazemi-Shirazi, 2000; Shakib, 2008, Breiteneder, 2009, Stewart, 2014, Matricardi 2016). Most allergen component proteins are enzymes, enzyme inhibitors, ligand-binding proteins, storage proteins, or are associated with cytoskeletal proteins, especially actin. In addition, some allergenic molecules have unique structures that facilitate their recognition and binding by cells of the innate immune system. In some cases, they may directly promote the synthesis of IgE antibodies by the adaptive immune system (Shakib, 2008). An example is Der p 1 allergen, which is released in fecal particles produced by the dust mite *Dermatophagoides pteronyssinus*. *D. pteronyssinus* sensitivity is important in the pathogenesis of allergic asthma. Der p 1 is a cysteine protease that acts in the airway to degrade protective surfactant molecules and α_1-antitrypsin, which normally provide a barrier to inhaled allergens. In addition, Der p 1 directly promotes mast cell degranulation and increased secretion of IL-4. It may also inhibit the development of Treg cells that dampen the Th2-driven response to Der p 1 antigen exposure.

Recombinant protein technology has enabled the development of a new generation of allergen component reagents for use in immunoassays of IgE antibodies. Studies of recombinant component proteins have enhanced our understanding of the molecular basis of cross-reactivity between common pollen and food allergens. Studies of the molecular structures of allergenic components have identified several families of allergenic proteins that commonly elicit allergic signs and symptoms (see Table 56.3). The following are of particular clinical importance: pathogenesis-related family 10 proteins (PR10 proteins) from plants and foods; nonspecific lipid transfer proteins (nsLTPs) from foods and pollens; profilin proteins from foods and pollens; heat-stable storage proteins from foods, including 2S albumin, 7S globulin, and 11S globulin proteins; parvalbumin proteins from freshwater and saltwater fish; tropomyosin from shellfish; lipocalins from cat and dog; serum albumin from cow's milk, beef, eggs and chicken; and cross-reactive carbohydrate determinants (CCDs) from glycoproteins in pollens, plant foods, and insect venoms. A complete discussion of these allergen component families is beyond the scope of this chapter. They are extensively discussed in the EAACI molecular allergology user guide, (Matricardi et al., 2016). However, it is important to comment on certain properties of these components that determine their allergenicity and cross-reactivity.

The PR10 and profilin component families are referred to as panallergens, as these proteins are widely conserved in different plant species. PR10 proteins feature a high degree of structural sequence homology, and are susceptible to degradation by heat and digestive enzymes. Bet v 1 from birch pollen was among the first of the PR10 components identified; subsequent studies have sequenced and synthesized Bet v 1 homologues from many different plant foods (Ballmer-Weber, 2011). PR10 proteins in plant foods commonly elicit local symptoms, such as oral allergy syndrome (OAS). Profilin components bind actin, are widely distributed in pollens and plant foods (including vegetables, fruits, and nuts), and share a high degree of sequence homology (Santos, 2011). Profilins are also susceptible to degradation by proteolytic enzymes and heat. Profilin sensitization does not usually cause clinical symptoms but may cause severe reactions in

TABLE 56.3

Allergen Component Families

Protein Family	Sensitivity to heat and proteases	Examples of Plant Food Allergen Sources	Clinical Expression
PR10 proteins (Birch pollen Bet v 1 homologues)	Sensitive*	Betulaceae: hazelnut* Rosaceae: e.g., apple, cherry, peach Apiaceae: e.g., carrot, celery,* fennel, parsley Fabaceae: e.g., peanut,* soybean,* mungbean	Oral allergy syndrome (OAS); Symptoms usually mild but may be severe, e.g., Gly m 4 (soybean)
nsLTPs (nonspecific lipid transfer proteins)	Stable	Betulaceae: hazelnut Rosaceae: e.g., apple, cherry, peach Other: maize, peanut, barley, grape, cabbage	Systemic reactions common
Profilins (Birch pollen Bet v 2 homologues)	Sensitive to intermediate	Profilins are widely distributed in plants and plant foods: including citrus, banana, tomato, vegetables, and nuts.	Mainly OAS Symptoms usually mild
Storage proteins (2S albumins, 7S/11S globulins)	Stable	Kernels/nuts/seeds: e.g., peanut/soybean, tree nuts, seeds, cereals	Systemic reactions common
Parvalbumin	Stable	Fish, freshwater and saltwater	Systemic reactions common
CCDs (cross-reactive carbohydrate determinants)	Stable	CCDs are widely distributed in plant foods. CCD allergenicity has been proposed for celery, tomato, and zucchini.	†

PR10 proteins, Pathogenesis-related family 10 proteins from plants.
*Bet v 1 homologues in hazelnut, celery, peanut, and soybean have been found to be partially heat stable, and systemic reactions may occur.
†Immunoglobulin (IgE) antibodies to profilins and CCDs in general are considered to have less clinical relevance than those to other allergen components.

some patients with allergic sensitization to citrus fruits, melon, banana, or tomato. Sensitization both to PR10 and profilin panallergen proteins often occurs through pollen exposure, with subsequent cross-reactive sensitization to homologues in foods. Panallergen sensitization and sensitization to ubiquitous CCD glycoprotein moieties accounts for the presence in some sera of IgE antibodies that cross-react widely with allergens of common pollens and foods. This finding can confound the interpretation of skin tests and in vitro tests for IgE antibodies, which can lead to the mistaken diagnosis of widespread allergy to multiple foods.

nsLTPs, storage proteins, and parvalbumin proteins are resistant to heat and proteolytic degradation. This property promotes stable 3-dimensional protein structures that greatly enhance the allergenicity of these proteins. nsLTP components are found in the outer layers of Rosaceae fruits, such as the peach, where they are responsible for severe reactions in allergic individuals. 2S albumin storage proteins are found in peanuts, tree nuts (e.g., cashews, walnuts, and pecans), soybeans, and a wide variety of seeds (Sharma et al., 2011; Beyer, 2015). 2S albumins from different species have a relatively low degree of sequence homology and there is limited cross-reactivity between distantly related botanical families—for example, IgE antibodies to 2S albumins from different tree nuts often cross-react but do not react with 2S albumin from the legume peanut. Parvalbumin is a major allergen in both freshwater and saltwater fish (Griesmeier, 2010). Parvalbumin components resist heat and proteolytic degradation and cause most severe allergic reactions to fish. Additional clinically important ingested, injected, and inhaled allergenic molecules have been produced by recombinant technology and are FDA cleared for use as diagnostic test reagents.

IN VIVO TEST TECHNIQUES: SKIN TESTS AND END-ORGAN CHALLENGE TESTS

In discussing the use of laboratory tests in the diagnosis and management of allergic diseases, it is important to mention commonly used in vivo tests, particularly the skin prick test and end-organ challenge tests. In vivo tests are regarded by many allergy specialists in the United States as standards of diagnostic accuracy and reliability. The ability to reproduce a specific allergic reaction by in vivo challenge is considered the most highly predictive technique for demonstrating sensitization and for defining allergic reactivity to aeroallergens, venoms, and drugs. Despite this widely held opinion, the results of skin tests can be highly variable (McCann, 2002). Sources of variability include lack of standardization for the majority of diagnostic skin testing extracts, differences in the potency of allergen extracts available for testing, and differences in the techniques employed by different operators.

Skin tests are performed by prick/puncture and intradermal injection methods (Demoly, 1998). The response to intradermal injection of an allergen extract is graded by measuring the diameter of the wheal and erythema reaction within 15 minutes following allergen injection. A 1+ reaction corresponds to a 5- to 10-mm wheal. A response of this magnitude is usually considered evidence of sensitization to an allergen. Highly sensitized individuals may develop wheal diameters greater than 15 mm with pseudopods.

Skin tests also are performed by the prick method. Skin prick testing makes use of more concentrated allergen extracts, up to 1000-fold greater concentrations than are used for intradermal testing. A mean wheal diameter of 3 mm is commonly considered the threshold for a positive reaction. The wheal size provides an estimate of the degree of sensitization. A more quantitative estimate of sensitization can be obtained by the technique of endpoint titration. Serial, tenfold dilutions of allergen extract are used, beginning with the most dilute solution (Turkeltaub, 2000). The endpoint is defined as the greatest dilution that produces a 1+ reaction.

End-organ challenge tests are useful both in the diagnosis and clinical management of the allergic patient. Adaptations include the bronchial provocation test in the evaluation of asthma; the double-blind, placebo-controlled food elimination and open food challenge test in the diagnosis of food allergy; and the rarely used sting challenge in the diagnosis of anaphylactic sensitivity to insect venom. Use of challenge tests in routine clinical situations is limited by the lack of well-standardized allergen extracts of defined potency and by the limited number of allergens that can be tested in an individual on a single occasion. As an example, double-blind food elimination and challenge procedures require periods of abstinence of several days between introduction of suspected foods (Sampson et al., 2012). Although generally regarded as the most reliable test for food allergy, the double-blind, placebo-controlled food challenge test is performed by relatively few practicing allergists.

MEASUREMENT OF TOTAL SERUM IMMUNOGLOBULIN E: ANALYTIC METHODS AND REFERENCE RANGES

Historically, a variety of immunochemical methods have been used to measure total serum IgE, including competitive displacement immunoassays, immunometric (sandwich) assays with radiolabeled and enzyme-labeled second-stage antibodies, and enhanced sensitivity nephelometry (Hamilton, 2014). Currently, autoanalyzer-based, nonisotopic immunometric assays are the most widely used in clinical laboratories. In brief, anti-IgE antibody (either polyclonal or monoclonal) is immobilized to a solid phase to capture IgE from serum. Following a buffer wash, bound IgE is detected with a second enzyme-labeled antibody that produces a response (optical density or fluorescence) that is proportional to the total IgE content in the test serum. Clinically used immunoassays for total serum IgE are capable of detecting as little as 1 kU/L of IgE in the pediatric assay format, with a working range of 2 to 5000 kU/L for the routine assay. One kU

TABLE 56.4
Serum Immunoglobulin E (IgE) Reference Ranges in Children and Adults

Age	Mean (kU/L)	+1 SD (kU/L)
6 weeks	0.6	2.3
3 months	1.0	4.1
6 months	1.8	7.3
9 months	2.6	10
12 months	3.2	13
2 years	5.7	23
3 years	8.0	32
4 years	10	40
5 years	12	48
6 years	14	56
7 years	16	63
8 years	18	71
9 years	20	78
10 years	22	85
*Adults	13.2	41

SD, Standard deviation.
*The +2 SD cutoffs for adults and children reported in different studies vary considerably (Data from Kjellman NI, Croner S: Cord blood IgE determination for allergy prediction—a follow-up to seven years of age in 1,651 children, Ann Allergy 53:167–171, 1984.)

equals approximately 2.4 μg of IgE. Assay calibrators used in commercial products are well standardized between manufacturers and are traceable to an international standard (World Health Organization preparation for human IgE) (Thorpe, 2014). Interlaboratory proficiency surveys indicate that measurement of total serum IgE by multiple methods is highly reproducible, with interlaboratory coefficients of variation <15% (Hamilton, 2006, 2016). A number of studies have examined the total serum IgE concentrations in healthy, nonallergic children and adults. Synthesis of IgE occurs in the human fetus as early as the 11th week of gestation, but cord serum typically contains less than 1 kU/L of IgE. Serum concentrations of IgE in children increase slowly with age and reach adult levels at approximately 10 years of age (Table 56.4). In both children and adults, studies of healthy subjects have yielded frequency histograms of IgE measurements that are strongly positively skewed, with upper 95th percentile confidence intervals that are seemingly high compared with mean levels of IgE. The distribution of IgE concentrations in allergic subjects significantly overlaps the skewed distribution of results in healthy controls. To adjust for this finding, many laboratories report reference ranges that are based on logarithmic transformations of the skewed normal distributions, and the upper limits of "normal" are portrayed as +1 standard deviation (SD) of age-related distributions of healthy controls (see Table 56.4). This convention is confusing to many clinicians who are not aware of the skewed histograms of serum IgE concentrations in healthy nonallergic subjects.

MEASUREMENT OF TOTAL SERUM IMMUNOGLOBULIN E: CLINICAL APPLICATIONS

The measurement of total IgE protein in serum has been thoroughly evaluated for (1) its clinical usefulness as a screening test in the diagnosis of various allergic diseases, (2) its predictive value as an indicator of the likelihood of development of allergic disease in asymptomatic infants and children, and (3) its utility as a prognostic indicator in adults with certain types of chronic allergic disease. Measurement of IgE may also be useful in the evaluation of patients suspected of having immunodeficiency diseases, parasitic diseases, allergic bronchopulmonary aspergillosis, or the rare hyper-IgE (Job) syndrome.

The hyper-IgE syndrome was described in 1972 by Buckley and colleagues, who reported two patients with greatly elevated serum IgE levels, diffuse dermatitis, recurrent furunculosis, and pneumonia with pneumatoceles secondary to *Staphylococcus aureus* infection. Subsequent reports of patients with this disorder have defined the clinical syndrome: elevations of serum IgE concentration are extreme (2000–50,000 kU/L), and patients have blood and tissue eosinophilia and strongly positive immediate wheal and flare reactions to inhalant allergens, pollens, foods, and bacterial and fungal antigens. Despite these findings, asthma is not common in patients with the hyper-IgE syndrome (Buckley, 1978).

The synthesis of IgE, as reflected by serum levels, has been studied in patients with a variety of primary immunodeficiency diseases. Increased IgE levels have been described in some patients with partial deficiencies of cellular immunity, including Di George syndrome, Omen syndrome and Wiskott-Aldrich syndrome. Immunodeficiency with increased IgE can be classified based on inheritance with autosomal-dominant disease, Job syndrome, caused by STAT3 mutations; and mutations of DOCK8 or Tyk2 associated with recessive inheritance (Xiong, 2012). Immunodeficiency diseases in which there is complete absence of synthesis of IgG, IgA, and IgM, such as severe combined immunodeficiency disease, characteristically show diminished IgE synthesis and markedly decreased serum IgE levels. Serum IgE levels are variable in patients with IgA deficiency; ataxia telangiectasia patients typically have diminished levels, but patients with isolated IgA deficiency may have normal or modestly increased levels.

Parasitic infiltration of the gastrointestinal tract or parenchymatous organs strongly stimulates IgE synthesis. Studies in laboratory animals suggest that specific IgE antibodies are important in the host defense against parasites such as *Nippostrongylus brasiliensis* and *Schistosoma mansoni*. Serum IgE concentrations greater than 1000 kU/L are regularly found in children in areas of endemic infestation with parasites. Other parasitic diseases known to be associated with increased serum IgE levels include visceral larva migrans (*Toxocara canis*), intestinal capillariasis (*Capillaria philippinensis*), schistosomiasis, ancylostomiasis, filariasis, and echinococcosis. In patients with intestinal parasitic disease, serum levels of IgE have been noted to decrease considerably following successful treatment with antiparasitic drugs.

In reviewing the usefulness of the total serum IgE measurements in the diagnosis of allergic diseases, it is appropriate to discuss its use in children and adults separately. Elevated IgE levels in serum at birth or during infancy often antedate the development of clinical allergy (Kjellman, 1984). Serum IgE levels above the 95th percentile are found in approximately 75% of children with a biparental family history of allergic disease. Among healthy children with IgE levels more than 1 SD above the mean for a given age, development of allergic disease during the following 18 months is increased more than tenfold compared with a group with lower IgE levels. Although predictive of future development of allergic disease, these data are mainly of epidemiologic interest.

Measurements of total serum IgE in infants and children are of limited value in the diagnosis of allergic disease. Serum IgE levels greater than the +1 SD cutoff support the diagnosis of an allergic disease, but normal IgE levels do not exclude the diagnosis of allergic disease during infancy or later in life. The results of other diagnostic tests, including tests for allergen-specific IgE antibodies, are more sensitive, specific, and have higher predictive values for allergic disease (see later discussion). If the presenting signs of allergic disease are unequivocal—for example, eczema and rhinitis in a child with an atopic family history—the total serum IgE level provides little additional information. In older children and adults, measurement of IgE in serum also has limited diagnostic sensitivity. In general, children with sensitization and allergy to several different allergens and multiple allergic diseases have elevated serum IgE levels, whereas children sensitized to fewer allergens with limited end-organ involvement often have normal levels. In atopic children, the presence of cutaneous disease and gastrointestinal manifestations increases the likelihood that the serum IgE level will be elevated. Children with allergic diseases that involve several target organs also tend to have elevations in serum IgE of greater magnitude than those with limited disease.

Measurement of total serum IgE also has limited diagnostic usefulness in adults suspected of having an allergic disease. Results of clinical studies of adult respiratory allergy indicate that approximately 50% of adults with allergic asthma and fewer than 5% of adults with nonallergic asthma have elevated serum IgE levels. Asthmatic adults sensitized to a limited number of allergens usually have normal levels. The highest IgE levels in adults typically occur in patients with allergic sensitization to several allergens and combinations of asthma, atopic dermatitis, and rhinitis. Just as in children, the limited diagnostic sensitivity of the serum IgE levels limits the clinical usefulness of this test in those situations in which the diagnosis of allergic disease is most uncertain (Klink, 1990). Despite limited sensitivity, the finding of an elevated concentration of total serum IgE in serum carries a high positive predictive value for allergic disease.

Allergic bronchopulmonary aspergillosis (ABPA) is associated with marked elevation in the serum concentration of IgE. This disease typically occurs in patients with allergic asthma, generally of long duration. The concentration of IgE in serum is elevated during times of acute pulmonary infiltration but may fluctuate considerably during the course of the disease. A normal IgE level in a patient with active lung disease virtually excludes the diagnosis of ABPA.

MEASUREMENT OF ALLERGEN-SPECIFIC IMMUNOGLOBULIN E ANTIBODIES: ANALYTIC METHODS

Two methods are commonly used in clinical practice to detect IgE antibodies: in vivo allergen skin testing by the prick/puncture method (see previous discussion) and in vitro testing by immunometric assays with solid-phase allergen immunosorbents. A third type of method measures release of histamine (leukocyte histamine release assay) or the expression of activation antigen markers (CD63) on the surface of blood basophils exposed to allergen in vitro (basophil activation assay) (Nolte, 1993). These basophil-based assays have not been widely adopted by clinical laboratories in the United States because they require a fresh whole-blood sample and are thus used principally in clinical research. Cellular assays require testing of blood samples within 24 hours, and cells from up to 15% of individuals called "nonresponders" do not release histamine in vitro. Assays that rely on the detection of activation markers may be subject to false-positive results from IL-3 priming that is required before exposure to allergen. The results of early clinical studies of commercial cell-based assays showed relatively poor diagnostic sensitivity compared with skin tests for several allergens, including foods and insect venoms (Maly, 1997). In more recent clinical studies, basophil activation results have shown improved efficacy for identifying allergy to foods and hapten drugs and may be useful to predict the severity of reactions in peanut allergic children (Santos, 2015).

Immunometric assays for IgE antibodies were introduced in the late 1960s (Wide, 1967). Original (first-generation) methods utilized solid-phase immunosorbents prepared by coupling allergen extracts covalently to cyanogen bromide–activated Sephadex, paper disks, or microcrystalline cellulose particles as capture reagents for IgE antibodies. After incubating with serum, the solid phase was washed with buffer and radiolabeled, affinity-purified, polyclonal anti-IgE antibody was added as a detection protein. These early methods were semiquantitative, with results determined by comparison to an arbitrary dose-response reference curve that interpolated binding of IgE antibodies in calibrator solutions to a birch pollen immunosorbent. Results were reported in arbitrarily defined classes from 0 (negative) to 5+ (strongly positive). The original commercial method, now obsolete, was referred to by the term *radioallergosorbent test* (*RAST*). First-generation tests for IgE antibodies had a number of limitations: the immunosorbents had limited capacity to bind IgE antibodies, which resulted in relatively poor analytic sensitivity; long incubations were required; and IgE binding to immunosorbents was susceptible to interference from competing IgG antibodies. In addition, the allergens used to prepare these early immunosorbents were poorly characterized and varied considerably from lot to lot and from one manufacturer to another.

The most widely used allergen-specific IgE antibody assays are currently computer-driven autoanalyzers that report quantitative results and address the performance and analytic sensitivity and specificity concerns of the earliest RAST (Yunginger et al., 2000; Hamilton et al., 2016). One important advancement is the use of higher-capacity allergen immunosorbents that have an increased antibody-binding capacity compared with earlier solid-phase reagents. Their calibration is now traceable to the third World Health Organization IgE Reference Preparation (Hamilton, 2016; Thorpe et al., 2014). A modified method of calibration is based on demonstrating parallelism between a simultaneously run dose-response curve for total serum IgE and the dose-response curves for IgE bound to each different allergen immunosorbent. This type of calibration scheme, called *heterologous interpolation*, permits reporting of results for IgE antibody tests in mass units, kUa/L, where 1 IU is equivalent to 2.4 ng/mL (Hamilton et al., 2016). Analytic sensitivity has been enhanced with detection of IgE antibodies at concentrations as low as 0.1 kUA/L (0.24 ng/mL). Sample sizes used in these instruments vary from 40 μL to as low as 4 μL with excellent precision. The expression of results in actual concentrations enables identification of more precise cutoffs for classifying clinical data. In addition, the current singleplex assays that analyze one IgE antibody specificity per analysis are more resistant to interference by allergen-specific IgG antibodies because of the higher binding capacity of the allergosorbent. Reproducibility has also been enhanced with the use of better characterized allergen extracts. Results are typically available within 6 hours with reduced turnaround times for clinical tests.

Significant improvements have been achieved in the production and quality control of reagent allergens used to measure IgE antibodies. As noted earlier, allergenic molecules from several protein families have been extensively characterized structurally. More than 100 recombinant protein components are now available for clinically important allergen specificities, including components of dust mites, cat, dog, and animal epithelia; mold allergens (e.g., *Alternaria tenuis*), pollen aeroallergens from trees, grasses, and weeds, and food allergens, including peanut, tree nuts, soybean, wheat, milk, egg, stone fruits, fish and shellfish; natural rubber latex; and insect venom allergens.

Although much improved over earlier versions, and despite FDA clearance as quantitative methods, IgE antibody assays from different manufacturers do not generate numerically equivalent test results. This is an important caveat, since published cutoffs for clinical decision making are method dependent (Hamilton, 2010, 2016; Wood et al., 2007). Assays from different commercial manufacturers differ in the composition of the allergen used in their allergosorbents and in the mathematical algorithms used in their calibration systems. Depending on the assay design, orally consumed biotin and naturally occurring carbohydrate (CCD)-specific IgE antibody may also interfere in some of the assays (Hemmer et al., 2018).

Test methods for IgE antibodies have also been adapted to detect multiple different antibodies simultaneously (so-called multi-allergen tests). By coupling several allergens to the same allergosorbent, it is possible to test an aliquot of serum for the presence of several different antibodies without losing analytic sensitivity (Ownby, 1984; Hamilton, 2016). The diagnostic sensitivity and negative predictive value of multiallergen tests exceeds that of other single analyte screening tests for allergy, including measurement of total serum IgE (Ownby, 1984). Multiallergen reagents can be used effectively in algorithms to test sera for antibodies to several allergens of a common class (e.g., grass pollens or foods). Testing for individual specificities as guided by the clinical history is indicated only if the screening test is positive.

There is active interest in developing a more rapid point-of-care diagnostic allergy test that could use a finger prick or small blood sample and provide IgE antibody levels in less than 30 minutes (Garib, 2018). The technical challenges of producing a quantitative IgE antibody level with the constraints on analytic sensitivity, less than ideal reproducibility, limited sample size and allergen specificity design restrictions make this goal elusive.

MEASUREMENT OF ALLERGEN-SPECIFIC IMMUNOGLOBULIN E ANTIBODIES: CLINICAL APPLICATIONS

At the outset, it is useful to note that in vitro testing for IgE antibodies has certain advantages compared with in vivo skin testing. It poses no risk to the patient, and results are not influenced by concomitant treatment with antihistamines, adrenergic bronchodilators, or brief courses of treatment with systemic corticosteroids. In addition, IgE antibody testing is preferable to skin testing in infants and patients with dermographism or widespread dermatitis. With the availability of molecular allergenic components, serologic measurements of IgE antibody can provide an indication of true versus cross-reactivity–induced sensitization. For select foods, it can aid in making decisions about the need for an open or controlled food challenge.

Disadvantages must also be noted. In vitro testing is more costly if large numbers of individual tests are ordered; it is often necessary to send tests to referral laboratories, and the results may not be available for several days.

Current recommendations for clinical use are based on the results of empirical studies in which the sensitivities and predictive values of IgE antibody results were compared with the results of skin tests and challenge tests.

It is clear from many published studies that the diagnostic sensitivity and specificity of IgE antibody results can vary considerably depending on the populations studied and the allergens and diseases in question. When considering a particular disease or allergen, results will vary depending on characteristics of the study cohorts, especially the patients' age, geographic location, affected target organs, and severity of disease. Results are also affected by the elapsed time between exposure to allergen and testing, along with the source of allergen tested. For the purposes of this chapter, it is useful to review the following clinical applications separately: allergic diseases of infants and children, including food allergies; adult allergic diseases; insect venom sensitivities; and drug and occupational allergies.

Atopic children commonly develop symptoms and signs of allergic disease in a predictable sequence. This concept has been called the *allergic march*. In genetically predisposed infants, eczema (atopic dermatitis) is often the first manifestation of allergic disease. Atopic infants and children younger than 3 years of age may also have gastrointestinal symptoms (colic, diarrhea, vomiting, and abdominal pain) or may suffer from chronic otitis. Very young children may suffer from recurrent wheezing. As the atopic child matures, cutaneous and gastrointestinal symptoms commonly give way to worsening respiratory symptoms with development of allergic

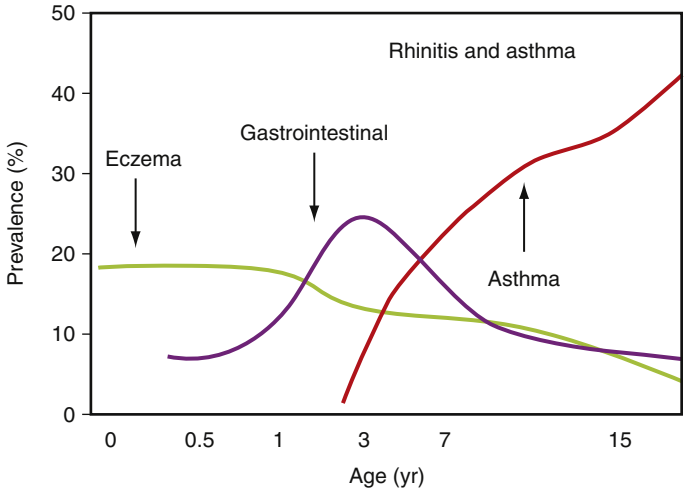

Figure 56.4 Relationship of age and clinical manifestations of allergic disease in children.

rhinitis and asthma (Wahn, 1998; Wahn, 2000; Hahn, 2005). The typical sequence of the allergic march is shown schematically in Figure 56.4.

The presenting symptoms of allergic diseases in infants and children are not specific and are easily mistaken for other etiologies. Increasingly, physicians have recognized that empirical therapy for suspected allergic diseases in children is not acceptable because it often results in unnecessary or inappropriate treatment with antihistamines, inhaled or systemic corticosteroids, leukotriene antagonists, and antibiotics. Empirical therapy may also allow the allergic march to proceed unchecked by missing the opportunity to lessen exposure to offending allergens. Although the results of clinical investigations are inconclusive, evidence suggests that avoidance of offending allergens and optimum pharmacotherapy may lessen the risk of sensitization to additional allergens and may mitigate the advance of allergic respiratory diseases later in childhood (Wahn, 1998; Platts-Mills, 2003; van Bever, 2008).

In a consensus document, the European Academy of Allergy and Clinical Immunology made the following recommendation (Host, 2003): generally, all individuals with severe, persisting, or recurrent possible "allergic symptoms" and individuals with need for continuous prophylactic treatment should be tested for specific allergy, irrespective of the age of the child. Included in this description are children with cutaneous disease, gastrointestinal symptoms (colic, diarrhea, vomiting, or failure to thrive), recurrent wheezing, otitis, rhinitis, or asthma. Laboratory tests for IgE antibodies and skin tests were considered essentially interchangeable for the purpose of evaluating symptomatic children (Host, 2003).

The selection of appropriate allergens for testing is determined by clinical signs and symptoms and by the age of the child. The most frequent offending allergens in infants and children younger than 3 years of age are foods, notably component protein allergens in cow milk, egg white, wheat, soy, peanut, fish and shellfish, and tree nuts (Nickel, 1997; Sampson, 2001; Salo, 2014). Immediate hypersensitivity to food allergens in infants is commonly associated with eczema, gastrointestinal symptoms, chronic otitis, and wheezing. Less commonly, atopic children younger than 3 years may be sensitized and have demonstrable IgE antibodies to house dust mites (*D. farinae* and *D. pteronyssinus*) and ubiquitous molds (e.g., *Alternaria tenuis*). These inhalant allergens are common asthmatic triggers in older children. Except for a child with systemic signs and symptoms (anaphylaxis or OAS) whose symptoms are strongly associated with ingestion of particular food(s) (e.g., peanuts or tree nuts), it is seldom necessary to test for IgE antibodies to multiple foods if the results of tests for the common food allergens mentioned earlier are negative. In addition, allergic respiratory disease caused by seasonal inhalant aeroallergens such as pollens is uncommon before age 5 years; routine testing for IgE antibodies to these allergens is not necessary. In the age group younger than 5 years, the presumptive diagnosis of an allergic disease can usually be established with tests for IgE antibodies to allergens in common foods, dust mites (*D. pteronyssinus* and *D. farinae*), and cat and dog dander, mouse urine, and/or cockroach if indicated by exposure history (Grant et al., 2017).

Positive test results for IgE antibodies to common food allergens in children less than 5 years have dual significance: they establish a substantial likelihood of allergic disease and they indicate an increased risk of sensitization to additional allergens later in childhood (Nickel, 1997; Wahn, 2009). For these reasons, the identification of IgE antibodies to common food allergens in symptomatic infants and children younger than 5 years is important for making proper treatment choices and for deciding whether to seek referral to an allergy specialist. The concentrations of IgE antibodies that predict clinically significant, immediate hypersensitivity with high positive predictive values (95% or greater) differ considerably for different foods and study populations, and the clinical significance of low levels of IgE antibodies to common foods is limited (Sampson, 1997, 2001). Nevertheless, it is clear from the relationships shown in Figure 56.5 that the higher the level of IgE antibodies, the greater the likelihood of an allergic reaction to each food allergen. The receiver operator characteristic curves depicted in Figure 56.5 indicate cutoff concentrations for several common food allergens that had high predictive values for positive responses on subsequent food challenge testing. As illustrated by the graphs, a distinct advantage is associated with reporting results in quantitative units compared with the obsolete convention of class scores.

Allergic diseases in children older than 3 years typically manifest with respiratory signs and symptoms: rhinitis, wheezing, and persistent cough (see Fig. 56.4). In atopic children and adults, it is useful to think of the entire respiratory tract as a single allergic target organ. Allergic rhinitis and asthma often accompany one another. Most asthmatic children suffer from rhinitis, and children with rhinitis often have asthma that may be clinically apparent or subclinical (Sly, 1999). With the development of disease affecting the respiratory tract, tests for IgE antibodies to inhalant aeroallergens become much more important for clinical decision making (Host, 2003; Stringari, 2014). Because a vast number of different inhalant aeroallergens are available for testing, it is important to be selective in the initial testing of children with respiratory signs and symptoms to avoid unnecessary testing.

The allergens chosen for testing in children with respiratory diseases depend on the age of the child and the scope of clinical manifestations (Table 56.5). After age 3 or 4 years, it is common for atopic children to develop IgE antibodies to indoor perennial aeroallergens, including house dust mites, animal epithelia (cat and dog), cockroach, rodent urine, and molds. The last antibody specificities to develop in children are common outdoor aeroallergens, including pollen inhalants of trees, grasses, and weeds. There is no agreement on the minimum number of inhalant allergens that should be tested when evaluating children with respiratory symptoms. However, by consensus, testing should include house dust mites, cat or dog epithelium, a ubiquitous mold species (e.g., *A. tenuis*), and appropriate pollen allergens (Host, 2003). Testing for IgE antibodies to pollen allergens is indicated in older children, especially when symptoms are seasonal and tests can be performed at the time symptoms are manifest. Concentrations of IgE antibodies to seasonal inhalants vary with seasons, and there is little utility in performing tests for IgE antibodies to pollen inhalants when the allergens are not present in the environment, as results may be falsely negative. The multiallergen IgE antibody test is an efficient option to screen initially for the presence of IgE antibodies to families of pollen allergens. A positive result indicates the presence of IgE antibodies to at least one of the 10 aeroallergens, but it is not specific for a particular allergen. As such, positive results are useful to identify patients for further testing with individual allergens.

Testing for IgE antibodies is indicated in children with symptoms of asthma. Longitudinal cohort studies and population-based studies of children point to the importance of IgE antibodies and exposure to allergens in predicting the severity of disease in children with wheezing. The likelihood of wheezing and exacerbations of disease increase directly with the summed concentrations of IgE antibodies to inhalant aeroallergens (Custovic, 2005). In addition, high concentrations of IgE antibodies to dust mite, animal, and rodent epithelia and urine and other common aeroallergens in children with wheezing predispose to greater morbidity and increase the likelihood of inpatient hospital treatment (Custovic, 2005; Arroyave, 2013). The probability of exacerbations of disease increases directly with the concentrations of IgE antibodies for several common aeroallergens (Arroyave, 2013). The development of asthma in a child is almost invariably accompanied by rhinitis and is classified commonly as allergic phenotype disease (Corren, 2013).

In adults with allergic rhinitis, tests for IgE antibodies are reliable for identifying individuals sensitized to all allergen specificities. The most prevalent sensitivities are to aeroallergens, including house dust mites, cockroach, animal epithelia, mold spores, pollens, and organic dust allergens (Hamilton, 2016). Testing is indicated if the results are likely to influence the mode of treatment (Gendo, 2004). In adults suspected of having allergic rhinitis, IgE antibody tests are most useful when the pretest probability of disease is relatively low (less than 30%) (Adkinson & Hamilton, 2015). Such patients typically do not have clinical findings that strongly suggest an allergic etiology. In this situation, positive test results greatly

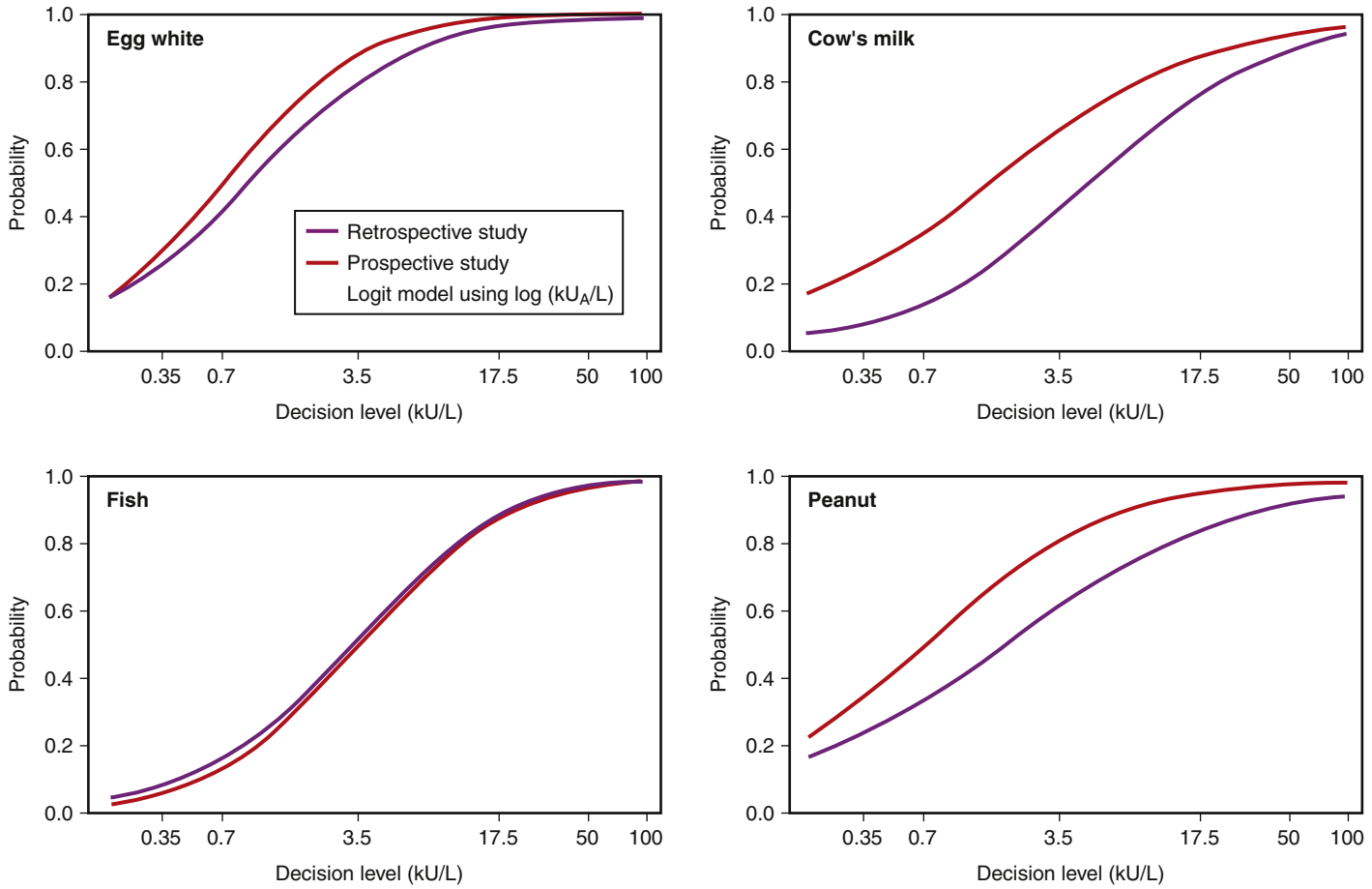

Figure 56.5 Probability of reacting to food allergens at increasing levels of immunoglobulin (Ig) E antibodies. kUa, kilounits of IgE per liter. (From Sampson HA: Utility of food-specific IgE concentrations in predicting symptomatic food allergy, *J Allergy Clin Immunol* 107:891–896, 2001.)

TABLE 56.5
Selected Immunoglobulin (Ig) E Antibody Tests for Evaluating Children With Clinical Signs of Allergy

Age, Years	Signs of Disease	Allergens
Younger than 3	Eczema with or without wheezing and otitis	Common foods: Egg white, milk, wheat, soy; house dust mites (*Dermatophagoides farinae* and *Dermatophagoides pteronyssinus*)
Older than 3 or 4	Rhinitis, wheezing, asthma	Common perennial inhalants: house dust mites, cat or dog, cockroach, *Alternaria tenuis*
Older than 3 or 4	Rhinitis, wheezing, asthma with seasonal exacerbations	Common perennial inhalants, as above, plus pollen inhalants (tree, grass, or weed pollens)

increase the posttest probability of allergic disease. Among patients with a strongly suggestive clinical history (prominent nasal symptoms and allergen triggers), testing is less likely to be useful and empirical treatment is often indicated. Skin tests and IgE antibody tests have essentially equivalent diagnostic utility in adults with allergic rhinitis; either test modality is helpful to identify allergens for inclusion in immunotherapy treatment regimens (Gendo, 2004).

Testing for IgE antibodies is also clinically indicated in the evaluation of adults with asthmatic symptoms to characterize the phenotype of disease and to identify allergen triggers, including occupational allergens. Unlike disease in children, adult-onset asthma is often nonatopic. Late (adult)–onset, nonatopic asthma is considered a distinct phenotype characterized by prominent neutrophilic inflammation of the airways with blood and sputum eosinophilia (Corren, 2013).

In addition to avoidance, pharmacotherapy, and immunotherapy, the treatment of severe persistent allergic asthma has been improved by the availability of anti-IgE pharmacotherapy (Busse, 2001; Soler, 2001; Lanier, 2003; Humbert, 2014). Therapeutic anti-IgE (omalizumab) is a recombinant humanized mouse monoclonal antibody to IgE that binds to the ε heavy chain of IgE, inhibits binding of IgE antibodies to Fc ε receptors on mast cells, and decreases antigen-induced mediator release from mast cells and basophils. Treatment with anti-IgE pharmacotherapy also decreases expression of Fc ε receptors on mast cells and decreases circulating IL-13. By interfering with binding of IgE antibodies to effector cells, anti-IgE antibody effectively blocks the release of inflammatory mediators that results from exposure to allergen. Results of clinical studies of anti-IgE pharmacotherapy for asthma have shown reduced rates of disease exacerbation and reduced requirements for corticosteroid drugs in treated patients. The dosage of anti-IgE is calculated based on body weight and serum IgE concentration. In patients with elevated serum IgE concentrations (30–700 kU/L in the United States; 30–1500 kU/L in the European Union) omalizumab is administered subcutaneously every 2 to 4 weeks to achieve a reduction in the circulating free IgE level to less than 50 ng/mL (approximately 25 kU/L). The duration of therapy required in patients with severe allergic asthma has not been determined. Caution should be exercised when interpreting IgE antibody data obtained by analyzing serum collected from a patient who has received omalizumab, as the presence of exogenous anti-IgE in the serum may compromise the accuracy of some clinically used IgE antibody assays (Hamilton, 2006; Hamilton et al., 2016).

As noted earlier, quantitative tests for IgE antibodies are widely used in the evaluation of suspected sensitization and allergy to foods (Sampson, 2001). The acknowledged gold standard for determining food allergy is the double-blind, placebo-controlled food challenge test (Sampson, 2014). Published empirical data indicate that the presence of IgE antibodies confirms food allergen sensitization. Serum concentrations of IgE antibodies may be useful to predict a positive response to food challenges for several common foods, including milk, egg, soy, and wheat (see Fig. 56.5). Concentrations of IgE antibodies were identified above which food challenges were likely to be positive and, therefore, not indicated. Subsequent studies indicated that caution is required in applying these published cutoffs in clinical practice. Attempts by different investigators to reproduce the

empirical cutoffs of earlier studies showed considerable differences for milk and egg allergens. It was not possible to define predictive cutoffs for soy or wheat. In addition, negative test results did not conclusively rule out reactivity to food challenge, and positive results did not reliably predict the severity of reactions in individual allergic patients. Despite these limitations, IgE antibody testing is recommended in the current food allergy practice parameter (Sampson, 2014). In contrast, testing for IgG4 antibodies specific for food allergens is not recommended as a diagnostic allergy test, as it has been shown to have no predictive value in demonstrating clinically relevant food sensitization (Stapel et al., 2008).

The recent availability of recombinant food allergen component proteins greatly facilitates identifying and differentiating cross-reactive sensitization from sensitization to species-specific food proteins (Hamilton & Kleine-Tebbe, 2015; Kleine-Tebbe et al., 2016). This advancement is important because patients sensitized to heat-stable, species-specific storage proteins (e.g., Ara h 2 in peanut; Cor a 14 in hazelnut) are likely to be at greater risk of systemic reactions. The overall prevalence of food sensitization as indicated by positive IgE antibody tests (or skin prick tests) greatly exceeds the prevalence of food allergy (Sicherer, 2013; Sicherer, 2014). For example, while approximately 8% to 10% of nonatopic children have positive tests for IgE antibodies detected by testing with whole-peanut allergen, fewer than 2% react to peanut ingestion. This finding is explained by noting that most peanut-sensitized children have antibodies to the highly cross-reactive PR10 protein Ara h 8 or a profilin homologue, are sensitized to homologous pollen panallergen(s), and do not have antibodies to species-specific, peanut storage proteins (Valcour et al., 2017). Antibodies to the 2S albumin storage protein Ara h 2 are strongly associated with systemic reactivity to peanut in most peanut-allergic children and adults (Nicolai, 2011; Klemans, 2013; Sicherer, 2014). Several studies have examined the sensitivity and specificity of IgE antibodies to Ara h 2 for identifying and predicting systemic reactivity to peanut. Although Ara h 2 antibodies are more specific for peanut allergy and have a much higher positive predictive value for peanut allergy, the results must be interpreted in the clinical context when assessing the risk of peanut allergy (Sicherer, 2013). Higher concentrations of IgE antibodies to Ara h 2 are associated with greater risk of systemic reactivity (Sicherer, 2013).

Testing for IgE antibodies to components is also useful for determining allergy to other foods. The situation is analogous to that described earlier for peanuts, that is, the prevalence of sensitization is much greater than the prevalence of severe allergy and many positive results in sensitized patients can be accounted for by the presence of antibodies to cross-reactive, heat-labile, panallergen components or to carbohydrate moieties (CCDs) on plant glycoproteins (Matricardi, 2016). Sensitization to panallergen PR10 or profilin components causes primarily mild allergic reactions to fruits and vegetables. While this is a useful generalization, there are some notable exceptions, such as soy, for which the PR10 homologue Gly m 4 is associated with severe systemic reactivity. The risk of allergic reactivity to several food components is summarized in Table 56.3.

Testing for IgE antibodies is also useful in a number of special situations. Exercise-induced anaphylaxis has been described in patients with IgE antibodies to the wheat components, omega-5-gliadin, or nsLTP (Pastorello, 2014). Delayed anaphylaxis occurring 3 to 6 hours after ingestion of red meat is associated with IgE antibodies to the cross-reactive carbohydrate determinant galactose-α-1,3-galactose (α-gal). Antibodies to α-gal are also associated with allergic reactions to cetuximab. The α-gal epitope is present on the Fab portion of cetuximab, a mouse-human monoclonal antibody against epidermal growth factor used to treat colon carcinoma and squamous cell carcinoma of the head and neck. Up to one-third of patients treated with cetuximab have allergic reactions. Sensitization to α-gal is believed to occur through tick bites and is more common in the southeastern United States (Commins, 2009; Berg, 2014).

Testing for IgE antibodies is useful in the evaluation of suspected allergy to Hymenoptera venom(s). Individuals sensitized to the venoms of honeybees and bumblebees, yellow jackets, hornets, or wasps may manifest signs of anaphylaxis following a sting, including urticaria, angioedema, bronchospasm, or cardiovascular collapse. The reported death rate from sting-induced systemic reactions is at least 40 cases annually. The incidence of venom-induced anaphylaxis is exceeded only by anaphylaxis caused by food or drug allergies (Wood, 2014). The natural history of untreated venom sensitivity varies from patient to patient. In many patients with documented venom allergy, it is possible to elicit a clinical history of progressively more severe reactions to successive stings. Anaphylaxis also can occur in individuals with no prior history of allergic reactions. Conversely, venom allergy apparently ameliorates spontaneously in many other cases. The decision to treat a patient with venom immunotherapy is based on clinical assessment of the risk of anaphylaxis to possible future stings. The most reliable indicator of venom allergy is the response to a deliberate sting challenge, but this test is seldom performed and is rarely required in previously untreated patients to establish the diagnosis of venom allergy. Venom skin tests and IgE antibody tests are useful to confirm the clinical impression of venom allergy and to define its specificity. Comparative studies indicate that skin testing is a more sensitive diagnostic modality, with only approximately 80% of skin test–positive patients having demonstrable IgE antibodies to whole-venom allergens (Golden, 2003). Venom IgE antibody tests are useful primarily to confirm the results of skin tests, to define the allergen specificity of venom hypersensitivity, and in selected patients to identify venom sensitivity when a positive clinical history is not confirmed by venom skin testing (Golden, 2003). Carbohydrate-free, species-specific major component allergens from bee venom (Api m 1), Vespula (hornet) venom (Ves v 1, phospholipase, and Ves v 5, antigen 5) and Polistes (wasp) venom have been used recently in clinical studies. These reagents have been shown to aid in differentiating allergy from cross-reactivity in patients with positive skin tests and IgE antibody tests to multiple whole-venom allergens (Muller, 2012; Ebo, 2013). The ability to identify cross-reactivity also is important in choosing appropriate allergens for immunotherapy. Recombinant venom components may also increase the diagnostic sensitivity of testing in patients with negative IgE antibody tests to whole-venom allergens (Kohler, 2014).

With the exception of the sting challenge, no in vitro or in vivo test reliably predicts the clinical response to an insect sting in a treated patient following venom immunotherapy. Although the concentrations of IgG antibodies in serum increase markedly with venom immunotherapy, no cutoff level has been defined that can be used to identify those patients who are no longer at risk. Quantitative estimates of IgG antibodies are not useful clinically, and levels of IgE antibodies following treatment bear no consistent relationship to clinical status. The decision to discontinue venom immunotherapy is based on clinical studies that show high protection rates after approximately 3 years of treatment (Yunginger, 1998).

Measurements of IgE antibodies have also been applied to the diagnosis of drug allergies. Although many drugs and their metabolites are capable of eliciting synthesis of antibodies, clinical data and the results of IgE antibody measurements are available for relatively few drugs, including the penicillins (β-lactam antibiotics) and insulin. Penicillin and its isomer, penicillenic acid, combine with serum proteins through amide linkages to create allergenic moieties. Penicilloyl-protein and penicillenic acid-protein comprise the so-called major and minor antigenic determinants, respectively (Fig. 56.6). Measurable levels of IgM and IgG antibodies specific for the penicilloyl determinant occur commonly in penicillin-treated patients. Although high titers of these antibodies persist in plasma for relatively short periods, lower titers can often be detected years after treatment (Shepherd, 1991). The diagnosis of hypersensitivity to penicillin has relied on skin testing with penicillin, penicilloyl-polylysine, and a minor antigen mixture. Positive skin test results occur infrequently, especially when testing is done remotely following treatment with penicillin. Fewer than 30% of patients with probable histories of immediate hypersensitivity to penicillin have positive skin tests, and immediate hypersensitivity reactions to penicillin therapy are rare in patients with negative skin tests (Blanca, 2009).

Using the results of skin tests as a diagnostic reference, clinical studies have reported IgE antibodies to the penicilloyl determinant in 65% to 85% of patients with positive skin tests (Fontaine, 2007). Antipenicilloyl antibodies were not detected in control subjects. On the basis of these data, it is reasonable to recommend in vitro testing for penicilloyl-IgE antibodies only in patients with a history of recent reactions. The absence of specific antibodies to penicilloyl-polylysine does not exclude the possibility of clinically significant IgE antibodies to other penicillin metabolites (Weiss, 1988; Fontaine, 2007; Blanca, 2009). There is considerable cross-reactivity between different β-lactam drugs. Nevertheless, some patients have unique antibodies that react with amoxicillin side chains. Testing with amoxicilloyl allergen is indicated to identify such cases (Blanca, 2001).

Allergic diseases, particularly asthma, may be caused by a wide variety of allergens encountered in the workplace. The list of causative agents associated with allergic occupational asthma is long and includes the following: animal proteins, enzymes, plant proteins, legumes, anhydrides, metallic salts, dyes, isocyanates, and wood dusts. Testing for IgE antibodies is available for many of these allergens. Considerable attention has been devoted to studies of natural rubber latex (*Hevea brasiliensis*) as an allergen in the health care workplace and for patients with spina bifida who have undergone multiple surgical procedures involving the use of latex gloves. Natural rubber latex is a complex allergen that contains multiple unique protein component allergens. Testing for IgE antibodies to latex whole allergen is useful for identifying sensitized individuals. Approximately 90% of skin test–positive patients have measurable IgE antibodies to latex allergens

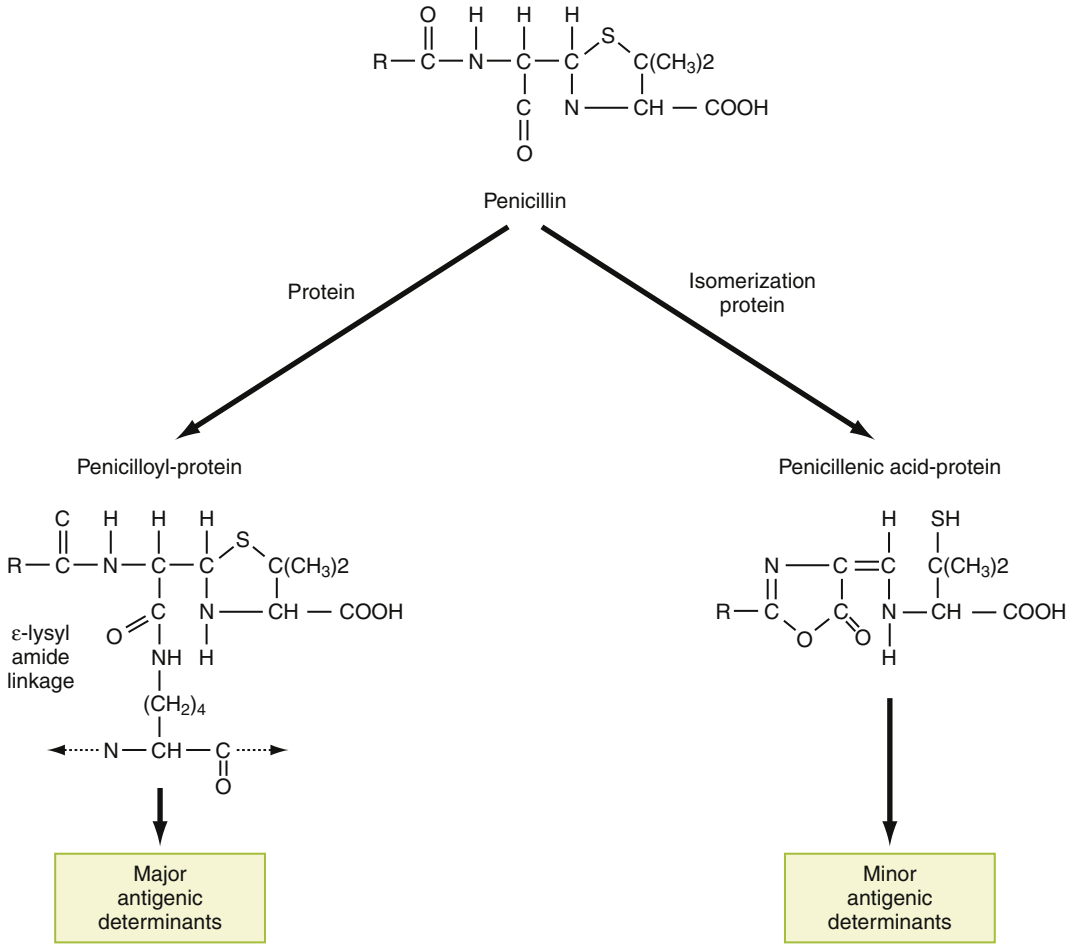

Figure 56.6 Allergens derived from penicillin.

(Hamilton, 2003). The majority of latex-sensitized patients who fail to react to exposure to latex are sensitized only to the profilin component Hev b 8 and do not have antibodies to other latex components (Ott, 2010).

In concluding this section on testing for IgE antibodies with currently available tests, it is appropriate to summarize some of the major points made earlier. Measurement of IgE antibodies is useful and can be recommended in the following clinical situations: (1) to evaluate children with early clinical signs of allergic disease, including children with eczema, gastrointestinal symptoms, wheezing, and rhinitis; (2) to evaluate children and adults suspected of having allergic respiratory disease to establish the diagnosis and to define the specificity of allergen sensitization to pollens, dust mites, rodent urine, mold allergens, and foods; (3) to confirm sensitization to food allergens in patients with signs of clinical food allergy; (4) to identify allergens for use in immunotherapy regimens in patients with severe allergic rhinitis; (5) to evaluate the specificity of sensitization to insect venom allergens; (6) to confirm the diagnosis of penicillin hypersensitivity in patients with recent clinical reactions; and (7) to confirm the presence of sensitization and possible allergy to occupational allergens. Testing for IgE antibodies is not routinely recommended for evaluating the effects of immunotherapy in treated patients or for excluding the diagnosis of anaphylactic sensitivity to insect venoms in treated patients. Testing for IgE antibodies is indicated only in patients who have had a thorough medical history and physical examination. Importantly, the presence of allergen-specific IgE antibody as detected either in the blood or skin of a patient is strictly an indication of sensitization and not verification of allergic disease. The clinical history of the patient must be the final arbiter used to interpret IgE antibody results in making the definitive diagnosis of allergic disease (Hamilton, 2014).

FUTURE DIRECTIONS: COMPONENT-RESOLVED DIAGNOSTICS AND TESTING BY MICROARRAY METHODS

As discussed earlier, it is important in clinical allergy practice to identify sensitization to an allergen and to differentiate cross-reactivity from probable allergy. As noted in Table 56.3, many allergens from seemingly unrelated sources (e.g., pollen aeroallergens and plant foods) share components from widely conserved protein and glycoprotein families (profilins, PR10 panallergens, and CCDs) with high degrees of structural similarity. Other allergenic proteins are unique to particular sources (e.g., food storage proteins). In several instances, panels of recombinant protein components from a single source have proven more useful than extracted whole allergens for determining sensitization to an allergen (e.g., peanut, hazelnut, and natural rubber latex) and will often reveal whether reactivity to the whole allergen is caused by sensitization to one or more unique allergen components or is attributable to cross-reactivity arising from sensitization to a panallergen (Kleine-Tebbe et al., 2016). This distinction is important, as the likelihood of severe reactivity or persistent allergy is usually greater with sensitization to unique allergen components (e.g., Ara h 2 in peanut or ovomucoid in egg white). Knowledge of cross-reactivity also may help to determine the optimum allergens to avoid or for use in planning treatment regimens. In a recent study, tests for IgE antibodies to recombinant component allergens failed to reveal antibodies to major allergens in up to 60% of children with allergic rhinitis who had positive tests to extracted pollen allergens (Stringari, 2014). It is not known at this time whether more selective immunotherapy based on component testing will improve the efficacy of immunotherapy treatment regimens. The use of allergen components in clinical testing has been called *component-resolved diagnosis* and *molecular allergy diagnosis*. It is safe to conclude that this type of testing will increase in use as its likely advantages are better defined and more components are cleared for clinical testing (Canonica, 2013).

Recombinant protein components have been paired with microarray technologies to enable testing for multiple IgE antibodies simultaneously (Hamilton, 2017). Up to 112 different recombinant allergen components from more than 50 different allergens have been used in a single microarray panel. Results of semiquantitative microarray tests are consistent with the results of established quantitative immunometric methods for IgE antibodies (Jahn-Schmid, 2003; Martinez-Aranguren, 2014). The results of a microarray analysis can be used to construct a serologic phenotype profile that displays sensitization to unique and cross-reactive allergen components. This type of analysis holds considerable promise for evaluating

patients prior to immunotherapy, for investigating suspected food allergy, for resolving cases of apparent sensitization to multiple different allergens, and for investigating cases of anaphylaxis in which the offending allergen is not apparent from the clinical history. At this time, microarray test platforms and many of the recombinant component reagents are not cleared for clinical use by the FDA. Limitations of the microarray include the fixed panel of allergens that may generate results that are difficult to interpret within the context of the patient's clinical history and the propensity of other types of antibody (e.g., IgG antiallergen) to compete (interfere) with IgE antibody for binding to small quantities of allergen on the chip and, thus, artifactually reduce the reported IgE antibody level (Hamilton, 2017).

TESTS FOR MEDIATORS OF IMMEDIATE HYPERSENSITIVITY REACTIONS

As noted earlier, a number of mediators of immediate hypersensitivity reactions—including histamine, tryptase, the cysteinyl leukotrienes, and prostaglandin D_2—have been identified. Each of these mediators promotes inflammation in human allergic disease or in animal models of allergy and anaphylaxis. Despite their proven roles in promoting allergic inflammation, measurements of mediators in body fluids are of limited usefulness clinically in the differential diagnosis of allergic diseases. Measurements of histamine in plasma or urine occasionally can be of value in patients with anaphylaxis when tests are performed immediately following an anaphylactic episode, but care is needed to obtain a suitable specimen (Friedman, 1989). Hemolysis can lead to falsely elevated histamine levels in the blood, and histamine-rich foods and bacterial colonization can lead to falsely elevated levels in urine. A more useful test in this clinical setting is measurement of mast cell tryptase in blood (Schwartz, 2006). Tryptase in serum consists primarily of protryptase and mature tryptase (previously referred to as *α-monomers* and *β-monomers*, respectively) released constitutively from mast cells. Following anaphylaxis, mature β-tryptase (tetramer) is released from sensitized mast cells and the level of tryptase increases rapidly (15 minutes to 2 hours), remaining elevated for up to 24 hours. An elevated concentration of tryptase measured in postmortem blood is consistent with the diagnosis of anaphylaxis (Schwartz, 2006). By comparison, histamine is cleared rapidly from blood with a half-life of minutes. The leukotrienes are active locally and are present in minute concentrations in body fluids. Measurement of leukotrienes may be informative in research applications, but testing is rarely used in the clinical evaluation of allergic patients.

SELECTED REFERENCES

Ballmer-Weber B, Hoffman-Sommergruber K: Molecular diagnosis of fruit and vegetable allergy, *Curr Opin Allergy Clin Immunol* 11(3):229–235, 2011.

This article provides information on allergen sensitization to fruit and vegetable components and is an example of the rapidly evolving knowledge around allergy to prevalent food components.

Bernstein I, Li J, Bernstein D: Allergy diagnostic testing: an updated practice parameter, *Ann All Asthma Immunol* s1:148, 2008.

This practice parameter provides an overview of current recommendations for diagnostic testing in patients suspected of having allergic diseases.

Bradding P, Saito H: Biology of mast cells and their mediators. In Adkinson F, Bochner B, Burks W, et al.: *Middleton's allergy principles and practice*, Philadelphia, 2014, Saunders, pp 228–237.

This chapter reviews mast cell biology, mast cell inflammatory mediators, and their roles in allergic inflammation.

Canonica G, Ansotegui I, Pawankar R, et al.: A WAO-ARIA-GALEN consensus document on molecular-based allergy diagnostics, *World Allergy Organ J* 6:17, 2013.

This document provides an overview of recommendations for performing component (molecular) testing for IgE antibodies in allergic disease diagnosis.

Gendo K, Larson EB: Evidence-based diagnostic strategies for evaluating suspected allergic rhinitis, *Ann Intern Med* 140:278–289, 2004.

This article is a meta-analysis of studies that compare in vitro and in vivo diagnostic methods in the evaluation of patients with respiratory allergies.

Hahn EL, Bacharier LB: The atopic march: the pattern of allergic disease development in childhood, *Immunol Allergy Clin North Am* 25:231–246, 2005.

This article reviews the sequence of sensitization to different allergen classes in children and the concomitant development and expression of allergic diseases in atopic children.

Hamilton RG: Proficiency survey-based evaluation of clinical total and allergen-specific IgE assay performance, *Arch Pathol Lab Med* 134:975–982, 2010.

This article is a comprehensive review of the evolution and performance of in vitro assays for IgE antibodies.

Hamilton RG, Matsson P, Chan S, et al.: Analytical performance characteristics, quality assurance and clinical utility of immunological assays for human immunoglobulin E (IgE) antibodies of defined allergen specificities; approved guideline. In *CLSI document I/LA20-A3*, ed 3, Wayne, PA, 2016, Clinical and Laboratory Standards Institute.

This concensus guideline presents an overview of laboratory tests for IgE and IgE antibodies with emphasis on analytic concepts and quality control of clinical assays.

Holloway J: Genetics and epigenetics of allergic diseases and asthma. In Adkinson F, Bochner B, Burks W, et al.: *Middleton's allergy principles and practice*, Philadelphia, 2014, Saunders, pp 343–360.

This chapter provides a comprehensive overview of the genetics and molecular genetics of IgE and accessory molecules important in promoting susceptibility to allergic diseases.

Host A, Andrae S, Charkin S, et al.: Allergy testing in children: why, who, when and how? *Eur J Allergy Clin Immunol* 58:1–11, 2003.

An excellent review of allergic diseases in children, this article presents the consensus recommendations of European allergy societies for evaluating children with suspected allergic diseases.

Matricardi P, Kleine-Tebbe J, Hoffman HJ, et al.: EAACI molecular allergology User's guide, *Pediatr Allergy Immunol Suppl* 23:1–250, 2016.

This comprehensive textbook covers all current aspects of molecular allergology, including assay methods, clinical utility of component-based IgE antibody testing and issues of cross-reactivity of panallergens. The authors are located across the globe and are all experts in their respective field of molecular allergology.

Oettgen H: Immunobiology of IgE and IgE receptors. In Adkinson F, Bochner B, Burks W, et al.: *Middleton's allergy principles and practice*, Philadelphia, 2014, Saunders, pp 364–375.

This article presents a comprehensive review of the immunobiology of IgE synthesis and the biology of IgE receptors.

Salo P, Arbes S, Jaramillo R, et al.: Prevalence of allergic sensitization in the United States: results from the national health and nutrition examination survey (NHANES) 2005–2006, *J Allergy Clin Immunol* 134:350–359, 2014.

This article presents data on the age-related and geographic prevalence of sensitization to common allergens in the United States. These demographic data are important for designing appropriate test offerings for allergic diseases in children of all ages.

Sampson HA: Utility of food-specific IgE concentrations in predicting symptomatic food allergy, *J Allergy Clin Immunol* 107:891–896, 2001.

This is a clinical article that discusses the use of IgE antibody levels to predict responses to double-blind, placebo-controlled food challenges. Decision levels for several common food allergens are presented.

Sampson H, Aceves S, Bock A, et al.: Food allergy: a practice parameter update—2014, *J Allergy Clin Immunol* 134:1016–1025, 2014.

This article is a comprehensive overview and update to the food allergy practice parameter. The practice parameter includes recommendations for evaluating suspected food allergies and sensitivities of all types.

Shakib F, Ghaemmaghami AM, Sewell HF: The molecular basis of allergenicity, *Trends Immunol* 29:633–642, 2008.

This review article presents a comprehensive discussion of the chemical properties of common allergens.

Wahn U: What drives the allergic march? *Allergy* 55:591–599, 2000.

Wahn U: Development and prevention of atopic disease in childhood. In Adkinson N, Bochner B, Busse W, et al.: *Middleton's allergy principles and practice*, St. Louis, 2009, Mosby, pp 779–786.

The article and chapter discuss the "allergy march." This concept is important for understanding the development of allergic diseases in children with age and sequential sensitization to allergens of different classes, including foods, perennial inhalants, and seasonal inhalants.

Access the complete reference list online at Elsevier eBooks for Practicing Clinicians.

REFERENCES

Adkinson Jr NF, Hamilton RG: Clinical history-driven diagnosis of allergic disease. Utilizing in vitro IgE testing, *J Allergy Clin Imunol Pract* 3:871–878, 2015.

Arroyave W, Rabito F, Carlson J, et al.: The relationship between a specific IgE level and asthma outcomes: results of the 2005–2006 National Health and Nutrition Examination Survey, *J Allergy Clin Immunol: In Pract* 1:501–508, 2013.

Ballmer-Weber B, Hoffman-Sommergruber K: Molecular diagnosis of fruit and vegetable allergy, *Curr Opin Allergy Clin Immunol* 11(3):229–235, 2011.

Beck L, Marcotte G, MacGlashan D, et al.: Omalizumab-induced reductions in mast cell Fc epsilon RI expression and function, *J Allergy Clin Immunol* 114:527–530, 2004.

Bennich H, Ishizaka K, Ishizaka T, et al.: A comparative antigenic study of gamma E-globulin and myeloma-IgND, *J Immunol* 102:826–831, 1969.

Berg E, Platts-Mills T, Commins S: Drug allergens and food-the cetuximab and galactose-alpha-1,3-galactose story, *Ann Allergy Asthma Immunol* 112:97–101, 2014.

Bernstein DI, Biagini RE, Karnani R, et al.: In vivo sensitization to purified *Hevea brasiliensis* proteins in health care workers sensitized to natural rubber latex, *J Allergy Clin Immunol* 111:610–616, 2003.

Bernstein I, Li J, Bernstein D: Allergy diagnostic testing: an updated practice parameter, *Ann All Asthma Immunol* 100:s1–148, 2008.

Beyer K, Grabenhenrich L, Härtl M, et al.: Predictive values of component-specific IgE for the outcome of peanut and hazelnut food challenges in children, *Allergy* 70:90–98, 2015.

Blanca M, Torres M, Reche M, et al.: Clinical evaluation of Pharmacia CAP system RAST FEIA amoxicilloyl and benzylpenicilloyl in patients with penicillin allergy, *Allergy* 56(9):862–870, 2001.

Blanca M, Romano A, Torres M: Update on the evaluation of hypersensitivity reactions to betalactams, *Allergy* 64:183–193, 2009.

Bradding P, Saito H: Biology of mast cells and their mediators. In Adkinson N, Bochner B, Burks W, et al.: *Middleton's allergy principles and practice*, Philadelphia, 2014, Saunders, pp 228–237.

Branum A, Lukacs S: Food allergies among children in the United States, *Pediatrics* 124:1549–1555, 2009.

Breiteneder H: Protein families: implications for allergen nomenclature, standardisation and specific immunotherapy, *Arb Paul Ehrlich Inst Bundesinstitut Impfstoffe Biomed Arzneim Langen Hess* 96:249–256, 2009.

Buckley R: Abnormalities in the regulation of human IgE synthesis, *Immunol Rev* 41:288, 1978.

Busse W, Corren J, Lanier BQ, et al.: Omalizumab, anti-IgE recombinant humanized monoclonal antibody, for the treatment of severe allergic asthma, *J Allergy Clin Immunol* 108:184–190, 2001.

Cairns JA, Walls AF: Mast cell tryptase is a mitogen for epithelial cells: stimulation of IL-8 production and intercellular adhesion molecule-1 expression, *J Immunol* 156:275–283, 1996.

Canonica G, Ansotegui I, Pawankar R, et al.: A WAO-ARIA-GALEN consensus document on molecular-based allergy diagnostics, *World Allergy Organ J* 6:17, 2013.

Centers for Disease Control and Prevention (CDC): *Behavioral risk factor surveillance system survey: current asthma prevalence data*, Atlanta, 2010, US Department of Health and Human Services, Centers for Disease Control and Prevention.

Chung CH, Mirakhur B, Chan E, et al.: Cetuximab-induced anaphylaxis and IgE specific for galactose-a-1, 3-galactose, *N Engl J Med* 358:1109–1117, 2008.

Coico R, Sunshine G, Benjamini E: The genetic basis of antibody structure. In *Immunology: a short course*, Hoboken, NJ, 2003, John Wiley & Sons, pp 79–89.

College of American Pathologists (CAP): Diagnostic allergy (SE-C) survey. Northfield, Il.

Commins S, Platts-Mills T: Anaphylaxis syndromes related to a new mammalian cross-reactive carbohydrate determinant, *J Allergy Clin Immunol* 124:652–657, 2009.

Corren J: Asthma phenotypes and endotypes, *Discov Med* 83:243–249, 2013.

Custovic A, Murray C, Simpson A: Allergy and infection: understanding their relationship, *Allergy* 60(suppl 79):10–13, 2005.

Defrance T, Carayon P, Billian G, et al.: Interleukin 13 is a B cell stimulating factor, *J Exp Med* 179:135–143, 1994.

Demoly P, Francois-Bernard M, Bousquet J: In vivo methods for study of allergy skin tests, techniques, and interpretation. In Middleton E, Reed C, Ellis E, et al.: *Allergy principles & practice*, vol. 1. St Louis, 1998, Mosby/Year Book, pp 430–439.

Devereux G, Matsui E, Burney P: Epidemiology of asthma and allergic airway diseases. In Adkinson N, Bochner B, Burks W, et al.: *Middleton's Allergy principles and practice*, Philadelphia, 2014, Saunders, pp 754–778.

Du Toit G1, Roberts G, Sayre PH, et al.: Randomized trial of peanut consumption in infants at risk for peanut allergy, *N Engl J Med* 372:803–813, 2015.

Ebo D, Faber M, Sabato V, et al.: Component-resolved diagnosis of wasp (yellow jacket) venom allergy, *Clin Exp Allergy* 43:255–261, 2013.

Ewan PW, Coote D: Evaluation of a capsulated hydrophilic carrier polymer (the ImmunoCAP) for measurement of specific IgE antibodies, *Allergy* 45:22–29, 1990.

Findlay SR, Barden JM, Easley CB, et al.: Effect of the oral leukotriene antagonist, ICI 204,219, on antigen-induced bronchoconstriction in subjects with asthma, *J Allergy Clin Immunol* 89:1040–1045, 1992.

Fontaine C, Mayorga C, Bousquet PJ, et al.: Relevance of the determination of serum-specific IgE antibodies in the diagnosis of immediate beta-lactam allergy, *Allergy* 62:47–52, 2007.

Friedman B, Steinberg S, Meggs W, et al.: Analysis of plasma histamine levels in patients with mast cell disorders, *Am J Med* 87:649, 1989.

Galli SJ: New insights into 'the riddle of the mast cells': microenvironmental regulation of mast cell development and phenotypic heterogeneity, *Lab Invest* 62:5–33, 1990.

Garib V, Rigler E, Gastager F, et al.: Determination of IgE and IgG reactivity to more than 170 allergen moleculse in paper dried blood spots, *J Allergy Clin Immunol*, 2018.

Gendo K, Larson EB: Evidence-based diagnostic strategies for evaluating suspected allergic rhinitis, *Ann Intern Med* 140:278–289, 2004.

Gether U: Uncovering molecular mechanisms involved in activation of G protein-coupled receptors, *Endocr Rev* 21:90–113, 2000.

Golden DB, Tracy JM, Freeman TM, et al.: Negative venom skin test results in patients with histories of systemic reaction to a sting, *J Allergy Clin Immunol* 112:495–498, 2003.

Grant T, Aloe C, Perzanowski M, et al.: Mouse sensitizationand exposure are associated with asthma severity in urban children, *J Allergy Clin Immunol Pract* 5:1008–1014, 2017.

Griesmeier U, Vazquez-Cortes M, Bublin C, et al.: Expression levels of parvalbumins determine allergenicity of fish species, *Allergy* 65:191–198, 2010.

Hahn E, Bacharier L: The atopic march: the pattern of allergic disease development in childhood, *Immunol Allergy Clin North Am* 25:231–246, 2005.

Hamilton R: Laboratory tests for allergic and immunodeficiency diseases. In *Middletons' allergy principles and practice*, Philadelphia, 2014, Saunders, pp 1187–1202.

Hamilton RG: Accuracy of US Food and Drug Administration-cleared IgE antibody assays in the presence of anti-IgE (omalizumab), *J Allergy Clin Immunol* 117:759–766, 2006.

Hamilton RG: Monitoring allergic patients on Omalizumab with free and total serum IgE measurements, *J Allergy Clin Immunol Pract* 4:366–368, 2016.

Hamilton RG: Allergic sensitization is a key risk factor for but not synonymous with allergic disease, *J Allergy Clin Immunol* 134:360–361, 2014.

Hamilton RG: Franklin Adkinson N Jr: in vitro assays for the diagnosis of IgE-mediated disorders, *J Allergy Clin Immunol* 114:213–225, 2004. quiz 226.

Hamilton RG, Rossi C, Yeang H, et al.: Latex specific IgE assay sensitivity enhanced using Hev b 5 enriched latex allergosorbent, *J Allergy Clin Immunol* 111(suppl):S174, 2003.

Hamilton RG, Matsson PNJ, Adkinson Jr NF, et al.: Analytical performance characteristics, quality assurance and clinical utility of immunological assays for human immunoglobulin E (IgE) antibodies of defined allergen specificities: in development. In *CLSI report I/LA20*, 3rd edition, Wayne, PA, USA, 2016, Clinical and Laboratory Standards Institute.

Hamilton RG, Kleine-Tebbe J: Molecular allergy diagnosis: analytical features that support clinical decisions, *Curr Allergy Asthma Rep* 9:57–80, 2015. Review..

Hamilton RG: Microarray technology applied to human allergic disease, *Microarrays* 6:1–20, 2017.

Hemmer W, Altmannb F, Holzweber F, et al.: ImmunoCAP cellulose displays cross-reactive carbohydrate determinant (CCD) epitopes and can cause false positive test results in patients with high anti-CCD IgE antibody levels, *J Allergy Clin Immunol* 141:372–381, 2018.

Holloway J: Genetics and epigenetics of allergic diseases and asthma. In Adkinson N, Bochner B, Burks W, et al.: *Middleton's allergy principles and practice*, Philadelphia, 2014, Saunders, pp 343–360.

Holloway J, Yang I, Holgate S: Genetics of allergic disease, *J Allergy Clin Immunol* 125:581–594, 2010.

Holloway J, Koppelman G: Identifying novel genes contributing to asthma pathogenesis, *Curr Opin Allergy Clin Immunol* 7:69–74, 2007.

Host A, Andrae S, Charkin S, et al.: Allergy testing in children: why, who, when and how? *Eur J Allergy Clin Immunol* 58:1–11, 2003.

Hsieh F, Lam B, Penrose J, et al.: T helper cell type 2 cytokines coordinately regulate immunoglobulin E-dependent cysteinyl leukotriene production by human cord blood-derived mast cells: profound induction of leukotriene C(4) synthase expression by interleukin 4, *J Exp Med* 193:123–133, 2001.

Humbert M, Busse W, Hanania N, et al.: Omalizumab in asthma: an update on recent developments, *J Allergy Clin Immunol: In Pract* 2:525–536, 2014.

Irani A, Schecter N, Craig S: In *Two types of mast cells that have distinct neutral protease compositions*, vol. 82. 1986, pp 1214–1218.

Irvine A, McLean W, Leung D: Filaggrin mutations associated with skin and allergic diseases, *N Engl J Med* 365:1315–1327, 2011.

Ishizaka K, Ishizaka T: Physicochemical properties of reaginic antibody. 1. Association of reaginic activity with an immunoglobulin other than gammaA- or gammaG-globulin, *J Allergy* 37:169–185, 1966.

Ishizaka K, Ishizaka T, Menzel AE: Physicochemical properties of reaginic antibody. VI. Effect of heat on gamma-E-, gamma-G- and gamma-A-antibodies in the sera of ragweed sensitive patients, *J Immunol* 99:610–618, 1967.

Jahn-Schmid B, Harwanegg C, Hiller R, et al.: Allergen microarray: comparison of microarray using recombinant allergens with conventional diagnostic methods to detect allergen-specific serum immunoglobulin E, *Clin Exp Allergy* 33:1443–1449, 2003.

Kabesch M, Schedel M, Carr D, et al.: IL-4/IL-13 pathway genetics strongly influence serum IgE levels and childhood asthma, *J Allergy Clin Immunol* 117:269–274, 2006.

Kazemi-Shirazi L, Pauli G, Purohit A, et al.: Quantitative IgE inhibition experiments with purified recombinant allergens indicate pollen-derived allergens as the sensitizing agents responsible for many forms of plant food allergy, *J Allergy Clin Immunol* 105:116–125, 2000.

Kjellman NI, Croner S: Cord blood IgE determination for allergy prediction—a follow-up to seven years of age in 1,651 children, *Ann Allergy* 53:167–171, 1984.

Klemans R, Otte D, Knol M, et al.: The diagnostic value of specific IgE to Ara h 2 to predict peanut allergy in children is comparable to a validated and updated diagnostic prediction model, *J Allergy Clin Immunol* 131:157–163, 2013.

Kleine-Tebbe J, Matricardi PM, Hamilton RG: Allergy work-up including component resolved diagnosis. How to make allergen-specific immunotherapy more specific, *Immunol Allergy Clin North Am* 36:191–203, 2016.

Klink M, Cline MG, Halonen M, et al.: Problems in defining normal limits for serum IgE, *J Allergy Clin Immunol* 85:440–444, 1990.

Kohler J, Blank S, Muller S, et al.: Component resolution reveals additional major allergens in patients with honeybee venom allergy, *J Allergy Clin Immunol* 133:1383–1389, 2014.

Korthauer U, Graf D, Mages HW, et al.: Defective expression of T-cell CD40 ligand causes X-linked immunodeficiency with hyper-IgM, *Nature* 361:539–541, 1993.

Lanier B, Corren W, Lumry J, et al.: Omalizumab is effective in the long-term control of severe allergic asthma, *Ann Allergy Asthma Immunol* 1:154–159, 2003.

Liu A: Hygiene hypothesis for allergy and asthma. In Martin RJ, Sutherland ER, L'enfant C, editors: *Infection and asthma*, Tampa, FL, 2010, Informa Healthcare USA.

Matricardi P, Kleine-Tebbe J, Hoffman HJ, et al.: EAACI molecular allergology User's guide, *Pediatr Allergy Immunol* Suppl 23:1–250, 2016.

Maly F, Marti-Wyss S, Blumber S, et al.: Mononuclear blood cell sulpholeukotriene generation in the presence of interleukin 3 and whole blood histamine release in honeybee and yellow jacket venom allergy, *J Invest Allergy Clin Immunol* 7:217–224, 1997.

McCann W, Ownby D: The reproducibility of the allergy skin test scoring and interpretation by board certified/board eligible allergists, *Ann Allergy Asthma Immunol* 89:368–371, 2002.

Martinez-Aranguren R, Lizaso M, Goikoetxea M, et al.: Is determination of specific IgE against components using ISAC 112 a reproducible technique? *PloS One* 9(2), 2014.

Metcalfe DD, Peavy RD, Gilfillan AM: Mechanisms of mast cell signaling in anaphylaxis, *J Allergy Clin Immunol* 124:639–648, 2009.

Miller JS, Moxley G, Schwartz LB: Cloning and characterization of a second complementary DNA for human tryptase, *J Clin Invest* 86:864–870, 1990.

Moffatt M, Gut I, Demenais F, et al.: A large-scale, consortium-based genomewide association study of asthma, *N Engl J Med* 363:1211–1221, 2010.

Muller U, Schmid-Grendelmeier P, Hausmann O, et al.: IgE to recombinant allergens Api m 1, Ves v 1, and Ves v 5 distinguish double sensitization from crossreaction in venom allergy, *Allergy* 67:1069–1073, 2012.

National Center for Health Statistics: *National hospital Ambulatory medical care survey (NHAMCS)*, US Department of Health and Human Services, Centers for Disease Control and Prevention, 2006.

Nickel R, Kulig M, Forster J, et al.: Sensitization to hen's egg at the age of twelve months is predictive for allergic sensitization to common indoor and outdoor allergens at the age of three years, *J Allergy Clin Immunol* 99:613–617, 1997.

Nicolaou N, Custovic A: Molecular diagnosis of peanut and legume allergy, *Curr Opin Allergy Clin Immunol* 11:222–228, 2011.

Nolte H: The clinical utility of basophil histamine release, *Allergy Proc* 14:251–254, 1993.

Oettgen H: Immunobiology of IgE and IgE receptors. In Adkinson N, Bochner B, Burks W, et al.: *Middleton's allergy principle and practice*, Philadelphia, 2014, Saunders, pp 364–375.

Oettgen HC, Geha RS: IgE regulation and roles in asthma pathogenesis, *J Allergy Clin Immunol* 107:429–440, 2001.

Ott H, Schroder C, Raulf-Heimsoth M, et al.: Microarrays of recombinant Hevea brasiliensis proteins: a novel tool for the component-resolved diagnosis of natural rubber latex allergy, *J Investig Allergol Clin Immunol* 20:129–138, 2010.

Ownby DR, Anderson JA, Jacob GL, et al.: Development and comparative evaluation of a multiple-antigen RAST as a screening test for inhalant allergy, *J Allergy Clin Immunol* 73:466–472, 1984.

Palmer C, Irvine A, Terron-Kwiatkowski A, et al.: Common loss-of-function variants of the epidermal barrier protein filaggrin are a major predisposing factor for atopic dermatitis, *Nat Genet* 38:441–446, 2006.

Pastorello E, Farioli L, Stafylaraki C, et al.: Wheat-dependent exercise-induced anaphylaxis caused by a lipid transfer protein and not by omega-5 gliadin, *Ann Allergy Asthma Immunol* 112:386–387, 2014.

Petersen LJ, Church MK, Skov PS: Histamine is released in the wheal but not the flare following challenge of human skin in vivo: a microdialysis study, *Clin Exp Allergy* 27:284–295, 1997.

Pieters J: MHC class II-restricted antigen processing and presentation, *Adv Immunol* 75:159–208, 2000.

Platts-Mills TA: Allergen avoidance in the treatment of asthma and rhinitis, *N Engl J Med* 349:207–208, 2003.

Ravetech J, Kinet J: Fc receptors, *Ann Rev Immunol* 9:457, 1991.

Salo P, Arbes S, Jaramillo R, et al.: Prevalence of allergic sensitization in the United States: results from the national health and nutrition examination survey (NHANES) 2005-2006, *J Allergy Clin Immunol* 134:350–359, 2014.

Sampson HA: Utility of food-specific IgE concentrations in predicting symptomatic food allergy, *J Allergy Clin Immunol* 107:891–896, 2001.

Sampson HA, Ho DG: Relationship between food-specific IgE concentrations and the risk of positive food challenges in children and adolescents, *J Allergy Clin Immunol* 100:444–451, 1997.

Sampson H, Aceves S, Bock A, et al.: Food allergy: a practice parameter update-2014, *J Allergy Clin Immunol* 134:1016–1025, 2014.

Sampson HA, Gerth van Wijk R, et al.: Standardizing double-blind, placebo-controlled oral food challenges: American Academy of allergy, asthma & Immunology-European Academy of allergy and clinical Immunology PRACTALL consensus report, *J Allergy Clin Immunol* 130:1260–1274, 2012.

Santos A, Van Ree R: Profilins mimickers of allergy or relevant allergens, *Int Arch Allergy Immunol* 155(3):191–204, 2011.

Santos A, Du Toit G, Douiri A, et al.: Distinct parameters of the basophil activation test reflect the severity and threshold of allergic reactions to peanut, *J Allergy Clin Immunol* 135:179–186, 2015.

Schwartz LB, Lewis RA, Austen KF: Tryptase from human pulmonary mast cells: purification and characterization, *J Biol Chem* 256:11939–11943, 1981.

Schwartz L: Diagnostic value of tryptase in anaphylaxis and mastocytosis, *Immunol Allergy Clin North Am* 26:451–463, 2006.

Sharma G, Irsigler A, Dhanarajan P: Cloning and characterization of 2S albumin, Car I 1, a major allergen of pecan, *J Agri Food Chem* 59(8):4130–4139, 2011.

Sicherer S, Wood R: Advances in diagnosing peanut allergy, *J Allergy Clin Immunol: In Pract* 1:1–13, 2013.

Sicherer S, Sampson H: Food allergy: epidemiology, pathogenesis, diagnosis and treatment, *J Allergy Clin Immunol* 133:291–307, 2014.

Shakib F, Ghaemmaghami AM, Sewell HF: The molecular basis of allergenicity, *Trends Immunol* 29:633–642, 2008.

Shepherd G: Allergy to β-lactam antibiotics, *Immunol Allergy Clin North Am* 11:611, 1991.

Smits HH, Engering A, van der Kleij D, et al.: Selective probiotic bacteria induce IL-10-producing regulatory T cells in vitro by modulating dendritic cell function through dendritic cell-specific intercellular adhesion molecule 3-grabbing nonintegrin, *J Allergy Clin Immunol* 115:1260–1267, 2005.

Soler M, Matz J, Townley R, et al.: The anti-IgE antibody omalizumab reduces exacerbations and steroid requirement in allergic asthmatics, *Eur Respir J* 18:254–261, 2001.

Stapel SO, Asero R, Ballmer-Weber BK, et al.: Testing for IgG4 against foods is not recommended as a diagnostic tool; EAACI Task Force Reprt, *Allergy* 63:793–796, 2008.

Stewart G, Richardson J, Zhang J, et al.: The structure and function of allergens. In Adkinson N, Bochner B, Burks W, et al.: *Middletons' allergy principle and practice*, Philadelphia, 2014, Saunders, pp 398–428.

Stringari G, Tripodi S, Caffarelli C, et al.: The effect of component-resolved diagnosis on specific immunotherapy prescription in children with hay fever, *J Allergy Clin Immunol* 134:75–81, 2014.

Thorpe SJ, Heath A, Fox B, et al.: The 3rd International Standard for serum IgE: international collaborative study to evaluate a candidate preparation, *Clin Chem Lab Med* 52:1283–1289, 2014.

Turkeltaub PC: Percutaneous and intracutaneous diagnostic tests of IgE-mediated diseases (immediate hypersensitivity), *Clin Allergy Immunol* 15:53–87, 2000.

Valenta R, Lidholm J, Hayek B, et al.: The recombinant allergen-based concept of component-resolved diagnostics and immunotherapy (CRD and DRIT), *Clin Exp Allergy* 29:896–904, 1999.

Valcour A, Jjones JE, Lidholm, et al.: Sensitization profiles to peanut allergaen across the United States, *Ann Allergy Asthma Immujol* 119:262–266, 2017.

Van Bever H, Samuel S, Lee B: Halting the allergic march, *W Allergy Org J* 1:57–62, 2008.

Van Eerdewegh P, Little R, Dupuis J, et al.: Association of ADAM 33 gene with asthma and bronchial hyperresponsiveness, *Nature* 418:426–430, 2002.

Vercelli D, Jabara HH, Arai K, et al.: Induction of human IgE synthesis requires interleukin 4 and T/B cell interactions involving the T cell receptor/CD3 complex and MHC class II antigens, *J Exp Med* 169:1295–1307, 1989.

Visness CM, London SJ, Daniels JL, et al.: Association of obesity with IgE levels and allergy symptoms in children and adolescents: results from the national health and nutrition examination survey 2005–2006, *J Allergy Clin Immunol* 123:1163–1169, 2009.

Wahn U: Allergic factors associated with the development of asthma and the influence of cetirizine in a double-blind, randomised, placebo-controlled trial: first results of ETAC. Early treatment of the atopic child, *Pediatr Allergy Immunol* 9:116–124, 1998.

Wahn U: Development and prevention of atopic disease in childhood. In Adkinson NF, Bochner BS, Busse WW, et al.: *Middleton's allergy principles & practice*, St Louis, 2009, Mosby, pp p779–786.

Wahn U: What drives the allergic march? *Allergy* 55:591–599, 2000.

Wang JH, Reinherz EL: Structural basis of T cell recognition of peptides bound to MHC molecules, *Mol Immunol* 38:1039–1049, 2002.

Wank SA, DeLisi C, Metzger H: Analysis of the rate-limiting step in a ligand-cell receptor interaction: the immunoglobulin E system, *Biochemistry* 22:954–959, 1983.

Weidinger S, Geiger C, Rodriguez E, et al.: Genome-wide scan on total serum IgE levels identifies FCERIA as novel susceptibility locus, *PLoS Genet* 4, 2008. e1000166, Epub Aug 22, 2008.

Weiss KB, Sullivan SD: The health economics of asthma and rhinitis. I. Assessing the economic impact, *J Allergy Clin Immunol* 107:3–8, 2001.

Weiss ME, Adkinson NF: Immediate hypersensitivity reactions to penicillin and related antibiotics, *Clin Allergy* 18:515–540, 1988.

Wess J: G-protein-coupled receptors: molecular mechanisms involved in receptor activation and selectivity of G-protein recognition, *FASEB J* 11:346–354, 1997.

Wide L, Bennich H, Johansson SG: Diagnosis of allergy by an in-vitro test for allergen antibodies, *Lancet* 2:1105–1107, 1967.

Wood R, Camargo C, Lieberman P, et al.: Anaphylaxis in America: the prevalence and characteristics of anaphylaxis in the United States, *J Allergy Clin Immunol* 133:461–467, 2014.

Wood RA, Segall N, Ahlstedt S, et al.: Accuracy of IgE antibody laboratory results, *Ann. Allergy Asthma Immujol* 99:34–41, 2007.

Wu L: Zarrin A: the production and regulation of IgE by the immune system, *Nature Reviews* 14:247–259, 2014.

Xiong H, Curotto de Lafaille M, Lafaille J: What is unique about the IgE response, *Adv Immunol* 116:113–141, 2012.

Yunginger JW: Insect allergy. In Middleton E, Reed C, Ellis E, et al.: *Allergy principles & practice*, vol. 2. St Louis, 1998, Mosby/Year Book, pp 1063–1072.

Yunginger JW, Ahlstedt S, Eggleston PA, et al.: Quantitative IgE antibody assays in allergic diseases, *J Allergy Clin Immunol* 105:1077–1084, 2000.

PART 7

Medical Microbiology

EDITED BY | Gail L. Woods, Richard A. McPherson

CHAPTER 57

MEDICAL BACTERIOLOGY

Christina M. Wojewoda, Lisa M. Stempak

SPECIMEN PROCESSING, 1130
Gram Stain, 1130
Culture Techniques, 1131
MEDICALLY IMPORTANT BACTERIA, 1131
Gram-Positive Cocci, 1131
Gram-Positive Rods, 1137
Gram-Negative Bacteria—Cocci, 1142
Gram-Negative Bacteria—Bacilli, 1144
Gram-Negative Bacteria—Nonfermentative Bacilli, 1147
Gram-Negative Bacteria—The HACEK Bacteria, 1153
Miscellaneous Gram-Negative Bacilli, 1154
Anaerobic Bacteria, 1160
SELECTED REFERENCES, 1165

KEY POINTS

- Bacteria can be categorized based on the Gram stain reaction (gram-positive or gram-negative), shape (cocci, bacilli, coccobacilli, spirochete), preferred atmosphere (aerobic, microaerophilic, anaerobic), and presence or absence of spores. They can be identified on the basis of key biochemical tests, antigenic components (e.g., cell wall antigens, toxins), and/or molecular features, including nucleic acid–based testing and proteomic detection.
- Among the gram-positive cocci, the most important human pathogens (and the infections that they commonly cause) are *Staphylococcus aureus* (skin and soft-tissue infections, bacteremia, septic arthritis), *Streptococcus pyogenes* (pharyngitis and its nonsuppurative complications, skin and soft-tissue infections), *Streptococcus agalactiae* (neonatal bacteremia and meningitis), *Streptococcus pneumoniae* (community-acquired pneumonia, meningitis), and *Enterococcus faecalis* and *E. faecium* (nosocomial urinary tract infections and bacteremia).
- Among gram-positive bacilli, the most important human pathogens (and the infections that they commonly cause) are *Listeria monocytogenes* (meningitis, bacteremia), *Nocardia* species (pneumonia, soft-tissue infections, brain abscess), *Bacillus anthracis* (skin and soft-tissue infections, pneumonia; a bioterrorism agent), and *Corynebacterium diphtheriae* (diphtheria), which is rarely encountered in the clinical laboratory in the United States.
- Among gram-negative cocci, the most important human pathogens (and the infections that they commonly cause) are *Neisseria meningitidis* (meningitis), *Neisseria gonorrhoeae* (gonorrhea), and *Moraxella catarrhalis* (upper and lower respiratory tract infections).
- Gram-negative bacilli include Enterobacterales, many of which are normal flora in the gastrointestinal tract; nonfermentative gram-negative bacilli (e.g., *Pseudomonas aeruginosa* and *Acinetobacter baumannii*), which are found in the environment and cause human infection when host defenses are compromised; halophilic organisms (*Vibrio* spp.); microaerophilic bacteria (*Campylobacter*, *Helicobacter*); fastidious organisms (*Legionella* spp., *Bordetella* spp., *Francisella tularensis*, *Brucella* spp., *Haemophilus* species); and miscellaneous infrequently encountered bacteria.
- Among the Enterobacterales, the most important human pathogens (and the infections that they commonly cause) are *Escherichia coli* (urinary tract infection, diarrhea, bacteremia), *Klebsiella pneumoniae* and *Klebsiella oxytoca* (urinary tract infection, pneumonia, bacteremia), *Proteus* spp. (urinary tract infection, wound infections), *Salmonella* spp. (diarrhea, typhoid fever), *Shigella* spp. (diarrhea), and *Enterobacter* spp. (nosocomial pneumonia, urinary tract infection, bacteremia).
- Among the anaerobes, the most important human pathogens (and the infections that they commonly cause) are the *Bacteroides fragilis* group (intraabdominal infections, abscesses); *Clostridium* spp., especially *Clostridium perfringens* (soft-tissue infections, food poisoning), *Clostridium tetani* (tetanus), and *Clostridioides difficile* (antibiotic-associated diarrhea); and non–spore-forming gram-positive anaerobes, such as *Actinomyces israelii* and *Cutibacterium acnes*.

A wide variety of bacterial species may be recovered from clinical specimens. To appropriately assess the clinical significance of these organisms, an understanding of the normal bacterial flora present at different anatomic locations is essential. In some cases, the number of organisms present can be extremely high—for example, 10^6 organisms/cm^2 of skin, 10^9 organisms/mL of oral secretions, and 10^{11} organisms/g of colon contents. It is important to obtain samples with minimal contamination from the normal flora (Miller et al., 2007; McElvania & Singh, 2019). This may be difficult but can be optimally achieved if proper procedures are followed. These procedures, along with processing techniques that serve to enhance recovery of pathogenic microorganisms, are discussed in Chapter 66.

SPECIMEN PROCESSING

GRAM STAIN

Direct examination of a specimen with a Gram stain is one of the most valuable procedures performed by the microbiology laboratory. The Gram stain result rapidly provides information that is used by the clinician for selecting appropriate antimicrobial therapy. It also helps the clinical laboratory scientist assess the quality of the specimen and the extent to which certain organisms recovered in culture will be worked up. Organisms present in abundant quantity in specimens containing many white blood cells are given more attention than those that are present in smaller numbers in the absence of white blood cells. Multiple specimens positive for similar organisms in smears and cultures contribute to increased clinical significance of the results.

To prepare a smear for staining, an aliquot of the most purulent or bloody portion of the specimen is placed on a clean microscopic slide in a manner that provides both thick and thin areas. For sterile body fluids such as cerebrospinal fluid (CSF), a cytocentrifuge should be used to concentrate the specimen by 10 to 100 times (McElvania & Singh, 2019). The material on the slide is allowed to air-dry, is fixed with methanol or gentle heat, and then is stained with Gram stain reagents (crystal violet, Gram iodine, alcohol, and safranin). Organisms that have a gram-positive cell wall will resist decolorization with methanol and will retain the purple color of the crystal violet. Organisms that have a gram-negative cell wall will be decolorized and will stain red with safranin counterstain.

Stained smears are initially examined using a low-power objective to look for large structures, such as nematode larvae, Curschmann spirals, large granules, grains, bacterial microcolonies, or fungal forms. An oil immersion lens is then used to assess the type of bacteria present. Because 10^5 organisms/mL must be present to see one organism per oil immersion field (1000×), smears must be examined carefully to detect small numbers of organisms.

The organisms observed should be evaluated for size, shape, and Gram reaction, which should be reported with as much description as possible. Reporting the presence of gram-positive cocci in pairs that resemble *S. pneumoniae* (Fig. 57.1) is more helpful than simply reporting gram-positive cocci in chains. White cells and squamous epithelial cells should be quantified and reported, along with any intracellular bacteria observed. Correlation of Gram stain observations with culture results is a good way to check

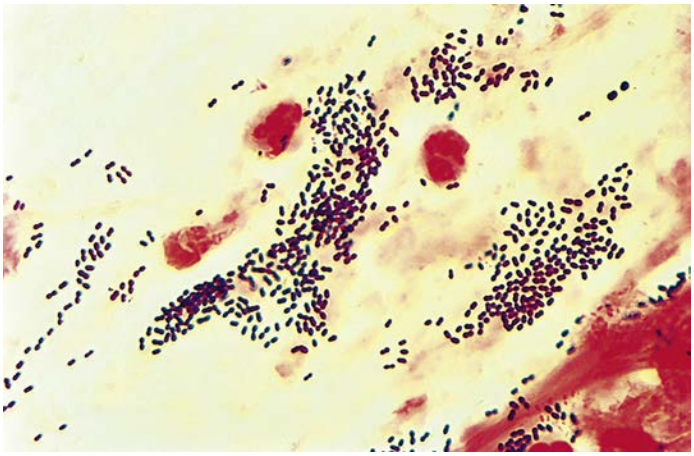

Figure 57.1 Gram stain of a sputum smear shows neutrophils, debris, and gram-positive diplococci, suggestive of pneumococcal infection (oil immersion).

on the quality of the stains and culture. Demonstration of many bacteria on Gram stain that do not grow out in culture may indicate unusual organisms that require more specialized media or culture conditions. Alternatively, it could suggest a false-positive Gram stain result caused by contamination of reagents or incorrect interpretation of Gram stain results. Gram stain results could indicate the need to inoculate additional media for a specific specimen. For example, finding many gram-negative coccobacilli in a respiratory specimen could indicate the need for a chocolate plate to recover *Haemophilus* spp., which would not be recovered on a blood agar plate. Other stains, such as the acridine orange stain, can be utilized for staining blood culture bottles, CSF, or buffy coat preparations. This fluorescent stain provides a rapid and, at times, more sensitive stain for bacteria and fungi (Mirrett et al., 1982; Adler et al., 2003). Bacteria and fungi will produce an orange fluorescence, and mammalian cells will stain green. Some experience is required for accurate interpretation of the acridine orange stain, and correct preparation of the smears is necessary to avoid excessive cellular material, which can result in too much cellular deoxyribonucleic acid (DNA) that can mask the presence of any bacterial DNA.

Rapid recognition of positive blood cultures and timely, appropriate therapy is imperative for improved patient outcomes for sepsis (MacVane & Nolte, 2016; Beganovic et al., 2017). Therefore, rapid identification of pathogens growing in positive blood culture bottles—and, in some cases, identification of markers of resistance—is becoming more common in clinical laboratories. Methods to do this include matrix-assisted laser desorption ionization–time-of-flight (MALDI-TOF), in situ hybridization, DNA-microarray hybridization, and nucleic acid amplification from positive blood culture bottles (Peker et al., 2018). Detection from patient blood samples without the need for incubation can also be accomplished using magnetic resonance technology (Charnot-Katsikas et al., 2017). These assays vary in how many pathogens can be detected and what susceptibility or resistance testing is performed.

CULTURE TECHNIQUES

Media for culture are selected to provide the optimal conditions for growth of pathogens commonly encountered at a particular site or in a particular type of specimen. Consideration is given to special growth requirements of bacteria associated with a given type of infection or to the necessity of selecting certain pathogenic bacteria from a mixed population of usual flora. Therefore, the media chosen may include selective and differential media in addition to standard enrichment agar.

Blood-supplemented agar is a good general growth medium that can be used to demonstrate the hemolytic action of colonies on the red blood cells. Antibiotics or chemicals can be added to create a selective medium, such as colistin–nalidixic acid (CNA) agar or phenylethyl alcohol agar (PEA), both of which are used to inhibit the growth of gram-negative bacilli while permitting gram-positive bacteria to grow. Heating the blood to make chocolate agar and adding vitamin supplements creates an enriched medium with available hemin (X factor) and nicotinamide adenine dinucleotide (V factor) for the isolation of *Haemophilus* spp. and other fastidious bacteria. Gram-negative bacilli may be separated from gram-positive bacilli by using bile salts and dye in a medium such as MacConkey agar, which additionally divides the colonies into lactose-positive and lactose-negative colonies, thus making it both selective and differential. Guidelines for the selection of media to be used with different types of specimens can be found in multiple references (McElvania, 2019; Linscott, 2016).

Bacterial cultures are generally incubated at 35°C. Addition of 5% to 10% carbon dioxide (CO_2) may be essential or stimulatory to the growth of *N. gonorrhoeae*, *Haemophilus influenzae*, and *S. pneumoniae*, and should be used whenever feasible. Exceptions to this recommendation are those cultures on differential and selective media in which the pH alteration (which can be affected by added CO_2) is used to differentiate colony types (e.g., xylose-lysine-deoxycholate [XLD] agar, Hektoen enteric [HE] agar).

For recovery of anaerobes, inoculated media should be placed into an anaerobic environment as quickly as possible. Several types of anaerobic culture systems are available. One of these is the anaerobic jar, in which water is added to a CO_2 and hydrogen (H_2) generator package, and oxygen (O_2) is catalytically converted to water with palladium-coated alumina pellets contained in a lid chamber. A modification of this system is a transparent plastic bag containing its own gas generator and palladium catalyst and designed to hold an agar plate; a version of this is the anaerobic BioBag. Another jar-based system uses an automated evacuation-replacement technique to control the anaerobic environment (Summanen et al., 1999; Shahin et al., 2003).

Another approach to anaerobic culture is the anaerobic glove box or chamber, which consists of a large, clear plastic, airtight chamber filled with an oxygen-free gas mixture of nitrogen, hydrogen, and carbon dioxide. Specimens, plates, and tubes are introduced into or removed from the chamber through a gas interchange lock. Anaerobiosis is maintained by palladium catalysts and the hydrogen gas in the chamber. All manipulations within the chamber are done with neoprene gloves sealed to the chamber wall or, for "gloveless" systems, through a hole with sleeves that seal tightly around the forearms. The chambers contain internal incubators that maintain the incubation temperature. Each of the anaerobe systems has its advantages and disadvantages, but all are equally effective in isolating clinically significant anaerobic bacteria from specimens.

Bacterial cultures should be examined routinely after 18 to 24 hours of incubation. The exception to this is the anaerobe culture, which is generally examined at 48 hours to allow these slower-growing bacteria to produce visible colonies. In general, solid media are held for 48 hours, with liquid media held for an additional 24 to 48 hours. Anaerobic media are incubated for at least 5 days. If this is different for specific organisms, it will be mentioned in the text.

A preliminary report is issued when the culture is first examined; this report is updated as additional information becomes available. Certain results (e.g., positive blood or CSF Gram stain, isolation of an organism requiring infection control measures) are reported to the health care provider as soon as the information becomes available. Final reports are issued when all work on a culture has been completed.

MEDICALLY IMPORTANT BACTERIA

GRAM-POSITIVE COCCI

Staphylococcus

Characteristics

Staphylococci are catalase-positive spherical organisms that often appear in grape-like clusters in stained smears (Fig. 57.2). They grow well on any peptone-containing nutrient medium under aerobic and anaerobic conditions and may produce hemolysis of various species of animal blood cells and yellow or orange pigment on certain types of agar. Growth of staphylococci is readily detected on blood agar plates or in various types of nutrient broth. A selective medium for the isolation of *S. aureus* is one containing 7.5% to 10% sodium chloride (NaCl) with mannitol (Becker, 2019).

S. aureus is differentiated from other species of staphylococci principally by its production of coagulases, which are capable of clotting plasma. In addition, many laboratories are now utilizing polymerase chain reaction (PCR) assays for detection of *S. aureus* in nasal swabs and directly from positive blood culture bottles. Many of these assays enable detection of methicillin-resistant *S. aureus* (MRSA) versus methicillin-susceptible *S. aureus*.

Clinical Manifestations and Pathogenesis

S. aureus may be present among the usual flora of the skin, eye, upper respiratory tract, gastrointestinal tract, urethra, and, infrequently, vagina. Therefore, infection may arise from an endogenous or an exogenous source. Factors of importance in the development of infection due to *S. aureus* include breaks in the continuity and integrity of mucosal and cutaneous surfaces, the presence of foreign bodies or implants, prior viral diseases, antecedent antimicrobial therapy, and underlying diseases with defects in cellular or humoral immunity.

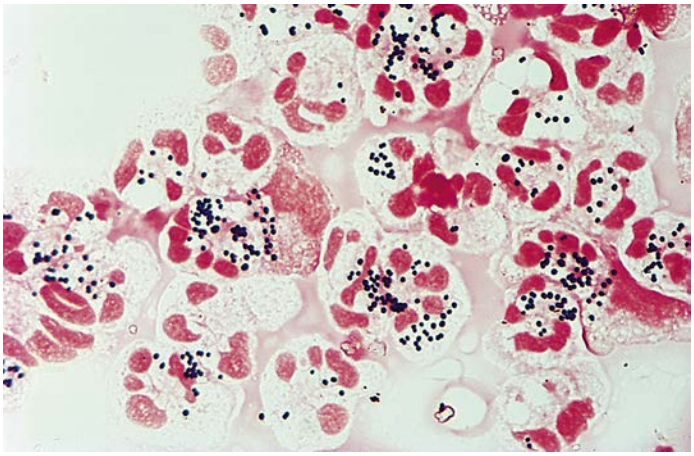

Figure 57.2 Cytocentrifuge preparation of cerebrospinal fluid stained with Gram stain shows many neutrophils, smooth amorphous material, and gram-positive cocci in pairs, short chains, and clusters, suggestive of staphylococcal infection (oil immersion).

Infections caused by *S. aureus* may affect multiple organ systems. Among the most common are those involving the skin and its appendages, such as impetigo, folliculitis, mastitis, and infection of surgical wounds. *S. aureus* is among the leading causes of bacteremia in hospitalized patients, and it may cause endocarditis, particularly in persons with left-sided valvular heart disease and in intravenous drug users. *S. aureus* is the most common cause of spinal epidural abscess and suppurative intracranial phlebitis, and it may be recovered from brain abscesses, typically following trauma. Meningitis caused by *S. aureus* is uncommon; it generally follows head trauma or a neurosurgical procedure.

S. aureus is responsible for many cases of osteomyelitis and is the most common cause of septic arthritis. *S. aureus* is an infrequent cause of community-acquired pneumonia but is a common cause of nosocomial pneumonia, which usually follows aspiration of endogenous nasopharyngeal organisms. Predisposing factors for staphylococcal pneumonia include infection with influenza A virus, cystic fibrosis, and immunodeficiency. Urinary tract infections caused by *S. aureus* are rare, but cases of pyelonephritis and intrarenal and perirenal abscesses can be found.

Several factors play a role in the virulence of *S. aureus*. The capsule, if present, has antiphagocytic properties. Cell wall peptidoglycans have endotoxin-like activity, stimulating the release of cytokines by macrophages, activation of complement, and aggregation of platelets. Protein A, an immunologically active substance in the cell wall, has antiphagocytic properties that are based on its ability to bind the Fc fragment of IgG. Other surface proteins, designated as microbial surface components recognizing adhesive matrix molecules, may play an important role in the ability of staphylococci to colonize host tissues (Speziale et al., 2009). The significant involvement of superantigens of *S. aureus* in sepsis, endocarditis, and acute kidney injury has been elucidated (Salgado-Pabón et al., 2013).

S. aureus produces numerous toxins. The exotoxin TSST-1 is responsible for toxic shock syndrome, and enterotoxins A to E are responsible for staphylococcal food poisoning. The exfoliative toxins—epidermolytic toxins A and B—cause skin erythema and separation, as seen in scalded skin syndrome. Various enzymes are also produced, including protease, lipase, and hyaluronidase, all of which destroy tissue and probably function to facilitate the spread of the infection.

Toxin-mediated diseases caused by *S. aureus* include scalded skin syndrome, food poisoning, and toxic shock syndrome. Scalded skin syndrome occurs in infants infected with a strain of *S. aureus* producing exfoliative toxin. The illness begins abruptly with erythema, followed in 2 to 3 days by the formation of flaccid bullae, which slough, leaving denuded areas that eventually resolve completely. Staphylococcal food poisoning, characterized by nausea, vomiting, abdominal cramps, and diarrhea, occurs 1 to 6 hours after ingestion of foods contaminated with preformed staphylococcal enterotoxin, which is usually introduced into the food product by food handlers who prepare and/or serve the food (Baumgartner et al., 2014).

Toxic shock syndrome is a multisystem disease affecting individuals who have no antibodies to TSST-1 and are colonized or infected with strains of *S. aureus* producing TSST-1 or, rarely, enterotoxin B or C. Toxic shock syndrome is primarily the result of a superantigen-mediated cytokine storm and M protein–mediated neutrophil activation, resulting in the release of mediators leading to respiratory failure, vascular leakage, and shock (Low, 2013). The illness occurs in women 15 to 25 years of age who use tampons during menstruation, male or female patients with a surgical wound or other focal infection, and individuals who have had a surgical procedure in the nose or sinuses (Sharma et al., 2018). Toxic shock syndrome begins abruptly with fever, myalgias, vomiting, and diarrhea, followed by hypotension, hypovolemic shock, and an erythematous rash that frequently involves the palms and soles and desquamates in 1 to 2 weeks. The diagnosis is clinical; isolation of *S. aureus* from any site is not required. Full recovery is the rule, although repeated episodes may occur (Becker, 2019).

Over the past 10 to 15 years, cases of community-acquired infection with *S. aureus* that are oxacillin resistant (CA-MRSA) have become more common. In these isolates, Panton-Valentine leukocidin toxin (PVL), which has rarely been associated with hospital-acquired strains of *S. aureus* (Becker, 2019), has been found. PVL has been shown to be responsible for necrotizing skin and soft-tissue infections and has been infrequently demonstrated to cause a necrotizing and occasionally fatal pneumonia (Hageman et al., 2006; MMWR, 2007a; Moskowitz & Wiener-Kronish, 2009; Toro et al., 2014). Individuals who were initially felt to be at greatest risk are children involved in contact sports and individuals in institutions such as prisons (MMWR, 2003; Pan et al., 2003). These CA-MRSA strains, unlike hospital-acquired strains of MRSA (HA-MRSA), are often susceptible to most non–β-lactam classes of antibiotics. HA-MRSA strains are usually resistant to all antibiotics except the glycopeptides, such as vancomycin. The mechanism of oxacillin resistance is the same in CA-MRSA and HA-MRSA—the presence of a *mecA* gene that is responsible for production of a new penicillin-binding protein (PBP-2a or PBP-2′). However, the chromosomal cassette that houses the CA-MRSA *mecA* gene is different from and much smaller than that containing the *mecA* gene of HA-MRSA. Many experts believe that, in time, blending of CA-MRSA and HA-MRSA strains will occur, and without molecular typing of any isolate, it will be difficult to distinguish them. Homologs of the *mecA* gene have been described, including *mecC*, which results in expression of a PBP2a homolog that has higher affinity for oxacillin than cefoxitin (Becker, 2019).

S. aureus bacteremia can be caused by community and nosocomial strains of *S. aureus*. A study compared the risk factors, morbidity, and mortality due to bacteremia related to HA-MRSA bacteremia versus CA-MRSA bacteremia. Patients with CA-MRSA bacteremia were likely to have diabetes mellitus, chronic liver disease, and HIV infection, perhaps reflecting the community nature of acquisition of the *S. aureus*. In those patients with bacteremia due to HA-MRSA occurring with 48 hours or more of hospitalization, the risk factors were found to include the presence of a central venous catheter, solid tumor, chronic renal failure, prior hospitalizations, and previous antibiotic therapy. Those with bacteremia caused by HA-MRSA that occurred with less than 48 hours of hospitalization were more prone to have had previous hospitalizations, to have been in long-term care facilities, and to have received corticosteroid therapy (Bassetti et al., 2012).

Infections caused by coagulase-negative *Staphylococcus* (CoNS) spp. usually occur in association with foreign bodies, especially implanted prosthetic valves, joints, and CSF shunts. Isolates of CoNS are usually considered less pathogenic than *S. aureus*, although that varies among the species and strains (Becker et al., 2014). The presence of biofilms and antibiotic resistance of CoNS appears to be associated with bacteremia, whereas specific adhesion capabilities of CoNS were associated with prosthetic joint infections (Giormezis et al., 2014). CoNS are one of the most common organisms associated with CSF shunt infections; they are rarely involved in urinary tract infections, pneumonia, or skin and soft-tissue infections. More than 20 species of CoNS are known, of which *S. epidermidis* is the species most frequently involved in such infections. *S. saprophyticus* is an important cause of bacteriuria, particularly among sexually active young women. *S. haemolyticus*, reported to rank second in frequency to *S. epidermidis* in clinical specimens, can be resistant to vancomycin, an agent to which most CoNS are susceptible (Giormezis et al., 2014). *S. lugdunensis* can appear morphologically similar to *S. aureus* (i.e., in production of a narrow zone of β-hemolysis on blood agar plates) and on occasion will test positive in some assays for coagulase. However, it is usually classified as a coagulase-negative staphylococcus. Clinically, it will act more aggressively than most other CoNS and in this way mimics *S. aureus* infection, including its role as an agent of endocarditis, osteomyelitis, and other more severe staphylococcal infections (Sabe et al., 2014). It is important to distinguish *S. lugdunensis* from other CoNS because the breakpoints to use (according to the Clinical Laboratory and Standards Institute [CLSI]) for the interpretation of susceptibility results versus oxacillin (or cefoxitin) should be those that are used to interpret *S. aureus* and not those used to interpret breakpoints for oxacillin (or cefoxitin) versus CoNS (CLSI, 2019).

Laboratory Diagnosis

The observation microscopically of gram-positive cocci in clusters in smears of material taken from previously unopened or undrained lesions, or in smears of broth from a positive blood culture, is indicative of staphylococcal infection. All staphylococci are catalase positive. This enzyme converts hydrogen peroxide to oxygen and water, which is detected by observing bubble production when mixing a bacterial colony with hydrogen peroxide.

S. aureus produces coagulase, an enzyme that binds plasma fibrinogen, causing the organisms to agglutinate or plasma to clot. Only rare strains of other staphylococci are coagulase positive. More than 95% of isolates of *S. aureus* are identified by the slide coagulase test, which detects cell-bound enzyme (clumping factor); nearly 100% of all isolates are identified by tube coagulase tests, which detect free coagulase (Becker, 2019).

The slide coagulase test is performed by mixing a dense emulsion of the organism with plasma on a glass slide. The test is positive if clumping occurs within 30 seconds. *S. lugdunensis* and *S. schleiferi* are two other staphylococci that may give a positive result with this slide coagulase test. A control that consists of emulsifying the suspect colony in saline should be run with each slide test to ensure that autoagglutination does not occur. If autoagglutination is present, slide test results should be considered insufficient for determination of the coagulase reaction of the isolate.

For the tube coagulase test, several colonies are transferred into a tube containing plasma that is incubated at 35°C for 4 hours and then is examined for clot formation. If no clot has formed, the tube is reincubated at room temperature and reexamined after a total of 24 hours of incubation. The test should be examined after 4 hours because most isolates of *S. aureus* produce a clot within this interval. However, some strains produce a fibrinolysin that can lyse the clot, thus producing a false-negative reaction if the test is observed only after 24 hours. *S. intermedius* and *S. hyicus* will also be positive with the tube coagulase test, but they are primarily pathogens of animals and are encountered only rarely in human specimens.

Several commercial latex agglutination assays are available for rapid identification of *S. aureus*. These assays detect protein A and clumping factor; some also detect capsular polysaccharide, which may improve the ability to detect methicillin (oxacillin)-resistant *S. aureus*. *S. saprophyticus* and *S. sciuri* are two other staphylococcus species that may be latex agglutination positive, along with the rare *Micrococcus* spp.; however, these should all be slide coagulase negative (Becker, 2019).

Many species of CoNS have been recognized. However, with the exception of *S. epidermidis*, *S. lugdunensis*, and *S. saprophyticus*, which is resistant to novobiocin, identification of these isolates to the species level is not practical or clinically indicated in every culture. Identification of the species may be needed if isolates are found repeatedly in sterile sites, if susceptibility testing is being performed, if *S. lugdunensis* is being ruled out, or if correlation between isolates in a patient is being sought to increase the likelihood that the two isolates are the same and, therefore, are potentially clinically relevant. If necessary, attempts to identify these isolates to the species level may be made using commercially available identification kits or with use of MALDI-TOF (Peel et al., 2014). Alternatively, isolates may be sent to a reference laboratory capable of performing standard biochemical assays or molecular assays such as 16S ribosomal ribonucleic acid (rRNA) analysis (Loonen et al., 2012). Staphylococci may be classified into strains for epidemiologic purposes to attempt to identify a common source of infection on the basis of their susceptibility to different bacteriophages, plasmid profiles, cellular fatty acids, electrophoresis of multilocus enzymes, or chromosomal molecular typing (pulsed field gel electrophoresis and repetitive PCR). These tests are generally available only through reference laboratories.

Antimicrobial Susceptibility

More than 90% of staphylococci are resistant to penicillin due to inducible plasmid-encoded β-lactamase. A penicillin disk diffusion zone edge test or a PCR for the *blaZ* gene should be performed to confirm a penicillin-susceptible minimum inhibitory concentration (MIC) (CLSI, 2019). Resistance to the penicillinase-resistant penicillins (methicillin, oxacillin, nafcillin) occurs in up to 80% of coagulase-negative staphylococci and in more than 50% of isolates of hospital-acquired *S. aureus*. Resistance to this group of antimicrobial agents is mediated by the *mecA* gene, which encodes an altered penicillin-binding protein, PBP2a. Detection of oxacillin resistance is best done by demonstrating resistance to cefoxitin (CLSI, 2019). When MIC testing for oxacillin is performed, the trays should be incubated for 24 hours at 35°C to detect resistance (CLSI, 2019). The *mecA* homolog, *mecC*, can be detected by some molecular *mecA* assays; *mecC* may be detected in tests for PBP2a (Paterson et al., 2014).

Several assays have been developed for rapid detection of oxacillin resistance. These include nucleic acid amplification, nucleic acid probe assays for *mecA*, and latex agglutination assays for PBP2a (Bowers et al., 2003; Chediac-Tannoury & Araj, 2003; Chapin & Musgnug, 2004; Nonhoff et al., 2012). For direct detection of MRSA in nasal swabs, two approaches can be used. Chromogenic media specific for the detection of MRSA require overnight incubation but allow easy detection of specific-colored colonies that are positive for the presence of *mecA* (Perry et al., 2004; Manickam et al., 2013; Veenemans et al., 2013). Chromogenic agars work well in detecting MRSA but are less sensitive than the available molecular assays. They are, however, less expensive than the molecular assays. Molecular assays that can detect MRSA directly in clinical specimens (nasal swabs, blood cultures, and wounds) are being routinely used in clinical laboratories (Warren et al., 2004; Al-Haj-Hussein et al., 2005; Frey et al., 2011; Buchan et al., 2014).

Clindamycin may be used to treat staphylococcal infection. Inducible resistance due to mechanisms involving *erm* genes may not be detected in routine susceptibility testing. This *erm* gene also confers cross-resistance to the macrolides (e.g., erythromycin) and streptogramins (quinupristin-dalfopristin). An isolate of *S. aureus* that is resistant to erythromycin but susceptible to clindamycin should be evaluated for inducible resistance to clindamycin by the "D-zone" test. A 15-μg erythromycin disk and a 2-μg clindamycin disk are placed 15 mm apart on the surface of a blood agar plate inoculated with the isolate in question. After overnight incubation, if there is inducible resistance to clindamycin, blunting of the clindamycin zone of inhibition will be seen on the side near the erythromycin disk, giving the appearance of a D zone (CLSI, 2019) (Fig. 57.3).

Vancomycin resistance, although rarely seen in *S. aureus*, is a serious issue that laboratories need to be aware of. Isolates of vancomycin intermediately susceptible *S. aureus* (VISA) have MICs in the intermediate range (4–8 μg/mL) (Cosgrove et al., 2004). In the early 2000s, 14 cases of vancomycin-resistant *S. aureus* were reported (MMWR, 2004). Because these have not been uniformly detected in automated systems for susceptibility testing, the Centers for Disease Control and Prevention (CDC) recommends that all *S. aureus* isolates that test resistant to vancomycin be sent to a public health laboratory for confirmation.

Newer antimicrobial agents have good activity against susceptible and resistant staphylococci. These include quinupristin/dalfopristin, a streptogramin; the lipopeptide daptomycin; linezolid; telavancin; and ceftaroline. The last is the only cephalosporin to which MRSA isolates are susceptible.

Streptococcus and Enterococcus

Characteristics

Streptococci are catalase-negative, gram-positive, spherical, ovoid, or lancet-shaped cocci, often seen in pairs or chains. They are facultatively anaerobic. Some strains require added CO_2 for their initial isolation but

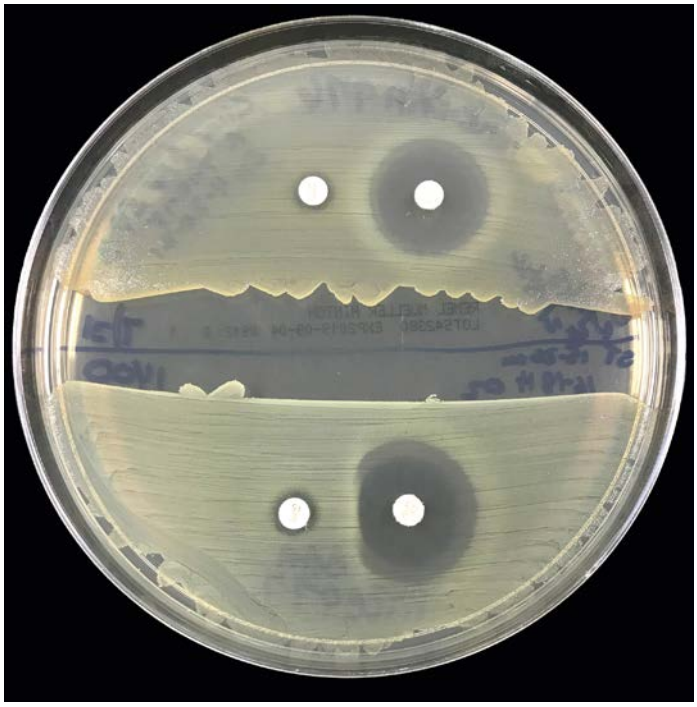

Figure 57.3 Positive D-zone test demonstrating inducible clindamycin resistance.

may lose this requirement in subcultures. Streptococci can be broadly classified according to the hemolytic reaction on blood agar (Table 57.1). Those strains that completely hemolyze the red cells around their colonies are called *β-hemolytic* and can be further categorized into the Lancefield groups based on serologically reactive carbohydrates. Important members of this group include *S. pyogenes* (group A) and *S. agalactiae* (group B). Figure 57.4 is a Gram stain of *S. pyogenes* (group A streptococcus) in a specimen from abscess material on the arm of a patient with cellulitis. The gram-positive cocci in chains that produce partial hemolysis (which cause "greening" of the agar) are α-hemolytic. An important member of this group is *S. pneumoniae*. Streptococci that do not hemolyze blood are γ-hemolytic. An important member of this group is the *S. bovis* complex. Some *S. agalactiae* may also be γ-hemolytic. Most of the remainder of the α- and γ-hemolytic streptococci are collectively called viridans streptococci, including *S. mutans*, *S. sanguis*, *S. mitis*, *S. salivarius*, and *S. anginosus*. The group of organisms previously referred to as nutritionally variant (pyridoxal or thiol dependent, satelliting) streptococci have now been assigned to the genus *Abiotrophia* or *Granulicatella*.

Members of the genus *Enterococcus*, previously designated as group D streptococci because their cell wall antigens reacted with group D antisera, are different molecularly as well as metabolically from the other members of the genus *Streptococcus*. These organisms are gram-positive cocci that occur singly, in pairs, and in short chains. They are facultatively anaerobic. Most enterococci are α- or γ-hemolytic on blood agar, but some may exhibit β-hemolysis. The most common species are *E. faecium* and *E. faecalis*; yellow motile strains of the enterococci, less commonly associated with infections, include *E. casseliflavus* and *E. gallinarum*. These latter two species are usually intrinsically vancomycin resistant; it is important to differentiate them from the vancomycin-resistant *E. faecium* or *E. faecalis* strains.

Other genera of catalase-negative gram-positive cocci that may be isolated from clinical specimens include *Leuconostoc*, *Pediococcus*, *Rothia*, *Gemella*, *Aerococcus*, *Lactococcus*, and other less rarely isolated species. These organisms are considered to have low virulence potential and generally are pathogenic only in the compromised host, with the exception of some species of *Aerococcus* (*A. urinae* and *A. sanguinicola*), which are known urinary tract pathogens. However, some of these isolates may be confused with viridans streptococci, in particular; their differentiation is important because of their lower virulence and potential for vancomycin resistance.

TABLE 57.1
Classification of *Streptococci* and *Enterococci*

Hemolysis	Lancefield Group	Species
β	A	*Streptococcus pyogenes*
	B	*Streptococcus agalactiae*
	C	*Streptococcus dysgalactiae*
	D	*Enterococcus* spp.
α or γ	D	*Enterococcus* spp.
	D	*Streptococcus bovis complex* (reclassified into many new species, as described in text)
	None	Viridans group*
α	None	*Streptococcus pneumoniae*

*Small colony variants of Lancefield group A, C, F, or G, or nongroupable strains, can be any hemolysis.

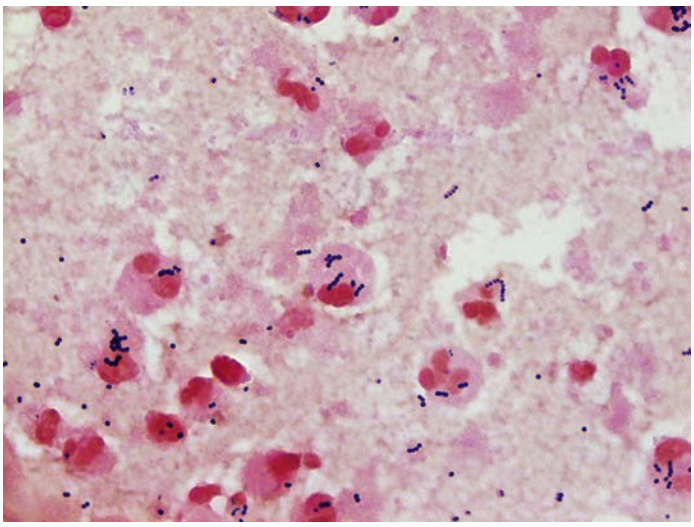

Figure 57.4 Gram stain of *Streptococcus pyogenes* (group A streptococcus) from a case of cellulitis (oil immersion).

Clinical Manifestations and Pathogenesis

One of the most common clinical manifestations of group A streptococci is pharyngitis. This may be accompanied by scarlet fever, a punctate exanthem overlying diffuse erythema that usually first appears on the neck or upper chest, becomes generalized, and then desquamates. Skin infections caused by group A streptococcus include cellulitis, erysipelas, and pyoderma. Acute rheumatic fever, characterized by carditis, polyarthritis, erythema marginatum, chorea, and subcutaneous nodules, may occur 1 to 5 weeks after group A streptococcal pharyngitis. Acute glomerulonephritis may develop 10 days to 3 weeks after group A streptococcal pharyngitis or pyoderma.

Beginning in the late 1980s, serious group A streptococcal clinical syndromes, including necrotizing fasciitis, myositis, malignant scarlet fever, bacteremia, and toxic shock–like syndrome, began to be seen with increasing frequency. These have been associated with high morbidity rates and mortality rates of up to 30% or more. The reason for this increase is not completely understood but appears to be related to changes in the prevalence of organisms having an enhanced virulence potential (Kaplan, 2005; Vucicevic et al., 2008; Lappin & Ferguson, 2009; Reglinski & Sriskandan, 2014).

S. pyogenes produces numerous virulence factors. One of the most important is the antiphagocytic cell wall M protein. Antibodies against the specific M protein confer lifelong type-specific immunity. However, because more than 60 M protein types exist, infection with a group A streptococcus possessing a different M protein may occur. Another important cell wall component is lipoteichoic acid, which permits bacterial adherence to the respiratory epithelium. *S. pyogenes* also elaborates about 20 extracellular products, including enzymes (streptolysins, hyaluronidase, streptokinase, deoxyribonucleases [DNases], and nicotinamide adenine dinucleotidase [NADase]) and erythrogenic toxins. Streptolysin O, an antigenic, oxygen-labile enzyme, produces subsurface hemolysis on blood agar plates; streptolysin S, a nonantigenic, oxygen-stable enzyme, produces surface hemolysis. Neither streptolysin has a proven role in the pathogenesis of human disease. Streptokinase promotes fibrinolytic activity by converting plasminogen to plasmin, and hyaluronidase may enhance the spread of the organism through connective tissue. The pathogenic significance of the DNases and of NADase is unknown. Pyrogenic (erythrogenic) toxins (serotypes A, B, C) are produced by isolates of *S. pyogenes* infected with a specific temperate bacteriophage. Their pyrogenicity is caused by a direct action on the hypothalamus. Streptococcus group A has also been found to possess superantigens with high mitogenic capabilities. They have been associated with cases of more severe streptococcal infection, such as necrotizing fasciitis or toxic shock syndrome (Kotb et al., 2002; Reglinski & Sriskandan, 2014).

The pathogenesis of acute rheumatic fever is not fully understood. Certain M protein types of *S. pyogenes* may be rheumatogenic. The presence of complexes of immunoglobulin and the C3 component of complement along the sarcolemmal sheaths of cardiac myofibers from individuals with rheumatic carditis suggests that myocarditis results from the production of antibodies directed against a streptococcal cell wall M protein that cross-reacts with myocardial tissue. Moreover, a heart or tissue cross-reactive antigen of *S. pyogenes* that shares immunologic epitopes with, but is distinct from, the M protein has been identified (Barnett & Cunningham, 1990). Renal damage in acute glomerulonephritis is caused by deposits of circulating streptococcal–antistreptococcal immune complexes in the glomeruli and subsequent activation of complement. Cell-mediated reactions to an altered glomerular basement membrane or activation of the alternate complement pathway also may be involved. Isolates of *S. pyogenes* have been linked to toxic shock syndrome, with a clinical picture very similar to *S. aureus*; streptococcal superantigens (Sags) are thought to be responsible for the toxic shock–like syndrome caused by strains of *S. pyogenes* (Reglinski & Sriskandan, 2014).

The most significant infections caused by Group B streptococci (GBS) are neonatal sepsis, pneumonia, and meningitis. Colonization of the maternal genital tract is associated with colonization of infants and risk of neonatal disease, with early-onset infections occurring within the first few days after delivery and late-onset infections appearing after 1 week of age. To reduce the incidence of neonatal disease, the CDC published

specific guidelines to facilitate early identification and treatment of women colonized with GBS and identification and treatment of neonates at risk for developing disease (ACOG, 2019; Verani et al., 2010). All pregnant women at 36 0/7 to 37 6/7 weeks of gestation should have vaginal/rectal specimens collected and processed for detection of GBS. These specimens can be cultured or have a nucleic acid amplification test (NAAT) performed on them after enrichment in a selective culture broth (ACOG, 2019). Results of this test should be available during labor so that appropriate prophylaxis can be given to the mother before delivery to prevent infection of the newborn. Isolation of $>10^4$ colony-forming units (CFUs) per milliliter of GBS from the urine of a pregnant female can also be used as a marker of GBS vaginal carriage. This information should be used to direct prophylaxis to mothers found to be positive. If urine is positive, screening of vaginal/rectal cultures may not be necessary. Molecular tests that can rapidly identify the presence of GBS during or right before delivery are available, although reported sensitivities vary and susceptibility testing for clindamycin in penicillin-allergic patients is not possible (ACOG, 2019; Feuerschuette et al., 2018). GBS infections in adults include postpartum endometritis, urinary tract infection, bacteremia, skin and soft-tissue infections, pneumonia, endocarditis, meningitis, arthritis, and osteomyelitis.

Group C and G streptococci are similar to *S. pyogenes* in that they cause a wide range of infections, including bacteremia, endocarditis, meningitis, arthritis, and respiratory and skin infections (Rantala, 2014). The pharyngeal infection caused by these streptococci is similar to that of group A streptococci except that the nonsuppurative sequelae of rheumatic fever do not occur.

Infections caused by *S. pneumoniae* include pneumonia, meningitis (especially in infants and the elderly), spontaneous bacteremia (in persons who do not have a spleen), otitis, sinusitis, and spontaneous peritonitis. *S. pneumoniae* is seen in the normal flora of the upper respiratory tract of 25% to 50% of preschool children, 36% of primary school–age children, and nearly 20% of adults, termed carriers with decreasing prevalence of invasive serotypes due to vaccination (Lopez et al., 1999; Devine et al., 2017). Its spread is enhanced by upper respiratory tract infections and crowding. Pneumonia may develop when the host immune defenses are impaired. Most cases are endogenous, following aspiration of oral secretions containing normal flora that includes *S. pneumoniae*. Person-to-person transmission during epidemics occurs by droplet aerosols. The major virulence factor of *S. pneumoniae* is its antiphagocytic polysaccharide capsule; strains with a thick, mucoid capsule are especially virulent. Vaccines designed to protect against infection by pneumococci of many of the predominant capsular polysaccharide types are available. The CDC recommends that infants receive the 13-valent conjugated vaccine starting at 2 months of age. It also is recommended that adults 65 years of age and older receive the 23-valent polysaccharide vaccine. Immunosuppressed patients of any age should receive both vaccines (Matanock et al., 2019).

Bacterial endocarditis is the most common infection caused by viridans streptococci; others include abscesses in the brain or liver, bacteremia, and dental caries. The *Streptococcus anginosus* group (*S. constellatus*, *S. intermedius*, and *S. anginosus*) consists of the most common viridans streptococci responsible for liver, spleen, and brain abscesses. They often are more susceptible to antibiotics than other strains of viridans streptococci, although resistance to penicillin is increasingly being recognized. *S. bovis* bacteremia has been associated with malignancies of the gastrointestinal tract. *S. bovis* is now recognized as a complex of seven subspecies broken down into four branches: *S. gallolyticus* (includes the subspecies *gallolyticus*, *pasteurianus*, and *macedonicus*); *S. equinus*; *S. infantarius* (includes subspecies *infantarius* and *coli*); and *S. alactolyticus*. *S. gallolyticus* subsp. *gallolyticus* is isolated from blood cultures of patients with colonic cancer more often than others in the group. *S. gallolyticus* subsp. *gallolyticus* is associated with prosthetic joint infections and infective endocarditis; *S. gallolyticus* subsp. *pasteurianus* is associated with meningitis in infants. *S. alactolyticus*, *S. equinus*, and *S. infantarius* are not often found in human disease (Jans et al., 2014; Vaska & Faoagali, 2009). In many laboratories, isolates are still reported as *S. bovis* because phenotypic identification may not be adequate for differentiation and physicians recognize the clinical significance of *S. bovis*. Other viridans group streptococci include the *Streptococcus mitis* group (commonly associated with endocarditis), the *Streptococcus mutans* group (etiologic agent of dental carries), and the *Streptococcus salivarius* group (isolated from the oral cavity and blood). As use of molecular methods or MALDI-TOF for bacterial identification increases, more of these differences may be appreciated (Vaska & Faoagali, 2009; Su et al., 2018).

Enterococci are not highly pathogenic; however, they are a common cause of urinary tract infection in hospitalized persons. They may also cause endocarditis, bacteremia, and wound infections. Vancomycin-resistant enterococci offer a greater potential for infection, especially in immunocompromised patients and patients with implanted foreign devices (Han et al., 2009; McBride et al., 2009).

Laboratory Diagnosis

Streptococci grow well on blood or chocolate agar. Blood agar is preferred because the hemolytic properties of the organism can be assessed. When culturing vaginal/rectal swabs from pregnant women for GBS, specimens should first be inoculated to a selective broth, such as Lim or carrot broth, or on to selective agar, such as Granada agar, to enrich for this organism (Church et al., 2008; Carvalho et al., 2009; Spellerberg, 2019). Tests that may be used in the clinical microbiology laboratory to presumptively name the β-hemolytic species of *Streptococcus* are shown in Figure 57.5. More than 99% of isolates of group A *Streptococcus* (GAS) are susceptible to bacitracin, but a very small percentage of isolates of GBS and 10% to 20% of isolates of groups C and G *Streptococcus* are also susceptible. Therefore, results of the bacitracin susceptibility test provide a presumptive identification. An isolate may be called GAS presumptively based on hydrolysis of L-pyrrolidonyl-β-naphthylamide (PYR) (Spellerberg, 2019). All isolates of GAS and more than 99% of isolates of *Enterococcus* are PYR positive. Identification of GAS is confirmed by bacitracin susceptibility or using latex agglutination for the Lancefield group A antigen.

GAS antigen may be detected directly in throat swab specimens by using commercial kits designed to generate a rapid result. These tests are highly specific but, given their low sensitivity, which varies among studies from 31% to 95% (Carroll & Reimer, 1996; Lean et al., 2014), a negative antigen test in children should be followed by culture or NAAT. More recently, clinical guidelines recommended that negative antigen assays in adults need not be followed up with culture (Dingle et al., 2014; Lean et al., 2014; Nakhoul & Hickner, 2013; Shulman et al., 2012). The use of NAAT for direct diagnosis of GAS pharyngitis can allow laboratories to perform single-tiered testing without reflex cultures (Durant et al., 2019). Serologic tests to detect streptolysin O and DNase B antibodies in acute and convalescent serum samples are used primarily to diagnose acute rheumatic fever and acute glomerulonephritis following infection with GAS.

Catalase-negative colonies that are β-hemolytic and hippurate hydrolysis positive and/or that have a positive CAMP test (named for researchers Christie, Atkins, and Munch-Petersen) reaction presumptively can be called group B *Streptococcus* (GBS). Isolates of presumed GBS from sterile body sites should be identified by serotyping (using latex agglutination or coagglutination tests) or MALDI-TOF. For culture of vaginal/rectal swab specimens from pregnant women during weeks 36 through 38 of gestation, it is recommended that a broth enrichment be used along with or as a replacement for agar-based media. Selective broth media, including Lim broth or selective Todd-Hewitt broth, can be used as enrichment media (Heelan et al., 2005). Chromogenic broth, including carrot broth media, can be used as enrichment broth; colonies of β-hemolytic GBS will convert the color of the tube from clear to yellow or orange. However, nonhemolytic GBS will not change the tube color and, when used, a negative broth would still need to be planted onto solid media for recovery of these strains. In addition, a selective nonchromogenic enrichment broth can be subcultured to Granada agar, on which colonies of GBS will appear yellow to orange for ease of detection. Nucleic acid amplification assays can be used to detect GBS directly in vaginal-rectal specimens or can be used to detect GBS in Lim or carrot broth cultures (Picard & Bergeron, 2004; Block et al., 2008; Gray et al., 2012). Current guidelines highlight the higher sensitivity of NAAT performed after enrichment culture (MMWR, 2010).

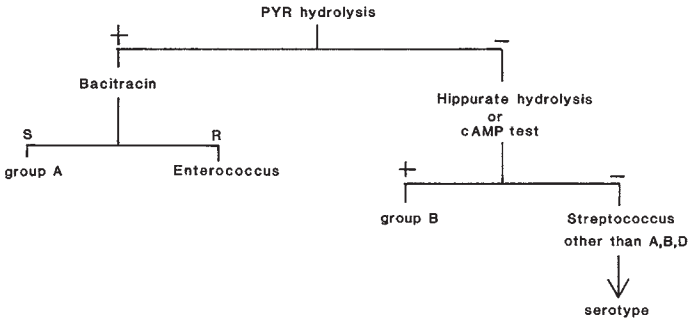

Figure 57.5 Decision tree of tests to presumptively name the β-hemolytic species of *Streptococcus*. +, Positive result; –, negative result; *R*, resistant; *S*, susceptible. (With permission from Woods GL, Gutierez Y: Diagnostic pathology of infectious diseases, Philadelphia, 1993, Lea & Febiger.)

Latex agglutination assays are available for direct detection of GBS (as well as *S. pneumoniae*, some serotypes of *N. meningitidis*, *E. coli*, and *H. influenzae* type b) in CSF, serum, and urine. These assays have been shown to have sensitivities equivalent to or lower than a Gram stain and may give false-positive results. The rapid bacterial antigen tests are much more expensive and labor-intensive than Gram stain, so most laboratories no longer offer these tests or strictly limit their use (Thomas, 1994). Nucleic acid amplification tests for detection of common pathogens in central nervous system infections have been developed and can decrease the time to detection of pathogens relative to cultures. These assays can have false-positive and false-negative results; thus, discussions with health care providers on how to best utilize this test are required (Tansarli & Chapin, 2019).

Tests used to presumptively identify α- and γ-hemolytic streptococci and enterococci are shown in Figure 57.6. α-Hemolytic colonies that are mucoid or flattened with a depressed center are suggestive of *S. pneumoniae*; they should be tested for susceptibility to optochin (P disk), and for bile solubility. *S. pneumoniae* is susceptible to both; other α-hemolytic streptococci are resistant to optochin and are variable in response to bile. A urinary antigen assay for detection of *S. pneumoniae* has been shown in some studies to be a nonculture diagnostic method for patients with severe pneumococcal infection, for diagnosis of pneumococcal exacerbation in chronic obstructive pulmonary disease patients, and as a tool for diagnosis of otitis media. Reported sensitivities compared with conventional diagnostic methods range between 50% and 80% with specificities of at least 90% (Roson et al., 2004). As with any antigen assay, caution needs to be taken in interpreting results in cases in which prior infection with *S. pneumoniae* may have occurred since the assay can remain positive for 1 to 6 months (Gisselsson-Solen et al., 2007; Smith et al., 2009; Couturier et al., 2014; Harris et al., 2014).

α-Hemolytic colonies that are not *S. pneumoniae* and γ-hemolytic colonies are tested for PYR hydrolysis; enterococci are PYR positive, and viridans streptococci are negative. Moreover, all enterococci grow in the presence of 6.5% NaCl, but viridans streptococci do not. Enterococci hydrolyze esculin in the presence of bile (causing visible growth and blackening of the agar), but up to 10% of viridans streptococci are also bile–esculin positive. Additional biochemical assays or MALDI-TOF are required to identify enterococci to the species level. A majority of vancomycin-resistant enterococci (VRE) are *E. faecium*.

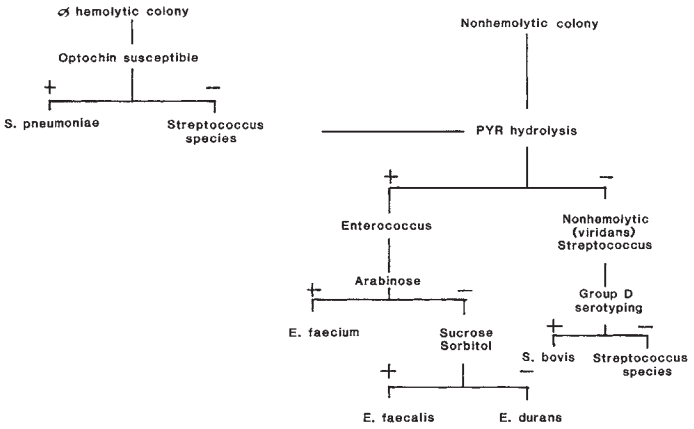

Figure 57.6 Decision tree of tests to presumptively name the α-hemolytic species of *Streptococcus* and *Enterococcus*. +, Positive result; –, negative result; *R*, resistant; *S*, susceptible. (*With permission from Woods GL, Gutierez Y:* Diagnostic pathology of infectious diseases, *Philadelphia, 1993, Lea & Febiger.*)

α-Hemolytic and γ-hemolytic streptococci that are not *S. pneumoniae* or *Enterococcus* are grouped as viridans streptococci. Identification of individual species of viridans streptococci requires conventional biochemical testing, molecular methods, or MALDI-TOF (Fang et al., 2012; Moon et al., 2013). Kit systems to identify these organisms are commercially available although they may lack accuracy for viridans group streptococci. Full identification of species members of viridans streptococci, however, is usually not necessary.

Leuconostoc and *Pediococcus* rarely cause disease, but it is important to correctly identify them as they are intrinsically resistant to vancomycin. Characteristics that can be used to identify and differentiate these organisms are listed in Table 57.2 (Facklam et al., 1989). Included in this table is *Aerococcus* spp., because of their morphologic similarity to *Enterococcus* spp. The clue that an isolate (especially from a urine culture) might be an *Aerococcus* sp. is the finding on Gram stain that a catalase-negative colony consists of gram-positive cocci in tetrads and clusters, not in pairs and chains. Some species of *Aerococcus* are PYR positive, which leads to further confusion with *Enterococcus* spp.

Members of the genus *Abiotrophia* and *Granulicatella* will not grow in the absence of pyridoxal. Often, they are first recognized as satelliting colonies growing around a colony of *S. aureus* or only growing on chocolate media (Christensen, 2019). Methods of performing susceptibility tests for strains of *Abiotrophia* and *Granulicatella* can be found in the third edition of CLSI document M45 (CLSI, 2015).

Antimicrobial Susceptibility

Groups A, B, C, and G streptococcus are all are susceptible to penicillin. Therefore, routine antimicrobial susceptibility testing of these organisms is unnecessary unless penicillin cannot be used, as in the case of a penicillin allergy. In those situations, testing for resistance to macrolides, clindamycin, and the tetracyclines may be warranted. Inducible resistance to clindamycin may occur with *Streptococcus* (i.e., GBS), and a D zone test as described earlier for *S. aureus* may be warranted if the streptococcal isolate is found resistant to erythromycin. Specific guidelines for streptococcal D–zone testing recommend that the clindamycin and erythromycin disks be separated by 12 mm instead of the 15 to 16 mm recommended for testing *S. aureus* (CLSI, 2019).

Because *S. pneumoniae* organisms with intermediate- or high-level resistance to penicillin are found worldwide, isolates should be tested for susceptibility to penicillin. A screening test using disk diffusion with a 1-μg oxacillin disk (≥20 mm = susceptible) may be performed. However, isolates that are not susceptible by this method must be further evaluated by macrodilution or microdilution testing using Mueller-Hinton broth supplemented with lysed horse blood or gradient diffusion testing to determine the penicillin MIC. There are breakpoints for penicillin and the cephalosporins for isolates from cases of meningitis versus those isolated from nonmeningitis sites (CLSI, 2019). Resistance to third-generation cephalosporins also occurs; therefore, isolates should be tested for susceptibility to these antimicrobial agents as well.

Susceptibility testing should be performed on isolates of nonhemolytic (viridans) streptococci from sterile body sites, because resistance to penicillin does occur. *Enterococcus* spp. should also be tested, primarily to identify high-level resistance to penicillin or ampicillin, high-level resistance to streptomycin and gentamicin, and resistance to vancomycin. Enterococci

TABLE 57.2
Characteristics Differentiating Enterococcus, Leuconostoc, Pediococcus, and Aerococcus

	Enterococcus	Aerococcus	Leuconostoc	Pediococcus
Gram stain	Pairs and short chains	Tetrads	Cocci, coccobacilli, and rods; pairs and chains	Tetrads and pairs; spherical cells
Hemolysis	β or α or γ	α or γ	α or γ	α or γ
Bile esculin	+	V	V	+
Growth in 6.5% NaCl	+	+	V	V
PYR	+	*	–	–
LAP	+	*	–	+
Vancomycin susceptibility	S/R	S	R	R

+, Positive result; –, negative result; *LAP*, leucine aminopeptidase; *PYR*, l-pyrrolidonyl-β-naphthylamide; *R*, resistant; *S*, susceptible; *V*, variable reactions.
**Aerococcus urinae* is PYR and LAP positive; *Aerococcus viridans* is PYR positive and LAP negative.

are resistant to vancomycin because of the presence of resistance genes, referred to as the *van* genes (CLSI, 2019). Although many of these genes have been described, the most common are *vanA*, *vanB*, and *vanC*. The *vanA* and *vanB* genes, conferring high-level resistance and predominantly found in *E. faecium* and less frequently in *E. faecalis*, are acquired, plasmid-borne genes that can create infection control problems involving transmission of this resistance. This vancomycin resistance should be differentiated from intrinsic and lower-level resistance (*vanC* genes) in the yellow, motile species of *Enterococcus*; this information should be reported to the infection control team (Teixeira et al., 2019).

Gemella and *Aerococcus*

Other nonstreptococcal gram-positive, catalase-negative cocci of increasing importance are those that belong to the genera *Gemella* and *Aerococcus*. *Gemella* spp. (*G. haemolysans* and *G. morbillorum*) resemble viridans streptococci, although they usually produce smaller colonies. *G. haemolysans* has been associated with endocarditis and meningitis. Gram stain usually demonstrates diplococci with adjacent sides flattened that can be confused with a *Neisseria* sp. because cells can easily become decolorized. *G. haemolysans* prefers an aerobic growth atmosphere. *G. morbillorum* usually appears as cocci in pairs or short chains. Both are PYR positive, 6% NaCl, and esculin–hydrolysis negative (to differentiate them from enterococci). *G. morbillorum* is leucine-aminopeptidase (LAP) positive as well. Both are usually susceptible to penicillin. As with other gram-positive cocci, if there is doubt about the morphology of the organism (i.e., whether it is a short rod or a coccus), Gram stain performed from a broth culture will usually resolve the difficulty. MALDI-TOF has been shown to be a useful tool in the correct identification of *Gemella* spp. (Schultness et al., 2013).

Two major species of *Aerococcus* may be clinically relevant and/or isolated from clinical specimens: *A. urinae* and *A. viridans*. Both resemble viridans streptococci or enterococci on agar plates. However, in Gram stains, they usually appear in tetrads. An increasing number of clinically relevant cases of *A. urinae* (and other species of aerococci) are being reported. Urinary tract infections are most common, but rare cases of more serious infection, including bacteremia, are seen (Christensen et al., 2019; Shelton-Dodge et al., 2011). *A. viridans* remains relatively uncommon as a pathogen when isolated from clinical samples; *A. sanguinicola* isolation is not always associated with clinical disease, but case numbers are increasing (Ibler et al., 2008; Shelton-Dodge et al., 2011).

A. urinae is PYR negative and LAP positive, in contrast to *A. viridans*, which is PYR positive and LAP negative (see Table 57.2). Both will grow in the presence of 6.5% NaCl. Neither are anaerobes, and *A. viridans* usually will not grow under anaerobic conditions. *A. urinae* is usually susceptible to penicillin and nitrofurantoin but may be resistant to sulfonamides. Variability in its response to trimethoprim has been noted (Christensen et al., 2019; Senneby et al., 2015). A newer member of the genus *Aerococcus*, *A. sanguinicola*, which is rarely recovered from clinical specimens, can be both LAP and PYR positive, although this is not a confirmatory identification. Use of MADLI-TOF can provide more reliable results. It can be responsible for urinary tract infections as well as bacteremia and infective endocarditis. Like *A. urinae*, isolates of *A. sanguinicola* are usually susceptible to penicillin and nitrofurantoin, but are variable in their response to sulfonamides and quinolones (Ibler et al., 2008; Rasmussen, 2013; Senneby et al., 2015).

GRAM-POSITIVE RODS

Corynebacterium and *Arcanobacterium*

Characteristics

The corynebacteria, also known as *diphtheroids*, appear in the gram-stained smear as slightly curved, gram-positive rods with nonparallel sides and sometimes wider ends, giving a clubbed appearance (Fig. 57.7). These organisms are catalase positive. More than 100 species of *Corynebacterium* are known. Most are rarely pathogenic in humans; notable exceptions are *C. diphtheriae* and its closely related species *C. ulcerans* and *C. pseudotuberculosis*. *C. pseudodiphtheriticum* has been implicated in respiratory tract infections, including pneumonia (Camello et al., 2009). Other medically relevant coryneform gram-positive rods include *Arcanobacterium haemolyticum*, *Trueperella pyogenes*, and *Trueperella bernardiae*. These organisms also appear as irregular gram-positive rods on Gram stain but can be easily differentiated from the corynebacteria by their negative catalase reaction.

Clinical Manifestations and Pathogenesis

At the initial site of infection on the epithelial cells of the tonsils and oropharynx, *C. diphtheriae* elaborates an exotoxin that causes local cell necrosis and subsequent inflammation. The exotoxin is encoded by a specific bacteriophage carrying the *tox* gene and is absorbed into the circulation. Distribution of exotoxin through the bloodstream can produce degenerative changes in the heart, nervous system, and kidneys. The toxin molecule consists of two fragments: A, containing the enzymatically active site, and B, comprising the receptor binding site. Once in the cell, protein synthesis is disrupted. The bacteria and exotoxin produce a serum exudate and cellular infiltrate of the mucous membrane in the pharynx. Exudative lesions coalesce, forming a grayish-black adherent pseudomembrane, which is characteristic of diphtheria. Although toxin production and pathogenicity are often considered to be synonymous, pseudomembranes may form in persons infected with nontoxigenic strains. Extension of the pseudomembrane superiorly into the nasopharynx or inferiorly into the larynx may be so marked as to produce respiratory obstruction. Although *C. diphtheriae* infections of other parts of the body do occur, those observed most frequently in the United States today are infections of the skin. Transmission of *C. diphtheriae* occurs by droplet nuclei from the respiratory tract or by contact from cutaneous foci of infection (Byard, 2013; Mattos-Guaraldi et al., 2003). Nontoxigenic strains of *C. diphtheriae* can cause skin and bloodstream infections (Wojewoda, 2012).

Because they are part of the normal flora of the skin and mucous membranes, it is difficult to establish the etiologic role of the other corynebacteria. Clinical significance is generally increased if the organism is observed in the gram-stained smear in association with leukocytes, is isolated from a sterile site, and is isolated from multiple samples. *C. jeikeium* has been clearly associated with infections of implanted prosthetic materials (e.g., heart valves, CSF, joints), has caused subacute bacterial endocarditis, and has been involved in a variety of opportunistic infections. *C. urealyticum* has been associated with urinary tract infection as well as with bacteremia, endocarditis, and wound infection (Nebreda-Mayoral et al., 1994). When identified, *C. striatum* and *C. amycolatum* are the most common normal flora skin coryneforms. They may become pathogenic, especially in cases of prosthetic joint infections and, of note, are often resistant to β-lactam antibiotics, a characteristic usually attributed only to *C. jeikeium* (Crabtree & Garcia, 2003; Cazanave et al., 2012).

A. haemolyticum has been associated with pharyngitis and wound and soft-tissue infections (Fernandez-Suarez et al., 2009). *T. pyogenes* and *T. bernardiae* are associated with abscess formation (Bernard, 2019).

Laboratory Diagnosis

Because of the relative rarity of diphtheria in the United States today, the diagnosis may be overlooked clinically, and the laboratory may easily fail to recognize it in cultures. When the diagnosis of diphtheria is suspected, the laboratory should be informed so that the specimen can be handled appropriately. Specimens should be obtained with a cotton- or polyester-tipped swab from inflamed regions of the nasopharynx and, if possible, beneath the pseudomembrane. If skin lesions are suspected of being positive for *C. diphtheriae*, the most appropriate specimen would be an aspirate of the lesion. Corynebacteria will grow on routine blood-containing agar; however, cystine-tellurite (CT) blood agar or Tinsdale medium is preferred. On CT medium, colonies of *C. diphtheriae* are gray or black after 48 hours of incubation. Colonies may be large or small and flat or convex. Colonies of species other than *C. diphtheriae* may produce black colonies on CT or Tinsdale media, although these will usually be smaller. If a laboratory does

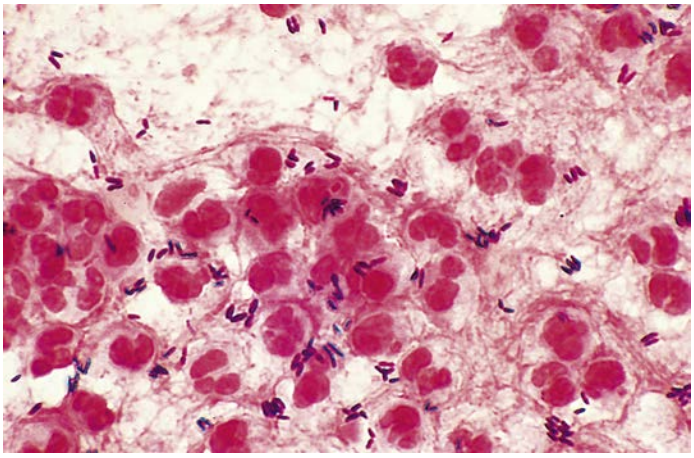

Figure 57.7 Sputum stained with Gram stain shows many neutrophils, amorphous debris, and coryneform gram-positive bacilli (oil immersion).

not have CT or Tinsdale medium and a request for *C. diphtheriae* is made, CNA can be used, although it will be more difficult to recognize possible *C. diphtheriae* strains (Bernard, 2019).

Classification of oral and skin corynebacteria or diphtheroids is difficult and confusing. Commercial identification systems, including MALDI-TOF, are available to identify many of the members of this group of organisms (Bernard, 2019). Isolates of suspected *C. diphtheriae* must be tested for production of exotoxin. The elaboration of toxin may be detected in vitro with the Elek immunodiffusion test. However, this generally is not done in a routine clinical laboratory. Isolates should be sent to a public health laboratory or a reference laboratory for an Elek immunodiffusion test. Alternatively, PCR-based tests available at reference or public health laboratories have been described that may be used for detection of the toxin gene (Mancini et al., 2012). *C. jeikeium* often produces a characteristic metallic sheen on the surface of blood agar plates. *C. striatum* and *C. amycolatum* are common skin flora that can be responsible for infection. Whether they need to be specifically identified is controversial, and identification can be difficult with biochemical methods. Species identification of *Corynebacterium* often requires a combination of commercial kit systems, cellular fatty acid analysis, MALDI-TOF, and/or sequencing (Van den Velde et al., 2006). *C. striatum* and *C. amycolatum* organisms are often resistant to many antibiotic agents—a characteristic that often is more typically associated with hospital-acquired strains, in particular, *C. jeikeium*. MALDI-TOF has been reported to be very useful in the identification of *Corynebacterium* spp. (Bernard, 2012; Vila et al., 2012).

Arcanobacterium spp. are β-hemolytic on sheep blood agar. Colonies on sheep blood agar are small after 48 hours of incubation, and the hemolysis may go unnoticed. Adequate growth and noticeable hemolysis are best demonstrated in a CO_2-enhanced environment. *Arcanobacterium* spp. are catalase negative. Biochemical reactions that are used to determine the species of corynebacteria are also useful in identifying the *Arcanobacterium* spp. (Bernard, 2019). *A. haemolyticum* produces phospholipase D, which is responsible for the reverse CAMP reaction with *S. aureus*. This organism inhibits hemolysis around the *S. aureus* streak, producing an inverted triangle of no hemolysis.

Antimicrobial Susceptibility

Although antitoxin remains the only specific method of treatment of diphtheria, antibiotics are administered to patients with disease and to asymptomatic carriers of toxigenic strains. *C. diphtheriae* is usually inhibited by penicillins and the macrolides. The antimicrobial susceptibilities of other species of corynebacteria or diphtheroids are far less predictable. *C. jeikeium* is usually resistant to the penicillins and cephalosporins, is variably susceptible to most other antibiotics, and is almost uniformly susceptible to vancomycin. Other species of *Corynebacterium*, however, may be similarly resistant to β-lactam antibiotics. Treatment of infection caused by these organisms is often complicated by the presence of compromised host defenses and implanted prosthetic materials. Arcanobacteria are sensitive to penicillin and other β-lactams, rifampin, tetracycline, and the macrolides. Growth of the organisms may be inhibited by fluoroquinolones and aminoglycosides (Bernard, 2019). Methods used for performing susceptibility tests on *Corynebacterium* spp. and interpretive criteria can be found in CLSI document M45-A3 (CLSI, 2015). Susceptibility patterns of *Corynebacterium* spp. have been recently described (Neemuchwala et al., 2018).

Prevention

Methods of prevention of diphtheria are almost exclusively active and passive immunization programs with supplemental antibiotics to eliminate the carrier state of toxigenic strains during epidemics. Vaccination for diphtheria is with a modified version of the toxin (a toxoid). Thus, colonization or infection with a no-toxigenic strain of *C. diphtheriae* is still possible in vaccinated individuals.

Listeria

Characteristics

Listeria spp. are nonbranching, non–spore-forming gram-positive rods. *L. monocytogenes* (Fig. 57.8) is the only species of *Listeria* that is pathogenic for humans, and *L. ivanovii* is the only species of the other five *Listeria* spp. that is pathogenic for animals. Optimal growth of *L. monocytogenes* is observed between 30°C and 37°C; however, growth may occur as low as 4° C. Colonies are small after 24 hours and exhibit a narrow zone of β-hemolysis on blood agar. A characteristic tumbling motility of saline suspensions of the colonies occurs at room temperature but rarely at 35°C. This same temperature-dependent motility is also noted in semisolid media, in which growth appears as an umbrella shape at the top of the medium (aerobic conditions), preferentially at lower temperatures.

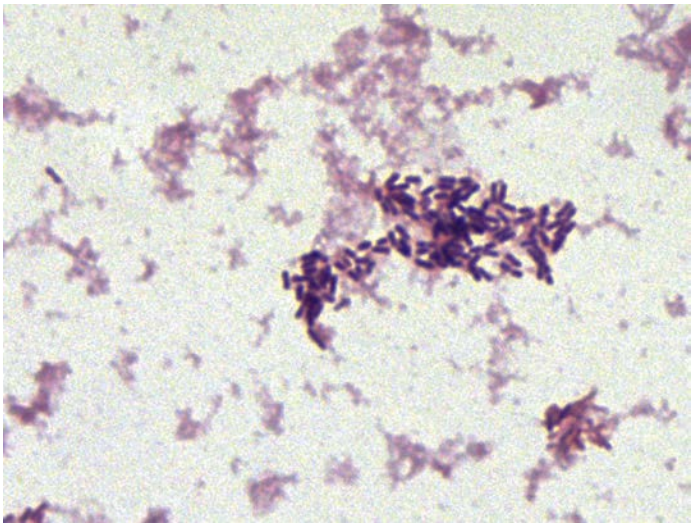

Figure 57.8 Gram stain of a cerebrospinal fluid sample that grew *Listeria monocytogenes*. The gram-positive rods are short and straight-sided (oil immersion).

Clinical Manifestations and Pathogenesis

L. monocytogenes is found in soil, dust, water, silage, sewage, and raw unpasteurized milk and in asymptomatic human and animal carriers. Transmission of the organism by foods such as coleslaw, pasteurized milk, soft cheeses, and cantaloupe has resulted in several major epidemics in North America and Europe (MacDonald et al., 2005; Cartwright et al., 2013; McCollum et al., 2013; Jackson et al., 2018). According to data from microbiological surveys of food, *L. monocytogenes* has been detected in 2% to 3% of dairy products, 20% of soft cheeses and processed meats, 30% of certain vegetables (cabbages, radishes), and up to 50% of raw meat and poultry (Wellinghausen, 2019; Simmons et al., 2014). About 1% to 10% of humans are fecal carriers.

Listeriosis is mainly a disease of industrialized countries, occurring sporadically or in epidemics. The primary mode of transmission is contaminated food products, although occasional non–food-related outbreaks have occurred in health care settings, primarily in nurseries, as the result of cross-infection. Contaminated mineral oil for bathing was implicated in one such outbreak (Schuchat et al., 1991). A meta-analysis of over 11,700 literature references pertaining to cases of listeriosis globally resulted in 23,150 illnesses and 5463 deaths in 2010. The proportion of perinatal cases was 20.7% (de Noordhout et al., 2014). The incidence rate of listeriosis in the United States was 0.27 cases per 100,000 between 2004 and 2009 and 0.29 per 100,000 from 2009 to 2011; in adults aged over 65 years, the incidence increased to 1.3 cases per 100,000 inhabitants (Hernandez-Milian & Payeras-Cifre, 2014).

Clinical manifestations of listeriosis differ among pregnant women, neonates, and immunocompromised individuals, which constitute the high-risk groups. Listeriosis during pregnancy, most common in the third trimester, presents as a flu-like illness. Bacteremia occurs concomitantly, during which time the uterine contents are infected. Progression to amnionitis may induce premature labor or septic abortion in 3 to 7 days. Infection in the mother is self-limited because the source of infection is removed with delivery of the infected fetus and placenta. Neonatal listeriosis may have an early or late onset. Early-onset disease, manifested at birth or a few days thereafter, results from in utero infection. Infants present with temperature instability, hemodynamic compromise, and respiratory distress. Widely disseminated granulomas, particularly involving the placenta, posterior pharynx, and skin, are characteristic of the illness but are not always present. Late-onset disease, affecting full-term infants of mothers with uncomplicated pregnancies, is assumed to be acquired postpartum, but in most cases the source is unknown. Clinical manifestations of meningitis become apparent several days to weeks after birth.

Nonperinatal listeriosis usually occurs in immunosuppressed individuals, but in about one-third of cases, no risk factor is identified. Tropism for *L. monocytogenes* for the central nervous system (CNS) is manifested predominantly as meningitis; other forms of CNS listeriosis include cerebritis and brainstem and spinal cord abscesses. Severe disease with high mortality rates (20% to 50%) and neurologic sequelae among survivors are common. Primary bacteremia or focal infections outside the CNS are uncommon. Primary cutaneous listeriosis has occurred occupationally in veterinarians and abattoir workers after exposure to infected animal tissues. Endocarditis,

TABLE 57.3

Differential Characteristics of *Listeria monocytogenes* and *Erysipelothrix rhusiopathiae*

Test	*L. monocytogenes*	*E. rhusiopathiae*
β-Hemolysis	+	–
Growth at 4°C	+	–
Catalase	+	–
Motility	+	–
Esculin hydrolysis	+	–
Gluconate utilization	+	–
Voges-Proskauer	+	–
H_2S in triple sugar iron agar	–	+

+, Positive; –, negative.

osteomyelitis, arthritis, endophthalmitis, and other focal infections have been reported rarely. Febrile gastrointestinal disease due to *L. monocytogenes* has been reported in nonimmunocompromised patients; implicated foods include chocolate milk, rice salad, and delicatessen meats and cheeses (Wellinghausen, 2019; Hernandez-Milian & Payeras-Cifre, 2014). Immunocompromised patients, such as those with leukemias or bone marrow transplants and patients on immunosuppressive therapies, are cautioned against eating uncooked deli meats to decrease the risk of infection with this organism.

The pathogenesis of listeriosis has been well elaborated in recent years. Host susceptibility, gastric acidity, inoculum size, and virulence properties of the organism, along with specific food products, are the most common factors that determine progression from infection to disease and the severity of that disease in the infected individual. *L. monocytogenes* can penetrate the epithelial cells of the gastrointestinal tract and grow within hepatic and splenic macrophages. From there, the organism can spread to the CNS or the pregnant uterus. Virulence factors—such as internalin and E-cadherin, a placental receptor—interact to result in infection in the pregnant female/fetus. Immunity to listeriosis relies on T cell–mediated activation of macrophages by lymphokines (Wellinghausen, 2019; Hernandez-Milian & Payeras-Cifre, 2014).

Laboratory Diagnosis

Colonies are small and grayish-blue, growing in 24 to 48 hours, and are surrounded by a narrow zone of β-hemolysis on blood agar. A positive catalase reaction differentiates *L. monocytogenes* from similarly appearing group B streptococci. Organisms are motile at room temperature and produce acid from glucose, trehalose, and salicin, and hydrolyze esculin. Other biochemical characteristics of *L. monocytogenes* and differences between *Listeria* and *Erysipelothrix* are listed in Table 57.3. Successful use of MALDI-TOF for the identification of *L. monocytogenes* has been reported (Farfour et al., 2012).

Antimicrobial Susceptibility

L. monocytogenes is usually susceptible to penicillin, ampicillin, erythromycin, chloramphenicol, tetracycline, and gentamicin. Isolates usually are only moderately susceptible to the quinolones. Cephalosporins are ineffective against *Listeria* spp.; isolates should not be tested against cephalosporins because they are ineffective in vivo regardless of the in vitro result. Methods of performing susceptibility tests for *Listeria* and interpretive criteria can be found in CLSI document M45-A3 (CLSI, 2015). Resistance to chloramphenicol, macrolides, and tetracyclines has been found in several clinical isolates (Wellinghausen, 2019; Hernandez-Milian & Payeras-Cifre, 2014). Ampicillin, alone or in combination with an aminoglycoside, has been used successfully in the treatment of infections caused by *L. monocytogenes*. Trimethoprim-sulfamethoxazole (TMP-SMX) may be used as alternative therapy in penicillin-allergic patients. Newer gram-positive antibiotics—such as daptomycin, linezolid, and tigecycline—appear susceptible in vitro, but limited clinical data document their in vivo effectiveness.

Erysipelothrix

Characteristics

Erysipelothrix rhusiopathiae is a catalase-negative, non–spore-forming, nonmotile, facultatively anaerobic gram-positive bacillus that has a worldwide distribution. Microscopically, they appear as short rods with rounded ends, occurring singly, in short chains, or in nonbranching filaments. *E. rhusiopathiae* is a recognized pathogen in humans, occasionally causing erysipeloid, a localized cutaneous infection of hands and fingers obtained after exposure to animals or animal products (Wellinghausen, 2019).

Clinical Manifestations and Pathogenesis

E. rhusiopathiae is usually transmitted to humans from animals by means of skin wounds produced by contaminated objects or in contact with blood, flesh, viscera, or feces of infected animals. *E. rhusiopathiae* is widespread in nature in wild and domestic animals, birds, fish, and decaying organic matter and causes infection in swine, sheep, rabbits, cattle, birds, and fowl. At risk of infection with this organism are butchers, abattoir workers, fishermen, fish handlers, poultry processors, and veterinarians. The most common form of erysipeloid is a local cutaneous infection manifested by pain, swelling, and a cutaneous eruption characterized by a slowly progressive, slightly elevated, violaceous zone around the site of inoculation. The swelling and erythema migrate peripherally, and the lesion involutes without desquamation. Systemic disease is rare, but numerous case reports describe septicemia and endocarditis. Also rarely reported have been cases of arthritis and brain abscess. Virulence factors include a hyaluronidase, a neuraminidase, and a heat-labile capsule (Wang et al., 2010).

Laboratory Diagnosis

Biopsy and tissue aspirates from erysipeloid lesions are the best specimens for culture. The organisms are located deep in the subcutaneous layer of the leading edge of the lesion; therefore, swabs of the surface of the skin are not useful. The organism will grow on blood or chocolate agar, but may require up to 7 days for growth. Conventional blood culture media are suitable for its isolation from blood.

E. rhusiopathiae is oxidase and catalase negative. It is considered nonhemolytic, although greenish discoloration of the media beneath the colonies is often observed after 2 days of incubation. Characteristically, it produces hydrogen sulfide (H_2S) in triple-sugar iron agar (TSIA) and ferments glucose and lactose. It is nonmotile, does not reduce nitrates to nitrites, and is negative for urease, gelatin, and esculin hydrolysis. A trait highly characteristic of *E. rhusiopathiae* is the "pipe cleaner" pattern of growth in gelatin stab cultures incubated at 22°C. This organism can be readily distinguished from *L. monocytogenes*, *Lactobacillus*, and *Bacillus* species by MALDI-TOF and biochemical characteristics (see Table 57.3) (Principe et al., 2016).

Antimicrobial Susceptibility

Erysipelothrix is susceptible to the penicillins, the cephalosporins, imipenem, erythromycin, clindamycin, chloramphenicol, the tetracyclines, and the fluoroquinolones but is resistant to sulfonamides, aminoglycosides, and vancomycin. Penicillin is the treatment of choice for localized and systemic infection (Wellinghausen, 2019). Methods used for performing susceptibility tests for *E. rhusiopathiae* and interpretive criteria can be found in CLSI document M45-A3 (CLSI, 2015).

Prevention

Prevention of human disease is recommended by control of animal disease through sound husbandry, herd management, good sanitation, and immunization procedures (Wang et al., 2010).

Bacillus

Characteristics

Members of this genus are strictly aerobic or facultatively anaerobic, rod-shaped, spore-forming, gram-positive, and catalase-positive organisms. Figure 57.9 shows a Gram stain of a *Bacillus* sp. seen in pleural fluid. With the notable exception of *B. anthracis*, they are usually motile by means of lateral or peritrichous flagella. They can easily over-decolorize, resulting in gram-variable rods and, because of their variable oxidase reactions, can be confused with gram-negative bacilli. The most reliable diagnostic characteristic of the genus is spore formation, which occurs optimally and on a variety of media under aerobic conditions at 25°C to 30°C. In gram-stained smears, endospores are detectable by the presence of unstained defects or holes within the cell.

Clinical Manifestations and Pathogenesis

Of the numerous species of *Bacillus*, *B. anthracis* is the only one that is uniformly and highly pathogenic. Great care must be exercised when handling material suspected of harboring this species. Work should be performed in biological safety cabinets by gloved, gowned, masked, and immunized personnel; work surfaces must be disinfected with 5% hypochlorite or 5% phenol; and all supplies, materials, and equipment must be decontaminated. Because *B. anthracis* spores have been used as a means of bioterrorism, cultures containing suspected *B. anthracis* should be handled only by reference or public health laboratories.

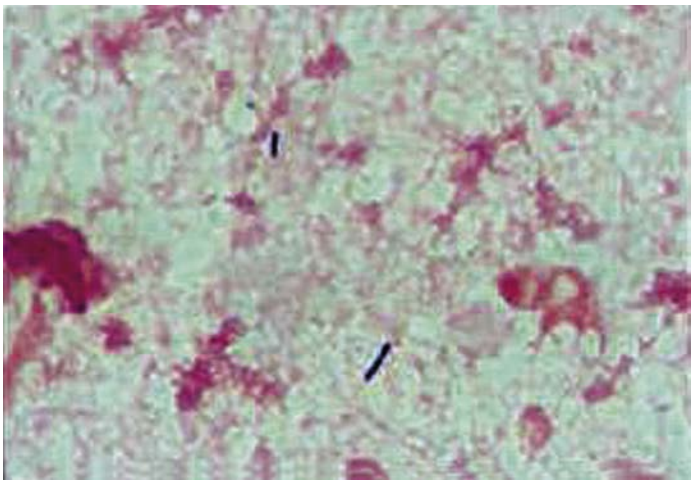

Figure 57.9 Gram stain of *Bacillus cereus* in pleural fluid (oil immersion).

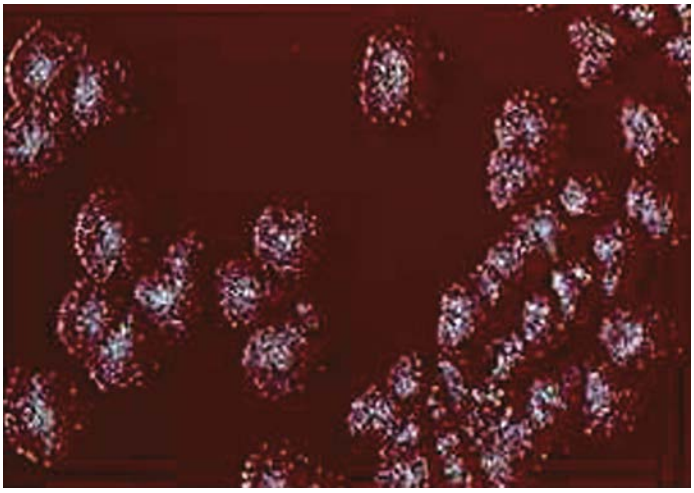

Figure 57.10 Colonies of *Bacillus anthracis* on blood agar. Note the irregular edges of the colonies.

Three forms of anthrax are recognized: cutaneous, inhalation, and intestinal. In its cutaneous form, anthrax produces a small, red, macular lesion that progresses to a vesicle and finally to necrosis, with formation of a characteristic black eschar. Regional lymphadenopathy and septicemia may occur. Mortality in untreated cases with this form of disease is approximately 20%. Inhalation of anthrax spores can lead to acute bronchopneumonia, mediastinitis, and septicemia ("woolsorter's disease"). The mortality in recognized cases of this form of disease is nearly 100%. Intestinal anthrax follows the ingestion of contaminated food and is manifested by nausea, vomiting, and diarrhea. In some cases, gastrointestinal bleeding is followed by prostration, shock, and death. Septicemia can occur in all three forms of anthrax and may lead to a fatal, purulent meningitis. More recently, a fourth type of anthrax, injectional anthrax, has been recognized in heroin addicts, resulting in severe soft-tissue infections with an increased risk of shock and higher level of mortality than is associated with cutaneous infections (Sweeney et al., 2011).

A major factor in the organism's pathogenic capabilities is its glutamyl polypeptide capsule, which inhibits phagocytosis; anticapsular antibodies do not protect against the disease. A complex toxin with three components (edema factor, protective antigen, and lethal factor) is responsible for the signs and symptoms of anthrax. The cell wall peptidoglycan is believed to produce a robust intravascular inflammatory response that can lead to hemodynamic and organ dysfunction, resulting in shock (Turenne et al., 2019; Sweeney et al., 2011).

Humans become infected with anthrax by contact with and inhalation or ingestion of infected animals, their carcasses, or their by-products. Cattle, sheep, horses, and goats are the animals most frequently infected and provide a ready source of vegetative organisms that sporulate and perpetuate the environmental contamination.

Although usually saprophytic, other species of *Bacillus* can cause disease. *B. cereus* has been associated with ear infection, pneumonia, posttraumatic ocular wound infection, septicemia, endocarditis, and meningitis. Patients with pneumonia and septicemia are often immunosuppressed. Bacteremia is frequently associated with intravenous drug use and with contaminated intravascular devices (Stevens et al., 2012).

Two forms of gastroenteritis are associated with *Bacillus* species. Food poisoning caused by *Bacillus* may occur within 1 to 6 hours following ingestion of food contaminated by *B. cereus* that has produced a preformed heat-stable toxin. Major manifestations of *Bacillus* food poisoning include nausea, vomiting, cramps, and occasionally diarrhea, but no fever. Typically, this form of *Bacillus* gastroenteritis results from the bulk preparation of foods that are not reheated before they are served. *B. cereus* type 1 grows particularly well in fried rice and is more heat resistant than other types; thus, this form of gastroenteritis is frequently seen in association with consumption of cooked rice in Chinese restaurants. The second form of gastroenteritis caused by *Bacillus* spp. results from contamination of poultry and vegetable dishes and is characterized by the onset of cramps and diarrhea 8 to 16 hours following ingestion of contaminated food. In this instance, the major manifestations of *B. cereus* infection are caused by the production of a heat-labile enterotoxin. From 1998 to 2008, 1229 foodborne outbreaks caused by *B. cereus* (rice dishes were implicated in 50% of the cases), *Clostridium perfringens*, and *S. aureus* were reported in the United States. In 2008, there were 17 to 18 suspected outbreaks of gastroenteritis associated with *B. cereus* as compared to over 40 outbreaks due to *S. aureus* and 10 or 11 outbreaks due to *C. perfringens* (Bennett et al., 2013).

The genus *Bacillus* contains more than 300 species; other than *B. anthracis* and *B. cereus*, common species include *B. subtilis*, *B. licheniformis*, *B. megaterium*, *B. pumilus*, and *B. thuringiensis*. Many species have been renamed, however, and more than 100 new genera of gram-positive spore-producing aerobic bacilli have been named. One of those genera, *Paenibacillus*, contains species that have been associated with clinical disease, including meningitis and endophthalmitis. Species of *Paenibacillus* have been implicated in infections associated with penetrating injuries and contaminated medical devices (Anikpeh et al., 2010; Turenne et al., 2019; Celandroni et al., 2016). *P. macerans* has been found in contaminated blood culture bottles in a neonatal intensive care unit, and *P. pasadenensis* has been isolated in spacecraft facilities and also as a cause of mediastinitis following heart surgery (Noskin et al., 2001; Anikpeh et al., 2010).

Laboratory Diagnosis

In cases of suspected cutaneous anthrax, vesicle fluid and material under the edge of the eschar should be collected with a swab for smear and culture. For suspected inhalation anthrax, sputum should be collected for smear and culture. Oropharyngeal and rectal swab cultures should be considered in the intestinal form. Smears and cultures of CSF should be requested in suspected meningitis. In the septicemic stage, blood cultures should be performed. Finding large, boxcar-shaped gram-positive cells in smears of any of these specimens should raise suspicion for the diagnosis.

Species of *Bacillus* grow well on sheep blood agar. Colonies of *B. anthracis* are usually flat, with an irregular margin ("Medusa head"), appear off-white with a ground-glass surface, and are usually nonhemolytic. Figure 57.10 demonstrates the colonial morphology of *B. anthracis* on blood agar. When touched with an inoculating loop, the colonies are tenacious and will stand up like a beaten egg white. The Medusa head colony may be seen with *B. cereus* and certain other *Bacillus* species. Anthrax bacilli are nonmotile in a hanging drop test or in semisolid media, whereas most other species of *Bacillus* are motile. Motility by the hanging drop method is a useful differential test between *B. anthracis* and *B. cereus* but must be carried out with a fresh broth culture of the organism. As mentioned earlier, because of the use of *B. anthracis* in terrorist attacks, sentinel laboratories (level A) should send any suspicious isolates of this organism to their public health laboratory or the CDC. A commercial system has been evaluated recently for identification of aerobic endospore-formers; 93% of the strains were correctly identified to species level in the genera *Bacillus*, *Paenibacillus*, *Aneurinibacillus*, *Brevibacillus*, *Geobacillus*, and *Virgibacillus* (Halket et al., 2010). *Bacillus* spp. other than *anthracis* have been correctly identified using MALDI-TOF (Farfour et al., 2012).

The diagnosis of *B. cereus* gastroenteritis cannot be accurately made by culture of stool because the organisms may be a component of the indigenous gut flora. Diagnosis, therefore, depends on quantitative culture of the suspected contaminated food. The presence of greater than or equal to 10^5 CFUs/g in the suspected food constitutes presumptive evidence of *B. cereus* food poisoning (Logan, 2011). This testing is usually not performed in a routine clinical microbiology laboratory.

Antimicrobial Susceptibility

Although susceptible to a variety of agents, antibiotic therapy of anthrax has centered on the use of fluoroquinolones. These agents are highly active

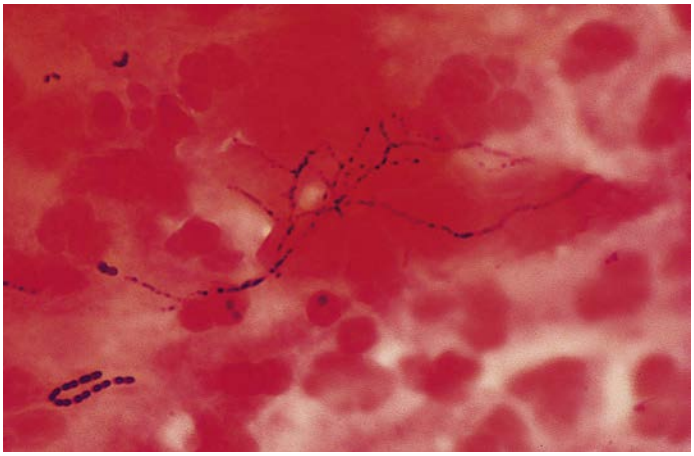

Figure 57.11 Sputum smear stained with Gram stain shows neutrophils, amorphous debris, and filamentous, beaded, branched gram-positive bacilli (oil immersion).

against *B. anthracis*, strains of which are typically susceptible to β-lactam antibiotics. However, many strains of *Bacillus* spp. elaborate β-lactamases in nature; thus, these agents usually are not considered as first-line drugs of choice until the specific susceptibility of the isolate is known. Most strains of *Bacillus* spp. are inhibited by fluoroquinolones, tetracyclines, aminoglycosides, and chloramphenicol at low concentrations (Turenne et al., 2019) and most are susceptible to vancomycin, but reports have described vancomycin resistance in *B. circulans* and *P. thiaminolyticus*. *Bacillus* strains have been demonstrated to carry genes similar to the *vanA* gene of the enterococci (Patel et al., 2000). Methods of performing susceptibility tests and of interpreting their results can be found in the third edition of the CLSI document M45 (CLSI, 2015).

Prevention

Prevention of anthrax in humans ideally depends on its control in animals. Prompt diagnosis of sick animals, their isolation and therapy, and cremation of carcasses are indicated when sporadic outbreaks occur. In enzootic areas, vaccination with nonencapsulated spore preparations is used. Occupationally exposed persons should also be immunized. Acute diarrheal disease caused by *B. cereus* may be prevented by proper cooking and refrigeration of foods prepared in bulk to prevent proliferation of vegetative forms of the bacteria and formation of the enterotoxin.

Nocardia

Characteristics

In gram-stained smears of clinical specimens, *Nocardia* spp. appear as long, thin, beaded, branching gram-positive bacilli (Fig. 57.11). The most distinguishing quality of the nocardiae is their partial acid fastness; cells stain positively with a modified acid-fast (Ziehl-Neelsen or Kinyoun) stain, differentiating them from *Actinomyces*, which may have a similar gram-stain appearance. Partial acid fastness may be difficult to demonstrate and can be enhanced by growing the organism for about 4 days on Middlebrook 7H10 agar or in litmus milk broth. Most clinical infections have been caused by *N. abscessus*, *N. brasiliensis*, *N. cyriageorgica*, *N. farcinica*, *N. nova*, *N. pseudobrasiliensis*, *N. veterana*, and *N. wallacei* (Cloud et al., 2004; Conville et al., 2019).

Clinical Manifestations and Pathogenesis

Nocardiae are found in soil and organic material worldwide, causing disease in many animals and in fish. It is usually acquired via inhalation of the organism but may occur following trauma and contact with contaminated soil, or the organism may enter the body via the gastrointestinal tract when contaminated material contacts an area of mucosal ulceration.

In the lungs, *Nocardia* spp. are phagocytosed by alveolar macrophages and grow intracellularly, eliciting a mixed inflammatory response (neutrophils, lymphocytes, and macrophages), eventually resulting in abscess or, occasionally, granuloma formation. In vitro studies of the host defenses against *Nocardia* spp. suggest that neutrophils, activated macrophages, and cytotoxic T cells are involved. Although neutrophils do not kill virulent *Nocardia* spp., they inhibit their growth, possibly suppressing the infection until macrophages are fully activated. If the infection is not contained within the lung, organisms spread to other tissues by advancing growth, thus producing empyema, chest wall involvement, and draining sinuses, or by hematogenous dissemination, resulting in abscess formation, especially in the brain, subcutaneous tissues, and kidneys. The primary host factor associated with increased risk of nocardiosis is cellular immune dysfunction, although many persons infected with *Nocardia* spp. have no recognized cellular or humoral immune defect (Budzik et al., 2012; Wilson, 2012).

Pulmonary disease, the most frequent manifestation of nocardiosis, is characterized by fever, anorexia, weight loss, cough, dyspnea, and pleuritic chest pain. Skin and subcutaneous disease may present as pyoderma, cellulitis, single or multiple abscesses, lymphocutaneous disease resembling sporotrichosis, or nodules. In Central and South America, primary infections of the skin with *N. brasiliensis* may produce an actinomycetoma (a localized indurated granulomatous mass with sinus tracts draining pus and "sulfur" granules), typically on the lower extremities. Disseminated disease is usually caused by members of the *N. asteroides* complex. It originates in the lung in most cases and typically is manifested as single or multiple abscesses involving the CNS (Anagnostou et al., 2014). The skin is the second most common site of dissemination, followed by kidney, liver, and lymph nodes (Conville & Witebsky, 2011).

Laboratory Diagnosis

Nocardia spp. grow aerobically on most nonselective media, such as sheep blood and chocolate agars, potato dextrose agar, Sabouraud dextrose agar, and Löwenstein-Jensen or Middlebrook media and in 7H9 broth used for mycobacterial culture. These organisms will grow on buffered charcoal-yeast extract (BCYE) agar used for the isolation of *Legionella* spp. as well. It is important to note that *Nocardia* spp. may not always survive the decontamination procedures used for recovery of mycobacteria. Incubation in the presence of 10% CO_2 enhances growth. *Nocardia* spp. may grow in 48 hours, but colonies typically appear in 5 to 10 days as waxy, bumpy, or velvety rugose forms, often with yellow to orange pigment, depending on the species. Observing branching filaments that stain only with a modified acid-fast stain distinguishes *Nocardia* spp. from mycobacteria. *Nocardia* spp. are differentiated from most other aerobic actinomycetes by testing resistant to the action of lysozyme (*Nocardia* spp. are resistant; *Streptomyces* spp., *Rhodococcus* spp., *Gordona* spp., and *Actinomadura* spp. are susceptible) and examining their morphology on tap water agar. For example, the latter can help in differentiating the branching *Nocardia* from nonbranching *Rhodococcus* spp. Because many new species of *Nocardia* have been recognized over the past several years, the use of biochemical tests (e.g., casein, hypoxanthine, tyrosine, xanthine) is not sufficient for identification. Molecular tests (e.g., 16S rDNA sequencing, PCR-restriction enzyme pattern analysis [PRA]) of MALDI-TOF (Farfour et al., 2012) are required for accurate species identification (Cloud et al., 2004; Patel et al., 2004). Identification to the species level is important because of the variability in antibiotic susceptibility patterns noted among species (Brown-Elliott et al., 2006; Schlaberg et al., 2014).

Antimicrobial Susceptibility

Sulfonamides (alone or in combination with trimethoprim—e.g., TMP-SMX) are usually the antimicrobial agents of choice. However, optimal antimicrobial therapy depends on the species of *Nocardia* present, the susceptibility pattern of the individual strain, and the type of infection. Other potential antimicrobial agents include amikacin, clarithromycin, imipenem, or a quinolone, depending on the species isolated. The CLSI has information about methods used for susceptibility testing and interpretation of results for *Nocardia* and other aerobic actinomycetes (CLSI, 2018).

Other Aerobic Actinomycetes

Other genera of actinomycetes that are medically relevant to humans include *Rhodococcus*, *Gordonia*, *Tsukamurella*, *Actinomadura*, and *Streptomyces*. One other member, *Tropheryma whippelei*, is nonculturable and is the causative agent of Whipple disease.

Clinical Manifestations and Pathogenesis

Members of this group of organisms are ubiquitous in the environment and have been isolated from soil, fresh water, marine water, and organic matter. *R. equi* is the most common *Rhodococcus* sp. pathogenic to humans. It is an opportunistic pathogen in severely immunocompromised hosts, causing a slowly progressive granulomatous pneumonia. It may be isolated from the blood of infected patients. The organism is likely acquired via the respiratory route, possibly as a result of exposure to infected animals. The organism's ability to persist in and ultimately destroy macrophages probably accounts for its ability to cause disease (Weinstock & Brown, 2002). Infections caused by *Gordonia* spp. and *Tsukamurella* spp. are increasingly being reported (Savini et al., 2012; Ramanan et al., 2013). *Tsukamurella*

spp. appear to be pathogenic only when certain clinical conditions are present (e.g., immunosuppression, presence of foreign body, active chronic infection, such as tuberculosis) (Woo et al., 2003). *Actinomadura* spp. are a frequent cause of actinomycotic mycetomas, a chronic infection of skin and subcutaneous soft tissues. Most of these infections are seen in tropical and subtropical countries, where walking barefoot increases the chance of exposure through repeated puncture wounds. *Streptomyces* spp. have traditionally been considered of little medical significance; however, one species, *S. somaliensis*, has been identified as an etiologic agent of actinomycotic mycetoma. Other *Streptomyces* spp. have only occasionally been reported to be of medical importance (Mossad et al., 1995).

Laboratory Diagnosis

Aerobic actinomycetes are slow growing and may require 2 to 3 weeks of incubation. These microorganisms grow on most of the nonselective media used to isolate bacteria, mycobacteria, and fungi. Species of *Rhodococcus* grow as coccobacilli in a zigzag fashion. Rudimentary branched filaments have been observed from liquid media. Colonies may be rough, smooth, or mucoid and have pigments ranging from buff to coral to orange to deep rose after several days of incubation. *R. equi* is usually pale pink, pale yellow, or coral and may appear slimy. *Gordonia* spp. range from smooth, mucoid colonies that are adherent to the media to dry, raised colonies. The pigment produced may be beige to salmon colored. *Tsukamurella* spp. are slightly acid fast by the modified Kinyoun. They appear as long rods that fragment into three parts. No aerial hyphae are produced. The colonies are circular, with entire or rhizoid edges. They may be dry or creamy, with a white to orange pigment. Rough colonies may be produced after 7 days of incubation. Species of *Actinomadura* form waxy, cerebriform, tough, membranous white, yellow, pink, or red colonies. Colonies of *Streptomyces* are dry to chalky, heaped or folded, gray-white to yellow, and have the odor of a musty basement. A wide variety of pigments are produced that color the substrate and hyphae. Some species do not produce aerial hyphae. As with the *Nocardia* spp., complete identification of these members of the aerobic actinomycetes often requires molecular sequencing methods or MALDI-TOF (Conville et al., 2019; Buckwalter 2016).

GRAM-NEGATIVE BACTERIA—COCCI

Neisseria

Characteristics

This genus is composed of species that are nonmotile and catalase and oxidase positive. These aerobic, gram-negative cocci are often arranged in pairs, with flattened adjacent surfaces, giving the appearance of kidney beans or coffee beans (Fig. 57.12). The organisms are somewhat fastidious, in some instances requiring the addition of blood, serum, cholesterol, or oleic acid to the medium to counteract growth inhibitors, such as fatty acids. *N. gonorrhoeae* and *N. meningitidis* generally require prompt incubation in CO_2 for growth. However, this is strain dependent, varies with the phase of the organism's growth curve, and is often lost in subcultures. *N. meningitidis* and most *N. gonorrhoeae* are not inhibited by the presence of vancomycin or lincomycin, colistin, and nystatin—a characteristic that is particularly useful in their selective isolation from specimens contaminated by other bacteria (Elias et al., 2019).

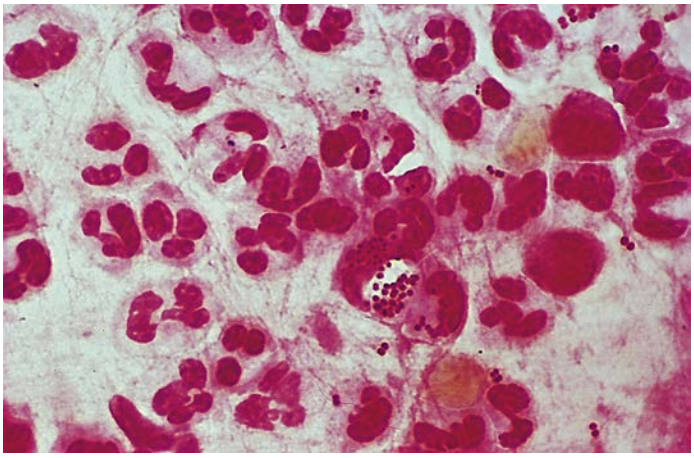

Figure 57.12 Sputum smear stained with Gram stain shows many neutrophils and intracellular gram-negative diplococci, suggestive of *Neisseria meningitidis* infection (oil immersion).

Clinical Manifestations and Pathogenesis

Although opportunistic infections caused by species of *Neisseria* other than *N. gonorrhoeae* and *N. meningitidis* have occasionally been reported in compromised hosts, these species are generally nonpathogenic. *N. meningitidis* may colonize the mucous membranes of the upper respiratory tract—an event that is usually followed in 7 to 10 days by the formation of bactericidal and hemagglutinating antibodies, which may not eliminate the carrier stage but convey group-specific immunity. In a few cases, disease results shortly after colonization, most frequently in the form of meningococcemia and meningitis. The organism also has a tendency to invade serous membranes and joint tissues, with the development of pleuritis, pericarditis, and arthritis. Carriage of *N. meningitidis* in the nasopharynx occurs in 5% to 15% of healthy individuals; this rate may be higher in confined groups such as military recruits. A direct correlation between carrier rates and incidence of disease has not been established, with the possible exception of members of large households or households with an infant or childhood case during epidemics of disease. *N. meningitidis* has also been isolated from genital sources, where its clinical significance is uncertain. When cultured from these sources, bacteria may be misidentified as *N. gonorrhoeae* unless appropriate tests for distinguishing these species are performed.

N. gonorrhoeae is always considered a pathogen, even in the absence of obvious clinical symptoms. In the United States, an estimated 820,000 new *N. gonorrhoeae* infections occur each year, and gonorrhea is the second most commonly reported communicable disease (MMWR, 2015). Urethral infections caused by *N. gonorrhoeae* among men produce symptoms that cause them to seek curative treatment soon enough to prevent sequelae but often not soon enough to prevent transmission. In male patients, local complications of urethral gonorrhea include epididymitis, penile edema, and abscesses of the urethral and/or bulbo-urethral glands.

In females, *N. gonorrhoeae* causes infection of the endocervix. Infections of the urethra, rectum, and the Bartholin and Skene glands can also occur. Asymptomatic infections due to *N. gonorrhoeae* are more common in female patients. Typical symptoms of *N. gonorrhoeae* infection in women include increased vaginal discharge, dysuria, and intermenstrual bleeding. Complications of untreated infection include ascension of the infection, potentially resulting in pelvic inflammatory disease (PID), including salpingitis, tubo-ovarian abscesses, endometritis, and peritonitis. PID can result in tubal scarring that can lead to infertility or ectopic pregnancy. Up to 80% of infected women are asymptomatic and, therefore, untreated. The lack of therapy may allow dissemination of the infection, manifesting as skin lesions and/or arthritis. Disseminated gonococcal infection (DGI) is relatively uncommon (0.5%–3.0%) but should be considered when infective arthritis occurs in young people. Two clinical presentations of DGI are typical: an early-stage polyarthritis/dermatitis and a later-stage septic arthritis. The dermatologic manifestations include hemorrhagic pustules and papules; hemorrhagic bullae or necrotic lesions can be seen. Polyarthritis of the knees and elbows is typical.

The principal virulence factor of *N. meningitidis* is a lipopolysaccharide–endotoxin complex. In experimental animals, it activates the clotting cascade, depositing fibrin in small vessels, producing hemorrhage in the adrenals and other organs, altering peripheral vascular resistance, which leads to shock and death. This can initially present as petechial lesions, which can coalesce and become ecchymotic. The pathogenesis and clinical manifestations of *N. gonorrhoeae* infections differ somewhat from those of *N. meningitidis*. Pathogenic types of *N. gonorrhoeae* adhere by means of pili, which are not produced by nonpathogenic types, to various human cells. These antigenically heterogeneous pili, which represent one of the principal virulence factors of *N. gonorrhoeae*, may inhibit phagocytosis and stimulate strain-specific antibody formation. Other possible virulence factors of *N. gonorrhoeae* are less clearly defined. Both *N. gonorrhoeae* and *N. meningitidis* produce an IgA protease, which may be important in their pathogenesis because IgA is the antibody class that predominates in secretions on mucous membranes (Elias et al., 2019).

Laboratory Diagnosis

The single most important element in the laboratory diagnosis of infection caused by *N. meningitidis* or *N. gonorrhoeae* is the specimen, including proper selection, collection, and transport to the laboratory. The pathogenic species are sensitive to drying and extremes of temperature, and material must be cultured promptly to enhance recovery. They are mesophilic and grow poorly, if at all, at room temperature. Many require prompt incubation in CO_2 (2%–8%) for primary isolation.

Chocolate media are commonly used for cultures of *N. gonorrhoeae* and should contain antibiotics (i.e., vancomycin or lincomycin, as well as colistin, nystatin or anisomycin, and trimethoprim) if the specimen is prone to be contaminated by normal flora. Vancomycin-susceptible gonococci will

grow on media containing lincomycin. However, because of the synergistic interaction of lincomycin and trimethoprim, the latter must be omitted from media containing lincomycin. Direct inoculation of specimens at the bedside followed by prompt incubation at 35°C in CO_2 is optimal. This can be accomplished in several ways: placing the medium into a candle jar; placing the medium in a sealed bag containing a citric acid bicarbonate tablet; or using a medium contained within a bottle having a CO_2 atmosphere. If any of these culture systems must be mailed to a reference laboratory for processing, they must first be incubated overnight to ensure growth of the organisms.

An isolate from a urogenital specimen showing the appropriate colony appearance on a selective medium presumptively may be called *N. gonorrhoeae* based on results of Gram stain and oxidase and catalase tests. Gram-stained smears prepared from colonies of *N. gonorrhoeae* should show typical gram-negative diplococci, but organisms may occur in tetrads, especially from young cultures. All species of *Neisseria* are oxidase positive, and all species except *N. elongata* are catalase positive. Because *Neisseria* other than *N. gonorrhoeae* may be recovered from urogenital sites, confirmatory testing is strongly recommended and is required for all isolates from extragenital sites and when sexual abuse is suspected (preferably by more than one method).

Confirmation of *N. gonorrhoeae* and identification of the other *Neisseria* spp. are based on growth and biochemical characteristics (Table 57.4) (Elias et al., 2019). The standard method of identification consists of detection of acid production from carbohydrates in a cystine trypticase acid (CTA) base medium and other conventional biochemical tests. However, given the drawbacks of conventional methods, more rapid identification tests are used in most clinical laboratories. Tests for direct detection of *N. gonorrhoeae* and *N. meningitidis* in clinical specimens are also available. Typing of isolates of *N. gonorrhoeae* and *N. meningitidis* is done primarily for epidemiologic studies.

With the standard method of identification, acid production from glucose, maltose, lactose, sucrose, and fructose in a CTA base medium and a carbohydrate-free control are tested. Tubes are inoculated, incubated at 35°C to 37°C in ambient air, and examined at 24-hour intervals until reactions are interpretable, or for 72 hours. Expected results for the species of *Neisseria* are shown in Table 57.4. Occasionally, however, an isolate of *N. meningitidis* yields aberrant carbohydrate reactions: glucose-negative, maltose-negative, or asaccharolytic. If *N. meningitidis* is strongly suspected in these cases, identification can be confirmed by slide agglutination using pooled polyvalent grouping antisera or sera specific for individual serogroups. In addition to conventional carbohydrate degradation tests, reduction of nitrates and nitrites and production of DNase should be evaluated. The latter is especially useful for identification of *Moraxella catarrhalis*, which is DNase positive (*Neisseria* spp. are DNase negative). Drawbacks to conventional tests are the requirement for a heavy inoculum, the need to work with pure cultures, long turnaround time, and failure of some fastidious strains of *N. gonorrhoeae* to grow.

Several commercial systems detect acid production from carbohydrates, usually in 1 to 4 hours (Elias et al., 2019). The inoculum must be prepared from a pure culture of the isolate; thus, identification is generally available 24 hours after isolation. Acid reactions of some *N. gonorrhoeae* and, to a lesser extent, *N. meningitidis* may be difficult to interpret or may be aberrant with some kits, and strains of *N. gonorrhoeae* that are weak producers of acid from glucose may appear to be glucose negative. Some strains of *N. cinerea*, which does not typically produce acid from glucose, can appear glucose positive in certain systems.

Enzyme substrate tests provide rapid identification (1–4 hours) only of isolates of oxidase-positive, gram-negative diplococci recovered on a selective medium (Elias et al., 2019). They are valuable for differentiating maltose-negative strains of *N. meningitidis* from *N. gonorrhoeae*. However, color changes may be subtle and if misinterpreted could cause isolates of *N. meningitidis* and other *Neisseria* spp. to be incorrectly called *N. gonorrhoeae*. Moreover, strains of *N. cinerea* and *Kingella denitrificans* that grow on gonococcus-selective media could be misidentified as *N. gonorrhoeae* if not confirmed by other procedures. Commercial products that combine enzyme substrate tests with modified conventional tests provide accurate identification of species of *Neisseria* and *Haemophilus*. Immunologic tests for *N. gonorrhoeae*—in particular, coagglutination—can be used to confirm the biochemical identification of *N. gonorrhoeae*. Both false-positive and false-negative results have been reported with these reagents. MALDI-TOF is able to identify both *N. meningitidis* and *N. gonorrhoeae*.

Culture detection of *N. gonorrhoeae* from urogenital sites has been largely replaced by NAAT. Many NAATs are available that simultaneously detect *N. gonorrhoeae* and *Chlamydia trachomatis* in vaginal, cervical, urethral, and urine samples with greater sensitivity than culture, and for which loss of viability of *N. gonorrhoeae* in particular is an issue. These tests are recommended by the CDC as the preferred test in symptomatic and asymptomatic individuals, although there are also recommendations that culture be available for both *N. gonorrhoeae* and *C. trachomatis* at least in some laboratories in situations of potential antimicrobial resistance and in some sexual assault situations (MMWR, 2015). These molecular techniques are described in other sections of this text.

Antimicrobial Susceptibility

Despite the occasional recovery of *N. meningitidis* strains with decreased susceptibility to penicillin, penicillin G remains the drug of choice for treatment of meningococcal meningitis (Elias et al., 2019). Decreased susceptibility of *N. meningitidis* to penicillin is thought to be due to decreased binding of penicillin by altered meningococcal cell wall penicillin-binding proteins PBP-2 and PBP-3. Other species of *Neisseria* have also demonstrated this lowered affinity to penicillin. Other agents that have good activity against *N. meningitidis* include the extended-spectrum cephalosporins and chloramphenicol. Rifampin and ciprofloxacin may be used for prophylaxis among household contacts. Standardized methods of susceptibility testing and breakpoints in the CLSI documents are available (CLSI, 2019). The CLSI recommends broth microdilution or agar dilution with cation-supplemented Mueller-Hinton Broth (with 2%–5% laked horse blood) or Mueller-Hinton agar (with 5% [vol/vol] sheep blood) if testing is done. In laboratories where susceptibility testing for *N. meningitidis* is not

TABLE 57.4
Differentiation of Species of *Neisseria* and *Moraxella catarrhalis*

	N. gonorrhoeae	*N. meningitidis*	*N. cinerea*	*N. lactamica*	*M. catarrhalis*
Growth					
Thayer-Martin medium	+*	+	–	+	†
Nutrient agar, 25°C	–	–	–	–	+
Oxidase	+	+	+	+	+
β-Galactosidase	–	–	–	+	–
Reduction of nitrate	–	–	–	–	+
DNase	–	–	–	–	+
Production of Acid from					
Glucose	+	+	–‡	+	–
Maltose	–	+	–	+	–
Lactose	–	–	–	+	–
Sucrose	–	–	–	–	–
Fructose	–	–	–	–	–

+, ≥90% of strains positive; –, ≥90% of strains negative; *DNase,* deoxyribonuclease.
*Most vancomycin-susceptible strains will not grow on Thayer-Martin medium.
†Some strains positive and others negative.
‡Weak reaction may occur in rapid carbohydrate utilization tests.

available, β-lactamase testing can be performed by using the chromogenic cephalosporin test, the cefinase nitrocefin disk test, if lowered susceptibility or clinical failure on penicillin is suspected. If positive, isolates can be shipped to a reference laboratory for further testing.

Because of widespread resistance of *N. gonorrhoeae* to penicillin and tetracycline, the current recommendation for treatment is ceftriaxone plus azithromycin. Although no resistance to the cephalosporins is apparent, resistance to the fluoroquinolones has been documented (MMWR, 2016). Therefore, susceptibility testing should be performed if symptoms persist after treatment. The CLSI document recommends the agar dilution method or a disk diffusion method for testing of *N. gonorrhoeae* (CLSI, 2019). For some agents, only a susceptible breakpoint is available because no resistant strains have yet been documented. If an isolate with a nonsusceptible result to a third-generation cephalosporin is identified, for example, confirmation tests and referral to a reference laboratory should be strongly considered (CLSI, 2019).

Prevention

Two meningococcal conjugate vaccines against *N. meningitidis* serogroups A, C, Y, and W135 are licensed in the United States and recommended for all adolescents at 11 to 12 years and 16 years (MMWR, 2007). There are also recommendations for some adult populations, such as microbiologists who routinely work with *N. meningitidis* (MMWR, 2017). There is also a conjugate vaccine against serogroup B, which is available for all adolescents and young adults, but specifically recommended for asplenic patients and patients with a complement deficiency. Antibiotic prophylaxis should be limited to household contacts and those who have had contact with patients' oral secretions. Rifampin is currently the drug of choice. Laboratory safety is very important when handling specimens and cultures positive for *N. meningitidis*. Borrow and colleagues (2014) wrote an article on the appropriate precautions for handling specimens and steps to take if accidents do occur.

The use of preexposure antibiotics to prevent gonococcal disease is discouraged because of the potential risks of sensitization and the emergence of resistant strains. The sole exception to this rule is the application of erythromycin ointment to the eyes of newborns to prevent gonococcal (and chlamydial) ophthalmia (U.S. Preventive Services Task Force, 2019).

Moraxella catarrhalis

M. catarrhalis may be carried in the oropharynx of healthy children and adults. It is an encapsulated organism, and extending from its outer membrane are pili that serve as adhesins. The most common infections caused by this organism are bronchitis, otitis, sinusitis, and pneumonia (especially in persons with underlying chronic lung disease) (Murphy & Parameswaran, 2009; Cools et al., 2019). More recently, molecular mechanisms have been described that demonstrate the virulence factors possessed by strains of *M. catarrhalis* responsible for otitis media (Hassan, 2013). *M. catarrhalis* is an infrequent cause of bacteremia, endocarditis, meningitis, urogenital infection, and ophthalmia neonatorum.

Figure 57.13 shows the Gram stain of sputum in which *M. catarrhalis* is seen in large quantities inside and outside the polymorphonuclear leukocytes. *M. catarrhalis* initially was part of the *Neisseria* genus and later was transferred to the *Branhamella* genus for a short time. *M. catarrhalis* is a coccus that morphologically resembles *Neisseria* spp., unlike other members of the genus *Moraxella* (e.g., *M. lacunata*, *M. osloensis*, *M. atlantae*), which appear as rods. *M. catarrhalis* bacteria are oxidase and catalase positive but can be differentiated from *Neisseria* spp. in their ability to grow readily on blood agar, their lack of oxidative metabolism (sugars will be negative), and their production of DNase. Nearly all isolates of *M. catarrhalis* produce β-lactamase, which can be detected using nitrocefin. Although they should be assumed to be resistant to penicillin because of this, these isolates generally remain susceptible to cephalosporins, TMP-SMX, and β-lactamase inhibitor combinations (Cools et al., 2019).

GRAM-NEGATIVE BACTERIA—BACILLI

The gram-negative bacilli make up a complex group. They are broken down into Enterobacterales, which are those found normally in the gastrointestinal (GI) tract or that colonize and cause infection there primarily; nonfermentative gram-negative bacilli, which usually are not found as part of the normal flora of humans but rather are environmental bacteria; non-Enterobacterales, which can cause GI infection, such as *Vibrio* or *Campylobacter*; agents of infections with specific epidemiologic characteristics, such as *Legionella* and *Francisella*; other gram-negative bacilli, including *Haemophilus* spp.; and miscellaneous genera. A good overview of how to approach the identification of the aerobic gram-negative rods can be found in Norskov-Lauritsen and Ridderberg (2019).

Enterobacterales

Characteristics

The Enterobacterales are facultatively anaerobic, non–spore-forming, nonmotile or peritrichously flagellated, oxidase-negative, gram-negative bacilli that produce acid fermentatively from glucose and reduce nitrates to nitrites. Figure 57.14 shows a Gram stain of *Escherichia coli*, but it could represent any member of the Enterobacterales. Common clinical genera included in this group are *Citrobacter*, *Enterobacter*, *Escherichia*, *Klebsiella*, *Morganella*, *Proteus*, *Providencia*, *Salmonella*, *Serratia*, *Shigella*, and *Yersinia* (Buchan et al., 2019).

Clinical Manifestations and Pathogenesis

Enterobacterales are found on plants, in soil, in water, and in the intestines of humans and animals. They have been associated with many clinical infections, including abscesses, pneumonia, meningitis, septicemia, and urinary tract infections. Those commonly associated with human infection include *E. coli*, *Klebsiella* spp., *Proteus* spp., *Enterobacter* spp., *Salmonella* spp., *Shigella* spp., *Serratia* spp., *Citrobacter* spp., and *Providencia* spp. In the urinary tract, those frequently isolated are *E. coli*, *Proteus mirabilis*, *Klebsiella pneumoniae*, and *K. oxytoca*. Gram-negative pneumonias associated with the Enterobacterales are frequently caused by *K. pneumoniae*. Gram-negative bacteremias related to the Enterobacterales are frequently caused by *E. coli*, *K. pneumoniae*, *Enterobacter* spp., and *P.*

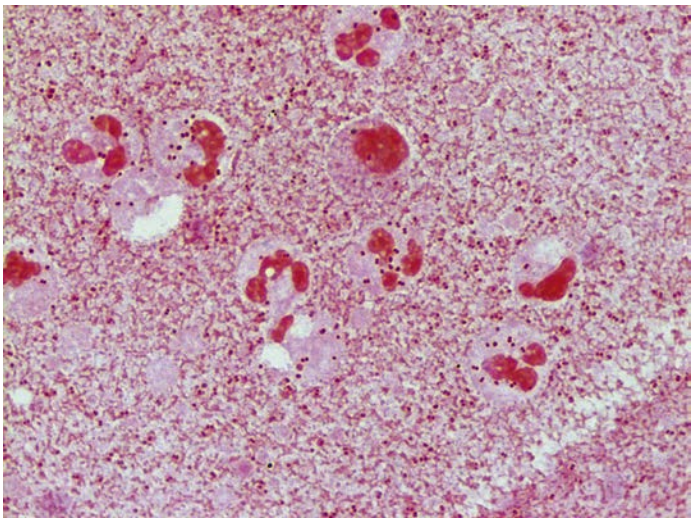

Figure 57.13 Gram stain of *Moraxella catarrhalis* in a sputum specimen. Note the intracellular gram-negative diplococci that resemble *Neisseria* spp. (oil immersion).

Figure 57.14 Gram stain of urine positive for *Escherichia coli*. The short, plump gram-negative rods are typical of any member of the Enterobacterales (oil immersion).

TABLE 57.5

Enteric Differential and Selective Media

Medium	Gram-positive Bacteriostatic Agent	Fermentable Carbohydrate	Indicator	Colony Color Fermenter	Nonfermenter	Category
Eosin methylene blue (EMB)	Eosin Y Methylene blue	Lactose*	Eosin Y Methylene blue	Red or black with sheen	Colorless	S, D
MacConkey	Crystal violet Bile salts	Lactose	Neutral red	Red	Colorless	S, D
Xylose-lysine-deoxycholate (XLD)	Bile salts	Xylose Lactose Sucrose	Phenol red	Yellow	Red	S, D
Hektoen enteric (HE)	Bile salts	Salicin Lactose Sucrose	Bromthymol blue	Yellow-orange	Green, blue-green	S, D
Salmonella shigella (SS)	Bile salts	Lactose	Neutral red	Red	Colorless	S
Bismuth sulfite (BS)	Brilliant green	Glucose	Bismuth sulfite	†	†	S
Thiosulfate citrate bile salts sucrose (TCBS)‡	Bile salts pH 8.6	Sucrose	Thymol blue Bromthymol blue	Yellow	Colorless	S, D

D, Differential; *S,* selective.
*Levine's formulation.
†H_2S-producing salmonellae have black colonies.
‡Used for isolation of vibrios.

mirabilis. Infections acquired in the hospital are likely to be caused by members of antibiotic-resistant genera, such as *Citrobacter*, *Enterobacter*, and *Serratia*. Enterobacterales associated with diarrhea include *Shigella* spp., *Salmonella* spp., *E. coli* (enterohemorrhagic [Shiga toxin producing], enterotoxigenic, enteroinvasive, enteropathogenic, enteroaggregative), and *Yersinia* spp. *Shigella* spp. are rarely isolated from sources other than the GI tract, whereas *Salmonella* spp. are more likely to be isolated from other sources, such as urine or blood. *Plesiomonas* spp. have been added to the Enterobacterales and remain as the only oxidase-positive member of this family. They also can be associated with infections of the GI tract. *Klebsiella granulomatis* is the causative agent of donovanosis or granuloma inguinale, a disease characterized by chronic genital ulcers (Forsythe et al., 2019).

Endotoxins that are present within the cell walls of the Enterobacterales, as well as other gram-negative bacilli, are responsible for much of the morbidity and mortality resulting from infections associated with these bacteria. Endotoxins consist of lipid and polysaccharide moieties with small quantities of amino acids and are often referred to as *lipopolysaccharides*. Lipopolysaccharides may elicit fever, chills, hypotension, granulocytosis, thrombocytopenia, disseminated intravascular coagulation, and activation of both classic and alternate complement pathways. Endotoxic shock is the result of gram-negative septicemia, with endotoxin reacting with macrophages, leukocytes, platelets, complement, and other serum proteins to increase the blood levels of proteolytic enzymes and vasoactive substances, resulting in pooling of blood, increased peripheral vasoconstriction, and diminution in cardiac output. It has become clear that the lethal effects of endotoxin are dependent on macrophage activation and responsiveness and that the production of cachectin from the activated macrophage plays a major role in causing profound shock and multiple-organ injury (Munford, 2006).

Other pathogenetic factors of the Enterobacterales include the K1 antigen, which is associated with a high percentage of strains of *E. coli*, causing neonatal meningitis; the capsule of *K. pneumoniae*, which, like that of the pneumococcus, inhibits phagocytosis; the Vi antigen of *Salmonella* serotype *typhi*, which may interfere with intracellular killing of this organism; and various surface antigens, such as fimbriae, that mediate adherence of the organism to mucosal surfaces.

Plasmid-mediated factors appear to play an important role in the invasive properties of *Salmonella*, *Shigella*, and enteroinvasive strains of *E. coli*. Moreover, the heat-labile enterotoxins (LT) and the heat-stable enterotoxins of *E. coli* are plasmid mediated. LT stimulates adenylate cyclase in mucosal cells of the small intestine, which, in turn, activates cyclic adenosine monophosphate (cAMP). This causes secretion of fluid and electrolytes into the intestinal lumen, producing watery diarrhea. In contrast, heat-stable (ST) enterotoxins appear to activate guanylate cyclase.

Laboratory Diagnosis

The isolation of gram-negative bacilli from contaminated specimens is greatly facilitated by the use of differential and selective media (Table 57.5). Eosin methylene blue (EMB) and MacConkey agar can be used interchangeably as minimally selective and differential media to initially select for and differentiate lactose-fermenting from non–lactose-fermenting gram-negative bacilli. XLD and HE agars are more selective differential media that are especially useful in selecting for *Salmonella* spp. and *Shigella* spp. in heavily contaminated specimens such as stool. Bismuth sulfite is a highly selective medium that is especially useful for the detection of salmonellae in endemics or epidemics. *Salmonella* spp. produce H_2S and are easily recognized by the production of colonies with black centers on XLD, HE, and bismuth sulfite agars. An enrichment medium, such as selenite-F or gram-negative (GN) broth, should be used to allow detection of low numbers of *Salmonella* spp. and *Shigella* spp. in stool. Cefsulodin-irgasan-novobiocin (CIN) agar incubated at room temperature is selective and differential for the recovery of *Yersinia enterocolitica*. Colonies will appear as bull's-eyes with red centers and transparent borders. MacConkey agar with sorbitol as the fermentable sugar is a differential medium that is capable of differentiating the sorbitol-fermentation–negative *E. coli* 0157:H7, which is associated with hemolytic uremic syndrome from most other *E. coli* (Buchan et al., 2019).

Multiple commercially available nucleic acid amplification tests can be used to detect bacterial stool pathogens (Zhang et al., 2015; Harrington et al., 2015). These assays can be more sensitive and provide results in a more timely manner than culture. Since public health departments often require stool pathogen isolates to be submitted for outbreak investigations, discussions with all parties should occur before bringing on one of these assays. In addition, the ability to culture bacterial stool pathogens should still be retained in case susceptibility testing is needed.

For some of the Enterobacterales, a few simple colonial characteristics or biochemical reactions can be used to presumptively identify an isolate. For example, *Proteus* spp. swarm on blood agar, *Klebsiella* spp. form lactose-positive mucoid colonies, *Serratia marcescens* may produce a red pigment, *Salmonella* spp. produce H_2S, and *E. coli* is indole positive. Definitive identification of these and other species requires additional biochemical testing and/or molecular methods. Innumerable schemes based on the use of conventional biochemical media have been described for identification of the Enterobacterales. Some differential characteristics of the Enterobacterales most commonly encountered in the clinical laboratory are shown in Table 57.6. Commercially prepared kits and automated devices are available that offer convenience and accuracy in identifying the vast majority of isolates belonging to the Enterobacterales. In some instances, identification is accurately made in a few hours. Semiautomated systems may combine identification and antimicrobial susceptibility testing in a single disposable unit. In general, accuracy of identification among these systems

TABLE 57.6
Differentiation of Aerobic Gram-Negative Bacilli

Test	*Escherichia coli*	*Klebsiella pneumoniae*	*Klebsiella oxytoca*	*Proteus mirabilis*	*Proteus vulgaris*	*Shigella* spp.	*Citrobacter freundii*	*Yersinia enterocolitica*	*Enterobacter cloacae*	*Serratia marcescens*	*Morganella morganii*	*Providencia alcalifaciens*	*Salmonella* Serotype *choleraesuis*	*Salmonella* Serotype *typhi*	*Salmonella* Serotype *paratyphi A*
Indole	+	–	+	–	+	D	–	D	–	–	+	+	–	–	–
H_2S (in triple sugar iron agar)	–	–	–	+	+	–	+	–	–	–	–	–	D	+	– or +
Urease	–	+	+	+	+	–	D	+	D	– or +	+	–	–	–	–
Motility	+ or –	–	–	+*	+*	–	+	+ + (25C)/– (37°C)	+	+	+ or –	+	+	+	+
Acid produced from lactose	+	+	+	–	–	–	+ or (+)	D	D	–	–	–	–	–	–

+, ≥90% positive reactions within 2 days; –, ≥90% negative reactions; *(+),* positive reactions in 3 to 7 days; + *or* –, reactions of most strains positive; – *or* +, reactions of most strains negative; *D,* different reactions [+, (+), or –].
*Swarm on blood and chocolate agar.

is very high and comparable. MALDI-TOF has been shown to be an excellent tool for the identification of members of the Enterobacterales with the exception of *Shigella* spp. and can usually provide results more quickly than traditional or semiautomated biochemical methods (Richter et al., 2013).

There are two species of *Salmonella*, *S. enterica* and *S. bongori* (rarely isolated from humans), each of which contains multiple subspecies. Six subspecies of *S. enterica* are known, with subspecies I (*S. enterica* subsp. *enterica*) being the most common human isolate. More than 2000 serotypes of *Salmonella* have been identified, most belonging in the subspecies *enterica*. Serotyping is based on immunologic reactivity of the heat-stable somatic "O" antigens, which are predominantly lipopolysaccharide in content, and the heat-labile flagellar "H" antigens. In the United States, *S.* serotypes *typhimurium* and *enteritidis* are the most common. *S.* serotype *typhi* also produces a heat-labile capsular polysaccharide Vi antigen. In practice, most clinical laboratories identify isolates as *Salmonella* spp. based on biochemical reactions and use group-specific immunologic reagents to assign isolates to a specific serogroup. Commercial slide agglutination tests to differentiate large serogroups—A, B, C, and D—are useful in differentiating typhoidal salmonella from nontyphoidal strains. *S.* serotype *typhi* carries the D serogroup and Vi antigen. Further identification of the specific serotype is generally performed only by state health departments or other reference laboratories (Buchan et al., 2019).

Isolates biochemically resembling *Shigella* are also classified by the reactivity of the "O" antigen, as are isolates of *E. coli* that are identified as potential causes of diarrhea and hemolytic uremic syndrome. Such *E. coli* are classified by the type of toxin produced as well. Commercial kits are available to identify *E. coli* O157 and to detect some types of toxins in culture or stool specimens. However, this type of testing can be sent out to referral laboratories or state health departments. The CDC has recommended that all laboratories consider testing stool samples for the presence of Shiga toxins I and II produced by certain strains of enterohemorrhagic *E. coli* (O157:H7 and other serotypes). Shiga toxin is also produced by *Shigella*, but by the species *S. dysenteriae*, which is not often seen in the United States. Antigen tests are available and are widely used in clinical laboratories for this toxin (Buchan et al., 2019).

Antimicrobial Susceptibility

The susceptibility of Enterobacterales to various antimicrobial agents is highly variable. Susceptibility to ampicillin was common among strains of *E. coli* and *P. mirabilis*, for example (although resistance in both has increased greatly over the past 10–20 years), but was not expected among most other clinically significant members of the Enterobacterales. Resistance to first-generation cephalosporins (cefazolin, cephalothin) is expected for *Enterobacter* spp., *Serratia* spp., *Citrobacter* spp., *Proteus vulgaris*, *Providencia* spp., *Morganella* spp., and *Yersinia* spp.; susceptibility to third-generation cephalosporins (e.g., ceftriaxone, cefotaxime, ceftazidime) continues for many members of the Enterobacterales. However, the presence of extended-spectrum β-lactamases and *Amp-C* genes, which are recognized by resistance of the bacteria to third-generation cephalosporins and all β-lactam antibiotics except carbapenems, is increasing in selected strains of *E. coli*, *K. pneumoniae*, *P. mirabilis*, and others. Most Enterobacterales are susceptible to aminoglycosides and fluoroquinolones. It had been very unusual for a member of the Enterobacterales to be resistant to carbapenems (e.g., imipenem, meropenem, ertapenem, doripenem). However, in the late 1990s, in a few U.S. states, isolates of *K. pneumoniae* were first recognized that produced a bla_{KPC} gene, resulting in production of carbapenemases that inactivate all carbapenems. These strains are often referred to as *KPCs* or *K. pneumoniae*–producing carbapenemases. These isolates are resistant to most classes of antibiotics, except for an aminoglycoside, colistin, and tigecycline. The spread of these KPC genes has continued (Peirano et al., 2014). Infection control procedures are essential to prevent the spread of these highly resistant strains.

Because the susceptibility pattern of the Enterobacterales is unpredictable, susceptibility testing should be performed as a general rule if antimicrobial therapy is being considered. No susceptibility testing need be performed if antimicrobial therapy is not instituted, as is the case for uncomplicated enteric infection due to *Salmonella*, for which therapy may actually prolong the carrier state, or when a mixed flora infection is present and individual susceptibilities may not be appropriate. Methods for performing susceptibility test interpretive criteria can be found in CLSI documents (CLSI, 2019).

Plesiomonas

Characteristics

Plesiomonas shigelloides, the only species in the genus *Plesiomonas*, is a facultatively anaerobic, oxidase- and catalase-positive, glucose-fermenting, gram-negative rod. Recent molecular genetic evidence demonstrates that the genus *Plesiomonas* is most closely related to the genus *Proteus*. Therefore, it has been placed into the Enterobacterales family (Forsythe et al., 2019) as the only oxidase-positive member of this group of gram-negative bacilli.

Clinical Manifestations and Pathogenesis

P. shigelloides is found in aquatic environments that are limited geographically by its minimum growth temperature of 8°C. It may be found in fresh and estuarine water, usually in tropical countries. It has been implicated as a cause of gastroenteritis, especially following the ingestion of uncooked shellfish. The diarrheal stool specimen frequently contains polymorphonuclear leukocytes and red blood cells, although a cholera-like illness may occur. Gastroenteritis may occur in sporadic cases as well as in outbreaks. Extraintestinal manifestations of infection with *P. shigelloides*

include meningitis, septicemia, cellulitis, arthritis, and endophthalmitis (Ampofo et al., 2001; Ozdemir et al., 2010). Virulence factors of *P. shigelloides* include hemolysins, cytotoxins, production of exoenzymes associated with pathogenicity, adhesive ability, and vacuolation of cell lines in vitro (Salerno et al., 2010).

Laboratory Diagnosis

P. shigelloides can be isolated on a variety of nonselective and enteric-selective media. Acid production from lactose is variable, but on enteric media the organism usually appears to be a non–lactose fermenter. It is indole positive; reduces nitrates to nitrites; produces catalase; is methyl red positive; and ferments glucose, maltose, and trehalose (Forsythe et al., 2019).

Antimicrobial Susceptibility

P. shigelloides is susceptible to a variety of antimicrobial agents, including cephalosporins, TMP-SMX, imipenem, and the quinolones (Forsythe et al., 2019). Susceptibility to the penicillins is variable because of the presence of a β-lactamase. Recommendations for testing are available in the CLSI M100 document (CLSI, 2019).

GRAM-NEGATIVE BACTERIA—NONFERMENTATIVE BACILLI

The group of "nonfermenters" is composed of gram-negative bacilli that do not ferment glucose and other sugars. They account for about 15% of the gram-negative bacilli isolated from hospitalized patients. Although many genera of nonfermenters are known, 75% of those that are clinically relevant are *Pseudomonas aeruginosa* and the majority of the remaining 25% are *Acinetobacter* spp., *Stenotrophomonas maltophilia*, and *Burkholderia cepacia*. As a group, they are environmental bacteria and are usually not considered as members of the normal flora of the human body, except as colonizers in hospitalized patients. They can be readily isolated from water, soil, vegetables, plants, and hospital surfaces. Although no uniform biochemical characteristics have been noted, they are often oxidase-positive (*Acinetobacter* spp. and the majority of *S. maltophilia* isolates are notable common exceptions), lactose-negative colonies on selective media such as MacConkey agar (although some of the species do not grow on this medium), and they are frequently resistant to many of the antibiotics that are effective against members of the Enterobacterales family. The four main species mentioned previously, as well as other common nonfermenters, are discussed in this chapter.

Pseudomonas

Characteristics

The genus *Pseudomonas* has undergone extensive revision. Now, many of the species that were previously classified in this genus have been reclassified into the genera *Burkholderia*, *Ralstonia*, *Comamonas*, *Acidovorax*, *Delftia*, *Hydrogenophaga*, *Brevundimonas*, and *Stenotrophomonas*. Of the 12 clinically significant species that remain, *P. aeruginosa* is the most important human pathogen. Figure 57.15 shows the Gram stain of *P. aeruginosa* in a sputum specimen.

Most *Pseudomonas* spp. are aerobic, catalase-positive, oxidase-positive, gram-negative bacilli. Their metabolism is mainly respiratory, with oxygen as the terminal electron acceptor, and rarely fermentative, utilizing arginine for anaerobic growth. Many *Pseudomonas* spp. are motile by means of polar flagella.

Clinical Manifestations and Pathogenesis

Pseudomonas spp. are typical inhabitants of moist environments and have been found in cosmetics, swimming pools, hot tubs, and the inner soles of shoes, leading to folliculitis, otitis externa, and diabetic foot infections. While *P. aeruginosa* causes the greatest morbidity and mortality today, other *Pseudomonas* spp., although often isolated from clinical specimens, are only occasionally involved in disease.

P. aeruginosa is ubiquitous in the hospital environment, existing almost anywhere there is moisture, including medical equipment and disinfectant solutions and soaps. It is only rarely found as part of the normal flora of healthy people, but in hospitalized patients, the rates of colonization increase with the length of hospitalization. *P. aeruginosa* may produce serious infection in patients with burns and traumatic and operative wounds, following urinary tract manipulation, in patients with diseases of the hematopoietic, reticuloendothelial, and lymphoid systems, and in those with impaired cellular or humoral defenses. Pulmonary infection occurs commonly in patients with cystic fibrosis (CF) or who are on mechanical ventilation. The mortality rate is highest in severely leukopenic patients.

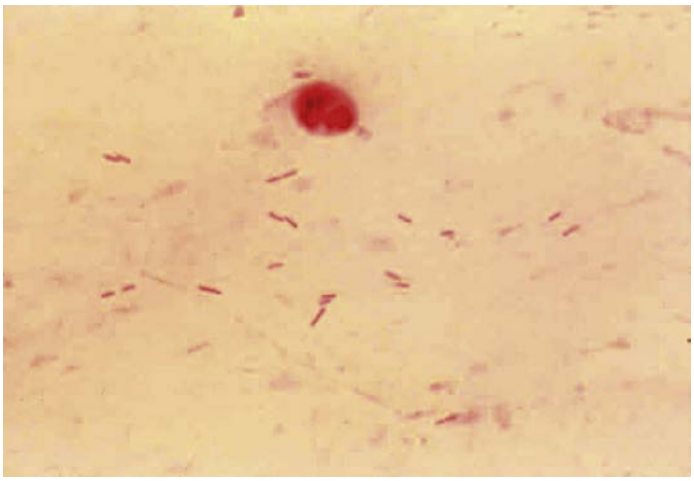

Figure 57.15 Gram stain of *Pseudomonas aeruginosa* in a sputum specimen. Note the longer, gram-negative bacilli compared with Figure 57.14 (oil immersion).

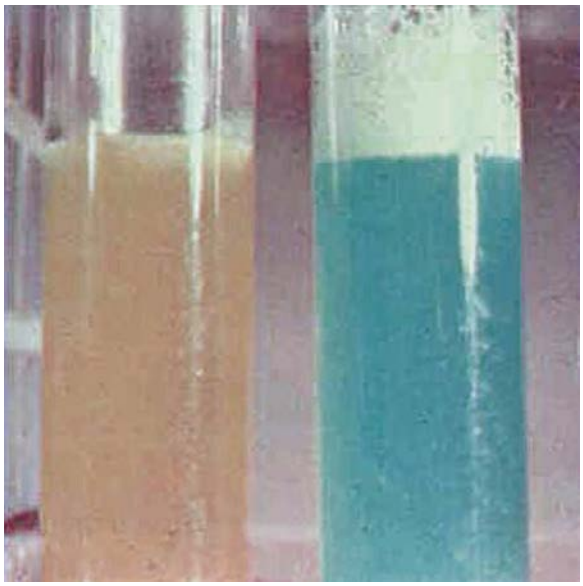

Figure 57.16 Extracted pyocyanin pigment from *Pseudomonas aeruginosa*.

P. aeruginosa produces a slime polysaccharide, an endotoxin, and proteases that inactivate components of complement, thereby inhibiting to some degree opsonization and the inflammatory response, and perhaps contributing to its invasiveness. Exotoxin A promotes cellular damage and tissue invasion and is toxic to macrophages.

Laboratory Diagnosis

The presence of *P. aeruginosa* in culture can often be suspected because of its grape-like or corn tortilla odor, the rough or ground-glass appearance of its colonies on sheep blood agar, and the presence of one or both of two pigments: a blue-green fluorescent pigment (Fig. 57.16) and/or a metallic sheen caused by pyoverdin pigment. It can be identified easily with a positive oxidase reaction, growth at 42°C, an alkaline slant/neutral butt reaction in a TSI agar, and the formation of sheen and/or pigment on the slants of TSI and *Pseudomonas* P agar. Additional tests are shown in Table 57.7. Tests of carbohydrate utilization should be carried out in O-F basal medium, which contains a minimal quantity of peptone and a relatively large quantity of carbohydrate; thus, it can allow detection of very small quantities of acid formed by this group of bacteria. Reactions are usually complete within 48 hours but may require as long as 7 days. MALDI-TOF is now routinely used to make the identification of *P. aeruginosa* due to improved turnaround times and less expense than traditional identification methods (Verroken et al., 2016).

Antimicrobial Susceptibility

Susceptibility testing should be performed for all clinically significant isolates of *P. aeruginosa*. The following antibiotic classes are often effective at treating *P. aeruginosa* infections and susceptibility testing should

TABLE 57.7
Differential Characteristics of Non-Fermentative Gram-Negative Bacilli Isolated from Clinical Specimens

	Pseudomonas aeruginosa	*Pseudomonas fluorescens*	*Pseudomonas putida*	*Acinetobacter baumannii*	*Burkholderi cepacia*	*Stenotrophomonas maltophilia*
Oxidase	+	+	+	–	+	–
Pyocyanin	+	–	–	–	–	–
Fluorescein	+	–	+	–	–	–
Glucose oxidation	+	+	+	+	+	+/–
42°C	+	–	–	+	+/–	+/–
DNase	–	–	–	–/+	–	+
Growth on MacConkey agar	+	+	+	+*	+	+
Motility	+	+	+	–	+	+

+, Positive; –, negative; +/–, variable results, most strains positive; –/+, variable results, most strains negative; *DNase,* deoxyribonuclease.
*Purplish color on MacConkey agar.

routinely be performed for the following agents: β-lactam combination agents (piperacillin-tazobactam, ceftazidime-avibactam, and ceftolozane-tazobactam), ceftazidime, cefepime, aztreonam, carbapenems, aminoglycosides, and fluoroquinolones. *P. aeruginosa* is intrinsically resistant to amoxicillin-clavulanate, ceftriaxone, TMP-SMX, and tetracyclines as well as newer broad-spectrum antibiotics ertapenem and tigecycline. Hospital strains of *P. aeruginosa* may be resistant to many classes of antibiotics and the incidence of multidrug-resistant *P. aeruginosa* is increasing, especially in intensive care units and among patients who have long-standing *Pseudomonas* infections, such as those with CF and other chronic syndromes (Tabak et al., 2019). When resistant isolates are encountered, additional susceptibility testing for colistin and polymyxin B are often performed. The CLSI has breakpoints for both of these antibiotics and MICs from colistin can be used to predict those for polymyxin B (CLSI, 2019).

Acinetobacter

Characteristics

Organisms in this genus are short, rod-shaped to spherical, nonmotile, oxidase-negative, strictly aerobic, and gram negative. In a gram-stained smear, they often appear in pairs and may be difficult to decolorize, resulting in *Acinetobacter* spp. mistakenly being classified as gram-positive organisms.

Clinical Manifestations and Pathogenesis

Acinetobacter spp. are found commonly in soil and water and uncommonly on the skin and mucous membranes of healthy people. Current research has elucidated several virulence factors in this group of organisms, as they are being more recognized as serious pathogens, especially in hospitalized patients. Although colonization is more common than infection, *Acinetobacter* spp. have been increasingly associated with nosocomial septicemia, pneumonia, bacteriuria, and wound infection, especially due to the increased antimicrobial resistance that has developed in many strains of *A. baumannii*. The mortality rate associated with *A. baumannii* infections can reach 35% in some populations (Wong et al., 2016).

Laboratory Diagnosis

Acinetobacter spp. can be distinguished readily from *Pseudomonas* spp. on the basis of their negative oxidase reaction, lack of motility, and inability to reduce nitrates. They may produce characteristic purplish colonies on MacConkey agar due to absorption of crystal violet, but they do not ferment lactose. More than 50 species are known, but historically their differentiation biochemically was difficult and they were often grouped together in the *A. calcoaceticus–A. baumannii* complex. The glucose-oxidizing (saccharolytic strains), nonhemolytic clinical strains were usually classified as *A. baumannii*; the asaccharolytic strains (nonglucose oxidizers) were classified as *A. lwoffi* if nonhemolytic or *A. haemolyticus* if hemolytic (Cools et al., 2019). Currently, routine use of MALDI-TOF in the clinical laboratory provides reliable species-level identification of *Acinetobacter* spp., especially as databases improve (Jeong et al., 2016). The most clinically relevant are members of the *A. baumannii* complex; these are the group most resistant to antimicrobials as well.

Antimicrobial Susceptibility

Susceptibility testing for *Acinetobacter* spp. should be performed for clinically significant isolates or upon request of the clinician. β-Lactam combination agents, ceftazidime, cefepime, carbapenems, aminoglycosides, fluoroquinolones, and tetracyclines are the recommended antibiotics for testing (CLSI, 2019). In some hospitals in the United States, *Acinetobacter* spp. have become the predominant nosocomial pathogen. Members of the *A. baumannii* complex have a propensity to develop resistance to multiple drug classes and while the carbapenems (excluding ertapenem) are considered the most active, resistance rates of up to 11% for this class have been described in nosocomial strains throughout the United States (Chopra et al., 2013). These resistant isolates are often referred to as carbapenem-resistant *A. baumannii* (CRAB) and are often resistant to all classes of antibiotics except colistin, polymyxin B, and tigecycline (Chopra et al., 2013). Increased attention has been focused on appropriate infection control measures, screening neighboring patients, and an emphasis on hand hygiene to prevent transmission (Guan et al., 2016).

Burkholderia

Characteristics

Burkholderia spp. are aerobic, non–spore-forming, gram-negative rods. These organisms are catalase positive and most are weakly or strongly oxidase positive. The majority of species grow well on MacConkey agar and produce lactose-negative colonies. All are motile due to the presence of a polar flagellum, except for *Burkholderia mallei*.

Clinical Significance and Pathogenesis

These organisms are found in the environment in water, in soil, and on plants. Because of their predilection for watery environments, *Burkholderia* spp. can be found in the hospital environment and have the potential to cause nosocomial acquired infections.

Two important human pathogens in the genus include the *B. cepacia* complex and *B. pseudomallei*. The *B. cepacia* complex is composed of organisms that are nosocomial pathogens and can cause bacteremia, urinary tract infections, septic arthritis, and respiratory tract infections due to contaminated medical equipment, medications, and disinfectants. These organisms are important pathogens in patients with CF and in those with chronic granulomatous disease (CGD). Patients with CF who become chronically infected with these organisms have a decreased rate of survival, even with lung transplantation. The *B. cepacia* complex is composed of at least 20 species, all of which have been recovered from patients with CF. In the United States, approximately 50% of strains are *B. multivorans* or *B. cenocepacia*. *B. cenocepacia* is most frequently associated with cepacia syndrome and has been shown in many studies to possess potent virulence factors that lead to increased mortality in CF patients versus those infected with other strains of *Burkholderia* (LiPuma et al., 2019). *B. pseudomallei*, which is acquired from the environment by inhalation or contact through cut or abraded skin, causes melioidosis. The infection can be asymptomatic, can become chronic, or can cause a fulminant sepsis. Melioidosis is most prevalent in Southeast Asia and Australia but may occur in other tropical and subtropical environments as well.

Laboratory Diagnosis

Burkholderia spp. grow well on standard laboratory media, including blood and chocolate agars. Isolation of *B. cepacia* from contaminated specimens such as sputa may be made easier through the use of selective media to inhibit *P. aeruginosa*, for example, *P. cepacia* selective agar (PC), oxidation-fermentative base-polymyxin B, bacitracin-lactose-agar (OFPBL) and *B. cepacia* selective agar (BCSA) (LiPuma et al., 2019). No good biochemical or commercial phenotypic methods are available to differentiate among

TABLE 57.8

Differential Characteristics of *Vibrio* Species

Test	*V. cholerae*	*V. mimicus*	*V. parahaemolyticus*	*V. alginolyticus*	*V. vulnificus*
Indole	+	+	+	+/–	+
Voges-Proskauer	+/–	–	–	+	–
Lysine decarboxylase	+	+	+	+	+
Ornithine decarboxylase	+	+	+	+/–	+/–
Arginine dihydrolase	–	–	–	–	–
Lactose	–	–/+	–	–	+
Sucrose	+	–	–	+	–/+
Mannitol	+	+	+	+	–/+
Maltose	+	+	+	+	+
Arabinose	–	–	+	–	–
$NO_3 \rightarrow NO_2$	+	+	+	+	+
Oxidase	+	+	+	+	+
Growth in Nutrient Broth Plus NaCl, %					
0	+	+	–	–	–
1	+	+	+	+	+
6	–/+	–/ +	+	+	+/–

+, Positive; –, negative; +/–, variable results, most strains positive; –/+, variable results, most strains negative.

the various members of the *B. cepacia* complex and related organisms, such as *B. gladioli* and *Ralstonia*, *Cupriavidus*, and *Pandoraea* spp., as they are all phenotypically similar. Molecular techniques are often required for confirmatory identification and should be pursued when a *B. cepacia* complex organism is suspected. The use of MALDI-TOF may also assist in further speciation, but the accuracy in identification of less common members of the *B. cepacia* complex is still an issue (Plongla et al., 2016). The CF Foundation (http://www.cff.org) has established a *B. cepacia* reference laboratory to confirm the identity of possible isolates in respiratory cultures from CF patients using phenotypic and genotypic methodologies (LiPuma et al., 2019).

Antimicrobial Susceptibility

The susceptibility of these organisms to antimicrobial agents varies considerably. Organisms in the *B. cepacia* complex are highly resistant to many antimicrobials but are usually susceptible to TMP-SMX, ceftazidime, meropenem, minocycline, and levofloxacin. CLSI recommends testing and reporting only these limited antibiotics (CLSI, 2019). However, isolates from CF patients who have been on repeated courses of antibiotics are likely to become resistant to these agents. All *B. cepacia* complex organisms are intrinsically resistant to aminoglycosides and polymyxins (colistin) and regularly develop resistance to β-lactam antibiotics.

Stenotrophomonas maltophilia

Characteristics

S. maltophilia is an opportunistic pathogen and a significant cause of nosocomial infections. Risk factors for colonization or infection with this organism are mechanical ventilation, use of broad-spectrum antibiotics, catheterization, and neutropenia (Brooke, 2012; Behnia et al., 2014). Like *P. aeruginosa* and the *B. cepacia* complex, *S. maltophilia* can colonize and cause respiratory infections in CF patients.

Laboratory Diagnosis

Important distinguishing biochemical reactions of *S. maltophilia* are its negative oxidase reaction and positive DNase activity. The colonies are lavender green on blood agar and MacConkey agar and may have an ammonia-like odor. The bacteria are motile and oxidatively ferment glucose and maltose.

Antimicrobial Susceptibility

S. maltophilia is intrinsically resistant to many antibiotic classes, including the carbapenems. TMP-SMX is the antibiotic of choice, although some strains have become resistant (Brooke, 2012). Many laboratories in the United States report susceptibility results for TMP-SMX and will only release results for ceftazidime, minocycline, and levofloxacin if TMP-SMX is resistant or upon clinician request (CLSI, 2019).

Other nonfermentative, gram-negative bacilli include members of the genera *Alcaligenes*, *Achromobacter*, *Flavobacterium*, *Cupriavidus*, *Pandoraea*, *Chryseobacterium*, *Acidovorax*, *Brevundimonas*, *Comamonas*, and *Ralstonia*, among others. These are infrequently isolated from clinical specimens and often represent contamination or colonization. They can be considered clinically significant, especially when isolated from sterile sites, on multiple occasions in immunosuppressed patients or patients with foreign devices in place.

Vibrio

Characteristics

Vibrio spp. are facultatively anaerobic, catalase-positive, oxidase-positive, straight, curved, or comma-shaped gram-negative bacilli that are usually motile by means of polar flagella. All *Vibrio* spp. require Na^+ for growth, ferment carbohydrates, and reduce nitrates to nitrites. Several species are medically important and are included in Table 57.8.

Clinical Manifestations and Pathogenesis

Cholera toxin-producing *V. cholerae* O1 is a well-known cause of epidemic cholera, which manifests itself by massive intestinal fluid loss and severe dehydration. The cholera toxin mediates this effect by binding to and activating the adenylate cyclase of cells in the small intestine, resulting in hypersecretion of electrolytes and water (Tarr et al., 2019). *Vibrio* spp. are abundant in aquatic environments—in particular, marine waters—and infection is acquired by drinking contaminated water in areas where there is poor sanitation. Other non-O1, non-O139 strains of *V. cholerae* can cause self-limited gastroenteritis but are not responsible for epidemics of disease. Nearly all non-O1, non-O139 strains of *V. cholerae* do not produce cholera toxin but do produce two types of hemolysins and a heat-stable enterotoxin.

V. mimicus and *V. parahaemolyticus* primarily cause gastroenteritis due to consumption of raw fish or shellfish, particular oysters. Outbreaks of acute diarrheal disease following ingestion of contaminated food have been especially common in Japan but have also occurred in the United States and other countries (Tarr et al., 2019). The mechanism of pathogenicity of the halophilic *V. parahaemolyticus* appears to be related to invasiveness rather than to enterotoxin production. More than 95% of isolates of *V. parahaemolyticus* isolated from patients with gastroenteritis produce a cell-free hemolysin that is lethal to mice when injected in high doses and is described as the *Kanagawa phenomenon*. *V. vulnificus* causes severe wound infections and septicemia and results in notably high mortality rates. Disease is usually associated with consumption of raw oysters or traumatic injuries incurred while exposed to marine waters. Middle-aged men with preexisting hepatic disease, increased available iron stores, and other immunosuppressive conditions are particularly susceptible to infection with *V. vulnificus*.

Laboratory Diagnosis

Although formerly of concern only to U.S. travelers to endemic areas, cases of *V. cholerae* disease have been described in the United States in

association with ingestion of contaminated shellfish. In 2014, the CDC reported 7 cases of toxigenic *V. cholerae*, all of which were serogroup 01 and travel related (cdc.gov/cholera/index.html). In addition, gastroenteritis caused by *V. parahaemolyticus* and by other halophilic *Vibrio* spp. in contaminated shellfish has been described in many parts of the country, particularly in coastal areas. In 2014, there were 1252 cases of *Vibrio* infection in the United States—48% by *V. parahaemolyticus*, followed by 19% *V. alginolyticus*, and 10% *V. vulnificus*. Of these, 14% of the *Vibrio* infections were isolated from patients in noncoastal states (cdc.gov/vibrio/index.html). Thus, it is important for clinical laboratories to have the capability to culture stool for *Vibrio* spp. when indicated on the basis of travel and dietary history.

With the exception of *V. cholerae* and *V. mimicus*, growth of this group of organisms requires media containing NaCl. Most solid and liquid media used for bacterial culture contain enough sodium that the use of special media in such instances is not necessary. Selective media containing sucrose, such as thiosulfate citrate bile salts-sucrose (TCBS) medium, is very useful for culturing stool specimens for *Vibrio* spp. *V. cholerae* and *V. alginolyticus* ferment sucrose and appear as yellow colonies on this medium. An enrichment medium, such as alkaline peptone water, may be used prior to subculture to solid medium to enhance recovery of *Vibrio* spp. from stool. *Vibrio* spp. can be differentiated among themselves and from other enteric gram-negative bacilli according to the reactions listed in Table 57.8. It may be necessary to carry out biochemical testing of the halophilic *Vibrio* spp. in media supplemented with 1% to 3% NaCl. If TSI and lysine iron agar (LIA) are inoculated for screening purposes, their reactions will be acid slant/acid butt with no gas (A/A) or H_2S and alkaline slant/alkaline butt (K/K), respectively (Tarr et al., 2019). Not all commercially available gram-negative identification systems are reliable for the identification of *Vibrio* spp. and they should be used only if they have proved accurate. Use of MALDI-TOF and molecular methods for identification have become more useful if full identification is needed (Erler et al., 2014).

Antimicrobial Susceptibility

Antimicrobial susceptibility testing can be performed using the disk diffusion method with Mueller-Hinton agar and broth microdilution using cation-adjusted Mueller-Hinton broth and incubation at 35°C for 16 to 18 hours. The CLSI has established interpretive standards for *V. cholerae* and recommends performing testing for ampicillin, azithromycin, chloramphenicol, sulfonamides, tetracycline or doxycycline, and TMP-SMX (CLSI, 2015). Interpretive standards for the other *Vibrio* spp. are also included in the CLSI M45-A3 document (CLSI, 2015).

Aeromonas

Characteristics

Members of this genus are facultatively anaerobic, oxidase- and catalase-positive, rod-shaped, gram-negative bacilli. They are usually motile by means of polar flagella, although some species may be nonmotile. They form acids from carbohydrates by oxidative and fermentative metabolism and reduce nitrates to nitrite.

Clinical Manifestations and Pathogenesis

Aeromonas spp. are mainly found in aquatic environments. They have been isolated from tap water, rivers, soil, and various foods, and may also be found in marine environments (brackish water). These organisms have been associated with both intestinal and extraintestinal disease. Although the role of *Aeromonas* spp. as the cause of gastroenteritis has been previously questioned, the presence of *Aeromonas* spp. in stool is more often associated with diarrhea than with an asymptomatic carrier state. Its role in producing diarrheal disease is possibly related to the production of an enterotoxin by some strains. A hemolysin and cytopathic factor have also been described. *Aeromonas* spp. may cause infection of traumatically acquired wounds or septicemia in patients who are immunocompromised (Janda & Abbott, 2010). The clinical presentation of wound infections can range from relatively benign cellulitis to severe necrotizing fasciitis. An unusual association has also been reported between *Aeromonas* wound infections and bacteremia and the use of medicinal leech therapy to decrease vascular congestion following reconstructive surgery. This is due to the fact that *A. veronii* biovar sobria is the main symbiont in the gut of leeches (Marden et al., 2016).

Laboratory Diagnosis

Isolation of a fermenting, oxidase-positive, gram-negative bacillus from an appropriate specimen should suggest the possibility of *Aeromonas* spp. Organisms grow readily on conventional laboratory media and produce colonies that have a greenish, ground-glass appearance similar to *Pseudomonas* spp. Most species are β-hemolytic on blood agar and may have a fruity odor. Isolation of *Aeromonas* spp. from stool specimens may be enhanced by inoculation of blood agar containing ampicillin or CIN medium. More than 36 species of *Aeromonas* are now recognized. *A. hydrophila* complex, *A. caviae* complex, and *A. veronii* complex are the most common isolates from human specimens. Esculin, Voges-Proskauer, gas from glucose fermentation, and L-arabinose are four biochemicals that can be used to separate *Aeromonas* spp. into one of these three complexes. A more definitive identification to the species level requires molecular sequencing methods (Lamy & Horneman, 2019). While MALDI-TOF may provide the shortest time to result, accurate identification of *Aeromonas* to the species level is hindered by incomplete databases, which lack some clinically relevant organisms (Vavrova et al., 2015).

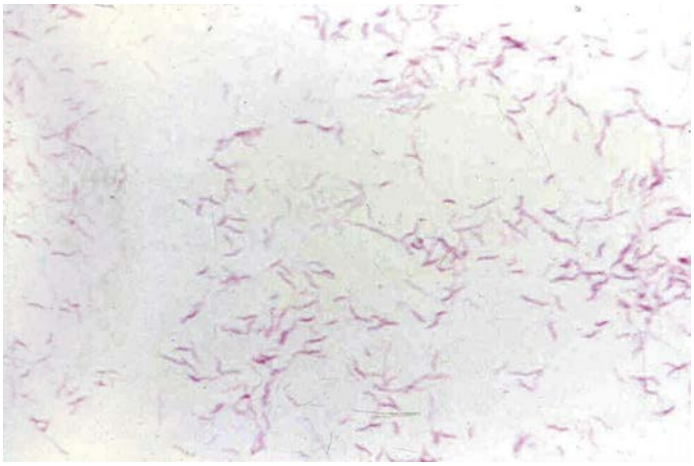

Figure 57.17 *Campylobacter jejuni* Gram stain. Note the comma-shaped appearance of the bacilli (oil immersion).

Antimicrobial Susceptibility

Aeromonas spp. are susceptible to fluoroquinolones, aminoglycosides, carbapenems, and TMP-SMX, but produce multiple, inducible β-lactamases that mediate resistance to the penicillins, first-generation cephalosporins, and some extended spectrum cephalosporins (Lamy & Horneman, 2019). Carbapenemases, although rare, may be difficult to detect by conventional susceptibility testing methods, including automated systems (Lamy & Horneman, 2019). Increases in cases of ciprofloxacin-resistant *Aeromonas* spp. following leech therapy have been noted (Giltner et al., 2013).

Campylobacter

Characteristics

Campylobacter spp. are small (0.5–5.0 μm long × 0.2–0.9 μm wide), motile, non–spore-forming, curved (comma-shaped) or S-shaped gram-negative bacilli that grow optimally in a microaerobic atmosphere containing 5% to 10% oxygen. Figure 57.17 shows a Gram stain of *C. jejuni* from culture. *C. jejuni* subsp. *jejuni* is one of the most common causes of bacterial enteritis in the United States. Other *Campylobacter* spp. associated with enteritis are *C. coli*, *C. lari*, and *C. upsaliensis*. *C. fetus* subsp. *fetus* is the most common cause of *Campylobacter* bacteremia and can also present as meningitis, osteomyelitis, vasculitis, or perinatal infections in those that are pregnant, elderly, or immunosuppressed (Wagenaar et al., 2014). *Arcobacter* are aerotolerant, *Campylobacter*-like, spiral-shaped bacteria that are frequently isolated from bovine and porcine products of abortion and feces of animals with enteritis (Nachamkin, 2019). *A. butzleri* and *A. cryaerophilus* have been shown to cause human infection and have been isolated from patients with diarrhea, bacteremia, endocarditis, and peritonitis. *A. skirrowii* has been isolated from stool of patient with chronic diarrhea, although clinical relevance is unclear (Nachamkin, 2019).

Clinical Manifestations and Pathogenesis

C. jejuni is found worldwide as a commensal of the GI tract of wild or domesticated cattle, sheep, swine, goats, dogs, cats, and poultry, especially turkeys and chickens. *Campylobacter* was the most commonly isolated enteric pathogen in the United States in 2018, with an incidence of 19.5 per 100,000 individuals (Tack et al., 2019). The incidence of infection in the United Kingdom and in other developed nations is similar to that in the United States; the incidence in underdeveloped countries is probably even higher. Infections generally occur in the summer and fall and are commonly the result of ingestion of improperly cooked foods, primarily

poultry. In addition, several outbreaks of *C. jejuni* enteritis have been linked to unpasteurized dairy products and to defects in municipal water systems. The spectrum of illness ranges from asymptomatic to severely ill. The stool from patients with diarrhea may contain blood or leukocytes. Symptoms can last up to 1 week and generally are self-limited. Extraintestinal infections, including bacteremia, reactive arthritis and Reiter syndrome, urinary tract infection, and meningitis, may also occur. *C. jejuni* is the most recognized antecedent cause of Guillain-Barré syndrome. The pathogenesis of this organism is not completely understood, but it appears to first adhere to the intestinal mucous layer and then translocate through the epithelial surface to the underlying tissue, causing invasive disease (Nachamkin, 2019).

The major habitat of *C. fetus* subsp. *fetus* is the intestine of sheep and cattle, but it also may be found in the genital tract of these animals, their placentas, and the gastric contents of their aborted fetuses and, less frequently, in other animals and birds. The mechanisms of transmission of infection to humans are not completely understood. Direct contact with an infected animal is possible, but less than one third of infected individuals have a history of environmental or occupational exposure. Contaminated food or water may be a vehicle for infection, or infection may originate from an endogenous source.

Laboratory Diagnosis

A single stool specimen is generally adequate to detect enteric pathogens, including *Campylobacter* spp. Examination for fecal leukocytes is not recommended because they may be present in as few as 25% of cases. Several enzyme immunoassays (EIAs) are available for direct detection of *C. jejuni* and *C. coli* antigens in stool specimens. Though convenient to use, however, test performance is documented to be highly variable among these kits (Fitzgerald et al., 2016). Various media can be used for the selective isolation of *Campylobacter* spp., including charcoal-cefoperazone deoxycholate agar (CCDA), charcoal-based selective medium (CSM), semisolid blood-free motility medium, Skirrow medium, and Campy-CVA (cefoperazone, vancomycin, amphotericin B). Most *Campylobacter* spp. require a microaerobic environment (5% O_2, 10% CO_2, and 85% N_2), which can be produced using commercially available gas generator packs or the Anoxomat automated system. The amount of oxygen in a candle jar is insufficient to support the growth of *Campylobacter* spp., thus should not be used. Incubation of the plates at 42°C for at least 72 hours increases selectivity for *C. jejuni* while suppressing the growth of normal fecal flora. Commercial multiplex PCR assays that detect multiple pathogens in stool are also available. If *Campylobacter* spp. are suspected in a blood culture based on clinical history or appearance of the organism on Gram stain, the broth should be subcultured to a nonselective blood agar plate and incubated at 37°C in a microaerobic environment.

In general, *Campylobacter* spp. grow as gray, flat, irregular, spreading colonies, which may become round, convex, and glistening as the moisture content in the media is reduced. A typical Gram stain appearance and a positive oxidase reaction from a colony growing on selective media at 42°C can be reported as *Campylobacter* spp. *C. jejuni* is able to hydrolyze hippurate and is susceptible to nalidixic acid and resistant to cephalothin. *C. coli* is hippuricase negative. *C. fetus* subsp. *fetus* is resistant to nalidixic acid, fails to hydrolyze hippurate, and does not ordinarily grow at 42°C. MALDI-TOF has been shown to reliably identify common *Campylobacter* species.

Antimicrobial Susceptibility

C. jejuni and *C. coli* are variably susceptible to antimicrobial agents. Most are not susceptible to penicillins or cephalosporins. For intestinal infection, macrolides are the drugs of choice, with fluoroquinolones used as alternative therapy. Treatment often is not warranted, however, for simple gastroenteritis with *Campylobacter* spp. in an otherwise healthy individual. Resistance to both agents has been encountered. The CLSI M45-A3 document provides standardized methods for susceptibility testing for this group of organisms; it recommends performing testing for erythromycin, ciprofloxacin, and tetracycline (CLSI, 2015).

Helicobacter

Characteristics

Helicobacter spp. are non–spore-forming, spiral-shaped or curved, gram-negative bacilli, measuring 0.3 to 0.6 μm wide and 1 to 10 μm long. They are motile by multiple bipolar or monopolar flagella, microaerophilic, and have a respiratory metabolism.

Clinical Manifestations and Pathogenesis

Helicobacter spp. are found in the GI tracts of mammals and birds. Transmission from one host to another is not completely understood, but there is evidence to support both oral-oral and fecal-oral spread. *H. pylori* is considered to be one of the gastric helicobacters. In the stomach, it lives within or beneath the mucous layer adjacent to the epithelium. It is also found transiently in the duodenum, saliva, and feces.

Infection with *H. pylori* results in acute gastritis with nausea and abdominal pain. Most infected patients develop chronic active gastritis, which may lead to nonulcer dyspepsia or duodenal ulcers. *H. pylori* has been associated with 90% of duodenal ulcers and nearly all gastric ulcers. Infection with *H. pylori* has also been associated with gastric adenocarcinoma and gastric mucosa–associated lymphoid tissue (MALT) lymphoma (Testerman & Morris, 2014). The prevalence of gastritis associated with *H. pylori* increases with age, suggesting that the organism is acquired over time as people age.

The enteric helicobacters, such as *H. cinaedi* and *H. fennelliae*, have been implicated in cases of gastroenteritis. Rarely, these organisms may invade the bloodstream and can be isolated from blood cultures, particularly in immunocompromised hosts.

Laboratory Diagnosis

Typically, nonculture methods, such as the urea breath test or stool antigen test, are utilized to diagnose *H. pylori* infection as well as assess eradication following treatment. The urea breath test is a noninvasive method to detect urease activity of *H. pylori* by measuring $^{13}CO_2$ in the patient's expelled air after ingestion of ^{13}C labeled urea. Enzyme-linked immunosorbent assay (ELISA)–based stool antigen tests using monoclonal antibodies have higher sensitivity and specificity than tests using polyclonal antibodies or immunoenzymatic point-of-care tests (Korkmaz et al., 2013). Serologic assays, while once widely used in symptomatic patients to detect antibodies against *H. pylori*, are no longer recommended by the American College of Gastroenterology (ACG) due to prolonged seropositivity after treatment. Also, because most adults have been exposed to *H. pylori*, detection of IgG antibodies is not helpful diagnostically but may be used as an epidemiologic or surveillance tool. In some cases, gastric biopsies from the affected tissues of the corpus and antrum are obtained and examined histologically using hematoxylin and eosin, Warthin-Starry, and/or *H. pylori*–specific antibody immunohistochemical stains for the presence of organisms with morphology typical of *H. pylori*. Because the organism rapidly hydrolyzes urea, a portion of the gastric biopsy may be placed directly into urea containing agar or onto urea containing paper strips to detect breakdown products of ammonia and carbonate over 1 to 24 hours.

If culture is requested, tissue specimens should be maintained at 4°C and transported to the laboratory within 2 hours of collection. Acceptable transport media include isotonic saline with 4% glucose, Stuart transport medium, *Brucella* broth with 20% glycerol, and *H. pylori*–selective semisolid transport medium. Processed specimens may be inoculated to one of several media, including brain-heart infusion, *Brucella*, trypticase soy agar, Columbia agar base with 10% defibrinated horse blood, or Wilkens-Chalgren agar. Inoculated media should be incubated in a microaerobic atmosphere (10% CO_2, 85% N_2, and 5% O_2) under high humidity at 35°C for a minimum of 10 days. Addition of 5% to 8% H_2 in the atmosphere enhances growth of *H. pylori*, which generally produces small, gray, translucent colonies that have a characteristic gram-negative spiral appearance on stained smears and are positive for oxidase, catalase, and urease. Stool is generally not cultured for the enteric helicobacters. *Helicobacter* spp. will grow and be detected by automated blood culture systems used in many laboratories but may require incubation for longer than the standard 5 days (Couturier, 2019). *Helicobacter* spp. are not included in the commercial databases of MALDI-TOF; therefore, they are not useful in the identification of these organisms. While it has been reported PCR is a sensitive method for detection of *H. pylori* and faster than culture, limitations such as false-positive results and lack of a commercial method preclude its use for routine patient care (Sugimoto et al., 2009; Couturier, 2019).

Antimicrobial Susceptibility

Multidrug regimens are used to treat *H. pylori* infection. First-line therapy consists of clarithromycin, either amoxicillin or metronidazole, and a proton pump inhibitor. Tetracycline, levofloxacin, and nitroimidazole are additional antibiotic options included in other treatment regimens. The latest clinical guidelines regarding the treatment of *H. pylori* gastritis were published by the ACG in 2017 (Chey et al., 2017). While routine susceptibility testing is not recommended, resistance to metronidazole and clarithromycin have been reported. Interpretive breakpoints for clarithromycin are provided in the CLSI M45-A3 document and should be tested in cases of apparent treatment failure (CLSI, 2015). The use of molecular methodologies to detect genotypic resistance to clarithromycin has also been successfully performed (Arevalo-Jaimes et al., 2019).

Haemophilus

Characteristics

Members of the *Haemophilus* genus are oxidase-positive, facultatively anaerobic, small, gram-negative, pleomorphic rods or coccobacilli with a potential requirement for X (hemin) and/or V (NAD) factors. Figure 57.18 shows an *H. influenzae* bacterium in a brain abscess specimen.

Clinical Manifestations and Pathogenesis

Most *Haemophilus* spp. are commensal bacteria of the mucous membranes of the oral cavity and upper respiratory tract. Some may reside in the gastrointestinal or urogenital tract. Person-to-person spread occurs by respiratory droplets. Infections caused by *Haemophilus* spp. range from conjunctivitis, otitis media, and sinusitis to epiglottitis, pneumonia, meningitis, and endocarditis. Species that are generally considered human pathogens are *H. influenzae*, *H. parainfluenzae*, *H. haemolyticus*, *H. ducreyi*, and *Aggregatibacter (Haemophilus) aphrophilus* (Gonzalez & Ledeboer, 2019).

The major virulence factor of *H. influenzae* is the polysaccharide capsule, of which there are six serotypes (a to f). Strains that do not possess a capsule are referred to as nontypeable. Endotoxin is not produced by *H. influenzae*, and this species is rapidly killed once ingested by macrophages unless antibody, complement, or phagocytic responses are deficient. The role of antibodies in immunity is poorly understood. Antibodies develop with age, presumably following natural infection with *H. influenzae* or with cross-reacting antigenic organisms. Thus, most persons older than 15 years have antibodies. Which antibodies are present and at what level those antibodies are protective remain unknown.

Since the introduction of the conjugate antigen vaccine for *H. influenzae* type b in the mid-1980s, there has been a sharp drop in the incidence of invasive infection, such as meningitis and epiglottitis, due to this organism. Figure 57.19 demonstrates the pleomorphic nature of the *H. influenzae* seen in a CSF specimen. Nontypeable strains of *H. influenzae* are most frequently associated with acute otitis media and acute exacerbations of chronic bronchitis and are currently the most prevalent strain causing invasive infections (Butler et al., 2018). *H. parainfluenzae* is usually a commensal in the pharynx and nasopharynx but may also cause illnesses similar to *H. influenzae* and, rarely, endocarditis. *A. aphrophilus*, another upper respiratory tract commensal, can cause endocarditis, brain abscess, pneumonia, meningitis, and bone and joint infections. *H. ducreyi* causes chancroid, a sexually transmitted disease most common in developing countries (Gonzalez & Ledeboer, 2019).

Laboratory Diagnosis

Isolation of *Haemophilus* spp. usually requires the presence of X and/or V factor in the culture medium. The former is most frequently supplied by the incorporation of heat-lysed ("chocolatized") blood cells in agar, although it may also be provided by whole human, horse, or rabbit blood cells. NAD is commonly supplied by the incorporation of yeast extract or other appropriate supplements in the medium or by a suspension of staphylococci, which is streaked across the agar surface and about which satellite colonies of dependent strains of *Haemophilus* spp. grow. The differential characteristics of members of this genus are listed in Table 57.9.

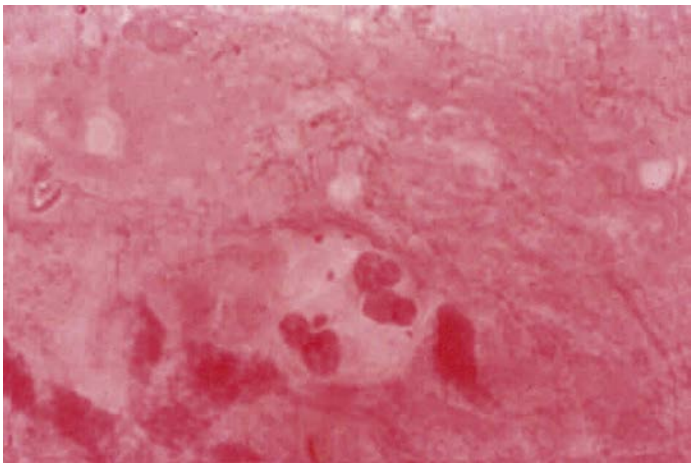

Figure 57.18 Gram stain of a *Haemophilus influenzae* coccobacillus in a brain abscess (oil immersion).

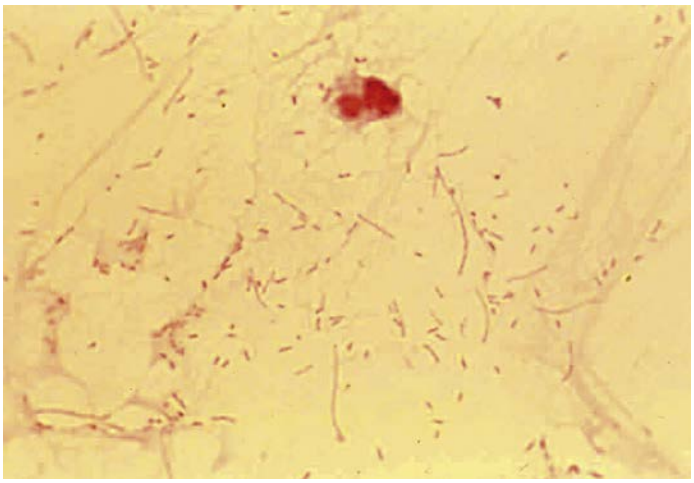

Figure 57.19 Note the pleomorphic nature of the *Haemophilus influenzae* seen in this Gram stain of cerebrospinal fluid (oil immersion).

TABLE 57.9

Differential Characteristics of Medically Important *Haemophilus* Species

	Porphyrin	X Factor Dependent	V Factor Dependent	Fermentation of Sucrose	Hemolysis*	Catalase
Haemophilus influenzae	–	+	+	–	–	+
Haemophilus haemolyticus	–	+	+	–	+	+
Haemophilus parahaemolyticus	+	–	+	+	+	V
Haemophilus ducreyi	–	+	–	–	–	–
Haemophilus parainfluenzae	+	–	+	+	–	V
Haemophilus pittmaniae	+	–	+	+	+	W
Haemophilus paraphrohaemolyticus	+	–	+	+	+	+

+, Positive; –, negative; *V*, variable; *w*, weak.
*On horse and rabbit blood.
Modified from Gonzalez MD, Ledeboer NA: Haemophilus. In Carroll KC, Pfaller MA, Landry ML, et al., editors: *Manual of clinical microbiology*, ed 12, Washington, DC, 2019, American Society for Microbiology, p 671.

Requirements for X and V factors are determined by the presence or absence of growth on media containing these factors. An alternative method to test for X factor dependence is the porphyrin test described by Kilian, which determines the ability of *Haemophilus* spp. to convert δ-aminolevulinic acid into porphobilinogen and porphyrins, which are the metabolic intermediates of X factor. The formation of porphobilinogen can be detected by adding Kovac's reagent to the reaction mixture and observing the development of a red color in the aqueous phase. Alternatively, the formation of porphyrins in the reaction mixture can be demonstrated by red fluorescence under a Wood's lamp. When the porphyrin test is positive, the organism is X factor independent; when the test is negative, the organism requires X factor for growth. Hemolytic properties of *Haemophilus* spp. can be determined on rabbit or horse blood agar.

A. aphrophilus must often be distinguished from species such as *A. actinomycetemcomitans*, *Cardiobacterium hominis*, and *Eikenella corrodens* (Table 57.10), all of which have been associated with subacute bacterial endocarditis. These organisms, as well as many clinically relevant *Haemophilus* spp., are able to be identified by commercial biochemical systems and MALDI-TOF (Couturier et al., 2011).

Cultivation of *H. ducreyi* from chancroid lesions is problematic. A gram-stained smear of material from the lesion may be helpful if gram-negative bacilli in pairs or in rows ("schools of fish") are seen. Figure 57.20 shows a typical Gram stain of *H. ducreyi* from a genital lesion. Material may be inoculated onto a GC medium base plus 1% hemoglobin, 5% fetal calf serum, 1% IsoVitaleX (BBL Microbiology Systems), and 3 μg/mL of vancomycin or Mueller-Hinton agar plus 5% horse blood, 1% cofactor-vitamin-amino acid enrichment, and 3 μg/mL vancomycin. These media should be incubated at 35°C with 5% CO_2 for 5 days to allow for growth of these fastidious organisms.

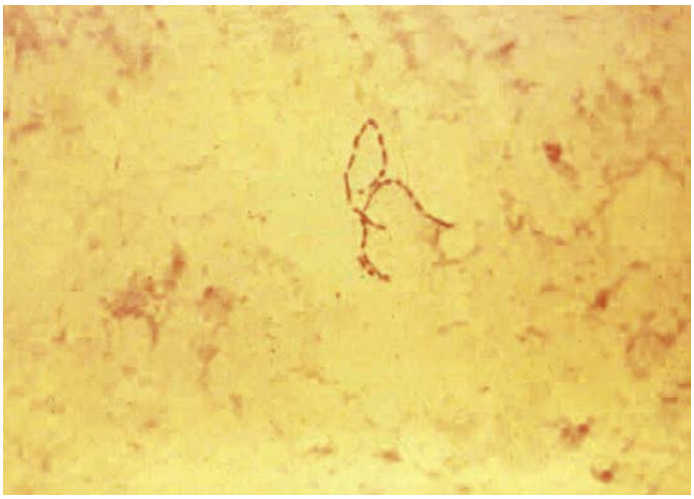

Figure 57.20 *Haemophilus ducreyi* bacilli from a genital lesion (oil immersion).

Antimicrobial Susceptibility

Currently, the CLSI recommends testing *H. influenzae* isolated from blood or CSF against ampicillin, chloramphenicol, a third-generation cephalosporin, and meropenem (CLSI, 2019). Resistance to ampicillin may be as high as 60% in the United States, varying geographically. Resistance to ampicillin is usually mediated by the production of a β-lactamase. However, rare isolates are resistant to ampicillin due to altered penicillin binding proteins and are classified as β-lactamase negative and ampicillin resistant (BLNAR). As β-lactamase producing strains of *H. influenzae* remain susceptible to cephalosporins, β-lactam combination agents, and carbapenems, susceptibility testing from respiratory isolates, outside of a β-lactamase assay, is often not necessary. Susceptibility testing of *H. influenzae* and *H. parainfluenzae* requires the use of *Haemophilus* test medium (HTM) and can be done by disk diffusion or broth microdilution. The recommended treatment for *H. ducreyi* infection is a single dose of azithromycin or ceftriaxone. Alternative regimens include ciprofloxacin or erythromycin, but resistance to both of these antibiotics has been reported.

GRAM-NEGATIVE BACTERIA—THE HACEK BACTERIA

The HACEK bacteria are a group composed of the following organisms: *Aggregatibacter aphrophilus*, *A. actinomycetemcomitans*, *Cardiobacterium hominis*, *E. corrodens*, and *Kingella* spp. As a result of taxonomic changes, some of the HACEK members previously in the *Haemophilus* genus have been reassigned to the *Aggregatibacter* genus (Norskov-Lauritsen & Kilian, 2006). The HACEK group are gram-negative coccobacilli that make up the microbiota of the nasopharynx and oral cavity and are known to cause subacute bacterial endocarditis. They spread endogenously to the bloodstream, settle on native or prosthetic heart valves, and cause a slowly progressive, indolent form of endocarditis. As a group, the HACEK organisms are fastidious, fail to grow on MacConkey agar, and require 5% to 10% CO_2 for enhanced growth. Differential characteristics of the members of the HACEK group are listed in Table 57.10.

Haemophilus

H. influenzae and *H. parainfluenzae* were discussed earlier in this chapter. *Aggregatibacter aphrophilus* is a member of the HACEK group and grows well on blood and chocolate agars, as it does not require X or V factors. Along with causing endocarditis, *A. aphrophilus* has been reported in cases of endophthalmitis following ophthalmic procedures, bone and joint infections, peritonitis, and brain abscess. In one study, 39% of patients who developed an *A. aphrophilus* infection reported undergoing prior dental procedures (Huang et al., 2005). Testing for the presence of β-lactamase is recommended and combination therapy with a β-lactam and an aminoglycoside may be required for successful treatment of serious infections.

Aggregatibacter

Characteristics

A. actinomycetemcomitans is a gram-negative, non–spore-forming coccobacillus or short rod. It is a facultative anaerobe whose growth is enhanced in the presence of 5% to 10% CO_2. Colonies are small, with an irregular edge on blood agar; with prolonged incubation, they become star-shaped in appearance.

TABLE 57.10

Differential Characteristics of HACEK Organisms Frequently Isolated from Clinical Specimens

Test	*A. aphrophilus*	*A. actinomycetemcomitans*	*C. hominis*	*E. corrodens*	*K. kingae*
Oxidase	V	–/w	+	+	+
Catalase	–	+	–	–	–
δ-ALA utilization	+	+	+	+	+
V requirement	V	–	–	–	–
Indole	–	–	+	–	–
Urease	–	–	–	–	–
Lysine decarboxylase	–	–	–	+	–
Acid from glucose	+	+	+	–	+
Sucrose	+	–	+	–	–
Lactose	+	–	–	–	–
Mannitol	–	V	+	–	–
Xylose	–	V	–	–	–

+, Positive; –, negative; *V*, variable; *w*, weak.
δ-ALA, δ-Aminolevulinic acid.

Clinical Manifestations and Pathogenesis

Aggregatibacter organisms are found in the mucous membranes of the respiratory and genitourinary tracts of humans and animals. They generally are considered nonpathogenic and cause disease only in immunocompromised individuals or when they are traumatically introduced into healthy tissues. *A. actinomycetemcomitans* is a major cause of juvenile and adult periodontitis and also causes soft-tissue infections, osteomyelitis, and endocarditis. As implied by its species name, there is a frequent association with *Actinomyces* spp. in sulfur granules. A leukotoxin is the main virulence factor described (Zbinden, 2019).

Laboratory Diagnosis

A. actinomycetemcomitans grows on blood and chocolate agar. After 24 to 72 hours, the colonies are 1 to 3 mm in diameter, with a central wrinkling. The organism is catalase positive, oxidase negative or weakly positive, and urease negative (Zbinden, 2019). Additional biochemical methods or MALDI-TOF must be used to differentiate *A. actinomycetemcomitans* from other slowly growing, somewhat fastidious gram-negative bacilli (see Table 57.10).

Antimicrobial Susceptibility

This organism is resistant to penicillin but is usually susceptible to many other antibiotics, including the cephalosporins, β-lactam combination agents, fluoroquinolones, and tetracycline. Macrolide and aminoglycoside resistance has been documented. Methods for performing susceptibilities and interpretation of results can be found in the CLSI M45-A3 document (CLSI, 2015).

Cardiobacterium hominis

Characteristics

C. hominis is a gram-negative, non–spore-forming bacillus that is part of the normal flora of the oral cavity and nasopharynx. It is a facultative anaerobe that does not require CO_2, although growth is enhanced in microaerobic conditions. Growth occurs on blood and chocolate agar but not on MacConkey agar and typically requires at least 48 hours of incubation.

Clinical Manifestations and Pathogenesis

C. hominis mainly causes subacute bacterial endocarditis, similar to other HACEK members, but it may rarely cause abscess and soft-tissue infections at other body sites. The usual habitat of *C. hominis* is the upper respiratory tract, but it may also be found in the gastrointestinal and genitourinary tracts (Zbinden, 2019).

Laboratory Diagnosis

After 48 hours of incubation, colonies are small and may have a yellow pigment, although most are white. The Gram stain of *C. hominis* shows gram-negative rods arranged in characteristic rosettes. The organism is generally oxidase and indole positive but negative for catalase, urease, esculin, and nitrate reduction.

Antimicrobial Susceptibility

Isolates are usually susceptible to penicillins, cephalosporins, carbapenems, and tetracyclines. Resistance to clindamycin is common. β-Lactamases have been rarely reported but can be overcome by a β-lactamase inhibitor (Lu et al., 2000). Methods for performing susceptibilities and interpretation of results can be found in the CLSI M45-A3 document (CLSI, 2015).

Eikenella

Characteristics

E. corrodens are facultative anaerobes whose colonies characteristically cause pitting of the agar surface. *E. corrodens* organisms are oxidase-positive, catalase-negative, nonfermentative, gram-negative bacilli. Growth is enhanced by 5% to 10% CO_2 and/or the presence of hemin (X factor) in the medium.

Clinical Manifestations and Pathogenesis

E. corrodens resides predominantly in the oral cavity and is isolated frequently from the upper respiratory tract of humans. Similar to other HACEK bacteria, it is responsible for subacute bacterial endocarditis, especially in intravenous drug users who clean the needles with saliva. It has been associated with periodontitis and recovered from abscesses, cellulitis, and wound infections, often following human bites. Infections are usually mixed with other organisms, particularly staphylococci and streptococci (Zbinden, 2019). Little is known about factors contributing to the organism's virulence in human disease, but *E. corrodens* is thought to induce inflammation in dental disease (Zbinden, 2019).

Laboratory Diagnosis

Growth is observed on blood or chocolate agar but not on MacConkey agar. The most striking features of *E. corrodens* in culture are the distinctive bleach-like odor and the characteristic pitting of the agar. Pitting does not occur with all strains, however. Colonies appear slowly after 2 to 4 days of incubation and are generally small (1–2 mm in diameter). *E. corrodens* usually must be distinguished from other fastidious, slowly growing gram-negative bacilli by biochemical or MALDI-TOF methodologies (see Table 57.10).

Antimicrobial Susceptibility

E. corrodens is susceptible to the penicillins, cephalosporins, fluoroquinolones, and tetracycline, with variable susceptibilities to aminoglycosides, and is often resistant to macrolides and clindamycin. β-Lactamases have been described in clinical strains, but resistance can be overcome with the use of a β-lactam combination agent (Zbinden, 2019).

Kingella

Characteristics

Kingella is composed of four species: *K. kingae* (the HACEK species), *K. oralis*, *K. denitrificans*, and *K. potus*. They are gram-negative coccobacilli to rods that require increased CO_2 for optimum growth. Colonies grow well on blood and chocolate agars but not on MacConkey agar, and exhibit a narrow but distinct zone of β hemolysis.

Clinical Manifestations and Pathogenesis

K. kingae is the most pathogenic of the genus and causes an indolent, slowly progressive endocarditis. In addition, it is associated with septic arthritis, osteomyelitis, and septicemia in otherwise healthy children between 6 months to 4 years of age (Yagupsky, 2015). *K. oralis* has been isolated from patients with periodontitis but with unclear clinical relevance. *K. denitrificans* is a rare clinical isolate that can be associated with endocarditis (Zbinden, 2019).

Laboratory Diagnosis

K. kingae is oxidase-positive, nonmotile, and produces acid from glucose, although in delayed fashion. Indole and catalase are negative. Both biochemical and MALDI-TOF methodologies can successfully identify *K. kingae*. Laboratory developed reverse transcriptase–polymerase chain reaction (RT-PCR) tests to detect *K. kingae* from pediatric clinical isolates are often performed due to increased sensitivity and specificity in this population (El Houmami, 2018).

Antimicrobial Susceptibility

K. kingae is susceptible to penicillin and most antibiotics to which other members of the HACEK group are susceptible. β-Lactamases have been described in clinical strains, but resistance can be overcome with the use of β-lactam combination agents (Zbinden, 2019). Methods for performing susceptibilities and interpretation of results can be found in the CLSI M45-A3 document (CLSI, 2015).

MISCELLANEOUS GRAM-NEGATIVE BACILLI

Legionella

Characteristics

Legionella spp. are obligately aerobic, faintly staining, small, gram-negative bacilli. *Legionella* spp. were first recognized to cause human disease during an epidemic of pneumonia that occurred among members of the Pennsylvania American Legion who had gathered in Philadelphia to celebrate the 1976 bicentennial. There are now more than 59 named species and a number of unnamed species as well. Most clinical cases have been due to *L. pneumophila* serogroup 1. Figure 57.21 demonstrates excellent staining of *Legionella* spp. with a Dieterle silver stain.

Clinical Manifestations and Pathogenesis

Legionella spp. are found in the environment in association with water. Growth within environmental protozoa, such as *Acanthamoeba* and *Naegleria*, is thought to be an important factor for survival of the organism in the environment. Transmission to humans occurs through the aerosolization of contaminated water from faucets, shower heads, and public fountains. *Legionella* spp. have been found in high concentrations in warm water from water heaters, cooling towers, and warm-water spas. Human-to-human infection and laboratory-acquired infections are not known to occur.

Infections can be subclinical, pulmonary, or extrapulmonary. Infection is usually manifested as an acute, fibrinopurulent pneumonia with lobular distribution. Histologically, there is an alveolar infiltrate of neutrophils

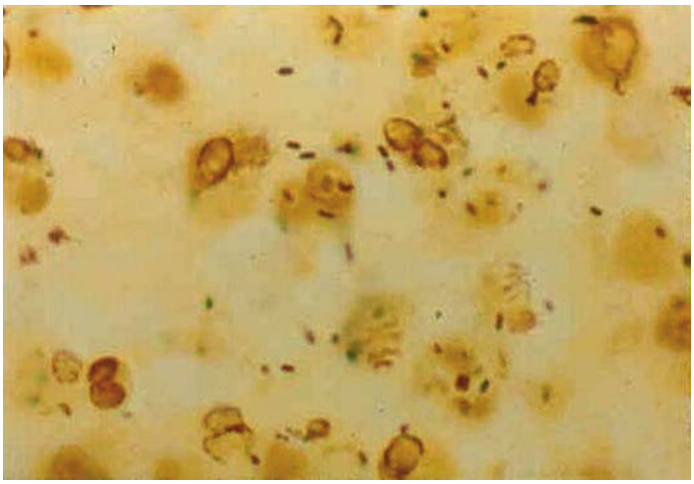

Figure 57.21 *Legionella pneumophila* in a clinical specimen stained with a Dieterle silver stain (oil immersion).

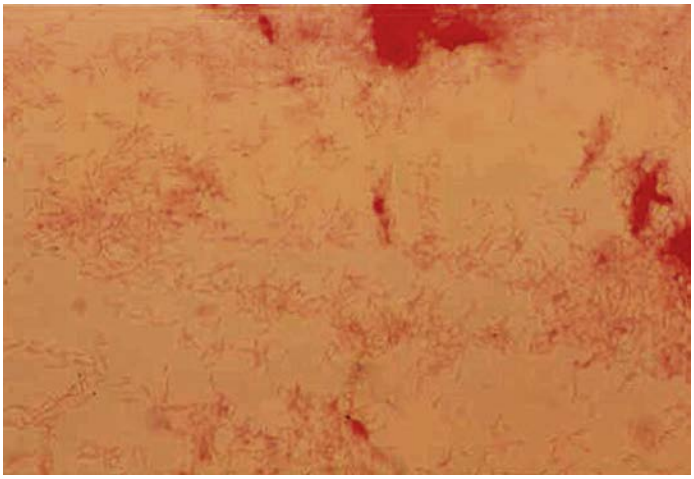

Figure 57.23 Gram stain of culture of *Legionella pneumophila* (oil immersion).

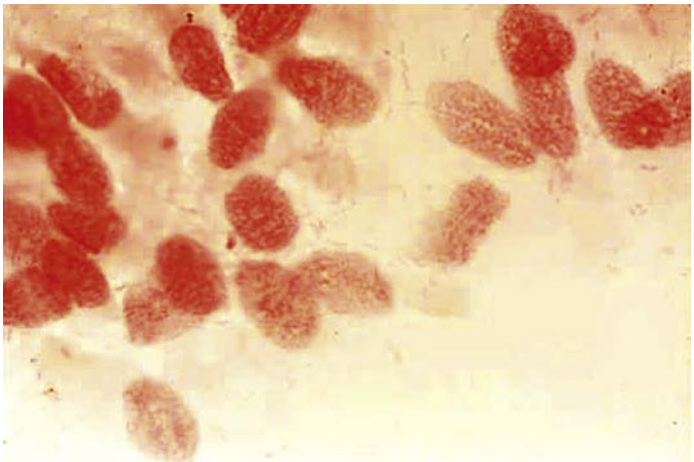

Figure 57.22 *Legionella pneumophila* faintly staining negative with Gram stain of pulmonary infiltrate (oil immersion).

and macrophages, accompanied by fibrin and red blood cell extravasation. *Legionella* spp. primarily causes disease by infecting the alveolar macrophages. Figure 57.22 shows the Gram stain of sputum of a patient with *L. pneumophila* pneumonia. *L. pneumophila* has been isolated from blood cultures as well.

Laboratory Diagnosis

Legionella spp. are isolated using BCYE agar supplemented with growth factors, including L-cysteine, ferric salt, and α-ketoglutarate. This medium may be made selective for culture from nonsterile body sites by the addition of cefamandole, polymyxin B, and anisomycin, or polymyxin B, anisomycin, and vancomycin (Edelstein, 2019). Chocolate agar may also support the growth of legionellae. Treatment of sputum with a weak acid (KCl-HCl, pH 2.2) for 4 minutes or with heat (50°C) for 30 minutes may help to reduce contamination from other organisms. However, care should be taken to strictly follow procedures, as the yield of *Legionella* spp. may be adversely affected. Performing a 1:10 dilution in tryptic soy broth or distilled water for respiratory tract specimens will increase the culture yield due to decreased inhibition by antibiotics and serum and tissue factors (Edelstein, 2019).

Inoculated media should be incubated for at least 5 days and up to 14 days in a humid atmosphere containing no more than 2% to 5% CO_2. Colonies often appear iridescent and have a sticky consistency. Isolates with typical Gram stain morphology should be subcultured to BCYE without cysteine or blood agar, where no growth should be observed due to the organism's dependence on cysteine. These organisms may be weakly oxidase and catalase positive and often are motile. Further identification of *Legionella* spp. is most accurately achieved using type-specific antibody assays or sequencing with appropriate primers. Potential drawbacks in the accurate identification of *Legionella* spp., especially those other than *L. pneumophila* serogroup 1, include the lack of commercial platforms, cross-reactivity, expense, and expertise necessary to perform testing. Referral to large reference laboratories with experience in *Legionella* identification procedures or public health laboratories may be necessary (Edelstein, 2019). Figure 57.23 shows a Gram stain of *L. pneumophila* from culture.

Previously, direct fluorescent antibody (DFA) staining was used to identify *Legionella* spp. directly from respiratory specimens, but the sensitivity is lower than newer detection methods and is rarely used. The urine antigen test for *L. pneumophila* serogroup 1 is often used as an initial diagnostic test due to high specificity, ease of use, and rapid results, but clinical sensitivity varies depending on subtype and severity of illness. Use of the urinary antigen test within the intensive care unit and for patients on ventilators has been shown to have a positive impact on patient cases (Couturier et al., 2014; Edelstein, 2019).

The diagnosis of legionellosis can also be established serologically by detecting a fourfold or greater rise in antibody titer to at least 1:128. A single antibody titer of 1:256 is presumptive evidence of past infection. However, the clinical utility of serologic tests is limited due to the need for acute and convalescent sera at multiple time points and the fact that not all patients seroconvert. PCR assays for direct detection of *Legionella* spp. in clinical specimens and for sequencing identification of cultured isolates have been developed. A meta-analysis of 9 studies that evaluated PCR tests reported a pooled sensitivity of 83% (95% confidence interval [CI]: 79%–87%) and specificity of 90% (95% CI: 88%–92%) (Cristovam et al., 2017). Use of these molecular assays can provide more rapid results, especially when direct clinical specimens are tested. In addition, sequencing-based identification has been successful in correctly identifying about 90% of *Legionella* spp. other than *L. pneumophila* to the species level. Recently, a multiplex PCR assay that is able to detect fastidious organisms such as *Mycoplasma pneumoniae*, *Chlamydia pneumoniae*, and *L. pneumophila* directly from lower respiratory tract isolates has become commercially available (FilmArray Pneumonia Panel, BioFire Diagnostics, Salt Lake City, UT).

Antimicrobial Susceptibility

Because of the intracellular nature of *Legionella* spp. in clinical infection, in vitro susceptibility test results do not predict the clinical response of antibiotics. As the media required to grow *Legionella* spp. inactivates many antibiotics, there are no published CLSI guidelines and susceptibility testing should not be routinely performed. Macrolide, tetracycline, and fluoroquinolone antibiotic agents are able to achieve adequate intracellular concentrations and are effective treatment for legionellosis (Valve et al., 2009; Edelstein, 2019). No β-lactam or aminoglycoside antibiotic has acceptable intracellular activity against *L. pneumophila*. Macrolides and fluoroquinolones are also efficacious against infection with *L. micdadei*, *L. longbeacheae*, *L. bozemanae*, or L. *dumoffi* (Muder & Yu, 2002).

Bordetella

Characteristics

Bordetella spp. are strictly aerobic, catalase-positive, small gram-negative coccobacilli that can oxidize amino acids but do not ferment sugars. Members of the genus *Bordetella* include *B. pertussis* and *B. parapertussis*, which are responsible for pertussis or a pertussis-like disease in humans, respectively. *B. bronchiseptica* and *B. avium*, which are primarily responsible for disease in dogs and birds, can rarely cause respiratory infections in humans. Other uncommon *Bordetella* spp., including *B. hinzii*, *B. trematum*, *B. holmseii*, *B. petri*, and *B. ansorpii*, have been found to be infrequent causes of

nonrespiratory infections in humans, particularly in immunocompromised hosts (Kilgore & Coenye, 2019).

Clinical Manifestations and Pathogenesis

Bordetella spp. are found in the respiratory tract of warm-blooded animals and humans. *B. pertussis*, the etiologic agent of whooping cough, is considered to be strictly a human pathogen. Infection initially presents as a runny nose, sneezing, and coughing (catarrhal phase), followed by coughing spasms, whooping, and vomiting (paroxysmal phase). Prolonged coughing for 3 to 6 weeks can occur (convalescent phase). In 2017, more than 18,000 cases of whooping cough were reported to the CDC, with approximately half of cases occurring in adolescents and adults. In California alone in 2014, an outbreak with nearly 10,000 cases was reported (cdc.gov/pertussis). Most of the cases in children less than 12 months old who were hospitalized during this epidemic were not vaccinated. Whooping cough is less easily diagnosed in adults, but there are indications that the number of cases is increasing in adults as well as children as protection from the vaccine wanes over time (McGuiness et al., 2013). *B. parapertussis*, which infects both humans and sheep, is less frequently identified as infection may be asymptomatic or may cause a pertussis-like illness or bronchitis. *B. bronchiseptica* primarily causes kennel cough in dogs, although it may rarely cause pertussis-like symptoms in immunocompromised human hosts.

Both *B. pertussis* and *B. parapertussis* can cause whooping cough, although cases due to the latter are usually milder and of shorter duration. They are transmitted via respiratory droplets from other infected individuals. In unvaccinated individuals, the transmission rate can be as high as 90%, whereas lower rates are seen in vaccinated populations. Protection against *B. pertussis* wanes over the years postinfection or vaccination. Thus, the World Health Organization (WHO) recommends that adolescents, pregnant women, and adults receive a booster dose of the acellular pertussis vaccine (Tdap) in order to reduce the burden of circulating *B. pertussis*, especially to newborns and infants (WHO, 2015). *B. holmseii* has been more recently described as causing bacteremia, endocarditis, meningitis, and arthritis in addition to pertussis-like illnesses (Pittet et al., 2014).

Bordetella spp. produce a number of virulence factors, including adhesions, filamentous hemagglutinin, fimbriae, pertactin, and toxins. *B. pertussis* produces pertussis toxin that induces lymphocytosis and suppresses chemotaxis oxidative responses and inhibits the activity of neutrophils and macrophages (Kilgore & Coenye, 2019). At the onset of a pertussis infection, the organism first attaches to the ciliated epithelium of the upper respiratory tract and a variety of virulence factors work together to inhibit the host's immune system and damage the respiratory epithelium, resulting in inflammation, epithelial necrosis, accumulation of secretions, cough, and ultimately bronchopneumonia and hypoxic episodes (Kilgore et al., 2016).

Laboratory Diagnosis

Nasopharyngeal aspirate is the optimal specimen for the isolation of *Bordetella* spp., especially in infants and young children. In older children, adolescents, and adults, a Dacron or rayon nasopharyngeal swab is acceptable if properly collected (Kilgore & Coenye, 2019). *B. pertussis* and *B. parapertussis*, in particular, are sensitive to transport and should be cultured as quickly as possible after collection or placed into special transport devices, such as Amies medium with charcoal. Routine transport conditions are acceptable for other *Bordetella* spp., which are not as fragile. Nasopharyngeal specimens for culture and PCR testing should be collected at the onset of illness as the rate of isolation of *B. pertussis* declines with the duration of disease.

In general, swabs or aspirates should be inoculated onto suitable media, such as Regan-Lowe or Bordet-Gengou agar, as quickly as possible after collection. The medium used is usually supplemented with an antibiotic such as cephalexin to suppress contaminating bacteria and is incubated for at least 7 days at 35°C to 37°C in an ambient atmosphere. Colonies of *B. pertussis* are small, smooth, round, and glistening, resembling a drop of mercury. *B. pertussis* does not grow on blood agar. Positive catalase and oxidase reactions and a negative urease can be used for the presumptive identification of *B. pertussis*. *B. parapertussis* grows more rapidly and will have variable growth on Columbia agar. *B. parapertussis* is oxidase negative and catalase and urease positive. *B. bronchiseptica* grows well on both blood and MacConkey agars and is catalase, oxidase, urease, and nitrate reduction positive. *B. holmseii* grows well on blood agar, variably on MacConkey agar, and is oxidase and urease negative. MALDI-TOF provides good identification of the common *Bordetella* spp. Isolation of *B. pertussis* from culture is very specific; thus, sensitivity will depend on the patient's age, vaccination status, the duration of the illness, and quality of specimen collected.

Direct detection of *B. pertussis* in clinical specimens by PCR is more sensitive than culture and stringent transport conditions are not needed. A number of commercial PCR assays are available that include *B. pertussis* and *B. parapertussis* in *Bordetella*-specific assays or as part of larger multiplex panels for the diagnosis of upper respiratory infections. PCR primers are directed against multitarget copies, IS481, IS1001, IS1002, and the pertussis toxin to provide high sensitivity and specificity in distinguishing between the most common clinical species of *Bordetella* (Roorda et al., 2017). PCR assays that can also detect *B. parapertussis* should be utilized as, in the case of some whooping cough outbreaks, *B. parapertussis* is a significant pathogen (Kilgore & Coenye, 2019). PCR assays are able to detect *Bordetella* spp. for a longer time period during clinical illness as compared with culture and may remain positive, even with appropriate antimicrobial therapy. Direct examination of smears stained with fluorescein-conjugated *B. pertussis* monoclonal or polyclonal antiserum may provide a rapid diagnosis, but these DFA assays suffer from low sensitivity (30%–71%) and low specificity. As such, they are no longer recommended for *B. pertussis* diagnosis (Kilgore & Coenye, 2019).

Serologic methods for *B. pertussis* and *B. parapertussis* may be used to make the diagnosis of whooping cough in older vaccinated children, adolescents, and adults and is especially helpful in making the diagnosis in later phases of disease. Quantitative enzyme immunoassays measuring pertussis toxin antibodies is the method of choice. Demonstration of seroconversion or a significant rise in concentration of IgG antibodies to greater than 100 IU/mL provides good sensitivity and specificity for pertussis diagnosis in these patient populations. Serology, however, should not be used for 1 year after a person is vaccinated with the acellular pertussis vaccine, as it cannot distinguish between vaccine- or infectious-immunologic responses. A recent study comparing culture, PCR, and serology for diagnosis of pertussis demonstrated that PCR was more sensitive than culture in the first 2 weeks of illness and serology's greatest sensitivity was noted after the second week of symptoms (Lee et al., 2018).

Antimicrobial Susceptibility

Although the role of antibiotics in the treatment of pertussis is not well documented, macrolides (azithromycin, clarithromycin, and erythromycin) are the drugs of choice for treatment and prophylaxis. TMP-SMX is an acceptable alternative in patients who are unable to tolerate macrolides or when the isolate is erythromycin resistant, which is a rare occurrence. Early treatment of *B. pertussis* may prevent bacterial complications in patients with the disease and may decrease spread to nonimmune contacts. Susceptibility testing is not recommended for *B. pertussis*, and methods are not standardized (Kilgore & Coenye, 2019). Vaccines to prevent *B. pertussis* infections are combined with those for diphtheria and tetanus. Children less than 7 years old should receive a three-part series of the DTaP vaccine; adolescents, pregnant females, and all other adults should receive the Tdap vaccine.

Brucella

Characteristics

Brucella spp. are small, gram-negative coccobacilli that measure 0.5 to 0.7 μm by 0.6 to 1.5 μm. In smears, they occur predominantly as single coccobacilli, but they may occur in pairs or short chains. They are nonmotile, strictly aerobic, catalase- and oxidase-positive organisms. They are nonfermenters. They can grow on a variety of laboratory media, but growth is often enhanced by the presence of 5% to 10% CO_2 and the addition of blood or serum. Of the recognized species, *B. melitensis*, *B. abortus*, *B. suis*, and *B. canis* are human pathogens. *B. ovis* is a pathogen of rams, and *B. neotomae* has been isolated from desert and wood rats. The two species that have been recovered from marine animals are *B. pinnipedialis*, and *B. ceti*. All *Brucella* spp. hydrolyze urea except *B. ovis*, which remains a significant characteristic of the genus (Araj, 2019).

Clinical Manifestations and Pathogenesis

Brucella spp. are intracellular bacteria that infect a wide range of animals and can cause infections in humans. They are important veterinary pathogens and most human infections are found in those with occupational hazards such as veterinarians and dairy and abattoir workers. Preferential hosts are sheep, goats, and camels for *B. melitensis*, cattle for *B. abortus*, swine for *B. suis*, and dogs for *B. canis*. However, each species may occasionally cross-infect other mammals. Humans become infected by inhalation of aerosolized particles, direct contact with infected material, including animal carcasses, fetal membranes, vaginal discharge, fetuses, skin, or mucous membranes, or through the consumption of unpasteurized milk or milk products from infected animals. To prevent infection with *Brucella* spp., the CDC recommends not consuming undercooked meats or unpasteurized milk, cheeses, or ice cream. If animals are handled, proper use of personal protective equipment is essential to prevent infection. Approximately

100 cases of human brucellosis are reported per year in the United States; in 2015, there were 126 reported cases, with the most cases occurring in California (29) and Texas (23). A common risk factor for brucellosis in the United States is consumption of imported cheese made from unpasteurized goat's milk. In addition, brucellosis is the most often reported disease associated with laboratory acquisition. Thus, appropriate precautions should be taken when working with specimens and cultures from suspected cases (cdc.gov/brucellosis).

Brucella organisms are located intracellularly within neutrophils and macrophages. They have a variety of virulence factors that inhibit phagosome killing and promote survival. Local lymphadenopathy often occurs with dissemination via the reticuloendothelial system and formation of granulomas in various organs, including the liver, spleen, bone marrow, genitourinary tract, and lungs. Signs and symptoms are often variable and nonspecific, with fever, chills, sweats, and anorexia frequently occurring. The fever is characteristically diurnal or undulant and may be mistaken for malaria or typhoid fever. The incubation period is generally considered to be 1 to 4 weeks. Urease, which is produced by most *Brucella* spp., serves as an important virulence factor that enables passage through the acidic environment of the stomach when infection occurs through ingestion. *Brucella*-containing vacuoles enable escape from the host immune system and provide an acidic environment to avoid antibiotic killing (Araj, 2019). Complications of brucellosis infections include septicemia and osteomyelitis, and, rarely, orchitis, salpingitis, and cardiac and neurologic manifestations of the disease.

Laboratory Diagnosis

Brucella spp. are recovered most often from blood and bone marrow. Less often, they are recovered from material obtained from spleen and liver abscesses and CSF. The organism grows slowly on standard laboratory media, including *Brucella*, blood, chocolate, and trypticase soy agar. Some isolates have variable growth on MacConkey agar. *Brucella* spp. will grow in media used in automated blood culture systems and should be held 10 to 14 days, although the majority are positive within 5 to 7 days (Araj, 2019). *Brucella* spp. are recognized as Category B bioterrorism agents; once presumptive identification of *Brucella* spp. is made by the clinical laboratory (sentinel laboratory), species-level identification and other confirmatory testing should be completed by public health laboratories within the Laboratory Response Network (LRN) and the CDC.

Solid media should be incubated in an atmosphere containing 5% to 10% CO_2. These organisms grow slowly—even after 48 hours of incubation, colonies may be difficult to see. Organisms can be presumptively identified as *Brucella* spp. based on a characteristic Gram stain appearance and are catalase, oxidase, and urease positive. Urease activity is manifested rapidly (15 minutes) by *B. suis* and more slowly (2–24 hours) by *B. melitensis* and *B. abortus*. Because brucellosis can be laboratory acquired, laboratory personnel should be notified if this organism is suspected and all manipulations of possible *Brucella* spp. should be conducted in a biological safety cabinet (Araj, 2019).

Identification of *Brucella* to the species level requires tests for CO_2 requirement, oxidative metabolic tests, urea hydrolysis, dye sensitivity, and phage lysis. Clinical laboratories should refer this testing to other laboratories within the LRN. While some *Brucella* spp. are included in the databases, MALDI-TOF and other automated systems should not be used to identify these organisms due to the risk of aerosolization and laboratory-acquired infections. Molecular methods such as PCR have become more effective means of identifying cases of brucellosis (Schmoock et al., 2011).

There are many serologic tests that are also helpful in the diagnosis of brucellosis, commonly available in areas where brucellosis is endemic. The serum agglutination test (SAT) is among the most widely used. However, it has limitations, including false-negative results in chronic or complicated cases, cross-reactivity with *Francisella tularensis*, and a 24-hour turnaround time. The slide agglutination test is easy to perform, providing results within 10 minutes. It is relatively good in acute cases although, similar to the SAT, it is prone to false-negative and false-positive reactions. The indirect Coombs test is more useful in chronic cases, but it requires 48 hours for a result. ELISA is the method of choice in most chronic, complicated cases and is very sensitive and specific, with results obtained in 4 to 6 hours. *Brucella* agglutination titers of greater than 1:160 are usually considered positive, although lower titers with SAT have been reported in positive cases. It is recommended that two of these tests be used in combination for diagnosis to ensure that chronic cases are not missed (Araj, 2019).

Antimicrobial Susceptibility

Several antibiotics are effective against *Brucella* spp., including doxycycline, aminoglycosides, rifampin, TMP-SMX, some fluoroquinolones, and cephalosporins. Combination with dual or triple therapy is recommended because studies have shown more treatment failure and relapses when monotherapy is used (Skalsky et al., 2008). For uncomplicated cases, the WHO recommends treatment with doxycycline and rifampin for 6 to 8 weeks. Longer treatment periods are recommended for cases of neurobrucellosis and patients with endocarditis (Araj, 2019). Although treatment failures do occur, they are not thought to be due to antimicrobial resistance. Thus, susceptibility testing is not recommended, although the CLSI describes a broth microdilution method using unsupplemented *Brucella* broth to determine the MICs for doxycycline, tetracycline, and TMP-SMX (CLSI, 2015). Such testing, if needed, should be performed by a public health laboratory or the CDC.

Pasteurella

Characteristics

Pasteurella spp. are facultatively anaerobic, oxidase- and catalase-positive, nonmotile, gram-negative bacteria that range morphologically from coccobacilli to rods arranged in short chains. There are eight species known to cause infections in humans (*P. multocida*, *P. canis*, *P. dagmatis*, *P. stomatis*, *P. oralis*, *P. aerogenes*, *P. bettyae*, and *P. caballi*), with *P. multocida* recognized as the most important human pathogen. There has been some flux in the taxonomy of the *Pasteurella* genus; the latter three species may be reclassified in the future.

Clinical Manifestations and Pathogenesis

Pasteurella spp., especially *P. multocida*, may be found as normal microbiota in the nasopharynx and gingiva of wild and domesticated animals, including cats and dogs. Humans most frequently develop wound or soft-tissue infections after animal bites, scratches, or licking of wounds. Cat bites more often become infected than dog bites. Local infections can become systemic; a number of reports have described septicemia, osteomyelitis, and dialysis-associated peritonitis. *Pasteurella* spp. have also been associated with respiratory tract infections, including sinusitis, peritonsillar abscess, mastoiditis, pulmonary abscess, pneumonia, empyema, and bronchitis, usually in patients with underlying chronic pulmonary disease (Zbinden, 2019). Common virulence factors of *P. multocida* in human infections include a capsule, lipopolysaccharide, hyaluronidase, and a potent mitogen toxin (Wilkie et al., 2012).

Laboratory Diagnosis

Pasteurella spp. grow well on blood and chocolate agars as they do not require hemin or CO_2 and do not grow on MacConkey agar. A mouse-like odor is produced by indole-positive isolates. The finding of a small gram-negative rod with these growth characteristics that is oxidase, catalase, and indole positive provides strong presumptive evidence of *P. multocida*. In addition, susceptibility to penicillin, as evidenced by a wide zone of inhibition around a penicillin disk on a blood agar plate, also supports the diagnosis of *P. multocida*. Both commercial biochemical methods and MALDI-TOF provide good identifications for clinically relevant *Pasteurella* spp.

Antimicrobial Susceptibility

Pasteurella spp. are usually susceptible to penicillin, broad-spectrum cephalosporins, tetracyclines, fluoroquinolones, TMP-SMX, and azithromycin. However, resistance to oxacillin, cephalexin, erythromycin, and clindamycin is common. Penicillin is the therapeutic drug of choice. Rare strains of *P. multocida* have produced a β-lactamase, but β-lactam combination agents are effective in these cases (Zbinden, 2019). As wound infections usually contain multiple organisms, susceptibility testing for *Pasteurella* spp. is not generally required and empiric treatment is sufficient. Susceptibility guidelines are found in the CLSI M45-A3 document and testing is recommended for isolates obtained from normally sterile sites (CLSI, 2015).

Francisella tularensis

Characteristics

F. tularensis is a strictly aerobic, tiny gram-negative coccobacillus that requires cysteine for growth. These organisms are nonmotile, weakly catalase positive and oxidase and urease negative. *F. tularensis* is a virulent pathogen with an extremely low infectious dose.

Clinical Manifestations and Pathogenesis

F. tularensis is found mainly in North America in rodents, rabbits, ticks (*Dermacentor* spp. and *Amblyomma americanum*), and animal feces. The primary reservoir for this organism is hares and rabbits. Transmission to humans occurs through the bite of tick or deerfly, direct cutaneous inoculation from the handling of an infected or dead animal, conjunctival inoculation,

inhalation, or ingestion of undercooked infected animal meat or contaminated water. Several forms of the disease occur, including ulceroglandular, glandular, oculoglandular, oropharyngeal, pneumonic, and typhoidal. There were 239 cases of tularemia reported to the CDC in the United States in 2017. The disease is most prevalent in the south central states of Arkansas, Oklahoma, Missouri, and Kansas (cdc.gov/tularemia). *F. tularensis* is a category A agent of bioterrorism. Because of this, workup of suspected cases is limited to approved laboratories. Most clinical laboratories are considered sentinel laboratories; if *F. tularensis* is suspected, isolates should be sent to public health laboratories within the LRN or the CDC for further testing and confirmation (Dietrich & Petersen, 2019).

Tularemia manifests in various forms after an incubation period of 1 to 21 days. Headache, fever, chills, vomiting, and malaise characteristically occur at the onset. In ulceroglandular disease, lymphadenitis and lymphadenopathy occur in the region draining the primary lesion following direct exposure or a tick bite. The lesion is initially papular and then develops into an ulcer. Oculoglandular disease is characterized by inflammation of the conjunctiva and usually a papule of the lower lid with lymphadenitis of the preauricular, parotid, submaxillary, and anterior cervical nodes. The oropharyngeal form of tularemia is characterized by ulcerative lesions of the mouth, throat, and upper gastrointestinal tract after ingestion of contaminated food or water. The pneumonic form occurs after inhalation of aerosols, typically acquired by landscaping activities, mowing over rabbits, or laboratory exposure, and is considered the most severe. The CDC recommends the use of insect repellent when outdoors in tick- and deerfly-infested areas, wearing gloves when handling potentially infected animals, and cooking game meat thoroughly before eating. While vaccines have been developed in the past to protect personnel conducting biodefense research, they are not available to the public (Mulligan et al., 2017).

Virulence of *F. tularensis* appears to be related to its ability for intracellular replication, especially within macrophages, and its ability to evade host recognition. The *F. tularensis* genome, as compared with other *Francisella* spp., has two copies of an atypical type VI secretion system that allow for intracellular growth and virulence (Broms et al., 2010). Tularemia should be suspected in anyone who has been in an endemic area, had contact with wild animals or livestock, has a history of tick bites, has consumed contaminated food or water, or has been exposed to cultures or infected animals in the laboratory. Trappers, hunters, fur and meat industry workers, landscapers, and laboratory personnel are at greatest risk. Because of its nonspecific manifestations, especially in typhoidal cases, tularemia can be confused with many other diseases, such as brucellosis, anthrax, sporotrichosis, typhoid fever, tuberculosis, cat scratch fever, and plague.

Laboratory Diagnosis

Specimens suitable for culture include tissue or fluid from the primary lesion, aspirates of enlarged regional lymph nodes, sputum, pharyngeal washes, and gastric aspirates. Due to the low dose of organisms required for infection and aerosolization risks, appropriate precautions by laboratory personnel when handling suspicious specimens is required. Clinicians should always notify the laboratory if *F. tularensis* is suspected to prevent exposures. Bacterial isolation of *F. tularensis* is challenging due to its fastidious nature and special growth requirements, which may allow for overgrowth of other organisms in the specimen. *F. tularensis* grows on chocolate, Thayer-Martin, and BCYE agars as well as cysteine heart agar supplemented with 9% chocolatized sheep blood (CHAB) (Dietrich & Petersen, 2019). If clinical material is contaminated by other organisms, selective agar with antibiotics and antifungals can be used to isolate *F. tularensis*.

Cultures are incubated at 35°C with or without added CO_2. Colonies usually appear within 2 to 4 days and are blue-gray to white, round, smooth, and slightly mucoid. On blood-containing agar, a small zone of α-hemolysis may be seen. Isolates are weakly catalase positive, oxidase negative, nonmotile, and react with only a few carbohydrates. Because working with the organism in the laboratory is dangerous, suspected isolates should be sent to public health laboratories or the CDC for confirmation. While commercial systems and MALDI-TOF could potentially identify *F. tularensis*, their use is not recommended due to the risk of misidentification and aerosol generation (Rudrik et al., 2017).

The diagnosis of *F. tularensis* can also be established serologically. Titers determined by tube agglutination (TA), microagglutination (MA), or ELISA are standard methods utilized for detection of antibodies to *Francisella*. In the United States, a single TA titer of 1:160 or greater or an MA titer of 1:128 or greater is considered positive (Dietrich & Petersen, 2019). As with other serologic assays, demonstration of a fourfold change in titers between an acute and convalescent serum is also considered positive. Cross-reactivity with *Brucella* antibodies has been observed but usually at a considerably lower level (Dietrich & Petersen, 2019).

Antimicrobial Susceptibility

All *F. tularensis* isolates are β-lactamase positive, rendering penicillins and cephalosporins not effective. The antibiotics recommended for treatment and prophylaxis include streptomycin, gentamicin, doxycycline, and ciprofloxacin. The CLSI has published a method utilizing cation-adjusted Mueller-Hinton broth supplemented with 2% defined growth supplement for broth microdilution (CLSI, 2015). However, due to safety concerns and the fact that antibiotic resistance has not been reported, performing susceptibility testing is not recommended.

Gardnerella

Characteristics

Gardnerella vaginalis is a thin, gram-variable rod or coccobacillus that makes up the normal biota of the vaginal tract of females who are of reproductive age. *G. vaginalis* exhibits a slow fermentative metabolism and is nonmotile and catalase negative. Growth is best observed after 48 hours of incubation in a 5% CO_2-enriched atmosphere. Colonies are small and exhibit faint β-hemolysis on media containing rabbit or human blood.

Clinical Manifestations and Pathogenesis

Extensive colonization with *G. vaginalis* and other anaerobes with a decrease in protective *Lactobacillus* spp. is characteristic of bacterial vaginosis (BV), which results in inflammation and vaginal discharge. BV has been linked to preterm birth, endometriosis, PIDs, and an increased risk of other sexually transmitted diseases (Zevin, 2016). Occasionally, *G. vaginalis* can cause septicemia in postpartum females and newborns. As more research is conducted regarding the pathogenesis of BV, there is increasing evidence to support that BV may be sexually transmitted (Muzny & Schwebke, 2016).

Laboratory Diagnosis

Traditionally, the gold standard for the diagnosis of BV is direct examination of vaginal secretions for the presence of "clue cells" (epithelial cells covered with bacteria on the cell margins) on a wet prep or the identification of an increase in small or curved gram-negative rods and coccobacilli in the absence of lactobacilli (gram-positive thin rods) on Gram stain. Standardized scoring criteria are available and used in many microbiology laboratories to diagnosis BV (Nugent et al., 1991). Other common features of BV include a vaginal pH greater than 4.5 and a fishy amine odor after addition of 10% potassium hydroxide (KOH) to vaginal secretions. A few point-of-care tests that detect a high level of sialidase produced by BV-associated organisms are also available. Additionally, there is a growing number of commercially available molecular multiplexed assays to detect BV as well as other infectious causes of vaginitis. While bacterial culture is not recommended to diagnose BV, *G. vaginalis* can be isolated from blood and other nongenital sites. *G. vaginalis* grows as small, β-hemolytic colonies (<0.5 mm) after 24 to 48 hours on medium containing human or rabbit blood (Bernard, 2019). The Gram stain of *G. vaginalis* is Gram variable rods or coccobacilli and the majority of isolates hydrolyze hippurate. Biochemical identification systems and MALDI-TOF provide accurate identifications of *G. vaginalis*.

Antimicrobial Susceptibility

Metronidazole is the drug of choice for bacterial vaginosis and other infections caused by *G. vaginalis*. Systemic infection may be treated with ampicillin or amoxicillin because this organism has not been found to produce β-lactamase (Bernard, 2019). Susceptibility testing of *G. vaginalis* is not recommended, and no guidelines presently exist.

Capnocytophaga

Characteristics

Capnocytophaga is a genus of facultatively anaerobic, nonmotile, long, gram-negative rods with a fusiform appearance. *C. ochraceus*, *C. gingivalis*, *C. sputigena*, and *C. granulosa* are all oxidase and catalase negative and represent normal oral flora in humans. *C. canimorsus* and *C. cynodegmi* are both oxidase and catalase positive and are predominantly found in the oral cavity of dogs.

Clinical Manifestations and Pathogenesis

The oxidase- and catalase-negative groups of *Capnocytophaga* spp. cause endogenous periodontal infections and are also associated with septicemia leading to endocarditis or osteomyelitis in both immunocompromised and immunocompetent patients (Zbinden, 2019). *C. canimorsus* and *C. cynodegmi* can cause wound infections and septicemia following a dog or cat bite. Patients who progress to fatal septicemia commonly had a history of prior splenectomy or alcoholism as predisposing risk factors (Oehler

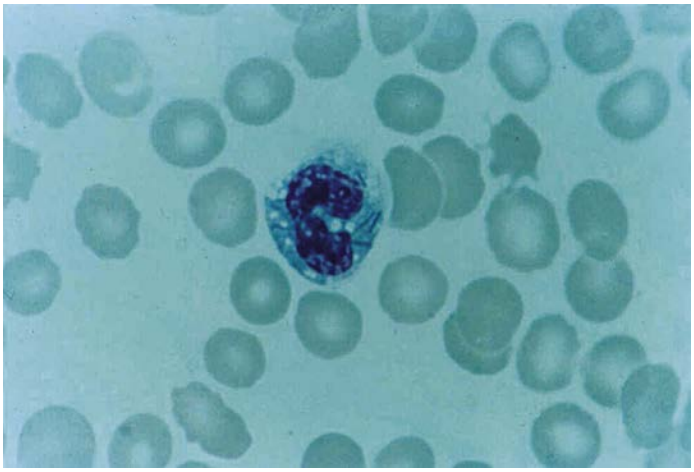

Figure 57.24 Blood smear positive for *Capnocytophaga canimorsus* in patient with septicemia (Wright stain; oil immersion).

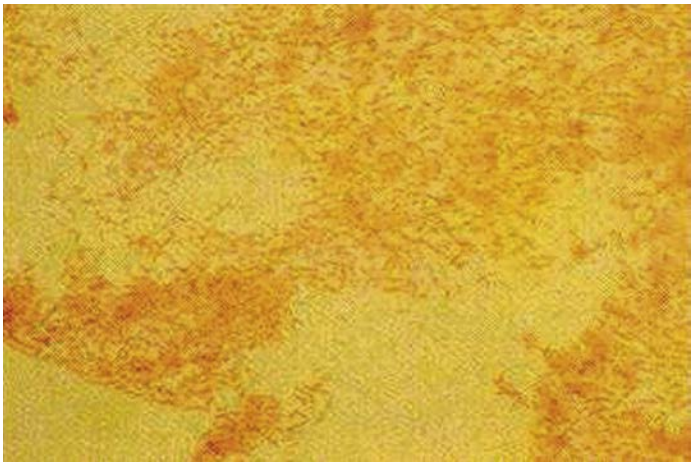

Figure 57.25 Gram stain of *Capnocytophaga ochraceus*. Note the fusiform bacilli (oil immersion).

et al., 2009; Gaastra & Lipman, 2010). Meningitis, endocarditis, arthritis, and eye infections have also been documented with *C. canimorsus* (Gasch et al., 2009). Figure 57.24 shows a Wright stain of *C. canimorsus* seen on a peripheral blood smear of a patient with *C. canimorsus* septicemia. Note the intracellular location of the bacilli.

Laboratory Diagnosis

Isolation of *Capnocytophaga* spp. requires inoculation of blood or chocolate agar and incubation in a 5% to 10% CO_2 environment, generally for longer than 24 hours. Thayer-Martin and Martin-Lewis agars are also helpful in isolating *Capnocytophaga* spp. from mixed infections. Automated blood culture instruments may not always detect *C. canimorsus*; blind subculture is recommended with a relevant clinical history (Zbinden, 2019). Colonies usually have a slight yellow or orange pigmentation and may spread because of a "gliding" motility. Gram stains often show long, thin, spindle-shaped cells with tapered ends that are fusiform in appearance. Figure 57.25 shows the Gram stain of *C. ochraceus*, demonstrating the fusiform nature of the bacilli. Due to similarities in biochemical reactions, automated phenotypic systems may only be able to identify *Capnocytophaga* spp., while MALDI-TOF can provide accurate species-level identifications.

Antimicrobial Susceptibility

Capnocytophaga spp. are usually susceptible to cephalosporins, carbapenems, tetracyclines, clindamycin, and fluoroquinolones, but are resistant to the aminoglycosides (Zbinden, 2019). There is a high prevalence of β-lactam and macrolide resistance in *Capnocytophaga* spp. obtained from the human oral cavity (Ehrmann et al., 2014).

Klebsiella granulomatis (*Calymmatobacterium granulomatis*)

Characteristics

K. granulomatis is a nonmotile, encapsulated, gram-negative rod that is found intracytoplasmically within macrophages and cannot be cultured on conventional agar. The organism possesses antigenic and molecular determinants similar to those of *Klebsiella* spp., leading taxonomists to now classify it among the Enterobacterales as *K. granulomatis* (Brisse et al., 2009).

Clinical Manifestations and Pathogenesis

K. granulomatis causes granuloma inguinale, also known as donovanosis, a rare sexually transmitted disease seen predominantly in tropical countries, characterized by ulcerogranulomatous lesions of the skin and mucosa of the genital and inguinal areas (O'Farrell, 2010). Humans are the only known reservoir.

Laboratory Diagnosis

The most effective way to establish the diagnosis of granuloma inguinale in the clinical microbiology laboratory is by a crush preparation made from a fragment of tissue at the margin of an ulcer and stained with Wright or Giemsa stains. The finding of small, straight or curved, pleomorphic rods with rounded ends and characteristic polar granules, giving a safety-pin appearance within mononuclear cells (Donovan bodies), is characteristic of *K. granulomatis*. While *K. granulomatis* does not grow on routine culture media, it has previously been cultured in embryonated eggs or a monocyte co-culture system (Kharsany et al., 1997). Molecular methods for detection of this organism along with other agents of genital ulcers have been developed but are not commercially available (Bialasiewicz et al., 2012).

Antimicrobial Susceptibility

Azithromycin therapy for at least 3 weeks or until all lesions have completely healed is the recommended treatment regimen for *K. granulomatis*. Alternative antibiotics include doxycycline, ciprofloxacin, erythromycin, or TMP-SMX (https://www.cdc.gov/std/tg2015/donovanosis.htm).

Streptobacillus

Characteristics

Streptobacillus is a facultatively anaerobic, nonmotile, pleomorphic gram-negative rod that frequently occurs in chains or long filaments, often with a series of oval to elongated bulbous swellings, giving a string-of-beads appearance on Gram stain. The microscopic morphology of the organism in culture varies with time, being more homogeneously filamentous in young cultures and becoming fragmented into irregular coccobacilli with age. L-phase colonies, which lack a cell wall, have a fried-egg appearance and may occur alongside the smooth, round wild-type colonies on agar. Figure 57.26 is a smear of *S. moniliformis* from the culture of a patient with rat-bite fever.

Clinical Manifestations and Pathogenesis

S. moniliformis is a member of the normal biota in the upper respiratory tract of wild and laboratory rats and other rodents. Infection in humans is acquired following rodent bites (known as rat bite fever) or from the ingestion of contaminated food or water (Haverhill disease). Local lymphangitis and lymphadenitis may develop up to 3 weeks later, followed by fever, chills, malaise, and, later, a general morbilliform maculopapular or petechial rash. Some patients develop a migratory polyarthritis, which may be suppurative in nature. Endocarditis has been reported, as have cases of myocarditis, pericarditis, meningitis, pneumonia, and abscess development due to *S. moniliformis* (Madhubashini et al., 2013).

Laboratory Diagnosis

Ideal specimens for recovery of *S. moniliformis* include blood, synovial fluid, and abscess material. The organism grows on media enriched with 15% sheep or rabbit blood, serum, or ascitic fluid. Inoculated media should be incubated at 37°C in a humid environment containing an atmosphere of 5% to 10% CO_2. Colonies on solid media are small and vaguely translucent to opaque, with slightly irregular edges. Coccal forms and Gram variability may occur; usually, though, colonies will demonstrate long filaments with granules and bulbs or banding forms on Gram stain. L-forms may be present in some cultures, along with the wild-type bacterial forms.

Colonies in liquid media form as "puff balls," usually at the bottom of the tube. In culture, the organism dies quickly and must be subcultured often. Because this organism is relatively inert, identification of *S. moniliformis* is difficult. Biochemical tests must be performed in heart infusion agar or broth supplemented with yeast extract and horse serum. 16S rRNA sequencing methods or fatty acid analysis is required for complete identification (Zbinden, 2019). Also, *S. moniliformis* is included in some MALDI-TOF databases. In addition, direct specimen testing with molecular methods may prove more sensitive than culture (Mackey et al., 2014).

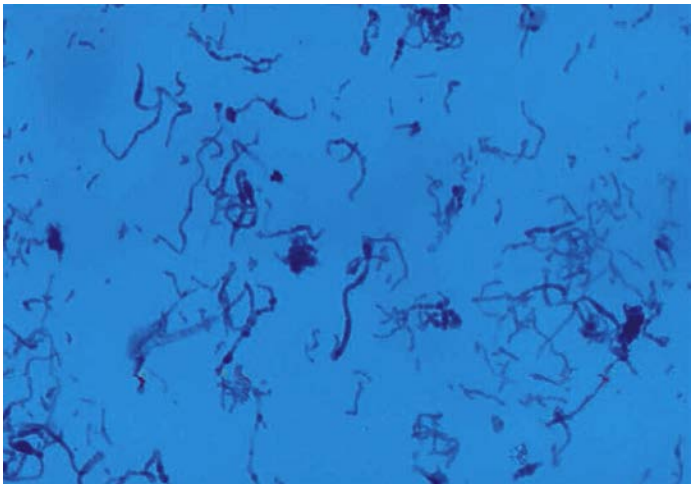

Figure 57.26 Gram stain of *Streptobacillus moniliformis* from culture (oil immersion). *(Courtesy Dr. Nancy Cornish.)*

Antimicrobial Susceptibility

S. moniliformis is susceptible to penicillins and tetracyclines, which are the recommended antibiotics for therapy. It is also susceptible to cephalosporins, carbapenems, clindamycin, macrolides, and aztreonam. Variable susceptibilities have been reported for the aminoglycoside and fluoroquinolone classes, and *S. moniliformis* is resistant to colistin and TMP-SMX (Elliott, 2007). Combination therapy with a high-dose penicillin and an aminoglycoside is recommended to treat endocarditis caused by *S. moniliformis*.

ANAEROBIC BACTERIA

Anaerobic bacteria comprise a major portion of the normal microbiota of the skin, mucous membranes, and gastrointestinal and genitourinary tracts of humans. Infections caused by anaerobic bacteria are often due to spread from their normal location (endogenous) or as a result of trauma, surgical procedures, or, rarely, from consumption of contaminated food or water (exogenous). Common infections caused by anaerobic bacteria include oral infections, wound infections, abscesses in various organs and body cavities, myonecrosis, gas gangrene, enteric diseases, joint infections, and bloodstream infections. Frequently, anaerobic infections are mixed with other anaerobic bacteria, facultatively anaerobic bacteria, and aerobes. Correctly distinguishing these groups from each other based on growth in different atmospheric conditions is an important first step in the identification of anaerobic bacteria. Other important considerations in the successful isolation and identification of anaerobic bacteria include proper selection and collection of specimens as well as prompt transport to the laboratory, as specimens can easily be contaminated with resident microbiota and die quickly when exposed to oxygen, even if only for a short period of time.

In the laboratory, commonly isolated anaerobes could traditionally be recognized on the basis of colony and Gram stain morphology and presumptively identified with a few additional tests. Definitive identification was based on biochemical reactions, physiologic and molecular characteristics, and, occasionally, pathogenicity and toxin neutralization tests. Previously, identification of anaerobes to the species level was challenging and time-consuming due to manual testing methods and the need for gas-liquid chromatography instrumentation that was not available at all laboratories. As commercial identification systems and MALDI-TOF have become routine platforms in most laboratories, the identification of anaerobic bacteria has improved substantially (Weintraub, 2019). It is important to consider the site of infection (sterile vs. nonsterile), quality of the specimen, and the presence and quantity of other organisms in order to determine the clinical significance of anaerobic bacteria isolated in culture. Historically, anaerobes were fairly consistent in their response to antibiotics, at least in vitro, but resistance is increasing and susceptibility patterns are becoming less predictable. While routine susceptibility testing of all anaerobic isolates is not recommended, testing should be performed for virulent pathogens with unpredictable susceptibility patterns, those isolated in pure culture from sterile sites, and in the case of suspected treatment failures (Brook et al., 2013).

Definitions and Characteristics

Anaerobes require an atmosphere with reduced oxygen tension for growth and fail to grow on the surface of solid media in an atmosphere of room air with 10% CO_2. Some anaerobes are classified as strict obligate anaerobes that cannot tolerate more than 0.5% O_2, whereas some show scant growth on solid agar in room air with 5% to 10% CO_2 and are considered aerotolerant. It is important to distinguish true anaerobes from other facultative anaerobic bacteria that are able to grow under aerobic or anaerobic conditions. Microaerophilic bacteria, such as *Campylobacter* and *Helicobacter* spp., preferentially grow in an atmosphere with reduced O_2 and increased CO_2.

Pathogenesis and Virulence Factors

Clostridium and *Bacteroides* spp. have a number of well-known virulence factors that contribute to the organism's pathogenicity. Clostridia produce the highest number of toxins of any bacteria, including potent exotoxins, neurotoxins, spore-forming toxins, and lethal toxins. In addition, Clostridia also possess collagenases, permeases, lecithinases, hemolysins, and hyaluronidases. Members of the *B. fragilis* group have a polysaccharide capsule that promotes abscess formation in addition to other virulence factors that have endotoxic, proteolytic, and heparinase activities. As more anaerobes are identified and studied in further detail, additional virulence properties are being discovered for a variety of anaerobes for which previously limited information was known.

Clostridium spp. are widespread in nature due to their ability to form resistant endospores and commonly cause exogenous infections due to traumatic injuries contaminated with soil or consumption of potent toxins or endospores. Also, many clostridial infections originate endogenously from indigenous anaerobic flora that spread from contiguous mucous membranes when their integrity has been disrupted by surgery, instrumentation, trauma, or malignancy. A decrease in the oxidation-reduction potential at the site of injury by bacterial multiplication and failure of blood supply is essential to the establishment of anaerobes in the infectious process.

Histotoxic clostridial species, including *C. perfringens*, *C. septicum*, and C. *sordellii*, are capable of causing aggressive disease ranging from crepitant cellulitis to myonecrosis with gas, shock, and death. Most *Clostridium* spp. associated with these infections result from wounds that are contaminated with soil containing endospores. The clostridia multiply in cellular debris, hematomas, and necrotic tissue, often without observable clinical symptoms. Anaerobic cellulitis is a necrotizing process of the soft tissues that is gradual but can progress rapidly and extensively. While gas is produced in anaerobic cellulitis, the process typically does not involve muscle or fascial tissue. In contrast to anaerobic cellulitis, clostridial myonecrosis or gas gangrene is an acute and rapidly progressive invasive process that presents with severe pain and foul-smelling discharge and produces marked necrosis of muscle with gas in the tissue. Even with appropriate antibiotic therapy, radical amputation is often necessary to prevent mortality. Distinguishing between anaerobic cellulitis and clostridial myonecrosis is critical to avoid performing unnecessarily aggressive and mutilating surgery in the former condition. *C. perfringens* has been the species most frequently involved in clostridial myonecrosis; however, *C. septicum* and *C. sordellii* are implicated in patients with gastrointestinal pathology or following abortions, vaginal deliveries, or cesarean section. Although clostridial infections are unquestionably of major medical importance, other anaerobic cocci and gram-negative bacilli may cause cellulitis and myonecrosis in addition to or instead of *Clostridium* spp.

C. botulinum causes botulism in humans that is characterized by a sudden flaccid paralysis due to an intoxication with the extremely potent botulism neurotoxin. Botulism is usually acquired by the ingestion of improperly preserved or canned foods containing the toxin. Infants less than 1 year old who ingest spores from soil, dust, or honey are also at risk for disease. Gastrointestinal symptoms and weakness in muscles of the face and pharynx usually occur between 18 and 36 hours following ingestion of contaminated food and can progress to paralysis of the diaphragm, requiring intubation. Of the eight antigenic types of botulinum toxin known, type A is the most common in foodborne and infant cases in the United States, followed by types B, E, and F, with the majority of cases occurring in California. The toxin is absorbed from the intestinal tract or, rarely, from an infected wound, into the bloodstream and attaches to motor nerve terminals, preventing acetylcholine release at the neuromuscular junction.

C. tetani causes tetanus. Its virulence is attributed to a potent neurotoxin, tetanospasmin, which is acquired by trauma or puncture wounds that are contaminated with soil. Symptoms typically occur within the first 2 weeks of injury, and a rigid paralysis and tonic spasms occur. Infrequently, cases have been reported to occur postoperatively, following dental work, childbirth, abortion, or in association with stasis and decubitus ulcers. The toxin is transported to gangliosides in the central nervous system in the lymphatics and bloodstream and blocks the inhibitory impulses, resulting in painful muscle contractions and trismus, or lockjaw. Tetanus can

be prevented by immunization with a tetanus toxoid vaccine and booster doses every 10 years.

Clostridioides (formerly *Clostridium*) *difficile* is a frequent cause of antibiotic-associated diarrhea and is now the most common health care–associated infection in North America (Kuikper & Barbut, 2019). Pseudomembranous colitis and toxic megacolon, which can be complicated by bowel perforation, are the most severe manifestations of *C. difficile* disease and may require surgical resection of portions of the colon. Disease is due to production of the enterotoxin TcdA and the cytotoxin TcdB, which work in concert to enter and damage the cytoskeleton of cells of the large intestine, leading to apoptosis. Recent studies have shown that TcdB serves as a major virulence factor by itself and can induce the inflammatory response and cause severe disease in the absence of TcdA (Carter et al., 2015). Use of molecular diagnostics in the clinical laboratory for detection of the TcdB gene alone or both the TcdA and TcdB genes have increased sensitivity and have a high negative predictive value. However, overdiagnosis is a concern if appropriate preanalytic considerations, such as testing only those with clinically significant diarrhea and no history of laxative use, are not followed (McDonald et al., 2018). There is a high prevalence of asymptomatic carriage of toxigenic *C. difficile*, reaching 50% or more, in neonates. However, disease is rare and testing is never recommended in this age group (McDonald et al., 2018). Colonization, with or without toxin production, may be maintained for several months, but when the adult flora becomes established at 6 to 12 months of age, colonization rates fall and only about 3% of normal, healthy adults are colonized with the organism. Colonization rates are higher in adults in acute care hospitals (3%–26%) and among elderly patients in long-term care facilities (5%–7%) (McDonald et al., 2018). Clindamycin, broad-spectrum cephalosporins, carbapenems, and fluoroquinolones have the highest risk of causing *C. difficile* infections, especially in the month following antibiotic therapy, although any antibiotic can cause disease. Although *C. difficile* is thought to be primarily acquired in the hospital setting by person-to-person spread via the fecal-oral route or by direct exposure to an environment contaminated with spores, more cases of community onset are being documented.

Other anaerobic bacteria, particularly anaerobic gram-negative bacilli and cocci, have been associated with anaerobic cellulitis and abscesses. These organisms are part of the normal microbiota of the mucous membranes of the oral cavity and of the gastrointestinal and genitourinary tracts. As such, they are encountered in abscesses of the abdominal cavity, pelvis, brain, and numerous sites of the head and neck, aspiration pneumonia, and bacteremia. Anaerobic abdominal infections commonly follow abdominal and colon surgeries and are most frequently associated with the *B. fragilis* group. Organisms in the *B. fragilis* group are more virulent, resistant to many antimicrobial agents, and are the most frequently isolated anaerobic pathogen from bloodstream infections. *Fusobacterium necrophorum*, another anaerobic gram-negative bacillum, is known for causing invasive disease in healthy individuals due to leukotoxin and plasminogen binding virulence factors (Conrads et al., 2019). Gram-positive anaerobes, *Finegoldia magna* and *Cutibacterium* (formerly *Propionibacterium*) *acnes*, possess adhesion factors and have the ability to form biofilms, especially on prosthetic materials in the case of *C. acnes*.

Laboratory Diagnosis

In the clinical laboratory, specimens for anaerobic culture are inoculated onto all-purpose media enriched with 5% sheep blood, vitamin K, and hemin such as *Brucella*, CDC, or Columbia agar as well as selective and differential agars, including kanamycin-vancomycin laked blood agar, *Bacteroides* bile esculin (BBE) agar, PEA or CNA agars, and a broth medium. Most laboratories use commercial pre-reduced anaerobically sterilized (PRAS) media instead of preparing their own in-house. Plates are placed into anaerobic bags, jars, or chambers that have an atmosphere composed of 80% to 90% nitrogen, 5% hydrogen, and 5% to 10% carbon dioxide and are incubated at 35°C for at least 48 hours before the first examination to prevent death of slower-growing anaerobes. Examination of the direct Gram stain for the presence of bacteria and inflammatory cells as well as assessment of aerotolerance by incubating a chocolate agar plate in CO_2 also provide valuable information to help in the identification of anaerobes. Identifying anaerobic bacteria to the species level can be a complex task, as detailed earlier; however, the extent to which isolates of anaerobic bacteria are identified varies. For example, mixed anaerobic flora from a site such as a decubitus ulcer, perirectal fistula, or intraabdominal abscess may simply be reported as mixed fecal flora (mentioning specifically whether there are aerobes and anaerobes or only anaerobes present) without specific identification of its components. Determining species-level identifications may be reserved for isolates present in pure culture from a normally sterile body fluid or site, which can be readily accomplished with the use

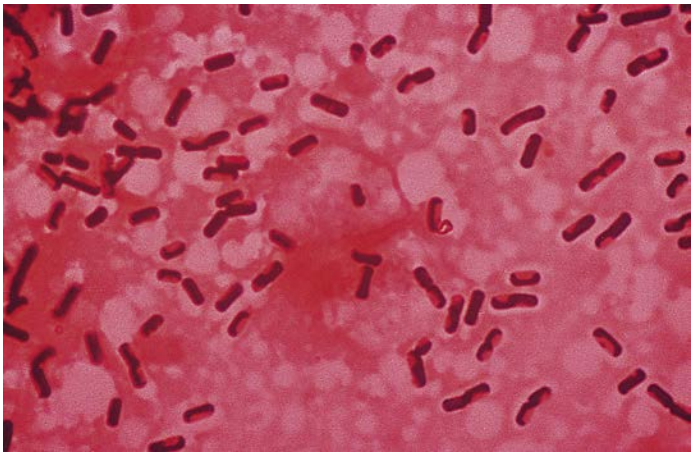

Figure 57.27 Gram stain of a smear of exudate from a wound that had gas bubbles shows large, boxcar-shaped, gram-positive bacilli, suggestive of clostridial disease (oil immersion).

of any of several commercially available biochemical kits, MALDI-TOF, or sequencing platforms. The clinical value of reporting the presence of anaerobic bacteria is directly related to the speed of identification, and procedures that require 1 to 2 weeks to complete are generally only for academic interest. Identification of every anaerobe isolated in a culture is often not appropriate; clinical relevance should be used to guide the workup of anaerobic cultures, similar to that of other culture types.

Because of their rapid progression and considerable morbidity and mortality, the initial diagnosis and management of diseases caused by clostridia species must be based on the patient's symptoms and clinical presentation. In some patients with tetanus, no primary wound is evident. When a wound is present, slender bacilli with terminal spores typical of *C. tetani* are seldom seen in stained smears even though they may be recovered from cultures. Moreover, because of this organism's widespread distribution in nature, its isolation from a wound is not necessarily indicative of the diagnosis of tetanus. Similarly, a negative culture or molecular test for detection of tetanospasmin does not exclude a tetanus diagnosis. Laboratory confirmation of botulism requires detection of the toxin in serum, wounds, gastric contents, stool, or the food suspected of causing the disease. Procedures for extracting the toxin and performing mouse bioassays and neutralization tests are complex but remain an important test for the diagnosis of botulism and are performed by public health laboratories or the CDC. ELISA and PCR assays are also available for the detection of botulism toxin, but the mouse bioassay is still the study of choice (Kuijper & Barbut, 2019). If botulism is suspected in the United States, the CDC should be notified immediately to ensure that proper specimens are collected to establish the diagnosis, start therapy, and investigate potential outbreaks.

In cases of suspected anaerobic cellulitis or gas gangrene, the clinical laboratory can provide a rapid diagnosis by performing Gram stains on multiple tissue specimens. The finding of numerous, large, boxcar-shaped, gram-positive or gram-variable bacilli in the absence of neutrophils (Fig. 57.27) provides a presumptive diagnosis of a clostridial infection. Spores are infrequently observed in tissue specimens. Gram stain may also be diagnostic of anaerobic streptococcal myositis. Cultures of exudate, tissue, and blood should be performed. *C. perfringens* is traditionally identified by its Gram stain morphology, the production of a double zone of β-hemolysis on blood agar, and a positive lecithinase reaction on egg yolk agar.

For many years, laboratory diagnosis of *C. difficile* infection was based on isolating the organism from culture and confirming toxin production or performing a cell culture cytotoxicity neutralization assay. While this was once considered the gold standard for *C. difficile* diagnosis, rapid antigen detection and molecular methods direct from stool have limited the utility of these culture methods for instances in which susceptibility testing or epidemiologic studies are needed. Presently, antigen tests that detect glutamate dehydrogenase (GDH), a metabolic enzyme expressed in high levels by all toxigenic and nontoxigenic *C. difficile*, toxin A and B enzyme immunoassays, and molecular methods to detect toxin genes are commonly used as part of multistep algorithms for the laboratory diagnosis of *C. difficile*. Stool toxin tests by themselves lack appropriate sensitivity and specificity and should be part of a two- or three-step algorithm, such as GDH plus toxin; GDH plus toxin, arbitrated by molecular toxin test; or molecular toxin test plus toxin (Crobach et al., 2016). When molecular toxin tests are used alone, there is a risk for poor positive predictive values if the testing is performed on patients without clinically significant diarrhea (McDonald et al., 2018). The

TABLE 57.11

Most Common Species of *Clostridium* and *Clostridioides* in Clinical Samples

Species	Colony	Gram Stain and Biochemicals	Common Clinical Infections
C. perfringens	Large, gray; double zone of β-hemolysis	Large rods with blunt ends, boxcar appearance; may be Gram variable; rare spores seen; nonmotile; lipase negative; lecithinase positive; indole negative; reverse CAMP positive	Most common isolate; skin and soft-tissue infections, including gas gangrene; bacteremia; also found in gastrointestinal tract as part of normal flora
C. ramosum	Large, spreading white colony	Often stain gram negative or variable; cells are more slender and longer than *C. perfringens*; rare, terminal spores	Commonly isolated in wounds and abscesses
C. sordellii	White; swarms	Large rods with subterminal spores seen; lecithinase positive; lipase negative; indole and urease positive	Gas gangrene of uterus following abortion, vaginal delivery, or cesarean section
C. tetani	Thin film of growth	Thin bacilli with terminal spores, drumstick or tennis racket appearance; lecithinase negative; lipase weak positive; indole variable and urease negative	Causes tetanus; neonates in developing countries and injecting drug users are at risk
C. septicum	Translucent, swarming colonies with irregular margins	Long, filamentous bacilli with rare subterminal spores; lecithinase, lipase, indole, and urease negative	Nontraumatic gas gangrene; when isolated from blood cultures, indicates a possible gastrointestinal pathology
C. difficile	White colonies with distinctive horse stable odor; selective CCFA media: yellow, ground-glass appearing colonies, chartreuse fluorescence	Thin, long bacilli with terminal spores seen	Cause of antibiotic-associated diarrhea and pseudomembranous colitis
C. tertium	Small, gray, translucent	Terminal spores; aerotolerant	Bacteremia in severely ill patients; resistant to many common anaerobic antibiotics

CCFA, Cycloserine cefoxitin fructose egg yolk agar.

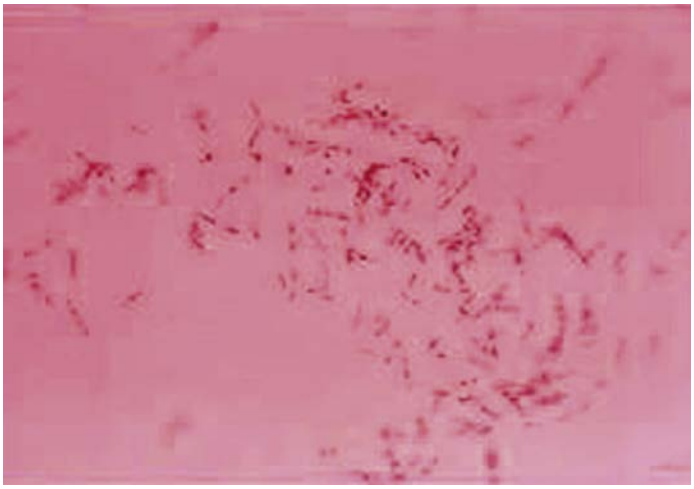

Figure 57.28 Gram stain of *Bacteroides fragilis* from broth culture (oil immersion).

optimum testing method and diagnostic algorithm is still a matter of debate and the diagnosis of *C. difficile* relies on clinical symptoms as well as laboratory testing. Regardless of the algorithm used, diagnostic accuracy will be improved when only symptomatic patients are tested (Kuijper & Barbut, 2019). Laboratory characteristics of the most common clinical isolated clostridia species are noted in Table 57.11.

Organisms in the *B. fragilis* group and *Parabacteroides* genus are frequently isolated anaerobic bacteria that commonly cause clinical disease. These isolates grow on selective BBE and kanamycin-vancomycin laked sheep blood agar plates, and have a characteristic Gram stain morphology, as seen in Figure 57.28. With rare exception, members of the *B. fragilis* group grow in the presence of 20% bile and hydrolyze esculin. Inclusion of a BBE agar plate for anaerobic culture is recommended for more rapid detection and identification of these organisms (Conrads et al., 2019). In addition to being resistant to vancomycin and kanamycin, these organisms are resistant to colistin disks. Common organisms in the *B. fragilis* group and *Parabacteroides* spp. and their biochemical characteristics and disease associations are listed in Table 57.12.

Fusobacterium spp., including *F. nucleatum* and *F. necrophorum*, have been found in recurrent tonsillitis, brain abscesses, bacteremia, and as the cause of infections in the female genital tract, including septic abortion. *F. necrophorum* is associated with Lemierre syndrome, which is an infectious thrombophlebitis of the internal jugular vein that commonly results from infections in the head and neck region. Bacteremia and septic emboli are known complications of Lemierre syndrome; blood cultures should be collected in addition to other tissue or fluid cultures if the disease is suspected. On Gram stain, *F. nucleatum* appears as long, thin, tapered (or pointed) gram-negative bacilli, as seen in Figure 57.29. *F. necrophorum* is more pleomorphic, with bizarre forms seen on Gram stain. Table 57.12 includes some of the common *Fusobacterium* spp. and provides distinguishing biochemical characteristics. Information about the pigmented anaerobic gram-negative bacilli, *Prevotella* spp. and *Porphyromonas* spp., can also be located in Table 57.12.

Previously, the majority of gram-positive anaerobic cocci were included in the *Peptostreptococcus* genus, but many taxonomic changes have now reclassified these organisms into the *Finegoldia*, *Parvimonas*, *Anaerococcus*, *Peptoniphilus*, and *Gallicola* genera. *Finegoldia magna* and *Parvimonas micra*, the predominant gram-positive anaerobic cocci of the skin flora and oral flora, respectively, are the most common anaerobic gram-positive cocci isolated from clinical specimens and the ones most often associated with disease. Gram-negative anaerobic cocci include the genera *Veillonella*, *Acidaminococcus*, *Negativicoccus*, *Megasphaera*, and *Anaeroglobus*. *Veillonella* spp. comprise the normal flora of the oral cavity and urogenital tract and are the most frequently isolated from mixed cultures (Veloo & Johnson, 2019). Gram stain and culture characteristics as well as common clinical manifestations of the most frequently isolated anaerobic cocci are included in Tables 57.12 and 57.13.

Actinomyces spp. are gram-positive anaerobic bacilli that make up the normal flora of mucosal surfaces, but when spread to deeper tissues through surgical procedures or trauma can cause infection. Actinomycosis is granulomatous disease that is characterized by the formation of sinus tracts and often contains sulfur granules, which can be identified microscopically. Commonly, abscesses form in response to oral and dental infections, aspiration events, and abdominal or pelvic infections, often due to bowel perforation or the presence of an intrauterine device (Bonnefond et al., 2016). Other sites frequently involved include the soft tissues, breast, liver, and brain. *Actinomyces* spp. can be differentiated from *Nocardia* spp. due to their anaerobic growth requirements and the lack of mycolic acid in their cell walls. *C.* (formerly *Propionibacterium*) *acnes* is another commonly isolated gram-positive anaerobic bacillus that is a component of the skin microbiota and can cause acne vulgaris. *C. acnes* also causes neurosurgical shunt infections, prosthetic joint infections, and endophthalmitis after cataract surgery due to the organism's ability to form biofilms. Figure 57.30 shows a Gram stain of *C. acnes* in vitreous fluid obtained from a patient months after cataract surgery. In order to successfully culture *C. acnes*, sonication of the prosthesis, inoculation of sonicate into anaerobic blood culture bottles, and an extended incubation of 10 to 14 days is recommended (Butler-Wu & She, 2019). Additional clinically relevant gram-positive anaerobic rods and selected diagnostic features are listed in Tables 57.13 and 57.14.

TABLE 57.12

Most Frequently Isolated Gram-Negative Anaerobic Bacteria

Species	Colony	Biochemicals	Other Characteristics
Bacteroides fragilis group*	Gray to white, round; requires 24–48 hours		
B. fragilis		Negative for indole; positive for catalase and esculin	Most common and most pathogenic of the group
B. thetaiotaomicron		Positive for indole, catalase, and esculin	
B. vulgatus		Negative for indole; usually negative for catalase and esculin	
B. ovatus		Positive for indole, catalase, and esculin	
*Parabacteroides distasonis***		Negative for indole; usually positive for catalase and esculin	Intraabdominal infections
*P. goldsteinii***		Negative for indole; usually positive for catalase and esculin	Intraabdominal infections
Bacteroides ureolyticus	Small, translucent; colonies often "pit" the agar	No growth in 20% bile; indole, catalase and esculin usually negative; urease positive	Not a member of the *B. fragilis* group; part of normal anaerobic oral flora
Bilophila wadsworthia		Grows in 20% bile; catalase positive; negative for indole and esculin	Polymicrobial intraabdominal infections, gangrenous appendicitis
Porphyromonas asaccharolyticus	Colonies fluoresce brick red with ultraviolet light exposure; black pigment with age	Bile sensitive; indole positive and catalase negative	Normal oral flora; decubitus ulcers, diabetic foot infections
Prevotella disiens and *P. bivia*		Bile sensitive; indole and esculin negative; saccharolytic and nonpigmented	Normal oral and genitourinary flora; can be involved in pelvic abscesses and bloodstream infections
Fusobacterium nucleatum	Breadcrumb-like and speckled colonies; long, tapered (pointed) bacilli	Bile sensitive; indole positive and esculin negative	Oral flora; can be involved in bacteremia, pulmonary infection; human bite wounds
F. necrophorum	Umbonate colonies; greening of agar; pleomorphic "bizarre" forms seen on Gram stain	Usually sensitive to bile; indole positive; lipase positive	Septic thrombophlebitis, Lemierre syndrome
F. mortiferum	"Fried egg" appearance of colonies; nontapered rods and "bizarre forms" on Gram stain	Grows on 20% bile; indole negative and esculin positive	Infrequent isolate
Gram-Negative Cocci			
Veillonella spp.	Small white colonies; Gram stain: round cocci, singly or in pairs; red fluorescence	Nitrate reduction positive; catalase variable	Common isolate, but rarely involved in clinical disease

*In addition to those listed, *B. fragilis* group includes *B. caccae, B. cellulosilyticus, B. calarus, B. coprocola, B. coprophilus, B. dorei, B. eggerthii, B. faecis, B. finegoldii, B. flexus, B. intestinalis, B. massiliensis, B. nordii, B. oleiciplenus, B. plebius, B. salyersiae, B. stercoris, B. uniformis,* and *B. xylanisolvens.*
**These organisms have been placed in the Parabacteroides genus along with *P. faecis, P. gordonii, P. johnsonii,* and *P. merdae.*

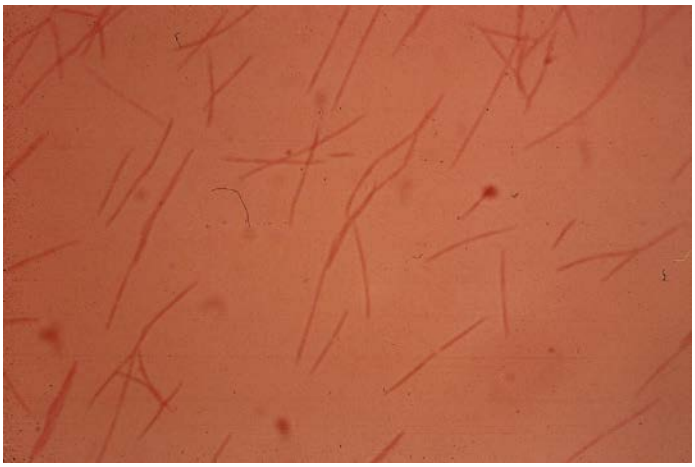

Figure 57.29 Gram stain of *Fusobacterium nucleatum* (oil immersion).

Antimicrobial Susceptibility

Previously, the majority of anaerobic infections were treated with empiric antibiotics and susceptibility testing was not performed. As more resistance is detected, this approach is no longer recommended. While performing susceptibility testing on all anaerobic isolates, especially those from mixed cultures, is not cost-effective or necessary, general criteria are suggested for what isolates to test. Susceptibility testing should be performed on isolates from normally sterile sites, those in pure culture, and for organisms that are highly virulent or have unpredictable susceptibility patterns. These organisms include *Clostridium*, *Bacteroides*, *Fusobacterium*, and *Prevotella* spp. Susceptibility testing should also be performed in the case of severe infections, such as brain abscess, endocarditis, prosthetic joint infection, and bacteremia, if infections fail to respond or relapse after empiric therapy, or when the patient requires prolonged therapy (Brook et al., 2013). CLSI guidelines endorse agar dilution, broth microdilution, and Etest to provide MIC breakpoints and interpretative criteria (CLSI, 2012, 2019). Penicillin, β-lactam combination agents, clindamycin, metronidazole, and carbapenems usually have good anaerobic coverage and are recommended as first-line antibiotics to test for anaerobic isolates. In addition to antibiotics, source control of the infection by drainage and debridement is important in the management of anaerobic infections. While metronidazole has good anaerobic coverage for a number of organisms, it is important to note that several species in the *Cutibacterium*, *Actinomyces*, and *Lactobacillus* genera are intrinsically resistant to this antibiotic. *B. fragilis* group organisms are some of the most resistant anaerobes and are intrinsically resistant to penicillin and ampicillin by β-lactamase activity. Regular review of anaerobic antibiogram data may serve as a useful tool to guide empiric therapy and monitor resistance patterns in health care systems (Boyanova et al., 2007).

TABLE 57.13

Most Frequently Isolated Gram-Positive Non–Spore-Forming Anaerobic Bacteria: Gram-Positive Cocci

Species	Gram Stain	Colony	Indole	PYR	Common Clinical Infections
Peptostreptococcus anaerobius	Large cocci, often in chains	Nonhemolytic; gray with raised center; sweet odor	–	–	Infections in abdominal cavity and female urogenital tract
Parviomonas micra	Clusters or short chains; <0.7 μm	Small; dull color; "halo" around colony	–	+	Endodontic disease, peritonsillar abscess
Finegoldia magna	Pairs, tetrads, and clusters; >0.6 μm	Small; white; convex	–	+	Skin, soft-tissue, bone, and joint infections
Peptoniphilus asaccharolyticus	"Clumps," pairs, or tetrads	Small; uniform; slight yellow pigment	Usually +	–	Predominant in skin flora, decubitus ulcers
Anaerococcus prevotii	Clumps and tetrads	Nonglistening; gray; convex	–	+	Infections in abdominal cavity and female urogenital tract
A. tetradius	Clumps and tetrads	Nonglistening; gray; convex	–	+	
Staphylococcus saccharolyticus	Clusters and tetrads	Nonhemolytic; catalase and coagulase negative	ND	ND	Skin, bone and joint infections, rare cases of endocarditis

+, Positive; –, negative; *ND,* not done; *PYR,* l-pyrrolidonyl-β-naphthylamide.

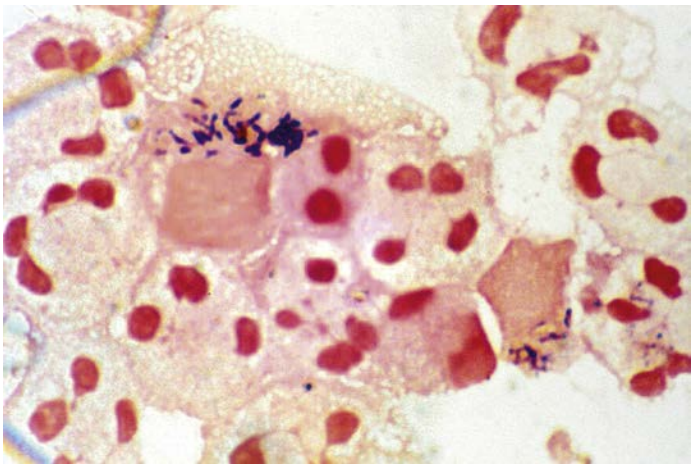

Figure 57.30 Gram stain of *Cutibacterium acnes* from vitreous fluid (oil immersion).

TABLE 57.14

Most Frequently Isolated Gram-Positive Non–Spore-Forming Anaerobic Bacteria: Gram-Positive Bacilli

Species	Gram Stain	Colony	Aerotolerance	Biochemicals	Common Clinical Infections
Actinomyces israelii	Short rods; branching or beading, associated sulfur granules	White, opaque; "molar tooth"	(+)	Catalase negative; esculin positive	Common cause of actinomycosis: genital, pulmonary, abdominal
A. naeslundii	Short rods; branching or beading	Gray-white; translucent	+++	Catalase negative; urease positive	Oral flora; IUD-associated infections
A. odontolyticus	Short rods; branching or beading	May produce pink to red colonies in ambient air	+++	Catalase negative; urease negative	Oral flora; IUD-associated infections
A. turicensis	Straight to curved rods	Glistening; opaque	++	Catalase, urease, and esculin negative	Commonly isolated species; abscesses; oral and IUD-associated infections
Cutibacterium acnes	Short, pleomorphic rods; may appear "spidery"	Small, white, round	+/–	Catalase positive; indole positive	Normal skin flora; ventricular shunt infections; prosthetic joint infections, particularly in the shoulder; endophthalmitis (post–cataract surgery) infrequent cause of endocarditis, osteomyelitis
Propionimicrobium lymphophilum	Diphtheroid-like or coccoid; singly, pairs, or short chains	Small, white, glistening	–	Catalase variable; esculin negative	Initially isolated from lymph nodes; urinary tract infections

Continued

TABLE 57.14

Most Frequently Isolated Gram-Positive Non–Spore-Forming Anaerobic Bacteria: Gram-Positive Bacilli—cont'd

Species	Gram Stain	Colony	Aerotolerance	Biochemicals	Common Clinical Infections
Bifidobacterium spp.	Diphtheroid-like; bifurcated or forked ends		–		Normal flora of GI and GU tract; dental caries; polymicrobial bacteremia
Eggerthella lenta	Straight rod with rounded ends	Grow in 20% bile; saccharolytic	–	Catalase positive; indole-negative	GI flora; abscesses; bacteremia in immunosuppressed
Mobiluncus spp.	Curved with tapered ends; Gram variable				Normal vaginal flora; bacterial vaginosis
Lactobacillus spp.	Long, slender rods; singly or in pairs and chains		+	Catalase negative; often vancomycin resistant	Beneficial vaginal flora; dental caries; rarely, bacteremia and endocarditis

+, ++, +++, Positive with increasing strength; –, negative, *GI,* gastrointestinal; *GU,* genitourinary; *IUD,* intrauterine device; *ND,* not done; *PYR,* L-pyrrolidonyl-β-naphthylamide.

SELECTED REFERENCES

Becker K, Skov RL, von Eiff C: *Staphylococcus*, *Micrococcus*, and other catalase positive cocci. In Carroll KC, Pfaller MA, Landry ML, et al.: *Manual of clinical microbiology*, ed 12, Washington, DC, 2019, American Society for Microbiology, pp 367–398.

Provides an excellent overview of the biochemical tests useful for identification of aerobic catalase-positive Gram-positive cocci. Additionally, it includes a discussion of the important resistance mechanisms and tests that allow detection of resistant isolates.

Clinical and Laboratory Standards Institute: *Performance standards for antimicrobial susceptibility testing, twenty-ninth informational supplement. CLS document M100-S29*, Wayne, PA, 2019, CLSI.

Essential for appropriate interpretation and reporting of antibacterial susceptibility test results.

Clinical and Laboratory Standards Institute: Methods for antimicrobial dilution and disk susceptibility testing of infrequently isolated or fastidious bacteria. In *CLSI document M45-A3*, ed 3, Wayne, PA, 2015, CLSI.

Essential for laboratories that perform antimicrobial susceptibility testing on fastidious or infrequently isolated bacteria.

Norskov-Lauritsen N, Ridderberg W: Approaches to the identification of aerobic gram-negative bacteria. In Carroll KC, Pfaller MA, Landry ML, et al.: *Manual of clinical microbiology*, ed 12, Washington, DC, 2019, American Society for Microbiology, pp 630–639.

Provides an excellent discussion of the biochemical, MALDI-TOF, and sequencing tests useful for identification of gram-negative bacteria. Includes algorithms for identification and tables of pertinent biochemicals for differentiating among the many organisms included in the Gram-negative aerobic bacteria.

Access the complete reference list online at Elsevier eBooks for Practicing Clinicians.

REFERENCES

Adler H, Baumlin N, Frei R: Evaluation of acridine orange staining as a replacement of subcultures for BacT/ALERT-positive, gram stain-negative blood cultures, *J Clin Microbiol* 41:5238–5239, 2003.

Al-Haj-Hussein BT, Al-Shehri MA, Azhar EA, et al.: Evaluation of 2 real-time PCR assays for the investigation of mecA gene in clinical isolates of MRSA in Western Saudi Arabia, *Saudi Med J* 26:759–762, 2005.

Ampofo K, Graham P, Ratner A, et al.: *Plesiomonas shigelloides* sepsis and splenic abscess in an adolescent with sickle-cell disease, *Pediatr Inf Dis J* 20:1178–1179, 2001.

Anagnostou T, Arvanitis M, Kourkoumpetis TK, et al.: Nocardiosis of the central nervous system: experience from a general hospital and review of 84 cases from the literature, *Medicine* 93:19–32, 2014.

Anikpeh YF, Keller P, Bloemberg GV, et al.: Spacecraft bacterium, Paenibacillus pasadenensis, causing wound infection in humans, *BMJ Case Rep* 2010.

Araj GF: Brucella. In Carroll KC, Pfaller MA, Landry ML, et al.: *Manual of clinical microbiology*, ed 12, Washington, DC, 2019, American Society for Microbiology, pp 883–892.

Arevalo-Jaimes B, Rojas-Rengifo DF, Jaramillo CA, et al.: Genotypic determination of resistance and heteroresistance to clarithromycin in *Helicobacter pylori* isolates from antrum and corpus of Colombian symptomatic patients, *BMC Infect Dis* 19:546, 2019.

Barnett LA, Cunningham MW: A new heart-cross-reactive antigen in *Streptococcus pyogenes* is not M protein, *JID (J Infect Dis)* 162:875–882, 1990.

Bassetti M, Trecarichi EM, Mesini A, et al.: Risk factors and mortality of healthcare-associated and community-acquired *Staphylococcus aureus* bacteraemia, *Clin Microbiol Infect* 18:862–869, 2012.

Baumgartner A, Niederhauser I, Johler S: Virulence and resistance gene profiles of *Staphylococcus aureus* strains isolated from ready-to-eat foods, *J Food Prot* 77:1232–1236, 2014.

Becker K, Heilmann C, Peters G: Coagulase-negative staphylococci, *Clin Microbiol Rev* 27:870–926, 2014.

Beganovic M, Costello M, Wieczorkiewicz SM: Effect of matrix-assisted laser desorption ionization-time of flight mass spectrometry (MALDI-TOF MS) alone versus MALDI-TOF MS combined with real-time antimicrobial stewardship Interventions on time to optimal antimicrobial therapy in patients with positive blood cultures, *J Clin Microbiol* 55:1437–1445, 2017.

Behnia M, Logan SC, Fallen L, et al.: Nosocomial and ventilator-associated pneumonia in a community hospital intensive care unit: a retrospective review and analysis, *BMC Res Notes* 7:232, 2014.

Bennett SD, Walsh KA, Gould LH: Foodborne disease outbreaks caused by *Bacillus cereus*, *Clostridium perfringens*, and *Staphylococcus aureus*—United States, 1998-2008, *Clin Infect Dis* 57:425–433, 2013.

Bernard K: The genus *Corynebacterium* and other medically relevant coryneform-like bacteria, *J Clin Micobiol* 50:3152–3158, 2012.

Bernard KA: Coryneform gram-positive rods. In Carroll KC, Pfaller MA, Landry ML, et al.: *Manual of clinical microbiology*, ed 12, Washington, DC, 2019, American Society for Microbiology, pp 488–524.

Bialasiewicz S, Mackay IM, Whiley DM, et al.: Protocol for the use of enzyme-linked hybridization assays for genital ulcer disease, *Methods Mol Biol* 903:225–233, 2012.

Block T, Munson E, Culver A, et al.: Comparison of carrot broth-and selective Todd-Hewitt broth-enhanced PCR protocols for real-time detection of *S. agalactiae* in prenatal vaginal/anorectal specimens, *J Clin Microbiol* 46:3615–3620, 2008.

Bonnefond S, Catroux M, Melenotte C, et al.: Clinical features of actinomycosis: a retrospective, multicenter study of 28 cases of miscellaneous presentations, *Medicine (Baltim)* 95, 2016. e3923.

Borrow R, Findlow J, Gray S, et al.: Safe laboratory handling of *Neisseria meningitidis*, *Infect* 68:305–312, 2014.

Bowers KM, Wren MW, Shetty NP: Screening for methicillin resistance in *Staphylococcus aureus* and coagulase-negative staphylococci: an evaluation of three selective media and Mastalex-MRSA latex agglutination, *Br J Biomed Sci* 60:71–74, 2003.

Boyanova L, Kolarov R, Mitov I: Antimicrobial resistance and the management of anaerobic infections, *Expert Rev Anti Infect Ther* 5:685–701, 2007.

Brisse S, Fevre C, Passet V, et al.: Virulent Clones of Klebsiella pneumoniae: identification and Evolutionary Scenario based on genomic and phenotypic characterization, *PloS One* 4, 2009. e4982.

Broms JE, Sjostedt A, Lavander M: The role of the *Francisella tularensis* pathogenicity Island in type VI secretion, intracellular survival, and Modulation of host cell Signaling, *Front Microbiol*, 2010, https://doi.org/10.3389/fmicb.2010.00136.

Brook I, Wexler HM, Goldstein EJ: Antianaerobic antimicrobials: spectrum and susceptibility testing, *Clin Microbiol Rev* 26:526–546, 2013.

Brooke JS: *Stenotrophomonas maltophilia*: an emerging global opportunistic pathogen, *Clin Microbiol Rev* 25:2–41, 2012.

Brown-Elliott BA, Brown JM, Conville PS, et al.: Clinical and laboratory features of the *Nocardia* spp. based on current molecular taxonomy, *Clin Microbiol Rev* 19:259–282, 2006.

Buchan BW, Allen S, Burnham CA, et al.: Comparison of the next generation Xpert MRSA/SA BC and GeneOhm StaphSR assays to routine culture for the identification of *Staphylococcus aureus* and MRSA in positive blood culture broths, *J Clin Microbiol*, 2014. pii: JCM.03108–14.

Buchan BW, Faron ML, Humphries RM, et al.: *Escherichia*, *Shigella*, and *Salmonella*. In Carroll KC, Pfaller MA, Landry ML, et al.: *Manual of clinical microbiology*, ed 12, Washington, DC, 2019, American Society for Microbiology, pp 688–723.

Buckwalter SP, Olson SL, Connelly BJ, et al.: Evaluation of matrix-assisted laser desorption ionization-time of flight mass spectrometry for identification of *Mycobacterium* species, *Nocardia* species, and other aerobic *Actinomycetes*, *J Clin Microbiol* 54:376–384, 2016.

Budzik JM, Hosseini M, Mackinnon Jr AC, et al.: Disseminated *Nocardia farcinica*: literature review and fatal outcome in an immunocompetent patient, *Surg Infect* 13:163–170, 2012.

Butler DF, Myers AL: Changing epidemiology of *Haemophilus influenzae* in children, *Infect Dis North Am* 32:119–128, 2018.

Butler-Wu SM, She RC: *Actinomyces*, *Lactobacillus*, *Cutibacterium*, and other non-spore-forming anaerobic gram-positive rods. In Carroll KC, Pfaller MA, Landry ML, et al.: *Manual of clinical microbiology*, ed 12, Washington, DC, 2019, American Society for Microbiology, pp 938–967.

Byard RW: Diphtheria: "The strangling angel" of children, *J Forensic Leg Med* 20:65–68, 2013.

Camello TC, Souza MC, Martins CA, et al.: *C. pseudodiphtheriticum* isolated from relevant clinical sites of infection: a human pathogen overlooked in emerging countries, *Lett Appl Microbiol* 48:458–464, 2009.

Carroll K, Reimer L: Microbiology and laboratory diagnosis of upper respiratory tract infections, *Clin Infec Dis* 23:442–448, 1996.

Carter GP, Chakravorty A, Pham Nguyen TA, et al.: Defining the roles of TcdA and TcdB in localized gastrointestinal disease, systematic organ damage, and the host response during *Clostridium difficile* infections, *mBio* 6, 2015. e00551–15.

Cartwright EJ, Jackson KA, Johnson SD, et al.: Listeriosis outbreaks and associated food vehicles, United States, 1998-2008, *Emerg Infect Dis* 19(1–9), 2013.

Carvalho G, Facklam R, Jackson D, et al.: Evaluation of three commercial broth media for pigment detection and identification of a group B Streptococcus (*S. agalactiae*), *J Clin Microbiol* 47:4161–4163, 2009.

Cazanave C, Greenwood-Quaintance KE, Hanssen AD, et al.: Corynebacterium prosthetic joint infection, *J Clin Microbiol* 50:1518–1523, 2012.

Celandroni F, Salvetti S, Gueye SA, et al.: Identification and pathogenic potential clinical *Bacillus* and *Paenibacillus* isolates, *PloS One* 31, 2016. e1052831.

Chapin KC, Musgnug MC: Evaluation of the PBP2a Latex agglutination assay for identification of methicillin resistant *Staphylococcus aureus* directly from blood cultures, *J Clin Microbiol* 42:1283–1284, 2004.

Charnot-Katsikas A, Tesic V, Love N, et al.: Use of the Accelerate Pheno System for identification and antimicrobial susceptibility testing of pathogens in positive blood cultures and impact on time to results and workflow, *J Clin Microbiol* 56, 2017. e01166–17.

Chediac-Tannoury R, Araj GF: Rapid MRSA detection by latex kit, *Clin Lab Sci* 16:198–202, 2003.

Chey WD, Leontiadis GI, Howden CW, et al.: ACG clinical guideline: treatment of *Helicobacter pylori infection*, *Am J Gastroenterol* 112:212–238, 2017.

Chopra T, Marchaim D, Awali RA, et al.: Epidemiology of bloodstream infections caused by *Acinetobacter baumannii* and the impact of drug resistance to both carbapenems and ampicillin-sulbactam on clinical outcomes, *Antimicrob Agents Chemother* 57:6270–6275, 2013.

Christensen JJ, Nielsen XC, Ruoff KL: *Aerococcus*, *Abiotrophia*, and other aerobic catalase-negative, gram-positive cocci. In Carroll KC, Pfaller MA, Landry ML, et al.: *Manual of clinical microbiology*, ed 12, Washington, DC, 2019, American Society for Microbiology, pp 436–450.

Church DL, Baxter H, Lloyd T, et al.: Evaluation of StrepB carrot broth versus Lim broth for detection of group B streptococcus colonization status of near-term pregnant women, *J Clin Microbiol* 46:2780–2782, 2008.

Clinical and Laboratory Standards Institute: *Methods for antimicrobial dilution and disk susceptibility testing of infrequently isolated or fastidious bacteria*, *Approved guideline*, 3rd edition, Wayne PA, 2015, CLSI document M45-A3. CLSI.

Clinical and Laboratory Standards Institute: *Susceptibility testing of Mycobacteria*, *Nocardiae*, *and other aerobic actinomycetes*, *Approved standard*, 3nd edition, Wayne, PA, 2018, CLSI document M24-A3. CLSI.

Clinical and Laboratory Standards Institute: *Methods for antimicrobial susceptibility testing of anaerobic bacteria*, *Approved standard*, 7th ed., Wayne, Pa., 2012, CLSI/NCCLS Publication M11-A8. CLSI.

Cloud JL, Conville PS, Croft A, et al.: Evaluation of partial 16S ribosomal DNA sequencing for identification of nocardia species by using the MicroSeq 500 system with an expanded database, *J Clin Microbiol* 42:578–584, 2004.

Conrads G, Nagy E, Kononen E, et al.: *Fusobacterium*, and other anaerobic gram-negative rods. In Carroll KC, Pfaller MA, Landry ML, et al.: *Manual of clinical microbiology*, ed 12, Washington, DC, 2019, American Society for Microbiology, pp 995–1023.

Cools P, Nemec A, Kampfer P, et al.: *Acinetobacter*, *Chryseobacterium*, *Moraxell*a, and other nonfermentative gram-negative rods. In Carroll KC, Pfaller MA, Landry ML, et al.: *Manual of clinical microbiology*, ed 12, Washington, DC, 2019, American Society for Microbiology, pp 829–857.

Conville PS, Brown-Elliot BA, Witebsky FG, et al.: *Streptomyces*, and other aerobic actinomycetes. In Carroll KC, Pfaller MA, Landry ML, et al.: *Manual of clinical microbiology*, ed 12, Washington, DC, 2019, American Society for Microbiology, pp 525–557.

Couturier MR: Helicobacter. In Carroll KC, Pfaller MA, Landry ML, et al.: *Manual of clinical microbiology*, ed 12, Washington, DC, 2019, American Society for Microbiology, pp 1044–1057.

Couturier MR, Graf EH, Griffin AT: Urine antigen tests for the diagnosis of respiratory infections: legionellosis, histoplasmosis, pneumococcal pneumonia, *Clin Lab Med* 34:219–236, 2014.

Couturier MR, Mehinovic E, Croft AC, et al.: Identification of HACEK clinical isolates by matrix-assisted laser desorption ionization-time of flight mass spectrometry, *J Clin Microbiol* 49:1104–1106, 2011.

Crabtree JH, Garcia NA: *Corynebacterium striatum* peritoneal dialysis catheter exit site infections, *Clin Nephrol* 60:270–274, 2003.

Cristovam E, Almeida D, Caldeira D, et al.: Accuracy of diagnostic tests for Legionnaires' disease: a systematic review, *J Med Micorbio* 66:485–489, 2017.

Crobach MJ, Phanche T, Eckert C, et al.: European Society of Clinical Microbiology and Infectious Diseases: update of the diagnostic guidance document for *Clostridium difficile* infection, *Clin Microbiol Infect* 22(Suppl 4):S63–S81, 2016.

de Noordhout CM, Devleesschauwer B, Angulo FJ, et al.: The global burden of listeriosis: a systematic review and meta-analysis, *Lancet Infect Dis* 14:1073–1082, 2014.

Devine VT, Cleary DW, Jefferies JM, et al.: The rise and fall of pneumococcal serotypes carried in the PCV era, *Vaccine* 35:1293–1298, 2017.

Dietrich EA, Petersen JM: Francisella. In Carroll KC, Pfaller MA, Landry ML, et al.: *Manual of clinical microbiology*, ed 12, Washington, DC, 2019, American Society for Microbiology, pp 871–882.

Dingle TC, Abbott AN, Fang FC: Reflexive culture in adolescents and adults with group a streptococcal pharyngitis, *Clin Infect Dis* 59:643–650, 2014.

Durant TJS, Merwede J, Reynolds J, et al.: Optimization of turnaround time for group A Streptococcus PCR, *J Clin Microbiol* 57, 2019. e00619–19.

Edelstein PH: Legionella. In Carroll KC, Pfaller MA, Landry ML, et al.: *Manual of clinical microbiology*, ed 12, Washington, DC, 2019, American Society for Microbiology, pp 905–920.

Ehrmann E, Handal T, Tamanai-Sharcoori Z, et al.: High prevalence of β-lactam and macrolide resistance genes in human oral *Capnocytophaga* species, *J Antimicrob Chemother* 69:381–384, 2014.

El Houmami N, Durand GA, Bzdrenga j, et al.: A new highly sensitive and specific real-time PCR assay Targeting the malate dehydrogenase gene of *Kingella kingae* and application to 201 pediatric clinical specimens, *J Clin Microbiol* 56, 2018, https://doi.org/10.1128/JCM.00505-18.

Elias J, Frosch M, Voge U: Neisseria. In Carroll KC, Pfaller MA, Landry MK, et al.: *Manual of clinical microbiology*, ed 12, Washington, DC, 2019, American Society for Microbiology, pp 640–655.

Elliott SP: Rat bite fever and *Streptobacillus moniliformis*, *Clin Microbiol Rev* 20:13–22, 2007.

Erler R, Wichels A, Heinemeyer EA, et al.: VibrioBase: a MALDI-TOF MS database for fast identification of *Vibrio* spp. that are potentially pathogenic in humans, *Syst Appl Microbiol*(14)00150–00157, 2014. pii: S0723-2020.

Facklam RR, Hollis D, Collins MD: Identification of gram-positive coccal and coccobacillary vancomycin-resistant bacteria, *J Clin Microbiol* 27:724–730, 1989.

Fang H, Ohlsson AK, Ullberg M, et al.: Evaluation of species-specific PCR, Bruker MS, VITEK MS and the VITEK 2 system for the identification of clinical Enterococcus isolates, *Eur J Clin Microbiol Infect Dis* 31:3073–3077, 2012.

Farfour E, Leto J, Barritault M, et al.: Evaluation of the Andromas matrix-assisted laser desorption ionization-time of flight mass spectrometry system for identification of aerobically growing gram-positive bacilli, *J Clin Microbiol* 50:2702–2707, 2012.

Fernandez-Suarez A, Benitez JM, Vidal AM, et al.: Lemierre's syndrome and septicemia caused soley by *Arcanobacterium haemolyticum* in a young immunocompetent patient, *J Med Microbiol* 58:1645–1648, 2009.

Feuerschuette OHM, Silveira SK, Cancelier ACL, et al.: Diagnostic yield of real-time polymerase chain reaction in the diagnosis of intrapartum maternal rectovaginal colonization by group B Streptococcus: a systematic review with meta-analysis, *Diagn Microbiol Infect Dis* 91:99–104, 2018.

Fitzgerald C, Patrick M, Gonzalez A, et al.: Multicenter evaluation of clinical diagnostic methods for detection and isolation of *Campylobacter* spp. from stool, *J Clin Microbiol* 54:1209–1215, 2016.

Forsythe SJ, Pitout J, Charnot-Katsikas A, et al.: *Klebsiella* and selected *Enterobacterales*. In Carroll KC, Pfaller MA, Landry ML, et al.: *Manual of clinical microbiology*, ed 12, Washington, DC, 2019, American Society for Microbiology, pp 724–750.

Frey AB, Wilson DA, LaSalvia MM, et al.: The detection and differentiation of methicillin-resistant and methicillin-susceptible *Staphylococcus aureus* endocarditis by using the BD GeneOhm StaphSR Assay, *Am J Clin Pathol* 136:686–689, 2011.

Gaastra W, Lipman LJ: Capnocytophaga canimorsus, *Vet Microbiol* 140:339–346, 2010.

Gasch O, Fernandex N, Armisen A, et al.: Community-acquired *Capnocytophaga canimorsus* meningitis in adults: report of one case with a subacute course and deafness, and literature review, *Enferm Infecc Microbiol Clín* 27:33–36, 2009.

Giltner CL, Bobenchik AM, Uslan DZ, et al.: Ciprofloxacin-resistant *Aeromonas hydrophila* cellulitis following leech therapy, *J Clin Microbiol* 51:1324–1326, 2013.

Giormezis N, Kolonitsiou F, Foka A, et al.: Coagulase-negative staphylococcal bloodstream and prosthetic device-associated infections: the role of biofilm formation, adhesin and toxin genes distribution, *J Med Microbiol*, 2014. pii: jmm.0.075259-0. doi: 10.

Gisselsson-Solen M, Bylander A, Wilhelmsson C, et al.: The Binax NOW test as a tool for diagnosis of severe acute otitis media and associated complications, *J Clin Microbiol* 45:L3003–L3007, 2007.

Gonzalez MD, Ledeboer NA: Haemophilus. In Carroll KC, Pfaller MA, Landry ML, et al.: *Manual of clinical microbiology*, ed 12, Washington, DC, 2019, American Society for Microbiology, pp 670–687.

Guan X, He L, Hu B, et al.: Laboratory diagnosis, clinical management and infection control of the infections caused by extensively drug-resistant gram-negative bacilli: a Chinese consensus statement, *Clin Microbiol Infect* 22:S15–S25, 2016.

Hageman JC, Uyeki TM, Francis JS, et al.: Severe community-acquired pneumonia due to *Staphylococcus aureus*, 2003–04 influenza season, *Emerg Infec Dis* 12(6):894–899, 2006.

Halket G, Dinsdale AE, Logan NA: Evaluation of the VITEK2 BCL card for identification of *Bacillus* sp. and other aerobic endosporeformers, *Lett Appl Microbiol* 50:120–126, 2010.

Han SH, Chin BS, Lee HS, et al.: Vancomycin-resistant enterococci bacteremia: risk factors for mortality and influence of antimicrobial therapy on clinical outcome, *J Infect* 58:182–190, 2009.

Harris AM, Beekmann SE, Polgreen PM, et al.: Rapid urine antigen testing for *Streptococcus pneumoniae* in adults with community-acquired pneumonia: clinical use and barriers, *Diagn Microbiol Infect Dis* 79:454–457, 2014.

Harrington SM, Buchan BW, Doern C, et al.: Multicenter evaluation of the BD MAX Enteric Bacterial Panel PCR assay for rapid detection of *Salmonella* spp., *Shigella* spp., *Campylobacter* spp. (*C. jejuni* and *C. coli*), and Shiga Toxin 1 and 2 genes, *J Clin Microbiol* 53: 1639–1347, 2015.

Hassan F: Molecular mechanisms of *Moraxella catarrhalis*-induced otitis media, *Curr Allergy Asthma Rep* 13:512–517, 2013.

Heelan JS, Struminsky J, Lauro P, et al.: Evaluation of a new selective enrichment broth for detection of Group B Streptococcus in pregnant women, *J Clin Microbiol* 43:896–897, 2005.

Hernandez-Milian A, Payeras-Cifre A: What is new in listeriosis? *BioMed Res Int* 358051:2014, 2014.

Huang ST, Lee HC, Lee NY, et al.: Clinical characteristics of invasive *Haemophilus aphrophilus* infections, *J Microbiol Immunol* 38:271–276, 2005.

Ibler K, Truberg Jensen K, et al.: Six cases of *Aerococcus sanguinicola* infection: clinical relevance and bacterial identification, *Scand J Infect Dis* 40:761–765, 2008.

Jackson KA, Gould LH, Hunter JC, et al.: Listeriosis outbreaks associated with soft cheeses, United States, 1998-2014, *Emerg Infect Dis* 24:1116–1118, 2018.

Janda JM, Abbott SL: The genus *Aeromonas*; Taxonomy, pathogenecity, and infection, *Clin Microbiol Rev* 23:35–73, 2010.

Jans C, Meile L, Lacroix C, et al.: Genomics, evolution, and molecular epidemiology of the *Streptococcus bovis/Streptococcus equines* complex (SBSEC), *Infect Genet Evol* 2014. pii: S1567-1348(14)00345-1.

Jeong S, Hong JS, Kim J, et al.: Identification of Acinetobacter species using matrix-assisted laser desorption ionization-time of flight mass spectrometry, *Ann Lab Med* 36:325–334, 2016.

Kaplan EL: Pathogenesis of acute rheumatic fever and rheumatic heart disease: Evasive after half a century of clinical, epidemiological, and laboratory investigations, *Heart* 91:3–4, 2005.

Kharsany AB, Hoosen AA, Kiepiela P, et al.: Growth and cultural characteristics of *Calymmatobacterium granulomatis*- the aetiological agent of granuloma inguinale (Donovanosis), *J Med Microbiol* 46:579–585, 1997.

Kilgore PE, Coenye T: *Bordetella* and related genera. In Carroll KC, Pfaller MA, Landry ML, et al.: *Manual of clinical microbiology*, ed 12, Washington, DC, 2019, American Society for Microbiology, pp 858–870.

Kilgore PE, Salim AM, Zervos MJ, et al.: Pertussis: microbiology, disease, treatment, and prevention, *Clin Microbiol Rev* 29:449–486, 2016.

Korkmaz H, Kesli R, Karabagli P, et al.: Comparison of the diagnostic accuracy of five different stool antigen tests for the diagnosis of *Helicobacter pylori* infection, *Helicobacter* 18:384–391, 2013.

Kotb M, Norrby-Teglund A, McGeer A, et al.: An immunogenetic and molecular basis for differences in the outcome of invasive Group A streptococcal infections, *Nat Med* 8:1398–1404, 2002.

Kuijper ED, Barbut F: *Clostridium* and *Clostridioides*. In Carroll KC, Pfaller MA, Landry ML, et al.: *Manual of clinical microbiology*, ed 12, Washington, DC, 2019, American Society for Microbiology, pp 968–994.

Lamy B, Horneman AJ: Aeromonas. In Carroll KC, Pfaller MA, Landry ML, et al.: *Manual of clinical microbiology*, ed 12, Washington, DC, 2019, American Society for Microbiology, pp 765–774.

Lappin E, Ferguson AJ: Gram positive toxic shock syndromes, *Lancet Infect Dis* 9:281–289, 2009.

Lean WL, Arnup S, Danchin M, et al.: Rapid diagnostic tests for group A streptococcal pharyngitis: a meta-analysis, *Pediatrics* 134:771–781, 2014.

Lee AD, Cassiday PK, Pawloski LC, et al.: Clinical evaluation and validation of laboratory methods for the diagnosis of Bordetella pertussis infection: culture, polymerase chain reaction (PCR) and anti-pertussis toxin IgG serology (IgG-PT), *PloS One* 13, 2018. e0195979.

Linscott AJ: Specimen collection, transport, and acceptability. In Leber AL, editor: *Clinical microbiology procedures handbook*, ed 4, Washington, DC, 2016, ASM Press, pp 2.0.1–2.1.29.

LiPuma JJ, Currie BJ, Peacock SJ, et al.: Burkholderia, Stenotrophomonas, Ralstonia, Cupriavidus, Pandoraea, Brevundimonas, Comomonas, Delftia, and Acidovorax. In Carroll KC, Pfaller MA, Landry ML, et al.: *Manual of clinical microbiology*, ed 12, Washington, DC, 2019, American Society for Microbiology, pp 807–828.

Loonen AJ, Jansz AR, Bergland JN, et al.: Comparative study using phenotypic, genotypic, and proteomics methods for identification of coagulase-negative staphylococci, *J Clin Microbiol* 50:1437–1439, 2012.

Lopez R, Cima MD, Vazquez F, et al.: Epidemiologic studies *of S. pneumoniae* carriage in healthy primary school aged children, *Eur J Clin Microbiol Infect Dis* 18:771–776, 1999.

Low DE: Toxic shock syndrome: major advances in pathogenesis, but not treatment, *Crit Care Clin* 29:651–675, 2013.

Lu PL, Hseuh PR, Hung CC, et al.: Infective endocarditis complicated with progressive heart failure due to a β-lactamase producing *Cardiobacterium hominis*, *J Clin Microbiol* 38:2015–2017, 2000.

MacDonald PD, Whitwam RE, Boggs JD, et al.: Outbreaks of listeriosis among Mexican immigrants as a result of consumption of illicitly produced Mexican-style cheese, *Clin Infect Dis* 40:677–682, 2005.

Mackey JR, Melendez EL, Farrell JJ, et al.: Direct detection of indirect transmission of *Streptobacillus moniliformis* rat bite fever infection, *J Clin Microbiol* 52:2259–2261, 2014.

MacVane SH, Nolte FS: Benefits of adding a rapid PCR-based blood culture identification panel to an established antimicrobial stewardship program, *J Clin Microbiol* 54:2455–2463, 2016.

Madhubashini M, George S, Chandrasekaran S: *Streptobacillus moniliformis* endocarditis: case report and review of literature, *Indian Heart J* 65:442–446, 2013.

Mancini F, Monaco M, Pataracchia M, et al.: Identification and molecular discrimination of toxigenic and nontoxigenic diphtheria *Corynebacterium* strains by combined real-time polymerase chain reaction assays, *Diagn Microbiol Infect Dis* 73:111–120, 2012.

Manickam K, Walkty A, Lagacé-Wiens PR, et al.: Evaluation of MRSASelect™ chromogenic medium for the early detection of methicillin-resistant *Staphylococcus aureus* from blood cultures, *Can J Infect Dis Med Microbiol* 24:e113–e116, 2013.

Marden JN, McClure EA, Beka L, et al.: Host matters: medicinal leech digestive-tract symbionts and their pathogenic potential, *Front Microbiol* 7:1569, 2016.

Matanock A, Lee G, Gierke R, et al.: Use of the 13-valent pneumococcal conjugate vaccine and 23-valent pneumococcal vaccine among adults aged >/= 65 years: updated recommendations of the Advisory Committee on Immunization Practices, *MMWR (Morb Mortal Wkly Rep)* 68:1069–1075, 2019.

Mattos-Guaraldi AL, Moreira LO, Damasco PV, et al.: Diphtheria remains a threat to health in the developing world—an overview, *Mem Inst Oswaldo Cruz* 98:987–993, 2003.

McBride SJ, Upton A, Roberts SA: Clinical characteristics and outcomes of patients with vancomycin-susceptible *Enterococcus faecalis* and *Enterococcus faecium* bacteremia in a five-year retrospective review, *Eur J Clin Microbiol Infect Dis*, 2009. epub Nov. 15.

McCollum JT, Cronquist AB, Silk BJ, et al.: Multistate outbreak of listeriosis associated with cantaloupe, *N Engl J Med* 369:944–953, 2013.

McDonald LC, Gerding DN, Johnson S, et al.: Clinical practice guidelines for *Clostridium difficile* infection in adults and children: 2017 update by the infectious diseases Society of American (IDSA) and Society for healthcare epidemiology of America (SHEA), *Clin Infect Dis* 66:987–994, 2018.

McElvania E, Singh K: Specimen collection, transport, and processing: Bacteriology. In Carroll KC, Pfaller MA, Landry ML, et al.: *Manual of clinical microbiology*, ed 12, Washington, DC, 2019, American Society for Microbiology, pp 302–330.

McGuiness CB, Hill J, Fonseca E, et al.: The disease burden of pertussis in adults 50 years old and older in the United States: a retrospective study, *MC Infect Dis* 13:32, 2013.

Mirrett S, Lauer BA, Miller GA, et al.: Comparison of acridine orange, methylene blue, and gram stain for blood cultures, *J Clin Microbiol* 14:562–566, 1982.

MMWR: Methicillin resistant *S. aureus* infections among competitive sports participants, *Morbid Mortal Wkly Rep* 52:793–798, 2003. 2000–2003.

MMWR: Vancomycin resistant *S. aureus*—New York, *Morbid Mortal Wkly Rep* 53:322–323, 2004. 2004.

MMWR: Severe methicillin-resistant *Staphylococcus aureus* community-acquired pneumonia associated with influenza—Louisiana and Georgia, December 2006–January 2007, *Morb Mort Wkly Rep* 56:325–329, 2007a.

MMWR: Neisseria gonorrhoeae antimicrobial susceptibility surveillance – the Gonococcal Isolate Surveillance Project, 27 sites, United States, 2014, *Morbid Mort Wkly Surveill Summ* 60:1–19, 2016.

MMWR: Sexually transmitted diseases treatment guidelines, *MMWR Recomm Rep (Morb Mortal Wkly Rep)* 64(RR–03), 2015.

MMWR: Revised recommendations of the Advisory Committee on Immunization Practices to vaccinate all persons aged 11-18 years with meningococcal conjugate vaccine, *Morbid Mort Wkly* 56:794–795, 2007.

MMWR: Updated recommendations of use of MenB-FHbp serogroup B meningococcal vaccine – Advisory Committee on immunization practices, 2016, *Morb Mortal Wkly Rep* 66:509–513, 2017.

Moon HW, Lee SH, Chung HS, et al.: Performance of the Vitek MS matrix-assisted laser desorption ionization time-of-flight mass spectrometry system for identification of gram-positive cocci routinely isolated in clinical microbiology laboratories, *J Med Microbiol* 62:1301–1306, 2013.

Moskowitz SM, Wiener-Kronish JP: Mechanisms of bacterial virulence in pulmonary infections, *Curr Opin Crit Care*, 2009. epub.

Mossad SB, Tomford JW, Stewart R, et al.: Case report of *Streptomyces* endocarditis of a prosthetic aortic valve, *J Clin Microbiol* 33:3335–3337, 1995.

Muder RR, Yu VL: Infection due to *Legionella* species other than *L. pneumophila*, *Clin Infect Dis* 35:990–998, 2002.

Mulligan MJ, Stapleton JT, Keitel WA, et al.: Tularemia vaccine: safety, reactogenicity, "Take" skin reactions, and antibody responses following vaccination with a new lot of the Francisella tularensis live vaccine strain - a phase 2 randomized clinical Trial, *Vaccine* 35:4730–4737, 2017.

Munford RS: Severe sepsis and septic shock: the role of gram-negative bacteremia, *Annu Rev Pathol* 1:467–496, 2006.

Murphy TF, Parameswaran GI: *Moraxella catarrhalis*—a human respiratory tract pathogen, *Clin Infect Dis* 49:124–131, 2009.

Muzny CA, Schwebke JR: Pathogenesis of bacterial vaginosis: discussion of current, *Hypotheses* 214(Suppl 1):S1–S5, 2016.

Nachamkin I: *Campylobacter* and *Arcobacter*. In Carroll KC, Pfaller MA, Landry ML, et al.: *Manual of clinical microbiology*, ed 12, Washington, DC, 2019, American Society for Microbiology, pp 1028–1043.

Nakhoul GN, Hickner J: Management of adults with acute streptococcal pharyngitis: minimal value for backup strep testing and overuse of antibiotics, *J Gen Intern Med* 28:830–834, 2013.

Nebreda-Mayoral T, Munoz-Bellido JL, Garcia-Rodriguez JA: Incidence and characteristics of urinary tract infections caused by *Corynebacterium urealyticum* (Corynebacterium group D2), *Eur J Clin Microbiol Infect Dis* 13:600–604, 1994.

Neemuchwala A, Soares D, Ravirajan V, et al.: *In vitro* antibiotic susceptibility patter of non-diphtheriae *Cornynebacterium* isolates in Ontario, Canada, from 2011 to 2016, *Antimicrob Agents Chemother* 27, 2018. e01776–17.

Nonhoff C, Roisin S, Hallin M, et al.: Evaluation of Clearview Exact PBP2a—a new immunochromatographic assay for detection of low-level methicillin-resistant *Staphylococcus aureus* (LL-MRSA), *J Clin Microbiol* 50:3359–3360, 2012.

Norskov-Lauritsen N, Kilian M: Reclassification of Actinobacillus actinomycetemcomitans, Haemophilus aphrophilus, H. paraprophilus and H. segnis as Aggregatibacter actinomycetemcomitans gen. nov., comb. nov., Aggregatibacter aphrophilus comb. nov. and Aggregatibacter segnis comb. nov., and emended description of Aggregatibacter aphrophilus to include V factor-dependent and V factor-independent isolates, *Int J Syst Evol Microbiol* 56:2135–2146, 2006.

Norskov-Lauritsen N, Ridderberg W: Approaches to the identification of aerobic gram-negative bacteria. In Carroll KC, Pfaller MA, Landry ML, et al.: *Manual of clinical microbiology*, ed 12, Washington, DC, 2019, American Society for Microbiology, pp 630–639.

Noskin GA, Suriano T, Collins S, et al.: *Paenibacillus macerans* pseudobacteremia resulting from contaminated blood culture bottles in a neonatal intensive care unit, *Am J Infect Control* 29:126–129, 2001.

Nugent RP, Krohn MA, Hillier SL: Reliability of diagnosing bacterial vaginosis is improved by a standardized method of Gram stain interpretation, *J Clin Microbiol* 29:297–301, 1991.

Oehler RL, Velez AP, Mizrachi M, et al.: Bite-related and septic syndromes caused by cats and dogs, *Lancet Infect Dis* 9:439–475, 2009.

O'Farrell N, Moi H: IUSTI/WHO European STD Guidelines Editorial Board. European guideline for the management of donovanosis, *Int J STD AIDS* 21:609–610, 2010. 2010.

Ozdemir O, Sari S, Terzioglu S, et al.: *Plesiomonas shigelloides* sepsis and meningoencephalitis in a surviving neonate, *J Microbiol Immunol Infect* 43:344–346, 2010.

Pan ES, Diep BA, Carlton HA, et al.: Increasing prevalence of MRSA infections in California jails, *Clin Infect Dis* 37:1384–1388, 2003.

Patel R, Piper K, Cockerill FR, et al.: The biopesticide *Paenibacillus popilliae* has a vancomycin resistance gene cluster homologous to the enterococcal VanA vancomycin gene cluster, *Antimicrob Agents Chemother* 44:704–709, 2000.

Patel JB, Wallace RJ, Brown-Elliott BA, et al.: Sequence-based identification of aerobic actinomycetes, *J Clin Microbiol* 42:2530–2540, 2004.

Paterson GK, Morgan FJ, Harrison EM, et al.: Prevalence and characterization of human mecC methicillin-resistant *Staphylococcus aureus* isolates in England, *J Antimicrob Chemother* 69:907–910, 2014.

Peel TN, Cole NC, Dylla BL, et al.: Matrix-assisted laser desorption ionization time of flight mass spectrometry and diagnostic testing for prosthetic joint infection in the clinical microbiology laboratory, *Diagn Microbiol Infect Dis*, 2014. pii: S0732-8893(14)00486–6.

Peirano G, Bradford PA, Kazmierczak KM, et al.: Global incidence of carbapenemase-producing Escherichia coli ST131, *Emerg Infect Dis* 20:1928–1931, 2014.

Peker N, Couto N, Sinha B, Rosen JW: Diagnosis of bloodstream infections from positive blood cultures and directly from blood samples: recent developments in molecular approaches, *Clin Microbiol Infect* 24:944–955, 2018.

Perry JD, Davies A, Butterworth LA, et al.: Development and evaluation of a chromagar media for methicillin resistant *S. aureus*, *J Clin Microbiol* 42:4519–4523, 2004.

Picard FJ, Bergeron MG: Laboratory detection of Group B streptococci for prevention of perinatal disease, *Eur J Clin Microbiol Infect Dis* 23:665–671, 2004.

Pittet LF, Emonet S, Schrenzel J, et al.: *Bordetella holmesii*: an under-recognised *Bordetella* species, *Lancet Infect Dis* 14:510–519, 2014.

Plongla R, Panagea T, Pincus DH, et al.: Identification of *Burkholderia* and uncommon glucose-nonfermenting gram-negative bacilli isolated from patients with cystic fibrosis by use of matrix-assisted laser desorption ionization-time of flight mass spectrometry (MALDI-TOF MS), *J Clin Microbiol* 54:3071–3072, 2016.

Principe L, Bracco S, Mauri C, et al.: Erysipelothrix rhusiopathiae bacteremia without endocarditis: rapid identification from positive blood culture by MALDI-TOF mass spectrometry. A case report and literature review, *Infect Dis Rep* 21:6368, 2016.

Ramanan P, Deziel PJ, Wengenack NL: *Gordonia* bacteremia, *J Clin Microbiol* 51:3443–3447, 2013.

Rantala S: *Streptococcus dysgalactiae* subsp. *equisimilis* bacteremia: an emerging infection, *Eur J Clin Microbiol Infect Dis* 33:1303–1310, 2014.

Rasmussen M: Aerococci and aerococcal infections, *J Infect* 66:467–474, 2013.

Reglinski M, Sriskandan S: The contribution of group A streptococcal virulence determinants to the pathogenesis of sepsis, *Virulence* 5:127–136, 2014.

Richter SS, Sercia L, Branda JA, et al.: Identification of Enterobacteriaceae by matrix-assisted laser desorption/ionization time-of-flight mass spectrometry using the VITEK MS system, *Eur J Clin Microbiol Infect Dis* 32:1571–1578, 2013.

Roorda L, Buitenwerf J, Ossewaarde JM, et al.: A real-time PCR assay with improved specificity for detection and discrimination of all clinically relevant *Bordetella* species by the presence and distribution of three insertion sequence elements, *BMC Res Notes* 4:11, 2011.

Roson B, Fernandez-Sabe N, Carratala J, et al.: Contribution of a urinary antigen assay (Binax NOW) to the early diagnosis of pneumococcal pneumonia, *Clin Infect Dis* 38:222–226, 2004.

Rudrik JT, Soehnlen MK, Perry MJ, et al.: Safety and accuracy of matrix-assisted laser desorption ionization-time of flight mass spectrometry for identification of highly pathogenic organisms, *J Clin Microbiol* 55:3513–3529, 2017.

Sabe MA, Shrestha NK, Gordon S, et al.: *Staphylococcus lugdunensis*: a rare but destructive cause of coagulase-negative staphylococcus infective endocarditis, *Eur Heart J Acute Cardiovasc Care* 3:275–280, 2014.

Salerno A, Cižnár I, Krovacek K, et al.: Phenotypic characterization and putative virulence factors of human, animal and environmental isolates of *Plesiomonas shigelloides*, *Folia Microbiol* 55:641–647, 2010.

Salgado-Pabón W, Breshears L, Spaulding AR, et al.: Superantigens are critical for Staphylococcus aureus infective endocarditis, sepsis, and acute kidney injury. Superantigens are critical for Staphylococcus aureus infective endocarditis, sepsis, and acute kidney injury, *mBio* 4, 2013. pii: e00494–13.

Savini V, Fazii P, Favaro M, et al.: Tuberculosis-like pneumonias by the aerobic actinomycetes *Rhodococcus*, *Tsukamurella* and *Gordonia*, *Microbes Infect* 14:401–410, 2012.

Schlaberg R, Fisher MA, Hanson KE: Susceptibility profiles of *Nocardia* isolates based on current taxonomy, *Antimicrob Agents Chemother* 58:795–800, 2014.

Schmoock G, Ehricht MF, Elschner M, et al.: Development of a diagnostic multiplex polymerase chain reaction microarray assay to detect and differentiate *Brucella* spp., *Diagn Microbiol Infect Dis* 71:341–353, 2011.

Schuchat A, Lizano C, Broome CV, et al.: Outbreak of neonatal listeriosis associated with mineral oil, *Pediatr Infect Dis* 10:183–189, 1991.

Schulthess B, Brodner K, Bloemberg GV, et al.: Identification of gram-positive cocci by use of matrix-assisted laser desorption ionization-time of flight mass spectrometry: comparison of different preparation methods and implementation of a practical algorithm for routine diagnostics, *J Clin Microbiol* 51:1834–1840, 2013.

Senneby E, Petersson AC, Rasmussen M: Epidemiology and antibiotic susceptibility of aerococci in urinary cultures, *Diagn Microbiol Infect Dis* 81:149–151, 2015.

Shahin M, Jamal W, Verghese T, et al.: Comparative evaluation of Anoxomat and conventional anaerobic GasPak jar systems for the isolation of anaerobic bacteria, *Med Princ Pract* 12:81–86, 2003.

Sharma H, Smith D, Turner CE, et al.: Clinical and molecular epidemiology of staphylococcal toxic shock syndrome in the United Kingdom, *Emerg Infect Dis* 24:258–266, 2018.

Shelton-Dodge K, Vetter EA, Kohner PC, et al.: Clinical significance and antimicrobial susceptibilities of *Aerococcus sanguinicola* and *Aerococcus urinae*, *Diagn Microbiol Infect Dis* 70:448–451, 2011.

Shulman ST, Bisno AL, Clegg HW, et al.: Clinical practice guideline for the diagnosis and management of Group A streptococcal pharyngitis: 2012 update by the Infectious Disease Society of America, *Clin Infect Dis* 55:e86–e102, 2012.

Simmons C, Stasiewicz MJ, Wright E, et al.: *Listeria monocytogenes* and *Listeria* spp. contamination patterns in retail delicatessen establishments in three U.S. states, *J Food Prot* 77:1929–1939, 2014.

Skalsky K, Yahav D, Bishara J, et al.: Treatment of human brucellosis: systematic review and meta-analysis of randomised controlled trials, *BMJ* 336:701–704, 2008.

Smith MD, Sheppard CL, Hogan A, et al.: Diagnosis of *S. pneumoniae* infections in adults with bacteremia and community acquired pneumonia: clinical comparison of pneumococcal PCR and urinary antigen detection, *J Clin Microbiol* 47:1046–1049, 2009.

Spellerberg B, Brandt C, Sendi P: Streptococcus. In Carroll KC, Pfaller MA, Landry ML, et al.: *Manual of clinical microbiology*, ed 12, Washington, DC, 2019, American Society for Microbiology, pp 399–417.

Speziale P, Pietrocola G, Rindi S, et al.: Structural and functional role of *Staphylococcus aureus* surface components recognizing adhesive matrix molecules of the host, *Future Microbiol* 4:1337–1352, 2009.

Stevens MP, Elam K, Bearman G: Meningitis due to *Bacillus cereus*: a case report and review of the literature, *Can J Infect Dis Med Microbiol* 23:e16–e19, 2012.

Su TY, Lee MH, Huang CT, et al.: The clinical impact of patients with bloodstream infection with different groups of Viridans group streptococci by using matrix-assisted laser desorption ionization-time of flight mass spectrometry (MALDI-TOF MS), *Medicine* 97, 2018. e13607.

Sugimoto M, Wu JY, Abudayyeh S, et al.: Unreliability of results of PCR detection of *Helicobacter pylori* in clinical or environmental samples, 47:738–742, 2009.

Summanen PH, McTeague M, Vaisanen ML, et al.: Comparison of recovery of anaerobic bacteria using the Anoxomat, anaerobic chamber, and GasPak jar systems, *Anaerobe* 5:5–9, 1999.

Sweeney DA, Hicks CW, Cui X, et al.: Anthrax infection, *Am J Respir Crit Care Med* 184:1333–1341, 2011.

Tabak YP, Merchant S, Ye G, et al.: Incremental clinical and economic burden of suspected respiratory infections due to multi-drug-resistant *Pseudomonas aeruginosa* in the United States, *J Hosp Infect*, 2019, https://doi.org/10.1016/j.jhin.2019.06.005.

Tack DM, Marder EP, Griffin PM, et al.: Preliminary incidence and trends of infections with pathogens transmitted commonly through food - foodborne Diseases Active Surveillance Network, 10 U.S. Sites, 2015–2018, *Am J Transplant* 19:1859–1863, 2019.

Tansarli GS, Chapin KC: Diagnostic test accuracy of the BioFire FilmArray meningitis/encephalitis panel: a systematic review and meta-analysis, *Clin Microbiol Infect*(19)30615–30619, 2019 Nov 21. pii: S1198–743X(19)30615–9, https://doi.org/10.1016/j.cmi.2019.11.016. [Epub ahead of print].

Tarr CL, Glover WA, Boucher Y, Farmer JJ: *Vibrio* and related organisms. In Carroll KC, Pfaller MA, Landry ML, et al.: *Manual of clinical microbiology*, ed 12, Washington, DC, 2019, American Society for Microbiology, pp 775–786.

Teixeira LM, Carvalho MGS, Facklam RR, Shewmaker PL: Enterococcus. In Carroll KC, Pfaller MA, Laundry ML, et al.: *Manual of clinical microbiology*, ed 12, Washington, DC, 2019, American Society for Microbiology, pp 418–435.

Testerman TL, Morris J: Beyond the stomach: an updated view of *Helicobacter pylori* pathogenesis, diagnosis, and treatment, *World J Gastroenterol* 20:12781–12808, 2014.

Thomas JG: Routine CSF antigen detection for agents associated with bacterial meningitis: another point of view, *Clin Microbiol Newsl* 16:89–95, 1994.

Toro CM, Janvier J, Zhang K, et al.: Community-associated methicillin-resistant *Staphylococcus* aureus necrotizing pneumonia without evidence of antecedent viral upper respiratory infection, *Can J Infect Dis Med Microbiol* 25:e76–e82, 2014.

Turenne CY, Alexander DC: *Bacillus* and other aerobic endospore-forming bacteria. In Carroll KC, Pfaller MA, Laundry ML, et al.: *Manual of clinical microbiology*, ed 12, Washington, DC, 2019, American Society for Microbiology, pp 455–476.

U.S. Preventive Services Task Force: Ocular prophylaxis for gonococcal ophthalmia neonatorum: US Preventative Services Task Force reaffirmation recommendation statement, *J Am Med Assoc* 321:394–398, 2019.

Valve K, Vaalasti A, Anttila VJ, et al.: Disseminated *L. pneumophila* infection in an immunocompromised patient treated with tigecycline, *Scand J Infect Dis*, 2009. epub Nov. 17.

Van den Velde S, Lagrou K, Desmet K, et al.: Species identification of corynebacteria by cellular fatty acid analysis, *Diagn Microbiol Infect Dis* 54:99–104, 2006.

Vaska VL, Faoagali JL: *Streptococcus bovis* bacteraemia: identification within organism complex and association with endocarditis and colonic malignancy, *Pathology* 41:183–186, 2009.

Vavrova A, Balazova T, Sedlacek I, et al: Evaluation of the MALDI-TOF MS profiling for identification of newly described *Aeromonas* spp. Folia Microbiol 60:375–383.

Veenemans J, Verhulst C, Punselie R, et al.: Evaluation of brilliance MRSA 2 agar for detection of methicillin-resistant *Staphylococcus aureus* in clinical samples, *J Clin Microbiol* 51:1026–1027, 2013.

Veloo AC, Johnson CN, Peptostreptococcus F, et al.: *Veillonella*, and other anaerobic cocci. In Carroll KC, Pfaller MA, Landry ML, et al.: *Manual of clinical microbiology*, ed 12, Washington, DC, 2019, American Society for Microbiology, pp 925–937.

Verroken A, Defourny L, le Polain de Waroux O, et al.: Clinical impact of MALDI-TOF MS identification and rapid susceptibility testing on adequate antimicrobial treatment in sepsis with positive blood cultures, *PloS One* 11, 2016. e0156299.

Vila J, Juiz P, Salas C, et al.: Identification of clinically relevant Corynebacterium spp., Acranobacterium haemolyticum, and Rhodococcus equi by matrix-assisted laser desorption ionization-time of flight mass spectrometry, *J Clin Microbiol* 50:1745–1747, 2012.

Vucicevic Z, Bencic IJ, Kruslin B, et al.: Toxic shock syndrome due to group A streptococcal pharyngitis and bacteremia in an adult, *J Microbiol Immunol Infect* 41:351–354, 2008.

Wagenaar JA, van Bergen MA, Blaster MJ, et al.: *Campylobacter fetus* infections in humans: exposure and disease, *Clin Infect Dis* 58:1579–1586, 2014.

Wang Q, Chang BJ, Riley TV: Erysipelothrix rhusiopathiae, *Vet Microbiol* 140:405–417, 2010.

Warren DK, Liao RS, Merz LR, et al.: Detection of methicillin resistant *S. aureus* directly from nasal swab specimens by a real-time PCR assay, *J Clin Microbiol* 42:5578–5581, 2004.

Weinstock DM, Brown AE: Rhodococcus equi: an emerging pathogen, *Clin Infect Dis* 34:1379–1385, 2002.

Weintraub A: Approaches to the identification of anaerobic bacteria. In Carroll KC, Pfaller MA, Landry ML, et al.: *Manual of clinical microbiology*, ed 12, Washington, DC, 2019, American Society for Microbiology, pp 921–924.

Wellinghausen N: *Listeria* and *Erysipelothrix*. In Carroll KC, Pfaller MA, Landry ML, et al.: *Manual of clinical microbiology*, ed 12, Washington, DC, 2019, American Society for Microbiology, pp 477–487.

Wilkie IW, Harper M, Boyce JD, et al.: *Pasteurella multocida*: diseases and pathogenesis, *Curr Top Microbiol Immunol* 361:1–22, 2012.

Wilson JW: Nocardiosis: Updates and clinical overview, *Mayo Clin Proc* 87:403–407, 2012.

Wojewoda CM, Koval CE, Wilson DA, et al.: Bloodstream infection caused by nontoxigenic *Corynebacterium diphtheriae* in an immunocompromised host in the United States, *J Clin Microbiol* 50:2170–2172, 2012.

Woo PC, Ngan AH, Lau SK, et al.: *Tsukamurella conjunctivitis*: a novel clinical syndrome, *J Clin Microbiol* 41:3168–3171, 2003.

Wong D, Nielsen TB, Bonomo RA, et al.: Clinical and Pathophysiological overview of *Acinetobacter* infections: a century of Challenges, *Clin Microbiol Rev* 30:409–447, 2017.

World Health Organization: Pertussis vaccines: WHO position paper, August 2015-Recommendations, *Vaccine* 34:1423–1425, 2015.

Yagupsky P: *Kingella kingae*: carriage, transmission, and disease, *Clin Microbiol Rev* 28:54–79, 2015.

Zbinden R, Aggregatibacter C, Eikenella K: *Pasturella*, and other fastidious or rarely encountered gram-negative rods. In Carroll KC, Pfaller MA, Landry ML, et al.: *Manual of clinical microbiology*, ed 12, Washington, DC, 2019, American Society for Microbiology, pp 656–669.

Zevin AS, Xie IY, Birse K, et al.: Microbiome composition and function drives wound-healing impairment in the female genital tract, *PLoS Pathog* 12, 2016. e1005889.

Zhang H, Morrison S, Tang YW: Multiplex polymerase chain reaction tests for detection of pathogens associated with gastroenteritis, *Clin Lab Med* 35:461–486, 2015.

CHAPTER 58

IN VITRO TESTING OF ANTIMICROBIAL AGENTS

Angella Charnot-Katsikas, Amanda Harrington

INTRODUCTION AND DEFINITIONS, 1166
Guidance Documents For In Vitro Testing of Antimicrobial Agents, 1166
TECHNICAL CONSIDERATIONS IN SUSCEPTIBILITY TESTING, 1167
Testing Media, 1167
Inoculum, 1167
Incubation Conditions, 1167
Test Interpretation, 1167
INHIBITORY METHODS FOR SUSCEPTIBILITY TESTING, 1168
Dilution Testing, 1168
Gradient Diffusion, 1169
Disk Diffusion, 1169
Other Phenotypic Methods, 1170
Direct Tests for β-Lactamase, 1170
BACTERICIDAL TESTING, 1170
COMMERCIAL AUTOMATED INSTRUMENT SYSTEMS, 1171
MOLECULAR-BASED AND NEWER METHODS OF ANTIMICROBIAL SUSCEPTIBILITY TESTING, 1172
Detection of Important Resistance Phenotypes, 1172
Molecular Antimicrobial Susceptibility Testing, 1177
INDICATIONS FOR SUSCEPTIBILITY TESTING, 1179
SELECTION OF ANTIBIOTICS FOR TESTING, 1180
SELECTING ANTIBIOTICS TO BE REPORTED, 1180
CUMULATIVE ANTIMICROBIAL SUSCEPTIBILITY REPORTS, 1181
SELECTED REFERENCES, 1181

KEY POINTS

- The minimum inhibitory concentration (MIC) is defined as the lowest concentration of antibiotic that inhibits the visible growth of an organism in vitro. It is distinguished from the breakpoint, which is the concentration of antibiotic that determines whether an isolate is categorized as susceptible, intermediate, or resistant.
- MIC values are determined by inhibitory methods in the laboratory, which include broth dilution, agar dilution, and gradient diffusion. Disk diffusion testing, which is a qualitative rather than a quantitative test, does not directly result in an MIC value; it is based on direct correlation of inhibitory zone sizes with MIC values. Molecular testing also does not result in an MIC; rather, it is increasingly being used to rapidly determine the presence of resistance genes in an organism. Whatever method of testing is chosen, it must be remembered that resistance mechanisms are complex and can evolve quickly. Therefore, it is imperative that the laboratory director remain informed of the most current literature and guidelines.
- Whatever method of susceptibility testing is used, standardized conditions related to media, inoculum concentration, incubation time, atmosphere, and temperature are necessary to produce accurate and reproducible results. Standards for these variables are published by the Clinical and Laboratory Standards Institute (CLSI) and represent standards of practice for microbiology laboratories.
- Commercial automated instrument systems are available for rapid, high-volume susceptibility testing. However, despite the advantages of speed and efficiency that these systems allow, it must be remembered that the systems may have weaknesses. In addition to the expense of the systems, some are associated with problems in accurately detecting specific resistance phenotypes. Expert rules can be programmed into the software to help streamline some of these issues for more accurate reporting. It is the responsibility of the laboratory director to be aware of the weaknesses in the systems used and to find alternative or supplemental approaches of testing, as appropriate.
- Both the indications for susceptibility testing and the selection of which antimicrobials to test and report should be determined by individual laboratories on the basis of recommendations published by the CLSI and in close consultation with the antimicrobial stewardship team, including pharmacists and infectious disease providers of the institution. In general, susceptibility testing is warranted when the susceptibility of an organism causing an infection cannot be predicted reliably from its identity.
- Cumulative antimicrobial susceptibility reports (antibiograms) should be published by laboratories, based on CLSI guidelines, on at least an annual basis. These compilations are important for use by physicians in initiating appropriate empirical treatment before testing results are available, are helpful for pharmacists in monitoring the use and need of specific antimicrobials and in attempting to control drug costs, and are helpful in trending susceptibility patterns in a particular hospital or region over time.

INTRODUCTION AND DEFINITIONS

In vitro **antibiotic susceptibility testing (AST)** in clinical laboratories is performed using a variety of methodologies, but phenotypic methods remain a primary method of testing at this time. Phenotypic methods have traditionally required isolation of the pathogen being tested, followed by exposure of the pathogen to the antimicrobial and subsequent evaluation of the expression, or lack of expression, of resistance to the antibiotic. This process can be labor-intensive and time-consuming, which may be disadvantageous under some circumstances to the patient, the laboratory, or both. Despite this fact, phenotypic methods—which include broth dilution, agar dilution, disk diffusion, and gradient diffusion—are at present the most prevalent and, in many cases, the most cost-effective way to accomplish susceptibility testing. Commercial systems, based on phenotypic methods, have reduced the labor and time necessary to detect the expression of antibiotic resistance and are used in many laboratories. Finally, newer methods of testing (primarily molecular), some of which can be performed directly on patient specimens, have become much more integrated into routine testing, as they eliminate the delay associated with pathogen isolation.

Phenotypic antimicrobial susceptibility tests may be categorized according to the endpoint used, that is, inhibition of growth or killing. In most cases, inhibition of growth is the parameter used in the laboratory, with only limited use of a killing endpoint (bactericidal) for very specific circumstances.

GUIDANCE DOCUMENTS FOR IN VITRO TESTING OF ANTIMICROBIAL AGENTS

Whichever method of dilution or disk-diffusion testing a laboratory selects (and laboratories usually select a combination of methods to accommodate

their needs), a standardized procedure is of the utmost importance in producing accurate and reproducible results. Various standards organizations in a variety of venues throughout the world have set and published these parameters. In the United States, the **Clinical and Laboratory Standards Institute (CLSI)** fulfills this role. Professional organizations (e.g., the American Society for Microbiology, Infectious Disease Society of America), private industry, and governmental organizations have worked together within the Subcommittee on Antimicrobial Susceptibility Testing under the Area Committee on Microbiology of the CLSI to establish the necessary standards. Testing conditions, quality control parameters, and interpretative guidelines—including clinical breakpoints for specific antibiotic-organism combinations—are set and published for use by clinical laboratories in the CLSI document M100 (CLSI M100, 2020) entitled *Performance Standards for Antimicrobial Susceptibility Testing*. Breakpoints established by the CLSI may differ for a variety of reasons from those set by the European Committee on Antimicrobial Susceptibility Testing (EUCAST) or other standards organizations. One such reason involves different dosing and administration schedules used for the same drugs in different countries. In the United States, challenges also arise when breakpoints differ between the CLSI and the U.S. Food and Drug Administration (FDA). The breakpoints and interpretations of the FDA regulate the manufacturers of the automated testing systems while the breakpoints and interpretations of the CLSI guide clinical microbiologists and are updated regularly based on the most recent and relevant literature. The CLSI has also published a series of documents that describe standardized procedures for susceptibility testing of fastidious and facultatively anaerobic bacteria (CLSI M45, 2016), anaerobic bacteria (CLSI M11, 2018), mycobacteria and aerobic actinomycetes (CLSI M24, 2018), filamentous fungi (CLSI M38, 2017), and yeasts (CLSI M27, 2017). The Subcommittee on Antimicrobial Susceptibility Testing revises the text of most documents on a 3-year cycle and reviews and revises on a yearly basis tables detailing MIC breakpoints or zone-diameter breakpoints. Standardized procedures published by the CLSI represent the standard of laboratory practice in the United States. Laboratories should ensure that the most current tables and texts are on hand and that revisions in the tables and texts are incorporated into the methods and policies of the laboratory when they become available.

TECHNICAL CONSIDERATIONS IN SUSCEPTIBILITY TESTING

TESTING MEDIA

It has been demonstrated that the testing components of susceptibility testing may have an effect on the results. With respect to testing media, the CLSI currently recommends Mueller-Hinton agar or broth because they demonstrate good batch-to-batch reproducibility; are low in sulfonamide, trimethoprim, and tetracycline inhibitors; and support the growth of most nonfastidious bacteria (CLSI M02 and M07, 2018). Stringent quality control must be adhered to in commercial or "in-house" preparation of media, as many physical properties of the media directly influence testing. Variations in ion concentrations and pH will also affect testing. For example, excess calcium and magnesium will cause *Pseudomonas aeruginosa* isolates to appear more resistant when tested against aminoglycosides, but decreased levels may demonstrate false susceptibility. The level of calcium will also affect daptomycin susceptibility results for those species against which the drug is tested, and zinc ion levels influence carbapenem results. As another example, the pH of the media will also directly affect testing; it must be between 7.2 and 7.4 for accurate results. A more acidic pH will cause some drugs—such as aminoglycosides, quinolones, and macrolides—to lose potency and drugs such as penicillin to have increased activity. A higher pH can have the opposite effect.

For some fastidious species, supplements must be added to the Mueller-Hinton media, or specialized media containing required growth factors are necessary. For example, streptococci do not grow well in or on unsupplemented Mueller-Hinton media. This problem can be overcome by adding defibrinated sheep blood to a final concentration of 5% for disk diffusion or lysed horse blood to the medium at a final concentration of 2.5% to 5.0% for broth dilution. *Haemophilus influenzae* requires *Haemophilus* test medium when performing broth dilution, and *Neisseria gonorrhoeae* testing requires GC agar base medium with growth supplement (CLSI M45, 2016). For susceptibility testing of anaerobes, *Brucella* agar supplemented with laked (i.e., defibrinated and hemolyzed by freezing) sheep blood, hemin, and vitamin K_1 (Wadsworth method) is necessary to allow testing using the agar dilution method (CLSI M11, 2018). An exception is seen with the *B. fragilis* group, which can be tested using the microbroth dilution method with *Brucella* broth with hemin, vitamin K_1, and 5% lysed horse blood.

Additional medium parameters may influence testing. For example, agar depth in plates used in disk-diffusion testing must measure 4 mm; otherwise, the diffusion gradient of the antibiotic will be affected. False resistance may occur if the agar is too deep, and false susceptibility may occur if the agar is not deep enough. When Mueller-Hinton is supplemented with blood, the zones of inhibition may be smaller by 2 to 3 mm than those obtained with unsupplemented agar.

INOCULUM

Intuitively, it is evident that the quantity of bacteria present will influence results of susceptibility testing when a finite amount of antibiotic is used in the testing process. To ensure consistency in the quantity of organisms inoculated into the test system, the CLSI has mandated that the prepared inoculum suspension must have a turbidity equivalent to a 0.5 McFarland turbidity standard, which contains approximately 1 to 4 × 10^8 colony-forming units/mL. These standards can be purchased commercially or a BaSO4 suspension can be prepared in the laboratory, the instructions for which are detailed in CLSI documents (CLSI M02 and M07, 2018).

Inoculum preparations can be made by several methods by directly suspending 18- to 24-hour-old colonies from nonselective media in broth or saline until turbidity of 0.5 McFarland is achieved or by suspending several colonies of the organism to be tested into nutrient broth and incubating for several hours until growth results in turbidity equivalent to 0.5 McFarland. The direct colony suspension method is necessary for very fastidious species that require special supplements or media for growth, although the growth method is preferable for species that are difficult to suspend uniformly and when 18- to 24-hour plates are not immediately available. For most commonly isolated species, the two methods are equivalent.

INCUBATION CONDITIONS

Test systems must be incubated under standardized temperature and atmospheric conditions to ensure uniform results. These conditions have been described and published by the CLSI and FDA for U.S. laboratories. General conditions for disk diffusion and broth dilution of bacteria include a temperature of 35°C ± 2°C with an atmosphere of ambient air for a period of 16 to 24 hours (CLSI M02 and M07, 2018). Many exceptions to this have been noted, however. For example, for disk diffusion, *Streptococcus* spp. and *Haemophilus* spp. require incubation in an atmosphere of 5% carbon dioxide. Although zones of inhibition of *Haemophilus* spp. are measured after 16 to 18 hours of incubation, those for *Streptococcus* spp. should not be determined until after 20 to 24 hours. Similarly, although susceptibility testing for most antibiotics against *Staphylococcus* spp. and *Enterococcus* spp. requires 16 to 18 hours, when oxacillin and vancomycin against *Staphylococcus* spp. and vancomycin against *Enterococcus* spp., respectively, are tested, a full 24 hours of incubation is necessary. Differences in testing and incubation parameters among aerobic, facultative anaerobic, anaerobic, mycobacterial, filamentous fungi, and yeast species require that the relevant CLSI documents be studied carefully prior to testing.

TEST INTERPRETATION

The inhibitory parameter that forms the basis for the majority of phenotypic susceptibility tests is the **minimum inhibitory concentration (MIC)**, which is the lowest concentration of antibiotic that inhibits the visible growth of an organism in an in vitro system (Fig. 58.1). MIC results are dependent not only on the interaction between the antimicrobial agent and organism but also on test conditions. These conditions include pH and ion concentrations of testing media, the temperature at which the test system is incubated, the incubation atmosphere, the amount of organism used in testing, and the length of time the system incubates.

Although the MIC is a very useful and reproducible indicator of the interaction of an antibiotic with a specific organism, the information it provides to a physician in the context of the infected patient by itself is limited. The MIC is a snapshot assessment of the interaction of a constant concentration of drug with the organism at a specific point in time under specified conditions in vitro. The MIC must be correlated with the complex and changing environment of the physiology of the patient to

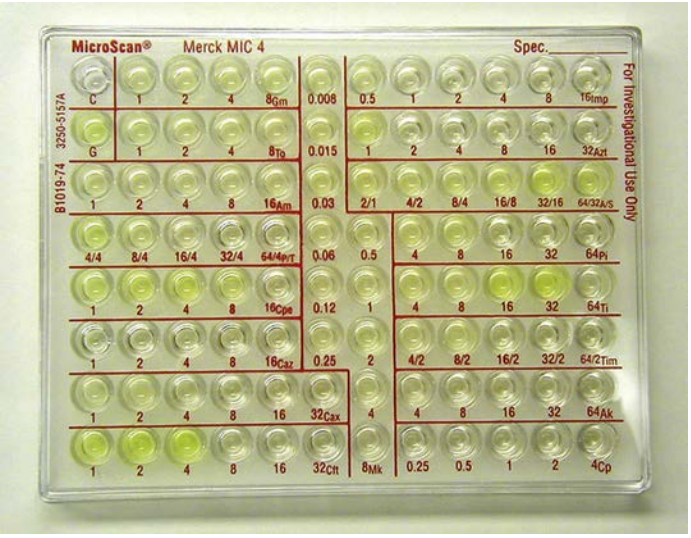

Figure 58.1 Minimum inhibitory concentration by broth microdilution. Seen in this figure is a commercially prepared microtiter tray containing different concentrations of antibiotics in the various sets of wells; the concentrations in mcg/mL are marked by the numbers listed under each well, and the different antimicrobial agents are indicated by abbreviations seen nearest the well with the highest drug concentration. The organism is manually inoculated into the wells and read by direct visualization. Growth is indicated by turbidity (in the present figure, there is also pigmentation seen), and the organism will grow in the wells containing concentrations of antibiotics to which it is resistant. The MIC value is determined by the lowest concentration without visible growth. In cases in which all wells in the series of a given antibiotic are negative, the MIC is resulted as lower than the lowest concentration of that drug; conversely, when there is growth in all wells in the series of a given antibiotic, the MIC is resulted as higher than the highest concentration of that drug. In the present figure, the last antibiotic agent in the lowest row on the right is Ciprofloxacin (Cp), with an MIC ≤0.25 mcg/mL. Cefotetan (Cft) is on the lower left, with clear growth in the wells marked 1, 2, and 4, and no growth in the wellmarked 8, making the MIC for this drug 8 mcg/mL. For comparison (as well as for use as an indicator of test validity), the negative (C) and positive control (G) wells can be seen on the upper left.

allow the physician to predict whether therapy with a particular antibiotic will be successful. This is accomplished through the use of **breakpoints**, which allow assessment of the efficacy of killing or inhibition of growth of the organism by the antimicrobial. Several types of breakpoints—including microbiological, pharmacokinetic/pharmacodynamic, and clinical—have been identified. Clinical breakpoints, which are intended to separate strains of organisms into categories that predict whether therapy in a patient will be successful, are breakpoints relevant to this short review and are the only type of breakpoint discussed here. Determining clinical breakpoints is complex, difficult, and subjective. The process can involve numerous clinical trials, and clinical breakpoints may vary with the determining standards organization. Breakpoints also change over time, as they are reassessed and revised according to the most recent guiding literature. Breakpoints also vary based on the clinical site of infection; for example, the breakpoint set for meningitis due to *S. pneumoniae* is different from that set for pneumonia caused by the same organism due to the fact that the concentration of antibiotic achieved varies between sites of clinical infection. Breakpoints are not perfectly clinically predictive for various reasons, such as differences in patient characteristics and immunity, as well as differences in organism virulence and type and site of infection. Excellent discussions of breakpoints and their determination, maintenance, and relevance can be obtained by referring to several review articles (Jenkins & Jerris, 2011; Jenkins & Schuetz, 2012).

Interpretive categories have been established that allow simplified and easily understood reporting of susceptibility results by laboratories. Many laboratories report these categories in addition to reporting an MIC or, in some cases, in lieu of reporting an MIC. Although highly knowledgeable infectious disease physicians may be able to make informed management decisions with the MIC, this is unlikely to be the case for physicians who do not specialize in this area. Treating physicians depend on guidance from the laboratory regarding interpretation of the actual breakpoints. The basic interpretative categories include **susceptible**, **intermediate**, and **resistant**. There is also a **nonsusceptible** category and, most recently, a **susceptible dose dependent** (**SDD**) category for antibacterial AST (CLSI M100, 2020). *Susceptible* implies that therapy with the recommended dosage of a particular antibiotic is likely to be effective in eradicating the infection, and *resistant* indicates that the antibiotic in the appropriate dose has not been shown to have a high likelihood of treatment success in clinical trials.

Reporting an interpretative category of intermediate has several implications. It suggests that the isolate tested may be less inhibited by the usual dose of the antibiotic than those isolates that are categorized as susceptible. It also implies that therapy with higher doses of antibiotic may be effective and that therapy may also be effective if used in anatomic sites in which the antibiotic is concentrated. An example of this latter situation is the use of β-lactam antibiotics in treating urinary tract infection. This category also includes a **buffer zone**, which is intended to prevent technical factors from resulting in a major interpretive error. An additional category of **SDD** implies that susceptibility of an isolate is dependent on a higher dosing regimen (higher doses and/or more frequent dosing intervals) than typically used and that the dose to which the patient is exposed is higher than that used when the susceptible breakpoint was established. This category has been in use for antifungal AST but is now used for antibacterial AST because it was noted that *intermediate* was often misinterpreted as *resistant* by clinicians, thereby limiting their choices for therapy.

The **nonsusceptible** category is intended for cases in which intermediate and resistant isolates have not been found or categories of intermediate and resistant have not been defined. It is utilized primarily for new antibiotics. If testing of an isolate yields an MIC value that is above the cutoff concentration established for the breakpoint for a susceptible category, the laboratory can report the isolate as nonsusceptible. This does not necessarily imply that resistance to the antibiotic exists, but it means that experience with isolates that demonstrate MICs at this level is limited; thus, no definitive assessment can be made.

Although reporting of antimicrobial susceptibility testing and categorization of an isolate into one of the interpretative categories are helpful to physicians in managing patients with infection, it must be remembered that antimicrobial activity in vivo depends on many factors. In addition to drug dosage, route of administration, pharmacokinetic/pharmacodynamic characteristics of the drug, and site of infection, patient-specific factors such as immune status, hepatic and renal function, diet, and concomitant therapy with other pharmaceuticals also determine a patient's response to therapy, thus must be considered in planning treatment. Therefore, antimicrobial susceptibility testing is an adjunct to patient management and does not in itself predict response to therapy.

INHIBITORY METHODS FOR SUSCEPTIBILITY TESTING

DILUTION TESTING

In dilution testing, a standardized amount of organism is inoculated into a series of tubes, wells, or dishes that contain a range of concentrations of antimicrobial in a vehicle, such as broth or agar, usually starting with an integral of 2 (e.g., 128 μg/mL) and decreasing on a $\log_2$ basis to the lowest concentration tested. For the purposes of convenience and economy, it has become common to limit the range of concentrations of each antimicrobial tested to those concentrations encompassing the breakpoints that distinguish between susceptible and resistant.

The broth macrodilution method is performed using standard test tubes. The tubes are viewed by the unaided eye to determine whether growth is present. The broth macrodilution system is no longer used by most laboratories because of its labor-intensive nature, but this method is the foundation of most modern susceptibility testing systems. Similarly, the agar dilution method, in which the antibiotic being tested is incorporated into solid agar in Petri dishes, is an older, labor-intensive method that is rarely used by modern laboratories for routine testing. However, because the isolate being tested is placed onto the agar as a single spot, the agar dilution method can allow the testing of multiple isolates on a single plate. Additionally, some species that do not grow well in broth, or for which the broth method has not been shown to be sufficiently reproducible, can be tested by this method. For example, with the exception of the *Bacteroides fragilis* group, agar dilution is the reference method recommended by the CLSI for susceptibility testing of anaerobic bacteria (CLSI M11, 2018).

Broth microdilution, considered the reference standard, is the most common dilution method used in the modern microbiology laboratory. This method is the basis for most commercial systems. Commercially prepared and disposable microtiter trays containing antibiotics exist as standalone devices, which are manually inoculated and read by visualization (see Fig. 58.1). Because of the labor associated with preparing microtiter trays

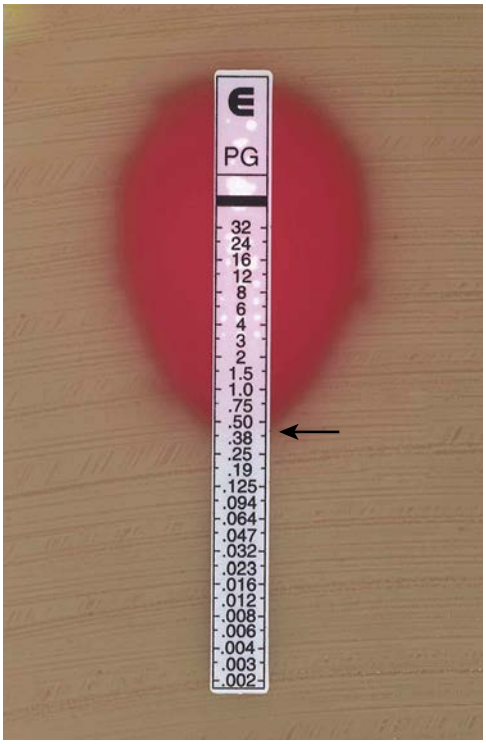

Figure 58.2 Epsilometer, or E-test. A gradient of antibiotic (penicillin in this example) is incorporated into the plastic strip, which is placed on the agar surface on which an organism has been streaked (*Streptococcus pneumoniae*). The intersection of the zone of inhibition with the numeric scale on the strip is read as the minimum inhibitory concentration (MIC) (*arrow*).

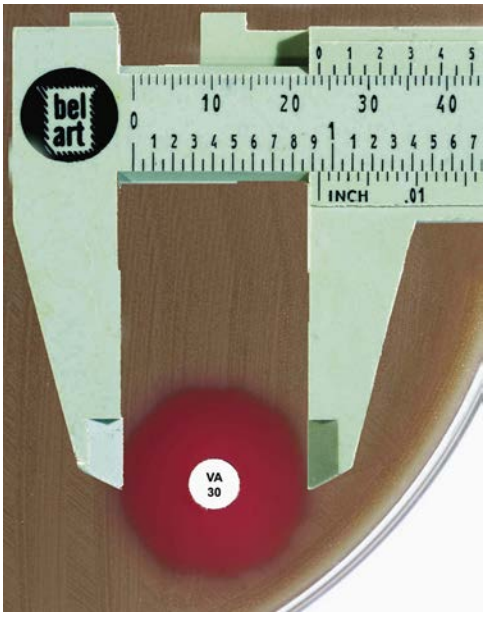

Figure 58.3 Disk diffusion. The zone of inhibition around the antibiotic disk (vancomycin in this case) on the agar surface on which the organism (*Streptococcus pneumoniae*) has been streaked is measured. The result may be susceptible, intermediate, or resistant, based on the zone size.

in-house, and the extensive quality assurance testing necessary when preparing the trays, commercially prepared trays and systems are very popular. They can be expensive, however, and the antibiotics available on a given tray may not conform to local needs. Customized trays may also be available but usually are associated with additional expense. The antibiotic-containing microtiter trays are also components of automated systems that are read by spectrophotometric and fluorometric methods. Several systems have been in existence for a number of years, have extensive databases built over the years, offer computerized software that allows collection of antibiogram data, and include "expert" systems that assist in interpretation of susceptibility results. **Expert systems** in the automated instruments allow for rules to be programmed into the software such that AST reporting can be as automated and as accurate as possible. These rules involve actions to be taken on the basis of defined susceptibility results. They are based on clinical breakpoints as well as a compilation of other important information, such as known intrinsic resistance of organisms, unusual resistance profiles, and interpretive rules (the inference of resistance mechanisms from AST results) (Leclercq et al., 2013).

GRADIENT DIFFUSION

There are two commercially available formats for testing via gradient diffusion, which is based on a combination of the concepts of both dilution and diffusion. The first is the Epsilometer, commonly referred to as the E-test (bioMérieux SA, Marcy-l'Etoile, France). The E-test strip is a plastic strip with a gradient of antibiotic on one side and a continuous MIC scale on the opposite side. The second is the MIC Test Strip, or MTS (Liofilchem, Inc. Waltham, MA), which is a paper-based strip. Both strips function similarly and, as with broth dilution, the MIC can be determined. The strip is placed on the surface of an agar plate that has been inoculated with the test isolate. Like disk diffusion, antibiotic from the strip will diffuse into the surrounding agar—the difference is that, in this method, diffusion will occur in a gradient corresponding to the gradient on the strip. If the isolate is susceptible, an ellipse of inhibition will occur in growth of the bacterium on the surface of the plate, and the point on the MIC scale of the strip where the ellipse of inhibition intersects is the MIC (Fig. 58.2). The results are most commonly interpreted using the unaided eye; readers should be aware of the challenges with reading the strip that are outlined in the product inserts. The MIC obtained using the strips has been shown to correlate well with the MIC obtained with the agar or broth dilution for many antibiotic–bacterial species combinations (Baker et al., 1991). This method is useful because it allows the testing of single antibiotics against isolates, which has particular utility if testing of an isolate against a drug not on the laboratory's preconstructed antibiotic panel is necessary, if testing of one or a few drugs against fastidious species that require special media is required (e.g., *H. influenzae*), or if the antibiotic has been newly introduced into the market. However, as with all newly introduced methods in the lab, a thorough verification of performance should be done before implementing this method into practice.

DISK DIFFUSION

In the disk diffusion test (Kirby-Bauer), largely limited to rapidly growing aerobic and facultatively anaerobic bacteria, a paper disk containing a specified amount (not concentration) of antimicrobial is applied to an agar surface that has been streaked with a standardized inoculum of the test isolate. Testing is done on a 150-mm–diameter agar plate that allows testing of up to 12 antibiotics at once. The antibiotic diffuses into the agar medium from the disk, resulting in a zone of growth inhibition at the point at which a critical concentration of the antimicrobial in the medium inhibits growth of the bacteria after a standardized time period (16–24 hours; Fig. 58.3). The diameter of the zone of growth inhibition has been shown to be inversely correlated with the MIC. The relationship between the two can be expressed as a linear regression line, and zone diameter equivalents of susceptible, intermediate, and resistant interpretations can be extrapolated from their intercepts on the regression line with corresponding MIC values. Of note, the diameters that correspond to the interpretive breakpoints differ for the various drug-bug combinations, such that a 13-mm diameter for one drug-bug combination may be interpreted as susceptible while for another it might be considered resistant.

Disk diffusion is a simple method that provides a qualitative susceptibility result. It allows easy modification of the choice of antibiotics being tested and is inexpensive relative to a number of other methods. It is primarily a manual method, although a video-assisted plate reader as part of a susceptibility data management system, the BIOMIC System (Giles Scientific, Santa Barbara, CA), has been available for a number of years. For laboratories with a high volume of testing, dependence on manual labor may prohibit the use of disk diffusion as the routine method of susceptibility testing. Additionally, certain fastidious species may require special media or conditions for performing disk diffusion that may prohibit routine testing in some laboratories, as it may not be cost-effective to keep the necessary media on hand for the infrequent times when testing is necessary. Referral of the isolate to a reference

laboratory for susceptibility testing is sometimes a more cost-effective approach in these situations.

OTHER PHENOTYPIC METHODS

There are many phenotypic methods used in AST. Some of these include using colorimetry, chromogenic media, latex agglutination, or lateral flow immunoassays. Many phenotypic assays use the diffusion and dilution methods described earlier to show growth inhibition of an organism in the presence of antibiotics to confirm the presence of a resistance mechanism. Some of these assays will be outlined further in the upcoming section Detection of Important Resistance Phenotypes.

DIRECT TESTS FOR β-LACTAMASE

Direct β-lactamase tests are not inhibitory tests but rather are phenotypic tests that detect the presence of β-lactamase production by an organism. They are mentioned with the inhibitory tests because they, like the inhibitory tests, are commonly used in clinical laboratories. These tests are useful in detecting penicillinase enzymes in gram-positive and a few gram-negative species. Three types of β-lactamase direct tests may be used: acidometric, iodometric, and chromogenic. The chromogenic test is the most sensitive, most specific, and easiest to use. It has replaced the other types in usual laboratory use and is the only type discussed here. The chromogenic test consists of a paper disk impregnated with a chromogenic cephalosporin (nitrocefin). A loopful of bacteria to be tested is simply smeared onto the disk; if the organism is producing β-lactamase, hydrolysis of the chromogenic cephalosporin will occur and the disk color will change from yellow to red, usually within 1 minute. However, a final observation of the disk at 15 minutes is necessary for slowly developing reactions. The test can be used to detect β-lactamase production in several species, including *Haemophilus* spp., *Moraxella catarrhalis*, *Staphylococcus* spp., *Enterococcus* spp., and gram-negative anaerobes (excluding the *B. fragilis* group, which are assumed to be β-lactamase producers). A positive test indicates that the organism will not be inhibited by a penicillinase-susceptible penicillin. A positive nitrocefin test for an isolate of *H. influenzae* or *M. catarrhalis* indicates that infection due to the isolate will not respond to ampicillin or amoxicillin. For many gram-positive species, the enzymes require induction by exposure to a β-lactam antibiotic before the enzyme is expressed and can be detected. For example, a simple and appropriate method for testing a staphylococcal isolate for β-lactamase production is accomplished by selecting growth from around the edges of a β-lactam–containing disk on a disk-diffusion plate. Further, for *S. aureus*, the induced nitrocefin β-lactamase test is less sensitive than other tests for the detection of penicillinase production. Therefore, a more sensitive test, such as the penicillin disk zone edge test, should be performed when the nitrocefin test is negative (CLSI M100, 2020). In the penicillin disk zone edge test, a sharply demarcated zone of inhibition around a penicillin disk along with individual colonies within the zone of inhibition indicates a positive test for β-lactamase production, whereas a "fuzzy," or gradually tapered zone, implies sensitivity to penicillin (CLSI M100, 2020). It should be noted that direct β-lactamase tests cannot be used to predict susceptibility to β-lactam antibiotics used in the treatment of infection caused by certain gram-negative aerobes or facultative anaerobes such as *Pseudomonas* spp. or the *Enterobacteriaceae*. Also, a negative β-lactamase test does not exclude resistance to penicillin because there are other mechanisms of β-lactam resistance, such as penicillin binding protein modifications, as found in *Neisseria gonorrhoeae*.

BACTERICIDAL TESTING

Bactericidal testing of antimicrobial agents is infrequently performed in the current clinical laboratory environment. Many tests are labor-intensive and complicated, and until relatively recently, the procedures were not standardized. The three major categories of bactericidal antimicrobial testing are (1) determination of the minimum concentration of an antimicrobial necessary to kill 99.9% of an inoculum of the isolate, that is, the minimum bactericidal concentration (MBC) or minimum lethal concentration (MLC); (2) determination of the killing rate (time-kill curve or killing curve) at which an antibiotic kills an inoculum of the isolate; and (3) determination of the highest dilution of the serum of a patient receiving antibiotic(s) necessary to kill 99.9% of an inoculum of isolate, otherwise known as the *serum bactericidal titer* (*SBT*) or *serum lethal titer*.

Publication of an approved guideline by the CLSI for performance of the MBC has addressed one of the criticisms leveled at the performance of this test—that it is not standardized (National Committee for Clinical Laboratory Standards [NCCLS], 1999a, 1998b). To determine the MBC, serially diluted (on a $\log_2$ basis) antimicrobial in broth is inoculated with a standardized suspension of the isolate of interest in the same way as when determining the MIC. After incubation at 35°C for 24 hours, those dilutions demonstrating no visible growth are subcultured onto antimicrobial-free agar medium. After incubation, the number of colonies on the agar medium is counted and the number of viable organisms per milliliter of antimicrobial dilution is calculated. The MBC or MLC is the lowest concentration of the antimicrobial agent that is lethal or bactericidal to the original inoculum, with the endpoint defined as a 99.9% decrease in viable organisms relative to the original inoculum.

Although, in theory, one could see how the MBC could be very useful for certain types of infection, determination of the MBC often is not straightforward and can be confounded by several factors. One such factor is the persistence of a small number of organisms of the inoculum ("persisters") that survive the antimicrobial exposure but remain susceptible if retested against the antimicrobial. In the case of cell wall–active agents, such as the β-lactams and vancomycin, at least some may represent cells that are in a dormant or nongrowing phase of the cell cycle. These cells have been termed *indifferent* to the effects of the antibiotic by some authors rather than *resistant* (Jayaraman, 2008). Second is the paradoxical effect (Eagle phenomenon), which is an unexplained increase in the number of surviving organisms as the concentration of the antimicrobial increases above the MBC. Third is tolerance, a phenomenon in which bactericidal agents have reduced bactericidal activity against a particular strain of a bacterial species. The mechanism behind tolerance currently is not understood. However, as pointed out by Jayaraman (2008), *tolerance* on the part of an isolate is clearly different from *indifference*, or dormancy. Some authors have given a more practical (at least for the laboratory) definition of *tolerance* on the part of an isolate, that is, if the MBC/MIC ratio is ≥32, the isolate is defined as tolerant to the test antimicrobial (Sherris, 1986).

In determining the time-kill curve, a single dilution of the test antimicrobial, usually at a concentration at or near what can maximally be achieved in a patient, is inoculated with a standardized inoculum of the isolate in question. Then, quantitative cultures are performed at regular intervals over a 24-hour period. The amount of bacterial growth evident on quantitative culture at each time period over 24 hours is graphed to generate the time-kill curve. The test essentially determines the rate and duration of killing by the antimicrobial at a specified concentration. This test is very useful in animal models of specific infections and in pharmacologic research, but its labor-intensive nature is one of the factors that make it difficult for laboratories to offer it as a clinical test.

The basic premise of the MBC and the time-kill study can be applied to the serum bactericidal titer, with the addition of serum from the patient receiving antibiotics to the test system. As with the MBC, serum bactericidal tests have been standardized by the CLSI (NCCLS, 1999b). The modification involves obtaining two serum specimens from the patient—a specimen when the antibiotic is at its lowest concentration in the body ("trough" specimen), usually just before the patient receives a dose of the antimicrobial, and a specimen when the antibiotic is at its highest ("peak specimen"), a specified time after a dose of the antimicrobial is given, with the time depending on the route of administration. Serial $\log_2$ dilutions are made of each specimen and are inoculated with a standardized inoculum of the isolate of interest. The dilutions are incubated at 35°C for 24 hours. Similar to the MBC, those dilutions in which no visible growth is seen are subcultured to agar medium for quantitative culture and are reincubated. The **serum bactericidal titer** is the lowest concentration of antimicrobial that results in a 99.9% decrease in viable organisms relative to the original inoculum. The theory behind the SBT is that it takes into account factors such as the effects of absorption and metabolism of the antimicrobial, effects of metabolites or breakdown products of the antimicrobial on the isolate, protein binding of the antimicrobial, and the effects of interaction with any other medications the patient is taking (NCCLS, 1999b). The SBT can provide an assessment of bactericidal activity by determining the antibiotic concentration relative to the MBC and can allow an assessment of how many half-lives of the antimicrobial bactericidal activity will persist in the patient's serum (NCCLS, 1999b). Finally, if a time-kill study is performed using the patient's serum, the serum bactericidal rate or the rate of killing over time can be determined. Alternatively, if the area under the curve is examined, the magnitude and duration of bactericidal activity can be ascertained (NCCLS, 1999b).

In addition to the labor-intensive nature of the bactericidal tests, which a laboratory must address if it is decided that these tests will be performed,

another consideration is the clinical relevance of the tests. At various times in the past, bactericidal tests have been recommended as contributory in the prediction of therapeutic success or failure in bacterial endocarditis, osteomyelitis, sepsis in immunocompromised patients, infected prosthetic implants, and infections for which therapeutic guidelines are poorly described (Petersen & Shanholtzer, 1992). Many of the studies supporting these recommendations were performed before standardization of the procedure; subsequent studies have failed to support the claim that the tests are directly predictive of therapeutic success or failure (Petersen & Shanholtzer, 1992). Despite this, studies suggesting that bactericidal tests have a role in predicting prognosis in specific infections or in infections in special patient populations continue to appear. Liao and colleagues (2007) suggest that for nosocomial infections with multidrug-resistant *Acinetobacter baumannii*, the SBT is useful in determining prognosis and the need for therapeutic alterations. Cahen and colleagues (1993) state that they demonstrated that the SBT is directly predictive of cure or failure in acute pulmonary exacerbation in cystic fibrosis patients. The clinical utility of the tests remains controversial; however, what is not controversial is the resources that the clinical microbiology laboratory must invest to accurately perform these tests. Based on this, the recommendation put forth by both Petersen and Shanholtzer (1992) and the CLSI (NCCLS, 1999a, 1999b) indicates that if consideration is given to requesting this test on the part of the clinical staff, the clinical microbiology laboratory director should be consulted to determine whether the test can be contributory to patient care, what method should be used, and how the results should be interpreted.

COMMERCIAL AUTOMATED INSTRUMENT SYSTEMS

Most microbiology laboratories in the United States use automated commercial microbroth dilution systems as their predominant testing systems (Jones, 2001). There is efficiency gained from replicate inoculation of combined systems for identification and susceptibility testing, and there are benefits of data management software that is an integral component of most of these instruments, such as the expert systems described in the previous sections. Another benefit is the ability of these instruments to directly communicate with the laboratory information system (LIS) such that results can automatically cross over into the patient's medical record without manual intervention. This increases workflow efficiency in larger laboratories and minimizes the chance of clerical errors associated with manually entering AST results. Additionally, these systems allow for expanded panels of antimicrobial agents as well as reporting of the MIC value, which may be preferred to simply reporting the interpretive categories generated by disk-diffusion testing. Though inhibitory zone measurements have been accurately correlated with MIC values statistically, most physicians, with the exception of infectious disease specialists, do not know how to utilize the MIC. Selection of the methods to be used for antibiotic susceptibility testing, whether automated or manual, can be done based on workflow, convenience, economic reasons, or preferences of the medical staff without significant differences in accuracy.

A variety of systems are available. Before deciding to purchase a system, the laboratory director should consider whether the advantages of replicate inoculation and of data management systems outweigh the costs of the commercial system, which involve both an up-front outlay of cash and an ongoing expense related to consumable components of the system compared with the economy and simplicity offered by the disk-diffusion test. The tendency is to consider the disk-diffusion test archaic and too unsophisticated for modern laboratory practice. However, this method can provide accurate results that are easily understood by health care providers and that suffice in many clinical situations; it is also economical and flexible. The labor-intensive nature of the test compared with automated systems may be limiting in high-volume laboratories, however.

Selection of a particular automated system is based on a list of considerations. Systems differ somewhat in terms of some of these parameters, and it is incumbent on laboratory directors to find the best fit for their laboratory. The list of parameters for evaluation includes the volume that the system can handle; the technical expertise required to operate the system; the utility and usability of the data management system; the cost of the hardware; the cost of disposable supplies, reagents, and service contracts; and the space occupied by the system. Information on performance characteristics of the system is imperative. With the Vitek System (Vitek bioMérieux Inc., Durham, NC), antimicrobial agents are contained in wells within a plastic card and are inoculated with the isolate in a filler-sealer module, placed in an incubator-reader, and read after incubation, with data managed by the computer module and displayed on the data terminal or printed, or both. The original system (Legacy system, bioMérieux) was very popular in clinical laboratories but now has been superseded by the Vitek 2 system. The updated system has automated some of the procedures in the original system that required manual performance and employs turbidimetric optics to repetitively monitor organism growth at 15-minute intervals, allowing results to be generated in hours.

Microscan (Beckman Coulter, Sacramento, CA) is a suite of systems that may be utilized in manual mode when frozen or lyophilized panels are inoculated and then may be read manually after overnight incubation. The semiautomated version, the Microscan Walkaway, can perform traditional overnight MIC testing in which the results are read with a spectrophotometer or a more rapid method can be used that is based on the generation of fluorescence from the utilization of substrates by inoculated organisms. The Phoenix system (Becton, Dickinson, Sparks, MD) uses a redox indicator to assess bacterial growth in inoculated wells. Similar to Vitek 2 and Microscan Walkaway, this system has the capability to provide results within hours. Finally, Sensititre (ThermoFisher Scientific, Lenexa, KS) panels use microtiter plates containing dried antimicrobial agents and can utilize systems such as the ARIS 2X to provide an MIC. Unlike some of the other systems, such as the Vitek2, MICs obtained from the Sensititre are direct (i.e., not calculated or extrapolated using growth curves and algorithms). Therefore, they can be read manually or automatically.

The ability to report antimicrobial susceptibility results faster is heavily promoted by manufacturers as a benefit of automated susceptibility systems. The concept behind this is that switching a patient to an antibiotic that has been demonstrated to be susceptible by in vitro susceptibility testing sooner rather than later will improve the outcome of treatment. In a widely cited retrospective cohort study of 2731 patients with septic shock in intensive care units, Kumar and colleagues (2006) found a time-dependent mortality; for every hour after the onset of hypotension that appropriate antimicrobial therapy was delayed (over a 6-hour time frame), patient survival decreased by 7.6%.

In theory, the faster that antibiotic susceptibility results are available, the greater is the potential for effective therapy and, hence, the greater is the likelihood of improving outcome. This potential, however, will vary with the disorder in question, specific pathogen, patient population, and rapidity of the response to the available results. In a randomized trial evaluating the impact of rapid multiplex polymerase chain reaction (PCR)–based blood culture identification and susceptibility testing, Banerjee and colleagues (2015) found that compared to a control group of standard organism identification (ID) and AST, the intervention (rapid test) group had decreased use of broad-spectrum and increased use of appropriate narrow spectrum antibiotics. In their study, the intervention group, which also included real-time antimicrobial stewardship consultation, demonstrated the shortest time (by nearly 1 day) to appropriate antimicrobial de-escalation or escalation.

The potential contribution of faster susceptibility testing in certain environments using other types of outcomes measures has been well demonstrated (e.g., reducing the cost of hospitalization), facilitating faster switching or focusing of antibiotic therapy as the most effective and/or least expensive alternative antimicrobial. This is of great importance in the current cost-conscious health care environment in the United States, and can also play a role in reducing the prevalence of resistant isolates in an institution and preventing the emergence of specific nosocomial pathogens, such as vancomycin-resistant enterococci (VRE) or *Clostridium difficile*. As newer molecular and proteomic technologies are becoming widely used, the reporting of susceptibility results is getting even faster.

Although there may be benefits of automated susceptibility systems in certain environments, it should be remembered that these systems, like all systems, are not infallible and do have weaknesses. Just as with any test offered, laboratorians must verify the performance of their automated AST systems, which must meet criteria acceptable for patient testing. Guidelines for such verification are provided by the CLSI (CLSI M52, 2015; Humphries, 2018). Briefly, evaluations of these assays must show acceptable levels (≥90%) of essential agreement (i.e., % of isolates showing agreement of the MIC within 1 doubling dilution) and categorical agreement (i.e., % of isolates showing agreement of the categorical interpretations S, I, and R) when compared with the reference, or comparator, method. Moreover, testing must show low rates of error. False-susceptible and false-resistant results are also known as "very major" and "major" errors, respectively. Acceptable error rates are further outlined by the CLSI (CLSI M52, 2015). Such evaluations must also occur when antimicrobial cards, formulations,

and software are changed on an existing automated AST instrument as well as when breakpoints are revised. In this way, laboratorians will be aware if their automated systems have difficulty producing accurate results for specific antimicrobial-pathogen combinations. Difficulties may be specific to a given system or common to many of the automated systems. In such cases, the laboratory may opt for alternative testing for the specific problematic agents.

MOLECULAR-BASED AND NEWER METHODS OF ANTIMICROBIAL SUSCEPTIBILITY TESTING

The methods described earlier refer to phenotypic methods of AST. There are also genotypic, or molecular-based methods (e.g., nucleic-acid amplification tests [NAATs]) that have good applicability in the clinical lab for the detection and identification of a number of AST genes. Low detection limits, quick speed of the test (hours in many cases, particularly when performed directly from patient specimens), and the ease with which the tests are adapted to high-volume testing have made them particularly useful when the pathogen in question grows in culture slowly, such as the *Mycobacterium tuberculosis* complex (MTBC), or when speed of detection is of great help in managing the patient, as in sepsis, when every hour counts for patient outcome. The ability to rapidly identify a pathogen and to determine its susceptibility profile can be critically important for patient management, infection-control measures, and antimicrobial stewardship efforts.

The use of NAAT and other molecular-based methods in attempting to detect the presence of antimicrobial resistance in an organism is rather more complicated than identification for a number of reasons. First, although identification can be accomplished by amplifying and detecting a particular species-specific segment of genome, resistance to a particular antimicrobial may be due to a variety of mechanisms. Therefore, testing for a number of genes may be required to exclude the potential for resistance. This is particularly true for resistance in gram-negative organisms. Second, the presence of a target resistance gene does not necessarily ensure that the gene is being expressed and manifesting the phenotype of drug resistance. Third, many NAATs require the use of specific primers and probes. Therefore, they will detect only known resistance mechanisms, not allowing for the ability to detect novel resistance mechanisms. However, there are now numerous molecular assays that, by using multiplex technology, have incorporated the detection of many known resistance markers. Some of these are discussed later in this chapter. Finally, detection of a resistance mechanism, though important, does not negate the need for an MIC-based approach for most antimicrobials, as the MIC is still needed for guidance among various potential treatment options.

Molecular methods of AST routinely used in the clinical laboratory include the amplification of single or multiple (multiplexing) resistance gene targets. There are numerous additional techniques, including fluorescence in situ hybridization (FISH) as well as spectrophotometric and proteomic techniques. These will be discussed further in the next section.

DETECTION OF IMPORTANT RESISTANCE PHENOTYPES

Methicillin-resistant *Staphylococcus aureus* (MRSA) and methicillin-resistant coagulase-negative staphylococci (CoNS) remain significant problems in hospital environments. *S. aureus* and CoNS consistently remain in the top five pathogens causing health care–associated infections (Weiner, 2016). However, between 2012 and 2017, the incidence for hospitalized patients in the United States decreased for MRSA infection (from 114.18 to 93.68 cases per 10,000 hospitalizations) (Jernigan, 2020). The increased prevalence of community-acquired MRSA has further increased the importance of detection of methicillin resistance in these species.

In some institutions, 25% to 50% of *S. aureus* and up to 75% of CoNS isolates are resistant to methicillin or oxacillin (Weiner, 2016; Mendes, 2018). These isolates are resistant to all currently available β-lactam antimicrobials (and β-lactam/β-lactamase inhibitor combinations) with the exception of some of the newer cephalosporins with anti-MRSA activity. Because of this, vancomycin is often used as empirical therapy for staphylococcal infections. Therefore, the proper detection of resistance in such isolates is crucial for therapeutic management. Most commonly, oxacillin resistance in *Staphylococcus* spp. is due to production of an altered PBP protein (PBP 2a, also called PBP2′) a product of the *mecA* gene that is involved in peptidoglycan synthesis. Therefore, testing for β-lactamase production will not predict methicillin susceptibility in these organisms.

Methicillin resistance may be expressed homogeneously or heterogeneously. Although isolates that express the gene homogeneously can be relatively easily detected, those that express it heterogeneously may be more problematic—they may appear phenotypically sensitive by dilution testing using oxacillin (Sakoulas 2001; Swenson 2001; Felten 2002). When a dilution technique is used, sensitivity for detecting these heteroresistant strains can be improved by adding NaCl (2% weight/volume to the medium) (CLSI M07, 2018).

Cefoxitin can be used to screen staphylococci for *mecA*-mediated resistance and is often tested as a surrogate for oxacillin for *S. aureus*, *S. lugdunensis*, *S. epidermidis*, and some of the other *Staphylococcus* spp. due to improved sensitivity and specificity for the detection of *mecA* mediated resistance. Cefoxitin dilution testing, but not disk testing, can be used for *S. aureus* and *S. lugdunensis*. This extends to the automated susceptibility systems, which have incorporated cefoxitin MIC testing for *S. aureus* into their testing and expert systems, with studies showing close to 100% agreement on detection of MRSA compared with reference methods such as *mecA* gene detection (Junkins, 2009; Kaase, 2009). Of note, oxacillin disk testing is only reliable for designated species and should not be used for *S. aureus*. However, for certain staphylococcal species, such as *S. pseudintermedius*, oxacillin is the most reliable predictor of resistance (CLSI M100, 2020).

In addition to traditional phenotypic inhibitory testing, there are several other methods that are routinely used to detect and differentiate the presence of MRSA among isolated bacteria and clinical specimens. Chromogenic media—which, in the case of MRSA select for cefoxitin-resistant strains and differentiate *S. aureus* from other species based on presence and color of the colony—are frequently used for MRSA surveillance (Denys, 2013). Direct detection of PBP 2a, encoded by the *mecA* gene, can be performed based on a latex agglutination (LA) format (MRSA-Screen, Denka Seiken Co., Tokyo, Japan; Oxoid PBP2′ latex agglutination test, Oxoid, Basingstoke, United Kingdom) or lateral flow (LFA) format (Alere PBP2A SA, Abbott Scarborough, ME) and have been approved for use with *S. aureus* colonies to separate MRSA from methicillin-susceptible isolates. Studies have shown sensitivities of 98.5% to 100% with a specificity of 100% for detecting MRSA (Louie, 2000; Arbique, 2001; Sakoulas, 2001, Arnold, 2016). LA can also be used to detect methicillin resistance in CoNS, though better results are obtained when testing is performed after induction of the *mecA* gene because of the heterogeneous expression of the gene in these species (Hussain, 2000).

Alterations in PBPs leading to resistance to penicillin and cephalosporins is also a problem in *S. pneumoniae*. A global surveillance study (the Tigecycline Evaluation and Surveillance Trial [TEST]) found 61.7% of *S. pneumoniae* isolates susceptible to penicillin globally. Penicillin-intermediate and -resistant isolates were found in 24.8% and 13.6% of *S. pneumoniae* tested (Zhang, 2019). The incidence of multidrug resistance (resistance to penicillin and two other antibiotics) remained at about 30% in the United States over this period. In 2010, the pneumococcal conjugate vaccine (PCV) was expanded to cover the 13 most common serotypes (PCV13). Utilization of this vaccine plays a role in the reduction of antibiotic-resistant infection caused by vaccine strains. The CDC has estimated that there are greater than 2 million cases and 6000 deaths due to multidrug-resistant *S. pneumoniae* in the United States annually (CDC, 2019).

Susceptibility testing of *S. pneumoniae* is mandatory when isolated from sterile sites. The oxacillin screen disk diffusion method can be used, with isolates having a zone of inhibition ≥20 mm, indicating that the isolate is susceptible to penicillin and to other β-lactams listed in the CLSI M100 (2020). This applies only to nonmeningitis isolates, as MIC testing is recommended for isolates from this source. Further, zone sizes <19 mm on the oxacillin screen require additional testing using an MIC method because a zone of inhibition of this size may be seen with isolates that are resistant, susceptible, or intermediate to penicillin. Therefore, it may be most effective to proceed directly to MIC testing when an isolate is obtained from a source (meningitis, blood) for which a delay in susceptibility testing may be potentially dangerous. It should be noted that interpretive standards for penicillin and the third-generation cephalosporins differ, depending on whether the isolate is a CSF isolate or not. The CLSI recommends that both interpretations be reported unless the isolate is obtained from the CSF, in which case only the meningitis interpretive category is reported. Testing methods are determined by the antibiotics tested for *S. pneumoniae*, as disk diffusion cannot be performed for drugs such as ampicillin, cefotaxime, ceftriaxone, imipenem, and meropenem, to name several (CLSI M100, 2020). The commercial automated systems—Phoenix (Becton, Dickinson Diagnostic Systems, Sparks, MD), Vitek 2 (bioMérieux Inc.), and MicroScan (Siemens Medical Solutions USA, Inc., Malvern,

PA)—offer antibiotic testing panels for *S. pneumoniae*. Their performance has been favorable in published studies (Ligozzi, 2002; Richter, 2007).

Penicillin or ampicillin resistance is of importance in enterococci; note, though, that the penicillin susceptibility profile will predict the profile of ampicillin, the reverse is not true (CLSI M100, 2020). Most penicillin resistance in the enterococci, usually seen in *Enterococcus faecium*, is due to the production of low-affinity PBPs; thus, testing for β-lactamase production in this genus will not predict ampicillin susceptibility (CLSI M100, 2020). In some cases, however, β-lactamase production is the cause of the resistance. It is important to note that dilution procedures will not detect β-lactamase production, which is the reason why the CLSI also recommends testing isolates from select cases, as in those from blood or CSF, with the nitrocefin β-lactamase test (CLSI M100, 2020). Additionally, a synergistic action of penicillin or ampicillin with aminoglycosides is often effective therapy for serious infections. This synergistic effect can occur even when the penicillin or ampicillin MIC is at a high level, above the resistant interpretive category.

Aminoglycosides are clinically ineffective against enterococci by themselves. Susceptibility testing with this class of drugs is performed only for the possible synergistic effect when combined with penicillin, ampicillin, or a glycopeptide. Testing is performed only with high concentrations of the aminoglycoside, 500 μg/mL gentamicin, or 1000 μg/mL of streptomycin, using broth dilution (different concentrations are used for disk diffusion). Therefore, enterococci causing serious infection require testing against penicillin or ampicillin, high-level aminoglycoside screening, and testing for susceptibility to a glycopeptide, which is usually vancomycin in the United States.

Enterococci can express two types of glycopeptide resistance. The first is intrinsic resistance, which is a low-level resistance to vancomycin seen in *E. gallinarum* and *E. casseliflavus/E. flavescens* isolates. This is a nontransferable type of resistance, which does not have implications for infection control. The second is acquired resistance because of plasmid-derived acquisition of genes. This type of resistance is seen most often in *E. faecium* and *E. faecalis*; it is less commonly seen in other species of enterococci.

Glycopeptide resistance in enterococci is mediated by the production of altered pentapeptide peptidoglycan precursors, which results in a greatly reduced affinity for binding of vancomycin by 1000-fold. Binding of vancomycin to the pentapeptide prevents cross-linking with other precursors, resulting in prevention of the production of a stable cell wall. Altered precursors are the result of specific genes; the two most relevant are *vanA* and *vanB*. When these genes are detected (typically in *E. faecium* and *E. faecalis*), the isolates are termed *vancomycin-resistant enterococci* (*VRE*). Isolates with *vanA* carry high-level resistance (high MICs) to vancomycin and teicoplanin. Those with *vanB* demonstrate lower-level vancomycin resistance and susceptibility to teicoplanin. Additional genes, *vanD* and *vanE*, have also been described to cause moderate resistance to these drugs. The *vanC* gene is usually found in *E. casseliflavus* or *E. gallinarum*, causing a low level of vancomycin resistance. In contrast to *vanA* and *vanB*, it is not transferable, is less frequently associated with serious infections, and has not been associated with large outbreaks.

Screening for VRE can be done using agar or broth dilution or a screening agar consisting of brain-heart infusion with 6 μg/mL of vancomycin. During testing, it is important that the previously mentioned testing systems be incubated for a full 24 hours, because reading at 16 to 20 hours may produce an erroneous result (CLSI M100, 2020). Modern commercial test systems have performed well in detecting VRE—all isolates with the VRE phenotype have been detected by the Phoenix (BD Diagnostic Systems) and the Vitek 2 (bioMerieux) in published studies (Ligozzi, 2002; Abele-Horn, 2006; Carroll, 2006).

Vancomycin susceptibility testing of *S. aureus* has become an important concern for clinical microbiology laboratories since the detection of isolates with reduced susceptibility to the drug (i.e., vancomycin-intermediate *S. aureus* [VISA] with MIC values of 4–8 μg/mL and vancomycin-resistant *S. aureus* [VRSA] with MIC ≥16 μg/mL). Although the mechanism of resistance in VRSA isolates appears to be linked to acquired *vanA* from enterococcal isolates harboring the gene (Walters, 2015), the mechanism associated with elevated MIC values appears to be linked to increased cell wall thickness and vancomycin-binding peptides (Cui, 2000). Detection of these isolates is important because most are also MRSA, and vancomycin is often used to treat these organisms. Additionally, increased vancomycin MICs have been associated with increased MICs to daptomycin, further limiting treatment options (Dhand & Sakoulas, 2012). In the United States, there have been 14 confirmed cases of VRSA infection from 2002 to 2015 (Walters 2015). Though rare, these remain important resistance threats. In fact, there have been reports of poorer clinical outcomes with infections caused by vancomycin-susceptible MRSA isolates with higher vancomycin MICs that fall within the susceptible range. This has been termed the *MIC creep* (Dhand & Sakoulas, 2012). More information is needed regarding the true impact of the MIC creep on patient outcomes.

VRSA isolates can be identified by microbroth dilution or vancomycin-screening agar. Brain-heart infusion agar with 6 μg/mL vancomycin can be used as long as the test systems are incubated a full 24 hours at 35°C ± 2°C (CLSI M100, 2020). For VISA, the issue is problematic because disk diffusion is not an effective screening method, and the vancomycin screening agar is not reliable for isolates that have MIC values on the lower end of the spectrum (CLSI M100, 2020; Swenson, 2009). Commercial automated and nonautomated systems similarly have difficulty detecting certain VISA isolates. These systems all have their own peculiarities with respect to testing these isolates; laboratories should be aware of these peculiarities if consideration is given to using a particular system (Riedel, 2014; Swenson et al., 2009). In the study by Swenson and colleagues (2009), manual microbroth dilution, which was the most reliable testing method for detecting VISA, had difficulty with VISA isolates with MIC values on the low end of the intermediate resistance spectrum. The E-test has also demonstrated MIC values 1 to 2 dilutions higher when compared with standard methods (Rybak, 2013). The issue of VISA is further complicated by the existence of vancomycin heteroresistant *S. aureus* (hVISA) isolates, which are vancomycin-susceptible isolates that contain subpopulations of organisms with MIC values in the VISA and VRSA ranges. Like VRSA and VISA, there are reports that hVISA appears to be associated with treatment failure when vancomycin is used (Tenover & Moellering, 2007). Additionally, although VRSA and VISA isolates are infrequent, studies have suggested that hVISA isolates are not rare and may account for up to 18% of isolates in some geographic locations (Tenover & Moellering, 2007). Unfortunately, no current susceptibility testing method is exceptionally reliable for detecting hVISA, making epidemiologic reports of hVISA difficult to establish.

For streptococci other than *S. pneumoniae* or the enterococci, antimicrobials to be tested and reported depend on the species. For *S. pyogenes* (Lancefield group A, also called group A *Streptococcus*), susceptibility testing for penicillin and other β-lactams and vancomycin is typically not warranted because resistant strains have not been reported (CLSI M100, 2020). Testing is necessary only if the patient is penicillin allergic and consideration is given to treatment with a macrolide/lincosamide, as infections caused by group B *Streptococcus* have demonstrated 40% resistance to clindamycin and 50% resistance to erythromycin (CDC, 2019). Resistance to erythromycin has been documented as an emerging threat (CDC, 2019). Moreover, results obtained with erythromycin may be generalized to azithromycin, clarithromycin, and dirithromycin (CLSI M100, 2020). Similarly, current recommendations are that β-lactam susceptibility testing for *S. agalactiae* (Lancefield group B, also called group B *Streptococcus*) is not necessary. However, recent literature has reported the occurrence of isolates with MIC values above the breakpoints for susceptibility for penicillin and cephalosporins from the Far East and the United States (Dahesh, 2008; Kimura, 2008) and resistance to vancomycin has been reported (Park, 2014). Altered PBPs, similar to those found in *S. pneumoniae*, were identified by molecular studies. Additional studies are necessary to determine the implications, both clinically and with respect to laboratory testing, before the clinical relevance of these reports is known.

It is also recommended that for pregnant women who are colonized with group B streptococci and who are allergic to penicillin, testing for clindamycin and erythromycin should be carried out (CLSI M100, 2020). Isolates that are resistant to erythromycin but susceptible to clindamycin should be tested for "inducible" resistance to clindamycin that is mediated by the *erm* gene (MLSB resistance: macrolide, lincosamide, streptogramin B), using broth microdilution or the **D-zone approximation test**, with closely approximated diffusion disks of both clindamycin and erythromycin (CLSI M100, 2020) (Fig. 58.4). Only clindamycin results should be reported. "Inducible" clindamycin resistance can also occur in staphylococci, β-hemolytic streptococci, and *S. pneumoniae*. The prevalence may vary between geographic areas (Desjardins, 2004; Richter, 2005) or with the origin of the isolate in a given geographic area, such as whether the *S. aureus* isolate is hospital or community acquired (Patel, 2006).

For the viridans streptococci, any isolate derived from a sterile body site and implicated in a serious infection, such as endocarditis or sepsis, should be tested for penicillin or ampicillin susceptibility (CLSI M100, 2020). Interpretive standards for diffusion testing of penicillin and ampicillin do not exist for viridans streptococci, as the method is unreliable for this pathogen-antimicrobial combination. Thus, testing is accomplished using an MIC method (CLSI M100, 2020). Viridans streptococci are important pathogens, causing sepsis in patients with neutropenia and native valve endocarditis, and studies have demonstrated increasing rates of their

Figure 58.4 Disk induction, or "D" test. The *Staphylococcus aureus* isolate on the left demonstrates erythromycin (E) resistance but susceptibility to clindamycin (CC). The *S. aureus* isolate on the right demonstrates inducible clindamycin resistance with blunting of the zone of inhibition around the clindamycin disk adjacent to the erythromycin disk.

resistance to penicillin and the cephalosporins (Gordon, 2002; Prabhu, 2004). Fluoroquinolones are often used prophylactically in neutropenic patients; since the development of fluoroquinolone resistance in viridans streptococci (Prabhu, 2005), testing of fluoroquinolones in this patient population is indicated despite an overall low prevalence of fluoroquinolone resistance in viridans streptococcal isolates in general (Gordon, 2002). This illustrates a situation wherein a specific patient population served by an institution dictates testing and reporting of specific antimicrobials.

Although resistance to the β-lactam antibiotics in gram-positive organisms in many cases involves altered PBPs, in gram-negative organisms, resistance is often mediated by the production of β-lactamase enzymes. For some gram-negative species, it may be possible to test for β-lactamase production using the chromogenic cephalosporin test. The prevalence of β-lactamase–positive *H. influenzae* in the United States is approaching 30%, while the prevalence of β-lactamase–negative, ampicillin-resistant (BLNAR) strains, which are not detected by the β-lactamase test, is low, though geographic variation has been noted (Tomic & Dowzicky, 2014; Zhang, 2019). For non–life-threatening infections with *H. influenzae*, the nitrocefin test will predict susceptibility to ampicillin and amoxicillin. It may be possible for a laboratory to utilize the nitrocefin test alone in this situation, saving time and money, because susceptibility testing of *Haemophilus* spp. requires specialized media (*Haemophilus* test medium), which have a short shelf life. In areas with a high prevalence of BLNAR, however, this strategy would not be effective. In the case of life-threatening infection, such as meningitis, the CLSI recommends that susceptibility testing be performed and that only ampicillin, a third-generation cephalosporin, chloramphenicol, and meropenem should be reported (CLSI M100, 2020).

In contrast to *H. influenzae*, penicillin resistance in *N. meningitidis* is due primarily to altered PBPs, although occasional isolates with β-lactamase production do occur (Jorgensen, 2005). Both MIC interpretive standards and disk diffusion breakpoints for susceptibility testing of *N. meningitidis* have been published in CLSI documents (CLSI M100, 2020). Although resistance to penicillin has been reported in the United States, resistance to cefotaxime and ceftriaxone, used in the treatment of infections due to this species, has not been reported. Resistance to rifampin, used for prophylaxis, is rare (Zouheir, 2019; Jorgensen, 2005). Therefore, testing protocols for this particular species may be determined with input from local medical staff or infectious disease specialists. It is important to remember that if testing is undertaken, because of the occurrence of laboratory-acquired meningococcal infection, which has a high fatality rate, appropriate safety precautions, including the use of a biological safety cabinet, must be utilized by testing personnel to avoid the occurrence of laboratory-acquired meningococcal infection, which has a high fatality rate (Weinstein & Singh, 2009).

Altered PBPs and β-lactamase production in *N. gonorrhoeae* have been responsible for penicillin resistance in the organism since the 1980s. Since then, *N. gonorrhoeae* has acquired additional genes and mechanisms of resistance, and reported rates of resistance to cephalosporins and fluoroquinolones have increased such that the recommended treatments for *N. gonorrhoeae* infections have been revised multiple times over the last decades. Today, antibiotic-resistant *N. gonorrhoeae* is considered an urgent threat by the Centers for Disease Control and Prevention, and the CLSI now recommends that culture and AST of *N. gonorrhoeae* should be considered in cases of treatment failure (CDC, 2019; CLSI M100, 2020).

β-Lactam antibiotics are used frequently for treatment of infections caused by the gram-negative *Enterobacteriaceae*. However, hundreds of β-lactamase enzymes have been identified in this group of organisms, with increasing number of infections caused by **extended-spectrum β-lactamases (ESBLs)**, AmpC β-lactamases, and carbapenemases, which are of global concern (Bush, 2020; CDC, 2019). Beta-lactamases can be classified by their structure (i.e., the amino acid motif in the enzyme's active site), known as the *Ambler method of classification*, or by their resistance phenotype, known as the *functional classification* (Bush & Jacoby, 2010; Bush, 2018). The Ambler method categorizes the enzymes into four molecular groups, A through D. Groups A, C, and D have a serine at their active site, while those in group B are metalloenzymes that use zinc at their active site (Table 58.1). ESBLs are plasmid derived and, hence, highly transferable enzymes that produce resistance to penicillins, the first- through third-generation cephalosporins, and aztreonam, but generally remain susceptible to inhibition by β-lactamase inhibitors (clavulanate, sulbactam, tazobactam, avibactam), the cephamycins (Paterson & Bonomo, 2005), and carbapenems. In the United States, they are found primarily in *K. pneumoniae*, *K. oxytoca*, *E. coli*, and *P. mirabilis*—species previously recommended by the CLSI to be screened for the presence of ESBLs—but they may be found in other species as well, including *Enterobacter* spp., *Citrobacter* spp., *Serratia* spp., and *Salmonella* spp. (Paterson & Bonomo, 2005; Moland, 2006). *Enterobacteriaceae* with ESBLs are common worldwide; in the United States, there are an estimated 197,400 cases and 9100 deaths in hospitalized patients annually (CDC, 2019) with a high predilection for intensive care unit environments. They are associated with prolonged hospital stays, indwelling medical devices, and prior therapy with a variety of antimicrobials (Paterson & Bonomo, 2005; Moland, 2006).

There are many families of ESBLs, the most common of which are CTX-M, SHV, and TEM, though prevalence of each type is geographically variable (Thomson, 2010; Bush, 2020). In vitro testing of ESBLs may show that they appear susceptible to antimicrobials that they are capable of hydrolyzing. Moreover, there is a chance of clinical failure when therapy using one of these antimicrobials is used, even when MIC values are in the susceptible range (Paterson & Bonomo, 2005; Livermore, 2012). Additionally, the different families of ESBLs vary in their preferred substrates. For example, many of the CTX-M enzymes are better at inactivating ceftriaxone and cefotaxime, while the TEM enzymes are better at inactivating ceftazidime (Bush & Jacoby, 2010). Some members of this group are also not as well inhibited by the β-lactamase inhibitors, complicating matters even further (Bush & Jacoby, 2010). For treatment of infections caused by ESBLs, use of β-lactamase inhibitors and cephamycins have yielded conflicting results, as results of in vitro testing do not always infer clinical success. This may be due in part to differences in the AST cards and systems used for testing as well as the inoculum effect. The latter refers to the fact that the MIC may be a function of the amount of bacteria used in the assay, which has been shown to impact the categorical interpretations given to an isolate (Smith, 2018). Therefore, for severe infections, such as those occurring in the bloodstream, carbapenems are regarded as the antibiotics of choice, leaving cephamycins and β-lactamase inhibitor combinations to be considered for the treatment of nonsevere urinary tract infections (Tamma, 2015; Tamma, 2017a).

Confirmation of ESBLs is no longer a requirement for laboratories using the current (lowered) CLSI breakpoints, as MIC interpretations are thought to sufficiently predict whether a drug would have activity against an organism regardless of whether the organism harbors a resistance gene or not. However, published reports evaluating the effects of applying the revised breakpoints provided shown conflicting information, and many organisms harboring ESBLs were still testing as susceptible to antimicrobials to which they would previously have been considered resistant, using confirmatory testing. McWilliams and colleagues (2014) reported that more than 89% of ESBL-producing *E. coli* would have been reported as susceptible or intermediate for aztreonam and/or ≥1 cephalosporin using the 2010 guidelines. Further, nearly 68% of ESBL-producing *K. pneumoniae* isolates would have been reported as susceptible or intermediate to aztreonam and/or ≥1 cephalosporin, though the subsequent lowered cefepime breakpoints of 2014 did help to increase the reporting of the resistant category for both species. Another report found that approximately 21% of *E. coli*, 25% of *K. oxytoca*, and 79% of

TABLE 58.1
Beta-Lactamase Classification

β-Lactamase Category	Molecular (Ambler) Class	Examples	Key Features of the Class*	Found In
ESBL	A (serine)	CTX-M SHV TEM	Resistant to penicillins, 1st- through 3rd-generation cephalosporins and aztreonam; **inhibited by β-lactamase inhibitors**	*Enterobacteriaceae*; other gram-negative organisms, such as *N. gonorrhoeae* and *H. influenzae*
AmpC	C (serine)	ACC, FOX LAT, MOX	Resistant to cephamycins (cefoxitin) and β-lactamase inhibitors; susceptible to carbapenems (if no additional resistance mechanisms); **inhibited by cefepime, boronic acid and cloxacillin;** can be induced by β-lactams and β-lactam/ β-lactamase inhibitor combinations	SPACE bugs and other gram-negative organisms (detailed discussion in text)
Carbapenemase (resistant to the carbapenems, cephamycins, and most β-lactamase inhibitors); all are serious infection-control threats	A (serine)	KPC, IMI, SME	**Inhibited by boronic acid and avibactam** (ceftazidime-avibactam may be effective); not inhibited by cloxacillin	*Enterobacteriaceae*, esp. *K. pneumoniae* and *E.coli*; SME in *Serratia marcescens*; *A. baumannii*; *P. aeruginosa*
	B (metallo β-lactamases, "MβLs"; zinc at active site)	NDM, VIM, IMP, GIM, SPM-1	Strongest carbapenemase hydrolyzers; do not inactivate aztreonam; **inhibited by EDTA and dipicolinic acid (DPA)** but not β-lactamase inhibitors (including avibactam) or boronic acid	*A. baumannii; P. aeruginosa*; *Enterobacteriaceae*
	D (serine)	OXA	Weak carbapenem hydrolysis; **inhibited by oxacillin and temocillin;** susceptible to aztreonam; not inhibited by EDTA, boronic acid, and β-lactamase inhibitors. May show in vitro susceptibility to the cephalosporins (if no co-production of ESBLs).	*A. baumannii; P. aeruginosa*; *Enterobacteriaceae*

Modified from Bush K, Jacoby GA: Updated functional classification of beta-lactamases, *Antimicrob Agents Chemother* 54(3):969–976, 2010.
Notes: This is not an all-inclusive table. It is meant to cover the highlights and more common trends seen among members of the various Ambler classes.
*Exceptions exist within groups as discussed in the text. Interpretations can also be challenging because of multiple resistance mechanisms in a given isolate (i.e., AMPCs that are also resistant to ertapenem not because of carbapenemase enzymes but rather because of porin mutations, the presence of efflux pumps, etc.). **Bolded text** in Key Features of the Class column includes features of various inhibitory tests that can be used to discriminate among the various β-lactamase classes.

Figure 58.5 E-test showing one possible phenotypic test for the detection of extended-spectrum β-lactamases. The left agar plate shows an ESBL-producing *K. pneumoniae* isolate. The right plate shows a non-ESBL–producing E. coli. On each plate, the E-test strip on the left contains cefotaxime (CT) on one end and cefotaxime with clavulanic acid (CTL) on the other. The E-test strip on the right contains ceftazidime (TZ) on one end and ceftazidime with clavulanic acid (TZL) on the other. ESBL production is determined by a ≥3 twofold-concentration decrease in the MIC of CT or TZ in the presence of clavulanic acid. A positive test also occurs when a "phantom zone" or deformed CT or TZ ellipse is present. In the *K. pneumoniae* example on the left, the CT is 0.75 and the CTL is 0.25 for a ratio of 3, not indicative of an ESBL; however, the TZ is >32 and the TZL is 0.75 for a ratio of 43; this is therefore a positive ESBL test because the TZ/TZL ratio is ≥8, indicating an effect of the β-lactamase inhibitor on the susceptibility of the test organism. The *E. coli* on the right does not show such an effect by clavulanic acid.

P. mirabilis isolates tested susceptible to ceftazidime but were ESBL positive, suggesting that the CLSI breakpoints might still have been too high to detect ESBLs (Morrissey et al., 2014). In other cases, rates of reported resistance increased following the revised CLSI breakpoints, particularly for third-generation cephalosporins. The concern in such cases would be that broad-spectrum antimicrobials would be used in cases in which narrower-spectrum therapies might be effective (Heil, 2016). This could ultimately limit therapeutic options longer term, adding to the selection of multidrug-resistant organisms (MDROs).

Therefore, laboratories may choose to perform confirmatory testing on *Enterobacteriaceae* isolates showing decreased susceptibility to the extended-spectrum cephalosporins (cefotaxime, ceftazidime, ceftriaxone) or the monobactams. One confirmatory test that can be used is the E-test, shown in Figure 58.5. The confirmatory test is based on the characteristic that ESBL producers are inhibited in vitro by β-lactamase inhibitors. Therefore, a positive confirmatory test results when the susceptibility of the test organism increases (therefore, the MIC decreases) in the presence of a β-lactamase inhibitor, compared with the result obtained using a third-generation cephalosporin alone. Notably, often two β-lactamase inhibitor combinations are used in confirmatory testing due to differences in the preferred substrate specificities of the β-lactamases, as discussed earlier. Of note, the phenotypic confirmatory tests could instead be included in the automated AST instrument used in the laboratory, such that ESBL screening (higher MICs to the third-generation cephalosporins) and confirmation could be performed at the same time by the instrument by comparing the MICs obtained from testing a third-generation cephalosporin with and without a β-lactamase inhibitor. This would result in a shorter turnaround time to results than would be possible by manual confirmatory tests. However, discrepancies in ESBL detection have been noted among commercial automated tests. This may be due to the antimicrobial AST cards used in such systems as well as other factors, such as the overlap of resistance mechanisms, making it difficult for an automated system to accurately detect ESBLs. This is especially true for isolates harboring AmpCs in addition to ESBLs (Robberts, 2009; Espinar, 2011; Jang, 2013; Bobenchik, 2015; Smith, 2017). Therefore, care must be taken to ensure accurate performance of a laboratory's chosen automated AST system.

AmpC enzymes can be thought of as extended-spectrum cephalosporinases and exist in two forms, chromosomal and plasmid mediated. Among the *Enterobacteriaceae*, chromosomally mediated and inducible AmpC enzymes are sometimes referred to by various acronyms, including ESCPM, SPICE, and SPACE, which stand for S*erratia marcescens*, *indole-positive* P*roteae (Providencia* spp., *Morganella morganii*),

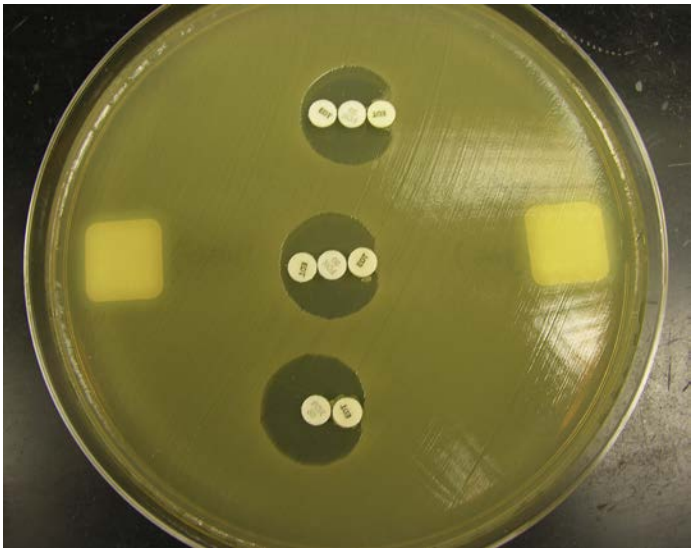

Figure 58.6 AmpC cefoxitin- ethylenediaminetetraacetic acid test. This AmpC test is performed as described by Black and colleagues (2005). Briefly, a lawn of cefoxitin-susceptible *E. coli* is inoculated onto the surface of a Mueller-Hinton agar plate. EDTA disks are moistened, and the test isolates are smeared on the surface of the disks, which are placed organism-side-down onto the agar down next to a 30 g cefoxitin disk. EDTA increases the permeability of the cell wall of the test isolate, allowing for release of β-lactamases into the agar. After an overnight incubation, if AmpC β-lactamase is present in the test isolate, the *E. coli* will grow in toward the cefoxitin disk, showing either an indentation or a flattening of the zone of inhibition, reflecting the enzymatic inactivation of cefoxitin (positive result). The absence of a distortion indicates that cefoxitin was not inactivated (negative result). In the figure, the top set of disks shows an AmpC-negative *E. coli* on the EDTA disk to the left of the cefoxitin disk and an AmpC-positive *E. cloacae* to the right. The middle set of disks shows an AmpC-negative *K. pneumoniae* on the EDTA disk to the left of the cefoxitin disk and an AmpC-positive *E. coli* to the right. The bottom set of disks shows a weak positive Amp-C producing *K. pneumoniae* on the EDTA disk to the right of the cefoxitin disk.

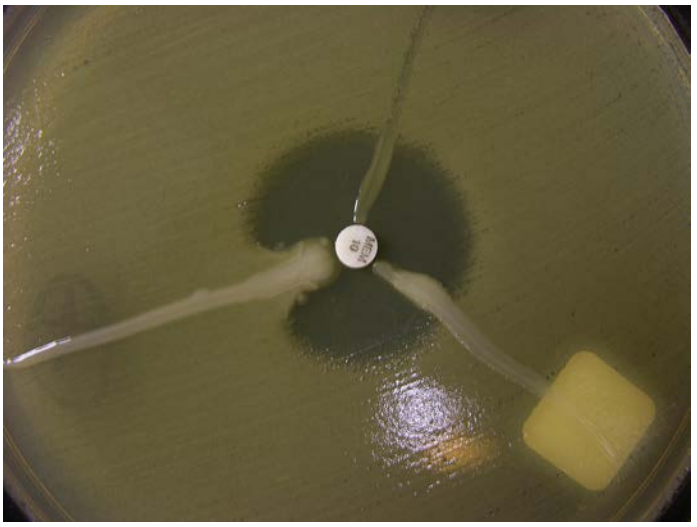

Figure 58.7 The Modified Hodge Test (MHT). This test is no longer recommended by the Clinical and Laboratory Standards Institute (CLSI). However, it is shown here because it is still being performed widely (57%–84%) in laboratories worldwide that have not yet implemented newer carbapenemase confirmation tests (Humphries, 2019). For detailed instructions (and illustrations) on how to perform the currently CLSI-endorsed carbapenemase confirmation tests (CarbaNP and mCIM), the reader is referred to the CLSI M100 (2020).

Aeromonas spp., *Citrobacter freundii*, *Enterobacter cloacae* complex, and *Klebsiella* (formerly *Enterobacter*) *aerogenes*. This is not an exhaustive list, as there are additional organisms that can harbor and express the chromosomal AmpC β-lactamase, such as *Hafnia alvei* and *P. aeruginosa* (Jacoby, 2009; Bush, 2018). Though AmpC expression may be low and though they may test as susceptible to some of the β-lactams listed, the SPACE organisms should be considered inherently resistant to broad-spectrum penicillins, the extended-spectrum cephalosporins except cefepime (at the conventionally tested inoculum), the monobactams, and, in contrast to ESBLs, the cephamycins. Therefore, testing for the presence of AmpC in these organisms is not necessary. In contrast to ESBLs, AmpC producers are not inhibited by commercially available β-lactamase inhibitors. In fact, the chromosomal AmpC enzyme can be induced by β-lactam antibiotics as well as β-lactamase inhibitors, leading to high levels of AmpC expression. For these intrinsically resistant organisms, the laboratory director may choose to include a statement of caution on the AST report—a warning to the effect that therapy with β-lactam and β-lactamase inhibitors may induce the AmpC enzyme present in the given pathogen. AmpCs may also be plasmid derived and are often found in *Klebsiella* spp., *E. coli*, *Salmonella* spp., *Citrobacter* spp., *and P. mirabilis*. It is important to recognize these because isolates that produce this enzyme will be resistant to the same antimicrobials as those expressing the chromosomal enzyme but, because these are plasmid borne, they are transferable to other organisms and, therefore, also infection-control risks.

The prevalence of AmpCs is unknown, as surveillance is limited to laboratories that choose to detect them. Though CLSI recommendations do not include testing for AmpCs, various phenotypic tests have been evaluated. Possible screens for the presence of an AmpC β-lactamase–producing isolate include the presence of cefoxitin resistance, a positive ESBL screen but a negative ESBL confirmatory test, and carbapenem susceptibility (Black, 2005; Polsfuss, 2012). Importantly, positive ESBL screens are nonspecific and are often due to AmpCs rather than ESBLs or to the co-occurrence of resistance mechanisms (Munier, 2010). Moreover, cefoxitin resistance may also be due to porin loss. Further, some AmpC producers that also have a porin mutation may test resistant to the carbapenems, confusing them with carbapenemase producers (Thomson, 2010). The complex nature of β-lactamase resistance and the many mechanisms that can result in similar phenotypes makes testing in the laboratory all the more challenging.

Cefoxitin-resistant non–AmpC β-lactamase–producing isolates may be separated from those producing AmpC β-lactamase by a few different methods that utilize the fact that AmpC producers (unlike ESBL producers) are reliably inhibited by cefepime, boronic acid, and cloxacillin. The E-Test (bioMérieux, Durham, NC) and disks that incorporate these antimicrobials can be used (Polsfuss, 2011; Maraskolhe, 2014; Tamma, 2019). There is also the AmpC cefoxitin-ethylenediaminetetraacetic acid (EDTA) double-disk test, which utilizes the ability of Tris-EDTA to permeabilize the test bacterium and release the resistance enzymes into the agar, causing inactivation of cefoxitin (Fig. 58.6) (Peter-Getzlaff, 2011). Notably, these manual tests may be prone to subjectivity and false-positive results may also be due to the presence of carbapenemases.

Finally, phenotypic tests cannot reliably differentiate between chromosomal and plasmid-mediated AmpC producers. In such cases, molecular identification can be used (Polsfuss, 2011; Tamma, 2019).

Enterobacteriaceae that produce an ESBL or AmpC β-lactamase (or both) may often be treated with a carbapenem antibiotic. Unfortunately, the prevalence of **carbapenemase-producing organisms (CPO)**, including **carbapenemase-producing carbapenem-resistant Enterobacteriaceae** (**CP-CRE**), is increasing worldwide (Tzouvelekis, 2012; Bonomo, 2018; CDC, 2019). Their presence is often associated with prior health care exposures, though they have also become endemic in many parts of the world. Though there is variability in which carbapenemases predominate in a given geographic region, one group of serine carbapenemases, the ***Klebsiella pneumoniae* carbapenemases (KPCs),** are some of the most common. KPCs are resistant to most β-lactams, including extended-spectrum cephalosporins and carbapenems, as well as to most β-lactamase inhibitors, dramatically decreasing treatment options. KPCs are found in many species of *Enterobacteriaceae* and other gram-negative organisms and are very often found in *K. pneumoniae* and *E. coli* in the United States. The genes for production of the enzymes are plasmid borne, and clonal expansion can occur easily. KPC enzymes first appeared in the United States in New York City, and a survey of four hospitals in Brooklyn, New York over 2 months in 2004 demonstrated that 24% of *K. pneumoniae* isolates had one of two *KPC* genes (Walther-Rasmussen & Høiby, 2007). The spread of KPC enzymes has since become a global epidemic (Tzouvelekis, 2012; Bonomo, 2018). In the United States alone, more than 13,000 infections and 1100 deaths are caused by carbapenem-resistant *Enterobacteriaceae* (CRE) bacteria each year. The CDC has labeled these "Nightmare Bacteria" (CDC, 2019). The prevalence of CP-CRE, especially KPC organisms, has exceeded 20%

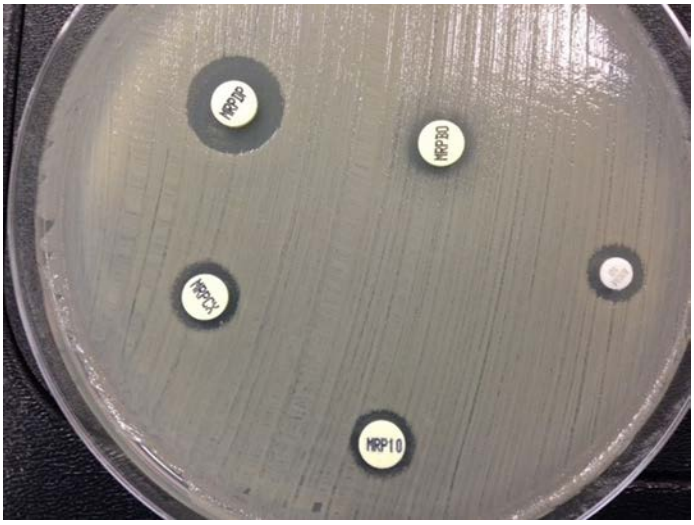

Figure 58.8 Inhibition test used to classify carbapenemases. The *Klebsiella pneumoniae* carbapenemase– metallo β-lactamase (KPC-MBL) confirm kit (Rosco Diagnostica, Taastrup, Denmark) uses carbapenem disks in combination with various inhibitors known to inhibit the different carbapenemases, allowing for the classification of carbapenemase type in an isolate (see also Table 58-1 for inhibitors). The figure shows an isolate inhibited by a combined meropenem-dipicolinic acid (MRP-DP) antibiotic disk. This same isolate is resistant to inhibition by the meropenem-boronic acid (MRP-BO), meropenem-cloxacillin (MRP-CX), and meropenem alone (MRP10).

to 40% in areas of endemicity (Tzouvelekis, 2012). CP-CRE are resistant to nearly all available antibiotics and are associated with increased length of stay in the hospital and increased mortality rates, ranging from 24% to 70% (Tzouvelekis, 2012; Tamma, 2016). Moreover, patients with CPO require that certain infection-control practices, including contact precautions and patient cohorting, must be implemented upon identification of the resistance mechanism. The CDC has published specific guidelines on practices for the control of CRE transmission in health care settings (CDC, 2015).

Though the CLSI recommends that clinical laboratories perform carbapenemase confirmatory testing only for epidemiologic and infection-control purposes, many believe that it is important to perform such testing for clinical management as well (CLSI M100, 2020). This is especially true now that newer antimicrobials are available that are effective against only a particular type of CPO. For example, the β-lactam/β-lactamase inhibitor combination ceftazidime-avibactam has shown activity against KPC-producing organisms but is ineffective against the metallo β-lactamases (MBLs). These newer β-lactam/β-lactamase inhibitors, among other newer antimicrobials, provide therapeutic options that were not available before (Lasko, 2020). Moreover, as also noted with the ESBLs, AST of carbapenemase producers by automated methods can give poor agreement depending on the methods of testing, isolates involved, and type of carbapenemases present (Thomson, 2011, 2017). Though the lowering of the CLSI carbapenem breakpoints has mitigated much of this problem, there remain discrepancies in which an MIC result falls in the susceptible range in one assay but in the resistant range in another. Therefore, care must be taken to mitigate erroneous interpretations and the possibility of inappropriate therapy.

There are numerous phenotypic and genotypic tests to confirm the presence of a carbapenemase. Though the modified Hodge test (Fig. 58.7) is no longer recommended by the CLSI, many laboratories worldwide continue to perform this test (Humphries, 2019; CLSI M100, 2020). This is a sensitive test for the detection of KPC-type carbapenemases but lacks specificity and cannot differentiate among the various types of carbapenemases. It is also subjective and can be difficult to interpret. False-positive results were seen with AmpCs, particularly with *Enterobacter* spp. (especially when these co-occurred with other mechanisms of resistance, such as porin alterations), and false negatives occurred with NDM-1 and other MBL-producing organisms that have weaker carbapenemase activity.

Supplementary phenotypic tests currently endorsed by the CLSI for the detection of carbapenemases in the *Enterobacteriaceae* and *P. aeruginosa* include the CarbaNP, a colorimetric assay, and the modified carbapenem inactivation method (mCIM), a disk-diffusion test. The CarbaNP detects carbapenem hydrolysis using special reagents. It can provide rapid results but suffers from suboptimal detection of OXA-type carbapenemases (Nordmann, 2012; CLSI M100, 2020). The mCIM is an indirect growth-based assay that requires an overnight incubation. It detects the growth of a meropenem-susceptible indicator organism in the presence of a meropenem disk that has been incubated with the test organism. If the latter expresses a carbapenemase, the indicator organism will grow in the presence of an inactivated meropenem disk. Importantly, neither assay can differentiate the type of carbapenemase present. Therefore, a positive result using either assay can be supplemented with the eCIM (an EDTA-based modified carbapenem inactivation assay) for the specific detection of MBLs (Pierce, 2017; Sfeir, 2019; CLSI M100, 2020).

Other methods utilize a carbapenem disk with and without various carbapenemase inhibitors to help differentiate among the various types of carbapenemases. For example, boronic acid can be used to inhibit and, therefore, detect class A while EDTA can similarly be used for class B carbapenemases (Fig. 58.8) (Tsakris, 2009; Stuart & Leverstein-van Hall, 2010). This is the premise of the KPC-MBL confirm kit (Rosco Diagnostica, Taastrup, Denmark), which includes combination antimicrobial disks containing meropenem with various carbapenemase inhibitors (e.g., boronic acid, EDTA). This test requires an overnight incubation. There are also lateral flow immunoassays, such as the NG-Test Carba 5 (NG Biotech, Guipry, France), which can discriminate among carbapenemases in under 30 minutes. All perform well but also have limitations. There are numerous phenotypic tests that have shown good overall performance in the detection of carbapenemases. Additional details regarding the performance of various phenotypic assays for carbapenemase detection are provided elsewhere (Doyle, 2012; Tamma, 2017b; Tamma & Simner, 2018).

MOLECULAR ANTIMICROBIAL SUSCEPTIBILITY TESTING

Antimicrobial resistance in gram-negative bacteria is complex, as resistance to a given drug may be due to multiple genes and alterations in cell porins, efflux pumps, drug-inactivating enzymes, or modifications of the target of the drug. Despite this, rapid tests using molecular techniques to detect antimicrobial resistance genes in gram-negative organisms have become increasingly used in clinical laboratories in recent years. Some target individual genes and some are multiplexed, targeting multiple genes in a single assay. Either type of assay can be used depending on the needs of the laboratory and the population served. For example, certain resistance genes may deserve more attention than others based on the frequency with which they are known to circulate in a given region (Lupo, 2013; Bonomo, 2018). The *CTX-M*, *SHV*, and *TEM* genes are important for the detection of ESBLs, *CMY* for the detection of AmpCs, and *KPC*, *NDM*, *VIM*, *IMP*, and *OXA* for the detection of CPOs. Laboratories may also want to include the *gyrA* and *parC* genes for the detection of quinolone resistance. The challenge is that there are hundreds of β-lactamases within the various classes listed such that testing for ESBLs may mean testing for hundreds of *CTX-M*, *SHV*, and *TEM* genes. Therefore, it would be beneficial to first understand the epidemiology of the more prevalent genes in a given region before implementing such testing in the lab. Further, unlike phenotypic tests that test for expression of resistance, molecular tests are limited to identifying only known targets.

Various rapid molecular AST assays for *Enterobacteriaceae* and other gram-negative organisms are commercially available. The BD Phoenix CPO detect (CPO detect) detects and classifies carbapenemases in the *Enterobacteriaceae*, *A. baumannii*, and *P. aeruginosa*. Accurate detection and classification of CPOs for the majority of isolates was noted in a multicenter evaluation of this assay (Whitley, 2020). The NucliSENS EasyQ KPC assay (bioMérieux SA, Marcy l'Etoile, France) is a real-time nucleic acid sequence–based amplification (NASBA) assay for the detection of *KPC* from stool samples and rectal swabs; results are available within about 2 hours. This assay has a reported a sensitivity and specificity of 93.3% to 100% and 99.0% to 100%, respectively (Spanu, 2012; McEwan, 2013). Other assays use multiplexing technology to interrogate numerous genes simultaneously. The eazyplex SuperBug CRE (Amplex Diagnostics GmbH, Gars, Germany) uses a loop-mediated isothermal amplification-based system to detect multiple carbapenemase types, including KPC (types 2–15), NDM (types 1–7), VIM (types 1–37), and OXA (types 48, 162, 181, 204, and 244), as well as the ESBLs CTX-M1 and CTX-M9. This test can be

performed directly from blood cultures, urine, rectal swabs, and bacterial cultures. One study found that the assay worked well in bronchoalveolar lavage specimens as well (Garcia-Fernandez, 2014; Fiori, 2019). Garcia-Fernandez et al. (2014) found that the assay correctly detected carbapenemase genes for 100% of their *Enterobacteriaceae* isolates, including those harboring ESBL genes. However, the assay has shown decreased specificity (~83%) for the OXA-48–like genes (Findlay, 2015; Sekyere, 2015). Sekowska et al. (2020) found that the assay also performed well in *P. aeruginosa*. Notably, the eazyplex series of assays also includes assays specific for other β-lactamases such as AmpC, and time to results can be available within 15 to 60 minutes (Sekyere, 2015). The Xpert Carba-R (Cepheid Inc., Sunnyvale, CA) detects five targets (KPC, NDM, VIM, OXA-48, and IMP-1) and is intended for use with rectal swab specimens. It has reported sensitivities and specificities of up to 100%. Though its specificity was initially lower (~83%) for OXA-48–like genes, version 2 showed improved detection of OXA-48 variants such as OXA-181 and OXA-232 (Findlay, 2015; Dortet, 2016).

The Check-Points assays (Check-Points Health, Wageningen, the Netherlands) are intended for the detection of resistance genes from rectal swabs. They consist of real-time PCR and detection using fluorescent DNA probes, and can provide results within approximately 2.5 hours. Two of these include the Check-Direct ESBL Screen, which detects the main genes encoding ESBLs (CTX-M1, CTX-M2, CTX-M9, and SHV-ESBL), and the Check-Points CPO, which detects KPC (types 2–37), NDM (types 1–24), VIM (types 1–6, 8–52, 54, 56–60), IMP (types 1–4, 6–8, 10, 19–20, 23–26, 30, 34, 38, 40, 42–43, 51–52, 55, 59–61, 66, 70, 73, 76–80) (it cannot distinguish between VIM and IMP), and OXA-48 like (48, 162, 163, 181, 204, 232, 244, 245, 370, 405, 438–439, 484, 505, 517, 519, 566). Check-Points also includes assays, like the Check-MDR CT103, that utilize microarray technology for simultaneous detection of up to 100 ESBL, AmpC, and carbapenemase resistance markers. These assays perform well, with reported sensitivities and specificities of up to 100%. However, they come with the limitations of microarray technology, such as higher costs and longer turnaround times (Cuzon, 2012; Sekyere, 2015; Wu, 2019).

Compared to the gram-negatives, fewer mechanisms for antimicrobial resistance exist in gram-positive organisms. In some cases, resistance to a particular drug is almost wholly due to the expression of a single gene. This has made this group more amenable for the initial development and deployment of molecular tests to detect antimicrobial resistance. Commercially available molecular tests to detect oxacillin or methicillin resistance in *S. aureus* are the best example. Molecular assays targeting the *mecA* resistance gene or the staphylococcal cassette chromosome *mec* (SCC*mec*)—a mobile genetic element that carries *mecA* in conjunction with a gene or genes specific for *S. aureus*—are increasingly used in the clinical laboratory, thereby differentiating MRSA from CoNS as well as MRSA from methicillin-sensitive *S. aureus* (MSSA). Updated and newer assays also detect the presence of *mecC*, which is a novel mecA gene ($mecA_{LGA\ 251}$) that was first identified in the United Kingdom and Denmark from cattle as well as humans (Garcia Alvarez, 2011). Isolates carrying *mecC* are phenotypically methicillin resistant (PBP2a positive and resistant to cefoxitin) but will not be detected by NAATs that have only the standard *mecA* target. Prevalence remains low at this time.

There are a number of commercially available molecular assays for the detection of MRSA in clinical samples, most using a real-time PCR method. Xpert MRSA (Cepheid, Sunnyvale, CA), BD MAX MRSA Assay (BD Diagnostics, Sparks, MD), Cobas MRSA/SA Test (Roche Molecular Systems, Pleasanton, CA), and ARIES MRSA Assay (Luminex, Austin, TX) have been approved for use in diagnosing infections or in screening patients for nasal colonization with *S. aureus* and MRSA depending on the specimen type and intended use approved by the FDA. These assays demonstrate high levels of sensitivity and specificity for the detection of both *S. aureus* and MRSA (Buchan, 2015; Silbert, 2017).

The performance studies using the various available molecular assays for detection of *S. aureus* have illustrated some of the issues associated with molecular testing for antibiotic resistance (e.g., whether identification of a specific but very focused genomic segment correlates with a particular species or resistance phenotype). In particular, false-positive results were noted from revertant MRSA isolates that had residual SCC*mec* extremity fragments but without functional *mecA* genes, commonly referred to as "*mecA* dropouts" (Blanc, 2011; Mehta, 2017; Mendes, 2016), as well as from a specimen with a mixture of a methicillin-resistant CoNS and an SCC*mec* empty cassette variant (Wolk, 2009; Blanc, 2011). The risk for false positives decreases when additional targets are used, for example, those that target not only *SCCmec* but also the presence of *mecA*, specifically. False-negative results can result from different *SCCmec* variants, the large diversity of the *orfX-SCCmec* junctions (*orfX* being a conserved open reading frame in *S. aureus* at which *SCCmec* inserts), as well as from those rare isolates that express *mecC*, a *mecA* homologue that also results in oxacillin resistance but is not detected by tests directed at *mecA* or PBP 2a. For these reasons, molecular assays must be reevaluated with some regularity to ensure continued optimal performance.

The issue of specificity for a particular gene has been particularly well illustrated with the BD GeneOhm VanR assay (BD Diagnostics, Spark, MD), an amplification test that detects the presence of the *vanA* and *vanB* genes associated with glycopeptide resistance in *Enterococcus* species. This assay is intended to allow screening of patients for VRE colonization. It is very effective for its intended purpose when screening in institutions with a high prevalence of VRE due to isolates with the *vanA* gene, but it suffers from specificity issues in situations in which *vanB* is highly prevalent because of the apparent ability of other species, such as *Clostridium* spp., to acquire the gene (Stamper, 2007). The Xpert vanA/vanB assay (Cepheid, Sunnyvale, CA) has also shown false positives for *vanB* but when performed on enriched inoculated broths with an adjusted cutoff cycle threshold value, the performance of the assay is greatly improved and false-positive results are limited (Zhou, 2014). Both assays can detect the genes within hours; Birgand and colleagues (2013) found that this led to a significant impact on infection-control measures and cost savings in a French hospital.

Multiplex panels often detect a combination of gram-positive and gram-negative AST resistance genes. The Verigene Gram Positive and Gram Negative Blood Culture Test (Luminex, Madison, WI) is a microarray-based assay that can identify bacteria and multiple resistance genes (*MRSA*, *KPC*, *NDM*, *OXA*, *VIM*, *IMP*, and *CTX-M*) directly from blood culture specimens. It has a reported sensitivity of greater than 95% for *S. aureus* (Liesenfeld, 2014). For the carbapenemases, sensitivities and specificities are >97% (Braun, 2014; Sullivan, 2014; Sekyere, 2015). Another rapid blood culture ID system that includes resistance gene determinants is the Biofire FilmArray (BioFire, Salt Lake City, UT), a closed system that performs multiplex PCR for the detection of multiple pathogens as well as the *KPC*, *mecA*, and *vanA/B* resistance genes. For the pathogens and resistance genes that they share, the Verigene and BioFire systems performed comparably well in a head-to-head comparison (Bhatti, 2014). The most recent introduction is the GeneMark Dx ePlex Blood Culture ID system, which consists of three panels: one for Gram positives, one for Gram negatives, and one for fungi. Overall performance was high (93%–100% positive agreement) when compared with routine culture methods (Huang, 2019; Carroll, 2020; Zhang, 2020). For such multiplex molecular assays to be optimized, they should provide rapid and accurate results, be relatively low cost and easy to use, and maintain a level of versatility to accommodate changes in resistance genes and patterns over time. Such assays should also have the ability to detect resistance genes expressed at low levels.

Studies have evaluated the use of whole-genome sequencing (WGS) to infer antimicrobial resistance from bacterial genomes (Ellington, 2017). A benefit of this approach is that it does not require prior knowledge of a resistance phenotype. Some studies show good correlation with phenotype, particularly the epidemiologic cutoff value (ECOFF) of an organism, which delineates it as wild-type versus not wild-type. This approach also allows for comparisons when breakpoints differ between organizations or when they are revised over time (Ellington, 2017). Some studies show that it may even be possible to predict the MIC of an antimicrobial by applying machine learning to genomic data (Nguyen, 2018; Nguyen, 2019; Hyun, 2020). This kind of surveillance may also make it possible to more accurately define multidrug resistance. For example, concordance of 95% to 99.7% between WGS and phenotypic AST was achieved for multiple classes of antimicrobials in studies involving *E. coli* and *K. pneumoniae* isolates as well as MRSA and VRE isolates (Stoesser, 2013; Gordon, 2014; Babiker, 2019). Studies evaluating WGS in the nonfermentative gram-negative bacteria, such as the opportunistic *P. aeruginosa* or *A. baumannii*, have shown inferior performance, achieving sensitivities and specificities of <95% (Kos, 2015). This could be due, in part, to their high and complex genomic diversity, their numerous intrinsic and acquired β-lactamases, and the interplay of multiple overlapping resistance mechanisms in these organisms that often include mutations affecting functions such as membrane permeability and efflux

that contribute to multidrug resistance (Kos, 2015; Breidenstein, 2011; Ellington, 2017).

Despite this, there are real limitations for the use of this technology to guide clinical decision making. In addition to the significant cost required, there are gaps in knowledge regarding novel mutations with unknown function (such as the unexpected emergence of the colistin resistance determinant gene *mcr-1*), and there is uncertainty regarding the interplay of multiple genes that may account for resistance (such as those involved in porin mutations and efflux pumps) as well as regarding the complex relationship between genotype and gene expression. Moreover, there are technological and bioinformatics barriers as well as a lack of standardization of this methodology for routine AST in the clinical lab (Liu, 2016; Suzuki, 2014; Ellington, 2017; Doyle, 2020). For all of these reasons, WGS has been used successfully in outbreak investigations and surveillance but is, at present, not used for routine AST in the clinical laboratory (Hendriksen, 2019). In their 2017 review, EUCAST determined that there are insufficient data to present a definitive document on the topic (Ellington, 2017).

Additional technologies being evaluated and gaining popularity in the world of AST include hybridization techniques, such as FISH as well as spectrophotometric and proteomic techniques. These have shown promise in being highly sensitive and specific, as well as rapid, compared with the phenotypic susceptibility tests.

FISH has been used in clinical laboratories for bacterial identification and is now increasingly being used for AST. The PhenoTest (Accelerate Diagnostics, Tucson, AZ) is a FISH-probe–based bacterial identification and AST system that can be performed directly from blood culture bottles. This assay employs time-lapse image analysis of bacterial cell growth in various antibiotic concentrations. A complete ID and an MIC result can be obtained in 1 and 7 hours, respectively, and results compare well (>95% agreement) with routine ID/AST methods (Charnot-Katsikas, 2018; Pancholi, 2018).

Non–nucleic acid-based technologies, such as Matrix Assisted Laser Desorption Ionization Time-of-Flight Mass Spectrometry (MALDI-TOF MS), are also showing promise for their use in rapid AST. MALDI-TOF identifies molecules based on their mass-to-charge ratio and time of flight as compared with a reference database. This methodology can identify molecules with a wide range of molecular masses and can detect a variety of molecules, including resistance enzymes, antibiotics and their products of hydrolysis, bacterial cell wall components, and antibiotic target sites. One of the advantages of MALDI-TOF is the detection of actual expression of resistance as opposed to detection of the potential for resistance (i.e., detection of a resistance gene). Using MALDI-TOF, Hrabak and colleagues (2011) detected carbapenemase activity in *Enterobacteriaceae* by meropenem degradation, reporting a sensitivity and specificity of 96.67% and 97.87%, respectively. Also, Kempf and colleagues (2012) determined that the use of imipenem to identify carbapenem resistance in *A. baumannii* isolates showed a sensitivity and specificity of 100%. However, this method cannot detect other carbapenem resistance mechanisms, such as porin alterations and efflux mechanisms. Nonetheless, it provides rapid results, which can allow for earlier directed therapy and avoidance of inappropriate empiric therapy, and may provide useful information for purposes of epidemiologic infection control.

There are newer technologies in various phases of research for AST. Some of these include biochemical, electrochemical, flow-cytometry, and live-imaging techniques. Some offer testing on a nanoscale level. With further optimization of newer technologies for AST, as well as decreasing costs and turnaround times, it is likely that their use for AST will become more mainstream in the clinical laboratory. Some of these techniques are culture independent and can be tested directly from the patient specimen, allowing for even more rapidity in generating results. However, until the full implications of detecting or not detecting a specific gene using a particular molecular technique are fully understood, these tests will serve in a supporting role to phenotypic antimicrobial susceptibility testing in many clinical laboratories. As this section is by no means a comprehensive review of all available commercial assays, the reader is referred to Puttaswamy (2018) and Maugeri (2019) for additional discussion on new and emerging technologies for AST.

Few studies have demonstrated that the rapidity of results coming from this newest generation of antimicrobial susceptibility tests have improved patient outcomes (Huang, 2013; Beuving, 2015; Banerjee, 2019); nonetheless, Huang and colleagues (2013) found that the rapid organism identification using MALDI-TOF along with AST intervention decreased time to effective and optimal antibiotic therapy. In a large randomized controlled trial, Banerjee et al. (2019) showed that rapid organism ID and AST using the PhenoTest resulted in faster changes in antibiotic therapy for gram-negative bacteremia. More studies are needed to assess the threshold at which rapid results are truly clinically impactful, as analytic turnaround time requires intervention by providers to truly impact patient outcomes, as shown in the reports in which rapid results have been combined with rapid stewardship interventions.

In summary, the use of molecular techniques—particularly amplification and hybridization-based techniques—to rapidly detect the presence of antimicrobial resistance genes is an important innovation that has led to standardized, commercially available tests for use by clinical laboratories. WGS is also a molecular technology that is being studied for its potential use in AST. However, at present, its use has primarily been epidemiologic strain typing in outbreak investigations. Additional methods abound and show promise for their possible incorporation into routine clinical AST in the not-so-distant future.

INDICATIONS FOR SUSCEPTIBILITY TESTING

Whether antimicrobial susceptibility testing on a particular isolate is necessary varies with the infecting species. If the susceptibility of a bacterial species to a particular antimicrobial is unpredictable, then testing is necessary. If the susceptibility profile is predictable, it is not necessary, in most cases, to do testing on an isolate. For example, resistance to penicillin in *S. pyogenes* pharyngitis has not been reported in the United States; thus, it is appropriate to treat a patient with *S. pyogenes* pharyngitis without susceptibility testing. However, if a patient is allergic to or cannot take the primary choice of antibiotic to treat an infection caused by a particular pathogen or if, for another reason, the susceptibility profile of the alternate-choice antibiotic is unpredictable, testing must be done. If the patient in the previous example were allergic to penicillin and the physician wished to treat the patient with a macrolide, such as azithromycin, susceptibility testing of the isolate against macrolides could be done because a high proportion of *S. pyogenes* isolates have tested resistant to macrolides for a number of years (Jacobs, 2003). It must also be remembered that testing should be limited to those isolates that are definite pathogens, because testing of isolates that are "contaminants" or "normal flora" is expensive, time-consuming, and may lead to unnecessary administration of antibiotics (Bates, 1991). With increasing numbers of severely immunocompromised patients, however, species generally considered to be normal flora or contaminants may be pathogenic. In these patients, susceptibility testing against these species may be warranted. Close consultation with infectious disease physicians is necessary in these cases.

Several years ago, antibiotic therapy for infections caused by anaerobes was often empiric, because the susceptibility profiles of these pathogens were thought to be relatively predictable, susceptibility testing was not standardized, and only limited proof suggested that susceptibility testing correlated with outcome. In recent years, however, it has been demonstrated that the susceptibility patterns of many anaerobic pathogens are changing and that, at least for some species, in vitro antibiotic susceptibility testing correlates with clinical outcome. This is particularly true of *Bacteroides fragilis* and closely related species (Nguyen, 2000; Boyanova, 2015). *B. fragilis*, the most frequently isolated species from anaerobic infections, has the greatest number of antimicrobial resistance mechanisms, as well as the highest rates of antimicrobial resistance, among anaerobic bacterial pathogens (Boyanova, 2015). For example, resistance to the cephalosporins, the β-lactam/β-lactamase inhibitor combinations, moxifloxacin, clindamycin, and even the carbapenems is increasing globally for *Bacteroides* and *Parabacteroides* species, as well as some of the other gram-negative anaerobes (Snydman, 2011; Boyanova, 2015). Resistance to moxifloxacin is also increasing in some *Clostridium* species, and many non–spore-forming gram-positive anaerobic rods are resistant to metronidazole. Further, multidrug-resistant *B. fragilis* strains have been identified, though these are still not frequently seen in the United States (Boyanova, 2015).

Though members of the *Bacteroides* group are presumed to be resistant to the penicillins and do not warrant β-lactamase testing, other anaerobes can be tested for the presence of β-lactamase with a chromogenic cephalosporin, though other mechanisms of resistance may also exist. The CLSI recommends testing of anaerobic isolates from specific types of infections, including brain abscess, endocarditis, osteomyelitis, joint infection, infection of prosthetic or vascular devices, and bacteremia (CLSI M11, 2018).

Additionally, certain species that have a high incidence of resistance or are highly virulent warrant testing, including species of *Bacteroides*, *Prevotella*, *Fusobacterium*, *Bilophila*, and *Sutterella*, and members of the *Clostridium* species. Despite this, in the United States, only 21% of laboratories performing anaerobic culture perform anaerobic susceptibility testing in-house; another 20% utilize reference laboratories for this purpose (Boyanova, 2015). Currently, the CLSI-recommended susceptibility testing method for anaerobes is the agar dilution method. The exception is the *B. fragilis* group, for which broth microdilution can also be performed (CLSI M11, 2018). As the agar dilution method is labor-intensive and time-consuming, laboratories may validate alternate methods, such as the E-Test, for the testing of anaerobes. Importantly, disk diffusion should not be used, as results do not correlate well with the CLSI reference method (CLSI M11, 2018).

For other isolates not already discussed, batch susceptibility testing of archived isolates of anaerobes can be performed, either locally or by a reference laboratory, on a periodic basis (recommended annually by the CLSI) in a surveillance protocol to detect local changes in resistance patterns. An effort should be made to include some of the more common anaerobic bacterial isolates in hospital antibiograms to assist in the choice of therapy for patients.

SELECTION OF ANTIBIOTICS FOR TESTING

In 2017 The Joint Commission, an accreditation organization for health care organizations, issued standards on performance regarding the utilization of antimicrobial agents in a document entitled New Antimicrobial Stewardship Standards. The goal of the implementation of these standards is the reduction of inappropriate antimicrobial use across health care organizations, including hospitals, nursing care centers, and ambulatory care centers. The implementation of these standards, known as an **antimicrobial stewardship program (ASP)**, is largely overseen by a multidisciplinary team of ID-trained physicians, pharmacists, and a member of the laboratory, and is commonly referred to as the antimicrobial stewardship team (Goff, 2017).

Selection of antimicrobial agents for testing is complicated by the expanding spectrum and number of antibiotics available and by the growing list of resistance phenotypes that are being identified in pathogenic bacteria. Testing of all agents available in an institution's formulary is neither practical nor warranted. The antimicrobial testing menu should be established in consultation with the antimicrobial stewardship team and the Pharmacy and Therapeutics Committee so that the therapeutic needs of the patient population can be best coordinated with the practical limitations of the institution, pharmacy, and clinical laboratory. This coordination is important for a variety of reasons. First, many laboratories utilize commercial automated testing systems for susceptibility testing. Manufacturers offer a variety of preconfigured antibiotic testing panels in systems designed to correspond to hospital formularies; however, disparities between the preconfigured panel and the hospital formulary often exist. The laboratory may be faced with an added expense of modifying a preconfigured panel or adding testing methods to the laboratory to accommodate testing of additional agents. Second, testing multiple representatives of the same antibiotic class is not usually necessary except for when it is required to deduce mechanisms of antimicrobial resistance or allow for flexibility in different routes of administration (e.g., intravenous, oral). In many cases, results derived by testing a representative drug of the class can be inferred for the other members of the class. Discussion and coordination with the medical staff and infectious disease specialists relative to which antibiotics are necessary to allow the providers to manage their patients may save the laboratory these added expenses. Also, for some drug-bug combinations, there are no established interpretive criteria. However, these drugs may still be considered for treatment as the last resort in cases of multidrug or pan-resistant infections. The handling of such cases also requires detailed discussion with the clinical providers.

The yearly CLSI informational supplement (CLSI M100, 2020) lists in a table the antimicrobial agents that are recommended for testing for highly prevalent and important nonfastidious pathogens, including *Enterobacteriaceae*, *P. aeruginosa*, *Staphylococcus* spp., *Enterococcus* spp., *Acinetobacter* spp., *Burkholderia cepacia*, and *Stenotrophomonas maltophilia*. A separate table lists recommended antibiotics for more fastidious pathogens, such as *Haemophilus* spp., *N. gonorrhoeae*, *S. pneumoniae*, *Streptococcus* β-hemolytic spp., and *Streptococcus* viridans group spp. The antibiotics are listed in four groups, with group A containing drugs recommended for testing and reporting on all isolates and group B containing agents suggested for testing against all isolates but reported only under certain circumstances (e.g., when the isolate is resistant to drugs in group A). Group C lists antibiotics that are considered supplemental and could be used in institutions that have a high prevalence of highly resistant isolates, when unusual pathogens are isolated, or by infection-control practitioners as epidemiologic tools. Finally, group U lists antimicrobials that should be tested and reported only on isolates from urine.

Within each group—A, B, C, or U—more antibiotics are listed than need be tested or reported. Within boxes in the tables, drugs that usually have similar interpretive results and clinical efficacy are grouped together. If an agent is listed with another agent separated by "or," this implies almost identical cross-resistance or susceptibility between drugs; the results of testing one drug will predict the susceptibility result for the other. In the absence of the "or," even though the antibiotics listed in the same box have similar clinical efficiency and similar interpretive results, stringent statistical criteria for comparable testing results were not met when a large number of isolates were tested with the antibiotics in question or the data were not available; thus, equivalence for testing results cannot be confidently inferred. For example, for *Enterobacteriaceae*, Table 2A (CLSI M100, 2020) notes that testing of cephalothin will predict the susceptibility profile of certain other first-generation cephalosporins but that cefazolin is the preferred agent to test for predicting results for oral cephalosporins for uncomplicated urinary tract infections. In contrast, in group B, the third-generation cephalosporins cefotaxime and ceftriaxone are separated by an "or," indicating that their susceptibility profiles are virtually interchangeable and that only one of the two needs to be tested if the isolate is a member of *Enterobacteriaceae*.

SELECTING ANTIBIOTICS TO BE REPORTED

Policies for reporting of antibiotics for isolates should take into account not only the results of testing but also a variety of factors. For example, the laboratory should not report susceptibility results for antimicrobials that are not effective in treating a given infection. As many drugs (including first- or second-generation cephalosporins, macrolides, clindamycin, fluoroquinolones, tetracyclines, and orally administered drugs) are not appropriate in the treatment of CSF infections, they should not be reported for isolates from the central nervous system (CLSI M100, 2020). Similarly, drugs that may test susceptible in vitro but have been shown to be ineffective in vivo for particular species, such as cephalosporins or trimethoprim-sulfamethoxazole for *Enterococcus* spp., also should not be reported (CLSI M100, 2020). Drugs that are effective only for urinary tract infection (e.g., nitrofurantoin) should not be reported on isolates from any site other than the urinary tract. Many institutions utilize **cascade** reporting to encourage the use of antimicrobials that are effective based on in vivo susceptibility testing but may be less expensive than the "newest" or most heavily commercially promoted drug to try to lower pharmacy costs. For example, third-generation cephalosporins might be reported, barring other considerations such as isolate source, only if first- or second-generation cephalosporins are resistant upon testing.

A close working relationship between the clinical microbiology laboratory and the infectious disease service is important in effective **antibiotic stewardship** programs that guide an institution's caregivers in the most appropriate use of antibiotics. These programs are instituted to save money or, more important, to combat the increasing problem of antibiotic resistance. They may involve the use of mandatory prescribing and treatment guidelines, reporting or nonreporting of specific antibiotics on susceptibility profiles, and **gatekeeper** providers such as infectious disease physicians, whose approval is required before specific antibiotics can be used. As an example, it has been demonstrated in prospective studies (Project ICARE: Intensive Care Antimicrobial Resistance Epidemiology) that the frequent use of vancomycin and third-generation cephalosporins is associated with increased prevalence of VRE in intensive care units and that by limiting the use of vancomycin, the prevalence can be decreased (Fridkin, 2001, 2002). Similarly, in a multicenter retrospective analysis, Pakyz and colleagues (2009) showed that restricting the use of carbapenems resulted in lower incidences of carbapenem-resistant *P. aeruginosa* than were seen in hospitals that did not restrict carbapenem use.

Selection of an antibiotic by a physician to treat an infection in a patient involves consideration of numerous factors, including, but not limited to, the known or most likely infecting organism(s), local patterns of drug

resistance on the part of the organism(s), the site of infection, pharmacodynamic and pharmacokinetic properties of the drug, overall health of the patient, and the cost of the antibiotic. Although initial selection of an antimicrobial agent is empiric in many cases, in vitro laboratory testing of the susceptibility of isolated pathogen(s) to antibiotics is an important aid in subsequent management of the patient. Modification of therapy may be desirable if (1) the infecting organism(s) is resistant to current therapy, (2) the dose of antibiotic is not appropriate, (3) an equally effective but less expensive agent can be used, or (4) de-escalation of antibiotic therapy can occur (i.e., if the organism is found to be more susceptible than anticipated).

Finally, reports from several centers in different parts of the world have detailed outbreaks of a highly virulent strain of *C. difficile* that resulted in high morbidity and mortality. These outbreaks have been determined to be associated with the use of specific antibiotics, particularly the fluoroquinolones, to which this particular strain is highly resistant. Containment of the outbreaks has required a number of measures, including strict antibiotic stewardship programs that completely prohibited fluoroquinolone use in some cases (Valiquette, 2007; Labbé, 2008; Debast, 2009). These examples demonstrate the importance of knowing how and what antibiotics are reported by the laboratory as well as the importance of the clinical laboratory working closely with the infectious disease service in addressing issues created by patterns of antibiotic use. A multicenter survey of U.S. hospitals showed that the most frequently prescribed antibiotic class from 2002 to 2006 was the fluoroquinolones and that carbapenem use was increasing significantly (Pakyz, 2008). These issues are directly relevant to the examples given here and show that the management of antibiotic use in hospitals, including what antibiotics the clinical laboratory reports, will be a continuing and increasingly complex issue in the coming years.

CUMULATIVE ANTIMICROBIAL SUSCEPTIBILITY REPORTS

Susceptibility patterns for specific species against antimicrobials can vary with geographic locale, type of medical institution, and antibiotic usage patterns. It is the responsibility of the clinical microbiology laboratory to monitor susceptibility patterns and keep the medical staff informed of current patterns. This is usually accomplished by monitoring susceptibility data on isolates over time, compiling these data for a specific time period, calculating the percentage of a specific species that is susceptible to a given drug, putting all the data into an easily accessible format, and making it available to the medical staff. These reports, usually referred to as *antibiograms*, can be used by the medical staff to treat infections empirically while awaiting specific culture and susceptibility results. They can also be used by hospital epidemiology and infection control to monitor resistance trends, identify outbreaks, and formulate infection-control policy. They may also be referred to by the pharmacy and therapeutics committee of the institution when making policy or formulary decisions (Zapantis, 2005). By including antibiotic cost data in the antibiogram, institutions may encourage providers to utilize less-expensive but still effective drugs.

The CLSI provides guidance to institutions on the preparation of antibiograms in CLSI document M39-A4 (2014). It includes suggestions on use of terminology; obtaining, analyzing, and presenting data; statistical considerations; and specific limitations of the antibiogram. Examples and templates are included in the document. Hindler and Stelling (2007) summarized many of the essential considerations discussed in the CLSI document, and they discussed issues that must be considered and decided on when compiling an institution's antibiogram. For example, how multiple isolates from a single patient are counted in compiling the data can have a marked effect on the percentage of a specific species that appears susceptible to a given antibiotic. If all isolates are counted, this will bias the result toward isolates that are submitted from patients who have multiple cultures submitted over time (e.g., those patients with infection due to resistant organisms, who remain hospitalized for long periods, or who do not respond to therapy) (Hindler & Stelling, 2007). Whether duplicate isolates from the same patient are all counted (isolate-based algorithm), whether they are excluded and only the first one counted (patient-based algorithm), are counted only if they represent a new clinical episode (episode-based algorithm), or are counted only if they show a new resistance phenotype (phenotype-based algorithm) directly affects the percentages of susceptibility for an antimicrobial. Which algorithm is best for a given institution should be decided upon consultation with the medical staff and/or the pharmacy and therapeutics committee and then adhered to during subsequent compilations so that comparisons between individual time periods are valid.

Data management associated with antibiograms and the information that can be obtained from these data may be complex and difficult to manage and manipulate. The World Health Organization (WHO) Collaborating Centre for Surveillance of Antimicrobial Resistance has made available a software program that can be downloaded and utilized at no charge to accomplish useful data management (WHO, 2006). The software program (WHONET) has a module that allows a laboratory to input which antimicrobials are reported and what patient care areas are served by the laboratory, and allows alerts for important organisms or phenotypes. A second module permits the entry, retrieval, correction, and printing of clinical reports. Finally, a third module allows a variety of analyses to be generated from the institution data, including, but not limited to, organism frequencies over time, antimicrobial susceptibility statistics, disk diffusion zone diameter or MIC histograms, antimicrobial scatterplots, and regression curves. Additionally, a software component, BacLink, can be obtained that can upload data from an institution's current system directly into WHONET, avoiding manual data entry. Both WHONET and BacLink software can be downloaded directly from the Internet at no cost (WHO, 2006). The WHONET software is being used by laboratories in more than 90 countries worldwide.

In conclusion, the CDC estimates that antibiotic-resistant bacteria and fungi cause more than 2.8 million infections and 35,000 deaths in the United States each year (CDC, 2019). Many more die from other conditions complicated by an antibiotic-resistant infection. MDROs add significant financial burden to patients, their families, and to the health care system. The yearly cost to the health care system of the United States alone due to MDROs has been estimated at nearly $34 billion, along with more than 8 million additional days in the hospital (WHO, 2014b). The use of antibiotics is the most important factor leading to antibiotic resistance. Moreover, at least 30% of outpatient antibiotics prescribed in the United States are unnecessary (Fleming, 2016). This is a critical time in the fight against drug resistance. The need is greater than ever for the most accurate susceptibility testing and reporting, as well as for the implementation of robust infection-control measures and antibiotic stewardship programs, in which the microbiology laboratory plays a key role.

SELECTED REFERENCES

Beuving J, Wolffs PF, Hansen WL, et al.: Impact of same-day antibiotic susceptibility testing on time to appropriate antibiotic treatment of patients with bacteraemia: a randomised controlled trial, *Eur J Clin Microbiol Infect Dis* 34:831–838, 2015.

This is an interesting study illustrating that rapid AST can significantly reduce the time to receipt of targeted therapy in patients with bacteremia. A clear clinical benefit regarding outcomes was not seen, however, which helps to highlight the fact that more than just a rapid result is needed to significantly impact patient outcomes. Rapid clinical intervention must accompany the rapid result in order for the latter to be significant.

Bush K: Past and present perspectives on β-lactamases, *Antimicrob Agents Chemother* 62(10), 2018. e01076–18.

This publication provides a comprehensive and current review of the evolution and burden of β-lactamases around the world. It discusses some of the nuances and complexities of their identification and categorization, providing a framework for categorizing these resistance genes to help understand them.

Centers for Disease Control and Prevention: *Antibiotic resistance threats in the United States, 2019. Atlanta, GA.* U.S. Department of Health and Human Services, CDC. Available at https://www.cdc.gov/drugresistance/pdf/threats-report/2019-ar-threats-report-508.pdf, 2019.

This publication outlines the current epidemiology and statistics of MDROs in the United States. It individually highlights the various MDROs that the CDC considers to be some of the most serious threats to public health.

Clinical and Laboratory Standards Institute: Performance standards for antimicrobial susceptibility testing. In *CLSI supplement M100*, 30, Wayne, PA, 2020, Clinical and Laboratory Standards Institute.

This document is a staple for any clinical microbiology laboratory. It is an important reference and is updated annually. Readers should familiarize themselves with this document, as it provides thorough and detailed guidance for the performance of AST.

Humphries RM, Ambler J, Mitchell SL, et al.: On behalf of the CLSI methods development and standardization working group of the Subcommittee on antimicrobial susceptibility testing. CLSI methods development and standardization working group best practices for evaluation of antimicrobial susceptibility tests, *J Clin Microbiol* 56(4), 2018. e01934–17.

This article discusses best practices for the evaluation of the performance of an AST system, including the analysis of data and investigation of errors, to avoid design and analysis flaws.

Puttaswamy S, Gupta SK, Regunath H, et al.: A comprehensive review of the present and future antibiotic susceptibility test (AST) systems, *Arch Clin Microbiol* 9(3):83, 2018.

This article provides an overview of current clinical laboratory practices for AST. It then discusses emerging as well as future AST technologies, along with their turnaround time to results and whether they can be performed directly from patient specimens.

Access the complete reference list online at Elsevier eBooks for Practicing Clinicians.

REFERENCES

Abele-Horn M, Hommers L, Trabold R, et al.: Validation of VITEK 2 version 4.01 software for detection, identification, and classification of glycopeptides-resistant enterococci, *J Clin Microbiol* 71:44, 2006.

Arbique J, Forward K, Haldane D, et al.: Comparison of the Velogene rapid MRSA screen assay, Denka MRSA-screen assay, and BBL Crystal MRSA ID system for rapid identification of methicillin-resistant Staphylococcus aureus, *Diagn Microbiol Infect Dis* 5:40, 2001.

Arnold AR, Burnham C-AD, Ford BA, et al.: Evaluation of an immunochromatographic assay for rapid detection of penicillin-binding protein 2a in human and animal Staphylococcus intermedius group, Staphylococcus lugdunensis, and Staphylococcus schleiferi clinical isolates, *J Clin Microbiol* 54:745–748, 2016, https://doi.org/10.1128/JCM.02869-15.

Babiker A, Mustapha M, Pacey MP, et al.: Use of online tools for antimicrobial resistance prediction by whole-genome sequencing in methicillin-resistant Staphylococcus aureus (MRSA) and vancomycin-resistant enterococci (VRE), *Journal of Global Antimicrobial Resistance* 19:136–143, 2019, ISSN 2213-7165, https://doi.org/10.1016/j.jgar.2019.04.006.

Banerjee R, Lauren Komarow MS, Virk A, et al.: Randomized clinical trial evaluating clinical impact of RAPid IDentification and antimicrobial susceptibility testing for Gram-negative bacteremia (RAPIDS-GN), open Forum infectious diseases, vol. 6. Issue Supplement_2, October 2019, Pages S296–S297. https://doi.org/10.1093/ofid/ofz360.708.

Banerjee R, Teng CB, Cunningham SA, et al.: Randomized trial of rapid multiplex polymerase chain reaction-based blood culture identification and susceptibility testing, *Clin Infect Dis* 61(7):1071–1080, 2015, https://doi.org/10.1093/cid/civ447.

Bates DW, Goldman L, Lee TH: Contaminant blood cultures and resource utilization. The true consequences of false-positive results, *J Am Med Assoc* 365:265, 1991.

Beuving J, Wolffs PF, Hansen WL, et al.: Impact of same-day antibiotic susceptibility testing on time to appropriate antibiotic treatment of patients with bacteraemia: a randomised controlled trial, *Eur J Clin Microbiol Infect Dis* 34:831–838, 2015.

Bhatti MM, Boonlayangoor S, Beavis KG, et al.: Evaluation of FilmArray and Verigene systems for rapid identification of positive blood cultures, *J Clin Microbiol* 52:3433–3436, 2014.

Birgand G, Ruimy R, Schwarzinger M, et al.: Rapid detection of glycopeptide resistant enterococci: impact on decision-making and costs, *Antimicrob Resist Infect Control* 2:30, 2013.

Black JA, Moland ES, Thomson KS: AmpC disk test for detection of plasmid-mediated AmpC β-lactamases in Enterobacteriaceae lacking chromosomal AmpC β-lactamses, *J Clin Microbiol* 3110:43, 2005.

Blanc DS, Basset P, Nahimana-Tessemo I, et al.: High proportion of wrongly identified Methicillin-resistant Staphylococcus aureus carriers by use of a rapid commercial PCR assay due to presence of staphylococcal cassette chromosome element lacking the mecA gene, *J Clin Microbiol* 49:722–724, 2011.

Bobenchik AM, Deak E, Hindler JA, et al.: Performance of Vitek 2 for antimicrobial susceptibility testing of Enterobacteriaceae with Vitek 2 (2009 FDA) and 2014 CLSI breakpoints, *J Clin Microbiol* 53:816–823, 2015.

Bonomo RA, Burd EM, Conly J, et al.: Carbapenemase-producing organisms: a global Scourge, *Clin Infect Dis* 66(8):1290–1297, 2018, https://doi.org/10.1093/cid/cix893.

Boyanova L, Kolarov R, Mitov I: Recent evolution of antibiotic resistance in the anaerobes as compared to previous decades, *Anaerobe* 31(4–10), 2015.

Braun SD, Monecke S, ThCurmer A, et al.: Rapid Identification of carbapenemase genes ingram-negative bacteria with an oligonucleotidemicroarray-based assay, *PloS One* 9, 2014. e102232.

Breidenstein EB, de la Fuente-Nunez C, Hancock RE: Pseudomonas aeruginosa: all roads lead to resistance, *Trends Microbiol* 19:419e26, 2011.

Buchan BW, Allen S, Burnham C-AD, et al.: Comparison of the next-generation Xpert MRSA/SA BC assay and the GeneOhm StaphSR assay to routine culture for identification of Staphylococcus aureus and methicillin-resistant S. aureus in positive-blood-culture broths, *J Clin Microbiol* 53:804–809, 2015, https://doi.org/10.1128/JCM.03108-14.

Bush K, Bradford PA: Epidemiology of β-lactamase-producing pathogens, *Clin Microbiol Rev*(2)33, 2020 Feb 26, pii: e00047-19., https://doi.org/10.1128/CMR.00047-19.

Bush K, Jacoby GA: Updated functional classification of beta-lactamases, *Antimicrob Agents Chemother* 54:969–976, 2010.

Bush K: *Past and Present Perspectives on β-Lactamases Antimicrobial Agents and Chemotherapy* 62(10), 2018, e01076-18, https://doi.org/10.1128/AAC.01076-18.

Cahen P, Le Bourgeois M, Delacourt C, et al.: Serum bactericidal test as a prognostic indicator in acute pulmonary exacerbations of cystic fibrosis, *Pediatrics* 451:91, 1993.

Carroll KC, Borek AP, Burger C, et al.: Evaluation of the BD Phoenix Automated Microbiology System for identification and antimicrobial susceptibility testing of staphylococci and enterococci, *J Clin Microbiol* 44, 2006. 2072.

Carroll KC, Reid JL, Thornberg A, et al.: Clinical performance of the novel GenMark Dx ePlex blood culture ID gram-positive panel, *J Clin Microbiol* 58(4), 2020 e01730-19. Published 2020 Mar 25, https://doi.org/10.1128/JCM.01730-19.

CDC: *Antibiotic resistance threats in the United States, 2019*, Atlanta, GA, 2019, U.S. Department of Health and Human Services, CDC. Atlanta, GA. Available at https://www.cdc.gov/drugresistance/pdf/threats-report/2019-ar-threats-report-508.pdf.

CDC: Facility guidance for control of carbapenem-resistant Enterobacteriaceae (CRE) – November 2015 update. CDC, Atlanta, GA. Available at https://www.cdc.gov/hai/pdfs/cre/cre-guidance-508.pdf.

Charnot-Katsikas A, Tesic V, Love N, Hill B, Bethel C, Boonlayangoor S, Beavis KG: Use of the Accelerate Pheno system for identification and antimicrobial susceptibility testing of pathogens in positive blood cultures and impact on time to results and workflow, *J Clin Microbiol* 56, 2018. e01166-17.

CLSI: Analysis and presentation of cumulative antimicrobial susceptibility test data; approved guideline. In *CLSI document M39-A4*, 4th ed., Wayne, PA, 2014, Clinical and Laboratory Standards Institute.

CLSI: Methods for antimicrobial dilution and disk susceptibility testing of infrequently isolated or fastidious bacteria. 3rd ed. CLSI guideline M45. Wayne, PA: Clinical and Laboratory Standards Institute; 2016.

CLSI: Methods for antimicrobial susceptibility testing of anaerobic bacteria. 9th ed. CLSI document standard M11. Wayne, PA: Clinical and Laboratory Standards Institute; 2018.

CLSI. Methods for dilution antimicrobial susceptibility tests for bacteria that grow aerobically. 11th ed. CLSI standard M07. Wayne, PA: Clinical and Laboratory Standards Institute; 2018.

CLSI. Performance Standards for antimicrobial disk susceptibility tests. 13th ed. CLSI standard M02. Wayne, PA: Clinical and Laboratory Standards Institute; 2018.

CLSI. Performance Standards for Antimicrobial Susceptibility Testing. 30th ed. CLSI supplement M100. Wayne, PA: Clinical and Laboratory Standards Institute; 2020.

CLSI. Reference method for broth dilution antifungal susceptibility testing of filamentous fungi. 3rd ed. CLSI standard M38. Wayne, PA: Clinical and Laboratory Standards Institute; 2017.

CLSI. Reference method for broth dilution antifungal susceptibility testing of yeasts. 4th ed. CLSI standard M27. Wayne, PA: Clinical and Laboratory Standards Institute; 2017.

CLSI. Susceptibility testing of Mycobacteria Nocardia spp., and other aerobic actinomycetes. 3rd ed. CLSI standard M24. Wayne, PA: Clinical and Laboratory Standards Institute; 2018.

CLSI. Verification of commercial microbial identification and antimicrobial susceptibility testing systems. 1st ed. CLSI guideline M52. Wayne, PA: Clinical and Laboratory Standards Institute; 2015.

Cui L, Murakami H, Kuwahara-Arai K, et al.: Contribution of a thickened cell wall and its glutamine nonamidated component to the vancomycin resistance expressed by Staphylococcus aureus Mu50, *Antimicrob Agents Chemother* 2276:44, 2000.

Cuzon G, Naas T, Bogaerts P, et al.: Evaluation of a DNAmicroarray for the rapid detection of extended-spectrum β-lactamases (TEM, SHV and CTX-M), plasmid-mediated cephalosporinases (CMY-2-like, DHA, FOX, ACC-1, ACT/MIR and CMY-1-like/ MOX) and carbapenemases (KPC, OXA-48, VIM, IMP and NDM), *J Antimicrob Chemother* 67:1865–1869, 2012.

Dahesh S, Hensler ME, Sorge NMV, et al.: Point mutation in the Group B streptococcal pbp2x gene conferring decreased susceptibility to β-lactam antibiotics, *Antimicrob Agents Chemother* 2915:52, 2008.

Daikos GL, Markogiannakis A, Souli M, et al.: Bloodstream infections caused by carbapenemase-producing Klebsiella Pneumoniae: a clinical perspective, *Expert Rev Anti-Infect Ther.* 10:1393–1404, 2012.

Debast SB, Vaessen N, Choudry A, et al.: Successful combat of an outbreak due to Clostridium difficile PCR ribotype 027 and recognition of specific risk factors, *Clin Microbiol Infect* 427(15), 2009.

Denys GA, Renzi PB, Koch KM, et al.: Three-way comparison of BBL CHROMagar MRSA II, MRSASelect, and spectra MRSA for detection of methicillin-resistant Staphylococcus aureus isolates in nasal surveillance cultures, *J Clin Microbiol* 51(1):202–205, 2013.

Desjardins M, Delgaty KL, Ramotar K, et al.: Prevalence and mechanisms of erthromycin resistance in Group A and Group B Streptococcus: implications for reporting susceptibility results, *J Clin Microbiol* 5620:42, 2004.

Dhand A, Sakoulas G: Reduced vancomycin susceptibility among clinical Staphylococcus aureus isolates ("the MIC Creep"): implications for therapy, *F1000 Medicine Reports* 4(4), 2012.

Dortet L, Fusaro M, Naas T: Improvement of the Xpert Carba-R kit for the detection of carbapenemase-producing Enterobacteriaceae, *Antimicrobial Agents and Chemotherapy May* 60(6):3832–3837, 2016, https://doi.org/10.1128/AAC.00517-16.

Doyle D, Peirano G, Lascols C, et al.: Laboratory detection of Enterobacteriaceae that produce carbapenemases, *J Clin Microbiol* 50:3877–3880, 2012, https://doi.org/10.1128/JCM.02117-12.

Doyle RM, O'Sullivan DM, Aller SD, et al.: Discordant bioinformatic predictions of antimicrobial resistance from whole-genome sequencing data of bacterial isolates: an inter-laboratory study, *Microb Genom* 6, 2020, https://doi.org/10.1099/mgen.0.000335.

Ellington MJ, Ekelund O, Aarestrup FM, et al.: The role of whole genome sequencing in antimicrobial susceptibility testing of bacteria: report from the EUCAST Subcommittee, *Clin Microbiol Infect* 23:2–22, 2017, https://doi.org/10.1016/j.cmi.2016.11.012.

Espinar MJ, Rocha R, Ribeiro M, et al.: Extended-spectrum beta-lactamases of Escherichia coli and Klebsiella pneumoniae screened by the Vitek 2 system, *J Med Microbiol* 60(Pt 6):756–760, 2011.

Felten A, Grandry B, Lagrange PH, et al.: Evaluation of three techniques for detection of low level methicillin-resistant Staphylococcus aureus (MRSA): a disk diffusion method with cefoxitin and moxalactam, the Vitek 2 system, and the MRSA-Screen latex agglutination test, *J Clin Microbiol* 2766:40, 2002.

Findlay J, Hopkins KL, Meunier D, et al.: Evaluation of three commercial assays for rapid detection of genes encoding clinically relevant carbapenemases in cultured bacteria, *J Antimicrob Chemother* 70:1338–1342, 2015, https://doi.org/10.1093/jac/dku571.

Fiori B, D'Inzeo T, Posteraro B, et al.: Direct use of eazyplex® SuperBug CRE assay from positive blood cultures in conjunction with inpatient infectious disease consulting for timely appropriate antimicrobial therapy in Escherichia coli and Klebsiella pneumoniae bloodstream infections, *Infect Drug Resist* 12:1055–1062, 2019, https://doi.org/10.2147/IDR.S206323.

Fleming-Dutra KE, Hersh AL, Shapiro DJ, et al.: Prevalence of inappropriate antibiotic prescriptions among U.S. ambulatory care visits, 2010–2011, *J Am Med Assoc* 315:1864–1873, 2016, https://doi.org/10.1001/jama.2016.4151.

Fridkin SK, Edwards JR, Courval JM, et al.: The effect of vancomycin and third-generation cephalosporins on the prevalence of vancomycin-resistant enterococci in 126 US adult intensive care units, *Ann Intern Med* 175:135, 2001.

Fridkin SK, Lawton R, Edwards JR, et al.: Monitoring antimicrobial use and resistance: comparison with a national benchmark on reducing vancomycin use and vancomycin-resistant enterococci, *Emerg Infect Dis* 8, 2002. 702.

Garcia-Alvarez L, Holden MT, Lindsay H, et al.: Meticillin-resistant Staphylococcus aureus with a novel mecA homologue in human and bovine populations in the United Kingdom and Denmark: a descriptive study, *Lancet Infect Dis* 11:595–603, 2011.

Garcia-Fernandez S, Morosini M-I, Marco F, et al.: Evaluation of the eazyplex® SuperBug CRE system for rapid detection of carbapenemases and ESBLs in clinical Enterobacteriaceae isolates recovered at two Spanish hospitals, *J Antimicrob Chemother* 70:1047–1050, 2014.

Goff DA, Kullar R, Bauer KA, et al.: Eight Habits of highly effective antimicrobial stewardship programs to meet the joint Commission standards for hospitals, *Clin Infect Dis* 64(8):1134–1139, 2017, https://doi.org/10.1093/cid/cix065.

Gordon KA, Beach ML, Biedenbach DJ, et al.: Antimicrobial susceptibility patterns of beta-hemolytic and viridans group streptococci: report from the SENTRY Antimicrobial Surveillance Program (1997-2000), *Diag Microbiol Infect Dis* 157:43, 2002.

Gordon NC, Price JR, Cole K, et al.: Prediction of Staphylococcus aureus antimicrobial resistance by whole-genome sequencing, *J Clin Microbiol* 52(4):1182–1191, 2014, https://doi.org/10.1128/JCM.03117-13.

Heil EL, Johnson JK: Impact of CLSI breakpoint changes on microbiology laboratories and antimicrobial stewardship programs, *J Clin Microbiol* 54(4):840–844, 2016, https://doi.org/10.1128/JCM.02424-15.

Hindler JF, Stelling J: Analysis and presentation of cumulative antibiograms: a new consensus guideline from the Clinical and Laboratory Standards Institute, *Clin Infect Dis* 867:44, 2007.

Hrabak J, Walkova R, Studentova V, et al.: Carbapenemase activity detection by matrix-assisted laser desorption ionization-time of flight mass spectrometry, *J Clin Microbiol* 49:3222–3227, 2011.

Huang AM, Newton D, Kunapuli A, et al.: Impact of rapid organism identification via matrix-assisted laser desorption/ionization time-of-flight combined with antimicrobial stewardship team intervention in adult patients with bacteremia and candidemia, *Clin Infect Dis* 57:1237–1245, 2013.

Huang TD, Melnik E, Bogaerts P, et al.: Evaluation of the ePlex blood culture identification panels for detection of pathogens in bloodstream infections, *J Clin Microbiol* 57(2), 2019: e01597-18. Published 2019 Jan 30, https://doi.org/10.1128/JCM.01597-18.

Humphries RM, Ambler J, Mitchell SL, et al.: On behalf of the CLSI methods development and standardization working group of the Subcommittee on antimicrobial susceptibility testing. CLSI methods development and standardization working group best practices for evaluation of antimicrobial susceptibility tests, *J Clin Microbiol* 56(4), 2018. pii: e01934-17. doi. org/10.1128/JCM.01934-17.

Humphries RM: CIM city: the Game continues for a better carbapenemase test, *J Clin Microbiol* 57(7), 2019, e00353-19, https://doi.org/10.1128/JCM.00353-19.

Hussain Z, Stoakes L, Garrow S, et al.: Rapid detection of mecA-positive and mecA-negative coagulase-negative staphylococci by an anti-penicillin binding protein 2a slide latex agglutination test, *J Clin Microbiol* 38:2051–2054, 2000.

Hyun JC, Kavvas ES, Monk JM, et al.: Machine learning with random subspace ensembles identifies antimicrobial resistance determinants from pan-genomes of three pathogens, *PLoS Comput Biol* 16(3), 2020 Mar 2, e1007608, https://doi.org/10.1371/journal.pcbi.1007608.

Jacobs MR, Felmingham D, Appelbaum PC, et al.: The Alexander project, 1998-2000: susceptibility of pathogens from community-acquired respiratory tract infection to commonly used antimicrobial agents, *J Antimicrob Chemother* 229:52, 2003.

Jacoby JA: AmpC β-lactamases, *Clin Microbiol Rev* 22:161–182, 2009.

Jang W, Park YJ, Park KG, et al.: Evaluation of MicroScan WalkAway and Vitek 2 for determination of the susceptibility of extended-spectrum beta-lactamase-producing Escherichia coli and Klebsiella pneumoniae isolates to cefepime, cefotaxime and ceftazidime, *J Antimicrob Chemother* 68:2282–2285, 2013.

Jayaraman R: Bacterial persistence: some new insights into an old phenomenon, *J Biosci* 795:33, 2008.

Jenkins SG, Jerris RC: Critical assessment of issues applicable to development of antimicrobial susceptibility testing breakpoints, *J Clin Microbiol* 49, 2011. S5–S10.

Jenkins SG, Schuetz AN: Current concepts in laboratory testing to guide antimicrobial therapy, *Mayo Clin Proc* 87:290–308, 2012.

Jernigan JA, Hatfield KM, Wolford H, et al.: Multidrug-resistant bacterial infections in U.S. Hospitalized patients, 2012-2017, *N Engl J Med* 382(14):1309–1319, 2020, https://doi.org/10.1056/NEJMoa1914433.

Jones RN: Method preferences and test accuracy of antimicrobial susceptibility testing: updates from the College of American Pathologists microbiology surveys, *Arch Pathol Lab Med* 1285:125, 2001.

Jorgensen JH, Crawford SA, Feibelkorn KR: Susceptibility of Neisseria meningitidis to 16 antimicrobial agents and characterization of resistance mechanisms affecting some agents, *J Clin Microbiol* 3162:43, 2005.

Junkins AD, Lockhart SR, Heilmann KP, et al.: BD Phoenix and VITEK 2 detection of mecA-mediated resistance in Staphylococcus aureus with cefoxitin, *J Clin Microbiol* 2897:47, 2009.

Kaase M, Baars B, Freidrich S, et al.: Performance of Microscan Walkaway and Vitek 2 for detection of oxacillin resistance in a set of methicillin-resistant Staphylococcus aureus isolates with diverse genetic backgrounds, *J Clin Microbiol* 2623:47, 2009.

Kempf M, Bakour S, Flaudrops C, et al.: Rapid detection of carbapenem resistance in Acinetobacter baumannii using matrix-assisted laser desorption ionization-time of flight mass spectrometry, *PloS One* 7, 2012. e31676.

Kimura K, Suzuki S, Wachino J, et al.: First molecular characterization of Group B streptococci with reduced penicillin susceptibility, *Antimicrob Agents Chemother* 2890:52, 2008.

Kos VN, Deraspe M, McLaughlin RE, et al.: The resistome of Pseudomonas aeruginosa in relationship to phenotypic susceptibility, *Antimicrob Agents Chemother* 59:427e36, 2015.

Kumar A, Roberts D, Wood KE, et al.: Duration of hypotension before initiation of effective antimicrobial therapy is the critical determinant of survival in human septic shock, *Crit Care Med* 34, 2006. 1589.

Labbé AC, Poirier L, Maccannell D, et al.: Clostridium difficile infections in a Canadian tertiary care hospital before and during a regional epidemic associated with the BI/NAP1/027 strain, *Antimicrob Agents Chemother* 3180:52, 2008.

Lasko MJ, Nicolau DP: Carbapenem-resistant Enterobacterales: considerations for treatment in the Era of new antimicrobials and evolving Enzymology, *Curr Infect Dis Rep* 22(3):6, 2020 Feb 7, https://doi.org/10.1007/s11908-020-0716-3.

Leclercq R, Canton R, Brown D, et al.: EUCAST expert rules in antimicrobial susceptibility testing, *Clin Microbiol Infect* 19:141–160, 2013.

Liao CH, Sheng WH, Chen YC, et al.: Predictive value of the serum bactericidal test for mortality in patients infected with multidrug-resistant Acinetobacter baumannii, *J Infect* 149(55), 2007.

Liesenfeld O, Lehman L, Hunfeld KP, et al.: Molecular diagnosis of sepsis: new aspects and recent developments, *Eur J Microbiol Immunol (Bp)* 4:1–25, 2014.

Ligozzi M, Bernini C, Bonora MG, et al.: Evaluation of the VITEK 2 system for identification and antimicrobial susceptibility testing of medically relevant Gram-positive cocci, *J Clin Microbiol* 1681:40, 2002.

Liu YY, Wang Y, Walsh TR, et al.: Emergence of plasmid-mediated colistin resistance mechanism MCR-1 in animals and human beings in China: a microbiological and molecular biological study, *Lancet Infect Dis* 16:161e8, 2016.

Livermore DM, Andrews JM, Hawkey PM, et al.: Are susceptibility tests enough, or should laboratories still seek ESBLs and carbapenemases directly? *J Antimicrob Chemother* 67:1569–1577, 2012, https://doi.org/10.1093/jac/dks088.

Louie L, Matsumura SO, Choi E, et al.: Evaluation of three rapid methods for detection of methicillin resistance in Staphylococcus aureus, *J Clin Microbiol* 38, 2000. 2170.

Lupo A, Papp-Wallace KM, Sendi P, et al.: Non-phenotypic tests to detect and characterize antibiotic resistance mechanisms in Enterobacteriaceae, *Diagn Microbiol Infect Dis* 77:179–194, 2013.

Maraskolhe DL, Deotale VS, Mendiratta DK, Narang P: Comparision of three laboratory tests for detection of AmpC β lactamases in Klebsiella species and E. Coli, *J Clin Diagn Res* 8(6):DC05–DC8, 2014, https://doi.org/10.7860/JCDR/2014/8256.4432.

Maugeri G, Lychko I: Identification and antibiotic-susceptibility profiling of infectious bacterial agents: a review of current and future trends, *Biotechnol J* 14(1), 2019. e1700750.

McEwan AS, Derome A, Meunier D, et al.: Evaluation of the NucliSENS EasyQ KPC assay for detection of Klebsiella pneumoniae carbapenemase-producing Enterobacteriaceae, *J Clin Microbiol* 51:1948–1950, 2013.

McWilliams CS, Condon S, Schwartz RM, et al.: Incidence of extended-spectrum-β-lactamase-producing Escherichia coli and Klebsiella pneumoniae isolates that test susceptible to cephalosporins and aztreonam by the revised CLSI breakpoints, *J Clin Microbiol* 52:2653–2655, 2014.

Mehta SR, Estrada J, Ybarra J, et al.: Comparison of the BD MAX MRSA XT to the Cepheid™ Xpert® MRSA assay for the molecular detection of methicillin-resistant Staphylococcus aureus from nasal swabs, *Diagn Microbiol Infect Dis* 87(4):308–310, 2017, https://doi.org/10.1016/j.diagmicrobio.2016.12.011.

Mendes RE, Sader HS, Castanheira M, et al.: Distribution of main Gram-positive pathogens causing bloodstream infections in United States and European hospitals during the SENTRY Antimicrobial Surveillance Program (2010-2016): concomitant analysis of oritavancin in vitro activity, *J Chemother* 30(5):280–289, 2018, https://doi.org/10.1080/1120009X.2018.1516272.

Mendes RE, Watters AA, Rhomberg PR, et al.: Performance of BD Max StaphSR for screening of methicillin-resistant Staphylococcus aureus isolates among a Contemporary and diverse collection from 146 institutions located in nine U.S. Census regions: prevalence of mecA dropout Mutants, *J Clin Microbiol* 54(1):204–207, 2016, https://doi.org/10.1128/JCM.02047-15.

Moland ES, Hanson ND, Black JA: Prevalence of newer β-lactamases in gram-negative clinical isolates collected in the United States from 2001 to 2002, *J Clin Microbiol* 3318:44, 2006.

Morrissey I, Bouchillon SK, Hackel M, et al.: Evaluation of the Clinical and Laboratory Standards Institute phenotypic confirmatory test to detect the presence of extended-spectrum β-lactamases from 4005 Escherichia coli, Klebsiella oxytoca, Klebsiella pneumoniae and Proteus mirabilis isolates, *J Med Microbiol* 63(Pt 4):556–561, 2014.

Munier GK, Johnson CL, Snyder JW, et al.: Positive extended-spectrum-b-lactamase (ESBL) screening results may be due to AmpC b-lactamases more often than to ESBLs, *J Clin Microbiol* 48:673–674, 2010.

National Committee for Clinical Laboratory Standards: *Methodology for the serum bactericidal test; Approved guideline*, Wayne, Pa., 1999b, CLSI document M21-A. CLSI.

National Committee for Clinical Laboratory Standards: *Methods for determining bactericidal activity of antimicrobial agents; approved guideline*, Wayne, Pa., 1999a, CLSI document M26-A. CLSI.

Nguyen M, Brettin T, Long SW, et al.: Developing an in silico minimum inhibitory concentration panel test for Klebsiella pneumoniae, *Sci Rep* 8:421–18972, 2018, https://doi.org/10.1038/s41598-017-18972-w.

Nguyen M, Long SW, McDermott PF, et al.: Using machine learning to predict antimicrobial MICs and associated genomic features for nontyphoidal salmonella, *J Clin Microbiol* 57, 2019 e01260-18, https://doi.org/10.1128/JCM.01260-18.

Nguyen MH, Yu VL, Morris AJ, et al.: Antimicrobial resistance and clinical outcome of Bacteroides bacteremia: findings of a multicenter prospective observational trial, *Clin Infect Dis* 870:30, 2000.

Nordmann P, Poirel L, Dortet L: Rapid detection of carbapenemase-producing Enterobacteriaceae, *Emerg Infect Dis* 18:1503–1507, 2012.

Pakyz AL, MacDougall C, Oinonen M, et al.: Trends in antibacterial use in US academic health centers: 2002 to 2006, *Arch Intern Med* 2254:168, 2008.

Pakyz AL, Oinonen M, Polk RE: Relationship of carbapenem restriction in 22 university teaching hospitals to carbapenem use and carbapenem-resistant Pseudomonas aeruginosa, *Antimicrob Agents Chemother* 53:2009, 1983.

Pancholi P, Carroll KC, Buchan BW, et al.: Multicenter evaluation of the Accelerate PhenoTest BC kit for rapid identification and phenotypic antimicrobial susceptibility testing using morphokinetic cellular analysis, *J Clin Microbiol* 56, 2018. e01329-17.

Park C, Nichols M, Schrag SJ: Two cases of invasive vancomycin-resistant group B streptococcus infection, *N Engl J Med* 370(9):885–886, 2014, https://doi.org/10.1056/NEJMc1308504.

Patel M, Waites KB, Moser SA, et al.: Prevalence of inducible clindamycin resistance among community- and hospital-associated Staphylococcus aureus isolates, *J Clin Microbiol* 2481:44, 2006.

Paterson DL, Bonomo RA: Extended-spectrum β-lactamases: a clinical update, *Clin Microbiol Rev* 657:18, 2005.

Peter-Getzlaff S, Polsfuss S, Poledica M, et al.: Detection of AmpC beta-lactamase in Escherichia coli: comparison of three phenotypic confirmation assays and genetic analysis, *J Clin Microbiol* 49:2924–2932, 2011.

Petersen LR, Shanholtzer CJ: Tests for bactericidal effects of antimicrobial agents: technical performance and clinical relevance, *Clin Microbiol Rev* 420(5), 1992.

Pierce VM, Simner PJ, Lonsway DR, et al.: Modified carbapenem inactivation method for phenotypic detection of carbapenemase production among Enterobacteriaceae, *J Clin Microbiol* 55:2321–2333, 2017, https://doi.org/10.1128/JCM.00193-17.

Polsfuss S, Bloemberg GV, Giger J, et al.: Comparison of European Committee on Antimicrobial. Susceptibility Testing (EUCAST) and CLSI screening parameters for the detection of extended-spectrum β-lactamase production in clinical Enterobacteriaceae isolates, *J Antimicrob Chemother* 67:159–166, 2012.

Polsfuss S, Bloemberg GV, Giger J, et al.: Practical approach for reliable detection of AmpC beta-lactamase-producing Enterobacteriaceae, *J Clin Microbiol* 49(8):2798–2803, 2011, https://doi.org/10.1128/JCM.00404-11.

Prabhu RM, Piper KE, Baddour LM, et al.: Antimicrobial susceptibility patterns among viridans group streptococcal isolates from infective endocarditis patients 1971 to 1986 and 1994 to 2002, *Antimicrob Agents Chemother* 4463:48, 2004.

Prabhu RM, Piper KE, Litzow MR, et al.: Emergence of quinolone resistance among viridans group streptococci isolated from the oropharynx of neutropenic peripheral blood stem cell transplant patients receiving quinolone antimicrobial prophylaxis, *Eur J Clin Microbiol Infect Dis* 832:24, 2005.

Puttaswamy S, Gupta SK, Regunath H, et al.: A comprehensive review of the present and future antibiotic susceptibility test (AST) systems, *Arch Clin Microbiol* 9(3):83, 2018.

Richter SS, Heilman KP, Beekmann SE, et al.: Macrolide-resistant Streptococcus pyogenes in the United States, 2002-2003, *Clin Infect Dis* 599:41, 2005.

Richter SS, Howard WJ, Weinstein MP, et al.: Multicenter evaluation of the BD Phoenix automated microbiology system for antimicrobial susceptibility testing of Streptococcus species, *J Clin Microbiol* 2863:45, 2007.

Riedel S, Neoh KM, Eisinger SW, et al.: Comparison of commercial antimicrobial susceptibility test methods for testing of Staphylococcus aureus and Enterococci against vancomycin, daptomycin, and linezolid, *J Clin Microbiol* 52:2216–2222, 2014.

Robberts F, Kohner P, Patel R: Unreliable extended-spectrum β-lactamase detection in the presence of plasmid-mediated AmpC in Escherichia coli clinical isolates, *J Clin Microbiol* 47:358–361, 2009.

Rybak MJ, Vidaillac C, Sader HS, et al.: Evaluation of vancomycin susceptibility testing for methicillin-resistant Staphylococcus aureus: comparison of Etest and three automated testing methods, *J Clin Microbiol* 51(7):2077–2081, 2013, https://doi.org/10.1128/JCM.00448-13.

Sakoulas G, Gold HS, Venkataraman L, et al.: Methicillin-resistant Staphylococcus aureus: comparison of susceptibility methods and analysis of mecA-positive susceptible strains, *J Clin Microbiol* 3946:39, 2001.

Sękowska A, Bogiel T, Gospodarek-Komkowska E: Evaluation of eazyplex® SuperBug CRE test for beta-lactamase genes detection in Klebsiella spp. and P. aeruginosa strains, *Curr Microbiol* 77(1):99–103, 2020, https://doi.org/10.1007/s00284-019-01806-5.

Sekyere JO, Govinden U, Essack SY: Review of established and innovative detection methods for carbapenemase–producing Gram–negative bacteria, *JALM* 119(5):1219–1233, 2015.

Sfeir MM, Hayden JA, Fauntleroy KA, et al.: EDTA-modified carbapenem inactivation method: a phenotypic method for detecting metallo-β-lactamase-producing Enterobacteriaceae, *J Clin Microbiol* 57(5), 2019, e01757-18, https://doi.org/10.1128/JCM.01757-18.

Sherris JC: Problems in the in vitro determination of antibiotic tolerance, *Antimicrob Agents Chemother* 633:30, 1986.

Silbert S, Gostnell A, Kubasek C, et al.: Evaluation of the BD Max StaphSR assay for detecting methicillin-resistant Staphylococcus aureus (MRSA) and methicillin-susceptible S. aureus (MSSA) in ESwab-collected wound samples, *J Clin Microbiol* 55(9):2865–2867, 2017, https://doi.org/10.1128/JCM.00641-17.

Smith KP, Brennan-Krohn T, Weir S, et al.: Improved accuracy of cefepime susceptibility testing for extended-spectrum beta-lactamase-producing Enterobacteriaceae with an on-demand digital dispensing method, *J Clin Microbiol* 55:470–478, 2017.

Smith KP, Kirby JE: The inoculum effect in the Era of multidrug resistance: Minor differences in inoculum have dramatic effect on MIC determination, *Antimicrob Agents Chemother* 62(8), 2018, e00433-18. Published 2018 Jul 27, https://doi.org/10.1128/AAC.00433-18.

Snydman DR, Jacobus NV, McDermott LA, et al.: Update on resistance of Bacteroides fragilis group and related species with special attention to carbapenems 2006-2009, *Anaerobe* 17:147–151, 2011.

Spanu T, Fiori B, D'Inzeo T, et al.: Evaluation of the New NucliSENS EasyQ KPC test for rapid detection of Klebsiella pneumoniae carbapenemase genes (blaKPC), *J Clin Microbiol* 50(8):2783–2785, 2012, https://doi.org/10.1128/JCM.00284-12.

Stamper PD, Cai M, Lema C, et al.: Comparison of the BD GeneOhm VanR assay to culture for identification of vancomycin-resistant enterococci in rectal and stool specimens, *J Clin Micro* 3360:45, 2007.

Stoesser N, Batty EM, Eyre DW, et al.: Predicting antimicrobial susceptibilities for Escherichia coli and Klebsiella pneumoniae isolates using whole genomic sequence data, *J Antimicrob Chemother* 68, 2013. 2234e44.

Stuart JC, Leverstein-van Hall MA: Dutch working party on the detection of highly resistant Microorganisms: guideline for phenotypic screening and confirmation of carbapenemases in Enterobacteriaceae, *Int J Antimicrob Agents* 36:205–210, 2010.

Sullivan KV, Deburger B, Roundtree SS, et al.: Pediatricmulticenter evaluation of the Verigene gram-negative blood culture test for rapid detection of inpatientbacteremia involving gram-negative organisms, extended-spectrum beta-lactamases, and carbapenemases, *J Clin Microbiol* 52:2416–2421, 2014.

Suzuki S, Horinouchi T, Furusawa C: Prediction of antibiotic resistance by gene expression profiles, *Nat Commun* 5:5792, 2014.

Swenson JM, Anderson KF, Lonsway DR, et al.: Accuracy of commercial and reference susceptibility testing methods for detecting vancomycin-intermediate Staphylococcus aureus, *J Clin Microbiol* 47:2009, 2013.

Swenson JM, Williams PP, Kilgore G, et al.: Performance of eight methods, including two rapid methods for detection of oxacillin resistance in a challenge set of Staphylococcus aureus organisms, *J Clin Microbiol* 3785:39, 2001.

Tamma PD, Goodman KE, Harris AD, et al.: Comparing the outcomes of patients with carbapenemase-producing and non-carbapenemase-producing carbapenem-resistant Enterobacteriaceae bacteremia, *Clin Infect Dis* 64:257–264, 2016.

Tamma PD, Doi Y, Bonomo RA, et al.: Antibacterial resistance Leadership group . A primer on AmpC β-lactamases: necessary knowledge for an increasingly multidrug-resistant world, *Clin Infect Dis* 69(8):1446–1455, 2019, https://doi.org/10.1093/cid/ciz173.

Tamma PD, Han JH, Rock C, et al.: Carbapenem therapy is associated with improved survival compared with piperacillin-tazobactam for patients with extended-spectrum β-lactamase bacteremia, *Clin Infect Dis* 60(9):1319–1325, 2015, https://doi.org/10.1093/cid/civ003.

Tamma PD, Opene BNA, Gluck A, et al.: 11 A comparison of eleven phenotypic assays for the accurate detection of carbapenemase-producing Enterobacteriaceae, *J Clin Microbiol*, 2017b, https://doi.org/10.1128/JCM.02338-16.

Tamma PD, Rodriguez-Baño J: The Use of Noncarbapenem β-lactams for the treatment of extended-spectrum β-lactamase infections, *Clinical Infectious Diseases 2017* 64(7):972–980, TAMMA, 2017a.

Tamma PD, Simner PJ: Phenotypic detection of carbapenemase-producing organisms from clinical isolates, *J Clin Microbiol* 56, 2018, e01140-18, https://doi.org/10.1128/JCM.01140-18. e01140-18.

Tenover FC, Moellering RC: The rationale for revising the clinical and laboratory standards institute vancomycin minimal inhibitory concentration interpretive criteria for Staphylococcus aureus, *Clin Infect* 44, 2007. Dis1208.

Thomson KS, Robledo IE, Vazquez GJ, et al.: KPC screening by updated BD Phoenix and Vitek 2 automated systems, *J Clin Microbiol* 49:3386–3387, 2011.

Thomson KS: The immaculate carbapenemase study, *J Clin Microbiol* 55:1608–1611, 2017, https://doi.org/10.1128/JCM.00430-17.

Thomson KS: Extended-spectrum beta-lactamase, AmpC, and carbapenemase issues, *J Clin Microbiol* 48:1019–1025, 2010.

Tomic V, Dowzicky MJ: Regional and global antimicrobial susceptibility among isolates of Streptococcus pneumoniae and Haemophilus influenzae collected as part of the Tigecycline Evaluation and Surveillance Trial (T.E.S.T.) from 2009 to 2012 and comparison with previous years of T.E.S.T. (2004-2008), *Ann Clin Microbiol Antimicrob* 13:52, 2014.

Tsakris A, Kristo I, Poulou A, et al.: Evaluation of boronic acid disk tests for differentiating KPC-possessing Klebsiella pneumoniae isolates in the clinical laboratory, *J Clin Microbiol* 362:47, 2009.

Valiquette L, Cossette B, Garant MP, et al.: Impact of reduction in the use of high-risk antibiotics on the course of an epidemic of Clostridium difficile-associated disease caused by the hypervirulent NAP1/027 strain, *Clin Infect Dis* 45(Suppl 2):S112, 2007.

Walters M, Lonsway D, Rasheed K, et al.: Investigation and control of vancomycin-resistant Staphylococcus aureus: a guide for health Departments and infection control personnel. Atlanta, GA 2015. Available at http://www.cdc.gov/hai/pdfs/VRSA-Investigation-Guide-05_12_2015.pdf.

Walther-Rasmussen J: Høiby N: class A carbapenemases, *J Antimicrob Chemother* 470:60, 2007.

Weiner LM, Webb AK, Limbago B, et al.: Antimicrobial-resistant pathogens associated with Healthcare-associated infections: summary of data reported to the national Healthcare safety Network at the centers for disease control and prevention, 2011-2014, *Infect Control Hosp Epidemiol* 37(11):1288–1301, 2016, https://doi.org/10.1017/ice.2016.174.

Weinstein RA, Singh K: Laboratory-acquired infections, *Clin Infect Dis* 49(1):142–147, 2009, https://doi.org/10.1086/599104.

Whitley V, Kircher S, Gill T, et al.: Multicenter evaluation of the BD Phoenix CPO detect test for detection and classification of carbapenemase-producing organisms in clinical isolates, *J Clin Microbiol* 58(5), 2020, e01752-19. https://doi.org/10.1128/JCM.01752-19.

Wolk DM, Struelens MJ, Pancholi P, et al.: Rapid detection of Staphylococcus aureus and methicillin-resistant S. aureus (MRSA) in wound specimens and blood cultures: multicenter preclinical evaluation of the Cepheid Xpert/SA skin and soft tissue and blood culture assays, *J Clin Microbiol* 823:47, 2009.

World Health Organization (WHO): Antimicrobial resistance global report on surveillance, 2014b Available at http://apps.who.int/iris/bitstream/10665/112642/1/9789241564748_eng.pdf?ua=1, ISBN 978 92 4 156474 8.

World Health Organization (WHO): WHONET software. 2006 Available at https://www.who.int/medicines/areas/rational_use/AMR_WHONET_SOFTWARE/en/.

Wu W, Feng Y, Tang G, et al.: NDM metallo-β-lactamases and their bacterial producers in health care settings, *Clin Microbiol Rev* 32(2), 2019, e00115-18. Published 2019 Jan 30, https://doi.org/10.1128/CMR.00115-18.

Zapantis A, Lacy MK, Horvat RT, et al.: Nationwide antibiogram analysis using NCCLS M39-A guidelines, *J Clin Microbiol* 2629:43, 2005.

Zhang SX, Carroll KC, Lewis S, et al.: Multicenter evaluation of a PCR-based digital Microfluidics and electrochemical detection system for the rapid identification of 15 fungal pathogens directly from positive blood cultures, *J Clin Microbiol* 58(5), 2020, e02096-19. Published 2020 Apr 23, https://doi.org/10.1128/JCM.02096-19.

Zhang Z, Chen M, Yu Y, Pan S, Liu Y: Antimicrobial susceptibility among Streptococcus pneumoniae and Haemophilus influenzae collected globally between 2015 and 2017 as part of the Tigecycline Evaluation and Surveillance Trial (TEST), *Infect Drug Resist* 12:1209–1220, 2019.

Zhou X, Arends JP, Kampinga GA, et al.: Evaluation of the Xpert vanA/vanB assay using enriched inoculated broths for direct detection of vanB vancomycin-resistant Enterococci, *J Clin Microbiol* 52:4293–4297, 2014.

Zouheir Y, Atany T, Boudebouch N: Emergence and spread of resistant N. meningitidis implicated in invasive meningococcal diseases during the past decade (2008–2017), *J Antibiot* 72:185–188, 2019, https://doi.org/10.1038/s41429-018-0125-0.

CHAPTER 59

MYCOBACTERIA

Kyle G. Rodino, Gail L. Woods, Nancy L. Wengenack

MYCOBACTERIUM TUBERCULOSIS COMPLEX, 1183

NONTUBERCULOUS MYCOBACTERIA, 1184
Mycobacterium Avium Complex, 1185
Mycobacterium Genavense, 1185
Mycobacterium Gordonae, 1185
Mycobacterium Haemophilum, 1185
Mycobacterium Kansasii, 1185
Mycobacterium Marinum, 1185
Mycobacterium Ulcerans, 1186
Mycobacterium Xenopi, 1186
Rapidly Growing Mycobacteria, 1186
Mycobacterium Leprae, 1186

TESTING FOR LATENT M. TUBERCULOSIS INFECTION, 1187

LABORATORY DIAGNOSIS, 1187
Specimens, 1187
Microbial Stains, 1188
Culture Methods, 1189
Tests For Identification of Mycobacteria, 1190
Susceptibility Testing, 1191

TREATMENT, 1192

PREVENTION, 1192
Mycobacterium Tuberculosis Complex, 1192
Mycobacterium Avium Complex, 1192

SELECTED REFERENCES, 1193

KEY POINTS

- The *Mycobacterium tuberculosis* complex is of public health importance because it is transmitted from person to person.
- The Mantoux skin test and interferon-γ release assays are useful for identifying persons with latent *M. tuberculosis* infection.
- For optimal detection of mycobacteria in clinical specimens, laboratories should use a fluorochrome stain and liquid culture system with a concomitant solid medium for culture.
- Nucleic acid amplification testing for direct detection of *M. tuberculosis* complex should be performed on respiratory specimens from patients with suspected tuberculosis.
- Susceptibility testing to the primary antituberculous agents (isoniazid, rifampin, ethambutol, and pyrazinamide) should be performed on all initial isolates of *M. tuberculosis* complex.
- Infections caused by nontuberculous mycobacteria are acquired from the environment (e.g., water).
- The nontuberculous mycobacteria most commonly encountered in the clinical laboratory are *Mycobacterium avium* complex, which causes pulmonary disease and, in immunocompromised patients, disseminated disease; the rapidly growing mycobacteria *M. chelonae* complex, *M. abscessus* complex and *M. fortuitum* group, which most often cause skin and soft-tissue infections; *M. kansasii*, which causes pulmonary infection; and *M. marinum*, which causes skin and soft-tissue infections.
- Molecular tests are the standard for identification of mycobacteria and an important adjunct to phenotypic methods for susceptibility testing of the *M. tuberculosis* complex.

Mycobacteria are aerobic, nonmotile, acid alcohol–fast, slightly curved or straight bacilli. The organisms contain high-molecular-weight (60–90 carbons) mycolic acids in their cell walls that on pyrolysis release C22 to C26 straight-chain saturated long-chain acids. Their guanine plus cytosine deoxyribonucleic acid (DNA)–based content ratios are in the range of 62 to 70 mol%. Mycobacteria can be divided into two groups: those in the *M. tuberculosis* complex and nontuberculous mycobacteria.

MYCOBACTERIUM TUBERCULOSIS COMPLEX

The tubercle bacilli that make up the *M. tuberculosis* complex (MTBC) include *M. tuberculosis*, *M. bovis*, *M. bovis* Bacille Calmette-Guérin strain (BCG), *M. caprae*, *M. pinnipedii*, *M. africanum*, *M. microti*, and *M. canettii*. The species that most commonly infects humans is *M. tuberculosis*. *M. bovis*, which infects many warm-blooded animals (e.g., cattle, dogs, cats, pigs, badgers, deer, elk, and some birds) as well as primates and humans, is responsible for a small fraction of tuberculosis (TB) cases today. *M. bovis* BCG is used for vaccine purposes in many countries outside the United States. It also is administered intravesically to induce immunostimulation against bladder cancer and, in such situations, rarely may cause disseminated disease. *M. africanum* causes TB in humans in tropical Africa but has been reported elsewhere, including the United States, primarily in persons who had lived in Africa. *M. caprae* predominantly infects goats, but also infects cattle and, rarely, humans (Kubica et al., 2003). *M. microti* was originally isolated from rodents but has caused TB in other warm-blooded animals and, rarely, in humans (Emmanuel et al., 2007). *M. canettii* was first collected in 1969 by Georges Canetti; it was recognized many years later as having the potential to cause disease in humans (Castets et al., 1968; Van Soolingen et al., 1997; Pfyffer, 1998). The natural host of *M. pinnipedii* is sea lions, but it can infect other animals and apparently may be transmitted to humans (Kiers et al., 2008).

Each year, the World Health Organization (WHO) issues the Global Tuberculosis Report, providing an update on the worldwide TB epidemic (World Health Organization, 2018). The 2018 report estimated 10 million (range, 9.0–11.1 million) new cases of TB: 1.0 million in children, 3.2 million in women, and 5.8 million in men. An estimated 558,000 of these cases (5%) were multidrug-resistant TB (MDR-TB), which is defined as resistance to at least isoniazid and rifampin. Two thirds of all cases were in eight countries: India (27%), China (9%), Indonesia (8%), the Philippines (6%), Pakistan (5%), Nigeria (4%), Bangladesh (4%), and South Africa (3%). Only 3% of cases occurred in the WHO European Region and 3% occurred in the WHO Region of the Americas. An estimated 1.6 million deaths were attributed to TB in 2017, with 300,000 of those occurring in the HIV-positive population. While the global burden of TB remains significant, the global incidence, absolute number of TB deaths, and TB mortality rate have all decreased since 2000 (World Health Organization, 2018).

In the United States, TB was the leading cause of death at the turn of the 20th century. Mortality then decreased, initially because of public health efforts and later because of the availability of antituberculous drugs. Between 1953, when TB became notifiable on a national basis, and 1984, the incidence of TB steadily decreased (Rieder, 1989). From 1985 to 1992, a resurgence of TB cases was seen, in large part because of the spread of the human immunodeficiency virus (HIV), deterioration of the health care infrastructure, and an increase in the number of cases reported among foreign-born persons. In addition to the resurgence, MDR-TB emerged and remains a concern, although to a much lesser degree than in developing countries. Since 1992, the incidence of TB in the United States has declined each year and MDR-TB has become uncommon (Alami et al., 2014). In 2018, the Centers for Disease Control and Prevention (CDC) received report of 9029 new cases of TB in the United States, down 5.9% from the 9588 cases in 2013 (Talwar et al., 2018). The 2018 national incidence was 2.8 cases per 100,000 persons, with the highest incidence reported in Alaska (8.5) and the lowest in Wyoming (0.2). California, Florida, New York, and Texas are home to more than half of the TB cases in the country (Talwar et al., 2018). Of the 9029 TB cases in 2018, two thirds occurred in individuals born outside the United States, with persons of Asian origin having the highest incidence. For U.S.-born persons, the populations at highest risk for TB included the homeless,

residents of correctional facilities, and residents of long-term care facilities. TB drug susceptibility data, available from 2017, showed 1.9% of U.S. TB cases classified as MDR-TB (Talwar et al., 2018).

Tubercle bacilli are transmitted primarily via inhalation of dried residues of small infectious droplets (1–10 μm in diameter). Infection also may be acquired by direct inoculation of abraded skin—an event most likely to occur when pathologists or other laboratory personnel handle infected tissues. In addition, *M. bovis* may be transmitted from cattle to humans by drinking contaminated raw milk or by respiratory exposure to live infected cattle or their carcasses, from humans to cattle via exposure to urine from persons with urinary tract infections due to *M. bovis*, and from cattle and wild reservoirs to cattle, probably by respiratory secretions.

The most important source of infection is an undiagnosed person with cavitary, sputum smear–positive pulmonary disease. The risk for active pulmonary disease is low after one exposure to the organism but increases under conditions of stress or in a confined environment where repeated exposures to the organism occur. Most persons who become infected with *M. tuberculosis* do not develop active disease. The lifetime risk for developing active disease is 5% to 10% for immunocompetent persons. For persons infected with both MTBC and HIV, in contrast, the risk for developing TB is 7% to 10% per year.

Persons at increased risk for MTBC infection are close contacts of those with known or suspected active TB, foreign-born persons from an area with a high incidence of active TB (e.g., Asia, Africa), persons who visit a country with a high prevalence of active TB, residents and employees of congregate settings whose clients are at increased risk for active TB (e.g., correctional facilities, homeless shelters), health care workers who care for patients at increased risk for active TB, and persons who abuse drugs or alcohol. Factors that increase the risk for progression of infection to active TB include HIV infection, age younger than 5 years, immunosuppressive therapy, infection with MTBC within the past 2 years, history of inadequately treated active TB, silicosis, diabetes mellitus, chronic renal failure, various cancers, gastrectomy or jejunoileal bypass, weight <90% of ideal body weight, cigarette smoking, and abuse of drugs and/or alcohol.

Based on analysis of its genomic sequence, *M. tuberculosis* does not appear to encode typical bacterial virulence factors (e.g., toxins). However, certain genes and gene products have been identified as key factors enabling *M. tuberculosis* to cause disease. PhoP, a transcription regulator, has been shown to have an important role in virulence because phoP mutants grow very poorly in macrophages and in mice (Ryndak et al., 2008). Phthiocerol dimycocerosates, which are lipids found at the outermost layers of the cell envelope, are required for optimal multiplication and persistence of *M. tuberculosis* in mice lungs, and phenolic glycolipids are thought to be involved in the hypervirulence of certain *M. tuberculosis* strains (Gordon et al., 2009). In addition, the ESX secretion systems, which are specialized secretion systems present in many gram-positive bacteria, are important in pathogenesis because mutants lacking the system or its substrates are attenuated in cultured macrophages and animal models of infection. Mutants with a deletion spanning much of the ESX-1 locus demonstrate defective cell-to-cell spread, altered cytokine profiles, and failure to inhibit phagolysosome fusion in cultured cells (Tobin & Ramakrishnan, 2008).

The usual host response to infection with MTBC is activation of the cell-mediated immune system. During primary (initial) infection, inhaled bacilli travel to the alveolar spaces, where they are ingested by resident macrophages. These macrophages are unable to kill the tubercle bacilli, which multiply intracellularly during the first several days after infection. Macrophages infected with mycobacteria migrate to regional tracheobronchial lymph nodes and present sensitizing antigen(s) to immunocompetent T cells or they enter the lymphatics and blood and travel back to the lungs (primarily the apices) and to distant organs such as lymph nodes, kidneys, epiphyseal areas of the long bones, vertebral bodies, and meninges, where bacilli continue to multiply until the cellular immune response is activated.

Immunocompetent T cells migrate from regional lymph nodes to the site of infection in the lung. There, they release chemotactic, migration-inhibitory, and mitogenic cytokines, which stimulate recruitment of blood-derived monocytes and lymphocytes, macrophage and lymphocyte division, and macrophage activation. Activated macrophages have enhanced microbicidal activity and produce cytokines such as interleukin-1, interferon-γ, and tumor necrosis factor, which stimulate or regulate other components of the immune system, properties that help control infection. The cytokines and lytic enzymes released by the macrophages also contribute to concomitant local tissue destruction. Over time, the activated T-cell population declines and is replaced by long-lived memory immune T cells, which protect against reinfection with MTBC and provide some cross-protection against infection with other mycobacteria. Despite the limitation of further mycobacterial multiplication in primary and metastatic foci by the activated macrophages and memory T cells, a residual nidus of infection remains indefinitely in the lung (most frequently in the apex, where the oxygen tension is high) and less often in distant sites. Therefore, the potential for reactivation of disease in these quiescent foci exists during periods of immunosuppression.

The primary focus of pulmonary infection, called the *Gohn lesion*, is usually subjacent to the pleura in the lower part of the upper lobes or in the upper part of the lower lobes of one lung, corresponding to areas of the lung that receive the greatest volume flow of inspired air. Lesions (tubercles) are well-circumscribed, 1- to 2-cm–diameter areas of grayish-white consolidation with soft to necrotic centers. Similar-appearing tubercles typically are found in the regional tracheobronchial lymph nodes; these plus the primary lung lesion are termed the *Gohn complex*. Microscopically, tubercles are composed of well-circumscribed caseating or noncaseating granulomas; organisms may be seen in sections stained with an acid-fast stain. Over time, these lesions are replaced by hyalinized fibrous tissue and eventually calcify. Lesions of miliary tuberculosis are small (one to several millimeters in diameter), distinct, yellow-white areas of consolidation without gross caseation that histologically resemble tubercles. The ability to form granulomas depends on the immunocompetence of the host. Individuals infected with HIV, for example, may have extensive necrosis, many neutrophils, microabscesses, and numerous acid-fast bacilli (AFB), without granulomas.

In the United States, pulmonary TB accounts for about 80% of cases of active disease. The clinical presentation may be insidious, with gradual onset of constitutional symptoms over months: catarrhal, with productive cough often attributed to a bad cold or lingering bronchitis; pneumonia- or flu-like, with high fever, aches and pains, and cough; hemoptoic, with acute-onset of blood-streaked sputum; or pleuritic. Extrapulmonary TB may be localized but more commonly involves multiple organs with or without concurrent lung infection. Multiorgan TB occurs predominantly in infants and young children, older adults, and immunocompromised individuals, especially those infected with both HIV and MTBC. Additionally, most infections with *M. bovis* in the United States are extrapulmonary, involving lymph nodes, the gastrointestinal tract, bones, and kidneys, and most commonly occur in children of Hispanic ethnicity (Hlavsa Michele et al., 2008; Rodwell et al., 2008). Infrequently, infection follows intravesical instillation of *M. bovis* BCG for treatment of superficial bladder carcinoma (Lamm et al., 1992; Kristjansson et al., 1993).

TABLE 59.1
Runyon's Classification of the Nontuberculous Mycobacteria

Classification	Description of Colonies
Photochromogen	Not pigmented unless exposed to light (optimally during their early growth and with good aeration of the surface)
Scotochromogen	Pigmented when grown in the dark and in light
Nonchromogen	Not pigmented when grown in the dark or in light
Rapid grower	Growth on solid media in ≤7 days

NONTUBERCULOUS MYCOBACTERIA

The nontuberculous mycobacteria (NTM; also called *mycobacteria other than tubercle bacilli*) may be categorized on the basis of colony pigmentation before and after exposure to light and growth rate on a solid medium as described by Runyon in 1959 (Table 59.1) (Runyon, 1959). This classification system, however, has limits. For example, *M. kansasii* is usually a photochromogen but rarely is nonchromogenic or scotochromogenic. Members of the *M. avium* complex are nonchromogenic in Runyon's scheme, but some isolates produce slightly pigmented colonies after prolonged incubation, potentially causing incorrect classification as a scotochromogen. *M. szulgai* is a scotochromogen at 37°C and a photochromogen at 25°C. Moreover, when a liquid medium is used for mycobacterial culture, as is currently recommended (discussed in the section regarding culture methods), growth rates used by Runyon for classification do not apply. *M. leprae* is unique among mycobacteria by virtue of the fact that it has not yet been cultivated in vitro.

In general, little is known about the antigens associated with virulence of the NTM, and the immune response to infection with these mycobacteria is poorly understood. With current molecular techniques, nearly 200 species of NTM have been identified. Select potential pathogens are reviewed in the following sections. An extensive description of the more recently described and infrequently isolated mycobacteria is found in the excellent review by Tortoli (Tortoli, 2003).

MYCOBACTERIUM AVIUM COMPLEX

The *M. avium* complex (MAC) is a heterogeneous group of mycobacteria classically composed of two taxa: *M. avium*, which clinically appears to be the more important pathogen in disseminated disease, and *M. intracellulare*, which appears to be more important in respiratory disease. However, with the availability of molecular tools, new species and subspecies have been discovered. Currently, the species *M. avium* consists of three subspecies: subsp. *avium*, subsp. *silvaticum*, and subsp. *paratuberculosis*. Other species in the complex are *M. ariosiense*, *M. bouchedurhonense*, *M. chimaera*, *M. colombiense*, *M. marseillense*, *M. paraintracellulare*, *M. timonense*, *M. vulneris*, and *M. yongonense*. These species have such similar growth characteristics and biochemical reactions that they often are not distinguished in the clinical microbiology laboratory; isolates commonly are reported as MAC. Should species identification be required, molecular methods can be utilized.

MAC bacilli are ubiquitous in the environment. They have been isolated from water, soil, food, house dust, and several animals. However, the specific environmental sources responsible for human infection are not known (Inderlied et al., 1993; Falkinham, 1996). The most likely portal of entry is the gastrointestinal tract, but transmission via the respiratory tract is also possible. From sites of colonization, organisms enter the blood and infect many organs, especially those of the monocyte-macrophage system. In many clinical microbiology laboratories in the United States today, MAC is the most frequently isolated mycobacterium.

For many years, pulmonary disease caused by MAC occurred most often in white older adult men who had underlying chronic lung disease or who had undergone gastrectomy. However, since the mid- to late 1980s, it has become more common in persons without predisposing factors, especially older women (Prince et al., 1989; Dhillon & Watanakunakorn, 2000; Griffith et al., 2007). Disseminated MAC occurs almost exclusively in immunosuppressed individuals, especially persons with advanced acquired immunodeficiency syndrome (AIDS). In the United States, MAC was the most common cause of systemic bacterial infection in patients with AIDS in the late 1980s and early 1990s (Horsburgh, 1991). The numbers of such infections, however, decreased since highly active antiretroviral therapy became widely available (Kaplan et al., 2009). The major risk factor for disseminated MAC in AIDS patients is the degree of immune dysfunction, indicated by the $CD4^+$ lymphocyte count, as the disease is rare in individuals whose $CD4^+$ lymphocyte count is over 50/μL.

Manifestations of disease caused by MAC depend on the site and extent of infection. Pulmonary disease may manifest as bronchiectasis or may mimic TB. Disseminated disease in persons without AIDS is manifested by fever, weight loss, bone pain, lymphadenopathy, hepatosplenomegaly, and skin lesions. In those with AIDS, persistent fever, weight loss, and diarrhea are most common. Anorexia, weakness, lymphadenopathy, or hepatomegaly also may occur (Inderlied et al., 1993; Griffith et al., 2007; Kaplan et al., 2009). Significant laboratory abnormalities include anemia and elevated alkaline phosphatase. Cervical lymphadenitis caused by MAC most often affects children but also occurs in adults. Other manifestations of infection with MAC are synovitis, genitourinary tract disease, cutaneous lesions, deep infection of the hand, osteomyelitis, meningitis, ulcer of the colon, and pericarditis (Inderlied et al., 1993; Wolinsky, 1979; Woods & Washington, 1987).

The histologic findings of lesions caused by MAC vary. Caseating granulomas with AFB, indistinguishable from TB; pulmonary interstitial fibrosis with organizing pneumonia; necrotizing granulomatous vasculitis resembling Wegener granulomatosis; and, especially in persons with AIDS, aggregates of foamy macrophages containing many intracellular AFB may be seen.

Recently, an outbreak of *M. chimaera* wound and disseminated infections was identified in patients following cardiac surgery over a 5-year period beginning in 2012 (van Ingen et al., 2017). The cause was traced to contaminated heater-cooler units used in cardiac bypass surgeries and the source of contamination was determined to have occurred at the manufacturing site of the heater-cooler units. Although the risk of infection was determined to be low at approximately 1 in 100 to 1 in 1000 surgeries, cases are still being detected years after the surgery. For this reason, MAC isolates from sterile sites should be identified to the species level in patients who had cardiac surgery in the years immediately prior to recognition of the heater-cooler unit contamination.

MYCOBACTERIUM GENAVENSE

M. genavense was first isolated in 1991 in Switzerland from the blood of a patient with AIDS (Bottger et al., 1992). Conditions for detection in the laboratory were described shortly thereafter (Coyle et al., 1992). Disease occurs predominantly in immunocompromised patients. The most common presentation is disseminated disease in HIV-infected patients, which clinically is very similar to disseminated MAC (Griffith et al., 2007; Maschek et al., 1994; Tortoli et al., 1998). Other manifestations include enteritis, genital and soft-tissue infections, and lymphadenitis.

MYCOBACTERIUM GORDONAE

M. gordonae is ubiquitous in the environment, commonly isolated from tap water, and the most common mycobacterial laboratory contaminant (Arnow et al., 2000; Hoefsloot et al., 2013). *M. gordonae* is a slow-growing scotochromogen, usually taking at least 3 weeks of incubation to produce colony growth, which can appear yellow to orange (Griffith et al., 2007). Laboratory isolation of *M. gordonae* can pose challenges in identification and interpretation. Early colony growth may lack pigment, making *M. gordonae* difficult to distinguish from MTBC (Tokars et al., 1990). Rapid differentiation can be accomplished via commercial DNA probes, providing valuable information to readily guide treatment decisions (Lebrun et al., 1992). Additionally, isolation of *M. gordonae* is routinely attributed to sample contamination (Arnow et al., 2000). However, numerous case reports have appeared describing infection with *M. gordonae*, primarily in immunocompromised populations (Mazumder et al., 2010; Youssef et al., 2014; Chen et al., 2017; Verma & Spencer, 2012; Weinberger et al., 1992; Bonnet et al., 1996). The significance of *M. gordonae* isolation should be determined in conjunction with the clinical presentation. Susceptibility testing is not routinely recommended (Woods et al., 2018).

MYCOBACTERIUM HAEMOPHILUM

M. haemophilum was first described in 1978 but very probably was the nonculturable AFB recognized in skin ulcers in 1972 and 1974 (Lomwardias & Madge, 1972; Feldman, 1974; Sompolinsky et al., 1978). The organism is unique among mycobacteria in its growth requirement for hemoglobin or hemin. Human infections caused by *M. haemophilum* are uncommon, usually seen in persons who have an underlying immunodeficiency, such as lymphoma, exogenous immunosuppression after organ transplantation, or AIDS. However, lymphadenitis in otherwise healthy children has been reported (CDC, 1991; Lindeboom et al., 2005). Disease most commonly is manifested by multiple cutaneous nodules, ulcers, or painful swellings, typically involving the extremities, which occasionally become abscesses and open fistulas draining purulent material. Microscopically, lesions show foci of necrosis without caseation surrounded by a polymorphous inflammatory infiltrate with occasional Langhans giant cells in the lower dermis. AFB are seen singly or in small clusters, often within cells.

MYCOBACTERIUM KANSASII

M. kansasii, first described as the *yellow bacillus*, accounted for 3% of mycobacterial isolates in the United States in 1979 and 1980. The highest numbers of cases were reported from California, Texas, Louisiana, Illinois, and Florida (Buhler & Pollak, 1953; Good & Snider, 1982). The natural reservoir of *M. kansasii* is unknown; however, it has been recovered from water samples (Falkinham, 1996). Pulmonary disease is most common in males 50 to 60 years of age living in urban areas, among certain occupational groups (miners, welders, sandblasters, and painters), and among individuals with pneumoconioses and chronic obstructive pulmonary disease. Disseminated disease generally affects persons with impaired cellular immunity.

The most common manifestation of disease caused by *M. kansasii* is chronic cavitary pulmonary lesions, usually involving the upper lobes (Griffith et al., 2007). Extrapulmonary manifestations include cervical lymphadenitis in children, cutaneous disease, musculoskeletal involvement (carpal tunnel syndrome, synovitis, arthritis, tendinitis and fasciitis, or osteomyelitis), disseminated disease, isolated genitourinary tract disease, and pericarditis. Histologic findings of lesions caused by *M. kansasii* vary and include caseating or noncaseating granulomas and, especially in skin lesions, necrosis or foci of acute and chronic inflammation without well-formed granulomas. AFB are common in lung and lymph node tissue but are seen less frequently in tissue from other sites.

MYCOBACTERIUM MARINUM

M. marinum was recognized as a human pathogen in 1951 (Nordén & Linell, 1951). It causes chronic granulomatous infections involving skin and soft tissue, often called *swimming pool granuloma* or *fish tank granuloma*, and occasionally bone (Griffith et al., 2007; Lewis et al., 2003; Aubry et al., 2002). Human infection is typically acquired via trauma to the skin during

contact with contaminated nonchlorinated fresh water or salt water, but it may be acquired via trauma unassociated with water contact or contact with water in the absence of preceding trauma. A single papulonodular lesion usually appears 2 to 3 weeks after inoculation, most commonly on the elbow, knee, foot, toe, or finger, and often becomes verrucous or ulcerated (Ang et al., 2000). Occasionally, an abscess forms at the site of inoculation, and several secondary nodules develop and progress centrally along the lymphatics, resembling sporotrichosis (see Chapter 60). In immunocompromised persons, cutaneous lesions may become disseminated. Synovitis, osteomyelitis, and ocular and laryngeal lesions have been reported (Woods & Washington, 1987).

The histology of skin lesions varies with the stage of infection. In early infection, neutrophil aggregates are surrounded by histiocytes. Later, lymphocytes, epithelioid histiocytes, occasional Langhans giant cells, and foci of fibrinoid necrosis are seen. In lesions present for longer than 6 months, aggregates of lymphocytes are found in the dermis. Stains for AFB are usually negative, but organisms may be seen within histiocytes.

MYCOBACTERIUM ULCERANS

M. ulcerans is endemic in areas of the Democratic Republic of the Congo, Uganda, Nigeria, Ghana, Cameroon, Malaysia, New Guinea, Guyana, Mexico, and Australia located between latitudes 25° N and 38° S (Debacker et al., 2004; Piersimoni & Scarparo, 2009). In all endemic areas, disease is more frequent among children younger than 15 years of age and is slightly more common in males (Debacker et al., 2004; Piersimoni & Scarparo, 2009). The natural reservoir of *M. ulcerans* and the usual route of its transmission to humans remain unknown.

Eponyms for disease caused by *M. ulcerans* include *Bairnsdale ulcer*, for the area in Australia where it was first recognized, and *Buruli ulcer* or *Buruli disease*, after the area of Uganda reporting the greatest number of cases (Amofah, 2002). The disease begins as one or, rarely, multiple painless boils or subcutaneous lumps on an exposed area, most often the leg, which possibly was a site of previous trauma. After several weeks, the lump ulcerates, and satellite nodules and ulcers may appear. Lymph nodes typically are not enlarged, and affected individuals are afebrile and without systemic symptoms unless lesions become secondarily infected with bacteria. Unless treatment is begun early and adherence is good, the infection spreads to the bone, causing deformities.

MYCOBACTERIUM XENOPI

M. xenopi was first isolated from a toad in 1957 and was recognized as a human pathogen in 1965 (Costrini et al., 1981). It has been cultured from hot- and cold-water faucets, hospital hot-water generators and storage tanks, and other environmental sources. Birds are a possible natural reservoir. Most pulmonary infections caused by *M. xenopi* have been reported from Canada, Europe, and Great Britain; it is an uncommon cause of mycobacterial disease in the United States. Disease has occurred only in adults, more frequently in males than females. Most persons have preexisting lung damage or another predisposing condition, such as an extrapulmonary malignancy, alcoholism, diabetes mellitus, or immunosuppressive therapy. Pulmonary disease may be chronic, subacute, or acute; symptoms are indistinguishable from those associated with disease caused by *M. kansasii*. Focal extrapulmonary infections (osteomyelitis, arthritis, lymphadenitis) and disseminated disease are uncommon, but the latter has been reported in persons with AIDS (Tecson-Tumang, 1984).

RAPIDLY GROWING MYCOBACTERIA

Rapidly growing mycobacteria are ubiquitous; they have been cultured from soil, freshwater lakes and rivers, seawater, wastewater from hospitals, reagents and wash solutions used in hospitals, drinking water, raw milk, and dust. The species of rapidly growing mycobacteria that most commonly cause human disease are the *M. fortuitum* group (predominantly *M. fortuitum*) and the *M. chelonae/M. abscessus* group (predominantly *M. chelonae* and *M. abscessus* subsp. *abscessus* [formerly *M. abscessus*]). Species within the *M. fortuitum* group are *M. fortuitum*, *M. peregrinum*, *M. senegalense*, *M. setense*, *M. septicum*, *M. porcinum*, *M. houstonense*, *M. boenickei*, *M. brisbanense*, and *M. neworleansense*. Identification to the species level requires molecular techniques, but in most cases has little clinical relevance. It may, however, be useful for certain epidemiologic applications. Species in the *M. chelonae/M. abscessus* group are *M. chelonae*, *M. immunogenum*, *M. abscessus* subsp. *abscessus*, *M. abscessus* subsp. *bolletii*, *M. abscessus* subsp. *massiliense*, and *M. salmoniphilum*. Differentiating *M. chelonae* from *M. abscessus* subsp. is recommended because the latter is more resistant to antimicrobial agents (Brown-Elliott et al., 2001). Other rapidly growing mycobacteria commonly associated with human disease are the *M. mucogenicum* group, *M. goodii*, *M. cosmeticum*, *M. neoaurum*, *M. peregrinum*, *M. canariasense*, and, rarely, *M. smegmatis* (Griffith et al., 2007; Brown-Elliott & Wallace, 2002).

The most common manifestation of disease due to rapidly growing mycobacteria is skin and soft-tissue infection, typically following a penetrating injury (trauma or surgical procedure) with possible soil or water contamination, although outbreaks have been associated with administration of diphtheria-pertussis-tetanus-polio vaccines, histamine injections, lidocaine administration using a jet injector, tattoos, use of foot baths in nail salons, and liposuction (Piersimoni & Scarparo, 2009; Brown-Elliott & Wallace, 2002; Wallace et al., 1983). Primary cutaneous/subcutaneous disease may present as localized cellulitis, draining abscesses, or minimally tender nodules, generally appearing 3 weeks to 12 months (most often 4–6 weeks) after the penetrating injury in persons with an intact immune system. Osteomyelitis is an occasional complication, especially following puncture wounds to the feet. Postoperative infections are characterized by a nonhealing wound or breakdown of a healed wound with serous drainage in a person with minimal systemic symptoms. They generally develop 3 weeks to 3 months after the procedure, especially median sternotomy, augmentation mammaplasty, or insertion of a percutaneous catheter. Disseminated skin and soft-tissue abscesses in which no primary source of infection is evident typically occur in immunocompromised adults, especially those receiving corticosteroid therapy.

A less common manifestation of infection with rapidly growing mycobacteria is chronic pulmonary disease. It is most often seen in patients with underlying cystic fibrosis or bronchiectasis, is usually caused by *M. abscessus*, and typically resembles disease due to *M. kansasii* or MAC, except that cavitation is uncommon. Endocarditis involving a prosthetic valve has been reported, usually becoming manifest 4 to 12 weeks after surgery. Rarely, rapidly growing mycobacteria cause keratitis and corneal ulceration after trauma, or cervical lymphadenitis. A very thorough description of disease caused by rapidly growing mycobacteria is found in the excellent review by Brown-Elliott and Wallace (2002).

Lesions caused by rapidly growing mycobacteria are characterized histologically by necrosis with minimal caseation and a mixed inflammatory infiltrate composed of neutrophils and granulomas with foreign body or Langhans giant cells; lipid-laden macrophages are seen occasionally. Clumps of extracellular AFB are found within aggregates of neutrophils in less than one third of cases. In lung tissue, foamy macrophages may be seen in a pattern resembling lipoid pneumonia.

MYCOBACTERIUM LEPRAE

M. leprae is an etiologic agent of leprosy, also called *Hansen disease* (Scollard et al., 2006). It is unique among the mycobacteria by virtue of the fact that it has not been cultivated. It can be propagated in the mouse footpad, but this requires an average of 6 months for growth. Animal hosts in the wild include the nine-banded armadillo in the United States, red squirrels in the United Kingdom, and chimpanzees and monkeys in other parts of the world. *M. leprae* has been recognized in nearly every part of the world at some time. The reported number of new cases worldwide registered each year remains between 500,000 and 700,000 (Lockwood & Suneetha, 2005). During 1994 to 2011, there were 2323 new cases of leprosy in the United States, with an average annual incidence rate of 0.45 cases per 1 million persons (0.13 cases per 1 million persons among U.S.-born persons versus 2.81 cases per 1 million persons among foreign-born persons (Nolen et al., 2014). Persons born in Oceania were the population with the highest rate of leprosy in the United States, with a rate of diagnosis more than 10 times that of any other region.

The mechanism of transmission of *M. leprae* is unknown, but person-to-person spread via aerosolization of organisms from the nose of a person with active lepromatous disease (see later discussion), which then contacts the nasal mucosa of another individual, is the favored theory. Transmission also may occur through intact skin or via penetrating wounds, such as thorns or the bite of an arthropod. Breast milk from lactating women with lepromatous disease contains bacilli that may be transmitted to infants, and transplacental transmission of *M. leprae* is possible. Cases of human leprosy following contact with armadillos have been reported (Lumpkin et al., 1983). Moreover, the discovery of a naturally occurring leprosy-like disease among armadillos and the fact that sporadic cases of leprosy occur in persons who have no known contact with human leprosy suggest that nonhuman sources of *M. leprae* may exist (Blake et al., 1987).

Most persons effectively resist infection with *M. leprae*. Resistance depends on an effective cell-mediated immune response to *M. leprae* antigens, as occurs in tuberculoid leprosy. In persons who lack specific

cell-mediated immunity to these antigens, bacilli multiply within macrophages, eventually resulting in widely disseminated lepromatous leprosy. The defect in cellular immunity, which may involve T-lymphocyte function or interaction of T lymphocytes with macrophages, is apparently specific for antigens to *M. leprae* rather than a generalized defect. The lesions of leprosy develop after a 2- to 5-year incubation period, varying in appearance depending on the host's immune response. Leprosy always involves peripheral nerves, almost always involves the skin, and frequently involves mucous membranes. The three cardinal signs of the disease are skin lesions, areas of cutaneous anesthesia, and enlarged peripheral nerves.

The system outlined by Ridley and Jopling (presented in the following section) is still used to classify the spectrum of clinical and histopathologic forms of leprosy (Ridley & Jopling, 1966). Indeterminate leprosy, the earliest sign of disease, is characterized by one or a few hypopigmented skin macules with minimal local sensory loss. In about 75% of cases, the disease heals spontaneously; in the rest, it progresses, often after a prolonged period.

The polar types of leprosy—lepromatous leprosy, the widespread anergic form of the disease, and tuberculoid leprosy, the localized form—are stable clinically. Lepromatous leprosy is characterized by cutaneous lesions ranging from diffuse generalized skin involvement to widespread, symmetrically distributed nodules (called *lepromas*) filled with organisms. Lesions generally involve the cooler parts of the body surface: the anterior third of the eye, the nasal mucosa, and the superficial peripheral nerve trunks. In advanced disease, lesions are accompanied by sensory loss from involvement of dermal nerve fibers. Microscopically, lesions show foamy histiocytes containing many AFB; few or no lymphocytes; minimal intraneural inflammation; and many AFB in nerves, the perineurium, blood vessel walls, and arrector muscles. In tuberculoid leprosy, one or a few well-circumscribed anesthetic macules or plaques develop, often accompanied by an enlarged peripheral nerve near the skin lesions. Histologically, lesions demonstrate noncaseating granulomas in the nerves and dermis, extending to involve the basal layer of the epidermis; few, if any, AFB are present. Borderline leprosy, a clinically unstable condition, encompasses the types of disease between the polar forms. It may develop features more closely resembling tuberculoid disease through a process termed *upgrading*, or features more like those of lepromatous disease, called *downgrading*.

A recently described species, *M. lepromatosis*, has been implicated as a second causative agent of leprosy. *M. lepromatosis* was found in patients from Mexico and Brazil with leprosy. Genomic analysis has confirmed that it is distinct from *M. leprae* (Han, 2017; Han et al., 2012).

TESTING FOR LATENT *M. TUBERCULOSIS* INFECTION

Two types of tests may be used to detect latent infection with MTBC: the tuberculin skin test (TST) and interferon-γ release assays (IGRAs). However, neither will differentiate active disease from latent infection. With the TST, persons infected with MTBC develop a hypersensitivity reaction to proteins of the bacilli, which make up the skin test reagent purified protein derivative (PPD). The preferred method of skin testing is the Mantoux test, performed by intracutaneous injection of 0.1 mL of intermediate-strength (5 tuberculin units) PPD-S. The reaction is interpreted after 48 to 72 hours by measuring the diameter of induration in millimeters (Huebner et al., 1993). Induration of 5 mm or greater is considered positive in persons infected with HIV, those who have had recent close contact with someone who has infectious TB, and those who have chest radiograph findings consistent with old healed TB. A reaction of 10 mm or greater is positive in persons who do not meet the previous criteria but who have other risk factors for TB. Included in this group are foreign-born persons from countries where the prevalence of TB is high; injection drug users; medically underserved, low-income populations; residents of long-term care institutions; and persons who have a medical condition associated with increased risk for TB (e.g., silicosis, gastrectomy, jejunoileal bypass, 10% or more below ideal body weight, chronic renal failure, diabetes mellitus, treatment with high-dose corticosteroids or with other immunosuppressive drugs, malignancies). A reaction of 15 mm or greater is positive in all other persons. Interpretation is difficult in those immunized with the BCG vaccine.

False-positive PPD reactions may occur in persons with NTM infection and in those immunized with BCG vaccine. False-negative reactions may be due to poor administration or reading technique or improper storage of the reagent. If the test is administered appropriately, false-negative reactions are uncommon in relatively healthy people but occur in up to 20% of individuals with known TB when they are first tested. Most of these false-negative reactions are attributed to the general illness and revert to positive after 2 to 3 weeks of therapy when health is restored. Factors causing a state of general anergy, such as protein malnutrition, concurrent viral infection, sarcoidosis, malignancy (especially lymphoma), immunosuppressive or corticosteroid therapy, and infection with HIV, also may cause a false-negative tuberculin reaction.

The Mantoux test generally remains positive as long as viable bacilli persist in quiescent foci. However, the reaction may wane below positive with increasing age, a phenomenon that occurs most frequently in those older than 55 years of age. In these individuals, the reaction will be boosted (or become positive) if retesting is performed as early as 1 week after the first test, a reaction termed the *booster effect*.

IGRAs became commercially available in the early 21st century (Pai et al., 2008; Lalvani & Pareek, 2010). These are in vitro tests that are based on the detection of interferon-γ released by T cells in response to *M. tuberculosis* proteins (ESAT-6, CFP-10, TB7.7) not present in *M. bovis* BCG or most NTM (except *M. kansasii*, *M. szulgai*, and *M. marinum*). The two most commonly used tests are the QuantiFERON-TB (Qiagen, Germantown, MD) and the T-Spot.TB (Oxford Immunotech, UK). In 2017, the updated QuantiFERON-TB Gold Plus was released. This replacement for the QuantiFERON-TB Gold In-Tube differs from its predecessor in two main aspects: the use of only two antigens (ESAT-6 and CFP-10) and the addition of tube designed to improve activation of CD8 T cells. These changes have been proposed to improve sensitivity of the assay, particularly in patients with HIV with low CD4 T-cell counts (Theel et al., 2018). Performance of IGRAs requires collection of blood during a single visit, and results are available within 24 hours. Advantages of IGRAs over the TST include improved sensitivity in immunosuppressed persons (although false-negative results may occur) and children, and much better specificity in persons who have been vaccinated with BCG (Mori, 2009; Ruhwald & Ravn, 2009). In 2017, the American Thoracic Society (ATS), Infectious Diseases Society of America (IDSA), and CDC released guidelines for the diagnosis of TB. In persons ≥5 years of age, the IGRA is the recommended testing modality in those with likely TB infection, low to intermediate risk of progression, and where testing is deemed warranted (Lewinsohn et al., 2017). Additionally, an IGRA is preferred for testing persons who have received BCG vaccine and persons from groups that have been shown to have a low rate of returning to have the TST read (e.g., homeless persons and illicit drug users) (Lewinsohn et al., 2017; Mazurek et al., 2010). A TST is preferred for testing children younger than 5 years of age, although use of both a TST and an IGRA may increase diagnostic sensitivity in this age group. More recent data have shown that using an IGRA as a substitute for TST to screen for latent MTBC infection in health care workers (HCWs) is problematic. For example, the Quantiferon Gold In-Tube assay has been shown to have an unacceptably high number of false-positive results, poor reproducibility, especially with values near the cutoff for a positive, and a low predictive value of conversions (i.e., negative to positive result from one year to the next) (Joshi et al., 2014; Joshi et al., 2012). In 2019, the CDC released new guidelines for TB screening in U.S. HCWs, no longer recommending serial screening for low-risk HCWs without evidence of latent tuberculosis infection (LTBI). Screening is still recommended to establish an initial baseline as part of a postexposure program and in populations deemed at higher risk due to some aspect of their occupation (Sosa et al., 2019).

LABORATORY DIAGNOSIS

SPECIMENS

Specimens recommended for diagnosis of mycobacterial infection are listed in Table 59.2. Samples from contaminated sites such as sputum and other respiratory secretions, gastric secretions, urine, and feces must be decontaminated prior to inoculation of media to prevent normal flora from overgrowing and masking the presence of mycobacteria, which grow more slowly. Concentrating the specimen after decontamination increases the sensitivity of smear and culture. Specimens from normally sterile body sites—such as blood, cerebrospinal fluid (CSF), pleural and peritoneal fluid, and tissues—may be inoculated directly without decontamination.

Processing and inoculation of specimens for mycobacterial culture should be performed in a biological safety cabinet. The *N*-acetyl-L-cysteine (NALC)–sodium hydroxide procedure (Fig. 59.1) is the most common method used in the clinical laboratory to liquefy, decontaminate, and concentrate specimens for detection of mycobacteria. Potentially contaminated specimens should be refrigerated if they cannot be processed immediately. Before proceeding to the steps outlined in Figure 59.1, additional handling is necessary for some specimens. Gastric lavage specimens should

TABLE 59.2
Mycobacterial Diseases and Specimens for Diagnosis

Disease	Common *Mycobacterium* Species	Specimens
Pneumonia	MTBC, *M. kansasii*, MAC, *M. abscessus* subsp. *abscessus*	Sputum (early morning, deep cough on 3 consecutive days), BAL fluid, lung tissue, pleural fluid, gastric contents
Disseminated	MTBC, MAC	Blood, bone marrow, involved tissue
Lymphadenitis	MTBC, MAC	Lymph node aspirate or biopsy
Skin, soft tissue	*M. fortuitum*, *M. abscessus*/*M. chelonae* group, *M. marinum*, *M. haemophilum*, *M. ulcerans*	Aspirate or biopsy of lesion
	M. leprae, *M. lepromatosis*	Smears of nasal secretions and skin slits, biopsy of lesion
Musculoskeletal	MTBC, *M. fortuitum*, *M. abscessus*/*M. chelonae* group, *M. marinum*, *M. kansasii*	Joint fluid, synovium, bone
Meningitis	MTBC	Cerebrospinal fluid
Brain abscess	MTBC	Abscess material
Genitourinary	*M. tuberculosis*, *M. bovis* BCG	Urine (early morning), involved tissue—kidney, bladder (*M. bovis* BCG), endometrium, fallopian tube, prostate, seminal vesicles, epididymis
Gastrointestinal	*M. tuberculosis*, *M. bovis*, MAC	Tissue, feces
Peritonitis	MTBC	Peritoneal biopsy, peritoneal fluid
Hepatitis	MTBC, MAC	Liver tissue
Pericarditis	MTBC, MAC	Pericardium, pericardial tissue
Catheter-related infection	Rapidly growing mycobacteria	Blood

Modified with permission from Woods GL: Mycobacteria. In Woods GL, Gutierrez Y, editors: *Diagnostic pathology of infectious diseases*, Philadelphia, 1993, Lea & Febiger, p 378.
BAL, Bronchoalveolar lavage; BCG, bacille Calmette-Guérin; *MAC, M. avium* complex; *MTBC, M. tuberculosis* complex.

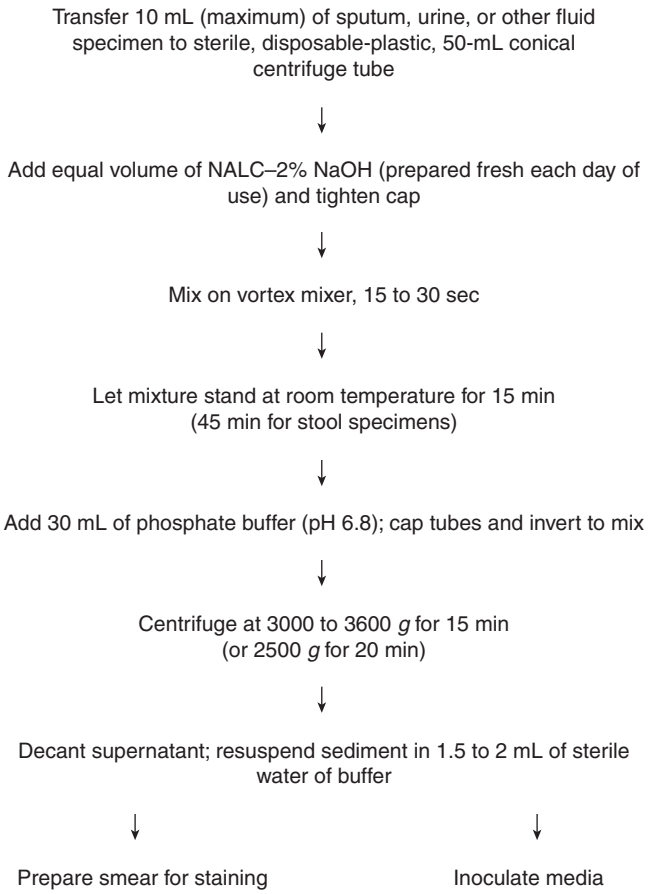

Figure 59.1 Protocol for decontamination, using 2% sodium hydroxide–*N*-acetyl-L-cysteine, and concentration of specimens for detection of mycobacteria by smear and culture.

be processed immediately. If a delay cannot be avoided, traditionally it has been recommended that 10% sodium hydroxide or 1% sodium bicarbonate should be added until the pH of the sample is neutral. However, data from one study suggest that neutralization may not be necessary (Parashar et al., 2013). If more than 10 mL of gastric secretions is collected, the sample is centrifuged at 3000 to 3600 *g* for 20 to 30 minutes, the supernatant

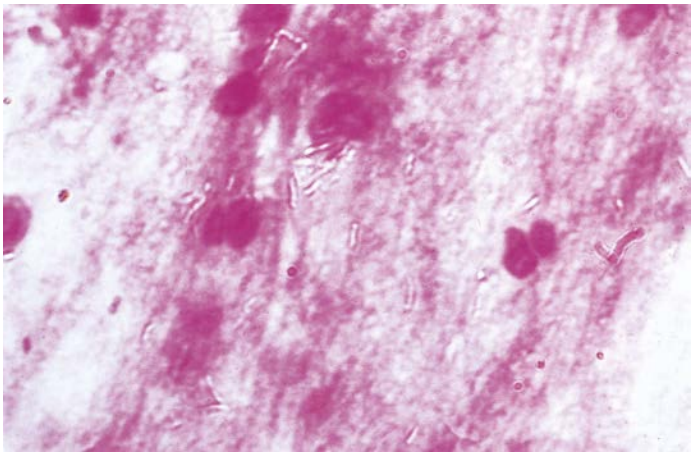

Figure 59.2 Smear of a sputum specimen stained with Gram stain shows "ghost cells" (mycobacterial culture grew *Mycobacterium tuberculosis*; Gram stain, 400×).

is decanted, and the sediment is processed as delineated in Figure 59.1. For feces, 1 to 2 g of a formed sample or 5 mL of a liquid specimen is placed in a 50-mL centrifuge tube, and sterile filtered distilled water is added to obtain a volume of 10 mL. The suspension is agitated on a vortex mixer, filtered through gauze, and then processed as outlined. Urine specimens are divided into two to four 50-mL centrifuge tubes and are centrifuged at 3000 to 3600 g for 30 minutes. The supernatant is decanted, leaving about 2 mL of sediment in each tube. Tubes are mixed on a vortex mixer, sediments are combined, and, if necessary, distilled water is added to obtain a volume of 10 mL, which then is decontaminated as outlined in Figure 59.1.

MICROBIAL STAINS

In smears stained with the Gram stain, most mycobacteria appear as slender, poorly stained, beaded gram-positive bacilli. However, sometimes the bacilli do not take up the crystal violet or safranin and appear "gram neutral" or as "Gram ghosts" (Fig. 59.2). Similar ghost images of bacilli may be found in macrophages in smears stained with the Wright or Papanicolaou stain. In general, specimens (except blood) collected from persons with suspected mycobacterial infection should be examined microscopically for organisms. However, to improve cost efficiency, many laboratories do not prepare smears of specimens in which AFB rarely are seen, such as CSF, urine, and bone marrow. To prepare a smear, two to three drops of the concentrated sediment are spread uniformly on a microscope slide, which

TABLE 59.3

Guidelines for Reporting Smears for Acid-Fast Bacilli

No. of AFB with Carbol Fuchsin Stain (1000×)	No. of AFB with Fluorochrome Stain (450×)	Report
0	0	No AFB seen
1–2/300 F (3 sweeps)	1–2/70 F (11/2 sweeps)	Doubtful; repeat
1–9/100 F	2–18/50 F (1 sweep)	1+
1–9/10 F	4–36/10 F	2+
1–9/F	4–36/F	3+
>9/F	>36/F	4+

Modified with permission from Kent PT, Kubica GP: *Public health mycobacteriology: A guide for the level III laboratory*, Atlanta, 1985, Department of Health and Human Services.
AFB, Acid-fast bacilli; *F,* field; *sweep,* scanning full length of a smear.

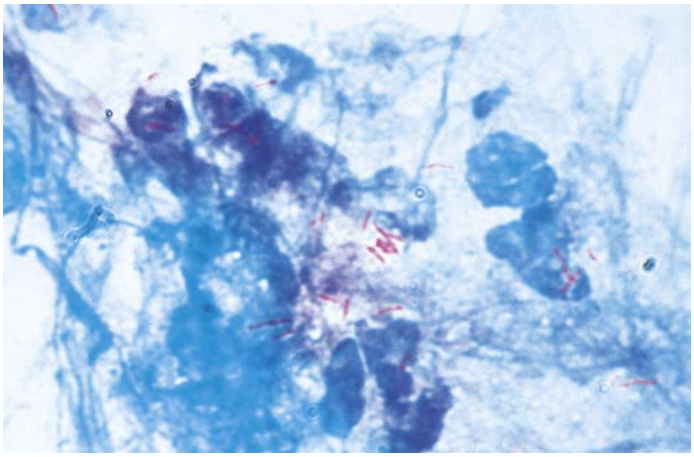

Figure 59.3 Smear of a sputum specimen shows acid-fast bacilli (*Mycobacterium tuberculosis*; Kinyoun, 400×).

then is fixed for 15 minutes at 80°C or for 1 to 2 hours at 65°C to 70°C on an electric hot plate.

Two types of stain detect AFB: carbol fuchsin (the classic Ziehl-Neelsen stain, which requires heating, and the cold Kinyoun stain) and the preferred fluorochrome stains (auramine-rhodamine and auramine-O), which is more sensitive. Smears stained with a carbol fuchsin stain are examined at 800× to 1000× magnification (oil immersion). Smears stained with a fluorochrome stain are examined at lower magnifications (250× and 400×). This allows visualization of more fields in less time. Cells of some rapidly growing mycobacteria stain poorly with fluorochromic stains and may not be detected. Therefore, when the latter organisms are suspected pathogens (e.g., in postsurgical wound infection), restaining negative fluorescent smears with a carbol fuchsin stain is reasonable. Results are reported after 100 fields are viewed and should include a statement indicating whether the smear was prepared directly from the specimen or after decontamination and concentration. Guidelines for reporting results of smears stained for AFB are shown in Table 59.3 (Kent & Kubica, 1985).

In smears stained with carbol fuchsin, AFB typically appear as purple to red, slightly curved rods (1–10 μm long and 0.2–0.6 μm wide), which often are beaded or banded (Fig. 59.3) but may also appear coccoid or filamentous. In general, the appearance of AFB does not provide species identification. However, cells of certain species have features that may be useful diagnostically. The formation of "cords" in smears of broth cultures is typical (but not diagnostic) of MTBC. Cells of *M. kansasii* often appear as cross-barred bacilli (Fig. 59.4), larger than *M. tuberculosis* and resembling a "shepherd's crook." Cells of MAC are typically pleomorphic and occasionally coccobacillary and stain positively with the periodic acid–Schiff stain. Cells of *M. marinum* are typically longer and broader than those of *M. tuberculosis* and often show cross-banding. Cells of *M. leprae* stain weaker than those of most other mycobacteria.

The specificity of stains for AFB typically is 99% or more, and the sensitivity ranges from about 25% to about 75% (Strumpf et al., 1979; Murray, 1980; Rickman & Moyer, 1980). False-positive results (positive stain, negative culture) may be caused by nonviable organisms that might occur in patients receiving antituberculosis therapy; prolonged

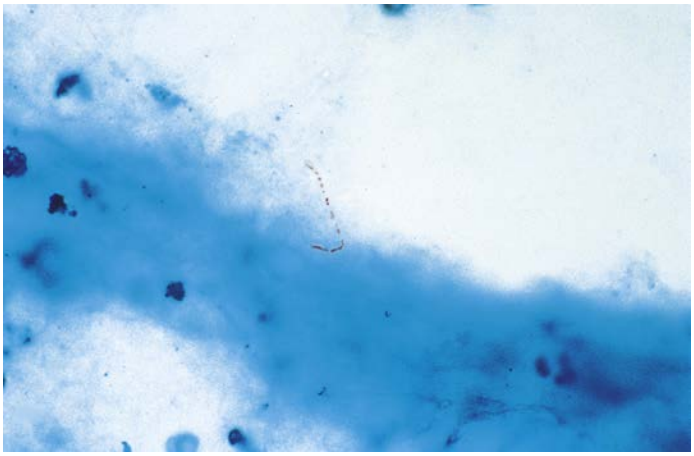

Figure 59.4 Smear of an aspirate from an enlarged cervical lymph node shows a large, cross-barred, acid-fast bacillus (*Mycobacterium kansasii*; Kinyoun, 400×). (Courtesy of Vicki J. Schnadig, MD, Department of Pathology, University of Texas Medical Branch, Galveston, TX)

decontamination, killing mycobacteria as well as contaminating bacteria; or cross-contamination during the staining procedure. Factors that influence the sensitivity of smear results include patient population (persons with cavitary lesions are more likely than those without cavities to have a smear-positive sputum) (Kubica et al., 2003), specimen type (respiratory specimens are more likely than other specimen types to be positive) (Emmanuel et al., 2007), the number of specimens examined (Castets et al., 1968), the number of AFB present in the sample (5000 to 10,000 organisms/mL of specimen are needed for a positive result) (Van Soolingen et al., 1997), the species present (specimens containing *M. tuberculosis* or *M. kansasii* are more likely to be positive than are those that contain other mycobacteria) (Pfyffer, 1998), observer experience (Kiers et al., 2008), and the stain used (Tenover et al., 1993). Fluorochromic stains are more sensitive and are easier to read than carbol fuchsin stains, and they are recommended by experts at the CDC (Tenover et al., 1993). The CDC also suggests that for respiratory specimens, results of stained smears should be reported within 24 hours of specimen receipt, which means processing 7 days a week.

CULTURE METHODS

For optimal recovery of mycobacteria from clinical specimens, inoculation of both a broth and a solid medium is recommended (Tenover et al., 1993) because broth is more sensitive than solid media and provides more rapid detection of mycobacterial growth (Anargyros et al., 1990; Stager et al., 1991; Abe et al., 1992). However, use of a broth system alone may be considered if data show that adding a solid medium does not enhance recovery of mycobacterial pathogens.

Two types of solid media are used for mycobacterial culture: egg based (Löwenstein-Jensen) and agar based (Middlebrook 7H10, 7H11, and selective 7H11). Specimens from cutaneous lesions should be inoculated to one egg- or agar-based medium, and to ensure recovery of *M. haemophilum* (see earlier discussion), the agar should be supplemented with hemin. To recover *M. genavense* (from specimens or subcultures of liquid to solid media), solid media must be supplemented with mycobactin J. All cultures should be incubated at 37°C in an atmosphere of 5% to 10% carbon dioxide (CO_2), and tubed media should be incubated in a slanted position with caps loose for at least 1 week to ensure even distribution of the inoculum over the surface. For specimens from cutaneous sites, a second set of cultures should be inoculated and incubated at 30°C, because some mycobacteria that cause skin lesions—*M. marinum*, *M. haemophilum*, the rapidly growing mycobacteria, and *M. ulcerans*—grow optimally at the lower temperature. All cultures should be examined weekly for at least 6 weeks.

The major advantage of culture on solid media is that it allows visualization of colony morphology and pigmentation, which is useful diagnostically, especially for distinguishing colonies of *M. tuberculosis* from those of some NTM. The colony appearance and growth characteristics of commonly encountered mycobacteria are outlined in Table 59.4. Disadvantages of conventional solid media include prolonged time to growth of mycobacteria (colonies often are not visible on tubed solid media for 3 to 4 weeks or longer) and low sensitivity. Inoculation of Middlebrook agar plates, which then are examined under the microscope, allows more rapid detection of colonies (Welch et al., 1993). However, this procedure is labor-intensive, prohibiting its use in many clinical laboratories.

TABLE 59.4

Colony Morphology and Growth Characteristics of Mycobacteria Commonly Isolated in the Clinical Laboratory

Mycobacterium Species	Colony Morphology	Pigment	Growth Rate, Weeks	Comments
Slowly Growing Mycobacteria				
M. tuberculosis	Rough	N (buff)	3–6	Generally niacin and nitrate positive
M. bovis	Rough; thin or transparent on LJ	N (colorless to buff)	4–6	Generally niacin and nitrate negative; resistant to pyrazinamide
MAC	Smooth; small, thin, transparent or large, opaque, domed; ± rough	N	3–6	Colonies of some isolates become lightly pigmented with prolonged incubation; grows at 42°C
M. kansasii	Rough, ± smooth, β-carotene crystals	P	3–6	Rare strains are N or S
M. gordonae	Smooth	S	3–6	Common laboratory contaminant; rare strains are N
M. marinum	Wrinkled, shiny; smooth, hemispherical; (rarely) rough, dry	P	2	Optimal growth, 30°C–33°C
M. xenopi	Smooth, filamentous extensions ("bird's nest")	S	3–6	Growth at 42° C
M. haemophilum	Rough, ± smooth	N	3–6	Optimal growth, 20°C–32°C; requires hemin for growth
M. szulgai	Smooth or rough	S, 37°C; P, 25°C	3–6	
Rapidly Growing Mycobacteria				
M. abscessus complex	Smooth; ± rough, wrinkled	N	<1	
M. fortuitum group	Wrinkled	N	<1	Branching filaments often are present on periphery of colonies
M. chelonae	Smooth	N	<1	

MAC, M. avium complex; *N,* nonchromogenic; *P,* photochromogenic; *S,* scotochromogenic.

For laboratories with a low number of requests for mycobacterial culture, the manually read MGIT tubes, which can be used to culture all specimen types except blood and urine, may be the most cost-effective option. These tubes contain modified 7H9 broth and have a fluorescent indicator embedded in silicone in the bottom. Tubes are inoculated with the specimen, an antibiotic mixture to inhibit growth of contaminating bacteria and a mycobacterial growth enrichment are added, and the tubes are capped and incubated at 37°C for at least 6 weeks. To detect mycobacterial growth, tubes are manually placed on top of a 365-nm ultraviolet transilluminator or in front of a Wood's lamp. The appearance of strong fluorescence in the sensor (a bright-orange color on the bottom of the tube and meniscus) indicates growth. For laboratories with a high volume of requests, the totally automated BACTEC 960 (or 320) instrument, which continuously monitors tubes for fluorescence and signals those that are positive, is more appropriate.

In addition to the BACTEC MGIT 960/320, two other fully automated continuously monitoring systems for growth and detection of mycobacteria in specimens are commercially available: the MB/BacT system (bioMérieux, Durham, NC) (Rohner et al., 1997; Brunello et al., 1999) and the VersaTrek (previously called ESP Culture System II, currently distributed by Thermo Scientific, Lenexa, KS) (Tholcken et al., 1997; Woods et al., 1997). With each system, bottles are inoculated with specimen, an antibiotic mixture, and a growth supplement. The MB/BacT has one bottle type for blood and another bottle for all other specimen types. Bottles are then incubated in the respective instrument, where they are monitored for changes in production or production and consumption of various gases, indicating growth of mycobacteria or other organisms.

TESTS FOR IDENTIFICATION OF MYCOBACTERIA

Identification of mycobacteria has traditionally been based on rate of growth on a solid medium, colony morphology (rough or smooth) and pigmentation with and without exposure to light, and results of biochemical tests, described in detail elsewhere (Kent & Kubica, 1985). Biochemical test results, however, are not usually available for several weeks to months after colonies appear on solid media; for identification of MTBC especially, more rapid methods are recommended (Tenover et al., 1993). Additionally, biochemical testing frequently does not provide unequivocal identification at the species level.

Currently, the most rapid method for diagnosis of pulmonary TB is the use of a nucleic acid amplification test (NAAT) for direct detection of MTBC in clinical specimens (Piersimoni & Scarparo, 2003). The CDC recommends direct-from-specimen NAAT testing, in conjunction with AFB smear and culture, from at least one sample for patients with a high suspicion for TB, where the test result will alter clinical management, and/or when TB control activities will be influenced by the result (CDC, 2009). Forbes et al. (2018) outline an ideal testing algorithm based on these recommendations for patients with high or low suspicion for TB infection. Two commercial NAATs for the detection of MTBC are available in the United States: the Amplified MTD (Mycobacterium Tuberculosis Direct) test (Hologic, Marlborough, MA) and the Xpert MTB/RIF (Cepheid, Sunnyvale, CA). The Hologic test is approved for testing smear-positive and smear-negative respiratory specimens following NALC-NaOH treatment, while the Cepheid assay is approved for smear-positive and smear-negative sputum or concentrated sputum sediments. Data suggest that NAATs may be useful in AFB smear-negative patients at high risk for TB (e.g., persons infected with HIV, incarcerated persons in correctional facilities), allowing more rapid diagnosis and earlier initiation of treatment (Gamboa et al., 1998; Bergmann et al., 1999). The sensitivity of NAATs is generally slightly lower for nonrespiratory specimens, but they may be useful for diagnosis of some cases of extrapulmonary TB, especially when the AFB smear is positive. Neither assay is able to differentiate the members for the MTBC (CDC, 2009).

The MTD test relies on transcription-mediated amplification (TMA) of a mycobacterial rRNA target followed by a hybridization protection assay (HPA). After amplification, a target-specific DNA probe linked to a chemiluminescent label hybridizes with MTBC ribonucleic acid (RNA) amplicons. The resulting complex is detected via luminometer with the result reported in relative light units (RLUs). Results are interpreted as follows: <30,000 RLU is negative, 30,000 to 499,999 RLU is equivocal, and ≥500,000 RLU is positive. According to the package insert, sensitivity compared with culture is 64% and 87.5% for smear-negative and smear-positive samples, respectively, with specificity ~100% for both sample types. The sensitivity is improved if more than one sample is tested (Hologic, 2013).

The Xpert MTB/RIF assay is technically much less demanding than other NAATs, and it has the added advantage of also detecting rifampin resistance. The assay has two components: a single-use cartridge containing liquid sample-processing and polymerase chain reaction (PCR) buffers and lyophilized real-time PCR reagents (Kubica et al., 2003), and the GeneXpert instrument, which performs sample processing and real-time PCR in a single hands-free step (Emmanuel et al., 2007). It simultaneously detects *M. tuberculosis* and rifampin resistance by PCR amplification of the 81-bp fragment of the *M. tuberculosis rpoβ* gene and subsequent probing for mutations associated with rifampin resistance. Approved specimen types are raw sputum and concentrated sputum sediments. Total hands-on time is less than 5 minutes per specimen, and results are available in less than 2 hours. The sensitivity versus culture for identifying

M. tuberculosis when testing sputum specimens is 98% to 100% for AFB smear-positive samples and 69% to 72% for smear-negative samples. Specificity in studies to date has been 100% (Boehme et al., 2010; Helb et al., 2010; Zeka et al., 2011).

Chemiluminescent DNA probes allow identification of a few species or a species complex of mycobacteria within 1 to 2 hours after sufficient growth is present on a solid or in a liquid medium (Lebrun et al., 1992; Evans et al., 1992; Goto et al., 1992; Reisner et al., 1994). Commercial probes specific for MTBC, MAC, *M. avium*, *M. intracellulare*, *M. gordonae*, and *M. kansasii* are currently available. Testing requires minimal equipment (i.e., luminometer, sonicator, and heating block). Disadvantages of the probes include failure to identify some isolates of MAC, especially when testing growth from a liquid medium; false-positive results with the MAC probe when testing aliquots of broth cultures (Cloud et al., 2005); and rare false-positive results with the MTBC probe (Lebrun et al., 1992; Cloud et al., 2005; Bull & Shanson, 1992; Butler et al., 1994).

The last decade has seen rapid adoption of matrix-assisted laser desorption ionization-time of flight mass spectrometry (MALDI-TOF MS) for organism identification in the clinical laboratory. Use of MALDI-TOF MS for identification of *Mycobacteria* has lagged but is increasingly employed as the databases used for spectral analysis improve (Buckwalter et al., 2016). The addition of a pre-extraction step, designed to disrupt the complex mycobacterial cell wall producing higher-quality spectra, has also improved the performance of MALDI-TOF MS. This step is also key to the inactivation of MTBC, allowing for safe analysis outside of a BSL-3 environment (Buckwalter et al., 2016; Mather et al., 2014). Performance of MALDI-TOF MS has traditionally required organism growth on solid media, but new studies have demonstrated the potential to identify organisms direct from broth media (Buchan et al., 2014; Lotz et al., 2010; Miller et al., 2018). While MALDI-TOF MS is able to differentiate a number of *Mycobacteria* spp., some complexes, including the MTBC and the subspecies of *M. abscessus*, are unable to be resolved (Saleeb et al., 2011). For more on the use of MALDI-TOF MS, see Chapter 5.

High-performance liquid chromatography allows identification of mycobacterial colonies on a solid medium or growth in a liquid medium in 2 to 4 hours. This technique was used in public health and some reference laboratories for many years but more recently has lost popularity due to the availability of other more accurate and less time-consuming techniques, such as reverse hybridization (line-probe) assays (Wu et al., 2007; Hofmann-Thiel et al., 2011; Mitarai et al., 2012), MALDI-TOF MS, and sequencing. Line-probe assays perform best using colonies on a solid medium or broth from a positive liquid culture, although direct testing of AFB smear-positive specimens is possible. With line-probe assays, the target sequences are first amplified by PCR using biotinylated primers. The amplified product is then applied to a nitrocellulose strip to which multiple probes are immobilized. Lines form at the site of amplicon-probe hybridization, and the pattern is compared with a key, allowing interpretation of the results and identification of the isolate.

The most accurate identification method for mycobacteria is sequencing. For the identification of *Mycobacteria*, a variety of genes may be needed to provide adequate differentiation to the species level. Sequencing of the 16S rRNA gene is the most common approach, but for many species, including the most clinically relevant, interrogation of additional genes such as *rpoB*, *secA*, *hsp65*, *gyrB*, or the internal transcribed spacer (ITS) may be necessary (Wu et al., 2007; Patel et al., 2000; Cloud et al., 2002; Hall et al., 2003; Zelazny et al., 2005; Roth et al., 1998; Zelazny et al., 2009; Pinsky & Banaei, 2008; Niemann et al., 2000). Beyond sequencing of individual genes, whole-genome sequencing (WGS) of *Mycobacteria* has become the newest frontier in the clinical lab. While WGS is currently costly and technically complex, limiting the application to larger reference laboratories, the wealth of information provided has significant appeal. WGS allows for greater resolution for species and subspecies identification by interrogation of multiple genes or comparison of the whole genome to a well-curated database of reference genomes. Simultaneously, assessment for known markers of resistance can be performed, providing rapid recognition of mutations or polymorphisms associated with drug resistance (Quan et al., 2018; Doyle et al., 2018). It should be cautioned that phenotypic antimicrobial susceptibility testing should accompany WGS analysis, as uncharacterized mutations responsible for antimicrobial resistance may exist (Mostowy et al., 2004).

SUSCEPTIBILITY TESTING

Susceptibility testing of mycobacteria should be performed according to guidelines of the Clinical and Laboratory Standards Institute (CLSI, 2018a, 2018b). Primary and secondary drugs that should be tested are listed in Table 59.5.

TABLE 59.5

Drugs Recommended for Susceptibility Testing of Mycobacteria

Mycobacterium Species	Indication	Drugs
MTBC	Primary	Isoniazid, rifampin, ethambutol, pyrazinamide
	Secondary	Capreomycin, ethionamide, amikacin, kanamycin, levofloxacin, linezolid, moxifloxacin, *p*-aminosalicylic acid, rifabutin
MAC	Primary	Clarithromycin, amikacin
	Secondary	Moxifloxacin, linezolid
M. kansasii	Primary	Clarithromycin, rifampin
	Secondary	Amikacin, ciprofloxacin, doxycycline, linezolid, minocycline, moxifloxacin, rifabutin, trimethoprim-sulfamethoxazole
Slowly growing mycobacteria other than MAC and *M. kansasii*	Primary	Amikacin, ciprofloxacin, clarithromycin, doxycycline, linezolid, minocycline, moxifloxacin, rifabutin, rifampin, trimethoprim-sulfamethoxazole
Rapidly growing mycobacteria	Primary	Amikacin, cefoxitin, ciprofloxacin, clarithromycin, doxycycline, imipenem, linezolid, meropenem, moxifloxacin, tigecycline, tobramycin, trimethoprim-sulfamethoxazole

MAC, M. avium complex; *MTBC, M. tuberculosis* complex.

For the MTBC, the initial isolate from every patient should be tested to all primary drugs. Testing should be repeated if specimens remain culture positive after 3 months of appropriate therapy or earlier if there is clinical evidence of treatment failure. Testing may be performed on isolated colonies or a positive broth culture (indirect test) or on sputum specimens that are AFB smear positive (direct test). Agar proportion is the standard method of testing susceptibility of the MTBC to antituberculosis agents. With this method, isolates showing greater than 1% resistance to a single concentration of drug are considered resistant to that drug. However, because the target turnaround time for results is an average of 28 days after specimens are received in the laboratory, use of a liquid-based system approved by the U.S. Food and Drug Administration (FDA) that provides results equivalent to those of agar proportion is recommended (Tenover et al., 1993; CLSI, 2018a) . With currently available liquid-based systems, results are generally available 5 to 7 days after bottles are inoculated with the MTBC isolate (Bergmann & Woods, 1998; Bergmann et al., 2000; Scarparo et al., 2004). Susceptibility to all secondary drugs should be tested when an isolate is resistant to rifampin alone or any two of the primary agents. Isolates resistant only to the critical concentration of isoniazid also should be tested for susceptibility to secondary agents if the planned treatment regimen will include a fluoroquinolone.

Given the importance of rapid identification of drug-resistant TB, molecular methods that can be used to test positive cultures (broth or colonies) or AFB smear–positive specimens for detection of mutations associated with resistance have been developed (Santos, 2012). Use of a molecular test to detect drug resistance directly in an AFB smear–positive specimen may be considered in a patient who has a history of prior treatment for TB, comes from a country or ethnic group known to have increased drug resistance, fails to respond to standard therapy, and/or has known exposure to MDR-TB. Probe-based molecular methods (e.g., Cepheid's GeneXpert MTB/RIF assay using molecular beacons and HAIN's MTBDR*plus* and MTBDR*sl* assays using line probes) detect the presence or absence of mutations. Sequence-based methods (e.g., Sanger sequencing and pyrosequencing) provide sequences of either wild-type isolates or mutants. Genetic loci commonly examined are drug-resistance determining regions of *rpoβ*, *emb*, and *gyrA*, promoters of *inhA* and *eis*, regions of *katG* and *rrs* with established mutations, and complete open reading frames of *tlyA* and *pncA* (Campbell et al., 2011). Because drug resistance can be caused by mutations other than those detected by these methods, failure to detect a mutation does not necessarily equate to a phenotypic result of susceptible. Additionally, because not all mechanisms of resistance are known, failure to detect a mutation does not unequivocally exclude resistance. Therefore, although molecular-based methods provide useful information quickly,

TABLE 59.6

Antimicrobial Agents Recommended for Primary Treatment of Common Mycobacterial Infections

Mycobacterium Species	Site of Infection	Antimicrobial Agents
MTBC	Any	Isoniazid, rifampin, ethambutol, pyrazinamide
MAC	Pulmonary	Clarithromycin,* rifampin, and ethambutol, inhaled amikacin
	Disseminated	Clarithromycin* and ethambutol ± rifabutin
	Lymphadenitis†	None
M. kansasii	Pulmonary	Rifampin, ethambutol, and isoniazid or clarithromycin
M. chelonae/*M. abscessus* group, *M. fortuitum* group‡	Nonpulmonary	Clarithromycin (if susceptible) and one or more additional agents§
M. abscessus¶	Pulmonary	Multidrug regimen,§ including clarithromycin
M. marinum	Skin/soft tissue	Clarithromycin, doxycycline or minocycline, trimethoprim-sulfamethoxazole, or rifampin and ethambutol

MAC, M. avium complex; *MTBC, M. tuberculosis* complex.
*Or azithromycin.
†Recommended management is surgery.
‡Surgical debridement often is necessary.
§Agent(s) selected should be based on results of susceptibility testing.
¶Currently, there are no drug regimens with proven efficacy, although antimicrobial therapy may provide symptomatic improvement and disease regression. If disease is limited, surgical resection plus multidrug therapy is optimal.

they are adjuncts to, not replacements for, phenotypic drug susceptibility testing (Campbell et al., 2011).

The GeneXpert MTB/RIF assay was described earlier in this chapter. With regard to detecting rifampin resistance in *M. tuberculosis*, Zeka and colleagues (2011) reported total agreement with agar proportion for 89 of the 429 specimens that were culture positive for *M. tuberculosis*: 88 were susceptible and 1 was resistant. In contrast, Marlowe and colleagues (2011) reported some false resistance. Of 217 specimens, 130 were culture positive for *M. tuberculosis*. All 130 were susceptible to rifampin by broth microdilution; however, 3 were initially rifampin resistant by GeneXpert and 1 remained resistant after retesting. Recent introduction of an updated cartridge, MTB/RIF Ultra has been reported to improve the sensitivity of the test but resulted in a slight reduction in specificity (Dorman et al., 2018).

The HAIN probe assays, which use reverse hybridization to detect mutations, are not FDA approved in the United States but have been used in several countries outside the United States. Both MTBDR*plus* and MTBDR*sl* assays include both wild-type probes and probes for several commonly encountered mutations. The absence of a wild-type band indicates that a mutation is present. The simultaneous presence of a mutant band indicates that a specific mutation is present in the specimen/isolate. The absence of both a wild-type band and a mutant band indicates the presence of a mutation but does not provide information regarding the identification of the mutation. The performance of these assays varies depending on the drug, performing best with rifampin and the quinolones. For both assays, specificity (drug is susceptible by both the line-probe assay and phenotypic drug susceptibility testing) is ≥95% and is greater than the sensitivity (drug is resistant by both the line-probe assay and phenotypic drug susceptibility testing), with the exception of rifampin (Mitarai et al., 2012; Kiet et al., 2010; Ignatyeva et al., 2012; Crudu et al., 2012).

Susceptibility testing of NTM should be performed on clinically significant isolates (Griffith et al., 2007). However, for some species, little correlation has been found between susceptibility test results for some drugs and clinical response to therapy. This is especially true for MAC and results for ethambutol and the rifamycins. The method recommended by the CLSI for susceptibility testing of rapidly and slowly growing NTM is broth microdilution (CLSI, 2018a; Woods et al., 1999). Media, incubation times and temperatures, and guidelines for interpretation of results are beyond the scope of this chapter but are described in detail for MAC, *M. kansasii*, and other slowly growing mycobacteria, and the rapidly growing mycobacteria in the most recent edition of CLSI M24 (Brown-Elliott et al., 2013). Recommended drugs to test are listed in Table 59.5. In addition to the drugs listed for MAC, recent data support initial testing of amikacin as well as clarithromycin (Brown-Elliott et al., 2013). For slowly growing mycobacteria other than those mentioned earlier, the CLSI recommends testing the same primary and secondary drugs listed for *M. kansasii* and using the same interpretive criteria. In general, both the minimum inhibitory concentration (MIC) and the interpretation (susceptible, intermediate, resistant) should be reported.

TREATMENT

The chemotherapeutic regimen currently recommended for treatment of TB (Table 59.6) should be initiated before susceptibility test results are available, but treatment should be altered based on those results if an isolate is found to be resistant. Medications should be administered by directly observed therapy. Regimens commonly used to treat infections caused by the most frequently encountered NTM also are listed in Table 59.6 (Griffith et al., 2007). For many NTM, however, neither the optimal regimen nor the duration of therapy is known.

PREVENTION

MYCOBACTERIUM TUBERCULOSIS COMPLEX

Four general strategies for controlling TB are described. The most important is early identification and adequate treatment of persons with infectious TB. This renders the infected person noncontagious within a few weeks and eventually results in cure. The second strategy entails identification and treatment of individuals with noncontagious TB: extrapulmonary disease, primary pulmonary disease in children, bacteriologically unconfirmed pulmonary disease, and latent infection with MTBC (i.e., positive TST or IGRA, normal chest radiograph, no symptoms).

The third strategy involves creation of a safe environment in situations in which the risk for transmitting infection is high: autopsy suites, sputum induction cubicles, chest clinic waiting areas, correctional institutions, some shelters for the homeless, and mycobacteriology laboratories. To accomplish this, several issues must be addressed (Segal-Maurer & Kalkut, 1994). Rooms housing infectious patients or in which potentially infectious specimens are handled should be under negative pressure, and air likely to be contaminated with infectious droplet nuclei should be exhausted to the outside. A single-pass ventilation system (best accomplished by locating air supply outlets at the ceiling level and exhaust inlets near the floor) and a minimum of six air changes per hour (12 exchanges per hour for autopsy suites) are recommended. Universal precautions must be followed when handling all specimens, and both specimens and cultures must be handled in a certified, class II biological safety cabinet. Moreover, a particulate respirator that filters out particles 1 to 5 μm in diameter should be worn, and personnel should be trained in a respiratory program; the standard surgical mask is not adequate.

The fourth strategy is vaccination with the BCG vaccine, an attenuated vaccine derived from a strain of *M. bovis* by Calmette and Guérin in France. This vaccine is used in many countries where the prevalence of TB is high to prevent TB meningitis and miliary TB in children but generally is not recommended in the United States, because the risk for infection with MTBC is low and the effectiveness of the vaccine in adults is variable. The BCG vaccine should not be given to immunocompromised persons, those likely to become immunocompromised, or pregnant women. Disseminated *M. bovis* in patients with AIDS and *M. bovis* lymphadenitis in symptomatic HIV-infected infants have occurred following BCG vaccination (CDC, 1985; Blanche et al., 1986). However, disseminated *M. bovis* has not been reported in asymptomatic persons infected with HIV. In populations where the risk for TB is high, the WHO recommends that the BCG vaccine be given to HIV-infected children at birth or soon thereafter. It should not be given to children with symptomatic HIV infection, to populations in which the risk for tuberculosis is low, or to persons known or suspected to be infected with HIV (WHO, 1987).

MYCOBACTERIUM AVIUM COMPLEX

Disseminated MAC in patients with AIDS is associated with considerable morbidity and a shortened duration of survival (Horsburgh et al., 1991; Nightingale et al., 1992). Therefore, prevention of the disease is desirable. Because MAC is ubiquitous in the environment, the most reasonable approach to prevention is chemoprophylaxis. Currently, the U.S. Public Health Service and the IDSA recommend clarithromycin or azithromycin prophylaxis in AIDS patients with $CD4^+$ cell counts lower than 50/μL (Kaplan et al., 2009). If neither of these drugs can be tolerated, rifabutin is an alternative prophylactic agent. Primary prophylaxis should be discontinued in patients who have responded to antiretroviral therapy with an increase in $CD4^+$ count of >100 cells/μL for at least 3 months.

SELECTED REFERENCES

Brown-Elliott AB, Wallace Jr RJ: Clinical and taxonomic status of pathogenic nonpigmented or late-pigmenting rapidly growing mycobacteria, *Clin Microbiol Rev* 15:716–746, 2002.

An excellent review of the taxonomy of rapidly growing mycobacteria. Also includes a discussion of laboratory tests for identification and the usual antimicrobial susceptibility patterns.

Clinical and Laboratory Standards Institute: *Susceptibility testing of mycobacteria, Nocardia, and other aerobic actinomycetes*, Wayne, PA, 2018, Clinical and Laboratory Standards Institute. Approved Standard M24.

Guidelines for testing susceptibility of M. tuberculosis complex, rapidly growing mycobacteria, and select slowly growing mycobacteria, including M. avium complex, M. kansasii, and M. marinum.

Falkinham III JO: Epidemiology of infection by nontuberculous mycobacteria, *Clin Microbiol Rev* 9:177, 1996.

An in-depth review of the epidemiology of more commonly encountered nontuberculous mycobacteria, including M. avium complex, M. kansasii, and M. marinum, as well as M. simiae and M. xenopi.

Griffith DE, Aksamit T, Brown-Elliott BA, et al.: An official ATS/IDSA statement: diagnosis, treatment, and prevention of nontuberculous mycobacterial diseases, *Am J Respir Crit Care Med* 175:367, 2007.

An excellent review of the laboratory diagnosis and treatment of commonly encountered nontuberculous mycobacteria, including M. avium complex, M. kansasii, M. marinum, and rapidly growing mycobacteria.

Madkukar P, Zwerling A, Menzies D: Systematic review: T-cell-based assays for the diagnosis of latent tuberculosis infection: an update, *Ann Intern Med* 149(1), 2008.

An excellent discussion of the value of T cell–based assays for diagnosis of latent tuberculosis infection.

Piersimoni C, Scarparo C: Relevance of commercial amplification methods for direct detection of *Mycobacterium tuberculosis* complex in clinical samples, *J Clin Microbiol* 41:5355–5365, 2003.

An excellent review of the commercial nucleic acid amplification tests for direct detection of M. tuberculosis complex in clinical specimens.

Runyon EH: Anonymous mycobacteria in pulmonary disease, *Med Clin North Am* 43:273, 1959.

A classic description of the different groups of nontuberculous mycobacteria.

Santos LC: Review: the molecular basis of resistance in *Mycobacterium tuberculosis*, *Open Journal Med Microbiol* 2:24–36, 2012.

An excellent summary of the molecular basis of resistance in M. tuberculosis.

Scollard DM, Adams LB, Gillis TP, et al.: The continuing challenges of leprosy, *Clin Microbiol Rev* 19:338, 2006.

An excellent up-to-date review of leprosy.

Tortoli E: Impact of genotypic studies on mycobacterial taxonomy: the new mycobacteria of the 1990s, *Clin Microbiol Rev* 16:319–354, 2003.

An excellent discussion of the more recently described species of slowly growing and rapidly growing mycobacteria. Includes information regarding epidemiology, clinical manifestations, phenotypic characteristics, and antimicrobial susceptibility.

Access the complete reference list online at Elsevier eBooks for Practicing Clinicians.

REFERENCES

Abe C, Hosojima S, Fukasawa Y, Kazumi Y, Takahashi M, Hirano K, et al.: Comparison of MB-Check, BACTEC, and egg-based media for recovery of mycobacteria*J*, *Clin Microbiol* 30:878–881, 1992.

Alami NN, Yuen CM, Miramontes R, Pratt R, Price SF, Navin TR, Centers for Disease C, Prevention: Trends in tuberculosis - United States, 2013, *MMWR Morb Mortal Wkly Rep* 63:229–233, 2014.

Amofah G: Buruli ulcer in Ghana: results of a national case Search, *Emerg Infect Dis* 8:167–170, 2002.

Anargyros P, Astill DS, Lim IS: Comparison of improved BACTEC and Lowenstein-Jensen media for culture of mycobacteria from clinical specimens, *J Clin Microbiol* 28:1288–1291, 1990.

Ang P, Rattana-Apiromyakij N, Goh C-L: Retrospective study of Mycobacterium marinum skin infections, *International J Dermatol* 39:343–347, 2000.

Arnow PM, Bakir M, Thompson K, Bova JL: Endemic contamination of clinical specimens by Mycobacterium gordonae, *Clin Infect Dis* 31:472–476, 2000.

Aubry A, Chosidow O, Caumes E, Robert J, Cambau E: Sixty-three cases of Mycobacterium marinum infection: clinical features, treatment, and antibiotic susceptibility of causative isolates, *Arch Intern Med* 162:1746, 2002.

Bergmann JS, Woods GL: Evaluation of the ESP culture system II for testing susceptibilities of Mycobacterium tuberculosis isolates to four primary antituberculous drugs, *J Clin Microbiol* 36:2940–2943, 1998.

Bergmann JS, Yuoh G, Fish G, Woods GL: Clinical evaluation of the enhanced Gen-Probe Amplified Mycobacterium Tuberculosis Direct Test for rapid diagnosis of tuberculosis in prison inmates, *J Clin Microbiol* 37:1419–1425, 1999.

Bergmann JS, Fish G, Woods GL: Evaluation of the BBL MGIT (Mycobacterial growth indicator tube) AST SIRE system for antimycobacterial susceptibility testing of Mycobacterium tuberculosis to 4 primary antituberculous drugs, *Arch Pathol Lab Med* 124:82–86, 2000.

Blake LA, West BC, Lary CH, Todd JR: Environmental nonhuman sources of leprosy, *Clin Infect Dis* 9:562–577, 1987.

Blanche S, Le Deist F, Fischer A, Veber F, Debre M, Chamaret S, et al.: Longitudinal study of 18 children with perinatal LAV/HTLV III infection: Attempt at prognostic evaluation, *J Pediatr* 109:965–970, 1986.

Boehme CC, Nabeta P, Hillemann D, Nicol MP, Shenai S, Krapp F, et al.: Rapid molecular detection of tuberculosis and rifampin resistance, *N Engl J Med* 363:1005–1015, 2010.

Bonnet E, Massip P, Bauriaud R, Alric L, Auvergnat JC: Disseminated Mycobacterium gordonae infection in a patient infected with human immunodeficiency virus, *Clin Infect Dis* 23:644–645, 1996.

Bottger EC, Teske A, Kirschner P, Bost S, Hirschel B, et al.: Disseminated "Mycobacterium genavense" infection in patients with AIDS, *Lancet* 340:76–80, 1992.

Brown-Elliott BA, Wallace RJ: Clinical and taxonomic status of pathogenic nonpigmented or late-pigmenting rapidly growing mycobacteria, *Clin Microbiol Rev* 15:716–746, 2002.

Brown-Elliott BA, Wallace RJ, Sanguinetti M, Fadda G: Clarithromycin resistance in Mycobacterium abscessus, *J Clin Microbiol* 39:2745–2746, 2001.

Brown-Elliott BA, Iakhiaeva E, Griffith DE, Woods GL, Stout JE, Wolfe CR, et al.: In vitro activity of amikacin against isolates of Mycobacterium avium complex with proposed MIC Breakpoints and finding of a 16S rRNA gene mutation in treated isolates, *J Clin Microbiol* 51:3389–3394, 2013.

Brunello F, Favari F, Fontana R: Comparison of the MB/BacT and BACTEC 460 TB systems for recovery of mycobacteria from various clinical specimens, *J Clin Microbiol* 37:1206–1209, 1999.

Buchan BW, Riebe KM, Timke M, Kostrzewa M, Ledeboer NA: Comparison of MALDI-TOF MS with HPLC and nucleic acid sequencing for the identification of Mycobacterium species in cultures using solid medium and broth, *Am J Clin Pathol* 141:25–34, 2014.

Buckwalter SP, Olson SL, Connelly BJ, Lucas BC, Rodning AA, Walchak RC, et al.: Evaluation of matrix-assisted laser desorption ionization-time of flight mass spectrometry for identification of Mycobacterium species, Nocardia species, and other aerobic Actinomycetes, *J Clin Microbiol* 54:376–384, 2016.

Buhler VB, Pollak A: Human infection with atypical acid-fast organisms: report of two cases with pathologic findings, *Am J Clin Pathol* 23:363–374, 1953.

Bull TJ, Shanson DC: Rapid misdiagnosis by Mycobacterium avium-intracellulare masquerading as tuberculosis in PCR/DNA probe tests, *Lancet* 340:1360, 1992.

Butler WR, O'Connor SP, Yakrus MA, Gross WM: Cross-reactivity of genetic probe for detection of Mycobacterium tuberculosis with newly described species Mycobacterium celatum, *J Clin Microbiol* 32:536–538, 1994.

Campbell PJ, Morlock GP, Sikes RD, Dalton TL, Metchock B, Starks AM, et al.: Molecular detection of mutations associated with first- and second-line drug resistance compared with conventional drug susceptibility testing of Mycobacterium tuberculosis, *Antimicrob Agents Chemother* 55:2032–2041, 2011.

Castets M, Boisvert H, Grumbach F, Brunel M, Rist N: [Tuberculosis bacilli of the African type: preliminary note], *Rev Tuberc Pneumol* 32:179–184, 1968.

Centers for Disease Control and Prevention: Updated guidelines for the use of nucleic acid amplification tests in the diagnosis of tuberculosis, *MMWR Morb Mortal Wkly Rep* 58:7–10, 2009.

Centers for Disease Control and Prevention: Mycobacterium haemophilum infections—New York City metropolitan area, 1990-1991, *MMWR Morb Mortal Wkly Rep* 40:636–637, 643, 1991.

Centers for Disease Control and Prevention: Disseminated Mycobacterium bovis infection from BCG vaccination of a patient with acquired immunodeficiency syndrome, *MMWR Morb Mortal Wkly Rep* 34:227–228, 1985.

Chen Y, Jiang J, Jiang H, Chen J, Wang X, Liu W: Mycobacterium gordonae in patient with facial ulcers, Nosebleeds, and positive T-SPOT.TB test, China, *Emerg Infect Dis* 23:1204–1206, 2017.

Clinical and Laboratory Standards Institute (CLSI): *Susceptibility Testing of mycobacteria*, Nocardia *spp. and other aerobic Actinomycetes*. 3rd ed. *CLSI Standard M24*. Clinical and Laboratory Standards Institute, 950 West Valley Road, Suite 2500, Wayne, PA 19087, USA, 2018a.

Clinical and Laboratory Standards Institute (CLSI): *Performance Standards for Susceptibility Testing of Mycobacteria, Nocardia spp. and Other Aerobic Actinomycetes*. CLSI Supplement M62. Clinical and Laboratory Standards Institute, 950 West Valley Road, Suite 2500, Wayne, PA 19087, USA, 2018b.

Cloud JL, Neal H, Rosenberry R, Turenne CY, Jama M, Hillyard DR, Carroll KC: Identification of Mycobacterium spp. by using a commercial 16S Ribosomal DNA sequencing Kit and additional sequencing Libraries, *J Clin Microbiol* 40:400–406, 2002.

Cloud JL, Carroll KC, Cohen S, Anderson CM, Woods GL: Interpretive criteria for Use of AccuProbe for identification of Mycobacterium avium complex directly from 7H9 broth cultures, *J Clin Microbiol* 43:3474–3478, 2005.

Costrini AM, Mahler DA, Gross WM, Hawkins JE, Yesner R, D'Esopo ND: Clinical and roentgenographic features of nosocomial pulmonary disease due to Mycobacterium xenopi, *Am Rev Respir Dis* 123:104–109, 1981.

Coyle MB, Carlson LC, Wallis CK, Leonard RB, Raisys VA, Kilburn JO, et al.: Laboratory aspects of "Mycobacterium genavense," a proposed species isolated from AIDS patients, *J Clin Microbiol* 30:3206–3212, 1992.

Crudu V, Stratan E, Romancenco E, Allerheiligen V, Hillemann A, Moraru N: First evaluation of an improved assay for molecular genetic detection of tuberculosis as well as rifampin and isoniazid resistances, *J Clin Microbiol* 50:1264–1269, 2012.

Debacker M, Aguiar J, Steunou C, Zinsou C, Meyers WM, Scott JT, et al.: Mycobacterium ulcerans disease: role of age and gender in incidence and morbidity, *Trop Med Int Health* 9:1297–1304, 2004.

Dhillon SS, Watanakunakorn C: Lady Windermere syndrome: Middle lobe bronchiectasis and Mycobacterium avium complex infection due to Voluntary cough Suppression, *Clin Infect Dis* 30:572–575, 2000.

Dorman SE, Schumacher SG, Alland D, Nabeta P, Armstrong DT, King B, et al.: Xpert MTB/RIF Ultra for detection of Mycobacterium tuberculosis and rifampicin resistance: a prospective multicentre diagnostic accuracy study, *Lancet Infect Dis* 18:76–84, 2018.

Doyle RM, Burgess C, Williams R, Gorton R, Booth H, Brown J, et al.: Direct whole-genome sequencing of sputum accurately Identifies drug-resistant Mycobacterium tuberculosis faster than MGIT culture sequencing, *J Clin Microbiol* 56, 2018.

Emmanuel FX, Seagar A-L, Doig C, Rayner A, Claxton P, Laurenson I: Human and animal infections with *Mycobacterium microti*, Scotland, *Emerg Infect Dis* 13:1924–1927, 2007.

Evans KD, Nakasone AS, Sutherland PA, de la Maza LM, Peterson EM: Identification of Mycobacterium tuberculosis and Mycobacterium avium-M. intracellulare directly from primary BACTEC cultures by using acridinium-ester-labeled DNA probes, *J Clin Microbiol* 30:2427–2431, 1992.

Falkinham JO: Epidemiology of infection by nontuberculous mycobacteria, *Clin Microbiol Rev* 9:177–215, 1996.

Feldman RA: Mycobacterial skin infection by an Unidentified species: a report of 29 patients, *Ann Intern Med* 80:445, 1974.

Forbes BA, Hall GS, Miller MB, Novak SM, Rowlinson MC, Salfinger M, et al.: Practice guidelines for clinical microbiology laboratories: mycobacteria, *Clin Microbiol Rev* 31, 2018.

Gamboa F, Fernandez G, Padilla E, Manterola JM, Lonca J, Cardona PJ, et al.: Comparative evaluation of initial and new versions of the Gen-Probe Amplified Mycobacterium Tuberculosis Direct Test for direct detection of Mycobacterium tuberculosis in respiratory and nonrespiratory specimens, *J Clin Microbiol* 36:684–689, 1998.

Good RC, Snider DE: Isolation of nontuberculous mycobacteria in the United States, 1980, *J Infect Dis* 146:829–833, 1982.

Gordon SV, Bottai D, Simeone R, Stinear TP, Brosch R: Pathogenicity in the tubercle bacillus: molecular and evolutionary determinants, *Bioessays* 31:378–388, 2009.

Goto M, Okuzumi K, Oka S, Kimura S, Shimada K: [Identification of mycobacteria by the acridinium-ester labeled DNA probes for M. tuberculosis and M. avium-intracellulare complex in culture and its clinical application], *Kansensbogaku Zasshi* 66:81–86, 1992.

Griffith DE, Aksamit T, Brown-Elliott BA, Catanzaro A, Daley C, Gordin F, et al.: An official ATS/IDSA statement: diagnosis, treatment, and prevention of nontuberculous mycobacterial diseases, *Am J Respir Crit Care Med* 175:367–416, 2007.

Hall L, Doerr KA, Wohlfiel SL, Roberts GD: Evaluation of the MicroSeq system for identification of mycobacteria by 16S Ribosomal DNA sequencing and its Integration into a routine clinical mycobacteriology laboratory, *J Clin Microbiol* 41:1447–1453, 2003.

Han XY, Sizer KC, Velarde-Felix JS, Frias-Castro LO, Vargas-Ocampo F: The leprosy agents Mycobacterium lepromatosis and Mycobacterium leprae in Mexico, *Int J Dermatol* 51:952–959, 2012.

Han XY: Detection of the leprosy agent Mycobacterium lepromatosis in South America and Europe, *Am J Trop Med Hyg* 96:260, 2017.

Helb D, Jones M, Story E, Boehme C, Wallace E, Ho K, et al.: Rapid detection of *Mycobacterium tuberculosis* and rifampin resistance by Use of on-Demand, near-patient Technology, *J Clin Microbiol* 48:229–237, 2010.

Hlavsa Michele C, Moonan Patrick K, Cowan Lauren S, Navin Thomas R, Kammerer JS, Morlock GP, et al.: Human tuberculosis due to *Mycobacterium bovis* in the United States, 1995–2005, *Clin Infect Dis* 47:168–175, 2008.

Hoefsloot W, van Ingen J, Andrejak C, Angeby K, Bauriaud R, Bemer P, et al.: The geographic diversity of nontuberculous mycobacteria isolated from pulmonary samples: an NTM-NET collaborative study, *Eur Respir J* 42:1604–1613, 2013.

Hofmann-Thiel S, Turaev L, Alnour T, Drath L, Müllerova M, Hoffmann H: Multicentre evaluation of the speed-oligo Mycobacteria assay for differentiation of Mycobacteriumspp. in clinical isolates, *BMC Infect Dis* 11:353, 2011.

Hologic: *Amplified mycobacteria tuberculosis direct test package insert — IN0014*. Rev001. Hologic, San Diego, CA, 2013.

Horsburgh CR, Havlik JA, Ellis DA, Kennedy E, Fann SA, Dubois RE, et al.: *Survival of Patients with acquired immune Deficiency Syndrome and disseminated <i>Mycobacterium avium* complex infection with and without antimycobacterial Chemotherapy, *Am RevRespir Dis* 144:557–559, 1991.

Horsburgh CR: *Mycobacterium avium* complex infection in the acquired immunodeficiency syndrome, *N Engl J Med* 324:1332–1338, 1991.

Huebner RE, Schein MF, Bass JB: The tuberculin skin test, *Clin Infect Dis* 17:968–975, 1993.

Ignatyeva O, Kontsevaya I, Kovalyov A, Balabanova Y, Nikolayevskyy V, Toit K, et al.: Detection of resistance to second-line antituberculosis drugs by Use of the Genotype MTBDRsl assay: a Multicenter evaluation and Feasibility study, *J Clin Microbiol* 50:1593–1597, 2012.

Inderlied CB, Kemper CA, Bermudez LE: The Mycobacterium avium complex, *Clin Microbiol Rev* 6:266–310, 1993.

Joshi M, Monson TP, Woods GL: Use of interferon-gamma release assays in a health care worker screening program: experience from a Tertiary care centre in the United States, *Can Respir J* 19:84–88, 2012.

Joshi M, Monson TP, Joshi A, Woods GL: IFN-γ release assay conversions and Reversions. Challenges with serial testing in U.S. Health care workers, *Annals of the American Thoracic Society* 11:296–302, 2014.

Kaplan JE, Benson C, Holmes KK, Brooks JT, Pau A, Masur H: Guidelines for prevention and treatment of opportunistic infections in HIV-infected adults and adolescents: recommendations from CDC, the national Institutes of health, and the HIV medicine association of the infectious diseases Society of America, *MMWR Recomm Rep (Morb Mortal Wkly Rep)* 58:1–207, 2009. quiz CE201–204.

Kent PT, Kubica GP: *: Public health mycobacteriology: a guide for the level III laboratory*, USDHHS, Centers for Disease Control, Atlanta, 1985.

Kiers A, Klarenbeek A, Mendelts B, Van Soolingen D, Koeter G: Transmission of Mycobacterium pinnipedii to humans in a zoo with marine mammals, *Int J Tuberc Lung Dis* 12:1469–1473, 2008.

Kiet VS, Lan NTN, An DD, Dung NH, Hoa DV, van Vinh Chau N, et al.: Evaluation of the MTBDRsl test for detection of second-line-drug resistance in Mycobacterium tuberculosis, *J Clin Microbiol* 48:2934–2939, 2010.

Kristjansson M, Green P, Manning HL, Slutsky AM, Brecher SM, von Reyn CF: Molecular Confirmation of Bacillus Calmette-Guerin as the cause of pulmonary infection following urinary tract instillation, *Clin Infect Dis* 17:228–230, 1993.

Kubica T, Rusch-Gerdes S, Niemann S: Mycobacterium bovis subsp. caprae caused one-third of human M. Bovis-associated tuberculosis cases reported in Germany between 1999 and 2001, *J Clin Microbiol* 41:3070–3077, 2003.

Lalvani A, Pareek M: A 100 year update on diagnosis of tuberculosis infection, *Br Med Bull* 93:69–84, 2010.

Lamm DL, Van Der Meijden APM, Morales A, Brosman SA, Catalona WJ, Herr HW, et al.: Incidence and treatment of complications of Bacillus Calmette-Guerin intravesical therapy in superficial bladder cancer, *J Urol* 147:596–600, 1992.

Lebrun L, Espinasse F, Poveda JD, Vincent-Levy-Frebault V: Evaluation of nonradioactive DNA probes for identification of mycobacteria, *J Clin Microbiol* 30:2476–2478, 1992.

Lewinsohn DM, Leonard MK, LoBue PA, Cohn DL, Daley CL, Desmond E, et al.: Official American Thoracic Society/infectious diseases Society of America/centers for disease control and prevention clinical Practice guidelines: diagnosis of tuberculosis in adults and children, *Clin Infect Dis* 64:e1–e33, 2017.

Lewis FMT, Marsh BJ, von Reyn CF: Fish tank exposure and cutaneous infections due to Mycobacterium marinum: tuberculin skin testing, treatment, and prevention, *Clin Infect Dis* 37:390–397, 2003.

Lindeboom JA, Prins JM, Bruijnesteijn van Coppenraet ES, Lindeboom R, Kuijper EJ: Cervicofacial lymphadenitis in children caused by Mycobacterium haemophilum, *Clin Infect Dis* 41:1569–1575, 2005.

Lockwood DN, Suneetha S: Leprosy: too complex a disease for a simple elimination paradigm, *Bull World Health Organ* 83:230–235, 2005.

Lomwardias S, Madge GE: Chaetoconidium and atypical acid-fast bacilli in skin ulcers, *Arch Dermatol* 106:875–876, 1972.

Lotz A, Ferroni A, Beretti JL, Dauphin B, Carbonnelle E, Guet-Revillet H, et al.: Rapid identification of mycobacterial whole cells in solid and liquid culture media by matrix-assisted laser desorption ionization-time of flight mass spectrometry, *J Clin Microbiol* 48:4481–4486, 2010.

Lumpkin LR, Cox GF, Wolf JE: Leprosy in five armadillo handlers, *J Am Acad Dermatol* 9:899–903, 1983.

Marlowe EM, Novak-Weekley SM, Cumpio J, Sharp SE, Momeny MA, Babst A, et al.: Evaluation of the Cepheid Xpert MTB/RIF assay for direct detection of Mycobacterium tuberculosis complex in respiratory specimens, *J Clin Microbiol* 49:1621–1623, 2011.

Maschek H, Georgii A, Schmidt RE, Kirschner P, Böttger EC: Mycobacterium genavense autopsy findings in three patients, *Am J Clin Pathol* 101:95–99, 1994.

Mather CA, Rivera SF, Butler-Wu SM: Comparison of the Bruker Biotyper and Vitek MS matrix-assisted laser desorption ionization-time of flight mass spectrometry systems for identification of mycobacteria using simplified protein extraction protocols, *J Clin Microbiol* 52:130–138, 2014.

Mazumder SA, Hicks A, Norwood J: Mycobacterium gordonae pulmonary infection in an immunocompetent adult, *N Am J Med Sci* 2:205–207, 2010.

Mazurek GH, Jereb J, Vernon A, LoBue P, Goldberg S, Castro K, Committee IE, Centers for Disease C, Prevention: Updated guidelines for using interferon gamma release assays to detect Mycobacterium tuberculosis infection - United States, 2010, *MMWR Recomm Rep (Morb Mortal Wkly Rep)* 59:1–25, 2010.

Miller E, Cantrell C, Beard M, Derylak A, Babady NE, McMillen T, et al.: Performance of Vitek MS v3.0 for identification of Mycobacterium species from patient samples by Use of automated liquid medium systems, *J Clin Microbiol* 56, 2018.

Mitarai S, Kato S, Ogata H, Aono A, Chikamatsu K, Mizuno K: Comprehensive Multicenter evaluation of a new line probe assay Kit for identification of Mycobacterium species and detection of drug-resistant Mycobacterium tuberculosis, *J Clin Microbiol 50*:**8**84–890, 2012.

Mori T: Usefulness of interferon-gamma release assays for diagnosing TB infection and problems with these assays, *J Infect Chemother* 15:143–155, 2009.

Mostowy S, Onipede A, Gagneux S, Niemann S, Kremer K, Desmond EP, et al.: Genomic analysis Distinguishes Mycobacterium africanum, *J Clin Microbiol* 42:3594–3599, 2004.

Murray PR: The acid-fast stain: a specific and predictive test for mycobacterial disease, *Ann Intern Med* 92:512, 1980.

Niemann S, Harmsen D, Rusch-Gerdes S, Richter E: Differentiation of clinical Mycobacterium tuberculosis complex isolates by gyrB DNA sequence polymorphism analysis, *J Clin Microbiol* 38:3231–3234, 2000.

Nightingale SD, Byrd LT, Southern PM, Jockusch JD, Cal SX, Wynne BA: Incidence of Mycobacterium avium-intracellulare complex bacteremia in human immunodeficiency virus-positive patients, *J Infect Dis* 165:1082–1085, 1992.

Nolen L, Haberling D, Scollard D, Truman R, Rodriguez-Lainz A, Blum L, Blaney D, Centers for Disease C, Prevention: Incidence of Hansen's disease—United States, 1994-2011, *MMWR Morb Mortal Wkly Rep* 63:969–972, 2014.

Nordén Å, Linell F: A new type of pathogenic Mycobacterium, *Nature* 168, 1951. 826–826.

Pai M, Zwerling A, Menzies D: Systematic review: T-cell-based assays for the diagnosis of latent tuberculosis infection: an update, *Ann Intern Med* 149:177–184, 2008.

Parashar D, Kabra SK, Lodha R, Singh V, Mukherjee A, Arya T, et al.: Does neutralization of gastric aspirates from children with suspected Intrathoracic tuberculosis affect mycobacterial Yields on MGIT culture? *J Clin Microbiol* 51:1753–1756, 2013.

Patel JB, Leonard DG, Pan X, Musser JM, Berman RE, Nachamkin I: Sequence-based identification of Mycobacterium species using the MicroSeq 500 16S rDNA bacterial identification system, *J Clin Microbiol* 38:246–251, 2000.

Pfyffer G: Mycobacterium canettii, the smooth variant of M. tuberculosis, isolated from a Swiss patient exposed in Africa, *Emerg Infect Dis* 4:631–634, 1998.

Piersimoni C, Scarparo C: Relevance of commercial amplification methods for direct detection of Mycobacterium tuberculosis complex in clinical samples, *J Clin Microbiol* 41:5355–5365, 2003.

Piersimoni C, Scarparo C: Extrapulmonary infections associated with nontuberculous mycobacteria in immunocompetent persons, *Emerg Infect Dis* 15:1351–1358, 2009.

Pinsky BA, Banaei N: Multiplex real-time PCR assay for rapid identification of Mycobacterium tuberculosis complex members to the species level, *J Clin Microbiol* 46:2241–2246, 2008.

Prince DS, Peterson DD, Steiner RM, Gottlieb JE, Scott R, Israel HL, et al.: Infection with *Mycobacterium avium* complex in patients without predisposing conditions, *N Engl J Med* 321:863–868, 1989.

Quan TP, Bawa Z, Foster D, Walker T, Del Ojo Elias C, Rathod P, et al.: Evaluation of whole-genome sequencing for mycobacterial species identification and drug susceptibility testing in a clinical setting: a large-Scale prospective assessment of performance against line probe assays and phenotyping, *J Clin Microbiol* 56, 2018.

Reisner BS, Gatson AM, Woods GL: Use of Gen-Probe AccuProbes to identify Mycobacterium avium complex, Mycobacterium tuberculosis complex, Mycobacterium kansasii, and Mycobacterium gordonae directly from BACTEC TB broth cultures, *J Clin Microbiol* 32:2995–2998, 1994.

Rickman TW, Moyer NP: Increased sensitivity of acid-fast smears, *J Clin Microbiol* 11:618–620, 1980.

Ridley DS, Jopling WH: Classification of leprosy according to immunity. A five-group system, *Int J Lepr Other Mycobact Dis* 34:255–273, 1966.

Rieder HL: Tuberculosis in the United States, *J Am Med Assoc: JAMA*, *J Am Med Assoc* 262:385, 1989.

Rodwell TC, Moore M, Moser KS, Brodine SK, Strathdee SA: Tuberculosis from *Mycobacterium bovis* in Binational Communities, United States, *Emerg Infect Dis* 14:909–916, 2008.

Rohner P, Ninet B, Metral C, Emler S, Auckenthaler R: Evaluation of the MB/BacT system and comparison to the BACTEC 460 system and solid media for isolation of mycobacteria from clinical specimens, *J Clin Microbiol* 35:3127–3131, 1997.

Roth A, Fischer M, Hamid ME, Michalke S, Ludwig W, Mauch H: Differentiation of phylogenetically related slowly growing mycobacteria based on 16S-23S rRNA gene internal transcribed spacer sequences, *J Clin Microbiol* 36:139–147, 1998.

Ruhwald M, Ravn P: Biomarkers of latent TB infection, *Expet Rev Respir Med* 3:387–401, 2009.

Runyon EH: Anonymous mycobacteria in pulmonary disease, *Med Clin North Am* 43:273–290, 1959.

Ryndak M, Wang S, Smith I: PhoP, a key player in Mycobacterium tuberculosis virulence, *Trends Microbiol* 16:528–534, 2008.

Saleeb PG, Drake SK, Murray PR, Zelazny AM: Identification of mycobacteria in solid-culture media by matrix-assisted laser desorption ionization-time of flight mass spectrometry, *J Clin Microbiol* 49:1790–1794, 2011.

Santos LC: Review: the molecular basis of resistance in *Mycobaterium tuberculosis</i&gt*, *Open J Med Microbiol* 02:24–36, 2012.

Scarparo C, Ricordi P, Ruggiero G, Piccoli P: Evaluation of the fully automated BACTEC MGIT 960 system for testing susceptibility of Mycobacterium tuberculosis to pyrazinamide, Streptomycin, isoniazid, rifampin, and ethambutol and comparison with the Radiometric BACTEC 460TB method, *J Clin Microbiol* 42:1109–1114, 2004.

Scollard DM, Adams LB, Gillis TP, Krahenbuhl JL, Truman RW, Williams DL: The continuing challenges of leprosy, *Clin Microbiol Rev* 19:338–381, 2006.

Segal-Maurer S, Kalkut GE: Environmental control of tuberculosis: continuing Controversy, *Clin Infect Dis* 19:299–308, 1994.

Sompolinsky D, Lagziel A, Naveh D, Yankilevitz T: Mycobacterium haemophilum sp. nov., a new pathogen of humans, *Int J Syst Bacteriol* 28:67–75, 1978.

Sosa LE, Njie GJ, Lobato MN, Morris SB, Buchta W, Casey ML, et al.: Tuberculosis screening, testing, and treatment of US health care personnel: recommendations from the national tuberculosis Controllers association and CDC, 2019, *Mmwr-Morbidity and Mortality Weekly Report* 68:439–443, 2019.

Stager CE, Libonati JP, Siddiqi SH, Davis JR, Hooper NM, Baker JF, et al.: Role of solid media when used in conjunction with the BACTEC system for mycobacterial isolation and identification, *J Clin Microbiol* 29:154–157, 1991.

Strumpf IJ, Tsang AY, Sayre JW: Re-evaluation of sputum staining for the diagnosis of pulmonary tuberculosis, *Am Rev Respir Dis* 119:599–602, 1979.

Talwar A, Tsang CA, Pricer SF, Pratt RH, Walker WL, Schmit KM, et al: Tuberculosis - United States, 2018. Mmwr-Morbidity and Mortality Weekly Report 68:257–262, 2019.

Tecson-Tumang FT: Mycobacterium xenopi and the acquired immunodeficiency syndrome, *Ann Intern Med* 100:461, 1984.

Tenover FC, Crawford JT, Huebner RE, Geiter LJ, Horsburgh Jr CR, Good RC: The resurgence of tuberculosis: is your laboratory ready? *J Clin Microbiol* 31:767–770, 1993.

Theel ES, Hilgart H, Breen-Lyles M, McCoy K, Flury R, Breeher LE, et al.: Comparison of the QuantiFERON-TB Gold plus and QuantiFERON-TB Gold in-tube interferon gamma release assays in patients at risk for tuberculosis and in health care workers, *J Clin Microbiol* 56, 2018.

Tholcken CA, Huang S, Woods GL: Evaluation of the ESP Culture System II for recovery of mycobacteria from blood specimens collected in isolator tubes, *J Clin Microbiol* 35:2681–2682, 1997.

Tobin DM, Ramakrishnan L: Comparative pathogenesis of Mycobacterium marinum and Mycobacterium tuberculosis, *Cell Microbiol* 10:1027–1039, 2008.

Tokars JI, McNeil MM, Tablan OC, Chapin-Robertson K, Patterson JE, Edberg SC: Mycobacterium gordonae pseudoinfection associated with a contaminated antimicrobial solution, *J Clin Microbiol 28*:2765–2769, 1990.

Tortoli E, Brunello F, Cagni AE, Colombrita D, Dionisio D, Grisendi L, et al.: Mycobacterium genavense in AIDS patients; report of 24 cases in Italy and reiew of the literature, *Eur J Epidemiol* 14:219–224, 1998.

Tortoli E: Impact of genotypic studies on mycobacterial taxonomy: the new mycobacteria of the 1990s, *Clin Microbiol Rev* 16:319–354, 2003.

van Ingen J, Kohl TA, Kranzer K, Hasse B, Keller PM, Katarzyna Szafranska A, et al.: Global outbreak of severe Mycobacterium chimaera disease after cardiac surgery: a molecular epidemiological study, *Lancet Infect Dis 17*:1033–1041, 2017.

Van Soolingen D, Hoogenboezem T, De Haas PEW, Hermans PWM, Koedam MA, Teppema KS, et al.: A Novel pathogenic Taxon of the Mycobacterium tuberculosis complex, Canetti: Characterization of an exceptional isolate from Africa, *Int J Syst Bacteriol* 47:1236–1245, 1997.

Verma N, Spencer D: Disseminated Mycobacterium gordonae infection in a child with cystic fibrosis, *Pediatr Pulmonol* 47:517–518, 2012.

Wallace RJ, Swenson JM, Silcox VA, Good RC, Tschen JA, Stone MS: Spectrum of disease due to rapidly growing mycobacteria, *Clin Infect Dis* 5:657–679, 1983.

Weinberger M, Berg SL, Feuerstein IM, Pizzo PA, Witebsky FG: Disseminated infection with Mycobacterium gordonae: report of a case and critical review of the literature, *Clin Infect Dis* 14:1229–1239, 1992.

Welch DF, Guruswamy AP, Sides SJ, Shaw CH, Gilchrist MJ: Timely culture for mycobacteria which utilizes a microcolony method, *J Clin Microbiol* 31:2178–2184, 1993.

Wolinsky E: Nontuberculous mycobacteria and associated diseases, *Am Rev Respir Dis* 119:107–159, 1979.

Woods GL, Washington JA: Mycobacteria other than Mycobacterium tuberculosis: review of microbiologic and clinical aspects, *Clin Infect Dis* 9:275–294, 1987.

Woods GL, Fish G, Plaunt M, Murphy T: Clinical evaluation of difco ESP culture system II for growth and detection of mycobacteria, *J Clin Microbiol* 35:121–124, 1997.

Woods GL, Bergmann JS, Witebsky FG, Fahle GA, Wanger A, Boulet B, et al.: Multisite reproducibility of results obtained by the broth microdilution method for susceptibility testing of Mycobacterium abscessus, Mycobacterium chelonae, and Mycobacterium fortuitum, *J Clin Microbiol* 37:1676–1682, 1999.

Woods GL, Wengenack NL, Lin G, Brown-Elliott BA, Cirillo DM, Conville PS: In *Susceptibility testing of mycobacteria*, *Nocardiae*, *and other aerobic Actinomycetes*, (Wayne (PA), 2018.

World Health Organization: *Global tuberculosis control 2018*, p. 15 volumes. Global Tuberculosis Programme, Geneva, 2018.

Wu X, Zhang J, Liang J, Lu Y, Li H, Li C, et al.: Comparison of three methods for rapid identification of mycobacterial clinical isolates to the species level, *J Clin Microbiol* 45:189–1903, 2007.

Youssef D, Shams WE, Elshenawy Y, El-Abbassi A, Moorman JP: Pulmonary infection with caseating mediastinal lymphadenitis caused by Mycobacterium gordonae, *Int J Mycobacteriol* 3:220–223, 2014.

Zeka AN, Tasbakan S, Cavusoglu C: Evaluation of the GeneXpert MTB/RIF assay for rapid diagnosis of tuberculosis and detection of rifampin resistance in pulmonary and extrapulmonary specimens, *J Clin Microbiol* 49:4138–4141, 2011.

Zelazny AM, Calhoun LB, Li L, Shea YR, Fischer SH: Identification of Mycobacterium species by secA1 sequences, *J Clin Microbiol* 43:1051–1058, 2005.

Zelazny AM, Root JM, Shea YR, Colombo RE, Shamputa IC, Stock F, et al.: Cohort study of molecular identification and typing of Mycobacterium abscessus, Mycobacterium massiliense, and Mycobacterium bolletii, *J Clin Microbiol* 47:1985–1995, 2009.

CHAPTER 60

MYCOTIC DISEASES

Peter C. Iwen, George R. Thompson III, Nathan P. Wiederhold

NOMENCLATURE, TAXONOMY, AND FUNGAL MORPHOLOGY, 1195
Overview, 1195
The Fungal Colony, 1195
Structure of Yeasts and Hyphae, 1195
Fungal Pigment, 1195
Reproductive Structures, 1196
Dimorphism, 1199

DIAGNOSTIC TECHNIQUES, 1200
Laboratory Safety, 1200
Specimen Collection and Transport, 1200
Direct Examination, 1200
Isolation in Culture, 1203
Growth Rate, 1203
Growth Temperature, 1203
Morphologic Identification, 1203
Biochemical Identification, 1204
Serologic Identification, 1205
Molecular Identification, 1205
MALDI-TOF Mass Spectrometry, 1206
Susceptibility Testing, 1206

CANDIDIASIS, CRYPTOCOCCOSIS, AND OTHER INFECTIONS CAUSED BY YEAST, 1207
The Genus Candida, 1207
The Genus Cryptococcus, 1209
The Genus Malassezia, 1210
Other Yeast and Yeastlike Pathogens, 1211

MYCOSES CAUSED BY DIMORPHIC FUNGI, 1211
The Genus Histoplasma, 1211
The Genus Blastomyces, 1213
The Genus Coccidioides, 1214
The Genus Sporothrix, 1215
Other Dimorphic Fungi, 1216

DERMATOPHYTOSES, 1216
Risk Factors, 1217
Clinical Diseases, 1217
Laboratory Diagnosis, 1217

MYCOSES CAUSED BY DEMATIACEOUS (MELANIZED) FUNGI, 1219
Clinical Diseases, 1219

MUCORMYCOSIS (ZYGOMYCOSIS), 1220
Risk Factors, 1221
Clinical Diseases, 1221
Pathology, 1221
Laboratory Diagnosis, 1221

ASPERGILLOSIS, FUSARIOSIS, AND OTHER MYCOSES CAUSED BY HYALINE FUNGI, 1222
The Genus *Aspergillus*, 1222
The Genus Fusarium, 1224
The Genera *Scedosporium* and Lomentospora, 1225
Other Septate Hyaline Molds, 1225

MICROSPORIDIOSIS, 1225
Risk Factors, 1225
Pathology, 1225
Laboratory Diagnosis, 1226

***PNEUMOCYSTIS* PNEUMONIA, 1226**
Risk Factors, 1226
Clinical Diseases, 1226
Laboratory Diagnosis, 1226

PROTOTHECOSIS, 1227

SELECTED REFERENCES, 1228

KEY POINTS

- Opportunistic fungal pathogens have emerged as common causes of invasive disease in the compromised host.
- Histopathologic examination of deep tissue is a major means used for the rapid detection and recognition of fungal pathogens causing invasive infection.
- Micromorphologic and phenotypic methods continue to be the general processes used in the clinical laboratory for the identification of fungal pathogens in culture.
- Molecular methods have advanced as techniques used for the confirmed identification of fungal pathogens from culture and are evolving as future methods for the rapid identification of fungal pathogens directly in clinical material.
- *Candida albicans* continues to be the most common fungal species associated with human disease; however, non-*albicans Candida* species are becoming more widespread in causing invasive disease with increased resistance to standard antifungal treatments.
- Dimorphic fungal pathogens are frequent causes of mild infection in people living in endemic areas; however, invasive disease, whether recurrent or primary, is becoming more common owing to the increase in immunocompromised hosts.
- Recent introduction of new antifungal agents and progression of resistance among molds and yeasts have added importance to the development and standardization of antifungal susceptibility testing.

Medical mycology is the science devoted to the study of fungi and their relationship to human disease. This scientific discipline encompasses single-celled yeasts and filamentous molds as agents of disease ranging from superficial skin infection (cutaneous mycosis) to disseminated deep-seated visceral disease (systemic mycosis). Fungal agents include the historically pathogenic fungi (true pathogens), as well as the saprophytic fungi elevated to the status of pathogen by modern therapies and diseases (opportunistic pathogens). Modern therapies such as high-dose chemotherapy to treat cancer and solid organ transplantation, as well as immunosuppressive infection such as acquired immunodeficiency syndrome (AIDS), have served as the impetus to allow fungi to emerge as major causes of human disease (Chen et al., 2011; Miceli & Lee, 2011; Petrikkos et al., 2012; Pfaller & Diekema, 2007; Shoham, 2013; Tuite & Lacey, 2013).

Although medical mycology education for the medical profession in general has been lacking, pathologists who have been nurtured in the surgical pathology suite have acquired a general understanding of the recognition of fungal pathogens. Overall, the general lack of education in this area is troublesome because most fungi are identified by skilled human observation rather than by machines.

The goal of this chapter is to present the fundamentals of medical mycology with an emphasis on practical issues and a description of those fungal pathogens encountered regularly in the laboratory. For a comprehensive atlas of the histopathology of fungal infections, refer to the book by Chandler and Watts (1987) and the articles by Guarner and Brandt (2011) and Roden and Schuetz (2017). Additionally, although not included in the fungal kingdom, infections caused by achlorophyllous algae are also discussed in this chapter because the characteristics of the algae and the diseases they produce resemble fungi more than other infectious agents.

Since this chapter reports specifically on fungal mycoses, other types of fungal diseases are not discussed. Reviews of these other diseases are available and include the topics of noninvasive allergic responses to fungi (Duggal & Wise, 2013; Schubert, 2009; Taxy et al., 2009), poisoning by the ingestion of poisonous fungi (mushroom poisoning or mycetismus) (White et al., 2019), intoxication by ingestion of fungal toxins (mycotoxicosis) (Alshannaq & Yu, 2017), and psychoactive drugs of fungal origin (Stebeiska, 2013).

NOMENCLATURE, TAXONOMY, AND FUNGAL MORPHOLOGY

OVERVIEW

The first hurdle for the beginning mycologist consists of nomenclature and its handmaiden, taxonomy. Members of the fungal kingdom (Eumycota) are eukaryotic cells that have the capability to reproduce by both sexual and asexual methods. Fungi are classified into phyla by the nature of their sexual reproductive structures or lack thereof (Hibbett et al., 2007), with fungi that have recognized sexual reproductive structures (perfect fungi) classified into the phylum *Zygomycota* (now split into the phylum *Glomeromycota* with four additional subphylums of uncertain placement), *Ascomycota*, or *Basidiomycota* based on the type of sexual reproductive structure produced (Kwon-Chung, 2012). Fungi that lacked recognized sexual reproductive structures were classified in the phylum *Deuteromycota*, also called the **imperfect fungi**, on the basis of their asexual reproductive structures. This classification, however, has complicated the naming and taxonomic positioning of fungi due to dual nomenclature to have two scientific names, mainly a species name for those producing asexual (anamorphic) structures and another species name for those with sexual (teleomorphic) structures. A major change in fungal systematics occurred at the July 2011 International Botanical Congress, where it was voted to abolish the dual system of fungal nomenclature and to rename the code regulating the naming of fungi the *International Code of Nomenclature for Algae, Fungi, and Plants* (previously called the *International Code of Botanical Nomenclature*) (Hawksworth, 2011; Hibbett & Taylor, 2013). These new rules meant that after January 1, 2013, one fungus can only have one name. Although many challenges remain with respect to acceptance of what constitutes a valid name for those fungal species that had this dual nomenclature, a regulatory mechanism is now in place to allow for addressing these challenges of naming fungi (Hawksworth, 2011). However, which names to use have not always been straightforward (Wiederhold & Gibas, 2018).

Historically, fungi were identified to species using a combination of morphologic and physiologic characteristics. Important terms, which are still commonly used today in the clinical laboratory to describe these characteristics of fungi, are displayed in Table 60.1. More recently, the development of molecular methods to identify fungi has led to the discovery of fungal species that are morphologically indistinguishable and described as cryptic species. In light of these recent developments, a polyphasic approach has been suggested for the identification of fungal species. This approach includes a combination of molecular sequencing (using at least two genomic targets) or proteomic analysis (i.e., matrix assisted laser-desorption ionization time-of-flight mass spectrometry [MALDI TOF MS]), morphologic features, and physiologic characteristics in the identification process. However, since many clinical microbiology laboratories may still rely on morphologic features for identification of species, recommendations now suggest using the name **species complex** when the identification is based on morphology or other means that cannot distinguish between closely related species (de Hoog et al., 2013, 2015). In this chapter, a simplified conceptual approach is used to recognize the pathogens most commonly encountered in the clinical laboratory. For practical purposes, a few general characteristics shown in Table 60.2 serve as the basis for identification of fungi in the laboratory.

THE FUNGAL COLONY

Two morphologic forms of fungi are recognized and include yeasts and molds. Yeasts are unicellular organisms that usually reproduce asexually by blastoconidia (also called **budding**) to produce a daughter cell. The colonial mass of yeast is a collection of distinct individual organisms that macroscopically may resemble bacterial colonies on the surface of the agar. Many yeast species have colonies that are usually smooth with a regular edge, although some species may be rough with irregular edges. When the colonies become heaped and dull, they may resemble those of staphylococci. Yeast produces catalase, so the noncautious microbiologist who does not perform a Gram stain or a wet preparation may mistake a yeast colony for a bacterium and provide a misleading report. The microscopic presence of "budding yeast" with or without pseudohyphae would be adequate to identify the colony as yeast. Furthermore, the pseudohyphae of yeast are often visible macroscopically as filamentous extensions from the edges of the colony, known colloquially as **feet** (Fig. 60.1).

In contrast to yeasts, molds are described as filamentous fungi that are multicellular in structure. Although the term **mold** is used to describe this morphologic type, the term **mould** is historically recognized and more commonly used by mycologists to describe this morphologic form. The filamentous nature of the mold gives colonies a woolly, fluffy, or velvety appearance, sometimes punctuated with a granular or powdery aspect that is produced by the formation of asexual reproductive structures (Fig. 60.2). At other times, the colony may have a glabrous (smooth) appearance.

The distinction between molds and yeasts is not firmly established. Some yeasts also develop a visually macroscopic filamentous component. For instance, *Trichosporon* spp. are yeasts that develop such filamentous extensions, whereas *Exophiala jeanselmei* is a dematiaceous yeast that develops a mycelium as it matures. Furthermore, dimorphic fungi can exhibit a mold form under some conditions and a yeast or yeastlike form in other circumstances. Clinically important dimorphic fungi are systemic pathogens that behave as molds in the environment and on agar media at 25° to 30°C. In contrast, the tissue form may be yeast (such as *Blastomyces*, *Histoplasma*, and *Sporothrix*) or, in the cases of *Coccidioides immitis* and *Coccidioides posadasii*, a structure called a **spherule** is observed. When cultivated in vitro at 37°C on appropriate media, the tissue form is reproduced by these fungi. Other agents also exhibit dimorphism but are less common in the clinical laboratory. For instance, black molds such as *Fonsecaea pedrosoi* and *Phialophora verrucosa* produce nonhyphal cells in tissue called **sclerotic bodies** but appear as molds when grown on solid media at room temperature. Reverse dimorphism is exemplified by *Malassezia furfur*, which produces both yeast cells and hyphae in the cutaneous lesions of patients with pityriasis versicolor.

STRUCTURE OF YEASTS AND HYPHAE

The morphology of the fungus is an important characteristic for the identification of both yeasts and molds. The filamentous structure of a mold is referred to as **hyphae** (singular, **hypha**), and a mass of hyphae is known as a **mycelium**. The mycelium growing on the surface of or within the agar is known as the **vegetative mycelium**, whereas filamentous extensions above the colony are called **aerial mycelium**. True hyphae may have cross-walls that contain pores for communication through the hyphae or cross-walls that are complete, dividing the hyphae into multiple cells. Hyphae that have cross-walls are called **septate**, whereas those without cross-walls are referred to as **aseptate**. Some fungi that have septate hyphae also have aseptate or septate specialized hyphae (conidiophores) that bear asexual reproductive structures. Conversely, some so-called **nonseptate fungi** have occasional cross-walls and perhaps would be better designated as sparsely septate.

The width of the hyphae and the angle of branching are important clues to fungal identity. Mucormycetes (also called **zygomycetes** and members of the order Mucorales), such as *Rhizopus* spp., have broad, ribbonlike hyphae that have haphazard branching (Fig. 60.3), whereas hyaline molds such as *Aspergillus* spp. have narrow hyphae that branch at acute angles (dichotomous branching) (Fig. 60.4). The designation of a fungus as *Aspergillus* on the basis of hyphal morphology in a smear or tissue section is, in truth, only a statement of the a priori odds for this pathogen group. Describing the characteristics of the hyphae is a better approach to reporting this observation.

Yeasts reproduce asexually by the formation of blastoconidia, where the daughter cell usually appears at one end of a yeast cell and eventually enlarges to form a new yeast cell. This process is also referred to in a more generic sense as budding. If a series of daughter cells do not detach fully from the originating cells, a **pseudohypha** (plural, **pseudohyphae)** is produced. Pseudohyphae are distinguished from true hyphae by the presence of a constriction at the junction of adjacent cells and by the restriction in size of the daughter cell to that of the parent (Fig. 60.5). In contrast, the walls of true hyphae are parallel without constrictions. *Candida albicans* and some strains of *C. tropicalis* may produce pseudohyphae that have the appearance of true hyphae, depending on growth conditions, and differentiation of *Candida* from hyaline molds such as *Aspergillus* in tissue sections on occasion may be problematic. In contradistinction, *Cryptococcus* spp. produces only budding yeast and rarely rudimentary or primitive pseudohyphae, but true hyphae are not formed.

FUNGAL PIGMENT

Some mold hyphae and yeast can be characterized by the production of a dark pigment. These fungi contain melanin, which imparts a brown coloration to the fungal element in microscopic preparations and causes colonies of the fungi to appear dark green, brown, or black. The terms **dematiaceous**, **melanized**, **dark**, and **phaeoid** have been used interchangeably to denote those fungal elements that contain melanin (Revankar & Sutton, 2010). Superimposed dyes in stained smears, wet preps, or histologic sections may partially obscure the color, which can be more obvious in unstained preparations. Those fungi that lack dark hyphal pigmentation

TABLE 60.1
Glossary of Terms Commonly Used in Medical Mycology

Term	Definition
Aerial mycelium	Hyphae produced above the surface of the agar media
Anamorph	Asexual form of fungal sporulation (imperfect state)
Arthroconidium	Conidium derived from the fragmentation of specialized hyphae
Ascocarp (ascoma)	Fruiting structure that contains asci (several types exist)
Ascospore	Sexual spore formed within an ascus following meiosis
Ascus (pl., asci)	Saclike structure that contains ascospores, characteristic of *Ascomycetes*
Basidiospore	Sexual spore formed as an outgrowth of a basidium
Basidium	Structure that contains basidiospores (e.g., mushroom)
Blastoconidium (pl., blastoconidia)	Asexual spore formed by budding of the hyphal, pseudohyphal, or yeast cell
Chlamydospore	Thick-walled resting or survival structure (also called *chlamydoconidia*)
Cleistothecium (pl., cleistothecia)	Enclosed ascocarp, composed of layers of hyphae that contain randomly dispersed asci
Collarette	Funnel-shaped structure at the apex of a phialide
Columella	An extension of the sporangiophore into the base of the sporangium
Conidiogenous cell	Cell that produces conidia
Conidiophore	Specialized hyphal structure that carries the conidia
Conidium (pl., conidia)	Asexual reproductive structure that forms on the side or the end of a hypha or conidiophore
Dematiaceous (phaeoid)	Pigmented conidia, spores, or hyphae due to the presence of melanin
Dimorphic	Displaying two morphologic types, one environmental (mold) and one in vivo (yeast)
Glabrous	Smooth, referring to colonial morphology
Heterothallic	Sexual reproduction requiring the interaction of two different thalli (mating strains)
Holomorph	Whole fungus; the anamorphic plus the teleomorphic state of the fungus
Homothallic	Sexual reproduction can take place within one thallus
Hyaline	Clear, colorless, or transparent
Hypha (pl., hyphae)	Septate or aseptate vegetative unit of a mold
Intercalary	Borne within a hypha
Macroconidium	Larger of two types of conidia produced by a mold
Microconidium	Smaller of two types of conidia produced by a mold
Mold	Filamentous fungus that reproduces by sexual or asexual means
Mycelium	Mass of hyphae that make up the thallus of a mold
Perithecium	Enclosed ascocarp with a pore at the top through which the ascospores are discharged
Phialide	Cell with opening through which conidia are produced
Pseudohyphae	Connected yeast cells (blastoconidia) that resemble a hypha but contain areas of constriction between adjacent cells
Sclerotic body (pl., sclerotia)	Thick-walled, dematiaceous, muriform, rounded cells found in tissue diagnostic for chromoblastomycosis
Septum (pl., septa)	Cross-wall in a hypha
Spherule	A round structure containing endospores characteristic of *Coccidioides* species in tissue
Sporangiophore	Stalk bearing the sporangium
Sporangiospore	Asexual spore produced within a sporangium
Sporangium	Saclike structure in which the asexual sporangiospores develop
Sterigmata	Slender outgrowth of a cell bearing conidia
Teleomorph	Sexual form of a fungal sporulation (perfect state)
Terminal	Borne at the end of a hypha
Thallus (pl., thalli)	Vegetative growth of a fungus; includes an interwoven mass of hyphae
Thermophilic	Fungi that grow at a high temperature
Vegetative mycelium	Hyphae produced on the surface or extending into the agar media
Vesicle	Enlarged or swollen cell, often at the end of a conidiophore or sporangiophore, which may also be within hyphae
Yeast	Single-cell fungus that reproduces by budding or by fission
Zygospore	A mucoraceous spore formed sexually by the union of two similar cells

are referred to as **hyaline** (clear or colorless). This term may not fully reflect the fungal species appearance, because in some cases a light pigmentation may produce colored colonies, and asexual reproductive structures of some hyaline molds may have green, brown, or black pigments that impart a color to the surface of the colony once the reproductive structures have formed. The true appearance of these molds usually can be discerned by observing the back of the colony, which maintains a light coloration. In contrast, both the front (obverse) and the back (reverse) of dematiaceous or highly melanized colonies usually demonstrate the dark pigment.

REPRODUCTIVE STRUCTURES

The primary means for identification of mold fungi is by characterization of asexual reproductive structures. For yeast, phenotypic studies are the mainstay in identification, with asexual reproductive structures serving as ancillary clues in the identification process. The two principal asexual structures are spores (which may also be present as sexual structures) and conidia. Asexual spores (called **sporangiospores**) are produced by cleavage within an encompassing structure called a **sporangium** (Fig. 60.6). **Conidia** (singular, **conidium**) are much more diverse and form by differentiation from the tip or side of a fertile hypha, such as a conidiophore, or by hyphal differentiation. Unfortunately, interchangeable use of the terms *conidium* and *spore* in the literature has led to confusion. *Sporulation* and *spores* often are used as general terms for asexual reproduction, and the term *spore* is sometimes used when *conidium* would have been more accurate.

The principal means of asexual reproduction in yeast is by the formation of blastoconidia (i.e., budding). A bud starts as a softening of the cell

TABLE 60.2
Characteristics Useful for the Identification of Fungi

Characteristic	Examples
Type of macroscopic growth	Colonies of unicellular organisms (yeast)
	Colonies of filamentous organisms (molds)
Morphology of yeast	Budding
	Budding with pseudohyphae
	Round yeast with capsules
	Budding yeast with collarets
Morphology of filamentous structures	True septate hyphae
	True nonseptate hyphae (or sparsely septate)
Pigment of hyphae	Hyaline (lightly pigmented or nonpigmented)
	Dematiaceous or phaeoid (darkly pigmented)
Morphology of asexual reproductive structures	Conidia
	Spores
Morphology of sexual reproductive structures	Ascospores
	Cleistothecia
	Perithecia
Growth rate	Slow (>10 days)
	Medium (4–10 days)
	Fast (<4 days)
Inhibition by cycloheximide	Many saprophytic fungi
Optimal growth temperature	25°–30°C
	35°–37°C
	40°–42°C
	50°–58°C
Biochemical tests	Assimilation
	Fermentation
	Enzymatic degradation (e.g., urease)
	Growth enhancement
Conversion from mold to yeast phase	Supplanted by DNA probe tests in most laboratories
Immunologic detection of antigens or antibodies	*Cryptococcus, Histoplasma, Coccidioides, Blastomyces, Aspergillus*
DNA probe	*Histoplasma, Coccidioides, Blastomyces*

DNA, Deoxyribonucleic acid.

Fig. 60.1 Filamentous extensions from the periphery of colonies of *Candida albicans* are known colloquially as "feet."

Fig. 60.2 Powdery surface of the colonies of *Aspergillus fumigatus* overlies white masses of mycelium. Adjacent bacterial colonies contrast with the filamentous fungus. (Sheep blood agar.)

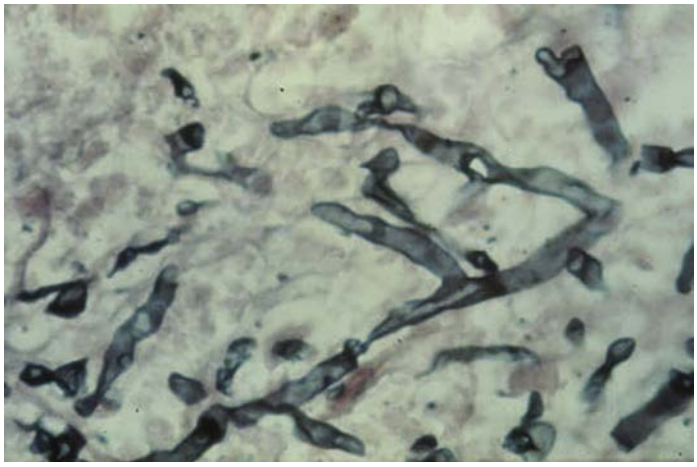

Fig. 60.3 Characteristic wide, nonseptate hypha of a mucormycete in lung tissue. (Gomori's methenamine silver stain, 400×.)

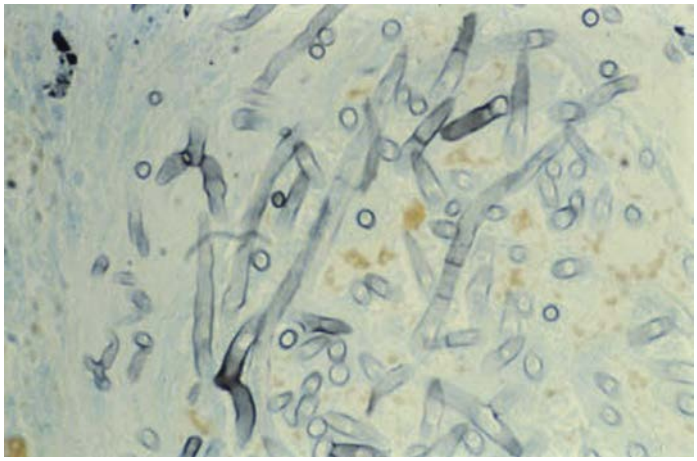

Fig. 60.4 Characteristic narrow branching, septate hyphae of a hyaline mold in tissue. (Gomori's methenamine silver stain, 400×.)

wall of the mother cell, followed by expansion of the cell wall (blown out) and migration of nucleus and cytoplasm to the swollen area. A septum seals the boundary between daughter and parent cells (Fig. 60.7). If separation does not occur, a pseudohypha results.

The portions of the vegetative mycelium that differentiate into conidia are referred to as **conidiogenous cells**. Specialized hyphae that support the conidia are termed **conidiophores**, which may be the conidiogenous cell itself arising from the vegetative mycelium or may be a supporting hypha. In *Aspergillus* spp., the conidiophore, which is aseptate, enlarges

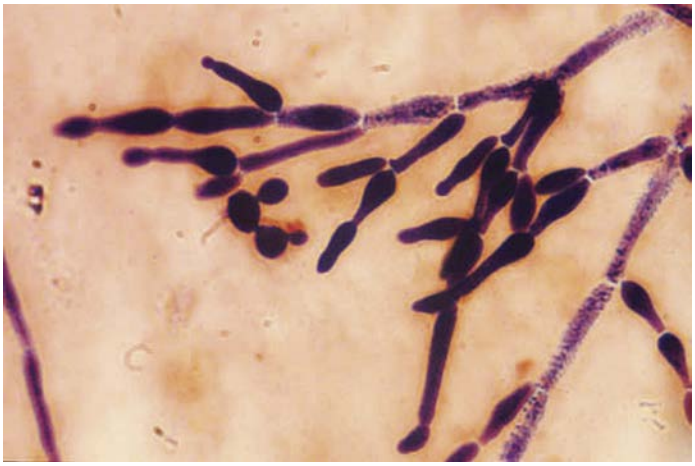

Fig. 60.5 Chains of elongated budding yeasts of *Candida albicans* producing pseudohyphae observed in sputum. (Gram stain, 1000×.)

Fig. 60.6 Sporangiophores of *Rhizopus* spp. supporting sporangia that contain sporangiospores. Rhizoids arise from the hyphae near the origin of the sporangiophores. (Lactophenol cotton blue stain, 100×.)

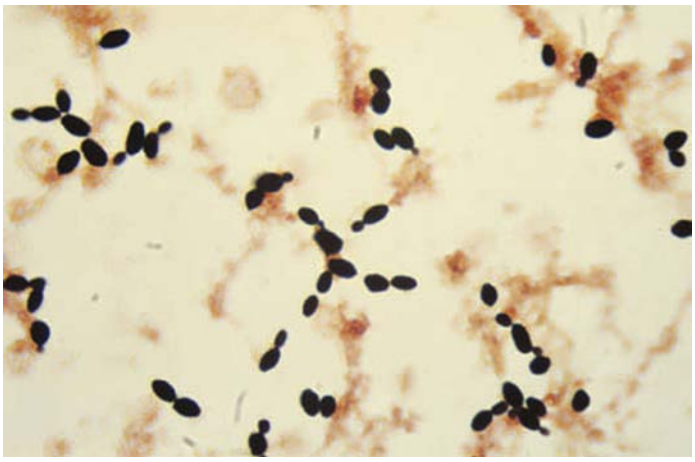

Fig. 60.7 Budding and nonbudding yeast cells detected in a blood culture bottle sample. (Gram stain, 1000×.)

at the tip to form a swollen vesicle (Fig. 60.8). Conidiogenous cells, now termed **phialides**, arise from the vesicle to support chains of conidia. Some species of *Aspergillus* produce a row of phialides, which occur on a row of sterile cells called **metulae**, with the conidia arising from the distal phialides. The mucormycetes produce structures called sporangiophores, which support the sporangium with enclosed sporangiospores (see Fig. 60.6). An extension of the apex of the sporangiophore into the sporangium is termed the **columella**.

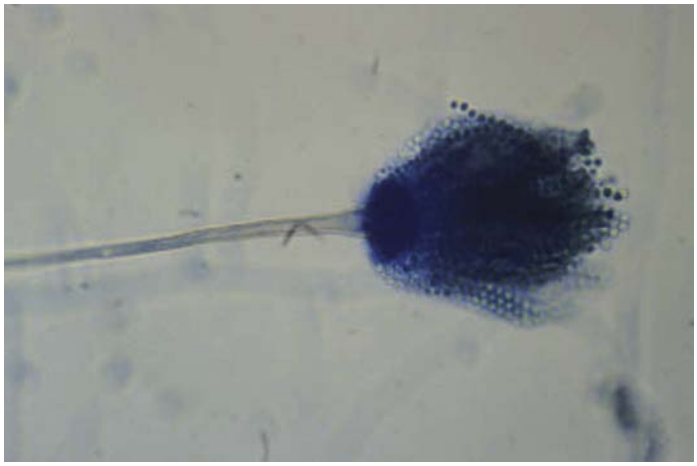

Fig. 60.8 Fruiting head of *Aspergillus fumigatus*. The conidiophore is swollen at the tip to form a vesicle, and phialides arise from the upper half of the vesicle with chains of conidia present that align parallel to the long axis of the conidiophore. (Lactophenol cotton blue stain, 400×.)

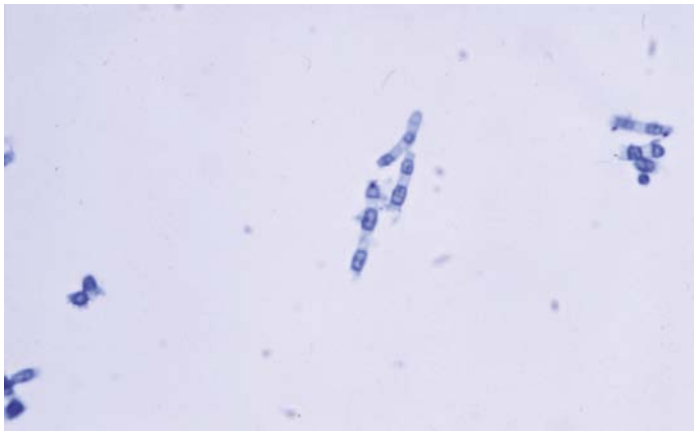

Fig. 60.9 Arthroconidia of *Coccidioides* spp. Alternating barrel-shaped arthroconidia are separated by thin-walled, empty disjunctor cells within portions of the hyphae. (Lactophenol cotton blue stain, 400×.)

Thallic conidiogenesis is a process in which the conidium does not develop until a septum is formed between the conidium and the parent cell. The conidium originates from the whole of the parent cell. The most important human pathogens that exhibit thallic conidiogenesis are the dermatophytes and the dimorphic fungi in the genus *Coccidioides*. As conidiogenesis progresses in these species, barrel-shaped conidia called **arthroconidia** are produced; these fragment easily and are disseminated with little difficulty, resulting in a high degree of infectivity demonstrated by these important human pathogens (Fig. 60.9). The thallic conidia of the dermatophytes are separated by size into two types: large septate macroconidia (Fig. 60.10) and small, one-celled microconidia that are simpler structures (Fig. 60.11).

The other type of conidiogenesis is called **blastic conidiogenesis**, whereby the protoplasm of the conidiogenous cell is blown out or blasted to form the conidium. The simplest form of blastic conidiogenesis is the budding process by which many types of yeast, including *Candida* spp., develop. As with thallic conidia, blastoconidia are divided into two types: one where the cell wall is involved in the process and the other where it is not. Further division of blastic conidiogenesis is made among those species in which the outer cell wall does not participate in the process (called **enteroblastic conidiogenesis**). In enteroblastic fungi, phialidic and annellidic conidiogenous cells have been recognized. Phialides are conidiogenous cells that often have a collarette at the apices, produced when the tip releases the first conidium. The collarette may be a conspicuous flask-shaped structure, as observed in *Phialophora* spp., or an inconspicuous structure, as seen in *Aspergillus* spp. In contrast, annellides are conidiogenous cells that rupture to leave a distinct ring of cellular material at the base of the conidium when it separates from the annellide. Formation of sequential conidia at the base pushes the oldest cell to the tip of the chain and leaves a series of rings or annellations at the apex of the annellide, providing a record of past events, like rings on a tree. Although important for

Fig. 60.10 Macroconidia of *Epidermophyton floccosum.* Typical blunt-ended macroconidia occur in aggregates along the hyphae with the absence of microconidia. (Lactophenol cotton blue stain, 400×.)

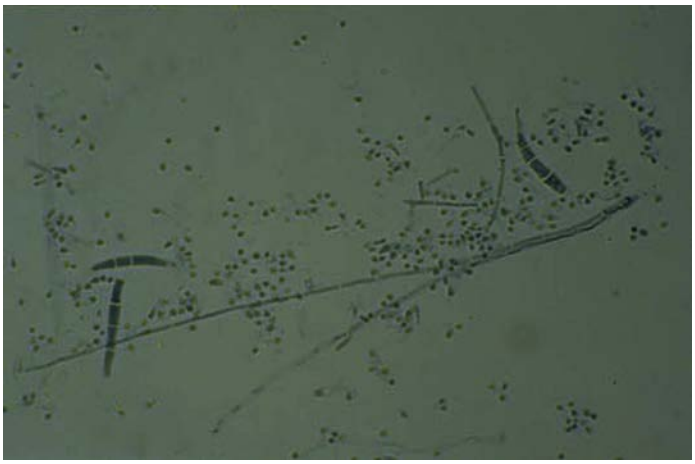

Fig. 60.11 Elongated macroconidia of *Trichophyton mentagrophytes* along with microconidia are lined up along the surface of the hypha. (Lactophenol cotton blue stain, 400×.)

the microscopic identification of some mold fungi, the fine details of these structures may be difficult to visualize using the light microscope.

Differentiation of the various conidial structures is important for the correct identification of many fungal isolates. In some cases, the pertinent morphologic features are easily discerned; however, as in surgical pathology, pattern recognition is an essential tool for identification of the most common pathogens and saprobes. The pathologist should always appreciate the salient features of the entire morphologic preparation without primarily focusing on outliers or aberrant structures. Developing conidial structures of *Aspergillus* or *Paecilomyces*, for instance, may resemble the structures of *Penicillium*, and the observer must not be misled into thinking that two molds are present. At the same time, the possibility of a mixed culture must be remembered. Mycologists must use a low-powered objective for initial observation from fungal culture; however, the details of cellular subsets in that low-powered picture must be appreciated for study at a higher magnification.

The fine art of mycologic diagnosis rests in the appreciation and differentiation of cellular details, and in some instances, the task requires great subtlety and considerable experience. Sometimes, the isolate must be coaxed to produce the necessary diagnostic structures by selection of appropriate media (Table 60.3). In general, enriched media favor the propagation of vegetative mycelium, whereas asexual reproductive structures are encouraged by basal (starving) media. Subculture onto water agar or potato flake agar is a general technique for encouraging the development of conidial structures. The colors of *Aspergillus* colonies are best studied on Czapek-Dox agar, whereas *Trichophyton rubrum* is encouraged to produce red pigment on potato dextrose or potato flake agar or on cornmeal agar with 1% glucose.

Experience also is important in determining whether a subculture has been incubated sufficiently long for diagnostic structures to form. Rootlike structures (rhizoids) that develop from the hyphae of some mucormycetes

TABLE 60.3
Media for the Identification and Isolation of Fungi

Medium	Main Function
Ascospore medium, V-8 agar	Ascospore development
Birdseed (niger) agar	Demonstration of melanin in *Cryptococcus neoformans*
Brain-heart infusion agar with blood	Enhanced recovery of dimorphic fungi
Christensen urea agar	Differentiation of *Trichophyton rubrum* and *T. mentagrophytes*
CHROMagar *Candida*	Chromogenic mixture to identify *Candida* species
Cornmeal agar with Tween 80	Visualization of yeast morphology
Czapek-Dox agar	Identification of *Aspergillus* species
Inhibitory mold agar	Selective medium that contains chloramphenicol and gentamicin
Potato dextrose agar or Potato flake agar	Pigment development of *Trichophyton rubrum* and mold morphology
Sabouraud dextrose (SAB) agar	General purpose fungal growth medium (traditional formulation or Emmon's modification)
SAB agar with antibiotics	Selective medium to inhibit saprophytic fungi (antibacterials such as chloramphenicol or gentamicin also included)
Slide culture (various agars)	Study of microscopic structure
Trichophyton agars	Differentiation of *Trichophyton* species

are important differentiating features, but they may not be detected if observation is terminated prematurely. Some of the techniques necessary for complete differentiation are difficult or even beyond the reach of most clinical laboratories. For instance, the melanized pathogen *Exophiala dermatitidis* produces blastic conidia with phialides and annellides. The presence of annellides was not recognized when the mold was studied with the light microscope, however, and this organism was once classified as *Phialophora dermatitidis.* Recognition that annellides were formed by the isolate led to a reassignment to a new genus, *Exophiala*, which contained both phialides and annellides.

Sexual reproductive structures are of occasional value for fungal identification in the general mycology laboratory. Although they are infrequently encountered in vitro, recognition of sexual structures for heterothallic fungi requires that a compatible mating strain be available for testing. Homothallic fungi, on the other hand, can produce sexual structures in culture without this mating process. The two structures most likely to be demonstrated in the laboratory from homothallic species are the naked asci of *Saccharomyces cerevisiae* and the cleistothecium of *Scedosporium boydii* (previously known as *Pseudallescheria boydii* and formerly considered to be the sexual phase of *Scedosporium apiospermum* but now recognized as a separate species) (Gilgado et al., 2008), *Aspergillus nidulans*, or the *Aspergillus glaucus* group of fungi. The naked asci of *Saccharomyces* resemble oval yeast cells in which one to four individual haploid ascospores are enclosed (Fig. 60.12). The ascospores in this species may be visualized in wet preparations but are detected more reliably using a Gram stain or an acid-fast stain. A cleistothecium is a sexual fruiting body (ascocarp) in which the ascospores are entirely enclosed and can be released only by rupture of the cleistothecial wall (Fig. 60.13). The wall is composed of single or multiple layers of specialized hyphae. A perithecium is a sexual structure similar to a cleistothecium, but it contains an opening at the apex of the pear-shaped structure.

Although asexual and rarely sexual reproductive structures are necessary for the identification of fungi, especially molds, some isolates refuse to produce either of these structures for diagnosis. The colonies consist only of vegetative and aerial hyphae morphologically and subsequently are described as **sterile hyphae** or **mycelia sterilia**. Identification under this circumstance requires molecular or proteomic methods that may not be readily available in most routine diagnostic laboratories (Gomez, 2014; Griffin & Hanson, 2014; Zhang, 2013).

DIMORPHISM

Demonstration of dimorphism is the traditional approach to definitive identification of endemic fungal pathogens. In most laboratories, the initial

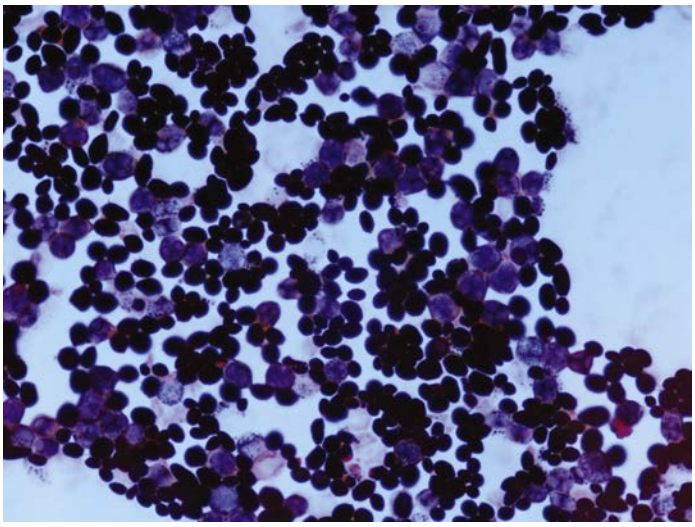

Fig. 60.12 Ascospores with asci (pale staining) along with budding yeast cells of *Saccharomyces cerevisiae.* (Gram stain, 1000×.)

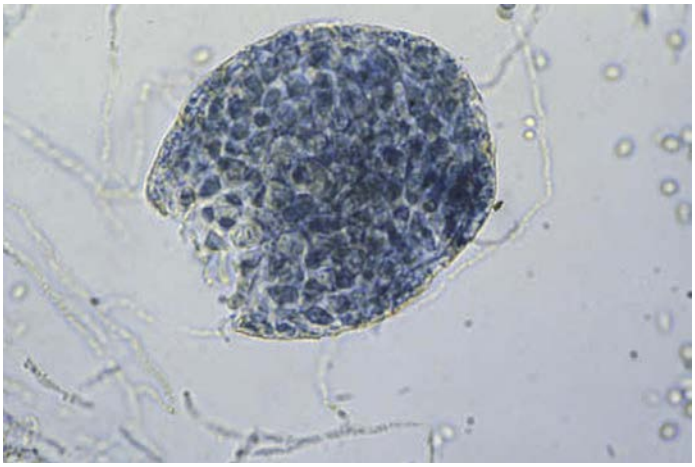

Fig. 60.13 Cleistothecium of *Scedosporium boydii.* This sexual reproductive structure is specifically referred to as an ascus containing ascospores. (Lactophenol cotton blue stain, 400×.)

isolate is the mold phase because culture plates usually are incubated at 25° to 30°C. Conversion to the tissue phase (yeast or yeastlike structure) is accomplished by incubating a subculture at 37°C. The transition from mold to yeast morphology may occur grudgingly, and hyphal forms are often intermixed with yeast cells. Some isolates may never be successfully converted. A rich medium, such as brain-heart infusion agar with a blood supplement, should be included with the primary isolation medium, particularly when *H. capsulatum* is suspected. Cysteine hemoglobin agar is a common medium used for the conversion of *B. dermatitidis.* Media for conversion of *Coccidioides* spp. have been described but are not often used. Similarly, inoculation of animals is infrequently employed in clinical laboratories, although this method is effective when used for conversion to the in vivo phase. The introduction of molecular probes has considerably simplified the task of definitive identification for these endemic fungi and has eliminated the need to demonstrate both phases of the dimorphic fungi in the laboratory (Reiss et al., 2000). Rapid deoxyribonucleic acid (DNA) probe tests, which utilize the technique of nucleic acid hybridization, are available for the identification of the three major dimorphic pathogens from culture (e.g., GenProbe AccuProbe, Hologic, Inc., San Diego, CA). Although demonstration of the characteristic yeast or yeastlike phase in tissue strongly supports the diagnosis of a dimorphic fungus, identification of the pathogen in culture is still necessary for disease confirmation (Sangoi et al., 2009).

DIAGNOSTIC TECHNIQUES

With the increased number of patients undergoing transplantation procedures or receiving aggressive immunosuppression and chemotherapy, the growing population of immunosuppressed hosts has dramatically increased, leading to a subsequent rise in the prevalence of invasive fungal infection (Chandrasekar, 2009). Early recognition of a fungal infection to optimize patient management is becoming more realistic with advances in diagnostic applications for the identification of fungal etiologic agents.

LABORATORY SAFETY

Biosafety considerations from specimen collection through culture conformation in the mycology laboratory are critical (Clinical and Laboratory Standards Institute [CLSI], 2012). Inoculation of specimens and manipulation of mold colonies should always be performed in a biologic safety cabinet to prevent dissemination of the highly mobile fungal conidia. Scrupulous attention to cleaning the surfaces of both the biologic safety cabinet and the incubator should be maintained. Separate safety cabinets for the study of isolated molds may minimize contamination of other clinical samples.

The greatest hazard for laboratory personnel comes from handling mold cultures of the dimorphic pathogens, *Coccidioides immitis/posadasii* and *H. capsulatum*. These isolates are classified as risk group 3 (RG3) pathogens, and biosafety level 3 practices, containment equipment, and facilities are highly recommended for propagating and manipulating cultures, as well as for processing soil or other environmental materials known or likely to contain infectious conidia from these agents (Department of Health and Human Services, 2004, 2009, 2019). Screw-capped tubes of culture media should be used for culture if these pathogens are suspected. Unfortunately, the diagnosis may not be appreciated before the pathogen is isolated in some cases. All work with molds, however, should be performed in a certified biologic safety cabinet.

Of special note is that the tissue phase of dimorphic pathogens is not infectious by the airborne route, thus little or no biohazard is involved in handling tissue specimens from patients with blastomycosis, histoplasmosis, or coccidioidomycosis. A possible exception to this rule might occur if a *Coccidioides* spp. grew as a mold within a lung cavity that connected with the bronchial tree, which would allow for in vivo sporulation.

SPECIMEN COLLECTION AND TRANSPORT

The correct specimen for submission to the mycology laboratory depends on the clinical presentation and the organ system affected (CLSI, 2012). A summary of the major categories of diseases produced by fungi along with suggested specimens is presented in Table 60.4.

Yeast, particularly *Candida* spp., may be recovered on occasion from swab specimens, especially from purulent lesions. Flocked swabs may be used for sampling oral or vaginal lesions suggestive of candidiasis and may be adequate for collecting specimens from patients with chronic external otitis, in which large numbers of *Aspergillus* conidia are usually present. However, swabs are decidedly inferior for collecting specimens in most areas of the infectious process. Particularly problematic is that swab fibers may be mistaken for hyphal elements upon direct examination of clinical specimens. A policy of rejecting swabs for fungal culture should be accompanied in most cases by assiduous and persistent educational efforts.

The best specimens for mycologic diagnosis are scrapings, curettings, aspirates, and lesion biopsies. Hairs infected with a dermatophytic fungus (e.g., *Microsporum canis*) fluoresce under a long-wavelength ultraviolet light (Wood's lamp) and can be specifically selected for examination. Cutaneous lesions of dermatophytosis (ringworm) are characterized by an active advancing edge with central healing, so that scrapings can be collected from the edge of the process. Hair, nails, scalp, and skin scrapings should be sent to the laboratory in a clean, dry container. Tissue samples should be sent in a sterile container with a small amount of sterile, preservative-free saline or a transport medium to prevent drying of the sample. Most samples can be handled as one would any other samples submitted for bacterial observation and culture.

DIRECT EXAMINATION

Most clinical specimens can be examined directly for the presence of a fungal pathogen, although negative results are not sensitive enough to rule out the presence of a fungus. Multiple techniques are employed for the direct examination of clinical material. As a reminder, multiple manipulations of specimen material in the laboratory may render the material not acceptable for culture, so in cases in which culture is warranted, specimens must be separated before this type of examination is performed.

TABLE 60.4

Major Clinical Syndromes and Commonly Associated Fungal Pathogens

Clinical Presentation/Organ System	Patient Group	Likely Pathogens	Specimen(s)
Skin, hair, or nail infection	All	Dermatophytes	Skin scraping
		Candida	Hair
		Malassezia	Nail clipping
Subcutaneous tissue infection	All	*Coccidioides*	Lesion biopsy
		Blastomyces dermatitidis	
		Sporothrix schenckii	
	Patient with mycetoma	*Scedosporium apiospermum*	
		Madurella	
		Actinomadura	
Primary pneumonia	All	*Histoplasma capsulatum*	Sputum
		Blastomyces dermatitidis	Bronchoalveolar lavage
		Cryptococcus neoformans	Transbronchial biopsy
		Coccidioides	Surgical lung biopsy
			Pleural fluid
			Thoracentesis fluid
	Immunodeficient	*Aspergillus*	
		Fusarium	
		Mucormycetes/Zygomycetes (Mucorales)	
		Scedosporium	
		Pneumocystis jirovecii	
Gastrointestinal infection	Immunodeficient	*Candida*	Scrapings
		Aspergillus	Curettings
		Mucormycetes/Zygomycetes (Mucorales)	Biopsy
Urinary tract infection	All	*Candida*	Urine
Endocarditis	All	*Candida*	Blood
		Fusarium	
Meningitis	Immunodeficient	*Cryptococcus neoformans/C. gattii*	Cerebrospinal fluid
		Candida	
		Coccidioides	
Encephalitis and brain abscess	Immunodeficient	Mucormycetes/Zygomycetes (Mucorales)	Brain biopsy
		Aspergillus	
		Cladophialophora bantiana	
Osteomyelitis	All	*Coccidioides*	Biopsy
		Blastomyces dermatitidis	
		Cryptococcus	
Keratitis	All	*Aspergillus*	Scraping
		Fusarium	
External otitis	All	*Aspergillus*	Scraping
			Swab
Sinusitis	All	*Aspergillus*	Biopsy
		Fusarium	Curettings
		Dematiaceous molds	
Burn wounds	All	*Aspergillus*	Biopsy
		Mucormycetes/Zygomycetes (Mucorales)	
		Fusarium	
		Scedosporium	
Vaginitis	All	*Candida*	Vaginal secretions
Intravenous catheter infection	Indwelling catheter	*Candida*	Catheter tip
		Malassezia (newborns)	Blood
Disseminated infection	All	*Histoplasma capsulatum*	Blood, bone marrow
		Blastomyces	Tissue biopsy
		Coccidioides	
	Immunodeficient	*Candida*	Blood
		Mucormycetes/Zygomycetes (Mucorales)	Tissue biopsy
		Aspergillus	
		Fusarium	
		Scedosporium	
		Cryptococcus	
		Potentially any fungus	

Wet Preparation

The simplest method for direct examination of a specimen is to observe a suspension placed on a slide and coverslip under reduced light. For those specimens that are dry or viscous, the addition of a wetting agent such as saline is necessary prior to observation. For specimens that contain distracting tissue debris and cells, such as vaginal secretions, nails, and skin scrapings, a solution of potassium hydroxide (KOH) may be used as a means to dissolve the tissue material, so that fungal elements are more visible (Box 60.1). Some preparations also contain dimethyl sulfoxide (DMSO), which facilitates more rapid breakdown of keratinized tissue, and chlorazole, a lipophilic dye that is attracted to and stains fungal elements an iridescent green-black (i.e., Chlorazole Black E) (CLSI, 2012).

Gram Stain

This commonly used microbiologic stain is particularly useful for the detection of yeast. Most yeasts stain partially or completely gram positive and are generally differentiated from bacteria by their larger size and by the presence of budding cells (see Fig. 60.5). The hyphae of molds may appear gram positive or gram negative by this stain but may stain less reliably than yeast cells and are easily missed in clinical specimens using this method.

Giemsa or Wright Stain

In cases in which histoplasmosis is suspected, these hematologic stains are useful for demonstrating yeast cells within macrophages.

India Ink Preparation

The polysaccharide capsule of species within the *Cryptococcus neoformans/C. gattii* species complex can be demonstrated by negative staining using India ink particles; it is especially evident when infected cerebrospinal fluid (CSF) is examined. When examined with the light microscope, the capsule stands out as a clear space around the fungal cell, with ink particles bouncing off the edge as brownian motion occurs (Fig. 60.14). When budding yeast cells are demonstrated along with the capsule in the CSF of an infected patient, the specificity of the diagnosis of cryptococcal meningitis is ensured. Other potentially encapsulated fungi, such as *Rhodotorula* spp., *Exophiala spinifera*, or other cryptococcal species are infrequent pathogens and can be eliminated from practical consideration under this circumstance. Although the capsules usually are large in direct examination of specimens, isolation of the pathogen on agar media is usually characterized by the production of a much-diminished capsule, which is not as obvious. Unfortunately, some *C. neoformans* strains are poorly encapsulated; thus the sensitivity of the India ink test is generally less than 50%, and the organism is especially evident in patients who are not infected with the human immunodeficiency virus (HIV). However, direct detection of antigen in CSF or serum using a latex agglutination or enzyme immunoassay technique has increased the sensitivity to close to 100%. These techniques basically have replaced the use of India ink as a direct diagnostic technique, although the India ink technique is still useful when the antigen test is not immediately available and for examination of capsules in cells from isolated colonies that suggest *C. neoformans/C. gattii* species complex.

Histopathologic Stains

Surgical pathologic examination of biopsy material is a common practice for the identification of suspected fungal infection (Guarner & Brandt, 2011). A number of stains have proved useful in recognizing fungal elements in tissue and in showing the immunologic response to infection. The periodic acid–Schiff (PAS) method is useful for demonstrating internal details. Gomori's methenamine silver (GMS) technique is considered one of the better stains for demonstrating fungi because it provides high contrast with minimal background staining, thus allowing for the demonstration of sparsely present fungal elements in the sample. The hematoxylin and eosin (H&E) stain is best used for studying the host reaction and for determining whether a fungus is hyaline (colorless) or dematiaceous (naturally pigmented). Other more specialized stains include Mayer's mucicarmine stain for demonstration of the mucoid capsule of *C. neoformans* and the Fontana-Masson stain for demonstration of melanin or melanin-like substances in the lightly pigmented agents of phaeohyphomycosis as well as the staining of minute amounts of melanin pigment in the cell wall of *C. neoformans/C. gattii* species complex. A book by Chandler and Watts (1987) provides greater detail on the utilization of stains to detect fungi in tissue.

Calcofluor White Stain

This fluorochrome compound, a whitener used in the textile and paper industries, binds to the chitin in the walls of fungal cells and fluoresces white (Fig. 60.15) or apple green (depending on the filter combination used) when exposed to short-wavelength ultraviolet light from a fluorescence microscope (Box 60.2) (Hageage & Harrington, 1984). Calcofluor white can also be mixed with potassium hydroxide to clear

BOX 60.1

KOH Preparation

1. Place 1 drop of 10% potassium hydroxide (KOH) on a clean glass slide.
2. Immerse an aliquot of the specimen in the drop of KOH on the slide.
3. Gently heat the mixture by passing the slide through a Bunsen burner flame several times. Do not allow the mixture to boil.
4. Coverslip the slide and examine at 100× and 400× magnification using reduced light. Excessively tenacious specimens may require additional heating.
5. KOH may also be used as a simple mounting medium without heating (the addition of Lactophenol [aniline] blue or Calcofluor white stain with the KOH will enhance the visibility of fungal elements).

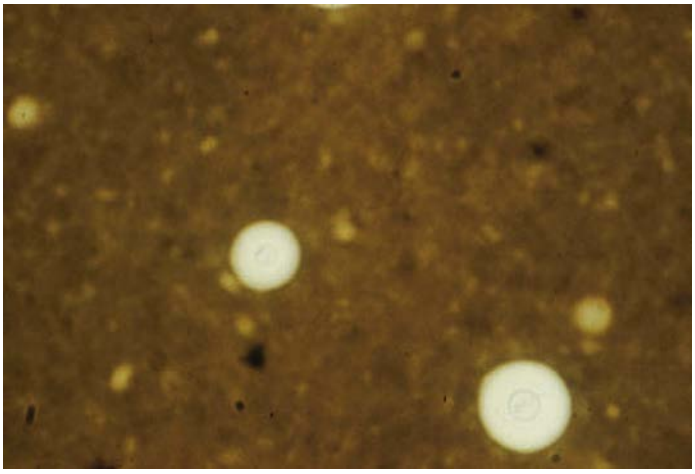

Fig. 60.14 India ink preparation of cerebrospinal fluid containing *Cryptococcus neoformans*. This yeast produces a characteristic polysaccharide capsule around the budding yeast cells. (400×.)

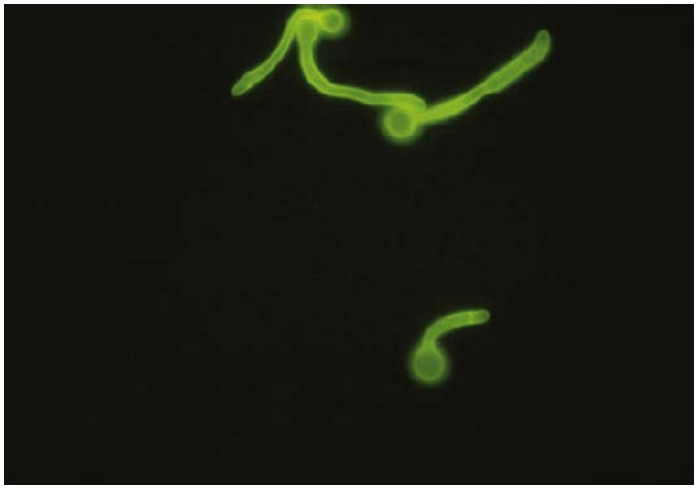

Fig. 60.15 Calcofluor white stain of *Candida albicans* in culture. When viewed with a fluorescence microscope, the chitinous walls of the fungus will fluoresce. Germ tubes shown are produced following incubation of the yeast in serum. (Courtesy Dr. Brian Harrington, Centers for Disease Control and Prevention Public Health Image Library.)

BOX 60.2

Calcofluor White Stain

1. Place specimen on a clean glass slide.
2. Mix with Calcofluor white reagent.
3. Using a fluorescence microscope, examine the preparation for fungal elements at 100× to 400× magnification (will typically appear bluish white against a dark background). (Calcofluor white may be substituted for Lactophenol [aniline] blue stain when microscopic morphology of culture isolates is studied.)

the specimen for easier observation of fungi. As is true with all fluorescent staining, care must be used in interpreting the results because nonspecific staining of substances that resemble fungal elements may also occur.

Immunohistochemical Stains

Immunohistochemistry has been used to identify a wide variety of infectious agents, including the fungi, in fresh, frozen, or paraffin-embedded tissues (Eyzaguirre & Haque, 2008). Although many fungi can be readily identified by standard histologic staining, some fungal elements appear atypical in tissue sections and in some cases cannot be distinguished morphologically. Monoclonal and polyclonal antibodies for *Aspergillus* spp. and *Candida albicans* have been previously available (AbD Serotec, Bio-Rad Laboratories, Inc, Hercules, CA); however, these are not US Food and Drug Administration (FDA) approved and would require in-house validation testing prior to patient use. Cross-reactivity with *Fusarium* spp. has been found using immunohistochemicals to detect *Aspergillus* spp. (Lackner & Lass-Florl, 2013).

ISOLATION IN CULTURE

Selection of Media

All specimens should be inoculated onto a general-purpose fungal growth medium (see Table 60.3). The medium used traditionally is Sabouraud dextrose agar, which has a pH of 5.5 to 5.6 and was designed for the isolation of dermatophytic fungi. Emmons modification of Sabouraud dextrose agar, which contains less glucose with a pH of 6.8 to 7.0, is more widely used in the clinical mycology laboratory as a general growth medium because of its wide application for the culture of fungi. Inhibitory mold agar and potato dextrose agar or potato flake agar are also utilized as general isolation media in the laboratory.

For specimens from nonsterile sites or from sites that are likely to be contaminated with other microbial flora, inoculation of a nonselective agar and a selective agar in tandem is recommended. The most commonly used selective agar employs cycloheximide (400 to 500 mg/L) to inhibit saprobic fungi and an antibacterial agent (usually chloramphenicol [50 mg/L] or gentamicin [50 mg/L]) to inhibit bacteria. For tissue specimens, especially when dimorphic fungi might be the etiologic agent, an enriched agar, such as brain-heart infusion agar with 5% to 10% sheep blood and supplemented with chloramphenicol and gentamicin or SABHI agar with antibiotics, may be added.

For the cultivation of yeast from clinical specimens the selective and differential medium called CHROMagar *Candida* (CHROMagar Company, Paris, France) may be used for the isolation and differentiation of major clinically significant *Candida* spp. This medium uses a chromogenic mixture to differentiate major *Candida* spp. by colony color: *C. albicans*, green; *Candida krusei*, pink; *Candida tropicalis*, metallic blue; and other species, white to mauve. Numerous reports have shown this medium to be useful for the isolation and presumptive identification of yeasts and to optimize detection of mixed cultures in clinical specimens (Ozcan et al., 2009; Perry & Freydiere, 2007; Raut & Varaiya, 2009).

Inoculation and Incubation

Processing of clinical specimens for fungal detection requires careful handling because some processes commonly used to prepare specimens for bacterial culture may be too disruptive for the fungal organism (e.g., grinding in a homogenizer). Inoculation of scrapings or curettings onto and into the agar at multiple points on the agar surface is a reliable technique for culture. Tissue should be teased or minced, after which the fragments are similarly inoculated.

Plates or tubes should be incubated in ambient air at 25° to 30°C. A controlled temperature incubator is essential. Although it is not necessary to incubate parallel plates or tubes at 37°C for recovery of the yeast phase of dimorphic fungi, in cases where strong suspicion of endemic fungi occurs, incubation at this temperature should be considered. Most fungi grow within a 2-week incubation period, and among commonly isolated fungi, only the dimorphic fungi such as *H. capsulatum* and *B. dermatitidis* are frequently detected after 14 days of incubation. General recommendations for incubation times are as follows: 7 days to detect the presence of yeast in mouth, throat, or vaginal specimens; 21 days to detect fungal pathogens in tissues and sterile body fluids other than blood; and up to 28 days for respiratory, bone marrow, and blood pathogens, and for specimens in which a dimorphic fungus is suspected. In general, all other specimens should be incubated for up to 14 days. Plates should be examined at least twice during the first week, when rapidly growing isolates may appear, and at least weekly thereafter.

Blood Cultures

Recovery of fungi from blood requires special attention and can be accomplished by inoculating broth media by using a biphasic broth-agar system or by using the lysis centrifugation technique (Isolator System; Wampole, Cranbury, NJ). The lysis centrifugation method consists of a tube containing a solution that lyses erythrocytes and leukocytes (Cockerill et al., 1996; Reimer et al., 1997). After the blood is drawn into the vacutainer tube, the lysed contents, including any microbes, are centrifuged into a pellet, which is removed and plated onto the surface of agar plates. Although the Isolator System is considered a sensitive method for detection of fungemia, this system is also more susceptible to contamination through handling of the tube or by airborne spores that settle onto the agar plates during processing. Because a high percentage of fungemias are caused by yeast, continuous-read automated-culture methods have become the mainstay for fungal detection. Two systems commonly used are the BACTEC System (Becton Dickinson Diagnostic Systems, Sparks, MD) and the BacT-Alert System (bioMerieux, Inc., Durham, NC). Because yeasts are aerobic organisms, aerobic culture bottles are used for detection. Two systems in combination (i.e., BACTEC MYCO/F Lytic blood culture bottles and the Isolator System) have been shown to optimize the recovery of fungi from blood (Vetter et al., 2001).

GROWTH RATE

The rate of growth of fungal isolates provides a useful clue to diagnostic possibilities. In general, the pathogenic dimorphic and dematiaceous fungi grow slower, requiring 1 week or longer for colonies to appear. Rapidly growing mold colonies that appear after prolonged incubation on mycologic media should be questioned as possible contaminants. However, many exceptions to this generalization have been noted, and laboratorians need to be aware that fungi such as the *Coccidioides* spp. may grow quickly on nonfungal medium. Protocols on how to handle fungal growth on bacterial cultures are needed to prevent unnecessary exposure of laboratory personnel to highly infectious fungal pathogens that may be encountered.

GROWTH TEMPERATURE

Most molds grow best at 25° to 30°C. Most yeasts, however, grow well at 35° to 37°C and are often recovered first on enriched blood agar plates in the bacteriology laboratory. In some cases, growth of a fungus at elevated temperatures is useful for differentiation of species.

MORPHOLOGIC IDENTIFICATION

Some of the morphologic studies necessary for the identification of fungal isolates can be accomplished with colonies from the original isolation plates. However, it is often necessary to transfer portions of colonies to new or different media (subculture) to demonstrate diagnostic structures. Table 60.3 describes some of the media commonly used for the identification of fungal species. One of the media more commonly used is cornmeal agar supplemented with Tween 80 (CM-T80) for the visualization of yeast morphology. Recognition of pseudohyphae with chlamydoconidia on this medium is considered confirmatory for *C. albicans* and *Candida dubliniensis*. Other morphologic features can help to categorize yeasts into groups to facilitate separation into species. Although biochemical tests are important for identifying yeast isolates, complementation of these with a morphologic examination provides an important check on the biochemical information, especially if a commercial identification system has been used.

Yeast Morphology

The germ tube test is an important initial step in the identification of yeast isolates. Germ tubes, which are elongated, fingerlike extensions from a yeast cell, represent the beginnings of a true hypha (Fig. 60.16). This structure can be differentiated from pseudohyphae by the lack of a constriction at the junction of germ tube and yeast cell and by the parallel cell walls in the germ tube. True germ tubes are formed by both *C. albicans* and *C. dubliniensis* after growth in serum at 37°C for up to 4 hours. In many laboratories with well-trained staff, the germ tube in combination with results of morphology on CM-T80 agar is considered confirmatory for the identification of *C. albicans/C. dubliniensis*.

The traditional germ tube test involves inoculation of a tube of serum (Box 60.3). After observation of the isolate for germ tubes at 37°C, incubation is continued for subsequent study of hyphal morphology and chlamydoconidia formation at 25° to 30°C. Thus all the information necessary for rapid identification can be collected in one procedure. The CM-T80 agar may be substituted, but regardless of the medium used, incubation

conditions must be carefully controlled and the test monitored with controls to achieve good results. The traditional Dalmau technique for demonstration of chlamydoconidia on cornmeal agar is detailed in Box 60.4.

Mold Morphology

A simple method for examination of molds is the cellophane tape mount, using clear tape and staining with lactophenol cotton (aniline) blue (LPCB) stain. If diagnostic structures are not observed, incubation can be continued and the process repeated. The established method used in observing mold morphology is to tease the mycelium apart with inoculating needles and examine the teased hyphae with LPCB stain.

Occasionally, a slide culture may be necessary to preserve easily disrupted conidial structures in their original relationships. The classic approach involves cutting a square of an appropriate agar medium (usually Sabouraud dextrose, potato dextrose, or potato flake agar), which is suspended on a glass slide and overlaid with a coverslip. The slide is supported by glass rods in a Petri dish, to which sterile water is added for maintenance of humidity. The coverslip subsequently can be removed after a few days of incubation, placed in a drop of LPCB, and observed for undisturbed reproductive structures.

When a mold isolate is suspected of being a dimorphic fungus (e.g., growth on cycloheximide-containing medium), a slide culture should not be performed, and a cellophane tape test or teased preparation should be examined only after the preparation has been sealed in a biosafety cabinet certified for use. Lactophenol cotton blue is fungicidal, but sealing the coverslip with nail polish before observation provides additional protection. Alternatively, the culture may be flooded with 10% formalin (4% formaldehyde solution) and incubated at room temperature overnight before the mold is manipulated.

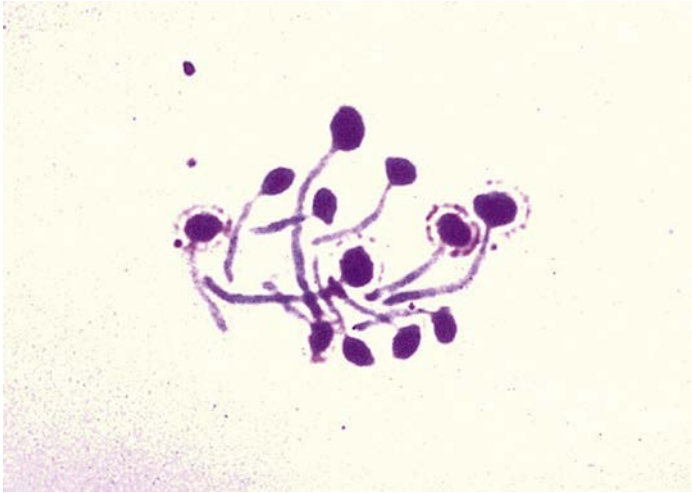

Fig. 60.16 Germ tubes have extended from the yeast cells of *Candida albicans*. No constriction is seen at the junction of yeast cell and germ tube. The walls of the germ tube are parallel. The yeast was incubated for 2 hours at 37°C in serum. (Gram stain, 400×.)

BOX 60.3

Serum Germ Tube Test

1. Aseptically transfer several colonies of yeast to a 12-mm × 75-mm test tube containing approximately 0.5 mL of serum (human, fetal calf, bovine, or rabbit).
2. Incubate the tube at 35°C for up to 3 hours.
3. Place 1 drop of the mixture on a clean glass slide and coverslip.
4. Examine under high dry (400×) magnification and reduced light for the presence of germ tubes.

BOX 60.4

Yeast Morphology Test

1. Streak a light inoculum of yeast onto a section of a cornmeal agar containing Tween 80.
2. Coverslip the area inoculated.
3. Incubate at 25° to 30°C for 24 to 72 hours.
4. Observe under 100× and 400× magnification using reduced light for morphologic structures.

BIOCHEMICAL IDENTIFICATION

Biochemical tests are at the core of identification schemes for yeast and occasionally are useful for identification of molds. A number of rapid tests for the presumptive identification of yeasts are described in Table 60.5.

Biochemical characterization of yeasts may be accomplished by study of fermentation or assimilation patterns. Assimilation testing, which is used more extensively in the laboratory, assesses the ability of an isolate to use a carbohydrate as the sole source of carbon needed for growth, or of nitrate as the sole source of nitrogen. Numerous commercial identification systems with varying incubation times from 4 to 72 hours are available and have become the mainstay for yeast identification. These systems include the API 20C AUX System and the VITEK 2 System (both from bioMérieux, Hazelwood, MO), the MicroScan System (Siemens Healthcare Diagnostics, West Sacramento, CA), the RapID Yeast Plus System (Remel, Thermo Fisher Scientific, Lenexa, KS), and the Phoenix Yeast ID Panel (Becton, Dickinson and Co., Franklin Lakes, NJ). All of these systems perform well, as judged by reports in the literature and by proficiency testing surveys of the College of American Pathologists (Bernal et al., 1998; Crist et al., 1996; Espinel-Ingroff et al., 1998; Fenn et al., 1994; Gayibova et al., 2014; Hata et al., 2007; Ramani et al., 1998; Riddle et al., 1994). However, because no one system is known to be 100% accurate for identification of yeast species, a combination of methods should be considered, especially when rare species are recognized (Pincus et al., 2007).

In addition to fermentation and assimilation studies, stimulation of growth by biochemical compounds is a secondary test used in the differentiation of certain *Trichophyton* spp. (Weitzman et al., 1983). Inclusion of inositol and thiamine in various combinations into agar media (*Trichophyton* agars) allows assessment of growth-stimulating properties. The endpoint of the test, relative growth in comparison with a basal medium, is subjective, and both positive and negative controls should be included.

The test for urease production in cryptococci is of general utility in the clinical laboratory to differentiate these species from *Candida* spp., particularly in respiratory specimens (Canteros et al., 1996). *C. neoformans* is a pulmonary and systemic pathogen, whereas *Candida* spp. are frequent inhabitants of the upper airways but uncommon causes of primary pneumonia. Urease, however, may be produced by other nonpathogenic species of *Cryptococcus*, by *Rhodotorula* spp., and by some isolates of *Trichosporon* spp. and *C. krusei*. Urease production can be tested by inoculation of the yeast isolate onto a slant of Christensen urea agar or into urea broth. Alkalinization of the medium after production of NH_3 by urea-splitting organisms is detected by inclusion of a pH indicator in the system. Colonies that have macroscopically visible pseudohyphae (feet) or that grow on cycloheximide-containing agar need not be tested, because *Cryptococcus* does not produce pseudohyphae in vitro and does not grow in the presence of cycloheximide.

Production of urease also is useful to differentiate the dermatophytes *Trichophyton mentagrophytes* (urease positive) from *T. rubrum* (urease negative). The isolate should be subcultured to a slant of Christensen urea agar and incubated at 25° to 30°C for at least 3 days.

Although commercial biochemical tests are used for the identification of yeast, confirmation of the identification by examination of yeast morphology on agar media should also be considered, as should molecular sequencing or proteomic analysis. Trusting the results of automated or packaged systems implicitly is problematic, as highlighted by the emerging pathogen *Candida auris*. Studies have demonstrated that biochemical assays and even early versions of MALDI-TOF MS clinical databases were unable to correctly identify yeast of increasing clinical importance (Kathuria et al., 2015; Mizusawa et al., 2017).

TABLE 60.5

Rapid Testing for Presumptive Identification of Yeast Following Colonial Formation

Urease production	*Cryptococcus gattii/C. neoformans*
Germ tube production	*Candida albicans/C. dubliniensis*
Pseudohyphae present	*Candida* species
Chlamydoconidia present	*Candida albicans/C. dubliniensis*
Lipid growth requirement	*Malassezia furfur* species complex
Red colonial pigmentation	*Rhodotorula* species
Ascospore formation	*Saccharomyces cerevisiae*
Trehalose assimilation	*Candida glabrata*

SEROLOGIC IDENTIFICATION

Immunologic tests are available for detection of both antigens and antibodies to selected fungal pathogens; these assays have been shown to be of value for diagnosing infection and for monitoring therapeutic response (Lau et al., 2009; Wheat, 2006a, 2009; Wheat & Walsh, 2008). Although antibody testing for fungal pathogens has historically been used in some instances for diagnostics, these tests are no longer widely accepted owing to low sensitivity and specificity. In addition, the benefit of antibody detection remains unclear if patients are under immune suppression or are heavily colonized but not infected (Einsele & Loeffler, 2008).

Tests to detect fungal antigens or metabolic byproducts in serum or other body fluids, on the other hand, have been shown to be more useful for the diagnosis and management of fungal disease. Multiple antigen-detection methods are used for the specific diagnosis of a variety of diseases, including aspergillosis, cryptococcosis, histoplasmosis, blastomycosis, paracoccidioidomycosis, and talaromycosis (formerly penicilliosis) caused by *Talaromyces marneffei* (formerly *Penicillium marneffei*). One antigen-detection test is the cryptococcal antigen test for the diagnosis of cryptococcal infection (Perfect et al., 2010). The polysaccharide capsule of *C. neoformans* becomes dissolved in the serum and CSF and can be detected by the latex-based agglutination test or the enzyme immunoassay. Although these tests have limitations, they have been shown to be helpful in monitoring therapy over time through quantitative measurement of the titer of *Cryptococcus* polysaccharide in CSF (Babady et al., 2009). A rapid, point-of-care lateral-flow device is now available for the diagnosis of cryptococcosis and can be performed on CSF or serum. This dipstick test (IMMY cryptococcal LFA, Immuno-Mycologics, Inc., Norman, OK) contains immobilized monoclonal antibodies to cryptococcal antigen and can provide results within 10 to 20 minutes without the use of specialized equipment (Boulware et al., 2014; McMullan et al., 2012).

Antigen detection for the diagnosis of histoplasmosis has also proved useful when serum, urine, or bronchoalveolar lavage (BAL) fluid is tested (Wheat, 2009; Wheat et al., 2007a). As a screening test, detection of *Histoplasma* antigen plays a special role in the diagnosis of disseminated and diffuse acute pulmonary histoplasmosis (Hage et al., 2019). Studies have shown that *H. capsulatum*–specific antigen can be detected in the urine of 90% of patients with disseminated infection and 80% of patients with acute histoplasmosis. Detection of antigen in BAL has also proved useful for the diagnosis of histoplasmosis, especially when the results of testing are combined with those obtained from cytopathology (Hage et al., 2007).

The Platelia *Aspergillus* Ag (Bio-Rad, Marnes-la-Coquette, France) is an immunoenzymatic sandwich microplate assay for the detection of the galactomannan antigen, a reliable marker for invasive aspergillosis (IA). This assay is available to screen serum and bronchoalveolar fluid samples of high-risk patients for IA. Although this test has been shown to only have moderate sensitivity for the diagnosis of IA, the test is highly specific and considered a reliable screening for the detection of IA when used with other clinical parameters (Hage et al., 2019; Heng et al., 2014; Morrissey et al., 2013). False-positive results have been reported in patients receiving piperacillin/tazobactam due to the presence of the galactomannan antigen in the preparation of this antibiotic, although some reports now suggest that the newer preparations no longer have this residual galactomannan present (Mikulska et al., 2012). The FDA, however, still recommends that when reporting a positive Platelia *Aspergillus* galactomannan test result, laboratories inform physicians of the limitations of the test with regard to potential interaction with piperacillin/tazobactam.

A commercial test to detect (1-3)-beta-D-glucan (BG) is available for the presumptive diagnosis of invasive fungal infection (Fungitell Assay; Associates of Cape Cod, Inc., East Falmouth, MA) (Pickering et al., 2005). This antigen is present in the cell walls of most pathogenic fungi (including *P. jirovecii*), with some notable exceptions such as *Cryptococcus* spp. and the Mucorales. Published studies have shown that BG may be useful as a screening tool for surveillance of invasive aspergillosis, as well as other invasive fungal diseases in populations at risk (Hage et al., 2019; Marty & Koo, 2009). Although false-positive results appear to limit the use of this test, additional studies are needed to further define its diagnostic utility (Onishi et al., 2012).

Skin tests have been used for the epidemiologic study of some infections, but they have limited utility for diagnostic purposes.

MOLECULAR IDENTIFICATION

Recent advances in molecular testing for the identification of fungal pathogens have had a significant impact on the diagnosis of fungal infections (Arvanitis et al., 2014; Borman et al., 2008; Griffin & Hanson, 2014; Preuner & Lion, 2009). Numerous reviews have addressed these changes, and the general consensus is that approaches to species identification of many fungi today should include both morphologic and molecular testing methods (Hibbett & Taylor, 2013).

One of the greatest needs for clinical medicine is the development of a rapid and reliable detection method that can identify fungal pathogens directly from clinical specimens. This need reflects not only the inability of current laboratory tests to provide a timely result, but also the fact that fungal infections in immunocompromised patients usually appear suddenly, progress rapidly, and are often fatal unless treatment is started earlier in the course of infection.

Numerous molecular assays using both probe-based and amplification-based technologies have been developed for the identification of fungal pathogens. With any of these approaches, an initial goal has been to define the genetic loci within the genome for use as the molecular target. Although multiple areas within the fungal genome have been evaluated, the targeted areas most commonly used are those found within the ribosomal DNA (rDNA) gene complex (Table 60.6) (Iwen et al., 2002). This section of the genome includes variable nucleotide sequence areas within the 18S gene and the 28S gene, as well as DNA sequence areas of the intervening internal transcribed spacer (ITS) regions called ITS1 and ITS2. Sequence homology within the rDNA genes and differences within the spacer regions are used as the genetic basis for the organization of fungi into taxonomic groups. The ITS regions of the nuclear rRNA gene had been proposed as the fungal barcode locus; however, more recent studies have now shown that other genetic markers are needed for the separation of species within many of the genera of fungi (Balajee, 2009; Guarro, 2013; Schoch et al., 2012)

Probe-based assays are commercially available and are commonly used in the mycology laboratory for the identification of *Histoplasma*, *Blastomyces*, and *Coccidioides* spp. from culture (GenProbe AccuProbe, Hologic, Inc., Bedford, MA). Another probe-based method called the peptide nucleic acid fluorescence in situ hybridization (PNA-FISH) assay was developed and has become commercially available for the qualitative identification of certain *Candida* spp. in blood culture bottles (Forrest, 2007; Wilson et al., 2005). This assay uses a fluorescent-labeled peptide nucleic acid probe that targets the species-specific ribosomal RNA of *Candida* spp. Two assays are available, and include the Yeast Traffic Light and QuickFISH diagnostic tests (OpGen, Inc., Gaithersburg, MD). The Yeast Traffic Light assay groups *Candida* spp. by color based on probable susceptibility to fluconazole. *Candida albicans* and *C. parapsilosis* fluoresce green since they are likely susceptible to this antifungal, *C. tropicalis* fluoresces yellow for variable susceptibility, and *C. glabrata* and *C. krusei* fluoresce red due to reduced susceptibility or resistance to fluconazole. The QuickFISH assay can detect *C. albicans* (green), *C. parapsilosis* (yellow/orange), and *C. glabrata* (red). The sensitivity and specificity of these tests have been shown to be greater than 97%, and the impact of

TABLE 60.6

Genetic Targets Utilized for the Detection and Identification of Fungal Pathogens

Gene Target	Fungal Species
Actin	*Candida albicans*
β-Tubulin	*Aspergillus* species, *Scedosporium* species
Calmodulin	*Aspergillus* species, *Fusarium* species, *Scedosporium* species
Chitin synthetase	Dermatophyte species
Cytochrome b	*Candida albicans*
Dihydrofolate reductase	*Pneumocystis jirovecii (carinii)*
Elongation factor (EF-1α gene)	*Fusarium* species
Mitochondrial rRNA	*Pneumocystis jirovecii*
rDNA complex (5S gene)	*Candida albicans, Pneumocystis jirovecii*
rDNA complex (18S gene)	Multiple
rDNA complex (28S gene)	*Aspergillus* species, *Candida* species
rDNA complex (IGS regions)	*Aspergillus* species
rDNA complex (ITS regions)	Multiple
RNA polymerase (RPB1 and RPB2)	*Fusarium* species

IGS, Intergenic spacer region; *ITS,* internal transcribed spacer region; *rDNA,* ribosomal deoxyribonucleic acid.

rapid identification of *Candida* in the blood can be seen in the significant reduction in the empirical use of antifungals (Abdelhamed et al., 2015; Farina et al., 2012; Hall et al., 2012; Stone et al., 2013). Incorporating the *Candida* PNA-FISH test as part of the initial identification algorithm for yeast recovered from blood can result in substantial savings for hospitals. Major drawbacks to this assay include the high costs of reagents, the need for fluorescent microscopy, and the changes in workflow required to incorporate testing in the laboratory.

Numerous amplification methods using both non–sequence-based and sequence-based approaches for analysis have been applied in identification of fungi. Most of the sequence-based analysis methods have used conventional polymerase chain reaction (PCR) with universal primers to target sequences within the *28S rDNA* gene, the *18S rDNA* gene, or the ITS1-5.8S-ITS2 target areas (Arvanitis et al., 2014; Irinyi et al., 2015).

The availability of a nucleotide-based sequence database that has the breadth of phylogenetics and the taxonomic accuracy needed to identify fungal species is desirable for sequence analysis alignment. The largest database currently used for sequence-based identification is the publicly available GenBank database (National Center for Biotechnology Information, Washington, DC). Unfortunately, because this is an open-source database, previous reports suggested that up to 20% of the sequenced entries listed for fungi may be associated with erroneously identified species (Balajee et al., 2007). Other publicly available databases include the International Society of Human and Animal Mycology (ISHAM) Barcoding database, which offers pairwise sequence alignments against reference ITS and translation elongation factor 1 alpha (TEF1α) sequences (Irinyi et al., 2015), and the Westerdijk Fungal Biodiversity Institute (formerly the Centraalbureau voor Schimmelcultures Fungal Biodiversity Centre). Additionally, there is a need for sequences from a variety of genomic targets in the database that is phylogenetically represented with accurate species identification. Although multiple locus sequencing and alignment comparisons have been done using a variety of fungal species, additional studies using sequence comparison analysis are needed to determine the optimal target or targets for fungal identification. Multiple target evaluations for the identification of aspergilli and fusaria have been done and show this approach to be valid for identification purposes (O'Donnell, Sutton et al., 2009; Peterson, 2008).

High-order multiplex PCR assays have been developed for the direct detection of microbial pathogens in positive blood cultures. The FilmArray Blood Culture ID (BCID) Panel (BioFire Diagnostics, Salt Lake City, UT) tests positive blood culture broth for a complex panel of 24 pathogens to include five *Candida* spp. (*C. albicans*, *C. glabrata*, *C. krusei*, *C. parapsilosis*, and *C. tropicalis*). This assay includes the ability to automatically carry out all steps of the identification process in a closed system from DNA extraction to the interpretation of the PCR data. Limited prospective studies have shown that the FilmArray panel was a reliable alternative to identify the most common yeast from positive blood cultures (Altun et al., 2013; Desoubeaux et al., 2014). A similar meningitis/encephalitis (ME) panel is available that tests for 15 pathogens, including *C. neoformans/C. gattii* directly on CSF. However, false negatives with this assay in patients with positive cryptococcal antigen tests have been reported in the literature (Leber et al., 2016). Additional studies are needed to determine how they will improve the management of patients by a reduction in the time of diagnosis and consequent length of hospitalization and mortality rates.

T2 Magnetic Resonance

A fully automated assay is now available for the detection of *Candida* spp. directly from whole blood, which eliminates the time needed for blood culture bottles to become positive. In the T2 *Candida* assay (T2Biosystems), red blood cells and pathogen cells are first lysed, and *Candida* DNA is amplified using primers targeted for the ITS2 region (Neely et al., 2013). The amplified DNA is then hybridized to supraparamagnetic nanoparticles coated with complimentary DNA, which agglomerate into microclusters and produce a signature T2 magnetic resonance signature. This signature is read and compared to a database for organism identification. This assay is able to detect between one and three colony-forming units/mL of whole blood of *Candida*, which is similar to the commercially available PNA-FISH assays, and groups species based on typical fungal susceptibility patterns (*C. albicans* grouped with *C. tropicalis*; *C. glabrata* grouped with *C. krusei*; and *C. parapsilosis* by itself) (Beyda et al., 2013). In a clinical study, the specificity of the assay was 99.4%, and the time to negativity was 4.2 hours (vs >120 hours for traditional blood cultures) (Mylonakis et al., 2015). By rapidly ruling out candidemia, the inappropriate use of antifungals may be reduced.

MALDI-TOF MASS SPECTROMETRY

Proteomics using matrix-assisted laser desorption/ionization time-of-flight mass spectrometry (MALDI-TOF-MS) has emerged as a reliable method for the rapid identification of microbial pathogens (Chalupova et al., 2014; Patel, 2019). This technology involves combining of the pathogen with a suitable energy-absorbent chemical matrix (e.g., α-cyano-4-hydroxycinnamic acid dissolved in acetonitrile and trifluoroacetic acid), pulsing the sample with a laser for ablation and desorption, followed by ionization using time-of-flight technology to create a mass spectrum fingerprint of the ribosomal proteins of the organisms that is detected by mass spectrometry. This mass spectrum is then compared with a database of known spectra to allow for organism identification. Prior to performing the assay, fungal cells must be lysed, which may occur either "on plate" or "off plate." Yeast typically undergo on plate extraction where cells are transferred to the target plate or slide from a growing culture, and this is followed by the addition of formic acid and drying, after which the matrix is applied. The preparation of filamentous fungi takes longer and may occur off plate. Success has been demonstrated with treating an appropriate amount of biomass with formic acid and acetonitrile prior to application to the target plate or slide (Rychert et al., 2018). Although the complexity of the composition of the fungal cell wall and the different protein compositions seen (e.g., between vegetative cells and spores and between young and mature colonies) has made the creation of reliable databases for analysis challenging, significant progress has been made, and two commercial systems are now FDA cleared for the identification of fungi. These include the Biotyper (Bruker Daltonics, Inc., Billerica, MA) and the VITEK MS (bioMerieux, Inc., Durham, NC).

Overall, both systems appear to have similar success rates in the identification of yeast species. One large study that included 1192 yeast isolates reported 97.6% correct species identification with the Bruker Biotyper and 96.1% with the bioMerieux MS (Bader et al., 2011). Similar rates of correct species identification of various yeasts can be found in the literature using this technology (range 92–99%) (Bizzini & Greub, 2010; Mancini et al., 2013; Marklein et al., 2009a, 2009b; Pence et al., 2014; Posteraro et al., 2012; Stevenson et al., 2010; van Veen et al., 2010; Westblade et al., 2013). Studies have also demonstrated that this technology can discriminate between closely related species where biochemical assays have had difficulty (McTaggart et al., 2011; Pinto et al., 2011; Posteraro et al., 2012). However, the success of MALDI-TOF MS is dependent upon the availability of a well-curated database that contains reference spectra for the organisms being identified (Patel, 2019). Neither of the FDA-cleared commercial systems was able to correctly identify *C. auris* when this species first began to be recognized as an emerging pathogen of clinical importance (Mizusawa et al., 2017). MALDI-TOF MS has also been evaluated for the identification of filamentous fungi with varying success. Both the Bruker Biotyper and bioMerieux VITEK MS FDA-cleared systems now contain molds within their databases, but the number is limited compared to yeast species, although more mold species are available within their research use only (RUO) databases (Patel, 2019).

One of the main advantages of MALDI-TOF MS is the rapidity by which results are available. One study estimated that the turnaround time for species identification of bacteria and yeasts was on average 1.45 days faster than conventional methods (Tan et al., 2012). However, access to available spectral databases is limited and those databases that are FDA cleared for use in clinical microbiology laboratories are maintained by the companies rather than publicly available like sequence databases (i.e., GenBank). Another limitation of MALDI-TOF MS is the need for a pure culture. Although MALDI-TOF MS has also been evaluated for the direct identification of yeast from positive blood culture bottles with accuracy in identification of greater than 90% in one study (Rosevinge et al., 2013), additional studies are needed. Studies have also been conducted to evaluate this technology for antifungal susceptibility testing (Johansson et al., 2014; Marinach et al., 2009; Oviano et al., 2014; Saracli et al., 2015; Vella et al., 2013a, 2013b). Some studies have reported good categoric agreement between MALDI-TOF MS methods and those obtained by broth microdilution (De Carolis et al., 2012; Vella et al., 2013b), although such agreement has not been universally reported (Saracli et al., 2015).

SUSCEPTIBILITY TESTING

For many years, few antifungal chemotherapeutic agents were available, with amphotericin B virtually the only agent effective against most systemic fungal pathogens. Although this potent antifungal agent was frequently toxic, resistance to therapy was rare. With the recent introduction of new antifungal agents and with the widespread use of antifungal

prophylaxis, the epidemiology of invasive fungal infections has changed, with non-*albicans Candida*, non-*fumigatus Aspergillus*, and molds other than *Aspergillus* becoming more common as causes of invasive disease (Alastruey-Izquierdo et al., 2013; Baddley et al., 2009; Kontoyiannis et al., 2010; Lai et al., 2008; Naggie & Perfect, 2009; Neofytos et al., 2009; Pappas et al., 2010; Rodriguez-Tudela et al., 2008). These emerging fungi are resistant to or less susceptible than other fungi to standard antifungal agents and thus become more difficult to treat. Furthermore, although the predictability of innate resistance frequently means that species identification is often sufficient to alert the clinician to the likelihood of in vitro and often associated in vivo resistance, the emergence of resistance in a previously susceptible strain during the course of treatment has become more problematic (Arikan, 2007; Johnson, 2008).

The Clinical and Laboratory Standards Institute has developed reference broth dilution methods for antifungal susceptibility testing of yeasts (CLSI, 2017c) and molds (CLSI, 2017b). Methods for antifungal disk diffusion susceptibility testing of yeasts (CLSI, 2009) and a method for antifungal disk diffusion susceptibility testing of nondermatophyte filamentous fungi (CLSI, 2017b) have also been developed.

The CLSI M27 document provides the reference methods for the testing of yeasts (CLSI, 2017c), and a new document (CLSI, 2017a) has now been published that includes quality control and reference performance standards for 24-hour and 48-hour reading times for broth microdilution testing of the antifungals against yeast species and the species- and drug-specific breakpoints for the echinocandins (anidulafungin, caspofungin, and micafungin), fluconazole, and voriconazole against common species of *Candida* (*C. albicans*, *C. glabrata*, *C. guilliermondii*, *C. krusei*, *C. parapsilosis*, and *C. tropicalis*) (CLSI, 2017a).

The CLSI M38 document provides the reference method for in vitro susceptibility testing of filamentous fungi that can cause invasive disease (CLSI, 2017b). Organisms included in this document for evaluation are *Aspergillus* spp., *Fusarium* spp., *Rhizopus oryzae (R. arrhizus)*, *Scedosporium apiospermum/S. boydii*, *Lomentospora* (*Scedosporium*) *prolificans*, and the mycelial form of *Sporothrix* spp., as well as the dermatophytes (*Epidermophyton*, *Microsporum*, and *Trichophyton* spp.). The CLSI M27 and M38 documents are reference standards developed through a consensus process to facilitate agreement among laboratorians in measuring the susceptibility of yeasts and molds to antifungal agents. Although the clinical relevance of testing yeasts is established and now included in treatment guidelines (Pappas et al., 2016), the need for testing filamentous fungi remains uncertain, and a breakpoint has been set for only one antifungal (voriconazole) against one species (*Aspergillus fumigatus*) (CLSI, 2020). The European Union Committee on Antimicrobial Susceptibility Testing (EUCAST), an organization similar in function to CLSI, has also published reference standards for susceptibility testing of fungi and have set breakpoints for antifungals against *Candida* spp. and some *Aspergillus* spp. (Arendrup et al., 2017; EUCAST, 2018).

Since both reference broth methods are time consuming to perform, simplified alternatives to these methods have been assessed to include the disk-diffusion method, the Etest agar-gradient MIC method (bioMérieux, Inc., Durham, NC) (Alexander et al., 2007), the Sensititre YeastOne method (Thermo Scientific, TREK Diagnostic Systems, Inc., Cleveland, OH) (Garcia-Agudao et al., 2012; Pfaller et al., 2012c), and the VITEK 2 method (bioMérieux, Durham, NC) (Cuenca-Estrella et al., 2010). The disk-diffusion method has also been approved for the testing of yeast, and studies have shown that results obtained from testing using this method are comparable with results obtained with the CLSI microdilution broth method (Diekema et al., 2007; Messer et al., 2007; Pfaller et al., 2003).

The Etest uses a plastic strip that contains a predefined stable gradient of antifungal concentrations to determine the on-scale minimum inhibitory concentration (MIC) of the antifungal agent tested. These strips are now commercially available for several antifungals. Studies have shown the Etest strips to be similar to the results obtained by the CLSI broth microdilution methods for in vitro susceptibility testing of both molds and yeasts (Alexander et al., 2007; Diekema et al., 2007; Pfaller et al., 2003).

The Sensititre YeastOne method uses a dried colorimetric microdilution panel in a microtiter format for antifungal testing. This method is the only FDA-cleared assay for in vitro diagnostic use in testing yeast susceptibility to fluconazole, itraconazole, 5-flucytosine, and voriconazole. Instead of reading the presence or absence of growth of the organism being tested, a change in color indicative of a change in the metabolism of the pathogen is used as the endpoint. Panels are also available for RUO in testing antifungal susceptibility to amphotericin B, anidulafungin, caspofungin, micafungin, and posaconazole. This testing platform has been shown to be dependable for the testing of yeasts (Castro et al., 2004; Pfaller et al., 2012b).

Although the key elements involved in selecting an appropriate antifungal agent include the type of patient (e.g., solid organ or stem cell transplant), the severity of immunosuppression, a history of prolonged exposure to antifungal drugs, and knowledge of the genera and species of the infecting pathogen, susceptibility testing may be warranted in some circumstances, including the following: (1) as part of periodic surveys that establish antibiograms for isolates in an institution; (2) to help in the management of refractory oropharyngeal candidiasis in patients with apparent therapeutic failure; and (3) to aid in the management of invasive candidiasis when the use of azole antifungal agents is uncertain (Cornely et al., 2014). Also, scant data are available regarding the clinical implications of in vitro susceptibility testing in many cases, and the refractile nature of many fungal pathogens to antifungal therapy makes susceptibility testing an option that needs to be considered. For instance, reports now show that resistance has emerged during treatment of *Aspergillus* infections, thus highlighting the potential need for in vitro susceptibility testing under this circumstance (Lass-Florl, 2010).

CANDIDIASIS, CRYPTOCOCCOSIS, AND OTHER INFECTIONS CAUSED BY YEAST

THE GENUS CANDIDA

Candida species are the most common recognized yeast pathogens and with increased use of immunosuppressive therapies, use of broad-spectrum antibiotics, and aging of the population, they have assumed a prominent place among nosocomial pathogens (Horn et al., 2009; Pappas et al., 2016; Pfaller et al., 2012a). These species are currently the fourth most common cause of hospital-acquired bloodstream infection in the United States and rank third among causes of bloodstream infection in the intensive care unit (Bassetti et al., 2019; Diekema et al., 2012). Although *C. albicans* accounts for about 50% of invasive infections caused by *Candida* spp., the non-*albicans Candida* spp. have emerged as more common causes of disease (Bassetti et al., 2019; Diekema et al., 2012; Pfaller et al., 2014). In a multicenter evaluation of patients with candidemia (Prospective Antifungal Therapy Alliance registry), *C. albicans* accounted for 42.1% of cases, followed by *Candida glabrata* (26.7%), *Candida parapsilosis* (15.9%), *Candida tropicalis* (8.7%), and *Candida krusei* (3.4%) (Pfaller et al., 2012a).

Risk Factors

Candida infections are limited in extent and severity, depending on the immune status of the host. Since *Candida* spp. are a part of the normal flora in the gastrointestinal (GI) tract, mucous membranes, and skin, infections generally occur as the result of an opportunity. For instance, the use of broad-spectrum antibacterial therapy upsets the balance of colonizing flora on the mucous membranes of the oral cavity, the skin, and the GI tract by eliminating the predominant competing bacterial flora, thus allowing overgrowth of yeast (Diekema et al., 2012; Patel et al., 2012).

Invasive disease by *Candida* spp. develops when host defenses are compromised. Diabetes, immunosuppressive disease or therapy, and neutropenia as a result of disease (e.g., AIDS) or treatment with high-dose chemotherapy are common risk factors. Bloodstream infections, including fungal endocarditis, are fostered by the use of indwelling vascular lines, which is common practice in the management of hospitalized patients (Baddley et al., 2008; Pappas et al., 2016).

Clinical Diseases

Although *C. albicans* is the most common pathogen within the genus *Candida*, the frequency of the non-*albicans* species associated with infections has increased over the last few decades (Diekema et al., 2012; Pfaller et al., 2014). Numerous reports describe invasive infections caused by *C. tropicalis* (Chai et al., 2010; Kothavade et al., 2010), *C. parapsilosis* (Pammi et al., 2013), *C. glabrata* (Rodrigues, Silva et al., 2014), *C. krusei* (Pelletier et al., 2005), and *C. lusitaniae* (Hawkins & Baddour, 2003). *C. auris* has recently emerged and represents a challenge to both infection control and treating clinicians alike (Spivak & Hanson, 2018).

Resistance to antifungal agents has emerged as a problem with the introduction of newer agents, which is especially problematic within the non-*albicans Candida* species (Pfaller et al., 2014). Resistance has been most notable within *C. glabrata* (resistance to the imidazoles [fluconazole, itraconazole, posaconazole, and voriconazole] and to the echinocandins) and within *C. krusei* (resistance to itraconazole), but also the recently recognized pathogen *C. auris* (resistance to triazoles, echinocandins, and polyenes in some cases) (Jeffery-Smith et al., 2018). Antifungal intrinsic resistance is also present in *C. krusei* and in *C. lusitaniae* to fluconazole and amphotericin B, respectively. The Infectious Diseases Society of America

has updated its clinical practice guidelines for the management of patients with invasive candidiasis and mucosal candidiasis to reflect changes noted with the addition of the new antifungals (Pappas et al., 2016).

Cutaneous Disease

Cutaneous disease is the most frequent infection caused by *Candida* spp. This disease presents topically as an erythematous lesion of the skin, sometimes accompanied by a creamy white exudate or scaling. Moist conditions, such as diaper rash in infants and infection of skin folds (intertrigo) in adults, are precursors to infection. Common sites are those in the groin, between fingers and toes, under the female breast, and in the axilla. Workers who immerse their hands in water for long periods of time are also at risk for infection of the skin of the hands, the nails (onychomycosis), or the nail bed (paronychia) (Jayatilake et al., 2009). Moreover, chronic cutaneous disease (referred to as chronic cutaneous candidiasis) is an uncommon manifestation of *Candida* infection in patients with defective cellular immunity, and the underlying genetic polymorphisms responsible are under active investigation (Lionakis & Netea, 2013).

Oral Candidiasis

Oral candidiasis usually manifests as the appearance of creamy white patches overlying erythematous buccal mucosa (thrush) although can also present with an erythematous form, particularly under dentures (Thompson et al., 2010). Although symptoms are usually minimal, dysphagia may result from heavy infection or with esophageal candidiasis. Fissuring at the corners of the mouth is common and may be the primary complaint. Oral candidiasis is a common initial infection in patients with HIV and frequently is a marker of immune failure in these patients (Patel et al., 2012). Especially notable is the prevalence of *C. dubliniensis* and the association with oral carriage and oropharyngeal infections in these patients with HIV (Perea et al., 2002; Thompson et al., 2010).

Gastrointestinal Candidiasis

Gastrointestinal candidiasis occurs most frequently as esophagitis and uncommonly as gastritis (Wilcox et al., 1996). Erosive lesions of the distal esophagus and stomach result in substernal pain, which is aggravated by swallowing. White plaques overlie the lesions when viewed by endoscopy. The differential diagnosis includes infection with herpes simplex virus, although these two processes may coexist. Esophageal candidiasis was previously described as a frequent opportunistic infection in persons infected with HIV; however, the use of highly active antiretroviral therapy has led to a striking decline in the prevalence of this disease (Raufman, 2005). Even though *Candida* spp. are seen frequently as flora of the lower GI tract, the significance of finding yeast in stool is uncertain. True invasive infection of the lower GI tract is less common than disease of the upper tract, although overgrowth of *Candida* spp. in the stool may accompany antimicrobial therapy.

Vaginal Candidiasis

Vaginal candidiasis afflicts postpubertal women; diabetes mellitus, utilization of antimicrobial therapy, pregnancy, and sexual activity are predisposing conditions (Donders & Sobel, 2017). Vaginal burning and itching, dyspareunia, and a discharge that is classically curdlike are associated with an infection that may be acute or chronic and difficult to eradicate.

Urinary Tract Infection

Urinary tract infection caused by *Candida* spp. is difficult to diagnose because these yeasts are frequently recovered from the urine as a result of vaginal contamination or colonization of the bladder in patients with indwelling catheters, especially when systemic antibiotics have been administered (Fisher et al., 2011; Pappas et al., 2016). Severe infection of the upper urinary tract, including necrosis of the renal papillae, is a serious complication that occurs particularly in patients who have obstructive uropathy. Quantitative cultures do not appear useful for assessing the significance of *Candida* spp. in the urinary tract.

Invasive Candidiasis

Invasive candidiasis often involves sources other than the skin or mucous membranes. Most invasive infections caused by *Candida* spp. result in bloodstream invasion with hematogenous spread of the organism although cultures are negative in a significant percentage of cases (Clancy & Nguyen, 2013, 2018). *Candidemia* is defined as the isolation of *Candida* spp. from at least one blood culture specimen with hematogenous spread of the yeast to one or more organs. Nonhematogenous *Candida* infection of a single deep organ (also called *disseminated* or *deep-seated* candidiasis) is often suspected as hematogenous spread to a single organ in which the manifestations of disease are seen or following trauma. Primary localized invasive infections occur normally after abdominal surgery and following perforation of the gut leading to contamination of the peritoneal cavity with *Candida*. Other forms of deep-seated infection include endophthalmitis, meningitis, pneumonia, osteomyelitis, and hepatitis. Fungal endocarditis resulting from a bloodstream infection is uncommon, but when present is most commonly caused by a *Candida* spp. Risk factors for this infection include prosthetic valve surgery, preexisting valvular heart disease, use of intravenous catheters or broad-spectrum antibiotics, intravenous drug abuse, and immunosuppression (Baddley et al., 2008).

Pathology

The tissue response to *Candida* is regularly purulent, resembling lesions of bacterial infection with abscess formation present. On occasion, the response to *Candida* infection is granulomatous. In tissue, most *Candida* organisms appear as mats of budding yeasts measuring 3 to 5 μm in diameter mixed with pseudohyphae. *C. glabrata*, which is noted for producing smaller-sized yeast cells (3 μm in diameter), does not produce pseudohyphae and must be differentiated from *Histoplasma* in tissue. Vascular invasion, as occurs with *Aspergillus* or the Mucorales, is also uncommon in yeast infection. Yeast can often be demonstrated with an H&E stain but may be more easily recognized in sections stained with GMS or PAS. Studies have also shown that a finding of *Candida* organisms on a Papanicolaou (PAP) smear is a reliable indicator of vaginitis (Heller et al., 2008).

Laboratory Diagnosis

Specimens for culture should be taken from affected organs and from lesions in which they can be visualized. Modern continuous-monitoring blood culture systems detect most clinically significant yeast isolates with the ability to directly identify the five most common *Candida* spp. in positive blood cultures using recently approved molecular tests (Salimnia et al., 2016). Detection from whole blood using a dedicated instrument via magnetic resonance is also performed at many centers following the development of the T2 *Candida* panel (Clancy et al., 2018). Tissue specimens, scrapings, and swabs from the mouth or vagina should be inoculated onto primary fungal isolation media with and without cycloheximide. The presence of filamentous extensions from the edges of the colony (feet) is a macroscopic indication that pseudohyphae are being produced (see Fig. 60.1). *C. glabrata* and *Cryptococcus* spp. do not form pseudohyphae in vitro, with some other *Candida* spp., such as *C. (Clavispora) lusitaniae* and *C. (Meyerozyma) guilliermondii*, also void of pseudohyphae formation.

The extent of the mycologic evaluation depends on the clinical setting and the specimen type. *Candida* spp. are frequently isolated from the respiratory and urinary tracts; however, interpretation of a finding of *Candida* spp. in these areas is difficult and frequently represents colonization rather than infection. Complete identification of isolates from these sites should be accomplished only selectively after consultation with the responsible clinician.

A preliminary report of *C. albicans/C. dubliniensis* may be issued if the germ tube test is positive (see Fig. 60.16). Additional study of yeast morphology using cornmeal agar to confirm the presence of chlamydoconidia can facilitate identification of *C. albicans/C. dubliniensis* within 24 to 48 hours if phenotypic characteristics alone are to be used (Fig. 60.17). Since both *C. albicans* and *C. dubliniensis* are germ tube positive, and because they

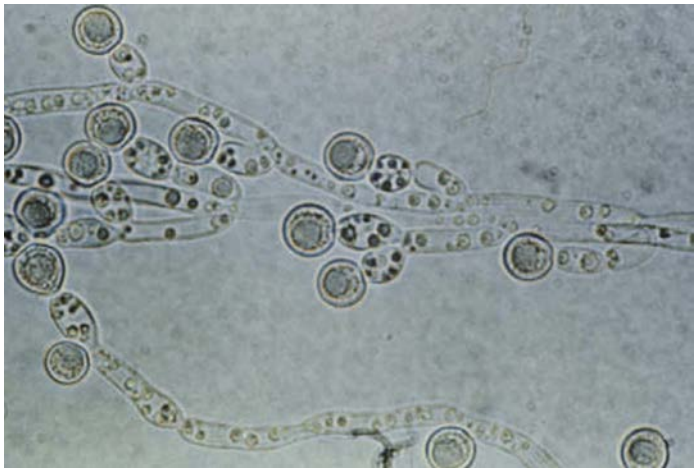

Fig. 60.17 Chlamydoconidia produced by *Candida albicans*. These thick-walled asexual reproductive structures that occur most commonly at the ends of pseudohyphae are characteristic for this species and for *Candida dubliniensis*. (Cornmeal agar plate, 400×.)

have a high degree of phenotypic similarity, distinguishing between these two species has been difficult. However, strict adherence to detail when it comes to growth at 42°C, the production of abundant chlamydoconidia, and the sugar assimilation pattern can be used to differentiate between them (Ells et al., 2011; Loreto et al., 2010). In addition, MALDI-TOF MS can also differentiate between these two species (Westblade et al., 2013, Roberts DMID 2016).

When germ tubes and chlamydoconidia are not demonstrated, a preliminary or presumptive identification of *Candida* spp. can be made only if pseudohyphae are present and arthroconidia are absent. Conventional methods for identification of *Candida* spp. based on morphologic and physiologic attributes are commonly used (see Table 60.6) (Neppelenbroek et al., 2014). For instance, a rapid assimilation trehalose test procedure has been suggested by the CLSI (document M35-A2) for the identification of *C. glabrata*, a species that has emerged as a common cause of invasive disease with known resistance to standard antifungal therapy (CLSI, 2008). An accurate identification, however, is often complex and time consuming, frequently requiring new techniques such as molecular typing to confirm the identification (Castanheira et al., 2013; Neppelenbroek et al., 2014).

THE GENUS CRYPTOCOCCUS

The *Cryptococcus* species complex consists of two species: *C. neoformans* and *C. gattii* (formerly called *C. neoformans* var. *gattii*) and a recent proposal would further subdivide these into eight distinct species (Kwon-Chung et al., 2017). These are known to cause systemic infection in both immunocompetent and immunocompromised individuals (Perfect et al., 2010). The environmental reservoir for *C. neoformans* (teleomorph, *Filobasidiella neoformans*) is primarily pigeon guano, and infections caused by this organism occur worldwide. *C. gattii*, on the other hand, was originally found predominantly in tropical and subtropical areas, especially those areas associated with eucalyptus trees, with infection apparently limited in distribution, primarily to northern Australia and Papua New Guinea (Chen et al., 2014). Infections have also been noted in individuals after exposure in the Vancouver and US Pacific Northwest regions, with recent emergence of this pathogen now identified in multiple states outside of these areas (Chen et al., 2014; Harris et al., 2013; Roe et al., 2018). Since both species are classified within the phylum *Basidiomycota*, they are capable of producing basidiospores under the right circumstances. This sexual stage of cryptococci occurs only when appropriate mating types are crossed; thus this stage is not generally recognized in the clinical laboratory. Sexual reproduction in the genus *Cryptococcus*, however, leads to increasing genetic diversity with the potential to produce strains that are hypervirulent and show increased antifungal resistance (Kozubowski & Heitman, 2012).

Risk Factors

Immunosuppressive therapy or disease is a risk factor for cryptococcosis (Perfect et al., 2010). Prior to the appearance of HIV infection, 30% to 50% of patients with cryptococcal infection were immunologically normal, as measured by available parameters. Risk factors for these patients include malignancy, diabetes mellitus, immunosuppressive therapy, and immunologic disease. The introduction of the HIV/AIDS-infected patient dramatically increased the number of cases of cryptococcosis, and although tremendous advances have been made in antiretroviral therapy, in antifungal treatment, and in intracranial pressure management in these patients, cryptococcosis continues to have a high rate of mortality. An estimate of the global burden of cryptococcal meningitis finds the numbers of cases and deaths to be excessive within areas of sub-Saharan Africa, where there is a high incidence of HIV-infected people (Vallabhaneni et al., 2016).

Clinical Disease

Primary cryptococcal disease generally occurs in the lungs following inhalation of the fungus from the environment. This disease can remain localized or can disseminate by hematogenous spread to other tissues, most frequently the central nervous system. The severity of the disease is dependent on the host's immune response, with severe disease most frequent in immunologically compromised patients. Practical guidelines for the management of cryptococcal diseases are available from the Infectious Diseases Society of America (Perfect et al., 2010).

Respiratory Tract

Cryptococcal infection of the respiratory tract exhibits a wide variety of presentations (Brizendine et al., 2011). Immunologically competent patients may exhibit no symptoms despite the presence of cryptococci in the lower respiratory tract, and the infection may be diffuse or localized, to include the formation of coin lesions that usually do not calcify. Immunocompromised patients on the other hand may have extensive infection that often is accompanied by other infectious agents, particularly *Pneumocystis (carinii) jirovecii* or cytomegalovirus. Extrapulmonary disease may appear weeks after a pulmonary infection has been documented (Campbell, 1966).

Skin Lesions

Skin lesions usually result from hematogenous dissemination from the respiratory tract in immunocompromised patients (Negroni, 2012). These lesions present as single or multiple papules, which enlarge and, in some cases, ulcerate, producing a thin exudate that contains the yeast.

Bone and Joint Infection

Bone and joint infection may occur as a result of dissemination from the respiratory tract (Bariteau et al., 2014). Osteolytic lesions are produced, with abscesses formed in adjacent soft tissue that contain a thin exudate with large numbers of cryptococci. Less commonly, joint spaces are involved.

Central Nervous System Infection

Cryptococcal meningitis is the most frequent and most serious focus of disseminated cryptococcal infection (Skipper et al., 2019). Onset of this disease may be acute, or presentation may be insidious and with few symptoms. Headache and changes in mental status and personality often dominate the clinical picture. Basilar meningitis, involvement of the cranial nerves, and invasion of the underlying cortex result in hydrocephalus and decreased visual acuity. Fever, if present, usually is of low grade, and typical signs of acute meningeal irritation, such as stiff neck and Kernig's and Brudzinski's signs, are often absent.

Pathology

The histologic response depends on the degree of encapsulation of the infecting cryptococcal strain. Most commonly, little or no inflammatory response is seen, and the cells of normal tissue are separated by large numbers of encapsulated cryptococci. Poorly encapsulated strains of *Cryptococcus* spp. elicit a granulomatous inflammatory response, and yeasts are found predominantly in the cytoplasm of macrophages. When CSF is examined, the only cells present may be the yeasts, which may be misinterpreted as mononuclear host cells if infection is not suspected clinically. Large capsules usually are demonstrated in positive India ink preparations; however, they are not always evident, and the cells may be confused with those of *Blastomyces* spp. or even immature spherules of *Coccidioides* spp.

Differentiation in tissue sections can be accomplished by staining of cryptococcal mucopolysaccharide with mucin stains or demonstration of melanin pigment with the Fontana-Masson stain. Mayer's mucicarmine stain and the GMS stain have been shown to be important for the diagnosis of cryptococcosis when atypical forms were present in an uncommon location (Gazzoni et al., 2009). The presence of a thick polysaccharide capsule gives these organisms the characteristic appearance of having a clear space around the yeast cells that can be seen in tissue sections using H&E stain. The encapsulated yeast is variable in size (3–10 μm in diameter) with a decidedly round nature and narrow-based budding are clues to the identification of this organism in tissue.

Fig. 60.18 Colonies of *Cryptococcus neoformans* usually appear mucoid when first isolated. Some strains are poorly encapsulated and lack the mucoid appearance. (Sabouraud dextrose agar.)

Laboratory Diagnosis

Possible cryptococci should always be identified as to the species complex level. Clues to the presence of this fungus include good growth on blood agar plates incubated in the bacteriology laboratory at 35° to 37°C, a mucoid appearance of the colonies (Fig. 60.18), a round appearance of the yeast cells without pseudohyphae in microscopic wet preps or stained preparations, and lack of growth on media that contain cycloheximide. Presumptive identification can be performed rapidly by examining an India ink preparation for capsules (see Fig. 60.14) and/or a positive urease test. Capsules may be diminished even in heavily encapsulated strains once they have been isolated on agar media; however, subcultures of isolates may restore the mucoid capsule. Definitive identification of the species complex can be accomplished by biochemical testing or genomic identification. Diagnosis from the CSF can now be obtained by the use of rapid molecular testing or antigen testing with results available prior to culture confirmation (Boulware et al., 2014; Leber et al., 2016; McMullan et al., 2012) although false negatives have been reported with molecular testing (Chew et al., 2018).

The differentiation between *C. gattii* and *C. neoformans* using standard phenotypic methods is difficult and generally not performed in the clinical laboratory (reported as *C. neoformans* species complex or *C. gattii/C. neoformans*). The incorporation of glycine into specialized medium (L-canavanine-glycine-bromthymol blue medium) has been shown to be a reliable method for the differentiation of these species, in that *C. gattii* readily assimilates glycine and *C. neoformans* does not (Klein et al., 2009). Molecular sequencing of the D1/D2 region of the 28S rDNA gene or the ITS regions of the rRNA genes has also been shown to be reliable in separating these two species (Georgi et al., 2009). More recently, MALDI-TOF MS has been shown to be a reliable method to rapidly discriminate between these two species (Firacative et al., 2012).

The polysaccharide antigen of the *C. neoformans* species complex can be detected in CSF and serum, using the latex agglutination test (Perfect et al., 2010) or the more recently developed lateral flow assay (Kabanda et al., 2014). The latex agglutination test exhibits a sensitivity of greater than 90%, although considerable variability in performance has been noted among different commercial kits. The frequency of erroneous results can be diminished by treatment of serum specimens with pronase. False-positive reactions appear to be less common in patients infected with HIV, perhaps because of the large numbers of organisms present. The lateral flow assay has the advantage of more rapid results, and does not require specialized equipment for sample preparation. Titration of positive results has been done traditionally to assess prognosis and to obtain a baseline for use in following the effects of treatment. Large amounts of antigen and persistence of antigen following therapy are poor prognostic signs in patients. Measurement of serum antigen appears to be a more sensitive test than testing of CSF in HIV-infected patients. However, both serum and CSF should be tested for optimal sensitivity. A negative India ink test on CSF is a good prognostic sign in non–HIV-infected patients but does not have the same implication for patients with AIDS.

THE GENUS MALASSEZIA

The history of the nomenclature used for the genus *Malassezia* is complicated. Currently, this genus is composed of one non–lipid-dependent species *(M. pachydermatis)* and 13 lipid-dependent species (Cabanes, 2014). *M. globosa* and *M. restricta* are considered the most common pathogens in this group among humans. Since differentiation of the *Malassezia* spp. requires molecular sequencing, most clinical laboratories prefer to report results as *Malassezia* spp.

Risk Factors

Malassezia yeasts are commensals of the normal skin, and cutaneous disease may occur in normal hosts. Systemic infection occurs primarily in neonates and is associated with intravenous hyperalimentation with lipid solutions (Cabanes, 2014). Although *Malassezia* spp. are not ordinarily present on the skin of healthy infants, the yeasts have been recovered from the skin of more than 35% of infants who were in intensive care units.

Clinical Diseases

Infection caused by *Malassezia* spp. can range from an asymptomatic lesion on the epidermis of normal individuals to systemic disease in the immunocompromised host.

Cutaneous Infection

Malassezia spp. are known causes of pityriasis (tinea) versicolor and seborrheic dermatitis, and evidence is accumulating that they play a significant role in atopic eczema/dermatitis syndrome (formerly called atopic dermatitis) (Cabanes, 2014; Pedrosa et al., 2014).

Pityriasis versicolor is a common infection of the epidermis in immunologically normal patients, resulting in hyperpigmentation or hypopigmentation of the skin, commonly on the trunk and upper arms. Fawn-colored macules are the most common presentation, but depigmenting lesions are more obvious in dark-skinned persons and may be accentuated by a suntan in light-skinned individuals. The ill effects are purely cosmetic but may be considerably troublesome. Hypopigmented lesions must be differentiated from vitiligo. Therapy consists of topical application of fungicidal creams or rinses, and systemic therapy is infrequently required.

Seborrheic dermatitis is a multifactor disease that requires both endogenous and exogenous predisposing factors for development. An inflammatory reaction against the yeast is considered the basis for the development of this disease.

Systemic Infection

Systemic infection occurs almost invariably in infants who have received intravascular infusions of lipid (the disease is also called *Malassezia* catheter–associated sepsis) (Tragiannidis et al., 2010). Diluted lipid solution supports the growth of lipid-dependent *Malassezia* spp. by supplying long-chain fatty acids that are also found on the skin and must be supplied in the laboratory for isolation of the yeast. Infected infants are often asymptomatic, but fever, leukocytosis, and thrombocytopenia may be present. Pneumonia is a common systemic manifestation of disease, probably resulting from emboli received from infected intravenous catheters. Removing the infected catheter is therapeutic.

Pathology of *Malassezia* Infection

The diagnosis of pityriasis versicolor usually is made clinically or by demonstrating yeast and short hyphal forms (similar in appearance to spaghetti and meatballs) in KOH preparations of skin scrapings (Fig. 60.19). The addition of Calcofluor white or another fungal stain enhances detection because the fungal cells are small and difficult to visualize when unstained. When biopsied, hyperkeratosis, acanthosis, and dermal mononuclear infiltrates may be seen. Little is known of the pathology of systemic infection with *Malassezia* spp. because biopsies are performed infrequently, and lethal infection is uncommon. In rare fatal cases, vasculitis, septic infarcts, and granulomatous inflammation have been described in many organs, including the lung, liver, and kidney.

Laboratory Diagnosis

Culture for *Malassezia* spp. is rarely requested in cutaneous disease, and direct observation of yeast in KOH preparations usually is done in the physician's office. This yeast should be sought in cultures of blood and intravenous catheter tips from neonates. Before inoculation, a drop of sterile olive oil is added to the surface of a suitable agar medium, such as Sabouraud dextrose agar or sheep blood agar. Within 2 to 3 days, colonies appear light brown and often have a very dry appearance in the oil overlay. An initial clue to this pathogen is lack of growth in the absence of oil or stimulation of growth by the presence of oil overlay (Fig. 60.20). In contrast, *M. pachydermatis* is not dependent on long-chain fatty acids for growth.

Identification of the genus can be suspected by microscopic examination of the yeast cells, which measure 3 to 7 μm in diameter. The budding process in *Malassezia* is unusual because it occurs as an enteroblastic

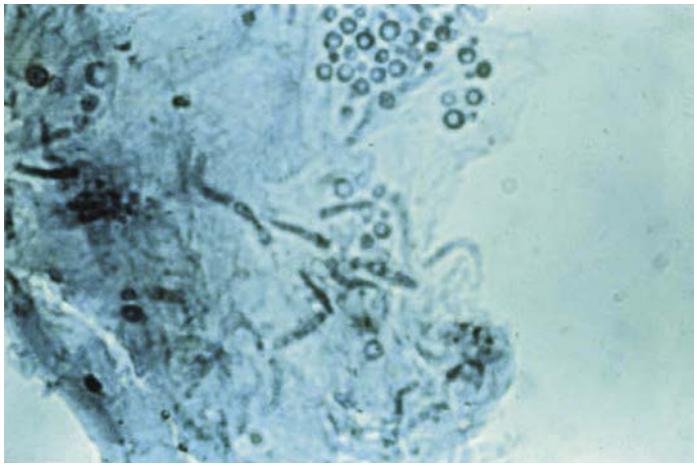

Fig. 60.19 Skin scrapings from a lesion of pityriasis versicolor. The yeast and short hyphal forms (spaghetti and meatballs appearance) are characteristic of *Malassezia furfur* species complex. (Lactophenol cotton blue stain, 400×.)

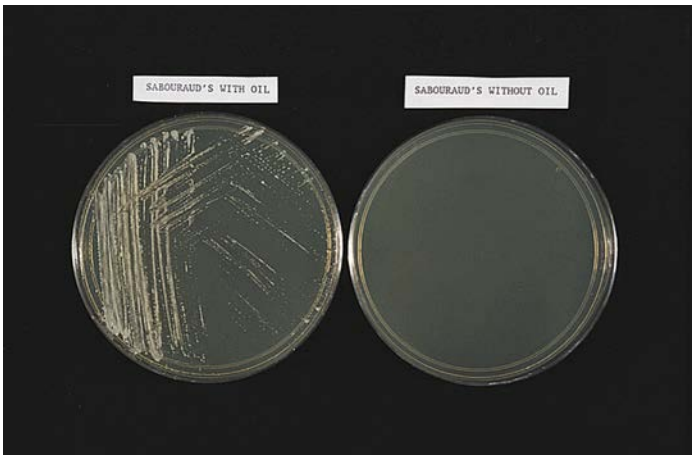

Fig. 60.20 Abundant growth of *Malassezia furfur* is evident on a plate that was overlaid with oil before the inoculum was applied. No growth is seen on a companion plate without oil. (Sabouraud dextrose agar.)

Fig. 60.21 Gram stain from culture demonstrating gram-positive yeast cells of *Malassezia* spp. showing the characteristic collarette (bud scar). (Gram stain, 1000×.)

process with the formation of phialides. The bud is broad based, and the collarettes of the phialides may be observed with the light microscope as a distinct dark ring separating the mother and daughter cells (Fig. 60.21). Species identification can be confirmed using molecular techniques that target regions within the rDNA complex (Cafarchia et al., 2011).

OTHER YEAST AND YEASTLIKE PATHOGENS

Invasive infection caused by rare yeast pathogens continues to increase due in part to the severe immunosuppressive conditions that predispose patients to infection. A panel of experts of the European Society of Clinical Microbiology and Infectious Diseases (ESCMID) and the European Confederation of Medical Mycology (ECMM) undertook a data review and compiled guidelines for the diagnostic tests and procedures for detection and management of rare invasive yeast infections (Arendrup et al., 2014). Their assessment showed that there are a number of non-*Candida* species that continue to emerge and cause disease. Notable examples of species associated with invasive disease included the *Trichosporon* spp., *Saprochaete capitata* (formerly *Geotrichum candidum*), and *Rhodotorula mucilaginosa* (Fig. 60.22). Currently, over 50 species of *Trichosporon* have been described with human disease remaining uncommon (Colombo et al., 2011). Of these *T. asahii*, *T. mucoides*, and *T. asteroids* are most commonly associated with invasive infection. The ability of these species to adhere to and form biofilms on implanted devices has been shown to account for the emergence of invasive trichosporonosis cases (Colombo et al., 2011). Both *S. capitata* and *R. mucilaginosa* have emerged as causes of life-threatening fungemia in severely immunocompromised patients (Arendrup et al., 2014). Resistance to regularly used antifungal agents is not uncommon with these pathogens and other rare yeast-causing disease, making the correct identification mandatory for appropriate management of the infected patient (Thompson et al., 2009).

Fig. 60.22 An aerial mycelium arises from the yeastlike colony of *Geotrichum candidum*. (Sabouraud dextrose agar.)

Demonstration of these rare yeasts in tissues, by histopathology with culture or isolation in culture from multiple specimens of a sterile site, is required to document the role of an unusual yeast in the infectious process. Species confirmation in these circumstances requires molecular sequencing of the isolated pathogen.

MYCOSES CAUSED BY DIMORPHIC FUNGI

Thermally dimorphic fungi are the most pathogenic organisms encountered in a clinical mycology laboratory. In the United States, the most important dimorphic pathogens are *Histoplasma*, *Blastomyces*, *Coccidioides* and *Sporothrix* spp. *Sporothrix* is widely distributed throughout the world, while the other organisms are found predominantly in North and South America, where they have distinct geographic distributions (Fig. 60.23). Epidemic disease is most common with *Histoplasma* and *Coccidioides* and less common with *Sporothrix* and *Blastomyces*, although outbreaks certainly occur. These endemic mycoses share several characteristics, including (1) the ability to cause disease in a healthy host, (2) association with a specific ecologic niche in the environment, and (3) demonstration of temperature dimorphism (mold in the environment at a temperature of 25° to 30°C and yeast or spherules [in the case of *Coccidioides*] at body temperature).

THE GENUS HISTOPLASMA

H. capsulatum has traditionally been divided into two varieties: *H. capsulatum* var. *capsulatum* (hereafter referred to as *H. capsulatum*) and *H. capsulatum* var. *duboisii*. Both of these fungal pathogens are geographically restricted, and acquisition of infection does not overlap in most cases. *H. capsulatum* is found primarily along the Ohio, Mississippi, and St. Lawrence rivers but may have worldwide distribution. A recent proposal has further subdivided *H. capsulatum* into additional species although these have not yet been uniformly accepted (Sepulveda et al., 2017). *H. capsulatum* var. *duboisii*, on the other hand, is limited to equatorial Africa and causes a disease referred to as African histoplasmosis. Distinguishing characteristics of the tissue phase can be observed to differentiate between these two pathogens; however, lack of travel to the endemic area in Africa generally can be used to rule out infection with *H.* var. *duboisii*.

Risk Factors

The primary risk factor for acquiring histoplasmosis is living in endemic regions of the United States. In some areas, more than 90% of the population reacts positively to histoplasmin skin testing. Growth of *H. capsulatum* in the soil is stimulated by bird guano, although the fungus does not infect the bird. Once growing in the soil, the fungus sporulates and produces conidia, which, during activities that generate aerosols, can be inhaled into the lungs. Occupationally acquired acute histoplasmosis has been reported, leading the US National Institute for Occupational Safety and Health (NIOSH) to issue a document outlining measures for protecting workers at risk (Department of Health and Human Services, 2004).

Epidemic acute disease has occurred in individuals exposed to areas endemic for this fungus. The Centers for Disease Control and Prevention (CDC) described 221 cases of histoplasmosis among students representing 37 colleges in 18 states who had vacationed in Acapulco, Mexico, in March 2001 and then returned to the United States (CDC, 2001) and a recent summary of past outbreaks has been published (Benedict & Mody, 2016).

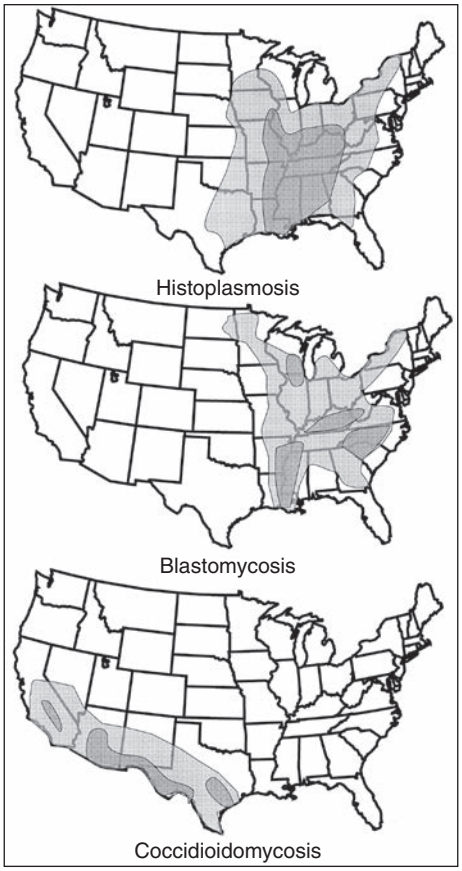

Fig. 60.23 Geographic distribution of dimorphic fungal infections in the United States. Areas of greatest endemicity *(dark shading)* and lesser endemicity *(light shading)* are illustrated. Sporadic cases may also occur in other areas outside of the endemic zones.

Occupationally, a CDC report described an outbreak of histoplasmosis wherein at least 25 workers at an agricultural processing plant in Nebraska developed disease following exposure to soil known to be contaminated with *H. capsulatum* (CDC, 2012).

Clinical Diseases

The magnitude of the exposure and the immune status of the host influence the clinical manifestations of disease, which can range from an asymptomatic infectious process to disseminated life-threatening disease (Azar & Hage, 2017; Wheat et al., 2007b). Exposure to low concentrations of spores from the environment in a normal host is typically asymptomatic. Therefore most adults living in an endemic area are seropositive and show immunologic evidence of infection; however, they remain asymptomatic to disease. Disseminated disease is usually reserved for individuals who are immunosuppressed.

Acute Pulmonary Infection

Individuals who are exposed to large numbers of conidia may develop a flulike syndrome with high fever, chills, fatigue, cough, and pleuritic or retrosternal chest pain. More severely affected individuals may be sick for several weeks, but resolution usually is complete even without antifungal therapy in the normal host (Wheat et al., 2007b). If focal granulomatous inflammation has occurred, calcification of the focus typically leaves a well-circumscribed coin lesion, which may be seen on the chest radiograph.

Granulomatous and Fibrosing Mediastinitis

These types of manifestations involve the lymph nodes in the mediastinum (Hammoud et al., 2009). Granulomatous disease is characterized by enlarged lymph nodes, which may obstruct the airways, pulmonary vessels, or esophagus. Fistulas can form within the lymph nodes and adjacent mediastinal structures. Fibrosing disease is a reaction that occurs in the mediastinum among individuals predisposed to an excessive response to *Histoplasma* antigens. Obstructions may form that involve the superior vena cava, the airways, the pulmonary arteries or veins, or the esophagus. Both granulomatous and fibrosing diseases are thought to progress independently.

Chronic Pulmonary Histoplasmosis

This debilitating disease occurs primarily in patients with chronic obstructive pulmonary disease (COPD), most of whom are middle-aged men (Goodwin et al., 1976). However, studies have shown that this disease is becoming more commonly recognized among females, and that females exhibited fewer cavities and presented with decreased numbers of smokers and reduced extent of smoking exposure, along with absence of COPD. In this disease, calcification and cavitation may occur, which may mimic chronic pulmonary tuberculosis and pulmonary neoplasia.

Disseminated Histoplasmosis

Dissemination of yeast through the reticuloendothelial system may occur as part of acute pulmonary histoplasmosis, resulting in healed granulomas that often calcify, especially in the spleen. Clinically disseminated infection occurs in two classes of patients. The first group consists of individuals at the extremes of age who do not have a recognized immunosuppressive condition but may have an immune system that is incompletely developed or is diminished by age in ways that are incompletely understood. The second group comprises patients with recognized immunosuppressive diseases or therapies. Before the 1980s, these diseases were predominantly hematologic neoplasms; however, in recent years, HIV and the receipt of tumor necrosis factor-α (TNF-α) blockers have dominated as major risk factors for severe infection (Vergidis et al., 2015; Wheat et al., 2007b). Progression of disease may be rapid or insidious.

Compromised patients may develop an infection of the reticuloendothelial system, resulting in lymphadenopathy, hepatosplenomegaly, or thrombocytopenia (Wheat et al., 2016). Destruction of the adrenal cortex by the granulomatous process may be sufficiently extensive to cause hormonal insufficiency. Central nervous system infection may be manifested as chronic meningitis, intracerebral granulomas, or both. Endovascular infection includes endocarditis with large, bulky vegetations. Any part of the GI tract may be affected, and ulcerating lesions may suggest a neoplasm macroscopically. The hallmark of disease is an oropharyngeal ulcer, which may cause hoarseness, dysphagia, or a painful lesion on the tongue or gingiva (Psevdos & Tanowitz, 2008; Young et al., 1972).

Pathology

As a facultative intracellular pathogen, *Histoplasma* is found predominantly in macrophages. Pathologic lesions consist of collections of infected macrophages, noncaseating granulomas, or caseating granulomas. Histopathologic lesions are similar to those produced by *Mycobacterium tuberculosis*, and these two pathogens should be considered at the same time in patient evaluation. Intracellular yeasts are often well demonstrated by H&E staining (Fig. 60.24). However, PAS and GMS stains are more sensitive, with the silver stain essential for demonstration of old yeast cells in healed granulomas. This yeast, presumably no longer viable, may be enlarged and distorted in morphology, making diagnosis difficult. Differential diagnosis of yeast forms includes small forms of *Blastomyces*, *Talaromyces (Penicillium marneffei)*, *Leishmania* spp., or *Candida* spp., especially *C. glabrata*. The yeasts of *Histoplasma* in caseating granulomas are sufficiently distinctive to provide a presumptive diagnosis, but unusual granulomatous presentations of *Pneumocystis (carinii) jirovecii* must be differentiated. Culture is generally required for disease confirmation; however, molecular tests for direct testing on tissue have shown promise for the confirmation of histoplasmosis without culture (Babady et al., 2011; Koepsell et al., 2012).

Laboratory Diagnosis

The yeast form in tissue may be demonstrated histologically or in preparations of respiratory secretions, fluids, peripheral blood, bone marrow, or tissue imprints. Wet preparations and Calcofluor white may be used, but the morphology of tissue and yeast cells is best seen with Giemsa staining because the details of nuclear morphology can be assessed. The yeast cells measure 3 to 5 μm in diameter, have a single nucleus, and bud with a narrow neck.

If disseminated infection is suspected, blood cultures for *Histoplasma* should be performed. The Isolator technique is a sensitive technique for recovering the yeast phase from blood, although other blood culture detection systems can also be used to detect this fungus. Other clinical specimens should be inoculated to an enriched agar, such as brain-heart infusion agar supplemented with sheep blood, which is incubated at 25° to 30°C.

Colonies of *Histoplasma* usually appear after incubation for 10 to 14 days but occasionally require incubation for up to 4 weeks. They are fluffy and vary from white to buff-brown. Diagnostic asexual forms include microconidia and macroconidia. Microconidia, which are produced first, are similar to the structures produced by *Blastomyces*. The more

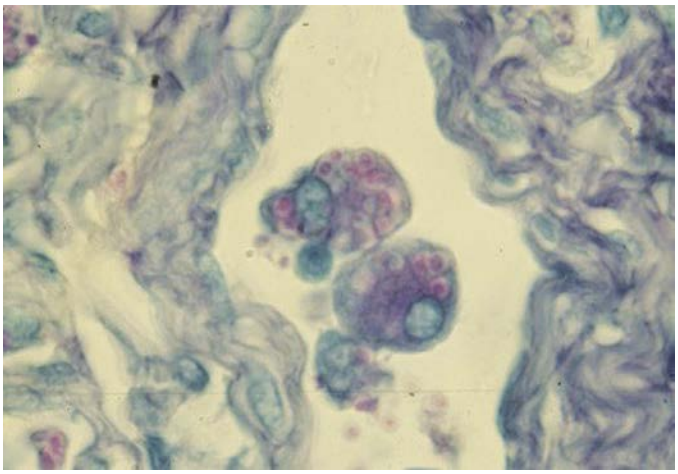

Fig. 60.24 Yeast cells of *Histoplasma capsulatum* in macrophages. The presence of intracellular small, round to oval yeastlike cells in tissue is a characteristic pathologic finding in histoplasmosis. (Hematoxylin and eosin stain, 1000×.)

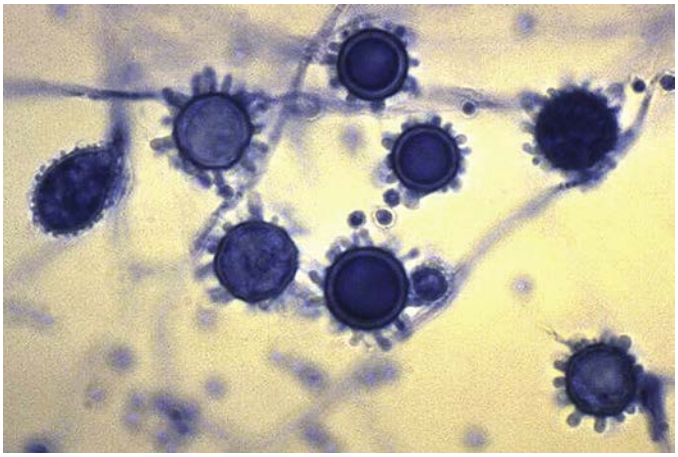

Fig. 60.25 Tuberculate macroconidia with microconidia of *Histoplasma capsulatum* in culture. These structures are characteristic of the environmental mold form of this dimorphic fungus. ((Lactophenol cotton blue stain, 400×.) (Courtesy Centers for Disease Control and Prevention Public Health Image Library.))

characteristic macroconidia have roughened projections from the periphery of the conidia, a configuration referred to as tuberculate (Fig. 60.25). The macroconidia of the saprobe, *Sepedonium*, may be confused with *Histoplasma*, so differentiation of these two fungi is important. The macroscopic appearance of the colonies, the rate of growth, the growth of *H. capsulatum* on media containing cycloheximide, the presence of yeast forms in tissue, and the clinical history usually are sufficient to diagnose histoplasmosis. Final confirmation most often is provided by nucleic acid hybridization probe testing from the culture isolate. Conversion of the mold to the yeast phase also confirms identification, but this is often difficult and has been supplanted in most clinical laboratories by the molecular probe technique (AccuProbe).

Serologic tests for the detection of anti-*Histoplasma* antibodies (i.e., immunodiffusion and complement fixation) have several limitations that need to be considered, making these tests suboptimal for the diagnosis of histoplasmosis. A 2- to 6-week delay after exposure is required for the production of antibodies, reducing the value of this testing for the diagnosis of acute disease. Once patients are infected with *Histoplasma*, antibody levels remain detectable for many years. Antibodies to *Histoplasma* and *Blastomyces* also may cross-react. Additionally, patients with immune dysfunction may not produce detectable levels of antibodies, and patients with previous exposure might have elevated levels of antibodies (Wheat, 2006b).

Antigen detection, on the other hand, has been shown to be useful for the diagnosis and management of histoplasmosis (Connolly et al., 2007; Hage et al., 2011). The sensitivity of urine antigen detection for diagnosis is greatest in patients with disseminated disease (up to 92%) or acute pulmonary histoplasmosis (75–80%) although is less helpful in other forms of histoplasmosis (Fandino-Devia et al., 2016). Antigen detection is also useful for following the effects of therapy on fungal burden; when antigen concentrations in urine or serum fall during therapy, treatment success is suggested. Moreover, increased antigen levels in a previously infected individual suggest a relapse of infection. Use of the antigen assay to detect *Histoplasma* antigen in bronchoalveolar fluid has been shown to complement antigen detection in serum and urine as an objective diagnostic test (Hage et al., 2010).

The histoplasmin skin test antigen has been useful for epidemiologic studies but should not be used for diagnosis. Not only does the high frequency of positive tests in endemic areas cloud interpretation, but the skin test can cause an individual to seroconvert to positive, further confusing the issue.

THE GENUS BLASTOMYCES

Blastomyces dermatitidis was previously the only species within the genus *Blastomyces;* however, several other species have since been proposed (Dukik et al., 2017). Endemic areas for this pathogen in the soil include the eastern part of the United States, mainly areas adjacent to the Mississippi and Ohio river basins and areas northwest of the Great Lakes in Canada; the newly described species *B. helicus* is found primarily in western states (Schwartz et al., 2019).

Risk Factors

Most cases of blastomycosis (also referred to as North American blastomycosis) are sporadic, and an environmental source is not often found. Small outbreaks do occur, and the fungus has been isolated from soil at outbreak sites (Roy et al., 2013). Few risk factors for blastomycosis are known, although severe cases in the Hmong population in Wisconsin have been associated with interleukin 6 (IL-6) polymorphisms (Merkhofer et al., 2019). HIV-infected patients who reside in endemic areas are particularly at risk for serious infection (Chapman et al., 2000).

Clinical Diseases

As is true with most other endemic dimorphic fungi, the portal of entry is the respiratory tract, where the infection may be asymptomatic, transient, or insidiously progressive (Bariola & Vyas, 2011; Saccente & Woods, 2010). Chronic pulmonary blastomycosis with low-grade fever, weight loss, and localized pulmonary infiltrates may suggest neoplastic disease, for which diagnostic studies, including BAL, fine-needle aspiration of the lung, or surgical lung biopsy, may be undertaken. Dissemination of yeast from the lung most commonly results in cutaneous or skeletal infection (Jain et al., 2014; Mason et al., 2008). The central nervous and genitourinary systems are involved less frequently. Cutaneous lesions often are hypertrophic or ulcerative and may be locally destructive. The lesions may be mistaken for squamous cell carcinoma of the skin. Secondary involvement of the skin over bony lesions also occurs. A delay in diagnosis is not uncommon, especially when patients have no history of exposure to an endemic area (Bradsher, 2014; Veligandla et al., 2002).

Pathology of Blastomycosis

The characteristic histologic response to *Blastomyces* is a mixture of acute inflammation with microabscess formation and granulomatous inflammation. In cutaneous lesions, pseudoepitheliomatous hyperplasia of the epidermis overlying the inflammation is characteristic. Yeast cells are most often found in the microabscesses or within multinucleated giant cells. The characteristic yeast can frequently be demonstrated in tissue sections stained with H&E, but the organism may be more readily visible when stained with PAS or GMS. The thick-walled yeast cells measure 8 to 15 μm in diameter and maintain a broad base during the budding process (Fig. 60.26). An artifactual separation of the cytoplasm from the cell wall in formalin-fixed preparations may give the appearance of a double wall. Although nonbudding yeast cells must be differentiated from yeast cells of *Cryptococcus* spp. and from developing spherules of *Coccidioides* spp., the diagnosis of blastomycosis can generally be proposed by observation of characteristic yeast forms in tissues by an experienced pathologist (Patel et al., 2010).

Surgical pathology and cytopathology have been reported as the primary means of diagnosis because positive culture may not always be recovered. However, microbiology culture and conventional morphologic assessment of routine samples have redundant utility in diagnosis and generally are required to make a confirmed disease diagnosis (Taxy, 2007). Advances in molecular diagnostics have shown promise for the identification of *Blastomyces* directly from clinical specimens (Babady et al., 2011).

Laboratory Identification

Direct demonstration of the yeast cells may be accomplished in tissue sections or in wet preparations of aspirated fluids and imprints of tissues.

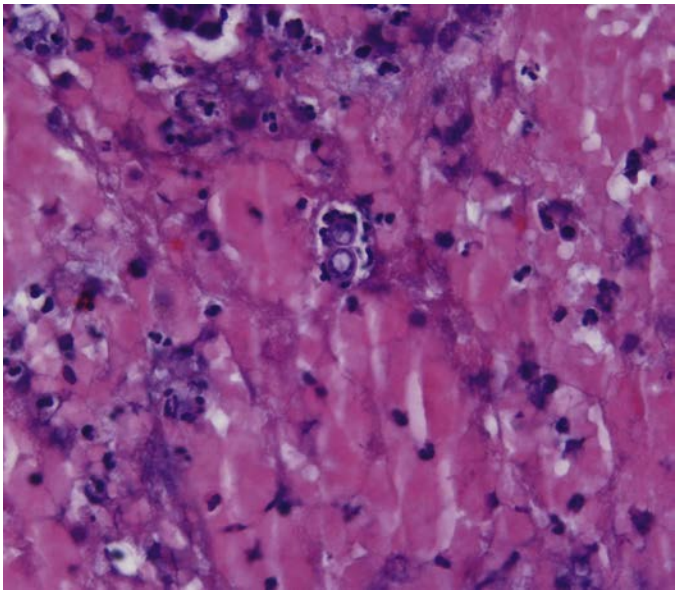

Fig. 60.26 *Blastomyces dermatitidis* in tissue showing characteristic large, broad-based, budding yeast cells with a thick refractile (double-contoured) wall. (Hematoxylin and eosin stain, 400×.)

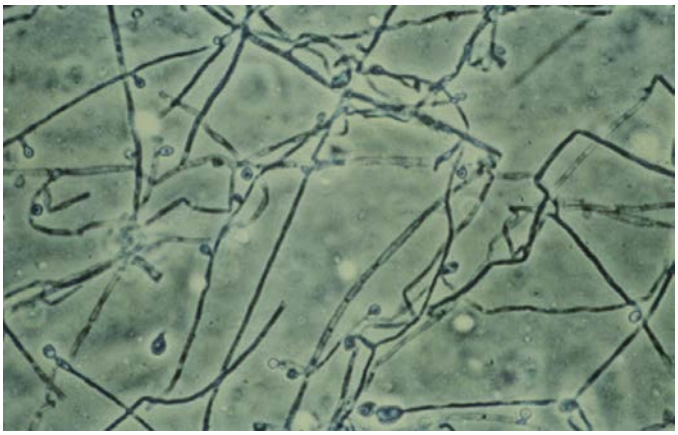

Fig. 60.27 Mold form of *Blastomyces dermatitidis* in culture. The lollipop appearance of the conidium on a conidiophore is characteristic of the environmental mold form for this dimorphic fungus. (Lactophenol cotton blue stain, 400×.)

Calcofluor white staining may enhance detection of the yeast. Growth is somewhat more rapid than that of *Histoplasma*, and fluffy white to buff colonies, which often cannot be distinguished from *Histoplasma*, usually appear within 1 to 2 weeks. The microconidia resemble those of *Histoplasma* (Fig. 60.27), but macroconidia are not formed. A saprobic mold, *Chrysosporium* resembles *Blastomyces* but does not develop a yeast phase and does not grow on media that contain cycloheximide. Conversion to the yeast phase may occur on routine media incubated at 37°C with hemoglobin and cysteine containing agar used specifically for this purpose (Fig. 60.28). Once again, demonstration of the yeast form in tissue serves as a reasonable substitute for demonstration of dimorphism in the laboratory. The nucleic acid probe hybridization test (AccuProbe) from culture material is the preferred method for confirmation of isolates in most laboratories, although false-positive results have been reported (Scalarone et al., 1992).

Although the complement fixation test has been used as a serologic test for the diagnosis of blastomycosis, this test has considerable limitations. A *Blastomyces* antigen test similar to the *Histoplasma* antigen test also is available in a reference laboratory; however, data regarding utility and reliability are lacking and considerable overlap exists with other endemic fungi limiting the specificity of this test.

THE GENUS COCCIDIOIDES

Until recently, *Coccidioides immitis* was considered the sole etiologic agent of coccidioidomycosis (valley fever, San Joaquin Valley fever, and desert fever). Phylogenetic studies now show the existence of two genetically distinct *Coccidioides* spp. (*C. immitis* and *C. posadasii*) with considerable population

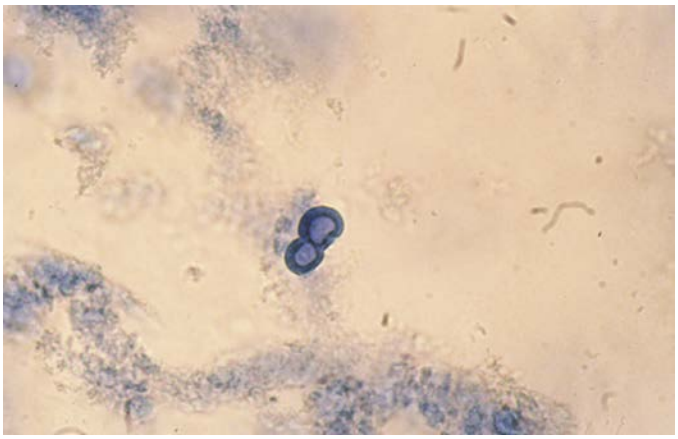

Fig. 60.28 Budding yeast cells of *Blastomyces dermatitidis* in culture. When cultures are incubated at 37°C, large, broad-based budding yeasts with a double-contoured wall are detected that are characteristic of the yeast phase of this dimorphic fungus. (Lactophenol cotton blue stain, 400×.)

differences between these (Engelthaler et al., 2016). Recent evidence has also found phenotypic differences between these species (Barker et al., 2019).

The coccidioidal organisms are soil-dwelling fungi found in the southern portions of California and in other areas of the southwestern United States (especially southern regions of Arizona, Utah, Nevada, and New Mexico, as well as western Texas), Washington state, northern Mexico, and Central and South America (especially Venezuela) (Brown et al., 2013). Arizona has seen a dramatic increase in cases over the years, with a disproportionate rate of infection occurring in people older than 65 years of age and in those with HIV infection, although California cases for the first time exceeded those in Arizona in 2018 (California Health Department, unpublished data). Although coccidioidomycosis is endemic to the hot, arid regions of the southwestern United States and Central America, recognition of exposure to contaminated soil outside of these endemic areas should be considered by health care providers and veterinarians (Benedict et al., 2015).

Risk Factors

Residence in an endemic area is the primary risk factor for the development of infection because the arthroconidia of the mold phase are in the soil and are easily disseminated through the air (Brown et al., 2013; Stockamp & Thompson, 2016). A classic example of epidemic coccidioidomycosis occurred among cast and crew members at an outdoor filming event in California in 2012 (Wilken et al., 2014). Five individuals within this group were laboratory-confirmed to have pulmonary coccidioidomycosis, with an additional five probable cases following an extensive outbreak investigation of this filming event. The dry, dusty conditions during the filming associated with substantial soil-disruptive work, including grading and digging, illustrated the risk to employees working outdoors in *Coccidioides*-endemic areas. The locations of military bases in the southwestern United States have also shown coccidioidomycosis to have a profound effect on military personnel training in these areas (Crum-Cianflone, 2007). The development of an effective vaccine for valley fever to protect both military members and civilians residing or training in endemic areas has been a suggested prevention strategy to avoid acquiring the disease (Kirkland, 2016).

Genetic factors have been suggested to influence the frequency of severe and disseminated infection, and current studies are ongoing (Hung et al., 2019). Disseminated infection is reportedly more common in blacks and Filipinos than in whites. Asians, Native Americans, and Hispanic patients also appear to be at increased risk for the disease.

Immunosuppressive infection or disease is a known risk factor for disseminated infection, with HIV-infected patients at particular risk for disseminated disease (Galgiani et al., 2016). Transplant recipients or others receiving immunosuppressive medications who travel to or reside part time or full time in endemic areas are also at risk for both primary and reactivation coccidioidomycosis (Blair et al., 2019). Clinicians in nonendemic areas should be aware of the potential for this disease and should know that early diagnosis followed by prompt antifungal therapy could be lifesaving in these patients.

Clinical Diseases

Primary coccidioidomycosis is most frequently asymptomatic, as indicated by the high prevalence of positive skin tests for coccidioidal antigens in

endemic areas. Symptomatic disease usually is manifested as fever with cough or chest pain, or both, and may mimic bacterial pneumonia clinically (Twarog & Thompson, 2015). Erythema nodosum and erythema multiforme, which may accompany the primary infection, are favorable prognostic signs of disease and represent an immunologic response to infection. Solitary pulmonary nodules may persist as consequences of the primary pulmonary infection, also similar in appearance to a neoplasm or to tuberculosis.

Disseminated infection most commonly affects the skin, the skeletal system, and the meninges. Skin lesions include papules, ulcers, draining sinuses, and subcutaneous abscesses. Arthritis most often results from involvement of adjacent bones. Meningitis may be acute but is more commonly indolent and chronic.

Pathology

The tissue response to *Coccidioides* spp. is granulomatous, with and without caseation. Developing immature spherules can be found in macrophages and multinucleated giant cells (Fig. 60.29). Endospores within the spherules measure 2 to 5 μm in diameter (Fig. 60.30). The spherules measure up to 100 μm in diameter, and developing spherules have a large range of sizes protecting them from phagocytosis by the host (Lee et al., 2015). The differential diagnosis of developing spherules primarily includes nonbudding forms of *Blastomyces* or *Cryptococcus*. The spherules must be differentiated from the fungal forms in adiaspiromycosis and rhinosporidiosis, both of which are uncommon infections in the United States. In early disease stages, spherules may not be readily observed, and the presence of only endospores may make the diagnosis of coccidioidomycosis difficult.

Laboratory Diagnosis

The diagnosis of coccidioidomycosis can involve a variety of direct microscopic methods (i.e., Calcofluor white stain of respiratory specimen and histopathology of tissue), as well as culture with specific molecular probes for identification (Saubolle, 2007). Spherules may be demonstrated in sputum or, more commonly, in BAL fluid, but the sensitivity of direct examination for these structures is generally low. Calcofluor white staining following digestion of the specimen with KOH may increase the sensitivity of testing. If cavitary disease is present, hyphae may be present in clinical specimens, although this is a rare finding. In contrast to the other dimorphic pathogens, the possibility of communicability of arthroconidia directly from the specimen to medical personnel exists under this circumstance.

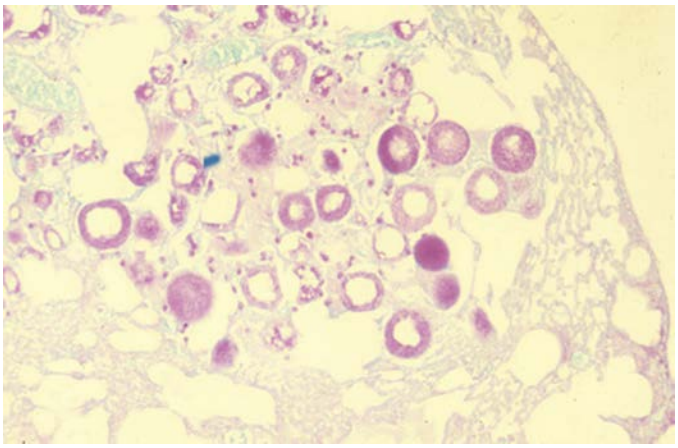

Fig. 60.29 Spherules of *Coccidioides* spp. in tissue. Observation of these large structures in tissue is a presumptive diagnosis for coccidioidomycosis. (Hematoxylin and eosin stain, 100×.)

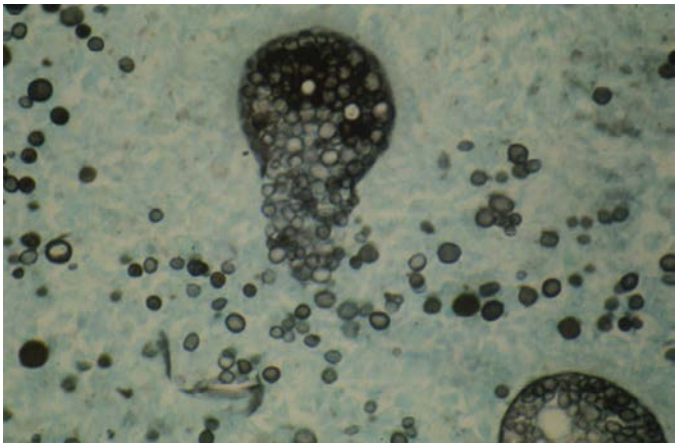

Fig. 60.30 Spherules of *Coccidioides* spp. in tissue showing release of endospores. At maturity, the spherule ruptures and releases endospores, which, in turn, mature to become spherules. When seen in tissue, these immature endospores may be confused with other smaller yeasts. (Gomori's methenamine silver stain, 1000×.)

Coccidioides spp. grows rapidly (within 1 week) and can appear on standard bacteriology media such as blood agar in the laboratory. Unfortunately, the arthroconidia of the *Coccidioides* are highly infectious and are easily transmitted by aerosolization. Infection of laboratory workers is a major concern, so inoculated cultures should be handled with great care in a biosafety cabinet. The National Institutes of Health has classified both *C. immitis* and *C. posadasii*, along with *Histoplasma* spp., as biosafety risk group 3 biologic agents (i.e., agents that are associated with serious or lethal human disease for which preventive or therapeutic interventions may not be available). Biosafety level 3 containment is suggested when specimens known or likely to contain this organism are handled. In a survey of laboratory-acquired infections, coccidioidomycosis was included in a list of the 10 most frequently reported infections (Singh, 2009).

Colonies of *Coccidioides* spp. are variable in appearance, ranging from velvety or cottony to granular or powdery. The colonial morphology may change as the colony and arthroconidia develop. Most isolates are white, but a variety of colors may be observed, and a diffusible pigment may be produced by some strains. Cultures often become gray with age. If a *Coccidioides* variety is suspected, some mycologists prefer to sterilize the culture before examination of the colonies by flooding the container with 10% formalin, followed by overnight incubation. In cases in which specimens are suspected to contain *Coccidioides*, screw-capped slants should be used instead of plates. The mold form is not routinely converted to the tissue form because specialized synthetic broth is generally required for this to occur, and it can be technically difficult. Separation of species into *C. immitis* and *C. posadasii* is best achieved by specialized molecular techniques, which normally are not available in routine clinical laboratories (Saubolle, 2007). Generally, laboratories will report the results as "*Coccidioides immitis/posadasii*" or as a "*Coccidioides* species."

Alternating barrel-shaped arthroconidia with empty disjuncture cells upon microscopic examination of culture material are distinctive (see Fig. 60.9) but must be differentiated from other organisms that produce arthroconidia, such as *Trichosporon*, *Saprochaete (Geotrichum)*, and some members of the family *Gymnoascaceae*. All size characteristics typically make this distinction straightforward. A presumptive identification is generally adequate to make a diagnosis of coccidioidomycosis in an individual who has been in an endemic area and in whom spherules with endospores have been detected in clinical material. A molecular-based genetic probe (AccuProbe) is the method of choice for identification of the fungus into *Coccidioides immitis/C. posadasii* (McGinnis et al., 2006).

In contrast to histoplasmosis and blastomycosis, serologic analysis with the complement fixation test is useful for assessing the extent and prognosis of coccidioidomycosis (McHardy et al., 2018). Of the serologic techniques available, complement fixation has been studied most extensively. Antibodies are detected approximately 2 to 6 weeks after infection. The height of the titer is an indication of the likelihood of disseminated disease, and a rising titer bodes a poor outcome. Skin testing does not confound the diagnosis by producing a seroconversion, as in histoplasmosis, but the sensitivity and specificity of the currently available skin test formulation has been questioned limiting its clinical utility (Ampel et al., 2019). Patients with disseminated infection may demonstrate anergy to the skin test antigen. In an update on diagnosis, Malo and colleagues (2014) provide examples of classic clinical and radiographic presentations, discuss the utility of serologic testing, and provide suggested algorithms that may aid in the diagnosis of coccidioidomycosis.

THE GENUS SPOROTHRIX

Historically, the only known species responsible for sporotrichosis was *Sporothrix schenckii*. However, molecular studies now demonstrate that *S. schenckii* is a complex of at least five distinct species (*S. schenckii*, *S. albicans*, *S. brasiliensis*, *S. globosa*, *S. luriei*, and *S. mexicana*) (Oliveira et al., 2014). Although methods for distinction among these species have been developed, most laboratories do not have the expertise to identify specific species and still refer to *S. schenckii* as the sole cause of sporotrichosis. More appropriately, laboratory reports should now consider identification as a complex of multiple species and should report results as "*Sporothrix schenckii* species complex."

Sporothrix spp. are dimorphic fungi present worldwide in soil, plants, and decaying vegetation. Although considered endemic dimorphic fungi, this complex of species exhibit epidemiologic differences that separate them from the other classic endemic dimorphic fungi. The mode of entry for these fungi is usually traumatic implantation (vs inhalation), the disease produced is usually a localized systemic infection (vs pulmonary), and the incidence of systemic infection is rare (Barros et al., 2011).

Risk Factors

Although *Sporothrix* spp. are common in vegetation throughout the world, they do not appear to be plant pathogens; however, epidemics have been caused by exposure to plant products (Rodrigues, de Hoog et al., 2014). One major outbreak occurred among florists and nursery and forestry workers who handled contaminated sphagnum moss grown in Wisconsin (Dixon et al., 1991). Another recent major outbreak involved infected cats in Rio de Janeiro, Brazil, where 759 human cases of cat-transmitted sporotrichosis were reported suggesting *S. brasiliensis* may have shifted from an environmental to a zoonotic disease in some locations (Gremiao et al., 2017). An unusual epidemic occurred among members of a college fraternity in Florida who were building a wall with bricks packed in contaminated straw (Sanders, 1971).

Clinical Diseases

The overwhelming predominant clinical form of sporotrichosis is involvement of cutaneous and subcutaneous tissues (Kauffman et al., 2007). A papule at the portal of entry may ulcerate and spread the pathogen through regional lymphatics, resulting in a series of lesions progressing up the affected limb (referred to as **lymphocutaneous sporotrichosis**). Dissemination to osteoarticular structures and viscera is uncommon and appears to occur more often in patients who have a history of alcohol abuse or immunosuppression, especially in patients with AIDS.

Pathology of Sporotrichosis

Histologic responses to *Sporothrix* and *Blastomyces* are similar with a mixed suppurative (including eosinophils) and granulomatous inflammation (Guarner & Brandt, 2011). In the skin, pseudoepitheliomatous hyperplasia of the epidermis is common. The yeast cells of *Sporothrix* are rarely seen in tissue, but when present are pleomorphic and round or elongated, resembling cigars 2 to 6 μm in diameter with narrow-based budding. A tissue reaction to the fungus may result in radiating eosinophilic material up to 10 μm in thickness around the yeast cell, known as the **Splendore-Hoeppli phenomenon** (asteroid bodies) (Hussein, 2008). This distinctive tissue reaction is uncommon, although the reaction is not specific for the diagnosis of sporotrichosis. The differential diagnosis of the skin lesions is primarily mycobacterial infection, especially *Mycobacterium marinum* (swimming pool granuloma) in the United States and cutaneous leishmaniasis in the tropics.

Laboratory Diagnosis

The preferred specimen is an aspirate, curetting, or biopsy of the skin lesion. *S. schenckii* grows well on primary isolation media with cycloheximide incubated at 25° to 30°C. The colonies, which may be moist or smooth (glabrous), are often light colored initially and may turn darker with increasing age. This organism produces two types of conidia: thin-walled hyaline conidia arranged as a rosette around the apex of a conidiophore, and thick-walled, dark, sessile conidia attached directly to the hyphae. These dark conidia account for a dematiaceous appearance of the fungus in culture (melanized fungus). The thin-walled microconidia are borne on conidiophores that arise at right angles from the hyphae. They may be arranged sympodially around an expanded vesicle at the tip of the conidiophore, producing an arrangement that has been described as a floret (Fig. 60.31). Similar structures are produced by *Acremonium* spp., which have rarely been reported as a cause of human disease. This mold is differentiated from *Sporothrix* by the absence of growth on cycloheximide agar and by the absence of a yeast phase. Conversion of the mold phase to yeast is accomplished by incubation of the isolate at 37°C in an atmosphere of 5% carbon dioxide on an enriched medium, such as brain-heart infusion agar supplemented with sheep blood or on chocolate agar. Phenotypic characteristics such as the morphology of sessile pigmented conidia; growth at 30°C, 35°C, and 37°C; and the assimilation of sucrose, raffinose, and ribitol have been used successfully to distinguish among species (Marimon et al., 2006). Molecular studies using the calmodulin gene sequence, the rRNA internal transcribed spacer sequence data, and the β-tubulin sequence have been shown to be reliable for differentiating among *Sporothrix* spp., although more recently whole genome sequencing has revealed significant structure within this genus (Barros et al., 2011; Teixeira et al., 2014).

OTHER DIMORPHIC FUNGI

H. capsulatum var. *duboisii* causes cutaneous and systemic diseases in Africa (African histoplasmosis). The yeast is larger than that of *H. capsulatum* var. *capsulatum*, and the walls are thicker, resembling the cells of *Blastomyces*, but without the broad-based buds. Fatty acid profiling has been shown to be useful for the differentiation between these two strains of *Histoplasma* (Zarnowski et al., 2007). This strain of *Histoplasma* is considered an emerging infectious agent in HIV-infected patients in Africa (Loulergue et al., 2007).

Paracoccidioidomycosis (also known as South American blastomycosis) is a relatively common disease in southern Mexico, parts of Central America, and South America (mainly Brazil, Venezuela, Colombia, Ecuador, and Argentina) caused by the dimorphic fungi *Paracoccidioides brasiliensis*, *P. lutzii*, *P. americana*, *P. restrepiensis*, and *P. venezuelensis* (de Macedo et al., 2019; Munoz et al., 2016). These organisms, which are generally acquired through the lungs, can cause a variety of clinical syndromes from acute infection (with a progressive lymphadenopathy) to a chronic infection that involves the lungs, skin and mucous membranes, lymph nodes, and adrenal glands (Bocca et al., 2013). The clinical manifestations can mimic such conditions as tuberculosis, Hodgkin lymphoma, several systemic and subcutaneous mycoses, and squamous cell carcinoma. The diagnosis is made by finding the organism in a biopsy specimen and isolating the organism in fungal culture (Marques, 2012). The characteristic tissue phase yeast cells of *Paracoccidioides* have multiple peripheral buds (ranging in size from 4–60 μm), producing an appearance that has been compared with a mariner's wheel (Guarner & Brandt, 2011).

Talaromyces marneffei (formerly *Penicillium marneffei*) is a common cause of disease in HIV-positive patients in Southeast Asia (Limper et al., 2017). This agent has also been found to be associated with the bamboo rat *(Rhizomys sinensis)*, which is thought to be the natural environmental reservoir for this fungus (Cao et al., 2011). The species was unique among the genus *Penicillium* as the only member growing as a mold form at 30°C and producing reproductive structures typical of *Penicillium* spp., and in tissue producing small oval-shaped yeasts (2–5 μm in diameter) with transverse septa (due to division by fission) and hence moved to its own genus (Guarner & Brandt, 2011).

Emergomyces (formerly *Emmonsia*) are a newly described genus first identified as a cause of disseminated disease in AIDS patients within South Africa *(Es. africanus)* (Kenyon et al., 2013). This dimorphic fungus is the most common endemic mycoses in South Africa, and presenting symptoms are most frequently fever, weight loss, elevated liver enzymes, and radiographic findings of the chest similar to those of tuberculosis. Skin disease is also common and presents concurrently with other clinical findings. Subsequent investigation has identified other *Emergomyces* spp., including *Es. orientalis*, *Es. canadensis*, *Es. europaeus*, and *Es. pasteurianus* (Dukik et al., 2017; Schwartz et al., 2018). Isolates are frequently misidentified as *Blastomyces*, and sequencing is often necessary to differentiate these organisms. Treatment of this infection has yet to be refined; however, initial therapy with amphotericin B until clinical improvement is observed followed by itraconazole, voriconazole, or posaconazole is recommended (Maphanga et al., 2017).

DERMATOPHYTOSES

Dermatophytic fungi are keratinophilic fungi that affect the hair, nail, and skin of humans with approximately 25% of the global human population

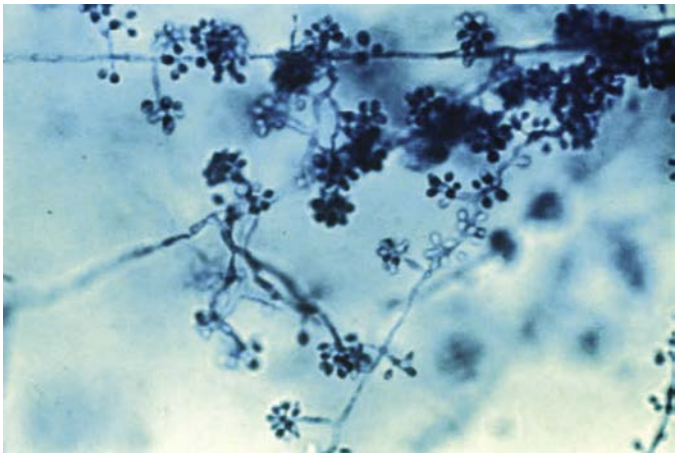

Fig. 60.31 Sympodial conidia of *Sporothrix schenckii* are borne in clusters at the tips of lateral conidiophores. (Lactophenol cotton blue stain, 400×.)

infected at least once in a lifetime (Dukik et al., 2019; Elavarashi et al., 2017). Generally, the infections are mild and rarely do the fungi associated with these infections cause invasive disease. With the introduction of molecular methods and the abandonment of the dual nomenclature in fungi, the dermatophyte taxonomy has undergone extensive revisions (de Hoog et al., 2017; Dukik et al., 2019; Zhan et al., 2018). Currently there are over 40 species of dermatophytes with three genera most recognized as the major causes of dermatophytosis (*Microsporum*, *Trichophyton*, and *Epidermophyton*) (White et al., 2014). As a group, the dermatophytic fungi are distributed worldwide, but individual species may have a more restricted geographic distribution. In addition, ecologic grouping of the dermatophytes is frequently done when studying these fungi to include those with a strict association with humans (anthropophilic), with animals (zoophilic), and with the soil (geophilic).

RISK FACTORS

Dermatophytic infections result from contact with the relevant source of the fungus, which may also provide a clue to the diagnosis. For instance, infection of the face in farmers who have contact with cows as they milk the animals is characteristically caused by *Trichophyton verrucosum*, a zoophilic dermatophyte found in cattle. Geographic variation in dermatophytic pathogens are also noted, with tinea pedis (athlete's foot) more prevalent in developed countries and likely caused by the anthropophilic fungus *T. rubrum*, while in poorer countries, scalp infections (tinea capitis) are caused by *T. soudanense* or *M. audouinii* (Havilickova et al., 2008). Skin disorders caused by dermatophytic fungi are also now recognized more often in sports in which there is direct contact between athletes, such as wrestling (called tinea gladiatorum) (Peterson et al., 2019).

CLINICAL DISEASES

Dermatophytes produce infection of the epidermis, hair, and nails (Seebacher et al., 2008). Infection is often referred to as **ringworm** (or **tinea**), a name derived from the advancing, serpiginous nature of the lesions (especially evident on the skin). Clinical terminology uses the Latin name *tinea* followed by the body part involved, such as tinea capitis (scalp), tinea barbae (beard), tinea corporis (trunk and limbs), tinea pedis (foot), tinea cruris (groin), and tinea unguium (nail, also called onychomycosis). With occasional exceptions, *Epidermophyton floccosum* infects primarily the skin, *Microsporum* spp. infect the scalp and skin, and *Trichophyton* spp. infect the skin, scalp, and nails. *Trichophyton tonsurans* is the most common cause of tinea capitis in North America, while *M. canis* is a common cause of scalp infection in children in Europe (Gupta et al., 2018). When deep infection of hair follicles occurs, a boggy inflammatory process called a *kerion* results. *T. mentagrophytes* and *T. verrucosum* are particularly associated with kerion formation. *T. mentagrophytes*, *T. rubrum*, and *M. canis* are commonly found to cause tinea corporis and tinea pedis, *E. floccosum* is a common cause of tinea cruris, and *T. rubrum* and *T. interdigitale* are common causes of tinea unguium.

LABORATORY DIAGNOSIS

Diagnosis of a dermatophyte infection generally involves both microscopic examination and culture, although treatment of dermatophyte infection is not directed by the specific identification of the isolate. Demonstration of hyphae in skin scrapings (using a KOH preparation) is frequently the only diagnostic technique performed before therapy is initiated (Fig. 60.32). The size and morphology of hyphae suggest the involvement of dermatophytes in the infection. Verification of the species is useful for confirming that the hyphae did in fact belong to a dermatophytic fungus, for assessing the probable source of the infection and for assessing the increased likelihood of chronic, relapsing infections (especially when *T. rubrum* is identified). Skin scrapings, nail clippings, and hair can be examined in KOH preparations, which may incorporate Calcofluor white to facilitate the detection of hyphae. Care must be taken when reading this type of preparation in that tissue fragments, fibers, and cholesterol crystals may be mistaken for hyphae by the inexperienced observer. Histopathology involving an invasive procedure to obtain a biopsy has limited value as a diagnostic procedure, except in cases where a diagnosis is warranted and cannot be obtained by the other noninvasive methods. The H&E stain is characterized by the formation of hyperkeratosis with the presence of fungal elements usually in the superficial layers. To better visualize the hyphae, which are generally septated, the Grocott methenamine silver or the PAS stains can be used.

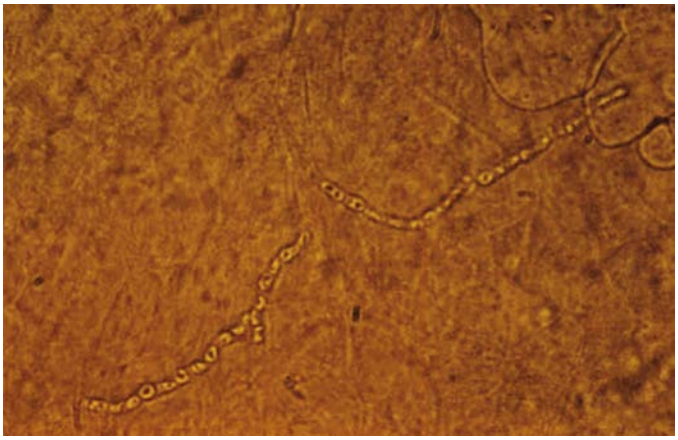

Fig. 60.32 Hyphae of a dermatophyte are demonstrated in a scraping from the edge of a tinea lesion. The presence of thin-segmented hyphae in this clinical setting establishes the diagnosis of dermatomycosis but does not define the specific cause. (Potassium hydroxide preparation, 400×.)

Fungi such as *M. audouinii*, *M. canis*, and *M. ferrugineum* are associated with hair infection and cause the hairs to fluoresce yellow-green with a long-wavelength ultraviolet light (Wood's lamp). In the United States, tinea capitis due to a fluorescing fungus is most likely caused by *M. canis*. *T. tonsurans* on the other hand does not show up with fluorescence and may lead to a misdiagnosis if a physician considers fluorescence to be synonymous with tinea capitis (Gupta et al., 2018). Microscopic examination of infected hair by an experienced observer may also suggest the etiologic agent, based on the appearance and location of the arthroconidia. In ectothrix colonization, as occurs with *M. canis* infection, arthroconidia are external to the hair shaft. Endothrix invasion, as seen in infection with *T. tonsurans*, is characterized by arthroconidia within the hair shaft. In favic infection, hyphae, air bubbles, or tunnels and fat droplets are present in the intrapilar area, which is more commonly observed with *T. schoenleinii*.

Infected hairs, nail scrapings, or scrapings of the edges of skin lesions should be submitted to the laboratory in a clean, dry container or placed on the surface of primary isolation medium supplied by the laboratory. Sabouraud dextrose agar was designed for recovery of dermatophytic fungi and is also effective for isolating *Candida* spp., especially *C. albicans*, which may produce similar infections of the skin and nails. Additionally, dermatophytes are not inhibited by cycloheximide, which will inhibit many saprobic fungi. All dermatophytic fungi have septate and hyaline hyphae, and they produce macroconidia and/or microconidia in various combinations. Arthroconidia and chlamydoconidia may also be produced, but the morphology of the macroconidia and especially of the presence of the microconidia is more important for identification. The combination of micromorphologic features with some phenotypic testing is most often used to differentiate the dermatophytes.

Microsporum species produce characteristic macroconidia, which are the key diagnostic structures. In some cases, microconidia, which are not as useful diagnostically, are produced. *M. canis*, the most frequently isolated zoonotic species of this genus, produces a characteristic lemon-yellow pigment in culture (Fig. 60.33), which is intensified by growth on potato flake agar. The macroconidia of this species are illustrated in Fig. 60.34.

The genus *Trichophyton* includes the important dermatophytic fungi *T. rubrum* (Fig. 60.35), *T. verrucosum*, *T. mentagrophytes* (see Fig. 60.11), and *T. tonsurans* (Fig. 60.36). The colonies may have a fluffy, granular, or (less commonly) glabrous appearance. Macroconidia, which are useful for identification, may be produced by this genus, especially in strains that produce powdery colonies, but unfortunately they usually are absent. Microconidia are formed more commonly. When present, the macroconidia are thin walled and smooth, and they contain variable numbers of septa. Interpretation of the microscopic morphology in some isolates can be difficult because overlap occurs frequently. Phenotypic testing using the *Trichophyton* agars is helpful in the characterization of nutritional requirements among members of the genus. Seven media have been described; however, four of these seem to be the most useful for identification purposes. These media include T1, basal medium agar (for a control to compare with other supplemented media); T2, basal medium with inositol (growth stimulated by inositol); T3, basal medium with inositol plus thiamine (growth stimulated by the addition of both inositol and thiamine); and T4, basal medium

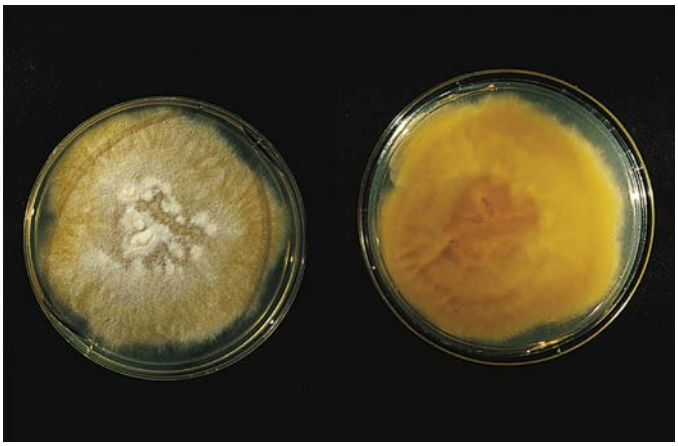

Fig. 60.33 The obverse of a *Microsporum canis* colony *(left)* showing the characteristic lemon-yellow pigment, which also may be seen on the reverse of the colony *(right)*. (Sabouraud dextrose agar with cycloheximide.)

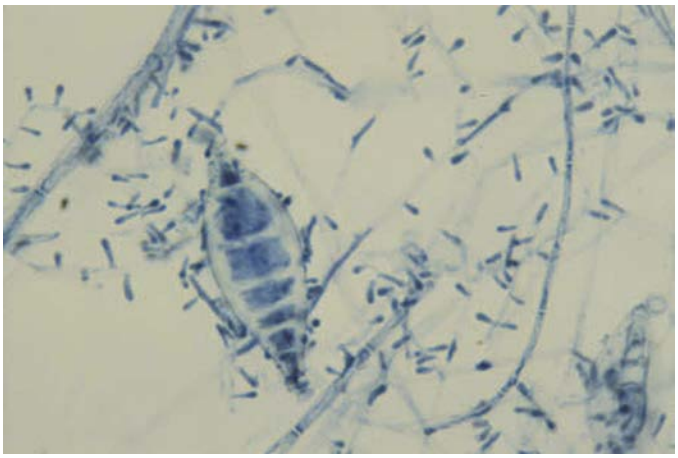

Fig. 60.34 Thick-walled, roughened, tapered, spindle-shaped macroconidia of *Microsporum canis* with thin, septate hyphae. (Lactophenol cotton blue stain, 400×.)

Fig. 60.35 Fluffy white colonies of *Trichophyton rubrum* with diffusible red pigment, which may also be seen on the reverse of the colony. (Potato dextrose agar.)

with thiamine (growth stimulated by thiamine only). In combination, these media allow assessment of dependency on inositol, thiamine, or both compounds together for growth.

Differentiation of *T. mentagrophytes* and *T. rubrum* is facilitated by several nonmorphologic tests as well (Ates et al., 2008). A diffusible pigment may be produced by both species, but the intensely red pigment of *T. rubrum* is encouraged by culture on potato dextrose agar or cornmeal agar with 1% dextrose. Production of urease within 3 to 5 days by *T. mentagrophytes* but not by *T. rubrum* also helps differentiate these two species. Finally, the hair penetration test can be used as a differential test wherein *T. mentagrophytes* produces wedge-shaped defects in hairs in vitro, whereas

Fig. 60.36 A flat colony showing pale yellow coloration with a reddish-brown pigmentation at the periphery characteristic of *Trichophyton tonsurans*. Radial furrowing of the thallus as seen is also common. (Sabouraud dextrose agar with cycloheximide.)

Fig. 60.37 The suedelike texture and yellowish green color of the mold colonies are characteristic of *Epidermophyton floccosum*. (Sabouraud dextrose agar with cycloheximide.)

T. rubrum grows on the outside of the hair without penetration. Use of both morphologic and nonmorphologic approaches provides the most accurate identification of isolates.

The only pathogen within the genus *Epidermophyton* is *E. floccosum*, an anthropophilic fungus that is an important cause of tinea cruris and, less commonly, tinea pedis. Colonies, which are initially brownish yellow, gray, or khaki brown, become velvety and folded as they mature (Fig. 60.37). *E. floccosum* produces no microconidia, but distinctive macroconidia provide clues to identification (see Fig. 60.10). These structures have smooth external walls, with up to four cross-walls and a club shape, and they tend to "flocculate," hence the epithet name.

Since species identification for dermatophytes is time consuming and requires knowledge and technical expertise because of morphologic similarity, variability, and polymorphism within dermatophytes, the addition of molecular methods using targeted sequencing has become the method of choice for identification purposes (Graser et al., 2012; Rich et al., 2013; Westerberg & Voyack, 2013). PCR-based methods using the internal transcribed spacer region locus have been shown to be reliable for the differentiation of the dermatophyte species from culture (Dukik et al., 2019). Additionally, direct testing of specimens has shown promise to detect and identify the dermatophytes in veterinary medicine (Cafarchia et al., 2013; Verrier et al., 2019). However, although many kit-based assays have been developed for direct specimen testing, they are not yet commercially available in the United States. More recently, MALDI-TOF MS has been shown to be a fast and useful approach to differentiate dermatophytes grown in culture (Intra et al., 2018; L'Ollivier & Ranque, 2017). However, there still remains a challenge in using this methodology partly due to the lack of clear species definition for some taxa to provide a reference system library that is adequate enough for dermatophyte identification.

MYCOSES CAUSED BY DEMATIACEOUS (MELANIZED) FUNGI

The dematiaceous (also referred to as **melanized**, **dark**, and **phaeoid**) fungi are a fascinating and complex group of fungi characterized by the formation of a dark pigment due to production of melanin in the cell walls of the fungal cell (Revankar & Sutton, 2010). Although these fungi are soil and plant saprobes and historically are considered rare causes of disease in humans, they appear to be emerging as more common fungal pathogens.

CLINICAL DISEASES

The clinical syndromes are typically distinguished on the basis of histologic findings into eumycotic mycetoma (also called **eumycetoma**), chromoblastomycosis (also called **chromomycosis**), and phaeohyphomycosis (Garnica et al., 2009; Seyedmousavi et al., 2013). These diseases are frequently diagnosed by a unique histologic picture in tissue followed by isolation of the fungus in culture and morphologic evaluation of the reproductive structures. The classification of black fungi has undergone numerous changes over the years, which adds difficulty to recognition of the etiologic agent.

Mycetoma

Mycetoma is a tropical disease causing a localized, chronic granulomatous infection characterized by the formation of a painless subcutaneous mass of chronic onset, with multiple sinuses draining pus and grains (also called granules) with extension to the bone (Garnica et al., 2009). The disease is most often confined to the hands or feet (also called Madura foot) in immunocompetent individuals such as farmers, field hands, and others in contact with contaminated soil-laden materials. This disease can be caused by bacteria (actinomycotic mycetoma) or by fungi (eumycotic mycetoma) that are dark pigmented (dematiaceous) or, rarely, nonpigmented (hyaline). Recently, mycetoma was listed by the World Health Organization as a neglected tropical disease, leading to development of key research priorities needed to combat infection (van de Sande et al., 2014).

A mycetoma occurs after a traumatic injury with a contaminated object such as a splinter, a thorn, or any other penetrating item. Although more than 25 fungal species have been known to cause eumycotic mycetoma, the most common causes are molds that include *Madurella mycetomatis*, followed by a variety of other dematiaceous and hyaline fungi. Members of the *Scedosporium apiospermum* species complex, which are hyaline fungi, are considered the most common cause of this disease in the United States.

A noninvasive disease involving the paranasal sinus has been described as a fungal mycetoma (also called a **fungus ball**) (Grosjean & Weber, 2007; Pagella et al., 2007; Robey et al., 2009). This condition involves the accumulation of dense fungal concrements in the sinus cavities, most often the maxillary sinus, and is associated with a variety of molds, including dematiaceous fungi. Although some categorize this infection as a mycetoma, others prefer to describe it as a fungal rhinosinusitis because this infection does not specifically fit the description of a mycetoma presented here (an absence of granule formation). Controversies on the categorization and definition of fungal rhinosinusitis occur because of the wide spectrum of immune and pathologic responses associated with this disease. Attempts are being made to develop a consensus on the terminology and disease classification for this condition (Chakrabarti et al., 2009).

A definitive diagnosis of a mycetoma can be achieved by the demonstration of grains (or granules) in a tissue biopsy, in draining exudates from a sinus tract, or in material aspirated from an unopened lesion (Fig. 60.38). These grains are microscopically composed of broad, interwoven, septate hyphae 2 to 5 μm in diameter that are lined with intense eosinophilic material (Splendore-Hoeppli phenomenon) (Fig. 60.39). For dematiaceous fungi, these grains are associated with a dark pigment and generally are called **black grains**; with fungi that are nondematiaceous and produce nonpigmented hyphae, these are called white grains. Identification of the etiologic agent requires culture on standard fungal media such as Sabouraud dextrose agar, which may take 4 weeks or longer to grow (Fig. 60.40). Once isolated, the fungal species is identified using gross colony morphology and pigmentation, along with close observation of the micromorphologic characteristics of reproductive structures following sporulation (Fig. 60.41). In cases in which sporulation does not occur, physiologic tests such as carbohydrate and nitrate utilization may aid in identification. Molecular assays using targets within the rDNA complex have been shown to be reliable for identification of dematiaceous fungi (Borman et al., 2008; Revankar & Sutton, 2010; Seyedmousavi et al., 2014).

Fig. 60.38 Image showing granules of various sizes *(black grains)* of the fungus *Madurella grisea* composed of black masses of hyphae. (Courtesy Centers for Disease Control and Prevention Public Health Image Library.)

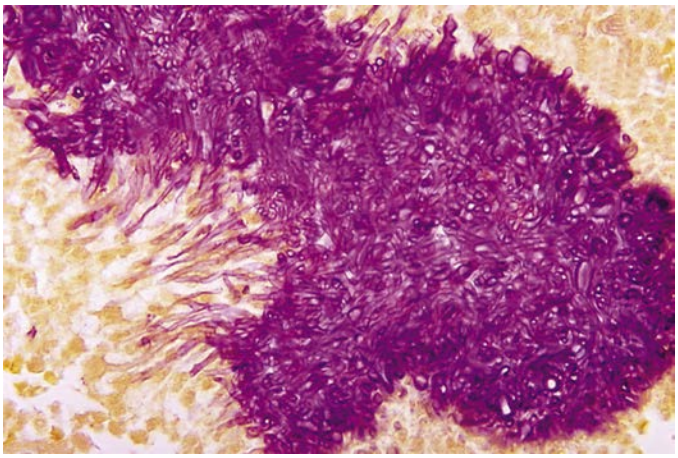

Fig. 60.39 Histologic appearance of "black grain mycetoma" due to *Madurella mycetomatis.* ((Gridley stain, 1000×.) (Courtesy Dr. Libero Ajello, Centers for Disease Control and Prevention Public Health Image Library.))

Fig. 60.40 Close-up of the surface of a dematiaceous (melanized) fungus growing on Sabouraud dextrose agar.

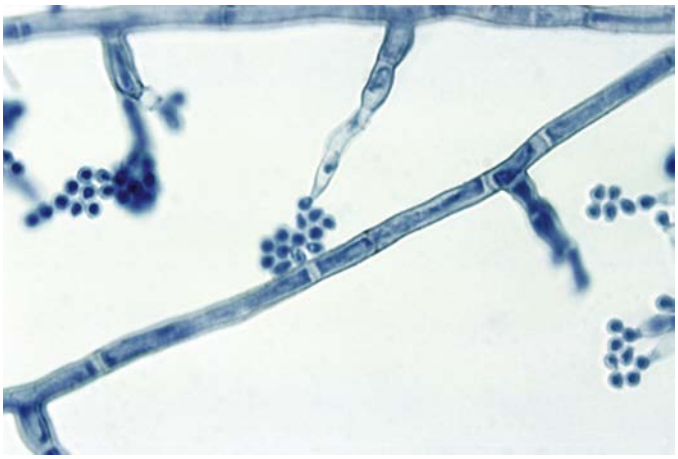

Fig. 60.41 Image showing phialides with terminal conidia of the *Madurella mycetomatis* fungus. ((Lactophenol cotton blue stain, 400×.) (Courtesy of Lucille George, Centers for Disease Control and Prevention Public Health Image Library.))

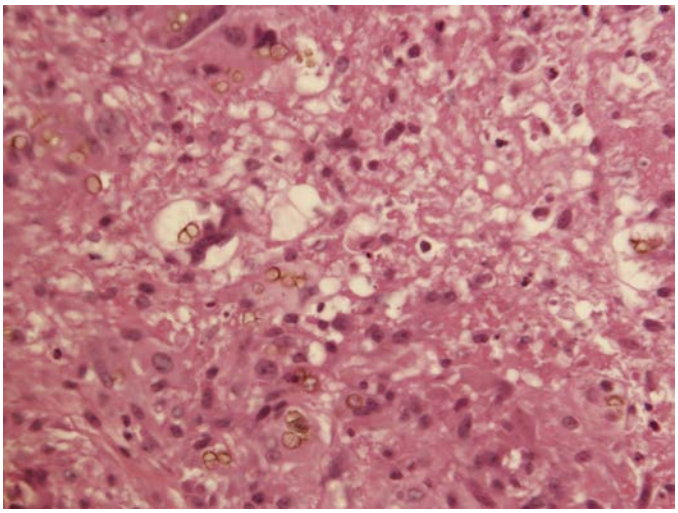

Fig. 60.42 Sclerotic cells observed in tissue that is characteristic of the etiologic agents of chromoblastomycosis. (Hematoxylin and eosin stain, 400×.)

Chromoblastomycosis

Chromoblastomycosis (chromomycosis) is a slowly progressing, chronic subcutaneous mycosis that is seen predominantly in tropical areas. The disease is characterized by the presence of large, muriform, thick-walled dematiaceous cells called **sclerotic bodies** (medular bodies or "copper pennies") within the infected tissues (Krzysciak et al., 2014; Revankar & Sutton, 2010). The disease affects immunocompetent individuals who most often live in tropical and subtropical areas and is distinguished by the formation of a painless verrucous plaque or nodule at the site of inoculation following a penetrating trauma, with healing areas of the lesion evident along with the formation of scar materials (Queiroz-Telles et al., 2009). The most common species causing this disease is *Fonsecaea pedrosi*, followed by *Phialophora verrucosa* and, less commonly, *Cladophialophora carrioni* and *Rhinocladiella aquaspersa*, although numerous other melanin-producing species may also be involved (Revankar & Sutton, 2010). The distinguishing feature is the presence of round, nonhyphal brown cells (sclerotic bodies) in tissues (Fig. 60.42). These structures, which divide by producing a septal plane, are diagnostic of the entity but do not provide a clue as to species identification of the mold. Culture and recognition of morphologic features of the isolate are needed to identify the infecting species. An additional characteristic is that both mycetoma and phaeohyphomycosis result in tissue necrosis, whereas chromoblastomycosis infections lead to excessive proliferation of host tissue (Seyedmousavi et al., 2014).

Phaeohyphomycosis

Phaeohyphomycosis (from the Greek word **phaeo**, meaning "dark") was a term originally proposed by Ajello as a histopathologic entity to cover all infections "caused by fungi that develop in tissue in the form of dark-walled dematiaceous septate mycelial elements" (Ajello et al., 1974). Over the years, phaeohyphomycosis has become more recognized as a cause of subcutaneous and systemic diseases characterized by the formation of brownish to olivaceous hyphal elements in tissue (Seyedmousavi et al., 2013). Although both chromoblastomycosis and eumycotic mycetoma are caused by dematiaceous fungi, they are distinguished from phaeohyphomycosis by the appearance in tissue of sclerotic bodies and mycotic granules, respectively.

Phaeohyphomycosis can arbitrarily be divided into allergic disease (including allergic fungal sinusitis and allergic bronchopulmonary mycosis); superficial infection (including onychomycosis and tinea nigra); deep local infection such as subcutaneous lesions, keratitis, bone and joint infections, and peritonitis; pulmonary infection; central nervous system infection; and disseminated infection (Revankar & Sutton, 2010). Allergic disease manifest as asthma is linked to exposure to *Alternaria* spp. and *Cladosporium* spp., while the bronchopulmonary form is most frequently due to *Bipolaris* or *Curvularia*. Superficial infections involve the keratinized tissues such as the fingernails and toenails and the stratum corneum (e.g., tinea nigra, a pigmented macule usually on the palms or soles). These asymptomatic infections are most commonly caused by *Hortaea (Phaeoannellomyces) werneckii*, *Scopulariopsis brevicaulis*, *Juxtiphoma (Phoma) eupyrena*, and *Chaetomium globosum*. The subcutaneous forms of the disease are characterized by the formation of a solitary asymptomatic subcutaneous nodule or cyst usually in an immunocompetent individual (Naggie & Perfect, 2009). The most common dematiaceous fungi associated with the subcutaneous cutaneous condition are *Exophiala jeanselmei*, *Exophiala (Wangilla) dermatitidis*, and *Bipolaris/Curvularia* spp. (Garnica et al., 2009). Disseminated infection is a rare complication of immunosuppression. One of the more common species associated with this condition is *Lomentospora (Scedosporium) prolificans*, an aggressive fungus that is generally resistant to all available antifungal agents. *Cladophialophora bantiana* is a neurotropic species capable of growth at 40°C and has been associated with numerous cases of cerebral phaeohyphomycosis, including disease in immunocompetent hosts (Chakrabarti et al., 2016; Kantarcioglu et al., 2017; Revankar & Sutton, 2010). Other etiologic agents of cerebral phaeohyphomycosis have included *Fonsecaea monophora* and *Verruconis (Ochroconis) gallopava* (Bagla et al., 2016; Doymaz et al., 2015; Surash et al., 2005).

The variety of disease manifestations and the range of species associated with phaeohyphomycosis were brought to light in a recent multistate outbreak of phaeohyphomycosis that was associated with injection of methylprednisolone acetate solution contaminated with the dematiaceous fungus, *Exserohilum rostratum*, from a single compounding pharmacy (Kainer et al., 2012; Ritter et al., 2013). Epidural and intraarticular injections of this contaminated solution resulted in over 700 confirmed drug-related infections (ranging from localized epidural, paraspinal, and peripheral joint infections to fatal fungal meningitis) resulting in over 50 deaths. *E. rostratum* had only rarely been reported as a cause of human disease prior to this outbreak.

In most cases of phaeohyphomycosis, diagnosis may be difficult because many of the etiologic agents are often considered contaminants when isolated from culture. In tissue, the presence of irregular, swollen, septate hyphal forms with yeastlike structures that stain with a melanin-specific Masson-Fontana stain is presumptive for the diagnosis of phaeohyphomycosis.

Sick Building Syndrome

Dematiaceous molds have also been associated with the condition known as **sick building syndrome**. The mold most commonly associated with this condition is *Stachybotrys chartarum*, and although the causative association of mold contamination within a building with disease has been questioned, health concerns to indoor mold exposure leading to persistent allergy symptoms or asthmalike symptoms have been documented (Al-Ahmad et al., 2010). Others have also suggested that toxins associated with molds such as *S. chartarum* are associated with health problems following exposure (Straus, 2009; Terr, 2009). NIOSH (2012) has provided a document that presents a comprehensive review on preventing occupational respiratory disease from exposures caused by dampness in office buildings, schools, and other nonindustrial buildings.

MUCORMYCOSIS (ZYGOMYCOSIS)

Current advances in molecular techniques have contributed to taxonomic reorganization with the group of fungi formally classified within the phylum Zygomycota and described as causative agents of the disease zygomycosis (also called **phycomycosis**). Phylogenetic analysis, however, confirmed that the phylum Zygomycota was polyphyletic, which led to a new phylum classification of Glomeromycota with four additional

subphyla of uncertain placement (*incertae sedis*) (Kwon-Chung, 2012). One of these subphyla is identified as Mucoromycotina (with no class designation), which contains the order Mucorales, where approximately 20 species that have caused human disease reside (Iwen et al., 2011). These changes in taxonomy led to the species within the order Mucorales to be called **mucormycetes** with the disease caused by these species to be identified as mucormycosis (Kwon-Chung, 2012).

In cases of mucormycosis where species were determined, *Rhizopus* spp. were the organisms most commonly isolated with *R. (oryzae) arrhizus* and *R. microsporus* recognized as causing a majority of cases (Jeong et al., 2019). Other less common species include *Lichtheimia (Absidia)* spp., *Apophysomyces* spp., *Cunninghamella* spp., *Mucor* spp., *Saksenaea* spp., and *Rhizomucor (Mucor) pusillus*.

RISK FACTORS

Most cases of mucormycosis generally result from inhalation of fungal sporangiospores that have been released in the environment or from direct inoculation of organism into disrupted skin. Uncontrolled diabetes, corticosteroid use, neutropenia, infant prematurity, stem cell or solid organ transplantation, and the use of deferoxamine are all well-described risk factors for the development of mucormycosis (Jeong et al., 2019; Roden et al., 2005). Diabetic ketoacidosis is the most common recognized underlying condition for the development of mucormycosis in humans; however, many of the other conditions described are associated with impairment of normal leukocyte immune function, which puts patients at increased risk for infection. Recognition of no underlying condition following penetrating trauma, surgery, and burns has also been seen at the time of infection (Neblett Fanfair et al., 2012; Roden et al., 2005).

CLINICAL DISEASES

Six distinct clinical syndromes of mucormycosis can occur in susceptible hosts, which have been classified as rhino-orbital-cerebral, pulmonary, cutaneous, gastrointestinal, disseminated, and uncommon presentation (such as endocarditis, bone and joint infection, peritonitis, and pyelonephritis) (Serris et al., 2019). The two major clinical presentations are sinus infection with or without cerebral or orbital involvement and localized pulmonary infection (Roden et al., 2005).

PATHOLOGY

The prerequisites for the diagnosis of mucormycosis are a high index of suspicion, recognition of host factors, and the proper assessment of clinical manifestations (Skiada et al., 2018). Additionally, the utilization of invasive procedures such as a tissue biopsy with histopathologic staining are frequently the primary means for diagnosis. This utility of histopathologic examination of tissue for diagnosis has been borne out by multiple studies (Jeong et al., 2019; Schuetz & Walsh, 2015; Skiada et al., 2018). The identification of hyphae in tissue also provides important evidence that a mold isolated in culture is not an environmental contaminant and thus dismissed as a saprobe, since the Mucorales often are considered common contaminants within the mycology laboratory. The tissue response is dominated by necrosis, regardless of the site of infection. The propensity for these molds to invade through the walls of arteries and veins, producing acute thrombosis, leads to extensive coagulative necrosis. The presence of broad, aseptate or pauciseptate hyphae with wide-angle branching with a variable width from 5 to 20 μm along with the angioinvasive property of these fungi are highly suggestive of a mucormycete-caused infection (see Fig. 60.3). Comparison of the histologic features of mucormycetes versus those of other nonpigmented hyphae in tissue is described in Table 60.7. The hyphae of these molds often stain better with the H&E stain than with the GMS method.

LABORATORY DIAGNOSIS

Direct microscopy and culture of various clinical specimens are common methods used for the confirmed diagnosis of mucormycosis. A presumptive method for diagnosis is the direct observation of characteristic hyphae in a clinical specimen using an optical brightener such a Calcofluor white. For a proven invasive mucormycosis, culture of sterile material with or without confirmation by pathology is still required (Hartnett et al., 2019). Broad, sparsely septate hyphae may be demonstrated in tissue sections or in imprint smears of tissue, using the Calcofluor white stain.

Most mucormycetes grow well on standard fungal medium. Unfortunately, recovery of these organisms from tissue may be difficult leading to a negative culture result even though histologic evidence of a mucormycete is present in the clinical material (Roden et al., 2005). Aggressive processing of a specimen has been indicated as a potential cause of this inability to grow leading to damage of the organism so it is no longer viable. To increase the likelihood of successful culture, it has been suggested that tissue be minced or teased, rather than homogenized, after which it is inoculated onto the surface of a primary isolation agar (Ribes et al., 2000). Mucormycetes are also inhibited by cycloheximide, so nonselective fungal medium should be included when fungal cultures are performed. Isolates grow rapidly (within 48–72 hours) and produce abundant aerial hyphae that rapidly reach the lid of the Petri dish, colloquially referred to as **lid lifters** (Fig. 60.43). The hyphae are characterized as woolly and initially white, turning gray to black as spores develop.

Since the mucormycetes have varying differences in antifungal susceptibility, the ability to provide species identification is required for appropriate patient management. The identification of micromorphologic characteristics from culture are helpful to at least broadly characterize the fungal species. *Rhizopus* spp. produce unbranched sporangiophores that support sporangia (60–350 μm) with an ellipsoidal columella containing sporangiospores. The sporangiospores are oval and frequently have a brown pigment (see Fig. 60.6). An important diagnostic feature for *Rhizopus* is the presence of hyaline-to-brown rootlike structures called **rhizoids**, which develop at the point where the sporangiophores arise. In contrast to *Rhizopus*, the rhizoids of *Lichtheimia (Absidia)* spp. arise from the stolons between conidiophores. The sporangiophores are pear shaped rather than round, and a collarette is visible around the columella when the sporangium disintegrates.

Mucor spp. on the other hand do not produce rhizoids; the conidiophores usually are more branched than other mucormycetes, and growth does not occur above 37°C. *Rhizomucor*, which is morphologically intermediate between *Rhizopus* and *Mucor*, has rudimentary rhizoids and branched conidiophores and grows at temperatures as high as 58°C. *Mucor* spp. were commonly thought to be the second most recognized causes of mucormycosis; however, they now have been described as a rare cause of human

TABLE 60.7

Histopathologic Features of the Mucormycetes/Zygomycetes in Comparison With Other Fungi That Occur as Nonpigmented Hyphae in Tissue[a]

Characteristic	Zygomycetes[b]	*Aspergillus*[c]	*Fusarium*
Hyphal characteristics			
Width (μm)	Variable (5–10)	Consistent (3–6)	Consistent (3–8)
Branching pattern	Haphazard	Dichotomous	Right angle
Septation frequency	Rare	High	High
Reproductive structures in tissue	Absent	May be present where infected area communicates with air	Chlamydoconidia sometimes present
Angioinvasiveness	Yes	Yes	Yes

[a]In all cases, a definitive diagnosis of the species requires isolation and identification of the fungus on synthetic media.
[b]Entomophthorales are included in this group with the hyphal fragments in tissue generally coated by anophous eosinophilic Splencore-Hoepple material and lack of angioinvasiveness noted.
[c]Because of hyphal degeneration or host immune response or both, the hyphae of the *Aspergillus* species may exhibit atypical morphologic forms that may cause problems in the differential diagnosis.
Modified with permission from Freifeld AG, Iwen PC: Zygomycosis. *Semin Respir Crit Care Med* 25:221–231, 2004.

disease (Iwen et al., 2007). This is due to the fact that *Mucor corymbifera* has been reassigned to the genus *Lichtheimia (Absidia)* as *L. corymbifera*, and *M. pusillus* has been reclassified in the genus *Rhizomucor* as *R. pusillus* (Iwen et al., 2011).

Although genera of the mucormycetes can be readily recognized in the mycology laboratory, unfortunately only a few laboratories have the expertise needed to identify specific species. Historically, one method used to accurately identify these organisms has been the observation of zygospores following mating studies because of the heterothallic nature of this group of organisms (Weitzman et al., 1995). Although this method has been used successfully, mating studies do not always yield a positive result. Additionally, the need to maintain a library of testing strains necessary to perform mating does not make this method realistic for most clinical laboratories.

More recently, molecular methods for the identification of fungal species from both clinical specimens and from culture isolates have been shown to be successful (Dadwal & Kontoyiannis, 2018; Scherer et al., 2018). The concept of using molecular targets in the form of short DNA sequences has provided for the reliable species identification of many fungal groups to include the mucormycetes as a "fungal barcoding" methodology (Prakash et al., 2017). A variety of molecular targets have been described for species identification of the mucormycetes (Iwen et al., 2011). Nucleotide sequence comparisons using the ITS regions of the rDNA complex and the variable D1/D2 region of the 28S gene have been shown to have the highest discriminatory capability for the identification of most Mucorales (Balajee et al., 2009). Other molecular approaches, such as multilocus sequence typing (MLST) have been shown to be reliable in discriminating among different species; however, this is highly dependent on the choice of the gene loci and accuracy of sequences (Prakash et al., 2017). Molecular testing on direct specimens to include formalin-fixed paraffin-embedded tissues has shown some success; however, they are currently limited by the lack of technique standardization and clinical validation (Scherer et al., 2018; Walsh et al., 2012). More recently MALDI-TOF MS has shown success for the rapid identification from culture of some common species of the mucormycetes; however, the libraries used for analysis of spectra results are currently limited (Dadwal & Kontoyiannis, 2018; Rychert et al., 2018; Sagiroglu et al., 2019; Shao et al., 2018).

ASPERGILLOSIS, FUSARIOSIS, AND OTHER MYCOSES CAUSED BY HYALINE FUNGI

This large group of saprobic fungi is frequently encountered in the clinical laboratory and contains some of the most important pathogenic molds. These molds are collectively classified as hyaline because they produce nonpigmented hyphae, and the disease is frequently called **hyalohyphomycosis**. The number of species within this group that are capable of causing human disease is large and continues to expand as immunosuppressive therapies become more common methods for the management of patients. By far the most recognized hyaline molds causing human disease are classified in the orders Eurotiales (*Aspergillus*, *Paecilomyces*, and *Penicillium*), Microascales (*Scedosporium* and *Scopulariopsis*), and Hypocreales (*Cylindrocarpon*, *Fusarium*, and *Trichoderma*). In this section, detailed consideration will be given to *Aspergillus* spp. and *Fusarium* spp., the hyaline molds most commonly identified as causing invasive human disease.

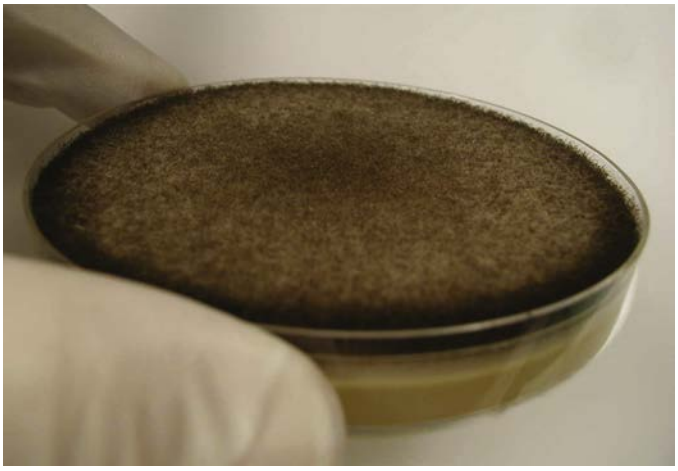

Fig. 60.43 A fluffy gray colony of *Rhizopus* spp. fills the space within the Petri dish (lid lifter). (Sabouraud dextrose agar.)

THE GENUS *ASPERGILLUS*

Invasive aspergillosis is the most common life-threatening opportunistic invasive mold infection in immunosuppressed patients (Patterson et al., 2016). The term **aspergillosis** is used to describe these infections, which are caused by species within the genus *Aspergillus*. This group of organisms has the ability to produce a wide spectrum of infections, which include mycotoxicosis, allergic manifestations, and superficial infection in the normal host; localized noninvasive infection in hosts with tissue damage or foreign-body obstruction; and invasive infection in the compromised host. Although they are not discussed further here, numerous reviews are recommended for additional information on intoxication by ingestion of *Aspergillus* toxin (Perrone & Gallo, 2017) and allergic manifestations associated with *Aspergillus* spore exposure (Chang et al., 2013; Thompson & Patterson, 2012).

The number of new *Aspergillus* spp. associated with human disease continues to expand with the utilization of genomic methods for identification (Bongomin et al., 2018; Gautier et al., 2016; Siqueira et al., 2018). Historically, the aspergilli were identified to species based on observable morphologic (e.g., reproductive structures and cultural characteristics) and physiologic (e.g., effect of temperature on growth) characteristics. However, the utilization of molecular sequencing has now shown that many of the fungal species are morphologically indistinguishable, leading to the concept described as **cryptic species** (Samson & Varga, 2009). A polyphasic approach has now been suggested for species identification to include morphologic, physiologic, and molecular characteristics (using a combination of multilocus sequence data). Since most clinical laboratories still utilize identification methods based on morphology, the recommendation for reporting to account for these cryptic species is to describe the identification as a "species complex" based on the major taxonomic section of the fungus (e.g., *Aspergillus fumigatus* species complex, *A. flavus* species complex, *A. terreus* species complex, *A. ustus* species complex, or *A. niger* species complex) (Balajee, 2009; Balajee et al., 2009; Hong et al., 2008). Antifungal resistance associated with these cryptic species may, however, in the future make more precise species identification useful to appropriately manage an infected patient (Alastruey-Izquierdo et al., 2014; Gautier et al., 2016).

Aspergillus fumigatus species complex is considered the most common group associated with invasive aspergillosis, followed by the *Aspergillus flavus* and *Aspergillus terreus* species complexes (Patterson et al., 2000). However, in some studies, the *A. flavus* species complex has emerged as a predominant pathogen group, especially when those patients with fungal sinusitis and fungal keratitis were evaluated in several institutions worldwide (Krishnan et al., 2009). Suggestions are that the bigger size of the *A. flavus* spores, in comparison with the spores of *A. fumigatus*, may favor their deposit in the upper respiratory tract and eye (Pasqualotto, 2009).

Aspergillus terreus species complex, as the third most common species complex recognized, is often refractory to therapy with the antifungal amphotericin B and has the propensity to disseminate (Posch et al., 2018; Risslegger et al., 2017). Multiple other species of *Aspergillus* have rarely been recognized as causing invasive disease (Gautier et al., 2016; Wiederhold, 2017).

Risk Factors

The aspergilli are ubiquitous fungi to which all people are exposed on a regular basis. These fungi reside in vegetation of all types and are ubiquitous in the environment. Nosocomial infections, although uncommon, have been linked to numerous cases associated with hospital construction in the literature (Haiduven, 2009; Suleyman & Alangaden, 2016). Engineering infection control through institution design to prevent high-risk patients from spore exposure has been done to provide a safer environment for patients.

The most important risk factors for invasive aspergillosis are immunosuppressive disease, high-dose chemotherapy with or without transplantation, and solid organ transplantation (Bays & Thompson, 2019; Ben-Ami et al., 2009; Patterson et al., 2000). Neutropenia is a prominent predisposing factor for disease; however, serious invasive disease may rarely occur in individuals who are not immunosuppressed by chemotherapy or malignancy. For instance, wound infection has been a problem in patients with extensive burn wounds and in individuals exposed to materials contaminated with conidia—a situation reminiscent of the Mucorales. A fungus ball may also occur in the lung of patients with chronic obstructive lung disease, bronchiectasis, and/or an old cavity caused by tuberculosis (Riscili & Wood, 2009; Thompson & Patterson, 2008).

Clinical Diseases

The spectrum of invasive disease caused by *Aspergillus* spp. is broad. Although these fungi have a low pathogenicity in humans and rarely cause

disease in the immunologically competent individual, immunocompromised patients are at risk for invasive disease. Those patients especially at risk are those with prolonged granulocytopenia or graft-versus-host disease and those undergoing immunosuppressive therapy or receiving corticosteroid treatment. Since *Aspergillus* spores are normally present in the environment, the most common primary sites of infection are the lower respiratory tract and, to a lesser extent, the paranasal sinuses (Cadena et al., 2016).

Ocular Infections

Keratomycosis usually follows trauma to the eye, especially in patients who have been treated with topical steroids. Pain and blurring of vision follow the traumatic episode, and if not treated, the infection may extend into the anterior chamber. Enucleation of the eye may be necessary if the process is not halted. The most common underlying disease recognized in a study of 15 patients with orbital invasive aspergillosis was diabetes mellitus, with all patients having a primary paranasal sinus infection (Thomas & Kaliamurthy, 2013). Ocular symptoms of this disease in the immunosuppressed patient include visual disturbances, periorbital swelling, and periorbital pain.

Otic Infections

Otomycosis is an infection of the external ear that is usually caused by members of the *Aspergillus niger* or *A. fumigatus* species complexes. Pain, decreased hearing, and discharge are accompanied by a fluffy green or black growth in the ear canal. Extension beyond the external ear is uncommon but may occur in immunosuppressed patients (Ho et al., 2006; Munguia & Daniel, 2008).

Sinus Infection

Invasive fungal sinusitis can be classified as an acute fulminant invasive disease or as a chronic indolent invasive disease (Thompson & Patterson, 2012). Spread of the fungus from the sinus into adjacent tissues is frequently dependent on the host immunologic response and on whether metabolic ketoacidosis is present, although invasive infection has also been reported in apparently healthy individuals (El Naderi et al., 2013).

Cutaneous Infection

Aspergillus spp. may infect the skin after dissemination from another site, usually pulmonary, or the infection may be a primary infection after direct cutaneous exposure to a contaminated environmental source (Bretagne et al., 1997; Bryce et al., 1996; McCarty et al., 1986). Recognized risk factors include immunosuppression, but local factors that abrogate defense mechanisms of the skin are also important, such as may occur with burn wounds and surgical wounds, especially if occlusive dressings are present. Dissemination to the skin from another primary source in the suppressed patient is difficult to treat and generally results in death. This condition is usually recognized by multiple lesions appearing over different areas of the body.

Primary Pulmonary Infection

Primary pulmonary aspergillosis is the most common invasive mold infection in immunocompromised patients, especially in those patients with hematologic malignancies who are undergoing intensive chemotherapy (Bays & Thompson, 2019), although antifungal prophylaxis in this group may cause a shift in the organisms responsible (Lamoth et al., 2017). Even though the disease is usually associated with severely immunocompromised persons, less invasive and noninvasive diseases that affect the lungs such as aspergilloma (fungus ball), chronic necrotizing pulmonary aspergillosis, semi-invasive aspergillosis, and chronic invasive pulmonary aspergillosis may also occur (Kosmidis & Denning, 2015). The predilection of aspergilli to invade blood vessels can lead to infarction and hemorrhage in the lungs and may involve hematogenous spread to other organs (Cadena et al., 2016; Thompson & Patterson, 2008).

Disseminated Infection

Dissemination from the lung or any other primary site of infection may affect any other organ system within the body. The propensity of hyphae to invade vascular structures and cause thrombosis leads to infarcts and abscesses in multiple organs. Single or multiple organs, including the brain, skin, kidneys, pleura, heart, esophagus, liver, or any other site, may be involved (Del Bono et al., 2008; Patterson et al., 2016).

Pathology of Aspergillosis

The histologic appearance of the aspergilli in tissue is similar to that observed with the other hyaline molds, and differentiation among genera and species usually is not possible, except in unusual cases in which sporulation within the tissue cavity has occurred (Guarner & Brandt, 2011). The tissue reaction may be granulomatous but is more commonly dominated by polymorphonuclear neutrophils unless the patient is severely neutropenic. Vascular invasion, thrombosis, and infarction often are prominent features. The hyphae are thin (2–5 μm) and septate and branch at acute angles (dichotomous) (see Fig. 60.4). The H&E stain often colors the hyphae, but the morphology may be demonstrated to advantage with the PAS or GMS technique. The histologic appearance of aspergilli in tissue and the Mucorales can typically be differentiated on the basis of size, hyphal characteristics, and the presence of septa (see Table 60.7).

When the pathologic process is a fungus ball, the hyphae may stain poorly using histopathologic stains. A cavity that is in contact with air, as in the lung or sinuses, may develop fruiting heads, an event that permits identification of the genera and possibly the species (Fig. 60.44). The conidiophores, which are not septate and may be wider than the vegetative hyphae, should not be confused with the Mucorales. Thick-walled Hülle cells and cleistothecia have also been described in vivo. When the patient is immunocompetent and the histologic response is granulomatous, the hyphae may be fragmented and confined to the cytoplasm of macrophages and multinucleated giant cells. The granulomatous response to *Aspergillus* in the lung may be mistaken for bronchocentric granulomatosis in patients who have allergic disease.

Laboratory Diagnosis

Aspergilli are saprobic fungi that should never be dismissed as contaminants without consultation with the attending physician. Isolation from a sterile site or repeated isolation from respiratory specimens suggests clinical significance. Hyphae may be demonstrated directly in clinical specimens in imprint preparations or wet preparations. Calcofluor white staining is useful for demonstrating the mold in specimens. Obtaining tissue, fluid, scrapings, or curettings for examination is important. Tissue should be teased or minced and inoculated directly onto the surface of the isolation medium. *Aspergillus* spp. grow rapidly, but most are inhibited or are partially inhibited by cycloheximide. The colonies of many of these molds teem with conidia. To prevent contamination of the worker and other cultures, the colonies should be manipulated carefully in a biologic safety cabinet, after which the surfaces of the safety cabinet should be thoroughly wiped with a fungicidal solution. Maintenance of isolated molds in plastic bags with continuing incubation also reduces the probability of contaminating other cultures.

Keeping in mind that cryptic species with similar morphologic features are common within the major groups of fungi, specific identification within the aspergilli complexes is made by study of the reproductive structures and the macroscopic appearance of the culture. Careful attention to details of the conidial head is needed for species complex identification. *A. fumigatus* species complex grows rapidly, producing colonies with a fluffy appearance and a blue-green appearance to the colony (see Fig. 60.2). Examination of the colony with a dissecting microscope reveals the conidiophores with their expanded vesicles as small globes projecting above the vegetative mycelium. The conidiophore is smooth, relatively short (300–500 μm), and expanded into a flask-shaped vesicle. The phialides develop in a single row (uniseriate), most commonly on only the upper two-thirds of the vesicle,

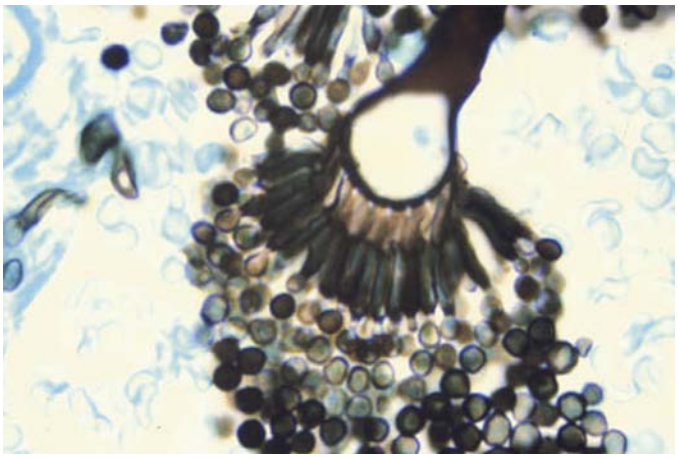

Fig. 60.44 A fruiting head of *Aspergillus* is demonstrated within a pulmonary mycetoma (fungus ball). The phialides and conidia are well demonstrated. Although the hyphae of *Aspergillus* are not etiologically diagnostic, demonstration of the fruiting head documents the presence of this genus. (Gomori's methenamine silver stain, 400×.)

parallel to the axis of the conidiophore (see Fig. 60.8). The conidia are roughened (echinulate) and are round to oval.

Colonies of *A. flavus* species complex have a velvety yellow to green appearance once fruiting heads develop (Fig. 60.45). The conidiophore is long (400–700 μm), ending in a vesicle that may be elliptical or round. The conidiophore is rough and stubbly. A single or double (biseriate) row of phialides occurs over the whole vesicle or the upper three quarters (Fig. 60.46). Round to oval conidia appear yellow-green en masse and measure 3 to 4.5 μm. *Aspergillus terreus* species complex can be differentiated from other species by the production of a cinnamon-brown colony with microscopic characteristics that include short conidiophores (<250 μm) and biseriate phialides.

Although the gold standard for making a diagnosis of invasive aspergillosis is to obtain a positive culture from sterile tissue with histologic evidence of mycelial invasion, the need for invasive techniques to obtain the specimen, the delayed time required for culture, and the rapidity by which the aspergilli can spread make diagnosis problematic. Serologic tests are available for the detection of galactomannan to rapidly diagnose invasive aspergillosis and for the detection of (1-3)-β-D-glucan for nonspecific diagnosis of an invasive fungal infection (Eigl et al., 2017; Hage et al., 2019; Koo et al., 2010; Richardson & Page, 2017; White et al., 2015). All of these tests have shown utility in the management of patients with invasive aspergillosis; however, limitations of the various assays need to be understood.

Although DNA sequencing of isolates has led to dramatic changes in the taxonomy of the *Aspergillus* spp., they will continue to be evaluated as methods for the rapid diagnosis of fungal infection from clinical material. Multiple molecular targets for the identification of the aspergilli have been evaluated, and targets showing greatest promise for identification appear to be the partial β-tubulin and calmodulin genomic areas (Powers-Fletcher & Hanson, 2016). The general consensus at the present time is that a combination of phenotypic and molecular testing needs to be considered for the accurate identification of *Aspergillus* spp.

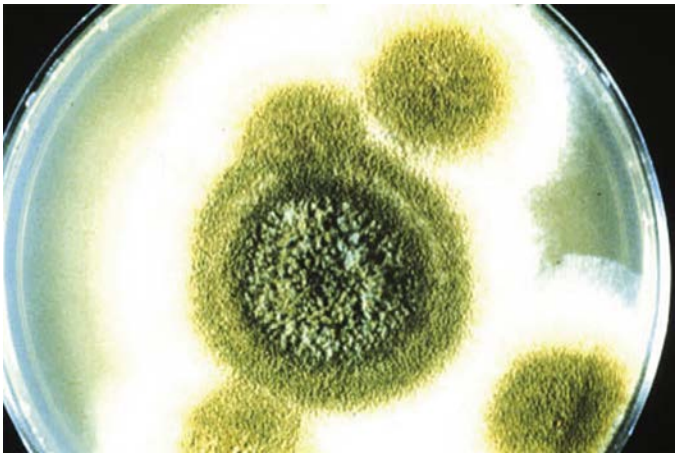

Fig. 60.45 Fluffy colonies with granular areas produced by fruiting heads of *Aspergillus flavus*. The development of yellow or green coloration within the white colonies is characteristic. (Sabouraud dextrose agar.)

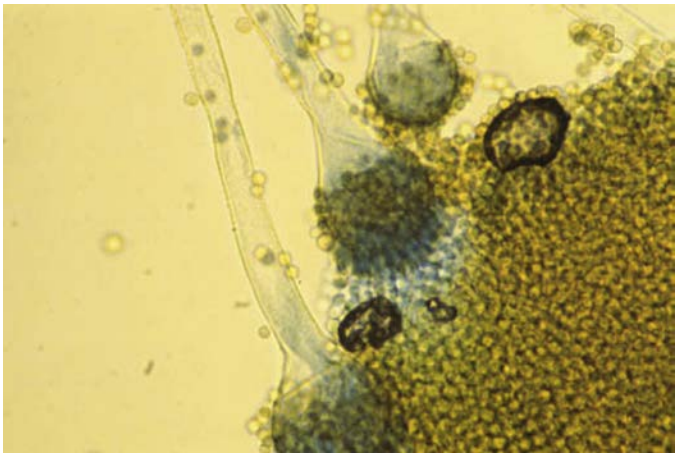

Fig. 60.46 The fruiting head of *Aspergillus flavus* species complex is uniseriate and biseriate. The phialides extend around much of the vesicle with a roughened (spiny) appearance of the conidiophore. (Lactophenol cotton blue stain, 400×.)

Multiple platforms for direct detection of *Aspergillus* DNA in clinical specimens have been evaluated with varying degrees of success (Powers-Fletcher & Hanson, 2016; White et al., 2017). A recent systematic review and meta-analysis done on the use of PCR tests for the diagnosis of invasive aspergillosis directly from blood, plasma, and serum samples concluded that a single PCR-negative result was sufficient to exclude a diagnosis of proven or probable aspergillosis (White et al., 2015). However, two or more positive tests were required to confirm the diagnosis because of increased specificity after testing of multiple samples and improved performance characteristics are seen when used in combination with other noninvasive tests. With advances in molecular testing, a formal evaluation of PCR needs to be considered to assess its use in patients most likely to benefit from testing.

THE GENUS FUSARIUM

Fusarium spp. have been implicated in a number of infectious diseases, including keratomycosis, burn wounds, and invasive disease in immunocompromised patients (Muhammed et al., 2013). Fusariosis is, after aspergillosis, the second most common mold infection in humans (Guarro, 2013). Although still considered a rare cause of human disease, a major outbreak of *Fusarium* keratitis was recently reported wherein 130 cases of eye infection were confirmed (Chang et al., 2006). An epidemiologic investigation showed that most infected patients wore contact lenses that had been cleaned with a lens solution obtained from one manufacturer that exhibited decreased efficacy killing fungi in vitro. This investigation led to the voluntary recall and permanent removal of the associated contact lens solution from the worldwide market.

The histopathologic picture for fusariosis is essentially identical to that observed with invasive aspergillosis (angioinvasive and acute branching septate hyphae). *Fusarium* spp. also have been shown to sporulate in tissues, and thus there may be a combination of yeastlike structures and hyphae in histopathologic preparations (Nucci & Anaissie, 2007). A differentiating feature from invasive aspergillosis is that fungemia is commonly described in fusariosis. *Fusarium*-positive blood cultures are frequently detected during disseminated disease; however, even in documented disseminated disease, detection of aspergilli in the blood is rare (Lionakis et al., 2004).

In culture, *Fusarium* colonies develop rapidly, producing a fluffy aerial mycelium, which often has a pink, lavender, or salmon color. Diffusible pigments may be seen in the surrounding agar. Simple or branched phialides develop directly from the hypha without a separate conidiophore. Short oval microconidia may be produced, but the distinctive structure is a canoe-shaped or crescent-shaped macroconidium, which may have one or more septa (Fig. 60.47). Identification of species in the mycology laboratory is difficult, usually requiring a reference laboratory with experience in recognition of subtle microscopic details related to the reproductive structures.

The taxonomy of *Fusarium* spp. has undergone extensive evaluation following whole genome sequencing (Salah et al., 2015). Most *Fusarium* isolates pathogenic to humans are members of the *F. solani* (now proposed to be within the genus *Neocosmospora*) or the *F. oxysporum* species complexes; however, the traditional taxonomic practice is to refer to members of these complexes as single species (i.e., *F. solani* and *F. oxysporum*). Recent molecular phylogenetic studies have begun to clarify species boundaries within evolutionary lineages

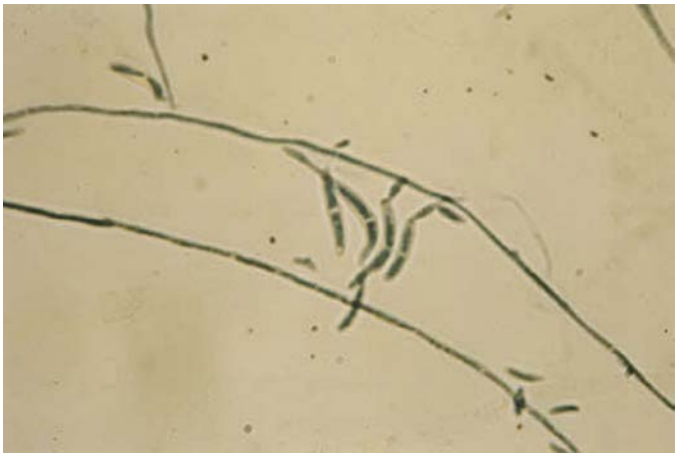

Fig. 60.47 Canoe-shaped conidia of *Fusarium* species. The conidia are often septate. (Lactophenol cotton blue stain, 400×.)

of *Fusarium* that contain human pathogens. Currently, however, recognition of the species, although important for epidemiologic purposes, does not have an impact on therapeutic decisions; thus many laboratories continue to report these as "*Fusarium* species." For molecular identification of the fusaria, three different loci have been recommended and include the translation elongation factor 1α (EF-1α), the largest subunit of RNA polymerase (RPB1), and the second largest subunit of RNA polymerase (RPB2) (Balajee et al., 2009; Guarro, 2013; O'Donnell, Gueidan et al., 2009).

THE GENERA *SCEDOSPORIUM* AND LOMENTOSPORA

Medically important species within these genera include *Scedosporium apiospermum*, *S. (Pseudallescheria) boydii*, *S. aurantiacum*, *S. dehoogii*, and *Lomentospora (Scedosporium) prolificans* (Chen et al., 2016; Cobo et al., 2018; Cortez et al., 2008; Seidel et al., 2019). These fungi are ubiquitous saprobic fungi found in the soil and in decaying vegetation. *L. prolificans* has been reported as a rare cause of disseminated infection, whereas *S. apiospermum*, although most often associated with a subcutaneous infection (eumycotic mycetoma), is the most common species associated with invasive disease in the immunocompromised patient. A distinctive clinical syndrome of sinopulmonary and central nervous system infections in immunocompetent individuals has been associated with near drowning in polluted waters, with *S. apiospermum* as the etiologic agent (Gilgado et al., 2009; Katragkou et al., 2007).

Scedosporium grows on isolation medium at 25°C, producing a fluffy colony that develops a brownish gray to dark gray ("mousy") color after incubation for several days. The culture darkens still further with continued incubation (Fig. 60.48). The asexual phase is characterized by single or small clusters of annelloconidia on a straight or branched conidiophore that may develop terminally or laterally from the vegetative hyphae. The conidia are light brown and have an oval, spermlike morphology (Fig. 60.49). In the sexual phase of *S. boydii*, brown cleistothecia are produced that contain ascospores (see Fig. 60.13). The cleistothecia (100–300 μm in diameter), which are found most readily at the edges of the colony, develop best on nutritionally deficient media, such as cornmeal agar, V-8 juice agar, or potato dextrose (potato flake) agar. Because this fungus is homothallic, recognition of brown cleistothecia in the clinical laboratory is common. Although both macroscopic and microscopic characteristics can be used to separate species within the genus *Scedosporium*, molecular studies now suggest a complex of multiple species (Chen et al., 2016).

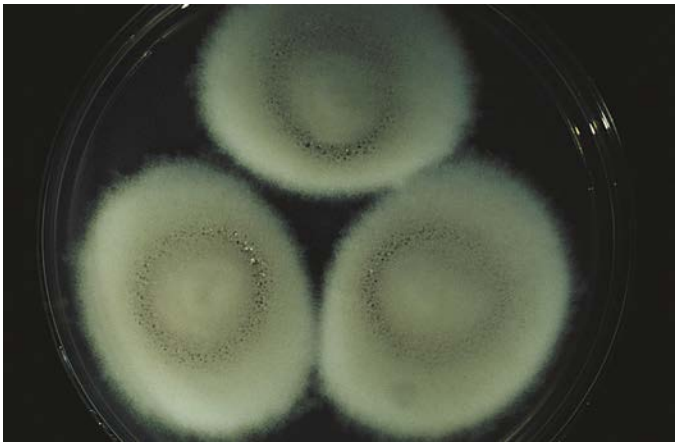

Fig. 60.48 A developing colony of *Scedosporium apiospermum* with the characteristic mousy gray coloration. (Sabouraud dextrose agar.)

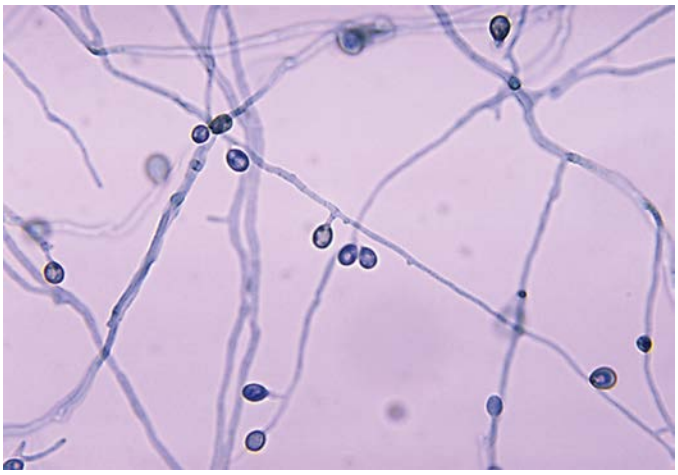

Fig. 60.49 Tadpole- or sperm-shaped microconidia of *Scedosporium apiospermum* are representative of this organism. (Lactophenol cotton blue stain, 400×.)

OTHER SEPTATE HYALINE MOLDS

Hyaline molds comprise a long list of environmental saprobic with low virulence that usually are not associated with clinical disease when isolated in the mycology laboratory (Douglas et al., 2016; Tortorano et al., 2014). This list includes *Acremonium*, *Paecilomyces*, *Purpeocillium*, among others, and any of these molds may be pathogenic under the right conditions. In most cases, the host defenses of the patient are compromised in some way, or the fungus is introduced into the body by trauma or medical manipulation. Increasing numbers of case reports document rare saprobic fungi producing infection of deep tissue and systemic organs. Demonstration of hyphae in tissue is extremely important for documenting the pathogenicity of these isolates, with culture necessary for species recognition. Molecular methods with sequence comparison analysis are becoming the standard for identification of these unusual pathogens given the difficulty with phenotypic differentiation alone (Balajee et al., 2007). MALDI-TOF MS has also demonstrated utility in the identification of these fungi (Rychert et al., 2018).

MICROSPORIDIOSIS

Microsporidia are obligate intracellular, spore-forming parasites that were previously considered "primitive" protozoa but are now classified as fungi in the phylum *Microspora* following phylogenetic analysis (Han & Weiss, 2017). Over 1400 described species of microsporidia, representing about 200 named genera, have been described with many having the capacity to infect a variety of animals, to include humans. Although a number of these species can cause disease in humans, the two most common are *Enterocytozoon bieneusi* and *Encephalitozoon intestinalis* followed by *Encephalitozoon cuniculi* and *Encephalitozoon hellem*.

The transmission to humans generally occurs through contaminated food or water but may also be transmitted by male-male sexual encounter or intravenous drug abuse (Didier, 2005). Once the spore is ingested or inhaled, the organism goes through two distinct life cycles in vivo (Han & Weiss, 2017). During the first stage (referred to as merogony or proliferating state), the spore germinates, forming a polar tube that leads to injection of the sporoplasm into the host cell cytoplasm. Once in the cytoplasm, the injected sporoplasm develops into meronts, which multiply forming multinucleate plasmodial forms. In stage 2 (referred to as sporogony or the infectious state), the meronts' cell membranes thicken, forming sporonts, which ultimately develop into mature spores. The host cells subsequently become distended and the spores are then released into the environment at which point the infectious spores are environmentally stable and can reside for long periods of time.

RISK FACTORS

The microsporidia are serious pathogens in immunocompromised hosts, especially those with AIDS, in whom they are responsible for a large percentage of otherwise unexplained diarrheal disease (Didier, 2005). They are generally associated with a chronic diarrhea leading to weight loss in the AIDS patient, similar to that caused by *Cryptosporidium*. In addition, the microsporidia are now recognized as emerging pathogens causing a variety of extraintestinal infections in the non-HIV immunosuppressed to include organ transplant recipients (La Hoz et al., 2019).

PATHOLOGY

Until recently, the diagnosis frequently occurred in the anatomic pathology laboratory following examination of tissues submitted for routine light and electron microscopy (Ramanan & Pritt, 2014). In histopathologic sectioning of tissue, the microsporidial spores stain pink using the H&E stain and may also be positive with the GMS and Ziehl-Neelsen acid-fast stains. The PAS stain also stains positive and produces a characteristic polar dotlike staining pattern, which is most evident in the larger spores. This appearance is unlike the staining pattern of yeasts, thus aiding in the differentiation. Additionally, size is also important when observing histopathologic

slides. The most common microsporidia (*E. bieneusi* and *Encephalitozoon* spp.) are small, measuring 0.8 to 1.5 μm in length by approximately 1 μm in width. This small size, however, can be challenging to interpret with the overlap in the size of small yeasts such as *Histoplasma capsulatum* and *Candida glabrata*. Also, these microscopic features allow only for the presumptive identification of the microsporidia but do not provide a definitive genus or species information.

LABORATORY DIAGNOSIS

In the clinical laboratory, the diagnosis of microsporidiosis is most widely performed using light microscopy and looking for characteristic spores in stool and body fluid stained samples (Garcia, 2002). The most common stain used is the modified trichrome stain methods, which are designed to detect microsporidial spores from centrifuged stool specimens. These staining methods have been modified from the classic Wheatley's modification of Gomori's trichrome stain by using a higher dye content of chromotrope 2R to enhance the stain penetration into the microsporidial spore and using a much longer staining time. Several of these stains are commercially available (e.g., Weber-Green modified trichrome stain, Ryan-Blue modified trichrome stain). With these methods, the small elliptic spores stain red against a faint green background (or blue depending on the method used) and some display a characteristic midbody cross-band (Fig. 60.50). Fluorochrome stains such as Uvitex 2B and Calcofluor white are also used and appear to be more sensitive in detecting spores and may be useful in the initial screening of specimens, although these methods will also stain yeasts. None of these methods, however, will identify the species.

More recently, molecular amplification using PCR has been used to detect the microsporidia and to identify the infecting species (Marcos & Gotuzzo, 2013). These methods are now becoming the test of choice to diagnose microsporidiosis. Molecular targets used include the intergenic spacer region gene and the small subunit ribosomal DNA (Verweij et al., 2007). These tests offer superior sensitivity and specificity over conventional microscopy-based methods, and although there are no FDA-approved assays available, numerous reference laboratories and public health labs now offer this testing.

PNEUMOCYSTIS PNEUMONIA

The taxonomic position of *P. (carinii) jirovecii* has undergone numerous changes over the years. This organism was originally described as a protozoan, with the morphologic forms identified as trophozoites, cysts, and sporozoites. This protozoan hypothesis remained predominant until DNA analysis showed this organism to be more closely related to the taxonomic kingdom of fungi (Edman et al., 1988). Molecular information has since shown that the organism had differing DNA sequences when identified from diverse mammal hosts. To address this issue, the *Pneumocystis* Working Group in 1994 proposed the name *P. carinii* f. sp. *hominis* as a special form *(formae specialis)* of the organism causing *P. carinii* pneumonia (PCP) in humans (Pneumocystis Working Group, 1994). Subsequently, those attending the International Workshop on Opportunistic Protists in 2001 began the process to rename the species to *P. jirovecii* (pronounced "yee row vet zee") (Stringer et al., 2002). Although initially controversial, the name has now become widely accepted as the "microbe that causes PCP in humans," with the acronym PCP now standing for "*Pneumocystis* pneumonia" (Hughes, 2003). More recently the correct and valid name under the International Code of Zoological Nomenclature was changed to *Pneumocystis jirovecii* (Stringer et al., 2009). It is now thought that most mammals have at least one species of *Pneumocystis* that is not found in any other mammal suggesting that hundreds or even thousands of species may be represented in this one genus (Cushion & Ali Rai, 2019).

RISK FACTORS

P. jirovecii (human-derived *Pneumocystis*) is a pathogen capable of causing a broad spectrum of clinical presentations. In the early 1980s, *Pneumocystis* became a major cause of life-threatening pneumonia in 60% to 80% of HIV-infected adults in the United States and Western Europe, and it subsequently became known as one of the AIDS-defining illnesses (Travis et al., 2009). Although still a serious problem within this patient population, the incidence of disease in people with AIDS has decreased to less than 10% of patients owing to the availability of highly active antiretroviral therapy (HAART), the increasing use of anti-PCP prophylaxis, and improved awareness of the infection (Limper et al., 2017). Thus this disease should also be considered in any immunosuppressed patient who presents with fever, respiratory symptoms, or infiltrate on chest radiograph (Fishman et al., 2019; Morris & Norris, 2012; Salzer et al., 2018).

CLINICAL DISEASES

Pneumonia is the most common manifestation of *P. jirovecii* infection (Salzer et al., 2018). Although the onset may be acute or insidious, symptomatic adults frequently present with dyspnea, a nonproductive cough, an inability to breathe deeply, chest tightness, and night sweats. Although no radiographic pattern is pathognomonic for *Pneumocystis* pneumonia and frequently dependent on the patient's state of immunosuppression, the findings of fine, bilateral, perihilar interstitial shadowing, however, may be present (Fishman et al., 2019). Often, radiographic infiltrates are much more extensive than would be suggested by the degree of symptoms. Concurrent infection with other agents, particularly cytomegalovirus and *C. neoformans*, is common. The most common extrapulmonary sites of infection are the thyroid gland, liver, bone marrow, lymph nodes, and spleen (Wazir & Ansari, 2004).

LABORATORY DIAGNOSIS

Since *P. jirovecii* does not grow on culture media in vitro, the definitive diagnosis of PCP generally requires the demonstration of cysts or trophozoites within lung tissues or respiratory tract specimens (Fig. 60.51). The initial diagnosis might include examination of BAL, sputum, or tracheal aspirate by a cytopathologist following staining with a modified PAP stain, Gram Wiegert, or Wright Giemsa stain for visualization of the cysts or trophozoite forms (Baldassarri et al., 2019).

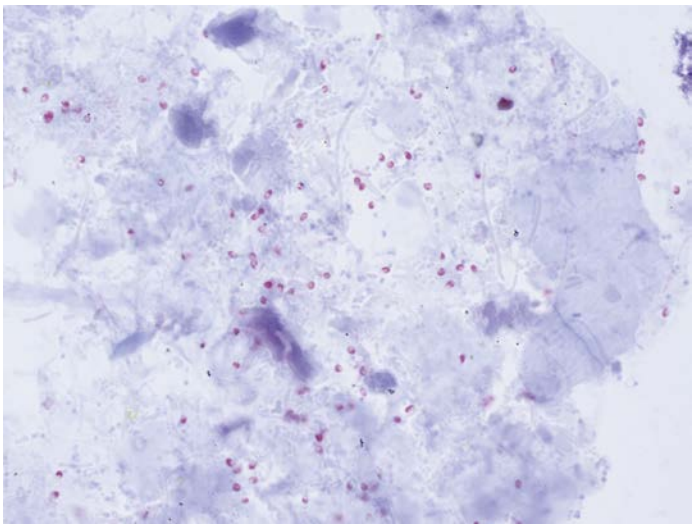

Fig. 60.50 Numerous microsporidial spores seen in feces. ((Ryan-Blue modified trichrome stain, 1000x.) (Courtesy Dr. Bobbi Pritt.))

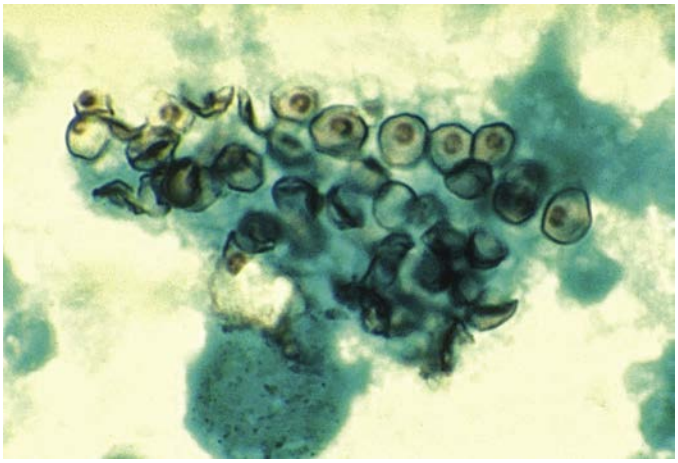

Fig. 60.51 Cysts of *Pneumocystis jirovecii* in a smear from bronchoalveolar lavage. (Gomori's methenamine silver stain, 400×.) (Courtesy Dr. Russell K. Brynes, Centers for Disease Control and Prevention Public Health Image Library.))

One of the standards for diagnosis is staining BAL fluid with an immunofluorescent monoclonal antibody directed against surface epitopes for *Pneumocystis* cysts and trophozoites (Cushion & Ali Rai, 2019). The life cycle of *P. jirovecii* involves development of sporozoites within a cyst, after which the sporozoites are released. In patients with HIV infection, sufficient numbers of organisms are produced that sputum induced with saline by a skilled respiratory therapist may provide the diagnosis. Experience with sputum has varied among centers, however, and the yield is very low in patients who have underlying disease other than HIV. Use of fluorescein-conjugated monoclonal antibodies to detect *P. jirovecii* in clinical specimens has proved to be a specific and sensitive method for identification (Fig. 60.52) (Fishman et al., 2019). The immunofluorescence assay has been more sensitive in histochemical stains in some reports, but the skill and care of the observers undoubtedly play a role in the comparative sensitivity of the techniques. The diagnostic accuracy of the serum or BAL (1-3)-beta-D-glucan assay has a high negative predictive value and is useful as a screening tool for this disease; however, positive beta-D-glucan results do not exclude other fungal infections, resulting in reflex to additional diagnostic testing (Karageorgopoulos et al., 2013). Cysts of *P. jirovecii* occasionally may also be encountered in Gram-stained preparations, although this technique is not a sensitive method for detection.

In cases where a diagnosis cannot be made from these specimens, a more invasive procedure might need to be considered, such as an open thorax lung biopsy, because of the low number of organisms present. Classic histopathologic findings of PCP in sections of lung stained with H&E include widening of the alveolar septa with an infiltrate of mononuclear cells and foamy exudate within the alveolar spaces (sometime referred to as **honeycombed exudates**) (Woods & Schnadig, 2003). This exudate consists of aggregated cysts and trophozoites with the cyst form of *P. jirovecii* illustrated in tissue using the GMS stain, 4 to 6 μm in diameter, staining brown to black and showing the characteristic oval, cup, crescent, or helmet shape. *Pneumocystis* cysts do not bud, and this feature can be used to distinguish this organism from other fungi found in tissue. The histologic differential diagnosis of *P. jirovecii* includes *Histoplasma capsulatum* (small oval yeast cells) and *Coccidioides* spp., when only the endospores are present (Roden & Schuetz, 2017).

Various PCR amplification strategies have also been described for detecting *P. jirovecii* in clinical specimens (Doyle et al., 2017; Rober-Gangneux et al., 2014). Some studies have suggested that PCR was the most sensitive method for the detection of *Pneumocystis* and should be the diagnostic test of choice (Doyle et al., 2017). Other studies, however, have shown that although PCR did have high negative predictive values, positive results were unable to decipher between infected and colonized individuals (Guegan & Robert-Gangneux, 2019). Studies are ongoing in the development of real-time quantitative PCR testing as compatible methods for *Pneumocystis* infection diagnosis (Salzer et al., 2018).

PROTOTHECOSIS

Protothecosis is an infection caused by achlorophyllic algae of the genus *Prototheca* (Hillesheim & Bahrami, 2011; Seok et al., 2013; Todd et al., 2012). Most human infections are caused by *Prototheca wickerhamii*; however, rare cases have also been caused by *Prototheca zopfii*. Although these species are classified as algae, they are included in this chapter because of the resemblance of the infections to fungal diseases. *Prototheca* are found in fresh and marine waters and probably gain entrance to the body through superficial wounds. Some patients are immunocompetent, but serious underlying diseases, such as diabetes mellitus, or immunosuppressive therapies often predispose patients to infection with these pathogens. Steroid overuse or iatrogenic adrenal insufficiency have been reported to predispose individuals to high-risk infections caused by the *Prototheca* (Tseng et al., 2018). Infections commonly involve the skin and subcutaneous tissue, with subsequent involvement of underlying tendons. Disseminated infection is also possible in immunocompromised individuals (Macesic et al., 2014; Ramirez et al., 2016).

Prototheca form large, nonbudding cells that can readily be seen in tissue. The appearance is a spheroid or ovoid cell with a thick, double-layered wall and a "morula-like" structure filled with endospores (Hillesheim & Bahrami, 2011). The organisms are readily apparent using the PAS and GMS stains (Fig. 60.53). *Prototheca* grow readily on fungal isolation media such as Sabouraud dextrose agar and inhibition mold agar at 30°C. The colonies are white to light tan within 48 hours of incubation (Fig. 60.54). A Gram stain from culture will show characteristic gram-positive staining endospores. *Prototheca* species can be identified to the species level by using commercial yeast identification systems, such as the API 20C System and the VITEK 2 System (bioMérieux). More recently, MALDI-TOF MS has been shown to be reliable for the rapid identification of *Prototheca* from culture to the species level (Todd et al., 2018).

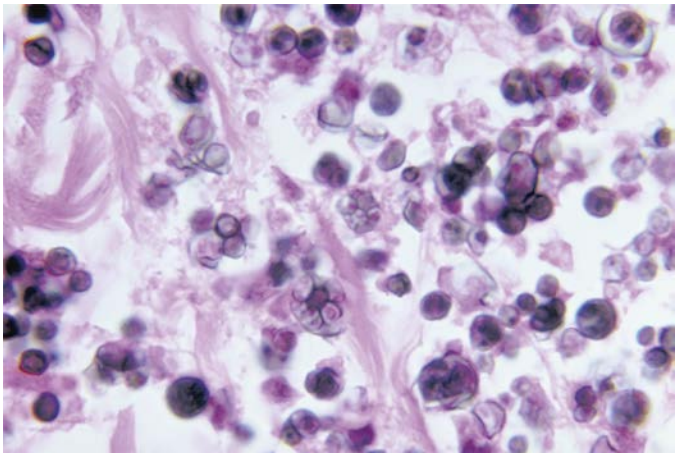

Fig. 60.53 Histopathologic changes in protothecosis of the skin and mucous membrane of the nose due to *Prototheca wickerhamii*. Septation of the algal cells leads to multiple intracellular bodies and structures known as *morula*. (Courtesy Dr. William Kaplan, Centers for Disease Control and Prevention Public Health Image Library.)

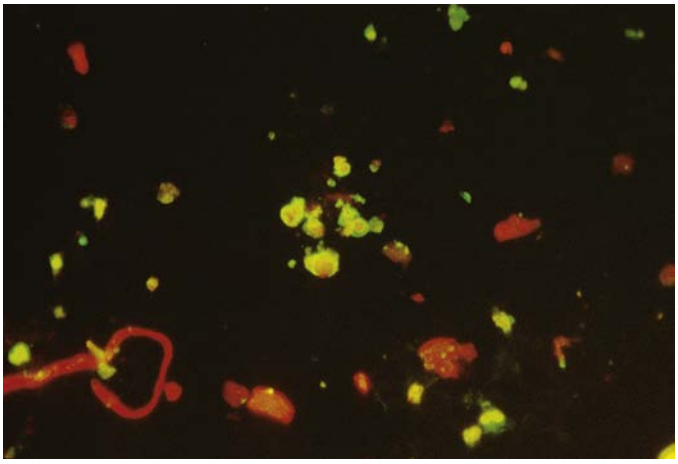

Fig. 60.52 Immunofluorescence microscopy showing the presence of *Pneumocystis jirovecii*. (561×.) (Courtesy Centers for Disease Control and Prevention Public Health Image Library, Lois Norman, provider.)

Fig. 60.54 Colonies of *Prototheca wickerhamii* are yeastlike in appearance. (Sabouraud dextrose agar.)

SELECTED REFERENCES

Arvanitis M, Anagnostou T, Fuchs BB, et al.: Molecular and nonmolecular diagnostic methods for invasive fungal infections, *Clin Microbiol Rev* 27:490–526, 2014.

This review highlights the different diagnostic approaches that are currently utilized or under development for invasive fungal infections and to identify their performance characteristics and the challenges associated with their use.

Balajee SA, Borman AM, Brandt ME, et al.: Sequence-based identification of *Aspergillus*, *Fusarium*, and *Mucorales* species in the clinical mycology laboratory: where are we and where should we go from here? *J Clin Microbiol* 47:877–884, 2009.

A minireview focusing on the molecular strategies available for evaluation of medically important fungi of the genera Aspergillus and Fusarium and the order Mucorales.

Chandler FW, Watts JC: *Pathologic diagnosis of fungal infections*, Chicago, 1987, ASCP Press.

This atlas provides a practical foundation for the pathologic diagnosis of diseases caused by fungi, actinomycetes, and algae.

Cornely OA, Cuenca-Estrella M, Meis JF, et al.: European society of clinical microbiology and infectious diseases (ESCMID) fungal infection study group (EFISG) and European Confederation of medical mycology (ECMM) 2013 joint guidelines on diagnosis and management of rare and emerging fungal diseases, *Clin Microbiol Infect* 20(Suppl 3):1–4, 2014.

This guideline serves as a recommendation for the diagnosis and management of rare and emerging fungi, to include mucormycosis, hyalohyphomycosis, phaeohyphomycosis, and emerging yeasts.

Griffin AT, Hanson KE: Update on fungal diagnostics, *Curr Infect Dis Rep* 16:415–425, 2014.

This review highlights recent laboratory developments in the diagnosis of invasive candidiasis, cryptococcosis, opportunistic molds, and endemic fungal infections.

Guarner J, Brandt ME: Histopathologic diagnosis of fungal infections in the 21st century, *Clin Microbio Rev* 24:247–280, 2011.

This report presents methods that can be used for diagnosis of specific yeasts and molds in formalin-fixed, paraffin-embedded tissue submitted for histopathologic diagnosis, as well as a series of scenarios that should help to guide the diagnosis and treatment of patients with mycoses.

Hibbett DS, Binder M, Bischoff JF, et al.: A higher-level phylogenetic classification of the fungi, *Mycol Res* 111:509–547, 2007.

This article provides a comprehensive phylogenetic classification of the fungal kingdom with reference to the recent molecular phylogenetic analyses used to derive this proposed classification.

Naggie S, Perfect JR: Molds: hyalohyphomycosis, phaeohyphomycosis, and zygomycosis, *Clin Chest Med* 30:337–353, 2009.

This review focuses on emerging fungal pathogens with an emphasis on microbiology, pathogenesis, clinical presentations, diagnosis, treatment, and outcomes.

Perfect JR: Fungal diagnosis: how do we do it and can we do better? *Cur Med Res Opin* 29 (Suppl 4):3–11, 2013.

This article provides better understanding of the strengths and weaknesses of currently available diagnostic tools and further devises linked strategies to best implement them either alone or in combination to improve early and accurate diagnosis of invasive fungal infections and improve their successful management.

Pfaller MA, Diekema DJ: Epidemiology of invasive candidiasis: a persistent public health problem, *Clin Microbiol Rev* 20:133–163, 2007.

This review provides an overview of the incidence, risk factors involved, and treatment strategies used for management of invasive candidiasis.

Queiroz-Telles F, Esterre P, Perez-Blanco M, et al.: Chromoblastomycosis: an overview of clinical manifestations, diagnosis and treatment, *Med Mycol* 47:3–15, 2009.

This article provides an overview of the diagnosis and management of the disease chromoblastomycosis.

Revankar SG, Sutton DA: Melanized fungi in human disease, *Clin Microbiol Rev* 24:884–928, 2010.

This review seeks to provide a broad, yet in-depth overview of melanized fungi in human disease as it currently stands, recognizing that the field will continue to evolve and expand with our increasing knowledge of and experience with these clinically important fungi.

Roden AC, Schuetz AN: Histopathology of fungal diseases of the lung, *Semin Diagn Pathol* 34:530–549, 2017.

This comprehensive review discusses the histopathology observed with various fungal pneumonias and the means by which these lung infections can be diagnosed.

Wiederhold NP, Gibas CFC: From the clinical mycology laboratory: new species and changes in fungal taxonomy and fungal nomenclature, *J Fungi* 4, 2010https://doi.org/10.3390/jof4040138.

This review provides information on changes in fungal nomenclature and taxonomy, including new species, what is driving these changes, how the changes may affect clinical laboratories, and suggestions and recommendations as to how clinical microbiology laboratories may deal with these changes.

Access the complete reference list online at Elsevier eBooks for Practicing Clinicians.

REFERENCES

Abdelhamed AM, Zhang SX, Watkins T, Morgan MA, Wu F, Buckner RJ, et al.: Multicenter evaluation of Candida QuickFISH BC for identification of Candida species directly from blood culture bottles, *J Clin Microbiol* 53:1672–1676, 2015, https://doi.org/10.1128/JCM.00549-15.

Ajello L, Geortg LK, Steigvigel RT, Want CJ: A case of phaeohyphomycosis caused by a new species of, *Phialophora*, *Mycologia* 66:490–498, 1974.

Al-Ahmad M, Manno M, Ng V, Ribeiro M, Liss GM, Tario SM: Symptoms after mould exposure including *Stachybotrys chartarum*, and comparison with darkroom disease, *Allergy* 65:245–255, 2010.

Alastruey-Izquierdo A, Alcazar-Fuoli L, Cuenca-Estrella M: : antifungal susceptibility profile of cryptic species of Aspergillus, *Mycopathologia* 178:427–433, 2014, https://doi.org/10.1007/s11046-014-9775-z.

Alastruey-Izquierdo A, Mellado E, Pelaez T, Peman J, Zapico S, Alvarez M, Rodriguez-Tudela JL, Cuenca-Estrella M, Group, F.S: population-based survey of filamentous fungi and antifungal resistance in Spain (FILPOP study), *Antimicrob Agents Chemother* 57:4604, 2013, https://doi.org/10.1128/AAC.01287-13.

Alexander BD, Byrne TC, Smith KL, et al.: Comparative evaluation of Etest and Sensititre YeastOne panels against the Clinical and Laboratory Standards Institute M27-A2 reference broth microdilution method for testing *Candida* susceptibility to seven antifungal agents, *J Clin Microbiol* 45:698–706, 2007.

Alshannaq A, Yu JH: Occurrence, Toxicity, and analysis of major mycotoxins in food, *Int J Environ Res Public Health* 14, 2017https://doi.org/10.3390/ijerph14060632.

Altun S, Almuhayawi M, Ullberg M, Ozenci V: Clinical evaluation of the FilmArray blood culture identification panel in identification of bacteria and yeasts from positive blood culture bottles, *J Clin Microbiol* 51:4130–4136, 2013.

Ampel NM, Robey I, Nguyen CT: An analysis of skin test responses to Spherulin-based Coccidioidin (Spherusol((R))) among a group of Subjects with various forms of active coccidioidomycosis, *Mycopathologia* 184:533–538, 2019, https://doi.org/10.1007/s11046-019-00356-5.

Arendrup MC, Boekhout T, Akova M, Meis JF, Cornely OA, Lortholary O, European Society of Clinical, M, Infectious Diseases Fungal Infection Study, G: European Confederation of Medical, M: ESCMID and ECMM joint clinical guidelines for the diagnosis and management of rare invasive yeast infections, *Clin Microbiol Infect* 20(Suppl 3):76–98, 2014, https://doi.org/10.1111/1469-0691.12360.

Arendrup MC, Meletiadis J, Mouton JW, Lagrou K, Hamal P, Guinea J: EUCAST Definitive Document E.Def 9.3.1: method for the determination of broth dilution minimum inhibitory concentrations of antifungal agents for conidia forming moulds, EUCAST, *Basel*, *Switzerland*, 2017.

Arikan S: Current status of antifungal susceptibility testing methods, *Med Mycol* 45:569–587, 2007.

Arvanitis M, Anagnostou T, Fuchs BB, Caliendo AM, Mylonakis E: Molecular and nonmolecular diagnostic methods for invasive fungal infections, *Clin Microbiol Rev* 27:490–526, 2014.

Ates A, Ozcan K, Ilkit M: Diagnostic value of morphological, physiological and biochemical tests in distinguishing *Trichophyton rubrum* from T*richophyton mentagrophytes* complex, *Med Mycol* 46:811–822, 2008.

Azar MM, Hage CA: Clinical perspectives in the diagnosis and management of histoplasmosis, *Clin Chest Med* 38:403–415, 2017, https://doi.org/10.1016/j.ccm.2017.04.004.

Babady NE, Bestrom JE, Jespersen DJ, Jones MF, Beito EM, Binnicker MJ, Wengenack NL: Evaluation of three commercial latex agglutination kits and a commercial enzyme immunoassay for the detection of cryptococcal antigen, *Med Mycol* 47:336–338, 2009.

Babady NE, Buckwalter SP, Hall L, Le Febre KM, Binnicker MJ, Wengenack NL: Detection of Blastomyces dermatitidis and Histoplasma capsulatum from culture isolates and clinical specimens by use of real-time PCR, *J Clin Microbiol* 49:3204–3208, 2011, https://doi.org/10.1128/JCM.00673-11.

Baddley JW, Benjamin Jr DK, Patel M, Miro J, Athan E, Barsic B, et al.: Candida infective endocarditis, *Eur J Clin Microbiol Infect Dis* 27:519–529, 2008, https://doi.org/10.1007/s10096-008-0466-x.

Baddley JW, Marr KA, Andes DR, Walsh TJ, Kauffman CA, Kontoyiannis DP: Patterns of susceptibility of *Aspergillus* isolates recovered from patients enrolled in the Transplant-Associated Infection Surveillance Network, *J Clin Microbiol* 47:3271–3275, 2009.

Bader O, Weig M, Taverne-Ghadwal L, Lugert R, Gross U, Kuhns M: Improved clinical laboratory identification of human pathogenic yeasts by matrix-assisted laser desorption ionization time-of-flight mass spectrometry, *Clin Microbiol Infect* 17:1359–1365, 2011, https://doi.org/10.1111/j.1469-0691.2010.03398.x.

Bagla P, Loeffelholz M, Blanton LS: Cerebral phaeohyphomycosis by Fonsecaea monophora: report in a patient with AIDS and a ring enhancing lesion, *Med Mycol Case Rep* 12:4–7, 2016, https://doi.org/10.1016/j.mmcr.2016.06.002.

Balajee SA: *Aspergillus terreus* complex, *Med Mycol* 47(Suppl 1):S42–46, 2009.

Balajee SA, Borman AM, Brandt ME, Cano J, Cuenca-Estrella M, Dannaoui E: sequence-based identification of *Aspergillus*, *Fusarium*, and *Mucorales* species in the clinical mycology laboratory: where are we and where should we go from here? *J Clin Microbiol* 47:877–884, 2009.

Balajee SA, Sigler L, Brandt ME: : DNA and the classical way: identification of medically important molds in the 21st century, *Med Mycol* 45:475–490, 2007.

Baldassarri RJ, Kumar D, Baldassarri S, Cai G: Diagnosis of infectious diseases in the lower respiratory tract: a Cytopathologist's Perspective, *Arch Pathol Lab Med* 143:683–694, 2019, https://doi.org/10.5858/arpa.2017-0573-RA.

Bariola JR, Vyas KS: Pulmonary blastomycosis, *Semin Respir Crit Care Med* 32:745–753, 2011, https://doi.org/10.1055/s-0031-1295722.

Bariteau JT, Waryasz GR, McDonnell M, Fischer SA, Hayda RA, Born CT: Fungal osteomyelitis and septic arthritis, *J Am Acad Orthop Surg* 22:390–401, 2014, https://doi.org/10.5435/JAAOS-22-06-390.

Barker BM, Litvintseva AP, Riquelme M, Vargas-Gastelum L: Coccidioides ecology and genomics, *Med Mycol* 57:S21–S29, 2019, https://doi.org/10.1093/mmy/myy051.

Barros MB, de Almeida Paes R, Schubach AO: Sporothrix schenckii and sporotrichosis, *Clin Microbiol Rev* 24:633–654, 2011, https://doi.org/10.1128/CMR.00007-11.

Bassetti M, Giacobbe DR, Vena A, Trucchi C, Ansaldi F, Antonelli M: Incidence and outcome of invasive candidiasis in intensive care units (ICUs) in Europe: results of the EUCANDICU project, *Crit Care* 23:219, 2019, https://doi.org/10.1186/s13054-019-2497-3.

Bays DJ, Thompson 3rd GR: : fungal infections of the stem cell transplant recipient and hematologic malignancy patients, *Infect Dis Clin North Am* 33:545–566, 2019, https://doi.org/10.1016/j.idc.2019.02.006.

Ben-Ami R, Lewis RE, Kontoyiannis DP: Invasive mould infections in the setting of hematopoietic cell transplantation: current trends and new challenges, *Curr Opin Infect Dis* 22:376–384, 2009.

Benedict K, Mody RK: Epidemiology of histoplasmosis outbreaks, United States, 1938-2013, *Emerg Infect Dis* 22:370–378, 2016, https://doi.org/10.3201/eid2203.151117.

Benedict K, Thompson 3rd GR, Deresinski S, Chiller T: : mycotic infections acquired outside areas of known endemicity, United States, *Emerg Infect Dis* 21:1935–1941, 2015, https://doi.org/10.3201/eid2111.141950.

Bernal S, Martin Mazuelos E, Chavez M, Coronilla J, Valverde A: Evaluation of the new API *Candida* system for identification of the most clinically important yeast species, *Diagn Microbiol Infect Dis* 32:217–221, 1998.

Beyda ND, Alam MJ, Garey KW: Comparison of the T2Dx instrument with T2Candida assay and automated blood culture in the detection of Candida species using seeded blood samples, *Diagn Microbiol Infect Dis* 77:324–326, 2013, https://doi.org/10.1016/j.diagmicrobio.2013.07.007.

Bizzini A, Greub G: Matrix-assisted laser desorption ionization time-of-flight mass spectrometry, a revolution in clinical microbial identification, *Clinical Microbiology and Infection* 16:1614–1619, 2010, https://doi.org/10.1111/j.1469-0691.2010.03311.x.

Blair JE, Ampel NM, Hoover SE: Coccidioidomycosis in selected immunosuppressed hosts, *Med Mycol* 57:S56–S63, 2019, https://doi.org/10.1093/mmy/myy019.

Bocca AL, Amaral AC, Teixeira MM, Sato PK, Shikanai-Yasuda MA, Soares Felipe MS: Paracoccidioidomycosis: eco-epidemiology, taxonomy and clinical and therapeutic issues, *Future Microbiol* 8:1177–1191, 2013, https://doi.org/10.2217/fmb.13.68.

Bongomin F, Moore CB, Masania R, Rowbotham E, Alastruey-Izquierdo A, Novak-Frazer L, Richardson MD: Sequence analysis of isolates of Aspergillus from patients with chronic and allergic aspergillosis reveals a spectrum of cryptic species, *Future Microbiol* 13:1557–1563, 2018, https://doi.org/10.2217/fmb-2018-0178.

Borman AM, Linton CJ, Miles SJ, Johnson EM: Molecular identification of pathogenic fungi, *J Antimicrob Chemother* 61(Suppl 1):i7–12, 2008.

Boulware DR, Rolfes MA, Rajasingham R, von Hohenberg M, Qin Z, Taseera K, Schutz C: Multisite validation of cryptococcal antigen lateral flow assay and quantification by laser thermal contrast, *Emerg Infect Dis* 20:45–53, 2014, https://doi.org/10.3201/eid2001.130906.

Bradsher Jr RW: The endemic mimic: blastomycosis an illness often misdiagnosed, *Trans Am Clin Climatol Assoc* 125:188–202, 2014. discussion 202–183.

Bretagne S, Bart-Delabesse E, Wechsler J, Kuentz M, Dhedin N, Cordonnier C: Fatal primary cutaneous aspergillosis in a bone marrow transplant recipient: nosocomial acquisition in a laminar-air flow room, *J Hosp Infect* 36:235–239, 1997.

Brizendine KD, Baddley JW, Pappas PG: Pulmonary cryptococcosis, *Semin Respir Crit Care Med* 32:727–734, 2011, https://doi.org/10.1055/s-0031-1295720.

Brown J, Benedict K, Park BJ, Thompson GR: 3rd: coccidioidomycosis: epidemiology, *Clin Epidemiol* 5:185–197, 2013, https://doi.org/10.2147/CLEP.S34434.

Bryce EA, Walker M, Scharf S, Lim AT, Walsh A, Sharp N, Smith JA: An outbreak of cutaneous aspergillosis in a tertiary-care hospital, *Infect Control Hosp Epidemiol* 17:170–172, 1996.

Cabanes FJ: Malassezia yeasts: how many species infect humans and animals? *PLoS Pathog* 10:e1003892, 2014, https://doi.org/10.1371/journal.ppat.1003892.

Cadena J, Thompson 3rd GR, Patterson TF: Invasive aspergillosis: current strategies for diagnosis and management, *Infect Dis Clin North Am* 30:125–142, 2016, https://doi.org/10.1016/j.idc.2015.10.015.

Cafarchia C, Gasser RB, Figueredo LA, Latrofa MS, Otranto D: Advances in the identification of Malassezia, *Mol Cell Probes* 25:1–7, 2011, https://doi.org/10.1016/j.mcp.2010.12.003.

Cafarchia C, Gasser RB, Figueredo LA, Weigl S, Danesi P, Capelli G, Otranto D: An improved molecular diagnostic assay for canine and feline dermatophytosis, *Med Mycol* 51:136–143, 2013, https://doi.org/10.3109/13693786.2012.691995.

Campbell GD: Primary pulmonary cryptococcosis, *Am Rev Respir Dis* 94:236–243, 1966, https://doi.org/10.1164/arrd.1966.94.2.236.

Canteros CE, Rodero L, Rivas MC, Davel G: A rapid urease test for presumptive identification of, *Cryptococcus neoformans*. *Mycopathologia* 136:21–23, 1996.

Cao C, Liang L, Wang W, Luo H, Huang S, Liu D, Xu J, et al.: Common reservoirs for Penicillium marneffei infection in humans and rodents, China, *Emerg Infect Dis* 17:209–214, 2011, https://doi.org/10.3201/eid1702.100718.

Castanheira M, Woosley LN, Diekema DJ, Jones RN, Pfaller MA: Candida guilliermondii and other species of candida misidentified as Candida famata: assessment by vitek 2, DNA sequencing analysis, and matrix-assisted laser desorption ionization-time of flight mass spectrometry in two global antifungal surveillance programs, *J Clin Microbiol* 51:117–124, 2013, https://doi.org/10.1128/JCM.01686-12.

Castro C, Serrano MC, Flores B, Espinel-Ingroff A, Martin-Mazuelos E: Comparison of the Sensititre YeastOne colorimetric antifungal panel with a modified NCCLS M38-A method to determine the activity of voriconazole against clinical isolates of *Aspergillus* spp, *J Clin Microbiol* 42:4358–4360, 2004.

Centers for Disease Control and Prevention: Update: outbreak of acute febrile respiratory illness among college students–Acapulco, *MMWR Morb Mortal Wkly Rep* 50:359–360, 2001. Mexico, March 2001.

Centers for Disease Control and Prevention: Histoplasmosis outbreak among day camp attendees–Nebraska, *MMWR Morb Mortal Wkly Rep* 61:747–748, June 2012. 2012.

Chai LY, Denning DW, Warn P: Candida tropicalis in human disease, *Crit Rev Microbiol* 36:282–298, 2010, https://doi.org/10.3109/1040841X.2010.489506.

Chakrabarti A, Denning DW, Ferguson BJ, Ponikau J, Buzina W, Kita H, Marple B, et al.: Fungal rhinosinusitis: a categorization and definitional schema addressing current controversies, *Laryngoscope* 119:1809–1818, 2009.

Chakrabarti A, Kaur H, Rudramurthy SM, Appannanavar SB, Patel A, Mukherjee KK, Ghosh A, Ray U: Brain abscess due to Cladophialophora bantiana: a review of 124 cases, *Med Mycol* 54:111–119, 2016, https://doi.org/10.1093/mmy/myv091.

Chalupova J, Raus M, Sedlarova M, Sebela M: Identification of fungal microorganisms by MALDI-TOF mass spectrometry, *Biotech Adv* 32:230–241, 2014.

Chandler FW, Watts JC: Zygomycosis. In Chandler FW, Watts JC, editors: *Pathologic diagnosis of fungal infections*, *Chicago*, 1987, American Society of Clinical Pathologists, pp 85–96.

Chandrasekar P: Invasive mold infections: recent advances in management approaches, *Leuk Lymphoma* 50:703–715, 2009.

Chang C, Gershwin ME, Thompson 3rd GR: fungal disease of the nose and sinuses: an updated overview, *Curr Allergy Asthma Rep* 13:152–161, 2013, https://doi.org/10.1007/s11882-012-0320-1.

Chang DC, Grant GB, O'Donnell K, Wannemuehler KA, Noble-Wang J, Rao CY, Jacobson LM, et al.: Multistate outbreak of Fusarium keratitis associated with use of a contact lens solution, *J Am Med Assoc* 296:953–963, 2006, https://doi.org/10.1001/jama.296.8.953.

Chapman SW, Bradsher Jr RW, Campbell Jr GD, Pappas PG, Kauffman CA: Practice guidelines for the management of patients with blastomycosis. Infectious Diseases Society of America, *Clin Infect Dis* 30:679–683, 2000, https://doi.org/10.1086/313750.

Chen M, Zeng J, De Hoog GS, Stielow B, Gerrits Van Den Ende AH, Liao W, Lackner M: The 'species complex' issue in clinically relevant fungi: a case study in Scedosporium apiospermum, *Fungal Biol* 120:137–146, 2016, https://doi.org/10.1016/j.funbio.2015.09.003.

Chen SC, Blyth CC, Sorrell TC, Slavin MA: Pneumonia and lung infections due to emerging and unusual fungal pathogens, *Semin Respir Crit Care Med* 32:703–716, 2011.

Chen SC, Meyer W, Sorrell TC: Cryptococcus gattii infections, *Clin Microbiol Rev* 27:980–1024, 2014, https://doi.org/10.1128/CMR.00126-13.

Chew KL, Lee CK, Cross GB, Lum LHW, Yan B, Jureen R: Culture-confirmed cryptococcal meningitis not detected by Cryptococcus PCR on the Biofire meningitis/encephalitis panel((R)), *Clin Microbiol Infect* 24:791–792, 2018, https://doi.org/10.1016/j.cmi.2018.02.024.

Clancy CJ, Nguyen MH: Finding the "missing 50%" of invasive candidiasis: how nonculture diagnostics will improve understanding of disease spectrum and transform patient care, *Clin Infect Dis* 56:1284–1292, 2013, https://doi.org/10.1093/cid/cit006.

Clancy CJ, Nguyen MH: Diagnosing invasive candidiasis *J Clin Microbiol* 56, 2018https://doi.org/10.1128/JCM.01909-17.

Clancy CJ, Pappas PG, Vazquez J, Judson MA, Kontoyiannis DP, Thompson 3rd GR, Garey KW: Detecting infections rapidly and easily for candidemia trial, Part 2 (DIRECT2): a prospective, multicenter study of the T2Candida panel, *Clin Infect Dis* 66:1678–1686, 2018, https://doi.org/10.1093/cid/cix1095.

CLSI: In *Abbreviated Identificaiton of bacteria and yeast*, Second Edition, Wayne, PA, 2008, Clinical and Laboratory Standards Institute.

CLSI: In *Method for antifungal disk diffusion susceptibility testing of yeasts: approved guideline*, 2nd edition, Wayne, PA, 2009, Clinical and Laboratory Standards Institute (M44–A2).

CLSI: *Principles and procedures for detection of fungi in clinical specimens - direct examination and culture; approved guideline (M54-A)*, Wayne, PA, 2012, Clinical and Laboratory Standards Institute.

CLSI: In *Performance standards for antifungal susceptibility testing of yeasts*, First Edition, Wayne, PA, 2017a, Clinical and Laboratory Standards Institute.

CLSI: In *Reference method for broth dilution antifungal susceptibility testing of filamentous fungi*, Third Edition, Wayne, PA, 2017b, Clinical and Laboratory Standards Institute.

CLSI: *Reference method for broth dilution antifungal susceptibility testing of yeasts; approved standard - fourth Edition*, Wayne, PA, 2017c, Clinical and Laboratory Standards Institute.

CLSI: *Performance standards for antifungal susceptibility testing of filamentous fungi*, 2nd edition, Wayne, PA, 2020, Clinical and Laboratory Standards Institute.

Cobo F, Lara-Oya A, Rodriguez-Granger J, Sampedro A, Aliaga-Martinez L, Navarro-Mari JM: Infections caused by Scedosporium/Lomentospora species: clinical and microbiological findings in 21 cases, *Med Mycol* 56:917–925, 2018, https://doi.org/10.1093/mmy/myx147.

Cockerill FRI, Torgerson CA, Reed GS, Vetter EA, Weaver AL, Dale JC, Roberts GD, Henry NK, Ilstrup DM, Rosenblatt JE: Clinical comparison of Difco ESP, Wampole isolator, and Becton Dickinson Septi-Chek aerobic blood culturing systems, *J Clin Microbiol* 34:20–24, 1996.

Colombo AL, Padovan AC, Chaves GM: current knowledge of Trichosporon spp. and trichosporonosis, *Clin Microbiol Rev* 24:682–700, 2011, https://doi.org/10.1128/CMR.00003-11.

Connolly PA, Durkin MM, Lemonte AM, Hackett EJ, Wheat LJ: detection of histoplasma antigen by a quantitative enzyme immunoassay, *Clin Vaccine Immunol* 14:1587–1591, 2007, https://doi.org/10.1128/CVI.00071-07.

Cornely OA, Cuenca-Estrella M, Meis JF, Ullmann AJ: European society of Clincal microbiology and Infedtious diseases (ESCMID), fungal infection study group (EFISG), and European Confederation of medical mycology (ECMM) 2013 joint guidelines on diagnosis and management of rare and emerging fungal diseases, *Clin Microbiol Infect* 20:1–4, 2014.

Cortez KJ, Roilides E, Quiroz-Telles F, Meletiadis J, Antachopoulos C, Knudsen T, et al.: Infections caused by *Scedosporium* spp, *Clin Microbiol Rev* 21:157–197, 2008.

Crist Jr AE, Johnson LM, Burke PJ: Evaluation of the Microbial Identification System for identification of clinically isolated yeasts, *J Clin Microbiol* 34:2408–2410, 1996.

Crum-Cianflone NF: Coccidioidomycosis in the U.S. Military: a review, *Ann N Y Acad Sci* 1111:112–121, 2007.

Cuenca-Estrella M, Gomez-Lopez A, Alastruery-Izquierdo A, et al.: Comparison of the Vitek 2 antifungal susceptibility system with the Clinical and Laboratory Standards Institute (CLSI) and European Committee on Antifungal Susceptibility Testing (EUCAST) broth microdilution reference methods and with the Sensititre YeastOne and Etest techniques for in vitro detection of antifungal resistance in yeast isolates, *J Clin Microbiol* 48:1782–1786, 2010.

Cushion MT, Ali Rai M: Pneumocystis. In Carroll KC, Pfaller MA, Landry ML, McAdam AJ, Patel R, Richter SS, Warnock DW, editors: *Manual of clinical microbiology*, Twelth Edition ed, Washington, DC, 2019, ASM Press, pp 2087–2102.

Dadwal SS, Kontoyiannis DP: Recent advances in the molecular diagnosis of mucormycosis, *Expert Rev Mol Diagn* 18:845–854, 2018, https://doi.org/10.1080/14737159.2018.1522250.

De Carolis E, Vella A, Florio AR, Posteraro P, Perlin DS, Sanguinetti M, Posteraro B: Use of matrix-assisted laser desorption ionization-time of flight mass spectrometry for caspofungin susceptibility testing of Candida and Aspergillus species, *J Clin Microbiol* 50:2479–2483, 2012, https://doi.org/10.1128/JCM.00224-12.

de Hoog GS, Chaturvedi V, Denning DW, Dyer PS, Frisvad JC, Geiser D, Graser Y, et al.: Name changes in medically important fungi and their implications for clinical practice, *J Clin Microbiol* 53:1056–1062, 2015, https://doi.org/10.1128/JCM.02016-14.

de Hoog GS, Dukik K, Monod M, Packeu A, Stubbe D, Hendrickx M, Kupsch C, Stielow JB, et al.: Toward a Novel multilocus phylogenetic taxonomy for the dermatophytes, *Mycopathologia* 182:5–31, 2017, https://doi.org/10.1007/s11046-016-0073-9.

de Hoog GS, Haase G, Chaturvedi V, Walsh TJ, Meyer W: Lackner, M: taxonomy of medically important fungi in the molecular era, *Lancet Infect Dis* 13:385–386, 2013, https://doi.org/10.1016/S1473-3099(13)70058-6.

de Macedo PM, Teixeira MM, Barker BM, Zancope-Oliveira RM, Almeida-Paes R, Francesconi do Valle AC: Clinical features and genetic background of the sympatric species Paracoccidioides brasiliensis and Paracoccidioides americana, *PLoS Negl Trop Dis* 13:e0007309, 2019, https://doi.org/10.1371/journal.pntd.0007309.

Del Bono V, Mikulska M, Viscoli C: Invasive aspergillosis: diagnosis, prophylaxis and treatment, *Curr Opin Hematol* 15:586–593, 2008.

Department of Health and Human Services: Histoplasmosis: protecting workers at risk. In *Centers for disease control and prevention*, Second Edition, Washington, 2004, D.D.

Department of Health and Human Services: In Richmond JY, McKinney RW, editors: *Biosafety in microbiological and Biomedical laboratories (ed 5th)*, 4th ed, Washington, D.C, 2009, U.S. Government Printing Office, p 403.

Department of Health and Human Services: *NIH guidelines for research involving Recombinant or synthetic nucleic acid Molecules Washington*, *DC*, 2019.

Desoubeaux G, Fanck-Martel C, Bailly E, Le Brun C, Gyan E, Aoudeau A, Chandenier J, Lanotte P: Prospective assessment of FilmArray technology for the rapid identification of yeast isolated from blood cultures, *J Microbiol Methods* 106:119–122, 2014.

Didier ES: Microsporidiosis: an emerging and opportunistic infection in humans and animals, *Acta Trop* 94:61–76, 2005, https://doi.org/10.1016/j.actatropica.2005.01.010.

Diekema D, Arbefeville S, Boyken L, Kroeger J, Pfaller, M: The changing epidemiology of healthcare-associated candidemia over three decades, *Diagn Microbiol Infect Dis* 73:45–48, 2012, https://doi.org/10.1016/j.diagmicrobio.2012.02.001.

Diekema DJ, Messer SA, Hollis RJ, Boyken LB, Tendolkar S, Kroeger J, Pfaller MA: Evaluation of Etest and disk diffusion methods compared with broth microdilution antifungal susceptibility testing of clinical isolates of Candida spp. against posaconazole, *J Clin Microbiol* 45:1974–1977, 2007.

Dixon DM, Salkin IF, Duncan RA, Hurd NJ, Haines JH, Kemna ME, Coles FB: Isolation and characterization of Sporothrix schenckii from clinical and environmental sources associated with the largest U.S. epidemic of sporotrichosis, *J Clin Microbiol* 29:1106–1113, 1991.

Donders GG, Sobel JD: Candida vulvovaginitis: a store with a buttery and a show window, *Mycoses* 60:70–72, 2017, https://doi.org/10.1111/myc.12572.

Douglas AP, Chen SC, Slavin MA: Emerging infections caused by non-Aspergillus filamentous fungi, *Clin Microbiol Infect* 22:670–680, 2016, https://doi.org/10.1016/j.cmi.2016.01.011.

Doyle L, Vogel S, Procop GW: Pneumocystis PCR: it is time to make PCR the test of choice, *Open Forum Infect Dis* 4, 2017https://doi.org/10.1093/ofid/ofx193. ofx193.

Doymaz MZ, Seyithanoglu MF, Hakyemez I, Gultepe BS, Cevik S, Aslan T: A case of cerebral phaeohyphomycosis caused by Fonsecaea monophora, a neurotropic dematiaceous fungus, and a review of the literature, *Mycoses* 58:187–192, 2015, https://doi.org/10.1111/myc.12290.

Duggal P, Wise SK: Chapter 8: invasive fungal rhinosinusitis, *Am J Rhinol Allergy* 27:S28–30, 2013.

Dukik K, de Hoog GS, Stielow JB, Freeke J, van den Ende BG, Vicente VA, Menken SBJ, Ahmed SA: Molecular and phenotypic characterization of Nannizzia (Arthrodermataceae), *Mycopathologia*, 2019https://doi.org/10.1007/s11046-019-00336-9.

Dukik K, Munoz JF, Jiang Y, Feng P, Sigler L, Stielow JB, Freeke J, Jamalian A, et al.: Novel taxa of thermally dimorphic systemic pathogens in the Ajellomycetaceae (Onygenales), *Mycoses* 60:296–309, 2017, https://doi.org/10.1111/myc.12601.

Edman JC, Kovacs JA, Masur H, Santi DV, Elwood HJ, Sogin ML: Ribosomal RNA sequence shows *Pneumocystis carinii* to be a member of the fungi, *Nature* 334:519–522, 1988.

Eigl S, Hoenigl M, Spiess B, Heldt S, Prattes J, Neumeister P, Wolfler A, Rabensteiner J, Prueller F, et al.: Galactomannan testing and Aspergillus PCR in same-day bronchoalveolar lavage and blood samples for diagnosis of invasive aspergillosis, *Med Mycol* 55:528–534, 2017, https://doi.org/10.1093/mmy/myw102.

Einsele H, Loeffler J: Contribution of new diagnostic approaches to antifungal treatment plans in high-risk haematology patients, *Clin Microbiol Infect* 4(14 Suppl):37–45, 2008.

El Naderi S, Rodriguez C, Devars Du Mayne M, Badoual: C: [Invasive fungal rhinosinusitis in an apparently immunocompetant patient], *Ann Pathol* 33:410–413, 2013, https://doi.org/10.1016/j.annpat.2013.10.001.

Elavarashi E, Kindo AJ, Rangarajan S: Enzymatic and non-Enzymatic virulence activities of dermatophytes on solid media, *J Clin Diagn Res* 11:DC23–DC25, 2017, https://doi.org/10.7860/JCDR/2017/23147.9410.

Ells R, Kock JL, Pohl CH: Candida albicans or Candida dubliniensis? *Mycoses* 54:1–16, 2011, https://doi.org/10.1111/j.1439-0507.2009.01759.x.

Engelthaler DM, Roe CC, Hepp CM, Teixeira M, Driebe EM, Schupp JM, Gade L, et al.: Local population structure and patterns of western Hemisphere Dispersal for Coccidioides spp., the fungal cause of valley fever, *mBio* 7, 2016https://doi.org/10.1128/mBio.00550-16. e00550–00516.

Espinel-Ingroff A, Stockman L, Roberts G, Pincus D, Pollack J, Marler J: Comparison of RapID yeast plus system with API 20C system for identification of common, new, and emerging yeast pathogens, *J Clin Microbiol* 36:883–886, 1998.

EUCAST: European Committee on antifungal susceptibility testing: antifungal agents breakpoints TAbles for interpretation of MICs, *European Union Committee on Antimicrobial Susceptibility Testing*, 2018.

Eyzaguirre E, Haque AK: Application of immunohistochemistry to infections, *Arch Pathol Lab Med* 132:424–431, 2008.

Fandino-Devia E, Rodriguez-Echeverri C, Cardona-Arias J, Gonzalez A: Antigen detection in the diagnosis of histoplasmosis: a meta-analysis of diagnostic performance, *Mycopathologia* 181:197–205, 2016, https://doi.org/10.1007/s11046-015-9965-3.

Farina C, Perin S, Andreoni S, Conte M, Fazii P, Lombardi G, Manso E, et al.: Evaluation of the peptide nucleic acid fluorescence in situ hybridisation technology for yeast identification directly from positive blood cultures: an Italian experience, *Mycoses* 55:388–392, 2012, https://doi.org/10.1111/j.1439-0507.2011.02166.x.

Fenn JP, Segal H, Barland B, Denton D, Whisenant J, Chun H, Christofferson K, Hamilton L, Carroll K: Comparison of updated Vitek yeast biochemical card and API 20C yeast identification systems, *J Clin Microbiol* 32:1184–1187, 1994.

Firacative C, Trilles L, Meyer W: MALDI-TOF MS enables the rapid identification of the major molecular types within the Cryptococcus neoformans/C. gattii species complex, *PloS One* 7:e37566, 2012, https://doi.org/10.1371/journal.pone.0037566.

Fisher JF, Sobel JD, Kauffman CA, Newman CA: Candida urinary tract infections–treatment, *Clin Infect Dis* 52(Suppl 6):S457–466, 2011, https://doi.org/10.1093/cid/cir112.

Fishman JA, Gans H, Practice, A.S.T.I.D.C.o: Pneumocystis jiroveci in solid organ transplantation: guidelines from the American society of transplantation infectious diseases community of practice, *Clin Transplant*e13587, 2019, https://doi.org/10.1111/ctr.13587.

Forrest GN: Pna FISH: present and future impact on patient management, *Expert Rev Mol Diagn* 7:231–236, 2007.

Galgiani JN, Ampel NM, Blair JE, Catanzaro A, Geertsma F, Hoover SE, Johnson RH, Kusne S, Lisse J, et al.: 2016 infectious diseases society of America (IDSA) clinical practice guideline for the treatment of coccidioidomycosis, *Clin Infect Dis* 63:e112–146, 2016, https://doi.org/10.1093/cid/ciw360.

Garcia LS: Laboratory identification of the microsporidia, *J Clin Microbiol* 40:1892–1901, 2002, https://doi.org/10.1128/jcm.40.6.1892–1901.

Garcia-Agudao L, Garcia-Martos P, Martos-Canadas J, Aznar-Marin P, Marin-Casanova P, Rodriguez-Iglesias M: Evaluation of the Sensititre Yeast One microdilution method for susceptibility testing of *Candida* species to anidulafungin, caspofungin, and micafungin, *Rev Esp Quimioter* 25:256–260, 2012.

Garnica M, Nucci M, Queiroz-Telles F: Difficult mycoses of the skin: advances in the epidemiology and management of eumycetoma, phaeohyphomycosis and chromoblastomycosis, *Curr Opin Infect Dis* 22:559–563, 2009.

Gautier M, Normand AC, Ranque S: Previously unknown species of Aspergillus, *Clin Microbiol Infect* 22:662–669, 2016, https://doi.org/10.1016/j.cmi.2016.05.013.

Gayibova U, Dalyan Cilo B, Agca H, Ener B: [Comparison of Phoenix Yeast ID Panel and API(R) ID 32C commercial systems for the identification of Candida species isolated from clinical samples], *Mikrobiyol Bul* 48:438–448, 2014.

Gazzoni AF, Severo CB, Barra MB, Severo LC: atypical micromorphology and uncommon location of cryptococcosis: a histopathologic study using special histochemical techniques (one case report), *Mycopathologia* 167:197–202, 2009.

Georgi A, Schneemann M, Tintelnot K, Calligaris-Maibach RC, Meyer S, Weber R, Bosshard PP: *Cryptococcus gattii* meningoencephalitis in an immunocompetent person 13 months after exposure, *Infection* 37:370–373, 2009.

Gilgado F, Cano J, Gene J, Serena C, Guarro J: different virulence of the species of the *Pseudallescheria boydii* complex, *Med Mycol* 47:371–374, 2009.

Gilgado F, Cano J, Gene J, Sutton DA, Guarro J: Molecular and phenotypic data supporting distinct species statuses for *Scedosporium apiospermum* and *Pseudallescheria boydii* and the proposed new species Scedosporium dehoogii, *J Clin Microbiol* 46:766–771, 2008.

Gomez BL: Molecular diagnosis of endemic and invasive mycoses: advances and challenges, *Rev Iberroam Micol* 31:35–41, 2014.

Goodwin Jr RA, Owens FT, Snell JD, Hubbard WW, Buchanan RD, Terry RT, Des Prez RM: : chronic pulmonary histoplasmosis, *Medicine (Baltim)* 55:413–452, 1976, https://doi.org/10.1097/00005792-197611000-00001.

Graser Y, Czaika V, Ohst T: Diagnostic PCR of dermatophytes: an overview, *J Dtsch Dermatol Ges* 10:721–726, 2012.

Gremiao ID, Miranda LH, Reis EG, Rodrigues AM, Pereira SA: Zoonotic epidemic of sporotrichosis: cat to human transmission, *PLoS Pathog* 13:e1006077, 2017, https://doi.org/10.1371/journal.ppat.1006077.

Griffin AT, Hanson KE: Update on fungal diagnostics, *Curr Infect Dis Rep* 16, 2014.

Grosjean P, Weber R: Fungus balls of the paranasal sinuses: a review, *Eur Arch Oto-Rhino-Laryngol* 264:461–470, 2007.

Guarner J, Brandt ME: Histopathologic diagnosis of fungal infections in the 21st century, *Clin Microbiol Rev* 24:247–280, 2011, https://doi.org/10.1128/CMR.00053-10.

Guarro J: Fusariosis, a complex infection caused by a high diversity of fungal species refractory to treatment, *Eur J Clin Microbiol Infect Dis* 32:1491–1500, 2013.

Guegan H, Robert-Gangneux F: Molecular diagnosis of Pneumocystis pneumonia in immunocompromised patients, *Curr Opin Infect Dis* 32:314–321, 2019, https://doi.org/10.1097/QCO.0000000000000559.

Gupta AK, Mays RR, Versteeg SG, Piraccini BM, Shear NH, Piguet V, Tosti A, Friedlander SF: Tinea capitis in children: a systematic review of management, *J Eur Acad Dermatol Venereol* 32:2264–2274, 2018, https://doi.org/10.1111/jdv.15088.

Hage CA, Carmona EM, Epelbaum O, Evans SE, Gabe LM, Haydour Q, et al.: Microbiological laboratory testing in the diagnosis of fungal infections in pulmonary and critical care practice. An Official American Thoracic society clinical practice guideline, *Am J Respir Crit Care Med* 200:535–550, 2019, https://doi.org/10.1164/rccm.201906-1185ST.

Hage CA, Davis TE, Egan L, Parker M, Fuller D, Lemonte AM, Durkin M, Connelly P, Joseph Wheat L, Blue-Hnidy D, Knox KS: Diagnosis of pulmonary histoplasmosis and blastomycosis by detection of antigen in bronchoalveolar lavage fluid using an improved second-generation enzyme-linked immunoassay, *Respir Med* 101:43–47, 2007.

Hage CA, Davis TE, Fuller D, Egan L, Witt 3rd JR, Wheat LJ, Knox KS: Diagnosis of histoplasmosis by antigen detection in BAL fluid, *Chest* 137:623–628, 2010, https://doi.org/10.1378/chest.09-1702.

Hage CA, Kirsch EJ, Stump TE, Kauffman CA, Goldman M, Connolly P, Johnson PC, Wheat LJ, Baddley JW: Histoplasma antigen clearance during treatment of histoplasmosis in patients with AIDS determined by a quantitative antigen enzyme immunoassay, *Clin Vaccine Immunol* 18:661–666, 2011, https://doi.org/10.1128/CVI.00389-10.

Hageage GJ, Harrington B: Use of calcofluor white in clincial mycology, *Lab Med* 15:109, 1984.

Haiduven D: Nosocomial aspergillosis and building construction, *Med Mycol* 47(Suppl 1):S210–216, 2009, https://doi.org/10.1080/13693780802247694.

Hall L, Le Febre KM, Deml SM, Wohlfiel SL, Wengenack NL: Evaluation of the Yeast Traffic Light PNA FISH probes for identification of Candida species from positive blood cultures, *J Clin Microbiol* 50:1446–1448, 2012, https://doi.org/10.1128/JCM.06148-11.

Hammoud ZT, Rose AS, Hage CA, Knox KS, Rieger K, Kesler KA: Surgical management of pulmonary and mediastinal sequelae of histoplasmosis: a challenging spectrum, *Ann Thorac Surg* 88:399–403, 2009.

Han B, Weiss LM: Microsporidia: obligate intracellular pathogens within the fungal kingdom, *Microbiol Spectr* 5, 2017. 10.1128/microbiolspec.FUNK-0018-2016.

Harris JR, Lockhart SR, Sondermeyer G, Vugia DJ, Crist MB, D'Angelo MT, Sellers B, et al.: Cryptococcus gattii infections in multiple states outside the US Pacific Northwest, *Emerg Infect Dis* 19:1620–1626, 2013, https://doi.org/10.3201/eid1910.130441.

Hartnett KP, Jackson BR, Perkins KM, Glowicz J, Kerins JL, Black SR, Lockhart SR, Christensen BE, Beer KD: A guide to investigating suspected outbreaks of mucormycosis in healthcare, *J Fungi (Basel)* 5, 2019, https://doi.org/10.3390/jof5030069.

Hata DJ, Hall L, Fothergill AW, Larone DH, Wengenack NL: Multicenter evaluation of the new VITEK 2 advanced colorimetric yeast identification card, *J Clin Microbiol* 45:1087–1092, 2007.

Havilickova B, Czaika VA, Friedrich M: Epidemiological trends in skin mycoses worldwide, *Mycoses* 51:2–15, 2008.

Hawkins JL, Baddour LM: Candida lusitaniae infections in the era of fluconazole availability, *Clin Infect Dis* 36:e14–18, 2003, https://doi.org/10.1086/344651.

Hawksworth DL: A new dawn for the naming of fungi: impacts of decisions made in Melbourne in July 2011 on the future publication and regulation of fungal names, *IMA Fungus* 2:155–162, 2011.

Heller DS, Pitsos M, Skurnick J: Does the presence of vaginitis on a Pap smear correlate with clinical symptoms in the patient? *J Reprod Med* 53:429–434, 2008.

Heng SC, Chen SC, Morrissey CO, Thursky K, Manser RL, De Silva HD, Halliday CL, Seymour JF, et al.: Clinical utility of *Aspergillus* galactomannan and PCR in bronchalveolar lavage fluid for the diagnosis of invasive pulmonary aspergillosis in patients with haematological malignancies, *Diagn Microbiol Infect Dis* 79:322–327, 2014.

Hibbett DS, Binder M, Bischoff JF, Blackwell M, Cannon PF, Eriksson OE, Huhndorf S, James T, Kirk PM, et al.: A higher-level phylogenetic classification of the Fungi, *Mycol Res* 111:509–547, 2007.

Hibbett DS, Taylor JW: Fungal systematics: is a new age of enlightenment at hand? *Nature Rev* 11:129–133, 2013.

Hillesheim PB, Bahrami S: Cutaneous protothecosis, *Arch Pathol Lab Med* 135:941–944, 2011.

Ho T, Vrabec JT, Yoo D, Coker NJ: Otomycosis: clinical features and treatment implications, *Otolaryngol Head Neck Surg* 135:787–791, 2006, https://doi.org/10.1016/j.otohns.2006.07.008.

Hong SB, Shin HD, Hong J, Frisvad JC, Nielsen PV, Varga J, Samson RA: New taxa of Neosartorya and Aspergillus in Aspergillus section Fumigati, *Antonie Leeuwenhoek* 93:87–98, 2008, https://doi.org/10.1007/s10482-007-9183-1.

Horn DL, Neofytos D, Anaissie EJ, Fishman JA, Steinbach WJ, Olyaei AJ, Marr KA, Pfaller MA, Chang CH, Webster KM: Epidemiology and outcomes of candidemia in 2019 patients: data from the prospective antifungal therapy alliance registry, *Clin Infect Dis* 48:1695–1703, 2009.

Hughes WT: *Pneumocystis carinii* vs. Pneumocystis jiroveci: another misnomer (response to Stringer et al.) *Emerg Infect Dis* 9:276–277, 2003.

Hung CY, Hsu AP, Holland SM, Fierer J: A review of innate and adaptive immunity to coccidioidomycosis, *Med Mycol* 57:S85–S92, 2019, https://doi.org/10.1093/mmy/myy146.

Hussein MR: Mucocutaneous Splendore-Hoeppli phenomenon, *J Cutan Pathol* 35:979–988, 2008.

Intra J, Sarto C, Tiberti N, Besana S, Savarino C, Brambilla P: Genus-level identification of dermatophytes by MALDI-TOF MS after 2 days of colony growth, *Lett Appl Microbiol* 67:136–143, 2018, https://doi.org/10.1111/lam.12997.

Irinyi L, Serena C, Garcia-Hermoso D, Arabatzis M, Desnos-Ollivier M, Vu D, Cardinali G, Arthur I, Normand AC, Giraldo A, da Cunha KC, et al.: International Society of Human and Animal Mycology (ISHAM)-ITS reference DNA barcoding database–the quality controlled standard tool for routine identification of human and animal pathogenic fungi, *Med Mycol* 53:313–337, 2015, https://doi.org/10.1093/mmy/myv008.

Iwen PC, Hinrichs SH, Rupp ME: Utilization of the internal transcribed spacer regions as molecular targets to detect and identify human fungal pathogens, *Med Mycol* 40:87–109, 2002.

Iwen PC, Sigler L, Noel RK, Freifeld AG: Mucor circinelloides was identified by molecular methods as a cause of primary cutaneous zygomycosis, *J Clin Microbiol* 45:636–640, 2007.

Iwen PC, Thapa I, Bastola D: Review methods for the identification of zygomycetes with an emphasis on advances in molecuar diagnostics, *Lab Med* 42:260–266, 2011.

Jain R, Singh K, Lamzabi I, Harbhajanka A, Gattuso P, Reddy VB: Blastomycosis of bone: a clinicopathologic study, *Am J Clin Pathol* 142:609–616, 2014, https://doi.org/10.1309/AJCPG2CFGHZ4URLN.

Jayatilake JA, Tilakaratne WM, Panagoda GJ: Candidal onychomycosis: a mini-review, *Mycopathologia* 168:165–173, 2009.

Jeffery-Smith A, Taori SK, Schelenz S, Jeffery K, Johnson EM, Borman A, Candida auris Incident Management, T, Manuel R, Brown CS: Candida auris: a review of the literature, *Clin Microbiol Rev* 31, 2018, https://doi.org/10.1128/CMR.00029-17.

Jeong W, Keighley C, Wolfe R, Lee WL, Slavin MA, Kong DCM, Chen SC: The epidemiology and clinical manifestations of mucormycosis: a systematic review and meta-analysis of case reports, *Clin Microbiol Infect* 25:26–34, 2019, https://doi.org/10.1016/j.cmi.2018.07.011.

Johansson A, Nagy E, Soki J: Instant screening and verification of carbapenemase activity in Bacteroides fragilis in positive blood culture, using matrix-assisted laser desorption ionization–time of flight mass spectrometry, *J Med Microbiol* 63:1105–1110, 2014, https://doi.org/10.1099/jmm.0.075465-0.

Johnson EM: Issues in antifungal susceptibility testing, *J Antimicrob Chemother* 61(Suppl 1):i13–18, 2008.

Kabanda T, Siedner MJ, Klausner JD, Muzoora C, Boulware DR: Point-of-care diagnosis and prognostication of cryptococcal meningitis with the cryptococcal antigen lateral flow assay on cerebrospinal fluid, *Clin Infect Dis* 58:113–116, 2014, https://doi.org/10.1093/cid/cit641.

Kainer MA, Reagan DR, Ngyuen DB, Wiese AD, Wise ME, Ward J, Park BJ: Kanago, M.L: fungal infections associated with contaminated methylprednisolone in Tennessee, *N Engl J Med* 367:2194–2203, 2012.

Kantarcioglu AS, Guarro J, De Hoog S, Apaydin H, Kiraz N: An updated comprehensive systematic review of Cladophialophora bantiana and analysis of epidemiology, clinical characteristics, and outcome of cerebral cases, *Med Mycol* 55:579–604, 2017, https://doi.org/10.1093/mmy/myw124.

Karageorgopoulos DE, Qu JM, Korbila IP, Zhu YG, Vasileiou VA, Falagas, M.E: Accuracy of beta-D-glucan for the diagnosis of Pneumocystis jirovecii pneumonia: a meta-analysis, *Clin Microbiol Infect* 19:39–49, 2013, https://doi.org/10.1111/j.1469--0691.2011.03760.x.

Kathuria S, Singh PK, Sharma C, Prakash A, Masih A, Kumar A, Meis JF, Chowdhary A: Multidrug-resistant Candida auris misidentified as Candida haemulonii: characterization by matrix-assisted laser desorption ionization-time of flight mass spectrometry and DNA sequencing and its antifungal susceptibility profile variability by vitek 2, CLSI broth microdilution, and etest method, *J Clin Microbiol* 53:1823–1830, 2015, https://doi.org/10.1128/JCM.00367-15.

Katragkou A, Dotis J, Kotsiou M, Tamiolaki M, Roilides E: Scedosporium apiospermum infection after near-drowning, *Mycoses* 50:412–421, 2007, https://doi.org/10.1111/j.1439-0507.2007.01388.x.

Kauffman CA, Bustamante B, Chapman SW, Pappas PG: Infectious diseases society of, A: clinical practice guidelines for the management of sporotrichosis: 2007 update by the infectious diseases society of America, *Clin Infect Dis* 45:1255–1265, 2007, https://doi.org/10.1086/522765.

Kenyon C, Bonorchis K, Corcoran C, Meintjes G, Locketz M, Lehloenya R, Vismer HF, Naicker P, et al.: A dimorphic fungus causing disseminated infection in South Africa, *N Engl J Med* 369:1416–1424, 2013, https://doi.org/10.1056/NEJMoa1215460.

Kirkland TN: The quest for a vaccine against coccidioidomycosis: a neglected disease of the Americas, *J Fungi (Basel)* 2, 2016, https://doi.org/10.3390/jof2040034.

Klein KR, Hall L, Deml SM, Rysavy JM, Wohlfiel SL, Wengenack NL: Identification of *Cryptococcus gattii* by use of L-canavanine glycine bromothymol blue medium and DNA sequencing, *J Clin Microbiol* 47:3669–3672, 2009.

Koepsell SA, Hinrichs SH, Iwen PC: Applying a real-time PCR assay for Histoplasma capsulatum to clinically relevant formalin-fixed paraffin-embedded human tissue, *J Clin Microbiol* 50:3395–3397, 2012, https://doi.org/10.1128/JCM.01705-12.

Kontoyiannis DP, Marr KA, Park BJ, Alexander BD, Anaissie EJ, Walsh TJ, Ito J, Andes DR, et al.: Prospective surveillance for invasive fungal infections in hematopoietic stem cell transplant recipients, 2001-2006: overview of the Transplant-Associated Infection Surveillance Network (TRANSNET) Database, *Clin Infect Dis* 50:1091–1100, 2010, https://doi.org/10.1086/651263.

Koo S, Bryar JM, Baden LR, Marty FM: Prognostic features of galactomannan antigenemia in galactomannan-positive invasive aspergillosis, *J Clin Microbiol* 48:1255–1260, 2010, https://doi.org/10.1128/JCM.02281-09.

Kosmidis C, Denning DW: The clinical spectrum of pulmonary aspergillosis, *Thorax* 70:270–277, 2015, https://doi.org/10.1136/thoraxjnl-2014-206291.

Kothavade RJ, Kura MM, Valand AG, Panthaki MH: Candida tropicalis: its prevalence, pathogenicity and increasing resistance to fluconazole, *J Med Microbiol* 59:873–880, 2010, https://doi.org/10.1099/jmm.0.013227-0.

Kozubowski L, Heitman J: Profiling a killer, the development of Cryptococcus neoformans, *FEMS Microbiol Rev* 36:78–94, 2012, https://doi.org/10.1111/j.1574--6976.2011.00286.x.

Krishnan S, Manavathu EK, Chandrasekar PH: *Aspergillus flavus*: an emerging non-*fumigatus Aspergillus* species of significance, *Mycoses* 52:206–222, 2009.

Krzysciak PM, Pindycka-Piaszczynska M, Piaszczynski M: Chromoblastomycosis, *Postepy Dermatol Alergo* 31:310–321, 2014.

Kwon-Chung KJ: Taxonomy of fungi causing mucormycosis and entomophthoramycosis (zygomycosis) and nomenclature of the disease: molecular mycologic perspectives, *Clin Infect Dis* 54:S8–15, 2012.

Kwon-Chung KJ, Bennett JE, Wickes BL, et al.: The case for Adopting the "species complex" nomenclature for the etiologic agents of cryptococcosis, *mSphere* 2, 2017, https://doi.org/10.1128/mSphere.00357-16.

L'Ollivier C, Ranque S: MALDI-TOF-Based dermatophyte identification, *Mycopathologia* 182:183–192, 2017, https://doi.org/10.1007/s11046-016-0080-x.

La Hoz RM, Morris MI, Practice, A.S.T.I.D.C.o: Intestinal parasites including Cryptosporidium, Cyclospora, Giardia, and microsporidia, Entamoeba histolytica, Strongyloides, Schistosomiasis, and Echinococcus: guidelines from the American society of transplantation infectious diseases community of practice, *Clin Transplant*e13618, 2019, https://doi.org/10.1111/ctr.13618.

Lackner M, Lass-Florl C: Up-date on diagnostic strategies of invasive aspergillosis, *Curr Pharm Des* 19:3595–3614, 2013, https://doi.org/10.2174/1381612811319999323.

Lai CC, Tan CK, Huang YT, Shao PL, Hsueh PR: Current challenges in the management of invasive fungal infections, *J Infect Chemother* 14:77–85, 2008.

Lamoth F, Chung SJ, Damonti L, Alexander BD: Changing epidemiology of invasive mold infections in patients receiving azole prophylaxis, *Clin Infect Dis* 64:1619–1621, 2017, https://doi.org/10.1093/cid/cix130.

Lass-Florl C: In vitro susceptibility testing in *Aspergillus* species: an update, *Future Microbiol* 5:789–799, 2010.

Lau A, Chen S, Sleiman S, Sorrell T: Current status and future perspectives on molecular and serological methods in diagnostic mycology, *Future Microbiol* 4:1185–1222, 2009.

Leber AL, Everhart K, Balada-Llasat JM, Cullison J, Daly J, Holt S, Lephart P, Salimnia H, Schreckenberger PC, et al.: Multicenter evaluation of BioFire FilmArray meningitis/encephalitis panel for detection of bacteria, Viruses, and yeast in cerebrospinal fluid specimens, *J Clin Microbiol* 54:2251–2261, 2016, https://doi.org/10.1128/JCM.00730-16.

Lee CY, Thompson Iii GR, Hastey CJ, Hodge GC, Lunetta JM, Pappagianis D, Heinrich V: Coccidioides endospores and spherules Draw strong Chemotactic, Adhesive, and phagocytic responses by individual human neutrophils, *PloS One* 10:e0129522, 2015, https://doi.org/10.1371/journal.pone.0129522.

Limper AH, Adenis A, Le T, Harrison TS: Fungal infections in HIV/AIDS, *Lancet Infect Dis* 17:e334–e343, 2017, https://doi.org/10.1016/S1473-3099(17)30303-1.

Lionakis MS, Bodey GP, Tarrand JJ, Raad II, Kontoyiannis DP: The significance of blood cultures positive for emerging saprophytic moulds in cancer patients, *Clin Microbiol Infect* 10:922–925, 2004, https://doi.org/10.1111/j.1469-0691.2004.00933.x.

Lionakis MS, Netea MG: Candida and host determinants of susceptibility to invasive candidiasis, *PLoS Pathog* 9:e1003079, 2013, https://doi.org/10.1371/journal.ppat.1003079.

Loreto ES, Scheid LA, Nogueira CW, Zeni G, Santurio JM, Alves SH: Candida dubliniensis: epidemiology and phenotypic methods for identification, *Mycopathologia* 169:431–443, 2010, https://doi.org/10.1007/s11046-010-9286-5.

Loulergue P, Bastides F, Baudouin V, Chandenier J, Mariani-Kurkdjian P, Dupont B, Viard JP, Dromer F, Lortholary O: Literature review and case histories of *Histoplasma capsulatum* var. *duboisii* infections in HIV-infected patients, *Emerg Infect Dis* 13:1647–1652, 2007.

Macesic N, Fleming S, Kidd S, Madigan V, Chean R, Ritchie D, Slavin M: Protothecosis in hematopoietic stem cell transplantation: case report and review of previous cases, *Transpl Infect Dis* 16:490–495, 2014, https://doi.org/10.1111/tid.12223.

Malo J, Luraschi-Monjagatta C, Wolk DM, Thompson R, Hage CA, Knox KS: Update on the diagnosis of pulmonary coccidioidomycosis, *Ann Am Thorac Soc* 11:243–253, 2014, https://doi.org/10.1513/AnnalsATS.201308-286FR.

Mancini N, De Carolis E, Infurnari L, Vella A, Clementi N, Vaccaro L, Ruggeri A, Posteraro B, Burioni R, Clementi M, Sanguinetti M: Comparative evaluation of the Bruker Biotyper and Vitek MS matrix-assisted laser desorption ionization-time of flight (MALDI-TOF) mass spectrometry systems for identification of yeasts of medical importance, *J Clin Microbiol* 51:2453–2457, 2013, https://doi.org/10.1128/JCM.00841-13.

Maphanga TG, Britz E, Zulu TG, Mpembe RS, Naicker SD, Schwartz IS, Govender NP: In vitro antifungal susceptibility of yeast and mold phases of isolates of dimorphic fungal pathogen Emergomyces africanus (formerly Emmonsia sp.) from HIV-infected South African patients, *J Clin Microbiol* 55:1812–1820, 2017, https://doi.org/10.1128/JCM.02524-16.

Marcos LA, Gotuzzo E: Intestinal protozoan infections in the immunocompromised host, *Curr Opin Infect Dis* 26:295–301, 2013, https://doi.org/10.1097/QCO.0b013e3283630be3.

Marimon R, Gene J, Cano J, Trilles L, Dos Santos Lazera M, Guarro J: Molecular phylogeny of, *Sporothrix schenckii*, *J Clin Microbiol* 44:3251–3256, 2006.

Marinach C, Alanio A, Palous M, Kwasek S, Fekkar A, Brossas JY, Brun S, Snounou G, Hennequin C, Sanglard D, Datry A, Golmard JL, Mazier D: MALDI-TOF MS-based drug susceptibility testing of pathogens: the example of Candida albicans and fluconazole, *Proteomics* 9:4627–4631, 2009, https://doi.org/10.1002/pmic.200900152.

Marklein G, Josten M, Klanke U, Muller E, Horre R, Maier T, Wenzel T, Kostrzewa M, Bierbaum G, Hoerauf A, Sahl HG: Matrix-assisted laser desorption ionization-time of flight mass spectrometry for fast and reliable identification of clinical yeast isolates, *J Clin Microbiol* 47:2912–2917, 2009a, https://doi.org/10.1128/JCM.00389-09.

Marklein G, Josten M, Klanke U, Muller E, Horre R, Maier T, Wenzel T, Kostrzewa M, Bierbaum G, Hoerauf A, Sahl HG: Matrix-assisted laser desorption ionization-time of flight mass spectrometry for fast and reliable identification of clinical yeast isolates, *J Clin Microbiol* 47:2912–2917, 2009b, https://doi.org/10.1128/Jcm.00389-09.

Marques SA: Paracoccidioidomycosis, *Clin Dermatol* 30:610–615, 2012, https://doi.org/10.1016/j.clindermatol.2012.01.006.

Marty FM, Koo S: Role of (1—>3)-beta-D-glucan in the diagnosis of invasive aspergillosis, *Med Mycol* 47(Suppl 1):S233–240, 2009.

Mason AR, Cortes GY, Cook J, Maize JC, Thiers BH: Cutaneous blastomycosis: a diagnostic challenge, *Int J Dermatol* 47:824–830, 2008.

McCarty JM, Flam MS, Pullen G, Jones R, Kassel SH: Outbreak of primary cutaneous aspergillosis related to intravenous arm boards, *J Pediatr* 108:721–724, 1986.

McGinnis MR, Smith MB: Hinson, E: use of the Coccidioides posadasii Deltachs5 strain for quality control in the ACCUPROBE culture identification test for Coccidioides immitis, *J Clin Microbiol* 44:4250–4251, 2006, https://doi.org/10.1128/JCM.01265-06.

McHardy IH, Dinh BN, Waldman S, Stewart E, Bays D, Pappagianis D, Thompson 3rd GR: Coccidioidomycosis complement fixation titer trends in the age of antifungals, *J Clin Microbiol* 56, 2018https://doi.org/10.1128/JCM.01318-18.

McMullan BJ, Halliday C, Sorrell TC, Judd D, Sleiman S, Marriott D, Olma T, Chen SC: Clinical utility of the cryptococcal antigen lateral flow assay in a diagnostic mycology laboratory, *PloS One* 7:e49541, 2012, https://doi.org/10.1371/journal.pone.0049541.

McTaggart LR, Lei E, Richardson SE, Hoang L, Fothergill A, Zhang SX: Rapid identification of Cryptococcus neoformans and Cryptococcus gattii by matrix-assisted laser desorption ionization-time of flight mass spectrometry, *J Clin Microbiol* 49:3050–3053, 2011, https://doi.org/10.1128/JCM.00651-11.

Merkhofer Jr RM, O'Neill MB, Xiong D, et al.: Investigation of genetic susceptibility to blastomycosis reveals interleukin-6 as a potential susceptibility locus, *MBio* 10, 2019, https://doi.org/10.1128/mBio.01224-19.

Messer SA, Diekema DJ, Hollis RJ, Boyken LB, Tendolkar S, Kroeger J, Pfaller MA: Evaluation of disk diffusion and Etest compared to broth microdilution for antifungal susceptibility testing of posaconazole against clinical isolates of filamentous fungi, *J Clin Microbiol* 45:1322–1324, 2007.

Miceli MH, Lee SA: Emerging moulds: epidemiological trends and antifungal resistance, *Mycoses* 54:e666–678, 2011.

Mikulska M, Furfaro E, Del Bono V, Raiola AM, Ratto S, Bacigalupo A, Viscoli C: Piperacillin/tazobactam (Tazocin) seems to be no longer responsible for false-positive results of the galactomannan assay, *J Antimicrob Chemother* 67:1746–1748, 2012.

Mizusawa M, Miller H, Green R, Lee R, Durante M, Perkins R, Hewitt C, Simner PJ, Carroll KC, Hayden RT, Zhang SX: Can Multidrug-resistant Candida auris Be reliably identified in clinical microbiology laboratories? *J Clin Microbiol* 55:638–640, 2017, https://doi.org/10.1128/JCM.02202-16.

Morris A, Norris KA: Colonization by Pneumocystis jirovecii and its role in disease, *Clin Microbiol Rev* 25:297–317, 2012, https://doi.org/10.1128/CMR.00013-12.

Morrissey CO, Chen SC, Sorrell TC, Milliken S, Bardy PG, Bradstock KF: Galactomannan and PCR versus culture and histology for directing use of antifungal treatment for invasive aspergillosis in high-risk hematologiy patients: a randomised controlled trial, *Lancet Infect Dis* 13:519–528, 2013.

Muhammed M, Anagnostou T, Desalermos A, Kourkoumpetis TK, Carneiro HA, Glavis-Bloom J, Coleman JJ, Mylonakis E: Fusarium infection: report of 26 cases and review of 97 cases from the literature, *Medicine (Baltim)* 92:305–316, 2013, https://doi.org/10.1097/MD.0000000000000008.

Munguia R, Daniel SJ: Ototopical antifungals and otomycosis: a review, *Int J Pediatr Otorhinolaryngol* 72:453–459, 2008, https://doi.org/10.1016/j.ijporl.2007.12.005.

Munoz JF, Farrer RA, Desjardins CA, Gallo JE, Sykes S, Sakthikumar S, Misas E, Whiston, et al.: Genome diversity, Recombination, and virulence across the major lineages of Paracoccidioides, *mSphere* 1, 2016, https://doi.org/10.1128/mSphere.00213-16.

Mylonakis E, Clancy CJ, Ostrosky-Zeichner L, Garey KW, Alangaden GJ, Vazquez JA, Groeger JS, et al.: T2 magnetic resonance assay for the rapid diagnosis of candidemia in whole blood: a clinical trial, *Clin Infect Dis* 60:892–899, 2015, https://doi.org/10.1093/cid/ciu959.

Naggie S, Perfect JR: Molds: hyalohyphomycosis, phaeohyphomycosis, and zygomycosis, *Clin Chest Med* 30:337–353, 2009, vii–viii.

National Institute for Occupational Safety and Health: Preventing occupational respiratory disease from exposures caused by dampness in office buildings, schools, and other nonindustrial buildings, *Department of Health and Human Services Publication Number 2013–102*, 2012.

Neblett Fanfair R, Benedict K, Bos J, Bennett SD, Lo YC, Adebanjo T, Etienne K, et al.: Necrotizing cutaneous mucormycosis after a tornado in Joplin, Missouri, in 2011, *N Engl J Med* 367:2214–2225, 2012, https://doi.org/10.1056/NEJMoa1204781.

Neely LA, Audeh M, Phung NA, Min M, Suchocki A, Plourde D, Blanco M, et al.: T2 magnetic resonance enables nanoparticle-mediated rapid detection of candidemia in whole blood, *Sci Transl Med* 5, 182ra154. 2013, https://doi.org/10.1126/scitranslmed.3005377.

Negroni R: Cryptococcosis, *Clin Dermatol* 30:599–609, 2012.

Neofytos D, Horn D, Anaissie E, Steinbach W, Olyaei A, Fishman J, Pfaller M, Chang C, et al.: Epidemiology and outcome of invasive fungal infection in adult hematopoietic stem cell transplant recipients: analysis of Multicenter Prospective Antifungal Therapy (PATH) Alliance registry, *Clin Infect Dis* 48:265–273, 2009.

Neppelenbroek KH, Seo RS, Urban VM, Silva S, Dovigo LN, Jorge JH, Campanha NH: Identification of Candida species in the clinical laboratory: a review of conventional, commercial, and molecular techniques, *Oral Dis* 20:329–344, 2014, https://doi.org/10.1111/odi.12123.

Nucci M, Anaissie E: Fusarium infections in immunocompromised patients, *Clin Microbiol Rev* 20:695–704, 2007, https://doi.org/10.1128/CMR.00014-07.

O'Donnell K, Gueidan C, Sink S, Johnston PR, Crous PW, Glenn A, Riley R, et al.: A two-locus DNA sequence database for typing plant and human pathogens within the *Fusarium oxysporum* species complex, *Fungal Genet Biol* 46:936–948, 2009a.

O'Donnell K, Sutton DA, Rinaldi MG, Gueidan C, Crous PW, Geiser DM: Novel multilocus sequence typing scheme reveals high genetic diversity of human pathogenic members of the *Fusarium incarnatum-F. equiseti* and *F. chlamydosporum* species complexes within the United States, *J Clin Microbiol* 47:3851–3861, 2009b.

Oliveira MM, Almeida-Paes R, Gutierrez-Galhardo MC, Zancope-Oliveira RM: molecular identification of the Sporothrix schenckii complex, *Rev Iberoam De Micol* 31:2–6, 2014, https://doi.org/10.1016/j.riam.2013.09.008.

Onishi A, Sugiyama D, Kogata Y, Saegusa J, Sugimoto T, Kawano S, Morinobu A, Nishimura K, Kumagai S: Diagnostic accuracy of serum 1,3-beta-D-glucan for *Pneumocystis jirovecii* pneumonia, invasive candidiasis, and invasive aspergillosis: systematic review and meta-analysis, *J Clin Microbiol* 50:7–15, 2012.

Oviano M, Fernandez B, Fernandez A, Barba MJ, Mourino C, Bou G: Rapid detection of enterobacteriaceae producing extended spectrum beta-lactamases directly from positive blood cultures by matrix-assisted laser desorption ionization-time of flight mass spectrometry, *Clin Microbiol Infect* 20:1146–1157, 2014, https://doi.org/10.1111/1469-0691.12729.

Ozcan K, Ilkit M, Ates A, Turac-Bicer A, Demirhindi H: Performance of Chromogenic *Candida* Agar and CHROMagar *Candida* in recovery and presumptive identification of monofungal and polyfungal vaginal isolates, *Med Mycol*1–6, 2009.

Pagella F, Matti E, De Bernardi F, Semino L, Cavanna C, Marone P, Farina C, Castelnuovo P: Paranasal sinus fungus ball: diagnosis and management, *Mycoses* 50:451–456, 2007.

Pammi M, Holland L, Butler G, Gacser A, Bliss JM: Candida parapsilosis is a significant neonatal pathogen: a systematic review and meta-analysis, *Pediatr Infect Dis J* 32:e206–216, 2013, https://doi.org/10.1097/INF.0b013e3182863a1c.

Pappas PG, Alexander BD, Andes DR, Hadley S, Kauffman CA, Freifeld A, Anaissie EJ, Brumble LM, et al.: Invasive fungal infections among organ transplant recipients: results of the Transplant-Associated Infection Surveillance Network (TRANSNET), *Clin Infect Dis* 50:1101–1111, 2010, https://doi.org/10.1086/651262.

Pappas PG, Kauffman CA, Andes DR, Clancy CJ, Marr KA, Ostrosky-Zeichner L, Reboli AC, Schuster MG, Vazquez JA, et al.: Clinical practice guideline for the management of candidiasis: 2016 update by the infectious diseases society of America, *Clin Infect Dis* 62:e1–50, 2016, https://doi.org/10.1093/cid/civ933.

Pasqualotto AC: Differences in pathogenicity and clinical syndromes due to *Aspergillus fumigatus* and *Aspergillus flavus*, *Med Mycol* 47(Suppl 1):S261–270, 2009.

Patel AJ, Gattuso P, Reddy VB: Diagnosis of blastomycosis in surgical pathology and cytopathology: correlation with microbiologic culture, *Am J Surg Pathol* 34:256–261, 2010, https://doi.org/10.1097/PAS.0b013e3181ca48a5.

Patel PK, Erlandsen JE, Kirkpatrick WR, Berg DK, Westbrook SD, Louden C, Cornell JE, et al.: The changing epidemiology of oropharyngeal candidiasis in patients with HIV/AIDS in the era of antiretroviral therapy, *AIDS Res Treat* 262471, 2012, https://doi.org/10.1155/2012/262471.

Patel R: A Moldy application of MALDI: MALDI-ToF mass spectrometry for fungal identification, *J Fungi (Basel)* 5, 2019, https://doi.org/10.3390/jof5010004.

Patterson TF, Kirkpatrick WR, White M, Hiemenz JW, Wingard JR, Dupont B, Rinaldi MG, Stevens DA, Graybill JR: Invasive aspergillosis. Disease spectrum, treatment practices, and outcomes. I3 Aspergillus Study Group, *Medicine (Baltim)* 79:250–260, 2000, https://doi.org/10.1097/00005792-200007000-00006.

Patterson TF, Thompson 3rd GR, Denning DW, Fishman JA, Hadley S, Herbrecht R, Kontoyiannis DP, Marr KA, Morrison, et al.: Practice guidelines for the diagnosis and management of aspergillosis: 2016 update by the infectious diseases society of America, *Clin Infect Dis* 63:e1–e60, 2016, https://doi.org/10.1093/cid/ciw326.

Pedrosa AF, Lisboa C, Goncalves Rodrigues A: Malassezia infections: a medical conundrum, *J Am Acad Dermatol* 71:170–176, 2014, https://doi.org/10.1016/j.jaad.2013.12.022.

Pelletier R, Alarie I, Lagace R, Walsh TJ: Emergence of disseminated candidiasis caused by *Candida krusei* during treatment with caspofungin: case report and review of literature, *Med Mycol* 43:559–564, 2005.

Pence MA, McElvania TeKippe E, Wallace MA, Burnham CA: Comparison and optimization of two MALDI-TOF MS platforms for the identification of medically relevant yeast species, *Eur J Clin Microbiol Infect Dis* 33:1703–1712, 2014, https://doi.org/10.1007/s10096-014-2115-x.

Perea S, Lopez-Ribot JL, Wickes BL, Kirkpatrick WR, Dib OP, Bachmann SP, Keller SM, Martinez M, Patterson TF: Molecular mechanisms of fluconazole resistance in Candida dubliniensis isolates from human immunodeficiency virus-infected patients with oropharyngeal candidiasis, *Antimicrob Agents Chemother* 46:1695–1703, 2002, https://doi.org/10.1128/aac.46.6.1695-1703.2002.

Perfect JR, Dismukes WE, Dromer F, Goldman DL, Graybill JR, Hamill RJ, Harrison TS, et al.: Clinical practice guidelines for the management of cryptococcal disease: 2010 update by the infectious diseases society of America, *Clin Infect Dis* 50:291–322, 2010, https://doi.org/10.1086/649858.

Perrone G, Gallo A: Aspergillus species and their associated mycotoxins, *Methods Mol Biol* 1542:33–49, 2017, https://doi.org/10.1007/978-1-4939-6707-0_3.

Perry JD, Freydiere AM: The application of chromogenic media in clinical microbiology, *J Appl Microbiol* 103:2046–2055, 2007.

Peterson AR, Nash E, Anderson BJ: Infectious disease in contact sports, *Sports Health* 11:47–58, 2019, https://doi.org/10.1177/1941738118789954.

Peterson SW: Phylogenetic analysis of *Aspergillus* species using DNA sequences from four loci, *Mycologia* 100:205–226, 2008.

Petrikkos G, Skiada A, Lortholary O, Roilides E, Walsh TJ, Kontoyiannis DP: Epidemiology and clinical manifestations of mucormycosis, *Clin Infect Dis* 54:S23–34, 2012.

Pfaller M, Neofytos D, Diekema D, Azie N, Meier-Kriesche HU, Quan SP, Horn D: Epidemiology and outcomes of candidemia in 3648 patients: data from the Prospective Antifungal Therapy (PATH Alliance(R)) registry, 2004-2008, *Diagn Microbiol Infect Dis* 74:323–331, 2012a, https://doi.org/10.1016/j.diagmicrobio.2012.10.003.

Pfaller MA, Andes DR, Diekema DJ, Horn DL, Reboli AC, Rotstein C, Franks B, Azie NE: Epidemiology and outcomes of invasive candidiasis due to non-albicans species of Candida in 2,496 patients: data from the Prospective Antifungal Therapy (PATH) registry 2004-2008, *PloS One* 9:e101510, 2014, https://doi.org/10.1371/journal.pone.0101510.

Pfaller MA, Chaturvedi V, Diekema DJ, Ghannoum MA, Holliday NM, Killian SB, Knapp CC, Messer SA, et al.: Comparison of the Sensititre YeastOne colorimetric antifungal panel with CLSI microdilution for antifungal susceptibility testing of the echinocandins against Candida spp., using new clinical breakpoints and epidemiological cutoff values, *Diagn Microbiol Infect Dis* 73:365–368, 2012b, https://doi.org/10.1016/j.diagmicrobio.2012.05.008.

Pfaller MA, Chaturvedi V, Diekema KJ, Ghannoum MA, Holliday NM, Killian SB, Knapp CC, Messer SA, et al.: Comparison of the Sensititre YeastOne colorimetric antifungal panel with CLSI microdilution for antifungal susceptibility testing of the echinocandins against *Candida* spp, using new clinical breakpoints and epidemiological cutoff values, *Diagn Microbiol Infect Dis* 73, 2012c.

Pfaller MA, Diekema DJ: Epidemiology of invasive candidiasis: a persistent public health problem, *Clin Microbiol Rev* 20:133–163, 2007.

Pfaller MA, Diekema DJ, Boyken L, Messer SA, Tendolkar S, Hollis RJ: Evaluation of the Etest and disk diffusion methods for determining susceptibilities of 235 bloodstream isolates of *Candida glabrata* to fluconazole and voriconazole, *J Clin Microbiol* 41:1875–1880, 2003.

Pickering JW, Sant HW, Bowles CA, Roberts WL, Woods GL: Evaluation of a (1->3)-beta-D-glucan assay for diagnosis of invasive fungal infections, *J Clin Microbiol* 43:5957–5962, 2005.

Pincus DH, Orenga S, Chatellier S: Yeast identification–past, present, and future methods, *Med Mycol* 45:97–121, 2007.

Pinto A, Halliday C, Zahra M, van Hal S, Olma T, Maszewska K, Iredell JR, Meyer W, Chen SC: Matrix-assisted laser desorption ionization-time of flight mass spectrometry identification of yeasts is contingent on robust reference spectra, *PloS One* 6:e25712, 2011, https://doi.org/10.1371/journal.pone.0025712.

Pneumocystis Working Group: Nomenclature of Pneumocystis, Eukaryot, *Microbiol* 41:1215–1225, 1994.

Posch W, Blatzer M, Wilflingseder D: Lass-Florl, C: Aspergillus terreus: Novel lessons learned on amphotericin B resistance, *Med Mycol* 56:73–82, 2018, https://doi.org/10.1093/mmy/myx119.

Posteraro B, Vella A, Cogliati M, De Carolis E, Florio AR, Posteraro P, Sanguinetti M: Tortorano, A.M: matrix-assisted laser desorption ionization-time of flight mass spectrometry-based method for discrimination between molecular types of Cryptococcus neoformans and Cryptococcus gattii, *J Clin Microbiol* 50:2472–2476, 2012, https://doi.org/10.1128/JCM.00737-12.

Powers-Fletcher MV, Hanson KE: Molecular diagnostic testing for Aspergillus, *J Clin Microbiol* 54:2655–2660, 2016, https://doi.org/10.1128/JCM.00818-16.

Prakash PY, Irinyi L, Halliday C, Chen S, Robert V, Meyer W: Online databases for taxonomy and identification of pathogenic fungi and proposal for a cloud-based Dynamic data Network platform, *J Clin Microbiol* 55:1011–1024, 2017, https://doi.org/10.1128/JCM.02084-16.

Preuner S, Lion T: Towards molecular diagnostics of invasive fungal infections, *Expert Rev Mol Diagn* 9:397–401, 2009.

Psevdos Jr G, Tanowitz HB: Oral histoplasmosis, *AIDS Read* 18:217–218, 2008.

Queiroz-Telles F, Esterre P, Perez-Blanco M, Vitale RG, Salgado CG, Bonifaz A: Chromoblastomycosis: an overview of clinical manifestations, diagnosis and treatment, *Med Mycol* 47:3–15, 2009.

Ramanan P, Pritt BS 2014: Extraintestinal microsporidiosis, *J Clin Microbiol* 52:3839–3844, 2009, https://doi.org/10.1128/JCM.00971-14.

Ramani R, Gromadzki S, Pincus DH, Salkin IF, Chaturvedi V: Efficacy of API 20C and ID 32C systems for identification of common and rare clinical yeast isolates, *J Clin Microbiol* 36:3396–3398, 1998.

Ramirez I, Nieto-Rios JF, Ocampo-Kohn C, Aristizabal-Alzate A, Zuluaga-Valencia G, Munoz Maya O, Perez JC: Protothecal bursitis after simultaneous kidney/liver transplantation: a case report and review, *Transpl Infect Dis* 18:266–274, 2016, https://doi.org/10.1111/tid.12496.

Raufman JP: Declining gastrointestinal opportunistic infections in HIV-infected persons: a triumph of science and a challenge for our HAARTs and minds, *Am J Gastroenterol* 100:1455–1458, 2005.

Raut SH, Varaiya A: Differentiation of *Candida dubliniensis* on chrom agar and Pal's agar, *Indian J Med Microbiol* 27:55–58, 2009.

Reimer LG, MWilson ML, Weinstein MP: Update on detection of bacteremia and fungemia, *Clin Microbiol Rev* 10:444–465, 1997.

Reiss E, Obayashi T, Orle K, Yoshida M, Zancope-Oliveira RM: Non-culture based diagnostic tests for mycotic infections, *Med Mycol* 38(Suppl 1):147–159, 2000.

Revankar SG, Sutton DA: Melanized fungi in human disease, *Clin Microbiol Rev* 23:884–928, 2010, https://doi.org/10.1128/CMR.00019-10.

Ribes JA, Vanover-Sams CL, Baker DJ: Zygomycetes in human disease, *Clin Microbiol Rev* 13:236–301, 2000.

Rich P, Elewski B, Scher RK, Pariser D: Diagnosis, clinical implications, and complications of onychomycosis, *Semin Cutan Med Surg* 32:S5–8, 2013.

Richardson MD, Page ID: Aspergillus serology: have we arrived yet? *Med Mycol* 55:48–55, 2017, https://doi.org/10.1093/mmy/myw116.

Riddle DL, Giger O, Miller L, Hall GS, Woods GL: Clinical comparison of the Baxter MicroScan yeast identification panel and the vitek yeast biochemical card, *Am J Clin Pathol* 101:438–442, 1994.

Riscili BP, Wood KL: Noninvasive pulmonary *Aspergillus* infections, *Clin Chest Med* 30:315–335, 2009, vii.

Risslegger B, Zoran T, Lackner M, et al.: A prospective international Aspergillus terreus survey: an EFISG, ISHAM and ECMM joint study, *Clin Microbiol Infect* 23:776 e771–776 e775, 2017, https://doi.org/10.1016/j.cmi.2017.04.012.

Ritter JM, Muehlenbachs A, Blau DM, et al.: *Exserobilum* infections associated with contaminated steroid injections: a clinicopathologic review of 40 cases, *Am J Pathol* 183:881–892, 2013.

Rober-Gangneux F, Belaz S, Revest M, Tattevin P, Jouneau S, Decaus O, Chevrier S, Le Tulzo Y, Gangneux JP: Diagnosis of *Pneumocystis jirovecii* pneumonia in immunocompromised patients by real-time PCR: a 4-year prospective study, *J Clin Microbiol* 52:3370–3376, 2014.

Robey AB, O'Brien EK, Richardson BE, Baker JJ, Poage DP, Leopold DA: The changing face of paranasal sinus fungus balls, *Ann Otol Rhinol Laryngol* 118:500–505, 2009.

Roberts AL, Alelew A, Iwen PC: Evaluation of matrix-assisted laser desorption ionization-time-of-flight mass spectrometry to differentiate between *Candida albicans and Candida dubliniensis. Diagn Microbiol Infect Dis* 85:73–76, 2016.

Roden AC, Schuetz AN: Histopathology of fungal diseases of the lung, *Semin Diagn Pathol* 34:530–549, 2017, https://doi.org/10.1053/j.semdp.2017.06.002.

Roden MM, Zaoutis TE, Buchanan WL, Knudsen TA, Sarkisova TA, Schaufele RL, Sein M, Sein T, Chiou CC, Chu JH, Kontoyiannis DP, Walsh TJ: Epidemiology and outcome of zygomycosis: a review of 929 reported cases, *Clin Infect Dis* 41:634–653, 2005.

Rodrigues AM, de Hoog G, Zhang Y, de Camargo ZP: : emerging sporotrichosis is driven by clonal and recombinant Sporothrix species, *Emerg Microbes Infect* 3:e32, 2014, https://doi.org/10.1038/emi.2014.33.

Rodrigues CF, Silva S: Henriques, M: Candida glabrata: a review of its features and resistance, *Eur J Clin Microbiol Infect Dis* 33:673–688, 2014, https://doi.org/10.1007/s10096-013-2009-3.

Rodriguez-Tudela JL, Alcazar-Fuoli L, Cuesta I, Alastruey-Izquierdo A, Monzon A, Mellado E, Cuenca-Estrella M: Clinical relevance of resistance to antifungals, *Int J Antimicrob Agents* 32(Suppl 2):S111–113, 2008.

Roe CC, Bowers J, Oltean H, et al.: Dating the Cryptococcus gattii Dispersal to the North American Pacific Northwest, *mSphere* 3, 2018https://doi.org/10.1128/mSphere.00499-17.

Rosevinge FS, Dzajic E, Knudsen E, Malig S, Andersen LB, Levig A, et al.: Performance of matrix-assisted laser desorption-time of flight mass spectrometry for identification of clinical yeast isolates, *Mycoses*229–235, 2013.

Roy M, Benedict K, Deak E, et al.: A large community outbreak of blastomycosis in Wisconsin with geographic and ethnic clustering, *Clin Infect Dis* 57:655–662, 2013, https://doi.org/10.1093/cid/cit366.

Rychert J, Slechta ES, Barker AP, et al.: Multicenter evaluation of the vitek MS v3.0 system for the identification of filamentous fungi, *J Clin Microbiol* 56, 2018, https://doi.org/10.1128/JCM.01353-17.

Saccente M, Woods GL: Clinical and laboratory update on blastomycosis, *Clin Microbiol Rev* 23:367–381, 2010, https://doi.org/10.1128/CMR.00056-09.

Sagiroglu P, Nedret Koc A, Atalay MA, Altinkanat Gelmez G, Canoz O, Mutlu Sariguzel F: mucormycosis experience through the eyes of the laboratory, *Infect Dis (Lond)* 51:730–737, 2019, https://doi.org/10.1080/23744235.2019.1645962.

Salah H, Al-Hatmi AM, Theelen B, Abukamar M, Hashim S, van Diepeningen AD, Lass-Florl C, Boekhout T, Almaslamani M, Taj-Aldeen SJ: Phylogenetic diversity of human pathogenic Fusarium and emergence of uncommon virulent species, *J Infect* 71:658–666, 2015, https://doi.org/10.1016/j.jinf.2015.08.011.

Salimnia H, Fairfax MR, Lephart PR, et al.: Evaluation of the FilmArray blood culture identification panel: results of a multicenter controlled trial, *J Clin Microbiol* 54:687–698, 2016, https://doi.org/10.1128/JCM.01679-15.

Salzer HJF, Schafer G, Hoenigl M, Gunther G, Hoffmann C, Kalsdorf B, Alanio A, Lange C: Clinical, diagnostic, and treatment Disparities between HIV-infected and non-HIV-infected immunocompromised patients with Pneumocystis jirovecii pneumonia, *Respiration* 96:52–65, 2018, https://doi.org/10.1159/000487713.

Samson RA, Varga J: What is a species in Aspergillus? *Med Mycol* 47(Suppl 1):S13–20, 2009, https://doi.org/10.1080/13693780802354011.

Sanders E: Cutaneous sporotrichosis. Beer, bricks, and bumps, *Arch Intern Med* 127:482–483, 1971.

Sangoi AR, Rogers WM, Longacre TA, Montoya JG, Baron EJ, Banaei N: Challenges and pitfalls of morphologic identification of fungal infections in histologic and cytologic specimens: a ten-year retrospective review at a single institution, *Anatomic Pathol* 131:364–375, 2009.

Saracli MA, Fothergill AW, Sutton DA, Wiederhold NP: Detection of triazole resistance among Candida species by matrix-assisted laser desorption/ionization-time of flight mass spectrometry (MALDI-TOF MS), *Med Mycol* 53:736–742, 2015, https://doi.org/10.1093/mmy/myv046.

Saubolle MA: Laboratory aspects in the diagnosis of coccidioidomycosis, *Ann N Y Acad Sci* 1111:301–314, 2007.

Scalarone GM, Legendre AM, Clark KA, Pusater K: Evaluation of a commercial DNA probe assay for the identification of clinical isolates of Blastomyces dermatitidis from dogs, *J Med Vet Mycol* 30:43–49, 1992.

Scherer E, Iriart X, Bellanger AP, et al.: Quantitative PCR (qPCR) detection of Mucorales DNA in bronchoalveolar lavage fluid to diagnose pulmonary mucormycosis, *J Clin Microbiol* 56, 2018, https://doi.org/10.1128/JCM.00289-18.

Schoch CL, et al.: Nuclear ribosomal internal transcribed spacer (ITS) region as a universal DNA barcode marker for fungi, *Proc Nati Acad Sci* 109:6241–6246, 2012.

Schubert MS: Allergic fungal sinusitis: pathophysiology, diagnosis and management, *Med Mycol* 47(Suppl 1):S324–330, 2009.

Schuetz AN, Walsh TJ: Importance of fungal histopathology in immunocompromised Pediatric patients: It's not Just "Aspergillus" Anymore, *Am J Clin Pathol* 144:185–187, 2015, https://doi.org/10.1309/AJCPE3NSJ2RYLENS.

Schwartz IS, Sanche S, Wiederhold NP, Patterson TF, Sigler L: Emergomyces canadensis, a dimorphic fungus causing fatal systemic human disease in North America, *Emerg Infect Dis* 24:758–761, 2018, https://doi.org/10.3201/eid2404.171765.

Schwartz IS, Wiederhold NP, Hanson KE, Patterson TF, Sigler L: Blastomyces helicus, a new dimorphic fungus causing fatal pulmonary and systemic disease in humans and animals in western Canada and the United States, *Clin Infect Dis* 68:188–195, 2019, https://doi.org/10.1093/cid/ciy483.

Seebacher C, Bouchara JP, Mignon B: Updates on the epidemiology of dermatophyte infections, *Mycopathologia* 166:335–352, 2008.

Seidel D, Meissner A, Lackner M, et al.: Prognostic factors in 264 adults with invasive Scedosporium spp. and Lomentospora prolificans infection reported in the literature and FungiScope((R)), *Crit Rev Microbiol* 45:1–21, 2019, https://doi.org/10.1080/1040841X.2018.1514366.

Seok JY, Lee Y, Lee H, Yi SY, Oh HE, Song JS: Human cutaneous protothecosis: report of a case and literature review, *Korean J Pathol* 47:575–578, 2013.

Sepulveda VE, Marquez R, Turissini DA, Goldman WE, Matute DR: Genome sequences reveal cryptic Speciation in the human pathogen histoplasma capsulatum, *MBio 8*, 2017, https://doi.org/10.1128/mBio.01339-17.

Serris A, Danion F, Lanternier F: Disease Entities in mucormycosis, *J Fungi (Basel)* 5, 2019, https://doi.org/10.3390/jof5010023.

Seyedmousavi S, Guillot J, De Hoog GS: Phaeohyphomycosis: emerging opportunistic diseases in animals, *Clin Microbiol Rev* 26:19–35, 2013.

Seyedmousavi S, Netea MG, Mouton JW, Melchers WJG, Verweij PE, De Hoog GS: Black yeasts and their filamentous relatives: principles of pathogenesis and host defense, *Clin Microbiol Rev* 27:527–542, 2014.

Shao J, Wan Z, Li R, Yu J: Species identification and Delineation of pathogenic Mucorales by matrix-assisted laser desorption ionization-time of flight mass spectrometry, *J Clin Microbiol* 56, 2018, https://doi.org/10.1128/JCM.01886-17.

Shoham S: Emerging fungal infections in solid organ transplant recipients, *Infect Dis Clin North Am* 27:305–316, 2013.

Singh K: Laboratory-acquired infections, *Clin Infect Dis* 49:142–147, 2009.

Siqueira JPZ, Wiederhold N, Gene J, Garcia D, Almeida MTG, Guarro J: Cryptic Aspergillus from clinical samples in the USA and description of a new species in section Flavipedes, *Mycoses* 61:814–825, 2018, https://doi.org/10.1111/myc.12818.

Skiada A, Lass-Floerl C, Klimko N, Ibrahim A, Roilides E, Petrikkos G: Challenges in the diagnosis and treatment of mucormycosis, *Med Mycol* 56:93–101, 2018, https://doi.org/10.1093/mmy/myx101.

Skipper C, Abassi M, Boulware DR: Diagnosis and management of central nervous system cryptococcal infections in HIV-infected adults, *J Fungi (Basel)* 5, 2019, https://doi.org/10.3390/jof5030065.

Spivak ES, Hanson KE: Candida auris: an emerging fungal pathogen, *J Clin Microbiol* 56, 2018, https://doi.org/10.1128/JCM.01588-17.

Stebeiska K: Fungal hallucinogens psilocin, ibotenic acid, and muscimol: analytical methods and biologic activities, *Ther Drug Monit* 35:420–442, 2013.

Stevenson LG, Drake SK, Shea YR, Zelazny AM, Murray PR: Evaluation of matrix-assisted laser desorption ionization-time of flight mass spectrometry for identification of clinically important yeast species, *J Clin Microbiol* 48:3482–3486, 2010, https://doi.org/10.1128/JCM.00687-09.

Stockamp NW, Thompson 3rd GR: Coccidioidomycosis, *Infect Dis Clin North Am* 30:229–246, 2016, https://doi.org/10.1016/j.idc.2015.10.008.

Stone NR, Gorton RL, Barker K, Ramnarain P, Kibbler CC: : evaluation of PNA-FISH yeast traffic light for rapid identification of yeast directly from positive blood cultures and assessment of clinical impact, *J Clin Microbiol* 51:1301–1302, 2013, https://doi.org/10.1128/JCM.00028-13.

Straus DC: Molds, mycotoxins, and sick building syndrome, *Toxicol Ind Health* 25:617–635, 2009.

Stringer JR, Beard CB, Miller RF: Spelling Pneumocystis jirovecii, *Emerg Infect Dis* 15:506, 2009, https://doi.org/10.3201/eid1503.081060.

Stringer JR, Beard CB, Miller RF, Wakefield AE: A new name (*Pneumocystis jiroveci*) for *Pneumocystis* from humans, *Emerg Infect Dis* 8:891–896, 2002.

Suleyman G, Alangaden GJ: Nosocomial fungal infections: epidemiology, infection control, and prevention, *Infect Dis Clin North Am* 30:1023–1052, 2016, https://doi.org/10.1016/j.idc.2016.07.008.

Surash S, Tyagi A, De Hoog GS, Zeng JS, Barton RC, Hobson RP: Cerebral phaeohyphomycosis caused by Fonsecaea monophora, *Med Mycol* 43:465–472, 2005, https://doi.org/10.1080/13693780500220373.

Tan KE, Ellis BC, Lee R, Stamper PD, Zhang SX, Carroll KC: Prospective evaluation of a matrix-assisted laser desorption ionization-time of flight mass spectrometry system in a hospital clinical microbiology laboratory for identification of bacteria and yeasts: a bench-by-bench study for assessing the impact on time to identification and cost-effectiveness, *J Clin Microbiol* 50:3301–3308, 2012, https://doi.org/10.1128/JCM.01405-12.

Taxy JB: Blastomycosis: contributions of morphology to diagnosis: a surgical pathology, cytopathology, and autopsy pathology study, *Am J Surg Pathol* 31:615–623, 2007.

Taxy JB, El-Zayaty S, Langerman A: Acute fungal sinusitis: natural history and the role of frozen section, *Amer J Clin Path* 132:86–93, 2009.

Teixeira MM, de Almeida LG, Kubitschek-Barreira P, et al.: Comparative genomics of the major fungal agents of human and animal Sporotrichosis: Sporothrix schenckii and Sporothrix brasiliensis, *BMC Genom* 15:943, 2014, https://doi.org/10.1186/1471-2164-15-943.

Terr AI: Sick Building Syndrome: is mould the cause? *Med Mycol* 47(Suppl 1):S217–222, 2009.

Thomas PA, Kaliamurthy J: Mycotic keratitis: epidemiology, diagnosis and management, *Clin Microbiol Infect* 19:210–220, 2013, https://doi.org/10.1111/1469-0691.12126.

Thompson 3rd GR, Patel PK, Kirkpatrick WR, Westbrook SD, Berg D, Erlandsen J, Redding SW, Patterson TF: Oropharyngeal candidiasis in the era of antiretroviral therapy, *Oral Surg Oral Med Oral Pathol Oral Radiol Endod* 109:488–495, 2010, https://doi.org/10.1016/j.tripleo.2009.11.026.

Thompson 3rd GR, Patterson TF: Pulmonary aspergillosis, *Semin Respir Crit Care Med* 29:103–110, 2008.

Thompson 3rd GR, Patterson TF: Fungal disease of the nose and paranasal sinuses, *J Allergy Clin Immunol* 129:321–326, 2012, https://doi.org/10.1016/j.jaci.2011.11.039.

Thompson 3rd GR, Wiederhold NP, Sutton DA, Fothergill A, Patterson TF: In vitro activity of isavuconazole against Trichosporon, Rhodotorula, Geotrichum, Saccharomyces and Pichia species, *J Antimicrob Chemother* 64:79–83, 2009, https://doi.org/10.1093/jac/dkp138.

Todd JR, King JW, Oberle A, Matsumoto T, Odaka Y, Fowler M, Posr RS, Shahan TA, Yin L, Sanusi ID: Protothecosis: report of a case with 20-year follow-up and review of previously published cases, *Med Mycol* 50:673–689, 2012.

Todd JR, Matsumoto T, Ueno R, Murugaiyan J, Britten A, King JW, Odaka Y, Oberle A, Weise C, Roesler U, Pore RS: Medical phycology 2017, *Med Mycol* 56:S188–S204, 2018, https://doi.org/10.1093/mmy/myx162.

Tortorano AM, Richardson M, Roilides E, et al.: ESCMID and ECMM joint guidelines on diagnosis and management of hyalohyphomycosis: Fusarium spp., Scedosporium spp. and others, *Clin Microbiol Infect* 20(Suppl 3):27–46, 2014, https://doi.org/10.1111/1469-0691.12465.

Tragiannidis A, Bisping G, Koehler G, Groll AH: Minireview: Malassezia infections in immunocompromised patients, *Mycoses* 53:187–195, 2010, https://doi.org/10.1111/j.1439-0507.2009.01814.x.

Travis J, Hart E, Helm J, Duncan T, Vilar J: Retrospective review of *Pneumocystis jirovecii* pneumonia over two decades, *Int J STD AIDS* 20:200–201, 2009.

Tseng HC, Chen CB, Ho JC, Cheng YW, Huang HW, Sun PL, Lee CH: Clinicopathological features and course of cutaneous protothecosis, *J Eur Acad Dermatol Venereol* 32:1575–1583, 2018, https://doi.org/10.1111/jdv.14804.

Tuite NL, Lacey K: Overview of invasive fungal infections, *Methods Mol Biol* 968:1–23, 2013.

Twarog M, Thompson 3rd GR: Coccidioidomycosis: recent updates, *Semin Respir Crit Care Med* 36:746–755, 2015, https://doi.org/10.1055/s-0035-1562900.

Vallabhaneni S, Mody RK, Walker T, Chiller T: The global burden of fungal diseases, *Infect Dis Clin North Am* 30:1–11, 2016, https://doi.org/10.1016/j.idc.2015.10.004.

van de Sande WW, Maghoub el S, Fahal AH, Goodfellow M, Welsh O, Zijlstra E: The mycetoma knowledge gap: identification of research priorities, *PLoS Negl Trop Dis* 27:e2667, 2014.

van Veen SQ, Claas ECJ, Kuijper EJ: High-throughput identification of bacteria and yeast by matrix-assisted laser desorption ionization-time of flight mass spectrometry in conventional medical microbiology laboratories, *J Clin Microbiol* 48:900–907, 2010, https://doi.org/10.1128/Jcm.02071-09.

Veligandla SR, Hinrichs SH, Rupp ME, Lien EA, Neff JR, Iwen PC: Delayed diagnosis of osseous blastomycosis in two patients following environmental exposure in nonendemic areas, *Am J Clin Pathol* 118:536–541, 2002.

Vella A, De Carlois E, Vaccaro L, Posteraro P, Perlin DS, Kostrzewa M: Rapid antifungal susceptibility testing by matrix-assisted laser desorption inoization-time of flight mass spectrometry analysis, *J Clin Microbiol* 51:2964–2969, 2013.

Vergidis P, Avery RK, Wheat LJ, et al.: Histoplasmosis complicating tumor necrosis factor-alpha blocker therapy: a retrospective analysis of 98 cases, *Clin Infect Dis* 61:409–417, 2015, https://doi.org/10.1093/cid/civ299.

Verrier J, Jeanneau-Imparato L, Guillet C, Bourdeau P, Bouchara JP: PCR-terminal restriction fragment length polymorphism for direct detection and identification of dermatophytes in veterinary mycology, *Med Mycol* 57:447–456, 2019, https://doi.org/10.1093/mmy/myy058.

Verweij JJ, Ten Hove R, Brienen EA, van Lieshout L: Multiplex detection of Enterocytozoon bieneusi and Encephalitozoon spp. in fecal samples using real-time PCR, *Diagn Microbiol Infect Dis* 57:163–167, 2007, https://doi.org/10.1016/j.diagmicrobio.2006.08.009.

Vetter E, Torgerson C, Feuker A, et al.: Comparison of the BACTEC MYCO/F Lytic bottle to the isolator tube, BACTEC Plus Aerobic F/bottle, and BACTEC Anaerobic Lytic/10 bottle and comparison of the BACTEC Plus Aerobic F/bottle to the Isolator tube for recovery of bacteria, mycobacteria, and fungi from blood, *J Clin Microbiol* 39:4380–4386, 2001.

Walsh TJ, Gamaletsou MN, McGinnis MR, Hayden RT, Kontoyiannis DP: Early clinical and laboratory diagnosis of invasive pulmonary, extrapulmonary, and disseminated mucormycosis (zygomycosis), *Clin Infect Dis* 54(Suppl 1):S55–60, 2012, https://doi.org/10.1093/cid/cir868.

Wazir JF, Ansari NA: *Pneumocystis carinii* infection. Update and review, *Arch Pathol Lab Med* 128:1023–1027, 2004.

Weitzman I, Salkin IF, Rosenthal SA: Evaluation of trichophyton agars for identification of Trichophyton soudanense, *J Clin Microbiol* 18:203–205, 1983.

Weitzman I, Whittier S, McKitrick JC, Della-Latta P: Zygospores: the last word in identification of rare or atypical zygomycetes isolated from clinical specimens, *J Clin Microbiol* 33:781–783, 1995.

Westblade LF, Jennemann R, Branda JA, et al.: Multicenter study evaluating the Vitek MS system for identification of medically important yeasts, *J Clin Microbiol* 51:2267–2272, 2013, https://doi.org/10.1128/JCM.00680-13.

Westerberg DP, Voyack MJ: Onychomycosis: current trends in diagnosis and treatment, *Am Fam Physician* 88:762–770, 2013.

Wheat LJ: Antigen detection, serology, and molecular diagnosis of invasive mycoses in the immunocompromised host, *Transpl Infect Dis* 8:128–139, 2006a.

Wheat LJ: Improvements in diagnosis of histoplasmosis, *Expert Opin Biol Ther* 6:1207–1221, 2006b, https://doi.org/10.1517/14712598.6.11.1207.

Wheat LJ: Approach to the diagnosis of the endemic mycoses, *Clin Chest Med* 30:379–389, 2009, viii.

Wheat LJ, Azar MM, Bahr NC, Spec A, Relich RF, Hage C: Histoplasmosis, *Infect Dis Clin North Am* 30:207–227, 2016, https://doi.org/10.1016/j.idc.2015.10.009.

Wheat LJ, Freifeld AG, Kleiman MB, Baddley JW, McKinsey DS, Loyd JE, Kauffman CA: Clinical practice guidelines for the management of patients with histoplasmosis: 2007 update by the Infectious Diseases Society of America, *Clin Infect Dis* 45:807–825, 2007a.

Wheat LJ, Freifeld AG, Kleiman MB, Baddley JW, McKinsey DS, Loyd JE, Kauffman CA: Infectious diseases society of, A: clinical practice guidelines for the management of patients with histoplasmosis: 2007 update by the infectious diseases society of America, *Clin Infect Dis* 45:807–825, 2007b, https://doi.org/10.1086/521259.

Wheat LJ, Walsh TJ: Diagnosis of invasive aspergillosis by galactomannan antigenemia detection using an enzyme immunoassay, *Eur J Clin Microbiol Infect Dis* 27:245–251, 2008.

White J, Weinstein SA, De Haro L, Bedry R, Schaper A, Rumack BH, Zilker T: Mushroom poisoning: a proposed new clinical classification, *Toxicon* 157:53–65, 2019, https://doi.org/10.1016/j.toxicon.2018.11.007.

White PL, Posso RB, Barnes RA: Analytical and clinical evaluation of the PathoNostics AsperGenius assay for detection of invasive aspergillosis and resistance to azole antifungal drugs directly from plasma samples, *J Clin Microbiol* 55:2356–2366, 2017, https://doi.org/10.1128/JCM.00411-17.

White PL, Wingard JR, Bretagne S, Loffler J, Patterson TF, Slavin MA, Barnes RA, Pappas PG, Donnelly JP: Aspergillus polymerase chain reaction: systematic review of evidence for clinical Use in comparison with antigen testing, *Clin Infect Dis* 61:1293–1303, 2015, https://doi.org/10.1093/cid/civ507.

White TC, Findley K, Dawson Jr TL, Scheynius A, Boekhout T, Cuomo CA, Xu J, Saunders CW: Fungi on the skin: dermatophytes and Malassezia, Cold spring Harb Perspect med, 4, 2014, https://doi.org/10.1101/cshperspect.a019802.

Wiederhold NP: Antifungal resistance: current trends and future strategies to combat, *Infect Drug Resist* 10:249–259, 2017, https://doi.org/10.2147/IDR.S124918.

Wiederhold NP, Gibas CFC: From the clinical mycology laboratory: new species and changes in fungal taxonomy and nomenclature, *J Fungi (Basel)* 4, 2018, https://doi.org/10.3390/jof4040138.

Wilcox CM, Alexander LN, Clark WS, Thompson 3rd SE: Fluconazole compared with endoscopy for human immunodeficiency virus-infected patients with esophageal symptoms, *Gastroenterology* 110:1803–1809, 1996, https://doi.org/10.1053/gast.1996.v110.pm8964406.

Wilken, J.A, Marquez, P, Terashita, D, McNary, J, Windham, G, Materna, B, Centers for Disease, C, Prevention: Coccidioidomycosis among cast and crew members at an outdoor television filming event–California, 2012, MMWR Morb Mortal Wkly Rep 63, 321–324, 2014.

Wilson DA, Joyce MJ, Hall LS, Reller LB, Roberts GD, Hall GS, Alexander BD, Procop GW: Multicenter evaluation of a Candida albicans peptide nucleic acid fluorescent in situ hybridization probe for characterization of yeast isolates from blood cultures, *J Clin Microbiol* 43:2909–2912, 2005.

Woods GL, Schnadig VJ: Histopathology of fungal infections. In Anaissie E, McGinnis MR, Pfaller MA, editors: *Clinical mycology*, Philadelphia, 2003, Churchill Livingstone, pp 80–95.

Young LL, Dolan CT, Sheridan PJ: Reeve, C.M: oral manifestations of histoplasmosis, *Oral Surg Oral Med Oral Pathol* 33:191–204, 1972, https://doi.org/10.1016/0030-4220(72)90389-1.

Zarnowski R, Miyazaki M, Dobrzyn A, Ntambi JM, Woods JP: Typing of Histoplasma capsulatum strains by fatty acid profile analysis, *J Med Microbiol* 56:788–797, 2007, https://doi.org/10.1099/jmm.0.47067-0.

Zhan P, Dukik K, Li D, et al.: Phylogeny of dermatophytes with genomic character evaluation of clinically distinct Trichophyton rubrum and T. violaceum, *Stud Mycol* 89:153–175, 2018, https://doi.org/10.1016/j.simyco.2018.02.004.

Zhang SX: Enhancing molecular approaches for diagnosis of fungal infections, *Future Microbiol* 8:1599–1611, 2013.

CHAPTER 61

SPIROCHETE INFECTIONS

Dejan Nikolic

***TREPONEMA*, 1229**
Classic Treponemal Disease, 1230
Laboratory Diagnosis of Treponematoses, 1233
Treatment of Treponematoses, 1235
Other Treponemal Diseases, 1236

***LEPTOSPIRA*, 1236**
Description, 1236
Epidemiology, 1236
Pathology and Pathogenesis, 1236
Clinical Manifestations, 1236
Laboratory Diagnosis, 1237
Treatment, 1237

***BORRELIA*, 1237**
Lyme and Lymelike Diseases, 1237
Relapsing Fever, 1243

AGENTS OF INTESTINAL SPIROCHETOSIS, 1244
Description, 1244
Epidemiology and Clinical Manifestations, 1244
Pathology and Pathogenesis, 1244
Laboratory Diagnosis, 1244
Treatment, 1244

SELECTED REFERENCES, 1245

KEY POINTS

- Human disease caused by spirochetes typically follows a clinical course that reflects three sequential phenomena: (1) early, local proliferation of the organisms at the site of introduction, (2) spirochetemia with systemic dissemination, and (3) persistence of small numbers of microbes at various, often immune, "privileged" sites.
- Direct detection of pathogenic spirochetes is sometimes possible by microbiologic culture, microscopy, or genomic amplification, but diagnosis more often relies upon the demonstration of a patient's serologic response to the offending agent.
- Venereal syphilis is a historic sexually transmitted disease caused by *Treponema pallidum* subsp. *pallidum* and its incidence is rising, including neonatal syphilis.
- In the early stages of disease, venereal syphilis may be diagnosed using direct microscopic visualization although today it is rarely performed.
- Serologic detection of syphilis, by far the most common mode of diagnosis, comprises methods that semiquantitatively measure antibody to various lipoproteins, as well as methods that detect antibody to treponeme-specific antigens. Serologic testing algorithms may begin with a nontreponemal assay, or with a treponeme-specific assay (referred to as the *reverse algorithm*).
- Yaws, endemic syphilis (bejel), and pinta are not sexually transmitted, are endemic to various tropical and Middle Eastern regions, and are caused by *T. pallidum* subsp. *pertenue, T. pallidum* subsp. *endemicum,* and *T. carateum,* respectively.
- Presumptive diagnosis of the endemic treponematoses can sometimes be made on the basis of clinical and epidemiologic data; however, as with venereal syphilis, serologic and direct microscopic techniques may prove useful.
- The most common tickborne disease in North America and Europe, Lyme disease is caused chiefly by *Borrelia burgdorferi* sensu stricto, *Borrelia garinii,* and *Borrelia afzelii.*
- Typical clinical manifestations of Lyme disease include erythema migrans (early localized disease), neuroborreliosis (early disseminated or late-stage disease), and/or Lyme arthritis (late-stage disease).
- Because no single laboratory test performs sufficiently in all clinical scenarios, a diagnosis of Lyme disease must be based on a combination of (1) clinicoepidemiologic characteristics, (2) host serologic response (as measured by enzyme-linked immunosorbent assay/immunofluorescence assay and immunoblot), (3) molecular evidence, and/or (4) culture results.
- Epidemic, louseborne relapsing fever has a worldwide distribution and is caused by *Borrelia recurrentis.*
- Endemic, tickborne relapsing fever has a limited geographic distribution and is caused by several *Borrelia* spp., including *Borrelia hermsi* and *Borrelia turicata.*
- Acute onset of high fever and constitutional symptoms followed by cycles of evanescence and recrudescence is frequently recognized in both forms of relapsing fever.
- Diagnosis of relapsing fever is most often established through the demonstration of spirochetes in peripheral blood smears stained by a Giemsa technique.
- One of the most common zoonotic diseases throughout the world, leptospirosis is caused by various serovars of different species within the genus *Leptospira.*
- Although leptospirosis is usually subclinical or mild and flulike, a small proportion of patients develop severe symptoms related to gastrointestinal/hepatic disease, meningitis, renal failure, and/or myocarditis (also referred to as Weil disease).
- Although *Leptospira* spp. can be cultivated in vitro, diagnosis is usually made by demonstrating seroconversion.
- *Brachyspira aalborgi* and *Brachyspira pilosicoli* have been demonstrated in and isolated from the colon of humans with diarrheal disease, but their pathogenicity has not been firmly established.
- Demonstration of spirochetes along the colonic epithelial cell borders using routine, immunohistochemical, or in situ hybridization microscopy from biopsy material is more commonly performed than cultivation or genomic amplification assays.

Spirochetes (*spiro*, "coiled"; *chaete*, "hair") are slender, spiral-shaped bacteria containing one or more complete rotations that form a helix. They are gram negative but can be visualized only by darkfield or phase microscopy, silver impregnation, and immunohistochemical stains in tissue sections. Flagella-like organelles called periplasmic fibrils or axial filaments are attached near the poles of the bacteria and permit a corkscrew-like motility. Many commensal and nonpathogenic species of spirochetes exist, and human disease is limited primarily to infection by members of three genera: *Treponema*, *Borrelia*, and *Leptospira*. Widely diverse from an epidemiologic standpoint, spirochetes within these genera demonstrate a number of pathogenic, and hence clinical, similarities upon acquisition by humans. Although *Brachyspira* spp. have been associated with gastrointestinal syndromes, definitive causation of disease by these bacteria has not been universally accepted.

TREPONEMA

The genus *Treponema* contains two species responsible for disease in humans. *Treponema pallidum* is divided into three subspecies, each of which is the etiologic agent of a distinct clinical entity: subspecies *pallidum*, *pertenue*, and *endemicum* are the etiologic agents of venereal syphilis, yaws, and endemic syphilis (bejel), respectively. Pinta is caused by the second closely related species, *Treponema carateum*. Controversy exists even to this day concerning the origins of the sexually transmitted form of infection. Previously, the debate focused largely on deducing geographic regions of disease occurrence (e.g., Old World vs New World) based on morphologic skeletal abnormalities of excavated remains that were presumably a result of *T. pallidum* subsp. *pallidum* infection. Work utilizing phylogenetic molecular methods seems to support the "Columbian" theory (i.e., that a form of venereal infection was acquired during exploration of the New World and was subsequently introduced into Europe) (Harper, Ocampo et al., 2008).

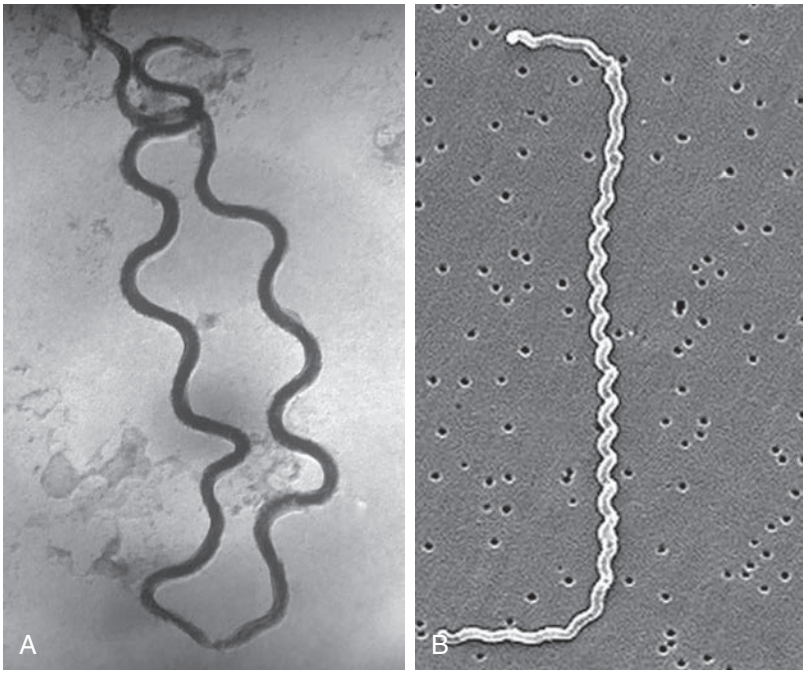

Fig. 61.1 Electron photomicrographs of pathogenic spirochetes. **A** Two spiral-shaped *Treponema pallidum* bacteria (36,000×). **B** *Leptospira interrogans* strain RGA bound to a 0.2-μm filter. (CDC/PHIL file photo.)

CLASSIC TREPONEMAL DISEASE

Syphilis

Description

T. pallidum subsp. *pallidum*, the etiologic agent of venereal syphilis, is a thin (0.2 μm) spirochete, 6 to 20 μm in length with 10 to 13 coils (Fig. 61.1, *A*). The disease appears to have spread rapidly throughout Europe during the 16th century, and its absence in the medical literature prior to this period suggests that the organism was brought from the New World.

Epidemiology

Man is the only natural reservoir for *T. pallidum* subsp. *pallidum*. Transmission occurs by direct contact with active lesions, largely through sexual contact. Vertical transmission across the placenta, the second most common mode of infection, may result when a latently infected female becomes pregnant or when a pregnant woman becomes infected (Wicher & Wicher, 2001; Workowski, 2015). Infection may also rarely be transmitted by nonsexual contact with an active lesion, by transfusion of fresh blood products from an infected person (although organisms do not survive >48 hours under typical blood bank storage conditions), by accidental needlestick, or when infectious specimens are handled in the laboratory.

The incidence of venereal syphilis in the United States declined dramatically with the advent of penicillin following World War II and remained stable until the mid-1980s, when the incidence began to increase once again, presumably as the result of increased intravenous drug use and sexual promiscuity. A continuous decline in infection rates was observed among women of childbearing age throughout the 1990s and was paralleled by a comparable decrease in the incidence of congenital syphilis. Following a nadir in disease incidence in 2000 that marked the lowest rate of syphilis in the United States during recorded history, the rate of primary and secondary syphilis has increased almost every year since 2013. In 2017, 30,644 cases of primary and secondary syphilis were reported, representing an increase of 76% compared to the number of cases in 2013, and yielding a rate of 9.5 cases/100,000 population compared to a rate of 5.3 cases /100,000 population in 2013 (Centers for Disease Control and Prevention [CDC], 2018d). Similarly, after a steady decline from 2008 to 2012, since 2013 the national rate of congenital syphilis has increased each year from 9.2 cases/100,000 live births to 23.3 cases/100,000 live births, representing a 153% increase during 2013 to 2017 (more than doubled) (Fig. 61.2). In 2017, 918 cases of congenital syphilis were reported, including 64 syphilitic stillbirths and 13 infant deaths. The increase in congenital syphilis rate reflects the increase in primary and secondary syphilis among all women, including reproductive-age women during 2013 to 2017 (increase in rates were 155.6% and 142.8%, respectively) (CDC, 2018d).

Pathogenesis and Pathology

T. pallidum subsp. *pallidum* penetrates an intact mucous membrane or gains access to tissue through abraded skin, multiplies at the inoculation site, and

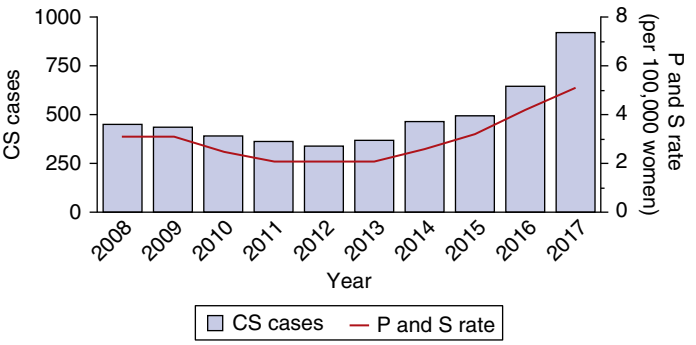

Fig. 61.2 Congenital syphilis. Reported cases by year of birth and rates of reported cases of primary and secondary syphilis among women aged 15–44 years, United States, 2008–2017. *CS,* Congenital syphilis; *P,* primary syphilis; *S,* secondary syphilis. (Centers for Disease Control and Prevention: Sexually transmitted diseases surveillance, 2018. https://www.cdc.gov/std/stats17/2017-STD-Surveillance-Report_CDC-clearance-9.10.18.pdf.)

then enters the lymphatic and circulatory system and spreads throughout the body. For the intradermal inoculation in humans, the 50% infectious dose has been calculated to be 57 organisms (Lukehart, 2018b). Clinical lesions appear when a critical mass of organisms is reached locally (≈10^7 spirochetes); therefore the incubation period is directly related to the size of the initial inoculum with the mean incubation period in humans of ~21 days, it rarely exceeds 6 weeks (Lukehart, 2018b).

The host immunologic response to *T. pallidum* subsp. *pallidum* is influenced by the structure of the bacterium. The outer membrane is a phospholipid bilayer that lacks lipopolysaccharide and has few demonstrable protein antigens. The lack of exposed outer membrane proteins as well as the presence of antigenetically unique organisms within *T. pallidum* subsp. *pallidum* populations are key factors in the organism's ability to evade opsonization and clearance by macrophages (Cruz et al., 2012).

This delayed and attenuated immune response allows *T. pallidum* subsp. *pallidum* to disseminate and to produce a chronic infection. The course of syphilis can be divided into predictable stages. Its primary stage, the development of a chancre, occurs at a median of 3 weeks postinoculation, although a primary lesion may not develop in all patients. Additionally, because of its painless nature, the lesion may go unnoticed in a proportion of cases. Upon healing within 2 to 8 weeks, the chancre gives rise to the secondary stage. Typically manifesting about 6 weeks after inoculation (range, 2–12 weeks), this stage is characterized by widespread dissemination of spirochetes via the bloodstream and the development of mucocutaneous and organ involvement with the presence of constitutional symptoms. Upon resolution of the secondary stage, the infection enters a period of latency, during which time the patient exhibits minimal manifestations of infection.

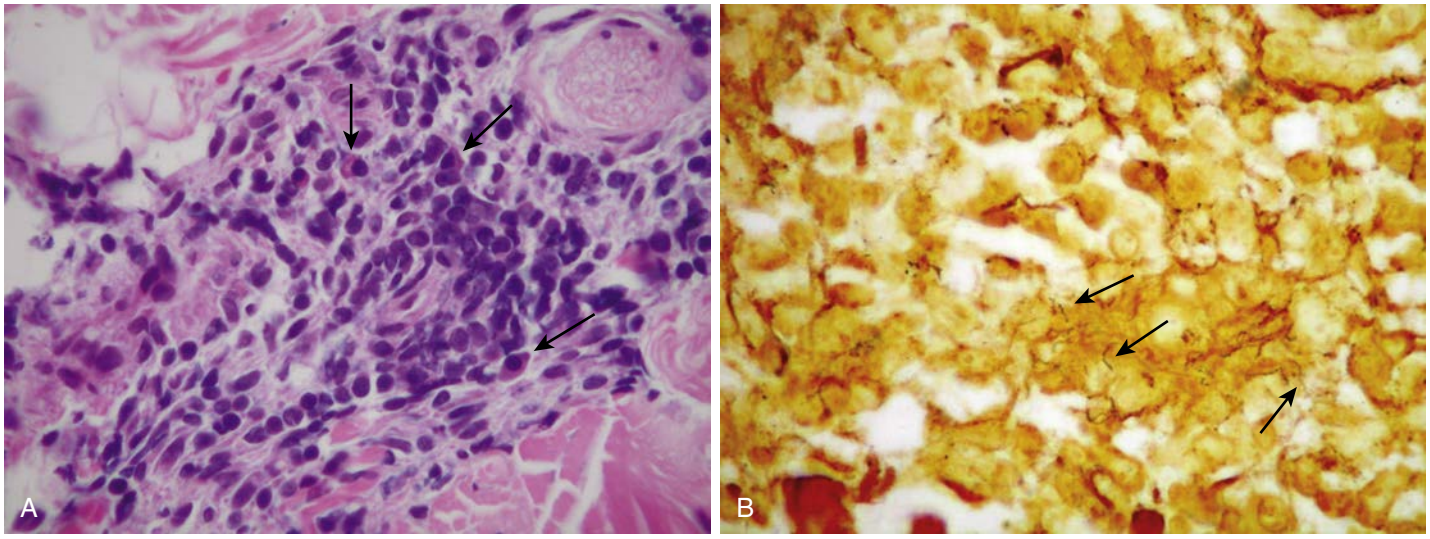

Fig. 61.3 Histologic photomicrographs of a secondary syphilis case. **A** Superficial dermis showing a dense, perivascular lymphomononuclear infiltrate containing many plasma cells *(arrows)* (hematoxylin & eosin [H&E], ≈400×), which was confirmed in **B** to contain numerous argyrophilic spirochetes *(arrows)* (Steiner silver impregnation technique, 400×). Patient was subsequently shown to have a high rapid plasma reagin (RPR) titer.

The first year of this stage, termed the early latent period, may be characterized by occasional relapses, whereas relapse is not common during the late latent period. Following a period of 10 to 25 years, approximately one-third of untreated patients develop tertiary syphilis, the most serious manifestations of which involve the cardiovascular system or the central nervous system (CNS).

Whatever organ is involved or whatever stage of the disease is reached, the histologic hallmark of syphilis is obliterative endarteritis, demonstrating concentric endothelial and fibroblastic proliferations with an associated mononuclear cell infiltrate rich in plasma cells (Fig. 61.3, *A*). Endarteritis results from the binding of spirochetes to endothelial cells via fibronectin molecules that have attached to the surface of the bacteria (Thomas et al., 1986). Treponemes may be demonstrable in tissues with silver impregnation (see Fig. 61.3, *B*) and immunohistochemical stains, particularly during the first and second stages of disease (Martin-Ezquerra et al., 2009). With progression, both the plasma cell infiltrate and the concentration of treponemes lessen in intensity. Although commonplace in the pretreatment era, syphilitic gummas, or large visceral necrotizing granulomas, develop as tertiary-stage manifestations but are now rarely seen (Fargen et al., 2009).

Elucidation of the complete genomic sequence of *T. pallidum* subsp. *pallidum* has provided insight into the pathogenesis and molecular epidemiology of this organism. Molecular typing tools have identified geographically specific strains (Smajs et al., 2012). The 12-member *T. pallidum* repeat (Tpr) gene family displays similarities to variable outer membrane antigens of other spirochetes. One member, *TprK*, contains a discrete variable region that could undergo an antigenic variation resulting in avoiding the immune surveillance of the host (Lukehart, 2018b).

Clinical Manifestations

Syphilis is a chronic infection with a multiplicity of expressions, primarily related to the stage at which it manifests. The primary chancre is characteristically ulcerated with raised, firm edges and a smooth base and is notable for absence of an exudate or pain (Fig. 61.4, *A*). Although these are typically solitary, multiple chancres can occur in up to one-third of patients. Patients with previous infection can present with atypical lesions, such as a small papule, or may not develop a lesion at all. Regional lymphadenopathy, with moderately enlarged, rubbery, nonsuppurative lymph nodes, is seen in some patients.

Dissemination marks the secondary stage, and patients present with signs and symptoms of a systemic illness. More than 90% develop a rash that begins on the trunk and extremities (although any body surface can be involved) as small macules that progress to papules, and in some patients to pustules, over a period of weeks. The appearance of the rash on the palms and soles is characteristic (see Fig. 61.4, *B*), and enlargement and coalescence of papules produce the pale plaques of condyloma lata (see Fig. 61.4, *C*). Approximately 90% of patients also exhibit generalized lymphadenopathy, and as many as three-fourths may suffer fever, malaise, anorexia, arthralgia, pharyngitis, and weight loss. Mucous patches are seen in up to one-third of cases. About 40% of persons develop CNS symptoms during this stage, particularly among those coinfected with human immunodeficiency virus (HIV), although only 1% to 2% present with acute meningitis (CDC, 2007; Lukehart, 2018b). The remainder may experience headache and meningismus, uveitis, sensorineural hearing loss, and cranial nerve involvement.

The tissue destruction of tertiary syphilis usually becomes evident decades after the primary infection. Cardiovascular syphilis occurs as a result of weakening of the tunica media and results in an aneurysm of the ascending aorta with aortic valve insufficiency and narrowing of the coronary artery ostia. Syphilitic gummas may involve the skin, brain, skeletal system, or mucocutaneous tissues, although any organ can be affected. Both cardiovascular syphilis and syphilitic gummas became much less frequent after the advent of antibiotic treatment. Meningovascular syphilis occurs 5 to 10 years after initial infection and clinically presents as seizures, stroke, and aphasia. Multiple small infarcts due to endarteritis in the CNS are the cause of this form. Parenchymatous neurosyphilis, which presents 15 to 30 years after initial infection, is a degenerative process with loss of neurons and myelinated tracts resulting in a complex of neurologic and psychiatric manifestations, including general paresis, tabes dorsalis, and pupillary abnormalities. Some patients lack clinical signs or symptoms altogether but demonstrate cerebrospinal fluid (CSF) abnormalities such as pleocytosis, increased protein, a reactive Venereal Disease Research Laboratory (VDRL) test, or antibody against *T. pallidum* indicating CNS infection.

Congenital syphilis occurs clinically as two forms: an early or infantile form (<2 years of age) and a late form following a period of latency (few years to several decades). Although transplacental passage of spirochetes can occur during any trimester, congenital acquisition during early gestational age results in stillbirth more often than does acquisition during late gestation or parturition (Harter & Bernischke, 1976). As may be expected, congenital transmission is more frequent during the primary, secondary, and early latent periods of maternal infection (Woods, 2009). Necrotizing funisitis, or inflammation of the umbilical cord, is characteristic of congenital syphilis, although it is typically present in only the most severe cases. In the infantile form, a diffuse rash with sloughing of the skin, osteochondritis, and periostitis are characteristic; however, affected newborns may be asymptomatic (Mahon et al., 2015). Diffuse fibrosis of the liver (hepar lobatum) and lung (pneumonia alba) is also seen. After a latent period, the late form presents in childhood or adulthood with a wide variety of signs and symptoms; however, the triad of interstitial keratitis, Hutchinson teeth, and eighth nerve deafness is classic. Periostitis, saber shins, and saddle deformity of the nose are also seen frequently.

Syphilis and HIV infection are increasingly seen as coinfections because these diseases share common risk factors and may even potentiate one another. Through several mechanisms, syphilis increases the risk for acquisition and transmission of HIV. The disrupted mucosal barrier at the chancre can facilitate HIV infection and transmission. The inflow of host immune cells to the site of syphilis infection increases the number of targets available for HIV infection. In addition, recruited monocytes express increased amounts of the HIV coreceptor CCR5 (Sheffield et al., 2007). While the clinical presentation of syphilis in HIV-infected persons is usually similar to that in individuals without HIV, cases of more severe

Fig. 61.4 Clinical manifestations of venereal syphilis. **A** Penile chancre. **B** Secondary syphilitic lesions involving the palms. **C** Condylomata lata lesions involving the vulvar and anal region. (CDC/PHIL file photos.)

primary and secondary lesions, as well as unusual presentations, have been reported (Stevenson & Heath, 2006). Patients with AIDS have a high incidence of eye involvement, with anterior uveitis being the most common manifestation of *T. pallidum* infection in this setting (Stevenson & Heath, 2006). HIV infection status may affect laboratory tests for syphilis, and vice versa. Early syphilis infection is associated with an increase in plasma HIV viral load and a decrease in the CD4 cell count (Buchacz et al., 2004). A multicenter prospective study showed that CSF nontreponemal tests were more likely to remain positive ("serofast") following syphilis therapy in HIV-infected individuals than in HIV-uninfected patients (Marra, Maxwell et al., 2004). It remains to be seen, however, if such laboratory evidence of treatment failure is a true reflection of potential clinical relapse. What does seem clear, as evidenced by multiple studies, is that anti-HIV therapy itself improves the likelihood of serologic response following syphilis treatment in HIV-positive patients (Marra et al., 2008; González-López et al., 2009).

Yaws

Yaws (also called *frambesia tropica*, *pian*, *parangi*, *paru*, *buba*, or *bouba*) is a chronic disease caused by *T. pallidum* subsp. *pertenue* and is the most prevalent of the nonvenereal treponematoses. This disease, which has afflicted residents of the tropics since antiquity, is common in rural areas of tropical countries with heavy rainfall. After a decline in the 1950s due to large campaigns to control the treponematoses, the incidence of yaws has increased in some areas. Following a massive azithromycin campaign during the past several years, there is an apparent lack of recent publications about yaws. However, it is not clear whether yaws transmission was actually interrupted; therefore more information is needed (Zoni et al., 2019).

Yaws is contracted chiefly during childhood by direct contact, with breaks in the skin allowing entry of treponemes. Early lesions generally appear about 3 weeks later but may not develop for months. One or several papules appear, most frequently on the lower extremities, and then ulcerate or progress to papillomatous lesions. Numerous treponemes are found in these lesions. Spontaneous resolution is usual; however, relapses preceded by malaise, fever, and generalized lymphadenopathy followed by disseminated skin lesions are common. Most patients enter a period of latency during which no clinical signs or symptoms are evident. For most, the disease shows no additional manifestations; however, the destructive lesions of tertiary yaws were previously reported to occur in up to 10% of untreated patients and they involve irreversible, destructive lesions of bone, cartilage, soft tissue, and the skin, which is the most commonly affected. However, the destructive lesions of tertiary yaws are now rarely seen (Marks et al., 2015). Cardiovascular and CNS lesions similar to those seen in syphilis, although rare, have been reported to occur (Giacani & Lukehart, 2014; Marks et al., 2015).

Endemic Syphilis

Endemic syphilis (bejel) is a nonvenereal chronic infection caused by infection with *T. pallidum* subsp. *endemicum*. The disease is ancient and, although no longer as widespread as it once was, still occurs in the Middle East and Africa in hot, dry climates. Because no recent data are available for the endemic syphilis (the most recent World Health Organization [WHO] global estimate was in 1995), the prevalence of the disease is unknown (Lukehart, 2018). Endemic syphilis is transmitted by direct contact with active lesions, contaminated fingers, and eating or drinking utensils. Crowded living conditions and poor hygiene are common associated factors. Children 2 to 15 years of age are primarily infected, although the disease can be found in adults in the same family, and those adults who did not suffer from the disease in childhood can be infected by their children. The inoculum is small, and the primary lesions of early endemic syphilis, most frequent on the oropharyngeal mucosa, often are not apparent. Initial clinical manifestations of the disease are usually seen in a secondary stage, with mucous patches, condyloma lata, angular stomatitis, generalized lymphadenopathy, and painful osteoperiostitis. This is followed by a latent period of variable length. The late stage is characterized by tissue

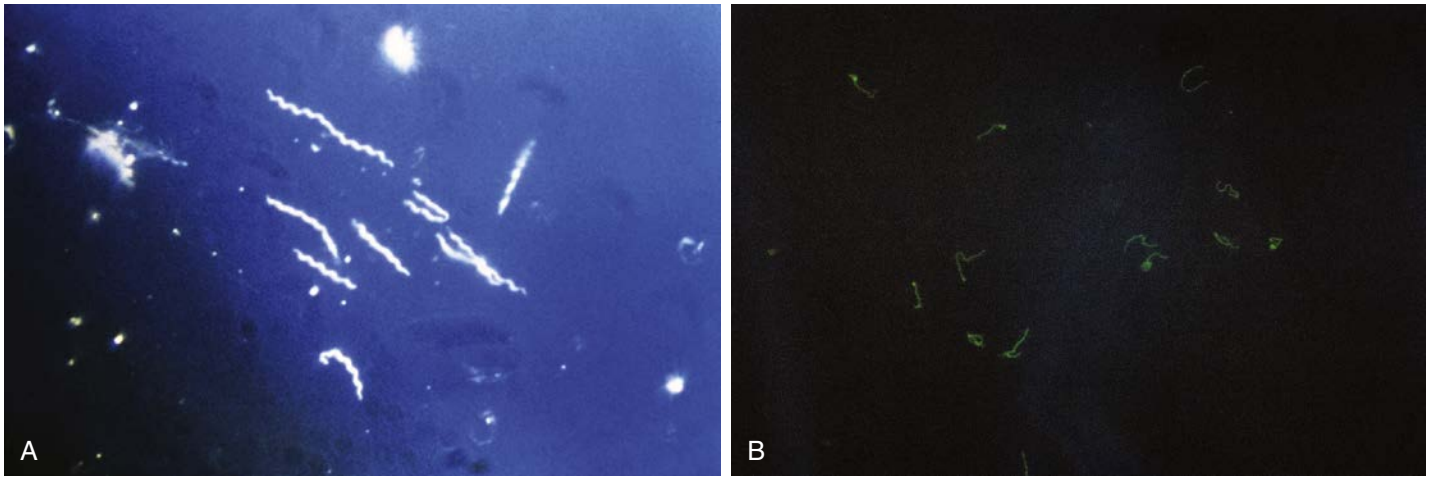

Fig. 61.5 In vitro diagnostic modalities for venereal syphilis detection. **A** Darkfield microscopy technique (400×) reveals the presence of motile spirochetes. **B** Positive fluorescent treponemal antibody absorption (FTA-ABS) test for antibody response in patient with syphilis. (CDC/PHIL file photo.)

destruction of the skin, bones, and cartilage, with a predilection for the nose and palate (so-called *gangosa*), and sometimes laryngeal involvement.

Pinta

Pinta (carate, mal de pinto, azul) is caused by infection with *T. carateum*. The disease is endemic in rural tropical Central America and northern South America, where it is found rarely and only in remote villages (Lukehart, 2018). Since no recent data are available, the prevalence of the disease is unknown (Lukehart, 2018). Children younger than 5 years of age are primarily infected. Inoculation is thought to occur via nonvenereal skin or mucous membrane contact. Characterization of the pathogenesis of the disease is difficult because, unlike other treponematoses that are pathogenic in humans, an animal model is unavailable and the treponeme cannot be cultured continuously. A primary papule or plaque develops at the site of inoculation after weeks to months, with or without localized lymphadenopathy. The primary lesion resolves, and several months to years later, disseminated secondary lesions, or pintids, which resemble scaly psoriasiform plaques, appear and remain for long periods or resolve and recur. In late pinta, lesions demonstrate hypopigmentation and skin atrophy or hyperkeratosis, which can persist for life. The skin appears to be the only organ affected in this disease (Giacani & Lukehart, 2014).

LABORATORY DIAGNOSIS OF TREPONEMATOSES

Because the etiologic agents of the human treponematoses cannot be isolated easily by routine culture methods, testing for disease generally is completed directly by visualization of the organisms in material from lesions or indirectly by immunologic methods. Consequently, different stages of the treponematoses often require a particular testing modality. In the early stages when lesions are present, highly specific microscopic techniques are used. Upon resolution of lesions, a variety of serologic tests are employed for diagnosis. It is important to remember that none of these laboratory tests is capable of distinguishing between the closely related species and subspecies of pathogenic treponemes, so differentiating between them requires clinical, epidemiologic, and, when possible, genomic information (Harper, Liu et al., 2008).

Darkfield Microscopy

When direct sampling of lesions is possible, such as in primary, secondary, or early congenital syphilis (chancres, mucous patches, or condyloma lata), the lesion should be cleansed with sterile water (no soap or antiseptic) and gently abraded. Pressure is applied, causing serous exudate to collect in the lesion. A drop of the fluid is placed on a slide, and a coverslip is placed over the fluid. The specimen must be examined within ~20 minutes, as visualization of motility is necessary for definitive identification. Because of their narrow width, treponemes cannot be visualized by conventional light microscopy. Instead, darkfield microscopy is necessary. This technique makes use of a patch stop, which creates the microscopist's "dark field," and a condenser lens that targets the spirochetes with light waves at an oblique angle, some of which are scattered into the objective, giving the appearance of bright organisms in a dark background (Fig. 61.5, *A*). The darkfield examination can be positive several weeks before a positive serologic test and has a sensitivity of 80% in diagnosing syphilis (Larsen et al., 1995). Highly skilled microscopists are required to avoid false positives. Because of possible confusion with commensal treponemes in the mouth, however, it is not recommended that this technique be utilized for oral lesions. Additionally, three *Treponema* spp. that are normal inhabitants of the genital region (*T. phagedenis*, *T. refringens*, and *T. minutum*) could potentially be confused with *T. pallidum* on darkfield examination. Careful cleaning of the area is important in reducing the likelihood of this occurrence. The characteristic motility of *T. pallidum* is an important feature that distinguishes it from saprophytic spirochetes.

Immunohistochemical Microscopy

Monoclonal and polyclonal antibodies with specificities for spirochetes, treponemes, or *T. pallidum* have been used by pathologists for detection in paraffin-embedded tissues (Martin-Ezquerra et al., 2009). With this technique, antitreponemal antibodies bound to spirochetes in tissue sections are detected after a series of immunologic reactions typically consisting of a primary, biotinylated antibody conjugate with organism specificity followed by an enzyme-conjugated streptavidin complex. After development of the enzyme with an appropriate chromogenic substrate, organisms are highlighted against a pale counterstained background. This allows for easy detection of rare bacteria and affords the capability for histologic localization. The procedure reportedly offers improvement in sensitivity and specificity over silver impregnation stains for the detection of treponemes, but this is largely dependent upon the source of primary antibody.

Nontreponemal Serologic Tests

The nontreponemal assays detect antibodies to lipoprotein material and cardiolipin released from cells damaged by treponemes. As a consequence, they are not specific for *Treponema*. These tests have been used traditionally to screen for syphilis and to monitor the course of the disease after treatment. Standard tests include the VDRL, manual rapid plasma reagin (RPR), unheated serum reagin (USR), and toluidine red unheated serum (TRUST). All these tests use a phospholipid antigen, some fortified with lecithin and cholesterol. Flocculation is the endpoint for the manual standard tests, whereas absorbance values are calculated spectrophotometrically in the enzyme-linked immunosorbent assay (ELISA). Serum is the preferred specimen for each. Heating of the serum to eliminate nonspecific reactions is required in the VDRL, whereas the addition of choline chloride to the RPR and USR eliminates the need for heating, making these popular choices among diagnostic laboratories. Antibody-antigen reactions in the VDRL and USR are assessed using a microscope at 100×, and the addition of charcoal to the RPR and dye to the TRUST makes the reactions macroscopically visible (Fig. 61.6).

In April 2019, the US Food and Drug Administration (FDA) cleared another fully automated system, the AIX1000 (Gold Standard Diagnostics, Davis, CA), for nontreponemal RPR testing. The AIX1000 automates the processing, analysis, result interpretation, and archiving of RPR screens and semiquantitative titers. This methodology reduces variation associated with manual testing and interpretation, and the images of each RPR result are stored digitally and are retrievable for review (Brusca, 2019).

Antibodies detected by the nontreponemal tests generally develop 1 to 4 weeks after the appearance of the primary chancre. The time at which the specimen is taken during the primary stage therefore will affect assay sensitivity. The titer rises, remains high during the first year of infection, and then gradually declines. The tests will ultimately revert to negative

in most patients in the absence of therapy, particularly during the late latent stage. Thus these tests are general markers of disease activity. False-negative nontreponemal tests may also be associated with very high titers of antibody (prozone phenomenon), which are seen most commonly in secondary syphilis. This condition is easily resolved by diluting the specimen prior to testing. False-positive results may occur with acute illnesses such as hepatitis, other viral infections, pregnancy; or chronically with the connective tissue diseases (Mahon et al., 2015; Lukehart, 2018).

Standard nontreponemal tests afford the capability of semiquantitative reporting by testing serial twofold specimen dilutions (i.e., titers). Follow-up titers are used to determine the efficacy of treatment, with a fourfold decrease in titer considered an adequate response (CDC, 2015). Follow-up testing by the same method is necessary because titers between different nontreponemal tests cannot be directly compared. Patients treated in early syphilis are more likely to revert to negative than those treated in late syphilis (Brown et al., 1985). In a small minority of patients, nontreponemal tests will remain positive despite adequate therapy—a situation known as the *serofast response*.

Reports have documented various aberrant nontreponemal test results with patients coinfected with HIV and syphilis, including delayed seroconversion; however, seronegative syphilis does not appear to be prevalent in AIDS patients (Flores, 1995). The false-positive rate is reportedly increased in AIDS patients (4% vs 1% in non-AIDS); however, the increased rate of positivity may be associated with intravenous drug abuse rather than HIV infection itself (Flores, 1995; Larsen et al., 1995; Hernandez-Aguado et al., 1998). False-negative results also occur in AIDS patients with syphilis because of an exaggerated nontreponemal antibody response that occurs in some patients, with the resultant prozone effect (Gourevitch et al., 1993). Furthermore, as mentioned previously, a small number of AIDS patients may experience minimal to no decline in nontreponemal antibody titers despite presumably adequate therapy, although this may be related to the stage at which treatment was initiated rather than HIV coinfection (Larsen et al., 1995). The sensitivity of nontreponemal tests varies based on the disease stage. During primary, secondary, latent, and late syphilis, sensitivity is approximately 75% to 88%, 100%, 88% to 100%, and 71% to 73%, respectively. Specificity varies based on population but is usually greater than 96% (Table 61.1).

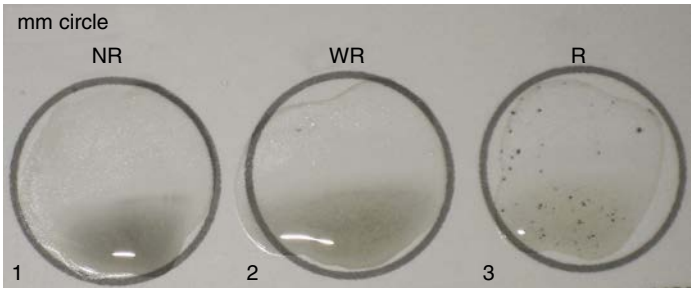

Fig. 61.6 Rapid plasmin reagin test card showing nonreactive, weakly reactive, and strongly reactive serum samples *(wells 1 to 3)* with their respective agglutination patterns.

Treponemal Serologic Tests

Treponemal tests detect the presence of antibodies to treponemal antigens and have traditionally been used to confirm a positive nontreponemal screening test, referred to as the traditional algorithm, or to confirm infection in the face of a negative nontreponemal test in late or latent disease stages, which can occur in up to 30% of patients with tertiary syphilis (Larsen et al., 1995). Treponemal tests have been used as a primary screening test, referred to as the reverse algorithm (CDC, 2008; Loeffelholz & Binnicker, 2012; Marangoni et al., 2009; Sena et al., 2010; Sokolovskiy et al., 2009). The fluorescent treponemal antibody absorption (FTA-ABS) test is an indirect fluorescent antibody test. It involves the addition of heated patient serum, which has been absorbed with antigen of the nonpathogenic Reiter treponeme for removal of cross-reactive antibodies to a slide on which *T. pallidum* subsp. *pallidum* (Nichols strain) has been fixed, followed by the addition of FITC-labeled antihuman globulin. Visible treponemes on fluorescent microscopy indicate the presence of antibody to the pathogenic treponemal species in the patient's serum (see Fig. 61.5, *B*). Another test, preferred by some laboratories because of its relative simplicity, is the microhemagglutination assay for antibodies to *T. pallidum* (MHA-TP). Absorbed serum is added to sheep red blood cells sensitized with *T. pallidum* (Nichols strain) sonicate in a microtiter tray. Agglutination of red blood cells is produced by syphilis-specific antibody. The *T. pallidum* particle agglutination (TPPA) test is based on the agglutination of gel particles sensitized with sonicated Nichols strain *T. pallidum* antigens. Anti–*T. pallidum* antibodies react with the gel particles to form a smooth mat in microtiter plate wells. In the absence of specific antibodies, the gel particles form a button at the bottom of the well. ELISA and chemiluminescent immunoassay (CLIA) test formats utilizing treponeme-specific antigens (e.g., sonicated lysates, recombinant proteins) have become available for use in clinical laboratories. These offer the advantages of automation for high-volume testing and an objective, numeric output to aide in interpretation.

In June 2017 the first completely automated assay for detection of both treponemal and nontreponemal (RPR) antibodies, the BioPlex 2200 Syphilis Total & RPR multiplex flow immunoassay (Bio-Rad Laboratories), was cleared by the FDA. By providing the capability of simultaneously detecting *Treponema pallidum*, RPR antibodies, and RPR titers, the BioPlex assay allows the full automation of testing following either the

TABLE 61.1
Sensitivities of Serologic Tests for Syphilis in Different Stages of Disease

Test	STATE OF SYPHILIS, % SENSITIVITY (RANGE)				% Specificity (Range)
	Primary	Secondary	Latent	Late	
Nontreponemal					
VDRL	78 (74-87)	100	95 (88-100)	71 (37-94)	98 (96-99)
RPR	86 (77-100)	100	98 (95-100)	73	98 (93-99)
Treponemal					
FTA-ABS	84 (70-100)	100	100	96	97 (94-100)
MHA-TP	76 (69-90)	100	97 (97-100)	94	99 (98-100)
TPPA	88 (86-100)	100	100	NA	96 (95-100)
IgG ELISA	100	100	100	NA	100
CLIA	98	100	100	100	99
Centaur CIA	94.5	100	100	94.1	95.5 (93.0-97.3)
Trep-Sure EIA	94.5	100	100	98.5	82.6 (78.4-86.1)
LIAISON CIA	96.4	100	97.6	92.6	94.5 (91.8-96.5)
Bioplex MBIA	96.4	100	95.1	94.1	96.7 (94.4-98.2)
INNO-LIA	96.4	100	100	91.1	98.5 (96.8-99.5)

CLIA, Chemiluminescent immunoassay; *EIA,* enzyme immunoassay; *ELISA,* enzyme-linked immunosorbent assay; *FTA-ABS,* fluorescent treponemal antibody absorption; *MBIA,* microbead immunoassay; *MHA-TP,* microhemagglutination assay for antibodies to *Treponema pallidum*; *NA,* not available; *RPR,* rapid plasma reagin; *TPPA, T. pallidum* particle agglutination; *VDRL,* Venereal Disease Research Laboratory.
Data from: Larsen SA, Steiner BM, Rudolph AH: Laboratory diagnosis and interpretation of tests for syphilis, *Clin Microbiol Rev* 8:1, 1995; Sena AC, White BL, Sparling PF: Novel *Treponema pallidum* serologic tests: a paradigm shift in syphilis screening for the 21st century, *Clin Infect Dis* 51:700, 2010; Park IU, Fakile YF, Chow JM, et al: Performance of treponemal tests for the diagnosis of syphilis, *Clin Infect Dis* 68(6):913, 2019.

traditional or reverse algorithm (Bio-Rad, 2017). Recent studies showed comparable performance, including the high negative percent agreement, of the Syphilis Total & RPR assay performed on BioRad BioPlex 2200 to those of the Treponema Assays and the manual RPR test (Arbefeville et al., 2019; Tesfazghi et al., 2019). The sensitivity and specificity of the BioPlex RPR assay were 90.5% and 97.2%, respectively, when compared to the manual RPR assay (Arbefeville et al., 2019).

The performance characteristics of seven treponemal assays, including four automated immunoassays, were recently evaluated and compared: (1) BioPlex 2200 (multiplex flow immunoassay), (2) ADVIA Centaur (CIA assay), (3) LIAISON (CIA), (4) Trep-Sure (EIA); and three nonautomated assays: (5) FTA-ABS, (6) TPPA, and (7) INNO-LIA (line immunoassay). During primary syphilis, sensitivities of six of the abovementioned assays were more than 94.5%. The exception was the FTA-ABS, which had a sensitivity of only 78.2%. During secondary, early latent, and late latent syphilis, the sensitivities of all immunoassays were 100%, 95.2% to 100%, and 86.8% to 98.5%, respectively (Park et al., 2019).

Generally, the MHA-TP, FTA-ABS, and TPPA tests are equivalent, except in the primary stage of syphilis, where the TPPA test shows higher sensitivity and specificity than FTA-ABS and is thus a preferred assay, for example, to arbitrate discordant results with the reverse algorithm (Park, 2019). IgG ELISA and CLIA formats are at least as sensitive and specific as the traditional treponemal tests. Importantly, they show improved sensitivity during the primary stage of syphilis (Sena et al., 2010). Sensitivities and specificities of the various nontreponemal and treponemal serologic tests are summarized in Table 61.1 (Larsen et al., 1995; Park et al., 2019). Since there are significant limitations associated with any type of serologic assay, including false-negative and false-positive results, utilizing only one type is not sufficient to diagnose syphilis.

Treponemal-specific antibody develops in primary syphilis and persists indefinitely in most patients, although as many as 20% may eventually serorevert (Romanowski et al., 1991). AIDS patients have shown a greater tendency to revert to seronegativity following treatment (Haas et al., 1990). The FTA-ABS usually is the first test to become positive, followed by the MHA-TP, and then the nontreponemal tests shortly thereafter. False-positive FTA-ABS results occur in ≈1% to 3% of patients, most often in older adults, in persons with connective tissue disease, and in those infected with related organisms such as *Borrelia* spp. (Larsen et al., 1995). The frequency of false-positive results with the MHA-TP is reportedly lower than with the FTA-ABS test and TPPA (Sena et al., 2010).

Because of the advantages offered by their automated formats, IgG ELISAs and CLIAs have been implemented as primary screening assays in some laboratories in the United States (the "reverse algorithm") (CDC, 2008; Loeffelholz & Binnicker, 2012) and Europe (Marangoni et al., 2009; Sokolovskiy et al., 2009). These tests, however, do not distinguish past from active infection. Therefore follow-up testing of positive specimens with a semiquantitative nontreponemal test is needed. As with all immunoassays, treponemal ELISAs and CLIAs may yield occasional false-positive results. The proportion of false positives relative to all positive results varies depending on the patient population tested (CDC, 2011a, 2011b). When follow-up RPR is nonreactive, further testing using a traditional treponemal assay is usually necessary. ELISA and CLIA formats generate a numeric value, the strength of which can be used with high accuracy to predict when the second treponemal assay will be positive, thereby reducing unnecessary follow-up testing (Loeffelholz et al., 2011; Yen-Lieberman et al., 2011).

Immunoassays with IgM-specific detection capability are also available and may have some utility in the diagnosis of congenital syphilis and primary infection (Larsen & Johnson, 1998; Sena et al., 2010). Finally, several rapid, point-of-care assays that incorporate treponemal or nontreponemal antigens have been described (Greer & Wendel, 2008). Their utility lies chiefly in areas with high prevalence rates and low likelihood of patient follow-up, where patients with positive results can be treated presumptively at the time of testing.

Other Diagnostic Test Methods

More complex tests, such as the immunoblot and the PCR, are available in some reference laboratories. The immunoblot has been integrated into the diagnosis of congenital syphilis or as confirmation for treponemal-specific antibody screening by some laboratories (Larsen et al., 1995; Wang & Li, 2009). PCR may be useful in the diagnosis of primary infection, when serologic tests are often still negative (Gayet-Agaron et al., 2013). PCR has been advocated for the diagnosis of neurosyphilis, particularly in AIDS patients, although some studies have not demonstrated advantages over currently used methods. Neither immunoblot nor PCR is used extensively in the diagnostic setting, as standardization remains poor. Although PCR-based assays have been demonstrated to be more sensitive and accurate than darkfield microscopy in cases of ulcerative lesions and/or tissues, the sensitivity of nucleic acid amplification tests (NAATs) when testing material collected with a swab is still only about 80% (Gayet-Ageron et al., 2015; Buder et al., 2019). For this reason, a negative NAAT result cannot rule out infection (Buder et al., 2019). However, PCR can be a helpful additional diagnostic aid under specific circumstances. For example, cases of seronegative secondary syphilis have been reported, and it has been suggested that direct detection of *T. pallidum* via NAATs, darkfield microscopy, and/or histology should be attempted under these circumstances (Furuhata et al., 2016; Montecinos et al., 2015; Buder et al., 2019). Additionally, PCR-based assay was capable of detecting *T. pallidum* deoxyribonucleic acid (DNA) in the aortic valve of a patient with infectious endocarditis, indicating the better performance of NAATs in these settings (Hijikata et al., 2019). *T. pallidum* is capable of displaying high-level resistance to macrolide antibiotics (Stamm, 2016; Buder et al., 2019) caused by mutations within 23S rRNA that in theory could be detected by NAATs (Chen et al., 2013). However, these NAATs are not yet FDA cleared.

Diagnosis of Congenital and Neurosyphilis

Currently, early screening for syphilis is recommended in all pregnant women (US Preventive Services Task Force, 2009; Curry et al., 2018). All women should be tested at least once during pregnancy; in high prevalence areas or among women with potential risk factors, repeat testing may be indicated in later trimesters. For diagnosis of congenital syphilis, antepartum maternal serum is the ideal specimen. Confirmation of congenital syphilis, however, may require a combination of clinical and radiologic examinations, placental analysis, and testing of neonatal serum. The latter is typically performed semiquantitatively using nontreponemal tests and is compared with maternal serologic titer to determine the source of the antibody (i.e., to exclude transplacentally derived maternal antibody).

The diagnosis of neurosyphilis requires a positive serum treponemal test in addition to a positive VDRL on CSF or some other CSF abnormality (e.g., pleocytosis, elevated protein level). A positive CSF VDRL is highly specific for the diagnosis of neurosyphilis but is also insensitive. It is negative in 22% to 69% of patients with active neurosyphilis, and its sensitivity in inactive neurosyphilis may be as low as 10%. By contrast, the CSF FTA-ABS is reported to have high sensitivity and negative predictive value for neurosyphilis, so some experts advocate using this as a means of excluding the diagnosis (Marra, Tantalo et al., 2004). Its low specificity limits its positive predictive value, however.

TREATMENT OF TREPONEMATOSES

T. pallidum subsp. and *T. carateum* are uniformly susceptible to penicillin and other β-lactam antibiotics. Treatment for primary, secondary, and early latent syphilis is a single intramuscular injection of benzathine penicillin G. The dosage and length of treatment depend on the stage of infection (CDC, 2015). For pregnant women with penicillin allergy, desensitization is recommended prior to penicillin therapy (CDC, 2015). In contrast to β-lactam antibiotics, *T. pallidum* could display high-level resistance to macrolide antibiotics due to mutations in 23S rRNA (Stamm, 2016).

Yaws, pinta, and endemic syphilis are treated with the same antibiotic, although often at a lower dose. Household contacts of patients with the latter three diseases usually are also treated. For patients who are allergic to penicillin, doxycycline or tetracycline may be used. A single oral dose of azithromycin, a currently recommended equivalent to benzathine penicillin according to the 2012 revised WHO policy, seems to be an efficient approach to eradicate yaws (Mitja et al., 2015). A pronounced worsening in clinical course, termed the Jarisch-Herxheimer reaction, may be seen upon treatment of venereal syphilis patients, although symptoms frequently are not as severe as in treatment of relapsing fever spirochetes (Griffin, 1998).

For late latent syphilis or syphilis of unknown duration, benzathine penicillin G is given in multiple doses in a course of several weeks. Stage of disease does not affect treatment for yaws, pinta, or endemic syphilis (Engelkens, Judanarson et al., 1991; Engelkens, Niemel et al., 1991). A 10- to 14-day course of high-dose intravenous aqueous penicillin G is indicated for neurosyphilis and congenital syphilis (CDC, 2015). For patients coinfected with HIV and *T. pallidum*, current CDC guidelines do not recommend any significant deviation in therapy (CDC, 2015). As indicated by large-scale prospective studies, patients with RPR titers of 1:32 and above are at high risk of having neurosyphilis (11-fold and 6-fold higher in HIV-infected and HIV-uninfected individuals, respectively), as are HIV-infected patients with CD4+ T-cell counts of 350/uL and below. It is important to identify those individuals at higher risk because penicillin G benzathine does not achieve treponemicidal levels in CSF (Lukehart, 2018).

Indeed, prospective studies have failed to show any benefit of "enhanced" or alternative therapies for early syphilis and neurosyphilis, respectively, among HIV-infected persons (Rolfs et al., 1997; Marra et al., 2000). On the other hand, some authorities suggest that given a propensity to develop neurosyphilis even in the face of treatment for primary syphilis, all coinfected patients should have CSF examined for the evidence of neurosyphilis regardless of the stage of syphilis, and if CSF abnormalities are found to be treated for neurosyphilis (Lukehart, 2018).

OTHER TREPONEMAL DISEASES

Description

A number of spirochetes belonging to the treponeme molecular group-1, previously referred to as pathogen-related oral spirochetes, and various species of *Treponema* (e.g., *T. denticola*, *T. socranskii*) have been recovered with increased frequency and in higher numbers from the gingiva of patients with ulcerative gingivitis and chronic periodontitis compared with patients with healthy gingiva (Riviere et al., 1995, 1996; Loesche & Grossman, 2001). Using very sensitive nucleic acid amplification coupled with electrospray ionization mass spectrometry analysis, *T. denticola* genes have also been reported in high proportions of patients undergoing prosthetic joint revisions, the significance of which remains to be determined (Jacovides et al., 2012). Although originally thought to resemble *T. pallidum* on the basis of immune cross-reactivity and in vitro invasive properties, these putative pathogens are rather genetically heterogeneous and only distantly related to *T. pallidum* (Choi et al., 1996; Riviere et al., 1999).

Pathogenesis

A definitive causal relationship between the spirochetes and these diseases has not been firmly established; however, their presence in significant numbers, more commonly in diseased than in healthy tissue, suggests at least an association with gingivitis/periodontitis. Because a number of other nontreponemal bacterial genera (e.g., *Prevotella*, *Actinobacillus*, *Porphyromonas*) have also been associated with these clinical manifestations, research continues as to whether culpability belongs to specific virulent organisms among them or rather to the overall diversity of organisms contained within the plaque biofilm (Loesche & Grossman, 2001).

Diagnosis

As with the commensal species of *Treponema* found in the genital area, some oral *Treponema* spp. can be cultured under strict anaerobic conditions using a variety of specialized, enriched broth media. Other species, including most of those associated with periodontal disease, have not been cultured in vitro. These organisms have been detected with monoclonal antibodies against *T. pallidum*, with which they cross-react. Other investigators have employed a variety of genetic amplification tools in an effort to identify and characterize them (Paster et al., 2001; Hutter et al., 2003). These "molecular expeditions" are conducted by using primers that target conserved bacterial sequences and either PCR to amplify ribosomal (rRNA) genes or reverse-transcriptase PCR to amplify the rRNA itself. Resultant products can then be cloned in *Escherichia coli* and sequenced to determine phylogenetic relationships.

Treatment

For years, treatment has been aimed primarily at reducing the overall bacterial burden by removing the plaque biofilm, both above and below the gumline, through physical manipulation (e.g., surgical debridement). Recently, the addition of various antimicrobial regimens, including systemic antibiotics and locally applied agents, has been shown to be a potentially beneficial adjunct. Of 11 antimicrobials tested in a recent study, doxycycline, minocycline, azithromycin, and erythromycin were all effective against *T. denticola* strains, *T. socranskii*, and *T. vincentii*, in contrast to quinolones or kanamycin, which were ineffective (Okamoto-Shibayama et al., 2017). A novel antimicrobial agent, amixicile (inhibitor of pyruvate-ferredoxin oxidoreductase), with effective in vitro activity against *T. denticola* and other oral spirochetes has been suggested as a selective agent to treat periodontal disease (Reed et al., 2018).

LEPTOSPIRA

DESCRIPTION

The genus *Leptospira* is composed of at least 20 genomic species, many containing both pathogenic and nonpathogenic strains, and more than 260 serovars (Ko et al., 2009). Previously, *Leptospira* was divided into only three species, *L. interrogans* (pathogenic), *L. biflexa* (nonpathogenic), and *L. parva* (nonpathogenic), based on biochemical properties. However, it has become evident that antigenic properties and pathogenic potential are not consistently predictive of genetic relatedness (Ko et al., 2009). Leptospires are members of the phylum *Spirochaetes* and exhibit tightly coiled forms that measure 0.1 μm in width by 6 to 20 μm in length and demonstrate spinning motility. Unique among the pathogenic spirochetes described in this chapter, leptospires have a characteristic hooklike or question mark–like appearance by electron microscopy (see Fig. 61.1, *B*) and have the ability to exist as free-living organisms in alkaline fresh water and moist soil.

EPIDEMIOLOGY

Leptospirosis is a leading zoonotic disease causing morbidity and mortality in humans, predominantly in tropical and subtropical regions (CDC, 2018b; Costa et al., 2015). Although it was identified nearly 100 years ago, it is still considered an important emerging disease. Individual serovars show geographic preferences as well as particular ecologic niches. The organism is carried by many rodents and feral and domestic animals; however, murids are among the most frequent reservoirs and serve as an important source of infection in man. Reservoir hosts harbor high concentrations of leptospires in renal tubules without significant untoward effect and shed high numbers in their urine. Contact with urine-contaminated water or soil followed by entry of bacteria through cuts or mucosal surfaces is a frequent mode of acquisition. Some occupations (e.g., miners, farmers and field workers, veterinarians, fish farmers, sewage workers) and recreational pursuits (e.g., camping near or swimming in infected waterways) increase exposure risk. The estimated probability of transmitting *Leptospira* spp. from dogs to humans is very low (Guagliardo et al., 2019). Approximately 100 to 150 cases occur in the United States each year, predominantly in Hawaii and Puerto Rico (CDC, 2018b); however, the disease is probably significantly underreported.

PATHOLOGY AND PATHOGENESIS

Upon entry, leptospires quickly gain access to the bloodstream and disseminate widely to sites such as the CNS, eye, liver, kidneys, lungs, and/or other viscera. Damage to endothelium in infected tissues may result in local ischemia, hemorrhage, and proinflammatory cytokine upsurge, potentially leading to end-organ (e.g., hepatocellular, renal tubular, alveolar) damage (Ko et al., 2009). The liver exhibits a characteristic yellow-green color, but histologic changes range from uninvolved to disorganization of liver cell plates, spotty necrosis, Kupffer cell hyperplasia, cholestasis, and portal infiltrates; submassive centrilobular hepatocellular necrosis associated with intense hemorrhage has been reported in Weil disease (Milner et al., 2015b). Acute interstitial nephritis, necrosis of proximal tubules with mixed inflammatory infiltrate of lymphocytes, plasma cells histiocytes, and eosinophils with breaks in the basement membrane are seen in leptospirosis (Milner et al., 2015b). Pulmonary findings include congestion and edema, pleural effusion, alveolar hemorrhage, and infrequent intraalveolar hemorrhage (may be massive), sometimes with hyaline membranes, rarely with organizing pneumonia. Myocarditis, meningitis/encephalitis, and myositis could also be seen (Milner et al., 2015b). Silver stain or immunohistochemistry (IHC) may reveal filamentous or granular aggregates of organisms (Milner et al., 2015b). The specific mechanisms for endothelial, hepatic, and renal damage are unknown but are likely immune mediated.

CLINICAL MANIFESTATIONS

Typically, infection with leptospires is subclinical or manifests as a mild, influenza-like illness (anicteric form) 2 to 20 days following organism acquisition. Symptomatic cases are often biphasic, characterized initially by the abrupt onset of nonspecific symptoms such as chills, fever, headache, myalgia, back pain, abdominal pain, anorexia, nausea, and vomiting. This phase lasts 4 to 7 days and is marked by bacteremia with systemic dissemination. Following a short remission of several days, the immune phase begins, which is characterized by the appearance of antibodies to the organism, uveitis, rash, and hepatic and renal damage. As many as one-half of patients have clinical signs of meningitis and a CSF pleocytosis during this second phase of illness. A more severe monophasic form of disease (called the icteric form or Weil disease) also affects a minority of patients. This is characterized by fever, jaundice, and bleeding, followed by oliguric renal failure, shock, and myocarditis. Mortality has been reported to range from 1% to 50% in Weil disease (Wagenaar & Goris, 2018) and more than 50% in severe hemorrhagic syndrome (CDC, 2018b).

LABORATORY DIAGNOSIS

Although not commonly performed in diagnostic laboratories, leptospires can be isolated from CSF, blood, and tissues early in the bacteremic phase (first 10 days) and from urine during the immune phase (second week to up to 30 days). Culture requires a specialized medium (e.g. Fletcher or Ellinghausen-McCullough-Johnson-Harris) and prolonged incubation at 25° to 30°C (Johnson, 2014). Leptospires growing below the surface of the medium may be detected by darkfield microscopic examination in which characteristic spinning leptospires with hooked ends are visualized.

The majority of leptospirosis cases are diagnosed serologically. Agglutinating antibodies appear during the first week of illness, peak at around 3 to 4 weeks, and may persist for years. Antibodies can be detected using bacterial antigens by a macroscopic or microscopic agglutination test, a hemagglutination test, or ELISA testing. The microscopic agglutination test, which employs antigen from live bacteria, is the established serologic reference method. Additionally, various rapid assays utilizing lateral flow, ELISA, or agglutination methodology have been developed with reasonable sensitivity and specificity. Some of these assays are commercially available and could be used in settings with limited laboratory facilities (Wagenaar & Goris, 2018). Molecular methods, including PCR and real-time PCR, provide the capability of confirming the diagnosis of leptospirosis during the first 5 days of illness with a high degree of accuracy. Although molecular methods are being more widely implemented, they are still not readily available in most clinical laboratories for leptospiral DNA detection (Wagenaar & Goris, 2018).

TREATMENT

Severe disease requires aqueous penicillin G or ampicillin given intravenously, and less severe disease can be treated with oral ampicillin, amoxicillin, or doxycycline. Prophylaxis with oral doxycycline or azithromycin (in pregnant women and children) provides protection for individuals in high-exposure environments (Wagenaar & Goris, 2018), including areas following floods, military personnel, and disaster workers (CDC 2018a; Schneider et al., 2017). Immunization of domestic livestock and pets has reduced the danger of infection from these animals to high-risk populations such as veterinarians and farmers. Risk is not completely eliminated, as infection has been shown to occur in immunized animals with successful transmission of the agent to humans (Wagenaar & Goris, 2018).

BORRELIA

The genus *Borrelia* contains several species that form two phylogenetic clades: the Lyme borreliosis group (or *Borrelia burgdorferi* sensu lato [s.l.]) and the relapsing fever group. The former has been divided into multiple genospecies by molecular analyses, three of which are clearly associated with human disease: *B. burgdorferi* sensu stricto (s.s.), *Borrelia garinii*, and *Borrelia afzelii*. The relapsing fever group contains many species that can be isolated from argasid (soft) ticks (e.g., *B. hermsii*, *B. turicatae*), ixodid (hard) ticks (e.g., *B. lonestari*, *B. miyamotoi*), and the human body louse *(B. recurrentis)*. Members of the *Borrelia* genus are helical bacteria ranging in size from 5 to 30 μm long by 0.2 to 0.5 μm wide; they are actively motile, containing 7 to 22 periplasmic flagella, and multiply by binary fission. Unlike *Treponema* spp., *Borrelia* exhibit a multitude of immunogenic proteins on their outer membrane surfaces, and many species can be cultivated in/on artificial media. Moreover, the intricacies of the *Borrelia* genome, with its 910 kB linear chromosome and 21 linear and circular plasmids, render it a more genetically complex genus than *Treponema* (Brisson et al., 2012).

What follows is a description of the two major clinical disease forms of human borreliosis, both of which are vectorborne. As a result, they must often be considered, both from an epidemiologic and from a clinical standpoint, in conjunction with other infectious agents transmitted by similar or identical vectors. Examples include the flaviviral agents of tickborne encephalitis and various bacteria of the *Rickettsiaceae*, *Ehrlichiaceae*, and *Francisellaceae* families, as well as the protist *Babesia microti*. Clinical and diagnostic information related to these and other vectorborne diseases may be found elsewhere in this volume.

LYME AND LYMELIKE DISEASES

Lyme disease is the most common tickborne illness in North America and Europe today (Steere, 2018). Lyme disease (Lyme borreliosis) was so named during the 1970s following an epidemic of oligoarticular arthritis encompassing several communities in eastern Connecticut, chief among them the town of Old Lyme (Steere, Malawista, Hardin et al., 1977; Steere, Malawista, Syndman et al., 1977). Epidemiologic inquiry quickly established an association between Lyme disease (then referred to as *Lyme arthritis*) and the hard tick *Ixodes scapularis* (formerly *Ixodes dammini*) (Steere et al., 1978). Within 4 years, Burgdorfer et al. (1982) had successfully (1) isolated a novel spirochete species from an *Ixodes* tick sp. collected in New York, (2) reproduced the characteristic primary dermal lesions of Lyme disease in tick-fed rabbit models, and (3) demonstrated seroreactivity to antigens of this novel spirochete both in the rabbit model and in convalescent sera from human cases, thus fulfilling a contemporary "immunologic" variation of Koch postulates (Fredricks & Relman, 1996). The implicated organism was subsequently recognized as a member of the genus *Borrelia* and named *B. burgdorferi* in recognition of its discoverer. In retrospect, different aspects of the multisystem inflammatory ailment now commonly known as Lyme disease had been recognized and described both in Europe (Afzelius, 1910; Bannwarth, 1941) and in the United States (Scrimenti, 1970) prior to the epidemic in Connecticut. Yet the present body of knowledge pertaining to Lyme borreliosis can be attributed largely to the establishment and identification of its infectious origin spawned by the New England outbreak.

Borrelia mayonii, a novel pathogenic species of bacteria, is capable of causing Lyme disease in North America in addition to *B. burgdorferi*, as recently discovered by members of the CDC and Mayo Clinic (Pritt et al., 2016). Of the 100,000 clinical samples screened for the presence of *B. burgdorferi*, six were flagged as a unique species, which the researchers called *Borrelia mayonii* (Pritt et al, 2016; Young & Hefner, 2016). Approximately 20 ticks were also positive for *B. mayonii* (Pritt et al., 2016). So far, *B. mayonii* has been found only in the upper Midwest portion of the United States, including Minnesota, Wisconsin, and North Dakota. The genetic similarities between *B. mayonii* and closely related *B. burgdorferi* spp. may explain why these two bacteria are both capable of causing similar clinical symptoms. In addition to typical symptoms of *B. burgdorferi* infection, *B. mayonii* has been demonstrated to cause nausea, vomiting, diffuse macular rashes rather than a bull's-eye rash, and unusually high spirochaetemia (Pritt et al, 2016; Young & Hefner, 2016). Neurologic symptoms, including confused speech, profound somnolence, and visual difficulties, were present in three patients (Pritt et al., 2016). According to the CDC, current tests and treatments for Lyme disease seem to be effective against *B. mayonii* infection.

Epidemiology and Pathogenesis

A total of 20 different genospecies of *Borrelia* that form the Lyme borreliosis group have been characterized (Steere, 2018). The well-established human pathogens include *B. burgdorferi* s.s., which causes Lyme disease in North America, Europe, and Asia; and *B. garinii*, *B. afzelii*, *B. spielmanii*, and *B. bavariensis*, which cause similar but subtly different illnesses in Europe and/or Asia (Stanek et al., 2012; Stanek & Reiter, 2011). Other *B. burgdorferi* s.l. species have been isolated from a variety of geographic locations and both vertebrate and invertebrate hosts, yet their role as etiologic agents of human disease remains in various stages of elucidation (Oliver et al., 2008; Rudenko et al., 2011).

In the United States, the incidence of Lyme disease varies with the geographic distribution and prevalence of causative *Borrelia* spp., which in turn are regionally dependent on natural transmission cycles and the number, type, and density of tick vectors, animal reservoirs, and incidental hosts. Disease onset exhibits a seasonal peak, which parallels the questing periods of the predominant tick vector in a given region (Falco et al., 1999). Cases of Lyme disease have almost tripled since the 1990s to the estimation of more than 300,000 annually (CDC, 2017b). Lyme disease is present in all 50 states (Quest Diagnostics, 2018). A total of 42,743 confirmed and probable cases of Lyme disease were passively reported in 2017, an increase of more than 17% from 2016 (CDC, 2017b). The actual incidence of Lyme disease is most probably up to 10 times higher as supported by the CDC report, which examined test results performed from seven large commercial laboratories, indicating that the actual annual incidence during 2008 may have exceeded 240,000 cases (Hinckley et al., 2014).

The vast majority of cases occur in the Northeast, Upper Midwest, and Northwest regions where *B. burgdorferi* s.s. is endemic. Here, incidence rates vary from 10 to 100 cases/100,000 population (Fig. 61.7). The relative lower incidence observed in the Northwest can be explained by different feeding habits of the two primary tick vectors there: *I. spinipalpis*, which maintains enzootic transmission but seldom feeds on or transmits to humans, and the Western black-legged tick, *I. pacificus* (Fig. 61.8, *A*), which more commonly feeds on humans but plays little role in the enzootic cycle (and hence is rarely infected) (Girard et al., 2009). In the Midwest and Northeast, the black-legged tick (or deer tick), *I. scapularis* (see Fig. 61.8, *B*), serves both these roles. Its promiscuous feeding habits permit it to transmit *B. burgdorferi* s.s. between primary reservoir hosts

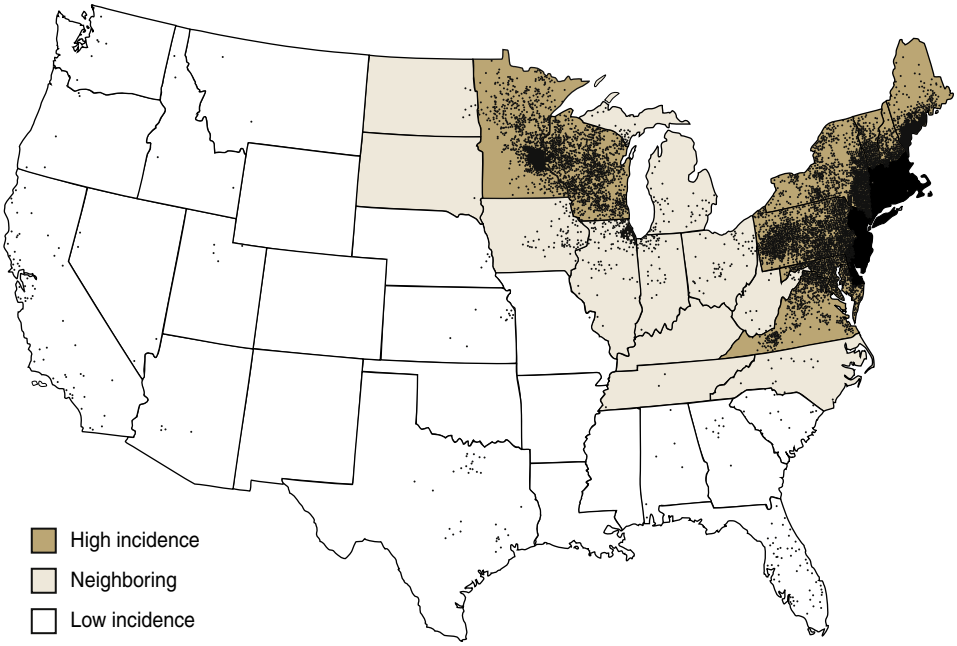

Fig. 61.7 Average annual number of confirmed Lyme disease cases, by county of residence—United States, 2008–2015. Each dot represents one confirmed case according to county of the patient's residence. *High incidence,* States with an average annual incidence ≥10 confirmed Lyme cases per 100,000 population; *neighboring,* states that share a border with high incidence states or are located between those states; *low incidence,* all other states. (Schwartz AM, Hinckley AF, Mead PS, et al: Surveillance for Lyme disease—United States, 2008-2015, MMWR Surveill Summ 66[22]:1–12, 2017.)

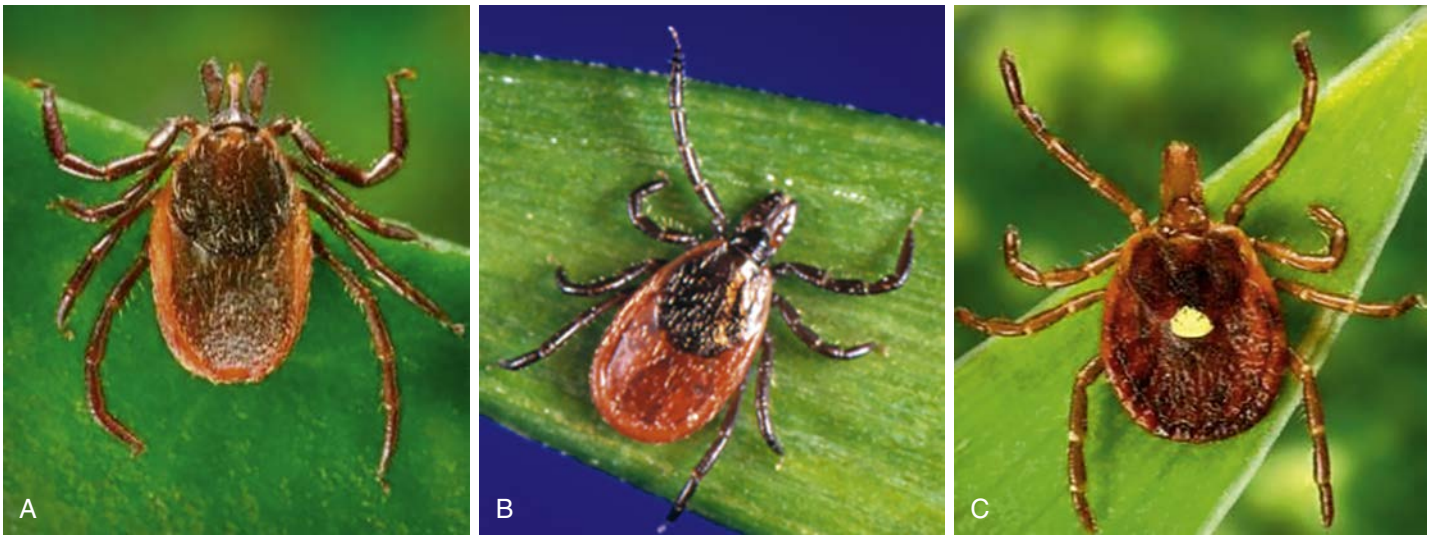

Fig. 61.8 Hard-tick vectors of *Borrelia* in the United States. **A** Adult female, Western black-legged tick, *Ixodes pacificus*. **B** Adult female, black-legged tick (or deer tick), *Ixodes scapularis*. **C** Adult female, lone star tick, *Amblyomma americanum.* (Courtesy James Gathany, CDC/PHIL file photos.)

(the white-footed mouse) as well as to humans. A number of recent studies report an expansion of *I. scapularis* geographic distribution, some with concomitant increases in *B. burgdorferi* s.s isolation and/or Lyme disease rates (Pepin et al., 2012; Wang et al., 2014; Brinkerhoff et al., 2014). In Europe and Asia, the most important tick vectors include *I. ricinus* (sheep tick) and *I. persulcatus*, respectively, and primary animal reservoirs for *B. afzelii* and *B. garinii* comprise small rodents, voles, and/or various avian species (Parola & Raoult, 2001).

Other important epidemiologic factors contributing to transmission dynamics of *B. burgdorferi* s.l. and incidence of Lyme disease include the density and infection rate of local vectors, the abundance and infectivity of reservoir hosts, and the likelihood and duration of human exposure to tick vectors (Parola & Raoult, 2001). Amplification hosts, such as the white-tailed deer in the northeastern United States, may also increase vector population density, thereby indirectly affecting disease rates regionally (Steere, 2015). Another key transmission variable relates to the developmental stage of the tick and its duration of attachment during feeding. Hard-tick life cycles consist of three stages (called instars)—larvae, nymphs, and adults. Each instar requires a single blood meal before molting to the next stage (or ovipositing, in the case of adult females). Because *B. burgdorferi* s.l. is not efficiently transmitted vertically in *Ixodes* spp., larvae acquire the spirochete from an infected host upon feeding and, hence, play no role in human transmission (Rollend et al., 2013). Rather, only nymphal and adult forms infected during a prior blood meal may transmit the spirochete to humans. Because nymphs are small and likely to go unrecognized while attached, they are believed to account for the greatest number of human infections (Falco et al., 1999; Nadelman et al., 2001). The process for tick transmission is most efficient with feeding durations exceeding 24 to 48 hours (Hojgaard et al., 2008), yet more rapid transmission has been documented (Cook, 2014).

As with *T. pallidum*, several complete genome sequences of *B. burgdorferi* s.l. have been characterized and compared (Fraser et al., 1997; Glöckner et al., 2006), revealing some fairly conserved genes important in survival, transmission, and virulence as well as some biosynthetic gaps. The former include a group of plasmid-encoded outer surface proteins (Osp A-F), which are differentially expressed in vector and mammal environments and are highly immune stimulatory (de Silva & Fikrig, 1997; Porcella & Schwan, 2001). The lipoprotein VlsE (for "variable major proteinlike sequence expressed") has the capability to undergo extensive antigenic variation (Zhang, 1998; Porcella & Schwan, 2001), although a conserved portion of this peptide forms the basis of some newer serologic tests (see later). Animal models of Lyme borreliosis have been useful for investigating the dynamics of *Borrelia* dissemination (e.g., tissue localization within heart, skin, and joints), specific cellular interactions, and details of immunologic responses and virulence mechanisms. In an investigation using Rhesus macaques to study spirochete persistence following antimicrobial therapy, Embers and colleagues (2012) described recovery of viable *Borrelia* (in addition to evidence of persistent DNA, RNA, and protein

antigen) from some ticks that fed on monkeys 7 to 11 months following treatment (so-called xenodiagnoses; see later). While these observations raise important questions regarding the potential use of xenodiagnosis for human disease and about the actual rate of *Borrelia* eradication following standard treatment regimens, the authors' study design, methodology, and interpretations have drawn sharp criticism (Wormser et al., 2012), so definitive conclusions should await further investigation. Xenodiagnosis using *Ixodes* ticks in humans is still an experimental method, requiring an approved clinical research protocol.

Both innate and adaptive host immune responses are required to eradicate *B. burgdorferi*. A variety of proinflammatory cytokines are being produced and released at the affected sites. An atypical form of peptidoglycan, a major constituent of the *B. burgdorferi* cell envelope, has been suggested to act as a potential immunogen exaggerating inflammatory response during Lyme infections, including Lyme arthritis (Jutras et al., 2019). Moreover, a systematic review of studies examining biomarkers among patients with antibiotic-resistant Lyme arthritis had identified several potential biomarkers, including the Th17 pathway–dependent chemokines and cytokines (e.g., interleukin 6 [IL-6], IL-8, IL-10, tumor necrosis factor α [TNF-α], interferon gamma [IFN-γ], CXCL9, CXCL10, CCL2, CCL3 and CCL4, CRP) as well as several miRNA species (miR-146a, miR-155, and let-7a), which could be potentially utilized in the future to predict antibiotic resistance (Badawi et al., 2019). In infected human skin tissues, *Borrelia* has been demonstrated to be capable of forming mixed biofilms with *Chlamydia* (Sapi et al., 2019), which could potentially provide a protective microenvironment from host responses and antibiotics. It is unclear whether *Borrelia* can play a synergistic role with *Chlamydia* in the etiopathogenesis of these diseases. Interestingly, a biofilm microcolony of *B. burgdorferi* caused more severe disease in a mouse model of Lyme arthritis than a regular microcolony of *B. burgdorferi*, providing a useful model for future studies (Feng et al., 2019).

Clinical Manifestations

Similar to syphilis, the clinical progression of Lyme borreliosis can be divided into three general stages: (1) an early localized phase in which a primary lesion develops at the inoculation site; (2) an early disseminated phase marked by spirochete spread systemically, producing a variety of cardiac, neurologic, and/or dermatologic manifestations; and (3) a late phase heralded by rheumatologic disease as well as further neurologic and/or dermatologic phenomena. Asymptomatic seroconversion or subclinical disease has also been reported to occur in as many as 7% of persons within endemic areas (Steere et al., 2003).

The earliest clinical stage begins ≈1 week following the bite of an infected tick, at which time a characteristic rash, descriptively termed erythema migrans, develops near the inoculation site in approximately 75% of patients. The lesion appears as a painless red macule or papule and subsequently expands to become an erythematous patch measuring up to 70 cm in extreme cases (Nadelman et al., 1996). An area of central pallor may develop, imparting a targetlike or bull's-eye appearance (Fig. 61.9), but only in a minority (37%) of patients (Nadelman et al., 1996). Lesions are often accompanied by nonspecific symptoms such as fever, fatigue, headache, and myalgia, as well as regional lymphadenopathy (Nadelman et al., 1996; 1998; Smith et al., 2002). If biopsied, histologic analysis reveals superficial and deep perivascular infiltrate with eosinophils centrally and plasma cells at periphery; also reported are peripheral neutrophils and eosinophils, lack of plasma cells, and spongiosis (Milner et al., 2015a). Unlike the lesions of syphilis, vasculitis is not a typical histologic feature of erythema migrans.

Dissemination of *Borrelia* portends the second stage of clinical illness, in which many organ systems may be affected. Smaller, secondary erythema migrans lesions arising in multiple sites are one of the more common signs of early dissemination (Murray & Shapiro, 2010). The probability of early hematogenous dissemination could be predicted by a particular genotype (Nadelman & Wormser, 1998; Brisson et al., 2008). A novel pathogenic *Borrelia* species, named *B. mayonii*, causing Lyme disease with unusually high spirochaetemia has been isolated from six patients and recently described (Pritt et al., 2016). Neurologic manifestations (neuroborreliosis) affect up to 15% of US patients, with symptoms including radiculopathy, cranial nerve palsy (including bilateral cranial nerve VII), lymphocytic meningitis, and a variety of peripheral neuropathies (Steere, 2018; Shah et al., 2018). These manifestations are collectively referred to as **Bannwarth syndrome** in some European countries. Interestingly, a cluster of five patients who presented with Bannwarth syndrome was recently described in the US Midwest (Shah et al., 2018). Somewhat rarer, cardiac involvement in the form of transient atrioventricular block or myocarditis is also reported in about 5% of US patients (Steere, 2001). Other sites potentially affected include the liver (e.g., mild, transient hepatitis) and eyes (e.g., conjunctivitis, neuroretinitis) (Steere, 2015).

Fig. 61.9 Characteristic bull's-eye lesion, erythema migrans, observed at the site of spirochete inoculation in ≈80% of patients with Lyme disease. (Courtesy James Gathany, CDC/PHIL file photo.)

In the United States, the most common manifestation of untreated, late-stage Lyme disease is arthritis, which develops in over half of untreated patients (Steere, 2018). Typically monoarticular or oligoarticular in extent, large joints such as the knee are frequently involved (Steere, 2018). Symptoms of pain and swelling begin acutely several weeks to months following spirochete inoculation and may last for days to months (median, 1 week). Some patients continue to experience intermittent recurrences of migratory arthritis followed by prolonged disease-free periods (Steere, 2018). Conversely, late-stage manifestations of persistent Lyme borreliosis in European patients more commonly involve neurologic or cutaneous organs. The former may overlap clinically with early disseminated neuroborreliosis and include lymphocytic meningitis and peripheral neuropathies (e.g., sensory polyneuritis, pareses). In addition, CNS manifestations such as myelitis and spastic-ataxic gait disturbances as well as short-term cognitive dysfunction have been noted (Kaiser, 1998; Halperin, 2008, 2019). A dermatologic phenomenon known as acrodermatitis chronica atrophicans has also been associated with late Lyme borreliosis in Europe. These lesions are present on hands, wrists, elbows, and feet; they are often symmetric and characterized histologically by a slight acanthosis with a dense, patchy, superficial and deep infiltrate with dilated and ectatic vessels with progressive epidermal thinning, hyperkeratosis, and dermal atrophy (Milner et al, 2015a). Other well-established or controversial long-term dermatologic manifestations include *Borrelia* lymphocytoma, cutaneous B-cell lymphoma, morphea, and lichen sclerosus et atrophicus (McGinley-Smith & Tsao, 2003; Milner et al, 2015a).

Some of the variations in late-stage clinical manifestations may be attributable to inherent traits of different *Borrelia* spp. themselves. For instance, *B. afzelii* has been disproportionately isolated from lesions of erythema migrans and acrodermatitis chronica atrophica in Europe as compared with other genospecies. By contrast, *B. garinii* is more frequently implicated in European cases of neuroborreliosis and it may cause borrelial encephalomyelitis (Steere, 2018). Other studies demonstrate that particular molecular subtypes of *B. burgdorferi* s.s. are more frequently associated with invasive properties and spirochetemia (Dykhuizen, 2008; Wormser et al., 1999). Additional observations corroborating the notion that disease course is influenced by virulence properties of the specific *Borrelia* strain include (1) serologic responses among patients with particular clinical symptoms may be preferential toward antigens from specific *Borrelia* spp., and (2) certain genospecies appear to have different properties in vitro.

In the vast majority of patients, clinical manifestations of Lyme disease respond to appropriate antibiotic therapy (Seltzer et al., 2000; Wormser et al., 2006; Aucott et al., 2013). Yet, a small subset may continue to experience persistent symptoms such as musculoskeletal pain, fatigue, and neurocognitive deficits despite treatment—a condition that has variably been

termed post–Lyme disease syndrome, chronic Lyme disease, or treatment-resistant borreliosis (Klempner, 2002; Halperin et al., 2011). Without exception, prospective studies have shown little benefit of prolonged antibiotic therapy over placebo in reducing the symptoms of this syndrome. Further, isolation of *Borrelia* or amplification of *Borrelia* genes is often unsuccessful among patients with this disorder (Klempner, 2002); and retrospective case-controlled studies illustrate that the frequency of objective signs among such patients is no different than that of age-matched controls without a history of Lyme disease (Seltzer et al., 2000). An international panel of subject experts has summarized the evidence, or lack thereof, in support of a link between *B. burgdorferi* and this chronic syndrome (Feder et al., 2007). It should be noted that despite the existence of only one body of medical literature, strong opposition to this viewpoint exists. Adamant dissent is evidenced not only by the many correspondence letters referencing the report by Feder and colleagues (2007), but also by the advocacy group International Lyme and Associated Diseases Society, which issued its own management recommendations distinct from those of the Infectious Disease Society of America (IDSA) (Cameron et al., 2014) and contributed testimony in an antitrust investigation brought against IDSA by the state of Connecticut. The investigation culminated in an agreement by IDSA to allow review of the guidelines by an independent arbiter, which ultimately upheld essentially all of the initial recommendations (Lantos et al., 2010).

A number of reports have documented erythema migrans–like lesions in patients residing in the US South, Midwest, and other areas beyond the Lyme-endemic regions (reviewed in Masters et al., 2008). Referred to as southern tick-associated rash illness (STARI) or Master disease, the skin lesions are preceded by the bite of the lone star tick, *Amblyomma americanum* (see Fig. 61.8, *C*) yet are clearly not caused by *B. burgdorferi* s.l. infection (James et al., 2001; Wormser, Masters, Liveris et al., 2005; Masters et al., 2008). Although a putative relapsing-fever group agent, *B. lonestari*, had been tentatively implicated (Varela et al., 2004), failure to reproduce this association in multiple subsequent studies suggests that the true etiology remains elusive. Given the clinical overlap of STARI and Lyme disease (Wormser, Masters, Nowakowski et al, 2005; Herman-Giddens & Herman-Giddens, 2017) as well as the distribution of *A. americanum* in many Lyme-endemic regions, misclassification of these entities may be especially problematic in the absence of confirmatory diagnostic testing (Feder et al., 2011; Fukushima et al., 2019; Herman-Giddens & Herman-Giddens, 2017).

Laboratory Diagnosis

In the United States, Lyme disease is a reportable disease, with both laboratories and clinical providers passively reporting to public health agencies (CDC, 2017a). According to the 2017 CDC surveillance definition, a confirmed case requires documentation of compatible clinical findings (e.g., erythema migrans, arthritis, myelitis) in combination with either (1) laboratory evidence of infection (i.e., positive serology or culture) or (2) potential tick exposure within a Lyme-endemic region (CDC, 2017a). In the absence of objective clinical signs/symptoms, laboratory data, and/or endemic exposure, cases may only be considered as "suspected." Accordingly, laboratory testing is not an acceptable standalone diagnostic modality, but should serve rather as a tool to assist in confirming or refuting clinical suspicions (Brown et al., 1999). Reports highlighting the concepts of pretest probability based on epidemiologic and clinical factors, as well as likelihood ratios and test predictive values, thoroughly demonstrate the futility and high cost of a standalone laboratory-based approach (Seltzer & Shapiro, 1996; Nichol et al., 1998). In fact, Lyme disease testing for patients with only nonspecific symptoms such as fatigue, headache, or myalgia, even in endemic areas using accurate laboratory assays, can lead to more false-positive than true-positive results (Steere, 2018). Exacerbated by widespread anxiety on the part of the public and a general misunderstanding by many health care providers, the current diagnostic confusion surrounding Lyme borreliosis can perhaps be best dealt with by taking a thorough look at the indications for and limitations of laboratory testing.

A recommended approach to the laboratory diagnosis of Lyme disease and other acute tickborne illnesses is shown in Fig. 61.10. Rocky Mountain spotted fever, ehrlichiosis, anaplasmosis, and babesiosis are discussed in Chapter 63. Relapsing fever is discussed later in this chapter.

Serologic Tests

Laboratory diagnosis of Lyme disease most often is based on results of serologic tests. Detection of *Borrelia*-specific antibodies may be accomplished using methods that express results in terms of total or class-specific IgG or IgM. Various ELISAs that may incorporate whole cell–derived or select antigens produced recombinantly or from partially purified extracts of *Borrelia* are typically utilized.

As with any serologic response to an infectious agent, several variables affect the performance of assays developed to detect them. Early in the course of Lyme disease, levels of antibody below the limit of detection cause false-negative results. This may be circumvented partially with assays that detect IgM specifically (Reed, 2002). As disease progresses, antibody test sensitivity increases. In fact, the duration of illness itself is of greater importance for serologic detection than is test method or format (Steere, 2018). Specificity of the ELISA may also be adversely affected by cross-reacting antibodies to other microorganisms and host-derived proteins, including pathogenic spirochetes (e.g., relapsing fever group of *Borrelia* and treponemes), other bacteria (e.g., *Helicobacter pylori*), viruses (e.g., Epstein-Barr), as well as antinuclear antigens present in autoimmune disorders such as systemic lupus erythematosus (Brown et al., 1999; Reed, 2002; Steere et al., 2008). Previous immunization with the OspA subunit Lyme disease vaccine may lead to false-positive ELISA results as well (Steere et al., 1998). Other factors that may contribute to test variability include the particular antigen composition of the assay, stringency of quality control, optical density or index value thresholds utilized, bacterial strain responsible for infection, and the patient's individual immune response.

In an effort to increase the accuracy of serologic testing, in 1994 the CDC proposed the use of a two-tiered standard algorithm in which all initial positive and indeterminate ELISA results are subsequently tested by immunoblot (CDC, 1995), which provides the capability to discern antibodies against particular *Borrelia* proteins, for confirmation. With the manual Western blot, interpretation is somewhat subjective; although strict criteria for defining positive results have been outlined by the CDC (1995) (Fig. 61.11), some laboratories use modified criteria, which alters overall performance (Fallon et al., 2014). In June 2018, the FDA cleared the Lyme disease IgG and IgM line immunoblot confirmatory testing as the second tier (Gold Standard Diagnostics Corp., Davis, CA) (Lima, 2018), which offers several improvements to Western blot technology. The antigens are evenly and consistently spaced, the native three-dimensional antigen structure is maintained, results are precisely defined, the presence of the bands is determined by scanning software that provides more objective and standardized results, and the methodology can be easily automated. Within 4 weeks of symptom onset, most patients with Lyme disease will have developed an IgG response, so diagnostic reliance upon IgM assays alone is not recommended beyond this time point (CDC, 2017a).

There are issues with the standard two-tiered testing algorithm utilizing immunoblot as the second tier. The major weakness is that the results are significantly influenced by the stage of disease during which testing is performed (Steere, 2018). In the early stages of Lyme disease, the sensitivity is only about 40% to 60%, depending on the study (Moore et al., 2016). Limitations of the Western blot include false-positive results, particularly with the IgM immunoblot, and a high degree of interlaboratory and intralaboratory variability (Aguero-Rosenfeld, 2005; Fallon et al., 2014; Seriburi et al., 2012; Moore et al., 2016). Moreover, due to wide ranges of sensitivities and specificities of various available assays, even the choice of a particular ELISA-immunoblot combination can have a profound effect on percentage of positive results obtained via the standard algorithm. Finally, it is impractical for most hospital clinical laboratories to offer Western blot in-house, so samples typically are sent out to a commercial reference laboratory for confirmation, prolonging the turnaround time of the results.

In July 2019, the Zeus Borrelia modified two-tiered testing algorithm, in which two enzyme immunoassays (EIAs) are run concurrently or sequentially, replacing immunoblot as the second tier of serologic testing, was cleared by the FDA for diagnosing Lyme disease (Kelley & DiFrancesco, 2019). The sensitivity of this modified two-tier serologic testing protocol is higher than the sensitivity of ELISA methods during the early stage of the disease. Depending on the combination of ELISAs used, sensitivity increases from 10% to 20% for modified algorithm versus standard algorithm. The modified algorithm is more feasible for hospital clinical laboratories than an ELISA followed by immunoblot (Paxton, Theel et al., 2020). Moreover, ELISAs are objectively interpreted, tend to have high throughput, and can easily be automated, thus reducing turnaround time. Additionally, it is less costly to perform two ELISAs than it is to perform an ELISA followed by an IgM/IgG Western blot (Paxton, Theel et al., 2020).

Some newer ELISAs utilize recombinant, highly conserved, and immunodominant VlsE antigen or portions thereof (i.e., 26-mer peptide from the sixth invariable region [C6 peptide]), which could increase test accuracy particularly during the early stages of disease (Embers et al., 2007; Branda et al., 2010, 2011, 2018; Wormser et al., 2013). The C6 ELISA has demonstrated an excellent performance in correctly identifying patients with noncutaneous Lyme disease (Nigrovic et al., 2019).

With the Zeus modified algorithm, the VlsE1/pepC10 IgG/IgM ELISA is the first-tier test. If this initial test is reactive (positive) or

Acute tick-borne disease testing algorithm[1]

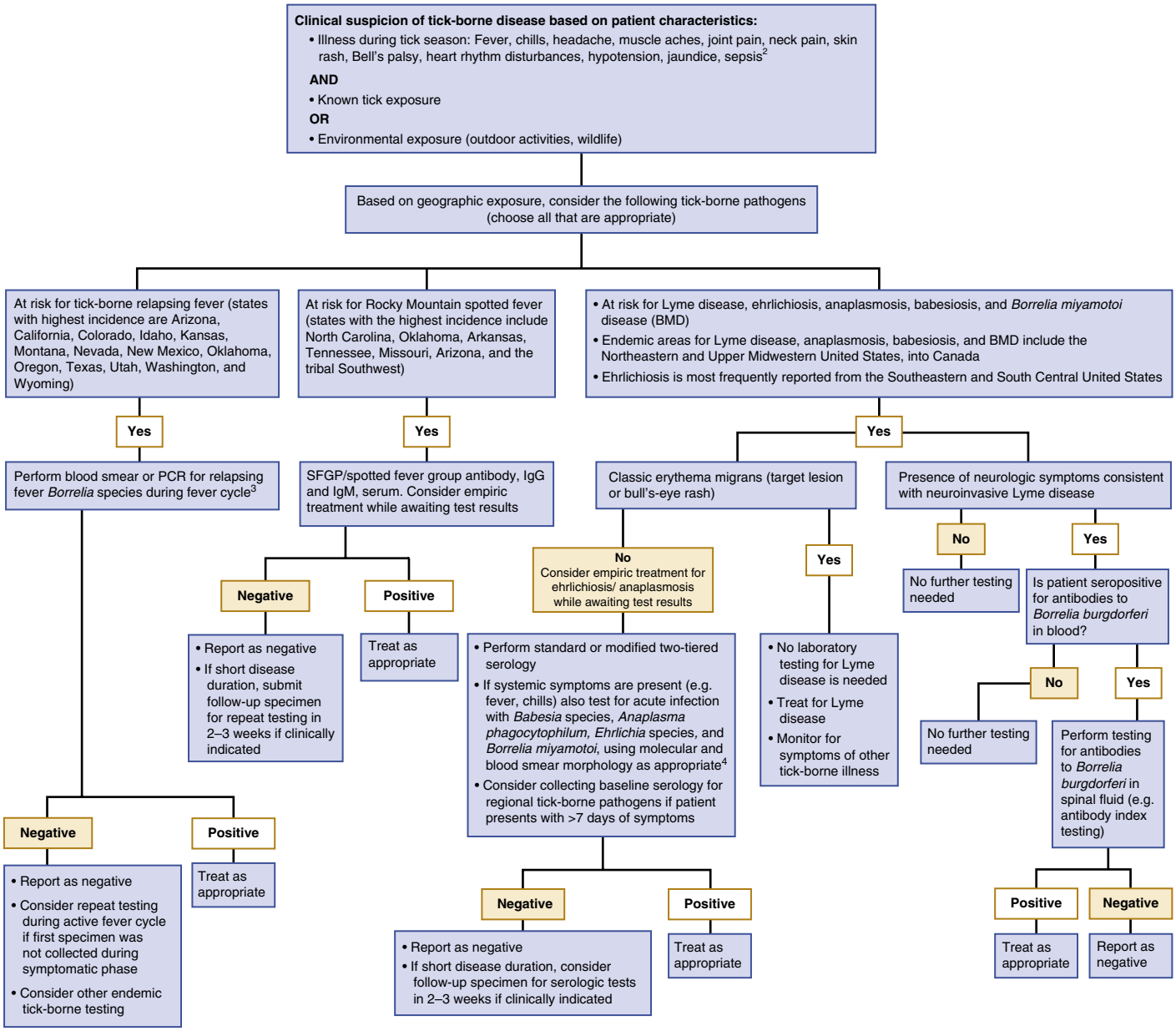

[1]Covers testing for the most common tick-borne pathogens in the United States. Not all inclusive.

[2]In the presence of severe neurologic symptoms, contact public health authorities for additional testing options (e.g. Powassan/deer tick virus, Heartland virus, Bourbon virus).

[3]If infection is thought to have been acquired outside the Americas, order both blood smear and PCR. Not all species of relapsing fever *Borrelia* may be detectable by a single PCR.

[4]Local test availability may vary. PCR testing of blood may be useful for detection of *Borrelia mayonii* in patients with exposure to ticks in Minnesota or Wisconsin.

Fig. 61.10 A recommended approach to the laboratory diagnosis of Lyme disease, relapsing fever, and other acute tickborne illnesses. Rocky Mountain spotted fever, ehrlichiosis, anaplasmosis, and babesiosis are discussed in Chapter 63.

equivocal, there are two options for second tier. In the first option, the second-tier assay is the Zeus whole cell antigen IgM/IgG ELISA, which detects total (IgG and/or IgM) result but does not differentiate antibody class. The other option of the modified algorithm involves performing two separate ELISAs as the second tier: one for IgM, the other for IgG, both of which use the whole cell antigen material (Paxton, Theel et al., 2020).

Although the modified two-tier testing has the potential to simplify interpretation in the majority of cases, there is still a role for the immunoblot in difficult or challenging cases of Lyme disease. In those cases, immunoblot can provide detailed information about the presence of an antibody response, indicate whether it is a predominantly IgM or IgG antibody response, and determine if it is a recent or past infection (Paxton, Theel et al., 2020).

Several other laboratory-based immunologic techniques have been evaluated for potential use in the diagnosis of Lyme disease. Reports have indicated that *Borrelia*-specific antibodies detected by ELISA and/or immunoblot in CSF and synovial fluid samples may be useful in confirming neuroborreliosis and Lyme arthritis, respectively, particularly when compared with serum levels (Cruz et al., 1991; Hansen & Lebech, 1991). For example, the CSF-to-serum anti-*Borrelia* antibody index, the favored assay to detect intrathecal production of anti-*Borrelia* antibodies for the diagnosis of neuroborreliosis in adults, has also shown an excellent performance in pediatric patients, with a reported 97% specificity and 75% sensitivity (Skogman et al., 2017). Moreover, the sensitivity could be further increased by measuring CSF early biomarkers, such as CXCL13 and/or total IgM index (Henningsson et al., 2016; Skogman et al., 2017).

Direct Methods of Detection

Given the relatively poor performance of serologic testing in the early presentation of Lyme disease, alternative testing methods for Lyme borreliosis have been highly sought after. Genomic amplification techniques for Lyme diagnostics surfaced in the early 1990s as a potential solution.

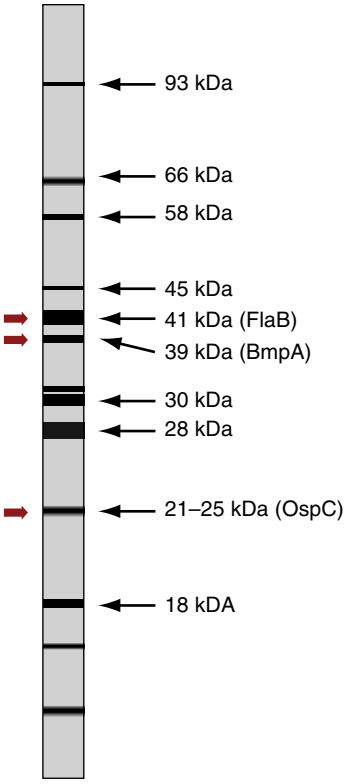

Fig. 61.11 Ten major bands and respective molecular weights of antibodies against *Borrelia burgdorferi* identified in immunoblot assays. For positivity according to Centers for Disease Control and Prevention (CDC) recommendations, immunoglobulin (Ig)G-specific blots require the presence of 5 of 10 bands, whereas IgM-specific assays require 2 of 3 *(red arrow)* bands. *BmpA,* Basic membrane protein A; *FlaB,* flagellin; *kDa,* kilodaltons; *OspC,* outer surface protein C.

Since that time, several modifications of the PCR using various genetic targets and amplicon detection methods have been applied to a variety of specimen types in search of *Borrelia* nucleic acids, though to date none have been cleared by the FDA for clinical use.

Samples from which *B. burgdorferi* s.l. could not be readily isolated were the focus of early investigations on PCR utility. Analyses on joint aspirate specimens from patients with Lyme arthritis demonstrated high sensitivity and specificity rates when several primer sets were used (Nocton et al., 1994; Dumler, 2001). After the results were compared with clinical information, it became apparent that (1) detection of *Borrelia* nucleic acids was more frequently associated with a history of absent or inadequate antimicrobial therapy, and (2) PCR positivity disappeared following appropriate treatment (Nocton et al., 1994). Further inquiry into a performance discrepancy of primer sets targeting genomic (e.g., *rRNA* genes) versus plasmid-derived (e.g., *OspA*, *OspB* genes) DNA revealed that the latter is present in higher quantities within joint spaces in Lyme arthritis (Persing et al., 1994). This phenomenon, termed target imbalance, seems to be unique to the inflammatory spirochete milieu of synovial fluid in Lyme arthritis and probably accounts for the higher sensitivity observed with primers targeting the *OspA* gene (Lebech, 2002).

Nucleic acid detection in tissue from erythema migrans lesions has been successful. However, although biopsy of the skin demonstrates a reasonably high sensitivity, this approach is very impractical (Dumler, 2001; Paxton, Theel et al., 2020). With the exception of erythema migrans lesions, the very low numbers of *B. burgdorferi* organisms that are present in tissues and body fluids, including blood and cerebrospinal fluid, are typically insufficient for detection by standard PCR-based assays (Schutzer et al., 2019). For this reason, studies of amplification assays did not work well on CSF or blood specimens regardless of the stage of Lyme disease or manifestations of suspected Lyme disease regardless of the PCR method utilized (Paxton, Theel et al., 2020). Increasing the volume of blood collected and/or performing an additional enrichment step have been suggested to improve the sensitivity during early Lyme disease (Hosono et al., 2003; Schutzer et al., 2019). In addition, several novel unconventional amplification assays capable of detecting significantly lower *B. burgdorferi* numbers than standard PCR assay (e.g., T2 magnetic resonance assay) are currently being developed and/or have been successfully utilized (Eshoo et al., 2012; Snyder et al., 2017; Schutzer et al., 2019).

Additionally, detection of *Borrelia* genetic material extracted directly from Ixodid tick vectors may be useful from an epidemiologic standpoint but cannot be relied upon for diagnosis or management of patients from whom the ticks were removed (Dumler, 2001; Wormser et al., 2006). As with most amplification techniques, use of PCR for diagnosis of Lyme disease is limited by many factors, including polymerase inhibitors, low target concentrations, potential for contamination, and choice of primer, among others. Whatever the application, the sensitivity and specificity of molecular tests are imperfect. Accordingly, negative results alone cannot be used to exclude a diagnosis, and positive results out of context do not confirm a diagnosis. Misinterpretations such as these may lead to dismal consequences if not resolved early (Patel et al., 2000; Molloy et al., 2001). It is important to note that because most patients with late manifestations of Lyme disease will have evidence of seroreactivity by the time of presentation (thereby fulfilling the CDC case definition), PCR studies probably are best used during early Lyme disease prior to seroconversion. Of utmost importance is the correlation of laboratory data with clinical impression, irrespective of whether such data are derived through serologic or molecular means.

Other methods for diagnosis of Lyme disease are under investigation. These include antigen-detection assays that as of this writing appear to have lower sensitivities than serologic testing, an INF-γ release assay, which shows promise for diagnosis of early Lyme disease, and metabolomics studies that evaluate the metabolic profile of patients infected with early disease for specific biosignature metabolites (Paxton, Theel et al., 2020).

Culture

Culture is the gold standard in diagnostic testing for many infectious diseases in which the causative agent does not also asymptomatically colonize humans. Cultivation of *Borrelia* spp. is achievable in the early phases of Lyme disease (Reed, 2002). Several modifications of the broth-based Barber-Stoenner-Kelly medium have been shown to be useful in the recovery of *Borrelia* spp. from biopsy tissue of erythema migrans lesions and large-volume plasma collections during the early, acute phase of disease (Nadelman et al., 1996; Wormser et al., 2001). However, reliance on subjective endpoints (e.g., darkfield microscopy or fluorescent antibodies) for the detection and identification of positive cultures, high media and reagent costs, wide reported sensitivity ranges, and a requirement that invasive procedures be performed on the patient (e.g., tissue biopsy) have all contributed to the test's general unpopularity outside research settings. Very importantly, recovery of *Borrelia* from CSF, synovial fluid, or other samples collected beyond the early phases of disease is rarely successful and therefore of little diagnostic utility.

Xenodiagnosis

In addition to culture of specimens collected from an infected person, recovery of *B. burgdorferi* s.s. can be accomplished by xenodiagnosis. In this technique, uninfected ticks are allowed to feed on patients with suspected infection. Upon repletion, ticks are then analyzed for viable *Borrelia*. While the method performs well in murine studies (Hua et al., 2003) and appears safe in human clinical trials (Marques et al., 2014), the ultimate value for diagnosing human infection remains to be determined given the marked differences in dissemination within murine (i.e., reservoir-like) and human (i.e., dead-end) hosts (Bockenstedt & Radolf, 2014). Xenodiagnosis using *Ixodes* ticks in humans is still only an experimental method.

Treatment and Prevention

The IDSA have published guidelines for the management of patients with suspected or proven Lyme borreliosis. To summarize, a large body of evidence confirms that a 10-day to 3-week course of oral doxycycline or amoxicillin is highly effective in the treatment of early, uncomplicated Lyme disease (Sanchez et al., 2016; Wormser et al., 2006; Young & Sadoughi, 2019) as some recent publications suggested the equal efficacy of shorter courses of treatment, such as 10 days (Kowalski et al., 2010; Stupica et al., 2012). In patients unable to tolerate any of these regimens, or for whom such regimens would be contraindicated, macrolide therapy may be an acceptable alternative. Extended treatment courses of this standard oral regimen are also considered to be effective in most patients with Lyme arthritis in the absence of neurologic manifestations (Sanchez et al., 2016). However, parenteral therapy with ceftriaxone (or penicillin as an alternative) may be used in cases of arthritis relapse. This same intravenous regimen is recommended for patients with third-degree heart block and/or neuroborreliosis. Of note, most of the prospective therapeutic trials upon which IDSA recommendations are based have endpoints defined in terms of clinical responses (i.e., disappearance of symptoms) rather than

the eradication of *Borrelia*. Cases of Lyme arthritis resistant to antibiotics could respond to symptomatic therapy (Steere & Angelis, 2006).

A somewhat more contested issue surrounds the use of prophylactic antibiotic therapy following recognition and removal of a feeding tick. Early prospective studies employing 10-day oral regimens of antimicrobial prophylaxis failed to establish any benefit over placebo (Warshafsky et al., 1996). Factors confounding the matter include (1) the extremely low success rate of *Borrelia* transmission to humans (1–3%), even in hyperendemic areas where tick infection rates may exceed 50% (Shapiro et al., 1992; Nadelman et al., 2001); (2) the frequency with which tick bites are not recognized among patients with Lyme disease (up to 75% of patients) (Nadelman et al., 1996); (3) the inaccuracy of tick species identification and estimates of feeding duration by nonentomologists (Falco et al., 1998); and (4) the potential costs of widespread antibiotic use (e.g., financial, unanticipated side effects, bacterial resistance). One investigation demonstrated that a single 200-mg dose of doxycycline administered after removal of an *I. scapularis* tick significantly reduced the incidence of subsequent development of erythema migrans (Nadelman et al., 2001). Although interpretations of the study were varied (Bellovin, 2001; Leenders, 2001; Shapiro, 2001), the most recent IDSA guideline states that prophylaxis "may be offered" if the epidemiologic findings (e.g., tick species, stage and duration of feeding, confirmed area of acquisition) are compelling. New draft guidelines for Lyme disease were issued in July 2019 by IDSA (Young & Sadoughi, 2019). One recommendation in the draft is, "Prophylactic antibiotics (a single dose of oral doxycycline) should be administered to patients within 72 hours of removing a tick after a high-risk bite, but not after lower-risk bites. High-risk bites must meet all of the following criteria: from an Ixodes tick, in a highly endemic area, and from a tick engorged and attached for 36 hours or more." The draft also states, "Additional antibiotics are not recommended in patients with persistent or recurring nonspecific symptoms, such as pain or fatigue, after treatment for Lyme disease but who don't have evidence of reinfection or treatment failure." Evaluation and management of patients presenting with "chronic" Lyme disease, who often have other underlying disorders, were also discussed in the guideline.

Primary Lyme disease prevention strategies that are generally agreed upon include interventions that decrease both the likelihood and the duration of vector attachment and feeding. Use of insect repellents, acaricides, and barrier clothing such as long pants and long-sleeved shirts and the performance of daily "tick checks" have a theoretical if not proven value in reducing human cases of Ixodid tickborne disease (Steere, 2018). The single most widely accepted and thoroughly tested prevention strategy, human vaccination, is no longer commercially available, however. This subunit vaccine containing a lipidized, recombinant OspA antigen was shown to significantly reduce the incidence of Lyme borreliosis following a three-step immunization schedule (Steere et al., 1998). Because of low sales and perhaps an unfounded fear of complications, the product was withdrawn from the market in 2002. This product, however, also seemed not to provide a long-lasting immunity (CDC, 2018c). As of this writing, no vaccine is commercially available.

RELAPSING FEVER

Relapsing fever can be divided into two categories based on microbiologic and epidemiologic features. Epidemic louseborne relapsing fever (LBRF) occurs worldwide, reflecting the ubiquitous distribution of its transmission vector, *Pediculus humanus*, the human body louse (Rhee & Johnson, 2005). Although the disease has been largely eradicated from most developed nations, documented occurrences persist in the Horn of Africa and parts of South America (Warrell, 2019). Humans are the only known reservoir for the causative agent, *B. recurrentis*. By contrast, endemic tickborne relapsing fever (TBRF) has a narrower geographic distribution, paralleling that of its primary transmission vectors, argasid ticks of the genus *Ornithodoros* (Fig. 61.12; Table 61.2). North American areas of disease endemicity include the Pacific Northwest, the Northern and Central Rocky Mountains, and parts of the Sierra range of California (*Ornithodoros hermsi* habitats), as well as the arid flatlands of Mexico, Texas, and New Mexico (*Ornithodoros turicata* habitats) (Dworkin et al., 2008) (see Table 61.2). The disease is also well documented in parts of Africa and Europe where *B. duttonii* and *B. crocidurae* are common pathogens (Parola & Raoult, 2001; Cutler, 2010). *Borrelia* spp. causing TBRF were traditionally named after the argasid tick species from which they were isolated (e.g., *B. hermsi* and *B. turicatae* associated with *O. hermsi* and *O. turicata*, respectively); yet, with the detection of several novel relapsing-fever group *Borrelia* spp., some from Ixodid ticks (e.g., *B. miyamotoi* and *B. lonestari*), such practice is no longer common (Barbour, 2014).

Fig. 61.12 Example of a member of the Argasidae family of "soft ticks," which are responsible for transmission of endemic relapsing fever *Borrelia.* (Courtesy James Gathany, CDC/PHIL file photo.)

Epidemiologic factors and transmission dynamics associated with TBRF are considerably different from those of Lyme disease. Argasid ticks feed nocturnally and for much shorter durations than Ixodid ticks (Parola & Raoult, 2001). As a result, TBRF *Borrelia* present in tick salivary secretions are successfully inoculated into a host within minutes of feeding (Dworkin et al., 2008; CDC, 2015b). While *Ornithodoros* ticks do not efficiently transmit *Borrelia* vertically (transovarial), they are able to maintain spirochetes in nature for extended periods due to their longevity (life spans of many years), their ability to persist for long durations in the absence of a blood meal, and by their multihost feeding habits (Dworkin et al., 2008). Human disease often occurs in small clusters following exposure to the vector while sleeping in rustic cabins or in seldom occupied rural dwellings *(O. hermsi)* or in caves *(O. turicata)* (Forrester et al., 2015). By contrast, relapsing fever group *Borrelia* spp. transmitted by Ixodid ticks would presumably share many epidemiologic features with the Lyme borreliosis group (Crowder et al., 2014), yet the overall impact on human health remains largely unknown. Although human infection caused by *B. miyamotoi* has been reported (Krause et al., 2013; Hovius et al., 2013), it remains unclear whether the paucity of cases relates to inadequate diagnostic methods or to rarity of infection.

Clinical features of TBRF and LBRF are similar in many ways. Following a 5- to 7-day incubation period, infected patients experience an acute onset of high fever (38.9°–40.0°C) accompanied by nonspecific symptoms such as headache, malaise, arthralgia, and fatigue (Southern, 1969; Dworkin et al., 2008; Barbour, 2018). Minor hemorrhagic manifestations, likely related to transient thrombocytopenia, may be noted. Hepatosplenomegaly is identified more frequently in patients with LBRF. The commonest sign is hepatic tenderness (in about 60%) and enlargement (50%) (Barbour, 2018; Warrell, 2019). Neurologic involvement in the form of meningitis, seventh nerve palsy, myelitis, and encephalitis has also been reported (Barbour, 2018). Almost as suddenly as they begin, symptoms subside after 3 to 6 days in most patients, only to relapse roughly 1 week later (Rhee & Johnson, 2005). Similar episodes of symptomatic recurrence may continue up to as many as 13 times but more typically resolve after two or three relapses (Southern & Sanford, 1969). These waves of recrudescence result from the organism's extraordinary ability to vary its surface protein antigenic makeup temporally under immune selective pressure, thus producing cycles of epitope variation and immune escape followed by new antibody production and organism suppression (Rich et al., 2001; Dworkin et al., 2008). Left untreated, LBRF appears to have a higher mortality rate than its tickborne counterpart, but the contributive effects of other factors (e.g., malnutrition, war) often accompanying LBRF may bias this observation; and self-limited cases of probable TBRF have been reported (Dworkin et al., 2008; Barbour, 2018).

Figure 61.10 illustrates a recommended approach to the laboratory diagnosis of relapsing fever (Paxton, Theel et al., 2020). Microscopic examination of peripheral blood samples obtained during febrile episodes remains the best laboratory approach for diagnosis of relapsing fever. *Borrelia* organisms may be visualized in wet mounts using a darkfield technique or in fixed smears stained with Wright-Giemsa, acridine orange, or specific fluorescent antibodies. Drawbacks to microscopy include (1) the requirement of a high spirochetemic burden for visualization, although this may be mitigated by collection of samples during febrile periods; (2) observer inexperience or unfamiliarity with morphology or clinical differential; and (3) the inability to identify causative

TABLE 61.2
Location by County of 504 Tickborne Relapsing Fever Cases Reported in the United States, 1990–2011.

		NONRESIDENTS	
County[a]	**Total no.**	**No.**	**(%)**
Kootenai, Idaho	**29**	29	(100)
Mono, California	**23**	14	(60.9)
Nevada, California	**20**	15	(75.0)
Spokane, Washington	**20**	1	(5.0)
Okanogan, Washington	**15**	5	(33.3)
Placer, California	**15**	13	(86.7)
El Dorado, California	**14**	10	(71.4)
Lake, Colorado	**13**	8	(61.5)
Fresno, California	**11**	5	(45.5)
McKinley, New Mexico	**11**	7	(63.6)

[a]Median elevation of the 10 counties was 3840 feet (range = 1178 – 7562 feet) (1170 m [range = 359 – 2305 m]).
From Forrester JD, Kjemtrup AM, Fritz CL, et al: Tickborne relapsing fever—United States, 1990–2011, *Morb Mortal Wkly Rep* 64:58–60, 2015.

Borrelia to the species level. Cultivation of the spirochetes is also possible, although difficult, and is rarely performed in clinical settings. Demonstration of serologic response using techniques such as IFA, ELISA, and Western blot has met with variable success. The degree of *Borrelia* antigenic variability limits serologic assay sensitivity, whereas cross-reactivity with other spirochetes, in particular those of the Lyme borreliosis group, affect specificity. Assays utilizing a 34 kDa recombinant protein, GlpQ, appear to be more specific for the relapsing fever spirochetes (Schwan et al., 2003; Porcella et al., 2000). A multiplex real-time PCR capable of detecting and differentiating four main *Borrelia* spp. from blood specimens in Africa has been developed and demonstrated excellent performance characteristics (100% sensitive and specific for *B. duttonii/B. recurrentis* and *B. hispanica* and 99% sensitive and specific for *B. crocidurae*) (Elbir et al., 2013). PCR is more sensitive than microscopy for detecting *Borrelia* spp., as demonstrated when several infected immigrants in Europe who were negative on microscopic examination were actually diagnosed by PCR (Hoch et al., 2015; Antinori et al., 2017). Point-of-care PCR testing to detect *B. crociduare* has been successfully utilized in rural Senegal (Sokhna et al., 2013). However, none of these assays are FDA cleared.

Successful treatment of LBRF may be accomplished using a single oral dose of tetracycline or erythromycin (Barbour, 2018; Warrell, 2019) whereas 10 days of therapy with either of these agents is recommended for TBRF (Barbour, 2018). Parenteral administration of a β-lactam may be considered in the case of meningitis or encephalitis (Barbour, 2018). Whatever the antibiotic, symptoms of the Jarisch-Herxheimer reaction may be observed and can be particularly severe in the louseborne form of disease. This reaction usually occurs within a few hours of antibiotic initiation and is typified by an increase in temperature (0.5°–1°C) with rigors, systemic hypotension, and leukopenia. As with other shocklike syndromes, the proposed mechanism of Jarisch-Herxheimer reaction involves a cytokine storm, with TNF-α, IL-6, and IL-8 as major orchestrating components (Barbour, 2018).

Although the experience in treating infections caused by *B. miyamotoi* is limited, it is thought that this organism likely has the same antibiotic susceptibilities as other *Borrelia* spp. and that the guidelines for Lyme disease therapy can be followed (Barbour, 2018).

Prevention strategies for TBRF include rodent-proofing rural cottages or cabins to avoid immigration and colonization by soft ticks, use of insecticides around such dwellings, use of topical repellents while sleeping, and altogether avoiding overnight excursions into known *Ornithodoros* habitats. Prevention of LBRF may be effected through good personal hygiene and delousing procedures (Barbour, 2018). No vaccine is currently available.

AGENTS OF INTESTINAL SPIROCHETOSIS

DESCRIPTION

Two species of spirochete, *Brachyspira aalborgi* and *Brachyspira pilosicoli* (formerly designated as a member of the genus *Serpulina*), have been identified in the human gastrointestinal tract. These organisms are gram negative, 0.2 to 0.4 μm in diameter, and 4 to 8 μm in length. Four to six flagella are present subterminally at each end near the pointed ends of the bacteria.

EPIDEMIOLOGY AND CLINICAL MANIFESTATIONS

B. pilosicoli and *B. hyodysenteriae* cause porcine intestinal spirochetosis, a diarrheal disease in young pigs; and similar organisms have been recovered from birds and other animals (Hampson, 2018). It is unknown whether animals act as reservoirs for human infection. In contrast, *B. aalborgi* was named after its isolation from the colon of a human patient but remains less well characterized overall. The association of intestinal spirochetes with disease is not firmly established, as the bacteria have been identified in both symptomatic and asymptomatic individuals. Prevalence rates appear higher among homosexual men and within different geographic populations (Tsinganou & Gebbers, 2010). Symptoms often attributed to intestinal spirochetosis include diarrhea, abdominal pain, and rectal bleeding and discharge (Tsinganou & Gebbers, 2010). Additionally, *B. pilosicoli* has been isolated from the blood of critically ill and immunocompromised patients, the clinical significance of which is uncertain (Kanavaki et al., 2002; Hampson, 2018). Although the true prevalence of the spirochetosis colonization in humans is not known, some targeted surveys suggested a relatively high prevalence of colonization in certain human population groups (e.g., patients with colonic adenomas, inflammatory polyps, inflammatory bowel disease, or HIV infection and in men who have sex with men) (Rojas et al., 2017).

PATHOLOGY AND PATHOGENESIS

The spirochetes are easily seen on biopsy specimens as a dark blue "fringe" on the surface of colonic epithelial cells with sparing of the goblet cells (Fig. 61.13, *A*). Silver impregnation stains demonstrate the organisms well (see Fig. 61.13, *B*). The epithelial cells appear normal without significant inflammatory infiltrate in the underlying lamina propria. Electron microscopy demonstrates that the bacteria attach to the surface of colonic epithelial cells end-on and are oriented perpendicular to the lumen (Teglbjaerg, 1990; Milner et al., 2015c). Invasion into epithelial and mucosal macrophages has been demonstrated in both symptomatic and asymptomatic patients (Korner & Gebbers, 2003). Pathogenic mechanisms have not been established. Interestingly, *Lactobacillus* spp. have been shown to have antagonistic in vitro activities against *B. pilosicoli* (Bernardeau et al., 2009).

LABORATORY DIAGNOSIS

Spirochetes can be detected in stool by darkfield microscopy and cultured from stool or biopsy specimens on trypticase soy agar with 5% to 10% horse or calf blood. The addition of spectinomycin and polymyxin B makes the media selective. On media incubated anaerobically, pinpoint, weakly β-hemolytic colonies develop in 3 days to 4 weeks, depending on the strain. MALDI-TOF MS has been used successfully to identify isolates of *Brachyspira* spp., including *B. pilosicoli* (Calderaro et al., 2012). Recently, fluorescent in situ hybridization assays in combination with 16S rRNA gene sequencing has been successfully used to correctly identify *P. pilosicoli* and *B. aalborgi* (Rojas et al., 2017).

TREATMENT

Although antimicrobial susceptibilities of *Brachyspira* spp. have been published, standardized testing of a large number of isolates has not been described (Karlsson et al., 2003; Brooke et al., 2003). Patients suffering from symptoms of intestinal spirochetosis have reportedly responded to metronidazole, a drug of choice (Umeda et al., 2017).

ACKNOWLEDGMENTS

I gratefully acknowledge the contribution of P. Rocco LaSala, Michael Loeffelholz, Mike Smith, Gail Woods, and others who authored this chapter in previous editions.

I also acknowledge Bobbi Pritt, Elitza Theel, Blake Buchan, and Anne Paxon for permission to use the acute tickborne disease testing algorithm that they published in *CAP Today* (Paxton, Pritt et al., 2020).

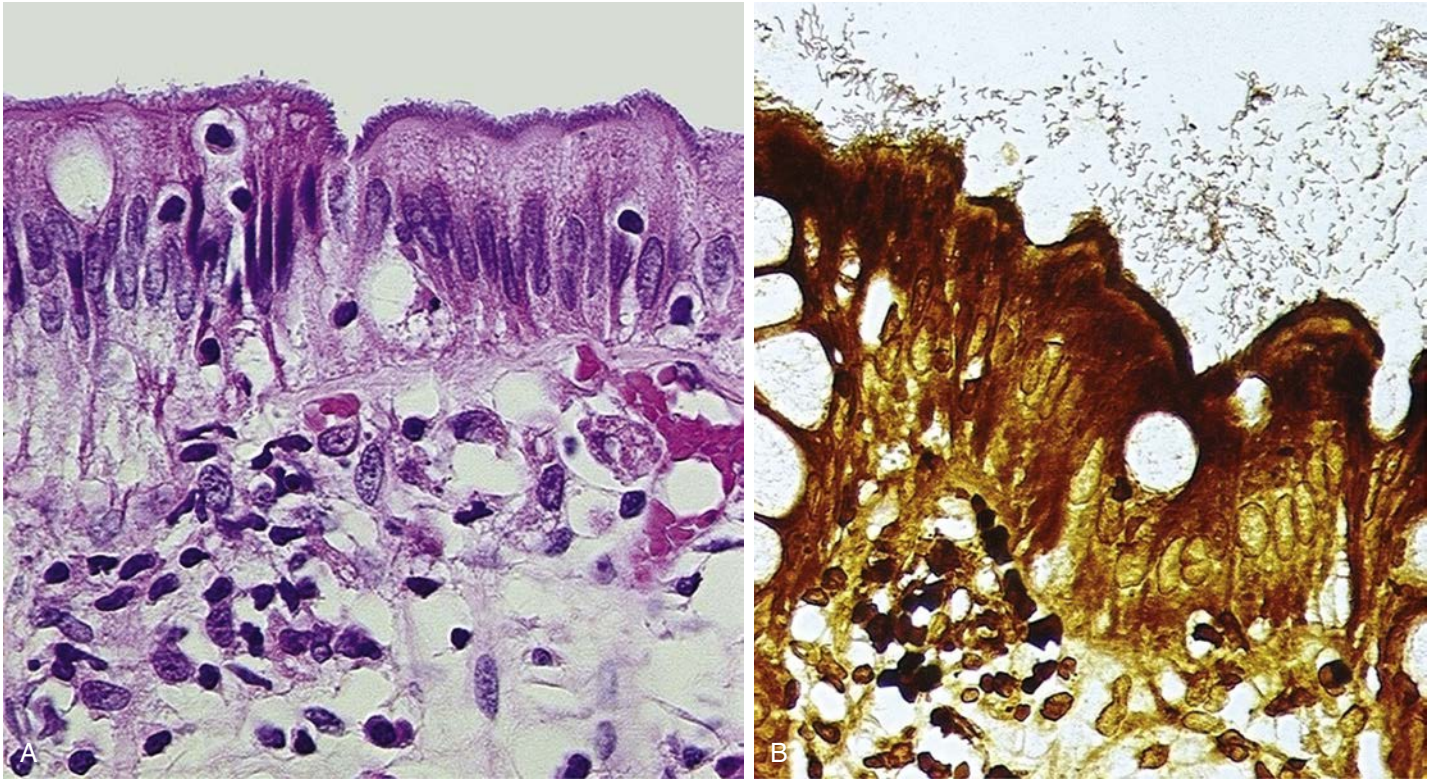

Fig. 61.13 Colonic epithelium demonstrating **A** basophilic discoloration along the bowel luminal surface (hematoxylin & eosin [H&E], ≈400×), which is confirmed in **B** to be numerous argyrophilic spirochetes, consistent with intestinal spirochetosis (Steiner silver impregnation technique, 400×). (Images courtesy Hagen Blaszyk, MD.)

SELECTED REFERENCES

Giacani L, Lukehart SA: The endemic treponematose, *Clin Microbiol Rev* 27:89, 2014.

This extensive review provides descriptions of the clinical manifestations of endemic treponematoses, including yaws, bejel, and pinta; their origin; diagnostic tools; past and current eradication programs; and the epidemiologic situation.

Halperin JJ: Lyme neuroborreliosis, *Curr Opin Infect Dis* 32(3):259, 2019.

This concise review goes over the recent evidence regarding symptomatology and diagnosis of nervous system Lyme disease with emphasis on CSF parameters that could be used to confirm CNS infection in Lyme neuroborreliosis.

Hampton DJ: The spirochete *Brachyspira pilosicoli*, enteric pathogen of animals and humans, *Clin Microbiol Rev* 31:e00087-17, 2018.

In-depth review of the spirochete Brachyspira pilosicoli, including the spectrum of diseases, pathogenesis, epidemiology, diagnosis, prevention, and treatment.

Krause PJ, et al.: *Borrelia miyamotoi* infection in nature and in humans, *Clin Microbiol Infect* 21:631, 2015.

This review of the spirochete Borrelia miyamotoi includes the clinical manifestations, etiologic diagnosis, confirmation by blood smear examination, PCR, antibody assays, in vitro cultivation, isolation by animal inoculation, and updated treatment options for this infection.

Park IU, Fakile YF, Chow JM, et al.: Performance of treponemal tests for the diagnosis of syphilis, *Clinic Infect Dis* 68(6):913, 2019.

Explores and compares the test performance characteristics of seven different immunoassays for the diagnosis of syphilis at various stages of the disease.

Picardeau M: Virulence of the zoonotic agent of leptospirosis: still terra incognita? *Nat Rev Microbiol* 15:297, 2017.

Systematic review of the epidemiology, taxonomy, genomics, pathogenesis, and molecular basis of virulence in leptospirosis.

Sanchez E, Vannier E, Wormser GP, et al.: Diagnosis, treatment, and prevention of Lyme disease, human granulocytic anaplasmosis, and babesiosis: a review, *J Am Med Assoc* 315(16):1767, 2016.

An excellent review packed with updated information on diagnosis, treatment, and prevention of abovementioned tick-borne illnesses.

Stamm LV: Syphilis: re-emergence of an old foe, *Microb Cell* 3(9):363, 2016.

A comprehensive yet concise review of etiologic, epidemiologic, diagnostic, and clinical features of syphilis, and updated information about treatment, prevention, and control measures.

Workowski KA, Bolan GA, Centers for Disease Control and Prevention, et al.: Sexually transmitted diseases treatment guidelines. US Department of Health and Human Services, *MMWR Recomm Rep (Morb Mortal Wkly Rep)* 64:1, 2015.

Developed as a tool to guide therapy of many sexually transmitted diseases, these recommendations also include many variable diagnostic considerations for a variety of presentations.

Access the complete reference list online at Elsevier eBooks for Practicing Clinicians.

REFERENCES

Afzelius A: Verhanlungen der dermatologischen Gesellschaft zu Stockholm, *Arch Dermatol Syphilis* 101:405, 1910.

Aguero-Rosenfeld ME, Wang G, Schwartz I, et al.: Diagnosis of lyme borreliosis, *Clin Microbiol Rev* 18:484, 2005.

Antinori S, Tonello C, Edouard S, et al.: Diagnosis of Louse-Borne relapsing fever despite negative microscopy in two asylum seekers from Eastern Africa, *Am J Trop Med Hyg* 97(6):1669, 2017.

Arbefeville S, Lynch M, Ferrieri P: Evaluation of a multiplex fully automated treponemal and nontreponemal (rapid plasma reagin) assay, *Am J Clin Pathol* 152(2):230, 2019.

Aucott JN, Crowder LA, Kortte KB: Development of a foundation for a case definition of post-treatment Lyme disease syndrome, *Int J Infect Dis* 17:e443, 2013.

Badawi A, Arora P, Brenner D: Biologic markers of antibiotic-refractory lyme arthritis in human: a systematic review, *Infect Dis Ther* 8:5, 2019.

Bannwarth A: Chronische lymphocytäre Meningitis, entzundliche polyneuritis und "rheumatismus", *Arch Psychiatr Nervenkr* 113:284, 1941.

Barbour AG: Phylogeny of a relapsing fever Borrelia species transmitted by the hard tick Ixodes scapularis, *Infect Genet Evol* 27:551, 2014.

Barbour AG: Relapsing fever. In Jameson JL, Fauci AS, Kasper DL, et al.: *Harrison's principles of internal medicine*, ed 20, New York, 2018, McGraw–Hill, pp 1295–1298. (chapter 180).

Bellovin SM: Correspondence, *N Engl J Med* 345:1349, 2001.

Bernardeau M, Gueguen M, Smith DGE, Corona-Barrera E, Vernoux JP: In vitro antagonistic activities of *Lactobacillus* spp. against *Brachyspira hyodysenteriae* and *Brachyspira pilosicoli*, *Vet Microbiol* 138:184, 2009.

Bio-Rad: *BioPlex® 2200 syphilis total & RPR instructions for use*, Hercules, CA, 2017, Bio-Rad Laboratories, Clinical Diagnostic Group.

Bockenstedt LK, Radolf JD: Xenodiagnosis for posttreatment Lyme disease syndrome: resolving the conundrum or adding to it? *Clin Infect Dis* 58:946, 2014.

Branda JA, Aguero-Rosenfeld ME, Ferraro MJ, et al.: 2-tiered antibody testing for early and late Lyme disease using only an immunoglobulin G blot with the addition of a VlsE band as the second-tier test, *Clin Infect Dis* 50:20, 2010.

Branda JA, Body BA, Boyle J, et al.: Advances in Serodiagnostic testing for lyme disease are at hand, *Clin Infect Dis* 19:1133, 2018. 66:7.

Branda JA, Linskey K, Kim YA, et al.: Two-tiered antibody testing for Lyme disease with use of 2 enzyme immunoassays, a whole-cell sonicate enzyme immunoassay followed by a VlsE C6 peptide enzyme immunoassay, *Clin Infect Dis* 53:541, 2011.

Brinkerhoff RJ, Gilliam WF, Gaines D: Lyme disease, Virginia, USA, 2000-2011, *Emerg Infect Dis* 20:1661, 2014.

Brisson D, Drecktrah D, Eggers CH, et al.: Genetics of *Borrelia burgdorferi*, *Annu Rev Genet* 46:515, 2012.

Brooke CJ, Hampson DJ, Riley TV: In vitro antimicrobial susceptibility of Brachyspira pilosicoli isolates from humans, 47(7):2354, 2003.

Brown ST, Zaidi A, Larsen SA, et al.: Serological response to syphilis treatment, *J Am Med Assoc* 253:1296, 1985.

Brown SL, Hansen SL, Langone JJ: Role of serology in the diagnosis of Lyme disease, *J Am Med Assoc* 282(1):62–66, 1999, https://doi.org/10.1001/jama.282.1.62. PMID: 10404913.

Brusca C: Gold standard diagnostics Corp. Announces issuance of U.S. Patent for the AIX1000®. Gold standard diagnostics Corp, *AP News*, May 15, 2019. Available at https://apnews.com/ad8482b5a0da4d82a28c2d039424979d. [Accessed 5 November 2019].

Buchacz K, Patel P, Taylor M, et al.: Syphilis increases HIV viral load and decreases CD4 cell counts in HIV-infected patients with new syphilis infections, *AIDS* 18:2075, 2004.

Buder S, Schofer H, et al.: Bacterial sexually transmitted infections, *JDDG* 1610, 2019.

Burgdorfer W, Barbour AG, Hayes SF, et al.: Lyme disease—a tick-borne spirochetosis? *Science* 216:1317, 1982.

Calderaro A, Piccolo G, Montecchini S, et al.: MALDI-TOF MS analysis of human and animal *Brachyspira* species and benefits of database extension, *J Proteom* 8:273, 2012.

Cameron DJ, Johnson LB, Maloney EL: Evidence assessments and guideline recommendations in Lyme disease: the clinical management of known tick bites, erythema migrans rashes and persistent disease, *Expert Rev Anti Infect Ther* 12:1103, 2014.

Centers for Disease Control and Prevention: Discordant results from reverse sequence syphilis screening—five laboratories, United States, 2006–2010, *Morb Mortal Wkly Rep* 60:133, 2011a.

Centers for Disease Control and Prevention: *Leptospirosis– Healthcare workers*, Atlanta, U.S, 2018a, Department of Health and Human Services. Available at https://www.cdc.gov/leptospirosis/pdf/fs-leptospirosis-clinicians-eng-508.pdf. [Accessed 5 November 2019].

Centers for Disease Control and Prevention: *Leptospirosis–risk of exposure*, Atlanta, U.S, 2018b, Department of Health and Human Services. Available at https://www.cdc.gov/leptospirosis/exposure/index.html. [Accessed 5 November 2019].

Centers for Disease Control and Prevention: *Lyme disease vaccine*, Atlanta, U.S, 2018c, Department of Health and Human Services. Available at https://www.cdc.gov/lyme/prev/vaccine.html. [Accessed 5 November 2019].

Centers for Disease Control and Prevention: *Lyme disease (Borrelia burgdorferi) 2017 case definition*, Atlanta, U.S, 2017a, Department of Health and Human Services. Available at https://wwwn.cdc.gov/nndss/conditions/lyme-disease/case-definition/2017/. [Accessed 5 November 2019].

Centers for Disease Control and Prevention: *National Notifiable diseases surveillance system, 2011b*. Available at http://wwwn.cdc.gov/NNDSS/script/casedef.aspx?CondYrID=752&DatePub=1/1/2011%2012:00:00%20AM. [Accessed 5 November 2019].

Centers for Disease Control and Prevention: Recommendations for test performance and interpretation from the second national Conference on serologic diagnosis of lyme disease, *J Am Med Assoc* 274:937, 1995.

Centers for Disease Control and Prevention: *Sexually transmitted disease surveillance, syphilis, 2017*, Atlanta, U.S, 2018d, Department of Health and Human Services. Available at https://www.cdc.gov/std/stats17/syphilis.htm. [Accessed 5 November 2019].

Centers for Disease Control and Prevention: Surveillance for lyme disease — United States, 2008–2015, Atlanta, U.S. Department of health and human Services, *Surveillance Summaries* 66(22):1, 2017b. Available at https://www.cdc.gov/lyme/stats/humancases.html. [Accessed 5 November 2019].

Centers for Disease Control and Prevention: Symptomatic early neurosyphilis among HIV-positive men who have sex with men—four cities, United States, January 2002–June 2004, *Morb Mortal Wkly Rep* 56:625, 2007.

Centers for Disease Control and Prevention: Syphilis testing algorithms using treponemal tests for initial screening—four laboratories, New York, 2005-2006, *Morb Mortal Wkly Rep* 57:872, 2008.

Centers for Disease Control and Prevention: Tickborne relapsing fever—United States. Atlanta, U.S. Department of health and human Services, 1990–2011, *MMWR (Morb Mortal Wkly Rep)* 64:58, 2015.

Chen CY, Chi KH, Pillay A, et al.: Detection of the A2058G and A2059G 23S rRNA gene point mutations associated with azithromycin resistance in *Treponema pallidum* by Use of a TaqMan real-time multiplex PCR assay, *J Clin Microbiol* 51(3):908, 2013.

Choi BK, Wyss C, Gobel UB: Phylogenetic analysis of pathogen-related oral spirochetes, *J Clin Microbiol* 34:1922, 1996.

Cook MJ: Lyme borreliosis: a review of data on transmission time after tick attachment, *Int J Gen Med* 8:1, 2014.

Costa F, Hagan JE, et al.: Global morbidity and mortality of leptospirosis: a systematic review, *PLoS Negl Trop Dis* 9(9):e0003898, 2015.

Crowder CD, Carolan HE, Rounds MA, et al.: Prevalence of Borrelia miyamotoi in Ixodes ticks in Europe and the United States, *Emerg Infect Dis* 20:1678, 2014.

Cruz AR, Ramirez LG, Zuluaga AV, et al.: Immune evasion and recognition of the syphilis spirochete in blood and skin of secondary syphilis patients: two immunologically distinct compartments, *PLoS Negl Trop Dis* 6:e1717, 2012.

Cruz M, Hansen K, Ernerudh J, et al.: Lyme arthritis: oligoclonal anti-*Borrelia burgdorferi* IgG antibodies occur in joint fluid and serum, *Scand J Immunol* 33:61, 1991.

Curry SJ, Krist AH, Owens DK et al: Screening for syphilis infection in pregnant women. US Preventive Services Task Force Reaffirmation Recommendation Statement, JAMA 320:9:911, 2018.

Cutler SJ: Relapsing fever—a forgotten disease revealed, *J Appl Microbiol* 108:1115, 2010.

de Silva AM, Fikrig E: Arthropod- and host-specific gene expression by *Borrelia burgdorferi*, *J Clin Invest* 99:377, 1997.

Dumler JS: Molecular diagnosis of lyme disease: review and meta-analysis, *Mol Diagn* 6(1):1, 2001.

Dworkin MS, Schwan TG, Anderson Jr DE, Borchardt SM: Tick-borne relapsing fever, viii *Infect Dis Clin Northb Am* 22(3):449–468, 2008, https://doi.org/10.1016/j.idc.2008.03.006. PMID: 18755384; PMCID: PMC3725823.

Dykhuizen DE, Brisson D, Sandigursky S, et al.: The propensity of different *Borrelia burgdorferi* sensu stricto genotypes to cause disseminated infections in humans, *Am J Trop Med Hyg* 78:806, 2008.

Elbir H, Henry M, Diatta G, Mediannikov O, et al.: Multiplex real-time PCR diagnostic of relapsing fevers in Africa, *PLoS Negl Trop Dis* 7(1):e2042, 2013.

Embers ME, Barthold SW, Borda JT, et al.: Persistence of Borrelia burgdorferi in rhesus macaques following antibiotic treatment of disseminated infection, *PloS One* 7:e29914, 2012.

Embers ME, Jacobs MB, Johnson BJ, et al.: Dominant epitopes of the C6 diagnostic peptide of Borrelia burgdorferi are largely inaccessible to antibody on the parent VlsE molecule, *Clin Vaccine Immunol* 14:931, 2007.

Engelkens HJ, Judanarson J, Orange AP, et al.: Endemic treponematoses. Part I. Yaws, *Int J Dermatol* 30:77, 1991.

Engelkens HJ, Niemel PL, van der Sluis JJ, et al.: Endemic treponematoses. Part II. Pinta and endemic syphilis, *Int J Dermatol* 30:231, 1991.

Eshoo MW, Crowder CC, Rebman AW, et al.: Direct molecular detection and genotyping of Borrelia burgdorferi from whole blood of patients with early lyme disease, *PloS One* 7(5):e36825, 2012.

Falco RC, Fish D, D'Amico V: Accuracy of tick identification in a Lyme disease endemic area, *J Am Med Assoc* 280:602, 1998.

Falco RC, McKenna DF, Daniels TJ, et al.: Temporal relation between *Ixodes scapularis* abundance and risk for Lyme disease associated with erythema migrans, *Am J Epidemiol* 149:771, 1999.

Fallon BA, Pavlicova M, Coffino SW, et al.: A comparison of lyme disease serologic test results from 4 laboratories in patients with persistent symptoms after antibiotic treatment, *Clin Infect Dis* 59:1705, 2014.

Fargen KM, Alvernia JE, Lin S, et al.: Cerebral syphilitic gummata: a case presentation and analysis of 156 reported cases, *Neurosurgery* 64:568, 2009.

Feder Jr HM, Johnson BJ, O'Connell S, et al.: A critical appraisal of "chronic Lyme disease, *N Engl J Med* 357:1422, 2007.

Feder HM, Hoss DM, Zemel L, et al.: Southern Tick-Associated Rash Illness (STARI) in the north: STARI following a tick bite in long Island, New York, *Clin Infect Dis* 53:e142, 2011.

Feng J, Li T, Yee R, et al.: Stationary phase persister/biofilm microcolony of Borrelia burgdorferi causes more severe disease in a mouse model of Lyme arthritis: implications for understanding persistence, Post-treatment Lyme Disease Syndrome (PTLDS), and treatment failure, *Discov Med* 148:125, 2019.

Flores JL: Syphilis: a tale of twisted treponemes, *West J Med* 163:552, 1995.

Forrester JD, Kjemtrup AM, Fritz CL, et al.: Tickborne relapsing fever—United States, 1990-2011, *MMWR Morb Mortal Wkly Rep* 64:58–60, 2015.

Fraser CM, Casjens S, Huang WM, et al.: Genomic sequence of a Lyme disease spirochete, *Borrelia burgdorferi*, *Nature* 390:580, 1997.

Fredricks DN, Relman DA: Sequence-based identification of microbial pathogens: a reconsideration of Koch's postulates, *Clin Microbiol Rev* 9:18, 1996.

Fukushima K, Yanagisawa N, et al.: Erythema migrans-like rash Mimicking lyme disease, *Jap Soc Intern Med* 58(15):2271, 2019.

Furuhata M, Yanagisawa N, Suganuma A: Atypical skin rash in seronegative secondary syphilis, *Intern Med* 55(23):3547, 2016.

Gayet-Agaron A, Lautenschlager S, Ninet B, et al.: Sensitivity, specificity and likelihood ratios of PCR in the diagnosis of syphilis: a systemic review and meta-analysis, *Sec Transm Infect* 89:251, 2013.

Gayet-Ageron A, Combescure C, Lautenschlager S, et al.: Comparison of diagnostic accuracy of PCR targeting the 47-kilodalton protein membrane gene of Treponema pallidum and PCR targeting the DNA Polymerase I gene: systematic review and metaanalysis, *J Clin Microbiol* 53(11):3522, 2015.

Girard YA, Travinsky B, Schotthoefer A, et al.: Population structure of Lyme borreliosis spirochete *Borrelia burgdorferi* in the Western black-legged tick *(Ixodes pacificus)* in Northern California, *Appl Environ Microbiol* 75:7243, 2009.

Glöckner G, Schulte-Spechtel U, Schilhabel M, et al.: Comparative genome analysis: selection pressure on the *Borrelia* vls cassettes is essential for infectivity, *BMC Genom* 7:211, 2006.

Gonzalez-Lopez JJ, Guerrero ML, Luján R, et al.: Factors determining serologic response to treatment in patients with syphilis, *Clin Infect Dis* 49:1505, 2009.

Gourevitch MN, Selwyn PA, Devanay K, et al.: Effects of HIV infection on the serologic manifestations and response to treatment of syphilis in intravenous drug users, *Ann Intern Med* 118:350, 1993.

Greer L, Wendel GD: Rapid diagnostic methods in sexually transmitted infections, *Infect Dis Clin North Am* 22:601, 2008.

Griffin GE: Cytokines involved in human septic shock—the model of the Jarisch-Herxheimer reaction, *J Antimicrob Chemother* 41(Suppl A):25, 1998.

Guagliardo SAJ, Iverson SA, Reynolds L, et al.: Despite high-risk exposures, no evidence of zoonotic transmission during a canine outbreak of leptospirosis, *Zoonoses Public Health* 66:223, 2019.

Haas JS, Bolan G, Larsen SA, et al.: Sensitivity of treponemal tests for detecting prior treated syphilis during human immunodeficiency virus infection, *J Infect Dis* 162:862, 1990.

Halperin JJ, Baker P, Wormser GP: Lyme disease: the great controversy. In Halperin JJ, editor: *Lyme disease: an evidence-based approach*, CAB International, 2011.

Halperin JJ: Lyme neuroborreliosis, *Curr Opin Infect Dis* 32(3):259, 2019.

Halperin JJ: Nervous system Lyme disease, *Infect Dis Clin North Am* 22:261, 2008.

Hampson DJ: The spirochete *Brachyspira pilosicoli*, enteric pathogen of animals and humans, *Clin Microbiol Rev* 31:e00087, 2018.

Hansen K: Lebech AM: lyme neuroborreliosis: a new sensitive diagnostic assay for intrathecal synthesis of *Borrelia burgdorferi*-specific immunoglobulin, *Ann Neurol* 30:197, 1991.

Harper KN, Liu H, Ocampo PS, et al.: The sequence of the acidic repeat protein (arp) gene differentiates venereal from nonvenereal *Treponema pallidum* subspecies, and the gene has evolved under strong positive selection in the subspecies that causes syphilis, *FEMS Immunol Med Microbiol* 53:322, 2008.

Harper KN, Ocampo PS, Steiner BM, et al.: On the origin of the treponematoses: a phylogenetic approach, *PLoS Negl Trop Dis* 2:e148, 2008.

Harter C, Bernischke K: Fetal syphilis in the first trimester, *Am J Obstet Gynecol* 124:705, 1976.

Henningsson AJ, Gyllemark P, Lager M, Skogman BH, Tjernberg I: Evaluation of two assays for CXCL13 analysis in cerebrospinal fluid for laboratory diagnosis of Lyme neuroborreliosis, *APMIS* 124(11):985, 2016.

Herman-Giddens ME, Herman-Giddens DM: Retrospective case reports of two central North Carolina residents: frequency of tick bites and associated illnesses, 2001-2014, *N C Med J* 78(3):156, 2017.

Hernandez-Aguado I, Bolumar F, Moreno R, et al.: False positive tests for syphilis associated with human immunodeficiency virus and hepatitis B virus infection among intravenous drug abusers, *Eur J Clin Microbiol Infect Dis* 17:784, 1998.

Hijikata S, Hongo I, Nakayama SI, et al.: A case diagnosed using polymerase chain reaction analysis of aortic valve, *Can J Cardiol* 35(1):104.e9, 2019.

Hinckley AF, Connally NP, Meek JI, et al.: Lyme disease testing by large commercial laboratories in the United States, *Clin Infect Dis* 59:676, 2014.

Hoch M, Wieser A, Löscher T, et al.: Louse-borne relapsing fever (Borrelia recurrentis) diagnosed in 15 refugees from northeast Africa: epidemiology and preventive control measures, Bavaria, Germany, July to October 2015, *Euro Surveill* 20(42):1, 2015.

Hojgaard A, Eisen RJ, Piesman J: Transmission dynamics of *Borrelia burgdorferi* s.s. during the key third day of feeding by nymphal *Ixodes scapularis* (Acari: Ixodidae), *J Med Entomol* 45:732, 2008.

Hosono S, Faruqi AF, Dean FB, et al.: Unbiased whole-genome amplification directly from clinical samples, *Genome Res* 13(5):954, 2003.

Hovius JW, de Wever B, Sohne M, et al.: A case of meningoencephalitis by the relapsing fever spirochaete Borrelia miyamotoi in Europe, *Lancet* 382:658, 2013.

https://www.cdc.gov/leptospirosis/pdf/fs-leptospirosis-clinicianseng-508.pdf.

Hua CM, Cheminade Y, Perret JL, et al.: Early detection of *Borrelia burgdorferi* sensu lato infection in Balb/c mice by co-feeding Ixodes ricinus ticks, *Int J Med Microbiol* 293:421, 2003.

Hutter G, Schlagenhauf U, Valenza G, et al.: Molecular analysis of bacteria in periodontitis: evaluation of clone libraries, novel phylotypes and putative pathogens, *Microbiology* 149:67, 2003.

Jacovides CL, Kreft R, Adeli B, et al.: Successful identification of pathogens by polymerase chain reaction (PCR)-based electron spray ionization time-of-flight mass spectrometry (ESI-TOF-MS) in culture-negative periprosthetic joint infection, *J Bone Joint Surg Am* 94:2247, 2012.

James AM, Liveris D, Wormser GP, et al.: *Borrelia lonestari* infection after a bite by an *Amblyomma americanum* tick, *J Infect Dis* 183:1810, 2001.

Johnson BJ, Pilgard MA, Russel TM: Assessment of new culture method for detection of Borrelia species from serum of Lyme disease patients, *J Clin Microbiol* 52:721, 2014.

Jutras BL, Lochhead RB, Kloos ZA, et al.: Borrelia burgdorferi peptidoglycan is a persistent antigen in patients with Lyme arthritis, *Proc Natl Acad Sci Unit States Am* 116(27):13498, 2019.

Kaiser R: Neuroborreliosis. *J Neurol* 245:247, 1998.

Kanavaki S, Mantadakis E, Thomakos N, et al.: *Brachyspira (Serpulina) pilosicoli* spirochetemia in an immunocompromised patient, *Infection* 30:175, 2002.

Karlsson M, Fellstrom C, Gunnarsson A, et al.: Antimicrobial susceptibility testing of porcine *Brachyspira (Serpulina)* species isolates, *J Clin Microbiol* 41:2596, 2003.

Kelley KJ, Di Francesco L: FDA clears marketing for "modified two-tiered" lyme disease tests, *NEJM, J Watch*, 2019.

Klempner MS: Controlled trials of antibiotic treatment in patients with post-treatment chronic Lyme disease, *Vector Borne Zoonotic Dis* 2:255, 2002.

Ko AI, Goarant C, Picardeau M: Leptospira: the dawn of the molecular genetics era for an emerging zoonotic pathogen, *Nat Rev Microbiol* 7:736, 2009.

Korner M, Gebbers JO: Clinical significance of human intestinal spirochetosis—a morphologic approach, *Infection* 31(5):341, 2003.

Kowalski TJ, Tata S, et al.: Antibiotic treatment duration and long-term outcomes of patients with early lyme disease from a lyme disease-hyperendemic area, *CID* 50:512, 2010.

Krause PJ, Narasimhan S, Wormser GP, et al.: Human Borrelia miyamotoi infection in the United States, *N Engl J Med* 368:291, 2013.

Lantos PM, Charini WA, Medoff G, et al.: Final report of the lyme disease review panel of the infectious disease Society of America, *Clin Infect Dis* 51:1, 2010.

Larsen SA, Johnson RE: Diagnostic tests. In Larson SA, Pope V, Johnson RE, et al.: *A manual of tests for syphilis*, ed 9, Washington, DC, 1998, American Public Health Association, p 1.

Larsen SA, Steiner BM, Rudolph AH: Laboratory diagnosis and interpretation of tests for syphilis, *Clin Microbiol Rev* 8:1, 1995.

Lebech AM: Polymerase chain reaction in diagnosis of Borrelia burgdorferi infections and studies on taxonomic classification, *Acta Pathol Microl Immunol Scand Suppl* 105:1, 2002.

Leenders AC: Correspondence, *N Engl J Med* 345:1349, 2001.

Lima A: FDA clears gold standard diagnostics' Borrelia burgdorferi IgG/IgM ELISA assay. Gold standard diagnostics Corp, *AP News*, June 12, 2018. Available at https://apnews.com/e30688a68b7b498baaaf1dfa1b94057e. [Accessed 5 November 2019].

Loeffelholz MJ, Binnicker MJ: It is time to use treponema-specific antibody screening tests for diagnosis of syphilis, *J Clin Microbiol* 50:1, 2012.

Loeffelholz MJ, Wen T, Patel JA: Analysis of Bioplex Syphilis IgG quantitative results in different patient populations, *Clin Vaccine Immunol* 18:2005, 2011.

Loesche WJ, Grossman NS: Periodontal disease as a specific, albeit chronic, infection: diagnosis and treatment, *Clin Microbiol Rev* 14:727, 2001.

Lukehart SA: Endemic treponematoses. In Jameson JL, Fauci AS, Kasper DL, et al.: *Harrison's principles of internal medicine*, 20th ed, New York, 2018a, McGraw-Hill, pp 1286–1290. (chapter 178).

Lukehart SA: Syphilis. In Jameson JL, Fauci AS, Kasper DL, et al.: *Harrison's principles of internal medicine*, ed 20, New York, 2018b, McGraw–Hill, pp 1279–1286. (chapter 177).

Mahon CR, Lehman DC, Manuselis G, et al.: Syphilis. In *Textbook of diagnostic Microbiology*, ed 5, Maryland Heights, MI, 2015, Saunders Elsevier, pp 914–917.

Marangoni A, Moroni A, Accardo S, et al.: Laboratory diagnosis of syphilis with automated immunoassays, *J Clin Lab Anal* 23:1, 2009.

Marks M, Mitjà O, Solomon AW, Asiedu KB, Mabey DC: Yaws, *Br Med Bull* 113(1):91–100, 2015, https://doi.org/10.1093/bmb/ldu037. Epub 2014 Dec 18. PMID: 25525120; PMCID: PMC4350436.

Marques A, Telford 3rd SR, Turk SP, et al.: Xenodiagnosis to detect Borrelia burgdorferi infection: a first-in-human study, *Clin Infect Dis* 58:937, 2014.

Marra CM, Boutin P, McArthur JC, et al.: A pilot study evaluating ceftriaxone and penicillin G as treatment agents for neurosyphilis in human immunodeficiency virus-infected individuals, *Clin Infect Dis* 30:540, 2000.

Marra CM, Maxwell CL, Tantalo L, et al.: Normalization of cerebrospinal fluid abnormalities after neurosyphilis therapy: does HIV status matter? *Clin Infect Dis* 38:1001, 2004a.

Marra CM, Maxwell CL, Tantalo LC, et al.: Normalization of serum rapid plasma reagin titer predicts normalization of cerebrospinal fluid and clinical abnormalities after treatment of neurosyphilis, *Clin Infect Dis* 47:900, 2008.

Marra CM, Tantalo LC, Maxwell CL, et al.: Alternative cerebrospinal fluid tests to diagnose neurosyphilis in HIV-infected individuals, *Neurology* 63:85, 2004b.

Martin-Ezquerra G, Fernandez-Casado A, Barco D, et al.: *Treponema pallidum* distribution patterns in mucocutaneous lesions of primary and secondary syphilis: an immunohistochemical and ultrastructural study, *Hum Pathol* 40:624, 2009.

Masters EJ, Grigery CN, Masters RW: STARI, or Masters disease: lone star tick-vectored lyme-like illness, *Infect Dis Clin North Am* 22:361, 2008.

McGinley-Smith DE, Tsao SS: Dermatoses from ticks, *J Am Acad Dermatol* 49:363, 2003.

Milner DA, Pecora N, et al.: Borrelia species infections. In *Diagnostic Pathology: infectious diseases*, Philadephia, PA, 2015a, Saunders Elsevier; II–2, pp 50–53.

Milner DA, Pecora N, et al.: Leptospira species infection. In *Diagnostic Pathology: infectious diseases*, Philadephia, PA, 2015b, Saunders Elsevier; II–2, pp 54–55.

Milner DA, Pecora N, et al.: Spirochetosis. In *Diagnostic Pathology: infectious diseases*, Philadephia, PA, 2015c, Saunders Elsevier; II–1, pp 24–25.

Mitja O, Houinei W, Moses P, et al.: Mass treatment with single-dose azithromycin for yaws, *N Engl J Med* 372:703, 2015.

Molloy PJ, Persing DH, Berardi VP: False positive results of PCR testing for Lyme disease, *Clin Infect Dis* 33:412, 2001.

Montecinos TM, González FMJ, Bassas-Vila J, et al.: Seronegative syphilis in a patient co-infected with HIV, *Int J Dermatol* 54(10):e439, 2015.

Moore A, Nelson C, Molins C, et al.: Current guidelines, common clinical pitfalls, and future directions for laboratory diagnosis of Lyme disease, United States, *Emerg Infect Dis* 22(7):1169, 2016.

Murray TM, Shapiro ED: Lyme disease, *Clin Lab Med* 30:311, 2010.

Nadelman RB, Nowakowski J, Fish D, et al.: Prophylaxis with single-dose doxycycline for the prevention of Lyme disease after *Ixodes scapularis* tick bite, *N Engl J Med* 345:79, 2001.

Nadelman RB, Nowakowski J, Forseter G, et al.: The clinical spectrum of early Lyme borreliosis in patients with culture-confirmed erythema migrans, *Am J Med* 100(5):502, 1996.

Nadelman RB, Wormser GP: Lyme borreliosis, *Lancet* 352:557, 1998.

Nichol G, Dennis DT, Steere AC, et al.: Test-treatment strategies for patients suspected of having Lyme disease: a cost effective analysis, *Ann Intern Med* 128:37, 1998.

Nigrovic LE, Lipsett SC, Molins CR, et al.: Higher C6 enzyme immunoassay index values correlate with a diagnosis of noncutaneous Lyme disease, *Diagn Microbiol Infect Dis* 94(2):160, 2019.

Nocton JJ, Dressler F, Rutledge BJ, et al.: Detection of *Borrelia burgdorferi* DNA by polymerase chain reaction in synovial fluid from patients with Lyme arthritis, *N Engl J Med* 330:229, 1994.

Okamoto-Shibayama K, Jin S, Kouki Y, et al.: Antimicrobial susceptibility profiles of oral *Treponema* species, *Anaerobe* 48:242, 2017.

Oliver JH, Gao L, Lin T: Comparison of the spirochete Borrelia burgdorferi S. L. isolated from the tick Ixodes scapularis in southeastern and northeastern United States, *J Parasitol* 94:1351, 2008.

Park IU, Fakile YF, Chow JM, et al.: Performance of treponemal tests for the diagnosis of syphilis, *Clinic Infect Dis* 68(6):913, 2019b.

Parola P, Raoult D: Ticks and tick-borne bacterial diseases in humans: an emerging infectious threat, *Clin Infect Dis* 32:897, 2001.

Paster BJ, Boshces SK, Galvin JL, et al.: Bacterial diversity in human subgingival plaque, *J Bacteriol* 183:3770, 2001.

Patel R, Grogg KL, Edwards WD, et al.: Death from inappropriate therapy for Lyme disease, *Clin Infect Dis* 31:1107, 2000.

Paxton A, Pritt B, Theel E, et al.: *Adapting test ordering to novel tick-borne disease rise*, CAP TODAY, College of American Pathologists, May issue, 2020.

Paxton A, Theel E, Branda JA, Rauch C, Gillim-Ross: *No-blot testing charts new course for Lyme diagnosis*, CAP TODAY, College of American Pathologists, Jan issue, 2020.

Pepin KM, Eisen RJ, Mead PS, et al.: Geographic variation in the relationship between human Lyme disease incidence and density of infected host-seeking *Ixodes scapularis* nymphs in the Eastern United States, *Am J Trop Med Hyg* 86:1062, 2012.

Persing DH, Rutledge BJ, Rys PN, et al.: Target imbalance: disparity of *Borrelia burgdorferi* genetic material in synovial fluid from Lyme arthritis patients, *J Infect Dis* 169:668, 1994.

Porcella SF, Schwan TG: *Borrelia burgdorferi* and *Treponema pallidum:* a comparison of functional genomics, environmental adaptations, and pathogenic mechanisms, *J Clin Invest* 107:651, 2001.

Porcella SP, Raffel SJ, Schrumpf ME, et al.: Serodiagnosis of louse-borne relapsing fever with glycerophosphodiester phosphodiesterase (GlpQ) from *Borrelia recurrentis*, *J Clin Microbiol* 38:3561, 2000.

Pritt BS, Mead PS, Johnson DKH, et al.: Identification of a novel pathogenic Borrelia species causing Lyme borreliosis with unusually high spirochaetaemia: a descriptive study, *Lancet Infect Dis* 16(5):556, 2016.

Quest Diagnostics: *Health Trends Lyme disease*, *Trends report*, 2018, pp 1–9. Available at https://questdiagnostics.com/dms/Documents/health-trends/Quest_LymeDiseaseTrendsReport_2018.pdf. [Accessed 5 November 2019].

Reed KD: Laboratory testing for Lyme disease: possibilities and practicalities, *J Clin Microbiol* 40:319, 2002.

Reed LA, O'Bier NS, Oliver Jr LD, et al.: Antimicrobial activity of amixicile against *Treponema denticola* and other oral spirochetes associated with periodontal disease, *J Periodontol* 89:1467, 2018.

Rhee KY, Johnson WD: *Borrelia* species (relapsing fever). In Mandell J, Bennett J, Dolin R, editors: *Principles and practice of infectious diseases*, ed 6, New York, 2005, Churchill Livingstone, p 2502.

Rich SM, Sawyer SA, Barbour AG: Antigen polymorphism in *Borrelia hermsii*, a clonal pathogenic bacterium, *Proc Natl Acad Sci U S A* 98:15038, 2001.

Riviere GR, Smith KS, Carranza N, et al.: Subgingival distribution of *Treponema denticola*, *Treponema socranskii*, and pathogen-related oral spirochetes: prevalence and relationship to periodontal status of sampled sites, *J Periodontol* 66:829, 1995.

Riviere GR, Smith KS, Tzagaroulaki E, et al.: Periodontal status and detection frequency of bacteria at sites of periodontal health and gingivitis, *J Periodontol* 67:109, 1996.

Riviere GR, Smith KS, Willis SG, et al.: Phenotypic and genotypic heterogeneity among cultivable pathogen-related oral spirochetes and *Treponema vincentii*, *J Clin Microbiol* 37:3676, 1999.

Rojas P, Petrich A, et al.: Distribution and phylogeny of Brachyspira spp. in human intestinal spirochetosis revealed by FISH and 16S rRNA-gene analysis, *Anaerobe* 47:25, 2017.

Rolfs RT, Joesoef MR, Hendershot EF, et al.: A randomized trial of enhanced therapy for early syphilis in patients with and without human immunodeficiency virus infection. The Syphilis and HIV Study Group, *N Engl J Med* 337:307, 1997.

Rollend L, Fish D, Childs JE: Transovarial transmission of *Borrelia* spirochetes by *Ixodes scapularis*: a summary of the literature and recent observations, *Ticks Tick Borne Dis* 4:46, 2013.

Romanowski B, Sutherland R, Fich GH, et al.: Serologic response to treatment of infectious syphilis, *Ann Intern Med* 114:1005, 1991.

Rudenko N, Golovchenko M, Grubhoffer L, et al.: Updates on Borrelia burgdorferi sensu lato complex with respect to public health, *Ticks Tick Borne Dis* 2:123, 2011.

Sapi E, Gupta K, Wawrzeniak K, et al.: Borrelia and Chlamydia can form mixed biofilms in infected human skin tissues, *Euro J Microbiol Immunol* 9(2):46, 2019.

Schneider MC, Velasco-Hernandez J, Min K, Leonel DG, et al.: The use of chemoprophylaxis after floods to reduce the occurrence and impact of leptospirosis outbreaks, *Intern J Envirom Res Public Health* 14:594, 2017.

Schutzer SE, Body BA, et al.: Direct diagnostic tests for lyme disease, *CID* 68:1052, 2019.

Schwan TG, Battisti JM, Porcella S, et al.: Glycerol-3-phosphate acquisition in spirochetes: distribution and biological activity of glycerophosphodiester phosphodiesterase (GlpQ) among Borrelia species, *J Bacteriol* 185:1346, 2003.

Scrimenti RJ: Erythema chronicum migrans, *Arch Dermatol* 102:104, 1970.

Seltzer EG, Gerber MA, Cartter ML, et al.: Long-term outcomes of persons with Lyme disease, *J Am Med Assoc* 283:609, 2000.

Seltzer EG, Shapiro ED: Misdiagnosis of Lyme disease: when not to order serologic tests, *Pediatr Infect Dis J* 15:762, 1996.

Sena AC, White BL, Sparling PF: Novel Treponema pallidum serologic tests: a paradigm shift in syphilis screening for the 21st century, *Clin Infect Dis* 51:700, 2010.

Seriburi V, Ndukwe N, Chang Z, Cox ME, et al.: High frequency of false positive IgM immunoblots for Borrelia burgdorferi in clinical practice, *Clin Microbiol Infect* 18:1236, 2012.

Shah A, O'Horo JC, Wilson JW, et al.: An unusual cluster of Neuroinvasive lyme disease cases presenting with Bannwarth syndrome in the Midwest United States, *Open Forum Infect Dis* 5(1):ofx276, 2018.

Shapiro ED, Gerber MA, Holabird NB, et al.: A controlled trial of antimicrobial prophylaxis for Lyme disease after deer-tick bites, *N Engl J Med* 327:1769, 1992.

Shapiro ED: Doxycycline for tick bites—not for everyone, *N Engl J Med* 345:133, 2001.

Sheffield JS, Wendel Jr GD, McIntire DD, et al.: Effect of genital ulcer disease on HIV-1 coreceptor expression in the female genital tract, *J Infect Dis* 196:1509, 2007.

Skogman BH, Lager M, Henningsson AJ, Tjernberg I: The recomBead Borrelia antibody index, CXCL13 and total IgM index for laboratory diagnosis of Lyme neuroborreliosis in children, *Eur J Clin Microbiol Infect Dis* 36(11):2221, 2017.

Smajs D, Norris SJ, Weinstock GM: Genetic diversity in Treponema palidum: implications for pathogenesis, evolution and molecular diagnostics of syphilis and yaws, *Infect Genet Evol* 12:191, 2012.

Smith RP, Schoen RT, Rahn DW, et al.: Clinical characteristics and treatment outcome of early Lyme disease patients with microbiologically confirmed erythema migrans, *Ann Intern Med* 136:421, 2002.

Snyder JL, Giese H, Bandoski-Gralinski C, et al.: T2 magnetic resonance assay based direct detection of three Lyme disease-related Borrelia species in whole blood samples, *J Clin Microbiol* 55:2453, 2017.

Sokhna C, Mediannikov O, Fenollar F, et al.: Point-of-care laboratory of pathogen diagnosis in rural Senegal, *PLoS Negl Trop Dis* 7:e1999, 2013.

Sokolovskiy E, Frigo N, Rotanov S, et al.: Guidelines for the laboratory diagnosis of syphilis in East European countries, *JEADV* 23:623, 2009.

Southern PMJ, Sanford JP: Relapsing fever: a clinical and microbiological review, *Medicine* 48:129, 1969.

Stamm LV: Syphilis: Re-emergence of an old foe, *Microb Cell* 3(9):363, 2016.

Stanek G, Wormser GP, Gray J, et al.: Lyme borreliosis, *Lancet* 379:461, 2012.

Stanek G, Reiter M: The expanding Lyme Borrelia complex—clinical significance of genomic species?, *Clin Microbiol Infect* 17(4):487–493, 2011, https://doi.org/10.1111/j.1469-0691.2011.03492.x. PMID: 21414082.

Steere AC, Angelis SM: Therapy for Lyme arthritis: strategies for the treatment of antibiotic-refractory arthritis, *Arthritis Rheum* 54(10):3079, 2006.

Steere AC, Broderick TF, Malawista SE: Erythema chronicum migrans Lyme arthritis: epidemiologic evidence for a tick vector, *Am J Epidemiol* 108:312, 1978.

Steere AC, Malawista SE, Hardin JA, et al.: Erythema chronicum migrans and Lyme arthritis: the enlarging clinical spectrum, *Ann Intern Med* 86:685, 1977a.

Steere AC, Malawista SE, Syndman DR, et al.: Lyme arthritis: an epidemic of oligoarticular arthritis in children and adults in three Connecticut communities, *Arthritis Rheum* 20:7, 1977b.

Steere AC, McHugh G, Damle N, et al.: Prospective study of serologic tests for Lyme disease, *Clin Infect Dis* 47:188, 2008.

Steere AC, Sikand VK, Meurice F, et al.: Vaccination against lyme disease with recombinant *Borrelia burgdorferi* outer-surface lipoprotein A with adjuvant. Lyme disease vaccine study group, *N Engl J Med* 339:209, 1998.

Steere AC, Sikand VK, Schoen RT, et al.: Asymptomatic infection with *Borrelia burgdorferi*, *Clin Infect Dis* 37:528, 2003.

Steere AC: *Borrelia burgdorferi* (Lyme disease, Lyme borreliosis). In Mandell J, Bennett J, Dolin R, editors: *Principles and practice of infectious diseases*, ed 6, New York, 2015, Churchill Livingstone, p 2798.

Steere AC: Lyme borreliosis. In Jameson JL, Fauci AS, Kasper DL, et al.: *Harrison's principles of internal medicine*, ed 20, New York, 2018, McGraw–Hill, pp 1298–1303. (chapter 181).

Steere AC: Lyme disease, *N Engl J Med* 345:115, 2001.

Stevenson J, Heath M: Syphilis and HIV infection: an update, *Dermatol Clin* 24:497, 2006.

Stupica D, Lusa L, et al.: Treatment of erythema migrans with doxycycline for 10 Days versus 15 Days, *CID* 55(3):343, 2012.

Teglbjaerg PS: Intestinal spirochetosis, *Curr Top Pathol* 81:247, 1990.

Tesfazghi MT, Anderson NW, Gronowski AM, Yarbrougha ML: Clinical performance of the BioPlex 2200 syphilis total & RPR assay at a tertiary medical center with a high rate of syphilis, *J Clin Microbiol* 57(1):pii:e01487, 2019, https://doi.org/10.1128/JCM.01487-18.

Thomas DD, Baseman JB, Alderete JF, et al.: Enhanced levels of attachment of fibronectin-primed *Treponema pallidum* to extracellular matrix, *Infect Immun* 52:736, 1986.

Tsinganou E, Gebbers JO: Human intestinal spirochetosis—a review, *Ger Med Sci* 8:1, 2010.

U.S. Preventive Services Task Force: Screening for syphilis infection in pregnancy: U.S. Preventive Task Force reaffirmation recommendation statement, *Ann Intern Med* 150:705, 2009.

Umeda S, Serizawa H, et al.: Clinical significance of human intestinal spirochetosis: a retrospective study, *The Japan J Gastro-enterol* 114(2):230, 2017.

US Preventive Services Task Force, Curry SJ, et al.: Screening for syphilis infection in pregnant women: US preventive Services Task Force reaffirmation recommendation statement, *J Am Med Assoc* 320(9):911, 2018.

Varela AS, Luttrell MP, Howerth EW, et al.: First culture isolation of *Borrelia lonestari*, putative agent of southern-tick associated rash illness, *J Clin Microbiol* 42:1163, 2004.

Wagenaar JFP, Goris MGA: Leptospirosis. In Jameson JL, Fauci AS, Kasper DL, et al.: *Harrison's principles of internal medicine*, ed 20, New York, 2018, McGraw–Hill, pp 1290–1295. (chapter 179).

Wang LN, Li JM: Evaluation of immunoglobulin M and G Western blot and ELISA for screening antibodies to *Treponema pallidum* in blood donors, *Sex Transm Dis* 36:413, 2009.

Wang P, Glowacki MN, Hoet AE, et al.: Emergence of *Ixodes scapularis* and *Borrelia burgdorferi*, the Lyme disease vector and agent, in Ohio, *Cell Infect Microbiol* 4:1, 2014.

Warrell DA: Louse-borne relapsing fever (Borrelia recurrentis infection), *Epidemiol Infect* 147:e106, 2019, https://doi.org/10.1017/S0950268819000116. PMID: 30869050; PMCID: PMC6518520.

Warshafsky S, Nowakowski J, Nadelman RB, et al.: Efficacy of antibiotic prophylaxis for prevention of Lyme disease, *J Gen Intern Med* 11:329, 1996.

Wicher V, Wicher K: Pathogenesis of maternal-fetal syphilis revisited, *Clin Infect Dis* 33:354, 2001.

Woods R: Congenital syphilis—persisting pestilence, *Pediatr Infect Dis J* 28:536, 2009.

Workowski KA, Bolan GA, et al.: Sexually transmitted diseases treatment guidelines, Centers for disease control and prevention, *Morb Mortal Wkly Rep* 64:RR3:1, 2015.

Wormser GP, Brisson D, Liveris D, et et al.: Borrelia burgdorferi genotype predicts the capacity for hematogenous dissemination during early Lyme disease, *J Infect Dis* 198:9:1358, 2008.

Wormser GP, Baker PJ, O'Connell S, et al.: Critical analysis of treatment trials of rhesus macaques infected with Borrelia burgdorferi reveals important flaws in experimental design, *Vector Borne Zoonotic Dis* 12:535, 2012.

Wormser GP, Bittker S, Cooper D, et al.: Yield of large-volume blood cultures in patients with early Lyme disease, *J Infect Dis* 184:1070, 2001.

Wormser GP, Brisson D, Liveris D, et al.: Borrelia burgdorferi genotype predicts the capacity for hematogenous dissemination during early Lyme disease, *J Infect Dis* 198(9):1358, 2008.

Wormser GP, Brisson D, Liveris D, et al.: *Borrelia burgdorferi* genotype predicts the capacity for hematogenous dissemination during early Lyme disease, *J Infect Dis* 198:1358, 2008.

Wormser GP, Dattwyler RJ, Shapiro ED, et al.: The clinical assessment, treatment and prevention of Lyme disease, human granulocytic anaplasmosis and babesiosis: clinical practice guidelines by the Infectious Disease Society of America, *Clin Infect Dis* 43:1089, 2006.

Wormser GP, Liveris D, Nowakowski J, et al.: Association of species subtypes of *Borrelia burgdorferi* with hematogenous dissemination in early Lyme disease, *J Infect Dis* 180:720, 1999.

Wormser GP, Masters E, Liveris D, et al.: Microbiologic evaluation of patients from Missouri with erythema migrans, *Clin Infect Dis* 40:423, 2005a.

Wormser GP, Masters E, Nowakowski J, et al.: Prospective clinical evaluation of patients from Missouri and New York with erythema migrans-like skin lesions, *Clin Infect Dis* 41:958, 2005b.

Wormser GP, Nowakowski J, Nadelman RB, et al.: Impact of clinical variables on *Borrelia burgdorferi*-specific antibody seropositivity in acute-phase sera from patients in North America with culture-confirmed early Lyme disease, *Clin Vaccine Immunol* 15:1519, 2008.

Wormser GP, Schriefer M, Aguero-Rosenfeld ME, et al.: Single-tier testing with the C6 peptide ELISA kit compared with two-tier testing for Lyme disease, *Diagn Microbiol Infect Dis* 75:9, 2013.

Yen-Lieberman B, Daniel J, Means C, et al.: Identification of false-positive syphilis antibody results using a semiquantitative algorithm, *Clin Vaccine Immunol* 18:1038, 2011.

Young K, Sadoughi S: Young new draft lyme disease guidelines issued, *NEJM J Watch*, June, 2019. https://www.jwatch.org/fw115560/2019/06/27/new-draft-lyme-disease-guidelines-issued.

Young K, Hefner JE: *New bacteria species that causes Lyme disease discovered*, *medical news Physician's first Watch*, Feb 9, 2016.

Zhang JR, Norris SJ: Genetic variation of the *Borrelia burgdorferi* gene vlsE involves cassette-specific, segmental gene conversion, *Infect Immunol* 66:3698, 1998.

Zoni AC, Saboya-Dı az MI, Castellanos LG, et al.: Epidemiological situation of yaws in the Americas: a systematic review in the context of a regional elimination goal, *PLoS Negl Trop Dis* 13(2):e0007125, 2019.

CHAPTER 62

CHLAMYDIAL AND MYCOPLASMAL INFECTIONS

Dejan Nikolic

CHLAMYDIAL INFECTIONS, 1246
Structure, 1246
Replication, 1246
Chlamydia Trachomatis, 1247
Chlamydophila (Formerly Chlamydia) Psittaci, 1248
Chlamydophila (Formerly Chlamydia) Pneumoniae, 1248
Laboratory Diagnosis, 1249
Treatment, 1250
MYCOPLASMAL AND UREAPLASMAL INFECTIONS, 1250
Mycoplasma Pneumoniae, 1251
Genital Mycoplasmas, 1252
Laboratory Diagnosis, 1252
Treatment, 1253
SELECTED REFERENCES, 1253

KEY POINTS

- *Chlamydia trachomatis*, the most common notifiable condition in the United States, is the most common bacterial cause of sexually transmitted disease in the United States and its prevalence is rising.
- The most sensitive method for detecting *C. trachomatis*, nucleic acid amplification, now is also commercially available for testing extragenital sites.
- *Chlamydophila pneumoniae* (formerly *Chlamydia pneumoniae*) is responsible for at least 10% of community-acquired pneumonias.
- Pneumonia due to *Mycoplasma pneumoniae* is often diagnosed on the basis of clinical manifestations alone. Definitive diagnosis requires detection of nucleic acid in a respiratory specimen by nucleic acid amplification.
- *M. genitalium*, thought to be the most common cause of nongonococcal nonchlamydial (NGNC) urethritis or the second most common cause of nongonococcal urethritis after *C. trachomatis*, contributes to an estimated 10% to 35% of acute or persistent/recurrent NGNC urethritis in men and to an estimated 10% to 30% of cases of clinical cervicitis in women in the United States.
- Commercially available nucleic acid amplification assays are the methodology of choice to detect *M. genitalium*. Treatment of *M. genitalium* could be complicated by development of resistance to multiple antimicrobial agents.

Human infections caused by chlamydias and mycoplasmas are discussed separately because the responsible pathogens differ from most other bacteria in several ways: The organisms are smaller, the structure of their cell walls is different, and chlamydias are obligately intracellular parasites.

CHLAMYDIAL INFECTIONS

The chlamydias have a tropism for columnar epithelial cells. They have a cell wall similar to that of gram-negative bacteria; they contain both deoxyribonucleic acid (DNA) and ribonucleic acid (RNA), have prokaryotic ribosomes, and synthesize their own proteins, nucleic acids, and lipids; they divide by binary fission; and they are susceptible to particular antibiotics. Unlike most bacteria, the chlamydias are "energy parasites"; they lack cytochromes and so cannot synthesize high-energy adenosine triphosphate (ATP) metabolites. For this reason, they are obligate intracellular bacteria and cannot replicate outside cells.

The chlamydias are classified in the order Chlamydiales, family Chlamydiaceae, the only family that contains human pathogens (Everett et al., 1999). Two genera and three species are pathogenic for humans: *Chlamydia trachomatis*, *Chlamydophila* (formerly *Chlamydia*) *psittaci*, and *Chlamydophila* (formerly *Chlamydia*) *pneumoniae*. Features useful for differentiating the three species are shown in Table 62.1. These genera also contain six other species that have not been associated with infection in humans. There are two biovars of *C. trachomatis:* lymphogranuloma venereum (LGV) (Biovar LGV) and trachoma (Biovar trachoma), which preferentially infect humans. Biovar LGV contains four serovars (L1, L2, L2a, and L3), and 15 serovars are included in Biovar trachoma: A, B, Ba, and C are associated with trachoma, whereas D to K, Da, Ia, and Ja are associated with genital infections. Mouse and hamster isolates that previously made up the third biovar of *C. trachomatis* have been reclassified as new species, *Chlamydia muridarum*, and the guinea pig inclusion conjunctivitis strain is now designated *C. caviae* (Gaydos & Quinn, 2018).

STRUCTURE

Two morphologically distinct forms of chlamydia are recognized. The elementary body is a dense, spherical form, 0.2 to 0.4 μm in diameter, that contains prokaryotic ribosomal RNA and has a rigid cell wall caused by extensive disulfide cross-linking of cell wall proteins. It is the infectious form of the organism, capable of limited extracellular survival. The reticulate body, 0.6 to 1.0 μm in diameter, is the intracellular, metabolically active form, incapable of surviving outside cells. The closed circular DNA of both forms is compactly organized in a central nucleoid and has a genome of 1.0 to 1.2 million nucleotide base pairs.

Two components of the outer membrane of the chlamydial outer membrane complex have diagnostic importance. The most prominent is the major outer membrane protein (MOMP), a transmembrane protein with serovar-, species-, genus-, and family-reactive epitopes defined by monoclonal antibodies. Infection with chlamydias induces MOMP-specific antibodies, but their role in protective immunity is unclear. The chlamydial outer membrane complex also contains a lipopolysaccharide (LPS) antigen, which is the major antigen detected in genus-specific serologic tests for chlamydial infection. Monoclonal antibodies and monospecific polyvalent antisera to the LPS or MOMP are used in direct fluorescent antibody (DFA) tests to detect chlamydial antigen in clinical specimens.

REPLICATION

Chlamydias replicate in the cytoplasm of infected host cells. The developmental cycle begins with attachment of the elementary body to a microvillus on a susceptible columnar cell via heparin bridges. The elementary body travels down the microvillus and localizes in indentations of the host cell plasma membrane. There, the chlamydia enters the host cell in an endosome, where *C. psittaci*, *C. pneumoniae*, and *C. trachomatis* remain during their intracellular development. Endosomes containing elementary bodies of *C. psittaci* do not become acidified or fuse with cellular lysosomes; those containing *C. trachomatis* elementary bodies fuse with one another and perhaps with lysosomes. Within 6 to 8 hours after the elementary body enters the host cell, changes in its cell wall result in a transition to the reticulate body and subsequent initiation of DNA, RNA, and protein synthesis and its division by binary fission. Host cell mitochondria migrate to and are positioned against the enlarging endosome, allowing the reticulate body to utilize host cell ATP. Reticulate bodies begin to reorganize 18

TABLE 62.1

Useful Features for Differentiating Species of *Chlamydia* and *Chlamydophila* Pathogenic for Humans

Parameter	SPECIES		
	Chlamydia trachomatis	***Chlamydophila psittaci***	***Chlamydophila pneumoniae***
Sulfa susceptibility	Susceptible	Resistant	Resistant
Glycogen staining of inclusion	Positive	Negative	Negative
Elementary body shape	Round	Round	Pear-shaped or round

to 24 hours after infection, and, presumably when nutrients are depleted, they mature into elementary bodies, which are released from the host cell. Cells infected with *C. psittaci* usually are severely damaged, and the organisms are released by cell lysis within 48 hours. In contrast, the inclusion of *C. trachomatis* appears to be extruded by fusion of the inclusion membrane with the plasma membrane 72 to 96 hours after infection, leaving a lesion in the surviving host cell membrane.

CHLAMYDIA TRACHOMATIS

C. trachomatis is the most common cause of sexually transmitted disease (STD) in the United States, and it is the primary infectious cause of blindness in trachoma-endemic regions of the Middle East, sub-Saharan Africa, and Asia. The disorder is endemic in more than 50 countries, and estimates indicate that 21 million people live with active trachoma, 7.3 million required surgery, and 2.2 million have visual impairment, including 1.2 million individuals that are blind due to trachoma (World Health Organization [WHO], 2018).

Epidemiology, Pathology, and Clinical Manifestations

Humans are the only known natural host for all strains of *C. trachomatis*. The clinical manifestations and organ specificity of human infections with *C. trachomatis* are determined by both the mechanism of transmission and the properties of the infecting strain. Epidemiologically, *C. trachomatis* infections are divided into three categories: classic trachoma, sexually transmitted infections of adults, and perinatal ocular and respiratory tract infections.

Classic trachoma is an important cause of blindness in areas where public sanitation is inadequate and personal hygiene is poor (Solomon et al., 2004; Gaydos & Quinn, 2018). The disease is due to repeated infections of the conjunctiva, resulting in a pathologic sequence over time of follicular conjunctivitis, subepithelial scarring, contraction of the scar resulting in turning inward of the eyelid (entropion), rubbing of the eyelashes on the cornea (trichiasis) with subsequent corneal injury, and corneal scarring with opacification and reduced vision. Typically, acute infection is transmitted among children via fingers, fomites, and probably flies, and most children become chronically infected within a few years of birth. Conjunctival scarring usually becomes evident by the second or third decade of life, and blindness can occur anywhere from 10 to 40 years after the first infection (Dean et al., 2008). It is interesting to note that other species of the Chlamydiaceae (*C. psittaci* and *C. pneumonia*) may also be involved in the pathogenesis of trachoma (Dean et al., 2008).

C. trachomatis–induced sexually transmitted infections of adults include LGV and urethritis/cervicitis and associated complications. LGV is endemic in Asia, Africa, and South America. In the United States, although approximately 500 cases are reported each year, the true incidence is much higher; the disease affects males more frequently than females and is most common in persons of low socioeconomic status living in the southeastern states, in men who have sex with men (MSM), and in persons who have visited LGV-endemic countries outside the United States. LGV is transmitted sexually, although transmission by fomites and by aerosols produced during laboratory accidents has caused pneumonitis, pleural effusions, and mediastinal or hilar lymphadenopathy (Jones & Batteiger, 2000). Reservoirs of infection probably are persons with asymptomatic or ignored symptomatic urethral, cervical, or anorectal infection.

LGV is the only infection caused by *C. trachomatis* that produces multisystem involvement and constitutional manifestations. During the primary phase, a small, painless vesicle or a nonindurated papule or ulcer develops, often on the external genitalia, 3 days to 3 weeks after exposure, and heals quickly without scarring. If transmission is rectal, an acute proctitis is often the first manifestation. An outbreak of LGV proctitis in MSM was first noticed in Europe at the beginning of this century and is due to infection with a unique LGV variant (labeled "L2b") (Spaargaren et al., 2005). Genomic similarity to isolates obtained from patients in the early 1980s in the United States suggests a silent ongoing epidemic in this population caused by this unique variant (Spaargaren et al., 2005). More recently several large outbreaks of LGV proctocolitis have been reported among MSM (Pallawela et al., 2014; de Vrieze et al., 2014; Koper et al., 2013; de Voux et al., 2016). Moreover, the rates of LGV infections among MSM in New York City clinics are continuously increasing, trends having almost doubled over an 8-year period (16.6% LGV positivity rate as determined by LGV-specific testing of submitted *C. trachomatis*–positive anorectal specimens in 2012–2015 vs 8.7% LGV positivity rate in 2008–2011) (Pathela et al., 2019). These data are consistent with the estimation that LGV-associated genotypes cause 10% to 20% of all *C. trachomatis*–positive anorectal cases among MSM. Given the fact that none of the LGV-specific tests are commercially available and the evidence that asymptomatic LGV infections are not uncommon (Haar et al., 2013; Van der Bij et al., 2006; de Vrieze et al., 2013; Saxon et al., 2016), it is likely that a significant proportion of LGV cases are currently underdiagnosed.

The secondary stage, characterized by suppurative regional lymphadenopathy, fever, chills, anorexia, headache, myalgias, and arthralgias, begins 2 to 6 weeks after exposure. The primary ulcer or papule often resolves before the secondary stage, but an acute proctitis may persist. Histologic examination of affected lymph nodes shows granulomas surrounding stellate abscesses. Involved lymph nodes become matted and eventually suppurate, producing draining fistulas that heal with scarring over several months. Fibrosis and resultant abnormal lymphatic drainage are responsible for the urethral or rectal strictures or induration and lymphedema of the genitalia that develop during the third stage.

Non-LGV *C. trachomatis* infection is the most common notifiable condition in the United States, the most common bacterial cause of STD in the United States, and its prevalence continues to rise (Centers for Disease Control and Prevention [CDC], 2018c). In 2017, 1,708,569 cases of the *C. trachomatis* infection were reported, resulting in a rate of 528.8 cases/100,000 population, an increase of 22% compared with a rate of 446.6 cases/100,000 population in 2013; and an increase of 6.8% compared to the rate in the previous year 2016. The rates have increased in all states, among both females and males, and among all racial and ethnic groups (CDC, 2017).

The clinical spectrum of sexually transmitted infections due to non-LGV strains of *C. trachomatis* is similar to disease caused by *Neisseria gonorrhoeae*. In men, *C. trachomatis* is responsible for 30% to 50% of cases of nongonococcal urethritis (NGU), but as many as 85% to 90% of men who harbor *C. trachomatis* in the urethra are asymptomatic (Peipert, 2003). Urethritis caused by *C. trachomatis* can present with dysuria and scant mucoid or mucopurulent discharge that rarely can progress to epididymitis. Among MSM, non-LGV strains of *C. trachomatis* have been associated with proctitis in up to 15% of all cases (Haar et al., 2013). Clinical manifestations of chlamydial proctitis, which can vary from asymptomatic to anorectal pain with mucopurulent discharge, have considerable overlap with manifestations of LGV proctitis. However, it is important to identify the specific pathogen, since a much longer duration of antibiotic therapy is required to treat genotypes associated with LGV.

In addition to occasionally causing reactive arthritis associated with HLA-B27, *C. trachomatis* can also sometimes cause eye and/or skin symptoms (Reiter syndrome) and rarely perihepatitis. Although more common in men, cases of Reiter syndrome have been reported in women and children. Genital infection with *C. trachomatis* is diagnosed more often in women than in men, with a rate of 687.4/100,000 reported for women in the United States in 2013, about twice the rate among men (CDC, 2017), a rate difference that is thought, at least in part, to reflect the greater number of women screened for this infection. Infection of the endocervix with *C. trachomatis* is often asymptomatic, but at least one-third of infected women have signs of infection on physical examination. The most common sign

is mucopurulent cervicitis, which can spread to the urethra and urinary bladder, resulting in the acute urethral syndrome of abacteriuric pyuria, or to the endometrium and fallopian tubes, producing endometritis or salpingitis. Untreated infections of the upper reproductive tract may progress to pelvic inflammatory disease (PID) or may cause scarring and dysfunction of the oviduct transport system, which could result in infertility, ectopic pregnancy, or chronic pelvic pain. Intraperitoneal spread of the infection may cause acute peritonitis, perihepatitis (Fitz-Hugh-Curtis syndrome), periappendicitis, or perisplenitis. A portion (1–5%) of patients with urogenital infection with *C. trachomatis* will develop a reactive sterile arthritis predominantly in large joints that is usually self-limited but may develop a chronic relapsing course (Rihl et al., 2006; Carter et al., 2009). Chlamydial infection in pregnancy has been associated with preterm labor, premature rupture of membranes, low birth weight, neonatal death, and postpartum endometritis. In women, it is not uncommon for *C. trachomatis* to spread to the rectum, causing chlamydial proctitis. A small percentage of adults with chlamydial genital infections develop inclusion conjunctivitis from autoinoculation.

In developed countries, where sexually transmitted infection with *C. trachomatis* is epidemic, the organism may be transmitted from infected mother to infant during passage through the birth canal. Data from studies in North America indicate that 60% to 70% of infants exposed to *C. trachomatis* during vaginal delivery become infected with the organism, whereas infection after cesarean section is uncommon (Jones & Batteiger, 2000). Rates of chlamydial infection are highest among adolescents and young adults. In 2017, almost two-thirds of reported cases were in individuals aged 15 to 24 years, and the rates were highest among women 15 to 19 years of age (3265.7 cases/100,000 women) and 20 to 24 years of age (3985.8 cases/100,000 women) (CDC, 2017). During 2013 to 2017, the infection rates in women 15 to 24 years of age increased 8.8%, and rates in men increased almost 40% (CDC, 2017). It is thought that reported cases for men are generally lower due to smaller numbers of men screened for *C. trachomatis* infection. It is unclear how much availability of commercial assays for urine (e.g., first-void urine) and extragenital testing (e.g., pharyngeal and rectal swabs) has contributed/will contribute to the better detection in men.

C. trachomatis is recovered from the conjunctiva of infected infants after 1 to 2 weeks and from the nasopharynx soon thereafter. The rate of isolation from the conjunctiva falls by 5 to 6 weeks, but *C. trachomatis* can be recovered from the nasopharynx, conjunctiva, rectum, and vagina (usually without producing symptoms) for several months.

Inclusion conjunctivitis, the most common manifestation of infection with *C. trachomatis* in infants, develops in nearly 80% of infants whose conjunctival culture or cytologic examination demonstrates the organism (Jones & Batteiger, 2000), and among those with conjunctivitis, approximately 50% will have a nasopharyngeal infection. A mucopurulent discharge appears 2 to 25 days after birth, and the conjunctiva becomes inflamed and edematous. Severity ranges from a mild infection with scant discharge to copious mucopurulent discharge with severe swelling and pseudomembrane formation.

Approximately 20% to 30% of infants who acquire infection with *C. trachomatis* at birth develop interstitial pneumonitis. The illness begins at between 2 weeks and 3 months of age (peak, 3–6 weeks) with nasal congestion, followed by a distinctive staccato cough with tachypnea and rales but no fever. Hyperinflation with interstitial or alveolar infiltrates on chest radiograph and peripheral eosinophilia are frequently seen. About one-half of patients have or have had conjunctivitis. Symptoms last several weeks, but inspiratory rales and chest roentgenographic changes may persist for months.

Recently, it was shown that *C. trachomatis* genital infection in women results in a shift in microbiota toward anaerobic bacteria, an increased production of lactoferrin, interleukin 6 (IL-6), IL-1α, interferon-α (IFN-α), and IFN-β, and decreased production of IFN-γ (Filardo et al., 2019). Another study examined and compared cytokines in cervical secretions from women with chlamydial infection involving only the cervix with those obtained from women with chlamydial infection involving both cervix and endometrium. It was proposed that polarization of the host immune response toward T-helper (Th) 1 phenotype and related cytokines is associated with protection against ascending infection and reinfection, while polarization toward humoral, type I interferon, Th 17 phenotype, and involved cytokines is associated with susceptibility to *C. trachomatis* (Poston et al., 2019). The unique LPS structure of *C. trachomatis*, which is capable of preventing initiation of both canonic and noncanonic innate immune signals, was suggested as a contributing factor to the high incidence of asymptomatic *C. trachomatis* infections (Yang et al., 2019).

CHLAMYDOPHILA (FORMERLY CHLAMYDIA) PSITTACI

Pneumonia associated with exposure to birds was described in Switzerland in 1879. The disease was rare in the United States and Europe until the late 1920s, when pet tropical birds became fashionable. The pathogen was isolated by Bedson from human and avian tissue in 1930 during an investigation of an outbreak at the London Zoo.

Epidemiology

Infection caused by *Chlamydophila* (formerly *Chlamydia*) *psittaci* (also called psittacosis, parrot fever, or ornithosis) occurs worldwide. *C. psittaci* has seven genotypes (A–F, E/B), all of which are infective for humans. Psittacine birds are considered the major reservoir, but most species of birds can be infected with the organism. Infected birds may be obviously ill and may die of the disease, but frequently they have mild signs such as anorexia, diarrhea, lethargy, and ruffled feathers. Human illness is sporadic and has been associated with exposure to parrots, canaries, pigeons, sparrows, ducks, cockatiels, fowl (especially turkeys), and occasionally mammals. Owners of pet birds account for about one-half of the cases reported in the United States each year. During the past decade, fewer than 10 confirmed cases were reported annually in the United States, which likely is an underrepresentation because patients with mild illness may not seek medical attention or be reported (CDC, 2018b). Pet shop employees, pigeon fanciers, zoo workers, veterinarians, and others who work with birds are at increased risk for infection. Outbreaks have occurred among poultry processing plant workers, principally among workers who killed the birds and plucked their feathers and those who eviscerated carcasses, with a mortality of about 1%, even with appropriate therapy (CDC, 1990; Petrovay & Balla, 2008). Before the discovery of antibiotics, the mortality rate for human infection was 15% to 20%. Over the past several decades, the prevalence of psittacosis in the United States has declined dramatically as a result of adding tetracycline to poultry feed, requiring medication of commercially imported psittacine birds before entering the country, and domestic breeding of parakeets.

C. psittaci is present in the blood, tissues, excreta, and feathers of infected birds and may be shed for months after acute infection. Transmission to humans occurs via inhalation of infectious aerosols derived from feces, fecal dust, and secretions of *C. psittaci*–infected birds, but may result from handling contaminated plumage or tissues, from bird bites, or from mouth-to-beak contact. Contact with birds does not have to be close or prolonged. Person-to-person spread of *C. psittaci* has never been demonstrated (Gaydos & Quinn, 2018).

Pathogenesis and Pathology

C. psittaci enters the body via the respiratory tract and is transported to the macrophages of the liver and spleen, where the organisms replicate. They then enter the blood and travel to the lungs, the primary target of infection, and other organs. Histologic examination of lung tissue shows lymphocytes in the alveolar and interstitial spaces and mucous plugging of the bronchioles. Small hemorrhages and macrophages with intracytoplasmic inclusions may be seen. The hilar lymph nodes, liver, and spleen may be enlarged and may contain foci of necrosis; in fatal cases, the myocardium, pericardium, meninges, brain, and adrenal glands may be involved.

Clinical Manifestations

After an incubation period of 1 to 2 weeks, psittacosis may begin abruptly with chills and fever, or it may begin more gradually with increasing fever and malaise. Persistent dry, hacking cough, occasionally productive of blood-streaked mucoid sputum, is prominent. The heart rate is often slow relative to body temperature, and a diffuse, severe headache is usual. Malaise, anorexia, painful myalgias, and arthralgias are common, and a macular rash (Horder spots) resembling the rose spots of typhoid fever may occur. Decreased mentation may develop at the end of the first week of illness, and some may have gastrointestinal complaints. *C. psittaci* is a rare cause of destructive endocarditis; most affected persons have a history of rheumatic heart disease or congenital valvular abnormalities (Jones et al., 1982). Myocarditis, hepatitis, and neurologic complications have been reported, some of which with fatal outcome (Gaydos & Quinn, 2018).

CHLAMYDOPHILA (FORMERLY CHLAMYDIA) PNEUMONIAE

In 1986, a unique chlamydial organism, initially considered to be a strain of *C. psittaci*, was associated with acute respiratory tract disease in humans. The organism was named TWAR for the laboratory identifying letters of

the first two isolates: TW-183, isolated in 1965 from the eye of a control child in a trachoma vaccine trial in Taiwan, and AR-39, recovered the same year from the throat of a student with pharyngitis at the University of Washington. Soon after its recognition, data from DNA homology and electron microscopic studies showed that this unique organism was a separate species, designated as *Chlamydia pneumoniae*, which has been reclassified as *Chlamydophila pneumoniae* (Campbell et al., 1987; Chi et al., 1987; Cox et al., 1988; Everett et al., 1999).

Epidemiology

The epidemiology of infection with *C. pneumoniae* is based on data from retrospective studies of sera collected during respiratory tract illnesses. About 50% of adults have antibodies to *C. pneumoniae*. Antibody prevalence rates are low in children, increase sharply in teenagers, continue to increase until middle age, and remain high into old age; rates are 10% to 25% higher for males. Data from retrospective and prospective serologic studies indicate that disease caused by *C. pneumoniae* is endemic in the United States and epidemic in Scandinavia and Finland, but does not occur with any consistent seasonal periodicity (Grayston et al., 1989, 1990). *C. pneumoniae* appears to be a primary human pathogen, transmitted from person to person without an avian or animal reservoir. The mechanism and place of transmission, incubation period, and infectiousness of the organism have not yet been determined.

Pathogenesis

The pathogenesis of infection with *C. pneumoniae* is unknown. Because the illness is generally mild and self-limited, autopsy studies are unavailable.

Clinical Manifestations

It is estimated that *C. pneumoniae* is responsible for at least 10% of community-acquired pneumonias (Grayston et al., 1990; Gaydos & Quinn, 2018). The pneumonia usually is mild with a single subsegmental infiltrate, but it may be severe, especially in older adults and in those with chronic disease. It often begins with pharyngitis and hoarseness, followed by persistent cough. Although pneumonia is the most common syndrome associated with *C. pneumoniae* infection, serologic studies during epidemics among military trainees have shown that only about 10% of infections with *C. pneumoniae* result in pneumonia, suggesting that infection is frequently mild or asymptomatic and unrecognized. Other manifestations of *C. pneumoniae* infection are bronchitis, pharyngitis, fever of undetermined origin, otitis, influenza-like illness, myocarditis, and endocarditis (Gaydos & Quinn, 2018). By enhancing inflammation, *C. pneumoniae* has been suggested to potentially play a role in the development and progression of several chronic inflammatory disorders (Di Pietro et al., 2019). Association between *C. pneumoniae* infection and atherosclerosis has been indicated (Zhu et al., 2000), with more evidence provided in the later studies (Sessa et al., 2014; Budzynski et al., 2016). By stimulating macrophages and other cell types, *C. pneumoniae* is capable of increasing production of proinflammatory cytokines and molecules necessary for atherosclerotic plaques formation (Di Pietro et al., 2019), potentially via Nod-like receptors (Tumurkhuu et al., 2018), Toll-like receptors (Chen et al., 2018), and systemic inflammation (Filardo et al., 2015). In laboratory animals, the *C. pneumoniae*–mediated accelerated progression of atherosclerosis could be abolished by use of antibiotics (Gaydos & Quinn, 2018). In humans, although the small trials suggested that antibiotics could reduce the incidence of cardiovascular complications, these findings were not confirmed by larger clinical trials (Campbell et al., 2014; Gaydos & Quinn, 2018). In Alzheimer disease, an inflammatory disorder of the brain (Di Pietro et al., 2019), *C. pneumoniae* has been shown to exaggerate chronic inflammation via stimulating production of proinflammatory cytokines by microglia and astrocytes, activating nitric oxide synthase (Balin et al., 2018) and inhibiting apoptosis (Appelt et al., 2008; Di Pietro et al., 2019). Despite the evidence, the antibiotics were ineffective against *C. pneumoniae* in the only clinical trial adding to the controversy (Loeb et al., 2004; Di Pietro et al., 2019). Although reactive arthritis is typically related to *C. trachomatis*, it has also been associated with *C. pneumoniae* (Zeidler & Hudson, 2016; Carter et al., 2017; Di Pietro et al., 2019). Despite the consistent detection of *C. pneumoniae* nucleic acid from synovial fluid and tissue (Contini et al., 2011; Rizo et al., 2012), the exact role of *C. pneumoniae* remains unclear (Di Pietro et al., 2019).

LABORATORY DIAGNOSIS

Non-LGV *Chlamydia Trachomatis*

Specimens for detection of *C. trachomatis* are determined by the type of disease suspected (Table 62.2). Screening women at risk for genital *C. trachomatis* infection (described earlier) has been shown to decrease the rate of PID, thus preventing subsequent reproductive sequelae (Nelson & Helfand, 2001). The transport system selected must be approved for the test method used. Specific collection techniques are discussed in Chapter 66. Most infections involve mucous membranes; specimens should be collected directly from the involved surface and must contain an adequate sample of infected epithelial cells. For females, both vaginal and endocervical specimens are acceptable. Purulent discharge is not an appropriate specimen and should be removed before a sample is collected with a swab or brush. Of the types of swabs available, Dacron- or rayon-tipped swabs with a plastic or wire shaft are preferred. Swabs with wooden shafts should be avoided because wood is toxic to the organism. Calcium alginate swabs may be toxic to the chlamydias or to the cells that support their growth. Cotton-tipped swabs are acceptable but are occasionally toxic to the chlamydias. Collection of urine and extragenital specimen sources, including pharyngeal and rectal sites for nucleic acid amplification testing, should follow manufacturer recommendations.

Nucleic Acid Amplification

Nucleic acid amplification tests (NAATs) have been shown in many studies to be highly specific and more sensitive than culture for detection of non-LGV *C. trachomatis* in urogenital specimens and thus are the diagnostic methodology of choice (Gaydos & Quinn, 2018). For this reason, NAATs that are cleared by the US Food and Drug Administration (FDA) currently are recommended by the CDC for detection of genital tract infections caused by non-LGV *C. trachomatis* in symptomatic and asymptomatic men and women (CDC, 2015). Because NAATs have increased sensitivity compared to other test methods (discussed later), the CDC also recommends that a NAAT be used for detection of rectal and oropharyngeal chlamydial infections. In May 2019, two NAATs (Aptima Hologic Combo 2 Assay and the GeneXpert Cepheid assay) were cleared by the FDA and thus are commercially available for detection of *C. trachomatis* (and *N. gonorrhoeae*) in extragenital sites, including oropharyngeal and rectal sites (FDA, 2019; Cepheid, 2019).

In the United States as of May 2019, five manufacturers (Abbott Molecular Inc., Des Plaines, IL; Hologic/Gen-Probe Inc., San Diego, CA; Becton Dickinson and Company, Sparks, MD; Cepheid, Sunnyvale, CA; and Roche Molecular Diagnostics, Pleasanton, CA) had FDA-cleared NAAT assay platforms for detection of *C. trachomatis* (and *N. gonorrhoeae*) in urogenital specimens. Nucleic acid targets, FDA-cleared specimen types, and specimen transport and storage conditions are nicely summarized elsewhere (CDC, 2015).

Interestingly, an estimated 6% to 10% of *C. trachomatis*–positive cases in Finland recently might have been missed due to false-negative/equivocal Aptima Combo 2 assay Hologic Inc. (Rantakokko-Jalava et al., 2019). The C1515T mutation in the *C. trachomatis* 23S rRNA gene was identified as a probable cause, and a kit containing a 23rRNA-mutant detection probe is currently being used as a research use only tool to better understand the geographic distribution of this mutant in Finland (Unemo et al., 2019). It is not an unexpected finding that an infectious agent, in this

TABLE 62.2
Specimens for Detection of *Chlamydia Trachomatis*

Disease	Specimen
Mucopurulent cervicitis	Endocervical swab, urine
Acute urethral syndrome (women)	Urethral swab, urine
Acute endometritis	Endometrial aspirate
Acute salpingitis	Fallopian tube biopsy
Nongonococcal urethritis (men)	Urethral swab, urine
Pharyngitis	Throat swab
Proctitis	Rectal swab
Inclusion conjunctivitis	Conjunctival scrapings/swab
Trachoma	Conjunctival scrapings/swab
Lymphogranuloma venereum	Lymph node aspirate, biopsy of ulcerated lesion, serum
Pneumonitis (infants)	Serum, tracheobronchial aspirate, nasopharyngeal swab

Urine is acceptable for the commercial nucleic acid amplification tests.
Specimens from pharyngeal and rectal sites, now US Food and Drug Administration approved for *C. trachomatis* nucleic acid amplification testing, must be collected with the appropriate swab collection kits according to the manufacturers.

case *C. trachomatis*, is changing and mutating under a strong selective pressure provided by NAAT identifying specific target so that mutated strain can no longer be detected (Unemo et al., 2019). More detailed molecular techniques, such as genotyping by sequencing of the OmpA gene or multilocus sequence typing, could allow greater differentiation between strains and thus provide better understanding of the molecular epidemiology of *C. trachomatis* infection.

Cell Culture

Cell culture currently is the recommended test method for diagnosis of chlamydial infections in cases of suspected sexual assault or abuse in boys and extragenital infections in girls. Culture also is the only method that can be used to properly assess test of cure. Cell lines most commonly used are McCoy or buffalo green monkey cells. Both have equivalent sensitivity, but the latter cells are easier to maintain and are more resistant to cytotoxic substances; they have been associated with more inclusions and larger inclusions (Krech et al., 1989). Adding cycloheximide (0.5–1.5 μL/mL) to the growth medium enhances sensitivity. Cell monolayers are grown on glass coverslips in shell vials or 24-well plates, or on the surface of polystyrene 96-well or 48-well culture dishes. To enhance recovery of *C. trachomatis*, specimens are sonicated or agitated on a vortex mixer before inoculation to release elementary bodies from host cells, and inoculated shell vials or culture dishes are centrifuged. After incubation for 48 to 72 hours, monolayers are fixed and stained with fluorescein-conjugated monoclonal antibodies. If a 96-well culture system is used, passaging specimens that are negative for *C. trachomatis* at 48 hours may enhance detection; however, passaging does not significantly increase detection in shell vials or 24-well plates. Although at one time considered the gold standard for detection of *C. trachomatis*, it is now recognized that because of the fastidious nature of the organism, sensitivity of cell culture is only in the 50% to 75% range, although with the use of monoclonal antibodies in the staining phase specificity should be 100% (Solomon et al., 2004; Carder et al., 2006).

Other Test Methods

Direct fluorescent antibody tests are the only FDA-cleared tests for detecting ocular chlamydial infections. They should not be used for routine testing of genital tract specimens. DFA allows direct visualization of *C. trachomatis* elementary bodies in smears of clinical specimens, and it is the only test that permits direct assessment of specimen adequacy. Antibodies directed against the species-specific MOMP of *C. trachomatis* appear to be more specific and produce more intense fluorescence than those directed against the chlamydial LPS (Cles et al., 1988). Occasionally, even the species-specific antibodies stain bacteria other than *C. trachomatis*, perhaps because of nonspecific immunoglobulin binding or cross-reactivity.

Serologic tests have little value for diagnosis of chlamydial genital infections for two reasons. First, antibodies to *C. trachomatis* persist after the infection resolves, so a positive serologic test does not necessarily correlate with active disease. Second, many serologic tests are not specific for *C. trachomatis* because they detect genus-specific antibodies. A possible exception is diagnosis of *C. trachomatis* pneumonitis in infants, in whom detection of IgM antibodies by microimmunofluorescence (MIF) may be useful. A single IgM titer greater than 1:32 when tested by MIF supports a diagnosis of chlamydial pneumonia. IgG is not useful in neonates because of circulating maternal antibody.

LGV *Chlamydia Trachomatis*

Diagnosis of LGV generally is based on clinical manifestations, consistent epidemiologic information, and excluding other causes of proctocolitis, inguinal lymphadenopathy, or genital or rectal ulcers. If available, testing for *C. trachomatis* also should be considered. Specimens that could be collected for diagnosis of LGV are exudate from a lesion or material aspirated from an involved lymph node. Tests to consider are culture, MIF, which are offered only in specialized laboratories, or the method of choice: nucleic acid amplification. MSM presenting with proctocolitis should be tested for chlamydia; preferred testing is NAAT performed on rectal specimen. The two commercially available NAATs approved for testing extragenital specimens detect both LGV and non-LGV *C. trachomatis* but cannot distinguish between them. Ideally, if one of these assays is positive in a patient suspected to have LGV, an additional LVG-specific NAAT could be used to differentiate LGV-associated strains from non-LGV *C. trachomatis* in rectal specimens, but none of these assays are FDA cleared.

Because LGV has a long latent period and clinical diagnosis often is delayed, chlamydial serology can support the diagnosis in a patient with a consistent clinical presentation. A single or stable complement fixation titer of 1:64 or greater supports a presumptive diagnosis.

Chlamydophila Psittaci

Since 1988 there has been a steady reduction in reported psittacosis cases in the United States, although the annual numbers can vary considerably due to periodic outbreaks (e.g., there was a multistate psittacosis outbreak among poultry plant workers in 2018) (CDC, 2018a). The CDC has established case definitions for *C. psittaci* infections, which are described as laboratory confirmed if (1) *C. psittaci* is cultured from respiratory material, or (2) antibody titers against *C. psittaci* increase fourfold or greater when tested by complement fixation or MIF at least 2 weeks apart, or (3) a single IgM titer greater than 1:16 when tested by MIF is present after the onset of symptoms (CDC, 1998; Gaydos & Quinn, 2018). *C. psittaci* can be grown in cell culture, but this is recommended only for specially equipped laboratories with experienced personnel, because the organism is especially virulent and has been associated with laboratory-acquired infection. Infection with *C. psittaci* is usually diagnosed serologically. Antibodies usually are detected by the end of the second week of illness, but early antibiotic therapy can delay their appearance for several weeks. The incidence of *C. psittaci* is likely underestimated due to insufficient diagnostic tools. In 2018, the first multiplex real-time polymerase chain reaction (PCR) assay to detect *C. psittaci* and *C. pneumoniae* in clinical specimens was developed at the CDC (Wolff et al., 2018), which displayed improved test performance characteristics, especially sensitivity, during acute phase of the disease. Although PCR can provide a rapid diagnosis, a limitation is insufficient sensitivity beyond the acute phase of disease (Nieuwenhuizen et al., 2018).

Chlamydophila Pneumoniae

Currently, a commercial FDA-cleared NAAT is the preferred test for diagnosis of *C. pneumoniae* infection. NAAT has demonstrated greater accuracy and speed in detecting etiology, especially in outbreak settings (Benitez et al., 2012). Previously, diagnosis had been based predominantly on serologic tests (Grayston et al, 1990; Kumar & Hammerschlag, 2007; Gaydos & Quinn, 2018), which still may occasionally be requested. IgM antibodies appear about 2 to 3 weeks after the onset of primary illness, usually decline over the next 2 to 6 months to an undetectable level, and may not reappear with reinfection. IgG antibodies are detected 6 to 8 weeks after onset of the primary illness, persist for life, and may rise 1 to 2 weeks following reinfection. The MIF test with the TWAR antigen, looking for a fourfold or greater IgG titer between acute and convalescent phase serum samples, is the serologic test method recommended by the CDC and the Infectious Disease Society of America (Kumar & Hammerschlag, 2007). A single IgM titer of 1:16 or above may also be helpful. Unfortunately, serologic tests have been shown to be insensitive, especially in children, and cross-reactions with *Mycoplasma*, *Bartonella*, and *Yersinia* species may occur. *C. pneumoniae* can be isolated in cell culture, but it is more difficult to grow than *C. trachomatis* (Roblin et al., 1992; Gaydos & Quinn, 2018).

TREATMENT

For genital infections due to *C. trachomatis*, recommended regimens include azithromycin (1 g orally, one dose) or doxycycline (100 mg orally twice a day for 7 days), which are equally efficacious (Lau & Qureshi, 2002). Ofloxacin and levofloxacin are also effective. Erythromycin generally is not recommended due to gastrointestinal side effects, which could interfere with the compliance (CDC, 2016). LGV requires the same daily dosage of doxycycline or erythromycin as genital infections, but for a period of 3 weeks. Ocular infections with *C. trachomatis* require systemic treatment with doxycycline or azithromycin for adults, and erythromycin for newborns; topical therapy suppresses symptoms but does not eradicate the organism. First-line therapy to treat infections caused by *C. pneumoniae* is a macrolide (azithromycin); acceptable alternative agents include tetracyclines and fluoroquinolones. For *C. psittaci*, the treatment of choice is tetracycline hydrochloride or doxycycline for 3 weeks. Erythromycin is an alternative but may be less effective in more severe cases as macrolide failures have been reported.

MYCOPLASMAL AND UREAPLASMAL INFECTIONS

Mycoplasmas were proved to cause human disease in 1962, when one mycoplasma (subsequently named *Mycoplasma pneumoniae*) was recognized as the etiologic agent of primary atypical pneumonia (Chanock et al., 1962). Mycoplasmas are the smallest free-living organisms. They are

pleomorphic, ranging from spherical cells 0.2 μm in diameter to filaments 0.1 μm wide by 1 to 2 μm long. Most are facultative anaerobes that replicate by binary fission. Mycoplasmas are unique among bacteria because they have no cell wall. They are unable to synthesize cell wall precursors, and they require cholesterol and related sterols for membrane synthesis. Mycoplasmas also lack the enzymatic pathways for purine and pyrimidine synthesis and, for this reason, require complex media (such as beef heart infusion broth supplemented with horse serum, yeast extract, and nucleic acids) for growth in vitro. The potential pathogens, *M. pneumoniae* and the genital mycoplasmas (*Mycoplasma hominis*, *Mycoplasma genitalium*, *Ureaplasma urealyticum*, and *Ureaplasma parvum*), are discussed.

MYCOPLASMA PNEUMONIAE

Epidemiology

Mycoplasma pneumoniae is found worldwide. Epidemics occur among confined populations such as children in schools, families, and military recruits, typically at 3- to 5-year intervals, and predominantly in late summer and fall. In nonepidemic years, infections occur year-round and in general spread slowly, possibly owing to the slow generation time of the bacterium (6 hours) and its low transmission rate, which apparently requires close contact with an ill person (Waites & Talkington, 2004). During epidemics, however, infection may spread rapidly, and the occurrence of point-source outbreaks in which close and prolonged exposure is not recognized suggests that *M. pneumoniae* may be transmitted via aerosols. Rates of infection with *M. pneumoniae* are greatest in school-age children and young adults, and pneumonia is seen most frequently in persons 5 to 20 years of age, especially in those between 15 and 19 years of age, although the infection can develop in individuals of any age (Marston et al., 1997; Miyashita et al., 2008; Gadsby et al., 2012). *M. pneumoniae* was detected in 8% of cases via real-time PCR in a recent prospective surveillance study of 2200 children hospitalized with community-acquired pneumonia, confirming *M. pneumoniae* as a significant pathogen. The prevalence was highest among older children (<5 years = 3%; 5–9 years = 17%; 10–17 years = 24%). Macrolide resistance was detected in only 4% of cases (Kutty et al., 2019).

Infection with *M. pneumoniae* occurs before 5 years of age but typically is asymptomatic or produces a mild illness with coryza and wheezing but no fever or pneumonia (Fernald et al., 1975). However, coinfections of *M. pneumoniae* with other bacterial and/or viral pathogens are common, especially in children less than 5 years of age; therefore, if the recovery is delayed, *M. pneumoniae* should be considered (Diaz et al., 2016; Kutty et al., 2019; Shah, 2019). Many patients with milder symptoms may not be seen by health professionals, and because NAATs are not available in all clinics and hospitals in the United States, it is likely that infection with *M. pneumoniae* is underdiagnosed. It is estimated that about 2 million cases of *M. pneumoniae* occur annually in the United States, including approximately 100,000 adults requiring hospitalizations (Marston et al., 1997; Winchell, 2013).

Pathogenesis and Pathology

M. pneumoniae, a surface parasite, colonizes the mucosa of the respiratory tract. Its ability to attach to respiratory mucosal cells, escape phagocytosis, and modulate the immune system is essential to initiation of disease. Its gliding motility may allow it to penetrate through respiratory secretions, and its filamentous, flexible form with terminal attachment organelle may facilitate localization in crypts and folds of the host cell membrane and between microvilli and cilia, where it is protected from phagocytosis. Attachment of *M. pneumoniae* to host cells is mediated by the P1 protein, which interacts with neuraminic acid–containing glycoproteins at the surface of the host cell membrane (Chandler et al., 1982; Geary & Gabridge, 1987; Waites et al., 2017). Hydrogen peroxide and superoxide produced by *M. pneumoniae* may injure mucosal cells, causing ciliostasis and sloughing of superficial cells (Almagor et al., 1984). Inhibition of catalase (which breaks down damaging peroxides) in host cells by bacterium-generated superoxides makes the cells more susceptible to damage (Waites et al., 2017). An adenosine diphosphate (ADP)–ribosylating protein (named community-acquired respiratory distress syndrome toxin [CARDS TX]) produced by *M. pneumoniae* has been identified and postulated to have an exotoxin function, as the protein has been demonstrated to induce vacuolization and ciliostasis in cultured host cells. Several potential downstream cellular targets for the CARDS TX have been identified, including the cytoplasmic molecules (NLRP3, PAMPs) and receptors (surfactant protein A, annexin A2) (Waites et al., 2017).

Based on the repetitive elements within P1 gene coding P1 protein, an essential virulence factor involved in adhesion to the host cells, isolates of *M. pneumoniae* can be divided into two major groups named subtype 1 and subtype 2, and several variants within each subtype. Although it has been suggested that a shift from one P1 subtype to the other may play some role in epidemics, the shift does not necessarily always happen (Waites et al., 2017).

Host-related factors also are involved in the pathogenesis of *M. pneumoniae* disease. The apparent high prevalence of *M. pneumoniae* infection in infants and young children, the mild nature of the disease in this age group, and the occurrence of more severe illness during infection at a later age suggest that severe disease may result from the host immune response to reinfection. *M. pneumoniae* has been demonstrated to induce cytokine production in vitro, suggesting that adherence of the bacterium to respiratory epithelial cells results in cytokine production, which in turn might both recruit inflammatory cells, including lymphocytes, to the site of infection and modulate the activity of the recruited cells (Waites et al., 2008). This cytokine production and influx of lymphocytes might be involved in fighting the infection by destroying the infecting organism or, conversely, might result in immune hypersensitivity that damages host cells. A more marked T-cell immune response may result in more severe disease (Waites et al., 2008). Moreover, extrapulmonary manifestations of disease (discussed later) are suspected to be immune mediated. The interaction of *M. pneumoniae* with the I antigenic determinant of human red blood cells, which contains the necessary 2,3-sialylated poly-*N*-acetylgalactosamine sequences, may alter the I antigen, converting it into a non–self-antigen that stimulates production of cold agglutinins. Other autoimmune antibodies produced during infection with *M. pneumoniae* (antibodies to lung, brain, smooth muscle, skin, joints, and lymphocytes) may have similar derivations. The ability of *M. pneumoniae* to form biofilms in a strain-dependent manner suggests that perhaps *M. pneumoniae* utilizes the protective microenvironment of biofilm to avoid host immune responses and antimicrobial agents (Kornspan et al., 2011; Simmons et al., 2013).

Few descriptions of the pathologic findings of disease caused by *M. pneumoniae* are available, because most infections are self-limited and tissue is rarely obtained. In fatal cases, patchy areas of consolidation are found in the lungs. Histologic examination of involved foci shows bronchitis, bronchiolitis, and interstitial and alveolar pneumonitis with peribronchiolar collections of lymphocytes and plasma cells, accompanied by macrophages and neutrophils if cellular necrosis is present.

Clinical Manifestations

The most common manifestation of disease caused by *M. pneumoniae* is tracheobronchitis, which occurs in about one-half of infected patients. After an incubation period of several weeks, sore throat, cough, coryza, fever, headache, myalgia, and sometimes conjunctivitis and myringitis are seen. The infection may resolve or may progress to pneumonia, the frequency of which is age dependent, with children 5 to 15 years of age most likely to develop lower respiratory involvement (Baum, 2000; Waites et al., 2017). Chest radiographs show unilateral lower lobe bronchopneumonia or occasionally bilateral feathery infiltrates. Additionally, pleural effusion (26% vs 12%) and hilar lymphadenopathy (10% vs 6%) are more commonly associated with *M. pneumonia* pneumonias than with viral pneumonias (Kutty et al., 2019). The peripheral white blood cell count is normal early and rises as the disease progresses. Maculopapular or, less commonly, vesicular skin eruptions occur in about 15% of cases a few days after disease onset. Without antimicrobial therapy, fever resolves in 2 to 14 days, but malaise, cough, and radiographic abnormalities persist for 2 to 6 weeks. In a small percentage of children and adults, pneumonia is severe enough to warrant hospitalization; these patients may develop lung abscess, pleural effusions, secondary bacterial infections, bronchiectasis, or clinical relapse.

Extrarespiratory manifestations such as clinically apparent hemolytic anemia (typically with very high titers of cold agglutinins); erythema multiforme, erythema nodosum, and urticaria; myocarditis and pericarditis; and arthralgias, arthritis, acute glomerulonephritis, tubulointerstitial nephritis, and IgA nephropathy may occur, but are not frequent (Waites & Talkington, 2004; Hardy, 2018). Among the most common extrapulmonary complications of *M. pneumonia* infection are dermatologic disorders, which are thought to be the result of both autoimmune host response and direct bacterial damage (Narita, 2010; Canavan et al., 2015) and could be quite severe (e.g., causing *M. pneumoniae*–associated Stevens-Johnson syndrome) (Watkins et al., 2017). In a small percentage of patients, delay in treatment can result in multiorgan failure, including acute respiratory distress syndrome (ARDS) and kidney failure (Cummiskey et al., 2019). Additionally, a small fraction of patients hospitalized with *M. pneumoniae* infection have neurologic manifestations, from minor to severe, including encephalitis and acute disseminated encephalomyelitis (Waites et al., 2017; Hardy, 2018).

Among 1988 patients referred to the California Encephalitis Project over a 9-year period, *M. pneumoniae* was implicated in 111 patients (5.6%) and was the single most common implicated infectious agent (Christie et al., 2007). Many cases of encephalitis associated with *M. pneumoniae* appear to be relatively mild; however, severe cases of acute disseminated encephalomyelitis that may even result in fatality can occur in association with the infection (Christie et al., 2007; Stamm et al., 2008; Waites et al., 2017).

GENITAL MYCOPLASMAS

Epidemiology

Ureaplasma spp. (*U. urealyticum* has been separated into *U. parvum*, formerly *U. urealyticum* biovar 1, and *U. urealyticum*, formerly *U. urealyticum* biovar 2) can be found colonizing the vagina and cervix in 40% to 80% of adult women, and *M. hominis* can be found in 21% to 53% of women (Waites et al., 2005). The frequency in men appears to be lower. *M. genitalium*, thought to be the most common cause of nongonococcal nonchlamydial (NGNC) urethritis or the second most common cause of NGU after *C. trachomatis*, contributes to an estimated 10% to 35% of acute or persistent/recurrent NGNC urethritis in men (Jensen et al., 2016) and to an estimated 10% to 30% of cases of clinical cervicitis in women in the United States. Recent prevalence studies of *M. genitalium* suggested that the prevalence of the infection ranges from 1.3% to 3.9% in the general population, with considerably higher rates in MSM, sex workers, and people attending STD clinics (Manhart et al., 2011; Bauman et al., 2018), and it continues to rise among these high-risk groups. A study from Great Britain showed that the prevalence was highest in men 25 to 34 years of age (2.1%) and in women 16 to 19 years of age (2.4%), with more than half of infections being asymptomatic, particularly in men. The prevalence of *M. genitalium* in youth clinics in Sweden was 9.6%, and a large study in Netherlands revealed a 4.5% prevalence. In the United States, a study among MSM revealed the urethral *M. genitalium* prevalence of 10.8%, and the rectal prevalence of 6.4% (Dionne-Odom et al., 2018).

Colonization of infants with genital mycoplasmas can occur during passage through the birth canal, but colonization appears to be temporary in many cases, and a lower rate of colonization has been noted in children (Klein et al., 1969; Hammerschlag et al., 1978). The increase in colonization by mycoplasmas after puberty indicates an association with sexual activity. In addition to passage through the birth canal, neonates can acquire infections due to *Ureaplasma* spp. and *M. hominis* hematogenously through the placenta or through an ascending infection, resulting in seeding of amniotic fluid (Waites et al., 2005).

Clinical Manifestations

Although simple vaginal colonization with the genital mycoplasmas in pregnant women is not associated with disease, the presence of mycoplasma (primarily *Ureaplasma* spp. and to a lesser extent *M. hominis*) in the placental membranes or amniotic fluid is consistently associated with chorioamnionitis, preterm birth, and adverse perinatal outcomes associated with several neonatal disorders, including perinatal pneumonia and sepsis in preterm infants (Waites et al., 2005; Goldenberg et al., 2008). Both *Ureaplasma* spp. and *M. hominis* are associated with postpartum fever. *Ureaplasma* spp. can cause urinary calculi and are a cause of NGU (Waites et al., 2005). *M. hominis* has been related to both PID and pyelonephritis and may have an association with bacterial vaginosis (Waites et al., 2005). Transmission of *M. genitalium* infections primarily occurs via direct mucosal genital-genital and genital-anal contact. *M. genitalium* has been linked to NGNC urethritis in males only relatively recently, but it is now firmly established as a significant cause of the disorder and is the etiologic agent in approximately 10% to 35% of cases (Ross & Jensen, 2006; Gaydos et al., 2009; Manhart et al., 2011; Jensen et al., 2016). In men, *M. genitalium* infections present with urethritis and less often with dysuria, discomfort, and mucopurulent urethral discharge. Among women, mucopurulent cervicitis is common, which can progress to endometritis, PID, and tubal infertility. In addition, proctitis, reactive arthritis, preterm birth, and spontaneous abortion have been reported (Haggerty et al., 2006; Short et al., 2009; Lis et al., 2015). Despite the fact that a causal relationship for *M. genitalium* infections and proctitis has not been demonstrated, *M. genitalium* was detected in 6.4% among MSM in the United States (Dionne-Odom et al., 2018) and in 12% of MSM with symptomatic proctitis in Australia (Bissessor et al., 2016). Moreover, the loads of *M. genitalium* were significantly higher among men with symptomatic proctitis than those among men with asymptomatic rectal *M. genitalium* infection (Bissessor et al., 2016).

LABORATORY DIAGNOSIS

Mycoplasma Pneumoniae

The optimal test for diagnosis of infection caused by *M. pneumoniae* is nucleic acid amplification. Both single assays and multiplex PCR assays, which detect several respiratory pathogens, are commercially available. In the United States, commercially available NAATs (such as Illumigene, Meridian, Cincinnati, OH; Filmarray, bioMerieux/Biofire Diagnostics, Salt Lake City, UT; and Chlamylege, Argene, Inc. Shirley, NY) have dramatically improved the diagnostic testing, especially during acute phase of the infection. Unfortunately, no point-of-care testing is commercially available for the rapid detection. MALDI–TOF MS (Bruker, Daltonics, Bremen, Germany) has demonstrated an excellent performance in rapid identification and subtyping of *M. pneumoniae;* however, growth in the culture is required, precluding rapid turnaround time (Xiao et al., 2014). Although currently macrolide resistance is moderate in the United States, it continues to increase and could be associated with more serious and prolonged infections.

The best specimen is a nasopharyngeal swab, but bronchoalveolar lavage fluid and lung tissue may be acceptable depending on the assay.

Diagnosis also may be made serologically. Detection of specific IgM in a single serum sample is diagnostic of acute infection. If IgG is measured, acute- and convalescent-phase samples must be tested, and the diagnosis is based on a fourfold or greater rise in titer. A variety of tests based on particle agglutination, enzyme immunoassay (EIA), or immunofluorescence are available; EIA, particularly with membrane-bound assays, is the most popular (Waites & Talkington, 2004). Serologic testing is not without problems as antibody titers vary with age, with children and younger individuals having consistently higher titers than adults (Daxboeck et al., 2002; Waites et al., 2017), and it is associated with both false-negative and false-positive results. Some experts consider the combined use of PCR on respiratory specimens and serology the optimum approach to obtain maximum sensitivity in diagnosing infection in children (Christie et al., 2007; Thurman et al., 2009; Waites et al., 2017) although this approach seems to be less effective in adults.

A nonspecific serologic test that may provide useful information is detection of cold agglutinins, which are IgM antibodies against the I antigen of human erythrocytes. The cold agglutinin response usually corresponds with the severity of pulmonary disease, as a titer of 1:32 or greater is found with severe pneumonia, whereas agglutinins are not detectable in mild disease (Waites et al., 2008). Cold agglutinins appear by the end of the first week or early in the second week of illness in at least half of infected persons, but their presence is not diagnostic of infection with *M. pneumonia*, as they may also be seen with other bacterial, rickettsial, or viral infections.

Circulating antibody-secreting cell (ASC) responses are thought to be more rapid and shorter lived than antibody responses to *M. pneumoniae*. In a recent observational study, IgM-ASCs to *M. pneumoniae* were measured by enzyme-linked immunospot (ELISpot), and the results of this study suggested a better discrimination between *M. pneumoniae* infection and carriage (Sauteur et al., 2019).

M. pneumoniae may be grown in culture, but it is cumbersome, time consuming, and rarely offers clinically relevant information, so few laboratories offer this option. However, it allows antimicrobial susceptibility testing and/or typing to be performed on the isolate when necessary. To isolate *M. pneumoniae*, special agar media, broth media, or a biphasic culture system is inoculated and incubated at 37°C in a sealed container for 3 weeks or more in 5% to 10% CO_2 or anaerobically. Cultures are examined microscopically (40×) each week for spherical colonies with a dense center and thin outer layer (resembling a "fried egg") embedded in the agar. Such colonies, consistent with *M. pneumoniae*, that demonstrate glycolysis (as demonstrated by color change in the media pH indicator), β-hemolysis, and hemadsorption of guinea pig erythrocytes are presumptively *M. pneumoniae*. Definitive speciation usually requires staining with monoclonal antibodies using immunofluorescence or immunoperoxidase, immunoblotting, or PCR.

Genital Mycoplasmas

Ureaplasma spp. *and M. hominis* may be recovered from urethral, vaginal, or endocervical swab specimens, blood, urine, abscess material, prostatic secretions, semen, or tissues. Traditionally, separate systems were used for each (U agar and U broth for *Ureaplasma* spp. *and* H agar and H broth for *M. hominis*) because the optimal pH for growth of the two organisms differs (pH 5.5–6.5 for *Ureaplasma* spp. and pH 6–8 for *M. hominis*), but single culture systems that effectively detect both ureaplasmas and *M. hominis* have been available for several years (Yajko et al., 1984; Wood et al., 1985;

Phillips et al., 1986). Broth cultures are incubated aerobically in sealed test tubes. Agar cultures are incubated anaerobically or in an atmosphere of 5% to 7% CO_2 and observed daily under a microscope. *M. hominis* also grows on sheep blood agar, producing nonhemolytic pinpoint colonies, and in most broth blood culture media, although no evidence of growth is visible.

Colonies of *M. hominis*, 200 to 300 μm in diameter with a typical fried-egg appearance, usually appear within 5 days. In broth containing phenol red and 0.1% arginine, *M. hominis* metabolizes arginine to ammonia, causing a color change from yellow to red. U agar plates are observed daily for 4 days, and on day 4 are stained with one to two drops of $CaCl_2$-urea solution. Colonies of *Ureaplasma* spp. have an irregular rather than circular umbonate morphology, are 15 to 60 μm in diameter, and stain dark brown in 5 minutes. In U broth, *Ureaplasma* spp. produce a shift in pH, and the color changes from yellow to red. A loopful of broth then is transferred to agar plates and is streaked for isolation.

M. genitalium grows very slowly, similar to *M. pneumoniae*, with which it shares many morphologic and antigenic similarities, and is difficult to isolate in culture. For clinical purposes, nucleic acid amplification is the only practical test. The Hologic Aptima 2 Combo assay, which was cleared by the FDA in 2019 for *M. genitalium* detection, has a reported sensitivity of 78% to 99% and specificity of 97.8% to 99.6% (Watts & Mazur, 2019). Acceptable specimens for Aptima Hologic assay include swabs (vaginal, endocervical, urethral, penile meatal) and female and male urine. For females, a vaginal swab is the preferred specimen type due to higher clinical sensitivity for detecting *M. genitalium* than other specimen types; however, female urine or clinician-collected endocervical swabs may be used as alternative specimens when vaginal swab specimens are not available (Hologic, 2019).

Mutations in 23S rRNA, particularly at positions 2058 and 2059 within the V domain, are responsible for the development of macrolide resistance. Molecular assays to detect the abovementioned mutations in 23S rRNA have been developed; however, none of these assays are FDA cleared, and thus the availability is very limited.

TREATMENT

A tetracycline, macrolide, or fluoroquinolone is effective treatment for *M. pneumoniae*, and azithromycin or clarithromycin is preferred because of dosing considerations. However, macrolide-resistant *M. pneumoniae* has been spreading and is currently very high in Asia (e.g., in some regions of China and Japan >90% of *M. pneumoniae* isolates are currently resistant to macrolides) (Waites et al., 2017). Although *M. pneumoniae* macrolide-resistant rates are currently moderate in Europe and in the United States, the prevalence appears to be increasing. In the United States, data from the CDC showed that between 2006 and 2013, 10% of isolates were macrolide resistant (Diaz et al., 2015), whereas an estimated 13.2% were resistant between 2012 and 2014 (Zheng et al., 2015). Patients infected with macrolide-resistant *M. pneumoniae* isolates could suffer a more severe and prolonged course of infection relative to those infected with susceptible isolates (Waites et al., 2017).

Generally, ureaplasmas are susceptible to tetracyclines, quinolones, and macrolides, with tetracycline resistance seen in approximately 10% of isolates (Waites et al., 2005). Resistance to the fluoroquinolones appears to be unusual, and *Ureaplasma* spp. are resistant to clindamycin. *M. hominis* is susceptible to clindamycin and the newer quinolones but is resistant to the macrolides. Some isolates also are susceptible to tetracyclines, although resistance to the tetracyclines is thought to be greater than in *Ureaplasma* spp., at approximately 40% (Waites et al., 2005). *M. genitalium* can be problematic because isolates can develop resistance to one or more antibiotics. Exposure to suboptimal macrolide (azithromycin) concentrations (e.g., doses used routinely to treat *N. gonorrhoeae* and/or *C. trachomatis* in asymptomatic individuals) can provide a selective pressure for macrolide resistance (Li et al., 2019) by inducing mutations at position 2058 and 2059 in the V domain of 23S rRNA gene. This can explain the wide range of macrolide resistance rates in various countries. In Europe, the reported rates of macrolide resistance were higher in men than women (22.2% vs 4.6%), and in MSM than in heterosexual men (32.5% vs 17.6%) (Pineiro et al., 2019). Results of a study of extragenital *M. genitalium* infections in Australia suggested that one in seven MSM treated for rectal *C. trachomatis* and/or *N. gonorrhoeae* have undiagnosed *M. genitalium* exposed to suboptimal azithromycin (Hughes et al., 2018; Latimer et al., 2019). Accordingly, MSM with *M. genitalium*–positive NGU are more likely to have a macrolide-resistant strain (McIver et al., 2019).

The preferred regimen for treatment of *M. genitalium* infections is azithromycin 500 mg orally given on the first day, followed by 250 mg on days 2 to 5 (CDC, 2015). However, recently, numerous studies have identified high rates of macrolide-resistant phenotype of *M. genitalium*. One study performed across a wide geographic area of the United States identified macrolide-resistant phenotype in 50.8% of females and 42% of males (Getman et al., 2016). These data indicate that the current treatment guidelines will need to be reevaluated. Doxycycline (100 mg orally twice a day for 7 days) has also been suggested, but a larger number of failures were seen with this regimen. However, replacing azithromycin with doxycycline and increasing dose of azithromycin for the initial treatment of STD syndromes has been recently reported to improve the cure rates with infrequent selection of macrolide resistance (Read et al., 2019).

In cases of treatment failure with azithromycin, moxifloxacin (400 mg orally for 7–10 days) is also recommended (Ross & Jensen, 2006; Bradshaw et al., 2008; Jernberg et al., 2008). However, fluoroquinolone resistance due to mutations in ParC gene are also becoming more common. Dual resistance infections are generally estimated at roughly 9% to 12%. In China, among men with symptomatic urethritis nearly 90% of *M. genitalium* infections were resistant to both macrolides and fluoroquinolones (Li et al., 2019).

The abovementioned studies indicate the need to develop assays capable of detecting both macrolide and quinolone resistance. Resistance-guided therapy using doxycycline followed by moxifloxacin are underway, and point-of-care assays with resistance targets are also in development (Sadiq et al., 2017; Read et al., 2019). Therapeutic options are very limited for multidrug-resistant cases of *M. genitalium* infections; potential antimicrobial agents are minocycline and pristinamycin, although the latter is not widely available (Glaser et al., 2019).

ACKNOWLEDGMENT

I gratefully acknowledge the contribution of Juan P. Olano, David H. Walker, Gail L. Woods, and others who authored this chapter in previous editions.

SELECTED REFERENCES

Centers for Disease Control and Prevention, Workowski KA, Bolan GA, et al.: Sexually transmitted diseases treatment guidelines, 2015, *MMWR Recomm Rep* 64(1), 2015. Atlanta, US Department of Health and Human Services.

Developed as a tool to guide therapy of many sexually transmitted diseases, these recommendations also include many variable diagnostic considerations for a variety of presentations.

Getman D, Jiang A, et al.: *Mycoplasma genitalium* prevalence, coinfection, and macrolide antibiotic resistance frequency in a multicenter clinical study cohort in the United States, *J Clin Microbiol* 54(9):2278, 2016.

Evaluates the prevalence of M. genitalium single infections, prevalence of coinfection with other sexually transmitted organisms, and rates of macrolide antibiotic resistance in a wide geographic area of the United States.

Kutty PK, Jain S, Taylor TH, et al.: Mycoplasma pneumoniae among children hospitalized with community-acquired pneumonia, *Clin Infect Dis* 68(1):5, 2019.

A recent prospective surveillance study of 2200 children hospitalized with community-acquired pneumonia that evaluated the clinical and epidemiologic features of M. pneumoniae, the prevalence of M. pneumoniae in different age groups, the prevalence of macrolide resistance, and prevalence of coinfections of M. pneumoniae with other bacterial and/or viral pathogens.

Nieuwenhuizen AA, Dijkstra F, Notermans DW, et al.: Laboratory methods for case finding in human psittacosis outbreaks: a systematic review, *BMC Infect Dis* 18(1):442, 2018.

Discusses the effectiveness and drawbacks of the current laboratory testing methods available for the rapid identification of cases in psittacosis outbreak investigations.

Read TRH, Fairley CK, et al.: Outcomes of resistance-guided sequential treatment of *Mycoplasma genitalium* infections: a prospective evaluation, *Clin Infect Dis* 68:554, 2019.

Prospective study evaluating outcomes of sequential antimicrobial therapy for M. genitalium guided by a macrolide resistance assay, suggesting that switching from azithromycin to doxycycline could improve the cure rates without significant selection of macrolide resistance.

Solomon AW, Peeling RW, Foster A, et al.: Diagnosis and assessment of trachoma, *Clin Microbiol Rev* 17:982, 2004.

An excellent review of trachoma, including a historical perspective and an overview of the developmental cycle, clinical presentation, and laboratory diagnosis.

Waites KB, Xiao L, Liu Y, et al.: *Mycoplasma pneumoniae* from the respiratory tract and beyond, *Clin Microbiol Rev* 30:747, 2017.

An excellent in-depth review of M. pneumoniae, including the updated information about infection epidemiology, pathogenesis and host defense, clinical manifestations and immunologic complications, laboratory detection, new developments in antimicrobial chemotherapy, molecular typing, and knowledge gained from comparative genomics.

Access the complete reference list online at Elsevier eBooks for Practicing Clinicians.

REFERENCES

Almagor M, Kahane I, Yatziv S: Role of superoxide anion in host cell injury induced by *Mycoplasma pneumoniae* infection, *J Clin Invest* 73:842, 1984.

Appelt DM, Roupas M, et al.: Apoptotic effects of *Chlamydophila pneumoniae* following infection of neuronal cells, *BMC Neurosci* 9(13), 2008.

Aptima H: *Aptima mycoplasma genitalium assay*, *Aptima Package insert*. Available at: https://www.hologic.com/sites/default/files/2019-01/AW-17946_001_01.pdf. [Accessed 6 August 2019], 2019.

Balin BJ, Hammond CJ, et al.: *Chlamydia pneumoniae*: an etiologic agent for late-onset Dementia, *Front Aging Neurosci* 10:302, 2018.

Baum SG: *Mycoplasma pneumoniae* and atypical pneumonia. In Mandell GL, Bennett JE, Dolin R, editors: *Principles and practice of infectious diseases*, ed 5, New York, 2000, Churchill Livingstone, p 2018.

Baumann L, Cina M, Egli-Gany D: Prevalence of Mycoplasma genitalium in different population groups: systematic review and meta-analysis, *Sex Transm Infect* 94(4):255, 2018.

Benitez AJ, Thurman KA, Diaz MH, et al.: Comparison of real-time PCR and a micro-immunofluorescence serological assay for detection of Chlamydophila pneumoniae infection in an outbreak investigation, *J Clin Microbiol* 50(1):151, 2012.

Bissessor M, Tabrizi SN, Bradshaw CS: The contribution of Mycoplasma genitalium to the aetiology of sexually acquired infectious proctitis in men who have sex with men, *Clin Microbiol Infect* 22:260, 2016.

Bradshaw CS, Chen MY, Fairley CK: Persistence of *Mycoplasma genitalium* following azithromycin therapy, *PloS One* 3, 2008. e3618.

Budzynski J, Wisniewska J, et al.: Association between bacterial infection and peripheral vascular disease: a review, *Int J Angiol* 25(3), 2016.

Campbell LA, Kuo CC, Grayston JT: Characterization of the new *Chlamydia* agent, TWAR, as a unique organism by restriction endonuclease analysis and DNA-DNA hybridization, *J Clin Microbiol* 25:1911, 1987.

Campbell LA, Kuo CC, Grayston JT: *Chlamydia pneumoniae* and cardiovascular disease, *Emerg Infect Dis* 4:571, 1998.

Campbell LA, Rosenfeld ME: Persistent *C. pneumoniae* infection in atherosclerotic lesions: Rethinking the clinical trials, *Front Cell Infect Microbiol* 4:34, 2014.

Canavan TN, Mathes EF, Frieden I, Shinkai K: *Mycoplasma pneumoniae*-induced rash and mucositis as a syndrome distinct from Stevens-Johnson syndrome and erythema multiforme: a systematic review, *J Am Acad Dermatol* 72:239, 2015.

Carder C, Mercey D, Benn P: Chlamydia trachomatis, *Sex Transm Infect* 82(Suppl IV):iv10, 2006.

Carter JD, Gérard HC, Espinoza LR, et al.: Chlamydiae as etiologic agents for chronic undifferentiated spondyloarthritis, *Arthritis Rheum* 60:1311, 2009.

Carter JD, Hudson AP: Recent advances and future directions in understanding and treating *Chlamydia*-induced reactive arthritis, *Expert Rev Clin Immunol* 13:197, 2017.

Centers for Disease Control and Prevention (CDC): Compendium of measures to control Chlamydia psittaci infection among humans (psittacosis) and pet birds (avian chlamydiosis), *MMWR 47:RR–10*, 1998. 1998.

Centers for Disease Control and Prevention (CDC): Psittacosis at a Turkey processing plant—North Carolina, *MMWR (Morb Mortal Wkly Rep)* 39:460, 1990. 1989.

Centers for Disease Control and Prevention, Papp JR, Schachter J, Gaydos C, et al.: Recommendations for the laboratory-based detection of Chlamydia trachomatis and Neisseria gonorrhoeae–2014, *MMWR Recomm Rep (Morb Mortal Wkly Rep)* 14(63):1, 2014.

Centers for Disease Control and Prevention: *Chlamydia treatment and care*, Atlanta, U.S, 2016, Department of Health and Human Services. Available at https://www.cdc.gov/std/chlamydia/treatment.htm. [Accessed 6 August 2019].

Centers for Disease Control and Prevention: Multistate psittacosis outbreak among poultry plant workers, 2018. In *Sexually Transmitted Disease Surveillance*, *2018*, Atlanta, 2018a, U.S. Department of Health and Human Services. (Available at: https://www.cdc.gov/pneumonia/atypical/psittacosis/surveillance-reporting/outbreaks/2018-poultry-multistate-investigation.html. [Accessed 6 August 2019].

Centers for Disease Control and Prevention: *Psittacosis*, *surveillance and reporting*, Atlanta, U.S, 2018b, Department of Health and Human Services. Available at: https://www.cdc.gov/pneumonia/atypical/psittacosis/surveillance-reporting/index.html. [Accessed 6 August 2019].

Centers for Disease Control and Prevention: *Sexually transmitted disease surveillance*, *Chlamydia*, Atlanta, U.S, 2017, Department of Health and Human Services. Available at https://www.cdc.gov/std/stats17/chlamydia.htm. [Accessed 6 August 2019].

Centers for Disease Control and Prevention: *Sexually transmitted disease surveillance*, *Chlamydia*, Atlanta, U.S, 2018c, Department of Health and Human Services. Available at: https://www.cdc.gov/std/stats18/chlamydia.htm. [Accessed 6 August 2019].

Centers for Disease Control and Prevention: *Sexually transmitted disease surveillance*, *lymphogranuloma venereum (LGV)*, Atlanta, U.S, 2015, Department of Health and Human Services. https://www.cdc.gov/std/tg2015/lgv.htm. [Accessed 6 August 2019].

Cepheid, Peterson D: *Cepheid Receives FDA clearance for extragenital Claims for Xpert® CT/NG test*, Cision PR Newswire May 29, 2019. Available at: (https://www.prnewswire.com/news-releases/cepheid-receives-fda-clearance-for-extragenital-claims-for-xpert-ctng-test-300858003.html . [Accessed 6 August 2019].

Chandler DKF, Grabowski MW, Barile MF: *Mycoplasma pneumoniae* attachment: competitive inhibition by mycoplasmal binding component and by sialic acid containing glycoconjugates, *Infect Immun* 38:598, 1982.

Chanock RM, Hayflick L, Barile MF: Growth on artificial medium of an agent associated with atypical pneumonia and its identification as a PPLO, *Proc Natl Acad Sci U S A* 48:41, 1962.

Chen S, Shimada K, et al.: Chlamydia and lipids engage a common signaling pathway that promotes atherogenesis, *J Am Coll Cardiol* 71:1553, 2018.

Chi EY, Kuo CC, Grayston JT: Unique ultrastructure in the elementary body of Chlamydia sp. strain TWAR, *J Bacteriol* 169:3757, 1987.

Christie LJ, Honarmand S, Talkington DF, et al.: Pediatric encephalitis: what role of *Mycoplasma pneumoniae? Pediatrics* 120:305, 2007.

Cles LD, Bruch K, Stamm WE: Staining characteristics of six commercially available monoclonal immunofluorescence reagents for direct diagnosis of *Chlamydia trachomatis* infections, *J Clin Microbiol* 26:1735, 1988.

Contini C, Grilli A, et al.: Detection of *Chlamydophila pneumoniae* in patients with arthritis: Significance and diagnostic value, *Rheumatol Int* 31:1307, 2011.

Cox RL, Kuo CC, Grayston JT, et al.: Deoxyribonucleic acid relatedness of *Chlamydia* sp. strain TWAR to *Chlamydia trachomatis* and *Chlamydia psittaci*, *Int J Syst Bacteriol* 38:265, 1988.

Cummiskey AG, Reardon M: Mycoplasma pneumonia: late treatment Leading to acute respiratory distress syndrome and Renal failure, *Eur J Case Rep Intern Med* 6(2):001003, 2019.

Daxboeck F, Kircher K, Krause R, et al.: Effect of age on antibody titer to *Mycoplasma pneumoniae*, *Scand J Infect Dis* 34:577, 2002.

De Voux A, Kent JB, Macomber K, et al.: *Notes from the Field*: Cluster of lymphogranuloma venereum cases among men who have sex with men – Michigan, *MMWR Morb Mortal Wkly Rep* 65:920, 2016. August 2015–April 2016.

de Vrieze NH, de Vries HJ: Lymphogranuloma venereum among men who have sex with men. An epidemiological and clinical review, *Expert Rev Anti Infect Ther* 12(6):697, 2014.

de Vrieze NH, van Rooijen M, et al.: Anorectal and inguinal lymphogranuloma venereum among men who have sex with men in Amsterdam, The Netherlands: trends over time, symptomatology and concurrent infections, *Sex Transm Infect* 89:548, 2013.

Dean D, Kandel RP, Adhikari HK, et al.: Multiple Chlamydiaceae species in trachoma: implications for disease pathogenesis and control, *PLoS Med* 5:e14, 2008.

Di Pietro M, Filardo S, Romano S, et al.: *Chlamydia trachomatis* and *Chlamydia pneumoniae* interaction with the host: Latest advances and future prospective, *Microorganisms* 16:140, 2019. 7:5.

Diaz MH, Benitez AJ, Winchell JM: Investigations of *Mycoplasma pneumoniae* Infections in the United States: trends in molecular typing and macrolide resistance from 2006 to 2013, *J Clin Microbiol* 53(1):124, 2015.

Diaz MH, Cross KE, Benitez AJ, et al.: Identification of bacterial and viral codetections with Mycoplasma pneumoniae using the TaqMan array card in patients hospitalized with community-acquired pneumonia, *Open Forum Infect Dis* 3(2), 2016. ofw071.

Dionne-Odom J, Geisler WM, Aaron KJ, et al.: High prevalence of multidrug-resistant Mycoplasma genitalium in human immunodeficiency virus-infected men who have sex with men in Alabama, *Clin Infect Dis* 66:796, 2018.

Everett KDE, Bush RM, Andersen AA: Emended description of the order Chlamydiales, proposal of Parachlamydiaceae fam. nov. and Simkaniaceae fam. nov., each containing one monotypic genus, revised taxonomy of the family Chlamydiaceae, including a new genus and five new species, and standards for the identification of organisms, *Int J Syst Bacteriol* 49:415, 1999.

Fernald GW, Collier AM, Clyde Jr WA: Respiratory infections due to *Mycoplasma pneumoniae* in infants and children, *Pediatrics* 55:327, 1975.

Filardo S, Di Pietro M, et al.: *Chlamydia pneumoniae*-mediated inflammation in atherosclerosis: a metaanalysis, *Mediators Inflamm*378658, 2015. 2015.

Filardo S, Di Pietro M, Tranquilli G, et al.: Selected immunological mediators and cervical microbial signatures in women with *Chlamydia trachomatis* infection, *mSystems* 4(4), 2019. e00094.

Gadsby NJ, Reynolds AJ, McMenamin J, et al.: Increased reports of Mycoplasma pneumoniae from laboratories in Scotland in 2010 and 2011—impact of the epidemic in infants, *Euro Surveill* 17(10):20110, 2012.

Gaydos C, Maldeis NE, Hardick P, et al.: *Mycoplasma genitalium* compared to chlamydia, gonorrhoea and trichomonas as an etiologic agent of urethritis in men attending STD clinics, *Sex Transm Infect* 85:438, 2009.

Gaydos CA, Quinn TC: Chlamydial infections. In Jameson JL, Fauci AS, Kasper DL, et al.: *Harrison's principles of internal medicine*, 20th ed, New York, 2018, McGraw–Hill, pp 1316–1325. (chapter 184.

Geary SJ, Gabridge MG: Characterization of a human lung fibroblast receptor site for *Mycoplasma pneumoniae*, *Isr J Med Sci* 23:462, 1987.

Glaser AM, Geisler WM, Ratliff AE, et al.: Two cases of multidrug-resistant genitourinary Mycoplasma genitalium infection successfully eradicated with minocycline, *Int J STD AIDS* 5:512, 2019.

Goldenberg RL, Andrews WW, Goepfert AR, et al.: The Alabama preterm birth study: umbilical cord blood *Ureaplasma urealyticum* and *Mycoplasma hominis* cultures in very preterm newborns, *Am J Obstet Gynecol* 198:43e–51e, 2008.

Grayston JT, Campbell LA, Kuo CC, et al.: A new respiratory pathogen: *Chlamydia pneumoniae* strain TWAR, *J Infect Dis* 161:618, 1990.

Grayston JT, Wang SP, Kuo CC, et al.: Current knowledge on *Chlamydia pneumoniae*, strain TWAR, an important cause of pneumonia and other acute respiratory diseases, *Eur J Clin Microbiol Infect Dis* 8:191, 1989.

Haar K, Dudareva-Vizule S, Wisplinghoff H, et al.: Lymphogranuloma venereum in men screened for pharyngeal and rectal infection, Germany, *Emerg Infect Dis* 3:488, 2013.

Haggerty CL, Totten PA, Astete SG, et al.: *Mycoplasma genitalium* among women with nongonococcal, nonchlamydial pelvic inflammatory disease, *Infect Dis Obstet Gynecol* 30184:2006, 2006.

Hammerschlag MR, Alpert S, Rosner I, et al.: Microbiology of the vagina in children: normal and potentially pathogenic organisms, *Pediatrics* 62(57), 1978.

Hardy RD: Infections due to mycoplasmas. In Jameson JL, Fauci AS, Kasper DL, et al.: *Harrison's principles of internal medicine*, 20th ed, New York, 2018, McGraw–Hill, pp 1313–1316. (chapter 183.

Hughes G, Saunders J: Mycoplasma genitalium: the next sexually transmitted superbug? *BMJ* 363(1), 2018.

Jensen JS, Cusini M, Gomberg M, et al.: European guideline on Mycoplasma genitalium infections, *J Eur Acad Dermatol Venereol* 30:1650, 2016.

Jernberg E, Moghaddam A, Moi H: Azithromycin and moxifloxacin for microbiological cure of *Mycoplasma genitalium* infection: an open study, *Int J STD AIDS* 19:676, 2008.

Jones RB, Batteiger BE: *Chlamydia trachomatis* (trachoma, perinatal infections, lymphogranuloma venereum, and other genital infections). In Mandell GL, Bennett JE, Dolin R, editors: *Principles and practice of infectious diseases*, ed 5, New York, 2000, Churchill Livingstone, p 1989.

Jones RB, Priest JB, Kuo C: Subacute chlamydial endocarditis, *J Am Med Assoc* 247:655, 1982.

Klein JO, Buckland D, Finland M: Colonization of newborn infants by mycoplasmas, *N Engl J Med* 280:1025, 1969.

Koper NE, van der Sande MA, Gotz HM: Lymphogranuloma venereum among men who have sex with men in The Netherlands: regional differences in testing rates lead to underestimation of the incidence, 2006-2012, *Euro Surveill* 18(34):20561, 2013.

Kornspan JD, Tarshis M, Rottem S: Adhesion and biofilm formation of *Mycoplasma pneumoniae* on an abiotic surface, *Arch Microbiol* 193(11):833, 2011.

Krech T, Bleckmann M, Paatz R: Comparison of buffalo green monkey cells and McCoy cells for isolation of *Chlamydia trachomatis* in a microtiter system, *J Clin Microbiol* 27:2364, 1989.

Kumar S, Hammerschlag MR: Acute respiratory infection due to *Chlamydia pneumoniae*: current status of diagnostic methods, *Clin Infect Dis* 44:568, 2007.

Latimer RL, Vodstrcil, De Petra V, et al.: Extragenital Mycoplasma genitalium infections among men who have sex with men, *Sex Transm Infect* 0(1), 2019.

Lau CY, Qureshi AK: Azithromycin versus doxycycline for genital chlamydial infections: a meta-analysis of randomized clinical trials, *Sex Transm Dis* 29(9):497, 2002.

Li Y, Su X, Le W, et al.: *Mycoplasma genitalium* in symptomatic male urethritis: macrolide Use is associated with increased resistance, *Clin Infect Dis pii* ciz294, 2019.

Lis R, Rowhani-Rahbar A, Manhart LE: Mycoplasma genitalium infection and female reproductive tract disease: a meta-analysis, *Clin Infect Dis* 61(3):418, 2015.

Loeb MB, Molloy D, et al.: A randomized, controlled trial of doxycycline and rifampin for patients with Alzheimer's disease, *J Am Geriatr Soc* 52:381, 2004.

Manhart LE, Broad JM, Golden MR: Mycoplasma genitalium: should We treat and how? *Clin Infect Dis* 53(Suppl 3):S129, 2011.

Marston BJ, Plouffe JF, File TM, et al.: Incidence of community-acquired pneumonia requiring hospitalization. Results of a population-based active surveillance study in Ohio. The Community-Based Pneumonia Incidence Study Group, *Arch Intern Med* 157(15):1709, 1997.

McIver R, Jalocon D, McNulty A: Men who have sex with men with Mycoplasma genitalium-positive nongonococcal urethritis are more likely to have macrolide resistant strains than men with only female partners: a prospective study, *Sex Trasm Dis* 46(8):513, 2019.

Miyashita N, Ouchi K, Kawasaki K, et al.: Mycoplasma pneumoniae pneumonia in the elderly, *Med Sci Monit* 14(8):CR387, 2008.

Narita M: Pathogenesis of extrapulmonary manifestations of Mycoplasma pneumoniae infection with special reference to pneumonia, *J Infect Chemother* 16:162, 2010.

Nelson HD, Helfand M: Screening for chlamydial infection, *Am J Prev Med* 20:95, 2001.

Pallawela SN, Sullivan AK, Macdonald N, et al.: Clinical predictors of rectal lymphogranuloma venereum infection: results from a multicentre case control study in the U.K., *Sex Transm Infect* 90(4):269, 2014.

Pathela P, Jamison K, Kornblum J, et al.: Lymphogranuloma venereum: an increasingly common anorectal infection among men who have sex with men attending New York city sexual health clinics, *Sex Transm Dis* 46(2):14, 2019.

Peipert JF: Genital chlamydial infections, *N Engl J Med* 349:2424, 2003.

Petrovay F, Balla E: Two fatal cases of psittacosis caused by *Chlamyophila psittaci*, *J Med Microbiol* 57:1296, 2008.

Phillips LE, Goodrich KH, Turner RM, et al.: Isolation of *Mycoplasma* species and *Ureaplasma urealyticum* from obstetrical and gynecological patients by using commercially available medium formulations, *J Clin Microbiol* 24:377, 1986.

Pineiro L, Idigoras P, de la Caba I, et al.: Guided antibiotic therapy for Mycoplasma genitalium infections: analysis of mutations associated with resistance to macrolides and fluoroquinolones, *Enferm Infecc Microbiol Clín* 37(6):394, 2019.

Poston TB, Lee DE, Darville T, et al.: Cervical cytokines associated with *Chlamydia trachomatis* susceptibility and protection, *J Infect Dis* 220(2):330, 2019.

Rantakokko-Jalava K, Hokynar K, Hieta N, et al.: Chlamydia trachomatis samples testing falsely negative in the Aptima Combo 2 test in Finland, *Euro Surveill* 24(22):1900298, 2019. 2019.

Rihl M, Köhler L, Klos A, et al.: Persistent infection of *Chlamydia* in reactive arthritis, *Ann Rheum Dis* 65:281, 2006.

Rizzo A, Domenico MD, et al.: The role of *Chlamydia* and *Chlamydophila* infections in reactive arthritis, *Intern Med* 51:113, 2012.

Roblin PM, Dumornay W, Hammerschlag MR: Use of HEp-2 cells for improved isolation and passage of *Chlamydia pneumoniae*, *J Clin Microbiol* 30:1968, 1992.

Ross JDC, Jensen JS: *Mycoplasma genitalium* as a sexually transmitted infection: implications for screening, testing, and treatment, *Sex Transm Infect* 82:269, 2006.

Sadiq ST, Mazzaferri F, et al.: Rapid accurate point-of-care tests combining diagnostics and antimicrobial resistance prediction for *Neisseria gonorrhoeae* and *Mycoplasma genitalium*, *Sex Transm Infect* 93:65, 2017.

Sauteur PMM, Seiler M, Truck J, et al.: *Diagnosis of Mycoplasma pneumoniae pneumonia with measurement of specific antibody-secreting cells AJRCCM 10.1164/rccm*, 2019, p 201904.

Saxon C, Hughes G, Ison C, ULC-F Group: Asymptomatic lymphogranuloma venereum in men who have sex with men, United Kingdom, *Emerg Infect Dis* 22:112, 2016.

Sessa R, di Pietro M, et al.: Infectious burden and atherosclerosis: a clinical issue, World, *J Clin Cases* 2:240, 2014.

Shah SS: *Mycoplasma pneumoniae* as a cause of community-acquired pneumonia in children, *Clin Infect Dis* 68(1):13, 2019.

Short VL, Totten PA, Ness RB, et al.: Clinical presentation of *Mycoplasma genitalium* infection versus *Neisseria gonorrhoeae* infection among women with pelvic inflammatory disease, *Clin Infect Dis* 48:41, 2009.

Simmons WL, Daubenspeck JM, Osborne JD, et al.: Type 1 and type 2 strains of *Mycoplasma pneumoniae* form different biofilms, *Microbiology* 159(4):737, 2013.

Spaargaren J, Schachter J, Moncada J, et al.: Slow epidemic of lymphogranuloma venereum L2b strain, *Emerg Infect Dis* 11:1787, 2005.

Stamm B, Moschopulos M, Hungerbuehler H, et al.: Neuroinvasion by *Mycoplasma pneumoniae* in acute disseminated encephalomyelitis, *Emerg Infect Dis* 14:641, 2008.

Thurman KA, Walter ND, Schwartz SB, et al.: Comparison of laboratory diagnostic procedures for detection of *Mycoplasma pneumoniae* in community outbreaks, *Clin Infect Dis* 48:1244, 2009.

Tumurkhuu G, Dagvadorj J, et al.: *Chlamydia pneumoniae* hijacks a host autoregulatory IL-1β loop to drive foam cell formation and accelerate atherosclerosis, *Cell Metab* 28:432, 2018.

Unemo M, Getman D, Hadad R, et al.: Letter to the editor: *Chlamydia trachomatis* samples testing falsely negative in the Aptima Combo 2 test in Finland, *Euro Surveill* 24(24):1900354, 2019. 2019.

United States Food and Drug Administration, Caccomo S: *FDA clears first diagnostic tests for extragenital testing for chlamydia and gonorrhea*, FDA News Release, May 23, 2019. Available at: https://www.fda.gov/news-events/press-announcements/fda-clears-first-diagnostic-tests-extragenital-testing-chlamydia-and-gonorrhea. [Accessed 6 August 2019].

United States Food and Drug Administration, Stark A: *FDA permits marketing of first test to aid in the diagnosis of a sexually-transmitted infection known as Mycoplasma genitalium*, FDA News Release, Jan 23, 2019. Available at: https://www.fda.gov/news-events/press-announcements/fda-permits-marketing-first-test-aid-diagnosis-sexually-transmitted-infection-known-mycoplasma. [Accessed 6 August 2019].

Van der Bij AK, Spaargaren J, Morré SA, et al.: Diagnostic and clinical implications of anorectal lymphogranuloma venereum in men who have sex with men: a retrospective case-control study, *Clin Infect Dis* 42(2):186, 2006.

Waites KB, Balish M, Atkinson TP: New insights into the pathogenesis and detection of *Mycoplasma pneumoniae* infections, *Future Microbiol* 3:635, 2008.

Waites KB, Katz B, Schelonka RL: Mycoplasmas and ureaplasmas as neonatal pathogens, *Clin Microbiol Rev* 18:757, 2005.

Waites KB, Talkington DF: *Mycoplasma pneumoniae* and its role as a human pathogen, *Clin Microbiol Rev* 17:697, 2004.

Waites KB, Xiao L, Liu Y, et al.: *Mycoplasma pneumoniae* from the respiratory tract and beyond, *Clin Microbiol Rev* 30:747, 2017.

Watkins LKF, Olson D, Diaz MH, et al.: Epidemiology and molecular characteristics of mycoplasma pneumoniae during an outbreak of M. Pneumoniae-associated Stevens-Johnson syndrome, *Pediatr Infect Dis J* 36(6):564, 2017.

Watts M, Mazur J: *New Hologic assay is first and only FDA-cleared diagnostic test to detect Emerging health Threat mycoplasma genitalium*, Hologic News, Jan 23, 2019. https://www.fda.gov/news-events/press-announcements/fda-permits-marketing-first-test-aid-diagnosis-sexually-transmitted-infection-known-mycoplasma. [Accessed 6 August 2019]. Available at:.

Winchell JM: Mycoplasma pneumoniae—a national public health perspective, *Curr Pediatr Rev* 9(4):324, 2013.

Wolff BJ, Morrison SS, Winchell JM: Development of a multiplex TaqMan real-time PCR assay for the detection of *Chlamydia psittaci* and *Chlamydia pneumoniae* in human clinical specimens, *Diagn Microbiol Infect Dis* 90(3):167, 2018.

Wood JC, Lu RM, Peterson EM, et al.: Evaluation of Mycotrim-GU for isolation of *mycoplasma* species and *Ureaplasma urealyticum*, *J Clin Microbiol* 22:789, 1985.

World Health Organization: *Trachoma–epidemiological situation*. Available at: https://www.who.int/trachoma/epidemiology/en. [Accessed 5 August 2019], 2018.

Xiao D, Zhao F, Zhang H, et al.: Novel strategy for typing *Mycoplasma pneumoniae* isolates by use of matrix-assisted laser desorption ionization-time of flight mass spectrometry coupled with ClinProTools, *J Clin Microbiol* 52:3038, 2014.

Yajko DM, Balston E, Wood D, et al.: Evaluation of PPLO, A7B, E, and NYC agar media for the isolation of *Ureaplasma urealyticum* and *Mycoplasma* species from the genital tract, *J Clin Microbiol* 19:73, 1984.

Yang C, Briones M, Chiou J, et al.: *Chlamydia trachomatis* lipopolysaccharide evades the canonical and noncanonical inflammatory pathways to subvert innate immunity, *mBio* 10(2), 2019. e00595.

Zeidler H, Hudson AP: Causality of *Chlamydiae* in arthritis and spondyloarthritis: a Plea for increased Translational research, *Curr Rheumatol Rep* 18(9), 2016.

Zheng X, Lee S, Selvarangan R, et al.: Macrolide resistant *Mycoplasma pneumoniae*, United States, *Emerg Infect Dis* 21:1470, 2015.

Zhu J, Quyyumi AA, Norman JE, Csako G, et al.: Effects of total pathogen burden on coronary artery disease risk and C-reactive protein levels, *Am J Cardiol* 85:140, 2000.

CHAPTER 63

RICKETTSIAE AND OTHER RELATED INTRACELLULAR BACTERIA

Juan P. Olano, David H. Walker

RICKETTSIAL INFECTIONS, 1254
Infections Caused By Organisms of The Genus *Rickettsia,* 1254
Scrub Typhus Caused By ***Orientia*** *Tsutsugamushi,* 1258
Infections Caused By Organisms of The Genera ***Ehrlichia*** And *Anaplasma,* 1259
Infections Caused By *Coxiella Burnetii,* 1261
Infections Caused By Organisms of The Genus *Bartonella,* 1263
SELECTED REFERENCES, 1265

KEY POINTS

- Treatable rickettsial infections, including life-threatening Rocky Mountain spotted fever, boutonneuse fever, epidemic typhus, murine typhus, scrub typhus, human monocytotropic ehrlichiosis, and human granulocytotropic anaplasmosis, are seldom diagnosed serologically during the acute stage of illness owing to absence of an early antibody response.
- Immunohistochemistry and molecular diagnostics are effective in diagnosing rickettsioses and ehrlichioses, respectively.
- Q fever endocarditis is a chronic infection that usually is diagnosed by detecting a high titer (≥1:800 by immunofluorescent antibody assay) of antibodies against *Coxiella burnetii* phase I antigen.
- The clinicoepidemiologic diagnosis of cat scratch disease can be confirmed serologically by antibodies to *Bartonella henselae* or by polymerase chain reaction testing of lymph node aspirates.

RICKETTSIAL INFECTIONS

More than 100 years ago, Dr. Arnold Theiler described the first rickettsial pathogen, namely *Anaplasma marginale*, a veterinary infectious agent that targets red blood cells. During the subsequent 4 decades, four major human rickettsial pathogens would be described: *Rickettsia prowazekii* (epidemic typhus), *R. rickettsii* (Rocky Mountain spotted fever), *R. conorii* (Mediterranean spotted fever), and *R. typhi* (endemic typhus) (Table 63.1). Rickettsia is a concept that developed historically as the molecular and physical nature of viruses was defined (Weiss, 1982). In contrast with human viral agents, which also require eukaryotic host cells for their intracellular replication, rickettsiae have a gram-negative bacterial cell wall, and their growth is inhibited by particular antibiotics. Rickettsiae are further differentiated from other obligately intracellular bacteria by their ecology and frequent transmission by arthropod vectors. The traditional taxonomic scheme of rickettsiae based on such phenotypic characteristics as intracellular growth and arthropod vector transmission has undergone substantial modification in light of contemporary gene sequence analyses. Based on extensive deoxyribonucleic acid (DNA) sequence analysis of several rickettsial organisms in the order Rickettsiales (one of eight major orders recognized in the class Alphaproteobacteria), the transition to the intracellular lifestyle occurred approximately 750 to 500 million years ago, followed by the transition to arthropods between 525 and 450 million years ago (Weinert et al., 2009; Diop et al., 2018; Munoz-Gomez et al., 2019). The genus *Rickettsia* is approximately 150 million years old (Weinert et al., 2009). Three major transitions occurred within the genus: sex ratio distorters in arthropods, arthropod-transmitted vertebrate pathogens, and arthropod-transmitted plant pathogens (Weinert et al., 2009). These transitions were accompanied by genomic degradation due to their endosymbiotic lifestyle, which provided them metabolic pathways from the eukaryotic host cell (Merhej, 2011). Two families contain most of the human pathogens in the order Rickettsiales: Anaplasmataceae and Rickettsiaceae. Genera that contain human pathogens in the former are *Ehrlichia*, *Anaplasma*, *Neorickettsia*, and *Neoehrlichia*. Genera in the latter are *Rickettsia* and *Orientia* (Gillespie et al., 2012; Dumler et al., 2001). Other genera included in this chapter include *Coxiella* and *Bartonella*. Despite their historical association with rickettsiology and arthropod transmission, *Bartonella* are cultivable in cell-free medium and do not belong in the order Rickettsiales (Brenner et al., 1993). Instead, they are included in the class Alphaproteobacteria, order Rhizobiales. *Coxiella* are also historically associated with rickettsiae, but they belong to the order Legionellales, class Gammaproteobacteria. Grouped by genus, the following diseases are presented in this chapter: *Rickettsia*—Rocky Mountain spotted fever, boutonneuse fever, *R. parkeri* infection, Pacific Coast spotted fever, African tick bite fever, rickettsialpox, and murine typhus; *Orientia*—scrub typhus; *Ehrlichia*—human monocytotropic ehrlichiosis caused by *E. chaffeensis* and human infections with *E. ewingii* and *E. muris eauclairensis*; *Anaplasma*, human granulocytotropic anaplasmosis; *Coxiella*—Q fever; and *Bartonella*—cat scratch disease, bacillary angiomatosis and peliosis, trench fever, and South American bartonellosis. The diseases caused by each genus comprise cohesive clinical and pathologic groupings, and overall the rickettsial diseases pose a similar set of diagnostic challenges with similar technical approaches to their solution. Several rickettsiae species have been isolated from tick vectors, but no human illness has been associated with them: *R. peacockii*, *R. montanensis*, *R. canadensis*, *R. tamura*, *R. gravesii*, *R. rhipicephali*, *R. hoogstrali*, *R. asemobonensis*, and *R. bellii* (Diop et al., 2018). So far their clinical importance lies in their possible role of inducing antibody production in humans, which would account for false-positive serologic tests.

INFECTIONS CAUSED BY ORGANISMS OF THE GENUS *RICKETTSIA*

Structure and Function

Spotted fever, transitional, and typhus group rickettsiae are genetically closely related bacteria that have a thin (0.3–0.5 by 1–2 μm) bacillary morphology and a gram-negative cell wall containing lipopolysaccharide with antigenic components that distinguish the spotted fever and typhus groups. All *Rickettsia* spp. reside free in the cytosol of the host cell and divide by binary fission. Rapid progress in bioinformatics and phylogenomics have elucidated secretion systems in rickettsiae, known as the *Rickettsia* secretome (Gillespie et al., 2015). Two Sec-dependent pathways (T5SS and Sec-TolC) are defined by the surface cell antigen (Sca) family and RARP-1 (*Rickettsia* ankyrin repeat protein 1), respectively. Two Sec-independent pathways are also conserved across *Rickettsia* spp.: T1SS and T4SS. An additional secretion system is the Twin-arginine translocation (Tat). The latter three have no known substrates (Gillespie et al., 2015). Rickettsiae attach to the host cell via Sca, a family of autotransporter proteins of which OmpA (Sca0, Sca1, Sca2) and OmpB (Sca5) have been very well characterized (Li & Walker, 1998; Uchiyama, 1999). OmpA and OmpB are both present in spotted fever group rickettsiae, whereas OmpA is absent in typhus group rickettsiae. OmpB is in fact the ligand of a ubiquitous cell surface receptor known as Ku70 (DNA-dependent protein kinase) (Martinez & Cossart, 2004; Martinez et al., 2005). Adhesion is followed by internalization, which requires ubiquitination of cholesterol-rich microdomains (lipid rafts) containing Ku70 (Samanta et al., 2017). Caveolin and clathrin further contribute to the endocytic process. Furthermore, once in the intracellular space, rickettsiae (and other obligate intracellular bacteria such as *Chlamydia*, *Coxiella*, *Anaplasma*, and *Ehrlichia*) can manipulate host cholesterol trafficking pathways to access intracellular vesicles in search of nutrients or obtain membrane

TABLE 63.1
Rickettsial Infections

Etiologic Agent	Disease	Geographic Distribution	Transmission
Spotted Fevers			
R. rickettsii	Rocky Mountain spotted fever	North, Central, and South America	Tick bite
R. conorii	Boutonneuse fever	Southern Europe, Africa, Russia, Georgia, Middle East, Indian subcontinent	Tick bite
R. africae	African tick bite fever	Southern, western and eastern Africa, Caribbean	Tick bite
R. parkeri	Maculatum disease	North and South America	Tick bite
R. sibirica	North Asian tick typhus	Russia, China, Mongolia, Pakistan, Europe, Africa	Tick bite
R. japonica	Japanese spotted fever	Japan, Korea, Thailand	Tick bite
R. honei	Flinders Island spotted fever	Australia, Asia	Tick bite
R. slovaca	TIBOLA/DEBONEL/SENLAT	Europe	Tick bite
R. aeschlimannii	Spotted fever	Sub-Saharan Africa, Europe	Tick bite
R. heilongjiangensis	Far-Eastern spotted fever	Russia, China, South Korea, Japan	Tick bite
R. massiliae	Spotted fever	Europe, Argentina	Tick bite
R. monacensis	Spotted fever	Europe	Tick bite
R. raoultii	TIBOLA/DEBONEL/SENLAT	Europe, Asia	Tick bite
Rickettsia strain 364D	Eschar-associated illness (mild)	California	Tick bite
Typhus Fevers			
R. prowazekii	Epidemic typhus	Potentially worldwide; in recent decades in Africa, South America, Central America, Mexico, Asia	Feces of human body louse
R. prowazekii	Brill-Zinsser disease	Worldwide; wherever persons with past epidemic typhus now reside	Recrudescence of latent infection
R. prowazekii	Flying squirrel typhus	United States	Presumably feces of flea or louse of flying squirrel
R. typhi	Murine typhus	Worldwide in tropics and subtropics	Flea feces
Transitional Group Rickettsial Fevers			
R. akari	Rickettsialpox	United States, Ukraine, Croatia, Korea, Turkey, Mexico	Mite bite
R. australis	Queensland tick typhus	Eastern Australia	Tick bite
R. felis	Fleaborne spotted fever	Worldwide	Presumably flea bite or feces

components for the bacteria or their vacuole (Samanta et al., 2017). On the other hand, OmpA has been shown to interact with the cell surface protein α2-β1 integrin through a discontinuous RGD motif in OmpA (Hillman et al., 2013). The roles of Sca1, Sca2, Sca3, Sca4, and Epac are far less well characterized. Disruption of Sca2 inhibits actin-based motility (Kleba et al., 2010). Furthermore, Sca2 has been shown to nucleate unbranched actin filaments via host profilin (actin-binding protein) (Haglund et al., 2010). Sca4 has been shown to activate vinculin (another actin-binding protein present in focal adhesions) (Park, Lee et al., 2011). Sca3 proteins are only present in typhus-group rickettsiae and *R. felis*.

Once internalized, rickettsiae escape the phagosome rapidly via phospholipase activity of rickettsial origin (Silverman et al., 1992; Whitworth et al., 2005). Phospholipase D and phospholipase A_2 are present in rickettsial genomes. Spotted fever group rickettsiae are propelled within cells and during release from the cell by stimulating polymerization of host cell F-actin at one pole (Gouin et al., 2004; Heinzen et al., 1993). Rickettsiae that manifest this activity (e.g., *Rickettsia rickettsii*) escape earlier from host cells and spread more quickly to other cells than those lacking this activity (e.g., *Rickettsia prowazekii*), which divide intracellularly to massive numbers before the host cell bursts and the organisms are released. According to the molecular phylogeny, *Rickettsia* spp. that are pathogenic for humans have evolved into three genogroups (Roux & Raoult, 1995). The typhus group includes *R. prowazekii* and *R. typhi*. The core spotted fever group contains *R. rickettsii*, *R. conorii*, *R. japonica*, *R. africae*, *R. parkeri*, *R. honei*, *R. sibirica*, *R. massiliae*, and *R. slovaca*, among others. A relatively newly recognized transitional clade contains *R. akari*, *R. australis*, and *R. felis*. *R. akari* and *R. australis* were traditionally considered to be relatively distant members of the spotted fever group, with which they share lipopolysaccharide antigens. As of 2018, 31 *Rickettsia* spp. have been validated; 5 more species added since 2013 (Diop et al., 2018; Jiang et al., 2013)

Rocky Mountain Spotted Fever

The most severe of all the rickettsioses, Rocky Mountain spotted fever has a substantial case fatality rate (5%) even among previously healthy, immunocompetent children and young adults with appropriate antibiotic treatment (Dalton et al., 1995; Paddock et al., 1999). *R. rickettsii* normally resides in nature in ticks: *Dermacentor variabilis*, the American dog tick, in the eastern two-thirds of the United States and California; *D. andersoni*, the Rocky Mountain wood tick, in the western United States; *Rhipicephalus sanguineus*, the brown dog tick, in Mexico, Brazil, and Arizona; and *Amblyomma cajennense* complex and *A. aureolatum* in South America. These ticks maintain *R. rickettsii* as they molt from stage to stage (larva, nymph, and adult) and transovarially from generation to generation. Fewer than 1 per 1000 ticks carries virulent *R. rickettsii*, which is pathogenic for ticks (Niebylski et al., 1999). New lines of ticks become infected by feeding on rickettsemic rodents or cofeeding with infected ticks, replenishing the population of organisms transovarially maintained in ticks (Gage et al., 1990).

Infections occur when and where humans encounter *R. rickettsii*–infected ticks (Helmick et al, 1984). Although Rocky Mountain spotted fever has been documented in recent years in nearly every state except Hawaii, Alaska, and Vermont, the highest incidence is in the south Atlantic states from Maryland to Georgia and the south central states of Oklahoma, Missouri, Arkansas, and Tennessee. Most cases occur in late spring and summer but, particularly in the southern latitudes, a few cases may occur even in winter. The highest incidence is in children, adults of retirement age, and others who are exposed to ticks during outdoor activities. Fatality/case ratios are higher for persons older than 30 years of age. Fulminant Rocky Mountain spotted fever (death by the fifth day of illness) occurs in association with moderate hemolysis (e.g., in black males with glucose-6-phosphate dehydrogenase [G6PD] deficiency) (Walker et al., 1983)

Rickettsiae are injected via the infected tick's salivary gland secretions into the patient's dermis after 6 to 10 hours of tick feeding and spread hematogenously throughout the body. The vascular endothelium is the target of intracellular infection, with some invasion into adjacent vascular smooth muscle cells. Infected endothelium is injured by reactive-oxygen-species-induced damage to cell membranes (Santucci et al., 1992). Damage to the endothelium (directly mediated by rickettsiae or indirectly mediated by cytokines/chemokines) results in increased vascular permeability leading to edema, hypovolemia, and hypotension (Colonne et al., 2013; Woods & Olano, 2008). The life-threatening consequences of vascular injury in the central nervous system (CNS) and lung are rickettsial meningoencephalitis and noncardiogenic pulmonary edema. Early in the course, lesions

show endothelial rickettsiae without thrombi or a cellular response. Late in the course, the characteristic lymphohistiocytic perivascular infiltrate appears as interstitial pneumonia, interstitial myocarditis, perivascular glial nodules of the brain, and similar vascular lesions in the dermis, gastrointestinal tract, liver, skeletal muscles, and kidneys. Severe injury may be accompanied by focal hemorrhages but seldom by microinfarcts, except in the white matter of the brain.

The clinical illness usually begins with fever, headache, and myalgia 2 to 14 days after a tick bite (Kaplowitz et al., 1983). Nausea, vomiting, abdominal pain and tenderness, and diarrhea occur more frequently in the first 3 days of illness. The rash, which usually appears between days 3 and 5, typically begins as macules around the wrists and ankles and, later, on the arms, legs, and trunk. The lesions become maculopapular, and in one-half of cases a central petechia appears in many of the maculopapules. Characteristic involvement of the palms and soles occurs in half of cases as a late manifestation. Renal failure is a feature of severe illness. CNS involvement is ominous; seizures and coma occur in 8% to 10% of cases overall, often preceding a fatal outcome. Thrombocytopenia occurs in half of cases, but disseminated intravascular coagulation is rare (Schmaier et al., 2001).

African Tick Bite Fever, Boutonneuse Fever, *Rickettsia Parkeri Infection,* and Other Spotted Fevers

R. conorii has been isolated in southern Europe; northern, eastern, and southern Africa; Israel; Turkey; India; Pakistan; Russia; Georgia; and Ukraine. The ecology of *R. conorii* and the epidemiology of boutonneuse fever are closely tied to ticks, especially *R. sanguineus*, which maintain the rickettsiae transovarially and transmit the infection to humans while feeding (Walker & Fishbein, 1991). Imported cases are diagnosed in travelers returning to the United States and northern Europe from the Mediterranean basin. The fatality rate among hospitalized patients is 1.4% to 5.6%, particularly in patients with underlying conditions such as diabetes and alcoholism. A milder disease caused by *R. africae* occurs with a high frequency in travelers returning from southern Africa (McQuiston et al., 2004). The clinical illness resembles that of the recently associated rickettsioses in the Americas caused by *R. parkeri*, which is very closely related to *R. africae* (Paddock et al., 2004, 2008). Tick bite eschars are often multiple; regional lymphadenopathy is observed frequently; and rash is typically sparse, sometimes vesicular, and often absent. *R. sibirica* has been isolated in Russia, China, Mongolia, and Pakistan; the distinct strain *R. sibirica mongolitimoniae* isolated in Asia, Europe, and Africa has been associated in one-half of the cases with lymphangitis extending proximally from the eschar. *R. japonica* has been documented in Japan, and infection with *R. japonica* occurs also in Korea, China, and Thailand. Human infections with *R. australis* occur only in Australia, and infection with *R. honei* has been documented in Australia and Asia. After an average incubation period of 7 days, these illnesses begin with fever, headache, and myalgias. Frequently, an eschar can be discovered by careful examination of the skin at this time. The pathology of these spotted fevers is well described in the tache noire or eschar at the site of tick bite inoculation of rickettsiae (Walker, 1989). Mononuclear phagocytes are the initial target cell in eschars of spotted fever rickettsioses.

The host defenses that effect killing of intracellular rickettsiae include nitric oxide, reactive oxygen species, and tryptophan limitation induced by cytokines secreted by T lymphocytes and macrophages, which infiltrate around the infected blood vessels and target cell apoptosis triggered by cytotoxic $CD8^+$ T lymphocytes (Herrero-Herrero et al., 1987; Valbuena et al., 2002; Walker et al., 2001). Activation of endothelial cells by cytokines, including γ-interferon and TNF-α, results in intracellular rickettsicidal activity, and ultimate clearance is mediated by cytotoxic T lymphocytes. Disseminated endothelial infection results in maculopapular rash, meningoencephalitis, and vascular lesions in the lungs, kidneys, gastrointestinal tract, and heart (Walker & Gear, 1985). Multifocal hepatocellular necrosis and granuloma-like lesions correlate with moderately increased concentrations of hepatic transaminases (Walker et al., 1986).

Other spotted fever rickettsiae that have been occasionally associated with human disease include *R. aeshlimannii*, *R. heilongjianensis*, *R. massiliae*, *R. monacensis*, *Rickettsia* strain 364D, *R. helvetica*, *R. raoultii*, *R. slovaca*, and *R. tamurae* (Parola et al., 2013).

Rickettsialpox

R. akari is maintained in nature by transovarial transmission in the gamasid mite, *Liponyssoides sanguineus*, an ectoparasite of the domestic mouse, *Mus musculus. R. akari* has been detected only in the United States, Croatia, the Ukraine, Turkey, Mexico, and Korea, perhaps more an indication of the paucity of rickettsial investigations than the actual distribution of this rickettsial species.

A papule develops during the approximately 10-day incubation period at the site of mite bite and progresses to become a 1- to 2.5-cm eschar. Illness begins with chills, fever, malaise, severe headache, and myalgia. Rash, which appears 2 to 6 days later, is initially maculopapular, later papular, and in classic cases pustular and/or vesicular. Some patients also suffer nausea, vomiting, pharyngitis, photophobia, splenomegaly, and nuchal rigidity.

Histopathologic examination of the eschar reveals coagulative necrosis of the epidermis, underlying vascular injury, and a perivascular lymphohistiocytic infiltrate in which mononuclear phagocytes appear to be the main target cell of infection (Brettman et al., 1981; Kass et al., 1994; Walker et al., 1999). Regional lymphadenopathy and cutaneous rash presumably reflect lymphogenous and hematogenous spread, respectively.

Fleaborne Spotted Fever

A widely dispersed organism, *R. felis* is maintained transovarially in cat fleas (*Ctenocephalides felis*). Human infections have been diagnosed in North America, Europe, Africa, Australia, and Asia only by nucleic acid amplification. *R. felis* DNA is also detected in blood samples of many healthy persons. There are no human isolates of *R. felis*, and serologic confirmation of diagnoses is lacking. Thus the role of *R. felis* in human disease is controversial (Schriefer, Sacci, Taylor et al., 1994; Zavala-Velazquez et al., 2000; Parola & Raoult, 2001; Raoult et al., 2001).

Murine Typhus and Louseborne Typhus

Endemic fleaborne *R. typhi* infection, murine typhus, is presently the most important typhus group infection in the United States and causes extensive morbidity throughout the warm regions of the world (Azad, 1990). Most of the cases in the United States are concentrated in Texas and California.

Historically, epidemic louseborne *R. prowazekii* infections have had a major impact on the outcome of military campaigns as well as scourging general populations disrupted by war, famine, and natural disasters (Zinsser & Castaneda, 1930; Patterson, 1993). *R. prowazekii* continues to cause disease in some poverty-stricken areas of the world and reappears in situations such as the civil war in Burundi, the extreme poverty of indigenous populations of the Andes, and other unsettled social and economic conditions (Houhamdi et al., 2005). An outbreak in Russia was also described in the 1990s (Tarasevich et al., 1998). Recrudescence of latent *R. prowazekii* infections can occur years after the primary infection in immigrants from typhus-afflicted areas (Brill-Zinsser disease). These cases are responsible for initiating outbreaks in populations with a high incidence of body louse infestation. Endemic transmission of *R. prowazekii* from a natural infectious cycle of flying squirrels *(Glaucoma volans volans)* and their ectoparasites occurs in the United States (McDade et al., 1980; Reynolds et al., 2003). The incubation period ranges from 10 to 14 days, and the disease is more severe than its counterpart endemic typhus. Rash occurs in a variable proportion of cases depending largely on light skin pigmentation for its recognition. Neurologic manifestations can occur in as many as 80% of cases. Respiratory manifestations occur in 40% to 70% of cases. Case fatality rates can be as high as 60% in the absence of antibiotic therapy and appropriate nursing care, and 15% in patients with previous good general health and good supportive care, and 4% when treated with appropriate antibiotics (Badiaga & Brouqui, 2012).

Murine typhus occurs particularly in tropical and subtropical coastal areas where *Rattus rattus*, *R. norvegicus*, and the Oriental rat flea abound (Azad, 1990). The fleas imbibe rickettsiae in the blood of infected rats and maintain the infection for their normal life span. Transovarian transmission occurs only at low levels; thus horizontal transmission to other rats is a key factor in maintenance of *R. typhi* in nature. Other mammal-arthropod cycles maintain the rickettsiae and result in transmission of infections to humans (e.g., the cat flea, *C. felis*, and the opossum in Texas and California [Los Angeles County and a few other southern counties]) (Schriefer, Sacci, Taylor et al., 1994). Hawaii also experienced an outbreak of endemic typhus in 2002 across five islands (Maui had the majority of cases), and the animal reservoir has not been identified. The disease remains endemic in Maui, Kauai, and Oahu, and serologic studies have revealed the presence of *R. typhi* in *R. rattus*, *R. norvegicus*, *R. exulans* (Polynesian rat), and *Mus musculus* (house mice) (Centers for Disease Control and Prevention [CDC], 2003).

Humans are believed to become infected by intradermal inoculation of infected flea feces into skin excoriated by scratching. However, inhalation of a rickettsial aerosol from dried infected flea feces or inoculation by flea bite may account for transmission in some cases. Flea bites are recalled in 0% to 40% of cases. After an incubation period of 1 to 2 weeks, illness begins with fever accompanied in some cases by severe headache, chills, myalgias, and nausea. A macular or maculopapular rash, most prominent on the trunk, is visualized on day 5 or 6 in 80% of patients with fair skin

and in 20% with darkly pigmented skin. A small proportion of patients have cough and pulmonary infiltrates. Severely ill patients may also suffer coma, seizures, and other neurologic signs. Approximately 10% of hospitalized patients require admission to the intensive care unit, and 1% to 2% of murine typhus patients die (Dumler et al., 1991). CNS complications occur in 2% to 10% of cases and appear late in the acute phase of the disease (10 days to 3 weeks).

The pathologic lesions of murine typhus include endothelial swelling and perivascular lymphohistiocytic infiltrates involving the blood vessels in the dermis, CNS, lungs, heart, gastrointestinal tract, and kidneys (Walker et al., 1989). The most serious consequences are meningoencephalomyelitis and diffuse alveolar injury.

Rickettsiae as Agents of Bioterrorism

R. prowazekii is a select agent, the possession of which is restricted by law to registered scientists in approved institutions where rigorous security and safety regulations are applied to the laboratories. This organism exists in nature, can be recovered and propagated, and is infectious via a stable aerosol with infectivity of as little as a single bacterium. *R. rickettsii* was formerly considered a select agent, but the CDC decided to remove it from the select agent list in 2012.

Case fatality rates of 15% to 25% in previously healthy persons would occur without prompt diagnosis and treatment. The potential for genetically engineered resistance to the effective antibiotics, tetracycline, and chloramphenicol would render these cases of epidemic typhus untreatable (Walker, 2003). Although the case fatality rates would be lower, bioterrorist-dispersed *R. typhi* or *R. conorii* could also create terror and overwhelm the medical and public health systems.

Laboratory Diagnosis

Unlike most infectious diseases for which precise diagnosis is sought during the acute phase of illness, when critical therapeutic decisions are made, rickettsial diseases are usually diagnosed acutely purely on clinicoepidemiologic suspicion and are treated empirically on a presumptive basis (Kaplowitz et al., 1983; Botelho-Nevers et al., 2012). Serologic diagnosis, which is often mistakenly sought early in the course of illness, provides the majority of laboratory confirmed diagnoses by demonstration of a fourfold or greater rise in titer only during convalescence. Even with the most sensitive serologic methods, fewer than 20% of patients have detectable specific antibodies to rickettsiae when presenting to the physician for medical attention. These antibodies may have been stimulated at an earlier time by organisms of low pathogenicity such as *R. amblyommatis*. Other approaches to diagnosis at the time of presentation include immunohistologic demonstration of rickettsiae in cutaneous lesions, immunocytologic identification of rickettsiae in circulating detached endothelial cells, detection of rickettsial DNA in blood and tissue specimens by polymerase chain reaction (PCR) (Furuya et al., 1995; Schriefer, Sacci, Taylor et al., 1994; Sexton et al., 1994; Tzianabos et al., 1989; Williams et al., 1994), and cultivation of rickettsiae from blood or tissue specimens; but these tests are not available in most clinical laboratories.

Rickettsiae were originally demonstrated in tissues of patients with Rocky Mountain spotted fever and epidemic louseborne typhus by Wolbach (1918) using Giemsa stain during and shortly after World War I. This method, essentially a lost art, requires careful attention to details of fixation and staining of rickettsiae and is not performed successfully in this manner in contemporary histology laboratories. A modified Brown-Hopps method stains a small fraction of organisms, which appear as thin bacilli within endothelial cells. A more sensitive and specific approach to visualization of rickettsiae in tissue sections is immunohistology, either immunofluorescence or immunoenzyme staining, using antibodies specific for the spotted fever or typhus group (Kaplowitz et al., 1983; Walker et al., 1989, 1997, 1999; Dumler et al., 1990). Staining of skin biopsies from patients with Rocky Mountain spotted fever by immunohistochemistry has a sensitivity of 60% to 80% and a specificity close to 100%. Patients with boutonneuse fever, African tick bite fever, murine typhus, and rickettsialpox have also been diagnosed by immunohistologic detection of rickettsiae in rash and eschar lesions. A monoclonal antibody to a spotted-fever-group–specific epitope on the cell wall lipopolysaccharide demonstrates *R. rickettsii*, *R. parkeri*, *R. conorii*, *R. akari*, *R. japonica*, *R. australis*, *R. africae*, *R. honei*, and *R. sibirica* in formalin-fixed, paraffin-embedded tissues, and a typhus group lipopolysaccharide-specific monoclonal antibody is similarly useful for detecting *R. typhi* and *R. prowazekii* (Walker et al., 1997). Currently, reagents for diagnostic immunohistology of rickettsioses are not commercially available, but it is feasible that kits could be developed for rickettsial-group–specific diagnosis using antibodies produced in research laboratories.

A unique diagnostic approach is the immunocytologic demonstration of *R. conorii* in detached, circulating endothelial cells captured from patient blood samples by immunomagnetic beads coated with a monoclonal antibody to a surface antigen of human endothelial cells (Drancourt et al., 1992; La Scola & Raoult, 1996a). In boutonneuse fever patients, this method has a sensitivity of 58% for examination of a single blood sample and may be used in patients prior to the onset of rash, which must be present for selection of the site of skin biopsy for immunohistologic diagnosis.

Nucleic acid amplification (NAA) tests used for spotted fever group and typhus group rickettsioses include PCR and its variants (nested, real-time, conventional) and loop-mediated isothermal amplification (LAMP). Abundant literature documents the use of several PCR targets, but the most commonly used genes include the 17 kDa lipoprotein gene, *gltA*, *rrs*, *groEL*, *ompA*, *ompB*, RC0338, and real-time PCR panrickettsia assays. Analytic sensitivity for PCR ranges from 10^3 to 10^5 genome equivalents/mL blood DNA for nested PCR (sensitivity is much lower for conventional PCR). For real-time PCR the sensitivity ranges from 100 to 5000 genome equivalents/mL of blood DNA. Reverse transcriptase real-time PCR targeting ribosomal RNA can increase analytic sensitivity of nucleic acid detection as much as 100X compared to regular PCR (as low as 9 copies per reaction) (Kato, 2013). LAMP assays for SFG and TG rickettsioses are not well evaluated. However, one study revealed low sensitivity in patients with endemic typhus, most likely due to low levels of bacteremia (Dittrich et al., 2014). In fact, detection of TG rickettsiae from blood samples using PCR is far lower when compared to SFG rickettsioses (2–10% vs 24–56%) (Paris & Dumler, 2016).

Samples for NAA include biopsy of eschar or rash, blood, buffy coat, necropsy tissue, and even arthropod vectors removed from patients. NAA tests may fail to detect rickettsial nucleic acids early in the course or after development of immunity or effective antimicrobial treatment (Tzianabos et al., 1989; Fournier & Raoult, 2004; Furuya et al., 1995; Leitner et al., 2002; Ndip et al., 2004; Roux & Raoult, 1999; Schriefer, Sacci, Dumler et al., 1994; Sexton et al., 1994; Walker, 2003; Kidd et al., 2008; Mendes do Nascimento et al., 2009; Stenos et al., 2005; Prakash et al., 2009). Isolation of rickettsiae is achieved frequently in antibiotic-free, centrifugation-enhanced shell vial cell culture in reference and research laboratories with biosafety level-3 containment and specialized expertise.

Serodiagnosis still remains the gold standard for rickettsioses (Abdad et al., 2018; Paris & Dumler, 2016). Test formats include immunofluorescent antibody (IFA), microimmunofluorescence (MIF) assay, and enzyme-linked immunosorbent assay (ELISA). MIF is very similar to IFA but allows simultaneous testing of several rickettsial antigens spotted in the testing wells. The indirect immunoperoxidase antibody test yields similar results. For spotted fever- and typhus-group rickettsial infections in the United States, IFA titers of 1:64 or greater are considered to indicate a probable diagnosis in a compatible clinicoepidemiologic situation. In countries where there is a high prevalence of persons with antibodies to these rickettsiae, due hypothetically to stimulation by nonpathogenic rickettsiae or subclinical or undiagnosed infection, higher titers are required to establish the diagnosis. In any event, a fourfold rise in IFA antibody titer to at least a titer of 1:64, but usually 1:256 or higher, is diagnostic. The sensitivity of the IFA for Rocky Mountain spotted fever is 94% to 100%, and the specificity is 100%. The sensitivity of IFA for spotted fever rickettsioses in general is 85% to 100%, and the specificity is 99% to 100% when detecting IgG antibodies. These values decrease slightly when using IgM. ELISA IgG testing has a sensitivity of 83% and specificity of 87% (Clements et al., 1983; Keysary & Strenger, 1997). Both sensitivity and specificity increase as the number of illness days also increase. By day 30, virtually all cases can be diagnosed serologically. With a cutoff titer for IgG of 1:128 and for IgM of 1:32, the indirect immunoperoxidase test yields similar results and has the advantage of requiring only a light microscope instead of an ultraviolet microscope.

Commercially available serologic tests include indirect immunofluorescence, latex agglutination, and standard solid-phase enzyme immunoassay (Kelly, Chan et al., 1995). Latex agglutination and solid-phase enzyme immunoassay provide diagnostically useful information, require less expensive equipment to perform, but generally are not considered as reliable as the IFA. The greatly increased reliance of reference laboratories on enzyme immunoassays has occurred in parallel with anomalous changes in public health reports of Rocky Mountain spotted fever. It has been suggested that a substantial portion of the tick-exposed population has standing titers of antibodies stimulated by spotted fever group rickettsiae of low pathogenicity (Graf et al., 2008). The Weil-Felix tests, which measure agglutination of *Proteus vulgaris* strains OX-19 and OX-2 (Kaplan & Schonberger, 1986), are insensitive and nonspecific and should not be used except in developing countries in which no other method can

be performed. Serology is seldom useful in assisting therapeutic decisions because antibodies appear later in the course.

A promising technology to detect low levels of rickettsia-specific circulating antibodies is by using protein microarrays produced from recombinant protein expression using ORF libraries, followed by fluorescent detection (Vigil et al., 2011).

Treatment

Well-controlled, double-blind randomized clinical trials are lacking for rickettsioses in general. However several in vitro susceptibility studies have been published mostly for the main pathogenic rickettsioses, although standardization is lacking, and therefore minimum inhibitory concentrations (MICs) are difficult to interpret. Studies in humans are mostly retrospective.

In general, rickettsiae are sensitive to tetracyclines, fluoroquinolones, chloramphenicol, and rifamycins. Less effective antibiotics are the macrolides (Raoult et al., 1991; Rolain et al., 1998). All Rickettsiales are inherently resistant to aminoglycosides, β-lactams, cephalosporins, and sulfa-derived medications. Sulfas are in fact contraindicated in any infection caused by Rickettsiales due to greater severity of disease and fatal outcomes. The presence of a toxin-antitoxin condition led to reconsideration of the use of fluoroquinolones. The gold standard treatment for all rickettsioses is doxycycline, even in patients younger than 8 years of age since the occurrence of discolored teeth and bone accumulation is minimal. When compared with other antimicrobial agents, doxycycline is associated with earlier defervescence and better protection against progression to severe forms of the disease. Alternatives include tetracycline, chloramphenicol, and selected macrolides and fluoroquinolones. Duration of treatment depends on the severity of the disease and rickettsial species. In general, Rocky Mountain spotted fever and epidemic typhus cases should be treated for several days compared with less severe rickettsioses, which can be treated even with single doses of doxycycline (Botelho-Nevers et al., 2012). Relapses are very common when patients with Rocky Mountain spotted fever or epidemic typhus are treated with a single dose. Reports of greater morbidity and mortality in patients with Rocky Mountain spotted fever treated with chloramphenicol compared with doxycycline have been published (Dalton et al., 1995). Alternatives in children and pregnant women include macrolides (azithromycin and clarithromycin) and rifampin for the treatment of less severe rickettsioses.

SCRUB TYPHUS CAUSED BY *ORIENTIA TSUTSUGAMUSHI*

O. tsutsugamushi's genome contains 2.1 megabases with 42% of repeated DNA (the most in the bacterial world) (Table 63.2). Genomic degradation has also occurred as in rickettsial genomes due to its intracellular lifestyle. It also contains genes coding for type I and greatly amplified type IV secretion systems, and intensive amplification of mobile elements (Cho et al., 2007; Nakayama et al., 2008). The gram-negative cell wall of *O.* (formerly *Rickettsia*) *tsutsugamushi* differs from that of spotted fever and typhus group rickettsiae; it has an ultrastructurally thicker outer leaflet and thinner inner leaflet of the outer envelope, has different major proteins, lacks lipopolysaccharide and lipid A, and has minimal peptidoglycan-like structure (Atwal et al., 2017; Tamura et al., 1995). *O. tsutsugamushi* attaches to host cell receptors (integrin α5-β1, fibronectin, and syndecan 4) via the major 56 kDa surface protein (TSA56 antigen), ScaC (autotransporter) and the 47kDa surface protein, followed by internalization through clathrin-dependent endosomal pathways and subsequent actin cytoskeleton rearrangements. *Orientia* escape the endosomal vacuole and are transported via microtubules (dynein-dynactin motor protein complex) to the perinuclear region where they multiply in a microcolony rich in polysaccharides (Ge & Rikihisa, 2011; Kim et al., 2001). *Orientia* are then released via a process involving pinching off a host cell membrane-bound rickettsia. This process needs cholesterol-rich lipid rafts and the bacterial surface protein HtrA (Kim et al., 2013). *O. tsutsugamushi* is transovarially and transstadially maintained in mites of the genus *Leptotrombidium* (Traub & Wisseman, 1978). Infected ova hatch into larvae, the only stage that feeds on an animal host. In fact, nymphs and adults only live in the soil and feed on insects' eggs. Rats become infected after rickettsia-containing larvae (chiggers) feed on the rats' tissue fluids, but feeding mite larvae that acquire rickettsiae do not pass the infection to their offspring. Thus humans and rats are only accidental, nonessential, dead-end hosts of scrub typhus rickettsiae. Scrub typhus occurs in countries within a triangular geographic area formed by Japan, Russia, and Korea to the north, Australia and Indonesia to the south, Pakistan to the west, and the Philippines and Micronesia to the east. Other countries within the triangle include Australia, China, India, Sri Lanka, Thailand, Vietnam, Taiwan, Maldives, Bangladesh, Malaysia, Nepal, Burma, Cambodia, and Laos (Bonell et al., 2017), and Chile (Balcells et al., 2011). Cases outside the "*O. tsutsugamushi* Triangle" have been described in the United Arab Emirates, sub-Saharan Africa (Kenya, Cameroon, Congo, Djibouti, Tanzania , and Chile) (Bonell et al., 2017). Infection is acquired in areas of dense vegetation where abundant rat populations harbor large populations of chiggers. It is estimated that 1 million cases occur every year and the population at risk is 1 billion people. The median case fatality rate is estimated at 6% without antibiotics and 1.4% in treated patients, but some reports place the case fatality rate as high as 30% to 70% (Bonell et al., 2017; Taylor et al., 2015; Varghese et al., 2006). Expansion of endemic areas in China, north of the Yangtse River, and in South Korea have already been documented. Currently, there are more than 70 recognized strains of *O. tsutsugamushi*, but studies correlating different strains with disease severity are lacking.

O. tsutsugamushi initially targets dendritic cells (DCs), which are then activated and attract monocytes/macrophages to the site of infection in the eschar via chemokines CCL5 and CCL3. Dissemination occurs via lymph nodes mostly by infected macrophages and some DCs followed by infection of endothelial cells more extensively than macrophages (Moron et al., 2001). The basic pathologic lesion is vascular injury with perivascular lymphohistiocytic inflammation, which is present in the cutaneous chigger-inoculation site of rickettsiae, the brain, lung, heart, gastrointestinal tract, and kidney.

After incubation for 6 to 21 days, illness begins with fever, headache, and (in some patients) myalgia, cough, and gastrointestinal symptoms. An eschar develops in half of Westerners, usually prior to the onset of fever, but less often in indigenous patients. Likewise, a macular or maculopapular rash occurs in half of Westerners with primary infection, 2 to 9 days after the onset of illness. Severely ill patients may develop hypotension, pneumonitis, meningoencephalitis, acute renal failure, and hemorrhagic phenomena. Unless treated with appropriate antimicrobial medications, 6% of cases are fatal. Greater severity is associated with greater bacterial loads (Sonthayanon et al., 2009). Scrub typhus may occur in trekkers and other travelers exposed to chiggers in endemic areas.

Diagnosis of scrub typhus on clinical grounds is difficult, especially if the classic eschar is absent (present in 7–97% of patients). Therefore the clinical laboratory has an important role in establishing a diagnosis of scrub typhus (Saraswati et al., 2018).

Serologic assays, despite their limitations, are still considered the best avenue to diagnose scrub typhus. Limitations are multiple, including difficulty in setting cutoff values (problematic in areas of high endemicity), high variability among available test formats, interobserver variability for tests that require interpretation such as IFA, lack of strong gold standards for comparison purposes among diagnostic tests, and in most cases rendering the diagnosis retrospectively when paired sera are obtained. NAA assays have been developed for the past 20 years or so and include conventional or real-time PCR for several gene targets (47 kDa, 56 kDa, *groEL*, and 16S rRNA) (Murai et al., 1992; Furuya et al., 1993; Kawamori et al., 1993; Sugita et al., 1993; Jiang et al., 2004) and have been demonstrated to be effective in practice, including on eschar specimens (Manosroi et al., 2003; Saisongkorh et al., 2004; Kim et al., 2006; Paris et al., 2008, 2009). The most evaluated NAA assay is the LAMP (Paris et al., 2011) that does not require a thermocycler and is easily performed in the point-of-care (POC) setting. Nucleic acid amplification also requires standardization since different assays target different genes, some of which are variable among strains, including the 56 kDa antigen. However, diagnosis in the acute phase of the disease remains problematic due to low levels of rickettsemia. Other POC tests include immunochromatographic serologic tests

TABLE 63.2
Infections by *Orientia*

Etiologic Agent	Disease	Geographic Distribution	Transmission
Scrub Typhus			
Orientia tsutsugamushi	Scrub typhus	Southeast Asia, Japan, China, Sri Lanka, India, Far-Eastern Russia, Indonesia, Indian Ocean and Western Pacific islands, Northern Australia, Africa, Chile	Chigger bite

(ICT) and dot-blot assays. All three POC tests have commercially available kits with great variability in sensitivity and specificity (Saraswati et al., 2018, 2019).

The sensitivity of IgM ICT ranged from 23.3% to 100% and the specificity from 73% to 100%. For total antibody ICT the sensitivity ranged from 20.9% to 99.1% and the specificity from 67.9% to 100% (Saraswati et al., 2018, 2019). For dot-blot tests the sensitivity and specificity ranged from 59.6% to 100% and 83% to 98.7%, respectively. LAMP's sensitivity and specificity ranged from 66.7% to 100% and 63.2% to 100%, respectively. These results are based on evaluations using different gold standards, varied populations, and both commercial and in-house developed tests (Saraswati et al., 2018, 2019)

IFA methods are considered the serologic gold standard. For the diagnosis of scrub typhus in an endemic region, the cutoff titer should be determined for the particular population, and for one region a titer of 1:400 or greater by IFA is 96% specific and 48% sensitive, and a fourfold rise in titer is the preferred serologic criterion for diagnosis (Blacksell et al., 2007). However, IFA cutoff titers are very difficult to determine due to the endemicity of the disease and the marked strain variability in the geographic areas affected by scrub typhus. Therefore standardization is highly desirable as to which antibodies and which antigens should be used for testing. Ideally, immunogenic antigens that are present broadly in *Orientia* and yet are specific for the genus would be excellent targets for immunoassays. Indirect immunoperoxidase is a similar method that does not require a fluorescent microscope. *Proteus mirabilis* strain OX-K agglutination is more readily available, but insensitive. Serologic assays using a recombinant 56 kDa antigen representing the major immunodominant surface protein, including a dipstick test, a rapid lateral flow assay, and a IgM capture enzyme immunoassay, yield excellent results (Ching et al., 2001; Coleman et al., 2002; Jang et al., 2003; Jiang et al., 2003). However, the 56 kDa antigen is highly variable among strains, and an assay that works in a certain area might not be as sensitive and specific in another area.

Undoubtedly, a combination of nucleic acid amplification and robust serologic assays is needed for the diagnosis of scrub typhus with high confidence (Saraswati et al., 2018, 2019). In 2011, criteria for diagnosis of scrub typhus were proposed: (1) cell culture isolate, (2) single admission IgM titer of 1:12,800 or greater using IFA, (3) fourfold increase in IgM IFA titer, and/or (4) detection of *O. tsutsugamushi* in at least two of three different target PCR assays (Paris et al., 2011). Doxycycline, tetracyclines, and azithromycin are considered first-line drugs for treatment of scrub typhus. Chloramphenicol, telithromycin, and rifampin are good alternatives. However, reports of chloramphenicol-nonresponsive cases in northern Thailand have been published, as well as sporadic reports of doxycycline resistance (Miyamura et al., 1985, 1989; Kelly, Salata et al., 1995; Strickman et al., 1995; Watt et al., 1996, 2000; Kim et al., 2004). In general, *O. tsutsugamushi* is inherently resistant to the fluoroquinolones (Tantibhedhyangkul et al., 2010)

INFECTIONS CAUSED BY ORGANISMS OF THE GENERA *EHRLICHIA* AND *ANAPLASMA*

Structure and Function

The family *Anaplasmataceae* (order Rickettsiales) consists of five genera, *Ehrlichia*, *Anaplasma*, *Neorickettsia*, *Neoehrlichia*, and *Wolbachia* (Dumler et al., 2001). Ehrlichieae and anaplasmae are small (0.5 μm), tickborne, obligately intracellular, gram-negative coccobacilli that reside in a cytoplasmic vacuole of leukocytes as dense-cored cells (infectious form) and reticulate cells (dividing form) (Popov et al., 2007) (Table 63.3). This intravacuolar microcolony of bacteria stained by the Wright-Giemsa method resembles a mulberry and thus is called a *morula* (Latin for *mulberry*). Neorickettsiae, similar small obligately intracellular bacteria, reside in trematode parasites in aquatic snails, insects, bats, and fish and are transmitted by ingestion of a parasitized host (e.g., *Neorickettsia helminthoeca* in trematode-parasitized salmon eaten by dogs in the Pacific Northwest). *Wolbachia* reside in arthropods and filarial worms (e.g., *Onchocerca volvulus*), in which they play a role in the pathogenesis of the human illness via arthropod biologic manipulation (feminization, male killing, parthenogenesis, cytoplasmic incompatibility).

Long known and studied as agents of veterinary diseases, *Ehrlichia* and *Anaplasma* have recently emerged as human pathogens. The reasons are primarily their recent discovery in humans, their rapid characterization with contemporary molecular tools, and increasing populations and geographic distribution of particular ticks that depend on deer as a host. The well-documented human pathogens in the United States are *E. chaffeensis*, *E. ewingii*, *A. phagocytophilum*, and in the upper Midwest *E. muris eauclairensis*-like agent (EMLA) due to its high genetic relatedness to *E. muris*, a murine pathogen (Anderson et al., 1991; Pritt et al., 2011; Allen et al., 2014; Buller et al., 1999). *Neorickettsia sennetsu* is the agent of a disease in Asia resembling infectious mononucleosis.

Ehrlichia and *Anaplasma* spp. have small genomes that range from 0.8 to 1.5 Mb, which target mononuclear phagocytes and neutrophils. Genomic reduction has occurred by gene degradation due to their intracellular lifestyle, similar to *Rickettsia* spp. Both genera lack LPS and peptidoglycan, which seems to provide survival advantage due to absence of some of the innate immune responses triggered by the interaction of LPS and peptidoglycan with pathogen-recognition receptors (PRRs) (Broz & Monack, 2011). Type I and IV secretion systems are well described for both genera, and several of the secreted proteins play important roles in intracellular survival. In *E. chaffeensis*, T1SS effector proteins are tandem-repeat proteins (TRP120, 32, 47, 75), which along with Ank200 are secreted into the intramorular space and translocated to the cytoplasm and nucleus (TRP120) where they modulate numerous cellular signaling pathways and gene transcription that favor intracellular survival (Luo et al., 2011; Wakeel et al., 2009, 2010, 2011; Zhu et al., 2009). T4SS plays a role during the exponential growth phase in monocytes and tick cells (Lina et al., 2016). Effector proteins in *A. phagocytophilum* include AnkA and Ats-1, both secreted through T4SS. AnkA (Ankyrin repeat domain-containing protein A) is translocated into the nucleus and functions as a nucleomodulin (targets include nuclear proteins, internucleosomal regions, ATC-rich sequences, and transcriptional regulatory regions) inhibiting the host cell innate immune response and downregulating reactive oxygen species (ROS) generation (Caturegli et al., 2000; Lin & Rikihisa, 2007; Lockwood et al., 2011; Park, Kim et al., 2004; Garcia-Garcia et al., 2009; Rennoll-Bankert & Dumler, 2012). Ats-1 (Anaplasma translocated substrate 1) contains a mitochondria-targeting presequence and it is translocated into the mitochondrial matrix and inhibits apoptosis (Niu et al., 2010).

Human Monocytotropic Ehrlichiosis

E. chaffeensis is transmitted by ticks, primarily *Amblyomma americanum*, the Lone Star tick, but also *D. variabilis* and *Ixodes pacificus* (Anderson, 1992; Ewing et al., 1995; Kramer et al., 1999). Cases are predominantly rural and seasonal (68% occur from May to July) (Fishbein et al., 1989; Olano et al., 2003, 2003a). Deer are a documented reservoir, and infected dogs and coyotes are also potential reservoir hosts. Ticks become infected when feeding as larvae or nymphs, carry the ehrlichiae as they molt from stage to stage, and transmit the infection during a subsequent blood meal. Ehrlichieae are not transmitted transovarially. Human monocytotropic ehrlichiosis has been reported in 47 states; most cases have occurred within the range of *A. americanum* in the third of the United States south of a line from New Jersey to Kansas. The number of reported cases is particularly high in Oklahoma, Missouri, Arkansas, Tennessee, North Carolina, and Maryland.

TABLE 63.3
Human Ehrlichiosis and Anaplasmosis

Etiologic Agent	Disease	Geographic Distribution	Transmission
E. chaffeensis	Human monocytotropic ehrlichiosis	United States, Africa, Asia	Tick bite
E. ewingii	Ehrlichiosis ewingii	United States, Africa, South America	Tick bite
Anaplasma phagocytophilum	Human granulocytotropic anaplasmosis	United States, Eurasia	Tick bite
Neorickettsia sennetsu	Sennetsu rickettsiosis	Asia	Unknown
Ehrlichia muris euclairensis	Monocytic ehrlichiosis	Upper Midwest, United States	Tick bite
Candidatus Neoehrlichia mykurensis	Granulocytic ehrlichiosis	Europe, Asia	Unknown
Anaplasma capra	Unnamed	Asia	Tick bite

Since the first case of human ehrlichiosis was reported in the United States in 1987, prospective studies documented an incidence of laboratory-confirmed *E. chaffeensis* infection that exceeds that of Rocky Mountain spotted fever and is two orders of magnitude greater than passive reporting suggests (Olano et al., 2003a; Demma et al., 2005). Human ehrlichiosis may represent the most serious tick-transmitted infection in the United States. Fatalities have occurred in approximately 3% of cases, a rate that would be much higher without effective antibiotic treatment in many patients (Fishbein et al., 1989; Olano et al., 2003, 2003a). The severity is reflected in the admission of 41% to 62% of patients to a hospital (Fishbein et al., 1989; Olano et al., 2003, 2003a). Although severe cases often affect older adults, children are also susceptible to the illness (Jacobs & Schutze, 1997; Schutze & Jacobs, 1997). The median duration of illness in a large CDC series, including treated cases, was 23 days. Signs and symptoms depict a systemic disease that has no clinically diagnostic features (percentages represent the average of six large series described in the medical literature: fever (98%), headache (63%), arthralgia (47%), malaise (61%), myalgia (58%), anorexia (47%), nausea (48%), vomiting (35%), rash (6% at onset, 25% during the first week, and 36% overall; 67% in children), regional lymphadenopathy (27%), cough (23%), pharyngitis (24%), diarrhea (21%), abdominal pain or tenderness (18%), hepatomegaly (9%), photophobia (17%), confusion (22%), stupor (7%), and coma (2%) (Fishbein et al., 1989; Jacobs & Schutze, 1997; Olano et al., 2003, 2003b; Schutze & Jacobs, 1997; Eng et al., 1990). Severe complications include adult respiratory distress syndrome, disseminated intravascular coagulation, and renal insufficiency. Several cases of hemophagocytic lymphohistiocytosis (HLH) have been reported to date (Naqah et al., 2017; Cheng et al., 2016; Otrock et al., 2015; Pandey et al., 2013; Hanson et al., 2010; Burns et al., 2010). This complication appears as a result of a "cytokine storm" of proinflammatory cytokines leading to widespread activation of the mononuclear-phagocytic system and subsequent phagocytosis of erythrocytes, leukocytes, and platelets leading to pancytopenia.

Clinical laboratory findings include leukopenia (60%), thrombocytopenia (68%), and elevated hepatic transaminases (86%). CNS involvement manifested by seizures and coma has been documented by cerebrospinal fluid (CSF) pleocytosis, increased protein concentration and *E. chaffeensis* in CSF, and the presence of cerebral lesions at autopsy (Dunn et al., 1992; Eng et al., 1990; Ratnasamy et al., 1996; Walker & Dumler, 1997). Severity is age-dependent, being worse in elderly individuals (Fishbein et al., 1989; Olano et al., 2003, 2003b). In immunocompromised patients, including those with acquired immunodeficiency syndrome (AIDS), human monocytotropic ehrlichiosis can be an overwhelming infection with massive growth of ehrlichiae and a fatal outcome (Paddock et al., 1993; Walker & Dumler, 1997). Mild and persistent infections have also been documented (Dumler, Sutker et al., 1993). After entry via tick bite, *E. chaffeensis* spreads by the lymphatic and/or hematogenous routes. Ehrlichial morulae have been identified in monocytes and macrophages in the bone marrow, peripheral blood (rarely), hepatic sinusoids, spleen, lymph nodes, meninges, kidney, gastrointestinal tract, and epicardium (Dumler, Dawson et al., 1993; Sehdev & Dumler, 2003; Walker & Dumler, 1997). Bone marrow examination frequently reveals granulomas, myeloid hyperplasia, and megakaryocytosis. Other reported lesions include perivascular lymphohistiocytic infiltrates in the kidney, meninges, brain, and heart; interstitial mononuclear pneumonitis; foci of apoptosis-like cell death in the liver, lymph node, and spleen; diffuse reticuloendothelial hyperplasia; erythrophagocytosis; and cholestasis.

Human Infection With *Ehrlichia ewingii*

Recognized first as a canine pathogen in 1971, *E. ewingii* also infects white-tailed deer and is transmitted by *A. americanum* ticks (Ewing et al., 1971; Anziani et al., 1990). It shares antigens with *E. chaffeensis* but infects mainly neutrophils. A high proportion of infected patients are immunocompromised (AIDS, organ transplantation), suggesting that immunocompetent patients may be relatively resistant to the illness (Buller et al., 1999; Paddock et al., 2001). However, a study based on passive surveillance shows that 55 cases were reported through the Nationally Notifiable Diseases Surveillance System (NNDSS) with a hospitalization rate of 77% and immunosuppressive conditions were reported in only 26% of cases (Nichols Heitman et al., 2016).

Human *Ehrlichia canis* Ehrlichiosis

To date, approximately 20 cases of human *E. canis* infection have been described in the literature (Perez et al., 1996, 2006). Signs and symptoms are very similar to the ones described for human monocytic ehrlichiosis (HME), although the disease is milder. "Healthy carriers" have been reported in a study performed in Costa Rica where *E. canis* was detected in 3.6% of blood samples from healthy blood bank donors (total sample: 280) by PCR targeting the *dsb* gene (Bouza-Mora et al., 2017).

Ehrlichia muris eauclairensis

All cases have been described in the upper Midwest, and few cases were receiving immunosuppressive therapy (Pritt et al., 2011). A large retrospective study performed across the nation tested 75,077 samples from all 50 states collected between 2007 and 2013. Sixty-nine of those samples (0.1%) were positive for the EML agent. States included Indiana, Michigan, Minnesota, North Dakota, and Wisconsin. All patients reported likely tick exposure in Minnesota and Wisconsin. All patients recovered and 23% were hospitalized. Immune status was documented in 24 patients and 50% of them were immunocompromised (Johnson et al., 2015). A murine animal model for this bacterium has been published, and the histopathology is very similar to what has been described in cases of HME (Saito et al., 2015). The pathogen is transmitted by *I. scapularis* ticks.

Human Granulocytotropic Anaplasmosis

Thousands of cases of human granulocytic anaplasmosis have been documented, with most of the cases in the upper Midwest (Wisconsin and Minnesota) and northeastern states (New York, Connecticut, Rhode Island, and New Jersey) of the United States but with confirmed autochthonous infections southward along the eastern seaboard and in California, Europe, and Asia (Aguero-Rosenfeld et al., 1996; Bakken et al., 1994; Horowitz et al., 1998; Petrovec et al., 1997). Infection is transmitted by *I. scapularis*, *I. pacificus*, and *I. ricinus* ticks. The white-footed mouse (*Peromyscus leucopus*) and other small mammals are likely reservoir hosts in the United States, and red deer, sheep, goats, and cattle in Europe (Hodzic et al., 1998). The pathology is poorly defined, with the observation of morula-containing neutrophils in peripheral blood and various organs, infiltrates of reticuloendothelial organs with foamy macrophages, multiorgan perivascular lymphohistiocytic infiltrates, and focal hepatocellular apoptosis (Walker & Dumler, 1997). Fatality may be associated with secondary opportunistic fungal and viral infections (Hardalo et al., 1995).

Human granulocytotropic anaplasmosis varies from asymptomatic to severe, with many diagnosed patients requiring hospitalization (Bakken et al., 1994). Infection is fatal in fewer than 1% of cases. The illness begins with chills, fever, headache, and myalgia. Thrombocytopenia occurs in most cases and leukopenia in nearly one-half. Hepatocellular injury is manifested as elevated hepatic enzymes, and severely ill patients may have septic shock–like illness with multiorgan involvement. Children are also affected by the disease although much less frequently (Sigurjonsdottir et al., 2017).

Human Infections Caused by "*Candidatus* Neoehrlichia mikurensis"

The first case was documented in Germany in 2010 (von Loewenich et al., 2010). Fourteen cases have been diagnosed in Europe as of 2016 (Silaghi et al., 2016) and seven cases in China (Li et al., 2012). In the European cohort, most cases occurred in immunosuppressed patients (Raoult, 2014; Andreasson et al., 2015; Grankvist et al., 2015). The cases in China revealed no evidence of immunosuppression. Five asymptomatic cases were documented in Poland (Welc-Faleciak et al., 2014). Cases were diagnosed by PCR using primers for the 16S rRNA gene. No isolates were obtained from any of the cases. Infection is transmitted by *Ixodes ricinus* ticks in Europe. The organisms belong to the family *Anaplasmataceae*, and their target cell appears to be endothelial cells. Neoehrlichial DNA has been detected in asymptomatic persons in the Netherlands and Norway who were bitten by ticks (Jahfari et al., 2016; Quarsten et al., 2017)

Laboratory Diagnosis

Isolation of ehrlichiae and anaplasmae from human blood in antibiotic-free cell culture has been accomplished more often for *A. phagocytophilum* (in HL-60 cells) than *E. chaffeensis* (in DH-82 cells), *E. muris eauclairensis* in ISE6 cells, only once for *E. canis* (in an asymptomatic person), and has yet to be reported for *E. ewingii* (Dawson et al., 1991; Edelman & Dumler, 1996; Childs et al., 1999; Goodman et al., 1996; Perez et al., 1996). Amplification of ehrlichial DNA by PCR using species-specific primers is an efficient diagnostic tool for all the human ehrlichioses (Anderson et al., 1992; Chen, Dumler et al., 1994; Buller et al., 1999; Comer et al., 1999; Everett et al., 1994). For human monocytotropic ehrlichiosis, the sensitivity of PCR is reported as 60% to 85% and for granulocytotropic anaplasmosis caused by *A. phagocytophilum*, 67% to 90% (Ismail & McBride, 2017). Later in the course there is a lower level of ehrlichemia, and tetracycline treatment reduces the sensitivity of detection of ehrlichiae by PCR. Target genes that have been validated clinically include *16S rRNA (rrs)*, *TRP120* (120 kDa tandem repeat protein), *groESL* heat shock operon, *dsb*, *nadA*, and *TRP 32* (*VLPT* gene) for *E. chaffeensis*; *rrs* and *dsb* for *E. ewingii*; and *rrs*, *ank-1*, *msp2*, and *ftsZ* for *A. phagocytophilum* (Doyle et al., 2005;

Dumler & Brouqui, 2004). Although in many cases a laborious task, detection of morulae in peripheral blood neutrophils provides a diagnosis of human anaplasmosis or ehrlichiosis and can be performed in any clinical laboratory. It is a more sensitive approach for *A. phagocytophilum* infection (30–80%) than for *E. chaffeensis* (7–17%) in immunocompetent patients and a very high proportion of immunocompromised patients (Hamilton et al., 2004). It is important to avoid false-positive interpretation caused by toxic granulations, Döhle bodies, superimposed platelets, apoptotic bodies, or contaminant particles. Immunohistochemical identification of both *E. chaffeensis* and *A. phagocytophilum* can be performed in tissue specimens (Dumler, Dawson et al., 1993; Nicholson et al., 1997; Yu et al., 1993).

Serologic diagnosis is the usual approach to the diagnosis of human ehrlichiosis, using cell-culture-propagated *E. chaffeensis* and *A. phagocytophilum* antigens in IFA assays (Walls et al., 1999; Childs et al., 1999; Eng et al., 1990; Olano et al., 2003, 2003b). This method is very sensitive for the demonstration of seroconversion to a titer of 1:64 or greater 2 to 4 weeks after disease onset. The expected serologic result on acute serum is absence of detected antibodies. Thus treatment should be initiated empirically on the basis of clinical and epidemiologic factors and not withheld pending laboratory confirmation. Opinion as to a diagnostic single serum titer for *E. chaffeensis* ranges from 1:64 to 1:256. Cross-reactivity of *A. phagocytophilum* and *E. chaffeensis* is observed in approximately 20% of patients with HME and human granulocytic anaplasmosis (HGA). Thus, particularly in geographic regions where these infections overlap and, indeed, if there is a possibility of travel-associated exposure, it is essential to determine antibody titers against both organisms. A fourfold difference in titer determines the infecting agent. Cases with twofold or less difference are classified as ehrlichiosis of indeterminate etiology.

Distinguishing *E. chaffeensis* from *E. ewingii* serologically is more problematic because the latter has yet to be cultivated. Western immunoblotting is a useful research tool at present for distinguishing infection with *E. chaffeensis* with its distinctive TRP120 protein and 28 kDa protein family from infection with *A. phagocytophilum* with its major 42 to 49 kDa protein patterns (Asanovich et al., 1997; Chen, Cullman et al., 1997; Chen, Yu et al., 1997; Rikihisa et al., 1997; Zhi et al., 1997). Serologic assays using these and other recombinant proteins show promise for future development (Knowles et al., 2003; Yu et al., 1999). The presence of antibodies reactive with *E. chaffeensis* in 10% or more of the healthy children in the geographic region of HME suggests the circulation of a less pathogenic cross-reactive organism in the population.

Treatment

Recommendations for treatment of ehrlichioses and anaplasmosis are based on limited retrospective human studies, in vitro susceptibility testing (if the agent is cultivable), and anecdotal reports. Prospective, randomized double-blind clinical studies have never been conducted. Doxycycline is the drug of choice for the treatment of HME followed by tetracyclines. *E. chaffeensis* is inherently resistant to β-lactams, macrolides, sulfonamides, aminoglycosides, and fluoroquinolones. Rifampin is a good alternative treatment (Bakken et al., 1994; Branger et al., 2004; Fishbein et al., 1989; Brouqui & Raoult, 1992; Klein et al., 1997). The use of chloramphenicol is not recommended as it has been associated with fatal outcomes, treatment failures (up to 13%), and delayed defervescence.

The in vitro susceptibility profile of *A. phagocytophilum* is very similar to that of *E. chaffeensis*. Perhaps the only differences are higher MICs for chloramphenicol and slightly lower MICs for levofloxacin, although their use in clinical practice is not recommended. Therefore the treatment recommendations are virtually the same. Rifampin has been used to treat a limited number of pregnant women and children successfully (Krause et al., 2003).

INFECTIONS CAUSED BY *COXIELLA BURNETII*

Structure and Function

C. burnetii is quite distant phylogenetically from other pathogenic rickettsiae and is the only one classified in the *γ-Proteobacteria* in the family *Coxiellaceae* and order Legionellales (closest relatives being *Legionella* and *Francisella*) (Table 63.4). These gram-negative bacteria vary morphologically from rods to cocci, and by electron microscopic examination there are two distinct forms: large cells (0.5–1.2 μm) and small, dense cells (0.5 μm), which have been proposed to represent a developmental cycle that includes a sporelike form that is resistant to harsh environmental conditions, which explains the persistence of *C. burnetii* in the environment and the ease of transmission between hosts and environment. The *C. burnetii* genome is approximately 2 million base pairs, larger than rickettsiae and ehrlichiae. Much emphasis has been placed on a laboratory phenomenon associated with cultivation of *C. burnetii* by prolonged passage in cell culture or eggs, namely, loss of the organism's ability to synthesize the entire lipopolysaccharide. This change from synthesis of the full to a truncated lipopolysaccharide, analogous to the conversion from smooth to rough phenotype by Enterobacteriaceae, has been designated phase variation from phase I to phase II. Phase I is found in nature and in infected persons and animals; phase II occurs in the laboratory owing to deletions of genes without selective advantage under conditions of passage outside of its hosts (Hoover et al., 2002; Omsland et al., 2013).

TABLE 63.4
Infections by *Coxiella*

Etiologic Agent	Disease	Geographic Distribution	Transmission
Coxiellosis			
C. burnetii	Q fever	Worldwide	Inhalation of aerosols from infected animals, possibly ingestion of animal products

Coxiella burnetii enters its target cell, the macrophage, by phagocytosis after interaction with α5/β3 integrin via RAC1-dependent phagocytosis and is highly adapted (e.g., synthesis of superoxide dismutase and acid phosphatase, and presence of several bacterial basic proteins) to the acidic conditions in the phagolysosome, where the switch from small, dense cells to large cells occurs and replication by binary fission takes place (Seshadri et al., 2003; Voth & Heinzen, 2007). In addition, four sodium-proton exchangers are coded in the bacterial genome (Seshadri et al., 2003).

Q Fever

The name *Q fever* was derived from its unknown etiology when the clinicoepidemiologic syndrome was first described as query fever after an outbreak in Queensland, Australia, among abattoir workers at Cannon Hill in 1937. The agent was isolated in guinea pigs a few weeks later by McFarlane Burnet in Melbourne. The ecology of *C. burnetii* includes silent infections in animals: many species of ticks, ungulates (particularly sheep, cattle, and goats, targeting placenta and mammary glands in females), other mammals (including cats and wild rabbits), fish, birds, reptiles, and marsupials (Marrie et al., 1988; Marrie & Raoult, 2002). Humans usually are infected by inhalation, especially of aerosols that originate in infected birth products of domestic livestock and pets and possibly also by ingestion of unpasteurized contaminated milk (Fishbein & Raoult, 1992; Raoult et al., 2005). Human-to-human transmission is rare but has been described through the respiratory route (infected aerosols). Many human infections occur as an occupational disease among abattoir workers, farmers, and veterinarians (McQuiston et al., 2006). However, urban nonoccupational cases are by no means rare in some populations in which they have been evaluated, such as among immunocompromised patients in France (Brouqui et al., 1993). The disease occurs worldwide, and the only areas where it has not been reported are New Zealand and Antarctica (Hilbink et al., 1993). A large outbreak (>4000 cases reported, possibly more than 40,000 cases) related to large numbers of infected goats occurred in the Netherlands illustrating the importance of this disease in both developed and underdeveloped countries (Delsing et al., 2010). Hyperendemicity occurs in Africa and an epidemic in Cayenne (French Guiana) has also been reported (Eldin et al., 2017). In the United States, the main reservoirs are sheep and goats (McQuiston & Childs, 2002). In 2000, 19 cases were reported to the CDC (Q fever became a notifiable disease in 1999). By 2017, approximately 156 cases of acute Q fever were reported and 196 cases of both acute and chronic Q fever (CDC).

The majority of human infections are asymptomatic (Marrie, 1989). The pathogenicity and virulence depend on route of infection, size of the inoculum, and bacterial strain (Glazunova et al., 2005). Several genes encoding type IV secretion system proteins have been described in *Coxiella* and are related to secretion system genes in Legionella (Segal & Shuman, 1999). Acute illness is often a self-limited, undifferentiated febrile illness, pneumonia, hepatitis, or meningoencephalitis (Drancourt et al., 1991; Eldin et al., 2017; Tissot Dupont et al., 1992). Individual patients with myalgias, anorexia, and headache are unlikely to be investigated diagnostically for Q fever, even though this syndrome is the most likely clinical presentation of this infection and accounts for a substantial proportion of patients with these symptoms in some populations. Manifestations of Q fever pneumonia vary: Cough may be nonproductive or absent, and the pneumonia may be severe and progress rapidly or be detected as multiple

rounded or segmental radiographic infiltrates without pulmonary symptoms. Q fever hepatitis may have a clinical presentation similar to acute viral hepatitis or the pathologic presentation of granulomatous hepatitis. A study of acute Q fever from the Basque region in Spain revealed that 80% of cases presented with pneumonitis; 50% of these patients were hospitalized. The study covered 21 years and 1261 cases. Ten patients were admitted to the intensive care unit (ICU), and only two patients went on to develop chronic Q fever (Montes et al., 2006; Sobradillo et al., 1989). Geographic variability certainly exists. For example in the Basque region, Maritime Canada, Croatia, and the Netherlands pneumonitis is the major manifestation. In Taiwan and France, hepatitis predominates (80% and 40%, respectively) (Marrie, 2010b). The most common clinical presentation in the epidemic in Cayenne was pneumonitis (Eldin et al., 2014). In fact, 24% of cases of community-acquired pneumonia were due to Q fever. It is worth noting that slightly more than half of humans become symptomatic after primary infection (Eldin et al., 2017). In pregnant women Q fever usually presents as an asymptomatic primary infection that leads to severe obstetric complications (including abortion) and fetal malformations (Million et al., 2009; Million & Raoult, 2015). Clearance of *Coxiella* in primary infections relies heavily on the innate and adaptive cell-mediated immunity, especially cytotoxic CD8 + T cells. One of the hallmarks of the immune response is the formation of granulomata driven primarily by secretion of γ-interferon, which stimulates bactericidal activity against *C. burnetii* via an oxygen-independent mechanism such as phagosome maturation, apoptosis, production of TNF-α and depletion of intracellular iron (Capo & Mege, 2012; Dellacasagrande et al., 1999, 2000, 2002). The humoral adaptive immune response is important for host protection against *C. burnetii* after the primary infection. Intracellular persistence is mostly due to blockage of maturation of late phagosomes into phagolysosomes by inhibition of Rab7 and cathepsin D recruitment (Ghigo et al., 2002, 2004).

Chronic Q fever is considered synonymous with *C. burnetii* endocarditis but also occurs less frequently as infection of an aneurysm or vascular prosthesis or osteomyelitis (Brouqui et al., 1993; Merhej et al., 2012). Chronic Q fever endocarditis usually involves previously damaged aortic or mitral valves as an afebrile illness that may manifest with heart failure, hepatosplenomegaly, changing cardiac murmurs, and weight loss. Disease associated with circulating immune complexes includes vasculitis-based purpuric rash (sometimes deep in the subcutis leading to erythema nodosum) and glomerulonephritis. Other associated clinical conditions include Guillain-Barré syndrome, mononeuropathies, optic neuritis, hemolytic anemia, hemophagocytic syndrome, and thrombocytopenia (Marrie, 2010b).

The first genome sequence of *C. burnetii* was published in 2003 (Seshadri et al., 2003). Since then several other strains have been sequenced. The genome contains approximately 1.9 to 2.2 Mbp. Like rickettsiae and ehrlichiae, genome reduction is common and in fact it seems to be related to highly epidemic strains (Merhej & Raoult, 2011). Other mutations related to high virulence were described in the Z3055 strain, which is very similar to the Netherlands strain (NL-Limburg) outbreak in which mutations of the ankyrin repeat domain proteins leading to changes in surface antigens that could not be recognized by the immune system in the population (D'Amato et al., 2014).

Other species of the *Coxiella* genus include *C. cheraxi* and *Candidatus Coxiella massiliensis* but no human illness has been documented in relation to these species (Angelakis et al., 2016; Smith et al., 2015).

The pathology of acute Q fever includes mixed interstitial-alveolar-bronchiolar pneumonia with mononuclear inflammatory cells and granulomatous inflammation of the liver and bone marrow. Q fever granulomas often contain a clear central vacuole and a surrounding ring of fibrin as well as epithelioid macrophages and multinucleated giant cells (Pellegrin et al., 1980; Srigley et al., 1985). These doughnut granulomas are neither pathognomonic lesions nor the only form of granuloma that occurs in the liver and bone marrow of Q fever patients. Neutrophils are sometimes present in granulomata and have been recently demonstrated to play a role in clearance of *Coxiella* in a mouse model (Elliott et al., 2015). The involved cardiac valves in Q fever endocarditis have a small vegetation and show a mixed subacute and chronic inflammation with many foamy macrophages having the cytoplasm filled with *C. burnetii*. Fibrosis, vascularization and dystrophic calcification can also be present (Lepidi et al., 2003). IL-10 seems to play an important role in the development of *Coxiella* persistence and Q fever endocarditis by downregulating TNF-α production (Ghigo et al., 2000). Preexisting valvulopathy also increases the risk of Q fever endocarditis. Patients with chronic Q fever have been shown recently at higher risk of developing diffuse large B-cell lymphomas and follicular lymphomas. IL-10 seems to play a role in the development of these lymphoid neoplasms (Melenotte et al., 2016).

Laboratory Diagnosis

The laboratory diagnosis of Q fever is most often accomplished by demonstration of antibodies to *C. burnetii* (Fournier et al., 1996, 1998). Serologic methods employ both phase I and phase II antigens and often evaluate class-specific antibody production. Enzyme immunoassay and indirect IFA tests are highly specific and are more sensitive than complement fixation. In acute Q fever, antibodies to phase II antigens appear earliest after infection, and antibodies to phase I may be detected 7 to 15 days after onset and decrease within 3 to 6 months (Anderson et al., 2013). In general, acute Q fever is associated with high titers to phase II antigens and lower titers to phase I antigens. By IFA, an antiphase II IgG titer of 1:200 or greater and antiphase II IgM titer of 1:50 or greater have a sensitivity of 58% and specificity of 92% in acute Q fever. A fourfold rise in titers is diagnostic when serum samples are taken 3 to 6 weeks apart. In chronic Q fever, antibodies to phase I are present at a higher titer (e.g., IgG-IFA antiphase I titer of ≥1:800), and antibodies to phase II are generally equal to or lower than the phase I titer. An IgA response to phase I antigens is often observed in patients with chronic Q fever. The higher the phase I IgG titers, the higher the PPV of Q fever endocarditis. Titers of 1:800 have a PPV of 37% whereas titers of 1:6400 have a PPV of 75% (Frankel et al., 2011). A titer of 1:128 or greater against phase I antigen by the complement fixation test is also considered diagnostic of chronic Q fever, although some patients have lower titers. Residual IgG antibodies at low titers can be detected for years or for life in some cases (Murphy & Field, 1970). Because of cross-reactivity of *Bartonella henselae* and *Bartonella quintana* with *C. burnetii*, a serologic diagnosis of *Bartonella* endocarditis should not be made until anti–*C. burnetii* titers have been determined (La Scola & Raoult, 1996b). In Q fever endocarditis, the anti–*C. burnetii* titer is substantially higher than the anti-*Bartonella* titer. An IFA containing both *C. burnetii* and *B. henselae* effectively distinguishes the infecting bacterium (Rolain et al., 2003). Cross-reactions with *Legionella micdadei* have also been demonstrated. Commercially available assay formats include IFA (the most sensitive), complement fixation, and ELISA, which is less prone to subjectivity. In fact, interobserver variability for IFA is very high with only 35% of concordance rates (Healy et al., 2011).

PCR assays have been developed against diverse target genes, and during the first 2 weeks of acute Q fever real-time PCR of serum is more sensitive (24%) than IFA serology (14%) (Fournier & Raoult, 2003). It is likely that PCR of blood or buffy coat would detect a greater proportion of cases with *Coxiella* than serum. PCR gene targets include 16S rRNA, 23S rRNA, superoxide dismutase, plasmid-based sequences, and the IS1111 multicopy insertion sequence. The latter target has multiple copies in the genome and therefore is more sensitive. During the Netherlands outbreak a qPCR assay showed sensitivity, specificity, PPV, and NPV of 92.2%, 98.9%, 99.2%, and 89.8%, respectively (Wielders et al., 2013). Analytic sensitivity can be further improved by lyophilization of sera, which concentrates DNA in the sample (Edouard et al., 2016).

Other methods for the diagnosis of chronic Q fever endocarditis include immunohistologic staining (sensitivity 32%), electron microscopy, culture (sensitivity 64%), and PCR (sensitivity 81%) detection of *C. burnetii* in a cardiac valve (Jaton et al., 2013). *C. burnetii* can be recovered from the blood or infected cardiac valves by in vitro cultivation using a centrifugation-enhanced shell vial HEL cell culture system. This method can identify the presence of coxiellae within 7 days but should be attempted only within cell culture institutions approved for biohazard containment level 3. In 2009, Omsland reported the first isolation in a cell-free medium for growth of *C. burnetii* using an acidified citrate cysteine medium under low oxygen tension (Omsland et al., 2009). Potential new tools include immune-PCR (ELISA combined with PCR) and IFN-γ and IL-2 measurements after stimulation of the patient's white blood cells with *Coxiella* antigens or whole inactivated organisms. IFN-γ/IL-2 ratios greater than 11 have been proposed as a marker for development of chronic Q fever (Schoffelen et al., 2013; Schoffelen, Limonard et al., 2014; Schoffelen, Sprong et al., 2014).

Criteria for the diagnosis of chronic Q fever were reevaluated extensively as a result of data analysis from the Dutch outbreak. Proven chronic Q fever requires positive PCR (blood or tissue) or IFA IgG titer greater than or equal to 1:1024 for *C. burnetii* phase I and definite endocarditis as defined by modified Duke criteria or proven large vessels or prosthetic infection by imaging. Probable chronic Q fever is defined as IFA titer of 1024 or greater IgG phase I antibodies and one or more of the following: valvulopathy not meeting major criteria or Duke criteria, known aneurysm or vascular or valvular prosthesis without signs of infection by imaging, suspected osteomyelitis or hepatitis, pregnancy, signs and symptoms of chronic infection, granulomatous inflammation (by histology), and immunosuppression.

Possible chronic Q fever is defined as IFA IgG titers for phase I greater than 1024 without any of the criteria for proven or probable chronic Q fever (Wegdam-Blans et al., 2012).

Treatment

In general, *C. burnetii* is susceptible to tetracyclines, rifampin, cotrimoxazole, and quinolones. Susceptibility to macrolides is variable, and the bacteria are resistant to β-lactams and aminoglycosides. Doxycycline is effective in shortening the course of acute Q fever when administered during the first 3 days after the onset of illness (Levy et al., 1991). A prospective, randomized double-blind study was performed in the Basque region to compare doxycycline and erythromycin for 10 days in the treatment of acute Q fever pneumonitis (Sobradillo et al., 1992). Patients treated with doxycycline had a faster defervescence and fewer gastrointestinal side effects. An effective macrolide is azithromycin. Prolonged fever has been described with clarithromycin. Ciprofloxacin or a combination of ciprofloxacin and rifampin are alternative medications for patients who cannot be treated with tetracycline. Treatment of chronic *C. burnetii* endocarditis requires prolonged administration (at least 1 year) of doxycycline and hydroxychloroquine or doxycycline and a quinolone (ofloxacin) for 3 years (Maurin & Raoult, 1999), which often does not eradicate the infection (Marrie, 2010a; Marrie & Raoult, 2002). Successful treatment is indicated by a slow fall in antiphase I IgG titer below 1:200, when discontinuation of treatment can be considered. Cardiac valve replacement is often performed for hemodynamic reasons. Q fever during pregnancy should be treated for the duration of pregnancy with cotrimoxazole.

C. burnetii is considered a category B select agent due to its easy dispersal as an aerosol, a very high infectivity rate with extremely low numbers of organisms, and resistance to harsh environmental conditions. Consequences to livestock and the environment in general would also be significant (Oyston & Davies, 2011).

INFECTIONS CAUSED BY ORGANISMS OF THE GENUS *BARTONELLA*

Structure and Function

For many years, *B. bacilliformis* (the agent of Carrion disease) was the only species in the genus *Bartonella*. The agent of trench fever was initially named *Rickettsia quintana* and renamed *Rochalimaea quintana* after its successful isolation in axenic medium in 1965. The *Rochalimaea* genus gained more notoriety in the early 1990s when both *R. quintana* and the newly described *R. henselae* were found in both HIV-infected patients and immunocompetent patients. In fact. *R. henselae* was found to be the agent of cat scratch disease. Genetic analysis based on DNA sequencing of the rRNA gene revealed very close similarity between the genera *Rochalimaea* and *Bartonella*. These two genera were merged into the *Bartonella* genus, and the family *Bartonellaceae* was removed from the order Rickettsiales and now belongs in the α2-Proteobacteria subdivision (Birtles & Raoult, 1996; Brenner et al., 1993). As of 2017 there are 45 species described in the genus, 13 of which have been associated with human disease (Okaro et al., 2017). The human pathogens, *B. quintana* (the etiologic agent of trench fever, a major louseborne disease in World Wars I and II and among homeless persons), *B. henselae* (the etiologic agent of cat scratch disease), *B. elizabethae* and *B. vinsonii* (associated with infective endocarditis), and *B. bacilliformis* (a sandfly-transmitted bacterium that causes febrile acute hemolytic anemia and chronic verruga peruana cutaneous lesions in South America), have been cultivated in blood-enriched media in the presence of 5% CO_2 and represent the main human pathogens. Several other *Bartonella* spp. have been associated with human disease (Table 63.5). These facultative intracellular gram-negative bacilli do not produce acid from carbohydrates and usually reside within erythrocytes in their natural mammalian hosts.

Bartonella exist in a wide range of animal reservoirs (humans, cats and rodents, and less frequently camels and wild carnivores such as lions, foxes, and bears) and circulate in nature from host to host through hematogenous arthropod vectors, including fleas, lice, ticks, biting flies, and sandflies. The main target cells for *Bartonella* spp are the endothelium and red blood cells. In red blood cells, *B. bacilliformis* deformin induces cytoplasmic membrane invaginations, and penetration is mediated by two invasion genes *(ialA/ialB)* and the flagella. All *Bartonella* spp. except for *B. bacilliformis* gain access into endothelial cells through Rho-GTPase activity mediated by two type IV secretion systems (Trw and VirB/VirD4). These protein effectors induce cytoskeletal rearrangements in endothelial cells so that bacterial internalization occurs in the form of bacterial clusters being internalized in a single endosomal vacuole (Angelakis & Raoult, 2014; Dehio, 2008; Pulliainen & Dehio, 2009). The genome of *Bartonella* spp. ranges from 1.45 Mbp *(B. bacilliformis)* to 2.64 Mbp *(B. tribocorum)*. Human-specific species reveal less horizontal gene transfer than rodent counterparts (Berglund et al., 2009)

Cat Scratch Disease, Bacillary Angiomatosis, and Bacillary Peliosis

B. henselae is transmitted to humans by the scratch, bite, or lick of infected kittens, which are bacteremic for many months while appearing healthy (Tappero & Koehler, 1993; Tappero et al., 1993; Bergmans, 1997; Chomel et al., 1995; Heller et al., 1997). The bacteria are transmitted from cat to cat by the cat flea (Chomel et al., 1996; Higgins et al., 1996). The nature of the disease is largely host-determined. In immunocompetent hosts, 80% are younger than 21 years of age and present with a cutaneous papule or pustule at the inoculation site and self-limited regional lymphadenopathy. Fewer than 2% of patients suffer complications such as hematogenously disseminated involvement of the liver, spleen, lung, bone, CNS, retina, conjunctiva, or skin (Liston & Koehler, 1996; Verdon et al., 2002; Wade et al., 2000). The histopathology of cat scratch disease lesions is granulomata surrounding stellate microabscesses. Less common agents of cat scratch disease are *B. clarridgeiae* and *B. grahamii* (Margileth & Baehren, 1998; Oksi et al., 2013). In severely immunocompromised patients,

TABLE 63.5
Infections Caused by *Bartonella*

Etiologic Agent	Disease	Geographic Distribution	Transmission
Bartonellosis			
B. bacilliformis	Oroya fever, verruga peruana	Western South America	Sandfly bite
B. henselae	Cat scratch disease, bacillary angiomatosis and peliosis, endocarditis, osteomyelitis, neuroretinitis, lymphadenitis	Worldwide	Kitten scratch or bite, cat flea
B. clarridgeiae	Cat scratch–like disease	Probably worldwide	Presumed cat scratch or bite
B. quintana	Trench fever, endocarditis, bacillary angiomatosis	Worldwide	Feces of *Pediculus* louse
B. koehlerae	Endocarditis, lymphadenitis	California, United States	Cat scratch
B. rochalimae	Bacteremia, fever, splenomegaly	United States	Unknown
B. vinsonii (subsp. *arupensis, vinsonii, berkhoffii*)	Bacteremia, endocarditis	United States	Dogs, rodents
B. washoensis	Myocarditis, meningitis	United States	Fleas
B. melophagi	Bacteremia	United States	Sheep
B. ancashi	Verruga peruana	Peru	Unknown
B. grahamii	Neuroretinitis	United Kingdom	Rodents, fleas
B. alsatica	Endocarditis, lymphadenopathy	Alsace, France	Rabbits
B. tamiae	Febrile illness	Khon Kaen, Thailand	Rodents, bats, chigger mites, ticks
Candidatus spp. *B. mayotimonensis*	Endocarditis	France	Bats
B. ancashi	Verruga peruana	Peru	Unknown

B. henselae infection is manifested by fever and bacteremia or by cutaneous or visceral angioproliferative lesions. The latter are characterized by lobular vascular proliferations of plump endothelial cells with clusters of small capillaries surrounding ectatic capillaries separated by edematous, mucinous, or fibrotic stroma containing clusters of neutrophils, neutrophil debris, and granular microcolonies of bartonella. In the skin, these lesions are designated *bacillary angiomatosis;* in the liver and spleen, they are designated *hepatic* and *splenic peliosis.* Dissemination to other sites may occur also. The angioproliferative lesions of *B. henselae* and *B. quintana* in immunocompromised patients are indistinguishable, and they are quite similar to the verruga peruana of *B. bacilliformis* (Koehler et al., 1997). *B. henselae*, *B. quintana*, *B. mayotimonensis*, *B. vinsonii* subsp. *berkhoffii* and subsp. *arupensis*, *B. alsatica*, *B. koehlerea*, and *B. elizabethae* have been documented as agents of infective endocarditis (Drancourt et al., 1995; Roux et al., 2000; Avidor et al., 2004; Fenollar et al., 2005; Jeanclaude et al., 2009; Raoult et al., 2006). Of all these, *B. quintana* (~70% of cases) and *B. henselae* (~20%) are the most common pathogens associated with *Bartonella*-endocarditis. The majority of cases have a clinical presentation similar to other cases of bacterial subacute endocarditis and includes fever, malaise, weight loss, cardiac murmurs, splenomegaly, heart failure, etc. The aortic valve is most commonly affected.

Trench Fever and Bacillary Angiomatosis

B. quintana causes prolonged bacteremia in convalescent humans, the apparent reservoir. Infections were recognized to be transmitted from person to louse *(Pediculus humanus corporis)* to another person in front-line trenches during World War I (Bruce, 1921). Among French homeless persons, 14% are bacteremic, of whom 80% are afebrile (Brouqui et al., 1999).

Louse feces laden with *B. quintana* are scratched into the skin, and approximately 8 days later an illness of variable severity begins. Manifestations include fever, generally lasting less than 1 week, headache, myalgias, pretibial pain, and an evanescent macular rash. Relapses often occur at 4- or 5-day (hence the name febris quintana, Latin for "fever five") intervals. Bacteremia persists for weeks, months, or longer, serving as a source for infecting lice, even when the person feels relatively healthy. Cases occur at present in alcoholic and homeless populations in American and European cities. These cases are sometimes known as "urban trench fever" (Foucault et al., 2002; Spach et al., 1995; Brouqui et al., 1999; Jackson & Spach, 1996).

Oroya Fever and Verruga Peruana

South American bartonellosis, manifested as an acute illness called Oroya fever or as chronic cutaneous lesions called verruga peruana, is transmitted by the bite of the *Lutzomyia* sandfly. Asymptomatic long-term human carriers are the reservoirs of *B. bacilliformis*. After an incubation period of approximately 3 weeks, Oroya fever begins insidiously with anorexia, headache, malaise, and low-grade fever, or abruptly with chills, high fever, headache, and mental status changes. Bartonellae invade the red blood cells and cause erythrocytic changes that result in erythrophagocytosis and anemia. Meningoencephalitis develops in up to 20% of cases. Verruga peruana, characterized by red to purple nontender nodules that appear in crops over 1 to 2 months and persist for months to years, follows Oroya fever or occurs without prior symptoms (Arias-Stella et al., 1986). Case fatality rates can be as high as 90% during the acute phase of the disease.

Possible autoimmune phenomena have been described in patients with *Bartonella* infections. The evidence so far is based on serologic data, and therefore strong causality has not been demonstrated. Autoimmune entities include juvenile arthritis and myositis, leukocytoclastic vasculitis, Henoch-Schönlein purpura, hemolytic anemia, and uveitis (Hayem et al., 1996; Al-Matar et al., 2002; Robinson et al., 2005; Van Audenhove et al., 2001; Kerkhoff & Rothova, 2000).

Laboratory Diagnosis

Direct examination of blood smears can be used in patients with suspected Carrion disease during the intraerythrocytic phase (Peters & Wigand, 1955). Giemsa-stained smears reveal red-violet rods or cocci in clusters or as single organisms associated with red blood cells. The bacteremia present in other bartonellosis is not high enough to be diagnosed on direct blood smears.

Serologic assays are the most practical in most laboratories to diagnose human bartonelloses (Okaro et al., 2017). However, the sensitivity of the assays is low in the acute phase of the disease due to low antibody titers. Acute and convalescent serum samples are required to confirm the diagnosis in most cases. However, patients with chronic *Bartonella* endocarditis or who have a prolonged clinical course with other clinical syndromes will reveal very high antibody titers, usually above 1/1600 (Edouard et al., 2015). Cutoff titers are determined in each laboratory. Techniques used include IFA and enzyme immunoassays (EIAs). The antigen used varies from bacterial whole cell antigens to recombinant proteins (VirB5, 17 kDa antigen) expressed in *Escherichia coli* (Anderson et al., 1995). Sensitivity and specificity vary widely and cross-reactions between *Bartonella* spp. is common, especially *B. henselae* and *B. quintana*. The use of recombinant antigens decreases cross-reactivity and therefore improves the specificity of the test. Cross reactions with *Coxiella* and *Chlamydia* have also been reported (Maurin et al., 1997; Rolain et al., 2003). Western immunoblotting is a powerful tool for diagnosis of bartonellae infections but it is available only in specialized laboratories (Edouard et al., 2015).

Molecular tools (conventional PCR and real-time PCR) have become more commonly used for the diagnosis of bartonellae infections (Gutierrez et al., 2017; Okaro et al., 2017). Their sensitivity depends mostly on the number of bacteria present in the sample (blood or solid tissues such as cardiac valves and lymph nodes). Specificity depends on the design of primers used for amplification (genus vs species specific). Real-time PCR assays are more sensitive than conventional PCR assays (Diaz et al., 2012; Gutierrez et al., 2013; Rampersad et al., 2005). Several target genes have been used but the most widely used genes are the citrate synthase (*gltA*), beta subunit of the RNA polymerase (*rpoB*)16S-23S internal transcribed spacer (ITS), 60 kDa heat shock protein (*groEL*), mtRNA (*ssrA*), and the 16S ribosomal RNA gene (Norman et al., 1995; Maggi & Breitschwerdt, 2005; Renesto et al., 2001; Bergmans et al., 1995; Marston et al., 1999; Diaz et al., 2012; Gutierrez et al., 2013; Morick et al., 2009). Positive results should be confirmed by sequencing of the amplicon for species identification.

Tissue sections from cardiac valves, lymph nodes, or other organs such as liver or spleen in cases of bacillary angiomatosis can be analyzed using immunohistochemical techniques with antibartonellae antibodies or silver-based stains such as Warthin-Starry, Dieterle, or Steiner.

In a large series of 106 cases on bartonellae endocarditis in France (Edouard et al., 2015), the overall sensitivity of IFA serology (IgG) was 91% (titers ≥1:100) and 100% for Western immunoblotting. Titers of 1:800 or more have a positive predictive value of 95% (58% sensitivity) whereas lower titers require confirmation by Western immunoblotting or PCR. Conventional PCR performed on valvular tissue has a sensitivity of 60% and no cases were detected by PCR on blood, whereas real-time PCR has a sensitivity of 92% on cardiac valves and 33% and 36% from blood and serum, respectively. The sensitivity of IHC in this series was 29% and 46% for Warthin-Starry. Silver stains are not specific, whereas IHC cannot discriminate among species of bartonellae.

Bartonellae are fastidious organisms that require blood-enriched media and increased CO_2 concentrations (5%) in the humid air they require to grow. Isolation from primary sources takes from 5 days up to 5 to 6 weeks depending on the number of bacteria present in the inoculum (Maurin & Raoult, 1999; Brenner et al., 1997; Tierno et al., 1995). If the sample consists of blood, lysis of red blood cells followed by centrifugation increases the chances of isolating bartonellae. Several agar media supplemented with 5% blood have been used for isolation of bartonellae, including Columbia, Brucella, BHI, and trypticase soy-based agars (Koehler et al., 1992; Regnery et al., 1992; Kosoy et al., 1997).

Treatment

Infections associated with local manifestations such as lymphadenitis in typical cat scratch disease do not require antibiotic treatment since its administration is not associated with increased cure rate or decreased time to achieve cure. This is based on meta-analysis of randomized controlled trials and observational studies (Angelakis & Raoult, 2014; Prutsky et al., 2013). Some people advocate for the use of antibiotics such as gentamicin, azithromycin, rifampin, or ciprofloxacin for 2 to 3 weeks, claiming that the lymphadenopathy subsides more quickly (Bass et al., 1998; Margileth, 1992).

Atypical cat scratch disease (severe systemic manifestations in 5–14% of cases of cat scratch disease with hepatosplenic disease and neuroretinitis) are treated with doxycycline and rifampin for 6 weeks (neuroretinitis), and for hepatosplenic disease rifampin alone, or with gentamicin for 4 to 6 weeks, is recommended (Reed et al., 1998; Rosen, 1999; Rosen et al., 1999; Wong et al., 1995; Arisoy et al., 1999).

Erythrocytic infections due to *B. bacilliformis* are treated with chloramphenicol for 2 weeks. *B. quintana* infections (also erythrocytic), bacteremia due to *B. henselae* and other *Bartonella* spp., and endocarditis are treated with gentamicin for 2 weeks followed by doxycycline for 4 weeks (a total of 6 weeks) (Foucault et al., 2003; Raoult et al., 2003). Angioproliferative lesions (verruga peruana, bacillary angiomatosis, and bacillary peliosis) are treated with erythromycin or doxycycline for 3 months or with doxycycline plus rifamycin for 3 months. Relapses are better treated with erythromycin or doxycycline for 4 to 6 months (Rolain et al., 2004).

SELECTED REFERENCES

Angelakis E, Raoult D: Pathogenicity and treatment of *Bartonella* infections, *Int J Antimicrob Agents* 44:16–25, 2014.

An excellent review of current treatment recommendations for Bartonella infections and their pathogenesis.

Ge Y, Rikihisa Y: Subversion of host cell signaling by *Orientia tsutsugamushi*, *Microbes Infect* 13:638–648, 2011.

Marrie TJ: Q fever pneumonia, *Infect Dis Clin North Am* 24:27–41, 2010.

A comprehensive review of Q fever, including epidemiology, pathogenesis, clinical manifestations, diagnosis, and treatment.

Parola P, Paddock CD, Socolovschi C, et al.: Update on tick-borne rickettsioses around the world: a geographic approach, *Clin Microbiol Rev* 26:657–702, 2013.

An excellent review of rickettsioses so far described worldwide, including newly described and unnamed rickettsial pathogens.

Walker DH, Paddock CD, Dumler JS: Emerging and re-emerging tick-transmitted rickettsial and ehrlichial infections, *Med Clin North Am* 92:1345, 2008.

Zinsser H, editor: *Rats, lice, and history*, New York, 1935, Little Brown.

A very readable historical account of the toll that disease takes, especially in times of conflict.

Access the complete reference list online at Elsevier eBooks for Practicing Clinicians.

REFERENCES

Abdad MY, Abou Abdallah R, Fournier PE, Stenos J, Vasoo S: A Concise review of the epidemiology and diagnostics of rickettsioses: Rickettsia and Orientia spp, *J Clin Microbiol* 56(8), 2018, https://doi.org/10.1128/JCM.01728-17.

Aguero-Rosenfeld ME, Horowitz HW, Wormser GP, McKenna DF, Nowakowski J, Munoz J: Human granulocytic ehrlichiosis: a case series from a medical center in New York State, *Ann Intern Med* 125(11):904–908, 1996, https://doi.org/10.7326/0003-4819-125-11-199612010-00006.

Al-Matar MJ, Petty RE, Cabral DA, Tucker LB, Peyvandi B, Prendiville J, et al.: Rheumatic manifestations of Bartonella infection in 2 children, *J Rheumatol* 29(1):184–186, 2002. Retrieved from https://www.ncbi.nlm.nih.gov/pubmed/11824958.

Allen MB, Pritt BS, Sloan LM, Paddock CD, Musham CK, Ramos JM, et al.: First reported case of Ehrlichia ewingii involving human bone marrow, *J Clin Microbiol* 52(11):4102–4104, 2014, https://doi.org/10.1128/JCM.01670-14.

Anderson A, Bijlmer H, Fournier PE, Graves S, Hartzell J, Kersh GJ: Diagnosis and management of Q fever—United States, 2013: recommendations from CDC and the Q fever working group, *MMWR Recomm Rep (Morb Mortal Wkly Rep)* 62(RR-03):1–30, 2013. Retrieved from https://www.ncbi.nlm.nih.gov/pubmed/23535757.

Anderson B: Etiologic agent of human ehrlichiosis, *Pediatr Infect Dis J* 11(7):597–598, 1992, https://doi.org/10.1097/00006454-199207000-00021.

Anderson B, Lu E, Jones D, Regnery R: Characterization of a 17-kilodalton antigen of Bartonella henselae reactive with sera from patients with cat scratch disease, *J Clin Microbiol* 33(9):2358–2365, 1995. Retrieved from https://www.ncbi.nlm.nih.gov/pubmed/7494028.

Anderson BE, Dawson JE, Jones DC, Wilson KH: Ehrlichia chaffeensis, a new species associated with human ehrlichiosis, *J Clin Microbiol* 29(12):2838–2842, 1991. Retrieved from https://www.ncbi.nlm.nih.gov/pubmed/1757557.

Anderson BE, Sumner JW, Dawson JE, Tzianabos T, Greene CR, Olson JG, et al.: Detection of the etiologic agent of human ehrlichiosis by polymerase chain reaction, *J Clin Microbiol* 30(4):775–780, 1992. Retrieved from https://www.ncbi.nlm.nih.gov/pubmed/1374076.

Andreasson K, Jonsson G, Lindell P, et al.: Recurrent fever caused by Candidatus Neoehrlichia mikurensis in a rheumatoid arthritis patient treated with rituximab, *Rheumatology* 54(2):369–371, 2015, https://doi.org/10.1093/rheumatology/keu441.

Angelakis E, Mediannikov O, Jos SL, Berenger JM, Parola P, Raoult D: Candidatus Coxiella massiliensis infection, *Emerg Infect Dis* 22(2):285–288, 2016, https://doi.org/10.3201/eid2202.150106.

Angelakis E, Raoult D: Pathogenicity and treatment of Bartonella infections, *Int J Antimicrob Agents* 44(1):16–25, 2014, https://doi.org/10.1016/j.ijantimicag.2014.04.006.

Anziani OS, Ewing SA, Barker RW: Experimental transmission of a granulocytic form of the tribe Ehrlichieae by Dermacentor variabilis and Amblyomma americanum to dogs, *Am J Vet Res* 51(6):929–931, 1990. Retrieved from https://www.ncbi.nlm.nih.gov/pubmed/2368951.

Arias-Stella J, Lieberman PH, Erlandson RA, Arias-Stella Jr J: Histology, immunohistochemistry, and ultrastructure of the verruga in Carrion's disease, *Am J Surg Pathol* 10(9):595–610, 1986, https://doi.org/10.1097/00000478-198609000-00002.

Arisoy ES, Correa AG, Wagner ML, Kaplan SL: Hepatosplenic cat-scratch disease in children: selected clinical features and treatment, *Clin Infect Dis* 28(4):778–784, 1999, https://doi.org/10.1086/515197.

Asanovich KM, Bakken JS, Madigan JE, Aguero-Rosenfeld M, Wormser GP, Dumler JS: Antigenic diversity of granulocytic Ehrlichia isolates from humans in Wisconsin and New York and a horse in California, *J Infect Dis* 176(4):1029–1034, 1997, https://doi.org/10.1086/516529.

Atwal S, Giengkam S, Chaemchuen S, Dorling J, Kosaisawe N, VanNieuwenhze M: Evidence for a peptidoglycan-like structure in Orientia tsutsugamushi, *Mol Microbiol* 105(3):440–452, 2017, https://doi.org/10.1111/mmi.13709.

Avidor B, Graidy M, Efrat G, Leibowitz C, Shapira G, Schattner A: Bartonella koehlerae, a new cat-associated agent of culture-negative human endocarditis, *J Clin Microbiol* 42(8):3462–3468, 2004, https://doi.org/10.1128/JCM.42.8.3462-3468.2004.

Azad AF: Epidemiology of murine typhus, *Annu Rev Entomol* 35:553–569, 1990, https://doi.org/10.1146/annurev.en.35.010190.003005.

Badiaga S, Brouqui P: Human louse-transmitted infectious diseases, *Clin Microbiol Infect* 18(4):332–337, 2012, https://doi.org/10.1111/j.1469-0691.2012.03778.x.

Bakken JS, Dumler JS, Chen SM, Eckman MR, Van Etta LL, Walker DH: Human granulocytic ehrlichiosis in the upper Midwest United States. A new species emerging?, *J Am Med Assoc* 272(3):212–218, 1994. Retrieved from https://www.ncbi.nlm.nih.gov/pubmed/8022040.

Balcells ME, Rabagliati R, Garcia P, Poggi H, Oddo D, Concha M: Endemic scrub typhus-like illness, Chile, *Emerg Infect Dis* 17(9):1659–1663, 2011, https://doi.org/10.3201/eid1709.100960.

Bass JW, Freitas BC, Freitas AD, Sisler CL, Chan DS, Vincent JM: Prospective randomized double blind placebo-controlled evaluation of azithromycin for treatment of cat-scratch disease, *Pediatr Infect Dis J* 17(6):447–452, 1998, https://doi.org/10.1097/00006454-199806000-00002.

Berglund EC, Frank AC, Calteau A, Vinnere Pettersson O, Granberg F, Eriksson AS, et al.: Run-off replication of host-adaptability genes is associated with gene transfer agents in the genome of mouse-infecting Bartonella grahamii, *PLoS Genet* 5(7):e1000546, 2009, https://doi.org/10.1371/journal.pgen.1000546.

Bergmans AM: Cat scratch disease: studies on diagnosis and identification of reservoirs and vectors, *Vet Q* 19(sup1):44–45, 1997, https://doi.org/10.1080/01652176.1997.9694804.

Bergmans AM, Groothedde JW, Schellekens JF, van Embden JD, Ossewaarde JM, Schouls LM: Etiology of cat scratch disease: comparison of polymerase chain reaction detection of Bartonella (formerly Rochalimaea) and Afipia felis DNA with serology and skin tests, *J Infect Dis* 171(4):916–923, 1995, https://doi.org/10.1093/infdis/171.4.916.

Birtles RJ, Raoult D: Comparison of partial citrate synthase gene (gltA) sequences for phylogenetic analysis of Bartonella species, *Int J Syst Bacteriol* 46(4):891–897, 1996, https://doi.org/10.1099/00207713-46-4-891.

Blacksell SD, Bryant NJ, Paris DH, Doust JA, Sakoda Y, Day NP: Scrub typhus serologic testing with the indirect immunofluorescence method as a diagnostic gold standard: a lack of consensus leads to a lot of confusion, *Clin Infect Dis* 44(3):391–401, 2007, https://doi.org/10.1086/510585.

Bonell A, Lubell Y, Newton PN, Crump JA, Paris DH: Estimating the burden of scrub typhus: a systematic review, *PLoS Negl Trop Dis* 11(9):e0005838, 2017, https://doi.org/10.1371/journal.pntd.0005838.

Botelho-Nevers E, Socolovschi C, Raoult D, Parola P: Treatment of Rickettsia spp. infections: a review, *Expert Rev Anti Infect Ther* 10(12):1425–1437, 2012, https://doi.org/10.1586/eri.12.139.

Bouza-Mora L, Dolz G, Solorzano-Morales A, Romero-Zuniga JJ, Salazar-Sanchez L, Labruna MB, et al.: Novel genotype of Ehrlichia canis detected in samples of human blood bank donors in Costa Rica, *Ticks Tick Borne Dis* 8(1):36–40, 2017, https://doi.org/10.1016/j.ttbdis.2016.09.012.

Branger S, Rolain JM, Raoult D: Evaluation of antibiotic susceptibilities of Ehrlichia canis, Ehrlichia chaffeensis, and Anaplasma phagocytophilum by real-time PCR, *Antimicrob Agents Chemother* 48(12):4822–4828, 2004, https://doi.org/10.1128/AAC.48.12.4822-4828.2004.

Brenner DJ, O'Connor SP, Winkler HH, Steigerwalt AG: Proposals to unify the genera Bartonella and Rochalimaea, with descriptions of Bartonella quintana comb. nov., Bartonella vinsonii comb. nov., Bartonella henselae comb. nov., and Bartonella elizabethae comb. nov., and to remove the family Bartonellaceae from the order Rickettsiales, *Int J Syst Bacteriol* 43(4):777–786, 1993, https://doi.org/10.1099/00207713-43-4-777.

Brenner SA, Rooney JA, Manzewitsch P, Regnery RL: Isolation of Bartonella (Rochalimaea) henselae: effects of methods of blood collection and handling, *J Clin Microbiol* 35(3):544–547, 1997. Retrieved from https://www.ncbi.nlm.nih.gov/pubmed/9041385.

Brettman LR, Lewin S, Holzman RS, Goldman WD, Marr JS, Kechijian P, et al.: Rickettsialpox: report of an outbreak and a contemporary review, *Medicine (Baltim)* 60(5):363–372, 1981, https://doi.org/10.1097/00005792-198109000-00004.

Brouqui P, Dupont HT, Drancourt M, Berland Y, Etienne J, Leport C, et al.: Chronic Q fever. Ninety-two cases from France, including 27 cases without endocarditis, *Arch Intern Med* 153(5):642–648, 1993, https://doi.org/10.1001/archinte.153.5.642.

Brouqui P, Lascola B, Roux V, Raoult D: Chronic Bartonella quintana bacteremia in homeless patients, *N Engl J Med* 340(3):184–189, 1999, https://doi.org/10.1056/NEJM199901213400303.

Brouqui P, Raoult D: In vitro antibiotic susceptibility of the newly recognized agent of ehrlichiosis in humans, Ehrlichia chaffeensis, *Antimicrob Agents Chemother* 36(12):2799–2803, 1992, https://doi.org/10.1128/aac.36.12.2799.

Broz P, Monack DM: Molecular mechanisms of inflammasome activation during microbial infections, *Immunol Rev* 243(1):174–190, 2011, https://doi.org/10.1111/j.1600-065X.2011.01041.x.

Bruce D: trench fever: Final report of the war Office trench fever investigation Committee, *J Hyg* 20(3):258–288, 1921, https://doi.org/10.1017/s0022172400034008.

Buller RS, Arens M, Hmiel SP, Paddock CD, Sumner JW, Rikhisa Y: Ehrlichia ewingii, a newly recognized agent of human ehrlichiosis, *N Engl J Med* 341(3):148–155, 1999, https://doi.org/10.1056/NEJM199907153410303.

Capo C, Mege JL: Role of innate and adaptive immunity in the control of Q fever, *Adv Exp Med Biol* 984:273–286, 2012, https://doi.org/10.1007/978-94-007-4315-1_14.

Caturegli P, Asanovich KM, Walls JJ, et al.: ankA: an Ehrlichia phagocytophila group gene encoding a cytoplasmic protein antigen with ankyrin repeats, *Infect Immun* 68(9):5277–5283, 2000, https://doi.org/10.1128/iai.68.9.5277-5283.2000.

Centers for Disease Control and Prevention: Murine typhus—Hawaii, 2002, *MMWR Morb Mortal Wkly Rep* 52(50):1224–1226, 2003. Retrieved from https://www.ncbi.nlm.nih.gov/pubmed/14681594.

Chen SM, Cullman LC, Walker DH: Western immunoblotting analysis of the antibody responses of patients with human monocytotropic ehrlichiosis to different strains of Ehrlichia chaffeensis and Ehrlichia canis, *Clin Diagn Lab Immunol* 4(6):731–735, 1997. Retrieved from https://www.ncbi.nlm.nih.gov/pubmed/9384299.

Chen SM, Dumler JS, Bakken JS, Walker DH: Identification of a granulocytotropic Ehrlichia species as the etiologic agent of human disease, *J Clin Microbiol* 32(3):589–595, 1994. Retrieved from https://www.ncbi.nlm.nih.gov/pubmed/8195363.

Chen SM, Yu XJ, Popov VL, Westerman EL, Hamilton FG, Walker DH: Genetic and antigenic diversity of Ehrlichia chaffeensis: comparative analysis of a novel human strain from Oklahoma and previously isolated strains, *J Infect Dis* 175(4):856–863, 1997, https://doi.org/10.1086/513982.

Childs JE, Sumner JW, Nicholson WL, Massung RF, Standaert SM, Paddock CD: Outcome of diagnostic tests using samples from patients with culture-proven human monocytic ehrlichiosis: implications for surveillance, *J Clin Microbiol* 37(9):2997–3000, 1999. Retrieved from https://www.ncbi.nlm.nih.gov/pubmed/10449489.

Ching WM, Rowland D, Zhang Z, Bourgeois AL, Kelly D, Dasch GA, et al.: Early diagnosis of scrub typhus with a rapid flow assay using recombinant major outer membrane protein antigen (r56) of Orientia tsutsugamushi, *Clin Diagn Lab Immunol* 8(2):409–414, 2001, https://doi.org/10.1128/CDLI.8.2.409-414.2001.

Cho NH, Kim HR, Lee JH, Kim SY, Kim J, Cha S, et al.: The Orientia tsutsugamushi genome reveals massive proliferation of conjugative type IV secretion system and host-cell interaction genes, *Proc Natl Acad Sci U S A* 104(19):7981–7986, 2007, https://doi.org/10.1073/pnas.0611553104.

Chomel BB, Abbott RC, Kasten RW, Floyd-Hawkins KA, Kass PH, Glaser CA, et al.: Bartonella henselae prevalence in domestic cats in California: risk factors and association between bacteremia and antibody titers, *J Clin Microbiol* 33(9):2445–2450, 1995. Retrieved from https://www.ncbi.nlm.nih.gov/pubmed/7494043.

Chomel BB, Kasten RW, Floyd-Hawkins K, Chi B, Yamamoto K, Roberts-Wilson J, et al.: Experimental transmission of Bartonella henselae by the cat flea, *J Clin Microbiol* 34(8):1952–1956, 1996. Retrieved from https://www.ncbi.nlm.nih.gov/pubmed/8818889.

Clements ML, Dumler JS, Fiset P, Wisseman Jr CL, Snyder MJ, Levine MM: Serodiagnosis of Rocky Mountain spotted fever: comparison of IgM and IgG enzyme-linked immunosorbent assays and indirect fluorescent antibody test, *J Infect Dis* 148(5):876–880, 1983, https://doi.org/10.1093/infdis/148.5.876.

Coleman RE, Sangkasuwan V, Suwanabun N, Eamsila C, Mungviriya S, Devine P, Lerdthusnee K: Comparative evaluation of selected diagnostic assays for the detec-

tion of IgG and IgM antibody to Orientia tsutsugamushi in Thailand, *Am J Trop Med Hyg* 67(5):497–503, 2002, https://doi.org/10.4269/ajtmh.2002.67.497.

Colonne PM, Sahni A, Sahni SK: Suppressor of cytokine signalling protein SOCS1 and UBP43 regulate the expression of type I interferon-stimulated genes in human microvascular endothelial cells infected with Rickettsia conorii, *J Med Microbiol* 62(Pt 7):968–979, 2013, https://doi.org/10.1099/jmm.0.054502-0.

Comer JA, Nicholson WL, Sumner JW, Olson JG, Childs JE: Diagnosis of human ehrlichiosis by PCR assay of acute-phase serum, *J Clin Microbiol* 37(1):31–34, 1999. Retrieved from https://www.ncbi.nlm.nih.gov/pubmed/9854059.

D'Amato F, Rouli L, Edouard S, Tyczka J, Million M, Robert C, et al.: The genome of Coxiella burnetii Z3055, a clone linked to The Netherlands Q fever outbreaks, provides evidence for the role of drift in the emergence of epidemic clones, *Comp Immunol Microbiol Infect Dis* 37(5–6):281–288, 2014, https://doi.org/10.1016/j.cimid.2014.08.003.

Dalton MJ, Clarke MJ, Holman RC, Krebs JW, Fishbein DB, Olson JG, et al.: National surveillance for Rocky Mountain spotted fever, 1981-1992: epidemiologic summary and evaluation of risk factors for fatal outcome, *Am J Trop Med Hyg* 52(5):405–413, 1995, https://doi.org/10.4269/ajtmh.1995.52.405.

Dawson JE, Anderson BE, Fishbein DB, Sanchez JL, Goldsmith CS, Wilson KH, et al.: Isolation and characterization of an Ehrlichia sp. from a patient diagnosed with human ehrlichiosis, *J Clin Microbiol* 29(12):2741–2745, 1991. Retrieved from https://www.ncbi.nlm.nih.gov/pubmed/1757543.

Dehio C: Infection-associated type IV secretion systems of Bartonella and their diverse roles in host cell interaction, *Cell Microbiol* 10(8):1591–1598, 2008, https://doi.org/10.1111/j.1462-5822.2008.01171.x.

Dellacasagrande J, Capo C, Raoult D, Mege JL: IFN-gamma-mediated control of Coxiella burnetii survival in monocytes: the role of cell apoptosis and TNF, *J Immunol* 162(4):2259–2265, 1999. Retrieved from https://www.ncbi.nlm.nih.gov/pubmed/9973502.

Dellacasagrande J, Ghigo E, Capo C, Raoult D, Mege JL: Coxiella burnetii survives in monocytes from patients with Q fever endocarditis: involvement of tumor necrosis factor, *Infect Immun* 68(1):160–164, 2000. Retrieved from https://www.ncbi.nlm.nih.gov/pubmed/10603382.

Dellacasagrande J, Ghigo E, Raoult D, Capo C, Mege JL: IFN-gamma-induced apoptosis and microbicidal activity in monocytes harboring the intracellular bacterium Coxiella burnetii require membrane TNF and homotypic cell adherence, *J Immunol* 169(11):6309–6315, 2002, https://doi.org/10.4049/jimmunol.169.11.6309.

Delsing CE, Kullberg BJ, Bleeker-Rovers CP: Q fever in The Netherlands from 2007 to 2010, *Neth J Med* 68(12):382–387, 2010. Retrieved from https://www.ncbi.nlm.nih.gov/pubmed/21209463.

Demma LJ, Holman RC, McQuiston JH, Krebs JW, Swerdlow DL: Epidemiology of human ehrlichiosis and anaplasmosis in the United States, 2001-2002, *Am J Trop Med Hyg* 73(2):400–409, 2005. Retrieved from https://www.ncbi.nlm.nih.gov/pubmed/16103612.

Diaz MH, Bai Y, Malania L, Winchell JM, Kosoy MY: Development of a novel genus-specific real-time PCR assay for detection and differentiation of Bartonella species and genotypes, *J Clin Microbiol* 50(5):1645–1649, 2012, https://doi.org/10.1128/JCM.06621-11.

Diop A, Raoult D, Fournier PE: Rickettsial genomics and the paradigm of genome reduction associated with increased virulence, *Microbes Infect* 20(7–8):401–409, 2018, https://doi.org/10.1016/j.micinf.2017.11.009.

Dittrich S, Castonguay-Vanier J, Moore CE, et al.: Loop-mediated isothermal amplification for Rickettsia typhi (the causal agent of murine typhus): problems with diagnosis at the limit of detection. *J Clin Microbiol* 52(3):832–838, 2014.

Doyle CK, Labruna MB, Breitschwerdt EB, Tang YW, Corstvet RE, Hegarty BC, et al.: Detection of medically important Ehrlichia by quantitative multicolor TaqMan real-time polymerase chain reaction of the dsb gene, *J Mol Diagn* 7(4):504–510, 2005, https://doi.org/10.1016/S1525-1578(10)60581-8.

Drancourt M, George F, Brouqui P, Sampol J, Raoult D: Diagnosis of Mediterranean spotted fever by indirect immunofluorescence of Rickettsia conorii in circulating endothelial cells isolated with monoclonal antibody-coated immunomagnetic beads, *J Infect Dis* 166(3):660–663, 1992, https://doi.org/10.1093/infdis/166.3.660.

Drancourt M, Mainardi JL, Brouqui P, Vandenesch F, Carta A, Lehnert F, et al.: Bartonella (Rochalimaea) quintana endocarditis in three homeless men, *N Engl J Med* 332(7):419–423, 1995, https://doi.org/10.1056/NEJM199502163320702.

Drancourt M, Raoult D, Xeridat B, Milandre L, Nesri M, Dano P: Q fever meningoencephalitis in five patients, *Eur J Epidemiol* 7(2):134–138, 1991, https://doi.org/10.1007/bf00237356.

Dumler JS, Barbet AF, Bekker CP, Dasch GA, Palmer GH, Ray SC, et al.: Reorganization of genera in the families Rickettsiaceae and Anaplasmataceae in the order Rickettsiales: unification of some species of Ehrlichia with Anaplasma, Cowdria with Ehrlichia and Ehrlichia with Neorickettsia, descriptions of six new species combinations and designation of Ehrlichia equi and 'HGE agent' as subjective synonyms of Ehrlichia phagocytophila, *Int J Syst Evol Microbiol* 51(Pt 6):2145–2165, 2001, https://doi.org/10.1099/00207713-51-6-2145.

Dumler JS, Brouqui P: Molecular diagnosis of human granulocytic anaplasmosis, *Expert Rev Mol Diagn* 4(4):559–569, 2004, https://doi.org/10.1586/14737159.4.4.559.

Dumler JS, Dawson JE, Walker DH: Human ehrlichiosis: hematopathology and immunohistologic detection of Ehrlichia chaffeensis, *Hum Pathol* 24(4):391–396, 1993, https://doi.org/10.1016/0046-8177(93)90087-w.

Dumler JS, Gage WR, Pettis GL, Azad AF, Kuhadja FP: Rapid immunoperoxidase demonstration of Rickettsia rickettsii in fixed cutaneous specimens from patients with Rocky Mountain spotted fever, *Am J Clin Pathol* 93(3):410–414, 1990, https://doi.org/10.1093/ajcp/93.3.410.

Dumler JS, Sutker WL, Walker DH: Persistent infection with Ehrlichia chaffeensis, *Clin Infect Dis* 17(5):903–905, 1993, https://doi.org/10.1093/clinids/17.5.903.

Dumler JS, Taylor JP, Walker DH: Clinical and laboratory features of murine typhus in south Texas, 1980 through 1987, *J Am Med Assoc* 266(10):1365–1370, 1991. Retrieved from https://www.ncbi.nlm.nih.gov/pubmed/1880866.

Dunn BE, Monson TP, Dumler JS, Morris CC, Westbrook AB, Duncan JL, et al.: Identification of Ehrlichia chaffeensis morulae in cerebrospinal fluid mononuclear cells, *J Clin Microbiol* 30(8):2207–2210, 1992. Retrieved from https://www.ncbi.nlm.nih.gov/pubmed/1500537.

Edelman DC, Dumler JS: Evaluation of an improved PCR diagnostic assay for human granulocytic ehrlichiosis, *Mol Diagn* 1(1):41–49, 1996, https://doi.org/10.1054/MODI00100041.

Edouard S, Nabet C, Lepidi H, Fournier PE, Raoult D: Bartonella, a common cause of endocarditis: a report on 106 cases and review, *J Clin Microbiol* 53(3):824–829, 2015, https://doi.org/10.1128/JCM.02827-14.

Eldin C, Mahamat A, Demar M, Abboud P, Djossou F, Raoult D: Q fever in French Guiana, *Am J Trop Med Hyg* 91(4):771–776, 2014, https://doi.org/10.4269/ajtmh.14-0282.

Eldin C, Melenotte C, Mediannikov O, Ghigo E, Million M, Edouard S, et al.: From Q fever to Coxiella burnetii infection: a paradigm change, *Clin Microbiol Rev* 30(1):115–190, 2017, https://doi.org/10.1128/CMR.00045-16.

Elliott A, Schoenlaub L, Freches D, Mitchell W, Zhang G: Neutrophils play an important role in protective immunity against Coxiella burnetii infection, *Infect Immun* 83(8):3104–3113, 2015, https://doi.org/10.1128/IAI.00042-15.

Eng TR, Harkess JR, Fishbein DB, Dawson JE, Greene CN, Redus MA, et al.: Epidemiologic, clinical, and laboratory findings of human ehrlichiosis in the United States, 1988, *J Am Med Assoc* 264(17):2251–2258, 1990. Retrieved from https://www.ncbi.nlm.nih.gov/pubmed/2214103.

Everett ED, Evans KA, Henry RB, McDonald G: Human ehrlichiosis in adults after tick exposure. Diagnosis using polymerase chain reaction, *Ann Intern Med* 120(9):730–735, 1994, https://doi.org/10.7326/0003-4819-120-9-199405010-00002.

Ewing SA, Dawson JE, Kocan AA, Barker RW, Warner CK, Panciera RJ, et al.: Experimental transmission of Ehrlichia chaffeensis (Rickettsiales: Ehrlichieae) among white-tailed deer by Amblyomma americanum (Acari: Ixodidae), *J Med Entomol* 32(3):368–374, 1995, https://doi.org/10.1093/jmedent/32.3.368.

Ewing SA, Roberson WR, Buckner RG, Hayat CS: A new strain of Ehrlichia canis, *J Am Vet Med Assoc* 159(12):1771–1774, 1971. Retrieved from https://www.ncbi.nlm.nih.gov/pubmed/5128792.

Fenollar F, Sire S, Raoult D: Bartonella vinsonii subsp. arupensis as an agent of blood culture-negative endocarditis in a human, *J Clin Microbiol* 43(2):945–947, 2005, https://doi.org/10.1128/JCM.43.2.945-947.2005.

Fishbein DB, Kemp A, Dawson JE, Greene NR, Redus MA, Fields DH: Human ehrlichiosis: prospective active surveillance in febrile hospitalized patients, *J Infect Dis* 160(5):803–809, 1989, https://doi.org/10.1093/infdis/160.5.803.

Fishbein DB, Raoult D: A cluster of Coxiella burnetii infections associated with exposure to vaccinated goats and their unpasteurized dairy products, *Am J Trop Med Hyg* 47(1):35–40, 1992, https://doi.org/10.4269/ajtmh.1992.47.35.

Foucault C, Barrau K, Brouqui P, Raoult D: Bartonella quintana bacteremia among homeless people, *Clin Infect Dis* 35(6):684–689, 2002, https://doi.org/10.1086/342065.

Foucault C, Raoult D, Brouqui P: Randomized open trial of gentamicin and doxycycline for eradication of Bartonella quintana from blood in patients with chronic bacteremia, *Antimicrob Agents Chemother* 47(7):2204–2207, 2003, https://doi.org/10.1128/aac.47.7.2204-2207.2003.

Fournier PE, Casalta JP, Habib G, Messana T, Raoult D: Modification of the diagnostic criteria proposed by the Duke Endocarditis Service to permit improved diagnosis of Q fever endocarditis, *Am J Med* 100(6):629–633, 1996, https://doi.org/10.1016/s0002-9343(96)00040-x.

Fournier PE, Marrie TJ, Raoult D: Diagnosis of Q fever, *J Clin Microbiol* 36(7):1823–1834, 1998. Retrieved from https://www.ncbi.nlm.nih.gov/pubmed/9650920.

Fournier PE, Raoult D: Comparison of PCR and serology assays for early diagnosis of acute Q fever, *J Clin Microbiol* 41(11):5094–5098, 2003, https://doi.org/10.1128/jcm.41.11.5094-5098.2003.

Fournier PE, Raoult D: Suicide PCR on skin biopsy specimens for diagnosis of rickettsioses, *J Clin Microbiol* 42(8):3428–3434, 2004, https://doi.org/10.1128/JCM.42.8.3428-3434.2004.

Frankel D, Richet H, Renvoise A, Raoult D: Q fever in France, 1985-2009, *Emerg Infect Dis* 17(3):350–356, 2011, https://doi.org/10.3201/eid1703.100882.

Furuya Y, Katayama T, Yoshida Y, Kaiho I: Specific amplification of Rickettsia japonica DNA from clinical specimens by PCR, *J Clin Microbiol* 33(2):487–489, 1995. Retrieved from https://www.ncbi.nlm.nih.gov/pubmed/7714214.

Furuya Y, Yoshida Y, Katayama T, Yamamoto S, Kawamura Jr A: Serotype-specific amplification of Rickettsia tsutsugamushi DNA by nested polymerase chain reaction, *J Clin Microbiol* 31(6):1637–1640, 1993. Retrieved from https://www.ncbi.nlm.nih.gov/pubmed/8315007.

Gage KL, Burgdorfer W, Hopla CE: Hispid cotton rats (Sigmodon hispidus) as a source for infecting immature Dermacentor variabilis (Acari: Ixodidae) with Rickettsia rickettsii, *J Med Entomol* 27(4):615–619, 1990, https://doi.org/10.1093/jmedent/27.4.615.

Garcia-Garcia JC, Barat NC, Trembley SJ, Dumler JS, et al.: Epigenetic silencing of host cell defense genes enhances intracellular survival of the rickettsial pathogen Anaplasma phagocytophilum, *PLoS Pathog* 5(6):e1000488, 2009, https://doi.org/10.1371/journal.ppat.1000488.

Ge Y, Rikihisa Y: Subversion of host cell signaling by Orientia tsutsugamushi, *Microbes Infect* 13(7):638–648, 2011, https://doi.org/10.1016/j.micinf.2011.03.003.

Ghigo E, Capo C, Amirayan N, Raoult D, Mege J: The 75-kD tumour necrosis factor (TNF) receptor is specifically up-regulated in monocytes during Q fever endocarditis, *Clin Exp Immunol* 121(2):295–301, 2000, https://doi.org/10.1046/j.1365--2249.2000.01311.x.

Ghigo E, Capo C, Tung CH, Raoult D, Gorvel JP, Mege JL: Coxiella burnetii survival in THP-1 monocytes involves the impairment of phagosome maturation: IFN-gamma mediates its restoration and bacterial killing, *J Immunol* 169(8):4488–4495, 2002, https://doi.org/10.4049/jimmunol.169.8.4488.

Ghigo E, Honstettre A, Capo C, Gorvel JP, Raoult D, Mege JL: Link between impaired maturation of phagosomes and defective Coxiella burnetii killing in patients with chronic Q fever, *J Infect Dis* 190(10):1767–1772, 2004, https://doi.org/10.1086/425041.

Gillespie JJ, Joardar V, Williams KP, Driscoll T, Hostetler JB, Nordberg E, et al.: A Rickettsia genome overrun by mobile genetic elements provides insight into the acquisition of genes characteristic of an obligate intracellular lifestyle, *J Bacteriol* 194(2):376–394, 2012, https://doi.org/10.1128/JB.06244-11.

Gillespie JJ, Kaur SJ, Rahman MS, Rennoll-Bankert K, Sears KT, Beier-Sexton M, et al.: Secretome of obligate intracellular Rickettsia, *FEMS Microbiol Rev* 39(1):47–80, 2015, https://doi.org/10.1111/1574-6976.12084.

Glazunova O, Roux V, Freylikman O, Sekeyova Z, Fournous G, Tyczka J, et al.: Coxiella burnetii genotyping, *Emerg Infect Dis* 11(8):1211–1217, 2005, https://doi.org/10.3201/eid1108.041354.

Goodman JL, Nelson C, Vitale B, Madigan JE, Dumler JS, Kurtti TJ, et al.: Direct cultivation of the causative agent of human granulocytic ehrlichiosis, *N Engl J Med* 334(4):209–215, 1996, https://doi.org/10.1056/NEJM199601253340401.

Gouin E, Egile C, Dehoux P, Villiers V, Adams J, Gertler F, et al.: The RickA protein of Rickettsia conorii activates the Arp2/3 complex, *Nature* 427(6973):457–461, 2004, https://doi.org/10.1038/nature02318.

Graf PC, Chretien JP, Ung L, Gaydos JC, Richards AL: Prevalence of seropositivity to spotted fever group rickettsiae and Anaplasma phagocytophilum in a large, demographically diverse US sample, *Clin Infect Dis* 46(1):70–77, 2008, https://doi.org/10.1086/524018.

Grankvist A, Moore ER, Svensson Stadler L, Pekova S, Bogdan C, Geissdorfer W, et al.: Multilocus sequence analysis of clinical "candidatus neoehrlichia mikurensis" strains from Europe, *J Clin Microbiol* 53(10):3126–3132, 2015, https://doi.org/10.1128/JCM.00880-15.

Gutierrez R, Morick D, Gross I, Winkler R, Abdeen Z, Harrus S: Bartonellae in domestic and stray cats from Israel: comparison of bacterial cultures and high-resolution melt real-time PCR as diagnostic methods, *Vector Borne Zoonotic Dis* 13(12):857–864, 2013, https://doi.org/10.1089/vbz.2013.1308.

Gutierrez R, Vayssier-Taussat M, Buffet JP, Harrus S: Guidelines for the isolation, molecular detection, and characterization of bartonella species, *Vector Borne Zoonotic Dis* 17(1):42–50, 2017, https://doi.org/10.1089/vbz.2016.1956.

Haglund CM, Choe JE, Skau CT, Kovar DR, Welch MD, et al.: Rickettsia Sca2 is a bacterial formin-like mediator of actin-based motility, *Nat Cell Biol* 12(11):1057–1063, 2010, https://doi.org/10.1038/ncb2109.

Hamilton KS, Standaert SM, Kinney MC: Characteristic peripheral blood findings in human ehrlichiosis, *Mod Pathol* 17(5):512–517, 2004, https://doi.org/10.1038/modpathol.3800075.

Hardalo CJ, Quagliarello V, Dumler JS: Human granulocytic ehrlichiosis in Connecticut: report of a fatal case, *Clin Infect Dis* 21(4):910–914, 1995, https://doi.org/10.1093/clinids/21.4.910.

Hayem F, Chacar S, Hayem G: Bartonella henselae infection mimicking systemic onset juvenile chronic arthritis in a 2 1/2-year-old girl, *J Rheumatol* 23(7):1263–1265, 1996. Retrieved from https://www.ncbi.nlm.nih.gov/pubmed/8823702.

Healy B, van Woerden H, Raoult D, Graves S, Pitman J, Lloyd G, et al.: Chronic Q fever: different serological results in three countries—results of a follow-up study 6 years after a point source outbreak, *Clin Infect Dis* 52(8):1013–1019, 2011, https://doi.org/10.1093/cid/cir132.

Heinzen RA, Hayes SF, Peacock MG, Hackstadt T: Directional actin polymerization associated with spotted fever group Rickettsia infection of Vero cells, *Infect Immun* 61(5):1926–1935, 1993. Retrieved from https://www.ncbi.nlm.nih.gov/pubmed/8478082.

Heller R, Artois M, Xemar V, De Briel D, Gehin H, Jaulhac B, et al.: Prevalence of Bartonella henselae and Bartonella clarridgeiae in stray cats, *J Clin Microbiol* 35(6):1327–1331, 1997. Retrieved from https://www.ncbi.nlm.nih.gov/pubmed/9163438.

Helmick CG, Bernard KW, D'Angelo LJ: Rocky Mountain spotted fever: clinical, laboratory, and epidemiological features of 262 cases, *J Infect Dis* 150(4):480–488, 1984, https://doi.org/10.1093/infdis/150.4.480.

Herrero-Herrero JI, Walker DH, Ruiz-Beltran R: Immunohistochemical evaluation of the cellular immune response to Rickettsia conorii in taches noires, *J Infect Dis* 155(4):802–805, 1987, https://doi.org/10.1093/infdis/155.4.802.

Higgins JA, Radulovic S, Jaworski DC, Azad AF: Acquisition of the cat scratch disease agent Bartonella henselae by cat fleas (Siphonaptera:Pulicidae), *J Med Entomol* 33(3):490–495, 1996, https://doi.org/10.1093/jmedent/33.3.490.

Hilbink F, Penrose M, Kovacova E, Kazar J: Q fever is absent from New Zealand, *Int J Epidemiol* 22(5):945–949, 1993, https://doi.org/10.1093/ije/22.5.945.

Hillman Jr RD, Baktash YM, Martinez JJ: OmpA-mediated rickettsial adherence to and invasion of human endothelial cells is dependent upon interaction with alpha2beta1 integrin, *Cell Microbiol* 15(5):727–741, 2013, https://doi.org/10.1111/cmi.12068.

Hodzic E, Fish D, Maretzki CM, De Silva AM, Feng S, Barthold SW: Acquisition and transmission of the agent of human granulocytic ehrlichiosis by Ixodes scapularis ticks, *J Clin Microbiol* 36(12):3574–3578, 1998. Retrieved from https://www.ncbi.nlm.nih.gov/pubmed/9817875.

Hoover TA, Culp DW, Vodkin MH, Williams JC, Thompson HA: Chromosomal DNA deletions explain phenotypic characteristics of two antigenic variants, phase II and RSA 514 (crazy), of the Coxiella burnetii nine mile strain, *Infect Immun* 70(12):6726–6733, 2002, https://doi.org/10.1128/iai.70.12.6726-2733.2002.

Horowitz HW, Aguero-Rosenfeld ME, McKenna DF, Holmgren D, Hsieh TC, Varde SA, et al.: Clinical and laboratory spectrum of culture-proven human granulocytic ehrlichiosis: comparison with culture-negative cases, *Clin Infect Dis* 27(5):1314–1317, 1998, https://doi.org/10.1086/515000.

Houhamdi L, Parola P, Raoult D: [Lice and lice-borne diseases in humans], *Med Trop* 65(1):13–23, 2005. Retrieved from https://www.ncbi.nlm.nih.gov/pubmed/15903070.

Ismail N, McBride JW: Tick-Borne emerging infections: ehrlichiosis and anaplasmosis, *Clin Lab Med* 37(2):317–340, 2017, https://doi.org/10.1016/j.cll.2017.01.006.

Jackson LA, Spach DH: Emergence of Bartonella quintana infection among homeless persons, *Emerg Infect Dis* 2(2):141–144, 1996, https://doi.org/10.3201/eid0202.960212.

Jacobs RF, Schutze GE: Ehrlichiosis in children, *J Pediatr* 131(2):184–192, 1997, https://doi.org/10.1016/s0022-3476(97)70152-5.

Jahfari S, Hofhuis A, Fonville M, van der Giessen J, van Pelt W, Sprong H, et al.: Molecular detection of tick-borne pathogens in humans with tick bites and erythema migrans, in The Netherlands, *PLoS Negl Trop Dis* 10(10):e0005042, 2016, https://doi.org/10.1371/journal.pntd.0005042.

Jang WJ, Huh MS, Park KH, Choi MS, Kim IS: Evaluation of an immunoglobulin M capture enzyme-linked immunosorbent assay for diagnosis of Orientia tsutsugamushi infection, *Clin Diagn Lab Immunol* 10(3):394–398, 2003, https://doi.org/10.1128/cdli.10.3.394-398.2003.

Jaton K, Peter O, Raoult D, Tissot JD, Greub G: Development of a high throughput PCR to detect Coxiella burnetii and its application in a diagnostic laboratory over a 7-year period, *New Microbes New Infect* 1(1):6–12, 2013, https://doi.org/10.1002/2052-2975.8.

Jeanclaude D, Godmer P, Leveiller D, Pouedras P, Fournier PE, Raoult D, et al.: Bartonella alsatica endocarditis in a French patient in close contact with rabbits, *Clin Microbiol Infect* 15(Suppl 2):110–111, 2009, https://doi.org/10.1111/j.1469--0691.2008.02187.x.

Jiang J, Chan TC, Temenak JJ, Dasch GA, Ching WM, Richards AL, et al.: Development of a quantitative real-time polymerase chain reaction assay specific for Orientia tsutsugamushi, *Am J Trop Med Hyg* 70(4):351–356, 2004. Retrieved from https://www.ncbi.nlm.nih.gov/pubmed/15100446.

Jiang J, Maina AN, Knobel DL, Cleaveland S, Laudisoit A, Wamburu K, et al.: Molecular detection of Rickettsia felis and Candidatus Rickettsia asemboensis in fleas from human habitats, Asembo, Kenya, *Vector Borne Zoonotic Dis* 13(8):550–558, 2013, https://doi.org/10.1089/vbz.2012.1123.

Jiang J, Marienau KJ, May LA, Beecham 3rd HJ, Wilkinson R, Ching WM, et al.: Laboratory diagnosis of two scrub typhus outbreaks at Camp Fuji, Japan in 2000 and 2001 by enzyme-linked immunosorbent assay, rapid flow assay, and Western blot assay using outer membrane 56-kD recombinant proteins, *Am J Trop Med Hyg* 69(1):60–66, 2003. Retrieved from https://www.ncbi.nlm.nih.gov/pubmed/12932099.

Johnson DK, Schiffman EKJ, Davis JP, et al.: Human infection with Ehrlichia muris-like pathogen, United States, 2007-2013(1). *Emerg Infect Dis* 21(10):1794–1799, 2015.

Kaplan JE, Schonberger LB: The sensitivity of various serologic tests in the diagnosis of Rocky Mountain spotted fever, *Am J Trop Med Hyg* 35(4):840–844, 1986, https://doi.org/10.4269/ajtmh.1986.35.840.

Kaplowitz LG, Lange JV, Fischer JJ, Walker DH: Correlation of rickettsial titers, circulating endotoxin, and clinical features in Rocky Mountain spotted fever, *Arch Intern Med* 143(6):1149–1151, 1983. Retrieved from https://www.ncbi.nlm.nih.gov/pubmed/6407418.

Kass EM, Szaniawski WK, Levy H, Leach J, Srinivasan K, Rives: Cet al: rickettsialpox in a New York city hospital, 1980 to 1989, *N Engl J Med* 331(24):1612–1617, 1994, https://doi.org/10.1056/NEJM199412153312403.

Kato CY, Chung IH, Levy H, Robinson LK, et al.: Assessment of real-time PCR assay for detection of Rickettsia spp. and Rickettsia rickettsii in banked clinical samples. *J Clin Microbiol* 51(1):314–317, 2013.

Kawamori F, Akiyama M, Sugieda M, Kanda T, Akahane S, Yamamoto S, et al.: Two-step polymerase chain reaction for diagnosis of scrub typhus and identification of antigenic variants of Rickettsia tsutsugamushi, *J Vet Med Sci* 55(5):749–755, 1993, https://doi.org/10.1292/jvms.55.749.

Kelly DJ, Chan CT, Paxton H, Thompson K, Howard R, Dasch G: Aet al: comparative evaluation of a commercial enzyme immunoassay for the detection of human antibody to Rickettsia typhi, *Clin Diagn Lab Immunol* 2(3):356–360, 1995. Retrieved from https://www.ncbi.nlm.nih.gov/pubmed/7664182.

Kelly DJ, Salata KF, Strickman D, Hershey JN: Rickettsia tsutsugamushi infection in cell culture: antibiotic susceptibility determined by flow cytometry, *Am J Trop Med Hyg* 53(6):602–606, 1995, https://doi.org/10.4269/ajtmh.1995.53.602.

Kerkhoff FT, Rothova A, et al.: Bartonella henselae associated uveitis and HLA-B27, *Br J Ophthalmol* 84(10):1125–1129, 2000, https://doi.org/10.1136/bjo.84.10.1125.

Keysary A, Strenger C: Use of enzyme-linked immunosorbent assay techniques with cross-reacting human sera in diagnosis of murine typhus and spotted fever, *J Clin Microbiol* 35(4):1034–1035, 1997. Retrieved from https://www.ncbi.nlm.nih.gov/pubmed/9157128.

Kidd L, Maggi R, Diniz PP, Hegarty B, Tucker M, Breitschwerdt E: Evaluation of conventional and real-time PCR assays for detection and differentiation of Spotted Fever Group Rickettsia in dog blood, *Vet Microbiol* 129(3–4):294–303, 2008, https://doi.org/10.1016/j.vetmic.2007.11.035.

Kim DM, Yun NR, Yang TY, Lee JH, Yang JT, Shim SK, et al.: Usefulness of nested PCR for the diagnosis of scrub typhus in clinical practice: a prospective study, *Am J Trop Med Hyg* 75(3):542–545, 2006. Retrieved from https://www.ncbi.nlm.nih.gov/pubmed/16968938.

Kim MJ, Kim MK, Kang JS: Involvement of lipid rafts in the budding-like exit of Orientia tsutsugamushi, *Microb Pathog* 63:37–43, 2013, https://doi.org/10.1016/j.micpath.2013.06.002.

Kim SW, Ihn KS, Han SH, Seong SY, Kim IS, Choi M: Set al: Microtubule- and dynein-mediated movement of Orientia tsutsugamushi to the microtubule organizing center, *Infect Immun* 69(1):494–500, 2001, https://doi.org/10.1128/IAI.69.1.494-500.2001.

Kim YS, Yun HJ, Shim SK, Koo SH, Kim SY, Kim S: A comparative trial of a single dose of azithromycin versus doxycycline for the treatment of mild scrub typhus, *Clin Infect Dis* 39(9):1329–1335, 2004, https://doi.org/10.1086/425008.

Kleba B, Clark TR, Lutter EI, Ellison DW, Hackstadt T: Disruption of the Rickettsia rickettsii Sca2 autotransporter inhibits actin-based motility, *Infect Immun* 78(5):2240–2247, 2010, https://doi.org/10.1128/IAI.00100-10.

Klein MB, Nelson CM, Goodman JL: Antibiotic susceptibility of the newly cultivated agent of human granulocytic ehrlichiosis: promising activity of quinolones and rifamycins, *Antimicrob Agents Chemother* 41(1):76–79, 1997. Retrieved from https://www.ncbi.nlm.nih.gov/pubmed/8980758.

Knowles TT, Alleman AR, Sorenson HL, Marciano DC, Breitschwerdt EB, Harrus S, et al.: Characterization of the major antigenic protein 2 of Ehrlichia canis and Ehrlichia chaffeensis and its application for serodiagnosis of ehrlichiosis, *Clin Diagn Lab Immunol* 10(4):520–524, 2003, https://doi.org/10.1128/cdli.10.4.520-524.2003.

Koehler JE, Quinn FD, Berger TG, LeBoit PE, Tappero JW: Isolation of Rochalimaea species from cutaneous and osseous lesions of bacillary angiomatosis, *N Engl J Med* 327(23):1625–1631, 1992, https://doi.org/10.1056/NEJM199212033272303.

Koehler JE, Sanchez MA, Garrido CS, Whitfeld MJ, Chen FM, Berger TG, et al.: Molecular epidemiology of bartonella infections in patients with bacillary angiomatosis-peliosis, *N Engl J Med* 337(26):1876–1883, 1997, https://doi.org/10.1056/NEJM199712253372603.

Kosoy MY, Regnery RL, Tzianabos T, Marston EL, Jones DC, Green D, et al.: Distribution, diversity, and host specificity of Bartonella in rodents from the Southeastern United States, *Am J Trop Med Hyg* 57(5):578–588, 1997, https://doi.org/10.4269/ajtmh.1997.57.578.

Kramer VL, Randolph MP, Hui LT, Irwin WE, Gutierrez AG, Vugia DJ: Detection of the agents of human ehrlichioses in ixodid ticks from California, *Am J Trop Med Hyg* 60(1):62–65, 1999, https://doi.org/10.4269/ajtmh.1999.60.62.

Krause PJ, Corrow CL, Bakken JS: Successful treatment of human granulocytic ehrlichiosis in children using rifampin, *Pediatrics* 112(3 Pt 1):e252–253, 2003, https://doi.org/10.1542/peds.112.3.e252.

La Scola B, Raoult D: Diagnosis of Mediterranean spotted fever by cultivation of Rickettsia conorii from blood and skin samples using the centrifugation-shell vial technique and by detection of R. conorii in circulating endothelial cells: a 6-year follow-up, *J Clin Microbiol* 34(11):2722–2727, 1996a. Retrieved from https://www.ncbi.nlm.nih.gov/pubmed/8897172.

La Scola B, Raoult D: Serological cross-reactions between Bartonella quintana, Bartonella henselae, and Coxiella burnetii, *J Clin Microbiol* 34(9):2270–2274, 1996b. Retrieved from https://www.ncbi.nlm.nih.gov/pubmed/8862597.

Leitner M, Yitzhaki S, Rzotkiewicz S, Keysary A: Polymerase chain reaction-based diagnosis of Mediterranean spotted fever in serum and tissue samples, *Am J Trop Med Hyg* 67(2):166–169, 2002, https://doi.org/10.4269/ajtmh.2002.67.166.

Lepidi H, Houpikian P, Liang Z, Raoult D: Cardiac valves in patients with Q fever endocarditis: microbiological, molecular, and histologic studies, *J Infect Dis* 187(7):1097–1106, 2003, https://doi.org/10.1086/368219.

Levy PY, Drancourt M, Etienne J, Auvergnat JC, Beytout J, Sainty JM, et al.: Comparison of different antibiotic regimens for therapy of 32 cases of Q fever endocarditis, *Antimicrob Agents Chemother* 35(3):533–537, 1991, https://doi.org/10.1128/aac.35.3.533.

Li H, Jiang JF, Liu W, Zheng YC, Huo QB, Tang K, Cao WC: Human infection with candidatus neoehrlichia mikurensis, China, *Emerg Infect Dis* 18(10):1636–1639, 2012, https://doi.org/10.3201/eid1810.120594.

Li H, Walker DH: rOmpA is a critical protein for the adhesion of Rickettsia rickettsii to host cells, *Microb Pathog* 24(5):289–298, 1998, https://doi.org/10.1006/mpat.1997.0197.

Lin M, Rikihisa Y: Degradation of p22phox and inhibition of superoxide generation by Ehrlichia chaffeensis in human monocytes, *Cell Microbiol* 9(4):861–874, 2007, https://doi.org/10.1111/j.1462-5822.2006.00835.x.

Lina TT, Farris T, Luo T, Mitra S, Zhu B, McBride JW: Hacker within! Ehrlichia chaffeensis effector driven phagocyte Reprogramming Strategy, *Front Cell Infect Microbiol* 6:58, 2016, https://doi.org/10.3389/fcimb.2016.00058.

Liston TE, Koehler JE: Granulomatous hepatitis and necrotizing splenitis due to Bartonella henselae in a patient with cancer: case report and review of hepatosplenic manifestations of bartonella infection, *Clin Infect Dis* 22(6):951–957, 1996, https://doi.org/10.1093/clinids/22.6.951.

Lockwood S, Voth DE, Brayton KA, Beare PA, Brown WC, Heinzen RA, et al.: Identification of Anaplasma marginale type IV secretion system effector proteins, *PloS One* 6(11):e27724, 2011, https://doi.org/10.1371/journal.pone.0027724.

Luo T, Kuriakose JA, Zhu B, Wakeel A, McBride JW: Ehrlichia chaffeensis TRP120 interacts with a diverse array of eukaryotic proteins involved in transcription, signaling, and cytoskeleton organization, *Infect Immun* 79(11):4382–4391, 2011, https://doi.org/10.1128/IAI.05608-11.

Maggi RG, Breitschwerdt EB: Potential limitations of the 16S-23S rRNA intergenic region for molecular detection of Bartonella species, *J Clin Microbiol* 43(3):1171–1176, 2005, https://doi.org/10.1128/JCM.43.3.1171-1176.2005.

Manosroi J, Chutipongvivate S, Auwanit W, Manosroi A: Early diagnosis of scrub typhus in Thailand from clinical specimens by nested polymerase chain reaction, *Southeast Asian J Trop Med Public Health* 34(4):831–838, 2003. Retrieved from https://www.ncbi.nlm.nih.gov/pubmed/15115096.

Margileth AM: Antibiotic therapy for cat-scratch disease: clinical study of therapeutic outcome in 268 patients and a review of the literature, *Pediatr Infect Dis J* 11(6):474–478, 1992. Retrieved from https://www.ncbi.nlm.nih.gov/pubmed/1608685.

Margileth AM, Baehren DF: Chest-wall abscess due to cat-scratch disease (CSD) in an adult with antibodies to Bartonella clarridgeiae: case report and review of the thoracopulmonary manifestations of CSD, *Clin Infect Dis* 27(2):353–357, 1998, https://doi.org/10.1086/514671.

Marrie TJ: Q fever pneumonia, *Semin Respir Infect* 4(1):47–55, 1989. Retrieved from https://www.ncbi.nlm.nih.gov/pubmed/2711056.

Marrie TJ: Q fever endocarditis, *Lancet Infect Dis* 10(8):507–509, 2010a, https://doi.org/10.1016/S1473-3099(10)70142-0.

Marrie TJ: Q fever pneumonia, *Infect Dis Clin North Am* 24(1):27–41, 2010b, https://doi.org/10.1016/j.idc.2009.10.004.

Marrie TJ, Durant H, Williams JC, Mintz E, Waag DM: Exposure to parturient cats: a risk factor for acquisition of Q fever in Maritime Canada, *J Infect Dis* 158(1):101–108, 1988, https://doi.org/10.1093/infdis/158.1.101.

Marrie TJ, Raoult D: Update on Q fever, including Q fever endocarditis, *Curr Clin Top Infect Dis* 22:97–124, 2002. Retrieved from https://www.ncbi.nlm.nih.gov/pubmed/12520650.

Marston EL, Sumner JW, Regnery RL: Evaluation of intraspecies genetic variation within the 60 kDa heat-shock protein gene (groEL) of Bartonella species, *Int J Syst Bacteriol* 49(Pt 3):1015–1023, 1999, https://doi.org/10.1099/00207713-49-3-1015.

Martinez JJ, Cossart P: Early signaling events involved in the entry of Rickettsia conorii into mammalian cells, *J Cell Sci* 117(Pt 21):5097–5106, 2004, https://doi.org/10.1242/jcs.01382.

Martinez JJ, Seveau S, Veiga E, Matsuyama S, Cossart P: Ku70, a component of DNA-dependent protein kinase, is a mammalian receptor for Rickettsia conorii, *Cell* 123(6):1013–1023, 2005, https://doi.org/10.1016/j.cell.2005.08.046.

Maurin M, Eb F, Etienne J, Raoult D: Serological cross-reactions between Bartonella and Chlamydia species: implications for diagnosis, *J Clin Microbiol* 35(9):2283–2287, 1997. Retrieved from https://www.ncbi.nlm.nih.gov/pubmed/9276403.

Maurin M, Raoult D: Q fever, *Clin Microbiol Rev* 12(4):518–553, 1999. Retrieved from https://www.ncbi.nlm.nih.gov/pubmed/10515901.

McDade JE, Shepard CC, Redus MA, Newhouse VF, Smith JD: Evidence of Rickettsia prowazekii infections in the United States, *Am J Trop Med Hyg* 29(2):277–284, 1980, https://doi.org/10.4269/ajtmh.1980.29.277.

McQuiston JH, Childs JE: Q fever in humans and animals in the United States, *Vector Borne Zoonotic Dis* 2(3):179–191, 2002, https://doi.org/10.1089/15303660260613747.

McQuiston JH, Holman RC, McCall CL, Childs JE, Swerdlow DL, Thompson HA: National surveillance and the epidemiology of human Q fever in the United States, 1978-2004, *Am J Trop Med Hyg* 75(1):36–40, 2006, https://doi.org/10.4269/ajtmh.2006.75.1.0750036.

McQuiston JH, Paddock CD, Singleton Jr J, Wheeling JT, Zaki SR, Childs JE: Imported spotted fever rickettsioses in United States travelers returning from Africa: a summary of cases confirmed by laboratory testing at the Centers for Disease Control and Prevention, 1999-2002, *Am J Trop Med Hyg* 70(1):98–101, 2004. Retrieved from https://www.ncbi.nlm.nih.gov/pubmed/14971705.

Melenotte C, Million M, Audoly G, Gorse A, Dutronc H, Roland G, et al.: B-cell non-Hodgkin lymphoma linked to Coxiella burnetii, *Blood* 127(1):113–121, 2016, https://doi.org/10.1182/blood-2015-04-639617.

Mendes do Nascimento EM, Colombo S, Nagasse-Sugahara TK, Angerami RN, Resende MR, da Silva LJ, et al.: Evaluation of PCR-based assay in human serum samples for diagnosis of fatal cases of spotted fever group rickettsiosis, *Clin Microbiol Infect* 15(Suppl 2):232–234, 2009, https://doi.org/10.1111/j.1469-0691.2008.02153.x.

Merhej V, Raoult D: Rickettsial evolution in the light of comparative genomics, *Biol Rev Camb Philos Soc* 86(2):379–405, 2011, https://doi.org/10.1111/j.1469-185X.2010.00151.x.

Merhej V, Tattevin P, Revest M, Le Touvet B, Raoult D: Q fever osteomyelitis: a case report and literature review, *Comp Immunol Microbiol Infect Dis* 35(2):169–172, 2012, https://doi.org/10.1016/j.cimid.2011.12.008.

Million M, Lepidi H, Raoult D: [Q fever: current diagnosis and treatment options], *Med Mal Infect* 39(2):82–94, 2009, https://doi.org/10.1016/j.medmal.2008.07.008.

Million M, Raoult D: Recent advances in the study of Q fever epidemiology, diagnosis and management, *J Infect* 71(Suppl 1):S2–9, 2015, https://doi.org/10.1016/j.jinf.2015.04.024.

Miyamura S, Ohta T, Tamura A: [Comparison of in vitro susceptibilities of Rickettsia prowazekii, R. rickettsii, R. sibirica and R. tsutsugamushi to antimicrobial agents], *Nihon Saikingaku Zasshi* 44(5):717–721, 1989, https://doi.org/10.3412/jsb.44.717.

Miyamura S, Sato N, Tamura A: [In vitro susceptibility of recent clinical isolates of Rickettsia tsutsugamushi to chemotherapeutic agents], *Kansenshogaku Zasshi* 59(5):486–488, 1985, https://doi.org/10.11150/kansenshogakuzasshi1970.59.486.

Montes M, Cilla G, Vicente D, Nieto V, Ercibengoa M, Perez-Trallero E: Gipuzkoa, Basque Country, Spain (1984-2004): a hyperendemic area of Q fever, *Ann N Y Acad Sci* 1078:129–132, 2006, https://doi.org/10.1196/annals.1374.020.

Morick D, Baneth G, Avidor B, Kosoy MY, Mumcuoglu KY, Mintz D, et al.: Detection of Bartonella spp. in wild rodents in Israel using HRM real-time PCR, *Vet Microbiol* 139(3–4):293–297, 2009, https://doi.org/10.1016/j.vetmic.2009.06.019.

Moron CG, Popov VL, Feng HM, Wear D, Walker DH: Identification of the target cells of Orientia tsutsugamushi in human cases of scrub typhus, *Mod Pathol* 14(8):752–759, 2001, https://doi.org/10.1038/modpathol.3880385.

Munoz-Gomez SA, Hess S, Burger G, Lang BF, Susko E, Slamovits CH, et al.: An updated phylogeny of the Alphaproteobacteria reveals that the parasitic Rickettsiales and Holosporales have independent origins, *Elife* 8, 2019https://doi.org/10.7554/eLife.42535.

Murai K, Tachibana N, Okayama A, Shishime E, Tsuda K, Oshikawa T, et al.: Sensitivity of polymerase chain reaction assay for Rickettsia tsutsugamushi in patients' blood samples, *Microbiol Immunol* 36(11):1145–1153, 1992, https://doi.org/10.1111/j.1348-0421.1992.tb02118.x.

Murphy AM, Field PR: The persistence of complement-fixing antibodies to Q-fever (Coxiella burneti) after infection, *Med J Aust* 1(23):1148–1150, 1970. Retrieved from https://www.ncbi.nlm.nih.gov/pubmed/5431751.

Nakayama K, Yamashita A, Kurokawa K, Morimoto T, Ogawa M, Fukuhara M, et al.: The Whole-genome sequencing of the obligate intracellular bacterium Orientia tsutsugamushi revealed massive gene amplification during reductive genome evolution, *DNA Res* 15(4):185–199, 2008, https://doi.org/10.1093/dnares/dsn011.

Ndip LM, Fokam EB, Bouyer DH, Ndip RN, Titanji VP, Walker DH, et al.: Detection of Rickettsia africae in patients and ticks along the coastal region of Cameroon, *Am J Trop Med Hyg* 71(3):363–366, 2004. Retrieved from https://www.ncbi.nlm.nih.gov/pubmed/15381820.

Nichols Heitman K, Dahlgren FS, Drexler NA, Massung RF, Behravesh CB: Increasing incidence of ehrlichiosis in the United States: a summary of national surveillance of Ehrlichia chaffeensis and Ehrlichia ewingii infections in the United States, 2008-2012, *Am J Trop Med Hyg* 94(1):52–60, 2016, https://doi.org/10.4269/ajtmh.15-0540.

Nicholson WL, Comer JA, Sumner JW, Gingrich-Baker C, Coughlin RT, Magnarelli LA, et al.: An indirect immunofluorescence assay using a cell culture-derived antigen for detection of antibodies to the agent of human granulocytic ehrlichiosis, *J Clin Microbiol* 35(6):1510–1516, 1997. Retrieved from https://www.ncbi.nlm.nih.gov/pubmed/9163471.

Niebylski ML, Peacock MG, Schwan TG: Lethal effect of Rickettsia rickettsii on its tick vector (Dermacentor andersoni), *Appl Environ Microbiol* 65(2):773–778, 1999. Retrieved from https://www.ncbi.nlm.nih.gov/pubmed/9925615.

Niu H, Kozjak-Pavlovic V, Rudel T, Rikihisa Y: Anaplasma phagocytophilum Ats-1 is imported into host cell mitochondria and interferes with apoptosis induction, *PLoS Pathog* 6(2):e1000774, 2010, https://doi.org/10.1371/journal.ppat.1000774.

Norman AF, Regnery R, Jameson P, Greene C, Krause DC: Differentiation of Bartonella-like isolates at the species level by PCR-restriction fragment length polymorphism in the citrate synthase gene, *J Clin Microbiol* 33(7):1797–1803, 1995. Retrieved from https://www.ncbi.nlm.nih.gov/pubmed/7545181.

Okaro U, Addisu A, Casanas B, Anderson B: Bartonella species, an emerging cause of blood-culture-negative endocarditis, *Clin Microbiol Rev* 30(3):709–746, 2017, https://doi.org/10.1128/CMR.00013-17.

Oksi J, Rantala S, Kilpinen S, Silvennoinen R, Vornanen M, Veikkolainen V, et al.: Cat scratch disease caused by Bartonella grahamii in an immunocompromised patient, *J Clin Microbiol* 51(8):2781–2784, 2013, https://doi.org/10.1128/JCM.00910-13.

Olano JP, Hogrefe W, Seaton B, Walker DH: Clinical manifestations, epidemiology, and laboratory diagnosis of human monocytotropic ehrlichiosis in a commercial laboratory setting, *Clin Diagn Lab Immunol* 10(5):891–896, 2003, https://doi.org/10.1128/cdli.10.5.891-896.2003.

Olano JP, Masters E, Hogrefe W, Walker DH: Human monocytotropic ehrlichiosis, Missouri, *Emerg Infect Dis* 9(12):1579–1586, 2003a, https://doi.org/10.3201/eid0912.020733.

Olano JP, Masters E, Hogrefe W, Walker DH: Human monocytotropic ehrlichiosis, Missouri. In *Emerg Infect Dis*, vol. 9. 2003b, pp 1579–1586. 2004/01/15.

Omsland A, Cockrell DC, Howe D, Fischer ER, Virtaneva K, Sturdevant DE, et al.: Host cell-free growth of the Q fever bacterium Coxiella burnetii, *Proc Natl Acad Sci U S A* 106(11):4430–4434, 2009, https://doi.org/10.1073/pnas.0812074106.

Omsland A, Hackstadt T, Heinzen RA: Bringing culture to the uncultured: Coxiella burnetii and lessons for obligate intracellular bacterial pathogens, *PLoS Pathog* 9(9):e1003540, 2013, https://doi.org/10.1371/journal.ppat.1003540.

Oyston PC, Davies C: Q fever: the neglected biothreat agent, *J Med Microbiol* 60(Pt 1):9–21, 2011, https://doi.org/10.1099/jmm.0.024778-0.

Paddock CD, Finley RW, Wright CS, Robinson HN, Schrodt BJ, Lane CC, et al.: Rickettsia parkeri rickettsiosis and its clinical distinction from Rocky Mountain spotted fever, *Clin Infect Dis* 47(9):1188–1196, 2008, https://doi.org/10.1086/592254.

Paddock CD, Folk SM, Shore GM, Machado LJ, Huycke MM, Slater LN, et al.: Infections with Ehrlichia chaffeensis and Ehrlichia ewingii in persons coinfected with human immunodeficiency virus, *Clin Infect Dis* 33(9):1586–1594, 2001, https://doi.org/10.1086/323981.

Paddock CD, Greer PW, Ferebee TL, Singleton Jr J, McKechnie DB, Treadwell TA, et al.: Hidden mortality attributable to Rocky Mountain spotted fever: immunohistochemical detection of fatal, serologically unconfirmed disease, *J Infect Dis* 179(6):1469–1476, 1999, https://doi.org/10.1086/314776.

Paddock CD, Suchard DP, Grumbach KL, Hadley WK, Kerschmann RL, Abbey NW, et al.: Brief report: fatal seronegative ehrlichiosis in a patient with HIV infection, *N Engl J Med* 329(16):1164–1167, 1993, https://doi.org/10.1056/NEJM199310143291605.

Paddock CD, Sumner JW, Comer JA, Zaki SR, Goldsmith CS, Goddard J, et al.: Rickettsia parkeri: a newly recognized cause of spotted fever rickettsiosis in the United States, *Clin Infect Dis* 38(6):805–811, 2004, https://doi.org/10.1086/381894.

Paris DH, Aukkanit N, Jenjaroen K, Blacksell SD, Day NP: A highly sensitive quantitative real-time PCR assay based on the groEL gene of contemporary Thai strains of Orientia tsutsugamushi, *Clin Microbiol Infect* 15(5):488–495, 2009, https://doi.org/10.1111/j.1469-0691.2008.02671.x.

Paris DH, Blacksell SD, Nawtaisong P, Jenjaroen K, Teeraratkul A, Chierakul W, et al.: Diagnostic accuracy of a loop-mediated isothermal PCR assay for detection of Orientia tsutsugamushi during acute Scrub Typhus infection, *PLoS Negl Trop Dis* 5(9):e1307, 2011, https://doi.org/10.1371/journal.pntd.0001307.

Paris DH, Blacksell SD, Newton PN, Day NP: Simple, rapid and sensitive detection of Orientia tsutsugamushi by loop-isothermal DNA amplification, *Trans R Soc Trop Med Hyg* 102(12):1239–1246, 2008, https://doi.org/10.1016/j.trstmh.2008.04.040.

Paris DH, Dumler JS: State of the art of diagnosis of rickettsial diseases: the use of blood specimens for diagnosis of scrub typhus, spotted fever group rickettsiosis, and murine typhus, *Curr Opin Infect Dis* 29(5):433–439, 2016, https://doi.org/10.1097/QCO.0000000000000298.

Park H, Lee JH, Gouin E, Cossart P, Izard T: The rickettsia surface cell antigen 4 applies mimicry to bind to and activate vinculin, *J Biol Chem* 286(40):35096–35103, 2011, https://doi.org/10.1074/jbc.M111.263855.

Park J, Kim KJ, Choi KS, Grab DJ, Dumler JS: Anaplasma phagocytophilum AnkA binds to granulocyte DNA and nuclear proteins, *Cell Microbiol* 6(8):743–751, 2011, https://doi.org/10.1111/j.1462-5822.2004.00400.x.

Parola P, Paddock CD, Socolovschi C, Labruna MB, Mediannikov O, Kernif T, et al.: Update on tick-borne rickettsioses around the world: a geographic approach, *Clin Microbiol Rev* 26(4):657–702, 2013, https://doi.org/10.1128/CMR.00032-13.

Parola P, Raoult D: Tick-borne bacterial diseases emerging in Europe, *Clin Microbiol Infect* 7(2):80–83, 2001, https://doi.org/10.1046/j.1469-0691.2001.00200.x.

Patterson KD: Typhus and its control in Russia, 1870-1940, *Med Hist* 37(4):361–381, 1993, https://doi.org/10.1017/s0025727300058725.

Pellegrin M, Delsol G, Auvergnat JC, Familiades J, Faure H, Guiu M, Voigt J: J: granulomatous hepatitis in Q fever, *Hum Pathol* 11(1):51–57, 1980, https://doi.org/10.1016/s0046-8177(80)80105-5.

Perez M, Bodor M, Zhang C, Xiong Q, Rikihisa Y: Human infection with Ehrlichia canis accompanied by clinical signs in Venezuela, *Ann N Y Acad Sci* 1078:110–117, 2006, https://doi.org/10.1196/annals.1374.016.

Perez M, Rikihisa Y, Wen B: Ehrlichia canis-like agent isolated from a man in Venezuela: antigenic and genetic characterization, *J Clin Microbiol* 34(9):2133–2139, 1996. Retrieved from https://www.ncbi.nlm.nih.gov/pubmed/8862572.

Peters D, Wigand R: *Bartonellaceae. Bacteriol Rev* 19(3):150–159, 1955. Retrieved from https://www.ncbi.nlm.nih.gov/pubmed/13260099.

Petrovec M, Lotric Furlan S, Zupanc TA, Strle F, Brouqui P, Roux V, Dumler JS: Human disease in Europe caused by a granulocytic Ehrlichia species, *J Clin Microbiol* 35(6):1556–1559, 1997. Retrieved from https://www.ncbi.nlm.nih.gov/pubmed/9163481.

Popov VL, Korenberg EI, Nefedova VV, Han VC, Wen JW, Kovalevskii YV, et al.: Ultrastructural evidence of the ehrlichial developmental cycle in naturally infected Ixodes persulcatus ticks in the course of coinfection with Rickettsia, Borrelia, and a flavivirus, *Vector Borne Zoonotic Dis* 7(4):699–716, 2007, https://doi.org/10.1089/vbz.2007.0148.

Prakash JA, Reller ME, Barat N, Dumler JS: Assessment of a quantitative multiplex 5' nuclease real-time PCR for spotted fever and typhus group rickettsioses and Orientia tsutsugamushi, *Clin Microbiol Infect* 15(Suppl 2):292–293, 2009, https://doi.org/10.1111/j.1469-0691.2008.02242.x.

Pritt BS, Sloan LM, Johnson DK, Munderloh UG, Paskewitz SM, McElroy KM, et al.: Emergence of a new pathogenic Ehrlichia species, Wisconsin and Minnesota, 2009, *N Engl J Med* 365(5):422–429, 2011, https://doi.org/10.1056/NEJMoa1010493.

Prutsky G, Domecq JP, Mori L, Bebko S, Matzumura M, Sabouni A, et al.: Treatment outcomes of human bartonellosis: a systematic review and meta-analysis, *Int J Infect Dis* 17(10):e811–819, 2013, https://doi.org/10.1016/j.ijid.2013.02.016.

Pulliainen AT, Dehio C: Bartonella henselae: subversion of vascular endothelial cell functions by translocated bacterial effector proteins, *Int J Biochem Cell Biol* 41(3):507–510, 2009, https://doi.org/10.1016/j.biocel.2008.10.018.

Quarsten H, Grankvist A, Hoyvoll L, Myre IB, Skarpaas T, Kjelland V, et al.: Candidatus Neoehrlichia mikurensis and Borrelia burgdorferi sensu lato detected in the blood of Norwegian patients with erythema migrans, *Ticks Tick Borne Dis* 8(5):715–720, 2017, https://doi.org/10.1016/j.ttbdis.2017.05.004.

Rampersad JN, Watkins JD, Samlal MS, Deonanan R, Ramsubeik S, Ammons DR: A nested-PCR with an Internal Amplification Control for the detection and differentiation of Bartonella henselae and B. clarridgeiae: an examination of cats in Trinidad, *BMC Infect Dis* 5:63, 2005, https://doi.org/10.1186/1471-2334-5-63.

Raoult D: Uncultured candidatus neoehrlichia mikurensis, *Clin Infect Dis* 59(7):1042, 2014, https://doi.org/10.1093/cid/ciu491.

Raoult D, Bres P, Drancourt M, Vestris G: In vitro susceptibilities of Coxiella burnetii, Rickettsia rickettsii, and Rickettsia conorii to the fluoroquinolone sparfloxacin, *Antimicrob Agents Chemother* 35(1):88–91, 1991, https://doi.org/10.1128/aac.35.1.88.

Raoult D, Fournier PE, Vandenesch F, Mainardi JL, Eykyn SJ, Nash J, et al.: Outcome and treatment of Bartonella endocarditis, *Arch Intern Med* 163(2):226–230, 2003, https://doi.org/10.1001/archinte.163.2.226.

Raoult D, La Scola B, Enea M, Fournier PE, Roux V, Fenollar F, et al.: A flea-associated Rickettsia pathogenic for humans, *Emerg Infect Dis* 7(1):73–81, 2001, https://doi.org/10.3201/eid0701.010112.

Raoult D, Marrie T, Mege J: Natural history and pathophysiology of Q fever, *Lancet Infect Dis* 5(4):219–226, 2005, https://doi.org/10.1016/S1473-3099(05)70052-9.

Raoult D, Roblot F, Rolain JM, Besnier JM, Loulergue J, Bastides F, Choutet P: First isolation of Bartonella alsatica from a valve of a patient with endocarditis, *J Clin Microbiol* 44(1):278–279, 2006, https://doi.org/10.1128/JCM.44.1.278-279.2006.

Ratnasamy N, Everett ED, Roland WE, McDonald G, Caldwell CW: Central nervous system manifestations of human ehrlichiosis, *Clin Infect Dis* 23(2):314–319, 1996, https://doi.org/10.1093/clinids/23.2.314.

Reed JB, Scales DK, Wong MT, Lattuada Jr CP, Dolan MJ, Schwab IR: Bartonella henselae neuroretinitis in cat scratch disease. Diagnosis, management, and sequelae, *Ophthalmology* 105(3):459–466, 1998, https://doi.org/10.1016/S0161-6420(98)93028-7.

Regnery RL, Anderson BE, Clarridge 3rd JE, Rodriguez-Barradas MC, Jones DC, Carr JH: Characterization of a novel Rochalimaea species, R. henselae sp. nov., isolated from blood of a febrile, human immunodeficiency virus-positive patient, *J Clin Microbiol* 30(2):265–274, 1992. Retrieved from https://www.ncbi.nlm.nih.gov/pubmed/1371515.

Renesto P, Gouvernet J, Drancourt M, Roux V, Raoult D: Use of rpoB gene analysis for detection and identification of Bartonella species, *J Clin Microbiol* 39(2):430–437, 2001, https://doi.org/10.1128/JCM.39.2.430-437.2001.

Rennoll-Bankert KE, Dumler JS: Lessons from Anaplasma phagocytophilum: chromatin remodeling by bacterial effectors, *Infect Disord - Drug Targets* 12(5):380–387, 2012, https://doi.org/10.2174/187152612804142242.

Reynolds MG, Krebs JS, Comer JA, Sumner JW, Rushton TC, Lopez CE, et al.: Flying squirrel-associated typhus, United States, *Emerg Infect Dis* 9(10):1341–1343, 2003, https://doi.org/10.3201/eid0910.030278.

Rikihisa Y, Zhi N, Wormser GP, Wen B, Horowitz HW, Hechemy KE: Ultrastructural and antigenic characterization of a granulocytic ehrlichiosis agent directly isolated and stably cultivated from a patient in New York state, *J Infect Dis* 175(1):210–213, 1997, https://doi.org/10.1093/infdis/175.1.210.

Robinson JL, Spady DW, Prasad E, McColl D, Artsob H: Bartonella seropositivity in children with Henoch-Schonlein purpura, *BMC Infect Dis* 5:21, 2005, https://doi.org/10.1186/1471-2334-5-21.

Rolain JM, Brouqui P, Koehler JE, Maguina C, Dolan MJ, Raoult D: Recommendations for treatment of human infections caused by Bartonella species, *Antimicrob Agents Chemother* 48(6):1921–1933, 2004, https://doi.org/10.1128/AAC.48.6.1921-1933.2004.

Rolain JM, Lecam C, Raoult D: Simplified serological diagnosis of endocarditis due to Coxiella burnetii and Bartonella, *Clin Diagn Lab Immunol* 10(6):1147–1148, 2003, https://doi.org/10.1128/cdli.10.6.1147-1148.2003.

Rolain JM, Maurin M, Vestris G, Raoult D: In vitro susceptibilities of 27 rickettsiae to 13 antimicrobials, *Antimicrob Agents Chemother* 42(7):1537–1541, 1998. Retrieved from https://www.ncbi.nlm.nih.gov/pubmed/9660979.

Rosen B: Management of B. henselae neuroretinitis in cat-scratch disease, *Ophthalmology* 106(1):1–2, 1999, https://doi.org/10.1016/S0161-6420(99)90031-3.

Rosen BS, Barry CJ, Nicoll AM, Constable IJ: Conservative management of documented neuroretinitis in cat scratch disease associated with Bartonella henselae infection, *Aust N Z J Ophthalmol* 27(2):153–156, 1999, https://doi.org/10.1046/j.1440--1606.1999.00174.x.

Roux V, Eykyn SJ, Wyllie S, Raoult D: Bartonella vinsonii subsp. berkhoffii as an agent of afebrile blood culture-negative endocarditis in a human, *J Clin Microbiol* 38(4):1698–1700, 2000. Retrieved from https://www.ncbi.nlm.nih.gov/pubmed/10747175.

Roux V, Raoult D: Phylogenetic analysis of the genus Rickettsia by 16S rDNA sequencing, *Res Microbiol* 146(5):385–396, 1995, https://doi.org/10.1016/0923-2508(96)80284-1.

Roux V, Raoult D: Body lice as tools for diagnosis and surveillance of reemerging diseases, *J Clin Microbiol* 37(3):596–599, 1999. Retrieved from https://www.ncbi.nlm.nih.gov/pubmed/9986818.

Saisongkorh W, Chenchittikul M, Silpapojakul K: Evaluation of nested PCR for the diagnosis of scrub typhus among patients with acute pyrexia of unknown origin, *Trans R Soc Trop Med Hyg* 98(6):360–366, 2004, https://doi.org/10.1016/j.trstmh.2003.10.012.

Saito TB, Thirumalapura NR, Shelite TR, Rockx-Brouwer D, Popov VL, Walker DH: An animal model of a newly emerging human ehrlichiosis, *J Infect Dis* 211(3):452–461, 2015, https://doi.org/10.1093/infdis/jiu372.

Samanta D, Mulye M, Clemente TM, Justis AV, Gilk SD: Manipulation of host cholesterol by obligate intracellular bacteria, *Front Cell Infect Microbiol* 7:165, 2017, https://doi.org/10.3389/fcimb.2017.00165.

Santucci LA, Gutierrez PL, Silverman DJ: Rickettsia rickettsii induces superoxide radical and superoxide dismutase in human endothelial cells, *Infect Immun* 60(12):5113–5118, 1992. Retrieved from https://www.ncbi.nlm.nih.gov/pubmed/1333449.

Saraswati K, Day NPJ, Mukaka M, Blacksell SD: Scrub typhus point-of-care testing: a systematic review and meta-analysis, *PLoS Negl Trop Dis* 12(3):e0006330, 2018, https://doi.org/10.1371/journal.pntd.0006330.

Saraswati K, Phanichkrivalkosil M, Day NPJ, Blacksell SD: The validity of diagnostic cut-offs for commercial and in-house scrub typhus IgM and IgG ELISAs: a review of the evidence, *PLoS Negl Trop Dis* 13(2):e0007158, 2019, https://doi.org/10.1371/journal.pntd.0007158.

Schmaier AH, Srikanth S, Elghetany MT, Normolle D, Gokhale S, Feng HM, Walker DH: Hemostatic/fibrinolytic protein changes in C3H/HeN mice infected with Rickettsia conorii—a model for Rocky Mountain spotted fever, *Thromb Haemost* 86(3):871–879, 2001. Retrieved from https://www.ncbi.nlm.nih.gov/pubmed/11583321.

Schoffelen T, Joosten LA, Herremans T, de Haan AF, Ammerdorffer A, Rumke HC, et al.: Specific interferon gamma detection for the diagnosis of previous Q fever, *Clin Infect Dis* 56(12):1742–1751, 2013, https://doi.org/10.1093/cid/cit129.

Schoffelen T, Limonard GJ, Bleeker-Rovers CP, Bouwman JJ, van der Meer JW, Nabuurs-Franssen M, et al.: Diagnosis of Coxiella burnetii infection: comparison of a whole blood interferon-gamma production assay and a Coxiella ELISPOT, *PloS One* 9(8):e103749, 2014, https://doi.org/10.1371/journal.pone.0103749.

Schoffelen T, Sprong T, Bleeker-Rovers CP, Wegdam-Blans MC, Ammerdorffer A, Pronk MJ, et al.: A combination of interferon-gamma and interleukin-2 production by Coxiella burnetii-stimulated circulating cells discriminates between chronic Q fever and past Q fever, *Clin Microbiol Infect* 20(7):642–650, 2014, https://doi.org/10.1111/1469-0691.12423.

Schriefer ME, Sacci Jr JB, Dumler JS, Bullen MG, Azad AF: Identification of a novel rickettsial infection in a patient diagnosed with murine typhus, *J Clin Microbiol* 32(4):949–954, 1994. Retrieved from https://www.ncbi.nlm.nih.gov/pubmed/8027348.

Schriefer ME, Sacci Jr JB, Taylor JP, Higgins JA, Azad AF: Murine typhus: updated roles of multiple urban components and a second typhuslike rickettsia, *J Med Entomol* 31(5):681–685, 1994, https://doi.org/10.1093/jmedent/31.5.681.

Schutze GE, Jacobs RF: Human monocytic ehrlichiosis in children, *Pediatrics* 100(1):E10, 1997, https://doi.org/10.1542/peds.100.1.e10.

Segal G, Shuman HA: Possible origin of the Legionella pneumophila virulence genes and their relation to Coxiella burnetii, *Mol Microbiol* 33(3):669–670, 1999, https://doi.org/10.1046/j.1365-2958.1999.01511.x.

Sehdev AE, Dumler JS: Hepatic pathology in human monocytic ehrlichiosis. Ehrlichia chaffeensis infection, *Am J Clin Pathol* 119(6):859–865, 2003, https://doi.org/10.1309/F7EA-B5P7-3217-16LJ.

Seshadri R, Paulsen IT, Eisen JA, Read TD, Nelson KE, Nelson WC, et al.: Complete genome sequence of the Q-fever pathogen Coxiella burnetii, *Proc Natl Acad Sci U S A* 100(9):5455–5460, 2003, https://doi.org/10.1073/pnas.0931379100.

Sexton DJ, Kanj SS, Wilson K, Corey GR, Hegarty BC, Levy MG, Breitschwerdt EB: The use of a polymerase chain reaction as a diagnostic test for Rocky Mountain spotted fever, *Am J Trop Med Hyg* 50(1):59–63, 1994. Retrieved from https://www.ncbi.nlm.nih.gov/pubmed/8304573.

Sigurjonsdottir VK, Feder Jr HM, Wormser GP: Anaplasmosis in pediatric patients: case report and review, *Diagn Microbiol Infect Dis* 89(3):230–234, 2017, https://doi.org/10.1016/j.diagmicrobio.2017.08.003.

Silaghi C, Beck R, Oteo JA, Pfeffer M, Sprong H: Neoehrlichiosis: an emerging tick-borne zoonosis caused by Candidatus Neoehrlichia mikurensis, *Exp Appl Acarol* 68(3):279–297, 2016, https://doi.org/10.1007/s10493-015-9935-y.

Silverman DJ, Santucci LA, Meyers N, Sekeyova Z: Penetration of host cells by Rickettsia rickettsii appears to be mediated by a phospholipase of rickettsial origin, *Infect Immun* 60(7):2733–2740, 1992. Retrieved from https://www.ncbi.nlm.nih.gov/pubmed/1612741.

Smith TA, Driscoll T, Gillespie JJ, Raghavan R: A Coxiella-like endosymbiont is a potential vitamin source for the Lone Star tick, *Genome Biol Evol* 7(3):831–838, 2015, https://doi.org/10.1093/gbe/evv016.

Sobradillo V, Ansola P, Baranda F, Corral C: Q fever pneumonia: a review of 164 community-acquired cases in the Basque country, *Eur Respir J* 2(3):263–266, 1989. Retrieved from https://www.ncbi.nlm.nih.gov/pubmed/2731605.

Sobradillo V, Zalacain R, Capelastegui A, Uresandi F, Corral J: Antibiotic treatment in pneumonia due to Q fever, *Thorax* 47(4):276–278, 1992, https://doi.org/10.1136/thx.47.4.276.

Sonthayanon P, Chierakul W, Wuthiekanun V, Phimda K, Pukrittayakamee S, Day NP, Peacock SJ: Association of high Orientia tsutsugamushi DNA loads with disease of greater severity in adults with scrub typhus, *J Clin Microbiol* 47(2):430–434, 2009, https://doi.org/10.1128/JCM.01927-08.

Spach DH, Kanter AS, Dougherty MJ, Larson AM, Coyle MB, Brenner DJ, et al.: Bartonella (Rochalimaea) quintana bacteremia in inner-city patients with chronic alcoholism, *N Engl J Med* 332(7):424–428, 1995, https://doi.org/10.1056/NEJM199502163320703.

Srigley JR, Vellend H, Palmer N, Phillips MJ, Geddie WR, Van Nostrand AW, Edwards V D: Q-fever: The liver and bone marrow pathology, *Am J Surg Pathol* 9(10):752–758, 1985. Retrieved from https://www.ncbi.nlm.nih.gov/pubmed/3904493.

Stenos J, Graves SR, Unsworth NB: A highly sensitive and specific real-time PCR assay for the detection of spotted fever and typhus group Rickettsiae, *Am J Trop Med Hyg* 73(6):1083–1085, 2005. Retrieved from https://www.ncbi.nlm.nih.gov/pubmed/16354816.

Strickman D, Sheer T, Salata K, Hershey J, Dasch G, Kelly D, Kuschner R: In vitro effectiveness of azithromycin against doxycycline-resistant and -susceptible strains of Rickettsia tsutsugamushi, etiologic agent of scrub typhus, *Antimicrob Agents Chemother* 39(11):2406–2410, 1995, https://doi.org/10.1128/aac.39.11.2406.

Sugita Y, Yamakawa Y, Takahashi K, Nagatani T, Okuda K, Nakajima H: A polymerase chain reaction system for rapid diagnosis of scrub typhus within six hours, *Am J Trop Med Hyg* 49(5):636–640, 1993, https://doi.org/10.4269/ajtmh.1993.49.636.

Tamura A, Ohashi N, Urakami H, Miyamura S: Classification of Rickettsia tsutsugamushi in a new genus, Orientia gen. nov., as Orientia tsutsugamushi comb. nov, *Int J Syst Bacteriol* 45(3):589–591, 1995, https://doi.org/10.1099/00207713-45-3-589.

Tantibhedhyangkul W, Angelakis E, Tongyoo N, Newton PN, Moore CE, Phetsouvanh R, et al.: Intrinsic fluoroquinolone resistance in Orientia tsutsugamushi, *Int J Antimicrob Agents* 35(4):338–341, 2010, https://doi.org/10.1016/j.ijantimicag.2009.11.019.

Tappero JW, Koehler JE: Rochalimaea infections, *Ann Intern Med* 119(6):535–536, 1993, https://doi.org/10.7326/0003-4819-119-6-199309150-00022.

Tappero JW, Mohle-Boetani J, Koehler JE, Swaminathan B, Berger TG, LeBoit PE, et al.: The epidemiology of bacillary angiomatosis and bacillary peliosis, *J Am Med Assoc* 269(6):770–775, 1993. Retrieved from https://www.ncbi.nlm.nih.gov/pubmed/8423659.

Tarasevich I, Rydkina E, Raoult D: Outbreak of epidemic typhus in Russia, *Lancet* 352(9134):1151, 1998, https://doi.org/10.1016/S0140-6736(05)79799-3.

Taylor AJ, Paris DH, Newton PN: A systematic review of mortality from untreated scrub typhus (Orientia tsutsugamushi), *PLoS Negl Trop Dis* 9(8):e0003971, 2015, https://doi.org/10.1371/journal.pntd.0003971.

Tierno Jr PM, Inglima K, Parisi MT: Detection of Bartonella (Rochalimaea) henselae bacteremia using BacT/Alert blood culture system, *Am J Clin Pathol* 104(5):530–536, 1995, https://doi.org/10.1093/ajcp/104.5.530.

Tissot Dupont H, Raoult D, Brouqui P, Janbon F, Peyramond D, Weiller PJ, et al.: Epidemiologic features and clinical presentation of acute Q fever in hospitalized patients: 323 French cases, *Am J Med* 93(4):427–434, 1992, https://doi.org/10.1016/0002-9343(92)90173-9.

Traub R, Wisseman CL: The ecology of murine typhus-a critical review, *Trop Dis Bull* 75(4):237–317, 1978. Retrieved from https://www.ncbi.nlm.nih.gov/pubmed/705902.

Tzianabos T, Anderson BE, McDade JE: Detection of Rickettsia rickettsii DNA in clinical specimens by using polymerase chain reaction technology, *J Clin Microbiol* 27(12):2866–2868, 1989. Retrieved from https://www.ncbi.nlm.nih.gov/pubmed/2512328.

Uchiyama T: Sequence analysis of the gene encoding the major outer membrane protein rOmp B of Rickettsia japonica, *Microbiol Immunol* 43(11):1061–1065, 1999, https://doi.org/10.1111/j.1348-0421.1999.tb01236.x.

Valbuena G, Feng HM, Walker DH: Mechanisms of immunity against rickettsiae. New perspectives and opportunities offered by unusual intracellular parasites, *Microbes Infect* 4(6):625–633, 2002, https://doi.org/10.1016/s1286-4579(02)01581-2.

Van Audenhove A, Verhoef G, Peetermans WE, Boogaerts M, Vandenberghe P: Autoimmune haemolytic anaemia triggered by Bartonella henselae infection: a case report, *Br J Haematol* 115(4):924–925, 2001, https://doi.org/10.1046/j.1365--2141.2001.03165.x.

Varghese GM, Abraham OC, Mathai D, Thomas K, Aaron R, Kavitha ML, Mathai E: Scrub typhus among hospitalised patients with febrile illness in South India: magnitude and clinical predictors, *J Infect* 52(1):56–60, 2006, https://doi.org/10.1016/j.jinf.2005.02.001.

Verdon R, Geffray L, Collet T, Huet H, Parienti JJ, Debruyne M, et al.: Vertebral osteomyelitis due to Bartonella henselae in adults: a report of 2 cases, *Clin Infect Dis* 35(12):e141–144, 2002, https://doi.org/10.1086/344791.

Vigil A, Chen C, Jain A, Nakajima-Sasaki R, Jasinskas A, Pablo J, et al.: Profiling the humoral immune response of acute and chronic Q fever by protein microarray, *Mol Cell Proteomics* 10(10), 2011https://doi.org/10.1074/mcp.M110.006304. M110 006304.

von Loewenich FD, Geissdorfer W, Disque C, Matten J, Schett G, Sakka SG, Bogdan C: Detection of "Candidatus Neoehrlichia mikurensis" in two patients with severe febrile illnesses: evidence for a European sequence variant, *J Clin Microbiol* 48(7):2630–2635, 2010, https://doi.org/10.1128/JCM.00588-10.

Voth DE, Heinzen RA: Lounging in a lysosome: the intracellular lifestyle of Coxiella burnetii, *Cell Microbiol* 9(4):829–840, 2007, https://doi.org/10.1111/j.1462--5822.2007.00901.x.

Wade NK, Levi L, Jones MR, Bhisitkul R, Fine L, Cunningham Jr ET: Optic disk edema associated with peripapillary serous retinal detachment: an early sign of systemic Bartonella henselae infection, *Am J Ophthalmol* 130(3):327–334, 2000, https://doi.org/10.1016/s0002-9394(00)00599-7.

Wakeel A, den Dulk-Ras A, Hooykaas PJ, McBride JW: Ehrlichia chaffeensis tandem repeat proteins and Ank200 are type 1 secretion system substrates related to the repeats-in-toxin exoprotein family, *Front Cell Infect Microbiol* 1:22, 2011, https://doi.org/10.3389/fcimb.2011.00022.

Wakeel A, Kuriakose JA, McBride JW: An Ehrlichia chaffeensis tandem repeat protein interacts with multiple host targets involved in cell signaling, transcriptional regulation, and vesicle trafficking, *Infect Immun* 77(5):1734–1745, 2009, https://doi.org/10.1128/IAI.00027-09.

Wakeel A, Zhu B, Yu XJ, McBride JW: New insights into molecular Ehrlichia chaffeensis-host interactions, *Microbes Infect* 12(5):337–345, 2010, https://doi.org/10.1016/j.micinf.2010.01.009.

Walker DH: Rickettsioses of the spotted fever group around the world, *J Dermatol* 16(3):169–177, 1989, https://doi.org/10.1111/j.1346-8138.1989.tb01244.x.

Walker DH: Principles of the malicious use of infectious agents to create terror: reasons for concern for organisms of the genus Rickettsia, *Ann N Y Acad Sci* 990:739–742, 2003, https://doi.org/10.1111/j.1749-6632.2003.tb07453.x.

Walker DH, Dumler JS: Human monocytic and granulocytic ehrlichioses. Discovery and diagnosis of emerging tick-borne infections and the critical role of the pathologist, *Arch Pathol Lab Med* 121(8):785–791, 1997. Retrieved from https://www.ncbi.nlm.nih.gov/pubmed/9278605.

Walker DH, Feng HM, Ladner S, Billings AN, Zaki SR, Wear DJ, Hightower B: Immunohistochemical diagnosis of typhus rickettsioses using an anti-lipopolysaccharide monoclonal antibody, *Mod Pathol* 10(10):1038–1042, 1997. Retrieved from https://www.ncbi.nlm.nih.gov/pubmed/9346184.

Walker DH, Fishbein DB: Epidemiology of rickettsial diseases, *Eur J Epidemiol* 7(3):237–245, 1991, https://doi.org/10.1007/bf00145672.

Walker DH, Gear JH: Correlation of the distribution of Rickettsia conorii, microscopic lesions, and clinical features in South African tick bite fever, *Am J Trop Med Hyg* 34(2):361–371, 1985, https://doi.org/10.4269/ajtmh.1985.34.361.

Walker DH, Hudnall SD, Szaniawski WK, Feng HM: Monoclonal antibody-based immunohistochemical diagnosis of rickettsialpox: the macrophage is the principal target, *Mod Pathol* 12(5):529–533, 1999. Retrieved from https://www.ncbi.nlm.nih.gov/pubmed/10349992.

Walker DH, Olano JP, Feng HM: Critical role of cytotoxic T lymphocytes in immune clearance of rickettsial infection, *Infect Immun* 69(3):1841–1846, 2001, https://doi.org/10.1128/IAI.69.3.1841-1846.2001.

Walker DH, Parks FM, Betz TG, Taylor JP, Muehlberger JW: Histopathology and immunohistologic demonstration of the distribution of Rickettsia typhi in fatal murine typhus, *Am J Clin Pathol* 91(6):720–724, 1989, https://doi.org/10.1093/ajcp/91.6.720.

Walker DH, Radisch DL, Kirkman HN: Haemolysis with rickettsiosis and glucose-6-phosphate dehydrogenase deficiency, *Lancet* 2(8343):217, 1983, https://doi.org/10.1016/s0140-6736(83)90194-0.

Walker DH, Staiti A, Mansueto S, Tringali G: Frequent occurrence of hepatic lesions in boutonneuse fever, *Acta Trop* 43(2):175–181, 1986. Retrieved from https://www.ncbi.nlm.nih.gov/pubmed/2874714.

Walls JJ, Aguero-Rosenfeld M, Bakken JS, Goodman JL, Hossain D, Johnson RC, Dumler JS: Inter- and intralaboratory comparison of Ehrlichia equi and human granulocytic ehrlichiosis (HGE) agent strains for serodiagnosis of HGE by the immunofluorescent-antibody test, *J Clin Microbiol* 37(9):2968–2973, 1999. Retrieved from https://www.ncbi.nlm.nih.gov/pubmed/10449483.

Watt G, Chouriyagune C, Ruangweerayud R, Watcharapichat P, Phulsuksombati D, Jongsakul K, et al.: Scrub typhus infections poorly responsive to antibiotics in northern Thailand, *Lancet* 348(9020):86–89, 1996, https://doi.org/10.1016/s0140-6736(96)02501-9.

Watt G, Kantipong P, Jongsakul K, Watcharapichat P, Phulsuksombati D, Strickman D: Doxycycline and rifampicin for mild scrub-typhus infections in northern Thailand: a randomised trial, *Lancet* 356(9235):1057–1061, 2000, https://doi.org/10.1016/S0140-6736(00)02728-8.

Wegdam-Blans MC, Wielders CC, Meekelenkamp J, Korbeeck JM, Herremans T, Tjhie HT, et al.: Evaluation of commonly used serological tests for detection of Coxiella burnetii antibodies in well-defined acute and follow-up sera, *Clin Vaccine Immunol* 19(7):1110–1115, 2012, https://doi.org/10.1128/CVI.05581-11.

Weinert, L. A., Werren, J. H., Aebi, A., Stone, G. N., & Jiggins, F. M: Evolution and diversity of Rickettsia bacteria. BMC Biol, 7, 6. doi:10.1186/1741-7007-7-6

Weiss E: 1982 The biology of rickettsiae, *Annu Rev Microbiol* 36:345–370, 2009, https://doi.org/10.1146/annurev.mi.36.100182.002021.

Welc-Faleciak R, Sinski E, Kowalec M, Zajkowska J, Pancewicz SA: Asymptomatic "Candidatus Neoehrlichia mikurensis" infections in immunocompetent humans, *J Clin Microbiol* 52(8):3072–3074, 2014, https://doi.org/10.1128/JCM.00741-14.

Whitworth T, Popov VL, Yu XJ, Walker DH, Bouyer DH: Expression of the Rickettsia prowazekii pld or tlyC gene in Salmonella enterica serovar Typhimurium mediates phagosomal escape, *Infect Immun* 73(10):6668–6673, 2005, https://doi.org/10.1128/IAI.73.10.6668-6673.2005.

Wielders CC, Wijnbergen PC, Renders NH, Schellekens JJ, Schneeberger PM, Wever PC, Hermans MH: High Coxiella burnetii DNA load in serum during acute Q fever is associated with progression to a serologic profile indicative of chronic Q fever, *J Clin Microbiol* 51(10):3192–3198, 2013, https://doi.org/10.1128/JCM.00993-13.

Williams WJ, Radulovic S, Dasch GA, Lindstrom J, Kelly DJ, Oster CN, Walker DH: Identification of Rickettsia conorii infection by polymerase chain reaction in a soldier returning from Somalia, *Clin Infect Dis* 19(1):93–99, 1994, https://doi.org/10.1093/clinids/19.1.93.

Wolbach SB: The etiology and pathology of Rocky mountain spotted fever : (third Preliminary report.) the occurrence of the parasite and the pathology of the disease in man. Additional Notes on the parasite, *J Med Res* 37(3):499–508, 1918. Retrieved from https://www.ncbi.nlm.nih.gov/pubmed/19972412.

Wong MT, Dolan MJ, Lattuada Jr CP, Regnery RL, Garcia ML, Mokulis EC, et al.: Neuroretinitis, aseptic meningitis, and lymphadenitis associated with Bartonella (Rochalimaea) henselae infection in immunocompetent patients and patients infected with human immunodeficiency virus type 1, *Clin Infect Dis* 21(2):352–360, 1995, https://doi.org/10.1093/clinids/21.2.352.

Woods ME, Olano JP: Host defenses to Rickettsia rickettsii infection contribute to increased microvascular permeability in human cerebral endothelial cells, *J Clin Immunol* 28(2):174–185, 2008, https://doi.org/10.1007/s10875-007-9140-9.

Yu X, Brouqui P, Dumler JS, Raoult D: Detection of Ehrlichia chaffeensis in human tissue by using a species-specific monoclonal antibody, *J Clin Microbiol* 31(12):3284–3288, 1993. Retrieved from https://www.ncbi.nlm.nih.gov/pubmed/7508458.

Yu XJ, Crocquet-Valdes PA, Cullman LC, Popov VL, Walker DH: Comparison of Ehrlichia chaffeensis recombinant proteins for serologic diagnosis of human monocytotropic ehrlichiosis, *J Clin Microbiol* 37(8):2568–2575, 1999. Retrieved from https://www.ncbi.nlm.nih.gov/pubmed/10405403.

Zavala-Velazquez JE, Ruiz-Sosa JA, Sanchez-Elias RA, Becerra-Carmona G, Walker DH: Rickettsia felis rickettsiosis in Yucatan, *Lancet* 356(9235):1079–1080, 2000, https://doi.org/10.1016/S0140-6736(00)02735-5.

Zhi N, Rikihisa Y, Kim HY, Wormser GP, Horowitz HW: Comparison of major antigenic proteins of six strains of the human granulocytic ehrlichiosis agent by Western immunoblot analysis, *J Clin Microbiol* 35(10):2606–2611, 1997. Retrieved from https://www.ncbi.nlm.nih.gov/pubmed/9316916.

Zhu B, Nethery KA, Kuriakose JA, Wakeel A, Zhang X, McBride JW: Nuclear translocated Ehrlichia chaffeensis ankyrin protein interacts with a specific adenine-rich motif of host promoter and intronic Alu elements, *Infect Immun* 77(10):4243–4255, 2009, https://doi.org/10.1128/IAI.00376-09.

Zinsser H, Castaneda MR: Studies on typhus fever : Ii. Studies on the etiology of Mexican typhus fever, *J Exp Med* 52(5):649–659, 1930, https://doi.org/10.1084/jem.52.5.649.

CHAPTER 64

VIRAL INFECTIONS

Catherine A. Hogan, M. Jana Broadhurst, Hannah Wang, Benjamin A. Pinsky

INTRODUCTION, 1266
CLINICAL VIRAL INFECTIOUS SYNDROMES, 1266
Pediatric and Adult Viral Respiratory Syndrome, 1266
Infectious Mononucleosis and Related Infections, 1270
Congenital and Perinatal Viral Infections, 1271
Viral Meningitis and Encephalitis, 1273
Viral Infections with Skin and Mucosal Manifestations, 1275
Viral Gastroenteritis, 1278
Viral Hepatitis, 1279
Human Immunodeficiency Virus, 1280
Virus-Associated Neoplasia, 1282
Viral Infections in Immunocompromised Hosts, 1283
Viral Infections in Returning Travelers, 1286
SUMMARY, 1289
SELECTED REFERENCES, 1289

KEY POINTS

- Viruses cause more human infections than any other group of microorganisms and produce diseases that range from benign to highly lethal. Viral pathogens, including SARS-CoV-2, influenza A subtypes, arboviruses, and hemorrhagic fever viruses, are continuously being discovered or identified in different geographic areas and have the potential to cause widespread disease.
- Accurate and timely viral diagnosis is essential to optimize patient management, enable appropriate use of antiviral drugs, reduce unnecessary laboratory testing and antibacterial therapy, implement appropriate infection control procedures, and provide effective outbreak response.
- Molecular methods for detection of viral DNA and RNA have largely replaced the traditional approaches of virus isolation in cell culture and viral antigen identification. Molecular testing is highly sensitive and specific and has become the new gold standard for viral testing for most viruses.
- Viral serology has two major applications: diagnosis of recent infection and determination of immunity. Demonstration of IgM-specific antibody during acute illness or a significant rise in IgG antibody between acute and convalescent sera defines acute infection. Serology is particularly helpful in cases where culture, antigen assays, or nucleic acid–based testing is not available or demonstrates limited test performance. Persistent specific IgG is a marker of immune status for measles, mumps, varicella zoster virus, and hepatitis A and B viruses.
- Nucleic acid amplification tests detect virus by recognizing specific and stable segments of the DNA or RNA viral genome. This testing is highly sensitive, specific, rapid, and can be used for both diagnosis and monitoring.
- Real-time polymerase chain reaction (PCR) amplification allows for accurate detection and quantitation of the viral load present in a variety of specimen types. Quantitative analysis is especially useful for monitoring response to therapy for viral pathogens such as human immunodeficiency virus (HIV), hepatitis C virus (HCV), hepatitis B virus (HBV), cytomegalovirus (CMV), Epstein-Barr virus (EBV), and BK virus.
- Point-of-care molecular technology is becoming an increasingly common feature of emergency room and admission decisions, providing diagnostic information about viral targets within hours. When properly utilized, rapid results generated through point-of-care testing have the potential to guide diagnostic testing, treatment decisions, and hospitalization and isolation needs.
- Syndromic multiplex diagnostic panels have greatly expanded the availability of molecular testing for viral infections. These assays generate comprehensive and reliable answers in a clinically actionable time frame and show potential to lead to improved clinical outcomes.
- Detection of antiviral resistance mutations is available for HIV, HBV, HCV, and CMV. Such testing is particularly informative for cases of suspected resistance, to inform treatment recommendations.
- Next-generation sequencing (NGS) is an evolving technique that can be used for viral detection and characterization of known and novel viruses, assessment of sequence variants for antiviral susceptibility, and in-depth exploration of viral outbreaks. Further work is required to understand how best to integrate NGS into routine clinical testing algorithms that are cost effective.

INTRODUCTION

The clinical virology laboratory plays a critical role in health care systems due to its impact on clinical management and public health interventions. Clinical virology encompasses a large range of viral agents, all of which are associated with their own biology, geographic distribution, clinical syndromes, testing modalities, and therapeutic options. In this chapter we present viruses through the lens of important clinical syndromes. For each virus or viral family, we describe the basic virology, epidemiology, clinical presentation, and laboratory diagnosis. Significant changes have occurred in the laboratory diagnosis of viruses in the last two decades due to a large shift toward molecular testing, including the use of near-patient and multiplexed panels. These and other diagnostic methods will be explored further, including discussion of pros and cons of each approach.

The reader should be reminded that viruses evolve constantly and that epidemiologic trends may change rapidly. Among the respiratory viruses, the recent emergence of the severe acute respiratory syndrome coronavirus 2 (SARS-CoV-2) pandemic serves as a stark reminder of the potential of viral agents to cause significant morbidity and mortality and shape major social events, as well as the need to be vigilant about the emergence and dissemination of novel viruses. Reviewing the most recent literature and data is thus paramount to secure the most up-to-date information on viral topics of interest.

CLINICAL VIRAL INFECTIOUS SYNDROMES

PEDIATRIC AND ADULT VIRAL RESPIRATORY SYNDROME

Respiratory tract infections, the majority of which are caused by viruses, are among the most common reasons for seeking health care (Renati & Linder, 2016). Clinical syndromes arising from respiratory viral infection can be grouped anatomically into upper respiratory tract infections (URTIs, involving the nasal cavities, sinuses, nasopharynx, throat, larynx, conjunctiva, and inner ear) and lower respiratory tract infections (LRTIs, involving the trachea and bronchoalveolar tree). URTIs commonly manifest as rhinosinusitis ("common cold"), acute sinusitis, acute laryngitis, conjunctivitis, and otitis media. LRTIs encompass more severe syndromes, including bronchitis, bronchiolitis, and pneumonia.

There is substantial overlap in the disease spectrum associated with each respiratory virus; as such, timely access to accurate testing is required to make a diagnosis. The respiratory viruses presented here may all cause upper and/or lower respiratory tract symptoms, in addition to systemic symptoms such as fever, chills, headache, myalgias, and generalized weakness. Furthermore, viruses that are typically associated with benign URTI may cause significant morbidity and mortality in patient populations at higher risk of complications, including children, the elderly, those with underlying pulmonary disease, and immunocompromised patients such as transplant recipients. Nosocomial transmission of respiratory viruses is well documented, and isolation precautions based on the primary mode of transmission are required. Moreover, a thorough travel and exposure history may be warranted to evaluate for epidemiologic risk factors associated with outbreak-prone emerging viruses and to guide appropriate infection control and biosafety precautions. In addition, several respiratory viruses demonstrate characteristic seasonality that can aid in risk assessment and clinical evaluation.

Diagnostic Methods

Diagnostic testing is an important tool to inform appropriate patient management decisions. Indeed, confirming the diagnosis of a respiratory viral infection may enable clinicians to avert unnecessary antibiotic use, guide the use of appropriate antiviral therapy (e.g., oseltamivir for confirmed influenza infection), and inform appropriate infection prevention and control strategies for a specific viral agent. Ideally, testing should be performed as early as possible in the disease course. Viral loads in respiratory specimens typically peak within the first 2 days following symptom onset and gradually decline to undetectable levels 5 to 8 days into the disease course; it could be longer in severely ill or immunocompromised individuals (Lee et al., 2009).

The specimen of choice will depend on the clinical presentation and the approved or validated specimen types for the available testing methods. For sampling the upper airway, nasopharyngeal aspirate (NPA) is traditionally considered the specimen type with the highest diagnostic yield (Sung et al., 2008). However, nasopharyngeal (NP) swabs are most commonly collected given the greater ease of sampling. Flocked swabs are recommended for optimal sampling and should be placed in viral or universal transport medium upon collection. For patients with isolated LRTI, sputum, endotracheal aspirate (ETA), or bronchoalveolar lavage (BAL) samples may contain higher viral loads and thus offer better sensitivity. However, these specimen types are off-label for many US Food and Drug Administration (FDA)–cleared assays and thus require laboratory validation for testing.

Several respiratory viruses can be cultured in routine cell lines; however, viral culture requires a high level of technical expertise and hands-on time, and results are typically not available in a clinically meaningful time frame. Shell vial culture reduces the turnaround time compared to conventional viral culture, but still requires 1 to 3 days and lacks sensitivity compared to molecular testing. Furthermore, viral culture may introduce the hazard of inadvertently propagating an emerging viral pathogen and placing laboratory personnel at risk.

Traditional antigen detection methods include direct and indirect fluorescent antibody staining that can be used to detect viral antigens directly in clinical specimens by fluorescence microscopy. These methods are relatively fast (<4 hours) but are labor intensive, and performance varies depending on specimen quality and technical expertise. Rapid antigen detection immunoassays have been developed for influenza viruses and respiratory syncytial virus (RSV), introducing the opportunity for Clinical Laboratory Improvement Amendment (CLIA)–waived testing at the point of care. While these assays have demonstrated good specificity, their sensitivity compared to molecular methods is poor (typically 50–70%) and thus cannot be used to rule out infection (Merckx et al., 2017). Due to performance concerns, these assays have recently been reclassified as class II (moderate risk) devices for the diagnosis of influenza by the FDA (2020).

In modern practice, many clinical laboratories in the United States have phased out viral culture and antigen detection for respiratory viruses in favor of rapid, highly sensitive and specific molecular testing. Over five FDA-cleared nucleic acid amplification test (NAAT) panels, including more than three targets for diagnosis of respiratory virus detection, are available and have modified the diagnostic approach for these viruses. These multiplex syndromic assays include between 8 and 21 viral and bacterial targets and present turnaround time as low as 1 hour (Ramanan et al., 2018). Overall test performance has been summarized for the most common platforms and has shown sensitivity greater than 84% and specificity greater than 99% (Ramanan et al., 2018). These automated platforms with integrated nucleic acid extraction bear high platform and reagent costs, but allow for minimal hands-on time, lower complexity (some CLIA-waived), higher throughput, and the possibility of near-patient testing to minimize turnaround time.

The uptake of multiplex syndromic panels has been the subject of many studies, including assessment of the possible benefits for both patients and health care systems. These include decreased time to virus identification, reduced hospital length of stay (LOS), and optimization of antimicrobial use in adults and children (Rappo et al., 2016; Subramony et al., 2016; Rogers et al., 2015). Randomized controlled trial (RCT) evidence has also supported reduction in LOS from implementation of point-of-care molecular testing compared to laboratory testing (Brendish et al., 2017); however, a separate RCT reported no such impact (Saarela et al., 2019). In addition, both of these studies demonstrated lack of impact on antimicrobial therapy (Brendish et al, 2017; Saarela et al., 2019). Thus the appropriate implementation and impact of multiplex NAAT panels depend on the health care setting and patient population, and the use of testing criteria or algorithms may facilitate appropriate uptake and utilization of these costly tests (Schreckenberger & McAdam, 2015; Charlton et al., 2019).

Finally, the clinical performance of any test for respiratory virus detection depends on the timing of specimen collection from symptom onset and the quality of the specimen collected. The predictive value of the test result will additionally depend on the seasonal prevalence of the circulating viruses.

Influenza Viruses

Virology

Influenza viruses (family: Orthomyxoviridae) are enveloped, segmented, single-stranded RNA viruses that include three main species in separate genera: *Alphainfluenzavirus* (species: *Influenza A virus*), *Betainfluenzavirus* (species: *Influenza B virus*), and *Gammainfluenzavirus* (species: *Influenza C virus*). Two types of surface glycoproteins, hemagglutinin (HA) and neuraminidase (NA), project from the virus envelope. Influenza A viruses are classified into subtypes based on HA and NA antigenic properties. Two clades of Influenza B are described, Yamagata and Victoria.

Epidemiology

Influenza infections peak during the winter months in temperate climates but may occur at any time of the year in the tropics (Moura, 2010). Each year in the United States, influenza causes 9 to 36 million illnesses, 140,000 to 710,000 hospitalizations, and 16,000 to 76,000 deaths (Rolfes et al., 2018). Universal immunity to influenza viruses is hampered by antigenic changes due to the accumulation of mutations (antigenic drift) and reassortment of genome segments (antigenic shift). Influenza vaccines are produced each year based on predictions of circulating strains. Live-attenuated, inactivated, and recombinant vaccine types are approved with multivalent formulations that include two Influenza A subtypes (H3N2 and H1N1) and one or both clades of Influenza B, though live-attenuated is thought to be relatively less effective (Piedra, 2019). Despite suboptimal efficacy (40–60%), influenza vaccines prevent an estimated 39,000 to 87,000 hospitalizations and 3000 to 10,000 deaths annually in the United States (Rolfes et al., 2018). Seasonal influenza is also an important cause of community and nosocomial outbreaks. Influenza A infects many species of birds and mammals in addition to humans, which can lead to spillover of novel reassortant strains from animal reservoirs to human populations. Influenza B and C are known to primarily infect humans.

Clinical Presentation

Symptoms of influenza usually manifest after a mean incubation period of 2 days (range, 1–4 days). The clinical presentation of influenza overlaps with other respiratory viruses and includes the abrupt onset of fever, myalgia, headache, generalized weakness, and URTI symptoms. In the elderly, the combination of acute onset of fever and cough significantly increases the likelihood of influenza, though other factors such as seasonality and local epidemiology should also be considered (Call et al., 2005). Secondary bacterial infection with *Staphylococcus aureus*, *Streptococcus pneumoniae*, and other organisms is a complication of influenza that is associated with significant morbidity and mortality (Rothberg & Haessler, 2010). Rarely, influenza infection can be associated with severe cardiac and neuromuscular complications, including pericarditis, myocarditis, myositis, rhabdomyolysis, Reye syndrome, transverse myelitis, and aseptic meningitis (Rothberg & Haessler, 2010).

Laboratory Diagnosis

As for other respiratory viruses, rapid molecular tests have shown high test performance for the diagnosis of influenza and are considered the current standard of care (Merckx et al., 2017). There are now several CLIA-waived test systems for rapid molecular detection of influenza, with clinical studies of point-of-care performance showing sensitivity ranging from 64% to 100%, and specificity greater than 95% to 100% across platforms (Babady et al., 2019). As discussed previously, rapid antigen detected tests (RADTs) for influenza have fallen out of favor given their lack of sensitivity compared to molecular assays.

Clinical Implications

Licensed antivirals for the treatment of influenza include neuraminidase inhibitors (oseltamivir, peramivir, and zanamivir) or the more recently approved cap-dependent endonuclease inhibitor (baloxavir). Another class of drugs, the adamantanes (amantadine, rimantadine) are no longer recommended for use in the United States owing to widespread resistance.

Parainfluenza Viruses

Virology

Parainfluenza viruses (PIVs) (family: Paramyxoviridae) are enveloped, nonsegmented, single-stranded RNA viruses. Four species causing human

respiratory infection are described: *Human parainfluenza virus 1* and *3* (PIV-1 and PIV-3) in the *Respirovirus* genus, and *Human orthorublavirus 2* and *4* (PIV-2 and PIV-4) in the *Orthorublavirus* genus.

Epidemiology

PIVs are an important cause of severe LRTI in young children, responsible for 2% to 17% of hospitalizations for respiratory illness in children less than 5 years of age, and in the elderly (Abedi et al., 2016, Jain et al., 2015a). Most hospitalizations are attributable to PIV-3 infection in infants less than 6 months of age. LRTI caused by PIV in hospitalized adults is associated with prolonged length of stay and rare fatalities (Russell et al., 2019). The seasonality of PIV outbreaks varies by species. PIV-1 outbreaks typically occur biennially, peaking in the autumn months of odd-numbered years. PIV-2 outbreaks are less predictable but tend to occur annually with highest prevalence in late autumn. PIV-3 circulates annually, peaking in late spring and summer months. Relatively few cases of PIV-4 are detected, and seasonality is not well defined.

Clinical Presentation

The majority of PIV infections manifest as mild URTIs following an incubation period of 2 to 6 days. Approximately 15% of infections involve the lower airways and occur typically in children. In hospitalized young children, PIV is responsible for nearly half of the cases of croup (laryngotracheitis; most commonly attributable to PIV-1) as well as a significant burden of bronchiolitis and pneumonia, which is most commonly attributable to PIV-3 (Abedi et al., 2016).

Laboratory Diagnosis

As for other respiratory viruses, multiplex viral nucleic acid tests, which include the Parainfluenza targets, are superior to both antigen assays and culture for clinical diagnosis, and are the standard of care for diagnosis (Mahony, 2008).

Clinical Implications

No targeted therapeutics are currently available for Parainfluenza, and treatment is supportive. Contact precautions are warranted to prevent nosocomial transmission and may be extended in young children and immunocompromised patients due to prolonged viral shedding (Centers for Disease Control and Prevention [CDC], 2020).

RSV

Virology

Human orthopneumovirus, commonly known as respiratory syncytial virus (family: Pneumoviridae; genus: *Orthopneumovirus*), is an enveloped, nonsegmented, single-stranded RNA virus. Two major antigenic groups in circulation are designated A and B, each with multiple known genotypes.

Epidemiology

RSV infections are extremely common worldwide, and most children have been infected by 3 years of age. In the United States, RSV is detected in more than a quarter of acute LRTIs in pediatric patients requiring hospitalization, with most cases in children less than 5 years old (Jain et al., 2015b). Subsequent infections are common and typically less clinically severe as protective immunity develops. However, loss of immune protection in older adults and immunocompromised patients is associated with severe respiratory infections requiring prolonged hospitalization, with the highest mortality rates occurring in patients over 65 years of age (Nam & Ison, 2019; Ison & Hirsch, 2019). Seasonal epidemics of RSV peak in the winter months in temperate climates. RSV is easily transmitted by large droplets from nasopharyngeal secretions; therefore droplet and contact isolation precautions are recommended for hospitalized patients.

Clinical Presentation

Following an incubation period of 4 to 8 days, RSV causes a typical URTI in healthy children and adults. RSV is an important cause of bronchiolitis and pneumonia in infants, the elderly, and immunocompromised patients, frequently requiring hospitalization. Premature newborns experience the most serious infections because their narrow terminal airways are more easily occluded. Acute symptoms usually resolve in a few days.

Laboratory Diagnosis

Several assays are now available for the rapid diagnosis of RSV and are more accurate compared to older RADT (Caya & Papenburg, 2018). As for influenza, at least two molecular tests can provide results for RSV in less than 30 minutes (Young et al., 2019). Syndromic multiplex panels are also frequently used for the diagnosis of RSV and are characterized by high sensitivity and specificity.

Clinical Implications

Most RSV infections are managed with supportive care; administration of oxygen and other supportive measures are often the only medical interventions needed. Ribavirin, in either aerosolized or intravenous formulation, may be used in severe cases. The monoclonal antibody palivizumab has been shown to prevent severe LRTI in high-risk pediatric patients; however, it is not an effective therapeutic for severe disease. Similar to other respiratory viruses, extended precautions are warranted in young children and immunocompromised patients, as these individuals exhibit prolonged viral shedding.

Human Metapneumovirus

Virology

Human metapneumovirus (hMPV) (family: Pneumoviridae; genus: *Metapneumovirus*) is an enveloped, nonsegmented, single-stranded RNA virus. Two antigenic groups, A and B, each with two distinct genetic lineages, have been described.

Epidemiology

hMPV is a common cause of respiratory infection in all age groups. Most children have had an initial infection by 5 years of age, and subsequent infections occur throughout life. hMPV is detected in 13% of severe LRTIs requiring hospitalization in pediatric patients in the United States (Jain et al., 2015b). Similar to RSV, severe LRTIs also occur in the elderly and immunocompromised patients (Ison & Hirsch, 2019). Infection rates are known to peak in the winter months in temperate climates, but transmission dynamics are not yet well described.

Clinical Presentation

hMPV infections in healthy children and adults are commonly asymptomatic or give rise to self-limited URTIs. LRTIs in the elderly and in immunocompromised patients may present as severe bronchitis or pneumonia warranting hospitalization and supportive care.

Laboratory Diagnosis

As with other respiratory viruses, NAAT is the diagnostic modality of choice given its high sensitivity and specificity.

Clinical Implications

No targeted therapeutics are available, and treatment is supportive. Appropriate contact precautions should be instituted (CDC, 2020).

Rhinovirus

Virology

Rhinoviruses (family: Picornaviridae; genus: *Enterovirus*) are nonenveloped, nonsegmented, single-stranded RNA viruses. Three species are described, *Rhinovirus A*, *B*, and *C*, with more than 150 serotypes.

Epidemiology

Rhinoviruses are the most common cause of respiratory viral infections globally and circulate year-round, with peak infection rates in late summer and early fall. Multiple serotypes cocirculate each year. During peak months, rhinoviruses are responsible for the large majority of URTIs. Among respiratory viruses, rhinoviruses show high rates of nosocomial transmission (Rahamat-Langendoen et al., 2013; Chow & Mermel, 2017).

Clinical Presentation

UTRI symptoms arise following an incubation period 2 to 3 days with pronounced watery nasal discharge. Common complications include acute otitis media and sinusitis. Rhinovirus infections, particularly *Rhinovirus C*, can cause severe LRTI in young children, the elderly, immunocompromised patients, and those with underlying lung disease, including asthma (Rahamat-Langendoen et al., 2013). Rhinoviruses are frequently identified as coinfections with other respiratory viruses, and asymptomatic viral shedding is common, presenting a challenge for interpreting the clinical significance of detection.

Laboratory Diagnosis

Rhinovirus is most commonly diagnosed on multiplex syndromic respiratory virus panels. Of note, given its high sequence homology with Enterovirus, testing on certain diagnostic panels may show Enterovirus or Rhinovirus, given the inability to differentiate the two.

Clinical Implications

Rhinovirus is the most common causal agent of the common cold. Clinical presentation varies based on age group, with a higher proportion of symptomatic children compared to adults (Pappas et al., 2008). Rhinovirus has also been linked to asthma exacerbations. Given its frequent detection, including in coviral infection, the causal role of Rhinovirus in acute illness remains to be elucidated.

Coronavirus

Virology

Seasonal coronaviruses (family: Coronaviridae) are enveloped, nonsegmented, single-stranded RNA viruses. Species from two genera are known to cause human infections. *Alphacoronavirus* genus includes *Human coronavirus (HCoV) 229E* and *HCoV NL63*. *Betacoronavirus* genus includes *HCoV HKU1* and *HCoV OC43* as well as three zoonotic species that may cause severe disease, *severe acute respiratory syndrome coronavirus* (SARS-CoV), *Middle East respiratory syndrome-related coronavirus* (MERS-CoV), and the recently described severe acute respiratory syndrome coronavirus 2 (SARS-CoV-2). SARS-CoV-2 will be described separately later. SARS-CoV and MERS-CoV are discussed in further detail under Viral Infections in Returning Travelers.

Seasonal Coronaviruses

Epidemiology. Seasonal CoV infections are widespread and collectively represent the most common cause of URTI behind Rhinoviruses. CoV can also cause LRTI and have been detected in up to 5% of pediatric patients and 11% of adult patients hospitalized for severe respiratory illness, frequently in the setting of underlying respiratory disease, immunocompromised state, or extremes of age (Jain et al., 2015b; Jain et al., 2015a; Ogimi et al., 2019; Walsh et al., 2013; Gaunt et al., 2010). Outbreaks of severe CoV disease with associated fatalities have been described in long-term care facilities warranting contact and droplet isolation precautions in high-risk health care settings (Hand et al., 1966). CoV circulation is restricted to winter months in temperate climates.

Clinical Presentation. Most coronaviruses are associated with minor URTI symptoms following an incubation period of 2 to 5 days. Severe LRTIs occasionally occur in vulnerable patient populations as noted earlier. Similar to rhinoviruses, coinfection with other respiratory viruses and asymptomatic shedding are common, complicating clinical interpretation of positive test results.

Laboratory Diagnosis. Seasonal coronaviruses are identified through molecular assays, which typically include the four most common species (*229E*, *NL63*, *HKU1*, and *OC63*); they do not include any of the three zoonotic species that require dedicated assays.

Clinical Implications. Coronaviruses have been implicated in both mild and severe clinical respiratory syndromes, and supportive care is the mainstay of therapy.

SARS-CoV-2

Virology. SARS-CoV-2 (family: Coronaviridae; genus: *Betacoronavirus*) is a recently described novel coronavirus that shares high sequence identity with bat coronavirus (96%) and SARS-CoV (up to 80%) (Zhou et al., 2020). Early phylogenetic analyses from China identified two major types of SARS-CoV-2: type L (70%) and type S (30%) (Xiaolu Tang et al., 2020). Since SARS-CoV-2 was first identified, several genetic variants have emerged. Those of concern are more transmissible, may cause more severe disease, and may reduce vaccine effectiveness. Cellular entry requires the viral spike (S) proteins to bind to cellular receptors, a process that is primed by host cell proteases (Hoffmann et al., 2020). Similarly to SARS-CoV, SARS-CoV-2 uses the angiotensin-converting enzyme II (ACE2) for host cell entry (Zhou et al., 2020). Furthermore, the TMPRSS2 protease in addition to other endosomal proteases prime the S protein (Hoffmann et al., 2020). Further discussion on this topic can be found in Chapter 21.

Epidemiology. SARS-CoV-2 emerged in December 2019 in Wuhan, China, in the context of a cluster of pneumonia cases of unknown viral etiology. The virus was subsequently identified as a novel member of the *Betacoronavirus* genus and was named SARS-CoV-2, causing coronavirus disease (COVID-19, numbered for the year in which it appeared, 2019). Epidemiologic work on the initial transmission of the virus linked a wet market in Wuhan, China, as an important risk factor, though person-to-person spread subsequently led to widespread transmission (Chen et al., 2020). The transmission dynamics of SARS-CoV-2 remain under study; however, both inhaled droplets and aerosol particles appear to be involved (Meselson, 2020; van Doremalen et al., 2020). Furthermore, environmental contamination such as through fomite spread may contribute to virus spread (Ong et al., 2020). SARS-CoV-2 subsequently disseminated globally to reach pandemic status in March 2020. As of mid-March 2021, over 118 million cases worldwide had been confirmed leading to over 2.5 million deaths, and these numbers continue to grow substantially (World Health Organization [WHO], 2021). Its origin has not yet been confirmed but cross-species transmission from a bat appears probable (Zhou et al., 2020).

Clinical Presentation. SARS-CoV-2 can lead to both asymptomatic and symptomatic infection. Symptoms appear after a median incubation period of 4 days postexposure, but cases have been reported over 2 weeks after exposure (Guan et al., 2020). In symptomatic individuals, the spectrum of clinical severity varies widely, ranging from mild URTI symptoms to acute respiratory distress syndrome (ARDS), multiorgan failure, and death. Interestingly, gastrointestinal symptoms, anosmia (loss of smell), and ageusia (loss of taste) have been noted as frequent clinical manifestations of SARS-CoV-2 (Xydakis et al., 2020; Cheung et al., 2020). Other clinical complications include mental status changes, hypotension, acute kidney injury, acute cardiac injury, liver dysfunction, and hypercoagulability (Yang et al., 2020; Bhatraju et al., 2020). Furthermore, lung imaging abnormalities are common with ground-glass and consolidative pulmonary opacities in bilateral and peripheral distributions as the most common findings, although imaging can appear within normal limits early on in the disease course (Bernheim et al., 2020). Estimates of disease severity from the early phase of the epidemic have shown case fatality ratios ranging from 1% to 4%, with significantly higher figures in elderly groups and in certain settings (Verity et al., 2020).

Laboratory Diagnosis. The diagnosis of acute SARS-CoV-2 infection is performed by molecular methods using reverse transcription polymerase chain reaction (RT-PCR). Multiple assays and platforms have received emergency use authorization (EUA) for this purpose in the first few months of the pandemic (Cheng et al., 2020). These assays span a large range of targets, including the envelope *(E)*, spike *(S)*, nucleocapsid (*N1* and *N2*), and RNA-dependent RNA polymerase *(RdRp)* genes, and the ORF1ab region of the replicase gene. Test performance of these assays has been largely comparable, with the highest sensitivity noted for the *E* and *N2* genes (Nalla et al., 2020). EUA molecular point-of-care testing has also been developed, including the Xpert Xpress SARS-CoV-2 (Cepheid, Sunnyvale, CA), ID NOW COVID-19 (Abbott, Chicago, IL), and Accula (Mesa Biotech, San Diego, CA). However, test performance and safety issues have been raised with the ID NOW, such that further improvements will be expected to facilitate access to near-patient testing in the future (Harrington et al., 2020).

Serologic testing identifying different immunoglobulins (IgA, IgM, and IgG) from whole blood, serum, or plasma has also emerged as a potentially useful diagnostic modality, especially to assess for evidence of previous exposure and to estimate population-level prevalence. Its role in the diagnosis of acute infection is likely limited given the median timeframe of 5 to 14 days required to detect an antibody response (Guo et al., 2020). Assays developed have mainly targeted the viral spike (S) and nucleocapsid (N) proteins. Laboratory-based testing is typically performed by enzyme-linked immunosorbent assays (ELISA). Several point-of-care serology immunoassays have appeared on the market and received EUA. Preliminary data show widely varying performance results comparing ELISA assays to point-of-care lateral flow tests, with sensitivities of 67% to 93% for ELISAs and 83% to 93% for point of care, and specificities of 93% to 100% for ELISAs and 80% to 100% for point of care (Lassaunière et al., 2020).

Antigen testing has also been suggested as a useful diagnostic modality, with preliminary data supporting good performance for certain assays, particularly for individuals with higher burden of infection (Pollock et al., 2021).

Clinical Implications. Prompt and accurate diagnosis of acute SARS-CoV-2 is crucial to implement appropriate infection control measures and limit onward transmission. Treatment is based on disease severity. Monoclonal antibodies designed to block viral attachment and entry into cells are recommended for nonhospitalized patients with mild to moderate COVID-19 disease. For hospitalized patients with more severe disease, treatment includes remdesivir, a novel nucleoside analogue administered parenterally (National Institute of Allergy and Infectious Diseases, 2020) alone or with dexamethasone or other immunomodulator. Hydroxychloroquine use as prophylaxis after exposure to SARS-CoV-2 has been shown to be ineffective to prevent COVID-19 (Boulware et al., 2020). The efficacy of other agents, including convalescent plasma, interleukin-6 inhibitors, and new antivirals remain under investigation. Supportive therapy also is needed for management of ARDS, clotting disorders, and acute renal failure if they occur. In the future, population-wide seroprevalence surveys will facilitate the identification of true burden of illness and confirm estimates of disease severity and mortality rates.

Adenovirus

Virology

Adenoviruses (family: Adenoviridae; genus: *Mastadenovirus*) are nonenveloped, double-stranded DNA viruses. Seven species infect humans, *Human*

mastadenovirus A–G, with more than 51 recognized serotypes currently recognized based on their resistance to neutralization.

Epidemiology

At least 15 serotypes within species B, C, and E cause respiratory tract infections, and certain serotypes (4, 7, 14, and 21) are associated with outbreaks of severe respiratory disease in crowded populations, such as in military recruits (Lion, 2014). Outbreaks of adenoviral keratoconjunctivitis are also an important concern. Adenoviruses do not demonstrate a distinct seasonality. Transmission occurs via aerosolized droplets or direct conjunctival inoculation, and contact and droplet isolation precautions are advised for hospitalized patients.

Clinical Presentation

The majority of adenoviral respiratory infections present as mild URTIs in children following an incubation period of 5 to 6 days. However, in one series, adenoviruses were detected in 11% of pediatric patients hospitalized for severe respiratory infection, mostly in children under 5 years of age (Jain et al., 2015b). Keratoconjunctivitis ("pink eye") may present with or without URTI symptoms. Severe pneumonia may develop in vulnerable patients, including young children. Adenoviruses are also an important cause of childhood diarrhea. Immunocompromised patients are at risk of severe multiorgan disease, including meningitis, myocarditis, encephalitis, and hepatitis, and are discussed further in Viral Infections in Immunocompromised Hosts later.

Laboratory Diagnosis

Multiple approaches are available for the diagnosis of adenovirus infection, including PCR, viral culture, and histopathologic studies. PCR represents the most useful and utilized modality due to its high sensitivity and specificity, capacity to detect early infection, utility in disease monitoring (including quantitative detection), and capacity to test multiple sample types. Adenovirus shedding may persist for an extended time period in the GI tract, and to a lesser extent in the respiratory tract, and confound result interpretation. As such, identification of adenovirus DNA by PCR from a normally sterile site is the most useful. Both laboratory-developed tests and commercial assays are available for testing.

During acute infection, adenovirus can be detected in respiratory secretions or stool by cell culture of epithelial cells such as A549. Cytopathic effect usually appears in 2 to 5 days but can take as long as 10 to 14 days. Moreover, Adenovirus 40 and 41 are fastidious and do not replicate in commonly used cell cultures; PCR from stool is typically performed for this diagnosis.

Clinical Implications

Most adenovirus infections are self-limited and will resolve with supportive management. However, patient populations such as immunocompromised hosts and young infants are at increased risk of severe disease and may require therapy. Cidofovir, an inhibitor of viral DNA polymerase, has been used for many years for adenovirus therapy but frequently induces nephrotoxicity limiting its use. An oral lipid ester of cidofovir, brincidofovir, has emerged as a therapeutic alternative with reduced toxicity. Limited data in support of these therapies have shown clinical improvement and suggestion of improved survival (Ljungman et al., 2003; Doan et al., 2007). Appropriate infection control procedures should also be implemented, including in subgroups of immunocompromised individuals with persistent shedding in stool.

INFECTIOUS MONONUCLEOSIS AND RELATED INFECTIONS

Introduction

Infectious mononucleosis (IM) is a febrile illness characterized by pharyngitis and lymphadenopathy, with associated atypical lymphocytosis (Dunmire et al., 2018). The incidence of IM in the United States is estimated to be about 500 cases per 100,000 per year (Williams-Harmon et al., 2016; Luzuriaga & Sullivan, 2000). The major etiologic agent of IM is Epstein-Barr virus (EBV), though other viruses, as well as bacteria and parasites, may present with a similar syndrome.

Epstein-Barr Virus

Epidemiology

EBV is among the most ubiquitous human viruses, infecting more than 90% of the world's adult population (de-The et al., 1975). Similarly, approximately 90% of IM cases are attributable to primary EBV infection (Hurt & Tammaro, 2007). IM is a disease of adolescence and early adulthood, with the highest annual incidence in individuals 15 to 24 years of age (Womack & Jimenez, 2015). College freshmen are at particularly high risk. Transmission in this age group is due to exposure to infected saliva, primarily via deep kissing (Dunmire et al., 2018). IM has no gender predisposition, yearly cycles, or seasonal variation. In adolescents and young adults, the rate of developing IM from primary EBV infection ranges from 26% to 74% (Dunmire et al., 2018; Womack & Jimenez, 2015). The incubation period is estimated to be 30 to 50 days (Dunmire et al., 2018; Luzuriaga & Sullivan, 2000).

In contrast to adolescence and young adults, primary EBV infection in early childhood typically manifests asymptomatically or with a nonspecific presentation. EBV exposure in early childhood is thought to be associated with close contact with household members and/or caregivers, and the mode of transmission is again likely to be through infected saliva. Transmission of EBV may also occur through transfusion or transplantation.

Virology

EBV or human gammaherpesvirus-4 (HHV-4) (family: Herpesviridae; subfamily: Gammaherpesvirinae; genus: *Lymphocryptovirus*) is an enveloped, double-stranded DNA virus comprised of a 172 kb genome and two major types, type 1 and type 2. During primary infection via the salivary route, EBV infects both epithelial cells of the oral cavity and B cells in pharyngeal lymphoid tissue. The initial binding of EBV to B cells is mediated by the high-affinity interaction of the gp350 envelope glycoprotein with CD21, complement receptor 2 (CR2) (Shannon-Lowe & Rowe, 2014). EBV establishes latency in resting memory-like B cells where it resides as an episome at 5 to 500 copies per cell (Dunmire et al., 2018).

Clinical Presentation

The classic clinical triad of IM, described originally in 1889 as glandular fever, is pharyngitis, fever, and lymphadenopathy. Fatigue, tonsillar enlargement, pharyngeal erythema, and palatal petechiae are also commonly observed. Other findings may include hepatomegaly, splenomegaly, nausea, vomiting, periorbital edema, and rash, though rash is most commonly associated with administration of β-lactam antibiotics. In a prospective study of undergraduate students, the median duration of acute illness was 18 days (range, 3–54 days) (Dunmire et al., 2018).

Laboratory Diagnosis

IM is associated with lymphocytosis, defined as an absolute count greater than 4500/μL or a differential count greater than 50% on peripheral smear. Significant atypical lymphocytosis may also be present, defined as more than 10% of total lymphocytes. As expected, these hematologic findings are neither sensitive nor specific for IM.

The diagnosis of IM continues to be made serologically through the identification of heterophile antibodies. Heterophile antibodies are defined by their property to agglutinate cells from species different from those of the source serum. The heterophile antibodies of IM, referred to in the literature as the Paul-Bunnell heterophile antibody after the discovering scientists (Paul & Bunnell, 1974), are primarily of the IgM isotype and agglutinate sheep and horse red blood cells. These cross-reacting antibodies are detected using red cell or latex agglutination rapid tests. One type of IM heterophile antibody test is the Monospot, a red cell agglutination assay that detects the presence of antibodies capable of binding to a surface component of equine erythrocytes (Marshall-Andon & Heinz, 2017). Heterophile antibody tests and Monospot are frequently used interchangeably to refer to tests that detect the heterophile antibodies of IM.

The sensitivity and specificity of heterophile antibody tests for the diagnosis of IM ranges from 63% to 84% and 84% to 100%, respectively (Linderholm et al., 1994). False negatives are of particular concern during the first week of symptoms, though sensitivity overall remains moderate (Hurt & Tammaro, 2007). Furthermore, heterophile antibody tests should not be used for the diagnosis of primary EBV infection in children 4 years and younger, as the sensitivity in this population is less than 40%. Importantly, false-positive heterophile antibodies may be associated with other pathogens, malignancy, or autoimmune disease (Dunmire et al., 2018). In addition, heterophile antibodies may persist for a year or more, so may not reflect acute EBV infection. Given these performance characteristics, the CDC does not recommend heterophile antibody tests for general use.

EBV-specific serology is useful to determine whether an individual is susceptible to EBV infection or has a recent or past infection. In practice, EBV-specific serology may be used to resolve questions regarding both heterophile-positive and heterophile-negative IM.

Several antibodies have been shown to provide important information regarding patients' EBV exposure status. IgM and IgG antibodies against

TABLE 64.1
Common Patterns of EBV-Specific Serologic Testing

VCA IgG	VCA IgM	EA IgG	EBNA-1 IgG	Interpretation
NEG	**NEG**	**NEG**	**NEG**	No serologic evidence of infection
NEG	**POS**	NEG	**NEG**	Current or recent infection
POS	**POS**	NEG	**NEG**	
POS	**POS**	POS	**NEG**	
NEG	**POS**	POS	**NEG**	
POS	NEG	NEG	**POS**	Past infection
POS	NEG	POS	**POS**	
POS	POS	NEG	**POS**	
POS	POS	POS	**POS**	

EA, Early antigen; *EBNA,* Epstein Barr nuclear antigen; *EBV,* Epstein Barr virus; *IgG,* immunoglobulin G; *IgM,* immunoglobulin M; *NEG,* negative; *POS,* positive; *VCA,* viral capsid antigen.

TABLE 64.2
Less Common Patterns of EBV-Specific Serologic Testing

VCA IgG	VCA IgM	EA IgG	EBNA-1 IgG	Interpretation
NEG	NEG	**POS**	NEG	False positive or uncertain timing
NEG	NEG	NEG	**POS**	Likely past infection
NEG	POS	NEG	**POS**	
NEG	NEG	POS	**POS**	
NEG	POS	POS	**POS**	
POS	**NEG**	NEG	**NEG**	Uncertain timing

EA, early antigen; *EBNA,* Epstein Barr nuclear antigen; *EBV,* Epstein Barr virus; *IgG,* immunoglobulin G; *IgM,* immunoglobulin M; *NEG,* negative; *POS,* positive; *VCA,* viral capsid antigen.

the viral capsid antigen (VCA IgM and VCA IgG) rise early in acute infection, and while VCA IgG persists for life, VCA IgM generally wanes over the 3 months following acute infection. IgG antibodies to early antigen (EA IgG), like VCA IgM, typically rise at the onset of clinical illness and wane after several months; however, this antibody persists in a significant percentage of patients. IgG antibodies to EBV nuclear antigen-1 (EBNA-1 IgG), a protein expressed after the establishment of viral latency, generally begin to appear 6 to 12 weeks after primary infection and persist for life. Given the different time courses of these antibodies' appearances in the immunologic response to EBV, their combinatorial serologic patterns can provide important information regarding the presence, absence, acuity, and chronicity of an EBV infection (Gartner et al.,2003; Hess, 2004; de Ory et al., 2011).

Table 64.1 describes common patterns of EBV-specific serologic testing. A susceptible individual is negative for all serologic markers. Current or recent infections are characterized by detection of VCA IgM antibodies in the absence of EBNA-1 IgG antibodies. In contrast, past infection is characterized by the presence of both VCA IgG and EBNA-1 IgG antibodies.

Table 64.2 shows less common patterns of EBV-specific serologic testing (e.g., the detection of EA IgG antibody alone may be a false positive or represent uncertain timing of exposure). The presence of EBNA-1 IgG in the absence of VCA IgG is consistent with a likely past infection. Finally, the presence of VCA IgG in the absence of both VCA IgM and EBNA-1 IgG indicates uncertain timing. This pattern may represent a past infection without a detectable EBNA-1 IgG response or a current/recent one, or infection without a detectable VCA IgM response. As demonstrated in these tables, EA IgG is of limited utility and can be safely removed from these EBV-specific antibody panels.

Traditionally, indirect immunofluorescence (IFA) has been used as a semiquantitative method to detect EBV-associated antibodies. In this method, an aliquot of a patient's serum is added to wells containing substrate, followed by the addition of a secondary fluorescently labeled antibody. The wells are then examined under fluorescent microscopy. Semiquantitative endpoint titers are determined by testing serial dilutions of positive specimens. Although this method is considered the gold standard, a major challenge arises in the qualitative determination by lab personnel of the presence or absence of fluorescence. Numerous immunoassays are also available that use enzyme-conjugated secondary antibody to produce a colored or fluorescent product that can then be detected.

Nucleic acid amplification testing for EBV DNA is not recommended for the diagnosis of IM.

Clinical Implications

IM is typically a self-limited disease. Treatment for individuals with IM is supportive care. Neither glucocorticoids nor acyclovir, a nucleoside analog with anti-EBV activity, is recommended for uncomplicated acute EBV infection, though steroids may be beneficial in cases of airway obstruction, a serious but uncommon complication of acute illness. Other complications include hemolytic anemia, thrombocytopenia, meningoencephalitis, and splenic rupture. To avoid splenic rupture athletes are recommended to abstain from contact sports for at least 3 weeks, though return to full activity may be longer if signs and symptoms have not resolved (Dunmire et al., 2018).

Some individuals develop enduring fatigue and other symptoms following primary EBV infection that meet the clinical criteria for Chronic Fatigue Syndrome/Myalgic Encephalomyelitis (CFS/ME) (Hickie et al., 2006). There is also a distinct syndrome called chronic active EBV (CAEBV), characterized by persistent and recurrent IM-like symptoms and detection of high levels of EBV DNA in tissues and peripheral blood (Okano et al., 2005). CAEBV is a rare, EBV-positive T/NK cell neoplasm that is primarily found in Japan and neighboring countries (Arai, 2019).

Additionally, latent EBV is associated with numerous malignancies, including Burkitt lymphoma, Hodgkin lymphoma, nasopharyngeal carcinoma, peripheral T-cell lymphoma, and gastric carcinoma (Shannon-Lowe & Rickinson, 2019). Furthermore, EBV is associated with malignancies of the immunocompromised host, including posttransplant lymphoproliferative disorder.

Other Causes of Infectious Mononucleosis

Approximately 10% of IM cases are caused by pathogens other than EBV (Hurt & Tammaro, 2007). The causative agents of these mononucleosis-like illnesses include primary infections with cytomegalovirus (CMV), human betaherpesvirus-6 (HHV-6), herpes simplex virus-1 (HSV-1), adenovirus, and human immunodeficiency virus-1 (HIV-1). Group A β-hemolytic *Streptococcus pyogenes*, the most common cause of acute bacterial pharyngitis, as well as primary infection with the protozoan parasite *Toxoplasma gondii*, may also present with an IM-like illness.

CONGENITAL AND PERINATAL VIRAL INFECTIONS

Introduction

Congenital and perinatal viral infections are important causes of fetal and neonatal mortality, and for those who survive through the neonatal period, these infections may significantly contribute to subsequent childhood morbidity. Congenital and perinatal viral infections are synonymous with the TORCH acronym, which was initially used to group five infections (**T**oxoplasmosis, Syphilis [**O**ther], **R**ubella, **C**MV, and **H**SV) that presented similarly with rash and ocular findings. Infections with *Toxoplasma gondii* and *Treponema pallidum* are covered elsewhere in this volume (see Chapters 65 and 61, respectively), and in this section rubella virus, CMV, and HSV will be covered in detail. A number of other viruses may be transmitted in utero, including HIV-1, hepatitis B, hepatitis C, Parvovirus B19, varicella zoster virus (VZV), enteroviruses, Zika virus, and the recently described SARS-CoV-2 (Neu et al., 2015; Leeper & Lutzkanin, 2018; Muldoon et al., 2020).

Rubella

Epidemiology

Rubella, also known as German measles or three-day measles, is a mild febrile rash illness transmitted through direct or droplet contact with infected nasopharyngeal secretions. Primary infection of a nonimmune mother with rubella virus during pregnancy may result in vertical transmission to the fetus and subsequent miscarriage or the development of congenital rubella syndrome (CRS). Risk of fetal infection is highest in the first trimester (>80%), with decreasing risk in the second trimester (~25%), then increasing risk in the third trimester up to term (60–100%) (Miller et al., 1982). The risk of severe birth defects is highest during the first trimester (~85%).

Rubella is a vaccine preventable disease and is a component of the live-attenuated MMR (measles, mumps, rubella) vaccine. Rubella was

declared eliminated in the United States in 2004 and the Americas in 2015. However, rubella-containing vaccines (RCVs) are not included in the national immunization program for many low- and middle-income countries (LMICs). Given the lack of vaccine coverage it was estimated that there were more than 100,000 new CRS cases annually worldwide in 2010 (Vynnycky et al., 2016). Since 2011, however, there has been accelerated progress toward control of rubella and CRS associated with the establishment of accelerated WHO rubella elimination goals and the availability of financial support for RCV introduction. This progress has been evidenced by the increase in the number of countries introducing RCV into national childhood immunization schedules and the increase in the global percent RCV coverage: 99 countries in 2000 (21% global RCV coverage), 132 countries in 2012 (40% coverage), and 168 countries in 2018 (69% coverage) (Grant et al., 2019).

Virology

Rubella virus (family: Matonaviridae; genus *Rubivirus*) is an enveloped, single-stranded, positive-sense RNA virus, comprised of a ~9.7 kb genome encoding five open reading frames, three structural proteins (Capsid [C] and envelope glycoproteins E1 and E2), and two nonstructural proteins (p90 and p150). Note that previously rubella virus was a member of the Togaviridae family; the taxonomy was changed in 2018 with the creation of the Matonaviridae family by the International Committee for the Taxonomy of Viruses (ICTV). Rubella virus has a single serotype. Based on E1 sequence, the virus is divided into two major clades, 1 and 2, composed of 10 and 3 genotypes, respectively (Update of standard nomenclature for wild-type rubella viruses, 2007).

Clinical Presentation

CRS is characterized by a small-for-gestational-age neonate with a constellation of congenital abnormalities that include cataracts, sensorineural hearing loss, and cardiac defects (Neu et al., 2015; Toizumi et al., 2019). Neonates with CRS also frequently present with a purpuric or "blueberry muffin" rash, hepatosplenomegaly, and thrombocytopenia. The clinical presentation of maternal rubella infection is typically mild and nonspecific (Bouthry et al., 2014).

Laboratory Diagnosis

The neonatal diagnosis of CRS is confirmed via the presence of rubella-specific IgM antibody in serum, the isolation of rubella virus in culture (e.g., in Vero cells, derived from kidney epithelial cells of the African Green Monkey), or the detection of rubella virus RNA by RT-PCR. For virus isolation or direct detection of the viral genome, the CDC recommends testing of both pharyngeal and urine specimens to increase the likelihood of virus detection.

Clinical Implications

There is no effective antiviral therapy for infection with rubella virus. Management of neonates with CRS is supportive.

Cytomegalovirus

Epidemiology

CMV is a common infection of women of reproductive age with seroprevalence ranging from 45% to approaching 100%, depending on the population (Cannon et al., 2010). Primary CMV infection is a mild febrile illness transmitted through direct contact with infected saliva or urine, though as described earlier in this chapter, primary CMV infection may also present with a mononucleosis-like syndrome similar to EBV. Primary infection of a nonimmune mother with CMV during pregnancy, as well as reactivation of latent virus or reinfection by a different CMV strain, may result in vertical transmission to the fetus and the sequelae of congenital CMV (cCMV) infection. However, the risk of vertical transmission is higher in primary infection (32%) compared to nonprimary infections (1.4%) (Kenneson & Cannon, 2007). In addition, the rate of vertical transmission increases as gestational age increases. In contrast, the risk of symptomatic cCMV disease is highest in the first trimester and decreases as gestational age increases (Bodeus et al., 2010; Picone et al., 2013). Globally, the prevalence of cCMV ranges from 0.2% to 2.5% of live-born neonates, and in developed countries the prevalence is 0.58% (Goderis et al., 2014).

Virology

CMV or human betaherpesvirus-5 (HHV-5) (family: Herpesviridae; subfamily: Betaherpesvirinae; genus: *Cytomegalovirus*) is an enveloped, double-stranded DNA virus comprised of a ~236 kbp genome, the largest of the herpes family viruses. Like other members of Herpesviridae, CMV establishes lifelong latency following primary infection.

Clinical Presentation

Neonates with symptomatic cCMV at birth are often small for gestational age and are characterized by the presence of a petechial rash, hepatosplenomegaly, thrombocytopenia, and jaundice. Symptomatic cCMV is associated with significant neurologic abnormalities, including microcephaly, chorioretinitis, and sensorineural hearing loss (SNHL) (Boppana et al., 2013). Approximately 40% to 60% of symptomatic neonates will develop long-term, permanent sequelae, including SNHL, visual impairment, and intellectual disabilities (Dollard et al., 2007). SNHL is the most well-studied of the long-term adverse neurologic outcomes associated with cCMV; 32.8% of symptomatic neonates will develop hearing loss, and of these cases 65.1% of the hearing loss will be bilateral and severe to profound (Goderis et al., 2014). However, only ~10% to 15% of congenitally infected neonates are symptomatic at birth. Nevertheless, asymptomatic neonates remain at risk for the development of long-term, permanent sequelae. In particular, 9.9% of asymptomatic congenitally infected neonates will develop SNHL, and of these cases over 40% of the hearing loss will be bilateral and severe to profound. Importantly, a subset of asymptomatic neonates experiences delayed onset hearing loss such that they pass newborn hearing screens.

Laboratory Diagnosis

The diagnosis of cCMV can be made prenatally by testing amniotic fluid or postnatally. Definitive postnatal diagnosis of cCMV can only be confidently made within 3 weeks of birth; subsequently, CMV detection may reflect either cCMV or postnatally-acquired infection. Laboratory abnormalities associated with cCMV include thrombocytopenia, elevated liver enzymes, and increased total and conjugated bilirubin. Infants with cCMV infection consistently shed high levels of virus in the urine and saliva, and these samples are optimal for testing (Gantt et al., 2017). Diagnostic modalities include PCR and viral culture, either traditional (requires 1–3 days or longer incubation) or shell vial (requires 1 day). Dried blood spots (DBS) can also be used for testing by PCR but are less sensitive. PCR is advantageous due to its rapid turnaround time, high sensitivity, and high testing availability (Gantt et al., 2017). Although viral culture has traditionally been the reference standard, reproducibly positive results by PCR are now accepted as virologically proven as well.

Clinical Implications

Early recognition and diagnosis of cCMV is crucial to guide initiation of therapy and reduce burden of disease. Treatment is indicated for symptomatic infants and asymptomatic infants with immune deficiency (Luck et al., 2017). The standard of care for treatment of mild disease is 6 months of valganciclovir, a prodrug of the DNA polymerase inhibitor ganciclovir. Infants with cCMV also require regular audiologic follow-up to assess for sensorineural hearing loss.

Many settings currently rely on clinical suspicion of cCMV alone to guide initiation of diagnostic testing. The implementation of targeted or universal newborn screening programs for earlier diagnosis of cCMV suggests better clinical outcomes could be achieved in a cost-effective manner (Gantt et al., 2016).

Herpes Simplex Virus

Epidemiology

Neonatal HSV infection (NHSV) is estimated to occur in 1 of every 3000 to 20,000 newborns and lead to significant morbidity and mortality (Mahnert et al., 2007). The risk of maternal to fetal transmission depends on the context of the genital HSV infection: primary versus recurrent infection and the preexisting presence of maternal antibody versus not. The highest risk corresponds to maternal infection that occurs for the first time in a nonimmune individual. Genital infection may be missed in asymptomatic cases, which is of important concern given that over 75% of NHSV cases are transmitted during delivery (Allen & Robinson, 2014). In contrast, in utero transmission occurs in less than 5% but can be associated with devastating outcomes (Allen & Robinson, 2014).

Virology

HSV (family: Herpesviridae; genus: *Simplexvirus*) is a double-stranded DNA virus divided in two genotypes: HSV-1 and HSV-2. Globally, HSV-2 is estimated to account for 75% of NHSV and HSV-1 for 25% (Kimberlin et al., 2018).

Clinical Presentation

In utero NHSV infection usually manifests with the triad of skin findings such as vesicles or scarring, eye damage, and severe central nervous system (CNS) findings such as microcephaly (Marquez et al., 2011). There are three main syndromes associated with NHSV: disease limited to the skin, eyes, and mouth (SEM); localized CNS disease; and disseminated disease (Allen & Robinson, 2014). Infected infants usually manifest symptoms within the first month of life and up to 6 weeks. Importantly, skin manifestations are not always present, and a high degree of clinical suspicion is required to send the appropriate testing.

Laboratory Diagnosis

Basic laboratory abnormalities in NHSV include thrombocytopenia and hepatitis. Similar to CMV, multiple diagnostic modalities are available for the diagnosis of HSV; however, PCR is the most widely used given its rapid turnaround time and high accuracy. All suspected NHSV cases should undergo mucous membrane testing (mouth, nasopharynx, and conjunctivae) in addition to vesicular fluid testing if skin lesions are present. Mucous membrane swabs should only be collected a minimum of 24 hours after delivery to prevent false-positive results from the mother (Allen & Robinson, 2014). Other sample types should be collected for PCR testing based on the clinical syndrome, including blood, nasopharyngeal swabs, and cerebrospinal fluid (CSF).

Clinical Implications

Prompt initiation of intravenous acyclovir therapy is required for cases of suspected or confirmed NHSV. The clinical syndrome dictates the duration of therapy, and ranges from 7 days to 3 weeks (Allen & Robinson, 2014). Close audiologic and developmental monitoring is also required given the significant morbidity associated with this illness.

VIRAL MENINGITIS AND ENCEPHALITIS

Viral Meningitis

Introduction

Meningitis refers to inflammation of any of the three meningeal layers (dura mater, arachnoid membrane, and pia mater) and is characterized by the presence of white blood cells (WBCs) in the CSF. Aseptic meningitis refers to clinical and laboratory evidence of meningeal inflammation with negative routine cultures and is often challenging to diagnose. The burden of aseptic meningitis is inversely proportional to age, with an estimated annual incidence of 219/100,000 in infants under age 1, 27.8/100,000 in children under age 14, and 7.6/100,000 in adults (Mount & Boyle, 2017; McGill et al., 2018; Logan & MacMahon, 2008). Multiple viruses can cause aseptic meningitis, most commonly enteroviruses, HSV-2, and VZV (Kupila et al., 2006; Jarrin et al., 2016; Shukla et al., 2017; Khetsuriani et al., 2003). Clinical presentation is not specific for any given viral etiology and is mainly differentiated from encephalitis by the absence of abnormal brain function, although significant overlap in these syndromes may occur. Most cases of viral meningitis are self-limited and associated with good outcome; however, considerable morbidity may occur with associated encephalitis (Logan & MacMahon, 2008).

Enteroviruses and Parechovirus

Epidemiology. Human enteroviruses (EVs) and human parechovirus (HPeV) are ubiquitous viruses associated with multiple diseases, including aseptic meningitis, myocarditis, febrile syndromes, exanthema, conjunctivitis, hepatitis, and other clinical syndromes, and are transmitted through the fecal-oral route. Although Enterovirus D68 was first identified in 1962, a countrywide outbreak of this serotype in 2014 drew heightened attention to its importance and potential for severe clinical presentation of acute flaccid myelitis (Cassidy et al., 2018). The incubation period for both genera is unclear, but it is recognized that viral shedding can persist for weeks in the gastrointestinal and respiratory tracts (Chung et al., 2001). Seasonality is an important factor to consider, with peak cases occurring in the summer or fall. Nonetheless, between 6% and 10% of cases occur during winter months and should still be considered in the differential (Pons-Salort et al., 2018). Infants, newborns, and immunocompromised hosts are considered at highest risk for meningitis.

Virology. Human enteroviruses (family: Picornaviridae; genus: *Enterovirus*) are single-stranded, nonenveloped RNA viruses and include over 100 genotypes spanning coxsackieviruses, echovirus, polioviruses, and other non-poliovirus enteroviruses. Parechovirus (family: Picornaviridae; genus: *Parechovirus*) shares similar viral organization to human enteroviruses and was recently reclassified in its own genus on the basis of genomic analyses and is classified into 19 genotypes (Hyypia et al., 1992; Olijve et al., 2018).

Clinical Presentation. The clinical presentation of viral meningitis is characterized by headache, fever, and nuchal rigidity. EV and HPeV may be associated with rash, diarrhea, and/or upper respiratory tract infection (URTI) symptoms.

Laboratory Diagnosis. Nucleic acid amplification testing on CSF is the diagnostic modality of choice for meningitis caused by EV and HPeV. Laboratory-developed RT-PCR assays have been developed with good test performance characteristics for these two viruses (Verstrepen et al., 2001; Selvaraju et al., 2013), in addition to a multiplex PCR panel (Leber et al., 2016). Other specimen types that can be used for the diagnosis of Enterovirus include nasopharyngeal and throat swabs, plasma, and stool. Given the possibility of persistent EV shedding, a positive result from the respiratory tract or stool testing does not necessarily imply active infection. In addition, as mentioned in the respiratory section of this chapter, cross-reactivity with Rhinovirus may be an issue when testing respiratory samples depending on the assay used.

Viral culture from multiple specimen types (including respiratory, tissue, fluids, and stool) can also be performed to isolate Enterovirus, but it is longer, less sensitive, and more labor intensive than molecular methods. Most species proliferate within 2 to 5 days in standard cell culture of primary monkey kidney cells (PMK) or human fibroblast cells. Preliminary identification can be performed with pan-EV immunofluorescence screening reagents, followed by type-specific monoclonal antibody identification. Cytopathic effect (CPE) for Enterovirus is characterized by small cells with the appearance of cytoplasmic tails, and the presence of large empty areas in the monolayer is typical (Leland & Ginocchio, 2007).

Clinical Implications. Access to prompt molecular testing can accelerate safe patient discharge from the emergency department and facilitate antibiotic and diagnostic stewardship by allowing cessation of antibiotics and reduction of additional unnecessary tests (Lafolie et al., 2018; Ramers et al., 2000; King et al., 2007). Supportive care is the mainstay of therapy for EV and HPeV meningitis.

HSV

Epidemiology. Herpes simplex virus type 2 (HSV-2) has been recognized as a frequent cause of viral meningitis, especially in young women. In contrast, HSV-1 is typically associated with encephalitis (Kupila et al., 2006).

Virology. HSV (family: Herpesviridae; genus: *Simplexvirus*) is a double-stranded DNA virus in the subfamily Alphaherpesviridae. It is divided in two genotypes: HSV-1 and HSV-2.

Clinical Presentation. Most cases of HSV meningitis are preceded by the appearance of genital lesions. Of persons who develop primary genital HSV infection, between 13% and 36% will develop symptoms consistent with meningitis (Schlesinger et al., 1995). Uniquely, HSV-2 can cause a form of recurrent benign lymphocytic meningitis named Mollaret meningitis, which self-resolves within a few days.

Laboratory Diagnosis. Molecular diagnosis is the modality of choice for the diagnosis of HSV meningitis and can be performed by laboratory-developed or commercial targeted PCR or by multiplex commercial PCR panel such as the BioFire FilmArray ME panel. Higher analytic sensitivity has been shown for laboratory-developed and FDA-cleared targeted HSV assays compared to the multiplex panel and is discussed in further detail in the context of HSV encephalitis later.

Clinical Implications. Diagnosis of HSV is important as it is one of the few aseptic meningitis viruses that is therapeutically actionable with intravenous acyclovir treatment. Controversy exists regarding the indication of treatment of HSV meningitis in previously healthy hosts, given lack of evidence of improved clinical outcomes in this setting (Noska et al., 2015). However, immunocompromised hosts should be treated. This is in stark contrast to HSV encephalitis, in which all patients should be treated promptly to limit adverse outcomes.

HIV

Epidemiology. Despite major advancements in reduction of HIV transmission, almost 70,000 new HIV infections were diagnosed in the United States in 2017 and 1.7 million worldwide in 2018 (UNAIDS, 2018: CDC, 2019). Neurologic symptoms are thought to occur in almost 20% of acutely infected individuals, resulting from underlying meningitis, meningoencephalitis, and encephalitis (Boufassa et al., 1995).

Virology. The human immunodeficiency virus (family: Retroviridae; genus: *Lentivirus*) is a single-stranded, enveloped RNA virus with a genome size of 9.75 kb, including two species: HIV-1 and HIV-2.

Clinical Presentation. HIV meningitis overwhelmingly occurs in the context of acute retroviral syndrome, characterized by fever, rash, malaise, lymphadenopathy, pharyngitis, weight loss, and diarrhea. Neurologic

symptoms vary and include headache, seizures, and cranial palsies (Wood et al., 2014). A high index of suspicion is required as this syndrome can be easily overlooked given the nonspecific nature of symptoms and the timing of neurologic symptoms, which can occur as late as 3 months after the onset of the acute retroviral syndrome. Interestingly, the presence of neurologic symptoms may be associated with risk of accelerated HIV disease progression (Newton et al., 2002).

Laboratory Diagnosis. HIV diagnosis in an individual with symptoms can usually be performed by the standard diagnostic algorithm, starting with a combined antigen/antibody immunoassay. HIV NAAT on CSF is possible in certain reference laboratories and may be useful to confirm HIV as the etiologic agent of meningitis in nongrossly bloody specimens (Almeida, 2015).

Clinical Implications. Prompt initiation of combination antiretroviral therapy is indicated in the setting of confirmed HIV infection.

Lymphocytic Choriomeningitis Virus (LCMV)

Epidemiology. LCMV is distributed worldwide. Despite likely underestimated disease burden, LCMV has been reported as the second most frequent cause of meningitis after human enteroviruses in certain settings (Khetsuriani et al., 2003). Multiple outbreaks have been reported, mainly involving pet shops (Gregg, 1975). Seasonality is an important clue to consider as most cases occur in the winter. LCMV is excreted in the urine and feces of rodents, including mice, rats, and hamsters. It is estimated that approximately 5% of house mice in the United States carry LCMV, of which most are asymptomatic. Although mortality is low (<1%), LCMV may be a cause for concern in the setting of pregnancy given potential for vertical transmission (Bonthius, 2012).

Virology. LCMV (family: Arenaviridae; genus: *Mammarenavirus*) is a negative-sense, single-stranded, enveloped RNA virus.

Clinical Presentation. LCMV is strongly neurotropic and thus neurologic symptoms predominate the clinical picture (Bonthius, 2012). Adults typically present meningitis symptoms that can last weeks, but prognosis overall is good. Vertical transmission of LCMV is associated with severe CNS disease and should be considered in the differential diagnosis of a fetus diagnosed with cerebral calcifications and/or hydrocephalus (Bonthius, 2012).

Laboratory Diagnosis. LCMV is unusual among viruses as it is associated with low glucose in CSF in 20% to 30% of cases (Adair et al., 1953). Serology is the recommended diagnostic method, including IgM and IgG in serum and CSF with the use of paired acute and convalescent samples. Testing is restricted to select reference laboratories.

Clinical Implications. Limited in vitro data support the use of ribavirin; however, it is not routinely recommended for clinical use. Confirmation of LCMV in pregnancy may entail closer follow-up by fetal ultrasound to assess and monitor the presence of fetal anomalies.

Other

Many other viruses causing meningitis or meningoencephalitis should be considered based on clinical presentation, epidemiologic risk features, and travel history. Such viruses can overlap in their presentation with meningoencephalitis, including multiple arboviruses further discussed later.

Viral Encephalitis

Introduction

Encephalitis refers to inflammation of the brain parenchyma itself, with or without associated meningitis, and is associated with significant morbidity and mortality. The burden of viral encephalitis in the United States is significant leading to almost 3000 hospitalizations per year, for an annual cost of hospitalization over $81 million (USD) (Khetsuriani et al., 2002). Etiologic diagnosis of encephalitis cases remains challenging with confirmation of an infectious etiology in less than half of cases (Khetsuriani et al., 2002). Of these, the most common etiologic organism is viral (38.2%), most frequently with HSV and VZV. Many other viruses have also been implicated, including multiple arboviruses, measles, mumps, LCMV, rabies, and others (Khetsuriani et al., 2003). Arboviral etiologies vary markedly geographically based on vector distribution. In North America, the most common arboviral etiologic agents are West Nile virus, eastern and western equine encephalitis, St. Louis and California encephalitis virus, La Crosse virus (Lindsey et al., 2014).

HSV

Epidemiology. HSV-1 is the most common etiologic agent of viral encephalitis worldwide and the leading cause of sporadic fatal encephalitis (Kupila et al., 2006). HSV-2 encephalitis can also occur in neonates (Corey et al., 1988). Encephalitis-related hospitalizations in the United States are estimated to occur in 10.3 cases/million neonates, 2.4/million children, and 6.4/million adults and lead to considerable in-hospital mortality ranging from 1% to 8% (Modi et al., 2017).

Virology. HSV (family: Herpesviridae; genus: *Simplexvirus*) is a double-stranded DNA virus in the subfamily Alphaherpesviridae; it is divided in two genotypes: HSV-1 and HSV-2. HSV encephalitis may occur through three routes of infection: (1) rapid CNS spread following primary infection (mainly in children), (2) CNS dissemination following viral reactivation, and (3) viral reactivation within the CNS itself (Levitz, 1998).

Clinical Presentation. HSV encephalitis (HSE) typically presents with the rapid onset of fever and focal neurologic signs, including altered mental status, cranial nerve palsies, seizures, and language and behavioral abnormalities (Levitz, 1998; Long, 2011). Other manifestations can occur, including rash, aseptic meningitis, loss of bladder or bowel control, and progression of neurologic symptoms such as memory impairment (Tunkel et al., 2008).

Laboratory Diagnosis. CSF is a valuable tool in the early assessment of suspected encephalitis and typically shows mild to moderate lymphocytic pleocytosis and elevated protein. An abnormally elevated number of red blood cells that does not normalize with subsequent CSF tube draws is also seen in the majority (84%) of cases (Levitz, 1998).

PCR is the modality of choice for the rapid and accurate diagnosis of HSV. The gold standard for HSE diagnosis is brain biopsy; however, given the invasive nature of this procedure, CSF is most commonly performed to enable a more rapid and less invasive diagnosis. Sensitivity and specificity of PCR reach 98% and 94%, respectively, when compared to brain biopsy–proven disease (Lakeman & Whitley, 1995). This can be performed by laboratory-developed or commercial targeted PCR, or by multiplex commercial PCR panel (FilmArray ME panel). Higher analytic sensitivity has been shown for laboratory-developed and FDA-cleared targeted HSV assays compared to this multiplex panel and should be considered when interpreting a negative result. For example, lower limit of detection (LLOD) comparison has shown an advantage of the FDA-cleared Simplexa HSV-1/2 Direct Assay (Focus Diagnostics, Cypress CA) (30 copies/mL [5 $TCID_{50}$/mL]) compared to the FilmArray ME panel (1500 copies/mL [250 $TCID_{50}$/mL]) (Gomez et al., 2017). However, early diagnosis can be missed even by the most sensitive molecular tests and thus testing should be repeated 3 to 7 days later if clinical suspicion persists or with temporal lobe involvement on CNS imaging and initial negative HSV testing (Tunkel et al., 2008; Weil et al., 2002). Furthermore, brain biopsy should be considered in cases when the diagnosis cannot be established through CSF testing alone as HSE may be detected only on brain biopsy (Rice et al., 2014). Viral culture shows very low sensitivity (5%) for detection of HSE (Levitz, 1998).

Clinical Implications. Early diagnosis and treatment of HSE is crucial to prevent morbidity, including serious sequelae and death (Tunkel et al., 2008). Intravenous acyclovir is the recommended treatment for HSE and should be administered for a 14- to 21-day course (Tunkel et al., 2008). Despite treatment, in-hospital mortality remains high at up to 12% in intensive care units (ICUs), and moderate to severe disability occurs in about half of survivors (Jouan et al., 2015).

VZV

Epidemiology. VZV can affect all age groups, but incidence gradually increases with age starting between the ages of 40 and 50 years (Johnson et al., 2015). Encephalitis is most commonly seen in immunocompromised hosts and is the second highest cause of viral encephalitis mortality after HSV (Johnson et al., 2015).

Virology. Like HSV, VZV is a double-stranded DNA virus (family: Herpesviridae; genus: *Varicellovirus*). VZV also establishes latency in the dorsal root ganglia and can reactivate in the CNS.

Clinical Presentation. The clinical presentation is similar to that of HSE, including a history of rash in most cases. However, absence of a rash does not exclude the diagnosis and can particularly be seen in immunocompromised hosts. In children, primary cerebellar involvement may be seen frequently leading to delirium and occasionally seizures. VZV-related vasculitis can present a wide range of symptoms, including acute hemiplegia, transient ischemic attacks (TIA), cerebral aneurysm, cerebral hemorrhage, or carotid dissection (Gilden et al., 2009).

Laboratory Diagnosis. CSF findings are similar to those described with HSV. As with HSV, VZV PCR is best diagnosed by laboratory-developed or commercial targeted PCR and can be diagnosed by the FilmArray ME panel (Leber et al., 2016; Liesman et al., 2018).

Clinical Implications. Intravenous acyclovir treatment is recommended for 10 to 14 days for the treatment of VZV encephalitis on the basis of limited clinical data (Tunkel et al., 2008).

TABLE 64.3

Other Important Arboviral Etiologies of Encephalitis

Viral Family	Virus	Geographic Distribution	Vector	Main Diagnostic Modality
Flaviviridae	Yellow fever	Sub-Saharan Africa, South America	Mosquito (*Aedes* spp., *Haemagogus* spp.)	Serology, NAAT
	Japanese encephalitis virus	Asia, Southeast Asia, Pacific Islands	Mosquito *(Culex tritaeniorhychnus)*	Serology
	St Louis encephalitis virus	North, Central and South America	Mosquito (*Culex* spp.)	Serology
	Murray Valley encephalitis virus	Australia, New Guinea	Mosquito *(Culex annulirostris)*	Serology
	Powassan virus	Russia, United States, Canada	Tick (*Ixodes* spp.)	Serology
	Tickborne encephalitis virus	Europe, Asia	Tick (*Ixodes* spp.)	Serology
Togaviridae	Eastern equine encephalitis	South America	Mosquito (*Culex* spp.)	Serology
	Western equine encephalitis	North, Central and South America	Mosquito (*Culex* spp, *Aedes* spp.)	Serology
	Venezuelan equine encephalitis	North, Central and South America	Mosquito (*Culex* spp, *Aedes* spp.)	Serology
Bunyaviridae	La Crosse	North America	Mosquito *(Aedes triseriatus)*	Serology

NAAT, Nucleic acid amplification test.

Other Viral Etiologies of Encephalitis

Arboviruses are the main next etiologic category of viral encephalitis. They vary widely based on geographic area and host risk factors.

West Nile Virus. In North America, the most common arboviral agent of encephalitis is West Nile virus (WNV) (family: Flaviviridae; genus: *Flavivirus*) with an incidence of 2647 cases in the United States in 2018 (CDC, 2019). Most cases occur between July and September, and are distributed throughout North America (Lindsey et al., 2014). Neuroinvasive disease represents less than 1% of WNV infections and occurs with highest incidence and case fatality ratio in older age groups (Lindsey et al., 2014).

Serology is the mainstay of diagnosis for WNV encephalitis and is performed by testing of both serum and CSF by IgM antibody-capture ELISA (MAC-ELISA) and/or immunofluorescence (IF) (Sambri et al., 2013). Cross-reactivity with other flaviviruses should be considered in patients with recent yellow fever vaccination or possible exposure to other flaviviruses such as zika and dengue, and confirmatory testing by plaque reduction neutralization assay (PRNT) should be performed. RNA detection of WNV has previously shown limited sensitivity from serum and CSF but may be higher in whole blood and urine (Lustig et al., 2016). Molecular detection may be useful in certain patient groups, including immunocompromised hosts with longer viremia and impaired antibody response. Management of WNV encephalitis is based on supportive care.

Other Arboviruses. Multiple other arboviruses can cause encephalitis, of which a selected list is presented stratified by vector type (Table 64.3). Many other viruses associated with encephalitis should be considered in the right epidemiologic and clinical context and include EBV, human herpesvirus 6 (HHV-6), John Cunningham virus, Herpesviridae B virus, HIV, measles, mumps, rabies, avian influenza, Nipah, and Hendra.

VIRAL INFECTIONS WITH SKIN AND MUCOSAL MANIFESTATIONS

Introduction

The majority of viral skin diseases are relatively benign and self-limiting in otherwise healthy individuals but are characterized by a high degree of infectivity by means of direct contact or airborne transmission. Although there is a wide range in their associated clinical syndromes, many pathognomonic associations exist that allow for clinical diagnosis without the need for laboratory confirmation (Ramdass et al., 2015). In general, viral or serologic diagnosis is pursued for diagnosis of immunocompromised hosts or in the perinatal setting to guide therapy or management or for purposes of infection control. The clinical syndromes caused by these viruses can be broadly divided into two categories: those caused by direct inoculation and those caused by hematogenous dissemination (Table 64.4).

Molluscum Contagiosum Virus

Epidemiology

Molluscum contagiosum virus (MCV) most commonly affects children and is transmitted through direct contact. When seen in adults, it is predominantly in the setting of sexual transmission or immunocompromise. Rare cases of vertical transmission have been reported (O'Connell et al., 2008). Incidence estimates vary widely due to likely selection bias in epidemiologic studies, but they average between 4% and 7% in children and 1% and 9% among HIV-infected individuals (Chen et al., 2013). There are four genotypes, among which MCV1 and MCV2 are the most common worldwide (Zorec et al., 2018).

Virology

MCV (family: Poxviridae; genus: *Molluscipoxvirus*) is an enveloped double-stranded DNA virus and is the only species member of its genus. It can only replicate in the human epidermis (Chen et al., 2013).

Clinical Presentation

MCV causes characteristic small (3–5 mm on average), skin-colored, dome-shaped, and umbilicated papules, some of which have a caseous center. The lesions typically number less than 20 and generally are not found on the palms and soles. However, lesions can present atypically as large ("giant molluscum") or widespread in immunocompromised patients.

Laboratory Diagnosis

This diagnosis is usually made clinically and can be confirmed through biopsy if necessary, as the histologic features are highly sensitive and specific (Fig. 64.1) (Ishikawa et al., 2015). No additional viral or serologic diagnostics are needed. Extensive and/or persistent molluscum disease in a patient without prior medical history should trigger testing for HIV or other causes of immunodeficiency such as autosomal recessive DOCK8 combined immunodeficiency (Zhang et al., 2009).

Clinical Implications

While individual lesions usually self-resolve within 2 months, autoinoculation from scratching or trauma extends the mean duration of infection to 8 to 13 months (Chen et al., 2013; Olsen et al., 2015). Lesions on the genital areas are indicative of sexual transmission in adults but are typically secondary to autoinoculation in children. There is no clear evidence to support treatment in immunocompetent individuals (van der Wouden et al., 2017).

Other Poxviruses

Since the eradication of smallpox (variola virus), MCV is thought to be the only poxvirus with a human reservoir. However, there are many other zoonotic poxviruses (e.g., monkeypox, cowpox, orf) that can infect humans. While uncommon, these infections are increasingly being recognized outside of their usual geographic distribution, with the 2003 US outbreak of monkeypox as a most notable example (Lewis-Jones, 2004). As such, these viruses are of concern from a bioterrorism and outbreak prevention perspective.

TABLE 64.4

Laboratory Diagnosis of Viruses With Typical Mucocutaneous Manifestations

Pathogenesis	Mucocutaneous Clinical Syndrome(s)	Virus	Viral Detection	Serologic Assays
Direct inoculation (clinically presents with mucocutaneous lesion[s])	Molluscum contagiosum	MCV	Not done	Not done
	Low-risk subtypes: cutaneous and genital warts, recurrent respiratory papillomatosis; high-risk subtypes: anogenital dysplasia and carcinoma, oropharyngeal carcinoma	HPV	NAAT, signal amplification methods, in situ hybridization (lowest sensitivity but advantageous for localization)	Not done
	Genital herpes, gingivostomatitis, herpes labialis	HSV-1 and HSV-2	NAAT (highest sensitivity), immunohistochemistry (not type specific)	Type specific IgG and IgM, not used for primary diagnosis (negative at acute presentation)
Both direct inoculation and hematogenous dissemination	Varicella (chickenpox) and zoster (shingles)	VZV	NAAT	IgG and IgM, used to assess immunity, though cannot reliably detect vaccine seroconversion
	HFMD, herpangina	Some Enterovirus serotypes	Not done except in atypical/complicated cases	Not done
Hematogenous dissemination (clinically presents with exanthem)	Measles	Measles morbillivirus	RT-PCR (most sensitive during early illness, best on throat/combined nasal and throat swab), viral culture (less sensitive, best on nasopharyngeal aspirate)	IgM (less sensitive than RT-PCR until >7 days after rash onset), or fourfold increase in IgG titer
	Rubella (German measles)	Rubella virus	RT-PCR, viral culture	IgM, or fourfold increase in IgG titer
	Erythema infectiosum (fifth disease)	Parvovirus B19	NAAT (most sensitive), in situ hybridization (most specific)	IgG and IgM, used in the setting of exposure during pregnancy
	Roseola infantum (exanthema subitum, sixth disease)	HHV-6	NAAT	IgG and IgM by immunofluorescence assay (of limited to no clinical utility given ubiquitous nature of virus)

DFA, Direct fluorescence antibody test; *HFMD,* hand, foot, and mouth disease; *HHV-6,* human herpesvirus 6; *HPV,* human papillomavirus; *HSV,* herpes simplex virus; *NAAT,* nucleic acid amplification test; *MCV,* molluscum contagiosum virus; *RT-PCR,* reverse transcriptase polymerase chain reaction; *VZV,* varicella-zoster virus.

Fig. 64.1 **A,** Molluscum contagiosum clinical lesions. These typical lesions are referred to as Mollusca and appear as skin-colored, umbilicated, painless raised lesions with a pearly appearance. **B,** Skin biopsy of molluscum contagiosum displaying the classic histologic features: lobulated endophytic epidermal hyperplasia with bright magenta viral inclusions also known as molluscum bodies or Henderson-Paterson bodies (hemoxylin and eosin [H&E] stain, 5x magnification). This endophytic growth pattern is what causes the characteristic umbilicated appearance of these lesions (From Centers for Disease Control and Prevention [CDC], 2020; Stanford Dermatopathology.)

Human Papillomaviruses

Epidemiology

Human papillomavirus (HPV) infections are ubiquitous, transmitted by direct contact, and usually spontaneously resolving. However, persistent infection with certain HPV types can lead to the development of cancer, accounting for 4.5% of all cancers globally. The majority of these are cervical cancers in low- and middle-income countries (de Martel et al., 2017). In high-income countries such as the United States, the incidence of HPV-related oropharyngeal carcinoma and anal cancer are rising while incidence of cervical cancer is falling (Viens et al., 2016). The epidemiologic landscape of HPV-related disease will continue to change rapidly as access to and indications for HPV vaccination expand.

Virology

HPVs (family: Papillomaviridae, genera: *Alpha-*, *Beta-*, *Gamma-*, *Mu-*, *and Nupapillomavirus*) are small, nonenveloped viruses with circular double-stranded DNA genomes. There are currently over 200 HPV genotypes, with new ones continually being discovered (Bzhalava et al., 2015). The *Alphapapillomavirus* genus contains HPV types with tropism to either mucosal or cutaneous sites, while the remaining four genera infect only cutaneous epithelium (Egawa et al., 2015). The HPV types with mucosal tropism are further classified into low-risk and high-risk (hrHPV) groups based on their oncogenic potential. Among hrHPVs, 12 HPV genotypes (16, 18, 31, 33, 35, 39, 45, 51, 52, 56, 58, and 59) are classified as group I carcinogens (International Agency for Research on Cancer [IARC] Working Group, 2012). While HPV16 and 18 account for the majority of

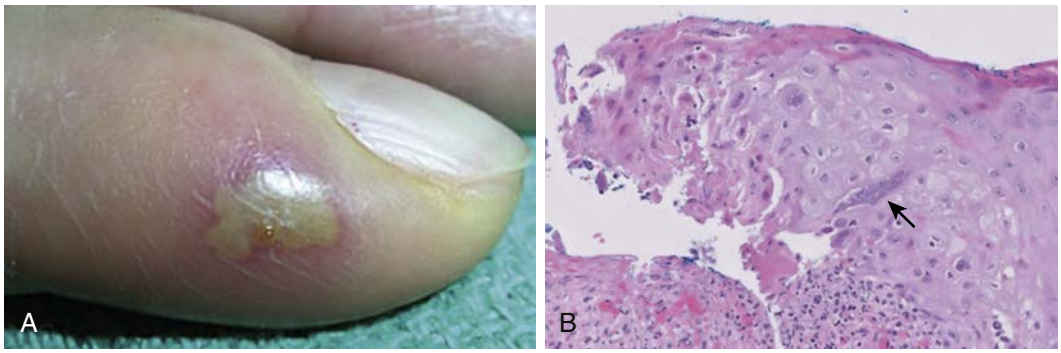

Fig. 64.2 **A,** Classic herpes simplex virus (HSV) skin lesions. A typical herpetic whitlow lesion is presented on the distal finger, with confluent vesicles on an erythematous base. These lesions are very painful. **B,** Skin biopsy in a patient with disseminated HSV-1 infection (hemoxylin and eosin [H&E] stain, 20x magnification). The *arrow* points to a keratinocyte displaying intranuclear inclusions with the characteristic "3 M's" associated with HSV infection: multinucleation, margination of the chromatin, and molding of the nuclei. While these features are classically associated with HSV infection, they are not entirely specific and can also be seen in varicella zoster virus (VZV) infection. Immunohistochemical stains for HSV are available but cannot distinguish between HSV-1 and HSV-2 (From Usatine RP, Tinitigan R: Nongenital herpes simplex virus. *Am Fam Physician* 82[9]:1075–1082, 2010.)

cervical carcinoma in the United States, other hrHPV types predominate in other countries (Fitzpatrick et al., 2019). The oncogenic potential of hrHPV is mediated primarily by viral proteins E6 and E7, which inhibit human tumor suppressor proteins p53 and Rb, respectively (Boyer et al., 1996; Scheffner et al., 1990).

Clinical Presentation

The clinical manifestations of cutaneous HPV infection depend on both the HPV type and the immune status of the host. While many of these infections are asymptomatic, some are associated with cutaneous warts/verrucae, often with features specific to the HPV type (i.e., plantar myrmecia warts with HPV-1, butcher's warts on the hand with HPV-7) (Egawa et al., 2015; Hsu et al., 2009). In patients with epidermodysplasia verruciformis, betapapillomavirus infection (particularly HPV-5 and -8) can lead to cutaneous squamous cell carcinoma (SCC). There are emerging data that betapapillomaviruses may be associated with development of cutaneous SCC in other patients as well (Rollison et al., 2019).

The majority of mucosal HPV infections are cleared spontaneously. Persistent low-risk HPV infection (HPV-6 and -11 predominantly) leads to anogenital warts, which are transmitted sexually. Low-risk HPV transmitted via the birth canal can result in recurrent respiratory papillomatosis, a benign but morbid laryngeal neoplasm in children (Derkay & Bluher, 2019). Persistent infection by hrHPV leads to dysplasia and carcinoma of the cervix and other anogenital sites (anus, vulva, vagina, penis) and is associated with head and neck SCCs (predominantly oropharyngeal carcinoma) in certain populations. The risk for malignant transformation is higher in all sites for HIV-positive patients despite antiretroviral therapy (Palefsky, 2009).

Laboratory Diagnosis

Laboratory diagnosis of cutaneous or low-risk mucosal HPV infections is of limited to no clinical utility. In contrast, diagnosis of hrHPV is a mainstay of cervical cancer screening programs and has contributed to the decline in cervical cancer incidence in many parts of the world. There are over 200 commercially available molecular HPV assays on the global market encompassing numerous technologies with varying performance characteristics, including nucleic acid amplification tests (i.e., PCR, transcription mediated amplification), signal amplification tests (i.e., hybrid capture, invader chemistry), and direct detection (in situ hybridization) (Poljak et al., 2020). Selection of method should be based upon indication for use (triage for equivocal cytology, adjunctive to Pap smear, or primary screening), need for genotyping, and desired throughput, among other factors. HPV serology testing is currently of no clinical diagnostic utility.

Clinical Implications

The results of HPV testing, in combination with age, prior history, and cytology (if performed), are used to guide management (Katki et al., 2013). Based on the associated risk for malignant progression, management options include continued routine screening, active surveillance, colposcopy, or surgical treatment (which can have a significant irreversible impact on fertility) (Perkins et al., 2019). HPV diagnostics can also be helpful in the setting of oropharyngeal carcinoma, as patients with HPV-associated disease are staged differently, have better prognosis, and may be candidates for future treatment deintensification (Amin, 2017).

HSV-1 and HSV-2

HSV is widespread in human adults, with a seroprevalence of 54% for HSV-1 and 16% for HSV-2 in the United States from 2005 to 2010 (Bradley et al., 2009). HSV-1 is classically transmitted nonsexually through oral secretions in childhood, while HSV-2 is primarily transmitted sexually in adolescence or adulthood. However, there is now significant overlap in the transmission mode of these two HSV types. Most infections are asymptomatic/subclinical (Fatahzadeh & Schwartz, 2007). When symptomatic, primary HSV-1 infection can result in gingivostomatitis in children or pharyngitis in young adults. Recurrent infection most commonly presents as cold sores (herpes labialis) (Spruance et al., 1977). In contrast, the most common clinical presentation of primary HSV-2 infection is genital ulceration. Reactivation can be either subclinical or result in recurrent symptomatic outbreak, though typically milder than seen at initial presentation. HSV-1 can also cause genital herpes, with higher incidence in high-income countries, and can be partially ascribed to decreased HSV-1 exposure in childhood in addition to varying sexual practices (Fatahzadeh & Schwartz, 2007). This is of particular concern because HSV-1 seroprevalence is declining in countries such as the United States, which is predicted to lead to increased prevalence of genital herpes as well as potential perinatal transmission (Bradley et al., 2009). Additional manifestations of HSV infection, as discussed in other sections of this chapter, include cutaneous presentations (Fig. 64.2), ocular disease, neurologic complications, and disseminated disease.

Viral diagnosis on lesional tissue is preferably made by NAAT, which has higher sensitivity and specificity compared to the Tzanck smear, viral culture, or direct fluorescence antibody testing (Legoff et al., 2014). Viral culture is useful in the setting of drug resistance, as only phenotypic testing is currently clinically available. Classic cytopathic effects seen on culture include refractile "ballooning" cells, or multinucleated giant cells, and typically appear within 1 to 3 days on a wide variety of cell lines (Motamedifar & Noorafshan, 2008). Accurate viral diagnosis informs management strategies, which include antiviral therapy and subsequent prophylaxis, symptom management, and prevention of transmission. Serologic diagnosis is typically not used for acute primary diagnosis, but rather in the setting of late presentation, to clarify the timing of infection, to determine risk to sexual partners of infected individuals, or to assess risk in transplant recipients.

VZV

Primary infection by VZV causes varicella (chickenpox), which classically presents as a diffuse vesicular rash with skin lesions in various stages of healing (Gershon et al., 2015). It is highly transmissible via both direct contact and inhaled aerosolized skin particles/vesicular fluid. While it is usually a benign self-limiting disease, complications, including CNS disease, can occur, especially in infants, adults, and immunocompromised hosts. The incidence of varicella has significantly decreased in countries with vaccination uptake, including the United States where varicella-related deaths have been reduced by up to 92% (Wutzler et al., 2017). After primary infection, VZV establishes latency in the sensory ganglia and can reactivate in older adults in the setting of diminished cell-mediated immunity (Hope-Simpson, 1965). This reactivation typically presents with a characteristic dermatomal rash known as herpes zoster (shingles) and can be complicated by postherpetic neuralgia and ocular disease, as well as meningoencephalitis and vasculitis as described earlier in this chapter. The burden of zoster disease is anticipated to decrease, both by primary varicella vaccination and

through the more recently developed zoster vaccine, though uptake of the latter has been low (Gershon et al., 2015).

While typical presentations of varicella and zoster can be diagnosed clinically, laboratory confirmation is often needed in atypical cases, immunocompromised individuals, or in those with a positive vaccination history. The preferred diagnostic method on lesional fluid or swabs is PCR due to higher sensitivity compared to shell vial or standard culture. Saliva may also have high sensitivity if sampled early during the infectious course (Leung et al., 2010). Rapid and accurate diagnosis of varicella can help in the triage of appropriate contact and airborne precautions, as well as indicate antiviral therapy in those at risk of complicated disease. In the setting of zoster, early antiviral therapy can reduce the risk of postherpetic neuralgia (Ramdass et al., 2015). Serologic assays are not used for primary diagnosis but can be used to identify at-risk nonimmune individuals. However, performance characteristics of VZV IgG assays vary widely, many of which cannot reliably identify vaccine seroconversion (Breuer et al., 2008).

Select Enteroviruses

Hand, foot, and mouth disease (HFMD) is predominantly a childhood disease characterized by an oral vesicular enanthem accompanied by a macular, maculopapular, or vesicular exanthema involving the hands, feet, arms, legs, and buttocks (Miller & Tindall, 1968). Herpangina similarly affects mostly children and is characterized by abrupt onset high fever with pharyngeal hyperemia and painful yellow-grey oral papulovesicular lesions without cutaneous lesions. Both are caused by enteroviruses. The most common causes of HFMD worldwide are coxsackievirus A16 and enterovirus A71, while herpangina association with specific enterovirus subtypes is more geographically variable (Solomon et al., 2010).

These diagnoses are typically made clinically, without the need for laboratory confirmation except in atypical or complicated cases. The clinical course of both these conditions is typically mild and self-resolves with supportive care. Neurologic and cardiovascular complications can rarely occur with HFMD and are associated with serotypes enterovirus A71 and coxsackievirus A6.

Measles Morbillivirus

Epidemiology

Measles is highly contagious and transmitted predominantly by respiratory droplets and aerosolized particles (Remington et al., 1985). Infection or vaccination generally provides robust immunity, and worldwide vaccination efforts have decreased global measles deaths by 73% (preventing an estimated 23.2 million deaths) from 2000 to 2018 (Patel, Dumolard et al., 2019). Despite this, measles still accounts for an estimated 100,000 deaths per year, predominantly occurring in the WHO African and Southeast Asia regions. Countries that have achieved measles elimination are still at risk of imported cases leading to outbreaks or reestablishment of endemic transmission (Moss, 2017). Measles incidence actually increased in five regions from 2016 to 2018 (Patel, Lee et al., 2019). Two sustained back-to-back measles outbreaks in underimmunized populations in New York resulted in almost 1000 infections and threatened the measles elimination status of the United States in 2019 (Patel, Lee et al., 2019).

Virology

Measles morbillivirus (family: Paramyxoviridae, genus: *Morbillivirus*) is an enveloped, negative-sense, single-stranded RNA virus. There are 24 genotypes recognized by the WHO, of which only 8 have been detected since 2009. Measles virus has one of the highest known basic reproductive numbers (i.e., number of new cases generated from a single case in a nonimmune population, R_o estimated at 9–18) and has a long incubation period of 11 to 13 days (Moss, 2017; Lessler et al., 2009).

Clinical Presentation

Measles classically presents with acute fever and cough/coryza/conjunctivitis (three Cs), followed by small white papules on the buccal mucosa (Koplik spots), and finally the characteristic maculopapular rash starting on the face and behind the ears, which coalesces and then spreads downwards to the trunk and extremities. Fever, cough, and coryza are most pronounced at the time of rash onset, which also corresponds with peak viral load. This constellation of symptoms can be altered or diminished in previously immunized children, adults, and immunocompromised individuals. Patients generally recover approximately 1 week after rash onset, although complications can occur, particularly in adults, pregnant women, the immunocompromised, undernourished children (especially vitamin A deficiency), and in infants/young children. These include respiratory tract disease (most commonly pneumonia), diarrhea, CNS disease (acute disseminated encephalomyelitis, measles inclusion body encephalitis, subacute sclerosing panencephalitis), keratoconjunctivitis, and adverse pregnancy outcomes (Moss, 2017).

Laboratory Diagnosis

While the diagnosis can be made clinically in endemic areas or outbreak situations, laboratory confirmation is necessary in most nonendemic settings to appropriately triage necessity of airborne precautions. Serology (detection of measles-specific IgM antibody) remains the most common method for laboratory confirmation of acute measles infection due to relatively low cost and complexity. Point-of-care serologic assays have shown promise in field tests but are not yet widely commercially available (Warrener et al., 2011). However, serum IgM is only 91% sensitive 0 to 3 days after rash onset, achieving 100% sensitivity only more than 7 days after rash onset. In contrast, RT-PCR was more sensitive during early infection and was persistently positive more than 7 days after rash onset. The optimal specimens for RT-PCR are throat swab/combined throat and nasal swab (100% sensitivity <0–3 days after rash onset), followed by urine (94.1%), nasopharyngeal aspirate (93.5%), and serum (81%). Nasopharyngeal aspirate had the highest sensitivity for viral culture (82%) but was still inferior to RT-PCR at every time point and presents additional aerosolization risk during collection (Woo et al., 2010).

Clinical Implications

Treatment of measles is largely supportive (hydration, vitamin A supplementation, treatment of secondary bacterial infection). Case fatality ratios are highly variable, ranging from less than 0.1% in high-income countries to 20% to 30% in migrant populations, and is consistently highest in unvaccinated children younger than 5 years (Wolfson et al., 2009). Prompt diagnosis is important from an infection control standpoint. Expanding two-dose measles vaccine coverage will be critical to the ultimate goal of global measles eradication.

Benign Pediatric Viral Exanthems

Rubella virus, parvovirus B19 (primate erythroparvovirus 1, family: Parvoviridae, genus: *Erythroparvovirus*), and HHV-6 are all causes of benign pediatric exanthems with characteristic clinical presentations. Rubella virus presents in children with a fine pink-red noncoalescing maculopapular rash that begins on the face and neck, spreads to the trunk and limbs within 24 hours, and usually resolves within 3 days. Although acquired rubella is typically transient and self-resolving, congenital infection can have devastating effects. While management is supportive, laboratory diagnosis is recommended in unvaccinated individuals as the clinical syndrome is nonspecific and of great public health concern. Parvovirus B19 infection causes erythema infectiosum, also known as fifth disease, and is characterized by a "slapped-cheek," bright red reticular facial rash that subsequently spreads symmetrically to the trunk and extremities. Laboratory diagnosis is typically not required except in the setting of aplastic anemia or other severe complications, or in pregnancy to evaluate for risk of hydrops fetalis and fetal loss. Primary infection by HHV-6, and less commonly HHV-7, results in roseola infantum (also known as exanthem subitum and sixth disease) and is characterized by a nonpruritic blanching macular/maculopapular rash that spreads from trunk to neck, face, and extremities. Laboratory diagnosis is unnecessary in the setting of primary infection but can be useful if reactivation is suspected in the setting of immunocompromise (Ramdass et al., 2015).

Other Nonspecific Viral Exanthems

Nonspecific exanthems can be a presenting clinical feature during infection by a variety of other viruses, including arboviruses (chikungunya, dengue, WNV), hemorrhagic fever viruses, HIV, EBV, and disseminated CMV or adenoviral infections in the immunocompromised host, among others.

VIRAL GASTROENTERITIS

Gastroenteritis represents one of the most common infectious diseases and accounts for significant morbidity and mortality worldwide that disproportionately affects those in low-income countries. Viruses are the most frequent etiologic agent of gastroenteritis and can lead to acute and chronic presentations in both children and adults. Treatment is predominantly supportive, as no specific antiviral agents are available.

Most of these nonenveloped viruses occur as a result of fecal-oral spread from contaminated food, water, or surfaces, although airborne transmission has been recently associated with hospital outbreaks of norovirus (Alsved et al., 2019). The most common viral agents causing gastroenteritis, summarized in Table 64.5, are detectable on stool syndromic PCR panels.

TABLE 64.5

Most Common Viral Etiologies of Gastroenteritis, Stratified by Clinical Features and Diagnostic Methods

Virus	Viral Family	Viral Nucleic Acid	Population	Peak Seasonality	Attributable Fraction of Diarrhea <2 Years (Platts-Mills et al., 2018)
Rotaviruses	Reoviridae	dsRNA	Pediatric	Winter/fall in some regions	6.9–9.5%
Norovirus	Caliciviridae	+ssRNA	All ages	Winter	4.8–7.2% (contrast to 17–20% in all ages) (Ahmed et al., 2014)
Sapovirus	Caliciviridae	+ssRNA	Pediatric	Winter	7.2–10.0%
Adenoviruses 40/41	Adenoviridae	dsDNA	Pediatric	None	7.1–8.9%
Astroviruses	Astroviridae	+ssRNA	Pediatric	Winter	4.5–7.1%

While laboratory confirmation is typically unnecessary in uncomplicated outpatients, these syndromic panels have been shown to decrease time on antibiotic therapy, time to discharge, and anticipated overall health care costs in inpatients and emergency department (ED) patients (Beal et al., 2018). Virus-specific antigen immunoassays and NAATs are also available but are of limited clinical utility when used individually, except in the setting of outbreak investigation.

Rotavirus is predominantly a childhood illness and is the principal cause of diarrhea-related mortality in children under 5 years of age globally. It accounts for 40% of hospital admissions and 200,000 deaths annually, most of which occur in low-income countries (Lanata et al., 2013; Tate et al., 2008). In these countries, rotavirus infections occur year-round, whereas in high-income countries, incidence of rotavirus infection notably peaks during the winter months. It is caused predominantly by species rotavirus A, for which two globally licensed oral vaccines have been available since 2006, now implemented in over 95 countries. These vaccines have lower efficacy in low-income countries compared to middle- and high-income countries, for unclear reasons. Still, vaccination of infants has significantly reduced rotavirus disease and is partially responsible for decreasing childhood mortality due to diarrhea by 34% between 2005 and 2015 (Bányai et al., 2018).

Norovirus (species, *Norwalk virus*) is the leading cause of acute gastroenteritis worldwide across age groups (Ahmed et al., 2014). It is highly transmissible due to its low infectious dose and extended viability in the environment (Teunis et al., 2008). For this reason it is a common cause of nosocomial as well as community and foodborne outbreaks. Norovirus can result in severe fatal infection in older adults and establish chronic infection in immunocompromised patients (Bányai et al., 2018).

Other viral agents that primarily cause gastroenteritis include sapovirus, adenovirus species F (types 40 and 41), and astroviruses. Using molecular methods, causative infectious agents have been identified in 65% to 89% of gastroenteritis cases; a minor fraction of cases still remain unaccounted for etiologically (Antonelli, 2013; Platts-Mills et al., 2018). While many novel viruses have been identified in gastroenteritis patients using next-generation sequencing in recent years, definite causality has not yet been confirmed for most of them (Page et al., 2019).

VIRAL HEPATITIS

Introduction

The five hepatitis viruses (Hepatitis A, B, C, D and E) are distributed in different viral families, but they all share a tissue tropism for the liver resulting in similar clinical presentation. Acute hepatitis can be caused by all five viruses, whereas chronic infection does not occur with hepatitis A. Most infections go unrecognized given their asymptomatic nature, but in those who develop disease manifestations can range from mild to life threatening.

Hepatitis A

Hepatitis A virus (HAV) (family: Picornaviridae; genus: *Hepatovirus*) is a nonenveloped, single-stranded RNA virus for which one serotype and multiple genotypes have been described (Ching et al., 2002). Worldwide there are approximately 1.4 million cases a year, making it the most commonly reported cause of acute hepatitis (WHO, 2019a). Contrary to the other viral hepatitis viruses, hepatitis A does not lead to chronic infection. Most cases resolve spontaneously, with hepatitis A accounting for only 0.5% of all viral hepatitis mortality. Transmission occurs through the fecal-oral route either through consumption of contaminated food and water or through direct person-to-person spread. The mean incubation period is 28 days (range, 15–50 days) (American Academy of Pediatrics [AAP], 2015). Multiple outbreaks in recent years have highlighted the increased risk of hepatitis A acquisition in specific populations, including persons experiencing unstable housing or homeless, persons who inject drugs, and men who have sex with men (MSM) (Plunkett et al., 2019; Wilson et al., 2019; CDC, 2019). In the United States alone, a total of 26,276 cases were reported from March 2017 to September 2019, of which 60% were hospitalized and 1% died (CDC, 2019).

Serology is the mainstay of diagnosis for hepatitis A as a detectable anti-HAV immunoglobulin M (IgM) response will typically be detectable at the onset of symptoms (Nainan et al., 2006). An anti-HAV IgG response can also be detected approximately 2 weeks postexposure. Serologic testing is most commonly performed by chemiluminescence and can target IgM anti-HAV only or total anti-HAV (IgM and IgG). Molecular methods have also been studied for the diagnosis of HAV given that viremia appears earlier than serology (within a few days postexposure) and persists throughout the period of liver enzyme abnormality (Nainan et al., 2006). Access to RT-PCR and HAV genotyping for the diagnosis of HAV can be performed in select laboratories such as the CDC.

Treatment of HAV consists of supportive care, with need for liver transplant in rare fulminant cases. Postexposure prophylaxis with hepatitis A vaccine for those aged 12 months and older (± HAV-specific immunoglobulin for specific populations) is recommended for previously unvaccinated individuals exposed to HAV in the preceding 2 weeks. A highly effective monovalent vaccine for HAV is available and should be considered preexposure for at-risk populations (Advisory Committee on Immunization et al., 2006).

Hepatitis B

Hepatitis B virus (HBV) (family: Hepadnaviridae; genus: *Orthohepadnavirus*) is an enveloped, partially dsDNA virus for which 10 genotypes have been described (Stuyver et al., 2000; Arauz-Ruiz et al., 2002). HBV can lead to both acute and chronic infection, with variable stages of disease depending on the host immune response to the virus. Chronic infection is defined as detection of hepatitis B surface antigen (HBsAg) for 6 months or longer. Individuals who acquire the infection in childhood are much more likely to develop chronic infection (up to 95%) compared to adulthood (3–5%) (Pan & Zhang, 2005). The WHO (2019b) estimates that globally there are 257 million people living with chronic HBV, with the highest prevalence rates in Africa and the Western Pacific. HBV is an important oncogenic virus leading to development of chronic hepatopathy and hepatocellular carcinoma (HCC) and was responsible for 887,000 deaths in 2015 (WHO, 2019b). HBV is transmitted through multiple different routes, including vertical transmission (mother-child), horizontal transmission in childhood, at-risk sexual intercourse, and intravenous drug use for which the relative importance of each varies by geographic settings. The mean incubation period for acute HBV is 90 days (range, 45–160 days) (AAP, 2015).

Diagnosis of acute hepatitis is based on detection of HBsAg and IgM antibody to the HBV core antigen (anti-HBc). HBV PCR can also be performed to confirm acute infection, particularly for increased sensitivity in immunocompromised hosts who may have impaired serologic response, or for individuals suspected to be in the window period of infection with negative surface antibody and antigen (HBsAg and anti-HBs). Chronic infection is diagnosed by HBsAg positivity, and infectivity is characterized by hepatitis B e antigen (HBeAg) and HBV viral load. Seroconversion in chronic infection can be monitored by both HBeAg and HBsAg, although the former is the most likely to convert on therapy (Terrault et al., 2016). HBV genotype may also be indicated for prognosis and to optimize therapeutic management (Sunbul, 2014).

Treatment of HBV in the acute phase is mainly supportive, though severe cases may require antiviral therapy. Treatment of HBV chronic infection includes different options, including tenofovir, entecavir, and telbivudine, and a review is beyond the scope of this chapter (Terrault et al., 2016). Vaccination against HBV is highly effective and is recommended per the routine childhood immunization schedule, in catch-up vaccination series for previously unvaccinated or partially vaccinated adolescents, and for vaccination of adults at risk (Schillie et al., 2018). Prevention of HBV vertical transmission is also highly effective when vaccination and hepatitis B immune globulin (HBIg) are administered within 12 hours of birth of the HBV-exposed infant (Schillie et al., 2018).

Hepatitis C

Hepatitis C virus (HCV) (family: Flaviviridae; genus: *Hepacivirus*) is a single-stranded RNA virus with seven described genotypes and multiple subtypes (Murphy et al., 2015). Worldwide, it is estimated that 71 million people are chronically infected with HCV, of which 3.5 million are in the United States (WHO, 2019c; Denniston et al., 2014). HCV was responsible for almost 400,000 deaths in 2016 (WHO, 2019c). Similar to HBV, HCV is a significant cause of preventable malignancy. HCV is transmitted mainly by the percutaneous (including intravenous drug use and contaminated blood products), sexual, and vertical routes. Upon HCV acute infection, between 15% and 45% will spontaneously clear the infection, and the remaining 55% to 85% will develop chronic infection. Of those who develop chronic infection, 20% to 30% will progress to cirrhosis within 30 years, and 1% to 4% per year will develop HCC (Lingala & Ghany, 2015). The incubation period averages 6 to 7 weeks but can last up to 6 months (AAP, 2015).

Diagnosis of HCV is initially made on detection of anti-HCV antibody; however, this result alone does not differentiate current infection from previously cleared infection. HCV RNA testing must thus be performed to assess for viral load, with an elevated result confirming active infection. Molecular testing should also be considered in immunocompromised patients, patients on hemodialysis, and persons at risk of acute HCV infection even in the presence of a negative antibody screen given the risk for false-negative results (American Association for the Study of Liver Diseases [AASLD], 2019). HCV genotyping should be performed for all confirmed cases of active HCV infection as this will inform therapeutic decision making (AASLD, 2019).

Treatment of HCV with direct-acting antivirals (DAAs) is recommended for all individuals with evidence of current HCV infection to achieve sustained virologic remission (SVR; defined as undetectable viral load at 12 weeks after completion of therapy), and prevent all-cause mortality, hepatocellular carcinoma, and liver-related complications (AASLD, 2019). There have been major developments in HCV therapy in the last decade, with multiple therapeutic agents showing greater than 95% SVR rates after 8- to 12-week regimens across all HCV genotypes. However, cost of these therapies remains high. No vaccine is currently available for HCV.

Hepatitis D

Hepatitis D virus (HDV; also known as hepatitis delta virus) (family: none; genus: *Deltavirus*) is a defective virus that requires HBV infection to provide envelope proteins necessary for viral replication. HDV can lead to acute HBV/HDV infection (highest risk of fulminant hepatic failure), acute HDV superinfection of an individual with chronic HBV, and chronic HDV infection (Noureddin & Gish, 2014). HBV/HDV coinfection is associated with higher risk of cirrhosis and HCC than HBV alone. Diagnosis is based on the presence of total (IgM and IgG) anti-HDV antibodies, or HDV PCR in reference laboratories. HDV genotyping is not currently available in the United States for routine clinical use.

Hepatitis E

Hepatitis E virus (HEV) (family: Hepeviridae; genus: *Orthohepevirus*) is a single-stranded, nonenveloped RNA virus with four genotypes infecting humans (Sridhar et al., 2017). HEV is distributed globally and is responsible for an estimated 20 million acute infections annually, of which only a minority are symptomatic (WHO, 2019d). The main mode of transmission of HEV is consumption of contaminated food and water, but transmission by blood transfusion in endemic areas and by the vertical route can also occur. HEV is mostly associated with acute infection; however, chronic infection can occur in immunocompromised hosts with genotypes 3 and 4 (WHO, 2019d). Women in the third trimester of pregnancy, immunocompromised hosts, and individuals with preexisting liver disease are at higher risk of severe disease (Chaudhry et al., 2015). Initial HEV diagnosis is based on the presence of anti-HEV IgM antibody. Test performance has been variable across anti-IgM assays, and confirmation testing by HEV RNA should be performed (Kamar et al., 2014). HEV RNA testing should also be considered in immunocompromised hosts even with negative HEV anti-IgM given impaired humoral response (Kamar et al., 2014). Treatment of acute and chronic HEV is mainly supportive, and reduction of immunosuppression as tolerated when applicable is recommended (Kamar et al., 2014). A HEV vaccine with high efficacy and a good safety profile has been developed and licensed in China but lacks data in high-risk groups and is not currently available in other countries (WHO, 2019d; Zhang et al., 2015).

HUMAN IMMUNODEFICIENCY VIRUS

Epidemiology

The human immunodeficiency virus (family: Retroviridae; genus: *Lentivirus*) includes two species: HIV-1 and HIV-2. Although both can lead to the acquired immunodeficiency syndrome (AIDS), HIV-1 has spread worldwide and is responsible for the HIV pandemic, whereas HIV-2 occurs infrequently and is mainly restricted to West Africa (Campbell-Yesufu & Gandhi, 2011). Globally there are 37.9 million persons estimated to be living with HIV, with approximately 1.7 million new cases a year (WHO, 2019e). Despite improvements in diagnostic methods and availability of potent antiretroviral therapy, HIV continues to account for significant morbidity and mortality worldwide (UNAIDS, 2018).

Pathogenesis

Upon primary infection, HIV reaches mucosal tissue first, then systemically spreads to lymphoid organs establishing a viral reservoir (Deeks et al., 2015). Providers should ensure proper understanding of the intervals between HIV exposure and positivity across HIV diagnostic assays to avoid missing acute HIV infection. The virus becomes detectable by NAAT at approximately 10 days of infection; time from infection to first detectability by molecular methods is referred to as the eclipse period (Fig. 64.3). Similarly, the time between HIV acquisition and immunoassay positivity is referred to as the window period and varies from 16 days for laboratory-based combination antigen/antibody assays to over 3 weeks for older-generation antibody-only assay (CDC, 2014). The acute phase of HIV infection is characterized by high viremia with a corresponding high risk of onward transmission and detectable p24 antigen; HIV antibody may not yet be detectable. This initial viremic peak stimulates an immune response in 50% to 90% of individuals, termed acute retroviral syndrome. This nonspecific clinical syndrome is characterized by fever, lymphadenopathy, pharyngitis, weight loss, and rash (Wood et al., 2014) and overlaps with other diagnoses such as EBV, CMV, toxoplasmosis, and HHV-6.

Following acute infection, the viral load decreases until attaining a set point, marking the onset of the *latent phase* of HIV, where most patients are asymptomatic. However, untreated HIV infection leads to progressive CD4 lymphocyte depletion and immunosuppression, culminating in well-characterized AIDS-defining infections, malignancy, or wasting or encephalopathy syndrome after a median time of 10 years (Bennett & Blaser, 2015). Progression to AIDS marks the *final phase* of HIV infection and is the most severe manifestation of HIV.

Laboratory Diagnosis

Multiple rapid (<40 min) HIV antibody single-use point-of-care diagnostic tests are available, including seven FDA-approved tests for use in nonclinical settings (CDC, 2019). Depending on the assay, testing may be performed using finger stick whole blood, venous whole blood, or oral fluid. An FDA-approved antigen-antibody point-of-care test is now available in the United States, after a period of backorder in 2019. Although considered less sensitive than laboratory-based assays, point-of-care tests may provide the most rapid preliminary result in time-sensitive settings such as the ED, labor and delivery, occupational postexposure prophylaxis assessment, and in clinical encounters historically associated with low follow-up adherence. Nonetheless, false-negative and false-positive results remain a concern with rapid point-of-care testing, especially with oral fluid testing (Stekler et al., 2013; Pilcher et al., 2013). As such, all reactive results should be confirmed using the recommended laboratory HIV testing algorithm for serum or plasma specimens (CDC, 2018a).

Laboratory diagnosis of HIV is performed as a two-step approach with an initial highly sensitive screening test, followed by confirmatory testing with a highly specific test (Fig. 64.4). Initial testing should be performed using an FDA-approved HIV-1/2 antigen/antibody immunoassay. If nonreactive, no further testing is recommended. If reactive, confirmatory testing should proceed with HIV-1/2 antibody differentiation assay. Discrepant results (antigen/antibody immunoassay positive and differentiation

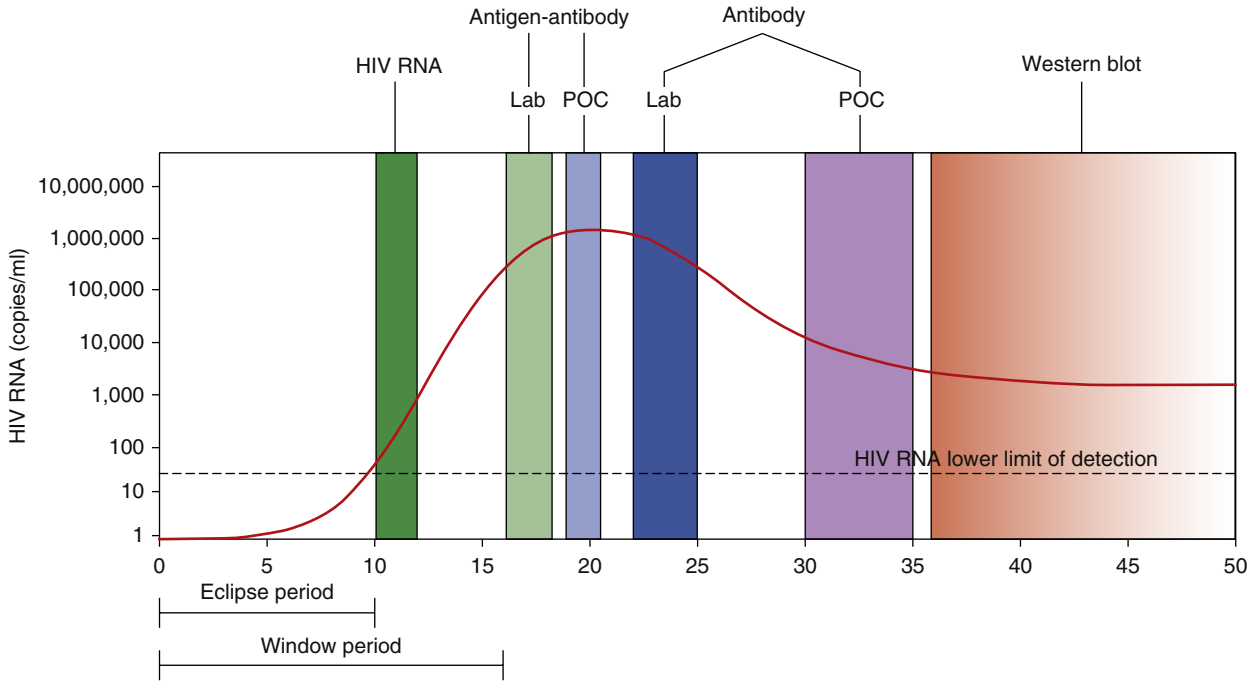

Fig. 64.3 Natural time course of untreated human immunodeficiency virus (HIV) infection. *POC,* Point of care; *RNA,* ribonucleic acid (Modified from the UW HIV Diagnostic Testing Curriculum.)

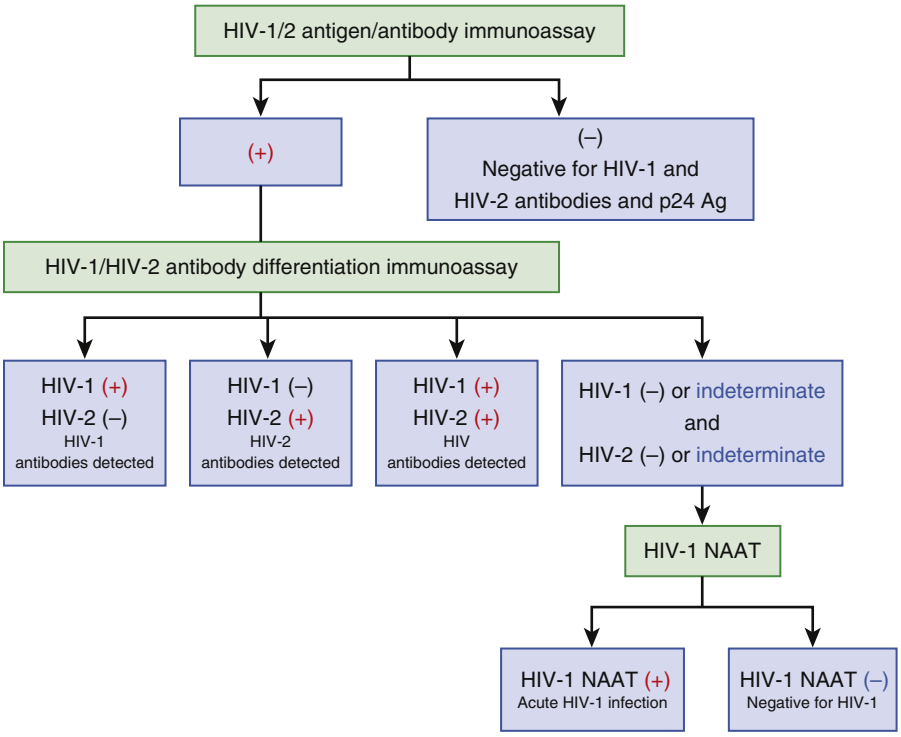

Fig. 64.4 Centers for Disease Control and Prevention (CDC) and the Association of Public Health Laboratories (APHL)–recommended algorithm for laboratory diagnosis of human immunodeficiency virus (HIV). *Ag,* Antigen; *NAAT,* nucleic acid amplification test; *(+),* positive; *(-),* negative (Modified from CDC and APHL.)

immunoassay negative) should be resolved by HIV-1 NAAT. The NAAT result is taken as final, and a positive result confirms acute HIV-1 infection. There are several FDA-cleared HIV Ag/Ab combination immunoassays available commercially, including the ARCHITECT (Abbott Diagnostics, Wiesbaden, Germany), the ADVIA Centaur (Siemens Healthcare Diagnostics, Tarrytown, NJ), and the BioPlex2200 (Bio-Rad Laboratories, Hercules, CA). In contrast, only a single confirmatory differentiation immunoassay is available, the Bio-Rad Geenius HIV1/2. Although multiple HIV NAATs are available, only one is FDA cleared for the diagnosis of HIV: the APTIMA HIV-1 RNA Qualitative Assay (Hologic, San Diego, CA).

A separate CDC algorithm is available for HIV diagnosis in individuals prior to the initiation of preexposure prophylaxis (PrEP) to more sensitively rule out acute HIV infection (CDC, 2019). PrEP represents a strategy to prevent HIV infection in high-risk individuals with the use of antiretroviral therapy. Prior to initiation of PrEP, HIV infection needs to be carefully excluded to avoid suboptimal treatment of previously unrecognized HIV infection and possible emergence of resistance. In this context, individuals with a syndrome consistent with acute HIV infection in the preceding four weeks and with a negative HIV screening should be considered for HIV-1 NAAT testing (CDC, 2019).

Although this diagnostic algorithm may appear straightforward, numerous examples from selected patient populations have revealed interpretation challenges, including in the context of PrEP use (Smith et al., 2018), long-term nonprogressors/elite controllers (LTNP/EC) (Joshi et al., 2017a, 2017b), and patients screened by NAAT after receipt of

TABLE 64.6
Selected List of Oncogenic Viruses

Viral Nucleic Acid Type	Viral Family	Virus	Malignancy	Mechanism	Oncogene/Oncoprotein	Preferred Diagnostic Method
DNA	Herpesviridae	EBV (HHV-4)	Burkitt lymphoma Hodgkin lymphoma Nasopharyngeal carcinoma Gastric adenocarcinoma	Oncogenic	*LMP-1*	NAAT, serology
		HHV-8	Kaposi sarcoma Primary effusion lymphoma Multicentric Castleman disease	Oncogenic	*vGPCR, vIL-6, vBc12, vMIPs, vFlip, vCyclin, LANA, Kaposin B*	NAAT
	Papillomaviridae	HPV-16/18	Cervical and anorectal cancer Oropharyngeal cancer	Oncogenic	E6/E7	NAAT, in situ hybridization
	Polyomaviridae	Merkel cell polyomavirus	Merkel cell carcinoma	Oncogenic	LT, sT	Histopathology
	Hepadnaviridae	HBV	HCC	Chronic inflammation	X-protein	Serology, NAAT
RNA	Flaviviridae	HCV	HCC	Chronic inflammation	None	Serology, NAAT
	Retroviridae	HTLV-1/2	Adult T-cell leukemia/lymphoma	Oncogenic	*Tax*	Serology, NAAT

EBV, Epstein Barr virus; *HBV,* hepatitis B virus; *HCC,* hepatocellular carcinoma; *HCV,* hepatitis C virus; *HHV,* human herpes virus; *HPV,* human papillomavirus; *HTLV-1/2,* human T lymphotropic virus type 1/2; *NAAT,* nucleic acid amplification test.

lentivirus-based genetically modified lymphocyte therapies such as chimeric antigen receptor (CAR T cell) (Ariza-Heredia et al., 2017; Laetsch et al., 2018; De Ravin et al., 2014). Use of alternative diagnostic assays such as HIV-1 NAATs with different viral targets or HIV-1 proviral testing may be useful in such cases.

Once a diagnosis of HIV has been established, plasma HIV-1 RNA viral load should be performed at entry into care and prior to initiation of therapy as this will help guide ART selection and be used to inform prognosis based on subsequent viral load response to ART (US Department of Health and Human Services [USDHHS], 2019). In addition, HIV genotyping should always be performed at entry into care to ensure selection of optimal ART regimen. Baseline serologic testing for multiple conditions, including hepatitis B and C, should be performed, as should tropism testing if treatment with a CCR5 antagonist is considered.

HIV NAAT testing also represents an important surrogate marker for follow-up in the care of persons living with HIV. Indeed, HIV viral load should be performed at 2 to 8 weeks after ART initiation or modification and regularly every 3 to 12 months thereafter depending on the clinical stability and viral load suppression history of the individual (USDHHS, 2019). HIV resistance testing is also an important component of diagnostic testing and should be performed for all persons with HIV at entry into care and in other settings such as virologic failure and suboptimal viral load reduction (USDHHS, 2019). A minimal HIV-1 viral load of 500 to 1000 copies/mL is typically required for this purpose. Although resistance testing can be performed by genotypic or phenotypic methods, the genotypic method is preferred as it provides more rapid turnaround time and a detailed assessment of mutations present in key HIV genome regions. Genotypic-phenotypic correlations are well established and documented in detail in the Stanford HIV Drug Resistance Database (Stanford University, 2020). Drug mutations occur in all HIV drug classes used, including nucleoside reverse transcriptase inhibitors (NRTI) (e.g., M184V, K65R), nonnucleoside reverse transcriptase inhibitors (NNRTI) (e.g., K103N, Y181C), protease inhibitors (PI) (e.g., I84V), and integrase strand transfer inhibitors (INSTI) (e.g., Q148H/K/R, Y143C) (Stanford University, 2015). In the future, advances in next-generation sequencing are likely to enable identification of low-abundance drug-resistant variants and provide more personalized results, although this strategy presents multiple complexities that remain to be addressed for clinical testing (Metzner, 2016).

Screening of blood transfusion products for HIV is also an important component of HIV testing. Potential donors are first administered a questionnaire to assess potential HIV risk factors. Two types of screening tests are performed: HIV-1 and HIV-2 antibody testing and minipool NAAT testing, where 6 to 16 specimens are combined to be tested at the same time to increase efficiency in low HIV-prevalence areas. These interventions have reduced the risk of transfusion-transmitted HIV to approximately 1 in 1.5 million units in the United States (Zou et al., 2010).

Vertical transmission (i.e., transmission from the mother to child) is estimated to occur in approximately 1.8 per 100,000 live births in the United States (USDHHS, 2018). Early HIV diagnosis in the mother is key to the successful management during pregnancy and prevention of HIV transmission. Standard HIV antigen/antibody immunoassay screening should be performed as early as possible in pregnancy and should be repeated in the third trimester if initial results are negative and there are risk factors for HIV acquisition. If HIV is detected, viral load should also be performed to inform management, including need for scheduled cesarean section in women with viral load greater than 1000 copies/mL. For women who present in labor with undocumented HIV status, rapid HIV testing should be performed with turnaround time of less than 1 hour to rapidly guide management (USDHHS, 2018).

HIV testing in the infant with perinatal HIV exposure needs to be performed by NAAT at 2 to 3 weeks, 1 to 2 months, and 4 to 6 months after birth. Antibody-based testing is not recommended until the age of 18 months given the risk of false-positive results from passive maternal antibody transfer (USDHHS, 2018). Additional testing at birth and after cessation of antiretroviral therapy should be performed for infants at high risk of HIV. The reader is referred to the DHHS guidelines on the management of HIV in pregnancy and perinatally for further detail (USDHHS, 2018).

VIRUS-ASSOCIATED NEOPLASIA

Oncogenic viruses are multiple and are thought to contribute causally to up to 20% of cancers worldwide (zur Hausen & de Villiers, 2014). These viruses vary significantly in their pathogenesis, geographic distribution, tissue tropism, and strength of association with cancer development. Most of these viruses promote tumor formation in humans through the complex modulation of normal cell growth mechanisms by targeting pathways of tumor suppression, host signaling, and DNA repair and by interfering with host immune response (Table 64.6) (Krump & You, 2018). In contrast, hepatocellular carcinoma-causing viruses exert their damage through chronic hepatic inflammation and progression to chronic liver disease. Oncogenic viruses represent a significant challenge to study as multiple

other factors, including host age, immunity, genetics, and environment, exert interdependent influences on the risk of malignant transformation (Krump & You, 2018; Chang et al., 2017).

There is important potential to reduce the incidence of virus-induced cancers through early detection, treatment, and management of these viruses. Indeed, accurate diagnostic methods for early detection are available for all of the listed oncogenic viruses. For example, early screening of nasopharyngeal carcinoma by circulating cell-free EBV DNA in plasma has been shown to lead to earlier diagnosis and improved clinical outcomes in asymptomatic individuals in endemic areas (Chan et al., 2017). In addition, advances in the development of highly effective therapy for HBV and HCV as described earlier in this chapter provide the tools to avert substantial potential cancer burden in the future. Nonetheless, such interventions are often associated with high costs that may be prohibitive in developing countries that are subject to a disproportionate burden of human oncogenic viruses. HTLV-1/2 continues to pose a significant conundrum as there are no specific therapies to prevent infection after confirmation of serologic status; as such, prevention efforts should focus on reducing transmission risk through exclusive bottle-feeding, promotion of safe sexual practices, and improvement of screening of donated blood products and organs (Martin et al., 1894). Eventual development of a vaccine would be highly beneficial to prevent development of adult T-cell leukemia and lymphoma (Tagaya et al., 2019).

VIRAL INFECTIONS IN IMMUNOCOMPROMISED HOSTS

Overview

The number of organ transplantations performed each year in the United States is steadily increasing, with 39,719 solid organ transplants (SOT) performed in 2019 and 22,863 hematopoietic stem cell transplants (HCT) in 2017 (United Network for Organ Sharing, 2020). Viral infections are an important cause of morbidity and mortality in transplant recipients due to the profound iatrogenic immune suppression required to facilitate engraftment and prevent donor tissue rejection. Sources of viral infections in transplant recipients include donor-derived viruses, reactivation of latent viruses, and transmission of community-acquired and healthcare-associated viruses. Infection risk for particular viruses varies with the type of organ transplanted, the nature and intensity of immunosuppression, the time posttransplant, and the availability of antiviral prophylaxis. Infection risk for SOT recipients is most pronounced in the first 6 months posttransplant (Fig. 64.5) correlating with the intensity of immunosuppressive therapy. In HCT recipients, infection risk is related to the timing of engraftment of donor stem cells and subsequent immune reconstitution (Fig. 64.6). Infection risk for many viral infections is highest in allogeneic HCT recipients due to the depletion of innate and adaptive immune function following myeloablative conditioning regimens.

Laboratory testing for transplant-associated viral infections begins with donor and recipient screening to assess risk and guide antiviral prophylaxis. Posttransplant virus detection and viral load testing by NAAT (typically single-target qPCR) may inform treatment decisions and be used to monitor treatment response. Phenotypic and/or genotypic testing to detect antiviral resistance in transplant-associated viruses is a growing need. In the following sections, we will review the clinical utilization and standard methods of laboratory testing in this arena. Emerging diagnostic technologies for transplant-associated viruses, including multiplex- and sequencing-based platforms, are in development and may have an important impact on clinical practice in the coming years.

Transplant Donor and Recipient Screening for Viral Infections

Common pretransplant screening tests are shown in Table 64.7. Additional testing may be included according to donor and recipient risk factors and/or the type of transplant. IgG serology testing is used to determine whether donors and recipients have had prior exposure to viruses associated with latent infection, most importantly herpesviruses, and in some cases to assess the immune status of the recipient. Seropositive donor status paired with seronegative recipient status denotes a higher risk for donor-transmitted infection, while seropositive recipient status predicts reactivation of latent viral infection. Antigen detection and NAAT may be used to evaluate for active infections. The most common clinically significant donor-derived viral infections are caused by CMV, EBV, and hepatitis viruses (Fischer et al., 2013). CMV serology is particularly helpful for risk stratification to guide patient management; high-risk patients (seropositive donor, seronegative recipient) may warrant closer viral load monitoring and/or more aggressive antiviral prophylaxis.

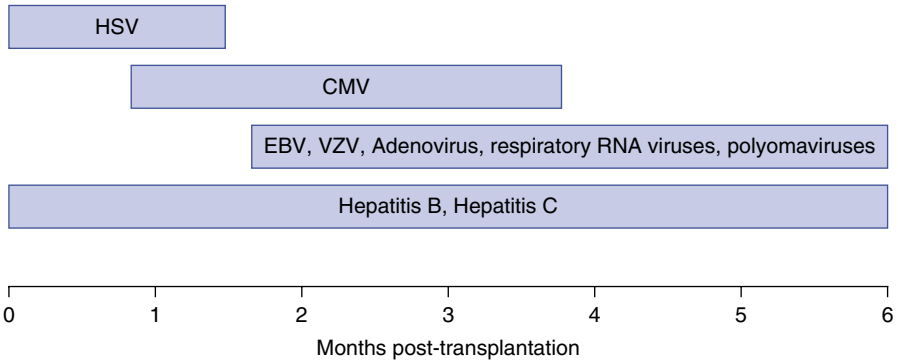

Fig. 64.5 Viral infections in solid-organ transplant recipients by time posttransplantation. *CMV,* Cytomegalovirus; *EBV,* Epstein Barr virus; *HSV,* herpes simplex virus; *VZV,* varicella zoster virus.

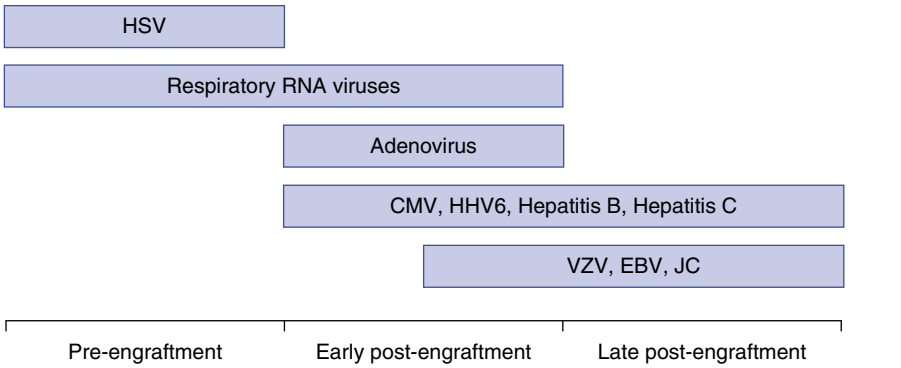

Pre-engraftment period: Begins with onset of conditioning therapy until approximately 20–40 days post-transplantation
Early post-engraftment period: Begins with neutrophil recovery until ~ 100 days post-transplantation (T/B cell recovery)
Late post engraftment period: Begins ~ 100 days post-transplantation until normal immune function is restored (18–36 months)

Fig. 64.6 Viral infection in allogeneic hematopoietic cell transplant recipients by time of engraftment. *CMV,* Cytomegalovirus; *EBV,* Epstein Barr virus; *HHV6,* human herpes virus 6; *HSV,* herpes simplex virus; *JC,* John Cunningham; *RNA,* ribonucleic acid; *VZV,* varicella zoster virus.

Transplant-Associated Viral Infections and Posttransplant Viral Load Testing

All of the DNA viruses discussed in this section have the ability to establish latent infections in select cell types following exposure. As discussed earlier in this chapter, CMV, EBV, HSV-1/2, VZV, and HHV-6 are ubiquitous herpesviruses that establish latency in a variety of tissues, and the majority of infections in the setting of immunosuppression represent reactivation of these endogenous viruses. NAAT testing of blood is the most common diagnostic method used for posttransplant viral load testing; other specimen types may also be evaluated when clinically warranted and a validated assay is available. Typical indications, methods, and specimen types for posttransplant virus testing are summarized in Table 64.8. The increasing availability of WHO international standards and FDA-cleared assays has allowed better standardization of quantitative NAAT assays and comparability between labs, but this remains an important challenge (Hayden et al., 2017). The frequency of asymptomatic viral reactivation and chronic shedding also presents a challenge for clinical interpretation of virus detection, and quantitative thresholds for clinical intervention are not well established.

TABLE 64.7

Routine Screening Tests for Viral Infections in Transplant Donors and Recipients

Virus	Screening Test
Routine testing	
CMV	Serology (D/R)
EBV	Serology (D/R)
HSV	Serology (R)
VZV	Serology (R)
HIV	Serology[a] (D/R)
HTLV	Serology (D)
HBV	sAg,[a] cAb, sAb (D/R)
HCV	Serology[a] (D/R)
Optional testing	
BK virus (kidney transplant)	Serology (D/R)
WNV	Serology, NAAT (D)
HHV-8	Serology (D)

cAb, Core antibody; *CMV,* cytomegalovirus; *D,* donor; *EBV,* Epstein Barr virus; *HBV,* hepatitis B virus; *HCV,* hepatitis C virus; *HHV,* human herpes virus, *HIV,* human immunodeficiency virus; *HSV,* herpes simplex virus; *HTLV,* human T lymphotropic virus; *R,* recipient; *sAb,* surface antibody; *sAg,* surface antigen; *VZV,* varicella zoster virus; *WNV,* West Nile virus.
[a]Positive result followed by NAAT to assess for active infection.

CMV

In the absence of antiviral prophylaxis, CMV reactivation occurs in a median of 37% of seropositive individuals postallogeneic HCT, and 12% of seropositive individuals postautologous HCT (Styczynski, 2018). Among SOT recipients, CMV reactivation occurs in a median of 30%, with the highest risk in donor-positive/recipient-negative individuals, and lung and small bowel transplant recipients (Styczynski, 2018). CMV disease in transplant recipients most commonly presents as undifferentiated fever. Severe CMV-associated pneumonitis, enteritis, hepatitis, and retinitis also occur. Prophylaxis with ganciclovir or valganciclovir is effective in preventing CMV reactivation; however, this approach can lead to unnecessary and prolonged drug exposure associated with myelosuppression and the promotion of antiviral resistance. As an alternative to prophylaxis, preemptive antiviral treatment can be used to mitigate the risk of symptomatic CMV disease in patients with detectable circulating virus (Kotton et al., 2018). Mutations in the CMV genome have been described that confer resistance to first-line (ganciclovir) and second-line (foscarnet, cidofovir) antivirals associated with treatment failure. Letermovir, a drug that inhibits CMV replication through a novel target on the CMV terminase complex, recently demonstrated efficacy against clinically significant CMV disease in HCT recipients with minimal toxicity (Lin et al., 2019; El Helou & Razonable, 2019). Routine viral monitoring by qPCR has largely replaced pp65 antigen detection testing and is typically performed during the first 3 to 6 months posttransplantation. Viral loads may be used to guide preemptive antiviral treatment and to monitor treatment response. The reproducibility and commutability of viral load quantitation by qPCR has benefited from the introduction of a WHO international calibration standard (Hayden et al., 2015) and the availability of commercial assays.

EBV

EBV infection in transplant recipients—resulting from reactivation in previously exposed patients or primary infection—is typically asymptomatic. However, high viral loads portend progression to posttransplantation lymphoproliferative disorder (PTLD), a dreaded outcome associated with

TABLE 64.8

Posttransplantation Laboratory Testing for Virus Detection

Virus	Indication(s) for Testing	Testing Method (Specimen)[a]	Clinical Action
CMV	• Prospective VL monitoring for all recipients • Monitor treatment response	NAAT, pp65 antigen (blood)	• Preemptive antiviral treatment • Antiviral resistance testing for nonresponsive infections
EBV	• Prospective VL monitoring for recipients at high risk for PTLD • Monitor treatment response	NAAT (blood)	• Further evaluation and/or preemptive treatment for PTLD • Reduction of immunosuppression • Consideration for investigational immunotherapies
HSV-1/2	• Diagnostic testing for symptomatic disease • Monitor treatment response	NAAT (lesion, CSF)	• Antiviral treatment • Antiviral resistance testing for nonresponsive infections
VZV	• Diagnostic testing for symptomatic disease • Monitor treatment response	NAAT (lesion, CSF)	• Antiviral treatment
HHV-6	• Diagnostic testing for symptomatic disease • Monitor treatment response	NAAT (blood, CSF)	• Antiviral treatment if clinically warranted
Adenovirus	• Prospective VL monitoring for high-risk patients • Diagnostic testing for symptomatic disease • Monitor treatment response	NAAT (blood)	• Supportive care, adjust immunosuppression, or antiviral treatment for severe disease
HBV/HCV	• Diagnostic testing in the setting of elevated liver enzymes in patients at risk	NAAT (blood)	• Antiviral treatment
BK virus	• Prospective VL monitoring for kidney transplant patients • Monitor treatment response	NAAT (blood)	• Adjust immunosuppression to mitigate risk of nephropathy
JC virus	• Diagnostic testing for symptomatic disease	NAAT (CSF)	• May pursue invasive diagnostic sampling for definitive diagnosis

CMV, Cytomegalovirus; CSF, cerebrospinal fluid; EBV, Epstein Barr virus; HBV, hepatitis B virus; HCV, hepatitis C virus; HHV, human herpes virus; HSV, herpes simplex virus; NAAT, nucleic acid amplification test; PTLD, posttransplantation lymphoproliferative disorder; VL, viral load; VZV, varicella zoster virus.
[a]For specimen type, blood includes whole blood or blood fraction.

high mortality. The risk of PTLD is highest for allogeneic HCT in seronegative (previously unexposed, typically pediatric) patients and those with more intensive T-cell suppression (Styczynski et al., 2016). Less common manifestations of EBV infection in transplant recipients include hepatitis, enteritis, encephalitis, and pneumonitis. qPCR of blood (or blood fraction) is recommended for prospective posttransplantation viral load monitoring in patients at high risk for PTLD (Styczynski et al., 2016; Chiereghin et al., 2019) and increasing viral loads may prompt preemptive treatment for PTLD and/or further diagnostic investigations, including imaging and histologic evaluation. The introduction of a WHO international calibration standard has allowed improved comparability of viral load quantitation between laboratories. No effective antiviral treatment has been established for EBV, and patients may be managed with B-cell–depleting antibodies (rituximab), reduction of immunosuppression, or investigational approaches such as adoptive T-cell transfer (Styczynski et al., 2016; Chiereghin et al., 2019; Kim et al., 2019).

HSV-1/2

Acyclovir prophylaxis reduces the rate of HSV reactivation significantly from historical rates of ~80% in seropositive allogeneic HCT recipients and 60% in seropositive SOT recipients (Shiley & Blumberg, 2011). HSV reactivation typically occurs earlier than other viruses in the posttransplant course, and symptomatic disease most commonly presents as oropharyngeal and genital ulcers. Less common disease presentations include encephalitis, hepatitis, and pneumonitis. Prospective viral monitoring for HSV is not necessary in the setting of prophylactic therapy. NAAT is the most sensitive method for diagnostic testing, and FDA-cleared qualitative assays are available for testing (Lee et al., 2019). Acyclovir is the first-line antiviral treatment.

VZV

VZV reactivation typically occurs in previously exposed transplant recipients and can be effectively prevented with acyclovir prophylaxis (Shiley & Blumberg, 2011). Infections typically arise several months posttransplantation, and only a minority are associated with symptomatic disease. Dermatomal zoster is the most common disease manifestation of reactivated infection; pneumonitis, hepatitis, and CNS disease also occur. Previously unexposed patients are at risk for primary infection with disseminated disease and are advised to avoid contact with individuals who have active varicella infections (chickenpox or shingles). NAAT is preferred for diagnostic testing, typically performed on lesion or CSF specimens (Pergam et al., 2019). Direct fluorescent antibody testing from lesion specimens offers an alternative option for rapid diagnosis. Acyclovir is the antiviral treatment of choice.

HHV-6

Reactivation of latent HHV-6 infection is common among all transplant recipients, and viral detection is seldom considered the causal agent responsible for the clinical syndrome of the patient (Hentrich et al., 2005). Occasionally, HHV-6 is the cause of posttransplantation fever, encephalitis, and pneumonitis and may warrant treatment with an antiviral such as foscarnet. Neither prophylactic therapy nor prospective monitoring are recommended. Of note, some individuals (<1% of the population) carry inherited chromosomally integrated HHV-6 resulting in high viral loads that may present a diagnostic challenge (Pellett et al., 2012). qPCR is highly sensitive for virus detection in blood and CSF, and quantitation may be helpful in determining clinical significance and monitoring treatment response.

Adenovirus

The frequency of adenovirus infection varies across age and transplant types—3% to 57% in SOT recipients and 3% to 42% in HCT recipients—with higher risk of severe disease in pediatric patients, allogeneic HCT recipients, and those with more intensive T-cell suppression (Lion, 2014; Matthes-Martin et al., 2012). Similarly, a wide range of organ involvement is observed, including pneumonitis, hepatitis, colitis, and rarely disseminated disease. Notably, adenovirus is associated with hemorrhagic cystitis in kidney transplant recipients. Due to the high rate of asymptomatic viral shedding, prospective viral load monitoring should be limited to patients at high risk of severe disease (Matthes-Martin et al., 2012). Quantitative PCR of blood is typically utilized for diagnosis of disseminated disease and monitoring treatment response (Florescu et al., 2019); testing of other specimen types may be warranted to investigate organ involvement. Treatment is typically supportive with consideration for adjustment of immunosuppression. Cidofovir is recommended when disease severity necessitates antiviral treatment (Dailey Garnes et al., 2019); however, nephrotoxicity is a major concern. Due to the high mortality of disseminated adenoviral disease and lack of desirable antiviral drugs, novel treatment options (including adoptive T-cell therapy) are under active investigation (Dailey Garnes et al., 2019).

Polyomaviruses

The majority of polyomavirus infections in transplant recipients represent viral reactivation in seropositive patients; however, community-acquired and donor-transmitted infections also occur. BK virus–associated nephropathy occurs in up to 15% of kidney transplant recipients and represents an important cause of graft dysfunction and failure (Hirsch et al., 2019). BK virus is also an important cause of hemorrhagic cystitis in HCT recipients. Circulating BK viral load correlates with the development of nephropathy in kidney transplant patients, and prospective viral load monitoring by qPCR in plasma is recommended (Hirsch et al., 2019; Kasiske et al., 2010). Interassay variability in viral load quantitation has hindered the definition of clinically actionable thresholds; however, the introduction of an international calibration standard by the WHO in 2016 is expected to improve interassay commutability (Tan et al., 2017). While antiviral treatment is not available, patients with persistently elevated viral loads are managed with adjustment of their immunosuppressive regimen (Hirsch et al., 2019; Kasiske et al., 2010). John Cunningham (JC) virus is a rare cause of disease in transplant recipients associated with fatal progressive multifocal leukoencephalopathy (PML). Brain biopsy is required for definitive diagnosis of PML; however, detection of JC virus DNA by PCR in CSF provides strong evidence in the context of a consistent clinical syndrome, especially when the viral load is high (Swinnen et al., 2019).

Hepatitis Viruses

HBV and HCV infections may arise from donor-derived transmission or reactivation of endogenous, chronic infections. Donor-derived HBV transmission occurs when recipients lack HBV core antibody and donors have an active or latent infection. HBV transmission risk is highest during active donor infection, and prophylactic treatment with antiviral agents (tenofovir or entecavir) may be indicated (Te & Doucette, 2019). HBV viral load testing by NAAT is indicated in the setting of elevated liver enzymes in patients at risk for reactivation or donor-transmitted infection and for monitoring treatment response (Te & Doucette, 2019). Historically, the risk of HCV transmission from a seropositive organ donor to an uninfected recipient has been high; however, recent data suggest this may now be a safe approach in the context of treatment with highly active direct-acting antiviral therapy (Luckett et al., 2019; Woolley et al., 2019). NAAT testing is indicated for diagnosis and monitoring treatment response.

Respiratory RNA Viruses

Community-acquired and healthcare-associated respiratory RNA viruses, including RSV, PIV, influenza, hMPV, coronaviruses, and rhinoviruses, cause significant morbidity and mortality in transplant recipients. Any of the respiratory RNA viruses may yield atypical clinical presentations in transplant recipients, including severe lower respiratory tract disease (Ison & Hirsch, 2019). Furthermore, respiratory viral infection may predispose to graft dysfunction, particularly for lung transplants (Peghin et al., 2019). General preventive measures include restricted access for visitors and staff with respiratory symptoms and immunization of transplant recipients and their families with the inactivated influenza vaccine. Prophylaxis for high-risk patients may include palivizumab for RSV and/or oseltamivir for influenza. Diagnostic evaluation of transplant recipients with respiratory symptoms using multiplex NAAT panel testing of nasopharyngeal specimens is recommended, providing high sensitivity, broad inclusivity, and short turnaround time (Manuel et al., 2019). Empiric treatment for influenza with oseltamivir is recommended while diagnosis is pending, as early antiviral treatment reduces influenza-related morbidity in transplant recipients (Kumar et al., 2018). Treatment for RSV in transplant recipients is not yet standardized; however, ribavirin therapy (oral or aerosolized) reduces mortality in HCT recipients (Shah et al., 2014), and ribavirin therapy is recommended in lung transplant recipients (Manuel et al., 2019). The development of targeted therapeutics for PIV, hMPV, rhinovirus, and coronaviruses remains an active area of investigation (Ison & Hirsch, 2019). These viruses are discussed in greater detail in an earlier section of this chapter.

Antiviral Resistance Testing

Development of antiviral resistance in CMV disease is an infrequent but growing challenge in transplant recipients. Resistance tends to occur more frequently in individuals with prolonged and/or incomplete antiviral exposure (Kotton et al., 2018). Specific mutations are associated with

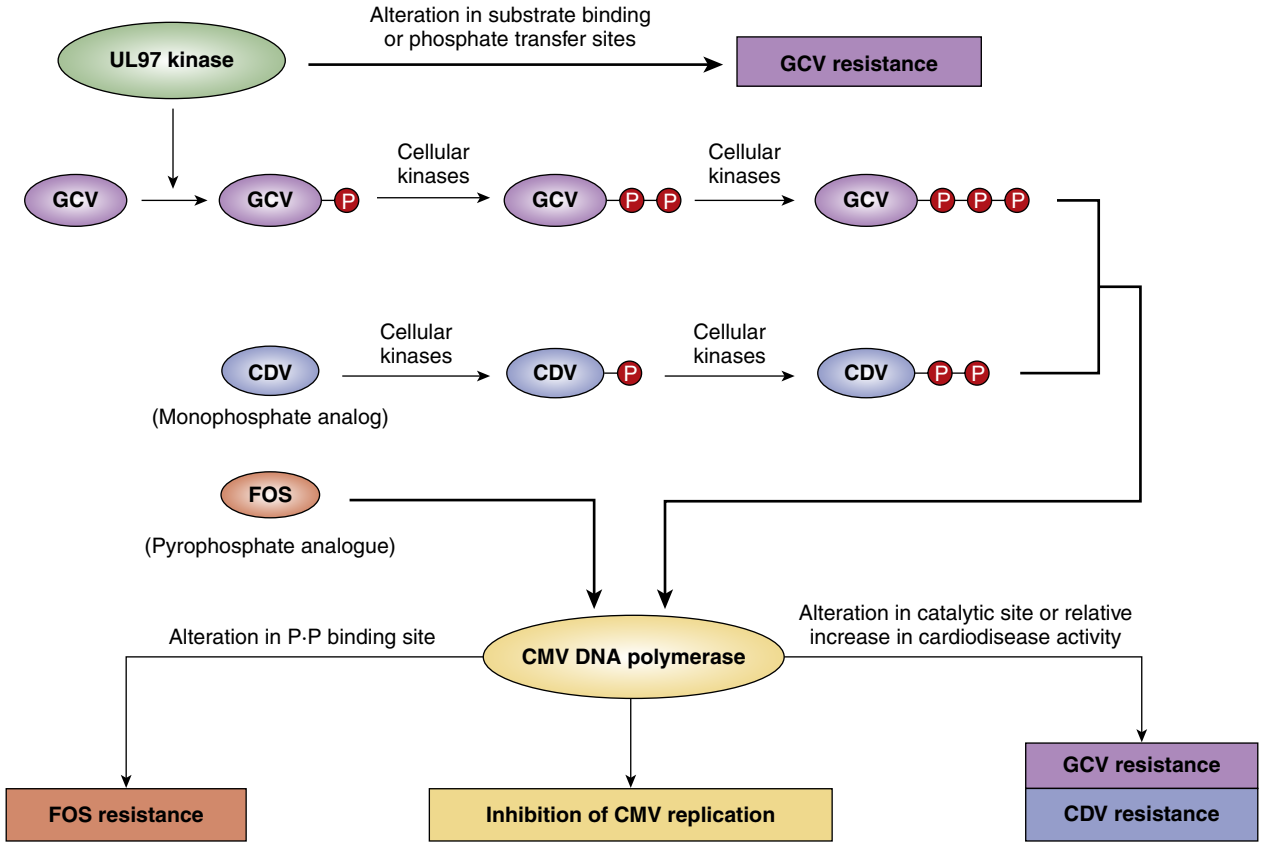

Fig. 64.7 Ganciclovir, foscarnet, and cidofovir anabolism. The UL97 kinase adds the initial phosphate to GCV. Cellular kinases add two additional phosphates. The active form of the drug, GCV triphosphate, is incorporated into viral deoxyribonucleic acid (DNA) by the viral DNA polymerase. CDV is a monophosphate analog and does not require initial viral kinase activity. Cellular kinases add additional phosphates to produce CDV diphosphate, the triphosphorylated form of the drug. Resistance is conferred only by DNA polymerase mutations. FOS is a pyrophosphatase analog, which does not require activation. Resistance is also conferred only by DNA polymerase mutations. The DNA polymerase is the ultimate target of all three drugs. *CDV,* Cidofovir; *CMV,* cytomegalovirus; *FOS,* foscarnet; *GCV,* ganciclovir (From Lurain NS, Chou S: Antiviral drug resistance of human cytomegalovirus. *Clin Microbiol Rev* 23[4]:689–712, 2010.)

typical antiviral resistance patterns and are described in a separate reference (Lurain & Chou, 2010). Genotypic antiviral resistance testing by Sanger sequencing is currently the most commonly used method for detection of these mutations and requires that a minimal CMV viral load be detected to be performed typically above 1000 copies/mL. The three main drugs used for CMV therapy include ganciclovir, foscarnet, and cidofovir. All of these agents target the viral DNA polymerase, but only ganciclovir requires UL97 viral kinase phosphorylation (Fig. 64.7). For individuals initially treated with ganciclovir, the most common resistance mutation to emerge is the UL97 kinase mutation, which confers resistance to ganciclovir. Subsequent mutation in the UL54 DNA polymerase gene may be seen, and confer high-level resistance to ganciclovir, in addition to variable resistance to foscarnet and/or cidofovir. In addition, although much more recently approved for the prophylaxis of CMV in HCT recipients, resistance to the terminase inhibitor letermovir has been described through UL56 terminase gene mutations (Chou et al., 2018).

Resistance of VZV to acyclovir has rarely been described in immunocompromised patients (Sauerbrei et al., 2011), However, testing for detection of VZV resistance is not currently available in commercial laboratories in the United States. Finally, detection of HSV acyclovir resistance is performed by phenotypic methods in reference laboratories. Acyclovir and/or foscarnet are typically tested and can only be performed in isolates with sufficient growth in cell culture. Once appropriate phenotypic-genotypic correlations have been performed, it is expected that future testing will also proceed by genotypic testing.

VIRAL INFECTIONS IN RETURNING TRAVELERS

Viral infections are frequently in the differential diagnosis of illness in returning travelers. A thorough evaluation of epidemiologic risk factors, exposure history, and incubation period is essential to guide targeted diagnostic testing for potentially serious viral infections. Although rarely encountered in the United States, several viruses that cause serious infections in travelers are highly transmissible person-to-person, warranting heightened biosafety and infection control measures and prompt reporting to public health authorities. Recent widespread outbreaks of high-consequence viruses, including SARS-CoV-2, MERS-CoV, SARS, Zika virus, and Ebolavirus, have demonstrated the increasingly global and rapidly evolving nature of infectious disease epidemiology. Clinical laboratory directors must work closely with clinical, infection control, and public health partners to maintain appropriate policies and procedures for specimen collection and laboratory testing in this arena.

In this section we present the key features of viruses responsible for serious and/or highly transmissible infections that are primarily acquired in endemic regions outside of the United States. Table 64.9 summarizes the epidemiology of these viruses and the incidence of cases documented in the United States, and Table 64.10 provides recommended diagnostic test methods and biosafety designations to guide safe specimen handling. Laboratory diagnosis often relies on laboratory-developed tests (LDTs) performed by commercial reference laboratories or CDC-designated assays performed by public health laboratories. Clinical diagnosis is challenged by the sporadic occurrence and nonspecific clinical presentation of these viral infections; thus improved access to timely laboratory testing is needed to guide urgent clinical and infection control interventions. Multiplexed molecular panels for use on automated NAAT platforms are in development to meet this need.

Serious Arboviral Infections

Dengue virus (DENV), Zika virus (ZIKV), and Chikungunya virus (CHIKV) are of increasing importance in the assessment of returning travelers with undifferentiated febrile illness and have overlapping epidemiologic and clinical features. DENV, ZIKV, and CHIKV are widespread in tropical and subtropical regions due to the expanding territory of their common vector, *Aedes* mosquitos. Transmission of these viruses by direct contact with infected body fluids or laboratory specimens is rare, and standard precautions are adequate for routine diagnostic procedures. Detection of viral RNA in blood by RT-PCR provides the most sensitive method for diagnosis during acute illness. IgM detection by capture ELISA is useful in the setting of viral clearance; however, extensive cross-reactivity among related viruses necessitates confirmatory testing for neutralizing

TABLE 64.9

Epidemiology of Severe Viral Infections in Returning Travelers

Syndrome	Virus	Geographic Distribution	Primary Mode(s) of Transmission	Incubation Period (Days)	US Cases Since 2010[a]
Arboviral febrile illness	**Dengue**	Africa, Asia, Americas, Europe	Mosquito (*Aedes* spp.)	3–14	5292
	Chikungunya	Africa, Asia, Americas	Mosquito (*Aedes* spp.)	1–12	4296
	Zika	Africa, Asia, Americas	Mosquito (*Aedes* spp.)	3–14	5703
Viral hemorrhagic fever	**Ebola**	Africa	Zoonotic exposure,[b] body fluids[c]	2–21	4
	Marburg	Africa	Zoonotic exposure,[b] body fluids[c]	2–21	0
	Lassa	West Africa	Rodent excreta, body fluids[b]	3–21	4
	CCHF	Europe, Asia, Africa	Tick (*Hyalomma* spp.), body fluids[b]	1–13	0
Severe viral respiratory illness	**CoV-MERS**	Middle East	Zoonotic exposure,[b] respiratory secretions[c]	2–13	2
	CoV-SARS	Asia	Zoonotic exposure,[b] respiratory secretions[c]	2–13	0
Viral encephalitis	**JE**	Asia, western Pacific	Mosquito (*Culex* sp.)	5–15	8
	Nipah	Southeast Asia	Zoonotic exposure,[b] respiratory secretions/body fluids[c]	4–14	0

CCHF, Crimean Congo hemorrhagic fever; COV, Coronavirus; *JE,* Japanese encephalitis virus.
[a]Indicates cases diagnosed in the United States and reported to the Centers for Disease Control and Prevention (CDC) since 2010. Notable cases prior to 2010 include 1 case of Marburg in 2008, 8 cases of SARS in 2003, and 4 additional cases of Lassa since 1969.
[b]See text for zoonotic source of transmission.
[c]Indicates mode of person-to-person transmission.

TABLE 64.10

Laboratory Testing and Biosafety for Severe Viral Infections in Returning Travelers

Virus	Primary Test Method (Specimen)[a]	Biosafety Level[b]	Select Agent[c] (Y/N)
Dengue	RT-PCR, NS1, IgM (blood)	2	N
Chikungunya	RT-PCR, IgM (blood)	3	N
Zika	RT-PCR, IgM (blood, urine)	2	N
Ebola	RT-PCR (blood)	4	Y
Marburg	RT-PCR (blood)	4	Y
Lassa	RT-PCR (blood)	4	Y
CCHF	RT-PCR (blood)	4	Y
CoV-MERS	RT-PCR (respiratory, blood, stool)	2/3	N
CoV-SARS	RT-PCR (respiratory, blood, stool)	2/3	Y
JE	IgM (CSF, serum)	3	N
Nipah	RT-PCR	4	Y

CCHF, Crimean congo hemorrhagic fever; *CoV, Coronavirus*; *CSF,* cerebrospinal fluid; *IgM,* immunoglobulin M; *JE,* Japanese encephalitis virus; *N,* no; *NS1,* nasopharyngeal swab; *RT-PCR,* reverse transcriptase polymerase chain reaction; *Y,* yes.
[a]Blood includes whole blood, serum, plasma.
[b]Biosafety levels: MERS/SARS specimens can be handled in BSL-2 facilities, testing procedures in class II BSC; propagation in culture is BSL3.
[c]Federal Select Agent Program.

antibodies. RT-PCR and IgM tests for DENV, ZIKV, and CHIKV are available in commercial reference laboratories; confirmatory testing is available from the CDC and certain public health laboratories.

Dengue

DENV (family: Flaviviridae) is an RNA virus with four genetically distinct serotypes (DENV1–4). DENV has caused human disease for centuries and continues to have vast global impact, with an estimated annual incidence as high as 400 million infections and 21,000 deaths annually (Guzman et al., 2016). Several hundred DENV infections are reported each year in the United States, and the large majority of these represent infections in returning travelers; however, a few small outbreaks with local transmission have been documented. Symptoms typically develop within 1 week of infection, ranging from mild febrile illness to severe disease characterized by hemorrhage and/or shock. In addition to RT-PCR, detection of nonstructural protein 1 (NS1) antigen by ELISA may be performed during acute illness.

Zika

ZIKV (family: Flaviviridae) is an RNA virus with three genetic clusters, two in Africa and one in Asia/Americas. ZIKV was first isolated in 1947 in Uganda and was not considered a public health concern until the first major outbreak was described in Yap in 2007. Local transmission in the Western Hemisphere was first documented in Brazil in 2015, leading to rapid spread through the Americas. More than 5700 cases have been reported in the United States, most of which occurred in 2016. The majority of cases result from mosquito-borne transmission; however, the recently described risks associated with sexual and maternofetal transmission raise new public health concerns. In symptomatic patients, ZIKV infection typically presents as a mild febrile illness 3 to 14 days after infection. Neurologic complications, including Guillain-Barre syndrome, are well described. Congenital Zika syndrome is notable for severe CNS malformations, including microcephaly. In symptomatic patients, the CDC currently recommends RT-PCR testing of paired serum and urine in the first week of illness and IgM testing after the first week (CDC, 2020). Both RT-PCR and IgM testing are recommended for symptomatic pregnant women as soon as possible and up to 12 weeks postsymptom onset.

Chikungunya

CHIKV (family: Togaviridae) is an RNA virus that was first isolated in 1952 in Tanzania. Historically CHIKV endemicity and outbreaks were restricted to the Eastern Hemisphere, but this changed in 2013 with the first documented outbreak in the Caribbean (Asian genotype) and subsequent spread through the Americas. Almost 4000 cases were reported in returning travelers in the United States between 2014 and 2016 (Lindsey et al., 2018). Following an average incubation period of 3 days, CHIKV infection is characterized by high fever and severe polyarthralgia. RT-PCR is recommended in the first week of symptoms, while IgM may be detected after 5 days of illness. Commercially available IgM testing kits vary considerably in sensitivity. Of note, bloodborne transmission during specimen collection and handling have been documented.

Viral Hemorrhagic Fever

The following section addresses highly pathogenic viruses associated with viral hemorrhagic fever syndrome that constitute major public health concerns when introduced into health care settings. Due to their severity, transmissibility, and lack of treatment, each of these viruses are designated as select agents requiring biosafety level 4 containment. Strict infection control precautions are warranted during specimen collection

and handling. High viral loads at the time of clinical presentation facilitate high clinical sensitivity of viral RNA detection by RT-PCR.

Ebola

The Ebolavirus genus (family: Filoviridae) comprises five species: *Zaire ebolavirus*, *Sudan ebolavirus*, *Bundibugyo ebolavirus*, *Tai Forest ebolavirus*, and *Reston ebolavirus*, collectively referred to here as EBOV. More than 30 EBOV outbreaks have been recorded in Africa since the virus was first isolated in 1976. An epidemic swept through West Africa in 2014 to 2016, with more than 28,600 cases and 11,300 deaths; 10 cases were treated in US hospitals, including four who were initially diagnosed in the United States. As of this writing, the second largest EBOV outbreak in history is ongoing in the Democratic Republic of Congo. EBOV outbreaks are triggered by zoonotic transmission events (likely involving exposure to bat excreta or bush meat) followed by person-to-person transmission via contact with infectious body fluids. A nonspecific febrile illness develops 2 to 21 days after exposure, which may progress to include severe gastrointestinal symptoms, hemorrhage, shock, and multiorgan failure. High viral loads are typically present at the time of clinical presentation and peak at 10^7 to 10^8 copies/mL for patients who ultimately survive; viral load continues to climb in fatal cases. Multiple NAAT and rapid antigen detection tests were granted emergency use authorization during the West Africa epidemic; currently in the United States, NAAT testing is available in public health laboratories and a few designated treatment hospitals. Confirmatory RT-PCR is performed at the CDC. With one vaccine against EBOV approved for compassionate use in the United States and another for use in Europe, several other vaccine candidates are currently in clinical trials.

Marburg

Marburgvirus (MARV) (family: Filoviridae) is an RNA virus related to EBOV. Two distinct lineages with more than 20% nucleic acid sequence variance have been implicated in human outbreaks: Ravn and Lake Victoria complex. MARV was first described in Germany in 1967 as the cause of a research laboratory–associated outbreak. Sporadic outbreaks have occurred over the past 50 years primarily in central Africa. The two largest outbreaks, which took place in the Democratic Republic of Congo in 1998 to 2000 and Angola in 2004 to 2005, incurred fatality rates greater than 80%. All outbreaks since 2007 have occurred in Uganda, and the only case reported in the United States was a traveler returning from Uganda in 2008. The primary reservoir for MARV is the African fruit bat, and zoonotic exposures have been linked to activities in caves where the bats reside. Infected body fluids mediate transmission from person-to-person and from infected nonhuman primates in veterinary or research settings. The incubation period and clinical presentation are similar to that of EBOV infection. RT-PCR testing is available at the CDC.

Lassa

Lassa mammarenavirus (LASV) (family: Arenaviridae) is a bisegmented RNA virus that was first isolated in 1969 in Nigeria. Six phylogenetic lineages have been described with 20% to 30% variation in gene sequences (Bowen et al., 2000). The geographic distribution of LASV spans West Africa, with most of the 100,000 to 300,000 annual cases occurring in Sierra Leone, Guinea, Liberia, and Nigeria. Eight LASV cases have been documented in returning travelers in the United States, with half occurring since 2010. The vast majority of LASV infections are transmitted from the main animal reservoir, *Mastomys natalensis* rats, through the inhalation or ingestion of rodent excreta (Lecompte et al., 1974). Person-to-person transmission also occurs with body fluid contact, and nosocomial spread is well documented (Fisher-Hoch et al., 1995). The incubation period ranges from 3 to 21 days, and up to 80% of infections are asymptomatic or characterized by mild febrile illness. In severe cases the clinical course may include ulcerative pharyngitis, conjunctivitis, pulmonary and CNS involvement, facial and neck swelling denoting vascular leakage, and signs of hemorrhage; 15% to 70% mortality is observed in hospitalized patients. Viral load peaks 4 to 9 days postsymptom onset, averaging 10^3 to 10^4 copies/mL at the time of diagnosis with higher viral loads predicting mortality (McCormick, 1986). Viral RNA detection in blood by quantitative RT-PCR is the cornerstone of diagnostic testing but remains challenged by suboptimal sensitivity when strain variance leads to mismatches in primer or probe targets (Panning et al., 2010). Utilization of multitarget RT-PCR assays and/or the addition of antigen and IgM detection is recommended to avoid false-positive results.

Crimean-Congo Hemorrhagic Fever

Crimean-Congo hemorrhagic fever orthonairovirus (CCHFV) (family: Nairoviridae) is a tri-segmented RNA virus first isolated in Congo in 1956, with recently increasing case detection in Europe, Asia, and Africa. The geographic distribution of CCHFV is determined by the range of its main reservoir and vector, *Hyalomma* ticks. The majority of infections occur via tick bite; however, CCHFV can also be transmitted by exposure to body fluids from infected people or animals (e.g., cattle, goats, sheep). Following an incubation period of 1 to 13 days and a nonspecific viral prodrome, hemorrhagic signs may rapidly develop leading to shock and multiorgan failure with high mortality. Viral loads peak during the first week of symptoms, and detection of viral RNA in blood by quantitative RT-PCR is recommended for initial diagnosis. Viral loads greater than 10^8 copies/mL portend a fatal outcome (Duh et al., 2007). The extensive sequence diversity across seven CCHFV clades may lead to false-negative results by some molecular assays (particularly if the assay relies on a single gene target), and inclusion of serologic assays for detection of protein antigens and IgM antibodies may increase overall diagnostic sensitivity (Mazzola & Kelly-Cirino, 2019; Bartolini et al., 2019).

Severe Respiratory Syndrome

Two novel, highly pathogenic viruses in the Coronaviridae family, severe acute respiratory syndrome–related coronavirus and Middle Eastern respiratory syndrome–related coronavirus recently gave rise to outbreaks of severe lower respiratory tract infections garnering international concern. In addition, the recent emergence of SARS-CoV-2 can also lead to a severe respiratory syndrome, which is discussed in further detail earlier. Bats are the primary reservoir for both SARS-CoV and MERS-CoV. Transmission from bats to other mammals ultimately leads to zoonotic exposures that cause human infection. Person-to-person transmission is responsible for the majority of cases, necessitating strict infection control precautions. Severe respiratory symptoms typically arise within 13 days of exposure (Assiri et al., 2013).

SARS

The emergence of SARS-CoV in 2002 to 2003 was linked to zoonotic transmission from palm civets at live animal markets in China. Over the course of a year, global travel and nosocomial spread gave rise to more than 8000 infections in 27 countries with a 10% fatality rate. Diagnostic RT-PCR assays were rapidly developed and made available in public health laboratories; however, no cases have been reported globally since 2004.

MERS

MERS-CoV was first described in 2012 (Zaki et al., 2012) and all human cases have been epidemiologically linked to the Middle East (Jordon, Saudi Arabia, United Arab Emirates, Yemen, Oman, Kuwait, Lebanon, Iran, and Qatar). Dromedary camels are a stable reservoir of MERS-CoV responsible for recurrent zoonotic transmission events. MERS-CoV infections are typically more severe that SARS-CoV, with a higher mortality rate of 35% (Alsolamy & Arabi, 2015). Approximately 2500 cases have been confirmed globally. Two cases were reported in the United States in 2014 associated with travel to Saudi Arabia. Most state public health laboratories are equipped to run the CDC RT-PCR assay for viral RNA detection in respiratory, serum, and stool specimens.

Severe Viral Encephalitis

Japanese Encephalitis

Japanese encephalitis virus (JEV) (family: Flaviviridae) is a neurotropic, mosquito-borne RNA virus that was first described in Japan in 1871. JEV is the most important cause of viral encephalitis in Asia, causing 68,000 symptomatic cases annually with a 30% mortality. JEV is primarily maintained in pigs and wading birds by *Culex* mosquito transmission; humans are accidental hosts and do not generate high enough viral load to propagate transmission. An effective vaccine was introduced in the United States in 1993, and since that time only 12 cases have been reported in returning travelers. Symptoms, including fever, vomiting, and signs of CNS involvement, develop 4 to 14 days following exposure. Due to low viral loads, direct virus detection methods, including NAAT, are considered insensitive and should not be used to rule out infection (Solomon et al., 2000). Virus-specific IgM may be detected in CSF or serum starting 3 days after the onset of symptoms, and this is the preferred diagnostic method. IgM capture ELISA is available in commercial reference laboratories, and confirmatory testing for neutralizing antibodies can be performed at the CDC.

Nipah

Nipah henipavirus (NiV) (family: Paramyxoviridae) is an emerging, highly pathogenic, zoonotic RNA virus. NiV was first isolated in 1999 in Malaysia and Singapore during an outbreak driven by close contact with infected pigs. Subsequent outbreaks have occurred regularly in Bangladesh and India, characterized by zoonotic transmission from the primary reservoir host, *Pteropus* bats, and person-to-person transmission presumed to involve close contact with respiratory secretions and body fluids. Febrile illness develops 4

to 14 days following exposure and may progress to severe pulmonary disease and/or CNS involvement with mortality rates ranging from 40% to 90% (Ang et al., 2018). Diagnostic tests for NiV are minimally developed and not widely available. Serology and RT-PCR testing for viral RNA detection in CSF, blood, and respiratory specimens is available at the CDC.

SUMMARY

In summary, we have shown throughout this chapter the great diversity in clinically relevant viral syndromes, including their virology, epidemiology, clinical presentation, laboratory diagnosis, and clinical implications. As described, clinical virology has largely shifted to molecular testing for many of these syndromes, although several applications of complementary diagnostic strategies remain in use. Significant laboratory diagnosis advances are expected in the coming years, particularly in the areas of next-generation sequencing and host-response markers. Finally, as the SARS-CoV-2 pandemic reminded us, there is need to constantly remain vigilant given that viruses may emerge and spread globally in a rapid timeframe and be associated with significant public health implications.

SELECTED REFERENCES

Antonelli G: Emerging new technologies in clinical virology, *Clin Microbiol Infect* 19(1):8–9, 2013.

This brief piece summarizes the progress made in clinical virology diagnostics, with a focus on emerging new technologies.

Chen N, Zhou M, Dong X, et al.: Epidemiological and clinical characteristics of 99 cases of 2019 novel coronavirus pneumonia in Wuhan, China: a descriptive study, *Lancet* 395(10223):507–513, 2020.

This retrospective study describes SARS-CoV-2 cases in the early phase of the pandemic in Wuhan, China and provides a clear picture of the demographic and clinical characteristics of infected individuals.

Kimberlin DW, Jackson MA, Long SS, editors: *Red book 2018: report of the committee on infectious diseases*, Elk Grove Village, IL, 2018, American Academy of Pediatrics.

This book is an essential reference for all paediatric infectious diseases matters, and spans epidemiology, diagnosis and management of a comprehensive list of pathogens and conditions.

Leber AL, Everhart K, Balada-Llasat JM, et al.: Multicenter evaluation of BioFire FilmArray meningitis/encephalitis panel for detection of bacteria, viruses, and yeast in cerebrospinal fluid specimens, *J Clin Microbiol* 54(9):2251–2261, 2016.

This study presents key data informing on test performance characteristics of the most commonly used panel for the diagnosis of meningitis and/or encephalitis from CSF specimens.

Leung J, Harpaz R, Baughman AL, et al.: Evaluation of laboratory methods for diagnosis of varicella, *Clin Infect Dis* 51:23–32, 2010.

This study presents a comprehensive test performance assessment of PCR for the diagnosis of varicella zoster virus, in both vaccine-modified and unmodified cases.

Lurain NS, Chou S: Antiviral drug resistance of human cytomegalovirus, *Clin Microbiol Rev* 23(4):689–712, 2010.

Excellent review summarizing the virological and clinical data pertaining to human cytomegalovirus antiviral drug resistance, supported by user-friendly diagrams.

Platts-Mills JA, Liu J, Rogawski ET, et al.: Use of quantitative molecular diagnostic methods to assess the aetiology, burden, and clinical characteristics of diarrhoea in children in low-resource settings: a reanalysis of the MAL-ED cohort study, *Lancet Global Health*, 2018.

Comprehensive review of the usefulness of quantitative molecular diagnostics to estimate pathogen-specific burdens of childhood diarrhea globally.

Ramanan P, Bryson AL, Binnicker MJ, et al.: Syndromic panel-based testing in clinical microbiology, *Clin Microbiol Rev* 31(1), 2018.

Excellent, well-written and comprehensive review of test performance and utilization of multiplexed molecular syndromic panels.

Schreckenberger PC, McAdam AJ: Point-counterpoint: large multiplex PCR panels should be first-line tests for detection of respiratory and intestinal pathogens, *J Clin Microbiol* 53(10):3110–3115, 2015.

Intellectually-stimulating discussion regarding the pros and cons of multiplexed molecular syndromic panels. Nicely complements Ramanan study above.

US Department of Health and Human Services: *Recommendations for the use of antiretroviral drugs in pregnant women with HIV infection and interventions to reduce perinatal HIV transmission in the United States*, 2018.

Indispensable resource and guidelines regarding all aspects of HIV management.

Access the complete reference list online at Elsevier eBooks for Practicing Clinicians.

REFERENCES

(UNAIDS) JUNPoHA: *DATA 2018. Geneva, Switzerland*, 2018.

Abedi GR, Prill MM, Langley GE, et al.: Estimates of parainfluenza virus-associated hospitalizations and cost among children aged less than 5 Years in the United States, 1998-2010, *J Pediatric Infect Dis Soc* 5(1):7–13, 2016.

Adair CV, Gauld RL, Smadel JE: Aseptic meningitis, a disease of diverse etiology: clinical and etiologic studies on 854 cases, *Ann Intern Med* 39(4):675–704, 1953.

Advisory Committee on Immunization P, Fiore AE, Wasley A, Bell BP: Prevention of hepatitis A through active or passive immunization: recommendations of the advisory Committee on immunization practices (ACIP), *MMWR Recomm Rep (Morb Mortal Wkly Rep)* 55(RR-7):1–23, 2006.

Ahmed SM, Hall AJ, Robinson AE, et al.: Global prevalence of norovirus in cases of gastroenteritis: a systematic review and meta-analysis, *Lancet Infect Dis*, 2014.

Allen UD, Robinson JL: Canadian Paediatric Society ID, Immunization C: prevention and management of neonatal herpes simplex virus infections, *Paediatr Child Health* 19(4):201–212, 2014.

Almeida SM: Cerebrospinal fluid analysis in the HIV infection and compartmentalization of HIV in the central nervous system, *Arq Neuropsiquiatr* 73(7):624–629, 2015.

Alsolamy S, Arabi YM: Infection with Middle East respiratory syndrome coronavirus, *Can J Respir Ther* 51(4):102, 2015.

Alsved M, Fraenkel C-J, Bohgard M, et al.: *Sources of airborne norovirus in hospital outbreaks*, Clinical Infectious Diseases, 2019.

Amin MB: In *AJCC cancer staging system*, 8th Edition, American Joint Commitee on Cancer, 2017.

American Association for the Study of Liver Diseases: https://aasldpubs.onlinelibrary.wiley.com/doi/full/10.1002/hep.31060.

Ang BSP, Lim TCC, Wang L: Nipah virus infection, *J Clin Microbiol* 56(6), 2018.

Antonelli G: Emerging new technologies in clinical virology, *Clin Microbiol Infect* 19(1):8–9, 2013.

Arai A: Advances in the study of chronic active Epstein-Barr virus infection: clinical features under the 2016 WHO classification and mechanisms of development, *Front Pediatr* 7(14), 2019.

Arauz-Ruiz P, Norder H, Robertson BH, Magnius LO, Genotype H: A new Amerindian genotype of hepatitis B virus revealed in Central America, *J Gen Virol* 83(Pt 8):2059–2073, 2002.

Ariza-Heredia EJ, Granwehr BP, Viola GM, et al.: False-positive HIV nucleic acid amplification testing during CAR T-cell therapy, *Diagn Microbiol Infect Dis* 88(4):305–307, 2017.

Assiri A, McGeer A, Perl TM, et al.: Hospital outbreak of Middle East respiratory syndrome coronavirus, *N Engl J Med* 369(5):407–416, 2013.

Babady NE, Dunn JJ, Madej R: CLIA-waived molecular influenza testing in the emergency department and outpatient settings, *J Clin Virol* 116:44–48, 2019.

Bányai K, Estes MK, Martella V, Parashar UD: Viral gastroenteritis, *Lancet* 392:175–186, 2018.

Bartolini B, Gruber CE, Koopmans M, et al.: Laboratory management of Crimean-Congo haemorrhagic fever virus infections: perspectives from two European networks, *Euro Surveill* 24(5), 2019.

Beal SG, Tremblay EE, Toffel S, Velez L, Rand KH: A gastrointestinal PCR panel improves clinical management and lowers health care costs, *J Clin Microbiol*, 2018.

Bennett JEDR, Blaser MJ: *Mandell, Douglas and Bennett's Principles and practice of infectious diseases*, Philadelphia, PA, 2015, Elsevier Saunders.

Bernheim A, Mei X, Huang M, et al.: Chest CT findings in coronavirus disease-19 (COVID-19): Relationship to duration of infection, *Radiology*, 2020. 200463.

Bhatraju PK, Ghassemieh BJ, Nichols M, et al.: *Covid-19 in critically ill patients in the Seattle region - case series*, N Engl J Med, 2020.

Bodeus M, Kabamba-Mukadi B, Zech F, Hubinont C, Bernard P, Goubau P: Human cytomegalovirus in utero transmission: follow-up of 524 maternal seroconversions, *J Clin Virol* 47(2):201–202, 2010.

Bonthius DJ: Lymphocytic choriomeningitis virus: an underrecognized cause of neurologic disease in the fetus, child, and adult, *Semin Pediatr Neurol* 19(3):89–95, 2012.

Boppana SB, Ross SA, Fowler KB: Congenital cytomegalovirus infection: clinical outcome, *Clin Infect Dis* 57(Suppl 4):S178–S181, 2013.

Boufassa F, Bachmeyer C, Carre N, et al.: Influence of neurologic manifestations of primary human immunodeficiency virus infection on disease progression. SEROCO Study Group, *J Infect Dis* 171(5):1190–1195, 1995.

Boulware DR, Pullen MF, Bangdiwala AS, et al.: *A Randomized trial of Hydroxychloroquine as postexposure prophylaxis for Covid-19*, N Engl J Med, 2020.

Bouthry E, Picone O, Hamdi G, Grangeot-Keros L, Ayoubi JM, Vauloup-Fellous C: Rubella and pregnancy: diagnosis, management and outcomes, *Prenat Diagn* 34(13):1246–1253, 2014.

Bowen MD, Rollin PE, Ksiazek TG, et al.: Genetic diversity among Lassa virus strains, *J Virol* 74(15):6992–7004, 2000.

Boyer SN, Wazer DE, Band V: *E7 protein of human papilloma virus-16 induces degradation of retinoblastoma protein through the ubiquitin-proteasome pathway*, Cancer Research, 1996.

Bradley H, Markowitz LE, Gibson T, McQuillan GM: Seroprevalence of herpes simplex virus types 1 and 2-United States, 1999-2010, *J Infect Dis* 209:325–333, 2014.

Brendish NJ, Malachira AK, Armstrong L, et al.: Routine molecular point-of-care testing for respiratory viruses in adults presenting to hospital with acute respiratory illness (ResPOC): a pragmatic, open-label, randomised controlled trial, *Lancet Respir Med* 5(5):401–411, 2017.

Breuer J, Schmid DS, Gershon Anne A: Use and Limitations of varicella–zoster virus–specific serological testing to evaluate Breakthrough disease in Vaccinees and to screen for susceptibility to varicella, *J Infect Dis* 197:S147–S151, 2008.

Bzhalava D, Eklund C, Dillner J: International standardization and classification of human papillomavirus types, *Virology* 476:341–344, 2015.

C AH, Caya C, Papenburg J: Rapid and simple molecular tests for the detection of respiratory syncytial virus: a review, *Expert Rev Mol Diagn* 18(7):617–629, 2018.

Call SA, Vollenweider MA, Hornung CA, Simel DL, McKinney WP: Does this patient have influenza? *J Am Med Assoc* 293(8):987–997, 2005.

Campbell-Yesufu OT, Gandhi RT: Update on human immunodeficiency virus (HIV)-2 infection, *Clin Infect Dis* 52(6):780–787, 2011.

Cannon MJ, Schmid DS, Hyde TB: Review of cytomegalovirus seroprevalence and demographic characteristics associated with infection, *Rev Med Virol* 20(4):202–213, 2010.

Cassidy H, Poelman R, Knoester M, Van Leer-Buter CC, Niesters HGM: Enterovirus D68 - the new Polio? *Front Microbiol* 9:2677, 2018.

Centers for Disease Control: *2018 Quick reference guide: recommended laboratory HIV testing algorithm for serum or plasma specimens*, 2018a.

Centers for Disease Control: *Rapid HIV tests suitable for use in non-clinical settings (CLIA-waived)*. Available at cdc.gov/hiv/pdf/testing/rapid-hiv-tests-non-clinical.pdf, 2018b. Accessed September 15th 2019.

Centers for Disease Control and Prevention (CDC): *Type and duration of precautions recommended for selected infections and conditions*. Available at https://www.cdc.gov/infectioncontrol/guidelines/isolation/appendix/type-duration-precautions.html. [Accessed 5 April 2020], 2018c.

Centers for Disease Control and Prevention (CDC): *Molluscum contagiosum*. Available at cdc.gov/poxvirus/molluscum-contagiosum/index.html. [Accessed 16 May 2020], 2015.

Centers for Disease Control and Prevention (CDC): *Testing guidance*, 2020.

Centers for Disease Control: https://www.cdc.gov/hiv/clinicians/transforming-health/health-care-providers/risk-reduction-strategies.html, 2019.

Centers for Disease Control: *Laboratory testing for the diagnosis of HIV infection : updated recommendations*, 2014.

Chan KCA, Woo JKS, King A, et al.: Analysis of plasma Epstein-Barr virus DNA to screen for nasopharyngeal cancer, *N Engl J Med* 377(6):513–522, 2017.

Chang Y, Moore PS, Weiss RA: Human oncogenic viruses: nature and discovery, *Philos Trans R Soc Lond B Biol Sci* 372(1732), 2017.

Charlton CL, Babady E, Ginocchio CC, et al.: Practical guidance for clinical microbiology laboratories: viruses causing acute respiratory tract infections, *Clin Microbiol Rev* 32(1), 2019.

Chaudhry SA, Verma N, Koren G: Hepatitis E infection during pregnancy, *Can Fam Physician* 61(7):607–608, 2015.

Chen N, Zhou M, Dong X, et al.: Epidemiological and clinical characteristics of 99 cases of 2019 novel coronavirus pneumonia in Wuhan, China: a descriptive study, *Lancet* 395(10223):507–513, 2020.

Chen X, Anstey AV, Bugert JJ: Molluscum contagiosum virus infection, *Lancet Infect Dis* 13:877–888, 2013.

Cheng MP, Papenburg J, Desjardins M, et al.: Diagnostic testing for severe acute respiratory syndrome-related coronavirus-2: a Narrative review, *Ann Intern Med*, 2020.

Cheung KS, Hung IF, Chan PP, et al.: Gastrointestinal manifestations of SARS-CoV-2 infection and virus load in fecal samples from the Hong Kong cohort and systematic review and meta-analysis, *Gastroenterology*, 2020.

Chiereghin A, Piccirilli G, Belotti T, et al.: Clinical utility of measuring Epstein-Barr virus-specific cell-mediated immunity after HSCT in addition to virological monitoring: results from a prospective study, *Med Microbiol Immunol* 208(6):825–834, 2019.

Ching KZ, Nakano T, Chapman LE, Demby A, Robertson BH: Genetic characterization of wild-type genotype VII hepatitis A virus, *J Gen Virol* 83(Pt 1):53–60, 2002.

Chou S, Satterwhite LE, Ercolani RJ: New Locus of drug resistance in the human cytomegalovirus UL56 gene revealed by in vitro exposure to letermovir and ganciclovir, *Antimicrob Agents Chemother* 62(9), 2018.

Chow EJ, Mermel LA: Hospital-acquired respiratory viral infections: incidence, morbidity, and mortality in pediatric and adult patients, *Open Forum Infect Dis* 4(1):ofx006, 2017.

Chung PW, Huang YC, Chang LY, Lin TY, Ning HC: Duration of enterovirus shedding in stool, *J Microbiol Immunol Infect* 34(3):167–170, 2001.

Corey L, Whitley RJ, Stone EF, Mohan K: Difference between herpes simplex virus type 1 and type 2 neonatal encephalitis in neurological outcome, *Lancet* 1(8575–6):1–4, 1988.

Dailey Garnes NJM, Ragoonanan D, Aboulhosn A: Adenovirus infection and disease in recipients of hematopoietic cell transplantation, *Curr Opin Infect Dis* 32(6):591–600, 2019.

de Martel C, Plummer M, Vignat J, Franceschi S: Worldwide burden of cancer attributable to HPV by site, country and HPV type, *Int J Canc* 141:664–670, 2017.

de Ory F, Guisasola ME, Sanz JC, Garcia-Bermejo I: Evaluation of four commercial systems for the diagnosis of Epstein-Barr virus primary infections, *Clin Vaccine Immunol* 18(3):444–448, 2011.

De Ravin SS, Gray JT, Throm RE, et al.: False-positive HIV PCR test following ex vivo lentiviral gene transfer treatment of X-linked severe combined immunodeficiency vector, *Mol Ther* 22(2):244–245, 2014.

Deeks SG, Overbaugh J, Phillips A, Buchbinder S: HIV infection, *Nat Rev Dis Primers* 1:15035, 2015.

Denniston MM, Jiles RB, Drobeniuc J, et al.: Chronic hepatitis C virus infection in the United States, national health and Nutrition Examination survey 2003 to 2010, *Ann Intern Med* 160(5):293–300, 2014.

Derkay CS, Bluher AE: *Update on recurrent respiratory papillomatosis*, Otolaryngologic Clinics of North America, 2019.

de-The G, Day NE, Geser A, et al.: Sero-epidemiology of the Epstein-Barr virus: preliminary analysis of an international study - a review, *IARC Sci Publ*(11 Pt 2)3–16, 1975.

Diseases AAftSoL: HCV guidance: recommendations for testing, managing, and treating hepatitis C. Available at: hcvguidelines.org/evaluate/testing-and-linkage. Accessed October 7 2019.

Doan ML, Mallory GB, Kaplan SL, et al.: Treatment of adenovirus pneumonia with cidofovir in pediatric lung transplant recipients, *J Heart Lung Transplant* 26(9):883–889, 2007.

Dollard SC, Grosse SD, Ross DS: New estimates of the prevalence of neurological and sensory sequelae and mortality associated with congenital cytomegalovirus infection, *Rev Med Virol* 17(5):355–3563, 2007.

Duh D, Saksida A, Petrovec M, et al.: Viral load as predictor of Crimean-Congo hemorrhagic fever outcome, *Emerg Infect Dis* 13(11):1769–1772, 2007.

Dunmire SK, Verghese PS, Balfour Jr HH: Primary Epstein-Barr virus infection, *J Clin Virol* 102:84–92, 2018.

Egawa N, Egawa K, Griffin H, Doorbar J: Human papillomaviruses; Epithelial tropisms, and the development of neoplasia, *Viruses* 7:3863–3890, 2015.

El Helou G, Razonable RR: Letermovir for the prevention of cytomegalovirus infection and disease in transplant recipients: an evidence-based review, *Infect Drug Resist* 12:1481–1491, 2019.

Fatahzadeh M, Schwartz RA: Human herpes simplex virus infections: epidemiology, pathogenesis, symptomatology, diagnosis, and management, *J Am Acad Dermatol*, 2007.

Fischer SA, Lu K, Practice ASTIDCo: Screening of donor and recipient in solid organ transplantation, *Am J Transplant* 13(Suppl 4):9–21, 2013.

Fisher-Hoch SP, Tomori O, Nasidi A, et al.: Review of cases of nosocomial Lassa fever in Nigeria: the high price of poor medical practice, *BMJ* 311(7009):857–859, 1995.

Fitzpatrick MB, Dube Mandishora RS, Katzenstein DA, et al.: hrHPV prevalence and type distribution in rural Zimbabwe: a community-based self-collection study using near-point-of-care GeneXpert HPV testing, *Int J Infect Dis*, 2019.

Florescu DF, Schaenman JM, Practice ASTIDCo: Adenovirus in solid organ transplant recipients: guidelines from the American Society of transplantation infectious diseases community of practice, *Clin Transplant* 33(9), 2019. e13527.

Gantt S, Bitnun A, Renaud C, Kakkar F, Vaudry W: Diagnosis and management of infants with congenital cytomegalovirus infection, *Paediatr Child Health* 22(2):72–74, 2017.

Gantt S, Dionne F, Kozak FK, et al.: Cost-effectiveness of universal and targeted newborn screening for congenital cytomegalovirus infection, *JAMA Pediatr* 170(12):1173–1180, 2016.

Gartner BC, Hess RD, Bandt D, et al.: Evaluation of four commercially available Epstein-Barr virus enzyme immunoassays with an immunofluorescence assay as the reference method, *Clin Diagn Lab Immunol* 10(1):78–82, 2003.

Gaunt ER, Hardie A, Claas EC, Simmonds P, Templeton KE: Epidemiology and clinical presentations of the four human coronaviruses 229E, HKU1, NL63, and OC43 detected over 3 years using a novel multiplex real-time PCR method, *J Clin Microbiol* 48(8):2940–2947, 2010.

Gershon AA, Breuer J, Cohen JI, et al.: Varicella zoster virus infection, *Nature Reviews Disease Primers* 1:1–41, 2015.

Gilden D, Cohrs RJ, Mahalingam R, Nagel MA: Varicella zoster virus vasculopathies: diverse clinical manifestations, laboratory features, pathogenesis, and treatment, *Lancet Neurol* 8(8):731–740, 2009.

Goderis J, De Leenheer E, Smets K, Van Hoecke H, Keymeulen A, Dhooge I: Hearing loss and congenital CMV infection: a systematic review, *Pediatrics* 134(5):972–982, 2014.

Gomez CA, Pinsky BA, Liu A, Banaei N: Delayed diagnosis of Tuberculous meningitis Misdiagnosed as herpes simplex virus-1 encephalitis with the FilmArray syndromic polymerase chain reaction panel, *Open Forum Infect Dis* 4(1):ofw245, 2017.

Grant GB, Desai S, Dumolard L, Kretsinger K, Reef SE: Progress toward rubella and congenital rubella syndrome control and elimination - worldwide, 2000-2018, *MMWR Morb Mortal Wkly Rep* 68(39):855–859, 2019.

Gregg MB: Recent outbreaks of lymphocytic choriomeningitis in the United States of America, *Bull World Health Organ* 52(4–6):549–553, 1975.

Guan WJ, Ni ZY, Hu Y, et al.: Clinical characteristics of coronavirus disease 2019 in China, *N Engl J Med* 382(18):1708–1720, 2020.

Guo L, Ren L, Yang S, et al.: Profiling early humoral response to diagnose novel coronavirus disease (COVID-19), *Clin Infect Dis*, 2020.

Guzman MG, Gubler DJ, Izquierdo A, Martinez E, Halstead SB: Dengue infection, *Nat Rev Dis Primers* 2:16055, 2016.

Hand J, Rose EB, Salinas A, et al.: Severe respiratory illness outbreak associated with human coronavirus NL63 in a long-term care facility, *Emerg Infect Dis* 24(10):1964–1966, 2018.

Harrington A, Cox B, Snowdon J, et al.: Comparison of Abbott ID Now and Abbott m2000 methods for the detection of SARS-CoV-2 from nasopharyngeal and nasal swabs from symptomatic patients, *J Clin Microbiol*, 2020.

Hayden RT, Preiksaitis J, Tong Y, et al.: Commutability of the first world health organization international standard for human cytomegalovirus, *J Clin Microbiol* 53(10):3325–3333, 2015.

Hayden RT, Sun Y, Tang L, et al.: Progress in quantitative viral load testing: variability and impact of the WHO quantitative international standards, *J Clin Microbiol* 55(2):423–430, 2017.

Hentrich M, Oruzio D, Jager G, et al.: Impact of human herpesvirus-6 after haematopoietic stem cell transplantation, *Br J Haematol* 128(1):66–72, 2005.

Hess RD: Routine Epstein-Barr virus diagnostics from the laboratory perspective: still challenging after 35 years, *J Clin Microbiol* 42(8):3381–3387, 2004.

Hickie I, Davenport T, Wakefield D, et al.: Post-infective and chronic fatigue syndromes precipitated by viral and non-viral pathogens: prospective cohort study, *BMJ* 333(7568):575, 2006.

Hirsch HH, Randhawa PS, Practice ASTIDCo: BK polyomavirus in solid organ transplantation-guidelines from the American Society of transplantation infectious diseases community of practice, *Clin Transplant* 33(9), 2019. e13528.

Hoffmann M, Kleine-Weber H, Schroeder S, et al.: SARS-CoV-2 cell entry depends on ACE2 and TMPRSS2 and is Blocked by a clinically proven protease inhibitor, *Cell* 181(2):271–280 e8, 2020.

Hope-Simpson RE: *The nature of herpes zoster: a long-term study and a new Hypothesis*, J Royal Soc Med, 1965.

Hsu JYC, Chen ACH, Keleher A, McMillan NAJ, Antonsson A: Shared and persistent asymptomatic cutaneous human papillomavirus infections in healthy skin, *J Med Virol*, 2009.

Hurt C, Tammaro D: Diagnostic evaluation of mononucleosis-like illnesses, *Am J Med* 120(10):911, 2007. e1–e8.

Hyypia T, Horsnell C, Maaronen M, et al.: A distinct picornavirus group identified by sequence analysis, *Proc Natl Acad Sci U S A* 89(18):8847–8851, 1992.

IARC Working Group on the Evaluation of Carcinogenic Risks to Humans: A review of human carcinogens. In *IARC Monographs on the evaluation of carcinogenic risks to humans. Lyon, France*, 2012, pp 255–314.

Ishikawa MK, Arps DP, Chow C, Hocker TL, Fullen DR: Histopathological features of molluscum contagiosum other than molluscum bodies, *Histopathology*, 2015.

Ison MG, Hirsch HH: Community-acquired respiratory viruses in transplant patients: diversity, impact, Unmet clinical needs, *Clin Microbiol Rev* 32(4), 2019.

Jain S, Self WH, Wunderink RG, et al.: Community-acquired pneumonia requiring hospitalization among U.S. Adults, *N Engl J Med* 373(5):415–427, 2015a.

Jain S, Williams DJ, Arnold SR, et al.: Community-acquired pneumonia requiring hospitalization among U.S. children, *N Engl J Med* 372(9):835–845, 2015b.

Jarrin I, Sellier P, Lopes A, et al.: Etiologies and management of aseptic meningitis in patients Admitted to an internal medicine department, *Medicine (Baltim)* 95(2), 2016. e2372.

Johnson RW, Alvarez-Pasquin MJ, Bijl M, et al.: Herpes zoster epidemiology, management, and disease and economic burden in Europe: a multidisciplinary perspective, *Ther Adv Vaccines* 3(4):109–120, 2015.

Joshi RP, Gomez CA, Steiner D, Aziz N, Pinsky BA: Closing the Brief case: confirmed positive HIV-1 serological screening but undetectable RNA virus load in a pregnant woman, *J Clin Microbiol* 55(12):3566–3567, 2017a.

Joshi RP, Gomez CA, Steiner D, Aziz N, Pinsky BA: The Brief case: confirmed positive HIV-1 serologic screening but undetectable RNA virus load in a pregnant woman, *J Clin Microbiol* 55(12):3316–3320, 2017b.

Jouan Y, Grammatico-Guillon L, Espitalier F, Cazals X, Francois P, Guillon A: Long-term outcome of severe herpes simplex encephalitis: a population-based observational study, *Crit Care* 19:345, 2015.

Kamar N, Dalton HR, Abravanel F, Izopet J: Hepatitis E virus infection, *Clin Microbiol Rev* 27(1):116–138, 2014.

Kasiske BL, Zeier MG, Chapman JR, et al.: KDIGO clinical practice guideline for the care of kidney transplant recipients: a summary, *Kidney Int* 77(4):299–311, 2010.

Katki HA, Schiffman M, Castle PE, et al.: Benchmarking CIN 3+ risk as the basis for incorporating HPV and pap cotesting into cervical screening and management guidelines, *J Low Genit Tract Dis*, 2013.

Kenneson A, Cannon MJ: Review and meta-analysis of the epidemiology of congenital cytomegalovirus (CMV) infection, *Rev Med Virol* 17(4):253–276, 2007.

Khetsuriani N, Holman RC, Anderson LJ: Burden of encephalitis-associated hospitalizations in the United States, 1988-1997, *Clin Infect Dis* 35(2):175–182, 2002.

Khetsuriani N, Quiroz ES, Holman RC, Anderson LJ: Viral meningitis-associated hospitalizations in the United States, 1988-1999, *Neuroepidemiology* 22(6):345–352, 2003.

Kim BK, Kang HJ, Hong KT, et al.: Successful preemptive therapy with single-dose rituximab for Epstein-Barr virus infection to prevent post-transplant lymphoproliferative disease after pediatric hematopoietic stem cell transplantation, *Transpl Infect Dis* 21(6), 2019. e13182.

Kimberlin DWBM, Jackson MA, Long SS, editors: *Red book 2018: report of the committee on infectious diseases*, Elk Grove Village, IL, 2018, American Academy of Pediatrics.

King RL, Lorch SA, Cohen DM, Hodinka RL, Cohn KA, Shah SS: Routine cerebrospinal fluid enterovirus polymerase chain reaction testing reduces hospitalization and antibiotic use for infants 90 days of age or younger, *Pediatrics* 120(3):489–496, 2007.

Kotton CN, Kumar D, Caliendo AM, et al.: The third international Consensus guidelines on the management of cytomegalovirus in solid-organ transplantation, *Transplantation* 102(6):900–931, 2018.

Krump NA, You J: Molecular mechanisms of viral oncogenesis in humans, *Nat Rev Microbiol* 16(11):684–698, 2018.

Kumar D, Ferreira VH, Blumberg E, et al.: A 5-year prospective Multicenter evaluation of influenza infection in transplant recipients, *Clin Infect Dis* 67(9):1322–1329, 2018.

Kupila L, Vuorinen T, Vainionpaa R, Hukkanen V, Marttila RJ, Kotilainen P: Etiology of aseptic meningitis and encephalitis in an adult population, *Neurology* 66(1):75–80, 2006.

Laetsch TW, Maude SL, Milone MC, et al.: False-positive results with select HIV-1 NAT methods following lentivirus-based tisagenlecleucel therapy, *Blood* 131(23):2596–2598, 2018.

Lafolie J, Labbe A, L'Honneur AS, et al.: Assessment of blood enterovirus PCR testing in paediatric populations with fever without source, sepsis-like disease, or suspected meningitis: a prospective, multicentre, observational cohort study, *Lancet Infect Dis* 18(12):1385–1396, 2018.

Lakeman FD, Whitley RJ: Diagnosis of herpes simplex encephalitis: application of polymerase chain reaction to cerebrospinal fluid from brain-biopsied patients and correlation with disease. National Institute of Allergy and Infectious Diseases Collaborative Antiviral Study Group, *J Infect Dis* 171(4):857–863, 1995.

Lanata CF, Fischer-Walker CL, Olascoaga AC, Torres CX, Aryee MJ, Black RE: *Global causes of diarrheal disease mortality in children <5 Years of age: a Systematic review*, PLoS ONE, 2013.

Lassaunière RFA, Harboe ZB, Nielsen ACY, Fomsgaard A, Krogfelt KA, Jørgensen CS: *Evaluation of nine commercial SARS-CoV-2 immunoassays*, medRxiv, 2020.

Leber AL, Everhart K, Balada-Llasat JM, et al.: Multicenter evaluation of BioFire FilmArray meningitis/encephalitis panel for detection of bacteria, viruses, and yeast in cerebrospinal fluid specimens, *J Clin Microbiol* 54(9):2251–2261, 2016.

Lecompte E, Fichet-Calvet E, Daffis S, et al.: Mastomys natalensis and Lassa fever, West Africa, *Emerg Infect Dis* 12(12):1971–1974, 2006.

Lee N, Chan PK, Hui DS, et al.: Viral loads and duration of viral shedding in adult patients hospitalized with influenza, *J Infect Dis* 200(4):492–500, 2009.

Lee SH, Chen SY, Chien JY, Lee TF, Chen JM, Hsueh PR: Usefulness of the FilmArray meningitis/encephalitis (M/E) panel for the diagnosis of infectious meningitis and encephalitis in Taiwan, *J Microbiol Immunol Infect* 52(5):760–768, 2019.

Leeper C, Lutzkanin 3rd A: Infections during pregnancy, *Prim Care* 45(3):567–586, 2018.

Legoff J, Péré H, Bélec L: Diagnosis of genital herpes simplex virus infection in the clinical laboratory, *Virol J*, 2014.

Leland DS, Ginocchio CC: Role of cell culture for virus detection in the age of technology, *Clin Microbiol Rev* 20(1):49–78, 2007.

Lessler J, Reich NG, Brookmeyer R, Perl TM, Nelson KE, Cummings DA: Incubation periods of acute respiratory viral infections: a systematic review, *Lancet Inf Dis*, 2009.

Leung J, Harpaz R, Baughman Andrew L, et al.: Evaluation of laboratory methods for diagnosis of varicella, *Clin Infect Dis* 51:23–32, 2010.

Levitz RE: Herpes simplex encephalitis: a review, *Heart Lung* 27(3):209–212, 1998.

Lewis-Jones S: *Zoonotic poxvirus infections in humans*, Current Opinion in Infectious Diseases, 2004.

Liesman RM, Strasburg AP, Heitman AK, Theel ES, Patel R, Binnicker MJ: Evaluation of a commercial multiplex molecular panel for diagnosis of infectious meningitis and encephalitis, *J Clin Microbiol* 56(4), 2018.

Lin A, Maloy M, Su Y, et al.: Letermovir for primary and secondary cytomegalovirus prevention in allogeneic hematopoietic cell transplant recipients: real-world experience, *Transpl Infect Dis* 21(6), 2019. e13187.

Linderholm M, Boman J, Juto P, Linde A: Comparative evaluation of nine kits for rapid diagnosis of infectious mononucleosis and Epstein-Barr virus-specific serology, *J Clin Microbiol* 32(1):259–261, 1994.

Lindsey NP, Lehman JA, Staples JE, Fischer M: Division of vector-borne diseases NCfE, zoonotic infectious diseases CDC. West nile virus and other arboviral diseases - United States, 2013, *MMWR Morb Mortal Wkly Rep* 63(24):521–526, 2014.

Lindsey NP, Staples JE, Fischer M: Chikungunya virus disease among travelers-United States, 2014-2016, *Am J Trop Med Hyg* 98(1):192–197, 2018.

Lingala S, Ghany MG: Natural history of hepatitis C, *Gastroenterol Clin North Am* 44(4):717–734, 2015.

Lion T: Adenovirus infections in immunocompetent and immunocompromised patients, *Clin Microbiol Rev* 27(3):441–462, 2014.

Ljungman P, Ribaud P, Eyrich M, et al.: Cidofovir for adenovirus infections after allogeneic hematopoietic stem cell transplantation: a survey by the infectious diseases working party of the European group for blood and Marrow transplantation, *Bone Marrow Transplant* 31(6):481–486, 2003.

Logan SA, MacMahon E: Viral meningitis, *BMJ* 336(7634):36–40, 2008.

Long SS: Encephalitis diagnosis and management in the real world, *Adv Exp Med Biol* 697:153–173, 2011.

Luck SE, Wieringa JW, Blazquez-Gamero D, et al.: Congenital cytomegalovirus: a European Expert Consensus Statement on diagnosis and management, *Pediatr Infect Dis J* 36(12):1205–1213, 2017.

Luckett K, Kaiser TE, Bari K, et al.: Use of hepatitis C virus antibody-positive donor livers in hepatitis C Nonviremic liver transplant recipients, *J Am Coll Surg* 228(4):560–567, 2019.

Lurain NS, Chou S: Antiviral drug resistance of human cytomegalovirus, *Clin Microbiol Rev* 23(4):689–712, 2010.

Lustig Y, Mannasse B, Koren R, et al.: Superiority of West Nile virus RNA detection in whole blood for diagnosis of acute infection, *J Clin Microbiol* 54(9):2294–2297, 2016.

Luzuriaga K, Sullivan JL: Infectious mononucleosis, *N Engl J Med* 362(21):1993–2000, 2010.

Mahnert N, Roberts SW, Laibl VR, Sheffield JS, Wendel Jr GD: The incidence of neonatal herpes infection, *Am J Obstet Gynecol* 196(5):e55–e56, 2007.

Mahony JB: Detection of respiratory viruses by molecular methods, *Clin Microbiol Rev* 21(4):716–747, 2008.

Manuel O, Estabrook M, American Society of Transplantation Infectious Diseases Community of P: RNA respiratory viral infections in solid organ transplant recipients: guidelines from the American Society of Transplantation Infectious Diseases Community of Practice, *Clin Transplant* 33(9), 2019. e13511.

Marquez L, Levy ML, Munoz FM, Palazzi DL: A report of three cases and review of intrauterine herpes simplex virus infection, *Pediatr Infect Dis J* 30(2):153–157, 2011.

Marshall-Andon T, Heinz P: How to use ... the Monospot and other heterophile antibody tests, *Arch Dis Child Educ Pract Ed* 102(4):188–193, 2017.

Martin F, Tagaya Y, Gallo R: Time to eradicate HTLV-1: an open letter to WHO. Lancet, 391(10133): 1893–1894.

Matthes-Martin S, Feuchtinger T, Shaw PJ, et al.: European guidelines for diagnosis and treatment of adenovirus infection in leukemia and stem cell transplantation: summary of ECIL-4 (2011), *Transpl Infect Dis* 14(6):555–563, 2012.

Mazzola LT, Kelly-Cirino C: Diagnostic tests for Crimean-Congo haemorrhagic fever: a widespread tickborne disease, *BMJ Glob Health* 4(Suppl 2), 2019. e001114.

McCormick JB: Clinical, epidemiologic, and therapeutic aspects of Lassa fever, *Med Microbiol Immunol* 175(2–3):153–155, 1986.

McGill F, Griffiths MJ, Bonnett LJ, et al.: Incidence, aetiology, and sequelae of viral meningitis in UK adults: a multicentre prospective observational cohort study, *Lancet Infect Dis* 18(9):992–1003, 2018.

Merckx J, Wali R, Schiller I, et al.: Diagnostic accuracy of novel and traditional rapid tests for influenza infection compared with reverse transcriptase polymerase chain reaction: a systematic review and meta-analysis, *Ann Intern Med* 167(6):394–409, 2017.

Meselson M: *Droplets and aerosols in the transmission of SARS-CoV-2*, N Engl J Med, 2020.

Metzner KJ: HIV whole-genome sequencing now: Answering still-open questions, *J Clin Microbiol* 54(4):834–835, 2016.

Miller E, Cradock-Watson JE, Pollock TM: Consequences of confirmed maternal rubella at successive stages of pregnancy, *Lancet* 2(8302):781–784, 1982.

Miller GD: Tindall JP: hand-foot-and-mouth disease, *J Am Med Assoc: J Am Med Associat*, 1968.

Modi S, Mahajan A, Dharaiya D, Varelas P, Mitsias P: Burden of herpes simplex virus encephalitis in the United States, *J Neurol* 264(6):1204–1208, 2017.

Moss WJ: Measles, *Lancet* 390:2490–2502, 2017.

Motamedifar M, Noorafshan A: *Cytopathic effect of the herpes simplex virus type 1 appears stereologically as early as 4 h after infection of Vero cells*, Micron, 2008.

Mount HR, Boyle SD: Aseptic and bacterial meningitis: evaluation, treatment, and prevention, *Am Fam Physician* 96(5):314–322, 2017.

Moura FE: Influenza in the tropics, *Curr Opin Infect Dis* 23(5):415–420, 2010.

Muldoon KM, Fowler KB, Pesch MH, Schleiss MR: SARS-CoV-2: is it the newest spark in the TORCH? *J Clin Virol* 127:104372, 2020.

Murphy DG, Sablon E, Chamberland J, Fournier E, Dandavino R, Tremblay CL: Hepatitis C virus genotype 7, a new genotype originating from central Africa, *J Clin Microbiol* 53(3):967–972, 2015.

Nainan OV, Xia G, Vaughan G, Margolis HS: Diagnosis of hepatitis a virus infection: a molecular approach, *Clin Microbiol Rev* 19(1):63–79, 2006.

Nalla AK, Casto AM, Huang MW, et al.: Comparative performance of SARS-CoV-2 detection assays using seven different primer/probe sets and one assay kit, *J Clin Microbiol*, 2020.

Nam HH, Ison MG: Respiratory syncytial virus infection in adults, *BMJ* 366:l5021, 2019.

National Institute of Allergy and Infectious Diseases: NIH clinical trial shows Remdesivir accelerates recovery from advanced COVID-19. Available at: https://www.nih.gov/news-events/news-releases/nih-clinical-trial-shows-remdesivir-accelerates-recovery-advanced-covid-19. Accessed May 3 2020.

Neu N, Duchon J, Zachariah P: TORCH infections, *Clin Perinatol* 42(1):77–103, 2015. viii.

Newton PJ, Newsholme W, Brink NS, Manji H, Williams IG, Miller RF: Acute meningoencephalitis and meningitis due to primary HIV infection, *BMJ* 325(7374):1225–1227, 2002.

Noska A, Kyrillos R, Hansen G, Hirigoyen D, Williams DN: The role of antiviral therapy in immunocompromised patients with herpes simplex virus meningitis, *Clin Infect Dis* 60(2):237–242, 2015.

Noureddin M, Gish R: Hepatitis delta: epidemiology, diagnosis and management 36 years after discovery, *Curr Gastroenterol Rep* 16(1):365, 2014.

O'Connell C, Oranje A, Van Gysel D, Silverberg NB: Congenital molluscum contagiosum: report of four cases and review of the literature, *Pediatr Dermatol*, 2008.

Ogimi C, Englund JA, Bradford MC, Qin X, Boeckh M, Waghmare A: Characteristics and outcomes of coronavirus infection in children: the role of viral factors and an immunocompromised state, *J Pediatric Infect Dis Soc* 8(1):21–28, 2019.

Okano M, Kawa K, Kimura H, et al.: Proposed guidelines for diagnosing chronic active Epstein-Barr virus infection, *Am J Hematol* 80(1):64–69, 2005.

Olijve L, Jennings L, Walls T: Human parechovirus: an increasingly recognized cause of sepsis-like illness in young infants, *Clin Microbiol Rev* 31(1), 2018.

Olsen JR GJ, Finlay AY, Piguet V, Francis NA: Time to resolution and effect on quality of life of molluscum contagiosum in children in the UK: a prospective community cohort study, *Lancet Infect Dis*, 2015.

Ong SWX, Tan YK, Chia PY, et al.: Air, surface environmental, and personal protective Equipment contamination by severe acute respiratory syndrome coronavirus 2 (SARS-CoV-2) from a symptomatic patient, *J Am Med Assoc*, 2020.

WHO: Hepatitis A. 2019a. https://www.who.int/immunization/diseases/hepatitisA/en/. Accessed March 13, 2021.

WHO: Hepatitis B. 2019b. https://wwwwho.int/news-room/fact-sheets/detail/hepatitis-b Accessed March 13, 2021.

WHO: Hepatitis C. 2019c. https://wwwwho.int/news-room/fact-sheets/detail/hepatitis-c. Accessed March 13, 2021.

WHO: *HIV/AIDS Data and statistics*. Available at who.int/hiv/data/en/, 2019e.

WHO 2021: Covid-19. https://covid19.who.int. 2021.

Page NA, Nadan S, Mans J: *Viral gastroenteritis*, Gastrointestinal Diseases and Their Associated Infections, 2019.

Palefsky J: Human papillomavirus-related disease in people with HIV, *Curr Opin HIV AIDS*, 2009.

Pan CQ, Zhang JX: Natural history and clinical consequences of hepatitis B virus infection, *Int J Med Sci* 2(1):36–40, 2005.

Panning M, Emmerich P, Olschlager S, et al.: Laboratory diagnosis of Lassa fever, Liberia, *Emerg Infect Dis* 16(6):1041–1043, 2010.

Pappas DE, Hendley JO, Hayden FG, Winther B: Symptom profile of common colds in school-aged children, *Pediatr Infect Dis J* 27(1):8–11, 2008.

Patel M, Lee AD, Clemmons NS, et al.: *National update on measles cases and outbreaks - United States, January 1-October 1, 2019*, MMWR Morbidity and mortality weekly report, 2019.

Patel MK, Dumolard L, Nedelec Y, et al.: *Progress toward regional measles elimination — worldwide, 2000–2018*, Morbidity and Mortality Weekly Report, 2019.

Paul JR, Bunnell WW: The presence of heterophile antibodies in infectious mononucleosis, *Am J Med Sci* 267(3):178–188, 1974.

American Academy of Pediatrics: In *Red book: 2015 report of the committee on infectious diseases*, 30th ed., 2015. (Elk Grove Village, IL..

Peghin M, Los-Arcos I, Hirsch HH, et al.: Community-acquired respiratory viruses are a risk factor for chronic lung Allograft dysfunction, *Clin Infect Dis* 69(7):1192–1197, 2019.

Pellett PE, Ablashi DV, Ambros PF, et al.: Chromosomally integrated human herpesvirus 6: questions and answers, *Rev Med Virol* 22(3):144–155, 2012.

Pergam SA, Limaye AP: Practice ASTIDCo: varicella zoster virus in solid organ transplantation: guidelines from the American Society of transplantation infectious diseases community of practice, *Clin Transplant* 33(9), 2019. e13622.

Perkins RB, Guido RS, Castle PE, et al.: ASCCP risk-based management Consensus guidelines for abnormal cervical cancer screening tests and cancer Precursors, *J Low Genit Tract Dis* 24:102–131, 2019.

Picone O, Vauloup-Fellous C, Cordier AG, et al.: A series of 238 cytomegalovirus primary infections during pregnancy: description and outcome, *Prenat Diagn* 33(8):751–758, 2013.

Piedra PA: Live attenuated influenza vaccine: will the Phoenix rise again? *Pediatrics* 143(2), 2019.

Pilcher CD, Louie B, Facente S, et al.: Performance of rapid point-of-care and laboratory tests for acute and established HIV infection in San Francisco, *PloS One* 8(12), 2013. e80629.

Platts-Mills JA, Liu J, Rogawski ET, et al.: Use of quantitative molecular diagnostic methods to assess the aetiology, burden, and clinical characteristics of diarrhoea in children in low-resource settings: a reanalysis of the MAL-ED cohort study, *Lancet Global Health*, 2018.

Plunkett J, Mandal S, Balogun K, et al.: Hepatitis A outbreak among men who have sex with men (MSM) in England, 2016-2018: the contribution of past and current vaccination policy and practice, *Vaccine X* 1:100014, 2019.

Poljak M, Oštrbenk Valenčak A, Gimpelj Domjanič G, Xu L, Arbyn M: Commercially available molecular tests for human papillomaviruses: a global overview, *Clin Microbiol Infect*, 2020.

Pollock NR, Savage TJ, Wardell W, et al.: Correlation of SARS-CoV-2 nucleocapsid antigen and RNA concentrations in nasopharyngeal samples from children and adults using an ultrasensitive and quantitative antigen assay, *J Clin Microbiol* 59(4):e03077–20, 2021.

Pons-Salort M, Oberste MS, Pallansch MA, et al.: The seasonality of nonpolio enteroviruses in the United States: patterns and drivers, *Proc Natl Acad Sci U S A* 115(12):3078–3083, 2018.

CfDCa P: *HIV surveillance Report*, 2019.

CfDCa P: *West Nile virus*, 2019.

CfDCa P: *Widespread person-to-person outbreaks of hepatitis A across the United States*, 2019.
Rahamat-Langendoen JC, Riezebos-Brilman A, Hak E, Scholvinck EH, Niesters HG: The significance of rhinovirus detection in hospitalized children: clinical, epidemiological and virological features, *Clin Microbiol Infect* 19(10):E435–E442, 2013.
Ramanan P, Bryson AL, Binnicker MJ, Pritt BS, Patel R: Syndromic panel-based testing in clinical microbiology, *Clin Microbiol Rev* 31(1), 2018.
Ramdass P, Mullick S, Farber HF: Viral skin diseases, *Prim Care Clin Off Pract* 42:517–567, 2015.
Ramers C, Billman G, Hartin M, Ho S, Sawyer MH: Impact of a diagnostic cerebrospinal fluid enterovirus polymerase chain reaction test on patient management, *J Am Med Assoc* 283(20):2680–2685, 2000.
Rappo U, Schuetz AN, Jenkins SG, et al.: Impact of early detection of respiratory viruses by multiplex PCR assay on clinical outcomes in adult patients, *J Clin Microbiol* 54(8):2096–2103, 2016.
Remington PL, Hall WN, Davis IH, Herald A, Gunn RA: Airborne transmission of measles in a Physician's office, *J Am Med Assoc: JAMA*, *J Am Med Assoc*, 1985.
Renati S, Linder JA: Necessity of office visits for acute respiratory infections in primary care, *Fam Pract* 33(3):312–317, 2016.
Rice CM, Yadav S, Boyanton B, Subedi P: Band J: clinical problem-solving. A creeping suspicion, *N Engl J Med* 371(1):68–73, 2014.
Rogers BB, Shankar P, Jerris RC, et al.: Impact of a rapid respiratory panel test on patient outcomes, *Arch Pathol Lab Med* 139(5):636–641, 2015.
Rolfes MA, Foppa IM, Garg S, et al.: Annual estimates of the burden of seasonal influenza in the United States: a tool for strengthening influenza surveillance and preparedness, *Influenza Other Respir Viruses* 12(1):132–137, 2018.
Rollison DE, Viarisio D, Amorrortu RP, Gheit T, Tommasino M: An emerging issue in oncogenic virology: the role of Beta human papillomavirus types in the development of cutaneous squamous cell carcinoma, *J Virol* 93:1–10, 2019.
Rothberg MB, Haessler SD: Complications of seasonal and pandemic influenza, *Crit Care Med* 38(4 Suppl):e91–e97, 2010.
Russell E, Yang A, Tardrew S, Ison MG: Parainfluenza virus in hospitalized adults: a 7-year retrospective study, *Clin Infect Dis* 68(2):298–305, 2019.
Saarela E, Tapiainen T, Kauppila J, et al.: Impact of multiplex respiratory virus testing on antimicrobial consumption in adults in acute care: a randomized clinical trial, *Clin Microbiol Infect*, 2019.
Sambri V, Capobianchi MR, Cavrini F, et al.: Diagnosis of west nile virus human infections: overview and proposal of diagnostic protocols considering the results of external quality assessment studies, *Viruses* 5(10):2329–2348, 2013.
Sauerbrei A, Taut J, Zell R, Wutzler P: Resistance testing of clinical varicella-zoster virus strains, *Antiviral Res* 90(3):242–247, 2011.
Scheffner M, Werness BA, Huibregtse JM, Levine AJ, Howley PM: The E6 oncoprotein encoded by human papillomavirus types 16 and 18 promotes the degradation of p53, *Cell*, 1990.
Schillie S, Vellozzi C, Reingold A, et al.: Prevention of hepatitis B virus infection in the United States: recommendations of the advisory Committee on immunization practices, *MMWR Recomm Rep (Morb Mortal Wkly Rep)* 67(1):1–31, 2018.
Schlesinger Y, Tebas P, Gaudreault-Keener M, Buller RS, Storch GA: Herpes simplex virus type 2 meningitis in the absence of genital lesions: improved recognition with use of the polymerase chain reaction, *Clin Infect Dis* 20(4):842–848, 1995.
Schreckenberger PC, McAdam AJ: Point-Counterpoint: large multiplex PCR panels should Be first-line tests for detection of respiratory and intestinal pathogens, *J Clin Microbiol* 53(10):3110–3115, 2015.
Selvaraju SB, Nix WA, Oberste MS, Selvarangan R: Optimization of a combined human parechovirus-enterovirus real-time reverse transcription-PCR assay and evaluation of a new parechovirus 3-specific assay for cerebrospinal fluid specimen testing, *J Clin Microbiol* 51(2):452–458, 2013.
Shah DP, Ghantoji SS, Ariza-Heredia EJ, et al.: Immunodeficiency scoring index to predict poor outcomes in hematopoietic cell transplant recipients with RSV infections, *Blood* 123(21):3263–3268, 2014.
Shannon-Lowe C, Rickinson A: The global landscape of EBV-associated tumors, *Front Oncol* 9:713, 2019.
Shannon-Lowe C, Rowe M: Epstein Barr virus entry; kissing and conjugation, *Curr Opin Virol* 4:78–84, 2014.
Shiley K, Blumberg E: Herpes viruses in transplant recipients: HSV, VZV, human herpes viruses, and EBV, *Hematol Oncol Clin North Am* 25(1):171–191, 2011.
Shukla B, Aguilera EA, Salazar L, Wootton SH, Kaewpoowat Q, Hasbun R: Aseptic meningitis in adults and children: diagnostic and management challenges, *J Clin Virol* 94:110–114, 2017.
Smith DK, Switzer WM, Peters P, et al.: A strategy for PrEP clinicians to manage Ambiguous HIV test results during follow-up visits, *Open Forum Infect Dis* 5(8):ofy180, 2018.
Solomon T, Dung NM, Kneen R, Gainsborough M, Vaughn DW, Khanh VT: Japanese encephalitis, *J Neurol Neurosurg Psychiatry* 68(4):405–415, 2000.
Solomon T, Lewthwaite P, Perera D, Cardosa MJ, McMinn P, Ooi MH: Virology, epidemiology, pathogenesis, and control of enterovirus 71, *Lancet Infect Dis* 10:778–790, 2010.
Spruance SL, Overall JC, Kern ER, Krueger GG, Pliam V, Miller W: The natural history of recurrent herpes simplex labialis: implications for antiviral therapy, *N Eng J Med*, 1977.
Sridhar S, Teng JLL, Chiu TH, Lau SKP, Woo PCY: Hepatitis E virus genotypes and Evolution: emergence of camel hepatitis E variants, *Int J Mol Sci* 18(4), 2017.
Stanford U: *HIV drug resistance Database*. Available at https://hivdb.stanford.edu/. [Accessed 18 May 2020], 2020.
Stanford U: *Major HIV-1 drug resistance mutations*. Available at https://hivdb.stanford.edu/pages/download/resistanceMutations_handout.pdf. [Accessed 18 May 2020], 2015.
Stekler JD, O'Neal JD, Lane A, et al.: Relative accuracy of serum, whole blood, and oral fluid HIV tests among Seattle men who have sex with men, *J Clin Virol* 58(Suppl 1), 2013. e119–e122.
Stuyver L, De Gendt S, Van Geyt C, et al.: A new genotype of hepatitis B virus: complete genome and phylogenetic relatedness, *J Gen Virol* 81(Pt 1):67–74, 2000.
Styczynski J, van der Velden W, Fox CP, et al.: Management of Epstein-Barr Virus infections and post-transplant lymphoproliferative disorders in patients after allogeneic hematopoietic stem cell transplantation: sixth European Conference on Infections in Leukemia (ECIL-6) guidelines, *Haematologica* 101(7):803–811, 2016.
Styczynski J: Who is the patient at risk of CMV recurrence: a review of the current Scientific evidence with a focus on hematopoietic cell transplantation, *Infect Dis Ther* 7(1):1–16, 2018.
Subramony A, Zachariah P, Krones A, Whittier S, Saiman L: Impact of multiplex polymerase chain reaction testing for respiratory pathogens on healthcare resource utilization for pediatric inpatients, *J Pediatr* 173:196–201, 2016. e2.
Sunbul M: Hepatitis B: virus genotypes: global distribution and clinical importance, *World J Gastroenterol* 20(18):5427–5434, 2014.
Sung RY, Chan PK, Choi KC, et al.: Comparative study of nasopharyngeal aspirate and nasal swab specimens for diagnosis of acute viral respiratory infection, *J Clin Microbiol* 46(9):3073–3076, 2008.
Swinnen B, Saegeman V, Beuselinck K, et al.: Predictive value of JC virus PCR in cerebrospinal fluid in the diagnosis of PML, *Diagn Microbiol Infect Dis* 95(3):114859, 2019.
Tagaya Y, Matsuoka M, Gallo R: 40 years of the human T-cell leukemia virus: past, present, and future, *F1000Res* 8, 2019.
Tan SK, Milligan S, Sahoo MK, Taylor N, Pinsky BA: Calibration of BK virus nucleic acid amplification testing to the 1st WHO international standard for BK virus, *J Clin Microbiol* 55(3):923–930, 2017.
Tate JE, Burton AH, Boschi-Pinto C, Steele AD, Duque J, Parashar UD: Estimate of worldwide rotavirus-associated mortality in children younger than 5 years before the introduction of universal rotavirus vaccination programmes: a systematic review and meta-analysis, *Lancet Infect Dis*, 2008. 2012.
Te H, Doucette K: Viral hepatitis: guidelines by the American Society of transplantation infectious disease community of practice, *Clin Transplant* 33(9), 2019. e13514.
Terrault NA, Bzowej NH, Chang KM, et al.: AASLD guidelines for treatment of chronic hepatitis B, *Hepatology* 63(1):261–283, 2016.
Teunis PFM, Moe CL, Liu P, et al.: Norwalk virus: how infectious is it? *J Med Virol*, 2008.
Toizumi M, Vo HM, Dang DA, Moriuchi H, Yoshida LM: Clinical manifestations of congenital rubella syndrome: a review of our experience in Vietnam, *Vaccine* 37(1):202–209, 2019.
Tunkel AR, Glaser CA, Bloch KC, et al.: The management of encephalitis: clinical practice guidelines by the Infectious Diseases Society of America, *Clin Infect Dis* 47(3):303–327, 2008.
U.S. Department of Health and Human Services: *Guidelines for the Use of antiretroviral agents in adults and adolescents with HIV*. Available at https://aidsinfo.nih.gov/guidelines/html/1/adult-and-adolescent-arv/37/whats-new-in-the-guidelines-. [Accessed 18 May 2020], 2019.
U.S. Department of Health and Human Services: *Recommendations for the Use of antiretroviral drugs in pregnant women with HIV infection and interventions to reduce perinatal HIV transmission in the United States*, 2018.
U.S. Food and Drug Administration: Microbiology devices; Reclassification of influenza virus antigen detection test systems Intended for Use directly with clinical specimens. Available at https://www.federalregister.gov/documents/2017/01/12/2017-00199/microbiology-devices-reclassification-of-influenza-virus-antigen-detection-test-systems-intended-for. [Accessed 5 April 2020].
United Network for Organ Sharing. Transplant trends. Accessed May 9 2020.
Update of standard nomenclature: Update of standard nomenclature for wild-type rubella viruses, *Wkly Epidemiol Rec* 82(24):216–222, 2007. 2007.
Usatine RP, Tinitigan R: Nongenital herpes simplex virus, *Am Fam Physician* 82(9):1075–1082, 2010.
van der Wouden JC, van der Sande R, Kruithof EJ, Sollie A, van Suijlekom-Smit LWA, Koning S: *Interventions for cutaneous molluscum contagiosum*, Cochrane Database of Systematic Reviews, 2017.
van Doremalen N, Bushmaker T, Morris DH, et al.: Aerosol and surface stability of SARS-CoV-2 as compared with SARS-CoV-1, *N Engl J Med* 382(16):1564–1567, 2020.
Verity R, Okell LC, Dorigatti I, et al.: Estimates of the severity of coronavirus disease 2019: a model-based analysis, *Lancet Infect Dis*, 2020.
Verstrepen WA, Kuhn S, Kockx MM, Van De Vyvere ME, Mertens AH: Rapid detection of enterovirus RNA in cerebrospinal fluid specimens with a novel single-tube real-time reverse transcription-PCR assay, *J Clin Microbiol* 39(11):4093–4096, 2001.
Viens LJ, Jane Henley S, Watson M, et al.: *Human papillomavirus-associated cancers — United States, 2008-2012*, Morbidity and Mortality Weekly Report, 2016.
Vynnycky E, Adams EJ, Cutts FT, et al.: Using seroprevalence and Immunisation coverage data to estimate the global burden of congenital rubella syndrome, 1996-2010: a systematic review, *PloS One* 11(3), 2016. e0149160.
Walsh EE, Shin JH, Falsey AR: Clinical impact of human coronaviruses 229E and OC43 infection in diverse adult populations, *J Infect Dis* 208(10):1634–1642, 2013.
Warrener L, Slibinskas R, Chua KB, et al.: *A point-of-care test for measles diagnosis: detection of measles-specific igM antibodies and viral nucleic acid*, Bulletin of the World Health Organization, 2011.
Weil AA, Glaser CA, Amad Z, Forghani B: Patients with suspected herpes simplex encephalitis: rethinking an initial negative polymerase chain reaction result, *Clin Infect Dis* 34(8):1154–1157, 2002.
Williams-Harmon YJ, Jason LA, Katz BZ: Incidence of infectious mononucleosis in Universities and U.S. Military settings, *J Diagn Tech Biomed Anal* 5(1), 2016.
Wilson E, Hofmeister MG, McBee S, et al.: Notes from the field: hepatitis A outbreak associated with drug Use and Homelessness - West Virginia, 2018, *MMWR Morb Mortal Wkly Rep* 68(14):330–331, 2019.
Wolfson LJ, Grais RF, Luquero FJ, Birmingham ME, Strebel PM: Estimates of measles case fatality ratios: a comprehensive review of community-based studies, *Int J Epidemiol*, 2009.
Womack J, Jimenez M: Common questions about infectious mononucleosis, *Am Fam Physician* 91(6):372–376, 2015.
Woo GKS, Wong AH, Lee WY, et al.: Comparison of laboratory diagnostic methods for measles infection and identification of measles virus genotypes in Hong Kong, *J Med Virol*, 2010.

Wood E, Kerr T, Rowell G, et al.: Does this adult patient have early HIV infection?: the Rational Clinical Examination systematic review, *J Am Med Assoc* 312(3):278–285, 2014.
Woolley AE, Singh SK, Goldberg HJ, et al.: Heart and lung transplants from HCV-infected donors to uninfected recipients, *N Engl J Med* 380(17):1606–1617, 2019.
World Health Organization: Coronavirus disease 2019 (COVID-19) situation Report - 101. Available at https://www.who.int/docs/default-source/coronaviruse/situation-reports/20200430-sitrep-101-covid-19.pdf?sfvrsn=2ba4e093_2. [Accessed 2 May 2020].
World Health Organization. Hepatitis E. 2019d.
Wutzler P, Bonanni P, Burgess M, Gershon A, Sáfadi MA, Casabona G: *Varicella vaccination - the global experience*, Expert Review of Vaccines, 2017.
Xiaolu Tang CW, Xiang L, Song Y, et al.: *On the origin and ongoing evolution of SARS-CoV-2*, National Science Review, 2020.
Xydakis MS, Dehgani-Mobaraki P, Holbrook EH, et al.: Smell and taste dysfunction in patients with COVID-19, *Lancet Infect Dis*, 2020.
Yang X, Yu Y, Xu J, et al.: Clinical course and outcomes of critically ill patients with SARS-CoV-2 pneumonia in Wuhan, China: a single-centered, retrospective, observational study, *Lancet Respir Med*, 2020.
Young S, Phillips J, Griego-Fullbright C, et al.: Molecular point-of-care testing for influenza A/B and respiratory syncytial virus: comparison of workflow parameters for the ID Now and cobas Liat systems, *J Clin Pathol*, 2019.
Zaki AM, van Boheemen S, Bestebroer TM, Osterhaus AD, Fouchier RA: Isolation of a novel coronavirus from a man with pneumonia in Saudi Arabia, *N Engl J Med* 367(19):1814–1820, 2012.
Zhang J, Zhang XF, Huang SJ, et al.: Long-term efficacy of a hepatitis E vaccine, *N Engl J Med* 372(10):914–922, 2015.
Zhang Q, Davis JC, Lamborn IT, et al.: Combined immunodeficiency associated with DOCK8 mutations, *N Engl J Med*, 2009.
Zhou P, Yang XL, Wang XG, et al.: A pneumonia outbreak associated with a new coronavirus of probable bat origin, *Nature* 579(7798):270–273, 2020.
Zorec TM, Kutnjak D, Hošnjak L, et al.: New insights into the evolutionary and genomic landscape of molluscum contagiosum virus (MCV) based on nine MCV1 and six MCV2 complete genome sequences, *Viruses* 10:1–24, 2018.
Zou S, Dorsey KA, Notari EP, et al.: Prevalence, incidence, and residual risk of human immunodeficiency virus and hepatitis C virus infections among United States blood donors since the introduction of nucleic acid testing, *Transfusion* 50(7):1495–1504, 2010.
zur Hausen H, de Villiers EM: Cancer "causation" by infections—individual contributions and synergistic networks, *Semin Oncol* 41(6):860–875, 2014.

CHAPTER 65

MEDICAL PARASITOLOGY

Blaine A. Mathison, Bobbi S. Pritt

PARASITE CLASSIFICATION AND TAXONOMY, 1292

LABORATORY METHODS, 1292
Examination of Blood, 1292
Examination of Fecal Specimens, 1294
Examination of Urogenital and Other Specimens (Sputa, Aspirates, Biopsies), 1297
Parasite Culture Techniques, 1297
Immunodiagnostic Methods, 1297
Molecular Diagnostic Methods, 1300
Quality Assurance, Quality Improvement, and Safety, 1300

BLOOD AND TISSUE PROTOZOA, 1301
Plasmodium Spp. (Malaria), 1301
Babesia Spp. (Babesiosis), 1304
Hemoflagellates, 1309
Toxoplasma Gondii (Toxoplasmosis), 1312
Opportunistic Free-Living Amebae, 1313
Intestinal and Urogenital Protozoa, 1315
Intestinal Amebae, 1315
Blastocystis spp., 1319
Flagellates, 1319
Ciliates, 1322

INTESTINAL HELMINTHS, 1326
Nematodes, 1326
Cestodes, 1330
Trematodes, 1335

TISSUE HELMINTHS, 1338
Nematodes, 1338
Other, 1341
Cestodes, 1342
Trematodes, 1344

MEDICALLY IMPORTANT ARTHROPODS, 1344
Biological Characteristics, 1344
Mechanisms of Injury, 1344
Laboratory Approaches to Arthropod Identification, 1346
Insects, 1346
Arachnids, 1347
Classes of Lesser Medical Importance, 1349

PARASITIC INFECTIONS AND THE IMMUNOCOMPROMISED HOST, 1351

SELECTED REFERENCES, 1351

KEY POINTS

- Accurate diagnosis of parasitic infection usually depends on macroscopic or microscopic examination of specimens that have been appropriately collected and preserved. Thick and thin blood smears are useful for detecting and characterizing organisms found in the blood. Fecal specimens may be fresh (if they can be examined rapidly) or may be placed into fixatives such as formalin and polyvinyl alcohol or single-vial commercial fixatives. Examination of at least three specimens, collected on separate days, provides the optimal sensitivity for parasite detection. In general, it is not useful to examine specimens from hospitalized patients who develop diarrhea after the third hospital day since parasites are an unlikely cause of their symptoms.
- Antigen detection methods serve as a useful adjunctive or alternative test for detecting select parasites in clinical specimens. Immunoassays are commercially available for detecting *Plasmodium* spp. in blood; *Giardia duodenalis*, *Cryptosporidium* spp., and *Entamoeba histolytica* in feces; and *Trichomonas vaginalis* in vaginal swabs.
- Serologic testing (i.e., detection of parasite-specific antibodies) is an important adjunct in recognizing parasitic infections that involve deep tissues, organs, and body spaces not readily amenable to routine morphologic testing methods.
- Molecular amplification methods generally offer high levels of sensitivity and specificity for diagnosis of parasitic disease. Most are laboratory developed tests (LDTs), although commercial options are available for some parasites, including multiplex panels that detect multiple gastrointestinal protozoan pathogens and nucleic acid amplification tests (NAATs) for *Trichomonas vaginalis.*
- Malaria is a protozoan parasite responsible for significant morbidity and mortality worldwide. The diagnosis of malaria should be considered in the differential diagnosis of unexplained fever with the history of travel in endemic geographic regions. Because of its high associated mortality, testing for acute disease should be done on a STAT basis. Thick and thin blood smears are complementary for detecting and identifying infecting *Plasmodium* spp., respectively, and are considered one of the gold standard laboratory methods. NAATs also offer high sensitivity and specificity but are rarely available on a STAT basis. Rapid antigen detection tests (RDTs) provide a quick presumptive diagnosis; however, they should be followed by more sensitive testing. Determination of parasite burden is used to direct initial therapy and monitor response to antimalarial treatment.
- Other important protozoal infections found in blood and/or tissue include babesiosis (blood), trypanosomiasis (blood, cerebral spinal fluid, and tissue), leishmaniasis (cutaneous, mucocutaneous, and visceral forms of disease), and toxoplasmosis. The latter often affects the central nervous system following congenital infection and in patients with acquired immunodeficiency syndrome (AIDS).
- Infection with intestinal amebae is acquired via ingestion of mature cysts, resulting in infection of the colon and passage of both cysts and trophozoites in the feces. Most amebae are nonpathogens. *Entamoeba histolytica* is a proven pathogen that may cause amebic dysentery, amebic colitis, and liver abscess. Diagnosis of amebiasis is made by microscopic examination of stool, antigen or nucleic acid testing of stool, and by serologic testing for antibodies in serum (for invasive disease).
- Flagellates include *Giardia duodenalis*, which causes diarrhea from ingestion of contaminated food or water and is diagnosed by the finding of trophozoites, cysts, and/or antigens in feces. *Trichomonas vaginalis* is acquired by sexual transmission and is detected in vaginal wet mounts by its characteristic motion or by more sensitive nucleic acid amplification techniques.
- *Cryptosporidium* and the coccidia (*Cystoisospora* and *Cyclospora*) can cause diarrhea in both immunocompetent and immunocompromised individuals. Symptoms are usually more protracted in immunocompromised individuals, such as those with AIDS. Special stains (e.g., modified acid-fast stain) are recommended for sensitive microscopic diagnosis; antigen and NAATs for *Cryptosporidium* spp. are also available and are more sensitive than microscopy.
- Helminths include nematodes (roundworms), cestodes (tapeworms), trematodes (flukes), and acanthocephalans (thorny-headed worms). These organisms reside as adults in the gastrointestinal tract or in other locations such as the liver, lung, and venous systems. Knowledge of their life cycles and zoogeography with intermediate hosts is important for understanding the clinical presentation and preventing transmission. Depending on the organism and its location(s) in the human host, eggs, larvae, or adult forms can be recovered from stool, urine, and/or sputum.
- Tissue helminths include filarial nematodes (adults in lymphatics, tissue and/or body cavities and larvae in blood or skin snips), *Trichinella* spp. (larvae are found in muscle), *Strongyloides stercoralis* (larvae in the lung, skin, and other organs during disseminated disease), and *Echinococcus* spp. (hydatidosis; cystic larval form in the liver, lungs, or other organs), among many others.
- Arthropods cause disease through direct tissue invasion, envenomation, vesication, blood loss, transmission of infectious agents, hypersensitivity reactions, and psychological manifestations. Characteristics necessary for identification can be maintained by preserving the organisms in alcohol (ticks, mites, fleas, lice, maggots) or by drying them (winged forms) after killing them with fumes of organic solvents.

TABLE 65.1

Taxonomic Relationships of the More Common Human Parasites

Modern Classification*	Representative Organisms
Protozoans	
Excavata: Metamonada (flagellates)	*Giardia duodenalis, Enteromonas hominis, Chilomastix mesnili, Retortamonas intestinalis, Dientamoeba fragilis, Trichomonas vaginalis, Pentatrichomonas hominis*
Excavata: Discicristata: Heterolobosea (free-living ameboflagellates)	*Naegleria fowleri*
Excavata: Discicristata: Euglenozoa: Kinetoplastea (hematoflagellates)	*Trypanosoma brucei, Trypanosoma cruzi, Leishmania* spp.
Amoebozoa: Discosea: Longamoebia (free-living amebae)	*Acanthamoeba* spp., *Balamuthia mandrillaris, Sappinia diploidea*
Amoebozoa: Archamoeba: Entamoebida (intestinal amebae)	*Entamoeba histolytica, E. dispar, E. moshkovskii, E. bangladeshi, E. coli, E. hartmanni, E. polecki, Endolimax nana, Iodamoeba buetschlii*
SAR: Apicomplexa: Conoidasida: Gregarinasina	*Cryptosporidium hominis, C. parvum*
SAR: Apicomplexa: Conoidasida: Coccidia (coccidians)	*Cystoisospora belli, Cyclospora cayetanensis, Toxoplasma gondii, Sarcocystis* spp.
SAR: Apicomplexa: Aconoidasida (malaria and babesiosis)	*Plasmodium falciparum, P. malariae, P. ovale, P. vivax, Babesia* spp.
SAR: Ciliophora (intestinal ciliates)	*Balantioides coli*
SAR: Stremenopiles (stremenopiles)	*Blastocystis* spp.
Trematodes	
Trematoda: Strigeatida (blood flukes)	*Schistosoma mansoni, S. haematobium, S. japonicum, S. mekongi, S. intercalatum, S. guineensis*
Trematoda: Echinostomida (intestinal and liver flukes)	*Echinostoma* spp., *Fasciola hepatica, F. gigantean, Fasciolopsis buski*
Trematoda: Opisthorchiida (small intestinal and liver flukes)	*Heterophyes heterophyes, Metagonimus yokogawai, Clonorchis sinensis, Opisthorchis* spp.
Trematoda: Plagiorchiida (lung and liver flukes)	*Paragonimus* spp., *Dicrocoelium dendriticum, Nanophyetus salmincola*
Cestodes	
Pseudophyllidea (pseudophyllidean cestodes)	*Dibothriocephalus latus, D. nihonkaiensis, Adenocephalus pacificus, Spirometra* spp.
Cyclophyllidea (cyclophyllidean cestodes)	*Taenia saginata, T. asiatica, T. solium, Echinococcus* spp., *Dipylidium caninum, Hymenolepis nana, H. diminuta*
Acanthocephalans	
Syndermata: Acanthocephala (acanthocephalans)	*Moniliformis moniliformis, Macracanthorhynchus hirudinaceus, M. ingens*
Nematodes	
Dorylaimia: Trichocephalida (trichuroid nematodes)	*Capillaria philippinensis, C. hepatica, Trichinella* spp., *Trichuris trichiura*
Chromadoria: Spururina: Ascarida (ascarid nematodes)	*Ascaris lumbricoides, Baylisascaris procyonis, Toxocara* spp., *Anisakis* spp., *Pseudoterranova* spp., *Contracaecum* spp.
Chromadoria: Spiruria: Oxyurida	*Enterobius vermicularis*
Chromadoria: Spiruria: Camallanida	*Dracunculus medinensis*
Chromadoria: Spiruria: Spirudida (spirudid and filarial nematodes)	*Brugia malayi, B. timori, Loa loa, Onchocerca volvulus, Wuchereria bancrofti, Mansonella perstans, M. ozzardi, M. streptocerca, Dirofilaria* spp., *Gnathostoma* spp., *Thelazia* spp.
Chromadoria: Rhabditina: Rhabditida (strongyles and hookworms)	*Strongyloides stercoralis, Ancylostoma duodenale, A. ceylanicum, Necator americanus, Angiostrongylus cantonensis, Trichostrongylus* spp.
Arthropods	
Crustacea: Maxillopoda: Pentastomida (tongueworms)	*Armillifer armatus, Linguatula serrata*
Arachnica: Acari (mites and ticks)	*Ixodes* spp., *Amblyomma* spp., *Dermacentor* spp., *Rhipicephalus* spp., *Hyalomma* spp., *Ornithodoros* spp., *Demodex* spp., *Sarcoptes scabiei*
Hexapoda: Insecta: Hemiptera (true bugs)	*Cimex lectularius, C. hemipterus, Triatoma* spp., *Rhodnius* spp., *Panstrongylus* spp.
Hexapoda: Insecta: Psocodea (lice)	*Pediculus humanus humanus, P. h. capitis, Pthirus pubis*
Hexapoda: Insecta: Siphonaptera (fleas)	*Ctenocephalides canis, C. felis, Pulex irritans, Xenopsylla cheopis, Tunga penetrans, T. trimamillata*
Hexapoda: Insecta: Diptera (myiasis-causing flies)	*Musca domestica, Phormia* spp., *Lucilia* spp., *Auchmeromyia senegalensis, Cochliomyia hominovorax, Chrysomya bezziana, Sarcophaga* spp., *Wohlfahrtia* spp., *Cuterebra* spp., *Dermatobia hominis, Cordylobia anthropophaga, Oestrus ovis*

Modified from Adl SM, Bass D, Lane CE, et al.: Revisions to the classification, nomenclature, and diversity of eukaryotes, *J Euk Microbiol* 66:4, 2019; and Adl SM, Mathison BA: Taxonomy and classification of human eukaryotic parasites. In: Carroll JC, Pfaller MA, Landry ML, et al., editors: *Manual of Clinical Microbiology*, ed 12, Washington, DC, 2019, ASM Press.

The study of parasitology has gained renewed importance in a world made smaller by the rapid movement of people and by the appearance of emerging and reemerging pathogens in immunocompromised individuals. Humans may be infected with a broad array of protozoan, helminthic, and arthropod parasites (Table 65.1). Various estimates have been put forth for the prevalence and related mortality figures of parasitic infections on a worldwide basis (Table 65.2). While the true incidence of many parasitic infections is unknown due to lack of public health reporting and limitations in clinical and laboratory expertise, it is clear that parasitic infections are an important cause of morbidity and mortality worldwide. Many important human parasitic diseases—such as malaria, leishmaniasis, trypanosomiasis, soil-transmitted helminthiases, and schistosomiasis—are concentrated in tropical and subtropical regions of the world, placing a tremendous burden on local health care resources while adversely affecting economic and societal development. Malaria, for example, was estimated by the World Health Organization (WHO) to infect 219 million people and cause 435,000 deaths in 2017 (WHO, 2018). Several additional parasitic infections have been classified as neglected tropical diseases (NTDs); combined, the NTDs are estimated to affect more than 1 billion people worldwide (WHO, 2019). Other parasitic diseases—such as scabies, giardiasis, enterobiasis (pinworm infection), toxoplasmosis, trichomoniasis, and pediculosis—have a broader distribution and may be found in temperate regions of the United States, Canada, and Europe. The United States Centers for Disease Control and Prevention (CDC) has targeted five neglected parasitic infections (NPIs) for public health action based on the number of individuals affected, the severity of infection, and the availability of adequate treatment and prevention modalities (CDC, 2018b). Regardless of geographic location, the ease and rapidity of global travel requires that clinicians and laboratorians be familiar with the array of important human parasites and their means of diagnosis.

This chapter provides an overview of the general approach used by laboratorians to recover and identify parasitic protozoa and helminths from human clinical specimens. Discussion of individual species of parasites focuses on essential clinical and biological information necessary to assist in diagnosis and management. For more extensive coverage of specific parasites, a number of excellent texts are available (Beaver et al., 1984; John & Petri, 2006; Ryan et al., 2019; Farrar et al., 2013; Roberts et al., 2013; Garcia, 2016; Mullen & Durden, 2018; among others). Some of these references are older and may be less accessible; however, they discuss classic disease presentations and historic perspectives in a way that is sometimes lacking in newer literature. Parasitology atlases are also important resources for any laboratorian performing parasitology examinations and should be readily available (Ash & Orihel, 2007; Pritt, 2014; Mathison & Pritt, 2015). Several texts specifically address the pathologic aspects of parasitic infections (Orihel & Ash, 1995; Meyers, 2000; Meyers et al., 2013; Pritt, 2018). The DPDx website hosted by the CDC (https://www.cdc.gov/dpdx/index.html) presents life cycles, epidemiology, clinical presentation, diagnostic methodologies, and image galleries for human parasitic infections. They also offer a telediagnostic service (https://www.cdc.gov/dpdx/contact.html) for medical and public health professionals.

PARASITE CLASSIFICATION AND TAXONOMY

Parasites are traditionally placed into one of three groups: the helminths (worms), protozoans, and arthropods. Historically, parasites within each group are then classified within hierarchical levels (i.e., Phylum, Class, Order, Family, and so on) based primarily on morphologic features and phenology (life cycle events and their relation to environmental factors). Unfortunately, the conventional classification scheme is somewhat subjective and does not always reflect phylogenetic relatedness between organisms within each grouping. Recent advances in biochemical and molecular methods, including whole-genome sequencing, have led to a revision of the classification of protozoans using a system based on hierarchical ranks (e.g., Super-group, First Rank, Second Rank) that reflect phylogenetic relatedness (Adl et al., 2012; Adl et al., 2019). Many of the familiar grouping names, such as *Apicomplexa*, *Entamoebidae*, and *Trypanosomatidae*—have been retained for ease of communication, but they are no longer linked to level descriptors such as *Order*, *Class*, and so on. However, this new classification is complex and used primarily in the research setting and by protozoologists studying nonparasitic organisms. While this system is gaining acceptance in the medical field for protozoa, the classic Linnaean hierarchal system of taxonomy is still commonly used for helminths and arthropods. An updated version of the traditional schemata incorporating the revised protozoan classification is presented in this chapter (Adl & Mathison, 2019).

LABORATORY METHODS

Numerous methods have been described for the recovery and identification of parasites in clinical specimens, some of which are useful for detection of a variety of organisms, whereas others detect only a particular species. It is preferable for the laboratory to offer a limited number of procedures that can be competently performed rather than a larger variety of infrequently performed tests for which competency cannot be reliably maintained provided that the laboratory is able to meet the clinical needs of the population it serves. At a minimum, most laboratories should be able to provide rapid detection of life-threatening parasitic infections such as malaria and primary amebic meningoencephalitis. Tests for detecting less serious infections may be sent to a reference laboratory if clinically applicable. As newer information becomes available on certain so-called emerging parasites, the laboratory may need to develop and use additional highly specific test methods or find competent referral laboratories where such tests are performed.

The types of specimens collected for laboratory evaluation depend on the species and stage of the parasite suspected. Knowledge of the life cycle of the parasite aids in determining the type, number, and frequency of specimens required for diagnosis. Analyses of blood and fecal specimens account for the largest share of clinician requests for parasitologic evaluation. A variety of additional specimens is submitted to the laboratory less frequently, including urogenital specimens, sputum, aspirates, and biopsy material. In addition to traditional microscopic examination, immunologic and molecular methods are useful in many instances and may be the only methods available in certain circumstances. Complete descriptions of general and esoteric laboratory procedures for the recovery and identification of parasites referred to here may be found in a variety of sources to which the reader is referred (Beaver et al., 1984; Ash & Orihel, 1987, 2007; Garcia, 2009, 2010, 2016; Garcia et al., 2018; Carroll et al., 2019). This chapter will focus on those that are most relevant for routine clinical use.

TABLE 65.2
Estimated Prevalence of Parasitic Infections Worldwide

Disease	Estimated Global Population Involved	Estimated Annual Number of Deaths
Protozoan		
Amebiasis	28 million illnesses/year	1470
African trypanosomiasis	<15,000 currently infected	NA
American trypanosomiasis (Chagas disease)	8 million currently infected	10,000
Cryptosporidiosis	8.5 million illnesses/year	3759
Echinococcosis	>1 million	19,300
Giardiasis	28 million illnesses/year	0
Leishmaniasis	1 million cutaneous illnesses/past 5 years; 300,000 cases of visceral leishmaniasis/year	26,000–65,000
Malaria	124–283 million illnesses/year	367,000–755,000
Toxoplasmosis	10.3 million illnesses/year	684
Helminthic		
Cestodiases (including cysticercosis)	340,864 illnesses/year	36,500
Clonorchiasis/opisthorchiasis	47,935 illnesses/year	7268
Dracunculiasis	28 illnesses/year	0
Fascioliasis	10,635 illnesses/year	0
Intestinal trematodiases	18,924 illnesses/year	0
Lymphatic filariasis	120 million	NA
Neurocysticercosis	2.56–8.30 million currently infected	NA
Soil-transmitted helminthiases (primarily hookworm infection, ascariasis, trichuriasis)	1.5 billion	>1000
Onchocerciasis	20.9 million	0
Paragonimiasis	139,238	250
Schistosomiasis	>166 million	200,000
Strongyloidiasis	30–100 million	NA
Trichinosis	4472 illnesses/year	4

Data from the Centers for Disease Control and Prevention, World Health Organization (WHO, 2015, 2019), and the GBD (GBD, 2017).
NA, Not available.

Familiarity with calibration and use of the ocular micrometer is necessary for any laboratory performing parasitologic examination, as measurement of the size of protozoal trophozoites and cysts and of helminth eggs and larvae is often required to make an accurate identification. For example, size is an important consideration for differentiating some of the intestinal protozoa (e.g., *Entamoeba histolytica* vs. *Entamoeba hartmanni*, *Cryptosporidium* spp. vs. *Cyclospora cayetanensis* oocysts), and morphologically similar helminth eggs (Ash & Orihel, 2007; Pritt, 2014).

EXAMINATION OF BLOOD

Parasites that may be detected in blood specimens include the agents of malaria (*Plasmodium* spp.), babesiosis (*Babesia* spp.), trypanosomiasis (*Trypanosoma* spp.), leishmaniasis (*Leishmania* spp.), and filariasis (*Wuchereria bancrofti*, *Brugia* spp., *Loa*, and *Mansonella* spp.). The most important techniques to be performed in the clinical laboratory to assist in the diagnosis of blood parasites include preparation, staining, and examination of thick and thin blood films. Other techniques used less frequently include the buffy coat smear (useful for detecting trypanosomes) and various concentration techniques reserved for recovery of microfilariae (WHO, 1987; Ash & Orihel, 2007; Garcia, 2016).

Thick and Thin Blood Films

Examination of permanently stained blood films is required to identify most blood parasites (Clinical and Laboratory Standards Institute [CLSI], 2000). Thin films are prepared in the same manner as for hematologic differential evaluation; blood is spread over the slide in a thin layer, yielding intact, nonoverlapping cellular elements (Fig. 65.1). Integrity of the blood cell membranes is important for determining the intracellular or extracellular nature of the infection and the size of the infected erythrocyte. In the thick film, blood is concentrated in a small area that is many cell layers deep. During staining, erythrocytes are dehemoglobinized and only leukocyte nuclei, platelets, and parasites (if present) are visible. The thick film is preferred for parasite *detection* because it contains 15 to 30 times more blood per microscopic field than does the thin film, thus increasing the chances of detecting light parasitemia and decreasing the time needed for reliable examination (Pritt, 2019). Although examination of thick films increases the likelihood of detecting an infection, species identification is usually performed by examination of thin films because morphology is often more definitive, especially for malarial parasites. For routine detection of malaria and babesiosis, both thick and thin films should be prepared (CLSI, 2000).

Preparation of Slides

Blood for examination may be obtained by fingerstick, earlobe puncture, or venipuncture. Fingerstick blood should flow freely to prevent dilution with tissue fluid, and it should not be contaminated with the alcohol disinfectant, which should be allowed to dry first. If obtained by venipuncture, the first drop of blood (anticoagulant-free) from the needle is used to prepare the films at the bedside (CLSI, 2000). Use of anticoagulants is discouraged when malaria is suspected because they may cause distortion of the parasites and interfere with staining. In practice, however, blood usually is submitted to the laboratory in an anticoagulant, which may be the only practical method to ensure that high-quality smears can be prepared. Ethylenediaminetetraacetic acid (EDTA)-anticoagulated blood is preferred in such cases; the specimen should be transported to the laboratory within the hour to prevent deterioration of organism morphology (CLSI, 2000). Anticoagulants do not interfere with the staining of microfilariae.

Both thin and thick films should be prepared on clean, grease-free slides. Thick films are prepared by placing 1 to 2 small drops of blood onto a slide and spreading them into an area the size of a dime (1.5 cm) with the edge of a second slide (CLSI, 2000; Pritt, 2019). The blood film is then allowed to dry flat at room temperature. Drying time may be decreased by placing the slides in a laminar flow hood. A proper thick film should be thin enough that newspaper print may be faintly readable through it (CLSI, 2000). If it is too thick, the film may peel from the slide. Adherence can be greatly improved by gently pushing (grinding) down with the corner of the second slide while spreading the droplet, creating minute scratches on the carrier slide that provide additional surface area for the blood film (see Fig. 65.1) (Norgan et al., 2013).

This method does not affect the microscopic morphology and allows the film to be stained as soon as it is dry (within 30–60 minutes). Heating the slides to decrease drying time is discouraged since excess heat may fix erythrocytes and prevent them from lysing when placed in the stain reagents (CLSI, 2000).

Staining

Blood begins to lose its affinity for stain in about 3 days, and the erythrocytes in older thick films do not lyse well. Therefore, slides stored for archival purposes should first be stained. Best staining results are achieved when using Giemsa stain, because host cell and parasite chromatin stains vividly while the hemoglobin in the erythrocytes is only a pale purple-red. When used at a neutral pH (7.0–7.2), this method also allows for optimal visualization of erythrocyte inclusions (e.g., Schüffner stippling, Maurer clefts) that occur with infection by certain malarial parasites (Pritt, 2019). Wright and Wright-Giemsa stains may also be used for thin films (as is common in the hematology lab), but they stain parasites less well than Giemsa and do not allow for visualization of erythrocyte inclusions due to the lower pH (<6.8). Because these stains incorporate alcohol as their fixative, thick films must be lysed in water before staining (CLSI, 2000; Pritt, 2019).

The Giemsa staining procedure requires somewhat more attention to preparation of reagents and staining protocol than does the Wright staining procedures, which are often automated. Generally, fresh Giemsa stain must be made each day of use by diluting stock solution into phosphate-buffered water (Garcia, 2016). Each new lot of stock Giemsa stain must be checked to determine optimal staining time and dilution because some variation is seen from lot to lot (Garcia, 2016).

Examination of Smears

Both thick and thin smears are examined in their entirety under the low-power (10×) objective to detect microfilariae, which rarely occur in large numbers. In particular, the feathered edge of thin smears should be examined, as microfilariae are often carried there during preparation of the smear (CLSI, 2000). Examination using a 50× oil immersion objective may subsequently be used to screen blood films for protozoa, although thorough examination using the 100× oil immersion objectives still is necessary to detect the smallest parasites, such as *Plasmodium* and *Babesia* spp. The optimal location for examining the thin film is the region of the feathered edge where there is minimal overlap of cells and the erythrocytes maintain their central pallor (Pritt, 2019). A common mistake is to examine regions of the thin film where the blood is too thick or too thin and the parasite morphology is distorted. An experienced microscopist should examine at least 100 oil immersion fields on both the thick and thin blood film and up to at least 300 fields for immunologically naïve patients who might present with more severe symptoms at a lower parasitemia (Mathison & Pritt, 2017).

Blood Concentration Techniques

A variety of special techniques have been described for the concentration of blood parasites—specifically, leishmaniasis, trypanosomes, and microfilariae—details of which may be found elsewhere (Beaver et al., 1984; CLSI, 2000; Ash & Orihel, 2007; Garcia, 2009, 2016).

Preparation of buffy coat smears, which most clinical laboratories can perform with existing resources, is helpful in the detection of *L. donovani*, trypanosomes, and microfilariae (CLSI, 2000). Following centrifugation of an anticoagulated blood sample, the layer of cells between plasma and packed erythrocytes is drawn off and used to prepare blood films for staining or for preparation of a wet mount to detect motile organisms (Ash & Orihel, 2007).

For detection of microfilariae, the Knott concentration technique or membrane filtration is helpful, particularly when the density of

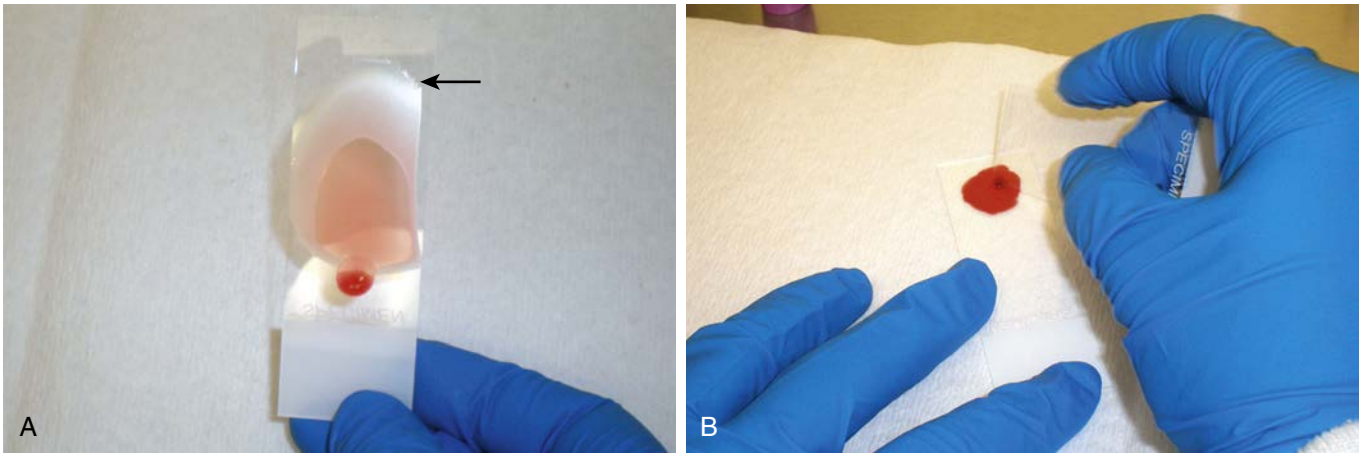

Figure 65.1 **A,** Thin blood film demonstrating a broad feathered edge *(arrow)*. **B,** Preparation of a thick blood film. Gentle pressure is used to create minute scratches in the carrier slide while spreading the blood into a 1.5- to 2.0-cm diameter film with the spreader slide. This method improves the adherence of the thick film to the carrier slide and prevents it from detaching during staining.

microfilariae in peripheral blood is very low. With the Knott concentration technique, anticoagulated blood is lysed with 2% formalin and centrifuged to concentrate the microfilariae in the sediment, which then may be examined as a wet preparation or stained with Giemsa or hematoxylin stain. In the membrane filtration procedure, blood is lysed and passed through a 5-μm membrane filter, which is subsequently stained with hematoxylin to reveal any microfilariae (WHO, 1987; CLSI, 2000; Ash & Orihel, 2007; Mathison et al., 2019).

Finally, use of the fluorochrome acridine orange in a microhematocrit centrifuge format (QBC Malaria test; Drucker Diagnostics, Port Matilda, PA) allows detection of *Plasmodium* spp. and other blood parasites. While it appears to be more sensitive than traditional thick and thin smears, it is not widely used due to the need for a fluorescent microscope (CLSI, 2000). Fluorescent attachments to traditional light microscopes may make this test more widely accessible. In positive cases of malaria or babesiosis, traditional blood films must be examined for *Plasmodium* spp. identification (if relevant) and calculation of parasite burden.

EXAMINATION OF FECAL SPECIMENS

The presence of intestinal parasites is primarily identified through the direct examination of feces using wet mounts, concentration techniques, and permanently stained smears. Microscopic examination of feces is commonly referred to as the "ova and parasite" exam, or O&P. Stages of helminths commonly recovered include eggs and larvae, although intact worms or portions thereof may occasionally be identified by gross examination. Intestinal protozoan infections are diagnosed by detection of trophozoites, cysts, or oocysts. Routine methods should include procedures that permit recovery of both protozoa and helminths, with the use of special procedures (e.g., stains for coccidians) limited to specific requests. Ideally, laboratories performing parasitologic examination should be capable of performing a concentration procedure and a permanent stain method, as many protozoan infections will be missed unless permanent stains are examined (Ash & Orihel 2007; Garcia, 2009, 2010, 2016; Garcia et al., 2018).

Specimen Collection, Handling, and Preservation

Recovery and subsequent identification of parasites in fecal specimens requires proper collection and handling. Old, poorly preserved, or contaminated specimens are of little value. Additionally, specimens should not be collected for 1 week after the patient has ingested any materials that leave a crystalline residue, such as nonabsorbable antidiarrheal compounds, antacids, bismuth, barium, or antimalarial agents. Oily laxatives such as mineral oil may also interfere with examination (CLSI, 2005). Use of antibiotics or contrast media may decrease the numbers of organisms, especially protozoa, in the intestinal tract for several weeks (Ash & Orihel, 2007; Garcia, 2009, 2016; Garcia et al., 2018).

Specimens may be submitted to the laboratory fresh or in appropriate preservatives. Fresh specimens should ideally be examined shortly after passage, with liquid specimens being examined within 30 minutes of passage, whereas semi-formed specimens should be examined within 1 hour, and solid specimens within 24 hours of passage (Garcia et al., 2018). Given that most labs cannot accommodate these time frames, it is best to place the specimen immediately into a suitable preservative to maintain parasite morphology and ensure that fragile protozoal trophozoites are not inadvertently destroyed (Garcia et al., 2018). Unpreserved specimens should be refrigerated if they cannot be examined immediately. Specimens in preservative can be stored at room temperature.

Specimens may be passed directly into clean, dry containers, or onto a specially designed wax or plastic collection sheet that is placed over the toilet bowl (CLSI, 2005; Garcia et al., 2018). Diarrheic specimens may also be collected in clean bedpans. Containers should have tight-fitting lids and should be placed in plastic bags before transport to the laboratory. Inadvertent introduction of urine or toilet water with the specimen may readily destroy protozoal trophozoites and should be avoided. Also, contamination with water or soil may accidentally introduce free-living organisms that may prove difficult to differentiate from parasitic ones (Garcia et al., 2018).

Kits consisting of vials of preservatives appropriate for performing direct examinations, concentration procedures, and preparation of stained smears are available from a number of commercial sources at relatively low cost. Aliquots of freshly passed stool should be immediately placed into these vials and mixed thoroughly. These kits are especially helpful for those patients who are unable to bring in a fresh sample in timely fashion or for those who will be collecting several specimens over the course of several days. With the classic two-vial technique, one portion of specimen is fixed in three parts of 5% to 10% buffered formalin and another portion in three parts of polyvinyl alcohol (PVA) fixative. Other available preservation systems include merthiolate-iodine-formalin (MIF) and sodium acetate–formalin (SAF; Table 65.3). SAF has an advantage in that it can be used for permanent stains as well as for direct mounts and concentration procedures and it does not contain mercury, which is present in Schaudinn and PVA fixatives. In addition to being poisonous, mercury presents disposal problems in an increasing number of states. However, the quality of permanent stains when SAF is used is not as good as when Schaudinn or PVA fixative is used. Zinc sulfate–based PVA and other newer commercial products such as single-vial multipurpose fixatives are gaining popularity, and their use may be indicated when mercury chloride–based compounds cannot be used (Garcia et al., 2018; Carroll et al., 2019).

Examination of three specimens collected on different days over a maximum 10-day period is considered the minimum necessary to perform an adequate O&P evaluation (Garcia, 2016; Garcia et al., 2018; Carroll et al., 2019). This procedure ensures an optimum interval for recovery of those parasites known to shed diagnostic forms intermittently. However, for certain parasites, such *Strongyloides stercoralis*, up to seven O&P examinations may be necessary for optimal detection. Additional sensitivity may be achieved in detecting these parasites, as well as *E. histolytica*, using antigen detection methods, nucleic acid amplification tests (NAATs) and concentration techniques (discussed later). In general, it is not useful to examine specimens from hospitalized patients who develop diarrhea after the third

TABLE 65.3

Commonly Used Stool Fixatives and Examination Techniques and Whether Fixatives are Appropriate for Antigen Detection or Molecular Assays

	EXAMINATION TECHNIQUE				
Fixative	**Direct Wet Mount**	**Wet Mount Concentration**	**Permanent Stained Smear**	**Antigen Detection**	**NAATs***
None (fresh stool)	Yes	Yes	Yes	Yes	Yes
10% formalin	Yes	Yes	No	Some	No
Schaudinn fluid	No	No	Yes	No	No
Polyvinyl alcohol (PVA)	No	No	Yes	No	No
Modified PVA†	No	Yes	Yes	No	Some
Merthiolate-iodine-formalin (MIF)	Yes	Yes	No‡	No	No
Sodium acetate–formalin (SAF)	Yes	Yes	Yes	No	No
Single-vial systems**	Yes	Yes	Yes	Some	Some

*NAATs: Nucleic acid amplification tests.
**Many commercially available single-vial fixatives are now available, for example, TOTAL-FIX (Medical Chemical Corporation, Torrance, CA), Para-Pak EcoFIX (Meridian Bioscience, Cincinnati, OH), ALCORFIX and APAFIX (Apacor, Berkshire, England), and may be used for both the concentration procedure and permanent stained smear as well as antigen detection and NAATs.
†Copper sulfate or zinc sulfate replaces the mercuric chloride.
‡Smears prepared from MIF-preserved specimens may be stained with polychrome IV stain.

hospital day since parasites are an unlikely cause of their symptoms. Once the specimens are received in the laboratory, they should undergo macroscopic and microscopic examination as detailed next.

Macroscopic Examination

Fecal specimens should be examined grossly for consistency (formed, soft, loose, or watery) and for the presence of mucus, blood, adult worms, and proglottids. Protozoan trophozoites are more likely to be found in watery or loose specimens, whereas cysts predominate in formed or soft specimens. Helminths or their eggs may be found in any type of fecal specimen. Most parasites are uniformly distributed in the stool as a result of the mixing action of the cecum, although some eggs (especially schistosomes) may enter the fecal stream in the lower colon and rectum and may be unevenly distributed, as may pinworm and *Taenia* spp. eggs. Protozoan trophozoites may be more numerous in the last portion of stool evacuated and should be specifically sought in mucus (Garcia, 2016).

Microscopic Examination

Specimens may be examined microscopically by direct wet mounts of fresh or preserved material, wet mounts of concentrated feces, or permanent stains. Each procedure has specific advantages and limitations, and not all may be routinely used in the clinical laboratory. Direct saline wet mounts of fresh feces allow detection and observation of motile protozoan trophozoites and helminth larvae. Direct mounts of preserved feces may allow detection of parasites that do not concentrate well. Concentration procedures increase the examiner's ability to detect protozoan cysts and helminth eggs and larvae but are unsatisfactory for detecting protozoan trophozoites. Permanent stains are useful for detection and morphologic examination of protozoan trophozoites and cysts.

The circumstances under which each procedure is performed vary depending on the workflow of the laboratory. As mentioned earlier, examination of unpreserved specimens allows for enhanced detection of motile parasites. Many protozoa can also be differentiated by their characteristic motility patterns. However, examination of unpreserved stool is useful only when specimens can be examined shortly after being passed. The direct wet mount may be omitted if the specimen is submitted in a preservative. At a minimum, fixed specimens should be examined by a concentration procedure, which provides increased sensitivity for detection of parasites. However, improved yield has been demonstrated when a permanent stain is also examined, as the two preparations are complementary. Therefore, the optimal stool examination includes both a concentrated wet prep and a permanently stained preparation (CLSI, 2005, Garcia, 2010, 2016; Garcia et al., 2018). The following provides detailed instructions for performing the direct wet mount, concentration techniques, and permanently stained preparations.

Direct Wet Mount

The direct wet mount is one of the most easily performed parasitologic tests, although proper interpretation requires careful examination and experience in using the microscope to full advantage. The test is most useful when fresh specimens, especially liquid stools or duodenal aspirates, are examined for motile trophozoites or helminth larvae, although it can also be performed using fixed specimens. A small amount of stool is mixed with a drop of 0.85% saline and covered with a coverslip.

Examination of the entire coverslip is performed systematically under the low-power (10×) objective, with the microscope diaphragm closed down to increase contrast. Suspicious objects and those that are refractile, such as protozoal cysts, should then be examined with the high-power (40×) objective. Detection of motility of slow-moving amebae requires that an object be examined for at least 15 seconds. In the absence of suspicious objects, up to a third of the preparation should be examined using the 40× objective. The oil immersion objective usually is not used unless the coverslip has been sealed with nail polish or Valspar (a 50:50 mixture of petroleum jelly and paraffin).

A second preparation may be made in identical fashion, except that a drop of a 1:5 dilution of Lugol iodine or an equivalent preparation is added in place of the saline. Use of straight Lugol or iodine causes clumping of material and is not recommended. Iodine is helpful in enhancing the visibility of nuclear structures in protozoal cysts and in detecting glycogen inclusions. Limitations, however, include loss of trophozoite motility and cyst refractivity, as well as difficulty in recognizing chromatoid bodies.

Concentration Techniques

Concentration procedures, which may be performed on fresh or preserved specimens (see Table 65.3), are more sensitive than direct wet mount examination for detection of protozoan cysts and helminth eggs and larvae because they decrease the amount of background material in the preparations and, in most circumstances, actually concentrate the organisms. A wet mount of the concentrated specimen is examined as described earlier for the direct wet mount. Although a variety of methods and modifications have been described, some are useful only for specific parasites (Ash & Orihel, 1987; Garcia, 2010, 2016; Garcia et al., 2018). For routine use, a method should be selected that allows reliable detection of both protozoan cysts and helminth eggs. Concentration methods are based on sedimentation or flotation principles. In sedimentation, the parasites settle to the bottom as a result of gravity or centrifugation. In flotation, the parasite cysts and eggs rise to the surface of a solution of high specific gravity. Flotation is less commonly used in the United States for human clinical specimens but is commonly used in veterinary medicine. Traditionally, concentration methods involved one or two-step processes involving formalin and ether or ethyl acetate. However, single-vial systems allow for concentration of fecal specimens, often by using less hazardous chemicals (Couturier et al., 2015).

The traditional formalin–ethyl acetate concentration is a biphasic sedimentation technique that is efficient in recovering most protozoan cysts and helminth eggs and larvae, including operculate eggs, and is moderately effective for schistosome eggs. Less distortion of protozoal cysts occurs with this technique than with zinc sulfate flotation. For proper concentration of coccidian oocysts, attention must be paid to the recommended speed and time of centrifugation (Garcia, 2010, 2016; Garcia et al., 2018). Despite these problems, the technique is used widely for both its simplicity and its suitability in most laboratory situations.

With the zinc sulfate flotation method, fresh stool is processed using zinc sulfate with a specific gravity of 1.18, and formalinized stool is processed with a solution of specific gravity of 1.20. Parasitic elements are recovered from the surface film of the solution following centrifugation. This method yields a cleaner preparation than is provided by formalin–ethyl acetate concentration, but it is unreliable for the recovery of nematode larvae, infertile eggs of *Ascaris*, and the eggs of most trematodes and large tapeworms. Problems with recovery also occur with stool specimens containing excessive amounts of fats. Use of formalinized stool specimens rather than fresh stool helps clear the specimen and prevents popping of opercula and distortion of the parasites (Bartlett et al., 1978).

Permanent Stains

Use of stained slide preparations provides a permanent record of a patient's specimen and allows review by consultants should difficulties arise in identification. These preparations are also amenable to whole-slide scanning for production of a digital image. Of the methods described for studying fecal specimens, only the permanent stain is designed for analysis using the oil immersion objective (100×). The permanent stain is most useful for detection of protozoal trophozoites and cysts, which may be recognized when direct and concentrated preparations are negative. Although they generally are not useful for detecting helminth eggs or larvae, permanent stains are inherently more sensitive for detecting protozoal infections, and their use has been recommended for every stool sample submitted for O&P examination (Garcia, 2016; Garcia et al., 2018).

A variety of staining techniques and modifications and their advantages and disadvantages have been described. The Wheatley trichrome stain and iron-hematoxylin stain are all-purpose methods that allow detection of amebae and flagellates. Unfortunately, most coccidia are not readily detected by these stains; thus, additional special stains (see next sections) must be employed. Technical problems may arise in the performance of any staining procedure; most are related to the age of the specimen, proper smear preparation and fixation, and the quality of the reagents. Positive control slides of known staining quality should be run with each batch of slides stained or, at the very least, once daily after reagents are changed. This is especially true in the performance of more specific stains for the coccidia. Less commonly used stains, such as polychrome IV stain for use with MIF-preserved specimens and chlorazol black E stain for use with fresh specimens, are not reviewed here. Details may be found elsewhere (Garcia, 2016; Garcia et al., 2018).

Wheatley Trichrome Stain. In the United States, the Wheatley modification of the trichrome method continues to find widespread acceptance because of its simplicity, reliability, and cost-effectiveness. Details of the procedure are available from a number of sources (Ash & Orihel, 2007; Garcia, 2010, 2016; Garcia et al., 2018). Appropriate specimens include those that have been fixed in Schaudinn fixative or PVA fixative; SAF- or MIF-preserved specimens may be stained with trichrome, but results are less satisfactory. Specimens preserved using single-vial commercial fixatives may also be stained with this or a slightly modified protocol. For example, EcoStain (Meridian Bioscience, Cincinnati, OH) is a modified trichrome stain that works well with non–mercury-based fixatives.

Iron Hematoxylin Stain. The traditional iron hematoxylin stains are technically more difficult to perform than the trichrome stain; thus, they are becoming increasingly rare in the United States. However, results generally are superior owing to enhanced definition of key nuclear and cytoplasmic characteristics, and most of the original descriptions of protozoan morphology are based on slides stained by these methods. A modified iron hematoxylin stain that incorporates carbol fuchsin has been described, which allows concurrent staining of acid-fast organisms such as *Cryptosporidium*, *Cyclospora*, and *Cystoisospora* (Garcia, 2010, 2016; Garcia et al., 2018). Specimens fixed in Schaudinn, PVA, or SAF fixative may be stained with iron hematoxylin stains (the preferred stain for SAF).

Modified Acid-Fast Stains. Oocysts of *Cryptosporidium*, *Cyclospora*, and *Cystoisospora* are difficult to recognize on concentrated wet preparations, trichrome- or iron hematoxylin–stained smears, but their presence may be detected by using an acid-fast staining technique such as the modified Kinyoun method, modified acid-fast dimethyl sulfoxide, or auramine-O or staining with safranin (hot method) (Cama & Mathison, 2015). Acid-fast stains are sensitive and cost-effective for detection of these protozoa, but they lack specificity. Close attention must be paid to defined morphologic criteria when these stains are used, and the use of positive control material is mandatory. For laboratories in which *Cryptosporidium* is rarely encountered, use of the highly specific and sensitive commercially available immunoassay reagents is recommended. Stool, sputa, biliary tract, and other appropriate specimens that are fresh, formalin fixed, or SAF fixed may be used with acid-fast stains.

Additional Techniques for Examination of Enteric Parasites

Cellulose Tape and Paddle Techniques for Pinworm

The female pinworm, *Enterobius vermicularis*, migrates from the cecum to the perianal skin, where she deposits typical eggs that are partially embryonated. The eggs or, occasionally, adult worms may be detected on examination of clear, adhesive cellophane tape or commercial collection kits that have been pressed on to the perianal skin (Fig. 65.2).

Eggs or adults are not commonly found in stool concentrates, which is considered to be an inappropriate specimen for detection of this parasite. Specimens should be collected first thing in the morning before bathing or defecation. Several specimens taken on different days should be examined before infection is ruled out. Commercial devices such as the SWUBE (Becton Dickinson, Franklin Lakes, NJ) use an adhesive paddle for collection and greatly simplify specimen collection and examination.

Egg Studies

Estimations of worm burden were historically requested to assist in the evaluation of therapeutic efficacy, identify patients with heavy infections that warrant anthelminthic therapy, or for following rates of reinfection with intestinal nematodes (*Ascaris*, *Trichuris*, and hookworms) or, occasionally, schistosomes. Quantification methods are less commonly used today in resource-rich settings since it is standard practice for all infected patients to be treated, regardless of the egg burden, and the currently available drugs are highly efficacious. Procedures for egg quantification include the direct smear method of Beaver, the Stoll dilution egg count, Kato thick smear, and various modifications (Beaver et al., 1984; Ash & Orihel, 1987, 2007). Large variations in results are inherent when these tests are performed, and levels of egg counts indicating clinical significance vary, depending on the infecting species and the person's age and nutritional status (Beaver et al., 1984).

Nematode Culture and Recovery Techniques

Several culture techniques (coproculture) assist in the detection and identification of certain nematode infections, including the Harada-Mori filter paper strip culture, filter paper/slant culture, and charcoal culture (Beaver et al., 1984; Ash & Orihel, 1987, 2007; Garcia, 2016; Garcia et al., 2018). Differentiation of hookworms and trichostrongyles on the basis of egg morphology is difficult, whereas infective-stage larvae are more readily identified. Such culture techniques may also prove useful in recovery of *Strongyloides* larvae, which may be few in number, and in differentiating them from those of hookworms. With all culture methods, feces are incubated in a humid environment to encourage egg hatching. With the Harada-Mori and filter paper/slant techniques, larvae migrate from the feces into a water phase, where they may be readily detected. In the charcoal culture, larvae first migrate into a dampened gauze pad, which is then placed in water, allowing the larvae to settle out. These methods are most commonly used in clinical laboratories in endemic settings.

The Baermann funnel technique and agar culture methods are sensitive and reliable methods for recovery of *Strongyloides* and other nematode larvae from a stool specimen. In the Baermann assay, feces are placed on several layers of gauze on top of a wire screen that is suspended in a funnel. The bottom of the funnel is clamped off, and water is added to the level of the gauze. Larvae actively migrate through the gauze and settle to the bottom of the funnel, where they may be drawn off for examination. Although this method provides increased sensitivity over the traditional O&P exam, it is labor-intensive and used infrequently in the clinical laboratory. The agar culture technique provides a simpler and more sensitive means for detecting *S. stercoralis* in feces. With this method, feces are plated on a nutrient agar and incubated at room temperature for several days. Over time, the larvae will migrate out of the feces into the agar and carry fecal bacteria with them. Growth of the bacteria in the larval tracks facilitates identification of larvae in the specimen (Fig. 65.3).

In latent *Strongyloides* infection, in which few larvae are being shed, several examinations over 1 week using a concentration technique may be required to detect the infection (Ash & Orihel, 1987, 2007; Garcia, 2009, 2016). It is important to note that filariform larvae of *S. stercoralis* and hookworms are highly infectious; therefore, testing must be performed using universal precautions.

Objects Resembling Enteric Parasites

A large variety of objects that closely resemble various parasite life cycle stages may be seen in feces and other specimens sent for O&P examination. Careful differentiation of these objects from real parasites is necessary to prevent inappropriate or unnecessary treatment. White blood

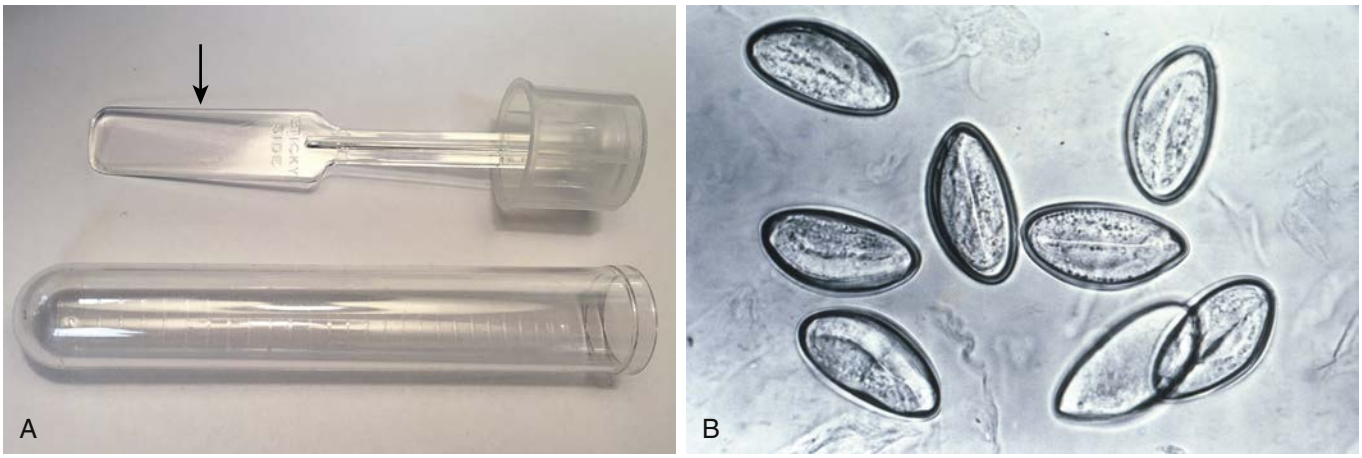

Figure 65.2 **A,** Commercial collection device (Swube) for detection of *Enterobius vermicularis* eggs and adult females from perianal skin. The paddle *(arrow)* has a sticky side that is applied to the perianal skin to collect the specimen. The paddle is then placed into the accompanying tube for safe transport to the laboratory. The clear paddle functions like a glass slide and can be viewed directly under the microscope. **B,** Positive specimens demonstrate *E. vermicularis* eggs and, less commonly, adult females. Eggs measure 50 to 60 μm long by 20 to 30 μm wide and are flattened on one side (unstained, 400×). (**B** courtesy of the Centers for Disease Control and Prevention Public Health Image Library.)

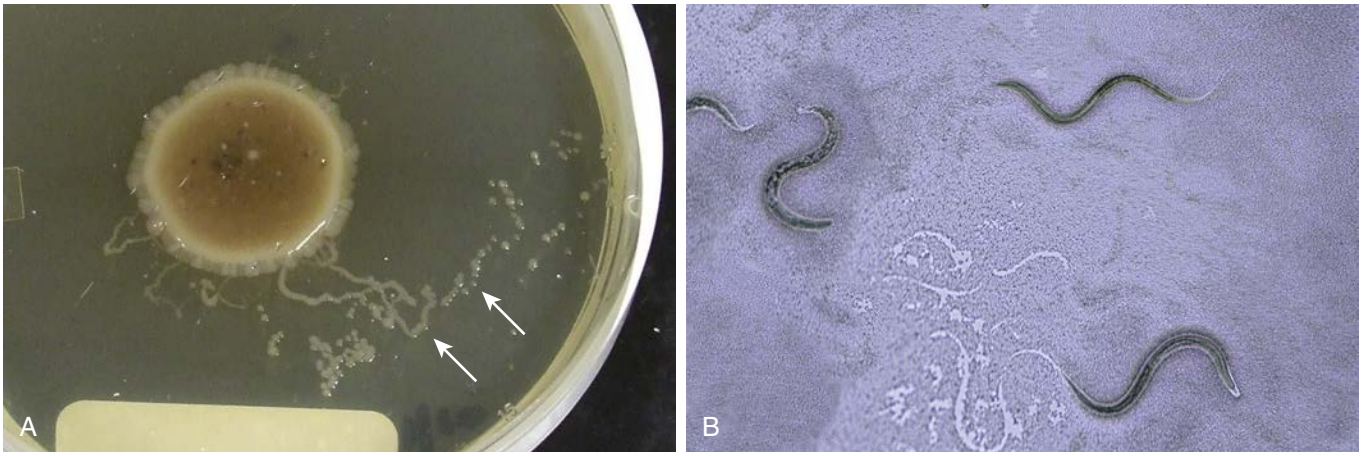

Figure 65.3 **A,** Stool agar culture method showing bacterial tracks *(arrows)* formed by migrating *Strongyloides stercoralis* larvae. **B,** Examination of the plate using a light microscope reveals multiple larvae and detail of the agar tracks (unstained, 100×).

cells, macrophages, and squamous and columnar epithelial cells may resemble amebae; yeasts and starch granules may resemble protozoal cysts or oocysts; pollen and fungal conidia may resemble helminth eggs; plant fibers may resemble nematode larvae; and pieces of vegetables or vegetable skins may resemble adult worms or proglottids. Examples of artifacts and pseudoparasites have been reviewed elsewhere (Ash & Orihel, 2007; Pritt, 2014; Garcia, 2016).

EXAMINATION OF UROGENITAL AND OTHER SPECIMENS (SPUTA, ASPIRATES, BIOPSIES)

Vaginal and urethral discharges, prostatic secretions, or urine may be submitted to the laboratory for detection of *Trichomonas vaginalis*. The most rapid and cost-effective method is the preparation of several wet mounts using a drop of specimen (urine should be centrifuged) diluted with a drop of saline, which is then covered with a coverslip. The slide is examined under the low-power (10×) objective using reduced lighting conditions for motile trophozoites, which display a jerky movement. High-power examination may reveal the beating flagella and the undulating membrane characteristic of the species. Unfortunately, wet mount microscopy is a relatively insensitive method (sensitivity 51%–65%) for detection of *T. vaginalis*; use of NAATs is now recommended for optimal detection (Workowski & Bolan, 2015). Use of culture, fluorescent antibody reagents, or a commercial deoxyribonucleic acid (DNA) probe technique also provides some improvement in sensitivity over wet mount microscopy (Peterman et al., 2006; Schwebke et al., 2011; Schwebke et al., 2018). Demonstration of metronidazole and tinidazole drug resistance requires culture of the organism (Workowski & Bolan, 2015; Clain et al., 2019).

Urine is also an important specimen for detecting the eggs of *Schistosoma haematobium* and, less commonly, microfilariae (Garcia, 2016). Urine can be examined directly for eggs and microfilariae; however, filtration through a membrane filter or examination of urine collected over a 24-hour period may increase the sensitivity of detection (Cheesbrough, 2005). *S. haematobium* eggs are shed sporadically; thus, examination of multiple specimens collected on different days is recommended, with specimens optimally collected between 10 AM and 2 PM (Cheesbrough, 2005).

A number of protozoal and helminthic parasites may be detected in sputum; the appropriate examination technique depends on the suspected organism. Generally, the technique required to detect a parasite from its usual site of infection is applied to sputum and most commonly involves a wet mount. When amebae are suspected, permanent stains should be performed. Acid-fast or specific antibody-based stains are appropriate for detection of *Cryptosporidium* oocysts. Identification techniques for the microsporidia and *Pneumocystis jiroveci* (formerly *Pneumocystis carinii*) are described elsewhere.

Examination of aspirates requires the use of stains as appropriate for the implicated organism. In addition to the methods used for sputum, Giemsa staining is often appropriate when examining for protozoa, especially the hemoflagellates. Biopsy material should be submitted for routine histology after imprint smears are prepared for staining with Giemsa or another appropriate permanent stain. Culture for *Leishmania* and trypanosomes also can be performed on tissues and may be important for demonstrating those infections. This testing is usually restricted to specialty reference and public health laboratories, such as the CDC. Skin snips sent for *Onchocerca* or *Mansonella streptocerca* examination should be teased apart in saline and the saline examined after 30 to 60 minutes for microfilariae. Muscle biopsy specimens for *Trichinella* spp. larvae may be examined by compressing the fresh specimen between two glass slides or by submitting it for routine histology. Likewise, rectal or bladder biopsies may be examined for schistosome eggs.

PARASITE CULTURE TECHNIQUES

Culture methods have been described for a wide variety of protozoan parasites, but few clinical laboratories undertake the task because of infrequent requests and lack of familiarity with methods. When culture requests are made, they are usually for *T. vaginalis*, *Leishmania* spp., *Trypanosoma cruzi*, *E. histolytica*, *Acanthamoeba* spp., or *Naegleria fowleri*. Methods are reviewed elsewhere (Ash & Orihel, 1987; Garcia, 2009, 2010, 2016; Garcia et al., 2018). The CDC may agree to provide this testing following consultation.

IMMUNODIAGNOSTIC METHODS

Several immunodiagnostic methods are available to identify the parasitic antigen or the antibody that is produced in response to the parasitic infection. Some signals are amplified, and others are direct detection methods. In general, laboratory methods employed are enzyme immunoassay (EIA), indirect immunofluorescence assay (IFA), direct fluorescence antibody assay (DFA), Western blot, radioimmunoassay, and immunodiffusion, among others.

Antigen Detection

Antigen detection methods are commercially available for several parasitic diseases, including amebiasis, cryptosporidiosis, giardiasis, malaria, and trichomoniasis (Table 65.4). These methods may be useful for initial testing or in instances in which traditional tests are negative, yet a high index of clinical suspicion remains. These tests offer the advantage of detecting current infection and can often be performed by someone other than an experienced morphologist (Garcia et al., 2018; Shimizu & Garcia, 2018).

Antigen detection in stool samples is usually performed using fecal immunoassays. A number of published studies have suggested that these assays have good or superior sensitivity and specificity when compared with routine ova and parasite examination (Cama & Mathison, 2015; Garcia et al., 2018). These immunoassays are easy to use and rapid, permit batch processing, and do not require experienced microscopists. Given the current shortage of medical technologists and individuals with specialized training in parasitology, use of immunoassays appears to be an attractive alternative. However, laboratories that use rapid cartridge-based immunoassays should be aware of potential problems with false-positive results and should closely monitor test performance. Currently, fecal immunoassays are marketed for *G. duodenalis*, *C. parvum*/*C. hominis*, the *E. histolytica*/*E. dispar* group, and *E. histolytica*. Antigen detection tests using blood or serum are also available for *Plasmodium* spp. and *W. bancrofti*. A latex agglutination test for *T. vaginalis* antigen detection in vaginal swabs has also been introduced. Immunoassays are usually available in three formats: EIA, DFA, and lateral flow (immunochromatography) cartridges. Fresh or preserved stool samples are appropriate for most antigen detection kits (Garcia et al., 2018). Although each kit has unique operating characteristics, most are generally comparable in performance (Garcia, 2016; Garcia et al., 2018).

TABLE 65.4

Select Antigen-Based Detection Assays for Parasites

Target Organism(s)	Test System	Manufacturer/Distributor	Format	FDA Approval/Clearance*
Cryptosporidium spp.	Xpect Cryptosporidium	Remel (Thermo Scientific)	LFA	Yes
	Crypto Cel	CeLLabs	DFA	Yes
	ProSpecT Cryptosporidium	Remel (Thermo Scientific)	EIA plate	Yes
	Cryptosporidium II	Tech-lab	EIA plate	Yes
	RIDASCREEN Cryptosporidium	R-Biofarm	EIA	No
	PARA-TEC Cryptosporidium	Medical Chemical Corporation	EIA	No
	UNI-GOLD Cryptosporidium	Trinity Biotech	LFA	Yes
	Crypto-Strip C-1005 (CRYPTO UNISTRIP, CRYPTO-CIT)	Coris BioConcept	LFA	No
	CRYPTO (card and blister formats)	CerTest Biotec	LFA	No
	Stick Crypto	Operon	LFA	No
Giardia duodenalis	Xpect GIARDIA	Remel (Thermo Scientific)	LFA	Yes
	Uni-Gold Giardia	Trinity Biotech	LFA	No
	Stick Giardia	Operon	LFA	No
	Giardia (dipstick and cassette)	Coris BioConcept	LFA	No
	Giardia lamblia (Giardia)	CerTest Biotec	LFA	No
	ProSpecT Giardia EZ	Remel (Thermo Scientific)	EIA plate	Yes
	Giardia lamblia ANTIGEN DETECTION MICROWELL ELISA	IVD Research	EIA plate	Yes
	Giardia Cel	CeLLabs	DFA	Yes
	ProSpecT Giardia	Remel (Thermo Scientific)	EIA plate	Yes
	RIDASCREEN Giardia	R-Biopharm	EIA plate	No
	PARA-TEC Giardia	Medical Chemical Corporation	EIA plate	No
	GIARDIA II	Tech-lab	EIA plate	Yes
	Giardia CELISA	CeLLabs	EIA plate	Yes
	Giardia lamblia II	Tech-lab	EIA plate	Yes
Entamoeba histolytica	E. histolytica QUIKCHEK	Tech-lab	LFA	Yes
	Entamoeba CELISA PATH	CeLLabs	EIA plate	Yes
	ProSpecT Entamoeba histolytica	Remel (Thermo Scientific)	EIA plate	Yes
	E. histolytica II	Tech-lab	EIA plate	Yes
Cryptosporidium/Giardia	Xpect Giardia/Cryptosporidium	Remel (Thermo Scientific)	LFA	Yes
	ImmunoCard STAT! Cryptospo-ridium/Giardia	Meridian Bioscience	LFA	No
	RIDA Quick Cryptosporidium/Giar-dia Combi (dipstick or cassette)	R-Biopharm	LFA	No
	CRYPTO-GIARDIA	CerTest Biotech	LFA	No
	MERIFLUOR Cryptosporidium/ Giardia	Meridian Bioscience	DFA	Yes
	Crypto Giardia DFA	IVD Research Inc.	DFA	Yes
	Crypto/Giardia Cel	CeLLabs	DFA	Yes
	PARA-TECT Cryptosporidium/ Giardia	Medical Chemical Corp.	DFA	No
	ColorPAC Giardia/Cryptosporidium	Becton Dickinson (BD)	LFA	Yes
	Giardia/Cryptosporidium CHEK	Tech-lab	EIA plate	Yes
	Giardia/Cryptosporidium QUI-KCHEK	Tech-lab	LFA	Yes
	ProSpecT Giardia/Cryptosporidium	Remel (Thermo Scientific)	EIA plate	Yes
Giardia duodenalis, *Cryptosporidium* spp., and *E. histolytica/dispar* combination	Alere Triage Parasite Panel	Alere	LFA	Yes
	TRI-COMBO Parasite Screen	Tech-lab	EIA plate	Yes
	RIDA Quick Cryptosporidium/Giar-dia/Entamoeba Combi (dipstick or cassette)	R-Biopharm	LFA	No
	CRYPTO-GIARDIA-ENTAMOEBA	CerTest Biotec	LFA	No
Plasmodium spp.*	BinaxNOW Malaria	Alere	LFA	Yes
	OptiMAL	BIO-RAD	LFA	No
	First Response Malaria Ag	Premier Medical Corp.	LFA	No
	CareStart Malaria COMBO	Apacor	LFA	No
	SD BIOLINE Malaria Ag	Alere	LFA	No
Wuchereria bancrofti	BinaxNOW Filariasis	Alere	LFA	No
	Filariasis Ab CELISA	CeLLabs	EIA plate	No

TABLE 65.4 —cont'd

Target Organism(s)	Test System	Manufacturer/Distributor	Format	FDA Approval/Clearance*
Trichomonas vaginalis	Light Diagnostic T. vaginalis	Nippon Chemicon	DFA	No
	OSOM Trichomonas Rapid Test	Sekisui Diagnostics	LFA	Yes
	XenoStrip-Tv	Xenotope Diagnostics	LFA	No

DFA, Direct fluorescence antibody assay; *Dipstick,* dipstick enzyme immunoassay; *EIA,* enzyme immunoassay; *LFA,* lateral flow assay.
*Many antigen detection tests are commercially available for *Plasmodium* spp. The tests listed here scored highly for detection of *P. falciparum* by the World Health Organization and the Foundation for Innovative New Diagnostics (FIND) product testing (FIND, 2012). Tests listed detect both *P. falciparum* and Pan-*Plasmodium* antigens.

Rapid antigen detection tests (RDTs) developed for malaria may detect histidine-rich protein II (HRP-II), parasite lactate dehydrogenase (pLDH), parasite aldolase, or a combination of these antigens in peripheral blood. HRP-II tests are specific for *Plasmodium falciparum*, and pLDH and aldolase tests detect all four human *Plasmodium* spp. These assays have highly variable performance characteristics, but in general are adequate for detecting moderate to heavy infections with *Plasmodium falciparum*. They are often significantly less sensitive for detecting lower levels of *P. falciparum* infection and infections with other *Plasmodium* spp. At the time of this writing, only the BinaxNow (Abbott Diagnostics, Chicago, IL) is cleared by the U.S. Food and Drug Administration (FDA) for clinical diagnosis of malaria in the United States (Mathison & Pritt, 2017).

Trichomonas vaginalis antigens from vaginal samples may also be detected using rapid antigen tests such as the OSOM Trichomonas Rapid Test (Sekisui Diagnostics, Burlington, MA), which is an FDA-cleared, Clinical Laboratory Improvement Amendments (CLIA)–waived test for detecting *T. vaginalis* antigen in vaginal swabs. These tests can be used for rapid detection of *T. vaginalis* infection in the clinical setting and may replace wet mount examinations, which generally have lower sensitivities (75%–96%) compared with NAATs (Association of Public Health Laboratories [APHL], 2016).

Most EIAs are available in microwell format (Shimizu & Garcia, 2019). Antigens from frozen, fresh, or 10% formalin–preserved stool samples are suitable for testing by this method. Concentrated or PVA samples are not suitable for testing with EIA kits. Parasite antigen is captured by immobilized antibodies coated on microwells and is detected by an enzyme-conjugated secondary antibody that is capable of producing a colored reaction following the addition of substrate. Although the colored wells can be read visually or with the use of a spectrometer, the latter seems to be the preferred option because of occasional ambiguous results obtained with some kits (Garcia et al., 2018). In general, EIA tests have good sensitivities and specificities. Garcia and colleagues evaluated nine immunoassay kits for detection of *G. duodenalis* and *Cryptosporidium* spp. in comparison with a reference DFA test that visualizes the parasite directly in the sample. Investigators found that all kits had high sensitivities, ranging from 94% to 99%, and 100% specificities (Garcia & Shimizu, 1997, 2000). This is in contrast to first-generation EIAs, which had been previously reported to produce false-positive results, resulting in their recall (Doing et al., 1999). Hence, a strong quality control (QC) pro and participation in proficiency test pros are required to ensure high-quality test results. Local epidemiology of the parasitic infection can help to determine whether additional confirmatory testing is required; consultation with local public health authorities may prove useful in characterizing which infections are being seen locally. Additionally, for some diseases such as giardiasis, examination of two specimens by EIA or microscopy may be necessary to achieve diagnostic sensitivity greater than 90% (Hanson & Cartwright, 2001).

Lateral flow cartridges are a popular format of immunoassay because of their ease of use and the minimal performance time required. These kits can be stored conveniently at room temperature and may be used in single or batch processing. The parasite antigen in the sample migrates through the membrane and binds to specific capture antibodies. Use of a secondary reagent results in development of a colored reaction. These kits also have an internal control to ensure that the colloidal dye conjugates used in the assay are intact and that proper capillary flow has occurred. To ensure complete migration of the specimen, only the supernatant of a well-mixed stool sample is used, and some samples may be diluted to a liquid state before testing. Any color visible at the reagent test zone (usually a band) is interpreted as positive. Some studies have demonstrated that cartridge assays are somewhat less sensitive than a microwell EIA plate assay (Pillai & Kain, 1999; Johnston et al., 2003). When lack of sensitivity is a concern, it may be necessary to perform alternative O&P or NAAT studies if the patient's symptoms persist.

DFA testing allows direct visualization of the parasites in stool specimen using antibodies conjugated to fluorescent dyes. These assays are easy to perform and to interpret, permitting rapid screening of slides when compared with some of the traditional stains used in parasitology (Garcia et al., 2018). A fluorescence microscope is necessary for this procedure, which is a limiting factor in some laboratories. Currently, kits are available for detection of cysts of *G. duodenalis* and oocysts of *Cryptosporidium* spp. Fixed stool specimens may be used for this procedure (10% formalin, SAF, or one of the mercury- or formalin-free products) (Garcia et al., 2018). Although fresh stool samples can be tested directly, the sensitivity of the assay can be improved by performing the test on centrifuged stool (500 *g* for 10 minutes). Occasionally, fluorescing bacteria and yeasts may be seen, but these are readily distinguished from *Giardia* and *Cryptosporidium* on the basis of their size and shape. The edges of the wells should be carefully examined to avoid missing the rare parasite in light infections. Given the relatively recent recognition of additional *Cryptosporidium* spp. that may infect humans, commercial assays currently available may not be adequate for detection of all infections.

Antibody Detection

Tests that are available from public health, hospital, or commercial laboratories to detect immunologic reactivity to parasitic diseases are summarized in Table 65.5. Historically, serologic procedures for parasitic diseases have been plagued by low sensitivity and specificity, primarily owing to the complex antigenic nature of parasites and the possibilities for cross-reactions from related species. However, newer test methods combined with the use of more highly defined antigenic components has provided more accurate results with greater predictive values. Many of the newer tests use the EIA or immunoblot (Western blot) format, although IFA, indirect hemagglutination (IHA), and complement fixation (CF) are still in use (Wilkins & Nutman, 2015).

In general, serologic diagnosis of parasitic infection is used as an adjunct to the usual diagnostic modalities or in special situations in which identification of the parasite itself or its antigen or nucleic acid from host tissue or excreta is not possible (Wilkins & Nutman, 2015). For example, parasitic infections such as toxoplasmosis and toxocariasis reside in deep tissues and cannot be readily diagnosed by morphologic means. Others such as cysticercosis and echinococcosis develop in organs, where invasive studies that may be required are not recommended in the initial patient evaluation. Additional conditions—such as filariasis, schistosomiasis, and strongyloidiasis—may remain subclinical because of light infections or because the clinical evaluation occurred during the prepatent period (interval from infection to demonstration of symptoms or recovery of organism). In these settings, serologic testing may be invaluable for making a presumptive diagnosis in correlation with the accompanying clinical and radiographic features. Other circumstances in which serologic evaluation may prove useful include diagnosis of extraintestinal amebiasis (e.g., amebic liver abscess), trichinellosis, and chronic stages of trypanosomiasis. Lastly, serologic studies serve as a powerful tool in enhancing our understanding of the epidemiology of diseases such as schistosomiasis, toxoplasmosis, amebiasis, Chagas disease, malaria, and babesiosis, and for screening blood donors for select infections (e.g., malaria, Chagas disease) (Wilkins & Nutman, 2015).

Interpretation of serologic testing may be challenging. Detection of antibodies, especially immunoglobulin (Ig) G, provides evidence of infection but may not be able to differentiate active from past exposure. High antibody levels are useful for diagnostic purposes if they occur in a patient with no previous exposure to the parasite and no recent history of travel to an endemic area. Unfortunately, positive antibody levels in persons living in endemic areas often do not help in the clinical diagnosis. In some parasitic diseases, levels of antibodies may decline slowly following successful therapy or self-cure and thus may be useful for monitoring response to treatment (Wilkins & Nutman, 2015).

Serologic tests for parasitic diseases generally evaluate IgG levels with the exception of toxoplasmosis and babesiosis, in which IgM- and IgA-specific antibodies may be helpful for determining the age of infection (Wilson & Nutman, 2015). Unfortunately, IgM and IgA may persist for as long as 2 years after the primary infection, thus limiting their utility for differentiating acute from past infection. When *Toxoplasma gondii* IgG

TABLE 65.5
Examples of Serologic Assays for Parasites Available from Reference Laboratories

Disease	Organism	Specimen Type	Assay
Amebiasis	*Entamoeba histolytica*	Serum	EIA, ID, IHA
Baylisascariasis	*Baylisascaris procyonis*	Serum, CSF	IB
Babesiosis	*Babesia microti*, *Babesia* sp. WA1	Serum	IFA
Chagas	*Trypanosoma cruzi*	Serum	IFA, EIA, CF, IB
Cysticercosis	*Taenia solium*	Serum, CSF	EIA, IB
Echinococcosis	*Echinococcus granulosus*	Serum	EIA, IB, IHA, IFA
Fascioliasis	*Fasciola hepatica*	Serum	IB
Filariasis	*Wuchereria bancrofti*	Serum	EIA
Leishmaniasis	*Leishmania braziliensis*, *Leishmania donovani*, *Leishmania tropica*	Serum	IFA, EIA, CF
Malaria	*Plasmodium* spp.	Serum	IFA
Paragonimiasis	*Paragonimus westermani*	Serum	EIA, IB
Schistosomiasis	*Schistosoma* spp.	Serum	EIA, IB
Strongyloidiasis	*Strongyloides stercoralis*	Serum	EIA
Toxoplasmosis	*Toxoplasma gondii*	CSF, serum	IFA, EIA
Trichinellosis	*Trichinella spiralis*	Serum	EIA, BF

BF, Bentonite flocculation; *CF,* complement fixation; *CSF,* cerebrospinal fluid; *EIA,* enzyme immunoassay; *IB,* immunoblot; *ID,* immunodiffusion; *IFA,* indirect immunofluorescence assay; *IHA,* indirect hemagglutination.

antibodies are detected, avidity testing may also be useful to distinguish recent from past infection, particularly during pregnancy (Wilson & Nutman, 2015; Robert-Gangneux & Dardé, 2012; McAuley & Singh, 2019). This testing is based on the principle that the initial host response results in the production of low-avidity antibodies. Over time, the antibodies gain higher avidity as the host immune response is enhanced.

Because serologic tests for most parasitic diseases are requested infrequently, specimens generally are submitted to public (CDC) or private reference laboratories. Some of the more commonly requested tests are available as commercial kits. However, many of these assays are developed in-house and, hence, lack correlation with universal standards. Interpretive criteria are established by reagent manufacturers or by the center performing the test; these criteria often vary from institution to institution. Individuals requesting such tests should inquire about the performance characteristics, including sensitivity and specificity, and should be aware that cross-reactions may occur. For example, antibody tests for Chagas disease are known to cross-react with antibodies produced in response to *Leishmania* infections. However, reactivity to homologous antigen is greater, and this test is useful in diagnosing chronic stages of the disease when parasitemia is generally low. Usually, serology for chronic Chagas disease correlates well with molecular diagnostic methods (Afonso et al., 2012). Helminthic parasites are well known to cross-react in serologic assays that use crude antigen preparations because of phylogenetic, hence antigenic, similarities.

Several factors that may influence the test performance of serologic assays include disease manifestation, test format, reagents used, and parasite viability, to name a few. The sensitivity of the test is increased in patients with invasive amebiasis but may be weak in intestinal amebiasis with minimal tissue invasion and absent for asymptomatic carriers. The type of serologic assay format may also determine the sensitivity, as in the diagnosis of toxoplasmosis (Wilkins & Nutman, 2015). The double-sandwich IgM enzyme-linked immunosorbent assay (ELISA) is known to be more sensitive and specific than IgM immunofluorescence for detecting recently acquired and congenital toxoplasmosis. IHA has been the primary test for serodiagnosis of amebiasis. The sensitivity of the assay is also dependent on the type or stage of parasite antigen used. For example, the sensitivity of cutaneous leishmaniasis can be improved by using amastigote antigens in place of promastigote antigens in the IFA test. Finally, serologic assays are also affected by parasite viability; hydatid cysts occurring in the lung and dead or calcified cysts are less frequently detected than active cysts in the liver. This also holds true for neurocysticercosis (larval infection with the cestode *Taenia solium*), in which sensitivity is low when only a single parenchymal cyst or calcified lesions are present (White et al., 2018).

MOLECULAR DIAGNOSTIC METHODS

Diagnostic methods using DNA and ribonucleic acid (RNA) amplification and nucleic acid probe techniques have been described for most of the common parasitic diseases and, in general, offer high levels of sensitivity and specificity. For more complete details on this topic, the reader is referred to more recent publications (Wilkins & Nutman, 2015; Pritt, 2015). Molecular methods offer some unique advantages, such as high sensitivity and specificity, and the ability to detect and differentiate species variants—all independent of the patient's underlying immune status, which is a potentially limiting feature of serologic assays. On the other hand, molecular amplification techniques—particularly those using "open" formats in which amplified nucleic acid is manipulated, are prone to cross-contamination if proper processing precautions are not strictly enforced.

The availability of molecular tests has been greatly enhanced by the introduction of multiple commercial assays, some of which are FDA cleared for in vitro diagnostic use (Wilkins & Nutman, 2015; Pritt, 2015). Among the FDA-cleared tests are assays for *T. vaginalis*, *G. duodenalis*, *Cryptosporidium* spp., *E. histolytica*, and *Cyclospora cayetanensis*. Laboratory-developed NAATs have also been developed for parasites such as *Plasmodium* spp., *Babesia* spp., *Leishmania* spp., *T. gondii*, and *Trypanosoma* spp. and are available through specialized reference and public health laboratories (Table 65.6). Most assays today are available in real-time format, wherein the kinetics of the nucleic acid amplification reaction is recorded and analyzed by computer algorithms to allow detection of amplicons (Wilkins & Nutman, 2015). The introduction of this technology has allowed for rapid detection and has lessened the risk for amplicon cross-contamination due to the closed nature of the steps involved in postamplification analysis. Isothermal methods—such as strand displacement amplification, transcription-mediated amplification, and loop-mediated isothermal amplification (LAMP) have also been described for some parasites and allow for rapid and highly sensitive detection of parasite nucleic acid. Because the innate nature of molecular methods is genotypic, polymerase chain reaction (PCR) assays have the ability to accurately detect to the species level depending on the gene being targeted, and may also be used for strain typing and outbreak investigation (Wilkins & Nutman, 2015). Molecular methods may also allow for detection of mutations associated with drug resistance (Wilkins & Nutman, 2015; Pritt, 2015; Clain et al., 2019).

QUALITY ASSURANCE, QUALITY IMPROVEMENT, AND SAFETY

A quality assurance program for the parasitology section of the laboratory is similar to that for the other laboratory sections. It covers all essential aspects of the operation, including, among others, a well-written and complete procedure manual that is reviewed annually, guidelines for maintaining all specimen and test result records, a complete QC program with appropriate technical supervision and review, and participation in an approved proficiency testing program. Laboratories also need to focus on customer satisfaction using a variety of available measures and should participate in the team approach to identifying problems and generating solutions as part of a continuous quality improvement process (Garcia, 2016).

TABLE 65.6

Examples of Nucleic Acid Amplification Assays for Parasites

Parasite	Common Target(s)	Specimen Type	FDA-Approved/Cleared Assay Available (Assay, Manufacturer)
Leishmania spp.	rDNA, kinetoplastid DNA, ITS1 and ITS2 genes	Whole blood, skin scrapings, tissue	Yes* (SMART Leish PCR, U.S. Army)
Plasmodium spp.	rDNA	Whole blood	No
Toxoplasma gondii	RE and B1 genes	Amniotic fluid, blood, cerebrospinal fluid, tissue, whole blood, ocular fluid	No
Entamoeba histolytica	rDNA	Stool	Yes† (FilmArray GI panel, BioMerieux; xTAG Gastrointestinal Pathogen Panel, Luminex Corporation; BD MAX Enteric Parasite Panel, BD)
Giardia duodenalis	rDNA, β-Giardia gene	Stool	Yes† (FilmArray GI panel, BioMeriux; xTAG Gastrointestinal Pathogen Panel, Luminex Corporation; BD MAX Enteric Parasite Panel, BD)
Cryptosporidium spp.	rDNA	Stool	Yes† (FilmArray GI panel, BioMerieux; xTAG Gastrointestinal Pathogen Panel, Luminex Corporation; BD MAX Enteric Parasite Panel, BD)
Cyclospora cayetanensis	rDNA	Stool	Yes† (FilmArray GI panel, BioFire Diagnostics)
Trichomonas vaginalis	rDNA, β-Tubulin gene	Vaginal, cervical and urethral (male) samples, urine, semen	Yes (Aptima Trichomonas vaginalis assay, Hologic; Xpert TV,‡ Cepheid; Solana Trichomonas assay, Quidel; BD Max CT/GC/TV, BD)

FDA, U.S. Food and Drug Administration; *PCR,* polymerase chain reaction; *rDNA,* ribosomal deoxyribonucleic acid.
*Restricted to U.S. Department of Defense use.
†Component of multiplex assays for gastrointestinal pathogens.
‡Only FDA-approved assay for testing both males and females.

The performance of individuals responsible for the parasitology section should be monitored periodically with both internal and external unknown specimens, and competency assessments should be up-to-date, especially for those laboratories that encounter positive specimens infrequently. A variety of reference materials should be readily available for use at the laboratory bench, including positive slides and fecal specimens, printed atlases, and slide atlases.

Unpreserved specimens for parasitologic examination should be considered potentially infectious. Thus, all blood and body fluids should be handled according to Standard Precautions as defined by the Final Rule on Blood-borne Pathogens by the Occupational Safety and Health Administration, as published in the *Federal Register*. In addition to blood-borne viral pathogens, malarial parasites and hemoflagellates may remain infective. A variety of parasites may remain infective in fresh stool specimens, including cysts of enteric protozoa; eggs of *Taenia solium*, *E. vermicularis*, and *H. nana*; and filariform larvae of *S. stercoralis*. *Trichuris trichiura*, *Ascaris lumbricoides*, and hookworm eggs may remain infective in older specimens, and *Ascaris* eggs can survive and embryonate while in 5% formalin. Fecal specimens also may contain pathogens such as *Salmonella*, *Shigella*, or viruses. Strict observance of proper specimen handling techniques and disposal is essential. Personal attention to hand washing is also necessary.

BLOOD AND TISSUE PROTOZOA

PLASMODIUM SPP. (MALARIA)

Malaria (from the Italian *mal' aria*, meaning "bad air") is an acute and sometimes chronic infection of the bloodstream characterized clinically by fever, anemia, and splenomegaly, and is caused by apicomplexan parasites of the genus *Plasmodium*. The defining clinical features of a malarial attack or paroxysm consist of, in order, shaking chills, fever (up to 40°C or higher), and generalized diaphoresis, followed by resolution of fever. The paroxysm occurs over 6 to 10 hours and is initiated by the synchronous rupture of erythrocytes with the release of new infectious blood stage forms known as *merozoites* (Fig. 65.4). The disease generally occurs throughout the tropics and subtropics and is spread exclusively by female anopheline mosquitoes. The four main species of *Plasmodium* causing human malaria are *P. vivax*, *P. falciparum*, *Plasmodium malariae*, and *Plasmodium ovale*. *P. falciparum* infection occurs principally in tropical areas worldwide, whereas *P. vivax* infections occur in both tropical and temperate zones, including the east horn of Africa, Central Asia and the Indian Subcontinent, Southeast Asia, and Latin America. *P. malariae* also occurs worldwide but to a much lesser extent than *P. falciparum* or *P. vivax*. *Plasmodium ovale* occurs primarily in western Africa and Southeast Asia; interestingly, *P. ovale* is the only species to date not to have been introduced to the Americas. Recently, human infection with *P. knowlesi*, a malarial parasite of Old World monkeys, has been described in several regions of Southeast Asia. These infections are potentially life-threatening but are difficult to distinguish from *P. malariae* microscopically, leading to misidentification. Use of PCR may be required to make the correct differentiation (Cox-Singh et al., 2008).

Because infection with *falciparum* malaria is potentially life-threatening, its presence must be considered in the differential diagnosis of unexplained fever, and history of travel in endemic geographic areas should always be sought. In an era of increasing world travel, the risk for acquiring malaria is not insignificant, and the rapid spread of drug-resistant strains poses particular problems when appropriate prophylaxis or therapy is considered.

Laboratory evaluation of patients suspected of having malaria continues to rely on timely examination of thick and thin blood films to demonstrate the intraerythrocytic parasites. Although they are straightforward in their approach, performance of these techniques may be problematic. Reliable identification of organisms requires continuous training to maintain expertise; therefore, those laboratories that rarely see positive specimens may choose to refer specimens to reference laboratories provided that processing and reporting are timely.

NAATs for detection of parasite-specific DNA (Mathison & Pritt, 2017) provide enhanced sensitivity and specificity but generally are not appropriate or available for smaller laboratories. They are also not typically performed on a STAT basis, as is necessary for detection of acute disease.

Within the past decade, antigen detection methods have become widely available for use in endemic and nonendemic settings (see Laboratory Methods section earlier in this chapter). They are now used in many moderate- to large-sized laboratories in nonendemic settings for rapid malaria diagnosis in resource-limited settings, particularly when skilled and experienced microscopists are not available (e.g., night shift). They are also an integral part of the WHO's malaria control efforts; an estimated 276 million malaria RDTs were sold worldwide in 2017, with an additional 245 million RDTs distributed at no cost by the National Malaria Programme (WHO, 2018). The WHO estimates that 75% of malaria tests conducted in malaria-endemic regions in sub-Saharan Africa were via RDTs (WHO, 2018). Most commercially available tests utilize a lateral flow format and detect *Plasmodium*-specific antigens such as lactate dehydrogenase, aldolase, and/or *P. falciparum* HRP-II. While they generally provide a high degree of sensitivity and specificity for the diagnosis of falciparum malaria, most suffer from inadequate sensitivity for detection of lower parasite loads and non–*P. falciparum* infections. The sensitivity, specificity, and invalid rates vary widely among the malaria RDTs. The WHO has performed 7 rounds of product testing on commercially available RDTs, the results of which are freely available online (WHO, 2017). It is generally recommended that antigen-based assay testing be followed by confirmatory conventional thick and thin film examination (Wilson, 2012; Mathison & Pritt, 2017).

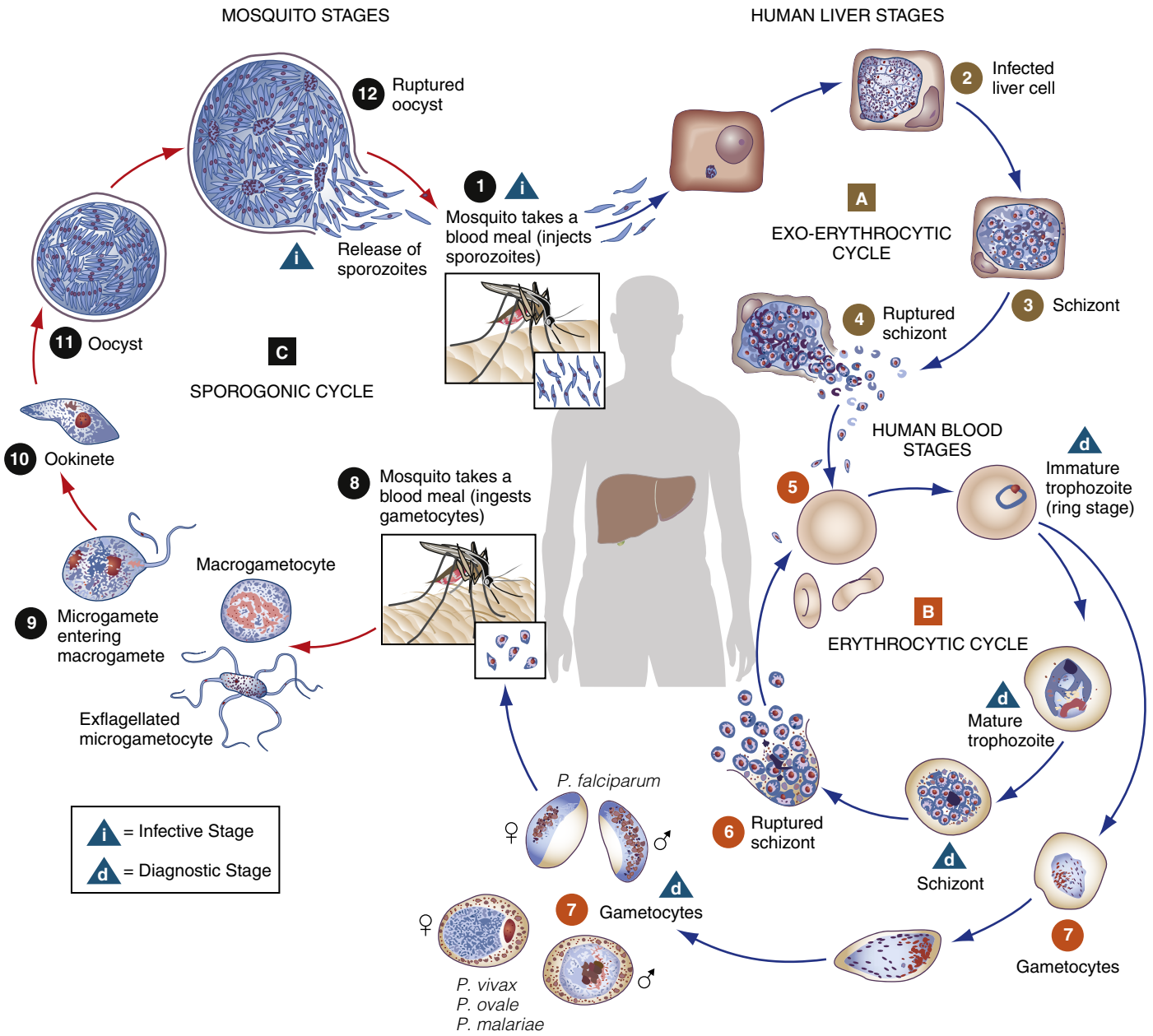

Figure 65.4 Life cycle of *Plasmodium* spp. Infection occurs when an infected female anopheline mosquito injects infectious sporozoites while taking a blood meal (1). Sporozoites are carried to the liver via the bloodstream, where they infect a hepatocyte (2) and divide asexually to form a hepatic schizont (3). The schizont ruptures (4), releasing infectious merozoites into the bloodstream that infect erythrocytes (5) and initiate the erythrocytic cycle. The early stage of the parasite is a "ring-form" trophozoite. As the trophozoite matures, it takes one of two pathways: it can become an erythrocytic schizont (6) that perpetuates the erythrocytic cycle or it can become a male or female gametocyte (microgametocyte or microgametocyte, respectively), (7). The gametocyte is a dead-end stage in the human host and is taken up by a mosquito when it takes a blood meal (8) to initiate the sexual cycle. In the mosquito host, microgametocytes (males) form microgametes and exflagellate, releasing the individual microgametes. A microgamete will fertilize a macrogamete (female) (9), resulting in the formation of an ookinete (10). The ookinete matures and becomes an oocyst in which proliferation of sporozoites occurs (11). The mature oocyte ruptures, releasing infectious sporozoites (12) which migrate to the salivary glands of the mosquito. The cycle continues when a female mosquito takes her next blood meal and injects sporozoites into the human host. (Courtesy of DPDx, Centers for Disease Control and Prevention, Atlanta.)

Life Cycle

Plasmodium spp. have a complex life cycle involving a mosquito definitive host and a vertebrate intermediate host (see Fig. 65.4). Human infection is initiated when a female *Anopheles* mosquito takes a blood meal and injects infectious sporozoites into the bloodstream. Sporozoites are carried to the liver and invade hepatic parenchymal cells, initiating a proliferative phase known as *extraerythrocytic sporogony*. Eventually, these hepatic schizonts rupture, releasing merozoites into the bloodstream, which infect erythrocytes. Developing parasites are known as *trophozoites*. Early trophozoites are usually characterized by a thin or thick vacuolated cytoplasm and one or two chromatin dots and are referred to as *rings* or *ring-form trophozoites*. Hemozoin pigment, a breakdown product of hemoglobin, is characteristic of erythrocytes containing mature stages of malarial parasites but is not usually evident in ring forms. As the trophozoites mature, they take one of two pathways.

In one pathway, trophozoites become *erythrocytic schizonts* that produce merozoites and perpetuate the erythrocytic cycle. The erythrocytic cycle takes approximately 48 hours (tertian periodicity) for *P. falciparum*, *P. ovale*, and *P. vivax* infections, and 72 hours (quartan periodicity) for *P. malariae* infection. Clinical symptoms of fever spikes are ties to the rupturing of erythrocytic schizonts. In the second pathway, trophozoites become macro- (female) or microgametocytes (male). Gametocytes are a dead-end stage in the human host; their sole purpose is to be picked up by a mosquito host to initiate the sexual cycle. In the mosquito host, microgametocytes exflagellate and the released microgametes fertilize a macrogamete, resulting in the formation of a motile *ookinete*. Ookinetes migrate outside the gut wall of the mosquito and become an oocyst. Within the oocyst, sporogony results in the formation of infectious sporozoites. The mature oocyst ruptures into the body cavity, releasing sporozoites, which then migrate through the tissues to the salivary glands, from which they are injected into the vertebrate host as the mosquito feeds. The time required for development in the mosquito ranges from 8 to 21 days.

Plasmodium vivax and *P. ovale* are unique in that true disease relapses may occur weeks to months following subsidence of previous attacks. This

occurs as a result of renewed extraerythrocytic and, eventually, erythrocytic schizogony from latent hepatic parasite forms known as *hypnozoites*. Recurrences of disease due to *P. falciparum* or *P. malariae*, called *recrudescences*, arise from increased numbers of persisting blood stage forms to clinically detectable levels and not from persisting liver stage forms. Liver cells are infected only by sporozoites from the mosquito; thus, transfusion-acquired *P. vivax* or *P. ovale* infection does not relapse (Pritt, 2019).

Epidemiology

Endemic transmission of malaria requires a reservoir of infection, an appropriate mosquito vector, and a susceptible host. Control of malaria is directed at elimination of mosquito hosts, treatment of active cases, and prophylaxis of susceptible persons. However, the emergence of mosquitoes resistant to insecticides, the development of resistance to prophylaxis and therapy by *P. falciparum* and *P. vivax* (WHO, 2018) and lack of adequate funding have made control difficult in endemic areas. Fortunately, renewed global efforts have dramatically decreased the morbidity and mortality of malaria worldwide, although further efforts are needed to achieve full control and elimination (WHO, 2018).

A number of hereditary erythrocyte genotypes offer some degree of protection against severe *P. falciparum* malaria, including sickle cell trait, glucose-6-phosphate dehydrogenase (G6PD) deficiency, hereditary ovalocytosis, and thalassemia (Mohandas & An, 2012; Uyoga et al., 2019). Alterations of erythrocyte cell membrane surface proteins may interfere with parasite invasion and confer a protective effect against malaria infection and severe disease. Individuals who lack the Duffy blood group antigen, for example, have a decreased likelihood of *P. vivax* infection since this is the primary protein used by *P. vivax* to bind and invade erythrocytes (Zimmerman, 2013). Alternate binding pathways have recently been identified for *P. vivax*, providing an explanation for the numerous reports of *P. vivax* malaria in Duffy blood group–negative individuals (Ntumngia et al., 2016).

Transfusion-acquired malaria may occur when blood donors have subclinical malaria and may prove fatal for the recipient. Similarly, congenital malaria may occur in infants born to mothers from endemic areas. The infant acquires the infection at birth as a result of rupture of placental blood vessels leading to maternal-fetal transfusion. Neither transfusion nor congenital malaria is expected to relapse because exoerythrocytic schizogony does not occur. The number of cases of malaria reported in the United States averages about 1700 cases per year (CDC, 2018a). The most recent surveillance summary from the CDC reported 1517 total cases in 2015 (Mace et al., 2018). Species causing infection were *P. falciparum* (67.4%), *P. vivax* (11.7%), *P. ovale* (4.1%), *P. malariae* (3.1%), and undetermined (12.9%), with less than 1% having infection with two species. Of reported cases, 17.1% were associated with severe disease, including the 11 persons who died. Only 4.7% of patients with malaria reported adhering to a CDC-recommended chemoprophylaxis malaria regimen. Patients acquired the infection in Africa (84.7%), Asia (8.6%), the Western Hemisphere (4.6%), or Oceania (2 cases). In patients for whom the reason for travel was known, the majority (68.4%) were visiting friends and relatives (VFRs). These individuals have long been known to be at higher risk for acquiring malaria than other travelers since they often do not seek pretravel counseling, do not take malaria chemoprophylaxis, travel to more rural areas, and often stay for longer periods of time.

Clinical Disease

Most patients who develop *P. falciparum* infection become symptomatic within 1 month of exposure, whereas a delay of up to 6 months or more may be seen with the other *Plasmodium* species. Common presenting symptoms of malaria include chills and fever, which often are associated with splenomegaly. In the early stages of the disease, febrile episodes occur irregularly but eventually become more synchronous, assuming the usual tertian (*P. vivax*, *P. falciparum*, and *P. ovale*) or quartan (*P. malariae*) periodicity. Patients with malaria may develop anemia and may have other manifestations, including diarrhea, abdominal pain, headache, and muscle aches and pains. *Plasmodium falciparum* malaria can result in high rates (50%) of parasitemia, which can lead to severe hemolysis with hemoglobinuria and profound anemia. Erythrocytes infected with growing trophozoites and schizonts of *P. falciparum* become sequestered in small vessels of the body, which may lead to occlusion of these vessels, causing symptoms related to capillary obstruction and tissue anoxia. Involvement of the brain is known as cerebral malaria, in which the patient becomes disoriented, progressing to delirium, coma, and often death.

The course of untreated malaria depends on the species. Most fatal cases of malaria are due to *P. falciparum*, although *P. knowlesi* can also cause fatalities. In nonfatal cases, the febrile paroxysms become less severe with time and the disease gradually subsides. Patients with *P. vivax* or *P. ovale* infection may have relapses after many months or, occasionally, years. Persons with *P. falciparum* and *P. malariae* infection may have symptom-free periods but suffer from sporadic recrudescences owing to persisting low-grade parasitemia. Relapses and recrudescences may be associated with changes in the host's defense mechanisms or possibly with antigenic changes in the infecting organisms.

Peripheral smears may show leukocytes that contain malaria pigment (hemozoin). Increased reticulocyte counts occur commonly and are associated with rapid erythrocyte turnover. The presence of greatly enlarged platelets may be noted on peripheral blood films and may occur as a result of their rapid turnover secondary to splenic sequestration. Malarial infection may interfere with certain serologic tests, producing false-positive results, especially those for syphilis.

Therapy and prophylaxis of malaria have become highly complex topics because of the widespread appearance of resistance by *P. falciparum* to chloroquine and other antimalarials and, to a lesser extent, resistance by *P. vivax* to chloroquine. Artemisinin combination therapy is now recognized as the preferred treatment by the WHO for treatment of *P. falciparum* infection and chloroquine-resistant *P. vivax* infection (WHO, 2018). Persons with *P. vivax* or *P. ovale* malaria should receive treatment with primaquine phosphate or tafenoquine in addition to standard primary treatment in order to eradicate hepatic hypnozoites and to prevent relapse. Use of primaquine or tafenoquine may be dangerous in patients who have G6PD deficiency. Screening of at-risk patients before therapy is initiated may be necessary (Drugs for Parasitic Infections, 2013; CDC, 2018a). Exchange transfusion may decrease morbidity and mortality in severe cases of *P. falciparum* infection in which the parasitemia is ≥10% (Pritt, 2019). While exchange transfusion is no longer recommended in this setting by the CDC (Tan et al., 2013), it is still supported in cases of severe malaria with high parasitemia by the American Society for Apheresis (Shaz et al., 2014).

Diagnosis

Malaria should always be included in the differential diagnosis of fever in patients who have a history of travel to or residence in endemic areas (Mathison & Pritt, 2017). Given the potentially life-threatening nature of infection, testing must be performed on a STAT basis. Diagnosis usually is established by demonstrating parasites in thick and thin blood films. Blood specimens ideally are collected just before the next anticipated fever spike or at the onset of fever. Specimens drawn several hours apart sometimes may be required to demonstrate infection or to diagnose the species because the number and morphologic stage of parasites vary during the cycle. Careful examination of thick films should reveal the presence of the parasites in almost all patients with clinically apparent malaria.

Identification of malarial parasites on thin blood films requires a systematic approach. Three major factors should be considered: appearance of infected erythrocytes, appearance of parasites, and stages found. Table 65.7 summarizes diagnostic characteristics of the species, which are illustrated in Figures 65.5 and 65.6. The size of the infected erythrocyte is a particularly useful feature for determining the infecting species; erythrocytes infected by *P. vivax* or *P. ovale* parasites often appear enlarged compared with adjacent uninfected cells, whereas *P. malariae* and *P. falciparum* parasites are usually found in erythrocytes of normal size. Erythrocytes infected with *P. ovale* are often oval or fimbriated (having irregular, usually polar or bipolar, projections of the cell margins), a feature rarely observed with *P. vivax*. Schüffner stippling, noted as numerous small uniform pink granules in the erythrocyte, is usually seen in cells infected with *P. vivax* and *P. ovale*, although it may not be evident in cells infected with early ring forms or on slides that have not been stained at the appropriate pH, such as the Wright-Giemsa stain, used widely in hematology laboratories (see the Laboratory Methods section earlier in the chapter). The presence of Schüffner stippling is helpful because it is not seen in *P. malariae* or *P. falciparum* infection.

As trophozoites grow in the infected cells, the amount of hemoglobin in the erythrocyte decreases and hemozoin pigment accumulates. The amount and appearance of the pigment vary among species. Ring forms of all parasites may have a similar appearance, and if only occasional ring forms are found, the species may not be identifiable. Young rings of *P. falciparum* tend to be smaller than those of the other species (one-sixth the diameter of the red blood cell compared with one-third the diameter of the red blood cell for the other species). Rings of *P. falciparum* that have grown are similar in size to those of the other species. Trophozoites that appear to be lying on the surface of the erythrocyte or protruding from it are called *appliqué* or *accolé* forms, most often seen in *P. falciparum* infection. Doubly infected cells and double chromatin dots in ring trophozoites occur most commonly in *P. falciparum* infection but can occur with the other species as well.

TABLE 65.7
Comparison of *Plasmodium* Species Affecting Humans

Species	Erythrocyte Size	Cytoplasmic Inclusions*	Parasite Cytoplasm	Parasite Pigment	Number of Merozoites	Stages Found in Circulating Blood
Plasmodium vivax	Enlarged; maximum size (attained with mature trophozoites and schizonts) may be 1–2 times normal erythrocyte diameter	Schüffner dots; all stages except early ring forms	Irregular and pleomorphic, ameboid in trophozoites; may have band forms	Golden brown	12–24; average is 16	All stages; wide range of stages may be seen on any given film
Plasmodium malariae	Normal to small	Ziemann dots rarely seen	Rounded, compact trophozoites with dense cytoplasm; band-form trophozoites occasionally seen	Dark brown, coarse, conspicuous	6–12; average is 8; "rosette" schizonts occasionally seen	All stages; wide range of stages usually not seen; relatively few rings or gametocytes generally present
Plasmodium ovale	Enlarged; maximum size may be 1.25 to 1.5 times normal red blood cell diameter; infected red blood cells may be oval and/or fimbriated (border has irregular projections)	Schüffner dots; all stages except early ring forms	Rounded, compact trophozoites; occasionally slightly ameboid; growing trophozoites have large chromatin mass	Dark brown, conspicuous	6–14; average is 8	All stages
Plasmodium falciparum	Normal; multiply infected red blood cells are common	Maurer clefts occasionally seen	Young rings are small, delicate, often with double chromatin dots; gametocytes are crescent or elongate	Black; coarse and conspicuous in gametocytes	6–32	Rings and/or gametocytes; other stages develop in blood vessels of internal organs but are usually not seen in peripheral blood except in severe infection

Modified from Ash LR, Orihel TC: *Atlas of human parasitology,* ed 5, Chicago, 2007, ASCP Press.
*A pH of 7.0–7.2 is optimal for visualization of cytoplasmic inclusions.

Growing trophozoites of *P. vivax* have irregular shapes and are termed *ameboid*. Those of *P. malariae* and *P. ovale* tend to remain compact, although vacuolated forms can occur (with *P. malariae*, these can take on a characteristic shape called the "basket-form" trophozoite). Mature trophozoites and schizonts of *P. falciparum* are usually sequestered in capillary beds secondary to cytoadherence to endothelial cells and are not seen in the peripheral blood except in very severe cases of infection. When schizonts are identified in the peripheral blood, determining the number of merozoites is helpful in identifying the various species. Gametocytes of *P. falciparum* are readily identified by their characteristic sausage shape. Gametocytes of *P. vivax*, *P. malariae*, and *P. ovale* have a similar shape. Thus, they are difficult to differentiate, although characteristics of infected red blood cells can aid in identification.

The varieties of developmental stages in the peripheral blood aid in diagnosis. In *P. falciparum* infection, ring forms predominate; finding numerous ring forms without more mature stages is highly suggestive for *P. falciparum* infection. In *P. vivax*, *P. malariae*, and *P. ovale* infections, various stages of parasites are found with some predominance of one stage depending on the phase of the cycle.

Thick films are preferred for detecting malarial infections because a greater quantity of blood is examined (see the Laboratory Methods section earlier in the chapter). Ring forms often have the appearance of punctuation marks rather than complete rings, and the presence of red chromatin and blue cytoplasm should be required to identify them as parasites (see Fig. 65.6A). Schüffner stippling still may be a helpful identifying characteristic, which may be recognized around growing trophozoites as a pink halo rather than as distinct granules seen in thin films. The ameboid character of *P. vivax* trophozoites is not as evident in thick films, but the number of merozoites in mature schizonts is helpful. Gametocytes usually cannot be differentiated. The distinctive sausage shape of *P. falciparum* gametocytes is still evident, although they may appear stubbier than in thin films. Gametocytes of the other species can be detected and are easily differentiated from host cell nuclei by the presence of refractile hemozoin pigment.

Mixed infections occur occasionally, but caution should be used in making such a diagnosis unless definite evidence reveals two separate populations of parasites. The most common mixed infections are *P. falciparum* and *P. vivax*. Finding gametocytes of *P. falciparum* in a person obviously infected with *P. vivax* is diagnostic, for example.

Multiple artifacts may be confused with malarial parasites on thick and thin films. The most common artifacts on thin films are blood platelets superimposed on red blood cells. These platelets should be readily identified because they do not have a true ring form, do not show differentiation of the chromatin and cytoplasm, and do not contain pigment. Clumps of bacteria or platelets may be confused with schizonts. At times, masses of fused platelets may resemble gametocytes of *P. falciparum* but do not show the differential staining or the pigment. Precipitated stain and contaminating bacteria, fungi, or spores may also be confused with these parasites.

Species-specific serologic tests for malaria are not useful for diagnosis of acute infection but may be useful for epidemiologic surveys and detection of infected blood donors (Mathison & Pritt, 2017). Such tests do not reliably differentiate current from past infection, however. Sensitive and specific IFA tests using antigens from the four human species are available from the CDC. Assays for the direct detection of malarial antigens in blood are especially useful (see the Laboratory Methods section earlier in the chapter) (Mathison & Pritt, 2017).

BABESIA SPP. (BABESIOSIS)

Similar to malarial parasites, etiologic agents of babesiosis are apicomplexan protozoa found nearly worldwide that infect erythrocytes, often producing febrile illness of variable severity. Unlike malaria, babesiosis is transmitted by ticks, is found in a variety of animal species that serve as reservoirs, and is primarily a disease of temperate regions. Less commonly, babesiosis is transmitted by blood transfusion and transplacentally.

Human infection in the United States occurs predominantly in the northeastern and Midwestern states, where the rodent parasite *Babesia microti* is responsible for infection. The *Ixodes scapularis*-complex, the "black-legged" or "deer ticks," are the usual vectors. *Babesia duncani* causes a smaller number of infections in northern California, Oregon, and Washington and is thought to be transmitted by the Western black-legged tick, *Ixodes pacificus* (Pritt, 2019). In Europe, babesiosis is caused primarily by *Babesia divergens*, with a smaller number of cases attributed to *Babesia venatorum* and *B. microti*. Infection with these agents is transmitted by *Ixodes ricinus*. Reports of *B. divergens* and *B. divergens*–like (*Babesia* MO-1) infections in the states of Kentucky, Missouri, and Washington expand the range of known human cases in the United States (Herwaldt et al., 2004). Other means of acquiring infection include blood transfusion and, rarely, congenital transmission. The FDA has approved the Imugen (Oxford Immunotec, Oxfordshire, UK) *Babesia microti*–arrayed fluorescent immunoassay for

A

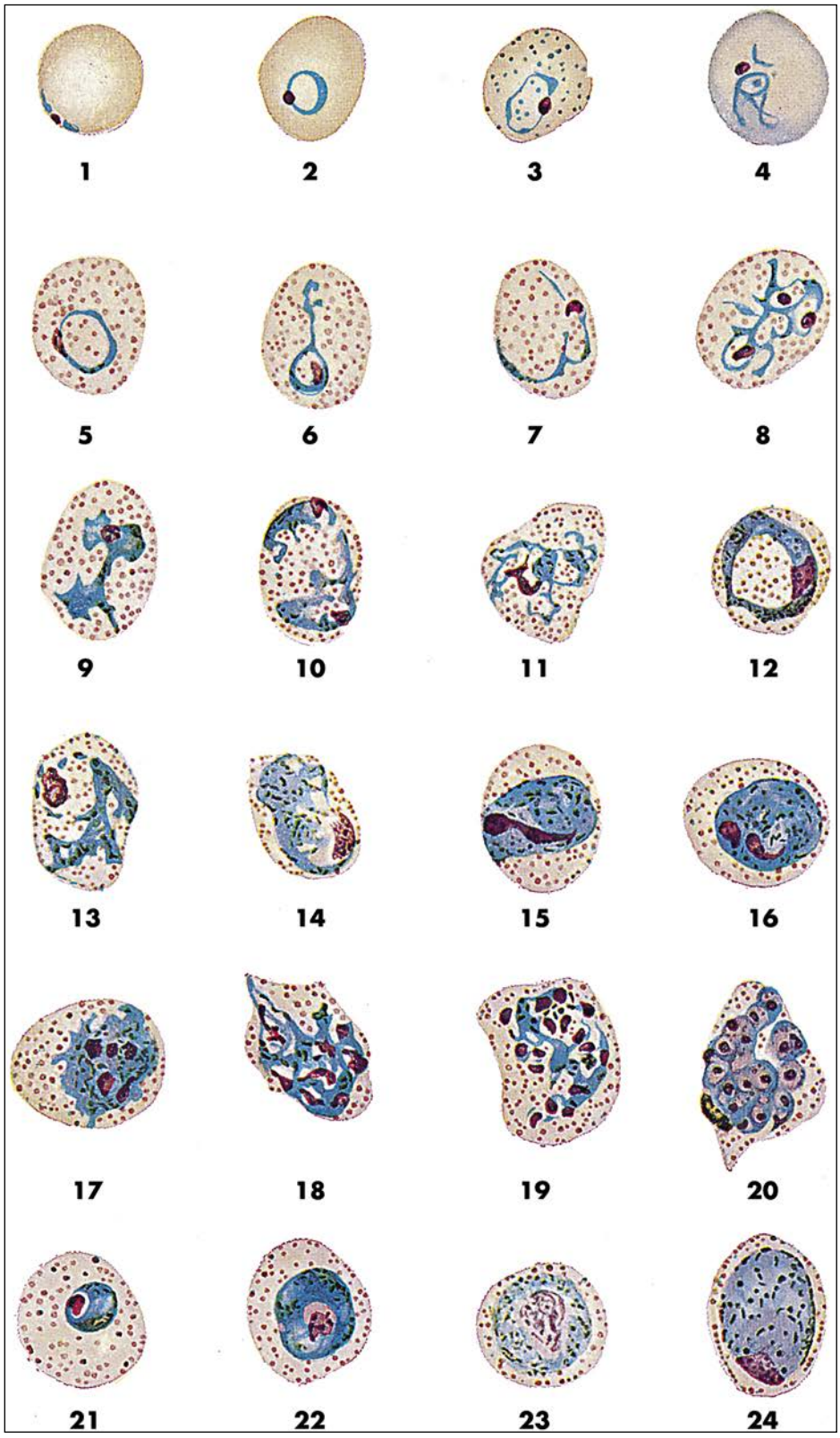

Figure 65.5 **A,** *Plasmodium vivax. 1,* Normal-size erythrocyte with marginal ring-form trophozoite. *2,* Young ring form (early trophozoite) in an enlarged erythrocyte (macrocyte). *3,* Slightly older ring form trophozoite in macrocyte showing Schüffner stippling. *4,* Polychromatophilic macrocyte containing late-stage trophozoite with pseudopodia (i.e., "ameboid" form). *5,* Ring form of trophozoite showing pigment in macrocyte with Schüffner stippling. This stippling does not appear in all cells containing the growing and older forms of *Plasmodium vivax*, but it can be found with any stage from the fairly young ring form onward. *6* and *7,* Ameboid trophozoite forms. *8,* Three ameboid trophozoites. *9* to *13,* Older ameboid trophozoites in the process of development. *10,* Two ameboid trophozoites in one cell. *14,* Mature trophozoite. *15,* Mature trophozoite with chromatin apparently in process of division. *16* to *19,* Schizonts showing progressive steps in division (early segmenting schizonts). *20,* Mature schizont. *21* and *22,* Developing gametocytes. *23,* Mature microgametocyte. *24,* Mature macrogametocyte. (From Wilcox A: *Manual for the microscopical diagnosis of malaria in man,* Bulletin No. 180, Bethesda, MD, 1942, National Institutes of Health.)

Continued

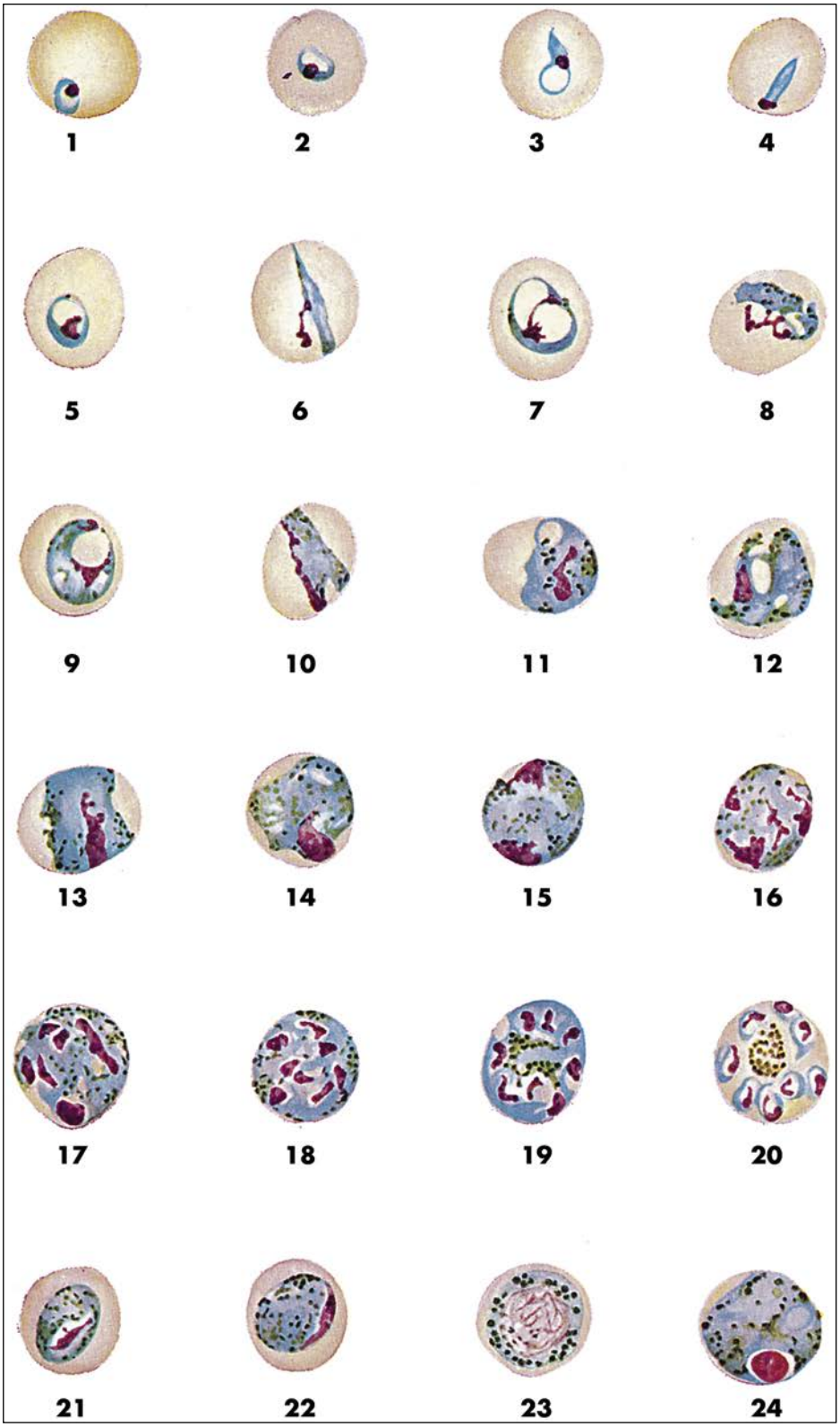

B

Figure 65.5—cont'd **B,** *Plasmodium malariae. 1,* Young ring form (early trophozoite). *2* to *4,* Young trophozoite forms of the parasite showing gradual increase in chromatin and cytoplasm. *5,* Developing ring form of trophozoite showing pigment granule. *6,* Early band form of trophozoite—elongate chromatin, some pigment apparent. *7* to *12,* Some forms that the developing (late-stage) trophozoite of *P. malariae* may take. *13* and *14,* Late-stage trophozoites—*13* shows a thick band form. *15* to *19,* Phases in the development of the schizont (early segmenting schizonts). *20,* Mature schizont containing a central hemozoin pigment granule and peripheral merozoites ("rosette" or "daisy head" arrangement). *21,* Immature microgametocyte. *22,* Immature macrogametocyte. *23,* Mature microgametocyte. *24,* Mature macrogametocyte. (From Wilcox A: *Manual for the microscopical diagnosis of malaria in man,* Bulletin No. 180, Bethesda, MD, 1942, National Institutes of Health.)

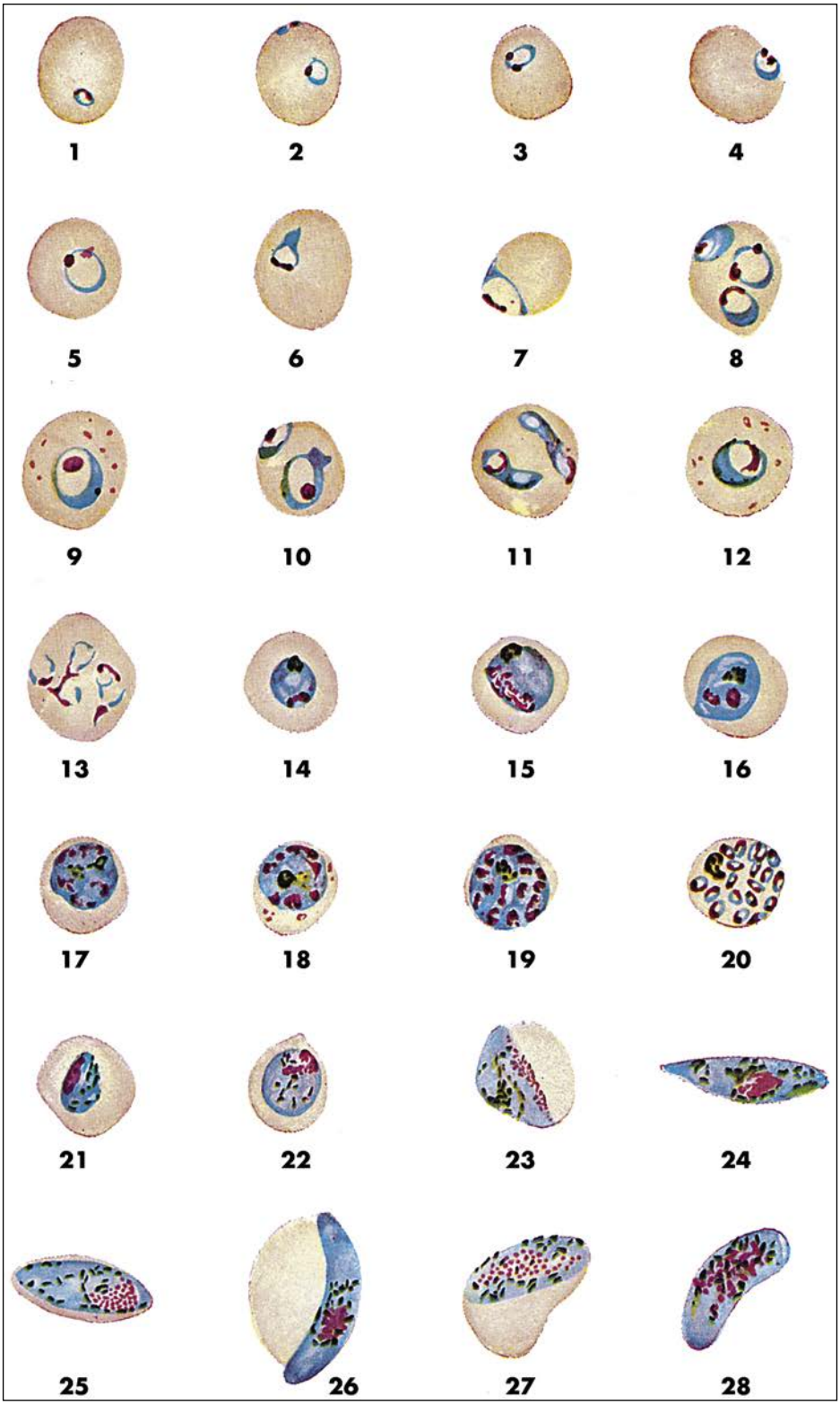

C

Figure 65.5—cont'd **C,** *Plasmodium falciparum. 1,* Very young ring form (early trophozoite). *2,* Double infection of single cell with young trophozoites—one a "marginal" or "applique" form, the other a "signet ring" form. *3* and *4,* Young trophozoites showing double chromatin dots ("headphone" forms). *5* to *7,* Developing trophozoite forms. *8,* Three late-stage trophozoites in one cell. Although these forms are not generally seen in freshly obtained peripheral blood with *P. falciparum* infection due to sequestration in the peripheral capillaries, they may be seen when there is a delay between collection and examination. *9,* Trophozoite showing pigment in a cell containing Maurer dots. These intracytoplasmic inclusions can be differentiated from the stippling seen with *P. vivax* and *P. ovale* infection in that the Maurer dots are larger and fewer in number. *10* and *11,* Two late-stage trophozoites in each of two cells, showing variation in forms that parasites may assume. *12,* Late-stage trophozoite showing haze of pigment throughout cytoplasm. Maurer dots are also present. *13,* Unusual slender forms of *P. vivax*. *14,* Mature trophozoite, showing clumped pigment. *15,* Parasite in the process of initial chromatin division to form a schizont (schizonts are not usually found in the peripheral circulation in *P. falciparum* infection). *16* to *19,* Various phases of development of the schizont (early segmenting schizonts). *20,* Mature schizont. *21* to *24,* Successive forms in development of the gametocyte—usually not found in the peripheral circulation. *25,* Immature macrogametocyte. *26,* Mature macrogametocyte. *27,* Immature microgametocyte. *28,* Mature microgametocyte. (Courtesy of United States Public Health Service, National Institutes of Health.)

Continued

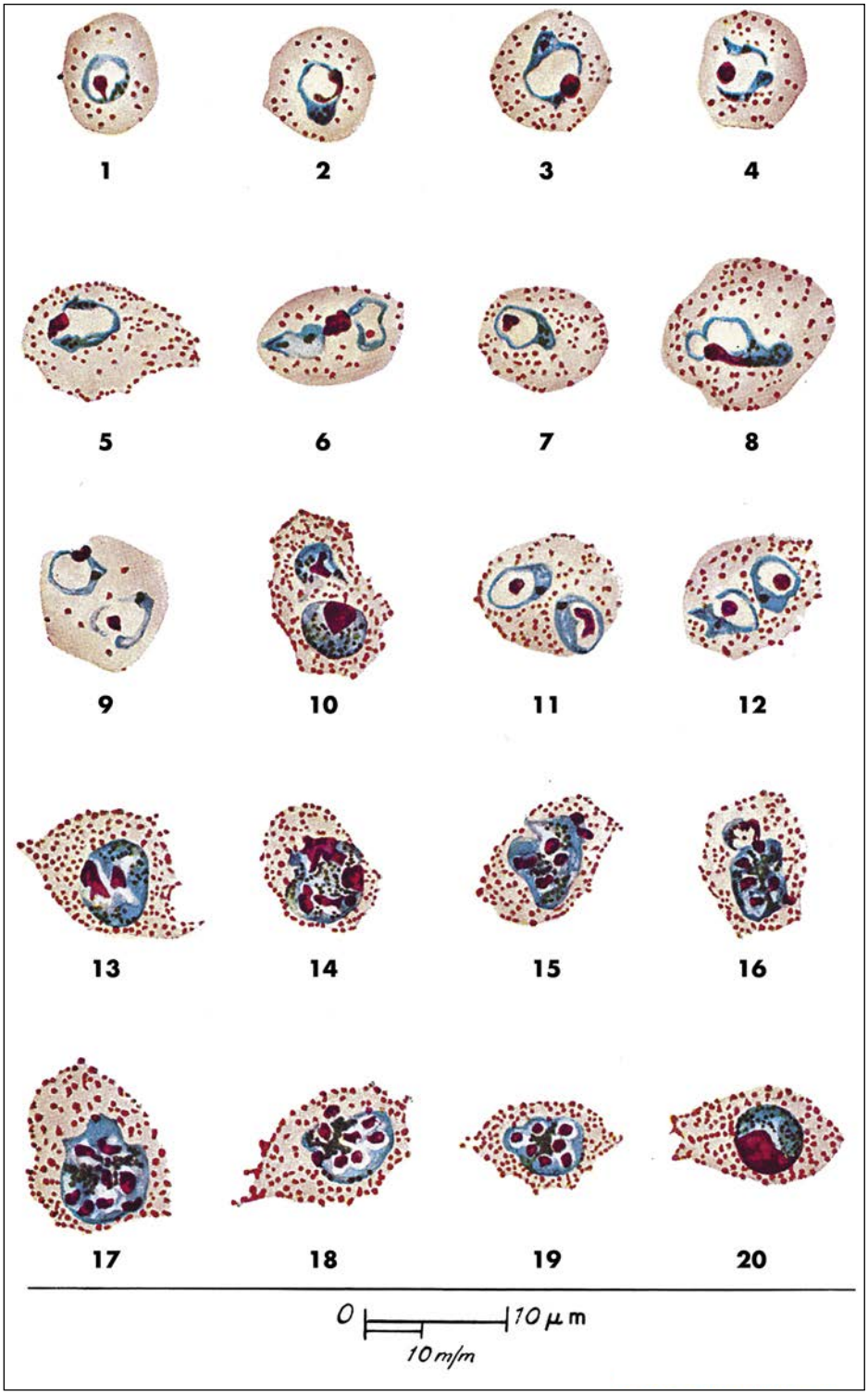

D

Figure 65.5—cont'd D, *Plasmodium ovale. 1,* Young ring form (early trophozoite). *2* to *5,* Older ring-shaped trophozoites. *6* to *8,* Older trophozoites, some with ameboid features reminiscent of *P. vivax* infection. Generally, *P. ovale* late-stage trophozoites have a more compact appearance than those of *P. vivax. 9, 11,* and *12,* Doubly infected cells, trophozoites. *10,* Doubly infected cell, young gametocytes. *13,* Early segmenting schizont with only 2 merozoites. *14* to *19,* Schizonts, progressive stages. *20,* Mature gametocyte. (Free translation of legend accompanying original plate in *Guide pratique d'examen microscopique du sang appliqué au diagnostic du paludisme* by Georges Villain. Reproduced with permission from Biologie Medicale Supplement, 1935. Courtesy of Aimee Wilcox, National Institutes of Health Bulletin No. 180, United States Public Health Service.)

detecting *B. microti* antibodies in human plasma samples as well as the Imugen *Babesia microti* nucleic acid test for detection of DNA in whole blood (https://www.fda.gov/news-events/press-announcements/fda-approves-first-tests-screen-tickborne-parasite-whole-blood-and-plasma-protect-us-blood-supply).

The spectrum of babesiosis varies from latent, subclinical infection to fulminant, hemolytic disease. Fatalities have been reported, especially in splenectomized or immunocompromised individuals. Immunocompetent persons may experience symptoms similar to those of malaria, including fever, chills, malaise, and anemia, although without recognizable periodicity. Investigation of an outbreak caused by *B. microti* on Nantucket Island in New England showed that some symptomatic patients harbored the parasite for months and others showed serologic evidence of infection without a history of clinical disease. Other evidence indicates that chronic subclinical infections may not be uncommon (Westblade et al., 2017). While asymptomatic infections in immunocompetent patients generally do not require treatment, symptomatic patients, including those at risk for severe disease (e.g., asplenic individuals), are generally treated using atovaquone plus azithromycin or clindamycin plus quinine (Drugs for Parasitic Infections, 2013).

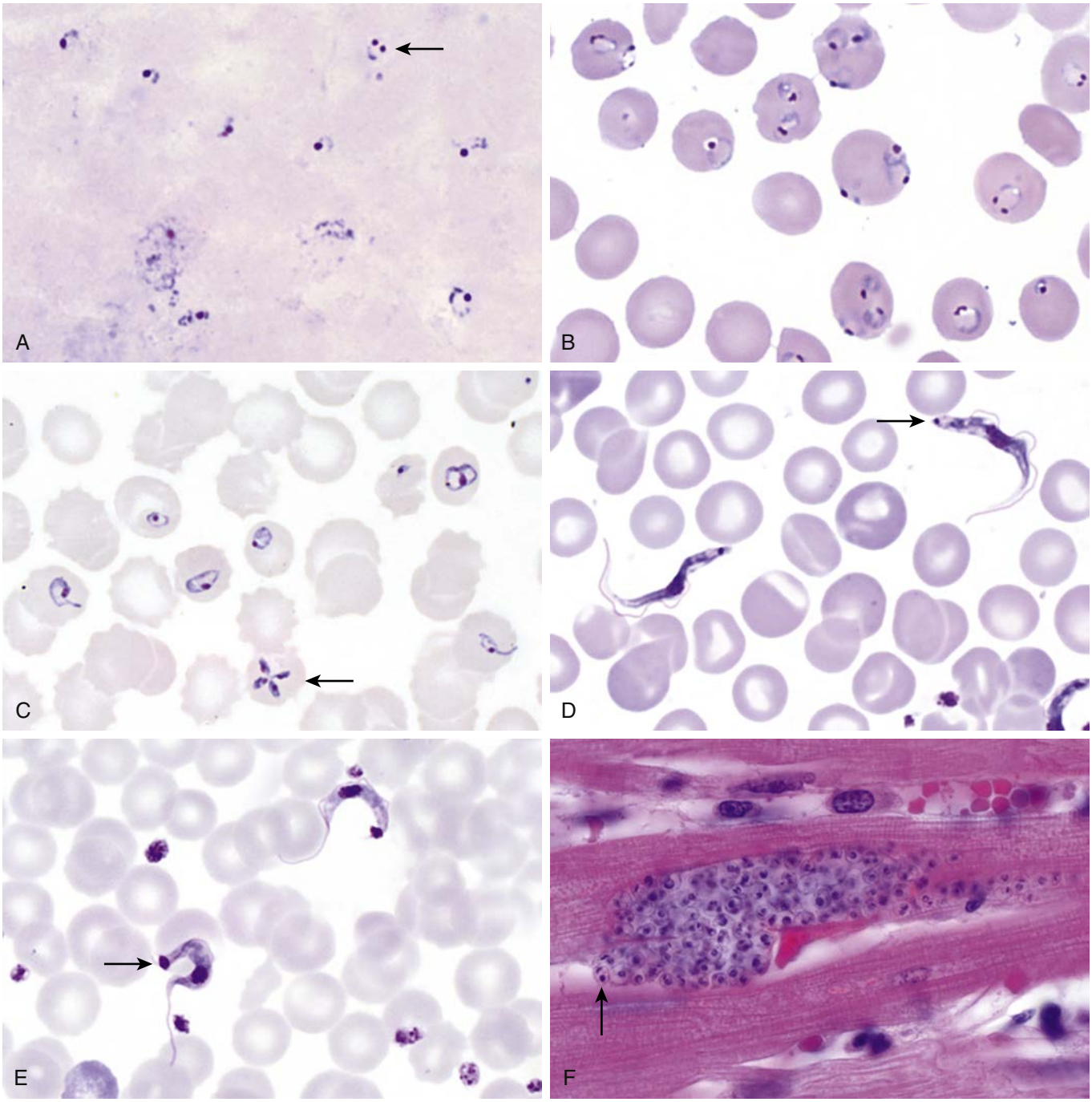

Figure 65.6 **A,** *Plasmodium falciparum* in Giemsa-stained thick blood film showing thin, delicate rings and a "headphone" form *(arrow)* (1000×). **B,** *Plasmodium falciparum* in Giemsa-stained thin blood film; note high parasitemia, multiply infected red blood cells, and delicate ring forms with appliqué and headphone forms (1000×). **C,** *Babesia microti* in Giemsa-stained thin blood film; note high parasitemia, multiply infected red blood cells with irregular forms, and Maltese cross configuration *(arrow)* (1000×). **D,** *Trypanosoma brucei* in thin blood film; note nucleus, small kinetoplast *(arrow)*, anterior flagellum, and undulating membrane (Giemsa stain; 1000×). **E,** *Trypanosoma cruzi* in thin blood film; note nucleus, large kinetoplast *(arrow)*, anterior flagellum, and undulating membrane (Giemsa stain; 1000×). **F,** *Trypanosoma cruzi* amastigotes in a cardiac biopsy; individual amastigotes with a small nucleus and rod-shaped kinetoplast *(arrow)* are visible (hematoxylin and eosin [H&E], 1000×).

Babesia parasites multiply in erythrocytes by binary fission, producing morphologically indistinguishable trophozoites and gametes. Although trophozoites of many species may be highly variable in size and shape, those of *B. microti* usually appear as delicate ring forms that may be easily confused with those of malarial parasites, especially *P. falciparum* (see Fig. 65.6C) (Westblade et al., 2017). *Babesia* can be differentiated from those of malarial parasites by the presence of a tetrad (Maltese cross) formation of the merozoites and the absence of large ameboid trophozoites and morphologically distinguishable gametocytes; extracellular forms may be seen in heavy infections. Also, *Babesia* species usually have a heterogeneous appearance with round, oval, spindled, and "racket" forms coexisting on the same peripheral blood smear. Finally, *Babesia*-infected cells lack hemozoin pigment, which is present in *Plasmodium*-infected cells. History of residence in or travel to endemic areas, or of a recent tick bite, might suggest *Babesia* infection. NAATs for *Babesia* species are available from the CDC on referral from state health departments and from some commercial laboratories. Serologic tests (e.g., IFA) may also be available but are generally not useful for detection of acute disease. However, they may be useful for screening blood donors in endemic settings. Serology tests for malaria are negative in babesiosis, although patients with malaria may cross-react in the *Babesia* serologies (Westblade et al., 2017; Pritt, 2019).

HEMOFLAGELLATES

The hemoflagellates of humans and animals are members of the group *Kinetoplastea* and are characterized by the presence of a kinetoplast, a complex of abundant circular DNA within a large mitochondrion, which can be seen by light microscopy when treated with Giemsa stain. Two genera

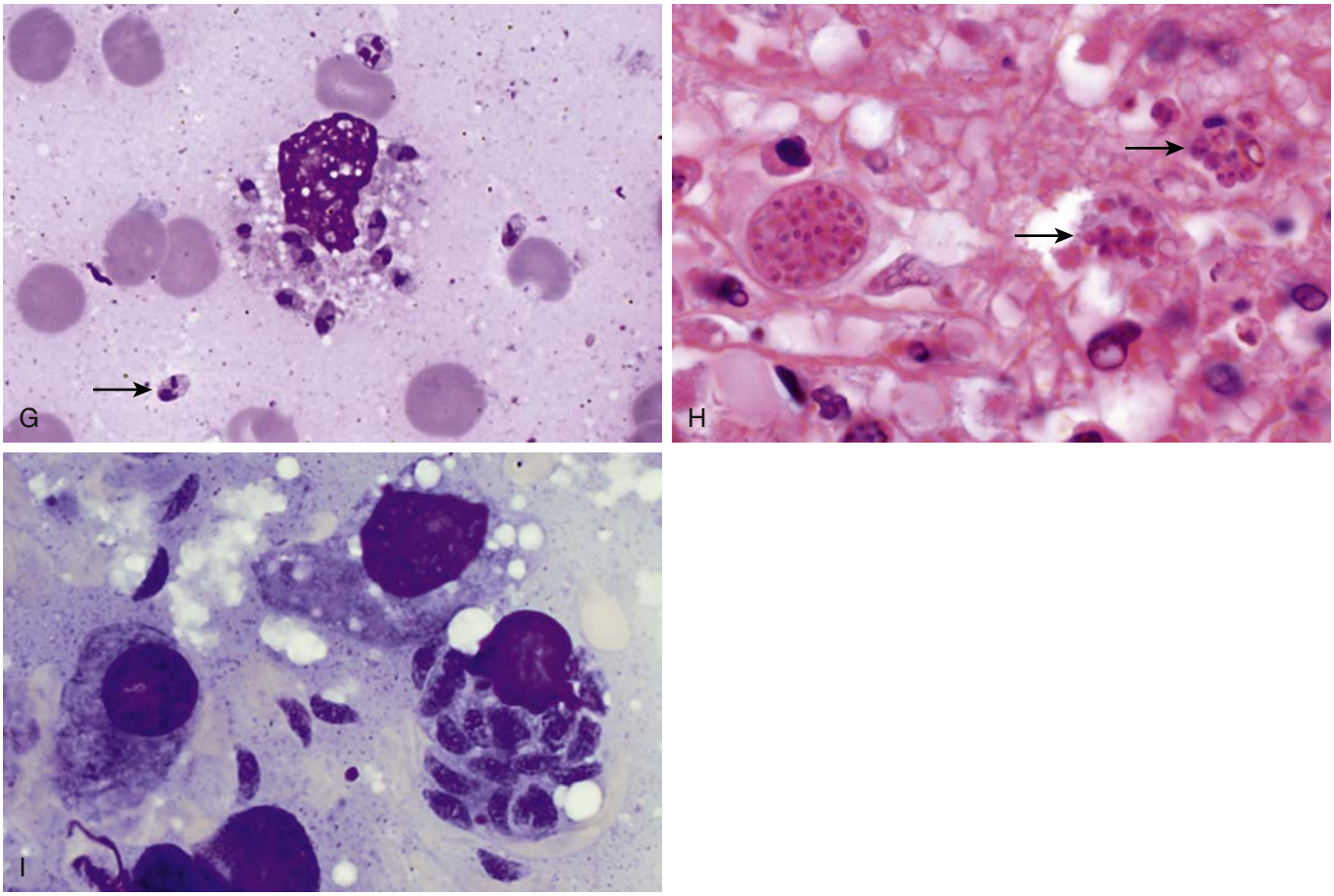

Figure 65.6—cont'd **G,** *Leishmania* sp. amastigotes in an impression smear of lymph node (Giemsa stain; 1000×). **H,** Pseudocyst *(left)* and free tachyzoites *(arrows)* of *Toxoplasma gondii* in brain tissue (H&E; 1000×). **I,** Intracellular and free *T. gondii* tachyzoites in an impression smear of brain tissue from an immunocompromised patient with reactivated disease (Giemsa; 1000×).

important in human disease are *Trypanosoma* and *Leishmania*. Members of both genera are transmitted by arthropod vectors and have animal hosts that serve as reservoirs.

Kinetoplastids assume different morphologic forms depending on their presence in vertebrate hosts, including humans, or in their insect vectors (Fig. 65.7). The amastigote stage is spherical, 2 to 5 μm in diameter, and displays a nucleus and kinetoplast. By definition, an external flagellum is lacking, although an axoneme (the intracellular portion of the flagellum) is apparent at the ultrastructural level. Amastigotes may be found in human or animal hosts infected with *T. cruzi* or *Leishmania* spp., where they multiply exclusively within cells, but not with *T. brucei*. The promastigote is an elongated and slender organism with a central nucleus, an anteriorly located kinetoplast and axoneme, and a free flagellum extending from the anterior end. This stage occurs in the insect vectors of *Leishmania* and is the stage detected in culture but is not detected in clinical specimens unless there is a substantial delay in processing. The epimastigote is similar to the promastigote, but the kinetoplast is found closer to the nucleus and has a small undulating membrane that becomes a free flagellum. All species of *Trypanosoma* that infect humans assume an epimastigote stage in the insect vector or in culture. Neither the promastigote nor epimastigote are seen in humans. In the trypomastigote, the kinetoplast is found at the posterior end and the flagellum forms an undulating membrane that extends the length of the cell, emerging as a free flagellum at the anterior end. Trypomastigote forms occur predominantly in the bloodstream of mammalian hosts infected with various *Trypanosoma* spp. Infectious stages found in appropriate insect vectors following transformation from the epimastigote form are known as *metacyclic trypomastigotes*.

Trypanosoma spp. (African and American Trypanosomiasis)

Infections with trypanosomes include those caused by *Trypanosoma brucei* (African trypanosomiasis) and *T. cruzi* (American trypanosomiasis, or Chagas disease). Both are of great importance in endemic areas. A third species, *Trypanosoma rangeli*, has been described in humans in the Americas but does not cause clinical illness. Bloodstream trypomastigotes of the *T. brucei* group (see Fig. 65.6D) are up to 30 μm long with graceful curves and a small kinetoplast. Those of *T. cruzi* are somewhat shorter (20 μm) and display a larger kinetoplast. Also, dividing forms may be seen in blood films with *T. brucei* but not *T. cruzi*, as the latter replicates only in the amastigote stage in the human host.

African Trypanosomiasis

In equatorial Africa, parasites of the *T. brucei* group infect both animals and humans and are transmitted by the bite of tsetse flies in the genus *Glossina*. Multiplication of organisms at the bite site often produces a transient chancre. East African trypanosomiasis is caused by *T. brucei rhodesiense*, which has a number of animal reservoir hosts. The disease is characterized by a rapidly progressive acute febrile illness with lymphadenopathy. Patients may die before central nervous system (CNS) involvement is prominent.

The infection in western Africa is caused by *T. brucei gambiense*, which is responsible for classic African sleeping sickness. The disease has a more chronic course that begins with intermittent fevers, night sweats, and malaise. Lymphadenopathy, especially of the posterior cervical lymph nodes (Winterbottom sign), may be pronounced. Involvement of the CNS becomes prominent with time. Somnolence, confusion, and fatigue progress, leading to stupor, coma, and eventual death. Humans are the primary reservoir for this disease (Bruckner & Labarca, 2019).

Treatment varies by stage of infection (hemolymphatic vs. late disease with CNS involvement) and is potentially toxic. The organoarsenic compound melarsoprol is the only drug available for treating *T. b. rhodesiense* late-stage disease and carries an associated 1% to 5% mortality rate (Drugs for Parasitic Infections, 2013; WHO, 2019). Consultation with the CDC or other public health experts is indicated in nonendemic settings.

The diagnosis is suspected on the basis of geographic history and clinical findings. Patients show high total IgM levels in blood and cerebrospinal fluid (CSF). Pleocytosis occurs with 50 to 500 mononuclear cells per microliter in CSF. The diagnosis is established by demonstrating the parasites on thick and thin films of peripheral blood, buffy coat preparations, or aspirates of lymph nodes or bone marrow, or in spun CSF that is stained with Giemsa (Bruckner & Labarca, 2019). Culture or animal inoculation may be helpful if it is available; a number of molecular methods have also been described.

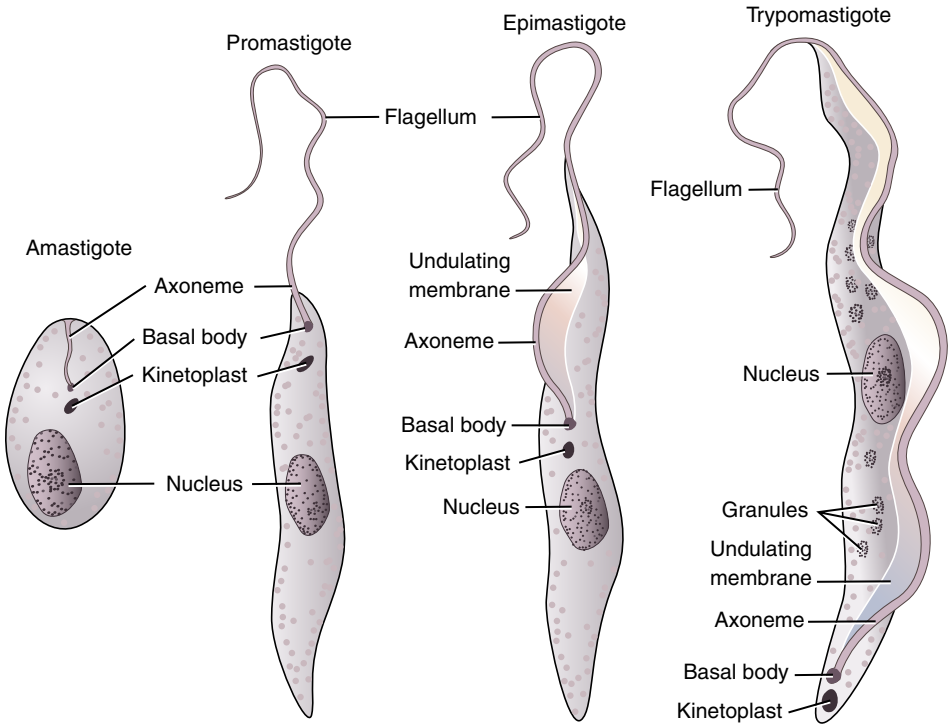

Figure 65.7 Morphology of hemoflagellates commonly infecting humans.

American Trypanosomiasis

American trypanosomiasis, or Chagas disease, is caused by *T. cruzi*. In its sylvatic form, the parasite occurs in the United States, Mexico, Central America, and most of South America. Human infections are common in parts of Mexico and Central and South America, where they are transmitted by kissing bugs in the family Reduviidae. In contrast, only rare cases of locally acquired Chagas have been documented in the United States. However, Chagas is now recognized as an important parasite in the United States due to the large number of immigrants that the country receives from endemic areas. As such, it has been designated as an NPI targeted for public health action (CDC, 2018b). The CDC and WHO estimate that more than 8 million individuals are infected worldwide and that greater than 300,000 infected individuals currently live in the United States (CDC, 2018b).

Genera and species of reduviid bugs involved in transmission vary from one country to another and among different ecologic niches. Some reduviids are responsible for maintaining the sylvatic cycle in animal reservoirs, whereas others are adapted to an anthropophilic life in which they infest poorly constructed houses, usually in rural areas. At the time of feeding, the reduviid bug defecates. The bug feces contain infective trypomastigotes that, as a result of scratching or rubbing, enter the body at the bite site or through intact mucosa of the mouth or conjunctiva. Infective forms actively enter nearby tissue cells, where they transform into dividing amastigotes. When the infected cell is filled with amastigotes, transformation to trypomastigotes occurs, followed by cell rupture. Trypomastigotes are released into the peripheral blood and reach distant tissues, where they transform into amastigotes and start the reproductive cycle de novo. Other important means of infection are vertical transmission, blood transfusion, organ transplantation from an infected donor, and, rarely, laboratory accident and through ingestion of contaminated food or drink (CDC, 2018b). Given the risk of transmission via blood transfusion, blood donor units are routinely screened in the United States for *T. cruzi* using FDA-approved serologic tests.

Chagas disease may cause acute or chronic infection. Acute disease is most common in children younger than 5 years of age and is characterized by malaise, chills, fever, hepatosplenomegaly, and myocarditis. Swelling of the tissues around the eye (Romaña sign) may be present if inoculation of the organisms occurs on the face. Swelling of tissues at other locations following the bite of an infected reduviid is called a *chagoma*. In older individuals, the acute course is milder and often asymptomatic, and the patient remains infected for life. Chronic manifestations of the infection, including megaesophagus, megacolon, and alterations in the conduction system of the heart, are related to destruction of the effector cells of the parasympathetic system by autoantibodies. Infection can be transmitted by blood transfusion, and quiescent infections may be exacerbated by immunosuppression.

Diagnosis of Chagas disease can be challenging. The trypomastigotes (Fig. 65.6E) can be observed in peripheral blood or CSF only during the acute stage of the disease or during reactivation. Amastigotes can also be identified in heart biopsies (Fig. 65.6 *F*), although this method is not commonly employed. Molecular diagnosis may be employed when morphologic diagnosis is inappropriate; examples of such clinical scenarios include (1) a person with a bug bite who has emigrated from or returned from an endemic area within 2 months, (2) monitoring organ transplant recipients after initial serologic testing, (3) laboratory accidents (e.g., accidental inoculation), and (4) suspected congenital cases. Often, more than one molecular assay is performed as different assays have different molecular targets (Qvarnstrom et al., 2012). Diagnosis of chronic Chagas disease is best achieved by antibody detection. Other clinical scenarios that may warrant antibody detection include (1) screening of blood and organ donors, (2) symptomatic patients with appropriate travel or exposure history, (3) initial transplant recipients with appropriate epidemiologic history or who received donated organs from an individual with appropriate epidemiologic history, and (4) possible congenital cases. No single serologic assay is sensitive and specific enough to be relied on alone. Therefore, per current recommended guidelines and the CDC, serologic confirmation of chronic *T. cruzi* infection requires reactivity on two tests using two different methodologies and/or two different *T. cruzi* antigen preparations. When results are discordant, a testing by a third assay is recommended to resolve the initial results or repeat testing on a new sample may be required. The CDC performs an ELISA (Chagatest, Wiener Laboratories, Rosario, Argentina) and a Trypomastigote-Excreted Secreted Antigen (TESA) immunoblot (LDT, CDC) for primary testing and an LDT immunofluorescence assay (IFA) for discordant results. A TESA blot can also be obtained commercially (BioMérieux, Rio de Janeiro, Brazil) (Bern et al., 2007; Afonso et al., 2012). In endemic areas, xenodiagnosis (examination of the gut contents of laboratory-raised reduviids that have been allowed to feed on a patient) may be used. In the chronic stage, serodiagnosis is the method of choice.

Management and treatment of Chagas disease is complex and varies with the age of the patient and stage of infection (CDC, 2018b; Drugs for Parasitic Infections, 2013). Antiparasitic therapy using nifurtimox or benznidazole is indicated for all cases of acute and reactivated disease and is also recommended for cases of chronic infection in children ≤18 years of age. Antiparasitic treatment is also strongly recommended for adults up to 50 years old with chronic disease in which advanced-stage cardiac involvement is not present. The potential benefits and risks of treatment for older individuals and those with advanced cardiomyopathy must be individually weighed prior to offering therapy (CDC, 2018b; Drugs for Parasitic Infections, 2013).

Leishmania spp. (leishmaniasis)

Leishmaniasis is a disease of the reticuloendothelial system caused by kinetoplastid protozoa of the genus *Leishmania*. All species that infect humans have animal reservoirs and are transmitted by sand flies belonging to the genera *Phlebotomus* in the Old World and *Lutzomyia* in the New World. The parasites assume the amastigote form in mammalian hosts and the promastigote form in insect vectors. Species of *Leishmania* cannot be differentiated by examination of amastigotes or promastigotes. Leishmaniasis may assume many different clinical forms; cutaneous, mucocutaneous, and visceral diseases are best known. The form and severity of disease vary with the infecting species, the particular host's immune status, and prior exposure (Bruckner & Labarca, 2019).

Cutaneous Leishmaniasis

Old World cutaneous leishmaniasis occurs in southern Europe, northern and eastern Africa, the Middle East, Iran, Afghanistan, India, and southern Russia. Infections are caused by *Leishmania tropica*, *Leishmania major*, and *Leishmania aethiopica*, although *L. donovani* and *Leishmania infantum* may also produce cutaneous lesions. The lesions of cutaneous leishmaniasis may be variable in appearance, with "wet," "dry," and warty appearances. Locally, they may be referred to by a variety of names such as oriental sore, Aleppo boil, desert boil, and Delhi boil. *Leishmania tropica* produces the "urban" dry ulcer, which is more long-lived than the "rural" wet ulcer of *L. major*. Ulcers caused by these species usually develop on an exposed area of the body and heal spontaneously. Infection produces long-lasting immunity. *L. tropica* may become viscerotropic, as was demonstrated in military personnel who participated in Operation Desert Storm (Magill et al., 1993). *Leishmania aethiopica* causes a more aggressive cutaneous infection, which in some individuals metastasizes to produce mucosal lesions or diffuse cutaneous leishmaniasis, the latter of which is characterized by multiple skin nodules resembling lepromatous leprosy.

Cutaneous leishmaniasis of the New World is caused by many species, including *Leishmania mexicana*, *Leishmania braziliensis*, *Leishmania amazonensis*, *Leishmania venezuelensis*, *Leishmania peruviana*, *Leishmania panamensis*, and *Leishmania guyanensis*, among others (Bruckner & Labarca, 2019). Lesions produced by *L. mexicana* often involve the earlobe (Chiclero ulcer), are self-limiting, and are not known to metastasize to the mucosa. However, *L. mexicana* and *L. amazonensis* may produce diffuse cutaneous lesions similar to those produced by *L. aethiopica*. A focus of cutaneous leishmaniasis exists in the southern part of Texas, where infections are caused by one or more species (McIlwee et al., 2018). *Leishmania peruviana*, which has been found on the western slopes of the Peruvian Andes, causes an infection called uta, a benign cutaneous lesion that occurs predominantly in children. *L. peruviana* is acquired in the home, where the main reservoirs are domestic dogs. This epidemiologic situation contrasts with other cutaneous leishmaniases, which usually are acquired in forests and have wild animals as reservoir hosts. Treatment of cutaneous leishmaniasis is based on the causative species and location and extent of disease. In endemic settings outside of the Americas, where there is no risk of mucosal dissemination, cosmetically unimportant lesions may be treated topically (e.g., cryotherapy) or allowed to self-heal. For individuals at risk of aggressive, disfiguring, or disseminated disease, systemic therapies with sodium stibogluconate, meglumine antimoniate, miltefosine, or paromomycin may be used (Drugs for Parasitic Infections, 2013). Topical paromomycin may also be used.

Mucocutaneous (Mucosal) Leishmaniasis

Mucocutaneous leishmaniasis (espundia) is caused primarily by *L. braziliensis* and species in the *Viannia* subgenus, which produce typical cutaneous lesions that generally are more aggressive, last longer, and often disseminate to mucous membranes, especially in the nasal, oral, or pharyngeal areas. In these locations, they may produce disfiguring lesions secondary to erosion of soft tissues and cartilage. *L braziliensis* is distributed in Mexico and Central and South America. Treatment is with sodium stibogluconate, meglumine antimoniate, amphotericin, or miltefosine (Drugs for Parasitic Infections, 2013).

Visceral Leishmaniasis

Visceral leishmaniasis of the Old World occurs sporadically over a wide geographic area and is caused by *L. donovani* or *L. infantum*. *L. donovani* predominates in Africa, India, and Asia, and *L. infantum* (syn. *L. chagasi*) occurs in the Mediterranean region, Middle East, Central Asia, and Central and South America. New World visceral leishmaniasis is caused by *L. chagasi* and occurs sporadically throughout Central and South America. On occasion, some species that cause cutaneous disease have been responsible for visceral disease, as demonstrated in some troops who participated in Operation Desert Storm (Magill et al., 1993). In some areas, humans may serve as the disease reservoir, although a variety of animals, including dogs and cats, usually assume this role.

The infection is usually benign and often subclinical, although some individuals, especially young children and malnourished individuals, have marked involvement of the viscera, especially liver, spleen, bone marrow, and lymph nodes. In some cases, death occurs after months to years unless it is treated appropriately. The infection is called *kala-azar* in India in reference to the darkening of the skin. Treatment is liposomal amphotericin B, sodium stibogluconate, meglumine antimoniate, miltefosine, amphotericin, or paromomycin (Drugs for Parasitic Infections, 2013). Visceral leishmaniasis is an opportunistic infection in individuals with concurrent human immunodeficiency virus (HIV); the condition responds poorly to therapy in such circumstances (Bruckner & Labarca, 2019).

Diagnosis of Leishmaniasis

The diagnosis usually is established by visualization of amastigotes in smears, imprints, or biopsies, or by growth of promastigotes in culture. In integumentary leishmaniasis, the border of the most active lesion should be biopsied and the fresh biopsy should be used to make imprints. The CDC provides instructions for specimen collection at https://www.cdc.gov/parasites/leishmaniasis/resources/pdf/cdc_diagnosis_guide_leishmaniasis_2016.pdf. Both the imprints and smears should be stained with Giemsa. Biopsies should be examined by histopathology and/or submitted for culture. Specimens that may be submitted when visceral leishmaniasis is suspected include buffy coat preparations, lymph node and bone marrow aspirates, spleen and liver biopsies, and antibody detection (Garcia, 2016).

A culture is desirable because it is more sensitive than microscopic examination and allows determination of the species or subspecies, a practice that may help in clinical management of the patient. Biopsy or aspirate specimens collected aseptically are cultured in Novy-MacNeal-Nicolle medium or in Schneider's *Drosophila* medium supplemented with fetal calf serum. Cultures usually begin to show promastigotes in 2 to 5 days but should be held for 4 weeks. The CDC provides culture collection kits after consultation and will perform culture and species identification using PCR and sequencing analysis (de Almeida et al., 2011).

Amastigotes found in imprints, smears, and tissue sections are recognized by their size (2–4 μm) and the presence of delicate cytoplasm, a nucleus, and a kinetoplast (see Fig. 65.6G). In tissue sections, they may appear smaller because of shrinkage during fixation. Amastigotes must be differentiated from other intracellular organisms, including yeast cells of *Histoplasma capsulatum* and trophozoites of *T. gondii*. *Leishmania* spp. have a kinetoplast and do not stain with Gomori methenamine silver (GMS) or periodic acid–Schiff (PAS). In contrast, *Histoplasma* lack the kinetoplast, and the cell wall stains with PAS and GMS. According to one study (Weigle et al., 1987), the sensitivity of histologic sections stained with hematoxylin and eosin (H&E) is 14%; imprints 19%, cultures 58%, and all methods combined, 67%. It should be noted that the amastigotes of *Leishmania* spp. and *T. cruzi* are morphologically indistinguishable.

TOXOPLASMA GONDII (TOXOPLASMOSIS)

Toxoplasma gondii is a protozoan parasite of the Apicomplexa clade that has a worldwide distribution in humans and in domestic and wild animals, especially carnivores. Infection in immunocompetent persons is generally asymptomatic or mild, but immunocompromised patients may experience serious complications. Infection in utero may result in serious congenital infection with sequelae or stillbirth (McAuley & Singh, 2019). The CDC estimates that more than 40 million individuals in the United States alone are infected with this parasite and have identified it as one of five NPIs targeted for public health action (CDC, 2018b).

The sexual stage in the life cycle of this coccidian parasite is completed in the intestinal epithelium of cats and other felines, which serve exclusively as definitive hosts. During this enteroepithelial cycle, asexual schizogony and sexual gametogony occur, leading to the development of immature oocysts that are passed in the feces. Oocysts mature to the infective stage (which contain two sporocysts with four sporozoites each) in the environment in 2 to 21 days. Ingestion of infective oocysts may lead to infection of a wide variety of susceptible vertebrate hosts in which actively growing trophozoites (tachyzoites) may infect any nucleated cells. Proliferation of tachyzoites results in cell death and injury to the host during acute infection. Once immunity has developed, the organisms form tissue cysts that may eventually contain hundreds or thousands of slowly growing bradyzoites. The presence of tissue cysts is characteristic of chronic infection. All stages of the life cycle occur in felines, but only trophozoite and cyst stages occur in humans and other intermediate hosts.

Humans acquire infection with *T. gondii* by ingestion of inadequately cooked meat, especially lamb or pork, that contains tissue cysts or by ingestion of infective oocysts from material contaminated by cat feces. Outbreaks have occurred from inhaling contaminated dust in an indoor riding stable (Teutch et al., 1979) and from drinking contaminated water or unpasteurized goat's milk (Benenson et al., 1982; Sacks et al., 1982; Bowie et al., 1997). Transmission via blood transfusion, organ transplantation, and transplacentally to the developing fetus also can occur.

Most acute infections are asymptomatic or mimic other infectious diseases in which fever and lymphadenopathy are prominent, such as infectious mononucleosis and acute HIV infection. Congenital infection may occur when the mother develops acute infection during gestation. The risk for infection to the neonate is unrelated to the presence or absence of symptoms in the mother, but severity of infection depends on the stage of gestation at which it is acquired. Intrauterine death, microcephaly, or hydrocephaly with intracranial calcifications may develop if infection is acquired in the first half of pregnancy. Infections in the second half of pregnancy are usually asymptomatic at birth, although fever, hepatosplenomegaly, and jaundice may appear. Chorioretinitis, psychomotor retardation, and convulsive disorders may appear months or years later (Montoya & Remington, 2008). Given the risks of congenital toxoplasmosis, expectant mothers are advised against handling cat feces (e.g., cleaning the cat litter box) if the cat spends times outdoors and eating undercooked meat.

In immunosuppressed individuals, especially those with acquired immunodeficiency syndrome (AIDS), infection with *T. gondii* usually manifests with CNS involvement. Other possible clinical and pathologic manifestations include pneumonitis, myocarditis, retinitis, pancreatitis, or orchitis (McAuley & Singh, 2019). Toxoplasmosis may be difficult to diagnose clinically and is often discovered at autopsy. These infections usually result from reactivation of a latent infection acquired months or years before but occasionally result from a primary infection. Treatment is based on numerous factors, including the immune status of the host and form of infection. Treatment is indicated for congenitally infected neonates and immunocompromised patients but not typically for acute infection in immunocompetent adults. Pyrimethamine is the standard therapy along with leucovorin to protect against bone marrow suppression (CDC, 2018b; Drugs for Parasitic Infections, 2013). Management during pregnancy varies with treatment center. Spiramycin may be administered to prevent spread to the fetus or when infection is diagnosed prior to 18 weeks' gestation; however, pyrimethamine, sulfadiazine, and leucovorin are recommended when infection of the fetus is suspected or when diagnosed at or after 18 weeks' gestation (CDC, 2018b; Drugs for Parasitic Infections, 2013).

Serology remains the primary approach in establishing a diagnosis of toxoplasmosis in immunocompetent hosts (Robert-Gangneux & Dardé, 2012; Wilson & Nutman, 2015; McAuley & Singh, 2019). The Sabin-Feldman dye test and the IFA test are standards against which other methods are compared, although the former is performed in only a few centers. EIA tests are commercially available and generally provide results similar to those of the IFA. Antibodies appear in 1 to 2 weeks, and titers peak at 6 to 8 weeks. Tests for IgM-specific antibodies are especially useful for diagnosis of congenital and acute infection, but knowledge of test limitations, specifically the occurrence of false-positive reactions, is extremely important. The persistence of IgM-specific antibodies, sometimes for 1 year or longer, also is problematic and must be interpreted in conjunction with IgG antibody results. Because many persons have had asymptomatic infection, low IgG titers have little significance. Titers in patients with chronic ocular infection may also be low. Immunocompromised patients, such as those with AIDS who have active *Toxoplasma* infection, almost always have preexisting specific IgG antibodies, although titers may be low and IgM antibodies are infrequently detected. As discussed in the Serologic Diagnosis section earlier in the chapter, IgG avidity testing may be useful for differentiating between acute and remote infection. Interpretation of IgG and IgM antibody titers varies by test method and by manufacturer. The laboratory performing the test should provide the necessary interpretive criteria (McAuley & Singh, 2019).

Diagnosis of toxoplasmosis may also be established by examination of tissues, blood, or body fluids (McAuley & Singh, 2019). Demonstration of tachyzoites or tissue cysts is definitive but may prove difficult to demonstrate in H&E-stained sections; fluorescence or immunohistochemical stains, if available, are useful. Giemsa is good for staining smears of body fluids and tissue imprints. Organisms may be demonstrated by inoculating appropriate material into tissue culture or uninfected mice, although this method is not widely available. Recovery in routine viral cultures also has been described but requires extended incubation. Isolation of organisms from blood or body fluid serves as evidence of acute infection, whereas recovery from tissues may reflect chronic infection. In smears, tachyzoites are crescent-shaped or oval, measuring approximately 3 × 7 μm; cysts measure up to 30 μm in diameter and are usually spherical, except in muscle fibers, where they appear elongate (McAuley & Singh, 2019) (see Figs. 65.6H and 65.6I).

In recent years, PCR has been increasingly used to detect toxoplasmic encephalitis, disseminated disease, and intrauterine infection. Testing is available from most reference laboratories, the CDC, and select research laboratories. PCR is now an important component of testing for pregnant women, neonates, and immunocompromised hosts (McAuley & Singh, 2019).

OPPORTUNISTIC FREE-LIVING AMEBAE

Amebae of the genera *Naegleria*, *Acanthamoeba*, and *Balamuthia* are inhabitants of soil, water, and other environmental substrates, where they feed on other microscopic organisms, especially bacteria and yeasts. All three genera have been associated with opportunistic infection of the CNS, and *Acanthamoeba* spp. can also cause keratitis (Visvesvara et al., 2007; Cope et al., 2019). There has also been a single report of *Paravahlkampfia francinae* being detected in the CSF of a patient with primary amebic meningoencephalitis (PAM) (Visvesvara, et al., 2009), and *Sappinia pedata* in a left temporal lobe brain biopsy in a patient with amebic encephalitis (Cope et al., 2019; Gelman et al., 2001; Qvarnstrom et al., 2009).

PAM, caused by the ameboflagellate *Naegleria fowleri*, typically affects children and young adults who have been swimming, jumping, or diving in warm freshwater lakes or pools, or people of any age by the improper use of nasal irrigation systems. The ameboflagellate enters the brain via the cribriform plate and olfactory bulbs and reaches the frontal lobes, where it produces an acute hemorrhagic meningoencephalitis that is usually fatal within 1 week of onset of symptoms. The disease has an extremely poor prognosis, despite vigorous therapeutic intervention, including induction of therapeutic coma. Drugs that have been used with limited success include amphotericin B, rifampin, fluconazole, azithromycin, and miltefosine (Drugs for Parasitic Infections, 2013). Antemortem diagnosis is made occasionally by identifying typical trophozoites in CSF on direct wet mounts, in stained preparations (Fig. 65.8A), or in culture. However, diagnosis is usually established at autopsy examination by the finding of trophozoites (only) in tissue sections (Fig. 65.8B). Trophozoites measure 10 to 35 μm; have a large, round, central karyosome; and if exposed to warm distilled water, convert to flagellated forms in 1 to 2 hours. Cysts are not seen in clinical specimens. Culture usually is performed on nonnutrient agar plates (1.5% agar, 0.5% sodium chloride, pH 6.6–7.0) seeded with a lawn of heat-killed or living *Escherichia coli* (Garcia, 2010, 2016). Amebae ingest the bacteria, leaving tracks in the bacterial lawn, which may be seen under low-power magnification using reduced light.

Granulomatous amebic meningoencephalitis (GAE) may be caused by several species of *Acanthamoeba*, including *A. castellani*, *A. culbertsoni*, *A. polyphaga*, and *A. astronyxis*, among others (Marciano-Cabral & Cabral, 2003). It is usually a subacute or chronic opportunistic infection of chronically ill, debilitated, and immunosuppressed individuals, leading to death weeks to months following onset of symptoms. Infection is thought to spread hematogenously from primary foci in skin, the pharynx, or the respiratory tract. Systemic infections occur in individuals with AIDS and may present as ulcerative skin lesions, subcutaneous abscesses, or erythematous nodules (Cope et al., 2019). Exposure to fresh water is not necessary because cysts of *Acanthamoeba* readily become airborne and may be recovered from the throat and nasal passages (Cope et al., 2019). The pathologic reaction in tissues is necrosis with acute inflammation. Despite the name of the disease, granulomas are not commonly seen but may be present in immunocompetent hosts. Trophozoites, and less commonly cysts, are seen within brain parenchyma, skin, and, rarely, lung sections. Organisms are commonly clustered around blood vessels, reflecting their hematogenous origin. Diagnosis usually is established at autopsy, but organisms may be recognized in brain biopsies or recovered using the culture technique described for *Naegleria*. Therapeutic drugs that have been used with some success are pentamidine, sulfadiazine, flucytosine, fluconazole, and miltefosine (Drugs for Parasitic Infections, 2013).

Acanthamoeba trophozoites are somewhat larger than *Naegleria*, measuring 15 to 45 μm, and display needlelike filamentous projections from the cell known as *acanthopodia*. Cysts measure 10 to 25 μm and are double-walled, displaying a wrinkled outer wall (ectocyst) and a polygonal, stellate, or round inner wall (endocyst). Identification to the species level is problematic and reflects uncertainty as to the validity of the 18 or more described species, although it is usually not required for clinical management. Currently, genotyping is the preferred approach used in differentiating types of *Acanthamoeba* (Marciano-Cabral & Cabral, 2003).

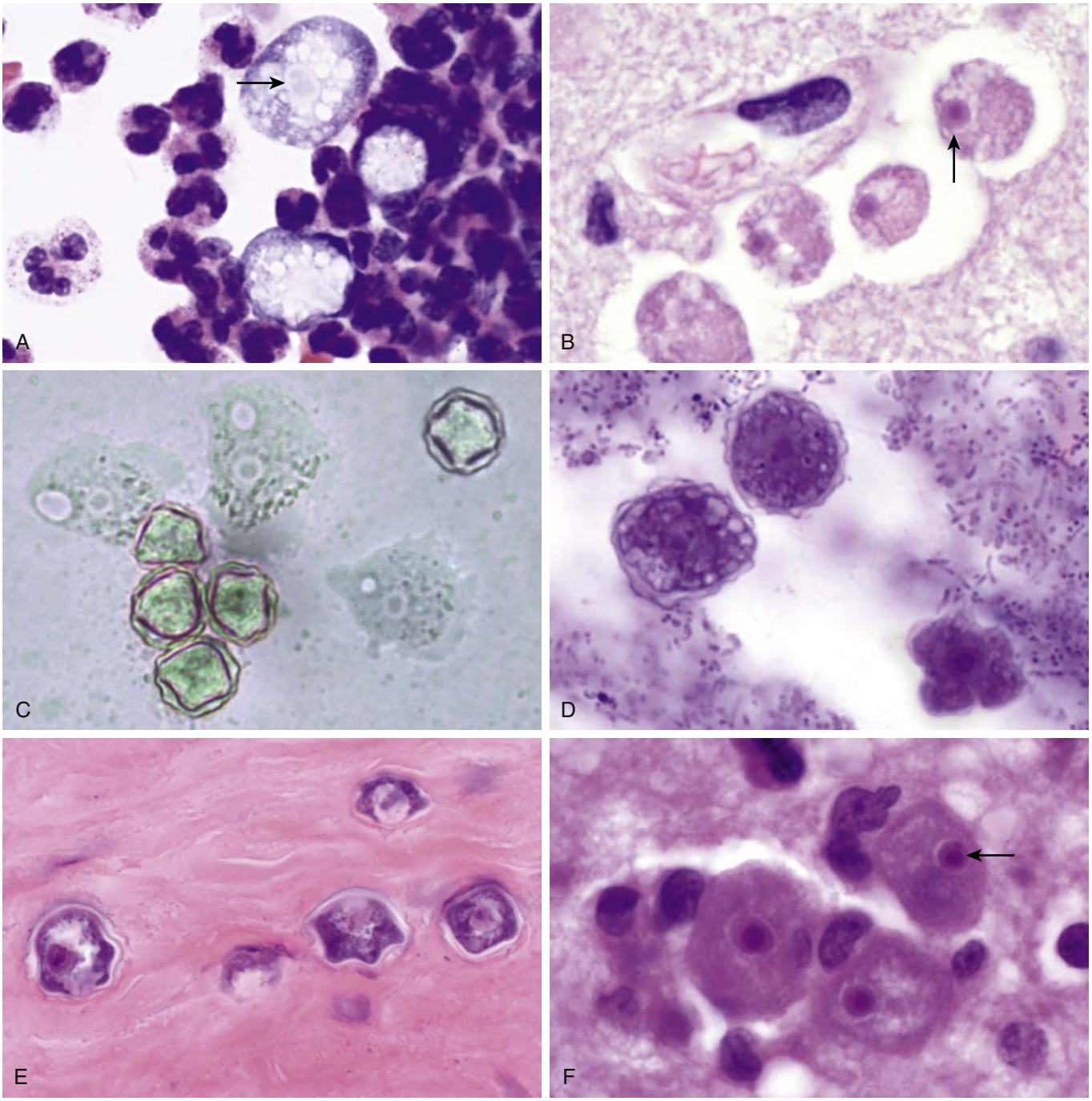

Figure 65.8 **A,** *Naegleria fowleri* trophozoites in the cerebrospinal fluid in a case of primary amebic meningoencephalitis (PAM). Note the pale nucleus with large karyosome *(arrow)* (Giemsa; 1000×). **B,** *Naegleria fowleri* trophozoites in an H&E-stained brain section in a case of PAM; note the small nucleus with large central karyosome *(arrow)* (1000×). **C,** *Acanthamoeba* sp. trophozoites and cysts on an agar culture (1000×). **D,** *Acanthamoeba* sp. cysts *(left)* and trophozoite *(right)* in contact lens fluid in a case of acanthamebic keratitis. There are abundant bacteria also present (H&E; 1000×). **E,** Double-walled cysts of *Acanthamoeba* sp. within corneal stroma (H&E; 1000×). **F,** Trophozoites in brain tissue in a case of *Balamuthia mandrillaris* granulomatous amebic encephalitis. The small nucleus with central large karyosome is highlighted *(arrow)* (H&E; 400×).

Immunofluorescence and immunoperoxidase techniques may prove useful in identifying and differentiating species and are available from the CDC (Cope et al., 2019).

GAE may also be caused by the leptomyxid ameba, *Balamuthia mandrillaris* (Cope et al., 2019). Treatment and prognosis are similar to GAE caused by *Acanthamoeba* spp. Morphologically, *Balamuthia* cannot be easily differentiated from *Acanthamoeba* by routine histology, although differences may be detected at the ultrastructural level. These organisms are antigenically distinct and may be identified using specific monoclonal or polyclonal antisera in DFA or immunoperoxidase assays (Cope et al., 2019). *Balamuthia* does not grow on agar plates used for *Naegleria* and *Acanthamoeba* but can be recovered in tissue culture using mammalian cell lines.

Acanthamoeba keratitis is an increasingly recognized painful infection of the cornea that is most likely to occur in persons who use daily-wear or extended-wear soft contact lenses or who have experienced trauma to the cornea. Incomplete or infrequent disinfection and use of homemade saline and multipurpose solutions are known risk factors for acquiring the infection (Cope et al., 2019). The disease is characterized by development of a paracentral ring infiltrate of the corneal stroma, which progresses to ulceration and possible perforation, with loss of the eye. The infection may be confused with fungal, bacterial, or herpetic keratitis but is characteristically refractory to commonly used antimicrobials. Optimal treatment varies based on the extent of disease, with topical biguanides and diamidines for uncomplicated disease (Clark et al., 2012; Drugs for Parasitic Infections, 2013). Keratoplasty is required in cases of extensive and refractory disease.

Diagnosis usually is established by demonstrating amebic trophozoites or cysts in corneal scrapings or biopsies (Fig. 65.8E). A variety of permanent stains can be used to highlight the organisms, including Giemsa, PAS, and trichrome. Use of the fluorochrome Calcofluor white is especially helpful in recognizing amebic cysts (Garcia, 2016). While cultures (described earlier, Fig. 65.8C) provide increased sensitivity over staining

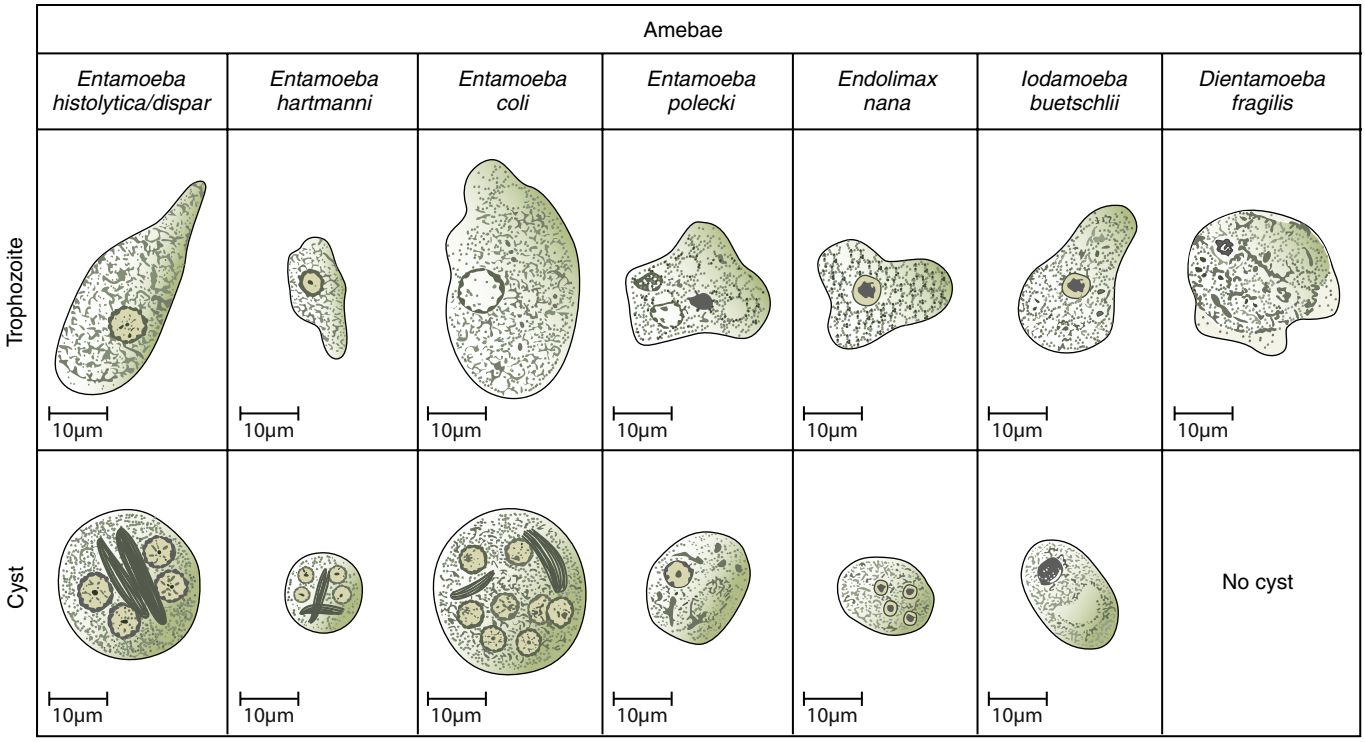

Figure 65.9 Amebae found in human stool specimens. (*Dientamoeba fragilis* is a flagellate but morphologically similar to amebae.)

methods and are often available from clinical laboratories, the sensitivity achieved by PCR may equal or exceed that of culture (Boggild et al., 2009).

INTESTINAL AND UROGENITAL PROTOZOA

Protozoa inhabiting the intestinal tract of humans include amebae, flagellates, ciliates, and coccidia, many of which are considered nonpathogens. Microsporidia also inhabit the human intestinal tract. They were historically grouped with the intestinal protozoa but are now known to be highly specialized fungi and are discussed elsewhere. Infection rates vary widely by population tested and the method employed. Most intestinal infections with protozoa are thought to be acquired by fecal-oral contamination directly from food handlers or indirectly via contaminated water.

For most laboratorians, identification of intestinal protozoa can be one of the more difficult aspects of parasitology. These organisms are small, and pathogenic species must be differentiated from nonpathogenic species and from inflammatory cells, epithelial cells, yeasts, pollen, and other confusing objects. Numerous characteristics assist in identifying intestinal protozoa. Motility patterns are classically described for many amebae, flagellates, and the ciliate *Balantioides coli,* but these are appreciated only when wet mount examination of fresh material is available. More importantly, features such as size, shape, and nuclear and cytoplasmic characteristics are used for identification in wet mounts of concentrated specimens and permanently stained preparations.

Size is an important feature (Figs. 65.9 and 65.10); thus, a properly calibrated ocular micrometer must be available for routine diagnostic use. Shape is also a helpful feature; flagellates generally are elongated and tapered, with a nucleus or nuclei at one end, whereas amebic trophozoites are rounded to oval with occasional pseudopod projections. Other important identifying morphologic features are the number and size of nuclei and the pattern of chromatin distribution, best seen in permanent stained preparations, and cytoplasmic structures such as fibrils in flagellates, ingested materials in amebic trophozoites, and glycogen masses and chromatoid bodies in amebic cysts.

During examination by any method, both nuclear and cytoplasmic characteristics should be assessed from a number of individual organisms to complete the identification. When reporting the presence of two or more species in a sample, the observer should be able to define distinct populations of organisms to prevent confusion with an occasional organism with an atypical appearance.

As mentioned in the previous section on Laboratory Methods, trophozoites typically predominate in liquid stool but degenerate within 30 minutes to 1 hour after passage unless the specimen is placed into a fixative. Cysts typically predominate in formed stool and are more resistant to degeneration. Formalin does not preserve trophozoites well; thus, parasites may be missed from formalin-based preparations unless permanent stained smears are also prepared and examined. Therefore, as mentioned previously, a complete stool examination should include examination of both a concentrated wet prep and permanently stained slide.

INTESTINAL AMEBAE

Three genera of amebae inhabit the intestinal tract of humans: *Entamoeba*, *Endolimax*, and *Iodamoeba*. Cysts are ingested and excyst in the small intestine. Resulting trophozoites proliferate by binary fission in the lumen of the colon. Both cysts and trophozoites may be passed in feces, but only mature cysts are infective. *Entamoeba histolytica* is the only ameba in which the trophozoites can invade tissues and cause clinical disease.

The genus *Entamoeba*, characterized by the presence of chromatin on the nuclear membrane, includes *E. histolytica*, the etiologic agent of amebiasis; *E. dispar*, a nonpathogenic species morphologically identical to *E. histolytica*; *E. hartmanni* and *E. coli*, two commensal species; and *Entamoeba polecki*, which is occasionally found in people who have contact with pigs or primates (Fig. 65.10) (Ash & Orihel, 2007). More recently, *E. moshkovskii* and *E. bangladeshi* have also been identified in human stool specimens and are morphologically indistinguishable from *E. histolytica*. Their potential pathogenicity is unknown at this writing. *Entamoeba gingivalis*, which does not have a known cyst stage, inhabits the oral cavity of people with poor oral hygiene (Ash & Orihel, 2007). *Entamoeba polecki* (Fig. 65.10F), *E. moshkovskii*, *E. bangladeshi*, and *E. gingivalis* are seen infrequently and are not described further. *Endolimax nana* and *I. buetschlii* are nonpathogenic species. *Dientamoeba fragilis* is recognized as a flagellate, although it lacks external flagella, and is discussed with the flagellates in the text but may be found with amebae in tables and figures because it is morphologically similar to them (Garcia, 2016).

Entamoeba histolytica (Amebiasis)

Most patients with *Entamoeba histolytica* infection are asymptomatic. However, *Entamoeba histolytica* may cause various clinical diseases, most commonly amebic dysentery, amebic colitis, and amebic liver abscesses (Meyers et al., 2013). General host defense mechanisms, previous contact with the parasite, diet, and the strain of *E. histolytica* may influence the severity of infection.

Amebic dysentery, which occurs infrequently in the United States, is an acute disease characterized by bloody diarrhea with abdominal pain and cramping. Trophozoite invasion of the intestinal mucosa occurs, producing ulceration that may lead to perforation and peritonitis. The more common form of disease seen in this country is amebic colitis, which may mimic

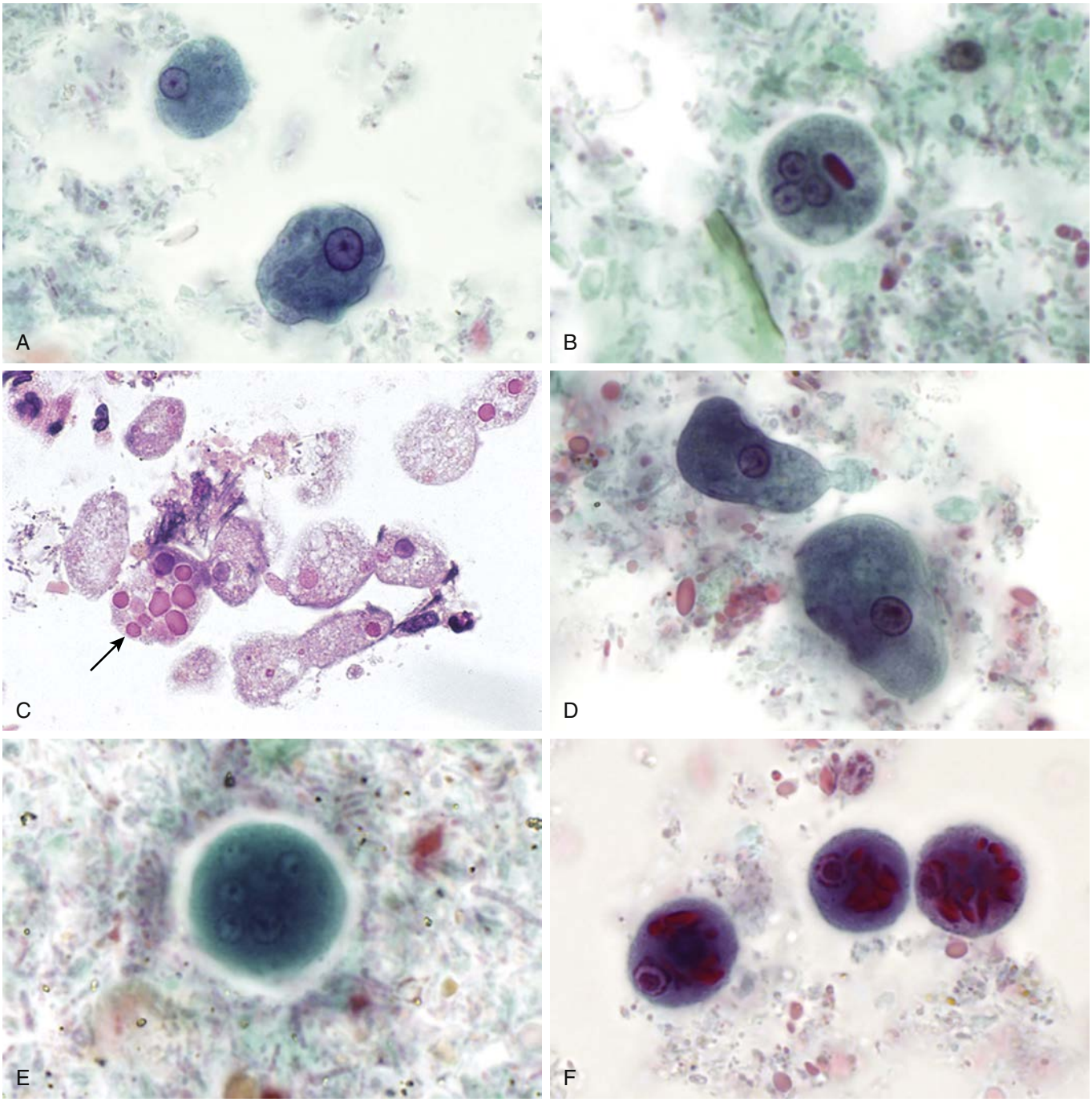

Figure 65.10 Intestinal protozoa, trichrome stain, oil immersion at 1000×, except as noted. **A,** Trophozoites of *Entamoeba histolytica/dispar*. **B,** Cyst of *E. histolytica/dispar* showing 3 of the 4 nuclei and a chromatoid bar with rounded ends. **C,** *E. histolytica* trophozoites with ingested red blood cells from a colonic lesion *(arrow)* (H&E). **D,** Trophozoites of *E. coli*. **E,** Cyst of *E. coli*. **F,** Cysts of *E. polecki* with numerous chromatoid bars.

Continued

ulcerative colitis and other forms of inflammatory bowel disease. Symptoms generally are less severe than in amebic dysentery but may include nonbloody diarrhea, constipation, abdominal cramping, and weight loss. Small, pinpoint mucosal ulcerations may develop and expand within the submucosa to form flask-shaped ulcers. All of the colon may be involved or only a portion, most commonly the cecum, rectosigmoid, or ascending colon. Less commonly, masses of granulomatous tissue, known as *amebomas*, may form in the intestine in response to the presence of amebae, producing a so-called *napkin ring lesion* that could be mistaken for a carcinoma (Meyers et al., 2013).

As *E. histolytica* trophozoites invade the intestinal wall, they may enter the bloodstream and disseminate via the portal blood supply to the liver and other organs. Amebic liver abscess (ALA) is the most common form of extraintestinal amebiasis, occurring in approximately 5% of patients with a history of intestinal amebiasis. Symptoms include fever and right upper quadrant pain. These liver abscesses are usually diagnosed by radiographic scans, ultrasound, and detection of parasite-specific host antibodies. It is important to note that *E. histolytica* cysts and/or trophozoites are present in the stool in less than half of patients at the time liver abscess is manifest; therefore, stool parasite examination is not a reliable means for diagnosis of infection. Rarely, amebic abscesses appear in other organs, such as the lung, brain, or skin, by hematogenous spread from the intestine or by contiguous spread from a liver abscess (e.g., across the diaphragm to the lungs). When the brain is involved, the trophozoites must be differentiated from those of the free-living amebae. This is usually accomplished by careful examination of the trophozoite morphology, associated host response, and clinical history. It is recommended that all patients with amebiasis be treated with suitable antiparasitic agents; asymptomatic individuals are treated with iodoquinol, paromomycin, or diloxanide furoate to eliminate the luminal stage of intestinal infection and prevent environmental shedding of infectious cysts (Drugs for Parasitic Infections, 2013). Patients with invasive or disseminated disease are first treated with metronidazole or tinidazole, both of which have good systemic penetration. This therapy should then be followed by either iodoquinol or paromomycin to eradicate any intestinal parasites (Drugs for Parasitic Infections, 2013).

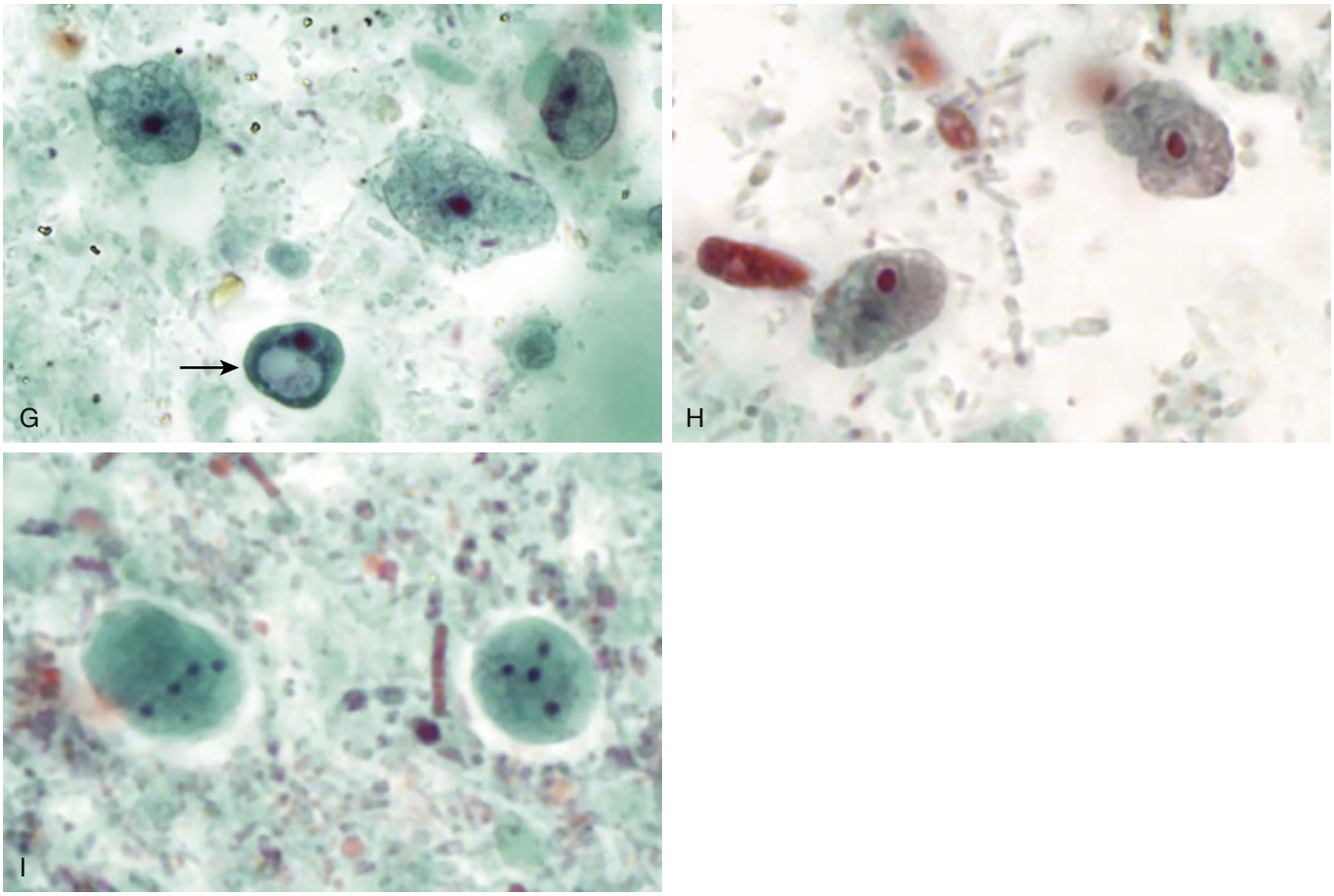

Figure 65.10—cont'd **G,** Trophozoites and cyst *(arrow)* of *Iodamoeba buetschlii*. The latter has a characteristic glycogen vacuole. **H,** Trophozoites of *Endolimax nana*. **I,** Cysts of *E. nana*.

Epidemiology

Most infections with *E. histolytica* are acquired by ingestion of contaminated food or water, although one historic outbreak was caused by a contaminated colonic irrigation machine (Istre et al., 1982). Infection may also be transmitted by oral-anal sexual activities (Pritt & Clark, 2008). Amebiasis is relatively uncommon in the United States, seen primarily in travelers and immigrants. In contrast, infection with the morphologically indistinguishable ameba, *E. dispar*, is thought to outnumber *E. histolytica* infection in the order of 9:1 (Pritt & Clark, 2008).

Diagnosis

Examination of a series of stool specimens should be sufficient for diagnosis of intestinal amebiasis in most cases, although differentiation of *E. histolytica* from *E. dispar*, *E. moshkovskii*, and *E. bangladeshi* requires additional molecular testing. The only exceptions to this are when ingested erythrocytes are seen within trophozoites in stool or trophozoites are observed in biopsy specimens or in extraintestinal sites since this is considered to be pathognomonic for invasive *E. histolytica* infection (Fig. 65.10C). If the patient has been given antibiotics or contrast media, the amebic infection may be masked for a period of time. Aspirated material from liver abscesses can be examined microscopically to detect trophozoites, although they are not commonly identifiable within the aspirated necrotic material. The last material aspirated is most likely to contain trophozoites and may be examined by direct microscopic examination or permanently stained slides. If tissue is available, sections may show organisms that stain prominently with PAS.

Culture procedures are not widely used for diagnosis but are useful for research. EIA antigen detection tests that are specific, sensitive, and able to differentiate *E. histolytica* from *E. dispar* are commercially available for stool specimens (see Table 65.4) (Garcia et al., 2018). Amplification techniques and DNA probes are also useful for differentiating *E. histolytica* from *E. dispar* (Qvarnstrom et al., 2005). At the time of this writing, there are three FDA-approved commercial molecular assays that can detect *E. histolytica*: (1) BioFire FilmArray Gastrointestinal GI Panel (BioMérieux, Marcy-l'Étoile, France), (2) BD MAX Enteric Parasite Panel (Becton Dickinson, Franklin Lakes, NJ), and (3) xTag Gastrointestinal Pathogen Panel (Luminex, Austin, TX). It is important to note that cross-reactivity with *E. dispar* may still occur with some molecular methods. The BioFire assay specifically mentions in its package insert that large numbers of *E. dispar* may result in a positive result for *E. histolytica*.

Unlike intestinal infection, ALA and other forms of disseminated disease are best detected by serologic testing. Approximately 95% of patients with ALA are seropositive; this decreases to 70% for patients with active intestinal infection and to 10% in asymptomatic carriers. Detectable titers may persist for months or years after successful treatment; as such, antibody detection cannot distinguish between past and present infection (Wilkins & Nutman, 2015).

Trophozoites of *E. histolytica* vary from 10 to 60 μm in diameter, with the nonpathogenic forms usually 15 to 20 μm and the invasive forms greater than 20 μm in greatest dimension (Table 65.8; see Figs. 65.9, 65.10A, and 65.10C) (Brooke, 1969). In direct wet mounts, trophozoites show progressive motility via rapidly formed hyaline pseudopodia that demonstrate a sharp demarcation between endoplasm and ectoplasm; unstained nuclei are not easily visible. In invasive disease, some trophozoites contain ingested erythrocytes (see Fig. 65.10C), a feature diagnostic of *E. histolytica* infection. In stained preparations, the peripheral nuclear chromatin is often evenly distributed along the nuclear membrane as fine granules. The karyosome is small and is often centrally located, with fine fibrils that generally are not visible, attaching it to the nuclear membrane. Variations in nuclear structure occur, with some karyosomes located eccentrically and peripheral chromatin irregularly distributed. As mentioned previously, the only characteristic that is pathognomonic for *E. histolytica* in stool is phagocytosis of erythrocytes. The cytoplasm is finely granular and, in cases of invasive disease, it is common to see only ingested erythrocytes. In contrast, the cytoplasm of noninvasive organisms may contain ingested bacteria or yeasts, which should not be mistaken for erythrocytes. In degenerating organisms, the cytoplasm may become vacuolated and nuclei may show abnormal chromatin clumping.

Cysts of *E. histolytica* are spherical and measure 10 to 20 μm (usually 12–15 μm) in diameter (Table 65.9; see Figs. 65.9 and 65.10B). The rounded precyst stage has a single nucleus but does not have a refractile cyst wall. As it matures, the cyst develops four nuclei, each approximately one-sixth the diameter of the cyst. Cyst nuclei appear similar to those of

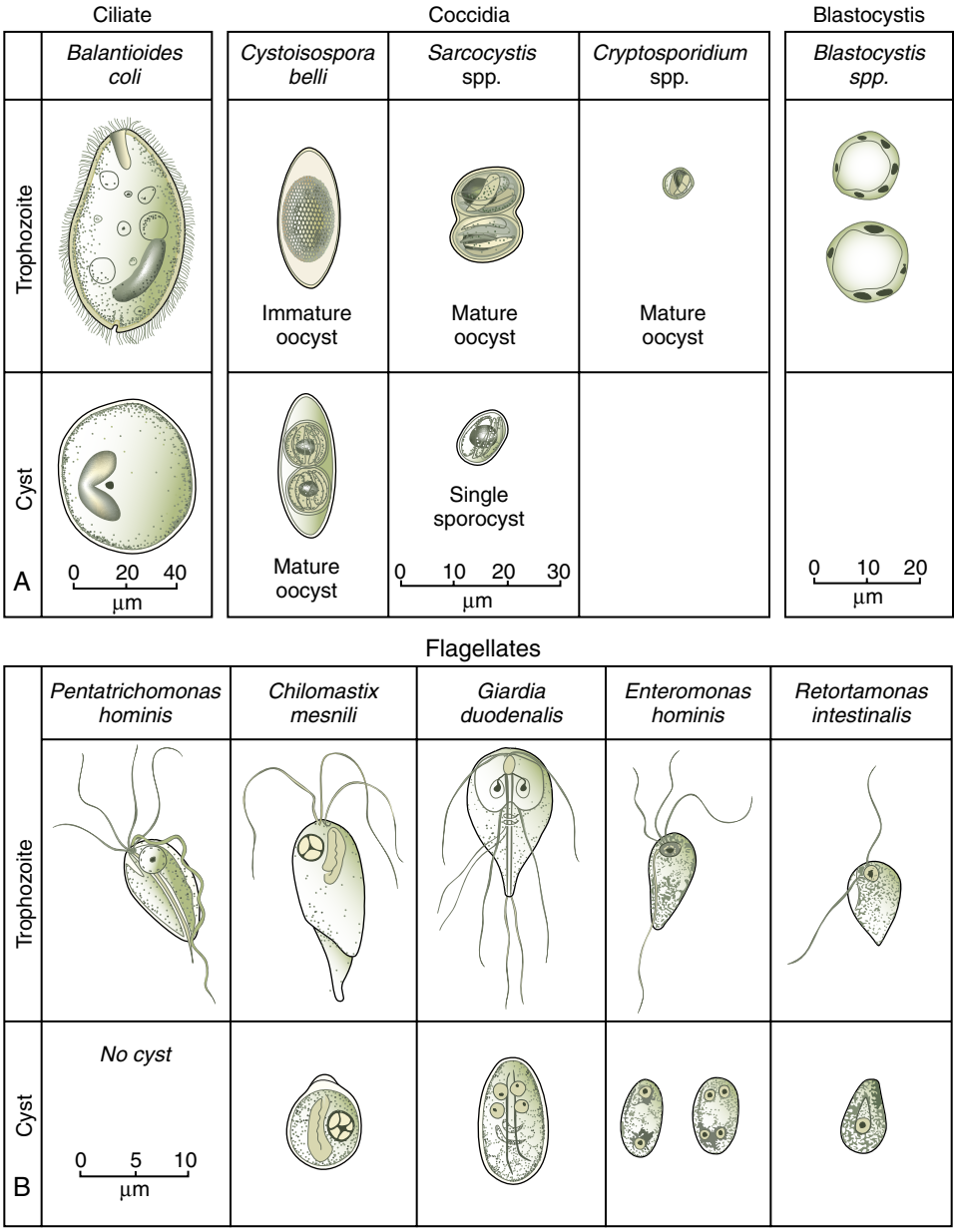

Figure 65.11 **A**, *Ciliate*, *Coccidia*, and *Blastocystis* spp. found in stool specimens of humans. **B**, Flagellates found in stool specimens of humans. (Modified from Brooke MM, Melvin DM: Morphology of diagnostic stages of intestinal parasites of man, Publication No. [CDC] 848116, Washington, DC, 1984, U.S. Department of Health and Human Services.)

trophozoites, but their smaller size makes them less useful as differentiating features. The cyst cytoplasm may contain glycogen vacuoles and chromatoid bodies with blunted or rounded ends. The number and size of nuclei and the appearance of chromatoid bodies are important diagnostic criteria for identifying cysts.

Those laboratories that do not use one of the immunologic or molecular methods to differentiate *E. histolytica* from *E. dispar* should report findings of *E. histolytica/E. dispar* or similar. A reporting comment may be added to suggest additional species-level testing if clinically indicated.

Nonpathogenic Amebae

Laboratory personnel must be able to differentiate nonpathogenic or commensal intestinal amebae from *E. histolytica/E. dispar* and *D. fragilis* (a flagellate), which are potential pathogens. Identification characteristics, best visualized in permanent stained sections, are summarized in Tables 65.8 and 65.9 and in Figures 65.9 and 65.10. Identification of trophozoites is based on size and nuclear and cytoplasmic characteristics; identification of cysts is based on size, number and characteristics of nuclei, and presence and character of chromatoid bodies and glycogen masses.

Entamoeba hartmanni has morphologic characteristics that are extremely similar to those of *E. histolytica* except that the trophozoites have a maximum diameter of 12 µm and cysts have a maximum diameter of 10 µm but are generally consistently less than 10 µm in diameter. Historically, *E. hartmanni* was called the *small race* of *E. histolytica* until it was recognized as a distinct species. Differentiation requires careful measurement of a representative sample of organisms with a properly calibrated ocular micrometer. The shrinkage of *E. histolytica/E. dispar* cysts and trophozoites in fixatives may result in an overreporting of *E. hartmanni*.

Entamoeba coli, a common lumen-dwelling ameba, may also be difficult to differentiate from *E. histolytica* given its morphologic similarities. In general, the cysts and trophozoites of *E. coli* are larger than those of *E. histolytica*, but significant size overlap exists and, therefore, size is not a reliable feature. The most definitive morphologic feature is the presence of 8 (or, rarely, 16) nuclei in mature cysts of *E. coli* compared with the usual 4 of *E. histolytica*, *E. dispar*, *and E. hartmanni.* Other helpful features are the characteristics of the cytoplasm. The cytoplasm of *E. coli* trophozoites stains somewhat more darkly than the cytoplasm of *E. histolytica* and is more vacuolated, containing numerous ingested bacteria, yeasts, and other materials. Chromatoid bodies, when present in *E. coli* cysts, are irregular in shape, with splintered or pointed ends rather than the rounded ends seen in *E. histolytica*. Although nuclear characteristics differ slightly from those of *E. histolytica* (see Figs. 65.10D and 65.10E), significant overlap may occur, especially in specimens that have not been promptly preserved. Therefore, distribution of peripheral chromatin and karyosomes should not be given great emphasis in identification of *Entamoeba* spp.

The nuclei of *I. buetschlii* trophozoites and cysts have a large, centrally located karyosome frequently surrounded by achromatic granules that may not be distinct but appear only as a muddy karyolymph space or halo. In

TABLE 65.8

Morphology of Trophozoites of Intestinal Amebae

Species	Size (in Diameter or Length)	Motility	Nucleus Number*	Peripheral Chromatin	Karyosomal Chromatin	Cytoplasm Appearance	Inclusions
Entamoeba histolytica/E. dispar	10–60 μm; usual range, 15–20 μm commensal form†; over 20 μm for invasive form‡	Progressive, with hyaline, fingerlike pseudopods	1 Not visible in unstained preparations	Fine granules; usually evenly distributed and uniform in size	Small, discrete; usually central but occasionally eccentric	Finely granular	Erythrocytes occasionally in invasive forms; noninvasive, contain bacteria
Entamoeba hartmanni	5–12 μm; usual range, 8–10 μm	Usually nonprogressive but may be progressive occasionally	1 Not visible in unstained preparations	Similar to *E. histolytica*	Small, discrete, often eccentric	Finely granular	Bacteria
Entamoeba coli	15–50 μm; usual range, 20-25 μm	Sluggish, nonprogressive with blunt pseudopods	1 Often visible in unstained preparation	Coarse granules, irregular in size and distribution	Large, discrete, usually eccentric	Coarse, often vacuolated	Bacteria, yeasts, or other materials
Endolimax nana	6–12 μm; usual range, 8–10 μm	Sluggish, usually nonprogressive with blunt pseudopods	1 Visible occasionally in unstained preparations	None	Large, irregularly shaped	Granular, vacuolated	Bacteria
Iodamoeba buetschlii	8–20 μm; usual range, 12–15 μm	Sluggish, usually nonprogressive	1 Not usually visible in unstained preparations	None	Large, usually central; surrounded by refractile, achromatic granules; these granules often are not distinct even in stained slides	Coarsely granular, vacuolated	Bacteria, yeasts, or other materials
Dientamoeba fragilis			2 (In approximately 20% of organisms, only 1 nucleus is present) Nuclei invisible in unstained preparations	None	Large cluster of 4–8 granules	Finely granular, vacuolated	Bacteria

Modified from Brooke MM, Melvin DM: *Morphology of diagnostic stages of intestinal parasites of man*, PHS Publication No. 1966, Bethesda, MD, 1969, U.S. Department of Health, Education, and Welfare.
*Visibility is for unfixed material. Nuclei sometimes may be visible in fixed material.
†Usually found in asymptomatic or chronic cases; may contain bacteria.
‡Usually found in acute cases; often contain red blood cells.

some nuclei, the halo is clear without evident achromatic granules, making the organism indistinguishable from *E. nana*. Cysts of *I. buetschlii* contain a single nucleus, in which the karyosome is often eccentric with a nearby crescent of achromatic granules (Fig. 65.10G). The cyst is characterized by a prominent vacuole of glycogen (Fig. 65.10G) that stains reddish brown in iodine-stained wet mounts. Glycogen is dissolved by aqueous fixatives and may not be demonstrable in material that has been stored.

Endolimax nana is the smallest ameba to infect humans. Trophozoites often have atypical nuclei that contain a triangular chromatin mass, a band of chromatin across the nucleus, or two discrete masses of chromatin on opposite sides of the nuclear membrane (Fig. 65.10H). A clear halo or karyolymph space surrounds the karyosome and extends to the nuclear membrane. Atypical nuclear forms may be helpful in differentiating *E. nana* from *I. buetschlii*, which is similar in appearance but larger. Cysts of *Endolimax* (Fig. 65.10I) usually contain four nuclei, although smaller numbers may be seen. Glycogen, when present, occurs diffusely in the cytoplasm rather than as a discrete mass.

BLASTOCYSTIS SPP.

Blastocystis is an enigmatic protozoan that inhabits the large bowel and is frequently found in stool specimens of asymptomatic individuals. Although appearing in stains as an ameba-like protozoan, it is now known to be a *Stramenopile* (a group that includes diatoms and algae) and is placed in the Stramenopiles-Alveolata-Rhizaria (SAR) clade (Adl et al., 2012, 2019). Traditionally, *Blastocystis* spp. have been described based on host data (*B. hominis* from humans, *B. ratti* from rats, etc.) and historically all isolates of humans were referred to as *B. hominis*. However, molecular analyses appear to demonstrate that there is no population unique to humans and all human isolates appear to have animal reservoirs. Nine (possibly 10) primary subtypes have been found in mammals and birds, with subtypes 1 and 3 making up most of the cases of human blastocystosis. It is becoming more common for clinical laboratories to report *Blastocystis* only at the genus level (Stensvold et al., 2007). Some studies have linked heavy infection to symptomatic intestinal disease, although this remains controversial (Coyle et al., 2012). Treatment options include metronidazole, trimethoprim/sulfamethoxazole, iodoquinol, and nitazoxanide (Drugs for Parasitic Infections, 2013).

Traditionally, the forms in human stool were referred to as cyst-like forms; however, those are not believed to be one of the different vaculoar forms seen in stool specimens (Fig. 65.12G). Occasionally, these forms may be seen dividing on stained slides. Because the morphologic separation of the various stages is not as clear-cut as with other protozoa, it is not common to identify and/or report the stages of *Blastocystis*. The forms in stool can vary greatly in size, from 5 to 40 μm in diameter. Characteristically, stool forms contain a large central body (similar to a vacuole) surrounded by a thin rim of cytoplasm that contains nuclei and other organelles. In a properly preserved specimen stained with trichrome, the central body is usually green while the surrounding organelles stain red (Fig. 65.12G). *Blastocystis* should be reported and quantified when present, especially when they are numerous (five or more per 1000× field), since quantity may correlate with clinical presentation (Garcia, 2016). This is the only protozoan parasite (and the only intestinal parasite in the United States) in which the quantity is routinely reported.

FLAGELLATES

Dientamoeba fragilis

Dientamoeba fragilis is an ameboid-appearing protozoan that infects the colon and has been associated with diarrheal disease, especially in young

TABLE 65.9

Morphology of Cysts of Intestinal Amebae

Species	Size	Shape	Nucleus Number	Peripheral Chromatin	Karyosomal Chromatin	Cytoplasm Chromatoid Bodies	Glycogen
Entamoeba histolytica/E. dispar	10–20 μm; usual range, 12–15 μm	Usually spherical	4 in mature cyst; immature cysts with 1 or 2 occasionally seen	Peripheral chromatin present; fine, uniform granules, evenly distributed	Small, discrete, usually central	Present; elongate bars with bluntly rounded ends	Usually diffuse; concentrated mass often present in young cysts; stains reddish brown with iodine
Entamoeba hartmanni	5–10 μm; usual range, 6–8 μm	Usually spherical	4 in mature cyst; Immature cysts with 1 or 2 often seen	Similar to *E. histolytica*	Similar to *E. histolytica*	Present; elongate bars with bluntly rounded ends	Similar to *E. histolytica*
Entamoeba coli	10–35 μm; usual range, 15–25 μm	Usually spherical; occasionally oval, triangular, or of another shape	8 in mature cyst; occasionally supernucleate cysts with 16 or more are seen; immature cysts with 2 or more occasionally seen	Peripheral chromatin present; coarse granules irregular in size and distribution, but often appear more uniform than in trophozoites	Large, discrete, usually eccentric, but occasionally central	Present; usually splinterlike with pointed ends	Usually diffuse, but occasionally well-defined mass in immature cysts; stains reddish brown with iodine
Endolimax nana	5–10 μm; usual range, 6–8 μm	Spherical, ovoid, or ellipsoidal	4 in mature cysts; immature cysts with fewer than 4 rarely seen	None	Large, usually centrally located	Occasionally, granules or small oval masses seen, but bodies as seen in *Entamoeba* spp. are not present	Usually diffuse; concentrated mass seen occasionally in young cysts; stains reddish brown with iodine
Iodamoeba buetschlii	5–20 μm; usual range, 10–12 μm	Ovoid, ellipsoidal, triangular, or of another shape	1 in mature cyst	None	Large, usually eccentric; refractile, achromatic granules on one side of karyosome	Granules occasionally present, but bodies as seen in *Entamoeba* spp. are not present	Compact, well-defined mass; stains dark brown with iodine

Modified from Brooke MM, Melvin DM: *Morphology of diagnostic stages of intestinal parasites of man*, PHS Publication No. 1966, Bethesda, MD, 1969, U.S. Department of Health, Education, and Welfare.

children (Stark et al., 2016). Although similar in appearance to amebae, *Dientamoeba* is considered a flagellate on the basis of ultrastructural details and antigenic and molecular similarities. Because of the similarity of *Dientamoeba* to amebae at the light microscope level, this species has traditionally been included in figures and diagnostic algorithms for amebae (Figs. 65.11 and 65.12 *F*).

Symptoms of *D. fragilis* infection include diarrhea and abdominal distention. Recent evidence suggests that dientamoebiasis is a more frequent cause of diarrhea than previously thought: 4.3% of patients in one study harbored this organism (Stark et al. 2016). Approximately 25% of persons infected with this parasite have been reported to have symptomatic disease; however, the exact role of *D. fragilis* in symptom causation is uncertain. Treatment options include paromomycin, iodoquinol, or metronidazole (Drugs for Parasitic Infections, 2013). *Dientamoeba fragilis* infection may be overlooked unless permanently stained slides are examined. Multiple specimens may need to be submitted because shedding varies from day to day. Commonly, organisms contain two nuclei that consist of a cluster of four to eight karyosomal granules, which may appear as one large irregular karyosome (see Fig. 65.12F). Uninucleate *D. fragilis* may be confused with trophozoites of *E. nana* or *I. buetschlii*. The cytoplasm is finely granular and often contains ingested bacteria and yeast. Classically, *D. fragilis* was not thought to have a cyst stage. Cyst forms have recently been described (Stark et al., 2014), although this has not gained wide acceptance in the protozoology community. Molecular phylogenetic analyses place *Dientamoeba fragilis* within the clade Trichomonadida, none of which are known to be cyst producers (Adl et al., 2018; Adl & Mathison, 2019).

Giardia duodenalis

Giardia duodenalis, historically known as *G. intestinalis* or *G. lamblia*, is a pathogenic intestinal protozoan that causes both endemic and epidemic disease worldwide. In the United States, it is especially problematic for travelers, campers, children attending day care, and homosexual men. It frequently causes disease in individuals drinking contaminated water, and a number of large water-borne outbreaks have been described (Cama & Mathison, 2015). Pathogenic protozoa are not always killed by the usual concentrations of chlorine in municipal water supplies. Therefore, unless the water supply is filtered, it may serve as a source of infection, as it did in the Rome, New York, outbreak (Craun, 1986).

Giardia duodenalis trophozoites multiply in the small bowel and attach to the mucosa by a ventral concave sucking disk. Infection may be asymptomatic or may cause disease ranging from mild diarrhea with vague abdominal complaints to a malabsorption syndrome with diarrhea and steatorrhea, similar to that of celiac disease (also known as *celiac sprue* and *gluten-sensitive enteropathy*). The pathogenesis is not fully understood, although disruption of the integrity of the brush border with resulting disaccharidase deficiency may occur from direct or indirect effects of the organism's presence (Meyers et al., 2013). Giardiasis should be considered in any patient presenting with diarrhea of longer than 10 days' duration. The drugs of choice for giardiasis are tinidazole, metronidazole, or nitazoxanide (Drugs for Parasitic Infections, 2013).

Diagnosis is commonly established by demonstration of *Giardia* trophozoites or cysts, or both, in fecal specimens, although antigen tests and NAATs provide increased sensitivity (see following discussion). Trophozoites predominate in diarrheic stool, whereas infectious cysts are more likely to be found in formed stool. The passage of organisms varies from day to day; therefore, examination of multiple specimens, collected on different days, may be necessary. Direct wet mounts may demonstrate the characteristic "falling leaf" motility of trophozoites in diarrheic or duodenal aspirate specimens. Both cysts and trophozoites can be seen in wet mounts and permanently stained slides. Historically, small bowel aspirates or so-called string tests (Enterotest) were used to provide increased sensitivity but are uncommonly used today.

Many antigen detection methods based on DFA or EIA are commercially available (see Table 65.4) and provide increased sensitivity for detection of *G. duodenalis* in stool specimens over routine O&P testing (Cama & Mathison, 2015). Antigen detection methods may be particularly useful for patients with diarrhea who have not traveled outside of the United States since they may be used in place of the labor-intensive and subjective O&P examination, often in combination with an antigen test for *Cryptosporidium*

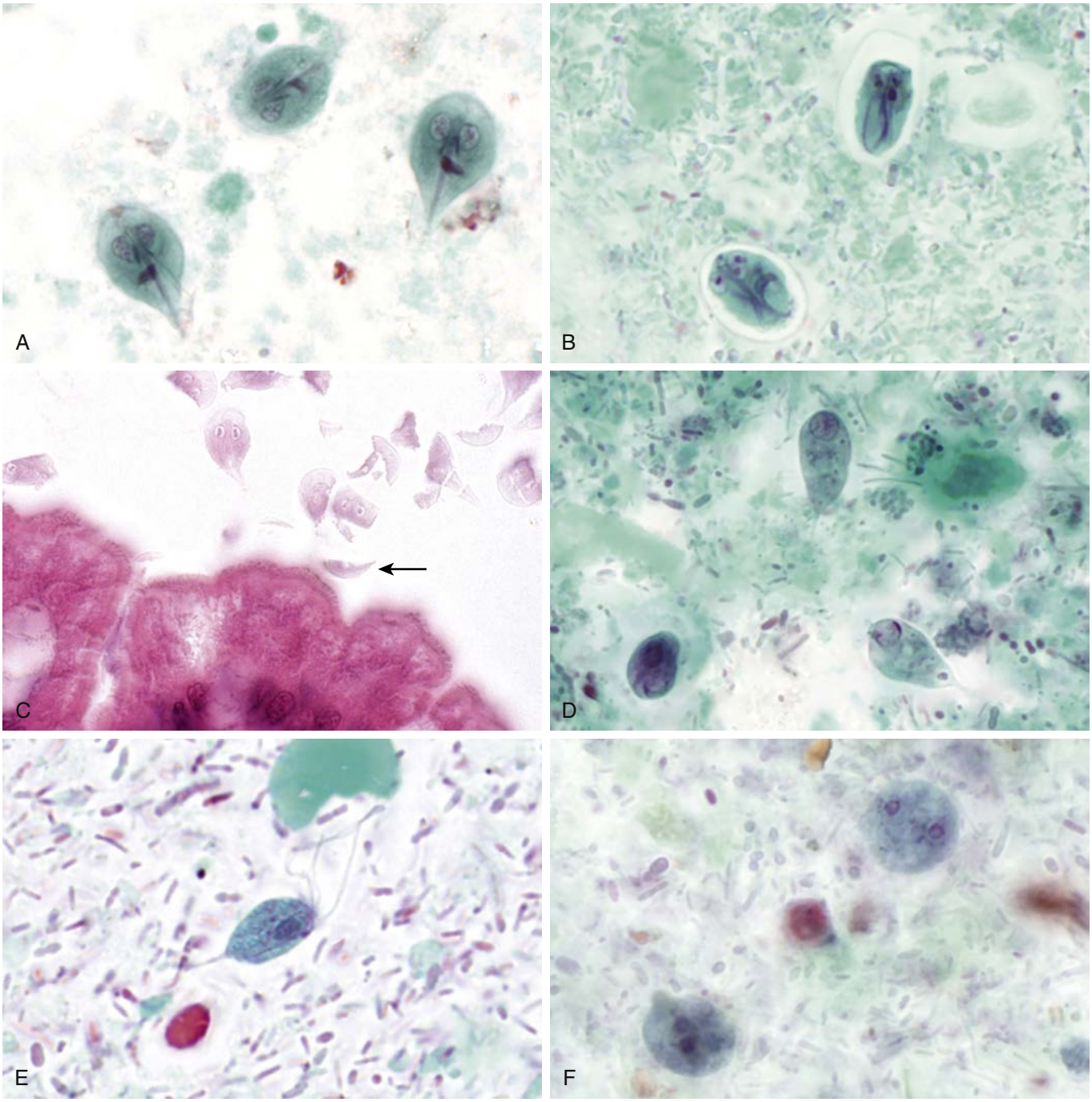

Figure 65.12 Intestinal protozoa, trichrome stain, oil immersion at 1000×, except as noted. **A,** Trophozoites of *Giardia duodenalis*. **B,** Cysts of *G. duodenalis*. **C,** Duodenal biopsy demonstrating multiple *G. duodenalis* trophozoites seen ventrally and laterally *(arrow)* (H&E). **D,** A lemon-shaped cyst of *Chilomastix mesnili (bottom left)* with visible nucleus and hyaline cap, and 2 *C. mesnili* trophozoites *(right)*. **E,** Trophozoite of *Pentatrichomonas hominis*. **F,** Trophozoites of *Dientamoeba fragilis*.

spp. However, they cannot replace the need for traditional morphologic examination of the specimen if other pathogenic intestinal parasites such as helminths are suspected. Also, use of an antigen detection method does not preclude the need for testing multiple separate stool specimens for sensitive detection of *G. duodenalis* (Hanson & Cartwright, 2001).

At the time of this writing, there are three FDA-approved multiplex NAATs that can detect *G. duodenalis* (see earlier Amebiasis section). All are components of multiplex NAATs that detect multiple bacterial, viral, and parasitic causes of diarrhea.

Giardia trophozoites are pear-shaped with a tapered posterior end, and possess a large sucking disc, two nuclei, and curved median bodies that give the appearance of a smiling face with two prominent eyes (Table 65.10; see Figs. 65.11, 65.12A, and 65.12C). When viewed from the side, the anterior end of the organism is thicker and tapers posteriorly; the anterior half to three-quarters consists of the sucking disk on the ventral surface (Fig. 65.12C). The four lateral, two ventral, and two caudal flagella are not usually evident in wet mounts or in stained preparations but are highlighted well using Giemsa-based stains. Cysts are oval and usually quadrinucleate when mature. Below the nuclei are dark-staining curved median bodies that cross the longitudinal fibrils (called *axonemes*), providing the appearance of a smiling mouth. The cytoplasm is sometimes retracted from the cyst wall.

Chilomastix mesnili

Chilomastix mesnili (see Table 65.10, Figs. 65.11, 65.12D, and 65.12E) is a nonpathogenic lumen-dwelling flagellate of humans that must be differentiated from trophozoites of amebae and *Giardia* in stained smears. The consistent location of the single nucleus at one end of the organism and the tapering of the end opposite the nucleus are helpful identifying features. If multiple organisms are examined, the cytostome and the spiral groove are commonly visible in some. The three external flagella usually are not visible in stained or formalin-fixed preparations. The lemon-shaped cysts contain a single nucleus and various curved cytostomal fibers with a safety pin–like appearance.

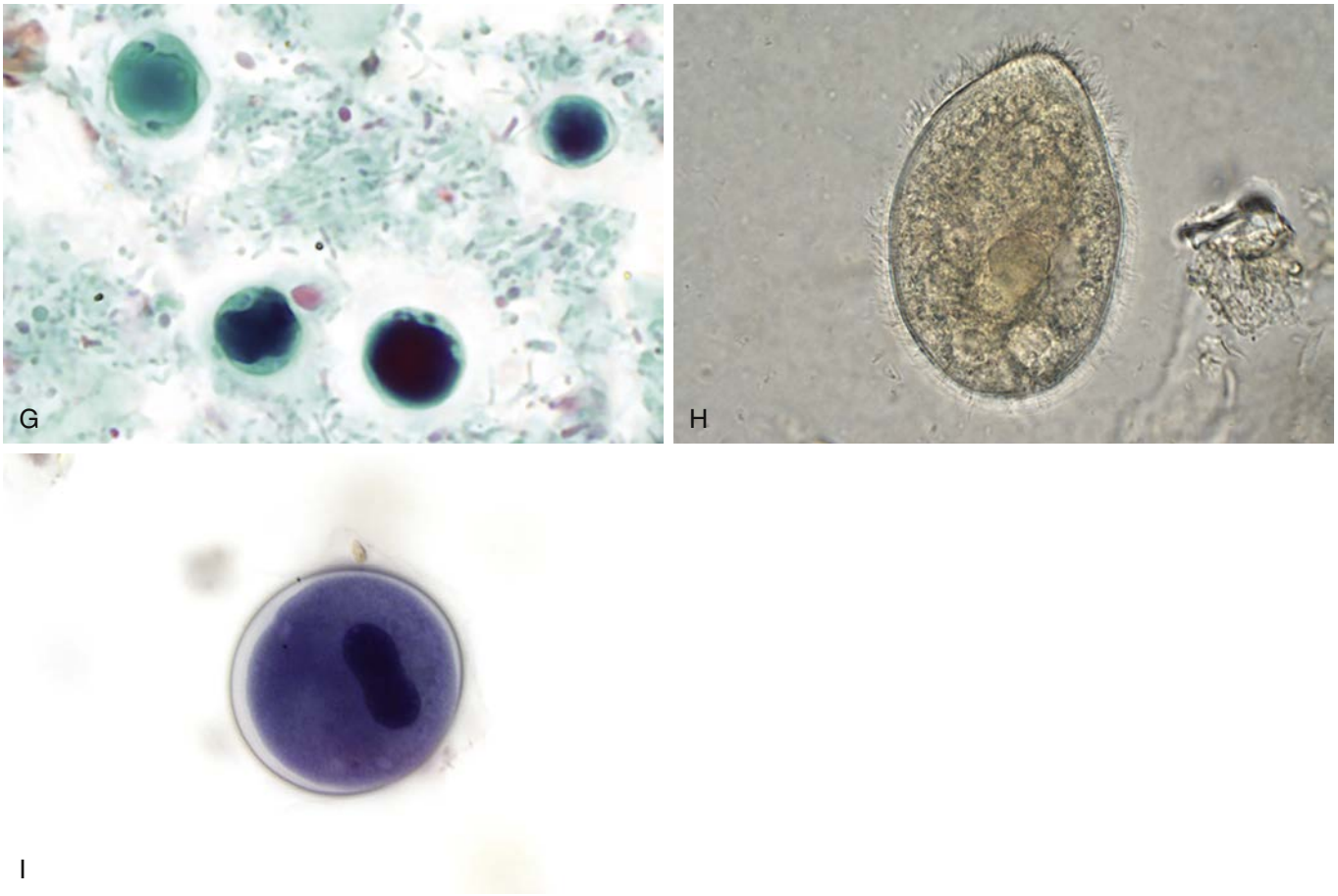

Figure 65.12—cont'd **G,** Multiple vacuolar forms of *Blastocystis* spp. **H,** Trophozoite of *Balantioides coli* in wet mount; note cilia covering the cell and the prominent macronucleus. **I,** Cyst of *B. coli* demonstrating a characteristic kidney-bean-shaped macronucleus (iron hematoxylin).

Pentatrichomonas hominis

Pentatrichomonas hominis, known previously as *Trichomonas hominis* (see Table 65.10 and Figs. 65.11 and 65.12E), is an infrequently seen, nonpathogenic intestinal flagellate that may be confused with *E. hartmanni*, small *E. histolytica* trophozoites, *E. nana*, *C. mesnili*, or *G. duodenalis*. Organisms do not stain particularly well and often are distorted in permanent smears. Several organisms may have to be examined in stained preparations to demonstrate the single nucleus, undulating membrane and associated costa, and flagella. A prominent rod-like object, the axostyle, runs through the organism and protrudes from the posterior end. No cyst stage has been described.

Trichomonas vaginalis

Trichomonas vaginalis is a common cause of vaginitis, characterized by inflammation, itching, vaginal discharge, and, occasionally, dysuria. The infection usually is spread by sexual intercourse, often to females from an asymptomatic male partner. Occasionally, males may have symptomatic prostatitis or urethritis. Trichomoniasis is the most common curable sexually transmitted infection (STI), estimated to infected 3.7 million individuals in the United States (CDC, 2018b). It is one of the five NPIs targeted by the United States for public health action. Complications of infection include preterm delivery and low birth weight in pregnant women, and increased risk of acquiring and spreading other STIs (CDC, 2018b). The drug of choice for trichomoniasis is tinidazole or metronidazole (Drugs for Parasitic Infections, 2013). Sexual partners should be simultaneously treated, regardless of symptoms.

Trichomonas vaginalis infections may be diagnosed in the physician's office by direct wet mount examination of vaginal fluid, prostatic fluid, or sediments of freshly passed urine. Morphologically, *T. vaginalis* resembles *P. hominis* but is larger (up to 23 μm), and the undulating membrane extends only half the length of the body. Because of the difference in habitat, it generally is not necessary to differentiate these trichomonads morphologically.

Despite its ease of use, direct wet mount examination is an insensitive method for detecting trichomoniasis (51%–65% sensitivity). Thus, NAATs are now the recommended method for detection (Workowski & Bolan, 2015; Meites et al., 2015). There are multiple FDA-cleared methods for detecting trichomoniasis, with sensitivities and specificities exceeding 95% (APHL, 2016; Nye, 2009). Most are cleared only for female specimens; the Xpert TV (Cepheid, Sunnyvale, CA), is the only NAAT that has FDA clearance for detection of *T. vaginalis* in both male and female specimens (Schwebke et al., 2018).

Other methods of testing include culture, antigen detection, and microscopic examination of stained smears (e.g., Papanicolaou, Giemsa) (APHL, 2016; Nye, 2009). Cultures, including use of a convenient commercial "pouch" system (In-Pouch TV, Biomed, White City, OR), were previously considered the gold standard prior to introduction of NAATs and reported sensitivities of 75% to 96% (APHL, 2016; Nye, 2009). The FDA-cleared nucleic acid probe test, BD Affirm VP III microbial identification system, also provides reasonable detection sensitivity (89.2%–92.8%) (APHL, 2016). Antigen tests generally have lower sensitivity than nucleic acid detection methods for trichomoniasis; the FDA-cleared OSOM Trichomonas Test (Sekisui Diagnostics, Burlington, MA) is a CLIA-waived EIA with reported sensitivities of 75% to 96% (APHL, 2016). Finally, Papanicolaou-stained gynecologic smears may reveal *T. vaginalis* on occasion but have poor sensitivity and specificity.

Other Flagellates

Enteromonas hominis and *Retortamonas intestinalis* are small, nonpathogenic intestinal flagellates that are seen infrequently but, when present, may occur in large numbers. Morphologic characteristics are reviewed in Table 65.10 (see also Fig. 65.11). *Trichomonas tenax*, a trichomonad that normally lives in the oral cavity of humans, has been isolated from the pleural fluid in patients with bacterial empyema. However, their presence is believed to be secondary to the bacteria, which is their normal food source (Leterrier et al., 2012).

CILIATES

Balantioides coli

The ciliate *Balantioides coli* (formerly *Balantidium coli*, syn. *Neobalantidium coli*; see Figs. 65.11, 65.12H, and 65.12I) may cause a dysentery-like syndrome with colonic ulcerations similar to that of amebiasis but only rarely disseminates outside of the intestine. Treatment is with tetracycline,

TABLE 65.10
Morphology of Intestinal Flagellates

Species	Size (Length)	Shape	Motility	Number of Nuclei	Number of Flagella*	Other Features
Trophozoites						
Pentatrichomonas hominis†	8–20 μm; usual range, 11–12 μm	Pear-shaped	Rapid, jerking	1 Not visible in unstained mounts	3–5 anterior; 1 posterior	Undulating membrane extending length of body
Chilomastix mesnili	6–24 μm; usual range, 10–15 μm	Pear-shaped	Stiff, rotary	1 Not visible in unstained mounts	3 anterior; 1 in cytostome	Prominent cytostome extending 1/3–1/2; spiral groove across ventral surface
Giardia duodenalis	10–20 μm; usual range, 12–15 μm	Pear-shaped	Falling leaf	2 Not visible in unstained mounts	4 lateral; 2 ventral; 3 caudal	Sucking disk occupying 1/2–3/4 of ventral surface
Enteromonas hominis	4–10 μm; usual range, 8–9 μm	Oval	Jerking	1 Not visible in unstained mounts	3 anterior; 1 posterior	One side of body flattened; posterior flagellum extending free, posteriorly or laterally
Retortamonas intestinalis	4–9 μm; usual range, 6–7 μm	Pear-shaped or oval	Jerking	1 Not visible in unstained mounts	1 anterior; 1 posterior	Prominent cytostome extending approximately 1/2 length of body
Dientamoeba fragilis†	5–15 μm; usual range, 9–12 μm	ameboid	Pseudopods are angular, serrated, or broad-lobed, and hyaline is almost transparent	1–2; typically binucleate forms predominate; not visible in unstained preparation	None	Cytoplasm may contain bacteria and yeast
Species	**Size**	**Shape**	**Number of Nuclei**	**Other Features**		
Cysts						
Chilomastix mesnili	6–10 μm; usual range, 8–9 μm	Lemon-shaped, with anterior hyaline knob or "nipple"	1 Not visible in unstained preparations	Cytostome with supporting fibrils. Usually visible in stained preparations.		
Giardia duodenalis	8–13 μm; usual range, 11–12 μm	Oval or ellipsoidal	Usually 4; not distinct in unstained preparations; usually located at one end	Fibrils or flagella longitudinally in cyst. Cytoplasm often retracts from a portion of cell wall.		
Enteromonas hominis	4–10 μm; usual range, 6–8 μm	Elongate or oval	1–4, usually 2 lying at opposite ends of cyst; not visible in unstained mounts	Resembles *E. nana* cyst. Fibrils or flagella usually are not seen.		
Retortamonas intestinalis	4–9 μm; usual range, 4–7 μm	Pear-shaped or slightly lemon-shaped	1 Not visible in unstained mounts	Resembles *Chilomastix* cyst. Shadow outline of cytostome with supporting fibrils extends above nucleus.		

Modified from Brooke MM, Melvin DM: *Morphology of diagnostic stages of intestinal parasites of man*, PHS Publication No. 1966, Bethesda, MD, 1969, U.S. Department of Health, Education, and Welfare.
*Not a practical feature for identification of species in routine fecal examinations.
†*Pentatrichomonas* hominis and *Dientamoeba fragilis* do not have a cyst form (see text for the latter).

metronidazole, or iodoquinol (Drugs for Parasitic Infections, 2013). Human infection, rare in the United States, is usually acquired from hogs, rodents, or nonhuman primates, which are commonly infected. *B. coli* is the largest protozoan and only ciliate to infect humans. Trophozoites are between 40 μm and more than 200 μm in greatest dimension (most measure 50 to 100 μm) and are uniformly covered with cilia that are slightly longer at the anterior end adjacent to the cytostome. A large macronucleus is readily seen in stained preparations, and a smaller micronucleus is infrequently visible. Numerous food vacuoles and contractile vacuoles are present in the cytoplasm. Cysts are rounded, measuring 50 to 70 μm in length. Cilia may be seen within younger cysts, and nuclear characteristics are similar to those of trophozoites (Ash & Orihel, 2007). Stool specimens that have been contaminated with stagnant water may contain free-living ciliates, which usually can be distinguished from *B. coli* by differences in their ciliary pattern. Ciliocytophthoria in respiratory specimens has resulted in incorrect presumptive identifications of *B. coli* (Hadziyannis et al., 2000; Pritt, 2018).

Cryptosporidium and the Coccidia

Cryptosporidium and the coccidia comprise a large group of apicomplexan parasites that have a sexual stage in the intestinal tract of invertebrate and vertebrate animals (Lindsay & Weiss, 2019; Xiao & Cama, 2019). Some species also develop asexually in extraintestinal sites in host tissues. Genera infecting the intestine of humans—such as *Cryptosporidium*, *Cyclospora*, *Cystoisospora*, and *Sarcocystis*—generally produce self-limited diarrheal disease in immunocompetent persons. Severe protracted diarrhea may develop in immunocompromised hosts following infection with *Cryptosporidium*, *Cyclospora*, and *Cystoisospora*. It should be noted that *Cryptosporidium* is no longer considered part of the Coccidia proper but is still grouped with the coccidians in the clinical realm for convenience (Adl et al., 2012, 2018; Xiao & Cama, 2019).

Cryptosporidium spp.

Cryptosporidium spp. use a single host in their life cycle. The two species most commonly implicated in human disease are *C. hominis* (a human parasite) and *C. parvum* (a livestock and ruminant parasite) (Cama & Mathison, 2015; Xiao & Cama, 2019). Parasites develop in the brush border of epithelial cells of the small and large intestine and occasionally spread to other sites, such as the gallbladder, pancreas, and respiratory tract, mainly in immunocompromised patients (Figs. 65.13A and 65.13E).

The epidemiology of cryptosporidiosis is similar to that of giardiasis. One of the largest known outbreaks of water-transmitted infection

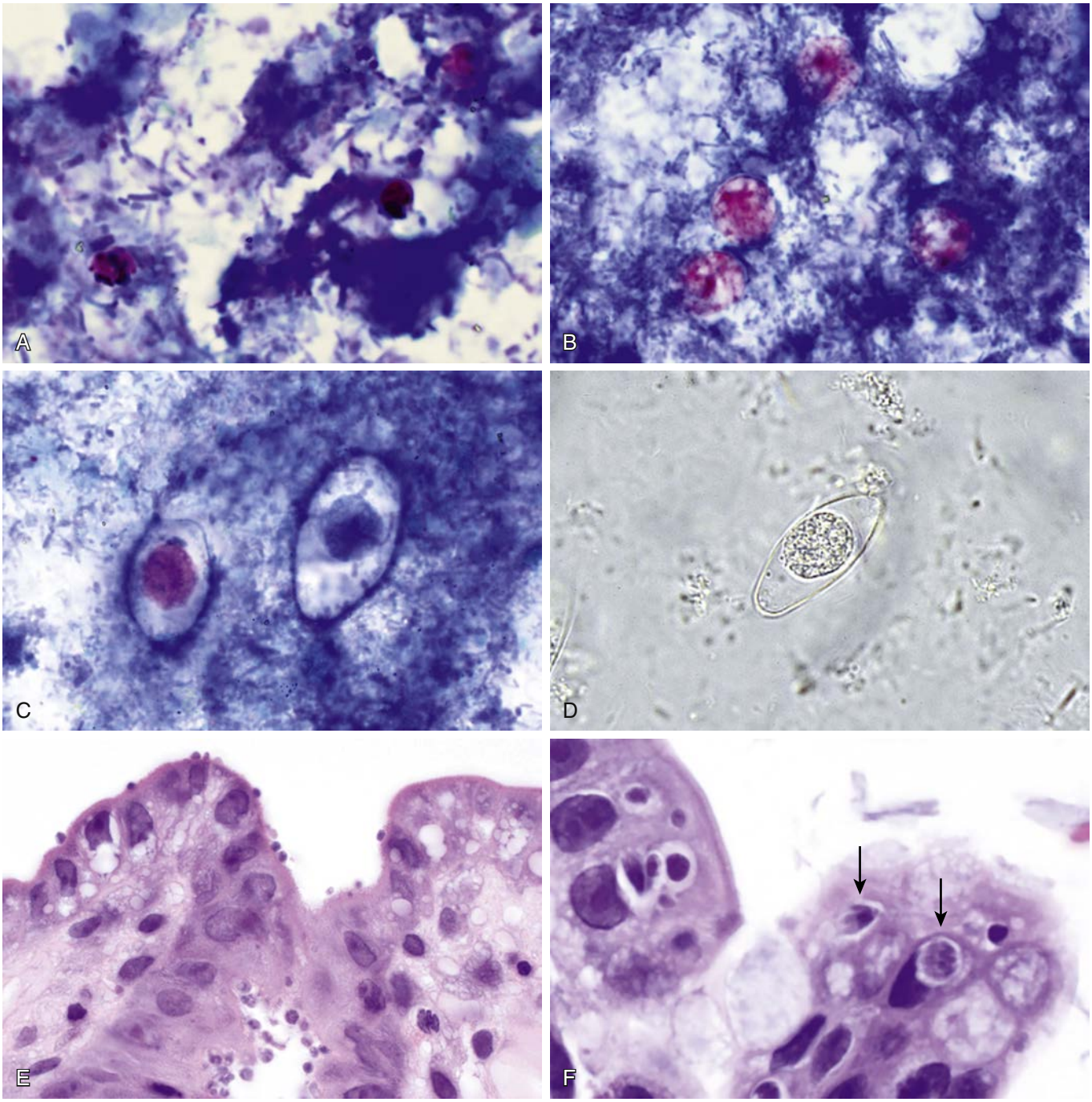

Figure 65.13 **A,** Modified acid-fast stain of a fecal smear demonstrating oocysts of *Cryptosporidium* sp. (1000×). **B,** Modified acid-fast stain of a fecal smear demonstrating oocysts of *Cyclospora cayetanensis* (1000×). **C,** Modified acid-fast stain of a fecal smear demonstrating two oocysts of *Cystoisospora belli*. Note that one is not stained, as is common with the oocysts of *C. cayetanensis* and *C. belli* (1000×). **D,** Oocyst of *C. belli* in feces (wet mount; 1000×). **E,** Small-bowel biopsy demonstrating development of *Cryptosporidium* sp. parasites within the brush border of enterocytes (H&E; 1000×). **F,** Small-bowel biopsy demonstrating development of *C. cayetanensis* parasites within enterocytes, including meronts *(arrows)* (H&E; 1000×).

Continued

occurred in Milwaukee, Wisconsin, in 1993. In that outbreak, an estimated 400,000 individuals became ill from tap water contaminated with farm runoff following heavy rains (MacKenzie et al., 1995). Similar to cysts of *Giardia*, *Cryptosporidium* oocysts are refractory to usual chlorination levels of drinking water; unless a community's water supply from a surface source is filtered, epidemics may occur.

Cryptosporidium is a common cause of acute, self-limited diarrhea in immunocompetent individuals, especially in children who attend day care. In patients with AIDS, *Cryptosporidium* may cause chronic secretory diarrhea that can last for months to years and may contribute to death. The incubation period is about 8 days; in previously healthy persons, the illness lasts 9 to 23 days. Patients may have malaise, fever, anorexia, abdominal cramps, and diarrhea (Xiao & Cama, 2019). Nitazoxanide is used to treat immunocompetent individuals, but no drug has proven efficacy in immunocompromised individuals (Drugs for Parasitic Infections, 2013); restoration of immunity, when possible, is the treatment of choice in the latter population.

Diagnosis can be made by stool examination, antigen detection, or molecular testing (see Tables 65.4 and 65.6). Various concentration methods, including formalin–ethyl acetate sedimentation and Sheather's sugar flotation, work well (Garcia, 2016). The availability of the formalin–ethyl acetate method makes this technique attractive, although centrifugation speed and times must be increased to maximize recovery (Garcia, 2010, 2016). A smear is prepared from the sediment and stained with an acid-fast stain or immunofluorescent reagents. Several acid-fast staining methods, including auramine-O, have been evaluated, but a modified cold Kinyoun method is used most widely. Spherical oocysts measure 4 to 6 μm in diameter and, when stained by the modified Kinyoun procedure, appear a deep fuchsia. However, some unevenness of staining intensity may occur, along with variability in the percentage of cysts that stain positive. Sporozoites may be visualized in the stained oocysts.

Commercial DFA and EIA reagents, which provide good sensitivity and specificity (Cama & Mathison, 2015), are especially good for laboratories where *Cryptosporidium* is infrequently encountered and where there is

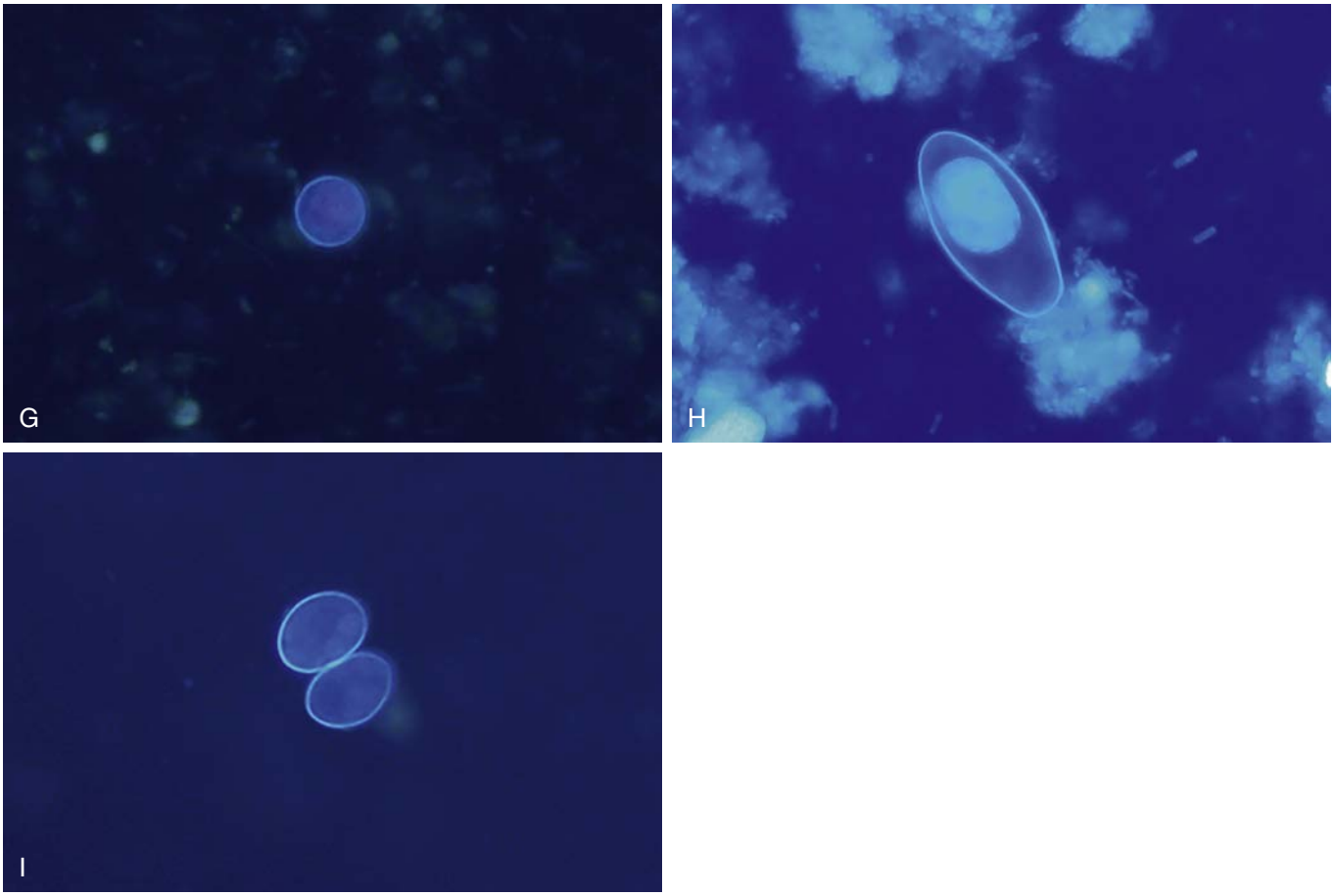

Figure 65.13—cont'd **G,** Oocyst of *C. cayetanensis* demonstrating autofluorescence (400×). **H,** Oocyst of *C. belli* demonstrating autofluorescence (400×). **I,** Oocyst of *Sarcocystis* spp. demonstrating autofluorescence. Note that sporocysts glow but the oocyst wall does not (400×). (**G-I** courtesy of Henry S. Bishop, DPDx Team, Centers for Disease Control and Prevention, Atlanta, GA.)

difficulty in maintaining expertise in the interpretation of acid-fast stains. As with *Giardia*, antigen testing is particularly useful for patients with diarrhea who have not traveled outside of the United States. In these patients, antigen testing (usually performed in conjunction with *Giardia* antigen testing) can supplement or replace the traditional subjective O&P examination with acid-fast staining (Cama & Mathison, 2015).

NAATs are also becoming more widely available and have been proven to be more sensitive than antigen testing (Cama & Mathison, 2015). At the time of this writing, three NAAT assays are FDA approved for use in the Unites States (see earlier Amebiasis section).

Cyclospora cayetanensis

Like *Cryptosporidium* spp. and the other coccidia, *C. cayetanensis* causes diarrheal disease in immunocompetent patients and severe, prolonged diarrhea and wasting in immunocompromised individuals (Lindsay & Weiss, 2019; Ortega & Sanchez, 2010). Unlike *Cryptosporidium*, it is a parasite of humans only. Therefore, infection is seen associated with ingestion of food or water that has been contaminated with human feces. The parasite has been recovered from patients in several countries, including the United States, and was initially described as a blue-green alga, a cyanobacterium-like body, or a coccidian-like body, among others (Ortega et al., 1993). Infection causes a flu-like illness with nausea, vomiting, weight loss, and explosive watery diarrhea lasting 1 to 3 weeks. The drug of choice for treatment is trimethoprim/sulfamethoxazole (Drugs for Parasitic Infections, 2013).

Oocysts, passed unsporulated, appear as nonrefractile spheres 8 to 10 μm in diameter that contain a cluster of refractile globules enclosed within a membrane when viewed by light microscopy. A total of 1 to 2 weeks is required for sporulation, after which the mature oocyst contains two sporocysts, each with two sporozoites. In trichrome-stained smears, the oocysts appear as clear, round, and somewhat wrinkled objects. Oocysts autofluoresce bright green to intense blue under ultraviolet epifluorescence; thus, this is a helpful method for locating oocysts in stool specimens (Fig. 65.13G). They stain acid-fast with modified acid-fast (Fig. 65.13B) or auramine-O staining techniques, although unstained oocysts ("ghost" forms) may predominate and could be overlooked by inexperienced microscopists. The hot safranin method provides more uniform staining but requires heating of the stain (e.g., via hot plate or microwave), (Visvesvara et al., 1997). Oocysts of *C. cayetanensis* must be differentiated from those of *Cryptosporidium* spp., which stain in a similar fashion but are smaller (4–6 μm) (Cama & Mathison, 2015).

Cystoisospora belli

Cystoisospora belli (formerly known as *Isospora belli*) undergoes both asexual and sexual development in the cytoplasm of small intestine epithelial cells. Sexual development results in the production of oocysts, which are passed in the stool and mature to the infective stage in the environment. Human infections cause diarrhea and malabsorption but are generally self-limited. In patients with AIDS or other immunosuppressive disorders, disease may persist for months or years and may contribute to death (Pritt, 2018; Lindsay & Weiss, 2019). The drug of choice for treatment is trimethoprim/sulfamethoxazole (Drugs for Parasitic Infections, 2013).

Diagnosis is made by finding the unsporulated or partially sporulated oocysts measuring 12 × 30 μm in fecal specimens, usually in direct wet mounts or concentration preparations (Fig. 65.13D). If the unfixed specimen is left at room temperature for 24 to 48 hours, sporulation can occur. The infectious oocyst contains two sporocysts, each with four sporozoites. These oocysts are similar to those of *Cryptosporidium* and *Cyclospora* in that they test positive by safranin and acid-fast (Fig. 65.13C) and, also like *Cyclospora*, the oocysts autofluoresce (Fig. 65.13H) (Cama & Mathison, 2015).

Sarcocystis spp.

Sarcocystis spp. are two-host coccidians in which the sexual phase develops in the intestinal mucosa of carnivorous animals and the asexual, extraintestinal phase occurs in the muscles and tissues of various intermediate hosts. Humans may serve as definitive or intermediate hosts depending on the species of *Sarcocystis*. Intestinal infection with *Sarcocystis hominis* and *Sarcocystis suihominis* is acquired by the ingestion of raw or incompletely cooked beef or pork, respectively, which contains tissue cysts (sarcocysts). Infection usually is asymptomatic, but occasional patients have transient

diarrhea, abdominal pain, or anorexia. Intestinal infection is self-limited because asexual multiplication occurs in the intermediate host and is not repeated in the definitive host. Treatment is not routinely recommended (Drugs for Parasitic Infections, 2013).

The diagnosis of intestinal infection is established by detection of sporulated 25 × 33 μm oocysts in stool; detection can be enhanced by using IV autofluorescence (Fig. 65.13I). Each mature oocyst contains two sporocysts, each of which contains four sporozoites. The oocyst wall is thin and often is not detectable, or has already ruptured, releasing the two sporocysts. These forms, best seen in wet mounts, appear larger than oocysts of *Cryptosporidium*. Trichrome stains are of little value in detecting these parasites. Humans also may serve as intermediate hosts for several unnamed animal species of *Sarcocystis*, in which cysts are found in skeletal and cardiac muscles (Fayer et al., 2015).

INTESTINAL HELMINTHS

Intestinal helminths discussed here include those nematodes (roundworms), cestodes (tapeworms), and trematodes (flukes) that reside as adults in the gastrointestinal tract or live in other locations (liver, lung, or blood) and produce eggs that exit the human body via the intestinal tract. A fourth group, the acanthocephalans (thorny-headed worms) cause rare to uncommon zoonotic disease in humans and will not be discussed further. Sizes for adult helminths vary from 1 mm to more than 10 m in length; sizes for eggs range from 25 to 150 μm (Fig. 65.14).

An understanding of helminth life cycles and zoogeography is critical in knowing which parasite stages may be present in a presumed infection, what organs or tissues may be involved, and when developmental stages may be expected to appear in clinical specimens. Although diagnosis usually depends on finding and identifying an appropriate developmental stage (egg, larva, or adult), some helminthic infections may be diagnosed chiefly on clinical grounds, on the basis of serologic or molecular evidence, or a combination thereof (Mathison & Pritt, 2018).

Certain species have developmental cycles whereby infectious stages can be transmitted directly from person to person (*Enterobius vermicularis* and *Hymenolepis nana*). In others (*Trichuris*, *Ascaris*, and *Trichostrongylus*), an additional maturation period in the environment is required before the parasite egg or larva (in the latter case) is infectious, thus making these latter parasites more common in settings with lack of adequate sanitary and waste treatment facilities. Ingestion of infective stages may also occur incidentally after the ingestion of insects or mollusks (*Dipylidium*, *Hymenolepis*, *Angiostrongylus*), plants (*Fasciolopsis*, *Fasciola*), or animal tissues (*Trichinella*, *Taenia*, *Dibothriocephalus*, *Clonorchis*, *Opisthorchis*, *Paragonimus*, *Heterophyes*, *Metagonimus*, and *Nanophyetus*). In some cases, larval parasite stages may directly penetrate the skin (hookworms, *Strongyloides*, *Schistosoma*).

Recovery and identification of helminth eggs and larvae in stool, urine, or sputum requires a systematic approach and appropriate training of the individuals performing the evaluations. The size of the eggs and larvae is an especially important characteristic; measurement often requires a properly calibrated ocular micrometer. External characteristics of eggs that should be documented include their shape, their wall thickness, and the presence or absence of a mamillated covering, operculum, opercular shoulders, abopercular knob, polar plugs, or spines. Egg development (embryonated, unembryonated) and the presence or absence of hooklets, which are characteristic of cestodes, should also be noted. The examiner also needs to have an appreciation for the large variety of artifacts detected in human feces that may mimic parasite eggs and larvae (Ash & Orihel, 2007; Pritt, 2014).

NEMATODES

Nematodes (roundworms) are common worms that inhabit the human intestinal tract, blood, and tissues. Some attach to intestinal mucosa by means of specialized mouthparts at the anterior end (e.g., hookworms, whipworm). Others move freely in the lumen of the bowel (e.g., pinworm, *Ascaris lumbricoides*); thus, they may be more likely to end up in ectopic locations. Nematodes have elongated, unsegmented bodies covered with an acellular cuticle and possess a full digestive tract. Most are dioecious (whereby male and female worms are individual animals), unlike the cestodes and some of the trematodes, which are hermaphrodites. Identification of characteristic eggs in stool is used for diagnosis of all intestinal nematode infections with the exception of *Strongyloides stercoralis*, in which only first-stage (rhabditiform) larvae are typically seen in stool, and pinworm, in which eggs are deposited onto the perianal skin folds and are not commonly found in stool. Of the intestinal nematodes, only the eggs of pinworm become infectious within 4 to 6 hours of being laid. The eggs of the other intestinal nematodes require an incubation period of several weeks in the soil to become infectious. Soil-transmitted helminth infections are identified as a neglected tropical disease and are seen in areas of

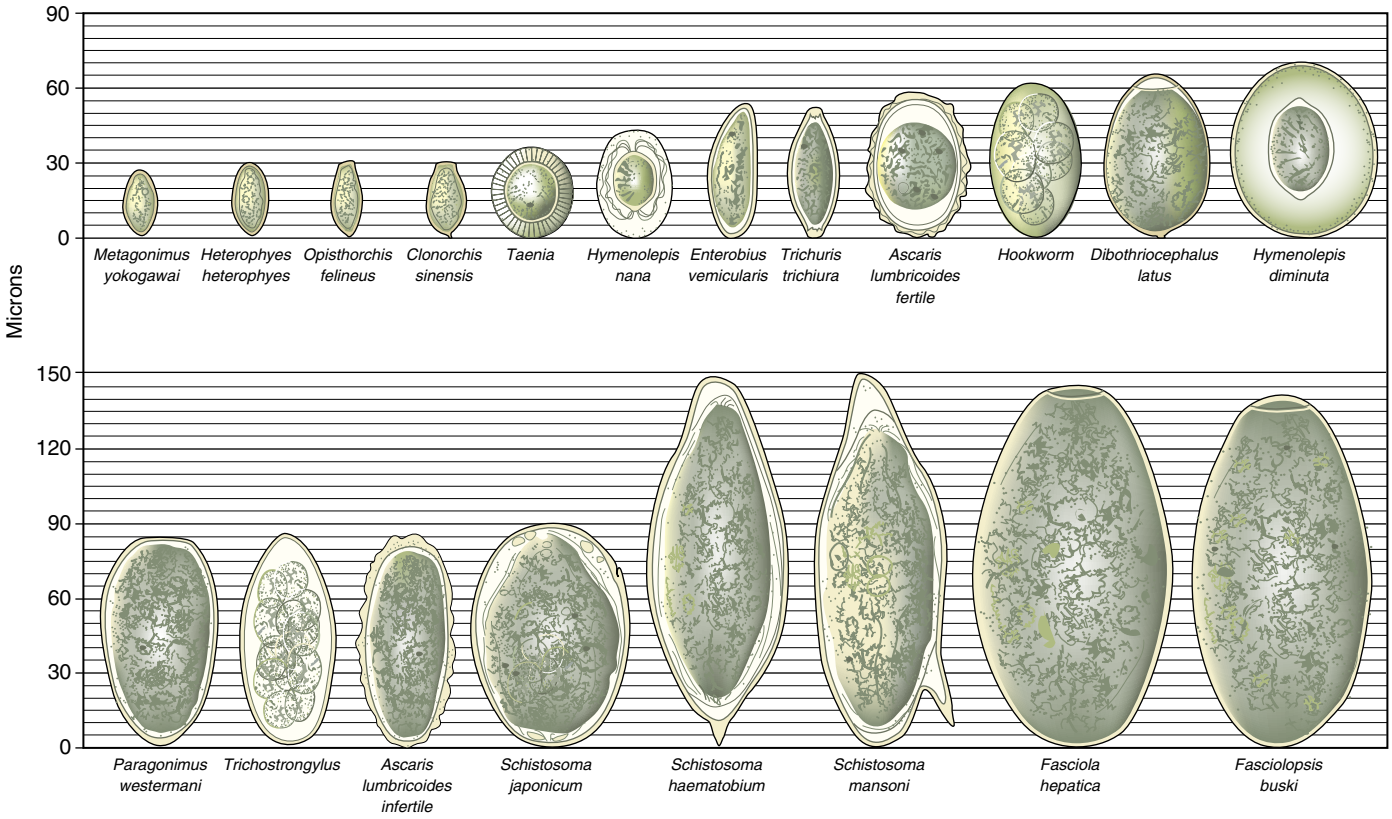

Figure 65.14 Relative sizes of helminth eggs. (Courtesy of Centers for Disease Control and Prevention, Parasitology Training Branch, Atlanta, GA.)

the world where sanitation is poor. Up to one-quarter of the world's population is estimated to be infected with soil-transmitted helminths (WHO, 2019). This section covers intestinal nematodes. Nematodes that are usually detected in intestinal biopsy specimens or extraintestinal sites are covered in the Tissue Helminths section later in the chapter.

Enterobius vermicularis (Pinworm Infection)

Enterobiasis is the most common helminthic infection in children of all social strata in the United States, Canada, and Europe. Although it is primarily a parasite of young children, rapid maturation of the egg allows it to be readily transmitted from person to person in both family and institutional settings. Male and female worms reside primarily in the cecum and adjacent areas. Females measure up to 13 mm in length and have a pointed posterior end that gives rise to their common name, the pinworm. Both sexes have lateral alae that are best seen in the cervical region and in cross-section as well as a prominent esophageal bulb (Figs. 65.15A and 65.15C).

Although males are rarely seen in clinical specimens, females may be found on the surface of a stool specimen or on the perianal skin, especially at night, where eggs are deposited. Eggs are colorless and ovoid with one side flattened and measure 20 to 40 μm wide by 50 to 60 μm long (see Fig. 65.15B). They are infective within hours and when ingested complete development to the gravid adult stage within 1 month (the prepatent period).

Although infection may be asymptomatic, children often suffer from nocturnal pruritus ani, irritability, and loss of sleep. Enterobiasis should be ruled out early in the evaluation of enuresis. Treatment is with albendazole, mebendazole, or pyrantel pamoate (Drugs for Parasitic Infections, 2013). Adult worms may also migrate to unusual sites, such as the vagina, fallopian tubes, or peritoneal cavity. Their egg-laying behavior and ultimate death in

Figure 65.15 All direct examination with brightfield illumination except as noted. **A,** Adult female pinworm, *Enterobius vermicularis*, with pointed "pin-like" posterior end. Prominent anterior inflations (alae) are also seen (4×). **B,** Numerous eggs of *E. vermicularis* as seen on a specialized "pinworm paddle" (400×). **C,** Cross-sections of adult *E. vermicularis* in the appendix; note characteristic lateral alae *(arrow)* (H&E; 100×). **D,** Adult whipworms, *Trichuris trichiura*; note females with straight tails and males with coiled tails. **E,** Egg of *T. trichiura* (400×). **F,** Adult female and male *Ascaris lumbricoides*, the largest human intestinal roundworm. The female has a straight tail, whereas the male has a coiled tail.

Continued

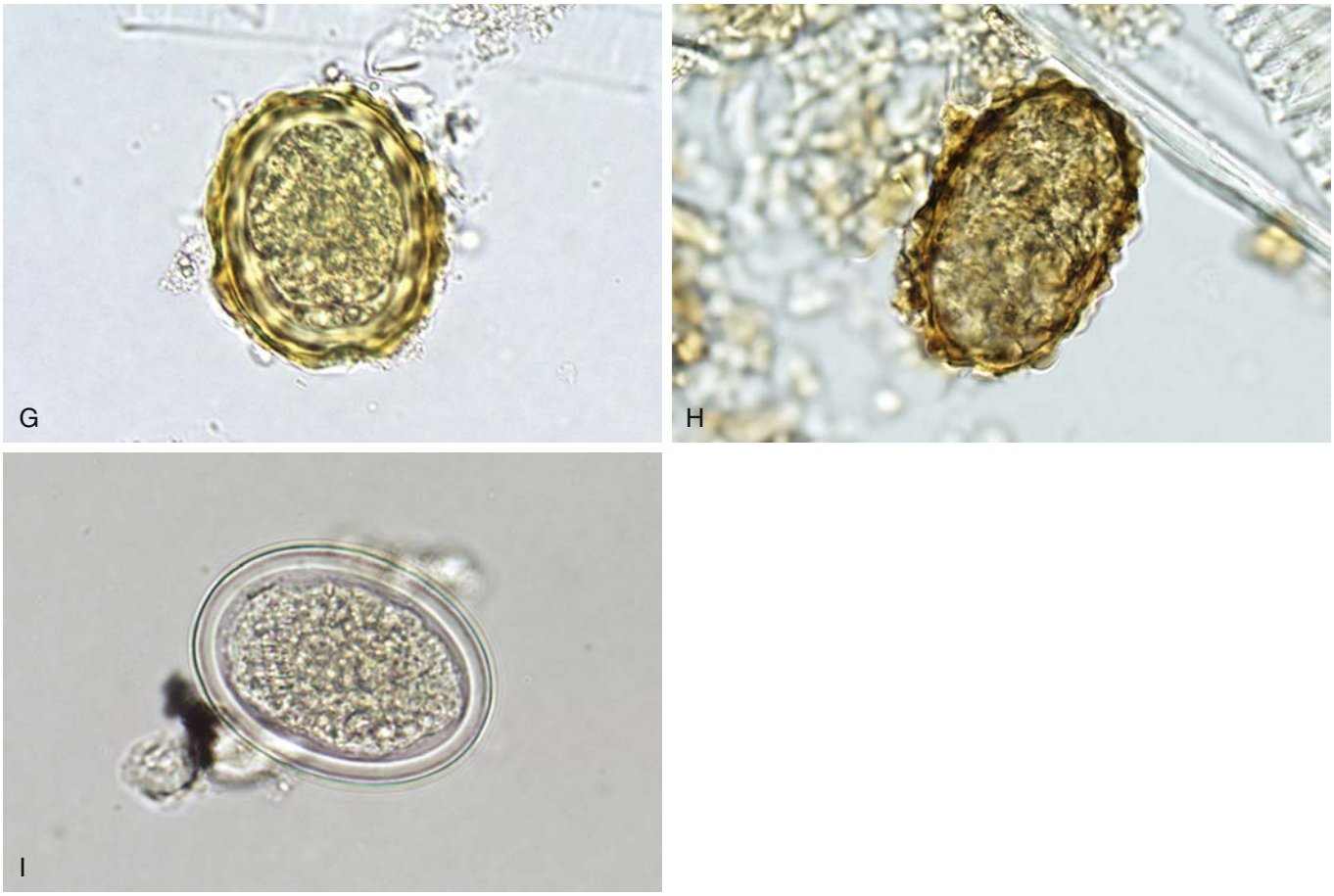

Figure 65.15, cont'd **G,** Fertile, unembryonated egg of *A. lumbricoides* (400×). **H,** Infertile egg of *A. lumbricoides* (400×). **I,** Decorticated fertile egg of *A. lumbricoide* (**D** and **F** from Zaiman H, editor: A pictorial presentation of parasites: a cooperative collection; https://www.astmh.org/education-resources/zaiman-slide-library.)

these locations may provoke inflammatory, granulomatous reactions (Orihel & Ash, 1995; Meyers, 2000; Pritt, 2018).

Recovery of eggs or, less commonly, adults from the perianal skin is usually done using the cellulose tape technique or commercially available collection kits (see Fig. 65.2) first thing in the morning before the patient bathes or defecates (Ash & Orihel, 2007; Garcia, 2016). Only 5% to 10% of cases are detected using routine stool examination since the eggs are laid on the skin rather than being secreted into the colonic lumen (Garcia, 2016).

Trichuris trichiura (Whipworm Infection)

Trichuriasis is common worldwide in tropical and subtropical regions with inadequate sanitation and waste treatment facilities. Adult worms are found in the large intestine, especially the cecum, but in heavy infections they can be found throughout the colon and rectum. Males and females measure up to 50 mm in length and remain attached to the intestinal mucosa by the long, slender anterior end, while the thicker posterior end hangs free in the lumen. Female worms are elongate, whereas the tails on males are coiled (Fig. 65.15D). *Trichuris* has a direct life cycle in which eggs are passed in stool unembryonated and require several weeks under appropriate soil conditions to mature to the infective stage. When fully embryonated eggs are ingested, larvae are released and mature into adults in the colon, where they attach and survive up to 10 years.

Light infection usually is asymptomatic, but when larger numbers (>300 worms) are present, diarrhea or symptoms of dysentery may develop in association with dehydration and anemia. Rectal prolapse may occur in heavily infected children (Bethony et al., 2006). Treatment is with albendazole, mebendazole, or ivermectin (Drugs for Parasitic Infections, 2013).

Diagnosis is made by finding typical eggs in direct fecal smears or with concentration techniques. The eggs are barrel shaped with refractile plugs at both ends and usually measure 50 to 55 μm long by 22 to 24 μm wide (Fig. 65.15E). Egg quantitation techniques occasionally may be requested, primarily in endemic settings, to assess infection intensity, therapeutic efficacy, and reacquisition rates of parasites.

Capillaria philippinensis

This parasite, normally found in fish-eating birds, infects humans who ingest raw or incompletely cooked fish that contain infective larvae in their flesh. Although first described in persons from the Philippines, and later Thailand, occasional cases have been reported in Asia, the Middle East, and South America (Cross, 1992; Ash & Orihel, 2007). The parasites can cause autoinfection, resulting in chronic diarrhea. Treatment is with mebendazole or albendazole (Drugs for Parasitic Infections, 2013). Infected individuals may pass eggs, larvae, and even adult worms in their feces. Eggs resemble those of *Trichuris*, although they measure 36 to 45 μm in length by 21 μm in width and have thick, radially striated shells and bipolar protuberances that are inconspicuous (Fig. 65.16F) (Ash & Orihel, 2007).

Ascaris lumbricoides (Ascariasis)

This is the largest nematode that infects the intestinal tract of humans and is one of the most common of the intestinal roundworms, infecting an estimated 1.3 billion individuals worldwide (John & Petri, 2006). Infection occurs primarily in areas with inadequate sanitation and waste treatment facilities. As with *Trichuris*, it is especially common in children, who are also more likely to harbor heavy infection. In the United States, infection is often associated with pigs, which serve as a reservoir host.

Adult *Ascaris* live primarily in the duodenum and proximal jejunum. Females measure up to 35 cm in length by 6 mm in diameter. The male is somewhat smaller and has a ventrally curved tail, unlike the female (Fig. 65.15F). Both adult and immature worms can be identified by the presence of three prominent lips at the anterior end.

Females produce approximately 200,000 eggs per day, which are unembryonated when passed and require 4 to 6 weeks in a satisfactory environment to become infective. Following ingestion, eggs hatch in the intestine, and larvae penetrate the mucosa to gain access to the bloodstream. They are carried to the lungs and mature briefly in the alveolar capillary bed before entering the alveoli. Respiratory clearance mechanisms move the larvae to the epiglottis, where they are swallowed and grow to adulthood in the small bowel. Development from embryonated egg to adult takes approximately 2 months.

Symptoms of ascariasis vary from asymptomatic infection to severe disease. Migration of large numbers of larvae through the lungs during the initial phase of infection can cause *Ascaris* pneumonitis or Loeffler syndrome, characterized by bilateral diffuse, mottled pulmonary infiltrates and mild

bronchitis associated with peripheral eosinophilia. The syndrome is rare and usually occurs in individuals who have been previously exposed to *Ascaris* (Orihel & Ash, 1995; Meyers, 2000; Pritt, 2018). Treatment is with albendazole, mebendazole, or ivermectin (Drugs for Parasitic Infections, 2013).

Light infections are usually asymptomatic, whereas heavy infection may produce varying degrees of abdominal pain and diarrhea. Intestinal obstruction may also occur with a mass of worms, especially in children. Even a small number of worms are cause for concern because of their ability to invade ectopic sites such as the common bile duct and liver, appendix, and stomach. Fever or drug therapy may stimulate migration. In endemic areas, anthelmintics often are prescribed before anesthetics are used in elective surgery.

Infection is diagnosed by demonstrating eggs in feces or on recovery of an adult that has been passed or vomited. The large number of eggs produced each day makes detection of even a single worm probable. A count of fewer than 20 eggs per slide (2 mg of feces) indicates light infection, and a count of more than 100 eggs per slide indicates heavy infection.

Fertile *Ascaris* eggs are round to slightly oval with a yellow-brown, irregular external mamillated layer and a thick shell. Eggs that have lost their mamillated layer are described as *decorticated* and may superficially resemble hookworm eggs. Fertile eggs are passed unembryonated and measure approximately 55 to 75 μm long by 35 to 50 μm wide (Figs. 65.15G and 65.15I). Single females may produce unfertilized eggs, which are larger and more elongate (up to 90 μm in length) and have a thinner shell with irregular mammillations (Fig. 65.15H). These eggs lack organized internal contents and are filled with irregularly sized globules.

Trichostrongylus spp.

Human disease caused by *Trichostrongylus* spp. represents a zoonotic infection because these parasites principally infect large herbivores, such as sheep, cattle, and goats. The genus occurs worldwide, and several species may infect humans, including *Trichostrongylus colubriformis*, *Trichostrongylus orientalis*, *Trichostrongylus axei*, and *Trichostrongylus brevis*. Adult worms inhabit the small bowel and produce eggs that mature outside of the body. Larvae emerge and crawl about on soil and vegetation, where they are available to be ingested by potential hosts. Unlike hookworms, they do not invade skin directly, nor does the life cycle involve a migratory phase through the lungs. Infection usually is light and asymptomatic, but heavy infection may produce abdominal pain and diarrhea, usually with eosinophilia. Treatment is with pyrantel pamoate, mebendazole, or albendazole (Drugs for Parasitic Infections, 2013). Eggs resemble those of hookworms but are longer and narrower, measuring 78 to 98 μm by 40 to 50 μm, and are slightly tapered at one end (Fig. 65.16B).

Necator americanus, Ancylostoma duodenale, and *A. ceylanicum* (Hookworm Infection)

Hookworms, which are among the more common helminths known to infect humans, occur in tropical and subtropical regions and some temperate areas where there are inadequate sanitation and waste treatment facilities. *Necator americanus* is found in the United States and in other areas of the world and frequently overlaps in distribution with *Ancylostoma duodenale*. In Southeast Asia, *A. ceylanicum* is a common cause of intestinal hookworm infection (Ngui et al., 2014). Given their overlapping distributions, it is inaccurate to classify *A. duodenale* as an "Old World" hookworm and *N. americanus* as a "New World" hookworm; use of these terms should be avoided.

Adult females measure up to 12 mm in length and the males slightly less. Males are readily distinguished by the fan-shaped copulatory bursa at the posterior end. The anterior end of hookworms is modified into a buccal capsule that contains teeth or cutting plates. Both sexes attach to the mucosa of the small intestine, where they may reside for up to 18 years (Ash & Orihel, 2007).

Eggs are passed in feces and develop rapidly, depending on prevailing conditions. Rhabditiform larvae are released and develop into the infective filariform stage in about 7 days. On contact with an appropriate host, the larvae penetrate the skin, gain access to the host's circulation, travel to the lungs, and move up the tracheobronchial tree to be swallowed. On maturation in the small intestine, oviposition begins. Although the life cycles of both species are similar, *Ancylostoma* can mature directly to the adult stage in the intestine if infective larvae are ingested.

Hookworms can produce clinical symptoms in the skin at the site of larval penetration. This condition, known as *ground itch*, is characterized by inflammation, redness, and blister formation, along with intense itching. Migration of large numbers of larvae through the lungs may produce Loeffler syndrome, as described earlier for *A. lumbricoides*. Depending on the worm burden, intestinal infection can result in gastroenteritis with abdominal pain, diarrhea, and nausea. Hookworms are known for their ability to produce chronic blood loss with secondary iron-deficiency anemia. The presence of each adult *A. duodenale* can result in the loss of 0.15 to 0.25 mL of blood per day compared with 0.03 mL for each *N. americanus*. Development of children can be severely affected by chronic infection. Blood loss and the number of hookworms present correlate with the number of eggs per gram of stool, which may help the clinician determine when to initiate therapy in individuals living in endemic areas (Farrar et al., 2013). Treatment is with albendazole, mebendazole, or pyrantel pamoate (Drugs for Parasitic Infections, 2013).

Diagnosis is made by finding the characteristic thin-shelled eggs in feces. These eggs are partially embryonated when passed and measure 58 to 76 μm in length by 36 to 40 μm wide (Fig. 65.16A). Embryonated eggs or free rhabditiform larvae may be found in unpreserved specimens that are not examined promptly, and the larvae must be differentiated from the similar-appearing larvae of *Strongyloides stercoralis*. This can be accomplished using morphologic features; hookworm rhabditiform larvae have a longer buccal canal than those of *S. stercoralis* and inconspicuous genital primordium (Fig. 65.17). Hookworm eggs may need to be differentiated from those of *Trichostrongylus* spp. (which are longer and more pointed) and those of plant parasitic nematodes, especially *Heterodera* spp. (which are longer, have blunt ends, and are often asymmetric).

Although adult hookworms can be differentiated on the basis of their mouthparts and the copulatory bursa in males, eggs of human hookworms are indistinguishable. In direct wet mounts, egg counts of fewer than five eggs per coverslip denote light infection that is unlikely to result in anemia, whereas more than 25 eggs per coverslip denotes heavy infection that is likely to be associated with symptoms.

Strongyloides stercoralis (Strongyloidiasis)

Strongyloidiasis occurs in many areas in the tropics and subtropics, but this infection also is reported in temperate zones and has historically been endemic in areas of southeastern United States (e.g., regions of Appalachia with lack of adequate sanitary facilities and indoor plumbing). Adult females are 2 to 3 mm long and live in the mucosa of the duodenum, where they reproduce parthenogenetically (i.e., without a male; Fig. 65.16E). Males do not occur in the parasitic phase of the life cycle. The eggs hatch primarily in the small bowel, releasing first-stage (L1) or rhabditiform larvae, which then are passed in the feces (eggs are rarely found in stool O&P examinations). In this direct cycle, the rhabditiform larvae metamorphose into infective third-stage (L3) filariform larvae in the soil. These infective larvae readily penetrate the skin of exposed individuals; they migrate randomly throughout the body, eventually settling in the small intestine, where they mature into adults. Under appropriate soil conditions of high humidity, an indirect cycle may appear transiently, in which the newly deposited larvae develop into a free-living generation consisting of reproductive males and females. Eggs produced by this generation develop into filariform larvae that again are infective for humans. A third variation in the life cycle of *Strongyloides* involves autoinfection, in which maturation to the filariform stage is completed within the intestinal tract, with subsequent reinvasion of bowel mucosa or perianal skin.

Disease presentation is variable and may depend on the strain acquired. Early migration of filariform larvae may produce irritation, redness, and pruritus at the site of entry. Later migration through the lungs may produce Loeffler syndrome as previously discussed, with *A. lumbricoides* and the hookworm (Purtilo et al., 1974). The presence of intestinal symptoms is related to the intensity of the infection. The affected individual may have symptoms of peptic ulcer, abdominal pain, and diarrhea. A malabsorption syndrome has been reported with chronic infection.

The ability of the parasite to autoinfect may result in persistence of the infection for decades, as was recognized in allied troops who were held as prisoners of war in Southeast Asia during World War II and found to have active infection decades later (Gill & Bell, 1979). In otherwise healthy patients, autoinfection is generally asymptomatic but may produce larva currens (linear urticarial lesions). In immunocompromised individuals (e.g., patients with human T lymphotropic virus type 1 [HTLV-1] infection, transplant recipients, those receiving chemotherapy, end-stage alcoholics, and severely malnourished individuals), autoinfection may result in a life-threatening hyperinfection syndrome caused by rapid multiplication of the parasite (Meyers et al., 2000). Severe pneumonia is often a presenting manifestation of hyperinfection, followed by marked diarrhea, enteritis, septicemia, and recurrent gram-negative meningitis. Bacteria and bacterial meningitis occur secondary to carriage of intestinal bacteria by migrating larvae into the bloodstream and tissues. Patients who have lived in endemic areas should be screened for *S. stercoralis* prior to receiving immunosuppressive therapy (CDC, 2018c). Unlike infection with the other intestinal nematodes, the drug of choice for strongyloidiasis is ivermectin (Drugs for Parasitic Infections, 2013).

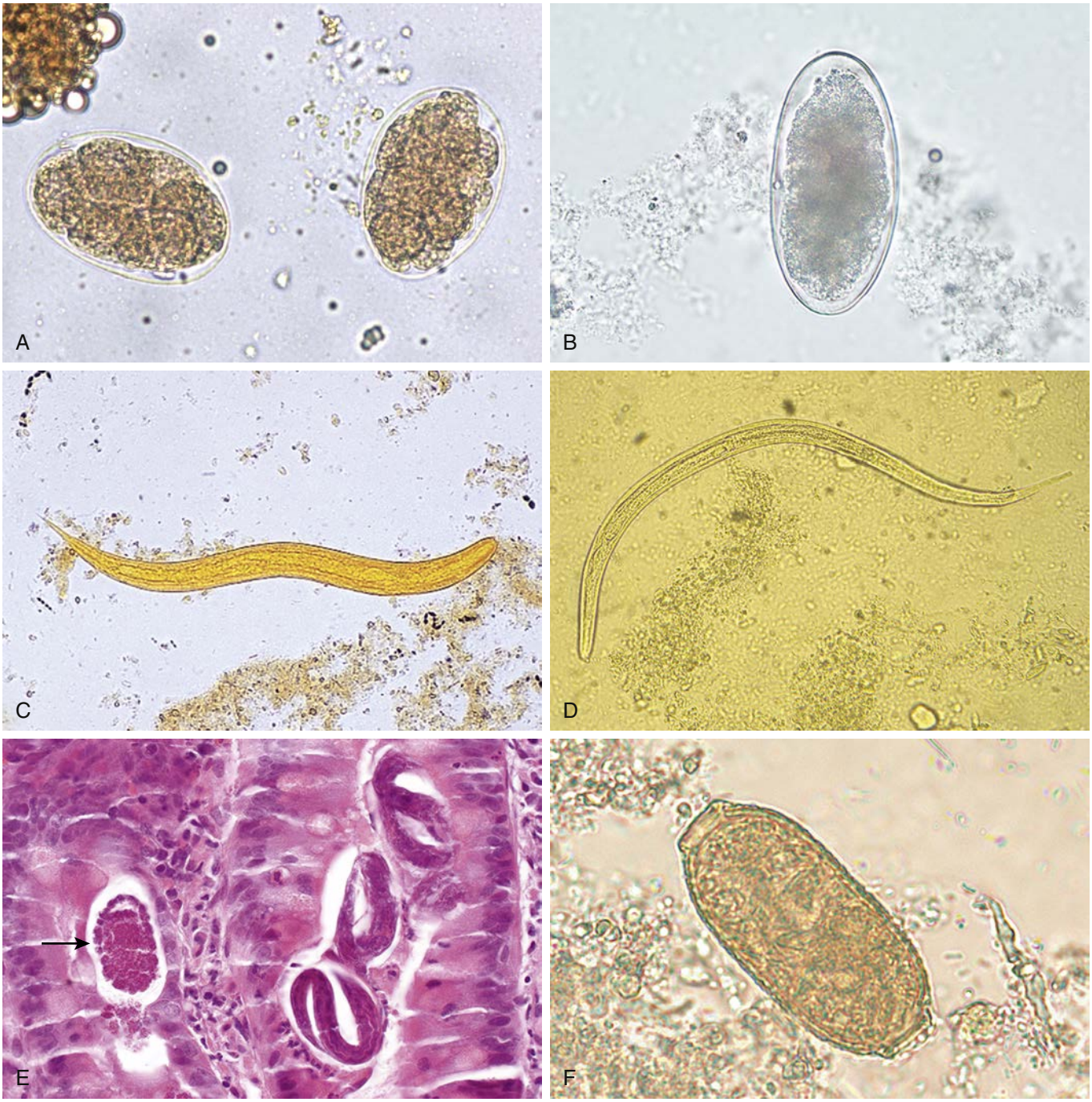

Figure 65.16 **A,** Hookworm (*Ancylostoma* sp. or *Necator americanus*) eggs (400×). **B,** Egg of *Trichostrongylus* sp. (400×). **C,** *Strongyloides stercoralis* rhabditiform (L1) larva in stool (iodine stain; 200×). **D,** Filariform (L3) larva of *S. stercoralis* in a bronchial wash (400×). **E,** Massive *S. stercoralis* infection in the duodenal mucosa. Note the presence of three larvae *(right)* and an egg *(arrow)* (H&E; 200×). **F,** *Capillaria philippinensis* egg in stool (400×).

Continued

Diagnosis is made on recovery and identification of typical rhabditiform larvae in stool specimens, although the routine O&P examination does not always reveal their presence and up to seven stool specimens may need to be examined for optimal sensitivity with this method (Garcia, 2016). When seen, *S. stercoralis* rhabditiform larvae must be differentiated from those of hookworms by their short buccal cavity and a prominent genital primordium (see Fig. 65.16C and 65.17). *S. stercoralis* filariform larvae may also be seen in respiratory and other extraintestinal specimens in disseminated disease. They have a notched tail and an esophagus approximately half the length of the body (Fig. 65.16D). Either stage of larvae is readily seen in fresh saline wet mounts under low power (e.g., 10×). If infective filariform larvae are detected in a recently passed stool specimen or in any extraintestinal specimens, superinfection should be suspected and reported immediately to the clinical team (Sheorey et al., 2019).

Examination of duodenal aspirates or string test specimens may be helpful in suspicious cases in which routine stool examinations are nonproductive, although they are not commonly used. The agar culture method (see Fig. 65.3) or one of the coproculture techniques (see the Laboratory Methods section earlier in the chapter) may also demonstrate the infection and provide highest sensitivity for detection of *S. stercoralis* from fecal specimens (Ash & Orihel, 2007; Garcia, 2016). Serologic tests are useful when infection is suspected but cannot be demonstrated by other methods; they are also useful for detecting evidence of prior infection. EIA and other tests display good sensitivity and specificity, although cross-reactions may appear with filariasis and some other nematode infections. These tests generally do not differentiate between past and current infection but may be useful in monitoring therapy (Wilkins & Nutman, 2015).

CESTODES

Cestodes, commonly referred to as tapeworms, are ribbon-like flatworms that live in the intestinal tract of vertebrate definitive hosts as adults and in the tissues or body cavities of various intermediate hosts as larvae. Depending on the species, humans can serve as definitive or intermediate

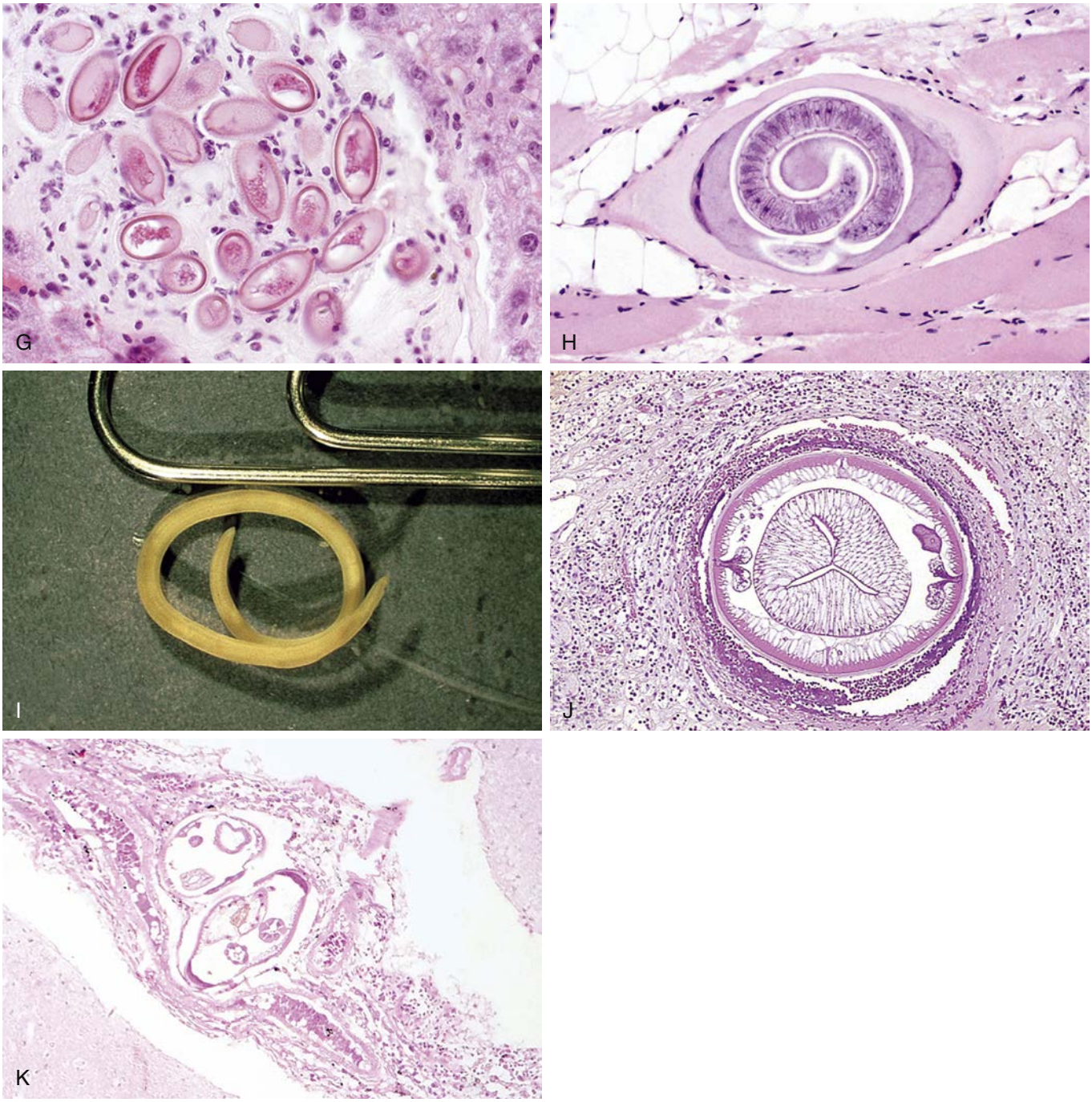

Figure 65.16 **G,** Eggs of *Capillaria hepatica* in a liver biopsy (H&E; 100×). **H,** *Trichinella* sp. cross-section of a larva in gastrocnemius muscle (H&E; 100×). **I,** Regurgitated anisakid nematode following consumption of fish. **J,** *Anisakis* sp., cross-section of larva found in small bowel following surgery for acute obstruction (H&E; 400×). **K,** Cross-sections of L4 larvae of *Angiostrongylus cantonensis* in brain tissue (H&E; 100×).

hosts and, in the case of *Taenia solium*, as both. Adult tapeworms attach to the intestinal mucosa by means of a scolex (head) that may display suckers, grooves (bothria), or a rostellum (knob-like protrusion) with hooks, depending on the species. The body of the worm (strobila) comprises an actively growing neck region that produces immature proglottids. These proglottids then undergo sequential development into mature and, eventually, gravid stages as they are pushed toward the posterior end with the formation of new immature proglottids. Each proglottid has a complete set of male and female gonads and is capable of producing fertile eggs, although sexual reproduction between two individual worms is the norm. Eggs of most cestodes infecting humans (*Dibothriocephalus* and related being the exception) may be readily differentiated from those of other helminths by the presence in each of a six-hooked embryo (oncosphere). Depending on the species, eggs are released directly into the fecal stream or are passed in intact proglottids. It is not uncommon in some species for long lengths of strobila to be passed intact or for proglottids to actively migrate out of the anus. Large species of *Taenia* and *Dibothriocephalus* may grow to 25 feet or longer and may live for 20 years. The treatment of choice for adult tapeworm infection is praziquantel, with niclosamide as an alternative drug (Drugs for Parasitic Infections, 2013).

Cestode larval stages develop to the infective stage in the tissues of invertebrate or vertebrate intermediate hosts, depending on the species, and complete their life cycle when ingested by a definitive host. Larval stages of several species may infect humans, causing cysticercosis, hydatidosis, sparganosis, and coenurosis. These conditions are covered more fully in the Tissue Helminths section later in the chapter. Unlike treatment for intestinal cestodes, treatment of larval tissue cestodes is with albendazole (Drugs for Parasitic Infections, 2013).

Taenia saginata (Taeniasis)

Humans are the sole definitive host for *Taenia saginata*, the beef tapeworm. Although it is distributed worldwide, infection is most common in the Middle East, Africa, Europe, Asia, and Latin America. It occurs rarely and sporadically in the United States, seen primarily in immigrants.

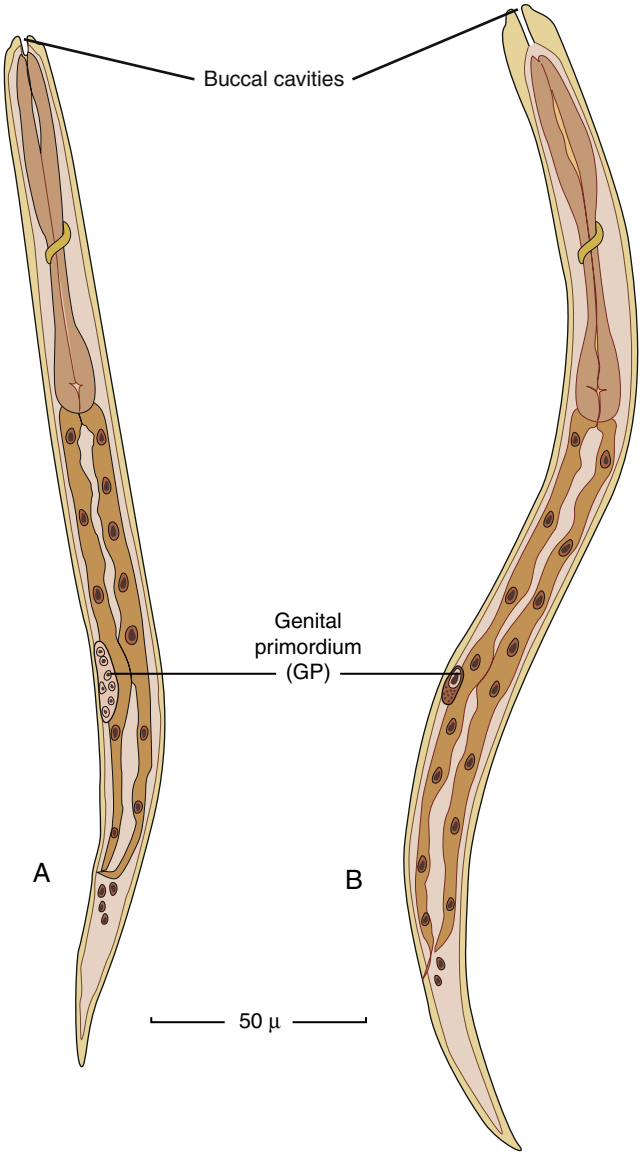

Figure 65.17 Hookworm and *Strongyloides stercoralis* larvae. **A,** *S. stercoralis* rhabditoid larva in human stools. Note the short size of the buccal cavity and the large genital primordium (GP). **B,** Hookworm rhabditoid larva as seen if there is a delay in processing stool stored at room temperature. The buccal cavity is longer and the GP is obsolete.

Larval cysticerci develop in the tissues of cattle that graze on land contaminated by human waste. When humans ingest infected raw or incompletely cooked beef, the cysticercus develops into a reproductive adult in the small intestine in 2 to 3 months. It uses a specialized scolex to attach to the small intestinal wall and then elongates as proglottids are produced, as described earlier. Most infected individuals are asymptomatic; when present, they commonly include abdominal discomfort and diarrhea. Unlike *T. solium* (discussed later), the eggs of *T. saginata* are not infectious to humans, and their ingestion does not result in human cysticercosis. Treatment is with praziquantel (Drugs for Parasitic Infections, 2013).

Diagnosis is made by finding characteristic eggs in the stool or shed proglottids. Eggs are spherical and measure 31 to 43 µm in diameter (Fig. 65.18A). The shell is thick, radially striated, and contains a six-hooked embryo. Eggs of all *Taenia* spp. are indistinguishable and should therefore be reported only as *Taenia* spp. eggs.

Species identification may only be made by microscopic examination of the proglottids or, more rarely, the scolex (following administration of an anthelminthic agent), or by NAATs. Proglottids of taeniids have a characteristic single lateral protrusion known as the *genital pore*. Careful injection of India ink through the genital pore using a tuberculin needle and syringe, following clearing in lactophenol, may succeed in outlining the uterus. In many circumstances, pressing an unpreserved proglottid between two slides, with or without prior clearing, will also adequately highlight the uterus and allow for species identification. The gravid uterus of *T. saginata* has 15 to 20 primary lateral branches (counted on one side only), whereas that of *T. solium* has 7 to 13 primary lateral branches (Figs. 65.18F and 65.19). Proglottids may also be cleared overnight in glycerol or stained with carmine or hematoxylin using published procedures (Ash & Orihel, 2007). If recovered, the scolex of *T. saginata* can be identified by the presence of four suckers and the absence of hooks on the crown or rostellum. When handling *Taenia* proglottids, it is important to remember that the eggs contained within may cause cysticercosis if ingested (if *T. solium*); thus, utmost care is warranted.

Taenia asiaticus (formerly considered a subspecies of *T. saginata*) cycles between humans and pigs in Southeast Asia. The proglottids of *T. asiaticus* are similar to those of *T. saginata* but the scolex has an armed rostellum, similar to *T. solium*. This species is not known to cause cysticercosis in humans (Ale et al., 2014).

Taenia solium (Taeniasis)

Taenia solium, the pork tapeworm, is most common in Europe, especially in Eastern Europe, Latin America, China, Pakistan, and India. It is encountered in the United States on occasion, most often in immigrants. Infection with the adult tapeworm (taeniasis) is acquired by eating raw or incompletely cooked pork containing cysticerci). Most patients with taeniasis due to *T. solium* are asymptomatic. Symptoms, if present, are identical to those of *T. saginata* infection. Treatment is with praziquantel (Drugs for Parasitic Infections, 2013). Importantly, accidental ingestion of *T. solium* eggs from one's own adult tapeworm or from contaminated food may result in cysticercosis. Past outbreaks of cysticercosis in the United States have been associated with food preparers with taeniasis due to *T. solium* (Schantz et al., 1992; CDC, 2018b). Additional details on cysticercosis may be found in the Tissue Helminths section later in the chapter.

Procedures used for diagnosis of intestinal *T. solium* infection are identical to those used for *T. saginata* infection, although certain morphologic differences are apparent. The scolex of *T. solium* has four suckers and, unlike *T. saginata*, a rostellum armed with two rows of hooks. Gravid proglottids have 7 to 13 primary lateral uterine branches on each side of the uterine stem (see Fig. 65.19).

Hymenolepis nana (Hymenolepiasis)

Hymenolepis nana, known as the dwarf tapeworm, has a worldwide distribution and is regarded as the most frequently recovered cestode species seen in the United States. It is a common parasite in mice and is the smallest cestode to infect humans, measuring up to 4.0 cm in length. The scolex has an armed rostellum containing a single row of hooks, and the proglottids have all of their genital pores located on the same side of the strobila (see Fig. 65.19). The life cycle may be direct, through the ingestion of infectious eggs, or indirect, through the ingestion of intermediate hosts (usually grain beetles) containing cysticercoid larvae. In the former instance, eggs may be passed directly from person to person, usually among children (highest likelihood), or may be ingested in food, such as grain products that are contaminated by grain beetles or possibly rodent droppings (Ash & Orihel, 2007).

Ingested eggs hatch in the intestine and embryos penetrate the mucosa, where they mature into cysticercoid larvae. They subsequently emerge and reattach to the intestinal wall to complete their development into adult tapeworms in 2 to 3 weeks. Therefore, humans serve as both the intermediate and definitive host for this parasite. Internal autoinfection may occur in some individuals in whom eggs hatch shortly after being discharged from the worm and rapidly invade the intestinal wall without leaving the body. Such a mechanism is thought to be responsible for the occasional case of massive infection.

Symptomatic infection, characterized by abdominal pain, diarrhea, anorexia, and irritability, may develop in patients with large numbers of worms. Treatment is with praziquantel (Drugs for Parasitic Infections, 2013). Diagnosis is made by recovery from stool of the oval, thin-shelled, colorless eggs, which measure 30 to 47 µm in diameter (Fig. 65.18B). They contain a centrally located, six-hooked embryo (oncosphere), which is separated from the outer shell by a clear space. This embryo displays two polar thickenings from which thin filaments arise and extend into the clear space between the embryo and outer shell. Rarely, intact strobila may be recovered if the stool is closely examined or by colonoscopy.

Hymenolepis diminuta (Hymenolepiasis)

The rat tapeworm, *Hymenolepis diminuta*, is cosmopolitan in distribution and rarely infects humans. Infection is infrequent because of the obligate need for an arthropod intermediate host, in which the cysticercoid larvae develop. Human infection usually occurs following the accidental ingestion of infected beetles that contaminate grain or cereal products. Adult

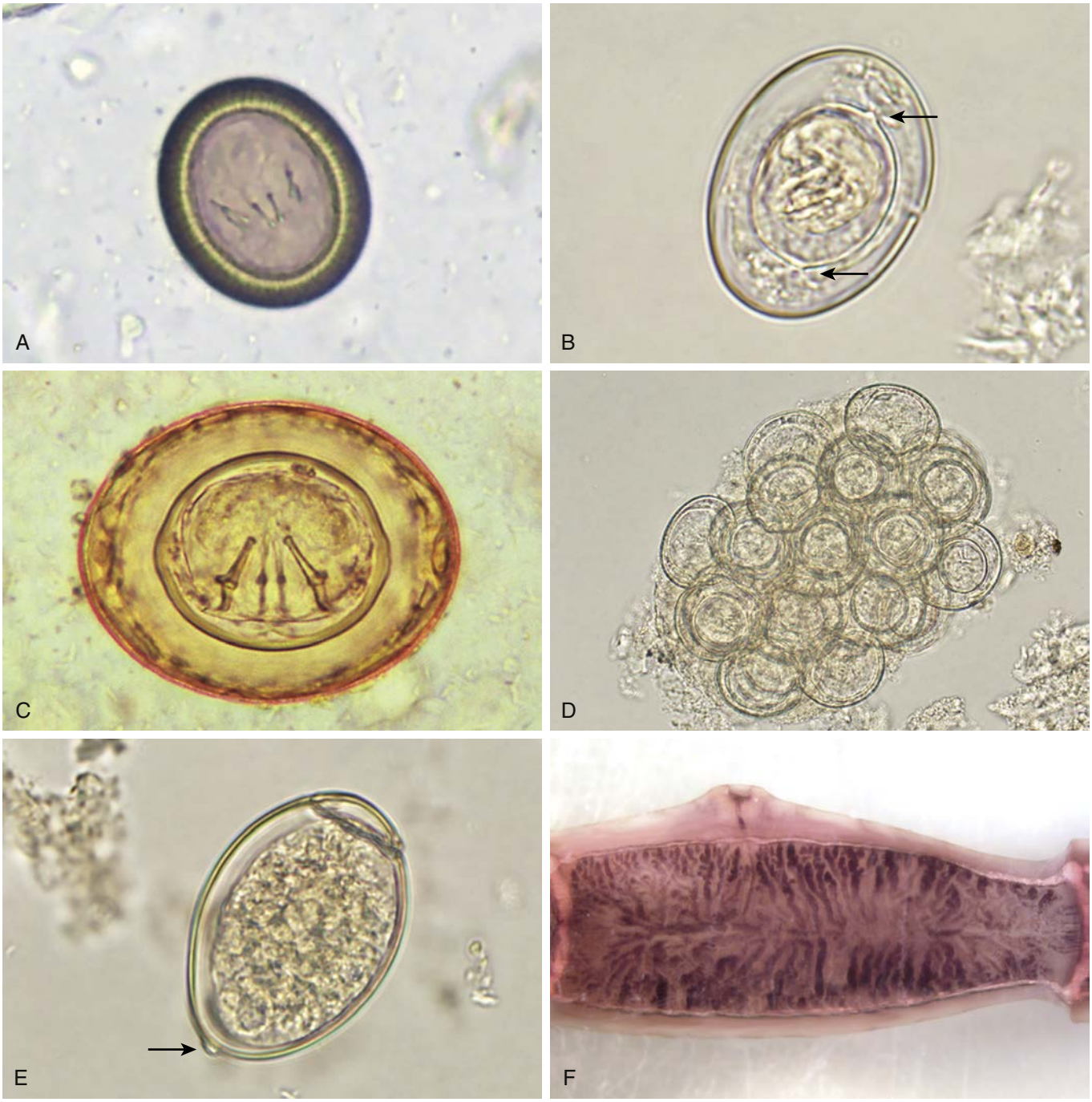

Figure 65.18 **A,** Egg of *Taenia* spp. Four of the six hooks of the oncosphere are visible (400×). **B,** Egg of *Hymenolepis nana*. Note the presence of hooklets and polar filaments *(arrows)* (400×). **C,** Egg of *Hymenolepis diminuta*. Note the lack of polar filaments. Hooks of the oncosphere are visible (iodine, 400×). **D,** Egg packet of *Dipylidium caninum* (400×). **E,** Egg of *Diphyllobothrium*/*Dibothriocephalus*/*Adenocephalus* spp. Note the operculum and small abopercular knob *(arrow)* (400×). **F,** Gravid proglottid of *T. saginata* injected through the genital pore with India ink to highlight the uterine branches (2×).

Continued

tapeworms develop in the small intestine, where they may grow to 60 cm in length. Similar to those of *H. nana*, the proglottids all have genital pores on one side; however, unlike that species, the scolex lacks an armed rostellum. Infection usually is asymptomatic because of the small number of worms likely to infect a single individual, although intestinal symptoms have occasionally been reported. Diagnosis is made by finding moderately thick-shelled, slightly ovoid, yellow-brown eggs measuring 70 to 85 µm by 60 to 80 µm in stool specimens (Fig. 65.18C). The eggs are most easily confused with those of *H. nana* but lack polar filaments.

Dibothriocephalus, Diphyllobothrium, and *Adenocephalus* (Diphyllobothriasis)

Humans may be infected by any of several species of diphyllobothriid cestodes, commonly collectively called the fish tapeworms. Historically, species implicated in human disease were placed in the genus *Diphyllobothrium*. However, the group has recently undergone taxonomic changes and most human infections are attributed to members of the genera *Dibothriocephalus* or *Adenocephalus* (Hernandez-Orts et al., 2015; Waeschenbach et al., 2017). These parasites are widely distributed in the temperate zones, especially northern Europe, Scandinavia, the former USSR, and Japan. Infection also occurs in Canada and in the north central states, the Pacific Coast states, and Alaska in the United States. Although *Dibothriocephalus latus* (formerly *Diphyllobothrium latum*) is the most common species implicated in human disease, differentiation of the infecting species cannot be made on the basis of egg morphology alone.

Diphyllobothriid cestodes inhabit the small intestine, where they can reach a length of 10 m or longer and can persist for years. Eggs are passed unembryonated in the feces and must reach a freshwater stream or lake to continue development. Following several weeks of embryonation, a ciliated larval form, the six-hooked coracidium, hatches and is ingested by a copepod, a type of microscopic crustacean. The coracidium develops into a procercoid larva, which is infective for the second intermediate host, a fish. In fish, the procercoid migrates into the tissues and develops into the plerocercoid larva. Plerocercoids may be passed up the food chain unchanged

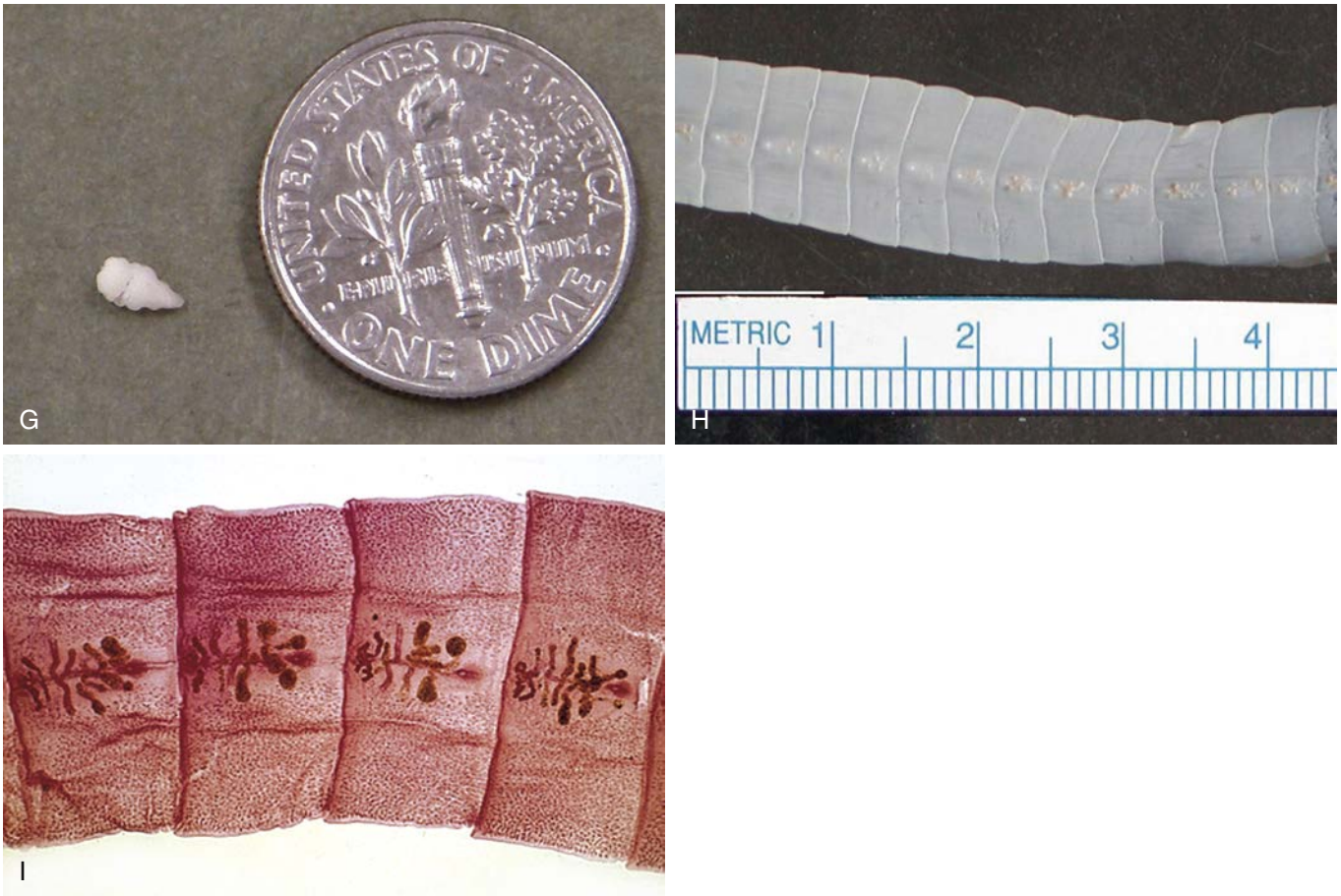

Figure 65.18—cont'd **G,** Proglottid of *Dipylidium caninum*. **H,** Proglottids of *Diphyllobothrium*/*Dibothriocephalus*/*Adenocephalus*. Note the centrally located uterus in each proglottid. **I,** Proglottids of *Dibothriocephalus* sp. (acetocarmine stain, 2×). (**G** courtesy of The College of American Pathologists Parasitology Benchtop Reference Guide.)

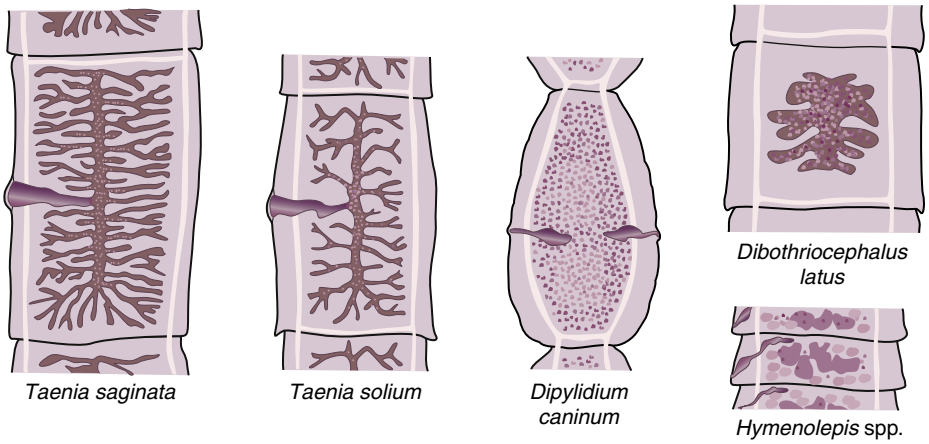

Figure 65.19 Gravid proglottids of different human tapeworms.

and accumulate in larger fish. Humans acquire these larvae through ingestion of raw or incompletely cooked fish that have spent at least part of their life in fresh water.

Adult worms mature and initiate egg production in approximately 1 month. Infection may be asymptomatic, with passage of a length of strobila being the initial complaint. In others, a variable degree of abdominal discomfort and diarrhea may be present. Rarely, intestinal obstruction occurs. In endemic areas in northern Europe, a small percentage of patients develop vitamin B_{12} deficiency and associated megaloblastic anemia due to the propensity of *Dibothriocephalus* to absorb B_{12} in the jejunum. Treatment is with praziquantel (Drugs for Parasitic Infections, 2013).

Diagnosis is made by the finding of typical yellow-brown, oval, operculate eggs (i.e., containing a lid-like opening called an operculum) in feces during O&P examination. Eggs measure 58 to 76 μm by 40 to 51 μm and, in addition to the operculum, have a small, round, knoblike projection on the abopercular end (i.e., the end opposite the operculum; Fig. 65.18E). The presence of the operculum is unique among those cestodes infecting humans. Care must be taken not to confuse these eggs with those of trematodes, especially *Paragonimus* or *Nanophyetus*, that are approximately the same size and also have an operculum. Identification of members of this complex is possible when a length of strobila (i.e., chain of proglottids) or an intact worm is passed. The scolex is rarely seen but may be recovered in the stool of patients treated with praziquantel; unlike the taeniids, it is elongate and has a pair of longitudinal grooves known as *bothria*, which replace the usual suckers of other human cestodes. Gravid proglottids are wider than they are long and have their genital pores located midventrally, adjacent to a centrally located rosette-shaped uterus (Figs. 65.18, *H*, *I*, and 65.19).

Dipylidium caninum

Dipylidium caninum is a common tapeworm of dogs and cats in most parts of the world that not infrequently infects humans, especially children.

In the usual life cycle, tapeworm eggs are ingested by flea larvae, which infest areas frequented by dogs or cats. The cysticercoid larvae persist as the flea undergoes metamorphosis to the adult stage. Accidental ingestion of the adult flea containing the infectious cysticercoid results in infection. Children are at highest risk for infection because of their close contact with pets and lack of hygiene. Worms mature in the small intestine and grow up to 70 cm in length. Infection produces few symptoms and generally causes concern only on detection of the actively moving proglottids (Cabello et al., 2011). Treatment is with praziquantel (Drugs for Parasitic Infections, 2013).

Detection is based on the finding of characteristic eggs, egg packets, or proglottids in the feces. The proglottids are rather hardy and are usually passed intact. As such, eggs or egg packets are less commonly detected in O&P examinations but can usually be expressed from proglottids in the laboratory. Spherical eggs, each containing a six-hooked embryo, measure from 24 to 40 μm in diameter and occur singly or in packets (Fig. 64.18D). The scolex is somewhat elongate, with four suckers and a small, retractable rostellum. Proglottids are barrel shaped and possess two genital pores, one on each lateral margin, which give rise to the common name *double-pored tapeworm* (see Fig. 65.19). They are commonly likened to a "grain of rice" or "cucumber seed" when seen intact in stool (Fig. 65.18G). Because they are often motile when passed, they are commonly noted by the child's caregiver.

TREMATODES

Trematodes, or flukes, are dorsoventrally flattened helminths that include both hermaphroditic forms (intestinal, liver, and lung flukes) and dioecious forms (separate sexes; seen with the blood flukes/schistosomes). Even with the hermaphroditic forms, sexual reproduction between two individual worms is the norm. All species that infect humans are characterized by the presence of an oral sucker through which the digestive tract opens and a ventral sucker (acetabulum) used for attachment. Adults vary in length from 1 mm (*Metagonimus*) to 70 mm (*Fasciola gigantica*).

Eggs reach the environment by being passed in the feces, sputum, or urine depending on the species. Hermaphroditic flukes produce operculate eggs, which may or may not be embryonated at the time of passage. Schistosome eggs are not operculated, and each contains a mature larva (miracidium) when passed. Miracidia are ciliated and are capable of penetrating the tissues of a molluscan host. Each species of trematode uses a particular species of freshwater or terrestrial snail as the first intermediate host. A complex asexual multiplication process within the snail results in the production of numerous free-swimming larvae called *cercariae*. Schistosome cercariae are capable of penetrating human skin directly, resulting in the disease schistosomiasis. Those of hermaphroditic flukes encyst on aquatic vegetation or invade the tissues of second intermediate hosts such as fish or crabs depending on the species. Ingestion of these encysted larval stages, known as *metacercariae*, results in human infection.

Human trematode infection may occur in many tropical and subtropical regions, involving considerably more species (mostly rare and sporadic intestinal infections) than can be presented here. Its presence depends on lack of adequate sewage treatment, availability of appropriate intermediate hosts, and, in the case of hermaphroditic species, dietary customs associated with ingestion of infective metacercariae in raw or undercooked plants or animals. Some of these diseases, especially schistosomiasis, expanded with the increased use of irrigation in endemic areas, which allowed for proliferation of the snail intermediate hosts. Symptoms vary depending on the number of worms parasitizing the host at a given time, the tissues and organs involved, and host responses. Many infections are asymptomatic. The treatment of choice for trematodiasis, with the exception of fascioliasis, is praziquantel (Drugs for Parasitic Infections, 2013).

The diagnosis of trematode infection is most commonly made by recovery and identification of the characteristic eggs in stool, sputum, urine, and, occasionally, tissues. Sedimentation concentration methods are most useful for recovery of these eggs. As mentioned in the prior Laboratory Methods section, zinc sulfate flotation methods are less satisfactory for detecting parasites with operculate eggs. Trematode eggs are usually shed in small numbers; thus, examination of multiple specimens is recommended for optimal detection sensitivity.

Fasciolopsis buski (Fasciolopsiasis)

This intestinal trematode is the largest species to infect humans, varying from 20 to 75 mm in length and from 8 to 20 mm in width. It occurs in many parts of China, Southeast Asia, and India and is frequently found in pigs, which serve as a natural reservoir host. Infection is acquired by ingesting infectious metacercariae on aquatic food plants such as water chestnuts and water caltrop. Worms attach to the wall of the duodenum and jejunum, where they mature to egg-laying adults in about 3 months. Symptoms such as diarrhea, epigastric pain, and nausea may develop if enough worms are present to produce ulceration of the superficial mucosa. Eosinophilia may be present, even in those who are asymptomatic. The treatment of choice for trematodiasis, with the exception of fascioliasis, is praziquantel (Drugs for Parasitic Infections, 2013).

Diagnosis is made by the finding of large (130–140 μm by 80–85 μm), yellow-brown, oval, thin-shelled eggs (Fig. 65.20C). The operculum may often be inconspicuous, and the eggs are passed unembryonated (i.e., there is no identifiable miracidium within, as is seen with schistosomes). Differentiation from *Fasciola* eggs generally is not possible, although these infections may be differentiated on the basis of geographic history and symptoms. Eggs of echinostome trematodes, which occasionally infect humans, are similar but smaller (Ash & Orihel, 2007).

Heterophyes and *Metagonimus*

These two genera include a number of species of minute (1–3 mm in length) intestinal worms that infect humans. *Heterophyes heterophyes* and *Metagonimus yokogawai* are common parasites in Asia but, along with other species, are found in other parts of the world as well. Infection is acquired by ingestion of metacercariae in raw or incompletely cooked freshwater fish. Although it is of minor medical importance, infection with these worms may produce diarrhea and abdominal pain. Infection is self-limited because the worms have a life span of only a few months. The treatment of choice for trematodiasis, with the exception of fascioliasis, is praziquantel (Drugs for Parasitic Infections, 2013).

Diagnosis is established by the finding of embryonated, operculate eggs that measure 20 to 30 μm in length by 15 to 17 μm in width. Differentiation of these eggs from those of *Clonorchis* and *Opisthorchis* may be difficult, although the operculum is more deeply seated with *Opisthorchis* and *Clonorchis* and heterophyid trematodes usually lack an abopercular knob. Such differentiation may be important for medical reasons.

Nanophyetus salmincola

Nanophyetus salmincola is a small (0.8–1.1 mm) intestinal fluke that has been reported in humans in areas of far eastern Siberia and the Pacific Northwest coast of the United States (Fritsche et al., 1989; Eastburn, 1987). These worms are acquired by ingesting raw, incompletely cooked, or home-smoked salmon or trout that contain infectious metacercariae. Symptoms are related to the number of worms present and may include abdominal pain and diarrhea, with or without eosinophilia. The treatment of choice for trematodiasis, with the exception of fascioliasis, is praziquantel (Drugs for Parasitic Infections, 2013). Eggs measuring 60 to 80 μm by 34 to 50 μm are broadly ovoid, operculate, and yellowish brown (Ash & Orihel, 2007). Thickening of the shell at the abopercular end should be differentiated from the knob seen on eggs of *Dibothriocephalus*. This fluke is the vector for a rickettsial species that produces a highly lethal infection in canines known as *salmon-poisoning disease*.

Fasciola hepatica (Fascioliasis)

Cattle, sheep, and goats in many parts of the world are infected with the liver fluke *Fasciola hepatica* and, less commonly in Africa and Asia, with the related species *Fasciola gigantica*. Adult parasites live in the biliary tree and lay eggs that are passed in the feces. Cercariae shed from the snail intermediate host encyst on aquatic vegetation, where infectious metacercariae then are available to herbivorous hosts. Humans usually acquire the infection by eating raw aquatic plants such as watercress or drinking fresh water contaminated with metacercariae. Once ingested, the larvae penetrate the intestinal wall and migrate through the peritoneal cavity to the liver. They burrow through the capsule and parenchyma, coming to reside within the bile ducts, where egg laying starts in about 2 months (Fig. 65.20F). Migration of the larvae through the liver elicits a painful inflammatory reaction both in the tissue and, later, in the bile ducts, which eventually become fibrosed. Clinical manifestations include colic, obstructive jaundice, abdominal pain and tenderness, cholelithiasis, and eosinophilia. Unlike the other trematodiasis, treatment is with triclabendazole rather than praziquantel (Drugs for Parasitic Infections, 2013).

Diagnosis is made by the finding of eggs in the stool. The unembryonated, yellow-brown, operculate eggs, 130 to 150 μm by 63 to 90 μm, cannot be distinguished from those of *Fasciolopsis* by morphology alone (see Fig. 65.20C); eggs of *F. gigantica* are typically larger, measuring 160 to 190 μm long by 70 to 90 μm wide. Spurious passage, which occurs by ingesting infected cattle or sheep liver, is diagnosed by obtaining a good history and performing a follow-up stool examination to look for elimination of the

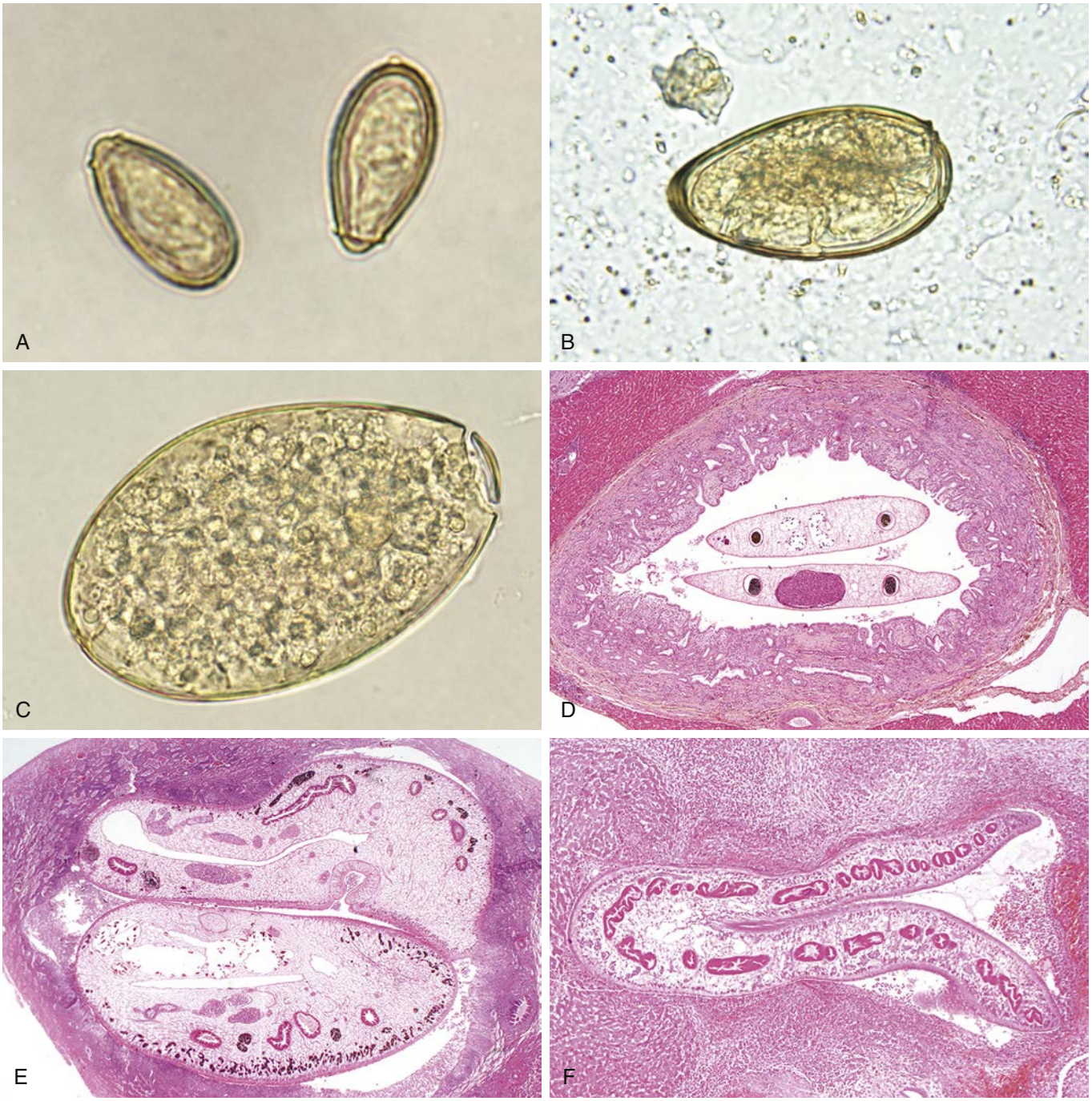

Figure 65.20 **A,** Egg of *Clonorchis sinensis* in stool. Note the prominent shouldered operculum, abopercular knob, and urn shape (1000×). **B,** Egg of *Paragonimus* sp. Note the prominent shouldered operculum and abopercular thickening (400×). **C,** Egg of *Fasciolopsis buski*, indistinguishable from that of *Fasciola hepatica*, in stool (400×). **D,** Two adult *Clonorchis sinensis* in bile duct (H&E; 40×). **E,** Pair of adult *Paragonimus* sp. in lung tissue with surrounding inflammatory reaction (H&E; 40×). **F,** Adult *Fasciola hepatica* in liver (H&E; 40×).

eggs. Serologic testing for *F. hepatica* is available in the United States at the CDC (Shin et al., 2016).

Clonorchis sinensis and *Opisthorchis* spp.

Clonorchis sinensis, the Oriental liver fluke, and a closely related species, *Opisthorchis viverrini*, inhabit the biliary system of humans and other piscivorous animals, including cats and dogs. *C. sinensis* occurs mainly in China, Taiwan, Korea, Japan, and Vietnam, whereas *O. viverrini* is found primarily in Southeast Asia, especially northern Thailand. Human infection is also known to occur with *Opisthorchis felineus* in Europe, *Amphimerus pseudofelineus* (syn. *Opisthorchis guayaquilensis*) in Ecuador, and *Metorchis conjunctus* in northern North America.

All of these parasites are acquired by the ingestion of infectious metacercariae in raw or uncooked freshwater fish. Unlike *F. hepatica*, the larvae reach the liver by migrating directly up the common duct into the liver bile ducts. Here, they can reside for 20 years and grow up to 25 mm in length (Fig. 65.20D). They produce small operculate eggs that are shed into the bile and subsequently are passed in stools.

Infection is often asymptomatic, although large numbers of flukes and repeated infection may cause inflammation of the bile ducts and subsequent hyperplasia and fibrosis (Drugs for Parasitic Infections, 2013). Of note, bile duct metaplasia and ultimate development of cholangiocarcinoma has been linked epidemiologically with long-standing infection of *Clonorchis sinensis* and *Opisthorchis* spp.

Diagnosis is made by recovering the small yellow-brown, embryonated, operculate eggs from stool (Fig. 65.20A). Eggs of *Clonorchis* cannot be readily differentiated from those of *Opisthorchis*. Both measure 25 to 35 μm by 12 to 20 μm and have a prominent, seated, or "shouldered" opercula and a small knob at the abopercular end. These eggs are difficult to differentiate from those of the *Heterophyes/Metagonimus* group, although the latter species do not have prominent, seated operculum or a small knob at the abopercular end. When specific identification is not possible, the

laboratory report should reflect this (i.e., could state, "*Clonorchis/Opisthorchis/Heterophyes/Metagonimus* eggs").

Paragonimus spp. (Paragonimiasis)

Several species of *Paragonimus* may parasitize the lungs of cats, dogs, and other carnivores, including humans. *Paragonimus westermani* and *P. heterotremus* cause human infection in many areas of Asia, whereas several species have been implicated in Central and South America, including *Paragonimus mexicanus*, *Paragonimus caliensis*, and *Paragonimus ecuadoriensis*. *Paragonimus kellicotti* has occasionally been implicated in cases from North America, and other species have been described from Africa (Ash & Orihel, 2007; Procop, 2009; Diaz, 2013).

Adult worms measure up to 12 mm by 6 mm and often are found in pairs in the lung parenchyma, where they reside encased in a host-derived fibrotic capsule (Fig. 65.20E). The capsule communicates with the bronchi, through which eggs pass to be eventually expelled in sputum or, if swallowed, the feces. A specific snail serves as the first intermediate host, while freshwater crabs and crayfish serve as second intermediates for infectious metacercariae. Humans become infected following ingestion of raw or undercooked crustaceans containing encysted metacercariae. Following ingestion, metacercariae excyst in the stomach and migrate through the intestinal wall into the peritoneal cavity, eventually reaching the lungs after penetrating the diaphragm. Maturation takes approximately 5 to 6 weeks, and worms may live for many years. Ectopic migration occurs not infrequently, resulting in infection of other organs, including the peritoneum, subcutaneous tissues, and the brain.

Symptoms, when present, may be caused by larvae migrating through tissues or by adults established in the lungs. The onset of lung infection is usually associated with fever, chills, and the appearance of eosinophilia. Once established, symptoms include chronic coughing with abundant mucus production, along with episodes of hemoptysis (Drugs for Parasitic Infections, 2013). Radiographs may show nodular shadows, calcifications, or patchy infiltrates. Eggs remaining in the lung tissues or in ectopic sites may cause an extensive granulomatous reaction.

Diagnosis is made by the finding of typical eggs in stool, sputum, or, occasionally, tissues. Eggs of the different *Paragonimus* spp. cannot be readily differentiated. Operculate, unembryonated eggs typically measure 80 to 120 μm by 45 to 70 μm and have a moderately thick, yellow-brown shell (Fig. 65.20B). The operculum is flattened and usually is set off from the rest of the shell by prominent shoulders (i.e., shouldered operculum). The abopercular end is somewhat thickened but does not have a knob. *Paragonimus* eggs may be differentiated from those of *Dibothriocephalus* and *Fasciola/Fasciolopsis*, which they superficially resemble, by size.

Schistosoma spp. (Schistosomiasis)

Schistosomiasis, or bilharzia, is among the most important parasitic diseases worldwide. As mentioned previously, this fluke is dioecious (i.e., male and female flukes are separate entities); adult flukes inhabit the veins of the mesentery or bladder; thus, they are referred to as *blood flukes*. The most important species infecting humans are *Schistosoma mansoni*, *S. japonicum*, *S. mekongi*, *S. haematobium*, *S. intercalatum*, and *S. guineensis*. Other zoonotic species infect humans less frequently.

Adult female schistosomes are slender, measuring up to 26 mm by 0.5 mm. Males, which are slightly shorter, enfold a female using the lateral margins of the body (the gynecophoral canal) to assist in sperm transfer. When examined *in situ*, schistosomes are often found together in this arrangement (i.e., *in copula*). They are generally monogamous throughout their existence. Within the blood vessels, blood flukes elicit little or no inflammatory response. However, eggs are deposited in the smallest venule that can accommodate the female worm, eliciting a strong granulomatous host response that results in extrusion of the egg through the intestinal or bladder wall and into the lumen for excretion in stool or urine, respectively. Eggs laid in the mesenteric vessels also commonly end up in the liver. The pathology associated with schistosomiasis is primarily related to the sites of egg deposition, the numbers deposited, and the host reaction to egg antigens.

Eggs are fully embryonated when passed and readily hatch when deposited in fresh water. The miracidia penetrate an appropriate species of snail host, where they undergo transformation and extensive asexual multiplication. After about 4 weeks, large numbers of fork-tailed cercariae emerge from the infected snail. These cercariae swim actively about for hours and readily penetrate the skin of susceptible hosts, including humans. After penetration, the cercariae lose their tail to become *schistosomulae* and enter the circulation, passing through the lungs and liver, to eventually reach the mesenteric-portal vessels. A female worm will not develop to maturity without the presence of a male.

Symptoms of schistosomiasis result primarily from penetration of cercariae (cercarial dermatitis or "swimmer's itch"), from initiation of egg laying (acute schistosomiasis or Katayama fever), and as a late-stage complication of tissue proliferation and repair in response to eggs in tissues (chronic schistosomiasis). In a matter of hours after cercarial penetration, a papular rash associated with pruritus may develop. This is a sensitization phenomenon resulting from prior exposure to cercarial antigens. The most severe form of dermatitis occurs in individuals who are repeatedly exposed to cercariae of nonhuman (primarily avian) schistosomes. Cercarial dermatitis occurs worldwide and is a well-recognized condition in parts of the United States (Brant & Loker, 2009).

Initiation of egg laying by mature worms 5 to 7 weeks after infection may result in acute schistosomiasis, or Katayama fever, a serum sickness–like syndrome that occurs with heavy primary infection, especially that of *S. japonicum*. The antigenic challenge to the host is thought to result in immune complex formation (Boros, 1989).

Chronic infection results in continued deposition of eggs, many of which remain in the body. Granulomas produced around these eggs in the intestine and in the bladder are gradually replaced by collagen, resulting in fibrosis and scarring. Eggs trapped in the liver may induce pipe-stem fibrosis with obstruction to portal blood flow. Occasionally, eggs are deposited in ectopic sites, such as the spinal cord, lungs, or brain (Orihel & Ash, 1995; Meyers, 2000; Pritt, 2018). Treatment is with praziquantel, which will kill the adult worms and prevent further damage (Drugs for Parasitic Infections, 2013). However, it will not reverse the scarring that previously occurred due to egg deposition.

Diagnosis is established by demonstrating eggs in feces or urine by direct wet mount or sedimentation-based concentration methods. Flotation concentration is not satisfactory for recovery of heavy schistosome eggs. Eggs also may be detected in biopsies of rectal, bladder, and, occasionally, liver tissues by crush preparation or in histologic sections (Fig. 65.21).

Serologic tests may be helpful in screening persons who have traveled to endemic areas and those with negative urine or stool examination who are at risk for infection, although it cannot be reliably correlated with worm burden, clinical status, egg production, or prognosis. Although not widely available, a limited number of reference laboratories and the CDC provide testing. Generally, serologic testing varies with the antigens used and test methods employed. The CDC uses the Falcon assay screening test in a kinetic enzyme-linked immunosorbent assay (FAST-ELISA). Sera that are positive by the screening test are further evaluated by immunoblot to improve specificity (Tsang & Wilkins, 1997).

Schistosoma mansoni

Schistosoma mansoni occurs in Africa, especially in the tropical areas and the Nile delta, southern Africa, and Madagascar, Brazil, Venezuela, Surinam, and certain Caribbean islands, including Puerto Rico. Adult *S. mansoni* live primarily in the portal vein and in the distribution of the inferior mesenteric vein. Initial deposition of eggs in the large intestine may produce abdominal pain and dysentery, with abundant blood and mucus in the stool. Eggs may be detected in feces at this time. Chronic infection may result in liver fibrosis and portal hypertension depending on the number of worms present; eggs may be more difficult to find in feces during this stage.

Eggs measure 116 to 180 μm by 45 to 58 μm, are oval, and possess a large distinctive lateral spine that protrudes from the side of the egg near one end (Figs. 65.21A and 65.21B). If the spine is not visible, the egg may be rotated by gently tapping the coverslip. Movement of the miracidium within the egg may be evident in unfixed material and, when seen, indicates active infection. Concentration techniques may be required to detect eggs because individuals with limited exposure or with chronic infection may pass few of them.

Schistosoma japonicum

Schistosoma japonicum, which occurs in China, southeast Asia, and the Philippines, causes disease that is clinically similar to that of *S. mansoni* but often more serious because many more (up to 10 times as many) eggs are produced by *S. japonicum*. The disease has been essentially eliminated from Japan, although animal reservoirs still exist. Adult worms live primarily in the distribution of the superior mesenteric vein, and eggs readily reach the liver, inducing fibrosis and portal hypertension as a common complication of chronic infection. The smaller size of the eggs is thought to predispose them to ectopic dissemination, especially to the brain and spinal cord. The eggs are broadly oval, measuring 75 to 90 μm by 60 to 68 μm, and have an inconspicuous lateral spine, which may be difficult to demonstrate (see Figs. 65.21C and 65.21D).

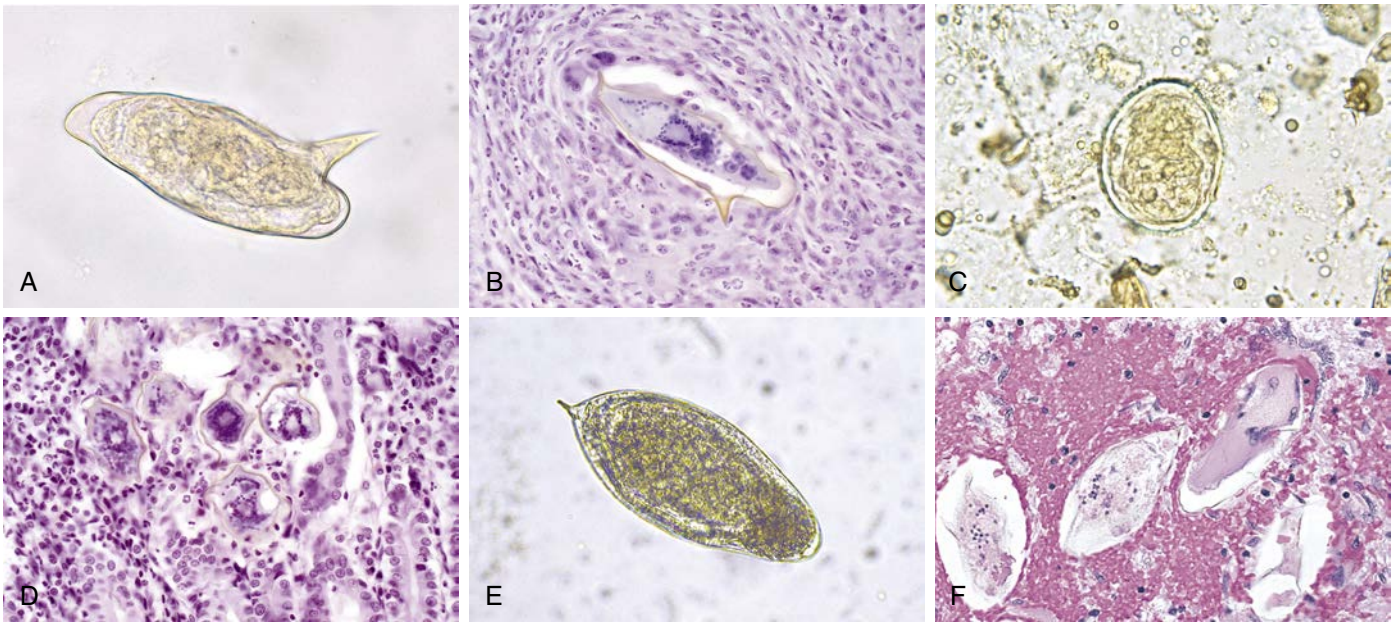

Figure 65.21 **A,** Egg of *Schistosoma mansoni*. Note the prominent lateral spine (400×). **B,** Egg of *S. mansoni* in an intestinal biopsy. Note the presence of a lateral spine (H&E; 400×). **C,** Egg of *Schistosoma japonicum*. Note the presence of a rudimentary lateral spine (400×). **D,** Eggs of *S. japonicum* in a small-bowel biopsy (H&E; 200×). **E,** Egg of *Schistosoma haematobium* found in urine sediment. Note the presence of a terminal spine (400×). **F,** Eggs of *S. haematobium* seen in a vulvar granuloma. Note the presence of a terminal spine (H&E; 400×).

Schistosoma mekongi

This species occurs in humans and animal reservoirs in countries along the Mekong River, especially Cambodia and Laos (Ash & Orihel, 2007). It is similar to *S. japonicum* but is differentiated from that species by several biological characteristics and by smaller eggs (60–70 μm by 52–61 μm), which otherwise are indistinguishable from those of *S. japonicum*.

Schistosoma haematobium

Urinary schistosomiasis occurs in many parts of Africa, the Middle East, and Madagascar, and has been introduced to Corsica, Italy (Ramalli et al., 2018). Parasites migrate via the hemorrhoidal veins to the venous plexuses of the urinary bladder, prostate, uterus, and vagina. One of the earliest and most common symptoms of infection is hematuria, especially at the end of micturition. Chronic infection may cause pelvic pain and bladder colic, with an increased desire to urinate. Accumulation of eggs in the tissues may result in hypertrophy of the urothelium, squamous metaplasia, and marked fibrosis, which may progress to obstruction and, ultimately, renal failure. Urinary schistosomiasis also has been associated with squamous cell carcinoma of the bladder (Meyers, 2000).

Eggs can be recovered from the urine by examination of spun sediment or through filtration. They are elongate, measuring 112 to 180 μm by 40 to 70 μm, and have a characteristic terminal spine (see Figs. 65.21E and 65.21F).

Schistosoma intercalatum and *S. guineensis*

These species occur in parts of central and western Africa and produce intestinal schistosomiasis. *Schistosoma guineensis* (formerly the "Lower Guinea strain" of *S. intercalatum*) occurs generally in central and western Africa while *S. intercalatum* proper (formerly the Zaire strain) is endemic to the Democratic Republic of the Congo. Eggs have a terminal spine, resembling those of *S. haematobium*, but they occur primarily in the feces and are larger (140–240 μm by 50–85 μm) (Webster et al., 2006).

TISSUE HELMINTHS

NEMATODES

Filarial Nematodes (Filariasis)

Filarial nematodes are arthropod-transmitted parasites of vertebrate animals. Adult male and female worms are long and slender, and are known to inhabit a variety of tissues, including subcutaneous tissues, lymphatics, blood vessels, peritoneal and pleural cavities, and the heart. All species produce larvae known as *microfilariae*, which may be recovered from blood or skin, depending on the species. The microfilariae of some species circulate in the blood with a well-defined periodicity (diurnal or nocturnal), whereas others do not. Microfilariae continue their development only in the appropriate arthropod vector, usually a mosquito or other fly, where they mature to the infective stage. Such larvae then are deposited in the tissues of a definitive host when the vector takes another blood meal.

The diagnosis of filariasis usually is made by the finding of microfilariae in the blood or skin because adult stages are often sequestered in the tissues. Use of Giemsa or hematoxylin-stained thick and thin smears of peripheral blood is routine. However, more sensitive procedures—such as membrane filter, Knott concentration, or saponin lysis—may also be required for detection (Ash & Orihel, 2007; Mathison et al., 2019). Microfilariae may also be seen moving in direct mounts of blood or tissue fluid.

Identification of the infecting filarial worm is important for directing therapy since it varies among the common human pathogens. Principal characteristics used for identification of microfilariae include the presence or absence of a sheath and its staining characteristics, the shape of the tail and the distribution of cell nuclei within, and the size of the cephalic space and appearance of its nuclear column (see organism-specific details in the following sections). An algorithm for identifying the common human-infecting microfilariae has recently been published (Mathison et al., 2019). Because microfilariae of *Wuchereria bancrofti* and *Brugia* spp. usually display a nocturnal periodicity, blood from patients suspected to be infected with these organisms should be drawn between the hours of 10 PM and 2 AM. *Loa* displays diurnal periodicity; thus, blood preferably should be drawn between 10:00 AM and 2 PM. *Mansonella ozzardi* and *M. perstans* are intrinsically nonperiodic; thus, blood can be obtained at any time for detection of these species. In contrast to the other filarial, the microfilariae of *Mansonella streptocerca* and *Onchocerca volvulus* are present in the skin and are detected by examination of skin snips or punch biopsies rather than blood films. Microfilariae in the skin do not exhibit periodicity.

Serologic tests for the diagnosis of lymphatic filariasis may prove helpful in select patients, especially those who are not native to endemic areas. Such methods are limited in their ability to distinguish between past exposure and current infection, however. Consequently, infection with other nematode species may result in the appearance of cross-reacting antibodies, with resultant false-positive results. Antigen detection tests also may be of value in the diagnosis of lymphatic filariasis but generally are not available in nonendemic settings and, to date, are not FDA approved for clinical diagnosis in the United States (Wilkins & Nutman, 2015; Norice-Tra & Nutman, 2019).

Wuchereria bancrofti (Lymphatic Filariasis)

This species, responsible for Bancroftian filariasis, is the most common filarial species to infect humans. Endemic areas include central and northern Africa, India, Southeast Asia, certain South Pacific islands, and portions of Central and South America and the West Indies. Adult worms reside in the lymphatic system, where chronic infection and reinfection result in lymphadenopathy and lymphangitis, which may progress to lymphedema

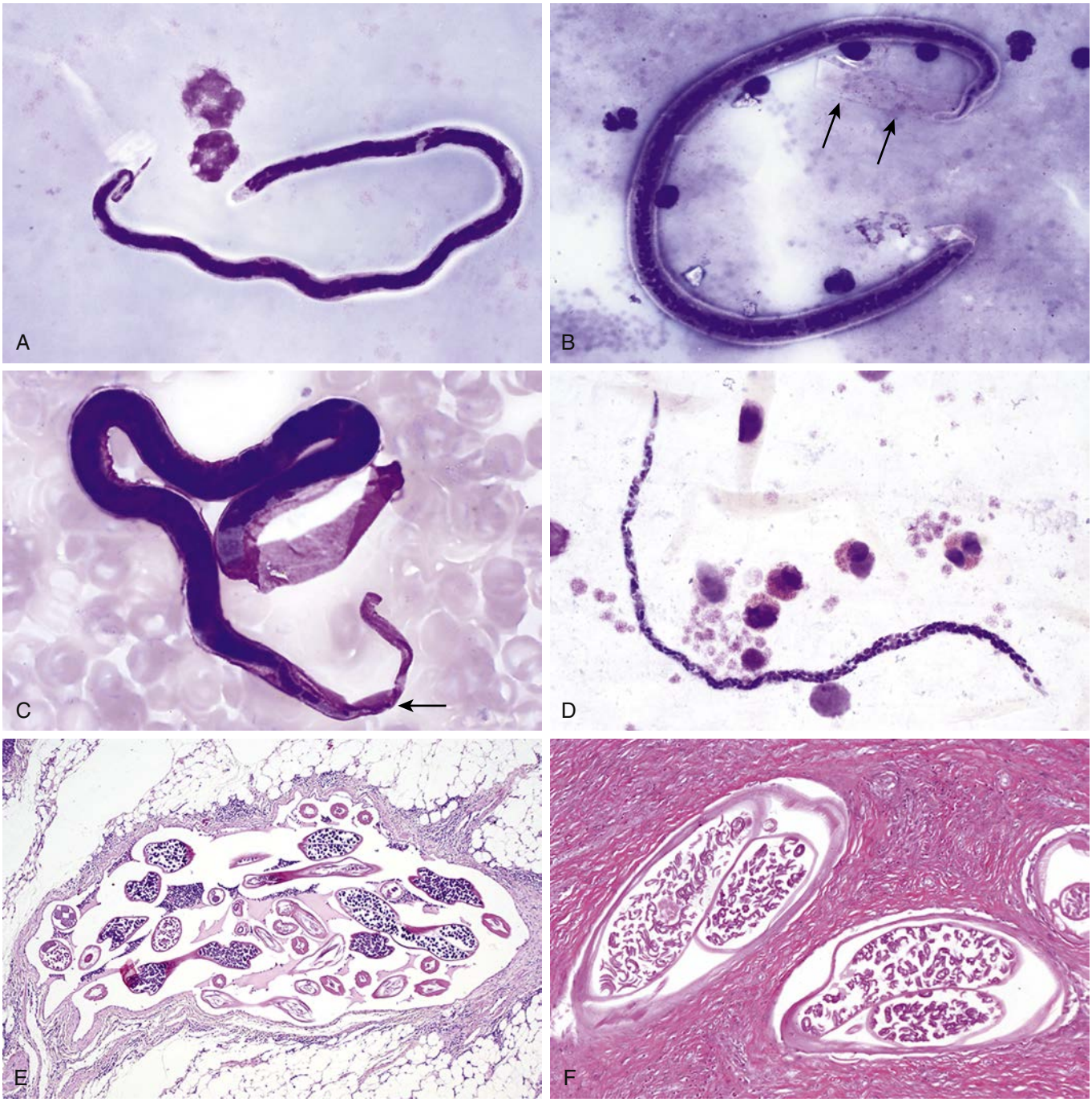

Figure 65.22 **A,** Sheathed microfilaria of *Loa*; cell nuclei extend to the tail tip. Note that the sheath is seen by its negative staining (Giemsa; 1000×). **B,** Sheathed microfilaria of *W. bancrofti*; cell nuclei do not extend to the tip of the tail. Note that the sheath *(arrows)* does not readily stain with Giemsa (1000×). **C,** Sheathed microfilaria of *Brugia malayi*; two solitary cell nuclei are seen in the tail tip. Note the deep pink–staining sheath (Giemsa; 1000×). **D,** Unsheathed microfilaria of *Mansonella perstans*; cell nuclei extend to the tail tip (Giemsa; 1000×). **E,** *Wuchereria bancrofti*, cross-section of adults in lymphatics. Note the associated fibrosis of the lymph vessel (H&E; 20×). **F,** *Onchocerca volvulus*, cross-section of adult in skin nodule, showing a classic "double-barrel" uterus (H&E; 100×).

and obstructive fibrosis (Fig. 65.22E). Severe involvement of the lower extremities and genitalia may result in a condition of enlarged limbs or scrotum referred to as *elephantiasis*. Diethylcarbamazine (DEC) is the drug of choice for *W. bancrofti* infection (Drugs for Parasitic Infections, 2013), but supportive care for irreversible edema and fibrosis may also be indicated.

In most areas, microfilariae circulate in peripheral blood with a nocturnal periodicity that corresponds with feeding activities of the usual vectors—*Culex*, *Aedes*, and *Anopheles* mosquitoes. Of note, infections originating in the South Pacific may be without periodicity, or subperiodic. The microfilariae are sheathed, although this may not always be obvious with Giemsa staining, in which the sheath may appear only as a negative outline. However, a hematoxylin stain will stain the sheath and allow for its ready identification (Mathison et al., 2019). The tail is pointed, and no nuclei are present in the tip. The cephalic space is not as long as it is wide, and the nuclei in the nuclear column are distinct (Figs. 65.22B and 65.23). Concentration procedures may be necessary for recovery because microfilariae may be present in small numbers.

Brugia malayi (Lymphatic Filariasis)

This species produces disease similar to that of *W. bancrofti*, although it is often milder and more frequently involves the lymphatics of the upper extremities. DEC is the drug of choice for infection (Drugs for Parasitic Infections, 2013), but supportive care for irreversible edema and fibrosis may also be indicated. The parasite occurs mainly in India, Southeast Asia, Korea, the Philippines, and Japan. Of note, human infection with related zoonotic *Brugia* spp. is encountered periodically in the Americas but is typically diagnosed by the finding of immature worms in biopsy specimens (Orihel & Ash, 2007). Surgical removal is curative for zoonotic *Brugia* infections.

The microfilariae circulate in the blood and are primarily nocturnally periodic. Microfilarial sheaths of *Brugia malayi* stain well with Giemsa

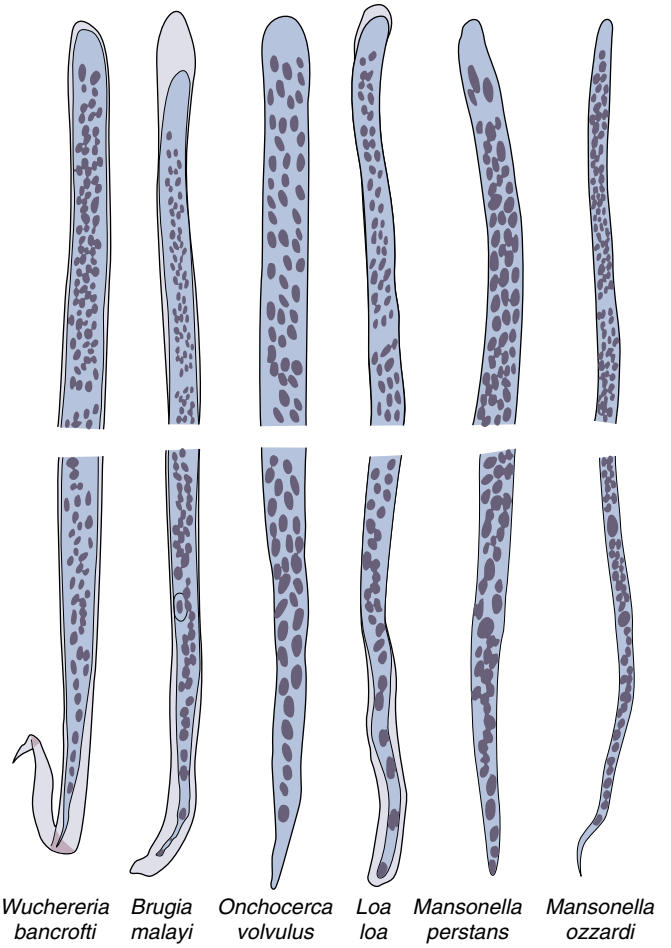

Figure 65.23 Anterior and posterior ends of microfilariae most commonly found in humans. All camera lucida drawings.

stain, often appearing bright pink. However, it should be noted that this phenomenon is not exclusive to *B. malayi* and may not be seen in some cases. Therefore, sheath staining should not be used as a sole diagnostic feature for *B. malayi*. The tail has a swelling at the tip and has two solitary nuclei located beyond the ends of the nuclear column separated by appreciable gaps (termed *subterminal* and *terminal* nuclei). The cephalic space may be much longer than it is wide (Figs. 65.22C and 65.23). *Brugia timori* is a distinct species occurring restricted to several islands in the Lesser Sunda archipelago, including the islands of Timor, Sumba, Lembata, Panta, and Alor. Microfilariae are very similar to those of *B. malayi*, although somewhat larger, and the sheath typically does not stain bright pink with Giemsa.

Loa (Loiasis)

Known as the African eye worm, the adult *Loa loa* lives in subcutaneous tissues. The nematodes migrate continuously, producing transient (2–3 days) local inflammatory reactions known as *Calabar* or *fugitive swellings*. Their occasional appearance in the conjunctiva allows them to be recognized and surgically excised. The presence of *L. loa* adults in the conjunctiva may cause a local inflammatory response but does not lead to blindness (compared with *O. volvulus*; see later discussion). DEC is the drug of choice, but caution must be used in cases of high microfilaremia (≥8000 microfilaria/mL) since rapid killing of circulating microfilariae may cause encephalitis. Upfront treatment with albendazole or apheresis is useful for reducing microfilaremia prior to DEC therapy (Drugs for Parasitic Infections, 2013). Loiasis occurs primarily in west and central Africa, where deer flies of the genus *Chrysops* serve as the vector. This parasite elicits strong eosinophilia.

Loiasis occasionally has been seen in the United States and other nonendemic settings in immigrants and travelers. In these settings, adult filarial nematodes recovered from the eye must be differentiated from *Dirofilaria* species that have a similar morphologic appearance. This can be accomplished by examining the cuticle of the retrieved worm. Adults of *L. loa* have random pimple-like cuticular projections called *bosses*, while *Dirofilaria* spp. have longitudinal cuticular ridges. The microfilariae, which circulate in the blood with diurnal periodicity, are sheathed. However, like the microfilariae of *W. bancrofti* and *B. timori*, the sheath does not stain with Giemsa stain. As with the others, a hematoxylin stain can be used to highlight the presence of the sheath. Nuclei in the tail extend to the rounded tip. The nuclear column is usually compact, and the cephalic space is short (Figs. 65.22A and 65.23) (Ash & Orihel, 2007; Mathison et al., 2019).

Onchocerca volvulus (Onchocerciasis)

Onchocerciasis due to *O. volvulus* is a leading cause of blindness in endemic areas, which include central Africa, Central America (Mexico and Guatemala), and northern South America. Vectors are black flies of the genus *Simulium*. Adult worms live in hard, fibrous nodules (onchocercomas) in subcutaneous and deeper tissues that can grow to be 40 mm in diameter (Fig. 65.22F). Nodules tend to occur on the upper half of the body in patients from Central America and on the lower half in those from Africa. Adult worms produce microfilariae that migrate continuously throughout the skin. Complications arise from the migratory activities of microfilariae, resulting in several forms of dermatitis. Movement of microfilariae through the surface of the eye may result in keratitis, corneal opacity, and damage to the anterior and posterior chambers and iris, leading to blindness with repeated infection over time. The drug of choice is ivermectin, which kills the circulating microfilariae and limits the morbidity associated with their migration. Unlike the other filariae, DEC should not be used for onchocerciasis since the rapid killing of microfilariae in the eye may lead to irreversible blindness (Drugs for Parasitic Infections, 2013). Ivermectin will not kill the adult *O. volvulus*; however, doxycycline may be coadministered with ivermectin to kill the obligate commensal bacterium, *Wolbachia*, found in the adult worms, and thus eliminate infection (Drugs for Parasitic Infections, 2013). Surgical removal of the onchocercoma may also be performed to eliminate individual infection.

In the United States, Europe, and northern Asia, human infection with the zoonotic species *O. lupi* can occur. Reported human cases in the Old World usually manifested with ocular involvement while cases in the United States involved periorbital, cervical, and subcutaneous nodules (Cantey et al., 2016). Removal is curative.

Diagnosis of *O. volvulus* infection is made by the finding of typical microfilariae in teased skin snips or skin biopsies, preferably taken from over the scapular region or from the iliac crest, when placed in saline. Alternatively, fluids expressed from scarified skin or aspirates of nodules may be examined (Garcia, 2016). Microfilariae in stained preparations lack both a sheath and nuclei in the tail tip (see Fig. 65.23). Detection of zoonotic infections with *O. lupi* is typically via histopathologic examination and identification of the adult worm in excised nodules (Cantey et al., 2016).

Mansonella spp.

Several species of *Mansonella* infect humans, but all are generally regarded as causing little pathology and must be differentiated from the truly pathogenic filarial species discussed previously. *Mansonella ozzardi* is found in Central and South America and in some areas of the Caribbean. Adult parasites reside in subcutaneous tissues. *Mansonella perstans* occurs in many areas of tropical Africa and sporadically in Central and South America and the Caribbean. Adults are thought to reside primarily in body cavities and the mesenteries. DEC is ineffective against *M. perstans* and *M. ozzardi*, but doxycycline may be useful for strains that contain *Wolbachia* as an obligate commensal bacterium (Drugs for Parasitic Infections, 2013). Microfilariae of both species are unsheathed and circulate in peripheral blood without evidence of periodicity. *M. ozzardi* microfilariae have a thin, pointed tail without nuclei, whereas the tail of *M. perstans* is broad and blunt with nuclei extending to the tip (Figs. 65.22D and 65.23). *Mansonella streptocerca*, which is found in tropical Africa, may be confused with *Onchocerca volvulus* because both adult and microfilarial stages occur in skin and subcutaneous tissues. Also, dermatitis may be produced by this species. DEC is the drug of choice (Drugs for Parasitic Infections, 2013). Microfilariae of this species, which may be recovered in skin snips, are unsheathed and have a crook in the tail with nuclei extending to the tip. All species of *Mansonella* are transmitted by midges (gnats) of the genus *Culicoides*, although *M. ozzardi* can also be transmitted by black flies of the genus *Simulium*.

Zoonotic Filarial Nematodes

Certain filarial nematodes of the genera *Dirofilaria*, *Brugia*, and *Onchocerca* that naturally parasitize wild and domestic mammals sporadically infect humans. Zoonotic infections with *Brugia* and *Onchocerca* species were discussed earlier. *Dirofilaria immitis*, commonly known as the canine heartworm, is widely distributed, and human infection is well documented. The mosquito-transmitted larval stage migrates to the right side of the heart. When the worm dies, it is swept into a small pulmonary artery, producing

a granulomatous nodule that appears as a coin lesion on a chest radiograph. Confirmatory diagnosis usually is made by histologic examination of the nodule following a positive chest radiograph (Pritt, 2018). Infected individuals are usually asymptomatic and disease is detected incidentally on radiologic imaging for some other indication. When present, symptoms include self-limited dyspnea, chest pain, fever, hemoptysis, and malaise. Treatment is not generally indicated.

Other species of *Dirofilaria*—including *D. tenuis*, *D. repens*, *D. ursi*, *D. striata*, and *D. subdermata*—commonly cause subcutaneous nodules in humans but usually fail to produce microfilariae. Such nodules have been reported from many body sites, including the face, conjunctiva, and breast, and usually are removed surgically. *D. tenuis* (southeastern United States) and *D. repens* (Europe and Asia) may also have ocular involvement and are diagnosed by the recovery of intact adult worms from the conjunctiva. Histologic examination often reveals a prominent mixed inflammatory reaction surrounding a dead worm. Criteria for identification of zoonotic filarial nematodes in tissue sections may be found elsewhere (Orihel & Ash, 1995; Meyers, 2000; Pritt, 2018). Surgical removal is curative.

OTHER

Dracunculus medinensis (Dracunculiasis)

Adults of *Dracunculus medinensis*, otherwise known as the Guinea worm, live in subcutaneous tissues and become clinically evident when the female worm migrates to the skin surface and produces a blister, usually on the lower extremities. When the extremity is immersed in water, the blister ruptures, releasing swarms of motile first-stage (L1) larvae from the female worm into the water. Freshwater copepods ingest the larvae, which then mature to the infective stage (L3 larvae) and are transmitted back to humans when copepods are accidentally swallowed in drinking water.

The disease was previously widespread, being found in areas of Africa, the Middle East, and Asia. Extensive control efforts have been made in recent years to eradicate this destructive parasite and success is thought to be close at hand, although the recent discovery of infected dogs in Chad, Ethiopia, and Mali has led to concerns that dogs may serve as an important disease reservoir (Eberhard et al., 2016; Hopkins et al., 2018). While not typically life-threatening, infection can result in disfiguring cutaneous scars and more serious secondary bacterial infection.

Diagnosis is made by identifying the female worm emerging at the skin surface with larvae in the discharge fluid. The worm is usually removed by gently pulling it out over a period of days, while winding it around a stick. Care must be taken not to damage it during removal. The long length of the worm (70–120 cm) generally precludes its surgical removal. Should the worm die in situ, pronounced inflammatory reaction along the length of the worm in its subcutaneous location and secondary bacterial infection may disable the affected individual.

Angiostrongylus cantonensis and *Angiostrongylus costaricensis* (Angiostrongyliasis)

Human eosinophilic meningoencephalitis, caused by *Angiostrongylus cantonensis*, occurs both in epidemics and sporadically in many areas of the South Pacific, Southeast Asia, and Taiwan. As the epidemiology becomes better understood, other cases have been reported from Australia, Cuba, Ecuador, Brazil, Puerto Rico, Madagascar, and mainland Africa. Human infection is rare in the continental United States. However, the disease has become problematic in Hawaii, where rats and terrestrial mollusks (snails, slugs, and invasive semi-slugs) have become serious pests. The mature parasite normally is found in the pulmonary arteries of rats. Larvae migrate up the trachea and are passed in the feces. They develop to the infective stage in slugs or land snails and, when eaten by the usual rodent host, migrate through the brain before maturing in the pulmonary arteries. Humans acquire the infection by eating large edible snails; raw or incompletely cooked shrimp or crabs, which may serve as paratenic hosts; or vegetables contaminated with infected mollusks. In humans, *A. cantonensis* larvae migrate to the CNS, producing generally nonfatal meningitis with high spinal fluid eosinophilia. Humans are a dead-end host for *A. cantonensis*; thus, further development does not occur. Neurologic symptoms begin with the death and inflammatory response to dying worms in the brain (Fig. 65.16L); the severity of symptoms is directly linked to worm burden. Treatment is not well defined; albendazole or mebendazole with or without corticosteroids may shorten the course of infection (Drugs for Parasitic Infections, 2013). Diagnosis is established both clinically and historically, although larvae occasionally have been recovered from spinal fluid (da Silva & Mathison, 2018). PCR is available at the CDC and the Hawaii Department of Public Health. Serologic tests are available in Asia but are not thought to be useful for clinical diagnosis, as there is high cross-reactivity with other nematode infections and high seroprevalence rates in asymptomatic individuals living in endemic settings have been reported.

Angiostrongylus costaricensis occurs widely in Central and South America (da Silva & Mathison, 2018). This parasite, which is responsible for the intestinal form of angiostrongyliasis, normally resides in the mesenteric arteries of the ileum and cecum of rodents. Human infection occurs in the same anatomic location but often results in granulomatous inflammation and symptoms of acute abdomen. Infection is self-limited, and treatment is not well defined (Drugs for Parasitic Infections, 2013). Diagnosis is made by histologic examination of surgical specimens and the finding of adults or eggs in the tissues (Orihel & Ash, 1995; Meyers, 2000; Pritt, 2018).

Trichinella species (Trichinosis or Trichinellosis)

Human trichinellosis occurs worldwide, although its incidence in the United States has been in steady decline, with fewer than 25 cases reported each year due to improved animal husbandry practices. Humans acquire the infection through ingestion of raw or incompletely cooked meat that contains infective larvae. Common sources of human infection in the United States are wild boar, bear, and occasionally walrus or domestic pigs raised on small, nonregulated personal or community farms (Mathison & Pritt, 2018). Ingested first-stage larvae mature in the small intestine, where gravid females produce new larvae for 2 to 3 weeks. During this stage, gastrointestinal symptoms occur, lasting several days. Larvae subsequently enter lymphatics and venules of the intestine, thus reaching the general circulation. They primarily invade the skeletal musculature, where they undergo further development and encapsulation. During the migratory and encapsulation phases, fever, muscle pain, respiratory difficulties, periorbital edema, and eosinophilia may develop, depending on the inoculating dose. During this stage of infection, treatment with albendazole and steroids may be indicated (Drugs for Parasitic Infections, 2013). After the parasites have encysted, few symptoms are noted. Encysted larvae may remain viable for several years, although they eventually become calcified. Perpetuation of the life cycle requires continuous cycles of carnivores and humans are typically a dead-end host.

Diagnosis is usually made on the basis of epidemiologic history and clinical symptoms and is confirmed by antibody detection by EIA (Wilkins & Nutman, 2015). *Trichinella* larvae may be observed in skeletal muscle biopsy specimens, particularly the gastrocnemius or deltoid muscles (see Fig. 65.16H), but the sensitivity is low.

Larval Migrans

Larval migrans is caused by prolonged wandering through body tissues of larvae of certain hookworms, ascarids, and *Strongyloides* species that normally infect wild or domestic animals. The syndrome varies with the species involved, the number of worms, and the tissues parasitized.

Cutaneous larva migrans, or ground itch, is produced by the cutaneous wanderings of cat or dog hookworms of the genus *Ancylostoma*, which penetrate the skin but cannot mature in the usual pattern. Serpiginous, erythematous, and pruritic tracks are apparent on the skin in areas where there has been contact with the ground. This is particularly problematic in warmer, humid climates, where eggs and larvae of these hookworms survive longer. Some species of *Strongyloides* that parasitize wild animals may cause a similar dermatitis (Beaver et al., 1984). Treatment is with albendazole (Drugs for Parasitic Infections, 2013).

Visceral larva migrans (VLM) is produced primarily by the random wanderings of the dog ascarid *Toxocara canis* and, to a lesser degree, by *Toxocara cati* from the domestic cat and *Baylisascaris procyonis* from the raccoon. Toxocariasis is one of 5 NPIs targeted by the CDC for public health action (CDC, 2018b). Children are usually infected following the accidental or intentional ingestion of eggs in soil contaminated with dog, cat, or raccoon feces. After hatching, the larvae are unable to complete their usual cycle and instead begin a prolonged migration through various tissues and organs. Children may present with failure to thrive and may display fever, hepatomegaly, pneumonitis, hypereosinophilia, and hypergammaglobulinemia. An inflammatory reaction in the retina from ocular larva migrans (OLM) may mimic retinoblastoma, a malignant tumor from which it must be differentiated. VLM is generally treated using albendazole or mebendazole. OLM is more difficult to treat due to the potential for ocular damage and may include surgical removal of the migrating larva and corticosteroids to decrease inflammation (Drugs for Parasitic Infections, 2013; CDC, 2018b).

Diagnosis of VLM is usually made on clinical grounds because the parasite is rarely recovered. Serologic tests may be helpful in confirming a presumptive diagnosis. The currently recommended procedure is an EIA that uses larval-stage excretory-secretory antigens (Rascoe et al., 2013; Wilkins, 2014).

A VLM-like syndrome may also be caused by species of *Gnathostoma* that infect the stomach of various mammals. Human infection is most common in Southeast Asia but has been reported in Mexico and Ecuador. These parasites use a copepod for the first intermediate host and fish and amphibians as secondary hosts. A variety of reptiles, birds, and mammals may serve as paratenic hosts. The larvae may migrate through subcutaneous tissues, causing transient swellings, and to deeper tissues, eventually invading the CNS. Treatment is with albendazole or ivermectin, with surgical removal of the migrating larva if possible (Drugs for Parasitic Infections, 2013). The occurrence of migratory lesions and a history of eating raw fish may be helpful in establishing a clinical diagnosis (Orihel & Ash, 1995).

Capillaria hepatica (Hepatic Capillariasis)

Although normally a parasite common to rodents, this species occasionally causes human disease, especially in children, in whom it may mimic VLM, hepatitis, amebic liver abscess, and other diseases. In the usual rodent host, eggs are ingested and resulting larvae migrate to the liver, where they mature and deposit eggs directly in the parenchyma. When the liver is eaten by a predator, the eggs are passed out in the feces and contaminate soil. Eggs may also be liberated into the environment by the natural death and decay of the rodent host. Children are at particular risk for acquiring the eggs if they eat dirt (Li et al., 2010). Diagnosis is usually made by examination of liver biopsies or tissue obtained at autopsy. Eggs are readily recognized in tissue biopsies as having thick, striated walls and plugs at both ends (Fig. 65.16G).

Anisakis, Pseudoterranova, and *Contracaecum* spp. (Anisakiasis)

Ingestion of raw fish, although considered by many to be a delicacy, has resulted in an increase in the number of reported cases of fish nematode infections. *Anisakis* spp., *Pseudoterranova* spp., and *Contracaecum* spp. are common gastrointestinal parasites of marine mammals and fish-eating birds. Small, shrimplike crustaceans (krill) serve as the first intermediate host and the infective stages (L3 larvae) are found in many saltwater fish and squid paratenic hosts. With little or no host specificity for fish and molluscan hosts, most commercial marine fish and squid are possible sources for human infection. When ingested by humans, these L3 larvae may attempt to penetrate the wall of the stomach or small bowel, causing acute abdominal pain. Treatment is with surgical or endoscopic removal (Drugs for Parasitic Infections, 2013). Anisakiasis may be presumptively diagnosed based on an appropriate history and clinical findings. The condition may be confirmed by the recovery of an intact worm at endoscopy or by the presence of an eosinophilic granuloma containing an identifiable, usually dead and degrading, nematode in a biopsy specimen. It is believed that species of *Anisakis* appear to be more prone to produce invasive disease and end up in ectopic locations, whereas *Pseudoterranova* spp. tend to be coughed up or vomited intact and often alive. The species-level identification of larval anisakids is not possible (Mathison & da Silva, 2018). Serologic diagnosis may be achieved by a positive skin prick test in conjunction with clinical manifestations and a recent history of consumption of seafood. Positive skin-prick tests should be confirmed by specific IgE assays and a negative reaction to host fish proteins (Audicana & Kennedy, 2008).

CESTODES

Several species of cestode infect humans in their larval stages and may produce serious disease. The more commonly encountered ones are readily distinguishable from each other and have unique patterns of transmission. When seen in tissue sections, larval and adult stages of cestodes contain basophilic-staining laminated bodies known as *calcareous corpuscles*, which are an important aid in their recognition.

Taenia solium (Cysticercosis)

Human infection with the larval stage of the pork tapeworm, *T. solium*, is found worldwide and occurs following unintentional ingestion of the eggs in food and fomites contaminated with human feces. The disease is especially prevalent in regions of Mexico, South and Central America, Africa, India, and Asia that have poor sanitation and where free-roaming pigs have access to human feces containing *T. solium* eggs (CDC, 2018b). Most cases in the United States originate from highly endemic areas; however, locally acquired cases may occur when individuals with intestinal *T. solium* infection (taeniasis) contaminate food with eggs that are shed in their stool). Cysticercosis is one of the 5 NPIs targeted for public health action in the United States (CDC, 2018b).

Eggs that are accidentally ingested in contaminated food or water subsequently hatch in the gastrointestinal tract, and the released oncosphere penetrates the intestinal mucosa and disseminates via the bloodstream to distant sites, including the skeletal muscle, heart, brain, or eye, where symptoms of infection and inflammation may become especially apparent. Seizures are a common complication of neurocysticercosis in endemic areas and are often the presenting symptom (CDC, 2018b; White, 2018). Treatment is complex and depends on the location of the lesion(s) and extent of disease. Guidelines were recently published for diagnosing and treating neurocysticercosis (White, 2018).

The diagnosis is usually made on clinical grounds in endemic areas but may be much more difficult to establish in nonendemic settings. Radiographs are helpful in recognizing the presence of calcified cysts but not in recognizing recent infection. Both brain noncontrast computed tomography (CT) and magnetic resonance imaging (MRI) are recommended for evaluating and classifying the form of neurocysticercosis (White et al., 2018). Laboratory confirmation is best achieved by antibody detection by enzyme-linked immunotransfer blot due to its superior sensitivity over routinely available ELISAs using crude antigens (White et al., 2018).

Recovery of an intact cysticercus at the time of surgery also confirms the diagnosis. However, in cases of neurocysticercosis, invasive procedures are not desirable. The cysticercus, or "bladder worm," is a translucent, fluid-filled, oval sac containing a single inverted protoscolex that measures 5 mm or more in diameter (Figs. 65.22A and 65.22B).

The occurrence of cysticercosis in someone from a nonendemic area and without an appropriate travel history should be investigated for accidental exposure to individuals involved in food preparation or for the possibility of infection with a different *Taenia* species (Schantz et al., 1992; CDC, 2018b).

Echinococcus spp. (Hydatidosis)

Human infection with larval stages of tapeworms of the genus *Echinococcus* may take one of three forms: (1) unilocular hydatid disease caused by *Echinococcus granulosus*, *E. canadensis*, and *E. ortleppi*; (2) multilocular or alveolar hydatid disease caused by *E. multilocularis*; or (3) polycystic hydatid disease caused by *E. vogeli* and *E. oligarthra* (Romig et al., 2015). Dogs and other canids are definitive hosts for these minute tapeworms (although *E. oligarthra* uses wild felids as its natural definitive hosts). What they lack in size they make up for in numbers, with many hundreds or thousands of worms producing large numbers of eggs in one host. Eggs are passed in the stools and are ingested by the intermediate hosts, which include sheep, cattle, pigs, rodents, and other herbivorous animals. Humans are infected following accidental ingestion of eggs from the environment.

Eggs hatch in the intestine; the released oncospheres penetrate the intestinal wall and then enter the bloodstream. Although most hydatids develop in the liver, some disseminate to other sites. Development of the cysts is slow—it may take many years for a cyst measuring 10 to 15 cm in diameter to form. In the usual secondary hosts, the cysts contain numerous protoscoleces, which proliferate from a germinal membrane.

Members of the *E. granulosus*-complex, the most important species producing human disease, are common in many sheep- and cattle-raising areas of the world, including small regions of the United States, where dogs are the usual definitive host. Unilocular hydatids develop as single cysts in the liver and secondarily in the lungs or other locations. The cysts are filled with clear fluid and may contain smaller "daughter" cysts. Within the parent and daughter cysts are brood capsules and protoscoleces, which can number in the thousands (Fig. 65.24C). Symptoms in humans include a slowly growing mass lesion, although infection in space-limited locations such as bone and the CNS may become apparent earlier than in other sites. The preferred treatment modality is dependent on the size, location, and complexity of the lesion. The drug of choice is albendazole; it is usually administered in conjunction with aspiration or surgical removal of the cyst (Drugs for Parasitic Infections, 2013). The PAIR procedure (puncture, aspiration, injection and re-aspiration) with ultrasound guidance is now a preferred method of choice for single liver cysts (Drugs for Parasitic Infections, 2013).

The diagnosis is suggested on the basis of clinical presentation and history plus the use of radiography, CT scans, and ultrasonography. Serologic tests are very useful in confirming a diagnosis and usually involve a screening test such as EIA or IHA followed, if positive, by a confirmatory assay such as immunoblot or gel diffusion (Brunetti et al., 2010; Wilkins & Nutman, 2015). Sensitivity varies from 60% to 90%, depending on the characteristics of the case. False-positive reactions may occur with cysticercosis, although disease presentation should prevent confusion. Aspiration of cyst contents is potentially dangerous because spillage of cyst contents may result in dissemination of disease or, possibly, anaphylactic

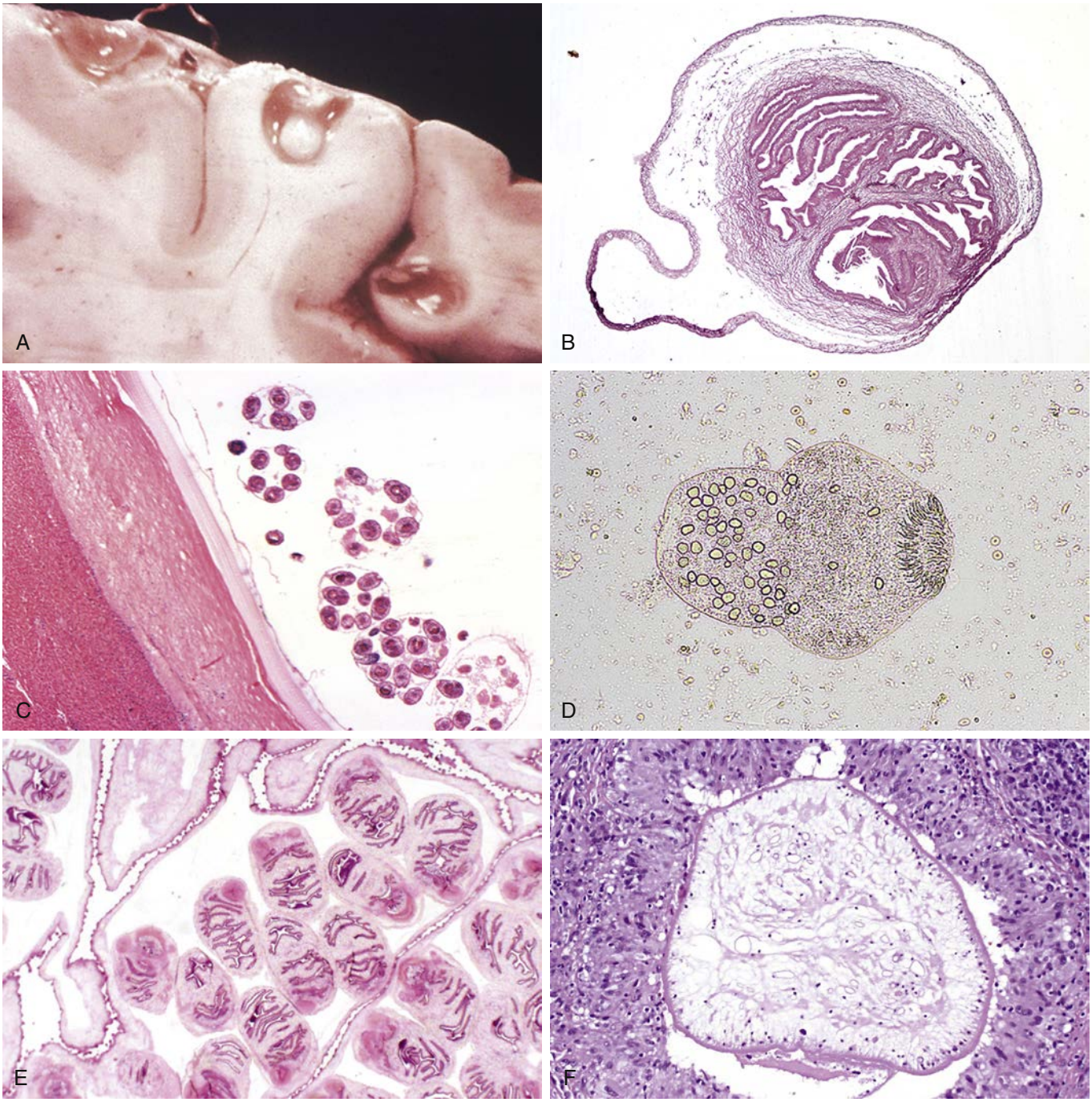

Figure 65.24 **A,** Gross specimen of neurocysticercosis. **B,** *Taenia solium* cysticercus (H&E; 10×). **C,** Hydatid cyst (*Echinococcus granulosus*) in the liver. Note the presence of multiple protoscoleces within brood capsules, a thin germinal membrane, a thicker laminated membrane, and the external fibrotic host reaction (10×). **D,** Protoscolex of *E. granulosus* found in aspirate fluid from a hepatic hydatid cyst. Note rostellar hooks and calcareous corpuscles (400×). **E,** Human infection with the larva of a canine *Taenia* (coenurus). Note the thin bladder membrane and numerous developing protoscoleces (10×). **F,** Sparganum (larva of *Spirometra* sp.) found in a lymph node. Note the surrounding granulomatous response (H&E; 100×). (**A** from Zaiman H: A pictorial presentation of parasites: a cooperative collection; https://www.astmh.org/education-resources/zaiman-slide-library. **C,** Courtesy of the Centers for Disease Control and Prevention Public Health Image Library.)

shock. However, if aspiration is performed, cyst contents usually reveal hydatid sand, a mixture of protoscoleces, disintegrating brood capsules, hooklets, and calcareous corpuscles (Fig. 65.24D). Aspiration performed under ultrasound or CT guidance seems to carry a lower risk and is now a commonly performed therapeutic method for patients with uncomplicated hydatid disease involving the liver.

Echinococcus multilocularis produces multilocular or alveolar hydatid disease in the northern regions of Europe and Russia, and in Alaska, Canada, and the northern tier of states in the United States. Intermediate hosts include several genera of small rodents; foxes, wolves, and dogs are definitive hosts. Human infection occurs in the liver, where the hydatid develops as an invasive cyst that insinuates itself within the tissue in an alveolar pattern without a surrounding outer capsule. Although the germinal membrane proliferates in the human liver, protoscoleces usually fail to develop. The pathologic picture is reminiscent of hepatic carcinoma. Given the more invasive nature of infection, surgical resection to the extent possible, in conjunction with prolonged albendazole administration, is the treatment of choice (Drugs for Parasitic Infections, 2013). Serologic assays that use *E. granulosus* antigens are useful in the diagnosis of this disease. The differential use of antigens from both parasites shows promise of discrimination between the two diseases (Brunetti et al., 2010; Wilkins & Nutman, 2015).

Echinococcus vogeli produces a polycystic hydatid cyst in humans that is invasive but, unlike *E. multilocularis*, produces both brood capsules and protoscoleces. The disease is limited to Latin America, where rodents, specifically the paca, and bush dogs complete the life cycle (D'Alessandro et al., 1979). Polycystic hydatid disease in South America may also be caused by *E. oligarthrus*, a parasite of felids and rodents. This species is similar morphologically to *E. vogeli* and cases have been misidentified (D'Alessandro et al., 1995). Treatment is not well defined for infection with these species.

Spirometra spp. (Sparganosis)

Sparganosis is caused by larval cestodes of the genus *Spirometra*, which are closely related to *Dibothriocephalus* spp. Adult stages commonly parasitize cats and dogs and their relatives in Asia (*Spirometra mansoni*) and North America (*Spirometra mansonoides*). Life cycles are similar to those of *Dibothriocephalus*: copepods serve as first intermediate hosts for procercoid larvae, and fish serve as second intermediate hosts for plerocercoid larvae. Humans become infected with the plerocercoid larval stage (also known as a sparganum) through ingestion of copepods in drinking water or ingestion of raw or incompletely cooked fish. Use of frogs and snakes as poultices may also result in the transfer of larvae to the human host. Sparganosis usually presents as localized or migratory subcutaneous swellings associated with erythema and pain, although brain infection may occur. Surgical exploration may reveal a delicate, slender, ivory-colored worm varying from a few to many centimeters in length. Cross-sections demonstrate a thick tegument with deep folds and parenchyma with prominent muscle bundles. No protoscolex is seen and calcareous corpuscles are numerous (Fig. 65.24F) (Orihel & Ash, 1995; Meyers, 2000; Pritt, 2018). Surgical removal is curative.

Taenia multiceps and *Taenia serialis* (Coenurosis)

Intestinal *Taenia* spp. of cats and dogs (primarily *Taenia multiceps* and *Taenia serialis*) produce a larval stage in intermediate hosts known as a *coenurus*. This stage consists of a large (up to 10 cm) transparent sac containing numerous scoleces that bud off from a germinal membrane and invaginate into the fluid-filled cyst (Fig. 65.24E). Sheep are the usual intermediate hosts for *T. multiceps*, and rodents, hares, and rabbits for *T. serialis*, although humans serve in this role through accidental ingestion of eggs originating from domestic cats and dogs. Similar to cysticerci, coenuri may develop in any organ, producing a similar disease. Most commonly, *T. multiceps* has a predilection for the CNS, while *T. serialis* is a predilection for subcutaneous tissues. Diagnosis is usually made by examination of the excised cyst or its demonstration in tissue sections. The presence of multiple invaginated scoleces within a single bladder differentiates the coenurus from the cysticercus of *T. solium*, which contains a single protoscolex. Surgical removal is curative.

TREMATODES

All liver-, lung-, and blood-inhabiting trematodes that mature in humans produce eggs that usually exit the body via stool, urine, or sputum. Because of their extraintestinal location, these flukes and their eggs may be found in tissues incidentally or in association with symptoms.

Adult *F. hepatica*, *C. sinensis*, and *O. viverrini* may be found in hepatic and biliary tissues, and occasionally in ectopic locations. The presence of typical eggs free in the tissues or within the uterus of the helminth often provides definitive identification. Adult *Paragonimus* spp. primarily reside in the lung but may be found in ectopic sites such as brain and subcutaneous tissue, where they produce abscesses, sometimes with large numbers of eggs. Adult schistosomes reside in blood vessels, primarily in the distribution of the inferior mesenteric vein (*S. mansoni*), the superior mesenteric vein (*S. japonicum* and *S. mekongi*), and the vesical plexus (*S. haematobium*). Although the adult stages are rarely encountered in tissue sections, eggs may be found in large numbers in tissues of the intestine, liver, and bladder (see Figs. 65.21B, 65.21D, and 65.21F). Eggs may disseminate via the bloodstream to other sites, including the brain, spinal cord, lungs, heart, kidneys, and spleen. The eggs of *S. japonicum* are especially prone to disseminate because of their smaller size and the large numbers typically produced. Identification of eggs is dependent on recognition of their typical sizes and morphologic characteristics (e.g., presence of a miracidium) in appropriate tissues.

MEDICALLY IMPORTANT ARTHROPODS

Arthropods comprise a large and diverse group of organisms, few of which have clinical or economic significance. Those that do, however, are important causes of morbidity and mortality in humans and their domestic animals and are responsible for serious economic losses to agriculture. Although perhaps best known among clinicians for their ability to transmit various infectious agents—including viruses, bacteria (rickettsia, spirochetes, and others), protozoa, and certain helminths—arthropods also cause serious disease by direct tissue invasion, envenomation, vesication, blood loss, and allergic reaction. Exaggerated fears of arthropods (entomophobia) and delusions of infestation (delusory parasitosis) are not uncommon neuroses, which may be disabling to some individuals. Species directly or indirectly responsible for human disease include representatives of all the major arthropod classes (Table 65.11).

In this section, an approach that the clinical laboratory may use when evaluating clinical specimens containing arthropods is presented, followed by a brief discussion of each of the arthropod groups of medical importance. A variety of general and specialized texts and guides are available for more complete coverage of the field of medical entomology (National Communicable Disease Center, 1969; Beaver et al., 1984; Lane et al., 1993; Moraru & Goddard, 2019; Mullen & Durden, 2018; Telford & Mathison, 2019), while a recent review (Mathison & Pritt, 2014) and bench guide (Mathison & Pritt, 2015) specifically discuss the identification of arthropods in the clinical microbiology laboratory.

BIOLOGICAL CHARACTERISTICS

Arthropods are characterized by a bilaterally symmetric, segmented body; several pairs of jointed appendages; and a rigid chitinous exoskeleton that is molted repeatedly during growth. Development proceeds from egg to adult through incomplete (hemimetabolous, with egg, nymph, and adult stages) or complete (holometabolous, with egg, larva, pupa, and adult stages) metamorphosis. Bedbugs, kissing bugs, lice, and cockroaches are examples of insects that undergo incomplete metamorphosis. Flies and mosquitoes, fleas, ants, bees, wasps, and beetles undergo complete metamorphosis; wormlike larval forms pupate to emerge as adults. Arachnids undergo developmental changes most similar to the process of gradual metamorphosis. The larval stages of those arthropods that undergo complete metamorphosis often prove to be the most difficult for clinical laboratorians to identify and should be referred to a medical entomologist if full identification is required for clinical management.

MECHANISMS OF INJURY

Direct Tissue Invasion

Invasion of superficial tissues (referred to as *infestation*) may occur with a variety of arthropods, of which scabies mites, chigoe fleas, and some dipteran larvae (maggots) are most common. Invasion of deeper body tissues and cavities (referred to as *infection*) occurs primarily with maggots and rarely with pentastomid larvae. Tissue invasion by dipteran larvae is referred to as *myiasis* and may occur in living or devitalized tissues depending on the involved species.

Envenomation

Many arthropods are capable of injecting venom with their bites or stings. For most individuals, these compounds cause only local tissue reactions, but serious, life-threatening reactions such as anaphylaxis may occur, often as a result of previous sensitization to the particular toxin. Hymenopteran (ants, bees, and wasps) and scorpion stings are among the greatest offenders (Moraru & Goddard, 2019). The bites of certain arthropods, especially centipedes; mosquitoes, flies, and biting midges; bedbugs, kissing bugs, and assassin bugs; sucking lice; fleas; and ticks and mites may also be toxic, causing local or systemic reactions. Almost all spiders are venomous, but only a few groups (widow spiders, violin spiders, and certain tarantulas, to name a few) pose significant health risks to humans. Less common but recognized causes of envenomation result from exposure to the urticating hairs of certain caterpillars and beetle larvae.

Vesication

Certain larger tropical millipedes are capable of spraying a vesicating (blister-causing) chemical substance from glands located on each body segment. These compounds are especially irritating should they reach the conjunctiva. Blister beetles are so named because of their ability to discharge vesicating fluids (cantharidin, the active ingredient in the aphrodisiac Spanish fly) from their bodies when handled.

Blood Loss

Arthropods responsible for producing significant irritation or blood loss to humans and domestic animals include bedbugs, kissing bugs, lice, fleas, flies, mosquitoes, biting midges, ticks, and mites. Although these activities are rarely life-threatening, the concurrent transmission of infectious agents may be.

Transmission of Infectious Agents

Many arthropods play an integral role in the mechanical or biological transmission of infectious disease agents. The common housefly, *Musca domestica*, may be responsible for the mechanical transmission of agents of bacillary dysentery, cholera, typhoid, viral diarrhea, amebic dysentery, and giardiasis, as well as pinworms and tapeworms. Mechanisms involved in the biological transmission of infectious agents vary from simple organism amplification in the arthropod vector to more complex life cycle changes in the involved parasite. Ticks and mites are involved in the transmission of certain bacteria (*Borrelia*, *Rickettsia*, *Ehrlichia*, *Anaplasma*, and others), protozoa (*Babesia*), and viruses. Among insects, lice are involved in the transmission of bacteria (*Rickettsia*, *Bartonella*, and *Borrelia*); kissing bugs

TABLE 65.11

Overview of the Medical Importance of Major Groups of Arthropods

Major Arthropod Groups	Medical Importance
Crustacea (crustaceans)	
Copepoda (copepods)	Intermediate host of *Spirometra*, *Gnathostoma*, *Dracunculus medinensis*
Decapoda (crabs, crayfish)	Intermediate hosts of *Paragonimus*
Pentastomida (tongueworms)	Causal agents of visceral pentastomiasis
Chilopoda (centipedes)	Envenomation
Diplopoda (millipedes)	Expulsion of noxious chemicals; intermediate hosts for acanthocephalans
Hexapoda (insects)	
Psocodea (lice)	
Pediculus (head and body lice)	Nuisance pests; vectors of agents of epidemic typhus, trench fever, louse-borne relapsing fever
Pthirus (pubic lice)	Nuisance pests
Blattodea (cockroaches)	Nuisance pests; intermediate hosts of acanthocephalans
Hemiptera (true bugs)	
Cimex (bed and bat bugs)	Nuisance pests
Triatoma, *Panstrongylus*, *Rhodnius* (kissing bugs)	Vectors of agent of Chagas disease
Siphonaptera (fleas)	
Xenopsylla (oriental rat flea)	Vector of agent of plague, murine (endemic) typhus
Ctenocephalides (cat and dog fleas)	Vectors of feline rickettsiae; intermediate host for *Dipylidium*, *Hymenolepis*
Pulex (human flea)	Nuisance pest; intermediate host of *Dipylidium*, *Hymenolepis*
Tunga (chigoe fleas)	Agents of tungiasis
Diptera (flies)	
Aedes, *Culex*, *Anopheles*, *Mansonia* (mosquitoes)	Vectors of agents of lymphatic filariasis, dirofilariasis, malaria, dengue, yellow fever, West Nile, chikungunya, SLE, EEE, WEE, many other arboviruses
Culicoides (biting midges)	Vectors of agents of mansonellosis
Phlebotemus, *Lutzomyia* (sand flies)	Vectors of agents of leishmaniasis, bartonellosis, phlebovirus
Simulium (black flies)	Vectors of agents of onchocerciasis, mansonellosis, dirofilariasis
Glossina (tse tse flies)	Vectors of agents of African sleeping sickness
Chrysops (deer flies)	Vectors of agents of loiasis, tularemia
Musca, *Fannia* (house, little house flies)	Vectors of agents of salmonellosis, shigellosis, *E. coli*–associated illness, cholera, bacterial conjunctivitis, thelaziasis; agents of myiasis
Dermatobia, *Oestrus*, *Cuterebra* (bot flies); *Sarcophaga*, *Wohlfahrtia* (flesh flies); *Cordylobia*, *Cochliomyia*, *Chrysomya*, *Lucilia*, *Phormia* (blow flies); others	Agents of myiasis
Hymenoptera (bees, ants, wasps)	Envenomation, allergic reactions to stings
Lepidoptera (butterflies and moths)	Caterpillars with urticating hairs
Coleoptera (beetles)	Expulsion of noxious chemicals; intermediate hosts for *Hymenolepis*, acanthocephalans
Arachnida	
Acari (ticks and mites)	
Amblyomma, *Ixodes*, *Hyalomma*, *Dermacentor*, *Rhipicephalus* (hard ticks)	Vectors of agents of Lyme disease, babesiosis, human granulocytic ehrlichiosis, Boutonneuse fever, human monocytic ehrlichiosis, Rocky Mountain spotted fever, tularemia, Crimean-Congo hemorrhagic fever, Colorado tick fever, relapsing fever borreliosis, human granulocytic anaplasmosis, tidewater spotted fever, Powassan virus, several others; implicated in tick paralysis and alpha-Gal syndrome
Ornithodoros, *Carios*, *Otobius* (soft ticks)	Vectors of agents of tick-borne relapsing fever
Sarcoptes scabiei	Agent of scabies
Demodex spp. (follicle mites)	Commensals on the human host
Various avian and rodent mites	Nuisance pests; vectors of agent of rickettsialpox
Chiggers	Nuisance pests; vectors of agent of scrub typhus
Scorpions	Envenomation
Spiders	Envenomation

Modified from Mathison BA, Pritt BS: Laboratory identification of arthropod ectoparasites, *Clin Microbiol Rev* 27:48–67, 2014; and Telford III SR, Mathison BA: Arthropods of medical importance. In Carroll JC, Pfaller MA, Landry ML, et al., editors: *Manual of clinical microbiology*, ed 12, Washington, D.C., 2019, ASM Press.

transmit trypanosomes; fleas transmit the agents of plague, typhus, and tapeworm infections; and dipterans transmit arboviruses, bacteria, and parasitologic agents of malaria, African trypanosomiasis, leishmaniasis, and filariases (see also Table 65.11).

Hypersensitivity Reactions

Most serious reactions to arthropod bites and stings result from allergic hypersensitivities. Hymenopteran stings alone are responsible for most arthropod-related deaths and usually result from the development of hypersensitivity following repeated exposure to venom. Allergies may be exacerbated following exposure to the saliva, excrement, or body parts of mites, ticks, lice, bedbugs, caterpillars, moths, and butterflies. Asthma and hay fever may also develop in response to the presence of the large variety of house, dust, and animal mites in the environment (Mullen & Durden, 2018).

Psychological Manifestations

Entomophobia refers to an unreasonable or excessive fear of seeing or touching arthropods. Although this fear may occasionally result in disruption of a

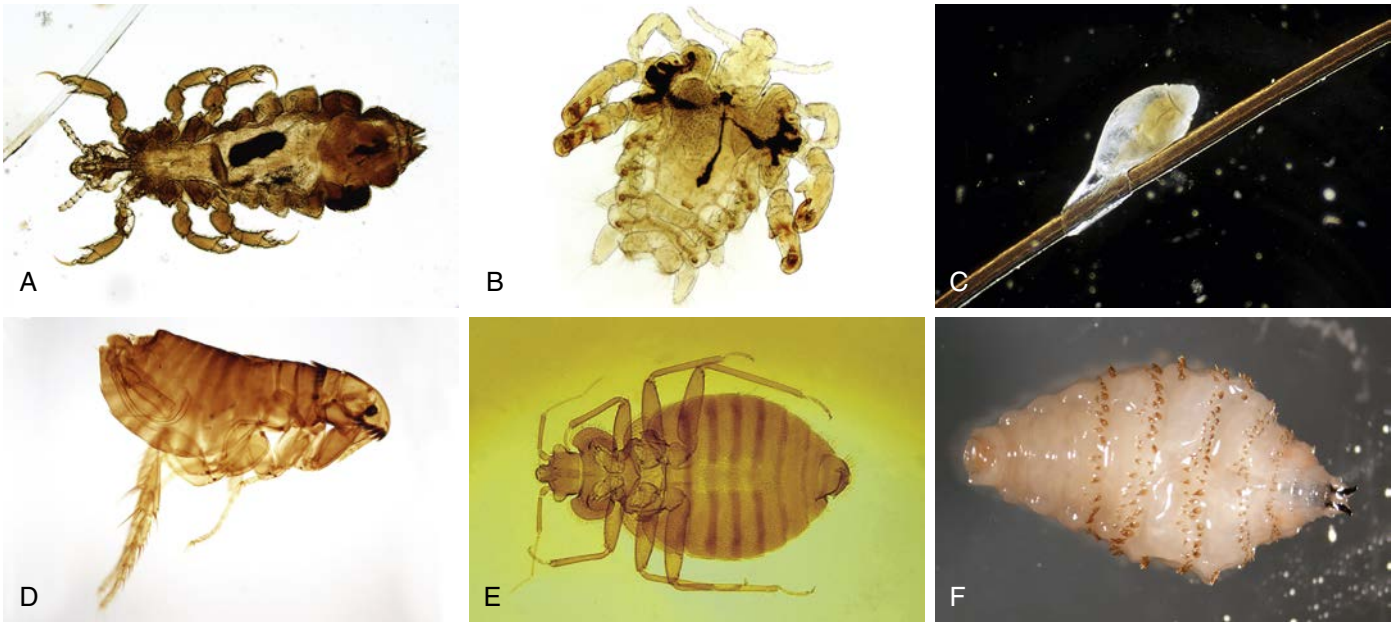

Figure 65.25 Medically important insects. **A,** *Pediculus humanus capitis*, the head louse, holding a strand of hair with one leg. **B,** *Pthirus pubis*, the crab louse. **C,** Intact egg (nit) of *P. pubis*. **D,** *Ctenocephalides* sp., the cat and dog fleas. Note the powerful hind legs. **E,** *Cimex lectularius*, the common bedbug. **F,** Larva of *Dermatobia hominis*, the "human" botfly. Note the two sclerotized hooks at the anterior end and numerous body spines (10×). (**D** *and* **F**, *with permission from the College of American Pathologists Arthropod Bench Reference Guide;* **E,** *with permission from Murray PR, Barron EJ, Pfaller MA, et al., editors:* Manual of clinical microbiology, *ed 6, Washington, DC, 1995, ASM Press.*)

person's normal activities, it rarely becomes incapacitating. Delusory parasitosis is a more serious emotional disorder in which an individual is convinced of being infected with parasites or arthropods despite objective evidence to the contrary. As the delusion progresses, the individual may report loss of employment, divorce, repeated use of pesticide services, and movement from house to house. Visits to health care providers are usually numerous and unsatisfactory. The problem may originate in the home or workplace and may be transferable from one to the other. The delusion may be so convincing that other family members or friends may believe it or acquire it themselves. The patient may submit to the laboratory numerous specimens, such as skin, fabric, lint, hair, and mucus. It is incumbent on laboratory personnel to examine these materials to rule out true infestation. The mysterious onset of irritation and itching may be due to bites from unrecognized scabies mites, lice, fleas, or bedbugs, or from insects and mites questing from an abandoned rodent or bird nest in an area of human habitation. Before such causes are dismissed, they must be looked for and their presence excluded. Patients with delusional parasitosis are difficult to treat, although the use of antipsychotics may provide some relief. The lack of clarity as to symptomatology, etiology, and diagnosis creates difficulty in management for both the patient and health care provider (Campbell et al., 2019).

LABORATORY APPROACHES TO ARTHROPOD IDENTIFICATION

Arthropod specimens are often directed to the clinical laboratory by both clinicians and patients with the expectation that they can be accurately identified, but few laboratory personnel receive more than a cursory exposure to entomology during training. Nonetheless, laboratorians should have access to texts and dichotomous keys, which should allow limited identification of the more commonly encountered medically important groups, especially ectoparasites (fleas, lice, mites, and ticks). Of greater importance is the ability of laboratory personnel to recognize those rare situations in which outside expertise should be sought. This specifically relates to those occasions when significant clinical decisions regarding therapy and prognosis are being made. State or local public health laboratories often have the expertise available or know of individuals trained in medical entomology who can be reached at regional educational institutions, museums, or other public or private agencies, including the CDC.

Specimens submitted to the laboratory are most often intact organisms, skin scrapings, tissues, sputum, urine, or stool. Inanimate objects, including foodstuffs, water, clothing, bedding, and carpeting, among others, may also be submitted. It is not uncommon for patients to submit arthropods recovered from the toilet bowl following urination or a bowel movement. In most cases, the presence of such organisms is incidental and is not related to infection.

Proper killing and preservation of arthropods is important to preserve those characteristics necessary for identification. Small, nonwinged arthropods—especially ectoparasites (lice, fleas, ticks, and mites), larval forms (maggots, grubs, and caterpillars), spiders, and scorpions—should be placed directly into 70% to 80% ethanol. Large larval forms are best killed in hot (not boiling) water to extend their bodies and prevent contraction before immersion in alcohol. Attached tissue or other debris should be gently removed or washed away prior to preservation. Smaller forms (mites, small ticks, fleas, and sandflies) may be prepared as permanent slide mounts (Mathison & Pritt 2014, 2015).

Winged insects—especially adult mosquitoes, midges, and flies—should be killed by exposure to the fumes of ethyl acetate or chloroform and preserved dry to retain the taxonomic information contained in the body and wing scales. Additional details regarding the collection, preservation, and preparation of arthropod specimens for examination are found elsewhere (Johnson & Triplehorn, 2005).

INSECTS

Insects account for more than 90% of all described arthropod species, although few are responsible for human disease. Members of this class are distinguished from other arthropods by having a body divided into three parts (head, thorax, abdomen); one pair of antennae; three pairs of legs; and one, two, or no pairs of wings. This is the only group of arthropods that has developed the ability of flight.

Parasitic Lice

Parasitic lice are dorsoventrally flattened, wingless insects that have characteristic claws on the ends of each leg that allow attachment to body hairs or clothing (Figs. 65.25A and 65.25B). All species suck blood intermittently, which may cause unexplained dermatitis. Eggs, known as *nits*, are deposited on hair shafts or clothing depending on the species. Although named for their primary site of attachment, they do not always remain confined to that location. The head louse, *Pediculus humanus capitis*, and the body louse, *Pediculus humanus humanus*, are indistinguishable to the nonspecialist and are thought to actually represent two ecotypes of the same species based on newly acquired molecular data. They are longer than they are wide and grow to about 3 mm in length. Biological differences are apparent; only *P. h. humanus* transmits the agents of epidemic typhus, trench fever, and relapsing fever (Moraru & Goddard, 2019). Infestations with *P. h. humanus* occurs primarily in settings of war, poverty, and homelessness, where bathing and laundering do not regularly occur. In comparison, *P. h. capitis* is much more common, particularly among children of school age. Children are at particular risk for acquiring head lice through the sharing of caps, clothing, and combs (Mullen & Durden, 2018). Nits of head lice are deposited primarily on hair shafts; those of body lice are deposited on clothing or other fomites. Because objects such as hair casts, dander, hair spray, and fungal hair infection may mimic nits, differentiation is important. Nits

are typically 1 mm long and when unhatched have intact opercula that are raised and flat anteriorly. Transmission occurs primarily through the sharing of infested clothing and bedding because body lice tend to lay their eggs in clusters, especially along seams or waistbands. The pubic louse, *Pthirus pubis*, is distinctly different from the others; it is wider (measuring up to 2 mm in width), the abdomen is more crablike, and the first pair of legs is significantly smaller and more slender than the other pairs (see Fig. 65.25B). Pubic lice and their nits, which are raised and conical (Fig. 65.25C) are found primarily on pubic hairs but may extend to other coarse hairs, including those on the chest, armpit, and facial hair. Transmission occurs primarily during sexual intercourse or other direct person-to-person contact. Lice infestation is treated with topical pediculicides.

Fleas

Fleas are small (1–2 mm), laterally compressed, wingless ectoparasites capable of sucking blood (Fig. 65.25D). Long, muscular legs are adapted for jumping great distances. Fleas that attack humans are parasites of other mammals or poultry and include both blood-sucking pests (many species) and tissue-penetrating jiggers. Infestations commonly occur with exposure to domestic animals and pets; the most pestiferous species are the dog flea (*Ctenocephalides canis*), the cat flea (*C. felis*), and the human flea (*Pulex irritans*). Some individuals become highly sensitized to flea bites, whereas others are unaffected. Cat and dog fleas are the usual intermediate hosts for the tapeworm *D. caninum* and less frequently for *H. diminuta* and *H. nana*. Because larvae of these species often develop in an animal's bedding or in carpets and furniture, eradication may require fumigation and cleaning of those articles. The Oriental rat flea, *Xenopsylla cheopis*, is an extremely important species because it transmits the agents of plague (*Yersinia pestis*) and murine typhus (*Rickettsia typhi*). Although normally parasitizing several species of rats, this flea readily attacks humans should the rodent host die. The jigger or chigoe fleas *Tunga penetrans* and *T. trimamillata* are found in both Central and South America, with *T. penetrans* having been introduced to regions of tropical Africa and Asia. The female flea attaches to and embeds itself in the skin, especially between the toes and under the toenails, where it grows to the size of a small pea. After eggs are discharged, the flea dies, prompting an inflammatory response and possible secondary bacterial infection or myiasis. Tungiasis is diagnosed by identifying the dark portion of the flea's abdomen (displaying the spiracles) protruding from the skin surface of an enlarging lesion (Moraru & Goddard, 2019) or by histopathologic examination of skin biopsies (Meyers et al., 2013; Pritt, 2018). Liberated eggs may be submitted to the clinical laboratory for identification (Mathison & Pritt, 2015).

Cockroaches

Cockroaches have closely adapted themselves to human habitation, sharing our food, shelter, and warmth. Although they are primarily nuisance pests, cockroaches are potential carriers of fecal pathogens owing to their ability to move quickly from sewers and drains to food preparation areas. In addition to transmitting pathogenic bacteria, they may spread hepatitis and poliovirus; intestinal protozoa, including *E. histolytica*; and several species of enteric nematodes. Allergies and asthma may develop in some individuals following exposure to the excreta, cast skins, or body parts of cockroaches (Moraru & Goddard, 2019).

Bed Bugs and Kissing Bugs

Bed bugs (family *Cimicidae*) and kissing bugs (family *Reduviidae*) are blood-sucking insects that have a long, narrow proboscis that is folded underneath the body when not in use. Bedbugs (*Cimex lectularius* and *C. hemipterus*) are reddish brown, dorsoventrally flattened, wingless insects approximately 5 mm in length (Fig. 65.25E). They are cosmopolitan in distribution and attack most any mammal, feeding primarily at night. During daylight hours, they hide under mattresses, loose wallpaper, and floorboards. Although they are not known to transmit disease-causing agents, bedbug bites may cause painful weals or bullae, depending on an individual's sensitivity to their saliva.

Kissing bugs (*Triatoma*, *Rhodnius*, *Panstrongylus*) have a cone-shaped head on a narrow neck and an abdomen that is widened in the middle. These insects are black or brown, and some have orange and black markings on the abdomen. They average 1 to 3 cm in length and, unlike bedbugs, have well-developed wings for flight. Similar to bedbugs, kissing bugs are relatively painless feeders on vertebrates and produce similar skin reactions. In Mexico and Central and South America, they transmit the agent of Chagas disease, *T. cruzi*, in the feces, which is secondarily inoculated into the skin by the human host while scratching (Moraru & Goddard, 2019). Although they are also found throughout the southern United States, autochthonous transmission of Chagas disease is thought to occur only rarely.

Bees, Wasps, and Ants

Hymenopterans are social insects that readily defend their nests when disturbed. In nonreproductive females, the ovipositor is modified as a stinger capable of injecting venom for use in the capture of prey or for defense. The venom of bees, wasps, hornets, and yellow jackets causes only transient swelling and discomfort in most individuals but may be responsible for systemic reactions, including anaphylaxis, in others who were previously sensitized (Moraru & Goddard, 2019). Up to 100 people in the United States die each year from hymenopteran stings. Many species of ant are problematic for humans because of their ability to sting. Some groups, such as harvester and fire ants, are capable of giving painful stings.

Beetles

Although beetles are perhaps best known as pests of agricultural crops, some species may give a painful bite. Others, especially blister beetles, may exude vesicating fluids (cantharidin) that cause dermatitis or blister formation. The larvae of certain larder beetles have urticating hairs that may be responsible for dermatitis or, if ingested, irritation of the gastrointestinal tract. Larval and adult larder and grain beetles also may serve as intermediate hosts for the rodent tapeworms *H. diminuta* and *H. nana*. Scarab beetles serve as intermediate hosts for the acanthocephalan, *Macracanthorhynchus hirudinaceus*.

Moths and Butterflies

Certain larvae (caterpillars) of *Lepidoptera* possess urticating hairs or spines capable of injecting venom when handled. Although most effects of these toxins remain localized to the skin, systemic effects such as shock and paralysis have been reported (Moraru & Goddard, 2019). Adult tussock and gypsy moths are known to have urticating scales and hairs that may cause dermatitis, eye irritation, or respiratory tract irritation, especially among forestry workers (Shama et al., 1982).

Flies, Mosquitoes, and Midges

Diptera are characterized by the presence of a single pair of membranous wings used for flight. Among all arthropods, they are responsible for the greatest share of human disease through blood-sucking activities, biological or mechanical transmission of infectious agents, and direct tissue invasion by larval forms (myiasis). Bites from a variety of flies, mosquitoes, and biting midges often cause local irritation from sensitivity to the saliva and, in some individuals, systemic reactions. In addition to blood-sucking activities, the repeated attacks themselves may be physically and psychologically damaging. Certain blood-sucking species are also responsible for the transmission of important human pathogens, including those that cause malaria, lymphatic filariasis, and arboviral disease by mosquitoes; onchocerciasis by black flies; loiasis by deer flies; leishmaniasis and bartonellosis by sandflies; and African trypanosomiasis by tsetse flies. Other viral, bacterial, and parasitic agents are readily transmitted mechanically by nonbiting flies such as house flies, flesh flies, and blow flies, which can easily contaminate human food.

Myiasis may occur in an accidental, facultative, or obligatory fashion. The housefly, *Musca domestica*, has no requirement for developing in mammalian tissue, yet may be found occasionally in dead tissue or under plaster casts. This type of accidental myiasis is not uncommon but rarely is clinically significant. Facultative myiasis is most often caused by blow flies and flesh flies, which ordinarily feed on dead tissues but may move into adjacent viable tissues. Obligatory myiasis is caused by certain species that develop only in living tissues. Those species that infect humans are all of zoonotic origin. The human bot fly, *Dermatobia hominis*, develops in boil-like subcutaneous lesions, with the posterior end of the maggot appearing at the skin surface (Fig. 65.25F). This species is most commonly found in individuals who have spent time in Central or South America. It is unusual in that its eggs are mechanically transported to the host by other flying insects, usually mosquitoes. The tumbu fly (*Cordylobia anthropophaga*), found in sub-Saharan Africa, causes a furuncular type of myiasis. Eggs of this species usually are laid on the ground or on hanging laundry, and larvae rapidly penetrate the skin on contact. The most serious myiasis is caused by the Old World screwworm, *Chrysomyia bezziana*, and the New World screwworm, *Cochliomyia hominivorax*. These species lay their eggs directly on their cattle hosts, usually on wounds or near the nostrils. The larvae actively feed on and move through living tissues. Human infection may be particularly destructive if larvae invade the eye, nose, or mouth. In North America, zoonotic furuncular or visceral myiasis caused by *Cuterebra* species (normally parasites of rodents and rabbits), is not rare. Other species may also be responsible for traumatic, obligatory myiasis in humans (Francesconi & Lupi, 2012).

ARACHNIDS

Medically important arachnids include scorpions, spiders, ticks, and mites. Scorpions and spiders have two body segments, the cephalothorax and the

Figure 65.26 Medically important arachnids. **A,** Scorpion. Note the forward-directed pincer claws and stinger on the tail tip. **B,** *Dermacentor variabilis* (dog tick), nonengorged adult female. **C,** *Ixodes scapularis* (black-legged tick or deer tick), nonengorged adult female. **D,** *Ornithodoros* sp. (soft tick), nonengorged adult, ventral view. **E,** *Sarcoptes scabiei* (itch mite) adult. Note the presence of adjacent eggs in skin scrapings. **F,** *Demodex folliculorum* (follicle mite) adult. (**A,** *With permission from Murray PR, Barron EJ, Pfaller MA, et al., editors:* Manual of clinical microbiology, *ed 6, Washington, DC, 1995, ASM Press.* **B** *and* **C,** *With permission from Northwest Infectious Disease Consultants.* **E,** *With permission from Spach DH, Fritsche TR: Norwegian scabies in a patient with AIDS,* N Engl J Med *331:777, 1994.*)

abdomen, whereas ticks and mites have only one. Members of the group have four pairs of legs as nymphs and adults; larval ticks and mites have three pairs of legs. All lack antennae, mandibles, and wings. Scorpions and spiders are best known for their ability to inject poisonous venom, whereas ticks and mites are best known as vectors for viral, bacterial, and protozoan pathogens.

Scorpions

Unlike other arachnids, scorpions have a pair of forward-directed pincer claws that impart a crablike appearance and a segmented tail with a bulbous stinging apparatus in the tip (Fig. 65.26A). They are predatory in nature and paralyze their intended victim with venom from the sting, which may also be used for defensive purposes. Toxicity to humans varies depending on the species; many elicit no more reaction than that of a bee sting, but some are deadly, causing more than 1000 deaths annually. Poisonous species are found in the Western Hemisphere, southern Europe, Africa, Australia, and the Middle East (Moraru & Goddard, 2019).

Spiders

Spiders lack a tail with an attached stinger but instead have fanglike chelicerae among their mouthparts, through which venom can be expressed. Although most spiders are venomous, few have chelicerae capable of penetrating human skin. Most spider bites cause only transitory irritation and pain. Widow spiders (genus *Lactrodectus*) are one group responsible for systemic arachnidism through the action of a potent neurotoxin capable of producing weakness, myalgia, paralysis, convulsions, and, occasionally, death. Published mortality rates vary from less than 1% to 6%. Five closely related species are found in the United States; the southern black widow (*Lactrodectus mactans*) is the most widespread. Female black widow spiders are glossy black with a characteristic red or orange hourglass-shaped marking on the underside of the abdomen and have a leg span of 3 to 4 cm. They live in protected locations such as woodsheds, basements, and outdoor privies (Moraru & Goddard, 2019).

Violin spiders (genus *Loxosceles*) are responsible for necrotic arachnidism or loxoscelism. In the United States, the brown recluse or fiddleback spider (*Loxosceles reclusa*) is most often involved, although other species are present. This species is 1 to 2 cm long and tan to dark brown; it has a darkened, violin-shaped marking oriented base forward on the dorsum of the cephalothorax. When present in homes, violin spiders are reclusive in their habits, preferring undisturbed areas such as closets, basements, and under porches. Their bite is painless and often goes unrecognized until several hours later, when the area becomes red, swollen, and painful. The venom is dermonecrotic and hemolytic, producing cutaneous necrosis and sloughing of involved skin over several days. The resulting lesion may be difficult to heal and subject to secondary infection. Systemic reactions such as hemolysis and acute renal failure are rare. Other spider genera have also been implicated in producing necrotic arachnidism (Moraru & Goddard, 2019).

Ticks

Ticks are one of the more common arthropods to be submitted to the clinical parasitology laboratory for identification. Unlike spiders and scorpions, ticks have a fused cephalothorax and abdomen, as well as a characteristic toothed hypostome for feeding. Tick development progresses through four stages: egg, larva, nymph, and adult (soft ticks may have multiple nymphal stages). Following hatching, a blood meal is required for progression to the subsequent stage. Humans usually acquire ticks in grassy or brushy areas in close proximity to the usual animal hosts. All species are obligate blood-sucking ectoparasites and are important vectors of viral, bacterial, and protozoan pathogens to humans and domestic animals. Their feeding activities may produce local tissue damage and blood loss, especially to livestock and wildlife, or tick paralysis, a syndrome caused by a neurotoxin secreted by a tick's salivary glands that produces ascending flaccid paralysis and toxemia. Symptoms may closely mimic those of Guillain-Barré syndrome, poliomyelitis, or botulism. Removal of the attached tick

usually results in resolution of symptoms within hours to days. Ticks have also been implicated in alpha-Gal syndrome, an allergic reaction to the carbohydrate Galα1-2Galβ1-(3)4GlcNAc-R (α-Gal) that is present in nonprimate mammals. When humans are bitten by a tick that has recently fed on a nonprimate mammal (e.g., deer), α-Gal can be injected into the bloodstream, resulting in antibody production to the carbohydrate. After this initial reaction, ingestion of animal meat with α-Gal causes an allergic reaction (de la Fuente et al., 2019; Wilson et al., 2019).

Species affecting humans include members of the family *Ixodidae* (hard ticks) and *Argasidae* (soft ticks). Hard ticks have anteriorly directed mouthparts and a sclerotized plate, or scutum, on the dorsum. The scutum covers the entire dorsum in the adult male but only the anterior portion in the adult female, larvae, and nymphs, allowing the body to swell when engorged (Figs. 65.26B and 65.26C). Argasid ticks have a soft leathery body lacking a scutum and ventrally directed mouthparts that are not visible when viewed from above (Fig. 65.26D). Unengorged ticks are generally 2 to 5 mm long but may enlarge to several times that size following engorgement.

Most ticks found crawling on or embedded in human skin are hard ticks. Soft ticks tend to feed only briefly and then often at night. Important species of hard ticks in North America include *Dermacentor variabilis* (American dog tick), *D. andersoni* (Rocky Mountain wood tick), *Amblyomma americanum* (Lone Star tick), *A. maculatum* (Gulf Coast tick), *Rhipicephalus sanguineus* (brown dog tick), *Ixodes scapularis* and *I. dammini* (black-legged or deer ticks), and *I. pacificus* (Western black-legged or deer tick). *Dermacentor* and *Amblyomma* ticks are called *ornate* ticks because of the presence of white markings on their scuta as adults; the other species are inornate ticks.

Dermacentor ticks transmit the agents of Rocky Mountain spotted fever, tularemia, Colorado tick fever, and, possibly, Q fever. *Ixodes* ticks are vectors of agents of Lyme disease, babesiosis, anaplasmosis, and Powassan virus. In other parts of the world, these ticks are responsible for the transmission of certain arboviruses. *Amblyomma* ticks are capable of transmitting agents of Rocky Mountain spotted fever, tidewater spotted fever, ehrlichiosis, and tularemia, and have been implicated in alpha-Gal syndrome. All these genera are capable of causing tick paralysis. *Rhipicephalus* ticks have been implicated in the transmission of agents of Rocky Mountain spotted fever and ehrlichiosis in North America, and of boutonneuse fever in the Mediterranean area. *Hyalomma* species transmit agents of Crimean Congo hemorrhagic fever in the Old World. Soft ticks of the genus *Ornithodoros* occur in many parts of the world, including the United States, and are important vectors of the relapsing fever spirochetes (*Borrelia recurrentis* and related species) (Moraru & Goddard, 2019; Mathison & Pritt, 2014; Muller & Durden, 2018).

Mites

Mites are arachnids of microscopic size (usually <1 mm) that are widely distributed in the environment. Medically important species may attack humans directly, serve as vectors for infectious disease, or cause dust allergies. Humans are commonly infested with both *Demodex folliculorum* and *D. brevis*, the follicle mites, and *Sarcoptes scabiei*, the itch or mange mite. Follicle mites are minute (0.1–0.4 mm), elongate parasites with stubby legs that can be recovered from hair follicles and sebaceous glands (Fig. 65.26F). They are common incidental findings on histologic skin preparations. Although their presence has been associated with various skin conditions, they are commonly found in healthy individuals as well, which makes their significance difficult to assess (Moraru & Goddard, 2019).

Sarcoptes scabiei mites are of greater medical importance because of their ability to create serpiginous tunnels through the upper layers of the epidermis. Transmitted through personal contact, these mites are found primarily in the interdigital spaces and the flexor surfaces of the wrists and forearms and less commonly in other areas, including the breasts, buttocks, and external genitalia. Inflammation and intense itching result from the tunneling activity and from the deposition of eggs and excreta. Clinical manifestations vary depending on the degree of sensitization to the parasites and their products. Lesions often become secondarily infected. Generalized dermatitis occurring in the presence of thousands of mites, typically in older adults or immunocompromised individuals, is known as *crusted* or *Norwegian* scabies. Classical scabies is commonly treated with topical 5% permethrin or 10% crotamiton, whereas oral ivermectin is added for cases of crusted scabies (Drugs for Parasitic Infections, 2013).

The diagnosis is made by placing skin scrapings collected from tunneled areas in 20% potassium hydroxide or mineral oil for clearing and examining under the microscope. Detection of eggs, six-legged larvae, and eight-legged nymphs or adults is diagnostic but may be difficult to demonstrate (Figs. 65.26E and 65.27). The diagnosis of scabies in an institutional or school setting may result in pseudoepidemics, in which numerous individuals develop itching without evidence of disease. Care must be exercised

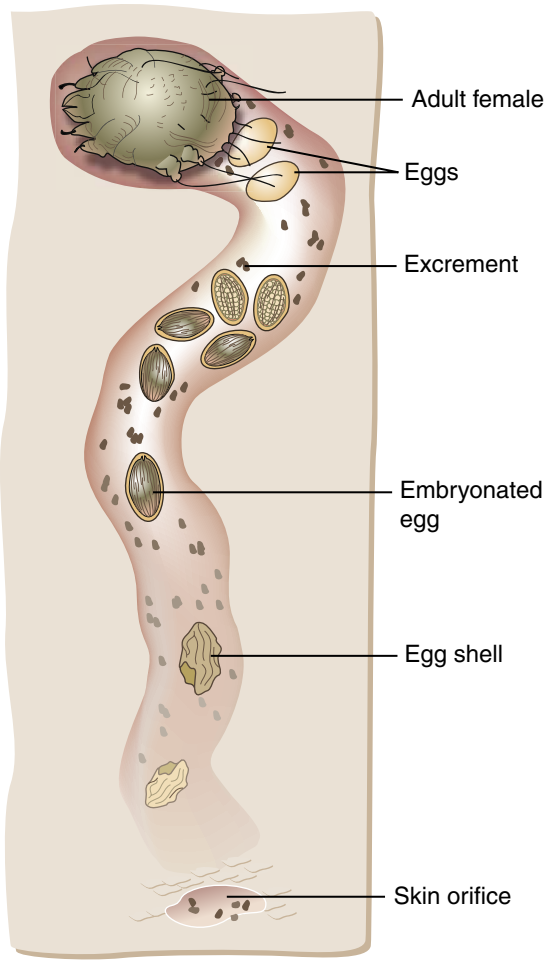

Figure 65.27 *Sarcoptes scabiei*. Diagram of a subcutaneous burrow.

to properly diagnose the disease to identify real cases and differentiate them from cases of delusory parasitosis (Moraru & Goddard, 2019).

A number of animal mite species may attack humans for a blood meal, either as larval forms or as adults, when normal mammalian or bird hosts are not available. Larval chigger mites (family *Trombiculidae*) are problematic in many parts of the world because their saliva can produce large wheal-and-flare reactions with intense itching. These tiny, six-legged larvae are often red and commonly attach to the skin in areas where clothing is restrictive, such as at the ankles, waistline, armpits, and wrists. In parts of Asia and Australia, trombiculid mites are vectors for the transmission of the agent of scrub typhus (Moraru & Goddard, 2019; Mullen & Durden, 2018). Avian and rodent mites in the genera *Ornithonyssus*, *Laelops*, *Dermanyssus*, and *Liponyssoides* (among others) will occasionally bite humans in the absence of, or during infestations of, their natural hosts. These mites cannot survive on human blood and are not vectors of disease-causing agents. One notable exception is the house mouse mite, *Liponyssoides sanguineus*, which has been implicated in the transmission of *Rickettsia akari* (rickettsialpox) in northeastern North America.

Certain nonbiting mites play a role in allergic rhinitis, asthma, and some skin conditions. The secretions, excreta, and body parts of the dust mites, *Dermatophagoides farinae* and *D. pteronyssinus*, and the house itch mite, *Glycyphagus domesticus*, are potent allergens that may occur in great numbers in the household environment (Calderón et al., 2015). Routine testing by an allergist may identify the offending agent.

Mites can have a very similar appearance to ticks, particularly in their larval form, but can be differentiated by their lack of a toothed hypostome (attachment organ used by ticks) and lack of Haller's organ on their forelegs.

CLASSES OF LESSER MEDICAL IMPORTANCE

Millipedes

Millipedes are cylindrical arthropods with numerous apparent body segments, each with two pairs of legs; they are commonly found in and around decaying vegetation. Although they lack mouthparts capable of producing serious bites, many species produce vesicating secretions from glands located on each body segment. When handled roughly, the larger tropical

TABLE 65.12
Parasitic Infections in Compromised Hosts

Infection	Predisposing Host Abnormalities	Comments	References
Intestinal Protozoa			
Cryptosporidiosis	AIDS (especially CD4+ <200/μL), transplantation, antineoplastic chemotherapy	Severe protracted diarrhea (up to 17 L/day). May have extraintestinal involvement, including pancreas, biliary tract, and lungs. Limited therapy available; is not curative.	Wang et al., 2018; Xiao & Cama, 2019
Cystoisosporiasis	AIDS, transplantation, antineoplastic chemotherapy	Severe protracted diarrhea. Extraintestinal involvement of regional lymph nodes may be seen. Effective therapy is available.	Lindsay & Weiss, 2019
Cyclosporiasis	AIDS, probably other immunosuppression	Severe protracted diarrhea clinically similar to cryptosporidiosis and isosporiasis. Responds to trimethoprim-sulfamethoxazole.	Ortega & Sanchez, 2010; Lindsay & Weiss, 2019
Giardiasis	Common variable immunodeficiency, X-linked agammaglobulinemia	Prolonged diarrhea with malabsorption. AIDS is not a predisposing factor.	Saurabh et al., 2017
Blood and Tissue Protozoa			
Granulomatous amebic encephalitis	AIDS and other immunocompromised states	Usually caused by amebae of the genera *Acanthamoeba* or *Balamuthia.* Produces subacute or chronic central nervous system infection but may be acute in severely immunosuppressed hosts with dissemination	Visvesvara et al., 2007; La Hoz et al., 2019
Toxoplasmosis	AIDS with CD4+ usually <100/μL and other immunocompromised states; heart transplant, donor seropositive and recipient seronegative	Usually result of reactivation of cysts from previous infection. Often disseminated disease with multiorgan involvement or multifocal central nervous system lesions. Can cause pneumonitis resembling that caused by *Pneumocystis jiroveci*. May cause chorioretinitis. Can occur after transplantation of bone marrow but usually mild. Heart transplant with donor serologically positive and recipient serologically negative may lead to severe, often fatal toxoplasmosis.	Dubey & Jones, 2008; La Hoz et al., 2019
Leishmaniasis	AIDS, other immunosuppression	Limited influence on cutaneous leishmaniasis. Susceptibility to visceral leishmaniasis increased, but not disease severity. More likely to relapse after treatment.	Herwaldt, 1999
American trypanosomiasis (Chagas disease)	AIDS, lymphoblastic lymphoma, cardiac transplantation, other immunosuppression	In AIDS, central nervous system often involved, myocarditis, skin lesions.	John & Petri, 2006; La Hoz et al., 2019
Babesiosis	Splenectomy	Usually subclinical infection in those with intact host defenses. Splenectomized patients usually develop clinically evident disease, which can be fatal.	Westblade et al., 2017
Helminth			
Strongyloidiasis	Immunosuppression for transplantation or by cancer chemotherapy or adrenal corticosteroids or lymphoma. AIDS is not a major predisposing factor	Because of endogenous autoinfection, hyperinfection or disseminated infection can develop and present as pneumonia or severe intestinal disease. Gram-negative sepsis or gram-negative meningitis can result from translocation of intestinal bacteria via invading larvae. Should check for strongyloidiasis before immunosuppressing patient from highly endemic areas.	Hayes & Nellore, 2018
Arthropod			
Scabies	Malignancy, transplant immunosuppression, antineoplastic therapy	AIDS leads to "Norwegian" or crusted scabies with widespread involvement by thick, crusted lesions. Sometimes has severe itching. Patient has numerous mites and is therefore highly contagious. Often less responsive to therapy.	Mullen & Durden, 2018; Sandoval et al., 2018

AIDS, Acquired immunodeficiency syndrome.

species are capable of squirting these fluids over a distance of several centimeters. Exposure of the skin or mucous membranes to these fluids may produce a burning sensation and blister formation. Millipedes may also serve as intermediate hosts for *Macracanthorhynchus ingens*, a thorny-headed worm that causes zoonotic infections in humans.

Centipedes

Centipedes are flatter than millipedes, have only one pair of legs per body segment and longer antennae. They are fast moving and can inflict a painful sting from a pair of forward-directed pincers that are modified from the first pair of legs. Although they are rarely responsible for serious injury to humans, the larger species (26–45 cm) found in southern United States and in tropical regions are able to penetrate human skin when handled, giving a painful, burning sting with local tissue reaction. Although systemic reactions may occur in individuals who have been previously sensitized, fatalities are rare (Moraru & Goddard, 2019).

Crustaceans

Crustaceans of medical importance are primarily those species that serve as hosts for larval stages of several different helminths. Several genera of crabs and crayfish are intermediate hosts for the metacercariae of various species of lung fluke (*Paragonimus* spp.) found around the world. Copepods are common microscopic zooplankton, certain species of which serve as first intermediate hosts for the nematodes *D. medinensis* and *Gnathostoma spinigerum* and for cestodes of the genera *Dibothriocephalus*, *Adenocephalus*, *Diphyllobothrium*, and *Spirometra*.

Pentastomes, or tongue worms, are a highly modified group of parasitic crustaceans. Adult stages are wormlike organisms that live in the nasal passages of certain predatory reptiles, birds, and mammals. Larval stages

resemble mites and reside in rodents, herbivores, and freshwater fish. Human liver and lung infections with larval stages of *Armillifer* spp. have been reported from Asia and Africa. Adult stages of *Linguatula serrata* have been recovered from the nasopharynx of individuals from the Middle East and Africa, where they are responsible for an obstructive condition known as *halzoun* (Tappe & Buttner, 2009).

PARASITIC INFECTIONS AND THE IMMUNOCOMPROMISED HOST

Immunocompromised hosts have abnormalities in their humoral or cellular immune systems resulting from disease, therapy, or congenital abnormality. Severe malnutrition may also compromise host defenses. In most instances, the predisposing host abnormalities are primarily of the cellular (T-cell) immune system and result from AIDS, malignancy, chemotherapy of malignancy, immunosuppression for transplantation, corticosteroid therapy, or a combination of these. The predisposing immune defect for giardiasis is with humoral immunity, and for babesiosis it is with splenectomy.

With the worldwide epidemic of HIV infection and AIDS being particularly severe in underdeveloped countries with a high incidence of parasitic infection such as malaria, schistosomiasis, ascariasis, amebiasis, and filariasis, it is fortunate that these infections do not cause particularly severe disease in AIDS patients. However, as comorbidities, their contribution to health care costs is enormous.

Some parasitic infections—such as cryptosporidiosis, toxoplasmosis, and strongyloidiasis—are more severe in immunocompromised hosts. However, there are differences depending on the type of immunosuppression. For example, although cryptosporidiosis and toxoplasmosis are particularly problematic in AIDS patients, strongyloidiasis is not a major problem in this population. However, it is a problem in transplant recipients, patients with HTLV-1 infection, and individuals receiving antineoplastic chemotherapy.

Table 65.12 lists parasitic infections that are more severe and/or frequent in immunocompromised patients. Clinical manifestations may be different from those seen in the general population, as is noted in the comment section.

ACKNOWLEDGMENT

The authors would like to acknowledge the contributions of Thomas Fritsche, MD to this chapter.

SELECTED REFERENCES

Adl SM, Bass D, Lane CE, et al.: Revisions to the classification, nomenclature, and diversity of eukaryotes, *J Euk Microbiol* 66:4–119, 2019.

This article by the International Society of Protistologists presents the most up-to-date version of the classification system for eukaryotes. It represents a revision of the system published in 2012 that introduced the concept of rankings based on phylogenetic relatedness rather than subjective morphologic features and phenology.

Ash LR, Orihel TC: In *Atlas of human parasitology*, ed 5, Chicago, 2007, ASCP Press.

This atlas is the go-to reference for diagnostic parasitologists. It covers the biology, life cycle, and morphologic features of human parasites, and provides high-resolution images of all parasites covered.

Carroll KC, Pfaller MA, Landry ML, et al.: *Manual of clinical microbiology*, ed 12, Washington, DC, 2019, ASM Press.

This is the most recent edition of the Manual of Clinical Microbiology, with detailed chapters on parasitic diseases by current experts in the field.

Clinical and Laboratory Standards Institute (CLSI): *Procedures for the recovery and identification of parasites from the intestinal tract; approved guideline*, Wayne, PA, 2005, CLSI Document M28-A2.

This consensus document contains a detailed, up-to-date presentation on the processing of gastrointestinal specimens for parasitic infections, including use of immunoassays and test characteristics.

Drugs for parasitic infections, *Med Lett (New Rochelle)* 11(suppl), 2013.

With increasing travel, immigration, use of immunosuppressive drugs and the spread of HIV, physicians anywhere may see infections caused by parasites. This publication is a large table that lists first-choice and alternative drugs for most parasitic infections. Also included are the principal adverse effects of these drugs and the known prenatal risks of antiparasitic drugs. It includes recommendations for both the United States and abroad.

Foundation for Innovative New Diagnostics (FIND): Special Programme for research and training in tropical diseases (TDR) and world health Organization (WHO): malaria rapid diagnostic test performance. In *Results of WHO product testing of malaria RDTs: round 4 (2012)*, Geneva, Switzerland, 2012, TDR/World Health Organization.

This publicly available study compares the performance of commercially available rapid diagnostic assays for malaria. It highlights the wide variation in performance characteristics among the different assays.

Garcia LS: In *Diagnostic medical parasitology*, ed 6, Washington, DC, 2016, American Society for Microbiology.

This textbook is a comprehensive guide to laboratory procedures for diagnostic parasitology.

Garcia LS, Arrowood M, Kokoskin E, et al.: Laboratory diagnosis of parasites from the gastrointestinal tract, *Clin Microbiol Rev* 17, 2018. e00025.

This Practical Guide for Clinical Microbiology document provides an overview on the recovery and identification of parasites of the gastrointestinal tract, including morphologic, molecular, and antigen detection methodologies.

Mace KE, Arguin PM, Tan KR: Malaria surveillance—United States, 2015, *MMWR Morb Mortal Wkly Rep* 67, 2018.

This presents the most recent data for malaria cases imported into the United States.

Mathison BA, Pritt BS: Laboratory identification of arthropod ectoparasites, *Clin Microbiol Rev* 27:48–67, 2014.

A detailed review describing the collection, proper handling, identification, and reporting of arthropods commonly submitted to the clinical microbiology laboratory.

Mathison BA, Pritt BS: *Arthropod benchtop reference guide*, Northfield, IL, 2015, College of American Pathologists.

This benchtop reference guide provides quick, easy, and reliable information on the morphologic identification of arthropod ectoparasites. It is handy to have on the bench scope-side for quick reference.

Mathison BA, Pritt BS: A systematic review of zoonotic helminths in North America, *Lab Medicine* 49:e61, 2018.

This review covers the epidemiology, biology, diagnosis, clinical presentation, pathology, and treatment of over 30 zoonotic helminth infections in North America.

Meyers WM, editor: *Pathology of infectious diseases* (vol. 1). Washington, DC, 2000, Armed Forces Institute of Pathology. (Helminthiases.

This atlas covers the biology, epidemiology, clinical presentation, pathology, and histopathologic identification of helminth infections.

Meyers WM, Firpo A, Wear DJ: *Topics on the pathology of protozoan and invasive arthropod diseases*, Washington, DC, 2013, Armed Forces Institute of Pathology.

This companion to the Meyers 2000 publication (above) covers protozoan and arthropod infections.

Mullen G, Durden L: *Medical and veterinary entomology*, ed 3, Cambridge, 2018, Academic Press.

This is the most recent edition of the premier textbook on medical entomology.

Orihel TC, Ash LR: *Parasites in human tissues*, Chicago, 1995, ASCP Press.

This is the companion to Ash and Orihel, 2007 (above), covering the histopathologic identification of human parasites.

Pritt BS: *Parasitology benchtop reference guide*, Northfield, IL, 2014, College of American Pathologists.

This benchtop reference guide provides quick, easy, and reliable information on the morphologic identification of intestinal and blood parasites. It is handy to have on the bench scope-side for quick reference.

Westblade LF, Simon MS, Mathison BA, Kirkman LA: *Babesia microti*: from mice to ticks to an increasing number of highly susceptible humans, *J Clin Microbiol* 55:2903, 2017.

This minireview covers the most recent information on the epidemiology, biology, and diagnosis of human babesiosis.

Wilkins P, Nutman TB: Immunological and molecular approaches for the diagnosis of parasitic infections. In Jorgensen JH, Pfaller MA, Carroll KC, et al.: *Manual of clinical microbiology*, ed 11, Washington, DC, 2015, ASM Press.

This is a comprehensive overview on serologic and molecular diagnostics for parasitic infections.

Access the complete reference list online at Elsevier eBooks for Practicing Clinicians.

REFERENCES

Adl SM, Simpson AGB, Lane CE, et al.: The revised classification of eukaryotes, *J Euk Microbiol* 59:429, 2012.

Adl SM, Bass D, Lane CE, et al.: Revisions to the classification, nomenclature, and diversity of eukaryotes, *J Euk Microbiol* 66:4, 2019.

Adl SM, Mathison BA: Chapter 135: taxonomy and classification of human eukaryotic parasites. In Carroll JC, Pfaller MA, Landry ML, et al.: *Manual of clinical microbiology*, ed 12, Washington, D.C., 2019, ASM Press.

Afonso AM, Ebdell MH, Tarleton RL: A systematic review of high quality diagnostic tests for Chagas disease, *PLoS Negl Trop Dis* 6:e1881, 2012.

Ale A, Victor B, Praet N, et al.: Epidemiology and genetic diversity of *Taenia asiatica*: a systematic review, *Parasit Vectors* 7:7, 2014.

Ash LR, Orihel TC: *Parasites: a guide to laboratory procedures and identification*, Chicago, 1987, ASCP Press.

Ash LR, Orihel TC: In *Atlas of human parasitology*, ed 5, Chicago, 2007, ASCP Press.

Association of Public Health Laboratories (APHL): *Advances in laboratory detection of Trichomonas vaginalis (updated)*, APHL, 2016. https://www.aphl.org/aboutAPHL/publications/Documents/ID_2016November-Laboratory-Detection-of-Trichomonas-update.pdf.

Audicana MT, Kennedy MW: *Anisakis simplex*: from obscure infectious worm to inducer of immune hypersensitivity, *Clin Microbiol Rev* 21:360, 2008.

Bartlett MS, Harper K, Smith N, et al.: Comparative evaluation of a modified zinc sulfate flotation technique, *J Clin Microbiol* 7:524, 1978.

Beaver PC, Jung RC, Cupp EW: In *Clinical parasitology*, ed 9, Philadelphia, 1984, Lea & Febiger.

Benenson MW, Takafuji ET, Lemon SM, et al.: Oocyst-transmitted toxoplasmosis associated with ingestion of contaminated water, *N Engl J Med* 307:666, 1982.

Bern C, Montgomery SP, Herwaldt BL, et al.: Evaluation and treatment of Chagas disease in the United States: a systematic review, *J Am Med Assoc* 298:2171, 2007.

Bethony J, Brooker S, Albonico M, et al.: Soil-transmitted helminth infections: ascariasis, trichuriasis, and hookworm, *Lancet* 367:1521, 2006.

Boggild AK, Martin DS, Lee TY, et al.: Laboratory diagnosis of amoebic keratitis: comparison of four diagnostic methods for different types of clinical specimens, *J Clin Microbiol* 47:1314, 2009.

Bowie WR, King AS, Werker DH, et al.: Outbreak of toxoplasmosis associated with municipal drinking water. The BC Toxoplasma Investigation Team, *Lancet* 350:173, 1997.

Brant SV, Loker ES: Schistosomes in the southwest United States and their potential for causing cercarial dermatitis or 'swimmer's itch', *J Helminthol* 83:191, 2009.

Brooke MM, Melvin DM: *Morphology of diagnostic stages of intestinal parasites of man. PHS Publication No. 1966*, Bethesda, Md, 1969, U.S. Department of Health, Education and Welfare.

Bruckner DA, Labarca JA: Chapter 140: *Leishmania* and *trypanosoma*. In Carroll JC, Pfaller MA, Landry ML, et al.: *Manual of clinical microbiology*, ed 12, Washington, D.C., 2019, ASM Press.

Brunetti E, Kern P, Vuitton DA: Writing panel for the WHO-IWGE, Expert consensus for the diagnosis and treatment of cystic and alveolar echinococcosis in humans, *Acta Trop* 14(1), 2010.

Cabello RR, Ruiz AC, Feregrino RR, et al.: *Dipylidium caninum* infection, *BMJ Case Rep*, 2011. bcr0720114510.

Calderón MA, Klein-Tebbe J, Linneberg A, et al.: House dust mite respiratory allergy: an overview of current therapeutic strategies, *J Allergy Immunol Pract* 3:843, 2015.

Cama V, Mathison B: Infections by intestinal coccidians and Giardia duodenalis, *Clin Lab Medicine* 35:423, 2015.

Campbell EH, Elston DM, Hawthorne JD, Beckert DR: Diagnosis and management of delusional parasitosis, *J Am Acad Dermatol* 80:1428, 2019.

Cantey PT, Weeks J, Edwards M, et al.: The emergence of zoonotic *Onchocerca lupi* infection in the United States – a case series, *Clin Infect Dis* 62:778, 2016.

Carroll KC, Pfaller MA, Landry ML, et al.: *Manual of clinical microbiology*, ed 12., Washington DC, 2019, ASM Press.

Centers for Disease Control and Prevention (CDC)a: Malaria. Atlanta, GA. https://www.cdc.gov/parasites/malaria/index.html [accessed November 26, 2018].

Centers for Disease Control and Prevention (CDC)b: Neglected Parasitic Infections (NPIs). Atlanta, GA. https://www.cdc.gov/parasites/npi/index.html [accessed August 25, 2019].

Centers for Disease Control and Prevention (CDC)c: *Strongyloides*. Atlanta, GA. https://www.cdc.gov/parasites/strongyloides/health_professionals/index.html#tx [accessed May 28, 2019].

Cheesbrough M: In *District laboratory practice in tropical countries. Part 1*, 2nd Edition, Cambridge, England, 2005, Cambridge University Press.

Clain J, Le Bras J, Secor WE: Susceptibility test methods. Chapter 154: pathogenic and opportunistic free-living amebae. In Carroll JC, Pfaller MA, Landry ML, et al.: *Manual of clinical microbiology*, ed 12, Washington, D.C., 2019, ASM Press.

Clark B, Sinha A, Parmar DN, Sykakis E: Advances in the diagnosis and treatment of *Acanthamoeba* keratitis, *J Ophthal* 484–892, 2012.

Clinical Laboratory Standards Institute. Laboratory diagnosis of blood borne parasitic diseases; approved guideline. CLSI, Wayne, PA:CLSI 2000, Clinical and Laboratory Standards Institute.

Cope JR, Ali IKM, Visvesvara GS: Chapter 142: pathogenic and opportunistic free-living amebae. In Carroll JC, Pfaller MA, Landry ML, et al.: *Manual of clinical microbiology*, ed 12, Washington, D.C., 2019, ASM Press.

Couturier BA, Jensen R, Arias N, et al.: Clinical and Analytical evaluation of a single-vial stool collection device with formalin-free fixative for improved processing and comprehensive detection of gastrointestinal parasites, *J Clin Microbiol* 53:2539, 2015.

Cox-Singh J, Davis TM, Lee KS, et al.: *Plasmodium knowlesi* malaria in humans is widely distributed and potentially life threatening, *Clin Infect Dis* 46:165, 2008.

Coyle CM, Varughese J, Weiss LM, Tanowitz HB: *Blastocystis*: to treat or not to treat, *Clin Infect Dis* 54:105, 2012.

Craun G: Waterborne giardiasis in the United States 1965-1984, *Lancet* 2:513, 1986.

Cross JH: Intestinal capillariasis, *Clin Microbiol Rev* 5:120, 1992.

D'Alessandro A, Ramirez LE, Chapadeiro E, et al.: Second recorded case of human infection by *Echinococcus oligarthrus*, *Am J Trop Med Hyg* 52(29), 1995.

D'Alessandro A, Rausch RL, Cuello C, et al.: *Echinococcus vogeli* in man, with a review of polycystic hydatid disease in Colombia and neighboring countries, *Am J Trop Med Hyg* 28:303, 1979.

da Silva AJ, Mathison BA: *Angiostrongylus* spp. of public health concern. In Ortega Y, Sterling CR, editors: *Foodborne parasites*, *food microbiology and food safety*, ed 2, New York, NY, 2018, Springer Nature, pp 139–158.

de Almeida ME, Steurer FJ, Koro O, et al.: Identification of *Leishmania* spp. by molecular amplification and DNA sequencing of a fragment of rRNA internal transcribed spacer 2, *J Clin Microbiol* 49:3143, 2011.

Diaz JH: Paragonimiasis acquired in the United States: native and nonnative species, *Clin Microbiol Rev* 26:493, 2013.

Doing KM, Hamm JL, Jellison JA, et al.: False-positive results obtained with the Alexon ProSpecT *Cryptosporidium* enzyme immunoassay, *J Clin Microbiol* 37:1582, 1999.

Drugs for parasitic infections, *Med Lett (New Rochelle)* 11(suppl), 2013.

Dubey JP, Jones JL: *Toxoplasma gondii* infection in humans and animals in the United States, *Int J Parasitol* 38:1257, 2008.

Eastburn RL, Fritsche TR, Terhune Jr CA: Human intestinal infection with *Nanophyetus salmincola* from salmonid fishes, *Am J Trop Med Hyg* 36:586, 1987.

Eberhard ML, Ruiz-Tiben, Hopkins DR: Dogs and Guinea worm eradication, *Lancet* 16:1225, 2016.

Farrar J, Hotez P, Junghanss T, Kang G, Lalloo D, White N: *Manson's tropical diseases*, ed 23, Philadelphia, 2013, Saunders Elsevier.

Fayer R, Esposito DH, Dubey JP: Human infections with *Sarcocystis* species, *Clin Microbiol Rev* 28:295, 2015.

Francesconi F, Lupi O, Myiasis: *Clin Microbiol Rev* 25:79, 2012.

Fritsche TR, Eastburn RL, Wiggins LH, et al.: Praziquantel for treatment of human *Nanophyetus salmincola* (*Troglotrema salmincola*) infection, *J Infect Dis* 160:896, 1989.

de la Fuente J, Pacheco I, Villar M, Cabezas-Cruz: The alpha-Gal syndrome: new insights into the tick-host conflict and cooperation, *Parasit Vectors* 12:154, 2010.

Garcia LS: In *Practical guide to diagnostic parasitology*, ed 2, Washington, DC, 2009, American Society for Microbiology.

Garcia LS: ed 3, *Clinical microbiology procedures handbook*, vols. 1–3. Washington, DC, 2010, American Society for Microbiology.

Garcia LS: In *Diagnostic medical parasitology*, ed 6, Washington, DC, 2016, American Society for Microbiology.

Garcia LS, Arrowood M, Kokoskin E, et al.: Laboratory diagnosis of parasites from the gastrointestinal tract, *Clin Microbiol Rev*, 2018. e00025-17.

Garcia LS, Shimizu RY: Evaluation of nine immunoassay kits (enzyme immunoassay and direct fluorescence) for detection of *Giardia lamblia* and *Cryptosporidium parvum* in human fecal specimens, *J Clin Microbiol* 35:1526, 1997.

Garcia LS, Shimizu RY: Detection of *Giardia lamblia* and *Cryptosporidium parvum* antigens in human fecal specimens using the ColorPAC combination rapid solid-phase qualitative immunochromatographic assay, *J Clin Microbiol* 38:1267, 2000.

Gelman BB, Rauf SJ, Nader R, et al.: Amoebic encephalitis due to *Sappinia diploidea*, *J Am Med Assoc* 285:2450–2451, 2005.

Gill GV, Bell DR: *Strongyloides stercoralis* infection in former Far East prisoners of war, *Br Med J* 2:572, 1979.

GBD 2016 Causes of Death Collaborators: global, regional, and national age-sex specific mortality for 264 causes of death, 1980-2016: A systematic analysis for the global burden of disease study 2016, Lancet vol. 390:1151–1210, 2017.

Goddard J: In *Physician's guide to arthropods of medical importance*, ed 6, Boca Raton, Fla, 2012, CRC Press.

Hadziyannis E, Yen-Lieberman B, Hall G, Procop GW: Ciliocytophthoria in clinical virology, *Arch Pathol Lab Med* 124:1220, 2000.

Hanson KL, Cartwright CP: Use of an enzyme immunoassay does not eliminate the need to analyze multiple stool specimens for sensitive detection of *Giardia lamblia*, *J Clin Microbiol* 39:474, 2001.

Hayes J, Nellore A: Management of *Strongyloides* in solid organ transplant recepients, *Infect Dis Clin North Am* 32:749, 2018.

Hernandez-Orts JS, Schotz T, Brabec J, et al.: High morphologic plasticity and global geographic distribution of the Pacific broad tapeworm *Adenocephalus pacificus* (syn. *Diphyllobothrium pacificum*): molecular and morphological survey, *Acta Trop* 149:168, 2015.

Herwaldt BL: Leishmaniasis, *Lancet* 354:1191, 1999.

Herwaldt BL, de Bruyn G, Pieniazek NJ, et al.: *Babesia divergens*-like infection, Washington State, *Emerg Infect Dis* 10:622, 2004.

Hopkins DR, Ruiz-Tiben E, Weiss AJ, et al.: Progress toward global elimination of dracunculiasis – January 2017-June 2018, *Morb Morth Wkly Rep* 67:1265, 2018.

Istre GR, Kreiss K, Hopkins RS, et al.: An outbreak of amebiasis spread by colonic irrigation at a chiropractic clinic, *N Engl J Med* 307:339, 1982.

John DT, Petri WA: In *Markell and Voge's medical parasitology*, ed 9, Philadelphia, 2006, Saunders Elsevier.

Johnson NF, Triplehorn CA: In *Borror and DeLong's introduction to the study of insects*, ed 7, Belmont, CA, 2005, Thompson Brooks/Cole.

Johnston SP, Ballard MM, Beach MJ, et al.: Evaluation of three commercial assays for detection of *Giardia* and *Cryptosporidium* organisms in fecal specimens, *J Clin Microbiol* 41:623, 2003.

La Hoz RM, Morris MI: Infectious diseases community of practice of the American society of transplantation: tissue and blood protozoa including toxoplasmosis, Chagas disease, leishmaniasis, *Babesia*, *Acanthamoeba*, *Balamuthia*, and *Naegleria* in solid organ transplant recipients – guidelines from the American society of transplantation infectious diseases community of practice, *Clin Transplant* e13546, 2019.

Lane RP, Crosskey RW: *Medical insects and arthropods*, London, 1993, Chapman & Hall.

Leterrier M, Morio F, Renard BT, et al.: Trichomonads in pleural effusion: case report, literature review and utility of PCR for species identification, *New Microbiol* 35:83, 2012.

Li CD, Yang HL, Wang Y: *Capillaria hepatica* in China, *World J Gasteroenterol* 16:698, 2010.

Linblade KA: The epidemiology of cercarial dermatitis and its association with limnological characteristics of a northern Michigan lake, *J Parasitol* 84(19), 1998.

Lindsay DS, Weiss LM: *Cystoisospora*, *Cyclospora* and *Sarcocystis*, chapter 144. In Carroll JC, Pfaller MA, Landry ML, et al.: *Manual of clinical microbiology*, ed 12, Washington, D.C., 2019, ASM Press.

MacKenzie WR, Schell WL, Blair KA, et al.: Massive outbreak of waterborne *Cryptosporidium* infection in Milwaukee, Wisconsin: recurrence of illness and risk of secondary transmission.

Mace KE, Arguin PM, Tan KR: Malaria surveillance – United States, 2015, *MMWR (Morb Mortal Wkly Rep)* 67, 2018.

Magill AJ, Grogl M, Gasser RA, et al.: Visceral infection caused by *Leishmania tropica* in veterans of Operation Desert Storm, *N Engl J Med* 328:1384, 1993.

McIlwee BE, Weis SE, Hosler GA: Incidence of endemic human cutaneous leishmaniasis in the United States, *JAMA Dermatol* 154:1032, 2018.

Marciano-Cabral F, Cabral G: *Acanthamoeba* spp. as agents of disease in humans, *Clin Microbiol Rev* 16:273, 2003.

Mathison BA, da Silva AJS: Anisakiasis. In: Ortega Y, Sterling CR, editors: *Foodborne Parasites*, *Food Microbiology and Food Safety*, ed 2, New York, NY, 2018, Springer Nature, pp 159–174.

Mathison BA, Couturier MR, Pritt BS: Diagnostic identification and differentiation of microfilariae, *J Clin Microbiol*, 2019. ONLINE VERSION ONLY AT THIS TIME.

Mathison BA, Pritt BS: Laboratory identification of arthropod ectoparasites, *Clin Microbiol Rev* 27:48, 2014.

Mathison BA, Pritt BS: *Arthropod benchtop reference guide*, Northfield, IL, 2015, College of American Pathologists.

Mathison BA, Pritt BS: Update on malaria diagnostics and test utilization, *J Clin Microbiol* 55:2009, 2017.

Mathison BA, Pritt BS: A systematic review of zoonotic helminths in North America, *Lab Medicine* 49:e61, 2018.

McAuley JB, Singh K: Chapter 141: *Toxoplasma*. In Carroll JC, Pfaller MA, Landry ML, et al.: *Manual of clinical microbiology*, ed 12, Washington, D.C., 2019, ASM Press.

Meites E, Gaydos CA, hobbs MM, et al.: A review of evidence-based care of symptomatic trichomoniasis and asymptomatic *Trichomonas vaginalis* infections, *Clin Infect Dis* 15:S837, 2015.

Meyers WM, editor: *Pathology of Infectious Diseases* (vol. 1). Washington, D.C., 2000, Armed Forces Institute of Pathology. (Helminthiases.

Meyers WM, Firpo A, Wear DJ: *Topics on the pathology of Protozoan and invasive arthropod diseases*, Washington, D.C., 2013, Armed Forces Institute of Pathology.

Miller GA, Klausner JD, Coates TJ, et al.: Assessment of a rapid antigen detection system for *Trichomonas vaginalis* infection, *Clin Diagn Lab Immunol* 10:1157, 2003.

Mohandas N, An X: Malaria and human red blood cells, *Med Microbiol Immunol* 201(4):593–598, 2012.

Montoya JG, Remington JS: Management of *Toxoplasma gondii* infection during pregnancy, *Clin Infect Dis* 47:554, 2008.

Moraru GM, Goddard J: *The Goddard guide to arthropods of medical importance ed 7*, Boca Raton, FL; CRC Press, 2019.

Mullen G, Durden L: *Medical and veterinary entomology*, ed 3., Cambridge, 2018, Academic Press.

National Communicable Disease Center: *Pictorial keys: arthropods, reptiles, birds, and mammals of public health significance*, Atlanta, 1969, Communicable Disease Center.

Ngui R, Lim YAL, Ismail WHW, et al.: Zoonotic *Ancylostoma ceylanicum* infection detected by endoscopy, *Am J Trop Med Hyg* 91:86, 2014.

Norgan AP, Arguello HE, Sloan LM, et al.: A method for reducing the sloughing of thick blood films for malaria diagnosis, *Malaria J* 12:231, 2013.

Norice-Tra C, Nutman TB: Chapter 147: filarial nematodes. In Carroll JC, Pfaller MA, Landry ML, et al.: *Manual of clinical microbiology*, ed 12, Washington, D.C., 2019, ASM Press.

Ntumngia FB, Thomas-Luque R, Torres Lde M, et al.: A novel erythrocyte binding protein of *Plasmodium vivax* suggests an alternate invasion pathway into Duffy-positive reticulocytes, *mBio* 7(4), 2016. e01261-16.

Orihel TC, Ash LR: *Parasites in human tissues*, Chicago, 1995, ASCP Press.

Orihel TC, Eberhard ML: Zoonotic filariasis, *Clin Microbiol Rev* 11:366, 1998.

Ortega YR, Sanchez R: Updates on *Cyclospora cayetanensis*, a food-borne and waterborne parasite, *Clin Microbiol Rev* 23:218, 2010.

Ortega YR, Sterling CR, Gilman RH, et al.: *Cyclospora* species: a new protozoan pathogen of humans, *N Engl J Med* 328:1308, 1993.

Peterman TA, Tian LH, Metcalf CA: High incidence of new sexually transmitted infections in the year following a sexually transmitted infection: a case for rescreening, *Ann Intern Med* 145:564, 2006.

Pillai DR, Kain KC: Immunochromatographic strip-based detection of *Entamoeba histolytica–E. dispar* and *Giardia lamblia* coproantigen, *J Clin Microbiol* 37:3017, 1999.

Pritt BS, Clark CG: Amebiasis, *Mayo Clinic Proc* 83:1154–1160, 2008.

Pritt BS: *Parasitology benchtop reference guide. Northfield, IL*, College of American Pathologists, 2014.

Pritt BS: Molecular diagnostics in the diagnosis of parasitic infection. In *Current and emerging Technologies for the diagnosis of microbial infections*, vol. 42. Cambridge, MA, 2015, Elsevier.

Pritt BS, editor: *Atlas of infectious diseases histopathology: a guide for daily Use*, Northfield, IL, 2018, College of American Pathologists.

Pritt BS: Chapter 139: *Plasmodium* and *Babesia*. In Carroll JC, Pfaller MA, Landry ML, et al.: *Manual of clinical microbiology*, ed 12, Washington, D.C., 2019, ASM Press.

Procop GW: North American paragonimiasis (caused by *Paragonimus kellicotti*) in the context of global paragonimiasis, *Clin Microbiol Rev* 22:415, 2009.

Purtilo DT, Meyers WM, Connor DH: Fatal strongyloidiasis in immunosuppressed patients, *Am J Med* 56:358, 1974.

Qvarnstrom Y, James C, Xayavong M, et al.: Comparison of real-time PCR protocols for the differential laboratory diagnosis of amebiasis, *J Clin Microbiol* 43:5491, 2005.

Qvarnstrom Y, da Silva AJ, Schuster FL, et al.: Molecular confirmation of *Sappinia pedata* as a causative agent of amoebic encephalitis, *J Infect Dis* 199:1139, 2009.

Qvarnstrom Y, Schijman AG, Vernon V, et al.: Sensitive and specific detection of *Trypanosoma cruzi* DNA in clinical specimens using a multi-target real-time PCR approach, *PLoS Negl Trop Dis* 6, 2012. e1689.

Ramalli L, Mulero S, Noël H, et al.: Persistence of schistosomal transmission liked to the Cavu river in southern Corsiva since 2013, *Euro Surveill* 23, 2018. pii=18-00017.

Rascoe LN, Santamaria C, Handali S, et al.: Interlaboratory optimization and evaluation of a serologic assay for diagnosis of human baylisascariasis, *Clin Vaccine Immunol* 20:1758, 2013.

Robert-Gangneux F, Dardé ML: Epidemiology of and diagnostic strategies for toxoplasmosis, *Clin Microbiol Rev* 25(2):264–296, 2012.

Romig T, Ebi D, Wassermann M: Taxonomy and molecular epidemiology of *Echinococcus granulosus sensu lato*, *Vet Parasitol* 213:76, 2015.

Roberts L, Janovy Jr J, Nadler S, Schmidt GD, Larry S: *Robert's Foundations of parasitology*, 9 ed., New York, 2013, McGraw-Hill.

Ryan ET, Hill DR, Solomon T, Endy TP, Aronson N: *Hunter's tropical medicine and emerging infectious diseases*, ed 10, Amsterdam, 2019, Elsevier.

Sacks JJ, Roberto RR, Brooks NF: Toxoplasmosis infection associated with raw goat's milk, *J Am Med Assoc* 248:1728, 1982.

Sandoval L, Cuestas D, Velandia A, et al.: Scabies herpeticum, an emerging clinical form of crusted scabies in AIDS patient: case report and literature review, *Int J Dermatol* 10, 2018. 1111/ijd.14256.

Saurabh K, Nag VL, Khera D, Elhence P: Giardiasis mimicking celiac disease in a patient with common variable immunodeficiency, *Trop Parasitol* 7:125, 2017.

Schantz PM, Moore AC, Munoz JL, et al.: Neurocysticercosis in an orthodox Jewish community in New York city, *N Engl J Med* 327:692, 1992.

Schwebke JR, Hobbs MM, Taylor SN, et al.: Molecular testing for *Trichomonas vaginalis* in women: results from a prospective U.S. clinical trial, *J Clin Microbiol* 49:4106–4111, 2011.

Schwebke JR, Gaydos CA, Davis T, et al.: Clinical evaluation of the Cepheid Xpert TV Assay for detection of *Trichomonas vaginalis* with prospectively collected specimens from men and women, *J Clin Microbiol* 56, 2018. e01091-17.

Shama SK, Etkind PH, Odell TM, et al.: Gypsy-moth-caterpillar dermatitis, *N Engl J Med* 306:1300, 1982.

Shaz BH, Schwartz J, Winters JL, et al.: American Society for Apheresis guidelines support use of red cell exchange transfusion for severe malaria with high parasitemia, *Clin Infect Dis* 58(2):302–303, 2014.

Sheorey H, Biggs BA, Ryan N: Chapter 146: nematodes. In Carroll JC, Pfaller MA, Landry ML, et al.: *Manual of clinical microbiology*, ed 12, Washington, D.C., 2019, ASM Press.

Shimizu RY, Garcia LS: Chapter 136: specimen collection, transport, and processing: parasitology. In Carroll JC, Pfaller MA, Landry ML, et al.: *Manual of clinical microbiology*, ed 12, Washington, D.C., 2019, ASM Press.

Shin SH, Hsu A, Chastain HM, et al.: Development of two FhSAP2 recombinant-based assays for immunodiagnosis of human chronic fascioliasis, *Am J Trop Med Hyg* 95:852, 2016.

Stark D, Garcia LS, Barratt JL, et al.: Description of *Dientamoeba fragilis* cyst and precystic forms from human samples, *J Clin Microbiol* 52:2680–2683, 2014.

Stark D, Barratt J, Chan D, Ellis JT: *Dientamoeba fragilis*, the neglected trichomonad of the human bowel, *Clin Microbiol Rev* 29:553, 2016.

Stensvold CR, Suresh GK, Tan KS, et al.: Terminology for *Blastocystis* subtypes – a consensus, *Trends Parasitol* 23:93, 2007.

Tan KR, Wiegand RE, Arguin PM: Exchange transfusion for severe malaria: evidence base and literature review, *Clin Infect Dis* 57(7):923–928, 2013.

Tappe D, Büttner DW: Diagnosis of human visceral pentastomiasis, *PLoS Negl Trop Dis* 3, 2009. e320.

Telford III SR, Mathison BA: Chapter 151: arthropods of medical importance. In Carroll JC, Pfaller MA, Landry ML, et al.: *Manual of clinical microbiology*, ed 12, Washington, D.C., 2019, ASM Press.

Teutch SM, Juranek DD, Sulzer A, et al.: Epidemic toxoplasmosis associated with infected cats, *N Engl J Med* 300:695, 1979.

Tsang VC, Wilkins PP: Immunodiagnosis of schistosomiasis, *Immunol Invest* 26:175, 1997.

Uyoga S, Macharia AW, Ndila CM, et al.: The indirect effects of malaria estimated from heath advantages of the sickle cell trait, *Nat Commun* 10:856, 2019.

Visvesvara GS, Moura H, Kovacs-Nace E, et al.: Uniform staining of *Cyclospora* oocysts in fecal smears by a modified safranin technique with microwave heating, *J Clin Microbiol* 35(3):730–733, 1997.

Visvesvara GS, Moura H, Schuster FL: Pathogenic and opportunistic free-living amebae: *Acanthamoeba* spp., *Balamuthia mandrillaris*, *Naegleria fowleri*, and *Sappinia diploidea*, *Immunol Med Microbiol* 50(1), 2007.

Visvesvara GS, Sriram R, Qvarnstrom T, et al.: *Paravahlkampfia francinae* n. sp. masquerading as an agent of primary amoebic meningoencephalitis, *J Eukaryot Microbiol* 56:357, 2009.

Waescbenbach A, Brabec J, Scholz T, et al.: The Catholic taste of broad tapeworms – multiple routes to human infection, *Int J Parasitol* 47:831, 2017.

Wang RJ, Li JQ, Chen YC, et al.: Widespread occurrence of *Cryptosporidium* infections in patients with HIV/AIDS: epidemiology, clinical feature, diagnosis, and therapy, *Acta Trop* 187:257, 2018.

Webster BL, Southgate VR, Littlewood DT: A revision of the interrelationships of *Schistosoma* including the recently described *Schistosoma guineensis*, *Int J Parasitol* 36:947, 2006.

Weigle KA, Davalos M, Heredia P, et al.: Diagnosis of cutaneous and mucocutaneous leishmaniasis in Colombia: a comparison of seven methods, *Am J Trop Med Hyg* 36:489, 1987.

Westblade LF, Simon MS, Mathison BA, Kirkman LA: *Babesia microti*: from mice to ticks to an increasingly number of highly susceptible humans, *J Clin Microbiol* 55:2903, 2017.

White Jr CA, Coyle CM, Rajshekhar V, et al.: Diagnosis and treatment of neurocysticercosis: 2017 clinical practice guidelines by the infectious diseases society of America (IDSA) and the American society of tropical medicine and hygiene (ASTMH), *Clin Infect Dis* 66(8):1159–1163, 2018.

Wilkins PP: Immunodiagnosis of human toxocariasis and prospects for improved diagnostics, *Curr Trop Med Rep* 1:44, 2014.

Wilkins P, Nutman TB: Immunological and molecular approaches for the diagnosis of parasitic infections. In Jorgensen JH, Pfaller MA, Carroll KC, et al.: *Manual of clinical microbiology*, ed. 11, Washington, D.C., 2015, ASM Press.

Wilson JM, Schuyler AL, Workman L, et al.: Investigatoin into the α-Gal syndrome: characteristics of 261 children and adults reporting red meat allergy, *J Allergy Clin Immunol Pract* S2213–2198(19):30314–30319, 2019.

Wilson ML: Malaria rapid diagnostic tests, *Clin Infect Dis* 54:1637, 2012.

World Health Organization: *Bench aids for the diagnosis of filarial infections*, Geneva, Switzerland, 1987, World Health Organization.

World Health Organization: *WHO estimates of the global burden of foodborne diseases*, Geneva, Switzerland, 2015, World Health Organization. https://www.who.int/foodborne_trematode_infections/resources/9789241565165/en/. [Accessed 6 September 2019].

World Health Organization: *WHO-FIND malaria RDT evaluation programme*, Geneva, Switzerland, 2017, World Health Organization. https://www.who.int/malaria/areas/diagnosis/rapid-diagnostic-tests/rdt-evaluation-programme/en/. [Accessed 25 August 2019].

World Health Organization: *World malaria report 2018*, Geneva, Switzerland, 2018, World Health Organization.

World Health Organization: *Neglected tropical diseases*. 2019. Geneva, Switzerland https://www.who.int/neglected_diseases/en/. [Accessed 25 August 2019].

Workowski KA, Bolan G: CDC Sexually transmitted diseases treatment guidelines, *MMWR (Morb Mortal Wkly Rep)* 64:72, 2015.

Xiao L, Cama V: Cryptosporidium. Chapter 145. In Carroll JC, Pfaller MA, Landry ML, et al.: *Manual of clinical microbiology*, ed 12, Washington, D.C., 2019, ASM Press.

Zimmerman PA, Ferreira MU, Howes RE, et al.: Red blood cell polymorphism and susceptibility to *Plasmodium vivax*, *Adv Parasitol* 81:27–76, 2013.

CHAPTER 66

SPECIMEN COLLECTION AND HANDLING FOR DIAGNOSIS OF INFECTIOUS DISEASES

Anna R. Plourde, Kathleen G. Beavis

GENERAL PRINCIPLES, 1352
Timing of Specimen Collection, 1352
Specimen Volume, 1352
Specimen Collection, 1352
Specimen Transport, 1352
Unacceptable Specimens, 1353
Standard Precautions, 1353
Referral Testing, 1353
BLOOD, 1353
Specimen Collection, 1353
Specimen Timing and Volume, 1353
Specimen Draws, 1354
Recovery of Microorganisms, 1354
Automated Blood Culture Systems, 1354
Detection and Notification of Positive Cultures, 1354
Detection of Viruses, 1355
Detection of Parasites, 1355
BODY FLUIDS, 1355
Cerebrospinal Fluid, 1355
Other Body Fluids, 1356
TISSUES, 1357
Specimen Collection and Processing, 1357
EYE, 1357
Conjunctival Specimens, 1357
Corneal Specimens, 1357
RESPIRATORY TRACT, 1358
Nasopharyngeal Specimens, 1358
Throat Specimens, 1358
Specimen Processing, 1358
Sputum and Tracheal Aspirates, 1359
Bronchoscopy Specimens, 1360
URINARY TRACT, 1361
Specimen Collection and Transport, 1361
Specimen Processing, 1361
GENITAL TRACT, 1362
Vaginal Secretions, 1362
Endocervical and Urethral Specimens, 1362
Vesicles, 1362
Ulcers, 1363
FECES, 1363
Viruses, 1363
Bacterial Pathogens, 1363
Parasites, 1364
SKIN AND SUBCUTANEOUS LESIONS, 1365
Fluid-Filled Lesions (Vesicles, Pustules, Bullae, and Abscesses), 1365
Wound Infections, 1365
Ulcers, 1366
SUMMARY, 1366
SELECTED REFERENCES, 1366

KEY POINTS

- Collect specimens from site of infection before initiating therapy.
- Collect an adequate volume of sample for testing required.
- Tissue, fluid, or aspirates are always superior to a swab specimen. The only exception is collecting culture material from a hard-to-reach spot such as a throat or cervix.
- Use required collection and transport materials to preserve specimen integrity.
- Communicate clear orders and source information.
- Expedite the transport of specimens to the laboratory and do not allow them to sit in collection areas.

Appropriate specimen collection, transport, and processing are crucial preanalytical steps in the accurate diagnosis of infectious diseases. Guidelines for specimen handling are discussed in this chapter. General principles are reviewed first followed by discussion of the most common types of specimens submitted to the clinical microbiology laboratory for testing.

GENERAL PRINCIPLES

TIMING OF SPECIMEN COLLECTION

For optimal detection of the pathogens responsible for an infectious disease, specimens should be collected at a time when the likelihood of recovering the suspected agent is greatest. For example, the likelihood of recovering most viruses is greatest in the acute phase of the illness. Specimens for recovery of bacteria should ideally be collected before antimicrobial therapy is started.

SPECIMEN VOLUME

The volume of specimen collected must be adequate for performance of the microbiological studies requested. If insufficient volume is received, the health care worker caring for the patient should be notified; either an additional sample can be obtained, or the physician must prioritize the requests.

Very little specimen is obtained with a swab, and much of the specimen is retained within the swab tip. Swabs should not be used as collection devices unless the specimen source is the throat, cervix, or other difficult-to-reach area. If a swab is used to collect the specimen, a polyester-tipped swab on a plastic shaft is acceptable for most organisms. Calcium alginate should be avoided for collection of samples for viral culture because it could inactivate herpes simplex virus (HSV), cotton may be toxic to *Neisseria gonorrhoeae*, and wooden shafts should be avoided because the wood may be toxic to *Chlamydia trachomatis*. Swabs are not optimal for detection of anaerobes, mycobacteria, or fungi, and they should not be used when these organisms are suspected. An actual tissue sample or fluid aspirate is always superior to a swab specimen for the recovery of pathogenic organisms.

SPECIMEN COLLECTION

Specimens should be obtained from the site of infection with minimal contamination from adjacent tissues and organ secretions, and with the exception of stool, should be collected in a sterile container. All specimens should be labeled with the name and identification number of the person from whom the specimen was collected, the source of the specimen, and the date and time it was collected.

SPECIMEN TRANSPORT

After collection, specimens should be placed in a biohazard bag and transported to the laboratory as soon as possible. If a delay is unavoidable, urine,

sputum and other respiratory specimens, stool, and specimens for detection of *C. trachomatis* or viruses should be refrigerated to prevent overgrowth of normal flora. Cerebrospinal fluid (CSF) and other body fluids, blood, and specimens collected for recovery of *N. gonorrhoeae* should be held at room temperature because refrigeration adversely affects recovery of potential pathogens from these sources.

UNACCEPTABLE SPECIMENS

Each laboratory director must establish criteria for rejecting specimens unsuitable for culture. Most clinical microbiologists agree that the following specimens should be rejected:

- Any specimen received in formalin
- 24-hour sputum collections
- Specimens in containers from which the sample has leaked
- Specimens that have been inoculated onto agar plates that have dried out or are outdated
- Specimens contaminated with barium, chemical dyes, or oily chemicals
- Foley catheter tips
- Duplicate specimens (except blood cultures) received in a 24-hour period
- Blood catheter tips submitted for patients without concomitant positive blood culture

The following specimens should be rejected for anaerobic culture:

- Gastric washings
- Urine other than suprapubic aspirate
- Stool (except for recovery of *Clostridium difficile* for epidemiologic studies or for diagnosis of bacteria associated with food poisoning)
- Oropharyngeal specimens except deep tissue samples obtained during a surgical procedure
- Sputum
- Swabs of ileostomy or colostomy sites
- Superficial skin specimens

STANDARD PRECAUTIONS

Safety is the responsibility of the laboratory director and, per the Clinical Laboratory Improvement Amendments (CLIA), cannot be delegated to others. The laboratory director should collaborate with infection control, institutional safety committees, environmental services, engineering, and others within the hospital and department to ensure that there are current and necessary policies and procedures, engineering controls, personal protective equipment (PPE), and a trained work force. The laboratory director is also responsible for making sure the policies and procedures are followed. Specimen processing can have additional challenges because this workforce often has the least amount of formal technical education.

Universal Precautions were designed to protect workers from infectious substances in blood and body fluids. Body Substance Isolation Precautions were designed to protect workers from transmission of organisms from moist body surfaces. In 1996, the US Hospital Infection Control Practices Advisory Committee unified these into "Standard Precautions." As described in *Biosafety in Microbiological and Biomedical Laboratories* (BMBL), Standard Precautions apply to (1) blood; (2) all body fluids, secretions, and excretions except sweat regardless of whether or not they contain visible blood; (3) nonintact skin; and (4) mucous membranes (Wilson, 2009). Standard Precautions must be followed when handling all specimens. A risk assessment should be performed in each laboratory area; it should detail the particular risks with each procedure. The safety recommendations for engineering controls, PPE, and work practices can be tailored to the risk (Callihan et al., 2014). Appropriate barriers are used to prevent exposure of skin and mucous membranes to the specimen. Gloves and a lab coat must be worn at all times when handling patient specimens, and masks, goggles (or working behind a plastic shield), and impermeable gowns or aprons must be worn when there is a risk for splashes or droplet formation. Optimally, all specimen containers, but at a minimum, those containing respiratory secretions and those submitted specifically for detection of mycobacteria or fungi should be opened in a biological safety cabinet. Specimens collected for virus isolation should be handled in a biological safety cabinet to prevent contamination of the cell cultures.

REFERRAL TESTING

When specimens or cultures must be shipped to a reference laboratory, they must be packaged according to dangerous goods shipping guidelines (see International Air Transport Association website, available at http://www.iata.org/whatwedo/cargo/dgr/Pages/index.aspx). Specimens must be limited to no more than 40 mL. Cultures of bacteria and fungi should be grown on solid media in tubes. The cap of the primary container (tube or vial) should be sealed with waterproof tape and inserted into a second container surrounded by sufficient packing material to absorb the entire volume of the culture or specimen if the primary container were to leak or break. If several primary tubes are placed in a second container, they must be either individually wrapped or separated so as to prevent contact between them, and there must be secondary packaging, which must be leakproof. The second container should be capped and placed in a shipping container made of corrugated fiberboard or hard plastic. An itemized list of contents must be enclosed between the secondary and outer packaging. The secondary and outer containers should be of sufficient strength to maintain their integrity at temperature and air pressures to which they will be subjected. If a specimen must be shipped on dry ice (which is considered to be a hazardous material), it must be marked "Dry ice, frozen medical specimen." The dry ice should be placed outside the second container with the packing material in such a way that the container does not become loose inside the outer container as the dry ice evaporates. All infectious shipping packages must be labeled with an official label containing the address and contents as well as the name and telephone number of the person responsible for the shipment. All laboratorians who package and ship materials that are known or reasonably expected to contain a pathogen must have documentation of training. There are several commercial and government-based resources for training.

BLOOD

The rapid identification and susceptibility testing of bloodborne pathogens is one of the most critical functions of the microbiology laboratory. Even with the increased use of molecular technologies capable of identifying organisms and some markers of resistance from either blood specimens or positive blood culture bottles, blood cultures are still the "gold standard" for identifying bacteria responsible for bacteremia, sepsis, infections of native and prosthetic valves, suppurative thrombophlebitis, mycotic aneurysms, and infections of vascular grafts. Blood cultures also are useful in diagnosing invasive or disseminated infections caused by certain fungi, especially *Cryptococcus neoformans*, *Candida* spp., *Fusarium* spp., and *Histoplasma capsulatum*. Serologic testing or nucleic acid amplification tests (NAATs) are needed to identify two important bacterial causes of culture-negative endocarditis, *Coxiella burnetii* and *Bartonella* spp. Parasites are usually detected in blood by microscopic examination of peripheral smears, but enzyme immunoassay (EIA) and NAATs are also used.

SPECIMEN COLLECTION

Timely detection and accurate identification of organisms in the blood depend on appropriate collection, transport, and processing of the specimen. In general, two to three sets of blood cultures should be collected for identification and susceptibility testing before antimicrobial therapy is initiated. Consensus guidelines recommend peripheral venipuncture rather than draws from intravascular catheters. Good skin cleaning and phlebotomy technique minimize the presence of skin contaminants in blood cultures (Miller et al., 2018). The use of iodine tincture, or chlorhexidine gluconate, is preferable to povidone–iodine solutions because the former require only about 30 seconds after application to achieve antiseptic effect; the latter requires up to 2 minutes. Each set of peripheral blood cultures must be drawn from a separate venipuncture site so that if a typical contaminating organism is present in one set and not the other, the organism can be more easily classified as a contaminant.

Compared with venipuncture, the risk for contamination is increased when blood cultures are drawn from an indwelling vascular device. Although it might seem advantageous to save the patient the discomfort of a venipuncture, a contaminated blood culture can cause even more diagnostic cultures, unnecessary antibiotics, and a prolonged stay in the hospital. If it is necessary to draw a culture through an intravenous line, another blood culture should be collected simultaneously from a venipuncture to aid in the interpretation of a contaminated line culture (Miller et al., 2018).

SPECIMEN TIMING AND VOLUME

The optimal time to draw blood for cultures when bacteremia or fungemia is suspected is just before a fever or chill, but this is not predictable. The single most important factor to detect bacteremia is volume of blood collected. In adults with bacteremia, the number of colony-forming units (CFUs) per milliliter of blood is frequently low. Therefore, for adults, collecting multiple sets of blood cultures with each bottle filled to optimal

volume is most important. (Washington & Ilstrup, 1986). In infants and children, the concentration of microorganisms in blood is higher, and collection of 1 to 5 mL of blood per culture is adequate. When blood cultures are drawn by personnel other than phlebotomists, it can be a challenge to obtain sufficient volumes in the culture bottles. With the current focus on detecting and treating sepsis, it behooves the pathologist to collaborate with clinical colleagues to optimize the amount of blood collected and improve the ability of the blood culture to detect bacteremia (Hazen et al., 2020; Khare et al., 2020).

SPECIMEN DRAWS

Recommendations concerning the number of blood specimens to collect are based on the nature of the bacteremia: transient, intermittent, or continuous. Transient bacteremia follows manipulation of a focus of infection (e.g., an abscess, a furuncle, or cellulitis), instrumentation of a contaminated mucosal surface (as occurs during dental procedures, cystoscopy, urethral catheterization, suction abortion, or sigmoidoscopy), or a surgical procedure in a contaminated site (e.g., transurethral resection of the prostate, vaginal hysterectomy, colon resection, and debridement of infected burns). Transient bacteremia also occurs early in the course of many systemic and localized infections such as meningitis, pneumonia, pyogenic arthritis, and osteomyelitis. Most intermittent bacteremias are associated with an undrained abscess, whereas continuous bacteremia is the hallmark of intravascular infection, such as bacterial endocarditis, mycotic aneurysm, or an infected intravascular catheter. Continuous bacteremia also occurs during the first few weeks of typhoid fever and brucellosis.

The optimal number of blood cultures for detection of bacteremia in patients without endocarditis is controversial. Most authorities agree that two or three 20-mL blood samples drawn over a 24-hour period and equally distributed into aerobic and anaerobic blood culture bottles will detect most bloodstream infections. One investigator demonstrated that 80% of bacteremias were detected with two blood cultures and 96% with three blood cultures. All bacteremias were detected with four blood cultures, but the routine collection of four blood cultures (up to 80 mL of blood) should be weighed against the risk for anemia (Cockerill et al., 2004). The optimal time interval between cultures is unknown, but 30 to 60 minutes for the first two sets has been suggested, with another one to two sets drawn over the remaining 24 hours if symptoms of septicemia persist (Cockerill et al., 2004). However, if initiation of antimicrobial therapy is deemed urgent, cultures should be collected before therapy is begun, from separate sites, within a few minutes.

Organisms such as the coagulase-negative staphylococci, viridans streptococci, *Corynebacterium* spp., *Bacillus* spp., and *Propionibacterium* spp. are frequent blood culture contaminants but may also be true pathogens. Collecting two sets of blood cultures per febrile episode helps distinguish probable pathogens from contaminants. If two sets are drawn from different venipuncture sites, the odds of both sets being contaminated by skin flora are very low. If two sets are drawn at the same time and only one set contains a skin contaminant, it is safe to assume that the culture was contaminated during collection. If only one set is drawn and a contaminant is present, it can be difficult to *not* treat the organism, especially if the patient has had recent surgery.

RECOVERY OF MICROORGANISMS

Host factors such as antibodies, complement, phagocytic white blood cells, and antimicrobial agents may impede recovery of microorganisms from blood; therefore, various approaches have been used to counteract these factors. Diluting the blood specimen in broth medium in a 1:10 ratio provides optimal neutralization of the serum bactericidal activity (Washington & Ilstrup, 1986). Incorporating 0.02% to 0.05% sodium polyanethol sulfonate in the blood culture medium inhibits coagulation, phagocytosis, and complement activation and inactivates aminoglycosides. Methods that counteract the presence of antimicrobial agents include using antibiotic-adsorbent resins or the lysis-centrifugation system.

AUTOMATED BLOOD CULTURE SYSTEMS

Three commercially available automated blood culture systems, each with advantages and disadvantages, are available. These continuously monitored automated detection systems have essentially replaced manual systems. All systems use nutritionally enriched liquid media, which are capable of supporting growth of most bacteria and many pathogenic yeasts. Traditionally, two bottles, an aerobic and an anaerobic, are inoculated.

Three major automated continuously monitoring blood culture systems are available commercially in the United States. With these systems, the usual incubation period is 5 days (Reisner & Woods, 1999). The BacT/ALERT 3D system (bioMerieux) is based on the colorimetric detection of carbon dioxide (CO_2) produced during microbial growth. A CO_2 sensor is bonded to the bottom of each blood culture bottle and is separated from the broth medium by a membrane that is impermeable to most ions and to components of media and blood but freely permeable to CO_2. Inoculated bottles are placed in cells in the instrument, which provides continuous rocking of both aerobic and anaerobic bottles. If bacteria are present, they generate CO_2, which is released into the broth medium; the pH then decreases, causing the sensor to change color from green to yellow. Color changes are monitored once every 10 minutes by a colorimetric detector. This system supports the growth of aerobic and anaerobic bacteria; bottles are available to support the growth of mycobacteria. This system has received Food and Drug Administration (FDA) clearance for monitoring bacterial contamination of platelets.

The BACTEC continuous-monitoring system (BD Diagnostics) is based on fluorescent technology. Bonded to the base of each vial is a CO_2 sensor that is impermeable to ions, medium components, and blood but freely permeable to CO_2. If organisms are present, they release CO_2 into the medium; it then diffuses into the sensor matrix and generates hydrogen ions. The subsequent decrease in pH increases the fluorescence output of the sensor, changing the signal transmitted to the optical and electronic components of the instrument. The computer generates growth curves, and data are analyzed according to growth algorithms. Inoculated bottles are placed in individual cells of the instrument and rocked continuously. Adult and pediatric aerobic and anaerobic bottles are available, as well as a bottle for the recovery of yeasts and mycobacteria.

The VersaTREK system (Trek Diagnostic Systems) detects growth of organisms in broth by measuring gas consumption and gas production. Each inoculated vial is fitted with a disposable connector that contains a recessed needle. The needle penetrates the bottle stopper and connects the bottle headspace to the sensor probe. The sensor monitors changes within the headspace in the consumption and production of all gases (CO_2, N_2, and H_2) by growing organisms and creates data points internally in the computer. Media are available to identify aerobic and anaerobic bacteria, including mycobacteria. Some clinicians continue to request extended incubation protocols for *Brucella* spp. and other bacteria known as the HACEK group (*Haemophilus*, *Aggregatibacter* [formerly *Actinobacillus*], *Cardiobacterium*, *Eikenella*, *Kingella* spp.). These organisms needed prolonged incubation times when manual methods predominated, but they can be detected during the routine incubation times of the automated instruments.

When mycobacteria or fungi are suspected, liquid medium developed by the manufacturer of automated and semiautomated broth culture systems can be used. These blood cultures are incubated for a prolonged period of 4 to 8 weeks.

DETECTION AND NOTIFICATION OF POSITIVE CULTURES

Positive blood cultures containing commonly isolated aerobic organisms are usually detected within 12 to 36 hours of incubation. Until recently, the initial report was limited to a Gram stain; identification and susceptibility results could be expected no sooner than 24 to 48 hours after the Gram stain report. Both the FilmArray blood culture identification panel (BioFire Diagnostics) and the Verigene system (Nanosphere) use molecular methods to identify more than 90% of the organisms in the time when a Gram stain would be reported. They can also identify the presence or absence of *mecA* and other resistance genes, allowing empiric therapy to be tailored (Bhatti et al., 2014a). The Accelerate Pheno system (Accelerate Diagnostics) can identify the organisms causing 90% of bacteremias and provide minimal inhibitory concentrations of key antimicrobial agents within 8 hours of a positive blood culture (Charnot-Katsikas et al., 2018). As these systems evolve and continue to provide even more rapid, clinically actionable information, laboratories should work with clinical colleagues to make sure these more expensive modalities have impact on patient care. "Pushing" information to clinicians has been shown to decrease the time to escalation or de-escalation of empiric antimicrobials (Banerjee et al., 2015).

The use of matrix-assisted laser desorption ionization–time of flight mass spectrometry (MALDI-TOF MS) has shortened the time to identification. Although most laboratories allow for overnight incubation before testing mature colonies, an aliquot of the positive culture can be centrifuged and the pellet inoculated onto prewarmed plates. About 95% of isolates can be identified with the MALDI-TOF after 4 hours of incubation (Bhatti et al., 2014b). Although more labor intensive, the reagents of

this method are much less expensive than the molecular methods. Cultures containing anaerobes are usually not detected for 48 to 72 hours, and identification is not available for 3 to 4 days. Fastidious organisms, such as those found in the HACEK group, may not be detected until 3 to 5 days.

In a small percentage of cases, no organisms will be seen on a Gram stain from a positive blood culture. It is very important to inoculate and monitor media in these cases. *Brucella* spp. can be difficult for an inexperienced eye to note on Gram stain; the colonies are visible on solid media a few days later. Conversely, some organisms are visible on Gram stain but not on routine media. These organisms grow on chocolate agar or sheep blood agar with a *Staphylococcus aureus* streak.

DETECTION OF VIRUSES

With regard to viruses, blood specimens are most commonly collected to monitor response of infection with human immunodeficiency virus (HIV), hepatitis C virus (HCV), hepatitis B virus (HBV), or cytomegalovirus (CMV) to antiviral therapy by using quantitative polymerase chain reaction (PCR) to measure viral load. Such assays are commercially available for each of these viruses, and in all cases, manufacturer's guidelines for specimen collection and transport should be followed. For HIV and HCV, blood specimens also may be collected for genotyping (commercial assays are available), and PCR (qualitative or quantitative PCR) generally is used to confirm an initial positive HCV antibody result. As with viral load, manufacturer's guidelines regarding specimen collection and transport should be followed.

In addition to assessing response to antiviral therapy, measuring viral load in a blood specimen is useful for monitoring disease and for diagnosis of disease in specific situations. In immunocompromised patients, especially transplant recipients but also patients with acquired immunodeficiency syndrome (AIDS), determining the level of CMV deoxyribonucleic acid (DNA) in blood is used to predict those at high risk for development of CMV disease and direct the initiation of preemptive therapy. Monitoring the level of BK virus and Epstein-Barr virus (EBV) DNA in serum or plasma by quantitative PCR is indicated in transplant recipients. If a commercially available NAAT assay is used, the package insert guidelines for specimen collection and transport should be followed. If, on the other hand, an assay developed and validated in house is used, guidelines published by that laboratory should be followed.

DETECTION OF PARASITES

Blood specimens are useful for diagnosis of malaria, babesiosis, trypanosomiasis, and some filariasis (Rosenblatt, 2009). Specimens should be collected in tubes with anticoagulant and transported promptly to the laboratory. If smears must be sent to a reference laboratory, they should follow the reference laboratory's instructions for fixation soon after they are made. The techniques used in the laboratory for detecting the aforementioned parasites are the same and are discussed here in order of the simplest to the most complicated.

Standard Precautions need to be used when preparing smears and reading fresh (unfixed) smears. Additional fixation time in methanol could be recommended depending on the patient's travel history. The simplest technique for detecting parasites in a sample of blood is the direct mount, prepared by placing 1 drop of blood on a glass slide, covering it with a cover glass, and examining it immediately. Direct mounts are excellent for diagnosis of trypanosomiasis or filariasis because the trypomastigotes and the microfilariae easily can be seen moving, often with low or medium power. Stained smears make the definitive diagnosis.

The thin smear, made as for hematologic work and stained in a similar manner, is the standard preparation for speciating *Plasmodium* spp., *Babesia* spp., *Trypanosoma* spp., and microfilaria. Thin smears for parasitologic work are fixed and then preferably stained manually with Giemsa stain, but automated hematologic staining is adequate. Smears are first scanned at low power to detect microfilariae, which are large objects (between 100 and 200 μm) and easily seen, usually at the lateral edges of the smear. After they are located, microfilariae should be studied under oil immersion for identification. After scanning with low power, the smear is examined with a high dry objective, searching for trypanosomes, and finally under oil immersion to find and identify *Plasmodium*, *Babesia*, and *Trypanosoma* spp.

Thick smears are useful for detecting all the parasites mentioned earlier and are part of the minimum laboratory workup for their diagnosis. One drop of blood is placed on a clean glass slide and, with the corner of another slide, is gently spread to cover 1 cm square. The preparation is allowed to dry and without fixation is stained with Giemsa stain, allowing for its dehemoglobinization.

BODY FLUIDS

CEREBROSPINAL FLUID

CSF is collected to diagnose meningitis and, less frequently, viral encephalitis. Infectious meningitis, a medical emergency requiring early therapy to prevent death or serious neurologic sequelae, is divided into acute, subacute, and chronic clinical syndromes, based on duration of symptoms. Potential pathogens are listed in Table 66.1. Enteroviruses are the agents most commonly responsible for meningitis, and they should be considered first in the differential diagnosis of meningitis in a child or adolescent during the late summer and early fall. The pyogenic bacteria responsible for meningitis vary with the age of the affected individual (Table 66.2).

Sample Collection and Transport

CSF is usually obtained by lumbar spinal puncture, but sometimes it is aspirated from the ventricles or collected from a shunt. As when collecting blood for culture, careful skin antisepsis is essential for collection of CSF, which typically is submitted to the laboratory in three or occasionally four tubes. The first tube filled should not be sent to Microbiology because it can contain skin flora. At least 0.5 to 1.0 mL should be sent to Microbiology for Gram stain and bacterial culture; ideally, the microbiology laboratory would receive 5 to 10 mL to accommodate requests for NAAT and cultures for mycobacteria and fungi (Miller et al., 2018). The parameters of normal CSF and the usual changes that occur during meningitis caused by different organisms are listed in Table 66.3.

CSF should be transported promptly to the laboratory and processed as rapidly as possible. If a brief delay in processing is unavoidable, the specimen should be held at room temperature unless viral culture is requested, in which case a portion (preferably 1 mL but no less than 0.5 mL) may be refrigerated for a short time. Specimen processing differs for bacteria, fungi, viruses, and parasites and is discussed separately for each group of organisms.

TABLE 66.1
Infectious Meningitis Syndromes

Syndrome	Onset or Duration	Probable Pathogens
Acute	<24 hours	Pyogenic bacteria
Subacute	1–7 days	Enteroviruses, pyogenic bacteria
Chronic	Persisting at least 4 weeks	*Mycobacterium tuberculosis*
		Treponema pallidum
		Brucella spp.
		Leptospira interrogans
		Borrelia burgdorferi
		Cryptococcus neoformans
		Coccidioides immitis
		Histoplasma capsulatum

TABLE 66.2
Common Bacterial Causes of Acute Meningitis by Age

Age	Organisms
Neonates–3 months	Group B streptococcus
	Escherichia coli
	Listeria monocytogenes[*]
	Streptococcus pneumoniae
4 months–6 years[†]	*Streptococcus pneumoniae*
6–45 years	*Neisseria meningitidis*
Older than 45 years	*Streptococcus pneumoniae*
	Listeria monocytogenes
	Group B streptococcus

[*]May cause meningitis in immunocompromised individuals in all age groups.
[†]Incidence of meningitis caused by *Haemophilus influenzae* type b in the United States has declined dramatically as a result of vaccination.

TABLE 66.3
Normal Cerebrospinal Fluid Parameters and Changes in Infectious Meningitis

Condition	WBCs (cells/μL)[a]	Protein (mg/dL)	Glucose (mg/dL)
Normal	5 (lymphocytes)	14–45	45–100 (2/3 serum)
Meningitis			
Acute or subacute bacterial	>500 (PMNs)	↑	↓
Chronic bacterial	200–2000	↑	↓
Tuberculous, fungal	(lymphocytes)	↑	↓
Enteroviral	200–2000 (PMNs early; lymphocytes later)	↑	Normal

[a]Cell type listed usually predominates.
↑, Increased; ↓, decreased; *PMN,* polymorphonuclear leukocyte; *WBC,* white blood cell.

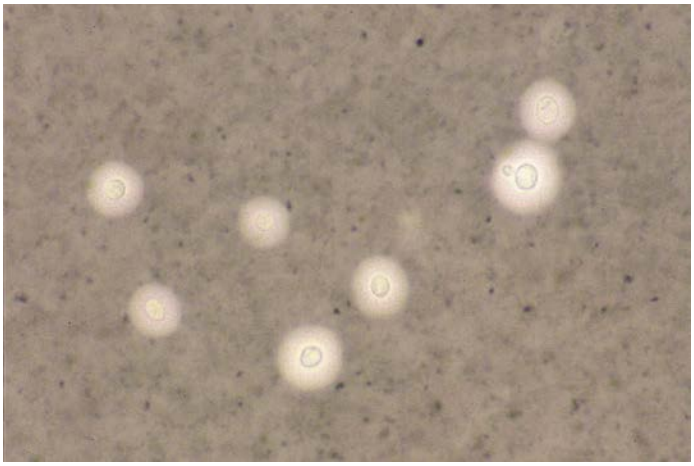

Figure 66.1 India ink preparation of cerebrospinal fluid showing encapsulated yeast forms of *Cryptococcus neoformans.* (400×.)

Sample Processing for Bacterial and Fungal Culture

Processing CSF for routine bacterial culture includes concentration (if 1 mL or more of specimen is received), preparation of a smear by cytocentrifugation for staining with Gram stain, and culture. The supernatant is decanted into a sterile tube, leaving about 0.5 mL of sediment and fluid, which is thoroughly mixed on a vortex mixer or by forcefully aspirating up and down into a sterile pipette.

Diagnosis of chronic bacterial meningitis requires specific requests because the CSF is handled differently for each entity. To diagnose brucellosis, the CSF is processed as described earlier for routine bacterial culture, but the media are incubated for 2 to 3 weeks. For leptospirosis, *Leptospira interrogans* may be cultured from the CSF during the first few weeks of illness, but the Centers for Disease Control and Prevention (CDC) can test using a NAAT. The diagnosis of neurosyphilis can be challenging and requires neurologic signs and symptoms, reactive serologic results, and CSF findings including pleocytosis, elevated protein, and a positive Venereal Disease Research Laboratory (VDRL) test result. If the CSF-VDRL result is negative in the presence of clinical and serologic support for neurosyphilis, a CSF fluorescent treponemal antibody absorption test might be useful. This test is more sensitive and less specific that the CSF-VDRL (https://www.cdc.gov/std/tg2015/syphilis.htm). The specimen should be refrigerated until it is tested. Involvement of the central nervous system by *Borrelia burgdorferi* (Lyme disease) also is diagnosed serologically by detection of specific immunoglobulin (Ig) M and IgG antibodies in CSF and serum.

At least 5 mL of CSF is recommended for mycobacterial culture; cytocentrifugation is required to make a smear and optimize the yield. A NAAT may be useful, but a negative result does not exclude mycobacterial infection.

Processing CSF for detection of fungi is similar to that described for detecting bacteria. Organisms are concentrated by filtration or by centrifugation. A cytocentrifuge preparation or a smear of the sediment stained with Gram or other stain is examined, and appropriate media (e.g., brain-heart infusion or SABHI agar without antibiotics) are inoculated for culture.

Additional Diagnostic Tests

In addition to culture, there is a commercially available molecular panel for meningitis including bacterial, viral, and fungal targets. This panel does not replace culture; the panel does not detect all CSF pathogens, and culture is still necessary for susceptibility results (Liesman et al., 2018; Tansarli & Chapin, 2020).

Two types of rapid tests are available for diagnosis of meningitis caused by *C. neoformans:* those specific for the capsular antigen (latex agglutination and enzyme-linked immunosorbent assay [ELISA]) and the nonspecific India ink preparation, which allow visualization of encapsulated yeast cells (Fig. 66.1). The sensitivity of the India ink stain, performed by mixing 1 drop of CSF sediment with 1 drop of India ink (available at art supply stores), is low, except in HIV-infected persons. Therefore, the cryptococcal latex agglutination test or the ELISA, both of which are highly specific and have sensitivities of more than 90%, is recommended for diagnosis. Supernatant of a centrifuged specimen or unspun CSF can be used for these latter two tests.

Cerebrospinal Fluid Sample Processing for Diagnosis of Viral and Parasite Infections

Currently, NAATs are used most often for diagnosis of viral infections of the central nervous system. Other diagnostic methods are conventional cell culture (primarily for detection of enteroviruses, although PCR is preferred) and serologic tests for viruses that cause encephalitis (western equine, eastern equine, Venezuelan equine, St. Louis, Japanese, La Crosse, and West Nile viruses).

CSF is occasionally sent to the laboratory for diagnosis of African trypanosomiasis (*Trypanosoma gambiense* and *Trypanosoma rhodesiense*) or infection with free-living amebae (*Naegleria fowleri* and *Acanthamoeba* spp.). When the specimen is received in the laboratory, it should be processed immediately. Wet preparations are prepared directly from the specimen and from the sediment by first shaking the tube gently (a step necessary because the parasites often stick to the wall of the tube) and then centrifuging the specimen at 250 *g* for 10 minutes. Preparations are examined under the microscope with the condenser in a low position to allow visualization of trophozoites or, preferably, by phase contrast microscopy.

Cultures of free-living amebae from CSF are done on nonnutrient agar plates covered with a suspension of *Escherichia coli* or *Enterobacter aerogenes*. The fluid is centrifuged at 250 *g* for 10 minutes, the supernatant is removed with a sterile pipette, and the sediment is mixed with 0.5 mL of saline solution and poured at the center of the plate. The culture is incubated at 37°C and examined for amebae daily for 10 days using a microscope under a 10× objective (Martinez & Visvesvara, 1991).

OTHER BODY FLUIDS

Fluid is collected from the pericardial, thoracic, or peritoneal cavity or from joint spaces by aspirating with a needle and syringe. A volume of 1 to 5 mL is adequate for isolating most bacteria, but 10 to 15 mL is optimal for recovery of mycobacteria and fungi, which are generally present in low numbers. Moreover, to diagnose peritonitis associated with chronic ambulatory peritoneal dialysis, collection of at least 50 mL of fluid may improve recovery of the responsible pathogen. To transport the fluid, it is aspirated into a sterile container and delivered promptly to the laboratory. Alternatively, peritoneal fluid may be directly inoculated into blood culture bottles at the patient's bedside; however, submission of fluid in blood culture bottles eliminates the possibility of direct Gram staining and delays the identification and susceptibility testing of any pathogens isolated. Clinicians should be advised to send fluid in a sterile container as well as in blood culture bottles to allow for the performance of a Gram stain and faster identification if the culture is positive.

Enteroviruses, primarily Coxsackie viruses A and B, are among the most common causes of infectious pericarditis. These viruses may be detected in pericardial fluid by NAAT or traditional cell culture, but because they are not recovered in all cases, collection of throat washings and stool (which are more likely to yield the virus), in addition to pericardial fluid, is strongly recommended for virus isolation from persons with suspected enteroviral pericarditis. Other viruses (HSV, varicella zoster virus [VZV], CMV, EBV, HBV, mumps virus, and influenza virus) are infrequent agents of pericarditis and usually are not detected in pericardial fluid.

Sample Processing for Bacterial Culture

Processing fluid from body cavities for detection of bacteria involves preparing a smear for Gram stain and inoculating appropriate media for culture. As mentioned earlier, the sample may be inoculated into blood culture bottles at the bedside, although this is not optimal unless additional specimen is sent for Gram stain and inoculation onto media. In the laboratory, the fluid is centrifuged, and the supernatant is removed, leaving about 0.5 mL of fluid in addition to the sediment, which is mixed thoroughly and then used to prepare smears and inoculate media. Alternatively, a small volume of noncloudy, nonviscous fluid (about 0.1 mL) may be removed before centrifugation and used to prepare a cytocentrifuged smear.

Fluid specimens submitted for detection of mycobacteria are processed as described earlier for CSF. Fluids for fungal culture should be concentrated by centrifugation as described for bacteria. The supernatant is removed, leaving 1.5 to 2.0 mL, in which the sediment is thoroughly mixed. A smear of the sediment is prepared for staining with Gram or Calcofluor white. Ideally, 0.5 to 1.0 mL of sediment is inoculated to primary fungal planting media (as for CSF), but lesser volumes are acceptable.

Parasitologic Examination

Body fluids are rarely collected for detection of parasites; however, *Entamoeba histolytica* may be found in the pericardial, pleural, or peritoneal cavity as a result of rupture of an abscess of the liver (into the peritoneal, pleural, or pericardial cavity) or of the lungs (into the pleural or pericardial cavity) or to perforation of amebic ulcers (into the peritoneal cavity). Hydatid cysts are infrequently diagnosed by examination of body cavity fluid, also caused by rupture of a cyst into a viscus contiguous to the cavity in question. The fluid collected is usually clear and contains hydatid sand (see Chapter 60) but rarely is turbid because of superimposed bacterial infection. Uncommonly, in individuals with a filarial infection, examination of wet preparations of a body cavity fluid may demonstrate the microfilariae; in patients with *Strongyloides* hyperinfection, larvae may be detected in body cavity fluids.

TISSUES

Tissue specimens obtained surgically are procured at great expense and at considerable risk to the patient; therefore, it behooves the surgeon to obtain an amount of material that is adequate for both histopathologic and microbiological examination. Swabs are rarely adequate for this purpose because of their limited capacity to hold specimen for culture. The histopathology of the lesion serves not only to differentiate between infection and malignancy but also to distinguish between a suppurative and a granulomatous process. In some cases, special stains are helpful in establishing the cause of the process. In chronic lesions, the differential diagnosis includes disease caused by actinomycetes, *Brucella* spp., mycobacteria, and fungi, any one of which may be present only in small numbers, again emphasizing the need to obtain adequate samples for examination and culture.

SPECIMEN COLLECTION AND PROCESSING

Tissue obtained surgically for culture should be placed into a sterile, wide-mouthed, screw-capped container. As a general rule, tissue should be bisected aseptically by the surgeon in the operating room, and material representative of the pathologic process should be submitted for both histopathologic and microbiological examination. Good communication between the anatomic pathologist and microbiologist is important, especially in cases of fever of unknown origin for which an exploratory laparotomy is being performed and multiple biopsy specimens are taken.

Tissue received in the laboratory is finely minced with sterile scissors or scalpels, added to a small volume of broth, and then rendered homogeneous either in a tissue grinder, mortar and pestle, or Stomacher to provide a 20% suspension. This suspension is used to inoculate all of the necessary culture media and is then stored under refrigeration for at least 2 weeks before being discarded.

Soft tissue specimens can be submitted after many injuries, including burns, animal or human bites, trauma, or surgery. The likely pathogens vary with the type of injury. When soft tissue specimens are received, there should be accompanying information to guide the workup in Microbiology. Human mouth flora is typically found in human bites; bites from animals are associated with organisms typical to the biting animal (e.g., *Pasteurella canis* from dogs and *Pasteurella multocida* from cats). Animal bites are typically polymicrobial and contain both aerobes and anaerobes. Soft tissue specimens after trauma can contain organisms depending on the type of trauma, including organisms usually thought of as environmental contaminants. Soft tissue specimens from burns can require quantitative cultures. These are best performed in concert with histopathologic examination to assess the true extent of the infection (Miller et al., 2018).

EYE

The most common ocular specimens received in clinical laboratories are conjunctival and corneal samples collected for the diagnosis of conjunctivitis and keratitis, respectively. Because specimen material is often scant, processing should be strategized based on the most likely etiologic organisms and informed by consultation with the clinician. The necessary collection materials, including culture media for direct inoculation or viral transport media (VTM), should be provided by the laboratory. Specimens should be labeled with the exact anatomic site (e.g., conjunctiva, cornea) to aid appropriate microbiological workup (Miller et al., 2018).

CONJUNCTIVAL SPECIMENS

Conjunctival scrapings or swab specimens are collected to determine the etiologic agent of conjunctivitis. Bacteria are the most common etiologic agents of infectious conjunctivitis, and those most frequently implicated are *Streptococcus pneumoniae* and *S. aureus* in adults; and *Haemophilus influenzae*, *S. pneumoniae*, and *S. aureus* in children. Trachoma, caused by the bacterium *C. trachomatis*, is a leading cause of blindness worldwide. *C. trachomatis* may also cause inclusion conjunctivitis in newborns and, less commonly, in adults. Viruses are responsible for about 15% to 20% of cases of acute infectious conjunctivitis, and in the United States, most epidemics of viral conjunctivitis (pinkeye) are caused by adenoviruses or herpes simplex virus. Rarely, parasites are causes of conjunctivitis.

Specimen Collection and Processing

Conjunctival cells are obtained from the superior and inferior tarsal conjunctiva by using a swab moistened with broth or a sterile platinum spatula. If a bacterial or fungal infection is suspected, culture media are inoculated directly by the individual collecting the sample to maximize the quantity and viability of organism recovered and the likelihood of detection. Media typically includes a chocolate agar plate for recovery of fastidious bacteria and fungi, with additional media as necessary based on suspected organisms (Das et al., 2010). Ideally, direct smears are also prepared, which may be useful in preliminary identification of the organism. If direct preparation of smears and inoculation of media is not possible, swab specimens may be obtained, though swabs yield minimal material. Smears should be air dried and promptly transported, with the inoculated media, to the laboratory. The conjunctiva and the eyelids of both the involved and uninvolved eye are often cultured concomitantly to characterize the normal flora, useful in assessing culture results from the involved eye.

If viral conjunctivitis is suspected, a second sample (swab or scrapings) should be collected and placed in viral transport medium. Viral conjunctivitis is now primarily diagnosed using NAATs because of their increased sensitivity and rapid turn-around time but require validation because there are no NAATs for any ocular source that are FDA approved to date. Viral culture remains an option if a NAAT is not available. A rapid diagnosis may also be provided by direct or indirect immunofluorescent staining of thin smears of conjunctival cells with virus-specific antibodies.

To detect *C. trachomatis*, NAATs are now the test of choice but, as for viral NAATs, require in-house validation (Dize et al., 2013). Alternative methods include examination of direct smear and culture. Specimens collected in viral or chlamydia transport medium are appropriate for all three types of methods (Miller et al., 2018). For direct examination, a smear prepared from conjunctival scrapings may be stained with Giemsa stain and examined for epithelial cells with basophilic intracytoplasmic inclusions diagnostic of *C. trachomatis* or preferably with monoclonal fluorescent antibodies, which are more sensitive and specific than Giemsa. The swab is rolled across the surface of the glass slide provided, the material is fixed, and the slide is transported promptly to the laboratory and held at room temperature or refrigerated briefly. Slides are stained and examined with a fluorescent microscope for elementary bodies (see Chapter 64). Specimens containing fewer than 10 columnar or metaplastic squamous cells are considered inadequate, and results should be reported as inconclusive, with an explanation, and another specimen should be requested. Culture of *C. trachomatis* should be performed when a diagnosis of chlamydial conjunctivitis is strongly suspected but other methods have produced negative results.

CORNEAL SPECIMENS

Corneal scrapings and biopsy specimens are useful in determining the etiologic agent of keratitis, an infection that can cause loss of vision and

requires immediate attention. Bacteria account for 65% to 90% of keratitis cases. In the United States, *S. aureus*, *S. pneumoniae*, *Pseudomonas aeruginosa*, and *Moraxella* spp. are most frequently implicated. Contamination of contact lens storage cases is a predisposing factor for keratitis; outbreaks have infrequently been caused by *Fusarium* spp. and *Acanthamoeba* spp. Viral keratitis is most commonly caused by recurrent HSV type 1, VZV, and EBV; the adenoviruses are less frequent causes. Postsurgical infections can be caused *S. aureus*, coagulase-negative staphylococci, and the *Mycobacterium chelonae–Mycobacterium abscessus* group. If keratitis follows a traumatic event, the laboratory should culture for environmental contaminants such as *Nocardia* spp., fungi, and *P. aeruginosa*, in addition to the organisms that often present as normal flora, such as *S. aureus*, coagulase-negative staphylococci, *S. pneumoniae*, and *Cutibacterium* spp (Gray et al., 2011).

Specimen Collection and Transport

Corneal scrapings are collected with a sterile platinum spatula and are used for preparation of smears by direct transfer to glass slides for staining and for inoculation to appropriate media for culture. Media typically include chocolate agar for recovery of fastidious bacteria, as well as brain–heart infusion agar with 10% sheep blood and inhibitory mold agar for fungal isolation (Leber, 2016). If evaluation for viral keratitis is requested, scrapings should be placed directly into VTM and delivered promptly to the laboratory. Viral keratitis is now diagnosed primarily with NAATs, though no FDA-approved assays are yet available. Viral culture remains an option if a NAAT is not available. Immunofluorescent staining of thin smears prepared directly from scrapings may be performed using virus-specific antibodies (Azher et al., 2017). When the culture of scrapings of a suspicious corneal ulcer is negative, a superficial keratectomy or corneal biopsy specimen may be obtained by the ophthalmologist, an approach especially useful for detection of fungi and *Acanthamoeba* spp.

RESPIRATORY TRACT

NASOPHARYNGEAL SPECIMENS

Nasopharyngeal aspirates, washings, and swab specimens are collected predominantly for diagnosis of viral respiratory infections, now typically diagnosed using rapid molecular methods (see Chapter 64). Nasopharyngeal specimens may also be submitted for workup of bacterial pneumonia caused by *Bordetella pertussis*, *C. trachomatis*, *Chlamydia pneumoniae*, or rarely *Corynebacterium diphtheriae* or to identify carriers of methicillin-resistant *S. aureus* (MRSA). Endoscopically or surgically collected specimens from the nasal sinuses are submitted for workup of sinusitis, typically in chronic or complicated cases, which are often associated with *S. aureus*, gram-negative bacilli, *Streptococcus* spp., anaerobes, or fungi (Miller et al., 2018).

Specimen Collection, Transport, and Processing

Nasopharyngeal aspirates and washings are superior to swabs for viral recovery, but swabs are frequently submitted because they are more convenient. Whereas washings or swab specimens are collected for detection of *B. pertussis*, swabs can be used for detection of *C. pneumoniae*. A swab is the preferred specimen for *C. trachomatis* and *C. diphtheriae*.

An aspirate is collected with a plastic tube (e.g., one used to feed premature infants) attached to a 1-mL syringe or a suction catheter with a mucus trap. A wash is obtained with a rubber suction bulb by instilling and withdrawing 3 to 7 mL of sterile phosphate-buffered saline. Swabs are obtained by removing all mucus from the nasal cavity, inserting a small flexible nasopharyngeal swab along the nasal septum to the posterior pharynx, and rotating against the mucosa several times. It is important to note that whereas cotton-tipped swabs and calcium alginate swabs inhibit PCR reactions, cotton-tipped swabs are toxic to *B. pertussis* (Cloud et al., 2002). Dacron or nylon swabs are preferable alternatives.

To detect viruses, nasopharyngeal specimens are placed into an appropriate transport medium, with or without antibiotics, and transported promptly to the laboratory or stored briefly in the refrigerator and packed in ice for transport as soon as possible. If a NAAT is used, the specimen must be collected as recommended by the manufacturer. Viral detection methods are discussed in more detail in Chapter 64.

The most sensitive method for detecting *B. pertussis* is PCR; a number of FDA-approved assays are commercially available (van der Zee et al., 2015; US FDA, 2020). If the sample must be transported to a reference laboratory for PCR, the swab should be shipped dry or in saline. To detect *B. pertussis* by culture, inoculation of washings or swab specimens at the bedside is optimal to preserve organism viability. If this is not possible, the sample is placed into sterile Casamino Acids broth, transported promptly to the laboratory, and processed within 2 hours for culture. If the sample must be sent to a reference laboratory for culture, the swab should be inoculated into a solid transport media such as Regan-Lowe or Bordet-Gengou agar, incubated at 37°C for 48 hours, and then shipped at ambient temperature. The direct fluorescent antibody (DFA) staining method, which provides a rapid diagnosis but is associated with false-positive and false-negative results, can be performed on a smear prepared from a nasopharyngeal swab or washing (van der Zee et al., 2015).

For detection of *C. trachomatis*, a nasopharyngeal swab specimen is collected with a polyester-tipped swab, which may be used for culture or for preparation of a smear for DFA staining. Detection methods are discussed in Chapter 62. For assessment of *C. trachomatis* or *C. pneumoniae*, the swab should be placed in an appropriate transport medium and transported to the laboratory as soon as possible or refrigerated for a short time. NAAT is recommended for detection of *C. pneumoniae* (Miller et al., 2018).

For culture of *C. diphtheriae*, swabbing multiple sites within the nasopharynx likely increases sensitivity. Any membranes present, as well as areas from beneath membranes, should be sampled for highest yield. Swabs should be immediately transferred to the microbiology laboratory. If delay is unavoidable, a semisolid transport medium (e.g., Amies) helps maintain bacterial viability (Efstratiou et al., 2000).

Carriers of MRSA may be detected within a few hours by commercial NAATs or after 24 to 48 hours using MRSA-specific chromogenic agar media (Bocher et al., 2008; Bischof et al., 2009; Tacconelli et al., 2009). Nasal secretions are collected from the anterior nares with a polyester-tipped swab, which is placed in a tube transport system and promptly delivered to the laboratory. If a NAAT is used, the specimen must be collected with the swab recommended by the manufacturer.

THROAT SPECIMENS

Throat swabs can be used to diagnose bacterial pharyngitis and Vincent's angina (caused by *Fusobacterium necrophorum* and other anaerobes). Group A streptococcus (GAS) is the cause of pharyngitis in less than one third of cases, but GAS needs to be identified and treated to prevent acute rheumatic fever, suppurative sequelae, transmission to others, and worsening of signs and symptoms. *C. diphtheriae* and *N. gonorrhoeae* are the other bacterial causes of pharyngitis for which antimicrobial therapy has been demonstrated to be effective. Other streptococci (group C and group G) also cause pharyngitis, but the utility of identifying them from culture is controversial. Antibiotics have been given to lessen the duration of symptoms, but controlled studies demonstrating evidence of a clinical response are lacking (Shulman et al., 2012).

Throat washings or swab specimens are also useful for detection of viruses shed in oral secretions without causing pharyngitis (HSV, CMV, or enteroviruses).

Because of the risk for respiratory obstruction, throat swabs are contraindicated for workup of epiglottitis (Rabinowitz, 1978).

Specimen Collection and Transport

Throat swab specimens are collected by depressing the tongue with a tongue blade, introducing the swab between the tonsillar pillars and behind the uvula without touching the lateral walls of the buccal cavity, and swabbing back and forth across the posterior pharynx. Swab specimens collected for detection of viruses should be placed in a viral transport medium, and those for detection of bacteria should be placed in a tube transport system containing modified Stuart's medium. For detection of *N. gonorrhoeae*, use of calcium alginate swabs should be avoided because they are toxic to the organism and can inhibit PCR (Lauer & Masters, 1988). Dacron-, rayon-, polyurethane-, and nylon-tipped swabs are acceptable alternatives. Specimens should be inoculated immediately to a selective medium, such as modified Thayer-Martin agar, or placed into charcoal-containing or other specific medium (Graver & Wade, 2004). Throat washings for diagnosis of viral infections are obtained by gargling with 5 mL of viral transport medium containing antibiotics. Throat washings and swab specimens should be delivered promptly to the laboratory or refrigerated for a short time if a delay in transport is unavoidable.

SPECIMEN PROCESSING

For diagnosis of GAS pharyngitis, culture is most sensitive; however, this requires overnight incubation. GAS grows well on horse and sheep blood agar, producing complete hemolysis (beta-hemolysis) of the agar. For rapid diagnosis of GAS, there are many commercially available point-of-care tests. These tests have a high specificity, so a throat culture does not need to follow a positive result. However, their sensitivity is lower. A commercial direct probe is the most sensitive of the rapid tests, but this test is not

usually used as a point-of-care test (Shulman et al., 2012). Other rapid, direct tests for GAS (several are commercially available) are less sensitive (as low as 70%); therefore, if one of these is used, two throat swab specimens should be collected. If the direct test result is positive, the second swab may be discarded, but if the direct test result is negative in children, a confirmatory culture must be performed using the second swab. In adults, because the incidence of streptococcal infection and the risk for rheumatic fever are low, confirmatory culture is optional (Shulman et al., 2012).

To detect *N. gonorrhoeae* in the throat, the swab specimen should be inoculated as soon as possible onto a selective medium, such as modified Thayer-Martin agar, to maximize yield. For diagnosis of diphtheria, both nasopharyngeal and throat swab specimens are collected and transported to the laboratory immediately. If laboratory personnel are not experienced in the recovery and identification of *C. diphtheriae*, the specimens should be sent in a semisolid transport media (e.g., Amies) to a reference laboratory. A differential inhibitory medium containing potassium tellurite, such as Tinsdale medium, is optimal for cultivating *C. diphtheriae*. However, this medium is expensive, has a short shelf-life, and is difficult to obtain from commercial vendors; therefore, it is seldom used in clinical laboratories. Colistin–nalidixic acid blood agar (CNA) is an acceptable alternative for the cultivation of *C. diphtheriae*, but because CNA is not a differential medium, all diphtheroid colony types must be evaluated to exclude *C. diphtheriae* when this agent is suspected. In addition, a sheep blood agar plate should be inoculated and examined for GAS.

Vincent's angina is an acute necrotizing ulcerative tonsillitis that may be caused by *F. necrophorum* and other anaerobes. A presumptive diagnosis may be made if gram-negative fusiform bacilli and spirochetes are seen in gram-stained smears prepared from a swab specimen of the ulcerated lesion. Cultures of the involved area are not usually helpful because many species of anaerobes are present in the oral cavity. However, blood cultures should be collected because the illness is commonly accompanied by sepsis.

SPUTUM AND TRACHEAL ASPIRATES

Microbiological studies of sputum (expectorated and induced) and tracheal aspirate specimens are done primarily to determine the etiologic agents of pneumonia and to assess mycobacterial infection. The Infectious Diseases Society of America and the American Thoracic Society have published guidelines for the diagnosis of community-acquired pneumonia (Metlay et al., 2019). Although routine sputum cultures are of questionable utility in many cases of community-acquired pneumonia, they should be performed if an unusual pathogen is suspected that would alter antimicrobial management. Clinical factors such as severe pneumonia requiring hospitalization or high risk for MRSA pneumonia, among others, support the utility of sputum culture (Metlay et al., 2019). Tracheal aspirates represent lower respiratory secretions collected in a Lukens trap from patients with tracheostomies. Patients with tracheostomies rapidly become colonized with gram-negative bacteria and other potential nosocomial pathogens and because bacteria colonizing the respiratory tract cannot be differentiated from bacteria causing invasive disease by culture of tracheal aspirates, interpretation of routine culture results is difficult. Culture for *Legionella* spp., mycobacteria, and fungi must be requested separately from routine culture because each of these requires special media for cultivation. *Pneumocystis jirovecii* cannot be cultured and is instead typically diagnosed using DFA staining; therefore, testing of *P. jirovecii* testing must also be requested separately (Miller et al., 2018).

Specimen Collection and Transport

Optimally, expectorated sputum is collected early in the morning before eating. The individual should rinse his or her mouth with water and then expectorate a specimen, preferably 5 to 10 mL, resulting from a deep cough. If mycobacteria are suspected, collection of three samples, at least one of which is an early morning specimen, is recommended. Additionally, the patient should not rinse his or her mouth before producing a specimen for mycobacterial workup because environmental mycobacteria that can be found in tap water such as *Mycobacterium gordonae* or *M. avium-intracellulare* could be introduced into the specimen. For persons with a nonproductive cough, a specimen may be induced by allowing the individual to breathe aerosolized droplets of a solution of 3% sodium chloride for about 20 minutes or until a cough reflex is initiated (Leber, 2016). Sputum and tracheal aspirate specimens should be collected into a sterile container and delivered promptly to the laboratory or refrigerated for a short time if a delay is unavoidable. If *Mycoplasma* is suspected, the specimen should be inoculated into liquid mycoplasmal growth media at the bedside if possible because the organism is very sensitive to environmental conditions such as drying (Leber, 2016).

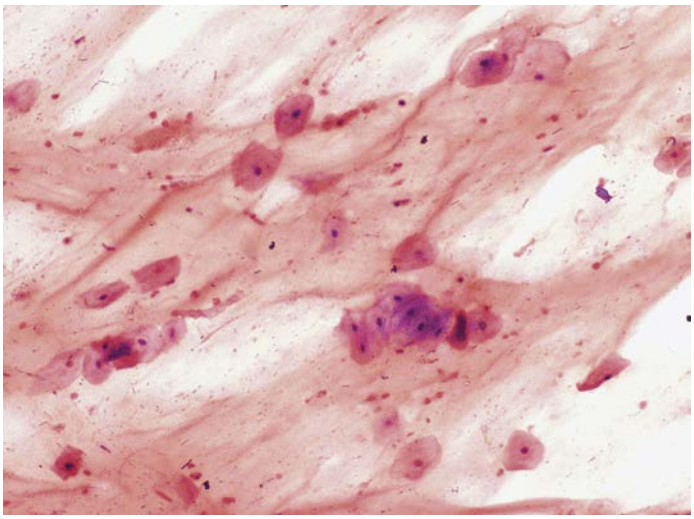

Figure 66.2 Gram stain of a sputum specimen demonstrating greater than 10 squamous epithelial cells per low-power field, which is unacceptable for culture. (10×.)

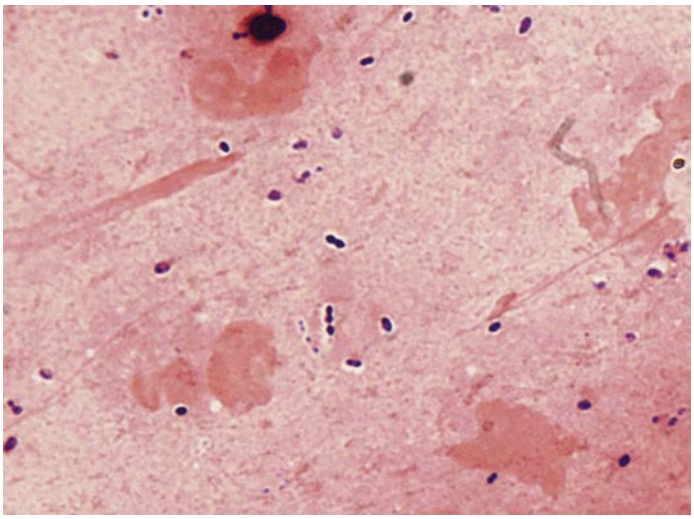

Figure 66.3 Gram stain of a sputum specimen showing encapsulated, lancet-shaped, gram-positive diplococci, consistent with *Streptococcus pneumoniae*. (100×.)

Specimen Processing

Sputum and tracheal aspirates for routine bacterial culture should be screened before they are plated to determine whether they are representative of lower respiratory secretions or of saliva. A smear prepared from a portion of the specimen consisting of purulent material is stained with the Gram stain. In general, specimens with more than 10 epithelial cells per low-power field (Fig. 66.2) are considered to have significant contamination with saliva and should be rejected. Specimens with fewer than 25 epithelial cells and more than 25 neutrophils per low-power field are probably acceptable (Murray & Washington, 1975). The number of neutrophils is not usually considered as a sole criterion when determining specimen quality because the individual from whom the sputum was collected may be neutropenic. Screening the quality of sputum samples submitted for detection of *M. pneumoniae*, *Legionella* spp., and mycobacteria is not generally required (Ingram & Plouffe, 1994; Havlik, 1995; McCarter & Robinson, 1996). The gram-stained smears prepared from specimens that are acceptable for culture are examined under oil immersion to determine the relative amounts of organisms. The quantity of organisms (rare, few, moderate, or many) is estimated for each kind of bacterium (e.g., gram-positive cocci in pairs [Fig. 66.3], chains, or clusters; gram-positive bacilli; gram-negative diplococci; and gram-negative rods), noting whether or not they are intracellular. Tracheal aspirates for which no organisms are observed in the gram-stained smear should probably be rejected (Morris et al., 1993). Portions of acceptable specimens containing purulent material are inoculated as outlined in Chapter 62. For specimens from persons with cystic fibrosis, also inoculating a medium selective for *Burkholderia cepacia* is recommended. The most sensitive method for detecting *B. pertussis* is PCR; a number of FDA-approved

assays are commercially available (van der Zee et al., 2015; US FDA, 2020). If PCR is not possible, *B. pertussis* culture should be performed as described above for nasopharyngeal samples.

When Legionnaires' disease is suspected, both *Legionella* culture and a rapid, direct test (e.g., fluorescent antibody on a respiratory specimen or *Legionella* antigen on a urine specimen) are recommended. DFA staining, which provides rapid results but is less sensitive than culture, can be used to supplement culture. Urinary antigen testing also provides rapid results but only detects *L. pneumophila* serotype 1 (Shimada et al., 2009). PCR can be performed but is considerably more expensive than culture, DFA, or urine antigen testing, and no FDA-approved assays are available yet (Benitez & Winchell, 2013). Culture, the most sensitive of these methods, can detect all *Legionella* spp. and serotypes and should always be performed. Decontaminating the specimens with acid (KCl-HCl buffer) before plating may enhance recovery of legionellae from sputum (Murdoch, 2003). Several drops of the specimen should then be inoculated onto each selective and nonselective buffered charcoal yeast extract agar plate. Use of the selective agar inhibits the growth of most other respiratory flora; however, some strains of *Legionella* spp. are susceptible to the medium's inhibitory agents. Thus, a nonselective plate should always be included.

For optimal detection of mycobacteria in sputum, the specimen must be decontaminated to prevent the normal respiratory flora from overgrowing the slower-growing mycobacteria. This process and detection methods are discussed in Chapter 61. All specimens submitted for mycobacterial workup should be processed in a biological safety cabinet, preferably in an isolated room with negative air pressure (Biosafety Level 3 laboratory).

All specimens submitted for fungal culture should also be handled as described for mycobacteria. The quality of the specimens should be determined by screening with smears stained with Gram stain (as described earlier for bacteria). Acceptable expectorated sputum, induced sputum, and tracheal aspirate specimens should be inoculated onto culture media for recovery of fungi. In general, to culture fungi, media with and without blood enrichment and media containing antimicrobial agents should be used. However, when making media selection, the laboratory director also should consider cost and the types of fungus usually encountered in the patient population served by the laboratory.

If viscous, sputum specimens for *P. jirovecii* detection by DFA staining are first treated with a mucolytic agent (e.g., N-acetyl-L-cysteine or dithiothreitol) and vigorously vortexed until the specimen is almost completely liquefied. After centrifugation, the sediment is smeared on glass slides and fixed, with fixation technique dependent on the stain manufacturer's instructions. Slides are then stained and examined microscopically (Leber, 2016).

BRONCHOSCOPY SPECIMENS

Bronchoalveolar lavage (BAL) fluid and protected brush specimens are useful for diagnosis of acute bacterial pneumonia, bacterial pneumonia in ventilated patients who have not received antimicrobial therapy and for detection of opportunistic pathogens in immunocompromised patients with pneumonia (Baselski & Wunderink, 1994; Carroll, 2002). BAL specimens may also be collected for suspected mycobacterial infection in patients who are unable to produce sputum (Holani et al., 2014). Although many have advocated quantitative cultures to improve the specificity of cultures from the lower respiratory tract, recent reviews have not shown an improvement in outcome for intubated patients compared with qualitative cultures (Caliendo et al., 2013). Only protected brush specimens are suitable for anaerobic culture (Baselski & Wunderink, 1994). For culture of *Legionella* spp., sputum specimens are preferable because BAL samples are diluted with saline and may contain small amounts of the anesthetic used locally, which inhibits the organism.

Specimen Collection and Transport

A protected brush sample is collected with a small brush that holds 0.001 to 0.01 mL of secretions, placed within a double-cannula enclosed catheter. The outer cannula has a displaceable polyethylene glycol plug at the tip. To obtain a specimen, the cannula is inserted to the desired area via bronchoscopy; the inner cannula is pushed out, dislodging the protective plug (water-soluble); and the brush is extended beyond the inner cannula. After the sample is taken, the brush is pulled back into the inner cannula, and both the brush and inner cannula are pulled into the outer cannula to prevent contamination of the brush when the catheter is removed. The brush is then placed into 1 mL of sterile saline or broth. The specimen should be transported immediately to the laboratory and processed as soon as possible. If a delay is unavoidable, the specimen should be stored in the refrigerator.

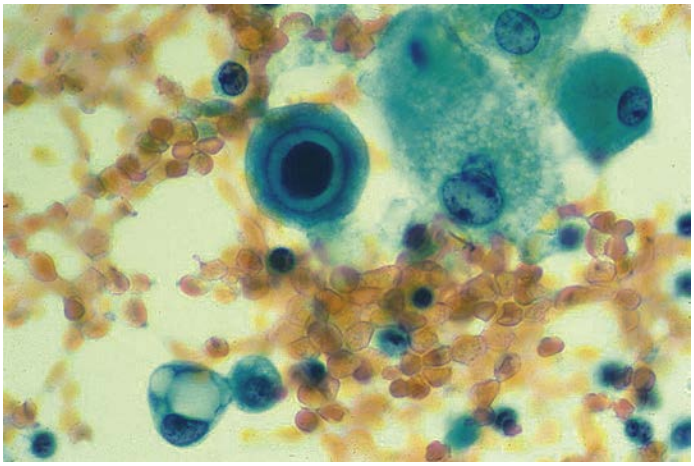

Figure 66.4 Cytologic preparation of bronchoalveolar lavage fluid shows an enlarged cell with intranuclear and intracytoplasmic inclusions, consistent with cytomegalovirus. (Papanicolaou stain, 250×.) (Courtesy of Vicki J. Schnadig, MD, Department of Pathology, University of Texas Medical Branch, Galveston, TX.)

To collect bronchoalveolar fluid, the tip of a bronchoscope is carefully wedged into an airway lumen. A volume of saline (usually >140 mL) in three to four aliquots is injected through the lumen, sampling an estimated 1 million alveoli. The total volume returned varies based on the volume instilled but is typically 10 to 100 mL. The specimen should be promptly transported to the laboratory (in <30 minutes) and processed as soon as possible because saline may be toxic to some respiratory pathogens (Leber, 2016). If a delay cannot be avoided, the fluid should be stored in the refrigerator. A number of FDA-approved NAATs for detection of respiratory viruses are available (US FDA, 2020). If a bronchoscopy specimen is being collected for testing by NAAT, the manufacturer's instructions for collection and processing should be followed.

Specimen Processing

To process the protected brush specimen, the fluid in which the brush is suspended is agitated on a vortex mixer, and the resulting suspension is used for a cytospin preparation and for culture inoculum. The BAL sample should be examined for small pieces of tissue; if present, they should be placed in a sterile container, kept moist with sterile saline, and processed in addition to the fluid (Sharp et al, 2004). If the specimen is viscous and fungi (including *P. jirovecii*) are suspected, treatment of the sample with a mucolytic agent (e.g., N-acetyl-L-cysteine or dithiothreitol) and subsequent centrifugation should be considered to concentrate contents and improve fungal recovery. The centrifuged specimen can then be used to prepare slides for staining (as discussed later) or inoculation to appropriate fungal culture media (outlined in Chapter 60).

Cytocentrifuge preparations can be useful for assessment of multiple types of respiratory pathogens. For bacterial detection, staining cytospin preparations with Gram stain is recommended because visualizing one or more bacteria per oil immersion field (in the absence of squamous epithelial cells) strongly suggests acute bacterial pneumonia (Kahn & Jones, 1987; Baselski & Wunderink, 1994). Examination of cytocentrifuge preparations stained with Papanicolaou stain allows detection of cytopathic changes, especially useful for diagnosis of CMV pneumonia (Fig. 66.4) (Woods et al., 1990). Cytospin preparations may also be stained with an acid-fast stain for detection of mycobacteria; with specific antibodies, such as those for detection of *Legionella* species or *P. jirovecii*; or with nonspecific stains (e.g., silver stain, Calcofluor white, or Giemsa) for detection of *P. jirovecii* or other fungi.

For bacterial culture, the laboratory may choose to inoculate plates quantitatively either by the serial dilution method or the calibrated loop method (Leber, 2016); however, the use of quantitative cultures is controversial, and pathologists should review their use with the clinical staff. The intent of this type of culture is to improve the specificity of the culture, with colony counts above a particular threshold appearing to correlate with infection.

For detection of mycobacteria, the specimen should be decontaminated and handled as described in Chapter 61. Viral detection methods from BAL specimens include NAAT and conventional cell culture, each further described in Chapter 64.

URINARY TRACT

The urinary tract above the urethra is sterile in healthy humans, but the urethra is normally colonized with many different bacteria, so urine specimens collected by a noninvasive method (e.g., clean-catch, midstream specimen) become contaminated during their passage. Growth of a predominant uropathogen in the quantity of 10^5 CFU/mL of bacteria or greater of urine has been considered highly indicative of infection. Quantitative cultures have been used to help differentiate between contaminants and presumed pathogens, but the entity of asymptomatic bacteriuria continues to confound culturing practices in the microbiology laboratory. Asymptomatic bacteriuria is the presence of bacteria in urine, with or without white cells, in patients (often women) who have no symptoms of urinary tract infection. This has led to the unnecessary use of antimicrobials. Some institutions have attempted to "screen" urine specimens, culturing only specimens meeting predetermined criteria often involving numbers of leukocytes or the presence of leukocyte esterase. Contemporary guidelines, bolstered by the *Choose Wisely* campaign to reduce inappropriate ordering of laboratory tests, instead focus on *not* culturing urine from nonpregnant, asymptomatic women (Nicolle, 2019). Growth of 10^5 CFU/mL of bacteria or greater of urine has been considered highly indicative of infection, but lower thresholds are relevant in certain populations. For example, in young, sexually active women with the acute urethral syndrome (dysuria, frequency, and urgency), as few as 10^2 CFU/mL is considered significant in the presence of concomitant pyuria (Stamm et al., 1982). True urinary infections associated with fewer than 10^5 CFU/mL may also occur in infants and children; in older men (Schaeffer & Nicolle, 2016); and in persons who are catheterized, were recently treated with antimicrobial agents, drink large amounts of fluids (which dilutes urine), have symptoms and concomitant pyuria, have urinary obstruction, or have pyelonephritis acquired from hematogenous spread (especially infections caused by yeast and *S. aureus*). Consequently, proper interpretation of urine culture results requires communication between clinicians and laboratory personnel.

SPECIMEN COLLECTION AND TRANSPORT

Acceptable methods of urine collection include midstream clean catch (preferably a first-voided morning specimen), catheterization, and suprapubic aspiration. In general, 24-hour urine specimens should be rejected except when detection of *Schistosoma haematobium* is requested specifically. Most commonly, the midstream flow of a clean-catch urine is collected. For women, the periurethral area and perineum should be cleaned before the specimen is collected (Nicolle, 2019). The first few milliliters of urine are passed into the toilet bowel or a bedpan to flush out bacteria normally colonizing the urethra, and the midstream portion is collected in a sterile container with a wide mouth and tightly fitting lid.

Catheterization is associated with the risk for inducing a nosocomial infection and should therefore be restricted to persons who are unable to produce a midstream sample, for example, individuals with an altered sensorium or those unable to void for neurologic or urologic reasons. Using strict aseptic technique, the catheter is inserted into the urethra, the first few milliliters of urine passed are discarded to clear organisms that may have entered the tip of the catheter during placement, and the midportion of the sample is obtained for culture. Urine may be collected from an indwelling catheter by aspirating with a 28-gauge needle and syringe through the rubber connector between the catheter and the collecting tubing, taking care to first disinfect the puncture site. Urine should not be collected from catheter bags, and Foley catheter tips should not be accepted for culture because they almost always are contaminated with urethral organisms.

Suprapubic aspiration is used primarily for neonates. The procedure requires a full bladder; the overlying skin is disinfected, the bladder is punctured above the symphysis pubis with a 22-gauge needle on a syringe, and about 10 mL of urine is aspirated.

All urine specimens should be transported promptly to the laboratory and should be processed within 2 hours after collection. If a delay in transport or processing cannot be avoided, specimens may be refrigerated up to 24 hours. Collection kits containing preservatives to maintain the bacterial population stable for 24 hours at room temperature are commercially available and advantageous if refrigeration cannot be guaranteed.

SPECIMEN PROCESSING

Quantitative bacterial culture of a urine specimen is done by inoculating appropriate media with a measured amount of urine, most commonly with a plastic or wire-calibrated loop designed to deliver a known volume.

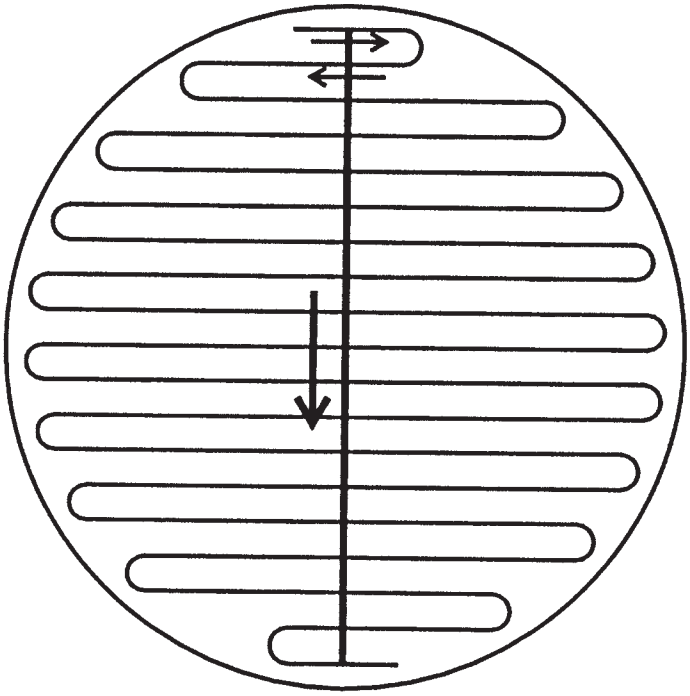

Figure 66.5 Technique for inoculating urine onto agar plates. (Redrawn from Woods GL, Gutierrez Y, editors: *Diagnostic pathology of infectious diseases,* Philadelphia, 1993, Lea & Febiger, p. 602.)

A 0.001-mL loop is used to inoculate all urine specimens except those collected from women with suspected acute urethral syndrome and suprapubic aspirates. Both the latter are inoculated with a 0.01-mL loop. The appropriate loop is inserted vertically into the well-mixed urine sample, and the loopful of urine removed is spread over the surface of the agar plate as illustrated in Figure 66.5. Without reflaming, the loop is again inserted vertically into the urine, and the removed sample is inoculated onto a second plate.

Some bacteria are not detected by routine culture of urine; when these pathogens are suspected, specific tests must be requested. For example, urine is an acceptable specimen for detection of *N. gonorrhoeae* and *C. trachomatis* by NAAT. The manufacturer's directions for urine collection and processing must be followed. *Leptospira interrogans* may be detected in urine after the first week of illness and for several months thereafter. To detect *L. interrogans* in urine, the specimen should be processed as soon as possible after collection because acidity may harm the organisms. One or 2 drops of undiluted urine and urine diluted 1:10 in broth are inoculated to 5 mL of Fletcher's medium or Ellinghausen-McCullough-Johnson-Harris medium containing 5-fluorouracil. Culture of urine for mycobacteria is discussed in Chapter 61. Yeasts may be recovered from urine on the media plated for routine bacterial culture, but if fungal culture is specifically requested, the sediment of a centrifuged urine specimen should be plated onto media such as inhibitory mold or SABHI agar containing antibacterial agents.

Urine specimens collected for culture of viruses should be submitted in liquid media containing antibiotics (e.g., penicillin, gentamicin, and amphotericin B), or antibiotics should be added to the sample when it is received in the laboratory to minimize bacterial contamination of cell cultures. PCR is more typically used than viral culture to identify viruses such as CMV, adenovirus, and HSV. Detection of BK virus in urine may be requested; however, PCR, rather than culture, is recommended. Because BK virus PCR is offered primarily by reference laboratories, it is best to contact that laboratory for collection and shipping requirements.

More than half of urine specimens submitted to the clinical laboratory for culture yield no growth or have bacterial counts below levels considered clinically significant. As discussed above, samples from asymptomatic, nonpregnant patients should not be cultured or screened for culture. Screening tests are used to quickly identify urine samples which are more likely to have "positive" culture results and to provide rapid results, eliminate negative specimens, and allow more time for positive specimens, improving efficiency and cost. In general, urine screen and culture results correlate well when 10^5 CFU/mL or greater is the reference, but they compare less favorably in the presence of lower colony counts. Commercial automated screening methods have been developed but are either no longer available or not actively marketed. Screening urine specimens by staining with

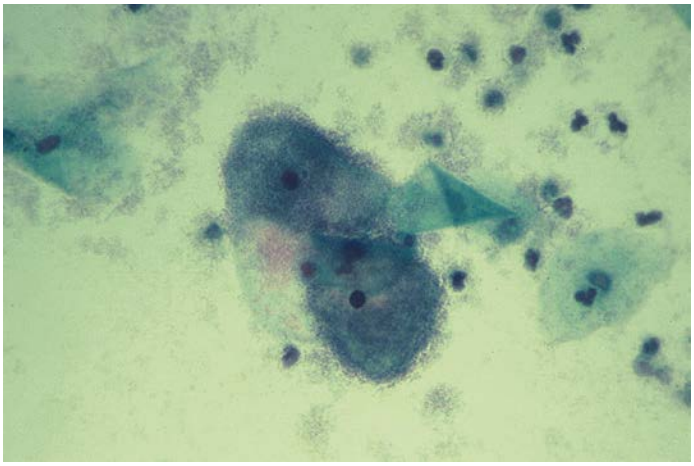

Figure 66.6 "Clue cells" in a smear of vaginal discharge. (Papanicolaou stain, 400×.) (Courtesy of Vicki J. Schnadig, MD, Department of Pathology, University of Texas Medical Branch, Galveston, TX.)

Gram stain is economical, but because examination of smears is tedious and time consuming, this approach rarely is adopted in the clinical laboratory. The commercial dipstick test that combines nitrate reductase (an enzyme present in most of the gram-negative bacilli that cause urinary tract infections) and leukocyte esterase (an enzyme produced by neutrophils) is rapid, inexpensive, and simple to perform and can suggest that a urinary tract infection is absent if both markers are negative, especially in symptomatic patients (Deville et al., 2004; St. John et al., 2006).

GENITAL TRACT

VAGINAL SECRETIONS

Vaginal secretions are useful in determining the etiologic agent of vulvovaginitis and bacterial vaginosis (BV). In women, the most common cause of BV is overgrowth of *Gardnerella vaginalis* (in association with a variety of anaerobes), whereas vulvovaginitis is most commonly caused by *Candida* spp. and *Trichomonas vaginalis*.

Regardless of the testing method, vaginal secretions should first be collected from the mucosal membrane of the vaginal wall using a sterile swab, with use of a manufacturer-provided swab if a testing kit is utilized.

Molecular assays are generally most sensitive for diagnosis of vulvovaginitis and BV. Three assays are currently available for simultaneous detection of *Candida* spp., *T. vaginalis*, and *G. vaginalis:* a DNA probe assay (Affirm VPIII microbial identification system, Becton Dickinson), a quantitative multiplex PCR assay (NuSwab, Laboratory Corporation of America Holdings), and an FDA-approved microbiome-based multiplex PCR assay (BD Max Vaginal Panel, Becton Dickinson) (Coleman & Gaydos, 2018). When testing by molecular methods, the manufacturer's protocol for specimen collection, transport, and processing should be followed.

If BV is suspected, a Gram stain of vaginal secretions should also be considered. When interpreted with a standardized scoring system (e.g., the Nugent score), the Gram stain is the most specific test for diagnosis of BV (Nugent et al., 1991). Culture is not recommended for diagnosis because *G. vaginalis* can be found in healthy women (Janulaitiene et al., 2017).

Although several rapid point-of-care tests exist for diagnosis of BV and vulvovaginitis (e.g., wet-mount preparations, vaginal pH test, whiff test), the sensitivity and specificity of these methods vary widely, and they are considered suboptimal (Miller et al., 2018). A wet mount is performed by placing a swab of the discharge in a tube containing about 1 mL of normal saline, removing the swab from the saline, and pressing the tip against a glass slide to express cellular material. The slide is coverslipped and examined for "clue cells" (epithelial cells covered with small coccobacillary bacteria) (Fig. 66.6), consistent with the diagnosis of nonspecific vaginosis; pseudohyphae, suggestive of candidiasis; and motile trichomonads. Other point-of-care tests include the vaginal pH test and the whiff test. The vaginal pH is usually about 4.5 in women with vulvovaginal candidiasis but is above 4.5 in those with bacterial vaginosis or trichomoniasis. A positive whiff test is the generation of a pungent, fishy odor after addition of 10% potassium hydroxide to 1 drop of vaginal discharge placed on a slide or on the speculum. This is associated predominantly with bacterial vaginosis but occasionally occurs with trichomoniasis.

ENDOCERVICAL AND URETHRAL SPECIMENS

Endocervical specimens are collected to determine the etiologic agents of cervicitis and to identify asymptomatic persons infected with an organism that cause sexually transmitted disease (e.g., *C. trachomatis*, *N. gonorrhoeae*). Endocervical specimens are obtained after the cervix is visualized with the aid of a speculum moistened only with warm water because lubricants may contain antibacterial agents. If a Papanicolaou smear is indicated, that sample should be collected first.

Specimens for microbiological studies are generally collected with a swab. Using a polyester-tipped swab with a plastic shaft is recommended. If a test kit is used for organism detection, the specimen must be collected with the swab specified by the manufacturer. Before collecting specimens for detection of *N. gonorrhoeae* and *C. trachomatis*, all discharge must be removed from the cervical os. The swab or brush then is inserted 1 to 2 cm into the endocervical canal (past the squamocolumnar junction), rotated firmly against the wall for 10 to 30 seconds, withdrawn without touching the surface of the vagina, and placed in the appropriate transport medium or tube system used to prepare a slide for DFA staining (for *C. trachomatis*) or used to immediately inoculate an agar medium for recovery of *N. gonorrhoeae*. Specimen handling varies based on the organism sought.

NAAT is recommended for detection of *N. gonorrhoeae* and *C. trachomatis*; several FDA-approved assays are available for simultaneous detection of both organisms (US FDA, 2020). If molecular methods are not available, culture may be performed, though sensitivity is lower (CDC, 2014). To isolate *N. gonorrhoeae*, direct inoculation of a selective agar medium, such as modified Thayer-Martin, within a container to which a CO_2-generating tablet is added, is optimal. Alternatively, the swab specimen can be placed in a tube transport system and delivered to the laboratory within 2 hours. If a delay in transport cannot be avoided, the swab should be left at room temperature and never refrigerated. Note that the viability of *N. gonorrhoeae* in Amies or modified Stuart medium substantially decreases after several hours (Miller et al., 2018). For chlamydial culture, the specimen should be transported in a transport medium containing antibiotics (e.g., M4 medium) to inhibit overgrowth of bacteria and fungi. To maintain the viability of *Chlamydia* organisms, the specimen should be transported to the laboratory and processed immediately. If delays in transport or processing are unavoidable, specimens should be stored in the refrigerator if they can be processed within 48 hours. Immunofluorescent staining (for chlamydial elementary bodies) and EIA are also available for chlamydial testing; the manufacturer's instructions for specimen handling must be followed.

To detect *C. trachomatis* and *N. gonorrhoeae* in men, a urethral swab specimen or first-voided urine sample, depending on the detection method used, should be obtained. Optimally, urethral swab specimens are collected at least 2 hours after the patient has voided. Samples for *N. gonorrhoeae* are obtained first, which maximizes the bacterial load and thus the likelihood of isolation (CDC, 2014). The conditions concerning types of swab and specimen transport are the same as those described for endocervical swab specimens, although the smaller urogenital swabs are used. The swab is inserted into the urethra for 2 to 4 cm, rotated in one direction for 5 seconds, withdrawn, and placed in the appropriate transport medium or used to prepare smears for DFA staining to detect *C. trachomatis* or for Gram staining to diagnose gonorrhea. Detection of intracellular gram-negative diplococci in a smear of urethral discharge from symptomatic men provides a presumptive diagnosis.

For optimal detection of HSV, NAAT is recommended, with specimen handling as per the test manufacturer or reference laboratory to which the sample is being sent. Alternatively, viral culture may be performed. The swab specimen is placed in viral transport medium such as M4 and transported as soon as possible to the laboratory. If immediate delivery is not feasible, the specimen should be stored in the refrigerator. For patients who have visible lesions on the cervix, a DFA may be performed on smears prepared from scrapings of the lesion base, though sensitivity is only about 70% compared with NAAT (Miller et al., 2018).

Genital tract infection with human papillomavirus (HPV) is diagnosed using nonculture methods; culturing the virus in vitro is not possible. Molecular techniques are most sensitive, with several available FDA-approved assays for testing of HPV genotypes associated with high risk for cervical cancer (US FDA, 2020). HPV-induced squamous cell changes may also be visualized on exfoliated cell samples (Papanicolaou smear).

VESICLES

Vesicular genital lesions are sampled to confirm HSV infection or (in children) atypical VZV infection. The vesicle fluid is aspirated with a small-gauge needle and syringe or capillary pipette. If only a small vesicle is

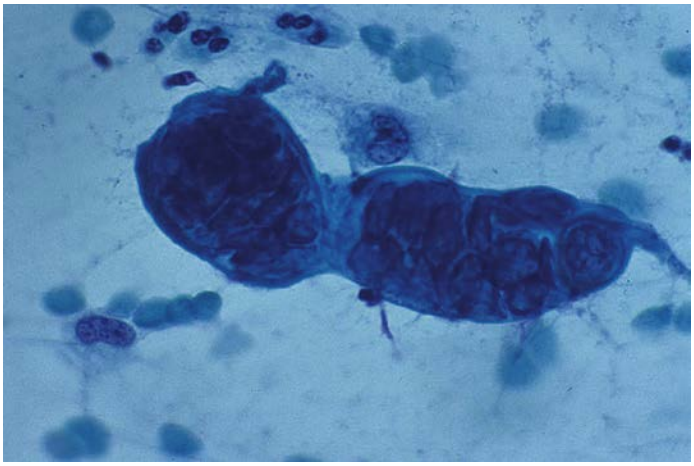

Figure 66.7 Multinucleate giant cell with intranuclear inclusions consistent with herpes simplex virus in a smear of endocervical cells. (Papanicolaou stain, 400×.) (Courtesy of Vicki J. Schnadig, MD, Department of Pathology, University of Texas Medical Branch, Galveston, TX.)

present, it is unroofed, and the base is firmly scraped with a Dacron swab to ensure collection of cells. Vesicle fluid or swab specimens should be placed in a viral transport medium. Testing by NAAT is optimal because it is most sensitive and can provide HSV typing information (Miller et al., 2018). HSV and VZV may also be detected in clinical specimens by viral cell culture or direct staining of smears, but these methods are less sensitive, and a negative result does not exclude the diagnosis. To make a smear, cells collected with a Dacron swab are spread on a glass slide, and the material is fixed in acetone for 5 to 10 minutes. The smear may be stained with Papanicolaou, Wright's, or Giemsa stain for detection of cytopathic changes (HSV and VZV have an identical appearance) (Fig. 66.7) or with specific monoclonal antibodies.

ULCERS

Material from genital ulcers is collected to identify the responsible pathogen; HSV, *Haemophilus ducreyi*, *Treponema pallidum*, *C. trachomatis* (serovars L1, L2, L3), and *Klebsiella granulomatis* should be considered.

For detection of HSV, specimen collection, transport and processing are identical to the protocol discussed for vesicles. In general, recovery of the virus and sensitivity of the tests previously described (i.e., NAATs, antigen detection, cell culture) are lower in ulcerative lesions compared to vesicular lesions.

Infection with *H. ducreyi* is typically diagnosed clinically (Workowski et al., 2015). If laboratory testing is deemed necessary, NAATs are generally most sensitive; several strategies have been developed for direct testing of clinical specimens, but there are currently no FDA-approved molecular assays for diagnosis of chancroid (West et al., 1995; Lewis, 2000; Chen & Ballard, 2012). Gram stain and culture are also possible but are less sensitive and not recommended unless the laboratory is experienced in these methods (Miller et al., 2018). For culture, a Dacron swab should be used to collect material from the base of the ulcer and directly inoculate a chocolate agar plate at the bedside. If bedside inoculation is not possible, the swab should be transported in modified Stuart's medium to the laboratory and held at room temperature until processed. A swab specimen may also be smeared onto a glass slide, Gram stained, and examined for small pleomorphic gram-negative coccobacilli in groups of chains resembling a "school of fish."

T. pallidum, the causative agent of syphilis, is usually diagnosed serologically. Spirochetes may be detected in genital or other lesions by darkfield microscopy or DFA, but these methods are unavailable in most laboratories. To collect specimens for spirochete detection, the surface of the lesion (if multiple lesions are present, the youngest should be selected) is cleaned with saline and blotted dry, and crusts are removed if present. The lesion is superficially abraded until slight bleeding occurs, and gentle pressure is applied to its base. The clear serum exudate from the subsurface is collected by directly touching the fluid with a glass slide or by aspiration with a 26-gauge needle (followed by drawing up 1 drop of saline into the syringe) with transfer of the fluid to a glass slide. A coverslip is placed on the fluid, and the specimen is examined immediately by darkfield microscopy for motile spirochetes or stained for DFA testing.

Lymphogranuloma venereum, caused by serovars L1, L2, or L3 of *C. trachomatis*, is typically diagnosed clinically. Serologic testing by microimmunofluorescence-IgG or complement fixation may be performed adjunctively (Stoner & Cohen, 2015). Although cell culture on biopsy or cellular material is possible, sensitivity is only 30%. Any overlying exudate is first removed from the lesion, and then a swab is firmly rotated against its base. Specimen transport and processing are the same as discussed for endocervical swab specimens.

K. granulomatis infection, which causes granuloma inguinale, is also typically diagnosed clinically. For laboratory examination, a scraping from an area of active granulation is taken, placed into formalin, and transported to the laboratory. The scrapings are then stained by Giemsa or Wright's stain for visualization of Donovan bodies, which appear as blue rods with prominent polar granules.

FECES

Feces and, in some cases, rectal swab specimens are useful for determining the etiologic agent of infectious diarrhea or food poisoning, confirming the diagnosis of diarrhea caused by *C. difficile* or *botulinum*, detecting certain sexually transmitted pathogens (e.g., *C. trachomatis*, *N. gonorrhoeae*), identifying carriers of bacterial pathogens for infection control purposes (e.g., vancomycin-resistant *Enterococcus* spp.), and in some instances, diagnosing helminths of the respiratory and biliary tracts. Collection, transport, and processing of specimens are different for viruses, bacteria, and parasites and are discussed separately for each group. Just as molecular and mass spectrometry methods have revolutionized the diagnosis of blood and respiratory specimens, they are similarly changing stool specimen diagnosis. There are numerous FDA-approved multiplex molecular methods for the rapid identification of bacterial, protozoal, and viral causes of diarrhea, as well as assays for identification of *C. difficile* and its toxin(s) (US FDA, 2020). Theoretically, this could eliminate routine stool cultures and ova and parasite examinations. However, as laboratories convert from culture-based to culture-independent methods, they must be aware of local regulations regarding submission of specimens or isolates of public health significance to public health laboratories and the need to perform susceptibility testing of certain pathogens (e.g., *Shigella* spp. and *Salmonella* spp. recovered from select age groups). Many jurisdictions ask that laboratories continue to send the patient's specimen for epidemiologic analysis.

VIRUSES

Specimen Collection and Transport

Stool is preferred for detection of enteroviruses and the viruses responsible for gastroenteritis (e.g., astrovirus, calicivirus, enteric adenovirus, rotavirus). Specimens should be collected in a clean container with a tight lid, or in VTM, depending on the type of testing to be performed. If feces cannot be obtained, a swab is inserted beyond the anal sphincter, rotated, withdrawn, and placed in VTM. Specimens should be delivered promptly to the laboratory; if this is not possible, fresh stool specimens can be stored at 4°C for up to 3 days and transported on wet ice. If the specimen must be mailed to a reference laboratory, it should be stored at –70°C and shipped on dry ice.

Specimen Processing

NAAT is recommended for detection of viral causes of gastroenteritis and enteroviruses because of their speed and accuracy of viral detection. A variety of laboratory-developed and commercial assays exist (US FDA, 2020). Viral culture remains an alternative method for adenovirus and enterovirus/parechovirus diagnosis, while EIA is an option for detection of rotavirus and adenovirus 40 and 41 (Miller et al., 2018). Specimens are processed according to the manufacturer's directions.

BACTERIAL PATHOGENS

Collection and Transport

The use of culture-independent diagnostic tests for bacterial stool pathogens is rapidly increasing because of their rapid turnaround time and improved sensitivity relative to culture (Shane et al., 2017). Many FDA-approved NAAT-based single- or multiplex assays are available (US FDA, 2020). Regardless of the testing method, stool is preferred for detection of pathogenic bacteria. Rectal swab specimens are an alternative but are less sensitive for culture in adults (Miller et al., 2018). Swabs should generally be reserved for detection of *N. gonorrhoeae*, *C. trachomatis*, and *Shigella* spp. and for assessment of vancomycin-resistant *Enterococcus* (VRE) carriage (Leber, 2016). Stool specimens should be collected in a clean container

with a tight lid, and the specimen should not be contaminated with urine, barium, or toilet paper because these substances can affect pathogen viability. Rectal swab specimens are obtained by inserting a swab past the anal sphincter (deep enough to become visibly stained with stool), gently rotated, withdrawn, and placed in a tube transport system containing appropriate transport media (e.g., Cary-Blair medium, manufacturer's transport medium for NAAT). All specimen types should be transported to the laboratory within 2 hours and quickly processed because the drop in pH that occurs as the stool cools may inhibit the growth of some pathogens, especially *Shigella* spp. If a delay in processing is unavoidable or if the specimen must be sent to a reference laboratory, transport of an aliquot of the specimen in transport media such as Cary-Blair is recommended.

Clinicians may consider testing a second stool specimen in adult patients who initially test negative for bacterial pathogens, but this is rarely necessary in pediatric patients. In adults, an enteric bacterial pathogen was detected in 87% of initial stool specimens, with a second specimen increasing this rate to 98% (Rohner et al., 1997). However, in pediatric patients, 98% of initial specimens were positive for a bacterial pathogen (Church et al., 1995).

Stool cultures for patients with diarrhea who have been hospitalized for more than 3 days are inappropriate unless the patient has been consuming food brought into the hospital. Offering *C. difficile* testing for health care–associated diarrhea may be considered instead. For diagnosis of *C. difficile* disease, 20 to 50 mL of liquid stool should be submitted in a sterile container. The stool specimen is stable for 2 days refrigerated or 1 week frozen. Testing should be performed only on patients with three or more unformed stools in 24 hours and who have not recently received laxatives. Unless the patient has ileus, testing of formed stool should be avoided because up to 15% of individuals are asymptomatic carriers, and testing may result in misdiagnosis and unnecessary treatment. Routine testing of children younger than 2 years old is not recommended because toxigenic *C. difficile* colonization is common in this age group (McDonald et al., 2018).

Specimen Processing

Processing stool or rectal swab specimens for detection of bacteria is based on the organism or group of organisms expected to be present. Specimens received for "routine" bacterial culture should be processed to allow recovery of *Shigella* spp., *Salmonella* spp., and *Campylobacter jejuni/coli* by plating to appropriate differential, inhibitory, and noninhibitory media. The microbiology laboratory director also might consider routinely examining stool for *Shiga* toxin–producing *E. coli* (STEC) and *Aeromonas* spp., depending on the prevalence of disease caused by these bacteria. The prevalence of gastroenteritis caused by *Yersinia enterocolitica*, *Vibrio cholerae*, or other *Vibrio* spp. or *Plesiomonas shigelloides* is low in most parts of the United States; therefore, specific requests for their detection are most cost effective. The patient population, season, and locale cause different laboratories to look for different pathogens. For this reason, every report from a stool culture should list the organisms that were identified or ruled out by the laboratory's protocol.

To detect STEC, *Shiga* toxin EIA or NAAT is preferred because they are more sensitive than culture and detect all serotypes of the organism (Pulz et al., 2003; Gavin et al., 2004). If culture is the only available method, the stool specimen is inoculated onto sorbitol-MacConkey agar (containing 1% D-sorbitol instead of lactose), a medium that differentiates isolates of STEC, which do not ferment sorbitol, from almost all other *E. coli*, which are sorbitol positive. When isolation of *Y. enterocolitica* is requested, cefsulodin-irgasan-novobiocin (CIN) agar is inoculated and incubated at room temperature. The organism also can be recovered by inoculating media typically used for routine bacterial culture. A MacConkey plate may be incubated at room temperature for 48 hours. Colonies of *Y. enterocolitica* are purple and pinhead in size. *Vibrio* spp. frequently grow on the media used for routine stool culture, but for their optimal recovery, thiosulfate citrate bile salts sucrose agar is inoculated. *Plesiomonas shigelloides* also grows on media used for routine culture, but because up to 30% of *P. shigelloides* isolates ferment lactose, their colonies do not appear sufficiently distinct to be recognized on these media, and screening all colonies for *Plesiomonas* is not cost effective. For this reason, culture of stool or rectal swab specimens for *P. shigelloides* should be requested specifically. Use of the selective-differential medium inositol brilliant-green bile salts agar has been suggested but is not essential.

Rectal swab specimens submitted for detection of *C. trachomatis* and *N. gonorrhoeae* are placed in transport medium and delivered promptly to the laboratory or are refrigerated for a short time. NAATs are recommended for detection of these organisms because they have superior sensitivity to culture and are highly specific (Schachter et al., 2008). Although NAATs are not FDA approved for extragenital site testing, they can be validated for this purpose.

Stool specimens or gastric contents collected from persons with short-incubation food poisoning should be evaluated for toxins from *S. aureus* and *Bacillus cereus*, and specimens from patients with long-incubation food poisoning should be evaluated for *Clostridium perfringens*. This testing is normally conducted by experts at public health laboratories, who should be contacted regarding appropriate specimen collection and transport. The clinical diagnoses of foodborne botulism and infant botulism may be confirmed by detecting botulinal toxin, *Clostridium botulinum*, or both in feces. Most clinical laboratories are not properly equipped to process specimens from persons with suspected botulism. In the United States, when a case of botulism is identified, investigators at the CDC should be notified to ensure appropriate specimen collection and transport, diagnosis, treatment, and investigation of the potential outbreak.

Diseases associated with *C. difficile* infection (CDI), such as pseudomembranous colitis and antibiotic-associated diarrhea, are caused by the toxins produced by the organism. In conjunction with clinical symptoms, several laboratory tests are available as diagnostic aids for CDI. These include toxigenic culture (TC); the cell cytotoxicity neutralization assay (CCNA); EIAs and immunochromatographic assays for detection of glutamate dehydrogenase (GDH) antigen, toxin A or B, or both toxins; and NAATs. TC and the CCNA serve as two reference methods for *C. difficile* diagnosis; however, both are slow and labor intensive. A testing algorithm that uses NAAT alone or in combination with GDH or toxin detection by immunoassay is recommended as an alternative approach for *C. difficile* detection (Kraft et al., 2019). NAAT-only testing has been shown to be highly sensitive and specific for detection of the *C. difficile* toxin genes A and B (Kraft et al., 2019). However, a NAAT-only approach may be cost prohibitive for laboratories, especially when testing volumes are high. Although immunoassays for GDH have low specificity for CDI because they do not distinguish isolates that produce toxin from those that do not, they have high sensitivity and a rapid turnaround time (15–45 minutes). Therefore, some have adopted a multistep algorithm by which samples are first screened with a GDH assay. Specimens yielding negative results require no further testing, whereas GDH-positive specimens are tested for toxin(s) using EIA or NAAT (Leber, 2016).

For epidemiologic studies, *C. difficile* may be isolated from stool or from rectal swab specimens placed in an anaerobic transport system. Because many bacteria are present in stool, procedures that select for *C. difficile* must be used. The most effective medium for this purpose is cycloserine cefoxitin fructose egg yolk agar (CCFA), with or without horse blood. The organism grows more quickly and luxuriantly on formulations containing horse blood. The medium is incubated anaerobically for 48 hours, and the plates are examined for colonies that have a peripheral fringe and a "horse stable" odor. Alternatively, *C. difficile* may be isolated by using an alcohol spore selection procedure, in which 1 mL of the original specimen is mixed with 1 mL of absolute ethanol. The mixture is allowed to stand for 1 hour at room temperature followed by subculture to CCFA and incubation anaerobically.

Swabs for assessment of VRE carriage can be inoculated to selective media containing vancomycin or VRE chromogenic agar, with subsequent NAAT-based testing to differentiate *vanA*- versus *vanB*-containing isolates (Leber, 2016).

With regard to mycobacterial culture, stool specimens usually are submitted for isolation of *Mycobacterium avium* complex (primarily from patients with AIDS), but *M. tuberculosis* complex and other *Mycobacterium* spp. also may be recovered. Processing the specimen (1–2 g of formed stool or 5 mL of liquid stool) involves decontamination and concentration, preparation of smears, and inoculation of media as discussed in Chapter 58.

PARASITES

The backbone of diagnostic parasitology in clinical laboratories is examination of stool samples for parasitic protozoa and helminth eggs or larvae. Laboratories performing such tests should have adequate facilities for handling stool samples and a good microscope with a calibrated micrometer to measure the organisms found. Staining of fecal smears is also required for identification of intestinal protozoa. In addition to morphologic examination, several antigen- or NAAT-based commercial assays have been developed for diagnosis of intestinal parasites (e.g., *Giardia* spp., *Cryptosporidium* spp.) as part of a gastrointestinal pathogen panel (US FDA, 2020).

Specimen Collection and Transport

The specimen (usually collected by the patient) can be collected in a clean, dry, wide-mouthed container. A portion of the sample is then aliquoted into two vials containing preservatives, one with modified polyvinyl alcohol (PVA) and the other with 10% formalin. Fecal specimens should not be

collected from the toilet bowl and should not be contaminated with urine, water, mineral or castor oil, antidiarrheal compounds, or radiologic contrast medium because these can destroy organisms or interfere with their detection (Garcia, 2016). After being collected and preserved, the sample should be delivered to the laboratory at the patient's convenience. The use of fresh stool is optimal for examination for motile trophozoites; however, it is usually very difficult to transport a fresh specimen to the laboratory and into the hands of the microbiologist within the 30 to 60 minutes after collection required to visualize motile trophozoites. Although it is rarely possible to perform wet mounts on fresh stools for motile trophozoites, they can still be identified on stained preparations, and the use of preserved specimens for examination minimizes the exposure of laboratory personnel to live organisms.

Several kits are commercially available for collection and transport of fecal samples; the choice depends on testing to be performed (e.g., special stains, immunoassays, NAAT) and the test manufacturer's recommendations for specimen fixative (Miller et al., 2018). The question of how many fecal specimens are required for identification of all individuals with intestinal protozoa or helminths is still without a definitive answer. It has been advised that a minimum of three specimens be examined, with one specimen collected every other day (Garcia et al., 2003; Clinical and Laboratory Standards Institute, 2005). For cost containment, the clinician should request examination of only one specimen because about 90% of all infections are diagnosed in the first sample (Montessori & Bischoff, 1987). If a parasite is not detected in the first sample, a second or third should be requested. If two or more specimens collected on different days are received in the laboratory at the same time, it has been suggested they be pooled and evaluated as one (Peters et al., 1988). This practice, however, is controversial. Stool examinations for parasites in patients who have been hospitalized for more than 3 days are inappropriate unless they are immunocompromised (Siegel et al., 1990).

Specimen Processing

The examination of stool samples for parasites includes preparation of saline solution and of iodine (Lugol's)-stained wet mounts of freshly collected samples (i.e., those that can be examined within a few hours of collection). This is followed by concentration of cysts and helminth eggs and finally by preparation of smears for staining with the trichrome stain. The wet preparations, if performed, should be made and examined before doing the concentration and trichrome staining. Even if a parasite is seen in the wet mount, examination of a concentrated specimen is recommended because specimens submitted for ova and parasite examination may contain multiple parasites. In particular, helminth eggs are often only visible in the concentrate.

The standard fecal smear is made from a fresh fecal sample as follows: 1 drop of saline solution is placed on a clear glass slide. With an applicator stick, a small amount of feces is picked up and with circular movements is mixed thoroughly with the saline (until enough sample is dissolved), and the mixture is covered with a 22-mm square cover glass. A good wet smear prepared as described, if placed on a paper with small print, should allow the print to be read through the smear. The smear stained with iodine is prepared in the same manner. Both the saline solution and the iodine solution wet preparations can be made on the same glass slide, at the same time mixing the feces with the saline solution first and then with the iodine solution. The saline solution smear will show trophozoites and cysts of protozoa, plus all the helminth eggs and larvae. In addition, the saline solution shows movement of trophozoites, which is useful for their identification. The smear stained with iodine does not show trophozoites because they are destroyed by the iodine unless the sample was previously fixed. The main advantage of the iodine stain is that it allows better visualization of some morphologic characteristics of cysts. To prepare wet mounts from formalin-fixed material, the contents are mixed well, and 1 drop is placed directly onto the glass slide and onto 1 drop of iodine solution.

Examination of the saline solution smear is carried out with medium power (10× objective) at first. Beginning at the upper-left corner of the cover slide, the slide is moved horizontally from right to left. The operation is repeated until the entire 22-mm square cover glass is examined. All helminth eggs or larvae and all protozoal cysts should be noted. Examination with the high-power objective is done next for detection and identification of protozoa, looking randomly for about 5 to 10 minutes per preparation. Note that pathogenic *E. histolytica* and nonpathogenic *Entamoeba dispar* cannot be distinguished based on morphology alone; an immunoassay or NAAT is needed for species-level identification (Tanyuksel & Petri, 2003).

The concentration technique, which can be done both on fresh and fixed specimens, is particularly useful because it allows detection of organisms present in low numbers. The concentration methods used for routine evaluation are described in detail in Chapter 60. Also discussed in that chapter are special stains required for detection of *Cryptosporidium* spp., microsporidia, and *Cyclospora* spp.

SKIN AND SUBCUTANEOUS LESIONS

FLUID-FILLED LESIONS (VESICLES, PUSTULES, BULLAE, AND ABSCESSES)

Fluid-containing lesions can be from viral, bacterial, or fungal causes; the appearance and distribution of the lesions suggest the most likely cause and should guide the specimen collection strategy. Vesicles are often viral, with HSV and VZV being common culprits. However, a bacterial cause should be considered if vesicles are limited to the face or extremities, as in nonbullous impetigo. Pustules are usually bacterial. Bullae that are generalized over the body are also typically associated with bacteria, especially *Staphylococcus* spp., whereas bullae limited to the foot are usually fungal. Finally, abscesses can be either bacterial or fungal, with anaerobic bacteria especially likely in the case of a closed abscess.

Specimen Collection and Transport

Regardless of the cause, aspirated fluid is the optimal specimen for testing fluid-filled lesions because this maximizes the concentration of viable pathogen while limiting contamination by extraneous microbes. Before fluid collection for bacterial or fungal testing, the overlying skin should be disinfected and allowed to dry completely. However, if viral testing is desired, skin disinfection should be avoided because antiseptic agents may inactivate viruses (Williamson et al., 2017).

Fluid can be aspirated using a needle and syringe. If viral testing is to be performed, the fluid should be immediately rinsed into VTM. Otherwise, the needle can be removed from the syringe and the syringe capped for transport to the laboratory.

If fluid aspiration is not possible, swabs may be used for sampling. Flocked swabs are preferable to nonflocked swabs because they yield greater organism recovery (Van Horn et al., 2008). Any overlying crust should first be gently removed and the lesion unroofed if necessary. One swab should then be used to absorb any fluid present, and a second swab should be used to vigorously rub the base and margins of the lesion. A minimum of two swab specimens should be collected: one for culture and the other for preparation of smears for staining. However, if more than one group of organisms (e.g., bacteria and fungi, fungi and viruses) is to be tested, collecting *at least* three swab specimens is recommended.

Swabs for bacterial or fungal testing may be placed into a commercially available swab transport system, with use of an anaerobic transport system if anaerobes are being considered. If viral causes are suspected, at least one swab should be placed into VTM. In addition, viral immunofluorescent staining (e.g., for HSV and VZV) may be helpful; slides should be prepared at the bedside by rolling the entire surface of the swab over a glass slide and allowing the material to air dry. All specimens should be promptly transported to the laboratory to limit loss of fastidious organisms and overgrowth of contaminants.

Specimen Processing

Processing specimens for detection of bacteria or fungi involves preparation of a smear for staining with Gram stain (for bacteria) or Calcofluor white (for fungi) and inoculation of appropriate media for culture. Additionally, if fungi are suspected, the fluid should be examined for grains or granules with a dissecting microscope because their presence indicates a mycetoma (Walsh et al., 2018). If present, grains and granules should be teased out of the specimen, washed in sterile solution, and examined for color (Leber, 2016). One portion should be crushed between two glass slides for examination for hyphae, and a second portion should be crushed and inoculated directly onto appropriate media.

Methods for viral detection include NAATs, antigen detection, and cell culture, any of which can be used to test fluid or swabs in VTM. Swab specimens received in VTM should be vigorously agitated on a vortex mixer, with removal and disposal of the swab. Specimens can be briefly refrigerated until they are processed.

WOUND INFECTIONS

Specimen Collection and Transport

Optimal wound sampling methods include aspiration (collected and transported as discussed earlier for fluid-filled lesions), tissue biopsy, and curettage. Swabs are far less helpful because they often are contaminated by skin commensal bacteria, leading to diagnostic confusion (Lipsky et al., 2012;

Nelson et al., 2018). All specimens should be delivered promptly to the laboratory. If transport will be delayed, inject a portion of the aspirate into an anaerobic transport tube. Tissue samples are transported in a sterile cup with moist sterile gauze to prevent desiccation. If a delay is unavoidable, specimens may be stored in the refrigerator, except those for anaerobe recovery, which should be maintained at room temperature.

Specimen Processing

Specimens should be Gram stained and inoculated to appropriate media for culture, as discussed in Chapters 59 and 62.

ULCERS

Ulcers may be primarily infected (e.g., those caused by viruses, *Bacillus anthracis*, *C. diphtheriae*, *Francisella tularensis*, *P. aeruginosa*, mycobacteria, or fungi) or secondarily colonized with aerobic and anaerobic bacteria, as is typical for chronic ulcers.

Specimens for viral detection from cutaneous ulcers are collected and transported identically to those described above for fluid-filled lesions. For bacterial, mycobacterial, or fungal isolation, handling of specimens differs by suspected cause.

B. anthracis is the cause of cutaneous anthrax, a rare disease in the United States that occurs among persons working with raw wool and other animal products contaminated with spores. For optimal diagnosis, specimens should be sent to a public health laboratory where NAAT can be performed. The public health laboratory's instructions for specimen collection and transport should be followed. If specimens are processed in the clinical laboratory, they must be handled in a biological safety cabinet. The swab is inoculated onto sheep blood agar and incubated in ambient air.

C. diphtheriae causes cutaneous diphtheria, an ulcerative lesion covered with a layer of necrotic debris resembling a membrane. For optimal diagnosis, a smear for staining with methylene blue is prepared from material from the edge of the membrane, and two swab specimens from the membrane itself are collected. One swab is used for routine bacterial culture and the other for inoculation of media selective for *C. diphtheriae* (e.g., cysteine tellurite agar) if available.

Ecthyma gangrenosum is an ulcerative cutaneous lesion that almost always occurs during bacteremia with *P. aeruginosa*. Ideally, two swab specimens are collected from the ulcer base; one is used to prepare a smear for Gram staining and the other for culture.

The diagnosis of the ulceroglandular form of tularemia, caused by *F. tularensis*, requires collection of a swab specimen from the ulcer base. The swab should be processed in a biological safety cabinet for routine bacterial culture, and the plates should be held for seven days because *F. tularensis* is a slowly growing bacterium that produces pinpoint colonies in 3 to 5 days on chocolate agar but does not grow on sheep blood agar. Suspicious isolates should be referred immediately to the nearest public health laboratory.

Mycobacteria most commonly isolated from cutaneous ulcers include *Mycobacterium fortuitum*, *Mycobacterium abscessus*, *Mycobacterium chelonae*, *Mycobacterium marinum*, and *Mycobacterium haemophilum*. *Mycobacterium ulcerans* is a common cause of skin lesions in some parts of the world but is difficult to culture. Exudate aspirated with a needle and syringe or a tissue sample is optimal for recovery of mycobacteria. Swab samples are not acceptable because mycobacteria become entrapped in the fibers of the swab and are difficult to dislodge. Transport of specimens is identical to that described earlier for wound infections. Specimens may be refrigerated for a short time until they are processed. Because some species of mycobacteria infecting the skin and extremities grow better at lower temperatures or with additional growth factors, it is important that personnel processing specimens are aware of the specimen source.

For fungal detection, an aspirate of the exudate (handled as described earlier for aspirates of fluid-filled lesions) or tissue sample from the active margin of the ulcer is optimal. A swab specimen of the exudate is suboptimal. Processing the specimen for detection of fungi involves preparing a smear for direct microscopic examination (potassium hydroxide or Calcofluor white preparation) and inoculation of appropriate media for culture.

Chronic skin ulcers are often colonized by aerobic, facultative, or anaerobic bacteria. To identify the responsible organisms, cultures of deep tissue biopsy (after thorough debridement) or deep aspiration of purulent material by needle and syringe are most useful. Surface cultures of such ulcers are not valuable because they usually represent colonizing bacteria rather than the causative agent (Miller et al., 2018). Transport and processing of tissue and aspirated material are identical to those described earlier for wound infections.

ACKNOWLEDGMENT

We gratefully acknowledge the contributions of Ann C. Croft and Gail L. Woods, who authored this chapter in previous editions.

SELECTED REFERENCES

Clinical and Laboratory Standards Institute: *Procedures for the recovery and identification of parasites from the intestinal tract; approved guideline, CLSI Document M28-A2*, Wayne, PA, 2005, Clinical and Laboratory Standards Institute.

Leber AL, editor: *Clinical microbiology procedures handbook*, ed 4, Washington, DC, 2016, ASM Press.

US Food and Drug Administration: Nucleic acid based tests. https://www.fda.gov/medical-devices/vitro-diagnostics/nucleic-acid-based-tests. Published 2020. Accessed 01/09/2020.

Access the complete reference list online at Elsevier eBooks for Practicing Clinicians.

REFERENCES

Azher TN, Yin XT, Tajfirouz D, et al.: Herpes simplex keratitis: challenges in diagnosis and clinical management, *Clin Ophthalmol* 11:185–191, 2017.

Banerjee R, Teng CB, Cunningham SA, et al.: Randomized trial of rapid multiplex polymerase chain reaction-based blood culture identification and susceptibility testing, *Clin Infect Dis* 61(7):1071–1080, 2015.

Baselski VS, Wunderink RG: Bronchoscopic diagnosis of pneumonia, *Clin Microbiol Rev* 7(4):533–558, 1994.

Benitez AJ, Winchell JM: Clinical application of a multiplex real-time PCR assay for simultaneous detection of Legionella species, Legionella pneumophila, and Legionella pneumophila serogroup 1, *J Clin Microbiol* 51(1):348–351, 2013.

Bhatti MM, Boonlayangoor S, Beavis KG, Tesic V: Evaluation of FilmArray and Verigene systems for rapid identification of positive blood cultures, *J Clin Microbiol* 52(9):3433–3436, 2014a.

Bhatti MM, Boonlayangoor S, Beavis KG, Tesic V: Rapid identification of positive blood cultures by matrix-assisted laser desorption ionization-time of flight mass spectrometry using prewarmed agar plates, *J Clin Microbiol* 52(12):4334–4338, 2014b.

Bischof LJ, Lapsley L, Fontecchio K, et al.: Comparison of chromogenic media to BD GeneOhm methicillin-resistant Staphylococcus aureus (MRSA) PCR for detection of MRSA in nasal swabs, *J Clin Microbiol* 47(7):2281–2283, 2009.

Bocher S, Smyth R, Kahlmeter G, et al.: Evaluation of four selective agars and two enrichment broths in screening for methicillin-resistant Staphylococcus aureus, *J Clin Microbiol* 46(9):3136–3138, 2008.

Caliendo AM, Gilbert DN, Ginocchio CC, et al.: Better tests, better care: improved diagnostics for infectious diseases, *Clin Infect Dis* 57(Suppl 3):S139–170, 2013.

Callihan DG, TJ; Beavis KG, et al.: Protection of laboratory workers from occupationally acquired infections; Approved Guideline. In *CLSI document M29-A4*, ed 4, Wayne, PA, 2014, Clinical and Laboratory Standards Institute.

Carroll KC: Laboratory diagnosis of lower respiratory tract infections: controversy and conundrums, *J Clin Microbiol* 40(9):3115–3120, 2002.

Centers for Disease Control and Prevention: Recommendations for the laboratory-based detection of Chlamydia trachomatis and Neisseria gonorrhoeae—2014, *MMWR Recomm Rep (Morb Mortal Wkly Rep)* 63(RR-02):1–19, 2014.

Charnot-Katsikas A, Tesic V, Love N, et al.: Use of the accelerate pheno system for identification and antimicrobial susceptibility testing of pathogens in positive blood cultures and impact on time to results and workflow, *J Clin Microbiol* 56(1):e01166–17, 2018.

Chen CY, Ballard RC: The molecular diagnosis of sexually transmitted genital ulcer disease, *Methods Mol Biol* 903:103–112, 2012.

Church DL, Cadrain G, Kabani A, et al.: Practice guidelines for ordering stool cultures in a pediatric population. Alberta Children's Hospital, Calgary, Alberta, Canada, *Am J Clin Pathol* 103(2):149–153, 1995.

Clinical and Laboratory Standards Institute: *Procedures for the recovery and identification of parasites from the intestinal tract; approved guideline*, *CLSI Document M28-A2*, Wayne, PA, 2005, Clinical and Laboratory Standards Institute.

Cloud JL, Hymas W, Carroll KC: Impact of nasopharyngeal swab types on detection of Bordetella pertussis by PCR and culture, *J Clin Microbiol* 40(10):3838–3840, 2002.

Cockerill 3rd FR, Wilson JW, Vetter EA, et al.: Optimal testing parameters for blood cultures, *Clin Infect Dis* 38(12):1724–1730, 2004.

Coleman JS, Gaydos CA: Molecular diagnosis of bacterial vaginosis: an update, *J Clin Microbiol* 56(9):e00342–18, 2018.

Das S, Sharma S, Kar S, Sahu SK, et al.: Is inclusion of Sabouraud dextrose agar essential for the laboratory diagnosis of fungal keratitis? *Indian J Ophthalmol* 58(4):281–286, 2010.

Deville WL, Yzermans JC, van Duijn NP, et al.: The urine dipstick test useful to rule out infections. A meta-analysis of the accuracy, *BMC Urol* 4:4, 2004.

Dize L, West S, Williams JA, et al.: Comparison of the Abbott m2000 RealTime CT assay and the Cepheid GeneXpert CT/NG assay to the Roche Amplicor CT assay for detection of Chlamydia trachomatis in ocular samples from Tanzania, *J Clin Microbiol* 51(5):1611–1613, 2013.

Efstratiou A, Engler KH, Mazurova IK, et al.: Current approaches to the laboratory diagnosis of diphtheria, *J Infect Dis* 181(Suppl 1):S138–S145, 2000.

Garcia LS, Smith JW, Fritsche TR: *Cumitech 30A*, *selection and use of laboratory procedures for diagnosis of parasitic infections of the gastrointestinal tract*, Washington, DC, 2003, ASM Press.

Garcia LS: In *Diagnostic medical parasitology*, ed 6, Washington, DC, 2016, ASM Press.

Gavin PJ, Peterson LR, Pasquariello AC, et al.: Evaluation of performance and potential clinical impact of ProSpecT Shiga toxin Escherichia coli microplate assay for detection of Shiga Toxin-producing E. coli in stool samples, *J Clin Microbiol* 42(4):1652–1656, 2004.

Graver MA, Wade JJ: Survival of Neisseria gonorrhoeae isolates of different auxotypes in six commercial transport systems, *J Clin Microbiol* 42(10):4803–4804, 2004.

Gray LDGPH, Fowler WC: *Cumitech 13B*, *Laboratory diagnosis of ocular infections*, Washington, DC, 2011, ASM Press.

Havlik DWGL: Screening sputum specimens for mycobacterial culture, *Lab Med* 26(6):411–413, 1995.

Hazen KC, Polage CR: Using data to optimize blood bottle fill volumes and pathogen detection: making blood cultures great again, *Clin Infect Dis* 70(2):269–270, 2020.

Holani AG, Ganvir SM, Shah NN, et al.: Demonstration of mycobacterium tuberculosis in sputum and saliva smears of tuberculosis patients using Ziehl Neelsen and fluorochrome staining—a comparative study, *J Clin Diagn Res* 8(7):ZC42–ZC45, 2014.

Ingram JG, Plouffe JF: Danger of sputum purulence screens in culture of Legionella species, *J Clin Microbiol* 32(1):209–210, 1994.

Janulaitiene M, Paliulyte V, Grinceviciene S, et al.: Prevalence and distribution of Gardnerella vaginalis subgroups in women with and without bacterial vaginosis, *BMC Infect Dis* 17(1):394, 2017.

Kahn FW, Jones JM: Diagnosing bacterial respiratory infection by bronchoalveolar lavage, *J Infect Dis* 155(5):862–869, 1987.

Khare R, Kothari T, Castagnaro J, et al.: Active monitoring and feedback to improve blood culture fill volumes and positivity across a large integrated health system, *Clin Infect Dis* 70(2):262–268, 2020.

Kraft CS, Parrott JS, Cornish NE, et al.: A laboratory medicine best practices systematic review and meta-analysis of nucleic acid amplification tests (NAATs) and algorithms including NAATs for the diagnosis of Clostridioides (Clostridium) difficile in adults, *Clin Microbiol Rev* 32(3):e00032-18, 2019.

Lauer BA, Masters HB: Toxic effect of calcium alginate swabs on Neisseria gonorrhoeae, *J Clin Microbiol* 26(1):54–56, 1988.

Leber AL, editor: *Clinical microbiology procedures handbook*, ed 4, Washington, DC, 2016, ASM Press.

Lewis DA: Diagnostic tests for chancroid, *Sex Transm Infect* 76(2):137–141, 2000.

Liesman RM, Strasburg AP, Heitman AK, et al.: Evaluation of a commercial multiplex molecular panel for diagnosis of infectious meningitis and encephalitis, *J Clin Microbiol* 56(4):e01927-17, 2018.

Lipsky BA, Berendt AR, Cornia PB, et al.: Infectious Diseases Society of America clinical practice guideline for the diagnosis and treatment of diabetic foot infections, *Clin Infect Dis* 54(12):e132–e173, 2012.

Martinez AJ, Visvesvara GS: Laboratory diagnosis of pathogenic free-living amoebas: Naegleria, Acanthamoeba, and Leptomyxid, *Clin Lab Med* 11(4):861–872, 1991.

McCarter YS, Robinson A: Quality evaluation of sputum specimens for mycobacterial culture, *Am J Clin Pathol* 105(6):769–773, 1996.

McDonald LC, Gerding DN, Johnson S, et al.: Clinical practice guidelines for Clostridium difficile infection in adults and children: 2017 update by the infectious diseases Society of America (IDSA) and Society for Healthcare Epidemiology of America (SHEA), *Clin Infect Dis* 66(7):987–994, 2018.

Metlay JP, Waterer GW, Long AC, et al.: Diagnosis and treatment of adults with community-acquired pneumonia. An official clinical practice guideline of the American Thoracic Society and Infectious Diseases Society of America, *Am J Respir Crit Care Med* 200(7):e45–e67, 2019.

Miller JM, Binnicker MJ, Campbell S, et al.: A guide to utilization of the microbiology laboratory for diagnosis of infectious diseases: 2018 update by the Infectious Diseases Society of America and the American Society for Microbiology, *Clin Infect Dis* 67(6):813–816, 2018.

Montessori GA, Bischoff L: Searching for parasites in stool: once is usually enough, *CMAJ (Can Med Assoc J)* 137(8):702, 1987.

Morris AJ, Tanner DC, Reller LB: Rejection criteria for endotracheal aspirates from adults, *J Clin Microbiol* 31(5):1027–1029, 1993.

Murdoch DR: Diagnosis of Legionella infection, *Clin Infect Dis* 36(1):64–69, 2003.

Murray PR, Washington JA: Microscopic and bacteriologic analysis of expectorated sputum, *Mayo Clin Proc* 50(6):339–344, 1975.

Nelson A, Wright-Hughes A, Backhouse MR, et al.: CODIFI (Concordance in Diabetic Foot Ulcer Infection): a cross-sectional study of wound swab versus tissue sampling in infected diabetic foot ulcers in England, *BMJ Open* 8(1):e019437, 2018.

Nicolle LE: Updated guidelines for screening for asymptomatic bacteriuria, *J Am Med Assoc* 322(12):1152–1154, 2019.

Nicolle LE, Gupta K, Bradley SF, et al.: Clinical practice guideline for the management of asymptomatic bacteriuria: 2019 update by the Infectious Diseases Society of America, *Clin Infect Dis* 68(10):1611–1615, 2019.

Nugent RP, Krohn MA, Hillier SL: Reliability of diagnosing bacterial vaginosis is improved by a standardized method of gram stain interpretation, *J Clin Microbiol* 29(2):297–301, 1991.

Peters CS, Hernandez L, Sheffield N, et al.: Cost containment of formalin-preserved stool specimens for ova and parasites from outpatients, *J Clin Microbiol* 26(8):1584–1585, 1988.

Pulz M, Matussek A, Monazahian M, et al.: Comparison of a shiga toxin enzyme-linked immunosorbent assay and two types of PCR for detection of shiga toxin-producing Escherichia coli in human stool specimens, *J Clin Microbiol* 41(10):4671–4675, 2003.

Rabinowitz M: Throat swabbing in epiglottitis, *J Am Med Assoc* 240(4):346–347, 1978.

Reisner BS, Woods GL: Times to detection of bacteria and yeasts in BACTEC 9240 blood culture bottles, *J Clin Microbiol* 37(6):2024–2026, 1999.

Rohner P, Pittet D, Pepey B, et al.: Etiological agents of infectious diarrhea: implications for requests for microbial culture, *J Clin Microbiol* 35(6):1427–1432, 1997.

Rosenblatt JE: Laboratory diagnosis of infections due to blood and tissue parasites, *Clin Infect Dis* 49(7):1103–1108, 2009.

Schachter J, Moncada J, Liska S, et al.: Nucleic acid amplification tests in the diagnosis of chlamydial and gonococcal infections of the oropharynx and rectum in men who have sex with men, *Sex Transm Dis* 35(7):637–642, 2008.

Schaeffer AJ, Nicolle LE: Urinary tract infections in older men, *N Engl J Med* 374(22):2192, 2016.

Shane AL, Mody RK, Crump JA, et al.: Infectious Diseases Society of America clinical practice guidelines for the diagnosis and management of infectious diarrhea, *Clin Infect Dis* 5(12):1963–1973, 2017.

Sharp SERA, Saubolle M, Santa Cruz M, et al.: *Cumitech 7B*, *lower respiratory tract infections*, Washington, DC, 2004, ASM Press.

Shimada T, Noguchi Y, Jackson JL, et al.: Systematic review and metaanalysis: urinary antigen tests for Legionellosis, *Chest* 136(6):1576–1585, 2009.

Shulman ST, Bisno AL, Clegg HW, et al.: Clinical practice guideline for the diagnosis and management of group A streptococcal pharyngitis: 2012 update by the Infectious Diseases Society of America, *Clin Infect Dis* 55(10):1279–1282, 2012.

Siegel DL, Edelstein PH, Nachamkin I: Inappropriate testing for diarrheal diseases in the hospital, *J Am Med Assoc* 263(7):979–982, 1990.

St John A, Boyd JC, Lowes AJ, Price CP: The use of urinary dipstick tests to exclude urinary tract infection: a systematic review of the literature, *Am J Clin Pathol* 126(3):428–436, 2006.

Stamm WE, Counts GW, Running KR, et al.: Diagnosis of coliform infection in acutely dysuric women, *N Engl J Med* 307(8):463–468, 1982.

Stoner BP, Cohen SE: Lymphogranuloma venereum 2015: clinical presentation, diagnosis, and treatment, *Clin Infect Dis* 61(Suppl 8):S865–S873, 2015.

Tacconelli E, De Angelis G, de Waure C, et al.: Rapid screening tests for methicillin-resistant Staphylococcus aureus at hospital admission: systematic review and meta-analysis, *Lancet Infect Dis* 9(9):546–554, 2009.

Tansarli GS, Chapin KC: Diagnostic test accuracy of the BioFire(R) FilmArray(R) meningitis/encephalitis panel: a systematic review and meta-analysis, *Clin Microbiol Infect* 26(3):281–290, 2020.

Tanyuksel M, Petri Jr WA: Laboratory diagnosis of amebiasis, *Clin Microbiol Rev* 16(4):713–729, 2003.

US Food and Drug Administration: Nucleic acid based tests. https://www.fda.gov/medical-devices/vitro-diagnostics/nucleic-acid-based-tests. Published 2020. Accessed 01/09/2020.

van der Zee A, Schellekens JF, Mooi FR: Laboratory diagnosis of pertussis, *Clin Microbiol Rev* 28(4):1005–1026, 2015.

Van Horn KG, Audette CD, Tucker KA, Sebeck D: Comparison of 3 swab transport systems for direct release and recovery of aerobic and anaerobic bacteria, *Diagn Microbiol Infect Dis* 62(4):471–473, 2008.

Walsh TH, Hayden RT, Larone DH: *Larone's medically important fungi: a guide to identification*, ed 6, Washington, DC, 2018, ASM Press.

Washington 2nd JA, Ilstrup DM: Blood cultures: issues and controversies, *Rev Infect Dis* 8(5):792–802, 1986.

West B, Wilson SM, Changalucha J, et al.: Simplified PCR for detection of Haemophilus ducreyi and diagnosis of chancroid, *J Clin Microbiol* 33(4):787–790, 1995.

Williamson DA, Carter GP, Howden BP: Current and emerging topical antibacterials and antiseptics: agents, action, and resistance patterns, *Clin Microbiol Rev* 30(3):827–860, 2017.

Wilson DC: Biosafety in microbiological and biomedical laboratories. In *HHS Publication No. (CDC) 21-1112*, Washington, DC, 2009, US Department of Health and Human Services.

Woods GL, Thompson AB, Rennard SL, Linder J: Detection of cytomegalovirus in bronchoalveolar lavage specimens. Spin amplification and staining with a monoclonal antibody to the early nuclear antigen for diagnosis of cytomegalovirus pneumonia, *Chest* 98(3):568–575, 1990.

Workowski KA, Bolan GA, Centers for Disease Control and Prevention: Sexually transmitted diseases treatment guidelines, *MMWR Recomm Rep (Morb Mortal Wkly Rep)* 4(RR-03):1–137, 2015.

PART 8

Molecular Pathology

EDITED BY | Martin H. Bluth, Matthew R. Pincus

CHAPTER 67

INTRODUCTION TO MOLECULAR PATHOLOGY

Martin H. Bluth, Matthew R. Pincus

INTRODUCTION, 1368
SPECIAL CONSIDERATIONS FOR MOLECULAR DIAGNOSTICS LABORATORIES, 1368
Infectious Disease, 1368
Cancer, 1368
Inherited Disorders, 1369
Informed Consent, Clinical Utilization, And Documentation, 1369
THE MOLECULAR BIOLOGY REVOLUTION AND ITS IMPACT ON THE PRACTICE OF PATHOLOGY, 1369
DISCUSSION OF DIAGNOSTIC MOLECULAR PATHOLOGY, 1370
Application Of Molecular Pathology To Detection Of Cancer, 1370
IMPLICATIONS OF MOLECULAR DIAGNOSTICS ON THE PRACTICE OF PATHOLOGY AND MEDICINE, 1371
Redefining Disease, 1371
Use Of Molecular Biology In The Treatment Of Disease, 1371
Data Analysis, 1371
QUALITY ASSURANCE, 1371
FINANCIAL MANAGEMENT REIMBURSEMENT FOR MOLECULAR DIAGNOSTICS TESTS, 1371
SOME CAVEATS, 1372
SELECTED REFERENCES, 1372

KEY POINTS

- The revolution in molecular biology continues to have a profound impact on the field of anatomic and clinical pathology (diagnostic medicine).
- Techniques, including polymerase chain reaction and other amplification and hybridization methods, are capable of detecting DNA in very small quantities in tissue and body fluids, enabling detection of various disease states, including cancer.
- The human genome project has created robust high-throughput and highly sensitive genetic methods for detecting abnormal genes in patient specimens and for establishing patterns of gene expression that are characteristic of specific diseases.
- Proteomic methods detecting protein expression in serum samples from patients allow for diagnosis of different types of cancers.
- Gene array high-throughput sequencing and proteomic methodologies require sophisticated mathematical methods of pattern recognition that allow for detection of disease.

INTRODUCTION

During the past decade, a vast amount of knowledge has been gained regarding genes, gene products, and their role in human disease. This knowledge has allowed us to better understand many disease processes and to start defining diseases and disease processes in terms of their molecular pathogenesis. Molecular pathology refers to the analysis of nucleic acids and proteins to diagnose disease, predict the occurrence of disease, predict the prognosis of diagnosed disease, and guide therapy. Molecular pathology–based diagnostics testing is a relatively recent specialty of laboratory medicine and is still in a state of flux at many levels, such as the choice of test, technology, automation, and reimbursement. The scope of molecular testing has expanded rapidly since its introduction in the late 1980s. This has led to the development of new clinical molecular assays for use in diagnosis, prognosis, selection of therapeutic modalities, and monitoring of disease in both general and personalized fashions (Bluth, 2018a, 2018b). The technologies that constitute molecular diagnostics—such as first-generation amplification, next-generation DNA sequencing, DNA probes, fluorescence in situ hybridization (FISH), second-generation biochips and microfluidics, next-generation signal detection, biosensors, and molecular labels—are influencing the discovery of therapeutic molecules, the screening and diagnosis of patients, and the optimization of drug therapy. In the past few years, this rapidly evolving field has seen several fascinating developments. There are many applications of this technology to different areas of the clinical laboratory. Whereas testing for inherited genetic diseases, cancer, viral load, and infectious diseases continues to predominate, the impact of pharmacogenomics on molecular diagnostics continues to evolve and impact diagnostics and prognostics of disease. The operation of a clinical molecular pathology laboratory requires integration of expertise in medical, scientific, and clinical molecular pathology; resources, including facilities, equipment, and personnel; and skills in organization, administration, management, and communication.

SPECIAL CONSIDERATIONS FOR MOLECULAR DIAGNOSTICS LABORATORIES

Whereas all molecular diagnostic tests share the use of nucleic acid technology, the different clinical applications may require different management considerations.

INFECTIOUS DISEASE

Increasing numbers of microorganisms are detected or characterized by molecular methods, including mass spectroscopy, as discussed in Part 7, which in many cases have become the standard of practice, especially for microorganisms that are difficult to culture or when subsequent culture is needed to identify drug resistance (Fairfax et al., 2018). As the volume of testing has grown, a need has arisen for automation of different steps of testing and standardized kits. There has been a surge of different automation platforms. Automated platforms perform nucleic acid extraction from different types of specimens, automated liquid handling systems set up reactions, and real-time technology monitors and quantifies nucleic acids as they are being amplified. In addition, quantitative molecular methods based on polymerase chain reaction (PCR) amplification and automated rapid sequencing techniques that are essential for viral speciation have become the standard of practice in monitoring response to therapy, especially in patients with human immunodeficiency virus (HIV), hepatitis B virus (HBV), and hepatitis C virus (HCV) infections. With these automated methodologies, the need for confidentiality, especially for patients undergoing HIV testing, has prompted specific federal and state regulations to ensure the protection of patients and their families. In addition, each state might have a list of different organisms that, if detected, must be reported to the state health department.

CANCER

Molecular methods are currently used for hematopoietic neoplasms as well as for solid tumors. The nucleic acid changes, either of DNA or ribonucleic acid (RNA), are present only in the affected populations of cells and are not part of the genetic makeup of the individual. Current technologies—such as real-time PCR, next-generation DNA sequencing, and microarray analysis—have provided greater diagnostic sensitivity and specificity for diagnostic testing, prognosis, treatment selection, monitoring response to

therapy, and detection of minimal residual disease. In addition, the exquisite sensitivity of these molecular methods has allowed the testing of very small amounts of nucleic acid from a wide range of sample types. Formalin-fixed paraffin-embedded tissue can provide good quality and quantity of DNA and RNA from processed tissues. However, very specific protocols either for DNA or RNA extraction must be followed. In contrast to inherited genetic testing that needs to be done once per lifetime, molecular oncology tests often are performed repeatedly (e.g., for initial diagnosis and during and after treatment for monitoring response to therapy). Molecular methods that identify rearrangements or mutations that cause specific tumor types may also be used to assess minimal residual disease. Molecular test results should be interpreted in the context of other laboratory testing, such as histopathology, flow cytometry, and clinical findings. The detection of a specific mutation in the tumor cells may also be used to determine the appropriate course of therapy. This is the case for metastatic colon cancer. A number of studies have shown that anti–epidermal growth factor receptor (anti-EGFR) monoclonal antibodies are effective treatments for metastatic colorectal cancer, but only in patients with the wild-type oncogene *KRAS*. The anti-EGFR monoclonal antibodies panitumumab and cetuximab are approved in the United States for treatment of metastatic colorectal cancer refractory to chemotherapy but are not recommended for use in patients with mutations in KRAS codon 12 or 13. Similarly, panitumumab is approved for the treatment of metastatic colorectal cancer only in patients with wild-type *KRAS* in Europe and Canada. It is clear that KRAS mutational analysis has become an important aspect of disease management in patients with metastatic colorectal cancer (Bhalla, 2018; Weindel & Bluth, 2016). Laboratory issues specific for hematopoietic neoplasms and solid tumor testing include the need for fresh or frozen tissue for RNA-based testing, the use of microdissection to reduce nonmalignant cell population in the specimens, and the need to work with small tissue specimens, such as needle biopsies.

INHERITED DISORDERS

All diseases have a genetic contribution, whether it is a specific genetic disease or an increased likelihood for developing a medical condition. Genetic disorders are primarily the result of a germline mutation or a mutation present in every cell of an individual. For this reason, genetic testing has far-reaching implications, because it could affect family members that might have inherited the same mutation. Molecular genetic testing is currently used for diagnosis, carrier status evaluation, and prenatal and presymptomatic DNA testing. Diagnostic testing is usually performed on affected individuals for establishing or confirming a clinical diagnosis.

Carrier testing is performed in an asymptomatic healthy individual to identify whether the individual is a carrier for an autosomal or X-linked recessive condition and whether the individual is at risk for having an affected child. This application can be used for individuals with a family history of a genetic disorder or for population screening, such as in screening for cystic fibrosis (CF). Carrier testing can be done first by testing an affected family member to identify the specific mutation present in the family. Once a specific mutation is identified, family members can be tested for that particular mutation, thus improving the accuracy of the risk assessment for the individuals in that family with a negative test result. In contrast, population screening focuses on the most common or prevalent mutation, most of the time with different rates of detection for different ethnic populations. Prenatal testing is performed to identify a fetus with a genetic disease or condition. Prenatal testing analyzes fetal cells obtained by amniocentesis or by chorionic villus sampling. Genomic technologies such as noninvasive prenatal testing (NIPT) are capable of detecting abnormalities in fetal DNA from maternal blood samples (Daley et al., 2014). This type of testing is usually initiated because family history or maternal factors suggest the need for it. In addition, some laboratories offer preimplantation genetic testing in the setting of in vitro fertilization for couples with a family history of a specific genetic disease. Presymptomatic testing is used primarily for the identification of adult onset of a genetic condition that will occur later in life, such as Huntington disease. Presymptomatic testing is the most problematic and challenging type of testing in terms of its psychological effect on the individual. Hence, it requires extensive protocols for pregenetic and postgenetic testing counseling.

INFORMED CONSENT, CLINICAL UTILIZATION, AND DOCUMENTATION

Several other issues are of critical relevance. Genetic testing requires special attention to informed consent, appropriateness, and urgency. A number of states have specific laws that govern the process of informed consent; each laboratory director should evaluate state laws to determine what the regulations stipulate. Many laboratories require documentation of informed consent before performing the genetic test. Informed consent can be documented by several means, such as requesting the actual signed informed consent or a copy of it, or by the physician or health care provider confirming on the requisition that the informed consent was obtained and is documented in the patient's chart. Until required documentation of informed consent is obtained, the laboratory can stabilize the patient specimen and extract and store the nucleic acid. The laboratory can start the testing once the required documentation is received. In addition to documentation of informed consent, the laboratory should review clinical indications for testing and determine whether the test is appropriate for a specific patient. Despite the tremendous advances in the understanding of the human genome, the full benefit of genetic testing for a particular patient is not always clear. Testing may be warranted even if the results are inconclusive or preventive strategies or treatments are not available. Genetic information raises critical ethical, legal, and social issues for both the individual being tested and family members. Special attention should be given to genetic testing in minors. For example, should carrier testing of minors be deferred until the minor is an adult? Similarly, a request for testing of an asymptomatic individual for a dominant disease should include arrangements for adequate genetic counseling. In addition, the laboratory should understand and communicate to health care providers the sensitivity and limitations of the test performed so that patients can be counseled appropriately as to the expectations of the testing and the significance of the testing results.

Genetic testing results often require interpretation using complex risk assessment calculations. Health care professionals must correctly interpret laboratory test results in the context of the particular patient and be able to convey the test results and interpretation to the patient and family members. Communication of genetic test results to patients and families can be complex and time-consuming. Clinicians trained in medical genetics as well as genetic counselors are well equipped to communicate the complex and involved information. Benefits of this approach have been well documented in the literature. Misinterpretation of negative genetic test results by inadequately trained physicians may result in inappropriately suggesting that patients discontinue recommended aggressive surveillance for the genetic condition. For these reasons, most genetic testing should be ordered through health care providers trained in genetics to ensure that the benefits and risks of testing have been explained to the patient during the informed consent process.

THE MOLECULAR BIOLOGY REVOLUTION AND ITS IMPACT ON THE PRACTICE OF PATHOLOGY

Molecular pathology refers to the analysis of nucleic acids and proteins to diagnose disease, predict the occurrence of disease, predict the prognosis of diagnosed disease, and guide therapy. It is the result of recent advances in molecular biology that have revolutionized the practice of medicine, especially diagnostic medicine. These revolutionary changes result from our abilities to clone disease-causing genes and the proteins that they encode and to detect the presence of these genes and proteins in the serum and other body fluids and tissues of patients, even though they may be present in minute quantities. This detection has been made possible by a veritable explosion of new, highly sensitive techniques involving amplification methods, such as PCR, branched-DNA (BDNA), FISH, and mass spectroscopy, the latter highly effective for the identification of proteins that are implicated in causing disease (Pincus & Friedman, 2003). Even more recent developments include first-generation amplification, next-generation DNA sequencing, second-generation biochips and microfluidics, next-generation signal detection, biosensors, and molecular labels.

Many of these techniques have been developed to the stage at which they are employed in so-called "high-throughput" processes that enable single patient samples to be analyzed for multiple genes or proteins. Some of these processes have already become completely automated.

A major consequence of the revolution in molecular biology has been the mapping of the human genome in the Human Genome Project (Venter et al., 2001) and the genomes of a number of other species. These projects identified numerous novel genes of unknown function whose functions can now be determined and whose expressions can be monitored in different disease states. In addition, the techniques employed in these projects have been proving exceptionally useful in studying patterns of gene expression in different disease states (see, for example, Golub et al., 1999, Anbazhagan et al., 1999).

All of these advances have led to the development of new clinical molecular assays for use in diagnosis, prognosis, selection of therapeutic modalities, and monitoring of disease in both general and personalized fashions (Bluth, 2018a; Bluth, 2018b). We note that, due to the rapidity of expansion of molecular diagnostic techniques, molecular pathology–based diagnostics testing is a relatively recent specialty of laboratory medicine and is still in a state of flux at many levels, such as the choice of test, technology, automation, and reimbursement. We here briefly discuss the impact of molecular pathology techniques in major areas of the medical laboratory.

DISCUSSION OF DIAGNOSTIC MOLECULAR PATHOLOGY

All of these molecular pathologic methods and approaches are described in Parts 8 and 9 of this book. In Part 8, we first discuss the principles that underlie the main diagnostic approaches used in clinical molecular biology. Chapter 68 describes the basic principles in gene hybridization, including use of Southern and Northern blots, gene cloning, gene sequencing, and next-generation DNA sequencing. Chapter 69 discusses amplification methodologies, including PCR and BDNA, that allow gene identification and quantification of gene expression. In Chapter 70, we discuss how the expression of multiple genes—in fact, of whole genomes—can now be assayed on microarrays.

One of the motivations for detecting genetic abnormalities in specific diseases is the finding that, in many such disease states, there are well-defined, reproducible chromosomal abnormalities. In fact, increasing numbers of genes that have been strongly implicated in causing disease can be identified on chromosomes using the FISH technique, which enables detection of gene rearrangements and gene deletions in a number of diseases, especially in cancers. In Chapter 71, we discuss the cytogenetics of human diseases and show how FISH technology has enabled major advances in diagnosis of disease. All of these diagnostic approaches constitute diagnostic or clinical molecular biology or molecular diagnostics. This is followed by a discussion of the use of molecular biological techniques to diagnose human disease in Chapter 72.

Quite recently, there has been a major surge of neuroscience studies of the genetics of neuropsychiatric disease, ranging from neuromuscular conditions and neurodegenerative diseases, such as Alzheimer and Parkinson disease, to psychoses such as bipolar disorders and schizophrenia. These studies have allowed application of molecular biological techniques to the detection of these diseases. Furthermore, treatment of many of these disorders can now be optimized using pharmacogenomic gene arrays to determine which drugs are best suited to patients on a personalized basis. These exciting new developments are discussed in Chapter 73, introduced for the first time in this 24th edition of the textbook.

One of the consequences of the genetic revolution has been the ability to identify single gene mutations in patients' DNA that may result in disease or may simply be polymorphisms. As discussed in Chapter 74, the latter can be taken advantage of in establishing the parentage of children and in the investigation of crime. Consequently, there has been a dramatic increase in the use of the molecular diagnostics laboratory for forensic purposes and for refining how to use single-nucleotide polymorphisms (SNPs) to establish parentage and the identities of the victims and perpetrators of crime.

Mapping of the human genome reveals that these polymorphisms occur in the human genome at approximately 1 per 1000 base pairs (bp). Some of these polymorphisms are in genes, principally those that encode cytochrome P450, whose functions are important in response of individual patients to therapy (Evans & Relling, 1999; Rodriguez-Antona et al., 2010).

Genes that encode drug-metabolizing enzymes, both activating and inactivating, and genes that encode ligands and receptors, may show polymorphisms that either decrease or increase the therapeutic effectiveness or toxicity of drugs already in wide use, accounting for some idiosyncratic responses previously not understood or predictable. Thus, there has been a major advance in testing patients for genetic expression of these isoforms, allowing prediction of which drugs would be most effective. This has revolutionized medical practice and has given rise to "personalized" medicine wherein patients are now tested genetically for the most appropriate drug therapy and to the field of pharmacogenomics in which this testing is performed. This burgeoning field has been applied with notable success to the area of anticoagulant and antiplatelet therapies (Gurbel & Tantry, 2012; Roberts et al., 2012). We describe the techniques and screening practices for the design of effective drug therapy in Chapter 75.

As more polymorphisms are identified and correlated with individual patients' response to treatment, the pathologist will be called upon increasingly to profile common polymorphisms in patients who are beginning therapy for common conditions such as coronary artery disease, congestive heart failure, diabetes, thrombosis, hypertension, cancer, and infections. The laboratory's identification of the individual patient's genotype/phenotype will determine the specific drugs and doses suitable for that patient. This evolution has placed the pathologist in a more definitive position to determine appropriate therapy than traditional prediction of disease behavior based on morphology of lesions or culture characteristics of infectious organisms.

As noted earlier, with respect to infectious organisms, the pathologist is being called upon to bring a wide variety of molecular pathology techniques into the diagnostic armamentarium to genotype infectious agents such as HIV, among others (Fairfax, 2013, 2018). Because different strains show markedly different drug susceptibilities, genotyping of infectious agents has major therapeutic implications in addition to facilitating diagnosis (Tozzi, 2010).

APPLICATION OF MOLECULAR PATHOLOGY TO DETECTION OF CANCER

Part 9 of this book is devoted to new developments in laboratory testing for cancer that capitalize on knowledge of molecular oncogenesis. It is now well established that particular genes, called *oncogenes*, and their encoded proteins, called *oncoproteins*, are active in carcinogenesis. Mutations in these genes, resulting from factors such as carcinogens and oncogenic viruses, may result in abnormal activation or overexpression of their encoded proteins.

Many of these oncogenic proteins are critical components of signal transduction pathways, in which ligands, such as growth factors, bind to cell membrane receptors, setting in motion a chain of protein activation cascades that are ultimately transmitted to the nucleus. This results in increased transcription and, ultimately, high levels of expression of promitotic proteins, such as the cyclins. When one or more of the proteins on mitogenic signal transduction pathways become mutated, the cells in which they are expressed become transformed into cancer cells. Once transformed, cancer cells express a number of proteins, in addition to the mutated or overexpressed oncoproteins, that are not expressed by normal cells even in the growth phase.

These findings have been translated into new clinical diagnostic methods for the detection of these abnormal proteins in the early detection of cancer in patients. Therefore, Part 9 of this book is devoted to the way in which these proteins are used in early tumor detection and to following the efficacy of the treatment of cancer. One of the major findings in this area has been that screening for cancer is most effective when multiple oncoproteins are assayed. Newly evolving mass-spectroscopic techniques enabling detection of protein expression patterns in serum that are unique to specific cancers, in a field known as *proteomics*, are showing great promise in screening for a number of different major human cancers (Khadir & Tiss, 2013). Screening for differential expression of specific patterns of genes that characterize a particular tumor, in combination with proteomics, has the potential to improve diagnosis and screening for a number of different types of tumors.

Many oncoproteins and oncogenes can be used very effectively as tumor markers when detected in serum, urine, and other body fluids. In Chapter 76, we discuss how proteins that are expressed predominantly in specific tissues can be used in cancer diagnosis and monitoring response to anticancer therapy. These tumor markers include prostate-specific antigen (PSA) for prostate cancer, carcinoembryonic antigen (CEA) for colon cancer and other gastrointestinal tumors, and α-fetoprotein (AFP) for hepatocellular carcinoma. Chapter 77 discusses how the proteins involved in mitogenic signal transduction pathways—such as epidermal growth factor receptor (EGFR), HER2/neu, ras-p21, raf, myc, and p53—can be employed very effectively as tumor markers. Chapter 78 includes the major advances in the molecular biology and diagnosis of hematopoietic neoplasia. There has been a veritable explosion of information on the genetics and molecular biology of a wide variety of solid tissue (epithelial cell) tumors and sarcomas over the past several years that complements the information concerning the serodiagnostic markers for a number of these tumors. Chapter 79 discusses the molecular genetics of these tumors and includes a summary of the major genetic findings for these tumors, which we hope will be a convenient reference for the reader.

The rapid pace of technological improvements in sequencing is quickly moving next-generation sequencing methods into the realm of clinical laboratories. In Chapter 80, we discuss the methodologies used in mapping the genome since these approaches are involved in screening for different diseases. As the functions of more genes become known, it

will become increasingly feasible to screen the genomes of patients for gene abnormalities, especially those causing or predisposing patients to develop cancer.

IMPLICATIONS OF MOLECULAR DIAGNOSTICS ON THE PRACTICE OF PATHOLOGY AND MEDICINE

REDEFINING DISEASE

Our understanding of health, disease susceptibility, disease, and disease precursors continues to change with increasingly detailed information about the human genome, protein coding genes, and gene regulation (Pandey & Mann, 2000). Increasingly, diagnoses that were made on the basis of morphology or other traditional laboratory data will require molecular analysis (Heller et al., 1997; Golub et al., 1999; Talaulikar & Dahlstrom, 2009). The clearest current example is the diagnosis of leukemias and lymphomas, for which identification of specific gene rearrangements and patterns of gene expression now enable distinction of different types (Bacher, 2009).

Gene sequencing and testing for mutations also leads to recognition that some diseases have a broader spectrum of presentation, ranging from mild symptoms previously unrecognized as part of the disease to full manifestation of the disease. For example, it is now recognized that mutations of the cystic fibrosis gene (*CFTR*) are associated with congenital bilateral absence of the vas deferens, chronic pancreatitis, and sinopulmonary complaints that are not always associated with the severe and milder pulmonary and pancreatic dysfunctions long accepted as cystic fibrosis (see Chapter 76). Recognition of diseases and definition of pathobiology on the basis of specific exon and intron mutations will result in recognition of novel symptom complexes associated with diseases and improved management of patients with milder or atypical forms of the disease (Ferrari, 1999).

USE OF MOLECULAR BIOLOGY IN THE TREATMENT OF DISEASE

As discussed earlier, genetic screening for the presence of isoforms of cytochrome P450 and other proteins involved in drug metabolism and the genotyping of infectious organisms has enabled the design of the effective treatment of patients on an individualized basis. Likewise, proteomic approaches to cancer detection have resulted in the development of new therapies. For example, many breast cancers express the neu/HER2 growth factor receptor that is detectable in serum with an immunoassay. Patients with neu/HER2-positive breast cancers are now treated with a cytotoxic antibody to this receptor, Herceptin (see Chapter 76).

DATA ANALYSIS

Molecular techniques are now producing data on many thousands of genes, including their expression and their sequences, which results in databases of unprecedented size and complexity. This has ushered in the age of "big data." As discussed in Chapter 80, the analytic challenge of organizing data into profiles of diseases or patients and relating profiles to meaningful clinical decisions has resulted in a tremendous growth in bioinformatics and the use of mathematical algorithms for pattern recognition, such as neural network theory (Klee, 2008; Khan et al., 2001; Bitner, 1999). These methods are now used in genome-wide association studies (GWAS) in which mutations in specific genes are identified in patients with a particular disease by comparing their genomic sequences with those of unaffected individuals. These studies are proving to be highly successful in identifying the molecular basis of neuropsychiatric disease, as discussed in Chapter 73.

QUALITY ASSURANCE

Molecular pathology requires the same attention to quality assurance as all laboratory methods to ensure that results are accurate and reliable. Two essential components of quality assurance, standardization of methods and interlaboratory comparison of test results, have been adapted for molecular pathology laboratories. Standardized methods for performance of the most common clinical molecular pathologic tests are published by the Clinical and Laboratory Standards Institute (CLSI) as guidelines on the current standards of excellent practice. Interlaboratory comparison of test performance is provided by the College of American Pathologists (CAP) (www.cap.org), currently including surveys for molecular microbiology, genetics, hematology, parentage and identity, and general forensic applications.

Applying established standards of quality assurance and using molecular pathologic techniques in the setting of quality laboratory management requires a thorough understanding of each method's assay strengths and limitations. The information provided in the chapters devoted to molecular pathology is designed to give pathologists the ability to capitalize on the opportunities these techniques offer for improved patient care and the understanding of basic pathobiology.

FINANCIAL MANAGEMENT REIMBURSEMENT FOR MOLECULAR DIAGNOSTICS TESTS

Reimbursement for laboratory tests is a complex process that can be broken down into three phases—coverage, coding, and payment. Coverage decisions are usually determined by each of the different health care plans. In the United States, health insurance coverage is provided by public programs such as Medicare and Medicaid or by private health plans purchased individually or through one's employer. In general, the scope of coverage provided by a health plan is outlined in broad benefits categories; decisions about specific services are made on a case-by-case basis during claims processing. Health plans may develop formal coverage policies that describe whether a particular service is covered and the conditions under which it will be covered. Medical directors, the federal and state governments, medical policy advisory committees, employers, and unions are among some of the entities involved in making coverage decisions. Medical necessity is the primary criterion used by health plans when making coverage decisions, although the definition of medical necessity is subject to different interpretations. Another criterion is that the service must have approval from the appropriate government regulatory body. Scientific evidence must permit conclusions concerning the effect of the technology on health outcomes.

Billing for molecular diagnostic testing follows the same procedure as any other laboratory tests. Generally, Current Procedural Terminology (CPT) codes (to document the procedure) and International Classification of Disease diagnostic codes (to document the medical condition that makes the procedure necessary) are required by the billing process to convey what services or procedures were performed and why. Beyond this, the reimbursement process is usually institution specific and relies on computerized and manual billing procedures. It is important to determine in advance the requirements regarding documentation and computer access needed in order to generate a bill (Weindel & Bluth, 2016).

The CPT codes for molecular pathology (MoPath) underwent significant changes, which took effect in January 2013. Further changes were made in subsequent years. The MoPath codes are divided into two general categories, referred to as tier 1 and tier 2. These codes are paid under the Medical Clinical Laboratory Fee Schedule. Tier 1 codes represent the most common single-analyte tests. Tier 2 codes represent less common tests and are organized into 9 levels based on the complexity of the assay and interpretive component. The tier 1 and tier 2 codes do not include molecular microbiology, for which a growing list of pathogen-specific codes are predominantly used (Weindel & Bluth, 2016). Codes for human leukocyte antigen (HLA) typing are listed separately. For tests not included in tier 1 or tier 2, the unlisted code 81479 is to be used. A new subsection was added: multianalyte assays with algorithmic analyses (MAAAs), referring to procedures that incorporate results from different assay types. Later, a subsection was added to cover genomic services and other molecular multianalyte assays. Furthermore, the Centers for Medicare and Medicaid Services created Healthcare Common Procedures Coding System (HCPCS) code G0452-26 for interpretation and reporting by a physician reimbursed through Medicare under the Physician Fee Schedule.

The tier 1 and tier 2 codes incorporate all of the technical components of the assays, such as cell lysis and nucleic acid extraction, amplification, and detection. These codes do not include procedures prior to extraction, such as microdissection. The codes cover procedures used to detect germline or somatic variants. Where guidance is available, the genes and variants are described in accordance with the Human Genome Organization (HUGO) and the Human Genome Variation Society (HGVS). Examples of tier 1 and tier 2 codes are given in Table 67.1. As noted earlier, tier 1 codes are designated based on specific genes. Tier 2 codes are designated based on 9 levels of complexity. Several genes/targets are associated with each level. The levels of complexity range from single germline variant for level 1 to analysis of >50 exons in a single gene by DNA sequence analysis at level 9. The recently added Genomic Sequencing Procedures and Other Molecular Multianalyte Assays cover procedures that simultaneously analyze multiple genes or genetic regions using technologies such as next-generation DNA sequencing. This includes whole exome and genome analysis as well as germline and somatic variant detection. Cytogenomic microarray analysis and multianalyte analysis with algorithms are covered with a different set of codes.

TABLE 67.1
Examples of CPT Code Billing for Molecular Tests

Test	CPT Code	Procedure
Tier 1		
APC	81201	Full gene sequence
EGFR	81235	Gene analysis, common variants (e.g., exon 19 LREA region, L858R, T790M, G719A, G719S, L861Q)
Factor 2 (prothrombin)	81240	Gene analysis, 20210 G>A variant
JAK2	81270	Val617Phe (V617F) variant
Tier 2		
Level 1	81400	Identification of a single germline variant (e.g., SNP)
		Factor 2, 1199 G>A variant
		SMN1, exon 7 deletion
Level 2	81401	2–10 SNPs, 1 methylated variant or 1 somatic variant or detection of a triplet repeat disorder
		ABL, T315I variant
		VWF common variants (T791M, R816W, R854Q)
Level 9	81408	Analysis of >50 exons in a single gene by DNA sequence analysis
		ATM full gene sequence

ABL, c-abl oncogene 1, receptor tyrosine kinase; *APC,* adenomatous polyposis coli; *ATM,* ataxia telangiectasia mutated; *CPT,* Current Procedural Terminology; *EGFR,* epidermal growth factor receptor; *JAK2,* janus kinase 2; *SMN1,* survival of motor neuron 1; *SNP,* single-nucleotide polymorphism; *VWF,* von Willebrand factor.

Reimbursement levels for individual tests are set by third-party payers and may bear little relationship to the actual cost of performing the test. Some third-party payers may reimburse at high levels, but others may follow laboratory fee schedules based on the Medicare Clinical Laboratory Fee Schedule or Physician Fee Schedule for the specific CPT codes. U.S. Food and Drug Administration (FDA) approval is not required for billing for these tests; a disclaimer for those tests not cleared by the FDA should be added to the final report to reflect this. While there is considerable economic advocacy for genetic testing reimbursement (Eisenberg & Varmus, 2017), some third-party payers will deny reimbursement for tests bearing such disclaimers because they believe that the cost of performing them should be borne by research grants even though the performance characteristics and clinical utility of the test have been validated by the clinical laboratory.

SOME CAVEATS

While molecular methods will continue to provide new insights into disease, optimal use often requires integration with traditional laboratory tests rather than complete replacement. For example, in the diagnostic workup of leukemias, the traditional morphologic and immunochemical testing must always be performed. Gene analysis becomes critical when there is a question as to the type of leukemia or the characterization of the types of gene rearrangement that have occurred. In cases of tissue pathology, the morphologic skills involved in histopathology and cytopathology must be employed to ensure that appropriate cells and tissues are analyzed molecularly. Otherwise, analysis of other than targeted cells/tissues, despite high-quality technical methods interpreted with skill and experience, can lead to erroneous, sometimes dangerously misleading, results.

In summary, molecular pathology continues to penetrate and permeate the entire clinical laboratory just as immunopathology did over 2 decades ago. Pathologists will be increasingly called upon to serve as "molecular shepherds" in this ever-changing landscape (Bluth, 2013). Section boundaries or barriers will continue to break down and dissolve in this transformation of laboratory medicine through the impact of this continuously evolving aspect of cellular and molecular biology.

SELECTED REFERENCES

Golub TR, Slonim DK, Tamayo P, et al.: Molecular classification of cancer: class discovery and class prediction by gene expression monitoring, *Science* 286:531–537, 1999.

A seminal paper that shows how analysis of multiple gene expression can be used to distinguish between different types of leukemia.

Khadir A, Tiss A: Proteomics approaches towards early detection and diagnosis of cancer, *J Carcinogen Mutagen* S14(2–16), 2013https://doi.org/10.4172/2157-2518.S14-002. open access.

An excellent review of the status of the discovery of biomarkers for cancer that provides an excellent evaluation of current problems in this area together with future directions.

Pincus MR, Friedman FK: Oncoproteins in the detection of human malignancies. In *Molecular diagnostics*, vol. 1. New York, 2003, Reed Business Information Publishers, pp 23–38.

A review of how multiple oncoproteins can be used serodiagnostically not only to screen for different types of cancer but, in some cases, to predict the future occurrence of cancers.

Access the complete reference list online at Elsevier eBooks for Practicing Clinicians.

REFERENCES

Anbazhagan R, Tihan T, Bornman DM, et al.: Classification of small cell lung cancer and pulmonary carcinoid by gene expression profiles, *Cancer Res* 59:5119–5122, 1999.

Bacher U, Kohlmann A, Haferlach T: Current status of gene expression profiling in the diagnosis and management of acute leukaemia, *Br J Haematol* 145:555–568, 2009.

Bitner M, Meltzer P, Trent J: Data analysis and integration: of steps and arrows, *Nat Genet* 22:213–214, 1999.

Bhalla A, Zulfiqar M, Bluth MH: Molecular diagnostics in colorectal carcinoma: advances and applications for 2018, *Clin Lab Med* 38(2):311–342, 2018 Jun.

Bluth MH: Molecular pathology in the modern era: revisiting Jacob's spotted sheep, *Clin Lab Med* 33:xi–xiii, 2013.

Bluth MH: Looking good in Your genes: Maximizing one's personalized molecular Fingerprint for optimal health, *Clin Lab Med* 38(2):xiii–xvi, 2018 Jun (a).

Bluth MH: Introduction: molecular medicine in the common era: applications and impact of molecular pathology in health and disease, *Clin Lab Med* 38(2):209–213, 2018 Jun (b).

Daley R, Hill M, Chitty LS: Non-invasive prenatal diagnosis: progress and potential, *Arch Dis Child Fetal Neonatal* Ed99(5):F426–F430, 2014 Sep.

Eisenberg R, Varmus H: Insurance for broad genomic tests in oncology, *Science* 358(6367):1133–1134, 2017 Dec 1, https://doi.org/10.1126/science.aao6708.

Evans WE, Relling MV: Pharmacogenomics: translating functional genomics into rational therapeutics, *Science* 286:487–491, 1999.

Fairfax MR, Bluth MH, Salimnia H: Diagnostic molecular microbiology: a 2018 Snapshot, *Clin Lab Med* 38(2):253–276, 2018 Jun.

Ferrari M, Cremonesi L: Genotype-phenotype correlation in cystic fibrosis patients, *Ann Biol Clin* 54:235–241, 1996.

Friedman KJ, Silverman LM: Cystic fibrosis syndrome: a new paradigm for inherited disorders and implications for molecular diagnostics, *Clin Chem* 45:929–931, 1999.

Gurbel PA, Tantry US: Do platelet function testing and genotyping improve outcome in patients treated with antithrombotic agents? Platelet function testing and genotyping improve outcome in patients treated with antithrombotic agents, *Circulation* 125:1276–1287, 2012.

Heller RA, Schena M, Chai A, et al.: Discovery and analysis of inflammatory disease-related genes using cDNA microarrays, *Proc Natl Acad Sci U S A* 94:2150–2155, 1997.

Khan J, Wei JS, Ringner M, et al.: Classification and diagnostic prediction of cancers using gene expression profiling and artificial neural networks, *Nat Med* 7:673–679, 2001.

Klee EW: Data mining for biomarker development: a review of tissue specificity analysis, *Clin Lab Med* 28:127–143, viii, 2008.

Pandey A, Mann M: Proteomics to study genes and genomes, *Nature* 405:837–846, 2000.

Roberts JD, Wells GA, Le May MR, et al.: Point-of-care genetic testing for personalisation of antiplatelet treatment (RAPID GENE): a prospective, randomised, proof-of-concept trial, *Lancet* 379:1705–1711, 2012.

Rodriguez-Antona C, Gomez A, Karlgren M, et al.: Molecular genetics and epigenetics of the cytochrome P450 gene family and its relevance for cancer risk and treatment, *Hum Genet* 127:1–17, 2010.

Talaulikar D, Dahlstrom JE: Staging bone marrow in diffuse large B-cell lymphoma: the role of ancillary investigations, *Pathology* 41:214–222, 2009.

Tozzi V: Pharmacogenetics of antiretrovirals, *Antiviral Res* 85:190–200, 2010.

Venter JC, Adams MD, Myers EW, et al.: The sequence of the human genome, *Science* 291:1304–1351, 2001.

Weindel MD, Bluth MH: Establishing a molecular diagnostics laboratory. In *McPherson and Pincus: Henry's clinical diagnosis and management by laboratory methods*, 23rd Edition, New York, June 2016, Saunders Publishing, pp 1360–1376.

CHAPTER 68

MOLECULAR DIAGNOSTICS: BASIC PRINCIPLES AND TECHNIQUES

Martin H. Bluth

NUCLEIC ACID BIOCHEMISTRY AND BIOLOGY, 1373
Molecular Composition And Structure, 1373
Nucleic Acid–Associated Enzymes, 1375
Replication Of DNA, 1375
Transcription Of DNA To RNA, 1376
Posttranscriptional Modification, 1376
Translation Of RNA To Protein, 1376
Transcriptional Control, 1376
Mechanisms Of DNA Repair, 1377
DNA Mutations, 1378
NUCLEIC ACID ANALYSES, 1379
Electrophoretic Separation, 1379
Nucleic Acid Hybridization, 1379
Hybridization Assays: Basic Components, 1380
Hybridization Assay Formats, 1381
Amplification Methods, 1383
Polymorphism Detection Assays, 1383
DNA Sequencing, 1384
Pyrosequencing, 1384
RELATIONSHIP TO LABORATORY EVALUATION OF DISEASE, 1385
Molecular Diagnosis, 1385
Beyond Diagnosis, 1385
SELECTED REFERENCES, 1385

KEY POINTS

- Familiarity with the basics of nucleic acid biochemistry and biology is required to understand molecular diagnostic testing.
- The chemical stability of double-stranded DNA stands in contrast to the lability of single-stranded RNA.
- Base pairing of nucleic acids is dictated by energetically favorable rules and forms the basis for DNA replication, RNA transcription, and hybridization assays.
- The chemical similarity of nucleic acid molecules, regardless of their source, means that methods of extraction, storage, and handling are often similar.
- Enzymes that synthesize and modify nucleic acids (e.g., polymerases, transcriptases, nucleases, ligases) may be harnessed as tools for molecular biology and molecular diagnostics.
- Nucleic acid analyses include electrophoresis, hybridization assays, amplification techniques, sequencing, and polymorphism detection. Complete assays or diagnostic tests often combine several of these techniques.
- Molecular diagnostics is now part of the mainstream of laboratory diagnostics.

Nucleic acids are the critical molecules of life. Deoxyribonucleic acid (DNA) resides in the nucleus of eukaryotic cells and maintains all the information necessary for maintenance of the organism and for transfer of the information to successive generations. Ribonucleic acid (RNA) carries information from DNA to the cytoplasm of a cell and directs synthesis of the proteins necessary for the function of the organism. The normal state of health depends on the stability of DNA and on accurate DNA duplication and translation into protein. Modern cell biology seeks to determine the basic mechanisms of cell structure and function. Studies are increasingly focused at the level of the gene, the protein-coding units of DNA. Therefore, diagnostic methods are also being directed toward nucleic acid evaluation. The goal of this chapter is to provide the conceptual framework for diagnostic applications of nucleic acid analyses.

NUCLEIC ACID BIOCHEMISTRY AND BIOLOGY

Nucleic acid biochemistry is central to modern cell biology and dictates many aspects of diagnostic applications. Many of the enzymes associated with in vivo nucleic acid synthesis, degradation, and repair have become basic laboratory tools for manipulation and analysis of DNA and RNA. Cellular mechanisms that operate to direct and control DNA replication, transcription, and translation address the basic biology of the cell in health and disease. Diagnosis, therapy, and research are all increasingly directed at a molecular level of cellular function. This chapter provides an overview of those aspects of nucleic acid biochemistry and biology that are required to understand the current diagnostic applications of molecular biology. Further details are available from textbooks on cell biology (e.g., Alberts et al., 2014).

MOLECULAR COMPOSITION AND STRUCTURE

DNA is a long, double-stranded polymeric molecule (dsDNA) that exists predominantly in the form of a right-handed double helix. Each single-stranded DNA molecule (ssDNA) is composed of a small number of building blocks. The backbone of the ssDNA polymer is the sugar deoxyribose connected by phosphate groups (Fig. 68.1A). Phosphodiester bonds between the 3′ carbon of one sugar ring and the 5′ carbon of the next give the backbone its invariant structure and its 5′ to 3′ directionality. Linked to the 1′ carbon of each sugar is one of four possible bases: thymine (T) and cytosine (C), which are pyrimidines, and adenine (A) and guanine (G), which are purines. The bases can occur in any sequence order and, thus, form the variable portion of ssDNA. The building blocks of the single-stranded polymer are the four deoxyribonucleotide triphosphates (dTTP, dCTP, dATP, dGTP), each consisting of a sugar molecule, a triphosphate group, and one base. During DNA synthesis, nucleotides are first stripped of two phosphate groups and then enzymatically linked together by phosphodiester bonds to form a chain.

DNA is an extraordinarily stable molecule, losing its normal conformational structure only at extremes of heat, pH, or in the presence of destabilizing agents. The double-stranded helix is the most energetically favorable state for DNA—an examination of the components of DNA explains this fact. Both sugar and phosphate groups are hydrophilic, forming stable hydrogen bonds with surrounding water molecules in solution. Bases, however, are hydrophobic and are not soluble in water at neutral pH. A stable molecule of DNA must ensure that the bases do not contact water. This is possible when two antiparallel ssDNA polymers (one running in the 3′ to 5′ direction, and the other 5′ to 3′) twist around the same axis. This arrangement allows planar hydrogen bonds to form between adenine and thymine, and between guanine and cytosine (see Fig. 68.1B). As long as the two chains have base sequences in complementary order, the strands of the helix have a ladder-like structure with rungs (base pairs [bp]) of consistent size. The flexibility of the carbon-oxygen linkages in the phosphodiester bond allows the ladder to twist, forming a regular helix such that the planar base pairs are stacked on top of each other, leaving no room for water molecules in between. The polymeric series of base pair hydrogen bonds holds the ssDNA chains tightly together, and the helical conformation protects the base pairs from water, exposing only the hydrophilic backbones.

Helical dsDNA is stable over a pH range of approximately 4 to 9. Solutions with pH outside these limits have the capacity to disrupt the base pair bonds and cause the DNA helix to denature or unwind into two

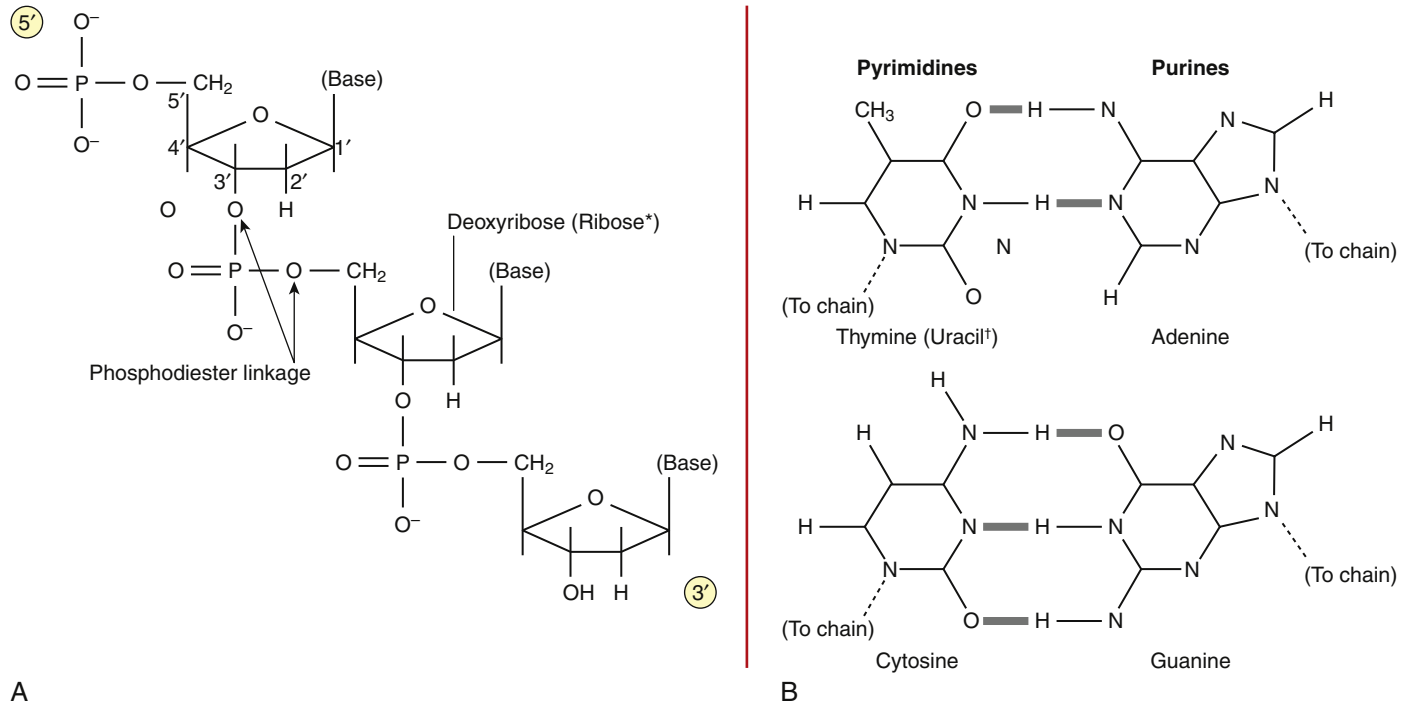

Figure 68.1 Repeating backbone of DNA and complementary base pairs. **A,** A single-stranded DNA chain. Repeating nucleotide units are linked by phosphodiester bonds that join the 5′ carbon of one sugar to the 3′ carbon of the next. **B,** Purine and pyrimidine bases and the formation of complementary base pairs. Shaded bars indicate the formation of hydrogen bonds. In RNA, the sugar is ribose, which has a 2′ hydroxyl added to deoxyribose. In RNA, thymine is replaced by uracil, which differs from thymine only in the lack of the methyl group. (*Modified from Piper MA, Unger ER:* Nucleic acid probes: A primer for pathologists*, Chicago, 1989, ASCP Press, with permission.*)

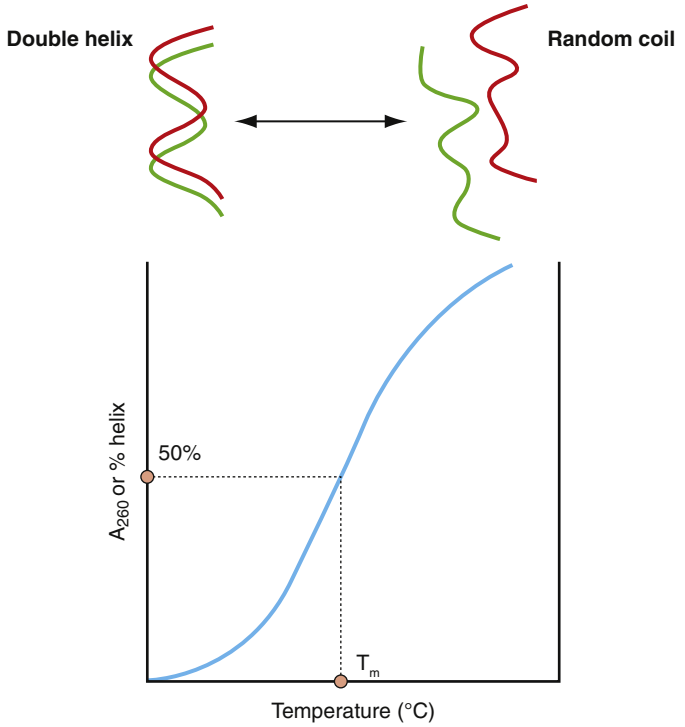

Figure 68.2 Melting/annealing curve of double-stranded helical nucleic acid. (*Modified from Piper MA, Unger ER:* Nucleic acid probes: A primer for pathologists*, Chicago, 1989, ASCP Press, with permission.*)

Figure 68.3 Photograph of purified DNA demonstrating stringy viscous nature of minimally sheared genomic DNA.

separate, random coils. Extreme heat and hydrogen bond disrupters, such as formamide, also have the same effect. This helix-to-coil transition can be followed spectrophotometrically at A_{260} (Fig. 68.2). The bases absorb ultraviolet (UV) light maximally at this wavelength but at a lower molar absorptivity in dsDNA; absorptivity increases 20% to 30% when dsDNA is converted to ssDNA. Because temperature is often used to effect this transition, the process has been referred to as *melting*, and the temperature at which 50% of dsDNA is converted to ssDNA is called the *melting point* or T_m of the DNA. The T_m of DNA molecules depends on the relative G-C versus A-T base pair content, because the three hydrogen bonds of G-C base pairs require more energy to disrupt than the two hydrogen bonds of A-T base pairs. Lowering the temperature can reverse the melting process, and the two complementary strands reform the original helix if the base pairs re-form in the correct linear conformation.

The length of a fully extended eukaryotic DNA molecule would be about 3 m per genome, much longer than the cell itself. Undegraded purified DNA forms a stringy viscous solution, reflecting the extreme length of genomic DNA (Fig. 68.3). In vivo, however, DNA is organized into highly compacted, regular units called *chromosomes*. A chromosome is composed

TABLE 68.1
Comparison of Key Features of DNA and RNA

Feature	DNA	RNA
Sugar	Deoxyribose	Ribose
Base pairs	Thymine–adenine	Uracil–adenine
	Cytosine–guanine	Cytosine–guanine
3D structure	Double-stranded	Single-stranded
	DNA duplex helix	Variable, determined by base sequence (see text)
Stability	Stable	Subject to base hydrolysis
	Degraded by DNase	Degraded by RNase
Function	Maintains genetic information in nucleus	Carries genetic information to cytoplasm

of its DNA strand wound around DNA-associated proteins in a highly structured fashion (chromatin). The chromosome structure involves several hierarchical levels of chromatin packing, from a "beads-on-a-string" nucleosome (146 nucleotide pairs wound around a histone core) to highly condensed loops, each containing about 100,000 bp of DNA. Each human cell nucleus contains two sets of 23 chromosomes of characteristic length and unique base pair sequence. Together, these chromosomes constitute the *human genome*. The complete sequence of the 3 billion chemical base pairs that make up the human genome was finished in 2001. (The Human Genome Project is discussed in Chapter 80.)

RNA differs from DNA in chemical composition, structure, and function (Table 68.1). In RNA, the sugar is ribose, containing a hydroxyl group at the 2′ position, and thymine is replaced by the methylated uracil (U). RNA exists predominantly as a single-stranded molecule and in much shorter lengths than DNA. The structure of RNA is more irregular, owing to the single-stranded nature of the molecule, but it may contain some helical sections and hairpin loops. However, RNA molecules of the same base sequence will form the same three-dimensional structure as a result of adopting the most energetically favorable conformation. These consistent three-dimensional structures are a requirement for RNA function. RNA is much less stable than DNA, due not only to the single-stranded structure but also to its susceptibility to alkaline hydrolysis via the 2′ hydroxyl group of the ribose moiety. Ubiquitous RNA-specific enzymes also rapidly degrade RNA.

NUCLEIC ACID–ASSOCIATED ENZYMES

DNA must be duplicated prior to cell division so that daughter cells retain an exact copy of the genetic information contained in parent chromosomes. RNA must be synthesized by all functioning cells to direct the synthesis of necessary proteins. DNA must be degraded during repair of damaged segments, and RNA is continually degraded and resynthesized. Enzymes that operate directly on nucleic acids affect these and other functions. Table 68.2 lists major categories of nucleic acid–specific enzymes and their in vivo functions. In vitro, purified enzymes have become laboratory *tools* for the molecular biologist, allowing genetic engineering and facilitating many nucleic acid assays for research and clinical use.

Nucleic acid–specific enzymes include polymerases, which catalyze the formation of phosphodiester bonds during synthesis, and nucleases, which hydrolyze these bonds. RNA-specific nucleases (RNases) are present virtually everywhere. Because of this, it requires much greater care in laboratory practice to work with RNA in vitro than with DNA. Restriction endonucleases are a special category of nucleases found only in bacteria, where they function to destroy foreign DNA. The recognition sites for restriction enzymes are located anywhere within the DNA molecules, are sequence specific, and can vary approximately 4 to 12 bp in length. At the recognition sequence or nearby restriction endonucleases make specific asymmetric or blunt end cuts in DNA molecules (Fig. 68.4). More than 3000 restriction endonucleases have been discovered and categorized according to the structure of their corresponding sequence recognition sites (Pingoud & Jeltsch, 2001). The in vivo function and in vitro utility of many of these enzymes are discussed in the following sections.

REPLICATION OF DNA

The DNA duplication process, known as *semiconservative replication*, uses each strand of the parent molecule to direct the synthesis of a daughter

TABLE 68.2
Nucleic Acid Enzymes and Associated Functions

Enzyme	In vivo function
Polymerases DNA polymerases RNA polymerases	Polymerases join DNA or RNA nucleotides together to form a single-stranded daughter molecule, using a stretch of single-stranded parent molecule as a template. These enzymes perform syntheses according to base pair rules and proceed in the 5′ to 3′ direction.
Reverse transcriptase	Mostly of viral origin, reverse transcriptase catalyzes the synthesis of DNA from either an RNA or DNA template.
DNA ligases	Joins DNA fragments formed by discontinuous synthesis in DNA replication or by DNA repair pathways.
Nucleases DNases, RNases	Nucleases "digest" nucleic acid molecules by breaking phosphodiester bonds.
Endonucleases Exonucleases	Endonucleases digest nucleic acids from the middle of the molecule, whereas exonucleases begin at a free end and may require a 3′ or 5′ end. Nucleases may have single-stranded, double-stranded, DNA, or RNA specificity. Some polymerases also have nuclease activity.
Restriction endonucleases	Bacterial endonucleases that recognize specific short DNA base pair sequences and cleave the DNA molecule only at the recognition site.

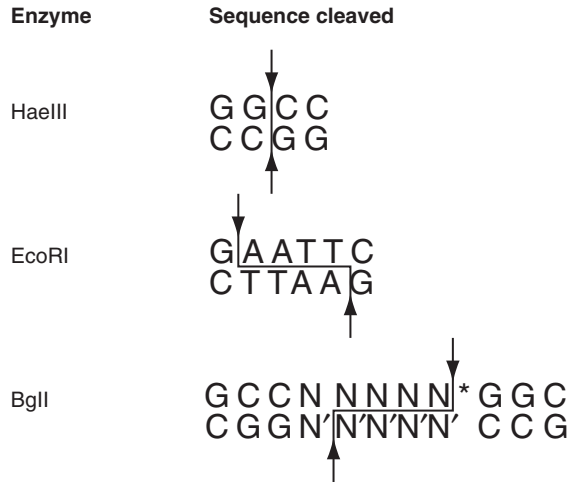

Figure 68.4 Examples of DNA restriction enzymes and their specificities. Enzymes are named for the bacteria from which they are isolated. (N* is any base, and N′ is its pairing counterpart.)

strand (Virshup, 1990). Because the base sequence of the parent strand dictates the sequence of the daughter strand, replication is faithful and the replication products consist of two dsDNA molecules composed of one parent strand and one daughter strand each, with exactly the same base pair sequence. Although this is conceptually simple, the process is complicated and involves a number of accessory proteins and enzymes. First, for synthesis to begin, a small single-stranded region must be produced at a point on the genome called an *origin*. This is not energetically favorable and must be accomplished using proteins—that is, helicases—that unwind and separate the strands of the helix. Next, at each origin, a short RNA primer is synthesized complementary to the single-stranded sequence. DNA polymerase III proceeds with DNA synthesis; later, the RNA primer is excised and replaced with DNA by DNA polymerase I. Chromosomal DNA contains many origins of replication. This process occurs simultaneously across the chromosome. Interestingly, DNA polymerase III is a directional enzyme and can synthesize DNA only in the 5′ to 3′ direction because it requires a free 3′OH end. This means that only one daughter strand, called the *leading strand*, can be synthesized continuously. The opposite strand,

called the *lagging strand*, is primed by RNA primase that does not require a free 3′OH end. It is synthesized discontinuously in short fragments (Okazaki fragments), each requiring an RNA primer, as the replication fork is opened up. These fragments are then joined together by DNA ligase after each primer is excised. DNA polymerase III is also unique in that it has *proofreading* and exonuclease activity. If an incorrect nucleotide is added to the growing chain, it is detected and excised by the nuclease portion of the enzyme; the correct nucleotide is then added. This helps explain the extraordinary fidelity of the DNA replication process. Postsynthesis repair mechanisms also contribute to the accuracy of replication (see Mechanisms of DNA Repair section). Finally, telomerase adds DNA repeat sequences to the 3′ end of each chromosome (the telomere) to prevent shortening of the lagging strand with each replication cycle.

TRANSCRIPTION OF DNA TO RNA

Sections of DNA that specify amino acid sequences of proteins are called *genes*. One gene contains the amino acid sequence code for one protein as well as the DNA sequences necessary for the regulation of the production of that protein. Within the 6 billion nucleotides of the human genome, there are about 20,000 to 25,000 protein-coding genes. Although these coding sequences are of paramount importance to the cell and to the function of the organism as a whole, they actually make up less than 2% of the nucleotides. The vast majority of the human genome is composed of noncoding DNA regions referred to in the past as *junk DNA*. While much of the function of noncoding DNA remains unknown, diverse roles of biological importance have been identified, such as regulation of gene expression, origins of replication, and coding of RNA (see later section on Gene Regulation Mediated by Small RNA and Cech & Steitz, 2014).

Protein synthesis begins with the activation of the appropriate gene. A copy of the gene is made from DNA in the form of RNA. Because the RNA copy carries the code from the DNA in the cell nucleus to the cytoplasm where amino acid synthesis takes place, this type of RNA is called *messenger RNA* (mRNA). mRNA is synthesized from only one strand (coding strand) of the DNA gene; the complementary DNA (cDNA) strand is not used. This is accomplished by a process called *transcription*. DNA promoter sequences present near the start of the gene to be transcribed promote the ability of RNA polymerases and associated proteins to recognize the nucleotide at which mRNA synthesis initiation begins. Synthesis of mRNA proceeds in much the same fashion as DNA replication, with the ssDNA sequence dictating the mRNA sequence using the same rules of base pair complementarity (uracil base pairs with adenine). When the end of the gene is reached, mRNA synthesis is terminated. Some genes are always expressed, while others are only active in certain physiologic situations. The rate of transcription also varies in different cells (see later section on Transcriptional Control).

POSTTRANSCRIPTIONAL MODIFICATION

Before export to the cytoplasm, the mRNA molecule is modified in several ways (Rosenthal, 1994). mRNA contains both amino acid coding sequences (exons) and noncoding sequences (introns); introns are excised from the mRNA molecule before protein synthesis. A molecular complex called a *spliceosome* (Sharp, 1988), which is composed of both low-molecular-weight RNA (including, at its catalytic core, a ribozyme; see Fica et al., 2013) and protein, recognizes mRNA sequences that identify the boundaries of an intron, joins the flanking exons, and releases the intron. Splicing must be exact, because the addition or subtraction of a single nucleotide at the splice junction would change the 3-nucleotide reading frame in the nucleotide sequences that follow.

Further modifications to the mRNA molecule include the addition of 7-methyl guanosine residues to the 5′ end in a unique 5′-5′ phosphodiester bond. This is called a *cap* and aids in the binding of the ribosome to the mRNA molecule for initiation of protein synthesis. A poly-A *tail*, which may be necessary for stability and transport to the cytoplasm, is added to the 3′ end. The polyadenylation locus is specified in part by the sequence AAUAAA, usually found in the 3′ untranslated region of the RNA transcript. At this point, the mRNA molecule is ready to direct the synthesis of its corresponding protein.

TRANSLATION OF RNA TO PROTEIN

Protein synthesis requires translation from the language of nucleotides to that of amino acids. Twenty-one different amino acids are used in protein synthesis; each amino acid is specified by one or more mRNA nucleotide triplets called *codons*. For example, AAG is the codon for lysine, and UCG is the triplet for serine. Thus, an amino acid coding sequence is read in groups of three nucleotides running in the 5′ to 3′ direction; this is the *reading frame* of a protein coding sequence. Three specific codons—UAG, UGA, or UAA—do not code for amino acids but instead signal the end of a gene (*stop* codons). Because an amino acid can be encoded by more than one codon, the code is referred to as a *degenerate code*.

Translation from the mRNA nucleotide code to protein is mediated by ribosomes in the cytoplasm of the cell. A ribosome binds to the 5′ end of the mRNA and provides a stable chemical environment for all molecules involved in protein synthesis. Amino acids are linked in the correct sequence by the action of small adaptor RNA molecules called *transfer RNAs* (tRNAs). Each tRNA molecule contains a region that is complementary to a particular mRNA codon: the *anticodon*. Linked to one end of the tRNA is the amino acid that corresponds to the complementary mRNA codon of the tRNA. A tRNA with the correct complementary anticodon binds to the first codon in the mRNA sequence, which is always AUG. When another specific tRNA binds to the next codon, ribosomal enzymes catalyze the formation of a peptide bond between the two amino acids linked to the tRNAs, removing the linkage between the first amino acid and its tRNA molecule. The first tRNA is ejected from the ribosome, and a new tRNA binds to the next codon. Protein synthesis proceeds from the N-terminus to the C-terminus. As this process continues, the ribosome moves along the mRNA molecule, completing the synthesis of the amino acid chain. When a stop codon is reached, the ribosome detaches from the mRNA. In reality, several ribosomes can move along the same mRNA molecule, each translating the mRNA code into a new protein molecule.

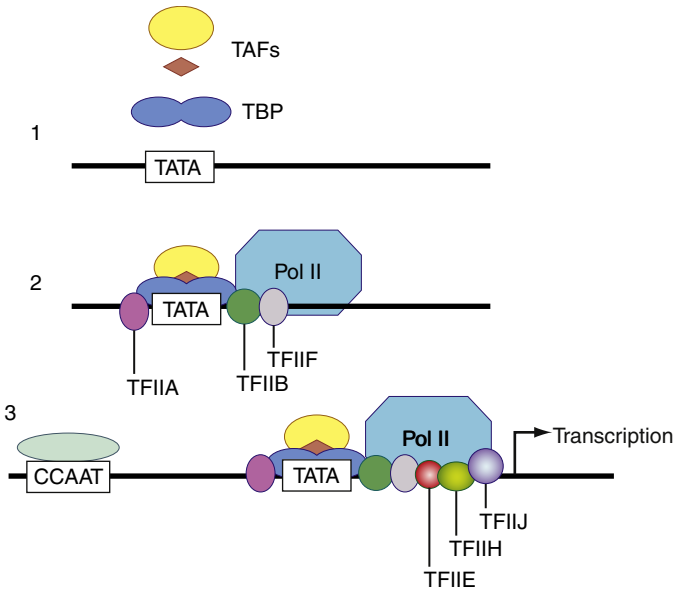

Figure 68.5 Assembly of the polymerase II transcription initiation complex. (1) The basal TFIID complex assembles as the TATA-box binding protein (TBP) and associated factors (TAFs) at the TATA box of the promoter region. (2) Additional transcription factors TFIIA and TFIIB are recruited to enable the polymerase II enzyme and TFIIF to bind. (3) The complex is stabilized with TFIIE, TFIIH, and TFIIJ. Typically, binding of additional factors to upstream enhancer sites like CCAAT or GGGCGG are required for effective RNA transcription.

TRANSCRIPTIONAL CONTROL

To allow for cellular differentiation and response to environmental stimuli, there must be mechanisms controlling the repertoire of gene transcription and protein translation. Some of these mechanisms operate at the level of DNA and control the transcription of mRNA (Rosenthal, 1994). As noted, promoters are important for the initiation of mRNA transcription and are found upstream (toward the 5′ end) at a relatively invariant distance from the beginning of the protein coding sequence. There are several different kinds of promoter consensus sequences (nucleotide sequences that are found in many examples). The most common promoters are rich in adenine and thymine and have been called *TATA boxes*. Because A-T base pair bonds are weaker than G-C base pair bonds, DNA unwinds more easily at repeat A-T sequences. After transcriptional activation, a local ssDNA region is produced and stabilized by the assembly of a complex of RNA polymerase and general transcription factors (Fig. 68.5). mRNA is synthesized from the local region of ssDNA, and the mRNA is quickly ejected as the DNA returns to its more energetically favorable double-stranded helical state.

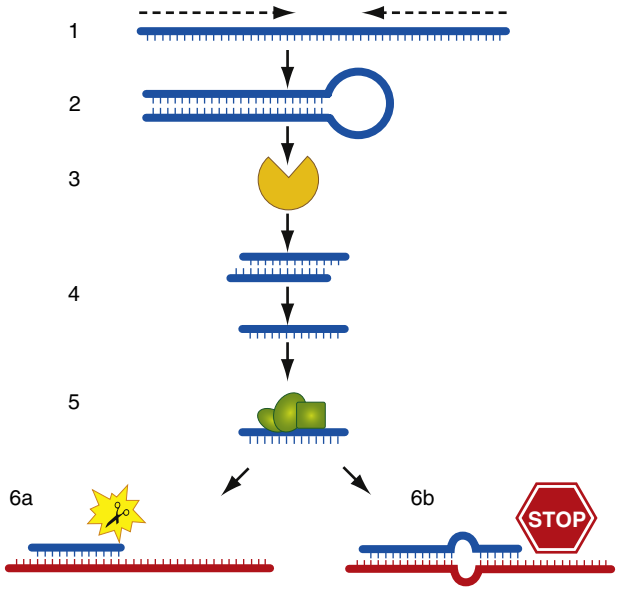

Figure 68.6 Diagram of the RNAi pathway. (1) Sense-antisense transcripts build a dsRNA with hairpin structure (2). This molecule is recognized by the Dicer complex (3) and processed into smaller fragments of 21 to 24 nucleotides (4). The RNA-induced silencing complex (RISC), a multiprotein complex, assembles with these molecules and unwinds them into single-strand oligos (5). Active RISC binds to target mRNAs with either perfect complementary sequence (6a), which initiates cleavage and degradation, or imperfect sequence match (6b), resulting in bulging, interference with translation, and subsequent silencing.

Enhancers are DNA sequences that can augment mRNA transcription and may be found in different locations relative to the gene that they affect. Gene-specific transcription factors are proteins that bind to enhancers and promoters and selectively stimulate or inhibit mRNA transcription (Papavassiliou, 1995). In eukaryotes, enhancers commonly contain multiple binding sites for several transcription factors, so it is the net effect of factors binding to these DNA elements that determines the activation and rate of expression. The availability of transcription factors, in turn, is controlled by cellular events such as phosphorylation or by other proteins such as hormones and growth factors. A network of intracellular and extracellular chemical communications can thus select and control the synthesis of necessary proteins.

Because mRNA is far less stable than DNA, the half-life of mRNA is very short. New mRNA molecules are continually transcribed from DNA. As the cell responds to changes in transcriptional signals, the genes that are transcribed into mRNA can be quickly changed, resulting in the immediate synthesis of new proteins. Thus, the cell has the ability to rapidly adjust its protein output in response to its environment.

Gene Regulation Mediated by Small RNA

An additional mechanism of gene regulation by another class of RNAs—small RNAs—is recognized as important. Small RNAs are short, noncoding ribonucleotides that function as posttranscriptional regulators of gene expression. First discovered in the 1990s, they were found in cells of many eukaryotic organisms, including mammals (Fire et al., 1998). The small RNAs are divided into several different subgroups, most notably small interfering RNA (siRNA) and microRNA (miRNA). Recently, next-generation sequencing has identified large numbers of noncoding RNAs of greater length (>200 nt). The function of these long noncoding RNAs (lncRNA) is an active area of research (Cech & Steitz, 2014).

The DNA sequences for siRNAs and miRNAs are often located in noncoding regions between genes. They generally have their own promoters, and transcription is mediated by polymerase II. The immediate product is an miRNA precursor that forms a double-stranded hairpin structure (Fig. 68.6, 6a). An enzyme called Dicer processes it to short RNA duplex molecules and further into single-stranded RNAs 22 to 26 nucleotides in length. The small RNA strand attaches to an RNA-induced silencing complex (RISC), which mediates binding to complementary sequences of mRNAs. siRNAs pair perfectly with the target mRNA and trigger a series of molecular mechanisms that lead to its degradation. This process is also called *RNA interference* (*RNAi*). miRNAs bind imperfectly to their target mRNA, causing conformational changes, bulging, and subsequent blockage of protein translation at the ribosome. Small RNAs are abundant in eukaryotic cells (several hundred); it is thought that each one can target multiple mRNAs either as siRNA or miRNA. They are often tissue specific and have been implicated in the regulation of all major cellular processes such as proliferation, differentiation, metabolism, and cell death. siRNAs have also been recognized as a new RNA-based immune system against viruses that is based on silencing through the RNAi mechanism. Furthermore, changes in miRNA expression patterns can be found in many malignancies, and specific miRNAs were found abundantly in certain tumors (Iorio & Croce, 2009).

miRNA research has advanced within a decade from one publication to thousands of publications describing the role of miRNAs in gene regulation. miRNA expression profiling has been recently evaluated as a reliable diagnostic biomarker for differentiating between normal and tumor specimens (Sethi, 2018). It has shown to be deregulated in multiple cancers in human and mouse models, and has proved to play a critical role in the development and progression of the tumor. Most of the miRNAs are differentially expressed, whereas some discriminate totally between normal and tumorigenic samples. The miRNA expression enhances (oncogenic miRNA) or reduces (tumor suppressor) as the tumor progresses and has been found to be associated with drug resistance. This discovery of miRNA a decade ago, as a diagnostic and prognostic marker, has now led to miRNA-based targeted therapy in vitro and may selectively predict better treatment outcome for patients with cancer. In addition, classification of an unknown tumor may be possible by the alteration of tumor-specific miRNA. The nomenclature for assigning names to novel miRNAs for publication in peer-reviewed journals is done by miRBase, which is the central repository for miRNA sequence information. It has an online database with all published miRNA sequences with links to the primary literature and to other secondary databases. Although some miRNAs are tumor specific, miR-21 has proved to be the global oncogenic miRNA in many solid tumors. The miRNAs with oncogenic potential include miR-155, miR-17-92, and miR-21 but it is not limited to these alone. The level of expression of miR-155 is upregulated in various carcinomas. However, they are specifically significant in pancreatic cancers, for which they have prognostic relevance.

Several synthetic small molecule inhibitors of miRNAs, such as chemically modified antisense oligonucleotides called "antagomiRs," are currently in use in vitro, targeting against specific oncogenic miRNAs. These antagomiRs silence the overexpressed oncogenic miRNAs in cancers by blocking their function. In animal experiments, antagomiRs against miR-16, miR-122, miR-192, and miR-194 were found to be efficacious in reducing the levels of miRNA in the liver, lung, kidney, and ovaries. Re-expression of tumor-suppressor miRNA, such as let-7, is another proposed miRNA therapeutic strategy to upregulate tumor-suppressor miRNA by exogenously transfecting let-7 that led to the inhibition of growth in vitro and in vivo. These characteristics of miRNA suggest their potential role as novel biomarkers for diagnostic, prognostic, and therapeutic targets (Fig. 68.6, 6b).

Epigenetics and Gene Regulation

Epigenetics refers to changes in gene expression that are not dependent on changes in DNA sequences. In most instances, this involves a change in the chromatin structure that facilitates or blocks gene transcription. This is a dynamic process involving enzymes that chemically modify DNA or histone proteins. A methyl group added to the fifth carbon of cytosine results in 5-methyl cytosine. This generally occurs on cytosines located next to guanines (CpG) that are often repeated in islands or patches located in the promoter region. DNA methylation tends to result in condensed chromatin and reduced transcription. DNA methyltransferases are the enzymes responsible for DNA methylation. Chromatin proteins may be acetylated, deacetylated, or methylated. There is evidence that small regulatory RNA may directly interact with a variety of epigenetic mechanisms (Moazed, 2009). Epigenetic changes are recognized to be important in tissue-specific gene transcription; alterations may be factors in cancers, aging, and stress response. The relationship of the microbiome has further been shown to promote epigenetic changes associated with disease and to modify gene expression patterns in a state of disturbed immunity (e.g., inflammatory bowel disease). To this end, poor dietary choices are encoded into the human gut and genetic make-up, which could be transferred to offspring in an epigenetic influential manner (Beaudet, 2008; Aleksanrova, 2017; Mochizuki, 2017).

MECHANISMS OF DNA REPAIR

Errors in DNA replication and damage to DNA during the normal cellular lifetime must be minimized to preserve the health of the entire organism. Several mechanisms operate to maintain the normal DNA sequence. First are the error-avoidance mechanisms that operate during DNA replication.

The DNA polymerase that synthesizes new DNA polymers selects each successive nucleotide monomer based on its complementarity to the next nucleotide in the template strand. Fidelity at this level is high, and most errors in synthesis are avoided at this stage. Nevertheless, an occasional base may be incorrectly added to the growing strand. To adjust for this, the proofreading activity of the polymerase can recognize the error, remove the incorrect base, and proceed again with synthesis. Together, the error avoidance mechanisms reduce base pair mismatches to approximately 1 in 10 million (Radman & Wagner, 1988). This represents a 100,000-fold increase in efficiency compared with the error rate of 1 in 160 bases for in vitro solid-phase oligonucleotide synthesis.

Despite the remarkable error avoidance in DNA replication, occasional mistakes do occur. In addition, DNA can be damaged by normal biochemical reactions and by nonphysiologic agents such as UV light and environmental carcinogens. Several repair mechanisms mend damaged DNA (Yu et al., 1999) (Table 68.3).

Direct repair mechanisms repair lesions in a single-step reaction. For example, O^6-methylguanine DNA methyltransferase repairs alkylation lesions by transferring the alkyl group from the lesion to the active site of the enzyme. Other direct repair mechanisms characterized in *Escherichia coli* may also exist in human cells (Yu et al., 1999).

Mismatch repair (MMR) functions immediately after DNA replication to replace mismatched bases with the correct ones (Modrich, 1994). Several MMR proteins recognize the error in the newly synthesized daughter strand and excise a region that includes the mismatch. DNA polymerase III and ligase restore the correct sequence and integrity of the daughter strand. The importance of this mechanism in stabilizing the genome is evidenced by recent studies associating Lynch syndrome with defects in MMR proteins.

Base excision repair targets small, nonhelix-deforming adducts such as those produced by methylation, oxidation, reduction, or base fragmentation by ionizing radiation. Base excision leaves three or four nucleotide sequence gaps that are then filled with the correct nucleotides; nicks are sealed with ligase. Larger, bulky adducts or dimers that distort the DNA helix may be caused by UV radiation, carcinogens, and therapeutic drugs, among other agents. Such damage is removed by the nucleotide excision repair (NER) pathway, which uses an enzyme system composed of many proteins to excise a single-stranded oligonucleotide containing the lesion (Sancar, 1994). The gap is then filled in by DNA polymerase and ligated. There are two NER pathways: one in which lesions that block transcription are rapidly removed (transcription-coupled repair; Hanawalt, 1994) and a global pathway that repairs bulk DNA, including the nontranscribed strand of active genes. Some of the possible consequences of the loss of NER activity are exemplified by the disease xeroderma pigmentosum (XP), which is caused by mutations in *NER*. XP results in extreme sensitivity to sunlight, with skin cancers occurring at an early age (Weeda et al., 1998).

Double-strand breaks that occur rarely or are produced by ionizing radiation and oxidative damage present significant repair problems. If unresolved, replication and transcription of involved sequences will be blocked. To maintain local and overall genomic integrity, double-stranded breaks are repaired by nonhomologous or allelic recombinational repair mechanisms. One of the genes associated with hereditary breast-ovarian cancer syndrome, *BRCA1*, encodes a protein involved in repairing double-strand breaks in DNA and illustrates the importance of this process.

It is now clear that DNA repair plays a central role in the life of the cell. Recent evidence also indicates that several primary repair proteins also function in transcription and in regulation of the cell cycle. Thus, the processes involving DNA appear to be highly integrated and are increasingly studied as a whole and in relation to human disease.

TABLE 68.3
DNA Repair Pathways

Repair Type	Function
Direct repair	Repairs certain types of DNA damage in a single-step reaction.
Mismatch repair	Checks for errors made when DNA is replicated. Any mispaired bases in the daughter strand are removed and replaced with the correct match.
Base excision repair	Repairs small, nonhelix-deforming adducts such as those produced by methylation, oxidation, reduction, or base fragmentation by ionizing radiation.
Nucleotide excision repair	Removes bulky DNA adducts such as thymine dimers and certain photoproducts as well as chemical adducts and cross-links.
Double-strand break repair	Repairs double-strand breaks that result from physiologic processes or from ionizing radiation and oxidative insults.

DNA MUTATIONS

Despite extensive repair mechanisms, alterations in DNA base sequence (mutations) occur. Yet, for an individual organism, some mutations are clearly harmful and can be associated with cancer and with inherited genetic disease. Studies of these diseases have led to the characterization of the various types of mutations that occur in the human genome (Weatherall, 1987). These can be conceptually grouped into a few major categories (Table 68.4). A point mutation is found in the β-globin gene in sickle cell anemia (Kan, 1992). A thymine base replaces an adenine base, causing a critical change in the structure of hemoglobin. As described in Chapter 72, muscular dystrophy is caused by deletions in the gene for the muscle protein dystrophin. In the Becker form of the disease, the deletions do not disrupt the reading frame. In most cases of the more severe Duchenne form, the reading frame is changed by the deletions, effectively abolishing the function of the protein (Liechti-Gallati et al., 1989).

Human DNA contains many short sequences of nucleotides (microsatellite DNA) that are sometimes grouped in tandem arrays and are repeated many times throughout the human genome. The number of tandem repeats at particular locations is a heritable trait. Some trinucleotide repeats have been found to increase in number in association with disease (Sutherland & Richards, 1994). In fragile X syndrome (see Chapter 72), expression of the disease is associated with amplification of the intragenic trinucleotide repeat sequence beyond a critical number of copies. The expansion of the trinucleotide repeats beyond this critical number disrupts expression of the gene.

A translocation, which is an exchange of a larger amount of chromosomal material between different chromosomes, may create a fusion gene, the combination of two different genes abnormally joined at the translocation site. This can create not only an altered gene transcript but may also bring the product of one gene under the transcriptional control of

TABLE 68.4
Types of DNA Mutations and Examples of Associated Diseases

Mutation	Description	Disease
Point	Single base pair substitution	Sickle cell anemia
Deletion/insertion	Subtraction/addition of amino acid codons in multiples of three. Reading frame is retained.	Becker muscular dystrophy
Deletion/insertion with frameshift	Subtraction/addition of amino acid codons in nonmultiples of three. Results in a shift of the reading frame and a completely different amino acid coding sequence from the mutation on.	Duchenne muscular dystrophy
Amplification/trinucleotide repeat	Increase in the number of repeat sequences in microsatellite DNA. Results in disruption of gene expression.	Fragile X syndrome
Translocation	Interchromosomal exchange of large chromosome segments. Results in an altered protein with altered function.	Chronic myelogenous leukemia

the other. For example, as discussed at length in Chapters 71 and 78, the Philadelphia chromosome, found in most cases of chronic myelogenous leukemia, results from a reciprocal translocation between the *c-abl* gene on chromosome 9 and a region termed the *breakpoint cluster region* (bcr) on chromosome 22. The fusion gene produced by this chromosomal rearrangement, consisting of most of the *c-abl* gene and a truncated bcr, codes for a c-abl protein that is larger than the normal product, has increased enzymatic activity, and is thought to interfere with signal transduction pathways normally involved in the control of cell death and proliferation.

It is both the type of mutation and its location in relation to the gene that determine the ultimate effect on the protein product. Mutations may have no effect on protein expression or functional activity; many human proteins exist in detectable variants that have no disease association. Mutations occurring in intron regions presumably have no effect at all. Even small mutations, however, in regions that code for key functional domains (exons) may drastically alter or eliminate function. "Nonsense mutations," mutations that change an amino acid codon to a stop codon, or vice versa, result in abnormally short or long protein products, respectively. *Missense mutations*, those that change the code from one amino acid to another, may or may not alter protein function depending on the change and function of the amino acid. Similarly, mutations within sequences that denote intron-exon splice sites could eliminate exons or introduce introns into the transcribed mRNA. Mutations may also occur in regulatory sequences, such as promoters or enhancers, producing dramatic effects on the levels of transcription.

NUCLEIC ACID ANALYSES

The unique biochemical properties of nucleic acids have been exploited to yield information about the biology or biochemistry of a system. While some of the assays, such as electrophoresis, are applicable to other biochemical building blocks, such as proteins and lipids, the majority are particular to nucleic acids. The following sections briefly describe the principles of the basic categories of analyses used to characterize DNA and RNA: electrophoretic separations, hybridization assays, amplification techniques, sequencing, and polymorphism-based analyses. In practice, the categories are often combined to produce novel variations of the same theme—for example, a complete assay may involve amplification, electrophoresis, and hybridization.

ELECTROPHORETIC SEPARATION

The repeating sugar-phosphate backbone of nucleic acids results in a net negative charge evenly distributed over these linear molecules. Therefore, DNA or RNA migrates toward the positive charge in response to an electric field. This property is used to characterize the size of nucleic acid fragments by electrophoretic separation. Samples are applied in separate wells at one end of a solid but porous separation medium. When an electric current is applied, the samples move toward the positive electrode in a linear fashion, each sample well forming one lane of migration. Comparison of the distance of migration of an unknown sample with that of a known standard allows size determination.

Density and length of the gel, as well as the strength of the electric current, can be varied to achieve resolution for different DNA fragment sizes. Commercial electrophoresis systems offer standardized conditions to ensure reproducibility. Traditionally, the gel was submerged in buffer; current systems offer enclosed gel cassettes that do not require additional liquids (Fig. 68.7). The simplest approach to visualizing the bands separated by electrophoresis is by staining with intercalating dyes (e.g., ethidium bromide), which insert between stacked bases, and viewing with UV transillumination. Direct visualization requires that the band attain a significant concentration. Increased sensitivity may be achieved in some applications that label the nucleic acid fragments with a radioactive or fluorescent tag.

The limitations in required sample concentration and detection sensitivity of classical gel electrophoresis have been addressed by capillary systems. The gel matrix is enclosed in capillary tubing 25 to 100 μm in diameter, with the electric poles on the opposite sites. Samples of nucleic acids enter the capillary on the side of the cathode and are separated according to base size while traveling through the gel. A camera measures light absorbed by fragments passing the end of the tube. Automated systems generate a chromatogram visualizing size and relative concentration as peaks. Capillary electrophoresis is precise enough to detect single-base differences and has been used routinely for Sanger sequencing (see DNA Sequencing later in this chapter).

A further advancement of this principle is the integration of the capillaries on a small cassette or chip. DNA or RNA molecules can be loaded into designated wells on the surface and are driven through polymer-filled microchannels inside the chip once the electrical circuits are closed inside an instrument (e.g., Bioanalyzer). Nucleic acids are measured and recorded as a chromatograph or electrograph (electronic image showing fragment size and separation speed). The system also measures purity and degradation by absorption of 260 and 280 nm wavelengths, providing several parameters of the quantity and quality of nucleic acid samples.

Electrophoretic resolution of high-molecular-weight genomic DNA requires controlled reduction in size through digestion with restriction enzymes. Restriction enzymes with a relatively simple recognition sequence produce fragments less than 50 kilobase pairs (kb) in length. Extremely large DNA fragments, measured in megabase pairs, are produced from digestion with enzymes with a complex recognition sequence and must be separated in special electrophoretic systems utilizing a pulsed electrical field. Most applications of DNA electrophoresis utilize nondenaturing conditions (i.e., the fragments resolved into bands are double-stranded). By contrast, most RNA separations utilize denaturing conditions (either formamide or glyoxal) to eliminate secondary structure of the single-stranded molecules. RNA molecules, as transcripts of DNA, are "presized" and relatively small so that no digestion is required before electrophoresis.

NUCLEIC ACID HYBRIDIZATION

Hybridization is a fundamental concept in nucleic acid biochemistry; it is defined as the interaction between two single-stranded nucleic acid molecules to form a duplex (double-stranded) molecule based on the complementary base pairing of their respective sequences. Hybridization is a direct consequence of the stable double-stranded structure of DNA under physiologic conditions. As discussed earlier, the helix is formed of two antiparallel strands of DNA held together by the combined strength of many specific hydrogen bonds between complementary base pairs as well as by hydrophobic shielding of bases from an aqueous environment. Central to the hybridization reaction is the fact that the binding between separate, complementary molecules (strands) is both reversible and base sequence specific.

When neither DNA strand is labeled, the process of re-forming the stable double-stranded structure is referred to as *annealing*. If one strand is labeled (i.e., has a marker that is capable of being detected in some fashion), the labeled strand is referred to as a *probe*, and the process is called *hybridization* because a hybrid molecule is formed between a labeled and unlabeled strand. RNA molecules can also participate in the hybridization process. Base pairing may occur between complementary strands of DNA, between DNA and RNA, and between complementary strands of RNA, resulting in DNA-DNA, DNA-RNA, and RNA-RNA duplex structures. Duplex molecules with exact complementarity in base sequence form the most stable structures. However, structures with varying degrees of base pair mismatch may form depending on the conditions. The relative instability of these mismatched duplexes is reflected in the lowered temperature of their disassociation (lower T_m; see Fig. 68.2).

Environmental conditions can be manipulated to control the degree of base pair mismatching that will be tolerated in a duplex structure (i.e., the *stringency* of the sequence match; Fig. 68.8). Low stringency refers to conditions such as high salt, low temperature, and no formamide, which favor shielding of hydrophobic bases from the aqueous environment

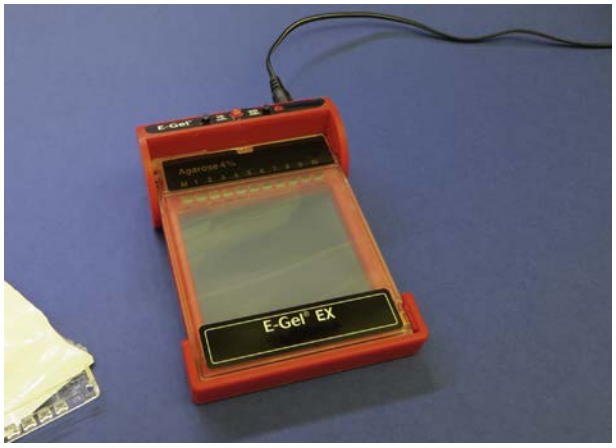

Figure 68.7 Photograph of precast agarose gel requiring no additional buffer for electrophoresis of DNA.

even without perfect alignment; the match need not be perfect. High-stringency conditions—high temperature (close to T_m), low salt, and high formamide—will allow only the most perfectly matched duplex structures to remain in a stable helix conformation.

HYBRIDIZATION ASSAYS: BASIC COMPONENTS

When the hybridization reaction is used to analyze the nucleic acid content of an unknown sample, the process is known as a *hybridization assay*. Hybridization assays include a wide variety of formats (see Hybridization Assay Formats), such as Southern blots, northern blots, in situ hybridization (FISH if fluorescence is used for detection), linear arrays, and microarrays ("DNA chips"). The property of complementary base pairing allows fragments of known composition (the probe) to interrogate an unknown for the presence of matching (complementary) sequences. Therefore, all hybridization assays require several basic elements: a probe, a sample, controlled conditions permissive to the desired degree of complementary base pairing, and a method for detection of specific probe-sample hybrids. Each of these elements is discussed in the coming sections, as well as the variations in formats that have been developed to allow hybridization assays to be performed and interpreted.

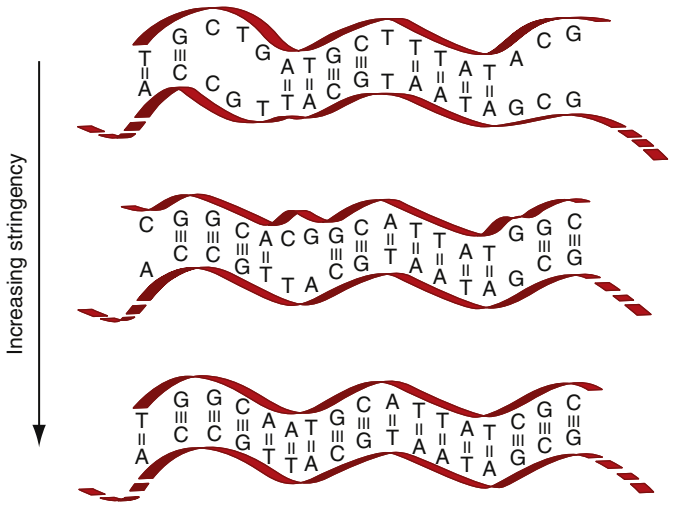

Figure 68.8 Illustration of stringency. As the stringency of the hybridization solution is increased, fewer mismatches are tolerated in a hybrid duplex. At very high stringency, even a single base pair mismatch disrupts the duplex.

Probe

The probe, a well-characterized fragment of nucleic acid, is central to a hybridization assay because it determines the specificity of the hybridization reaction. In most assay formats, the probe carries the reporter group for detection of hybridized molecules into the reaction. Reporter groups may be radioactive or nonradioactive (i.e., affinity label).

Many probes are produced through recombinant nucleic acid technology, as illustrated in Figure 68.9. Plasmids—short, circular, double-stranded segments of DNA—are harnessed as vectors to propagate desired sequences in bacteria. The segment of interest is introduced into the plasmid using restriction enzyme digestion and ligation, resulting in a new "recombined" molecule that retains the ability to be propagated in bacteria and includes the DNA sequence of interest. Bacteria containing the recombinant plasmid can be grown in culture, and the small circular plasmids can be easily separated from the bacterial genome on the basis of size. Many identical copies are obtained; thus, the DNA is often referred to as *cloned*. Purified plasmid may be used as a probe in assays where vector sequences do not interfere with the specificity of the reaction. In many applications, the inserted DNA sequence is separated from the vector sequence by digesting the isolated plasmid with the same restriction enzyme originally used in construction of the recombinant molecule. The probe resulting from either of these approaches is a double-stranded DNA molecule. Double-stranded probes must be denatured prior to use, and probe reannealing limits the extent of hybridization of the probe with the target. Plasmid vector that does not contain cloned DNA is a commonly used negative control for this type of probe.

Plasmid vectors have been constructed to include RNA promoter regions adjacent to the inserted DNA sequence. These recombinant plasmids are used to produce RNA transcripts of the DNA insert. The result is a single-stranded RNA probe that will not undergo self-hybridization. Controlling the orientation of the DNA insert with respect to the RNA promoter allows production of transcripts in the *sense* (same as mRNA) or *antisense* (complementary to mRNA) direction. In many applications, the sense transcripts form ideal negative control probes for hybridization reactions with antisense probes. Nonspecifically bound RNA probes (i.e., RNA not in a stable duplex structure) can be removed with the use of RNase specific for single-stranded RNA. The lability of RNA requires that the probes be handled with extreme care to prevent degradation (sterile technique, treated water, and glassware).

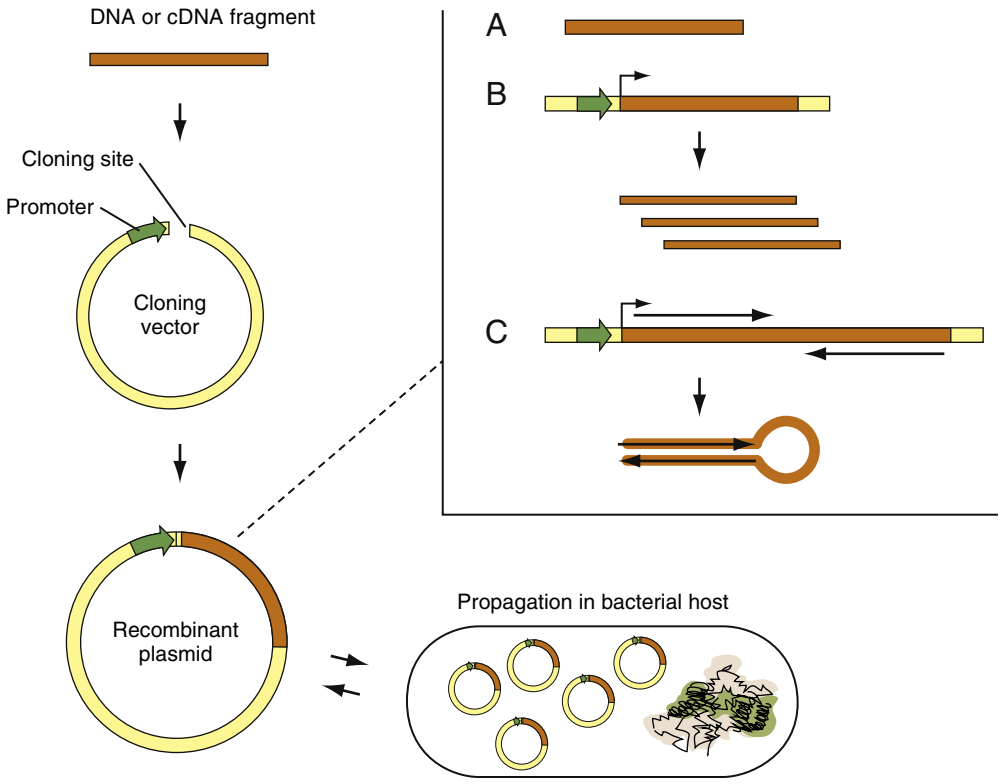

Figure 68.9 Production of cloned DNA or RNA. A DNA fragment or RNA that was converted into cDNA can be inserted into a cloning vector. The recombinant plasmid is transfected into a bacterial host, where it is rapidly propagated to millions of copies. The multiplied DNA fragment can either be isolated by excision through restriction enzymes that recognize sequences at the borders of the insert (A) or can be used to initiate RNA in vitro transcription with a promoter sequence in the plasmid (B). Such systems are also used to produce double-stranded RNA by cloning two complementary sequences in sense and antisense direction, typically with a spacer that forms a stabilizing loop in the dsRNA fragment (C).

Recombinant probes, whether DNA or RNA, are genetically complex—that is, they may include many kilobases of genetic information. By contrast, probes produced by synthetic methods are relatively short segments of DNA. Oligonucleotide probes produced by automated chemical reactions are usually 15 to 45 bases in length, synthesized to produce a specified base sequence. Probes with very high specificity of hybridization can be designed on the basis of sequence information available in data banks. They can be generated in a sense or antisense direction at a relatively low cost. These short probes are single stranded, diffuse into target, and hybridize rapidly because of their small size, and they are extremely sensitive to even single–base pair mismatches. The final sensitivity achieved with oligonucleotide probes is lower than that achieved with recombinant probes because of their limited genetic complexity. Multiple oligonucleotide probes directed to different areas of the same target have been used in some instances to increase the sensitivity by increasing the representation of the target sequence in the probe mixture. This approach is analogous to the use of a blend of monoclonal antibodies that react to different epitopes of the same complex antigen.

Probes longer than those obtained by direct chemical synthesis may be generated with the polymerase chain reaction (PCR) or other amplification technology (see later discussion and Chapter 69). These probes may be single stranded or double stranded depending on the conditions employed and may be as long as the product of the amplification reaction—in most cases, 100 bp to 1 kb in length.

Sample

Whereas probe selection and preparation are central to determining the sensitivity and specificity of the hybridization assay, the contribution of sample preparation to a successful assay cannot be overlooked. In clinical applications, samples of interest may be quite diverse. For example, a microbiology laboratory could anticipate testing specimens of blood, urine, stool, and sputum. Integrity of RNA targets may be difficult to maintain under such conditions, and even DNA may be degraded with improper handling. The goal of sample preparation is to maintain nucleic acid integrity and make the target genetic information available for interaction with the probe. For some applications, the requirement of target integrity will dictate immediate snap freezing or addition of lysis buffers containing potent RNase and DNase inhibitors. In other applications, more routine methods of sample collection will allow adequate target preservation.

The physical and chemical similarities of nucleic acids, regardless of source, allows for uniform methods of extraction and purification. For many assays, it is preferable to extensively purify DNA or RNA to remove inhibitors of enzymes to be added to the assay (e.g., a restriction enzyme or polymerase) and to maximize accessibility of the target to the probe. Complete purification schemes, however, are time-consuming and require a relatively large amount of starting sample. In many applications, relatively abbreviated sample purifications can be used. Purifications commonly use cell lysis (mechanical, chemical, or both), protease treatment, and organic or inorganic extractions. Automated methods standardize and streamline sample extraction.

Controlled Conditions Permissive for Complementary Base Pairing

The sensitivity and specificity of the hybridization reaction are greatly influenced by the physical-chemical environment during the reaction and subsequent detection/collection of hybrid molecules. In practice, the hybridization cocktail is the medium used to control the environment of the hybridization reaction. Empirically designed, the *hybridization cocktail* is a mixture of reagents selected to favor interaction of nucleic acids through sequence-specific hydrogen bonds rather than via charge. The components vary widely but include buffers, salts, denaturants such as formamide, high-molecular-weight polymers, carrier DNA or RNA, and various components added to reduce background (such as detergents, bovine serum albumin, Ficoll). Such a complex mixture is conveniently referred to as a *cocktail*. The ionic strength of both the hybridization cocktail and subsequent washes is most often modulated by the concentration of a saline sodium citrate (SSC) buffer, composed of 0.15 mol/L sodium chloride, 0.015 mol/L trisodium citrate, pH 7.0. The shorthand notation for these conditions refers to the strength of SSC—that is, 2 × SSC, 0.1 × SSC. The final stringency of the hybridization reaction is controlled by the formamide and salt concentration of the hybridization cocktail, the temperature of the hybridization reaction, and the temperature and salt concentration of the washing steps.

Detection of Hybrids

A wide variety of techniques have been applied to collection and analysis of specific nucleic acid hybrids, discussed briefly later under Hybridization Assay Formats. Once specific hybrids have been collected, methods of detection are obviously linked to methods of labeling. The first methods used radioactive labels such as phosphorus-32 (^{32}P), iodine-125 (^{125}I), sulfur-35 (^{35}S), carbon-14 (^{14}C), and tritium (^{3}H) that were detected through autoradiography or scintillation counting. Because radioactive probes are unstable due to their relatively short half-life, are hazardous to laboratory personnel, and generate expensive waste disposal problems, they have been replaced by nonradioactive methods. Nonisotopically labeled probes are stable reagents, greatly facilitating the commercial production and standardization that are crucial for assay reproducibility.

Nonisotopic labeling and detection methods for nucleic acids have many similarities to immunochemical assays developed for nonisotopic protein detection. In some applications, nucleic acids are directly linked to a signal-generating compound, usually a fluorochrome but occasionally an enzyme. This situation is analogous to immunoassays in which the primary antibody is labeled. More commonly, nucleic acids are indirectly detected in a multistep assay similar in concept to an indirect antibody reaction. Biotin, a commonly used affinity label for immunoassays, was the first affinity label introduced into nucleic acids (Langer et al., 1981). Many other functional groups have been developed as nonisotopic labels, such as bromodeoxyuridine, digoxigenin, and sulfone. Detection is achieved with high-affinity antibodies directed against the functional group or, in the case of biotin, with avidin or streptavidin. The antibody or avidin/streptavidin is linked to a signal-generating enzyme or fluorochrome, functioning like a labeled secondary antibody in an immunohistochemistry reaction. Because affinity labels are detected with large bulky proteins, availability of the label to the detection reagent is a crucial factor in determination of sensitivity. Increasing the number of affinity tags will not necessarily increase the number of detecting molecules that will be bound to the nucleic acid. In addition, because affinity labels are themselves bulky, overincorporation into the nucleic acid molecule can lead to steric hindrance of the hybridization reaction. For these reasons, the specific activity of the affinity label does not directly control the sensitivity of the detection.

One advantage of the indirect detection of affinity labels is that a variety of detection methods can be used for the same label (Fig. 68.10). For example, the affinity label biotin may be detected by binding to avidin linked to an enzyme with subsequent color or chemiluminescent detection, or avidin with a fluorescent tag or a labeled antibiotin antibody. For all nonradioactive methods, the detection portion of the assay is crucial in obtaining optimal sensitivity. Detection reagents with poor background and suboptimal signal generation can mar an effective hybridization reaction. The choice of the enzyme labels (peroxidase vs. alkaline phosphatase), enzyme substrate (colorimetric vs. chemiluminescent), and even source of reagents are critical for optimal results.

HYBRIDIZATION ASSAY FORMATS

A wide variety of hybridization assay formats have been developed, each designed to solve the methodologic problems of the hybridization assay: conditions permitting specific complementary base pairing, a method to

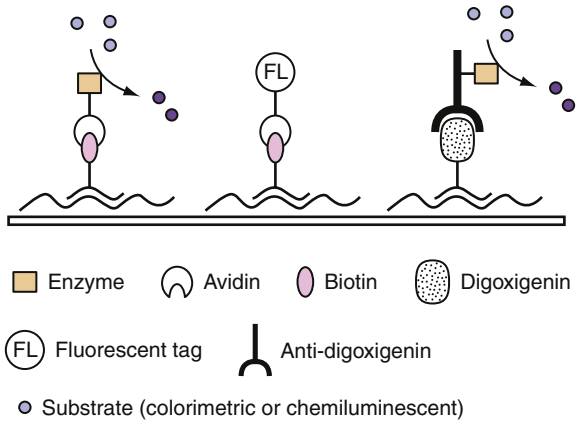

Figure 68.10 Examples of affinity-labeled probe detection systems. Dark purple circles in the first and third complexes are products of the enzyme-catalyzed reaction. (*From Unger ER, Piper MA: Nucleic acid biochemistry and diagnostic applications. In Burtis CA, Ashwood ER, editors:* Tietz textbook of clinical chemistry, *ed 2. Philadelphia, 1994, WB Saunders, with permission.*)

detect hybrids, and interpretation of the result. Each method has particular strengths and weaknesses, and the clinical setting and particular diagnostic question dictate selection of format. There is no one perfect assay. Several of the basic formats are briefly described herein, along with their particular strengths and weaknesses.

Each hybridization assay requires both positive and negative controls for validation. A positive sample control is one known to contain sequences complementary to the probe. This is used to establish that sample preparation is adequate to release the target for the hybridization assay and to ensure that the probe will hybridize with the specific target under the assay conditions. The sample control may also be used to monitor the sensitivity of the assay if the positive control is chosen near the lower limits of detection. A negative sample control (i.e., one known not to contain sequences complementary to the probe) is used to monitor specificity of the probe target interactions. Controls for the probe include vector sequences or unrelated probes labeled, hybridized, and detected under identical assay conditions. These latter controls allow monitoring of the background signal generated by localization of the probe through nonhybridized interactions, such as charge or trapping. In clinical practice, additional controls may be employed to monitor each step of the hybridization assay.

Liquid or Solution Phase Hybridization

In liquid hybridization assays, both the sample and probe interact in solution, which maximizes the kinetics of the reaction. The sample nucleic acids are generally purified from contaminating proteins and lipids, which could interfere with the collection of hybrids at the end of the assay, and some sample degradation is tolerated by the assay. The sample is denatured and randomly sheared before addition of a single-stranded probe lacking the ability to self-hybridize.

Hybridization may be detected by the specific binding of hybrids to a solid matrix such as hydroxyapatite, which binds only duplex structures. Once hybrids are bound, unhybridized probe may be efficiently removed by washing. Detection of the label on the bound probe permits quantitation of the hybridization reaction. In a variation of this approach, one commercial assay (Digene Hybrid-Capture, Qiagen USA, Valencia, CA) uses an antibody specific for RNA-DNA hybrids to specifically bind duplex structures formed of the DNA target and RNA probe. An alternative analysis involves digestion of the hybridization reaction mixture with S1 nuclease, an enzyme that acts only on single-stranded nucleic acid. Duplex structures resistant to digestion may then be precipitated by treatment with trichloroacetic acid. In the hybridization protection assay, label on the probe is protected from chemical degradation only when the probe is involved in a duplex structure.

Optimal kinetics, toleration for abbreviated purification steps, and some sample degradation make the assay adaptable for clinical application. Quantitation of the reaction product may be achieved depending on the detection system. The solution phase format does not permit identification of the size of the hybridizing product. Low positive reactions are difficult to interpret because low levels of specific target and high levels of weakly cross-reacting target will yield similar results. Solution phase hybridization is adaptable to the 96-well format with an enzyme-linked immunosorbent assay–type readout, and increasing automation and miniaturization of the assay using microfluidic devices can be anticipated.

Solid-Support Hybridization

Variations of the solid-support hybridization assays include dot or linear array hybridization, Southern and northern hybridization, microarray hybridizations ("DNA chips" or "bead arrays"), and in situ hybridization. In these assays, the hybridization occurs in a biphasic environment—a solid phase (usually sample) and a liquid phase (usually probe). The kinetics of hybridization to a nucleic acid bound to a solid support is greatly slowed, and the extent of the hybridization reaction is limited. These disadvantages are often outweighed by the convenience of having a solid medium to carry through multiple steps of the assay.

Dot or Linear Array Hybridization

In this assay format, multiple samples are immobilized in a geometric array on a nitrocellulose or nylon membrane. The name of the assay comes from the shape of each sample on the membrane. The solid matrix allows multiple samples to be processed through all steps of the assay simultaneously. The fact that all samples and controls are exposed to exactly the same reagents and conditions increases the standardization of the assay.

The extent of sample preparation varies from complete purification of nucleic acids before application to the filter, to direct application of unpurified sample. Some degree of sample degradation is tolerated by the assay. Purified nucleic acids have the advantage of being most available for interaction with the probe and having the least problems with background. Individual sample purification, however, is time-consuming and labor-intensive. Applications using direct application of unpurified sample take the entire array through an abbreviated purification procedure, which usually involves lysis and denaturation, protein digestion, and washing with detergent. The advantages of this approach are that it is applicable to small amounts of starting material and minimizes sample preparation time. However, the final sensitivity of the reaction is lower, and background from nonspecific probe interactions can make the assay unreliable.

Interpretation of the results of a dot/blot hybridization assay is relatively straightforward. If hybridization has occurred, a signal is generated in the specified spot. Depending on the label used for signal generation, results may be quantitated. However, usually a simple yes/no interpretation is given (i.e., the sample has more or less signal than adjacent samples and known positive and negative controls). Weak signals, which may result from a very small amount of specific target or from a large amount of weakly cross-reacting target, may cause problems in interpretation. No information is available about the size of the hybridizing fragments.

The reverse line blot assay is an important variation in which the sample is tested with many different probes. In this format, the sample carries the label into the assay and the unlabeled probes, or targets, are fixed to the solid support in a linear or matrix array. Areas of specific hybrid formation are identified and interpreted as in the standard dot assay. This assay format is a convenient means of identifying the product of an amplification assay (see later discussion and Chapter 69), such as in human leukocyte antigen analysis (Bugawan et al., 1994) or human papillomavirus typing (Gravitt et al., 1998).

Southern and Northern Hybridizations

Both Southern and northern hybridizations combine electrophoretic separation of test nucleic acid with transfer to a solid support and subsequent hybridization. Therefore, these assays not only give information about the presence of hybridization but also permit determination of the molecular weight of the hybridizing species.

The original procedure was termed *Southern blot hybridization* or *Southern blotting*, after its inventor, E. M. Southern (Southern, 1975). In this assay, the sample is DNA. Northern blotting was named by analogy for the technique using RNA samples. Sample preparation is time-consuming and labor-intensive for both of these techniques. Degradation of sample nucleic acids is not tolerated by the assays, and a relatively large amount of starting material is required. For Southern hybridizations, the DNA must be purified with minimal shearing. This is because sizing of the DNA fragments is achieved through digestion with one or more restriction enzymes. Shearing and degradation introduce random breaks in the sample, reducing the quantity available to be specifically cut at appropriate restriction enzyme recognition sequences. Impurities in the sample may interfere with the activity and sequence specificity of the restriction enzyme. Partially or improperly digested samples can produce spurious band sizes or result in such a reduced concentration of the specific band that it is no longer detected during hybridization. For northern hybridizations, the starting material is RNA, and extreme care must be taken to avoid degradation during sample collection and preparation because of the ubiquitous nature of RNases. RNA is composed of fragment sizes determined by transcription and processing of message and ribosomal RNA. It is not digested before electrophoresis but is separated under denaturing conditions to remove secondary structure.

The size-separated fragments in the agarose gel are then transferred to a nylon or nitrocellulose filter. As originally designed, the transfer occurred passively through capillary action, but vacuum or pressure can be used to speed the transfer. After transfer, baking or UV cross-linking immobilizes the nucleic acids, and the entire membrane is hybridized with a labeled probe, followed by detection to identify bands containing sequences complementary to the probe. Interpretation involves both detection and determination of the molecular weight of the hybridizing molecule. These technically demanding assays require several days to perform but were used in clinical laboratories before amplification methods were refined sufficiently to replace them.

Microarray Hybridization ("DNA Chip Technology" or "Bead Arrays")

Microarray hybridizations can be thought of as a variation of the dot blot format, in which the dotted material is arranged in a regular grid-like pattern, with each feature reduced to a very small size so that hundreds to thousands of features can be placed on one solid surface, currently most often a glass microscope slide. By convention in these applications, the sample is labeled and the arrayed features are referred to as *probes*. Microarrays allow

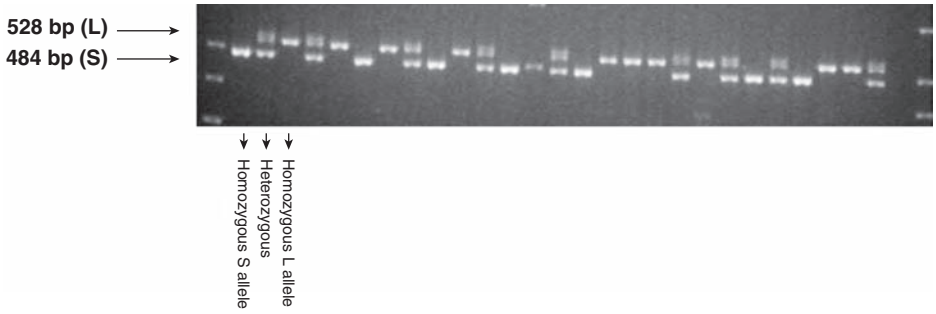

Figure 68.11 Example of polymorphism analysis by gel electrophoresis (allelic typing of the serotonin transporter gene [*5-HTTLPR*]). A polymorphism consisting of a 44-bp insertion/deletion polymorphism in the 5′ regulatory region is suggested to be associated with major depressive disorder. The presence of the two different alleles can be screened using PCR primers upstream and downstream of the site, producing fragments of distinct length. The amplicons are then separated by gel electrophoresis and stained with ethidium bromide. An individual is either homozygous for the long version (L allele = upper band), heterozygous with both alleles (two bands), or homozygous for the short version (S allele = lower band). *PCR,* Polymerase chain reaction. (*Photo courtesy Dr. I. Dimulescu and Dr. M. Rajeevan.*)

genome-wide transcription profiling or sequence determination in a single experiment. Probes can also be bound to microbeads coded by embedded fluorescence and detected with flow techniques, similar to bead-based immunoassays. The technique and applications are described in greater detail in Chapter 70.

In Situ Hybridization

In situ hybridization is simply detection of specific genetic information within a morphologic context. This specialized type of solid-support assay involves taking morphologically intact tissue, cells, or chromosomes affixed to a glass microscope slide through the hybridization process. Autoradiographic, colorimetric, and fluorescent methods of detection have been applied. Evaluation of the final product is very analogous to evaluation of immunohistochemistry and requires experience in histopathology. The strength of the method lies in linking microscopic morphologic evaluation with detection of hybridization.

The method also has applications in cytogenetic analysis of metaphase chromosome spreads or of interphase nuclei (see Chapter 71). In this context, the detection is usually fluorescent, and the technique is referred to as FISH. Detecting numerical aberrations or translocations of chromosomal regions can be achieved rapidly using probes for specific targets. FISH avoids some of the difficulties of conventional cytogenetics and may have greater sensitivity for some targets. Although FISH cannot completely replace karyotyping, it can complement and reduce the need for the frequency of cytogenetic analysis. Newer variations of FISH (Luke & Shepelsky, 1998) are exploiting the possibilities of automation (fast-FISH) and expanding the information that can be obtained in a single assay. FICTION (fluorescence immunophenotyping and interphase cytogenetics as a tool for investigation of neoplasms) combines immunophenotyping with FISH; fiber FISH makes it possible to simultaneously detect and map chromosomal breakpoints. In situ hybridization can be very labor-intensive and tedious. Recent improvements resulting in automated processing of slides through the assay hold much promise for more widespread adoption of this technique.

AMPLIFICATION METHODS

It is virtually impossible to read any medical journal without encountering at least one application of PCR technology. The PCR has forever changed the scope of research questions that can be addressed by virtually eliminating the problem of limited sample size. The importance and elegance of the concept has been recognized through awarding of the Nobel Prize in Chemistry to its inventor, Kary Mullis, less than 10 years after publication of the first practical application of PCR (Saiki et al., 1985). There are now other methodologies that result in multiplication of target, probe, or signal. These may be grouped together as amplification technologies and are described in Chapter 69.

A unique hybrid amplification approach that combines PCR (see Chapter 69) and flow cytometry (see Chapter 35) is xTAG technology (Luminex Corp, Austin, TX). This represents a next-generation form of multiplexing that overcomes the resolution limits of multiplex PCR by combining the methods of multiplex amplification with particle-based flow cytometry. Like multiplex PCR, multiple reactions can be carried out in a single reaction. However, because of the added flow component, many more tests can be run and resolved at the same time.

Using a viral panel as an example, after obtaining a biological sample, the mRNA is reverse transcribed to cDNA. The cDNA is then amplified using a panel of primers that can specifically amplify many different pathologic/pathogenic nucleic acid sequences at the same time. Each pathogen-specific primer used is tagged with a unique oligonucleotide sequence (called the *tag*) as well as a fluorophore. After the multiplex amplification step is completed, the reaction is mixed with microscopic beads that are internally tagged with varying amounts of fluorescent molecules at the time of production. Each different type of bead is also labeled with a unique oligonucleotide sequence that is complementary to the unique tag on the pathogen-specific primer (called the *anti-tag*). If both the tag and the anti-tag are present, then hybridization occurs, binding the fluorophore-labeled amplicon to its appropriate fluorophore-labeled bead. The beads are then processed and placed in a special flow-enabled luminometer equipped with 2 lasers for reading. The first of the 2 lasers identifies the bead based on its internal dye content and the second laser detects how much, if any, tagged amplicon is bound to its surface (Merante et al., 2007). This technology allows for the resolution of 100 or more tests from one sample at one time in one tube. It is adaptable to perform tests on nucleic acids, peptides, and proteins in a variety of sample matrices.

POLYMORPHISM DETECTION ASSAYS

Although greater than 99% of the human genome is identical in all individuals, there are still millions of regions in which there is some variability in DNA sequence among individuals. While polymorphisms are not always associated with a recognized functional consequence, changes in promoter or enhancer regions may result in altered transcription regulation, cause variation in the mRNA splice products if present in intron-exon junctions or produce altered amino acid sequences if an exon is affected. The serotonin transporter gene, for instance, exists in two alternative allelic variants characterized by a 44-bp insertion/deletion polymorphism in the promoter region. This polymorphism has been associated with major depressive disorders (see Chapter 73), and the two allelic versions can be distinguished by PCR amplification of the relevant DNA region, resulting in two different-sized products (Fig. 68.11). Most of the variations occur in the form of an individual base change known as *single-nucleotide polymorphisms* (*SNPs*). An example would be the alteration of a DNA fragment ACGT to ACTT by replacement of the third base from a guanine to a thymine. Two unrelated individuals will have approximately 3 million SNPs that differ between them.

The method used to assess such restriction fragment length polymorphism (RFLP) analysis includes restriction endonuclease digestion of DNA and subsequent gel electrophoretic separation of the resulting fragments. This technique allows the study of such polymorphisms that occur in the DNA sequences between individuals of the same species. These variances can occur in the form of differing numbers of small sequence repeats of DNA—called tandem repeats, minisatellites, and microsatellites—that are normally found in the noncoding regions of DNA. Polymorphisms can occur as a result of mutations—deletions, inversions, additions, substitutions, and translocations—to the DNA sequence.

Briefly, DNA is carefully isolated (to cause as little degradation and mechanical fragmentation as possible) and then digested with a particular endonuclease. The digested DNA is electrophoretically separated in an agarose gel. At this point, the separated DNA samples can be viewed using DNA binding dyes, such as ethidium bromide, to compare the banding patterns. Alternatively, the DNA fragments can be Southern blotted (see earlier discussion), hybridized with labeled probes, and then analyzed.

Therefore, if one were to digest DNA from 2 individuals (excluding identical twins and clones) and separate the resulting fragments by gel electrophoresis, some differences may be found in the 2 resulting banding patterns because of the differing number of tandem repeats between restriction sites from one individual to another. Analysis of the banding of an individual yields what is commonly known as a "genetic fingerprint." Using RFLP analysis, one may also observe a difference in the RFLP patterns between normal and diseased tissue (i.e., tumor) from the same individual. If a tumor arises from a genetic alteration (mutation), that alteration may lead to in a change in the size of one or more bands as a result of

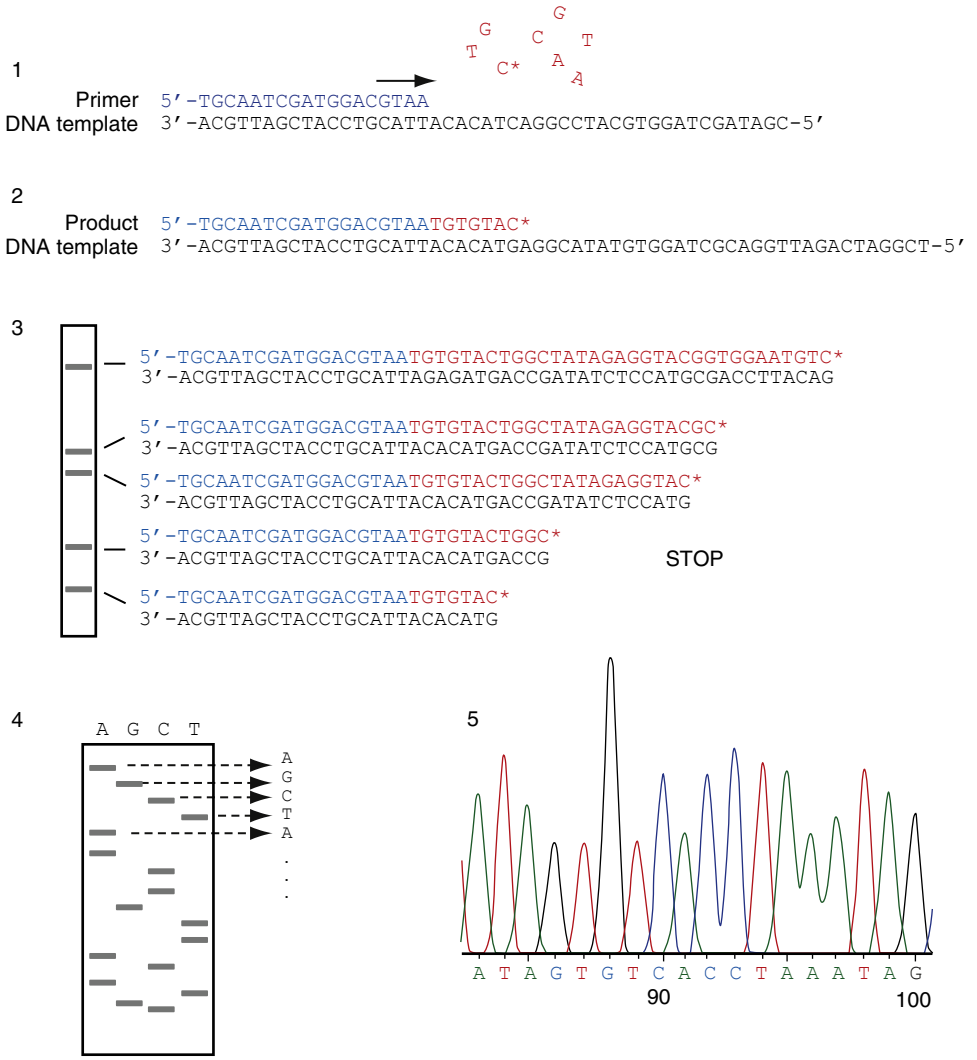

Figure 68.12 Principle of the Sanger DNA sequencing method. (1) A short primer *(in blue)* is annealed to a known sequence in the DNA template. In the presence of the four "usual" deoxynucleotides (dATP, dCTP, dGTP, dTTP) and an additional dideoxynucleotide at a low concentration, here ddCTP *(marked with an asterisk)* DNA polymerase initiates synthesis. (2) When ddCTP is incorporated, further polymerization cannot occur because it lacks the 3′-OH group required to accommodate another nucleotide (see Fig. 68.1) and the chain is terminated. (3) Random incorporation of ddCTP generates a series of DNA strands of different sizes, all ending at "C." These products start with the same primer sequence and are sized by electrophoresis to determine the position of each "C." (4) Dividing the reaction into four tubes, each with a different dideoxynucleotide, and electrophoresing all four reactions in parallel allow the complete sequence to be read from the order of the bands in each of the ladders of each lane. The example shown is not for the preceding example in the chain elongations in parts 1-3 above. (5) Most current applications use fluorescently tagged ddNTPs, each with a different-color dye. With this approach, the reaction is in a single tube and products are separated in a single lane. A laser is used to record the wavelength and order of the bands. A typical fluorescence scan is shown in this figure.

additions or deletions of DNA. In addition, single-nucleotide alterations may be observable via RFLP analysis if the alteration occurs within the sequence of just one of the endonuclease restriction sites, rendering that particular site unrecognizable to and uncut by the enzyme, which ultimately changes the banding pattern.

Because of the tremendous potential of polymorphism assays to predict inheritance of altered alleles and changes that predict drug interactions (see Chapter 75), considerable effort has been made in recent years to improve the speed, precision, and cost-effectiveness of these methods. The completion of the Human Genome Project in 2001 provided a reference against which all other sequencing data can be compared. Researchers are also systematically screening the genome to discover new SNPs. High-throughput SNP analysis methods have been developed that simultaneously scan thousands of SNPs in thousands of samples. Comprehensive mapping of an individual's SNP pattern is termed *genotyping*. Genotyping is somewhat easier, in that one form of the known gene sequence (allele) can be compared with an alternative form at a specific predetermined site. Currently, there are a wide variety of approaches for allelic discrimination that typically use a combination of molecular techniques (Chen & Sullivan, 2003; Bluth & Bluth 2018).

DNA SEQUENCING

The first methods for directly determining the base sequence of DNA became available in the 1970s. Until recently, almost all sequencing was based on the Sanger method, which utilizes enzymatic incorporation of chain terminating dideoxynucleotides (Fig. 68.12). Originally prohibitively time-consuming and expensive for diagnostic applications, automation and miniaturization have resulted in instrumentation capable of more rapidly and less expensively sequencing segments of DNA. Sequencing the first human genome was completed by the Human Genome Project in 2001 using the Sanger method.

The rapidly evolving field of next-generation sequencing (NGS) has produced a variety of different platforms and sequencing chemistries that allow extremely-high-throughput sequencing based on massively parallel sequencing in flow cells (Voelkerding et al., 2009; see Chapter 80). Consequently, NGS technology has revolutionized genomic research through increased throughput and decreased costs. It is now becoming possible to sequence an entire genome at a turnaround time acceptable for clinical applications. Currently, the diagnostic clinical utility of a complete human genome sequence is still being evaluated, but the knowledge of genetic and genomic sequence alterations has great potential to impact clinical pathology. Direct sequencing is being used to determine viral types (e.g., human papillomavirus), bacteria, and other pathogens. The greatest advances are being made in cancer oncology to identify key mutations in oncology (e.g., *BRCA1* and *BRCA2*), to define the causes of inherited diseases, and to use genome-wide mutation profiles for individualized medicine, care, and treatment. Further explorations of how to use an individual's genome for clinical management are underway (Ashley et al., 2010). NGS methods can also be applied to evaluate the transcriptome and are beginning to rival microarray technology in many applications.

PYROSEQUENCING

Pyrosequencing is a method of DNA sequencing based on sequencing by the principle of synthesis (Ahmadian, 2006). First, a sequencing primer is hybridized to a single-stranded DNA template in the presence of the enzymes DNA polymerase, adenosine triphosphate (ATP) sulfurylase, luciferase, and apyrase, and the substrates adenosine 5′ phosphosulfate (APS) and luciferin (Fig 68.13A) (Nyrén, 2007).

The first of 4 deoxynucleoside triphosphates (dNTPs) are then added to the reaction and DNA polymerase incorporates it only if it is complementary to the base in the template strand. Each incorporation event is

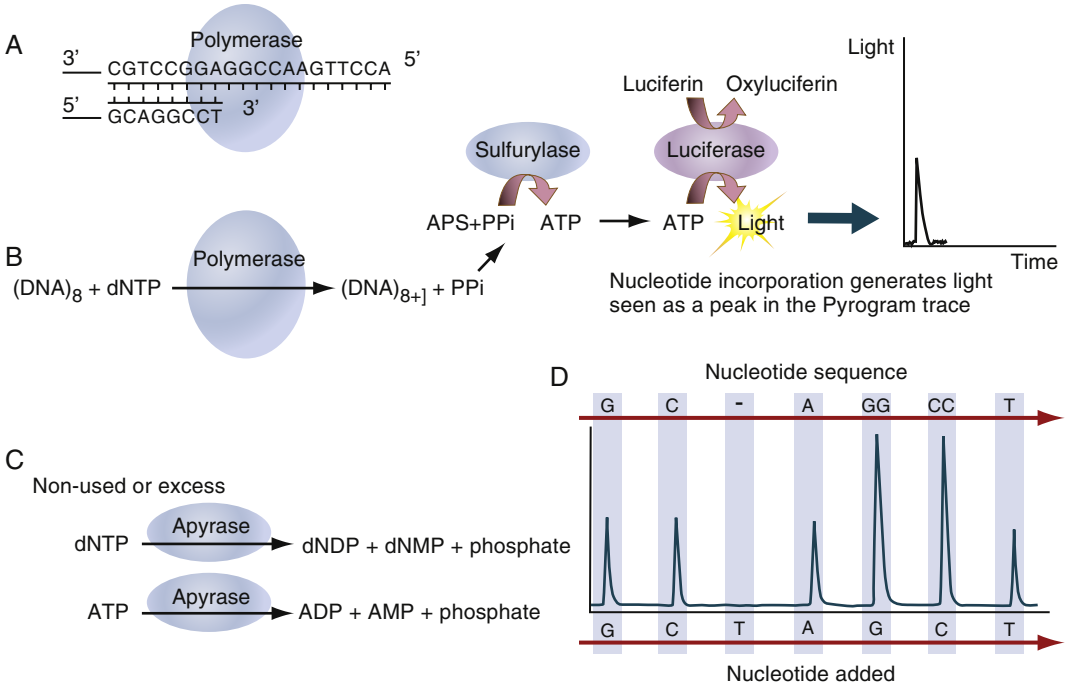

Figure 68.13 Stepwise illustration of the pyrosequencing method. The enzyme cascade of pyrosequencing technology. **A,** Incorporation of a nucleotide by polymerase. **B,** The conversion of the released PPi to light by enzymatic cascade followed by detection of the generated light by CCD sensors and represented as a peak in the raw data output. **C,** Continuous degradation of unincorporated nucleotides and ATP by apyrase. **D,** Representation of sequence quantitative decoding according to the sequential addition of nucleotides and the intensity of light, represented by the height of each peak, which is proportional to the number of nucleotides incorporated. (Modified from Qiagen; image kindly provided by QIAGEN, all rights reserved.)

accompanied by the release of pyrophosphate (PPi) in a quantity equimolar to the amount of incorporated nucleotide (Fig. 68.13B).

ATP sulfurylase quantitatively converts PPi to ATP in the presence of APS. This ATP drives the luciferase-mediated conversion of luciferin to oxyluciferin, which generates visible light in amounts proportional to the ATP generated. The light produced in the luciferase-catalyzed reaction is detected by a charge-coupled device camera and seen as a peak in a pyrogram. The height of each peak is proportional to the number of a specific nucleotide incorporated (Fig. 68.13C).

Apyrase, a nucleotide degrading enzyme, continuously degrades ATP and unincorporated dNTPs. Apyrase switches off the light-promoting reaction and regenerates the reaction solution. The next dNTP is then added (Fig. 68.13D). The addition of dNTPs is performed one at a time (G, then C, then T, then A, then G, then C, then T, and so on). As the process continues, the cDNA strand is built up and the nucleotide sequence is determined from the signal peaks in the pyrogram. Deoxyadenosine α-thiotriphosphate is used as a substitute for dATP because it is used efficiently by DNA polymerase but is not recognized by luciferase.

RELATIONSHIP TO LABORATORY EVALUATION OF DISEASE

Subsequent chapters describe the current applications of molecular diagnostics. It is clear that these new technologies have impacted all areas of laboratory diagnosis. Molecular methods also have the potential to redefine laboratory evaluation of disease to include issues beyond disease diagnosis.

MOLECULAR DIAGNOSIS

The advantages of a molecular approach to diagnosis are described in detail for each aspect of current application. Increased automation and commercially designed methods have reduced costs and the level of technical expertise required to perform the tests. Increasingly, molecular technology is being integrated into the mainstream of laboratory testing.

Detecting mutations and associating them with disease are at the heart of the current explosion of information in medical science and of many applications in molecular diagnostics. One of the most important consequences of the revolution in molecular genetics has been the ability to locate a gene responsible for a disease without knowing the protein product. Termed *positional cloning*, this process uses genomic mapping and linkage analysis of families that carry and express the disease to locate markers increasingly closer to the disease gene until it is ultimately located. Closely linked genomic changes markers that tend to segregate with disease may be used in clinically useful diagnostic tests even before the gene is completely characterized and the protein product finally identified. In this scenario, molecular diagnostic tests are developed and used first, to be replaced by simpler, more cost-effective methods directed at the level of the gene product when the consequence of mutation is fully understood.

BEYOND DIAGNOSIS

Molecular analyses have the potential to greatly expand the role of the laboratory in areas beyond disease diagnosis (Bluth, 2018). Molecular analysis of the somatic mutations in cancer has the potential to provide prognostic information, guide selection of optimal therapy, and monitor response to therapy. The implications of using molecular markers to detect neoplastic cells in the absence of clinical or morphologic evidence of disease, known as *minimal residual disease*, are now being explored in a variety of malignancy types (see Chapter 76). This approach of using molecular markers for disease detection can also be anticipated to impact secondary methods of cancer prevention (screening) and assessment of adequacy of surgical resection (evaluation of margins). Gene therapy for inherited genetic disease as well as cancer is being introduced based on a detailed understanding of the underlying disease. Monitoring these patients for the presence and activity of the introduced therapeutic gene will add another aspect to the laboratory evaluation of disease as the application to personalized medicine continues to develop.

SELECTED REFERENCES

Alberts B, Johnson A, Lewis J, et al.: *Molecular biology of the cell*, ed 6, New York, 2014, Garland Publishing.
An excellent, clearly written textbook of molecular biology. The fourth edition is available in searchable format through the NCBI bookshelf website: http://www.ncbi.nlm.nih.gov/entrez/query.fcgi?db=Books.

Cech TR, Steitz JA: The noncoding RNA revolution—Trashing old rules to forge new ones, *Cell* 157:77–94, 2014.
Review of noncoding RNA.

Fire A, Xu S, Montgomery MK, et al.: Potent and specific genetic interference by double-stranded RNA in *Caenorhabditis elegans*, *Nature* 391:806–811, 1998.
First description of RNAi in animal cells.

Langer PR, Waldrop AA, Ward DC: Enzymatic synthesis of biotin-labeled polynucleotides: novel nucleic acid affinity probes, *Proc Natl Acad Sci U S A* 78:6633–6637, 1981.
First description of affinity-labeled nucleotides that achieved sensitivity of detection required for eventual replacement of radioactive methods.

Papavassiliou AG: Transcription factors, *N Engl J Med* 332:45–47, 1995.
From the "Molecular Medicine" series in the New England Journal of Medicine, a brief review of transcription factors and their importance in medicine.

Rosenthal N: Regulation of gene expression, *N Engl J Med* 331:931–933, 1994.
From the "Molecular Medicine" series in the New England Journal of Medicine, a brief review of the regulation of gene expression and relevance to disease.
Saiki RK, Scharf S, Faloona F, et al.: Enzymatic amplification of β-globin genomic sequences and restriction site analysis for the diagnosis of sickle-cell anemia, *Science* 230:1350–1354, 1985.
Original description of the polymerase chain reaction.
Southern EM: Detection of specific sequences among DNA fragments separated by gel electrophoresis, *J Mol Biol* 98:503–517, 1975.
Original description of electrophoretic separation of DNA fragments, transfer to filter, and hybridization for identification.

Access the complete reference list online at Elsevier eBooks for Practicing Clinicians.

REFERENCES

Ahmadian A, Ehn M, Hober S: Pyrosequencing: history, biochemistry and future, *Clin Chim Acta* 363(Issues 1–2):83–94, January 2006.

Aleksandrova K, Romero-Mosquera B, Hernandez V: Diet, gut microbiome and epigenetics: Emerging links with inflammatory bowel diseases and Prospects for management and prevention, *Nutrients* 30(9):9, 2017 Aug, https://doi.org/10.3390/nu9090962. pii: E962.

Ashley EA, Butte AJ, Wheeler MT, et al.: Clinical assessment incorporating a personal genome, *Lancet* 375:1525–1535, 2010.

Beaudet AL: Epigenetics and complex human disease: is there a role in IBD? *J Pediatr Gastroenterol Nutr* 46:E2, 2008.

Bluth MH: Introduction: molecular medicine in the common Era: applications and impact of molecular pathology in health and disease, *Clin Lab Med* 38:209–213, 2018.

Bluth MJ, Bluth MH: *Clin Lab Med* 38:215–236, 2018.

Bugawan TL, Apple R, Erlich H: A method for typing polymorphism as the HLA-A locus using PCR amplification and immobilized oligonucleotide probes, *Tissue Antigens* 44:137–147, 1994.

Chen X, Sullivan PF: Single nucleotide polymorphism genotyping: biochemistry, protocol, cost and throughput, *Pharmacogenomics J* 3:77–96, 2003.

Fica SM, Tuttle N, Novack T, et al.: RNA catalyses nuclear pre-mRNA splicing, *Nature* 503:229–234, 2013.

Gravitt PE, Peyton CL, Apple RJ, et al.: Genotyping of 27 human papillomavirus types by using L1 consensus PCR products by a single-hybridization, reverse line blot detection method, *J Clin Microbiol* 36:3020–3027, 1998.

Hanawalt PC: Transcription-coupled repair and human disease, *Science* 266:1957–1958, 1994.

Iorio MV, Croce CM: MicroRNAs in cancer: small molecules with a huge impact, *J Clin Oncol* 27:5848–5856, 2009.

Kan YW: Development of DNA analyses for human diseases: sickle cell anemia and thalassemia as paradigm, *J Am Med Assoc* 267:1532–1536, 1992.

Liechti-Gallati S, Koenig M, Kunkel LM, et al.: Molecular deletion patterns in Duchenne and Becker type muscular dystrophy, *Hum Genet* 81:343–348, 1989.

Luke S, Shepelsky M, FISH: Recent advances and diagnostic aspects, *Cell Vis* 5:49–53, 1998.

Merante F, Yaghoubian S, Janeczko R: Principles of the xTAG respiratory viral panel assay (RVP Assay), *J Clin Virol* 40(S31–5), 2007.

Moazed D: Small RNAs in transcriptional gene silencing and genome defence, *Nature* 457:413–420, 2009.

Mochizuki K, Hariya N, Honma K, Goda T: Relationship between epigenetic regulation, dietary habits, and the developmental origins of health and disease theory, *Congenit. Anom*, 2017https://doi.org/10.1111/cga.12213.

Modrich P: Mismatch repair, genetic stability, and cancer, *Science* 266:1959–1960, 1994.

Nyre´n P: The history of pyrosequencing, *Methods Mol Biol* 373:1–14, 2007.

Pingoud A, Jeltsch A: Structure and function of type II restriction endonucleases, *Nucleic Acids Res* 29:3705–3727, 2001.

Radman M, Wagner R: The high fidelity of DNA duplication, *Sci Am* 259:40–46, 1988.

Sancar A: Mechanisms of DNA excision repair, *Science* 266:1954–1956, 1994.

Sethi S, Sethi S, Bluth MH: Clinical implication of MicroRNAs in molecular pathology: an Update for 2018, *Clin Lab Med* 38(2):237–251, 2018 Jun, https://doi.org/10.1016/j.cll.2018.02.003. Review.

Sharp PA: RNA splicing and genes, *J Am Med Assoc* 260:3035–3041, 1988.

Sutherland GR, Richards RI: Dynamic mutations, *Sci Am* 82:157–163, 1994.

Virshup DM: DNA replication, *Curr Opin Cell Biol* 2:453–460, 1990.

Voelkerding KV, Dames SA, Durtschi JD: Next-generation sequencing: from basic research to diagnostics, *Clin Chem* 55:641–658, 2009.

Weatherall DJ: Molecular pathology of single gene disorders, *J Clin Pathol* 40:959–970, 1987.

Weeda G, de Boer J, Donker I, et al.: Molecular basis of DNA repair mechanisms and syndromes, *Rec Results Cancer Res* 154:147–155, 1998.

Yu Z, Chen J, Ford BN, et al.: Human DNA repair systems: an overview, *Environ Mol Mutagen* 33:3–20, 1999.

CHAPTER 69

POLYMERASE CHAIN REACTION AND OTHER NUCLEIC ACID AMPLIFICATION TECHNOLOGY

Julie Woolworth Hirschhorn, Cynthia A. Schandl, Frederick S. Nolte

TARGET AMPLIFICATION METHODS, 1387
Polymerase Chain Reaction, 1387
Transcription-Based Amplification, 1393
Strand-Displacement Amplification, 1394
Loop-Mediated Isothermic Amplification, 1395
Helicase-Dependent Amplification, 1397
Nicking Endonuclease Amplification Reaction, 1397
PROBE AND SIGNAL AMPLIFICATION METHODS, 1397
Cleavase/Invader Technology, 1397
Branched DNA, 1399
Hybrid Capture Assays, 1399
SUMMARY, 1399
SELECTED REFERENCES, 1399

KEY POINTS

- Although the polymerase chain reaction is the most mature and widely used nucleic acid amplification method, other methods have diagnostic applications with unique properties and advantages.
- These techniques have analytic sensitivity unparalleled in laboratory medicine, creating new opportunities for the clinical laboratory to impact patient care.
- Clinical applications of the technology cut across the traditional disciplines in laboratory medicine.
- An understanding of the basic principles and relative strengths and limitations of the nucleic amplification methods is important for all involved in the practice of clinical pathology.

TARGET AMPLIFICATION METHODS

Polymerase chain reaction (PCR), transcription-mediated amplification (TMA), strand displacement amplification (SDA), loop-mediated amplification (LAMP), helicase-dependent amplification (HDA) and nicking endonuclease amplification (NEAR) are all examples of target amplification methods used in clinical laboratories. These methods share certain fundamental characteristics. They are enzyme-mediated processes in which a single enzyme or multiple enzymes synthesize copies of target nucleic acid. The amplification products in all of these techniques are defined by oligonucleotide primers that bind to complementary sequences on opposite strands of double-stranded targets. All result in the production of millions to billions of copies of the targeted sequence in a matter of hours and, in each case, the amplification products can serve as templates for subsequent rounds of amplification. Consequently, all techniques are sensitive to contamination with product molecules from previous amplifications, which can lead to false-positive reactions. However, special laboratory design, practices, and workflow have been developed to reduce the possibility of false-positive reactions to acceptable levels.

POLYMERASE CHAIN REACTION

The development of PCR by Mullis and colleagues (Saiki et al., 1985; Saiki et al., 1988) was a milestone in biotechnology that heralded the beginning of molecular diagnostics. PCR is a simple in vitro chemical reaction that permits the synthesis of essentially limitless quantities of a targeted nucleic acid sequence. This is accomplished through the action of a deoxyribonucleic acid (DNA) polymerase that, under the right conditions, can copy a strand of DNA. At its simplest, a PCR consists of target DNA, a molar excess of two oligonucleotide primers, a heat-stable DNA polymerase, an equimolar mixture of deoxyribonucleotide triphosphates (dATP, dCTP, dGTP, and dTTP), $MgCl_2$, KCl, and a Tris-HCl buffer. The two primers flank the sequence to be amplified, are typically 18 to 30 bases long, and are complementary to opposite strands of the target.

To initiate a PCR, the reaction mixture is heated to separate the two strands of target DNA (denaturation) and then cooled to permit the primers to anneal to the target DNA in a sequence-specific manner (annealing; Fig. 69.1). The DNA polymerase then initiates extension of each primer at its 3′ end (extension). The primer extension products are dissociated from the target DNA by heating. Each extension product, as well as the original target, can serve as a template for subsequent rounds of primer annealing and extension.

A PCR cycle typically consists of three steps at different temperatures: denaturation, annealing, and extension, although two-step cycling with a combined annealing/extension step is also common in diagnostic assays. When the annealing temperature is close enough to the extension step temperature, these can be combined into a single step to create the two-step cycling. At the end of each cycle, the PCR products are theoretically doubled. Thus after n PCR cycles, the target sequence can be amplified 2^n-fold. The whole procedure is carried out in a programmable thermal cycler that precisely controls the temperature at which the steps occur, the length of time that the reaction is held at the different temperatures, and the number of cycles. Ideally, after 20 cycles of PCR, a million-fold amplification is achieved, and after 30 cycles, a billion-fold. In practice, the amplification may not be completely efficient because of failure to optimize the reaction conditions or the presence of inhibitors of the DNA polymerase. In such cases, the total amplification is best described by the expression $(1 + e)^n$, where e is the amplification efficiency ($0 < e < 1$) and n is the total number of cycles.

After amplification, the products can be detected by various methods, including sequencing or analysis. Gel electrophoresis with intercalating dye staining is a classical method that separates products by size and may be sufficient for some applications. For finer size discrimination, capillary electrophoresis can be used. PCR amplification products can also be accurately sized using mass spectrometry. Alternatively, probe hybridization methods can be used to verify or analyze the reaction product. Closed tube methods, in which the amplified products are never released to the environment, avoid contamination of future reactions with products from prior positive reactions and mitigate problems with false positives. Adding a fluorescent dye or probe before amplification to the reaction mixture allows optical monitoring to follow the accumulation of reaction product as it progresses (real-time PCR) or after the reaction is complete (melting curve analysis) with the need to process the sample for a separate analysis step.

Reverse-Transcriptase Polymerase Chain Reaction

PCR, as it was originally described, was a technique for DNA amplification. Reverse-transcriptase PCR (RT-PCR) was developed to amplify ribonucleic acid (RNA) targets. In this process, complementary DNA (cDNA) is first produced from RNA targets by reverse transcription, and then the cDNA is amplified by PCR. RT-PCR, as originally described, employed

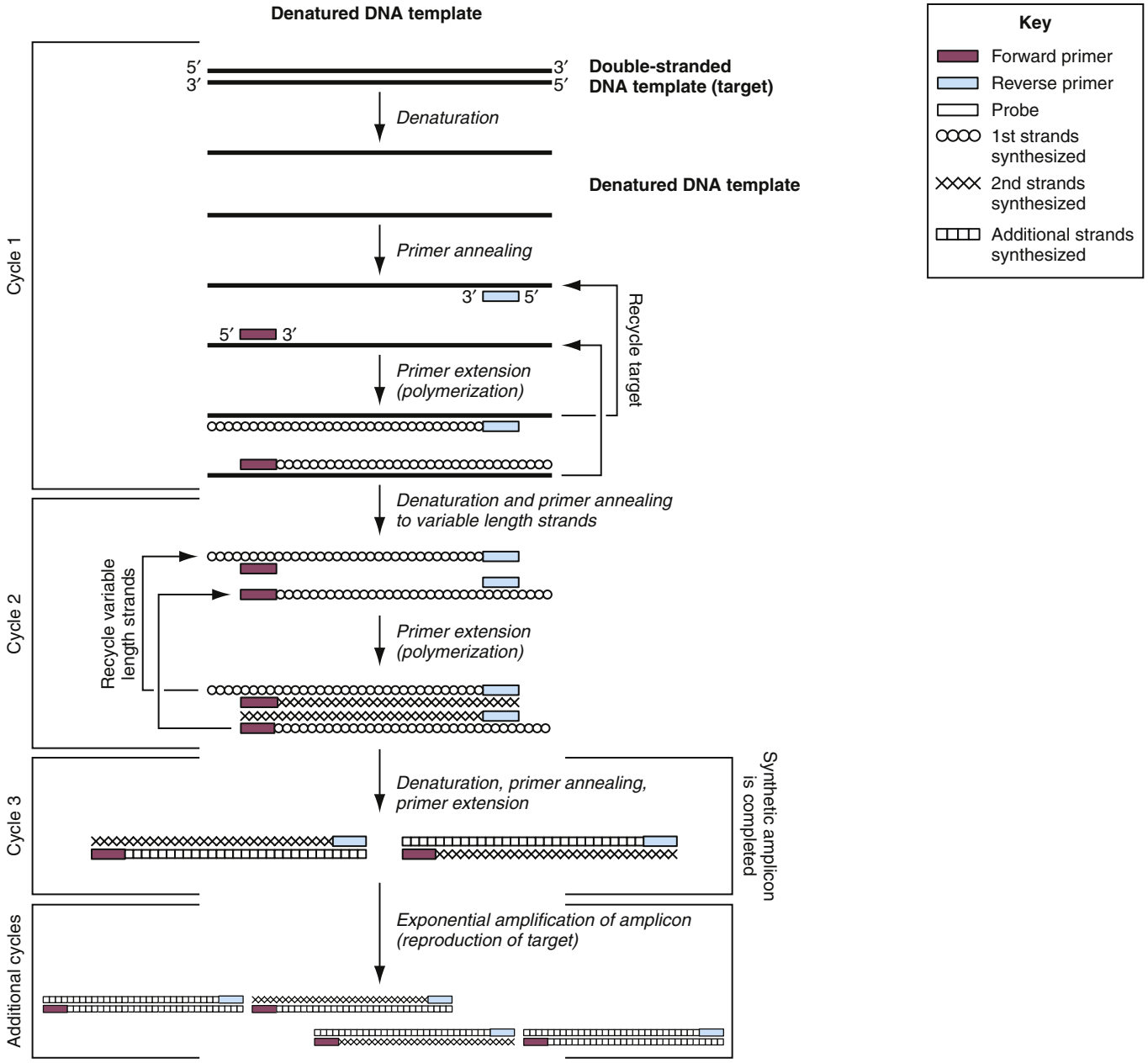

Figure 69.1 Polymerase chain reaction (PCR). (Redrawn from Wolk D, Mitchell S, Patel R: Principles of molecular microbiology testing methods. Infect Dis Clin N Am 15:1157–1204, 2008.)

two enzymes: a heat-labile RT, such as avian myeloblastosis virus reverse transcriptase (AMV-RT), and a thermostable DNA polymerase. Because of the temperature requirements of the heat-labile enzyme, cDNA synthesis had to occur at lower temperatures. This presented problems both in terms of the nonspecific primer annealing and inefficient primer extension due to formation of RNA secondary structures. These problems have been largely overcome by the development of thermostable DNA polymerases derived from *Thermus* spp., which, under the proper conditions, can function efficiently as both an RT and a DNA polymerase (Myers & Gelfand, 1991; Schönbrunner et al., 2006). RT-PCRs using these enzymes are more specific and efficient than previous protocols using conventional heat-labile RT enzymes. Commercially available kits employing this single-enzyme RT-PCR are available for detection of a variety of RNA targets in clinical specimens. RNA targets may present problems due to secondary or tertiary structure that may require special conditions or alternative target sites for efficient cDNA synthesis.

While the single enzyme RT-PCR has improved specificity and efficiency for problematic targets, there remain many applications that use a two-enzyme system. Modified heat-labile RT enzymes and optimized mixtures of reverse transcriptases with improved specificity and efficiency are now commercially available. Performing a separate RT reaction with random sequence primers allows PCR analysis of multiple targets from a single RT reaction. The RT reaction may be performed with oligo-dT primers providing cDNA of the messenger RNAs only. This scheme also allows PCR to be performed for multiple targets from a single RT reaction.

Nested Polymerase Chain Reaction

Nested PCR was developed to increase both the sensitivity and specificity of PCR (Haqqi et al., 1988). It employs two pairs of amplification primers and two successive rounds of PCR. Typically, one primer pair is used in the first round of PCR of 15 to 30 cycles. The products of the first round of amplification are then subjected to a second round of amplification using the second set of primers, which anneal to a sequence internal to the sequence amplified by the first primer set. The increased sensitivity arises from the high total cycle number. The increased specificity arises from the annealing of the second primer set to sequences found only in the first-round products, verifying the identity of the first-round product. In hemi-nested PCR, one of the primers in the second PCR is identical to the first.

The major disadvantage of nested PCR is the high rate of contamination that can occur during the transfer of first-round products to the second tube for the second round of amplification. This can be avoided either by physically separating the first- and second-round amplification mixtures with a layer of wax or oil or by designing closed-tube amplification and detection protocols.

The Cepheid (Sunnyvale, CA) assay for detection of *Mycobacterium tuberculosis* and the *rpoB* gene associated with rifampin resistance (Helb et al., 2010) and the BioFire Diagnostics FilmArray syndromic panels (see following section) use hemi-nested and nested PCR, respectively.

Multiplex Polymerase Chain Reaction

In multiplex PCR, two or more primer sets designed for amplification of different targets are included in the same reaction mixture (Chamberlain et al., 1988). With this technique, more than one target sequence in a clinical specimen can be co-amplified in a single tube. The success of a multiplex PCR reaction is dependent on the design of the specific primers used. It is preferred that primers have similar annealing temperatures and must be noncomplementary to each other to avoid primer-dimers and inefficient reactions. Multiplex PCRs are more complicated to develop and are often less sensitive than single-primer-set PCR reactions, but they allow multiple targets to be detected from a single specimen in one reaction. Multiplex PCR is analyzed by massively parallel sequencing, separating products by size by gel electrophoresis or capillary electrophoresis, by spatial separation on a surface or bead, or by probe color in real-time PCR. Real-time PCR is typically limited to 2 to 6 colors, but greater multiplexing is possible by combining color with the melting temperature of probes. Recent technological advances in decoding highly multiplex PCR reactions are described later. These innovations have led the way to development of large syndromic panels for infectious disease diagnosis (Ramanan et al., 2018).

One of the first highly multiplexed platforms for PCR analysis was the xMAP system (Luminex Corp., Austin, TX). The xMAP system incorporates a proprietary process to internally dye polystyrene microspheres with two spectrally distinct fluorochromes. By using precise ratios of these fluorochromes, an array is created consisting of 100 different microsphere sets with specific spectral addresses. Each microsphere set can possess a different reactant on its surface. For nucleic acid analysis, oligonucleotide probes would be covalently bound to the microsphere surface by carbodiimide coupling. Because each microsphere set can be distinguished by its spectral address, the sets can be combined, allowing up to 100 different analytes to be measured simultaneously in a single reaction vessel. A third fluorochrome coupled to a reporter molecule quantifies the biomolecular interaction that occurs at the microsphere surface.

Microspheres are interrogated individually in a rapidly flowing liquid stream as they pass by two separate lasers in the Luminex xMAP flow cytometer. High-speed digital signal processing classifies each microsphere based on its spectral address and quantifies the reaction on its surface. Thousands of microspheres are investigated per second, resulting in an analysis system capable of analyzing and reporting up to 500 different reactions in a single reaction vessel in a few seconds.

Multiplex assays run on the Luminex platform typically consist of three major steps: nucleic acid amplification by PCR, target-specific extension, and liquid bead array decoding (Merante et al., 2007). After PCR amplification, the amplicons are mixed with a second set of tagged primers specific for each target. If the target is present, the tagged primer will be extended through a process called *target-specific extension*. During this extension, a label is incorporated into the extension product. The color-coded beads are added to identify the tagged and labeled extension products. Attached to each differently colored bead is an oligonucleotide complementary to the tag sequence for each target. Samples are then placed in the Luminex xMAP flow cytometer, where the beads are read by two color lasers. One laser identifies the color of the bead; the other laser detects the presence or absence of a labeled extension product on that bead. U.S. Food and Drug Administration (FDA)–cleared assays for cystic fibrosis mutations, human leukocyte antigen (HLA) testing, respiratory virus and gastrointestinal pathogens, and pharmacogenetics are available from Luminex using this technology.

Luminex also has multiplex assays for respiratory pathogens, enteric pathogens, and identification of Gram-positive and Gram-negative bacteria from positive blood cultures based on Verigene NanoGrid technology (Scott, 2013). In this closed system, nucleic acids are extracted and/or amplified, denatured, and hybridized with target-specific oligonucleotides covalently bound to a glass microarray slide inside the test cartridge. Additional steps include hybridization with mediator oligonucleotides and gold nanoparticle-labeled probes. These bound gold nanoparticle probes are then coated in silver to form silver-enhanced gold nanoparticle aggregates that scatter light with high efficiency. The silver-enhanced gold nanoparticles are detected optically at relative positions on the microarray, using the Verigene Reader.

Another technology for high-order multiplex PCR is the FilmArray developed by BioFire Diagnostics (bioMérieux, Salt Lake City, UT). It is a completely automated, integrated, and self-contained lab-in-a-pouch system (Poritz et al., 2011). The film portion of the pouch has stations for cell lysis, nucleic acid purification, reverse transcription to detect RNA targets, first-stage PCR multiplex PCR, and an array of up to 120 second-stage nested PCRs. After extracting and purifying nucleic acids from the unprocessed sample, the FilmArray performs a nested multiplex PCR that is executed in two stages. During the first-stage PCR, the FilmArray performs a single large-volume, massively multiplexed reaction. The products from the first-stage PCR are then diluted and combined with a fresh, primer-free master mix. Aliquots of this second master mix solution are then distributed to each well of the array. Each well of the array is prespotted with a single set of primers. In the second stage, small-volume PCR is performed in singleplex fashion in each well of the array. Even though this assay uses nested PCR, the entire test is performed within a sealed pouch, eliminating concerns of carryover contamination. Using amplification and melting curve data, the FilmArray software automatically generates a result for each target. FilmArray panels for detection of respiratory, gastrointestinal, and bloodstream and central nervous system pathogens have been cleared for clinical use by the FDA. In addition, a FilmArray for detection of Ebola Zaire virus, as part of a biothreat panel, was given Emergency Use Authorization by the FDA during the 2014 Ebola outbreak.

GenMark Diagnostics (Carlsbad, CA) eSensor technology couples multiplex PCR with solution hybridization to ferrocene-labeled, target-specific signal probes and a microarray of gold-plated electrodes, each coated with different capture probes specific for the targets (Pierce & Hodinka, 2012). Target DNA-signal probe complexes present in the sample hybridize to the capture probes, bringing the ferrocene label in close proximity to the gold electrode. An electrical current is applied to each electrode and a captured DNA target is analyzed by electrochemical detection using voltammetry with a signal of 3 nA or greater for a given analyte considered positive. Panels for respiratory viruses, cystic fibrosis genotyping, thrombophilia risk, and warfarin sensitivity are FDA-cleared panels available on the original semiautomated XT8 system. Other panels not FDA cleared include hepatitis C genotyping and cytochrome P450 2C19 genotyping. The ePlex system automates all aspects of nucleic acid testing, including extraction, amplification, and detection, combining electrowetting and GenMark's eSensor technology in a single-use cartridge. It provides results in less than 2 hours, with minimal hands-on time. FDA-cleared panels for respiratory virus and blood culture identification are available on this system, with central nervous system and gastrointestinal panels in development (Babady et al., 2018). The ePLEX RP2 cartridge can detect a multitude of respiratory pathogens in addition to COVID-19.

Endpoint Quantitative Polymerase Chain Reaction

A linear relationship should exist between the quantity of input template and the amount of amplification product. However, because the final amount of PCR product depends on exponential amplification of the initial quantity of template, minor differences in amplification efficiency may lead to very large and unpredictable differences in the final product yield (Clementi et al., 1993). The tube-to-tube differences may depend on sample preparation and nucleic acid purification procedures, nucleic acid quality (e.g., formalin-fixed tissues), presence of inhibitors, and thermal cycler performance. For these reasons, simple quantification of product accumulated at the end of the reaction and the use of external standard curves do not provide reliable quantification of the amount of the template initially present in the sample.

A variety of PCR-based strategies have been developed to accurately quantify DNA and RNA targets in clinical specimens, but the competitive PCR (cPCR) approach has proved reliable and robust for clinical applications (Gilliland et al., 1990; Piatak et al., 1993). The basic concept behind cPCR is the coamplification in the same reaction tube of two different templates of equal or similar lengths and with the same primer binding sequences. Because both templates are amplified with the same primer pair, identical thermodynamics and amplification efficiency are ensured. The amount of one of the templates must be known; after amplification, products from both templates must be distinguishable.

Endpoint PCR has largely been replaced in the clinical laboratory by homogeneous kinetic (real-time) methods for product detection (see next section). These methods provide for more precise measurements of initial template concentrations because the analysis is performed early in the log phase of product accumulation and, as a result, are less prone to error resulting from differences in sample-to-sample amplification efficiency.

Real-Time (Homogeneous, Kinetic) Polymerase Chain Reaction

Real-time PCR describes methods by which the target amplification and detection steps occur simultaneously in the same tube (homogeneous). These methods require special thermal cyclers with precision optics that can monitor the fluorescence emission from the sample wells. The computer software supporting the thermocycler monitors the data throughout the PCR at every cycle (kinetic) and generates an amplification plot for each reaction. A typical amplification plot is shown in Figure 69.2. The amplification plot shows the normalized fluorescence signal from the reporter (R_n) at each cycle number. In the initial cycles, there is little change in the amount of fluorescence, which defines the baseline of the plot. Detection of accumulated PCR product is indicated by an increase above the baseline. A fixed fluorescence threshold can be set above the baseline to call positive samples. The PCR cycle at which the fluorescence passes the threshold is defined as the *cycle threshold* (C_T). There is an inverse linear relationship between the log of the initial target concentration and the C_T. Alternatively, the cycle number corresponding to the maximal rate change in fluorescence, the second derivative maximum, has a similar relationship to initial target concentration.

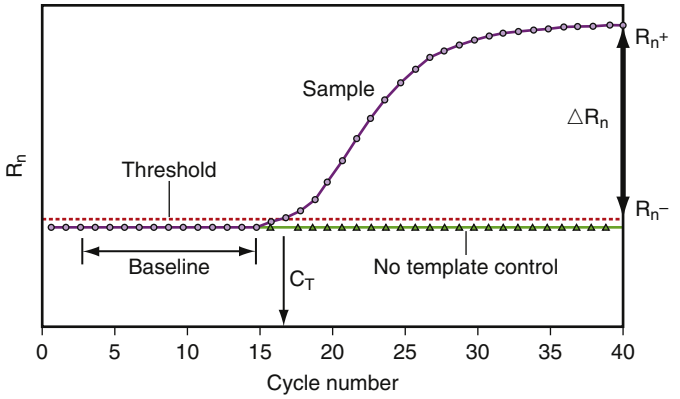

Figure 69.2 Real-time PCR amplification plot. *PCR,* Polymerase chain reaction. (*Courtesy Applied Biosystems.*)

In the simplest format, the PCR product is detected as it is produced using fluorescent dyes that preferentially bind to double-stranded DNA (dsDNA). SYBR Green I is one such dye that has been used in this application (Morrison et al., 1998). In the unbound state, the fluorescence is relatively low, but when bound to dsDNA, the fluorescence is greatly enhanced (Fig. 69.3A). The DNA-binding dye will affix to any dsDNA; therefore, it will bind both specific and nonspecific PCR products equally well. The specificity of the detection can be improved through melting curve analysis.

The specific amplified product will have a characteristic melting peak at its predicted melting temperature (T_m), whereas the primer-dimers and other nonspecific products should have a different T_m or give broader peaks (Ririe et al., 1997).

The specificity of real-time PCR can also be increased by including hybridization probes in the reaction mixtures. These probes are labeled with fluorescent dyes or with a combination of fluorescent and quencher dyes. In the 5′ nuclease (TaqMan) PCR assay, the 5′ to 3′ exonuclease activity of Taq DNA polymerase is used to cleave a nonextendable

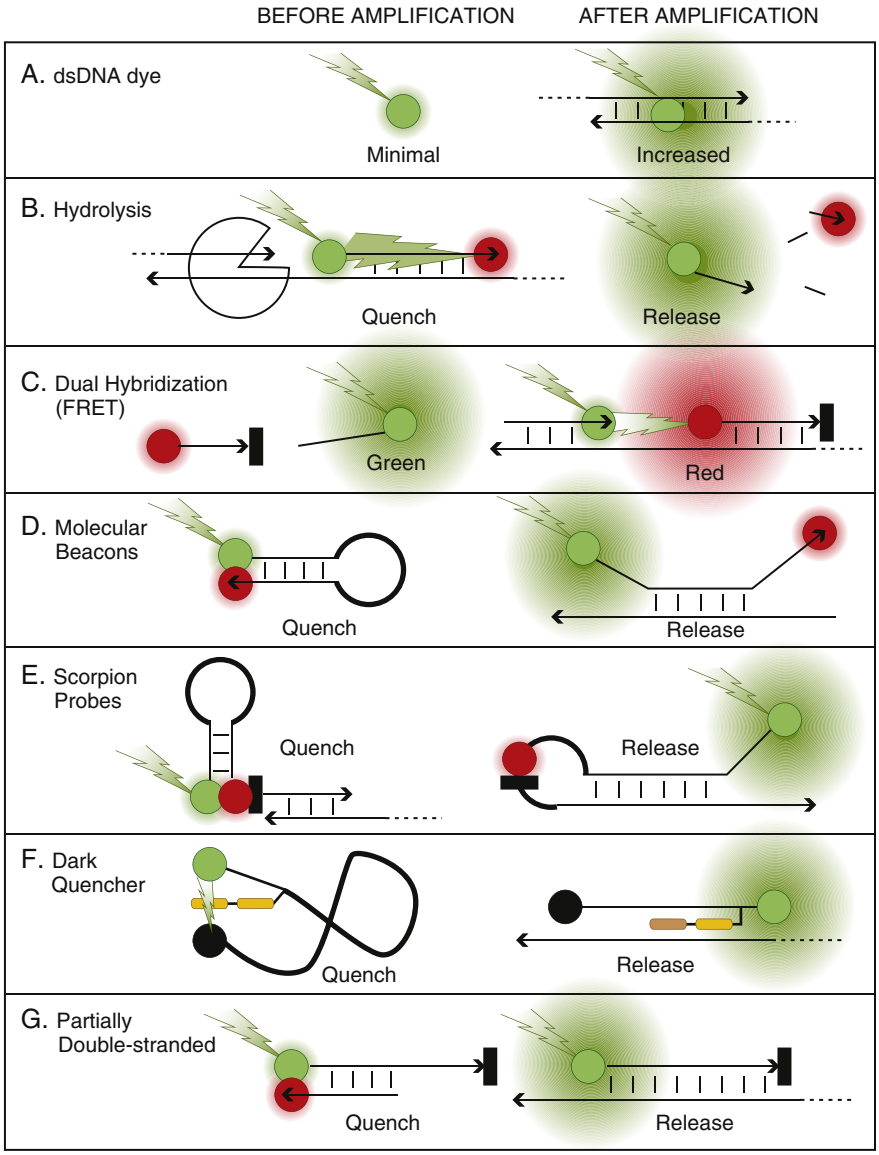

Figure 69.3 Common probes and dyes for real-time PCR. The *green lightning bolt* is the excitation light. The *green circles* are fluorophores, the *dark-red circles* are quenchers, and the *black circles* are dark quenchers. The *large gray circle* is a polymerase with 5′-to-3′ exonuclease activity. The *thin black squares* are blockers, and the *orange cylinders* are minor groove binders. **A,** Double-stranded DNA dyes show a significant increase in fluorescence when bound to DNA. **B,** Hydrolysis probes between a fluorescent reporter and a quencher are cleaved by polymerase activity, resulting in increased fluorescence. **C,** Dual-hybridization probes change color by resonance energy transfer when hybridized. **D,** The molecular beacon hairpin quenches fluorescence until target binding that separates the quencher from the fluorophore. **E,** Scorpion probes are quenched in the native conformation but increase in fluorescence when the original hairpin loop is hybridized to its extension product. **F,** Dark quencher probes are initially quenched by a minor groove binder and the dark quencher. Hybridization to the target releases the fluorescence. **G,** The short strand of partially double-stranded probes is displaced in the presence of target, releasing fluorescence from quenching. (Reprinted with permission from Nolte FS, Wittwer CT: Nucleic acid amplification methods overview. In Persing DH, Tenover FC, Hayden RT, Ieven M, Miller MB, Nolte FS, Tang Y-W, Belkum A, editors: *Molecular microbiology: diagnostic principles and practice*, ed 3, Washington, DC, 2016, ASM Press, pp 3–18,)

hybridization probe during the primer extension phase of PCR (Holland et al., 1991). This approach uses dual-labeled fluorogenic hybridization probes. One fluorescent dye serves as reporter, and its emission spectrum is quenched by the second fluorescent (quencher) dye. The nuclease degradation of the hybridization probe releases the reporter dye, resulting in an increase in its peak fluorescent emission (Fig. 69.3B). The increase in fluorescent emission indicates that a specific PCR product has been made, and the intensity of the fluorescence is related to the amount of product (Heid et al., 1996). Specificity is increased because the signal is generated only when the primer and probe are bound to the same template strand.

Fluorescence resonance energy transfer (FRET), also known as dual hybridization probes, can also be used to detect PCR product as it is generated (Lay & Wittwer, 1997). This method requires two specially designed sequence-specific oligonucleotide probes. These hybridization probes hybridize next to each other on the product molecule. As shown in Figure 69.3C, the 3′ end of one probe is labeled with a donor dye, and the 5′ end of the other probe is labeled with an acceptor dye. The donor dye is excited by an external light source and, instead of emitting light, transfers its energy to the acceptor dye by FRET. The excited acceptor dye emits light at a longer wavelength than the unbound donor dye, and the intensity of the acceptor dye light emission is proportional to the amount of PCR product.

Real-time detection and quantification of PCR product can also be accomplished using molecular beacons (Tyagi et al., 1998). Molecular beacons are hairpin-shaped oligonucleotide probes with an internally quenched fluorophore whose fluorescence is restored when they bind to a target nucleic acid (Fig. 69.3D). They are designed in such a way that the loop portion of the probe molecule is complementary to the target sequence. The stem is formed by the annealing of complementary arm sequences on the ends of the probe. A fluorescent dye is attached to one end of one arm, and a quenching molecule is attached to the end of the other arm. The stem keeps the fluorophore and quencher in close proximity such that no light emission occurs. When the probe encounters a target molecule, it forms a hybrid that is longer and more stable than the stem and undergoes a conformational change that forces the stem apart and causes the fluorophore and quencher to move away from each other, restoring the fluorescence.

Scorpion probes combine a PCR primer with a molecular beacon (Thelwell et al., 2000). Intramolecular hybridization of the loop structure to a downstream portion of the amplification product separates the reporter and quencher dyes (Fig 69.3E). The hybridization kinetics of scorpion probes is generally faster than those of molecular beacons because the primer and the probe are located on the same molecule.

It is not absolutely necessary to have a stem loop structure to use nonhydrolyzable probes in real-time PCR applications. Dark quencher probes contain a fluorophore on the 5′ end and a nonfluorescent quencher molecule on the 3′ end (Afonina et al., 2002). The fluorescence is quenched when the probe is in a random coil configuration and emitted when the probe anneals to the target sequence (Fig 69.3F). Because the dark quencher is not fluorescent, it does not contribute to the background signal. This has the advantage of improved signal-to-noise ratio for the detection system, which may improve sensitivity. These probes also incorporate a hybridization-stabilizing compound known as a *minor groove binder*. It is a small, crescent-shaped molecule that is covalently linked to the 3′ end of the probe that spans about 3 to 4 nt and snugly fits into the minor groove of DNA, where it forms hydrogen bonds with the template. The minor groove binder allows the use of shorter probes and enables improved T_m leveling, which improves the specificity of the detection reaction (Kutyavin et al., 2000).

Partially double-stranded (ds) linear probes consist of a hybridization probe labeled with a fluorescent probe and a shorter complementary quencher (Fig.69.3G). The asymmetry in strand length of the ds-probes correlates with an increased capacity for mismatch tolerance, and the length of both the hybridization probe and the quencher strand affect the mismatch tolerance efficiency (Luk et al., 2007). This ds-probe design can be useful to evaluate genetically polymorphic targets compared with other probe types, such as molecular beacons or TaqMan probes, for which nucleotide mismatches can result in reduced efficiency of probe hybridization. These probes can be created to tolerate or discriminate polymorphic targets, such as human immunodeficiency virus type 1 (HIV-1). In the absence of target, the ds-probe remains in a duplex that places the fluorophore in close proximity to the quencher and prevents a fluorescent signal. Presence of a target results in hybridization of the probe to the target, displacing the complementary quencher and leading to emission of the fluorescent signal. The hybridization probe is not destroyed during the amplification process, allowing for later melting curve analysis.

Melt curve analysis is a way to assess an amplicon sequence or complementarity by using a slow increase in temperature to dissociate dsDNA. The ability to break a double hydrogen bond between two nucleic acids during melt curve analysis depends on the length, the GC content, and the complementarity of the amplicon. A melt curve analysis can be measured with both intercalating dye reactions and with fluorescently labeled probes that are not degraded during the PCR reaction. Intercalating dyes, such as SYBR green, slot into the minor groove of dsDNA so that dissociation results in reduction of fluorescence. By slowly increasing the temperature in a melt curve reaction, characteristics of the sequence of the amplicon can be inferred from the temperature of the dissociation, which is reflected by a loss of fluorescence. The melting temperature of the amplicon is predictable based on the nucleic acid bases that make up the amplicon so that the shape and temperature at which the amplicon or probes dissociate are reliable and reproducible. A mutation in that amplicon sequence will result in a different melting temperature. The data are transformed and analyzed by plotting the first derivative of fluorescence on the y-axis and temperature on the x-axis (Fig. 69.4). The specific amplified product will have a characteristic melting peak at its predicted T_m, whereas the primer-dimers and other nonspecific products should have a different T_m or give broader peaks (Ririe et al., 1997).

Another approach to detection, characterization, and quantification of real-time PCR amplicons involves the use of a nonstandard DNA base pair constructed from isoG and isoC (Sherrill et al., 2004). These synthetic bases pair with each other but not with the natural bases guanine and cytosine and can be covalently coupled to a wide variety of reporter groups. In the MultiCode-RTx assays (Luminex), the target is amplified using a forward primer with a single isoC nucleotide with a fluorescent label at the 5′ end and an unlabeled standard base reverse primer. Amplification is performed in the presence of isoG coupled to a fluorescence quencher molecule. Site-specific incorporation of the isoG molecule by the DNA polymerase places the quencher in close proximity to the fluorophore, resulting in a decrease of fluorescence with every PCR cycle. The number of cycles in which the fluorescence change can be detected depends on the initial number of target molecules in the reaction. The decrease in fluorescence is easily monitored by a number of standard real-time PCR instruments. Postreaction amplicon melting curve analysis can be performed to confirm the identity of the amplicon and to detect sequence variants.

Real-time PCR methods decrease the time required to perform nucleic acid assays because there are no post-PCR processing steps. Also, because amplification and detection occur in the same closed tube, these methods eliminate the post-amplification manipulations that can lead to laboratory contamination with amplicon. In addition, real-time PCR methods lend themselves well to quantitative applications because analysis is performed early in the log phase of product accumulation and as a result is less prone to errors that may result from differences in amplification efficiency among samples.

Relative concentrations of DNA present during the exponential phase of the reaction are determined by plotting fluorescence against cycle number on a logarithmic scale (so that an exponentially increasing quantity will give a straight line). A threshold for detection of fluorescence above the background is determined, and the C_T is determined. Because all sets of primers do not work equally well, one has to calculate the reaction efficiency first. Reaction efficiency is the rate at which the PCR product is generated. A perfectly doubling PCR reaction would have an efficiency of 2 because the quantity of DNA theoretically doubles every cycle during the exponential phase, and relative amounts of DNA can be calculated (e.g., a sample whose C_T is three cycles earlier than another's has $2^3 = 8$ times more template). The equation to determine a reaction's efficiency is $E = 10^{(-1/slope)}$. One way to calculate efficiency is by using the slope of a standard curve from a dilution series. This is done by plotting the C_T values versus the $\log_{10}$ of the serial dilution and performing a linear regression to get the slope. This dilution series should cover a minimum of 5 logs and contain replicates. A second method to calculate efficiency can be done for each individual reaction by plotting fluorescence on a log scale and performing a linear regression on the exponential phase to get the slope. Both methods of determining efficiency have been shown to be comparable in measuring accuracy, although the second method was found to be more robust and required fewer PCRs than the first method (Karlen et al., 2007). If reaction efficiency was found to be 1.96 and we used the previous example of a C_T of 3 times earlier, then the starting template would be calculated by $1.96^3 = 7.53$ times more template.

Amounts of RNA or DNA are determined by comparing the results to a standard curve produced by a real-time PCR of serial dilutions (e.g.,

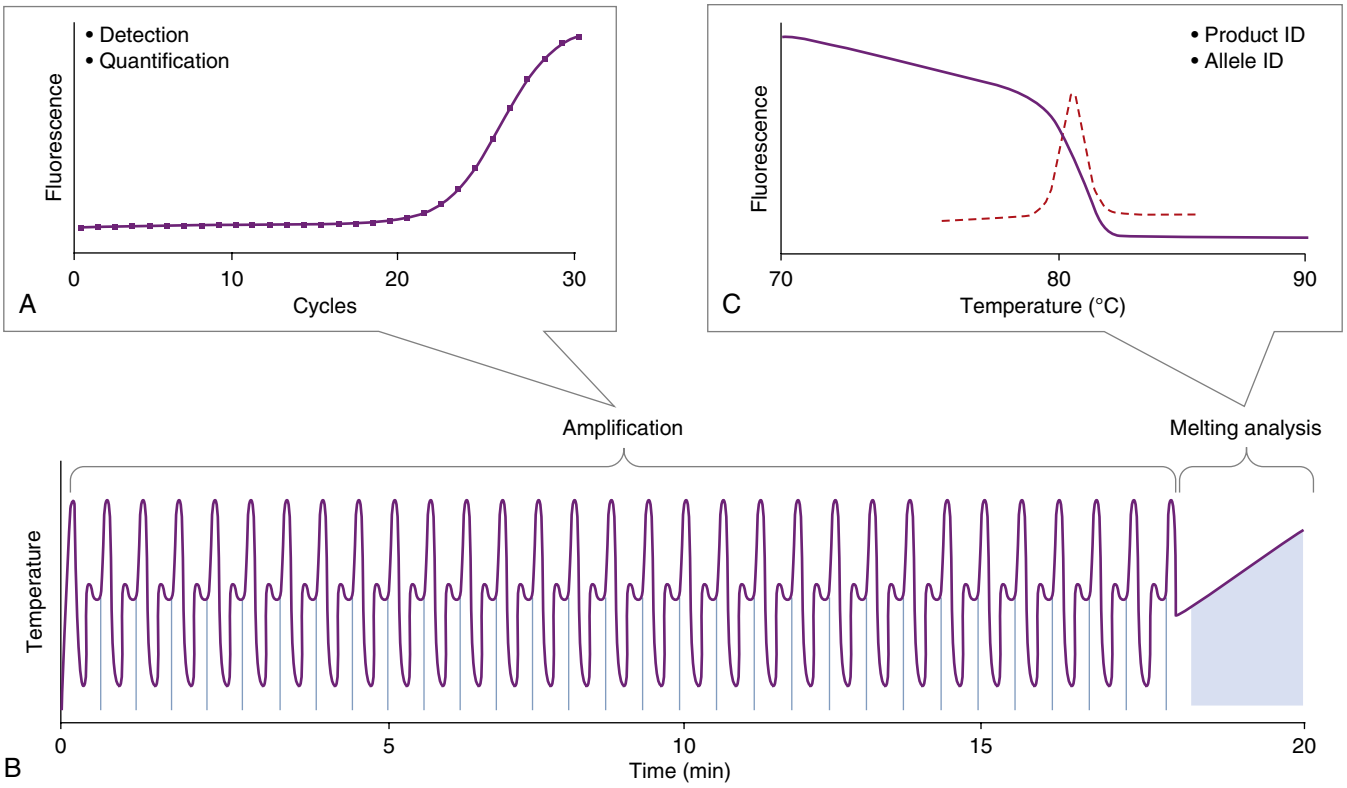

Figure 69.4 Real-time PCR with melting analysis. **A,** Detection and quantification are enabled by monitoring fluorescence at the end of extension of each cycle *(solid squares)*. **B,** Amplification is immediately followed by melting-curve acquisition after a defined number of amplification cycles (30, as shown in **B**). Melting-curve analysis identifies PCR products, microbial strains, and sequence alterations by melting temperature. **C,** The original melting-curve data *(solid line)* can also be plotted as a derivative melting curve *(dotted line)*. For the latter, the y-axis becomes the first derivative of fluorescence at each time point. (Reprinted with permission from Lyon E, Wittwer CT: LightCycler technology in molecular diagnostics, *J Mol Diagn* 11:93–101, 2009.)

undiluted, 1:4, 1:16, and 1:64) of a known amount of RNA or DNA. As mentioned earlier, to accurately quantify gene expression, the measured amount of RNA from the gene of interest is divided by the amount of RNA from a housekeeping gene measured in the same sample to normalize for possible variation in the amount and quality of RNA among the samples. This normalization permits accurate comparison of expression of the gene of interest between different samples, as long as the expression of the reference (housekeeping) gene used in the normalization is very similar across all samples. Therefore, choosing a reference gene that fulfills this criterion is of high importance and often can be challenging because only a very few genes show equal levels of expression across a range of different conditions or tissues.

Real-time PCR can be used to quantify nucleic acids by two strategies: relative quantification and absolute quantification (VanGuilder et al., 2008). Relative quantification measures the fold-difference (2×, 3×, etc.) in the target amount. For gene expression analysis, relative concentrations may be determined by the $2^{-\Delta\Delta CT}$ method in which, for each sample, the difference in C_T values for the gene of interest and the endogenous gene control is calculated (ΔC_T). Next, subtraction of the control-condition ΔC_T from the treated-condition ΔC_T yields the $\Delta\Delta C_T$. The negative value of this subtraction, $-\Delta\Delta C_T$, is used as the exponent of 2 in the equation and represents the difference in the corrected number of cycles to threshold. This value is often referred to as the *relative quantity value*.

Absolute quantification gives the exact number of target molecules present by comparing with known standards. The quality of standard is important for accurate quantification. MIQE guidelines defining the "minimal information for publication of quantitative real-time PCR experiments" provide the framework for more uniform, more comparable, and ultimately more reliable quantitative real-time PCR results (Bustin et al., 2009).

Rapid-Cycle Polymerase Chain Reaction

While real-time PCR methods have had a significant impact on assay time, a great deal of emphasis continues to be placed on further reducing the assay time for various PCR formats. Rapid-cycle PCR is not chemically different from any of the standard PCR formats (Wittwer & Garling, 1991). The polymerases used in PCR are capable of incorporating 35 to 100 nucleotides per second. Most of the time consumed in performing PCR is temperature equilibration for the solution so that efficient annealing and extension occur, as well as a significant amount of time changing the temperature. By reducing the thermal profile of the solution using thin-walled tubes or capillaries that force the reaction solution into thin columns or sheets of fluid, it is possible to improve thermal transfer rates as well as equilibration rates such that thermocycling time can be significantly reduced. In highly optimized systems, it is possible to approach the ideal processivity rate of the polymerase such that a 40-cycle PCR may be performed in 30 minutes or less using standard or real-time PCR chemistries. In fact, by increasing the primer and polymerase concentrations 10- to 20-fold over typical concentrations with temperature cycles of 0.4 to 2.0 seconds in thin-walled reaction capillaries, efficient, specific, and high-yield PCR is possible in 15 to 60 seconds (Farrar & Wittwer, 2015). This so-called "extreme PCR" highlights the considerable future potential of PCR for point-of-care applications if suitable instruments can be designed.

Digital Polymerase Chain Reaction

PCR exponentially amplifies nucleic acids and the subsequent number of amplification cycles, and detected amount of amplicon product allows for computation of the starting quantity of targeted nucleic acid. However, many factors can complicate this calculation, such as the quality and source materials of the standard curve, choice for signal threshold, and interlaboratory variation. These factors can often create uncertainties and inaccuracies, particularly when the starting concentration of the target is low. Digital PCR attempts to overcome these difficulties by transforming the exponential data from conventional PCR to digital signals that indicate whether or not amplification occurred (Vogelstein & Kinzler, 1999).

Digital PCR is accomplished by partitioning nucleic acid template molecules into master mix reactions in numerous individual but equal volume compartments or droplets. The smaller the size of the droplet and the more dilute the DNA, the more likely that only a single nucleic acid will be placed in a single droplet. The size of the droplet will determine the number of target molecules that can fit within each individual droplet. If the target is present in the droplet, it will undergo PCR and be amplified. The droplets are quantified in order to accurately calculate the number of negative versus positive reactions. The term *digital* refers to this fact: each droplet is considered positive or negative and, ideally, accounts for a single target molecule. The distribution of target nucleic acid is random;

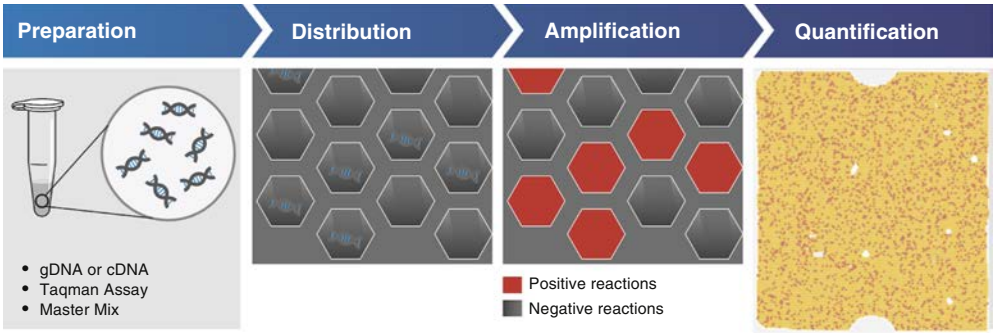

Figure 69.5 Digital PCR. Digital PCR is accomplished by partitioning individual nucleic acid target molecules into separate, equal volume, self-contained PCR reactions. Reaction compartments containing the target of interest may be counted by various detection methods and more than one target may be identified. In this example, the *green compartments* indicate a positive reaction (e.g., presence of a mutation), the *red compartments* indicate a negative reaction (e.g., presence of wild-type template), and no signal indicates absence of the DNA target region. Ideally, the resulting counts represent absolute quantification of the target (Image owned by Life Technologies Corporation, a part of Thermo Fisher Scientific Inc. www.thermofisher.com © 2020 Thermo Fisher Scientific Inc.)

thus, some droplets may contain no target nucleic acid. Depending on the design of the assay and size of the compartment or droplet, some individual reactions may not contain any nucleic acid and, therefore, are empty or have no target compartments or droplets. After PCR amplification, a count of the individual partitioned reactions is a direct measure of the absolute quantity of nucleic acid in the sample. The capture or isolation of individual nucleic acid molecules may be done in capillaries, microemulsions, arrays of miniaturized chambers, or on surfaces that bind nucleic acids (Fig. 69.5). The figure shows an application wherein the mutated target demonstrates one signal (green) while the wild-type target demonstrates a second signal (red).

Digital PCR has many applications, including detection and absolute quantification of low levels of pathogens or viral load, rare mutation detection, copy number variation, and clonal amplification of nucleic acids for sequencing mixed nucleic acid samples. Because digital PCR does not depend on a standard curve for absolute quantification, it is ideally suited to establish quantitative reference materials (Haynes et al., 2013). However, Poisson correction may be needed depending on the partition size and the associated likelihood of housing more than a single target molecule. The basic steps of the Poisson correction statistics are that the negatives are counted first, then the positive copies per event are estimated, and the original sample copies are calculated (dilution factor). Target amplification using digital PCR can be included as part of next-generation sequencing methods. Microfluidic or microdroplet technology can be used in combination with digital PCR to automate and improve the partitioning with high-throughput and/or low-volume reactions (Taly et al., 2012). MIQE guidelines emphasize the unique requirements of digital PCR (Huggett et al., 2013).

Allele-Specific Polymerase Chain Reaction

Allele-specific PCR relies on primer design in which the 3′ primer end is specific for the allele of interest. In this way, only the DNA with the mutation or polymorphism interrogated is amplified. Mutations may include single nucleotide changes or small insertions and deletions (Bottema & Sommer, 1993). Specificity and reproducibility are excellent and sensitivity enhanced to up to 0.1%. This methodology may be used when the DNA input is low or the mutational burden of low frequency makes it a reasonable option for testing of heterogeneous specimens such as tumor tissue. As an example, this methodology has been used for high-sensitivity identification of IDH1 and TERT promoter mutations important for diagnosis and prognosis in glioma (Diplas et al., 2019). In addition to the advantages described, the technique is amenable to multiple downstream applications, including real-time PCR and multiplex PCR (Broude et al., 2001), and can be both cost-effective and employed when fast turnaround times are needed for clinical decision making.

Other strategies available for the detection of minor alleles include the following: TamSeq (tagged-amplicon deep sequencing) (Forshew et al., 2012), COLD PCR (co-amplification at lower denaturation temperature-PCR) (Milbury et al., 2011), ARMS (amplification refractory mutation system) (Newton et al., 1989), BEAMing (beads, emulsion, amplification, and magnetics) (Li et al., 2006), PAP (pyrophosphorolysis-activated polymerization) (Liu & Sommer, 2000), and the previously described digital PCR.

TRANSCRIPTION-BASED AMPLIFICATION

Transcription-based amplification includes transcription-mediated amplification (TMA) and nucleic acid sequence-based amplification (NASBA). Both TMA and NASBA are isothermal nucleic acid amplification techniques that, although slightly different in practice, are identical in concept and are described together (Kwoh et al., 1989; Compton, 1991). TMA and NASBA are the intellectual properties of Hologic (San Diego, CA) and bioMérieux (Durham, NC), respectively. These techniques essentially recapitulate retroviral replication in vitro, converting RNA into DNA and then using the DNA as a template for transcription of multiple copies of RNA.

The process begins with an RNA target, which exists as a single-stranded entity in most cases, removing the need for thermal denaturation of the template before amplification (Fig. 69.6). A sequence-specific DNA primer binds to the RNA target. Reverse transcriptase then extends the primer, creating a DNA–RNA heteroduplex. The 5′ end of the sequence-specific primer contains the promoter for a T7 bacteriophage polymerase. The presence of this T7 promoter in the 5′ end of the primer results in the synthesis of a DNA strand complementary to the initial RNA target containing the T7 promoter at its 5′ end. In the case of TMA, the reverse-transcriptase enzyme itself degrades the initial RNA template as it synthesizes its complementary DNA. In NASBA, a separate enzyme, RNAse H, degrades the initial RNA template. RNAse H selectively cleaves RNA, which is heteroduplex-bound to DNA but not RNA alone. In either case, the resultant single-stranded, complementary DNA with the T7 promoter sequence binds to a second primer at its 3′ end. The DNA polymerase extends from this second primer, resulting in the synthesis of a dsDNA molecule containing an intact T7 promoter. This DNA molecule can now serve as a template for T7 polymerase, a bacteriophage enzyme that specifically recognizes the T7 promoter and synthesizes multiple copies of RNA. Each of these newly synthesized RNA molecules is antisense to the initial target, allowing it to hybridize to the second primer. The reverse-transcriptase, second primer, RNAse H, and DNA polymerase then use this antisense RNA molecule as a template to synthesize new dsDNA templates, which, in turn, make more RNA template. A 10^9-fold amplification of target RNA can be achieved with these methods in 2 hours or less.

TMA and NASBA have several distinct advantages over other RNA amplification techniques. Perhaps the most significant of these advantages is that no initial denaturation is required for the amplification to occur. Hence, dsDNA sequences are not denatured and, thus, are incapable of binding to primers in the reaction. DNA contamination can be particularly problematic when techniques such as PCR are used to assay for the RNA transcripts of retroviral or intron-less eukaryotic genes. NASBA and TMA eliminate the problem of DNA contamination giving a falsely elevated determination of RNA. A second advantage is that this technology uses isothermal processes that obviate the need for sophisticated thermocyclers because the whole process occurs at a single temperature. Combining this technology with molecular beacons or other sequence-specific probes that can be added directly to the amplification mixture creates a closed-tube system, which aids in preventing amplicon cross-contamination in the laboratory.

NASBA and TMA have been used successfully in a wide variety of clinical qualitative and quantitative applications, primarily in infectious diseases. FDA-cleared tests based on TMA are available from Hologic for qualitative detection of a variety of sexually transmitted infections, including *Neisseria gonorrhoeae*, *Chlamydia trachomatis*, *Trichomonas vaginalis*, herpes simplex virus (HSV), and human papillomavirus (HPV), quantitative tests for HIV-1, hepatitis C virus (HCV) and hepatitis B virus (HBV), and two vaginitis panels. BioMérieux developed an FDA-cleared HIV-1 quantitative assay based on NASBA and offered basic kits for design of laboratory-developed assays.

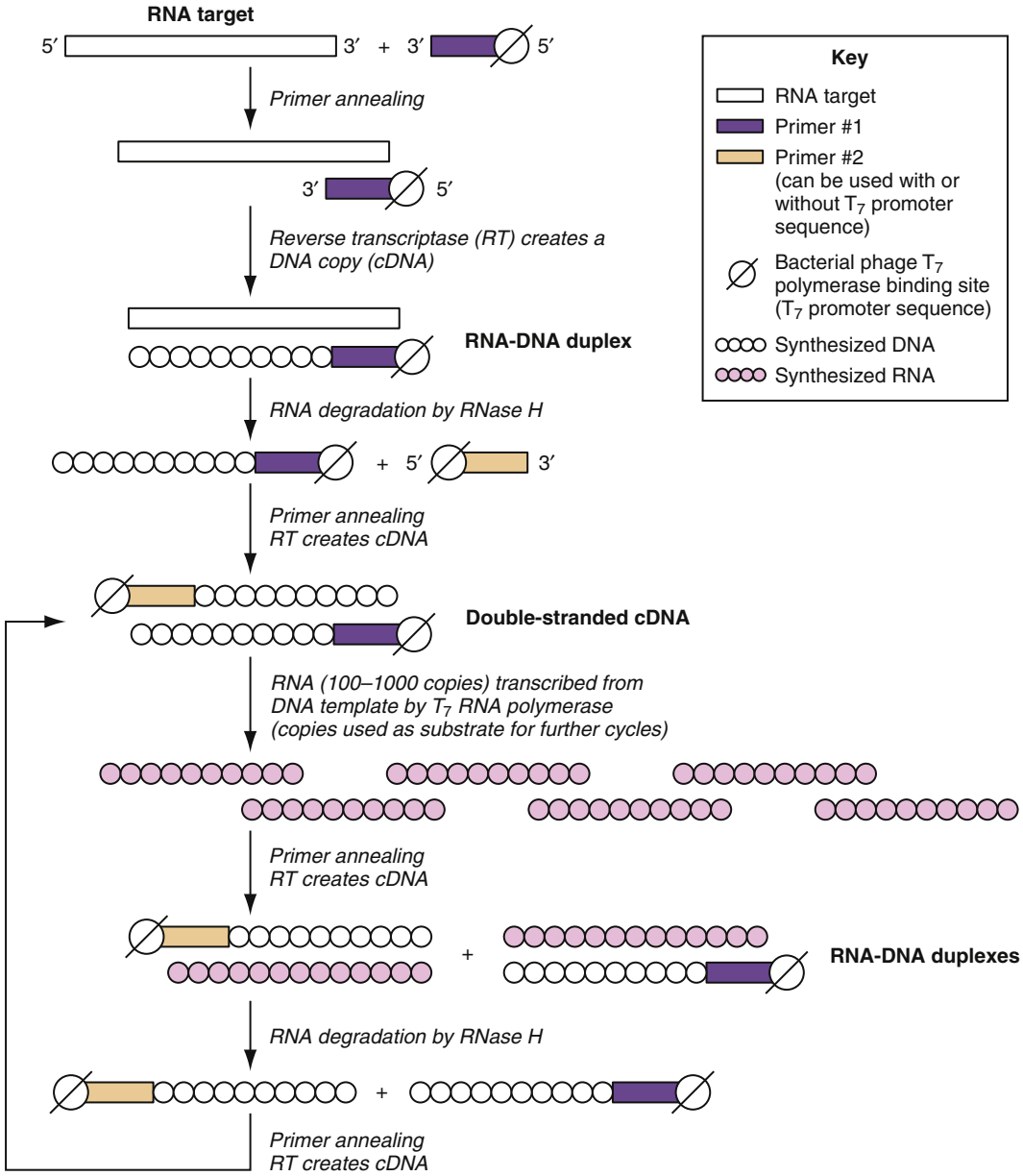

Figure 69.6 Transcription-mediated amplification (TMA). (*Redrawn from Wolk D, Mitchell S, Patel R: Principles of molecular microbiology testing methods,* Infect Dis Clin N Am *15:1157–1204, 2008.*)

TMA and NASBA are isothermal RNA amplification techniques with a widespread applicability and several unique advantages over other amplification methods. Combining these techniques with fluorescent probes allows one-step, closed-tube, real-time amplification without the need for thermal cycling.

STRAND-DISPLACEMENT AMPLIFICATION

Strand-displacement amplification (SDA) is an isothermal template amplification technique that can be used to detect trace amounts of DNA or RNA of a particular sequence. SDA as it was first described was a conceptually straightforward amplification process with some technical limitations (Walker et al., 1992a; Walker et al., 1992b). Since its initial description, however, it has evolved into a highly versatile tool that is technically simple to perform but conceptually complex. In its current iteration, SDA occurs in two discrete phases: target generation and exponential target amplification (Little et al., 1999). In the target generation phase, a dsDNA target is denatured and hybridized to two different primer pairs, designated as *bumper* and *amplification* primers (Fig. 69.7). The amplification primers include the single-stranded restriction endonuclease enzyme sequence for BsoB1 located at the 5′ end of the target binding sequence. The bumper primers are shorter and anneal to the target DNA just upstream of the region to be amplified. In the presence of BsoB1, an exonuclease-free DNA polymerase, and a dNTP mixture consisting of dUTP, dATP, dGTP, and thiolated dCTP (Cs), simultaneous extension products of both the bumper and amplification primers are generated. This process displaces the amplification primer products, which are available for hybridization with the opposite-strand products with the opposite-strand bumper and amplification primers.

The simultaneous extension of opposite-strand primers produces strands complementary to the products formed by extension of the first amplification primer with Cs incorporated into the BsoB1 cleavage site. This product enters the exponential target amplification phase of the reaction. The BsoB1 enzyme recognizes the double-stranded site; however, because one strand contains Cs, it is nicked rather than cleaved by the enzyme. The DNA polymerase then binds to the nick and begins synthesis of a new strand while simultaneously displacing the downstream strand. This step recreates the double-stranded species with the hemi-modified restriction endonuclease recognition sequence, and the iterative nicking and displacement process repeats. The displaced strands are capable of binding to opposite-strand primers, which produces exponential amplification of the target sequences.

These single-stranded products also bind to detector probes for real-time detection. The detector probes are single-stranded DNA (ssDNA) molecules with fluorescein and rhodamine labels. The region between the labels includes a stem-loop structure. The loop contains the recognition site for the BsoB1 enzyme. The target-specific sequences are located 3′ to the rhodamine label. In the absence-specific target, the stem-loop structure is maintained with the fluorescein and rhodamine labels in close proximity. The net effect is that very little emission for the fluorescein is detected after excitation. After SDA, the probe is converted to a double-stranded species, which is cleaved by BsoB1. The cleavage causes physical separation of the fluorescein and

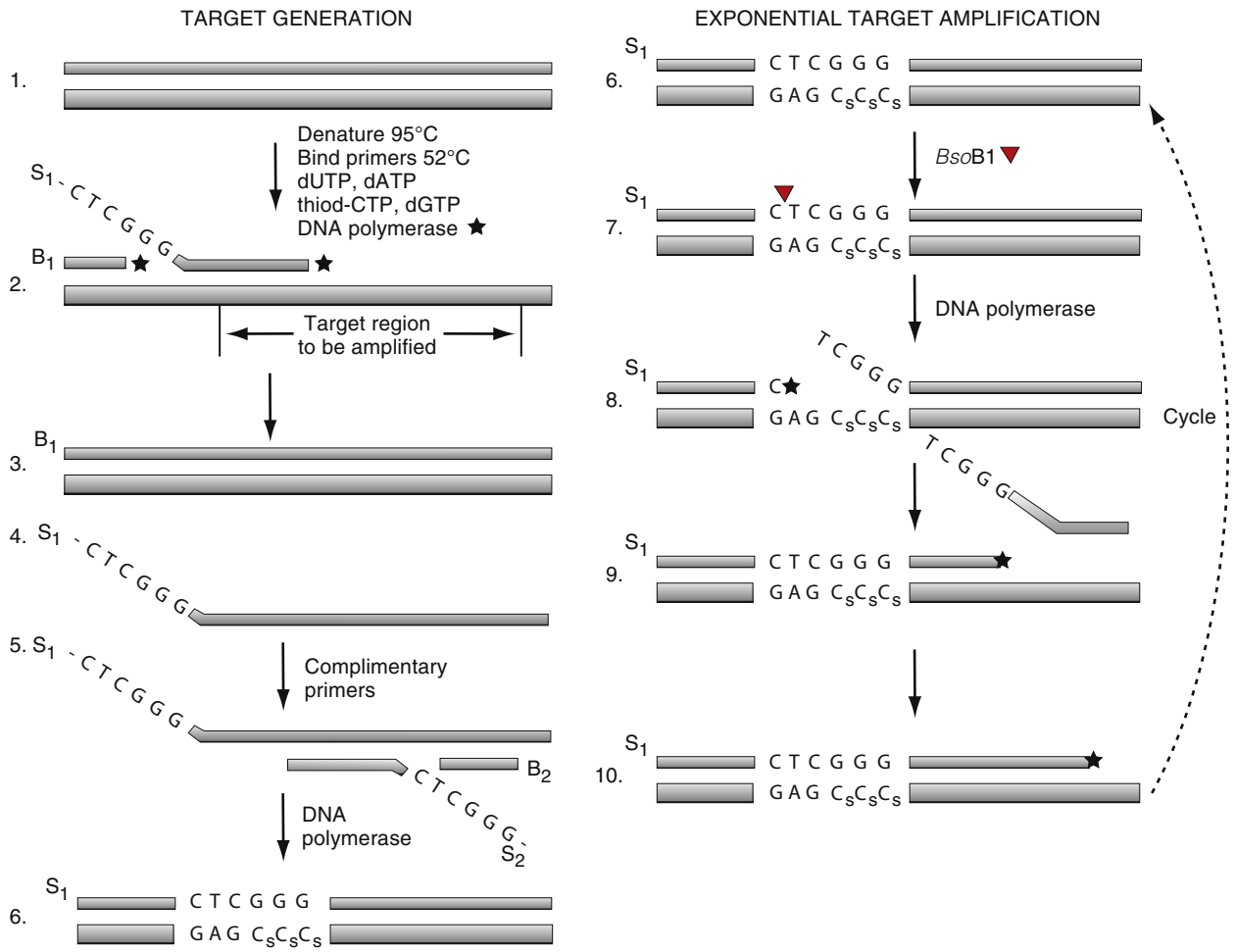

Figure 69.7 Strand displacement amplification (SDA). The process is shown for only one strand of a double-stranded DNA target, but amplification occurs on both strands simultaneously. B_1 and B_2 are bumper primers; S_1 and S_2 are amplification primers. (*Redrawn from Wolk D, Mitchell S, Patel R: Principles of molecular microbiology testing methods,* Infect Dis Clin N Am *15:1157–1204, 2008.*)

rhodamine labels, which results in an increase in emission from the fluorescein label.

The main advantage of SDA is that it is an isothermal process that, unlike PCR, can be performed at a single temperature after initial target denaturation. This eliminates the need for expensive thermocyclers. Furthermore, samples can be subjected to SDA in a single tube, with amplification times varying from 30 minutes to 2 hours. The main disadvantage of SDA lies in the fact that, unlike PCR, the relatively low temperature at which SDA is carried out (52.5°C) can result in nonspecific primer hybridization to sequences found in complex mixtures such as genomic DNA. Hence, when the target is in low abundance compared with background DNA, nonspecific amplification products can swamp the system, decreasing the sensitivity of the technique. However, the use of organic solvents to increase stringency at low temperatures and the recent introduction of more thermostable polymerases capable of strand displacement have alleviated much of this problem. FDA-cleared assays for detection of *N. gonorrhoeae*, *Chlamydia trachomatis*, HSV types 1 and 2, and *T. vaginalis* using SDA are available from BD Diagnostics (Franklin Lakes, NJ) on their Viper system.

LOOP-MEDIATED ISOTHERMIC AMPLIFICATION

Loop-mediated isothermal amplification (LAMP) is an isothermal method that relies on autocycling strand displacement DNA synthesis by *Bst* DNA polymerase and a set of four to six primers (Notomi et al., 2000). Two inner and two outer primers define the target sequence; an additional set of loop primers is added to increase the speed of amplification (Fig. 69.8). This is classically a two-step process, with the first step involving the production of the self-hybridizing loop structures and the second step being cycle amplification. The final products of the LAMP reaction are multimeric DNA molecules, with a cauliflower-like structure of multiple loops consisting of repeats of the target sequence. There are multiple ways to visualize the products created by LAMP. Amplification products can be visualized in agarose gels after electrophoresis and staining with ethidium bromide or SYBR Green. The products can also be analyzed in real time by monitoring turbidity since a precipitate is created when the pyrophosphate ion released from deoxynucleotide triphosphate incorporation by DNA polymerase precipitates with magnesium ions included in the reaction buffer. Real-time monitoring using fluorescence and quencher technologies has also been leveraged for LAMP.

Because LAMP is an isothermal process and positive reactions can be detected by simple turbidity measurements or direct visualization, it can be performed using no expensive equipment. For the detection of fluorescence, portable isothermal fluorometers are commercially available. These attributes make it an attractive technology for resource-poor settings and field use. However, primer design for LAMP is more complex than for PCR and specialized training and software may be required for optimal results. Meridian Bioscience, Inc. (Cincinnati, OH) has licensed LAMP technology from Eiken Chemical Company, Ltd. (Japan) for the development of infectious disease diagnostics in the United States including *Clostridium difficile*, group A and group B β-hemolytic streptococci, *Mycoplasma pneumoniae*, *Bordetella pertussis*, and HSV type 1 and type 2.

Historically, the majority of LAMP assays have been developed for the detection of infectious human pathogens. However, recently there has been an exploration of the technology for mutation screening for human genetic and genomic disease diagnosis, methylation status, and cancer therapy selection. LAMP is a compelling choice as an alternative testing strategy since it may provide significant reductions in both turnaround times and costs, leading to quicker treatment decisions in cancer care and improved test availability in resource-poor settings (Srividya et al., 2019; Mori & Notomi, 2019; Cao et al., 2018). The LAMP assay can be modified based on specimen type and target. Divergent LAMP test strategies include reverse-transcription LAMP, proofreading LAMP, in situ LAMP, allele-specific LAMP, mutation-oriented

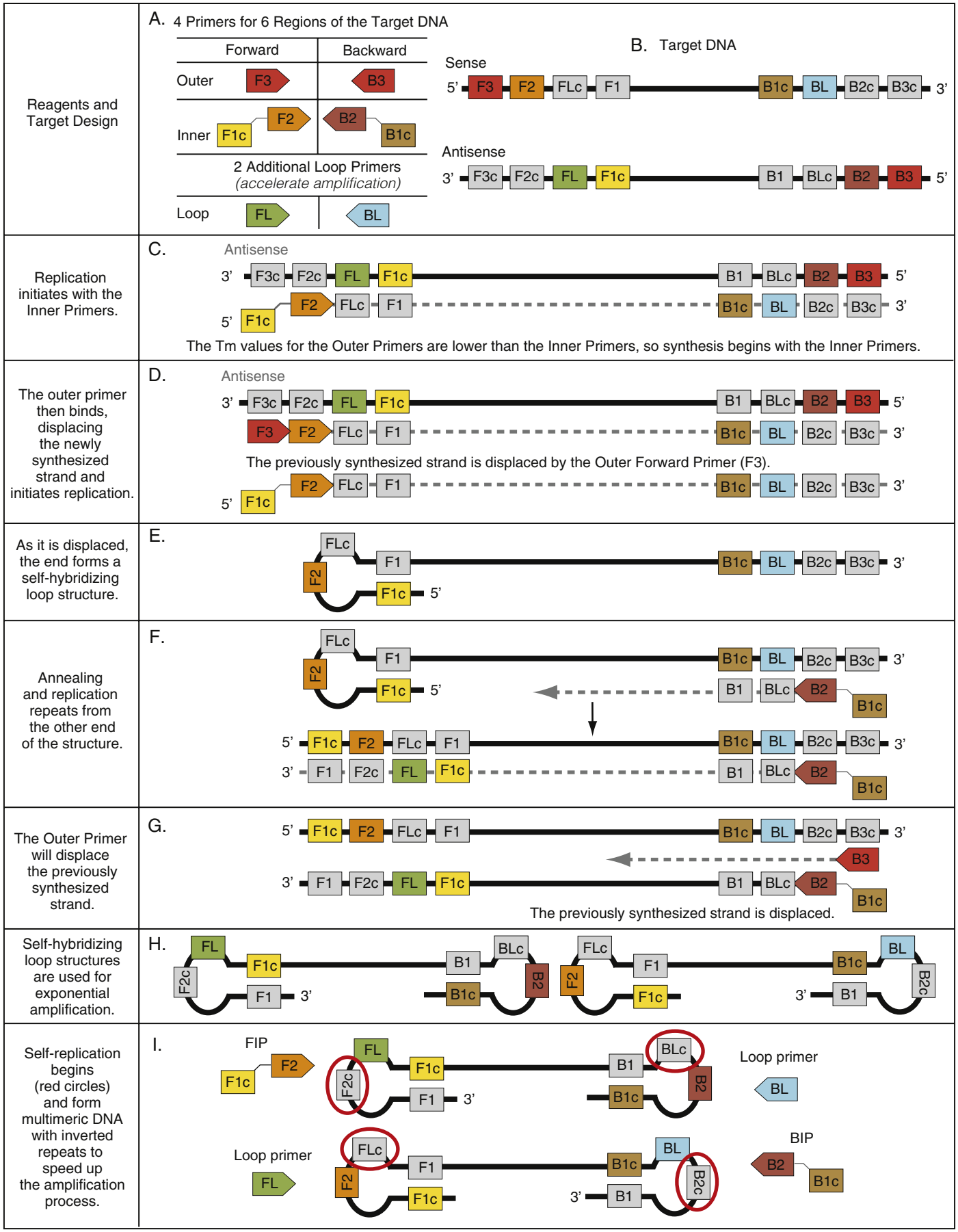

Figure 69.8 Loop-mediated isothermic amplification (LAMP). **A,** Four primers are necessary for LAMP, the forward and backward outer primers (F3 and B3) and the forward and backward inner primers (F2 and B2). Forward and backward loop primers (FL and BL) may be included to accelerate the amplification process. **B,** The sense and antisense strands are targets for amplification. The lowercase "c" indicated complementarity. Complementary regions are essential for formation of the loop structures created as strands are displaced during extension. **C,** Replication initiates with the forward inner primer (F2) due to its relatively higher T_m as compared with the outer primers. **D,** The forward outer primer (F3) displaces the newly synthesized strand from the template DNA. **E,** Following strand displacement, a self-hybridizing loop structure is formed (F1 to F1c) at one end of the strand. **F,** Annealing and replication by the backward inner primer (B2) is shown. **G,** The backward outer primer (B3) displaces the newly synthesized strand. **H,** Self-hybridizing loop structures are now present on both sides of the amplicon and cycle-amplification can begin. **I,** Self-replication originates from multiple sites *(circled in red)*, resulting in multimeric DNA that differs in the number of loops and length of the stem loop.

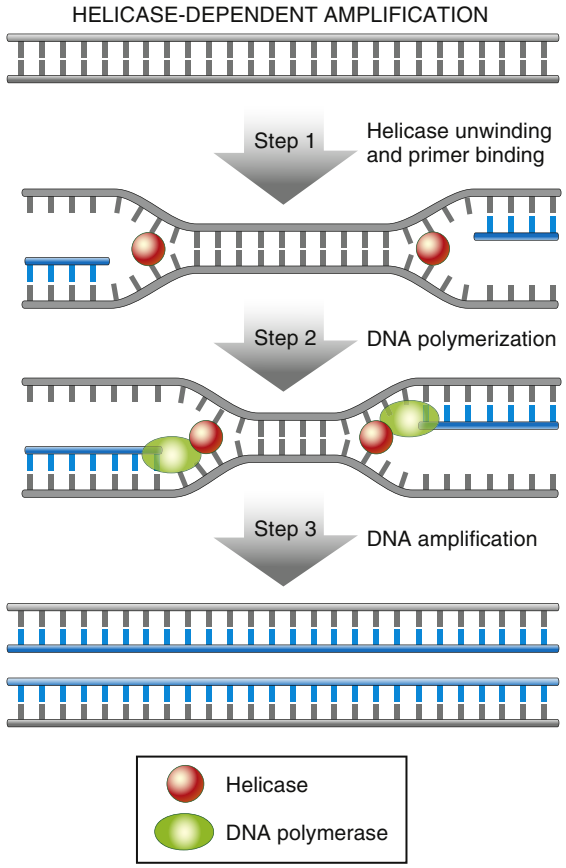

Figure 69.9 Helicase-dependent amplification (HDA). This method amplifies target sequences using two sequence-specific primers flanking the fragment to be amplified and a mixture of enzymes for DNA strand separation and polymerization. In the first step of the HDA reaction, the helicase enzyme loads on to the template and traverses along the target DNA, disrupting the hydrogen bonds linking the two strands. Exposure of the single-stranded target region by helicase allows primers to anneal. The DNA polymerase then extends the 3′ ends of each primer using free deoxynucleotides (dNTPs) to produce two DNA replicates. The two replicates independently enter the next cycle of HDA, resulting in exponential amplification of the target sequence. (Reprinted with permission from https://www.neb.com/products/h0110-isoamp-ii-universal-thda-kit#Product%20Information.)

LAMP, peptide nucleic acid LAMP, and ligation-initiated LAMP (Srividya et al., 2019).

HELICASE-DEPENDENT AMPLIFICATION

HDA is an isothermal process that uses helicase to separate dsDNA and generate single-stranded templates for primer hybridization and subsequent extension by a DNA polymerase (Vincent et al., 2004). As the helicase enzymatically unwinds dsDNA, the initial heat denaturation and subsequent thermocycling steps required by PCR can all be omitted (Fig. 69.9). In HDA, strands of dsDNA are separated by the DNA helicase and the ssDNA-coated ssDNA-binding proteins. Two sequence-specific primers hybridize to each border of the target sequence, and a DNA polymerase extends the primers annealed to the target sequence to produce dsDNA. The two newly synthesized products are used as substrates by the helicase in the next round of amplification. Thus, a simultaneous chain reaction proceeds, resulting in exponential amplification of the selected target sequence. The use of reverse transcription can be used to evaluate RNA (RT-HDA).

HDA is compatible with multiple detection technologies, including qualitative and quantitative fluorescent technologies and with instruments designed for real-time PCR (Tong et al., 2008). Furthermore, HDA has shown potential for the development of simple, portable DNA diagnostic devices to be used in the field or at the point of care. FDA-cleared tests for detection of *Bordetella*, *C. difficile*, group A and B β-hemolytic streptococci, HSV type 1 and type 2, *Trichomonas vaginalis*, varicella-zoster virus, influenza A + B, respiratory virus A/B and human metapneumovirus based on HDA and RT-HDA are available from Quidel (San Diego, CA).

NICKING ENDONUCLEASE AMPLIFICATION REACTION

NEAR is an isothermal process that begins with nicking of a double-stranded DNA template by a nicking enzyme to expose binding sites for primers (Nie et al., 2014). It also employs certain DNA polymerases that are able to bind short oligonucleotide primers in solution prior to binding to the target. This complex then binds to the target sequence and the extension reaction is carried out above the T_m because the chosen polymerase stabilizes the duplex during primer extension. In PCR, the primer binds the target first and then the polymerase binds to the stable duplex and extends the primer. This is a potential rate-limiting step in PCR avoided by NEAR and provides for improvements in reaction speed. Since the reaction occurs above the T_m of the primer-target, their annealing is a transient event that does not require the use of strand-displacing bumper primers used in SDA.

The NEAR mechanism of amplification is shown in Fig. 69.10. The T2 primer that includes the nicking enzyme binding site (NEBS) binds loosely to the template and is extended by polymerase. A second T2 primer binds to the same target and is extended, displacing the first T2. The recognition region (RR) of the T1 primer binds to its complement on the released strand and is extended to the 5′ end, creating the double-stranded NEAR amplification duplex. The stabilizing regions (SRs) serve to stabilize the NEAR amplification duplex and the nicking enzyme cut sites (NECSs) within primers allow for the process to repeat for rapid amplification of products.

NEAR is the basis of the FDA-cleared tests for direct detection of influenza A and B viruses, respiratory syncytial virus and group A streptococci in respiratory specimens that is available from Abbott (formerly Alere) for use in point-of-care settings by nonlaboratory personnel. As such, these tests represent a milestone in molecular diagnostics as the first Clinical Laboratory Improvement Amendments–waived nucleic acid amplification tests.

PROBE AND SIGNAL AMPLIFICATION METHODS

Probe and signal amplification methods differ from target amplification in that the amplifications are either probes or label molecules, not the target nucleic acid itself. These methods are becoming largely obsolete as target amplification methods have become more sensitive and specific over time, but they remain in use in several assays, which will be described. Cleavase/invader technology is an example of probe amplification while the other examples provided are of signal amplification. Multiple enzymes, multiple probes, multiple layers of probes, and strategies for reduction of background noise have been used to enhance target detection (Kricka, 1999). Either larger probes or more probes are employed in signal amplification; thus, these assays are less susceptible to errors resulting from target sequence heterogeneity. Since the number of target molecules is not altered, the signal is directly proportional to the amount of target sequence present in the clinical specimen. Signal amplification methods are also not affected by the presence of enzyme inhibitors, unlike target amplification methods. Finally, RNA can be measured directly, without the synthesis of a cDNA intermediate. Branched DNA and hybrid capture are examples of signal amplification systems leveraged in the design of diagnostic tests.

CLEAVASE/INVADER TECHNOLOGY

Cleavase/invader technology is an example of a probe amplification method currently used for the detection of high-risk genotypes of HPV in cervical samples (Ginocchio et al., 2008). It relies on the specific recognition and cleavage of the 5′ single-stranded flap of a branched base-paired duplex by members of the flap endonuclease-1 family of DNA polymerases called *cleavases* (Lyamichev et al., 1999). The enzyme recognizes the molecular structure of the DNA substrate without regard to the sequence of nucleic acids and *in vivo* likely plays a role in elimination of these structures during DNA replication and repair (Lieber, 1997).

In cleavase/invader assays, two primers (signal and invader) hybridize to the target sequence in an overlapping fashion (Fig. 69.11) such that the invader hybridizes upstream of the signal probe with a region of overlap between the 3′ end of the invader and the 5′ end of the signal probe. This overlap of primer binding sites results in a displacement equilibrium between the primers. Cleavase cleaves the 5′ flap, and the 5′ end of the signal probe is released. Since the DNA structure that serves as the cleavase

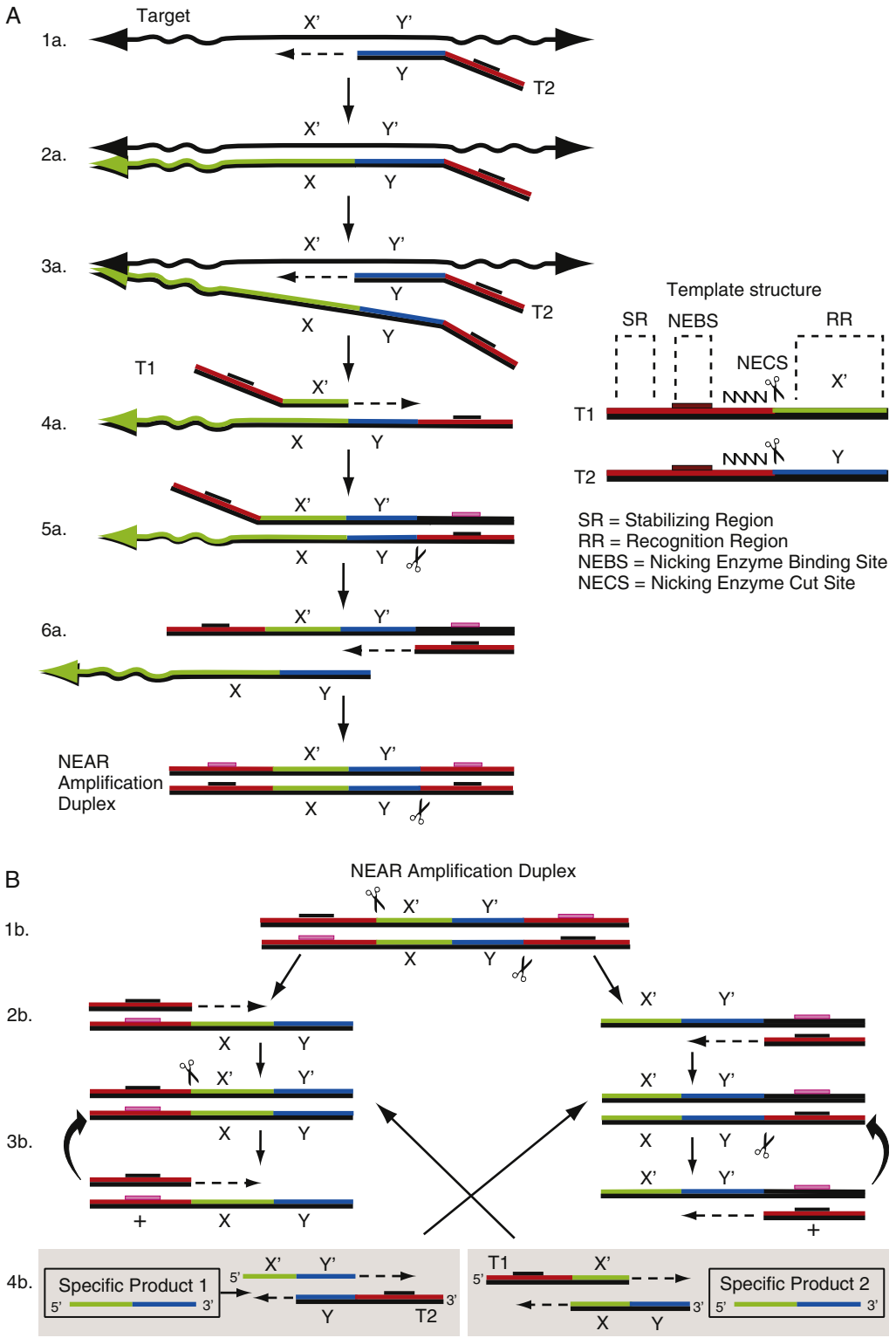

Figure 69.10 Nick endonuclease amplification reaction (NEAR). **A**, Mechanism of NEAR amplification duplex formation. (1a and 2a) The recognition region of T2 binds to the complementary target region and is extended by polymerase along the target. (3a) A second T2 binds to the same target and is extended, displacing the first T2. (4a) The recognition region of T1 binds to its complement in the released strand and is extended to the 5′ end, creating a double-stranded nicking enzyme recognition site. (5a) Nicking enzyme binds and nicks (indicated by scissors). (6a) Polymerase synthesizes off the cleaved 3′ OH along T1, displacing the remaining target complement and the final extended double-stranded complex is termed the NEAR amplification duplex. **B**, Mechanism of product formation. (1b and 2b) Nicking enzymes bind to both nicking enzyme binding sites on the NEAR duplex; cleavage and strand displacement amplification at both sites creates two complexes, each consisting of a duplex stability region, a nicking enzyme recognition region, and a single-stranded target. (3b and 4b) Repeated nicking, polymerization, and strand displacement result in the amplification of products 1 and 2. Cleaved complexes are regenerated (3b), while products 1 and 2 can anneal to T1 and T2 primers, respectively (4b), resulting in bidirectional extension and creating duplexes that generate the opposite product upon cleavage. The products continue to recycle until the templates, deoxynucleoside triphosphates (dNTPs), or enzymes are depleted. (Reprinted with permission from Nie S, Roth RB, Stiles J, et al.: Evaluation of Alere I Influenza A&B for rapid detection of influenza viruses A and B, *J Clin Microbiol* 52:3339–3344, 2014.)

substrate occurs only in the presence of the target sequence, the generation of cleavage products indicates the presence of the target. The cleaved product is detected by binding to and serving as an invader probe for a FRET probe. The 5′ end of the FRET probe is cut by cleavase, releasing the reporter molecule in the same way that it releases the 5′ end of the signal probe.

Multiple cleavase products are formed from a single target molecule since the cleavase reaction can occur at a temperature high enough for a primer exchange equilibrium due to the thermostable nature of the enzyme. Hence, the invader assay can be run under isothermal conditions, removing the need for thermal cycling. This technology has been used for detection, quantification, and characterization of a variety of microbial and human nucleic acid targets (Rossetti et al., 1997; Ryan et al., 1999; Wong et al., 2008).

Since the overlap in the invader probe need only be one base pair, single nucleic acid changes can be identified if the overlap region encompasses the point mutation of interest. Unlike target amplification techniques, the invader assay is less prone to false-positive results from amplicon cross-contamination. Cleavase can also generate fragment-length polymorphisms (in a fashion analogous to restriction fragment-length polymorphism). Melting genomic DNA and cooling it rapidly creates highly reproducible hairpin-loop secondary structures that can serve as substrates for cleavase. Digestion results in a distinct pattern that has been successfully employed to screen for interferon-α–resistant hepatitis C (Sreevatsan et al., 1998) in the past and to detect specific mutations in human genes (Rossetti et al., 1997). Hairpin loops are more diverse than most restriction enzyme recognition sites and offer a versatile fragmentation analysis pattern.

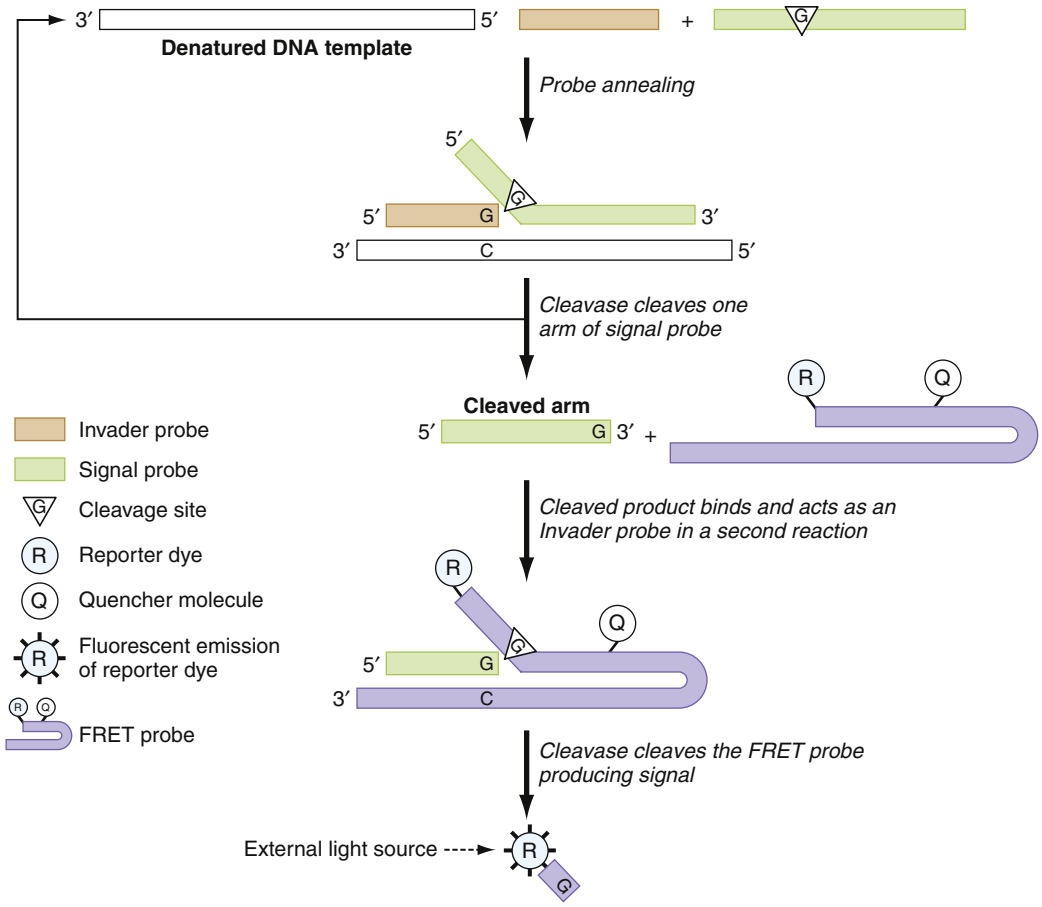

Figure 69.11 Cleavase/invader technology. Invasive cleavage and detection of an oligonucleotide probe using a FEN-1 DNA polymerase. *FEN-1,* Flap endonuclease-1; *FRET,* fluorescence resonance energy transfer. (*Redrawn from Wolk D, Mitchell S, Patel R: Principles of molecular microbiology testing methods,* Infect Dis Clin N Am *15:1157–1204, 2008*)

FDA-cleared assays for HPV and various mutations associated with thrombophilia (factor II, factor V, MTHFR 677, and MTHFR 1298) based on cleavase/invader technology are available from Hologic/Gen-Probe.

BRANCHED DNA

Branched DNA (bDNA) is a solid-phase, sandwich hybridization assay incorporating multiple sets of synthetic oligonucleotide probes (Nolte, 1998). The key to this technology is the amplifier molecule, a DNA molecule with 15 identical branches, each of which can bind three labeled probes.

Target-specific probes capture the target nucleic acid on to the surface of a microtiter well while a second set of target-specific probes also bind to the target. Preamplifier molecules bind to the second set of target probes and up to eight bDNA amplifiers. Three labeled probes hybridize to each branch of the amplifier. Detection of the bound labeled probes is achieved by various methods depending on the probes used (e.g., chemiluminescence, fluorescence, electrochemiluminescence). The resulting signal is directly proportional to the quantity of target in the sample, which is determined from an external standard curve. Strategies to decrease nonspecific hybridization are frequently employed (Collins et al., 1995; Piccirilli et at., 1990). The detection limit of the third-generation bDNA assay for HIV-1 RNA is 50 copies/mL (Kern et al., 1996). bDNA assays for the quantification of HBV DNA, HCV RNA, and HIV-1 RNA are commercially available (Bayer Diagnostics); automated platforms are available as well.

HYBRID CAPTURE ASSAYS

In hybrid capture, the target DNA is denatured and hybridized with a specific RNA probe and the DNA–RNA hybrids are captured by antibodies specific for such hybrids that are coated onto the surface of a tube. Signal amplification results from the large number of antibody binding sites and the efficiency of the enzyme–substrate reaction. Alkaline-phosphatase–conjugated antihybrid antibodies bind to the immobilized hybrids, the conjugate is detected with a chemiluminescent substrate, and the light emitted is measured in a luminometer. The intensity of the emitted light is proportional to the amount of target DNA in the specimen. Hybrid capture assays for detection of HPV (Cope et al., 1997) and CMV (Mazzulli et al., 1999) in clinical specimens are commercially available (Digene, Gaithersburg, MD).

SUMMARY

This chapter provides a basis for understanding the principles underlying the various nucleic acid amplification methods and their relative strengths and limitations. The technology has already had a tremendous impact on the diagnosis of infectious diseases and genetic disorders and promises to revolutionize the diagnosis and management of patients with cancer. The real power of the technology lies in its ability to cut across traditional disciplines in laboratory medicine. Consequently, a thorough understanding of the basic principles of nucleic acid amplification technology is important for all involved in the practice of laboratory medicine.

SELECTED REFERENCES

Afonina IA, Reed MW, Lusby E, et al.: Minor groove binder-conjugated DNA probes for quantitative DNA detection by hybridization-triggered fluorescence, *Biotechniques* 32:940–944, 2002.

This paper describes the development of second-generation real-time PCR probes employing DNA minor groove binders and a dark quencher and their use in single-nucleotide polymorphism detection, viral load determination, and gene expression analysis.

Holland PM, Abramson RD, Watson R, et al.: Detection of specific polymerase chain reaction product by utilizing the 5′ to 3′ exonuclease activity of *Thermus aquaticus* DNA polymerase, *Proc Natl Acad Sci U S A* 88:7276–7280, 1991.

This paper describes how the 5′ exonuclease activity of a DNA polymerase can be used to detect PCR products, which was a key factor in the development of real-time PCR.

Myers TW: Gelfand DH: reverse transcription and DNA amplification by a *Thermus thermophilus* DNA polymerase, *Biochemistry* 30:7661–7666, 1991.

This paper is another milestone in the enzymology of PCR. It describes the use of a single thermostable enzyme to accomplish both the reverse-transcriptase and cDNA amplification, facilitating the development of one-step, closed-tube RT-PCR for RNA targets.

Ririe K, Rasmussen RP, Wittwer CT: Product differentiation by analysis of DNA melting curves during the polymerase chain reaction, *Anal Biochem* 245:154–160, 1997.

This paper describes how melting curve analysis using a microvolume fluorometer integrated with a thermal cycler can be used to differentiate and identify PCR products by monitoring the double-stranded DNA binding dye SYBR green.

Saiki RK, Gelfand DH, Stoffel S, et al.: Primer-directed enzymatic amplification of DNA with a thermostable DNA polymerase, *Science* 239:487–491, 1988.

This seminal paper describes the use of a thermostable DNA polymerase to catalyze the polymerase chain reaction. This development made PCR much more "user friendly" and paved the way for automation of the process.

Access the complete reference list online at Elsevier eBooks for Practicing Clinicians.

REFERENCES

Afonina IA, Reed MW, Lusby E, Shishkina IG, Belousov YS: Minor groove binder-conjugated DNA probes for quantitative DNA detection by hybridization-triggered fluorescence, *Biotechniques* 940–944, 2002.

Babady N, England MR, Jurcic Smith KL, et al.: Multicenter evaluation of the ePlex respiratory pathogen panel for the detection of viral and bacterial respiratory Tract pathogens in Nasopharyngeal Swabs, *J Clin Microbiol* 56(2), 2018. e01658–17.

Bottema CD, Sommer SS: PCR amplification of specific alleles: rapid detection of known mutations and polymorphisms, *Mutat Res* 93–102, 1993.

Broude NE, Zhang L, Woodward K, Englert D, Cantor CR: Multiplex allele-specific target amplification based on PCR suppression, *Proc Natl Acad Sci Unit States Am* 206–211, 2001.

Bustin SA, Benes V, Garson JA, et al.: The MIQE guidelines: minimum information for publication of quantitative real-time PCR experiments, *Clin Chem* 611–622, 2009.

Cao G, Kong J, Xing Z, et al.: Rapid detection of CALR type 1 and type 2 mutations using PNA-LNA clamping loop-mediated isothermal amplification on a CD-like microfluidic chip, *Anal Chim Acta*123–125, 2018.

Chamberlain JS, Gibbs RA, Ranier JE, Nguyen P, Caskey C: Deletion screening of the Duchenne muscular dystrophy locus via multiplex DNA amplification, *Nucleic Acids Res* 16(23):11141–11156, 1988.

Clementi M, Menzo S, Bagnarelli P, Manzin A, Valenza A, Varaldo PE: Quantitative PCR and RT-PCR in Virology, *PCR Methods Appl* 191–196, 1993.

Collins ML, Zayati C, Detmer JJ, Daly B, Kolberg JA, Cha T-A, Irvine BD, Tucker J, Urdea MS: Preparation and characterization of RNA standards for use in quantitative branched DNA hybridization assays, *Anal Biochem* 226:120–129, 1995.

Compton J: Nucleic acid sequence-based amplification, *Nature* 350(6313):91–92, 1991.

Cope JU, Hildesheim A, Schiffman MH, Manos M, Lorincz AT, Burk RD, Glass AG, Greer C, Buckland J, Helgesen K: Comparison of the hybrid capture tube test and PCR for detection of human papillomavirus DNA in cervical specimens, *J Clin Microbiol* 35(9):2262–2265, 1997.

Diplas BH, Liu H, Yang R, Hansen LJ, Zachem AL, Zhao F, Yan H: Sensitive and rapid detection of TERT promoter and IDH mutations in diffuse gliomas, *Neuro Oncol*440–450, 2019.

Farrar JS, Wittwer CT: Extreme PCR: efficient and specific DNA amplification in 15-60 seconds, *Clin Chem*145–153, 2015.

Forshew T, Murtaza M, Parkinson C, Gale D, Tsui DW: Noninvasive identification and monitoring of cancer mutations by targeted deep sequencing of plasma DNA, *Sci Transl Med* 30(4):136ra68, 2012.

Gilliland G, Perrin S, Blanchard K, Bunn H: Analysis of cytokine mRNA and DNA: detection and quantitation by competitive polymerase chain reaction, *Proc Natl Acad Sci Unit States Am*2725–2729, 1990. April 1.

Ginocchio CC, Barth D, Zhang F: Comparison of the Third Wave Invader human papillomavirus (HPV) assay and the digene HPV hybrid capture 2 assay for detection of high-risk HPV DNA, *J Clin Microbiol* 46(5):1641–1646, 2008.

Haqqi TM, Sarkar G, David CS, Sommer SS: Specific amplification with PCR of a refractory segment of genomic DNA, *Nucleic Acids Res* 16(24):11844, 1988.

Haynes RJ, Kline MC, Toman B, Scott C, Wallace P, Butler JM, Holden MJ: Standard reference material 2366 for measurement of human cytomegalovirus DNA, *J Mol Diagn*177–185, 2013.

Heid CA, Stevens J, Livak KJ, Williams P: Real time quantitative PCR, *Genome Res* 986–994, 1996.

Helb D, Jones M, Story E, Boehme C, Wallace E, Ken H, Kop J, Owens MR, Rodgers R, Banada P, Safi H, et al.: Rapid detection of Mycobacterium tuberculosis and rifampin resistance by Use of on-Demand, Near-patient technology, *J Clin Microbiol* 48(1):229–237, 2010.

Holland PM, Abramson RD, Watson R, Gelfand DH: Detection of specific polymerase chain reaction product by utilizing the 5'—3' exonuclease activity of Thermus aquaticus DNA polymerase, *Proc Natl Acad Sci Unit States Am* 7276–7280, 1991.

Huggett JF, Foy CA, Benes V, et al.: The digital MIQE guidelines: minimum information for publication of quantitative digital PCR experiments, *Clin Chem* 892–902, 2013.

Karlen Y, McNair A, Perseguers S, Mazza C, Mermod N: Statistical significance of quantitative PCR, *BMC Bioinf* 131, 2007.

Kern D, Collins M, Fultz T, et al.: An enhanced-sensitivity branched-DNA assay for quantification of human immunodeficiency virus type 1 RNA in plasma, *J Clin Microbiol* 34(12):3196–3202, 1996.

Kricka LJ: Nucleic acid detection technologies — labels, strategies, and formats, *Clin Chem* 45(4):453–458, 1999.

Kutyavin IV, Afonina IA, Mills A, et al.: 3'-minor groove binder-DNA probes increase sequence specificity at PCR extension temperatures, *Nucleic Acid Research* 655–661, 2000.

Kwoh DY, Davis GR, Whitfield KM, Chappelle HL, MiMichele LJ, Gingeras TR: Transcription-based amplification system and detection of amplified human immunodeficiency virus type 1 with a bead-based sandwich hybridization format, *Proc Natl Acad Sci U S A* 86(4):1173–1177, 1989.

Lay MJ, Wittwer CT: Real-time fluorescence genotyping of factor V Leiden during rapid-cycle PCR, *Clin Chem*2262–2267, 1997.

Li M, Diehl F, Dressman D, Vogelstein B, Kinszler KW: BEAMing up for detection and quantification of rare sequence variants, *Nat Methods* 3:95–97, 2006.

Lieber MR: The FEN-1 family of structure-specific nucleases in eukaryotic DNA replication, recombination and repair, *Bioessays* 19(3):233–240, 1997.

Little MC, Andrews J, Moore R, et al.: Strand displacement amplification and homogeneous real-time detection incorporated in a second-generation DNA probe system, BDProbeTecET, *Clin Chem* 45(6):777–784, 1999.

Liu Q, Sommer SS: Pyrophosphorolysis-activated polymerization (PAP): application to allele-specific amplification, *Biotechniques* 29(5):1072–1076, 2000.

Luk KC, Devare SG, Hackett Jr JR: Partially double-stranded linear DNA probes: novel design for sensitive detection of genetically polymorphic targets, *J Virol Methods*1–11, 2007.

Lyamichev V, Mast AL, Hall JG, et al.: Polymorphism identification and quantitative detection of genomic DNA by invasive cleavage of oligonucleotide probes, *Nat Biotechnol* 17(3):292–296, 1999.

Mazzulli T, Drew LW, Yen-Lieberman B, et al.: Multicenter comparison of the digene hybrid capture CMV DNA assay (version 2.0), the pp65 antigenemia assay, and cell culture for detection of cytomegalovirus viremia, *J Clin Microbiol* 37(4):958–963, 1999.

Merante F, Yaghoubian S, Janeczko R: Principles of the xTAG^{TM} respiratory viral panel assay (RVP Assay), *J Clin Virol*S31–S35, 2007.

Milbury CA, Li J, Liu P, Makrigiorgos G: COLD-PCR: improving the sensitivity of molecular diagnostics assays, *Expert Rev Mol Diagn* 11(2):159–169, 2011.

Mori Y, Notomi T: Loop-mediated isothermal amplification (LAMP): expansion of its practical application as a tool to achieve universal health coverage, *J Infect Chemother*30231–30234, 2019.

Morrison TB, Weis JJ, Wittwer CT: Quantification of low-copy transcripts by continuous SYBR Green I monitoring during amplification, *Biotechniques*954–958, 1998.

Myers TW, Gelfand DH: Reverse transcription and DNA amplification by a Thermus thermophilus DNA polymerase, *Biochemistry* 30(31):7661–7666, 1991.

Newton CR, Graham A, Heptinstall LE, Powell SJ, Summers C, Kalsheker N, Smith JC, Markham AF: Analysis of any point mutation in DNA. The amplifICation refractory mutation system (ARMS), *Nucleic Acids Res* 17(7):2503–2516, 1989.

Nie S, Roth RB, Stiles J, et al.: Evaluation of Alere i Influenza A&B for rapid detection of influenza viruses A and B, *J Clin Microbiol* 52(9):3339–3344, 2014.

Nolte FS: Branched DNA signal amplification for direct quantitation of nucleic acid sequences in clinical specimens, *Advanced Clinical Chemistry* 33:201–235, 1998.

Notomi T, Okayama H, Masubuchi H, Yonekawa T, Watanabe K, Amino N, Hase T: Loop-mediated isothermal amplification of DNA, *Nucleic Acid Research* 28(12):e63, 2000.

Piatak M, Luk KC, Williams B, Lifson JD: Quantitative competitive polymerase chain reaction for accurate quantitation of HIV DNA and RNA species, *Biotechniques* 14(1):70–81, 1993.

Piccirilli JA, Krauch T, Moroney SE, Benner SA: Enzymatic incorporation of a new base pair into DNA and RNA extends the genetic alphabet, *Nature* 343(6253):33–37, 1990.

Pierce VM, Hodinka RL: Comparison of the GenMark diagnostics eSensor respiratory viral panel to real-time PCR for detection of respiratory viruses in Children, *J Clin Microbiol* 50(11):3458–3465, 2012.

Poritz MA, Blaschke AJ, Byington CL, et al.: FilmArray, an automated nested multiplex PCR system for Multi-Pathogen detection: development and application to respiratory Tract infection, *PloS One* e26047, 2011.

Ramanan P, Bryson AL, Binnicker MJ, Pritt BS, Patel R: Syndromic panel-based testing in clinical microbiology, *Clin Microbiol Rev* 31(1), 2018, Jan. e00024–17.

Ririe KM, Rasmussen RP, Wittwer CT: Product differentiation by analysis of DNA melting curves during the polymerase chain reaction, *Anal Biochem* 154–160, 1997.

Rossetti S, Englisch S, Bresin E, Pignatti P, Turco AE: Detection of mutations in human genes by a new rapid method: cleavage fragment length polymorphism analysis (CFLPA), *Mol Cell Probes* 11:155–160, 1997.

Ryan D, Nuccie B, Arvan D: Non-PCR-dependent detection of the factor V Leiden mutation from genomic DNA using a homogeneous invader microtiter plate assay, *Molecular Diagnostics* 4(2):135–144, 1999.

Saiki RK, Gelfand DH, Stoffel S, et al.: Primer-directed enzymatic amplification of DNA with a thermostable DNA polymerase, *Science* 487–491, 1988.

Saiki RK, Scharf S, Faloona F, et al.: Enzymatic amplification of Beta-Globin genomic sequences and restriction site analysis for diagnosis of Sickle cell anemia, *Science* 230(4732):1350–1354, 1985.

Schönbrunner NJ, Fiss EH, Budker O, Stoffel S, Sigua CL, Gelfand DH, Myers TW: Chimeric thermostable DNA polymerases with reverse transcriptase and attenuated 3′-5′exonuclease activity, *Biochemistry* 45(42):12786–12795, 2006.

Scott LJ: Verigene Gram-positive blood culture nucleic acid test, *Mol Diagn Ther* 17(2):117–122, 2013.

Sherrill CB, Marshall DJ, Moser MJ, Larsen CA, Daude-Snow L, Prudent JR: Nucleic acid analysis using an expanded genetic alphabet to quench fluorescence, *J Am Chem Soc* 4550–4556, 2004.

Sreevatsan S, Bookout JB, Ringpis FM, et al.: Algorithmic approach to high-throughput molecular screening for alpha interferon-resistant genotypes in hepatitis C patients, *J Clin Microbiol* 36(7):1895–1901, 1998.

Srividya A, Maiti B, Chakraborty A, Chakraborty G: *Loop mediated isothermal amplification: a promising tool for screening genetic mutations*, Molecular Diagnosis & Therapy, 2019. epub.

Taly V, Pekin D, El Abed A, Laurent-Puig P: Detecting biomarkers with microdroplet technology, *Trends Mol Med* 405–416, 2012.

Thelwell N, Millington S, Solinas A, Booth J, Brown T: Mode of action and application of Scorpion primers to mutation detection, *Nucleic Acid Research* 3752–3761, 2000.

Tong Y, Tang W, Kim H-J, Pan X, Ranalli TA, Kong H: Development of isothermal TaqMan assays for detection of biothreat organisms, *Biotechniques* 45(5):543–547, 2008.

Tyagi S, Bratu DP, Kramer FR: Multicolor molecular beacons for allele discrimination, *Nat Biotechnol*49–53, 1998.

VanGuilder HD, Vrana KE, Freeman WM: Twenty-five years of quantitative PCR for gene expression analysis, *Biotechniques* 619–626, 2008.

Vincent M, Xu Y, Kong H: Helicase-dependent isothermal DNA amplification, *EMBO Rep* 5(8):795–800, 2004.

Vogelstein B, Kinzler KW: Digital PCR, *Proc Natl Acad Sci Unit States Am* 9236–9241, 1999.

Walker GT, Fraiser MS, Schram JL, Little MC, Nadeau JG, Malinowski DP: Strand displacement amplification—an isothermal, in vitro DNA amplification technique, *Nucleic Acids Res* 20(7):1691–1696, 1992a.

Walker GT, Little MC, Nadeau JG, Shank DD: Isothermal in vitro amplification of DNA by a restriction enzyme/DNA polymerase system, *Proc Natl Acad Sci U S A* 89(1):392–396, 1992b.

Wittwer CT, Garling DJ: Rapid cycle DNA amplification: time and temperature optimization, *Biotechniques*76–83, 1991.

Wong AK, Chan RC, Nichols S, Bose S: Human papillomavirus (HPV) in atypical squamous cervical cytology: the Invader HPV test as a new screening assay, *J Clin Microbiol* 46(3):869–875, 2008.

CHAPTER 70

HYBRIDIZATION ARRAY TECHNOLOGIES

Martin H. Bluth

ARRAY TECHNOLOGIES, 1401
Macroarrays, 1402
Microarrays, 1402
Microarray Substrates, 1402
Microarray Fabrication, 1402
Oligonucleotide Microarrays, 1403
cdna Microarrays, 1404
Sequencing Arrays, 1404
Hybrid Capture, 1404
Reverse Line-Blot Hybridization, 1405
Hybridization, Detection, and Image Analysis, 1405
Bioinformatics, 1406
Intellectual Property Issues, 1407
CLINICAL APPLICATIONS OF ARRAY TECHNOLOGY, 1408
Array Technology in the Clinical Laboratory, 1408
Array Technology in Clinical Disease, 1408
Emerging Technologies: Exosomes, 1408
Limitations, 1410
SELECTED REFERENCES, 1410

KEY POINTS

- Array technology provides a unique and powerful approach to screen a sample for dozens to thousands of genes.
- Current array fabrications allow for diverse platforms with better detection and reduced cost for high-density applications.
- Positive signals are generated when a tagged nucleic acid moiety hybridizes with its complementary probe localized on a solid support (i.e., "chip").
- Care must be taken when performing and interpreting microarray experiments because numerous factors must be considered in analysis.
- Numerous applications of array technology have been proposed in the past few years, ranging from molecular staging of tumors to the identification and characterization of microbial agents.
- Improvement of quality and yield of nucleic acid extraction from fixed and frozen tissues combined with continued miniaturization and cost reduction of platforms are making array technology more commonplace and user friendly.

In only a few short years, hybridization array technology, which enables the performance of thousands of simultaneous hybridization reactions on a solid substrate within a single analytical procedure, has gone from theoretical construct to practical reality. Such massively parallel determinations offer previously unimaginable opportunities for diagnostic application, ranging from gene sequencing and detection of genetic polymorphisms to measurement of gene expression profiles in cancer cells. Microarray-based systems offer a platform for quantifying the expression of thousands of genes at the same time. Therefore, an unprecedented advantage of this technology is that it affords analysis of whole cassettes of genes, or patterns of gene expression, rather than analysis of one, two, or three genes at a time. The general schema for microarray processing includes the generation of nucleic acid (i.e., deoxyribonucleic acid [DNA]) complementary to genes of interest that is laid out in microscopic quantities on solid surfaces at defined positions (the "probe") nucleic acid (genomic DNA or complementary DNA [cDNA]) from samples is added over the surface—cDNA binds and the presence of bound DNA is detected by fluorescence after laser excitation (for a general review, see Friend & Stoughton, 2002).

It is clear that hybridization array technology has revolutionized the way we approach the study of disease. The one gene–one protein–one function approach is no longer the mainstay of scientific design. Array technology introduced a complicated mirror image of this approach—in other words, multiple functions, multiple proteins, multiple genes. The power of this technology lies in the "screening" capability that it provides. Under-defined experimental conditions, one now has the ability to determine changes in the patterns of genes, identifying multiple genes acting in concert. These patterns can then be "mined" through various computer algorithms, grouped into functional categories (e.g., respiratory genes, inflammatory genes), and used to derive signatures diagnostic of disease or to generate novel hypotheses about pathogenesis and cell function. The relationship of these genes to one another (increased versus decreased expression) are determined and generally expressed as fold-change. Microarray findings of differential gene expression require confirmation by other techniques such as quantitative reverse transcriptase polymerase chain reaction (RT-PCR) or additional independent microarray studies.

After candidate genes or groups of genes are identified, classic approaches to gene function (i.e., gene knockout or gene knockdown) can then be employed to elucidate or validate gene function. More important, hybridization array technology, with subsequent data mining, allows genes not previously known to be associated with the disease to be considered, generating new paradigms for future study. Similar platforms can be used to sequence large genes and to scan the genome for single nucleotide polymorphisms and methylation sites. This chapter reviews the theoretical basis for the various matrix hybridization platforms and provides a perspective on their clinical application, both currently and in the future.

ARRAY TECHNOLOGIES

A hybridization array is the molecular equivalent of a spreadsheet, on which each cell or address reveals a specific piece of data, usually inferred from the binding of a ligand to its specific target. The first array-based methods were exploited in immunoassays (Ekins & Jackson, 1987; Ekins & Chu, 1999), and arrays also have been proposed for parallel studies of diverse targets such as proteins, lipids, carbohydrates, and small molecules (Fodor et al., 1991; Pirrung et al., 1992; Southern, 1996a; Guschin et al., 1997; Schena et al., 1998). Similar to antigen–antibody interactions on immunoarrays, the fundamental principle of nucleic acid arrays is detection of specific hybridization between complementary strands. The principles of nucleic acid hybridization and an overview of various platforms are covered in Chapter 68. The effectiveness of solid-support hybridization formats was pioneered with the use of nitrocellulose membranes (Gillespie & Spiegelman, 1965) for dot blots (Kafatos et al., 1979), line probes, and Southern blots (Southern, 1975). Changing the labeled entity from the probe to the sample was first referred to as *reverse line-blot* (or *dot blot*) hybridization and led to the beginning of interrogating one sample for multiple potential targets. Moving from dozens to thousands of targets has come about rapidly over the last few years, driven in part by the unique convergence of microfabrication, robotics, and bioinformatics technologies and the demand for high-throughput genetic analysis resulting from the Human Genome Project.

The field is bursting with potential, and many investigators foresee diagnostic and prognostic applications in tumor classification, chemotherapeutic responsiveness, pathogen detection, monitoring antibiotic resistance, and characterizing inflammatory responses. Array technology may make the dream of personalized molecular medicine, in which the genes of an individual patient may be assessed for risk factors and disease susceptibility and to predict response to therapy, a reality. Studies using

gene expression profiling to predict diseases include identifying which trauma and burn patients will develop sepsis and multisystem organ failure (www.gluegrant.org) genes involved in the pathogenesis of chronic obstructive pulmonary disease (Wang et al., 2008), and which patients would likely have recurrence of cancer (Potti et al., 2006), among others. However, challenges of reproducibility and laboratory quality control remain to be addressed before this enormous potential is realized.

MACROARRAYS

The term *macroarray* has been applied to formats in which areas of probe localization, often called *features*, are large enough to be visualized without magnification. These have been manufactured on nylon or nitrocellulose membranes or as plastic strips with linear arrays of bound target. Because of the size of the features, the density of macroarrays is much lower than microarrays, ranging from a few dozen to hundreds or even thousands of probes. They are usually deposited onto the membrane by printing or dot blotting and then dried and stored for future use.

Nylon, plastic, and glass (silicon wafer) are standard supports to make macroarrays. Nylon suffers several drawbacks compared with silicon, which is a preferred matrix for hybridization arrays. Besides its porous nature, nylon displays high autofluorescence, limiting the sensitivity of fluorescence-based detection because of high background values. The latter also precludes the possibility to develop ratiometric (or two-color) assays. This approach uses two targets, each labeled with a different fluor. Most commonly, one is a constant reference control used in direct comparison with the unknown sample, with results expressed as a ratio of the two emitted fluorescent signals (Duggan et al., 1999).

Macroarrays are currently used for targeted applications. For example, some commercial arrays target all the known cytokine genes or those within specific signal transduction pathways that are activated during infectious and inflammatory processes. Other arrays, targeting the genes altered during oncogenesis, have been used in cancer research (e.g., Atlas Human Arrays, Clontech ; GeneFilters, Research Genetics). Other commercial applications, usually in kit format, are used to detect and type specific PCR products, such as in the cystic fibrosis mutation screen, human leukocyte antigen typing, or human papillomavirus (HPV) typing. Furthermore, nylon-based arrays have been used to detect bacterial colony–based gene expression (Barsalobres-Cavallari et al., 2006) and thyroid cancer detection (Durand et al., 2008). The advantages of macroarrays include the ability to use standard hybridization equipment, simplified reading or scanning, and affordability.

Some groups have been successful in producing high-density nylon arrays on a custom basis for gene discovery purposes (Gress et al., 1992; Takahashi et al., 1995; Granjeaud et al., 1996; Pietu et al., 1996; Clark et al., 1999; Durand et al., 2008). Even in high-density configurations, the size of the nylon arrays requires a relatively large volume of hybridization fluid, a practical limitation with respect to generating a probe from small amounts of diagnostic material. Because microarrays, rather than macroarrays, represent the high-density, high-throughput platform of choice, the bulk of this chapter focuses on applications of microarrays.

MICROARRAYS

Assay miniaturization saves time while cutting costs in biomedical diagnostic applications and research. Working with smaller volumes reduces reagent consumption, increases sample concentration, and improves reaction kinetics. These improvements allow the investigator to determine hundreds or thousands of results in the time formerly required for a single experiment. Microarrays are now available from several commercial suppliers, along with reading and fabrication equipment for custom manufacture of dedicated arrays for specific research or diagnostic applications.

MICROARRAY SUBSTRATES

A major distinction between microarrays and macroarrays consists of the choice of a nonporous solid support. By preventing diffusion of the target nucleic acids, nonporous surfaces (plastic, glass, or silicon substrates) allow faster hybridization kinetics and easier washing steps. To allow spatial discrimination of numerous reactions performed simultaneously, the molecular probes are bound to a solid surface in defined arrays. Deposition of probes on a solid substrate is also more amenable to automation and enables higher array densities with optimal image definition. These features apply to any type of microarray, from synthetic oligonucleotides to cloned cDNAs or PCR products (Southern et al., 1999). Most microarrays are now developed on glass. As opposed to plastic derivatives, glass transparency and lack of autofluorescence allows low-background, fluorescence-based detection. However, as materials science becomes more involved in array technologies, alternative substrates, including coated glass and plastic substrates, may become available.

MICROARRAY FABRICATION

3′-End functionalization (i.e., chemical modification) of nucleic acids—oligonucleotides, PCR products, cDNAs, or peptide nucleic acid oligomers—is required for covalent immobilization on either glass or polypropylene surfaces (Matson et al., 1995; Beier & Hoheisel, 1999). For example, treatment of glass slides with silane allows amino-covered glass to bind amino-linked probes, using bifunctional molecules such as a dialdehyde or a diisothiocyanate (Case-Green & Southern, 1994; Guo et al., 1994). Alternatively, glass coating with a polycation (e.g., polylysine) allows direct charge-coupled binding of polyanionic DNA probes (Maskos & Southern, 1993a); an ultraviolet photo-cross-linking step adds covalent bonds to the ionic interaction. Covalent binding is essential to permit stringent washes and therefore accurate discrimination of hybridized species. Several protocols have been published to address surface activation (Maskos & Southern, 1992; Beattie et al., 1995; Matson et al., 1995; Beier & Hoheisel, 1999). An interesting alternative consists of deposition of small patches of activated polyacrylamide to which presynthesized oligonucleotides are attached by microinjection (Khrapko et al., 1991; Yershov et al., 1996; Guschin et al., 1997).

The packing density of probes attached to solid surfaces influences greatly the performance of hybridization matrices. Poor coupling efficiency, which is often encountered on glass matrices, can result in low probe density and low signal-to-noise ratios. On the other hand, overly dense packing of oligonucleotides onto a solid surface causes spatial hindrance. This problem may be even more formidable with longer biomolecules such as cDNAs. Hybridization yields can be increased by up to two orders of magnitude by introducing spacers between the surface and the oligonucleotides (Southern et al., 1999). The longer the spacer, the better the hybridization, but, interestingly, there is an optimal spacer length beyond which hybridization yield declines (Shchepinov et al., 1997; Duggan et al., 1999). For example, a 40-carbon atom spacer provides a reported 150-fold hybridization enhancement (Shchepinov et al., 1997). The density of oligonucleotides is approximately 0.1 pmol/mm^2 on a glass surface, two orders of magnitude less than on aminated polypropylene. Thus, a potential advantage of glass over plastic matrices at present is an optimal oligonucleotide density associated with lower spatial hindrance (Southern et al., 1999). Improved surface chemistries may one day allow production of arrays on plastic sheets or films, which may dramatically reduce production costs. To this end, film-based chip arrays have recently been described (Erali et al., 2009).

The terminal composition (5′ end) of the oligonucleotides influences their duplex yield as measured by relative intensity. As expected, G:C-rich 5′ extremities lead to a better yield than their homologues (same composition but different sequences) (Maskos & Southern, 1993b). Approaches to modify the 5′ end of oligonucleotides (e.g., covalent addition of a degenerated linker) can therefore be considered to minimize this contribution. Alternatively, knowledge that mismatches at the ends are less destabilizing and therefore more difficult to discriminate by hybridization (Southern et al., 1999) has led to clever improvements for detection of hybridization events. Because polymerases and ligases are most sensitive to terminal (as opposed to internal) mismatches, enzymatic methods have been developed with improved detection stringency (solid-phase minisequencing [Pastinen et al., 1997; 1998; Syvanen, 1999], genetic-bit analysis [Nikiforov et al., 1994], or ligation-assays [Landegren et al., 1988; Nickerson et al., 1990]).

Commercially available arrays have been previously reviewed by Marshall and Hodgson (1998). Fabrication of microarrays falls into two broad categories: those made by direct probe delivery onto the solid surface and those made by in situ synthesis. A third method, which was developed by Nanogen (San Diego), consists of prefabricated oligonucleotides captured onto electroactive spots on silicon wafers (Edman et al., 1997; Sosnowski et al., 1997; Cheng et al., 1998; Heller et al., 1998; Jang et al., 2009). Modification of the electric field through independent, spatially addressable electrodes can speed up hybridization and, when the polarity is reversed, provide stringent washing (Edman et al., 1997). Recently, large single-stranded, circular-sense molecules were used as probes for DNA microarrays and showed stronger binding signals than those of PCR-amplified cDNA probes (Doh et al., 2010).

Delivery Technologies

Deposition of presynthesized biomolecules was initiated by Pat Brown and colleagues (Schena et al., 1995; Shalon et al., 1996). Biochemical substances

(e.g., proteins, peptides, oligonucleotides, cDNAs) are prepared, purified, and stored in microtiter plates. Small quantities of molecules are mechanically delivered on precisely defined locations on a solid surface using different precision robotic systems. This method is very flexible in terms of biochemical composition, microarray topology (e.g., size and density of the spots, replicate spots for each molecule), and ease of prototyping, allowing for design alteration for different applications. Mechanical methods allow the synthesis of moderate- to high-density microarrays (≤~16,000 probes/cm^2 [Graves, 1999]). It is the method of choice when large numbers of microarrays are needed with the same composition, as well as for long sequences using PCR products. Several companies are now manufacturing and selling premanufactured arrays (e.g., MicroMax, NEN Life Science) or arrayers based on deposition (Cheung et al., 1999) as an alternative to building an arrayer (Brown et al., 2000).

Delivery procedures consist of different microprinting systems. Most arrayers use fountain pen–like microdispensing tips (e.g., Cartesian Technologies), but some original systems such as the pin-and-ring technique have been developed (Genetic MicroSystems). In general, because of surface tension, static, and other effects, the reproducibility of printed arrays is lower than in situ synthesis and must be corrected by separate experiments (repeats), replicate spots (on the same slide), multicolor fluorescence detection, or other specific detection algorithms (Chen et al., 1997; Jang et al., 2009). Because of its flexibility and availability, printed array technology will probably have the largest impact on research and clinical laboratories over the next few years.

In Situ Synthesis

In situ synthesis allows higher yields, lower chip-to-chip variation, and higher probe densities. These methods also permit the manufacture of true "random access" arrays, meaning that each oligonucleotide in any position can have any chosen sequence (Southern et al., 1999). *Combinatorial strategies* refer to methods developed to make microarrays containing all sequences of a given length (also referred to as *generic arrays*). Combinatorial arrays have been promoted mostly to study large-scale hybridization behavior (Southern et al., 1994) or for solid-state nucleic acid sequencing (Macevicz, 1991; Strezoska et al., 1991; Drmanac & Crkvenjakov, 1993; Drmanac et al., 1993; Lipshutz, 1993; Drmanac et al., 1998; Drmanac & Drmanac 1999).

Manufacturing techniques include photolithographic masks to control chemical activation by photodeprotection steps (Fodor et al., 1991), ink-jet deposition (Stimpson et al., 1998), and physical barriers to sequential flooding of precursors (Maskos & Southern, 1993c). Affymetrix has coupled photochemical deprotection to solid-phase DNA synthesis by adapting techniques from the semiconductor industry (Pease et al., 1994; Lockhart et al., 1996; Lipshutz et al., 1999). Synthetic linkers modified with photochemically removable protecting groups are attached to silicon wafers. By shining ultraviolet light through a photolithographic mask, localized photodeprotection occurs and permits specific chemical building blocks (hydroxyl-protected deoxynucleosides) to react with the deprotected groups (Fodor et al., 1991) (Fig. 70.1). Cycles alternating photodeprotection and incubation with different chemical building blocks allow light-directed synthesis of polydeoxynucleotides (Fig. 70.2). The synthesized oligonucleotides have a maximum practical length because of the limited efficiency of the photodeprotection (80%–95% at each cycle) (Forman et al., 1999). Therefore, the proportion of 20-mers displaying the predefined sequence is between 1% and 36% (0.8E20 and 0.95E20) (Fodor et al., 1991).

Mechanical masks or barriers permit confinement of surface areas before flooding with defined precursors. Physical masks of different shapes (circular, diamond) allow in situ synthesis of a given precursor in known locations. Sequential displacement of masks followed by the flooding of another precursor allows synthesis of large combinatorial deoxynucleotide arrays (Southern et al., 1992; Southern, 1996b; Maskos & Southern, 1993c). To date, Affymetrix is able to synthesize up to 400,000 different polydeoxynucleotides in a 1.6-cm^2 area (Fodor et al., 1991). Critical to this step is the precise alignment of the mask with the wafer before each synthesis step. To ensure that this critical step is accurately completed, chrome marks on the wafer and on the mask are perfectly aligned. Although the process is highly efficient, some activated molecules fail to attach the new nucleotide. To prevent these outliers from becoming probes with missing nucleotides, a capping step is used to truncate them. In addition, the side chains of the nucleotides are protected to prevent the formation of branched oligonucleotides (www.affymetrix.com). Despite the high cost, this is the method of choice for large-scale differential gene expression studies because of sensitivity, reproducibility, and redundancy of information.

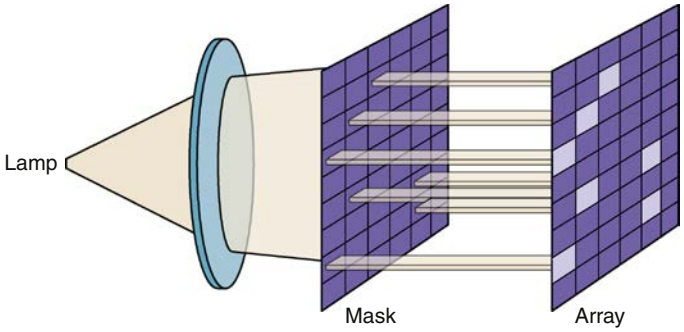

Figure 70.1 Photolithographic synthesis. Ultraviolet light is transmitted through a photolithographic mask, allowing localized photodeprotection of specific chemical building blocks. (Courtesy of Affymetrix.)

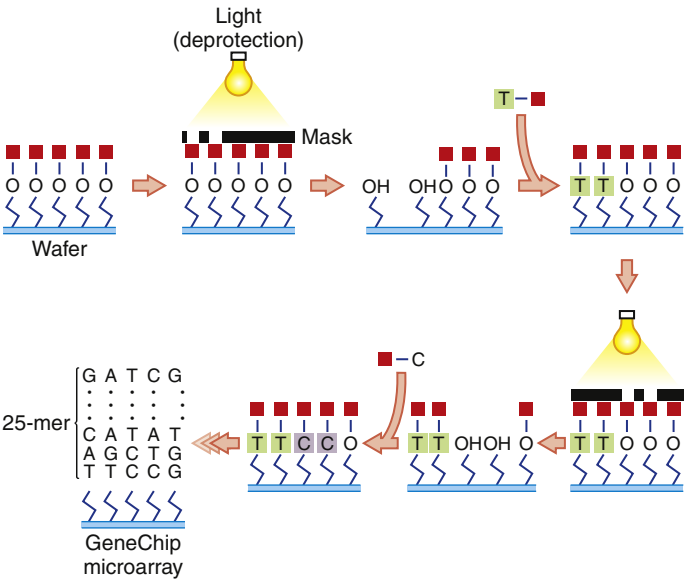

Figure 70.2 Diagram of GeneChip array manufacture using a unique combination of photolithography and combinatorial chemistry. (Courtesy of Affymetrix.)

Ink-jet technologies owe their development to the printer industry and are in continuous development by several companies such as Incyte Pharmaceuticals, Protogene, and Rosetta Inpharmatics (Blanchard et al., 1996). This technology is also commercially available (Ink-Jet, Packard Instruments; Piezoelectric pump, GeSiM). This technology gave rise to the ability to place an oligonucleotide or other entity (i.e., small molecule or tag) in two-dimensional space. Such an approach offers versatility in the biomolecules being delivered and eliminates the need for physical contact with the surface of the array; this last property may be of relevance for the development of arrays coated with thin layers of metals and using different detection methods (Heyse et al., 1998; Schmid et al., 1998). Light scattering from microparticles tagging target sequences can be detected as an evanescent wave immediately above the surface of the glass. This method allows real-time affinity measurement with a very low background (Stimpson & Gordon, 1996).

OLIGONUCLEOTIDE MICROARRAYS

Thermodynamics, kinetics of hybridization, and quantitative aspects of oligonucleotide hybridization have been extensively studied (reviewed by Wetmur, 1991; Hoheisel, 1996; Pozhitkov et al., 2007). Oligonucleotide arrays have a lower sensitivity than cDNA arrays for detection of rare messages or hybridization targets and poor predictability of hybridization characteristics because hybridization potential, and therefore the expected signal intensity, does not correlate well with the G:C content or the melting temperature (Lockhart et al., 1996; Graves, 1999). On the other hand, oligonucleotide arrays are easier to construct using deposition of synthesized product or in situ synthesis described earlier. In addition, hybridization conditions can be more homogeneous than on a cDNA array, provided that the array is designed with oligonucleotides of equivalent sizes.

Oligonucleotide arrays have applications in gene expression profiling as well as in DNA sequencing. For sequencing applications, they can be divided into two fields: generic arrays (representing a random oligonucleotide matrix) or dedicated arrays (for molecular variants of a predetermined target). Generic arrays have been proposed as an inexpensive alternative to sequencing. Using all possible combinations of an n-mer allows "walking" at every position along a nucleotide sequence. This type of array is the only one capable of detecting sequences that are lacking in large electronic libraries. In contrast, dedicated arrays are used for repetitive sequencing (resequencing) of the same target for detection of nucleotide polymorphisms or functional mutations. This implies knowledge of the targets and their most frequent variants in order to incorporate predetermined sets of oligonucleotides on the diagnostic array. This approach has been used for detection of genetic polymorphisms associated with human immunodeficiency virus (HIV) drug resistance and other polymorphisms. Oligonucleotide arrays can also be used to define single nucleotide polymorphisms (Guo et al., 1994), even by comparing two samples with multicolor fluorescence (Chee et al., 1996). Further examples and applications of polymorphism to disease diagnosis, treatment, and management are described later in this chapter and in Chapters 73 to 75.

The search for oligomers of higher affinity has opened the way for chemical modifications of the oligonucleotide probe and template to improve the kinetics and thermodynamics of binding. Peptide nucleic acid probes (PNAs) allow hybridization to be performed at a higher stringency because of the high-stability of PNA–DNA duplexes (Corey, 1997) and are able to recognize exclusively single strands of DNA and ribonucleic acid (RNA) in antiparallel fashion (Moggio et al., 2007). Methylated RNA probes (Corey, 1998) display relatively similar affinities. However, PNAs display more rapid hybridization conditions than their nucleic acid counterparts, primarily because of their neutral backbone structure (Freeman & Gioia, 1999). Overall, it can be said that although the reduction of the hybridization time from hours to minutes would be a clear asset, the problem of unpredictability of the melting points of these high-affinity oligomers must be overcome before implementation on microarrays (Weiler et al., 1997). In addition to probes, targets can be chemically modified to locally enhance signals. Pyrimidine-rich target regions can generate higher hybridization signals by incorporating 5-methyluridine during in vitro transcription (Woski et al., 1998).

cDNA MICROARRAYS

Microarrays of cDNA sequences allow hybridization-based monitoring of the expression of the cognate genes. Therefore, this strategy implies access to clones or the possibility of generating PCR products. To date, the best strategies use two-color fluorescence detection to discriminate between a sample and its control and check for differential level of expression. This method has been pioneered and validated by Pat Brown and colleagues at Stanford University (Schena et al., 1995; 1996; Shalon et al., 1996). Advantages of this approach are calculating a ratio on every probe to control for the quality of the probe, the specific hybridization properties of each target–probe pair, and the labeling efficacy. Synteni (a subsidiary of Incyte) has developed its Gene Expression Micro-arrays for this purpose (Schena et al., 1998). NEN Life Science is selling glass slides prespotted with 2400 known human genes (MicroMax), and continuous miniaturization is allowing for greater gene representation in a smaller area.

Although they appear to be inherently less reproducible, cDNA microarrays currently offer the greatest versatility in terms of probe deposition and accessibility of the technology. Several companies now offer equipment for array manufacture and reading of hybridized matrices. It is likely that cDNA arrays and high-density oligonucleotide arrays will play complementary roles in research laboratories over the next few years; high-density arrays will be used primarily for the discovery of diagnostically relevant loci, and dedicated arrays will be used increasingly for the medium- to low-density analysis of diagnostically relevant loci discovered by high-density array analysis.

SEQUENCING ARRAYS

Nucleic acid sequence data are fundamental to modern molecular biology. Conventional methods (Maxam & Gilbert, 1977; Sanger et al., 1977) are time consuming, labor intensive, and costly. Alternative sequencing methods using solid-phase hybridization were proposed on a theoretical basis (Bains & Smith, 1988; Khrapko et al., 1989) within 15 years of the discovery of these methods (Southern, 1975). The theoretical articles were followed shortly by data confirming the principles of array-based sequencing for short artificial templates (Southern et al., 1992; Pease et al., 1994; Parinov et al., 1996). A well-written review of microarray sequencing methods was published in 1999 (Hacia, 1999). Readers might note, however, that much of the work published and cited in this area is provided by researchers with some financial interest in one or more of the proprietary devices evaluated in these publications. Rather than endorsing a particular device or method, this chapter acquaints readers with basic principles involved in the assay.

Any nucleic acid sequence can in theory be broken down into subsets of length n. All the possible oligonucleotides of length n (n-mers) can then be placed at fixed locations on a solid surface. Nucleic acid to be sequenced (the template) is amplified if necessary, labeled with a direct (fluorescent, luminescent, radioactive) or indirect (affinity) label, and allowed to hybridize to the bound collection of n-mers. Detection of a label allows the sequencer to verify a match with an n-mer at a particular locus on the solid surface. The intensity of the signal at that locus should be directly proportional to the number of domains in the template corresponding to the n-mer at that locus. Methods for all these steps are outlined in preceding sections of this chapter.

For sequencing applications, the n-mers that match the template are then assembled into a definite order by analysis of n-mers with overlapping sequence, similar in principle to the arrangement of contigs by large-scale sequencing programs. Consider a nonanucleotide template that, under stringent conditions, is bound only to the loci containing the following four tetramers on an array with all 256 possible tetramers:

Tetramer	Intensity
5′ ACTG	2
5′ CTGA	2
5′ TGAC	1
5′ GACT	1

It is possible to reason from the areas of overlap that the nonanucleotide template was 5′ ACTGACTGA. Computational analysis of this kind is straightforward. Because the computation, the scanning of the array to detect the label, the labeling itself, and to some extent even the extraction and amplification of the DNA can be automated, it is lovely to envision a "black box" that accomplishes all this in an afternoon. Consider, however, a nonanucleotide that binds to loci containing the following tetramers:

Tetramer	Intensity
5′ TCTA	1
5′ CTAC	1
5′ TACT	1
5′ ACTT	1
5′ CTTC	1
5′ TTCT	1

This could represent 5′ TCTACTTCT or 5′ TTCTACTTC; there is no computational way to resolve it. Where n is less than half the length of the template, repeats of the same length as n/2 can render the data ambiguous. Computation becomes increasingly difficult as template length becomes an increasingly higher multiple of n, so it is desirable to have as long an n as possible for sequencing unknown domains. The practical length of n remains limited by technology, however, because 4^n (the number of loci required for universal representation) exceeds 1 million for $n = 10$. This approaches the current limits of the number of distinct oligonucleotides that can be differentiated on a photolithographic chip (Lipshutz et al., 1999).

HYBRID CAPTURE

Hybrid capture is a nucleic acid hybridization technology that can precede signal amplification and often uses fluorophore or chemiluminescent detection. To date, HPV cannot be cultured in vitro, and immunologic tests are inadequate to determine the presence of HPV cervical infection. Indirect evidence of anogenital HPV infection can be obtained through physical examination and by the presence of characteristic cellular changes associated with viral replication in Papanicolaou smears or biopsy specimens. Alternately, biopsies can be analyzed by nucleic acid hybridization to detect the presence of HPV DNA directly. In the case of modern molecular-based HPV tests, specimens containing the target DNA hybridize with a specific HPV RNA probe cocktail. The resultant RNA:DNA hybrids are captured onto the surface of a solid medium (i.e., a microplate well coated with antibodies specific for RNA:DNA hybrids or covalently linked to beads). Immobilized hybrids are then reacted with alkaline phosphatase–conjugated antibodies specific for the RNA:DNA hybrids that

bind to a different nonoverlapping determinant site recognized by the capture antibody and detected with a chemiluminescent substrate.

Several alkaline phosphatase molecules are conjugated to each antibody. Multiple conjugated antibodies bind to each captured hybrid, resulting in substantial signal amplification. As the substrate is cleaved by the bound alkaline phosphatase, light is emitted that is measured as relative light units on a luminometer. The intensity of the light emitted denotes the presence or absence of target DNA in the specimen. In the case of HPV, although this technique can elucidate the presence and load of the virus, it cannot determine which specific types of HPV are present. For the identification of the HPV strains present in the sample, PCR with HPV strain–specific primers is required (for a review, see Bluth & Bluth, 2018)

REVERSE LINE-BLOT HYBRIDIZATION

Reverse line-blot hybridization, also called "spacer oligonucleotide typing" (spoligotyping), is a method that can detect and identify pathogens based on the presence and comparison of pathogen-specific genes and is useful for confirming the presence of specific pathogens and a proper course of treatment based on possible multidrug resistance. For example, wild-type *Mycobacterium tuberculosis* is a slow-growing bacterium, requiring 2 to 6 weeks to culture, and is sensitive to treatment with rifampicin (RIF). Mutations in the *rpoB*gene can render it resistant to RIF. Using this information, the mutation hot-spot region of the *rpoB* gene is first amplified by mpPCR using as many as 20 different biotinylated primers, which yield labeled amplified products. The PCR products are hybridized to a set of wild-type and mutant oligonucleotide probes, which are covalently bound to a membrane, by reverse line blotting. It is called "reverse" because in contrast to Southern or northern blotting in which the sample is transferred onto a membrane and then probed, the probe is first systematically bound to the membrane, and the sample is then hybridized to it.

Positive hybridization is detected on film after streptavidin-peroxidase incubation and enhanced chemiluminescence. RIF-sensitive strains only hybridize with the wild-type probes, whereas resistant strains fail to hybridize with one or more wild-type probes and show additional hybridization signals for the mutant probes. The resultant hybridization pattern elucidates the genotype of the *M tuberculosis* and thus a proper treatment protocol (for a review, see Bluth & Bluth, 2013).

HYBRIDIZATION, DETECTION, AND IMAGE ANALYSIS

A critical component of microarray assays is the quality and labeling of the probe. Because the sample carries the label, sample-to-sample variation in probe preparation and labeling can be anticipated. When microarrays are used for gene expression profiling, this step is even more critical because of the difficulties in obtaining high-quality messenger RNA (mRNA). Insufficient, degraded, or poor-quality RNA can deliver erroneous results that lead, after data mining, to improper conclusions (Russo et al., 2003). Although many protocols are available for high yield of RNA, a final yield of at least a few micrograms of mRNA per experiment has been desirable in most applications, although protocols have used smaller amounts of RNA with subsequent amplification using cDNA intermediates that incorporate an RNA promoter and allow amplification with an RNA polymerase. Initial approaches (Auffray & Rougeon, 1980) converted mRNA to a fluorescent cDNA probe with direct incorporation of fluorescent nucleotides. Currently, most approaches use total RNA, and there are numerous variations of incorporation of a label into cDNA or RNA probes, including indirect affinity labels such as biotin with detection using antibody, avidin, or streptavidin tagged with fluors or light-scattering gold particles (Figs. 70.3 and 70.4). Each step of probe preparation from extraction through labeling must be carefully controlled to ensure reproducible results.

The usual consideration of time, temperature, stringency, and probe concentration determine the conditions of the microarray hybridization. Arrays often include negative control probes to allow optimal stringency to be determined. Because of the extremely high complexity of the probe used in gene expression profiling, hybridization times are generally extended to allow low-abundance messages to hybridize. Washes are designed to remove nonspecifically bound probe and reduce background. All steps need to be optimized and standardized. After a successful hybridization, labeled nucleic acid is bound to complementary sequences that are tethered to the array (Fig. 70.5). Some form of image analysis is used to capture a signal. In most approaches, the entire slide is scanned (fluorescence, autoradiographic, or light scattering), and an algorithm is used to link features with intensities and gene lists. Software associated with the scanner can generate a "mask" to align the image with a grid used to construct

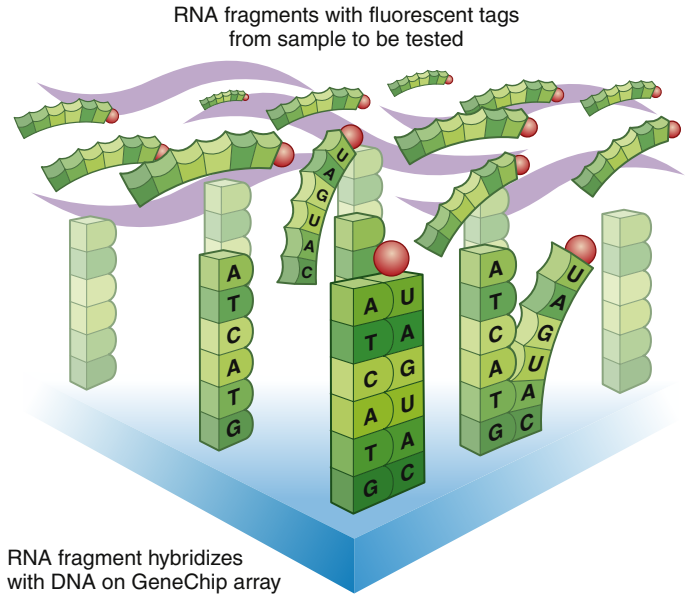

Figure 70.3 Schematic depicting hybridization of tagged probes to Affymetrix GeneChip microarray. (Courtesy of Affymetrix.)

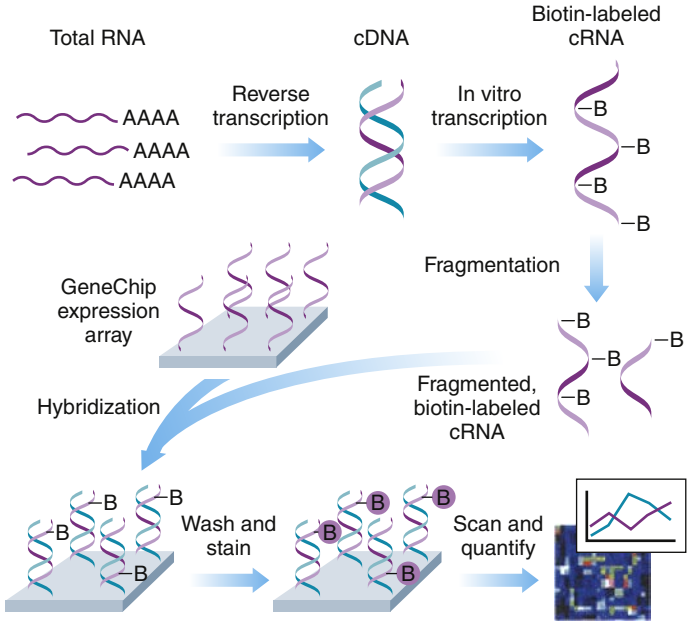

Figure 70.4 Standard eukaryotic gene expression assay. Labeled complementary DNA or RNA targets derived from the messenger RNA (mRNA) of an experimental sample are hybridized to nucleic acid probes attached to the solid support. By monitoring the amount of label associated with each DNA location, it is possible to infer the abundance of each mRNA species represented. *B,* biotin. *(Courtesy of Affymetrix.)*

the array. Data acquisition generates large data sets (one image uses typically 10–50 MB) that have to be stored under standard formats (e.g., BMP, GIF, JPG). Image processing software will become increasingly automated to ensure proper grid adjustment, detect artifacts, and identify features to extract meaningful information.

Microarray technology has grown over the past decade to incorporate miniaturization of fabrication platforms, enhancement of high-throughput automation (see also Chapter 80), and cost reduction. Many platforms exist to support individual user needs whether they be interrogation of an entire genome, exonic mRNA expression, or limited to a subset of genes involved in specific pathways of interest. Affymetrix pioneered mass application of array technology to the scientific community and continues as a leader in the field. Illumina (www.illumina.com) has facilitated RNA analysis of specific genes or regions of interest, with the development of its cDNA-mediated annealing, selection, extension, and ligation (DASL) assay (Fan et al., 2004). This assay reportedly allows for RNA profiling of up to 1536 targets using partially degraded RNA as found in

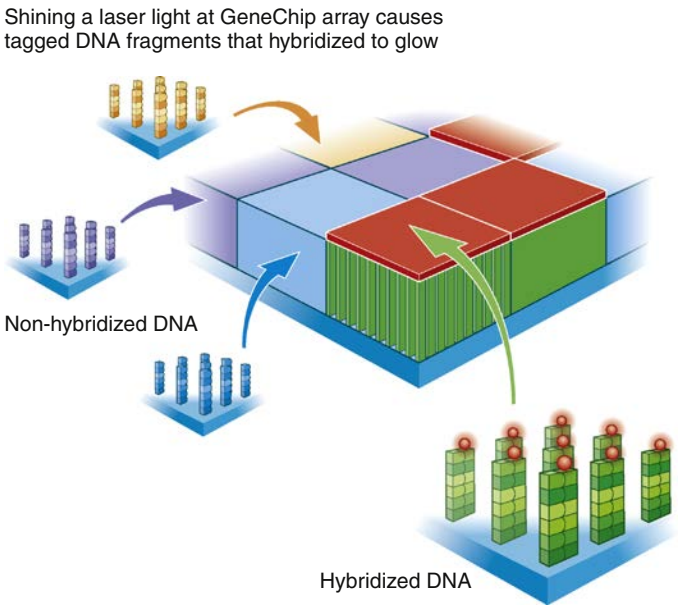

Figure 70.5 Scanning of tagged and untagged probes on an Affymetrix GeneChip microarray. (Courtesy of Affymetrix.)

formalin-fixed, paraffin-embedded (FFPE) samples. Array technology has also been adapted to interrogate single nucleotide polymorphisms, copy number variations, and structural variants, which differ among individuals and populations (Coulombe-Huntington et al., 2009; Stankiewicz & Lupski, 2010). Such variations influence how individuals differ in their risk of disease and their response to therapeutic treatments (see Chapter 75). Other improvements across the industry include the ability to detect low-abundance transcripts, reduced requirements for the quantity of a sample to a few hundred nanograms or less of total RNA (versus micrograms), automation for low per-sample pricing, and improved consistency in methodology and quality control (Yauk et al., 2005). As a result of the variations in array technologies and differences in sample preparation and signal processing, the Minimal Information About a Microarray Experiment (MIAME) guidelines have been implemented to ensure that all relevant experimental information is presented in a consistent and complete manner that will ensure that published data and publicly available microarray data sets can be interpreted accurately (Yauk et al., 2004).

BIOINFORMATICS

The most challenging aspect of microarrays starts here, when large data sets have been assembled and purged of artifacts and background noise and are awaiting analysis (Draghici, 2003; Parmigiana et al., 2003; Gopalappa et al., 2009; Zhang et al., 2009). The approach depends on the nature of the question and design of the experiment. An initial exploration of the data set is used to evaluate the quality, usually including an assessment of background and mean intensity of the features on the array. To facilitate statistical comparisons between arrays, intensities are commonly log transformed and arrays are "normalized" to each other.

A popular approach to normalizing gene expression is predicated on the assumption that the conditions being compared (e.g., normal versus tumor or infected versus noninfected) would affect the gene expression of relatively few genes, leaving most unaffected. In the absence of systematic bias, the median intensity of all features on the array should be unchanged. Thus, a common normalization method is to divide each intensity measurement on the array by the median intensity of the array (Kano et al., 2003). These assumptions are reasonable when the array contains a large number of genes that represent a wide range of biological function.

One caveat of the total intensity normalization methods arises from its implicit assumption that systematic variation is constant across the entire range of expression intensities of the array. However, as data from technical replicate arrays show, systematic variation is often intensity dependent, or nonlinear. In other words, systematic variation observed at low expression intensities differs from systematic variation observed at medium and high intensities (Simon, 2005). Thus, linear adjustments, such as dividing each measurement on an array with the median intensity of the array, would not be appropriate for some genes. For perhaps 80% of the arrays, systematic variation is close enough to linear so that total intensity normalization methods are sufficient. However, for the remaining 20% of the arrays, nonlinear normalization methods are required (Genomics and Bioinformatics Group, 2005).

Quantile normalization is a nonlinear normalization method that is often performed on microarrays. In addition to assuming that most genes are unchanged in their expression across experimental conditions, quantile normalization also makes the strong assumption that the distribution of gene expression intensities must also be invariant across the arrays (Irizarry et al., 2003). Thus, not only should the median intensity be the same for each array, but the intensity at every quantile of the array should also be the same. Given this assumption, quantile normalization sorts all intensity values on the array by increasing intensity values and adjusts the intensities so that the smallest intensity value on each array is identical, the second smallest values are identical, and so forth. The gene with the smallest intensity value on one array may be different from the gene with the smallest intensity value on another array.

Intensity-dependent systematic variation has also been shown for two-color technology arrays. Intensity-dependent dye bias was first identified by Terry Speed's laboratory, where it was observed that low-abundance genes appear to be upregulated in the Cy5 channel and that moderately expressed genes appear to be upregulated in the Cy3 channel (Yang et al., 2002). This systematic artifact can be effectively corrected by performing a locally weighted linear regression (lowess) (Fig. 70.6). The validity of using housekeeping genes for normalization has been called into question in the past few years. In this method, it is assumed that the expression levels of housekeeping genes are constant across experimental conditions. Thus, intensity measurements of an array can be normalized to the mean intensities of these genes. However, the expression levels of some housekeeping genes have been shown to vary considerably across some experimental conditions (Thellin et al., 1999).

After data have been normalized, quality control is performed at both the sample level and the gene level. Sample-level quality control assesses sample data globally to identify outliers or, in cases in which replicate reproducibility is generally observed, one or a few samples that may represent outliers. Potential outliers may be identified as those that do not cluster with replicate samples or those that do not correlate highly with replicate samples. Hierarchical clustering, principal component analysis, class prediction algorithms, and similarity metrics are often used to perform sample-level quality control (Grewal et al., 2003).

Gene-level quality control filters out genes for which the large proportion of measurements fall within the noise range to create a restricted set of genes for further analysis. Genes that are removed correspond to those that are not expressed in the tissues of concern or whose expression levels are so low that the technology is not sufficiently sensitive to detect differences in expression. Removal of such genes generally reduces noise, the likelihood of false-positive reactions in subsequent differential expression filters, and the severity of multiple testing corrections required in downstream statistical analyses.

After normalization and quality control of imported data have been completed, one can perform analyses to isolate the genes of interest. One basic objective in a microarray experiment is to identify genes that may be differentially expressed among the different experimental conditions. Researchers rely on many different variants of common statistical tests to identify differentially expressed genes. One caveat to using statistical tests to identify differentially expressed genes is that the number of false-positive reactions from the statistical analysis is proportional to the number of tests that are performed. Because hundreds or thousands of genes are often tested at once, the number of false-positive reactions from the analysis can potentially dominate the list of candidate genes that are thought to be differentially expressed. Thus, it is important to limit the number of false-positive reactions in a statistical analysis by performing multiple testing correction. Two categories of multiple testing correction are those that determine the family-wise error rate (FWER) and those that determine the false discovery rate (FDR). FWER tests control the overall chance that at most one gene is incorrectly identified as being differentially expressed after the statistical analysis and after performing the multiple testing correction (Grewal et al., 2003). Examples of FWER tests are the Bonferroni, Holms–Bonferroni step-down, and Westfall and Young Permutation. FDR tests confine the probability of false-positive reactions to be proportional to the number of genes that pass the statistical test instead of the total number of genes tested by the statistical analysis. An example of an FDR test is the Benjamini and Hochberg false discovery rate (Benjamini & Hochberg, 1995). Several excellent statistical packages are available online (e.g., BRB Tools, SAM, Focus, D Chip, R Bioconductor Library, PAM).

Clustering analysis (Fig. 70.7) is suitable for grouping genes that behave similarly across multiple conditions of an experiment. Clustering has many applications in expression data analysis. It allows one to infer the previously

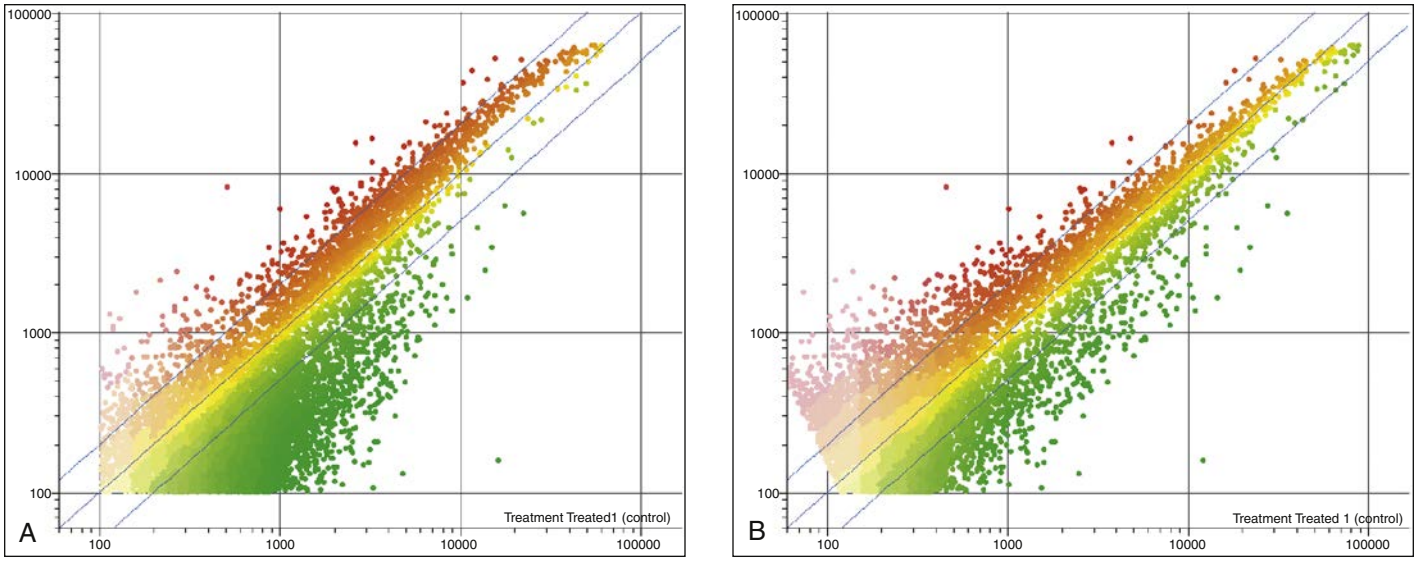

Figure 70.6 Locally weighted linear regression (lowess) intensity-dependent normalization is used for two-color data. A type of within-slide normalization scheme adjusts for intensity-dependent variation due to dye properties. Dye bias is caused by inconsistencies in the relative fluorescence intensity between Cy5 and Cy3. These inconsistencies often result in nonlinear relationship between the two dyes and a curve occurs in a scatter plot. **A**, Data before normalization. **B**, By applying lowess normalization, a locally weighted regression is fitted to the data to adjust the control value for each measurement. As a result, the plot of signal versus control value will be linear. (Courtesy of Agilent Technologies.)

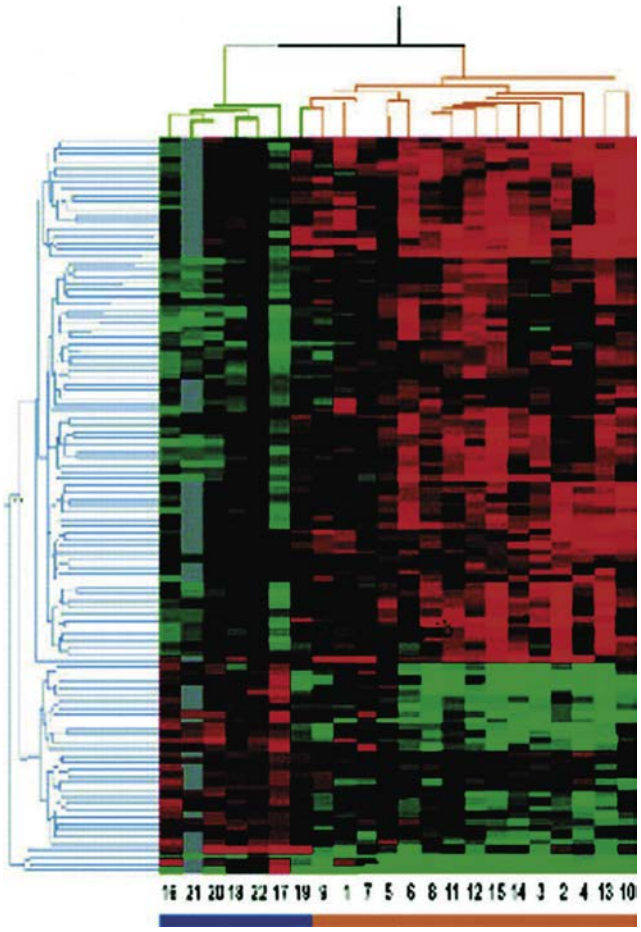

Figure 70.7 Hierarchical clustering dendrogram of duodenal genes from different celiac disease *(orange bar)* and control *(blue)* biopsy samples. Clustering of 109 genes across 22 samples clusters the seven control samples *(blue bar)* separately from the 15 celiac disease patients *(orange bar)*. Each column represents a celiac disease or a control sample, and each row represents an individual gene. For each gene, a *green signal* represents underexpression, *black signals* denote similarly expressed genes, a *red signal* represents overexpressed genes, and *gray signals* denote missing data. (Adapted with permission of the BMJ Publishing Group from Diosdado B, Wapenaar MC, Franke L, et al: A microarray screen for novel candidate genes in coeliac disease pathogenesis, Gut 53:944, 2004.)

unknown function of a gene from the functions of the genes that it clusters with. This is based on the assumption that genes that share similar functions share similar expression behavior across experimental conditions. Clustering may also be useful in finding genes that may be coregulated. This is based on the assumption that genes that are coregulated share similar expression profiles. Thus, it may be useful to analyze the promoter regions of genes that cluster together to find common regulatory elements (Grewal et al., 2003; Gollub & Sherlock, 2006).

The generated genes of interest can then be integrated with known biology. The ability to cross-reference gene lists from differential expression analysis and/or clustering analysis against gene ontology or other gene function lists to ascertain significance of overlap is available in some programs (e.g., Agilent/GeneSpring). Other popular programs include Bioconductor—an open source and open development software project for the analysis and comprehension of genomic data, based on the R programming language (Zhang et al., 2009); the oligonucleotide centric DChip (www.Dchip.org); TIGRsuite (www.tigr.org); and BeadStudio (array platform and manufacturer specific; www.illumina.com). (For a review, see Gollub & Sherlock, 2006; Platts et al., 2006). In addition, genes can be referenced to known biological pathways or public databases (GenBank, LocusLink, UniGene, serial analysis of gene expression [SAGE]).

Thus, because of the intensive need for pattern recognition, multidimensional data interpretation, and cross-platform comparison, microarray technology will enjoy a close relationship with bioinformatics, and coevolution of both hardware and software appears to be inevitable (see Chapter 79).

INTELLECTUAL PROPERTY ISSUES

Patents can cover a specific method of testing for an analyte, any method of testing for an analyte, or a mutation-gene-disease association in general. The vast majority of the in vitro amplification procedures are patented processes, and a license agreement for the use of these procedures must be obtained or the laboratory using the procedure is liable for patent infringement. Traditionally, licensure is obtained for a particular procedure by purchasing a Food and Drug Administration (FDA)–approved set of reagents sold by a manufacturer who holds the patent to the amplification process. The number of FDA-approved and -cleared tests is limited and does not cover all molecular tests currently performed in molecular diagnostics laboratories. Thus, a laboratory using a particular patented process must first negotiate a license agreement with the patent holder. Importantly, depending on the complexity of the institution seeking the agreement and the complexity of the agreement, it may take from 3 months to 1 year to obtain a license to perform and bill the procedure for clinical purposes.

Similar consideration must be given to developing assays for specific genes and disorders. The Supreme Court provided granularity to the gene patent discussion in the landmark ruling on June 13, 2013, in the case *Association for Molecular Pathology et al vs Myriad Genetics, Inc., et al.*

The Supreme Court held that "A naturally occurring DNA segment is a product of nature, and not patent eligible merely because it has been isolated, but cDNA is patent eligible because it is not naturally occurring." The *BRCA1* and *BRCA2* genes, mutations that are implicated in hereditary breast and ovarian cancer, were the subjects of the ruling. However, it was made clear that the ruling applies to all human genes. It was emphasized that the ruling does not apply to synthetic or non-naturally occurring DNA. Therefore, it is important to consider disease or gene specific patents before assay development. The terms and conditions offered by the patent holder vary greatly. Internet resources provided by the U.S. Patent and Trademark Office (www.uspto.gov) allow laboratories to perform searches on granted or pending patents in the United States.

Microarray technology is a rapidly moving field with fierce competition. It is therefore important to emphasize that numerous patents have been filed, some of which are directly relevant to clinical diagnosis. Therefore, intellectual property remains an important concern in this ever-evolving field (Rouse & Hardiman, 2003). For instance, Affymetrix possesses broad patent rights on high-density oligonucleotide arrays (Chee et al., 1998; Holmes, 1998), regardless of the means by which they are made. Assuming that a laboratory decides to develop in-house moderate-density arrays for tumor testing and to charge for such a service, this array might infringe Affymetrix's patents if it exceeds 400 features/cm^2 regardless of the synthesis method (Fodor et al., 1998). Array technologies using micromatrices of polyacrylamide gel pads (three-dimensional gel elements) represent a new approach that might not infringe on Affymetrix claims (Khrapko et al., 1991; Yershov et al., 1996; Guschin et al., 1997). Furthermore, the intellectual property related to the methodology and application of DNA array technology to identify medicinal versus toxic components in natural remedies, species-specific fingerprinting, and identification of unknown DNA has generated additional patent applications (Shaw et al., 2009). It is hoped that, as occurred with nucleic acid amplification technologies, competition among manufacturers will bring down costs of high- and medium-density arrays and allow for the democratization of this powerful technology.

CLINICAL APPLICATIONS OF ARRAY TECHNOLOGY

Numerous applications of microarray technology have been proposed in the past few years, ranging from molecular staging of tumors to the identification and characterization of microbial agents. This has led many to speculate that array technology represents the next wave of technologic advances to have a practical impact on the diagnosis of human disease, second only to PCR as a core technology in the clinical molecular diagnostics laboratory. This section focuses on current and future applications of array technology.

ARRAY TECHNOLOGY IN THE CLINICAL LABORATORY

Although not currently widespread, clinical laboratory utilization of array technology appears to be on the horizon. Roth and colleagues (2004) have employed array analysis to detect common respiratory pathogens and compared this with conventional culture from middle ear fluid samples. The sensitivities of the array assay compared to culture for *Haemophilus influenzae*, *Moraxella catarrhalis*, *Streptococcus pyogenes*, and *Streptococcus pneumoniae* were 96% (93% for culture), 73% (93% for culture), 93% (80% for culture), and 100% (78% for culture), respectively. Furthermore, tissue microarrays have been used as a tool for internal quality control to improve the interpretation of immunohistochemical staining (Packeisen et al., 2002; Gulmann et al., 2004). The FDA has granted 501(k) clearance to Roche Molecular Systems to market its AmpliChip CP450 Genotyping test to determine cytochrome P450 2D6 and 2C19 genotypes using the Affymetrix instrumentation system (Malone, 2005). Because cytochrome genes code for liver enzymes important in drug metabolism, clinicians will use the results to optimize drug dosing and minimize side effects on the basis of individual genotype. This is the first time a microarray chip has been given marketing clearance as a diagnostic device for use in the clinical laboratory, heralding the potentially new era of personalized medicine. Furthermore, recent reports demonstrate the promise of applying hybridization array technology to pre-, peri-, and postnatal screening and pediatrics diagnosis (Kang & Koo, 2012; Wei et al., 2013).

Small-scale, automated, microfluidic array instruments that have the technical discrimination and dynamic range required to detect RNA species at a frequency of 1 in 100,000 with a short turnaround time and low coefficient of variation (0.09–0.11) have also been described (Baum et al., 2003). However, methodologic consistency, quality control, and disease-specific application will have to be addressed prior to implementation as a routine test to the clinical laboratory.

ARRAY TECHNOLOGY IN CLINICAL DISEASE

Microarray technology has provided the ability to screen genes that are differentially regulated in experimental and clinical disease and allow further correlation of select genes with their function. For example, Ji and colleagues (2003) used microarray technology to screen for genes that are upregulated in the early stage of acute pancreatitis using two different experimental models of the disease. Many genes were upregulated in both experimental systems, suggesting their importance in the human condition. However, one gene in particular, *EGR1*, further analyzed through classical approaches (gene knockout), was shown to be a key regulator that may be important in the development of early acute pancreatitis. Others (Iacobuzio-Donahue et al., 2003) have performed a comprehensive evaluation and comparison of gene expression profiles of 39 samples of pancreatic cancer and identified between 6 and 40 genes that were highly expressed when examined by multiple methods (oligonucleotide arrays, cDNA arrays, or SAGE). These may eventually be translated into clinically useful targets for therapy or diagnosis.

Microarray analysis of cells and tissues as a means to identify key therapeutic candidates continues to evolve. Malignancies or their tissue components that have been analyzed in the quest for identifying key targets, diagnostic or prognostic indicators (Ma et al., 2009), or novel pathways include melanoma (Nambiar et al., 2004), leukemias (Moos et al., 2002; Jaakson et al., 2003; Shivarov & Bullinger, 2014), lymphomas (Hedvat et al., 2002; Kobayashi et al., 2003; Azambuja et al., 2009), myelodysplastic syndromes (Pellagatti et al., 2004; Ahmad & Iqbal, 2012), and carcinomas of the prostate (Pettus et al., 2004), bladder (Dyrskjot, 2003), kidney (Moch et al., 1999), colon or rectum (Frederiksen et al., 2003), breast (Jeffrey et al., 2002; Wilson & Dering, 2004), ovary (Rosen et al., 2004; Yang et al., 2009), and endometrium (Saidi et al., 2004; DeRycke et al., 2009).

Other clinical applications that utilize the gene screening capability of microarray technology include the study of the effect of ionizing radiation (Amundson et al., 1999); detection of microbial (Dunbar et al., 2013), viral (Sun et al., 2004; Striebel et al., 2003), and other pathogens (Hanson et al., 2004); karyotyping of cell-free DNA in amniotic fluid (Larrabee et al., 2004); providing molecular markers for allergic (Jahn-Schmid et al., 2003), urologic (Cheung et al., 2009), cardiac (Bostjancic et al., 2009), and inflammatory disorders (Bennett et al., 2003); Alzheimer disease (Pasinetti, 2001); multiple sclerosis (Whitney et al., 1999); dystonia (Walter et al., 2010); diabetes (Sreekumar et al., 2002; Mootha et al., 2003); transplant rejection (Flechner et al., 2004); and pulmonary hypertension (Geraci et al., 2001). The ability to predict adverse drug reactions (Guzey & Spigset, 2002), response to therapy (Sotiriou et al., 2002), drug sensitivity (Stein et al., 2004), and toxicity profiles (Waring et al., 2001), among others (Cox, 2001; Day et al., 2009; Stankiewicz & Lupski, 2010), have also been reported.

EMERGING TECHNOLOGIES: EXOSOMES

Exosomes are small (30–150 nm) vesicles containing mRNA, miRNA, lncRNA, lipid and protein cargo, that are constantly secreted by all cells in vitro and in vivo (Fig. 70.8A). The contents are different depending on the origin of the secreting cells (Fig. 70.8B) (Jalalian, 2019). Exosomes have many intriguing functions within the human body, including intercellular communication and signaling. These extracellular vesicles have become the focus of exponentially growing interest, both aimed at understanding their biological functions and using them toward practical applications such as development of noninvasive diagnostics and advanced therapeutics. Inappropriate release or dysregulation of exosomal miRNAs may lead to significant alterations in certain biological processes that influence disease development and progression. Therefore, exosome-encapsulated miRNAs may serve as potential diagnostic and prognostic biomarkers (and therapeutic targets) for select disease states (Yan, 2017).

To this end, serum profiles of exosome-encapsulated miRNAs in colorectal cancer demonstrated that there are 39 differentially expressed miRNAs detected by microarray analysis. Subsequent quantitative RT-PCR validation identified five exosome-encapsulated miRNAs including miR-638, miR-5787, miR-8075, miR-6869-5p, and miR-548c-5p to be significantly downregulated, whereas two exosome-encapsulated miRNAs including miR-486-5p and miR-3180-5p were significantly upregulated in exosome containing serum samples from patients with colorectal cancer. In addition, miRNAs of miR-638, miR-5787, miR-8075, miR-6869-5p, and miR-548c-5p may regulate the metabolism of glucose, thus playing critical roles in tumorigenesis and tumor progression.

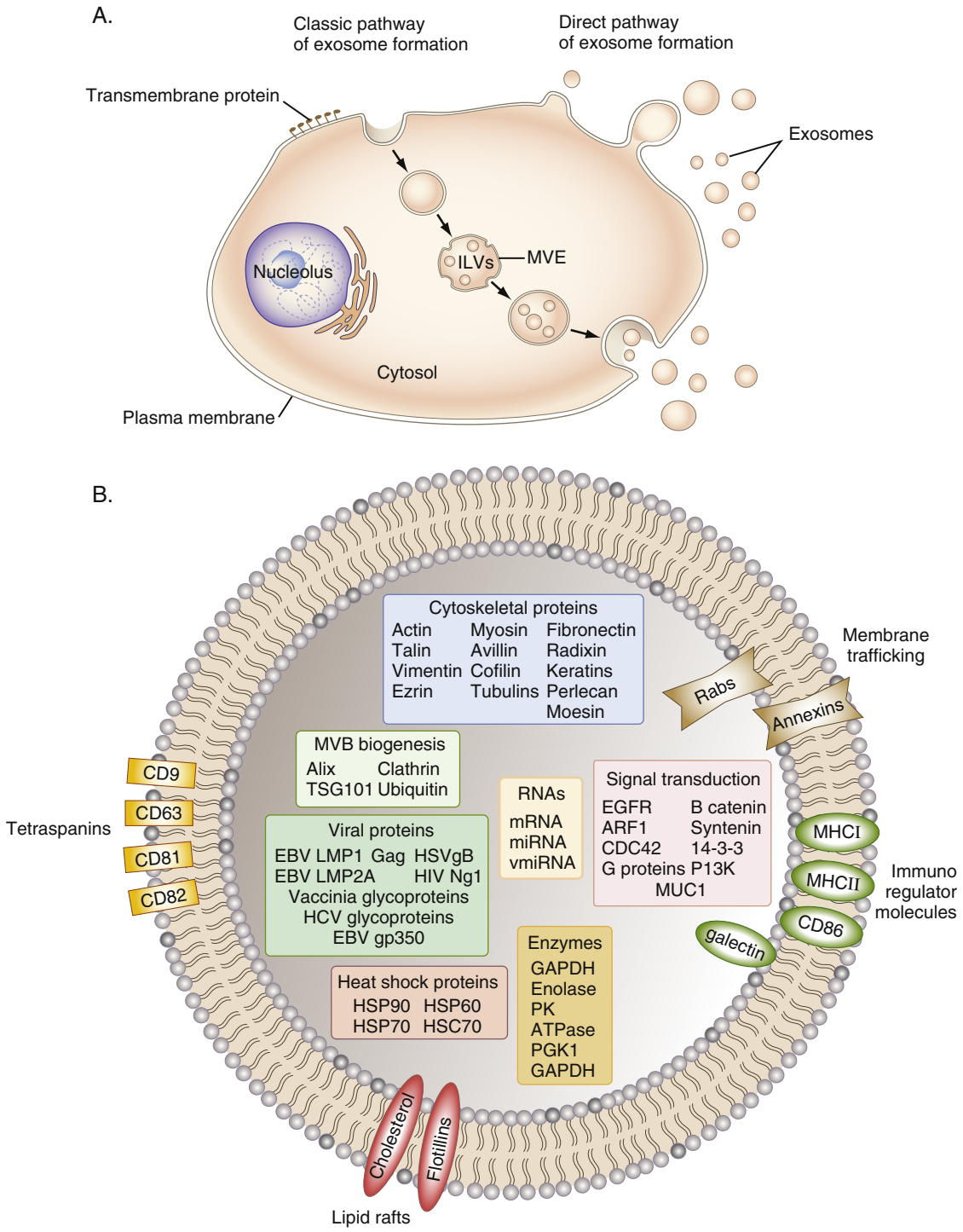

Figure 70.8 **A**, Pathways of exosome formation. **B**, Exosome biomarkers. (**A** from van der Pol E, Böing AN, Harrison P, Sturk A, Nieuwland R: Classification, functions, and clinical relevance of extracellular vesicles, *Pharmacol Rev* 64(3):676-705, 2012; **B** from Meckes DG, Raab-Traub N. Microvesicles and viral infection. *J Virol* 85(24):12844-12854, 2011.)

Exosomes as biomarkers in other disease states, including diabetic kidney, Alzheimer, and cardiovascular diseases, have been reported (Zang, 2019; Chen 2019; Xu, 2019; Wang, 2019), and other cancers (bladder, ovary, pancreas) have been studied as well (Taylor and Gercel-Taylor, 2008; Elsharkawi, 2019; Lux, 2019). For example, probes have been developed to miRNAs of patients with ovarian cancer. In a comprehensive study (Taylor & Gercel-Taylor, 2008) using microarrray probes to 467 different exosomal miRNAs from patients with ovarian cancers, expression of these miRNAs was studied in cohorts of normal female patients, patients with benign ovarian disease, and patients with ovarian cancer. The exosomes from all of these patients were isolated using cell-sorting techniques based on the expression of anti–epithelial cell adhesion molecule (EpCAM) on the surface of the exosomes. It was found that the patterns of miRNA expression in patients with ovarian cancers differed dramatically from those in patients with benign disease and that all normal patients were found not to express any exosomal miRNA.

miRNA from ovarian tumor cells and exosomes from the same patients were assessed using microarrays containing probes for 467 human mature miRNAs (Taylor and Gercel-Taylor, 2008). Although miRNA has been reported as a promising biomarker for tissue and serum based assessment of disease (Sethi, 2018), in studies by Taylor and Gercel-Taylor (2008), tumor-derived *miRNA-containing exosomes* were specifically isolated by a modified magnetic activated cell sorting (MACS) procedure using EpCAM and were positive for 218 of 467 mature miRNAs analyzed. Although EpCAM-positive exosomes were detectable in both patients with benign ovarian disease and ovarian cancer, exosomal microRNA from patients with ovarian cancer exhibited similar profiles but were significantly distinct from profiles observed in benign disease; exosomal miRNA was not detected in normal control participants.

In addition to the cells that *form* extracellular vesicles, such as exosomes, having diagnostic value, cells that *receive* these vesicles can be interrogated for biomarker value as well. Tumor cell-derived exosomes *transfer* some crucial material (RNA and protein species) to other cells in the cancer microenvironment, such as epithelial cells, macrophages, endothelial cells, and fibroblasts. This contributes to inflammatory cell infiltration, angiogenesis, obtainment of tumor-associated cell phenotypes, and tumor innervation. Exosomes communicating with fibroblasts also trigger reprogramming of recipient cells into cancer-associated phenotypes (Tian, 2019). Future studies will further elucidate the diagnostic and prognostic potential of exosomes and other extracellular vesicle constructs.

LIMITATIONS

Despite the excitement and increase in the potential clinical application of microarray technology, care must be taken in its interpretation. Clinical application will require procedures for quality control and quality assurance. The challenge to ensuring reproducibility of the high-density data presented in microarrays is unprecedented in the clinical laboratory. Each of the large number of steps from sample extraction, labeling, hybridization, image analysis, and data analysis contributes to difficulties in data reproducibility and can differ among commercially available systems (Kothapalli et al., 2002; Yauk et al., 2004; Pozhitkov et al., 2007). Furthermore, factors such as varying the method used for nucleic acid isolation (Feezor et al., 2004) or detection, tissue type (solid, glandular, or blood derived), type of specimen (FFPE vs frozen tissue) (Penland et al., 2007), and time to processing can affect results of gene expression profiling.

Approaches to further validate and confirm array-based results include verification of each clone sequence before printing the microarray; performing experiments in duplicate or triplicate where possible; and verification of candidate genes by classic methods (e.g., PCR, northern blotting, RNase protection assay). Some investigators (Rajeevan et al., 2001) have shown that the majority of array results were qualitatively accurate in cross-validation experiments using real-time RT-PCR. However, for genes showing less than a fourfold difference on the arrays, consistent cross-validation with real-time RT-PCR was not achieved. It is also very important to determine whether the difference in mRNA expression translates to a difference in the expression levels of the corresponding protein products. Currently, how frequently a difference in mRNA level translates to a difference in protein expression level is not clear.

Caution must also be exercised in interpreting differentially regulated genes during tumor progression (staging microarray). Any nucleic acid source derived from biopsy tissue is made up of many different cell populations and may represent homogeneous tissue only after the tumor mass has reached a large enough size (i.e., late stage). Although certain methods are available to isolate specific cells of interest in smaller tumors (e.g., laser capture microdissection), they are technically demanding, time consuming, and not universally available.

Like all sequencing strategies, microarrays have limited sensitivity for minority alleles, although newer platforms and analysis approaches claim to improve detection in this regard (Coulombe-Huntington et al., 2009; Stankiewicz & Lupski, 2010). An example of sequence-based identification of drug resistance in HIV will be particularly instructive. Microarray sequencing of clinical isolates can correctly predict some instances of drug resistance on the basis of specific mutations (Race et al., 1998) and is evolving toward standard practice (Perez-Olmeda et al., 1999). Even making the optimistic assumption that sequencing can detect a resistance allele when represented in 1% of the viral population or more, however, there is reason to doubt the predictive value of a test that is negative for resistance. Few virologists would argue that 0.5% prevalence of drug resistance is unimportant in a virus that generates more than a billion copies a day. Therefore, it should be understood that the power of this technology currently lies in its ability to screen for the regulation of genes in defined parameters (Russo et al., 2003) with the incorporation of appropriate standardization (Enkemann, 2010).

Further advances in diagnosis, classification, and prognosis await discovery by microarray-based methods in the near future. As emphasized earlier, it is not merely improvements in apparatus that make this possible but more sophisticated analytic strategies, detection sensitivity, throughput, automation, miniaturization, ease of use, and cost also evolve to keep up with the more complex data generated by these devices (Bassett et al., 1999; Zhang et al., 2009).

SELECTED REFERENCES

Bluth MJ, Bluth MH: Molecular pathology techniques; advances in 2018, *Clin Lab Med* 38:215–236, 2018.

Provides a comprehensive review of commonly utilized molecular pathology techniques employed in the clinical laboratory for elucidating disease pathophysiology in addition to diagnosis, prognosis, and therapeutic monitoring for patient management.

Jalalian SH, Ramezani M, Jalalian SA, et al.: Exosomes, new biomarkers in early cancer detection, *Anal Biochem* 571:1–13, 2019.

A comprehensive overview of exosome formation content and application to human disease diagnosis.

Ji B, Chen XQ, Misek DE, et al.: Pancreatic gene expression during the initiation of acute pancreatitis: identification of EGR-1 as a key regulator, *Physiol Genomics* 14:59, 2003.

An example of how microarray is employed to screen for regulation of gene expression in two models of experimental pancreatitis, with subsequent validation of select genes (EGR-1) by conventional methods.

Kothapalli R, Yoder SJ, Mane S, et al.: Microarray results: how accurate are they? *BMC Bioinf* 3(22), 2002.

Discusses problems associated with microarray in great detail and evaluates data obtained from two different commercially available systems.

Russo G, Zegar C, Giordano A: Advantages and limitations of microarray in human cancer, *Oncogene* 22:6497, 2003.

Highlights some of the recent developments and clinical applications of microarray technology and discusses potentially problematic areas associated with this technology.

Stein WD, Litman T, Fojo T, et al.: A serial analysis of gene expression (SAGE) database analysis of chemosensitivity: comparing solid tumors with cell lines and comparing solid tumors from different tissue origins, *Cancer Res* 64:2805, 2004.

Investigates the relationship of gene expression profiles for a given tumor type to its drug sensitivity or resistance to provide insights into the molecular basis of tumor intractability to chemotherapy.

Access the complete reference list online at Elsevier eBooks for Practicing Clinicians.

REFERENCES

Ahmad A, Iqbal MA: Significance of genome-wide analysis of copy number alterations and UPD in myelodysplastic syndromes using combined CGH–SNP arrays, *Curr Med Chem* 19:3739–3747, 2012.

Amundson SA, Bittner M, Chen Y, et al.: Fluorescent cDNA microarray hybridization reveals complexity and heterogeneity of cellular genotoxic stress responses, *Oncogene* 18:3666, 1999.

Auffray C, Rougeon F: Purification of mouse immunoglobulin heavy-chain messenger RNAs from total myeloma tumor RNA, *Eur J Biochem* 107:303, 1980.

Azambuja D, Lossos IS, Biasoli I, et al.: Human germinal center-associated lymphoma protein expression is associated with improved failure-free survival in Brazilian patients with classical Hodgkin lymphoma, *Leuk Lymphoma* 50:1830–1836, 2009.

Bains W, Smith GC: A novel method for nucleic acid sequence determination, *J Theor Biol* 135:303, 1988.

Barsalobres-Cavallari C, De Rosa Júnior V, Nogueira F, et al.: A novel system for large-scale gene expression analysis: bacterial colonies array, *Appl Microbiol Biotechnol* 71:963–969, 2006.

Bassett Jr DE, Eisen MB, Boguski MS: Gene expression informatics—it's all in your mine, *Nat Genet* 21:51–55, 1999.

Baum M, Bielau S, Rittner N, et al.: Validation of a novel, fully integrated and flexible microarray benchtop facility for gene expression profiling, *Nucleic Acids Res* 31:e151, 2003.

Beattie WG, Meng L, Turner SL, et al.: Hybridization of DNA targets to glass-tethered oligonucleotide probes, *Mol Biotechnol* 4:213, 1995.

Beier M, Hoheisel JD: Versatile derivatisation of solid support media for covalent bonding on DNA-microchips, *Nucl Acids Res* 27:1970, 1999.

Benjamini Y, Hochberg Y: Controlling the false discovery rate: a practical and powerful approach to multiple testing, *J R Statist Soc B* 57:2889, 1995.

Bennett L, Palucka AK, Arce E, et al.: Interferon and granulopoiesis signatures in systemic lupus erythematosus blood, *J Exp Med* 197:711, 2003.

Blanchard AP, Kaiser RJ, Hood LE: High-density oligonucleotide arrays, *Biosens Bioelectron* 11:687, 1996.

Bostjancic E, Zidar N, Glavac D: MicroRNA microarray expression profiling in human myocardial infarction, *Dis Markers* 27:255–268, 2009.

Brown MP, Grundy WN, Lin D, et al.: Knowledge-based analysis of microarray gene expression data by using support vector machines, *Proc Natl Acad Sci U S A* 97:262–267, 2000.

Case-Green SC, Southern EM: Studies on the base pairing properties of deoxyinosine by solid phase hybridisation to oligonucleotides, *Nucl Acids Res* 22:131, 1994.

Chee M, et al.: *Arrays of nucleic acid probes on biological chips*, Patent US1995000441887, 1998. Nov 17.

Chee M, Yang R, Hubbell E, et al.: Accessing genetic information with high-density DNA arrays, *Science* 274:610, 1996.

Chen Y, Dougherty ER, Bittner ML: Ratio-based decisions and the quantitative analysis of cDNA microarray images, *Biomed Optics* 2:364, 1997.

Cheng J, Sheldon EL, Wu L, et al.: Preparation and hybridization analysis of DNA/RNA from *E. coli* on microfabricated bioelectronic chips, *Nat Biotechnol* 16:541, 1998.

Cheung W, Bluth MJ, Johns C, et al.: Peripheral blood mononuclear cell gene array profiles in patients with overactive bladder, *Urology* 75(4):896–901, 2009.

Cheung VG, Morley M, Aguilar F, et al.: Making and reading microarrays, *Nat Genet* 21(Suppl 1):1, 1999.

Clark MD, Panopoulou GD, Cahill DJ, et al.: Construction and analysis of arrayed cDNA libraries, *Methods Enzymol* 303:205, 1999.

Corey DR: Peptide nucleic acids: Expanding the scope of nucleic acid recognition, *Trends Biotechnol* 15:224, 1997.

Corey DR: *DNA/RNA diagnostics*, Washington, DC, May 1998, Cambridge Healthtech Institute, pp 19–21.

Coulombe-Huntington J, Lam KC, Dias C, et al.: Fine-scale variation and genetic determinants of alternative splicing across individuals, *PLoS Genet* 5, 2009. e1000766.

Cox JM: Applications of nylon membrane arrays to gene expression analysis, *J Immunol Meth* 250(3), 2001.

Day A, Dong J, Funari VA, et al.: Disease gene characterization through large-scale co-expression analysis, *PloS One* 4, 2009. e8491.

DeRycke MS, Andersen JD, Harrington KM, et al.: S100A1 expression in ovarian and endometrial endometrioid carcinomas is a prognostic indicator of relapse-free survival, *Am J Clin Pathol* 132:846–856, 2009.

Diosdado B, Wapenaar M, Franke L, et al.: A microarray screen for novel candidate genes in coeliac disease pathogenesis, *Gut* 53:944, 2004.

Doh KO, Lee YH, Han KH, et al.: Fabrication of a microarray using a combination of the large circular sense and antisense DNA, *Int J Mol Med* 25:113–120, 2010.

Draghici S: *Data analysis tools for DNA microarrays*, Boca Raton, Fla, 2003, Chapman & Hall/CRC Press.

Drmanac R, Crkvenjakov R: *Method of sequencing of genomes by hybridization of oligonucleotide probes*, Patent US5667972, Apr 13, 1993. http://www.freepatentsonline.com/5667972.html.

Drmanac R, Drmanac S: cDNA screening by array hybridization, *Methods Enzymol* 303:165–178, 1999.

Drmanac R, Drmanac S, Strezoska Z, et al.: DNA sequence determination by hybridization: a strategy for efficient large-scale sequencing, *Science* 260:1649, 1993.

Drmanac S, Kita D, Labat I, et al.: Accurate sequencing by hybridization for DNA diagnostics and individual genomics, *Nat Biotechnol* 16:54, 1998.

Duggan DJ, Bittner M, Chen Y, et al.: Expression profiling using cDNA microarrays, *Nat Genet* 21(10), 1999.

Dunbar SA, Zhang H, Tang YW: Advanced techniques for detection and identification of microbial agents of gastroenteritis, *Clin Lab Med* 33:527–552, 2013.

Durand S, Ferraro-Peyret C, Selmi-Ruby S, et al.: Evaluation of gene expression profiles in thyroid nodule biopsy material to diagnose thyroid cancer, *J Clin Endocrinol Metab* 93:1195–1202, 2008.

Dyrskjot L: Classification of bladder cancer by microarray expression profiling: towards a general clinical use of microarrays in clinical diagnostics, *Expert Rev Mol Diagn* 3:635, 2003.

Edman CF, Raymond DE, Wu DJ, et al.: Electric field directed nucleic acid hybridization on microchips, *Nucl Acids Res* 25:4907, 1997.

Ekins RP, Chu FW: Microarrays: their origins and applications, *Trends Biotechnol* 17:217, 1999.

Ekins RP, Jackson TM: *Free ligand assay, UK Patent CA1227425 8 803 000*, 1987.

Elsharkawi F, Elsabah M, Shabayek M, Khaled H: Urine and serum exosomes as novel biomarkers in detection of bladder cancer, *Asian Pac J Cancer Prev* 20(7):2219–2224, 2019.

Enkemann SA: Standards affecting the consistency of gene expression arrays in clinical applications, *Cancer Epidemiol Biomarkers Prev* 19:1000–1003, 2010.

Erali M, Pattison DC, Wittwer CT, et al.: Human papillomavirus genotyping using an automated film-based chip array, *J Mol Diagn* 11:439–445, 2009.

Fan JB, Yeakley JM, Bibikova M, et al.: A versatile assay for high-throughput gene expression profiling on universal array matrices, *Genome Res* 14:878–885, 2004.

Feezor RJ, Baker HV, Mindrinos M, et al.: Whole blood and leukocyte RNA isolation for gene expression analysis, *Physiol Genomics* 19:247, 2004.

Flechner SM, Kurian SM, Head SR, et al.: Kidney transplant rejection and tissue injury by gene profiling of biopsies and peripheral blood lymphocytes, *Am J Transplant* 4:1475, 2004.

Fodor SP, Read JL, Pirrung MC, et al.: Light-directed, spatially addressable parallel chemical synthesis, *Science* 251:767, 1991.

Fodor SP, Stryer L, Read J, et al.: *Arrays of materials attached to a substrate*, Patent US1995000466632, Apr 28, 1998. http://www.freepatentsonline.com/5744305.html.

Forman JE, Walton ID, Stern D, et al.: *Molecular modeling of nucleic acids*, Washington, DC, 1999, American Chemical Society.

Frederiksen CM, Knudsen S, Laurberg S, et al.: Classification of Dukes' B and C colorectal cancers using expression arrays, *J Cancer Res Clin Oncol* 129:263, 2003.

Freeman WM, Gioia L: The maturation of nucleic acid technologies, *Trends Biotechnol* 17:44, 1999.

Friend SH, Stoughton RB: The magic of microarrays, *Sci Am* 286:44, 2002.

Genomics and Bioinformatics Group: *Microarray data analysis. low-level analysis of Affymetrix chips*, Bethesda, MD, 2005, National Institute of Health. http://discover.nci.nih.gov/microarrayAnalysis/Affymetrix.Preprocessing.jsp.

Geraci MW, Moore M, Gessell T, et al.: Gene expression patterns in the lungs of patients with primary pulmonary hypertension: a gene microarray analysis, *Circ Res* 88:555–562, 2001.

Gillespie D, Spiegelman SA: A quantitative assay for DNA-RNA hybrids with DNA immobilized on a membrane, *J Mol Biol* 12:829, 1965.

Gollub J, Sherlock G: Clustering microarray data, *Methods Enzymol* 411:194–213, 2006.

Gopalappa C, Das TK, Enkemann S, et al.: Removal of hybridization and scanning noise from microarrays, *IEEE Trans NanoBioscience* 8:210–218, 2009.

Granjeaud S, Nguyen C, Rocha D, et al.: From hybridization image to numerical values: a practical, high-throughput quantification system for high-density filter hybridizations, *Genet Anal* 12:151, 1996.

Graves DJ: Powerful tools for genetic analysis come of age, *Trends Biotechnol* 17:127, 1999.

Gress TM, Hoheisel JD, Lennon GG, et al.: Hybridization fingerprinting of high-density cDNA-library arrays with cDNA pools derived from whole tissues, *Mamm Genome* 3:609, 1992.

Grewal A, Lambert P, Stockton J: *Current protocols in informatics*, New York, 2003, John Wiley, p 7.1.1.

Gulmann C, Loring P, O'Grady A, et al.: Miniature tissue microarrays for HercepTest standardisation and analysis, *J Clin Pathol* 57:1229, 2004.

Guo Z, Guilfoyle RA, Thiel AJ, et al.: Direct fluorescence analysis of genetic polymorphisms by hybridization with oligonucleotide arrays on glass supports, *Nucl Acids Res* 22:5456, 1994.

Guschin D, Yershov G, Zaslavsky A, et al.: Manual manufacturing of oligonucleotide, DNA, and protein microchips, *Anal Biochem* 250:203, 1997.

Guzey C, Spigset O: Genotyping of drug targets: a method to predict adverse drug reactions? *Drug Saf* 25:553, 2002.

Hacia JG: Resequencing and mutational analysis using oligonucleotide microarrays, *Nat Genet* 21:42, 1999.

Hanson EH, Neimeyer DM, Folio L, et al.: Potential use of microarray technology for rapid identification of central nervous system pathogens, *Mil Med* 169:594, 2004.

Hedvat CV, Hegde A, Chaganti RS, et al.: Application of tissue microarray technology to the study of non-Hodgkin's and Hodgkin's lymphoma, *Hum Pathol* 33:968, 2002.

Heller MJ, O'Connell JP, Juncosa RD, et al.: *Methods for hybridization analysis utilizing electronically controlled hybridization*, Patent US5849486, Dec 15, 1998. http://www.freepatentsonline.com/5849486.html.

Heyse S, Ernst OP, Dienes Z, et al.: Incorporation of rhodopsin in laterally structured supported membranes: Observation of transducin activation with spatially and time-resolved surface plasmon resonance, *Biochemistry* 37:507, 1998.

Hoheisel JD: Sequence-independent and linear variation of oligonucleotide DNA binding stabilities, *Nucl Acids Res* 24:430, 1996.

Holmes CP: *Cyclic nucleic acid and polypeptide arrays*, Patent US1996000647618, 1998. Jun 23.

Iacobuzio-Donahue CA, Ashfaq R, Maitra A, et al.: Highly expressed genes in pancreatic ductal adenocarcinomas: a comprehensive characterization and comparison of the transcription profiles obtained from three major technologies, *Cancer Res* 63:8614, 2003.

Irizarry RA, Bolstad BM, Collin F, et al.: Summaries of Affymetrix GeneChip probe level data, *Nucleic Acids Res* 31:e15, 2003.

Jaakson K, Zernant J, Kulm M, et al.: Genotyping microarray (gene chip) for the ABCR (ABCA4) gene, *Hum Mutat* 22:395, 2003.

Jahn-Schmid B, Harwanegg C, Hiller R, et al.: Allergen microarray: comparison of microarray using recombinant allergens with conventional diagnostic methods to detect allergen-specific serum, *Immunoglobulin E, Clin Exp Allergy* 33:1443, 2003.

Jalalian SH, Ramezani M, Jalalian SA, et al.: Exosomes, new biomarkers in early cancer detection, *Anal Biochem* 571:1–13, 2019.

Jang H, Cho M, Kim H, et al.: Quality control probes for spot-uniformity and quantitative analysis of oligonucleotide array, *J Microbiol Biotechnol* 19:658–665, 2009.

Jeffrey SS, Fero MJ, Borresen-Dale AL, et al.: Expression array technology in the diagnosis and treatment of breast cancer, *Mol Interv* 2:101, 2002.

Kafatos FC, Jones CW, Efstratiadis A: Determination of nucleic acid sequence homologies and relative concentrations by a dot hybridization procedure, *Nucl Acids Res* 7:1541, 1979.

Kang JU, Koo SH: Evolving applications of microarray technology in postnatal diagnosis, *Int J Mol Med* 30:223–228, 2012.

Kano M, Kashima H, Shibuya T, et al.: A method for normalization of gene expression data, *Genome Informatics* 14:336, 2003.

Khrapko KR, Lysov YP, Khorlyn AA, et al.: An oligonucleotide hybridization approach to DNA sequencing, *FEBS Lett* 256:118, 1989.

Khrapko KR, Lysov YP, Khorlin AA, et al.: A method for DNA sequencing by hybridization with oligonucleotide matrix, *DNA Seq* 1:375, 1991.

Kobayashi T, Yamaguchi M, Kim S, et al.: Microarray reveals differences in both tumors and vascular specific gene expression in de novo CD5+ and CD5−′ diffuse large B-cell lymphomas, *Cancer Res* 63:60, 2003.

Landegren U, Kaiser RJ, Sanders J, et al.: A ligase-mediated gene detection technique, *Science* 241:1077, 1988.

Larrabee PB, Johnson KL, Pestova E, et al.: Microarray analysis of cell-free fetal DNA in amniotic fluid: a prenatal molecular karyotype, *Am J Hum Genet* 75:485, 2004.

Lipshutz RJ: Likelihood DNA sequencing by hybridization, *J Biomol Struct Dyn* 11:637, 1993.

Lipshutz RJ, Fodor SP, Gingeras TR, et al.: High density synthetic oligonucleotide arrays, *Nat Genet* 21:20, 1999.

Lockhart DJ, Dong H, Byrne MC, et al.: Expression monitoring by hybridization to high-density oligonucleotide arrays, *Nat Biotechnol* 14:1675–1680, 1996.

Lux A, Kahlert C, Grützmann R, et al.: c-Met and PD-L1 on circulating exosomes as diagnostic and prognostic markers for pancreatic cancer, *Int J Mol Sci* 20(13), 2019.

Ma S, Huang J, Moran MS: Identification of genes associated with multiple cancers via integrative analysis, *BMC Genom* 10:535, 2009.

Macevicz SC: *Nucleic acid sequence determination by multiple mixed oligonucleotide probes*, Patent US5002867, Mar 26, 1991. http://www.freepatentsonline.com/5002867.html.

Malone B: FDA clears first gene chip for pharmacogenomics, *Clin Lab News* 31:14, 2005.

Marshall A, Hodgson J: DNA chips: an array of possibilities, *Nat Biotechnol* 16:27, 1998.

Maskos U, Southern EM: Oligonucleotide hybridizations on glass supports: a novel linker for oligonucleotide synthesis and hybridization properties of oligonucleotides synthesised in situ, *Nucl Acids Res* 20:1679, 1992.

Maskos U, Southern EM: A novel method for the parallel analysis of multiple mutations in multiple samples, *Nucl Acids Res* 21:2269, 1993a.

Maskos U, Southern EM: A study of oligonucleotide reassociation using large arrays of oligonucleotides synthesised on a glass support, *Nucleic Acids Res* 21:4663, 1993b.

Maskos U, Southern EM: A novel method for the analysis of multiple sequence variants by hybridisation to oligonucleotides, *Nucl Acids Res* 21:2267, 1993c.

Matson RS, Rampal J, Pentoney SLJ, et al.: Biopolymer synthesis on polypropylene supports: oligonucleotide arrays, *Anal Biochem* 224:110, 1995.

Maxam AM, Gilbert W: A new method for sequencing DNA, *Proc Natl Acad Sci U S A* 74:560, 1977.

Moch H, Schraml P, Bubendorf L, et al.: High-throughput tissue microarray analysis to evaluate genes uncovered by cDNA microarray screening in renal cell carcinoma, *Am J Pathol* 154:981, 1999.

Moggio L, Romanelli A, Gambari R, et al.: Alternate PNA-DNA chimeras (PNA-DNA)(n): synthesis, binding properties and biological activity, *Biopolymers* 88:815–822, 2007.

Moos PJ, Raetz EA, Carlson MA, et al.: Identification of gene expression profiles that segregate patients with childhood leukemia, *Clin Cancer Res* 8:3118, 2002.

Mootha VK, Lindgren CM, Eriksson KF, et al.: PGC-1alpha-responsive genes involved in oxidative phosphorylation are coordinately downregulated in human diabetes, *Nat Genet* 34:267, 2003.

Nambiar S, Mirmohammadsadegh A, Bar A, et al.: Applications of array technology: melanoma research and diagnosis, *Expert Rev Mol Diagn* 4:549, 2004.

Nickerson DA, Kaiser RJ, Lappin S, et al.: Automated DNA diagnostics using an ELISA-based oligonucleotide ligation assay, *Proc Natl Acad Sci U S A* 87:8923, 1990.

Nikiforov TT, Rendle RB, Goelet P, et al.: Genetic bit analysis: a solid phase method for typing single nucleotide polymorphisms, *Nucl Acids Res* 22:4167, 1994.

Packeisen J, Buerger H, Krech R, et al.: Tissue microarrays: a new approach for quality control in immunohistochemistry, *J Clin Pathol* 55:613, 2002.

Parinov S, Barsky V, Yershov G, et al.: DNA sequencing by hybridization to microchip octa- and decanucleotides extended by stacked pentanucleotides, *Nucl Acids Res* 24:2998, 1996.

Parmigiana G, Garret ES, Irizarry RA, et al.: *The analysis of gene expression data: methods and software*, New York, 2003, Springer-Verlag.

Pasinetti GM: Use of cDNA microarray in the search for molecular markers involved in the onset of Alzheimer's disease dementia, *J Neurosci Res* 65:471, 2001.

Pastinen T, Kurg A, Metspalu A, et al.: Minisequencing: a specific tool for DNA analysis and diagnostics on oligonucleotide arrays, *Genome Res* 7:606, 1997.

Pastinen T, Perola M, Niini P, et al.: Array-based multiplex analysis of candidate genes reveals two independent and additive genetic risk factors for myocardial infarction in the Finnish population, *Hum Mol Genet* 7:1453, 1998.

Pease AC, Solas D, Sullivan EJ, et al.: Light-generated oligonucleotide arrays for rapid DNA sequence analysis, *Proc Natl Acad Sci U S A* 91:5022, 1994.

Pellagatti A, Esoof N, Watkins F, et al.: Gene expression profiling in the myelodysplastic syndromes using cDNA microarray technology, *Br J Haematol* 125:576, 2004.

Penland SK, Keku TO, Torrice C, et al.: RNA expression analysis of formalin-fixed paraffin-embedded tumors, *Lab Invest* 87:383–391, 2007.

Perez-Olmeda M, Rodriguez-Rosado R, Gomez-Cano M, et al.: Usefulness of genotypic analysis of resistance to nucleoside analogues in the clinical setting, *Eur J Clin Microbiol Infect Dis* 18:448, 1999.

Pettus JA, Cowley BC, Maxwell T, et al.: Multiple abnormalities detected by dye reversal genomic microarrays in prostate cancer: a much greater sensitivity than conventional cytogenetics, *Cancer Genet Cytogenet* 154:110, 2004.

Pietu G, Alibert O, Guichard V, et al.: Novel gene transcripts preferentially expressed in human muscles revealed by quantitative hybridization of a high density cDNA array, *Genome Res* 6:492, 1996.

Pirrung MC, Read JL, Fodor SPA, et al.: *Large scale photolithographic solid phase synthesis of polypeptides and receptor binding screening thereof*. Patent US51438542 http://www.freepatentsonline.com/5143854.html, Sep 1, 1992.

Platts AE, Dix DJ, Krawetz SA: Considerations when using array technologies for male factor assessment. In Carrell DT, editor: *The genetics of male factor infertility*, Totowa NJ, 2006, Humana Press, pp 37–54.

Potti A, Mukherjee S, Petersen R, et al.: A genomic strategy to refine prognosis in early-stage non-small-cell lung cancer, *N Engl J Med* 355:570–580, 2006.

Pozhitkov AE, Tautz D, Noble PA: Oligonucleotide microarrays: Widely applied—poorly understood, *Brief Funct Genomic Proteomic* 6:141–148, 2007.

Race E, Gilbert SM, Sheldon JG, et al.: Correlation of response to treatment and HIV genotypic changes during phase III trials with saquinavir and reverse transcriptase inhibitor combination therapy, *AIDS* 12:1465, 1998.

Rajeevan MS, Vernon SD, Taysavang N, et al.: Validation of array-based gene expression profiles by real-time (kinetic) RT-PCR, *J Mol Diagn* 3:26, 2001.

Rosen DG, Huang X, Deavers MT, et al.: Validation of tissue microarray technology in ovarian carcinoma, *Mod Pathol* 17:790, 2004.

Roth SB, Jalava J, Ruuskanen O, et al.: Use of an oligonucleotide array for laboratory diagnosis of bacteria responsible for acute upper respiratory infections, *J Clin Microbiol* 42:4268, 2004.

Rouse R, Hardiman G: Microarray technology—an intellectual property retrospective, *Pharmacogenomics* 4:623–632, 2003.

Saidi SA, Holland CM, Kreil DP, et al.: Independent component analysis of microarray data in the study of endometrial cancer, *Oncogene* 23:6677, 2004.

Sanger F, Nicklen S, Coulson AR: DNA sequencing with chain-terminating inhibitors, *Proc Natl Acad Sci U S A* 74:5463, 1977.

Schena M, Heller RA, Theriault TP, et al.: Microarrays: Biotechnology's discovery platform for functional genomics, *Trends Biotechnol* 16:301, 1998.

Schena M, Shalon D, Davis RW, et al.: Quantitative monitoring of gene expression patterns with a complementary DNA microarray, *Science* 270:467–470, 1995.

Schena M, Shalon D, Heller R, et al.: Parallel human genome analysis: microarray-based expression monitoring of 1000 genes, *Proc Natl Acad Sci U S A* 93:10614, 1996.

Schmid EL, Tairi AP, Hovius R, et al.: Screening ligands for membrane protein receptors by total internal reflection fluorescence: the 5-HT3 serotonin receptor, *Anal Chem* 70:1331, 1998.

Sethi S, Sethi S, Bluth MH: Clinical implication of microRNAs in molecular pathology: an update for 2018, *Clin Lab Med* 38(2):237–251, 2018.

Shalon D, Smith SJ, Brown PO: A DNA microarray system for analyzing complex DNA samples using two-color fluorescent probe hybridization, *Genome Res* 6:639, 1996.

Shaw PC, Wong KL, Chan AW, et al.: Patent applications for using DNA technologies to authenticate medicinal herbal material, *Chin Med* 4:21, 2009.

Shchepinov MS, Case-Green SC, Southern EM: Steric factors influencing hybridisation of nucleic acids to oligonucleotide arrays, *Nucl Acids Res* 25:1155, 1997.

Shivarov V, Bullinger L: Expression profiling of leukemia patients: key lessons and future directions, *Exp Hematol* 42:651–660, 2014.

Simon S: *STATS—Steve's attempt to teach statistics: normalization for microarray data*, . http://www.cmh.edu/stats/model/datamining/arrayNormalization.htm, 2005.

Sosnowski RG, Tu E, Butler WF, et al.: Rapid determination of single base mismatch mutations in DNA hybrids by direct electric field control, *Proc Natl Acad Sci U S A* 94:1119, 1997.

Sotiriou C, Powles TJ, Dowsett M, et al.: Gene expression profiles derived from fine needle aspiration correlate with response to systemic chemotherapy in breast cancer, *Breast Cancer Res* 4:R3, 2002.

Southern EM: Detection of specific sequences among DNA fragments separated by gel electrophoresis, *J Mol Biol* 98:503, 1975.

Southern EM: High-density gridding: techniques and applications, *Curr Opin Biotechnol* 7:85, 1996a.

Southern EM: DNA chips: analysing sequence by hybridization to oligonucleotides on a large scale, *Trends Genet* 12:110, 1996b.

Southern EM, Case-Green SC, Elder JK, et al.: Arrays of complementary oligonucleotides for analysing the hybridisation behaviour of nucleic acids, *Nucl Acids Res* 22:1368, 1994.

Southern EM, Maskos U, Elder JK: Analyzing and comparing nucleic acid sequences by hybridization to arrays of oligonucleotides: evaluation using experimental models, *Genomics* 13:1008, 1992.

Southern EM, Mir KU, Shchepinov MS: Molecular interactions on microarrays, *Nat Genet* 21:5, 1999.

Sreekumar R, Halvatsiotis P, Schimke JC, et al.: Gene expression profile in skeletal muscle of type 2 diabetes and the effect of insulin treatment, *Diabetes* 51:1913, 2002.

Stankiewicz P, Lupski JR: Structural variation in the human genome and its role in disease, *Annu Rev Med* 61:437–455, 2010.

Stimpson DI, Cooley PW, Knepper SM, et al.: Parallel production of oligonucleotide arrays using membranes and reagent jet printing, *Biotechniques* 25:886, 1998.

Stimpson DI, Gordon J: The utility of optical waveguide DNA array hybridization and melting for rapid resolution of mismatches, and for detection of minor mutant components in the presence of a majority of wild type sequence: statistical model and supporting data, *Genet Anal* 13:73, 1996.

Strezoska Z, Paunesku T, Radosavljevic D, et al.: DNA sequencing by hybridization: 100 bases read by a non-gel-based method, *Proc Natl Acad Sci U S A* 88:10089, 1991.

Striebel HM, Birch-Hirschfeld E, Egerer R, et al.: Virus diagnostics on microarrays, *Curr Pharm Biotechnol* 4:401, 2003.

Sun ZH, Zheng WL, Zhang B, et al.: Detection of hepatitis D virus by cDNA microarray method, *Hepatobiliary Pancreat Dis Int* 3:423, 2004.

Syvanen AC: From gels to chips: "Minisequencing" primer extension for analysis of point mutations and single nucleotide polymorphisms, *Hum Mutat* 13(1), 1999.

Takahashi N, Hashida H, Zhao N, et al.: High-density cDNA filter analysis of the expression profiles of the genes preferentially expressed in human brain, *Gene* 164:219, 1995.

Taylor DD, Gercel-Taylor C: MicroRNA signatures of tumor-derived exosomes as diagnostic biomarkers of ovarian cancer, *Gynecol Oncol* 110(1):13–21, 2008.

Thellin O, Zorzi W, Lakaye B, et al.: Housekeeping genes as internal standards: use and limits, *J Biotechnol* 75:291, 1999.

Tian W, Liu S, Li B: Potential role of exosomes in cancer metastasis, *BioMed Res Int* 4649705, 2019.

Walter M, Bonin M, Pullman RS, et al.: Expression profiling in peripheral blood reveals signature for penetrance in DYT1 dystonia, *Neurobiol Dis* 38(2):192–200, 2010.

Wang I-M, Stepaniants S, Boie Y, et al.: Gene expression profiling in patients with chronic obstructive pulmonary disease and lung cancer, *Am J Respir Crit Care Med* 177:402–411, 2008.

Wang W, Wang Y, Piao H, et al.: Circular RNAs as potential biomarkers and therapeutics for cardiovascular disease, *PeerJ* 7, 2019. e6831.

Waring JF, Jolly RA, Ciurlionis R, et al.: Clustering of hepatotoxins based on mechanism of toxicity using gene expression profiles, *Toxicol Appl Pharmacol* 175:28, 2001.

Wei Y, Xu F, Li P: Technology-driven and evidence-based genomic analysis for integrated pediatric and prenatal genetics evaluation, *J Genet Genomics* 40:1–14, 2013.

Weiler J, Gausepohl H, Hauser N, et al.: Hybridisation based DNA screening on peptide nucleic acid (PNA) oligomer arrays, *Nucl Acids Res* 25:2792, 1997.

Wetmur JG: DNA probes: applications of the principles of nucleic acid hybridization, *Crit Rev Biochem Mol Biol* 26:227, 1991.

Whitney LW, Becker KG, Tresser NJ, et al.: Analysis of gene expression in multiple sclerosis lesions using cDNA microarrays, *Ann Neurol* 46:425, 1999.

Wilson CA, Dering J: Recent translational research: microarray expression profiling of breast cancer-beyond classification and prognostic markers? *Breast Cancer Res* 6:192, 2004.

Woski SA, Fidanza J, McGall G, et al.: Enhanced high density oligonucleotide array-based sequence analysis using modified nucleoside triphosphates, *Nucl Acids Res* 26:4975, 1998.

Xu L, Wu LF, Deng FY: Exosome: an emerging source of biomarkers for human diseases, *Curr Mol Med* 19(6):387–394, 2019.

Yan S, Han B, Gao S, Wang X, et al.: Exosome-encapsulated microRNAs as circulating biomarkers for colorectal cancer, *Oncotarget* 8(36):60149–60158, 2017.

Yang YH, Dudoit S, Luu P, et al.: Normalization for cDNA microarray data: a robust composite method addressing single and multiple slide systematic variation, *Nucl Acids Res* 30:e15, 2002.

Yang GF, Li XM, Xie D: Overexpression of clusterin in ovarian cancer is correlated with impaired survival, *Int J Gynecol Cancer* 19:1342–1346, 2009.

Yauk CL, Berndt ML, Williams A, et al.: Comprehensive comparison of six microarray technologies, *Nucleic Acids Res* 32:e124, 2004.

Yauk C, Berndt L, Williams A, et al.: Automation of cDNA microarray hybridization and washing yields improved data quality, *J Biochem Biophys Methods* 64:69–75, 2005.

Yershov G, Barsky V, Belgovskiy A, et al.: DNA analysis and diagnostics on oligonucleotide microchips, *Proc Natl Acad Sci USA* 93:4913, 1996.

Zang J, Maxwell AP, Simpson DA, et al.: Differential expression of urinary exosomal microRNAs miR-21-5p and miR-30b-5p in individuals with diabetic kidney disease, *Sci Rep* 29(1):10900, 2019. 9.

Zhang Y, Szustakowski J, Schinke M: Bioinformatics analysis of microarray data, *Methods Mol Biol* 573:259–284, 2009.

CHAPTER 71

APPLICATIONS OF CYTOGENETICS IN MODERN PATHOLOGY

Mary Ann Perle, Constance H. Stein

DEFINITIONS, 1411
CYTOGENETICS, 1412
Chromosomes, 1412
Chromosome Abnormalities, 1418
CLINICAL APPLICATIONS, 1423
Constitutional Cytogenetics, 1423
Cancer Genetics, 1425
Cytogenetic Disorders, 1427
Other Cytogenetic Phenomena, 1431
SUMMARY, 1432
SELECTED REFERENCES, 1432

KEY POINTS

- Identification of chromosomal abnormalities often correlates to disease and phenotypic abnormalities and thus will aid in clinical diagnosis and treatment.
- Identification of a cytogenetically abnormal clone in a cancer can provide information on diagnosis, prognosis, treatment, and disease progression.
- Standard morphology and a specific banding pattern have been established for all human chromosomes. A variety of different technologies, including karyotype analysis, fluorescence in situ hybridization (FISH), microarray analysis, and deoxyribonucleic acid (DNA) sequencing, are used to uniquely identify chromosomes and determine if anomalies exist.
- The two basic categories of cytogenetic abnormality are numeric and structural.
- Many syndromes have been specifically linked to particular chromosomal anomalies (e.g., trisomy 21 in Down syndrome; 45,X in Turner syndrome; and deletion of 22q11.2 in velocardiofacial syndrome).
- Cytogenetic abnormalities may be either de novo or inherited. Detection may occur at any stage of a person's life from prenatal to adulthood.
- FISH, a targeted assay that combines technologies from both cytogenetics and molecular genetics, can provide important diagnostic information about specific genes.
- Cytogenetic analysis can be used in nearly every medical specialty and is an important element in clinical laboratory medicine.
- Microarray analysis and DNA sequencing have identified new genetic syndromes. These technologies are key to optimizing genetic testing and treatment currently and in the future.

Genetics is broadly defined as the scientific study of heredity, but in clinical laboratory medicine interest is focused on two subspecialties of this field: human genetics, the study of heredity in humans, and medical genetics, the study of human genetic variation of medical significance. Medical genetics can be further subdivided into five groups, two primarily clinical fields (clinical genetics and genetic counseling) and three laboratory sciences (cytogenetics, molecular genetics, and biochemical genetics).

Groundbreaking discoveries in the field of medicine can be attributed to genetics. Research and the development of new techniques in molecular genetics and cytogenetics have identified new genes and mutations directly related to disease. Knowing the underlying cause of a disease aids in diagnosis, provides new options for therapy, and allows the possibility of curing some genetic diseases in the future. This chapter focuses on cytogenetics; discussion of molecular diagnostics is found in Chapter 72.

DEFINITIONS

As in all areas of medicine, genetics relies on the proper use of specific terms for communication. The following definitions provide a basic vocabulary for this field:

Gene: a sequence of nucleotides that represents a functional unit of inheritance; a region of DNA that codes for a product, either RNA or protein.

Chromosome: a highly ordered structure composed of DNA and proteins that carries the genetic information. In humans, there are 46 chromosomes ordered in pairs.

Autosome: all chromosomes other than the X and Y chromosomes, which are designated the *sex chromosomes*.

Homologous chromosomes or *homologues:* sister chromosomes, the members of a pair of chromosomes in which one is inherited from the mother and the other from the father.

Locus: the position of a gene on a chromosome.

Allele: an alternative form of a gene occupying the same locus. An allele may be the result of a mutation. There is a maximum of two alleles per diploid chromosome complement (one allele per chromosome), but multiple alleles may exist within a population.

Mutation: a permanent heritable change in the sequence of genomic DNA. This may manifest at both the molecular and cytogenetic levels. Not all mutations are negative events. Many are benign (e.g., blue eye color), and some have positive effects (e.g., sickle cell trait in countries with a significant risk of malaria). Individuals with a *constitutional mutation* (i.e., a mutation present in every cell of the body) may pass that mutation on to their progeny by germline transmission. In some cases, notably cancer, an *acquired mutation* may arise in a single somatic cell, which then divides mitotically, giving rise to a new clone of cells. The mutation will be limited to this clone and will not be transmitted to progeny of the individual. In rare instances of *gonadal mosaicism*, a de novo acquired mutation, may arise in the gonads, resulting in a mixed population of normal and mutant gametes. Progeny receiving the new mutation may display a phenotype not present in either parent.

Karyotype: the chromosome constitution of an individual.

Karyogram: a figure showing the paired chromosomes from a cell arrayed in a standard sequence.

Diploid: the presence of two copies of each unique chromosome per cell. In humans, the chromosomes occur in pairs and the diploid ($2N$) number is 46.

Haploid: one copy of each unique chromosome. In humans, the gametes are haploid ($N = 23$).

Homozygous: both alleles at a locus are the same. (In the ABO system, an AA complement represents homozygosity.)

Heterozygous: the two alleles at a locus are different. (In the ABO system, an AO complement represents heterozygosity.)

Hemizygous: the presence of only one chromosome or chromosome segment rather than the usual two (e.g., males with a single X chromosome).

Genotype: the genetic constitution of an individual or organism (i.e., what alleles are present). (In the ABO system, AA, AO, BB, BO, AB, and OO are genotypes.)

Phenotype: the appearance of an individual that results from the interaction of environment and genotype. (In the ABO system, A, B, and O blood types represent the phenotypic expression of the alleles for a given individual.)

Dominant allele: an allele that is expressed when present in only a single dose (i.e., it "dominates" over the other allele present). (In the ABO system, A is dominant over O such that an AO genotype results in an A blood type phenotype. Similarly, the presence of pigment [T] is dominant to the absence of pigment [t] [i.e., albinism], such that Tt results in pigmentation.)

Recessive allele: in a diploid organism, an allele that is only expressed when homozygous. (In the ABO system, the O blood group is only seen with a OO genotype; O is recessive to A and B. Similarly, t is recessive to T, and an albino phenotype only occurs with a tt genotype.)

Codominant alleles: in a diploid organism, alleles that show no dominance or recessivity to each other, but when present together they are both fully expressed. (In the ABO system, A and B are codominant such that an AB genotype expresses both A and B antigens.)

Independent assortment: random assortment of chromosomes (paternal and maternal) in the gametes; there is a 50:50 chance of inheriting a given chromosome from one parent.

Linkage: the presence of two or more genes on the same chromosome that tend to be inherited together.

Crossing over: the physical exchange of genetic material between homologous chromosomes.

Recombination: the generation of new allelic combinations on chromosomes, usually by crossing over.

Mitosis: somatic cell division in which the DNA replicates and is evenly distributed to two equal daughter cells.

Meiosis: cell division in the gonads that produces the gametes. A single DNA replication is followed by two cell divisions that reduce the total DNA content of a cell from 2N to N. Recombination occurs to increase genetic diversity within a population.

Nondisjunction: failure of chromosomes or chromatids to separate to opposite poles in cell division. Usually results in one too many or one too few chromosomes in a cell.

CYTOGENETICS

Cytogenetics is defined as the science that combines the methods and findings of cytology and genetics, allowing the investigation of heredity at the cellular level. This involves careful evaluation of the chromosomes, structures composed of double-stranded DNA complexed with histone and nonhistone proteins. Chromosomes were first observed in tumor cells by Walther Fleming in 1882, only 16 years after Mendel established genetics as a new field of science. Thus cytogenetics is one of the oldest fields of genetics. Just after the turn of the century, the importance of the sex chromosomes was established, and in 1959, cytogenetic studies were first used in clinical laboratory studies. The ability to detect changes in chromosome structure and directly correlate them to disease and phenotypic anomalies in individuals proved a major advancement in clinical diagnosis. Over the years, the number and types of studies have grown, and many of the tests performed have become the gold standard for diagnosis. As more and more genes are being identified and linked to particular diseases, molecular testing, including direct mutation analysis, microarray, and sequencing, are becoming increasingly prevalent (see Chapters 69, 70, and 72). However, cytogenetics continues to be the most cost-effective and straightforward test to detect chromosomal numerical and structural rearrangements. Consequently, clinical applications for cytogenetic analysis can be found in all age groups and genetic specialties, ranging from prenatal diagnosis to cancer evaluation (Arsham et al., 2016; Nussbaum et al., 2016).

CHROMOSOMES

To recognize abnormalities, it is important to first understand what makes up a "normal" chromosome set. The human chromosome complement includes 46 chromosomes ordered in 23 pairs (Fig. 71.1). One member of each pair is inherited from an individual's mother and the other comes from the father. Twenty-two pairs are known as *autosomes* and appear as homologs of each other (i.e., they are indistinguishable from each other). The 23rd pair includes the sex chromosomes, which are homologous in a female, who has two X chromosomes, and are nonhomologous (structurally different) in a male, with one X and one Y chromosome (see Fig. 71.1). Genes are encoded in the DNA and are arrayed along the length of the chromosomes. During the cell cycle, the absolute lengths of the chromosomes vary, with the most condensed form reached in metaphase. This is the point when chromosomes can most easily be observed, so metaphase chromosomes are the basis for most cytogenetic studies. Complete evaluation of a set of chromosomes is known as *karyotype analysis* and an ordered image of the chromosomes from a cell is called a *karyogram*.

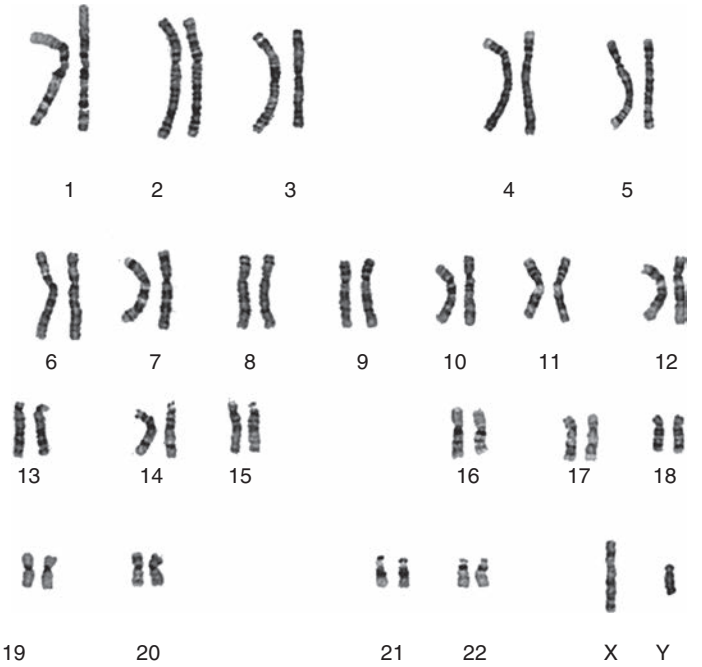

Fig. 71.1 Karyogram of male human chromosome complement, with 46 total chromosomes ordered in pairs. Note the nonhomologous pair of sex chromosomes with one X and one Y chromosome *(lower right)*.

Chromosome Structure

A single metaphase chromosome is composed of two DNA double helices associated with proteins. Each double helix is termed a *chromatid*, and the two chromatids are held together by an as yet unreplicated region of DNA known as the *centromere*, or primary constriction. In addition to its function in cell division, the centromere acts as a landmark and divides the chromosome into two distinct regions known as *arms* (Fig. 71.2A). The shorter of the two arms is designated the *p arm*, and the longer arm is known as the *q arm*. When the centromere is approximately equidistant from both ends, the chromosome is said to be metacentric, but if it is closer to one end than the other, the chromosome is submetacentric (see Fig. 71.2B). Five pairs of acrocentric chromosomes have modified short arms with stalks containing only multiple copies of rRNA genes that are capped by a modified telomere termed a *satellite* (see Fig. 71.2A).

The end of a chromosome is the *telomere*. These regions are known to be composed of tandemly repeated DNA with the sequence $(TTAGGG)_n$ that functions to stabilize the chromosomes. The mechanics of DNA replication are such that not all of the telomere DNA can be replicated at each division, so there is a shortening of the telomeres over time. It has been postulated that total loss of the telomeres leads to an increase in chromosomal aberrations that may, in part, be responsible for carcinogenesis and the human aging process (Harley et al., 1990; Wright & Shay, 1992; De Lange, 1998; Raynaud et al., 2008).

Cell Culture

To obtain metaphase cells for a chromosome analysis, cells from a patient must be cultured in vitro. The average human cell divides once every 24 hours, so only about 1% of the cell population is dividing at any given time. However, some cells, such as lymphocytes in a normal healthy individual, do not divide at all. Special culture techniques have therefore been developed to stimulate the cells to divide and increase the yield of metaphase cells.

Specimens

Virtually any viable, nucleated cell sample can be used for cytogenetic analysis. However, certain types of cells are easier to obtain and culture and are therefore favored for chromosomal preparations. For routine cytogenetic studies of adults and children, heparinized peripheral blood

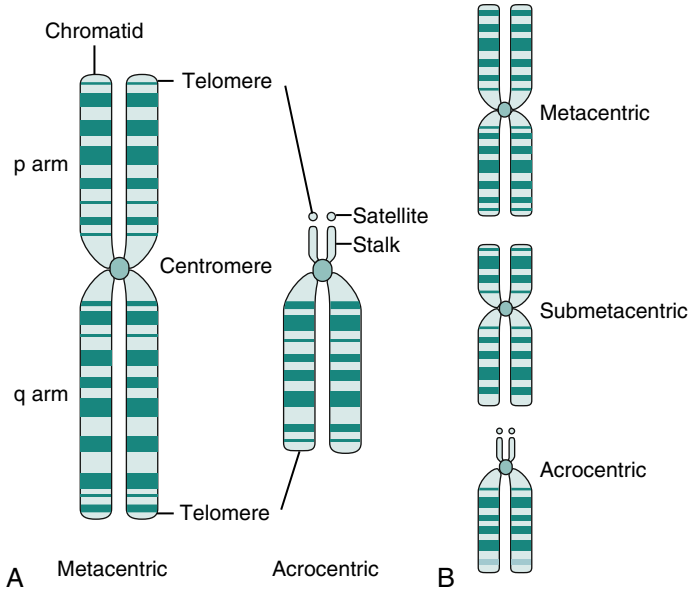

Fig. 71.2 Chromosome structure. **A** Schematic of metaphase chromosome anatomy showing major landmarks. Each chromosome is composed of two chromatids held together by the centromere. The telomere is the end structure of the chromosome. A typical metacentric form is contrasted with an acrocentric having a modified short arm structure composed of stalks and satellites. In all cases, the shorter, or p, arm is oriented up and the longer, or q, arm is oriented down. **B** The relative position of the centromere can vary, resulting in metacentric (centromere near the middle), submetacentric (centromere closer to one end), and acrocentric (modified short arm) chromosomes.

Fig. 71.3 Metaphase chromosome spread. Chromosomes from a single cell as seen on a microscope slide.

is the preferred specimen. Obtaining a sample via standard phlebotomy is usually easy to arrange and relatively painless for the patient. In hematologic disorders, the best results are obtained from bone marrow samples because this is the origin of the disease. Fibroblast cultures from skin biopsies or skin punches provide an adequate source of metaphase cells. Tissues such as liver, kidney, lung, and muscle are not routinely used because of the invasive nature of acquiring such specimens; however, these tissues can be useful to evaluate a fetal loss or an autopsy. Products-of-conception samples may contain a mix of maternal and fetal tissue and so require extra care in establishing a culture (De Martinville et al., 1984).

The most common specimen for prenatal analysis is amniotic fluid collected by amniocentesis. Under ultrasound guidance, the physician passes a needle through the mother's abdomen and uterus into the amniotic sac. This is typically done between 16 and 18 weeks of gestation, at which time 20 to 30 mL of amniotic fluid (fetal urine) can be withdrawn without endangering the fetus. Cells present in the sample are derived from the fetus and provide a source of material for cytogenetic, molecular genetic, and biochemical assays. The fluid itself contains alpha fetoprotein (AFP), as well as other proteins and enzymes, and forms the substrate for other prenatal assays. The risk of fetal loss due to amniocentesis is approximately 0.2% to 0.3%.

Another prenatal procedure is chorionic villus sampling (CVS), which provides tissue from the developing placenta (chorionic villi) (Blakemore, 1988; Rhoads et al, 1989). The transabdominal or transvaginal procedure is performed at 10 to 13 weeks of gestation and has a risk of fetal loss of approximately 1%. Because no amniotic fluid is collected, no AFP or related testing can be done, although standard cytogenetic, biochemical, and molecular analyses are possible.

Cordocentesis, or percutaneous umbilical blood sampling (PUBS), results in a fetal blood specimen that can be used for rapid karyotyping or molecular studies. This procedure is done at later gestational ages (≥20 weeks) and carries a higher risk of fetal loss (2–5%).

All clinical samples for cytogenetic analysis must be collected in a sterile manner. The presence of bacteria or fungi severely compromises the study because prokaryotic cells usually outcompete and overgrow any human cells that are present. To maximize the number of viable cells, specimens should be transported to the laboratory as soon as possible after collection. Blood, bone marrow, amniotic fluid, and chorionic villi should be maintained at room temperature, whereas solid tissue is transported on wet ice. The difference in temperature of transport is due to the native conditions of the sample. Blood, bone marrow, and amniotic fluid cells exist as individual cells in a fluid substrate, and the integrity of the sample will not be compromised as long as its temperature is maintained close to body temperature. However, collection of tissues such as skin requires cells to be excised from the body, leaving broken and dying cells at the periphery of the sample. The resultant release of lysosomal enzymes facilitates degradation of the dead cells, but the enzymes will also attack and destroy adjacent living cells. If the temperature is dropped to near 4°C, enzyme activity will be inhibited, and the viability of the sample is maintained.

Cell Culture Technique

Depending on the cell type, either a suspension (floating) or monolayer (fixed to a surface) culture technique may be employed. Blood and bone marrow cells are grown in suspension, so cells from the sample can be aliquoted directly into an appropriate culture medium. Bone marrow is typically cultured for 24 to 48 hours, whereas lymphocytes require 3 to 4 days in culture for maximum yield. Furthermore, because lymphocytes do not normally divide in culture, they must be induced using a mitogen, usually phytohemagglutinin. The resultant metaphase cells can then be collected by the use of a mitotic inhibitor, such as colcemid. Amniotic fluid cells, chorionic villi, and solid tissue are all grown as a monolayer in situ. Tissue and chorionic villi are first disaggregated using a mild collagenase treatment, and the individual cells are then seeded onto glass coverslips and covered with culture medium or placed into culture flasks. In an amniotic fluid sample, the cells must first be separated from the fluid by centrifugation before being plated in dishes or flasks and allowed to form in situ colonies. Typical culture times are 5 to 7 days for chorionic villi and amniocytes and up to 2 weeks for solid tissue culture.

Once maximum growth has been achieved, all cell types are harvested using similar techniques. The cells are swelled hypotonically (to the point that the cell membrane is stretched but not broken) and are then fixed, typically using a methanol:acetic acid fixative. Gentle blowing on the coverslip containing the fixed cells from in situ cultures results in the rupture of the cell membrane and a spreading of the metaphase chromosomes. For suspension cultures, the fixed cells must be dropped onto a clean microscope slide, which mechanically breaks the membranes and leaves the chromosomes separated slightly from each other but in a discrete region occupied by a single cell (Fig. 71.3). After air drying, the slides are suitable for staining. In some cases, artificial aging of the cells at approximately 65°C for 30 to 60 minutes improves the quality of the staining. Although most laboratories still perform these steps manually, an automated robotic harvester has been developed that can process large numbers of cultures quite efficiently.

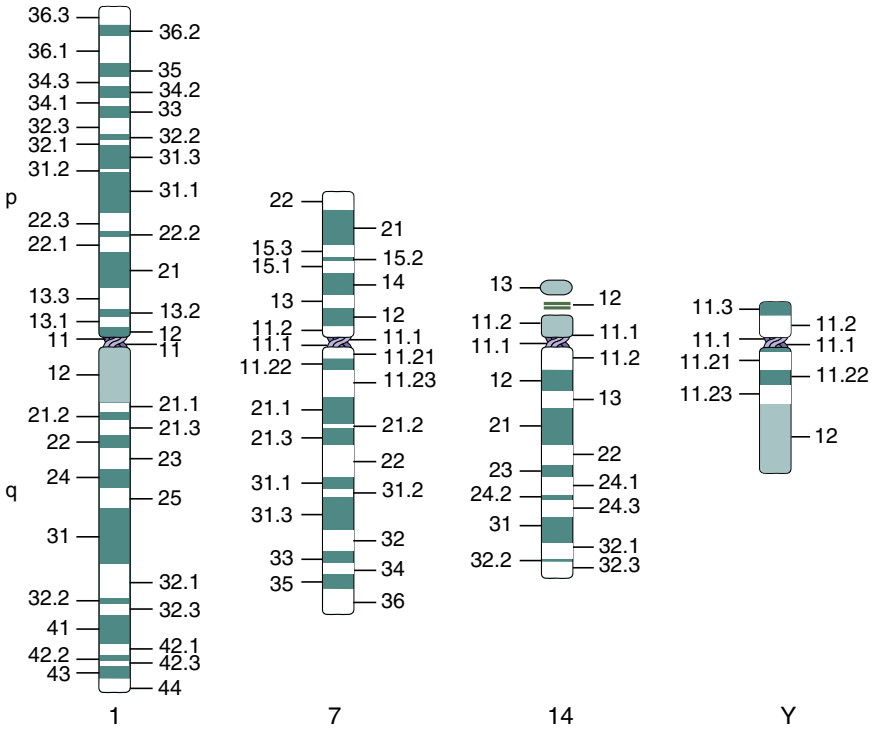

Fig. 71.4 Examples of ideograms for chromosomes 1, 7, 14, and Y showing the expected pattern of alternating light and dark bands.

Staining

Chromosomes are routinely stained using Giemsa or Wright stain, positively charged dyes that bind to the negatively charged DNA molecule. Mild trypsinization of the chromosomes before staining apparently weakens the DNA-protein interactions, yielding a defined pattern of alternating light and dark regions after the stain is applied. This is called the *banding pattern* (G-banding for Giemsa banding) (Yunis & Sanchez, 1973; Burkholder & Weaver, 1977; Holmquist et al., 1982). Each pair of chromosomes has a unique band pattern that is schematically represented as an ideogram (International System for Human Cytogenomic Nomenclature [ISCN], 2016) (Fig. 71.4), and this is used to identify each chromosome and the chromosomal subregions.

Although rarely used today, additional information about chromosome structure can be obtained with other special staining technologies. The most common special stains include Q-banding, C-banding, and R-banding. *Q-banding*, or quinacrine fluorescence staining, was originally used in routine chromosome analysis (Comings et al., 1975). However, because the fluorescence is transient, it has been replaced by G-banding, which allows a permanently stained preparation (Sumner et al., 1973). The current major application of Q-banding is for rapid identification of the Y chromosome. The distal end of the long arm of the Y chromosome is composed of heterochromatin and is the most brightly fluorescent region in a human metaphase (Fig. 71.5A).

C-banding, constitutive or centromere banding, may be used to evaluate constitutive heterochromatin or to determine whether a chromosome has two centromeres (dicentric). Normally, a centromere appears as a single dark spot on an overall pale-staining chromosome (Holmquist, 1979). In the case of a dicentric chromosome, the presence of two dark regions clearly identifies the two centromeres (see Fig. 71.5B). *R-banding*, or reverse banding, results in chromosomes with the same banding pattern as that seen in G-banding, but the light and dark bands are reversed, hence the name. Because the telomeres of the chromosomes tend to be small, light-staining bands, a deletion may not be easily detected using standard G-banding. In R-banding, however, the telomeres should appear as dark bands, and their absence as the result of a deletion is more obvious.

Karyotype Analysis

To perform a cytogenetic (karyotype) analysis, it is essential to be able to rapidly and accurately identify each chromosome and determine when chromosome abnormalities are present. The first step is to count the number of chromosomes present in the cell being evaluated. The number of active centromeres defines the total number of chromosomes and will total 46 in a normal human diploid cell. Too many or too few chromosomes indicate a potential numerical abnormality. In vitro culture can result in

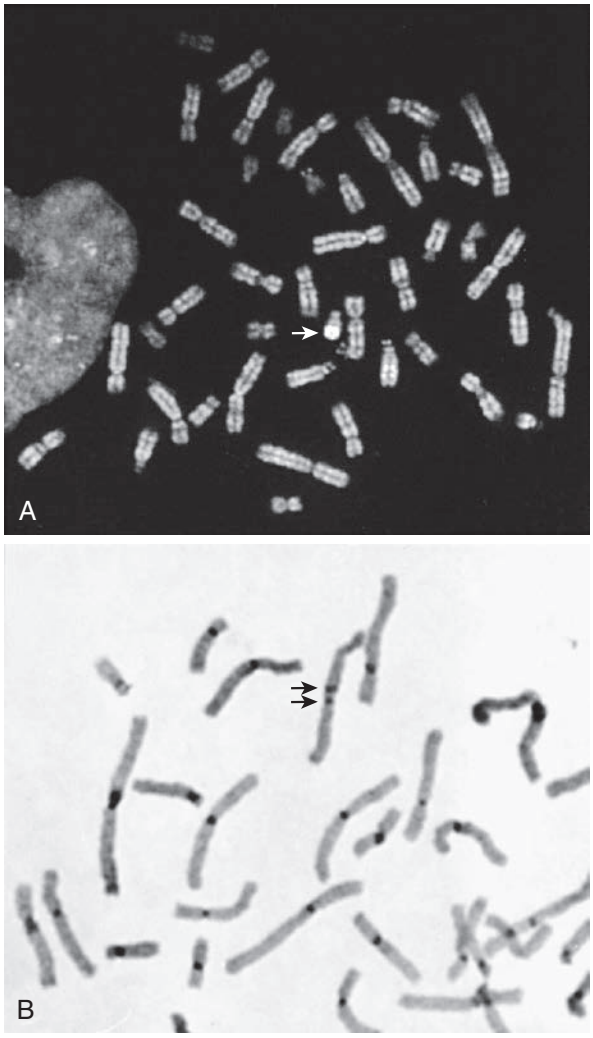

Fig. 71.5 **A** Q-banded metaphase showing bright fluorescence of the Y chromosome *(arrow)*. **B** C-banded chromosomes showing the dark staining centromeres. A dicentric chromosome was detected with two dark bands *(arrows)*.

culture artifacts, so no single cell is used to define an individual's chromosome complement. A typical clinical study requires analysis of 15 to 20 cells. Single cells with abnormalities are considered artifacts. Three or more cells with the same chromosome loss or two or more cells with the same additional chromosome or structural rearrangement define a true abnormality. In cases of mosaicism or for other special situations, 10 to 30 additional cells may be evaluated.

Individual chromosomes are identified based on the overall size of each chromosome, the position of its centromere, and the banding pattern. Any variation in chromosome structure should be detected at this time. In most circumstances, routine G-banding of metaphase chromosomes is sufficient for clinical diagnostic purposes. However, some disorders are associated with very small deletions of chromosomal material that may not be resolved at this level, so high-resolution analysis is used. Special culture conditions are employed, and the cells are harvested at prometaphase, a slightly earlier stage of cell division. At this point in the cell cycle, the chromosomes are less condensed and physically longer, making the presence of small abnormalities easier to detect. Please note that even at high resolution, the ability to detect very small chromosome abnormalities is limited. A duplication or deletion of about 3 MB is the smallest that can be seen using conventional karyotype analysis.

The analysis is performed by a technologist viewing the cells at the microscope, and once the study is complete, a determination is made as to whether the chromosome complement is normal or abnormal. For documentation, representative metaphase cells are captured, and karyograms (illustrations of the chromosomes of a given cell) (see Fig. 71.1) are prepared. The homologous pairs are arrayed from large to small, with special placement for the pair of sex chromosomes. By convention, the shorter arm, the p arm, is oriented up, and the longer q arm is oriented down.

Computer-Assisted Imaging

To capture the images, cytogenetics laboratories now use computer-assisted imaging. A CCD (charge-coupled device) video camera is used in combination with specially designed software to capture an image of a metaphase cell, which is digitized and displayed on the computer monitor. The image can be modified by lightening, darkening, or changing the contrast, and a variety of manipulations of the chromosomes are possible, including straightening and importing chromosomes from other fields. A karyogram can then be generated using a pattern-recognition subroutine that will automatically identify the chromosomes and place them in their proper places on a karyogram form. Depending on the software and the quality of the image, the accuracy of this process can vary from 10% to 85%. After the computer has taken its "best guess," a trained cytogenetic technologist must make the appropriate corrections, and the final version of the karyogram can be printed out by a high-resolution printer and then archived. A routine karyogram from capture to printing should take a trained technologist on average 15 to 20 minutes.

Fluorescence in Situ Hybridization

FISH, a combination of molecular and cytogenetic technologies, has expanded the ability to investigate chromosome anomalies. This technique requires a molecular probe (i.e., a fragment of DNA) that is labeled with a fluorescent dye. To create a probe, a target DNA of interest is chosen, the relevant DNA is isolated, and a single stranded copy of that DNA is labeled with a fluorescent dye. This probe can be hybridized to denatured metaphase or interphase cells and should bind to the homologous region of the chromosome from whence it was derived. The presence or absence of the signal can be seen using a fluorescence microscope (Ledbetter & Cavenee, 1989).

In clinical applications of FISH, the most common goal is to determine whether a gene, a specific mutation, or a particular chromosomal rearrangement is present, so the molecular probes used must be well characterized and specific to the locus in question. There are three basic types of probes. *Chromosome painting* probes are actually a cocktail of many unique DNA fragments from along the entire length of a chromosome, so that, following hybridization, the entire chromosome fluoresces (Fig. 71.6A). *Repeat sequence* probes are usually used in chromosome enumeration (i.e., to detect the gain or loss of specific chromosomes) (Lichter et al., 1990). Chromosome-specific pericentromeric and subtelomeric probes are typically used for this purpose (see Figs. 71.6, *C* and *D*). A *unique sequence* probe is usually isolated from cloned DNA of a disease-causing gene or a fragment of DNA of known location associated with a particular gene. This type of probe is used to identify the presence or absence of a gene, gene region, or chromosomal rearrangement of interest (Cherif et al., 1989; Lindsay et al., 1993). *Subtelomere* probes are a subset of this category, and chromosome-specific subtelomere probes have been used to characterize cryptic subtelomeric deletions or rearrangements that have been associated with unexplained mental retardation (see Fig. 71.6B) (Flint et al., 1995; Flint & Knight, 2003; National Institutes of Health and Institute of Molecular Medicine Collaboration, 1996; Rosenberg et al., 2001; Irons, 2003). Although accurate and useful, the subtelomere FISH assay has now been largely replaced by chromosome microarray studies.

Technique

FISH can be performed on either metaphase or interphase cells. For metaphase FISH, cells are cultured and harvested as for a routine karyotype analysis, but no culture is required for interphase FISH. Fixed cells are collected, and slides are made as described for karyotyping. The DNA on the slides is then denatured, and a fluorescently labeled single-stranded molecular probe is allowed to hybridize to the chromosomal DNA using an annealing temperature that favors hybridization of homologous regions of DNA (Fig. 71.7A). After an appropriate period of hybridization, excess probe is washed away and the nonhybridized DNA is counterstained with another fluorochrome to allow visualization of the entire chromosome complement. A fluorescent microscope with light from a 100-watt mercury bulb in combination with appropriate sets of exciter filters allows evaluation of the cells. Due to the optical limitations of the glass filters, a maximum of three colors can be visualized on a typical fluorescent microscope. For documentation, images are captured using a computer-assisted system.

One of the most critical elements in FISH is the selection of a specific probe(s) that will help to answer a clinical question. For example, one of the most useful clinical applications of FISH is the detection of microdeletions too small to be seen using classical cytogenetics (see Fig. 71.7B-D). The gene must be known, and the probe used must be homologous to the critical region of the gene that is usually deleted. Hybridization with the probe should result in a fluorescent signal only at the target locus. If a signal is present, DNA complementary to the probe is present, so there is no deletion (see Fig. 71.7B). However, the absence of signal indicates that a deletion exists (i.e., there is no DNA sequence present on the chromosome that is complementary to the probe, so no hybridization can occur) (see Fig. 71.7D). A control probe to a different region of the chromosome being tested is usually used as a hybridization control (see Fig. 71.7C). Therefore, when evaluating a disease-related probe, an unaffected individual should have two signals per cell for each autosomal gene: one signal for each chromosome of the pair (Fig. 71.8A). An affected individual with a deletion should have a single signal per cell, showing one normal and one deleted chromosome (see Fig. 71.8B). For both affected and unaffected individuals, the control probe should show two signals per cell in all cells that are scored. In a metaphase cell, the chromosomes may be short and condensed, with each chromatid individually visible, resulting in a discrete FISH signal on each chromatid. In these cells, there may appear to be two signals per chromosome, for a total of four signals, but in actual scoring only complete chromosomes are considered so a signal on one or both chromatids would be counted as just one positive signal.

One of the problems with this detection system is that the lack of signal is the positive indication of a deletion. Technical failure of hybridization may also result in absence of a signal. To eliminate this as a source of error, a minimum of 20 cells must be evaluated, and all cells must agree in signal count. If mosaicism is suspected, additional cells may be surveyed. In addition, unique sequence probes are currently used in combination with a second probe—a control probe—that is localized to a different locus on the same arm of the target chromosome (see Fig. 71.7C). The two probes are usually labeled with fluorochromes of different colors. In all cells evaluated, two clear control signals must be seen, and then the corresponding signals for the disease locus can be recorded. This provides a hybridization control as well as a marker for the chromosome of interest (see Fig. 71.7D). If a dual-color system is used, results may be obtained in interphase as well as metaphase cells.

Chromosome painting probes are most useful in identifying complex rearrangements or marker chromosomes. If an individual has an abnormal chromosome with extra material of unknown origin, it may be possible to use chromosome painting to identify the source of the extra DNA. This may help in either diagnosis or prognosis of the individual. For example, in the case of a patient with only one identifiable X chromosome and a small, unidentified marker chromosome, it will be important to determine if the origin of the marker is an X or a Y chromosome. This can be accomplished using chromosome paints for the X and Y chromosomes labeled with different fluorochromes.

FISH is a targeted assay. The probes will only provide information about the locus from which they are derived. Thus when interpreting results, it is critical to know which probe was used. When using metaphase cells, the necessary data can usually be obtained from viewing about 20 cells.

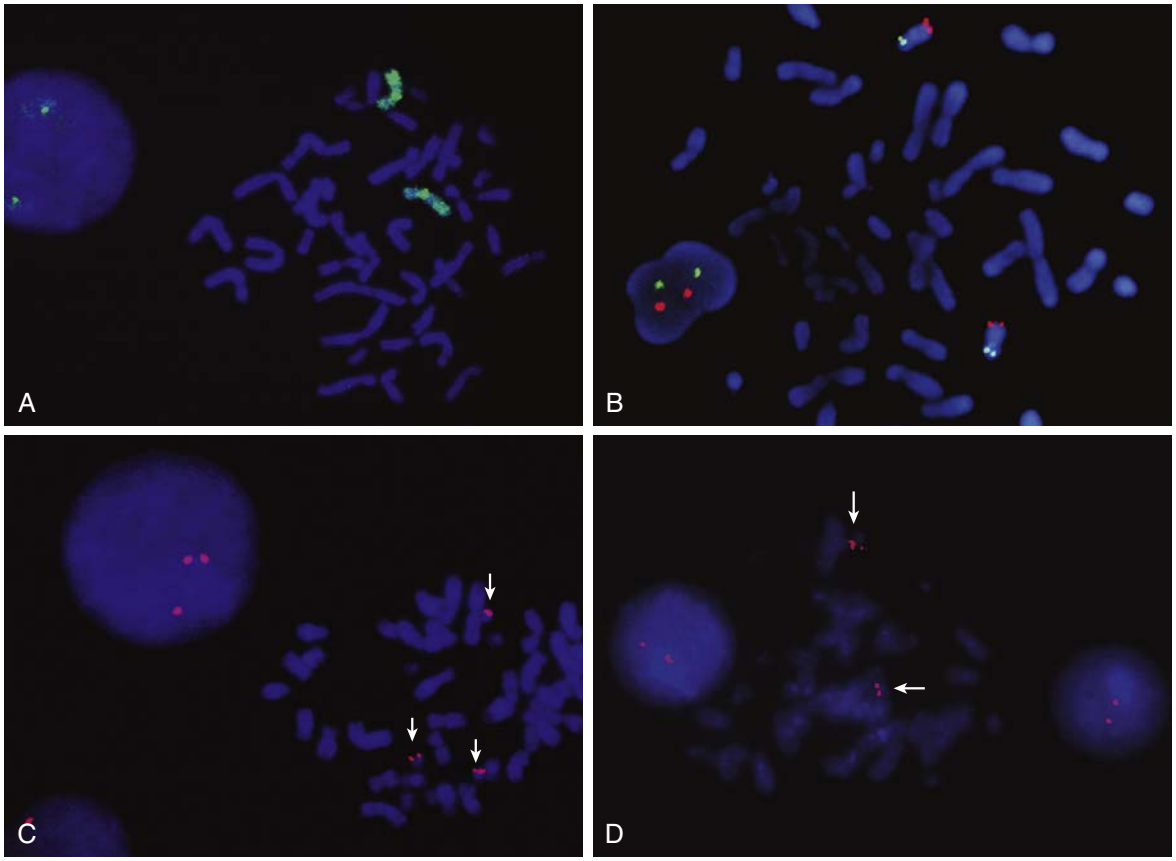

Fig. 71.6 Fluorescence in situ hybridization. **A** Whole chromosome paint probe highlighting the two X chromosomes in a female cell. **B** Chromosomes showing hybridization with subtelomere probes. The p arm subtelomere is indicated by the green signals, and the q arm subtelomere is indicated by the red signals. Paired red and green signals are seen in the interphase nucleus to the *left*. **C** and **D** Repeat sequence centromere probe for chromosome 21. **C** Trisomy 21 seen at *left* in an interphase nucleus and at *right* in a metaphase *(arrows)*. **D** Normal complement of two copies of chromosome 21 *(arrows)* seen in interphase (*left* and *right*) and in a metaphase *(center)*.

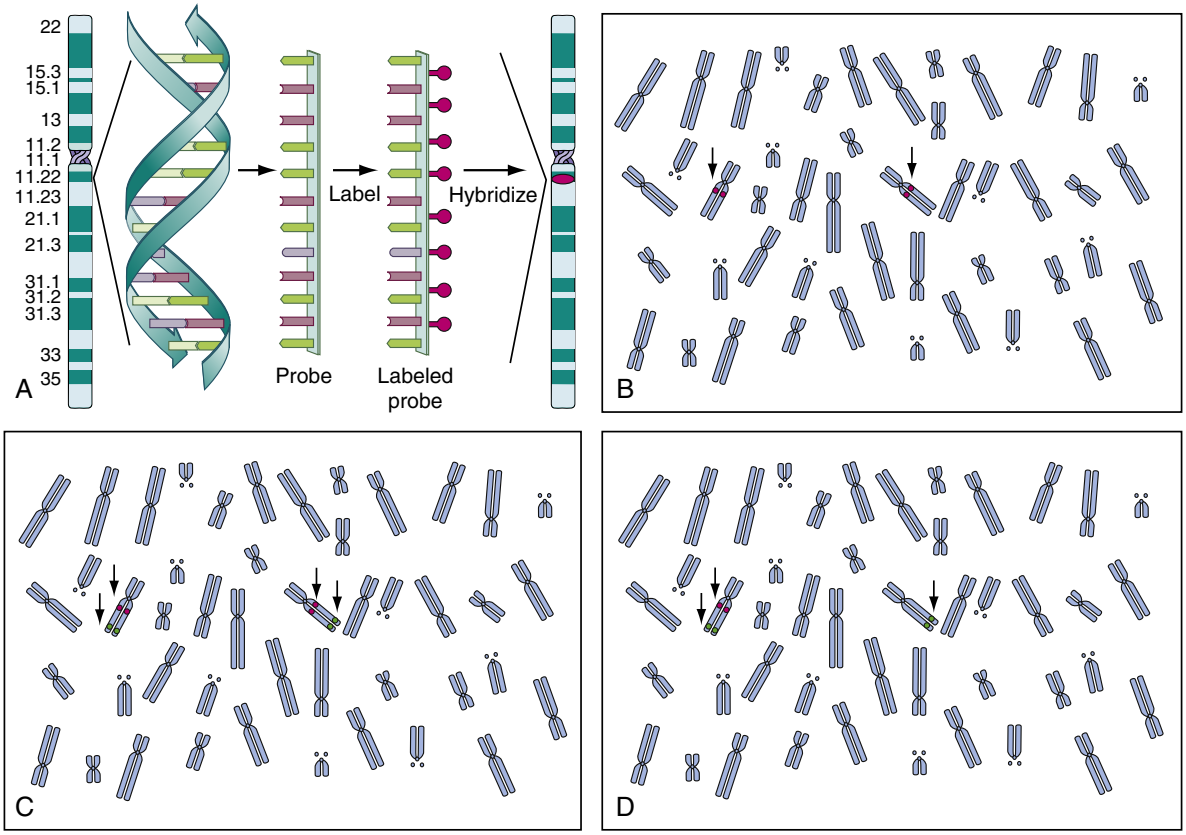

Fig. 71.7 **A** Schematic of fluorescence in situ hybridization (FISH) technology. DNA derived from a known gene is rendered single stranded, labeled with a fluorescent tag, and then hybridized back to the chromosomes of a metaphase cell. **B** to **D** Depiction of a metaphase cell with 46 chromosomes that has been processed using FISH technology. The labeled probes hybridized to targets are indicated with *arrows*. **B** Dual signals indicating hybridization to both alleles of target gene. **C** Target gene indicated by *red* signal and a control probe indicated in *green*. Complete hybridization to all alleles. **D** Hybridization of both controls *(green)* but presence of only a single target gene, indicating deletion of one allele.

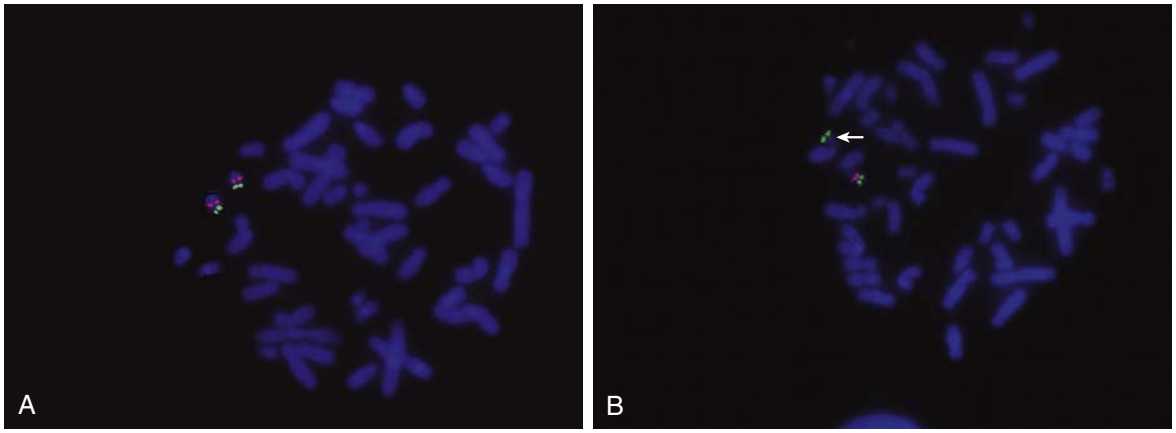

Fig. 71.8 Fluorescence in situ hybridization detection of a microdeletion of chromosome 22 associated with velocardiofacial syndrome. **A** An individual with no deletion showing the presence of one *red* (gene locus) and one *green* (control locus) signal for each chromosome 22. **B** Patient with a deletion seen as a chromosome with only a single *green* (control) signal. The homologous chromosome 22 is "normal" with one *red* and one *green* signal.

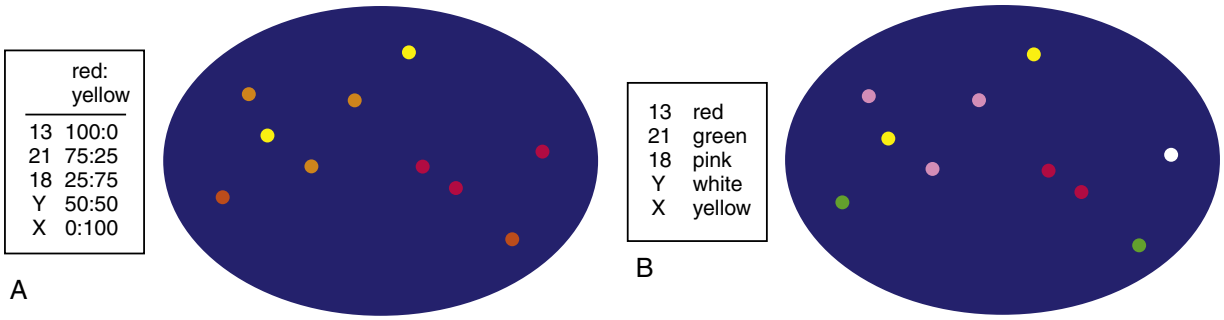

Fig. 71.9 Multicolor fluorescence in situ hybridization. **A** Diagram of the staining pattern for five probes (chromosomes 13, 18, 21, X, and Y) in an interphase cell. *(Table at the left shows relative proportions of the red and yellow fluorochromes used for each probe.)* **B** The same cell depicted in **A** now showing the computer-derived artificial color assignments *(key shown in box to left).* This cell can now be interpreted as having two copies each for chromosomes 13, 21, and X; three copies of chromosome 18; and one Y chromosome.

A larger sample of interphase cells (200–500) can yield statistically significant data about the frequencies of disease clones.

Multicolor Fluorescence in Situ Hybridization

Another advantage of FISH is the ability to hybridize multiple probes to a single slide to obtain a better understanding of chromosome rearrangements (Schrock et al., 1996; Speicher et al., 1996). For most fluorescent microscopes, the maximum number of FISH probe colors is three (one target sequence, one control sequence, and one counterstain). If more than three colors are needed, a computer-assisted imaging system is required. This is because a fluorescent image is the result of the light from the mercury bulb passing through an exciter filter, hitting the fluorochrome on the slide, and transmitting an image of the appropriate color to the eyepiece for viewing. Each fluorochrome requires its own filter, so for each additional color desired, the light must pass through additional thicknesses of glass. The optical properties of glass and light limit the total number of viewable colors to three. However, with a computer-assisted system, detection of multiple colors becomes possible. The computer does not actually "see" more colors, but it can detect subtle differences in shades better than the human eye. In a relatively simple example, two fluorochromes are used and mixed in varying proportions to give a range of colors. In the example in Fig. 71.9A, a red fluorochrome is mixed with a yellow fluorochrome, generating intermediate colors from red to yellow. Eight signals are seen, but as viewed through the microscope it is impossible to be absolutely sure which signal corresponds to a particular chromosome. Although difficult to distinguish by the human eye, the computer can register each color as a different shade of gray, and then the software assigns a unique color to that shade for display on the computer monitor. Figure 71.9B shows the final multicolor version using many different colors now easily distinguishable but very different from the original presentation (see Fig. 71.9A). Using the key to the left, the following chromosomes are detected: two each for chromosomes 13, 21, and X; three chromosomes 18; and one Y chromosome. This cell is therefore trisomic for chromosome 18 with an XXY sex chromosome complement. This is an example from prenatal genetic diagnosis (PGD). In PGD, a single blastomere is removed from an embryo at the eight-cell stage. With one cell, limited testing is possible, but using a multicolor FISH approach it is possible to do a single hybridization that will detect common abnormalities such as aneuploidies for chromosomes 13, 18, 21, and the sex chromosomes. In cancer studies, combinations of fluorochromes have been developed that allow detection of each of the 24 different chromosomes, followed by a unique color assignment by the computer (Reid, Baldini et al., 1992; Reid, Landes et al., 1992; Divane et al., 1994).

Microarray Technology

The gene level sensitivity of targeted FISH (~150 Kb) greatly increased the detection rate of chromosomal abnormalities formerly only sensitive to ~ 5 Mb, but some individuals who present with findings suggestive of a chromosome defect have an apparently normal karyotype, and a FISH assay only has very limited probe specificity. To obtain more detailed information on the chromosomes of these patients, use of microarray analysis has proven to be very valuable in genetic diagnosis. In 2010 a consensus paper was published that supported chromosomal microarray analysis (CMA) as a "first-tier clinical diagnostic test for individuals with developmental disabilities or congenital anomalies" (Miller et al., 2010). This was quickly followed by many additional publications showing the relevance of microarray for the detection of genetic abnormalities in both constitutional cases (Shaffer et al., 2012; Wapner et al., 2012) and, more recently, oncology cases (Cooley et al., 2013; Mikhail et al., 2019). Updated consensus standards for both prenatal and postnatal CMA testing continue to guide clinical applications for array testing (Riggs et al., 2019; South et al., 2013). CMA is now widely recommended in the postnatal setting as a first-tier test for patients with unexplained developmental delay, intellectual disability, autism spectrum disorder, neurodevelopmental disorders, and/or congenital anomalies (Silva et al., 2019).

A chromosomal microarray is a genome-wide diagnostic DNA test to detect copy number variations (CNVs) in the DNA sequence such as deletions, duplications, aneuploidies, and unbalanced translocations with a gain or loss of sequences (Fig. 71.10). (See Chapter 70 for a discussion of the technology behind microarray analysis.) Various array platforms are available, and most currently utilize either array comparative genomic hybridization or, more commonly, single nucleotide polymorphisms (SNPs). For diagnostic SNP-based arrays, criteria for reporting changes is expected to be 400 to 600 kb for prenatal and 200 to 400 kb for postnatal tests.

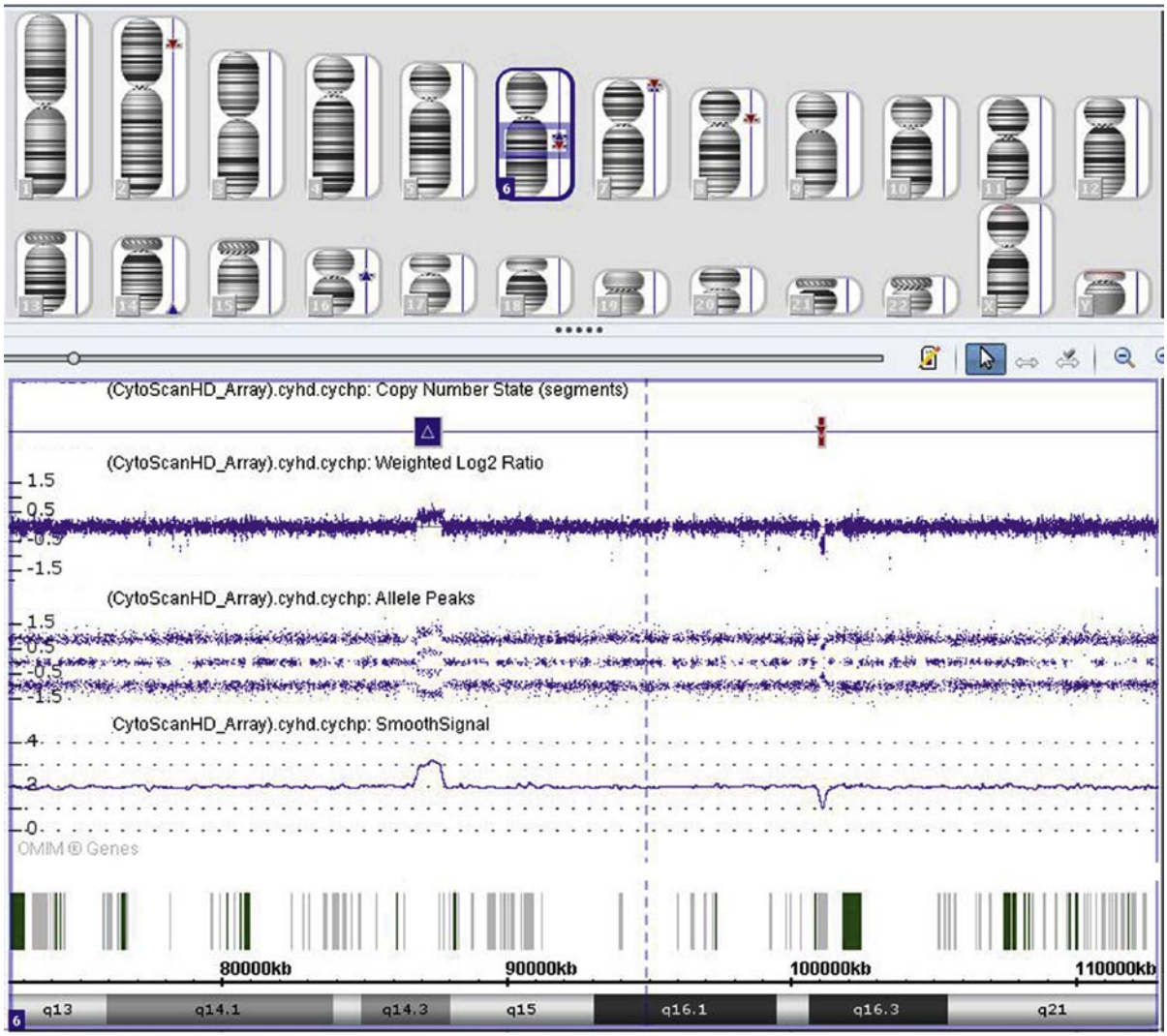

Fig. 71.10 Example of data from a microarray analysis. The upper panel shows the set of chromosomes from which chromosome 6 was chosen for examination in detail. The bands for that chromosome are shown horizontally at the bottom. In this case, the proximal long arm of chromosome 6 shows two anomalies: a duplication and a deletion. The duplication is identified by the blue box just below the chromosome panel, and the red bar denotes the smaller deletion. These are confirmed by the thick line at the top *(weighted log2 ratio),* series of three midweight lines in the middle *(allele peaks),* and the single line below that *(smooth signal).* For the duplication, the smooth signal deflects upward, showing three copies in that region and four copies for the allele peaks. For the deletion, the smooth signal deflects downward, indicating the presence of a single copy at that locus. (These data were collected using the Affymetrix CytoScanHD System.)

Genome-wide chromosomal microarray analysis provides identification of genomic lesions too small or too cryptic to be detected by other types of assays, leading to a diagnosis for many patients for whom the cause of their anomalies had previously been unknown. In addition, many new genetic syndromes have been recognized and added to the known catalogue of genetic disorders.

However, as with all technologies, microarray is not a perfect solution for all situations. Array-based tests do not detect balanced chromosome rearrangements, including translocations and inversions, and some may not detect low-level mosaicism or independent cell lines; some SNP-based arrays may detect uniparental disomy (UPD) and identity by descent (IBD; consanguinity, incest, inbreeding). Some CNVs found will be polymorphic variants for which the clinical significance is unknown. Thus it may not be possible to state for certain that the anomaly detected is related to the patient's clinical problem. It is important in all these cases to obtain parental follow-up studies, which may help in interpretation. For patients with a benign or apparently normal CMA and normal conventional karyotype result, testing using next-generation sequencing (NGS) technology (whole genome, whole exome, gene panel sequencing) may provide additional diagnostic information (Dharmadhikari et al., 2019; Lindstrand et al., 2019; Srivastava et al., 2019; Waggoner et al., 2018). Sequencing tests are currently not widely available for use in the clinical setting but are rapidly gaining recognition as an additional strategy for whole genome evaluation. To collect as much data as possible and to share the information among practicing geneticists, international databases have been set up, and clinical laboratories performing microarray analyses are encouraged to report their findings. These searchable databases will aid in better interpretation of CNVs and CMA variants.

CHROMOSOME ABNORMALITIES

Clinical cytogenetic testing is an integral part of clinical medicine. Finding a particular chromosome anomaly may be directly associated with a disease diagnosis, or it might explain a physical problem or phenotypic abnormality in the patient. It is therefore critical to determine whether an affected individual has a chromosome complement that differs from the standard pattern of 23 pairs of chromosomes with known morphology. There are two basic categories of cytogenetically detectable variation: numeric and structural change.

Numeric Abnormalities

In humans and other mammals, the chromosomes occur in pairs. Of the 46 human chromosomes per cell, there are only 24 uniquely different chromosomes. A set of 23 comprises the haploid (N) number of chromosomes, which is the number of chromosomes in a gamete. At fertilization, two haploid complements join to form a zygote with 46 chromosomes, the diploid ($2N$) complement. Errors in division can give rise to chromosome complements that have more or less than 46 chromosomes. Having exact multiples of the haploid set of chromosomes is called *euploidy*. Gain or loss of one or a few chromosomes is known as *aneuploidy*.

Euploidy

Diploidy, the normal state of human cells, is a form of euploidy. Abnormal euploidies include triploidy ($3N$ = 69 chromosomes) and tetraploidy ($4N$ = 92 chromosomes), but in humans these are not compatible with life and are detected primarily in neoplasia or spontaneous abortus tissues. Triploidy

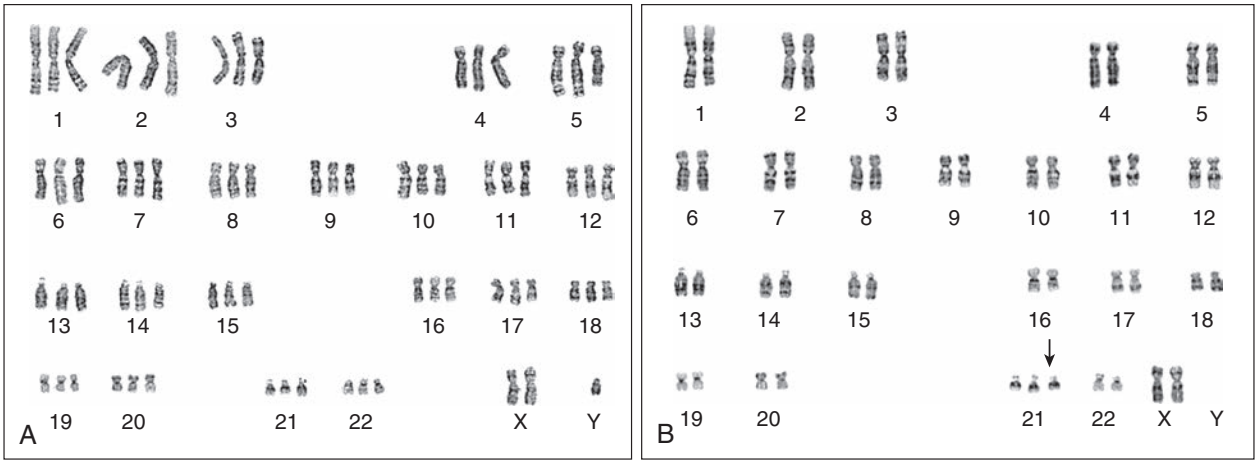

Fig. 71.11 Numerical chromosome abnormalities. **A** Triploid (3N) chromosome complement with three copies of each chromosome (69,XXY). **B** Trisomy 21 (47,XX,+21) with one extra chromosome 21 *(arrow)*.

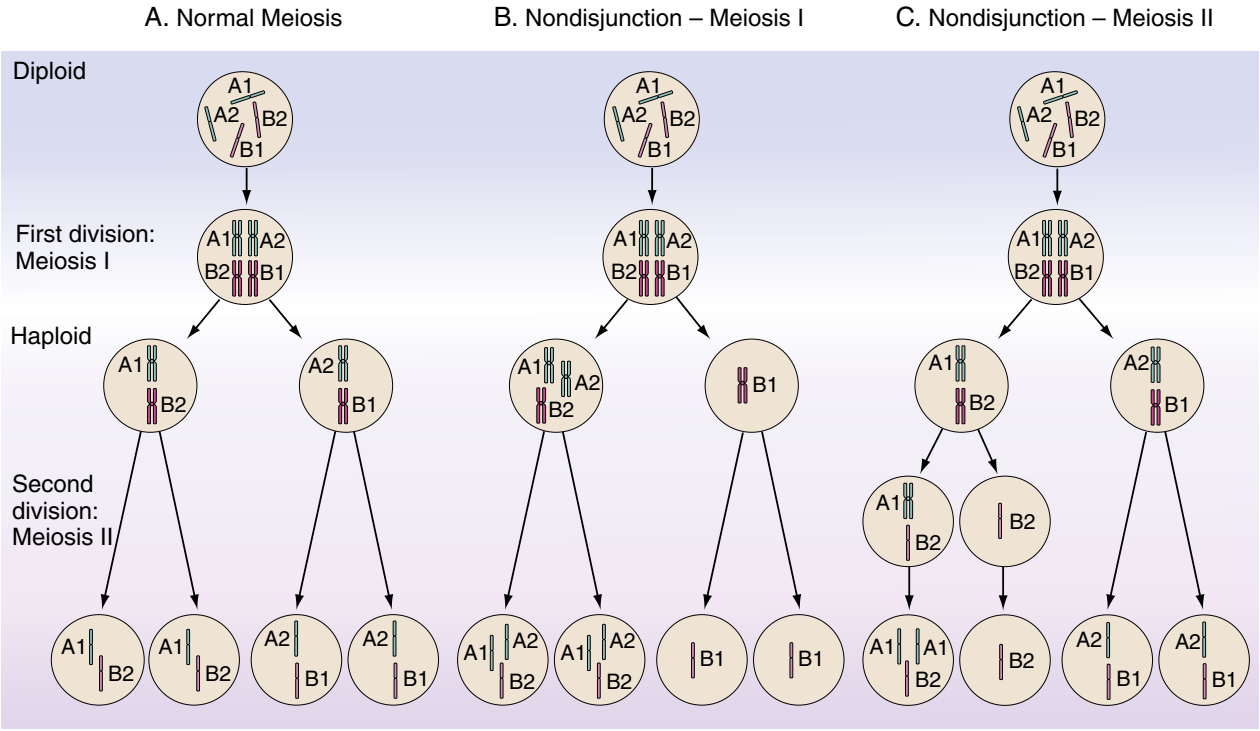

Fig. 71.12 Meiosis and meiotic nondisjunction errors, resulting in aneuploid gametes. **A** Normal meiosis generating four gametes with a haploid chromosome set. **B** Nondisjunction in meiosis I, leading to an extra copy of chromosome A (heterodisomy) in two gametes *(left)* but the lack of any A chromosome (nullisomy) in the remaining two gametes *(right)*. **C** Nondisjunction in meiosis II results in two gametes with a normal chromosome complement *(right)*, one gamete missing an A chromosome *(left center)*, and one gamete with an extra duplicated chromosome (two copies of A1), resulting in isodisomy for chromosome A1 *(left)*.

(Fig. 71.11A) may be due to the failure in gametogenesis of one of the meiotic divisions, giving rise to a 2*N* gamete that, when combined with a haploid gamete from the other parent, produces a triploid zygote. Alternatively, a 3*N* complement may be derived from dispermy, the fertilization of a haploid egg by two sperm, and this generally results in a nonviable partial hydatidiform mole. Tetraploidy, on the other hand, is usually a postmeiotic event and presents as a duplication of a diploid complement (XXXX or XXYY) probably due to failure of an early mitotic cleavage division in the zygote. Triploidy and tetraploidy seen in neoplasia usually result from a somatic division error.

Aneuploidy

More common are nondisjunctional errors resulting in aneuploidy. Here, a single pair of chromosomes fails to disjoin properly in division, giving rise to one extra chromosome or one missing chromosome per cell. Occasionally, more than one pair of chromosomes may be involved, but these cases are extremely rare in normal somatic tissues. Nondisjunction errors may occur in either meiosis or mitosis. Early mitotic nondisjunction in a zygote may result in an individual with the aberrant chromosome complement in all cells of the body, but a latter division error usually produces a *mosaic*, an individual with two cell lines that differ only by a single chromosome. Mitotic division errors in neoplasia can lead to aneuploidy for multiple chromosomes.

In normal meiosis, one DNA replication is followed by two cell divisions, resulting in four haploid (*N*) gametes (one copy of each chromosome) (Fig. 71.12A). The first meiotic division is the reduction division, in which the total number of chromosomes per cell is reduced by half. The second meiotic division is a simple mitotic type of division with a separation of the centromeres and distribution of the chromosomes to daughter cells. Meiotic errors may result in gametes with either an extra or missing chromosome (Angell et al., 1994). A nondisjunction error in the first meiotic division (see Fig. 71.12B) leads to two gametes that are disomic for one chromosome and two gametes that are missing that chromosome (nullisomic). When fertilized, the former will give a trisomic conception for the nondisjoined chromosome (e.g., trisomy 21 in Fig. 71.11B), and the latter will result in a monosomy. Similarly, Fig. 71.12C shows an error in the second meiotic division, resulting in two normal haploid gametes, one disomic gamete, and one nullisomic gamete.

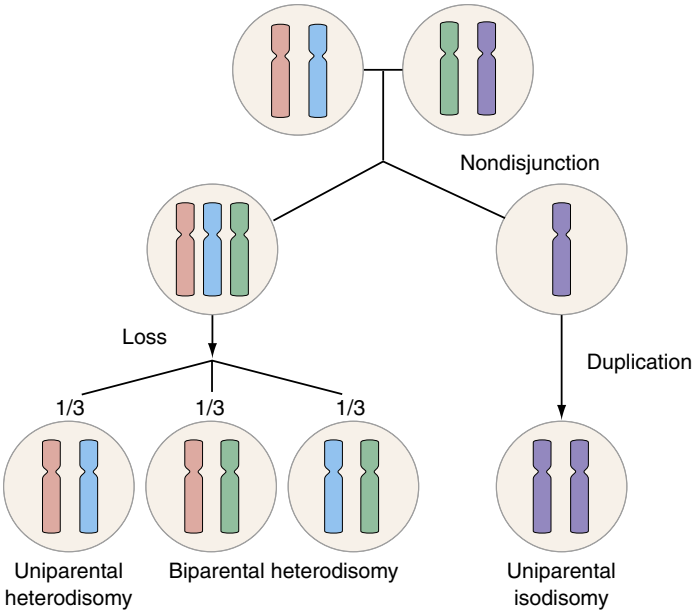

Fig. 71.13 Generation of uniparental disomy from nondisjunction errors. *(Left)* Heterodisomy resulting from reduction of a trisomy to a disomy is seen. *(Right)* Isodisomy as the result of monosomy rescue (duplication of a single existing chromosome) is seen.

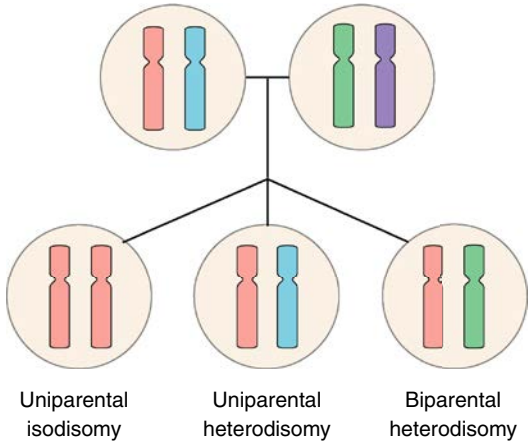

Fig. 71.14 Isodisomy versus heterodisomy. The expected conformation of a cell is biparental heterodisomy *(right)*—that is, one chromosome from each parent. Division errors can result in an aberrant distribution of parental chromosomes such that two copies of one chromosome from one parent (uniparental isodisomy) *(left)* or two different chromosomes from the same parent (uniparental heterodisomy) *(center)* occur.

Trisomy or monosomy may occur for any chromosome, but most of these occurrences are incompatible with life and will terminate spontaneously. Trisomy 16, for example, is the most commonly detected trisomy in spontaneous abortus tissue but is not reported in liveborn individuals. Liveborn autosomal trisomies include chromosomes 13, 18, and 21. Infrequently, patients with a mosaic chromosome complement for trisomies 8, 9, or 22 are identified. Sex chromosome trisomies are viable and well documented (see later). The only viable monosomy is of the X chromosome (45,X). Examples of clinically significant aneuploidies are discussed later in this chapter.

Because trisomies and monosomies are largely incompatible with life, it had been assumed that these would always result in fetal wastage. However, molecular analyses have shown that a small fraction of these aneuploid conceptions are "rescued" and go on to produce liveborn children. In the case of a monosomy, the rescue is accomplished by duplication of the single existing chromosome, resulting in a chromosome complement with *uniparental isodisomy* for that chromosome (two copies of the same chromosome inherited from one parent) (Fig. 71.13, *right*) (Ledbetter & Engel, 1995). This is exemplified by several reported cases in the literature in which a child affected with cystic fibrosis was shown to be homozygous for the ΔF508 mutation, although molecular tests on both parents revealed that only one was a carrier of ΔF508 (Spence et al., 1988; Voss et al., 1989). The interpretation is that the conception was a nonviable monosomy 7 rescued by duplication of the existing chromosome 7 that happened to be carrying the mutation for cystic fibrosis. A similar situation is possible in the case of a trisomy. Again, most trisomies are nonviable, but if one of the three chromosomes is lost, a disomy for that chromosome pair is reinstated (see Fig. 71.13, *left*). In a set of three chromosomes, loss of a single chromosome results in a complement with one maternal and one paternal chromosome *(biparental heterodisomy)* two of three times. One-third of the time, the two remaining chromosomes are from a single parent (i.e., uniparental disomy). In this situation, it makes a difference in which meiotic division the error occurred. A first-division nondisjunction results in heterodisomy, which is two homologous but heterozygous chromosomes (one grandmaternal and one grandpaternal); however, a second division error results in duplicate copies of a single chromosome: isodisomy (Fig. 71.14; see Fig. 71.12B,C).

In the past it was thought that having two chromosomes per pair was sufficient, but it has been shown that in some cases it is essential for the pairs to consist of one maternal and one paternal chromosome. This issue, including the problems of uniparental versus biparental disomy and isodisomy versus heterodisomy, is of major importance in understanding issues of *imprinting*, a topic discussed in detail in Chapter 72 (Nicholls et al., 1998; Hall, 1990; Cassidy et al., 1992; Petersen et al., 1992; Lobo, 2008).

Structural Chromosome Abnormalities

Chromosomes are not static structures but undergo recombination in both meiosis and mitosis. This is a natural process that is critical in generating variation in the species so a highly developed regulatory system is in place to prevent error from occurring. Nevertheless, errors do occur, sometimes resulting in chromosome rearrangements that change the structure of one or more chromosomes. Such abnormalities are quite varied and are often patient specific. Rearrangements may be *balanced*, if all the chromosomal material is present and functional but simply arranged in a different conformation, or *unbalanced*, if there is loss and/or duplication of some chromosomal material. Constitutional balanced rearrangements are usually clinically benign and tend to be stably transmitted, but they may increase the risk of errors in meiosis, resulting in chromosomal imbalances in fetuses or liveborn children. Unbalanced chromosome complements are generally associated with an abnormal clinical phenotype that often includes developmental delay and mental retardation. In cancer, chromosome instability may give rise to apparently balanced and unbalanced rearrangements. These anomalies may be an indirect or direct cause of the disease if important structural genes are damaged, duplicated, or inactivated by the rearrangement.

A *deletion* is the loss of a part of a chromosome that leads to partial monosomy of the chromosome involved (Fig. 71.15B). Deletions vary in size from quite large to very small and may be *terminal*, which is loss of a portion of one end of the chromosome, or *interstitial*, which is loss of an internal piece of chromosome. Chromosome breakage, unequal crossing over, or nondisjunction errors involving chromosome rearrangements may result in a deletion. In general, larger deletions result in more severe clinical abnormalities because of the greater number of gene loci that are missing.

A *duplication* is the presence of an additional copy of a chromosome segment and leads to partial trisomy for that chromosome (see Fig. 71.15C). Duplications may be *terminal* or *interstitial* and are generated by the same mechanisms as deletions. In fact, many duplications have been shown to be the reciprocal product of a deletion event (i.e., DNA sequences lost on one chromosome may be transferred to the homolog as a duplication) (see Fig. 71.25). As is true of deletions, the larger the duplicated piece of chromosome, the greater the genomic imbalance, and the more severe the clinical abnormalities tend to be. With the advent of microarray testing, the frequency of detectable duplications in clinically abnormal patients has increased significantly.

An *inversion* is a reversal of a chromosomal segment with respect to the normal gene arrangement and requires a minimum of two breaks in one chromosome (see Fig. 71.15D). Inversions are classified as either *paracentric*, where the two breaks occur on the same side of the centromere (i.e., in the same arm), or *pericentric*, where the breaks occur on opposite sides of the centromere and the inversion involves both arms (Fig. 71.16A; see Fig. 71.15D). The majority of inversions are balanced, but if the chromosome breaks within a gene and disrupts normal production of a required gene product, clinical abnormalities may be detected. During reproduction, there is an increased risk of meiotic error for inversion carriers who may exhibit infertility or early spontaneous fetal loss due to unbalanced chromosome products.

For a paracentric inversion carrier, meiosis begins with the pairing of the homologous chromosomes and loci, forming a structure known as an

inversion loop (see Fig. 71.16B). If no recombination occurs within the loop, the chromosomes separate, producing normal gametes. However, crossing over within the inversion loop can lead to acentric and dicentric chromosomes that are nonviable, unbalanced meiotic products. Thus there is an apparent suppression of recombination because the only viable gametes produced are from nonrecombined chromosomes (see Fig. 71.16B). For pericentric inversions, if recombination occurs within the inversion loop, gametes with a chromosome duplication and/or deletion may be derived. In general, larger pericentric inversions result in smaller duplications/deficiencies and increase the likelihood that a child will be liveborn with a chromosome imbalance and phenotypic abnormalities. Once an inversion carrier has been identified, prenatal diagnosis can be used to assess the chromosomes for each future conception.

Translocations are rearrangements involving two or more nonhomologous chromosomes. Each chromosome breaks once, and the pieces exchange places, establishing two (or more) derivative chromosomes (see Fig. 71.15E). As with inversions, a majority of translocations are balanced, and only when one or more important structural genes are disrupted does the translocation have clinical ramifications.

The primary danger of a balanced translocation is that carriers are at increased risk for chromosomally abnormal liveborn children. In the first meiotic division, translocated chromosomes assume a cross-shaped structure in order for all alleles to pair properly (Fig. 71.17). At anaphase, the alternate chromosomes must segregate together to generate balanced gametes. Up to one-third of the time, the chromosomes will not segregate in this manner and the resulting gametes will be unbalanced. The most common errors are termed *adjacent-1* and *adjacent-2 segregation*. Although both of these patterns result in duplication/deficiency of chromosomal material in the gametes, adjacent-2 is more deleterious because it is characterized by the unnatural occurrence of homologous centromeres in a single cell. Viability of a fetus receiving an unbalanced gamete is dependent on the chromosomes and genes involved in the translocation and the size of the duplication and/or deletion. Chromosomes may also follow a 3:1 segregation pattern (see Fig. 71.17, *right*), in which three chromosomes separate to one cell, with the remaining chromosome in the second cell. This results in gross imbalances of chromosomal material and is usually lethal in utero. Once a translocation carrier has been identified, prenatal diagnosis for future pregnancies is possible.

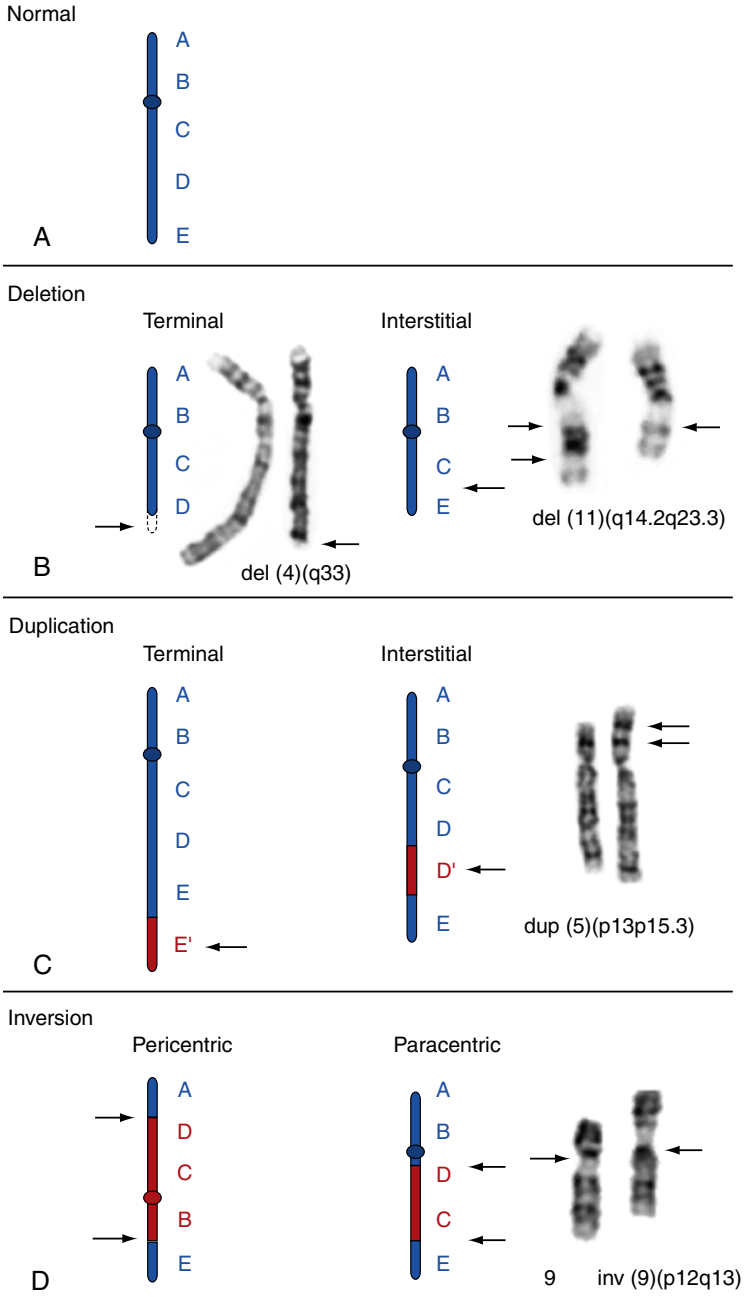

Fig. 71.15 Schematic representations of different structural chromosome anomalies described in the text associated with examples of each anomaly. **A** The normal configuration of a generalized chromosome, where A to E represent different gene loci, and the centromere is represented by a dot located between the B and C loci. **B** Deletion: Chromosome deletion showing terminal (loss of E locus) and interstitial (loss of D locus) configurations. Examples: Terminal deletion of the long arm of chromosome 4 and an interstitial deletion of the long arm of chromosome 11. **C** Duplication: Chromosome duplication showing terminal (gain of E′) and interstitial (gain of D′) configurations. Example: Terminal duplication of the short arm of chromosome 5 (*double arrows* indicate duplicated band). **D** Inversion: Chromosome inversion showing pericentric and paracentric forms. Example: Pericentric inversion of chromosome 9 (*arrows* indicate centromeres).

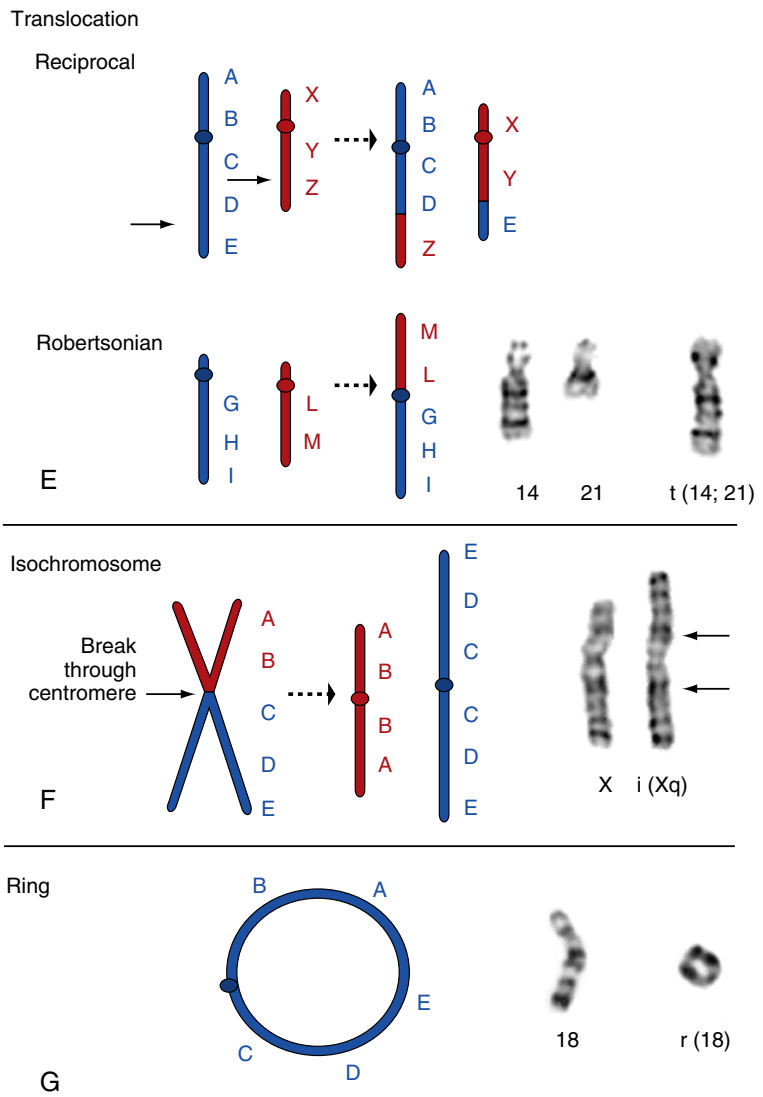

Fig. 71.15 cont'd **E** Translocation: Reciprocal translocation, where the E and Z loci exchange places. Below is a Robertsonian translocation shown by the fusion of two acrocentric chromosomes at the centromere. Example: Chromosomes 14 and 21 followed by the 14;21 Robertsonian translocation. **F** Isochromosome: Results from a misdivision of the centromere, generating inverted duplications of the long and short arms of the original chromosome. Example: Isochromosome of the long arm of the X chromosome. **G** Ring chromosome. Example: Chromosome 18 and ring 18.

Robertsonian translocations are a variation of the classic translocation. They occur only between two acrocentric chromosomes and appear to be a fusion of the long arms at the centromere, with the resulting loss of both short arms (see Fig. 71.15E). An individual who is a Robertsonian translocation carrier has a chromosome count of 45 because two chromosomes have functionally become one and share one centromere. Loss of the acrocentric short arms is not deleterious because multiple copies of the rRNA genes present there are also located on the remaining acrocentric chromosomes. However, Robertsonian translocation carriers are at increased risk for meiotic nondisjunction errors, resulting in children who are trisomic for one of the rearranged chromosomes. The most common example of this is an individual with a Robertsonian translocation involving chromosomes 13 and 14 who has liveborn children with trisomy 13 (Fig. 71.18). The affected child will have 46 chromosomes, including two free copies of chromosomes 13 plus the Robertsonian translocation that includes the third chromosome 13. Another common rearrangement is a Robertsonian 14;21 translocation (see Fig. 71.15E), which could give rise to trisomy 21 progeny.

Although the most common Robertsonian translocations occur between nonhomologous acrocentric chromosomes, it is possible to have such a rearrangement between homologous chromosomes. For example, an individual with a Robertsonian 21;21 translocation would have a total of 45 chromosomes, including the translocation in which the two 21s are joined at the centromere. This type of rearrangement is virtually always de novo, because carriers of the abnormality are unlikely to have normal progeny. Possible gametes include a cell with the Robertsonian translocation (two copies of chromosome 21), which, if fertilized, will give rise to a Down syndrome child, or a cell with no copies of chromosome 21, which, if fertilized, will result in a monosomy 21, which is not compatible with life.

An *isochromosome* results from misdivision of the centromere during cell division, generating two copies of one chromosome arm but missing the other arm (see Fig. 71.15F). This mechanism can result in two derivative chromosomes: one with an inverted duplication of the short arm and one with an inverted duplication of the long arm. If both derivative chromosomes are retained in the cell, it would be trisomic for that chromosome, a condition that is usually lethal. In a living individual therefore it is most common that one of the two derivative chromosomes is lost, resulting in a carrier who is trisomic for only one duplicated arm and monosomic for the other arm. The best-known example is the isochromosome of the long arm of the X. A patient with Turner syndrome (see later under Sex Chromosome Aneuploidies) may have one intact X chromosome and one isochromosome Xq (trisomy for the long arm but a monosomy for the short arm of the X). Because two functional copies of the X short arm are required for normal female development, this chromosome arrangement results in abnormal development. Acrocentric chromosomes may also form isochromosomes (inverted duplication of the long arm), but the resulting homozygosity of all loci present could lead to expression of recessive disorders that would otherwise not have been evident.

A *ring chromosome* occurs when both telomeres of a chromosome are lost and the remaining portion of the chromosome circularizes to reestablish chromosome stability (see Fig. 71.15G). Unfortunately these constructs are usually unstable because replication can result in interlinked circles that lead to chromosome breakage and loss when the homologs attempt to separate at anaphase. Under certain circumstances, however, rings can be

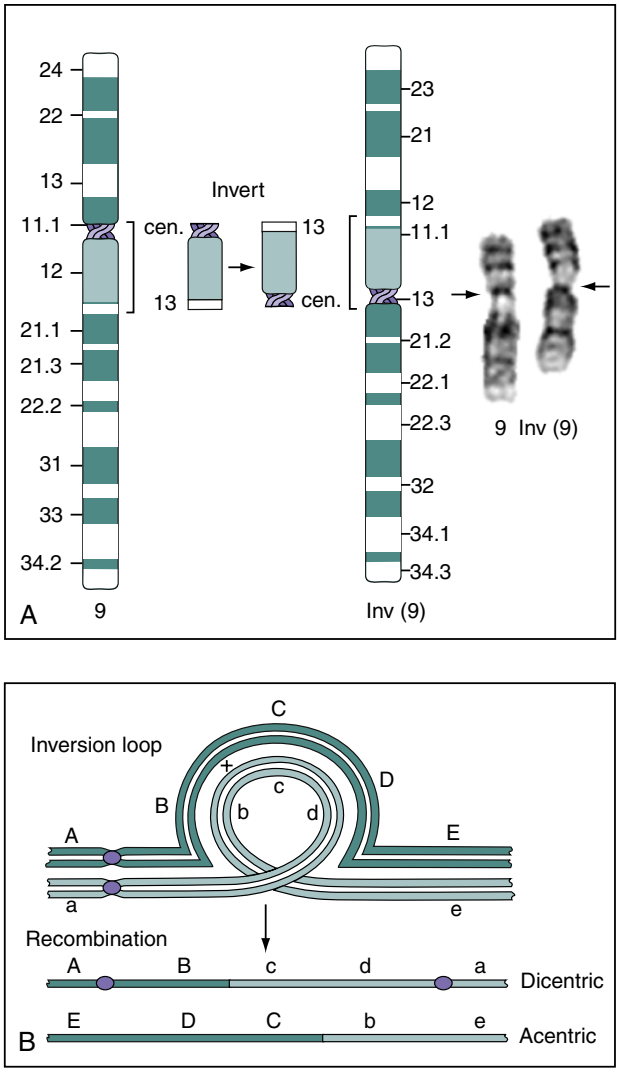

Fig. 71.16 Chromosome inversion. **A** Diagram of a pericentric inversion of chromosome 9 using ideograms to illustrate the mechanism of inversion. Banded chromosomes demonstrating this inversion are shown to the *right*. **B** Inversion loop showing the pairing of homologs in meiosis for one normal chromosome *(dark green)* and one with a paracentric inversion *(light green)*. If recombination occurs at the point indicated by the X in the loop, recombinant chromosomes would be generated as shown at the bottom. In the case of a paracentric inversion, the recombined chromosomes produced would be either dicentric or acentric.

stably transmitted in cell lines. This usually occurs when the ring contains genetic material that is essential for normal cell function.

A *marker* chromosome is a chromosome with a centromere that is stably transmitted to daughter cells but cannot be clearly identified because it is either too small or the banding pattern is too ambiguous. In a constitutional karyotype, a marker is often a benign finding, though it could represent a partial trisomy or tetrasomy and thus result in an abnormal clinical phenotype. Microarray studies can now identify most marker chromosomes. In cancer, marker chromosomes may be generated as a result of chromosome instability.

Conclusions

Chromosome abnormalities, either numeric or structural, that result in an unbalanced chromosome complement are usually associated with some type of abnormal clinical finding, and the size of the imbalance tends to be proportional to the severity of the problem. Most individuals with a constitutional chromosome abnormality have only a single chromosome defect. However, there are rare instances in which one person may have two or more chromosomal errors. Acquired chromosome abnormalities (seen in cancer cells) may be more complex and may have multiple numeric and structural changes in a single cell line.

Nomenclature

With such a broad range of chromosome variation, it was necessary to develop a system of classification that would allow each individual's chromosome complement to be succinctly described and understood worldwide. The first cytogenetic nomenclature provided a framework, and the "language" has been evolving ever since. Currently, the International System of Cytogenetic Nomenclature is recognized as the standard (ISCN, 2016).

The nomenclature describing a chromosome complement can be broken down into three basic parts: the total number of chromosomes, the sex chromosome complement, and any chromosome abnormalities. These units are listed in order, separated by commas. So an apparently normal female would be coded as 46,XX, and a male would be 46,XY. If two or more cell lines are present, they are listed sequentially, separated by a slash, with a normal diploid clone, if present, always listed last (45,X/46,XX). Other clones are ordered by size, with the largest clone placed first. The number of cells in each clone is indicated by a number enclosed in brackets (45,X[15]/47,XXX[3]/46,XX[12]). For numerical anomalies, the total number of chromosomes would be increased or decreased to indicate the overall change, and the specific chromosome gained or lost would be noted at the end. For example, trisomy 13 in a female would be written as 47,XX,+13, and monosomy 8 in a male would be written 45,XY,–8. However, for a sex chromosome variation that is known to be constitutional, it is not necessary to use a + or – sign, because the change in chromosome complement can be noted directly. Monosomy X becomes 45,X, and gain of a sex chromosome would be 47,XXY, 47,XXX, or 47,XYY. On the other hand, if the sex chromosome change is acquired, as in some cancer cell lines, a + or – indicating this would be required (e.g., 45,X,–Y for a male whose Y chromosome has been lost as a result of his disease).

Balanced structural changes in the chromosomes usually do not affect the total number of chromosomes present but should be noted at the end of the nomenclature to clarify the status of the rearranged chromosomes. To streamline the nomenclature, a series of abbreviations for the common structural anomalies has been generated that shortens the overall nomenclature (Table 71.1). A structural abnormality is indicated by the abbreviation of the abnormality, followed by the chromosome involved and breakpoints on the chromosome. For rearrangements in which two chromosomes are involved, a first set of parentheses gives the chromosomes (lowest numbered or sex chromosome first), followed by the breakpoints of the rearrangement in the same relative order—that is, t(4;9)(q21.2;p22) is a translocation between chromosomes 4 and 9 with breakpoints 4q21.2 and 9p22.

Examples include the following:

Deletion:	46,XX,del(4)(p15)	Terminal deletion of the short arm of 4 at band 15
Duplication:	46,XX,dup(11)(q13q23)	Interstitial duplication of the long arm of 11 involving the region from q13 to q23
Translocation:	46,XY,t(4;9)(q21.2;p22)	Translocation between 4q21.2 and 9p22
Inversion:	46,XY,inv(9)(p11q21.1)	Pericentric inversion in 9 between bands p11 and q21.1

CLINICAL APPLICATIONS

CONSTITUTIONAL CYTOGENETICS

Cytogenetic abnormalities may be found in apparently normal individuals, patients with phenotypic anomalies and/or a diagnosed genetic disorder, and individuals with other diseases such as cancer. Diagnosis may occur at any stage of life. When the same set of features is seen in several unrelated individuals, it may be possible to establish a syndrome. The characteristics associated with a syndrome are assumed to have a common basis, which can often be shown to be a specific chromosome abnormality. However, although a syndrome is defined by a certain set of characters, not all affected individuals have all of the known abnormalities so there is variability in phenotype within a population of affected individuals.

Prenatal

Studies have shown that 1 in 13 conceptuses has a chromosomal abnormality, but of these only 6 in 1000 are liveborn, indicating that most errors are biologically recognized and eliminated. For example, of all 45,X conceptions, greater than 95% will spontaneously terminate. Similar frequencies of termination are recorded for the liveborn trisomies (90% of trisomy 13

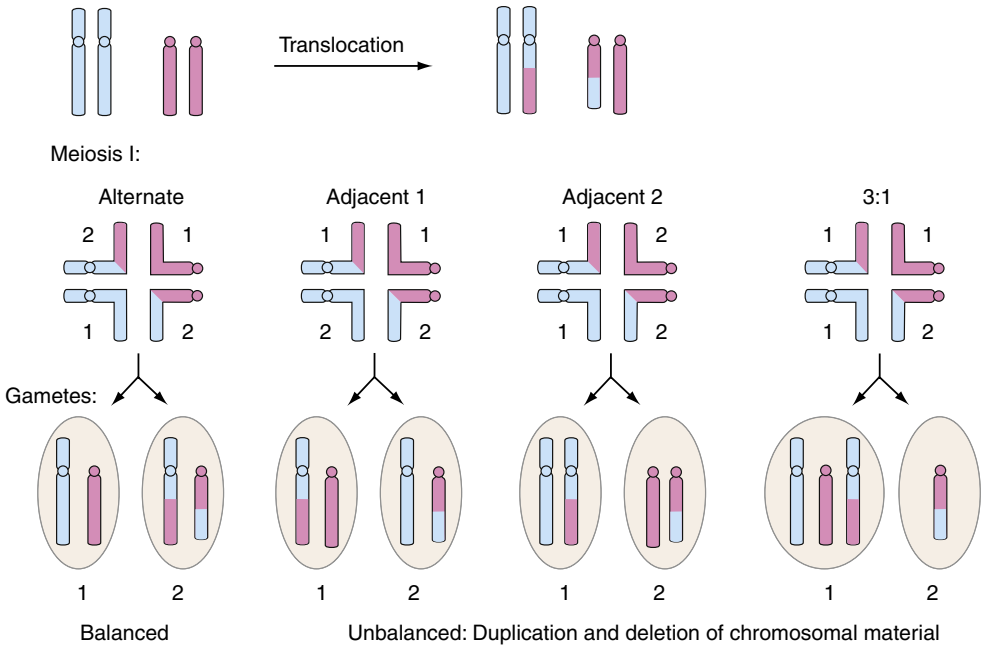

Fig. 71.17 Chromosome translocation. Generation of gametes from a hypothetical translocation in meiosis is diagrammed. The chromosomes pair in a cross-shaped configuration in meiosis I. Alternate segregation will result in balanced gametes. Adjacent 1, adjacent 2, or 3:1 segregation will produce unbalanced gametes, which may give rise to an abnormal liveborn child. (Only one of several possible 3:1 segregations is shown.)

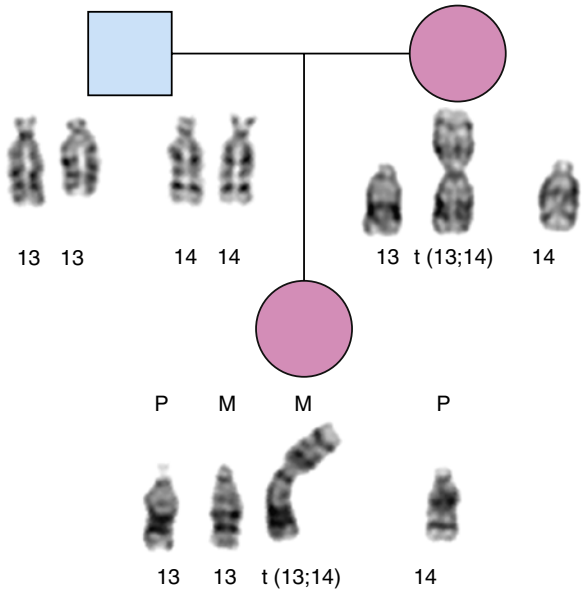

Fig. 71.18 Pedigree and banded chromosomes showing inheritance of a Robertsonian translocation of chromosomes 13 and 14. The mother carries the 13;14 translocation in a balanced form, but a meiotic error results in the transmission of both the Robertsonian translocation chromosome and the chromosome 13 from the mother to the child. The child has trisomy 13 and the Robertsonian translocation. Note: The second copy of chromosome 14 is not missing, but it is present as part of the Robertsonian rearrangement. *M,* Maternal chromosomes; *P,* paternal chromosomes.

conceptions, 80% of trisomy 18 conceptions, and 65% of trisomy 21 conceptions terminate). On average, 15% of all recognized pregnancies end in a spontaneous fetal loss, with 80% of these occurring in the first trimester. Of all spontaneous abortions, 60% are chromosomally abnormal (Table 71.2); of these, 52% are autosomal trisomies. The most common trisomy seen in abortus material is trisomy 16, but the most frequent class of chromosome error in spontaneous losses is 45,X.

There is a direct correlation between advanced maternal age and births with chromosomal abnormalities. Population studies have shown that women older than age 35 years have an increased risk for a chromosomally abnormal conception (Hassold & Chiu, 1985), with the most common abnormality being Down syndrome (trisomy 21) (Fig. 71.19; see Fig. 71.11B). This becomes important in a society in which women are delaying childbearing until later in life, and prenatal diagnosis has become a

TABLE 71.1
Common Abbreviations for Chromosome Abnormalities

Abbreviation	Meaning
Cen	Centromere
del	Deletion
dup	Duplication
ins	Insertion
inv	Inversion
i	Isochromosome
mar	Marker
r	Ring
rob	Robertsonian translocation
t	Translocation

TABLE 71.2
Chromosome Abnormalities in Spontaneous Fetal Losses and in Liveborn Infants

Abnormality	Chromosome	Spontaneous Fetal Losses (%)	Incidence in Live Births
45,X		18.0	1/4000
Triploidy		17.0	1/60,000
Tetraploid		6.0	0
Trisomy	16	16.4	0
	22	5.7	0
	21	4.7	1/830
	15	4.2	0
	14	3.7	0
	18	3.0	1/7500
	13	2.0	1/5000
	Other	12.3	1/10,000
Unbalanced rearrangement		3.0	1/2000
Balanced rearrangement		4.0	3/1000

Data from Hook & Hamerton, 1977; Jacobs et al., 1992; Nussbaum et al., 2007; Turnpenny & Ellard, 2011.

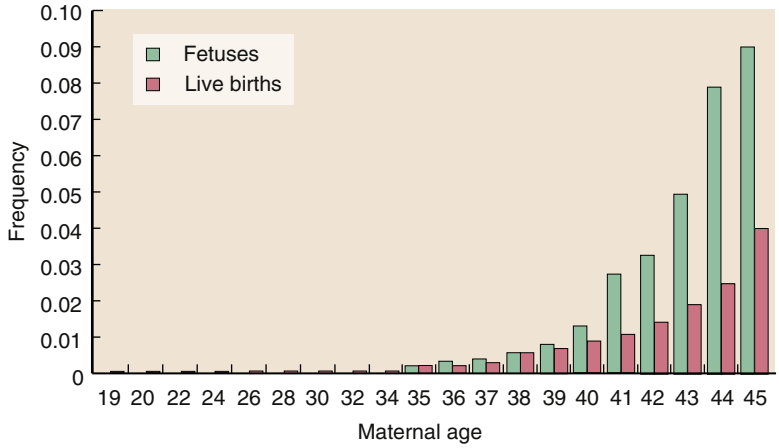

Fig. 71.19 Increased risk of a Down syndrome conception with increased maternal age. The number of live births is lower at older ages due to the intervention of prenatal diagnosis followed by termination of abnormal pregnancies.

major area of clinical cytogenetic study. In addition to screening for an age-related risk, other common reasons for referral include a family history of or previous child with a chromosome abnormality, abnormal levels of AFP in a screening test, or an abnormality detected by ultrasound.

The most common chromosome abnormalities detected in prenatal testing are the liveborn trisomies and the sex chromosome aneuploidies. Because these are usually the result of a meiotic nondisjunction error, there is a very low risk of recurrence. Occasionally, a child with a balanced or unbalanced structural chromosome abnormality will be identified. In these circumstances, karyotype analysis for both biologic parents is used to differentiate between an inherited rearrangement and a de novo anomaly in the child. For example, a child with an inherited balanced translocation has a less than 1% risk that the chromosome rearrangement will pose any problem. However, if the apparently balanced translocation seen in the fetus is not detected in either biologic parent, it must have arisen de novo in the child, and there is a 5% to 10% risk of related impairment for the infant. Unfortunately, finding an *unbalanced* translocation in a fetus, regardless of the carrier status of the parents, is a serious situation and almost always results in some type of genetic defect for the child. Follow-up to determine whether one of the parents is a balanced translocation carrier will provide information about recurrence risk for future pregnancies.

In addition to karyotype analysis, FISH studies may be used to identify chromosomal abnormalities in prenatal samples. FISH to detect the common aneuploidies (chromosomes 13, 18, 21, X, and Y) has been a primary tool in prenatal diagnosis for many years, and in 1997 the US Food and Drug Administration (FDA) cleared one version of this assay for general use (Aneuvysion by Abbott Molecular, Des Plaines, IL). In addition, certain ultrasound findings may suggest particular genetic syndromes, such as cardiac abnormalities associated with velocardiofacial syndrome (VCFS) (see Fig 71.8), and FISH may be used to confirm or rule out the diagnosis.

Since 2012 amnioctye FISH for aneuploidy detection has largely been replaced by an assay known as noninvasive prenatal screening (NIPS) or noninvasive prenatal testing (NIPT). It is noninvasive because rather than drawing amniotic fluid or taking a placental biopsy the study is performed on a sample of the mother's blood collected at 10 to 22 weeks of gestation (Wright & Burton, 2009). From this, cell-free DNA (cfDNA: free-floating DNA fragments, not the DNA in cells) is isolated. Maternal plasma contains both cell-free "fetal" DNA fragments originating from the placental trophoblast mixed with cell-free maternal DNA fragments. As this placental-derived DNA is usually the same as fetal DNA, it can be used to screen for fetal chromosomal aneuploidies using various molecular technologies. Note that samples may be noninformative for reasons such as fetoplacental mosaicism, nonidentical vanishing twins, multiple gestations, maternal obesity, maternal malignancy, and inadequate fetal/placental DNA levels. As a screening test for detection of trisomies 18 (Edwards syndrome), 21 (Down syndrome), and 13 (Patau syndrome), accuracy is being reported as approximately 98% to 99%. Sex chromosome aneuploidies are more problematic with high false-positive rates for Turner syndrome detection (Chen et al., 2019; Ehrich et al., 2017; Gil et al., 2017; Guy et al., 2019; Norton et al., 2012, 2015; Schwartz et al., 2018; Shaffer & Norton, 2018). Due to its advantages, in particular as a noninvasive, early, and accurate method, the American College of Medical Genetics and Genomics (ACMGG) recently released an updated position statement recommending the use of NIPS not only for detection of trisomies 13, 18, and 21 but also expanding its use for sex chromosome aneuploidy screening and selected copy-number variants (CNVs). Genome-wide screening for microdeletions or other autosomal trisomies, although tests are currently available, is not recommended for the general obstetric population (Gregg et al., 2016). The American College of Obstetricians and Gynecologists (ACOG) also recommended prenatal fetal aneuploidy screening (Committee on Practice Bulletins, 2016). However, it is important to understand that this is not a diagnostic study. It is a highly accurate screening test that provides a risk estimate for a chromosomal abnormality. Therefore any abnormal findings must be confirmed by an appropriate diagnostic test such as karyotype analysis, FISH, or microarray, which is performed on amniocytes following amniocentesis rather than CVS due to the potential for placentofetal discordance. Many of the cases of discrepant results, however, are actually both accurate due to the considerable potential for a pregnancy to normalize through selection. Many of these are so-called trisomy rescues, which when involving imprinted chromosomes run the risk of imprinting disorders associated with UPD.

Postnatal

Approximately 0.6% of newborns have a chromosome abnormality. If an infant presents with signs or symptoms of a defined syndrome, karyotype and/or FISH analysis may confirm a diagnosis. If the newborn has clinical anomalies unrelated to a specific disorder, karyotype or microarray analysis may provide information on a chromosome abnormality related to the clinical findings. Ambiguous genitalia may be related to an abnormal sex chromosome complement, but if the chromosomes are shown to be normal the physician knows that another cause for the patient's abnormality must be sought. If the child dies shortly after birth, cytogenetic analysis may provide information critical in understanding the demise, and these data should be correlated with autopsy results to substantiate a diagnosis. If a chromosome abnormality is found in the child, testing of both biologic parents should be considered to determine if the anomaly was inherited.

Childhood and Adult

A common misconception about genetic disorders is that because they are inherited, the diagnosis will be obvious at birth. In fact, the full clinical presentation of many disorders takes time to develop and may not be fully expressed until later in life. Consequently, some of the most difficult diagnostic problems occur in children and adults. In addition to considering the full range of cytogenetic possibilities, molecular and biochemical options must also be taken into account.

CANCER GENETICS

Another area of medicine in which cytogenetics is increasingly important is oncology (Heim & Mitelman, 2015). Although most solid tumors are difficult to culture and analyze cytogenetically, excellent clinical data exist for leukemias and lymphomas, including specific chromosome rearrangements that are directly associated with tumorigenesis (Table 71.3) (see also Chapters 76 and 77). The majority of these studies are performed on bone marrow or peripheral blood. Karyotype findings were originally used primarily as confirmation of a clinical diagnosis, but the role of genetics in patient management changed dramatically in 2001 when the World Health Organization (WHO) first published a revised classification for leukemias

TABLE 71.3
Common Cytogenetic Rearrangements in Leukemia and Lymphoma

Disorder	Chromosome Rearrangement(s)	Genes Involved
Chronic myelogenous leukemia	t(9;22)(q34.1;q11.2)	*BCR;ABL1*
Chronic myelogenous leukemia (accelerated or blast phase)	+8, i(17q), +19, +Ph′	
Polycythemia vera	+8, +9, del(20q), del(13q)	
Chronic idiopathic myelofibrosis	+8, –7 del(7q), del(11q), del(13q), del(20q)	
Essential thrombocythemia	+8, del(13q)	
Myelodysplastic syndrome with isolated del(5q)	del(5)(q13q33), del(5)(q22q33)	
Chronic myelomonocytic leukemia	–7, del(7q),+8, abnormalities of 12p	
Refractory anemia, refractory anemia with ringed sideroblasts, refractory anemia with excess blasts	–5, del(5q), –7, del(7q), +8, del(20q)	
AML with t(8;21)	t(8;21)(q22;q22)	*RUNX1; RUNX1T1*
AML with inversion or translocation 16	inv(16)(p12q22), t(16;16)(p13;q22)	*CBFβ; MYH11*
Acute promyelocytic leukemia	t(15;17)(q22;q12)	*PML; RARα*
AML with 11q23 (*MLL*) abnormalities	t(9;11)(p21;q23), t(11;19)(q23;p13.1), t(11;19)(q23;p13.3),	*AF9; KMT2A* *KMT2A; ENL*
AML with multilineage dysplasia	–5, del(5q), –7, del(7q), +8, del(11q), del(20q), +21, translocations involving 3q21 and 3q26, t(9;22)(q34.1;q11.2)	
Precursor B-lymphoblastic leukemia/lymphoma	t(1;19)(q23;p13.3)	*PBX1; TCF3*
	t(9;22)(q34;q11.2)	*ABL1; BCR*
	11q23 rearrangements, including:	*KMT2A*
	t(1;11)(p32;q23)	*AF1P; KMT2A*
	t(4;11)(q21;q23)	*AF4; KMT2A*
	t(11;19)(q23;p13)	*KMT2A; ENL*
	t(12;21)(p13q22)	*ETV6; RUNX1*
	Hyperdiploidy (modal number 50-56)	
Precursor T-lymphoblastic leukemia/lymphoma	Rearrangements at 14q11.2, 7q35, and 7p14-15	T-cell receptor loci
	del(9p)	*CDKN2A*
	Translocations at 1p32	*TAL1*
Mature B-Cell Neoplasms		
Chronic lymphocytic leukemia/small lymphocytic leukemia	+12, del13q, del11q23-24, 14q+, del17p13	
Lymphoplasmacytic lymphoma/Waldenström macroglobulinemia	t(9;14)(p13;q32)	*PAX5; IGH*
Multiple myeloma	t(11;14)(q13;q32)	*CCND1;IGH*
Marginal zone B-cell lymphoma (MALT)	t(11;18)(q21;q21), +3	*BIRC3;MALT1*
Follicular lymphoma,	t(14;18)(q32;q21), +7, +18, t(18;22)(q21;q11.2), del(6q), del/t(3)(q27)	*IGH; BCL2 BCL2;IGL*
Diffuse large B-cell lymphoma		*BCL6*
Mantle cell lymphoma	t(11;14)(q13;q32)	*CCND1; IGH*
Burkitt lymphoma	(8;14)(q24;q32)	*MYC; IGH*
	t(2;8) (p12;q24)	*IGK; MYC*
	t(8;22)(q24;q11.2)	*MYC; IGL*

and lymphomas (latest revision: Swerdlow et al., 2017). The data collected had shown a direct correlation between disease-causing mutations, the presence of specific chromosomal abnormalities, and response to therapy. Thus in the revised classification system, the importance of the genetic findings, either cytogenetic or molecular, became a key element for final diagnosis in most hematologic disorders. Cytogenetics had suddenly been pushed to the forefront of testing for oncology patients.

In addition to diagnosis, karyotype analysis can provide other valuable information regarding a cancer patient's disease. In general, prognosis and severity of disease are directly correlated to the number and type of chromosome abnormalities seen. Furthermore, once a chromosome abnormality has been detected, the progress of the disease can be monitored. If treatment is successful, most chromosome abnormalities are no longer evident in the bone marrow, and as long as the karyotype appears to be "normal," the patient is said to be in cytogenetic remission. However, if the treatment does not eliminate the aberrant cell line completely, remission may be merely an interlude in which the disease-causing cells are suppressed to such low levels that they are not detectable by routine analysis. Then at relapse, the same chromosome anomalies will reappear and may be accompanied by additional abnormalities and/or more complex cell lines, findings consistent with disease progression. An increase in complexity over time is known as *karyotype evolution.*

FISH has become a valuable tool in clinical oncology studies, with many probes commercially available (Cremer et al., 1988; Anastasi, 1991; Abbott Molecular, Inc. [www.abbottmolecular.com]; Cytocell, Ltd. [www.cytocell.com]). Studies can be done on either interphase or metaphase cells, with the choice resting on the type of data desired. Using interphase cells is often preferred because it provides a much larger sample that can be quickly assayed, giving results with a higher level of statistical significance (Werner et al., 1997).

For translocations, combination FISH probes have been developed that hybridize to the opposite sides of the translocation breakpoints. There are two common strategies employed to detect a translocation. Splitting of the signals may occur if the translocation separates a two-color fusion probe, generating two separated different-colored signals in place of the original dual-color fusion signal (a so-called breakapart probe). Alternatively, fusion may occur if the translocation results in relocation of the probes, bringing two different probes into proximity and generating a two-color fusion that creates a new color.

A primary example of the FISH fusion technology is the 9;22 translocation in leukemia. This rearrangement is characterized by a translocation between the *ABL1* proto-oncogene on chromosome 9 (9q34.1) and the *BCR* gene on chromosome 22 (22q11.2) (Fig. 71.20A), which produces a disease-associated chimeric gene usually on the derivative chromosome 22,

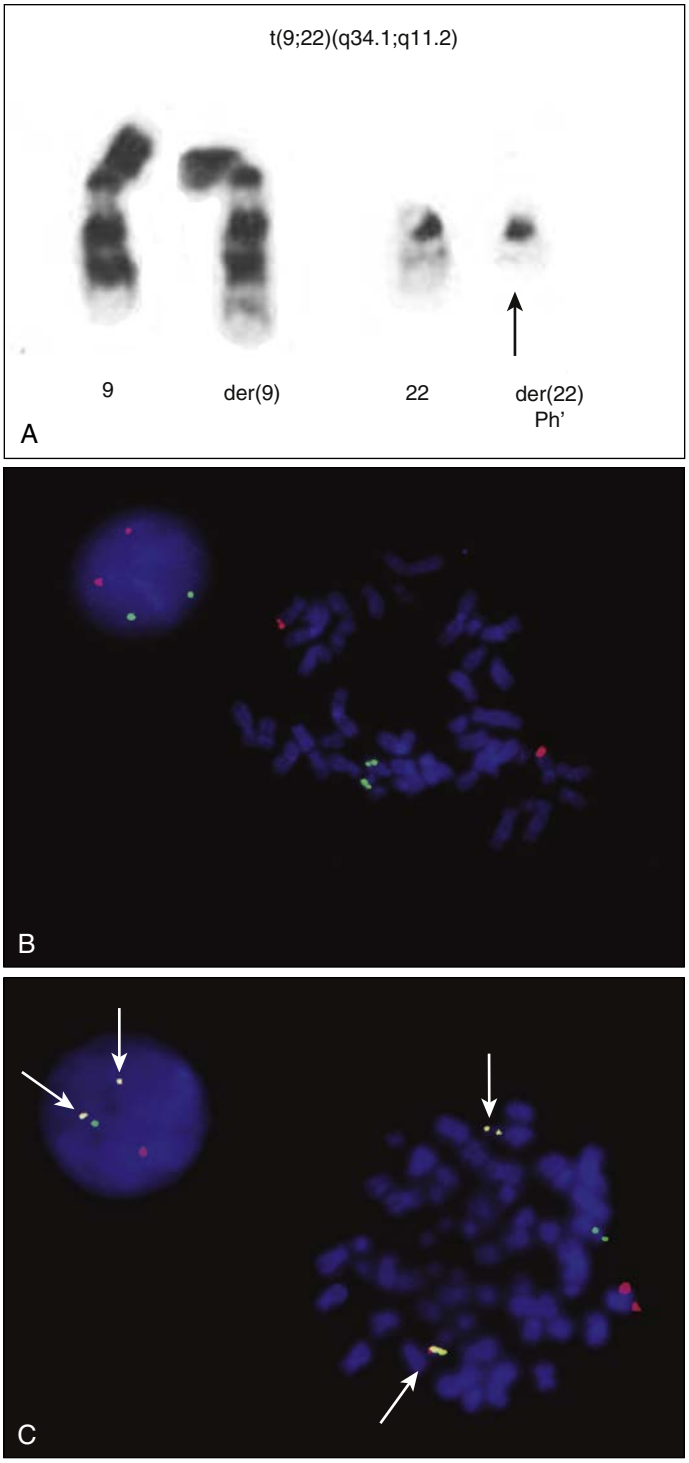

Fig. 71.20 Fluorescence in situ hybridization (FISH) detection of the 9;22 translocation in chronic myeloid leukemia (CML). **A** Banded chromosomes showing the 9;22 translocation. The derivative chromosome 22 is known as the *Ph′*, or *Philadelphia chromosome*. **B** and **C** Actual FISH images. **B** No translocation is present, as seen by two copies each of the chromosome 9 *(red)* and chromosome 22 *(green)* probes in both interphase *(left)* and metaphase *(right)* cells. **C** Cells with an m-BCR translocation as detected by two yellow fusion signals *(arrows)* plus one green and one red signal (metaphase on the *right* and interphase on the *left*).

also known as the *Philadelphia chromosome* (Ph′) (see also Chapter 77). The translocation is seen in chronic myelogenous leukemia (CML), acute myeloid leukemia (AML), and acute lymphoblastic leukemia (ALL) (see Table 71.3). A FISH assay is available to detect the *BCR/ABL1* fusion (i.e., Abbott Molecular). A pair of probes is used: red, which is localized to the *ABL1* locus on chromosome 9, and green, which is located at the *BCR* locus (chromosome 22). When no translocation is present, two green signals (detecting each *ABL1* allele) and two red signals (detecting each *BCR* allele) should be present in each cell (see Fig. 71.20B). When the BCR/ABL1 rearrangement occurs, the translocation splits the green *BCR* signal such that one portion of the green signal will remain on chromosome 22 but the distal portion will move to the derivative chromosome 9. On chromosome 9, the translocation splits the red *ABL1* signal such that part of the red signal is left on the derivative chromosome 9 and the distal part moves to the derivative chromosome 22. This reciprocal translocation thus results in two yellow fusion signals (derivative 9 is red fused to green, and derivative 22 is green fused to red). The net result of this FISH assay is four probe signals: one green (chromosome 22), one red (chromosome 9), and two yellow fusion signals detecting the 9;22 translocation (see Fig. 71.20C). Approximately 15% to 20% of cases have a variant FISH pattern. These are primarily due to three- or four-way translocations, partial or complete loss of the nononcogenic portion of the reciprocal exchange at either the *ABL1* and/or *BCR* loci, or cryptic insertions resulting in *BCR/ABL1* fusions. None of these FISH variant cases are clinically significant but are important in establishing the baseline for follow-up of residual disease in these patients. Other FISH detection assays using other disease gene–specific probes are available to evaluate a wide array of different cancer-related chromosome rearrangements.

In addition, chromosomal aneuploidies in cancer cells can be easily detected (e.g., use of a chromosome 12–specific centromere probe to screen an interphase cell population for trisomy 12 cells indicative of CLL, use of a chromosome 7 probe to detect monosomy 7 in myelodysplastic syndrome and AML, and use of a chromosome 8 probe to identify trisomy 8 in both chronic and acute disorders). The use of different-colored X and Y probes in evaluating the success of a bone marrow transplant when the donor and recipient are of opposite sexes has also been highly successful. Following transplantation, a male who has received female donor cells should have an XX complement. Failure of the engraftment may be signaled by the presence of a high frequency of XY cells. The FISH can be repeated at regular intervals to monitor the progress and provide an early warning if the patient's leukemic cell population begins to proliferate.

Initially, clinicians were concerned about apparently discrepant results from karyotype analysis and FISH on the same patient sample. For example, by karyotype, a patient with CML may show all cells with a t(9;22), but only 30% of cells will be positive for the translocation by interphase FISH. These data are actually consistent. Karyotype can only be performed on dividing cells, and, because cancer cells tend to divide frequently, a karyotype analysis could show 100% leukemic cells. FISH, on the other hand, detects all nucleated cells, but not all cells in a bone marrow sample are necessarily from the same clone because an affected individual usually has both a disease and a normal cell population. Interphase FISH can quantify the relative numbers of normal and disease cells, thus providing a more accurate estimate of disease involvement within the total population. This can be used advantageously to monitor a patient's response to treatment. Testing sequential samples over time can show a reduction in the disease cell population, and relapse will be reflected by a rise in the leukemic cell population. Thus it is important to perform both karyotype analysis and FISH on a diagnosis specimen. The karyotype will define the chromosomal abnormalities present, and the FISH will establish the baseline frequency of the leukemic clone(s). These data can then be used as a reference point for all future testing for the patient.

Multicolor FISH has also been used to evaluate leukemic cell lines, and the data have suggested that cancer cells actually undergo a significantly greater degree of chromosome rearrangement than was previously appreciated (Veldman et al., 1997). Exciting recent advances in chromosomal microarray analysis are now being employed to provide additional diagnostic and prognostic information as well as direct therapy choices (Cooley et al., 2013; Kanagal-Shamanna et al., 2018; Mikhail et al., 2019; Peterson et al., 2018; Schoumans et al., 2016; Xu et al., 2018).

CYTOGENETIC DISORDERS

Chromosomal Aneuploidy Syndromes

Autosomal Aneuploidies

The most common cause of mental retardation is trisomy 21, or Down syndrome. This disorder has a birth incidence of 1 in 700 and is characterized by hypotonia, flat facies, slanted palpebral fissures, small ears, protruding tongue, transverse palmar crease, heart defects, hypogonadism, and probable infertility. Down syndrome individuals also have an increased susceptibility to infectious diseases and increased risks for cancer and early onset Alzheimer disease. Approximately 92.5% of all Down syndrome individuals have 47 chromosomes, including three copies of chromosome 21 resulting from a nondisjunction error in parental meiosis. Just under 3% of patients tend to express a milder phenotype and have been shown to be mosaics with two cell lines (47,XX,+21/46,XX or 47,XY,+21/46,XY),

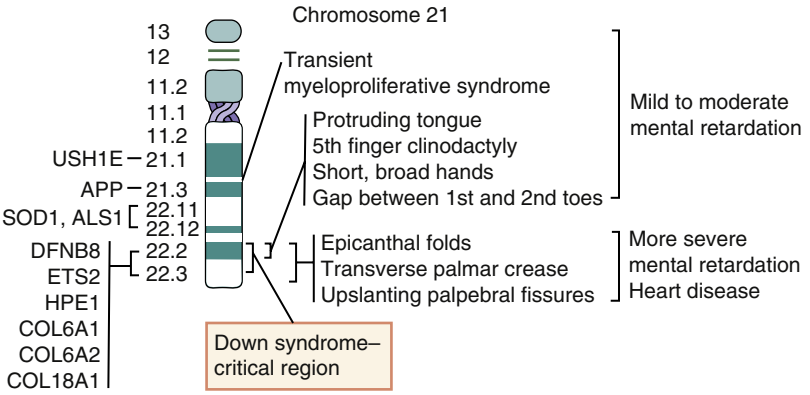

Fig. 71.21 Map of chromosome 21 showing the Down syndrome–critical region and relative positions of loci associated with various clinical features to the right. On the left, other mapped loci are shown. *ALS1*, Amyotrophic lateral sclerosis; *APP*, amyloid β-precursor protein (associated with Alzheimer disease); *COL6A1/COL6A2/COL18A1*, collagen genes; *DFNB8*, deafness 8; *ETS2*, oncogene ETS-2; *HPE1*, alobar holoprosencephaly-1; *SOD1*, superoxide dismutase-1; *USH1E*, Usher syndrome. (Data from Korenberg et al., 1990; Delabar et al., 1993; OMIM, website.)

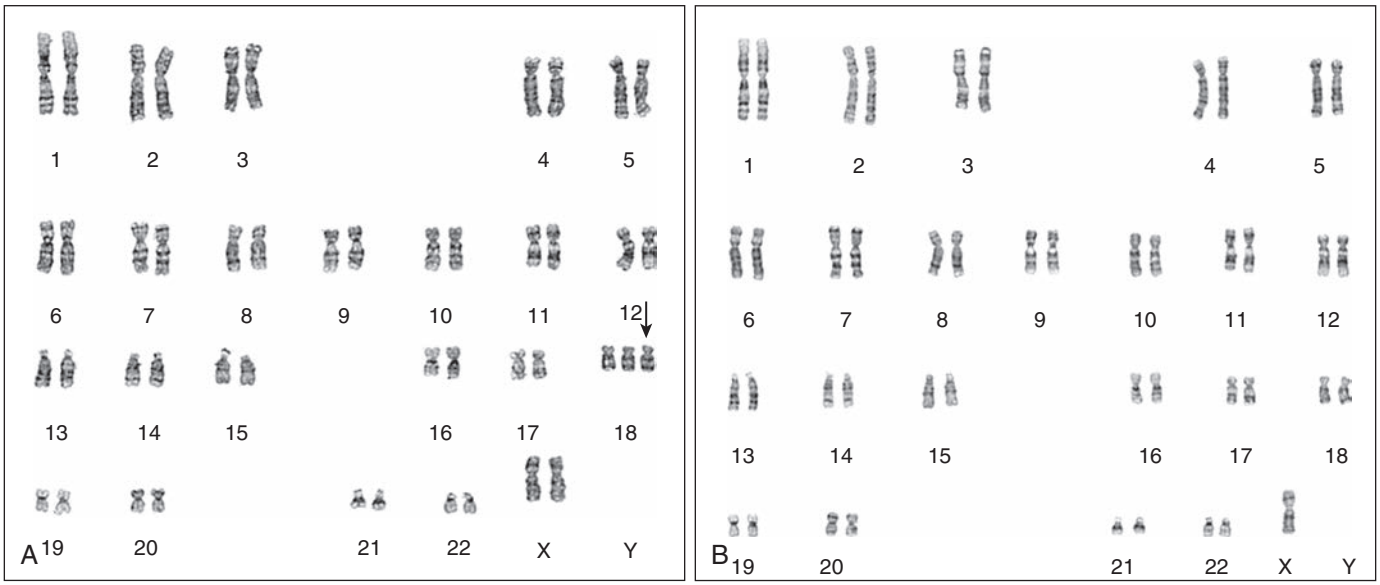

Fig. 71.22 Karyotypes from numerical chromosome syndromes. **A** Edwards syndrome (trisomy 18): 47,XX,+18. **B** Turner syndrome (monosomy X): 45,X.

and about 5% of Down syndrome patients have only 46 chromosomes because the extra 21 is part of a Robertsonian or other translocation. A child with a translocation is often indicative of the presence of a translocation carrier parent, so in these cases karyotype analysis of both parents is appropriate to determine whether the couple is at increased risk of having additional Down syndrome children in future pregnancies. Although it is most common for a Down syndrome patient to have three complete copies of chromosome 21, molecular studies of individuals with chromosome 21 rearrangements have clearly shown that it is only necessary to have three copies of the region of chromosome 21 encompassing bands 21q22.12 to 21q22.3, the Down syndrome–critical region (Fig. 71.21) (Korenberg et al., 1990; Delabar et al., 1993).

The other two liveborn trisomies are trisomy 13 and trisomy 18. *Trisomy 13*, or Patau syndrome, with a birth incidence of 1 in 4000 to 1 in 10,000, is characterized by a small head, cleft lip and/or cleft palate, cyclopia, transverse palmar crease, polydactyly of the hands and/or feet, prominent heel, ventricular septal defect, and punched-out scalp. *Trisomy 18*, or Edwards syndrome (Fig. 71.22A), is seen in approximately 1 in 8000 newborns, with features including a low birthweight, small mouth and jaw, ventricular septal defect, hypoplasia of the muscles, a prominent occiput, low-set malformed ears, rocker-bottom feet, and crossed fingers.

Despite its often severe clinical consequences, Down syndrome is usually manageable, and patients live into the second or third decade of life. Trisomy 13 and trisomy 18 are considerably less compatible with life, and patients usually die within the first month of life. If an individual survives the first year, the outlook is bleak, because patients do not learn to talk, walk, or care for themselves. Because of this, counseling for prenatally diagnosed cases of trisomy 13 or 18 includes the option of termination of pregnancy.

Sex Chromosome Aneuploidies

Sex chromosome aneuploidies are relatively common (overall frequency of 1 in 500 births) and are phenotypically milder than autosomal aneuploidies because of the effect of X inactivation and the limited number of genes present on the Y chromosome. Four disorders, including three trisomies and one monosomy, account for a majority of cases. All are the result of nondisjunction errors in meiosis, and, except for XYY, which is exclusively paternal, the other disorders may result from either maternal or paternal error.

The aberrant karyotypes of individuals with three X chromosomes (47,XXX females) or with one X and two Y chromosomes (47,XYY males) often go undetected throughout life. The birth incidence is relatively high (1 in 1000), but other than being somewhat taller than average, there are no striking features that would indicate a chromosomal abnormality. Some individuals have generalized learning difficulties and so may be identified by school screening programs. XXX females and XYY males may also be identified during infertility testing, though the cytogenetic abnormality is not usually related to the reason for referral. XYY males do have an increased risk of behavioral problems, and early studies suggested that they also had criminal tendencies because there was a higher than expected incidence of XYY in inmates of penal institutions (Jacobs et al., 1968; Price & Jacobs, 1970). However, subsequent work has shown that (1) the conclusions of the original study were biased because of a sampling error, (2) criminality is most probably due to a combination of multiple causes, and (3) XYY males are no more prone to criminal behavior than any other male (Witkin et al., 1976; Pitcher, 1982; Theilgaard, 1984).

Klinefelter syndrome (47,XXY) males tend to be tall and thin with relatively long legs, although early in life these findings seldom set them apart from their peers. Some individuals are identified in school because of their learning difficulties, but the most common reason for referral is postpubertal hypogonadism, femalelike breast development, and infertility due to small testicles, hyalinized testicular tubules, and azoospermia. A milder form of Klinefelter syndrome with the potential for fertility due to normal testicular development is seen in individuals with a mosaic chromosome complement, including a 46,XY cell line (47,XXY/46,XY). The relative proportion of XY and XXY cells during sex determination in the

TABLE 71.4

Distribution of Different Chromosome Complements That Give Rise to Turner Syndrome

Occurrence (%)	Chromosome Anomaly
50	45,X
20	46,X,i(Xq)
15	X chromosome deletions or rings, or the presence of a Y chromosome
10	Mosaics: 45,X/46,XX; 45,X/46,XY

early zygote and in the testes is the key for fertility. An excess of XXY cells will push the individual toward a true Klinefelter presentation, whereas higher numbers of XY cells should moderate the phenotype and increase the likelihood of fertility.

The most commonly recognized sex chromosome aneuploidy presenting with a female phenotype is 45,X: Turner syndrome (see Fig. 71.22B). This is also the only human viable liveborn monosomy. In sex determination, normal female development is dependent on the presence of two active X chromosomes. The critical region for female differentiation has been narrowed to a region of the short arm of the X just proximal to the centromere. If that region is missing or inactive, an individual with Turner syndrome will result. About half of all Turner syndrome patients have the classic 45,X chromosome complement, and the single X chromosome is usually maternal in origin, indicating that a paternal meiotic nondisjunction is the most common source of error. In addition to 45,X, more complex karyotypes are also possible (Table 71.4) (Palmer & Reichmann, 1976). The greatest concern is for individuals who possess a complete or partial Y chromosome in at least one cell line because these patients are at increased risk for gonadoblastoma.

The phenotype for Turner syndrome is highly variable. Affected individuals are typically short (<150 cm), with gonadal dysgenesis and learning difficulties. Other common features include webbed neck resulting from cystic hygroma in utero, low posterior hairline, heart and renal anomalies, cubitus valgus (increased carrying angle of the elbow), and shield chest. At birth, patients may present with edema of the hands and feet. Turner syndrome patients are usually of normal intelligence, although some individuals do have learning disabilities. Furthermore, although infertility used to be accepted as the standard in Turner syndrome, it is now known that some patients, usually those with mosaic karyotypes, can reproduce successfully. Furthermore, the reproductive problem is primarily related to nonfunctioning ovaries. Because the uterus is capable of normal function, using donor egg technologies a Turner syndrome patient can complete a full pregnancy and deliver a normal child. Due to the variability of phenotypes, prenatal counseling for a couple with an identified Turner syndrome fetus is extremely difficult. In general, however, most liveborn Turner syndrome patients can live productive lives, and mildly affected individuals may not know that they are affected with the disorder until puberty.

Other Sex Chromosome Abnormalities

Sex determination in humans is the result of a complex biochemical pathway involving the interaction of proteins produced by genes present on the autosomes and the X and Y chromosomes. The default sex in humans is female, so in the absence of any male-determining stimuli, a female individual will develop. The primary trigger for male development is a gene located on the short arm of the Y chromosome designated *TDF*, the testes determining factor, which is located in the sex-determining region of the Y chromosome *(SRY)* (Fig. 71.23).

The protein produced by *TDF* initiates the male developmental pathway. A number of disorders associated with mutations in different genes within this pathway have been identified and can result in ambiguous genitalia or genotype/phenotype mismatch (phenotypic male with an XX sex chromosome complement or a phenotypic female with an XY complement).

An XX male can usually be attributed to one of two causes. The more common of the two is virilization of a female fetus as a result of the autosomal recessive disorder congenital adrenal hyperplasia (CAH). The defect in CAH is the lack of the enzyme 21-hydroxylase. Without this enzyme, the normal biosynthetic pathway is blocked, and androgens accumulate in the body. Excessive levels of male hormones in the female circulation may result in a male-appearing infant despite a female chromosome complement. Furthermore, because androgens are capable of crossing the placenta, a normal female fetus may develop ambiguous genitalia due to exposure to excess hormones from a CAH-affected mother.

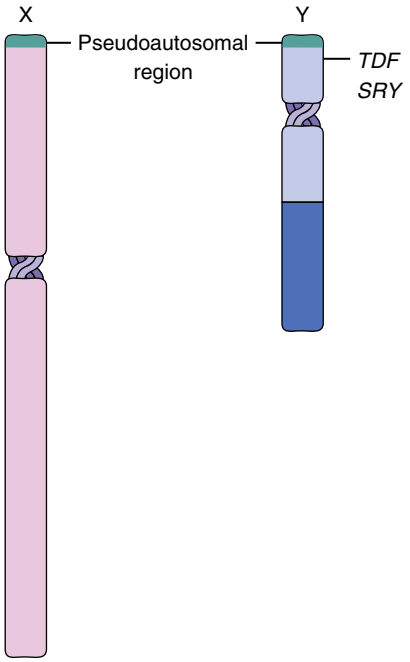

Fig. 71.23 Diagram of relative locations of TDF, SRY, and the pseudoautosomal regions of the X and Y chromosomes. *TDF*, Testes determining factor; *SRY*, sex-determining region of the Y chromosome.

A phenotypic male with an XX sex chromosome complement may also result from a cryptic translocation between the X and Y chromosomes. The distal ends of the short arms of the X and Y chromosomes are homologous and comprise what is termed the *pseudoautosomal regions* (see Fig. 71.23). This is the primary site of X and Y chromosome pairing during meiosis, and recombination may occur between X and Y alleles. Rarely, a recombination event outside the boundaries of the pseudoautosomal region takes place, resulting in the transfer of unique Y loci, including *SRY*, to the tip of the X chromosome. The amount of chromosome material involved in such an exchange is extremely small and cannot be cytogenetically detected. In a male with such a balanced translocation, there would be no clinical abnormalities, because the genes are all present, although in alternate locations. However, if this male transmits his rearranged X chromosome to an offspring who has received an X from the mother, the resultant child will have an apparent XX chromosome complement but a phenotype that is male or Klinefelter male due to the presence of the TDF protein that triggers the male developmental pathway.

The reciprocal of the aforementioned translocation may result in a Turner female with an apparent XY complement. If the rearranged Y chromosome is transmitted to a child, the male developmental pathway will not be initiated in that individual because there is no *TDF*/*SRY*, and sex determination will default to female. Unfortunately, these individuals also lack two intact copies of the proximal X short arm, and this will prevent normal female development, giving rise to a Turner syndrome individual. This situation is quite rare. The more common finding for an XY female is androgen insensitivity, also known as *testicular feminization*. In these individuals, the Y chromosome is intact, and *TDF* is present and functional. The problem is a mutation of the androgen receptor gene located on the long arm of the X chromosome (Xq21.3) that results in no androgen receptor protein being produced. The TDF protein will initiate male development, but the pathway will be blocked at the point where the androgen receptor protein is required to form a complex between testosterone and dihydrotestosterone. Without this critical step, further male differentiation is not possible, and the phenotype will default back to female. However, these individuals are infertile because of the lack of any functional internal genitalia, and they commonly present with a blind vagina and testes in the abdomen or inguinal canal.

Structural Chromosome Anomalies

A reasonable number of syndromes directly related to a structural chromosome abnormality have been described. Most of these are quite rare. The following is a discussion of some of the more common syndromes (see also Jones et al., 2013). The abnormalities can be detected by karyotype analysis, FISH, or microarray analysis.

TABLE 71.5
Microdeletion and Contiguous Gene Syndromes

Disorder	Location	Genes	Clinical Findings
Angelman syndrome	15q11.2	*UBE3A*	Severe MR, developmental delay, large mouth, prognathia, ataxia, seizures, DiGeorge syndrome
DiGeorge syndrome	22q11.2, 10p	*DGS1, DGS2*	Characteristic facies, cleft palate, heart defect, hypoplasia of the thymus and parathyroids, severe hypocalcemia, seizures
Ichthyosis	Xp22.32	*STS*	Scaly skin, short stature, hypogonadism, MR
Kallmann syndrome	Xp22.3	*KAL1*	Hypogonadism, inability to smell
Langer-Giedion syndrome	8q24.11-q24.13	*TRPSI* *EXT1*	Craniofacial dysmorphism, skeletal abnormalities, mild to severe mental deficiency
Lissencephaly	17p13.3	*LIS1*	Smooth brain, profound retardation, seizures
Miller-Dieker syndrome	17p13.3	*LIS1* and others	Lissencephaly, microcephaly, high forehead, small nose, micrognathia, low-set ears
Prader-Willi syndrome	15q11.2	*SNRPN* *NDN* and others	Hypotonia at birth, almond-shaped eyes, moderate to severe MR, absent sense of satiation leading to overeating, small hands and feet, hypogonadism
Retinoblastoma	13q14.1-q14.2	*RB1*	Tumors of the retinoblast cells of the eye
Rubinstein-Taybi syndrome	16p13.3	*CREBBP*	Beaked nose, prominent columella, hypoplastic maxilla, down-slanted palpebral fissures, broad thumbs and first toes, MR, speech delay
Smith-Magenis syndrome	17p11.2	*RAI1*	Brachycephaly, midface hypoplasia, broad nasal bridge, prominent jaw, short broad hands, hyperactivity, delayed speech, self-destructive behavior, MR
Velocardiofacial syndrome	22q11.2	*TBX1* and others	Palatal defects, hypoplastic alae nasi with long nose, learning disability, congenital heart disease
WAGR	11p13.3	*WT1, PAX6*	Wilms tumor, aniridia, genitourinary defects, and mental retardation
Williams syndrome	7q11.2	*ELN*	Low IQ, hypersensitivity to sound, blue eyes with stellate pattern in the iris, prominent lips, hoarse voice, supravalvular aortic stenosis or other cardiac defect, hypercalcemia, premature aging of the skin

MR, Mental retardation.

Wolf-Hirschhorn syndrome, also known as *4p– syndrome*, is due to a terminal deletion of the short arm of chromosome 4, del(4)(p16). Clinical findings include microcephaly, micrognathia, hypotonia, epicanthal folds, and developmental delay. The characteristic facial appearance has been likened to a Greek warrior's helmet because of the arched eyebrows and long nose. Individuals with this disorder require special education and are at increased risk of seizures.

Cri-du-chat, or *5p– syndrome*, del(5)(p15), is characterized by a distinctive high-pitched, catlike cry in infancy. Other features include low birthweight and subsequent slow growth, hypotonia, microcephaly, hypertelorism, epicanthal folds, cardiac anomalies, and mental retardation. Affected children have delayed development and may reach the cognitive and social level of a 5- or 6-year-old.

Microdeletion Syndromes and Contiguous Gene Syndromes

By definition, a *microdeletion* is a very small deletion, usually only a fraction of a single chromosome band. Cytogenetic microdeletions can be confused with molecular deletions, so it is important to recognize that although cytogenetic microdeletions are small, they are significantly larger (>500 kb) than the typical molecular deletion (1 base pair [bp] to several hundred bp), which can only be resolved by molecular technology (see Chapter 73). Although some chromosome microdeletions are large enough to identify by karyotype analysis, most will require FISH or microarray analysis for detection. Although originally thought to be deletions within single genes, it has now been shown that certain syndromes are actually due to deletions that encompass portions of several adjacent, unrelated genes. The clinical presentation may therefore be a combination of features due to the absence of several different gene products. The size of the deletion and number of genes affected may vary, such that the phenotype expressed may differ significantly between individuals. Collectively, these are called *contiguous gene syndromes*. Included in this group are many of the microdeletion syndromes (Table 71.5), as well as the larger, classic deletion syndromes such as Wolf-Hirschhorn and cri-du-chat.

Miller-Dieker syndrome clearly illustrates the overlap between microdeletion and contiguous gene syndromes. The disorder has been associated with a microdeletion of the distal short arm of chromosome 17 (17p13.3), and the cardinal clinical features are lissencephaly (smooth brain) and craniofacial anomalies. Isolated lissencephaly has also been recognized as an independent entity, so Miller-Dieker syndrome is a more complex presentation that couples the brain defect with characteristic facial features. Molecular analysis has shown there are at least two genes involved in Miller-Dieker syndrome, so it is a true contiguous gene syndrome resulting from a microdeletion. A smaller deletion of the *LIS1* gene only would result in isolated lissencephaly (Ledbetter et al., 1992).

Prader-Willi syndrome and *Angelman syndrome* are the best-known microdeletion syndromes. The same interstitial deletion of the proximal long arm of chromosome 15, del(15)(q11.2q11.2), can be found in both disorders, but the clinical presentations are significantly different. Prader-Willi patients are small and hypotonic at birth but change within the first year of life and begin to gain weight rapidly. If not placed on a controlled diet, they can become quite obese through overeating. Other characteristics include small hands and feet, hypogonadism, and a bad temper. Although they are developmentally delayed, most do well in special education classes. Because of their temper and difficulty in controlling their diet, Prader-Willi patients may be placed in special group homes that provide the proper environment. Angelman syndrome patients, on the other hand, are severely mentally handicapped. Although they are friendly, they usually cannot carry on a normal conversation, and discourse is often punctuated by bursts of inappropriate laughter. The disorder is also characterized by hyperactivity, short stature, microcephaly, seizures, and ataxia.

By routine or high-resolution cytogenetic analysis, the 15q deletion can be detected in about 60% of Prader-Willi individuals but only 10% to 20% of Angelman syndrome patients. Use of FISH has provided a much better diagnostic tool, and for both syndromes deletions can now be established in 80% to 85% of cases. Although it was accepted that not all deletions would be visible at the cytogenetic level, it was considered odd that FISH was unable to detect a deletion in 100% of cases. This, in addition to the fact that Prader-Willi syndrome and Angelman syndrome appear to share the same deletion but have such entirely different phenotypes, suggested that there might be another cause for the disorders. It is now known that Prader-Willi syndrome and Angelman syndrome are examples of genetic imprinting and that the mutational processes resulting in the diseases are much more complex than a simple deletion of DNA (Nicholls et al., 1989; Robinson et al., 1991) (see Chapter 72 for a discussion of imprinting and molecular detection of imprinted genes).

Williams syndrome has been associated with a deletion of the elastin gene *(ELN)* on the proximal long arm of chromosome 7 (7q11.23). The disorder is characterized by cardiac abnormalities, hypertension, hoarse voice, premature aging of the skin, and behavioral anomalies. Because elastin is known to be an important protein lending elasticity to tissues such as the heart, blood vessels, skin, and vocal cords, its absence explains many of the physical anomalies associated with this syndrome. The behavioral problems, however, could not be attributed to the lack of elastin, and further

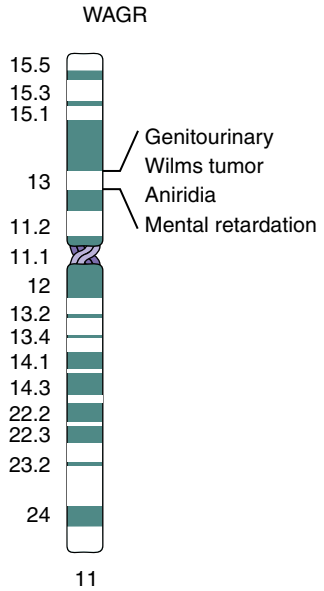

Fig. 71.24 Diagram of the contiguous gene syndrome WAGR showing relative positions of the different genes on the short arm of chromosome 11. *WAGR, W*ilms tumor, *a*niridia, *g*enitourinary defects, and mental *r*etardation.

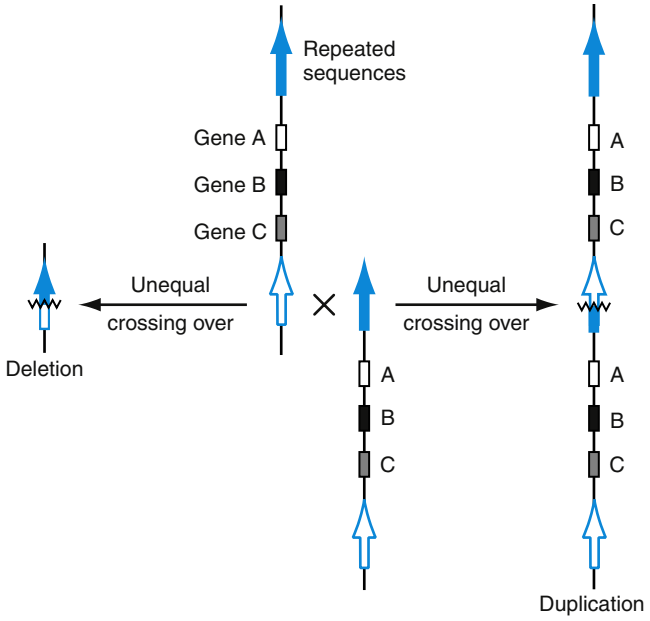

Fig. 71.25 Diagram of the possible outcomes of mispairing and recombination at the velocardiofacial syndrome locus on chromosome 22 (22q11.2). Two chromosomes that have mispaired by association of repeat sequences are seen in the middle of the figure. Recombination may or may not occur. If it does occur, one outcome is a deletion *(left)* resulting from the complete loss of both gene sequences from both original chromosomes (indicated as genes *A–C*). The reciprocal event would be a tandem repeat of both gene sequences, one derived from each of the original chromosomes *(right)*.

investigations have shown that Williams syndrome is actually a contiguous gene syndrome and that the variability of the phenotype is related to the number of adjacent genes deleted in combination with *ELN*.

A very-well-characterized contiguous gene syndrome is located on the short arm of chromosome 11 (11p13) and is known as *WAGR* (*W*ilms tumor, *a*niridia, *g*enitourinary defects, and mental *r*etardation). Except for the genitourinary defects, which appear to be due to a variant mutation in the Wilms tumor locus, each of the other three anomalies has been associated with a particular gene, and these are arranged in tandem on the short arm of chromosome 11 (Fig. 71.24). The phenotype of an affected individual will vary, depending on the size of the deletion. Statistically, about one in three children diagnosed with aniridia will also develop Wilms tumor. Conversely, only 1 in 50 Wilms patients has aniridia. With larger deletions, mental retardation and genitourinary defects may also be seen.

Velocardiofacial syndrome is possibly the most common microdeletion syndrome in humans, but it is often not recognized because it has a broad spectrum of clinical features and a presentation that can be mild. The disorder is usually diagnosed in the newborn period because of feeding difficulties, cardiac defects, and characteristic facial dysmorphologies. Learning disabilities, short stature, and conductive hearing loss are noted as the individual ages. Interestingly, 10% to 15% of patients will have a much more mildly affected parent with the same deletion. The 1.5- to 3-Mb deletion on the proximal long arm of chromosome 22 (22q11.2q11.2) is thought to be due to recombination errors between direct repeats that flank the common deletion region. The similarity in the repeats can result in slippage and mispairing between the chromosomes (Fig. 71.25). If recombination occurs between the misaligned chromosomes, two recombinant products are possible: a chromosome missing the region associated with a diagnosis of velocardiofacial syndrome, or a chromosome with a duplication of the 1.5- to 3-Mb region, which is associated with the microduplication 22q11.2 syndrome that has a completely different clinical presentation (McDermid & Morrow, 2002).

A similar mechanism resulting in the classic Williams syndrome deletion has also been reported (Bayes et al., 2003). Recombination following mispairing of the chromosomes is a recognized mutation strategy that explains deletion and duplication formation in a variety of other diseases.

OTHER CYTOGENETIC PHENOMENA

Fragile X Syndrome

Fragile X syndrome is the second leading cause of mental retardation and is the primary cause of inherited mental retardation. The disorder was first described by Herbert Lubs in 1969, when he noted the correlation between retardation and a "marker X" in affected family members (Lubs, 1969). The marker X has subsequently become known as the *fragile X*, characterized by a break or gap in the structure of the X chromosome that can be detected cytogenetically (Fig. 71.26) by culturing cells in the appropriate

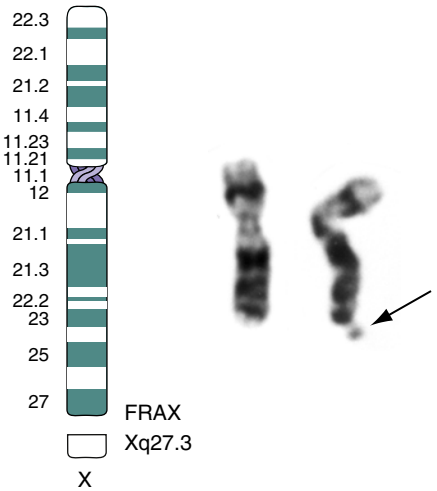

Fig. 71.26 Fragile X. Ideogram of the fragile X (left) and a representative pair of G-banded chromosomes showing the fragile X (right).

induction medium. However, not all affected individuals express the fragile X cytogenetically, so clinical diagnosis was significantly improved when the fragile X gene *(FMR1)* was cloned in 1991 and the causative mutation was identified as an amplification of a trinucleotide repeat sequence. This mutation is detectable at the molecular level, so cytogenetic analysis has been replaced by direct mutation analysis for fragile X syndrome (Rousseau et al., 1991; Verkerk et al., 1991) (see Chapter 72).

Breakage Syndromes

Chromosomal breakage syndromes (Table 71.6) are a set of autosomal recessive disorders that were originally grouped together because of the common finding of chromosome instability or fragility (Arlett & Lehmann, 1978). Consequently, cytogenetic testing was possible as an aid in diagnosis. Molecular studies have shown an additional commonality among the disorders in that the primary mutation in each is a defect in a DNA repair gene. This helped explain the other features of the syndromes because inability to repair the DNA can lead to chromosome breakage or increased recombination as well as widespread mutation and defects in DNA sequences that can lead to cancer.

TABLE 71.6
Chromosome Breakage Syndromes

Disorder	Clinical Features	Gene Locus	Cytogenetic Manifestation	Type of Cancer	DNA Repair Defect	Miscellaneous
Fanconi anemia	Pancytopenia, prenatal or postnatal growth retardation, hypoplastic or missing thumbs, possible arm deformation, brownish pigmentation of skin	1. Group A: 16q24.3 2. Group C: 9q22.3 3. Group D: -3p22-p26 4. Group E—6p21-p22 5. Groups B, F, H unmapped	Increased chromosome breakage detected by treatment with mitomycin C and diepoxybutane	Increased risk of AML, and progressive bone marrow failure		Current therapy: bone marrow transplantation
Bloom syndrome	Growth retardation, butterfly rash on face, possible malignancy	15q26.1	Increased SCE in response to UV light or BrdU incorporation		Abnormal DNA ligase I activity	High frequency in Ashkenazi Jewish population: 1/110 carrier frequency
Ataxia telangiectasia	Ataxia with degeneration of central nervous system, telangiectasia on face, deficiency in cellular immunity, degenerative, growth retardation	11q22.3	Increased spontaneous breakage, increased rings, triradials, and translocations, particularly with 7 and 14, induced with bleomycin or ionizing radiation	Various leukemias and solid tumors		
Xeroderma pigmentosum	Sensitivity to sun, neurologic abnormalities, ataxia and spasticity	Incidence: 1 in 250,000 1. A: 9q22.3 2. C: 653p25 3. D: 19q13.2-q13.3 4. E: 11p11–p12 5. F: 16p13.1-13.2, 16p13.13-p13.3 6. G: 13q33	Increase in SCE and chromosome rearrangement in response to UV light	Increased incidence of skin cancer	1. Lack of excision of thymine dimers 2. Postreplication repair defect	
Cockayne syndrome	Dwarfism, premature aging, microcephaly, neurologic deficit, pigmentary degeneration, deafness, sensitivity to sunlight, MR	Chr. 5	UV sensitivity	Increased incidence of skin cancer	Possible DNA ligase deficiency or defect of transcription coupled repair	

AML, Acute myeloid leukemia; *MR,* mental retardation; *SCE,* sister chromatid exchange; *UV,* ultraviolet.

SUMMARY

Cytogenetics is one of the oldest clinical laboratory sciences still in active use. It has grown and changed over time, keeping pace with the changes in the field of genetics. FISH and microarray technology have bridged the gap between cytogenetics and molecular diagnostics such that the two areas provide complementary information in many cases. Although cytogenetics is no longer the only clinical assay that can provide a quick overview of the entire human genome, karyotype analysis continues to be a clinically important tool in assessing numeric and structural chromosome anomalies and is still the gold standard for diagnosis of many neoplasia and inherited disorders.

SELECTED REFERENCES

Abbott Molecular. http://www.abbottmolecular.com/us/home.html.

Developer and manufacturer of FISH probes. The website provides information on the probes available and the biology behind the detection assay.

Arsham MS, Barch MJ, Lawce HJ: *The AGT cytogenetics laboratory manual*, ed 4, Hoboken, NJ, 2016, John Wiley & Sons.

An excellent reference covering laboratory protocols and principles for constitutional disorders, hematologic diseases and solid tumors, microscopy, FISH, microarray, and laboratory management.

Heim S, Mitelman F: *Cancer cytogenetics*, ed 4, West Sussex, UK, 2015, John Wiley & Sons.

This is an excellent source of information covering all aspects of cancer genetics. It includes molecular, cytogenetic, and clinical aspects of leukemias, lymphomas, and solid tumors.

ISCN 2016: In McGowan-Jordan J, Simons A, Schmid M, editors: *An international system for human cytogenetic nomenclature*, Basel, 2016, S Karger.

This reference provides the standard ideograms, the accepted cytogenetic nomenclature and how it is to be applied, and examples of usage of terminology.

Nussbaum RL, McInnes RR, Willard HF: *Thompson and Thompson—genetics in medicine*, ed 8, Philadelphia, 2016, Elsevier Inc.

Excellent textbook covering all aspects of medical genetics. It provides a basic introduction to the field, followed by detailed descriptions of subspecialties, including cytogenetics, molecular genetics, cancer genetics, immunogenetics, prenatal genetics, and genetic counseling.

OMIM (Online Mendelian Inheritance in Man). http://www.ncbi.nlm.nih.gov/Omim/.

The best source of information on genes related to diseases. Each entry includes data on the discovery of the gene, cytogenetic and molecular aspects of the disorder, possible genetic testing, related diseases, and references to the scientific literature.

Swerdlow SH, Campo E, Harris NL, et al.: *WHO classification of tumours of haematopoietic and lymphoid tissues*, ed 4, Lyon, 2017, IARC Press.

This is an important guide, providing the pathology (i.e., descriptions, molecular and clinical findings) associated with leukemias and lymphomas.

FURTHER READING

De Grouchy J, Turleau C: *Clinical atlas of human chromosomes*, ed 2, New York, 1984, John Wiley & Sons.

Fletcher CDM, Bridge JA, Hogendoorn PCW, et al.: *WHO classification of tumors of soft tissue and bone*, ed 4, Lyon, 2013, IARC Press.

Gelehrter T, Collins FC, Ginsburg D: *Principles of medical genetics*, ed 2, Baltimore, 1998, Williams & Wilkins.

McKusick V: *Mendelian inheritance in man: a catalog of human genes and genetic disorders*, ed 12, Baltimore, 1998, Johns Hopkins Press.

Mitelman F: *Catalog of chromosome aberrations in cancer*, ed 5, New York, 1994, Wiley-Liss.

Rooney DE, Czepulkowski BH: *Human cytogenetics—a practical approach*, ed 3, New York, 2001, Oxford University Press.

Jorde LB, Carey JC, Bamshad MJ, editors: *Medical genetics*, ed 5, Philadelphia, 2016, Elsevier.

Access the complete reference list online at Elsevier eBooks for Practicing Clinicians.

REFERENCES

Anastasi J: Interphase cytogenetic analysis in the diagnosis and study of neoplastic disorders, *Am J Clin Pathol* 95(Suppl 1):S22–S28, 1991.

Angell RR, Xian J, Deith J, et al.: First meiotic division abnormalities in human oocytes: mechanism of trisomy formation, *Cytogenet Cell Genet* 65:194–202, 1994.

Arlett CF, Lehmann AR: Human disorders showing increased sensitivity to the induction of genetic damage, *Ann Rev Genet* 12:95–115, 1978.

Bayes M, Magano LF, Rivera N, et al.: Mutation mechanisms of Williams-Beuren syndrome deletions, *Am J Hum Genet* 73:131–151, 2003.

Blakemore KJ: Prenatal diagnosis by chorionic villus sampling, *Obstet Gynecol Clin North Am* 15:179–213, 1988.

Burkholder GC, Weaver MG: DNA–protein interactions and chromosome banding, *Exp Cell Res* 110: 251–262, 1977.

Cassidy SB, Lai L-W, Erickson RP, et al.: Trisomy 15 with loss of the paternal 15 as a cause of Prader-Willi syndrome due to maternal disomy, *Am J Hum Genet* 51:701–708, 1992.

Chen Y, Yu Q, Mao X, et al.: Noninvasive prenatal testing for chromosome aneuploidies and subchromosomal microdeletions/microduplications in a cohort of 42,910 single pregnancies with different clinical features, *Hum Genom* 13:60–68, 2019.

Cherif D, Bernard O, Berger R: Detection of single-copy genes by nonisotopic in situ hybridization on human chromosomes, *Hum Genet* 81:358–362, 1989.

Chiu RWK, Akolekar R, Zheng YWL, et al.: Noninvasive prenatal assessment of trisomy 21 by multiplexed maternal plasma DNA sequencing: large-scale validity study, *BMJ* 342:c7401, 2011.

Comings DE, Kovacs BW, Avelino E, et al.: Mechanism of chromosome banding. V. Quinacrine banding, *Chromosoma* 50:111–145, 1975.

Committee on Practice Bulletins—Obstetrics: Committee on genetics, and society for maternal-fetal medicine. Screening for fetal aneuploidy. Practice Bulletin No. 163. American College of Obstetricians and Gynecologists, *Obstet Gynecol* 127: e123–e137, 2016.

Cooley LD, Lebo M, Li MM, et al.: A working group of the American College of medical genetics and genomics (ACMG) laboratory quality Assurance Committee: American College of medical genetics and genomics technical standards and guidelines: microarray analysis for chromosome abnormalities in neoplastic disorders, *Genet Med* 15:484–494, 2013.

Cremer T, Lichter P, Borden J, et al.: Detection of chromosome aberrations in metaphase and interphase tumor cells by in situ hybridization using chromosome-specific library probes, *Hum Genet* 80:235–246, 1988.

Delabar J-M, Theophile D, Rahmani Z, et al.: Molecular mapping of the twenty-four features of Down syndrome on chromosome 21, *Eur J Hum Genet* 1:114–124, 1993.

De Lange T: Telomeres and senescence: ending the debate, *Science* 279:334–335, 1998.

De Martinville B, Blakemore KJ, Mahoney MJ, et al.: DNA analysis of first-trimester chorionic villous biopsies: test for maternal contamination, *Am J Hum Genet* 36:1357–1368, 1984.

Dharmadhikari AV, Ghosh R, Yuan B, et al.: Copy number variant and runs of homozygosity detection by microarrays enabled more precise molecular diagnoses in 11,020 clinical exome cases, *Genome Med* 11:30, 2019.

Divane A, Carter NP, Spathas DH, et al.: Rapid prenatal diagnosis of aneuploidy from uncluttered amniotic fluid cells using five-colour fluorescence in situ hybridization, *Prenat Diagn* 14:1056–1069, 1994.

Ehrich M, Tynan J, Mazloom A, et al.: Genome-wide cfDNA screening: clinical laboratory experience with the first 10,000 cases, *Genet Med* 19(12):1332–1337, 2017.

Flint J, Knight S: The use of telomere probes to investigate submicroscopic rearrangements associated with mental retardation, *Curr Opin Genet Devel* 13:310–316, 2003.

Flint J, Wilke AOM, Buckle VJ, et al.: The detection of subtelomeric chromosomal rearrangements in idiopathic mental retardation, *Nat Genet* 9:132–139, 1995.

Gil MM, Accurti V, Santacruz B, et al.: Analysis of cell-free DNA in maternal blood in screening for aneuploidies: updated meta-analysis, *Ultrasound Obstet Gynecol* 50(3):302–314, 2017.

Gregg AR, Skotko BG, Benkendorf JL, et al.: On behalf of the ACMG noninvasive prenatal screening work group: noninvasive prenatal screening for fetal aneuploidy, 2016 update: a position statement of the American College of medical genetics and genomics, *Genet Med* 18(10):1056–1065, 2016.

Guy C, Haji–Sheikhi F, Rowland CM, et al.: Prenatal cell–free DNA screening for fetal aneuploidy in pregnant women at average or high risk: results from a large US clinical laboratory, *Mol Genet Genomic Med* 7:e545, 2019.

Hall JG: Genomic imprinting: review and relevance to human diseases, *Am J Hum Genet* 46:857–873, 1990.

Harley CB, Futcher AB, Greider CW: Telomeres shorten during ageing of human fibroblasts, *Nature* 345:458–460, 1990.

Hassold T, Chiu D: Maternal age-specific rates of numerical chromosome abnormalities with special reference to trisomy, *Hum Genet* 70:11–17, 1985.

Holmquist G: The mechanism of C-banding: depurination and beta-elimination, *Chromosoma* 72:203–224, 1979.

Holmquist G, Gray M, Porter T, et al.: Characterization of Giemsa dark- and light-band DNA, *Cell* 31:121–129, 1982.

Hook EB, Hamerton JL: The frequency of chromosome abnormalities detected in consecutive newborn studies—differences between studies—results by sex and by severity of phenotypic involvement. In Hook EB, Porter IH, editors: *Population cytogenetics. New York State department of health, birth defects institute symposium 1975*, New York, 1977, Academic Press, p 63.

Irons M: Use of subtelomeric fluorescence in situ hybridization in cytogenetic diagnosis, *Curr Opin Pediatr* 15:594–597, 2003.

Jacobs PA, Browne C, Gregson N, et al.: Estimates of the frequency of chromosome abnormalities detectable in unselected newborns using moderate levels of banding, *J Med Genet* 29:103–108, 1992.

Jacobs PA, Price WH, Court Brown WM: Chromosome studies on men in a maximum security hospital, *Ann Hum Genet* 31:339–358, 1968.

Jones KL, Jones MC, Del Campo M, editors: *Smith's recognizable patterns of human malformation*, ed 7, Philadelphia, 2013, Elsevier.

Kanagal-Shamanna R, Hodge JC, Tucker T, et al.: Assessing copy number aberrations and copy neutral loss of heterozygosity across the genome as best practice: an evidence based review of clinical utility from the Cancer Genomics Consortium (CGC) working group for myelodysplastic syndrome, myelodysplastic/myeloproliferative and myeloproliferative neoplasms, *Cancer Genet* 228–229:197–217, 2018.

Korenberg JR, Kawashima H, Pulst S-M, et al.: Molecular definition of a region of chromosome 21 that causes features of the Down syndrome phenotype, *Am J Hum Genet* 47:236–246, 1990.

Ledbetter DH, Cavenee WK: Molecular cytogenetics: interface of cytogenetics and monogenic disorders. In *The metabolic basis of inherited disease*, ed 6, New York, 1989, McGraw-Hill, pp 343–371.

Ledbetter DH, Engel E: Uniparental disomy in humans: development of an imprinting map and its implications for prenatal diagnosis, *Hum Mol Genet* 4:1757–1764, 1995.

Ledbetter SA, Kuwano A, Dobyns WB, et al.: Microdeletions of chromosome 17p13 as a cause of isolated lissencephaly, *Am J Hum Genet* 50:182–189, 1992.

Lichter P, Jauch A, Cremer T, et al.: Detection of Down syndrome by in situ hybridization with chromosome 21 specific DNA probes. In Patterson D, editor: *Molecular genetics of chromosome 21 and down syndrome*, New York, 1990, Wiley-Liss.

Lindsay EA, Halford S, Wadey R, et al.: Molecular cytogenetic characterization of the DiGeorge syndrome region using fluorescence in situ hybridization, *Genomics* 17:403–407, 1993.

Lindstrand A, Eisfeldt J, Pettersson M, et al.: From cytogenetics to cytogenomics: wholegenome sequencing as a first-line test comprehensively captures the diverse spectrum of disease-causing genetic variation underlying intellectual disability, *Genome Med* 11:68, 2019.

Lobo I: Genomic imprinting and patterns of disease inheritance, *Nature Education* 1:66, 2008.

Lubs HA: A marker X chromosome, *Am J Hum Genet* 31:231–244, 1969.

McDermid HE, Morrow BE: Genomic disorders on 22q11, *Am J Hum Genet* 70:1077–1088, 2002.

Mikhail FM, Biegel JA, Cooley LD, et al.: Technical laboratory standards for interpretation and reporting of acquired copy-number abnormalities and copyneutral loss of heterozygosity in neoplastic disorders: a joint consensus recommendation from the American College of Medical Genetics and Genomics (ACMG) and the Cancer Genomics Consortium (CGC), *Genet Med* 21(9):1903–1916, 2019.

Miller DT, Adam MP, Aradhya S, et al.: Consensus statement: chromosomal microarray is a first-tier clinical diagnostic test for individuals with developmental disabilities or congenital anomalies, *Am J Hum Genet* 86:749–764, 2010.

National Institutes of Health and Institute of Molecular Medicine Collaboration: A complete set of human telomeric probes and their clinical application, *Nat Genet* 14:86–89, 1996.

Nicholls RD, Knoll JHM, Butler MG, et al.: Genetic imprinting suggested by maternal heterodisomy in non-deletion Prader-Willi syndrome, *Nature* 342:281–285, 1989.

Nicholls RD, Saitoh S, Horsthemke B: Imprinting in Prader-Willi and Angelman syndromes, *Trends Genet* 14:194–198, 1998.

Norton ME, Brar H, Weiss J, et al.: Non-invasive chromosomal evaluation (NICE) study: results of a multicenter prospective cohort study for detection of fetal trisomy 21 and trisomy 18, *Am J Obstet Gynecol* 207:1.e1–1.e8, 2012.

Norton ME, Jacobsson B, Geeta K, et al.: Cell-free DNA analysis for noninvasive examination of trisomy, *N Engl J Med* 372:1589–1597, 2015.

Palmer CG, Reichmann A: Chromosomal and clinical findings in 110 females with Turner syndrome, *Hum Genet* 35:35–49, 1976.

Petersen MB, Bartsch O, Adelsberger PA, et al.: Uniparental isodisomy due to duplication of chromosome 21 occurring in somatic cells monosomic for chromosome 21, *Genomics* 13:269–274, 1992.

Peterson JF, Van Dyke DL, Hoppman NL, et al.: The utilization of chromosomal microarray technologies for hematologic neoplasms: an ACLPS critical review, *Am J Clin Pathol* 150(5):375–384, 2018.

Pitcher DR: Chromosome and violence, *Practitioner* 226:497–501, 1982.

Price WH, Jacobs PA: The 47,XXY male with special reference to behavior, *Semin Psychol* 2:30–39, 1970.

Raynaud CM, Sabatier L, Philipot O, et al.: Telomere length, telomeric proteins and genomic instability during the multistep carcinogenic process, *Crit Rev Oncol Hematol* 66:99–117, 2008.

Reid T, Baldini A, Rand TC, et al.: Simultaneous visualization of seven different DNA probes by in situ hybridization using combinatorial fluorescence and digital imaging microscopy, *Proc Natl Acad Sci U S A* 89:1388–1392, 1992.

Reid T, Landes G, Dackowski W, et al.: Multicolor fluorescence in situ hybridization for the simultaneous detection of probe sets for chromosomes 13, 18, 21, X and Y in uncultured amniotic fluid cells, *Hum Mol Genet* 1:307–313, 1992.

Rhoads GG, Jackson LG, Sachlesselman SE, et al.: The safety and efficacy of chorionic villus sampling for early prenatal diagnosis of cytogenetic abnormalities, *N Engl J Med* 320:609–617, 1989.

Riggs ER, Andersen EF, Cherry AM, et al.: Technical standards for the interpretation and reporting of constitutional copy-number variants: a joint consensus recommendation of the American College of Medical Genetics and Genomics (ACMG) and the Clinical Genome Resource (ClinGen), *Genet Med*, 2019. [Epub ahead of print.

Robinson WP, Bottani A, Yagang X, et al.: Molecular, cytogenetic and clinical investigations of Prader-Willi syndrome patients, *Am J Hum Genet* 49:1219–1234, 1991.

Rosenberg MJ, Killoran C, Dziadzio L, et al.: Scanning for telomeric deletions and duplications and uniparental disomy using genetic markers in 120 children with malformations, *Hum Genet* 109:311–318, 2001.

Rousseau F, Heitz D, Biancalana V, et al.: Direct diagnosis by DNA analysis of the fragile X syndrome of mental retardation, *N Engl J Med* 325:1673–1681, 1991.

Schoumans J, Suela J, Hastings R, et al.: Guidelines for genomic array analysis in acquired haematological neoplastic disorders, *Genes Chromosomes Cancer* 55:480–491, 2016.

Schrock E, du Manoir S, Veldman T, et al.: Multicolor spectral karyotyping of human chromosomes, *Science* 273:494–497, 1996.

Shaffer LG, Dabell MP, Fisher AJ, et al.: Experience with microarray-based comparative genomic hybridization for prenatal diagnosis in over 5000 pregnancies, *Prenat Diagn* 32:976–985, 2012.

Shaffer BL, Norton ME: Cell-free DNA screening for aneuploidy and microdeletion syndromes, *Obstet Gynecol Clin* 45(1):13–26, 2018.

Schwartz S, Kohan M, Pasion R, et al.: Clinical experience of laboratory follow–up with noninvasive prenatal testing using cell–free DNA and positive microdeletion results in 349 cases, *Prenatal Diag* 38(3):210–218, 2018.

Silva M, de Leeuw N, Mann K, et al.: European guidelines for constitutional cytogenomic analysis, *Eur J Hum Genet* 27(1):1–16, 2019.

South ST, Lee C, Lamb AN, et al.: Working Group for the American College of Medical Genetics and Genomics Laboratory Quality Assurance Committee: ACMG standards and guidelines for constitutional cytogenomic microarray analysis, including postnatal and prenatal applications: revision 2013, *Genet Med* 15(11):901–909, 2013.

Speicher MR, Ballard SG, Ward DC: Karyotyping human chromosomes by combinatorial multi-fluor FISH, *Nat Genet* 12:368–375, 1996.

Spence EJ, Perciaccante RG, Greig GM, et al.: Uniparental disomy as a mechanism for human genetic disease, *Am J Hum Genet* 42:217–226, 1988.

Srivastava S, Love-Nichols JA, Dies KA, et al.: Meta-analysis and multidisciplinary consensus statement: exome sequencing is a first-tier clinical diagnostic test for individuals with neurodevelopmental disorders, *Genet Med* 21:2413–2421, 2019.

Sumner AT, Evans HJ, Buckland RA: Mechanisms involved in the banding of chromosome with quinacrine and Giemsa I. The effects of fixation in methanol–acetic acid, *Exp Cell Res* 81:214–222, 1973.

Theilgaard A: A psychological study of the personalities of XYY- and XXY-men, *Acta Psychiatr Scand Suppl* 315:1–133, 1984.

Turnpenny P, Ellard S: *Emery's elements of medical genetics*, ed 14, Edinburgh, 2011, Churchill Livingstone.

Veldman T, Vignon C, Schrock E, et al.: Hidden chromosome abnormalities in haematological malignancies detected by multicolour spectral karyotyping, *Nat Genet* 15:406–410, 1997.

Verkerk AJMH, Pieretti M, Sutcliffe JS, et al.: Identification of a gene (FMR-1) containing a CGG repeat coincident with a breakpoint cluster region exhibiting length variation in fragile X syndrome, *Cell* 65:905–914, 1991.

Voss R, Ben-Simon E, Avital A, et al.: Isodisomy of chromosome 7 in a patient with cystic fibrosis: could uniparental disomy be common in humans? *Am J Hum Genet* 45:373–380, 1989.

Wapner RJ, Martin CL, Levy B, et al.: Chromosomal microarray versus karyotyping for prenatal diagnosis, *N Engl J Med* 367(23):2175–2184, 2012.

Werner M, Ewig M, Nasarek A: Value of fluorescence in situ hybridization for detecting the *bcr/abl* gene fusion in interphase cells of routine bone marrow specimens, *Diagn Mol Pathol* 6:282–287, 1997.

Witkin HA, Mednick SA, Schulsinger F, et al.: Criminality in XYY and XXY men, *Science* 193:547–555, 1976.

Wright CF, Burton H: The use of cell-free fetal nucleic acids in maternal blood for non-invasive prenatal diagnosis, *Hum Reprod Update* 15:139–151, 2009.

Wright WE, Shay JW: Telomere positional effects and the regulation of cellular senescence, *Trends Genet* 8:193–197, 1992.

Xu X, Bryke C, Sukhanova M, et al.: Assessing copy number abnormalities and copy-neutral loss-of-heterozygosity across the genome as best practice in diagnostic evaluation of acute myeloid leukemia: an evidence-based review from the Cancer Genomics Consortium (CGC) myeloid neoplasms working group, *Cancer Genet* 228– 229:218–235, 2018.

Yunis JJ, Sanchez O: G-banding and chromosome structure, *Chromosoma* 44:15–23, 1973.

CHAPTER 72

MOLECULAR DIAGNOSIS OF GENETIC DISEASES

Wayne W. Grody

INTRODUCTION, 1434
CHOICE OF TECHNIQUES, 1435
CHOICE OF APPLICATIONS, 1435
SPECIAL CONCEPTS UNIQUE TO MOLECULAR GENETIC DISORDERS, 1437
Molecular Heterogeneity, 1437
Variable Penetrance and Expressivity, 1437
Uniparental Disomy, 1437
Imprinting, 1437
Anticipation, 1438
Epigenetic Influences and Nonmendelian Inheritance, 1438
Allele Frequencies and Mass Population Screening, 1438
Predictive Genetic Testing, 1438
SPECIFIC DISEASE EXAMPLES, 1438
Cystic Fibrosis, 1438
Duchenne Muscular Dystrophy, 1439
Spinal Muscular Atrophy, 1440
Sickle Cell Anemia and Other Hemoglobinopathies, 1440
Hereditary Thrombophilias, 1440
Hereditary Hemochromatosis, 1441
Trinucleotide Repeat Expansion Disorders, 1441
Prader-Willi and Angelman Syndromes, 1445
Familial Cancers, 1445
Mitochondrial DNA Disorders, 1448
Other Targets of Molecular Genetic Testing, 1449
THE NEW FRONTIER OF DIAGNOSTIC MOLECULAR GENETICS: GENOME-LEVEL DNA SEQUENCING, 1449
SELECTED REFERENCES, 1449

KEY POINTS

- Molecular testing for inherited disorders is one of the most rapidly growing areas of molecular pathology owing to the plethora of disease genes discovered through the Human Genome Project and the introduction of exome and genome sequencing.
- The mutations for single-gene disorders, whether dominant or recessive, can be detected by a variety of molecular diagnostic techniques, either specific to the mutation in question, if it is known, or by a panel of the more common mutations or by comprehensive gene sequencing if the mutation is not known.
- Certain disorders, such as cystic fibrosis, have sufficiently high mutation carrier frequencies that they have become targets for large-scale population screening programs. With the advent of massively parallel ("next-generation") DNA sequencing, the potential mutation, gene, and disease targets for individual, couple, or population screening have greatly expanded.
- Late-onset dominant disorders, such as Huntington disease and familial cancers, are appropriate targets of presymptomatic testing provided that sufficient attention is paid to the associated genetic counseling and ethical concerns.
- Next-generation sequencing has revolutionized this field in the last few years, with exome or genome sequencing, or large gene panel testing, tending to replace or supplement single-gene testing. This approach has been especially fruitful in providing answers to patients with ultra-rare or undiagnosed disorders.
- Ethical issues raised by each of these applications involve genetic privacy, informed consent, pregnancy termination, reporting of off-target findings, duty to reanalyze and recontact test subjects, potential stigmatization, and theoretical risk of insurance or employment discrimination.

INTRODUCTION

Diagnostic molecular genetics shows promise of becoming the most powerful diagnostic and screening tool of the 21st century, spurred on by the introduction of high-throughput DNA sequencing technologies and the ever-growing description of gene-disease associations in the human genome. With this progress has come the recognition that virtually all diseases, including neoplastic and even infectious ones, have some genetic component, with the result that the clinical utility of this subspecialty can only continue to expand. Moreover, its unique capability to diagnose disease both prenatally and presymptomatically should confer on it a primary role in preventive medicine, a focus of increasing urgency in the present era of medical care cost containment. This goal will truly be brought home when researchers identify the genetic causes of the so-called "common complex" diseases: atherosclerosis, diabetes, hypertension, dementia, and so on. Even beyond that, diagnostic molecular genetics leads naturally into therapeutic molecular genetics because essentially the same normal gene sequences used to detect molecular genetic defects by deoxyribonucleic acid (DNA) hybridization could theoretically be used to correct such defects by gene replacement therapy or gene editing. Such therapies, in turn, will come under the purview of the molecular diagnostics laboratory, which will have the responsibility of confirming proper insertion and appropriate expression of the replaced or edited gene.

Yet such progress does not come unencumbered by appreciable obstacles. Aside from the considerable technical sophistication, expense, and complexity of these procedures, they are inextricably bound up with a number of thorny ethical dilemmas. Dissecting a patient's most fundamental constitutional makeup and the inborn errors therein raises problematic questions about genetic discrimination, stigmatization, ethnic differences, privacy, informed consent, and confidentiality. Since at the molecular genetic level everything becomes a preexisting condition, the very definition of insurability may need to be revised. Instances of insurance and employment discrimination as a result of genetic testing, although rare (Hall & Rich, 2000), have been reported (Billings et al., 1992). It is reassuring that in the United States, where privately insured health care is most vulnerable to such abuses, we now have federal legislation—the Genetic Information Nondiscrimination Act (GINA)—prohibiting discrimination in health insurance and employment based on genetic test results, although certain limitations still remain (Baruch & Hudson, 2008). Furthermore, discovery of any such heritable mutations in an individual has profound implications far beyond the immediate patient who is the target of the DNA test (the *proband*), extending to all the other members of that person's family, none of whom may have consented to exploring or revealing this type of information. Indeed, with the almost unlimited power of DNA testing afforded by amplification techniques such as the polymerase chain reaction (PCR) and high-throughput genomic analysis technologies (see Chapters 69, 70 and 80), it becomes quite easy to perform genetic analysis without the patient's consent or even knowledge because the testing can be done on minute portions of tissue or fluid samples obtained for other unrelated purposes. Prenatal diagnosis—and, by extension, preconception genetic carrier screening of couples—has become caught up in the fevered ethical and religious debates over abortion. In addition, gene therapy/gene editing, despite general consensus that it should be directed only at somatic rather than germline cellular targets (with high-profile violations of this

rule already occurring) (Cyranoski, 2020), raises the specter of eugenics among those who do not have to remember back all that far to times when such notions were not only accepted but actively espoused.

Much of diagnostic molecular genetics involves the assessment of risk for occurrence or recurrence of a disorder in an individual or family. For reasons described more fully later in this chapter, the test results obtained are often expressed not in terms of a numerical concentration or as a yes/no answer, but rather as a probability, which sometimes is derived by multifactorial Bayesian analysis (Ojino & Wilson, 2004) or a complex variant interpretation algorithm (Richards et al., 2015). The accurate and meaningful conveyance of such uncertainties to patients and even referring physicians can be quite difficult and time-consuming. For this reason, this area of laboratory medicine, perhaps more than most others, requires very close communication between the laboratory and the referring clinician or genetic counselor. In fact, some of these tests, particularly the emotionally charged predictive ones, should be ordered only through a medical geneticist or genetic counselor or through some alternative method of informed pretest counseling. Many large academic and commercial reference laboratories specializing in this type of testing employ their own genetic counselors on staff as a further safeguard to ensure appropriate test selection and communication with primary care physicians who may not be well-versed in these matters.

CHOICE OF TECHNIQUES

With so many genetic disease genes, loci, and mutational mechanisms known, diagnostic molecular genetics must take advantage of the entire spectrum of modern molecular biological techniques available. These include, among others (see Chapters 68, 69 and 80):

- PCR
- Southern blotting
- Allele-specific probe hybridization
- DNA sequencing (Sanger method)
- Real-time PCR
- Nucleic acid microarrays
- Multiplex ligation-dependent probe amplification (MLPA)
- Mass spectrometry
- Massively parallel (next-generation) DNA sequencing (NGS)
- RNA sequencing

To make such tests practical and affordable, a number of *multiplexing strategies* for simultaneous mutation detection have been devised. All of these involve some compromise as to overall test sensitivity. Indeed, the field of molecular genetic testing tolerates, by necessity, a number of screening tests with clinical sensitivities noticeably below those that would be considered acceptable in other areas of the clinical laboratory. The decision of just how low the acceptable sensitivity cutoff should be often comes down to public health considerations. Most geneticists have reasoned that, at least for screening tests, the potential public health benefits of offering an inexpensive and technically feasible test of admittedly suboptimal sensitivity outweigh the arguments for withholding it, as long as sufficient education and counseling are provided to patients so that they understand the residual risk inherent in a negative test result. It is important to keep in mind that this discussion is about clinical sensitivity, not analytical sensitivity. It is assumed (as validated by the laboratory) that the test is capable of detecting a given mutation whenever it is present; it is just that many rarer mutations will not be targeted by the assay, so that some proportion of carriers will be "missed"—a sort of "clinical false-negative" (Palomaki et al., 2004). *Direct mutation tests* were simplified immeasurably by the advent of PCR in the mid-1980s. Through the judicious choice of primers, this technique allows the laboratory to home in on the precise mutation of interest, or a "hot spot" within a gene containing several possible mutation sites, using minute amounts of starting material. Once the region containing the suspected mutation is amplified, it can be analyzed by gel or capillary electrophoresis, sequencing, or DNA probe hybridization. For a deletion or insertion that would be expected to alter the length of the amplicon, accurate molecular sizing of the PCR products by electrophoresis will be sufficient. For point mutations, a common approach is to hybridize the PCR products with allele-specific oligonucleotide (ASO) probes, short DNA fragments that are precisely complementary to either the normal or mutant target sequence. As discussed in Chapter 70, if the hybridization is performed under sufficiently stringent conditions, target DNA containing the mutation will hybridize only with the mutant probe and vice versa for wild-type target DNA. Several mutation hot spots in a gene can be amplified together by multiplex PCR. As a variation on this approach, any number of allelic probes can be spread out on a solid support for subsequent hybridization with the specimen DNA (or amplicons) in the form of a microarray or in suspension on microbeads. Lastly, a number of commercial reagents and instruments are available that detect point mutations by differential probe/quencher hybridization or by capillary electrophoresis and other sophisticated techniques, as described in Chapters 68 and 70.

Disorders caused by expansion of a trinucleotide (or other short tandem) repeat are typically diagnosed by PCR followed by sizing on a capillary electrophoresis instrument and observing a larger-than-normal target DNA fragment. Disorders caused by large deletions may be diagnosed by Southern blot by observing loss or decrease in size of a target fragment, or by PCR through loss of a product normally amplified from that site or appearance of a new "junction" fragment, or by MLPA or microarray. It should be noted that a weakness of the newer next-generation DNA sequencing (NGS) techniques is their inability to identify either repeat expansions or sizeable deletions (except for deletions on the X chromosome in a male), though this deficiency is starting to be overcome, especially through whole-genome sequencing (Pirooznia et al., 2015).

When the diagnostic investigation must go beyond a single gene, in cases of broad differential diagnosis, we turn to high-density oligonucleotide microarray platforms or NGS. The former was the first to enter routine use in clinical genetics in the form of array comparative genomic hybridization, now usually called *chromosomal microarray* (CMA). This technique employs a high number (500,000 to > 5,000,000) DNA probes on the array, chosen so that their complementary genomic sequences span the entire genome at regular intervals. Total genomic DNA from the patient is compared by hybridization to the array against what a "normal" total genomic control sample would produce (i.e., no pathologic gains or losses of hybridization signal). If the patient's DNA contains a deletion on a certain chromosome, this will be indicated by a decrease or absence of hybridization signal to the probes spanning that region (Fig. 72.1). Conversely, if the patient's DNA contains a duplication (insertion) of a chromosomal region, an excess of hybridization signal will be seen for that region. The resolution for detecting these *copy number variants* (CNVs) is much finer than can be achieved by classic karyotype analysis under the light microscope and is continually improving as ever greater numbers of probes at ever diminishing base-pair intervals are added to the arrays. As such, it has rapidly become a predominant technique for detecting deletions/duplications in patients with congenital problems that do not readily suggest a particular known genetic syndrome, including those with nonspecific physical malformations/dysmorphisms, developmental delay, and/or autism. In fact, it is now considered standard of practice for these indications instead of ordering a karyotype (Manning & Hudgins, 2010; Miller et al., 2010). However, it does have some limitations. First, because all it does is examine differences in hybridization intensity across the total genomic DNA, balanced translocations and inversions with no gain or loss of genetic material will not be detected. Second, all human genomes contain a great many CNVs that are nonpathogenic (i.e., benign). Some of these are well-known polymorphisms and, thus, can be discounted as etiologic if observed in a patient. However, many others are not yet known or studied extensively, producing the challenging "CNV of uncertain clinical significance." Aside from using intuition based on the particular genes encompassed by the deletion or insertion, testing of the parents may also be helpful. If a normal parent carries the same deletion, it is less likely to be pathogenic (though there are exceptions). More detailed discussion of microarray technology can be found in Chapter 70.

Of course, the ultimate gold standard for identifying all possible mutations would be whole-genome sequencing. It took 13 years to completely sequence the consensus human genome under the Human Genome Project using conventional Sanger sequencing platforms (see Chapter 68). We now have a new generation of automated DNA sequencers based on radically different chemistries involving sequencing of millions of short fragments of the patient's genome in parallel, which are then assembled into the full genome by analytic and bioinformatic software. These instruments are capable of sequencing billions of bases per day at relatively reasonable cost (with costs diminishing all the time), at last putting the whole human genome in reach for routine analysis. At present, the major clinical application of this technology in genetics is for the diagnosis of syndromic-appearing conditions for which standard single-gene and other clinical laboratory tests have been unrevealing (see later discussion for detailed description of this process). It is also being applied to oncology, with NGS of tumor DNA to detect so-called "druggable" somatic mutations (see Chapters 78 and 79). Further discussion of NGS in present and future applications can be found in Chapter 80.

CHOICE OF APPLICATIONS

To some extent, the choice of technique will also depend on the application or clinical indication. In medical genetics, these applications fall into

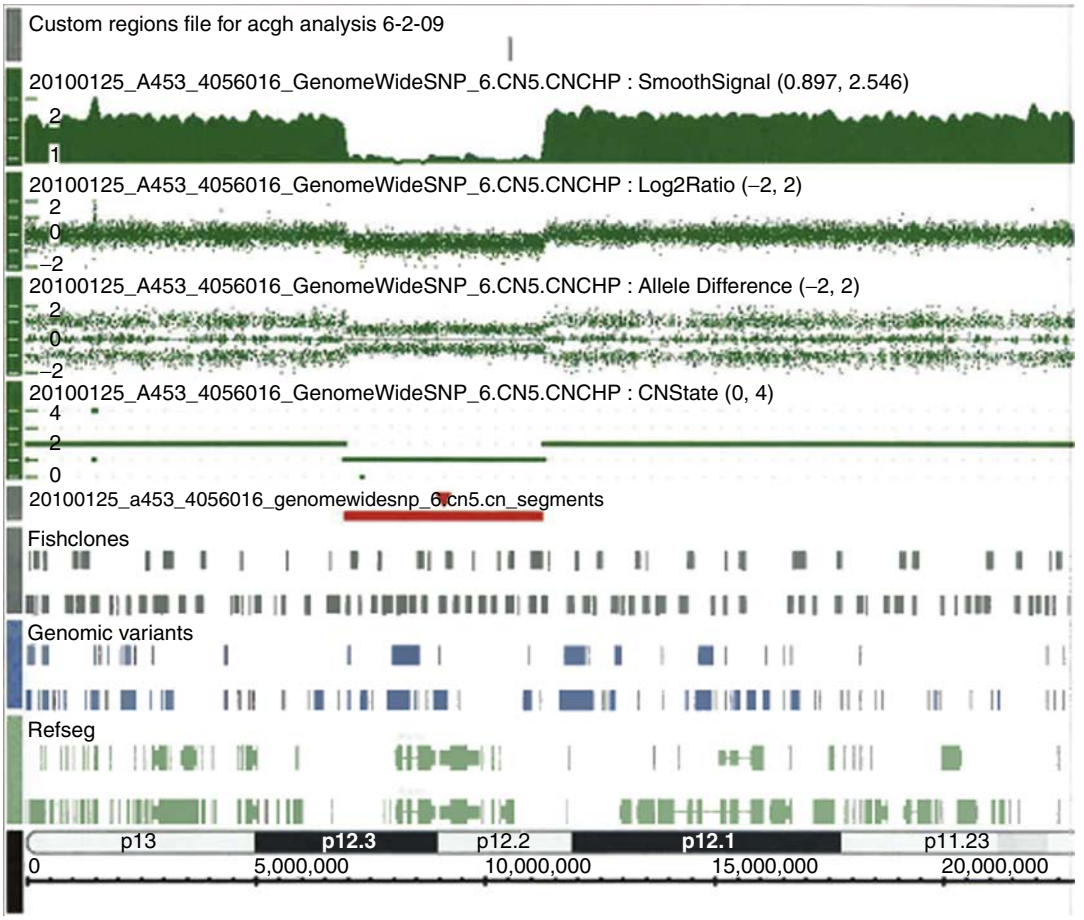

Figure 72.1 Example of a typical deletion result by array comparative hybridization. The gap in hybridization signal demarcated by the red line indicates a 4.329 Mb hemizygous deletion on chromosome 20p12.2-12.3 (6975661–11you 304543 bp). This deletion encompasses multiple genes, including *JAG1*, the gene implicated in Alagille syndrome, which was the clinical diagnosis in the tested patient (Courtesy of Dr. Xinmin Li.)

five major areas: carrier screening, newborn screening, diagnostic testing, presymptomatic DNA testing, and prenatal testing.

Carrier screening is the term applied to detection of recessive mutations in healthy individuals for purposes of genetic counseling and family planning. This application is further subdivided into screening of those individuals with a family history of the disorder and population-based screening of large numbers of individuals who have negative family history but who may be at risk for the disorder because of its prevalence within their ethnic group or in the population at large. In either case, the ultimate purpose is to identify couples at risk (i.e., both the father and mother are heterozygous for mutations within the gene) who would then have a 25% chance of having an affected child with each pregnancy. The testing strategies chosen for the two groups will differ, however. A person whose sibling has the disorder is at much higher risk of being a carrier than someone in the general population. That person may therefore warrant more aggressive testing (e.g., screening for a greater number of mutations or possibly complete gene sequencing) than would be cost-effective for the general population. On the other hand, access to the affected sibling's DNA may allow prior identification of the familial mutation, which would render subsequent testing of other family members much easier and straightforward. Population-based screening, in contrast, typically strives to keep the testing procedure as rapid and inexpensive as possible, focusing on perhaps a few of the more prevalent mutations, sacrificing clinical test sensitivity for cost-effectiveness and expediency. With a negative family history, there are no affected family members to make either single-site mutation testing or linkage analysis an option. In recent years, NGS has allowed for carrier screening in many more genes (into the hundreds) at reasonable cost. This approach is agnostic to the long-standing previous indications for targeted carrier screening: positive family history and/or ethnic risk. While uptake has been high in prenatal clinics, there remains some controversy as to its utility. On the positive side, it will detect mutations in genes for ultra-rare disorders that would not have been cost-effective to screen in large populations before, thus offering the opportunity for couples to avoid the birth of a child with a completely unexpected disorder for which they did not know they were at risk (Ben-Shachar et al., 2019). On the negative side, the addition of diseases and genes to construct the expanded panels has been rather arbitrary, with a number of diseases included for which little is known of the natural history, severity, or genotype-phenotype associations of the many novel sequence variants that may be detected (Grody, 2016). In addition, the inclusion of so many genes means that a significant proportion of the tested individuals (up to 30% or more) and couples will be positive for something (Guo & Gregg, 2019), creating a downstream burden on genetic counseling resources.

Like population-based carrier screening, *newborn screening* aims to identify relatively prevalent (as genetic diseases go) inherited defects in otherwise asymptomatic individuals. The most important disease targets—such as phenylketonuria, galactosemia, sickle cell disease, and cystic fibrosis (CF)—are likewise autosomal-recessive disorders. In the case of newborn screening, however, the goal is to ascertain affected babies early in life so that treatment (dietary or pharmaceutical) can be initiated before irreversible damage occurs. Currently, molecular genetic methods in this setting are employed mainly as a backup for confirmation of positive results ascertained by less expensive and more comprehensive biochemical or enzymatic methods, but this situation could reverse itself as molecular methods become increasingly cost-effective, high-throughput, and comprehensive. Ascertaining the actual mutations in the affected gene can offer additional information as to potential severity and drug response beyond the mere diagnosis produced through biochemical methods. Moreover, as NGS becomes increasingly less costly, it is not such a stretch to predict that all newborns may someday undergo a full-genome analysis as a matter of course—though whether and which results get reported out at that age will be a subject of intense debate.

Diagnostic genetic testing is, by definition, performed on a symptomatic individual. Because the single-gene DNA tests are absolutely disease-specific and the diseases themselves quite rare, these procedures do not cast a wide enough net to be used for extensive differential diagnosis. The symptoms must be sufficiently suggestive of the disorder in question to justify ordering the test. Also, one must weigh the DNA test against more traditional methods with regard to cost, convenience, and utility. For example, hemoglobin (Hb) electrophoresis may be more convenient and comprehensive for sorting out a suspected hemoglobinopathy than the specific DNA test for the sickle cell disease or thalassemia mutations alone.

On the other hand, molecular testing may be more advantageous for early or atypical clinical presentations. For example, molecular testing CF mutations can be performed in the newborn period when traditional sweat chloride analysis is either inconvenient or unreliable. In such cases, it is also important to determine that the mutation spectrum of the test represents the appropriate demographic. If not, a "negative" test may not be truly accurate. DNA tests also have the advantage of working well postmortem, when classic biochemical analytes can no longer be assessed.

Presymptomatic DNA testing is applied primarily to late-onset dominant disorders, in which the offspring of an affected parent are aware that they are at 50% risk of having inherited the disease gene and desire to know their status before its clinical onset to make informed reproductive, employment, and lifestyle decisions or to initiate surveillance or preventive interventions. The prototypic disorders in this group are Huntington disease and the heritable cancer syndromes, although such diseases as neurofibromatosis, Marfan syndrome, adult polycystic kidney disease, and tuberous sclerosis are also relevant. This sort of testing has been the most problematic, from a psychosocial and ethical standpoint, of any in diagnostic molecular genetics, with a risk of severe adverse consequences of results reporting, including insurance and employment discrimination and even suicide. Because of this, established testing protocols include stipulations for proper informed consent, concurrent clinical assessment, extensive pretest and posttest genetic counseling, and psychosocial support (Huntington's Disease Society of America, 1989; American College of Medical Genetics, 1999).

Finally, there is the clinical application, which accounts for a large proportion of medical genetics services: *prenatal testing*, or the detection of genetic disease in the fetus. With a few exceptions (e.g., hydrops fetalis in homozygous β-thalassemia, thanatophoric dwarfism and other skeletal dysplasias, and type I osteogenesis imperfecta), most Mendelian disorders, especially inborn errors of metabolism, are not expressed either visibly (by ultrasound) or biochemically in the fetus. Thus, predictive diagnosis can be made only at the DNA level. Even for those disorders that might be detected biochemically, DNA often proves to be a far more accessible substrate, from an obstetric point of view, than the affected protein products or metabolic substrates. Whereas molecular analysis can be performed on minute amounts of amniotic fluid or chorionic villus samples collected by routine methods, even if obtained for other purposes, unless the protein product is expressed in fibroblasts (and thus amniocytes), biochemical analysis will require invasive biopsy of deep fetal tissues or fetal blood sampling. For example, assay of phenylalanine hydroxylase activity to diagnose phenylketonuria would require fetal liver biopsy, and quantitation of dystrophin to diagnose Duchenne muscular dystrophy (DMD) would require fetal muscle biopsy.

The primary objective in prenatal diagnosis is the identification of an affected fetus in a timely manner so that a practical option of pregnancy termination can be offered to the couple. Even though some may argue an advantage for obtaining diagnosis prenatally so that therapy can be instituted promptly at birth or for psychological reassurance of a couple if the fetus is found to be unaffected, it may be difficult to justify the risk (albeit low) of miscarriage from amniocentesis and chorionic villus sampling performed for these other purposes. For an affected fetus, unless one intends to initiate therapy *in utero*, provisional treatment at birth while awaiting confirmatory neonatal testing is perfectly acceptable.

Although prenatal genetic counseling is always nondirective, with moral and/or religious objections to abortion respected, both the clinician and the DNA testing laboratory have a legitimate right and, indeed, responsibility to question the appropriateness of a prenatal test request, with its attendant risk and expense, from a couple for whom termination is not an option (the same would apply to requests coming too late in pregnancy for termination to be performed). It is because of these problems that invasive prenatal testing is not offered as a general population screening tool in women with no family history or known carrier status for the disorder in question. The power of PCR to enable single-cell genetic analysis has opened the way for preimplantation diagnosis, usually approached by performing in vitro fertilization and microdissection of a single blastomere from the early embryo. This strategy, initially applied to selected cases at risk for CF (Handyside et al., 1992) and other disorders, could potentially be offered to any at-risk couple for whom abortion is not an option, although it is not without its own ethical (and economic) considerations. More recently, it has begun to be used to diagnose adult-onset diseases such as familial breast/ovarian cancer (*BRCA1* and *BRCA2* genes), which, because they are late onset, incompletely penetrant, and potentially treatable, would otherwise raise uncomfortable objections to traditional amniocentesis and pregnancy termination among some groups (Sagi et al., 2009).

Despite all of these medical and moral dilemmas, when performed in appropriate circumstances, prenatal molecular genetic testing can offer at-risk couples, many of whom have already suffered the trauma of at least one affected child, one of the most valuable and life-changing services in all of clinical medicine.

SPECIAL CONCEPTS UNIQUE TO MOLECULAR GENETIC DISORDERS

Whereas the DNA analysis techniques discussed in this chapter for diagnosis of genetic disease are generally the same as those used for molecular diagnosis of cancer or infectious diseases, their application in the former has revealed a number of unusual phenomena that one must keep in mind when dealing with particular hereditary disorders. Some of these phenomena have been known since Mendel's time but can now be understood mechanistically at the DNA level. Others have emerged much more recently as unexpected by-products of the molecular dissection of specific disease genes.

MOLECULAR HETEROGENEITY

Few genetic disorders are associated with a single mutation consistently identified in all affected cases (e.g., the missense mutation in codon 6 of the β-globin gene causing sickle cell disease). The vast majority of genetic disorders can be caused by more than one—sometimes hundreds or thousands—of different mutations within the disease gene (e.g., the *CFTR* gene of CF), and sometimes even by more than one gene (e.g., the *TSC1* and *TSC2* genes of tuberous sclerosis or the *BRCA1* and *BRCA2* genes of familial breast/ovarian cancer). Obviously, identifying the causative mutations in such disorders is technically much more difficult or sometimes impossible. A corollary of such molecular heterogeneity is that not all of the mutations will produce equally severe disease. Some may cause only mild forms or related syndromes, with little resemblance to the classic phenotype (e.g., isolated congenital absence of the vas deferens caused by certain mutations in the *CFTR* gene, or either multiple endocrine neoplasia or Hirschsprung disease caused by different mutations in the *RET* gene). All of this variability adds greatly to the complexity of genetic counseling and genetic testing.

VARIABLE PENETRANCE AND EXPRESSIVITY

Penetrance refers to the proportion of individuals who, having inherited a mutant disease gene, will actually display the disease phenotype. Usually applied to dominant disorders, it can produce the striking appearance of generation-skipping in disease pedigrees. This can complicate both molecular diagnostics and genetic counseling, because it may not be clear whether the proband inherited the disease from a parent or instead represents a new mutation in the family. It is a feature of such relatively common genetic disorders as Marfan syndrome and neurofibromatosis.

Variable expressivity refers to the appearance of different signs, symptoms, and severity of a disorder in individuals inheriting the same mutation(s). Like penetrance, it is probably a reflection of differential gene effects within dissimilar genetic backgrounds (in other words, the modulation of phenotypic expression by other nonallelic or *modifier* genes). It, too, makes ascertainment and counseling difficult, and raises ethical challenges in considering pregnancy termination for diseases of variable and unpredictable severity (see earlier discussion of expanded carrier screening).

UNIPARENTAL DISOMY

This unusual cause of a recessive single-gene disorder was first discovered in a CF patient, only one of whose parents was a carrier (Spence et al., 1988). By DNA haplotyping using polymorphic markers, it was shown that the patient had inherited two copies of the carrier parent's chromosome 7 containing the mutant *CFTR* gene and no chromosome 7 from the other parent. The phenomenon has since been observed in other cases of CF and diseases involving other chromosomes as well. For some diseases, such as Prader-Willi and Angelman syndromes (see later discussion), the incidence of uniparental disomy approaches that of classic mutation mechanisms in the molecular pathogenesis, justifying routine testing for this phenomenon (typically by haplotyping the pair of chromosomes for shared polymorphic markers or, in some cases, by methylation analysis).

IMPRINTING

Imprinting refers to the differential expression of a gene in an offspring depending on whether it was inherited from the mother or the father, or

sometimes on other epigenetic influences. Some genes are expressed—or, conversely, turned off—only when they pass through the oocyte lineage and others only when they pass through the spermatocyte line. If an individual inherits the normal allele through the nonexpressing parental line, it cannot counteract a recessive mutation inherited from the other parent. In at least some cases, the molecular mechanism appears to be differential methylation of chromosome regions and regulatory elements. This is the basis for both the deletional and uniparental disomy cases of Prader-Willi and Angelman syndromes, as discussed in more detail later (Gurrieri & Accadia, 2009).

ANTICIPATION

Anticipation refers to a progressive increase in severity and/or decrease in age of onset of a genetic disorder in subsequent generations of a family. It is typically associated with the trinucleotide repeat disorders, such as myotonic dystrophy and Huntington disease, in which the increasing severity can be correlated with further expansion of the repeat region. In the former disease, especially severe cases with childhood or infantile onset, they have been born to affected mothers, while in the latter disease the phenomenon occurs solely with affected paternal transmission, invoking a parent-of-origin effect similar to imprinting (Koshy & Zoghbi, 1997). It is for these reasons that accurate molecular sizing of trinucleotide repeat lengths is so important for diagnosis, prognosis, and genetic counseling in these disorders.

EPIGENETIC INFLUENCES AND NONMENDELIAN INHERITANCE

Epigenetic changes are heritable but potentially reversible changes in gene expression that do not represent a change in the sequence of the cell's genomic DNA. The most striking examples of epigenetic inheritance are genomic imprinting (discussed previously) and mammalian X-chromosome inactivation, both involving transcriptional silencing of genes by methylation of cytosines at CpG dinucleotides. The methylation status of DNA is maintained following DNA replication by methylases, which act on hemimethylated double-stranded DNA to methylate the newly synthesized DNA strand as well. The process is perpetuated indefinitely in succeeding cell divisions. We now know that de novo methylation of CpG doublets can occur in the promoters of some tumor suppressor genes, silencing these genes and in essence constituting one or both of the "hits" in a tumor suppressor gene that leads to tumor development (Jacinto & Esteller, 2007).

Another category of epigenetic inheritance that is less clearly understood involves the property of some proteins to influence the conformation of newly synthesized or assembled proteins in a self-perpetuating manner. The most notable examples in mammals are the prion diseases, responsible for scrapie and bovine spongiform encephalopathy in animals and kuru and Creutzfeldt-Jakob disease in humans. The disease-producing prion protein, which may result from a coding sequence mutation in familial cases, is folded into an abnormal conformation and exerts an effect on newly synthesized prions in such a way that it perpetuates and proliferates the conformational abnormality that produces disease (Cobb & Surewicz, 2009).

ALLELE FREQUENCIES AND MASS POPULATION SCREENING

Reference has already been made to the application of carrier screening for recessive mutations on a population-wide basis. To justify, from a public health standpoint, the effort and expenditure required to perform a DNA test on thousands or millions of people, the incidence of the disease must be sufficiently high either in the whole population or in the particular racial or ethnic groups being selected for screening. For any autosomal-recessive disease of appreciable incidence, the law of Hardy-Weinberg equilibrium predicts that the carrier frequency will be a good deal higher than the prevalence of affected individuals. In addition, the candidate disease target must be sufficiently severe and/or amenable to some medical intervention upon identification. Several disorders appear to fit these criteria. Mutations associated with hereditary hemochromatosis and activated protein C resistance (factor V Leiden) are found in 5% to 10% of the white population, while the carrier frequency of the sickle cell mutation approaches 10% in the African American population. Unfortunately, controversies over disease penetrance in the first two and complex socioeconomic issues in the third have limited the application of these genes to screening (U.S. Preventive Services Task Force, 2006; Zhang et al., 2018). Screening for thalassemia in Mediterranean and Asian populations, and for a panel of recessive disorders such as Tay-Sachs disease and Gaucher disease in the Ashkenazi-Jewish population, is similarly justified by allele frequencies in the target group. CF mutations, while of lower frequency, potentially place such a large majority of North American couples at risk that they have been chosen as the first target for general molecular genetic population screening in the United States (see later discussion). Other disease targets proposed for large-scale screening include spinal muscular atrophy, fragile X syndrome, and hereditary hearing loss. This migration of molecular genetic screening out of the realm of rare or esoteric diseases and into the setting of common traits will have a profound effect on preventive medicine and public health, and will continue to drive new developments in DNA test automation in the coming years.

PREDICTIVE GENETIC TESTING

Unique among molecular pathology tests—and, indeed, among clinical laboratory tests in general—molecular genetic tests possess the ability to predict future disease in individuals with no signs or symptoms of the disorder at the time of testing. This predictive ability exceeds that imparted to such tests as human immunodeficiency virus antibody screening in individuals with no symptoms of acquired immunodeficiency syndrome, cholesterol levels as a risk factor for future atherosclerosis, or detection of abnormal metabolites by newborn screening. For those tests, one could argue that the serologic, microbiological, or biochemical signs of the disorder are already present, even if the patient does not yet experience any symptoms. Molecular genetic testing, in contrast, enables prediction of future disease even in the absence of *any* biochemical or physiologic abnormalities: Huntington disease can be predicted decades before there is any brain degeneration, and breast cancer risk years or decades before even a single breast epithelial cell has turned malignant. The potential psychosocial impact of revealing such information to a healthy individual cannot be overemphasized. For that reason, it is highly recommended that predictive or presymptomatic genetic testing be accompanied by pretest and posttest genetic counseling and psychiatric support, as already mentioned. Furthermore, such tests should be restricted to those who truly have an actionable need for them, in the sense that a positive DNA test will prompt some sort of early surveillance or preventive interventions or, at the very least, some guided lifestyle or life-planning changes. Because it is difficult to imagine such conditions existing in the case of a child tested for an unpreventable adult-onset disease, there is a strong convention in the field that healthy children younger than 18 years of age should not be offered predictive genetic tests for adult-onset disorders unless there is a demonstrated preventive intervention that needs to be acted upon in childhood. This will avoid potential stigmatization, discrimination, or adverse psychosocial effects of genetic information that is of no medical use to the child (Holtzman et al., 1997).

SPECIFIC DISEASE EXAMPLES

CYSTIC FIBROSIS

Because of its high carrier frequency in North America and northern Europe, its serious clinical nature, its straightforward Mendelian (autosomal-recessive) inheritance pattern, and its well-studied yet complex gene, CF has emerged as the paradigmatic disorder for large-scale molecular genetic screening. Within its scope can be found the full panoply of applicable molecular genetic techniques and the full spectrum of scientific and ethical dilemmas arising from the clinical variability of the disease, the extreme molecular heterogeneity of the causative mutations, and the advent of novel treatments, including mutation-specific targeting drugs (Egan, 2020) and, eventually, gene replacement therapy. With a carrier frequency as high as 1 in 29 in whites of northern European ancestry (and progressively less in southern Europeans, Hispanics, African Americans, and Asians), there was ample motivation to screen the general population in order to identify couples at 1-in-4 risk of having an affected child with each pregnancy. But because carriers are asymptomatic and have normal sweat chloride levels, this screening could only be done after isolation of the gene in 1989 (Kerem et al., 1989; Riordan et al., 1989). Even though the gene had been mapped to chromosome 7 some years earlier, allowing for prenatal diagnosis by linkage analysis in informative families, screening and testing in others, especially those with no family history of the disorder, could only be considered once the gene was cloned and the mutations identified.

Even with that laudable accomplishment, however, the history of DNA testing for CF has been fraught with challenges and controversies. The gene is more than 250,000 bp long and encodes a large ion channel protein

TABLE 72.1

Recommended Core Mutation Panel for General Population Cystic Fibrosis Carrier Screening

ΔF508	ΔI507	G542X	G551D	W1282X	N1303K
R553X	621+1G>T	R117H	1717–1G>A	A455E	R560T
R1162X	G85E	R334W	R347P	711+1G>T	1898+1G>A
2184delA	1078delT*	3849+	2789+5G>A	3659delC	I148T*
10kbC>T3120+1G>A					

Panel recommended by the American College of Medical Genetics (Grody, 2001a).
*Mutations subsequently removed from the panel (Watson, 2004).

called the cystic fibrosis transmembrane conductance regulator (CFTR) (Collins, 1992). Most notably, the spectrum of mutations observed is remarkably heterogeneous. Whereas a three-nucleotide deletion of phenylalanine codon 508 (designated ΔF508 or F508del) accounts for about 70% of the mutations in non-Hispanic whites (and less in other ethnic/racial groups), more than 2000 additional mutations have been reported so far. Most of these are so rare that it is neither feasible nor cost-effective to include them in testing panels. Only about 7 (in addition to ΔF508) account for more than 1% each of CF mutations in most white populations (Tsui, 1992) (Table 72.1). The sensitivity of carrier screening with mutation panels of between 6 and 25 alleles ranges from a high of 97% in Ashkenazi Jews (Abeliovich et al., 1992) to 75% to 90% in non–Ashkenazi North American whites, about 60% in Hispanic Americans, 50% in African Americans, and less than 10% in Asians (Ober et al., 1992; Grebe et al., 1994; Macek et al., 1997). Such variable and suboptimal sensitivity in an ethnically heterogeneous population such as that of the United States and the difficulties involved in counseling patients as to the residual carrier risk of negative test results made population-based carrier screening for CF mutations a controversial subject (Grody, 1999). After much debate and several pilot screening studies, a consensus conference recommended that screening be offered to all pregnant couples and those planning pregnancy (NIH Consensus Statement Online, 1997). A steering committee representing the American College of Medical Genetics (ACMG), the American College of Obstetricians and Gynecologists (ACOG), and the National Human Genome Research Institute decided on a core screening panel of the 25 most prevalent mutations in the general mixed population (Grody et al., 2001a). The same group produced accompanying educational materials providing guidance to obstetricians on how the screening test should be offered, patient education brochures, and tables for determining the residual risk in those whose test results are negative.

With the launch of these guidelines in 2001 and given the number of births every year, *CFTR* mutation analysis instantly became the highest volume molecular genetic test and one of the highest in all of molecular diagnostics. A wide variety of molecular methods, which incorporate at least the core panel of 25 mutations (revised downward to 23 in 2004 by Watson et al., 2004), and sometimes more, include ASO probe hybridization, microbead arrays, allele-specific PCR, Sanger sequencing and, most recently, NGS (Grosu et al., 2014; Brennan & Schrijver, 2016). The last technique has enabled complete gene sequencing to be used for both carrier screening and diagnosis by either a targeted or comprehensive approach. In fact, the first U.S. Food and Drug Administration–approved in vitro diagnostic using NGS for a genetic disorder was a targeted assay for 139 *CFTR* mutations (Grosu et al., 2014). The power of NGS has proven difficult to resist and has compelled ACMG itself to revisit the core mutation panel and open the option for untargeted full-gene sequencing in the carrier screening setting (full-gene sequencing has long been accepted for diagnosis of symptomatic or atypical patients) (Deignan et al., 2020). However, this unavoidably raises the question of whether and how to report variants of uncertain significance (VUSs) in the gene to a pregnant couple with little time to make an irreversible decision (Grody et al., 2007). The same challenge has arisen with ever-expanding gene panels used for universal carrier screening beyond CF (Grody, 2016) (see later discussion).

Another problem with genetic counseling for CF is the variable clinical severity of the disorder and the inconsistency of genotype–phenotype correlations. Beyond the finding that ΔF508 homozygotes tend to have pancreatic insufficiency, there is little about disease severity or complications that can be predicted reliably from knowing an affected individual's two mutations (Moskowitz et al., 2008). Even homozygotes for ΔF508, considered the prototypical severe mutation, can show a range in their degree of pulmonary compromise (Burke et al., 1992). Conversely, there are mutations that cause pulmonary disease yet maintain normal sweat chloride levels (Highsmith et al., 1994), and there are mutations and polymorphisms (e.g., R117H coupled with certain lengths of an intronic polythymidine tract) that do not cause CF at all but rather male infertility due to congenital absence of the vas deferens (Anguiano et al., 1992; Gervais et al., 1993). Taken together with the ever-increasing median lifespan of CF patients and the advent of new biological therapies, these factors render genetic counseling and reproductive decision-making for the disorder difficult. However, a powerful resource now exists, called CFTR2, a database resulting from the meticulous study—by phenotypic, genetic, and physiologic methods—of over 400 known variants in the *CFTR* gene and their predicted pathogenicity and expressivity (Raraigh et al., 2018; https://cftr2.org/). It would be wonderful if other important genetic disease genes had such a resource, but for now this remains the only one that is so comprehensive. CF is one of the targets of universal newborn screening in all 50 states, along with a large panel of metabolic disorders. Protocols vary by state but, in most cases, begin with a biochemical screen for immunoreactive trypsinogen followed by (in positive specimens) molecular testing for anywhere from one to more than 30 mutations. It is important to remember that the mutation panels chosen for newborn screening are up to the individual states and are not tied in any way to the ACMG/ACOG panel developed for population carrier screening. Likewise, mutations tested in the course of diagnostic workup of a symptomatic patient are also flexible (in the sense that they have never been defined by professional guidelines) and may range from just a few ethnic-specific mutations to complete gene sequencing.

CF is one of the first genetic diseases for which specific mutation-targeted therapies have come to market. These drugs, which are designed to circumvent the biochemical or posttranslational process defect caused by the mutation(s), are collectively called "CFTR modulators" (Derichs, 2013). They represent an elegant example of "personalized medicine" in that the treatment is tailored to the patient's specific, personal mutation(s). For this reason, the precise identification of a patient's mutations becomes even more important. Using a cocktail of targeted drugs, the majority of CF patients are now candidates for such treatment. Their promise can alter couples' attitudes toward prenatal carrier screening and prenatal diagnosis as they begin to see CF as a more treatable disease (Massie et al., 2014).

DUCHENNE MUSCULAR DYSTROPHY

This X-linked progressive myopathy was the first disorder whose causative gene was isolated by the process of positional cloning (Rowland, 1988). Before that discovery, the only tests that could be offered to at-risk families were detection of some female carriers by the finding of elevated serum creatine phosphokinase levels, followed by prenatal sex determination with the option to terminate a male fetus (even though 50% of these pregnancies would be normal). Genetic counseling was rendered even more problematic because about one-third of cases of DMD arise from new mutations.

Even after its discovery, translation to clinical application was not easy because the gene, dubbed *dystrophin*, proved to be one of the largest yet discovered, spanning 2.4 million bp and composed of 79 exons (Ahn & Kunkel, 1993). Use of full-length or partial cDNA probes to detect the variety of deletions accounting for two-thirds of cases was labor-intensive and time-consuming (Darras et al., 1988; Prior, 1991). It was only with the advent of multiplex PCR, described in Chapter 69, that a system was developed for rapid and inexpensive identification of more than 98% of dystrophin deletions and their localization to specific exons of the gene (Beggs et al., 1990; Multicenter Study Group, 1992). In this system, a deletion is identified by absence of one or more of the multiple expected amplicons on ethidium bromide–stained electrophoresis gels or capillary electrophoresis instruments (because a target gene deletion will abolish the hybridization site[s] of one or more primers, causing PCR failure; Fig. 72.2). Such fine-structure mapping combined with sequencing has also revealed important insights into the molecular pathogenesis of DMD and the milder allelic variant, Becker muscular dystrophy (BMD). Both are most often caused by large dystrophin deletions, but those in BMD typically preserve the

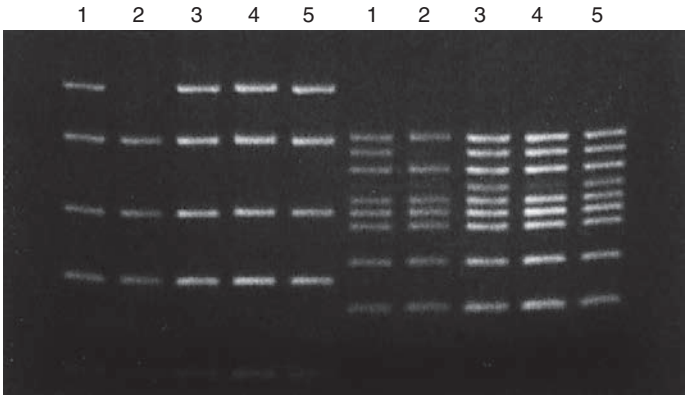

Figure 72.2 Multiplex polymerase chain reaction (PCR) analysis for dystrophin gene deletions in Duchenne muscular dystrophy. DNA samples from five patients were amplified simultaneously with five primer pairs (*left half of gel*) and nine primer pairs (*right half of gel*) and the products were analyzed by polyacrylamide gel electrophoresis. Absence of an expected PCR product band is indicative of a deletion. Patient 2 lacks the top band in the five-plex and the second-from-top band in the nine-plex. These correspond to deletions in exons 50 and 48, respectively, in the dystrophin gene. (Band 4 in the nine-plex is light but present in all of the samples.) (Courtesy of Dr. Kathryn E. Kronquist.)

correct reading frame in the resulting processed transcript, while deletions in DMD more often produce frameshift mutations and a more truncated protein product (Monaco et al., 1988).

The remaining one-third of patients with DMD and 15% of patients with BMD in whom no deletion is detected usually have point mutations or microdeletions/insertions. Because the gene is so large, it was until recently not an easy matter to identify these lesions directly, but now it is readily accomplished by NGS (Nallamilli et al., 2014). Alternatively, studies at the protein level can be performed by observing decreased or absent dystrophin in DMD and dystrophin of abnormal molecular weight in BMD by Western blot or immunohistochemistry in muscle biopsy tissue (Hoffman et al., 1988). This procedure has serious limitations for prenatal diagnosis, for which a fetal muscle biopsy would be required, but it can be used for proband diagnosis. Thus, the molecular diagnosis of DMD has come full circle: from identification of the gene without knowing the protein product (formerly called *reverse genetics*) to identification and diagnostic use of the protein product from knowing the gene. This sort of evolution occurred with a number of other genetic diseases prior to the completion of the Human Genome Project, when *forward genetics*, starting with the gene itself, became feasible. Furthermore, as in CF, our knowledge of the gene and its protein product have led to the development of mutation-targeted drugs for DMD. Since the dystrophin gene is so large, a prime therapeutic target has been the spliceosome, using antisense oligonucleotides to produce "skipping" of the exon containing the mutation, as the gene can remain functional even with that loss (Dzierlega & Yokota, 2020).

SPINAL MUSCULAR ATROPHY

Spinal muscular atrophy (SMA) is a neuromuscular disorder, the second most common lethal autosomal-recessive disorder after CF in Western countries, with carrier frequency ranging from 1 in 40 to 1 in 80 depending on ethnicity. As such, it has long been discussed as a potential target for universal carrier screening along the lines of CF. Progress has been hindered, however, by both technical and clinical challenges. The most common mutation is homozygous deletion of exon 7 of the *SMN1* gene, which is difficult to determine by DNA sequencing because of the presence of one or more copies of a highly homologous pseudogene called *SMN2*. Furthermore, the number of copies of *SMN2* can modify the severity of the symptoms (since that gene can produce a partially active protein product), requiring copy-number analysis of the pseudogene for genotype-phenotype prediction. For those reasons, there was hesitancy among professional organizations to mandate widespread population carrier screening. It was first recommended by the ACMG in 2008 (Prior, 2008), while the ACOG did not fully endorse it until 2017 (American College of Obstetricians and Gynecologists, 2017). At the time of this writing, it is still not commonly offered, at least as a standalone screening test (it may be included in some expanded carrier screening panels). Detection of the *SMN1* deletion and the *SMN2* copy number usually requires some form of quantitative and allele-specific PCR and/or MLPA (Ojino & Wilson, 2004; Prior, 2010), but recent refinements in genomic sequencing can now enable a one-step procedure (Chen et al., 2020). NGS also enables detection of the small percentage of SMA patients who carry a small intragenic mutation in one allele.

SICKLE CELL ANEMIA AND OTHER HEMOGLOBINOPATHIES

Given the long history of study of the protein product, diagnosis of molecular defects in the genes encoding the globin polypeptides did not come about through techniques of reverse genetics. Rather, these genes were cloned by classic methods, using antiglobin antibodies for polysome precipitation to isolate the relevant messenger ribonucleic acids (mRNAs). As such, Hb mutations, and the one causing sickle cell anemia in particular, were among the very first to be diagnosed at the DNA level, even though most large-scale screening and diagnosis of these disorders continues to be done by hemoglobin electrophoresis and isoelectric focusing (see Chapter 33). The sickle cell point mutation in codon 6 of the β-globin gene lies within (and, thus, destroys) a restriction endonuclease cleavage site (for *Mst*II, *Mnl*I or *Dde*I), providing a rapid method of detection using either Southern blot or restriction enzyme digestion of β-globin PCR products (Hatcher et al., 1992). Alternatively, the HbS and HbA sequences can be distinguished by dot blot using allele-specific oligonucleotide probes complementary to either the normal or mutant sequence (Conner et al., 1983). At present, higher-throughput techniques have come to predominate, such as real-time PCR, MLPA, and DNA sequencing (Sabath, 2017). These DNA-based techniques can be used for diagnosis, carrier screening, or prenatal diagnosis on amniocytes, in the latter case obviating the need for invasive fetal blood sampling and classic Hb electrophoresis. In addition, with sickle cell disease now a target of universal newborn screening programs, even if done by biochemical methods, the DNA test becomes important for backup confirmation of positives and ambiguous screening results, as in compound heterozygous states involving HbS and a thalassemia mutation (Hoppe, 2013). Several studies have shown that these DNA tests can be done on the same filter-paper blood spots collected for the initial newborn screening (McCabe & McCabe, 2004). A different mutation in codon 6, causing HbC disease, does not abolish the *Mst*II restriction endonuclease recognition sequence but can be detected by any of the other methods noted.

The thalassemias involve both qualitative and quantitative alterations in one or more globin chains with hundreds of sequence variants known, and their diagnosis at the molecular level is correspondingly more complex than that of sickle cell anemia. α-Thalassemia is the more straightforward because it is usually caused by deletion of either or both of the two contiguous α (*HBA*) genes on one or the other or both chromosomes 16. This can be detected by Southern blot, MLPA, or quantitative PCR, allowing differentiation of the silent carrier state (one α gene missing) from the very severe hydrops fetalis (all four genes missing) and the two intermediate states (Zhou et al., 2013). For the minority of cases caused by point mutations, Sanger sequencing or allele-specific probe hybridization can be used.

Molecular diagnosis of β-thalassemia is more complicated because of the wide variety of promoter, missense, termination, deletion, splice site, and frameshift mutations that have been documented. However, within each at-risk population (Mediterranean, Asian, African), a limited subset of mutations (usually ≤10) accounts for the majority of cases and carriers. Therefore, testing with a panel of mutation-specific probes/primers, along the lines of CF screening, is reasonable (Naja et al., 2004; Patrinos et al., 2005). In addition, the β-globin gene is not that large; thus, Sanger sequencing can be employed for nontargeted diagnostic testing. While both classes of thalassemia can also be diagnosed at the protein level by hemoglobin electrophoresis, molecular analysis is especially helpful for those patients with indeterminate electrophoresis profiles and to conclusively distinguish heterozygotes from homozygotes.

HEREDITARY THROMBOPHILIAS

CF is not the only disorder with sufficiently high mutation frequency to prompt consideration for population screening using molecular methods. Several other disease genes have revealed carrier frequencies several times higher than that for CF. Included in this group are genes involved in the anticoagulant system, which, as discussed in Part 5, keeps the clotting cascade in check. The most common such allele is the factor V Leiden mutation, a single-nucleotide change causing an amino acid substitution (R506Q) in the clotting factor V protein, rendering it resistant to cleavage by activated protein C (APC) (Bertina et al., 1994). The allele is carried in 5% to 7% of the white population and is responsible for more than 90% of clinical APC resistance, resulting in a tendency toward idiopathic venous thromboembolism (Ridker et al., 1997a). It produces a relative risk of thrombosis of about 7-fold in the heterozygous state and about 80-fold

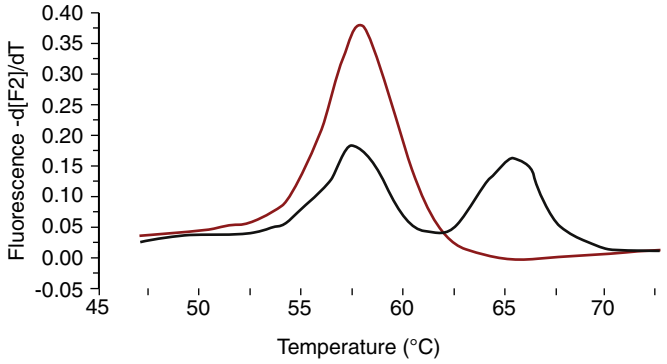

Figure 72.3 Detection of the factor V Leiden mutation by real-time polymerase chain reaction (PCR) and melting curve analysis. Mismatch of the amplified mutant allele lowers the melting temperature when hybridized with a wild-type DNA probe. The *black line* indicates the melting curve profile for an R506Q heterozygote, whereas the *red line* represents a homozygous mutant sample.

in the homozygous state. It is also associated with pregnancy complications such as recurrent miscarriage. Automated methods for high-throughput testing have been developed, such as real-time PCR (Fig. 72.3), microarray hybridization, and rapid sequencing platforms.

As for CF, however, there are controversies over which patients should be offered screening. Despite the dramatically increased relative risk, the absolute risk conferred by this mutation is rather low, with a lifetime penetrance for thrombotic symptoms of about 10%. Therefore, most carriers would not be candidates for anticoagulant therapy, with its risks of hemorrhage and stroke. Thus, it is uncertain whether such screening would alter patient management in a meaningful way. Some have proposed screening individuals with environmental risk factors known to act synergistically with the factor V Leiden risk, such as women on oral contraceptives. Yet here, too, it could be argued that obligating such women with positive test results to turn to less effective methods of birth control might cause more harm than good. For example, this could increase the pregnancy rate, with its own attendant complications, some of which are thrombotic in nature (Kupferminc et al., 1999). At present, most requests received by molecular genetics laboratories for factor V Leiden testing are on patients who have already experienced an otherwise unexplained thromboembolic event. Two professional consensus statements, by the ACMG and the College of American Pathologists (CAP), have designated this (in otherwise healthy patients under 50 years old) as the primary unequivocal indication for testing (Grody et al., 2001b; Press et al., 2002; Zhang et al., 2018).

Along with factor V Leiden, there are other inherited mutations of high allele frequency that confer thrombotic risk (also discussed in Part 5). The prothrombin 20210A variant, a single nucleotide change in the 3′ gene now more properly designated factor II c.*97G>A, results in increased circulating prothrombin levels and a phenotype similar to that of factor V Leiden. It is present in 1% to 2% of the general population (Poort et al., 1996). The 677C→T variant of methylenetetrahydrofolate reductase, an enzyme involved in the folate cycle of homocysteine metabolism, is carried by 30% to 40% of the general population and is associated with elevated plasma homocysteine levels and theoretical risk of vascular (including coronary artery) thrombosis. Indications for this test are even more nebulous because not everyone with the variant has hyperhomocysteinemia, and not all hyperhomocysteinemia is caused by this variant. Thus, biochemical measurement of plasma homocysteine levels may be a more effective screening method. Also, folate fortification of foods may make the genetic factor less relevant by broadly reducing homocysteine levels in the population. More recent studies have even called into question whether there is any relationship at all between homocysteine levels and thrombotic risk (Ducros et al., 2009), with the result that many molecular pathology laboratories have dropped the MTHFR test from their menus. Still, it continues to be ordered by some clinicians, even for putative risk for conditions beyond thrombophilia, such as migraine and psychiatric disorders (Wan et al., 2018). Furthermore, mutations in each of these genes can act synergistically; thus, patients carrying two or even three of these defects, including the rarer deficiencies of protein S and C, may find themselves at significantly increased risk (Koeleman et al., 1994; Ridker et al., 1997b).

HEREDITARY HEMOCHROMATOSIS

Hereditary hemochromatosis, first recognized in its full clinical expression as the triad of cirrhosis, diabetes mellitus, and bronzing of the skin, was originally thought to be a rare disorder of iron overload affecting about 1 in 5000 or fewer whites. However, when genetic studies linked the disease-causing gene to the HLA locus on chromosome 6, and biochemical tests of iron overload (principally, transferrin saturation) were utilized, it was recognized that the underlying genetic predisposition to iron overload was extremely common. Hereditary hemochromatosis is now recognized as an autosomal-recessive disorder with a carrier frequency as high as one in eight in people of northern European descent, making it the most common genetic disorder in the U.S. white population. The incidence of at-risk homozygotes is 1 in 250, but only a fraction of these accumulate sufficient excess iron to produce the tissue injury associated with the classic disorder.

Our understanding of hereditary hemochromatosis entered a new era with the identification of the *HFE* gene (initially called *HLA-H*) within the major histocompatibility locus on chromosome 6 (Feder et al., 1996). The HFE protein, although it is a major histocompatibility complex class I-like molecule, does not bind and present endogenous peptides and is not thought to have an immunologic function. Rather, evidence indicates that the HFE protein interacts with the transferrin receptor and modulates enteric absorption of dietary iron (Waheed et al., 1999). Mutations in *HFE* impair this regulatory function, leading to excess iron absorption and storage in tissues.

A single missense mutation in *HFE*, C282Y, which results in a tyrosine substitution for cystine at amino acid 282 in the HFE protein, is present in the homozygous state in 80% to 90% of whites with hemochromatosis. An additional small percentage of patients with hemochromatosis are compound heterozygotes, carrying one allele with the C282Y mutation and another with an H63D mutation. H63D is a common variant, with a carrier frequency of approximately 20%; its association with iron overload is very low (1%–2%) in the compound heterozygous state and probably even lower when homozygous (Gochee et al., 2002). Over the years since its discovery, the penetrance of the C282Y homozygous state has also been questioned and may be appreciably lower than the 80% quoted earlier, perhaps as low as 10% or even 1% (Beutler et al., 2002; Pietrangelo, 2004). For this reason, population screening for these mutations in individuals with no clinical or biochemical signs of hemochromatosis has not been recommended. Similar to what was discussed for factor V Leiden earlier, the DNA test is best reserved for differential diagnosis in patients already exhibiting the clinical disorder or elevated transferrin saturation detected on biochemical screening. The C282Y and H63D mutations are single-nucleotide substitutions and may be analyzed easily by a variety of PCR, real-time PCR, microarray, microplate, or sequencing methods. There are a number of other genes involved in iron metabolism, such as hepcidin, ferroportin, and hemojuvelin, but mutations in these genes are not common enough to justify widespread testing at present (Kowdley et al., 2019).

TRINUCLEOTIDE REPEAT EXPANSION DISORDERS

An important class of disease-causing mutations was revealed in 1991 with the discovery that X-linked spinal and bulbar muscular atrophy (SBMA; Kennedy's disease) and fragile X syndrome (FRAXA) are associated with tandem expansion of unstable trinucleotide repeat sequences in the androgen receptor (*AR*) and *FMR1* (fragile X mental retardation) genes, respectively. Since that time, similar disease-producing mutations have been associated with an ever-increasing number of additional neurologic and muscle disorders (Table 72.2). The affected gene in each of these disorders normally contains a repeated sequence of 3 bp: for example, $(CGG)_n$ in the *FMR1* gene, where *n* is variable but normally limited in its range. In the disease state, however, the size of the triplet repeat is expanded outside the normal range, sometimes only slightly and in other instances markedly. The mechanisms by which these expanded repeat sequences produce disease are various, and include gene silencing, inhibition of RNA processing, and toxic gain-of-function by mutant proteins.

Fragile X Syndrome

Fragile X syndrome (FRAXA) is said to be the most common single-gene defect causing moderate to severe mental retardation. Affected males with this X-linked disorder typically also exhibit dysmorphic features, including large ears, a long face, prominent jaw, and (at puberty) macroorchidism. Approximately 1 in 2500 females are heterozygous carriers of the FRAXA mutation, and one-third of these may show evidence of mental impairment or learning disability in the absence of the classic dysmorphism seen in affected males.

As explained in Chapter 71, the cytogenetic hallmark of FRAXA is a fragile site on the X chromosome at Xq27.3 resulting from a failure of normal chromatin condensation during mitosis. Although the inheritance pattern of the disease is clearly X-linked, it does not correspond in a

straightforward manner to either a recessive or dominant pattern of gene expression. Before the molecular mechanism was elucidated, the most puzzling feature had been the presence of phenotypically normal men (transmitting males) who are obligate carriers of the genetic abnormality. These men are sons of proven FRAXA carriers, they pass the carrier state to all of their daughters, and their daughters, in turn, transmit the fully expressed disease to a high proportion of their sons.

The discovery in 1991 of the genetic abnormality that causes FRAXA immediately explained its unusual pattern of inheritance, which had been dubbed the "Sherman Paradox" (Macpherson & Murray, 2016). The 5′-untranslated region of the *FMR1* gene at chromosome Xq27.3 carries a $(CGG)_n$ triplet repeat of variable size. In normal individuals, *n* ranges up to about 54, but in individuals with clinically apparent FRAXA, *n* is greater than 200 (referred to as a *full mutation*). Both men and women who carry an X chromosome where *n* is between 55 and 199 (referred to as a *premutation*) do not show signs of classic fragile X syndrome but are at risk of passing an allele of even larger size to their children. This is because of the instability of the premutation alleles and their tendency to increase in size during the meiotic cell divisions that produce the female gametes. Alleles of normal size are not unstable and generally pass unchanged, although there is now recognized a so-called "gray area" of repeats between 45 and 54 that has a low risk of slight expansion into the premutation range (Kronquist et al., 2008). Thus, it appears that there is a pool of small premutation (and gray area) alleles in the population, possibly of ancient origin, that is at risk of undergoing further expansion with each passage through another generation. As the premutation allele increases in size, the likelihood that it will expand further in the next generation increases, ranging from very low likelihood for repeats in the 60s to almost 100% for repeats above 100 (Nolin et al., 2003). In addition, interruptions of the CGG repeat by one or more AGG units serves to stabilize the permutation and inhibit its expansion into the full mutation range (Nolin et al., 2014), though testing for this requires DNA sequencing rather than simple sizing of the repeat length and is not offered routinely by molecular diagnostic laboratories. Curiously, expansion to a full mutation occurs only in female meiosis, never in males, which corresponds to the observation that the daughters of normal transmitting males are always phenotypically normal. Fig. 72.4B illustrates a family with FRAXA: a premutation allele is transmitted from the first to the second generation and then expands to a full mutation in the third generation.

The mechanism by which the expanded triplet repeat in the 5′-noncoding region of the *FMR1* gene produces the FRAXA phenotype is under active investigation. As the size of the repeat expands, there is progressive methylation of the regulatory region of the *FMR1* gene and decreased expression of FMR-1 protein. This RNA-binding protein is widely expressed in the developing brain and in other tissues. Its loss of expression in FRAXA presumably disturbs normal brain development and leads to mental retardation. Rare patients with typical fragile X syndrome do not have triplet repeat expansion or gene hypermethylation but do have inactivating point mutations or deletions leading to loss of FMR1 protein expression. Conversely, rare phenotypically normal or high-functioning males with full *FMR1* gene repeat expansions and cytogenetically visible fragile sites, but with no gene hypermethylation and normal FMR1 protein expression, have been described (Hagerman et al., 1994; Smeets et al., 1995). These findings all support the hypothesis that it is lack of FMR1 protein expression, usually caused by hypermethylation-related down-regulation of gene transcription, that is responsible for the disease phenotype.

Because the premutation is not methylated and the phenomenon of "normal" transmitting males was widely observed, it was long assumed that these alleles had no direct phenotypic effect. It was therefore quite surprising when more recent studies documented cases of premature ovarian failure and an unusual tremor-ataxia-dementia syndrome in female and male premutation carriers, respectively. The penetrance appears to be about 20% for the former (Sherman, 2000) and as high as 75% (by age 80 years) for the latter (Jacquemont et al., 2004), although it is difficult to accurately define such numbers in the absence of molecular screening of normal populations. The molecular mechanism may be related to premutation *FMR1* mRNAs being translated less efficiently and/or interfering with translation of the normal allele or other interacting genes. These revelations have made genetic counseling for fragile X syndrome even more complicated. They also raise additional concerns regarding the ethical merits of population screening for fragile X premutations or routine testing of pregnant women, which appears to be increasing despite the absence of professional guidelines to do so (Grody, 2011). Babies born to women who have undergone testing may be identified with a potentially devastating adult-onset disease for which no known preventive intervention is possible, something that is not done for predictive genetic testing of other late-onset disorders in children for the reasons discussed in the earlier section on Predictive Genetic Testing.

Neurodegenerative Disorders: Huntington Disease, X-linked Spinal and Bulbar Muscular Atrophy, Spinocerebellar Ataxias, and Dentatorubral-Pallidoluysian Atrophy

Huntington disease, X-linked spinal and bulbar muscular atrophy (SBMA), the spinocerebellar ataxias (SCAs) and dentatorubral-pallidoluysian atrophy (DRPLA) are autosomal-dominant or X-linked (SBMA) diseases characterized by selective neuronal degeneration in the central nervous system. In each of these disorders, there is expansion of a $(CAG)_n$ trinucleotide repeat in the coding region of the respective gene that produces abnormal elongation of a polyglutamine tract. The resultant abnormal protein produces intranuclear neuronal inclusions. It is postulated that the expanded polyglutamine sequences in each of these proteins leads to alterations in their folding and binding characteristics and a gain in function that is toxic to neurons in a selective manner, causing apoptosis (Everett & Wood, 2004).

In common with the other triplet repeat disorders, the expanded repeats in the neurodegenerative disorders are unstable and tend to increase in size in subsequent generations. There is an inverse correlation between increasing repeat size and earlier age of symptomatic onset. In contrast to fragile X and myotonic dystrophy, in which the most dramatic increases in repeat size occur in maternal meioses, paternal transmission produces the largest expansions in the exonic repeat neurodegenerative disorders. Consequently, juvenile-onset cases of Huntington disease, DRPLA, and the spinocerebellar ataxias, while rare, can occur in families in which there is successive paternal transmission of the mutant gene for several generations.

Molecular diagnosis of these disorders is used for either diagnostic or, because they are late-onset, predictive purposes. Because they have no documented treatment or preventive interventions (though this may be changing with the advent of some novel clinical trials), the emotions involved in the testing and fear of a positive result are considerable, with an attendant suicide risk in some cases. For that reason, it is mandatory that presymptomatic testing for these disorders be accompanied by pre- and posttest genetic counseling along with mental health support if indicated. In those settings, it is often observed that the at-risk relatives seeking predictive genetic testing are concerned about potential insurance or employment discrimination if the result is positive. Some of these people will insist on paying for the testing out of pocket and using a pseudonym. This approach, while allowed, can cause problems down the road with identity mix-ups, inability to retrieve the result in the medical record, and so on. In addition, most patients testing positive will wish to enter one of the new clinical trials using antisense or other inhibitory small molecules to reduce the intracellular levels of the abnormal gene product. It goes without saying that in order to be candidates, they will need to produce a positive test result with their real name on it. This is yet another important topic to be discussed during the pretest counseling session, as many centers are rethinking the traditional strictly confidential approach to this testing (Eno et al., 2020).

Myotonic Dystrophy

Myotonic dystrophy, type 1, is an autosomal-dominant, multisystem disorder with a wide range of clinical expression. In late childhood or early adulthood, the most typical patients develop progressive myotonia and weakness and atrophy of the muscles of the distal extremities and face. Cataracts, cardiac conduction defects, and testicular atrophy are also common. However, the disease may be so mild as to consist solely of cataracts developing at advanced age or so severe as to present at birth with marked muscle degeneration and mental retardation proceeding to early death. Sometimes the full spectrum of the disease can be observed in the same family, occurring in a pattern that clearly reflects the phenomenon of anticipation. As noted, anticipation is present in virtually all of the trinucleotide repeat disorders, but it is most striking in myotonic dystrophy, in which the clinical phenotype can progress from cataracts to severe congenital disease in three generations.

Myotonic dystrophy is caused by expansion of a $(CTG)_n$ repeat in the 3′-untranslated region of the myotonin protein kinase (*DMPK*) gene on chromosome 19q13.3 (Fu et al., 1992; Mahadevan et al., 1992). In normal individuals, this repeat ranges in size from 5 to 35 and is genetically stable. CTG repeats greater than 50 are genetically unstable and prone to expansion as they are passed to subsequent generations. In the range of 50 to

TABLE 72.2

Disorders Characterized by Unstable Expansions of DNA Trinucleotide Repeats

Disorder	Chromosome Location	Normal Alleles, Intermediate Alleles	Expanded Alleles	Anticipation	Transmission Sex Bias	Position of Repeat	Gene Product
Fragile Site/Mental Retardation Associated with CGG or GCC Expansion (X-Linked)							
Fragile X syndrome (CGG), FRAXA	Xq27	6–54 55–200	>200	Yes	Maternal, premutation	5′-UTR	FMRP
Diseases Associated with CAG Repeat Expansion (Autosomal Dominant Except for X-Linked Kennedy Disease)							
Spinobulbar muscular atrophy (Kennedy disease)	Xq11–12	9–36	38–62		Coding	Androgen receptor	
Huntington disease	4p16	6–35 36–39	40– >150	Marked in juvenile cases	Paternal, early onset	Coding	Huntingtin
Dentatorubral-pallidoluysian atrophy	12p13	3–35	49–88	Yes	Paternal	Coding	Atrophin
Spinocerebellar ataxia 1	6p23	6–35	40–88	Marked in juvenile cases	Paternal, early onset	Coding	Ataxin 1
Spinocerebellar ataxia 2	12q24	16–31	36–77	Yes	Paternal	Coding	Ataxin 2
Spinocerebellar ataxia 3 (Machado-Joseph disease)	l4q24–q31	12–41	55–86	Yes	Paternal	Coding	Ataxin 3
Spinocerebellar ataxia 6	19p13	6–17	21–30	Yes	Paternal	Coding	CACNA1A
Spinocerebellar ataxia 7	3p21–pl2	7-17	37–>200	Yes	Paternal	Coding	Ataxia-7
Spinocerebellar ataxia 12	5q31–q33	7–28	66–78	Yes	Paternal	5′-UTR	PPP2R2B
Spinocerebellar ataxia 17	6p27	25–42	45–63	Yes	Paternal	Coding	TBP
Diseases Associated with CTG Expansion (Autosomal Dominant)							
Myotonic dystrophy	19q13	5–35	50– >1000	Yes	Maternal congenital form	3′-UTR	Myotonin protein kinase
Spinocerebellar ataxia 8	13q21	16–35	75–250	Yes	Maternal	Noncoding	
Disease Associated with GAA Expansion (Autosomal Recessive)							
Friedreich ataxia	9q13	6–36	200–>900	No		Intron	Frataxin

Adapted from Rotilla (2017) and other sources

100, these repeats are often asymptomatic or produce minimal symptoms. When more than 100 repeats are present, the typical myotonic dystrophy phenotype is likely. Although there is a general correlation between repeat length and clinical severity, the size of the repeat is not a reliable prognostic indicator in the individual case. The extreme expansions to 1000 to 2000 repeats seen in congenital myotonic dystrophy occur only with female transmission of the unstable repeat. Thus, congenital myotonic dystrophy is always inherited from an affected mother.

The mechanism by which the expanded trinucleotide repeat in the myotonin protein kinase gene produces the myotonic dystrophy phenotype is not known. Because the repeat is not located in the coding region of the gene, it is possible that protein expression is altered or that RNA processing interactions are perturbed, though many other potential pathogenetic mechanisms have been proposed (Sznajder & Swanson, 2019).

Friedreich Ataxia

Friedreich ataxia is the most common of the hereditary ataxias, with an incidence of 2 per 100,000. Unlike all of the other trinucleotide repeat disorders, Friedreich ataxia is inherited as an autosomal-recessive disease and shows no evidence of anticipation. The expanded $(GAA)_n$ repeat is located in the first intron of the *FRDA* gene and reduces the expression of frataxin, a mitochondrial-targeted protein, probably through some interference with transcription or RNA processing. Frataxin is involved in mitochondrial respiration, iron balance, and response to oxidative stress. Some 97% of mutant *FRDA* alleles are due to $(GAA)_n$ expansions; the remaining alleles are due to other inactivating mutations, including point mutations (Lodi et al., 1999).

Other Tandem Repeat Expansion Disorders

While not discussed in specific detail in this chapter nor included in Table 72.2, it is worth noting that new disorders caused by tandem repeat expansions continue to be discovered, and not all of them are trinucleotides. For example, a gene with the unusual name *C9orf72* ("orf" referring to "open reading-frame") is a cause of some forms of frontotemporal dementia and amyotrophic lateral sclerosis due to expansion of a hexanucleotide repeat, GGGGCC; a zinc-finger gene, *ZNF9*, is responsible for myotonic dystrophy, type 2, owing to expansion of a tetranucleotide repeat, CCTG; and SCA type 10 is caused by an intronic pentanucleotide repeat, ATTCT, in the gene *ATXN10* (Rohilla & Gagnon, 2017).

Laboratory Testing for Trinucleotide Repeat Disorders

Depending on the length of the repeat segment, expansions of trinucleotide repeats are readily demonstrated by either Southern blot or PCR. PCR, followed by sizing of the products on an electrophoretic gel or capillary, is generally preferred for most of these disorders because of its speed, simplicity, and ability to resolve alleles differing in size by just one repeat unit. This is of particular importance when it is necessary to differentiate stable alleles at the upper size limit from small premutation or disease-causing alleles. For example, it is critically important to distinguish a 40-repeat from a 39-repeat in Huntington disease because of the dramatically different clinical implications and the psychosocial impact of a positive result. PCR is also the method of choice for accurate sizing of FRAXA premutation alleles, which is necessary for graded risk counseling of female carriers. However, where triplet expansions are very large, as in fully expressed FRAXA or myotonic dystrophy, it may not be possible to amplify the greatly expanded DNA segment by PCR. In this case,

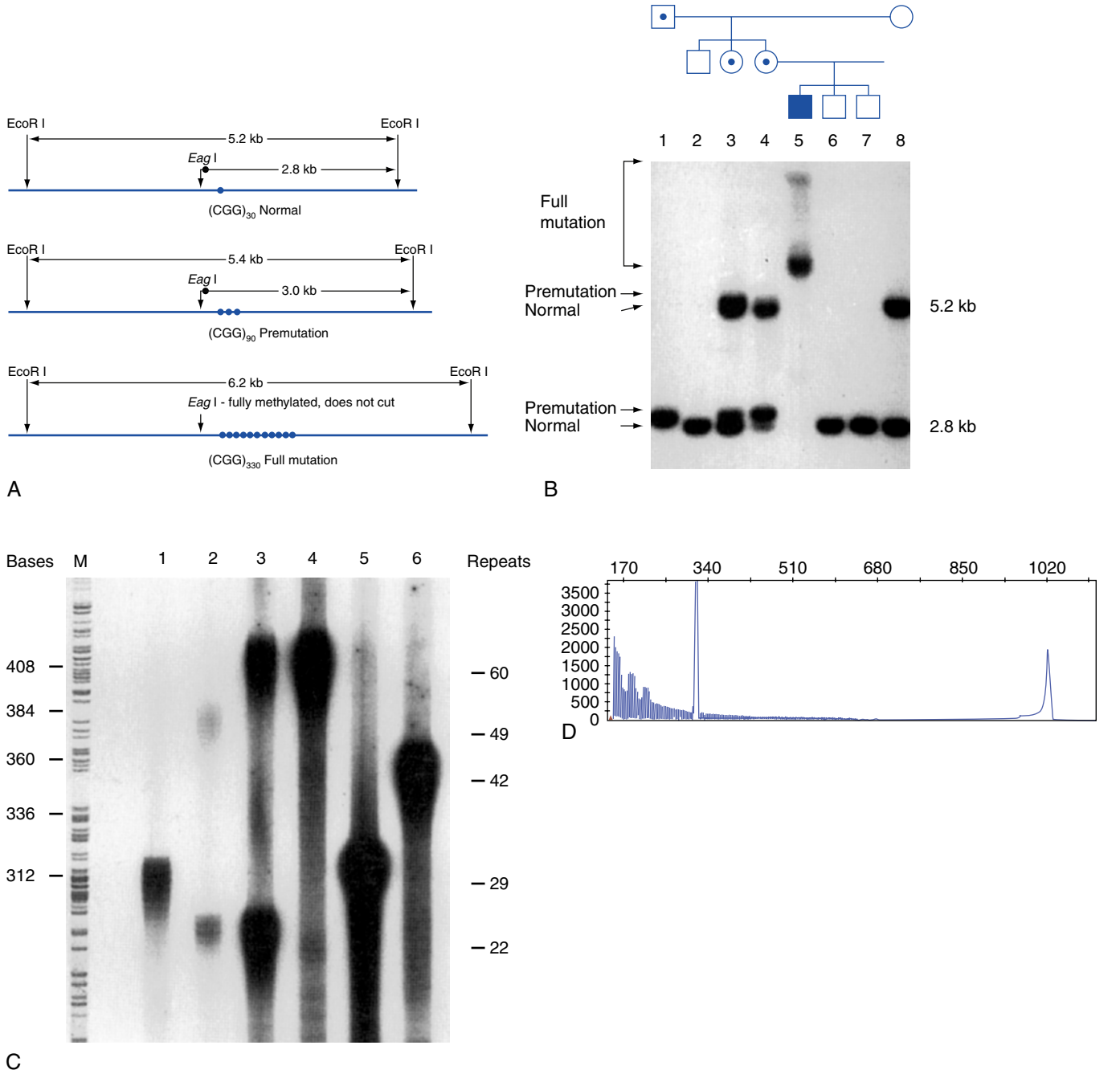

Figure 72.4 Detection of the $(CGG)_n$ repeat expansion in fragile X syndrome. **A,** Diagram of normal, premutation, and full-mutation alleles at the FRAXA locus. When expansion of the repeat to a full mutation occurs, the *Eag* I restriction enzyme site becomes methylated and does not cut with the enzyme. **B,** Family of a patient (*darkened square*) with fragile X syndrome. A Southern blot of *Eco*RI/*Eag* I-digested DNA from each individual in the pedigree was examined with a labeled DNA probe that hybridizes 3′ to the repeat. The three individuals on the right of the figure are normal (*open squares and circles*). Note that the two males each have a single 2.8-kb band, while the female has both a 2.8- and a 5.2-kb band. This is the expected result. The 5.2-kb band in the female is from the normal inactive (therefore methylated) X chromosome in each of her cells. Because the DNA on this chromosome is methylated, it is not cut by *Eag*I. The 2.8-kb band, however, is from the normal unmethylated active X chromosome (*Eag*I will cut the DNA in this case) in the female and in the males. The affected male has a greatly enlarged band. This is a consequence of marked expansion of the trinucleotide repeat as well as methylation of the *Eag*I restriction enzyme site. The three individuals marked by *bold dots* are carriers of premutation alleles. In the females, the distinction between normal and expanded alleles is seen most clearly in DNA from their active (unmethylated) X chromosomes. Here, there are distinct bands of 2.8 and 3 kb. Higher in the gel the resolution is not as good, and the 5.2- and 5.4-kb alleles are barely separated. Note that in this peripheral blood sample from the mother of the affected patient, X chromosome inactivation is skewed with respect to the repeat expansion: a greater proportion of normal X chromosomes in this cell population have randomly been inactivated compared with the X chromosomes carrying the premutation allele. **C,** Sizing of trinucleotide repeats by gel electrophoresis following amplification of the locus by the polymerase chain reaction (PCR). Lanes 1 through 6 represent six different individuals; lane M contains a size marker. The PCR products were labeled by incorporation of 32P-dCTP during the amplification reaction and the dried gel was exposed to X-ray film. Heterozygous females show two alleles; males and homozygous females show single alleles. The multiple bands produced with each allele are due to "slippage" of the DNA polymerase during the PCR reaction; the most intense band is taken as representative of the actual size of the allele. **D,** Successful PCR amplification of both the normal (*left peak*, 30 CGG repeats) and full-mutation (*right peak*) alleles in a female heterozygote, using reagents from Asuragen, Austin, Texas) (**C** courtesy of Dr. Anne Maddalena; **D** courtesy of Dr. Joshua Deignan.)

Southern blotting has traditionally been required. Southern blotting is also helpful in determining the methylation status of FRAXA full mutations through the use of methylation-sensitive restriction endonucleases and in ensuring that a large Huntington disease or FRAXA allele has not been missed in a patient who appears homozygous normal by PCR. Similarly, it more reliably identifies mosaic males whose cells show a mixture of premutation and full mutation alleles. More recently, however, methods for analyzing large premutations and even the full mutation of *FMR1* by PCR alone have entered routine practice, supported by the availability of commercial reagents (Hantash et al., 2010). Fig. 72.4 illustrates the use of both Southern blotting and PCR to detect full FRAXA mutations and FRAXA premutation alleles. In addition, PCR can be adapted to detect methylated regions following sodium bisulfite treatment of the target DNA (Tassone, 2015), as also utilized for the disorders discussed in the next section.

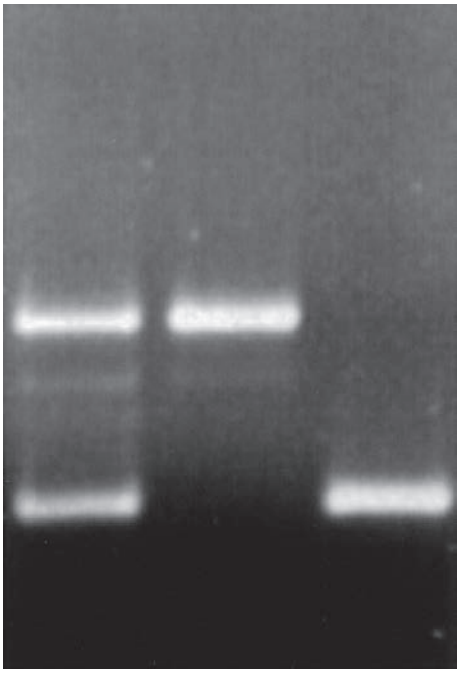

Figure 72.5 Polymerase chain reaction–based electrophoretic analysis of methylation patterns in Prader-Willi and Angelman syndromes using the sodium bisulfite method of Kosaki et al. (1997). In Prader-Willi syndrome, only the methylated maternal allele (*upper band*) is present due to either deletion of the paternal allele or uniparental disomy for the maternal allele. In Angelman syndrome, only the unmethylated paternal allele (*lower band*) is present due to either deletion of the maternal allele or uniparental disomy for the paternal allele. Similar analysis can also be done by Southern blot using methylation-sensitive restriction enzymes.

PRADER-WILLI AND ANGELMAN SYNDROMES

Prader-Willi and Angelman syndromes, whose genes lie at approximately the same locus on chromosome 15, are almost always discussed together, even though they are caused by different genes and have almost nothing in common phenotypically. Prader-Willi syndrome is characterized by obesity, mental retardation, hypoplastic genitalia, and dysmorphic features, while Angelman syndrome exhibits ataxia, puppet-like facies, mental retardation, paroxysmal laughter, and seizures. What they do share, remarkably, is a powerful imprinting mechanism determining disease expression. Both disorders are almost always sporadic. Prader-Willi syndrome, whose precise causative gene(s) is not yet known, is most often caused by a deletion at 15q12 in the paternally inherited chromosome only; this is pathologic because only the paternal PWS gene(s) is expressed. The opposite is true for Angelman syndrome, which is most often caused by deletion of a known gene (*UBE3A*) exclusively on the maternally inherited chromosome, which is the only allele normally expressed (Knoll et al., 1989; Matsuura et al., 1997). Alternatively, Prader-Willi syndrome can be caused by uniparental disomy for the maternal chromosome 15, which carries only the nonexpressing copy of the gene. Likewise, Angelman syndrome can be caused by uniparental disomy for the paternal chromosome 15. These phenomena can be detected by fluorescent in situ hybridization (FISH), chromosome haplotyping with microsatellite markers, or Southern blotting with methylation-sensitive restriction enzymes that can distinguish the methylated maternal critical region from the unmethylated paternal critical region. A differential PCR scheme that amplifies either the methylated or unmethylated allele of the nearby *SNRPN* gene within the critical region, based on resistance of methylated cytosines to chemical modification by sodium bisulfite (Kosaki et al., 1997), is also available (Fig. 72.5). Neither the Southern blot nor the PCR method will distinguish between the deletional or uniparental disomy mechanisms, nor will they detect cases (more frequent in Angelman syndrome) due to point mutations within the causative gene. These methods also will not distinguish rare cases of Angelman syndrome or Prader-Willi syndrome due to primary imprinting defects (resulting from aberrant methylation caused by a mutation in the chromosome 15 imprinting center) (Smith & Hung, 2017), which would have a much higher recurrence risk.

FAMILIAL CANCERS

All cancers are genetic disorders at the cellular level, caused by mutations in genes that control cell proliferation and differentiation. These genes may be divided broadly into two groups, those that promote proliferation (proto-oncogenes or, simply, oncogenes) and those that restrain cell growth (tumor suppressor genes). Most often, mutations in these genes occur in somatic cells, usually requiring cumulative alterations over many cell cycles in several oncogenes or tumor suppressor genes before a cancer develops. However, in some individuals, the initial mutation in this progression may be a germline lesion, inherited from a parent and present in every cell of that individual's body.

As discussed in Chapters 78 and 79, heritable cancer-causing mutations have been found most often in tumor suppressor genes, including several groups of genes that encode proteins with DNA repair functions, but have also been found in a few oncogenes. The inherited mutation should be viewed as the initiating event in tumor development, not in itself sufficient to cause cancer but merely the first step in a series of mutations that ultimately lead to uncontrolled cell growth, analogous to the first somatic mutation that initiates tumor development in a sporadic cancer. It is likely that most of the heritable mutations that contribute to cancer development have not been identified, because they are by themselves not highly penetrant and require the interaction of other genetic and environmental factors to initiate tumor development—a complex situation that is difficult to unravel. However, a number of highly penetrant genes have been identified that are major initiators of tumor development in what are recognizable heritable cancer syndromes (see Table 72.3).

Compared with their sporadic counterparts, hereditary cancers often develop at an earlier age, are more often multifocal, and appear bilaterally in paired organs. Noting these distinguishing features in sporadic retinoblastoma and familial retinoblastoma, Knudson postulated that at least two mutational events are necessary to produce a tumor (Knudson, 1971). In the case of a sporadic tumor, two independent mutational events in the same cell are necessary to initiate tumor development, whereas in the case of a hereditary tumor, the first mutation is already present at birth in every cell of the body, making it more likely that a second mutational event will occur at an earlier age and often in more than one cell. Knudson's "two-hit hypothesis" is an important concept that has guided many studies of the genetic basis of cancer. Elucidation of the heritable mutations in the hereditary cancer syndromes has been enormously informative, not only in understanding these rare disorders but also in understanding the fundamental changes responsible for common sporadic malignancies.

In the following discussion, some fundamental concepts of hereditary cancer syndromes are explained in the context of a disorder caused by a tumor suppressor gene—retinoblastoma—and a disorder caused by an oncogene—multiple endocrine neoplasia type 2. This is followed by descriptions of hereditary breast–ovarian cancer (HBOC) and hereditary colorectal cancer, the most common hereditary cancer syndromes, for which more than a million individuals in the United States are at risk. The section ends with a discussion of current approaches to genetic testing for these disorders.

Tumor Suppressor Genes: Retinoblastoma as a Paradigm

Although familial cancer syndromes due to mutations in tumor suppressor genes follow a dominant pattern of inheritance, at the cellular level the changes often appear recessive because tumorigenesis is initiated (in most cases) only when both copies of the tumor suppressor gene are inactivated. Loss of the normal gene inherited from the unaffected parent may occur as the result of a second novel pathogenic mutation, by large-scale deletion (appearing in certain molecular assays as loss-of-heterozygosity), by replacement with a duplicated copy of the mutant gene inherited from the affected parent by genetic mechanisms such as chromosomal nondisjunction, gene conversion or mitotic recombination, or by gene silencing due to hypermethylation. These events occur in retinoblastoma, a tumor of the retina caused by functional loss of both copies of the *RB1* gene, which encodes the RB protein that is involved in cell cycle and transcriptional regulation. In sporadic cases, both of these mutational events occur somatically and a solitary, sporadic tumor develops. In the hereditary cases, however, the first *RB1* mutation is present in the germline of the affected child, having been inherited from a similarly affected parent or occurring as a new mutation during gametogenesis. When this is the case, the likelihood that the remaining normal *RB1* gene will undergo mutation in at least one retinal precursor cell is greater than 90%. As Knudson observed, in most patients with familial disease, the tumors are bilateral and multifocal (Knudson, 1971), implying that several cells have sustained additional *RB1* mutations. It is not known whether *RB1* mutations alone are sufficient for tumorigenesis, but they certainly appear to be the initiating or key event.

Familial retinoblastoma has served as a model in guiding important cancer research. This has led to the discovery of a large number of tumor

TABLE 72.3
Hereditary Cancer Syndromes

Disorder	Associated Tumors	Population Incidence	GENE	Chromosome Location
Tumor Suppressor Genes (Autosomal Dominant Mode of Inheritance)				
Basal cell nevus (Gorlin) syndrome	Basal cell carcinoma, medulloblastoma	1/40,000	*PTCH*	9q22
Cowden syndrome	Breast, thyroid carcinoma	1/200,000	*PTEN*	10q23
Familial adenomatous polyposis	Colorectal, duodenal carcinoma	1/10,000	*APC*	5q21
Hereditary breast–ovarian cancer syndrome	Breast, ovarian, pancreatic, prostate carcinoma	1/300–1/500	*BRCA1*	17q21
			BRCA2	13q12
Hereditary diffuse gastric carcinoma	Gastric carcinoma	Rare	*CDH1*	16q22
Hereditary leiomyomatosis and renal cell carcinoma	Cutaneous and uterine leiomyomas, papillary renal cell carcinoma	Rare	*FH*	1q42
Hereditary melanoma	Melanoma, pancreatic carcinoma	Unknown	*CDKN2A*	9p21
			CDK4	12q14.1
Hereditary paraganglioma	Paraganglioma, pheochromocytoma	Rare	*SDHD*	11q23
			SDHB	1p35–36
			SDHC	1q21
			SDHAF2	11q12.2
Juvenile polyposis syndrome	Gastrointestinal cancer	1/10,000	*SMAD4*	18q21
			BMPR1A	10q22
Tumor Suppressor Genes (Autosomal-Dominant Mode of Inheritance)				
Li-Fraumeni syndrome	Sarcomas, breast carcinoma, leukemia, brain tumors	Rare	*p53*	17p13
Multiple endocrine neoplasia, type 1 (MEN1)	Pancreatic islet cell, pituitary, parathyroid tumors	1/100,000	*MEN1*	11q13
Neurofibromatosis type 1	Neurofibroma/sarcoma, pheochromocytoma	1/3000	*NF1*	17q11
Neurofibromatosis, type 2	Acoustic neuroma, meningioma	1/40,000	*NF2*	22q12
Peutz-Jeghers syndrome	Gastrointestinal tumors	1/200,000	*STK11*	19p13
Retinoblastoma, hereditary	Retinoblastoma, osteosarcoma	1/20,000	*RB1*	13q14
Von Hippel-Lindau disease	Hemangioblastoma, renal cell carcinoma, pheochromocytoma	1/40,000	*VHL*	3p25
Oncogenes (Autosomal-Dominant Mode of Inheritance)				
Hereditary melanoma	Melanoma	Rare	*CDK4*	12q13
Multiple endocrine neoplasia type 2A and type 2B	Medullary thyroid carcinoma, pheochromocytoma, parathyroid hyperplasia/adenoma; multiple mucosal neuromas (type 2B)	1/30,000	*RET*	10q12
Hereditary papillary renal carcinoma	Papillary renal carcinoma	Rare	*MET*	7q31
DNA Repair Genes (Autosomal-Dominant Mode of Inheritance)				
Hereditary nonpolyposis colorectal cancer (Lynch syndrome)	Colorectal, endometrial, ovarian carcinoma	1/400–1/700	*MSH2*	2p16
			MLH1	3p21
			MSH6	2p16
			PMS2	7p22
DNA Repair Genes (Autosomal-Recessive Mode of Inheritance)				
Ataxia telangiectasia	Lymphomas, others	1/40,000–1/100,000	*ATM*	11q22
Bloom syndrome	Various	Rare	*BLM*	15p26
Fanconi anemia	Acute myelogenous leukemia, others	1/100,000	*FANCA-G*	Various
MYH-associated polyposis	Colorectal carcinoma, duodenal polyposis	1/10,000	*MYH*	1p34
Xeroderma pigmentosum	Cutaneous basal carcinoma and squamous carcinoma	Rare	*XPA-G, POLH*	Various

Data from various sources, including Garber & Offit (2005).

suppressor genes that are key determinants of the pathogenesis of several hereditary cancer syndromes, including HBOC and hereditary colorectal cancer. These same tumor suppressor genes are also critical to the development of many common sporadic cancers.

Oncogenes: Multiple Endocrine Neoplasia Type 2 as a Paradigm

There are just a few familial cancer syndromes that are known to be caused by a heritable mutation in an oncogene (see Table 72.3). Of these, multiple endocrine neoplasia type 2A (MEN2A) and its variants, familial medullary thyroid carcinoma (FMTC) and multiple endocrine neoplasia type 2B (MEN2B), are best known. Single activating mutations in just one allele of the proto-oncogene *RET* are sufficient to initiate tumorigenesis in these disorders (Eng, 1999).

All three of these syndromes are characterized by hyperplasia of thyroid C cells and medullary thyroid carcinoma. In families afflicted with MEN2A, pheochromocytomas and/or parathyroid adenomas or parathyroid hyperplasia are also present. MEN2B is further characterized by the presence of multiple mucosal neuromas of the lips, mouth, and gastrointestinal tract, a marfanoid habitus, a particularly aggressive clinical course, and a high proportion of affected individuals due to new *RET* mutations.

RET is a signaling molecule with extracellular receptor and intracellular tyrosine kinase domains. With few exceptions, the known FMTC and MEN2A mutations are single base substitutions in one of five codons in the extracellular domain, in each case producing substitution of cystine by another amino acid. More than 95% of cases of MEN2B exhibit the same missense mutation, M918T.

Hereditary Breast–Ovarian Cancer

HBOC is caused predominantly by germline mutations in *BRCA1* and *BRCA2*, autosomal tumor suppressor genes with roles in DNA repair, transcription regulation, and cell cycle control. The combined carrier prevalence of abnormal variants of these two genes in the general U.S. population is estimated to be 1/500 to 1/300. Three founder mutations in the Ashkenazi-Jewish population are responsible for increasing the prevalence tenfold (1/40) in this ethnic group. HBOC accounts for 5% to 10% of female breast cancer cases and 12% of ovarian cancer cases. Whereas the lifetime risks to women of developing breast or ovarian cancer in the general population are 11% and 1%, respectively, the risk to mutation carriers is 50% to 85% for breast cancer (the risk of a second, contralateral cancer approaches 60%) and 25% to 45% for ovarian cancer. Other cancers, especially breast cancer in men, pancreatic cancer, colon cancer, and prostate cancer, are more prevalent as well, though not to the same extent as female breast and ovarian cancer. Characteristically, tumors occur at an earlier age than their sporadic counterparts, with average age of diagnosis of breast cancer in the 40s compared to the average age of diagnosis of sporadic breast cancer in the mid-60s. Development of breast cancer at an early age is one of the strongest predictors of the presence of HBOC.

BRCA1 and *BRCA2* are both large genes, encoding proteins of 1863 amino acids and 3418 amino acids, respectively. Disease-causing mutations, mostly frameshift or nonsense mutations that cause protein truncation, are distributed widely across both genes. Many thousands of unique deleterious mutations and variants have been identified. Although the presence of founder mutations permits a targeted approach to mutation identification in Ashkenazi-Jews (with just two common mutations in *BRCA1* and one in *BRCA2*), whole-gene sequencing is required for mutation detection in the heterogeneous general U.S. population at large. This approach has a high yield of detecting mutations (as long as they exist within the coding regions of the genes) but, analogous to the caveat about CMA testing discussed earlier, also reveals novel missense variants of undetermined clinical significance, which then have to be dealt with. Also, some HBOC patients have large deletions in one of the genes rather than a point mutation. These will be missed by Sanger sequencing and require an alternate approach, such as MLPA or modified NGS (Schmidt et al., 2017).

Genetic testing for *BRCA1* and *BRCA2* mutations in high-risk patients and family members is now a high-profile service in clinical genetics and oncology practice. Effective cancer prevention strategies for mutation carriers (increased surveillance, chemoprevention, prophylactic surgery) have markedly reduced the incidence of ovarian cancer and primary and secondary breast cancers (Nelson et al., 2014). Individuals at high risk can be identified by their personal history of ovarian or early-onset breast cancer in women or breast cancer in men and/or by a family history of these cancers in either the paternal or maternal lineages (National Comprehensive Cancer Network, 2005). Because HBOC is an autosomal-dominant disorder, first-degree relatives of mutation carriers have a 50% risk of carrying the same mutation. Once the familial mutation is known, testing of at-risk relatives no longer requires whole-gene sequencing but rather can be targeted to the particular nucleotide, saving significant time and expense. With next-generation DNA sequencing now enabling the cost-effective analysis of larger numbers of genes, laboratories have begun to offer gene panels for HBOC, adding loci such as *CHEK2*, *CDH1*, *PTEN*, *MUTYH*, and as many as 15 others in addition to *BRCA1* and *BRCA2* (Hart et al., 2020).

The Hereditary Colorectal Cancer Syndromes

Hereditary nonpolyposis colorectal cancer (HNPCC, or Lynch syndrome), as its name implies, is a hereditary colorectal cancer syndrome that is not associated with an abundance of adenomatous polyps. In contrast, familial adenomatous polyposis (FAP) and MYH-associated polyposis (MAP) are hereditary disorders in which variable and sometimes large numbers of adenomatous polyps may be present. This useful, if imperfect, clinical distinction is an important guide to the evaluation of individuals who are at risk for these disorders.

Hereditary Nonpolyposis Colorectal Cancer

HNPCC is the second most common hereditary cancer syndrome, affecting almost as many individuals as are affected by HBOC. However, because it is almost equally penetrant in both sexes, its public health impact is equivalent to that of HBOC. Notably, and often unrecognized, endometrial cancer is a prominent part of the syndrome in women. HNPCC accounts for 3% to 5% of all colorectal cancers and 2% to 3% of all endometrial cancers. The disease is caused by germline mutations in any of at least five DNA mismatch repair genes—*MSH2*, *MLH1*, *MSH6*, *PMS2*, and *PMS1*—each contributing roughly 50%, 40%, 10%, <1%, and <1%, respectively, to the overall incidence of the disorder. The combined carrier prevalence of abnormal variants of *MSH2* and *MSH1*, which account for approximately 90% of HNPCC, is estimated to be between 1/700 and 1/400. Colorectal cancer in HNPCC is characterized by early age of onset (average 44 years, compared with 72 years for sporadic colorectal cancer), locations predominantly on the right side of the colon, and frequent occurrence as multiple primary tumors simultaneously or over a period of time (synchronous or metachronous). The lifetime risk to male and female mutation carriers of developing colorectal cancer is approximately 80% (compared with a 2% lifetime general population risk), while the lifetime risk of endometrial cancer is 40% to 60% (compared with a 1.5% lifetime general population risk). The lifetime risks of gastric cancer (13%) and of ovarian cancer (12%) are also increased (compared with 1% in the general population).

A number of guidelines for identifying individuals at risk for HNPCC have been described that use a combination of personal and family history of cancer: for example, the Amsterdam Criteria and Bethesda Guidelines, which have gone through several revisions (Lipton et al., 2004). In practice, one need not hold dogmatically to these schemes, because a detailed personal and family history will usually suggest which patients are at risk, and over-adherence to the traditional criteria will result in missing a proportion of Lynch syndrome families (Moreira et al., 2012). Early-onset colorectal cancer and/or endometrial cancer are the strongest predictors of the disorder, particularly when they are seen together in an individual or family, are accompanied by other tumors associated with the disease, and occur in more than one generation of the family.

Another predictor of HNPCC in an affected patient is the presence of microsatellite instability (MSI) in the DNA of that individual's colorectal cancer (see Chapter 79). The term describes an alteration in the length of short tandem repeat DNA sequences (microsatellites) in the tumor due to mismatch repair errors during DNA replication. Microsatellite instability is highly sensitive but not entirely specific in identifying a colorectal tumor as due to HNPCC, because about 15% of sporadic colon cancers will also demonstrate MSI. Recent consensus guidelines have been published covering the molecular pathologic workup of colon tumors and the indications for subsequent germline testing for the mismatch repair genes if MSI is present (Sepulveda et al., 2017).

The DNA mismatch repair genes are moderately large genes, with *MSH2* encoding a protein of 935 amino acids and *MLH1* encoding a protein of 757 amino acids. Although there are a few mutations that have a high relative prevalence in some populations due to founder effects, the vast majority are distributed widely across both genes. Most mutations are frameshift or nonsense mutations that cause loss of gene expression due to RNA instability, protein instability or protein truncation. In addition, large deletions of single or multiple exons account for approximately one-third of the mutations present in *MSH2* and for a smaller fraction of the mutations in *MLH1*.

Genetic testing for mutations in the Lynch syndrome genes in high-risk patients and family members has moved into clinical practice in a manner similar to that which has occurred for *BRCA1* and *BRCA2* testing for HBOC. As in the latter, NGS technology has led to ever larger numbers of genes offered in hereditary colon cancer panels. For those individuals who are identified as carrying deleterious mutations, complete colonoscopy, beginning at an early age and at regular intervals, is very effective at identifying premalignant adenomatous polyps (the term *HNPCC* should not be taken to imply that there are no polyps involved in the syndrome), while endometrial biopsy and transvaginal ultrasound may identify early endometrial cancer. If colorectal cancer does develop, subtotal colectomy may be considered as an alternative to segmental resection because of the high rate of synchronous and metachronous tumors in patients with HNPCC. Prophylactic hysterectomy–bilateral salpingo-oophorectomy may be considered in women who have completed their families. As in all autosomal-dominant disorders, first-degree family members of mutation carriers have a 50% risk of also carrying that same mutation. Thus, their testing becomes relatively straightforward.

Familial Adenomatous Polyposis and Attenuated Familial Adenomatous Polyposis

Familial adenomatous polyposis is a hereditary colorectal cancer syndrome that can present with a striking phenotype in the colon—multifocal colorectal cancer in a background of thousands of adenomatous polyps. It is now recognized that the FAP phenotype is diverse and the number of colonic polyps can vary markedly. Accordingly, *classic* FAP is now diagnosed when an individual develops at least 100 adenomatous polyps over one's lifetime, whereas *attenuated* FAP (AFAP) is the term applied to a patient whose lifetime polyp burden is in the range of 20 to 100 polyps. The distinction is entirely clinical, because both disorders are caused by germline mutations in the *APC* (adenomatous polyposis coli) gene, a tumor suppressor gene

with several important cellular functions and a likely initiator of sporadic colorectal cancer development as well, though the location of mutations in the attenuated form tends to be clustered in the early and late exons of the gene (Talseth-Palmer, 2017). Germline *APC* mutations are carried by 1/10,000 to 1/5000 individuals. Most of these mutations have been inherited from a similarly affected parent, but 20% to 30% are de novo mutations. Accordingly, FAP or AFAP cannot be ruled out because of an absence of a positive family history, which is particularly important to keep in mind when assessing a patient with a low polyp burden.

Since FAP can have its onset in childhood, close clinical monitoring and surveillance starting at a young age is essential for individuals determined to be at risk by family history and/or genetic testing. Screening colonoscopies should be started at age 10 years and prophylactic colectomy performed when polyps have developed and become dysplastic. For individuals at risk for the less florid AFAP, screening may begin later in the teens. Colectomy is performed when the polyp burden is no longer manageable by polypectomy or when dysplastic features become more worrisome. Upper gastrointestinal surveillance is also indicated because gastric and small-bowel polyps can develop as part of the syndrome. This is particularly important in the duodenum, especially in the periampullary region, where the lifetime risk of progression to cancer is 5% to 12%.

Patients with FAP and AFAP are also at higher risk for a number of other cancers (pancreatic, biliary tract, thyroid) and frequently have other clinical findings: desmoid tumors, osteomas, dental abnormalities, epidermoid cysts, and congenital hypertrophy of the retinal pigmented epithelium (CHRPE). Of these, desmoid tumors, affecting approximately 10% of patients with FAP, are the most important. These clonal proliferations of myofibroblasts form in the abdominal wall or the abdominal cavity and are locally invasive, compress abdominal organs, and may cause serious morbidity and mortality.

APC is a large gene, encoding a protein of 2843 amino acids. Most disease-causing mutations are frameshift or nonsense variants producing protein truncation. These mutations are distributed widely along the gene, requiring full-gene sequencing unless the familial mutation is already known.

MYH-Associated Polyposis

MYH-associated polyposis is an autosomal-recessive hereditary cancer syndrome caused by mutations in the human homolog of the bacterial *mutY* gene, *MYH* (Wang et al., 2004). The clinical phenotype is very similar to that of AFAP or the less florid variants of FAP: that is, a polyp burden in the tens to hundreds, not thousands. As with FAP/AFAP, patients are at risk for duodenal polyposis and some have been reported to have extraintestinal manifestations, such as CHRPE and osteomas as well. Because of the autosomal-recessive nature of this disorder, MAP families typically show no evidence of vertical transmission of the disease, as would be true for the autosomal-dominant FAP/AFAP, but might include affected siblings. It is estimated that the carrier frequency for mutant *MYH* alleles is approximately 2%, which implies a 1/10,000 frequency of biallelic (affected) individuals. This is very similar to the number of patients who have FAP/AFAP. The close similarity of the MAP and FAP/AFAP phenotypes, and the fact that as many as 30% of individuals with FAP have no evidence of vertical transmission in the family because they carry de novo *APC* mutations, can make differential diagnosis difficult, especially when the polyp burden is not large. In many cases, it is necessary to perform mutation analysis for both *APC* and *MYH* to arrive at a diagnosis.

Laboratory Testing for Familial Cancer Mutations

DNA analysis for heritable, cancer-predisposing mutations has enormous potential for disease prevention and early treatment. If a very high proportion of the cancer-causing mutations in a particular gene or ethnic group is known, and these mutations are relatively few in number, direct analysis for these mutations may be simple and inexpensive. Fortunately, this may sometimes be the case with an oncogene, because activation of the gene can be achieved in only a limited number of ways. As mentioned earlier, the spectrum of mutations in *RET* that are responsible for MEN2 is quite small, with just a handful of well-defined mutations accounting for more than 95% of the total.

If, on the other hand, the gene is large, and cancer-causing mutations are numerous and widely dispersed (which is commonly the case with tumor suppressor genes because they can be inactivated in many different ways), then mutation analysis of necessity must be less targeted and capable of screening large stretches of DNA. In that case, direct DNA sequencing must be used. In addition, whole exon deletions or duplications, or even whole gene deletions, which are not detectable by standard sequencing, may constitute a significant percentage of the deleterious mutations in a particular gene. In this case, techniques that are capable of assessing gene dosage—such as some variation of quantitative PCR, MLPA, or a hybridization platform that is capable of measuring sequence dosage in a comparative way—must be used.

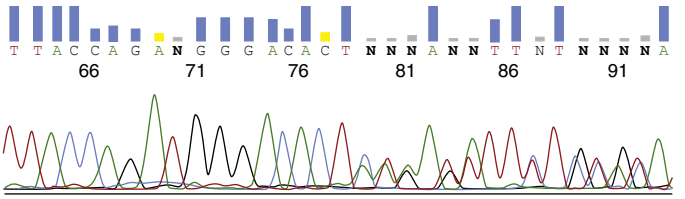

Figure 72.6 Detection of the Ashkenazi-Jewish founder mutation 185delAG in the *BRCA1* gene by DNA sequencing. Because familial breast–ovarian cancer is a dominant disorder, the mutation is heterozygous. In addition, because it results in the deletion of two nucleotides from one of the alleles, the sequence profile is "out of frame" from the mutation site onward (starting at nucleotide 79 in this particular readout). This causes overlapping of different nucleotides between the two alleles, which the automated sequencer has trouble identifying (hence, the frequent notation "N" for the nucleotide calls).

Fig. 72.6 illustrates the Sanger sequence tracing of the Ashkenazi-Jewish founder mutation 185delAG in *BRCA1*, which is an example of a common ethnic-specific mutation in an otherwise mutationally heterogeneous tumor suppressor gene. As mentioned earlier, NGS now allows for efficient testing of panels of genes associated with particular forms of familial cancer, of which a large number have been reported.

MITOCHONDRIAL DNA DISORDERS

In addition to the 6 billion bp of DNA that comprise the human nuclear diploid genome, vital genetic information is also encoded in DNA molecules carried by the mitochondria in the cytoplasm. These 16,500-bp, double-stranded, circular DNA molecules are present in 2 to 10 copies in each of the up to several hundred mitochondria of the cell. Mitochondrial DNA (mtDNA) codes for 13 of the proteins of the respiratory chain and adenosine triphosphate (ATP) synthase, 22 transfer RNAs required for their translation, and two ribosomal RNAs. mtDNA is self-replicating and is transmitted strictly by maternal inheritance because the mitochondria of a spermatozoon are not incorporated into the zygote upon fertilization of an ovum.

Disease-causing abnormalities of mtDNA may result from several different mechanisms (Ruiz-Pesini et al., 2007). Single large deletions (and, rarely, duplications) that apparently occur sporadically in oogenesis are typical of Kearns-Sayre syndrome, a myopathy characterized principally by progressive external ophthalmoplegia and pigmentary retinopathy. Most of the classic mitochondrial diseases are due to point mutations in one of the tRNA respiratory chain genes: for example, myoclonic epilepsy with ragged red fibers (MERRF); mitochondrial myopathy, encephalopathy, lactic acidosis, and strokelike episodes (MELAS), and Leber hereditary optic neuropathy (LHON). The most distinctive feature of these disorders from a genetic point of view is that they follow a pattern of strict maternal inheritance, never showing transmission from an affected male and passing from an affected female equally to her sons and daughters.

Often, the clinical presentation will guide the choice of mutation panel testing in a stepwise fashion because particular mutations are associated with each of the major syndromes (e.g., missense mutations G11778A, T14484C, and G3460A with LHON). If these tests are negative, one can proceed to a second-tier panel or to complete mtDNA sequencing. The situation is complicated by the finding that some mutations are found in more than one syndrome and by the phenomenon of heteroplasmy—the occurrence of different proportions of mutant and normal mitochondria in different tissues. For this latter reason, mtDNA testing may require biopsy of the involved tissue (e.g., muscle) because the mutation may not be represented highly enough in blood to be detectable. Recently, the advent of NGS has circumvented some of these challenges in that it allows sequencing of the complete mtDNA genome in a short time while also detecting minor populations of mutant mitochondria, even outside the affected tissue (Dames et al., 2015). In addition to the inherited encephalomyopathies, there is growing evidence that tissue-specific accumulations of somatic mitochondrial mutations may contribute to the development of many common late-onset degenerative disorders, and perhaps to aging itself. These, too, may be observed at minor allele frequency in NGS tests.

It must be kept in mind that the majority of "mitochondrial" disorders are actually due to mutations in nuclear genes that encode proteins destined for transport into the mitochondria or associated with mitochondrial metabolism or replication. To encompass these conditions in the diagnostic testing, larger gene panel sequencing by NGS is the best approach. A convenient quirk of the technology is that mitochondrial DNA is present in such higher copy numbers than the nuclear genome that it gets included in exome sequencing even though not specifically targeted in the exon-capture step.

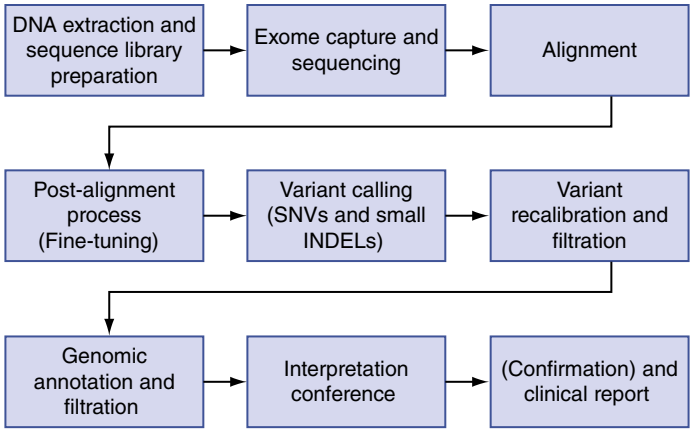

Figure 72.7 Workflow for clinical exome sequencing, from DNA isolation to final interpretation and reporting (Courtesy of Dr. Hane Lee.)

OTHER TARGETS OF MOLECULAR GENETIC TESTING

The specific disease examples covered in this chapter are among those tested most widely by clinical molecular genetics laboratories, a market that is reflected by their inclusion in the CAP/ACMG proficiency testing programs. This, in turn, has been dictated largely by their mutation carrier frequency or disease prevalence in the general population and by their clinical severity. As previously described, if the carrier frequency of a recessive mutation is sufficiently high in the target population, general screening may be justified. For these and other disorders, the application of the test to differential diagnosis, prenatal diagnosis, or presymptomatic diagnosis may also be of value. With more than 20,000 genetic diseases catalogued, there are obviously many others that could be considered. Currently, there are tests for about 10,000 of these available as listed in the online Genetic Test Registry (https://www.ncbi.nlm.nih.gov/gtr/). Many of these are esoteric and offered by only one or a few laboratories. Tests for extremely rare, or *orphan*, genetic diseases may be available only in the research laboratory that cloned the gene or studies the disease from a mechanistic level. This has led to some problems because such laboratories, although performing a vital service to the small number of families at risk, are not Clinical Laboratory Improvement Amendments (CLIA)–certified and on legal grounds should not be releasing test results for medical management. A number of solutions have been proposed, such as modifying certain CLIA requirements for such settings, partnering of the research laboratory with a clinical laboratory in their own institution, or establishing a network of dedicated orphan disease laboratories that can offer so-called "custom sequencing" of any gene or locus (Grody & Richards, 2008).

THE NEW FRONTIER OF DIAGNOSTIC MOLECULAR GENETICS: GENOME-LEVEL DNA SEQUENCING

Any chapter on molecular genetic testing in a contemporary textbook would be highly remiss if sufficient attention were not paid to the impact of next-generation DNA sequencing on the approach to molecular diagnosis of patients with novel, rare, or unclear phenotypic presentations. While already alluded to several times, it is appropriate that we conclude the chapter with a more thorough discussion of the ways in which, in a few short years, this powerful technology had completely changed the approach to molecular genetic diagnosis, especially for those patients with undiagnosed or ultra-rare diseases. Indeed, this remarkable advance in sequencing speed, capacity, cost-efficiency and throughput probably represents the most dramatic sea change in the molecular testing landscape since the advent of PCR in the mid-1980s. The combination of these new instrumentation platforms with our now-complete knowledge of the human genome sequence is proving to be a tool of incredible power, at last opening the gateway to true personalized medicine, especially in the areas of genetics and oncology. NGS, or *massively parallel* DNA sequencing, goes well beyond the specific targeting of a single region of a single gene that is characteristic of Sanger sequencing. Instead, the entire genome is targeted for sequencing, using a series of defined steps (Fig. 72.7). First,

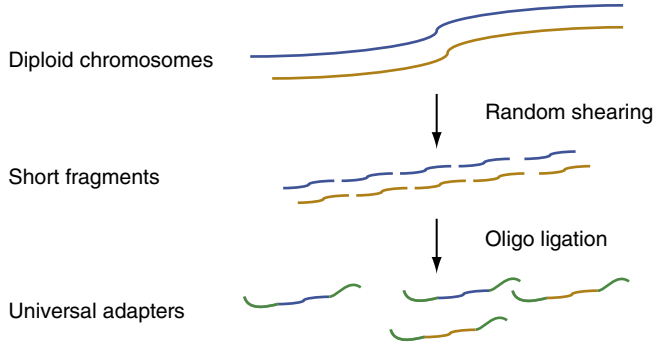

Figure 72.8 Shearing of genomic DNA into small fragments, followed by adapter ligation, the first steps in library preparation for next-generation sequencing (Courtesy of Dr. Sam Strom.)

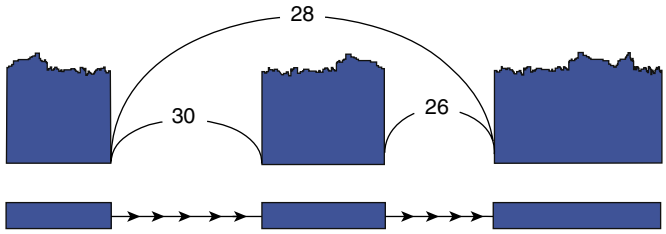

Figure 72.9 Visual representation of RNAseq data by means of the so-called "sashimi plot," in which read-densities of transcripts along the exons are plotted as histograms. In the example shown, 28 of the RNA reads counted in the analysis skip the middle exon, presumably due to a mutation affecting RNA splicing, compared with 30 and 26 reads that correctly splice together the first and second, and second and third, exons, respectively (RNAseq reads [from the derived cDNA] are typically about 150 bp long and do not individually cover the entire mRNA). Thus, this example would be consistent with the presence of a heterozygous mutation affecting RNA processing. The result can be correlated with results of whole-genome sequencing to further characterize the nature of the mutation in the patient's DNA (Lee et al., 2020) (Courtesy of Dr. Hane Lee.)

the genomic DNA isolated from the patient is sheared into hundreds of millions of short (usually 50–100 bp) fragments. These are then linked to adapters (Fig. 72.8) that provide universal primer sites for sequencing, "bar-coding" (for accurate cataloguing of every fragment in a mixed population by the computer analysis software), and attachment to a solid substrate (either a microarray-like surface or microbeads). The aggregate of all of the fragments with their adapters is called the *library*. Most clinical NGS laboratories also include an intermediate step of exon capture (using exonic probes on some type of solid support) so that only the coding regions of the genome (equal to about 1.5% of the total genome content) are sequenced. This test is then designated *exome* (rather than *genome*) sequencing. The rationale behind it is that the coding regions (about 230,000 exons in total for about 22,000 genes) likely account for most of the sites of mutations causing Mendelian disorders. Also, the extensive degree of population variation in the nonexonic (intronic and intergenic) regions is so high and poorly characterized that interpreting them becomes an almost insurmountable challenge. However, as described elsewhere in this book (e.g., Chapter 73), it should be kept in mind that genome-wide association studies (GWAS) of a number of diseases indicate that mutations affecting intronic DNA are closely associated with these diseases and may be involved in causing differences in levels of expression of protein products of associated exonic DNA and its transcription RNA product. Nevertheless, most experts predict that whole-genome sequencing will eventually replace exome sequencing as the standard procedure, as it offers advantages such as universal coverage across all the genes, detection of mutations outside the coding regions, and the capability of detecting larger deletions and insertions. It can also be combined with mRNA sequencing (*RNAseq* or *transcriptomics*) to define the nature of mutations in regulatory and splice-junction regions causing abnormalities in gene expression or RNA processing (Lee et al., 2020) (Fig. 72.9).

The technical details of the actual sequencing process vary by manufacturer of the instruments, but most of those in current use take "snapshots" of repeated sequencing cycles, adding one nucleotide at a time, with each of the four nucleotides identified by a certain fluorescent color or other chemical method (Fig. 72.10). Each fragment in the library is sequenced many times in both directions (so-called *paired-end* sequencing), typically

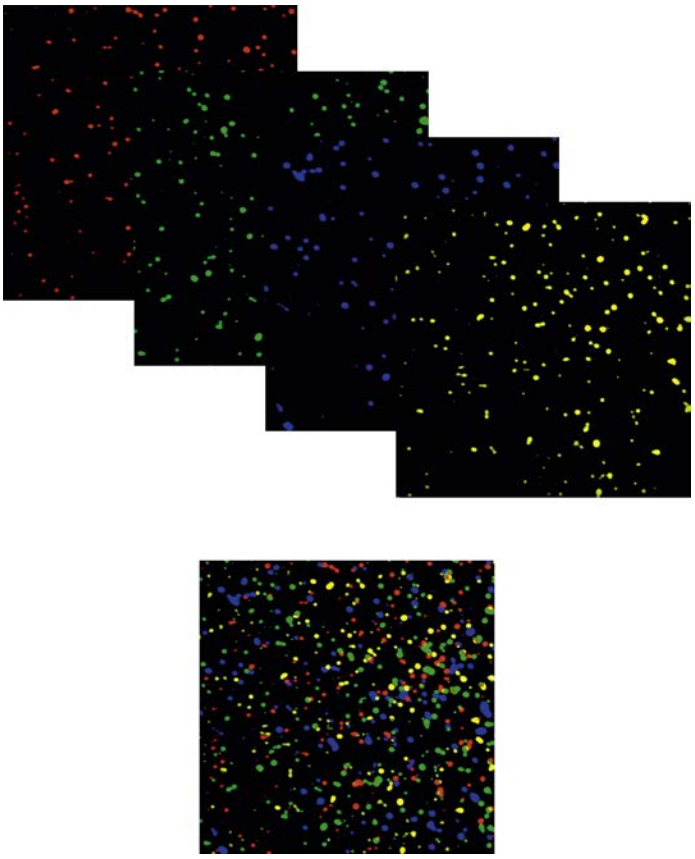

Figure 72.10 Examples of cluster arrays, the raw data from next-generation DNA sequencing. Shown are snapshots of nucleotide addition signals for each of the four bases independently and mixed together as read by the instrument (Courtesy of Dr. Sam Strom.)

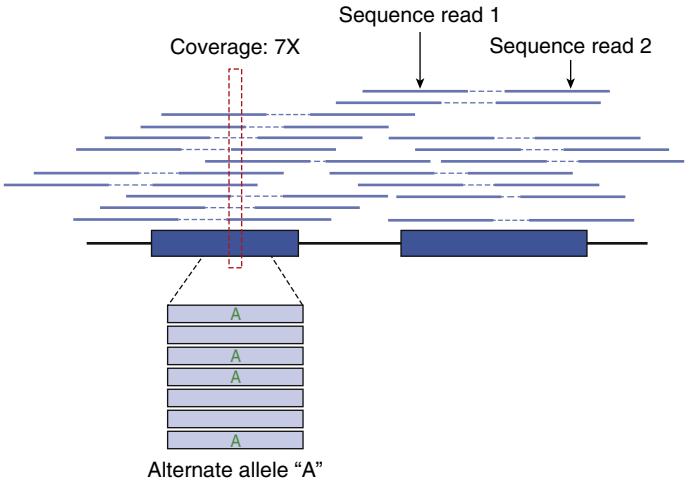

Figure 72.11 Alignment and variant calling of next-generation sequencing "reads." Fragments are overlapped by partial homology and the nucleotides at each position compared to the reference genome. In this example, an alternate nucleotide ("A") is observed in about half the aligned reads covering the left exon, consistent with a heterozygous variant. (Courtesy of Dr. Hane Lee.)

10 to 100×, but potentially even more—hence, the description "massively parallel." The greater the number of these "reads," the more accurate will be the sequence output since individual reactions may have random errors, but these will be statistically ignored if enough consensus reads are present.

After all of the sequencing is completed, the computer software must *align* each of the read fragments to the reference human genome sequence in order to be confident of which gene/exon it came from and whether it contains any sequence variants that do not agree with the reference sequence. The latter process is the *variant calling* step (Fig. 72.11). Next, each variant is examined for its potential biological/clinical significance (the *annotation* step). Then, these are *filtered* according to predetermined software criteria in order to reduce the huge number of sequence variants not matching the reference genome (20,000–30,000 for each exome, 3–4 million for each genome) down to a more manageable number. Typical parameters used to eliminate variants from consideration are "synonymous" nucleotide substitutions (which do not alter the amino acid encoded by the codon), relatively common polymorphisms in the healthy population, and heterozygous variants for disorders that are known to be recessive, while aspects favoring pathogenicity include association with known disease states, *in silico* prediction algorithms for effect on the protein structure, and known intolerance of the gene to missense or loss-of-function variants (Fig. 72.12). It must be admitted that some aspects of the filtering step are somewhat arbitrary, but there is simply no way for anyone to evaluate so many variants manually.

Once the variants are filtered down to a few tens or hundreds of potentially pathogenic changes, the challenge of *interpretation* begins. This may be the most difficult aspect of exome/genome sequencing, requiring extraordinarily sophisticated and broad expertise. Most centers employ a multidisciplinary group, including laboratory directors, geneticists, bioinformaticists and clinicians, to discuss and come to conclusions about which variants to report and whether to designate them as pathogenic, likely pathogenic, or unknown (usually called "variants of uncertain significance," or VUS). Guidelines have been promulgated by the ACMG and other groups to assist in the clinical interpretation of novel sequence variants (Richards et al., 2015).

Clinical exome sequencing has clearly delivered on its initial promise in the form of high diagnostic yields (most centers reporting 25%–50%) (Lee et al., 2014), cost savings by ending the lengthy and expensive "diagnostic odyssey" that many patients with rare disorders endure, and discovery of new disease genes. But it has also uncovered a significant ethical challenge in the form of "incidental" or "off-target" findings. These are pathogenic mutations identified in the course of sequencing that are unrelated to the clinical indication for performing the test but are potentially life-threatening or "actionable" (e.g., incidental identification of a *BRCA1* mutation in a 4-year-old girl undergoing exome sequencing because of autism). Debate has raged between those who feel that all such actionable findings should be mandatorily reported in both adults and children and those who feel that the patient (or parent) should have the ability to "opt out" of receiving such findings. The ACMG developed a list of about 25 diseases that are felt to be of sufficiently high penetrance, severity, and actionability that routine reporting of mutations found incidentally should be considered (Green et al., 2013; Kalia et al., 2017). It is intended that the list be periodically revisited and modified in light of new knowledge. While developed solely in the context of incidental (also called *secondary*) findings from diagnostic exome or genome sequencing, some have adapted it as the foundation for genomic screening in healthy people to assess risk of future disease, though the ACMG has cautioned against this (ACMG, 2019). For one thing, the potential clinical significance of both incidental findings and VUSs is best determined in the context of the patient's phenotype or positive family history, which often will not exist or be known in the healthy screening population (Grody, 2019). Similar considerations will apply to the application of exome sequencing to prenatal testing of a normal-appearing fetus, along with the additional burden of facing an irreversible pregnancy decision based on a VUS. These ethical dilemmas are likely to become even more commonplace as noninvasive prenatal screening, made possible by massively parallel sequencing of cell-free fetal DNA in the pregnant mother's blood, moves beyond detection of gross aneuploidies to sequence variants in the whole exome (Hashiloni-Dolev et al., 2019).

One way to avoid confronting off-target mutations is to limit the sequencing to genes already known to be associated with the patient's phenotype. Quite a few genetic conditions are caused by families of genes, with difficulty distinguishing the various subtypes based on clinical presentation alone. Examples include cardiomyopathies, hearing loss, and the other conditions listed in Box 72.1. Such conditions may be caused by anywhere from 10 to 100 or more different genes; NGS now allows for the efficient sequencing of such large amounts of DNA. However, experience has shown that as many as half of the patients with these disorders will be missed using existing gene panels (Lee et al., 2014) simply because the panels cannot keep up with all of the newly discovered or candidate (or thus far unknown) genes associated with the condition.

The applications presented in this chapter are all single-gene defects because that is all our current knowledge and technology can handle. In the future, it is hoped that molecular genetic testing will also be applied to the most common chronic diseases of medicine, which are all polygenic:

Variant info	**Chr:Pos**	7: 6426860
	Ref/Alt	A/G
Consequence	**Gene name**	RAC1
	Sequence ontology	missense_variant
	HGVS c.	NM_018890.4:c.53G>A
	HGVS p.	NP_061485.1:p.Cys18Tyr
Allele frequency	**Alt allele count (AC)**	Not in gnomAD
	Homozygous count	Not in gnomAD
	Hemizygous count	Not in gnomAD
Disease association	**Disorders (ID)**	Mental retardation autosomal dominant 48 (617751)
	Disorders inheritance	Autosomal dominant
Gene constraint	**gnomAD pLI**	0.7623
	gnomAD missense Z	3.1347
In silico prediction	**SIFT Pred (C)**	Tolerated
	Polyphen2 HVAR Pred (C)	Possibly damaging
Variant classification	**Clinvar (ID)**	Pathogenic (445280)
	HGMD (ID)	DM? (CM1713218)

Figure 72.12 Annotation of a variant observed in the *RAC1* gene by next-generation sequencing in a child with developmental delay. The missense variant, causing replacement of cystine by tyrosine at codon 18, is not observed in healthy population databases (gnomAD), but is listed in symptomatic databases (ClinVar, HGMD) as pathogenic or likely pathogenic. *In silico* prediction algorithms (SIFT, PolyPhen) are not in agreement, which is not unusual. The final exome report listed this variant as the likely cause of the child's delay from autosomal-dominant mental retardation, type 48. HGVS, Human Genome Variation Society. (Courtesy of Dr. Hane Lee.)

BOX 72.1

Some Conditions Tested Using Next-Generation Sequencing of Gene Panels

- Hypertrophic cardiomyopathy
- Dilated cardiomyopathy
- Hereditary arrhythmias (channelopathies)
- Retinitis pigmentosa
- Albinism
- Mental retardation
- DNA repair defects
- Skeletal dysplasias
- Disorders of sexual development
- Hearing loss
- Familial cancers
- Autoinflammatory disorders
- Immunodeficiencies

atherosclerosis, diabetes mellitus, hypertension, schizophrenia, and more. Since these conditions are likely caused by a great many genes (in addition to environmental factors), with each one contributing perhaps only incrementally to overall risk, NGS could theoretically be applied to address all of them at once. It is toward this end that a tremendous effort is being expended to identify single-nucleotide polymorphisms and other variants within candidate genes that may in aggregate produce quantitative trait effects on homeostasis, vascular tone, lipid metabolism, and so on. Many of these SNPs are the products of years of genome-wide association studies (GWAS). Once a sufficient number are known and clinically validated, they can be converted into a targeted genotyping test to produce what is now being called a *polygenic risk score* (Lewis & Vassos, 2020). It is hoped that the discovery of these determinants will enable population risk screening programs followed by targeted therapies and preventive interventions. In this way, molecular genetic testing will become the central modality behind an ever-greater proportion of medical practice and "precision medicine" in the 21st century, and virtually every patient, whether healthy or ill, will feel its impact.

SELECTED REFERENCES

GeneticTesting Registry. https://www.ncbi.nlm.nih.gov/gtr/.
This useful Internet site provides a worldwide searchable laboratory directory listing the locations where specific testing for each disease can be obtained, with over 500 testing laboratories included.

Green RC, Berg JS, Grody WW, Kalia SS, Korf BR, Martin CL, et al.: ACMG recommendations for reporting of incidental findings in clinical exome and genome sequencing, *Genet Med* 15:565–574, 2013.
This publication presents the initial guidelines developed by the American College of Medical Genetics and Genomics for which conditions should be reported when mutations are discovered "incidentally" in the course of exome or genome sequencing. Subsequent modifications and revisions continue to be issued.

Grody WW, Cutting G, Klinger K, et al.: Laboratory standards and guidelines for population-based cystic fibrosis carrier screening, *Genet Med* 3:149–154, 2001.
This article presents the recommendations from the American College of Medical Genetics and the American College of Obstetricians and Gynecologists for implementation of nationwide cystic fibrosis population carrier screening using a core panel of 25 CFTR mutations (later reduced to 23).

Grody WW: The transformation of medical genetics by clinical genomics: hubris meets humility, *Genet Med* 21:1916–1926, 2019.
Overview by the author of the power and challenges of clinical exome and genome sequencing.

Lee H, Deignan JL, Dorrani N, et al.: Clinical exome sequencing for genetic identification of rare Mendelian disorders, *J Am Med Assoc* 312:1880–1887, 2014.
One of numerous publications demonstrating the high diagnostic yield of genome-level DNA sequencing for patients with rare or undiagnosed disorders.

Miller DT, Adam MP, Aradhya S, et al.: Consensus statement: chromosomal microarray is a first-tier clinical diagnostic test for individuals with developmental disabilities or congenital anomalies, *Am J Hum Genet* 86:749–764, 2010.
This expert guideline was the first to recommend chromosomal microarray in place of standard karyotype for identification of deletions and duplications in the workup of patients with developmental delay, autism, or congenital malformations.

Richards S, Aziz N, Bale S, et al.: Standards and guidelines for the interpretation of sequence variants: a joint consensus recommendation of the American College of medical genetics and genomics and the association for molecular pathology, *Genet Med* 17:405–423, 2015.
The consensus guideline provides a detailed approach for assessing the pathogenicity of DNA sequence variants identified by either traditional testing or genome-level sequencing. It is now used universally by laboratories performing clinical exome and genome sequencing.

Access the complete reference list online at Elsevier eBooks for Practicing Clinicians.

REFERENCES

Abeliovich D, Lavon IP, Lerer I, et al.: Screening for five mutations detects 97% of cystic fibrosis (CF) chromosomes and predicts a carrier frequency of 1:29 in the Jewish Ashkenazi population, *Am J Hum Genet* 51:951–956, 1992.

ACMG Board of Directors: The use of ACMG secondary findings recommendations for general population screening: a policy statement of the American College of Medical Genetics and Genomics (ACMG), *Genet Med* 21:1467–1468, 2019.

Ahn AH, Kunkel LM: The structural and functional diversity of dystrophin, *Nat Genet* 3:283–291, 1993.

American College of Medical Genetics: *Genetic susceptibility to breast and ovarian cancer: assessment, counseling and testing guidelines—executive summary*, Albany, NY, 1999, American College of Medical Genetics and New York State Department of Health.

American College of Obstetricians and Gynecologists: Carrier screening for genetic conditions, *Committee Opinion No. 691, Obstet Gynecol 129*, 2017. e41–55.

Anguiano A, Oates RD, Amos JA, et al.: Congenital bilateral absence of the vas deferens: a primarily genital form of cystic fibrosis, *J Am Med Assoc* 267:1794–1797, 1992.

Baruch S, Hudson K: Civilian and military genetics: nondiscrimination policy in a post-GINA world, *Am J Hum Genet* 83:435–444, 2008.

Beggs AH, Koenig M, Boyce FM, Kunkel LM: Detection of 98% of DMD/BMD gene deletions by polymerase chain reaction, *Hum Genet* 86:45–48, 1990.

Ben-Shachar R, Svenson A, Goldberg JD, Muzzey D: A data-driven evaluation of the size and content of expanded carrier screening panels, *Genet Med* 21:1931–1939, 2019.

Bertina RM, Koeleman BPC, Koster T, et al.: Mutations in blood coagulation factor V associated with resistance to activated protein C, *Nature* 343:1535–1536, 1994.

Beutler E, Felitti VJ, Koziol JA, et al.: Penetrance of 845G-A (C282Y) HFE hereditary haemochromatosis mutation in the USA, *Lancet* 359:211–218, 2002.

Billings PR, Kohn MA, de Cuervas M, et al.: Discrimination as a consequence of genetic testing, *Am J Hum Genet* 50:476–482, 1992.

Brennan ML, Schrijver I: Cystic fibrosis: a review of associated phenotypes, use of molecular diagnostic approaches, genetic characteristics, progress, and dilemmas, *J Mol Diagn* 18:3–14, 2016.

Burke W, Aitken ML, Chen S-H, Scott CR: Variable severity of pulmonary disease in adults with identical cystic fibrosis mutations, *Chest* 102:506–509, 1992.

Cobb NJ, Surewicz WK: Prion diseases and their biochemical mechanisms, *Biochemistry* 48:2574–2585, 2009.

Chen X, Sanchis-Juan A, French CE, Connell AJ, Delon I, Kingsbury Z, et al.: Spinal muscular atrophy diagnosis and carrier screening from genome sequencing data, *Genet Med* 22:945–953, 2020.

Collins FS: Cystic fibrosis: molecular biology and therapeutic implications, *Science* 256:774–780, 1992.

Conner BJ, Reyes AA, Morin C, et al.: Detection of sickle beta-globin allele by hybridization with synthetic oligonucleotides, *Proc Natl Acad Sci U S A* 80:278–282, 1983.

Cyranoski D: What CRISPR-baby prison sentences mean for research (Editorial), *Nature* 577:154–155, 2020.

Dames S, Eilbeck K, Mao R: A high-throughput next-generation sequencing assay for the mitochondrial genome, *Methods Mol Biol* 1264:77–88, 2015.

Darras BT, Koenig M, Kunkel LM, Francke U: Direct method for prenatal diagnosis and carrier detection in Duchenne/Becker muscular dystrophy using the entire dystrophin cDNA, *Am J Med Genet* 29:713–726, 1988.

Deignan JL, Astbury C, Cutting GR, Del Gaudio D, Gregg AR, Grody WW, et al.: CFTR variant testing: a technical standard of the American College of Medical Genetics and Genomics (ACMG), *Genet Med* 22:1288–1295, 2020.

Derichs N: Targeting a genetic defect : cystic fibrosis transmembrane conductance regulator modulators in cystic fibrosis, *Eur Resp Rev* 22:58, 2013.

Ducros V, Barro C, Yver J, et al.: Should plasma homocysteine be used as a biomarker of venous thromboembolism? A case-control study, *Clin Appl Thromb Hemost* 15:517–522, 2009.

Dzierlega K, Yokota T: Optimization of antisense-mediated exon skipping for Duchenne muscular dystrophy, *Gene Ther*, 2020.

Egan ME: Cystic fibrosis transmembrane conductance receptor modulator therapy in cystic fibrosis, an update, *Curr Opin Pediatr* 32:384–388, 2020.

Eng C: RET proto-oncogene in the development of human cancer, *J Clin Oncol* 17:380–393, 1999.

Eno CC, Barton SK, Dorrani N, Cederbaum SD, Deignan JL, Grody WW: Confidential genetic testing and electronic health records: a survey of current practices among Huntington disease testing centers, *Mol Genet Genomic Med* 8, 2020. e1026.

Everett CM, Wood NW: Trinucleotide repeats and neurodegenerative disease, *Brain* 127:2385–2405, 2004.

Feder JN, Gnirke A, Thomas W, et al.: A novel MHC class I-like gene is mutated in patients with hereditary haemochromoatosis, *Nat Genet* 13:399–408, 1996.

Fu Y-H, Pizzuti A, Fenwick RG, et al.: An unstable triplet repeat in a gene related to myotonic muscular dystrophy, *Science* 255:1256–1258, 1992.

Garber JE, Offit K: Hereditary cancer predisposition syndromes, *J Clin Oncol* 23:276–292, 2005.

Gervais R, Dumur V, Rigot J-M, et al.: High frequency of the R117H cystic fibrosis mutation in patients with congenital absence of the vas deferens (letter), *N Engl J Med* 328:446–447, 1993.

Gochee PA, Powell LW, Cullen DJ, et al.: A population-based study of the biochemical and clinical expression of the H63D hemochromatosis mutation, *Gastroenterology* 122:646–651, 2002.

Grebe TA, Seltzer WK, DeMarchi J, et al.: Genetic analysis of Hispanic individuals with cystic fibrosis, *Am J Hum Genet* 54:443–446, 1994.

Green RC, Berg JS, Grody WW, Kalia SS, Korf BR, Martin CL, et al.: ACMG recommendations for reporting of incidental findings in clinical exome and genome sequencing, *Genet Med* 15:565–574, 2013.

Grody WW: Cystic fibrosis: molecular diagnosis, population screening, and public policy, *Arch Pathol Lab Med* 123:1041–1046, 1999.

Grody WW, Cutting G, Klinger K, et al.: Laboratory standards and guidelines for population-based cystic fibrosis carrier screening, *Genet Med* 3:149–154, 2001a.

Grody WW, Griffin JH, Taylor AK, et al.: American College of Medical Genetics consensus statement on factor V Leiden mutation testing, *Genet Med* 3:139–148, 2001b.

Grody WW, Cutting GR, Watson MS: The cystic fibrosis mutation "arms race": when less is more, *Genet Med* 9:739–744, 2007.

Grody WW, Richards CS: New quality assurance standards for rare disease testing, *Genet Med* 10:320–324, 2008.

Grody WW: Expanded carrier screening and the law of unintended consequences: from cystic fibrosis to fragile X, *Genet Med* 13:996–997, 2011.

Grody WW: Where to draw the boundaries for prenatal carrier screening, *J Am Med Assoc* 316:717–719, 2016.

Grody WW: The transformation of medical genetics by clinical genomics: hubris meets humility, *Genet Med* 21:1916–1926, 2019.

Grosu DS, Hague L, Chelliserry M, et al.: Clinical investigational studies for validation of a next-generation sequencing in vitro diagnostic device for cystic fibrosis testing, *Expert Rev Mol Diagn* 14:605, 2014.

Guo MH, Gregg AR: Estimating yields of prenatal carrier screening and implications for design of expanded carrier screening panels, *Genet Med* 21:1940–1947, 2019.

Gurrieri F, Accadia M: Genetic imprinting: the paradigm of Prader-Willi and Angelman syndromes, *Endocr Dev* 14:20–28, 2009.

Hagerman RJ, Hull CE, Safanda JF, et al.: High functioning fragile X males: demonstration of an unmethylated fully expanded FMR-1 mutation associated with protein expression, *Am J Med Genet* 51:298–308, 1994.

Hall MA, Rich SS: Laws restricting health insurers—use of genetic information: impact on genetic discrimination, *Am J Hum Genet* 66:293–307, 2000.

Handyside AH, Lesko JG, Tarin JJ, et al.: Birth of a normal girl after in vitro fertilization and preimplantation diagnostic testing for cystic fibrosis, *N Engl J Med* 327:905–909, 1992.

Hantash FM, Goos DG, Tsao D, et al.: Qualitative assessment of FMR1 (CGG)n triplet repeat status in normal, intermediate, premutation, full mutation, and mosaic carriers in both sexes: implications for fragile X syndrome carrier and newborn screening, *Genet Med* 12:162–173, 2010.

Hart SN, Polley EC, Yussuf A, Yadav S, Goldgar DE, Hu C, et al.: Mutation prevalence tables for hereditary cancer derived from multigene panel testing, *Hum Mutat* 41:e1–e6, 2020.

Hashiloni-Dolev Y: Nov-Klaiman T, Raz A: Pandora's pregnancy: NIPT, CMA, and genome sequencing-A new era for prenatal genetic testing, *Prenat Diagn* 39:859–865, 2019.

Hatcher SL, Trang QT, Robb KM, et al.: Prenatal diagnosis by enzymatic amplification and restriction endonuclease digestion for detection of haemoglobins A, S and C, *Mol Cell Probes* 6:343–348, 1992.

Highsmith WE, Burch LH, Zhou Z, et al.: A novel mutation in the cystic fibrosis gene in patients with pulmonary disease but normal sweat chloride concentrations, *N Engl J Med* 331:974–980, 1994.

Hoffman EP, Fischbeck KH, Brown RH, et al.: Characterization of dystrophin in muscle-biopsy specimens from patients with Duchenne's or Becker's muscular dystrophy, *N Engl J Med* 318:1363–1368, 1988.

Holtzman N, Murphy P, Watson M, Barr P: Predictive genetic testing: from basic research to clinical practice, *Science* 278:602–605, 1997.

Hoppe CC: Prenatal and newborn screening for hemoglobinopathies, *Int J Lab Hematol* 35:297–305, 2013.

Huntington's Disease Society of America: *Guidelines for predictive testing for Huntington's disease*, New York, 1989, Author.

Jacinto FV, Esteller M: Mutator pathways unleashed by epigenetic silencing in human cancer, *Mutagenesis* 22:247–523, 2007.

Jacquemont S, Hagerman R, Leehey MA, et al.: Penetrance of the fragile X-associated tremor/ataxia syndrome in a premutation carrier population, *J Am Med Assoc* 291:460–469, 2004.

Kalia SS, Adelman K, Bale SJ, Chung WK, Eng C, Evans JP, et al.: Recommendations for reporting of secondary findings in clinical exome and genome sequencing, 2016 update (ACMG SF v2.0): a policy statement of the American College of Medical Genetics and Genomics, *Genet Med* 19:249–255, 2017.

Kerem B-S, Rommens JM, Buchanan JA, et al.: Identification of the cystic fibrosis gene: genetic analysis, *Science* 245:1073–1080, 1989.

Knoll JHM, Nicholls RD, Magenis RE, et al.: Angelman and Prader-Willi syndromes share a common chromosome 15 deletion but differ in parental origin of the deletion, *Am J Med Genet* 32:285–290, 1989.

Knudson AG: Mutation and cancer: statistical study of retinoblastoma, *Proc Natl Acad Sci U S A* 68:820–823, 1971.

Koeleman BPC, Reitsma PH, Allaart CF, Bertina RM: Activated protein C resistance as an additional risk factor for thrombosis in protein C-deficient families, *Blood* 84:1031–1035, 1994.

Kosaki K, McGinniss MJ, Veraksa AN, et al.: Prader–Willi and Angelman syndromes: diagnosis with a bisulfite-treated methylation-specific PCR method, *Am J Med Genet* 73:308–313, 1997.

Koshy BT, Zoghbi HY: The CAG/polyglutamine tract diseases: gene products and molecular pathogenesis, *Brain Pathol* 7:927–942, 1997.

Kowdley KV, Brown KE, Ahn J, Sundaram V: ACG clinical guideline: hereditary hemochromatosis, *Am J Gastroenterol* 114:1202–1218, 2019.

Kronquist KE, Sherman SL, Spector EB: Clinical significance of tri-nucleotide repeats in fragile X testing: a clarification of American College of Medical Genetics guidelines, *Genet Med* 10:845–847, 2008.

Kupferminc MJ, Eldor A, Steinman N, et al.: Increased frequency of genetic thrombophilia in women with complications of pregnancy, *N Engl J Med* 340:9–13, 1999.

Lee H, Deignan JL, Dorrani N, Strom SP, Kantarci S, Quintero-Rivera F, et al.: Clinical exome sequencing for genetic identification of rare Mendelian disorders, *J Am Med Assoc* 312:1880–1887, 2014.

Lee H, Huang AY, Wang LK, Yoon AJ, Renteria G, Eskin A, et al.: Diagnostic utility of transcriptome sequencing for rare Mendelian diseases, *Genet Med* 22:490–499, 2020.

Lewis CM, Vassos E: Polygenic risk scores: from research tools to clinical instruments, *Genome Med* 12:44, 2020.

Lipton LR, Johnson V, Cummings C, et al.: Refining the Amsterdam Criteria and Bethesda Guidelines: testing algorithms for the prediction of mismatch repair mutation status in the familial cancer clinic, *J Clin Oncol* 22:4934–4943, 2004.

Lodi R, Cooper JM, Bradley JL, et al.: Deficit of in vivo mitochondrial ATP production in patients with Friedreich ataxia, *Proc Natl Acad Sci U S A* 96:11492–11495, 1999.

Macek M, Mackova A, Hamosh A, et al.: Identification of common cystic fibrosis mutations in African-Americans with cystic fibrosis increases the detection rate to 75%, *Am J Hum Genet* 60:1122–1127, 1997.

Macpherson JN, Murray A: Development of genetic testing for fragile X syndrome and associated disorders, and Estimates of the prevalence of FMR1 expansion mutations, *Genes* 7:110, 2016.

Mahadevan M, Tsilfidis C, Sabourin L, et al.: Myotonic dystrophy mutation: an unstable CTG repeat in the 3′ untranslated region of the gene, *Science* 255:1253–1255, 1992.

Manning M, Hudgins L: ACMG Professional Practice and Guidelines Committee: array-based technology and recommendations for utilization in medical genetics practice for detection of chromosomal abnormalities, *Genet Med* 12:742–745, 2010.

Massie J, Castellani C, Grody WW: Carrier screening for cystic fibrosis in the new era of medications that restore CFTR function, *Lancet Resp Med* 383:923–925, 2014.

Matsuura T, Sutcliffe JS, Fang P, et al.: De novo truncating mutations in E6-AP ubiquitin-protein ligase gene (UBE3A) in Angelman syndrome, *Nat Genet* 15:74–77, 1997.

McCabe LL, McCabe ERB: Genetic screening: carriers and affected individuals, *Annu Rev Genomics Hum Genet* 5:57–69, 2004.

Miller DT, Adam MP, Aradhya S, et al.: Consensus statement: chromosomal microarray is a first-tier clinical diagnostic test for individuals with developmental disabilities or congenital anomalies, *Am J Hum Genet* 86:749–764, 2010.

Monaco AP, Bertelson CJ, Liechti-Gallati S, et al.: An explanation for the phenotypic differences between patients bearing partial deletions of the DMD locus, *Genomics* 2:90–95, 1988.

Moreira L, Balaguer F, Lindor N, de la Chapelle A, Hampel H, Aaltonen LA, et al.: Identification of Lynch syndrome among patients with colorectal cancer, *J Am Med Assoc* 308:1555–1565, 2012.

Moskowitz SM, Chmiel JF, Sternen DL, et al.: Clinical practice and genetic counseling for cystic fibrosis and CFTR-related disorders, *Genet Med* 10:851–868, 2008.

Multicenter Study Group: Diagnosis of Duchenne and Becker muscular dystrophies by polymerase chain reaction: a multicenter study, *J Am Med Assoc* 267:2609–2615, 1992.

Naja RP, Kaspar H, Shbaklo H, et al.: Accurate and rapid prenatal diagnosis of the most frequent East Mediterranean beta-thalassemia mutations, *Am J Hematol* 75:220–224, 2004.

Nallamilli BR, Ankala A, Hegde M: Molecular diagnosis of duchenne muscular dystrophy, *Curr Protoc Hum Genet* 83:9–25, 2014.

National Comprehensive Cancer Network: Genetic/familial high-risk assessment: breast and ovarian, *Clinical Practice Guidelines in Oncology* v.1, 2005. Available at http://www.nccn.org/professionals/physician_gls/PDF/genetics_screening.pdf.

NIH Consensus Statement Online: Genetic testing for cystic fibrosis. Available at http://text.nlm.nih.gov/nih/cdc/www/106txt.html.

Nelson HD, Pappas M, Zakher B, Mitchell JP, Okinaka-Hu L, Fu R: Risk assessment, genetic counseling, and genetic testing for BRCA-related cancer in women: a systematic review to update the U.S. Preventive Services Task Force recommendation, *Ann Intern Med* 160:255–266, 2014.

Nolin SL, Brown WT, Glicksman A, et al.: Expansion of the fragile X CGG repeat in females with premutation or intermediate alleles, *Am J Hum Genet* 72:454–464, 2003.

Nolin SL, Glicksman A, Ersalesi N, Dobkin C, Brown WT, Cao R, et al.: Fragile X full mutation expansions are inhibited by one or more AGG interruptions in premutation carriers, *Genet Med* 17:358–364, 2015.

Ober C, Lester LA, Mott C, et al.: Ethnic heterogeneity and cystic fibrosis transmembrane regulator (CFTR) mutation frequencies in Chicago-area CF families, *Am J Hum Genet* 51:1344–1348, 1992.

Ojino S, Wilson RB: Bayesian analysis and risk assessment in genetic counseling and testing, *J Mol Diagn* 6:1–9, 2004.

Ojino S, Wilson RB: Spinal muscular atrophy: molecular genetics and diagnostics, *Expert Rev Mol Diagn* 4:15–29, 2004.

Palomaki GE, FitzSimmons SC, Haddow JE: Clinical sensitivity of prenatal screening for cystic fibrosis via CFTR carrier testing in a United States panethnic population, *Genet Med* 6:405–414, 2004.

Patrinos GP, Kollia P, Papadakis MN: Molecular diagnosis of inherited disorders: lessons from hemoglobinopathies, *Hum Mutat* 26:399–412, 2005.

Pirooznia M, Goes FS, Zandi PP: Whole-genome CNV analysis: advances in computational approaches, *Front Genet* 6:138, 2015.

Pietrangelo A: Hereditary hemochromatosis—a new look at an old disease, *N Engl J Med* 350:2383–2397, 2004.

Poort SR, Rosendaal FR, Reitsma PH, Bertina RM: A common genetic variation in the 3′-untranslated region of the prothrombin gene is associated with elevated plasma prothrombin levels and an increase in venous thrombosis, *Blood* 88:3698–3703, 1996.

Press RD, Bauer KA, Kujovich JL, Heit JA: Clinical utility of factor V Leiden (R506Q) testing for the diagnosis and management of thromboembolic disorders, *Arch Pathol Lab Med* 126:1304–1318, 2002.

Prior TW: Genetic analysis of the Duchenne muscular dystrophy gene, *Arch Pathol Lab Med* 115:984–990, 1991.

Prior TW: ACMG professional practice and guidelines committee: carrier screening for spinal muscular atrophy, *Genet Med* 10:840–842, 2008.

Prior TW: Perspectives and diagnostic considerations in spinal muscular atrophy, *Genet Med* 12:145–152, 2010.

Raraigh KS, Han ST, Davis E, Evans TA, Pellicore MJ, McCague AF, et al.: Functional assays are essential for interpretation of missense variants associated with variable expressivity, *Am J Hum Genet* 102:1062–1077, 2018.

Richards S, Aziz N, Bale S, Bick D, Das S, Gastier-Foster J, et al.: Standards and guidelines for the interpretation of sequence variants: a joint consensus recommendation of the American College of medical genetics and genomics and the association for molecular pathology, *Genet Med* 17:405–423, 2015.

Ridker PM, Miletich JP, Hennekens CH, Buring JE: Ethnic distribution of factor V Leiden in 4047 men and women: implications for venous thromboembolism screening, *J Am Med Assoc* 227:1305–1307, 1997a.

Ridker PM, Hennekens CH, Selhub J, et al.: Interrelation of hyperhomocyst(e)inemia, factor V Leiden, and risk of future venous thromboembolism, *Circulation* 95:1777–1782, 1997b.

Riordan JR, Rommens JM, Kerem B-S, et al.: Identification of the cystic fibrosis gene: cloning and characterization of complementary DNA, *Science* 245:1066–1073, 1989.

Rohilla KJ, Gagnon KT: RNA biology of disease-associated microsatellite repeat expansions, *Acta Neuropathol Commun* 5:63, 2017.

Rowland LP: Dystrophin: a triumph of reverse genetics and the end of the beginning (editorial), *N Engl J Med* 318:1392–1394, 1988.

Ruiz-Pesini E, Lott MT, Procaccio V, et al.: An enhanced MITOMAP with a global mtDNA mutational phylogeny, *Nucleic Acids Res* 35, 2007. D823–D828.

Sabath DE: Molecular diagnosis of thalassemias and hemoglobinopathies: an ACLPS critical review, *Am J Clin Pathol* 148:6–15, 2017.

Sagi M, Weinberg N, Eilat A, et al.: Preimplantation genetic diagnosis for BRCA1/2—a novel clinical experience, *Prenat Diagn* 29:508–513, 2009.

Schmidt AY, Hansen TVO, Ahlborn LB, Jønson L, Yde CW, Nielsen FC: Next-generation sequencing-based detection of germline copy number variations in BRCA1/BRCA2: validation of a one-step diagnostic workflow, *J Mol Diagn* 19:809–816, 2017.

Sepulveda AR, Hamilton SR, Allegra CJ, Grody W, Cushman-Vokoun AM, Funkhouser WK, et al.: Molecular Biomarkers for the evaluation of colorectal cancer: guideline from the American Society for clinical pathology, College of American Pathologists, association for molecular pathology, and American Society of clinical oncology, *J Mol Diagn* 19:187–225, 2017.

Sherman SL: Premature ovarian failure in the fragile X syndrome, *Am J Med Genet* 97:189–194, 2000.

Smeets HJM, Smits APT, Verheij CE, et al.: Normal phenotype in two brothers with a full FMR1 mutation, *Hum Mol Genet* 4:2103–2108, 1995.

Smith A, Hung D: The dilemma of diagnostic testing for Prader-Willi syndrome, *Transl Pediatr* 6:46–56, 2017.

Spence JE, Perciaccante RG, Greig GM, et al.: Uniparental disomy as a mechanism for human genetic disease, *Am J Hum Genet* 42:217–226, 1988.

Sznajder LJ, Swanson MS: Short tandem repeat expansions and RNA-mediated pathogenesis in myotonic dystrophy, *Int J Mol Sci* 20:3365, 2019.

Talseth-Palmer BA: The genetic basis of colonic adenomatous polyposis syndromes, *Hered Cancer Clin Pract* 15(5), 2017.

Tassone F: Advanced technologies for the molecular diagnosis of fragile X syndrome, *Expert Rev Mol Diagn* 15:1465–1473, 2015.

Tsui L-C: The spectrum of cystic fibrosis mutations, *Trends Genet* 8:393–398, 1992.

U.S. Preventive Services Task Force: Screening for hemochromatosis: recommendation statement, *Ann Intern Med* 145:204–208, 2006.

Waheed A, Parkkila S, Saarnio J, et al.: Association of HFE protein with transferrin receptor in crypt enterocytes of human duodenum, *Proc Natl Acad Sci U S A* 96:1579–1584, 1999.

Wan L, Li Y, Zhang Z, Sun Z, He Y, Li R: Methylenetetrahydrofolate reductase and psychiatric diseases, *Transl Psychiatry* 8:242, 2018.

Wang L, Baudhuin LM, Boardman LA, et al.: MYH mutations in patients with attenuated and classical polyposis and with young onset colorectal cancer without polyps, *Gastroenterology* 127:9–16, 2004.

Watson MS, Cutting GR, Desnick RJ, et al.: Cystic fibrosis couple carrier screening: 2004 revision of ACMG's mutation panel, *Genet Med* 6:387–391, 2004.

Zhang S, Taylor AK, Huang X, Luo B, Spector EB, Fang P, et al.: Venous thromboembolism laboratory testing (factor V Leiden and factor II c.*97G>A), 2018 update: a technical standard of the American College of Medical Genetics and Genomics (ACMG), *Genet Med* 20:1489–1498, 2018.

Zhou W, Wang G, Zhao X, Xiong F, Zhou S, Peng J, et al.: A multiplex qPCR gene dosage assay for rapid genotyping and large-scale population screening for deletional α-thalassemia, *J Mol Diagn* 15:642–651, 2013.

CHAPTER 73

MOLECULAR GENETICS OF NEUROPSYCHIATRIC DISORDERS: CURRENT RESEARCH AND PERSPECTIVES

Jacquelyn L. Meyers, Roseann E. Peterson, Tim B. Bigdeli, Ayman Fanous, Bo Lin, Shabnam Seydhafkan, Matthew R. Pincus

INTRODUCTION, 1452
GENOME-WIDE ASSOCIATION STUDIES, 1452
NEUROPSYCHIATRIC DISEASES, 1453
Schizophrenia, 1453
Bipolar Disorder, 1456
Substance Use Disorders, 1459
Major Depression Disorder, 1461
Posttraumatic Stress Disorder and Anxiety Disorders, 1463
Other Neuropsychiatric Disorders, 1464
FUTURE DIRECTIONS AND CONCLUDING REMARKS, 1466
SELECTED REFERENCES, 1467

KEY POINTS

- Genome-wide association studies (GWAS) on neuropsychiatric disorders have been expanding to increasingly large populations and are now including multiethnic groups.
- These studies are aimed at identifying specific single nucleotide polymorphisms (SNPs) that may be associated with specific diseases at high frequencies.
- Characteristic high-frequency SNPs seem to occur in schizophrenia, bipolar disorder (BD), substance use, major depression disorder (MDD), posttraumatic stress disorder (PTSD), Alzheimer disease (AD), and autism.
- Characteristic SNPs found for each disorder occur either in exons or introns.
- These SNPs occur in or near genes that encode a variety of proteins, which are receptors, channel proteins, transcription factors, central nervous system developmental proteins, and proteins involved in metabolism, especially fatty acid and carbohydrate metabolism.
- Many of these SNPs appear to be unique to each disease type, but there are overlaps such as SNPs involved with calcium channel proteins in both schizophrenia and bipolar disorder.
- Several GWAS have uncovered hitherto unknown feedback pathways involved in disease causation and suggest new therapeutic modalities for these diseases.

INTRODUCTION

Psychiatric and substance use disorders are extremely prevalent worldwide (Kessler et al., 2005). Many of these disorders are highly disabling and associated with many physical comorbidities; they also contribute substantially to global morbidity and mortality (Whiteford et al., 2013). Mental health conditions impair productivity and interpersonal functioning and are associated with significant psychological and financial costs. In view of the seriousness of these conditions, current epidemiologic studies integrating data from multiple levels (e.g., psychosocial, neurobiological, genomic) to identify risk and protective factors are needed to identify points prior to the onset of such disorders in which preventative action could be focused.

Twin and family studies have demonstrated that there are both genetic and environmental components in the inheritance of psychiatric and substance use disorders (Polderman et al., 2015). Twin studies provide an estimation of a trait's heritability in a population (i.e., what proportion of phenotypic variation is due to genetic variation underlying the trait). Twin studies accomplish this by comparing trait similarity between monozygotic twins, who share all of their genetic variation, with dizygotic twins, who share (on average) half of their genetic variation. Since measures of heritability are a function of the specific population, the estimates can vary among populations, age, sex, ancestry, and culture.

The search for specific risk and protective loci began with linkage studies, which localized chromosomal regions of interest transmitted by affected individuals in large extended families. While these linkage studies provided the first clues toward many specific chromosomal regions of interest, and in some cases genes of interest, early linkage studies lacked the resolution required to identify specific genetic variants. In addition, the resources required to study large pedigrees of affected individuals made the scaling up of genetic studies of psychiatric illness challenging. Thus the field moved away from large family-based linkage studies and on to candidate gene association studies, which compare a specific candidate gene (or specific candidate loci within genes) among affected and unaffected individuals. Candidate genes or variants were historically chosen based on prior knowledge of their involvement in specific biological pathways or systems, often as a follow-up of promising genes in linkage regions. For example, genes that are part of the dopaminergic system (e.g., dopamine receptor, *DRD2*) are considered candidate genes for several mental illnesses, at least in part because of the role of dopamine in the reward pathway. While the candidate gene strategy has been successful in some studies, this approach was largely limited by the scope of our understanding of human biology, publication biases, and generally small (statistically underpowered) samples typically conducted during the 1990s and 2000s, leading to a large number of nonreplicable genetic association findings (Duncan et al., 2019).

GENOME-WIDE ASSOCIATION STUDIES

In part due to the limitations of candidate gene studies, but also due to advances in genotyping technologies that made genome arrays accessible to researchers, the field turned to genome-wide association studies (GWAS) that could be conducted in related or unrelated individuals and, importantly, were hypothesis free. That is, they did not require prior understanding of the biological mechanisms underlying a given disorder but instead scanned the entire genome for variants that differed significantly among individuals with and without a particular disorder or trait of interest.

The basic object of this method in its simplest form is to sequence the genomes of large numbers of individuals (see Chapter 80) or to determine chromosomal changes in a group who have a particular disease and a second set of individuals who do not have the disease (control group). These sequences or chromosomes are then analyzed for single nucleotide polymorphisms (SNPs) at specific genomic sites or for chromosomal deletions, duplications, etc. Then the ratio of the number of individuals who have

SNPs of chromosomal changes and disease to the number of individuals who have SNPs or chromosomal changes but no disease is computed. This is divided by the ratio of the number of individuals who do not have SNPS but have disease to number of individuals who do not have SNPs and have no disease. This quotient is termed the odds ratio. The statistical significance of the odds ratio is computed using appropriate statistical tests such as the chi-square test. The *p* value for this computation is usually on the order of 5×10^{-8}; *p* values less than this value indicate statistical significance (i.e., the SNP or chromosomal pattern is unique to the disease). These *p* values can then be plotted (often as bar graphs) versus the specific SNPs or chromosomal changes identified for the specific disease. In these plots, -log of the *p* value is plotted on the *y*-axis, and the corresponding individual genes with significant SNPs or chromosome numbers on which changes occur are plotted on the *x*-axis. These plots are referred to as Manhattan plots because they resemble the Manhattan skyline in New York City, New York.

However, an early GWAS conducted by the Wellcome Trust Case Control Consortium quickly showed the field that this new method for novel gene discovery would prove challenging, particularly for complex, multifactorial, and psychiatric traits. A decade of mostly unsuccessful GWAS taught researchers that extremely large sample sizes would be necessary to detect the subtle genetic influences on psychiatric illnesses. Over the past several years, researchers have joined forces in forming large consortia and biobanks to compile the sample sizes needed for gene discovery in psychiatric and behavioral conditions. For example, the Psychiatric Genomics Consortium (PGC), iPSYCH, the UK Biobank, 23andMe, GSCAN, and most recently a US Department of Veterans Affairs effort, the Million Veterans Project (MVP). In the past few years, several landmark studies from these consortia and biobanks have been published in the area of psychiatric and substance use genomics. Additionally, as robust and replicable genomic risk factors for psychiatric disorders emerge, it becomes crucial to understand the biological mechanisms underlying these statistical associations and important interactions with aspects of the psychosocial environment. Also of note, the largest GWAS have disproportionately focused on cohorts of European descent. This European bias is not unique to psychiatric genetics research but systemic within the GWAS literature. Although the proportion of non-Europeans included in analyses has since been increasing, this remains a critical issue that the field must address. In the next section we discuss some of the latest findings in key psychiatric and substance use disorders.

NEUROPSYCHIATRIC DISEASES

SCHIZOPHRENIA

Schizophrenia affects ~0.6% to 1% of the population worldwide. It is a chronic and debilitating neuropsychiatric syndrome, which can include symptoms such as hallucinations, delusions, disorganized thought and speech, as well as deficits in social interaction and motivation (negative symptoms). Most of the variability in liability to illness is attributable to genetic factors, with ~80% heritability estimated by twin studies (Sullivan et al., 2003). While rare genetic variants play a role in the underlying liability, most of the currently explained liability is harbored in common variation. The past decade has seen the successes of psychiatric GWAS abound, including the first definitive demonstration of polygenic influences on schizophrenia risk and its shared basis with bipolar disorder, and ever-increasing numbers of robustly associated, replicated SNP associations culminating in the identification of 108 physically distinct risk loci for schizophrenia, a number that has since grown to 145 (Schizophrenia Working Group, 2014). This progress can be credited to collaborative enterprise on an unprecedented scale, as exemplified by the PGC, and a philosophy of data sharing that has enabled widespread meta-analysis and replication. Notable findings include dopamine receptor *DRD2* and glutamatergic and synaptic plasticity genes (e.g., *GRM3*, *GRIN2A*, *SRR*, *GRIA1*), which are highly relevant to current pharmacologic treatment of schizophrenia and correspond with long-standing etiopathogenic theories. In addition, genes that encode voltage-gated calcium channel subunits (*CACNA1C*, *CACNB2*, and *CACNA1I*) have consistently been associated with schizophrenia in GWAS; interestingly, *CACNA1C* was first robustly associated with bipolar disorder, an illness known to have significant genetic overlap with schizophrenia, as discussed later. We now describe these three classes of proteins further. A summary of these proteins and their functions is presented in Table 73.1.

TABLE 73.1
Proteins Associated With Characteristic SNPs in Schizophrenia

Protein/Chromosomal Changes	Function
D2 (dopamine) receptor	Nerve transmission, blocks cAMP pathways.
iGluR NMDA receptors: GRIA1 and Grin2A	Nerve conduction, direct channel proteins.
Serine racemase (SRR gene)	Catalyzes conversion of L- to D-serine that binds to NMDA receptor.
mGluR receptor	Coupled to G0 protein and initiate activation of phospholipase C, IP3, diacylglycerol, Akt. Causes calcium ion fluxes into cells and is involved in depolarization at synapse. Involved with synaptic plasticity.
CACNA1C	CaV1.2 calcium channel protein. Channel activity controlled by α-1 subunit. Interacts with calmodulin in its IQ domain. Promotes L-type currents at synapses.
CACNB2	Calcium voltage-gated channel auxiliary subunit β
CACNA1I	α-1 subunit of a voltage-gated calcium channel involved with T (transient) currents in rhythmic depolarization. Found in thalamic reticular nucleus (TRN) involved in sleep.
Neurexin	Transmembrane synaptic structural protein; also called "handshake" protein because it is involved in holding the axonal and dendritic components of the synapse together.
ARC protein (activity-regulated cytoskeleton-associated protein)	Involved in synaptic plasticity mainly at NMDA receptor locations; implicated in learning and memory.
Fragile X mental retardation syndrome protein (FMRP)	Involved in synaptic plasticity. CGG repeats in the genome for this protein can cause diminished expression.
Chromosomal deletions	15q13.3 and 1q21.1
Chromosomal changes	1q21.1, 2p16.3 (neurexin, see text), 3q29, 7q11.2, 15q13.3, 16p11.2, and 22q11.2

Gene-Encoded Dopamine Receptors

There are two types of receptors involved in synaptic transmission in neural pathways: ionotropic and metabotropic. The first type are ion channels that respond directly and rapidly to effectors resulting in immediate ion currents that are either excitatory (excitatory postsynaptic potentials [EPSPs]) or inhibitory (inhibitory postsynaptic potentials [IPSPs]), and the second type are more slowly responsive because they require activation of G proteins, which are proteins that become activated by binding guanosine triphosphate (GTP) in place of guanosine diphosphate (GDP) (see later; also see Chapter 77). These GTP-activated proteins, in turn, activate downstream targets on signal transduction pathways that ultimately end in the nucleus. These events result in the synthesis of proteins that affect the postsynaptic ion channels resulting in either EPSPs or IPSPs. Dopamine receptors are of the metabolomic type or G protein–coupled receptors (GPCRs).

There are at least five forms of the dopamine receptor that have strong sequence homology to one another but nonetheless differ significantly in sequences in specific domains. In fact, dopamine receptors are located and encoded by different genes. D1 receptor encoding is by the gene 5q31-q34. The genes encoding the D2 and D4 receptors are on chromosome 11, while the gene encoding the D3 receptor is located on chromosome 3 and the D5 receptor on chromosome 4. Activation of each of these receptors results in different regulation of ion channels and ion currents. Each type of dopamine receptor is associated with specific functions (i.e., D1: memory, attention, impulse control, regulation of renal function, locomotion; D2: locomotion, attention, sleep, memory, learning; D3: cognition, impulse control, attention, sleep; D4: cognition, impulse control, attention, sleep; D5: decision making, cognition, attention, renin secretion) (Mishra et al., 2018). Despite these differences all dopamine receptors are large, almost all α-helical proteins that span the membrane at seven locations, and they contain both amino and carboxyl termini as components of the extracellular domain of the receptor.

There are four G proteins downstream of the dopamine receptor: Gα,0; Gα,i; β; and ϒ. Gα,0 is an activator of downstream targets such as cyclic adenosine monophosphate (cAMP), while Gα,i inhibits this activation. β and ϒ proteins activate phospholipase C and induce the synthesis of inositol triphosphate (IP3), an important downstream target that activates further downstream targets such as induction of calcium ion release and activation of the all-important kinase, Akt (see Chapter 77). When activated by binding dopamine, the D2 receptor activates Gi in a signal transduction pathway that ultimately results in the inhibition of adenyl cyclase activity and activation of potassium channels.

Dopamine receptors, like epinephrine receptors (described in Chapter 24), exist on both sides of the synaptic cleft (i.e., presynaptic autoreceptors and postsynaptic receptors). The latter, when bound to dopamine in the presence of calcium ions from calcium channels, induce EPSPs or IPSPs. The former, presynaptic autoreceptors, downregulate the amount of dopamine released into the synaptic cleft and are therefore inhibitory.

Glutamate and *N*-Methyl-D-Aspartate (NMDA) Receptors

These receptors are activated by the binding of L-glutamate or NMDA to these receptors. As found for dopamine receptors, glutamate receptors can be ionotropic (iGluR) or metabotropic (mGluR).

iGluR receptors, of which GRIA1 and Grin2A are members, are ion channels consisting of dimeric protein receptors with their amino termini containing the ligand (e.g., glutamate) binding domain on the extracellular surface connected to four transmembrane domains and relatively short intracytosolic carboxyl terminal domains. This complex is illustrated in Panel 1A of Figure 73.1. Upon binding to the appropriate ligand, each of the two dimers is displaced such that they line an open cation channel allowing for an influx of a cation such as sodium, potassium, or calcium, as illustrated in panel 1B of Figure 73.1. This influx leads to depolarization and action potentials. The fastest action potentials with this system are achieved with NMDA receptors in the retina and parts of the central and peripheral nervous systems. Signaling is regulated by transport proteins that clear the synapse of the ligand.

A strong ligand that binds to the NMDA receptor is D-serine, which is produced by the action of serine racemase on L-serine in the presence of vitamin B_6, pyridoxal phosphate. Serine racemase is encoded by the SRR gene.

mGluR exists as 12 splice variants encoded by eight genes (Willard et al., 2013). The 12 splice variants can be classified into three groups based on sequence homology, specific agonist binding, and downstream targets of the activated receptor protein. Thus mGluR1a and mGluR5a are placed in group 1. Both receptors are coupled to Gα protein and are activated when two glutamate molecules bind to each of two neighboring receptors. Activated mGluR1a initiates a series of signal transduction pathways (see Panel 2 of Fig. 73.1). These pathways result in activation of calcium mobilization from intracellular organelles or in activation of pathways concerned with cell survival (antiapoptosis) and growth.

Signal Transduction Pathways; Cell Growth Pathways

Panel 2 of Figure 73.1 shows that activated receptor activates Gα protein that is involved probably through activation of the serine-threonine kinase, raf, that in turn activates MEK that activates MAP kinase, which, when activated, crosses the nuclear membrane and activates transcription factors such as fos that ultimately induces transcription of cell growth genes. This pathway is discussed more extensively in Chapter 77.

Calcium Mobilization Pathways

G protein activation also results in activation of an important downstream target protein, phosphoinositide-3-hydroxy kinase (PI3K), that results in the synthesis of 1,4,5-triphosphoinositide (IP3). This molecule is critical for mobilization of calcium ions from intracellular stores shown for the endoplasmic reticulum (ER) in Figure 73.1B (left lower portion of the figure). The released calcium activates an important calcium binding protein, calmodulin, discussed later, which in turn activates calmodulin kinase II that is involved in long-term potentiation.

In a second activation pathway (see Panel 2 of Fig. 73.1) the scaffold protein HOMER1 binds to the carboxyl terminal end of the intracytoplasmic domain of mGluR at a specific amino acid sequence. This results in the attachment of a second scaffold protein, SHANK, that induces release of calcium ions from the rough ER (RER). Both HOMER and SHANK proteins are of importance in bipolar disorders, as discussed later.

Pathway Interactions

IP3 is also synthesized from the action of phospholipase C on the phosphoinositol ester of a diglyceride yielding IP3 and diacylglycerol (DAG) that activates protein kinase C (PKC; *not shown in Fig. 73.1*). PKC can activate MEK and MAPK in the presence of raf, although it is not clear that this occurs in the mGluR pathway.

Antiapoptosis Cell Survival Pathways

Besides cell growth pathways, as in the MAPK pathway, there are other pathways that block apoptosis. As can be seen in Panel 2 of Figure 73.1, PI3K activates the protein Akt, also known as protein kinase B, that is both a cell growth-inducing pathway and an antiapoptosis protein. Phosphorylated Akt blocks the protein BAD from promoting apoptosis and, at the same time, promotes growth by activating mTOR protein (target of rapamycin protein, discussed in Chapter 24). In addition, phosphorylated Akt activates the protein IKK that in turn activates the protein NFκB that crosses into the nucleus and activates transcription of growth proteins.

It should be noted that there appear to be two endpoints for these G protein–induced pathways. The first is mobilization of calcium ions from stores in organelles. It must be remembered that these pathways occur in dendritic neurons at whose membranes EPSPs and IPSPs occur. Mobilization of calcium ions into the cytosol would have a tendency to lower the transmembrane potential in the dendrite likely leading to EPSPs and nerve conduction. Second is transcription of proteins involved in cell growth and survival, including inhibition of pathways involved in apoptosis. These pathways, such as MAPK- and BAD-induced pathways, assure survival of neurons, which cannot be replaced.

In contrast, mGluR2 and R3 (Grm3) in group 2 activate Gi and inhibit synthesis of cAMP (see earlier). Group 3, the largest group, contains mGluR4, R6, R7A, and R8A, which likewise activate Gi.

The overall structure of mGluR is similar to that of the dopamine receptor since it is a GPCR and has seven transmembrane domains with its amino terminus and the ligand-binding site located extracellularly. However, it is considered to be an atypical GPCR since it has a large extracellular domain ligand binding site (most GPCR have small ligand binding domains). In addition the receptors are paired such that one glutamate binds to the ligand binding domain of each of the monomers in the pair; in this process groups of sulfhydryl groups of cysteine residues become paired as disulfides upon ligand binding.

Importantly, glutamate neural pathways are involved in synaptic plasticity. This is the ability of synapses to increase or decrease their activities (e.g., number of EPSPs or IPSPs over time). This phenomenon is thought to be important in learning and memory. Changes in plasticity can result from changes in the number of postsynaptic receptors, alteration of the number of neurotransmitter quanta released into the synapse, and changes in the affinities of postsynaptic receptors for the neurotransmitter. Plasticity is also dependent on postsynaptic release of calcium ions.

Calcium Channel Proteins

Ion channels are formed by multisubunit proteins that form transmembrane pores or channels, which can allow ions to pass through these pores. In the resting state, these pores are closed. At specific changes in the transmembrane voltage, the subunits change their disposition and conformation such as to allow ions to flow through the channels. Depending on the type of ion that passes through the pores, the cell may become depolarized or hyperpolarized as, for example, the EPSPs and IPSPs in the postsynaptic dendritic membrane at synapses discussed earlier. These channels are referred to as voltage-gated channels.

CACNA1C

Voltage-dependent calcium channels mediate the entry of calcium ions into cells and calcium release from cellular organelles in a variety of calcium-dependent processes, such as muscle contraction, hormone or neurotransmitter release, and gene expression. Calcium channel proteins are composed of α-1, β, α-2/δ, and ϒ subunits. Channel activity is controlled mainly by the α-1 subunit, while the other subunits help to regulate this activity. Calcium channels differ from one another principally with respect to α isoforms (i.e., α-1A, B, C, D, E, and S). CACNA1A encodes the α-1A isoform of calcium channel protein that occurs almost exclusively in neuronal tissue.

Mutations in the CACNA1A gene are associated with multiple neurologic disorders, many of which are episodic, including familial hemiplegic migraine, ataxia, and epilepsy. This gene has been found to have (CAG) n-repeats in open reading frames, which encode polyglutamine, which has been associated with spinocerebellar ataxia.

The CACNA1C (α-1C) gene encodes the CaV1.2 channel protein, which is expressed usually in clusters of eight in smooth muscle, pancreas, fibroblasts, and neurons. It is also present in the myocardium where it mediates L (long-lasting)–type currents and helps define the shape of the action potential in cardiac muscle.

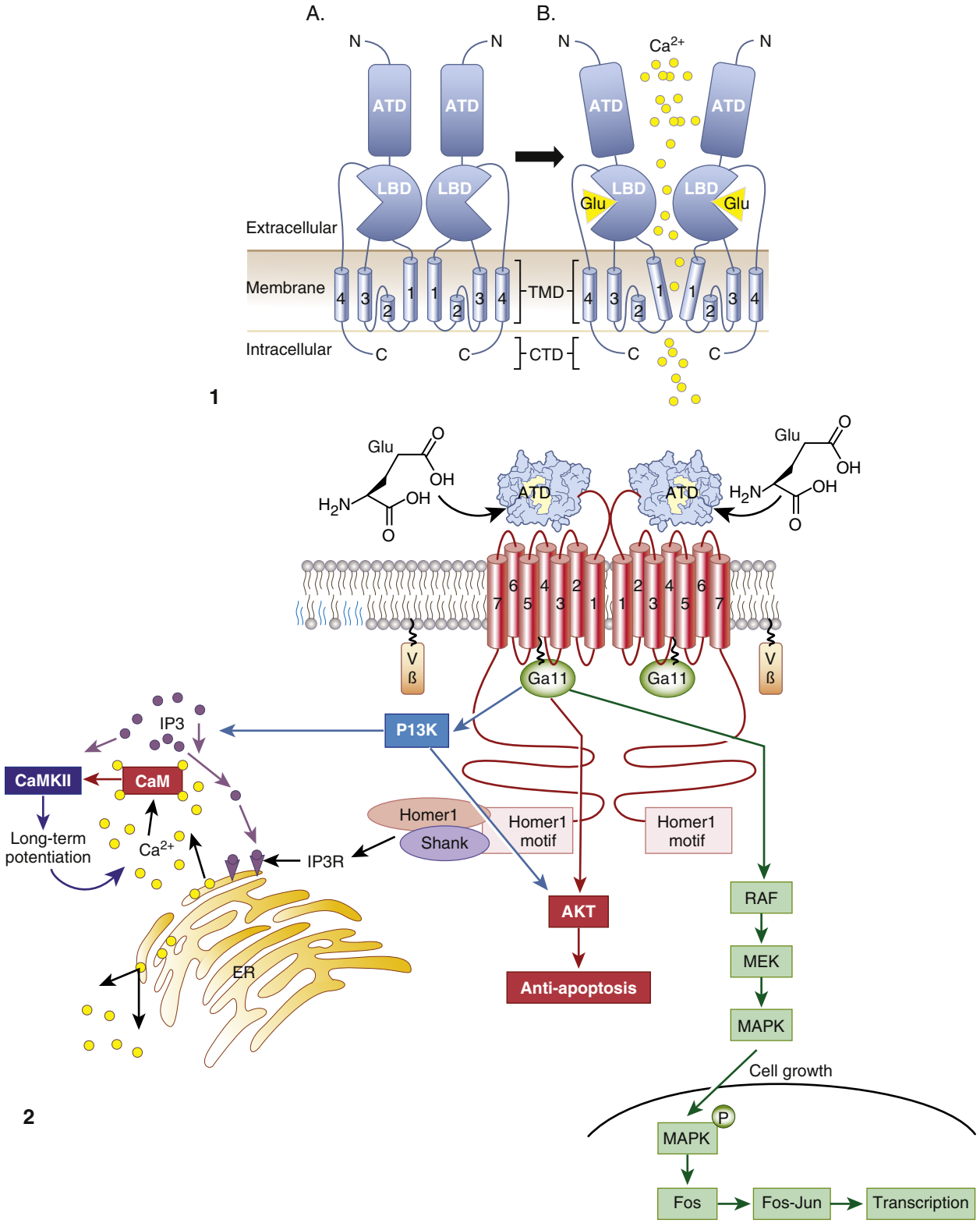

Fig. 73.1 **Panel 1,** iGluR structure and activation of this receptor. The receptor is shown as a dimer, represented by two symmetrically arranged polypeptide chains (subunits) in mirror-image fashion. Although this figure shows a dimeric structure, the actual receptor is a tetramer that lines an ion channel. Beginning at the N terminus *(N),* the amino terminal domain *(ATD)* is followed by the ligand binding domain *(LBD),* constituting the extracellular domain *(Extracellular).* This is followed by the four transmembrane domains (*TMD*; numbered 1–4) and the C-terminal domain *(CTD).* Panel 1A shows the resting conformation of iGluR. Panel 1B shows that when Glu binds to the Glu ligand binding site, the subunits rearrange such as to cause opening of the channel allowing calcium ions to diffuse into the cell. **Panel 2,** mGluR schematic structure and signal transduction pathways induced by it. This receptor is activated when two glutamate molecules bind to each of two extracellular domains of two adjacent receptors. This promotes dimerization of the two receptors resulting in activation of the intracytoplasmic domain of the receptor resulting in its binding to a G protein α-β-ϒ complex. The Gα subunit is activated and induces activation of a series of signal transduction pathways. Proceeding from left to right, this protein binds to two scaffolding proteins, Homer and Shank. This trimeric complex activates phosphoinositide-3-hydroxykinase *(PI3K),* which induces synthesis of inositol-3-phosphate *(IP3R)* that binds to a receptor *(purple triangles)* in the endoplasmic reticulum *(yellow/brown structures)* resulting in release of calcium ions *(yellow circles).* IP3 also activates CaMKII (calcium-calmodulin-dependent protein kinase II), that promotes long-term calcium-dependent potentiation. PI3K also activates Akt, a cell proliferation-promoting protein, which also blocks apoptosis. Activated Gα also activates the serine-threonine kinases, raf, MEK (mitogenic extracellular receptor-dependent kinase) and MAPK (mitogen activated protein kinase). The latter, when phosphorylated, transfers across the nuclear membrane into the nucleus where it activates (phosphorylates) the centrally important transcription factor, fos. Activated fos forms a heterodimeric complex with activated jun, another centrally important transcription factor, activated separately by jun kinase (JNK) to form an active transcription factor, fos-jun, that induces transcription and translation of multiple mitogenic proteins. (Adapted from Willard SS, Koochekpour S: Glutamate, glutamate receptors, and downstream signaling pathways. *Int J Biol Sci* 9:948–959, 2013 [fig. 7]. https://doi.org/10.7150/ijbs.6426.)

This protein is tightly regulated by calcium ions. Increase in intracellular concentration of calcium ions induces increased CaV1.2 channel–associated calcium ion influx into the cell. However, the influx of calcium ions itself induces a change in the structure of this channel protein such that it blocks further entry of calcium ions. These effects are governed by the interaction of the protein calmodulin with the carboxyl terminal segment of the CaV1.2 protein in its so-called IQ domain, an 11–amino acid residue segment. This event seems to induce interactions between the CaV1.2 units in the eight-member complex that allow simultaneous opening and reflex closing of these channels.

A single-nucleotide polymorphism in the third intron of the Cav1.2 gene (SNP rs1006737) is associated with cardiac arrhythmias, bipolar disorder, and schizophrenia (Imbrici et al., 2013; Smedler et al., 2019; Calabro et al., 2016). Also, a CACNA1C risk allele has been further associated with patients diagnosed with bipolar disorder that is not generally present in their unaffected relatives or healthy controls.

CACNB2 is a calcium voltage-gated channel auxiliary subunit β (see earlier). Polymorphisms in the gene encoding this channel protein are associated with cardiac arrhythmias (e.g., Brugada syndrome), autism, attention deficit-hyperactivity disorder (ADHD), bipolar disorder, major depressive disorder, and schizophrenia (Cross-Disorder Group of the Psychiatric Genomics Consortium, 2013).

CACNA1I is the α-1 subunit of a voltage-gated calcium channel. It is the channel associated with T (transient) calcium currents that occur in repolarized or hyperpolarized cells that lead to depolarization. It is this channel that occurs in the sinoatrial (SA) node in the heart and is a pacemaker channel. In the central nervous system (CNS) CACNA1I channels occur in neurons of the thalamic reticular nucleus (TRN) involved in sleep. Abnormalities of sleep and different patterns of neuronal activity in the thalamus have been found in patients with schizophrenia, a finding that suggests thalamocortical dysfunction (Andrade et al., 2016).

New GWAS

We have recently undertaken the largest GWAS of admixed African individuals to date, with a combined sample size of 6152 schizophrenia and schizoaffective disorder cases and 3918 screened controls from the Genomic Psychiatry Cohort (GPC). Meta-analysis of African ancestry results with PGC-SCZ2 (Psychiatric Genomics Consortium–Study of Schizophrenia) summary statistics yielded 94 associated loci, of which 11 were not among the 108 previously reported, and 7 were newly genome-wide significant (Bigdeli et al., 2017).

Copy Number Variants

In addition to the aforementioned common variant studies, another major class of genomic risk factors has been uncovered using the same technology that underlies GWAS—namely, copy number variants (CNVs), including both deletions and duplications. An increased burden of CNVs genome-wide was first reported in 2008.

Cytogenetic Findings

Several large CNVs were reported, most notably deletions on both 15q13.3 and 1q21.1. Subsequently, large-scale "mega-analysis" in the PGC confirmed this and showed a more or less specific increase in burden in genes with synaptic function as well as those implicated in animal models of illness. Furthermore, a number of specific loci showed significant enrichment in CNVs, including 1q21.1, 2p16.3 (neurexin1), 3q29, 7q11.2, 15q13.3, 16p11.2, and 22q11.2 (Marshall et al., 2017).

The involvement of neurexin 1 is significant since this protein is involved in synapse formation. It is expressed as a one-pass transmembrane protein on the presynaptic membrane and is vital for connections made between nerve endings at the synapse. It binds to the protein neuroligin in the synaptic cleft. Its intracytoplasmic domain is involved in exocytosis and is presumably involved in neurotransmitter release. Neurexins in general regulate signaling across the synapse and therefore control the interactions of neural networks at synapses. Besides being implicated as being involved with schizophrenia, they have further been implicated in other cognitive disorders such as Tourette syndrome and autism.

Rare Variant Studies

Rare variant studies utilizing both whole-genome sequencing (WGS) or whole-exome sequencing (WES) are in a relatively early phase, in part due to the inherently lower power to detect significant effects for lower frequency variants. Currently, there are a number of large-scale case control studies ongoing in both European and non-European ancestry populations. An early report utilizing WES showed that cases are enriched for rare (<1 in 10,000) disruptive mutations in coding regions. This study confirmed the involvement of gene sets previously implicated in GWAS and CNV studies. Furthermore, it additionally implicated gene sets, including the voltage-gated calcium ion channel and the ARC (activity-regulated cytoskeleton-associated) protein and targets of the fragile X mental retardation protein (FMRP) (Purcell et al., 2014). Both of these proteins are involved in synaptic plasticity. ARC protein expression seems to occur at NMDA receptor locations and has been implicated in learning and memory. FMRP is encoded on the X chromosome and has been found to be required for formation of synapses. Absence or low expression of this protein causes the so-called fragile X mental retardation syndrome. Individuals with this condition are found to have intellectual disabilities, a long and narrow face, large ears, flexible fingers, and (in males) enlarged testicles. Many of those affected have features of autism (see below), including problems with social interactions and delayed speech. The cause of the low protein expression is the occurrence of more than 200 repeats of CGG on the gene encoding this protein (normal is up to 40 repeats). Overall, the results of these more recent cytogenetic and rare variant studies suggest that abnormalities in synaptic proteins may contribute importantly to the occurrence of schizophrenia.

Use of GWAS in Pharmacogenomics

Adequately powered GWAS of the beneficial and adverse effects of psychotropic medications are limited by the considerable difficulty and expense of conducting longitudinal drug trials, which require valid and reliable symptom assessment over the course of an adequate trial. This is usually defined as 6 weeks of treatment at a therapeutic dose. The largest GWAS of antipsychotic efficacy to date examined the landmark CATIE (Clinical Antipsychotic Trials of Intervention Effectiveness) study (McClay et al., 2011), which included 738 patients.

In these studies, responses to both positive and negative symptoms of schizophrenia were determined. Positive symptoms include hallucinations, delusions, and racing thoughts; negative symptoms include apathy, lack of emotion, poor or nonexistent social functioning, disorganized thoughts, and difficulty in concentrating or following instructions. Only one SNP was genome-wide significant (on 4p15) and associated with positive symptom response to ziprasidone. However, two other SNPs exhibited low q values and were therefore deemed of interest. A SNP in ANKS1B (a postsynaptic scaffold protein involved in long-term potentiation) was associated with olanzapine effects on negative symptoms, while a SNP in CNTNAP5 (a neurexin protein; see earlier) was associated with risperidone effects on negative symptoms.

An analysis of metabolic side effects, which can be associated with significant morbidity and mortality, was also performed in the CATIE study (Adkins et al., 2012). This reported two genome-wide significant findings: two SNPs in GPR98 (a large adhesion GPCR protein with 6300 amino acids) were associated with elevated hemoglobin A_{1c} (HbA_{1c}) in olanzapine use, and a SNP in MEIS2 (a transcription regulator protein) was associated with increased hip circumference in risperidone use. A number of other SNPs were suggestively significant in analyses of measures that also included total cholesterol, high-density lipoprotein (HDL), and triglyceride levels. It is hoped that the availability of genomic data in large-scale registry-based cohorts will make it possible to conduct naturalistic pharmacogenomic studies of antipsychotic effects.

BIPOLAR DISORDER

Similar to schizophrenia, BD has been shown to have a prevalence of 1% to 2% and heritability of >70% (Smoller & Finn 2003). It is diagnosed on the basis of episodes of both mania and depression. In addition, about one-third of patients have psychotic symptoms, which can be very similar to those seen in schizophrenia. Indeed, the diagnostic distinction between the two disorders has been a subject of much discussion for more than a century. Furthermore, there are significant distinctions between different subgroups of BD (i.e., BD1 and BD2, schizoaffective disorder, and manic depression) that tend to complicate genomic analysis (Ikeda et al., 2018a, 2018b; Stahl et al., 2019).

However, the total sample size of the PGC-Bipolar Disorder Working Group has enlarged significantly since and is currently comprised of 20,352 cases and 31,358 controls. This study reported a total of 30 genome-wide significant loci, 20 of which had previously not been reported. In addition, recent large-scale studies were performed on Japanese and trans-European Japanese populations (2964 bipolar patients and 61,887 controls) (Ikeda et al., 2018a, 2018b). Gene sets that were significantly associated included ion channels, neurotransmitter transporters, synaptic components, nerve transmission, transcription and regulation of the cell cycle, neuronal stability, and immune and energy metabolism components (Stahl et al., 2019). The most prominent genes and their encoded proteins that were found thus far to be significantly associated with bipolar disorder are summarized in Table 73.2 and are discussed later.

TABLE 73.2

Proteins Associated With Characteristic SNPs in Bipolar Disorder

Protein	Function
	CHANNEL PROTEINS
CACNA1C	Calcium channel protein (see Table 73.1).
	PROTEINS CRITICAL FOR NEURAL/SYNAPSE DEVELOPMENT AND NERVE TRANSMISSION
ODZ4-Teneurins	Sequence conserved one-pass transmembrane glycoproteins expressed in neural pattern formation and development.
SHANK2	Important protein in synaptogenesis. It links mGlu receptors to NMDA receptors by binding to attachment protein PSD-95 that binds to mGlur and to HOMER1 scaffold protein, that attaches to the NMDA receptor. For other scaffold proteins, see ANK3.
ADCY2	G protein–coupled protein that has strong adenyl cyclase activity and transduces signaling via cAMP. Vital for functioning of neocortex, hippocampus, amygdala, and corpus striatum.
ZNF804A	Zinc finger protein involved in neurite outgrowth, dendritic branching, and synapse formation. Vital for differentiation of oligodendroglia.
NCAN (NeuroCAN)	Modulates neuronal adhesion, migration, and axon guidance. Also associated with abnormalities in lipid metabolism. See also FADS below.
	PROTEINS CRITICAL FOR TRANSCRIPTION AND REGULATION OF THE CELL CYCLE
POU3F2	CNS transcription factor that binds to DNA at ATGCAAAT sequences and regulates mammalian neurogenesis by regulating their diverse patterns of gene expression.
DDN (Dendrin)	Transcription factor and RNA polymerase.
NEK4	Regulates entry of cells into senescence.
GNL3	GTP-binding protein involved with cell cycle and cell differentiation.
Mad1L1	Mitotic spindle assembly check point protein.
ERBB-2 (Neu/HER2)	Growth factor that transmits mitotic signaling via ras-p21.
	PROTEINS INVOLVED IN NEURONAL STABILITY
ANK3/Ankrin	Scaffolding protein that binds neuronal cell membrane and spectrin that itself binds to the cell membrane. Thus this is a membrane anchoring protein. See also TRANK1 below.
SYNE1	Encodes the protein Nesprin-1α that links membrane proteins and receptors to the cytoskeleton.
	PROTEINS WITH OTHER FUNCTIONS (MAINLY IMMUNE AND ENERGY METABOLISM)
ITIH3, ITIH4	Alpha trypsin inhibitors with three heavy and one light chain called bikunin. Important in modulating the neural inflammatory response.
FADS (fatty acid desaturase)	Enzyme that regulates levels of unsaturated fatty acids in lipid metabolism.
DGKH (diacylglycerol kinase eta)	Major enzyme in lithium-sensitive phosphatidyl inositol pathway.
TRANK1	Structural protein of unknown function. It contains a tetratricopeptide sequence (tandem repeats of 34 amino acids) and contains an ankyrin domain.

Calcium Channel Protein

Interestingly, the calcium channel protein CACNA1A (discussed earlier, as being a major protein implicated in schizophrenia) overlaps with bipolar disorder pointing to a possible common ion channel protein involved in both diseases.

Proteins That Are Critical for Neural Development and Nerve Transmission

ODZ Gene-Encoded Teneurins

ODZ gene-encoded teneurins are transmembrane proteins that may interact with signal transduction molecules and are crucial in the regulation of neuronal and synaptic connectivity during brain development. They have been found to be involved with organization of the development and differentiation of oligodendrocytes and the myelination of neuronal axons during brain maturation. The common variant rs12576775 in an intron of gene *ODZ4* has been associated with bipolar disorder in large studies. This gene has a minor allele frequency (10% across all ethnic populations with the exception of European populations; in European individuals the minor allele occurs in about 20% of individuals) (Ikeda et al., 2018a, 2018b; Heinrich et al., 2013).

SHANK2

SHANK2 is a scaffold protein involved in signal transduction involving mGluR-induced calcium mobilization (see earlier, including Figure 73.1B). It is also involved in cross-linking mGluR and iGluR.

ADCY2

ADCY2(5p15.31) is a key enzyme in cAMP signaling pathway. There are two genome-wide significant SNPs located in ADCY2. The ADCY2 gene on chromosome 5p15.31 is expressed in the brain and encodes a cell membrane–bound enzyme for the synthesis of the second-messenger molecule, cAMP, which is involved in nerve conduction. ADCY2 plays a key role in cAMP-dependent GPCR pathways and is regulated by PKC and raf kinase (see preceding section and Chapter 77). Disturbed neurotransmission in cAMP pathways is considered to be important in the pathogenesis of psychiatric illnesses (Huang et al., 2020; van Hulzen et al., 2017).

ZNF804A

The human *ZNF804A* gene is located on chromosome 2q32.1 and codes for a protein consisting of 1210 amino acids, containing a zinc finger domain, which binds to and regulates the activities of transcription factors. This protein is expressed in the brain and regulates genes involved in neurodevelopmental processes, cell adhesion, neurite outgrowth, dendritic branching and synapse formation, and differentiation of oligodendrocytes and proliferation of oligodendrocyte progenitors. It has been found that a single nucleotide polymorphism rs1344706 that is strongly associated with bipolar disease occurs in an intronic region of the *ZNF804A* gene (substitution of A for C). This results in expression of altered messenger ribonucleic acid (mRNA) that encodes a protein that has altered affinity for nuclear proteins, including transcription factors, in the CNS that results in disrupting myelination and reduction of white matter integrity (Muhleisen et al., 2014; Wang et al., 2018).

NCAN (NeuroCAN)

NCAN (NeuroCAN) is a large gene located on chromosome 19p13.11. The SNP rs1064395, which is found in an intronic region of the gene, has been associated with bipolar disorder in one study. Rs1064395 affects only one of five alternative transcripts of the gene. This gene has significant differences in allele frequencies across all ethnic populations. The overall frequency of the A allele (or disease-associated allele) is about 23%. It is the major allele in 51% of African populations, 12% in Asia, and 15% in Europe. Postmortem brain studies in bipolar patients show increased cortical folding in some brain regions of patients with the A allele compared with healthy controls.

The gene *NCAN* codes for a large secreted neurocan protein that is found predominantly in the extracellular space, the lumen of the Golgi apparatus, and lysosomal cavities. There are 741 known variants in the gene, but coding variants have not been associated with any mendelian disorder. Neurocan protein modulates neuronal adhesion, migration, and axon guidance and has been associated with abnormalities in lipid metabolism (Ikeda et al., 2018a, 2018b; Wang et al., 2018).

Proteins Critical for Transcription and Regulation of the Cell Cycle

These proteins have known functions related to transcription and regulation of the cell cycle, but the relationship of these functions to bipolar disorder is not clear. As with other proteins that have been identified as being involved with this disease, some of the SNPs in the genes coding for these proteins occur in introns or in intergenic domains of the genome rather than with direct gene expression.

POU3F2

POU3F2 on chromosome 6q16 is a transcription factor that binds to specific deoxyribonucleic acid (DNA) sequences (ATGCAAAT) and regulates expression of neurogenic proteins. It occurs downstream of *MIR2113* (microRNA 2113) gene. In the spanning intronic region, the genome-wide significant SNP in this region (rs12202969) appears to be associated with neocortex development in mice and with a cognitive phenotype and speed of information processing (Muhleisen et al., 2014; Prata et al., 2019).

DDN

DDN located on chromosome 12 (12q13.12) encodes the protein Dendrin, which serves as both a transcription factor and an RNA polymerase. The SNP RS1054442A in the DDN gene is associated with bipolar disorder (Gaudet et al., 2011).

NEK4, GNL3, and MAD1L1

NEK4, GNL3, and MAD1L1 (see Table 73.2) are all involved in control of the cell cycle. NEK4 is a serine threonine kinase that promotes cell cycle arrest in response to double-stranded DNA damage and is required for inducing replicative cell senescence (Scott et al., 2009). GNL3 is a G protein that promotes cell differentiation (Yang et al., 2020; Scott et al., 2009; Han et al., 2005; Tsai & McKay, 2002), and MAD1L1 is a mitotic checkpoint protein that blocks anaphase if the chromosomes are not aligned correctly (Zhao et al., 2018; Ikeda et al., 2018a, 2018b; Hara et al., 2017).

ERB-B2

ERB-B2, also called Neu/HER2, is a growth factor that binds to a growth factor receptor very much analogous to the epidermal growth factor receptor. This binding process causes receptor dimerization resulting in activation of a tyrosine kinase on the intracytoplasmic domain of the receptor. This kinase ultimately activates the critically important G protein, ras-p21, implicated as a causative factor in a large number of human cancers (see Chapter 77). ras-p21 activates raf that activates MEK that, in turn, activates MAP kinase in a signal transduction cascade described earlier (and in Chapter 77).

Proteins Involved in Neuronal Stability

Ankyrin 3 (ANK3)

The most prominent among these is ankyrin 3 or ANK3, which is a membrane-stabilizing protein. The *ANK3* gene occurs on chromosome 10q21 and was the first gene discovered and confirmed to have most significant association with bipolar disorder. This gene encodes the protein ankyrin, a large scaffolding adapter protein consisting of two major domains: the ankyrin repeats and the ZU5 and UPA domains. The ankyrin repeats bind membrane proteins, and ZU5 and UPA domains bind β-spectrin, which itself is a scaffold protein that binds to a number of proteins in the cell membrane. It has several alternatively spliced exons. The largest spliced axon is known as "neuronal" exon. This exon is spliced in three different ways, giving rise to large isoforms that occur in neurons at the nodes of Ranvier, the axon initial segment and dendritic spines, and in oligodendrocytes at the paranodal axoglial junction. An elevated expression of this isoform has been proposed as occurring with relatively high frequency in bipolar pathogenesis. In addition, a rare loss-of-function splice-site SNP (rs41283526*G) in a minor isoform of *ANK3* (incorporating exon ENSE00001786716) is protective against this disorder in some studies. The corresponding risk alleles in *ANK3* located near the transcription start site of this isoform are significantly associated with its elevated expression (Goulding et al., 2019; Roby, 2017).

SYNE1

This gene encodes the Nesprin-1α protein. The *SNP* rs9371601occurs in this gene and is associated with bipolar disorder. Nesprin-1α is an outer nuclear membrane intracellular protein, which connects the nucleus to the cytoskeleton via its N-terminal region and is involved in signal transduction between cell membranes and the cytoskeleton (Orru & Carta, 2018; Hughes et al., 2018).

Proteins With Other Functions

These are proteins that are associated with inflammation or fatty acid metabolism. Again, the relationship of these proteins to bipolar disorder is not known. In the inflammatory category, the *ITIH3* and *ITIH4* genes encode the inflammation-associated protein inter-α-trypsin inhibitor (IαI) that contains either three or four heavy chains and one light chain encoded on a separate gene (Psychiatric, GWAS Consortium Bipolar Disorder Working Group, 2011; Finseth et al., 2014). These proteins bind to hyaluronan, a polysaccharide involved in inflammation to form a serum-derived hyaluronan-associated protein (SHAP)-HA complex that has been implicated in modulating the inflammatory response.

A recent GWAS discovery identified the *FADS* gene encoding the enzyme fatty acid desaturase that catalyzes the desaturation of fatty acids to form double bonds (Mallas et al., 2016; Zhao et al., 2018). When desaturation occurs at the omega position (i.e., between carbons 3 and 4 from the terminal methyl group) of a long straight chain fatty acid, omega-3-unsaturated fatty acids result. From these results it appears that fatty acid metabolism may be involved with bipolar disorder especially since the neurocan protein has been implicated as being involved with lipid metabolism. Omega-3-unsaturated fatty acids have been used in the treatment of bipolar disorder.

In keeping with the recent GWAS findings of associations between bipolar disorder and lipid metabolism, SNPs in the gene encoding the enzyme diacylglycerol kinase eta (DGKH) have been found to be located within the bipolar disorder linkage region on chromosome 13q14. This enzyme is a key protein in the lithium-sensitive phosphatidyl inositol pathway (Baum et al., 2008; Hains & Arnsten, 2008).

Although TRANK1 protein was known from original GWAS as being associated with bipolar disease (Prata et al., 2019), the function of this protein is unknown but is thought to have ankyrin-like activity.

Copy Number Variants in Bipolar Disorder

Unlike the case of schizophrenia, the most highly powered CNV studies of bipolar disorder have not supported a significant role for CNV burden. However, cases of schizoaffective disorder, bipolar type, which are often included in case definitions in genetic studies of bipolar disorder, did show an increase in burden compared to controls. While CNV burden has not been strongly associated, several recurrent CNVs have demonstrated association. These include a duplication at 1q21.1, a deletion at 3q29, and a duplication at 16p11.2, with the latter having the strongest association of the three (Green, 2016). A more definitive understanding of the role of CNVs in the etiology of bipolar disorder awaits the kind of large-scale consortium-based mega-analysis that has been completed for schizophrenia.

WES and WGS studies of bipolar disorder are currently in the process of being meta- and mega-analyzed and have not yielded definite findings to date. However, a number of smaller studies in both family- and population-based samples have been published. These have reported an enrichment of rare variants in postsynaptic density genes (Goes et al., 2019; Toma et al., 2018) and GPCRs (Cruceanu et al., 2018) as well as a number of individual genes, although there remain no strongly replicated risk genes identified by these studies at the time of writing.

Pharmacogenomic Studies

Currently, lithium is the only mood stabilizer that has been thoroughly examined in pharmacogenomic studies. While several GWAS have been published, only one has reported genome-wide significant findings. The International Consortium on Lithium Genetics (ConLiGen) examine >2500 patients and reported genome-wide significant association at two genes encoding long noncoding RNAs (lnc-RNAs), which have an important role in gene expression (Hou et al., 2016). This finding was replicated in a small independent sample of 75 patients. As is the case with schizophrenia, pharmacogenomic studies of bipolar disorder will benefit from the study of large registry-based datasets, which are coming online at the time of writing as they are approaching sample sizes of tens of thousands of patients. While these approaches are very promising and have the advantage of being naturalistic, they face challenges in phenotyping. This could benefit from increasingly sophisticated analytic methods, which could incorporate machine learning, artificial intelligence, and natural language processing.

Bipolar Disorder and Schizophrenia

Since even before Emil Kraepelin, the diagnostic entities we currently refer to as schizophrenia and bipolar disorder were thought to be the same disorder until Kraepelin distinguished them as *dementia praecox* and *manic-depressive illness* on the basis of course. Psychosis, as well as both depressive and manic symptoms, can be seen in both disorders at various points in their course. A large epidemiologic study in Sweden demonstrated an increased risk of both disorders in the relatives of probands with either disorder, suggesting significant genetic overlap. This was subsequently corroborated in a large cross-disorder GWAS. Furthermore, genetic influences on symptomatic dimensions in both illnesses have been shown to affect corresponding dimensions in the other. For example, schizophrenia cases with high polygenic risk scores for bipolar disorder had elevated levels of manic symptoms (Bipolar Disorder and Schizophrenia Working Group of the Psychiatric Genomics Consortium, 2018).

SUBSTANCE USE DISORDERS

In contrast to psychotic illnesses such as schizophrenia, alcohol and other substance use disorders are quite common. Recent estimates of *Diagnostic and Statistical Manual of Mental Disorders*, Fifth Edition (DSM-5) alcohol use disorder and cannabis use disorder show lifetime prevalence of 29.1% and 6.3%, respectively (Grant et al., 2015; Hasin et al., 2016). The dramatic increase in opioid use and opioid-related overdose deaths in the last decade has resulted in a US public health state of emergency. According to the Centers for Disease Control and Prevention, opioid-related deaths quadrupled between 1999 and 2014 and have continued to rise; estimates of DSM-5 opioid use disorder from 2012 to 2013 showed a lifetime prevalence of 2.1% (i.e., ~4.8 million US citizens), which is a substantial increase from 1.4% in 2001 to 2002 (Rhee & Rosenheck 2019). These disorders substantially impact the physical and mental health of those who abuse substances, as well as their families and communities through impaired interpersonal and professional functioning, and overdose deaths.

Based on the largest and most recent twin study of alcohol use disorder conducted, heritability estimates range between 30% and 50%. Similar heritability estimates are reported in twin studies of cannabis and other substance use disorders. In addition to providing estimates of heritability, twin methodology has also been used to demonstrate the genetic relationships among disorders or traits that often co-occur clinically. For example, a landmark study by Kendler and colleagues used the Virginia Twin Registry sample to identify common genetic factors underlying a range of comorbid psychiatric and substance use disorders and found that a common genetic factor accounted for 34% of the variance in DSM-4 alcohol dependence and a substantial proportion of the variance in other externalizing disorders (Schizophrenia Working Group, 2014). Since that time, other studies have found that this latent externalizing factor, constructed of measures of conduct disorder, adult antisocial behavior, alcohol and drug abuse/dependence, and disinhibitory personality traits, appears to be more heritable than the individual disorders themselves.

Alcohol Use

As mentioned in the introduction of this chapter, linkage studies were used to identify the first molecular genetic risk factors for many substance use disorders. Some of the first linkage studies on alcohol use disorder from the Collaborative Study on the Genetics of Alcoholism (COGA) and a sibling study from a Southwest American Indian tribe reported a broad risk locus on chromosome 4q that harbors the alcohol metabolism genes, alcohol dehydrogenase *(ADH)* and aldehyde dehydrogenase *(ALDH)* (Edenberg & McClintick 2018). Despite the large number of spurious findings that emerged from linkage and candidate gene studies, subsequent studies focusing on these functional candidates (e.g., *ALDH2*, *ADH1B* and *ADH1C*, *ADH4*, *KLB* and *GCKR*) for alcohol-related phenotypes were quite successful; the influence of genetic polymorphisms at loci encoding *ALDH* and *ADH* on risk for alcohol use disorder in specific populations is now well established, and the mechanism is tractable (Edenberg & McClintick 2018). Other notable substance use disorder candidate genes identified through linkage, and candidate gene studies, include a class of opioid receptors: *OPRM1*, *OPRD1*, and *OPRK1* (Berrettini 2019). These receptors are discussed in Chapter 24. Here we discuss the most recently identified proteins of interest mentioned earlier.

ADH and ALDH (Dodge et al., 2016)

These enzymes are discussed in Chapter 24. Briefly, alcohol dehydrogenase (ALD) is a zinc-dependent enzyme, expressed mainly in hepatocytes and catalyzes the oxidation of ethanol to acetaldehyde. This intermediate is further oxidized to acetate by a separate enzyme, acetaldehyde dehydrogenase (ALDH2), also in the liver. In each of these reactions, nicotinamide adenine dinucleotide (NAD) is reduced to NAD plus hydrogen (NADH). Acetate is then condensed with pantothenic acid to form acetyl-CoA, which is a substrate for the Krebs cycle. ADH is a heterotrimer of three polypeptide chains (A, B, and C) encoded, respectively, by *ADH1A*, *ADH1B*, and *ADH1C* genes. An important and frequent SNP is the substitution of Arg for His at position 48 in the amino acid sequence of the B chain. (This assumes that the sequence begins with the start codon–encoded amino acid Met. If this is omitted then the position is 47, not 48.) This substitution results in a gain-of-function mutation such as to increase the rate of catabolism of ethanol resulting in increased alcohol consumption. Often there is a concurrent SNP in ALDH2, substitution of Lys for Glu 487 in ALDH2, which significantly diminishes the activity of this enzyme. There is thus an accumulation of acetaldehyde that results in flushing especially in the face and in nausea, vomiting, and a variety of other detrimental side effects. Interestingly, it has been found there are two sites involved in a linkage disequilibrium involving the His to Arg 48 in ADH1B and Ile for Val 349 in ADH1C. ADH1C has been implicated in modulation of the association between alcohol consumption and levels of expression of HDL (and risk of myocardial infarction) in men. Another form of ADH, ADH4 (Edman & Marer 1993) that consists of a homodimer of two so-called pi subunits has also been found to have SNPs associated with alcohol abuse.

Oxidation of ethanol to acetaldehyde is also promoted in the liver by the cytochrome p450 system, in particular CYP 2E1. SNPs and/or mutations in this protein may also be associated with alcohol abuse.

KLB Gene (rs11940694)

This gene encodes the β-klotho protein, characteristic SNPs for which were found in a major study to be associated with alcohol abuse (Schumann et al., 2016). This protein is an obligate coreceptor for the hormone fibroblast growth factor 21 (FGF21) synthesized in the liver and which has been implicated in macronutrient preference for sweet nutrients (mainly carbohydrates) in humans in prior nutritional GWAS. It has been found to suppress sweet preference in the CNS, thereby lowering consumption of carbohydrates. Its synthesis and secretion by hepatocytes have now further been found to be strongly induced by alcohol. Similar to its suppression of carbohydrate intake, it likewise suppresses alcohol consumption. Strikingly, it has been found that knockout mice that do not express β-klotho have increased alcohol consumption and are refractory to the inhibitory effects of FGF21. β-klotho has been found in abundance in regions of the brain associated with reward behavior, including the ventral tegmental area and the nucleus accumbens. FGF21 has been found to reduce dopamine in the latter area. These findings all suggest that FGF21 may be an effective therapeutic agent for treating alcohol abuse and binge drinking (Schumann et al., 2016). These findings represent a major advance in our understanding of the mechanisms involved in alcohol abuse and discovery of potential effective agents for treatment of this condition as a result of this GWAS.

GCKR (Glucokinase Regulator Protein) Gene (rs1260326)

This protein is an inhibitor of hexokinase that phosphorylates glucose on its C6-OH group to yield glucose-6-phosphate that enters glycolysis in liver and pancreatic islet cells (Iynedjian, 2009). It is considered a susceptibility gene for development of type 2 diabetes mellitus due to the buildup of unphosphorylated glucose. The missense SNP is associated with over 25 metabolic traits, including type 2 diabetes, fasting insulin levels, and total cholesterol levels.

Recently, the number of large GWAS of substance use and problems has been increasing, particularly in the area of alcohol use behavior. In 2019, Sanchez-Roige et al. combined three of the largest GWAS of alcohol-related behavior conducted to date (UK Biobank, 23andMe, and PGC-alcohol use disorder) in a meta-analysis of 141,932 individuals; previously identified signals in the genes *ADH1B*, *ADH1C*, *KLB*, and *GCKR* as discussed earlier were replicated and novel associations localized to genes, including *JCAD* and *SLC39A13* (Sanchez-Roige et al., 2019). GSCAN has implicated 200+ alcohol and nicotine consumption variants (Liu 2018). Most recently, a very large GWAS of alcohol use disorder from the MVP has been published (Gelernter et al., 2019a, 2019b). The MVP GWAS of alcohol use disorder (International Classification of Diseases [ICD] 9/10 diagnoses) include large numbers of individuals of African and Hispanic/Latino ancestries (African ancestry N=57,340; Latino ancestry N=14,425; European ancestry N=209,020). Meta-analysis across the populations identified three loci previously associated with alcohol dependence (*ADH1B*, *ADH1C*, and *ADH4*) and six novel loci (*GCKR* [discussed earlier], *SIX3*, *SLC39A8*, *DRD2*, intergenic variant on chr10q25.1 (rs7906104), and *FTO*). We consider these newly discovered proteins in turn.

TABLE 73.3
Proteins Associated With Characteristic SNPs in Substance Use Disorders

Disease	Protein	Function
Alcohol	ADH1A/B/C polypeptide chains of alcohol dehydrogenase	Metabolize ethanol to acetaldehyde. H48R mutation increases rate in ADH1B; V349I causes inhibition of ADH1C.
	ALDH2, acetaldehyde dehydrogenase	Oxidizes acetaldehyde to acetate. E487K causes inhibition of the ALDH2 enzyme.
	KLB	β-Klotho protein coreceptor for FGF21. Decreases desire for alcohol in hypothalamus and in mesolimbic system.
	GCKR	Glucokinase regulator protein. Blocks hexokinase, leads to buildup of glucose, leading to diabetes mellitus.
	SIX3	Transcription factor critical in the development of the eye and forebrain. Inhibits proliferation signal transduction protein wnt1.
	SLC39A8 and 13	Zinc-binding proteins that transport zinc across cell membranes.
	DRD2	Dopamine receptor involved in synaptic signaling (see Table 73.1).
	FTO	Fat mass and obesity-associated protein. It is an α-ketoglutarate-dependent dioxygenase and an alkB family RNA demethylase.
Cannabinoids		**Cell Adhesion Proteins**
	CADM2 (cell adhesion molecule 2)	Binds to oligodendrocytes and nectin-like family members; causes cell aggregation and is important for synapse organization. Involved in long-term signal depression and potentiation and neuroactive ligand-receptor interaction.
	NCAM1 (neural cell adhesion molecule 1)	Involved with neurogenesis and dopaminergic neurotransmission. Implicated in multiple use conditions.
		Proteins Involved With Intracellular Processes
	ZNF704 (zinc finger protein 704)	Zinc finger transcription factor enhancer. Induces transcription of critical muscle proteins.
	RABEP2 (rab GTPase-binding effector protein 2 or rabaptin)	Membrane-bound G protein that promotes transporting proteins across the membranes of cellular organelles.
	ATP2A1 (sarcoplasmic/endoplasmic reticulum calcium ATPase 1)	Induces calcium ions to move from the cytosol into the sarcoplasmic reticulum to promote muscle contraction.
Opiates	KCNC1 (potassium voltage-gated channel subfamily C member 1)	Expressed in neurons that fire at high frequency, including auditory and fast-spiking GABAergic interneurons, retinal ganglion cells. Regulates action potential duration in presynaptic terminals.
	KCNG2 (gamma subunit of the voltage-gated potassium channel)	Involved with delayed-rectifier type channels and neurotransmitter release regulation.
	RGMA (repulsive guidance molecule A)	Coreceptor for bone morphogenic proteins and effector for activation of RHO and inhibition of ras-p21 resulting in blockade of cell growth and division.

SIX3 (Granadino et al., 1999)

The SIX homeobox 3 *(SIX3)* gene is a critical transcription factor involved in embryonic development of the forebrain and eye. It inhibits the growth factor wnt1 that induces cell division and has been implicated as a causative factor in several human cancers. It is involved in proper growth of the posterior brain and in blocking its extension into anterior brain areas, a direct effect of its blocking wnt1. It also activates the protein Pax6, important in eye development, and the protein SOX2, a protein that induces pluripotency of cells.

SLC39A8 and 13 (Jeong & Eide 2013)

These are zinc-binding transport proteins. A possible relationship of these proteins to alcohol abuse may relate to zinc transport since ADH requires zinc to function. A SNP that would change the efficacy of SLC39 in transporting zinc could have a major effect on ADH activity.

DRD2 is the D2 dopamine receptor discussed earlier. Alcohol disrupts the ability of D2 receptors to modulate dopaminergic nerve conduction.

FTO is the fat mass and obesity-associated chromosome 16 gene that encodes the protein α-ketoglutarate-dependent dioxygenase, an alkB family RNA demethylase that has also been found to contain significant expression of SNPs in major depression disorder (Sanchez-Pulido et al., 2007).

The functions of all of these proteins that are associated with alcohol use are summarized in Table 73.3.

Cannabis Use

Cannabinoids are discussed in Chapter 24. Large GWAS of cannabis initiation have also been published; the International Cannabis Consortium published a "cannabis ever use" meta-analysis (*N:* 184,765) that implicated genes encoding the adhesion proteins, *CADM2* and *NCAM1*, and additional genetic risk loci, including *ZNF704*, *RABEP2/ATP2A1*, and *ALDH2* (Pasman et al., 2018a). We discuss the protein products of these genes that may underlie the pathophysiology of cannabis use. These proteins seem to fall into two categories: cell adhesion proteins and proteins involved with intracellular processes, especially, unexpectedly, in myocytes, and their functions are summarized in Table 73.3.

Cell Adhesion Proteins

CADM2 (Cell Adhesion Molecule 2). This gene encodes a cell adhesion protein that is a synaptic cell adhesion molecule (Thomas et al., 2008) and is member of the immunoglobulin superfamily that has been shown to be widely expressed in the developing and adult brain in laboratory mice. The top SNPs related to cannabinoid use in this gene are on chromosome 3 (rs2875907, rs1448602, rs7651996). This gene has been previously identified in several behavioral disorders and personality traits. It has been found to bind preferentially to oligodendrocytes and engages in interactions with nectinlike family members and leads to cell aggregation; it is important for synapse organization through regulated transsynaptic adhesion (Pellissier et al., 2007). CADM2 proteins are involved in long-term signal depression and potentiation and neuroactive ligand-receptor interaction (Thomas et al., 2008). Studies have shown that *CADM2* is expressed in normal hippocampal tissue (obtained postmortem), and SNPs in the *CADM2* gene are involved in glutamatergic and GABA-ergic transmission (Ibrahim-Verbaas et al., 2016) (see Fig. 73.1).

NCAM1 (Neural Cell Adhesion Molecule 1). This gene encodes another neuronal adhesion molecule, NCAM1, which is located in the *NCAM1-TTC12-ANKK1-DRD2* gene cluster on chromosome 11q23. This protein is thought to be involved with neurogenesis and dopaminergic neurotransmission and has been implicated in the pathogenesis of smoking, alcohol use, illicit drug users, and other psychiatric disorders (Pasman et al., 2018b; Thoulouze et al., 1998).

Proteins Involved With Intracellular Processes, Including Protein Trafficking

ZNF704 (Zinc Finger Protein 704). This gene occurs on chromosome 8q21.13 and belongs to the genes encoding metal-binding proteins. It is a zinc finger transcription factor enhancer (i.e., it induces transcription of sets of genes encoding DNA-binding proteins, including, among others, p53, c-Myb, and MyoD). The latter gene encodes the myoD protein, which is a transcription factor itself that induces transcription of whole sets

of genes that encode proteins vital for myocyte differentiation and development (Yamamoto et al., 2007).

RABEP2 (Rab GTPase-Binding Effector Protein 2 or Rabaptin). This is a membrane-bound G protein in the ras family (see Chapter 77 for a discussion of the ras-p21 protein). It is activated by binding GTP and is inactivated in the presence of GAP (GTPase activating protein). When activated, it plays a role transporting proteins across the membranes of various cellular organelles such as the Golgi bodies, endoplasmic reticulum, lysosomes, and endosomal structures and may be involved in early endosome fusion (Gournier et al., 1998; Stenmark & Olkkonen 2001; Kofler et al., 2018). It is also a substrate for glycogen synthase kinase (GSK3) (Gourlay et al., 2017).

ATP2A1 (Sarcoplasmic/Endoplasmic Reticulum Calcium ATPase 1). This protein belongs to the family of so-called SERCA (sarcoplasmic/endoplasmic reticulum calcium-induced ATPase), which is involved in the reuptake of cytosolic Ca^{2+} into the sarcoplasmic reticulum while catalyzing the hydrolysis of ATP. This protein causes calcium sequestration and is a regulator of striated muscle excitation/contraction (Odermatt et al., 2000; Logie et al., 2017).

Opioid Use

In 2014, a GWAS on DSM-4 opioid dependence conducted in 5697 participants identified genes involved in potassium signaling pathways *KCNC1* and *KCNG2*. In 2017 a GWAS conducted in 3058 opioid-exposed participants (1290 met criteria for a DSM-4 opioid dependence) identified a variant on chromosome 15, near *RGMA* (Cheng et al., 2019). Against this backdrop, the National Institute of Drug Abuse (NIDA) Genetics Consortium GWAS of opioid addiction began working toward a collaborative meta-analysis across 19 GWAS of opioid abuse (case *N*=13,555; all controls *N*=48,238; opioid exposed controls *N*=3779) and frequency of opioid use among users (opioid user *N*=14,403) (Cates et al., 2019). This effort parallels the PGC–Substance Use Disorder's GWAS of DSM-4 opioid dependence.

Newly Identified Proteins From Opioid Addiction GWAS

The functions of these proteins are summarized in Table 73.3.

KCNC1 and KCNG2

KCNC1 (potassium voltage-gated channel subfamily C member 1) and KCNG2 (potassium voltage-gated channel subfamily G member 2) are voltage-gated potassium channels that are prominently expressed in neurons that fire at high frequency. These channels are important for the high-firing frequency of auditory and fast-spiking GABAergic interneurons, retinal ganglion cells, and the regulation of action potential duration in presynaptic terminals. A missense mutation c.959G>A (p.Arg320His) in KCNC1 causes progressive myoclonus epilepsy (Muona et al., 2015).

KCNC1 protein forms functional homotetrameric and heterotetrameric channels with variable proportions of different KCNC family members. There are two transcript variants encoding isoforms that differ at their C-termini by an alternative splicing: The longer isoform is called both "b" and "alpha" and the shorter isoform "a" and "beta" (Yokoyama et al., 1989; Grissmer et al., 1992; Park et al., 2019).

KCNG2 protein is a gamma subunit of the voltage-gated potassium channel and has diverse functions, including neurotransmitter release regulation, heart rate, neuronal excitability, epithelial electrolyte transport, smooth muscle contraction, and cell volume. This subunit forms the delayed-rectifier type channels, which were previously known to contribute to cardiac action potential repolarization (Grissmer et al., 1992; Gelernter et al., 2014).

RGMA

The *RGMA* gene encodes the repulsive guidance molecule A. This is a dual function protein that acts both as a coreceptor of the repulsive guidance molecule family for bone morphogenetic protein (BMP) and as an effector protein that binds to cellular receptors as described next. When it binds BMPs, it activates the intracellular SMAD1/5/8 signaling pathway (Corradini et al., 2009). The SMAD1/5/8 signaling plays an important role in the patterning of dorsal spinal cord through dorsoventral gradient of BMPs (Hegarty et al., 2013). Repulsive guidance molecules have been implicated to play an important role in the developing brain and in the scar tissue that forms after a brain injury. Further research has shown that RGMA is an inhibitor of axonal outgrowth. These findings highlight the importance of RGMA in axonal guidance and outgrowth (Severyn et al., 2009).

RGMA-Promoted Signal Transduction Pathways Block Cell Growth

RGMA has also been found to be involved as an effector protein in regulating closure of the cephalic neural tube, inhibition of neurite outgrowth, and cortical neuron branching, and the formation of mature synapses. These effects have been found to be mediated by induction of inhibition of signal transduction pathways that stimulate cell growth and division. RGMA binds to its cellular receptor neogenin, which has as a coreceptor the protein UNC5b. This results in activation of a tyrosine kinase on the intracytoplasmic portion of the receptor complex that activates SOS or guanine nucleotide exchange factor that induces the G protein RHO to exchange GDP for GTP, resulting in its activation ultimately resulting in collapse of the neuronal growth cone.

In this process, the enzyme focal adhesion kinase (FAK) is activated by the tyrosine kinase of the neogenin-UNC5b receptor, and it performs the actual phosphorylation and activation of the guanine nucleotide exchange factor of RHO. The UNC5b coreceptor is associated with the protein GAP (see the previous discussion of the RABEP2 protein in the cannabis use section). This protein induces hydrolysis of GTP to GDP in G proteins, including ras-p21, a strong promoter of mitosis (see Chapter 77) causing their inactivation. However, when bound to FAK, GAP is inactive; but when RGMA binds to the neogenin-UNC5b receptor, FAK dissociates from GAP, allowing it to interact with ras, thereby inactivating it and other cell growth and mitosis-inducing proteins. Thus RGMA blocks cell growth both by activation of RHO and inhibition of ras (Hata et al., 2009; Endo & Yamashita, 2009; Lah & Key, 2012; Cheng et al., 2018).

Future Studies

Forthcoming findings from these consortia-based efforts will be highly informative for gene discovery regarding alcohol use behavior. However, deeply phenotyped samples are needed to characterize findings emerging from these large genomic studies of alcohol use patterns with respect to related brain functioning. Polygenic risk scores (PRS) aggregate genetic information from GWAS (Purcell et al., 2009) permitting characterization of genomic findings from these large consortia-based studies in independent well-characterized samples, including measures of brain functioning. Greater understanding of how genetic risk factors for alcohol use behavior influence brain functioning and how such effects may differ among men and women in different developmental stages, will provide important context to findings emerging from large-scale genomic studies of alcohol problems.

MAJOR DEPRESSION DISORDER

MDD is a common mood disorder with cross-national lifetime rates ranging from 1.5% to 19% and is characterized by persistent feelings of sadness and loss of interest or pleasure in most things (anhedonia) for at least a 2-week period (Ferrari et al., 2013; Kessler et al., 2013). It is frequently accompanied by additional symptoms such as changes in appetite, weight, sleep, and energy, as well as reduced concentration, feelings of worthlessness, and suicidal thoughts. Given the chronic and recurrent nature of MDD it is associated with considerable morbidity, impairment, disability, excess mortality, and substantial costs. It is also often comorbid with other psychiatric disorders such as anxiety and substance use disorders as well as other medical conditions, including obesity, cardiovascular disease, and diabetes.

Twin studies estimate the heritability of major depression as 37% (Sullivan et al., 2000), supporting a complex etiology with both genetic and environmental factors. While initial genetic studies of major depression met difficulties in identifying individual-associated genetic variants, recent studies have been more successful. The first replicated genome-wide significant associations for major depression were reported by the CONVERGE Consortium (2015) from a study of severe, recurrent cases and carefully screened controls, all of whom were Han Chinese women, and identified two genetic loci, one close to *SIRT1* (Silent Information Regulator 1; SNP rs10997875), encoding the protein sirtuin 1, and the other in an intron (rs35936514) of the *LHPP* gene encoding the enzyme lysine-histidine pyrophosphate phosphatase (Yokoi et al., 2003; Hindupur et al., 2018), both on chromosome 10, both contributing strongly to the risk of MDD. We discuss these two major proteins identified as being potential markers for MDD and several other genes that likewise seem to be associated with this disorder.

Sirtuin

The sirtuins are a family of enzymes that catalyze the transfer of an acyl group (acetyl group for Sirt2) from the ε-amino group of Lys residues to the

–OH group of the ribose ring of NAD. They are thought to control transcription through deacylation of lysine residues in histone proteins thereby increasing histone-DNA binding and therefore may be involved in gene silencing. They have also been implicated in regulation of the cell cycle, fat and glucose metabolism, cellular oxidative stress, and senescence. They are further involved in glial activation, neurogenesis, circadian control, and potential signaling molecules. This gene has been the main target in antidepressant medical therapy (Lu et al., 2018; Sur et al., 1998). Animal model studies suggest that chronic stress can reduce Sirt1 levels in the cerebral cortex, and reduction of this enzyme in the cortex can induce depression-like states. Importantly, serum levels of sirtuin have been found to be significantly lower in patients diagnosed with MDD than in normal controls, suggesting a serodiagnostic role of this protein in MDD. Therapeutically, the agent resveratrol activates SIRT1 directly and indirectly and has been found to improve depression-like behavior in mice (Lu et al., 2018).

LHPP

LHPP has been found to be highly expressed in the CNS as a brain-specific transcript. It has been hypothesized that the *LHPP* rs35936514 polymorphism moderates brain regional activity in MDD. The MDD association with this gene is dependent on HTR1A (5-HT1a receptor). 5-hydroxytryptamine (serotonin) receptor 1A is a G protein–coupled guanine nucleotide-binding regulatory protein-coupled receptor (Cui et al., 2016).

Serotonin-Related Genes (SERT)

Serotonin (5-hydroxytryptamine)–dependent neural pathways are discussed in Chapter 24. There are seven genes known to encode key proteins in the serotonin system in which SNPs or variable numbers of tandem repeats (VNTRs) have been implicated in mood disorder pathology. These genes are implicated in the synthesis of tryptophan hydroxylase (TPH), which is critical in the synthesis of serotonin, the transport of serotonin, vesicular monoamine transporter 2 (VMAT2) and serotonin transporter, serotonin receptors (2A [*5-HTR2A*], 1A [*5-HTR1A*], and 1B [*5-HTR1B*]), and the degradation (monoamine oxidase A [*MAOA*]) of serotonin (Christiansen et al., 2007).

TPH1 and TPH2 encode tryptophan hydroxylase 1 and 2. These are the enzymes that add the hydroxyl group to tryptophan, in the initial and rate-limiting step in the synthesis of serotonin, to create the amino acid 5-hydroxytryptophan (5-HT) that is decarboxylated to yield 5-hydroxytryptamine or serotonin. This neurotransmitter along with its receptors play a role in depression. It is proposed that single nucleotide polymorphisms of tryptophan hydroxylase genes modulate the risk of depression (Wigner et al., 2018).

SERT1, or serotonin transporter, is a member of the sodium- and chloride-dependent monoamine transporter, which is involved in transport of serotonin, the monoamines dopamine (DAT) and norepinephrine (NET), and gamma aminobutyric acid. This serotonin transporter is an oligomeric glycoprotein with two sialic acid residues on each of two complex oligosaccharide molecules. Posttranslational modifications, including phosphorylation, glycosylation, serotonylation, and disulfide bond formation, influence SERT formation and efficient functioning. Translational modifications affect the structure, maturation, and serotonin (5-HT) uptake ability of SERT. The SERT uptake mechanism acquires energy for active transport via ATP hydrolysis or via movement against electrochemical gradient (Cooper et al., 2019).

SLC6A4 (Sodium-Dependent Serotonin Transporter)

The primary function of this protein includes regulation of serotonergic signaling via a sodium-dependent recycling process of serotonin molecules in the synaptic cleft. An upstream gene-linked polymorphic region, 5-HTTLPR genotype has been linked to susceptibility to depressive disorders. There are short (S) or long (L) alleles of this gene, which are the result of insertion/deletion VNTRs. The S allele results in lower *SLC6A4* transcriptional levels and therefore reduced reuptake of serotonin (Lam et al., 2018; Brandl et al., 2014; Calabro et al., 2016; Sur et al., 1998).

HTR2A

This gene encodes serotonin 2A receptors, the serotonin transporter gene. 5HTR2A is a modulator of the excitability of the prefrontal cortex network. In pyramidal cells, stimulation of this receptor increases both the frequency and amplitude of glutamatergic spontaneous excitatory postsynaptic potentials/spontaneous excitatory postsynaptic currents (sEPSCs) (Beique et al., 2007; Brandl et al., 2014). Polymorphisms in the promoter region of the serotonin transporter gene (5-HTTLPR) are implicated as moderators of the stress-depression relationship (Conway et al., 2010).

Tryptophan Metabolic Pathways Related to MDD

Recently, neuroinflammation and the immune-kynurenine pathway have received increased attention in the psychoimmunology field of major depressive disorder. Tryptophan (TRY) metabolism involves two major pathways: the methoxyindoles pathway and the kynurenine pathway. Approximately 1% to 5% of the available TRY in the body is synthesized as serotonin (5-HT) through the methoxyindoles pathway, primarily in the enterochromaffin cells of the gut, and less in the brain through the blood brain barrier (BBB). The availability of TRYs is an important rate-limiting factor for serotonin synthesis and, along with the tryptophan catabolites (TRYCATs) pathway, may play a role in pathogenesis of depressive disorders. The TRYCATs in the kynurenine pathway can be imbalanced due to stress or inflammation, which causes serotonin deficiency. TRYCATs can also act as endogenous anxiogens or anxiolytics, an NMDA (see earlier) agonist or antagonist, or a free radical generator (Kim & Jeon, 2018). Tryptophan metabolites include kynurenine, xanthurenic acid, and quinolinic acid. Quinolinic acid is toxic to postsynaptic structures and neurons via apoptosis in the hippocampus and induces selective necrosis of granular cells and reduces levels of dopamine, choline, and γ-aminobutyric acid (GABA) (Wigner et al., 2018).

COMT Gene

This gene encodes the enzyme catechol-O-methyltransferase (COMT), which catalyzes O-methylation and breaks down catecholamines (Brandl et al., 2014; Chen et al., 2011). COMT genotype can affect the strength of 5-HTTLPR in gene and environmental interaction and is linked to stress sensitivity and depressive disorders (Conway et al., 2010).

Further GWAS on MDD

Following this, GWAS that increased sample size by using a broader depression phenotype have identified additional genetic variants among individuals of European descent. For example, the consumer company 23andMe reported 15 genetic loci associated with self-report of clinical depression (75,607 cases and 231,747 reporting no history of depression) (Hyde et al., 2016), an analysis in the UK Biobank (n=322,580) identified 17 independent loci associated with broad depression phenotypes (Hodson et al., 2018), and the PGC-Major Depressive Disorder Working Group (130,664 cases and 330,470 controls) reported 44 independent loci (Wray et al., 2018). Subsequently, Howard et al. (2019) combined all three studies in a meta-analysis (246,363 cases and 561,190 controls) and identified 102 independent variants of which 87 replicated in an independent sample, including variants in and near DRD2 (the dopamine receptor discussed earlier), CELF4 (which regulates translation and concentration of large sets of mRNAs and is expressed in excitatory neurons, mainly in pyramidal cells of the cerebral cortex and hippocampus) (Wagnon et al., 2012), ELAVL2 (on chromosome 9p21 that encodes the Hel-N1 protein, which is an evolutionarily conserved neuronal RNA-binding protein expressed in CNS neurons) (Han et al., 1996), and FTO described in the preceding section on substance abuse (Howard et al., 2019). However, these loci account for only ~2% of the variance in liability (among European ancestry individuals), underscoring the importance of further research on the genetic architecture of depression, particularly in diverse ancestries (Peterson et al., 2019; McIntosh et al., 2019). The functions of these proteins implicated as being involved in MDD are summarized in Table 73.4.

The largest population genetic studies of major depression have demonstrated a highly complex genetic architecture, and progress in identifying robustly associated risk loci has lagged behind parallel efforts in more highly heritable neuropsychiatric disorders such as schizophrenia. This may reflect the extensive clinical and etiologic heterogeneity of major depression. For example, twin studies estimate the genetic correlation of major depression between males and females as +55%, suggesting genetic liability is only partially shared between the sexes. Although recent progress has yielded modest insight into the genetic architecture of major depression, a deeper understanding of causal processes will require applying novel approaches across development integrating multiple data types (e.g., environmental, clinical, neuroimaging, and genomic data).

Pharmacogenomics of MDD

For major depression, nonresponse to treatment, incomplete treatment symptom remission, and medication side effects are common (+30%). Pharmacogenetics has the potential to improve these outcomes by using genetic information to provide guidance on treatment choice and potential drug tolerance and side effects. Functional variants in two cytochrome P450 enzyme genes, CYP2D6 and CYP2C19 (see Chapter 75) can be used to predict antidepressant drug (tricyclics, selective serotonin reuptake inhibitors [SSRIs]) metabolizing status of an individual (e.g., poor

TABLE 73.4

Proteins Associated With Characteristic SNPs in Major Depressive Disorder

Protein	Function
SIRT (Silent Information Regulator 1 (SIRT1)–encoded SIRTUIN	Deacetylase utilizing NAD+, is involved in gene silencing, cell cycle, fat and glucose metabolism, cellular oxidative stress, and senescence.
LHPP (phospholysine phosphohistidine inorganic pyrophosphate phosphatase)	A protein phosphatase that cleaves phospholysine and/or phosphohistidine bonds in brain tissue. Its function is dependent on HTR1A (5-HT1a receptor).
SERT1	Serotonin transporter. A member of the sodium- and chloride-dependent monoamine transporter, involved in transport of serotonin, the monoamines dopamine (DAT) and norepinephrine (NET) and gamma aminobutyric acid.
Tryptophan hydroxylase 1 and 2	An enzyme that adds the hydroxyl group to tryptophan to create amino acid 5-hydroxytryptophan (5-HT). 5-HT is involved in the initial and rate-limiting step in the synthesis of serotonin.
5HTR2A (serotonin 2A receptors)	Modulator of the excitability of the prefrontal cortex network. In pyramidal cell, stimulation of this receptor increases both the frequency and amplitude of glutamatergic spontaneous excitatory postsynaptic potentials/spontaneous excitatory postsynaptic currents (sEPSCs).
SLC6A4 (sodium-dependent serotonin transporter)	The primary function of this protein includes regulation of serotonergic signaling via a sodium dependent recycling process of serotonin molecules in the synaptic cleft.
Catechol-O-methyltransferase (COMT)	An enzyme that catalyzes O-methylation and breaks down catecholamine.
CYP2D6 and CYP2C19	Highly pleomorphic enzymes, belonging to the cytochrome P450 superfamily and are involved in lipid, hormone, toxin, and drug metabolism, including the antipsychotics and TCAs.
BDNF (brain-derived neurotrophic factor)	A member of the neurotrophin (NT) family, known for its function as cell survival–promoting factor for sensory neurons, along with two other recently identified neurotrophins: neurotrophin 3 (NT3) and neurotrophin 4 (NT4).

metabolizer, ultra-rapid metabolizer). The Clinical Pharmacogenetics Implementation Consortium (CPIC) and the Dutch Pharmacogenetics Working Group (DPWG) report 13 antidepressant drugs with pharmacogenomic biomarkers in CYP2D6 and CYP2C19. However, standardized guidelines are needed for whom pharmacogenetic testing should be recommended and when. Implementation of pharmacogenetic testing into psychiatric clinics is underway but is not yet standard protocol. Current testing practices include patients with major depression who have not responded to, or tolerated, at least one prior pharmacotherapy (Fabbri & Serretti 2020; Bousman et al., 2019). It should be noted that CYP2D6 is highly polymorphic, having multiple alleles and other gene variations (e.g., deletions, duplication, and pseudogenes). Normal enzyme activity is coded by alleles 1, 2, 33, and 35 (Dean et al., 2012).

POSTTRAUMATIC STRESS DISORDER AND ANXIETY DISORDERS

Anxiety disorders are relatively common, often disabling conditions with lifetime prevalence of over 20%. GWAS of specific anxiety and related disorders such as generalized anxiety disorder, posttraumatic stress disorder, panic disorder, obsessive compulsive disorder, and phobias have also been published over the past several years. A recent meta-analysis across several anxiety disorders (Hettema et al., 2019) combined results across the nine samples for over 18,000 unrelated individuals, with the following markers showing the strongest association: for case control contrasts, rs1709393 located in an uncharacterized noncoding RNA locus on chromosomal band 3q12.3 and rs1067327 within *CAMKMT* on 2p21.

The *CAMKMT* gene encodes the enzyme lysine methyltransferase (calmodulin-lysine-N-methyltransferase) that transfers methyl groups from S-adenosyl methionine to lysine residues of calmodulin (CaM) resulting in activation of this protein. Defects in expression of this gene result in atypical hypotonia-cystinuria syndrome and mild to moderate mental retardation (Cloutier et al., 2013).

Changes in calmodulin-lysine-N-methyltransferase can therefore affect calmodulin activity. This protein, despite its small size (148 amino acid residues), is vital in modulating the actions of multiple intracellular proteins. It is involved in the mobilization of calcium ions from intracellular stores as shown in Panel 2 of Figure 73.1, regulation of ion channels and aquaporins (see Chapter 14), and muscle contraction. With regard to the latter function, CaM induces muscle contraction by inducing calcium-stimulated phosphorylation of myosin head groups allowing for interactions with actin. It itself is a calcium-binding protein that binds four calcium ions to four sites separated by long interbinding site segments that contain patches of exposed hydrophobic sequences that enable it to interact with corresponding hydrophobic and amphipathic domains of multiple proteins (Vetter & Leclerc 2003). Thus the preponderance of effects of SNPs and/or mutations in the CAMKMT gene may be due to changes in CaM activity.

A GWAS of general anxiety disorder (GAD) symptoms in a large, population-based sample of Hispanic/Latino adults (Dunn et al., 2017) identified intronic thrombospondin 2 (THBS2) variant rs78602344. This protein is a trimer of disulfide-linked glycoproteins that mediate cell-to-cell and cell-to-matrix protein interactions, including cell adhesion and migration. Importantly, thrombospondin promotes the formation of new synapses, mediated by the interaction between astrocyte-secreted thrombospondins and their neuronal receptor, calcium channel subunit α2δ-1 (see section on schizophrenia for discussion of calcium channel proteins) (Risher & Eroglu 2012). The effects of thrombospondin include protection of synapses from toxic damage (e.g., ammonia toxicity) (Jayakumar et al., 2014).

Recently, the PGC-PTSD working group has published a GWAS of PTSD in a multiethnic cohort, including over 30,000 PTSD cases and 170,000 controls; this study demonstrated SNP-based heritability estimates of 5% to 20%, varying by sex (generally higher heritability was observed in female cohorts) (Nievergelt et al., 2019). Three genome-wide significant loci were identified, two in European and one in African ancestry analyses. Analyses stratified by sex implicate three additional loci in men. Along with other novel genes and noncoding RNAs, a Parkinson disease gene, PARK2, was associated with PTSD.

This gene encodes the Parkin RBR (ring between ring) E3 ubiquitin protein ligase, which is abundantly expressed in the brain and which induces ubiquitination of misfolded proteins and targets them for proteolysis in the proteosome (Shimura et al., 2000). It further appears to be involved in mitochondrial function and may act as a tumor suppressor protein and has been implicated in the release of neurotransmitter from the axonal side of synapses. Loss of function of this protein can result directly in diminished release of dopamine at synapses and in the accumulation of misfolded and/or unneeded proteins that are toxic to axonal end plates resulting in further diminished release of dopamine at these synapses.

GWAS of PTSD reexperiencing symptoms in the MVP (Gelernter et al., 2019a, 2019b) dataset conducted on 146,660 European ancestry participants and 19,983 African ancestry participants found eight loci, including a chromosome 3 locus with top variant rs2777888. This variant is located in an intron of the *CAMKV* gene (CaM kinase-like vesicle associated), which is highly expressed in the brain, especially in dendrites. This protein, which is considered to be a pseudokinase, is vital for maintenance of dendritic spine stabilization (Liang er al., 2016). Dendritic spines are small membranous protrusions from dendrites that receive electrical inputs from single axons at a synapse and which then transmit electrical signals to the neuron cell body. Synthesis of this protein is regulated by neuronal activity. Its activity is blocked by cyclin-dependent kinase 5 (Cdk5), which induces inactivating phosphorylation of CAMKV at Thr345. Knockdown of this protein in the hippocampal CA1 pyramidal neurons in mice resulted in reduced synaptic transmission and plasticity and hyperactivity and spatial memory impairment. Thus this protein is critical for synaptic transmission.

An extended locus on chromosome 17 was also identified, with lead SNP rs2532252 closest to the KANSL1 gene, also called KAT8 regulatory NSL complex subunit 1. This gene encodes a subunit for two protein complexes involved with histone acetylation, the MLL1 complex and the NSL1 complex. Insufficiency of expression of this gene results in intellectual disability, agenesis of the corpus callosum, hypotonia, cardiac anomalies, hydronephrosis, skin dyspigmentation, and abnormal facies, a condition

referred to as the cardiofaciocutaneous (CFC) syndrome. Interestingly, there is evidence that the KANSL1 gene might have an effect on the Ras-p21 protein-induced activation of the MAP kinase pathway referred to earlier and discussed fully in Chapter 77 (Moreno-Igoa et al., 2015).

The abovementioned locus also encompasses the CRHR1 gene (corticotropin-releasing hormone receptor 1), a previous candidate gene for PTSD. This gene encodes the corticotropin-releasing hormone or factor (CRH or CRF) receptor (CRHR). It contains 14 exons and encodes a receptor protein of 444 amino acids. There are multiple splice variants due to selective deletions of single exons giving rise to different receptor activities in different tissues or even in the same tissue (Hillhouse & Grammatopoulos 2006). Binding of CRH to CRHR in the pituitary results in secretion of ACTH. In the CNS, CRF is found abundantly in the cerebral cortex, cerebellum, hippocampus, amygdala, and brainstem areas. From studies in mice (CRF knockouts or treated with CRF antagonists) it has been found that there is a blunted stress response, suggesting that CRF is anxiogenic (Henckens et al., 2016). In the CNS, CRF1 activation mediates fear learning; in the brainstem, it regulates arousal.

A third locus on chromosome 18 is located in a locus previously associated with schizophrenia, in the TCF4 gene that encodes the TCF4 proteins. These proteins act as transcription factors for a variety of genes encoding immunoglobulins (IgM), the somatostatin receptor and genes involved in neural development. It occurs in the CNS, somites, and gonadal ridge in infancy. In adulthood it is found in lymphocytes, muscles, and the gastrointestinal system. Mutations of TCF4 can give rise to the Pitt-Hopkins syndrome, in which these proteins do not bind to DNA properly and therefore do not control the differentiation of the nervous system. The phenotype is wide mouth, gastrointestinal problems, developmental delay of motor skills and of speech, and difficulty in breathing (Amiel et al., 2007; Zweier et al., 2007). The functions of the proteins implicated as being involved in PTSD and anxiety disorders are summarized in Table 73.5.

TABLE 73.5
Proteins Associated With Characteristic SNPs in Posttraumatic Stress Disorder

Protein	Function
	Calcium Activation Proteins
CAMKMT (calmodulin-lysine-N-methyltransferase)	Activates calmodulin
Calmodulin	Mobilization of calcium ions from intracellular stores; regulation of ion channels and aquaporins
	Synaptic Stabilization Proteins
Thrombospondin	Mediates cell-to-cell and cell-to-matrix protein interactions, including cell adhesion and migration.
	Promotes the formation of new synapses, mediated by the interaction between astrocyte-secreted thrombospondins and their neuronal receptor, calcium channel subunit α2δ-1
Parkin protein encoded by PARK2 gene	E3 ubiquitin protein ligase that removes unneeded proteins at synapse and promotes neurotransmitter (dopamine) release. Release of neurotransmitter from the axonal side of synapses.
CaMKV	Dendritic spine stabilization. Enhances synaptic plasticity.
	Transcriptional Proteins/Histone Acetylation
KANSL/KAT8 encoding MLL1 and NSL1 transcriptional proteins	Important for expression of synaptic proteins and neural development.
TCF4 proteins	Transcription of genes involved in neural development.
Stress protein CRF (corticotropin releasing hormone) and CRF receptor	Fear and anxiety effects in the central nervous system, including cortex, hippocampus, amygdala, and brainstem.

OTHER NEUROPSYCHIATRIC DISORDERS

Alzheimer Disease

Alzheimer disease is a progressive, neurodegenerative disease characterized by a continuous decline in thinking and memory that eventually disrupts a person's ability to function independently (Hodson, 2018). AD is the most common form of dementia in elderly people accounting for over 60% of all cases. Most cases of AD present with symptoms after the age of 65, termed late-onset or sporadic AD. A portion of AD cases occur before the age of 65 (<10%), known as early-onset AD. AD brains are characterized by the presence of the following pathologies: neuronal loss, the accumulation of amyloid-beta (Aβ) peptides in the extraneuronal space (plaques) and in the walls of the cerebral vessels (cerebral amyloid angiopathy), and the intracellular accumulation of hyperphosphorylated tau protein (neurofibrillary tangles).

In general, there are two genetic mechanisms of disease: an autosomal dominant mechanism associated with early-onset AD and a polygenic mechanism associated with late-onset AD. Linkage analysis identified highly penetrant mutations in three genes that cause early-onset AD: Aβ precursor protein *(APP)* and presenilin genes *PSEN1* and *PSEN2*. However, these mutations are rare and only account for 1% of cases.

APP and Presenilins

APP is an integral membrane protein expressed in many tissues and concentrated in the synapses of neurons. Although its primary function is still unclear, it is best known as the precursor molecule whose proteolysis generates Aβ. Mutations in critical regions of amyloid precursor protein, including the region that generates Aβ, cause familial susceptibility to Alzheimer disease (Goate et al., 1991). APP undergoes extensive posttranslational modification, including many types of proteolytic processing to generate peptide fragments (De Strooper & Annaert 2000). It is commonly cleaved by proteases in the secretase family. Cleavage by gamma secretase within the membrane-spanning domain after beta-secretase cleavage generates the Aβ fragment. Gamma secretase is a large multisubunit complex whose components have not yet been fully characterized but include presenilin, whose genes have also been identified as a major genetic risk factor for AD (Chen et al., 2006). Vertebrates have two presenilin genes, *PSEN1* and *PSEN2*. Both genes show conservation between species. Presenilins play a key role in the modulation of intracellular Ca^{2+} involved in presynaptic neurotransmitter release and long-term potentiation induction (Zhang et al., 2009). Gamma secretase can cut APP at several points within a small region of the protein, which results in Aβ of various lengths. The lengths associated with AD are 40 and 42 amino acids long. Aβ 42 is more likely to aggregate to form plaques in the brain than Aβ 40. Presenilin mutations lead to an increase in the ratio of Aβ 42 produced compared to Aβ 40 due to various effects of the mutations on gamma secretase, although the total quantity of Aβ produced remains constant (Citron et al., 1997; Bentahir et al., 2006).

APOE

The sporadic form of AD is considered a complex disease with late onset and a polygenic nature. Apolipoprotein E (APOE), discussed at length in Chapter 18, is a polymorphic protein with three isoforms: E2, E3, and E4. Although these isoforms differ from each other by only one or two amino acids at positions 112 and 158, these differences alter APOE structure and function (Zuo et al., 2006). The E4 allele is the strongest genetic risk factor for AD: Up to 50% of early-onset AD and 80% of late-onset AD are associated with APOE. Those carrying one copy of the E4 allele have an increased AD risk of 2- to 5-fold, while individuals carrying two copies have a 12- to 15-fold increase in risk compared to noncarriers. Approximately 30% of the homozygous carriers of E4 will develop AD by the age of 75 and more than 50% by the age of 85 (Clarimon et al., 2020).

APOE belongs to a family of fat-binding proteins called apolipoproteins, which transport lipids, fat-soluble vitamins, and cholesterol. In peripheral tissues, APOE is primarily produced by the liver and macrophages, and mediates cholesterol metabolism. In the CNS, APOE is mainly produced by astrocytes and transports cholesterol to neurons via APOE receptors. APOE was initially recognized for its importance in lipoprotein metabolism and cardiovascular disease. Defects in APOE result in familial dysbetalipoproteinemia. More recently, the E4 variant was found to be the largest known genetic risk factor for late-onset sporadic AD in a variety of ethnic groups (Sadigh-Eteghad et al., 2012). This may be caused by the interaction with amyloid. APOE enhances proteolytic breakdown of Aβ, both within and between cells. The E4 isoform is not as effective as the others at promoting these reactions, resulting in increased vulnerability to AD in individuals with that allele (Jiang et al., 2008).

Newer Genetic Loci

It was 20 years after the identification of the association of APOE with AD that GWAS began identifying other genetic loci associated with late-onset AD, including PICALM, CLU, and CR1. PICALM (phosphatidylinositol

binding clathrin assembly protein) is a clathrin-adaptor protein and plays critical roles in clathrin-mediated endocytosis and in autophagy. PICALM protein levels were decreased in AD brains. PICALM regulates clathrin-dependent internalization of Aβ bound to the low-density lipoprotein receptor related protein-1, leading to Aβ endothelial endocytosis and clearance (Zhao et al., 2015).

Clusterin (CLU) is an apolipoprotein and a stress-activated chaperone protein that functions in apoptosis, complement regulation, lipid transport, membrane protection, and cell-cell interactions (Jones & Goate 2002). Prior to the identification of risk alleles in LOAD, clusterin was implicated in AD pathogenesis. Clusterin mRNA expression is elevated in AD brains and is detected in amyloid plaques. Thus clusterin likely influences Aβ clearance, amyloid deposition, and neuritic toxicity. Clusterin is also associated with the complement system and modulates the membrane attack complex, where it inhibits the inflammatory response associated with complement activation. Because neuroinflammation is a hallmark of AD, SNPs that alter clusterin expression or its functions as an amyloid response agent could impact AD pathogenesis and downstream effects.

Complement receptor 1 (CR1) is located on chromosome 1q32 in a cluster of complement-related proteins. *CR1* encodes four isoforms that differ based on genetic duplication and deletions. CR1 expression on phagocytic cells, such as erythrocytes, results in the ingestion and removal of complement activated particles (Liu et al., 2009). CR1 is an interesting AD risk gene, as expression of complement factors are reportedly upregulated in affected regions of AD brains. Neurons and glia are sources of complement in the brain. Additionally, material isolated from neurofibrillary tangles and amyloid plaques activates the complement system (Shen et al., 2001). *CR1* encodes high expression and low expression alleles.

Individuals who are homozygous for the low expression *CR1* allele have fewer than 200 copies of CR1 per cell, while individuals who are homozygous for the high expression allele express nearly 1400 copies per cell. Higher CR1 protein expression is associated with a higher clearance rate of immune complexes. Clearance of plasma Aβ42 is dependent on C3b binding to CR1. It is also hypothesized that Aβ42 activates the complement system (Velazquez et al., 1997). Because elevated complement cascade activity could exacerbate AD pathology, individuals with CR1 variants that induce lesser complement response may be at lower risk of developing AD pathology.

The largest late-onset AD GWAS to date, from the International Genomic Alzheimer's Project (IGAP), comprises 35,274 cases and 59,163 controls, reporting 25 loci, including HLA, IQCK, and ACE.

The human leukocyte antigen (HLA) encodes proteins for the major histocompatibility complex (MHC) and is discussed at length in Chapter 50. Genes in this region are involved in a variety of pathways such as inflammation, the complement cascade, histocompatibility, and ligands for immune cell receptors. The MHC can be divided into three subgroups: MHC classes I, II, and III, in which the class II MHC locates at the centromeric end and encodes genes, including HLA-DRA, -DRB1, -DRB3, -DRB4, -DRB5, -DQA1, -DQB1, -DPA1, and -DPB1. The HLA-DRB5/DRB1 are associated with AD. The class II HLA-DR antigens are expressed by antigen-presenting cells, including microglia in the brain, and they can interact with T-cell receptors.

It has been reported that HLA-DR positive activated microglia are found in the substantia nigra of Parkinson disease individuals (Orr et al., 2005). The experimental evidence of how HLA-DR associates with AD is extremely limited, but it is speculated that, as another important neurodegenerative disease, the situation of HLA-DR in AD may be similar to that in Parkinson disease.

The IQCK gene encodes proteins with IQ domains like the CACNA-A1 calcium channel protein (see Table 73.1) that bind to the EF-hand domains of proteins like calmodulin. It is considered a candidate gene for obsessive-compulsive disorder.

Angiotensin-Converting Enzyme (ACE)

Interestingly, in addition to converting angiotensin I to angiotensin II, ACE also converts neurotoxic Aβ42 to Aβ40. Because of its neurotoxicity, Aβ42 is believed to play a causative role in the development of AD, whereas Aβ40 has neuroprotective effects against Aβ42 aggregation and against metal-induced oxidative damage. A recent study has shown that decrease in ACE levels promoted Aβ42 deposition and increased the number of apoptotic neurons in mouse model, and inhibition of ACE activity is a risk factor for impaired human cognition and for triggering AD onset (Liu et al., 2019).

Results From Next-Generation Sequencing

The application of next-generation sequencing technologies has enabled the identification of rare variants associated with AD risk in PLD3, TREM2, UNC5C, AKAP9, and ADAM10. These are briefly described next.

PLD3. *Phospholipase D3* is a poorly characterized "nonclassical" member of the PLD protein family with no reported catalytic activity. WES in LOAD families was coupled with genotyping in large case control series to identify *PLD3 V232M* as an AD risk factor (Cruchaga et al., 2014). Classical PLD proteins catalyze the hydrolysis of phosphatidylcholine to generate phosphatidic acid, which acts as an effector for clathrin-mediated endocytosis and have been implicated in AD pathogenesis. PLD3 is highly expressed in neurons in the hippocampus, entorhinal cortex, and frontal cortex. In vitro coexpression of PLD3 with APP produces significantly lower extracellular Aβ levels by a mechanism that remains unknown (Cruchaga et al., 2014).

TREM2. TREM2 is a receptor expressed on microglia that stimulates phagocytosis and suppresses inflammation. Homozygous mutations in *TREM2* are associated with autosomal recessive forms of dementia with bone cysts and fractures. Recently, rare missense mutations in *TREM2* have been reported to increase AD risk. In European descent populations, *TREM2* R47H is reported to increase AD risk approximately twofold (Guerreiro et al., 2013). Variants in the *TREM2* region are also associated with cerebrospinal fluid (CSF) tau levels. Interestingly, after trafficking to the cell surface, TREM2 is cleaved by γ-secretase (Wunderlich et al., 2013).

UNC5C. Emerging studies on cell and animal models identified that aberrant UNC5C may contribute to AD by activating death-associated protein kinase 1 (DAPK1), which is a new component involved in AD pathogenesis with an extensive involvement in aberrant tau, Aβ, and neuronal apoptosis/autophagy (Li et al., 2018). *UNC5C* is a member of UNC-5 family, including *UNC5A*, *UNC5B*, *UNC5C*, and *UNC5D*, which are widely expressed in the nervous system as well as the heart and seem to be enriched in the hippocampus of AD brain. So far, among these members, only *UNC5C* is reported to be associated with AD. *UNC5C* is a transmembrane protein known as the receptor of neurin-1, playing a crucial role in mediating axon repulsion of neuronal growth cones and cell migration in the developing nervous system. It is also responsible for the regulation of neuronal apoptosis. Aberrant *UNC5C* induces neuronal death by activating a DAPK1 pathway, independent of Aβ (Hashimoto et al., 2016).

AKAP9. *AKAP9* encodes A kinase-anchoring protein 9, which is ubiquitously expressed in the CNS and periphery. It is a scaffold protein that interacts with protein kinase A (PKA) and enhances its sensitivity to cAMP. PKA promotes the activity of glycogen synthase kinase-3β (GSK3β) and enhances tau phosphorylation. Two rare specific variants of *AKAP9* were identified in African American AD cases, and they were shown to increase phosphorylation of the tau protein (Ikezu et al., 2018).

ADAM10. *ADAM10* is the major α-secretase involved in shedding of the APP extracellular domain (Kuhn et al., 2010). *ADAM10* risk variants, Q170H and R181G, increase Aβ levels in vitro. In a mouse model, *ADAM10* Q170H and R181G disrupt α-secretase activity and shift APP processing toward amyloidogenic cleavage, yielding increased plaque load (Suh et al., 2013).

Taken together, genetic studies have confirmed 36 AD loci containing common or rare alleles, and, in addition to previously established hypotheses of AD, including those related to amyloid deposition and tau pathology, these studies are also pointing to the role of lipid processing, cardiovascular risk factors, and immunity in disease progression (D'Argenio & Sarnataro 2020; Kunkle et al., 2019). Figure 73.2 shows the AD-associated genes in terms of their AD risks, frequency in population, and function classes (modified from Karch & Goate 2015).

To date, there is still no effective treatment to cure or slow the progression of AD, nor are there effective preventative interventions. There are only four US Food and Drug Administration (FDA)–approved medications that target cognitive impairment: donepezil, rivastigmine, and galantamine for enhancing cholinergic transmission and memantine for protecting neurons against glutamate excitotoxicity. Despite efforts, there have been no new drugs for the treatment of AD registered since 2003. Clarifying the biological mechanisms underlying AD remains a priority, as it should lead to the identification of potential drug targets and to the design of an effective therapy (Clarimon et al., 2020; Kunkle et al., 2019).

Autism Spectrum Disorders

Autism spectrum disorder (ASD) is among the most common neurodevelopmental disorders, affecting >1% of all children. ASD is characterized by impaired social interactions, repetitive behavior, and a widely variable spectrum of comorbidities. These comorbidities may include developmental delay, gastrointestinal problems, cardiac disorders, immune and autoimmune dysregulation, neurologic manifestations (e.g., epilepsy, intellectual disability), and other clinical features. This wide phenotypic heterogeneity is difficult to predict and manifests across a wide range of ages and with a high degree of difference in severity, making disease management and prediction of a successful intervention very difficult. It has been shown that genetic factors play an important role in the development

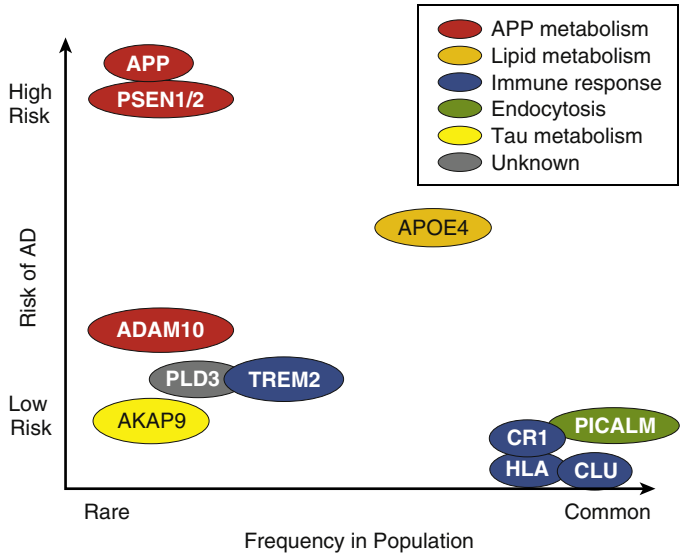

Fig. 73.2 Common and rare gene SNP variants contribute to Alzheimer disease risk. Risk is plotted against frequency of occurrence. Each gene is labeled on the plot. Around each label is a colored ellipse. Each color is reproduced in the table on the right side of the figure, which explains gene function for each gene.

of this disease, with a high heritability of approximately 80% (Bai et al., 2019), and recent advances in genomics and other molecular technologies have enabled the study of ASD on a molecular level, illuminating genes and pathways whose perturbations help explain the clinical variability among patients, and whose impairments provide possible opportunities for better treatment options. Both rare and common variants have been considered associated with ASD (Sullivan et al., 2019). However, recent GWAS of ASD have reported several associated genomic loci with modest contributions of common variants to ASD (Grove et al., 2019).

For example, a GWAS meta-analysis of 18,381 ASD cases and 27,969 controls yielded 93 genome-wide significant markers in three separate loci. Each locus was strongly supported by independent replication samples (iPSYCH and the PGC family-based data). The strongest signal among 294,911 markers analyzed on chromosome X was $P = 7.8 \times 10^{-5}$. They further explored the functional implications of these results with complementary functional genomics data, including Hi-C analyses of fetal brains and brain transcriptome data. Findings highlighted the involvement of processes relating to brain development and neuronal function. Notably, a number of genes located in the identified loci have previously been linked to ASD risk in studies of de novo and rare variants, including *PTBP2*, *CADPS*, and *KMT2E*, which were found to interact with credible SNPs in the Hi-C analysis *(PTBP2*, *CADPS)* or contain a loss-of-function credible SNP *(KMT2E)*. These proteins are further described later in this discussion.

PTBP2 (polypyrimidine tract binding protein 2) is an RNA-binding protein that governs alternative splicing in neurons, and alterations in alternative splicing have been identified in brains from individuals diagnosed with ASD (Parikshak et al., 2016). It has also been shown to coordinate axonogenesis (Zhang et al., 2019).

CADPS (calcium-dependent activator protein for secretion) functions to prime dense-core vesicles for Ca^{2+}-triggered exocytosis in neurons. Aberrant splicing of CADPS' sister gene CADPS2, which has almost identical function, has been found in autism cases, and Cadps2 knockout mice display behavioral anomalies with translational relevance to autism (Sadakata et al., 2007).

KMT2E is a member of the lysine-N-methyltransferase 2 (KMT2) family (see CAMKMT, earlier). This family of enzymes plays a vital role in regulating posttranslational histone methylation of histone 3 on lysine 4 (H3K4). Heterozygous variants in KMT2E cause a spectrum of neurodevelopmental disorders, including autism. One study showed most affected individuals with protein-truncating variants presented with mild intellectual disability. One-quarter of the individuals met criteria for autism (O'Donnell-Luria et al., 2019).

Table 73.6 summarizes the genes that are involved in ASD and the functions of their encoded proteins. As noted earlier, CACNB2, the auxiliary voltage-gated calcium channel protein, has also been implicated as being associated with ASD.

Interestingly, aberrant splicing of CADPS' sister gene CADPS2, which has almost identical function, has been found in autism cases, and Cadps2 knockout mice display behavioral anomalies with translational relevance to autism (Sadakata et al., 2007). PTBP2 encodes a neuronal splicing factor, and alterations in alternative splicing have been identified in brains from individuals diagnosed with ASD (Parikshak et al., 2016).

TABLE 73.6
Proteins Associated With Characteristic SNPs in Autism Spectrum Disorders

Protein	Function
PTBP2	RNA binding protein involves in RNA alternative splicing
CADPS	Ca^{2+} dependent exocytosis of dense-core vesicles
KMT2E	Methylation of histone H3K4

FUTURE DIRECTIONS AND CONCLUDING REMARKS

This chapter summarized recent genomic research on several psychiatric, neurologic, and substance use disorders. However, there are several important related areas of research that were not discussed in this chapter. While we mentioned some important comorbidities among key psychiatric and substance use disorders, such as those observed among schizophrenia and bipolar disorder, major depression and generalized anxiety disorder, and among substance use disorders, a recent publication from the Brainstorm Consortium has further demonstrated the large degree of common genetic variation shared among psychiatric disorders, some of which is distinct from our neurologic disorders and neurocognitive measures. In addition, while we have focused on individual findings from recent GWAS, these loci serve as the starting point for our understanding of how genetic variation impacts risk for psychiatric illness. As robust and replicable genomic risk factors for psychiatric disorders emerge, the next step is to understand the biological mechanisms underlying these statistical associations, as well as important interactions with aspects of the psychosocial environment.

Recent research has demonstrated that adverse life events (e.g., trauma exposure, stressful life events) (Peterson et al., 2018; Meyers et al., 2019; Trotta et al., 2016) moderate genomic influences on psychiatric and substance use disorders, and conversely social support (e.g., neighborhood social cohesion, social aspects of religiosity) (Meyers et al., 2013, 2019) has been shown to attenuate genomic risk. The future of the field will involve unpacking the genomic information emerging from GWAS and other large genetic studies focused on gene discovery and conducting research on deeply phenotyped samples to understand how, when, and in whom these genetic risk factors lead to the onset and course of illness.

In parallel, functional studies conducted in the laboratory are needed to further our understanding of biological mechanisms, and studies of brain function are needed to further our understanding of the neural and cognitive profiles of individuals at risk for these disorders. As discussed throughout this chapter, the implementation of pharmacogenetic testing in psychiatric clinics is underway. For example, pharmacogenetic dosing guidelines support the use of *CYP2C9*, *CYP2C19*, *CYP2D6*, *HLA-A*, and *HLA-B* information for the selection and dosing of certain psychotropic medications (Bousman et al., 2019). However, genomic understanding of the beneficial and adverse effects of psychotropic medications is limited by the considerable difficulty and expense of conducting longitudinal drug trials. Future, large-scale genomic studies will hopefully make it possible to conduct naturalistic pharmacogenomic studies to more precisely inform clinical decisions regarding the use of medication in treating neuropsychiatric illness.

Furthermore, a critical current limitation is that a disproportionate majority of participants in published GWAS of psychiatric disorders are of European descent (Peterson et al., 2019) https://paperpile.com/c/mjsgrG/mPdV. It is essential that diverse populations become better represented. The integration of genomics into health care has the potential to improve disease prediction and optimize treatments, whereas a lack of diversity will limit the utility of precision medicine efforts. For example, benefits of pharmacogenetics cannot be fully realized until there is equitable representation, as some therapeutics may be more effective or safer in certain populations because of differences in allele frequency, effect size, and penetrance of variants associated with drug metabolism (Roden et al., 2011). Increasing diversity among study participants will advance our understanding of genetics architecture in all populations and ensure that genetics research is broadly applicable.

SELECTED REFERENCES

Clarimon J, Moreno-Grau S, Cervera-Carles L, et al.: Genetic architecture of neurodegenerative dementias, *Neuropharmacology* 168:108014, 2020.

This is an important up-to-date summary of genes and proteins involved with dementias, including APOE in lipid metabolism.

Ikeda MT, Kondo SK, Iwata N: Genome-wide association studies of bipolar disorder: a systematic review of recent findings and their clinical implications, *Psychiatry Clin Neurosci* 72:52–63, 2018a.

This is an excellent review of GWAS studies on bipolar disorders with highly informative summary tables showing genes that have high probabilities of association with this disorder.

Schumann G, Liub C, O'Reilly P, et al.: KLB is associated with alcohol drinking, and its gene product β-klotho is necessary for FGF21 regulation of alcohol preference, *Proc Natl Acad Sci USA* 113:14372–14377, 2016.

This landmark paper identifies β-klotho protein to be a critical receptor for FGF21 that reduces desire for alcohol and a new endocrine pathway that is involved in alcohol consumption regulation.

Willard SS, Koochekpour S: Glutamate, glutamate receptors, and downstream signaling pathways, *Int J Biol Sci* 9:948–959, 2013, https://doi.org/10.7150/ijbs.6426.

By IvySpring International Publishers, this is a clear, concise, and extensive review of glutamate i and m receptors that gives an excellent background for drug discovery.

Access the complete reference list online at Elsevier eBooks for Practicing Clinicians.

REFERENCES

Adkins DE, Khachane AN, McClay JL, et al.: SNP-based analysis of neuroactive ligand–receptor interaction pathways implicates PGE2 as a novel mediator of antipsychotic treatment response: data from the CATIE study, *Schizophr Res* 135:200–201, 2012.

Amiel J, Rio M, de Pontual L, et al.: Mutations in TCF4, encoding a class I basic helix-loop-helix transcription factor, are responsible for Pitt-Hopkins syndrome, a severe epileptic encephalopathy associated with autonomic dysfunction, *Am J Human Genet* 80:988–993, 2007.

Andrade A, Hope J, Allen A, et al.: A rare schizophrenia risk variant of *CACNA1I* disrupts CaV3.3 channel activity, *Nature Scientific Reports* 6, 2016.

Bai D, Yip BHK, Windham GC, et al.: Association of genetic and environmental factors with autism in a 5-Country cohort, *JAMA Psychiatry* 76:1035, 2019.

Baum AE, Akula N, Cabanero, I. M, et al.: A genome-wide association study implicates diacylglycerol kinase eta (DGKH) and several other genes in the etiology of bipolar disorder, *Mol Psychiatry* 13:197–207, 2008.

Beique JC, Imad M, Mladenovic L, et al.: Mechanism of the 5-hydroxytryptamine 2A receptor-mediated facilitation of synaptic activity in prefrontal cortex, *Proc Natl Acad Sci U S A* 104:9870–9875, 2007.

Bentahir M, Nyabi O, Verhamme J, et al.: Presenilin clinical mutations can affect gamma-secretase activity by different mechanisms, *J Neurochem* 96(3):732–742, 2006.

Berrettini W: A brief review of the genetics and pharmacogenetics of opioid use disorders, *Dialogues Clin Neurosci* 19:229–236, 2017.

Bigdeli TB, Genovese G, Georgakopoulos P, et al.: Contributions of common genetic variants to risk of schizophrenia among individuals of African and Latino ancestry, *Mol. Psychiatry* 387:1085–1093, 2019.

B. Disorder and Schizophrenia Working Group of the Psychiatric Genomics Consortium, McQuillin A, Boocock J, et al.: Genomic Dissecti/on of bipolar disorder and schizophrenia, including 28 Subphenotypes, *Cell* 173:1705–1715, 2018. e16.

Bousman C, Maruf AA, Müller DJ: Towards the integration of pharmacogenetics in psychiatry: a minimum, evidence-based genetic testing panel, *Curr. Opin. Psychiatry* 32:7–15, 2019.

Brandl EJ, Tiwari AK, Zhou, J. X, et al.: Influence of CYP2D6 and CYP2C19 gene variants on antidepressant response in obsessive-compulsive disorder, *Pharmacogenomics J* 14:176–181, 2014.

Cahalan, Chandy KG: 'The Shaw-related potassium channel gene, Kv3.1, on human chromosome 11, encodes the type l K+ channel in T cells', *J Biol Chem* 267:20971–20979, 1992.

Calabro M, Mandelli L, Crisafulli C, et al.: Genes involved in neurodevelopment, Neuroplasticity, and bipolar disorder: CACNA1C, CHRNA1, and MAPK1, *Neuropsychobiology* 74:159–168, 2016.

Cates HM, Benca–Bachman CE, Guglielmo G, et al.: National Institute on Drug Abuse genomics consortium white paper: Coordinating efforts between human and animal addiction studies, *Genes, Brain Behav.* 18, 2019. e12577.

Chen F, Hasegawa H, Schmitt-Ulms G, et al.: TMP21 is a presenilin complex component that modulates gamma-secretase but not epsilon-secretase activity, *Nature* 440(7088):1208–1212, 2006.

Chen J, Song J, Yuan P, et al.: Orientation and cellular distribution of membrane-bound catechol-O-methyltransferase in cortical neurons: implications for drug development, *J Biol Chem* 286:34752–34760, 2011.

Cheng Z, Zhou H, Sherva R, et al.: Genome-wide association study identifies a regulatory variant of RGMA associated with opioid dependence in European Americans, *Biol. Psychiatry* 84:762–770, 2008.

Christiansen L, Tan Q, Iachina M, et al.: Candidate gene polymorphisms in the serotonergic pathway: influence on depression symptomatology in an elderly population, *Biol Psychiatry* 61:223–230, 2007.

Citron M, Westaway D, Xia W, et al.: Mutant presenilins of Alzheimer's disease increase production of 42-residue amyloid beta-protein in both transfected cells and transgenic mice, *Nat Med* 3(1):67–72, 1997.

Clarimon J, Moreno-Grau S, Cervera-Carles L, et al.: Genetic architecture of neurodegenerative dementias, *Neuropharmacology* 168:108014, 2020.

Cloutier P, Lavallee-Adam M, Faubert D, et al.: A newly uncovered group of distantly related lysine methyltransferases preferentially interact with molecular chaperones to regulate their activity, *PLoS Genet* 9, 2013. e1003210.

CONVERGE Consortium: Sparse whole-genome sequencing identifies two loci for major depressive disorder, *Nature* 523:588–591, 2015.

Conway CC, Hammen C, Brennan PA, et al.: Interaction of chronic stress with serotonin transporter and catechol-O-methyltransferase polymorphisms in predicting youth depression, *Depress Anxiety* 27:737–745, 2010.

Cooper A, Woulfe D, Kilic F: Post-translational modifications of serotonin transporter, *Pharmacol Res* 140:7–13, 2019.

Corradini E, Babitt JL, Lin HY: The RGM/DRAGON family of BMP co-receptors, *Cytokine Growth Factor Rev* 20(5–6):389–398, 2009.

Cross-Disorder Group of the Psychiatric Genomics Consortium: Identification of risk loci with shared effects on five major psychiatric disorders: a genome-wide analysis, *Lancet* 381(9875):1371–1379, 2013.

Cruceanu C, Schmouth J-F, Torres-Platas SG, et al.: Rare susceptibility variants for bipolar disorder suggest a role for G protein-coupled receptors, *Mol. Psychiatry* 23:2050–2056, 2018.

Cruchaga C, Karch CM, Jin SC, et al.: Rare coding variants in the phospholipase D3 gene confer risk for Alzheimer's disease, *Nature* 505(7484):550–554, 2014.

Cui L, Gong X, Tang Y, et al.: Relationship between the LHPP gene polymorphism and resting-state brain activity in major depressive disorder, *Neural Plast*, 2016. 9162590, 2016.

D'Argenio V, Sarnataro D: New insights into the molecular Bases of familial Alzheimer's disease, *J. Pers. Med.* 10:26, 2020.

Dean LVM, Pratt HL, McLeod WS, et al.: *Malheiro Imipramine therapy and CYP2D6 and CYP2C19 genotype*, Bethesda (MD)), 2012, Medical Genetics Summaries.

De Strooper B, Annaert W: Proteolytic processing and cell biological functions of the amyloid precursor protein, *J Cell Sci* 113(11):1857–1870, 2000.

Dodge NC, Jacobson JI, Jacobson SW: *Alcohol dehydrogenase alleles and impact on neuropathology in Neuropathology of drug addictions and substance Misuse*, Volume 1 VR Preedy. Philadelphia, 2016, Elsevier, pp 510–519.

Duncan LE, Ostacher M, Ballon J: How genome-wide association studies (GWAS) made traditional candidate gene studies obsolete, *Neuropsychopharmacology* 44:1518–1523, 2019.

Dunn EC, Sofer T, Gallo LC, et al.: Genome-wide association study of generalized anxiety symptoms in the Hispanic community health study/study of Latinos, *Am. J. Med. Genet. B. Neuropsychiatr. Genet.* 174:132–143, 2017.

Edenberg HJ, McClintick JN: Alcohol dehydrogenases, aldehyde dehydrogenases, and alcohol Use disorders: a critical review, *Alcohol Clin Exp Res* 42:2281–2297, 2018.

Edman K: Maret W Alcohol dehydrogenase genes: restriction fragment length polymorphisms for ADH4 (pi-ADH) and ADH5 (chi-ADH) and construction of haplotypes among different ADH classes, *Hum Genet* 90:395–401, 1993.

Endo M, Yamashita T: 'Inactivation of Ras by p120GAP via focal adhesion kinase dephosphorylation mediates RGMa-induced growth cone collapse, *J Neurosci* 29:6649–6662, 2009.

Fabbri C, Serretti A: Genetics of treatment outcomes in major depressive disorder: present and future, *Clin. Psychopharmacol. Neurosci.* 18:1–9, 2020.

Ferrari AJ, Charlson FJ, Norman RE, et al.: Burden of depressive disorders by Country, sex, age, and Year: findings from the global burden of disease study 2010, *PLoS Med* 10, 2013. e1001547.

Finseth PI, Sonderby IE, Djurovic S, et al.: Association analysis between suicidal behaviour and candidate genes of bipolar disorder and schizophrenia, *J Affect Disord* 163:110–114, 2014.

Gaudet P, Livstone MS, Lewis SE, et al.: Phylogenetic-based propagation of functional annotations within the Gene Ontology consortium, *Brief Bioinform* 12:449–462, 2011.

Gelernter J, Sun N, Polimanti R, et al.: Genome-wide association study of Maximum Habitual alcohol intake in 140,000 U.S. European and African American veterans yields novel risk loci, *Biol. Psychiatry* 86:365–376, 2019a.

Gelernter J, Sun N, Polimanti R, et al.: Genome-wide association study of post-traumatic stress disorder reexperiencing symptoms in 165,000 US veterans, *Nat Neurosci* 22:1394–1401, 2019b.

Gelernter J, Kranzler HR, Sherva R, et al.: 'Genome-wide association study of opioid dependence: multiple associations mapped to calcium and potassium pathways, *Biol Psychiatry* 76:66–74, 2014.

Goate A, Chartier-Harlin MC, Mullan M, et al.: Segregation of a missense mutation in the amyloid precursor protein gene with familial Alzheimer's disease, *Nature* 349(6311):704–706, 1991.

Goes FS, Pirooznia M, Tehan M, et al.: De novo variation in bipolar disorder, *Mol. Psychiatry*, 2019.

Goulding DR, Nikolova VD, Mishra L, et al.: Inter-alpha-inhibitor deficiency in the mouse is associated with alterations in anxiety-like behavior, exploration and social approach, *Genes Brain Behav* 18, 2019. e12505.

Gourlay AP,JD,WF, Sutherland C: Rab-GTPase binding effector protein 2 (RABEP2) is a primed substrate for Glycogen Synthase kinase-3 (GSK3), *Sci Rep* 7:17682, 2017.

Gournier H, Stenmark H, Rybin V, et al.: 'Two distinct effectors of the small GTPase Rab5 cooperate in endocytic membrane fusion, *EMBO J* 17:1930–1940, 1998.

Granadino B, Gallardo ME, López-Ríos J, et al.: Genomic cloning, structure, expression pattern, and chromosomal location of the human SIX3 gene, *Genomics* 55:100–105, 1999.

Grant BF, Goldstein RB, Saha TD, et al.: Epidemiology of DSM-5 alcohol Use disorder: results from the national epidemiologic Survey on alcohol and related conditions III, *JAMA psychiatry* 72:757–766, 2015.

Green EK, Rees E, Walters JTR, et al.: Copy number variation in bipolar disorder, *Mol. Psychiatry* 21:89–93, 2016.

Grissmer, S., S. Ghanshani, B. Dethlefs, et al..

Grove, J.; Ripke, S.; Als, T.D.; et al..

Andreassen OA, Anney R, et al.: Identification of common genetic risk variants for autism spectrum disorder, *Nat Genet* 51:431–444, 2019.

Guerreiro R, Wojtas A, Bras J, et al.: TREM2 variants in Alzheimer's disease, *N Engl J Med* 368(2):117–127, 2013.

Hains AB, Arnsten AF: Molecular mechanisms of stress-induced prefrontal cortical impairment: implications for mental illness, *Learn Mem* 15:551–564, 2008.

Han C, Zhang X, Xu W, et al.: Cloning of the nucleostemin gene and its function in transforming human embryonic bone marrow mesenchymal stem cells into F6 tumor cells, *Int J Mol Med* 16:205–213, 2005.

Han J, Knops JF, Longshore JW: King PH Localization of human elav-like neuronal protein 1 (hel-n1) on chromosome 9p21 by chromosome microdissection polymerase chain reaction and fluorescence in situ hybridization, *Genomics* 36:189–191, 1996.

Hara K, Taharazako S, Ikeda M, et al.: Dynamic feature of mitotic arrest deficient 2-like protein 2 (MAD2L2) and structural basis for its interaction with chromosome alignment-maintaining phosphoprotein (CAMP), *J Biol Chem* 292:17658–17667, 2017.

Hashimoto Y, Toyama Y, Kusakari S, et al.: An Alzheimer disease-linked rare mutation Potentiates Netrin receptor Uncoordinated-5C-induced signaling that Merges with amyloid β precursor protein signaling, *J Biol Chem* 291(23):12282–12293, 2016.

Hasin DS, Kerridge BT, Saha TD, et al.: Prevalence and Correlates of DSM-5 cannabis Use disorder, 2012-2013: findings from the national epidemiologic Survey on alcohol and related conditions–III, *Am. J. Psychiatry* 173:588–599, 2016.

Hata K, Kaibuchi K, Inagaki S, et al.: 'Unc5B associates with LARG to mediate the action of repulsive guidance molecule', *J Cell Biol* 184:737–750, 2009.

Hegarty SV, O'Keeffe GW, Sullivan AM: BMP-Smad 1/5/8 signalling in the development of the nervous system, *Prog Neurobiol* 109:28–41, 2013.

Heinrich, A., A. Lourdusamy, J. Tzschoppe, et al..

Heinz B, Ittermann E, Loth K, et al.: The risk variant in ODZ4 for bipolar disorder impacts on amygdala activation during reward processing, *Bipolar Disord* 15:440–445, 2013.

Henckens MJ, Deussing JM, Chen A Region-specific roles of the corticotropin-releasing factor-urocortin system in stress Nat Rev Neurosci: 17, 636–651. doi:10.1038/nrn.2016.94.PMID.27586075.

Hettema JM, Verhulst B, Chatzinakos C, et al.: Genome-wide association study of shared liability to anxiety disorders in Army STARRS, *Am. J. Med. Genet. B. Neuropsychiatr. Genet. ajmg.b.* 32776, 2019.

Hillhouse EW: Grammatopoulos the molecular mechanisms underlying the regulation of the biological activity of corticotropin-releasing hormone receptors: implications for physiology and pathophysiology, *Endocr Rev* 27:260–286, 2006, https://doi.org/10.1210/er.2005-0034.PMID.16484629.

Hindupur SK, Colombi M, Fuhs SR, et al.: The protein histidine phosphatase LHPP is a tumour suppressor, *Nature* 555:678–682, 2018.

Hodson R: Alzheimer's disease, *Nature* 559, 2018. S1–S1.

Hou L, Heilbronner U, Degenhardt F, et al.: Genetic variants associated with response to lithium treatment in bipolar disorder: a genome-wide association study, *Lancet (London, England)* 387:1085–1093, 2016.

Hodson DM, Adams MJ, Shirali M, et al.: Genome-wide association study of depression phenotypes in UK Biobank identifies variants in excitatory synaptic pathways, *Nat Commun* 9:1470, 2018.

Howard DM, Adams MJ, Clarke T-K, et al.: Genome-wide meta-analysis of depression identifies 102 independent variants and highlights the importance of the prefrontal brain regions, *Nat Neurosci* 22:343–352, 2019.

Huang CB, Shi WJ, Wang CJ, et al.: Association of adenylate cyclase-2 gene polymorphism with bipolar disorder, *Asian J Psychiatr* 52:102150, 2020.

Hughes T, Sonderby IE, Polushina T, et al.: Elevated expression of a minor isoform of ANK3 is a risk factor for bipolar disorder, *Transl Psychiatry* 8:210, 2018.

Hyde CL, Nagle MW, Tian C, et al.: Identification of 15 genetic loci associated with risk of major depression in individuals of European descent, *Nat Genet* 48:1031–1036, 2016.

Ibrahim-Verbaas CA, Bressler J, Debette S, et al.: 'GWAS for executive function and processing speed suggests involvement of the CADM2 gene, *Mol Psychiatry* 21:189–197, 2016.

Imbrici P, Camerino DC: Tricarico D Major channels involved in neuropsychiatric disorders and therapeutic perspectives, *Front Genet* 4:1–19, 2013.

Ikeda M, Saito T, Kondo K, Iwata N: Genome-wide association studies of bipolar disorder: a systematic review of recent findings and their clinical implications, *Psychiatry Clin Neurosci* 72:52–63, 2018a.

Ikeda M, et al.: A genome-wide association study identifies two novel susceptibility loci and trans population polygenicity associated with bipolar disorder, *Mol Psychiatr* 23:639–647, 2018b.

Ikezu T, Chen C, DeLeo AM, et al.: Tau phosphorylation is impacted by rare AKAP9 mutations associated with Alzheimer disease in African Americans, *J Neuroimmune Pharmacol* 13(2):254–264, 2018.

Iynedjian PB: Molecular physiology of mammalian glucokinase, *Cell Mol Life Sci* 66:27–42, 2009.

Jayakumar AR, Tong XY, Curtis KM, et al.: Decreased astrocytic thrombospondin-1 secretion after chronic ammonia treatment reduces the level of synaptic proteins: *in Vitro* and *in Vivo* Studies, *J Neurochem* 131:333–347, 2014.

Jiang Q, Lee CY, Mandrekar S, et al.: ApoE promotes the proteolytic degradation of Abeta, *Neuron* 58(5):681–693, 2008.

Jeong J, Eide DJ: The SLC39 family of zinc transporters, *Mol Aspects Med:* 34:612–619, 2013.

Jones SE, Jomary C: *Clusterin. Int J Biochem Cell Biol.* 34(5):427–431, 2002.

Karch CM, Goate AM: Alzheimer's disease risk genes and mechanisms of disease pathogenesis, *Biol Psychiatry* 77(1):43–51, 2015.

Kessler RC, Chiu WT, Demler O, et al.: Prevalence, severity, and comorbidity of 12-Month DSM-IV disorders in the national comorbidity Survey replication, *Arch. Gen. Psychiatry* 62:617, 2005.

Kessler RC, Bromet EJ: The epidemiology of depression across cultures, *Annu. Rev. Public Health* 34:119–138, 2013.

Kim YK, Jeon SW: Neuroinflammation and the immune-kynurenine pathway in anxiety disorders, *Curr Neuropharmacol* 16:574–582, 2018.

Kofler N, Corti F, Rivera-Molina F, et al.: 'The Rab-effector protein RABEP2 regulates endosomal trafficking to mediate vascular endothelial growth factor receptor-2 (VEGFR2)-dependent signaling, *J Biol Chem* 293:4805–4817, 2018.

Kuhn PH, Wang H, Dislich B, et al.: ADAM10 is the physiologically relevant, constitutive alpha-secretase of the amyloid precursor protein in primary neurons, *EMBO J* 29(17):3020–3032, 2010.

Kunkle BW, Grenier-Boley B, Sims R, et al.: Genetic meta-analysis of diagnosed Alzheimer's disease identifies new risk loci and implicates Aβ, tau, immunity and lipid processing, *Nat Genet* 51:414–430, 2019.

Lah GJ, Key B: 'Dual roles of the chemorepellent axon guidance molecule RGMa in establishing pioneering axon tracts and neural fate decisions in embryonic vertebrate forebrain, *Dev Neurobiol* 72:1458–1470, 2012.

Lam D, Ancelin ML, Ritchie K, et al.: Genotype-dependent associations between serotonin transporter gene (SLC6A4) DNA methylation and late-life depression, *BMC Psychiatr* 18:282, 2018.

Li Q, Wang BL, Sun FR, et al.: The role of *UNC5C* in Alzheimer's disease, *Ann Transl Med* 6(10):178, 2018.

Liang Z, Zhan Y, Shen Y, et al.: NY the pseudokinase CaMKv is required for the activity-dependent maintenance of dendritic spines, *Nature Commun* 7:13282, 2016.

Liu S, Ando F, Fujita Y, et al.: A clinical dose of angiotensin-converting enzyme (ACE) inhibitor and heterozygous ACE deletion exacerbate Alzheimer's disease pathology in mice, *J Biol Chem* 294(25):9760–9770, 2019.

Liu DJ, Brazel DM, Turcot V, et al.: Exome chip meta-analysis elucidates the genetic architecture of rare coding variants in smoking and drinking behavior, *Biol Psychiatry* 85(11):946–955, 2019.

Liu D, Niu ZX: The structure, genetic polymorphisms, expression, and biological functions of complement receptor type 1 (CR1/CD35), *Immunopharmacol Immunotoxicol* 31(4):524–535, 2009.

Logie, L., L. Van Aalten, A. Knebel, et al..

Lu G, Li J, Zhang H, et al.: Role and possible mechanisms of Sirt1 in depression, *Oxid Med Cell Longev*2018, 2018. 8596903.

Mallas EJ, Carletti F, Chaddock CA, et al.: Genome-wide discovered psychosis-risk gene ZNF804A impacts on white matter microstructure in health, schizophrenia and bipolar disorder, *PeerJ* 4, 2016. e1570.

Marshall CR, Howrigan DP, Merico D, et al.: Contribution of copy number variants to schizophrenia from a genome-wide study of 41,321 subjects, *Nat Genet* 49:27–35, 2017.

McClay JL, Adkins DE, Åberg K, et al.: Genome-wide pharmacogenomic analysis of response to treatment with antipsychotics, *Mol. Psychiatry* 16:76–85, 2011.

McIntosh AM, Sullivan PF, Lewis CM: Uncovering the genetic architecture of major depression, *Neuron* 102:91–103, 2019.

Meyers JL, Salvatore JE, Aliev F, et al.: Psychosocial moderation of polygenic risk for cannabis involvement: the role of trauma exposure and frequency of religious service attendance, *Transl Psychiatry* 9:269, 2019.

Meyers JL, Cerdá M, Galea S, et al.: Interaction between polygenic risk for cigarette use and environmental exposures in the Detroit neighborhood health study, *Transl Psychiatry* 3, 2013.

Mishra A, Singh S, Shukla S: Physiological and functional basis of dopamine receptors and their role in neurogenesis: possible implication for Parkinson's disease, *J Exp Neurosci* 12, 2018. 1179069518779829.

Moreno-Igoa M, Hernandez H-C, Bengoa-Alonso A, et al.: KANSL1 gene disruption associated with the full clinical spectrum of 17q21.31 microdeletion syndrome, *BMC Med Genet* 16:68, 2015.

Muona M, Berkovic SF, Dibbens LM, et al.: A recurrent de novo mutation in KCNC1 causes progressive myoclonus epilepsy, *Nat Genet* 47(1):39–46, 2015.

Muhleisen TW, Leber M, Schulze TG, et al.: 'Genome-wide association study reveals two new risk loci for bipolar disorder', *Nat Commun* 5:3339, 2014.

Nievergelt CM, Maihofer AX, Klengel T, et al.: International meta-analysis of PTSD genome-wide association studies identifies sex- and ancestry-specific genetic risk loci, *Nat Commun* 10:4558, 2019.

Odermatt A, Barton K, Khanna VK, et al.: 'The mutation of Pro789 to Leu reduces the activity of the fast-twitch skeletal muscle sarco(endo)plasmic reticulum Ca2+ ATPase (SERCA1) and is associated with Brody disease, *Hum Genet* 106:482–491, 2000.

O'Donnell-Luria AH, Pais LS, Faundes V, et al.: Heterozygous variants in KMT2E cause a spectrum of neurodevelopmental disorders and epilepsy, *Am J Hum Genet* 104(6):1210–1222, 2019.

Orr CF, Rowe DB, Mizuno Y, et al.: A possible role for humoral immunity in the pathogenesis of Parkinson's disease, *Brain* 128(Pt 11):2665–2674, 2005.

Orru G, Carta MG: Genetic variants involved in bipolar disorder, a Rough Road Ahead, *Clin Pract Epidemiol Ment Health* 14:37–45, 2018.

Parikshak NN, Swarup V, Belgard TG, et al.: Genome-wide changes in lncRNA, splicing, and regional gene expression patterns in autism, *Nature* 540:423–427, 2016.

Park J, Koko M, Hedrich UBS, et al.: 'KCNC1-related disorders: new de novo variants expand the phenotypic spectrum, *Ann Clin Transl Neurol* 6:1319–1326, 2019.

Pasman JA, Verweij KJH, Gerring Z, et al.: Genome-wide association analysis of lifetime cannabis use (N=184,765) identifies new risk loci, genetic overlap with mental health, and a causal influence of schizophrenia on cannabis use, *BioRxiv* 234294, 2018a.

Pasman JA, Verweij KJH, Gerring Z, et al.: 'GWAS of lifetime cannabis use reveals new risk loci, genetic overlap with psychiatric traits, and a causal influence of schizophrenia, *Nat Neurosci* 21:1161–1170, 2018b.

Pellissier F, Gerber A, Bauer C, et al.: 'The adhesion molecule Necl-3/SynCAM-2 localizes to myelinated axons, binds to oligodendrocytes and promotes cell adhesion, *BMC Neurosci* 8:90, 2007.

Peterson RE, Kuchenbaecker K, Walters RK, et al.: Genome-wide association studies in Ancestrally diverse populations: opportunities, methods, Pitfalls, and Recommendations, *Cell* 179:589–603, 2019.

Peterson RE, Cai N, Dahl AW, et al.: Molecular genetic analysis Subdivided by Adversity exposure suggests etiologic heterogeneity in major depression, *Am. J. Psychiatry* 175:545–554, 2018.

Polderman TJC, Benyamin B, de Leeuw CA, et al.: Meta-analysis of the heritability of human traits based on fifty years of twin studies, *Nat Genet* 47:702–709, 2015.

Prata DP, Costa-Neves B, Cosme G, et al.: Unravelling the genetic basis of schizophrenia and bipolar disorder with GWAS: a systematic review, *J Psychiatr Res* 114:178–207, 2019.

Psychiatric, GWAS Consortium Bipolar Disorder Working Group: Large-scale genome-wide association analysis of bipolar disorder identifies a new susceptibility locus near ODZ4, *Nat Genet* 43:977–983, 2011.

Purcell SM, Moran JL, Fromer M, et al.: A polygenic burden of rare disruptive mutations in schizophrenia, *Nature* 506:185–190, 2014.

Purcell SM, Wray NR, Stone JL, et al.: Common polygenic variation contributes to risk of schizophrenia and bipolar disorder, *Nature* 460:748–752, 2009.

Rhee TG, Rosenheck RA: Association of current and past opioid use disorders with health-related quality of life and employment among US adults, *Drug Alcohol Depend* 199:122–128, 2019.

Risher WC, Eroglu C: Thrombospondins as key regulators of synaptogenesis in the central nervous system Matrix, *Biol:* 31:170–177, 2012.

Roby Y: ANK3 gene polymorphisms and bipolar disorder: a meta-analysis, *Psychiatr Genet* 27:225–235, 2017.

Roden DM, Wilke RA, Kroemer HK, et al.: Pharmacogenomics: the genetics of variable drug responses, *Circulation* 123:1661–1670, 2011.

Sadakata T, Washida M, Iwayama Y, et al.: Autistic-like phenotypes in Cadps2-knockout mice and aberrant CADPS2 splicing in autistic patients, *J Clin Invest* 117:931–943, 2007.

Sadigh-Eteghad S, Talebi M, Farhoudi M: Association of apolipoprotein E epsilon 4 allele with sporadic late onset Alzheimer's disease. A meta-analysis, *Neurosciences* 17(4):321–326, 2012.

Sanchez-Pulido L, Andrade-Navarro MA: The FTO (fat mass and obesity associated) gene codes for a novel member of the non-heme dioxygenase superfamily, *BMC Biochem* 8:23, 2007.

Sanchez-Roige S, Palmer AA, Fontanillas P, et al.: Genome-wide association study meta-analysis of the alcohol Use disorders identification test (AUDIT) in two population-based cohorts, *Am. J. Psychiatry* 176:107–118, 2019.

Schizophrenia Working Group of the Psychiatric Genomics Consortium: Biological insights from 108 schizophrenia-associated genetic loci, *Nature* 511:421–427, 2014.

Schumann G, Liub C, O'Reilly P, et al.: KLB is associated with alcohol drinking, and its gene product β-Klotho is necessary for FGF21 regulation of alcohol preference, *Proc Natl Acad Sci USA* 113:14372–14377, 2016.

Scott LJ, Muglia P, Kong XQ, et al.: Genome-wide association and meta-analysis of bipolar disorder in individuals of European ancestry, *Proc Natl Acad Sci U S A* 106:7501–7506, 2009.

Severyn CJ, Shinde U, Rotwein P: Molecular biology, genetics and biochemistry of the repulsive guidance molecule family, *Biochem J* 422(3):393–403, 2009.

Shen Y, Lue L, Yang L, et al.: Complement activation by neurofibrillary tangles in Alzheimer's disease, *Neurosci Lett* 305(3):165–168, 2001.

Shimura H, Hattori N, Kubo S., et al.. Familial Parkinson disease gene product, parkin, is a ubiquitin-protein ligase. Nat Genet 25: 302-305, Jul; (3):302-5, 2000.

Smedler E, Abe C, Palsson E, et al.: CACNA1C polymorphism and brain cortical structure in bipolar disorder, *J Psychiatry Neurosci* 45:182–187, 2019.

Smoller JW, Finn CT: Family, twin, and adoption studies of bipolar disorder, *Am. J. Med. Genet. C. Semin. Med. Genet.* 123C:48–58, 2003.

Stahl EA, Breen G, Forstner AJ, et al.: Genome-wide association study identifies 30 loci associated with bipolar disorder, *Nat Genet* 51:793–803, 2019.

Stenmark H: Olkkonen VM the Rab GTPase family, *Genome Biol* 2:1–7, 2001.

Suh J, Choi SH, Romano DM, et al.: ADAM10 missense mutations potentiate β-amyloid accumulation by impairing prodomain chaperone function, *Neuron* 80(2):385–401, 2013.

Sullivan PF, Kendler KS, Neale MC: Schizophrenia as a complex trait, *Arch. Gen. Psychiatry* 60:1187, 2003.

Sullivan PF, Neale MC, Kendler KS: Genetic epidemiology of major depression: review and meta-analysis, *Am. J. Psychiatry* 157:1552–1562, 2000.

Sullivan PF, Geschwind DH: Defining the genetic, genomic, cellular, and diagnostic architectures of psychiatric disorders, *Cell* 177:162–183, 2019.

Sur C, Betz H, Schloss P: Distinct effects of imipramine on 5-hydroxytryptamine uptake mediated by the recombinant rat serotonin transporter SERT1, *J Neurochem* 70:2545–2553, 1998.

Thomas LA, Akins MR, Biederer T: 'Expression and adhesion profiles of SynCAM molecules indicate distinct neuronal functions, *J Comp Neurol* 510:47–67, 2008.

Thoulouze MI, Lafage M, Schachner M, et al.: 'The neural cell adhesion molecule is a receptor for rabies virus, *J Virol* 72:7181–7190, 1998.

Toma C, Pierce KD, Shaw AD, et al.: Comprehensive cross-disorder analyses of CNTNAP2 suggest it is unlikely to be a primary risk gene for psychiatric disorders, *PLoS Genet* 14, 2018. e1007535.

Trotta A, Iyegbe C, Di Forti M, et al.: Interplay between schizophrenia polygenic risk score and childhood Adversity in first-Presentation psychotic disorder: a Pilot study, *PloS One* 11, 2016. e0163319.

Tsai RY, McKay RD: A nucleolar mechanism controlling cell proliferation in stem cells and cancer cells, *Genes Dev* 16:2991–3003, 2002.

van Hulzen KJE, Scholz CJ, Franke B, et al.: Reif. Genetic overlap between attention-deficit/hyperactivity disorder and bipolar disorder: evidence from genome-wide association study meta-analysis, *Biol Psychiatry* 82:634–641, 2017.

Vetter SW, Leclerc E: Novel aspects of calmodulin target recognition and activation, *Eur J Biochem* 270:404–414, 2003.

Velazquez P, Cribbs DH, Poulos TL, et al.: Aspartate residue 7 in amyloid beta-protein is critical for classical complement pathway activation: implications for Alzheimer's disease pathogenesis, *Nat Med* 3(1):77–79, 1997.

Wagnon JL, Briese M, Sun W, et al.: Frankel WN CELF4 regulates translation and local abundance of a vast set of mrnas, including genes associated with regulation of synaptic function, *PLoS Genet* 8(11), 2012. e1003067.

Wang L, Liu W, Li X, et al.: Further evidence of an association between NCAN rs1064395 and bipolar disorder, *Mol Neuropsychiatry* 4:30–34, 2018.

Whiteford HA, Degenhardt L, Rehm J, et al.: Global burden of disease attributable to mental and substance use disorders: findings from the Global Burden of Disease Study 2010, *Lancet* 382:1575–1586, 2013.

Wigner P, Czarny P, Synowiec E, et al.: Association between single nucleotide polymorphisms of TPH1 and TPH2 genes, and depressive disorders, *J Cell Mol Med* 22:1778–1791, 2018.

Willard SS: Koochekpour S Glutamate, glutamate receptors, and downstream signaling pathways, *Int J Biol Sci* 9:948–959, 2013.

Wray NR, Ripke S, Mattheisen M, et al.: Genome-wide association analyses identify 44 risk variants and refine the genetic architecture of major depression, *Nat Genet* 50:668–681, 2018.

Wunderlich P, Glebov K, Kemmerling N: Sequential proteolytic processing of the triggering receptor expressed on myeloid cells-2 (TREM2) protein by ectodomain shedding and γ-secretase-dependent intramembranous cleavage, *J Biol Chem* 288(46):33027–33036, 2013.

Yamamoto M, Watt CD, Schmidt RJ, et al.: 'Cloning and characterization of a novel MyoD enhancer-binding factor, *Mech Dev* 124:715–728, 2007.

Yang Z, Zhou D, Li H, et al.: The genome-wide risk alleles for psychiatric disorders at 3p21.1 show convergent effects on mRNA expression, cognitive function, and mushroom dendritic spine, *Mol Psychiatry* 25:48–66, 2020.

Yokoi F, Hiraishi H, Izuhara K: Molecular cloning of a cDNA for the human phospholysine phosphohistidine inorganic pyrophosphate phosphatase, *J Biochem* 133:607–614, 2003.

Yokoyama S, Imoto K, Kawamura T, et al.: 'Potassium channels from NG108-15 neuroblastoma-glioma hybrid cells. Primary structure and functional expression from cDNAs, *FEBS Lett* 259:37–42, 1989.

Zhang C, Wu B, Beglopoulos V, et al.: Presenilins are essential for regulating neurotransmitter release, *Nature* 460(7255):632–636, 2009.

Zhang M, Ergin V, Lin L, et al.: Axonogenesis is coordinated by neuron-specific alternative splicing Programming and splicing regulator PTBP2, *Neuron* 101(4):690–706, 2019. e10.

Zhao L, Chang H, Zhou DS, et al.: Replicated associations of FADS1, MAD1L1, and a rare variant at 10q26.13 with bipolar disorder in Chinese population, *Transl Psychiatry* 8:270, 2018.

Zhao Z, Sagare AP, Ma Q, et al.: Central role for PICALM in amyloid-β blood-brain barrier transcytosis and clearance, *Nat Neurosci* 18(7):978–987, 2015.

Zuo L, van Dyck CH, Luo X, et al.: Variation at APOE and STH loci and Alzheimer's disease, *Behav Brain Funct* 2(1):13, 2006.

Zweier C, Peippo MM, Hoyer J, et al.: Haploinsufficiency of TCF4 causes syndromal mental retardation with intermittent hyperventilation (Pitt-Hopkins syndrome), *Am J Human Genet* 80:994–1001, 2007.

CHAPTER 74

IDENTITY TESTING: USE OF DNA ANALYSIS IN PARENTAGE, FORENSIC, AND MISSING PERSONS TESTING

Rhonda K. Roby, Samuel W. Kaskovich, Victor W. Weedn

HISTORICAL BACKGROUND, 1468
ADVANTAGES OF DNA, 1469
SAMPLES AND SPECIMEN COLLECTION, 1469
DNA EXTRACTION AND QUANTIFICATION, 1470
GENETIC MARKER SYSTEMS AND TEST METHODS, 1470
Short Tandem Repeats, 1470
X and Y chromosome Markers, 1471
Mitochondrial Dna Sequencing, 1471
Single Nucleotide Polymorphisms and Next-Generation Sequencing, 1472
SOFTWARE SYSTEMS, 1472
USE OF TEST DATA, 1473
DNA in the Crime Laboratory, 1473
DNA in the Pathology Laboratory, 1474
EXCLUSION OF PARENTAGE, 1475
Probability of Exclusion, 1475
Combined Probability of Exclusion, 1475
INCLUSION OF PARENTAGE, 1475
Paternity Index Calculation, 1476
Likelihood of Parentage, 1476
Parentage with an Absent Parent, 1477
Reconstruction of Families, 1477
QUALITY ASSURANCE STANDARDS, 1477
CONCLUSION, 1478
SELECTED REFERENCES, 1478

KEY POINTS

- Standardized marker systems are used in testing panels to generate allelic phenotypes; short tandem repeats (STRs) form the basis of commercially available kits.
- Forensic testing requires documentation of all steps taken during collection, extraction, and testing so results can withstand legal challenges.
- Deoxyribonucleic acid (DNA) can be obtained from any sample that contains cellular material. The stability of DNA allows it to withstand harsh environmental conditions and long postmortem intervals.
- Care must be taken to maintain the integrity of DNA evidence and to avoid contact or exposure of the evidence to any conditions that may contaminate and/or further degrade the original evidence.
- Mitochondrial DNA can be extracted from bone, teeth, and hair after hundreds and even thousands of years because it is small and present at hundreds to thousands of copies per cell. Mitochondrial DNA is maternally inherited and can be useful for identifying remains.
- DNA is used in identification of remains and can be used to link a suspect to a crime, to exculpate falsely accused suspects, to recognize serial crimes, to distinguish copycat crimes, and to aid in accident reconstruction (e.g., to determine who was driving a car by the identification of the bloodstains on the driver's side of the windshield).
- Pathology laboratories can use DNA testing to resolve specimen mixups, such as samples inadvertently switched or pathologic material floats onto a histologic or cytologic slide.
- Standards and quality assurance guidelines for identity testing laboratories have been developed by the American Association of Blood Banks (for parentage testing), the US Department of Justice Federal Bureau of Investigation's Scientific Working Group on DNA Analysis Methods, the Quality Assurance Standards for Forensic DNA Testing Laboratories, and the Quality Assurance Standards for DNA Databasing Laboratories and the National Institute of Standards and Technology's Organization of Scientific Area Committees for Forensic Science.

The authors would like to acknowledge Herbert Polesky MD for material from chapters in previous editions.

HISTORICAL BACKGROUND

The discovery of the ABO blood group system by Karl Landsteiner in 1900 (Landsteiner, 1901) and the recognition that these measurable characteristics follow the genetic rules described by Gregor Mendel (Mendel, 1866) provided objective evidence from laboratory results that could be used by courts to aid in parentage and criminal casework. In the United States, laws addressing the use of genetic markers for proving nonpaternity were enacted in 1935 (Schatkin, 1952). In the ensuing years, knowledge about useful genetic marker systems increased dramatically. By 1976, joint guidelines developed by an American Medical Association–American Bar Association committee recommended seven systems for routine blood group investigations in cases of disputed parentage: ABO, Rh, MNSs, Kell, Duffy, Kidd, and HLA (Miale et al., 1976). Other genetic systems such as polymorphic serum proteins and red cell enzymes were also recognized as useful. At the time, a variety of the aforementioned genetic markers were used to compare crime scene evidence with suspects or victims; however, DNA testing is used almost exclusively in the current era.

In 1980, Botstein and colleagues described DNA restriction fragment length polymorphism (RFLP) (Botstein et al., 1980). Sir Alec Jeffreys is credited with the first report in the scientific literature to suggest that DNA typing might be useful for forensic identification, and coined the term "DNA fingerprinting" in his *Nature* articles in 1985 (Jeffreys et al., 1985a, 1985b). Commercial laboratories began using DNA testing for parentage and criminalistic casework in 1986, and government crime laboratories began using DNA testing in 1989 (Weedn & Roby, 1993). Today, hundreds of laboratories worldwide use DNA testing for the criminal justice system. In 1990, when the first edition of *Standards for Parentage Testing Laboratories* (American Association of Blood Banks [AABB], 1990) was published, specific requirements for RFLP testing were included alongside those for more traditional serologic methods (red blood cell surface

antigens, human leukocyte antigens, red cell enzymes, and polymorphic serum proteins). DNA testing has since replaced these techniques.

The forensic DNA testing community has endured many iterations of DNA methods and technologies, and has standardized its testing with a core set of short tandem repeat (STR) loci as the current mainstay of testing to build its international offender databases. The national offender database, the Combined DNA Index System (CODIS), includes hardware and software systems that network crime laboratories at the local, state, and national levels. It links all 50 states and territories for laboratories to upload and search profiles for case-to-case matches and matches to offender samples. Additionally, CODIS houses the Missing Persons index to search for missing persons against family members' DNA samples for kinship testing. The core loci were expanded to include 7 additional loci in 2017 for a total of 20 CODIS core loci. This expansion was necessary to reduce the number of adventitious matches, increase international capability, and increase the power of discrimination for criminal and missing persons cases (Hares, 2015, 2012a, 2012b). The 20 CODIS core loci are often supplemented by other DNA testing. This supplemental data includes testing on allosomes, or sex chromosomes, which includes gender analysis (amelogenin is a protein with a single copy on the X and Y chromosomes and has been used in sex determination of samples) and X and Y chromosome markers. Other supplemental data commonly used is mitochondrial DNA (mtDNA) testing. Currently, capillary electrophoresis with fluorescence detection is the main instrument platform; however, next-generation sequencing (NGS) will likely supplant this method in the forensic laboratories of the future.

These same technologies are used to identify victims of war or mass disasters (Budowle et al., 2005), whether the disaster is natural, man-made, or industrial, and in cases of wildlife forensics. DNA testing is also used for accident reconstruction, in medical cases of sample mixups, and in animal husbandry. DNA technology is here to stay; newer technologies will be adopted that offer higher powers of discrimination, lower costs, enhanced sensitivity, increased efficiency, and even information on origin of ancestry and the physical traits (e.g., eye color, hair color) (Lippert et al., 2017) of remains or biological material left at a crime scene. As these newer technologies evolve and are validated, so will the field of forensic science and the demand for their use.

ADVANTAGES OF DNA

DNA permits the direct identification of the source; it is individual, or unique, and manifests biological variation. The human genome is approximately 99.9% the same between individuals; it is the 0.1% difference of the human genome that forensic scientists interrogate to identify stains, recovered remains from accidents and mass disasters, and biological relatives. DNA is useful as an identity marker because it is (1) present throughout all cells of the body, (2) the same in all cells of the body, (3) the same throughout life from the time of conception, and (4) different in all individuals. There are exceptions to the previously mentioned points, in order: (1) DNA is not recovered from mature red blood cells, (2) haploid sex gametes have half of the DNA material as compared to the other cells in the body, (3) progenitor stem cell transplantation can result in the presence of the donor's DNA rather than the recipient's inherited DNA, and (4) identical twins have the same DNA. DNA tests have a sensitivity that is far superior to the previously mentioned traditional serological markers. With the use of polymerase chain reaction (PCR)–based testing, DNA results can be obtained from minute samples and even invisible trace DNA deposits (trace DNA). DNA is a robust molecule resistant to strong acids, alkalis, detergents, and environmental factors (Kobilinsky, 1992). The typing information from DNA is found within the sequence of nucleotides. Consequently, DNA results are more successfully attained than serology tests on specimens that are older and have been exposed to greater environmental insults, and DNA results are possible to attain from many sample types.

Much of the casework for crime laboratories in the United States is from sexual assaults, most often a female victim with a male perpetrator. Hereto, a collected vaginal swab may contain female epithelial cells and bacteria as well as the male sperm. DNA from sperm can be separated from nonsperm DNA by a differential lysis procedure because of the protective capsule of spermatozoa. This procedure allows for individualization of the source of the semen without the confounding data of the nonsemen evidence. DNA targets are also generally human or primate specific, so the presence of bacterial DNA is of no consequence.

Additionally, other advantages to DNA testing include Y chromosome testing where a mixture of female and male DNA will reveal only the male's DNA type from the male contributor's Y chromosome. This testing technique is extremely useful in the presence of mixed DNA when predominantly female DNA is present in the sample. Mitochondrial DNA testing is advantageous for those cases where there are highly degraded remains such as burned skeletal remains or where only a single shed hair is recovered. Additionally, mtDNA testing is important when making a comparison to a close or even a distant maternal relative.

BOX 74.1

Anticoagulants to Use for Blood Collection

Ethylenediaminetetraacetic acid (EDTA; "purple top tubes") and citrate phosphate dextrose (CPD; "yellow top tubes") are often the anticoagulants used and requested for DNA testing. Heparin-anticoagulated blood ("green top tubes") is not recommended for DNA testing. Tubes with no anticoagulants are not recommended.

SAMPLES AND SPECIMEN COLLECTION

Buccal swabs and, less often, bloodstains on filter paper or fresh whole blood are used for parentage testing, reference standards, and databases. For forensic evidence recovered from a crime scene (e.g., property from a vehicle exam) or for biological samples recovered from the victim's body in the emergency department or from an autopsy, identifying the proper sample to collect is extremely important to the success of the case. To visualize the biological fluids and stains, oftentimes alternate light sources or presumptive chemical tests are used. Blood spatter pattern analysis is also employed to help the investigator interpret and intelligently collect specimens from large pools of blood and bloodstains. When a biological fluid has been deposited on a surface or an item that cannot be collected, the fluid should be sampled with a clean sterile swab. For large items where the biological fluid is dry, the sterile swab should be moistened with sterile distilled water, the evidence wiped with the swab, and allowed to air dry prior to packaging. For collection of DNA from bitemarks on bodies and also dried biological material, a double swab technique (Sweet et al., 1997) that involves rubbing the evidentiary area with a wet swab followed by a dry swab is often used. These items (e.g., blood on clothing, collection swab) should be collected one item at a time, packaged separately, clearly labeled, and itemized.

Even though mature red blood cells are devoid of DNA (both nuclear and mitochondrial) from blood for postmortem processing, ample DNA is present from the circulating white blood cells in the blood for DNA testing. The appropriate blood sample collection tubes with anticoagulants are listed in Box 74.1. Further, sources of DNA other than blood are preferred if there is significant decomposition. Virtually any tissue may be successfully used for DNA typing purposes. Some tissues that may be intuitively thought to be better sources of DNA because they are more densely cellular and would contain higher concentrations of DNA are, in fact, less optimal because of higher rates of postmortem degradation (Kobilinsky, 1992). Among soft tissues, the DNA recovered from liver tissue degrades quickly due to the presence of autolytic enzymes, whereas brain tissue is a relatively good source in the intermediate postmortem period. Bone, teeth, and nails (fingernails and toenails) (Anderson et al., 1999) are stable sources of postmortem tissue DNA. Informative DNA is routinely obtained from skeletal remains that are decades old. Generally, the greater the body decomposition and the longer the postmortem period, the greater the degradation of the DNA from cadaveric tissues.

Great care should be taken to prevent contamination of potentially significant specimens and stains by other sources of DNA. Examiners should collect evidence and specimens using single-use gloves, clean instruments, and masks; these methods are to protect the evidentiary item from first responders, the examiner, and cross-contamination of other evidence. When possible, nonexposed tissue should be collected by an incisional biopsy technique. Proper storage of specimens can be critical for the outcome of the DNA results. Many samples can be stored at room temperature while others are best preserved either at 4°C or -20°C (National Institute of Standards and Technology [NIST], 2013). Tissues in formalin are not optimal; however, results can usually be obtained with PCR-based testing techniques (see Chapter 69). No tissues or biological fluids and stains should be discarded as inadequate without first attempting DNA testing.

DNA in most specimens will undergo progressive random fragmentation or degradation, reducing the high molecular weight DNA to lower

BOX 74.2

Additional Requirements When Obtaining a Sample for Parentage Testing

AABB-accredited laboratories are required to obtain a history of any recent transfusion (in the preceding 3 months) or a hematopoietic stem cell transplant. A photographic identification and appropriate informed consent must also accompany each sample. The consent for a minor should be from an individual with legal rights to the custody of the child.

AABB, American Association of Blood Banks.

molecular weight DNA (Kobilinsky, 1992). As time progresses, high molecular weight DNA can become degraded even after a short time from fresh tissues and fluids. Residual smaller DNA fragments may persist despite considerable degradation. In contrast, high molecular weight DNA may be obtained for years after a fresh sample has been frozen or desiccated. Because of its high copy number (hundreds to tens of thousands of copies per cell), mtDNA often survives when no nuclear DNA is recovered. Consequently, mtDNA testing is routinely used to identify older skeletal remains (Ivanov et al., 1996; Núnéz et al., 2011).

Rapid DNA degradation or damage may occur under certain conditions (Parsons & Weedn, 1997). Chemical hydrolysis of DNA is normally quite slow. Tests have shown that mixing DNA with detergents, oil, gasoline, and other adulterants does not alter the DNA result. However, metal ions may catalyze oxidative hydrolysis (Gaydosh Combs et al., 2015). Ultraviolet radiation is known to cause thymidine dimerization; fragmentation of ancient DNA sequences is primarily due to depurination that creates abasic sites leading to DNA breaks.

Results from testing evidence are often used in legal proceedings. Thus all aspects of the specimen collection procedures should be well documented (i.e., chain of custody) since they may be subject to legal challenges. It is important to ensure clear documentation of the identification of the tested individuals, the collection of the evidence, and the labeling of samples. Although many parentage disputes are civil actions, some jurisdictions require documents showing the chain of custody of samples similar to those used in criminal matters and other required information. Likewise, the forensic sample must be properly collected, packaged, sealed, and stored and demonstrate evidence of proper chain-of-custody documentation. Typical requirements are summarized in Box 74.2.

DNA EXTRACTION AND QUANTIFICATION

The first and most critical step for DNA testing of evidence is the extraction, or purification, of the DNA from blood, biological stains, or other biological sources. DNA from a bloodstain, a vaginal swab, or other sources must be isolated from other cell components and environmental contaminants. Numerous DNA extraction methods are used in both parentage and forensic laboratories. Solid-phase column extraction methods and magnetic resin particles are most often used for DNA extraction since these methods are highly amenable to automated techniques (see Chapter 67). The column extraction and magnetic particle methods yield DNA that is highly purified for forensic samples. Contaminants such as those found in cigarette butts and certain dyes may be removed. Silicon beads are another excellent method to purify DNA when inhibitors need to be removed. Many laboratories eliminate the extraction step altogether, for reference and databasing samples, by performing direct PCR from a punch or small sample of a buccal collector or bloodstain.

As mentioned earlier, vaginal swabs require special conditions for extraction using a differential lysis procedure because of the need to separate the male DNA in sperm from the female DNA in epithelial cells (Crouse et al., 1993). The female fraction (the vaginal epithelial cells) is separated by standard extraction procedures. The male fraction (spermatozoa) is then extracted by centrifugation and breaking the disulfide bridges of the protective capsule of spermatozoa with a dithiothreitol or other reducing agent solution. Sensitive PCR-based systems often exhibit female source DNA in the male fraction, producing mixed DNA profiles.

Once the samples are extracted, quantification is performed. The forensic standards require quantification of forensic evidence for STR testing. When performing quantification and knowing the amount of DNA in a sample, amplification is usually more successful. Too little or too much DNA in a PCR-based assay results in nonoptimal amplification, which can produce poor results. In addition, having a priori information on the total human male DNA and a qualitative assessment of the total human DNA is extremely useful in determining which assays to perform in the downstream analysis. Today, real-time quantitative PCR is multiplexed to simultaneously obtain quantitative and qualitative assessment of total human and human male DNA in a single assay. Further, many laboratories have adopted a "stop-at-quant" procedure; since the quantification methods are sensitive enough to detect low levels of DNA, samples are oftentimes stopped at quantification if insufficient DNA is present. Furthermore, sexual assault cases, as described previously with a female victim and a male perpetrator, may stop at quantification if no male or insignificant amounts of male DNA are present.

GENETIC MARKER SYSTEMS AND TEST METHODS

Multiple genetic systems are used for parentage and identity testing. Ideally, the system should have multiple alleles distributed in the population so that there is a high power of exclusion and the least common phenotype has a frequency that can be determined reliably. All markers in the system should be expressed (i.e., with few to no null alleles) as codominant, mutation rates should be known, and phenotypes should be stable under usual storage conditions. Methods for detecting the markers should be reliable, reproducible, and feasible for a large number of laboratories. The genetics of the system must be known and follow established inheritance patterns (Mendelian laws). The system should be independent of other markers routinely tested. If the system is intended for calculating estimates of paternity or identity, the gene frequencies in various populations must be established (Budowle et al., 2001).

The DNA from every human (except identical twins) is unique because of the presence of polymorphisms, which are differences in the DNA between individuals. However, the vast preponderance of the DNA sequence is identical between individuals. On average, only 1 in 1300 nucleotide bases differs between individuals. Nonetheless, this amounts to an average of 3 million bases that differ between any two individuals and accounts for the tremendous genetic variation among individuals. Although the diversity in the coding regions of DNA (genes) is significant, the noncoding regions of DNA also provide for a great deal of diversity.

Length-based polymorphisms are found in repetitive DNA. More than 90% of the human genome is composed of noncoding, or "junk," DNA, of which approximately 20% to 30% is composed of repetitive regions. Many of the repetitive regions vary in the number of core repeats between individuals—so-called variable number of tandem repeat (VNTR) loci. DNA fragments containing VNTRs vary in length and are thus useful for analysis. Dinucleotide repeats are most common, but larger core repeats (i.e., tri-, tetra-, penta-, sextanucleotide repeats) are more useful for forensic purposes since interpretation is much easier than the dinucleotide repeats that exhibit an extremely high amount of reproducible artifacts from amplification (see Chapter 69). RFLP, amplified DNA fragment length polymorphisms, and STRs are examples of fragment length-based analytic techniques. Sequence polymorphisms exist within the DNA sequence of similarly sized DNA fragments. Sequence polymorphisms consist of differences in one or more bases in the DNA sequence at a particular location in the genome. Sequence variations can manifest as regions of alternative alleles or base substitutions, additions, or deletions. Most sequence polymorphisms are mere point mutations within repetitive and nonrepetitive regions and are known as single nucleotide polymorphisms (SNPs). SNPs, sequence-specific oligonucleotides, and mtDNA tests are examples of sequence-based tests as well as the introduction of NGS for forensic genomics. Identity testing has not yet widely adopted the power of the more than 2 million SNPs in the human genome, but the use of this technology is clearly on the horizon for forensic DNA testing.

SHORT TANDEM REPEATS

Loci typically used in commercial assays consist of repeat units of three to seven nucleotides; these short tandem repeats occur throughout the genome (Weber & May, 1989). Alleles at these STR loci are defined by the number of repeat units in the PCR-amplified product (see Chapter 69). Extracted sample DNA is added to a PCR reaction mix containing *Thermus aquaticus* (Taq) polymerase, or another enzyme, with specific forward and reverse primers for each locus tested, deoxynucleoside triphosphates, magnesium, a buffer solution, and typically bovine serum albumin. The PCR reaction mixture is amplified in a thermal cycler using carefully defined parameters to maximize detection of the alleles. Primers with different fluorescent labels are used in a multiplex reaction to detect alleles at many

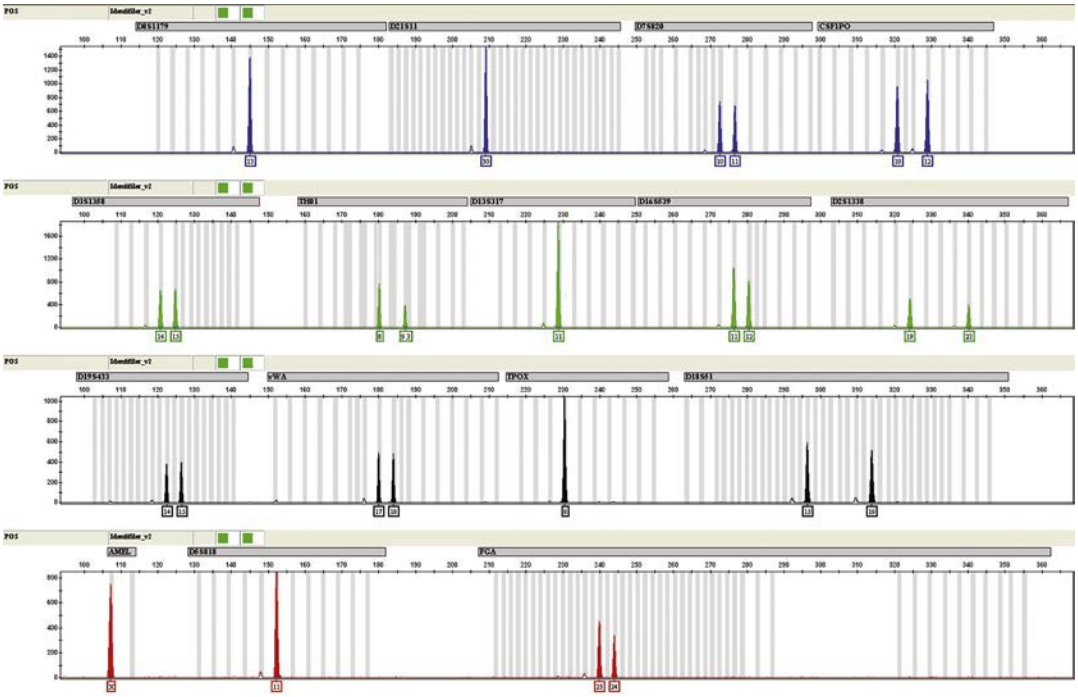

Fig. 74.1 The results of the kit-included positive control 9947A amplified with the AmpFLSTR Identifiler PCR Amplification Kit and electrophoresed on the ABI PRISM 3130*xl* Genetic Analyzer (Applied Biosystems) and typed with GeneMapper *ID* Software v.3.1.2 (Applied Biosystems). The results for the 15 autosomal STR loci and amelogenin, a sexing marker, are visualized. This image displays the phenotype of the positive control amplified in this multiplex. The locus name is shown in the gray bar above the peaks; the allele call(s) for each locus is just below the highlighted peak. The reader may wish to enlarge this figure so that gene identification is clear. The amelogenin peak is labeled "AMEL" on far left of bottom-most scan (first peak on left). (Applied Biosystems, Foster City, CA.) (From Collins P, Hennessy L, Leibelt C, et al: Developmental validation of a single-tube amplification of the 13 CODIS STR loci, D2S1338, D19S433 and amelogenin: the AmpFLSTR Identifiler PCR Amplification Kit, *J Forensic Sci* 49:1265–1277, 2004.)

loci in a single amplification. The PCR products, which vary in length, are separated by capillary electrophoresis. (See Chapter 24 for a discussion of this technique.) Detection is performed using a laser to excite the labeled fluorophore that has been incorporated in the primer. The loci in the multiplex reaction differ by size and color (Fig. 74.1). Sizing is accomplished by including a size standard with each sample injected in the capillary and using sizing software algorithms; phenotyping of each peak is achieved by comparing the peaks in the sample to an allelic ladder accounting for most alleles for each locus and using sophisticated genotyping software algorithms for allele calls that adjust for minor variations in electrophoresis for each injection (Fig. 74.2).

The most commonly used markers in forensic and parentage laboratories in the United States are the 20 core STR loci for CODIS (Table 74.1) that have been standardized for use in obtaining genetic profiles of individuals who have been convicted of various criminal offenses (Hares, 2015). The STR marker systems have discrete alleles. An STR locus may have three or four common alleles (frequencies of 0.15–0.25) and several rare alleles (frequencies of <0.01). Thus, to obtain a high cumulative probability of exclusion (CPE) and combined paternity index (CPI), it is usually necessary to test at least six or more STR loci. In a series of 50 paternity cases tested in parallel by both RFLP and nine STR loci, Alford et al. (1994) reported that both methods excluded the same 13 alleged fathers (based on two or more loci). The likelihood of paternity for the 37 nonexcluded men based on the STR systems was more than 99% in 36 cases. When 13 CODIS STR loci are obtained, the average random match probability is rarer than 1 in 1 trillion among unrelated individuals (Chakraborty et al., 1999). With 20 CODSI STR loci, it is not uncommon to obtain a random match probability rarer than 1 in 1 nonillion among unrelated individuals.

X AND Y CHROMOSOME MARKERS

Sex determination is commonly performed using the amelogenin locus (see Fig. 74.1). The primer for this locus amplifies an X-specific band (Xp22.1 to 22.3) and a Y-specific band (Yp11.2). This locus is coamplified and coanalyzed with most multiplexed STR systems designed for human identity testing. Sex determination marks a departure from all other routine identity markers, in that it provides specific phenotypic information about the source individual (i.e., male or female). It may also be important in the investigation of potential suspects as well as in the categorization of specimens as originating from a victim or suspect.

Although polymorphic Y chromosome markers (Fig. 74.3) are not used for sex determination, they are extremely useful in the typing of casework when there is a mixture of a male and female and a mixture of males. For example, an excellent use of Y-STRs is sexual assault evidence that displays a mixture of both the female epithelial cell DNA and male sperm DNA. When the quantity of male DNA is much less than the female DNA, Y-STRs are excellent in obtaining a profile of the male subject with no interference from the female subject since Y-STR results are only obtained from males. They also are used to characterize the paternal lineage in human remains identifications (Box 74.3). A haplotype is generated from Y-STRs versus a phenotype in autosomal STRs; haplotypes do not afford the same level of discrimination as autosomal STR profiles.

MITOCHONDRIAL DNA SEQUENCING

Mitochondrial DNA sequencing is most applicable when extremely small quantities of sample DNA are present or when the DNA is extremely degraded, such as in shed hairs (which have virtually no detectable nuclear DNA) and skeletal remains (Butler & Levin, 1998; Holland & Parsons, 1999). Hundreds to thousands of copies of mtDNA are present within a single cell with only one copy of nuclear DNA. Accordingly, an mtDNA profile can often be obtained when a nuclear DNA profile cannot. Further, mtDNA testing is used when references from distant relatives are available to compare to an evidentiary sample. A single distant relative in the maternal line may be used as a reference when reference samples are limited because nuclear DNA testing generally requires multiple close relatives.

Mitochondrial DNA is composed of a circular piece of DNA 16,569 base pairs (bp) in length. The region of mtDNA that is analyzed for human identification is the noncoding displacement loop (D-loop), also known as the control region. This locus spans approximately 1200 bp and contains two hypervariable regions. Mitochondria are maternally inherited; hence, mtDNA has no paternal contribution. Unlike nuclear DNA, which is present in pairs of chromosomes, generally only a single mtDNA sequence is present in the cell (homoplasmic) and consequently no genetic recombination occurs. An exact mtDNA sequence match can be traced through the maternal lineage of a family for many generations. However, the

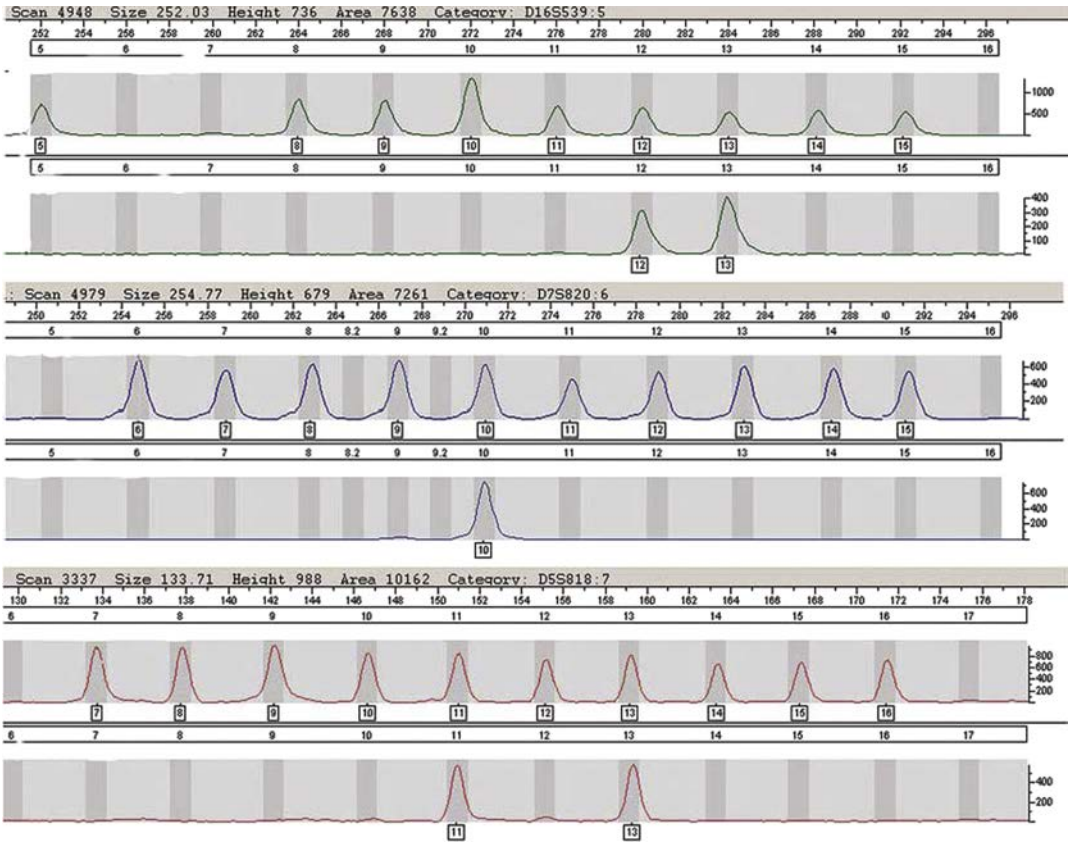

Fig. 74.2 The results of a sample electrophoresed on the ABI PRISM 3100 Genetic Analyzer (Applied Biosystems) and amplified with the AmpFLSTR Identifiler PCR Amplification Kit. The ladders and accompanying results for three loci, D16S539 (alleles 12, 13), D7S820 (allele 10), and D5S818 (alleles 11, 13), are visualized in these images. The images demonstrate excellent resolution in the electrophoresis.

TABLE 74.1
Twenty Core CODIS STR Loci and Amelogenin

Locus Designation	Repeat Sequence 5′ → 3′	Chromosome Location
Amelogenin	NA	Xp22.1–22.3 and Yp11.2
CSF1PO	AGAT	5q33.1 (149.436Mb)
D1S1656	TAGA Complex	1q42 (228.972Mb)
D2S1338	TGCC/TTCC	2q35 (218.705Mb)
D2S441	TCTA	2p14 (68.214Mb)
D3S1358	TCTA Complex	3p21.31 (45.557Mb)
D5S818	AGAT	5q23.2 (123.139Mb)
D7S820	GATA	7q21.11 (83.433Mb)
D8S1179	TCTA Complex	8q24.13 (125.976Mb)
D10S1248	GGAA	10q26.3 (130.567Mb)
D12S391	AGAT/AGAC Complex	12p12 (12.341Mb)
D13S317	TATC	13q31.1 (81.62Mb)
D16S539	GATA	16q24.1 (84.944Mb)
D18S51	AGAA	18q21.33 (59.1Mb)
D19S433	AAGG Complex	19q12 (35.109Mb)
D21S11	TCTA Complex	21q21.1 (19.476Mb)
D22S1045	ATT	22q12.3 (35.779Mb)
FGA	TTTC Complex	4q28 (155.866Mb)
TH01	AATG	11p15.5 (2.149Mb)
TPOX	AATG	2p25.3 (1.472Mb)
vWA	TCTA Complex	12p13.31 (5.963Mb)

discriminatory power of mtDNA sequencing is limited—on the order of one in a few thousand. This testing is expensive and time consuming. NGS may prove to eliminate some of the costs and time for mtDNA testing.

SINGLE NUCLEOTIDE POLYMORPHISMS AND NEXT-GENERATION SEQUENCING

Methods to detect SNPs are used to determine a single base change in a sequence at a specific location. Because of the limited variability at these loci, as many as 70 SNPs need to be tested to obtain the same level of information about relatedness, power of discrimination, and mixture resolution as provided by a multiplex of several STR loci. There are millions of SNPs in the human genome. SNPs are also very powerful for identity testing. SNPs provide information when traditional STRs may not because they can be designed to amplify smaller amplicons. In addition, specific SNPs may be used to provide information regarding the physical traits of an individual, and they can be designed to predict ethnic origin (Wollstein & Lao, 2015).

Today, whole-genome sequencing is being conducted at a greater rate and reduced cost than was imagined at the time of sequencing of the first human genome (Venter et al., 2001). The traditional Sanger sequencing methods have progressed to high throughput sequencing, or next-generation sequencing. NGS technology (see Chapter 80) was first released in 2005 (Margulies et al., 2005); it was introduced as the massively parallel pyrosequencing method. It is anticipated that the NGS technology and instrumentation will be incrementally adopted into some forensic laboratories in place of more traditional techniques. (Box 74.4). NGS can further discriminate STR alleles of the same size with a different sequence by reporting not only its length but also its internal variation. It is able to simultaneously amplify several hundred forensically relevant STRs and SNPs in a single multiplex reaction. SNPs can be detected and STRs can be measured with a precision not available with size-based capillary electrophoresis since the sequence variation is known for the STRs using NGS. Other applications such as molecular autopsies can also be performed.

SOFTWARE SYSTEMS

Parentage and forensic laboratories use genotyping software to size the alleles and make allele calls and computer programs to perform kinship statistical analyses. Most of these software systems also include expert systems programs that display rule firings, or flags, when specific laboratory-defined thresholds have not been met. Currently, expert systems are used

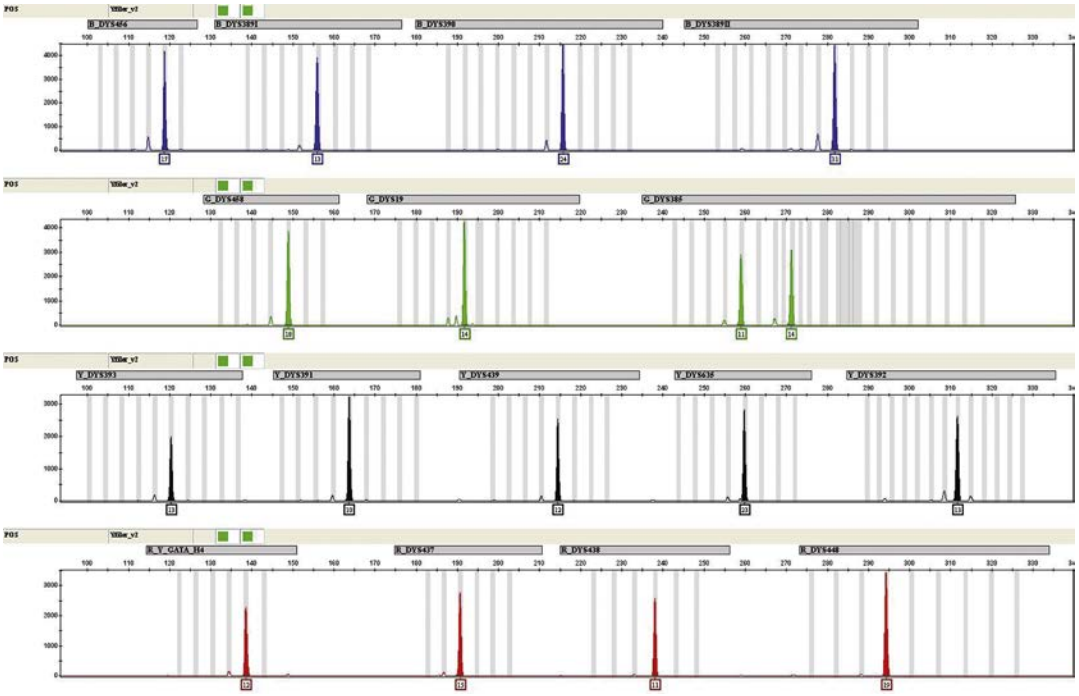

Fig. 74.3 The results of the kit-included positive control 9948 amplified with the AmpFLSTR Yfiler PCR Amplification Kit, electrophoresed on the ABI PRISM 3130*xl* Genetic Analyzer, and typed with GeneMapper *ID* Software v.3.1.2. The results for the 17 Y-STR loci are visualized. This image displays the phenotype of the positive control amplified in this mega-multiplex. The locus name is shown in the gray bar above the peaks; the allele call for each locus is just below the highlighted peak. (Applied Biosystems, Foster City, CA.) (From Mulero JJ, Chang CW, Calandro LM, et al: Development and validation of the AmpFLSTR Yfiler PCR Amplification Kit: a male specific, single amplification 17 Y-STR multiplex system, *J Forensic Sci* 51:64–75, 2006.)

BOX 74.3

Historical and Ethnic Y Chromosome Casework

The characterization of the Thomas Jefferson family lineage was accomplished using Y chromosome markers (Foster et al., 1998), an example of an historical and genealogic study. Data from extensive Y-STR typings have demonstrated that certain haplotypes are indicative of ethnic origin and can be used for human migration and evolutionary studies.

BOX 74.4

Forensic NGS Method

Verogen (San Diego, CA) has introduced a next-generation sequencing (NGS) system, the ForenSeq DNA Signature Prep Kit, used in conjunction with the MiSeq FGx™ Forensic Genomics System to evaluate short tandem repeats (STRs) (autosomal, Y-STRs, and X-STRs) and 173 single nucleotide polymorphisms (SNPs). Included in these SNPs are phenotypic-informative SNPs for eye color and hair color and ancestry-informative SNPs (Jäger et al., 2017).

by laboratories for the review of single-source reference standard samples. In addition, some forensic laboratories use mixture deconvolution software tools to assist the forensic analyst in the review of mixed data as is often observed with sexual assault evidence. The manual review of mixed data is time consuming and oftentimes difficult for the analyst to fully consider each mixture combination. Probabilistic genotyping software is available that calculates the probability of potential genotype combinations for a genotype result. There are two probabilistic genotyping models, semicontinuous and fully continuous. Both models report likelihood ratios by comparing two results: the probability of the result given the prosecution hypothesis over the probability of the result given the defense hypothesis, or a similar comparison. The semicontinuous model reports genotype combinations based on the allele calls. However, the fully continuous probabilistic genotyping model, which has gained special popularity, reports genotype combinations based on the allele calls and peak height ratios, mixture ratios, stutter, dropin, and dropout. This software tool assists the analyst in the interpretation of forensic DNA typing results, especially with mixtures and with low template DNA results. Probabilistic genotyping software combines biologic modeling with mathematical processes to interpret complex DNA profiles.

USE OF TEST DATA

DNA IN THE CRIME LABORATORY

DNA evidence is routinely admitted into court. In the United States, a large percentage of criminal DNA tests involve sexual assault, and a significant proportion involve homicide. DNA tests exonerate wrongfully accused suspects (Fig. 74.4), match the DNA of a suspect to a crime, or are reported as inconclusive due to no, or partial, DNA results being obtained, profiles showing high levels of degradation or inhibition, and complex interpretation issues. Only a fraction of the cases in which DNA evidence is tested are actually litigated because most cases result in a plea bargain. In the criminalistics context, DNA can be used to link a suspect to a crime, to exculpate falsely accused suspects, to recognize serial crimes and to distinguish copycat crimes, or to aid in accident reconstruction (e.g., to determine who was driving a car by the identification of the bloodstains on the driver's side of the windshield). In addition to the use of DNA for associative evidence at crime scenes, DNA is used in the identification of human remains.

Familial and Genealogy Testing

Familial testing was introduced in July 2010 by its success of identifying a match for the Grim Sleeper case. Lonnie Franklin Jr. is a convicted serial killer; he murdered at least 10 women in the 1980s and again, after a long hiatus, in 2007. Familial testing searches the database for close relatives of the perpetrator. Y-STRs have been used to narrow the list of possible matches as they could include a full-sibling, a son, a father, or paternal relative in that list if, in fact, they were in the database. Then, it uses likelihood ratios as indicators of possible relationships (Myers et al., 2010). In this case, there was a full Y-STR match and a partial autosomal STR hit to the Grim Sleeper; the partial hit would show that half of the DNA (obviously from a parent to child) matched, for other obvious reasons—the Y-STR match—to the perpetrator's son or father. The sample in the database was the son of the Grim Sleeper and led investigators to consider Mr. Franklin as a suspect.

The field of forensic genealogy surfaced as frontpage news in April 2018. The Golden State Killer was identified. The Golden State Killer, also known as the East Area Rapist and the Original Night Stalker, was responsible for terrorizing the California Bay Area from 1974 to 1986. He preyed upon innocent people, raped more than 50 women, and killed at least 12 people (Fuller & Hauser, 2018; Stanton et al., 2018). Forensic genealogy has been in use for many years. The military has used forensic genealogy in identifying the missing from military war conflicts. But this

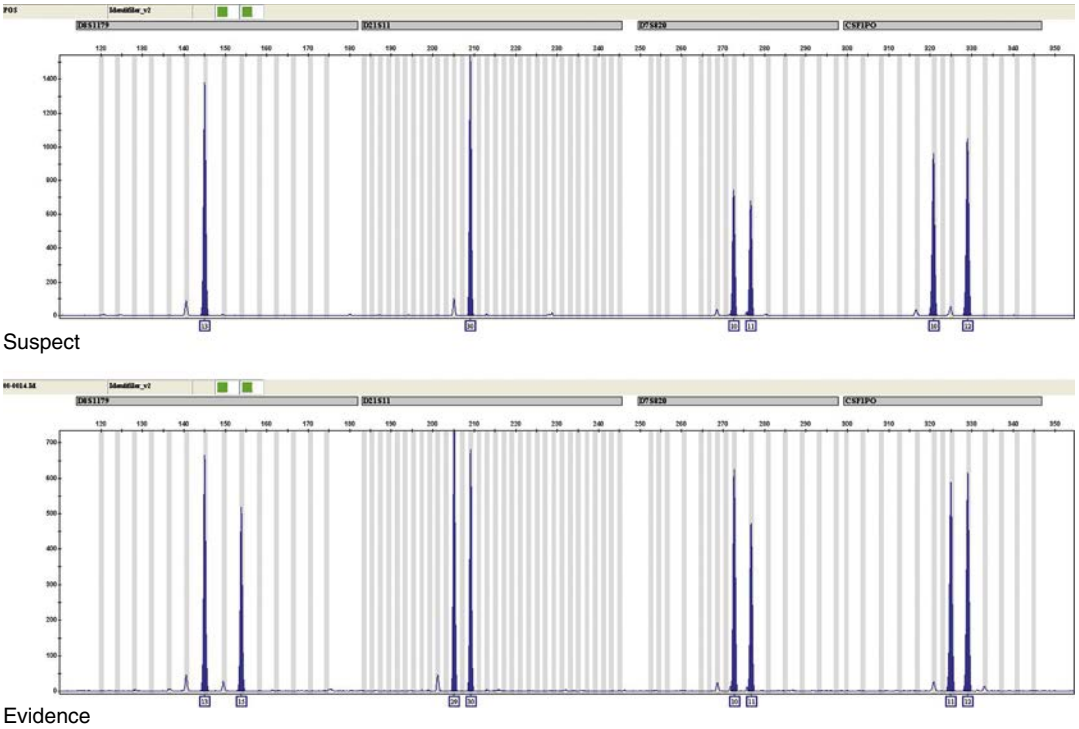

Fig. 74.4 Exclusion of suspect when compared to crime scene evidence. The profile for the evidence at D8S1179, D21S11, and CSF1PO is clearly different from the suspect's profile. The evidence could not have been contributed by the suspect.

TABLE 74.2
Identification of a Possible "Floater"

STR Locus	Floater	Tissue Block	Patient Sample	Frequency of Patient's Phenotype
CSF1PO	10,12	10,12	10,12	0.1910
D3S1358	15,16	16,17	16,17	0.0990
D5S818	11	11,12	11,12	0.0240
D7S820	9,11	11	11	0.0529
D8S1179	13	12,14	12,14	0.0976
D13S317	11	11	11	0.0798
D16S539	9,11	11,12	11,12	0.1764
D18S51	14,15	14,15	14,15	0.0477
D21S11	30	28, 31.2	28, 31.2	0.0341

Shaded results indicate the DNA from the floater is different than the DNA from the patient and the tissue block. The chance that the tissue block has the same genetic markers as the patient compared to a random Caucasian individual is less than 1 in 1.86×10^{10}.

case was different. The investigators in the Golden State Killer case turned to forensic genealogy since there had not been a match of this case in the National DNA Index System (NDIS), and there were no other investigative leads.

How did they catch the Golden State Killer? With the decreasing costs of DNA tests, the general public has turned to public domain consumer-type DNA testing where customers and their family members can submit a cell-filled saliva sample to manage information on their own ancestry, markers for health status, and databasing to find lost or unknown relatives where almost a million SNPs are stored. In turn, in this infamous case, the DNA from a crime scene sample was uploaded into a consumer-filled database used primarily for family members to search for known and unknown relatives; a relatively small list of potential relatives was generated for investigators to track (Greytak et al., 2019). Since this case, dozens of other cases have been solved in a similar fashion. The use of these databases has been challenged due to ethical and privacy concerns. This new era of testing must weigh the rights of all people versus the safety of a community. Procedures need to be put in place, training conducted on the proper use of databases, and access to case and database information should be controlled and limited (Wickenheiser, 2019).

Future DNA Testing: DNA Testing at Booking Stations

DNA testing is ever evolving. There are new chemistries and instruments that fully automate the process of generating a DNA profile from reference standards without human intervention called rapid DNA testing. The goal of the rapid DNA analysis is to have the instruments housed at booking stations; while an arrestee is in police custody it will be possible to develop a DNA profile within a couple of hours, the profile will be uploaded to NDIS, and then searched against unsolved crimes.

DNA IN THE PATHOLOGY LABORATORY

DNA identity tests can be used to resolve specimen mixups (Weedn, 1993), such as when samples are inadvertently switched or pathologic material floats onto a histologic or cytologic slide. A small fragment of cancerous tissue ("floater") on a glass microscope slide can be determined to be from someone other than the patient (Table 74.2). DNA testing may be used to confirm or refute mislabeling of biopsy specimens. In addition, urine drug tests that have been challenged on the basis of alleged sample switching may be resolved by DNA testing (Weedn et al., 1996). STR markers are also used to evaluate engraftment of marrow after transplantation (Scharf

TABLE 74.3

Exclusion of Parentage: Phenotype (Genotype)

Type of Exclusion	Mother	Child	Tested Man	Obligatory Gene(s)
Direct	A (aa, a?)	AB (ab)	C (cc, c?)	b
	AB (ab)	AC (ac)	AD (ad)	c
	C (cc, c?)	AB (ab)	AC (ac)	b (maternal)
Two-haplotype	A (aa, a?)	A (aa, a?)	BC (bc)	a or ?
	AB (ab)	A (aa, a?)	BC (bc)	a or ?
	AB (ab)	AB (ab)	CD (cd)	a or b
	Not available	AB (ab)	CD (cd)	a or b
Indirect*	A (aa, a?)	A (aa, a?)	B (bb, b?)	a or ?
	AB (ab)	B (bb, b?)	A (aa, a?)	b or ?
	C (cc, c?)	B (bb, b?)	AB (ab)	b or ? (maternal)
	Not available	B (bb, b?)	A (aa, a?)	b or ?

Examples of direct, two-haplotype, and indirect exclusions of the tested man. The capital letters represent the phenotype, and the small letters in parentheses represent the possible genotype. The question mark (?) represents a possible null, or silent, allele.
*Mutation must be considered with indirect exclusions.

et al., 1995). When the donor is related to the recipient, testing of multiple markers may be required to find informative loci since related people share many alleles.

EXCLUSION OF PARENTAGE

The primary goal of genetic marker testing in cases of disputed parentage is to identify the biological parent of a given child. Although this cannot be done with absolute certainty, genetic marker tests can provide objective evidence of nonparentage. By using multiple genetic systems, it is possible to exclude most (>99%), but not all, nonparents.

In systems that follow the rules of mendelian genetics, exclusions are identified by finding exceptions to the expected inheritance pattern. Interpretation of test results when paternity is in question usually depends on assuming that the sample defined as maternal is from the child's biological mother. The mother's and child's phenotypes should be compared to determine whether results are consistent with expected patterns of inheritance. An allele present in the child but not in the mother is referred to as the obligatory paternal gene (OG), or the obligatory paternal allele. If both alleles in the child and mother are identical, then there are alternative, or two, possibilities for the paternal gene.

If the tested man does not have the possibility of passing the OG, and the marker for the gene is absent in the presumed mother, the exclusion observed is termed direct exclusion (Table 74.3). An exclusion at a single locus is not considered sufficient evidence to establish nonpaternity (AABB, 2019) due to the mutation rate observed in DNA testing. A direct exclusion also occurs when the child or the tested male is heterozygous (two alleles present) and the two markers are absent in the other person. This type of direct exclusion sometimes is referred to as a two-haplotype exclusion. When only the child and one alleged parent are available for testing, if the tested individual or child has two haplotypes, neither of which is in the other, it is possible to establish nonparentage.

Absence of an expected genetic marker in a child when the parent in question appears to be homozygous (one allele present) for the gene is called an indirect exclusion. This is sometimes also known as reverse homozygosity. One indirect exclusion is not sufficient evidence to conclude that the tested individual is not the parent. Interpretation of reverse homozygosity as an indirect exclusion presumes that the tested subjects both have two identical alleles at the locus. In PCR testing of STRs, this absence of an expected allele may occur if there is a binding site mutation (Harrison et al., 2004; Leibelt et al., 2003) in one of the tested individuals, or it is possible that a rare null allele (or other undetected allele) or mutation is present in the child as well as the parent in question. The finding of indirect exclusions in at least two independent systems usually is sufficient evidence to reach a conclusion of nonpaternity.

PROBABILITY OF EXCLUSION

Before testing, it is possible to provide an estimate of the average chance that testing will prove nonparentage if the accused is not the parent. This is referred to as the probability of exclusion (PE), defined as the probability of excluding a random individual from the population given the alleles of the child and the mother; the genetic information of the tested man is not considered. For each genetic system, an average PE can be calculated based on the gene frequencies (p and q) for the alleles in the system. Weiner reported the general equation for a two-allele system (Wiener et al., 1930). When a system has multiple alleles, more complex formulas are required (Walker, 1978). A highly polymorphic system has a greater power of exclusion than a system with only a few alleles or one that has one or two common alleles and many rare alleles.

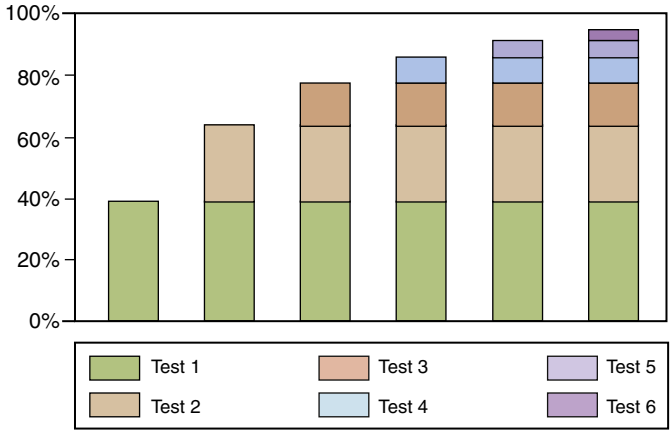

Fig. 74.5 Combined probability of exclusion (each added test; PE = 0.4). The percentage of the population excluded by each additional test becomes smaller and smaller. The overall exclusion probability of the six tests is 95.3%. If a seventh test with PE = 0.5 was performed, only an additional 2.4% of the population would be excluded ([1 – 0.953] × 0.5 = 0.0235).

COMBINED PROBABILITY OF EXCLUSION

The individual PE is calculated for each of the genetic systems (for each locus) analyzed. The overall combined PE (CPE), or the probability of excluding a falsely accused man in a given case, can be calculated by using the following formula:

$$CPE = 1 - [(1 - PE_1) \times (1 - PE_2) \times (1 - PE_3) \times \ldots \times (1 - PE_N)]$$

where PE is the probability of exclusion for each system used. As shown in Fig. 74.5, as more and more systems are used, fewer and fewer individuals are excluded by each additional test. With an appropriately selected battery of genetic systems, a CPE of 0.995 or greater is easily achieved.

INCLUSION OF PARENTAGE

If, after testing multiple independent systems, the parent in dispute is not excluded (Fig. 74.6), then an estimate of the possibility that the tested person could be the biological parent should be calculated. If the tested male is not excluded, it always can be argued that the amount of testing was inadequate, that evidence for exclusion will be found by testing another genetic system, or that the true parent is a close relative of the tested man. This line of reasoning could be correct only if the tested male has been falsely accused. In addition to the average probability of exclusion described previously, it also is possible to calculate the frequency with which a random male will not be excluded based on a mother-child pair exhibiting the observed phenotypes (Salmon, 1983). This value is related to the actual probability of exclusion for the tests performed.

In providing estimates of inclusion of paternity, appropriate gene frequency tables are used. In general, this means that a population of random persons of the same race has been phenotyped, that the size of the sample is large enough to provide gene frequencies with minimum errors of estimation for the alleles in the system, and that the tested male and biological father are from the same population. When multiple systems have been tested, the differences observed in gene frequencies in populations from various geographic locations become unimportant in calculations of the likelihood of paternity (Hummel & Claussen, 1981). When the tested male is of mixed racial background or from a population for which there are inadequate frequency tables, it may be impossible to provide a precise estimate of paternity. However, when multiple systems with a high power of exclusion have been used and the paternity index (PI) value using a reference population is high, there is a minimal chance that frequencies from

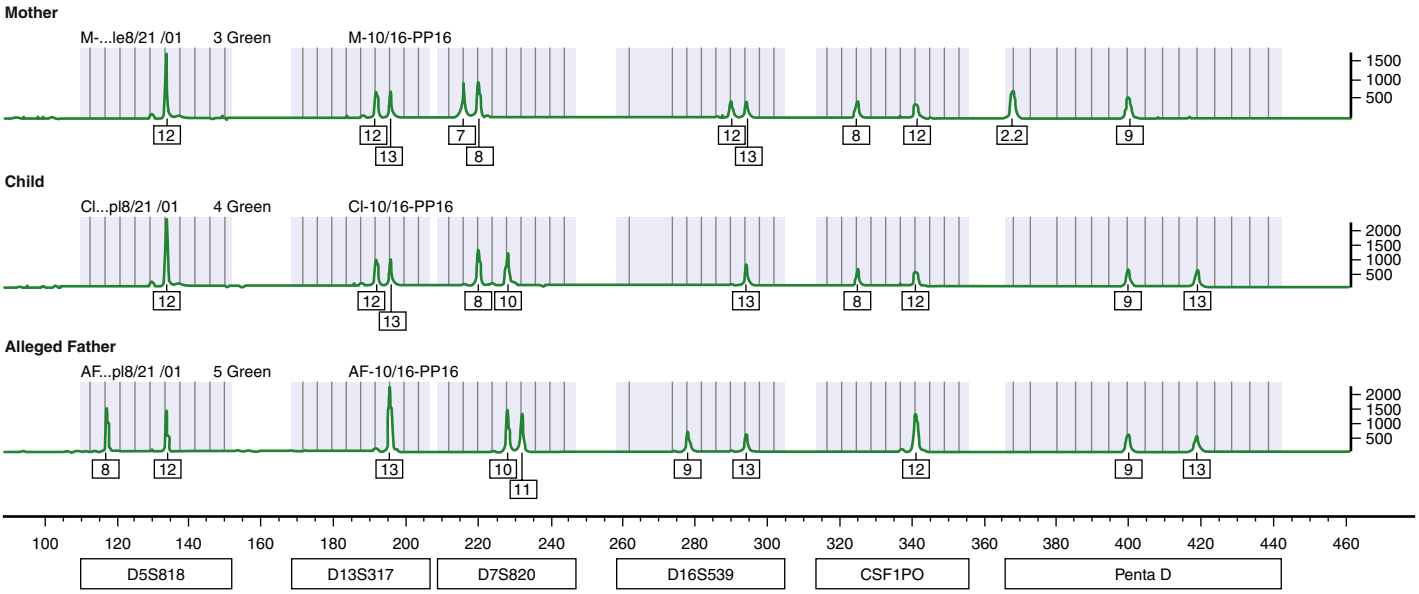

Fig. 74.6 Example of family analysis using short tandem repeats testing. Note the alleles shared between the mother *(top panel)* and the child *(middle panel)*. The alleles from the tested man *(bottom panel)* also match the child. The tested man is not excluded as the biological father of this child.

TABLE 74.4
Calculation of the System* Likelihood Ratio (Paternity Index)

Mother	Child	Obligatory Gene(s)	Tested Man	X	Y	Formula for Y Frequency	X/Y
A	A	a	A	1	0.25	p	4
A	A	a	AB	0.5	0.25	p	2
A	AB	b	B	1	0.4	q	2.5
A	AB	b	AB	0.5	0.4	q	1.25
AB	AB	a or b	A	1	0.65	p + q	1.54
AB	AB	a or b	B	1	0.65	p + q	1.54
AB	AB	a or b	AB	1	0.65	p + q	1.54
AB	AC	c	AC	0.5	0.3	r	1.67
BC	BC	b or c	BC	1	0.7	q + r	1.43
AC	AD	d	BD	0.5	0.05	s	10

X, Chance that tested male is the biological father; *Y,* chance that an untested male in the random population is the biological father; *X/Y,* likelihood ratio.
*Hypothetical locus with four codominant alleles A, B, C, and D with gene frequencies a=p, b=q, c=r, and d=s.

a more-defined population will have a significant effect on the conclusion of parentage. In these situations, comparisons with frequencies for several defined racial groups may also be helpful.

PATERNITY INDEX CALCULATION

In cases in which a trio has been tested, a general approach referred to as the comparison of sperm method is usually applied (Walker, 1978). This calculation compares the chance (x) that a sperm from a male of the phenotype of the tested male could have fertilized the ovum of the presumed mother to the chance (y) that a sperm from an untested male in the random population could have produced the child. Likelihood ratios (x/y) are calculated for each independent genetic system by comparing the tested male to the frequencies for the obligatory gene or alternate paternal genetic contribution in the random population of the same race of the tested male. These values are then multiplied to derive the PI, which reflects the genetic odds in favor of paternity, given the phenotypes of the trio. Table 74.4 displays the formulas for calculating the indexes with various phenotype combinations. Table 74.5 is an example using these formulas to determine the possible father of a fetus in a possible rape case. In this example, Tested Man 2 is clearly excluded as the biological father of this fetus.

PI values in cases where no exclusion is observed can have a numeric value greater than zero to a number approaching infinity. The AABB Standards (2019) require that, to determine parentage, the testing should result in a PI of at least 100. This means that the odds (likelihood ratio) for the tested man being the father are 99 to 1.

LIKELIHOOD OF PARENTAGE

Another useful estimate, the likelihood of parentage, combines the genetic testing with assumptions about prior events. Essen-Möller (1938) described this calculation based on Bayes theorem (Box 74.5). The estimate uses the PI to summarize the genetic information and p (a value for the prior probability) to account for the following assumptions:

1. The tested man was not sterile.
2. The tested man had access during the conceptive period.
3. The tested man is not a close (first-degree) relative of the father.
4. Other possible fathers are from a population with similar gene frequencies.

If a p of 0.5 is used, this assigns an equal prior chance to the tested man and one untested man. Using this value, the likelihood of paternity *(W)* is equal to

$$\frac{\text{PI}}{(\text{PI}+1)}$$

Other values for the prior probability can be used in this calculation but they introduce a bias against the tested man if greater than 0.5 and against the mother if less than 0.5.

TABLE 74.5

Determining Parentage From Fetal Tissue

STR Locus	Mother	Fetal Tissue*	Tested Man 1 (TM 1)	Tested Man 2 (TM 2)	Paternity Index TM 1	Paternity Index TM 2
CSF1PO	10	10	10	10, 12	3.74	1.87
D3S1358	15	15, 16	16	14	4.49	0†
D5S818	12, 13	11, 12, 13	10, 11	10	1.27	0†
D7S820	8, 9	8, 9	8, 9	10, 11	3.31	0†
D8S1179	11, 15	11, 15	12, 15	11, 15	2.60	5.19
D13S317	12, 13	10, 12, 13	10	11, 12	14.81	0†
D16S539	13	9, 13	9, 12	9, 14	4.65	4.65
D18S51	12	12, 17	12, 17	17	4.76	9.52
D21S11	31	31	31	31	18.18	18.18
vWA31/A	16, 18	16, 17, 18	14, 17	14, 18	2.00	0†
				CPI	2.19×10^6	0†

*Fetal tissue sample is contaminated with maternal tissue; mixture present.
†Tested man excluded at that locus.

BOX 74.5

Formula for the Likelihood of Parentage (W)

Bayes theorem is used to combine *p* with PI:

$$W = \frac{(p)\,(PI)}{[(p)\,(PI) + (1 - p)]}$$

where *p* = prior probability of nongenetic events, and PI (paternity index) = summary of testing results.

TABLE 74.6

Calculation of the System* Likelihood Ratio (Parentage Index) When Only One Parent Is Tested

Child	Tested Parent	Parental Gene(s) in Child	Obligatory Gene(s) in Other Parent	Formula to Calculate System Ratio
A	A	a	a	1/p
A	AB	a	a	1/2p
A	BC		a	Exclusion
AB	B	b	a or b	1/2q
AB	AB	a or b	a or b	(p+q)/4pq
AC	AB	a	a or c	1/4p
BC	A		b or c	Exclusion
AD	BD	d	a or d	1/4s

*Hypothetical locus with four alleles A, B, C, and D (frequency of genes a = p, b = q, c = r, and d = s).

The mathematical values obtained from the calculation of the PI or likelihood have special significance because in many jurisdictions the reported value may change the legal standing of the parties. For example, the Minnesota Statute Section 257.55 (Parentage Act, 2004) shifts the burden of disproving paternity to the man if the testing indicates a greater than 99% likelihood that he is the father.

PARENTAGE WITH AN ABSENT PARENT

If one of the parents is unavailable for testing, it is still possible to provide an estimate of parentage. The most common situation is one in which a sample is available from the child and alleged father, but not the mother. In this situation, the child must share at least one gene at each locus with the tested man. Formulas (Table 74.6) to estimate the paternity index and likelihood of paternity are similar to those used when a trio is tested (see Table 74.4) except that the estimates must include an adjustment for the frequency of the allele passed by the absent mother (Brenner, 1993). The calculation is more complicated if the missing mother and untested man are of different races (Traver, 1996). If the tested man or child has two alleles at a locus, neither of which is present in the other tested individual, then the tested man is excluded. If reverse homozygosity is present in the child and tested man, this also suggests nonpaternity.

RECONSTRUCTION OF FAMILIES

Many situations occur in which it is important to establish a relationship between individuals. This happens when individuals are trying to gain status as an immigrant or discover whether they share a parent, or when there is a question related to inheritance. DNA testing can be informative in identifying parents of fetal material found in a dumpster or products of conception in rape cases. Reconstruction is also very important when trying to identify bodies or body parts following a mass disaster. Because only a parent and child will share at least one allele at each locus, relatives may have systems in which they do not share any alleles. Formulas taking into account that alleles may be shared by descent are used to estimate the closeness of the relationship of two individuals (Wenk et al., 1986). Full siblings have a 0.25 chance of not sharing an allele in a system, whereas half-siblings, aunts, or uncles have a 0.5 chance. In cases in which the alleged father is deceased, his probable phenotype can be reconstructed if testing is performed with his biological parents (Mayr, 1983). The child and putative grandparents must share the obligatory paternal genes in all systems. A PI can be calculated using a frequency for *x* that takes into account the chance that the deceased could pass the allele (Fig. 74.7). Reconstructions can also be conducted by using data from multiple presumed relatives as shown in Fig. 74.8.

QUALITY ASSURANCE STANDARDS

Laboratories that perform forensic (parentage and criminalistic) DNA testing must follow appropriate standards, obtain accreditation, and participate in proficiency testing programs. The possibility of significant judicial scrutiny of every step of the procedures and practices used from collection of samples to reporting of results is to be expected. Challenges to the validation of the methods, the source of the databases used in statistical reports, and the qualification of the personnel are not uncommon. There is general agreement as to proper laboratory procedures that should be used in DNA testing and, although the DNA typing methods are not specifically standardized, procedures are remarkably uniform.

The Federal Bureau of Investigation's (FBI's) Technical Working Group on DNA Analysis Methods, now known as the Scientific Working Group on DNA Analysis Methods, promulgated early guidelines for DNA analytic procedures that became de facto standards (Technical Working Group, 1989, 1995). These standards were modified by the DNA Advisory

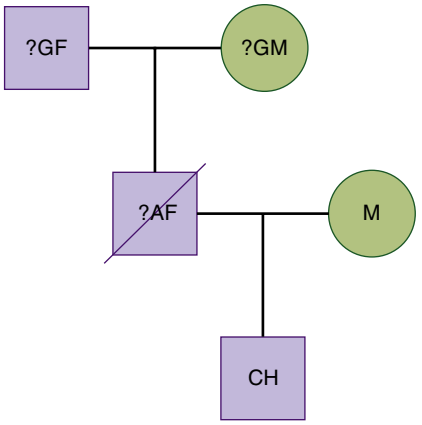

System	Child	Mother	OG	?GF	?GM*	Possible phenotypes of ?AF	Formula to calculate system index
CSF1PO	10,12	9,12	*10*	10,13	10,11	10;10,11; 10,13; 11,13	0.5/*p*
D3S1358	14,15	14,17	*15*	15,16	16,17	15,16; 15,17; 16,17;16	0.25/*p*
D7S820	10,11	10,11	*10* or *11*	8,9	11	8,11; 9,11	0.5/*p*+*q*
D16S539	9,12	9,13	*12*	10,12	12	10,12;12	0.75/*p*
TPOX	8	8, 11	*8*	8	8	8	1/*p*
vWA31/A	18	18	*18*	18	18	18	1/*p*

Fig. 74.7 Family testing to establish paternity. Interpretation assumes that the deceased ?AF is the child of the persons tested *(?GF, ?GM)* and *p* and *q* are the frequencies of the obligatory paternal gene(s). In this case, the presumed parents of the deceased alleged father were tested to reconstruct his probable phenotype. In each of the systems tested, the obligatory paternal gene *(OG)* is present in one of the child's presumed grandparents. Note: For D7S820, either allele in the child could be the maternal obligatory gene. The combined paternity index and likelihood of paternity are obtained by multiplying the values for the individual systems.

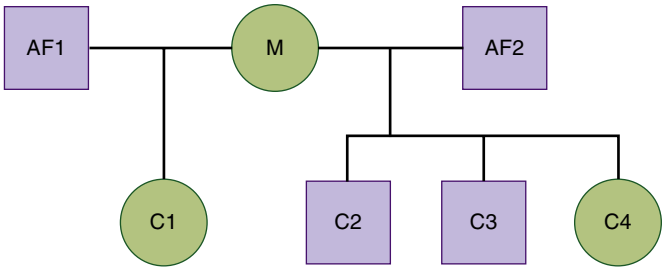

System	AF1	AF2	Child 1	Child 2	Child 3	Child 4
CSF1PO	10, 11	11, 12	10, **14**	12, **14**	**9,** 12	11, **14**
D3S1358	15, 17	15, 17	**14, 17**	**17**	**14,** 16	**14,** 15
D5S818	13, 14	11, 12	**10,** 14	**10, 12**	**12**	**12**
D7S820	8, 9	10, 13	8, **11**	10, **11**	10, **14**	13, **14**
D13S317	11, 12	8, 10	12, **14**	8, **10**	10, **14**	**10**
D16S539	12, 15	9, 11	**8,** 15	**8,** 11	11, **13**	9, **13**
vWA31/A	14, 20	16, 17	**15,** 20	**15,** 17	16,**18**	17, **18**
TH01	8, 9	6, 9	8, **9.3**	6, **9.3**	8, **9.3**	9, **9.3**
TPOX	8, 11	8, 10	**8**	**8, 12**	**8, 12**	**8**
Amelogenin	Male	Male	Female	Male	Male	Female
DYS390	23	23		23	23	
DYS391	10	11		11	11	

Fig. 74.8 Family study—presumed mother *(M)* is deceased. All four children in this family study could have the same mother. The probable maternal allele in each system is shown in bold. Note: In some systems, either marker could be maternal in one of the children (D3S1358 in child 1). Alleged father 1 *(AF1)* shares an allele with child 1 in all systems and is excluded as the possible father of children 2, 3, and 4 in several systems. AF2 is excluded as the father of child 1 in every system except D3S1358 and TPOX. AF2 is also excluded as the father of child 3 in two systems (D3S1358 and TH01). The finding of a possible match in 9 of 11 systems, including two Y-STRs, suggests that the true father of child 3 might be a relative of AF2, or two mutations have occurred.

Board and adopted by the FBI director pursuant to the DNA Identification Act, a component of the Crime Bill passed in 1994. These standards apply to crime laboratories that submit DNA results to the FBI's NDIS or that accept certain federal grants. There are different working groups managed by the FBI, the National Institute of Justice (NIJ), and NIST. A new version of the "Quality Assurance Standards for Forensic DNA Testing" has been released and took effect July 1, 2020. A nongovernmental organization that provides accreditation services to crime laboratories is the ANSI National Accreditation Board, also known as ANAB. The American Board of Criminalists certifies criminalists and has a subspecialty category for DNA analysts. Analysts who work on casework samples must have college coursework in genetics, biochemistry, molecular biology, and statistics. Each of these standards calls for proficiency testing by each analyst twice a year.

The AABB began developing standards and accrediting parentage testing laboratories in 1984. The 14th edition of *Standards for Relationship Testing Laboratories* was published in 2019 (AABB, 2019). All aspects of parentage testing from laboratory organization to process control and improvement are covered. The *Standards* includes requirements for documents and records, report content, and interpretation of results. Laboratories are required to participate in graded proficiency testing.

CONCLUSION

Scientific evidence that will aid in resolving cases of disputed parentage, questions of relatedness, and identity can be obtained from testing multiple DNA systems. Current technology provides test results that exclude more than 99.9% of falsely accused individuals in parentage and criminal cases. It is not possible to prove paternity or guilt by laboratory tests. The mathematical estimates derived from genetic marker tests when no exclusion is found or there is a match between sample and suspect are a significant source of data that can be used to establish parentage or guilt.

SELECTED REFERENCES

American Association of Blood Banks: *Standards for relationship testing laboratories*, ed 14, Arlington, VA, 2019, AABB.

The AABB periodically provides standards for accredited parentage testing laboratories that is updated and includes key elements of QA/QC, testing, reporting, and validation requirements. With each edition of Standards, a companion Guidance for Standards is published that has detailed explanations of the requirements, and appendices with useful tables and formulas.

Steffen CR, Coble MD, Gettings KB, Vallone PM: Corrigendem to "U.S. Population Data for 29 Autosomal STR Loci" [*Forensic Sci Int Genet* 7:e82-e83, 2013.] *Forensic Sci Int Genet* 31:e36-e40, 2017.

A reference for frequency data used to calculate parentage results as well as population frequencies for the chance that a matching sample is from a random individual. Several manufacturers also have websites with frequency tables based on results from their reagents.

Butler JM, Reeder DJ: Short tandem repeat DNA internet database. Available at: http://www.cstl.nist.gov/strbase/.

This website is supported by the National Institute of Standards and Technology (NIST) and has updated information

on STR loci, including new variants. It also contains links to other useful sites.

The Quality Assurance Standards for Forensic DNA Testing Laboratories, effective July 1, 2020 and the Quality Assurance Standards for DNA Databasing Laboratories, effective July 1, 2020. Available at www.swgdam.org.

Basic QA/QC requirements for forensic testing laboratories.

National Research Council: *The evaluation of forensic DNA evidence*, Washington, DC, 1996, National Academy of Sciences.

This monograph is a comprehensive evaluation of testing and statistical evaluation of data intended for use in legal proceedings.

Walker RH: Probability in the analysis of paternity test results. In Silver H, editor: *Paternity testing*, Washington, DC, 1978, American Association of Blood Banks, pp 69–135.

The proceedings of the Airlie Conference contain numerous papers dealing with methods of calculating data from paternity testing using the classical systems. Though pre-DNA testing, the principles apply to STR systems.

Access the complete reference list online at Elsevier eBooks for Practicing Clinicians.

REFERENCES

Alford RL, Hammond HA, Coto I, et al.: Rapid and efficient resolution of parentage by amplification of short tandem repeats, *Am J Hum Genet* 55:190–195, 1994.

American Association of Blood Banks: *Standards for relationship testing laboratories*, ed 14, Arlington, Va, 2019, AABB.

Anderson T, Ross J, Roby RK, et al.: A validation study for the extraction and analysis of DNA from human nail material and its application to forensic casework, *J Forensic Sci* 44:1053–1056, 1999.

Botstein D, White RL, Skolnick M, et al.: Construction of a genetic linkage map in man using restriction fragment polymorphisms, *Am J Hum Genet* 32:314–331, 1980.

Brenner CH: A note on paternity computation in cases lacking a mother, *Transfusion* 33:51–54, 1993.

Budowle B, Bieber FR, Eisenberg AJ: Forensic aspects of mass disasters: Strategic considerations for DNA-based human identifications, *Legal Med* 7:230–243, 2005.

Butler JM, Levin BC: Forensic applications of mitochondrial DNA, *Trends Biotechnol* 16:158–162, 1998.

Butler JM, Shen Y, McCord BR: The development of reduced size STR amplicons as tools for analysis of degraded DNA, *J Forensic Sci* 48:1054–1064, 2003.

Chakraborty R, Stivers DN, Su B, et al.: The utility of short tandem repeat loci beyond human identification: implications for development of new DNA typing systems, *Electrophoresis* 20:1682–1696, 1999.

Collins P, Hennessy L, Leibelt C, et al.: Developmental validation of a single-tube amplification of the 13 CODIS STR loci, D2S1338, D19S433 and amelogenin: the AmpFLSTR Identifiler PCR amplification kit, *J Forensic Sci* 49:1265–1277, 2004.

Crouse CA, Ban JD, D'Alessio JK: Extraction of DNA from forensic-type sexual assault specimens using simple, rapid sonication procedures, *Biotechniques* 15:641–646, 1993.

Essen-Möller E: Die Beweiskraft der Ähnlichkeit in Vaterschaftsnachweis: theoretische Grundlagen, *Mitt Anthrop Ges (Wien)* 68:9–53, 1938.

Foster EA, Jobling MA, Taylor PG, et al.: Jefferson fathered slave's last child, *Nature* 396:27–28, 1998. Also see Nature 396:13–14, 1998.

Fuller T, Hauser C: Search for 'Golden state killer' leads to arrest of ex-cop, *The New York Times*, *April 25*, 2018.

Gaydosh Combs L, Warren JE, Huynh V, et al.: The effects of metal ion PCR inhibitors on results obtained with the Quantifiler® Human DNA Quantification Kit, *Forensic Sci Int Genet* 19:180–189, 2015.

Green RL, Roinestad IC, Boland C, et al.: Developmental validation of the quantifiler real-time PCR kits for the quantification of human nuclear DNA samples, *J Forensic Sci* 50:809–825, 2005.

Greytak EM, Moore C, Armentrout SL: Genetic genealogy for cold case and active investigations. Forensic Sci Int 299:103-113, 2019.

Hares DR: Expanding the CODIS core loci in the United States, *Forensic Sci Int Genet* 6, 2012a. e52–e54.

Hares DR: Addendum to expanding the CODIS core loci in the United States, *Forensic Sci Int Genet* 6:e135, 2012b.

Hares DR: Selection and implementation of expanded CODIS core loci in the United States, *Forensic Sci Int Genet* 17:33–34, 2015.

Harrison C, Allen R, Eisenberg A, et al.: Phenotype versus genotype reporting for DNA polymorphisms, *Prog Forensic Genet* 10:526–528, 2004.

Holland MM, Parsons TJ: Mitochondrial DNA sequence analysis—validation and use for forensic casework, *Forensic Sci Rev* 11:21–50, 1999.

Hummel K, Claussen M: Exclusion efficiency and biostatistical value of conventional blood group systems in European and non-European populations; suitability of Central European tables from non-German speaking populations. In Hummel K, Gerchow J, editors: *Biomathematical evidence of paternity*, Berlin, 1981, Springer-Verlag, pp 97–108.

Ivanov P, Wadhams M, Roby R, et al.: Mitochondrial DNA sequence heteroplasmy in the Grand Duke of Russia Georgij Romanov establishes the authenticity of the remains of Tsar Nicholas II, *Nat Genet* 12:417–420, 1996.

Jäger AC, Alvarez ML, Davis CP, Guzmán E, et al.: Developmental validaton of the MiSeq FGx Forensic Genomics System for targeted next generation sequencing in forensic DNA casework and database laboratories, *Forensic Sci Int Genet* 28:52–70, 2017.

Jeffreys AJ, Wilson V, Thein SL: Hypervariable "minisatellite" regions in human DNA, *Nature* 314:67–73, 1985a.

Jeffreys AJ, Wilson V, Thein SL: Individual specific "fingerprints" of human DNA, *Nature* 316:76–79, 1985b.

Kobilinsky L: Recovery and stability of DNA in samples of forensic science significance, *Forensic Sci Rev* 4:67–87, 1992.

Landsteiner K: Über Agglutinationserscheinungen normalen menschlichen Blutes, *Wien Klin Wochenschr* 14:1132–1134, 1901.

Leibelt C, Budowle B, Collins P, et al.: Identification of a D8S1179 primer binding site mutation and the validation of a primer designed to recover null alleles, *Forensic Sci Int* 133:220–227, 2003.

Lippert C, Sabatini R, Maher MC, et al.: Identification of individuals by trait prediction using whole-genome sequencing data, *Proc Natl Acad Sci Unit States Am* 114:10166–10171, 2017.

Margulies M, Egholm M, Atlman WE, Attiya S, Bader JS, Bemben LA, et al.: Genome sequencing in microfabricated high-density picolitre reactors, *Nature* 437:376–380, 2005.

Mayr WR: Paternity testing with unavailable putative father or mother. In Walker RH, editor: *Inclusion probabilities in parentage testing*, Arlington, Va, 1983, American Association of Blood Banks, pp 373–379.

Mendel G: Versuche über Pflanzen-Hybriden, *Verhandlung Nat Forsch Verein Brunn* 4:3–47, 1866.

Miale JB, Jennings ER, Rettberg WAH, et al.: Joint AMA-ABA guidelines: present status of serologic testing in problems of disputed parentage, *Family Law Q* 10:247–285, 1976.

Mulero JJ, Chang CW, Calandro LM, et al.: Development and validation of the AmpFLSTR Yfiler PCR Amplificaiton Kit: a male specific, single amplification 17 Y-STR multiplex system, *J Forensic Sci* 51:64–75, 2006.

Mulero JJ, Chang CW, Lagacá RE, et al.: Development and validation of the AmpFLSTR MiniFiler PCR Amplification Kit: a miniSTR multiplex for the analysis of degraded and/or PCR inhibited DNA, *J Forensic Sci* 53:838–852, 2008.

Myers SP, Timken MD, Piucci ML et al: Searching for first-degree familial relationships in California's offender DNA database: validation of a likelihood rato-based approach, Forensic Sci Intl Genet 5:493-500.

National Institute of Standards and Technology: *The biological evidence preservation handbook: best practices for evidence handlers*, 2013https://doi.org/10.6028/NIST.IR.7928.

Núnéz C, Sosa C, Baeta M, et al.: Genetic analysis of 7 medieval skeletons from the Aragonese Pyrenees, *Croat Med J* 52:336–343, 2011.

Parentage Act: *Minnesota Statutes*, 2004, 257.55 Presumption of paternity.

Parsons TJ, Weedn VW: Preservation and recovery of DNA in postmortem specimens and trace samples. In Haglund WD, Sorg MH, editors: *Forensic taphonomy: the postmortem fate of human remains*, Boca Raton, Fla, 1997, CRC Press.

Salmon D: The random man not excluded expression in paternity testing. In Walker RH, editor: *Inclusion probabilities in parentage testing*, Arlington, Va, 1983, American Association of Blood Banks, pp 281–292.

Scharf SJ, Smith AG, Hansen JA, et al.: Quantitative determination of bone marrow transplant engraftment using fluorescent polymerase chain reaction primers for human identity markers, *Blood* 85:1954–1963, 1995.

Schatkin SB: *Disputed paternity proceedings*, vol. 3. Albany, NY, 1952, Banks & Co, pp 233–234.

Sprouse M, Kavlick M, Phillips N, et al.: Internal validation of a real-time quantitative polymerase chain reaction assay for human mitochondrial DNA, *J Forensic Sci* 59:1049–1056, 2014.

Stanton S, Egel B, Lillis R: *Update: East Area rapist suspect captured after DNA match, authorities say: Sacramento Bee*, 2018. April 25.

Sweet D, Lorente M, Lorente JA, et al.: An improved method to recover saliva from human skin: the double swab method, *J Forensic Sci* 42:320–322, 1997.

Technical Working Group on DNA Analysis Methods: Guidelines for a quality assurance program for DNA restriction fragment length polymorphism analysis, *Crime Lab Dig* 17:40–59, 1989.

Technical Working Group on DNA Analysis Methods: Guidelines for a quality assurance program for DNA Analysis, *Crime Lab Dig* 22:21–43, 1995.

Traver M: Paternity calculations: special situations. In *Statistics workshop*, Madison, Wisc, 1996, Promega Corporation.

Venter JC, Adams MD, Myers EW, et al.: The sequence of the human genome, *Science* 291:1304–1351, 2001.

Walsh PS, Varlaro J, Reynolds R: A rapid chemiluminescent method for quantitation of human DNA, *Nucleic Acids Res* 20:5061–5065, 1992.

Weber JL, May PE: Abundant class of human DNA polymorphisms which can be typed using the polymerase chain reaction, *Am J Hum Genet* 44:388–396, 1989.

Weedn VW: Where did this come from? Identification of sample mix-ups by DNA testing, *Am J Clin Pathol* 100:592–593, 1993.

Weedn VW, Lee DA, Roby RK, et al.: DNA analysis. In Wong SHY, Sunshine I, editors: *Handbook of analytical therapeutic drug monitoring and toxicology*, Boca Raton, Fla, 1996, CRC Press, pp 35–50.

Weedn VW, Roby RK: Forensic DNA testing, *Arch Pathol Lab Med* 117:486–491, 1993.

Wenk RE, Traver M, Chiafari FA: Determination of sibship in any two persons, *Transfusion* 36:259–262, 1986.

Wickenheiser RA: Forensic genealogy, bioethics and the Golden state killer case, *Forensic Sci Int Syn* 1:114–125, 2019.

Wiener AS, Lederer M, Polayes SH: Studies in isohemagglutination. IV: on the chances of proving non-paternity: with special reference to blood groups, *J Immunol* 19:259–282, 1930.

Wollstein A, Lao O: Detecting individual ancestry in the human genome, *Investig Genet* 6(7), 2015.

CHAPTER 75

PHARMACOGENOMICS AND PERSONALIZED MEDICINE

Jing Li, Martin H. Bluth

OVERVIEW, 1480
BASIC CONCEPTS, 1480
DRUG-METABOLIZING ENZYME PHARMACOGENOMICS, 1481
Phase I Enzymes, 1481
Phase II Enzymes, 1483
DRUG-TRANSPORTER PHARMACOGENOMICS, 1486
ATP-Binding Cassette Transporters, 1487
Solute Carrier Transporters, 1489
DRUG TARGET PHARMACOGENOMICS, 1489
DNA Repair Genes, 1489
Thymidylate Synthase, 1493
Epidermal Growth Factor Receptor, 1494
HUMAN LEUKOCYTE ANTIGEN PHARMACOGENOMICS, 1495
PHARMACOGENOMICS IN CANCER CHEMOTHERAPY, 1496
Thiopurines, 1496
Fluoropyrimidines (5-Fluorouracil and Capecitabine), 1496
Irinotecan, 1497
Tamoxifen, 1499
Molecular Targeted Agents, 1501
PHARMACOGENOMICS IN OTHER DISEASES, 1501
Diabetes, 1501
Human Immunodeficiency Virus, 1502
Osteoporosis, 1502
Psychiatric and Cognitive Disorders, 1502
Epigenomics, 1503
CONCLUSION, 1504
SELECTED REFERENCES, 1505

KEY POINTS

- High-throughput array technologies such as genomics and proteomics have provided unprecedented ability to personalize output of biomarkers implicated in select disease states.
- Pharmacogenomics, through utilization of novel technologies, can detect unique genomic alterations to serve as diagnostic, prognostic, or predictive biomarkers, which relate to an individual or group response to particular therapies.
- Elucidation of unique genomic markers related to personal responses can tailor therapy to the individual, thereby maximizing efficacy and minimizing side effects.
- Interpretation of pharmacogenomics data can be discretionary in that many genotypic and phenotypic variables are often involved.

OVERVIEW

Pharmacogenomics is the study of how genetic variations influence individual response to drugs, in terms of efficacy and risk for adverse drug reactions. This relatively new field combines pharmacology (the study of drugs and their uses, effects, and mode of action) and genomics (the study of genes and their functions) to develop effective, safe medications and doses that are tailored to a person's genetic makeup. Genetic variations influencing individual response to drugs can be generally grouped into germline genetic polymorphisms and somatic mutations as occur in tumor tissues. Germline genetic polymorphisms in genes encoding drug-metabolizing enzymes, transporters, drug targets, and human leukocyte antigens (HLAs) have been associated with interindividual differences in the pharmacokinetics, efficacy, and adverse drug reactions of many drugs. Somatic mutations in tumor tissues are important determinants of the tumor sensitivity or resistance to many molecular targeted agents. The knowledge of how inherited differences in genes affect the body's response to medications will allow the development of personalized medicine that will provide greater efficacy and safety in drug development and therapy. This chapter summarizes recent important findings on pharmacogenomics of drug-metabolizing enzymes, transporters, drug targets (including germline genetic polymorphisms and somatic mutations), and HLAs, and discusses their implications in the development of personalized medicine to treat a wide range of health problems.

BASIC CONCEPTS

The concept of a relationship between a substance and its effect on genes, rudimentary pharmacogenetics, has been present since the early 1900s. Dr. Archibald Garrod described that genetic variations could cause adverse biological reactions when chemical substances were ingested (Garrod, 1902). Garrod's work on alcaptonuria constituted the first proof of mendelian genetics in humans. As a result of these studies, he advanced the hypothesis that genetically determined differences in biochemical processes could affect outcome after drug administration (Mancinelli et al., 2000). The idea of *pharmacogenomics*, also referred to as *toxogenomics*, is considered to have matured from *pharmacogenetics*, a discipline comprising genetics, pharmacology, and biochemistry, as a fusion of pharmacogenetics and genomics. Whereas pharmacogenetics classically investigates the hereditary impacts upon the action of drugs, pharmacogenomics extends pharmacogenetics to include the multifactorial drug responses caused by many genetic alterations plus environmental factors (Kalow, 2008). The recognition of these complex interactions and the advance of genetics into genomics via high-throughput analysis of gene interrogation algorithms have given rise to the application of this science as a means of personalizing drug effects to a group or individual. The term *personalized medicine* has been coined toward the promise of making therapy safer and more effective, and by giving drugs that fit a person's genes.

The events following a drug administration can be divided into two phases: *pharmacokinetics* and *pharmacodynamics*. Pharmacokinetics relates a dosage regimen to drug concentrations achieved with time; pharmacokinetics concerns drug absorption, distribution, metabolism, and excretion. Pharmacodynamics relates drug concentrations to the magnitude of the desired or adverse effects produced with time; pharmacodynamics concerns drug target interaction, downstream signaling events, and pharmacologic response. Each drug, after it enters the body, interacts with numerous proteins, including carrier proteins, transporters, metabolizing enzymes, and target receptors. These protein interactions determine the pharmacokinetics (i.e., absorption, distribution, metabolism, and excretion) and pharmacodynamics (i.e., target site of action and pharmacologic effects) of a drug. As a result, the overall response to a drug is determined by the interplay of multiple genes that are involved in the pharmacokinetic and pharmacodynamic pathways of a drug (Fig. 75.1). The topics that follow summarize recent findings with regard to the functional and clinical relevance of genetic variations of drug-metabolizing enzymes, transporters, drug targets, and HLAs.

DRUG-METABOLIZING ENZYME PHARMACOGENOMICS

Drug-metabolizing enzymes are proteins that catalyze the biochemical modifications of xenobiotics (e.g., drugs) and endogenous chemicals (e.g., hormones, neurotransmitters). Drug metabolism can result in the activation (toxication) or deactivation (detoxication) of the chemical. Even though both occur, the majority of metabolites of most drugs are deactivation products. Broadly, drug-metabolizing enzymes are divided into two categories: phase I (functionalizing) enzymes that introduce or remove functional groups in a substrate through oxidation, reduction, or hydrolysis; and phase II (conjugating) enzymes that transfer moieties from a cofactor to a substrate. Essentially all of the major human metabolizing enzymes exhibit genetic polymorphisms at the genomic level, and many of these enzymes have clinically relevant genetic polymorphisms (Fig. 75.2). A gene is considered to be polymorphic when the frequency of a variant allele in a specific population is at least 1%.

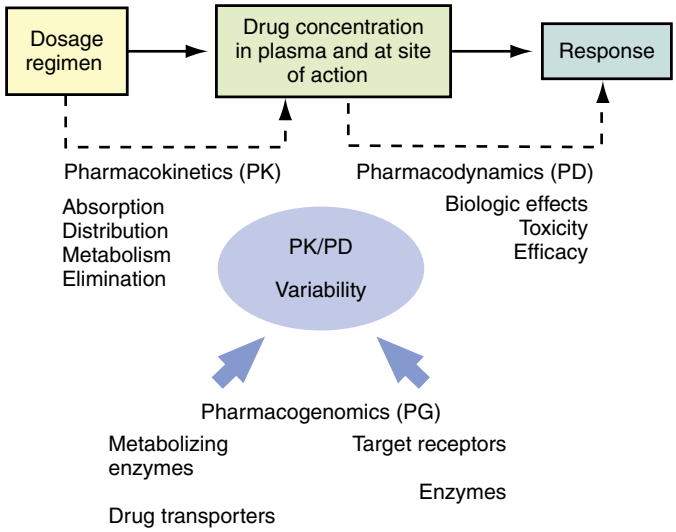

Fig. 75.1 Schematic illustration of interactions between pharmacokinetics (PK), pharmacodynamics (PD), and pharmacogenomics (PG). The PK relates a dosage regimen to drug concentration–time course in the body, and the PD relates the drug concentration to the magnitude of the desired or adverse effects produced. Genetic variations in the genes involved in drug disposition (e.g., drug-metabolizing enzymes, transporter genes) and drug action (e.g., target receptors, enzymes) contribute to the interindividual PK/PD variability.

PHASE I ENZYMES

Phase I metabolizing enzymes include those involved in oxidation (e.g., cytochrome P450 [CYP], alcohol dehydrogenase, aldehyde dehydrogenase, dihydropyrimidine dehydrogenase, monoamine oxidase, and flavin-containing monooxygenase), reduction (e.g., nicotinamide adenine dinucleotide phosphate [NADPH]-cytochrome P450 reductase and reduced cytochrome P450), and hydrolysis (e.g., epoxide hydrolase, esterases, and amidases).

The most important phase I enzymes that exhibit clinically relevant genetic polymorphisms are in the CYP superfamily, which represents the most important system responsible for catalyzing the oxidation of a large number of endogenous and exogenous compounds, including drugs, toxins, and carcinogens. In this superfamily, 57 genes and 58 pseudogenes have been identified, which are divided into 18 families and 43 subfamilies. Among them, three CYP subfamilies—CYP1, CYP2, and CYP3—are the main ones contributing to the oxidative metabolism of more than 90% of clinically used drugs.

The human *CYP* genes are highly polymorphic. The polymorphisms within the *CYP* genes, which include gene deletions, missense mutations, deleterious mutations creating splicing defects or premature stop codon, and gene duplications, can result in abolished, reduced, normal, or enhanced enzyme activity. Based on the level of CYP enzyme activity, patients can be classified into four phenotypes: poor metabolizer (abolished activity), intermediate metabolizer (reduced activity), extensive metabolizer (normal activity), and ultrarapid metabolizer (enhanced activity). Poor metabolizers may have higher concentrations of a drug that is inactivated by that enzyme pathway, thereby requiring a lower dose to avoid adverse reactions; whereas ultrarapid metabolizers may require a higher dose to achieve effective therapeutic drug concentrations. The opposite pattern of reactions occurs in response to a prodrug that requires metabolic activation to exert its pharmacologic effect. A prodrug may have little therapeutic effect in poor metabolizers while producing toxic levels of active form in ultrarapid metabolizers.

It is evident that genetic polymorphisms within the *CYP* genes have significant impact on drug disposition and/or response. The common functional polymorphisms in the major human *CYP* genes and their clinical relevance are summarized in Table 75.1. Comprehensive reviews on the pharmacogenetics of CYPs have been published (Ingelman-Sundberg, 2004; Andersson et al., 2005; van Schaik, 2005; Rodriguez-Antona & Ingelman-Sundberg, 2006; Zhou et al., 2009). Notably, the most pharmacologically and clinically relevant polymorphisms are found in *CYP2D6*, *CYP2C9*, and *CYP2C19*. Of the US Food and Drug Administration (FDA)–approved drug labels referring to human genomic biomarkers, 62% pertain to polymorphisms in the CYP enzymes, with CYP2D6 (35%), CYP2C19 (17%), and CYP2C9 (7%) being the most common (Frueh et al., 2008). For a review, see Li and Bluth (2011).

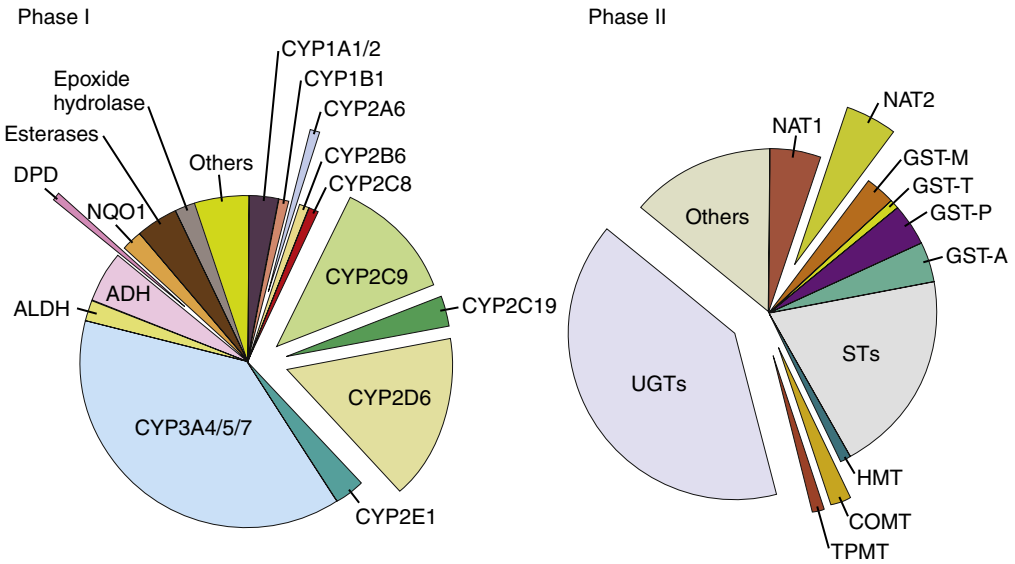

Fig. 75.2 Phase I and II drug-metabolizing enzymes that exhibit common genetic polymorphisms. The percentage of phase I and phase II metabolism of drugs that each enzyme contributes is estimated by the relative size of each section of the corresponding chart; those enzyme polymorphisms that have already been associated with changes in drug effects are separated from the corresponding pie charts. *ADH*, Alcohol dehydrogenase; *ALDH*, aldehyde dehydrogenase; *COMT*, catechol *O*-methyltransferase; *CYP*, cytochrome P450; *DPD*, dihydropyrimidine dehydrogenase; *GST*, glutathione *S*-transferase; *HMT*, histamine methyltransferase; *NAT*, *N*-acetyltransferase; *NQO1*, NAD(P)H dehydrogenase, quinone 1; *STs*, sulfotransferases; *TPMT*, thiopurine methyltransferase; *UGTs*, uridine 5′-triphosphate glucuronosyltransferases. (Adapted from Evans WE, Relling MV: Pharmacogenomics: translating functional genomics into rational therapeutics, Science 286:487–491, 1999.)

TABLE 75.1

Most Common Naturally Occurring Functional Polymorphisms in the Major Human Cytochrome P450 Genes: Allele Frequency, Functional Effect, and Highlights of Clinical Relevance

Common Allelic Variants	Polymorphism/ Substitution	ALLELE FREQUENCY (%)[a]			Functional Effect[b]	Highlights of Clinical Relevance[c]
		Ca	As	Af		
CYP1A1						Mainly expressed in extrahepatic tissues.
CYP1A1*2A	3698T>C(MspI)	6.6-19	33-54	22-28	↑Inducibility	CYP1A1, 1A2, and 1B1 play an important role in the bioactivation of a variety of carcinogens.
CYP1A1*2B	I462V; 3698T>C(MspI)	–	–	–	↑Inducibility	↑Lung cancer risk generally associated with highly inducible or active CYP1A1 polymorphisms such as CYP1A1*2C.
CYP1A1*2C	I462V	2.2-8.9	28-31	0-2.7	↑Activity	CYP1A1 genotypes also associated with risk for breast, prostate, and ovarian cancers that are possibly related to estrogen activation.
CYP1A1*3	3204T>C	0	0	7.6-14	Normal	
CYP1A1*4	T461N	2.0-5.7	–	–	Normal	
CYP1A2						CYP1A2 accounts for ~13% of total hepatic CYP content.
CYP1A2*1C	–3860G>A				↓Inducibility	High inducible *1F genotype associated with ↑clearance of CYP1A2 substrates (e.g., caffeine) after smoking or omeprazole treatment.
CYP1A2*1F	–163C>A	33	68		↑Inducibility	*1K associated with ↓in vivo caffeine metabolism.
CYP1A2*1K	Haplotype (–63C>A, –739T>G, –729C>T)	0.5			↓Inducibility ↓Activity	CYP1A2 genotypes are associated with cancer risk.
CYP2A6						CYP2A6 accounts for 1% to 10% of total hepatic CYPs.
CYP2A6*1X2	Gene duplication	1.7		0.4 <1	↑Activity ↓Activity	The frequency of CYP2A6 alleles has marked ethnic differences. CYP2A6*4 accounts for the majority of PMs in Asians.
CYP2A6*2	L160H	1-3	7-22	15-20	Abolished activity	Because nicotine is converted to cotinine by CYP2A6, a high expression/activity of CYP2A6 is proposed to increase the susceptibility to nicotine addiction and the risk for tobacco-related cancers. Therefore CYP2A6 genetic variation could play a role in nicotine addiction and tobacco-related cancer risks.
CYP2A6*4	Gene deletion	0.5-1				
CYP2B6						CYP2B6 is mainly expressed in the liver, accounting for 6% of total CYPs.
CYP2B6*4	K262R	5			↑Activity	The anticancer drug cyclophosphamide (CPA) is bioactivated by CYP2B6. CYP2B6 polymorphisms would likely affect the PK and/or PD of CPA. For example, CYP2B6*6 carriers exhibited ↑CPA clearance and CPA 4-hydroxylation activity.
CYP2B6*5	R487C	11-14	1		↓Expression	CYP2B6 polymorphisms may affect the PK and therapeutic outcome of anti-HIV agents such as efavirenz and nevirapine. For example, the CYP2B6 Q172H variant is associated with ↑plasma concentrations of efavirenz and nevirapine.
CYP2B6*6	Q172H; K262R	16-26	16		↑Activity	
CYP2B6*7	Q172H; K262R; R487C	13	0		↑Activity	
CYP2C8						CYP2C8 accounts for ~7% of total hepatic CYP contents.
CYP2C8*2	I269F	0.4	0	18	↓Activity	CYP2C8*3 is associated with ↓clearance of both R- and S-ibuprofen.
CYP2C8*3	R139K; K399R	13		2	↓Activity	
CYP2C8*4	I264M	7.5			↓Activity	
CYP2C9						CYP2C9 accounts for ~20% of total hepatic CYP contents.
CYP2C9*2	R144C	13-22	0	3	↓Activity	CYP2C9*2 and *3 have been shown to affect the oral clearance of at least 17 different CYP2C9 substrate drugs (e.g., S-warfarin, celecoxib, ibuprofen, and phenytoin).
CYP2C9*3	I359L	3-16	3	1.3	↓Activity	
CYP2C9*5	D360E	0	2	0	↓Activity	
CYP2C19						The PM phenotype of CYP2C19 occurs in 12% to 23% of the Asian population, 1% to 6% of Caucasians, and 1% to 7.5% of black Africans.
CYP2C19*2	Splicing defect; I331V	15	30	17	Abolished activity	Polymorphisms in the *CYP2C19* gene are known to affect the PK and/or response of several classes of drugs, including proton pump inhibitors (e.g., omeprazole) and barbiturates.
CYP2C19*3		0.04	5	0.4	Abolished activity	
CYP2C19*17	W212X; I331V I331V	18	4		↑Transcription	
CYP2D6						CYP2D6 accounts for ~2% of total hepatic CYP contents. However, it is involved in the metabolism of ~25% of all drugs in clinical use.
CYP2D6*3	Frameshift	1-2	<1		Abolished activity (PM)	Unlike other CYPs, CYP2D6 is not inducible, and thus genetic polymorphisms are largely responsible for the variation in enzyme expression and activity.
CYP2D6*4	Splicing defect	20-25	1	6-7	Abolished activity (PM)	CYP2D6 genotypes exhibit large interethnic differences: low frequency of PM in Asian (~1%) and African (0–5%) populations, compared to Caucasians (5–14%).

Continued

TABLE 75.1

Most Common Naturally Occurring Functional Polymorphisms in the Major Human Cytochrome P450 Genes: Allele Frequency, Functional Effect, and Highlights of Clinical Relevance_Cont'd

Common Allelic Variants	Polymorphism/ Substitution	ALLELE FREQUENCY (%)[a]			Functional Effect[b]	Highlights of Clinical Relevance[c]
		Ca	As	Af		
CYP2D6*5	Gene deletion	4-6	4-6	4-6	Abolished activity (PM)	The CYP2D6 genotype is of great importance for the PK and response of many drugs, including tricyclic antidepressants, antiarrhythmics, neuroleptics, analgesics, antiemetics, and anticancer drugs.
CYP2D6*10	P34S; S486T	<2	50	3-9	↓Activity (IM)	
CYP2D6*17	T107I; R296C; S486T	<1		20-34	↓Activity (IM)	
CYP2D6*41	R296C; splicing defect; S486T	1.3	2	5.8	↓Activity (IM)	
CYP2D6*1×N, N≥2	Gene duplication				↑Activity (UM)	
CYP2D6*2×N, N≥2	Gene duplication				↑Activity (UM)	
CYP3A4						CYP3A4 has the highest abundance in the human liver (~40%) and metabolizes over 50% of all currently used drugs.
CYP3A4*1B	5′ flanking region	2-9	0	35-67	Altered expression	Genetic polymorphisms in CYP3A4 appear to be more prevalent in Caucasians than in Asians.
CYP3A4*2	S222P	2.7-4.5	0	0	Substrate-dependent altered activity	There is no consensus on a direct functional or clinical association of CYP3A4 polymorphism. CYP3A4 polymorphism may have minor or moderate clinical relevance.
CYP3A4*3	M445T	1.1			↓Activity	
CYP3A4*17	F189S	2.1			↓Activity	
CYP3A4*18	L293P	0		1	↑Activity	
CYP3A5						The clinical relevance of the CYP3A5 polymorphism is demonstrated by the fact that the PK of the immunosuppressive drug tacrolimus is associated with the CYP3A5 genotype.
CYP3A5*3	Splicing defect	90	75	50	Abolished activity	
CYP3A5*6	Splicing defect	0	0	7.5	Severely ↓activity	
CYP3A5*7	346 frameshift	0	0	8	Severely ↓activity	
CYP3A7						CYP3A7 is a predominantly fetal enzyme.
CYP3A7*1C	Promoter	3	28	6	↑Expression	The in vivo functional effect of CYP3A7 polymorphism is demonstrated by the fact that carriers of the CYP3A7*1C allele had a significantly decreased endogenous level of dehydroepiandrosterone sulfate, a specific substrate of CYP3A7.
CYP3A7*2	T409R	8		62	↑Activity	

Af, African; *As,* Asian; *Ca,* Caucasian; ↑ indicates increased; ↓ indicates decreased.
[a]Allele frequency data are obtained from Xie et al. (2001), Bradford (2002), Mizutani (2003), Solus et al. (2004), Roy et al. (2005), Suarez-Kurtz (2005), Sistonen et al. (2007).
[b]Functional effect data are obtained from the Human Cytochrome P450 (CYP) Allele Nomenclature Committee website (http://www.cypalleles.ki.se/).
[c]Comprehensive reviews were written by Ingelman-Sundberg (2004), Bozina et al. (2009), Zhou et al. (2009).

Unlike other CYPs, CYP2D6 is not inducible. Therefore variations in the enzyme expression and activity are largely attributable to the genetic polymorphisms. The *CYP2D6* gene is highly polymorphic with more than 63 functional variants identified to date (https://www.pharmvar.org/). These alleles result in abolished, decreased, normal, or ultrarapid CYP2D6 enzyme activity. The most important null alleles are *CYP2D6*4* (splicing defect) and *CYP2D6*5* (gene deletion); the common alleles with severely reduced enzyme activity are represented by *CYP2D6*10*, **17*, and **41*; ultrarapid enzyme activity is derived from duplication or multiduplications of active *CYP2D6* genes (e.g., *CYP2D6*1* × N [N ≥2]) (see Table 75.1). The distributions of *CYP2D6* alleles exhibit notable interethnic differences. The nonfunctional allele *CYP2D6*4* is prevalent in Caucasians (allelic frequency, ~25%); the reduced function allele *CYP2D6*10* is common in Asians (allelic frequency, ~40%); and *CYP2D6*17* is common in Africans (allelic frequency, ~34%) (Bradford, 2002). As a result, CYP2D6 poor metabolizers, mainly derived from null allele *CYP2D6*4*, have a high frequency in Caucasians (5–14%) compared with Africans (0–5%) and Asians (0–1%). In contrast, CYP2D6 ultrarapid metabolizers due to gene duplication or multiduplications have a high frequency in Saudi Arabians (20%) and black Ethiopians (29%) compared with Caucasians (1–10%) (Bradford, 2002). The interethnic difference in the *CYP2D6* genotypes may contribute to the interethnic variation in the disposition and response of substrate drugs. Although it accounts for ~2% of total hepatic CYP contents, CYP2D6 is involved in the metabolism of ~25% of all drugs in clinical use. *CYP2D6* genotype is of great importance to the pharmacokinetics and response of many drugs, including tricyclic antidepressants, antiarrhythmics, neuroleptics, analgesics, antiemetics, and anticancer drugs (for a review, see Zhou et al. [2009]). A representative example is the implication of CYP2D6 phenotypes to the pharmacokinetics and clinical efficacy of tamoxifen, a prodrug requiring metabolic activation primarily mediated by CYP2D6. The pharmacogenetics of tamoxifen is discussed in detail later.

The human *CYP2C9* and *CYP2C19* genes are highly homologous at the nucleotide level. The most common nonsynonymous *CYP2C9* polymorphisms, *CYP2C9*2* and *CYP2C9*3*, result in the enzyme with differing affinity or intrinsic clearance for different substrates. *CYP2C9*2* effect appears substrate specific, while *CYP2C9*3* variant generally leads to reduced catalytic activity toward the majority of CYP2C9 substrates. The clinical importance of *CYP2C9* polymorphisms is exemplified by the CYP2C9 genotype-guided dosing of an oral anticoagulant warfarin. Patients carrying either *CYP2C9*2* or *CYP2C9*3* require significantly smaller daily dose of warfarin to maintain desired therapeutic effects while avoiding severe toxicity, as compared with patients carrying the wild-type *CYP2C9* (Higashi et al., 2002). For *CYP2C19*, a splice site mutation in exon 4 *(CYP2C19*2)* and a premature stop codon in exon 4 *(CYP2C19*3)* represent the two most predominant null alleles. By genotyping for *CYP2C19*2* and **3*, ~84%, ~100%, and >90% of poor CYP2C19 metabolizers could be detected in Caucasians, Asians, and Africans, respectively. CYP2C19 poor metabolizers are found in 12% to 23% of Asians, 1% to 6% of Caucasians, and 1% to 7.5% of Africans. *CYP2C19* genotypes are clinically relevant to the pharmacokinetics and response of several classes of drugs, including proton pump inhibitors (e.g., omeprazole) and barbiturates (for a review, see Zhou et al. [2009]).

PHASE II ENZYMES

The most important phase II enzymes that exhibit functional and clinically relevant genetic polymorphisms are uridine diphosphate glucuronosyltransferase (UGT), sulfotransferase (SULT), glutathione S-transferase (GST), *N*-acetyltransferase (NAT), and thiopurine methyltransferase (TPMT) (see Fig. 75.2). Table 75.2 summarizes common functional polymorphisms in these phase II enzymes and highlights their clinical significance.

TABLE 75.2

Most Common Naturally Occurring Functional Polymorphisms in Major Human Phase II Drug-Metabolizing Enzymes: Allele Frequency, Functional Effect, and Highlights of Clinical Relevance

Allelic Variants	Polymorphism/ Substitution	ALLELE FREQUENCY (%)			Functional Effect	Highlights of Clinical Relevance
		Ca	As	Af		
UGT1A1[a]						UGT1A1 low promoter activity alleles (e.g., UGT1A1*28) are significantly associated with ↓glucuronidation of SN-38 (the active metabolite of irinotecan), thereby resulting in ↑risk for irinotecan-induced toxicity.
UGT1A1*6	G71R	0	13-23	–	↓Activity	Genetic variations in UGT1A1 may modify susceptibility to steroid-related cancers including breast, ovarian, endometrial, and prostate cancers.
UGT1A1*28	(TA)6>(TA)7 in promoter	29-40	13-16	36-43	↓Expression	
UGT1A1*33	(TA)6>(TA)5 in promoter	0-0.7	0	3-8	↑Expression	
UGT1A1*34	(TA)6>(TA)8 in promoter	0-0.7	0	0.9-7	↓Expression	
UGT1A6[a]						UGT1A6 catalyzes the glucuronidation of aspirin and acetaminophen.
UGT1A6*2	T181A, R184S	30	23		↓Activity	"Low activity" UGT1A6 variants, leading to increased salicylate levels in aspirin users, are associated with a lower risk for colon cancer.
UGT1A6*3	R184S	1-2	1.6		Unknown	
UGT1A6*4	T181A	2.4			Unknown	
UGT1A7[a]						
UGT1A7*2	N129K, R131K	24-34	15	39	Similar activity	UGT1A7 is an important extrahepatic UGT that inactivates a variety of carcinogens.
UGT1A7*3	N129K, R131K, W208R	23-36	26	23	↓Activity	Low-activity UGT1A7 variants increase the risk of developing tobacco-related cancers, specifically orolaryngeal cancer.
UGT1A7*4	W208R	1-1.7	0	1	↓Activity	
UGT2B7[a]						UGT2B7 is of major significance for the glucuronidation of a number of clinically important drugs (e.g., morphinan derivatives, epirubicin, and zidovudine).
UGT2B7*2	H268Y	49-54	27		Similar or decreased activity	Further studies are needed to elucidate the clinical impact of the UGT2B7 polymorphism.
UGT2B15[a]						UGT2B15 is the most efficient UGT2B involved in the inactivation of steroid hormones, mainly androgens.
UGT2B15*2	D85Y	52-55	36-49	39	↑Activity	UGT2B15 polymorphisms have a potential role in a modified risk for prostate cancer.
SULT1A1[b]						SULT1A1 is the most highly expressed hepatic SULT.
SULT1A1*2	R213H	25-36	4.5-17	27-29	↓Activity and ↓thermal stability	SULT1A1 plays an important role in the sulfation of the metabolites of tamoxifen, 4-hydroxy-tamoxifen, and endoxifen. SULT1A1*2 is associated with decreased survival of breast cancer patients treated with tamoxifen.
SULT1A1*3	M223V	1.2	0.6	23	Similar activity	
GST[c]						
GSTA1*B	Promoter point mutation (T-631G, T-567G, C-69T, G-52A)	40		41	↓Expression	GSTA1 is involved in glutathione conjugation of the active metabolites of cyclophosphamide (CPA). GSTA1*B allele is associated with higher survival rate of breast cancer patients treated with CPA-containing chemotherapy.
GSTM1*0	Gene deletion	42-58		27-41	Abolished activity	The GSTM null genotype is associated with an increased risk for lung, colon, and bladder cancer.
						AML patients carrying GSTM*0 appear to have a better response to adriamycin and cyclophosphamide treatment.
GSTP1*B	I105V	6-40		54	↓Activity	The GSTP1*B allele is associated with lower clearance of etoposide and reduced risk for relapse in childhood ALL patients.
						The GSTP1*B allele is associated with increased survival rate in patients with advanced colorectal cancer or breast cancer.
GSTT1*0	Gene deletion	2-42			Abolished activity	The GSTT1 deletion is associated with reduced risk for relapse in childhood ALL patients.
						The GSTT1 deletion is a poor prognostic factor for survival in adult ALL.
NAT[d]						NAT1*14 and *17 are associated with slow acetylator phenotype.
NAT1*4	Wild-type				Normal	NAT2*5, *6, *7, *10, *14, and *19 lead to slow acetylator phenotype.
NAT1*14	R187Q	1.3-3.7			↓Activity	NAT2 slow acetylator phenotype is associated with increased susceptibility to hydralazine- and isoniazid-induced toxicity.
NAT1*14	R187Stop				↓Activity	NAT2 slow acetylator phenotype is associated with increased risk for bladder cancer.
NAT1*17	R64W				↓Activity	
NAT1*19	R33Stop				↓Activity	

Continued

TABLE 75.2

Most Common Naturally Occurring Functional Polymorphisms in Major Human Phase II Drug-Metabolizing Enzymes: Allele Frequency, Functional Effect, and Highlights of Clinical Relevance_Cont'd

Allelic Variants	Polymorphism/ Substitution	ALLELE FREQUENCY (%)			Functional Effect	Highlights of Clinical Relevance
		Ca	As	Af		
NAT1*22	D251V				↓Activity	
NAT2*4	Wild-type				Normal	
NAT2*5	I114T				↓Activity	
NAT2*6	R197Q				↓Activity	
NAT2*7	G286E				↓Activity	
NAT2*10	E167K				↓Activity	
NAT2*14	R64Q				↓Activity	
NAT2*17	Q145P				↓Activity	
NAT2*19	R64W				↓Activity	
TPMT[e]						TPMT is involved in the methylation reaction of mercaptopurine, an anticancer drug used in the treatment of childhood ALL.
TPMT*2	A80P	0-0.5	0	0-0.4	↓Activity	The TPMT genotype correlated well with in vivo enzyme activity and is clearly associated with a risk for mercaptopurine-induced toxicity. Patients with poor or intermediate TPMT activity may tolerate only one-tenth to half of the average mercaptopurine dose.
TPMT*3A	A154Y, Y240C	0-0.6	0-1	0-0.8	Abolished activity	
TPMT*3B	Y240C	–	0	–	9-fold ↓Activity	
TPMT*3C	A154Y	0.2-3.3	0-0.2	2.4-7.6	1.4-fold ↓ Activity	

Af, African; *ALL,* acute lymphoblastic leukemia; *AML,* acute myeloid leukemia; *As,* Asian; *Ca,* Caucasian; *GST,* glutathione S-transferases; *NAT,* N-acetyltransferase; *SULT,* sulfotransferase; *TPMT,* thiopurine methyltransferase; *UGT,* uridine diphosphate glucuronosyltransferase; ↑ indicates increased; ↓ indicates decreased.
[a]Data on *UGT* SNP allele frequencies, function effect, and clinical relevance are summarized from Guillemette (2003), Nagar and Remmel (2006).
[b]Data on *SULT1A1* SNP allele frequencies, function effect, and clinical relevance are summarized from Glatt and Meinl (2004), Nowell and Falany (2006).
[c]Data on *GST* SNP allele frequencies, function effect, and clinical relevance are summarized from McIlwain et al. (2006), Lo and Ali-Osman (2007).
[d]Data on *NAT* SNP allele frequencies, function effect, and clinical relevance are summarized from Hein (2002), Agundez (2008), Sim et al. (2008).
[e]Data on *TPMT* SNP allele frequencies, function effects, and clinical relevance are summarized from Hamdy et al. (2003), Zhou (2006).

Uridine Diphosphate Glucuronosyltransferase

The human UGT superfamily is a group of conjugating enzymes that catalyze the transfer of the glucuronic acid group of uridine diphosphoglucuronic acid to the functional group (e.g., hydroxyl, carboxyl, amino, sulfur) of a specific substrate (Guillemette, 2003). UGTs are membrane-bound enzymes localized in the endoplasmic reticulum of liver and many other extrahepatic tissues. Seventeen human *UGT* genes have been identified and are classified into two subfamilies (*UGT1* and *UGT2*). Glucuronidation increases the polarity of the substrates and facilitates their excretion in bile or urine. Genetic polymorphisms have been identified for almost all the UGT family members. These genetic variations may alter the function or expression of the enzyme, and consequently modify the glucuronidation capacity of the enzyme toward the substrates. There is evidence that genetic variations in the *UGT* genes contribute to differential susceptibility to diseases (e.g., cancer) and influence the pharmacokinetics and clinical outcome of substrate drugs (for reviews, see Guillemette [2003] and Nagar & Remmel [2006]). A representative example is that the *UGT1A1* low promoter activity alleles (i.e., *UGT1A1*28*) are associated with decreased glucuronidation of SN-38 (an active metabolite of irinotecan), thereby leading to increased risk for irinotecan-induced toxicity. The pharmacogenetics of irinotecan is discussed in detail later. The most common functional polymorphisms in the major UGT enzymes and their clinical relevance are summarized in Table 75.2 (for comprehensive reviews, see Guillemette [2003] and Nagar & Remmel [2006]).

Sulfotransferases

Cytosolic SULTs are phase II enzymes that catalyze the transfer of the sulfonyl group from the cofactor 3′-phosphoadenosine 5′-phosphosulfate to the nucleophilic sites of a variety of substrates, including hormones and xenobiotics. Sulfo conjugation of xenobiotics leads to formation of polar, excretable products as well as reactive, potentially mutagenic and carcinogenic metabolites (Glatt & Meinl, 2004). Eleven SULT proteins encoded by 10 genes have been identified in humans. They differ in substrate specificity and tissue distribution. Single nucleotide polymorphisms (SNPs) have been identified in most of the human *SULT* genes. Functional SNPs in *SULTs*, which result in altered enzymatic activity, have the potential to influence therapeutic response and modify cancer susceptibility (see Table 75.2) (see reviews in Glatt & Meinl [2004] and Nowell & Falany [2006]). A most commonly occurring SNP, *SULT1A1*2* (Arg213His), exhibits reduced enzymatic activity and thermal stability.

Glutathione S-Transferases

The superfamily of human GST catalyzes the conjugation of glutathione (GSH) to a large variety of endogenous metabolites and xenobiotics, including alkylating and free radical–generating anticancer drugs such as cyclophosphamide, anthracyclines, and topoisomerase II inhibitors (Lo & Ali-Osman, 2007). Human GSTs are categorized into three main families: cytosolic/nuclear, mitochondrial, and microsomal GSTs. The cytosolic GSTs are further divided into seven classes: alpha, mu, omega, pi, sigma, theta, and zeta. Their typical function is to detoxify reactive metabolites, while they may also play a role in the formation of cytotoxic metabolites (Hayes et al., 2005). Besides enzymatic function, GSTs also possess nonenzymatic functions, in which they act as regulators of cell signaling (Adler et al., 1999; Chie et al., 2004) and posttranslational modification pathway in response to stress, growth factors, and deoxyribonucleic acid (DNA) damage, and in cell proliferation, cell death, and other processes that ultimately lead to tumor growth and drug resistance. These multiple functionalities establish the importance of GSTs as determinants of cancer susceptibility and prognosis, as well as therapeutic response (see reviews in McIlwain et al. [2006] and Lo & Ali-Osman [2007]). The human genes encoding GSTs are highly polymorphic. A homozygous deletion (GST-null genotype) of *GSTM1* or *GSTT1* occurs in about 50% or 25%, respectively, of most populations (Relling & Dervieux, 2001). *GST* polymorphisms have been linked to cancer incidence, treatment outcome, and prognosis (Table 75.3) (for comprehensive reviews, see McIlwain et al. [2006] and Lo & Ali-Osman [2007]).

N-Acetyltransferase

The human NATs catalyze the transfer of an acetyl group from acetylcoenzyme A to arylamines, arylhydroxylamines, and arylhydrazines (Blum et al., 1990). The two human NAT genes, *NAT1* and *NAT2*, carry functional polymorphisms that influence the enzyme activity. Based on the level of NAT activity, patients can be classified into two phenotypes: fast acetylator (wild-type NAT acetylation activity) and slow acetylator (reduced NAT enzyme activity). For example, polymorphisms or haplotypes in *NAT1* (e.g., *NAT1*14*, **15*, **17*, **19*, and **22*) and *NAT2* (e.g., *NAT2*5*, **6*, **7*, **10*, **14*, and **17*) lead to slow acetylation phenotype (see Table 75.3) (for a review, see Sim et al. [2008]). NAT2 plays an important role in the activation and/or deactivation of a large and diverse number of aromatic amine and hydrazine drugs used in clinic, and therefore the *NAT2* genotype is particularly relevant to the response to these drugs. One representative example is the association of the NAT2 slow-acetylator phenotype with increased risk for an antituberculosis drug (isoniazid)–induced hepatitis (Huang et al., 2002).

TABLE 75.3
Pharmacologically Most Important Efflux and Uptake Drug Transporters, Tissue Distribution, and Representative Substrate Drugs

Gene	Protein	Tissue Distribution	Polarity	Representative Drug Substrates
ABC Transporters				
ABCB1	MDR1 (P-gp)	Liver, intestine, kidney, blood-brain barrier, lymphocytes, placenta	AP	Anthracyclines, taxanes, vinca alkaloids, imatinib, etoposide, levofloxacin, erythromycin, cyclosporine, tacrolimus, digoxin, quinidine, verapamil, diltiazem, ritonavir, saquinavir, talinolol, phenytoin, cimetidine, simvastatin, morphine, hydrocortisone
ABCC1	MRP1 (GS-X)	Ubiquitous	BL	Anthracyclines, vinca alkaloids, irinotecan, SN-38, methotrexate, camptothecins, saquinavir, ritonavir, difloxacin, drug-glucuronate/-glutathione/-sulfate conjugates
ABCC2	MRP2 (cMOAT)	Liver, kidney, intestine	AP	Anthracyclines, vinca alkaloids, methotrexate, camptothecins, rifampin, pravastatin, and drug-glucuronate/-glutathione/-sulfate conjugates
ABCG2	BCRP	Liver, intestine, placenta, breast	AP	Anthracyclines, irinotecan, SN38, SN38G, imatinib, tamoxifen
SLC Transporters				
OATP Family				
SLC21A3	OATP1A2 (OATP-A)	Ubiquitous, with highest expression in brain and testis	BL	Rosuvastatin, methotrexate, ouabain, D-penicillamine
SLC21A6	OATP1B1 (OATP-C)	Liver	BL	Statins, pravastatin, fexofenadine, repaglinide, rosuvastatin, ouabain, D-penicillamine, rifampin
SLC21A8	OATP1B3 (OATP8)	Liver	BL	Digoxin, rifampin, ouabain, methotrexate, D-penicillamine, rosuvastatin, cyclosporine
SLC21A9	OATP2B1 (OATP-B)	Ubiquitous	BL	Benzylpenicillin, rosuvastatin
OCT Family				
SLC22A1	OCT1	Liver	BL	Metformin, cisplatin, oxaliplatin, imatinib, procainamide, citalopram, cimetidine, quinidine, verapamil, acyclovir
SLC22A2	OCT2	Kidney	BL	Metformin, cisplatin, oxaliplatin, imatinib, procainamide, citalopram, cimetidine, quinidine, amantadine
SLC22A3	OCT3	Brain, liver, kidney, heart, muscle, placenta, and blood vessels	BL	Cimetidine, agmatine, adefovir, catecholamines
OAT Family				
SLC22A6	OAT1	Kidney, brain	BL	Methotrexate, salicylate, antiviral agents (e.g., acyclovir)
SLC22A7	OAT2	Liver, kidney,	BL	Methotrexate, salicylate, tetracyclines
SLC22A8	OAT3	Kidney, brain, muscle	BL	Methotrexate, antiviral agents (e.g., acyclovir), cimetidine, pravastatin, salicylate
SLC22A11	OAT4	Kidney, placenta	AP	Methotrexate, cimetidine, salicylate, tetracyclines

AP, Apical; *BCRP*, breast cancer resistance protein; *BL*, basolateral; *GS-X*, glutathione S-conjugate pump; *MDR1,* multidrug resistance 1; *MOAT,* multispecific organic anion transporter; *MRP*, multidrug resistance-related protein; *OAT,* organic anion transporter; *OATP*, organic anion transporting peptides; *OCT*, organic cation transporter; *P-gp,* P-glycoprotein.

In addition, because NAT1 and NAT2 catalyze the bioactivation (via *O*-acetylation) of aromatic and heterocyclic amine carcinogens, genetic variations in *NAT1/2* genes may modify the cancer risk related to exposure to these carcinogens (Hein, 2002). For instance, the NAT2 slow-acetylator phenotype has been linked to a higher risk for bladder cancer, particularly in cigarette smokers (Cartwright et al., 1982; Garcia-Closas et al., 2005).

Thiopurine *S*-Methyltransferase

TPMT is best known for its key role in the metabolism of the thiopurine drugs (e.g., 6-mercaptopurine, azathiopurine, and 6-thioguanine) by catalyzing the *S*-methylation of thiopurine drugs via *S*-adenosyl-L-methionine as the *S*-methyl donor. These drugs are clinically used to treat cancers, in particular acute lymphoblastic leukemia (ALL), or as immunosuppressants. The *TPMT* gene exhibits significant genetic polymorphisms across all ethnic groups studied, with 18 *TMPT* alleles identified to date. The three main *TPMT* alleles, namely *TMPT*2* (reduced activity), **3A* (abolished activity), and **3C* (reduced activity), account for 80% to 95% of the intermediate and poor metabolizers (see Table 75.3) (for a review, see Zhou et al. [2006]). About 90% of individuals have two wild-type *TPMT* alleles (*TPMT*1*) (resulting in high TPMT activity); about 10% of individuals have one wild-type *TPMT* allele and one nonfunctional variant allele (resulting in intermediate activity); and rare (1 in 300) individuals inherit two nonfunctional variant alleles (resulting in complete TMPT deficiency) (Schaeffeler et al., 2004). Individuals who inherit defective *TPMT* alleles or *TPMT* deficiency (i.e., two nonfunctional alleles) are at significantly increased risk for thiopurine-induced hematopoietic toxicity. Indeed, patients with absent TPMT activity (~0.3% prevalence) or low activity (~10% prevalence) may tolerate only 5% to 50% of the average mercaptopurine dose. Clinical diagnostic tests are now available for the detection of the SNPs in the human *TPMT* gene that lead to decreased or abolished enzyme activity. *TPMT* variant pharmacogenetic testing is recommended before treating patients with azathiopurine, mercaptopurine, and thioguanine.

DRUG-TRANSPORTER PHARMACOGENOMICS

In addition to drug-metabolizing enzymes, uptake and efflux transporters that facilitate the movement of drugs into and out of cells are important determinants of drug disposition and response. Broadly, drug transporters are classified into two families: efflux transporters of the adenosine-5′-triphosphate (ATP)–binding cassette (ABC) family and uptake transporters of the solute carrier (SLC) family. In the ABC transporter family, 49 genes have been identified and classified into seven subfamilies from ABCA through ABCG based on the sequence homology. The ABC transporters are responsible for transport of diverse substrates out of cells using ATP as an energy source. Among these, *ABCB1*, *ABCC1/2*, and *ABCG2* have been well characterized for their roles in drug disposition and response. In the SLC family, 360 genes have been identified and classified into 46

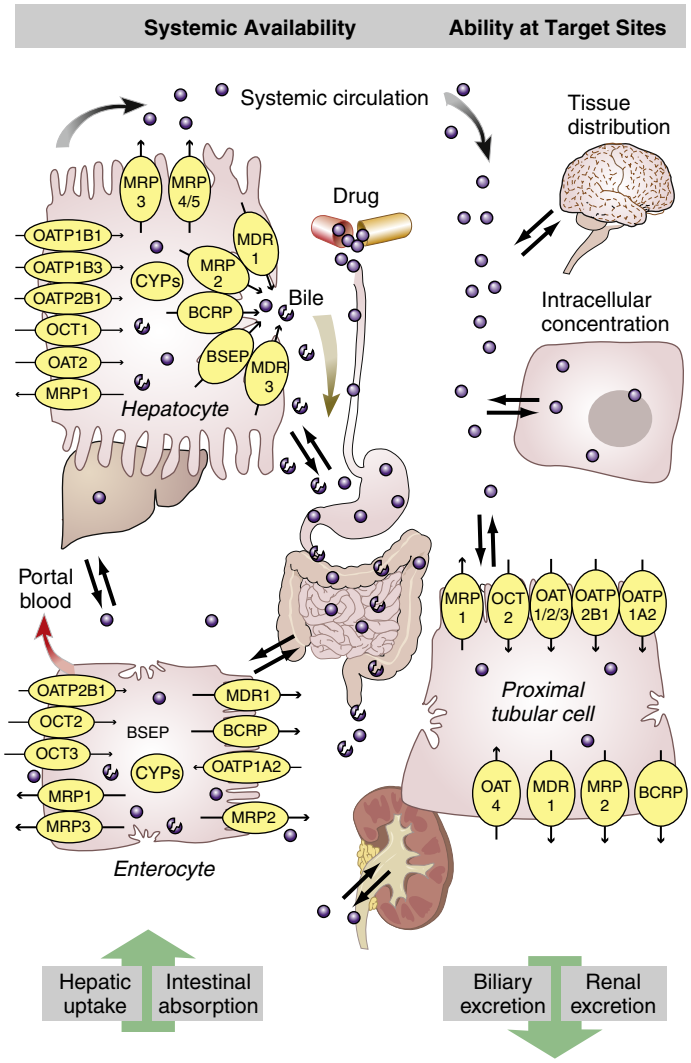

Fig. 75.3 Schematic representation of drug uptake and efflux transporters as determinants of drug disposition. Abbreviations are explained in Table 75.3. *BSEP*, bile salt export pump protein encoded by the ABCB11 gene. (Modified from Kerb R: Implications of genetic polymorphisms in drug transporters for pharmacotherapy, Cancer Lett 234:4–33, 2006.)

subfamilies. Of particular relevance to drug disposition are organic anion–transporting polypeptides (OATPs), organic cation transporters (OCTs), and organic anion transporters (OATs).

The pharmacologically most important ABC transporters (including ABCB1, ABCC1/2, and ABCG2) and SLC transporters (including OATP, OCT, and OAT families), their tissue distributions, and representative drug substrates are summarized in Table 75.3. These transporters play a crucial role in the intestinal absorption, biliary excretion, renal excretion, and tissue/cellular penetration of a wide variety of therapeutic drugs, and therefore they are important determinants of drug exposure in the system and at the site of action (Fig. 75.3). Genetic polymorphisms in transporter genes may influence the expression, subcellular localization, substrate specificity, and intrinsic transport activity of transporter proteins, and consequently may influence the disposition and response of substrate drugs. The sections that follow highlight the functional and clinical significance of the most commonly naturally occurring genetic polymorphisms within the pharmacologically most important ABC and SLC transporters. A comprehensive list of genetic variants in the ABC and SLC transporters and related information are available in Pharmacogenetics Research network databases at http://www.pharmGKB.org.

ATP-BINDING CASSETTE TRANSPORTERS

ABCB1

The *ABCB1* gene, also named as the multidrug resistance 1 *(MDR1)* gene, encodes a polypeptide (P-glycoprotein) that has two halves, each containing six hydrophobic transmembrane domains and an ATP-binding domain. ABCB1 is expressed in the intestinal epithelium, canalicular membrane of hepatocyte, brush border of the renal tubule, pancreatic ductile cell, trophoblast of placenta, capillary endothelial cells of brain and testes, and peripheral blood lymphocytes (see Table 75.3). ABCB1, located on the apical or luminal surface of the epithelial cells, functions as an efflux transporter in restricting intestinal absorption, facilitating hepatobiliary excretion and renal excretion, and protecting the brain and fetus from xenobiotics (see Fig. 75.3). In addition, ABCB1 overexpression in cancer cells is implicated in multidrug resistance to chemotherapeutic agents (Gottesman et al., 2002). ABCB1 transports a broad spectrum of structurally and functionally diverse drugs, including anticancer agents, antibiotics, immunosuppressants, cardiac drugs, calcium channel antagonists, and human immunodeficiency virus (HIV) protease inhibitors (see Table 75.3). Notably, there is a large overlap in substrate specificity and tissue distribution for ABCB1 and CYP3A4/5 (Wacher et al., 1995).

More than 50 SNPs have been identified in the human *ABCB1* coding region. The most common SNPs are the synonymous *1236C>T* and *3435C>T* and the nonsynonymous *2677G>T* (Ala899Ser). The allele frequencies of these three SNPs vary in different ethnic populations (Table 75.4). The *3435C>T* SNP has strong linkage disequilibrium with other SNPs in the *ABCB1* gene, creating common haplotypes consisting of *3435C>T* combined with *2677G>T* and/or *1236C>T*.

Given the important role of ABCB1 in drug absorption and disposition, genetic polymorphisms in the *ABCB1* gene may influence the outcome of pharmacotherapy. The first investigation of the functional and clinical effect of *ABCB1* polymorphism was reported in 2000 for a silent SNP *3435C>T*, which was associated with decreased duodenal expression of ABCB1 and increased digoxin plasma concentration after oral administration in humans (Hoffmeyer et al., 2000). In the past decade, a number of preclinical and clinical studies have been conducted investigating association of the ABCB1 genotype with its tissue expression and function, as well as with the pharmacokinetics and pharmacodynamics of a wide variety of substrate drugs (see Table 75.4) (for a review, see Ieiri et al. [2004]). However, data reported on the functional and clinical impact of ABCB1 polymorphisms are often inconsistent (for reviews, see Ieiri et al. [2004], Marzolini, Paus et al. [2004], Pauli-Magnus & Kroetz [2004], Sakaeda [2005], and Kerb [2006]). The discrepancy could be due to the lack of standardized methodology and assays among different studies. In addition, a particular SNP may often result in a very subtle functional outcome. It has been shown that the 3435C>T SNP affects the timing of cotranslational folding and insertion of ABCB1 into the membrane, thereby altering substrate specificity (Kimchi-Sarfaty et al., 2007). Interestingly, the *1236C>T-2677G>T-3435C>T* haplotype did not result in a change in substrate transport per se but influenced the inhibition of transport by a small subset of modulators (Kimchi-Sarfaty et al, 2007). Furthermore, conflicting results could be attributable to confounding factors from other transporters or metabolizing enzymes given the multiple disposition pathway of the substrate drug. For example, the commonly used in vivo ABCB1 probe drugs (e.g., digoxin, fexofenadine, and talinolol) are the dual substrates for both ABCB1 and OATP transporters; cyclosporine is not only transported by ABCB1 but also metabolized by CYP3A4. Thus the impact of *ABCB1* polymorphisms on the pharmacokinetics of these substrate drugs could be obscured by the activity of OATP or CYP3A4. Hence, a systemic analysis of polymorphisms in multiple genes known or suspected to contribute to drug disposition and response will be essential to better understanding of the genetic impact on pharmacotherapy. In addition, the ABCB1 has multiple polymorphisms, some of which are in linkage disequilibrium, and therefore a haplotype approach would allow a more accurate prediction of clinical phenotypes.

ABCC1 and ABCC2

ABCC1/2, also called *multidrug resistance-related proteins*, play an essential role in transport and excretion of organic anions, including physiologic metabolites, carcinogens, and drugs. They also contribute to multidrug resistance to chemotherapeutic agents (Hinoshita et al., 2000). ABCC1 and ABCC2 have overlapping substrate specificities, typically glutathione, glucuronate, and sulfate conjugated and unconjugated drugs, including many anticancer agents (e.g., vincristine and doxorubicin), HIV protease inhibitors (e.g., ritonavir and saquinavir), and antibiotics (e.g., difloxacin and grepafloxacin) (see Table 75.3). Both ABCC1 and ABCC2 require cotransport of reduced glutathione to transport some of their substrates (Rothnie et al., 2006). ABCC1 is located in basolateral membranes of polarized cells, whereas ABCC2 is located in the apical domain. While ABCC1 is ubiquitously expressed, ABCC2 is mainly expressed in the liver, renal proximal tubules, intestine, and brain (see Table 75.3).

The human *ABCC1* gene appears to be a conserved gene because many of the naturally occurring genetic variants in *ABCC1* are relatively rare.

TABLE 75.4

Most Common Functional Polymorphisms in Human *ABCB1*, *ABCC1/2*, and *ABCG2*: Allele Frequency and Functional Effects

Allele Variants	Polymorphism/Substitution	ALLELE FREQUENCY (%)*			Functional Effects
		Ca	As	Af	
ABCB1					
1236C>T	Silent	34-42	60-72	15-21	Affects cotranslational folding in nearby amino acids that are essential for ATP-binding and ATP hydrolysis (Fung & Gottesman, 2009)
2677G>T/A	A893S/T	38-47/1-10	32-62/3-22	15/ND	Affects ABCB1 expression or function, but data are inconsistent (Marzolini, Paus et al., 2004)
3435C>T	Silent	48-59	37-66	10-27	Affects cotranslational folding in nearby amino acids, thereby altering substrate specificity (Kimchi-Sarfaty et al., 2007)
ABCB1*13	1236C>T/2677G>T/3435C>T haplotype	23-42	28-56	4.5-8.7	Affects the inhibition of ABCB1 by a small subset of modulators (Kimchi-Sarfaty et al., 2007)
ABCC1					
128G>C	C43S		1		Reduced plasma membrane localization, ↓vincristine resistance in transfected cells (Leslie et al., 2003)
1299G>T	R433S	1.4			Changes in transport and resistance (Conrad et al., 2002)
2012G>T	G671V	2.8			Associated with anthracycline-induced cardiotoxicity (Wojnowski et al., 2005)
ABCC2					
1271A>G	R412G				DJS; ↓ in methotrexate elimination (Hulot et al., 2005)
1249G>A	V417I	22-26	13-19	14	Changes in ABCC2 expression and localization (Vogelgesang et al., 2004; Merino et al., 2005; Meyer zu Schwabedissen et al., 2005)
3563T>A	V1188E	4-7	1		Associated with anthracycline-induced cardiotoxicity (Wojnowski et al., 2005)
4544G>A	C1515Y	4-9			Associated with anthracycline-induced cardiotoxicity (Wojnowski et al., 2005)
ABCG2					
34G>A	V12M	2-10	15-18	4-6	Changes in transport and resistance (Mizuarai et al., 2004; Tamura et al., 2007)
376C>T	Q126stop	0	0.9-1.7	0	Loss of transport activity (Tamura et al., 2006)
421C>A	Q141K	9-14	27-35	1-5	Affects the ATP-binding domain, thereby leading to reduced transport activity (Mizuarai et al., 2004; Tamura et al., 2007)

Af, African; *As,* Asian; *ATP,* adenosine-5′-triphosphate; *Ca,* Caucasian; ↑ indicates increased; ↓ indicates decreased.
*Data of allele frequencies are obtained from Marzolini C, Paus E, Buclin T, et al.: Polymorphisms in human MDR1 (P-glycoprotein): recent advances and clinical relevance, *Clin Pharmacol Ther* 75:13–33, 2004; Gradhand U, Kim RB: Pharmacogenomics of MRP transporters (ABCC1-5) and BCRP (ABCG2), *Drug Metab Rev* 40:317–354, 2008.

Of the identified SNPs in the noncoding and coding region of *ABCC1*, 16 are known to result in amino acid changes, and some of them exhibit functional effects on either expression or function of the protein (see Table 75.4) (for a review, see Gradhand & Kim [2008]). However, data regarding the impact of *ABCC1* polymorphisms on in vivo physiology, clinical drug resistance, or toxicity are rather limited. Notably, one study has identified significant associations of *ABCC1 2012G>T* (Gly671Val) and a haplotype of *ABCC2* with anthracycline-induced cardiotoxicity among patients with non-Hodgkin lymphoma treated with doxorubicin (Wojnowski et al., 2005).

Mutations in the *ABCC2* gene have been initially identified in Dubin-Johnson syndrome, a relatively rare recessive disorder characterized by conjugated hyperbilirubinemia resulting from loss of expression and function of ABCC2 in the liver (see Chapter 22). However, the impact of this loss of hepatic ABCC2-mediated transport on the pharmacokinetics of substrate drugs in humans remains to be determined. Among more commonly occurring *ABCC2* SNPs, the most widely studied is *1249G>A* (Val417Ile). The effect of this SNP on ABCC2 expression is different depending on the tissue examined. For example, *1249G>A* was associated with lower *ABCC2* mRNA and protein levels in preterm placenta, but not in duodenum and liver (Meyer zu Schwabedissen et al., 2005; Meier et al., 2006). Of note, a possible association of *1249G>A* variant with tenofovir-induced renal proximal tubulopathy has been demonstrated, suggesting this SNP may influence renal excretion of some ABCC2 substrates (Izzedine et al., 2006). In addition, *1249G>A* has been associated with the change of ABCC2 localization in neuroepithelial tumors (Vogelgesang et al., 2004). A number of other nonsynonymous and synonymous SNPs have been studied for their potential functional influence on ABCC2 expression and transport activity (see Table 75.4). *ABCC2* SNPs appear to have varying effects on different organs or substrates, or between in vitro and in vivo studies (for a review, see Gradhand & Kim [2008]).

ABCG2

The ABCG2 (also known as BCRP) protein is an ATP-binding cassette half-transporter that bears six transmembrane domains and one ATP-binding domain. The protein actively extrudes a wide variety of chemically unrelated hydrophobic or partially hydrophobic compounds from the cells, including cytotoxic compounds (e.g., mitoxantrone, topotecan, SN-38, flavopiridol, and methotrexate), fluorescent dyes (e.g., Hoechst 33342), and toxic compounds found in normal food (e.g., pheophorbide A) (see Table 75.3). ABCG2 is expressed in the canalicular membrane of hepatocytes; in the epithelia of small intestine, colon, placenta, lung, kidney, adrenal glands, and sweat glands; as well as in the endothelia of the central nervous system vasculature. It is responsible for host detoxification and protection against potentially toxic xenobiotics (Jonker et al., 2000, 2002; Krishnamurthy & Schuetz, 2005). ABCG2 transporter–mediated efflux can confer drug resistance and also modulate drug absorption and disposition (Burger & Nooter, 2004; Hirano et al., 2005; Kondo et al., 2005; Merino et al., 2005; Sparreboom et al., 2005).

More than 80 polymorphisms in the *ABCG2* gene have been identified in different ethnic populations (Iida et al., 2002; Imai et al., 2002; Zamber et al., 2003; Ishikawa et al., 2005). Several naturally occurring SNPs in ABCG2 have been found to affect the function and/or expression of its encoded protein (Imai et al., 2002; Mitomo et al., 2003; Kobayashi et al., 2005; Lepper et al., 2005) and therefore may alter the pharmacokinetics and pharmacodynamics of substrate drugs. In particular, a functional SNP in exon 5 of the *ABCG2* gene, in which a C→A nucleotide transition at position 421 (*ABCG2* 421C>A), results in a nonsynonymous variant protein with a glutamine-to-lysine amino acid substitution in codon 141 (Q141K) (Imai et al., 2002). The *ABCG2 421C>A* variant has been associated with low ABCG2 expression levels and altered substrate specificity (Imai et al., 2002) and has been shown to modify the pharmacokinetics of substrate drugs such as diflomotecan and topotecan (Sparreboom et al., 2004, 2005). The clinical relevance of this polymorphism was further exemplified by

more recent findings that cancer patients carrying the *ABCG2 421A* allele, who were treated with the epidermal growth factor receptor (EGFR) tyrosine kinase inhibitor gefitinib, tended to have a greater drug systemic accumulation at the steady-state and higher incidence of gefitinib-induced diarrhea, as compared to patients carrying the wild-type *ABCG2* (Cusatis et al., 2006; Li et al., 2007b).

SOLUTE CARRIER TRANSPORTERS

Organic Anion Transporting Polypeptides (OATPs)

OATPs are membrane influx transporters that facilitate cellular uptake of a wide range of endogenous compounds (e.g., bile salts, hormones, and steroid conjugates) and clinically important drugs (e.g., HMG-CoA-reductase inhibitors, cardiac glycosides, anticancer agents, and antibiotics) (see Table 75.3). Of the 11 human OATP transporters, OATP1A2, OATP1B1, OATP1B3, and OATP2B1 are best characterized for their roles in drug pharmacokinetics. OATP1A2, expressed on the luminal membrane of small-intestinal enterocytes and at the blood-brain barrier, facilitates the intestinal absorption and brain penetration of its substrates. OATP1B1, OATP1B3, and OATP2B1, mainly expressed on the sinusoidal membrane of hepatocytes, facilitate the hepatic uptake of their substrate drugs for metabolism and biliary excretion (Niemi, 2007).

A number of SNPs and other genetic variations have been identified in the *SLCO1B1* gene (encoding OATP1B1), and their allele frequencies vary markedly across different populations (Table 75.5) (for a review, see Meyer zu Schwabedissen & Kim [2009] and Marzolini, Tirona et al. [2004]). Several *SLCO1B1* SNPs and haplotypes have been associated with impaired transport activity in vitro toward different substrates (Tirona et al, 2001; Kameyama et al, 2005; Nozawa et al, 2005). These functionally impaired OATP1B1 variants may limit the uptake of the substrate drugs into the hepatocytes, thereby resulting in decreased biliary excretion or hepatic metabolism and, consequently, increased systemic exposure. For instance, a common variant, *SLCO1B1 521T>C*, has been associated with increased systemic exposure to OATP1B1 substrate drugs, including repaglinide and statins (e.g., pravastatin) (Niemi et al., 2005, 2006) in humans. Genome-wide association studies have identified a noncoding SNP, rs4363657, which is in nearly complete linkage disequilibrium with the *SLCO1B1 521T>C*, to be a strong predictive marker for simvastatin-induced myopathy (Link et al., 2008). *OATP1B1*15* (a haplotype of *388A>G* and *512T>C*) has been linked to increased systemic exposure to pravastatin (Nishizato et al., 2003) and SN-38 (Xiang et al., 2006; Han et al., 2008). *OATP1B1*17* (a haplotype of *–11187G>A*, *388A>G*, and *512T>C*) has been associated with a better pharmacodynamic effect of pravastatin on cholesterol synthesis.

Several nonsynonymous polymorphisms have been identified in the *SLCO1A2* gene (encoding OATP1A2), and some of them demonstrate decreased in vitro transport activity toward OATP1A2 substrates (see Table 75.5) (for a review, see Franke et al. [2009]). However, the impact of these functional SNPs on the pharmacokinetics and clinical outcome of therapeutic drug use remains poorly explored and understood. For OATP1B3 and OATP2B1, there are few data on the clinical relevance of *SLCO1B3* and *SLCO2B1* polymorphisms, although some genetic variations within these two genes have been associated with altered in vitro transport activity of the protein (see Table 75.5) (Nozawa et al., 2002; Letschert et al., 2004; Konig, 2006; Zair et al., 2008).

Organic Cation Transporters

The OCTs belong to the solute carrier SLC22A family that mediate intracellular uptake of a broad range of structurally diverse small organic cations (molecular weight <400). Three isoforms, OCT1, OCT2, and OCT3, with partially overlapping substrate spectrum, are identified in humans (see Table 75.3). OCT1 is primarily expressed in the sinusoidal membrane of hepatocytes; OCT2 is predominantly expressed in the basolateral membrane of kidney proximal tubules; and OCT3 is expressed in many tissues, including placenta, heart, liver, and skeletal muscle (see Table 75.3). The expression of OCTs was also detected in cancer cell lines and tumor tissue samples (Hayer-Zillgen et al., 2002; Zhang et al., 2006).

A number of nonsynonymous SNPs have been identified in the *SLC22A1*gene (encoding OCT1) and *SLC22A2* (encoding OCT2) from different ethnic groups, and some of them have demonstrated altered (mostly impaired) transport function in vitro (see Table 75.5) (Choi & Song, 2008). By contrary, several synonymous SNPs have been identified in the *SLC22A3* gene (encoding OCT3); however, their functional impact remains to be determined. Functional polymorphisms in *OCT* genes could influence the clinical pharmacokinetics and response of substrate drugs, as exemplified by metformin, a drug used as a primary therapy for type 2 diabetes mellitus (Song et al., 2008).

Metformin is not metabolized and is excreted unchanged in the urine. Active tubular secretion in the kidney is the principal route of metformin elimination in humans (Pentikainen et al., 1979). The uptake of metformin from circulation into renal epithelial cells is primarily facilitated by OCT2, which is expressed predominantly at the basolateral membrane in the renal tubules. Renal excretion of metformin from the tubule cell to the lumen is mediated through MATE1 *(SLC47A1)* and MATE2-K *(SLC47A2)*, which are expressed in the apical membrane of the renal proximal tubule cells. OCT1 is also expressed on the apical and subapical domain side of both the proximal and distal tubules in kidney and may play important roles in metformin reabsorption in kidney tubules (Tzvetkov et al., 2009). Studies in humans suggest that genetic variants in OCT1 and OCT2 modulate the renal clearance and pharmacokinetics of metformin. Low-function OCT1 variants R61C, G401S, M420del, and G465R have been associated with significantly higher renal clearance of metformin (Tzvetkov et al., 2009). Genetic variants of *OCT2* (c.596C > T, c.602C> T, and c.808G > T [rs316019]) were associated with an increase in metformin systemic exposure and a decrease in renal clearance, compared with the reference genotype, in healthy Chinese participants (Choi & Song, 2008; Wang et al., 2008). In addition, OCT1, expressed on the basolateral membrane of hepatocytes, plays a key role in mediating the hepatic uptake of metformin. Low-activity *OCT1* alleles, including R61C (rs12208357), G401S (rs34130495), 420del (rs142448543, rs34305973, or rs35191146), and G465R (rs34059508), have been associated with decreased hepatic uptake and, consequently, diminished pharmacodynamic effect of metformin in the liver (i.e., glucose-lowering effect) (Shu et al., 2007; Christensen et al., 2011). However, no validated genetic factors are currently available for the prediction of metformin pharmacokinetics or response. In light of multiple transporters and target proteins involved in the pharmacokinetic and pharmacodynamic pathway of metformin, investigation of gene-gene and gene-environment interactions may provide a better understanding of the interindividual variability in metformin pharmacokinetics and response.

Organic Anion Transporters

The OATs belong to the SLC22 family of solute carriers that mediate cellular uptake of a broad range of structurally diverse small hydrophilic organic anions. OAT substrates include many clinically important anionic drugs, such as β-lactam antibiotics, diuretics, nonsteroidal antiinflammatory drugs, nucleoside/nucleotide antiviral drugs, and anticancer agents (see Table 75.3). There are at least six OAT members (OAT1–6). OAT1–3 localize to the basolateral membrane of the renal proximal tubule mediating the uptake of drug substrates from blood into the proximal tubule cells, and OAT4 localizes to the apical side of the renal proximal tubule functioning in the secretion of drug substrates into urine. Together, these transporters are responsible for the movement of drug substrates from the blood to the urine. Genetic variations in the genes encoding OATs may modify the renal clearance of substrate drugs. A number of polymorphisms have been reported in the coding region and 5′ regulatory region of the human *SLC22A6* (encoding OAT1), *SLC22A7* (encoding OAT2), *SLC22A8* (encoding OAT3), and *SLC22A11* gene (encoding OAT4) (see Table 75.5). Some of these polymorphisms lead to altered transporter activity in vitro (Xu et al., 2005; Bhatnagar et al., 2006). Notably, the coding region polymorphisms in these genes are rare (~1%), whereas the regulatory region polymorphisms of these genes, particularly *SLC22A8* (OAT3), may be important in accounting for variation in the renal clearance of substrate drugs (Bhatnagar et al., 2006). The functional and clinical relevance of these coding and regulatory region polymorphisms remains especially unexplored and understood.

DRUG TARGET PHARMACOGENOMICS

DNA REPAIR GENES

DNA repair is crucial to an organism's ability to maintain its genome integrity and function. Multiple DNA repair pathways exist to cope with a broad range of different DNA lesions or adducts induced by DNA damaging agents or radiation. Major DNA repair pathways include direct repair of alkyl adducts by methylguanine methyl transferase, repair of base damage and single-strand breaks by base excision repair, repair of bulky DNA adducts by nucleotide excision repair, repair of double-strand breaks by homologous recombination and nonhomologous end-joining repair, and repair of mismatches and insertion/deletion loops by DNA mismatch repair (Fig. 75.4).

At least 130 human genes have been identified in DNA repair pathways (Wood et al., 2001). Key genes associated with human DNA repair

TABLE 75.5

Most Common, Naturally Occurring Nonsynonymous SNPs in Genes Encoding Human OATP, OCT, and OAT Transporters: Allele Frequency and Functional Effects

Allele Variant	Polymorphism/Substitution	ALLELE FREQUENCY (%)[a] Ca	As	Af	Functional Effect[b]
OATP					
SLCO1A2 (OATP1A2)					
38T>C	I3T	11.1	0	2.1	↑Transport activity
516A>C	E172D	5.3	0	2.1	↓Transport activity
833A	N278del	0	0	0.6	↓Transport activity
SLCO1B1 (OATP1B1)					
217T>C	F73L	2	0	0	↓Transport activity
388A>G	N130D	30	54	74	↓Transport activity
463C>A	P155T	16	0	2	No alteration
521T>C	V174A	14	0.7	2	↓Transport activity
1463G>C	G488A	0		9	↓Transport activity
2000A>G	E667G	2		34	↓Transport activity
SLCO1B3 (OATP1B3)					
334T>G	S112A	74			Unknown
699G>A	M233I	71			Unknown
1564G>T	G522C	1.9			Affect localization and ↓transport activity
SLCO2B1 (OATP2B1)					
1457C>T	S486F	1.2	30.9		↓Transport activity
OCT					
SLC22A1 (OCT1)					
41C>T	S14F	0	0	3.1	↓Transport of metformin but ↑transport of MPP
480C>G	G160L	0.65	8.6-13	0.5	No alteration
1022C>T	P341L	0	16	8.2	↓Transport of MPP but not metformin
1201G>A	G401S	1.1	0	0.7	↓Transport activity
1222A>G	M408V	60	74-81	74	No alteration
1256delATG	M420del	18	0	2.9	↓Transport of metformin but not MPP
1393G>A	G465R	4	0	0	↓Transport activity
SLC22A2 (OCT2)					
596C>T	T199I	0	1	0	↓Transport activity
602C>T	T201M	0	1.3-2	0	↓Transport activity
808G>T	A270S	16	14-17	11	↓Transport activity
1198C>T	R400C	0	0	1.5	↓Transport activity
1294A>C	K432Q	0	0	1	↓Transport activity
OAT					
SLC22A6 (OAT1)					
20T>C	L7P	1	<1	1	
149G>A	R50H	1	1	1	↑Transport activity
1361G>A	R454Q	0	0	<1	↓Transport activity
SLC22A7 (OAT2)					
329C>T	T110I	1	1	1	Unknown
571G>A	V192I	1	1	1	Unknown
1520G>A	G507D	1	1	1	Unknown
SLC22A8 (OAT3)					
523A>G	I175V	1	1	1	Unknown
829C>T	R277W				↓Transport activity
SLC22A11 (OAT4)					
37G>A	V13M	1	1	1	Unknown
142C>T	R48Ter	1	1	1	Unknown
185C>G	T62R	1	1	1	Unknown
463G>A	V155M	1	1	1	Unknown
732C>T	A244V	1	1	1	Unknown

Continued

TABLE 75.5

Most Common, Naturally Occurring Nonsynonymous SNPs in Genes Encoding Human OATP, OCT, and OAT Transporters: Allele Frequency and Functional Effects_Cont'd

Allele Variant	Polymorphism/Substitution	ALLELE FREQUENCY (%)[a]			Functional Effect[b]
		Ca	As	Af	
832G>A	E278K	1	1	1	Unknown
1015G>A	V339M	1	1	1	Unknown
1175C>T	T392I	1	1	1	Unknown

Af, African; *As,* Asian; *Ca,* Caucasian; *MPP,* 1-methyl-4-phenylpyridinium; *OAT,* organic anion transporter; *OATP,* organic anion transporting polypeptides; *OCT,* organic cation transporter; *SNPs,* single nucleotide polymorphisms; ↑ indicates increased; ↓ indicates decreased.
[a]Allele frequency data are obtained from Xu G, Bhatnagar V, Wen G, et al: Analyses of coding region polymorphisms in apical and basolateral human organic anion transporter (OAT) genes [OAT1 (NKT), OAT2, OAT3, OAT4, URAT (RST)], *Kidney Int* 68:1491–1499, 2005; Kerb R: Implications of genetic polymorphisms in drug transporters for pharmacotherapy, *Cancer Lett* 234:4–33, 2006; Konig J, Seithel A, Gradhand U, et al: Pharmacogenomics of human OATP transporters, *Naunyn Schmiedebergs Arch Pharmacol* 372:432–443, 2006; Choi MK, Song IS: Organic cation transporters and their pharmacokinetic and pharmacodynamic consequences, *Drug Metab Pharmacokinet* 23:243–253, 2008.
[b]Functional effect data are summarized from Marzolini C, Tirona RG, Kim RB: Pharmacogenomics of the OATP and OAT families, *Pharmacogenomics* 5:273–282, 2004b; Zhou F, You G: Molecular insights into the structure-function relationship of organic anion transporters (OATs), *Pharm Res* 24:28–36, 2007; Choi MK, Song IS: Organic cation transporters and their pharmacokinetic and pharmacodynamic consequences, *Drug Metab Pharmacokinet* 23:243–253, 2008; Zair ZM, Eloranta JJ, Stieger B, et al: Pharmacogenetics of OATP (SLC21/SLCO), OAT and OCT (SLC22) and PEPT (SLC15) transporters in the intestine, liver and kidney, *Pharmacogenomics* 9:597–624, 2008; Franke RM, Scherkenbach LA, Sparreboom A: Pharmacogenetics of the organic anion transporting polypeptide 1A2, *Pharmacogenomics* 10:339–344, 2009.

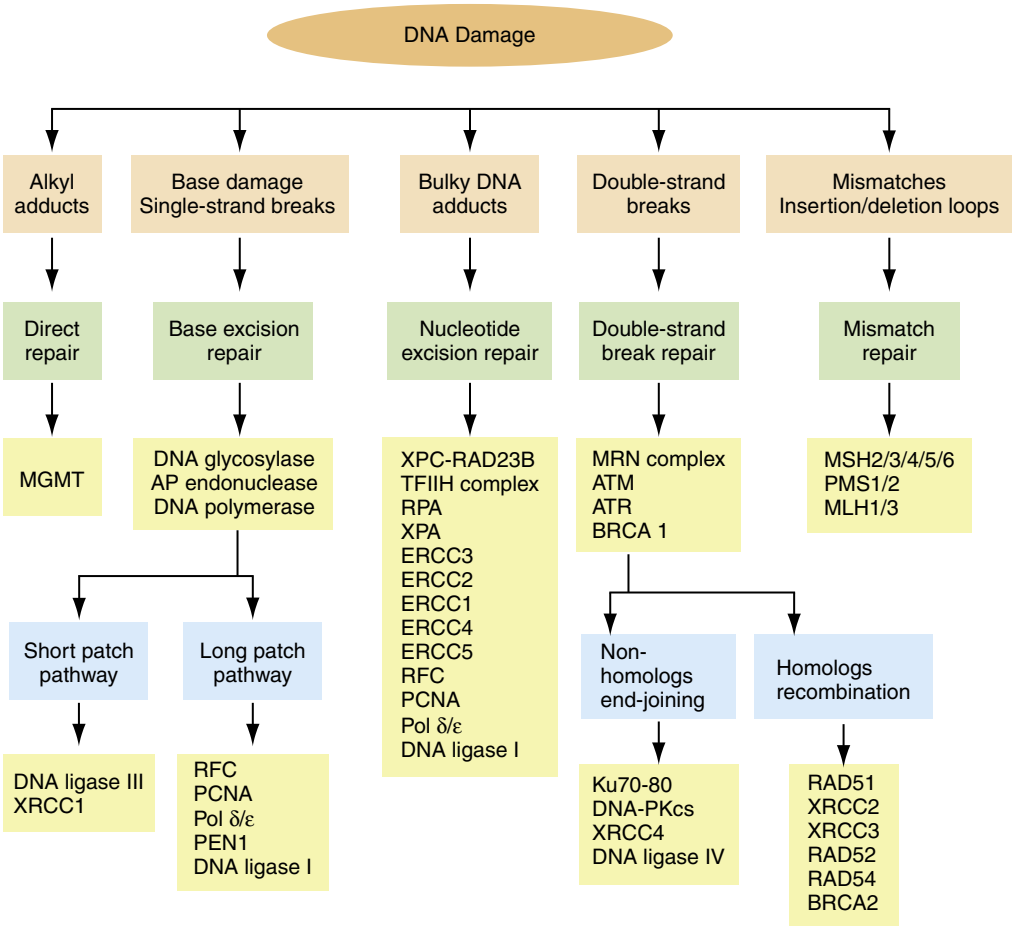

Fig. 75.4 Key players in mammalian DNA repair pathway. *AP,* Apurinic/apyrimidinic; *ATM,* ataxia telangiectasia mutated; *ATR,* ataxia telangiectasia and RAD3 related; *BRCA1/2,* breast cancer 1 and 2, early-onset gene; *DNA-PKcs,* DNA-dependent protein kinase catalytic subunit; *ERCC1/2/3/4/5,* excision repair cross-complementing group genes; *FEN1,* flap structure-specific endonuclease 1; *Ku70-80,* Ku antigen, 70 and 80 KDa subunits (XRCC6 and XRCC5); *MSH2/3/4/5/6,* mutS homolog genes; *PCNA,* proliferating cell nuclear antigen; *PMS1/2,* postmeiotic segregation increased 1 and 2; *Pol δ/ε,* DNA polymerase delta/epsilon; *RAD23B/51/52/54,* homologs of *S. cerevisiae* RAD (recombination protein) genes; *RFC,* replication factor C; *RPA,* replication protein A; *TFIIH,* transcription factor IIH; *XPA,* xeroderma pigmentosum complementation group A gene; *XRCC1/2/3/4,* X-ray repair, cross-complementing genes. (Modified from Gossage L, Madhusudan S: Cancer pharmacogenomics: role of DNA repair genetic polymorphisms in individualizing cancer therapy, Mol Diagn Ther 11:361–380, 2007.)

are listed in Fig. 75.4. Among these, apurinic endonuclease 1 *(APEX1);* x-ray repair cross-complementing group 1 *(XRCC1);* excision repair cross-complementing enzyme group 1 *(ERCC1);* excision repair cross-complementing rodent repair group 2 *(ERCC2);* breast cancer 1, early onset *(BRCA1);* and x-ray repair cross-complementing protein 3 *(XRCC3)* are the most widely reported DNA repair genes for which genetic polymorphisms have been associated with the therapeutic response (efficacy or toxicity) to chemotherapy or radiotherapy (Table 75.6) (for a review, see Gossage & Madhusudan [2007]).

Chemotherapy and radiotherapy are designed to induce DNA damage, thus causing cell cycle arrest and cell death. The efficacy of DNA damage–based cancer therapy can be compromised by DNA repair mechanisms that operate in cancer cells to recognize and rectify DNA damage. On the other hand, DNA repair activity may affect normal tissue tolerance to DNA damaging agents or radiation. Inefficient DNA repair in normal cells would result in inefficient removal of damaged DNA, thus leading to accumulation of DNA damage within normal tissues and increased normal tissue toxicity. Genetic variations within the DNA repair genes may modify the activities of DNA repair pathways within both cancer cells and normal cells, thereby influencing therapeutic resistance and normal tissue tolerance to chemotherapy and radiotherapy (see Table 75.6). Specifically, low-function variants that cause insufficient DNA repair may enhance the cytotoxic effect in cancer cells, thus reducing normal cell tolerance. However, data reported on the functional and clinical impact of genetic variants of DNA repair genes are not always consistent and are even contradictory in some instances (for a review, see Gossage & Madhusudan [2007]). The discrepancies could be due to (1) heterogeneity in study settings (e.g., different tumor types or stages, different treatment regimens, or different patient populations); (2) the presence of other untested SNPs that confound the data interpretation; and (3) small sample size. Large prospective clinical trials are needed to systematically assess the combined impact of multiple polymorphisms involved in several relevant DNA repair pathways on treatment outcome.

TABLE 75.6

Most Widely Reported DNA Repair Gene Polymorphisms That Have Demonstrated Associations With the Response (Efficacy and Toxicity) to Chemotherapy or Radiotherapy

DNA Repair Pathway/Gene	Gene Functions	SNP(s)	Association with Efficacy	Association with Toxicity
Base Excision Repair (BER)				
Apurinic endonuclease 1 *(APEX1)*	APEX1 is a critical protein involved in BER that hydrolyzes the phosphodiester backbone immediately 5′ to an apurinic/apyrimidinic (AP) site following removal of the damage base by a DNA glycosylase.	Asp148Glu (most common SNP of APEX1)	↓Overall survival for 148Glu/Glu homozygotes in pancreatic cancer (Cx/RT/Both) (Li et al., 2007a)	↓Risk for acute skin reactions for 148Glu allele in normal-weight breast cancer patients (adjuvant RT) (Chang-Claude et al., 2005)
X-ray repair cross-complementing group 1 *(XRCC1)*	XRCC1 interacts with DNA ligase III, polymerase beta, and poly (ADP-ribose) polymerase, and seals the remaining nick in DNA after DNA Pol β performs its one-nucleotide gap-filling reaction. XRCC1 is involved in the efficient repair of DNA single-strand breaks.	Arg194Trp	↑Response rate for 194Trp variants in advanced NSCLC (platinum Cx) (Wang et al., 2004) ↑Survival for 194Trp/Trp homozygotes in pancreatic cancer (Cx/RT/Both) (Li et al., 2007a)	↑Risk for hematologic toxicity for 194Arg/Arg homozygotes in NSCLC (gemcitabine and docetaxel Cx) (Petty et al., 2007) ↑Risk for early/late adverse reaction for 194Trp allele in breast cancer (adjuvant RT) (Moullan et al., 2003) ↓Risk for late reactions for 194Trp allele in cervical or endometrial cancer (RT) (De Ruyck et al., 2005)
		Arg399Gln	↑Response rate and ↑survival for 399Arg/Arg homozygotes in mCRC (FOLFOX), advanced NSCLC (platinum Cx), and esophageal (platinum Cx, RT, and surgery) (Stoehlmacher et al., 2001; Gurubhagavatula et al., 2004; Wu et al., 2006) ↓Breast cancer–free survival and progression-free survival for Gln399 variant allele in metastatic breast cancer (high-dose Cx and stem-cell transplantation) (Bewick et al., 2006)	↓Risk for acute skin reactions for 399Glu allele in normal-weight breast cancer patients (adjuvant RT) (Chang-Claude et al., 2005) ↑Risk for late skin toxicity for 399Arg/Arg homozygotes in breast cancer (adjuvant RT) (Andreassen et al., 2003)
Nucleotide Excision Repair *(NER)*				
Excision repair cross-complementing rodent repair group 2 *(ERCC2)*	ERCC2 is an ATP-dependent 5′-3′ DNA helicase, and a component of the core-TFIIH basal transcription factor. It is involved in NER by opening DNA in the 5′ to 3′ direction around the damage.	Asp312Asn	↓Survival for 312Asn variant allele in advanced NSCLC (platinum) (Gurubhagavatula et al., 2004) No association with response in advanced NSCLC (platinum) (Camps et al., 2003)	
		Lys751Gln	751Lys/Lys homozygotes more likely to relapse in stage 3 and 4 gastric cancer (surgery and chemoradiation) (Zarate et al., 2006) ↑Response rate and median survival for 751Lys/Lys homozygotes in mCRC (FOLFOX) (Park et al., 2001) ↑Disease-free and 1-year survival for 751Lys/Lys homozygotes in AML (Cx) (Allan et al., 2004) No association with response in advanced NSCLC (platinum Cx) (de las Penas et al., 2006)	ERCC2 genotype/haplotype associated with GI, GU, and liver toxicities in AML (daunorubicin and cytosine arabinoside Cx) (Kuptsova et al., 2007) ↓Risk for neutropenia for 751Gln/Gln homozygotes in NSCLC (gemcitabine and docetaxel Cx) (Petty et al., 2007)
Excision repair cross-complementing enzyme group 1 *(ERCC1)*	ERCC1 is a two-domained, non-catalytic protein that associates with ERCC4 (XPF) endonuclease to form an ERCC1-XPF heterodimer, whose role is to cleave DNA 5′ to the lesion. ERCC1-XPF is the last factor to join the mammalian NER incision complex and is also known to be involved in recombinational DNA repair and in the repair of interstrand cross-links.	19007T>C	↑Response rate or ↑survival for 19007C/C homozygotes for advanced NSCLC (platinum or cisplatin/docetaxel Cx) and mCRC (FOLFOX) (Isla et al., 2004; Ryu et al., 2004; Park et al., 2003) ↑Prognosis for 19007T/T homozygotes for CRC (adjuvant FU based) (Moreno et al., 2006) ↓Risk for platinum resistance in 19007T/C and T/T genotypes for ovarian cancer (Kang et al., 2006)	
		8092C>A	↑Survival in 8092C/C homozygotes for NSCLC (platinum Cx) (Zhou et al., 2004)	↑Risk for GI toxicity for 8092A allele in NSCLC (platinum Cx) (Suk et al., 2005) ↓Risk for metabolic toxicity for 8092C/A heterozygotes and ↓risk for lung toxicity for 8092A/A homozygotes in AML (daunorubicin and cytosine arabinoside Cx) (Kuptsova et al., 2007)

Continued

TABLE 75.6

Most Widely Reported DNA Repair Gene Polymorphisms That Have Demonstrated Associations With the Response (Efficacy and Toxicity) to Chemotherapy or Radiotherapy_Cont'd

DNA Repair Pathway/Gene	Gene Functions	SNP(s)	Association with Efficacy	Association with Toxicity
Double-Strand Break (DSB) Repair				
Breast cancer 1, early onset *(BRCA1)*	BRCA1 is a nuclear phosphoprotein that plays a role in maintaining genomic stability, and it also acts as a tumor suppressor. BRCA1 is associated with other tumor suppressors, DNA damage sensors, and signal transducers to form a large multisubunit protein complex known as the *BRCA1-associated genome surveillance complex (BASC).* It plays a role in transcription, DNA repair of double-stranded breaks, and recombination.	BRCA1 mutations	↑Clinical and pathologic complete response for BRCA1 mutation in breast cancer (anthracycline-based Cx) (Chappuis et al., 2002) ↑Response rate for BRCA heterozygotes in ovarian cancer (platinum-based Cx) (Cass et al., 2003)	
X-ray repair cross-complementing protein 3 *(XRCC3)*	XRCC3 participates in homologous recombination to maintain chromosome stability and repair DNA damage. It is involved in DSB repair, and functionally complements Chinese hamster irs1SF, a repair-deficient mutant that exhibits hypersensitivity to a number of different DNA-damaging agents.	Thr241Met	↑Time to treatment failure for 241Met variant genotype in multiple myeloma (autologous bone marrow transplantation) (Vangsted et al., 2007) ↑Survival for 241Met/Met homozygotes in advanced NSCLC (platinum Cx) (de las Penas et al., 2006) ↓Survival for 241Met variant genotype in breast cancer (high-dose Cx and stem cell transplantation) (Bewick et al., 2006) No association in advanced gastric cancer (platinum Cx) (Ruzzo et al., 2006)	↓Risk for 214Met variant in AML (daunorubicin and cytosine arabinoside Cx) (Kuptsova et al., 2007) ↑Risk for late skin toxicity for 241Thr/Thr homozygotes in breast cancer (adjuvant RT) (Andreassen et al., 2003)

AML, acute myeloid leukemia; *CRC,* colorectal cancer; *Cx,* chemotherapy; *FOLFOX,* fluorouracil/oxaliplatin chemotherapy; *FU,* fluorouracil; *GI,* gastrointestinal; *GU,* genitourinary; *mCRC,* metastatic colorectal cancer; *NSCLC,* non–small cell lung cancer; *RT,* radiotherapy; *SNPs,* single nucleotide polymorphisms; ↑ indicates increased; ↓ indicates decreased.

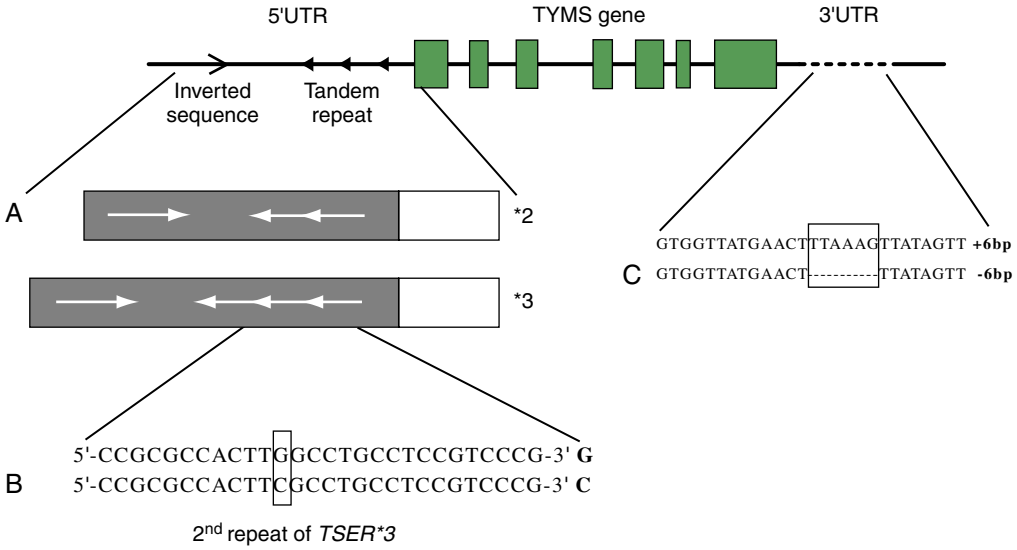

Fig. 75.5 Three functional genetic polymorphisms in the 5′ and 3′ untranslated regions (5′UTR and 3′UTR) of the thymidylate synthase *(TS)* gene, including the following: **A,** polymorphic tandem repeat of a 28-bp sequence that is present in either duplicate (2R) or in triplicate (3R) in the TS promoter enhancer region (TSER 2R>3R polymorphism); **B,** a G to C SNP within the second repeat when three repeats are present (TSER 3R G>C SNP); **C,** a 6-bp deletion in the 3′UTR of the *TS* gene (TS 1494del6bp). (Adapted from Marsh S: Thymidylate synthase pharmacogenetics, Invest New Drugs 23:533–537, 2005.)

THYMIDYLATE SYNTHASE

Thymidylate synthase (TS) catalyzes the conversion of deoxyuridylate (dUMP) and 5,10-methylenetetrahydrofolate to deoxythymidine monophosphate (dTMP) and 7,8-dihydrofolate. This reaction is the sole de novo biosynthesis of thymine in DNA. Given the essential role of TS in DNA synthesis, inhibition of TS by drugs such as 5-fluorouracil (5-FU) and capecitabine (orally bioavailable 5-FU prodrug) represents an efficacious treatment for a variety of human cancers (Danenberg, 1977). 5-FU is the mainstay of therapeutic regimens for treating colorectal cancer and other human malignancies. However, there is a large interindividual variability in the clinical outcome (efficacy and toxicity) of 5-FU–based chemotherapy.

There is substantial evidence that intratumoral TS expression (either mRNA or protein) is inversely associated with clinical benefit from 5-FU–based chemotherapy regimens (Johnston et al., 1995; Leichman et al., 1997; Aschele et al., 1999; Salonga et al., 2000). This association was validated by a meta-analysis of 887 patients with metastatic colorectal cancer and 2610 patients with localized colorectal cancer, which indicates that patients with high TS tumor levels have poorer overall survival compared with those with low TS tumor levels (Popat et al., 2004).

TS expression is modulated by three functionally significant germline polymorphisms in the 5′ and 3′ untranslated regions (5′UTR and 3′UTR) of the *TS* gene. These include a polymorphic tandem repeat of a 28–base pair (bp) sequence that is present in either duplicate (2R) or in triplicate (3R) in the *TS* promoter enhancer region (TSER 2R>3R polymorphism), a SNP (G>C) in the second repeat when three repeats are present (TSER 3R G>C SNP), and a 6-bp deletion in the 3′UTR of the *TS* gene (*TS* 1494del6bp) (Fig. 75.5). The 28-bp TSER tandem repeats contain elements that bind upstream stimulating factor and therefore act to enhance transcriptional activity of the *TS* gene. Patients with metastatic colorectal

cancer homozygous for the triple repeat (TSER 3R/3R) exhibit significantly higher intratumoral *TS* gene expression (Kawakami et al., 1999; Pullarkat et al., 2001). On the contrary, the presence of a G>C SNP within the second repeat of the 3R allele leads to decreased transcriptional activity by abolishing the binding of upstream stimulating factor within the repeat (Mandola et al., 2003). The 6-bp deletion in the 3′UTR of the *TS* gene is linked to decreased TS mRNA stability and lower intratumoral TS mRNA level in patients (Mandola et al., 2004). Of note, the allele frequencies of these polymorphisms vary among different ethnic populations (Table 75.7) (Marsh, 2005).

Genetic polymorphisms of the *TS* gene are not only the prognostic factor for disease-free survival and overall survival, but also the predictor of clinical benefit from 5-FU–based chemotherapy (for a review, see Lurje et al. [2009]). Most studies have consistently agreed that colorectal cancer patients carrying high-expression *TS* alleles (i.e., TSER-2R/3G, –3C/3G, –3G/3G, 3′-UTR +6bp/+6bp) generally have a poorer prognosis and worse clinical outcome to 5-FU–based chemotherapy, as compared with those carrying low-expression *TS* alleles (i.e., TSER-2R/2R, –2R/3C, –3C/3C, 3′-UTR +6bp/-6bp, -6bp/-bp) (for a review, see Lurje et al. [2009]).

TABLE 75.7

Functional Polymorphisms of the Thymidylate Synthase (TS) Gene

Polymorphism	ALLELE FREQUENCY Ca	As	Af	Functional Effect[a]
TSER 2R>3R repeat	52-69	62-82	52	↑TS mRNA for 3R allele
TSER 3R G>C SNP	56	37	28	↓Transcriptional activity of TS for C allele
TS 1494del6b	27-29			↓Stability of TS mRNA for –6-bp deletion

Af, African; *As,* Asian; *Ca,* Caucasian; *mRNA,* messenger ribonucleic acid; *TSER,* TS promoter enhancer region; ↑ indicates increased; ↓ indicates decreased.
[a]Summarized from Marsh S: Thymidylate synthase pharmacogenetics, *Invest New Drugs* 23:533–537, 2005; Lurje G, Manegold PC, Ning Y, et al: Thymidylate synthase gene variations: predictive and prognostic markers, *Mol Cancer Ther* 8:1000–1007, 2009.

EPIDERMAL GROWTH FACTOR RECEPTOR

EGFR activation plays a key role in cell proliferation and tumor growth, with effects on tumor cell motility, adhesion, invasion, survival, and angiogenesis (Woodburn, 1999; Raymond et al., 2000). EGFR is a transmembrane cell surface receptor tyrosine kinase that is found in the majority of epithelial tissues. Upon binding of the extracellular ligand (e.g., epidermal growth factor or transforming growth factor-α), the EGFR dimerizes, either homodimerizing with another EGFR or heterodimerizing with other members of the human EGFR family, leading to the activation of cytoplasmic tyrosine kinase (TK) activity (see Chapter 77, Fig. 77.2). The activation of receptor TK leads to the autophosphorylation of the intracellular domain of EGFR, resulting in the activation of downstream signaling pathways (e.g., Ras/mitogen-activated protein kinase pathway and the PI3K/Akt pathway and Janus-activated kinase signal transducers and activator of transcription) that are involved in tumor growth and metastasis. Receptor dimerization and signal transduction pathways are discussed further in Chapter 77. The reversible EGFR TK inhibitors, such as gefitinib and erlotinib, target the adenosine-5′-triphosphate (ATP) cleft within the EGFR-TK to prevent autophosphorylation of the receptor, thus inhibiting tumor growth and metastasis (Anderson et al., 2001; Ciardiello et al., 2001). Treatment with gefitinib or erlotinib results in dramatic clinical response in ~10% to 30% of patients with non–small cell lung cancer (NSCLC) depending on ethnic origin, sex, and smoking history (Fukuoka et al., 2003; Kris et al., 2003; Shepherd et al., 2005; Thatcher et al., 2005). There is solid evidence that certain somatic mutations of the *EGFR* gene confer sensitivity or resistance to EGFR TK inhibitors (for reviews, see Kumar et al. [2008] and Gazdar [2009]).

Somatic *EGFR*–activating mutations are found in the first four exons (18–21) of the TK domain (Fig. 75.6) (Lynch et al., 2004; Paez et al., 2004; Pao et al., 2004). These mutations fall into three broad classes. Class I mutations are in-frame deletions in exon 19 that almost always include amino acid residues leucine-747 to glutamic acid-749 (ΔLRE) and

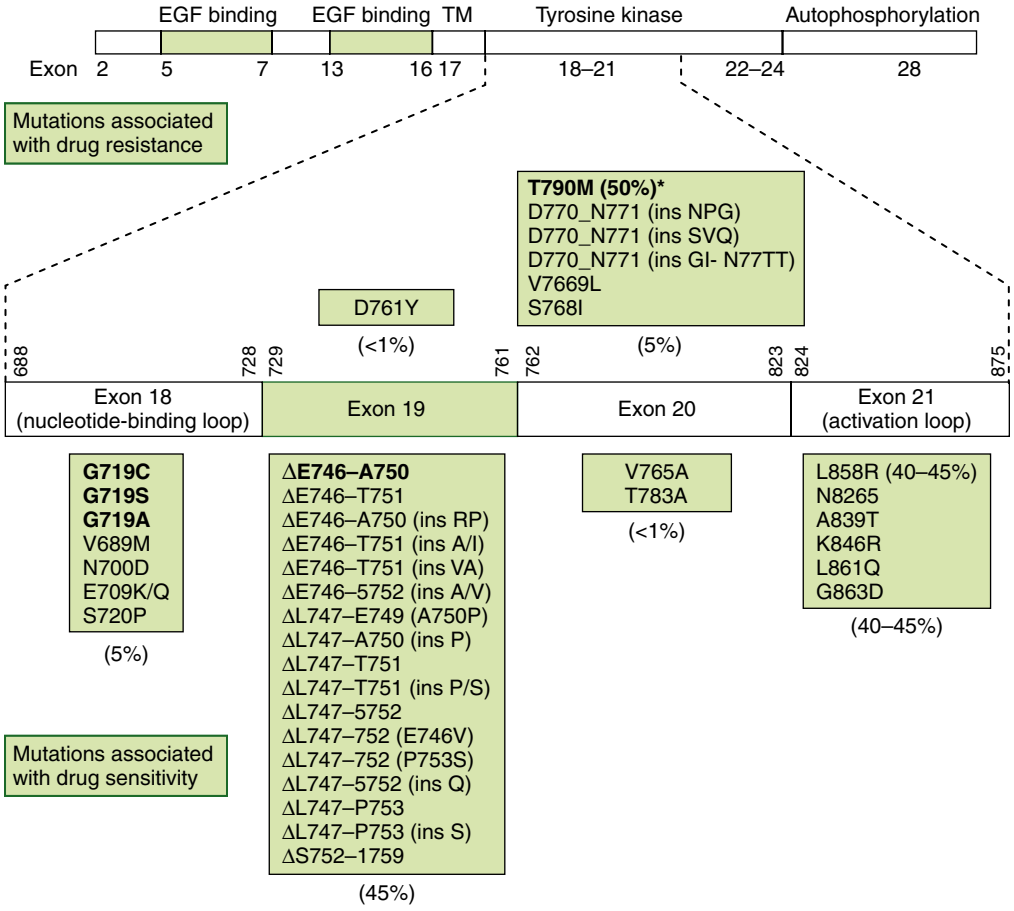

Fig. 75.6 Schematic presentation of the epidermal growth factor receptor (EGFR) tyrosine kinase (TK) domain mutations as important determinants of sensitivity or resistance to EGFR TK inhibitors. The most prevalent activating EGFR kinase domain mutations in non–small cell lung cancer (NSCLC) include in-frame deletions in exon 19 (accounting for 45% of EGFR mutations), an L858R substitution in exon 21 (accounting for 40–45% of EGFR mutations), nucleotide substitutions in exon 18 (e.g., G719C or G719S) (5%), and in-frame insertions in exon 20 (<1%). The most noteworthy clinically relevant mutations associated with resistance to EGFR TK inhibitors include T790M in exon 20, and D761Y, a T790M-like secondary mutation in exon 19. The main mutations in each class are shown in bold type. (Adapted from Sharma SV, Bell DW, Settleman J, et al.: Epidermal growth factor receptor mutations in lung cancer, Nat Rev Cancer 7:169–181, 2007.)

account for approximately 44% of all EGFR TK–activating mutations. Class II mutations are single nucleotide substitutions that cause an amino acid alteration. The most prevalent single-point mutation is L858R (an arginine changed to leucine at codon 858) in exon 21, accounting for about 41% of all EGFR TK–activating mutations; other class II mutations include G719 (a glycine changed to serine, alanine, or cysteine) in exon 18 (4% of all EGFR TK–activating mutations) and other missense mutations. Class III mutations are in-frame duplications and/or insertions in exon 20, accounting for about 5% of EGFR TK–activating mutations. Overall, the frequency of EGFR TK–activating mutations is 5% to 20%, occurring more commonly in East Asians, women, never smokers, and patients with adenocarcinoma (Janne & Johnson, 2006). This mirrors the clinically defined subsets of patients who were most likely to respond to EGFR TK inhibitors. NSCLC patients whose tumors present with EGFR TK–activating mutations show better overall response, longer progression-free survival, and overall survival after chronic gefitinib or erlotinib treatment, as compared to those without these activating mutations (Gazdar, 2009).

Acquired resistance occurs in virtually all NSCLC tumors that initially respond to EGFR TK inhibitors. The emergence of acquired resistance is conferred by a second point mutation in the TK domain. The most noteworthy, clinically relevant mutation T790M in exon 20 is detected in 50% of cases as a second site mutation rendering acquired resistance to EGFR TK inhibitors (Sharma et al., 2007). It is proposed that the T790M mutation affects the gatekeeper residue in the catalytic domain of the TK that weakens the interaction of the inhibitor with its target (Blencke et al., 2004). In addition, D761Y, a T790M-like secondary mutation in exon 19, was also associated with resistance to gefitinib and erlotinib in NSCLC cells that contain the L858R-EGFR mutation (Balak et al., 2006).

In summary, somatic mutations in the EGFR kinase domain are important determinants of sensitivity and resistance to EGFR TK inhibitors. EGFR mutation testing is currently implemented into routine clinical practice for personalized therapy of NSCLC patients.

HUMAN LEUKOCYTE ANTIGEN PHARMACOGENOMICS

The HLA gene family is the locus of genes that reside on chromosome 6 and encode cell-surface antigen-presenting proteins responsible for regulation of the immune system in humans (Rudolph et al., 2006). The *HLA* genes belong to the family of major histocompatibility complex (MHC) genes, which are classified as HLA class I complex (consisting the *HLA-A*, *HLA-B*, and *HLA-C* genes) and HLA class II complex (consisting of the *HLA-DP*, *HLA-DQ*, and *HLA-DR* genes). HLA molecules encoded by the HLA genes bind endogenous and exogenous peptides that result from the breakdown of self-cells or foreign proteins and present these bound peptide antigens to T cells, thereby eliciting an adaptive immune response. HLA class I molecules present peptides derived from proteins inside the cells to killer T cells (also called CD8-positive or cytotoxic T cells), whereas HLA class II molecules present antigens encountered outside of the cells to T-helper cells (referred to as CD4-positive T cells) (Parham & Ohta, 1996).

The HLA molecules play an important role in type B adverse drug reactions (ADRs), which accounts for ~15% of ADRs and are referred to as unpredictable, dose-independent, idiosyncratic, drug-induced hypersensitivity reactions. Type B reactions can be severe cutaneous adverse reactions (e.g., Stevens-Johnson syndrome [SJS], toxic epidermal necrolysis [TEN]), drug-induced hypersensitivity syndrome (referred to as drug reaction with eosinophilia and systemic symptoms), or single-organ drug hypersensitivity syndrome (e.g., drug-induced liver injury, pancreatitis, and tubulointerstitial nephritis). There are mainly three hypotheses to explain how T-cell receptors and HLA interact with drugs and peptides, leading to an immune response and type B ADRs. These include the hapten hypothesis, p-i concept, and altered repertoire model (Pavlos et al., 2012). The hapten hypothesis is based on the ability of a drug or metabolite to act as a hapten that covalently binds to endogenous proteins or MHC-bound peptides. These haptenated peptides or proteins are then presented on HLA molecules and recognized by T cells, thereby leading to HLA-restricted T-cell activation. Reexposure of sensitized individuals will result in proliferation of memory T cells and an inflammatory response within 24 to 72 hours. A representative example is penicillin derivatives that bind covalently to the lysine residue of serum albumin, eliciting penicillin allergy (Padovan et al., 1997). The p-i concept (direct pharmacologic interaction of a drug with immune receptors) proposed that drugs are capable of activating T-cell immune response by directly and noncovalently binding to T-cell receptors or forming HLA-drug complexes without the requirement for a specific peptide ligand. For example, carbamazepine interacts directly with HLA-B*15:02 to elicit cytotoxic T-cell activation without formation of drug-modified peptide (Wei et al., 2012). The altered repertoire model proposes that steric complementarity and noncovalent interactions between a drug molecule and the HLA antigen-binding cleft can modify the shape and chemistry of the antigen-binding cleft, thus leading to an altered repertoire of self-peptide presented to T cells and T-cell activation. It has been demonstrated that the altered repertoire model is a mechanism underlying abacavir-induced hypersensitivity syndrome (Illing et al., 2012; Norcross et al., 2012; Ostrov et al., 2012), and it is also one important mechanism involved in the pathogenesis of carbamazepine-induced severe cutaneous adverse reactions (Ko et al., 2011; Illing et al., 2012; Wei et al., 2012).

Because HLA proteins present a wide variety of peptides for immune recognition, the *HLA* genes are among the most highly polymorphic genes in the human genome. Currently, there are more than 3000 identified *HLA-A* alleles and more than 4000 identified *HLA-B* alleles (Phillips et al., 2018). There is substantial evidence linking specific HLA genetic alleles to drug-induced hypersensitivity reactions. To date, the best characterized HLA-associated drug-induced hypersensitivity reactions are for abacavir, carbamazepine, allopurinol, and nevirapine.

Abacavir, a potent nucleoside reverse transcriptase inhibitor, is indicated for the treatment of HIV infection. Abacavir hypersensitivity syndrome, which is characterized by skin rash, fever, gastrointestinal symptoms, and internal organ involvement, occurs in approximately 5% to 8% of patients during the first 6 weeks of treatment (Cutrell et al., 2004). Though it may be relatively mild initially and alleviated by withdrawal of the drug, a subsequent rechallenging can result in life-threatening reactions (Shapiro et al., 2001). There is substantial evidence linking the presence of *HLA-B*57:01* and abacavir hypersensitivity. In 2002, two groups independently reported the initial association between *HLA-B*57:01* and abacavir hypersensitivity syndrome in Australian and British populations (Hetherington et al., 2002; Mallal et al., 2002). The association between *HLA-B*57:01* and abacavir hypersensitivity was further confirmed in a randomized, double-blind controlled study enrolling ~2000 patients, which demonstrated the 100% negative-predictive value of *HLA-B*57:01* for abacavir hypersensitivity syndrome (Mallal et al., 2008). Notably, abacavir hypersensitivity occurs at a high frequency in Caucasians and at a low frequency in Asian and African American populations. This is consistent with the highest prevalence of *HLA-B*57:01* in Caucasians (5–8%) as compared to Asians and African Americans (2.4%) (Cao et al., 2001). Based on the strong evidence for the high risk of *HLA-B*57:01*–associated abacavir hypersensitivity, the FDA recommended that all patients should be screened for *HLA-B*57:01* alleles prior to the initiation of abacavir treatment (including those who had previously tolerated this drug and were being retreated) and that abacavir should be avoided in carriers of *HLA-B*57:01*. The screening significantly reduces the incidence of abacavir hypersensitivity reactions and is cost effective (Hughes et al., 2004; Mallal et al., 2008; Schackman et al., 2008).

Carbamazepine (CBZ), an aromatic amine anticonvulsant, is used for the treatment of epilepsy, trigeminal neuralgia, and bipolar disorder. CBZ-related drug reactions with eosinophilia and systemic symptoms (DRESS), which usually occurs 2 to 8 weeks after the initiation of the drug, presents as fever, rash, internal organ involvement, and lymphadenopathy. In addition, approximately 10% of patients develop mild-to-moderate cutaneous adverse drug reactions without internal organ involvement or fever, which is referred to as *maculopapular eruption*. CBZ-induced severe cutaneous adverse reactions (i.e., SJS and TEN) occur with an incidence rate of ~0.2/10,000 in the United States and ~5.9/10,000 in Taiwan (China).

There is evidence linking the *HLA-B*15:02* genotype with the risk of CBZ-induced SJS/TEN and linking the *HLA-A*31:01* genotype with CBZ-induced SJS/TEN, DRESS, and maculopapular eruption (MPE). These two alleles have distinct ethnic and geographic distributions. The *HLA-B*15:02* has the highest frequency in East Asian (6.9%), Oceania (5.4%), and South/Central Asian (4.6%) population, a lower frequency in Japanese (<1%) and Korean (<2.5%) population, and this allele is very rare in other ethnic populations. In contrast, the frequency of the *HLA-A*31:01* allele is more common in Caucasians (3%) and Hispanic/South Americans (6%), Japanese (8%), South Koreans (5%), and South/Central Asians (2%) (Phillips et al., 2018).

Consistent with the ethnic and geographic distribution of the *HLA-B*15:02* allele, the *HLA-B*15:02* has been strongly associated with CBZ-induced SJS/TEN in Chinese and other Southeast Asian populations (including Thai, Malaysian, Indian, Vietnamese, and Cambodian) (Chung et al., 2004; Mehta et al., 2009; Tassaneeyakul et al., 2010; Then et al., 2011; Kulkantrakorn et al., 2012). However, the *HLA-B*15:02* allele has not been observed in cases of CBZ-induced SJS/TEN in Japanese and Korean

populations or non-Asian descendants in Europe or North America (Lonjou et al., 2006). Based on the strong evidence linking *HLA-B*15:02* to CBZ-induced SJS/TEN, the FDA recommended that genetic screening of *HLA-B*15:02* should be performed prior to initiating CBZ in patients with Asian ancestry and that carriers of this allele should not be treated with CBZ unless the benefit clearly outweighs the risk (Phillips et al., 2018).

Unlike *HLA-B*15:02*, the *HLA-A*31:01* allele has been identified as the important genetic determinant for all types of CBZ-induced hypersensitivity reactions, including drug-induced hypersensitivity syndrome, MPE, and SJS/TEN across different ethnic populations (e.g., Chinese, Japanese, Koreans, and Europeans) (Hung et al., 2006; Kim et al., 2011; McCormack et al., 2011; Ozeki et al., 2011; Genin et al., 2014). The US Clinical Pharmacogenetics Implementation Consortium (CPIC) recommends that if a patient is CBZ-naïve and *HLA-A*31:01* positive, CBZ should be avoided due to the greater risk of SJS/TEN, DRESS, and MPE. If a CBZ-naïve patient is *HLA-B*15:02* positive, CBZ should be avoided regardless of the *HLA-A*31:01* genotype (Phillips et al., 2018).

Allopurinol, a xanthine oxidase inhibitor, has been used for decades to lower serum urate levels in patients with gout. The greatest safety concern with allopurinol is an estimated 0.1% to 0.4% risk of allopurinol hypersensitivity syndrome or SCAR, which is manifested by SJS, TEN, or drug reaction with eosinophilia and systemic symptoms (Hetherington et al., 2002). There is substantial evidence linking *HLA-B*58:01* genotype to allopurinol hypersensitivity syndrome. This association was first identified in the Chinese population (Chan & Tan, 1989; Hung et al., 2005), and later confirmed in other Asian ethnic groups, including Japanese, Thai, and Koreans (Dainichi et al., 2007; Kaniwa et al., 2008; Tassaneeyakul et al., 2009; Kang et al., 2011; Somkrua et al., 2011). A meta-analysis that consolidated all the published studies provided the odds ratios for allopurinol-induced SCAR in *HLA-B*58:01* carriers as 73 and 165 as compared to healthy controls and allopurinol-tolerant controls, respectively (Zineh et al., 2011). Notably, the association between *HLA-B*58:01* and allopurinol-induced SCAR is weaker in Caucasians than in Asians, which could be explained by the lower allele frequency of *HLA-B*58:01* in Caucasians (<6%) as compared to Asians (~15%) as well as other yet unknown risk factors. In addition to SJS/TEN, allopurinol also causes a mild cutaneous adverse reaction, maculopapular eruption, with an incidence rate of 2% to 3% (Hetherington et al., 2002). A strong association between *HLA-B*58:01* and allopurinol-induced maculopapular eruption has been found in the Chinese population (Cao et al., 2012). Based on the strong association of the *HLA-B*58:01* allele with allopurinol hypersensitivity reactions, the American College of Rheumatology's new guidelines on gout recommend genetic testing for *HLA-B*58:01* before initiating allopurinol treatment, especially in patients with Asian ancestry (Khanna et al., 2012). The CPIC recommends that allopurinol should not be prescribed to patients who have tested positive for *HLA-B*58:01* (Hershfield et al., 2013).

Nevirapine (NVP) is a nonnucleoside reverse transcriptase inhibitor that is used in combination with other drugs for the treatment of HIV infection. NVP-related hypersensitivity reactions, characterized by a combination of rash, fever, and/or hepatitis, occur in ~5% of patients initiating NVP treatment within the first 6 weeks and become more severe with NVP rechallenge (Pollard et al., 1998; Gangar et al., 2000). NVP hypersensitivity reactions have been associated with different class I and class II HLA alleles across different populations. Associations appear to be population and phenotype specific. The class II *HLA-DRB1*01:01* allele has been associated with NVP-induced hepatic and cutaneous reaction in Caucasian populations (Martin et al., 2005; Vitezica et al., 2008; Yuan et al., 2011). The class I *HLA-B*35:05* and *HLA-Cw*04* alleles are linked with NVP-induced cutaneous reactions in African American and Chinese populations, and these alleles are also associated with NVP-induced rash in Thai populations (Chantarangsu et al., 2009; Likanonsakul et al., 2009; Yuan et al., 2011; Gao et al., 2012). The *HLA-Cw8-HLA-DRB1:01:01* haplotype is linked to NVP hypersensitivity reactions in Sardinians (Littera et al., 2006) and Japanese (Gatanaga et al., 2007). In addition to HLA alleles involved in the immune response to NVP, genes outside of the MHC have been identified as additional risk factors for NVP-induced hypersensitivity reactions. For example, in African Americans, the risk for cutaneous reactions is highest for individuals carrying both *HLA-Cw*04* and *CYP2B6 516TT* alleles (Yuan et al., 2011). CYP2B6 is a main isozyme responsible for the metabolism of NVP. The *CYP2B6 516TT* allele is associated with decreased CYP2B6 expression and activity and thus results in higher NVP systemic concentrations (Mahungu et al., 2009). Therefore genes involved in immunologic and metabolic pathways, and their varying allele frequencies in different ethnic populations, will all have an impact on the susceptibility to NVP-induced hypersensitivity reactions in a phenotype- and population-specific manner.

In summary, significant progress has been made in understanding the HLA genotype as a genetic risk factor for immunologically mediated, idiosyncratic adverse drug reactions. Clinical integration of HLA genotyping into routine medical practice to prevent drug-induced hypersensitivity reactions has occurred in the cases of *HLA-B*57:01* and abacavir, *HLA-B*15:02/ HLA-A*31:01* and carbamazepine, and *HLA-B*58:01* and allopurinol.

PHARMACOGENOMICS IN CANCER CHEMOTHERAPY

THIOPURINES

The thiopurine drugs mercaptopurine and thioguanine, which are analogues of the purine nucleosides hypoxanthine and guanine, respectively, are commonly used for the treatment of leukemia and lymphoma. After cellular uptake, which is partly mediated through nucleoside transporters (e.g., SLC23A and SLC29A), mercaptopurine is metabolized mainly through phosphoribosylation and S-methylation in cells. Phosphoribosylation activates mercaptopurine through the purine salvage pathway to the principal active metabolite, thioguanine nucleotides, which are subsequently incorporated into DNA thus inducing cytotoxicity. S-methylation catalyzed by TPMT is the principal mechanism of intracellular inactivation of mercaptopurine.

The link between polymorphisms in *TPMT* and mercaptopurine toxicity has been well established. Three variant alleles (*TPMT*2*, *TPMT*3A*, and *TPMT*3C*), which account for >95% of low or intermediate TPMT enzyme activity, lead to increased levels of mercaptopurine and severe toxicity. The FDA has recommended genotyping of these three *TPMT* SNPs prior to mercaptopurine therapy. Individuals who are heterogenous for a nonfunctional *TPMT* variant allele are at intermediate risk of dose-limiting toxicity and may require a modest dose reduction of about 35% to 50%, while TPMT-deficient individuals require a dose reduction of >90% (Cheok & Evans, 2006). On the other hand, the TPMT genotype has been linked to early acute lymphoblastic leukemia response, where patients with two functional TPMT alleles had a 2.9-fold higher risk of positive minimum residual disease than did TPMT-heterozygous patients after remission-induction therapy (Stanulla et al., 2005). This is consistent with lower mercaptopurine exposure as a result of high TPMT activity in patients with wild-type *TPMT*, and it remains to be determined whether dose escalation in these patients would yield better efficacy.

FLUOROPYRIMIDINES (5-FLUOROURACIL AND CAPECITABINE)

Since its introduction more than 50 years ago (Heidelberger et al., 1957), fluoropyrimidines 5-fluorouracil and capecitabine are the backbone of treatments for gastrointestinal, breast, and head and neck cancers. 5-FU is a prodrug that undergoes multiple metabolic pathways that lead to activation and pharmacodynamic actions of the drug or detoxification and elimination of the drug (Fig. 75.7). Capecitabine is the oral prodrug of 5-FU, which is rapidly absorbed after oral administration and converted to 5-FU in tumor tissues.

The main mechanism of 5-FU activation is the conversion to fluorodeoxyuridine monophosphate (FdUMP), which inhibits the enzyme thymidylate synthase (TS), an important part of the folate-homocysteine cycle and purine and pyrimidine synthesis. The conversion of 5-FU to FdUMP can occur via three pathways: oratate phosphoribosyltransferase (OPRT) (pathway 1), uridine phosphorylase (pathway 2), and thymidine phosphorylase (TP) (pathway 3) (see Fig. 75.7) (Omura, 2003). Enzyme expression or activity in these pathways could influence activation and pharmacodynamic actions of 5-FU. High expression of OPRT (at mRNA or protein level) has been associated with better clinical response to 5-FU–based chemotherapy in patients with metastatic colorectal cancer (Ichikawa et al., 2003). In addition, genetic polymorphisms in the *OPRT* gene could modify OPRT enzyme activity and, consequently, impact the clinical outcome. For example, copresence of the *OPRT* Gly213Ala variant and *TS* 2R/2R genotype has been related to a higher incidence of grade 3/4 5-FU–induced neutropenia and diarrhea (Ichikawa et al., 2006).

The rate-limiting step of 5-FU catabolism and detoxification is the dihydropyrimidine dehydrogenase (DPD)–mediated conversion of 5-FU to dihydrofluorouracil (FUH_2), which is subsequently converted to fluoro-beta-alanine (FBAL) by dihydropyrimidinase (DHP) (see Fig. 75.7). Deficiency in enzymes in this pathway can result in severe and even fatal 5-FU toxicity. DPD expression has been linked to the tolerance and response

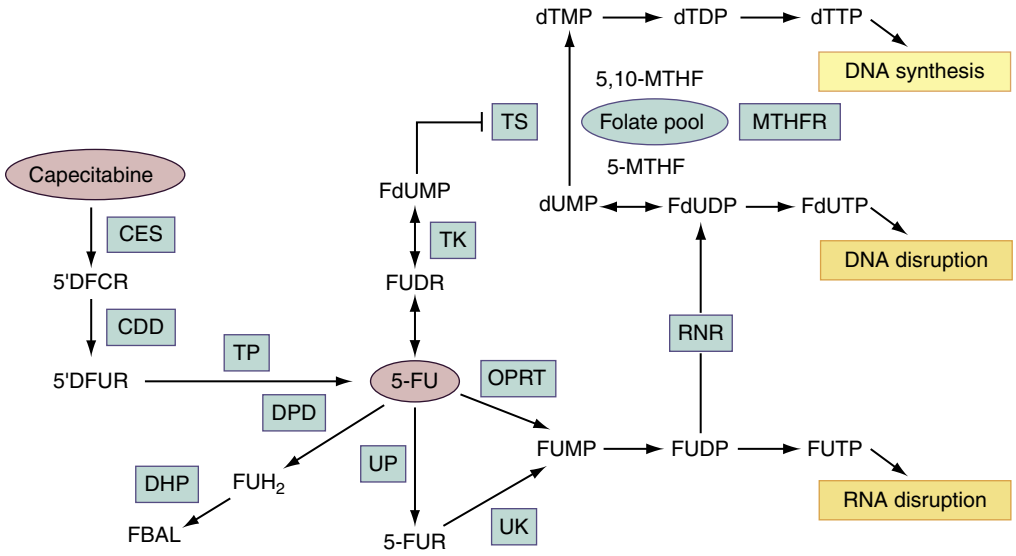

Fig. 75.7 Schematic illustration of pharmacokinetic and pharmacodynamic pathways that affect 5-fluorouracil (5-FU) efficacy. Genetic polymorphisms within the genes that are involved in 5-FU metabolic activation (e.g., *OPRT*), detoxification (e.g., *DPD*), and target interaction (e.g., *TS*) are important determinants of the efficacy and safety of 5-FU treatment. *5′DFCR,* 5′deoxy-5-fluorocytidine; *5′DFUR,* 3′deoxy-5-fluorouridine; *5-FUR,* 5-fluorouridine; *CDD,* cytosine deaminase; *CES,* carboxylesterase; *DHP,* dihydropyrimidinase; *DPD,* dihydropyrimidine dehydrogenase; *FBAL,* fluoro-b-alanine; *FUH2,* dihydro-5-fluorouracil; *MTHFR,* methylenetetrahydrofolate reductase; *OPRT,* orotate phosphoribosyltransferase; *RNR,* ribonucleotide reductase; *TK,* thymidine kinase; *TP,* thymidine phosphorylase; *TS,* thymidylate synthase; *UK,* uridine-cytidine kinase 2; *UP,* uridine phosphorylase 1. (Adapted from Walther A, Johnstone E, Swanton C, et al.: Genetic prognostic and predictive markers in colorectal cancer, Nat Rev Cancer 9:489–499, 2009.)

to 5-FU–based chemotherapy. Specifically, low expression or absence of DPD leads to the accumulation of 5-FU and, consequently, increased risk for severe toxicities, whereas high expression or activity of DPD is associated with poor response to 5-FU (Salonga et al., 2000; Soong et al., 2008). Approximately 3% to 5% of patients are partially or completely deficient in DPD enzyme activity (Lu et al., 1993). A substantial proportion of the cases of DPD deficiency result from deleterious polymorphisms in the gene *DPYD*. The most well-established deleterious *DPYD* variants associated with fluoropyrimidine toxicity are *DPYD*2A* (IVS14+1G>A, c.1905+1G>A, or rs3918290), c.2846A>T, c.1679T>G, and HapB3 (c.1129-5923C>G) (Morel et al., 2006; Amstutz et al., 2018). Among these, *DPYD*2A* and c.1679T>G result in the most significantly reduced DPD activity, whereas c.2846A>T and c.1129-5923C>G lead to moderately reduced DPD activity. *DPYD*2A*, a G-to-A point mutation within the 5′-splicing site of intron 14, results in a mutant DPD that lacks amino acids 581 to 635 and, consequently, loses catalytic activity. The variants c.1679T>G and c.2846A>T are missense mutations that affect protein function. The variant c.1129-5923C>G introduces a cryptic splice site and partial production of a nonfunctional transcript. In Europeans, the allele frequency of c.1129-5923C>G, *DPYD*2A*, and c.2846A>T is 4.7%, 1.6%, and 0.7%, respectively (Amstutz et al., 2018).

Taken all four variants together, ~7% of Europeans carry at least one reduced function *DPYD* variant. There is strong evidence linking *DPYD* genotype with variabilities in DPD enzyme activity and fluorodeoxyuridines-associated toxicity, which provides the basis for the dosing recommendations (Amstutz et al., 2018; Meulendijks et al., 2015). The likely DPD phenotype can be assigned based on *DPYD* genotype (Amstutz et al., 2018). Briefly, individuals carrying two nonfunction alleles are classified as DPD poor metabolizer; individuals carrying one nonfunction or decreased function allele are classified as DPD intermediate metabolizer; and those with only normal function variants are classified as DPD normal metabolizer. The genetic-based dosing recommendations for fluoropyrimidine are available from the FDA, the CPIC, and the Dutch Pharmacogenetics Working Group (Amstutz et al., 2018). Specifically, DPD intermediate metabolizers should receive 25% to 50% dose reduction. For DPD poor metabolizers, it is strongly recommended to avoid use of fluoropyrimidines, or if unavoidable, 5-FU should be administered at a significantly reduced dose combined with early therapeutic drug monitoring (Amstutz et al., 2018). *DPYD* genotype-guided dose reduction has been shown to reduce occurrence of severe 5-FU toxicity and eliminate toxicity-related deaths in carriers of *DPYD*2A* in a prospective study (Deenen et al., 2016). Nevertheless, it should be noted that not all individuals carrying *DPYD* decreased/nonfunction variants develop severe toxicity at standard doses, and thus these individuals may not receive full clinical benefit of fluoropyrimidine therapy. To maintain efficacy, the dose is recommended to be increased in patients with no toxicity or with subtherapeutic 5-FU plasma concentrations (Amstutz et al., 2018).

In addition to genes involved in 5-FU pharmacokinetic pathways, genetic polymorphisms in genes involved in pharmacodynamic actions of 5-FU also impact the clinical outcome of 5-FU treatment. In particular, variants in the *TS* gene have been linked to TS expression and response to fluorouracil chemotherapy (see detailed discussion earlier). In spite of contradictory findings from heterogeneous studies, most studies generally support the notion that colorectal cancer patients with a high TS-expression genotype appear to have poor prognosis and worse response to 5-FU–based chemotherapy, but possibly less severe toxicities, compared with those with a low TS-expression genotype (for a review, see Lurje et al. [2009]). A recent study of copy number variation in *TS* in colorectal tumor samples showed that high copy numbers were associated with disease relapse and death (Jensen et al., 2008), indicating that simple genotyping may not provide the whole picture. In addition, there have been some publications implicating variants in the methylenetetrahydrofolate reductase (MTHFR), DNA repair enzymes, and cell cycle pathways in the pharmacogenomics of fluoropyrimidines (Huang et al., 2008; Ruzzo et al., 2008; De Mattia & Toffoli, 2009).

In summary, several of the candidate genes in 5-FU metabolic activation (e.g., *OPRT*), detoxification (e.g., *DPYD*), and target interaction (e.g., *TS*) have been shown to influence clinical outcomes. There is strong evidence linking *DPYD* genotype with variabilities in DPD enzyme activity and 5-FU-associated toxicity, which provided the basis for *DPYD* genotype-guided dose adjustment. It should be recognized, however, that other genetic variations (e.g., additional rare deleterious *DPYD* variants) and patient characteristics (e.g., sex, age, and disease status) may also influence the overall risk of toxicity. A genetic test of only selected deleterious *DPYD* variants does not fully rule out DPD defect.

IRINOTECAN

The topoisomerase I inhibitor irinotecan is widely used in the treatment of metastatic colorectal cancer, either in combination with 5-FU in the first-line treatment setting or as monotherapy in the second-line setting (Saltz et al., 2000; Douillard et al., 2000). Irinotecan acts as a prodrug and undergoes complex metabolic pathways in humans (Fig. 75.8). Specifically, irinotecan is metabolized by human carboxylesterase 1 and 2 (hCE1 and hCE2) in the liver and plasma to form 7-ethyl-10-hydroxycamptothecin (SN-38), an active metabolite that targets topoisomerase I to inhibit DNA replication in cancer cells. SN-38 also contributes to the major dose-limiting toxicities, including neutropenia and diarrhea. In the liver, SN-38 is detoxified by UGT1A1-mediated glucuronidation to form SN-38 glucuronic acid (SN-38G) (Slatter et al., 1997). SN-38G is released by biliary excretion into the intestines for elimination, where bacterial beta-glucuronidases transform inactive SN-38G back into the active SN-38, leading to severe delayed diarrhea. In addition, irinotecan undergoes CYP3A-mediated oxidation to form the inactive metabolites 7-ethyl-10-(4-N-(5-aminopentanoic acid)-1-piperidino) carbonyloxycamptothecin (APC) and 7-ethyl-10-(4-amino-1-piperidino) carbonyloxycamptothecin (NPC); the latter can be further metabolized by hCE1 and hCE2 to form SN-38 (Rivory et al., 1996; Dodds et al., 1998). Uptake and efflux transporters, such as OATP1B1, ABCB1, ABCC1/2, and ABCG2, are involved in the hepatic uptake and biliary excretion of irinotecan, SN-38, and SN-38G (see Fig. 75.8) (Schellens et al., 2000; Luo et al., 2002).

Irinotecan exhibits substantial interindividual variability in its pharmacokinetics, efficacy, and toxicity profiles in cancer patients (Mathijssen et al., 2001; Ratain et al., 2002). This variability is attributable, at least in

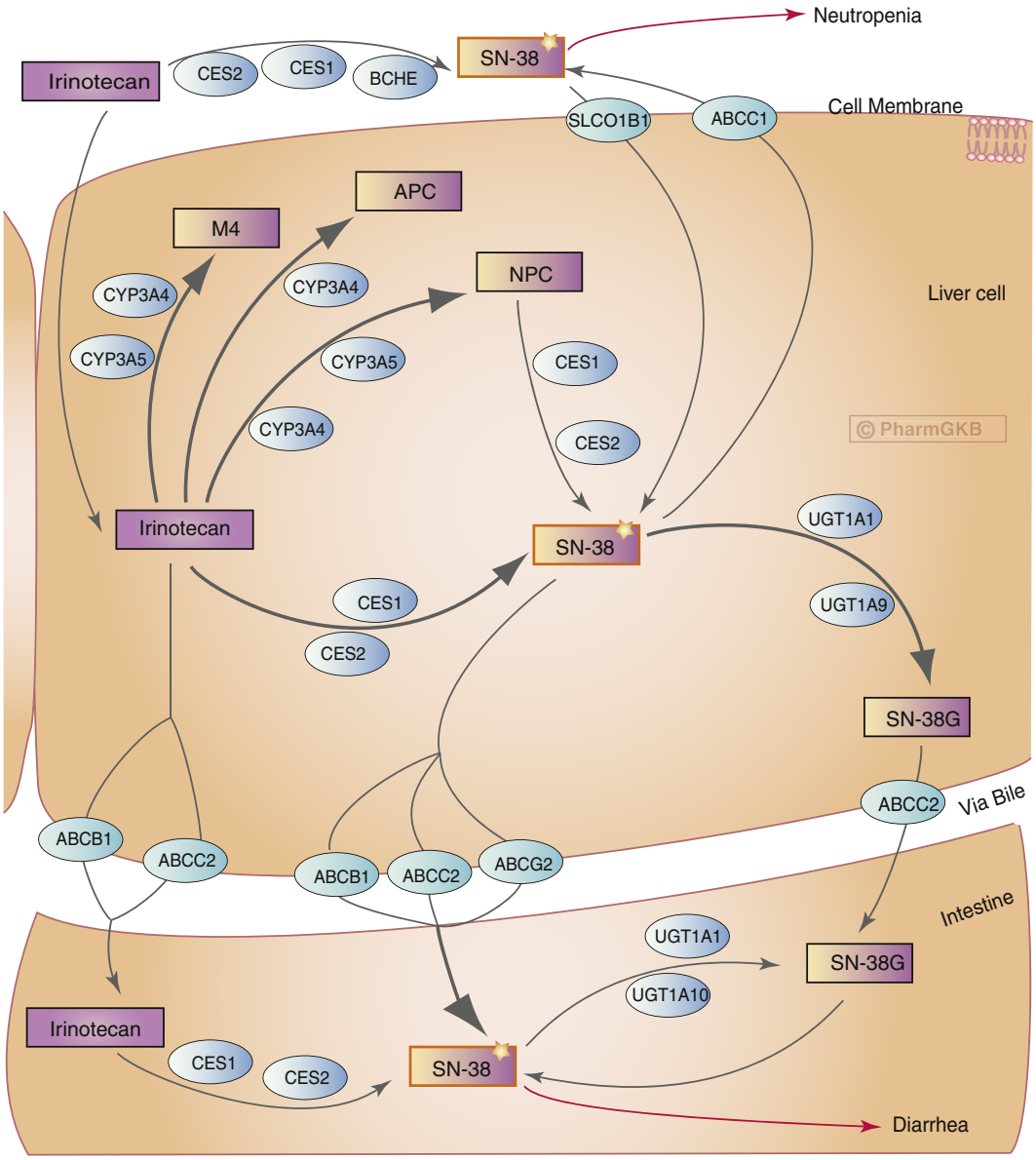

Fig. 75.8 Schematic illustration of irinotecan pharmacokinetic pathway. Irinotecan is activated to 7-ethyl-10-hydroxycamptothecin (SN-38) by human carboxylesterase 1 and 2 (hCE1 and hCE2), and SN-38 is subsequently detoxified by UGT1A1 to a β-glucuronide derivative, SN-38G. In addition, irinotecan undergoes CYP3A4-mediated oxidation to form the inactive metabolites 7-ethyl-10-(4-*N*-(5-aminopentanoic acid)-1-piperidino) carbonyloxycamptothecin (APC) and 7-ethyl-10-(4-amino-1-piperidino) carbonyloxycamptothecin (NPC), and NPC also undergoes a subsequent conversion by hCE2 to SN-38. Irinotecan and its metabolites (i.e., SN-38 and SN-38G) are also transported by the ABC transporters, including ABCB1, ABCC1/2, or ABCG2 or the organic anion transporting polypeptide 1B1 (OATP1B1). (Adapted from PharmGKB [https://www.pharmgkb.org/pathway/PA2001], with permission.)

part, to genetic variations in the genes encoding metabolizing enzymes, transporters, and targets that are involved in irinotecan pharmacokinetic and pharmacodynamic pathways (Marsh & Hoskins, 2010).

Up to 36% of patients treated with irinotecan develop severe, potentially life-threatening toxicities, particularly neutropenia and diarrhea. The most comprehensively studied genetic polymorphisms linked to irinotecan-induced toxicity are in UDP-glucuronosyltransferase 1A1 (*UGT1A1)*, which encodes a key enzyme responsible for the inactivation of SN-38 to SN-38G in the liver. The *UGT1A1*28* (rs8175347) allele is characterized by the presence of seven dinucleotide repeats in the TATA sequence of the *UGT1A1* promoter, as opposed to the *UGT1A1*1* allele with six repeats. *UGT1A1*28* results in decreased enzyme expression and activity and, consequently, reduced SN-38 glucuronidation and detoxification. Patients homozygous or heterozygous for the UGT1A1*28 allele commonly have greater susceptibility to dose-limiting severe neutropenia and diarrhea (Iyer et al., 2002; Tukey et al., 2002; Innocenti et al., 2004). The frequency of the *UGT1A1*28* ranges from 0.09 to 0.16 in Asians, 0.26 to 0.38 in Caucasians and Hispanics, to 0.42 to 0.56 in Africans (Marsh & Hoskins, 2010). In Asians where the frequency of *UGT1A1*28* is low, the exon 1 polymorphism *UGT1A1*6* (rs4148323) has a frequency of 0.23 in the Korean and Chinese populations. The *UGT1A1*6* allele causes decreased enzyme activity (Premawardhena et al., 2003). Patients homozygous for the UGT1A1*6 allele are at a higher risk for grade 4 neutropenia (Han et al., 2006). The most recent review suggests that the UGT1A1 polymorphisms *28 and *6 have been validated, by meta-analysis and multiple models, as the risk factors for irinotecan-induced neutropenia and diarrhea (Campbell et al., 2017). This association persists for neutropenia regardless of irinotecan dose; however, at low doses of irinotecan, there is evidence that irinotecan-induced diarrhea is not significantly associated with *UGT1A1*28* at least (dose subgroup analyses were not conducted for *UGT1A1*6*) (Campbell et al., 2017). Interestingly, the up-to-date systematic reviews found that *UGT1A1*28* was not associated with clinical response to irinotecan therapy (including objective response rate, progression-free or overall survival) regardless of irinotecan dose (Dias et al., 2012, 2014).

Besides *UGT1A1*, genetic polymorphisms in *UGT1A7* and *UGT1A9* genes have also been associated with SN-38 glucuronidation and irinotecan toxicities, particularly diarrhea (Carlini et al., 2005; Han et al., 2006). UGT1A7 is located in the intestine and is responsible for detoxifying SN-38. Patients homozygous for the *UGT1A7*2* have a higher enzyme activity as compared to carriers of *UGT1A7*3* and *UGT1A7*1*. By contrast, patients with *UGT1A7*3* and *UGT1A7*4* haplotypes display less UGT1A1 enzyme activity and impaired SN-38 conjugation. UGT1A9, expressed in the liver, is the principal enzyme catalyzing the glucuronidation of SN-38 to inactive SN-38G. *UGT1A9*22* is found predominantly in Eastern Asian populations and leads to higher enzyme expression and glucuronidation rates. Patients carrying *UGT1A9*9* or *UGT1A9*22* (rs3832043) are at a lower risk for severe diarrhea than patients homozygous for the wild-type *UGT1A9*.

In light of the important role of transporters in irinotecan pharmacokinetics, associations of genetic polymorphisms within the genes encoding ABCB1, ABCC1, ABCG2, and OATP with irinotecan pharmacokinetics or toxicity have been reported, even though the data are limited (for a review, see de Jong et al. [2006] and Marsh & Hoskins [2010]). ABCB1 is

involved in facilitating the biliary excretion of irinotecan and SN-38. The *ABCB1* 3435C>T variant was related to higher irinotecan plasma concentration in Chinese (Zhou et al., 2005), and *ABCB1* 1236C>T resulted in higher systemic exposure to irinotecan and SN-38 in Caucasians (Mathijssen et al., 2003). The clinical relevance of single *ABCB1* SNP to irinotecan treatment remains to be elucidated. ABCC2 plays a key role in facilitating secretion of irinotecan and its metabolites (SN-38 and SN-38G) from hepatocytes to the intestine. The *ABCC2*2* haplotype is beneficial in that it is associated with lower incidence of irinotecan-induced diarrhea, while the *ABCC2 3972 C>T* (rs3740066) variant results in a higher systemic exposure to irinotecan and its metabolites and higher risk for grade 3 diarrhea (Kim, 2002). ABCG2 is expressed in the intestine and colon and actively transports irinotecan and SN-38. The *ABCG2 34G>A* (rs2231137) variant has a diminished efflux activity, resulting in prolonged exposure of SN-38 to the intestines. Patients with at least one *ABCG2 34A* allele have a greater risk for grade 3 diarrhea as compared to the G allele carriers (Han et al., 2007). OATP1B1 is an important uptake transporter facilitating the uptake of SN-38 from blood circulation to hepatocytes. Genetic polymorphisms in the *OATP1B1* gene, such as *521T>C*, –11187G>A, *388A>G*, and the *OATP1B1*15* haplotype, have been associated with a lower clearance and higher systemic exposure of SN-38 and irinotecan (Xiang et al., 2006; Han et al., 2008).

In addition to the pharmacogenetic influence of genes involved in irinotecan pharmacokinetics, polymorphisms in genes encoding drug targets such as topoisomerase I (TOP1) and downstream effectors (such as XRCC1, ADPRT, TDP1, CDC45L) in the DNA repair and cell death pathways may influence patient outcomes to irinotecan treatment. For example, a retrospective analysis of 107 advanced colorectal cancer patients suggest that TOP1 and TDP1 htSNPs were related to grade 3/4 neutropenia and the *TDP1* variant and an *XRCC1* haplotype is associated with response to irinotecan (Hoskins et al., 2008).

In summary, neutropenia and diarrhea are the major dose-limiting, potentially life-threatening toxicities from irinotecan chemotherapy. *UGT1A1*28* and *UGT1A1*6* are validated risk factors for irinotecan-induced neutropenia regardless of irinotecan dose. *UGT1A1*28* and *UGT1A1*6* are also related to irinotecan-induced diarrhea; however, the *UGT1A1*28* association with diarrhea appears to be dose dependent. There is now an FDA-approved genetic test for *UGT1A1*28*, and the irinotecan package insert contains warnings regarding *UGT1A1*28* and risk of toxicity. A reduced initial dose of irinotecan is recommended for patients homozygous for the *UGT1A1*28* allele. The true clinical significance of genetic variations within other genes involved in the pharmacokinetics and pharmacodynamics of irinotecan with respect to clinical outcome remains to be validated.

TAMOXIFEN

Tamoxifen, a selective estrogen receptor (ER) modulator, is a standard endocrine therapy for the treatment and prevention of ER-positive breast cancer. ER-positive breast cancers are often dependent on estrogen for growth. Selective ER modulators bind to the ligand-binding domain of an ER and block the binding of estrogen. This prevents conformational changes of the ER that it requires for its association with coactivators, thus blocking transcriptional activation functions of the ER and subsequently reducing or eliminating estrogen-driven proliferation of ER-positive tumors.

Tamoxifen is a weak antiestrogen that is extensively metabolized to metabolites with less, similar, or more potent antiestrogenic activity. Tamoxifen undergoes extensive phase I and II liver metabolism by phase I enzymes (including CYP3A4, CYP3A5, CYP2C9, CYP2C19, CYP1A2, CYP2B6, and CYP2D6, as well as flavin-containing monooxygenase 1 and 3) and phase II enzymes (including SULTs and UGTs) (Fig. 75.9) (Dehal & Kupfer, 1997; Desta et al., 2004; Parte & Kupfer, 2005). The two predominant metabolic pathways, N-demethylation (catalyzed primarily by CYP3A4/5) and 4-hydroxylation (catalyzed primarily by CYP2D6), account for approximately 92% and 7% of tamoxifen metabolism, respectively (Desta et al., 2004; Della-Morte et al., 2004). 4-hydroxy-tamoxifen and N-desmethyltamoxifen are further metabolized, mainly by CYP3A4 and CYP2D6, respectively, to form the very potent secondary metabolite, endoxifen (Desta et al., 2004). Endoxifen and 4-hydroxytamoxifen show much greater affinity for the estrogen receptor than tamoxifen. While 4-hydroxytamoxifen and endoxifen have similar potencies in terms of antiestrogenic activity (Desta et al., 2004; Crewe et al., 2002), endoxifen plasma concentrations are up to 10-fold higher than 4-hydroxytamoxifen and exhibit large interpatient variability (Stearns et al., 2003). These data suggest that endoxifen is the predominant and crucial active metabolite responsible for the in vivo pharmacologic activity of tamoxifen.

Given the key role of CYP2D6 in catalyzing the hydroxylation of N-desmethyltamoxifen to endoxifen, genetic variations on *CYP2D6* may have a direct impact on endoxifen concentrations and consequently therapeutic benefit of tamoxifen. As mentioned earlier, *CYP2D6* functional alleles result in abolished, decreased, normal, or ultrarapid enzyme activity (see Table 75.1). As a result, patients can be classified as four phenotypes: poor metabolizer (PM) (abolished activity), intermediate metabolizer (IM) (reduced activity), extensive metabolizer (EM) (normal activity), and ultrarapid metabolizer (UM) (enhanced activity). It has been demonstrated that patients with low CYP2D6 enzyme activity, as a result of CYP2D6 genetic polymorphisms or the coadministration of strong CYP2D6 inhibitors, exhibit significantly lower endoxifen concentrations when treated with tamoxifen (Schroth et al., 2017; Stearns et al., 2003). CYP2D6 genotype explains 34% to 52% of the variability in absolute endoxifen concentrations (Schroth et al., 2017).

There are, however, conflicting clinical data on the association between *CYP2D6* genotypes and endoxifen concentrations with tamoxifen treatment outcome (Brauch et al., 2013; Province et al., 2014). Some studies suggest that, compared to those with normal enzyme activity, CYP2D6 PMs have worse clinical outcome after tamoxifen treatment or higher incidence of breast cancer when tamoxifen is used as a preventive agent (Hoskins et al., 2009; Higgins & Stearns, 2010; Goetz et al., 2005; Bonanni et al., 2006; Borges et al., 2006; Lim et al., 2007; Wegman et al., 2007; Schroth et al., 2009). On the contrary, other studies report contradictory results (Nowell et al., 2005; Wegman et al., 2005, 2007). Particularly, data from 5-year tamoxifen prospective trials, including ATAC, GIGI-98, and ABCSG8, do not support a role for the *CYP2D6* genotype in the activation of tamoxifen and likelihood of therapeutic benefit from testing for the *CYP2D6* genotype (Rae et al., 2012; Regan et al., 2012; Goetz et al., 2013). A more recent meta-analysis indicates an association between CYP2D6 genotype and disease-free survival, but only in patients who received tamoxifen as adjuvant therapy at a dose of 20 mg/day for 5 years (Province et al., 2014).

Several confounding factors could contribute to the conflicting results regarding *CYP2D6* genotype as a predictor for tamoxifen response. For example, *CYP2D6* copy number is not always assessed and rare CYP2D6 variants may not be included, which may cause a misclassification of CYP2D6 phenotype (Skierka et al., 2012). Environmental factors (such as menopausal status or coadministration of CYP2D6 inhibitors) are not always considered but can cause a big change in phenotype (Brauch et al., 2013). In addition, genetic variations in other metabolizing enzymes could also contribute to the interindividual variability in tamoxifen pharmacokinetics.

The *CYP2C19*17* higher-functioning variant has been associated with better responses to treatment, lower adverse reactions, and increased disease-free survival (Schroth et al., 2007; Gjerde et al., 2010). In addition, variants of phase I enzymes have also been associated with tamoxifen treatment outcome. Interestingly, the lower-functioning allele, *SULT1A1*2*, is associated with worse clinical outcome as compared to the higher-functioning allele *SULT1A1*1* (Nowell et al., 2002). One possible explanation for this observation is that further metabolism of tamoxifen metabolites (4-hydroxy-tamoxifen and endoxifen) by SULT1A1 forms highly reactive products, leading to DNA adducts (Dasaradhi & Shibutani, 1997; Davis et al., 1998), and therefore individuals with a low-activity *SULT1A1* genotype have poor clinical outcome. Variants in UGT2B15, known for metabolizing steroids as well as xenobiotics, have also been shown to affect survival and disease recurrence after tamoxifen treatment. *UGT2B15*2*, the higher-functioning variant, has been associated with decreased overall survival and increased disease recurrence (Nowell et al., 2005). This association is much stronger when both *SULT1A1* and *UGT2B15* genotypes are evaluated together (Nowell et al., 2005). In addition, genetic variations within the target genes (*ESR1* and *ESR2)* have been associated with altered susceptibility to tamoxifen-induced hot flashes and hormone-resistance (Zhang et al., 1997; Jin et al., 2008).

In conclusion, tamoxifen is bioactivated by CYP2D6 to 4-hydroxytamoxifen and endoxifen, both with greater antiestrogenic potency than the parent drug. Despite some conflicting results, there is substantial evidence that patients with reduced CYP2D6 enzyme activity, due to genetic polymorphisms or coadministration of CYP2D6 inhibitors, exhibit lower endoxifen concentrations and a higher risk of disease recurrence in studies of adjuvant tamoxifen therapy of early breast cancer. The CPIC recently published guidelines to provide therapeutic recommendations (Goetz et al., 2018). Briefly, for CPY2D6 PMs and IMs, it is recommended to use alternative hormonal therapy (e.g., aromatase inhibitors) for postmenopausal women or aromatase inhibitors combined with ovarian function suppression in premenopausal women. Should aromatase

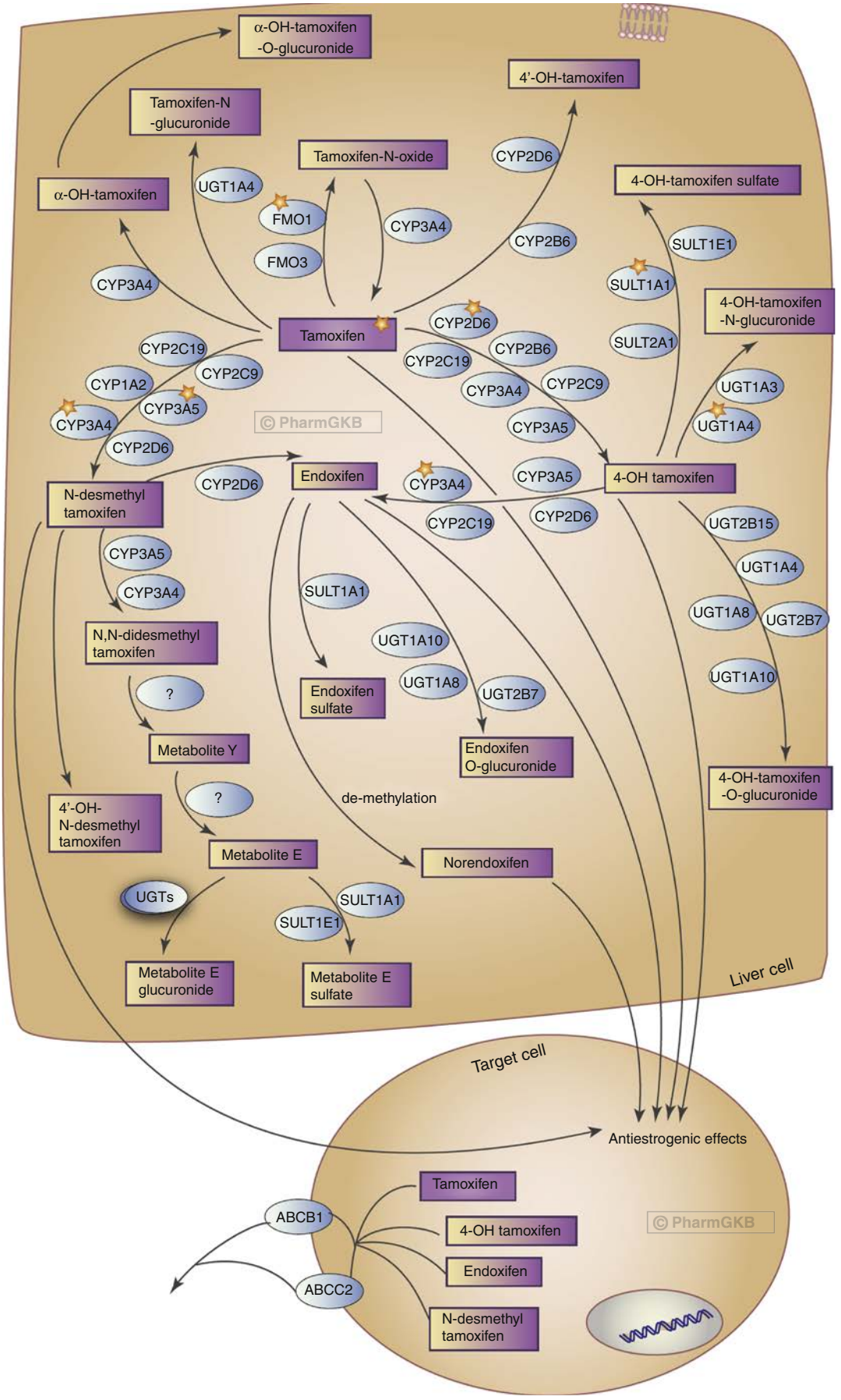

Fig. 75.9 Schematic illustration of tamoxifen pharmacokinetic pathway. Tamoxifen is extensively metabolized by hepatic phase I enzymes, including CYP3A4, CYP3A5, CYP2C9, CYP2C19, CYP1A2, CYP2B6, CYP2D6, and flavin-containing monooxygenase (FMO) 1 and 3, as well as phase II enzymes (including SULTs and UGTs). Tamoxifen metabolism mostly occurs via two pathways, 4-hydroxylation (catalyzed primarily by CYP2D6) and *N*-demethylation (catalyzed primarily by CYP3A4/5), and both are further metabolized to form the very potent secondary metabolite, endoxifen. (Adapted from PharmGKB [https://www.pharmgkb.org/pathway/PA145011119], with permission.)

inhibitors be contraindicated in either case, tamoxifen 40 mg/day can be considered for CYP2D6 PMs or IMs. Individuals who are CYP2D6 NM or UM should have tamoxifen initiated at 20 mg/day. In addition to germline polymorphisms, there are well-accepted tumor somatic factors that are associated with endocrine response. It should be recognized that the CYP2D6 genotype is one of multiple pieces of information that needs to be considered when making therapeutic choices for individual patients.

MOLECULAR TARGETED AGENTS

A better understanding of driver molecular mechanisms involved in cancer initiation, progression, and resistance has promoted the discovery and development of novel molecular targeted agents for cancer treatment. The response (efficacy or resistance) to molecular targeted agents has often been associated with specific tumor genomic alterations. Identifying the actionable genomic alterations in a patient's tumor and selecting matching targeted therapies represent a significant advance of personalized cancer therapy. Representative examples for tumor somatic mutations as predictive biomarkers of treatment efficacy or resistance to molecular targeted agents include *EGFR* mutations in non–small cell lung cancer for small molecule EGFR inhibitors (gefitinib and erlotinib), *EML4-ALK* fusion gene in NSCLC for ALK inhibitors (crizotinib and ceritinib), *BRAF* mutations in melanoma for vemurafenib, *BCR-ABL* fusion gene in chronic myeloid leukemia for imatinib, and *KRAS* mutations in colorectal cancer for anti-EGFR monoclonal antibodies (cetuximab and panitumumab).

EGFR Mutations and EGFR Inhibitors

As described earlier under "Epidermal Growth Factor Receptor", specific somatic mutations in EGFR are important determinants of sensitivity or resistance to small molecule EGFR TK inhibitors (gefitinib and erlotinib) in the treatment of NSCLC. Activating mutations in exons 18 to 21 of the TK domain in EGFR, which include in-frame deletions in exon 19 (delE746-A750), missense mutations in exon 21 (L858R) and exon 18 (G719), and in-frame duplications and/or insertions in exon 20, are predictors of the therapeutic response to gefitinib and erlotinib in NSCLC patients (Lynch et al., 2004; Paez et al., 2004; Pao et al., 2004). Deletions in exon 19 (delE746-A750) and a missense mutation in exon 21 (L858R) account for >90% of all EGFR mutations. In 2013, the FDA approved the first-line use of erlotinib in patients with EGFR-mutated metastatic NSCLC and a companion diagnostic test for erlotinib (cobas EGFR Mutation Test). Acquired resistance occurs in virtually all NSCLC tumors that initially respond to EGFR TK inhibitors. Two primary resistance mechanisms include secondary point mutation in EGFR (T790M or D761Y) and activation of bypass signaling (e.g., MET amplification) (Sharma et al., 2007; Balak et al., 2006). The T790M mutation, occurring in about two-thirds of resistance cases, reduces the binding affinity of erlotinib to the EGFR-TK domain. Osimertinib, a novel potent inhibitor of the EGFR with T790M mutation, received accelerated FDA approval in 2015 for the treatment of patients who have developed resistance to prior EGFR inhibitor therapy.

EML4-ALK Fusion Gene and ALK Inhibitors

The abnormal fusion gene, *EML4-ALK*, leads to constitutive activation of ALK and various growth stimulatory signaling pathways, including PI3K/AKT1/mTOR and RAS/RAF1/MAP2K1 pathways. EML4-ALK fused oncogene is present in 3% to 7% of NSCLC patients. The small molecule, competitive inhibitor of ALK, crizotinib, showed significantly improved overall response rate in patients with ALK-positive NSCLC as compared to standard chemotherapy (Kwak et al., 2010; Shaw et al., 2013). In 2011, the FDA approved crizotinib for the treatment of ALK-positive locally advanced or metastatic NSCLC alongside a companion diagnostic test to detect ALK positive (Vysis ALK Break Apart FISH [fluorescence in-situ hybridization] Probe Kit). Acquired resistance often occurs in patients who initially respond to crizotinib. Common mechanisms of resistance include secondary ALK mutations, ALK gene amplification, and aberrant activation of other kinases (e.g., KIT and EGFR) (Katayama et al., 2012). The next generation of ALK inhibitors (including ceritinib and alectinib), which have a higher potency against mutated ALK, received accelerated FDA approval for the treatment of ALK-positive metastatic NSCLC patients who have progressed on or are intolerant to crizotinib.

BRAF Mutations and BRAF Inhibitors

Activating *BRAF* mutations, occurring in ~50% of metastatic melanoma cases, lead to constitutive activation of downstream signaling of the MAPK pathway. A missense mutation *V600E* accounts for ~90% of *BRAF* mutations. Vemurafenib, a potent inhibitor of BRAF V600E, showed significantly improved survival benefit in patients with BRAF mutated metastatic melanoma as compared to standard chemotherapy (Chapman et al., 2011). In 2011, vemurafenib received accelerated FDA approval along with a companion diagnostic test (cobas 4800 BRAF V600 mutation test) to detect *BRAF* mutations.

BCR-ABL Fusion Gene and Imatinib

The *BCR-ABL* fused oncogene occurs in >95% of chronic myeloid leukemia (CML), leading to constitutive activation of signaling pathways associated with enhanced cell proliferation and tumor growth. Imatinib (Gleevec), the first tyrosine kinase inhibitor approved by the FDA for the treatment of BCR-ABL positive CML, principally inhibits BCR-ABL kinase activity by exclusively binding to the inactive conformation of BCR-ABL, and in addition it inhibits KIT, ARG, and PDGFR kinases. Approximately 10% to 15% of CML patients show primary resistance to imatinib and ~20% to 25% develop acquired imatinib resistance. The most common mechanism of imatinib resistance is the occurrence of point mutations in the kinase domain (drug binding site), P-loop (ATP binding site), catalytic domain, or activation loop of BCR-ABL (Milojkovic & Apperley, 2009). The *T315I* point mutation in the *c-ABL* is one of the most frequent mutations rendering acquired imatinib resistance and is resistant to all ABL kinase inhibitors. A single amino acid change caused by T315I mutation results in steric hindrance thus preventing imatinib binding to the ATP binding pocket (Gorre et al., 2001).

KRAS Mutations and Anti-EGFR Monoclonal Antibodies

Cetuximab and panitumumab are monoclonal antibodies that were designed to inhibit EGFR kinase by binding the extracellular domain of EGFR. It is evident that genomic alterations (in most instances point mutations) of *KRAS* are causally linked to the primary and acquired resistance to anti-EGFR treatment in colorectal cancer (Misale et al., 2012). KRAS is a membrane GTPase that can activate kinases such as c-Raf and PI3K in the EGFR signaling pathway. If *KRAS* is actively mutated, the inhibition of EGFR by cetuximab and panitumumab would not be adequate for blocking the EGFR pathway. The most common *KRAS* mutations in colorectal cancer (with a frequency of 40%) are mutations in exon 2 at G12 and G13 of *KRAS*, which lead to aberrant activation of KRAS. The FDA recommends a genetic test on the *KRAS* gene at these positions before prescribing cetuximab and panitumumab for the treatment of colorectal cancer. Based on the drug labels, cetuximab and panitumumab should be used only for colorectal cancer patients with EGFR expression and wild-type KRAS.

PHARMACOGENOMICS IN OTHER DISEASES

DIABETES

Pharmacogenomic investigations of diabetes mellitus have yielded variations in genomic loci containing common variants with translational consequences of altering disease susceptibility risk, clinical course, and response to standard therapy. This is becoming increasingly important in light of the prospected increased prevalence type 2 diabetes (T2D) to over 300 million cases in the year 2025 (Jiang, 2008; Zimmet, 2001). To this end, polymorphisms in genes related to β-cell function, glucose tolerance, insulin uptake, and other aspects of glucose metabolism are being actively investigated toward effective drug design and personalized responses. To this end, genome-wide association studies (GWAS) have identified >120 T2D risk loci where common and rare variants with varying effects could account for ~15% of the total risk of developing T2D (Zhou, 2016). One of the many classes of antidiabetic agents is the glitazones (such as thiazolidinedione [TZD]), which can be prescribed alone or in combination with sulfonylureas, metformin, or insulin. TZD pharmacologically act by agonizing the nuclear peroxisome proliferator-activated receptor gamma (PPAR-γ) to form heterodimers with the retinoid X receptors (RXR), which bind the PPAR-response elements and regulate target gene transcription. Pro12Ala, polymorphism in the PPAR-γ2, has a frequency of roughly 12% to 15% in the general population, making it the most common PPAR-γ variant. A meta-analysis showed that Ala12 allele displayed a protective effect with regard to developing T2D, reducing the risk in carriers by 19% (Ludovico, 2007). Although one study demonstrated that patients with the Pro12Al genotype receiving rosiglitazone for 12 weeks were significantly better when compared with patients with the homozygous Pro12 (PPAR-γ2) genotype (86.7% and 43.7%, respectively) (Kang et al., 2005), other studies have been inconsistent (Bluher, 2003). TZDs, including pioglitazone, rosiglitazone and troglitazone, have shown pleiotropic effects in reducing vascular risk factors and atherosclerosis. Of note, however, troglitazone was removed from the market due to its hepatoxicity, and rosiglitazone and pioglitazone both have particular warnings due to being

associated with heart diseases. It is thought that specific genetic variations in genes involved in the pathways regulated by TDZs can pose variability in treatment with these drugs (Della-Morte et al., 2014). Polymorphisms in genes associated with TZD toxicity include CYP2C19, CYP2D6, CYP2C8, CYP2C9, and CYP3A4 (Aquilante, 2007); however, the strengths of these relationships vary. Other polymorphisms related to patient responses to antidiabetic agents such as sulfonylureas (tolbutamide [Orinase], glipizide [Glucotrol], glibenclamide [Glyburide], and glimepiride [Amaryl]), biguanides (metformin), meglitinides (nateglinide [Starlix], repaglinide [Prandin]) are reviewed by Avery (2009) and others (Holstein, 2009; Pearson, 2009; Pawlyk, 2014). Furthermore, genetic variations of several membrane transporters, including SLC22A1/2 and SLC47A1/2 genes, are implicated in the highly variable glycemic response to metformin, and cytochrome P450 (CYP) enzymes are implicated in variation of sulfonylurea and meglitinide metabolism (Semiz, 2013). Other allelic polymorphisms (such as TCF7L2, the K allele of the E23K variant in KCNJ11, CTRB1/2, NFATC2, ABCC8) and their relationship to drug efficacy, function, and adverse drug reaction events have also been reported (Zhou, 2016; Pearson 2018). Various genomic consortia, including, including Pharmacogenomics Research Network (www.pgrn.org) and EMERGE network (www.genome.gov/Funded-Programs-Projects/Electronic-Medical-Records-and-Genomics-Network-eMERGE) are providing remarkable bioresourcing opportunities for unique gene-drug-function interrogation (Pearson, 2018).

HUMAN IMMUNODEFICIENCY VIRUS

HIV can be challenging to treat due to the mutational nature of the virus (Wolinski, 1996). Toward this end, common degenerate pathways common to HIV mutants and strains have been targets of drug design such as highly active antiretroviral therapy (HAART), which represents a combination of substances directed against various steps in the viral life cycle. Pharmacogenomic approaches are providing additional information toward devising therapies to decrease morbidity and mortality associated with HIV infections. Earlier studies by Liu et al. (1996) described resistance to HIV-1 infection in cells, obtained from multiply exposed individuals. Those studies found that such patients were homozygous defective for CC-CKR5 and therefore resistant to infection. Polymorphisms in the cytochrome P450 system, which is involved in drug clearance, has also been shown to be of value. The CYP3A4*20 null allele contains a premature stop codon yielding a truncated protein. Subjects of this genotype might be susceptible to side effects during drug therapy with substrates or inhibitors of CYP3A4, and this may have pharmacokinetics and pharmacodynamic application to antiretroviral drug design (Lakhman, 2009; Westlind-Johnsson, 2006). Adverse effects to antiviral medications have also been linked to polymorphisms. The HLA-DRB1*0101 haplotype may determine the susceptibility to Nevirapine (NPV) hypersensitivity, and the 3434T allele at the MDR1 gene is associated with a decreased risk of NPV-induced hepatotoxicity. Genetic polymorphisms in the human leukocyte antigen haplotypes HLD HLA-B*5701, HLA-DR7, and/or HLA-DQ3 have been correlated with susceptibility to Abacavir (ABC) allergic reactions. The presence of a TA insertion into the UGT1A1 promoter (Gilbert syndrome) has been associated with increased occurrence of hyperbilirubinemia of atazanavir (ATZ) and indinavir (IDV). Polymorphism in the *APOC3* gene has been associated with antiretroviral-induced hyperlipidemia; polymorphism at the serine protease kinase inhibitor Kazal-1 (SPINK-1) that encodes a trypsin inhibitor in the cytoplasm of pancreatic acinar cells and the cystic fibrosis transmembrane conductance regulator (CFTR) have been associated with some treatment regimens. Furthermore, many of these responses differ with respect to race (for review, see Clarke & Mousa [2009]). Polymorphisms in specific alleles can also vary among populations. Variations in CYP2B6, CYP2A6, and UGT2B7 alleles in African populations have been reported to have an effect on the metabolism of HIV-1 inhibitors efavirenz and nevirapine (Čolić et al., 2015), and the CYP2B6 c.983T>C polymorphism has been reported to be associated with nevirapine-induced hypersensitivities, including SJS and TEN in Malawian and Ugandan HIV populations (Carr, 2014). Recent studies have assessed the pharmacogenetics on antiretroviral pharmacokinetics and its relationship toward precision dosing for older HIV-infected patients, suggesting that age-related dosage adjustment may be dependent on genetic background since age and p16INK4a (a cellular aging marker) expression interacted with pharmacogenetics on atazanavir and tenofovir disposition (Chen et al., 2018).

OSTEOPOROSIS

Osteoporosis is an increasingly common disorder found in elderly patients often resulting from decreased bone mineral density (BMD) with subsequent enhanced bone fragility collectively leading to an increased incidence of fracture. Genetic susceptibility and hormonal and environmental factors are thought to influence bone mass, and as such polymorphisms and their reciprocal effects on therapeutic interventions are actively sought to design the most efficient medications. The VDR gene codes for the vitamin D receptor, which is the target for the active form of vitamin D, 1,25-dihydroxyvitamin D3 [1,25(OH)2D3]. Polymorphisms in the VDR gene can affect stability and expression of the mRNA. Restriction fragment length polymorphism (RFLP) and linkage disequilibrium analysis have highlighted polymorphisms in the VRD gene (TaqI, ApaI, BsmI, and FokI), some of which have been correlated with increased BMD measurements in certain patients taking antiresorptive drugs, alendronate, or raloxifene as hormone replacement therapy (Massart, 2008), and these responses were allele specific (Nguyen, 2008). Bone density regulation, by hormones such as estrogens, are also subject to the effects of genetic polymorphisms and allelic variation. Studies on the estrogen receptors ERα and ERβ, which are coded for by ESR1 and ESR2 genes, respectively, have shown that women with a particular polymorphism (Xba1) had greater spine and hip BMD and that genetic variations of ESR1 relates to bone structure and strength (Ferrari, 2008). The CYP19 gene codes for an enzyme (aromatase), which catalyzes the conversion of androstenedione to estrone and testosterone to estradiol. Mutations in this gene have been found to correlate with decreased BMD. In addition, enzymes involved in the biogenesis of estrone and estradiol have attracted attention as well as polymorphisms in the regulatory region of the type I collagen gene, COLIA1, affecting the binding site for the transcription factor specificity protein 1 (Sp1) (Thijssen, 2006). The relationship of farnesyl diphosphate synthase (FDPS) polymorphisms on BMD and the response to antiosteoclastic antiresorptive drugs (i.e., aminobisphosphonates such as pamidronate, alendronate, risedronate, ibandronate, and zoledronate) have demonstrated that rs2297480 or rs11264359 alleles were associated with variances in the BMD responses (Olmos, 2012). Other novel genes associated with osteoporosis-related pathways and their relationship to therapeutic intervention, by way of GEFOS/GENOMOS consortia and other modalities, have also been reported (Marini and Brandi, 2014; Riancho & Hernández, 2012; Riancho & Pérez-Campo, 2014).

PSYCHIATRIC AND COGNITIVE DISORDERS

This area of pharmacogenomics has become a burgeoning one and is discussed further in Chapter 73. Here we summarize some of the major advances in this field. Medications prescribed for psychiatric disorders are often administered on a trial-and-error basis (Lin et al., 2006). Furthermore, although depression and other disorders have been linked to certain genetic predispositions, the multifactorial nature of this disease class is wanting for better understanding of causal relationships. As such, clinical correlation studies employing methods such as SNP and linkage studies to facilitate efficiency of antidepressants/antipsychotics with genetic variants have been described (Hamilton, 2015; Lin et al., 2008). As an example, brain-derived neurotrophic factor (BDNF) gene encodes a protein of the nerve growth factor family that regulates synaptic plasticity and connectivity in the brain. A variation of this gene, which codes for a methionine (Met) substitution for valine (Val) at codon 66 (Val66Met), is associated with alterations in brain anatomy and memory (Chen, 2006). Patients with depressive disorder with polymorphisms in this gene have been shown to respond more efficiently to antidepressants such as citalopram, milnacipran, and fluvoxamine in select populations (Choi et al., 2006; Yoshida et al., 2007). Furthermore, BDNF stimulates the release of acetylcholine (ACH). Alzheimer disease (AD) is associated with defective ACH, and recent data demonstrate decreased expression BDNF and its receptor, trk B, in AD patients. As such, agents that serve to upregulate BNDF and/or trk B expression are being investigated with respect to genetic polymorphisms and responses to select drug classes (Fumagalli et al., 2006). Similarly in bipolar disorders, genetic factors and polymorphisms have been attributed to efficient response to drugs such as lithium and clozapine. These include variations in serotonin transporter genes and responses to serotonin reuptake inhibitors among others (Mansour et al., 2002). Regarding autism spectrum disorders (ASD), over 50 ASD-associated copy number variants (CNV) and at least 61 ASD-risk associated genes have been identified. Of the 61 ASD-associated genes, 36 (59%) are associated with known syndromes/phenotypes in OMIM (Online Mendelian Inheritance in Man, www.omim.org), with CHD8, SHANK2, and NLGN3 associated only with ASD (Hoehe & Morris-Rosendahl, 2018). In addition, CNVs have been associated with schizophrenia. Approximately 2.5% of schizophrenia patients will carry one of the associated CNVs (i.e., SETD1A, involved in histone methylation,

among others), and many more genes may be associated through more powerful sequencing studies (Singh et al., 2016; Hoehe & Morris-Rosendahl, 2018). Furthermore, to this end, the Consortium on Genetics of Schizophrenia (COGS) was established to better understand and simplify, where possible, the architecture of such mental disorders, as discussed in Chapter 73. The term *endophenotype* is defined as a trait intermediate between genes and a disorder where a trait "must co-segregate with the illness within a family, and it must be independent of the clinical state" (Gottesman & Gould, 2003). For example, electrophysiologic deficits in prepulse inhibition (linked to FABP7, CHRNA7) and P50 sensory gating or a decline in working memory (linked to RELN) have been considered as endophenotypic intermediate traits in schizophrenia (Demkow & Wolańczyk, 2017; Braff, 2015).

Nucleic variations in other psychiatric disease states have also been described. Studies of Glubb et al. (2009) examined whether a SNP (rs11042725) in the promoter of the adrenomedullin gene (Adm) was associated with mood disorders or selective serotonin reuptake inhibitor (SSRI) antidepressant response. They found that the only significant result was an association of the C/C genotype with a lower likelihood of response to paroxetine (Glubb, 2009). Other genes involved in affective disorders that correlate with selective treatment include variants at the tryptophan hydroxylase gene, 5-HT2a receptor, G protein β3, and inositol polyphosphate 1-phosphatase, among others (Serretti et al., 2002). Furthermore, altered activity of drug-metabolizing enzymes such as CYP2C19, TPMT, and CYP2D6 are becoming important with regard to drug dosing as they can affect steady-state drug levels and effectiveness requiring significant dose reductions in patients who possess the poor metabolizer phenotype (Hamilton, 2015). Attention to polymorphisms such as genetic variations of the CYP450 genotype (CYP2D6, CYP2C9, and CYP2C19) among other variables (substrate drugs and doses, coprescribed inhibitors and inducers, and patient age) have been proposed due to reports of associated akathisia/serotonin toxicity, homicidal or violent behavior, or other deleterious side effects, after taking antidepressant medications (Lucire & Crotty, 2011). Further, studies related to treatment with antipsychotics show a significantly increased risk for tardive dyskinesias in particular for CYP2D6-poor metabolizers, whereas CYP2D6-ultrarapid metabolizers do not appear to have an overall significant influence on antipsychotic drug response (Hoehe & Morris-Rosendahl, 2018). Such genetic element–related response concerns prompted the FDA to issue "black box" warnings on certain medications to alert the physician to determine if a patient carried a specific polymorphism prior to prescribing pharmacopeia to avoid such negative side effects (see http://www.fda.gov/Drugs/ScienceResearch/ResearchAreas/Pharmacogenetics/ucm083378.htm). In addition, the "Genetic Testing Statement" of the International Society of Psychiatric Genetics (ISPG; https://ispg.net/genetic-testing-statement/) is being periodically updated to reflect advances in clinical research as it relates to patient management in this regard.

Addiction Medicine

The opioid epidemic has created critical issues with respect to prescription of narcotic analgesics and pharmaceuticals in general. Recent data have shed light on the unique characteristics that genetic polymorphisms may have on the conversion of parent drug to metabolite. This can have a profound effect when a component of a drug requires processing such as oxidation/reduction (phase I) and/or conjugation (phase II) to be converted to the active form, functionally speaking, and is directly related to the enzyme activity responsible for such conversion. Various polymorphisms within the CYP system have been described that relate to such clinical observations (Schwarz et al., 2016). These include CYP2C19, CYP2D6, CYP2C9, CYP3A4, CYP3A5, CYP1A2, and CYP2B6, among others. For example, the CYP2D6 variant 6*10 corresponds to *decreased* enzymatic activity and is found most commonly among Asians (50%) when compared with African and Caucasian populations, thus warranting consideration of modifying the dosing of opiates such as codeine. Furthermore, the urine drug toxicology (UDT) results of such a patient prescribed codeine may only detect the presence of codeine and not show the characteristic metabolites of hydrocodone and morphine. This is in contrast to the 2D6 variant (*1/*2), representing a gene duplication, translating into *increased* enzymatic activity (ultrametabolizer) with respect to codeine to hydrocodone and morphine conversion. Such a UDT result may have no presence of codeine—rather only hydrocodone, morphine, and hydromorphone—thus posing the inappropriate suspicion of diversion of codeine and surreptitious administration of morphine. Genetic analysis in addition to the relationship of the patient's dose and timing of codeine administration in addition to a complete accounting of polypharmacy (prescribed and nonprescribed) would help clarify any such inconsistencies (Bluth, 2016, 2018; Schwarz et al., 2016).

EPIGENOMICS

The term *epigenetics* (*epi*, Greek "over; above" + *genetics*) refers to changes that occur outside the scope of a gene's DNA sequence. These changes result in phenotypic (appearance) or genotypic expression modulation caused by mechanisms other than changes in the underlying DNA sequence (Russo et al., 1996). Examples of epigenetic phenomena include DNA methylation status, histone coding, single nucleotide polymorphisms, CNVs, and chromatin remodeling, which can affect transcription and subsequent translation of a given gene irrespective of its sequence. As such, epigenetics can be used to describe any aspect other than DNA sequence that influences the development of an organism. Epigenomics can be considered an extension of this concept to convey overall epigenetic states of a cell across the entire genome. An important feature of epigenomics is DNA methylation that has been found to cause differences in protein expression in cells (Zhang et al., 2008), as illustrated in Fig. 75.10. However, other factors, not all of which are clearly understood, appear also to be involved (see below). These concerns make the development of diagnostic tests that could predict an individual's response to a particular drug rather difficult. Profiling the variation in DNA methylation can provide new insights into the regulation of gene expression as well as the mechanisms of individual drug response at a new level of complexity. To this end the National Institutes of Health has published a roadmap to better understand the relationship of epigenomics to the clinical marketplace (https://www.niehs.nih.gov/funding/grants/announcements/roadmap/index.cfm). Their proposition is to study a variety of human cell types, including human embryonic stem cells, differentiating cells, selected differentiated cell lines representative of human disease, and select human primary cells that are relevant to complex human disease. Epigenomes derived from these studies will serve as a reference and resource to identify potential therapeutic targets, enhance understanding of disease mechanisms, provide additional insights to genetic susceptibility of disease, pursue therapeutic opportunities in stem cell–based and tissue regeneration strategies, and understand normal differentiation, development, and aging/senescence. The initiative is intended to elucidate fundamental epigenomic changes or mechanisms underlying specific diseases, conditions of development or aging, or response to exposures (physical, chemical, behavioral, and social factors).

To this end, epigenomics holds potential to shed light on mental disorders (cognitive decline, AD, and schizophrenia) (Hack, 2019; Bennett et al., 2015; Yu et al., 2015; Gomase, 2008), drug addiction and

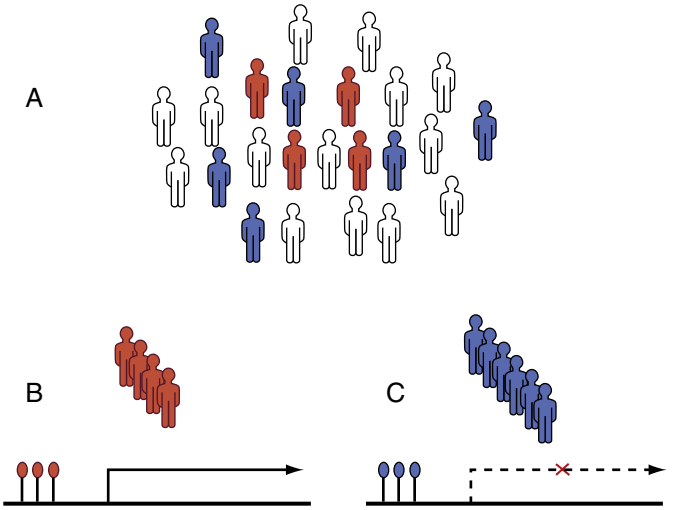

Fig. 75.10 DNA methylation status can affect variation in gene expression and drug response. **A,** For a particular drug response–related gene, there could be people with different epigenetic signatures within a population. *Orange,* sensitive people; *blue,* nonrespondent people; *white,* all others. **B,** Sensitive people have an epigenetic signature that causes overexpression of the gene. **C,** In contrast, nonrespondent people have an epigenetic signature that inhibits gene expression. (From Zhang W, Huang RS, Dolan E: Integrating epigenomics into pharmacogenomic studies, Pharmgenomics Pers Med 1:7–14, 2008, with permission.)

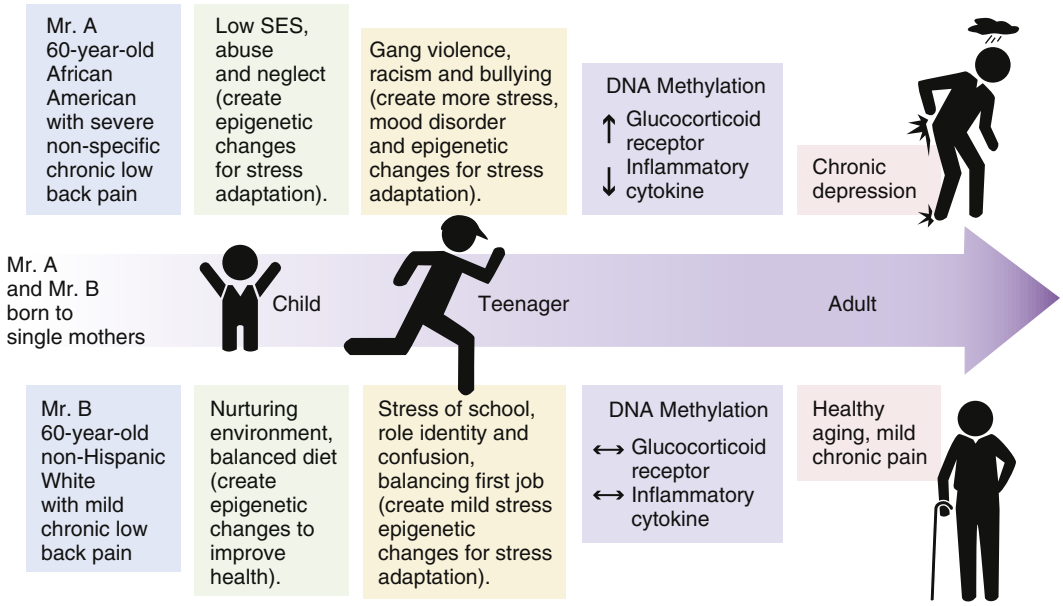

Fig. 75.11 Hypothetical cases of epigenetic changes in chronic pain. (Adapted from Aroke EN, Joseph PV, Roy A, et al.: Could epigenetics help explain racial disparities in chronic pain? *J Pain Res* 12:701–710, 2019, with permission.)

dependence (Mews & Calipari, 2017; Coller et al., 2009), diabetes (Izquierdo & Crujeiras, 2019; Berná et al., 2014; Maier & Olek, 2002), prostate cancer (Gu et al., 2015), autoimmune disorders (Jeffries & Sawalha, 2015), and respiratory diseases (Forno & Celedon, 2019; Bowman et al., 2009), among others. As an example with respect to drug dependence, the mu opioid receptor has a clear involvement in mediating the analgesic and rewarding effects of endogenous and exogenous opioids (Glatt et al., 2007). The most frequently studied of these receptors is the OPRM1 variant, a SNP A118G (recently renamed 304A/G10) in exon 1 that causes an Asn40Asp substitution at a putative glycosylation site in the extracellular domain and occurs at an allelic frequency of between 10% and 40% depending on ethnicity, and epigenetic studies have elucidated potential differences among ethnicities that may have a role in personalizing drug development. Furthermore, intronic SNP (rs9479757) in the OPRM1 locus showed that mild heroin addiction was associated with the AG genotype, whereas severe heroin addiction was associated with the GG genotype among Chinese heroin addicts (Xu et al., 2014). It is important to note that although meta-analyses of such studies may not yield conclusive differences (Coller et al., 2009), there may be differences in gender or in certain ethnicities (Gelernter et al., 1999; Hoehe et al., 2000; Kapur et al., 2007) that may not be apparent when combined with other studies.

Recent studies have postulated epigenetic mechanisms that may be involved in chronic pain where environmental factors such as childhood stress, racial discrimination, economic hardship, and depression can affect gene expression without altering the underlying genetic sequence (Aroke et al., 2019) (Fig. 75.11). To this end, studies of epigenetic changes in chronic pain may interface with altered DNA methylation in the glucocorticoid (stress response) receptor gene, NR3C1, in addition to 11b-HSD2 and FKBP5, in concert with the hypothalamic-pituitary-adrenal (HPA) axis. These changes have been associated with depression, childhood stress, low socioeconomic status, and/or chronic pain. Furthermore, race-related epigenetic alteration may be associated with DNA methylation changes and may play an essential role in the severity of chronic pain (Aroke et al., 2019).

Direct-to-Consumer Genetic Testing

Over the last decade, a new paradigm of direct-to-consumer (DTC) genetic testing has emerged. This happened in part because of the decreased cost of consumables (primer/probe sets, etc.) involved in genetic assessment, the relative ease of multiplex analysis that has developed in light of improved computer processing power, and insurance company denials due to stringent justification and prior authorization requirements as a result of inflated costs for such tests. Part of the insurance companies' reasoning to withhold reimbursement for genetic testing is due to a variegated approach to results, including (a) the variety of available options and methodologies, (b) the complexity of interpreting results, (c) the understanding that many of these tests are "laboratory developed" and do not require FDA premarket approval, and (d) the inability to provide clear distinction regarding new technologies that remain investigational and proven technologies for which scientific evidence is adequate to conclude that the intervention improves health outcomes (Eisenberg & Varmus, 2017; Pezalla, 2016). To this end, genetic counselors are often employed to provide additional clinical value of such tests for patient management.

Nonetheless, this has availed an opportunity for consumers to interrogate their genes for reasons ranging from risk aversion to marriage contemplation to biohacking one's biology toward achieving optimum health (Crow, 2019; Blell & Hunter, 2019). This has spurred a cornucopia of private companies (e.g., 23andMe) availing purchase of home-based kits at commercial drug stores and online retailers where the consumer can provide fluid (blood, saliva) for testing dozens to hundreds of genetic markers and polymorphisms for a fee. Although there have been reports demonstrating that, in certain cases, consumer (vs insurance)–based payment for genetic testing more often shared their results with their physician (Liu et al., 2018) and may appear more involved in their management, there are some downsides with the DTC testing gestalt. These include patients bringing their DTC results to their clinician for interpretation (Artin et al., 2019), the marketing of uniqueness of select testing options to highlight ancestry, wellness, health traits, and athleticism, among others, without the consumer truly understanding the limitations of such tests as well as applications to their health (Wysocki & Osier, 2019). To remedy this, many agree that extensive expansion of pharmacogenomics education is necessary to provide appropriate knowledge to both consumers and clinicians, with respect to methodology and application, toward effective and substantive patient care (Ta et al., 2019).

CONCLUSION

It is clear that the field of pharmacogenomics has heralded a new way of thinking about the relationship of a disease to the individual and the individual's response to a disease state encompassing the spectrum of disease pathophysiology, diagnosis, prognosis, and treatment. As such, the methodologies employed such as single nucleotide polymorphism (SNP), restriction fragment length polymorphism (RFLP), loss of heterozygosity (LOH), genome-wide association studies (GWAS), and hybridization array–based profiling (see also Chapter 70), among others, are as important as the study design, patient demographics, characterization, stratification, comorbidities, and data interpretation. Nonetheless, pharmacogenomics provides a unique approach toward investigating, appreciating, and therapeutically serving the individual patient. Continued investigation and adaptation of pharmacogenomics in clinical medicine should likely provide mankind with improved risk-versus-benefit ratios with respect to therapeutic efficacy versus side-effect profiles and effective reevaluation of drug design toward the generation of novel and specific therapies for disease.

SELECTED REFERENCES

Choi MK, Song IS: Organic cation transporters and their pharmacokinetic and pharmacodynamic consequences, *Drug Metab Pharmacokinet* 23:243–253, 2008.

This review provides an update of our current knowledge on organic cation transporters in terms of their roles in drug pharmacokinetics and pharmacodynamics.

Gossage L, Madhusudan S: Cancer pharmacogenomics: role of DNA repair genetic polymorphisms in individualizing cancer therapy, *Mol Diagn Ther* 11:361–380, 2007.

This review provides an overview on DNA repair pathways and the influence of DNA repair genetic polymorphisms on the clinical outcome (efficacy and toxicity) of DNA-damaging agents and radiotherapy.

Gradhand U, Kim RB: Pharmacogenomics of MRP transporters (ABCC1-5) and BCRP (ABCG2), *Drug Metab Rev* 40:317–354, 2008.

This review provides an overview on ABCC1-5 and ABCG2 transporters with regard to the functional and clinical relevance of their genetic polymorphisms.

Kumar A, Petri ET, Halmos B, et al.: Structure and clinical relevance of the epidermal growth factor receptor in human cancer, *J Clin Oncol* 26:1742–1751, 2008.

This article provides a comprehensive review on the epidermal growth factor receptor (EGFR) with regard to its structure, implication in cancer treatment, and genetic mutations as the determinant of sensitivity or resistance to small-molecule EGFR inhibitors.

Zhang W, Huang RS, Dolan E: Integrating epigenomics into pharmacogenomic studies, *Pharmgenomics Pers Med* 1:7–14, 2008.

This review provides an overview of the effect and relationship of epigenomics—genetic and nongenetic factors—and how they may contribute to pharmacogenomic influence and clinical outcomes.

Zhou SF, Liu JP, Chowbay B: Polymorphism of human cytochrome P450 enzymes and its clinical impact, *Drug Metab Rev* 41:89–95, 2009.

This article provides a comprehensive review on human CYP enzymes with regard to their distribution, substrates, genetic polymorphisms, and clinical relevance.

Access the complete reference list online at Elsevier eBooks for Practicing Clinicians.

REFERENCES

Adler V, Yin Z, Fuchs S, et al.: GSTpi-a regulator of JNK signaling, *EMBO J* 18:1321–1334, 1999.

Agundez JA: Polymorphisms of human N-acetyltransferases and cancer risk, *Curr Drug Metab* 9:520–531, 2008.

Allan JM, Smith AG, Wheatley K, et al.: Genetic variation in XPD predicts treatment outcome and risk of acute myeloid leukemia following chemotherapy, *Blood* 104:3872–3877, 2004.

Amstutz U, Henricks LM, Offer SM, et al.: Clinical pharmacogenetics Implementation Consortium (CPIC) guideline for dihydropyrimidine dehydrogenase genotype and fluoropyrimidine dosing: 2017 update, *Clin Pharmacol Ther* 103:210–216, 2018.

Anderson NG, Ahmad T, Chan K, et al.: ZD1839 (Iressa), a novel epidermal growth factor receptor (EGFR) tyrosine kinase inhibitor, potently inhibits the growth of EGFR-positive cancer cell lines with or without erbB2 overexpression, *Int J Cancer* 94:774–782, 2001.

Andersson T, Flockhart DA, Goldstein DB, et al.: Drug-metabolizing enzymes: evidence for clinical utility of pharmacogenomic tests, *Clin Pharmacol Ther* 78:559–581, 2005.

Andreassen CN, Alsner J, Overgaard M, et al.: Prediction of normal tissue radiosensitivity from polymorphisms in candidate genes, *Radiother Oncol* 69:127–135, 2003.

Aquilante CL: Pharmacogenetics of thiazolidinedione therapy, *Pharmacogenomics* 8:917–931, 2007.

Aroke EN, Joseph PV, Roy A, et al.: Could epigenetics help explain racial disparities in chronic pain? *J Pain Res* 12:701–710, 2019.

Artin MG, Stiles D, Kiryluk K, Chung WK: Cases in precision medicine: when patients present with direct-to-consumer genetic test results, *Ann Intern Med*, 2019 Apr 30https://doi.org/10.7326/M18-2356. [Epub ahead of print].

Aschele C, Debernardis D, Casazza S, et al.: Immunohistochemical quantitation of thymidylate synthase expression in colorectal cancer metastases predicts for clinical outcome to fluorouracil-based chemotherapy, *J Clin Oncol* 17:1760–1770, 1999.

Avery P, Mousa SS, Mousa SA: Pharmacogenomics in type II diabetes mellitus management: steps toward personalized medicine, *Pharmacogenomics Personalized Med* 2:79–91, 2009.

Avery P, Mousa SS, Mousa SA: Pharmacogenomics in type II diabetes mellitus management: steps toward personalized medicine, *Pharmgenomics Pers Med* 2:79–91, 2009.

Balak MN, Gong Y, Riely GJ, et al.: Novel D761Y and common secondary T790M mutations in epidermal growth factor receptor-mutant lung adenocarcinomas with acquired resistance to kinase inhibitors, *Clin Cancer Res* 12:6494–6501, 2006.

Bennett DA, Yu L, Yang J, et al.: Epigenomics of Alzheimer's disease, *Transl Res* 165:200–220, 2015.

Berná G, Oliveras-López MJ, Jurado-Ruíz E, et al.: Nutrigenetics and nutrigenomics insights into diabetes etiopathogenesis, *Nutrients* 6:5338–5369, 2014.

Bewick MA, Conlon MS, Lafrenie RM: Polymorphisms in XRCC1, XRCC3, and CCND1 and survival after treatment for metastatic breast cancer, *J Clin Oncol* 24:5645–5651, 2006.

Bhatnagar V, Xu G, Hamilton BA, et al.: Analyses of 5' regulatory region polymorphisms in human SLC22A6 (OAT1) and SLC22A8 (OAT3), *J Hum Genet* 51:575–580, 2006.

Blell M, Hunter MA: Direct-to-Consumer genetic Testing's red Herring: "genetic ancestry" and personalized medicine, *Front Med* 6:48, 2019.

Blencke S, Zech B, Engkvist O, et al.: Characterization of a conserved structural determinant controlling protein kinase sensitivity to selective inhibitors, *Chem Biol* 11:691–701, 2004.

Bluher M, Lubben G, Paschke R: Analysis of the relationship between the Pro12Ala variant in the PPAR-gamma2 gene and the response rate to therapy with pioglitazone in patients with type 2 diabetes, *Diabetes Care* 26:825–831, 2003.

Blum M, Grant DM, McBride W, et al.: Human arylamine N-acetyltransferase genes: isolation, chromosomal localization, and functional expression, *DNA Cell Biol* 9:193–203, 1990.

Bluth MH: Drug testing and toxicology: redefining the Plague of Darkness, *Clin Lab Med* 36:xi–xx, 2016.

Bluth MH: Introduction: molecular medicine in the common era: applications and impact of molecular Pathology in health and disease, *Clin Lab Med* 38:209–213, 2018.

Bonanni B, Macis D, Maisonneuve P, et al.: Polymorphism in the CYP2D6 tamoxifen-metabolizing gene influences clinical effect but not hot flashes: data from the Italian Tamoxifen Trial, *J Clin Oncol* 24:3708–3709, 2006. author reply 3709.

Borges S, Desta Z, Li L, et al.: Quantitative effect of CYP2D6 genotype and inhibitors on tamoxifen metabolism: implication for optimization of breast cancer treatment, *Clin Pharmacol Ther* 80:61–74, 2006.

Bowman RV, Wright CM, Davidson MR, et al.: Epigenomic targets for the treatment of respiratory disease, *Expert Opin Ther Targets* 13:625–640, 2009.

Bozina N, Bradamante V, Lovric M: Genetic polymorphism of metabolic enzymes P450 (CYP) as a susceptibility factor for drug response, toxicity, and cancer risk, *Arh Hig Rada Toksikol* 60:217–242, 2009.

Bradford LD: CYP2D6 allele frequency in European Caucasians, Asians, Africans and their descendants, *Pharmacogenomics* 3:229–243, 2002.

Braff DL: The importance of endophenotypes in schizophrenia research, *Schizophr Res* 163:1–8, 2015.

Brauch H, Schroth W, Goetz MP, et al.: Tamoxifen use in postmenopausal breast cancer: CYP2D6 matters, *J Clin Oncol* 31:176–180, 2013.

Burger H, Nooter K: Pharmacokinetic resistance to imatinib mesylate: role of the ABC drug pumps ABCG2 (BCRP) and ABCB1 (MDR1) in the oral bioavailability of imatinib, *Cell Cycle* 3:1502–1505, 2004.

Campbell JM, Stephenson MD, Bateman E, et al.: Irinotecan-induced toxicity pharmacogenetics: an umbrella review of systematic reviews and meta-analyses, *Pharmacogenomics J* 17:21–28, 2017.

Camps C, Sarries C, Roig B, et al.: Assessment of nucleotide excision repair XPD polymorphisms in the peripheral blood of gemcitabine/cisplatin-treated advanced non-small-cell lung cancer patients, *Clin Lung Cancer* 4:237–241, 2003.

Cao K, Hollenbach J, Shi X, et al.: Analysis of the frequencies of HLA-A, B, and C alleles and haplotypes in the five major ethnic groups of the United States reveals high levels of diversity in these loci and contrasting distribution patterns in these populations, *Hum Immunol* 62:1009–1030, 2001.

Cao ZH, Wei ZY, Zhu QY, et al.: HLA-B*58:01 allele is associated with augmented risk for both mild and severe cutaneous adverse reactions induced by allopurinol in Han Chinese, *Pharmacogenomics* 13:1193–1201, 2012.

Carlini LE, Meropol NJ, Bever J, et al.: UGT1A7 and UGT1A9 polymorphisms predict response and toxicity in colorectal cancer patients treated with capecitabine/irinotecan, *Clin Cancer Res* 11:1226–1236, 2005.

Carr DF, Chaponda M, Cornejo Castro EM, et al.: CYP2B6 c.983T T>C polymorphism is associated with nevirapine hypersensitivity in Malawian and Ugandan HIV populations, *J Antimicrob Chemother* 69:3329–3334, 2014.

Cartwright RA, Glashan RW, Rogers HJ, et al.: Role of N-acetyltransferase phenotypes in bladder carcinogenesis: a pharmacogenetic epidemiological approach to bladder cancer, *Lancet* 2:842–845, 1982.

Cass I, Baldwin RL, Varkey T, et al.: Improved survival in women with BRCA-associated ovarian carcinoma, *Cancer* 97:2187–2195, 2003.

Chan SH, Tan T: HLA and allopurinol drug eruption, *Dermatol* 179:32–33, 1989.

Chang-Claude J, Popanda O, Tan XL, et al.: Association between polymorphisms in the DNA repair genes, XRCC1, APE1, and XPD and acute side effects of radiotherapy in breast cancer patients, *Clin Cancer Res* 11:4802–4809, 2005.

Chantarangsu S, Mushiroda T, Mahasirimongkol S, et al.: HLA-B*3505 allele is a strong predictor for nevirapine-induced skin adverse drug reactions in HIV-infected Thai patients, *Pharmacogenet Genomics* 19:139–146, 2009.

Chapman PB, Hauschild A, Robert C, et al.: Improved survival with vemurafenib in melanoma with BRAF V600E mutation, *N Engl J Med* 364:2507–2516, 2011.

Chappuis PO, Goffin J, Wong N, et al.: A significant response to neoadjuvant chemotherapy in BRCA1/2 related breast cancer, *J Med Genet* 39:608–610, 2002.

Chen J, Akhtari FS, Wagner MJ, et al.: Pharmacogenetic analysis of the model-based pharmacokinetics of five anti-HIV drugs: how does this influence the effect of aging? *Clin Transl Sci* 11:226–236, 2018.

Chen ZY, Jing D, Bath KG, et al.: Genetic variant BDNF (Val66Met) polymorphism alters anxiety-related behavior, *Science* 314:140–143, 2006.

Cheok MH, Evans WE: Acute lymphoblastic leukaemia: a model for the pharmacogenomics of cancer therapy, *Nat Rev Cancer* 6:117–129, 2006.

Chie L, Friedman FK, Chung DL, Pincus MR: An effector peptide from glutathione-s-transferase-pi strongly and selectively blocks mitotic signaling by oncogenic *ras*-p21, *Protein J* 23:235–238, 2004.

Choi MJ, Kang RH, Lim SW, et al.: Brain-derived neurotrophic factor gene polymorphism (Val66Met) and citalopram response in major depressive disorder, *Brain Res* 1118:176–182, 2006.

Choi MK, Song IS: Organic cation transporters and their pharmacokinetic and pharmacodynamic consequences, *Drug Metab Pharmacokinet* 23:243–253, 2008.

Christensen MM, Brasch-Andersen C, Green H, et al.: The pharmacogenetics of metformin and its impact on plasma metformin steady-state levels and glycosylated hemoglobin A1c, *Pharmacogenet Genomics* 21:837–850, 2011.

Chung WH, Hung SI, Hong HS, et al.: Medical genetics: a marker for Stevens-Johnson syndrome, *Nature* 428:486, 2004.

Ciardiello F, Caputo R, Bianco R, et al.: Inhibition of growth factor production and angiogenesis in human cancer cells by ZD1839 (Iressa), a selective epidermal growth factor receptor tyrosine kinase inhibitor, *Clin Cancer Res* 7:1459–1465, 2001.

Clarke H, Mousa SA: The implications of pharmacogenomics in the treatment of HIV-1-infected patients of African descent, *Pharmacogenomics Personalized Med* 2:93–99, 2009.

Čolić A, Alessandrini M, Pepper MS: Pharmacogenetics of CYP2B6, CYP2A6 and UGT2B7 in HIV treatment in African populations: focus on efavirenz and nevirapine, *Drug Metab Rev* 47:111–123, 2015.

Coller JK, Beardsley J, Bignold J, et al.: Lack of association between the A118G polymorphism of the mu opioid receptor gene (OPRM1) and opioid dependence: a meta-analysis, *Pharmgenomics Pers Med* 2:9–19, 2009.

Conrad S, Kauffmann HM, Ito K, et al.: A naturally occurring mutation in MRP1 results in a selective decrease in organic anion transport and in increased doxorubicin resistance, *Pharmacogenetics* 12:321–330, 2002.

Crewe HK, Notley LM, Wunsch RM, et al.: Metabolism of tamoxifen by recombinant human cytochrome P450 enzymes: formation of the 4-hydroxy, 4'-hydroxy and N-desmethyl metabolites and isomerization of trans-4-hydroxytamoxifen, *Drug Metab Dispos* 30:869–874, 2002.

Crow D: A new Wave of genomics for all, *Cell* 177:5–7, 2019.

Cusatis G, Gregorc V, Li J, et al.: Pharmacogenetics of ABCG2 and adverse reactions to gefitinib, *J Natl Cancer Inst* 98:1739–1742, 2006.

Cutrell AG, Hernandez JE, Fleming JW, et al.: Updated clinical risk factor analysis of suspected hypersensitivity reactions to abacavir, *Ann Pharmacother* 38:2171–2172, 2004.

Dainichi T, Uchi H, Moroi Y, et al.: Stevens-Johnson syndrome, drug-induced hypersensitivity syndrome and toxic epidermal necrolysis caused by allopurinol in patients with a common HLA allele: what causes the diversity? *Dermatology* 215:86–88, 2007.

Danenberg PV: Thymidylate synthetase—a target enzyme in cancer chemotherapy, *Biochim Biophys Acta* 473:73–92, 1977.

Dasaradhi L, Shibutani S: Identification of tamoxifen-DNA adducts formed by alpha-sulfate tamoxifen and alpha-acetoxytamoxifen, *Chem Res Toxicol* 10:189–196, 1997.

Davis W, Venitt S, Phillips DH: The metabolic activation of tamoxifen and alpha-hydroxytamoxifen to DNA-binding species in rat hepatocytes proceeds via sulphation, *Carcinogenesis* 19:861–866, 1998.

de Jong FA, de Jonge MJ, Verweij J, et al.: Role of pharmacogenetics in irinotecan therapy, *Cancer Lett* 234:90–106, 2006.

de las Penas R, Sanchez-Ronco M, Alberola V, et al.: Polymorphisms in DNA repair genes modulate survival in cisplatin/gemcitabine-treated non-small-cell lung cancer patients, *Ann Oncol* 17:668–675, 2006.

De Mattia E, Toffoli G: C677T and A1298C MTHFR polymorphisms, a challenge for antifolate and fluoropyrimidine-based therapy personalisation, *Eur J Cancer* 45:1333–1351, 2009.

De Ruyck K, Van Eijkeren M, Claes K, et al.: Radiation-induced damage to normal tissues after radiotherapy in patients treated for gynecologic tumors: association with single nucleotide polymorphisms in XRCC1, XRCC3, and OGG1 genes and in vitro chromosomal radiosensitivity in lymphocytes, *Int J Radiat Oncol Biol Phys* 62:1140–1149, 2005.

Deenen MJ, Meulendijks D, Cats A, et al.: Upfront genotyping of DPYD*2A to individualize fluoropyrimidine therapy: a safety and cost analysis, *J Clin Oncol* 34:227–234, 2016.

Dehal SS, Kupfer D: CYP2D6 catalyzes tamoxifen 4-hydroxylation in human liver, *Cancer Res* 57:3402–3406, 1997.

Della-Morte D, Palmirotta R, Rehni AK, et al.: Pharmacogenomics and pharmacogenetics of thiazolidinediones: role in diabetes and cardiovascular risk factors, *Pharmacogenomics* 15:2063–2082, 2014.

Demkow U, Wolańczyk T: Genetic tests in major psychiatric disorders-integrating molecular medicine with clinical psychiatry-why is it so difficult?, *Transl Psychiatry* 7, 2017. e1151.

Desta Z, Ward BA, Soukhova NV, et al.: Comprehensive evaluation of tamoxifen sequential biotransformation by the human cytochrome P450 system in vitro: prominent roles for CYP3A and CYP2D6, *J Pharmacol Exp Ther* 310:1062–1075, 2004.

Dias MM, McKinnon RA, Sorich MJ: Impact of the UGT1A1*28 allele on response to irinotecan: a systematic review and meta-analysis, *Pharmacogenomics* 13:889–899, 2012.

Dias MM, Pignon JP, Karapetis CS, et al.: The effect of the UGT1A1*28 allele on survival after irinotecan-based chemotherapy: a collaborative meta-analysis, *Pharmacogenomics J* 14:424–431, 2014.

Dodds HM, Haaz MC, Riou JF, et al.: Identification of a new metabolite of CPT-11 (irinotecan): pharmacological properties and activation to SN-38, *J Pharmacol Exp Ther* 286:578–583, 1998.

Douillard JY, Cunningham D, Roth AD, et al.: Irinotecan combined with fluorouracil compared with fluorouracil alone as first-line treatment for metastatic colorectal cancer: a multicentre randomised trial, *Lancet* 355:1041–1047, 2000.

Eisenberg R, Varmus H: Insurance for broad genomic tests in oncology, *Science* 358:1133–1134, 2017.

Ferrari S: Human genetics of osteoporosis, *Best Pract Res Clin Endocrinol Metab* 22:723–735, 2008.

Forno E, Celedón JC: Epigenomics and Transcriptomics in the prediction and diagnosis of childhood Asthma: are We there yet? *Front Pediatr* 7:115, 2019.

Franke RM, Scherkenbach LA, Sparreboom A: Pharmacogenetics of the organic anion transporting polypeptide 1A2, *Pharmacogenomics* 10:339–344, 2009.

Frueh FW, Amur S, Mummaneni P, et al.: Pharmacogenomic biomarker information in drug labels approved by the United States food and drug administration: prevalence of related drug use, *Pharmacotherapy* 28:992–998, 2008.

Fukuoka M, Yano S, Giaccone G, et al.: Multi-institutional randomized phase II trial of gefitinib for previously treated patients with advanced non-small-cell lung cancer (The IDEAL 1 Trial) [corrected], *J Clin Oncol* 21:2237–2246, 2003.

Fumagalli F, Racagni G, Riva MA: The expanding role of BDNF: a therapeutic target for Alzheimer's disease? *Pharmacogenomics J* 6:8–15, 2006.

Fung KL, Gottesman MM: A synonymous polymorphism in a common MDR1 (ABCB1) haplotype shapes protein function, *Biochim Biophys Acta* 1794:860–871, 2009.

Gangar M, Arias G, O'Brien JG, et al.: Frequency of cutaneous reactions on rechallenge with nevirapine and delavirdine, *Ann Pharmacother* 34:839–842, 2000.

Gao S, Gui XE, Liang K, et al.: HLA-dependent hypersensitivity reaction to nevirapine in Chinese Han HIV-infected patients, *AIDS Res Hum Retroviruses* 28:540–543, 2012.

Garcia-Closas M, Malats N, Silverman D, et al.: NAT2 slow acetylation, GSTM1 null genotype, and risk of bladder cancer: results from the Spanish Bladder Cancer Study and meta-analyses, *Lancet* 366:649–659, 2005.

Garrod AE: The incidence of alcaptonuria: a study in chemical individuality, *Lancet* ii:1616–1620, 1902.

Gatanaga H, Yazaki H, Tanuma J, et al.: HLA-Cw8 primarily associated with hypersensitivity to nevirapine, *AIDS* 21:264–265, 2007.

Gazdar AF: Activating and resistance mutations of EGFR in non-small-cell lung cancer: role in clinical response to EGFR tyrosine kinase inhibitors, *Oncogene* 28(Suppl 1):S24–S31, 2009.

Gelernter J, Kranzler H, Cubells J: Genetics of two mu opioid receptor gene (*OPRM1*) exon 1 polymorphisms: population studies, and allele frequencies in alcohol- and drug-dependent subjects, *Mol Psychiatry* 4:476–483, 1999.

Genin E, Chen DP, Hung SI, et al.: HLA-A*31:01 and different types of carbamazepine-induced severe cutaneous adverse reactions: an international study and meta-analysis, *Pharmacogenomics J* 14:281–288, 2014.

Gjerde J, Geisler J, Lundgren S, et al.: Associations between tamoxifen, estrogens, and FSH serum levels during steady state tamoxifen treatment of postmenopausal women with breast cancer, *BMC Canc* 10:313, 2010.

Glatt H, Meinl W: Pharmacogenetics of soluble sulfotransferases (SULTs), *Naunyn-Schmiedeberg's Arch Pharmacol* 369:55–68, 2004.

Glatt SJ, Bousman C, Wang RS, et al.: Evaluation of *OPRM1* variants in heroin dependence by family-based association testing and meta analysis, *Drug Alcohol Depend* 90:159–165, 2007.

Glubb DM, McHugh PC, Deng X, et al.: Association of a functional polymorphism in the adrenomedullin gene (ADM) with response to paroxetine, *The Pharmacogenomics Journal advance online publication*, 28 July 2009, https://doi.org/10.1038/tpj.2009.33.

Glubb DM, McHugh PC, Deng X, et al.: Association of a functional polymorphism in the adrenomedullin gene (ADM) with response to paroxetine, *Pharmacogenomics J* 10:126–133, 2010.

Goetz MP, Rae JM, Suman VJ, et al.: Pharmacogenetics of tamoxifen biotransformation is associated with clinical outcomes of efficacy and hot flashes, *J Clin Oncol* 23:9312–9318, 2005.

Goetz MP, Sangkuhl K, Guchelaar HJ, et al.: Clinical pharmacogenetics Implementation Consortium (CPIC) guideline for CYP2D6 and tamoxifen therapy, *Clin Pharmacol Ther* 103:770–777, 2018.

Goetz MP, Suman VJ, Hoskin TL, et al.: CYP2D6 metabolism and patient outcome in the Austrian breast and colorectal cancer study group trial (ABCSG) 8, *Clin Cancer Res* 19:500–507, 2013.

Gomase VS, Tagore S: Epigenomics, *Curr Drug Metab* 9:232–237, 2008.

Gorre ME, Mohammed M, Ellwood K, et al.: Clinical resistance to STI-571 cancer therapy caused by BCR-ABL gene mutation or amplification, *Science* 293:876–880, 2001.

Gossage L, Madhusudan S: Cancer pharmacogenomics: role of DNA repair genetic polymorphisms in individualizing cancer therapy, *Mol Diagn Ther* 11:361–380, 2007.

Gottesman MM, Fojo T, Bates SE: Multidrug resistance in cancer: role of ATP-dependent transporters, *Nat Rev Cancer* 2:48–58, 2002.

Gottesman II, Gould TD: The endophenotype concept in psychiatry: etymology and strategic intentions, *Am J Psychiatry* 160(4):636–645, 2003.

Gradhand U, Kim RB: Pharmacogenomics of MRP transporters (ABCC1-5) and BCRP (ABCG2), *Drug Metab Rev* 40:317–354, 2008.

Gu L, Frommel SC, Oakes CC, et al.: BAZ2A (TIP5) is involved in epigenetic alterations in prostate cancer and its overexpression predicts disease recurrence, *Nat Genet* 47:22–30, 2015.

Guillemette C: Pharmacogenomics of human UDP-glucuronosyltransferase enzymes, *Pharmacogenomics J* 3:136–158, 2003.

Gurubhagavatula S, Liu G, Park S, et al.: XPD and XRCC1 genetic polymorphisms are prognostic factors in advanced non-small-cell lung cancer patients treated with platinum chemotherapy, *J Clin Oncol* 22:2594–2601, 2004.

Hack LM, Fries GR, Eyre HA, et al.: Moving pharmacoepigenetics tools for depression toward clinical use, *J Affect Disord* 249:336–346, 2019.

Hamdy SI, Hiratsuka M, Narahara K, et al.: Genotype and allele frequencies of TPMT, NAT2, GST, SULT1A1 and MDR-1 in the Egyptian population, *Br J Clin Pharmacol* 55:560–569, 2003.

Hamilton SP: The promise of psychiatric pharmacogenomics, *Biol Psychiatry* 77:29–35, 2015.

Han JY, Lim HS, Shin ES, et al.: Comprehensive analysis of UGT1A polymorphisms predictive for pharmacokinetics and treatment outcome in patients with non-small-cell lung cancer treated with irinotecan and cisplatin, *J Clin Oncol* 24:2237–2244, 2006.

Han JY, Lim HS, Shin ES, et al.: Influence of the organic anion-transporting polypeptide 1B1 (OATP1B1) polymorphisms on irinotecan-pharmacokinetics and clinical outcome of patients with advanced non-small cell lung cancer, *Lung Canc* 59:69–75, 2008.

Han JY, Lim HS, Shin ES, et al.: Comprehensive analysis of UGT1A polymorphisms predictive for pharmacokinetics and treatment outcome in patients with non-small-cell lung cancer treated with irinotecan and cisplatin, *J Clin Oncol* 24:2237–2244, 2006.

Han JY, Lim HS, Yoo YK, et al.: Associations of ABCB1, ABCC2, and ABCG2 polymorphisms with irinotecan-pharmacokinetics and clinical outcome in patients with advanced non-small cell lung cancer, *Cancer* 110:138–147, 2007.

Hayer-Zillgen M, Bruss M, Bonisch H: Expression and pharmacological profile of the human organic cation transporters hOCT1, hOCT2 and hOCT3, *Br J Pharmacol* 136:829–836, 2002.

Hayes JD: Flanagan JU and Jowsey IR: glutathione transferases, *Annu Rev Pharmacol Toxicol* 45:51–88, 2005.

Heidelberger C, Chaudhuri NK, Danneberg P, et al.: Fluorinated pyrimidines, a new class of tumour-inhibitory compounds, *Nature* 179:663–666, 1957.

Hein DW: Molecular genetics and function of NAT1 and NAT2: role in aromatic amine metabolism and carcinogenesis, *Mutat Res* 506–507:65–77, 2002.

Hershfield MS, Callaghan JT, Tassaneeyakul W, et al.: Clinical Pharmacogenetics Implementation Consortium guidelines for human leukocyte antigen-B genotype and allopurinol dosing, *Clin Pharmacol Ther* 93:153–158, 2013.

Hetherington S, Hughes AR, Mosteller M, et al.: Genetic variations in HLA-B region and hypersensitivity reactions to abacavir, *Lancet* 359:1121–1122, 2002.

Higashi MK, Veenstra DL, Kondo LM, et al.: Association between CYP2C9 genetic variants and anticoagulation-related outcomes during warfarin therapy, *J Am Med Assoc* 287:1690–1698, 2002.

Higgins MJ, Stearns V: CYP2D6 polymorphisms and tamoxifen metabolism: clinical relevance, *Curr Oncol Rep* 12:7–15, 2010.

Hinoshita E, Uchiumi T, Taguchi K, et al.: Increased expression of an ATP-binding cassette superfamily transporter, multidrug resistance protein 2, in human colorectal carcinomas, *Clin Cancer Res* 6:2401–2407, 2000.

Hirano M, Maeda K, Matsushima S, et al.: Involvement of BCRP (ABCG2) in the biliary excretion of pitavastatin, *Mol Pharmacol* 68:800–807, 2005.

Hoehe MR, Kopke K, Wendel B, et al.: Sequence variability and candidate gene analysis in complex disease: association of mu opioid receptor gene variation with substance dependence, *Hum Mol Genet* 9:2895–2908, 2000.

Hoehe MR, Morris-Rosendahl DJ: The role of genetics and genomics in clinical psychiatry, *Dialogues Clin Neurosci* 20:169–177, 2018.

Hoffmeyer S, Burk O, von Richter O, et al.: Functional polymorphisms of the human multidrug-resistance gene: multiple sequence variations and correlation of one allele with P-glycoprotein expression and activity in vivo, *Proc Natl Acad Sci U S A* 97:3473–3478, 2000.

Holstein A, Beil W: Oral antidiabetic drug metabolism: pharmacogenomics and drug interactions, *Expert Opin Drug Metab Toxicol* 5:225–241, 2009.

Hoskins JM, Carey LA, McLeod HL: CYP2D6 and tamoxifen: DNA matters in breast cancer, *Nat Rev Cancer* 9:576–586, 2009.

Hoskins JM, Marcuello E, Altes A, et al.: Irinotecan pharmacogenetics: influence of pharmacodynamic genes, *Clin Cancer Res* 14:1788–1796, 2008.

Huang YS, Chern HD, Su WJ, et al.: Polymorphism of the N-acetyltransferase 2 gene as a susceptibility risk factor for antituberculosis drug-induced hepatitis, *Hepatology* 35:883–889, 2002.

Huang ZH, Hua D, Li LH, et al.: Prognostic role of p53 codon 72 polymorphism in gastric cancer patients treated with fluorouracil-based adjuvant chemotherapy, *J Cancer Res Clin Oncol* 134:1129–1134, 2008.

Hughes DA, Vilar FJ, Ward CC, et al.: Cost-effectiveness analysis of HLA B*5701 genotyping in preventing abacavir hypersensitivity, *Pharmacogenetics* 14:335–342, 2004.

Hulot JS, Villard E, Maguy A, et al.: A mutation in the drug transporter gene ABCC2 associated with impaired methotrexate elimination, *Pharmacogenet Genomics* 15:277–285, 2005.

Hung SI, Chung WH, Jee SH, et al.: Genetic susceptibility to carbamazepine-induced cutaneous adverse drug reactions, *Pharmacogenet Genomics* 16:297–306, 2006.

Hung SI, Chung WH, Liou LB, et al.: HLA-B*5801 allele as a genetic marker for severe cutaneous adverse reactions caused by allopurinol, *Proc Natl Acad Sci U S A* 102:4134–4139, 2005.

Ichikawa W, Takahashi T, Suto K, et al.: Orotate phosphoribosyltransferase gene polymorphism predicts toxicity in patients treated with bolus 5-fluorouracil regimen, *Clin Cancer Res* 12:3928–3934, 2006.

Ichikawa W, Uetake H, Shirota Y, et al.: Both gene expression for orotate phosphoribosyltransferase and its ratio to dihydropyrimidine dehydrogenase influence outcome following fluoropyrimidine-based chemotherapy for metastatic colorectal cancer, *Br J Cancer* 89:1486–1492, 2003.

Ieiri I, Takane H, Otsubo K: The MDR1 (ABCB1) gene polymorphism and its clinical implications, *Clin Pharmacokinet* 43:553–576, 2004.

Iida A, Saito S, Sekine A, et al.: Catalog of 605 single-nucleotide polymorphisms (SNPs) among 13 genes encoding human ATP-binding cassette transporters: ABCA4, ABCA7, ABCA8, ABCD1, ABCD3, ABCD4, ABCE1, ABCF1, ABCG1, ABCG2, ABCG4, ABCG5, and ABCG8, *J Hum Genet* 47:285–310, 2002.

Illing PT, Vivian JP, Dudek NL, et al.: Immune self-reactivity triggered by drug-modified HLA-peptide repertoire, *Nature* 486:554–558, 2012.

Imai Y, Nakane M, Kage K, et al.: C421A polymorphism in the human breast cancer resistance protein gene is associated with low expression of Q141K protein and low-level drug resistance, *Mol Cancer Ther* 1:611–616, 2002.

Ingelman-Sundberg M: Pharmacogenetics of cytochrome P450 and its applications in drug therapy: the past, present and future, *Trends Pharmacol Sci* 25:193–200, 2004.

Innocenti F, Undevia SD, Iyer L, et al.: Genetic variants in the UDP-glucuronosyltransferase 1A1 gene predict the risk of severe neutropenia of irinotecan, *J Clin Oncol* 22:1382–1388, 2004.

Ishikawa T, Tamura A, Saito H, et al.: Pharmacogenomics of the human ABC transporter ABCG2: from functional evaluation to drug molecular design, *Naturwissenschaften* 92:451–463, 2005.

Isla D, Sarries C, Rosell R, et al.: Single nucleotide polymorphisms and outcome in docetaxel-cisplatin-treated advanced non-small-cell lung cancer, *Ann Oncol* 15:1194–1203, 2004.

Iyer L, Das S, Janisch L, et al.: UGT1A1*28 polymorphism as a determinant of irinotecan disposition and toxicity, *Pharmacogenomics J* 2:43–47, 2002.

Izquierdo AG, Crujeiras AB: Role of epigenomic mechanisms in the onset and management of insulin resistance, *Rev Endocr Metab Disord* 20:89–102, 2019.

Izzedine H, Hulot JS, Villard E, et al.: Association between ABCC2 gene haplotypes and tenofovir-induced proximal tubulopathy, *J Infect Dis* 194:1481–1491, 2006.

Janne PA, Johnson BE: Effect of epidermal growth factor receptor tyrosine kinase domain mutations on the outcome of patients with non-small cell lung cancer treated with epidermal growth factor receptor tyrosine kinase inhibitors, *Clin Cancer Res* 12:4416s–4420s, 2006.

Jeffries MA, Sawalha AH: Autoimmune disease in the epigenetic era: how has epigenetics changed our understanding ofdisease and how can we expect the field to evolve? *Expert Rev Clin Immunol* 11:45–58, 2015.

Jensen SA, Vainer B, Witton CJ, et al.: Prognostic significance of numeric aberrations of genes for thymidylate synthase, thymidine phosphorylase and dihydrofolate reductase in colorectal cancer, *Acta Oncol* 47:1054–1061, 2008.

Jiang WJ: Sirtuins: novel targets for metabolic disease in drug development, *Biochem Biophy Res Commun* 373:341–344, 2008.

Jin Y, Hayes DF, Li L, et al.: Estrogen receptor genotypes influence hot flash prevalence and composite score before and after tamoxifen therapy, *J Clin Oncol* 26:5849–5854, 2008.

Johnston PG, Lenz HJ, Leichman CG, et al.: Thymidylate synthase gene and protein expression correlate and are associated with response to 5-fluorouracil in human colorectal and gastric tumors, *Cancer Res* 55:1407–1412, 1995.

Jonker JW, Buitelaar M, Wagenaar E, et al.: The breast cancer resistance protein protects against a major chlorophyll-derived dietary phototoxin and protoporphyria, *Proc Natl Acad Sci U S A* 99:15649–15654, 2002.

Jonker JW, Smit JW, Brinkhuis RF, et al.: Role of breast cancer resistance protein in the bioavailability and fetal penetration of topotecan, *J Natl Cancer Inst* 92:1651–1656, 2000.

Kalow W: Pharmacogenomics: historical perspective and current status. From: Methods in molecular biology. In *Pharmacogenomics: methods and protocols*, vol. 311. Totowa, NJ, 2008, F. Innocenti © Humana Press Inc., pp 3–15.

Kameyama Y, Yamashita K, Kobayashi K, et al.: Functional characterization of SLCO1B1 (OATP-C) variants, SLCO1B1*5, SLCO1B1*15 and SLCO1B1*15+C1007G, by using transient expression systems of HeLa and HEK293 cells, *Pharmacogenet Genomics* 15:513–522, 2005.

Kang ES, Park SY, Kim HJ, et al.: Effects of Pro12Ala polymorphism of peroxisome proliferator-activated receptor gamma2 gene on rosiglitazone response in type 2 diabetes, *Clin Pharmacol Ther* 78:202–208, 2005.

Kang HR, Jee YK, Kim YS, et al.: Positive and negative associations of HLA class I alleles with allopurinol-induced SCARs in Koreans, *Pharmacogenet Genomics* 21:303–307, 2011.

Kang S, Ju W, Kim JW, et al.: Association between excision repair cross-complementation group 1 polymorphism and clinical outcome of platinum-based chemotherapy in patients with epithelial ovarian cancer, *Exp Mol Med* 38:320–324, 2006.

Kaniwa N, Saito Y, Aihara M, et al.: HLA-B locus in Japanese patients with anti-epileptics and allopurinol-related Stevens-Johnson syndrome and toxic epidermal necrolysis, *Pharmacogenomics* 9:161–1622, 2008.

Kapur S, Sharad S, Singh RA, et al.: A118G polymorphism in mu opioid receptor gene (OPRM1): association with opiate addiction in subjects of Indian origin, *J Integr Neurosci* 6:511–522, 2007.

Katayama R, Shaw AT, Khan TM, et al.: Mechanisms of acquired crizotinib resistance in ALK-rearranged lung Cancers, *Sci Transl Med* 4, 2012. 120ra117.

Kawakami K, Omura K, Kanehira E, et al.: Polymorphic tandem repeats in the thymidylate synthase gene is associated with its protein expression in human gastrointestinal cancers, *Anticancer Res* 19:3249–3252, 1999.

Kerb R: Implications of genetic polymorphisms in drug transporters for pharmacotherapy, *Cancer Lett* 234:4–33, 2006.

Khanna D, Khanna PP, Fitzgerald JD, et al.: American College of Rheumatology guidelines for management of gout. Part 2: therapy and antiinflammatory prophylaxis of acute gouty arthritis, *Arthritis Care Res* 64:1447–1461, 2012.

Kim RB: MDR1 single nucleotide polymorphisms: multiplicity of haplotypes and functional consequences, *Pharmacogenetics* 12:425–427, 2002.

Kim SH, Lee KW, Song WJ, et al.: Carbamazepine-induced severe cutaneous adverse reactions and HLA genotypes in Koreans, *Epilepsy Res* 97:190–197, 2011.

Kimchi-Sarfaty C, Oh JM, Kim IW, et al.: A "silent" polymorphism in the MDR1 gene changes substrate specificity, *Science* 315:525–528, 2007.

Ko TM, Chung WH, Wei CY, et al.: Shared and restricted T-cell receptor use is crucial for carbamazepine-induced Stevens-Johnson syndrome, *J Allergy Clin Immunol* 128:1266–1276, 2011. e11.

Kobayashi D, Ieiri I, Hirota T, et al.: Functional assessment of ABCG2 (BCRP) gene polymorphisms to protein expression in human placenta, *Drug Metab Dispos* 33:94–101, 2005.

Kondo C, Onuki R, Kusuhara H, et al.: Lack of improvement of oral absorption of ME3277 by prodrug formation is ascribed to the intestinal efflux mediated by breast cancer resistant protein (BCRP/ABCG2), *Pharm Res (N Y)* 22:613–618, 2005.

Konig J, Seithel A, Gradhand U, et al.: Pharmacogenomics of human OATP transporters, *Naunyn-Schmiedeberg's Arch Pharmacol* 372:432–443, 2006.

Kris MG, Natale RB, Herbst RS, et al.: Efficacy of gefitinib, an inhibitor of the epidermal growth factor receptor tyrosine kinase, in symptomatic patients with non-small cell lung cancer: a randomized trial, *J Am Med Assoc* 290:2149–2158, 2003.

Krishnamurthy P, Schuetz JD: Role of ABCG2/BCRP in biology and medicine, *Annu Rev Pharmacol Toxicol* 46:381–410, 2005.

Kulkantrakorn K, Tassaneeyakul W, Tiamkao S, et al.: HLA-B*1502 strongly predicts carbamazepine-induced Stevens-Johnson syndrome and toxic epidermal necrolysis in Thai patients with neuropathic pain, *Pain Pract* 12:202–208, 2012.

Kumar A, Petri ET, Halmos B, et al.: Structure and clinical relevance of the epidermal growth factor receptor in human cancer, *J Clin Oncol* 26:1742–1751, 2008.

Kuptsova N, Kopecky KJ, Godwin J, et al.: Polymorphisms in DNA repair genes and therapeutic outcomes of AML patients from SWOG clinical trials, *Blood* 109:3936–3944, 2007.

Kwak EL, Bang YJ, Camidge DR, et al.: Anaplastic lymphoma kinase inhibition in non-small-cell lung cancer, *N Engl J Med* 363:1693–1703, 2010.

Lakhman SS, Ma Q, Morse GD: Pharmacogenomics of CYP3A: considerations for HIV treatment, *Pharmacogenomics* 10:1323–1339, 2009.

Leichman CG, Lenz HJ, Leichman L, et al.: Quantitation of intratumoral thymidylate synthase expression predicts for disseminated colorectal cancer response and resistance to protracted-infusion fluorouracil and weekly leucovorin, *J Clin Oncol* 15:3223–3229, 1997.

Lepper ER, Nooter K, Verweij J, et al.: Mechanisms of resistance to anticancer drugs: the role of the polymorphic ABC transporters ABCB1 and ABCG2, *Pharmacogenomics* 6:115–138, 2005.

Leslie EM, Letourneau IJ, Deeley RG, et al.: Functional and structural consequences of cysteine substitutions in the NH2 proximal region of the human multidrug resistance protein 1 (MRP1/ABCC1), *Biochemistry* 42:5214–5224, 2003.

Letschert K, Keppler D, Konig J: Mutations in the SLCO1B3 gene affecting the substrate specificity of the hepatocellular uptake transporter OATP1B3 (OATP8), *Pharmacogenetics* 14:441–452, 2004.

Li D, Li Y, Jiao L, et al.: Effects of base excision repair gene polymorphisms on pancreatic cancer survival, *Int J Cancer* 120:1748–1754, 2007a.

Li J, Bluth MH: Pharmacogenomics of drug metabolizing enzymes and transporters: implications for cancer therapy, *Pharmgenomics Pers Med* 4:11–33, 2011.

Li J, Cusatis G, Brahmer J, et al.: Association of variant ABCG2 and the pharmacokinetics of epidermal growth factor receptor tyrosine kinase inhibitors in cancer patients, *Cancer Biol Ther* 6:432–438, 2007b.

Likanonsakul S, Rattanatham T, Feangvad S, et al.: HLA-Cw*04 allele associated with nevirapine-induced rash in HIV-infected Thai patients, *AIDS Res Ther* 6:22, 2009.

Lim HS, Ju Lee H, Seok Lee K, et al.: Clinical implications of CYP2D6 genotypes predictive of tamoxifen pharmacokinetics in metastatic breast cancer, *J Clin Oncol* 25:3837–3845, 2007.

Lin E, Chen PS: Pharmacogenomics with antidepressants in the STAR*D study, *Pharmacogenomics* 9:935–946, 2008.

Lin E, Hwang Y, Tzeng CM: A case study of the utility of the HapMap database for pharmacogenomic haplotype analysis in the Taiwanese population, *Mol Diagn Ther* 10:367–370, 2006.

Lin E, Hwang Y, Tzeng CM: A case study of the utility of the HapMap database for pharmacogenomic haplotype analysis in the Taiwanese population, *Mol Diagn Ther* 10:367–370, 2006.

Link E, Parish S, Armitage J, et al.: SLCO1B1 variants and statin-induced myopathy–a genomewide study, *N Engl J Med* 359:789–799, 2008.

Littera R, Carcassi C, Masala A, et al.: HLA-dependent hypersensitivity to nevirapine in Sardinian HIV patients, *AIDS* 20:1621–1626, 2006.

Liu R, Paxton WA, Choe S, et al.: Homozygous defect in HIV-1 coreceptor accounts for resistance of some multiply-exposed individuals to HIV-1 infection, *Cell* 86:367–377, 1996.

Liu W, Outlaw JJ, Wineinger N, Boeldt D, Bloss CS: Effect of co-payment on behavioral response to consumer genomic testing, *Transl Behav Med* 8:130–136, 2018.

Lo HW, Ali-Osman F: Genetic polymorphism and function of glutathione S-transferases in tumor drug resistance, *Curr Opin Pharmacol* 7:367–374, 2007.

Lonjou C, Thomas L, Borot N, et al.: A marker for Stevens-Johnson syndrome: ethnicity matters, *Pharmacogenomics J* 6:265–268, 2006.

Lu Z, Zhang R, Diasio RB: Dihydropyrimidine dehydrogenase activity in human peripheral blood mononuclear cells and liver: population characteristics, newly identified deficient patients, and clinical implication in 5-fluorouracil chemotherapy, *Cancer Res* 53:5433–5438, 1993.

Lucire Y, Crotty C: Antidepressant-induced akathisia-related homicides associated with diminishing mutations in metabolizing genes of the CYP450 family, *Pharmgenomics Pers Med* 4:65–81, 2011.

Ludovico O, Pellegrini F, Di Paola R, et al.: Heterogeneous effect of peroxisome proliferator-activated receptor gamma2 Ala12 variant on type 2 diabetes risk, *Obesity* 15:1076–1081, 2007.

Luo FR, Paranjpe PV, Guo A, et al.: Intestinal transport of irinotecan in Caco-2 cells and MDCK II cells overexpressing efflux transporters Pgp, cMOAT, and MRP1, *Drug Metab Dispos* 30:763–770, 2002.

Lurje G, Manegold PC, Ning Y, et al.: Thymidylate synthase gene variations: predictive and prognostic markers, *Mol Cancer Ther* 8:1000–1007, 2009.

Lynch TJ, Bell DW, Sordella R, et al.: Activating mutations in the epidermal growth factor receptor underlying responsiveness of non-small-cell lung cancer to gefitinib, *N Engl J Med* 350:2129–2139, 2004.

Mahungu T, Smith C, Turner F, et al.: Cytochrome P450 2B6 516G–>T is associated with plasma concentrations of nevirapine at both 200 mg twice daily and 400 mg once daily in an ethnically diverse population, *HIV Med* 10:310–317, 2009.

Maier S, Olek A: Diabetes: a candidate disease for efficient DNA methylation profiling, *J Nutr* 132:2440S–2443S, 2002.

Mallal S, Nolan D, Witt C, et al.: Association between presence of HLA-B*5701, HLA-DR7, and HLA-DQ3 and hypersensitivity to HIV-1 reverse-transcriptase inhibitor abacavir, *Lancet* 359:727–732, 2002.

Mallal S, Phillips E, Carosi G, et al.: HLA-B*5701 screening for hypersensitivity to abacavir, *N Engl J Med* 358:568–579, 2008.

Mancinelli L, Cronin M, Sadée W: Pharmacogenomics: the promise of personalized medicine, *AAPS PharmSci* 2(1), 2000. Article 4 http://www.aapspharmsci.org/.

Mandola MV, Stoehlmacher J, Muller-Weeks S, et al.: A novel single nucleotide polymorphism within the 5' tandem repeat polymorphism of the thymidylate synthase gene abolishes USF-1 binding and alters transcriptional activity, *Cancer Res* 63:2898–2904, 2003.

Mandola MV, Stoehlmacher J, Zhang W, et al.: A 6 bp polymorphism in the thymidylate synthase gene causes message instability and is associated with decreased intratumoral TS mRNA levels, *Pharmacogenetics* 14:319–327, 2004.

Mansour HA, Alda M, Nimgaonkar VL: Pharmacogenetics of bipolar disorder, *Curr Psychiatry Rep* 4:117–123, 2002.

Marini F, Brandi ML: Pharmacogenetics of osteoporosis, *Best Pract Res Clin Endocrinol Metab* 28:783–793, 2014.

Marsh S, Hoskins JM: Irinotecan pharmacogenomics, *Pharmacogenomics* 11:1003–1010, 2010.

Marsh S: Thymidylate synthase pharmacogenetics, *Invest New Drugs* 23:533–537, 2005.

Martin AM, Nolan D, James I, et al.: Predisposition to nevirapine hypersensitivity associated with HLA-DRB1*0101 and abrogated by low CD4 T-cell counts, *AIDS* 19:97–99, 2005.

Marzolini C, Paus E, Buclin T, et al.: Polymorphisms in human MDR1 (P-glycoprotein): recent advances and clinical relevance, *Clinical Pharmacol Ther* 75:13–33, 2004.

Marzolini C, Tirona RG, Kim RB: Pharmacogenomics of the OATP and OAT families, *Pharmacogenomics* 5:273–282, 2004b.

Massart F, Marcucci G, Brandi ML: Pharmacogenetics of bone treatments: the VDR and ERalpha gene story, *Pharmacogenomics* 9:733–746, 2008.

Mathijssen RH, Marsh S, Karlsson MO, et al.: Irinotecan pathway genotype analysis to predict pharmacokinetics, *Clin Cancer Res* 9:3246–3253, 2003.

Mathijssen RH, van Alphen RJ, Verweij J, et al.: Clinical pharmacokinetics and metabolism of irinotecan (CPT-11), *Clin Cancer Res* 7:2182–2194, 2001.

McCormack M, Alfirevic A, Bourgeois S, et al.: HLA-A*3101 and carbamazepine-induced hypersensitivity reactions in Europeans, *N Engl J Med* 364:1134–1143, 2011.

McIlwain CC, Townsend DM, Tew KD: Glutathione S-transferase polymorphisms: cancer incidence and therapy, *Oncogene* 25:1639–1648, 2006.

Mehta TY, Prajapati LM, Mittal B, et al.: Association of HLA-B*1502 allele and carbamazepine-induced Stevens-Johnson syndrome among Indians, *Indian J Dermatol Venereol Leprol* 75:579–582, 2009.

Meier Y, Pauli-Magnus C, Zanger UM, et al.: Interindividual variability of canalicular ATP-binding-cassette (ABC)-transporter expression in human liver, *Hepatology* 44:62–74, 2006.

Merino G, Jonker JW, Wagenaar E, et al.: The breast cancer resistance protein (BCRP/ABCG2) affects pharmacokinetics, hepatobiliary excretion, and milk secretion of the antibiotic nitrofurantoin, *Mol Pharmacol* 67:1758–1764, 2005.

Meulendijks D, Henricks LM, Sonke GS, et al.: Clinical relevance of DPYD variants c.1679T>G, c.1236G>A/HapB3, and c.1601G>A as predictors of severe fluoropyrimidine-associated toxicity: a systematic review and meta-analysis of individual patient data, *Lancet Oncol* 16:1639–1650, 2015.

Mews P, Calipari ES: Cross-talk between the epigenome and neural circuits in drug addiction, *Prog Brain Res* 235:19–63, 2017.

Meyer zu Schwabedissen HE, Jedlitschky G, Gratz M, et al.: Variable expression of MRP2 (ABCC2) in human placenta: influence of gestational age and cellular differentiation, *Drug Metab Dispos* 33:896–904, 2005.

Meyer zu Schwabedissen HE, Kim RB: Hepatic OATP1B transporters and nuclear receptors PXR and CAR: interplay, regulation of drug disposition genes, and single nucleotide polymorphisms, *Mol Pharm* 6:1644–1661, 2009.

Milojkovic D, Apperley J: Mechanisms of resistance to imatinib and second-generation tyrosine inhibitors in chronic myeloid leukemia, *Clin Cancer Res* 15:7519–7527, 2009.

Misale S, Yaeger R, Hobor S, et al.: Emergence of KRAS mutations and acquired resistance to anti-EGFR therapy in colorectal cancer, *Nature* 486:532–536, 2012.

Mitomo H, Kato R, Ito A, et al.: A functional study on polymorphism of the ATP-binding cassette transporter ABCG2: critical role of arginine-482 in methotrexate transport, *Biochem J* 373:767–774, 2003.

Mizuarai S, Aozasa N, Kotani H: Single nucleotide polymorphisms result in impaired membrane localization and reduced ATPase activity in multidrug transporter ABCG2, *Int J Cancer* 109:238–246, 2004.

Mizutani T: PM frequencies of major CYPs in Asians and Caucasians, *Drug Metab Rev* 35:99–106, 2003.

Morel A, Boisdron-Celle M, Fey L, et al.: Clinical relevance of different dihydropyrimidine dehydrogenase gene single nucleotide polymorphisms on 5-fluorouracil tolerance, *Mol Cancer Ther* 5:2895–2904, 2006.

Moreno V, Gemignani F, Landi S, et al.: Polymorphisms in genes of nucleotide and base excision repair: risk and prognosis of colorectal cancer, *Clin Cancer Res* 12:2101–2108, 2006.

Moullan N, Cox DG, Angele S, et al.: Polymorphisms in the DNA repair gene XRCC1, breast cancer risk, and response to radiotherapy, *Cancer Epidemiol Biomarkers Prev* 12:1168–1174, 2003.

Nagar S, Remmel RP: Uridine diphosphoglucuronosyltransferase pharmacogenetics and cancer, *Oncogene* 25:1659–1672, 2006.

Nguyen TV, Center JR, Eisman JA: Pharmacogenetics of osteoporosis and the prospect of individualized prognosis and individualized therapy, *Curr Opin Endocrinol Diabetes Obes* 15:481–488, 2008.

Niemi M, Backman JT, Kajosaari LI, et al.: Polymorphic organic anion transporting polypeptide 1B1 is a major determinant of repaglinide pharmacokinetics, *Clin Pharmacol Ther* 77:468–478, 2005.

Niemi M, Pasanen MK, Neuvonen PJ: SLCO1B1 polymorphism and sex affect the pharmacokinetics of pravastatin but not fluvastatin, *Clin Pharmacol Ther* 80:356–366, 2006.

Niemi M: Role of OATP transporters in the disposition of drugs, *Pharmacogenomics* 8:787–802, 2007.

Nishizato Y, Ieiri I, Suzuki H, et al.: Polymorphisms of OATP-C (SLC21A6) and OAT3 (SLC22A8) genes: consequences for pravastatin pharmacokinetics, *Clin Pharmacol Ther* 73:554–565, 2003.

Norcross MA, Luo S, Lu L, et al.: Abacavir induces loading of novel self-peptides into HLA-B*57: 01: an autoimmune model for HLA-associated drug hypersensitivity, *AIDS* 26:F21–F29, 2012.

Nowell S, Falany C: Pharmacogenetics of human cytosolic sulfotransferases, *Oncogene* 25:1673–1678, 2006.

Nowell S, Sweeney C, Winters M, et al.: Association between sulfotransferase 1A1 genotype and survival of breast cancer patients receiving tamoxifen therapy, *J Natl Cancer Inst* 94:1635–1640, 2002.

Nowell SA, Ahn J, Rae JM, et al.: Association of genetic variation in tamoxifen-metabolizing enzymes with overall survival and recurrence of disease in breast cancer patients, *Breast Cancer Res Treat* 91:249–258, 2005.

Nozawa T, Minami H, Sugiura S, et al.: Role of organic anion transporter OATP1B1 (OATP-C) in hepatic uptake of irinotecan and its active metabolite, 7-ethyl-10-hydroxycamptothecin: in vitro evidence and effect of single nucleotide polymorphisms, *Drug Metab Dispos* 33:434–439, 2005.

Nozawa T, Nakajima M, Tamai I, et al.: Genetic polymorphisms of human organic anion transporters OATP-C (SLC21A6) and OATP-B (SLC21A9): allele frequencies in the Japanese population and functional analysis, *J Pharmacol Exp Ther* 302:804–813, 2002.

Olmos JM, Zarrabeitia MT, Hernández JL, et al.: Common allelic variants of the farnesyl diphosphate synthase gene influence the response of osteoporotic women to bisphosphonates, *Pharmacogenomics J* 12:227–232, 2012.

Omura K: Clinical implications of dihydropyrimidine dehydrogenase (DPD) activity in 5-FU-based chemotherapy: mutations in the DPD gene, and DPD inhibitory fluoropyrimidines, *Int J Clin Oncol* 8:132–138, 2003.

Ostrov DA, Grant BJ, Pompeu YA, et al.: Drug hypersensitivity caused by alteration of the MHC-presented self-peptide repertoire, *Proc Natl Acad Sci U S A* 109:9959–9964, 2012.

Ozeki T, Mushiroda T, Yowang A, et al.: Genome-wide association study identifies HLA-A*3101 allele as a genetic risk factor for carbamazepine-induced cutaneous adverse drug reactions in Japanese population, *Hum Mol Genet* 20:1034–1041, 2011.

Padovan E, Bauer T, Tongio MM, et al.: Penicilloyl peptides are recognized as T cell antigenic determinants in penicillin allergy, *Eur J Immunol* 27:1303–1307, 1997.

Paez JG, Janne PA, Lee JC, et al.: EGFR mutations in lung cancer: correlation with clinical response to gefitinib therapy, *Science* 304:1497–1500, 2004.

Pao W, Miller V, Zakowski M, et al.: EGF receptor gene mutations are common in lung cancers from "never smokers" and are associated with sensitivity of tumors to gefitinib and erlotinib, *Proc Natl Acad Sci U S A* 101:13306–13311, 2004.

Parham P, Ohta T: Population biology of antigen presentation by MHC class I molecules, *Science* 272:67–74, 1996.

Park DJ, Stoehlmacher J, Zhang W, et al.: A Xeroderma pigmentosum group D gene polymorphism predicts clinical outcome to platinum-based chemotherapy in patients with advanced colorectal cancer, *Cancer Res* 61:8654–8658, 2001.

Park DJ, Zhang W, Stoehlmacher J, et al.: ERCC1 gene polymorphism as a predictor for clinical outcome in advanced colorectal cancer patients treated with platinum-based chemotherapy, *Clin Adv Hematol Oncol* 1:162–166, 2003.

Parte P, Kupfer D: Oxidation of tamoxifen by human flavin-containing monooxygenase (FMO) 1 and FMO3 to tamoxifen-N-oxide and its novel reduction back to tamoxifen by human cytochromes P450 and hemoglobin, *Drug Metab Dispos* 33:1446–1452, 2005.

Pauli-Magnus C, Kroetz DL: Functional implications of genetic polymorphisms in the multidrug resistance gene MDR1 (ABCB1), *Pharm Res (N Y)* 21:904–913, 2004.

Pavlos R, Mallal S, Phillips E: HLA and pharmacogenetics of drug hypersensitivity, *Pharmacogenomics* 13:1285–1306, 2012.

Pawlyk AC, Giacomini KM, McKeon C, et al.: Metformin pharmacogenomics: current status and future directions, *Diabetes* 63:2590–2599, 2014.

Pearson ER: Pharmacogenetics and future strategies in treating hyperglycaemia in diabetes, *Front Biosci* 14:4348–4362, 2009.

Pearson ER: Pharmacogenetics and target identification in diabetes, *Curr Opin Genet Dev* 50:68–73, 2018.

Pentikainen PJ, Neuvonen PJ, Penttila A: Pharmacokinetics of metformin after intravenous and oral administration to man, *Eur J Clin Pharmacol* 16:195–202, 1979.

Petty WJ, Knight SN, Mosley L, et al.: A pharmacogenomic study of docetaxel and gemcitabine for the initial treatment of advanced non-small cell lung cancer, *J Thorac Oncol* 2:197–202, 2007.

Pezalla EJ: Payer view of personalized medicine, *Am J Health Syst Pharm* 73:2007–2012, 2016.

Phillips EJ, Sukasem C, Whirl-Carrillo M, et al.: Clinical pharmacogenetics Implementation Consortium guideline for HLA genotype and Use of carbamazepine and Oxcarbazepine: 2017 update, *Clin Pharmacol Ther* 103:574–581, 2018.

Pollard RB, Robinson P, Dransfield K: Safety profile of nevirapine, a nonnucleoside reverse transcriptase inhibitor for the treatment of human immunodeficiency virus infection, *Clin Ther* 20:1071–1092, 1998.

Popat S, Matakidou A, Houlston RS: Thymidylate synthase expression and prognosis in colorectal cancer: a systematic review and meta-analysis, *J Clin Oncol* 22:529–536, 2004.

Premawardhena A, Fisher CA, Liu YT, et al.: The global distribution of length polymorphisms of the promoters of the glucuronosyltransferase 1 gene (UGT1A1): hematologic and evolutionary implications, *Blood Cells Mol Dis* 31:98–101, 2003.

Province MA, Goetz MP, Brauch H, et al.: CYP2D6 genotype and adjuvant tamoxifen: meta-analysis of heterogeneous study populations, *Clin Pharmacol Ther* 95:216–227, 2014.

Pullarkat ST, Stoehlmacher J, Ghaderi V, et al.: Thymidylate synthase gene polymorphism determines response and toxicity of 5-FU chemotherapy, *Pharmacogenomics J* 1:65–70, 2001.

Rae JM, Drury S, Hayes DF, et al.: CYP2D6 and UGT2B7 genotype and risk of recurrence in tamoxifen-treated breast cancer patients, *J Natl Cancer Inst* 104:452–460, 2012.

Ratain MJ: Irinotecan dosing: does the CPT in CPT-11 stand for "Can't Predict Toxicity"? *J Clin Oncol* 20:7–8, 2002.

Raymond E, Faivre S, Armand JP: Epidermal growth factor receptor tyrosine kinase as a target for anticancer therapy, *Drugs* 60(Suppl 1):15–23, 2000. discussion 41-42.

Regan MM, Leyland-Jones B, Bouzyk M, et al.: CYP2D6 genotype and tamoxifen response in postmenopausal women with endocrine-responsive breast cancer: the breast international group 1-98 trial, *J Natl Cancer Inst* 104:441–451, 2012.

Relling MV, Dervieux T: Pharmacogenetics and cancer therapy, *Nat Rev Cancer* 1:99–108, 2001.

Riancho JA, Hernández JL: Pharmacogenomics of osteoporosis: a pathway approach, *Pharmacogenomics* 13:815–829, 2012.

Riancho JA, Pérez-Campo FM: Pharmacogenomics of osteoporotic fractures, *Methods Mol Biol* 1175:661–670, 2014.

Rivory LP, Riou JF, Haaz MC, et al.: Identification and properties of a major plasma metabolite of irinotecan (CPT-11) isolated from the plasma of patients, *Cancer Res* 56:3689–3694, 1996.

Rodriguez-Antona C, Ingelman-Sundberg M: Cytochrome P450 pharmacogenetics and cancer, *Oncogene* 25:1679–1691, 2006.

Rothnie A, Callaghan R, Deeley RG, et al.: Role of GSH in estrone sulfate binding and translocation by the multidrug resistance protein 1 (MRP1/ABCC1), *J Biol Chem* 281:13906–13914, 2006.

Roy JN, Lajoie J, Zijenah LS, et al.: CYP3A5 genetic polymorphisms in different ethnic populations, *Drug Metab Dispos* 33:884–887, 2005.

Rudolph MG, Stanfield RL, Wilson IA: How TCRs bind MHCs, peptides, and coreceptors, *Ann Rev Immunol* 24:419–466, 2006.

Russo VEA, Martienssen RA, Riggs AD: *Epigenetic mechanisms of gene regulation*, Plainview, N.Y, 1996, Cold Spring Harbor Laboratory Press.

Ruzzo A, Graziano F, Kawakami K, et al.: Pharmacogenetic profiling and clinical outcome of patients with advanced gastric cancer treated with palliative chemotherapy, *J Clin Oncol* 24:1883–1891, 2006.

Ruzzo A, Graziano F, Loupakis F, et al.: Pharmacogenetic profiling in patients with advanced colorectal cancer treated with first-line FOLFIRI chemotherapy, *Pharmacogenomics J* 8:278–288, 2008.

Ryu JS, Hong YC, Han HS, et al.: Association between polymorphisms of ERCC1 and XPD and survival in non-small-cell lung cancer patients treated with cisplatin combination chemotherapy, *Lung Canc* 44:311–316, 2004.

Sakaeda T: MDR1 genotype-related pharmacokinetics: fact or fiction? *Drug Metab Pharmacokinet* 20:391–414, 2005.

Salonga D, Danenberg KD, Johnson M, et al.: Colorectal tumors responding to 5-fluorouracil have low gene expression levels of dihydropyrimidine dehydrogenase, thymidylate synthase, and thymidine phosphorylase, *Clin Cancer Res* 6:1322–1327, 2000.

Saltz LB, Cox JV, Blanke C, et al.: Irinotecan plus fluorouracil and leucovorin for metastatic colorectal cancer. Irinotecan Study Group, *N Engl J Med* 343:905–914, 2000.

Schackman BR, Scott CA, Walensky RP, et al.: The cost-effectiveness of HLA-B*5701 genetic screening to guide initial antiretroviral therapy for HIV, *AIDS* 22:2025–2033, 2008.

Schaeffeler E, Fischer C, Brockmeier D, et al.: Comprehensive analysis of thiopurine S-methyltransferase phenotype-genotype correlation in a large population of German-Caucasians and identification of novel TPMT variants, *Pharmacogenetics* 14:407–417, 2004.

Schellens JH, Maliepaard M, Scheper RJ, et al.: Transport of topoisomerase I inhibitors by the breast cancer resistance protein. Potential clinical implications, *Ann N Y Acad Sci* 922:188–194, 2000.

Schroth W, Antoniadou L, Fritz P, et al.: Breast cancer treatment outcome with adjuvant tamoxifen relative to patient CYP2D6 and CYP2C19 genotypes, *J Clin Oncol* 25:5187–5193, 2007.

Schroth W, Goetz MP, Hamann U, et al.: Association between CYP2D6 polymorphisms and outcomes among women with early stage breast cancer treated with tamoxifen, *J Am Med Assoc* 302:1429–1436, 2009.

Schroth W, Winter S, Murdter T, et al.: Improved prediction of endoxifen metabolism by CYP2D6 genotype in breast cancer patients treated with tamoxifen, *Front Pharmacol* 8:582, 2017.

Schwarz DA, George MP, Bluth MH: Precision medicine in toxicology, *Clin Lab Med* 36:693–707, 2016.

Semiz S, Dujic T, Causevic A: Pharmacogenetics and personalized treatment of type 2 diabetes, *Biochem Med* 23:154–171, 2013.

Serretti A, Lilli R, Smeraldi E: Pharmacogenetics in affective disorders, *Eur J Pharmacol* 438:117–128, 2002.

Shapiro M, Ward KM, Stern JJ: A near-fatal hypersensitivity reaction to abacavir: case report and literature review, *AIDS Read* 11:222–226, 2001.

Sharma SV, Bell DW, Settleman J, et al.: Epidermal growth factor receptor mutations in lung cancer, *Nat Rev Cancer* 7:169–181, 2007.

Shaw AT, Kim DW, Nakagawa K, et al.: Crizotinib versus chemotherapy in advanced ALK-positive lung cancer, *N Engl J Med* 368:2385–2394, 2013.

Shepherd FA, Rodrigues Pereira J, Ciuleanu T, et al.: Erlotinib in previously treated non-small-cell lung cancer, *N Engl J Med* 353:123–132, 2005.

Shu Y, Sheardown SA, Brown C, et al.: Effect of genetic variation in the organic cation transporter 1 (OCT1) on metformin action, *J Clin Invest* 117:1422–1431, 2007.

Sim E, Lack N, Wang CJ, et al.: Arylamine N-acetyltransferases: structural and functional implications of polymorphisms, *Toxicology* 254:170–183, 2008.

Singh T, Kurki MI, Curtis D, et al.: Rare loss-of-function variants in SETD1A are associated with schizophrenia and developmental disorders, *Nat Neurosci* 19:571–577, 2016.

Sistonen J, Sajantila A, Lao O, et al.: CYP2D6 worldwide genetic variation shows high frequency of altered activity variants and no continental structure, *Pharmacogenet Genomics* 17:93–101, 2007.

Skierka JM, Walker DL, Peterson SE, et al.: CYP2D6*11 and challenges in clinical genotyping of the highly polymorphic CYP2D6 gene, *Pharmacogenomics* 13:951–954, 2012.

Slatter JG, Su P, Sams JP, et al.: Bioactivation of the anticancer agent CPT-11 to SN-38 by human hepatic microsomal carboxylesterases and the in vitro assessment of potential drug interactions, *Drug Metab Dispos* 25:1157–1164, 1997.

Solus JF, Arietta BJ, Harris JR, et al.: Genetic variation in eleven phase I drug metabolism genes in an ethnically diverse population, *Pharmacogenomics* 5:895–931, 2004.

Somkrua R, Eickman EE, Saokaew S, et al.: Association of HLA-B*5801 allele and allopurinol-induced Stevens Johnson syndrome and toxic epidermal necrolysis: a systematic review and meta-analysis, *BMC Med Genet* 12:118, 2011.

Song IS, Shin HJ, Shim EJ, et al.: Genetic variants of the organic cation transporter 2 influence the disposition of metformin, *Clin Pharmacol Ther* 84:559–562, 2008.

Soong R, Shah N, Salto-Tellez M, et al.: Prognostic significance of thymidylate synthase, dihydropyrimidine dehydrogenase and thymidine phosphorylase protein expression in colorectal cancer patients treated with or without 5-fluorouracil-based chemotherapy, *Ann Oncol* 19:915–919, 2008.

Sparreboom A, Gelderblom H, Marsh S, et al.: Diflomotecan pharmacokinetics in relation to ABCG2 421C>A genotype, *Clin Pharmacol Ther* 76:38–44, 2004.

Sparreboom A, Loos WJ, Burger H, et al.: Effect of ABCG2 genotype on the oral bioavailability of topotecan, *Cancer Biol Ther* 4:650–658, 2005.

Stanulla M, Schaeffeler E, Flohr T, et al.: Thiopurine methyltransferase (TPMT) genotype and early treatment response to mercaptopurine in childhood acute lymphoblastic leukemia, *J Am Med Assoc* 293:1485–1489, 2005.

Stearns V, Johnson MD, Rae JM, et al.: Active tamoxifen metabolite plasma concentrations after coadministration of tamoxifen and the selective serotonin reuptake inhibitor paroxetine, *J Natl Cancer Inst* 95:1758–1764, 2003.

Stearns V, Johnson MD, Rae JM, et al.: Active tamoxifen metabolite plasma concentrations after coadministration of tamoxifen and the selective serotonin reuptake inhibitor paroxetine, *J Natl Cancer Inst* 95:1758–1764, 2003.

Stoehlmacher J, Ghaderi V, Iobal S, et al.: A polymorphism of the XRCC1 gene predicts for response to platinum based treatment in advanced colorectal cancer, *Anticancer Res* 21:3075–3079, 2001.

Suarez-Kurtz G: Pharmacogenomics in admixed populations, *Trends Pharmacol Sci* 26:196–201, 2005.

Suk R, Gurubhagavatula S, Park S, et al.: Polymorphisms in ERCC1 and grade 3 or 4 toxicity in non-small cell lung cancer patients, *Clin Cancer Res* 11:1534–1538, 2005.

Ta R, Cayabyab MA, Coloso R: Precision medicine: a call for increased pharmacogenomic education, *Per Med* 16:233–245, 2019.

Tamura A, Wakabayashi K, Onishi Y, et al.: Re-evaluation and functional classification of non-synonymous single nucleotide polymorphisms of the human ATP-binding cassette transporter ABCG2, *Cancer Sci* 98:231–239, 2007.

Tamura A, Watanabe M, Saito H, et al.: Functional validation of the genetic polymorphisms of human ATP-binding cassette (ABC) transporter ABCG2: identification of alleles that are defective in porphyrin transport, *Mol Pharmacol* 70:287–296, 2006.

Tassaneeyakul W, Jantararoungtong T, Chen P, et al.: Strong association between HLA-B*5801 and allopurinol-induced Stevens-Johnson syndrome and toxic epidermal necrolysis in a Thai population, *Pharmacogenet Genomics* 19:704–709, 2009.

Tassaneeyakul W, Tiamkao S, Jantararoungtong T, et al.: Association between HLA-B*1502 and carbamazepine-induced severe cutaneous adverse drug reactions in a Thai population, *Epilepsia* 51:926–930, 2010.

Thatcher N, Chang A, Parikh P, et al.: Gefitinib plus best supportive care in previously treated patients with refractory advanced non-small-cell lung cancer: results from a randomised, placebo-controlled, multicentre study (Iressa Survival Evaluation in Lung Cancer), *Lancet* 366:1527–1537, 2005.

Then SM, Rani ZZ, Raymond AA, et al.: Frequency of the HLA-B*1502 allele contributing to carbamazepine-induced hypersensitivity reactions in a cohort of Malaysian epilepsy patients, *Asian Pac J Allergy Immunol* 29:290–293, 2011.

Thijssen JH: Gene polymorphisms involved in the regulation of bone quality, *Gynecol Endocrinol* 22:131–139, 2006.

Tirona RG, Leake BF, Merino G, et al.: Polymorphisms in OATP-C: identification of multiple allelic variants associated with altered transport activity among European- and African-Americans, *J Biol Chem* 276:35669–35675, 2001.

Tukey RH, Strassburg CP, Mackenzie PI: Pharmacogenomics of human UDP-glucuronosyltransferases and irinotecan toxicity, *Mol Pharmacol* 62:446–450, 2002.

Tzvetkov MV, Vormfelde SV, Balen D, et al.: The effects of genetic polymorphisms in the organic cation transporters OCT1, OCT2, and OCT3 on the renal clearance of metformin, *Clin Pharmacol Ther* 86:299–306, 2009.

van Schaik RH: Cancer treatment and pharmacogenetics of cytochrome P450 enzymes, *Invest New Drugs* 23:513–522, 2005.

Vangsted A, Gimsing P, Klausen TW, et al.: Polymorphisms in the genes ERCC2, XRCC3 and CD3EAP influence treatment outcome in multiple myeloma patients undergoing autologous bone marrow transplantation, *Int J Cancer* 120:1036–1045, 2007.

Vitezica ZG, Milpied B, Lonjou C, et al.: HLA-DRB1*01 associated with cutaneous hypersensitivity induced by nevirapine and efavirenz, *AIDS* 22:540–541, 2008.

Vogelgesang S, Kunert-Keil C, Cascorbi I, et al.: Expression of multidrug transporters in dysembryoplastic neuroepithelial tumors causing intractable epilepsy, *Clin Neuropathol* 23:223–231, 2004.

Wacher VJ, Wu CY, Benet LZ: Overlapping substrate specificities and tissue distribution of cytochrome P450 3A and P-glycoprotein: implications for drug delivery and activity in cancer chemotherapy, *Mol Carcinog* 13:129–134, 1995.

Wang ZH, Miao XP, Tan W, et al.: Single nucleotide polymorphisms in XRCC1 and clinical response to platin-based chemotherapy in advanced non-small cell lung cancer, *Ai Zheng* 23:865–868, 2004.

Wang ZJ, Yin OQ, Tomlinson B, et al.: OCT2 polymorphisms and in-vivo renal functional consequence: studies with metformin and cimetidine, *Pharmacogenet Genomics* 8:637–645, 2008.

Wegman P, Elingarami S, Carstensen J, et al.: Genetic variants of CYP3A5, CYP2D6, SULT1A1, UGT2B15 and tamoxifen response in postmenopausal patients with breast cancer, *Breast Cancer Res* 9:R7, 2007.

Wegman P, Vainikka L, Stal O, et al.: Genotype of metabolic enzymes and the benefit of tamoxifen in postmenopausal breast cancer patients, *Breast Cancer Res* 7:R284–R290, 2005.

Wei CY, Chung WH, Huang HW, et al.: Direct interaction between HLA-B and carbamazepine activates T cells in patients with Stevens-Johnson syndrome, *J Allergy Clin Immunol* 129:1562–1569, 2012. e1565.

Westlind-Johnsson A, Hermann R, Huennemeyer A, et al.: Identification and characterization of CYP3A4*20, a novel rare CYP3A4 allele without functional activity, *Clin Pharmacol Ther* 79:339–349, 2006.

Wojnowski L, Kulle B, Schirmer M, et al.: NAD(P)H oxidase and multidrug resistance protein genetic polymorphisms are associated with doxorubicin-induced cardiotoxicity, *Circulation* 112:3754–3762, 2005.

Wolinski SM, Korber BTM, Neumann AU, et al.: Adaptive evolution of human immunodeficiency virus-type 1 during the natural course of infection, *Science* 272:537–542, 1996.

Wood RD, Mitchell M, Sgouros J, et al.: Human DNA repair genes, *Science* 291:1284–1289, 2001.

Woodburn JR: The epidermal growth factor receptor and its inhibition in cancer therapy, *Pharmacol Ther* 82:241–250, 1999.

Wu X, Gu J, Wu TT, et al.: Genetic variations in radiation and chemotherapy drug action pathways predict clinical outcomes in esophageal cancer, *J Clin Oncol* 24:3789–3798, 2006.

Wysocki K, Osier N: Direct to consumer versus clinical genetic testing, *J Am Assoc Nurse Pract* 31:152–155, 2019.

Xiang X, Jada SR, Li HH, et al.: Pharmacogenetics of SLCO1B1 gene and the impact of *1b and *15 haplotypes on irinotecan disposition in Asian cancer patients, *Pharmacogenet Genomics* 16:683–691, 2006.

Xie HG, Kim RB, Wood AJ, et al.: Molecular basis of ethnic differences in drug disposition and response, *Annu Rev Pharmacol Toxicol* 41:815–850, 2001.

Xu G, Bhatnagar V, Wen G, et al.: Analyses of coding region polymorphisms in apical and basolateral human organic anion transporter (OAT) genes [OAT1 (NKT), OAT2, OAT3, OAT4, URAT (RST), *Kidney Int* 68:1491–1499, 2005.

Xu J, Lu Z, Xu M, et al.: A heroin addiction severity-associated intronic single nucleotide polymorphism modulates alternative pre-mRNA splicing of the μ opioid receptor gene OPRM1 via hnRNPH interactions, *J Neurosci* 34, 2014. 11048–66.

Yoshida K, Higuchi H, Kamata M, et al.: The G196A polymorphism of the brain-derived neurotrophic factor gene and the antidepressant effect of milnacipran and fluvoxamine, *J Psychopharmacol* 21:650–656, 2007.

Yu L, Chibnik LB, Srivastava GP, et al.: Association of brain DNA methylation in SORL1, ABCA7, HLA-DRB5, SLC24A4, and BIN1 with pathological diagnosis of Alzheimer disease, *JAMA Neurol* 72:15–24, 2015.

Yuan J, Guo S, Hall D, et al.: Toxicogenomics of nevirapine-associated cutaneous and hepatic adverse events among populations of African, *Asian, and European descent*, *AIDS* 25:1271–1280, 2011.

Zair ZM, Eloranta JJ, Stieger B, et al.: Pharmacogenetics of OATP (SLC21/SLCO), OAT and OCT (SLC22) and PEPT (SLC15) transporters in the intestine, liver and kidney, *Pharmacogenomics* 9:597–624, 2008.

Zamber CP, Lamba JK, Yasuda K, et al.: Natural allelic variants of breast cancer resistance protein (BCRP) and their relationship to BCRP expression in human intestine, *Pharmacogenetics* 13:19–28, 2003.

Zarate RN, Arias F, Bandres E, et al.: Xeroderma pigmentosum group D 751 polymorphism as a predictive factor in resected gastric cancer treated with chemoradiotherapy, *World J Gastroenterol* 12:6032–6036, 2006.

Zhang QX, Borg A, Wolf DM, et al.: An estrogen receptor mutant with strong hormone-independent activity from a metastatic breast cancer, *Cancer Res* 57:1244–1249, 1997.

Zhang S, Lovejoy KS, Shima JE, et al.: Organic cation transporters are determinants of oxaliplatin cytotoxicity, *Cancer Res* 66:8847–8857, 2006.

Zhang W, Huang RS, Dolan E: Integrating epigenomics into pharmacogenomic studies, *Pharmacogenomics Personalized Med* 1, 2008. 7–1.

Zhang W, Huang RS, Dolan E: Integrating epigenomics into pharmacogenomic studies, *Pharmgenomics Pers Med* 1:7–14, 2008.

Zhou F, You G: Molecular insights into the structure-function relationship of organic anion transporters OATs, *Pharm Res (N Y)* 24:28–36, 2007.

Zhou K, Pedersen HK, Dawed AY, Pearson ER: Pharmacogenomics in diabetes mellitus: insights into drug action and drug discovery, *Nat Rev Endocrinol* 12:337–346, 2016.

Zhou Q, Sparreboom A, Tan EH, et al.: Pharmacogenetic profiling across the irinotecan pathway in Asian patients with cancer, *Br J Clin Pharmacol* 59:415–424, 2005.

Zhou S: Clinical pharmacogenomics of thiopurine S-methyltransferase, *Curr Clin Pharmacol* 1:119–128, 2006.

Zhou SF, Liu JP, Chowbay B: Polymorphism of human cytochrome P450 enzymes and its clinical impact, *Drug Metab Rev* 41:89–295, 2009.

Zhou W, Gurubhagavatula S, Liu G, et al.: Excision repair cross-complementation group 1 polymorphism predicts overall survival in advanced non-small cell lung cancer patients treated with platinum-based chemotherapy, *Clin Cancer Res* 10:4939–4943, 2004.

Zimmet P, Alberti KG, Shaw J: Global and societal implications of the diabetes epidemic, *Nature* 414:782–787, 2001.

Zineh I, Mummaneni P, Lyndly J, et al.: Allopurinol pharmacogenetics: assessment of potential clinical usefulness, *Pharmacogenomics* 12:1741–1749, 2011.

This page intentionally left blank

PART 9

Clinical Pathology of Cancer

EDITED BY Matthew R. Pincus, Martin H. Bluth, Wilbur B. Bowne, Richard A. McPherson

CHAPTER 76

DIAGNOSIS AND MANAGEMENT OF CANCER USING SEROLOGIC AND OTHER BODY FLUID MARKERS

Peng Lee, Shilpa Jain, Matthew R. Pincus, Marian Khalili, Wilbur B. Bowne, Martin H. Bluth, Richard A. McPherson

SERUM MARKERS AS AN EFFECTIVE TOOL FOR DIAGNOSIS AND MONITORING OF CANCER, 1509

FUNCTIONAL CLASSIFICATION OF TUMOR MARKERS, 1509
Oncoproteins are Markers for Cell Proliferation, 1509
Next-Generation Sequencing, 1510
Tumor Suppressors/Cell Differentiation, 1510
Adhesion Molecules and Metastasis, 1510
Monoclonal Antibody–Defined Tumor Markers, 1510
Other Markers, 1511

CLINICAL APPLICATIONS, 1511
Screening, 1511
Diagnosis, 1511
Prognosis: Recurrence, Metastasis, and Survival, 1511
Monitoring Treatment Response, 1511

RECOMMENDATIONS FOR ORDERING TUMOR MARKER TESTS, 1512

INDIVIDUAL TUMOR MARKERS, 1515
α-Fetoprotein, 1515
Angiogenic Factors, 1515
β_2-Microglobulin, 1515
Serum Free Light Chain Determinations, 1515
Carcinoembryonic Antigen, 1516
CA 15-3 and CA 27.29, 1516
CA 19-9, CA 50, and CA 19-5, 1516
CA 125, 1516
CA 72-4, 1517
Calcitonin, 1517
Chromogranin A, 1517
Cytokeratin 19 Fragment, 1517
Human Chorionic Gonadotropin, 1517
Her2/*neu* (c-*erbB*-2) Oncoprotein, 1517
p53, 1518
Parathyroid Hormone–Related Peptide, 1518
Serum Markers for Prostate Cancer, 1518

CIRCULATING TUMOR CELLS IN PERIPHERAL BLOOD, 1520

CIRCULATING NUCLEIC ACIDS IN PERIPHERAL BLOOD, 1521
Cell-Free Nucleic Acid Testing in Cancer, 1521
Gene Arrays Detecting Oncoprotein Abnormalities, 1521
Circulating microRNA, 1522
Gene Mutations, 1522
Microsatellite Alterations, 1522
Promoter Hypermethylation, 1522
Cell DNA Testing for Cancer Using Fluorescence in Situ Hybridization, 1522

MARKERS IN OTHER BODY FLUIDS, 1523
Urine Markers for Prostate Cancer, 1523
Urine Metabolic Test for Adenomatous Polyps of Colon, 1524
Fecal Occult Blood Testing and Mutant Protein Markers in Stool, 1524

CONCLUSIONS, 1524

SELECTED REFERENCES, 1524

KEY POINTS

- This chapter discusses the use of proteins, whose serum levels are often elevated in patients with malignancies, in the diagnosis and management of cancer.
- Many of these are so-called *oncofetal antigens*—that is, proteins that are expressed in fetal tissue during development but are not normally found in the tissues of adults. These include α-fetoprotein and carcinoembryonic antigen, whose serum levels are frequently elevated in hepatocellular and colon cancers, respectively.
- Other proteins, such as CA 19-9, CA 125, and CA 15-3, are expressed in epithelial cells and are also often present in the sera of patients with pancreatic, ovarian, and breast cancers, respectively.
- Because these "tumor marker" proteins are not tissue specific and can also be expressed in diseases other than cancer, their sensitivities and specificities are not sufficiently high that they can be used as cancer-screening proteins. Their use is predominantly in following patients who are being treated for known malignancies.
- The exception to this is prostate-specific antigen (PSA), a chymotrypsin-like enzyme that is expressed almost exclusively in prostate tissue and is elevated in the sera of most patients with prostate cancer. Therefore, elevated serum PSA levels have a high sensitivity for diagnosing prostate cancer. Because PSA is also elevated in other prostate diseases, such as benign prostatic hyperplasia, it has a lower specificity but nonetheless can still be used very effectively to screen patients for this disease.
- New developments in the field of early tumor detection using serum markers are also introduced in this chapter. These include use of mitogenic proteins, such as HER2/Neu, known to function as signal transduction proteins whose levels are elevated in many types of cancers; detection of genes encoding these proteins in body fluids; and proteomic approaches involving patterns of expression of multiple proteins that typify specific cancers. These specific approaches are also discussed in depth in Chapter 77.
- The identification of a circulating tumor cell (CTC) as a biomarker is a fast-growing area of research. This chapter updates the recent advances on CTCs that are or will be applied in clinical application for diagnostic and prognostic values.
- Another area of growing research and translation to clinical application in cancer biomarkers is circulating nucleic acid, including the levels as well as mutation and methylation status.

Although cancer mortality has decreased over the past seventy years by about 21%, it is still a leading cause of death despite the advancement of multidisciplinary treatment modalities. In contrast, dramatic decreases in mortality due to cardiovascular and infectious disease have been achieved. Studies have shown that early detection of cancer can lead to superior long-term survival. Thus, there is an urgent need to search for cancer biomarkers with high sensitivity and specificity to allow for early cancer detection, effective treatment, and decreased mortality. Much effort has been devoted to the discovery, characterization, and clinical application of tumor markers to detect the presence of cancer at an early stage. As a result, increasing numbers of biomolecules, mainly specific proteins and some specific ribonucleic acids (RNAs) and deoxyribonucleic acids (DNAs), have been identified and employed as markers potentially for screening purposes and for prognostic purposes in the daily clinical management of cancer patients. These markers can further be used not only to classify cancers but also to monitor response to neoadjuvant therapy. For example, estrogen receptor (ER), progesterone

receptor (PR), and HER2/*neu* oncogene protein are used in the diagnosis and management of breast cancer patients using surgical specimens. ER has been shown to be a prognostic marker for breast cancer and a predictive marker for hormonal treatment (Jensen & Jordan, 2003). HER2/*neu* amplification and overexpression were shown to be associated with poor prognosis and to be a predictor for therapeutic response in breast cancer (Wilmanns et al., 2004). PR has been shown to be associated with a good prognosis in ovarian cancer (Munstedt et al., 2000; Lee et al., 2005).

Among these markers are a number of tumor markers present in circulating body fluids, including blood. Broadly, body fluid tumor biomarkers (principally, serum and urine) are divided into three categories: tumor-associated proteins, such as the oncofetal antigens, which seem to be expressed in many cancers but have also been found to be present in other nonneoplastic conditions; oncoproteins, which are involved in the regulation of the cell cycle and become overexpressed or mutated almost exclusively in neoplastic conditions; and recently discovered patterns of protein expression in serum that appear to be unique to specific types of cancer (i.e., proteomics). This chapter emphasizes the use of the first two classes of tumor marker. Chapter 77 discusses oncoproteins and the use of multiple protein profiles on body fluids, or proteomics, as biomarkers for early tumor detection.

SERUM MARKERS AS AN EFFECTIVE TOOL FOR DIAGNOSIS AND MONITORING OF CANCER

Ideally, a tumor marker should become elevated in the serum only of patients with a malignant tumor and should not be elevated in the serum of disease-free individuals or of individuals with nonmalignant diseases such as inflammatory or infectious diseases. Also, a tumor marker protein should become elevated in the serum of cancer patients at an early stage, thereby enabling early tumor detection and the initiation of appropriate therapy. Although no one tumor marker has been found to meet all of these characteristics, progress toward the discovery of such markers is continuously being made.

In fact, studies show that one or more cancer biomarkers, including DNA, protein, or tumor cells, are almost always present in the serum of patients with cancer. These findings provide the rational basis for early detection of cancer using serum samples. Any circulating cell products, including DNA, RNA (including microRNA), proteins (enzymes, serum proteins, metabolites, receptors, carcinoembryonic proteins, oncoprotein, and proteins encoded by suppressor genes), and tumor cells, can be used as tumor markers if they are associated with events related to tumor formation and/or growth (Fig. 76.1). Such events include malignant transformation, proliferation, dedifferentiation, and metastasis. The blood levels of serum tumor markers are determined by tumor proliferation, tumor volume, proteolytic activities in the tumor cell, and release from necrotic tumor cells. The recent improvement of instrumentation, especially in consolidation of specialized testing instruments as immunoassay analyzers to a more general chemistry analyzer, facilitated the analysis of a wide range of analytes with the same degree of accuracy, specificity, and precision. The improved sensitivities of the assays made serologic tests far superior to other clinical examinations based on physical methods. An additional advantage of serum testing over tissue-based methods is the noninvasive nature, more accurate quantification, and lack of interobserver difference as opposed to tissue-based methods. Because of these benefits, serum markers are frequently used to screen for, diagnose, and predict the behavior of many cancers.

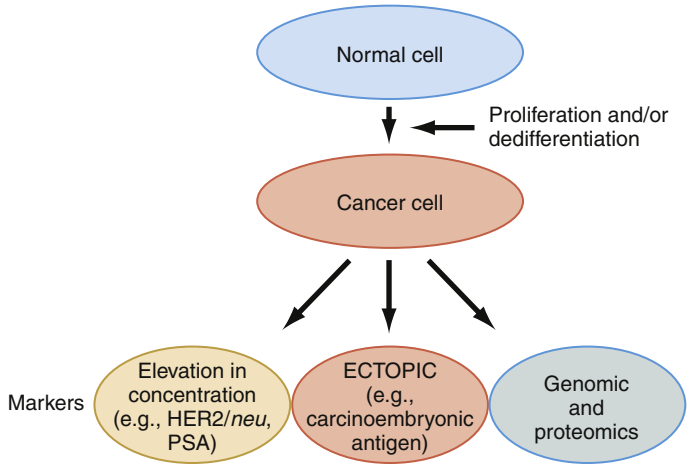

Figure 76.1 Different types of serum tumor markers are used to detect cancer. HER2 and prostate-specific antigen (PSA) reflect increased cellular proliferation. Carcinoembryonic antigen represents the dedifferentiation process of cancer. Current genomic and proteomics focus on collective changes in malignant cells.

The clinical value of any given tumor marker will depend on its specificity and sensitivity, as well as its intended clinical use. For example, prostate-specific antigen (PSA) can be used in the screening of prostate cancer, resulting in early detection and treatment. Serum HER2/*neu* is used as a marker of prognosis and monitoring therapy for breast cancer. The difference in their usefulness is due to their difference in tissue specificity and cancer sensitivity: PSA is organ specific but not cancer specific, whereas HER2/*neu* is cancer specific but not tissue specific and is found to be increased in breast cancers as well as lung and other epithelial cell tumors. The use of tumor markers as prognostic and risk factors has gained more popularity in recent years. Measurement of the level of risk factors has been found to be valuable in the assessment of the aggressiveness of a tumor and is helpful in selecting treatment strategies. The utility of tumor markers is adjunctive to medical and surgical management of malignancies, serving to help detect recurrences as well as predict prognosis.

FUNCTIONAL CLASSIFICATION OF TUMOR MARKERS

To learn how to identify, select, and utilize tumor markers for the diagnosis of cancer and the management of cancer patients, it is essential to be familiar with the function of each individual or group of cancer serum markers. This chapter emphasizes the role of three specific classes of tumor markers that are commonly used in the diagnosis of human malignancies: oncofetal antigens, such as α-fetoprotein (AFP) and carcinoembryonic antigen (CEA), which are normally expressed during fetal development but do not occur normally in the tissues or sera of children and adults; proteins occurring in epithelial cells that become elevated in tissue and serum in adenosquamous and squamous cell carcinomas, such as the CA 19-9, CA 125, and CA 15-3 proteins; and polypeptide hormones, such as the β chain of human chorionic gonadotropin (β hCG), and specific enzymes, such as the placental isoform of alkaline phosphatase (ALP), that become elevated in the serum of patients with specific tumors. These latter two tumor markers are frequently elevated in the sera of patients with germ cell tumors. Additionally, hormone-like proteins are found in the sera of patients with different cancers, such as parathyroid hormone–like protein that induces hypercalcemia as part of the so-called *paraneoplastic syndrome* in such cancers as renal cell carcinomas.

Most of these proteins have been discovered on the basis of having been observed in the sera of cohorts of patients with specific types of cancer. However, many are also found in the sera of patients with nonmalignant (e.g., inflammatory) conditions. In addition, they may not occur in significant numbers of patients in whom these cancers have been diagnosed. The sensitivities and specificities of these tumor marker proteins are often low; thus, they are not useful for screening purposes. On the other hand, all of these proteins are quite useful for *monitoring* specific cancers. For example, CEA is often elevated in the sera of patients with colon cancer. Thus, if CEA serum levels are found to be elevated in patients who have had a colon cancer resected, this is evidence of tumor recurrence. As discussed later, the one exception is PSA, a chymotrypsin-like enzyme that occurs almost uniquely in the prostate gland and has proved exceptionally useful in screening for prostate cancer and in monitoring patients who are being treated for this disease.

Standard assays for all of these proteins are now well developed and have received approval from the U.S. Food and Drug Administration (FDA) for use in the monitoring of treatment of known cancers but not, except for PSA, for screening for human cancers. Investigations are currently focused on searching for proteins that are expressed only in cancer cells (see Chapter 77). This chapter summarizes some of the more recently discovered proteins that are almost always expressed in cancerous but less commonly in noncancerous diseases and are promising for screening for the occurrence of cancer and for monitoring therapy.

ONCOPROTEINS ARE MARKERS FOR CELL PROLIFERATION

Oncoproteins are proteins that are directly or indirectly involved in the control of mitosis and are altered such that they continuously signal the cell to divide. These proteins either lie on signal transduction pathways

carrying mitogenic signals from growth factors at the cell membrane to the nucleus or are involved in the regulation of transcription, activating the genes ultimately causing cell growth and mitosis (see Chapter 77). For example, as discussed in Chapter 77, HER2/*neu* is a transmembrane receptor with an extracellular domain (ECD), a transmembrane domain, and an intracytoplasmic domain containing a tyrosine kinase. Upon binding of extracellular growth factors, the intracellular kinase becomes activated, causing dimerization of the receptor and interaction with a cytosolic adapter protein, Grb-2, to relay the message next to a guanine nucleotide exchange factor, SOS. SOS, in turn, binds to the critically important protein Ras-p21 (Barbacid, 1987). Oncogenic c-Myc is an example of a different type of oncogene transcriptional factor, which functions via the activation of its target genes, inducing synthesis of mitogenic proteins.

Often, these proteins can be detected in the serum of patients with abnormal cell growth (i.e., cancer or precancerous states). Extensive testing for the presence of oncoproteins has revealed that many oncoproteins are detected in the serum and/or other body fluids of cancer patients. A detailed discussion of each oncoprotein is found in Chapter 77.

NEXT-GENERATION SEQUENCING

Malignancy is a disorder of the genome. Oncogenesis implicates intricate interactions between forces at the level of the DNA (including sequence and epigenetic framework), RNA processing, and the final protein product. Sanger DNA sequencing, also known as *chain terminator sequencing*, was developed in 1997 and has been the sequencing standard until the late 2000s (Kamps, 2017). More recently, next-generation sequencing (NGS) integrates the complex processes involved in oncogenesis by identifying recurrent patterns at the level of the genome and exploiting them for clinical gain (Rubinstein, 2019). NGS is a novel DNA sequencing technology that generates hundreds of millions of short DNA reads that can sequence a human genome quickly with lower expense, permitting determination of point mutations, genomic rearrangements, deletions, amplifications, inversions, translocations, and gene fusions (Sabour, 2017).

Clinical utility of NGS in cancer includes diagnosis, prognosis, prevention, and treatability. NGS-based gene panels have provided us with diagnostic tools enabling individualized care of cancer patients. It is now possible to determine the genomic changes related to disease in each individual patient. Although more than 20,000 genes have been identified in the human genome, only 500 genes are potentially related to cancer. An NGS-based gene panel test can identify gene alterations that are targetable by molecular target drugs (Nagahashi, 2019). An NGS-based gene panel test has been successful in identifying targetable driver mutations in lung adenocarcinoma such as EGFR, ROS1, and ALK (Mano, 2012). Furthermore, patients with RET-rearranged non–small cell lung cancer can benefit from vandetanib, which targets RET (Yoh, 2017).

TUMOR SUPPRESSORS/CELL DIFFERENTIATION

Separate from oncogenes but equally important is a group of suppressor genes. Proteins encoded by suppressor genes are responsible for suppressing cell growth, either causing cell growth arrest in the cell cycle or apoptosis. Frequently, these suppressor genes undergo deletions or mutations, resulting in the production of inactive gene products. Among the tumor suppressor genes, the antioncogene protein p53 has been widely investigated and best characterized for its role in various cancers. It is involved in apoptosis, cell-cycle arrest, cell senescence, and DNA damage response. Deletions or mutations of the p53 gene greatly predispose cells to malignant transformation. p53 mutations have been identified in nearly 50% of human malignancies (Soussi & Beroud, 2001). Molecular assays are available to detect mutations in the serum DNA of tumor suppressor genes. In addition, antibodies against the abnormal tumor suppressor proteins can be used as a biomarker for cancer.

Molecular methods, such as PCR-SSCP (polymerase chain reaction single-strand conformation polymorphism) and DHPLC (denaturing high-performance liquid chromatography), have been described to detect serum p53 mutations in cancer. Recently, detection and quantification of tumor-specific p53 mutations using droplet digital PCR at the level of circulating tumor DNA has shown promise in the posttreatment surveillance of head and neck cancer patients (van Ginkel, 2017). More significantly, antibodies against the abnormal tumor suppressor p53 proteins have been detected in the serum of cancer patients (Soussi, 2000). Interestingly, the presence of p53 antibodies is correlated with the p53 mutation (Guinee et al., 1995; Hammel et al., 1999). In breast cancer, several studies indicated that the presence of p53 antibody in the serum correlated with increased proliferation antigen (Ki-67) and lack of ER expression, indicating that it may serve as a breast cancer prognostic marker (Schlichtholz et al., 1992; Sangrajrang et al., 2003).

The discovery of two breast cancer susceptibility genes (or tumor-suppressor genes), *BRCA1* and *BRCA2*, has generated tremendous interest. Studies suggest that mutations in *BRCA1* are responsible for approximately half of all cases of inherited breast cancer (Easton et al., 1993; Miki et al., 1994; Wooster et al., 1994). In addition, carriers of *BRCA1* mutations are also at an increased risk for ovarian, colon, and prostate cancer (Futreal et al., 1994). *BRCA2*, the second susceptibility gene for breast cancer, is thought to account for approximately 70% of cases of inherited breast cancer that are not due to *BRCA1* mutations and is associated with an increased risk of breast cancer in men.

The suppressor genes and their products are potentially useful as tumor markers for the screening and identification of families or high-risk individuals. Development of immunoassays to measure both *BRCA1*- and *BRCA2*-encoded proteins are under development and may be useful for the identification of high-risk individuals and their families.

ADHESION MOLECULES AND METASTASIS

Tumor metastases involve several major steps (Liotta, 1987). First, the tumor cells have to penetrate their adjacent surroundings, after which they invade vascular or lymphatic vessels. The tumor cells are then carried to distant sites until they are lodged in the venous or capillary beds of a distant organ. In this new environment, these tumor cells must again penetrate the vascular walls in order to grow at the distant site. Cell adhesion molecules, including integrins, selectins, cadherins, and cell adhesion molecules of immunoglobulin gene families, regulate many steps of the metastatic process. The changes in their levels of expression reflect the malignant behavior of cancer cells. For example, serum levels of E-selectin, intercellular adhesion molecule (ICAM), and vascular cell adhesion molecule (VCAM) are increased, in particular, in late-stage breast cancer patients (O'Hanlon et al., 2002; Sheen-Chen et al., 2004). Elevated serum VCAM level may be used to predict a shorter survival. Another study indicated that postchemotherapeutic levels of serum E-selectin and ICAM are associated with a response to treatment of patients with Hodgkin disease (Syrigos et al., 2004). Furthermore, increased E-selectin, ICAM-1, and VCAM are suggested to be a prognostic factor for survival in patients with gastric cancer (Alexiou et al., 2003). Therefore, the appearance of these cell adhesion molecules in blood circulation might indicate the risk or occurrence of metastases or a poor prognosis.

MONOCLONAL ANTIBODY–DEFINED TUMOR MARKERS

The development of hybridoma technology has greatly impacted the identification of tumor markers (Milstein & Cuello, 1983). Rather than dealing with a whole molecule of known protein structure, it is now possible to focus on only a small surface area, an epitope or antigenic determinant, using monoclonal antibodies. It is no longer necessary to purify the antigen for the preparation of polyclonal antibodies in animals. The complete characterization and identification of the molecule carrying the epitope is also no longer needed. A hybridoma can be prepared by injecting a mouse with an enriched fraction of the tumor cell membrane or the whole tumor cell. Hybridomas producing the monoclonal antibodies of interest are selected through the subsequent screening procedure. Once a hybridoma is established, there will be an unlimited and consistent supply of monoclonal antibody (MAb) for various uses.

By combining the MAbs with the solid-phase sandwich test design, new assays have been developed that have eliminated many problems associated with polyclonal assays, involving poor reproducibility, lot-to-lot variations, poor specificity, and nonspecific cross-reactivity (Diamond et al., 1981). It also reduces the differences between different kits and widens the linear concentration range for the assay. Whenever an MAb is available, its use is recommended. To achieve higher test sensitivity, the use of a combination of multiple MAbs has been found to improve the affinity between solid-phase-absorbed-multiple MAbs and the soluble antigen.

Tests for the MAb-defined tumor markers have been demonstrated to have a higher sensitivity and specificity than those using polyclonal antibodies. For example, CA 19-9, CA 125, and CA 15-3 are much more sensitive and specific than CEA for pancreatic, ovarian, and breast carcinomas, respectively. These markers are recommended to replace the polyclonal

CEA test for the diagnosis and management of patients with these carcinomas. Various tumor markers derived from different tumors also share many tumor-associated epitopes. For example, CA 19-9, CA 15-3, and CA 125 are expressed by almost all carcinomas in varying degrees. In addition to the sharing of any given epitope by more than one carcinoma, it is also possible for a single molecule to express more than one epitope (Yu et al., 1991). For example, it is likely that CA 15-3 and CA 125 are expressed by the same mucin molecule.

OTHER MARKERS

Many hormones (e.g., hCG, epinephrine, dopamine, and serotonin), serum proteins, enzymes (lactate dehydrogenase, ALP), and their metabolites, such as the metabolites of the neuroendocrine hormones (e.g., vanillylmandelic acid, homovanillic acid, and 5-hydroxyindoleacetic acid), may become elevated in tumors because of the high proliferation rate of tumor cells. Their serum levels rise to even higher levels when a benign tumor becomes malignant and metastasizes. Benign and nonmalignant diseases may also involve elevated levels of markers. Thus, these markers are not suitable for screening or for cancer diagnosis because of the large numbers of false-positive results that would be generated. These markers are more appropriately used for monitoring patient response during treatment.

One exception relates to the enzyme ALP discussed in Chapter 21. There are multiple isozymes of this enzyme, one of which is the placental isozyme placental ALP (PLAP). This form becomes elevated in the serum of patients who have germ cell tumors. One particular use of PLAP is in the serum or, more effectively, in the cerebrospinal fluid (CSF) of patients with a mass in the pineal region with a differential diagnosis of germ cell tumor versus pinealoma. If PLAP is elevated in the CSF of a patient with a mass in the pineal area, a diagnosis of germ cell tumor can be made. As it happens, radiation therapy is curative, obviating the need for surgery.

The enzymatic activities of various tissue-specific glycosyltransferases are altered in tumor cells. Some of the elevated glycosyltransferases have been used as tumor markers. The sugar sequence and composition of the carbohydrate moiety of many serum glycoproteins, including blood group substances and mucins, such as CA 19-9, are tumor markers resulting from altered glycosyltransferase activity. The AFP isolated from patients with primary hepatocellular carcinoma has an additional fucose compared with the AFP from benign liver disease, an example of altered fucosyltransferase in hepatocellular carcinoma cells (Wu, 1990).

Ectopic proteins are often expressed in cancer. Carcinoembryonic proteins, which are detectable in both fetal and tumor tissues but not in normal adult tissues, usually lack any known physiologic function and have blood concentrations at nanogram-per-milliliter levels. Therefore, measurements of carcinoembryonic proteins in the circulation must rely on immunoassays. The specificity and sensitivity associated with these proteins, although not 100%, are much higher than those of enzymes and metabolites that have been used as tumor markers in the past. The serum concentration of these carcinoembryonic proteins not only correlates well with tumor activity but can also be used to predict prognosis. However, carcinoembryonic proteins in general are not suitable for screening because the polyclonal antibodies directed against these proteins often cross-react with other, normal proteins, and these carcinoembryonic proteins do not appear sufficiently early in the blood from cancer patients to detect the tumors at initial stages. However, they have been used as adjunct tests for cancer diagnosis and are extremely useful for monitoring the success of treatment and for detecting recurrence.

CLINICAL APPLICATIONS

The serum tumor markers are currently used for screening, diagnosing, and predicting prognosis and treatment response. Use of tests for screening of disease, even those with high sensitivity and specificity, should be confined as much as possible to populations at risk for the disease. This is because the positive predictive value depends on the prevalence of the disease. Because most of the tumor markers described in this chapter are expressed both in neoplastic and benign conditions, their use is confined to following possible tumor recurrence in patients being treated for specific types of tumor.

SCREENING

The recommendation of screening for prostate cancer by the measurement of serum PSA in combination with a digital rectal examination (DRE) in men older than age 50 years is due to the high tissue specificity of PSA (Wu, 1994) and the high prevalence of prostate cancer. Combination of the PSA test and DRE provides the least costly approach to the early detection of prostate cancer (Littrup et al., 1993). PSA screening is especially recommended for African American men because the incidence of prostate cancer for African Americans is nearly twice that of the general population and the death rate is up to three times higher. Screening permits the treatment of organ-confined, potentially curable prostate cancer discovered in men with a life expectancy of longer than 10 years.

Although not approved for screening for hepatocellular carcinoma in the United States, AFP has been used to screen for primary hepatocellular carcinoma in China because of the high incidence of liver cancer in that country. The diagnosis of ovarian cancer has traditionally relied on imaging and discovery at surgery (e.g., exploratory laparotomy). However, in most cases, at the time of detection, the tumor has advanced to a stage at which the possibility of cure is low. The feasibility of screening for ovarian cancer in women by measuring serum CA 125 is being investigated.

DIAGNOSIS

Several approaches have been suggested recently to improve the diagnostic yield of many tumor markers. The use of multiple markers is one approach that has received wide acceptance. As is also noted in Chapter 77, specific patterns of multiple tumor markers seem to be associated with individual malignant diseases. Another approach to improving both the specificity and sensitivity of tumor markers, as in the case of a serum PSA test, involves the measurement of the velocity (the rate of increase in PSA concentration over time) and the density (e.g., by dividing the serum PSA concentration by the volume of the prostate gland, determined by transrectal ultrasound) (Benson et al., 1992). These efforts aim at a better discrimination between benign and malignant states. For example, a mildly elevated serum PSA level associated with a small prostate gland may indicate cancer, whereas the same PSA value in a patient with a large gland may indicate benign prostatic hypertrophy (BPH).

PROGNOSIS: RECURRENCE, METASTASIS, AND SURVIVAL

The assessment of tumor aggressiveness and the prognosis for the outcome of a cancer patient has received much attention in recent years. The knowledge of tumor aggressiveness helps in the development of a proper therapy for the patient. For example, the detection of tumor markers, highly associated with malignancy and metastases, will suggest a more rigorous and systemic treatment. Monitoring tumor markers for the detection of recurrence following the surgical removal of the tumor is the second most useful application of tumor markers. It is well known that the appearance of most of the circulating tumor markers has a lead time of several months (3–6 months) before the stage at which many of the physical procedures could be used for the detection of cancer. The specificity of tumor markers does not present a problem for this application. The ease of drawing blood and the sensitivity of tumor marker tests make this noninvasive monitoring process now widely accepted.

Most tumor markers become increasingly elevated when the tumor metastasizes. Very few tumor markers have a clear-cut boundary between benign and malignant stages. Proteins that reflect the risk factors associated with the process of tumor metastases, such as proteases and adhesion molecules, are usually better markers for predicting prognosis. However, most of these markers are still measured in tumor tissues and tissue lysates. The finding of the ECD of c-*erb*B-2 protein in the serum of cancer patients (Fig. 76.2) and the correlation of the serum ECD with the levels of other serum tumor markers are encouraging. Another area of intensive study is to explore the use of serum marker surrogates in the prediction of cancer patient survival.

MONITORING TREATMENT RESPONSE

One of the most useful applications of tumor markers involves monitoring the course of the disease, especially during treatment. The serum level of tumor markers reflects the success of surgery or the efficacy of chemotherapy. Detecting elevated levels of a tumor marker after surgery would indicate incomplete removal of the tumor, recurrence, or the presence of metastases. The measurement of serum tumor markers during chemotherapy also gives an indication of the effectiveness of the antitumor drug used and a guide for the selection of the most effective drug for each individual case.

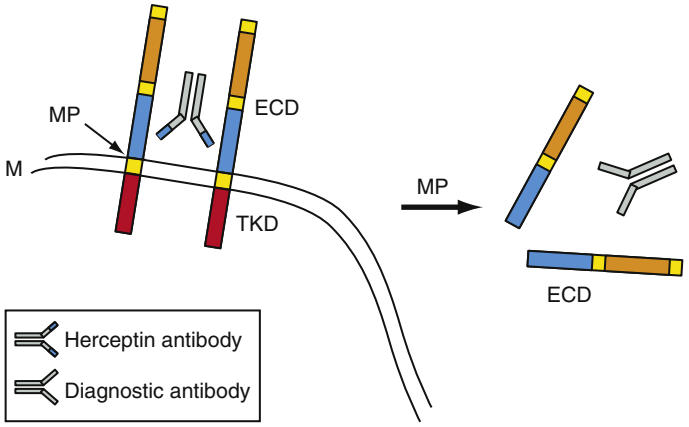

Figure 76.2 HER2/*neu* monoclonal antibodies are used both therapeutically and diagnostically in breast cancer. Humanized HER2 monoclonal antibody trastuzumab (Herceptin), shown with a *dark blue* complementarity determining region (CDR), reacts with a specific region of HER2 epitope *(dark blue)*, causes the death of malignant breast cells, and is often effective in the treatment of breast cancer. On the other hand, different monoclonal antibodies, which do not cross-react with the trastuzumab determinant, recognize the extracellular domain (ECD) (*orange-colored* domain in the figure) of HER2/*neu* in serum after it is cleaved off this growth factor receptor by metalloprotease. Because trastuzumab and diagnostic monoclonal antibodies recognize different epitopes of HER2, there is no interference in detecting serum levels of HER2 in trastuzumab-treated patients. *M,* Cell membrane; *MP,* metalloprotease; *TKD,* tyrosine kinase domain.

RECOMMENDATIONS FOR ORDERING TUMOR MARKER TESTS

When ordering tumor markers as an adjunct diagnostic test for managing cancer patients, the following recommendations should be kept in mind in order to avoid misinterpretation of the test results:

1. Never rely on the result of a single test. Because of low specificity associated with most tumor markers, it is difficult to differentiate between malignant and benign diseases on the basis of a single test result. Most tumor marker elevations found in nonmalignant diseases may be transient, whereas with cancer, the level often either remains elevated or rises continuously. Ordering serial testing can help detect falsely elevated levels due to transient elevation. For example, elevated serum AFP can be detected in patients with either primary hepatocellular carcinoma or benign liver disease. On a subsequent testing 2 weeks later, the serum AFP will remain elevated in patients with cancer, whereas in patients with benign conditions, the serum AFP may return to normal levels.
2. When ordering serial testing, be certain to order every test from the same laboratory using the same assay kit. Each different commercial kit may generate different results even though all are designed for the same tumor marker. Ordering from the same laboratory also ensures a more consistent performance. It is important to ensure that any change observed during the monitoring process is due to a change of tumor volume or other tumor activities and not to laboratory variability.
3. Be certain that the tumor marker selected for monitoring recurrence was elevated in the patient before surgery. Because none of the tumor markers are 100% sensitive to the detection of any particular cancer, it is important to be certain that the tumor marker ordered to detect recurrence was elevated before surgery. Otherwise, multiple markers should be measured before the surgery in order to select the tumor marker showing the highest elevation as the marker for monitoring the disease activity. Multiple markers may be used to monitor the therapeutic effects for increased sensitivity.
4. Consider the half-life of the tumor marker when interpreting the test result. Before surgery, estimate the time required for the level to decline to the normal or, in the case of PSA, to an undetectable level, based on the known half-life of the tumor marker. It is important that the success of surgical removal of a tumor as determined by tumor marker concentrations is not assessed earlier than 2 weeks postoperatively. If possible, it is preferable to wait 1 month to allow the preexisting tumor marker in the serum adequate time to decline to lower levels. For example, the half-life of serum PSA is approximately 3 to 4 days. Therefore, it takes 30 days for a serum PSA at 50 ng/mL to drop to an undetectable level following successful surgery.
5. Consider how the tumor marker is removed from or metabolized in the blood circulation. Elevated serum tumor markers are frequently detected in patients with renal or liver disease depending on whether the tumor marker is removed through the kidney or metabolized by the liver. For example, serum CEA is often elevated in patients with liver disease because the impaired liver fails to remove CEA efficiently from the blood circulation, whereas an elevated serum β_2-microglobulin (β_2M) has been frequently found in patients with renal failure in which even the small β_2M molecule has difficulty passing through the glomerular membrane in a normal fashion.

TABLE 76.1
Monoclonal Antibody–Defined Tumor Markers

Tumor Marker	Major Malignant Disease
CA 125	Ovarian carcinoma
CA 19-9	Pancreatic carcinoma
CA 15-3	Breast carcinoma
CA 72-4	Gastric carcinoma
HER2/*neu*	Breast carcinoma

6. Consider ordering multiple markers to improve both the sensitivity and the specificity for diagnosis. Tumors are made of heterogeneous types of cells. Some may still be normal, while others may be heterogeneous tumor cells as a result of different sequences of multiple mutations. Each type of cell may express a single marker, such as those shown in Table 76.1, or a number of characteristic tumor markers. The same marker may also be produced by different types of cells. Some cells may never produce any unique marker. Certain types of cancer are heterogeneous in their cellular composition. Consequently, more than one tumor marker may be required to provide a high sensitivity of detection. The heterogeneity in cell composition and the percentage of cell distribution of each tumor explains why a number of tumor markers may be required to reach a high (>90%) detection sensitivity and is the reason that the sensitivity of an individual marker differs among cancer patients. Multiple tumor markers associated with individual malignant diseases are listed in Table 76.2; the appearance of individual tumor markers in various malignancies is listed in Table 76.3. This explains why none of the tumor markers presently employed is 100% sensitive and specific and why the use of multiple markers will improve the sensitivity of detection. However, a unique pattern of multiple markers may be identified with tumors derived from the same tissues. Therefore, ordering multiple tumor markers may also improve test specificity. For example, a specific pattern seems to be associated with colon, breast, ovarian, and pancreatic carcinomas when all four MAb-defined tumor markers—CEA, CA 19-9, CA 15-3, and CA 125—are measured simultaneously. This information is clinically important, because more than 60% of diagnosed human cancers are epithelial-cell-derived carcinomas (Wu, 1989). Multiple markers were used to develop a more specific screening strategy for ovarian cancer. The use of CA 15-3 and CA 72-4 in combination with CA 125 can increase the apparent specificity of the CA 125 assay for distinguishing malignant from benign ovarian disease (Bast et al., 1991). Another example is the combination of CEA, CA 19-9, and CA 72-4. Use of this combination improves the diagnostic accuracy of gastrointestinal cancers (Carpelan-Holmstrom et al., 2002). During the selection of multiple tumor markers, only markers that are complementary to one another should be selected. Many tumor markers, which run parallel to one another when correlated with tumor activities, should not be selected for this purpose.
7. Be aware of the presence of ectopic tumor markers. The expression of tumor markers is under genetic regulation. For benign tumors, there are often proteins produced by the tumor that are cell specific and related to normal cell products at an elevated concentration (see Fig. 76.1). However, if a benign tumor becomes malignant, synthesis of these cell-specific proteins may no longer occur in the malignant cells. Conversely, proteins that are normally found at an early fetal stage and not in normal cells or in benign tumors of these cells may become constitutively expressed in the malignant cells. This is the reason that carcinoembryonic proteins and ectopic tumor markers are usually expressed in malignant cancers, often at advanced stages. Thus, the appearance of ectopic tumor markers is often associated with poor prognosis or metastasis. For example, elevated serum concentrations of AFP may be detected in patients with cancers of the gastrointestinal tract involving metastases even though the liver function tests are normal. Table 76.4 lists some of the known ectopic markers and their associated malignant diseases. One should be aware of the guidelines on gastrointestinal and breast cancer marker use published by the American Society of Clinical Oncology (Smith et al., 1999). They recommend monthly breast self-examination, annual mammography of the preserved and contralat-

TABLE 76.2

Serologic Tumor Markers Associated with Individual Malignant Diseases

Malignant Disease	Major Marker	Other Markers
Neuronal Tumors		
Brain tumor	Desmosterol	Polyamines
Neuroblastoma	VMA	HVA, NSE, cystathionine, ferritin, metanephrines
Head and Neck Tumors		
Squamous cell carcinoma	CYFRA 21-1	
Endocrine System		
Pituitary tumors	Growth hormone	IGF-I
Adrenal pituitary tumors	Cortisol	Free catecholamines, DHEA, 17-ketosteroids, prolactin
Cushing syndrome	ACTH	Endorphin, lipotropin
Hypercalcemia of malignancy	PTH-related peptide	
Endocrine pancreatic tumors:	Pancreatic polypeptide:	Chromogranin AC-peptide, IGF-I binding protein I
Gastrinoma	Gastrin	
Glucagonoma	Glucagon	
Insulinoma	Insulin	
Medullary carcinoma of thyroid	Calcitonin	NSE
Microadenomas (pituitary)	Prolactin	
Multiple endocrine neoplasias	Chromogranin A	
Papillary and follicular thyroid cancer	Thyroglobulin	
Parathyroid tumors	PTH-intact	
Zollinger-Ellison syndrome	Gastrin	
Pheochromocytoma	Metanephrine	Chromogranin A, plasma catecholamines
Pituitary tumors	Free β hCG	FSH, LH, prolactin, TSH
Bone and Skeletal Muscle System		
Osteosarcomas	Alkaline phosphatase	
Breast Cancer		
Breast cancer	HER2/*neu*, CA 15-3	CYFRA 21-1, CEA, calcitonin
Pulmonary System		
Bronchogenic carcinoma	Prolactin	
Lung cancer (NSC)	CYFRA 21-1, NSE	ACTH, CK-BB, calcitonin, CA 72-4, CEA, AFP, ferritin, LASA-P, TPA
Carcinoid tumors	Histamine, ADH, bradykinin	
Oat cell cancer	ACTH, ADH, CEA, CK-BB, NSE, bombesin, calcitonin	
Gastrointestinal System		
Colorectal cancer	CEA	CA 19-5, CA 19-9, CA 72-4, NSE
Gastric carcinoma	CA 72-4	CA 19-9, CA 50, CEA, ferritin, CK-BB, hCG, LASA-P, pepsinogen II
Hepatocellular carcinoma	AFP	CEA, ferritin, ALP, TPA, γ-glutamyltranspeptidase (GGT)
Pancreatic carcinoma	CA 19-9	CA 19-5, CA 50, CA 72-4, CEA, CK-BB, ADH, ALP
Vipoma (pancreas)	VIP	
Genitourinary System		
Bladder cancer	T-antigen, urokinase inhibitor, TPA, cytokeratins	Glycosaminoglycans, uroplakins
Nonseminomatous testicular tumor	AFP	hCG
Prostate carcinoma	PSA	PAP, racemase
Renal cell carcinoma	Renin, erythropoietin, IL-4, PGA	
Testicular cancer	hCG	PLAP, Oct3/4
Gynecological Tumors		
Cervical cancer	SCC	CA 125, CEA, TPA
Ovarian carcinoma	CA 125	UGF, inhibin, AFP, amylase isoenzyme, CEA, CK-BB, hCG
Choriocarcinoma	hCG	
Placental tumors	hCG	Free α hCG, CA 15-3, PTH, NSE, prolactin
Uterine cancer	SCC	
Teratoblastoma	AFP	hCG, ferritin
Hematologic Malignancies and Lymphomas		
B-cell chronic lymphocytic leukemia	TdT	Serum β_2M, LASA-P
B-cell malignancies	β_2M	
Chronic myelogenous leukemia	TdT	
Hairy cell leukemia	IL-2 receptor	
Hodgkin disease	LASA-P, ferritin	
Leukemia	TdT	ALP, β_2M, ferritin, LD, myelin basic protein, adenosine deaminase, PNP

Continued

TABLE 76.2 —cont'd

Malignant Disease	Major Marker	Other Markers
Lymphoma	β_2M	TdT, Ki-67, LASA-P
Multiple myeloma	Ig heavy and light chain	Bence-Jones protein, β_2M, IgA, serum free light chain
Waldenström disease	IgM	β_2M, serum free light chain
Melanoma		
Melanoma antigen	Melanoma-associated LASA-P, L-dopa	C-reactive protein
Endoreticular System		
Spleen tumors	Ferritin	
Other		
Sarcoma	β_2M	

ACTH, Adrenocorticotropic hormone; *ADH,* antidiuretic hormone; *AFP,* α-fetoprotein; *ALP,* alkaline phosphatase; *β_2M,* β_2-microglobulin; *CEA,* carcinoembryonic antigen; *CK-BB,* brain isozyme of creatine phosphokinase; *CYFRA 21-1,* cytokeratin subunit 19; *DHEA,* dihydroepiandrosterone; *FSH,* follicle-stimulating hormone; *hCG,* human chorionic gonadotropin; *HVA,* homovanillic acid; *Ig,* immunoglobulin; *IGF,* insulin-like growth factor; *IL,* interleukin; *ki67,* cell proliferation marker; *LASA-P,* lipid-associated sialic acid in plasma; *LD,* lactate dehydrogenase; *LH,* luteinizing hormone; *NSC,* non–small cell; *NSE,* neuron-specific enolase; *Oct3/4,* transcription factor in stem cells and germ cells required for pluripotency; *PAP,* prostate acid phosphatase; *PGA,* prostaglandin A; *PLAP,* placental alkaline phosphatase; *PNP,* purine nucleotide phosphorylase; *PTH,* parathyroid hormone; *SCC,* squamous cell carcinoma; *TdT,* terminal deoxynucleotide transferase; *TPA,* tissue plasminogen activator; *TSH,* thyroid-stimulating hormone; *UGF,* uterine growth factor; *VIP,* vasoactive intestinal polypeptide; *VMA,* vanillylmandelic acid.

TABLE 76.3

Malignant Disease Associated with Individual Serologic Tumor Markers

	ASSOCIATED MALIGNANT DISEASE	
Tumor Marker	**Major Disease**	**Minor Disease**
α-Fetoprotein	Primary hepatocellular carcinoma	Teratoblastomas of the ovary and testes
β hCG	Pituitary tumors	Yolk sac tumor or mixed germ cell tumor
β_2-Microglobulin	B-cell neoplasias	Multiple myeloma, B-cell lymphoma, B-cell chronic lymphocytic leukemia, and reticulum cell sarcoma; Waldenström macroglobulinemia
β hCG	Choriocarcinoma	Testicular cancers (nonseminomatous), trophoblastic tumors
Bence-Jones protein	Multiple myeloma	
Bombesin	Oat-cell cancer	
C-reactive protein	Melanoma	
CA 15-3	Breast cancer	Various carcinomas
CA 19-9	Pancreatic and gastric carcinoma	Various carcinomas
CA 72-4	Gastric carcinoma	Various carcinomas
CA 125	Ovarian carcinoma	Various carcinomas
CA 549	Breast cancer	
CA M26	Breast cancer	
Calcitonin	Medullary carcinoma	Cancer of the thyroid, liver cancer, renal cancer
Carcinoembryonic antigen	Colorectal carcinoma	Various carcinomas
c-*erb*B-2 oncoprotein	Breast carcinoma	Various carcinomas
Chromogranin A	Pheochromocytoma, neuroblastoma	Multiple endocrine neoplasias, small cell lung cancer, carcinoid tumors
CYFRA 21-1	Squamous cell carcinoma of the lung	
DHEA	Adrenal/pituitary cancer	
Ferritin	Acute myelocytic leukemia	Hodgkin lymphoma, neuroblastoma and various carcinomas, teratoblastoma
Galactosyltransferase	Ovarian cancer	
Galactosyltransferase isoenzyme II	Pancreatic cancer	
Gastrin	Gastrinoma	Zollinger-Ellison syndrome
Her2/*neu*	See c-*erb*B-2 oncoprotein	
Human chorionic gonadotropin	Choriocarcinoma	Gastric, ovarian, and breast carcinoma, trophoblastic or germ cell tumors, testicular cancer
Hyaluronic acid	Mesothelioma	
Immunoglobulin A	Multiple myeloma	
Insulin-like growth factor-I	Pituitary cancer	Insulinoma
Interleukin-2 receptor	Leukemia	
Immunoglobulins	Multiple myeloma	Mediterranean lymphoma, Waldenström macroglobulinemia, malignant lymphoma
Inhibin	Granulosa-cell tumors	
17-ketosteroids	Adrenal/pituitary cancer	

β hCG, β chain of human chorionic gonadotropin; *CYFRA 21-1,* cytokeratin subunit 19; *DHEA,* dihydroepiandrosterone; *hCG,* human chorionic gonadotropin.

eral breast, and a careful history and physical examination every 3 to 6 months for 3 years, then every 6 to 12 months for 2 years, and annually thereafter. They do not recommend the use of tumor markers (e.g., CEA, CA 15-3, and CA 27.29) for screening, nor do they recommend routine bone scans, chest radiographs, hematologic blood counts, liver ultrasonograms, or computed tomography for screening. The American College of Physicians has also published clinical guidelines concerning the early detection of prostate cancer. They emphasize the importance of both screening PSA and performing DRE for the early detection of prostate cancer. Even though DRE is not as sensitive as PSA screening, it can detect cancer that would otherwise be missed by PSA measurement (Coley et al., 1997a; 1997b).

TABLE 76.4

Ectopic Tumor Markers

Marker	Tumor
α-Fetoprotein	Gastrointestinal, renal, bladder, and ovarian carcinoma
Calcitonin	Endocrine tumors (islet cell, carcinoid, medullary thyroid, pheochromocytoma); lung, breast, and ovary carcinoma
Chromogranin A	Endocrine tumors (islet cell, carcinoid, medullary thyroid, pheochromocytoma), prostate cancer
Free α hCG	Colorectal carcinoma and pancreatic endocrine tumors
hCG	Gastric and pancreatic carcinoma, hepatoma, ovarian carcinoma, germ cell tumor of testis
PTH	Renal cell carcinoma, breast, squamous cell carcinoma, bladder and ovarian carcinomas
Thyroglobulin	Differentiated thyroid carcinoma

hCG, Human chorionic gonadotropin; *PTH,* parathyroid hormone.

8. Heterophilic antibody. The use of MAbs in immunoassays and the increasing clinical application of mouse MAbs for targeted imaging and immunotherapy create a new problem. Treated individuals apparently produce heterophilic antibodies against murine antibodies that interfere with many of the immunoassays for tumor markers (Nahm & Hoffmann, 1990) although this is not a common encounter. The interference by the heterophilic antibodies in human sera can either increase or decrease the results of an immunoassay. These antibodies react in a way similar to antigens in terms of binding to both solid-phase-associated and signal-labeled antibodies. These heterophilic antibodies may bind to a site other than the analyte-binding site, cross-linking the signal antibody with the capture antibody and, thus, generating a false assay response. Conversely, they may block antibodies used in immunoassays from binding to the antigen (tumor marker), giving a falsely low result. Fortunately, interfering heterophilic antibodies in immunoassays are uncommon. The standard approach for reducing heterophilic antibody interference is to include excess mouse sera or nonspecific mouse immunoglobulins in the immunoassay or to avoid using mouse antibodies.

INDIVIDUAL TUMOR MARKERS

α-FETOPROTEIN

AFP is a major fetal serum protein and is also one of the major carcinoembryonic proteins. AFP resembles albumin in many physical and chemical properties. In the fetus, AFP is synthesized by the yolk sac and fetal hepatocytes and, to a lesser extent, by the fetal gastrointestinal tract and kidneys. Elevated AFP can be found in patients with primary hepatocellular carcinoma and yolk sac–derived germ cell tumors (mainly endodermal sinus tumor) and is the most useful serum marker for these cancers (Lamerz, 1997). However, AFP is also transiently elevated during pregnancy and in many benign liver diseases. Because of the high prevalence of liver cancer in China and other countries in Southeast Asia, AFP testing has been used successfully in screening for hepatocellular carcinoma in that region of the world. Tests for both AFP and hCG are helpful in reducing clinical staging errors in patients with some testicular tumors and aid in the differential diagnosis of various germ cell tumors. Because an increase of fucosylation of AFP (hence, the lentil lectin reactivity of serum AFP) has been found in primary hepatocellular carcinoma, the determination of lentil lectin reactivity of serum AFP was found to be helpful not only to differentiate between primary hepatocellular carcinoma and benign liver diseases but also to provide an early signal indicating that hepatocellular carcinoma may begin to develop in patients with liver disease. Although the necessity for routine AFP screening needs further study, one study indicates that combined screening with AFP and ultrasonography results in increased sensitivity—from 75% to near 100%—in detecting hepatocellular carcinoma of patients with hepatitis B and hepatitis C (Izzo et al., 1998; Gebo et al., 2002). Finally, AFP is currently offered for prenatal screening for neural tube defects and, in conjunction with free β hCG and unconjugated estriol, for Down syndrome (triple test) (Cuckle, 2000; Yamamoto et al., 2001). (See also Chapter 26.)

ANGIOGENIC FACTORS

Angiogenesis is the formation of blood vessels in situ, involving the orderly migration, proliferation, and differentiation of vascular cells. Blood vessel formation is also important in the pathogenesis of rapid growth and metastasis of solid tumors. Several angiogenic factors have been identified, including acidic and basic fibroblast growth factor (bFGF), described in Chapter 77; angiogenin; and vascular endothelial growth factor (VEGF) (Folkman & Shing, 1992). Both angiogenic and antiangiogenic factors have been found in the serum of patients with malignant disease (Morelli et al., 1998). Serum levels of bFGF and VEGF reflect their expression in individual tumors (Poon et al., 2003; Granato et al., 2004). The significance of elevated serum VEGF in cancer patients has been evaluated in several studies, including breast, ovarian, hepatocellular, colorectal, and renal cell carcinomas and soft-tissue sarcoma. Elevated serum VEGF values in ovarian cancer patients were correlated with cancer differentiation, metastasis, and, more significantly, shorter average survival time (Alvarez Secord et al., 2004; Harlozinska et al., 2004; Li et al., 2004). Furthermore, elevated serum VEGF has been associated with shorter survival in renal cell carcinoma (Ljungberg et al., 2003) and colon carcinoma (De Vita et al., 2004).

β_2-MICROGLOBULIN

β_2M is the constant light chain of the human histocompatibility locus antigen expressed on the surface of most nucleated cells. The molecular weight of β_2M is only 11.8 kDa. β_2M is shed into the extracellular fluid and is elevated not only in solid tumors but also in lymphoproliferative diseases (including B-cell chronic lymphocytic leukemia, non-Hodgkin lymphoma, and, importantly, multiple myeloma) (Wu et al., 1986). Serum concentration of β_2M correlates with lymphocyte activity, making β_2M a good marker for lymphoid malignancies of the B-cell line. It has been used as an indicator of the patient's response to treatment (Haferlach & Loffler, 1997). CSF levels of β_2M are useful for detecting metastases in the central nervous system. It is reported that serum β_2M level is elevated in 75% of patients with multiple myeloma (Kyle et al., 2003) and is useful in following the efficacy of the treatment of this disease, although currently serum free light chain (FLC) assay has been found to be more effective in following this disease (see later discussion).

SERUM FREE LIGHT CHAIN DETERMINATIONS

In Chapters 20 and 47 on specific serum proteins, the use of serum protein electrophoresis was discussed as an important method for detecting monoclonal gammopathies. These are conditions in which single clones of B cells or plasma cells proliferate and overproduce a specific monoclonal immunoglobulin. These are detected as monoclonal spikes in the Ig region of the electrophoretogram. Immunofixation reveals the type of immunoglobulin that is being overexpressed. Monoclonal gammopathies involving IgG and IgA result in the condition of multiple myeloma, a cancer of B or plasma cells in which the proliferation of these cells causes lytic lesions in bone marrow, leading to pathologic fractures and resulting in hypercalcemia and elevations of serum alkaline phosphatase (see Chapter 21). Monoclonal gammopathies involving IgM give rise to Waldenström macroglobulinemia, also a cancer of B or plasma cells in which high levels of IgM are expressed in serum. IgM immunoglobulins are Ig pentamers with 10 antigen binding sites and are, therefore, very large proteins. These monoclonal proteins are highly hygroscopic, giving rise to the so-called *hyperviscosity syndrome* in which the relative viscosity of blood is much higher than that for blood from normal individuals, reaching as high as five times that of normal viscosity. This can lead to sludging of blood in capillaries, with resulting infarcts of tissues. In addition, monoclonal gammopathies occur that do not involve malignant transformation of B or plasma cells but involve overproduction of the monoclonal antibodies and light chains. Most of these conditions are referred to as *monoclonal gammopathy of undetermined significance* (*MGUS*). However, some of these conditions result in polymerization of the monoclonal light chains that are deposited in multiple different tissues, a condition called *primary*, or *AL*, *amyloidosis*. Irrespective of the specific condition, it is vital to diagnose and to follow these conditions in a quantitative manner.

All immunoglobulins involve the association of two heavy with two light chains, which are of the κ or λ types. Light chains are encoded on genes on chromosome 2 and are present in excess of heavy chains. In most monoclonal gammopathies, light chains are produced in substantial excess of heavy chains and are themselves monoclonal—that is, they have a single unique amino acid sequence. Light chains have constant, variable and hypervariable domains, the latter forming the complementarity-determining domain involved in antigen recognition. Each chain type has sequences that are type specific. Parts of these sequences are "buried" when the light chains are complexed with their counterpart heavy chains. Mono- and polyclonal antibodies have been developed that recognize each chain type uniquely and will bind to each only if the light chain is not bound to the heavy chain. This allows quantitation of free κ and λ light chains in serum.

The reference range for serum κ light chains is 0.33 to 1.94 mg/dL; for λ light chains, it is 0.57 to 2.63 mg/dL. Values of one or the other light chain that substantially exceed the upper reference range, while the level of the counterpart chain either remains in the reference range or is slightly elevated, suggest a monoclonal gammopathy. Another way of quantitating FLCs is to measure the ratio of κ to λ chain levels. The reference range for the κ/λ ratio is 0.57 to 2.63. Values below 0.57 suggest a λ gammopathy, while values that exceed 2.63 suggest a κ light chain gammopathy.

Serum FLC (SFLC) determinations are currently the most sensitive method for following the course of treatment of specific monoclonal gammopathies and have replaced serum protein electrophoresis and immunofixation and β-microglobulin levels for this purpose. They are also excellent predictors of the prognosis for patients being treated for these conditions and for patients with MGUS (Rajkumar et al., 2005).

Further studies indicate the importance of performing free light chain analysis. In one study (Kim et al., 2014), it was found that serum FLC assays had sensitivities of 64% to 72% depending on the assay, and 93% to 100% specificities. The reference method was immunofixation. The limitations of the serum FLC assay in diagnosing monoclonal gammopathy were very low levels of monoclonal protein, chronic kidney disease, polyclonal gammopathy, biclonal gammopathy, and IgM gammopathy. Another study (Kagan et al., 2016) similarly found that SFLC had a sensitivity of 69%, a specificity of 95%, a positive predictive value of 84%, and a negative predictive value of 90%. Importantly, SFLC identified gammopathy in 22% of cases for which the SPEP results were negative. The high values for the sensitivity and specificity are encouraging findings suggesting that FLC assays will become useful in detecting B and plasma cell tumors at an early stage.

CARCINOEMBRYONIC ANTIGEN

CEA is a glycoprotein with a molecular weight of approximately 200 kDa. It is the first of the so-called carcinoembryonic proteins and was discovered by Gold and Freedman in 1965. CEA is still the most widely used tumor marker for gastrointestinal cancer, but most CEA assays have replaced polyclonal with monoclonal anti-CEA antibodies.

CEA was originally thought to be a specific marker for colorectal cancer, but it turned out to be a nonspecific marker on further studies. CEA levels can be elevated in breast, lung, and liver cancers, among others. CEA studies demonstrated that tumor markers could be used to follow patients during therapy and to detect recurrence after successful surgery. The association between highly elevated serum tumor marker concentration and metastases and poor prognosis was also discovered through CEA studies. Elevated CEA levels before resection of colon cancer may suggest a worse prognosis. Declining levels during therapy suggest response to therapy, whereas increasing levels suggest disease progression. However, clinical decisions regarding management of disease cannot be based on CEA levels alone (Mitchell, 1998). As the liver metabolizes CEA, liver damage can impair CEA clearance and lead to increased levels in the blood circulation. Increased CEA concentrations have been observed in some patients following radiation treatment and chemotherapy. It was recommended that CEA should form part of the American Joint Committee on Cancer staging system (Compton et al., 2000). CEA can be used as a marker for monitoring colorectal cancer (Bast et al., 2001). However, a low positive predictive value for diagnosis in asymptomatic patients limits its widespread use in screening.

Other genetic tumor markers are being used with increased frequency. For example, transforming growth factor–α, fibroblast growth factor, and Ras oncoprotein are all increased in colorectal cancer and decreased after surgical resection. More recently, mutations of DNA mismatch repair genes (e.g., *hMSH2*, *hMLH1*, and *hMSH6*) are shown to be associated with hereditary nonpolyposis colorectal cancer. Further clinical studies to correlate the serum levels of expression and mutation in these genes might yield a better diagnostic/prognostic tool.

CA 15-3 AND CA 27.29

These antigens correspond to sequences of mucins called polymorphic epithelial mucins (PEMs), which are often overexpressed on the cell surfaces of malignant glandular cells such as those occurring in breast cancer, and increasing amounts are shed into the circulation, where they can be detected, making them useful as tumor markers. The polypeptide core of PEM contains a 69-amino acid cytoplasmic domain and a much larger ECD, consisting of 20 amino acid tandem repeats that vary among individuals; different alleles of the human *MUC1* gene may code for between 25 and 100 or more tandem repeats. A large part of the molecule is carbohydrate, and the degree of glycosylation is variable, making PEM very heterogeneous in structure (Klee & Schreiber, 2004).

The CA 15-3 determinant is identified by two distinct monoclonal antibodies. The assay uses a solid-phase conjugated MAb—MAb 115D8—to capture the MAM-6 antigen in human plasma and a labeled MAb DF3 as detecting antibody. MAb 115D8 was prepared against human defatted milk fat globule, and MAb DF3 was prepared against the breast carcinoma cell line MCF-7. The CA 15-3 antigen is present in a variety of adenocarcinomas, including breast, colon, lung, ovary, and pancreas.

CA 15-3 is a more sensitive and specific marker for monitoring the clinical course of patients with metastatic breast cancer (Canizares et al., 2001). CA 15-3 levels increase with higher stages of breast cancer (Bast et al., 2001). In addition, CA 15-3 can be used to predict adverse outcomes in breast cancer patients (Gion et al., 2002; Kumpulainen et al., 2002; Duffy et al., 2004). However, the relative low sensitivity (23%) and specificity (69%) (Chan & Sell, 2001) in detecting breast cancer have limited its use. CA 15-3 can also be elevated in chronic hepatitis, liver cirrhosis, sarcoidosis, tuberculosis, and systemic lupus erythematosus, and in patients who smoke (Tondini et al., 1988). CA 27.29, another mucin marker MUC1-associated antigen, is a slightly more sensitive breast cancer marker than CA 15.3. The FDA has approved both CA 15-3 and CA 27.29 for monitoring therapy of advanced or recurrent breast cancer. Patients with ovarian carcinoma have significantly elevated MUC1 serum concentrations as compared with those with benign ovarian diseases with high variability. Results from immunohistochemistry (IHC) indicate that mucin-1 has a prognostic relevance in ovarian carcinomas when evaluating the expression by VU4H5 antibody (Engelstaedter et al., 2012).

CA 19-9, CA 50, AND CA 19-5

CA 19-9 is the first tumor marker of a group of newer epitopes, including CA 125, CA 15-3, and CEA, defined by monoclonal antibodies. These new monoclonal kits detect more newly discovered epitopes and were designed to replace polyclonal CEA measurements for various carcinomas. The assay for CA 19-9 measures a carbohydrate antigenic determinant expressed on a high-molecular-weight mucin. CA 19-9 is an epitope, defined as sialylated lacto-*N*-fucopentose II, recognized by the MAb 1116NS-199. The molecule, carrying the CA 19-9 epitope, appears as mucin in the sera of cancer patients but as a ganglioside in tumor cells. CA 19-9 is also related to Lewis blood group substances. Only serum antigen from cancer patients belonging to the Le (a^-b^+) or Le (a^+b^-) blood group will be CA 19-9 positive. In addition to CA 19-9, CA 19-5 and CA 50 have been defined by monoclonal antibodies that are only slightly different from CA 19-9. CA 19-9 can be elevated in patients with colorectal cancer, gastric cancer, and pancreatic cancer. The epitope related to CA 50 is very similar to that of CA 19-9 but lacks a fucose residue, the same epitope found in Lewis-negative Le (a^-b^-) individuals. Serum CA 19-9 concentrations not only are frequently highly elevated in both gastric and pancreatic carcinomas but also are useful for monitoring the success of therapy and for detecting recurrence in these cancer patients. However, it has been reported that CA 19-9 and CA 50 complement each other in pancreatic and other carcinomas—their simultaneous use may improve the sensitivity in detecting these malignant diseases. CA 19-9 is the most widely studied and the only FDA-approved biomarker for pancreatic ductal carcinoma (Winter et al., 2013). Elevated perioperative serum CA 19-9 levels are independent predictors of poor survival in patients with resectable cholangiocarcinoma (Kondo et al., 2014). CA 19-5 is detected by mouse MAb CC3C-195 and reacts with both Le^a and sialyl-Le^a epitopes. CC3C-195 binds with high affinity to the sialylated Le^a blood group antigen but exhibits a lower affinity to the nonsialylated form. Elevated serum levels of CA 50 and CA 19-5 can also be found in patients with colon, pancreatic, and hepatocellular carcinomas. False-positive findings may occur in patients with benign liver disease and may be due to cholestasis in these patients (Wu & Carlisle, 1992).

CA 125

CA 125 is another antigenic determinant defined by an MAb and is also associated with a high-molecular-weight (>200 kDa) mucin-like glycoprotein. CA 125 is expressed by more than 80% of nonmucinous epithelial ovarian carcinomas and is found in most serous, endometrioid, and clear-cell carcinomas of the ovary (Jacobs & Bast, 1989). However, patients undergoing chemotherapy may show a false decline of CA 125 antigen and a negative result does not always rule out tumor recurrence. CA 125 is also used clinically for follow-up on uterine tumors (>60% are elevated) and benign tumors, including endometriosis. Recent studies showed greatly improved sensitivity of serum CA 125 in combination with other markers using proteomics techniques (discussed in detail in succeeding chapters) (Jacobs & Menon, 2004; Lu et al., 2004; Zhang et al., 2004). Studies for the application of serum CA 125 in other cancerous (e.g., non-Hodgkin lymphoma, lung cancer) and nonmalignant (e.g., liver cirrhosis) diseases

have been performed (Ando et al., 2003; Xiao & Liu, 2003; Zidan et al., 2004) and showed increased levels of CA 125 in the sera of these patients.

Recently, human epididymis protein 4 (HE4) has been studied to improve the sensitivity and specificity of ovarian cancer diagnosis. HE4 is primarily expressed in the reproductive and respiratory tracts (Bingle et al., 2002; Galgano et al., 2006) and is overexpressed in epithelial ovarian cancer (Schummer et al., 1999). The HE4 gene product is an *N*-glycosylated protein, which is secreted into the extracellular environment and can be detected in the bloodstream of patients with ovarian cancer (Moore et al., 2008). HE4 was found to be elevated in more than half of ovarian tumors that do not express CA 125 (Moore et al., 2008). This finding prompted the development of a dual marker algorithm that combined HE4 and CA 125 with the pre- and postmenopausal statuses of the patient, known as Risk of Ovarian Malignancy Algorithm (ROMA) (Moore et al., 2009). ROMA has been shown in several studies to better predict the presence of a malignant ovarian mass than other markers, with high sensitivity and specificity (Moore et al., 2009).

CA 72-4

The CA 72-4 assay detects a mucin-like human adenocarcinoma-associated antigen—TAG-72—which is a high-molecular-weight (>10^6 kDa) mucin-like complex molecule. Because TAG-72 can be detected in both fetal epithelia and sera from patients with various carcinomas, it is also considered to be a carcinoembryonic protein. However, only moderately elevated serum CA 72-4 levels are found in most carcinomas. Currently, CA 72-4 is considered to be a useful marker for the management of patients with gastric and colorectal carcinoma. CA 72-4 has been proposed as a specific marker for tumor occurrence of resectable gastric cancer (Marrelli et al., 2001) and a prognostic marker for survival (Gaspar et al., 2001). CA 72-4 has been reported to be an independent prognostic marker for survival in colorectal cancer (Louhimo et al., 2002) in multivariate analysis together with β hCG and CEA.

CALCITONIN

Calcitonin is one of the circulating peptide hormones that may become elevated in patients with increased bone turnover rate associated with skeletal metastases. Calcitonin can be ectopically elevated in bronchogenic carcinomas and is also elevated in medullary carcinoma of the thyroid (see Table 76.4). Serum procalcitonin, having comparable diagnostic accuracy, has great potential to replace serum calcitonin as a new standard of care in the management of medullary carcinoma of the thyroid because it does not need to be kept cool on ice or frozen and is easier to manage at the community level (Machens et al., 2014).

CHROMOGRANIN A

Chromogranin A is a major soluble protein of the chromaffin granule. Chromogranin A and catecholamines are released from the adrenal medulla upon stimulation of the splanchnic nerve. However, chromogranin A is not confined to chromaffin cells of the adrenal medulla and sympathetic neurons. It is also present in various neuroendocrine organs. Elevated serum chromogranin A levels can be detected in pheochromocytoma (Giovanella & Ceriani, 2002), medullary carcinoma of the thyroid, and small cell lung carcinoma (Ma et al., 2003). Interestingly, increased serum chromogranin A levels are detected in epithelial cancers with neuroendocrine differentiation, including prostate, breast, ovary, pancreas, and colon (Wu et al., 2000).

Prostate cancer with neuroendocrine differentiation has been an active area of study. Higher levels of serum chromogranin A are associated with poorly differentiated prostate cancer (Isshiki et al., 2002). It is also increased after androgen blockade therapy and systemic radionucleotide therapy (Ferrero-Pous et al., 2001) for prostate cancer. Furthermore, an association between increased chromogranin A and prostate cancer metastasis has been observed (Tarle et al., 2002). Intermittent androgen deprivation therapy can reduce the levels of chromogranin A and, thus, the neuroendocrine differentiation of prostate cancer (Sciarra et al., 2003). Chromogranin A is not only a reliable serum diagnostic biomarker for pancreatic neuroendocrine tumors but also can predict overall survival and treatment response, especially in Asian patients (Chou et al., 2014).

CYTOKERATIN 19 FRAGMENT

Cytokeratin 19 fragment (CYFRA 21-1) is a fragment of the cytokeratin 19 intermediate filament found in the serum. It is a subunit of a cytokeratin intermediate filament expressed in simple epithelia and their malignant counterparts. Studies of elevated serum CYFRA 21-1 have concentrated on breast cancer and squamous cell carcinoma of the lung. CYFRA 21-1 was reported to have a sensitivity of 60%, 64.2%, and 89% for the detection of stage IV breast cancer, recurrence, and metastasis, respectively. Probability of survival for primary cancer patients, recurrence after surgery, and response after chemotherapy were correlated with elevated preoperative serum CYFRA 21-1 in breast cancer patients (Nakata et al., 2000, 2004). CYFRA 21-1 was also shown to reflect the tumor mass in multiple studies with correlation to tumor stage, survival, predictive role in surgical treatment for early-stage disease, and chemotherapy for advanced-stage non–small cell lung cancer (NSCLC). In one study of head and neck squamous cell carcinoma (SCC), increased postradiotherapeutic or chemotherapeutic CYFRA 21-1 has been explored as an early indicator for distant metastasis (Kuropkat et al., 2002). CYFRA 21-1 is not increased in patients with nonneoplastic lung disease, including pneumoconiosis and obstructive airway disease (Schneider et al., 2003).

HUMAN CHORIONIC GONADOTROPIN

Human chorionic gonadotropin (hCG), a member of the glycoprotein hormone family, is synthesized and secreted by trophoblast cells of the placenta and is a heterodimeric hormone composed of noncovalently linked α and β subunits internally linked by disulfide bonds. The current assays using monoclonal antibodies are available to detect intact hCG, "nicked" hCG, or hCGn (which is partially degraded hCG that is missing peptide bonds between amino acids 44 and 45 or 47 and 48); hCG α subunit; hCG β subunit; and hCG β core (residual hCG β, residues 6–40 joined by disulfide bond to hCG β, residues 55–92) (Berger et al., 2002; Birken et al., 2003). Both malignant and nonmalignant trophoblast cells synthesize and secrete not only the biologically active α and β dimer but also the uncombined (or free) α and β subunits. In addition to the intact dimer, a free β subunit of hCG has been detected in the serum of women during early pregnancy and in patients with malignant tumors (see Chapter 26).

Measurement of the free β subunit is useful for the detection of recurrence or metastasis for choriocarcinoma when the intact hCG may remain normal. Analysis of serum hCG subunits is especially useful for managing patients with germ cell tumors (Von Eyben, 2003). However, elevated hCG can be found in trophoblastic tumors, choriocarcinoma, and testicular tumors. More than 60% of patients with nonseminomatous germ cell tumors and 10% to 30% with seminomas have elevated free β hCG.

Seminomatous testicular cancer contains both intact hCG and β hCG or free α subunits in equal amounts. Therefore, only one assay is needed for monitoring these patients. On the other hand, only hCG or β hCG subunits may be found in patients with nonseminomatous cancers. The measurement of both free subunits and intact hCG will increase the test sensitivity for these patients with nonseminomatous cancers.

Ectopic free β hCG production occurs in approximately 30% of patients with other cancers, including urothelial cancer, but only the free β hCG and its respective breakdown product, β core, have been detected in these clinical samples. Ectopic α hCG is a marker of malignancy in pancreatic endocrine tumors (Ma et al., 2003). Recent efforts in preparation of the new World Health Organization reference reagent for hCG (HCG, hCG-α, and hCG-β) and its related molecules may decrease the nonspecific reaction and increased accuracy of clinical hCG testing (Bristow et al., 2005).

HER2/*NEU* (C-*ERB*B-2) ONCOPROTEIN

In addition to lung adenocarcinoma, another successful example of individualized medicine using gene sequencing is anti-human epidermal growth factor receptor (HER2) using trastuzumab and other drugs targeting tumors overexpressing HER2 in breast cancer (Nagahashi, 2019). The HER2/*neu* (c-*erb*B-2) oncogene is a 185-kDa transmembrane protein of the tyrosine kinase receptor family, discussed extensively in Chapter 77. It shows structural and functional homology with the epidermal growth factor receptor (EGFR) containing intracellular, transmembrane, and ECDs (see Fig. 76.2). HER2/*neu* has been found to be elevated in the sera of patients with a number of different epithelial cell cancers, including breast cancer (Mori et al., 1990; Leitzel et al., 1992; Ali et al., 2002; Tsigris et al., 2002a, 2002b). In patients with breast cancer, serum HER2/*neu* is very important as a prognostic and predictive marker. At the time of initial diagnosis, serum HER2/*neu* is elevated in only 5% to 10% of breast cancer patients. Increased serum HER2/*neu* before adjuvant therapy has been shown to be associated with increased tumor size, tumor grade, and positive lymph nodes. The serum HER2/*neu* test is indicated for follow-up and monitoring of patients with metastatic breast cancer whose initial serum HER2/*neu* level is greater than 15 ng/mL. Schippinger and colleagues (2004) reported that a decrease of elevated serum HER2/*neu* to

levels below 15 ng/mL and levels continuously 15 ng/mL or less during the course of disease correlated significantly with longer survival. The serum HER2 level as assessed by the chemiluminescence immunoassay method is the most sensitive marker of HER2-positive metastatic breast cancer compared with the CEA and CA 15-3 levels (Kan et al., 2009). Prechemotherapy and postchemotherapy HER2/*neu* levels could serve as a prognostic marker for disease-free survival and overall survival (Hayes et al., 2001; Saghatchian et al., 2004). In addition, serum HER2/*neu* levels correlate with response to chemotherapy, including hormonal and Herceptin (trastuzumab) treatment; higher levels predict incomplete response, while low levels suggest longer or complete treatment responses (Colomer et al., 2000; Harris et al., 2001; Lipton et al., 2002; Bethune-Volters et al., 2004; Luftner et al., 2004).

HER2 overexpression is typically determined by IHC and fluorescent in situ hybridization (FISH). The enzyme-linked immunosorbent assay (ELISA) measures the levels of the circulating c-*erb*B-2, referred to as p105 or serum HER2, constituting the ectodomain (see Fig. 76.2). Three FDA-approved ELISA tests for serum circulating HER2 using monoclonal antibodies are available: one for microtiter plate assay—Oncogene Science/Siemens—and two for automated instrument—Bayer Immuno 1 HER2/neu assay (Siemens) and ADVIA Centaur HER2/*neu* immunoassay (Siemens). The ADVIA Centaur HER2/neu immunoassay kit is similar to the Bayer/Siemens Immuno 1 HER2/*neu* kit in indication for use, format, performance characteristics, and results. The ADVIA differs mainly in the signal system, which is chemiluminogenic instead of the ALP-catalyzed color reaction in the Siemens/ADVIA Immuno 1 assay. More important, there is no interference with the serum HER2/*neu* test by heterophile antibodies and, more significantly, the therapeutic MAb trastuzumab, because different antigen epitopes are targeted (see Fig. 76.2).

HER2/*neu* is also overexpressed and/or amplified in oral squamous cell carcinoma (Chen et al., 2007), NSCLC (Papila et al., 2009), gastric cancer (Tsigris et al., 2002b), colorectal cancer (Tsigris et al., 2002a), urothelial carcinoma (Hussain et al., 2007), prostate cancer (Kehinde et al., 2008), and ovarian cancers in association with advanced stage and poor prognosis. Thus, it can be used as a therapeutic target in these cancers (Agus et al., 2000). Recently, serum levels of HER2 extracellular domain have been highly correlated with tissue HER2 status in metastatic gastric cancer; thus, this assay can be considered as a potential alternative for tissue HER2 status (Peng et al., 2014).

NGS-based gene panel testing enables detection of HER2 gene amplification. IHC, FISH, and gene panel testing have demonstrated equivalent utility identifying candidates for anti-HER2 therapies in colorectal cancer (Shimada, 2017). It has recently been demonstrated that breast cancer patients with somatic HER2-activating mutations can benefit from anti-HER2 therapies although they lack HER2 amplification (Bose, 2013). NGS-based gene panel tests have the added advantage of detecting gene alterations that cause drug resistance. For example, NGS-based panels can examine the PI3K/mTOR pathway, MAPK pathway, and other receptor tyrosine kinases (RTKs) that have been implicated in resistance to anti-HER2 therapy (Nagahashi, 2019).

p53

p53 (see Chapter 77) is a 53-kDa nuclear phosphoprotein and a negative regulator of cell growth. It functions as a tumor suppressor by inducing the expression of gene products that are responsible for inhibiting or arresting cell growth and proliferation. The ability of p53 protein to regulate transcription of its target genes is based on its sequence-specific DNA binding activity and the presence of a domain that can activate transcription when attached to the DNA-binding domain of p53 target protein. It is the DNA-binding domain that appears to be sensitive to disruption by mutation, and most lesions associated with human cancers occur within this domain. The encoding gene for p53 has been found to be mutated in about half of almost all types of cancer arising from a wide spectrum of tissues. Because of its short half-life (20 minutes), the wild-type p53 protein in the blood circulation is not detectable (Malkin et al., 1990; Harris & Hollstein, 1993). However, current molecular techniques, such as PCR/SSCP (detailed in Part 8) can detect serum p53 gene mutations. The presence of p53 antibody in serum facilitated the detection of abnormal p53 serologically. Significantly, the presence of p53 antibody in serum is associated with the expression of p53 mutations and positively correlates with the degree of cancer malignancy (discussed in Chapter 77).

PARATHYROID HORMONE–RELATED PEPTIDE

Plasma concentrations of parathyroid hormone–related peptide (PTH-RP) are elevated in the majority of patients with cancer-associated hypercalcemia. PTH-RP is secreted by tumors associated with hypercalcemia. The circulatory forms of PTH-RP in these patients include both a large amino terminal peptide and a carboxyl terminal peptide with close sequence homology to parathyrin (PTH). The mechanism by which PTH-RP induces hypercalcemia involves binding and activating receptors that also bind PTH. Measuring the concentrations of PTH-RP may be useful in the differential diagnosis of hypercalcemia related to malignancy and associated either with primary hyperparathyroidism, sarcoidosis, vitamin D toxicity, or various malignancies (including squamous cell, renal, bladder, and ovarian carcinomas). Patients with impaired renal function but without hypercalcemia or cancer may have increased plasma concentrations of PTH-RP (Burtis et al., 1990).

SERUM MARKERS FOR PROSTATE CANCER

Serum Prostate-Specific Antigen

PSA is a member of the kallikrein family of serine proteases that is synthesized uniquely in the epithelial cells of the prostate gland. Its expression in these cells is regulated by the androgen receptor. Because of its high degree of tissue specificity, it is perhaps the most widely used tumor marker discovered thus far. The normal reference range is 0 to 4 ng/mL. The cancer sensitivity and tissue specificity of PSA make it the most useful tumor marker available for the screening and management of prostate cancer. Lack of cancer specificity in distinguishing prostate cancer and nonmalignant prostate lesions is the main drawback with PSA. Benign conditions such as BPH, acute prostatitis, and infarction can also be correlated with elevated serum PSA levels.

PSA serves as an excellent cancer marker in prostate cancer screening, diagnosis, prediction of cancer risk, and recurrence. Since its discovery in prostate cancer serum in 1980 (Papsidero et al., 1980), PSA has been subjected to intensive research and clinical usage in the screening, detection, and monitoring of prostate cancer. PSA and its various forms are used to guide clinical decisions for further tissue biopsy diagnosis, resulting in increased prostate cancer detection, especially in young men. Use of PSA in prostate cancer detection has also resulted in a reduction in the number of prostate cancers discovered only at late stages in which metastases occurred, from about 30% of all newly diagnosed cases to about 10% of all such cases (Cooperberg et al., 2004). Annual PSA screening is recommended by both the American Urological Association (AUA) and the American Cancer Society for all men over the age of 50 years. The AUA issued new guidelines during its 104th annual meeting (Greene et al., 2009). The new guidelines have lowered the age for beginning PSA screening to 40 years for relatively healthy, well-informed men who want to be tested. In addition, because of its tissue specificity, the PSA assay is particularly useful for monitoring the success of surgical prostatectomy. Complete removal of the prostate should result in an undetectable PSA level, while incomplete resection of the gland (not persistent disease) might result in measurable levels of PSA. However, it should remain unchanged on extended follow-up. Any increase in measurable PSA after a successful radical prostatectomy would indicate prostate cancer recurrence or metastasis. A transient and modest increase of PSA may occur during radiation therapy, which should not be misinterpreted as disease progression.

Multiple studies suggest that diagnosis is made in more than 80% (in some studies, >90%—e.g., DeSoto-LaPaix et al., 2003) of patients with prostate cancer from serum PSA levels that are greater than 4 ng/mL. Because BPH and acute prostatitis also induce elevated serum PSA levels, approximately half of patients with PSA values greater than 4 ng/mL are not found to have prostate cancer on biopsy, even at significantly elevated levels (i.e., >10 ng/mL). These studies suggest that PSA has a sensitivity of a minimum of 80% and a specificity of around 50%. However, it has also been found that about 20% of initially negative biopsies, when repeated over a 3-year period, become positive (DeSoto-LaPaix et al., 2003). Thus, the specificity of PSA may be higher assuming that the biopsies missed a malignant lesion and that a new malignancy did not occur over the 3-year time period, leading to the current practice of saturation biopsy.

On the other hand, the cutoff value of 4 ng/mL does not sufficiently distinguish patients with and without prostate cancer, including more aggressive cancers (Schröder et al., 2000; Horninger et al., 2002; Punglia et al., 2003; Thompson et al., 2004). In a review of the Prostate Cancer Prevention Trial, 2950 men who never had a PSA level greater than 4 ng/mL or an abnormal DRE had a final PSA determination and underwent a prostate biopsy after being in the study for 7 years (Thompson et al., 2004). There was a 15.2% (n = 449) biopsy-proven prevalence of prostate cancer in men with PSA levels no greater than 4 ng/mL. High-grade prostate cancer (defined as a Gleason score ≥7) was seen in 15.8% (n = 71) of these men. Size of the tumor was not reported. In the placebo arm of

the Prostate Cancer Prevention Trial, there was no cutpoint of PSA with simultaneous high sensitivity and high specificity for detection of prostate cancer in healthy men, but rather a continuum of prostate cancer risk at all values of PSA (Thompson et al., 2005). These studies appear to confirm the results of other studies that the sensitivity of PSA, using the 4 ng/mL cutoff, in diagnosing prostate cancer is on the order of 80% to 85%. The finding that using a cutoff of 4 ng/mL for PSA to diagnose this disease results in 15.2% false-negative results in the patient population subjected to biopsies is compatible with this conclusion (i.e., 84.2% of patients with prostate cancer had serum PSA levels greater than 4 ng/mL).

The issue of using lower cutoffs for serum PSA to identify more patients with prostate cancer has been further explored (Punglia et al., 2003), especially in view of the development of more sensitive assays for PSA, now commercially available in PSA test kits, that are capable of detecting serum PSA less than 0.1 ng/mL. Based on considerations from the Prostate Cancer Prevention Trial, European guidelines were issued in 2008 recommending a PSA cutoff value of 2.5 ng/mL or a PSA velocity of 0.6 ng/mL per year as a biopsy indication (Heidenreich et al., 2008).

In addition to the issue of cutoffs for PSA in the diagnosis of prostate cancer, the issue of the efficacy of diagnosis of this disease has been raised, as it has been for a number of other cancers, including breast cancer. The question is whether early diagnosis of prostate cancer saves patients' lives. To address this question, a major study by the European Randomized Study of Screening for Prostate Cancer (ERSPC) was carried out over approximately the past decade, involving 182,000 men between the ages of 50 and 74 years in 7 European countries who were randomly assigned to a group that was offered PSA screening at an average of once every 4 years or to a control group that was treated according to current practice standards and was not subjected to the regular screening procedure. Most participating centers in this study used a lower PSA cutoff value as an indicator of abnormality than the usual 4 ng/mL (i.e., 3 ng/mL vs. 4 ng/mL). Prostate cancer was detected in 8.2% of the men in the screening group, while 4.8% was detected in the control group. The absolute death risk difference between the control group and the screening group was 0.71 patient per 1000 patients, implying that 1410 patients must be screened in order to prevent 1 death from prostate cancer. Overall, this study found that screening resulted in a lower death rate from prostate cancer by 20% (Schröder et al., 2008, 2009). The study concluded that this significant reduction in the number of deaths from prostate cancer was accompanied by a high risk of overdiagnosis, which, nonetheless, seems to be a small price to pay for the significant number of lives saved.

Contrary to the results of this investigation, another study by the Prostate, Lung, Colorectal, and Ovarian Cancer Screening Trial on patients assigned to be screened with PSA and DRE and control groups found that whereas 20% more prostate cancer was diagnosed in the screened group than in the control group, the death rate among both groups was the same (Grubb et al., 2008). The conclusion was that screening for prostate cancer does not save lives but rather subjects patients to unnecessary procedures that do not affect outcome. However, it was recognized that increasing the length of the study might show differences in death rates between the two groups. Possibly also, the lower cutoff value of 3 ng/mL used in many of the centers in the ERSPC study identified more patients with significant disease.

Methods to Improve the Performance of Serum PSA Measurement for the Early Detection of Prostate Cancer

Several approaches have been developed to increase the sensitivity and specificity of PSA in detecting prostate cancer. First, as noted previously, use of serum PSA in combination with either DRE or transrectal ultrasound of the prostate results in increases in both sensitivity and specificity (Catalona et al., 1991; Brawer et al., 1992). In addition, the PSA fractions (i.e., free and bound) have been used to increase the sensitivity and specificity of elevated serum PSA in the diagnosis of prostate cancer.

Free PSA, Complex PSA, and Percentage of Free PSA

PSA is capable of complexing with various endogenous protease inhibitors, including α_1-antichymotrypsin (ACT), α_2-macroglobulin (to which it binds covalently), and α-protease inhibitor (API). These stable forms are collectively known as complexed PSA (cPSA). Serum PSA exists in the serum largely (up to 90% of total PSA) (Vessella & Lange, 1997) in the form of a PSA-ACT (PSA–α_1-antichymotrypsin) complex (Christensson et al., 1993), which is readily detectable by most immunoassays, whereas complexes with α_2-macroglobulin escape detection by commercial PSA. The noncomplexed forms, known as free PSA (fPSA), are unreactive with plasma protease inhibitors. In prostate cancer, there is generally an increase in the serum concentration of cPSA and a corresponding decrease in unbound or free PSA (Parsons et al., 2004). On the other hand, the relative amount of free PSA is higher in BPH than in prostate cancer. Thus, immunoassays have been developed that quantify either cPSA or fPSA. The epitopes exposed by fPSA but not by cPSA enabled the development of these assays specifically measuring fPSA or cPSA as complements to the conventional PSA assay, which measures total PSA (tPSA) (Lilja et al., 1991; Stenman et al., 1991). Based on these assays, it has been found that measuring cPSA with ACT (PSA-ACT) directly eliminates many technical problems associated with PSA assays and improves the differentiation of BPH from prostate cancer (Wu, 1994; Wu & Liu, 1998), thereby increasing test specificity (Parsons et al., 2004). The specificity of PSA has been enhanced by using molecular forms of PSA and fPSA, such as percent free PSA (%fPSA), proPSA, intact PSA, or benign prostatic hyperplasia–associated PSA, and/or new serum markers (Stephan et al., 2009).

Conversely, measurement of fPSA and the calculation of percentage of fPSA (%fPSA = [fPSA/tPSA] × 100), which has an inverse relationship with prostate cancer risk (Polascik et al., 1999), have been used to help to differentiate BPH from prostate cancer, also increasing test specificity and reducing unnecessary biopsies for BPH patients. More important, the fPSA ratio improves the specificity for prostate cancer detection in men with PSA between 4 and 10 ng/mL, also reducing unnecessary biopsies. In addition, fPSA may be useful as a prostate cancer morbidity predictor (Polascik et al., 1999; Ito et al., 2003). Some studies also showed that %fPSA can be used to predict prostate cancer in patients with PSA less than 4 ng/mL (Djavan et al., 1999; Horninger et al., 2002). One caveat is that fPSA is subject to quick degradation at 4°C or above. The recommended time interval from sample collection and assay should be less than 3 hours, and the sample should be stored and shipped at –70° C (Woodrum et al., 1996). Overall, prostate cancer is associated with elevated cPSA and low %fPSA (<6%) (Catalona et al., 1995), and higher ratios of fPSA (>23%) are usually associated with BPH.

The Bayer cPSA assay, which measures both PSA-ACT and PSA-API, was initially proposed as a single-assay alternative to the fPSA and tPSA assays (Brawer et al., 1998; Mitchell et al., 2001). However, only the ratio of cPSA to tPSA can reach equivalent results compared with %fPSA (Lein et al., 2003; Roddam et al., 2005).

fPSA has recently been shown to exist in at least three molecular forms: proPSA (Mikolajczyk et al., 1997), BPSA (Mikolajczyk et al., 2000), and inactive "intact" PSA (iPSA). Recently, the FDA approved the Dimension FPSA (free PSA) Flex (Dade Behring, Newark, DE) and AxSYM (Abbott, North Chicago, IL) Free Prostate Specific Antigen tests, which are typically performed along with a tPSA test and a DRE and helps to determine whether a prostate biopsy is needed to rule out the risk (in percent) of cancer in men 50 years or older with a tPSA of 4 to 10 ng/mL. The smaller the %fPSA, the more likely the patient is to have prostate cancer.

In 2007, the FDA gave approval to a new test, Immulite 1000/2000 Free PSA assay (Siemens, Tarrytown, NY), a third-generation PSA assay based on the solid-phase sequential chemiluminescent immunometric method for the quantitative measurement of fPSA that is used in conjunction with tPSA. The routine sample preparation and refrigerated (2°C–8°C) storage of samples for 24 hours or frozen storage at –70°C is acceptable for the measurement of fPSA.

Principles of Measurement. There are several different assays for fPSA and cPSA, one of which is summarized in Figure 76.3. When PSA is bound, certain antigenic determinants are "buried" by the protein to which it binds (mainly, ACT). These are exposed on fPSA; thus, antibodies to the buried determinants of cPSA will detect only fPSA. On the other hand, there are determinants that are exposed on both fPSA and cPSA and can be detected by antibodies to these determinants, allowing for determination of tPSA. Finally, antibodies to the buried PSA determinant are available that also block the common exposed determinant. These antibodies react only with fPSA by binding to the buried determinant but also block the exposed common site. Now, in the presence of this blocking antibody, another antibody is added that reacts only with the common exposed determinant. The only available common exposed determinants are on cPSA. Thus, this double antibody approach, using a blocking antibody and a detection antibody, quantifies the level of cPSA.

proPSA and Prostate Health Index

proPSA, which contains a seven amino acid pro peptide, is a molecular form of fPSA and is more likely to be associated with prostate cancer. Truncated forms of proPSA also exist in serum, which contain five, four, or two more amino acids than PSA. The proPSA (p2PSA) form has been identified as the most prevalent form in tumor extracts, which suggests a role for these molecular forms of PSA for the early detection of prostate cancer and for possibly identifying aggressive prostate cancer (Hori et al., 2013; Lazzeri

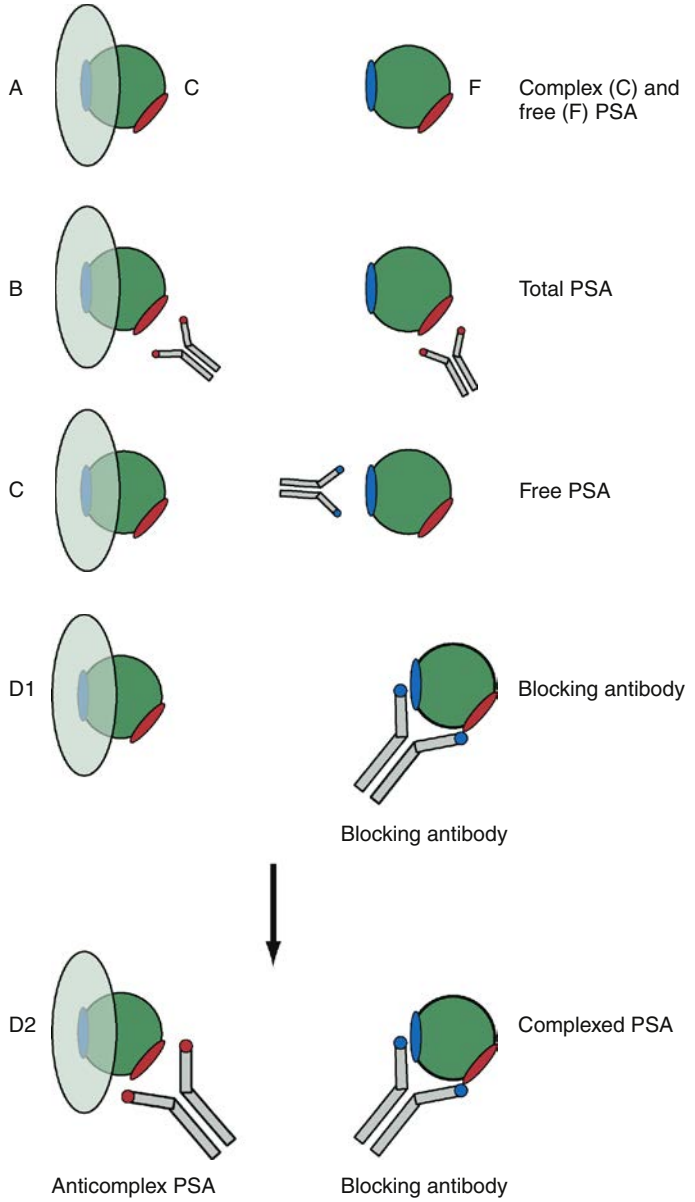

Figure 76.3 Three different assays for prostate-specific antigen (PSA). **A,** PSA is shown to exist in the free (F) or complexed (C) states. Some of its antigenic determinants (*blue* in the figure) are buried in the complexed state. These are exposed in the free state. On the other hand, as shown in **B**, there are common determinants (*red* in the figure) that are exposed in both complexed and free PSA. Antibodies to these common determinants will detect total PSA (free + complexed). Because the blue determinants are exposed only in free PSA, as shown in **C**, antibodies to these determinants will detect only free PSA. Finally, as shown in D1, antibodies have been developed against the blue determinant of free PSA that also block the red determinant. Thus, antibodies to the red determinant, which is common to both free and complexed PSA, will react only with complexed PSA, as shown in D2. This is the basis for the Siemens/Bayer assay for complexed PSA.

et al., 2013, 2014; Loeb et al., 2013; Scattoni et al., 2013; Heidegger et al., 2014). The Prostate Health Index (PHI) developed by Beckman Coulter, Inc., in partnership with the National Cancer Institute Early Detection Research Network was approved by the FDA in 2012. This new test is actually a mathematical formula of three biomarkers: (p2PSA/fPSA) × PSA1/2. Using this calculation, the clinician will be able to see each individual result and make a potentially better-informed recommendation to the patient. The intended use of the PHI is to distinguish prostate cancer from benign prostatic conditions in men aged 50 years and older with a total serum PSA between 4 and 10 ng/ml and in whom the DRE is not suspicious for cancer (Sokoll et al., 2010). Two recent studies published by Lazzeri and colleagues (2013, 2014) demonstrated that the use of p2PSA and the PHI significantly improved the predictive accuracy for detection of prostate cancer. In the first study of about 650 men from 5 European centers, patients had PSA levels between 2 and 10 ng/mL. The researchers demonstrated that p2PSA and the PHI improved the detection of prostate cancer with a Gleason score of greater than or equal to 7 diseases compared with PSA and fPSA. In the second study, in a small cohort of about 150 men with a positive family history of prostate cancer, the PHI significantly outperformed tPSA and %fPSA (areas under the curve [AUCs] 0.73, 0.55, and 0.60, respectively) for the detection of aggressive prostate cancer.

PSA Doubling Time, Velocity, and Density

Cancer is a growth process, and it seems reasonable to suppose that the rate of change of a tumor marker would be a more sensitive marker of disease aggressiveness than an absolute level. Thus, the concept of PSA doubling time and PSA velocity came forward in the last decade. The time (in months) required for the PSA value to double is known as the *PSA doubling time*. It has been shown that the PSA doubling time can predict recurrence after radical prostatectomy in androgen-independent prostate cancer patients (Lee, 2003; Loberg et al., 2003).

The rate of PSA increase over time—PSA velocity (PSAV) (Carter et al., 1992)—is the PSA difference divided by the number of years, typically given as nanograms per milliliter per year. It has been shown that a PSAV of 0.75 ng/year or greater is a strong predictor of cancer, with a specificity of 95% (Carter et al., 1992). More recently, it has been shown that PSAV may be useful in predicting prostate cancer risk when PSA levels are between 2 and 4 ng/mL (Fang et al., 2002). This is especially useful in predicting the risk of cancer and guiding the necessity of prostate biopsy in patients with low/normal PSA value (2–4 ng/mL). Moul et al. (2007) suggested that by analogy with serum PSA levels, which are age dependent, PSAV should be age adjusted. They noted that biopsy-guideline threshold levels (PSA ≥4 ng/mL, or PSAV ≥0.75 ng/mL per year) underestimated the cancer risk in men aged 50 to 59 years and, therefore, should be decreased to 2 ng/mL and 0.40 ng/mL per year, respectively. A sharp rise in the PSA level increases suspicion of a fast-growing cancer, but another important confounder is prostatitis. Thus, a repeat PSA measurement following a trial of antibiotics is a reasonable option. A 2006 study found that men who had a PSAV greater than 0.35 ng/mL per year had a higher relative risk of dying of prostate cancer than men who had a PSAV of less than 0.35 ng/mL per year (Carter et al., 2006). The National Comprehensive Cancer Center Network (www.nccn.org) 2007 guidelines for prostate cancer detection include a recommendation that men with a PSAV greater than 0.35 ng/mL per year should consider biopsy even if their PSA level is low. This is a notable finding because prostate cancer causes significant mortality, although a large number of prostate cancer patients die of other causes. Whereas these studies demonstrate a method of identifying aggressive forms of prostate cancer, randomized larger cohort studies are needed to validate these observations. Preoperative PSAV velocity is not a good parameter for prostate cancer grade, stage, or recurrence (Freedland et al., 2001). PSA density is a measure of the ratio of tPSA to prostate gland volume as measured by transurethral ultrasonography. PSA densities of greater than 0.15 indicate an increased probability of prostate cancer rather than BPH (Polascik et al., 1999).

PSA is still a gold standard biomarker for prostate cancer. It can be made even more useful diagnostically both by employing it in conjunction with other methods such as DRE and by quantifying its fractions (complexed and free) or various molecular markers in the urine.

CIRCULATING TUMOR CELLS IN PERIPHERAL BLOOD

Hematogenous spread of cancer cells is the main venue for cancer metastases (Eccles & Welch, 2007). Thus, the detection of these disseminating primary cancer cells in peripheral blood cannot only act as a tool for monitoring early metastases but it also can predict the prognosis and treatment outcome of novel therapies.

The major obstacle in successful detection of circulating tumor cells (CTCs) is their paucity in peripheral blood, approximately one or fewer CTC cells in 10^5 to 10^6 peripheral blood mononuclear cells. Thus, various enrichment techniques are used to capture the CTCs based on cell size. These include membrane microfilter devices or micro-electromechanical systems, isolation by the size of the epithelial tumor, cell density (density-gradient centrifugation), and specific antibodies to the cell surface proteins based on the use of immunomagnetic beads technique (see Chapter 45) and flow-assisted cell sorting (see Chapter 35). The enriched CTC can further be characterized by additional detection techniques. The two main approaches for the detection of CTCs are immunologic assays using monoclonal antibodies directed against specific proteins with the use of fluorescence microscopy and flow cytometry and by measuring tissue-specific transcripts by using PCR-based molecular assays (e.g., reverse transcriptase–polymerase chain reaction [RT-PCR] and methylated DNA

PCR) (Molnar et al., 2003). The Cellsearch (Johnson & Johnson) system, the first FDA-approved test based on the immunologic approach, has gained considerable attention because it allows both standardized automated immunomagnetic enrichment using antibodies targeting epithelial cell adhesion molecules (EpCam) and subsequent labeling of CTCs with fluorescent antibodies specific for epithelial cells (cytokeratins 8, 18, and 19) and leukocytes (CD45) (Cristofanilli et al., 2004; Eccles & Welch, 2007; Riethdorf et al., 2007; Pantel & Riethdorf, 2009). This system can provide clinically useful information on the prognosis of patients with metastatic breast, colon, and prostate cancer (Moreno et al., 2005; Cohen et al., 2006; Hayes et al., 2006) and has the potential to evaluate CTCs in pharmacodynamic studies that test new targeted therapies (Moreno et al., 2005; de Bono et al., 2007). A microfluidics microchip technology has been developed that uses a silicon microchip containing thousands of microspots staining with anti-EpCAM (CTC-chip). In this technique, microfluidics are used to pneumatically push whole blood over the surface of the CTC-chip. Then, EpCAM-positive CTCs are captured and confirmed as CTC via fluorescence microscopy (Nagrath et al., 2007; Uhr, 2007). CTC chips identified high numbers of cytokeratin-positive CTCs in nearly all tested patients with lung, prostate, pancreatic, breast, and colon cancer, including those without metastatic disease. Surprisingly, patients with localized prostate cancer had more CTCs than patients with overt metastasis. Future studies are required to test whether these cells are viable CTCs with tumor-specific genomic characteristics (Uhr, 2007).

The amount of EpCAM on tumor cells varies widely based on tumor type (Thurm et al., 2003). Therefore, alternative devices based on fiber-optic array scanning technology, an ultra-speed automated digital microscopy with laser printing techniques, has been developed to circumvent the rare-cell detection problem (He et al., 2007). By this method, laser-printing optics has been used to excite 300,000 cells per second, which have been decorated by fluorescent dye–conjugated antibodies directly on the slide. Another completely different antibody-based approach is the EPISPOT assay to detect proteins released by CTCs. Using the EPISPOT method, only viable, protein-excreting cells are detected. Nevertheless, the clinical utility of all of these new approaches needs to be validated in large-scale studies in cancer patients (Alix-Panabières et al., 2007a, 2007b).

As summarized, various clinical studies have provided evidence for an association between the presence of CTCs detected at the time of tumor resection and postoperative metastatic relapse in patients with cancers of the breast, prostate, lung, and gastrointestinal tract. The present research data strongly support that CTCs are indicators for cancer progression into metastatic disease and can be used to adjust treatment modality. A recent study indicates that CTC detection predicts the prognosis in clinically relevant subgroups of early-stage breast cancer patients (Ignatiadis et al., 2007). Recently, the first comprehensive meta-analysis of published literature on the prognostic relevance of CTC in patients with early-stage and metastatic breast cancer (MBC) clearly indicated that the detection of CTC is a reliable prognostic factor (Zhang et al., 2012). Keeping this in mind, the American Joint Committee on Cancer has proposed a new category, M0(i+), for TNM staging in breast cancer defined as "no clinical or radiographic evidence of distant metastases, but deposits of molecularly or microscopically detected tumor cells (no larger than 0.2 mm) in blood, bone marrow, or other nonregional nodal tissue in a patient without symptoms or signs of metastases." Despite the general belief that only invasive cancers are assumed to shed isolated tumor cells into the bloodstream and infiltrate lymph nodes, the latest studies indicated that tumor cell dissemination may occur before stromal invasion—that is, in the DCIS (ductal carcinoma in situ) stage. The reason for this is that these cells have already started to disseminate from preinvasive mammary lesions or represent the earliest step of microinvasion in a preinvasive lesion (Banys et al., 2012; Sanger et al., 2011). The clinical relevance of these cells has to be further evaluated.

Moreover, in other tumor entities such as gastrointestinal cancer, a disease in which overt bone marrow metastases are rare, CTC analyses have generated prognostic information. Therefore, they might become helpful indicators of early systemic tumor cell spread to other distant organs, such as the lung or liver. A recent systematic review and meta-analysis based on data from 12 studies representing 1329 patients showed that the detection of CTCs in peripheral blood of patients with resectable colorectal liver metastases or widespread metastatic colorectal cancer is associated with disease progression and poor survival (Groot et al., 2013). Gazzaniga and colleagues (2013) came to the conclusion that CTC detection might help in the selection of high-risk stage II colorectal cancer patient candidates for adjuvant chemotherapy after enumerating CTCs with the FDA-cleared CellSearch system. They detected CTCs in 22% of patients with a significant correlation with regional lymph node involvement and stage of disease.

Resel and colleagues (2012) analyzed the correlation among CTC and PSA levels, Gleason score, and TNM stage in patients with metastatic hormone-sensitive prostate cancer and reported that the CTC count in peripheral blood could provide a method for correctly staging prostate cancer and for assessing the prognosis of metastatic hormone-sensitive cancer. Monitoring of bone marrow and peripheral blood during and after systemic adjuvant therapy for CTCs might provide unique information for the clinical management of the individual cancer patient and allow an early change in therapy years before the appearance of overt metastasis signals incurability. Further research on the molecular characterization of CTC will provide important information for the identification of therapeutic targets and understanding resistance to therapies. Although large-scale clinical data are still lacking with regard to how molecular characterization of CTCs could be used as a clinical decision-making tool, this type of analysis holds tremendous promise for improved stratification of patients and the prospective development of tailored, targeted therapy.

CIRCULATING NUCLEIC ACIDS IN PERIPHERAL BLOOD

CELL-FREE NUCLEIC ACID TESTING IN CANCER

Protein tumor markers and histopathologic staging have been the cornerstones of diagnosis and prognosis of malignancy. Over the past decade, the discovery of cell-free nucleic acids in serum, plasma, urine, or other body fluids has promoted investigation of oncogenes encoding oncoproteins as a means to detect malignancy in a variety of cancers with potentially greater sensitivity (Schmidt et al., 2004), including melanoma (Kopreski et al., 1999; Board et al., 2009), lung (Fleischhacker, 2001; Schmidt et al., 2004; He et al., 2009; Ulivi & Silvestrini, 2013), stomach (Park et al., 2009), colon (Silva et al., 2002; Mansour, 2014), breast (Chen et al., 2000; Gal et al., 2001; Joosse et al., 2014), prostate (Goessl et al., 2000, 2002a, 2002b; Sita-Lumsden et al., 2013), ovary (Hickey et al., 1999), Epstein-Barr virus–positive lymphomas (Lechowicz et al., 2002; Lei et al., 2002), leukemia (Schwarz et al., 2009), intracranial neoplasms (Rhodes et al., 1994), and bladder (Goessl et al., 2000, 2002a, 2002b; Utting et al., 2002; Guo et al., 2009).

The basic concept is that tumor-derived nucleic acid can be detected in cell-free sources, such as serum, plasma, urine, lavage fluid, and so on, using amplification methods such as RT-PCR or other detection methods (Goldshtein et al., 2009; Lou et al., 2015). As discussed further in Chapter 77, this approach has been used successfully in detection of mutated oncogenes. Normally, DNA is isolated from tissue through standard procedures using phenol chloroform extraction, followed by ethanol precipitation. However, DNA can also be obtained directly from serum, plasma, or other body fluids by centrifugation, separating it from cells and platelets. It has been posited that cell-free nucleic acids actually serve an active biological role in tumor progression by host cell oncogenesis (García-Olmo & García-Olmo, 2013). Recent data suggest that nucleic acids obtained from apoptotic versus cancer cells, preanalytic variables, and intertumor versus intratumor burden can further differ in size, integrity, and tumor subclone representation, which may affect clinical utility as biomarkers (El Messaoudi et al., 2013; Marzese et al., 2013; Yu et al., 2014; Devonshire et al., 2014). In addition to detection of gene levels (including miRNA), the methodology of cell-free nucleic acid–based detection includes detection of microRNA, gene mutations, microsatellite alterations, and promoter hypermethylation.

GENE ARRAYS DETECTING ONCOPROTEIN ABNORMALITIES

Circulating DNA from mutated oncogenes can be readily detected in the serum of cancer patients (Sorenson et al., 1994; de Kok et al., 1997), and use of PCR methodology has successfully identified p21ras in the stool of patients with colorectal cancer, altered p53 in the urine of patients with bladder cancer (Sidransky et al., 1991), and ras, neu/HER2, and platelet-derived growth factor (PDGF) in the bile of patients with biliary tract cancer (Su et al., 2001). Microchips containing entire genomes now exist that can be hybridized with the total RNA of cells to detect different levels of gene expression. Studies using such chips on which different oncogenes are present may be effective in detecting expression of specific oncogenes present in body fluids from patients with different cancers.

It has been shown that these types of studies are feasible in a study on the tissue of 20 squamous cell esophageal carcinomas (Arai et al., 2003). A total of 57 oncogenes were present on the array and included many of the oncogenes discussed here, including FGF, erb-B2 (HER2/*neu*), and myc. In 9 of the 20 specimens, expression of eight oncogenes, including erb-B2 and myc, was two to four times higher than in normal, control

tissue. Comparison of these results with those obtained using conventional hybridization methods revealed that this gene amplification frequently was found not to be due to an increase in copy number. As noted earlier, the p53 gene is frequently overexpressed and/or mutated in squamous cell carcinomas of the esophagus and in head and neck squamous cell carcinomas. Unfortunately, p53 was not included on this array. In addition, this study did not include hybridization assays for mutant genes.

Nonetheless, these studies illustrate that oncogenes are frequently overexpressed in human cancers and can be detected on gene arrays. The earlier PCR studies on body fluids illustrate that gene amplification and mutation can also be readily detected in these body fluids. Therefore, gene arrays containing large numbers of different oncogenes, allowing for rapid assays, appear to hold great promise in tumor detection on body fluids.

CIRCULATING MICRORNA

miRNA constructs consist of small noncoding RNA molecules (of ≈19–25 nucleotides) and are found in most biological entities. They have been shown to function as regulators of gene expression via posttranscriptional effects and in RNA silencing. Cell-free miRNAs are highly stable in body fluids. Recent data suggest that cancer cells also secrete unique cell-free miRNAs into the extracellular environment and to cancer progression. They are thought to enter body fluids via mechanisms including passive release from broken, injured, and dead cells; active secretion through microvesicles; and/or active secretion via a microvesicle-free protein-dependent route (Javidi et al., 2014). Several miRNAs with oncogenic potential have been demonstrated to be upregulated in cancers, and miRNAs with a tumor-suppressive effect are downregulated in malignancies. Translating the application of miRNAs in the clinical context has been enhanced by the applicability of several novel high-throughput multiplex technologies on a wide variety of patient samples, including blood, serum, tissues (fresh and formalin-fixed paraffin embedded), and cerebrospinal fluid (Sethi et al., 2013).

miRNA biomarkers can be used for disease diagnosis, prognosis, surveillance during treatment, and follow-up. They hold much promise toward use in targeted therapies, including miR-27, a regulation of MET, EGFR (lung cancer), miR-215 (osteosarcoma), miR-205BP/S3 (melanoma), and miR-34a (hepatocellular carcinoma). Some miRNAs appear to possess global oncogenic potential in many tissues, including—but not limited to—miR-21, miR-155, and miR-17-92 (Sethi et al., 2013; Yang et al., 2013), and they appear to have prognostic relevance.

GENE MUTATIONS

These normally involve nucleic acid sequencing and can detect single base changes in genomic or mitochondrial DNA (gDNA and mtDNA, respectively). mtDNA can have 20 to 200 copies of DNA compared with 2 copies of gDNA. Mutated mtDNA was detected in 100% of patients with prostate cancer (Jeronimo et al., 2001a), whereas others have reported a lower mtDNA detection rate in patients with colorectal cancer (Anker et al., 1997; Hibi et al., 2001). Tumor and plasma DNA of 25 patients with breast or small cell lung cancer were analyzed for the presence of p53 gene mutations. Six patients had detectable mutations in their tissue, and three of these six had mutations detected in their plasma (Silva et al., 1999). Furthermore, although gene mutations have been detected in tissue obtained from malignant and healthy patients, the same is not true for plasma. Mutations detected in plasma are very specific for malignancy (Johnson & Lo, 2002). To this end, recent studies that analyzed plasma DNA of patients with hepatocellular carcinoma for p53 codon 249 by restriction fragment length polymorphism demonstrated that 6 of 79 samples (7.6%) from the hepatocellular carcinoma patients had amplifiable plasma DNA, whereas none of the 73 samples with amplifiable plasma DNA from the controls had this mutation (Igetei et al., 2008). In addition to detection, recent studies have demonstrated the utility of cell-free DNA (cfDNA) as a means to monitor efficacy of therapy. Spindler and colleagues (2014) showed that plasma levels of mutated cfDNA, encoding KRAS and BRAF, could be used to monitor patients during treatment with cetuximab and irinotecan. Others have reported that cfDNA analysis for the BRAF V600E mutation showed 100% specificity and sensitivity, whereas seven KRAS point mutations exhibited 98% specificity and 92% sensitivity, with a concordance value of 96%, using a PCR-based method of detection (Thierry et al., 2014).

MICROSATELLITE ALTERATIONS

These are polymorphic repetitive nucleic acid sequences, varying from 2 to 6 base pairs, that form variable stretches of DNA that appear as loss of heterozygosity (LOH) and are detectable by microsatellite analysis using PCR. A panel of four to six appropriate markers to detect these microsatellites can be used to profile tumors. LOH requires at least 20% of tumor DNA within normal DNA. Microsatellite instability refers to detection of additional PCR products and requires a ratio of tumor to normal DNA of greater than 0.5% (Goessl et al., 2000, 2002a, 2002b). Microsatellite alterations performed on cell-free bronchial lavage specimens from lung cancer patients revealed tumor-associated genes in 47% if DNA was used as the source material (n = 30) and in 100% if RNA was used (n = 25) (Schmidt et al., 2004). In addition, four microsatellite loci were detected in the sera of 17 of 34 breast cancer patients; LOH at various loci was observed in 16 patients, and microsatellite instability was detected in 1 patient (Schwarzenbach et al., 2004). However, no correlation was found between circulating tumor DNA and the level of tumor-associated protein marker CA 15-3 (Schwarzenbach et al., 2004). Plasma LOH has also been found in patients with recurrent bladder cancer, for which it appears to be a reliable marker (Dominguez et al., 2002). Furthermore, microsatellite alterations were detected in plasma DNA obtained from patients with malignant melanoma (Nakamoto et al., 2008). Metastasis or recurrence was confirmed in 3 out of 17 patients (17.6%); all were found to have LOH at four microsatellite markers, further encouraging the use of such loci markers as a screening tool.

PROMOTER HYPERMETHYLATION

Methylation of CpG islands, located in the promoter region of many genes, is associated with their transcriptional inactivation. Thus, aberrant hypermethylation of key tumor suppressor genes can permit expression of otherwise quiescent oncogenes. Promoter hypermethylation can be detected by methylation-specific PCR (MSP), and the reduced protein expression can be determined by IHC. MSP requires a ratio of tumor to normal DNA of 0.1% to 0.001% (Goessl et al., 2000, 2002a, 2002b; Bearzatto et al., 2002). Another method, quantitative methylation analysis of minute DNA amounts after whole bisulfitome amplification (qMAMBA) allows quantitative and sensitive detection of DNA methylation in minute amounts of DNA present in body fluids (Vaissière et al., 2009). Aberrant methylation of at least one of four tumor suppressor genes was detected in tissue biopsies from 15 of 22 patients (68%) with non–small cell lung cancer. Of the 15 patients with positive non–small cell lung cancer, 11 (73%) also had abnormal methylated DNA in their serum samples (Esteller et al., 1999). In addition, 17 of 27 bladder cancer patients (63%) displayed alterations in tumor suppressor genes in cell- and serum-derived DNA (Dominguez et al., 2002).

Interpretation of results obtained from cell-free testing warrants caution because results may vary depending on the detection method (promoter hypermethylation, gene rearrangements, microsatellite alterations, PCR, RT-PCR), the sample tested (Lee et al., 2001), and the nucleic acid source used (RNA, DNA) (Fleischhacker, 2001; Garcia et al., 2001; Johnson & Lo, 2002; Schmidt et al., 2004). Nonetheless, this remains a promising new modality for early cancer detection (Chan & Lo, 2002; Lechowicz et al., 2002; Board et al., 2009; Goldshtein et al., 2009).

Recent advances in immunotherapy appear to be able to identify predictive biomarkers of responsiveness to immunotherapy. NGS has made the determination of tumor burden possible. *Tumor burden* is defined as the rate of peptide-changing single-nucleotide variants per million pairs. Hypermutated tumors have an increased tumor burden and a higher rate of somatic mutations. This is associated with the development of neoantigens as well as responsiveness to immune checkpoint inhibitors. Along with exogenous and endogenous mutagens, microsatellite instability (MSI) is a leading mechanism resulting in hypermutation. Detection of MSI is vital in the assessment of hypermutation, particularly in colorectal and gastric cancers (Nagahashi, 2019).

CELL DNA TESTING FOR CANCER USING FLUORESCENCE IN SITU HYBRIDIZATION

This technique is described in Chapter 71 on cytogenetics. In brief, DNA oligonucleotide probes containing sequences known to occur uniquely on specific chromosomes are incubated with cells concentrated from body fluids, including blood and urine. These probes are so constructed that they hybridize either to specific normally occurring DNA sequences on specific chromosomes or to known abnormally occurring spliced chromosomal sequences (usually the result of translocations). The latter often produce either overexpressed mitogenic proteins or mutated constitutively activated mitogenic proteins. This methodology has potential application to many disease states, including malignancies (Goldshtein et al., 2009).

An example of the application of this technique is in the diagnosis of bladder cancer for which the Vysis-Abbott UroVysion detection system has been developed and has been FDA approved. A critical and common chromosomal lesion in this disease is the 9p21 homozygous deletion, perhaps the most constant genetic finding in bladder cancer. This results in deletion of a tumor suppressor gene that codes for the p16 antioncogene protein, again resulting in loss of control of mitotic rate (Halling, 2003).

An oligonucleotide probe, labeled with a gold fluorescent dye, has been developed to a sequence of 9p21. In addition, several other oligonucleotide probes have been prepared, linked to other colored fluorescent dyes, that hybridize to specific sequences in the centromeres of other "control" chromosomes. A mixture of these probes is incubated with cells obtained from the urinary sediments of patients and subjected to fluorescence microscopy. If the cells are normal, duplicate colored spots, from diploid normal chromosomes, appear in these cells.

On the other hand, absence of one or both yellow spots for chromosome 9p21 but the presence of duplicate fluorescent spots for the control probes is a strong indication of 9p21 deletion and the presence of urothelial (most probably bladder) cancer. It should be noted that this hybridization procedure is also capable of detecting malignant aneuploid bladder epithelial cells (with multiple copies of chromosomes) directly.

This method has a sensitivity of 36% for grade 1 cancers, 76% for grade 2, and almost 100% for grade 3 cancers, and an overall specificity of 97% (Halling, 2003; 2004). Therefore, it has great potential in detecting bladder cancer, especially if it is combined with probes for other genetic lesions known to occur in this disease, as discussed in the bladder cancer markers section earlier. In addition, multiple probes for known chromosomal lesions in a variety of lymphomas and leukemias have been prepared and are promising for the detection of these diseases in body fluids and tissue.

MARKERS IN OTHER BODY FLUIDS

URINE MARKERS FOR PROSTATE CANCER

Numerous promising prostate cancer biomarkers have been identified. These markers have allowed exploration of a new diagnostic approach based on the identification of cancer cells or shed material in the urine obtained after digital examination of the prostate (Fradet, 2009; Ploussard & de la Taille, 2010).

Urine Prostate Cancer Antigen 3

Prostate cancer antigen 3 (PCA3) is a prostate-specific gene that is an average of 66 times overexpressed in prostate cancer cells compared with normal prostate cells (de Kok et al., 2002). Assays were developed to measure the relative amount of PCA3 RNA over PSA RNA using quantitative RT-PCR or direct RNA amplification (Hessels et al., 2003; Fradet et al., 2004). A commercially available test by GeneProbe Inc. (San Diego, CA), referred to as the *Aptima PCA3 assay*, is based on the principle of target capture followed by transcription-mediated amplification and uses calibrators to quantify the PCA3 and PSA RNA copy number to provide a PCA3 score (ratio of PCA3 RNA/PSA RNA) (Groskopf et al., 2006). In a large European prospective multicenter study, this test clearly demonstrated a greater probability of a positive repeat biopsy with increasing PCA3 scores (Haese et al., 2008). Indeed, the proportion of patients with positive biopsy went from as low as 10% to as high as 70% in a linear fashion with the increasing PCA3 score. Moreover, using a PCA3 score cutoff of 35 provided similar results in men with serum PSA of 4 or less, 4 to 10, or more than 10 ng/mL, with sensitivities of 50% to 61% and specificity of 71% to 80% (Hoque et al., 2005). Furthermore, compared with PSA, PCA3 has the advantage that it is independent of prostate volume (Hoque et al., 2005), is correlated with tumor volume (Nakanishi et al., 2008; Whitman et al., 2008), and may even predict extracapsular tumor extension (Roupret et al., 2007).

The Progensa PCA3 assay is an in vitro nucleic acid amplification test. The assay measures the concentration of prostate cancer gene 3 (PCA3) and PSA RNA molecules and calculates the ratio of PCA3 RNA molecules to PSA RNA molecules (PCA3 score) in post-DRE urine specimens. Gen-Probe, Inc. obtained FDA approval in 2012 with the intended use for men who have a suspicion of PCa based on PSA level and/or DRE and/or one or more negative biopsy results. A PCA3 score less than 25 is associated with a decreased likelihood of PCa (Vlaeminck-Guillem et al., 2010; Auprich et al., 2011; Crawford et al., 2012). Seven of the studies used the currently available FDA-approved test kit (Progensa). AUC values ranged from 0.66 to 0.75. Sensitivity ranged from 53% to 69%, with specificity ranging from 71% to 83%. For patients who had a previous negative biopsy, sensitivity averaged 52.6% and specificity averaged 71.6%, which gives a positive predictive value (PPV) of about 40% and a negative predictive value (NPV) of about 80%. The overall accuracy is about 66%. Overall, PCA3 appears promising, and the specimen for PCA3 analysis is easily obtained after DRE.

Urine TMPRSS2:ERG and Mi-Prostate Score

A remarkable discovery of a family of new genes resulting from the fusion between the androgen-regulated transmembrane serine protease gene (TMPRSS2) with gene members of the E26 transformation-specific (ETS) family of oncogenes was made using a new biostatistical method called *cancer outlier profile analysis* (Kumar-Sinha et al., 2008). The TMPRSS2-E26 transformation specific-related gene (ERG) fusion transcripts have been identified in 40% to 80% of prostate cancers (see Chapter 79). More recently, TMPRSS2 has been found to be an androgen- and estrogen-regulated gene and is more commonly associated with a Gleason score greater than 7 (41% vs. 12%) and more prostate cancer–related deaths and/or metastatic disease development (53% vs. 23%) (Demichelis et al., 2007; Bhavsar et al., 2013; Falzarano & Magi-Galluzzi, 2013; Truong et al., 2013). The TMPRSS2-ERG (or T2-ERG) fusion has a low sensitivity of 37% but a high specificity of 93%, which gives a PPV of 94% after a DRE. Even though the specificity is high, most prostate cancer tumors have multiple foci, which make T2-ERG more heterogeneous. One way to overcome this heterogeneity is to combine T2-ERG with other markers (Cornu et al., 2013; Salami et al., 2013; Leyten et al., 2014). Several studies have investigated the association of T2-ERG with the aggressiveness of prostate cancer. In one study, among 1180 men who were treated by a radical prostatectomy, T2-ERG was found in 49% of the cases (Leyten et al., 2014). A significant correlation with high-stage tumor ($p < 0.01$) was found, but there was little correlation with Gleason score ($p = 0.58$), lethality ($p = 0.99$), and biochemical reoccurrence ($p = 0.60$). Earlier studies found correlations with higher Gleason score ($p = 0.01$) and lethality ($p < 0.01$) in a smaller group of men (n = 111) who were diagnosed with low-grade prostate cancer. In another study, T2-ERG was highly expressed in patients with T3-T4, Gleason score greater than or equal to 7 disease ($p = 0.003$ and $p < 0.01$, respectively).

The Mi-Prostate Score (University of Michigan Health System) combines the urine tests for PCA3 from Progensa, T2-ERG, and serum PSA levels to produce a risk assessment of prostate cancer that potentially indicates the likelihood of aggressive cancer. This test has been validated on approximately 2000 urine specimens (Cornu et al., 2013; Salami et al., 2013; Leyten et al., 2014).

Prostarix

Prostarix is a laboratory-developed test performed by the Clinical Laboratory Improvement Amendments (CLIA) lab at Metabolon, Inc. and offered through Bostwick Laboratories. The test aids clinicians in the decision for initial or repeat prostate biopsy in men with negative DRE and modestly elevated PSA levels. The Prostarix DRE urine test is based on a proprietary metabolic signature of four metabolites determined by liquid chromatography–mass spectrometry (LC-MS) on the pellet obtained from a centrifuged urine specimen. Similar to the PCA3 test, the urine needs to be collected immediately after a vigorous DRE (Saylor et al., 2012; Jung et al., 2013; McDunn et al., 2013). McDunn and colleagues (2013) analyzed over 500 prostate tissue samples (331 prostate tumors and 178 cancer free). Through the use of gas chromatography–mass spectrometry and liquid chromatography with tandem mass spectrometry (LC-MS/MS), the study was able to find significantly different metabolite profiles between tissue that contained prostate cancer and tissue that was cancer free. The profile improved prediction of organ confinement (AUC from 0.53 to 0.62) and 5-year recurrence (AUC from 0.53 to 0.64).

Urine Hypermethylated Glutathione *S*-Transferase pi 1 Gene

DNA hypermethylation has been demonstrated to be one of the most common molecular alterations in prostate cancer, with more than 90% of cancers with hypermethylated promoters in one or more genes (Jeronimo et al., 2001b; Woodson et al., 2004; Yegnasubramanian et al., 2004; Bastian et al., 2005). In 2001, Cairns and colleagues used a DNA-based test to detect the hypermethylation of the glutathione *S*-transferase pi 1 (GSTP1) gene in urinary sediments after prostatic massage and found an overall sensitivity of 73% and a specificity of 98% in a small cohort of patients (Cairns et al., 2001). Several groups have evaluated the usefulness of gene hypermethylation as a biomarker by testing for its presence in freely voided urine after prostatic massage, in ejaculates, in directly sampled prostatic secretions, and in serum (Goessl et al., 2000; Gonzalgo et al., 2003, 2004; Gonzalgo et al., 2004; Hoque et al., 2005; Roupret et al., 2007; Crocitto, 2004). A study by

Woodson and colleagues (2008) concluded that the methylation of GSTP1 in urine specimens had 75% sensitivity and 98% specificity for prostate cancer. GSTP1 methylation in the biopsy had 88% specificity and 91% sensitivity. Also, an observation of a higher frequency of GSTP1 methylation in the urine of men with stage III versus stage II disease (100% vs. 20%; $p = 0.05$) suggests increased frequency of hypermethylation with increased stage. This study and other initial studies suggest that GSTP1 methylation and other genes in urine may not have much impact on increasing the sensitivity of PSA screening but may improve the specificity of PSA and help distinguish men with prostate cancer from those with BPH.

URINE METABOLIC TEST FOR ADENOMATOUS POLYPS OF COLON

A new urine spot test was recently studied based on metabolic technology that can distinguish patients with colon adenomatous polyps from those without polyps. This test has superior accuracy to fecal-based tests. The top 10 metabolites that separated the normal participants from those participants with colonic adenomatous polyps were butyrate, serine, methanol, β-alanine, π-methylhistidine, 3-hydroxybutyrate, asparagine, trigonelline, 3-hydroxyphenylacetate, and histidine (Wang et al., 2014).

FECAL OCCULT BLOOD TESTING AND MUTANT PROTEIN MARKERS IN STOOL

Perhaps the most familiar test to screen for cancer in patients is the fecal occult blood test, which is performed in the physician's office on stool samples obtained from a DRE. It is performed routinely on most patients as part of annual checkups. In the hospital outpatient setting, it is more common to have the patient obtain a stool sample for testing after a bowel movement. If blood is present in the stool, it may be due to a colonic tumor. Thus, further workup, such as a colonoscopy, is strongly recommended. The actual test for occult blood is based on the ability of the heme moiety of hemoglobin to catalyze the oxidation of the colorless compound guaiaconic acid (hence, the name *guaiac test*) in the presence of H_2O_2 to a highly conjugated, blue-colored quinone. Usually, the guaiaconic acid is impregnated on a strip or solid support and the stool specimen is placed on a discrete section of the strip. In this nonspecific test, blood in stool can be caused by a number of nonmalignant causes such as hemorrhoids, colitis, diverticulitis, and local trauma to the perianal area, diminishing the specificity of this test. False-positive results for this test are also caused by exogenous factors such as the presence of meat fibers from meat ingestion or of bismuth, which is present in antacid preparations such as Pepto-Bismol. In addition, the ability of this method to detect the presence of colon cancer depends on such factors as whether and to what extent a cancer hemorrhages, its location (the closer to the rectum, the greater the likelihood of detection), and its pattern of growth (e.g., exophytic tumors are more likely to be detected than nonexophytic ones). The sensitivity of the fecal occult blood test is between 15% and 30%. It is much less effective than colonoscopy, the definitive mode of colon cancer detection. However, it offers the advantage of being noninvasive, although with "virtual colonoscopy" based on computed tomography scanning of the colon, this advantage is diminished.

As a result, efforts have been made to devise new noninvasive tests on stool specimens that have higher sensitivity and specificity than fecal occult blood tests. As discussed in Chapter 77, several mutant genes that code for proteins that are involved with control of the cell cycle have been strongly implicated as vitally important causative factors of colon cancer. These include mutant *ras* (of the Kirsten or K variety), mutant p53, the adenomatous polyposis coli (*APC*) gene, and the gene product BAT-26, associated with microsatellite instability. All of these mutant genes are oncogenes in colon cancer. Standardized RT-PCR techniques, discussed in Chapter 69, are available to detect mutations in any or all of these proteins. In addition, "long" DNA, thought to result from disordered apoptosis of cancer cells in colon cancer, has also been found to occur in a number of colon cancers. If sufficient numbers of cancer cells from a colon cancer are sloughed off into the lumen, one or more of the mutant genes (and/or long DNA) can be discovered, allowing for the noninvasive detection of colon cancer.

Using this approach, a cooperative study involving the Colorectal Cancer Study Group was conducted in which more than 5000 patients were entered and more than 2000 were completely evaluated for colon cancer using fecal occult blood testing, multioncogene testing on stool, and colonoscopy (Imperiale et al., 2004). All of the patients were 50 years of age or older (mean, 69.5 years). The results showed that the genetic RT-PCR–based methodology results in significantly higher rates of detection than fecal occult blood testing. Overall, the rate of detection of adenocarcinoma was 51.6% for the genetic screening but 12.9% for fecal occult blood screening. Interestingly, advanced adenomas were detected in 15.1% of cases in the genetic screening and 10.7% in the fecal occult blood screening. Because this condition may be regarded as a precursor for frank malignancy, both methods seem to have similar rates of early detection. On the other hand, the rate of detection of TNM stage I colon cancer by genetic screen was 53.3%, while that for fecal occult blood screening was 6.7%, suggesting that genetic screening is substantially more effective in detecting true colon cancer in its early stages. Surprisingly, both tests were found to have similar apparent false-positivity rates in conditions of minor polyps (7.6% vs. 4.8% for genetic and occult blood tests, respectively) and the condition of no polyps found on colonoscopy (5.6% vs. 4.8% for genetic and occult blood tests, respectively). Although this study has certain drawbacks, such as too few patients with cancers and advanced adenomas with high-grade dysplasia, skewing of the age of the population to 65 years of age and older, and lack of information as to appropriate testing intervals for the genetic approach, these results are encouraging and warrant further systematic studies using this approach.

M2 is an isomer of the enzyme pyruvate kinase (M2-PK) that has an important role in glycolysis. M2-PK can be isolated in stool. Most studies looking at a possible role for colorectal cancer screening have been performed in patients with known cancers or an increased risk for colorectal cancer. These studies suggest a sensitivity of about 80% for the detection of colorectal cancer (Tonus et al., 2012). The sensitivity for advanced adenomas is lower, with 22% reported in one prospective study (Haug et al., 2008). Due to the lack of a large study in the asymptomatic population, the exact efficacy of this test for colorectal cancer is currently unknown.

CONCLUSIONS

In summary, a molecule, protein, or nucleic acid could be used as a tumor marker as long as its changing concentration reflects tumor cell activity. The assessment of clinical utility for an individual tumor marker is based on its sensitivity and specificity. There has been a clear trend toward improving the test specificity and sensitivity by ordering multiple tumor markers. However, controversy exists concerning which and how many tumor markers should be included in a panel for individual malignant diseases. Several new tumor markers, discussed in Chapter 77, are now on the horizon. These tumor markers consist of oncoproteins, suppressor proteins, adhesion molecules, cyclins, and angiogenic factors. They mainly differ from currently used tumor markers in their association with specific known metabolic pathways or physiologic reactions. Most tumor markers employed currently for patient management are not associated with any known specific biological reaction. Conceivably, measuring these new tumor markers will provide information on more specific defects, which will help in the design of better treatments. The best example is the successful use of Herceptin (a humanized MAb against the ectodomain of the c-*erb*B-2 receptor) for metastatic breast cancer patients.

SELECTED REFERENCES

Djavan B, Zlotta A, Kratzik C, et al.: PSA, PSA density, PSA density of transition zone, free/total PSA ratio, and PSA velocity for early detection of prostate cancer in men with serum PSA 2.5 to 4.0 ng/mL, *Urology* 54:517–522, 1999.

The usage of PSA has changed the management of prostate cancer patients. This article points out the dilemma of using current PSA cutoff values and summarizes various PAS parameters to increase the specificity of PSA.

Lipton A, Ali SM, Leitzel K, et al.: Elevated serum Her-2/neu level predicts decreased response to hormone therapy in metastatic breast cancer, *J Clin Oncol* 20:1467–1472, 2002.

Provides evidence that serum HER2/neu may be useful in the prognosis of and monitoring the treatment of breast cancer patients.

Rouprêt M, Hupertan V, Yates DR, et al.: Molecular detection of localized prostate cancer using quantitative methylation-specific PCR on urinary cells obtained following prostate massage, *Clin Cancer Res* 13:1720–1725, 2007.

Serves as an example and a summary of the identification of biomarkers using current serum proteomics technology and how it will be the trend for future biomarkers.

Saghatchian M, Guepratte S, Hacene K, et al.: Serum HER-2 extracellular domain: relationship with clinicobiological presentation and prognostic value before and after primary treatment in 701 breast cancer patients, *Int J Biol Markers* 19:14–22, 2004.

Provides evidence that serum HER2/neu may be useful in the prognosis and monitoring of the treatment of breast cancer patients.

Zhang Z, Bast Jr RC, Yu Y, et al.: Three biomarkers identified from serum proteomic analysis for the detection of early stage ovarian cancer, *Cancer Res* 64:5882–5890, 2004.

Serves as an example and summary of the identification of biomarkers using current serum proteomics technology and how it will be the trend for future biomarkers.

Access the complete reference list online at Elsevier eBooks for Practicing Clinicians.

REFERENCES

Agus DB, Bunn Jr PA, Franklin W, et al.: HER-2/neu as a therapeutic target in non–small cell lung cancer, prostate cancer, and ovarian cancer, *Semin Oncol* 27(Suppl 11):53–63, 2000.

Alexiou D, Karayiannakis AJ, Syrigos KN, et al.: Clinical significance of serum levels of E-selectin, intercellular adhesion molecule-1, and vascular cell adhesion molecule-1 in gastric cancer patients, *Am J Gastroenterol* 98:478–485, 2003.

Ali SM, Leitzel K, Chinchilli VM, et al.: Relationship of serum HER-2/neu and serum CA 15-3 in patients with metastatic breast cancer, *Clin Chem* 48:1314–1320, 2002.

Alix-Panabières C, Müller V, Pantel K: Current status in human breast cancer micrometastasis, *Curr Opin Oncol* 19:558–563, 2007a.

Alix-Panabières C, Vendrell JP, Pellé O, et al.: Detection and characterization of putative metastatic precursor cells in cancer patients, *Clin Chem* 53:537–539, 2007b.

Alvarez Secord A, Sayer R, Snyder SA, et al.: The relationship between serum vascular endothelial growth factor, persistent disease, and survival at second-look laparotomy in ovarian cancer, *Gynecol Oncol* 94:74–79, 2004.

Ando S, Kimura H, Iwai N, et al.: Positive reactions for both Cyfra21-1 and CA125 indicate worst prognosis in non–small cell lung cancer, *Anticancer Res* 23:2869–2874, 2003.

Anker P, Lefort F, Vasioukhin V, et al.: K-ras mutations are found in DNA extracted from the plasma of patients with colorectal cancer, *Gastroenterology* 112:1114–1120, 1997.

Arai H, Ueno T, Tangoku A, et al.: Detection of amplified oncogenes by genome DNA microarrays in human primary esophageal squamous cell carcinoma: comparison with conventional comparative genomic hybridization analysis, *Cancer Genet Cytogenet* 146:16–21, 2003.

Auprich M, Bjartell A, Chun FK-H, et al.: Contemporary role of prostate cancer antigen 3 in the management of prostate cancer, *Eur Urol* 60:1045–1054, 2011.

Banys M, Gruber I, Krawczyk N, et al.: Hematogenous and lymphatic tumor cell dissemination may be detected in patients diagnosed with ductal carcinoma in situ of the breast, *Breast Cancer Res Treat* 131:801–808, 2012.

Barbacid M: *Ras* genes, *Annu Rev Biochem* 56:779–827, 1987.

Bast Jr RC, Knauf S, Epenetos A, et al.: Coordinate elevation of serum markers in ovarian cancer but not in benign disease, *Cancer* 68:1758–1763, 1991.

Bast Jr RC, Ravdin P, Hayes DF, et al.: 2000 Update of recommendations for the use of tumor markers in breast and colorectal cancer: clinical practice guidelines of the American Society of Clinical Oncology, *J Clin Oncol* 19:1865–1878, 2000.

Bastian PJ, Ellinger J, Wellmann A, et al.: Diagnostic and prognostic information in prostate cancer with the help of a small set of hypermethylated gene loci, *Clin Cancer Res* 11:4097–4106, 2005.

Bearzatto A, Conte D, Frattini M, et al.: p16^{INK4A} hypermethylation detected by fluorescent methylation-specific PCR in plasmas from non–small cell lung cancer, *Clin Cancer Res* 8:3782–3787, 2002.

Benson MC, Whang IS, Pantuck A, et al.: Prostate specific antigen density: a means of distinguishing benign prostatic hypertrophy and prostate cancer, *J Urol* 147:815–816, 1992.

Berger P, Sturgeon C, Bidart JM, et al.: The ISOBM TD-7 Workshop on hCG and related molecules. Towards user-oriented standardization of pregnancy and tumor diagnosis: assignment of epitopes to the three-dimensional structure of diagnostically and commercially relevant monoclonal antibodies directed against human chorionic gonadotropin and derivatives, *Tumour Biol* 23:1–38, 2002.

Bethune-Volters A, Labroquere M, Guepratte S, et al.: Longitudinal changes in serum HER-2/neu oncoprotein levels in trastuzumab-treated metastatic breast cancer patients, *Anticancer Res* 24:1083–1089, 2004.

Bhavsar T, McCue P, Birbe R: Molecular diagnosis of prostate cancer: are we up to age? *Semin Oncol* 40:259–275, 2013.

Bingle L, Singleton V, Bingle CD: The putative ovarian tumor marker gene HE4 (WFDC2) is expressed in normal tissues and undergoes complex alternative splicing to yield multiple protein isoforms, *Oncogene* 21:2768–2773, 2002.

Birken S, Yershova O, Myers RV, et al.: Analysis of human choriogonadotropin core 2 o-glycan isoforms, *Mol Cell Endocrinol* 204:21–30, 2003.

Board RE, Ellison G, Orr MC, et al.: Detection of BRAF mutations in the tumour and serum of patients enrolled in the AZD6244 (ARRY-142886) advanced melanoma phase II study, *Br J Cancer* 101:1724–1730, 2009.

Bose R, Kavuri SM, Searleman AC, et al.: Activating HER2 mutations in HER2 gene amplification negative breast cancer, *Cancer Discov* 3:224–237, 2013.

Brawer MK, Chetner MP, Beatie J, et al.: Screening for prostatic carcinoma with prostate specific antigen, *J Urol* 147:841–845, 1992.

Brawer MK, Meyer GE, Letran JL, et al.: Measurement of complexed PSA improves specificity for early detection of prostate cancer, *Urology* 52:372–378, 1998.

Bristow A, Berger P, Bidart JM, et al.: Establishment, value assignment, and characterization of new WHO reference reagents for six molecular forms of human chorionic gonadotropin, *Clin Chem* 51:177–182, 2005.

Burtis WJ, Brady TG, Orloff JJ, et al.: Immunochemical characterization of circulating parathyroid hormone-related protein in patients with humoral hypercalcemia of cancer, *N Engl J Med* 322:1106–1112, 1990.

Cairns P, Esteller M, Herman JG, et al.: Molecular detection of prostate cancer in urine by GSTP1 hypermethylation, *Clin Cancer Res* 7:2727–2730, 2001.

Canizares F, Sola J, Perez M, et al.: Preoperative values of CA 15-3 and CEA as prognostic factors in breast cancer: a multivariate analysis, *Tumour Biol* 22:273–281, 2001.

Carpelan-Holmstrom M, Louhimo J, Stenman UH, et al.: CEA, CA 19-9 and CA 72-4 improve the diagnostic accuracy in gastrointestinal cancers, *Anticancer Res* 22:2311–2316, 2002.

Carter HB, Ferrucci L, Kettermann A, et al.: Detection of life-threatening prostate cancer with prostate-specific antigen velocity during a window of curability, *J Natl Cancer Inst* 98:1521–1527, 2006.

Carter HB, Pearson JD, Metter EJ, et al.: Longitudinal evaluation of prostate-specific antigen levels in men with and without prostate disease, *J Am Med Assoc* 267:2215–2220, 1992.

Catalona WJ, Smith DS, Ratliff TL, et al.: Measurement of prostate-specific antigen in serum as a screening test for prostate cancer, *N Engl J Med* 324:1156–1161, 1991.

Catalona WJ, Smith DS, Wolfert RL, et al.: Evaluation of percentage of free serum prostate-specific antigen to improve specificity of prostate cancer screening, *J Am Med Assoc* 274:1214–1220, 1995.

Chan DW, Sell S: *Tumor markers*, Philadelphia, 2001, WB Saunders.

Chan KC, Lo YM: Circulating nucleic acids as a tumor marker, *Histol Histopathol* 17:937–943, 2002.

Chen CH, Tsai TL, Yang YS, et al.: Studies of the serum HER-2/neu and squamous cell carcinoma-related antigen expression in patients with oral squamous cell carcinoma, *J Oral Pathol Med* 36:83–87, 2007.

Chen XQ, Bonnefoi H, Pelte MF, et al.: Telomerase RNA as a detection marker in the serum of breast cancer patients, *Clin Cancer Res* 6:3823–3826, 2000.

Chou WC, Chen JS, Hung YS, et al.: Plasma chromogranin A levels predict survival and tumor response in patients with advanced gastroenteropancreatic neuroendocrine tumors, *Anticancer Res* 34(10):5661–5669, 2014.

Christensson A, Bjork T, Nilsson O, et al.: Serum prostate specific antigen complexed to alpha 1-antichymotrypsin as an indicator of prostate cancer, *J Urol* 150:100–105, 1993.

Cohen SJ, Alpaugh RK, Gross S, et al.: Isolation and characterization of circulating tumor cells in patients with metastatic colorectal cancer, *Clin Colorectal Cancer* 6:125–132, 2006.

Coley CM, Barry MJ, Fleming C, et al.: Early detection of prostate cancer. Part II: Estimating the risks, benefits, and costs. American College of Physicians, *Ann Intern Med* 126:468–479, 1997a.

Coley CM, Barry MJ, Fleming C, et al.: Early detection of prostate cancer. Part I: Prior probability and effectiveness of tests. American College of Physicians, *Ann Intern Med* 126:394–406, 1997b.

Colomer R, Montero S, Lluch A, et al.: Circulating HER2 extracellular domain and resistance to chemotherapy in advanced breast cancer, *Clin Cancer Res* 6:2356–2362, 2000.

Compton C, Fenoglio-Preiser CM, Pettigrew N, et al.: American Joint Committee on cancer prognostic factors Consensus Conference: colorectal working group, *Cancer* 88:1739–1757, 2000.

Cooperberg MR, Broering JM, Litwin MS, et al.: The contemporary management of prostate cancer in the United States: Lessons from the cancer of the prostate strategic urologic research endeavor (CapSURE), a national disease registry, *J Urol* 171:1393–1401, 2004.

Cornu JN, Cancel-Tassin G, Egrot C, et al.: Urine TMPRSS2:ERG fusion transcript integrated with PCA3 score, genotyping, and biological features are correlated to the results of prostatic biopsies in men at risk of prostate cancer, *Prostate* 73:242–249, 2013.

Crawford ED, Rove KO, Trabulsi EJ, et al.: Diagnostic performance of PCA3 to detect prostate cancer in men with increased prostate specific antigen: a prospective study of 1962 cases, *J Urol* 188:1726–1731, 2012.

Cristofanilli M, Budd GT, Ellis MJ, et al.: Circulating tumor cells, disease progression, and survival in metastatic breast cancer, *N Engl J Med* 351:781–791, 2004.

Crocitto LE, Korns D, Kretzner L, et al.: Prostate cancer molecular markers GSTP1 and hTERT in expressed prostatic secretions as predictors of biopsy results, *Urology* 64:821–825, 2004.

Cuckle H: Biochemical screening for Down syndrome, *Eur J Obstet Gynecol Reprod Biol* 92:97–101, 2000.

de Bono JS, Attard G, Adjei A, et al.: Potential applications for circulating tumor cells expressing the insulin-like growth factor-I receptor, *Clin Cancer Res* 13:3611–3616, 2007.

de Kok JB, van Solinge WW, Ruers TJ, et al.: Detection of tumor DNA in serum of colorectal cancer patients, *Scand J Clin Lab Invest* 57:601–604, 1997.

de Kok JB, Verhaegh GW, Roelofs RW, et al.: DD3 (PCA3)—a very sensitive and specific marker to detect prostate tumors, *Cancer Res* 62:2695–2698, 2002.

De Vita F, Orditura M, Lieto E, et al.: Elevated perioperative serum vascular endothelial growth factor levels in patients with colon carcinoma, *Cancer* 100:270–278, 2004.

Demichelis F, Fall K, Perner S, et al.: TMPRSS2:ERG gene fusion associated with lethal prostate cancer in a watchful waiting cohort, *Oncogene* 26:4596–4599, 2007.

DeSoto-LaPaix F, Bluth MH, Rong Y, et al.: Detecting prostate cancer: how useful is prostate specific antigen testing? *Fed Pract* 20:84–90, 2003.

Devonshire AS, Whale AS, Gutteridge A, et al.: Towards standardisation of cell-free DNA measurement in plasma: controls for extraction efficiency, fragment size bias and quantification, *Anal Bioanal Chem* 406:6499–6512, 2014.

Diamond BA, Yelton DE, Scharff MD, et al.: Monoclonal antibodies—a new technique for producing serologic reagents, *N Engl J Med* 304:1344–1349, 1981.

Dominguez G, Carballido J, Silva J, et al.: p14ARF promoter hypermethylation in plasma DNA as an indicator of disease recurrence in bladder cancer patients, *Clin Cancer Res* 8:980–985, 2002.

Duffy MJ, Duggan C, Keane R, et al.: High preoperative CA 15-3 concentrations predict adverse outcome in node-negative and node-positive breast cancer: study of 600 patients with histologically confirmed breast cancer, *Clin Chem* 50:559–563, 2004.

Easton DF, Bishop DT, Ford D, et al.: Genetic linkage analysis in familial breast and ovarian cancer: results from 214 families. The Breast Cancer Linkage Consortium, *Am J Hum Genet* 52:678–701, 1993.

Eccles SA, Welch DR: Metastasis: recent discoveries and novel treatment strategies, *Lancet* 369:1742–1757, 2007.

El Messaoudi S, Rolet F, Mouliere F, et al.: Circulating cell free DNA: Preanalytical considerations, *Clin Chim Acta* 424:222–230, 2013.

Engelstaedter V, Heublein S, Schumacher AL, et al.: Mucin-1 and its relation to grade, stage and survival in ovarian carcinoma patients, *BMC Canc* 12:600–608, 2012.

Esteller M, Sanchez-Cespedes M, Rosell R, et al.: Detection of aberrant promoter hypermethylation of tumor suppressor genes in serum DNA from non–small cell lung cancer patients, *Cancer Res* 59:67–70, 1999.

Falzarano SM, Magi-Galluzzi C: ERG protein expression as a biomarker of prostate cancer, *Biomarkers Med* 7:851–865, 2013.

Fang J, Metter EJ, Landis P, et al.: PSA velocity for assessing prostate cancer risk in men with PSA levels between 2.0 and 4.0 ng/mL, *Urology* 59:889–893, 2002.

Ferrero-Pous M, Hersant AM, Pecking A, et al.: Serum chromogranin-A in advanced prostate cancer, *BJU Int* 88:790–796, 2001.

Fleischhacker M: The 2nd International Symposium on circulating nucleic acids in plasma and serum (CNAPS-2), Hong Kong, February 20-21, 2001, *Eur J Med Res* 6:364–368, 2001.

Folkman J, Shing Y: Angiogenesis, *J Biol Chem* 267:10931–10934, 1992.

Fradet Y, Saad F, Aprikian A, et al.: uPM3, a new molecular urine test for the detection of prostate cancer, *Urology* 64:311–316, 2004.

Fradet Y: Biomarkers in prostate cancer diagnosis and prognosis: beyond prostate-specific antigen, *Curr Opin Urol* 19:243–246, 2009.

Freedland SJ, Dorey F, Aronson WJ: Preoperative PSA velocity and doubling time do not predict adverse pathologic features or biochemical recurrence after radical prostatectomy, *Urology* 57:476–480, 2001.

Futreal PA, Liu Q, Shattuck-Eidens D, et al.: BRCA1 mutations in primary breast and ovarian carcinomas, *Science* 266:120–122, 1994.

Gal S, Fidler C, Lo YM, et al.: Detection of mammaglobin mRNA in the plasma of breast cancer patients, *Ann N Y Acad Sci* 945:192–194, 2001.

Galgano MT, Hampton GM, Frierson Jr HF: Comprehensive analysis of HE4 expression in normal and malignant human tissues, *Mod Pathol* 19:847–853, 2006.

Garcia JM, Silva JM, Domiguez G, et al.: Heterogeneous tumour clones as an explanation of discordance between plasma DNA and tumor DNA alterations, *Genes Chromosomes Cancer* 31:300, 2001.

García-Olmo DC, García-Olmo D: Biological role of cell-free nucleic acids in cancer: the theory of genometastasis, *Crit Rev Oncog* 18:153–161, 2013.

Gaspar MJ, Arribas I, Coca MC, et al.: Prognostic value of carcinoembryonic antigen, CA 19-9 and CA 72-4 in gastric carcinoma, *Tumour Biol* 22:318–322, 2001.

Gazzaniga P, Gianni W, Raimondi C, et al.: Circulating tumor cells in high-risk non-metastatic colorectal cancer, *Tumour Biol* 34:2507–2509, 2013.

Gebo KA, Chander G, Jenckes MW, et al.: Screening tests for hepatocellular carcinoma in patients with chronic hepatitis C: a systematic review, *Hepatology* 36(Suppl 1):S84–S92, 2002.

Gion M, Boracchi P, Dittadi R, et al.: Prognostic role of serum CA15.3 in 362 node-negative breast cancers. An old player for a new game, *Eur J Cancer* 38:1181–1188, 2002.

Giovanella L, Ceriani L: Serum chromogranin-alpha immunoradiometric assay in the diagnosis of pheochromocytoma, *Int J Biol Markers* 17:130–134, 2002.

Goessl C, Krause H, Müller M, et al.: Fluorescent methylation-specific polymerase chain reaction for DNA-based detection of prostate cancer in bodily fluids, *Cancer Res* 60:5941–5945, 2000.

Goessl C, Muller M, Heicappell R, et al.: DNA-based detection of prostate cancer in blood, urine, and ejaculates, *Ann N Y Acad Sci* 945:51–58, 2002a.

Goessl C, Muller M, Straub B, et al.: DNA alterations in body fluids as molecular tumor markers for urological malignancies, *Eur Urol* 41:668, 2002b.

Gold P, Freedman SO: Specific carcinoembryonic antigens of the human digestive system, *J Exp Med* 122:467–481, 1965.

Goldshtein H, Hausmann MJ, Douvdevani A: A rapid direct fluorescent assay for cell-free DNA quantification in biological fluids, *Ann Clin Biochem* 46:488–494, 2009.

Gonzalgo ML, Nakayama M, Lee SM, et al.: Detection of GSTP1 methylation in prostatic secretions using combinatorial MSP analysis, *Urology* 63:414–418, 2004.

Gonzalgo ML, Pavlovich CP, Lee SM, et al.: Prostate cancer detection by GSTP1 methylation analysis of post biopsy urine specimens, *Clin Cancer Res* 9:2673–2677, 2003.

Granato AM, Nanni O, Falcini F, et al.: Basic fibroblast growth factor and vascular endothelial growth factor serum levels in breast cancer patients and healthy women: useful as diagnostic tools?, *Breast Cancer Res* 6, 2004. R38–R45.

Greene KL, Albertsen PC, Babaian RJ, et al.: Prostate specific antigen best practice statement: 2009 update, *J Urol* 182:2232–2241, 2009.

Groot KB, Rahbari NN, Buchler MW, et al.: Circulating tumor cells and prognosis of patients with resectable colorectal liver metastases or widespread metastatic colorectal cancer: a metaanalysis, *Ann Surg Oncol* 20(7):2156–2165, 2013.

Groskopf J, Aubin SM, Deras IL, et al.: APTIMA PCA3 molecular urine test: development of a method to aid in the diagnosis of prostate cancer, *Clin Chem* 52:1089–1095, 2006.

Grubb 3rd RL, Pinsky PF, Greenlee RT, et al.: Prostate cancer screening in the Prostate, Lung, Colorectal and Ovarian Cancer Screening Trial: update on findings from the initial four rounds of screening in a randomized trial, *BJU Int* 102:1524–1530, 2008.

Guinee Jr DG, Travis WD, Trivers GE, et al.: Gender comparisons in human lung cancer: analysis of p53 mutations, anti-p53 serum antibodies and C-erbB-2 expression, *Carcinogenesis* 16:993–1002, 1995.

Guo B, Luo C, Xun C, et al.: Quantitative detection of cytokeratin 20 mRNA in urine samples as diagnostic tools for bladder cancer by real-time PCR, *Exp Oncol* 31:43–47, 2009.

Haese A, de la Taille A, van Poppel H, et al.: Clinical utility of the PCA3 urine assay in European men scheduled for repeat biopsy, *Eur Urol* 54:1081–1088, 2008.

Haferlach T, Loffler H: Prognostic factors in multiple myeloma: practicability for clinical practice and future perspectives, *Leukemia* 11(Suppl 5), 1997. S5–S9.

Halling KC: Vysis UroVysion for the detection of urothelial carcinoma, *Expert Rev Mol Diagn* 3:507–519, 2003. Erratum in Expert Rev Mol Diagn 4:266, 2004.

Hammel P, Leroy-Viard K, Chaumette MT, et al.: Correlations between p53-protein accumulation, serum antibodies and gene mutation in colorectal cancer, *Int J Cancer* 81:712–718, 1999.

Harlozinska A, Sedlaczek P, Kulpa J, et al.: Vascular endothelial growth factor (VEGF) concentration in sera and tumor effusions from patients with ovarian carcinoma, *Anticancer Res* 24:1149–1157, 2004.

Harris CC, Hollstein M: Clinical implications of the p53 tumor-suppressor gene, *N Engl J Med* 329:1318–1327, 1993.

Harris LN, Liotcheva V, Broadwater G, et al.: Comparison of methods of measuring HER-2 in metastatic breast cancer patients treated with high-dose chemotherapy, *J Clin Oncol* 19:1698–1706, 2001.

Haug U, Hundt S, Brenner H: Sensitivity and specificity of faecal tumour M2 pyruvate kinase for detection of colorectal adenomas in a large screening study, *Br J Cancer* 99:133–135, 2008.

Hayes DF, Cristofanilli M, Budd GT, et al.: Circulating tumor cells at each follow-up time point during therapy of metastatic breast cancer patients predict progression-free and overall survival, *Clin Cancer Res* 12:4218–4224, 2006.

Hayes DF, Yamauchi H, Broadwater G, et al.: Circulating HER-2/erbB-2/c-neu (HER-2) extracellular domain as a prognostic factor in patients with metastatic breast cancer: cancer and Leukemia Group B Study 8662, *Clin Cancer Res* 7:2703–2711, 2001.

He C, Liu M, Zhou C, et al.: Detection of epidermal growth factor receptor mutations in plasma by mutant-enriched PCR assay for prediction of the response to gefitinib in patients with non–small-cell lung cancer, *Int J Cancer* 125:2393–2399, 2009.

He W, Wang H, Hartmann LC, et al.: In vivo quantitation of rare circulating tumor cells by multiphoton intravital flow cytometry, *Proc Natl Acad Sci U S A* 104:11760–11765, 2007.

Heidegger I, Klocker H, Steiner E, et al.: [–2]proPSA is an early marker for prostate cancer aggressiveness, *Prostate Cancer and Prostatic Disease* 17:70–74, 2014.

Heidenreich A, Aus G, Bolla M, et al.: European Association of Urology. EAU guidelines on prostate cancer, *Eur Urol* 53:68–80, 2008.

Hessels D, Klein Gunnewiek JM, van Oort I, et al.: DD3(PCA3)-based molecular urine analysis for the diagnosis of prostate cancer, *Eur Urol* 44:8–15, 2003.

Hibi K, Nakayama H, Yamazaki T, et al.: Detection of mitochondrial DNA alterations in primary tumors and corresponding serum of colorectal cancer patients, *Int J Cancer* 94:429, 2001.

Hickey KP, Boyle KP, Jepps HM, et al.: Molecular detection of tumour DNA in serum and peritoneal fluid from ovarian cancer patients, *Br J Cancer* 80:1803, 1999.

Hoque MO, Topaloglu O, Begum S, et al.: Quantitative methylation-specific polymerase chain reaction gene patterns in urine sediment distinguish prostate cancer patients from control subjects, *J Clin Oncol* 23:6569–6575, 2005.

Hori S, Blanchet JS, McLoughlin J: From prostate-specific antigen (PSA) to precursor PSA (proPSA) isoforms: a review of the emerging role of proPSAs in the detection and management of early prostate cancer, *BJU Int* 112:717–728, 2013.

Horninger W, Cheli CD, Babaian RJ, et al.: Complexed prostate-specific antigen for early detection of prostate cancer in men with serum prostate-specific antigen levels of 2 to 4 nanograms per milliliter, *Urology* 60(Suppl 1):31–35, 2002.

Hussain MH, MacVicar GR, Petrylak DP, et al.: National Cancer Institute. Trastuzumab, paclitaxel, carboplatin, and gemcitabine in advanced human epidermal growth factor receptor-2/neu-positive urothelial carcinoma: results of a multicenter phase II National Cancer Institute trial, *J Clin Oncol* 25:2218–2224, 2007.

Igetei R, Otegbayo JA, Ndububa DA, et al.: Detection of p53 codon 249 mutation in Nigerian patients with hepatocellular carcinoma using a novel evaluation of cell-free DNA, *Ann Hepatol* 7:339–344, 2008.

Ignatiadis M, Xenidis N, Perraki M, et al.: Different prognostic value of cytokeratin-1 mRNA positive circulating tumor cells according to estrogen receptor and HER2 status in early-stage breast cancer, *J Clin Oncol* 25:5194–5202, 2007.

Imperiale TF, Ransohoff DF, Itzkowitz SH, et al.: Colorectal Cancer Study Group: fecal DNA versus fecal occult blood for colorectal-cancer screening in an average-risk population, *N Engl J Med* 351:2704–2714, 2004.

Isshiki S, Akakura K, Komiya A, et al.: Chromogranin-A concentration as a serum marker to predict prognosis after endocrine therapy for prostate cancer, *J Urol* 167:512–515, 2002.

Ito K, Yamamoto T, Ohi M, et al.: Free/total PSA ratio is a powerful predictor of future prostate cancer morbidity in men with initial PSA levels of 4.1 to 10.0 ng/mL, *Urology* 61:760–764, 2003.

Izzo F, Cremona F, Ruffolo F, et al.: Outcome of 67 patients with hepatocellular cancer detected during screening of 1125 patients with chronic hepatitis, *Ann Surg* 227:513–518, 1998.

Jacobs I, Bast Jr RC: The CA 125 tumour-associated antigen: a review of the literature, *Hum Reprod* 4:1–12, 1989.

Jacobs IJ, Menon U: Progress and challenges in screening for early detection of ovarian cancer, *Mol Cell Proteomics* 3:355–366, 2004.

Javidi MA, Ahmadi AH, Bakhshinejad B, et al.: Cell-free microRNAs as cancer biomarkers: the odyssey of miRNAs through body fluids, *Med Oncol* 31:295, 2014.

Jensen EV, Jordan VC: The estrogen receptor: a model for molecular medicine, *Clin Cancer Res* 9:1980–1989, 2003.

Jeronimo C, Nomoto S, Caballero OL, et al.: Mitochondrial mutations in early stage prostate cancer and bodily fluids, *Oncogene* 20:5195, 2001a.

Jeronimo C, Usadel H, Henrique R, et al.: Quantitation of GSTP1 methylation in non-neoplastic prostatic tissue and organ-confined prostate adenocarcinoma, *J Natl Cancer Inst* 93:1747–1752, 2001b.

Johnson PJ, Lo YM: Plasma nucleic acids in the diagnosis and management of malignant disease, *Clin Chem* 48:1186, 2002.

Joosse SA, Müller V, Steinbach B, et al.: Circulating cell-free cancer-testis MAGE-A RNA, BORIS RNA, let-7b and miR-202 in the blood of patients with breast cancer and benign breast diseases, *Br J Cancer* 111:909–917, 2014.

Jung K, Reszka R, Kamlage B, et al.: Tissue metabolite profiling identifies differentiating and prognostic biomarkers for prostate carcinoma, *Int J Cancer* 133:2914–2924, 2013.

Kagan J, Cabanero M, Wieczorek R, Pincus MR: Can serum free light chains be used for the early diagnosis of monoclonal immunoglobulin-secreting B-cell and plasma-cell diseases? *Fed Pract* 33(suppl 5):36S-39S, 2016.

Kamps R, Brandão RD, Bosch BJ, et al.: Next-generation sequencing in Oncology: genetic diagnosis, risk prediction and cancer Classification, *Int J Mol Sci* 18(2):308, 2017, Published 2017 Jan 31 https://doi.org/10.3390/ijms18020308.

Kan N, Yoshikawa S: Serum HER-2 determination using a centauer HER-2/neu kit (CLIA method) in metastatic breast cancer, *Gan to Kagaku Ryoho* 36:779–783, 2009.

Kehinde EO, Maghrebi MA, Anim JT: The importance of determining the aggressiveness of prostate cancer using serum and tissue molecular markers, *Can J Urol* 15:3967–3974, 2008.

Kim H-S, Kim HS, Sin K-S, et al.: 2014 Clinical comparisons of two free light chain assays to immunofixation electrophoresis for detecting monoclonal gammopathy, *BioMed Res Int*1–7, 2014.

Klee GG, Schreiber WE: MUC1 gene-derived glycoprotein assays for monitoring breast cancer (CA 15-3, CA 27.29, BR): are they measuring the same antigen? *Arch Pathol Lab Med* 128:1131–1135, 2004.

Kondo N, Murakami Y, Uemura K, et al.: Elevated perioperative serum CA 19-9 levels are independent predictors of poor survival in patients with resectable cholangiocarcinoma, *J Surg Oncol* 110(4):422–429, 2014.

Kopreski MS, Benko FA, Kwak LW, et al.: Detection of tumor messenger RNA in the serum of patients with malignant melanoma, *Clin Cancer Res* 5:1961, 1999.

Kumar-Sinha C, Tomlins SA, Chinnaiyan AM: Recurrent gene fusions in prostate cancer, *Nat Rev Cancer* 8:497–511, 2008.

Kumpulainen EJ, Keskikuru RJ, Johansson RT: Serum tumor marker CA 15.3 and stage are the two most powerful predictors of survival in primary breast cancer, *Breast Cancer Res Treat* 76:95–102, 2002.

Kuropkat C, Lippert BM, Werner JA: Follow-up with serum Cyfra 21-1 in patients with squamous cell carcinomas of the head and neck, *Oncology* 63:280–285, 2002.

Kyle RA, Gertz MA, Witzig TE, et al.: Review of 1027 patients with newly diagnosed multiple myeloma, *Mayo Clin Proc* 78:21–33, 2003.

Lamerz R: AFP isoforms and their clinical significance (overview), *Anticancer Res* 17:2927–2930, 1997.

Lazzeri M, Abrate A, Lughezzani G, et al.: Relationship of chronic histologic prostatic inflammation in biopsy specimens with serum isoform [–2]proPSA (p2PSA), %p2PSA, and prostate health index in men with a total prostate-specific antigen of 4 to 10 ng/mL and normal digital rectal examination, *Urology* 38:606–612, 2014.

Lazzeri M, Haese A, Abrate A, et al.: Clinical performance of serum prostate specific antigen isoform [–2]proPSA (p2PSA) and its derivatives %p2PSA and the prostate health index (phi) in men with a family history of prostate cancer: results from a multicenter European study, the PROMEtheuS project, *BJU Int* 112:313–321, 2013.

Lechowicz MJ, Lin L, Ambinder RF: Epstein-Barr virus DNA in body fluids, *Curr Opin Oncol* 14:533, 2002.

Lee D: Prostate-specific antigen doubling time predicts disease progression and survival, *Clin Prostate Cancer* 1:208–211, 2003.

Lee P, Rosen DG, Zhu C, et al.: Expression of progesterone receptor is a favorable prognostic marker in ovarian cancer, *Gynecol Oncol* 96:671–677, 2005.

Lee TH, Montalvo L, Chrebtow V, et al.: Quantitation of genomic DNA in plasma and serum samples: higher concentrations of genomic DNA found in serum than in plasma, *Transfusion* 41:276, 2001.

Lei KI, Chan LY, Chan WY, et al.: Diagnostic and prognostic implications of circulating cell-free Epstein-Barr virus DNA in natural killer/T-cell lymphoma, *Clin Cancer Res* 8:29, 2002.

Lein M, Kwiatkowski M, Semjonow A, et al.: A multicenter clinical trial on the use of complexed prostate specific antigen in low prostate specific antigen concentrations, *J Urol* 170:1175–1179, 2003.

Leitzel K, Teramoto Y, Sampson E, et al.: Elevated soluble c-erbB-2 antigen levels in the serum and effusions of a proportion of breast cancer patients, *J Clin Oncol* 10:1436–1443, 1992.

Leyten GH, Hessels D, Jannick SA, et al.: Prospective multicentre evaluation of PCA3 and TMPRSS2:ERG gene fusions as diagnostic and prognostic urinary biomarkers for prostate cancer, *Eur Urol* 65:534–542, 2014.

Li L, Wang L, Zhang W, et al.: Correlation of serum VEGF levels with clinical stage, therapy efficacy, tumor metastasis and patient survival in ovarian cancer, *Anticancer Res* 24:1973–1979, 2004.

Lilja H, Christensson A, Dahlén U, et al.: Prostate-specific antigen in serum occurs predominantly in complex with alpha 1-antichymotrypsin, *Clin Chem* 37:1618–1625, 1991.

Liotta LA: Biochemical mechanisms of tumor invasion and metastases, *Clin Physiol Biochem* 5:190–199, 1987.

Littrup PJ, Goodman AC, Mettlin CJ: The benefit and cost of prostate cancer early detection. The Investigators of the American cancer Society–national prostate cancer detection project, *CA Cancer J Clin* 43:134–149, 1993.

Ljungberg B, Jacobsen J, Haggstrom-Rudolfssson S, et al.: Tumour vascular endothelial growth factor (VEGF) mRNA in relation to serum VEGF protein levels and tumour progression in human renal cell carcinoma, *Urol Res* 31:335–340, 2003.

Loberg RD, Fielhauer JR, Pienta BA, et al.: Prostate-specific antigen doubling time and survival in patients with advanced metastatic prostate cancer, *Urology* 62(Suppl 1):128–133, 2003.

Loeb S, Sokoll L, Broyles DL, et al.: Prospective multicenter evaluation of the Beckman Coulter prostate health index using WHO calibration, *J Uro* 189:1702–1706, 2013.

Lou X, Hou Y, Liang D, et al.: A novel Alu-based real-time PCR method for the quantitative detection of plasma circulating cell-free DNA: sensitivity and specificity for the diagnosis of myocardial infarction, *Int J Mol Med* 35:72–80, 2015.

Louhimo J, Carpelan-Holmstrom M, Alfthan H, et al.: Serum HCG beta, CA 72-4 and CEA are independent prognostic factors in colorectal cancer, *Int J Cancer* 101:545–548, 2002.

Lu KH, Patterson AP, Wang L, et al.: Selection of potential markers for epithelial ovarian cancer with gene expression arrays and recursive descent partition analysis, *Clin Cancer Res* 10:3291–3300, 2004.

Luftner D, Henschke P, Flath B, et al.: Serum HER-2/neu as a prediction and monitoring parameter in a phase II study with weekly paclitaxel in metastatic breast cancer, *Anticancer Res* 24:895–906, 2004.

Ma PC, Blaszkowsky L, Bharti A, et al.: Circulating tumor cells and serum tumor biomarkers in small cell lung cancer, *Anticancer Res* 23:49–62, 2003.

Machens A, Lorenz K, Dralle H: Utility of serum procalcitonin for screening and risk Machens stratification of medullary thyroid cancer, *J Clin Endocrinol Metab* 99(8):2986–2994, 2014.

Malkin D, Li FP, Strong LC, et al.: Germ line p53 mutations in a familial syndrome of breast cancer, sarcomas, and other neoplasms, *Science* 250:1233–1238, 1990.

Mano H: ALHoma: a cancer subtype with a shared target, *Cancer Discov* 2:495–502, 2012.

Mansour H: Cell-free nucleic acids as noninvasive biomarkers for colorectal cancer detection, *Front Genet* 5:182, 2014.

Marrelli D, Pinto E, De Stefano A, et al.: Clinical utility of CEA, CA 19-9, and CA 72-4 in the follow-up of patients with resectable gastric cancer, *Am J Surg* 181:16–19, 2001.

Marzese DM, Hirose H, Hoon DS: Diagnostic and prognostic value of circulating tumor-related DNA in cancer patients, *Expert Rev Mol Diagn* 13:827–844, 2013.

McDunn JE, Li Z, Adam KP, et al.: Metabolomic signatures of aggressive prostate cancer, *Prostate* 73:1547–1560, 2013.

Miki Y, Swensen J, Shattuck-Eidens D, et al.: A strong candidate for the breast and ovarian cancer susceptibility gene BRCA1, *Science* 266:66–71, 1994.

Mikolajczyk SD, Grauer LS, Millar LS, et al.: A precursor form of PSA (pPSA) is a component of the free PSA in prostate cancer serum, *Urology* 50:710–714, 1997.

Mikolajczyk SD, Millar LS, Wang TJ, " BPSA, et al.: A specific molecular form of free prostate-specific antigen, is found predominantly in the transition zone of patients with nodular benign prostatic hyperplasia, *Urology* 55:41–45, 2000.

Milstein C, Cuello AC: Hybrid hybridomas and their use in immunohistochemistry, *Nature* 305:537–540, 1983.

Mitchell EP: Role of carcinoembryonic antigen in the management of advanced colorectal cancer, *Semin Oncol* 25(Suppl 11):12–20, 1998.

Mitchell ID, Croal BL, Dickie A, et al.: A prospective study to evaluate the role of complexed prostate specific antigen and free/total prostate specific antigen ratio for the diagnosis of prostate cancer, *J Urol* 165:1549–1553, 2001.

Molnar B, Sipos F, Galamb O, et al.: Molecular detection of circulating cancer cells. Role in diagnosis, prognosis and follow-up of colon cancer patients, *Dig Dis* 21:320–325, 2003.

Moore RG, Brown AK, Miller MC, et al.: The use of multiple novel tumor biomarkers for the detection of ovarian carcinoma in patients with a pelvic mass, *Gynecol Oncol* 108:402–408, 2008.

Moore RG, McMeekin DS, Brown AK, et al.: A novel multiple marker bioassay utilizing HE4 and CA125 for the prediction of ovarian cancer in patients with a pelvic mass, *Gynecol Oncol* 112:40–46, 2009.

Morelli D, Lazzerini D, Cazzaniga S, et al.: Evaluation of the balance between angiogenic and antiangiogenic circulating factors in patients with breast and gastrointestinal cancers, *Clin Cancer Res* 4:1221–1225, 1998.

Moreno JG, Miller MC, Gross S, et al.: Circulating tumor cells predict survival in patients with metastatic prostate cancer, *Urology* 65:713–718, 2005.

Mori S, Mori Y, Mukaiyama T, et al.: In vitro and in vivo release of soluble erbB-2 protein from human carcinoma cells, *Jpn J Cancer Res* 81:489–494, 1990.

Moul JW, Sun L, Hotaling JM, et al.: Age adjusted prostate specific antigen and prostate specific antigen velocity cut points in prostate cancer screening, *J Urol* 177:499–503, 2007.

Munstedt K, Steen J, Knauf AG, et al.: Steroid hormone receptors and long-term survival in invasive ovarian cancer, *Cancer* 89:1783–1791, 2000.

Nagahashi M, Schimada Y, Ichikawa H, et al.: Next generation sequencing-based gene panel tests for the management of solid tumors, *Cancer Sci* 110(1):6–15, 2019.

Nagrath S, Sequist LV, Maheswaran S, et al.: Isolation of rare circulating tumour cells in cancer patients by microchip technology, *Nature* 450:1235–1239, 2007.

Nahm MH, Hoffmann JW: Heteroantibody: Phantom of the immunoassay, *Clin Chem* 36:829, 1990.

Nakamoto D, Yamamoto N, Takagi R, et al.: Detection of microsatellite alterations in plasma DNA of malignant mucosal melanoma using whole genome amplification, *Bull Tokyo Dent Coll* 49:77–87, 2008.

Nakanishi H, Groskopf J, Fritsche HA, et al.: PCA3 molecular urine assay correlates with prostate cancer tumor volume: implication in selecting candidates for active surveillance, *J Urol* 179:1804–1809, 2008.

Nakata B, Ogawa Y, Ishikawa T, et al.: Serum CYFRA 21-1 is one of the most reliable tumor markers for breast carcinoma, *Cancer* 89:1285–1290, 2000.

Nakata B, Takashima T, Ogawa Y, et al.: Serum CYFRA 21-1 (cytokeratin-19 fragments) is a useful tumour marker for detecting disease relapse and assessing treatment efficacy in breast cancer, *Br J Cancer* 91:873–878, 2004.

O'Hanlon DM, Fitzsimons H, Lynch J, et al.: Soluble adhesion molecules (E-selectin, ICAM-1 and VCAM-1) in breast carcinoma, *Eur J Cancer* 38:2252–2257, 2002.

Pantel K, Riethdorf S: Pathology: are circulating tumor cells predictive of overall survival? *Nat Rev Clin Oncol* 6:190–191, 2009.

Papila C, Uzun H, Balci H, et al.: Clinical significance and prognostic value of serum sHER-2/neu levels in patients with solid tumors, *Med Oncol* 26:151–156, 2009.

Papsidero LD, Wang MC, Valenzuela LA, et al.: A prostate antigen in sera of prostatic cancer patients, *Cancer Res* 40:2428–2432, 1980.

Park KU, Lee HE, Park do J, et al.: MYC quantitation in cell-free plasma DNA by real-time PCR for gastric cancer diagnosis, *Clin Chem Lab Med* 47:530–536, 2009.

Parsons JK, Brawer MK, Cheli CD, et al.: Complexed prostate specific antigen (PSA) reduces unnecessary prostate biopsies in the 2.6 to 4.0 ng/mL range of total PSA, *BJU Int* 94:47–50, 2004.

Peng Z, Liu Y, Li Y, et al.: Serum HER2 extracellular domain as a potential alternative for tissue HER2 status in metastatic gastric cancer patients, *Biomark Med* 8(5):663–670, 2014.

Ploussard G, de la Taille A: Urine biomarkers in prostate cancer, *Nat Rev Urol* 7:101–109, 2010.

Polascik TJ, Oesterling JE, Partin AW: Prostate specific antigen: a decade of discovery—what we have learned and where we are going, *J Urol* 162:293–306, 1999.

Poon RT, Lau CP, Cheung ST, et al.: Quantitative correlation of serum levels and tumor expression of vascular endothelial growth factor in patients with hepatocellular carcinoma, *Cancer Res* 63:3121–3126, 2003.

Punglia RS, D'Amico AV, Catalona WJ, et al.: Effect of verification bias on screening for prostate cancer by measurement of prostate-specific antigen, *N Engl J Med* 349:335–342, 2003.

Rajkumar SV, Kyle RA, Therneau TM, et al.: Serum free light chain ratio is an independent risk factor for progression in monoclonal gammopathy of undetermined significance, *Blood* 106:812–817, 2005.

Resel FL, San Jose ML, Galante RI, et al.: Prognostic significance of circulating tumor cell count in patients with metastatic hormone-sensitive prostate cancer, *Urology* 80:1328–1332, 2012.

Rhodes CH, Honsinger C, Sorenson GD: Detection of tumor-derived DNA in cerebrospinal fluid, *J Neuropathol Exp Neurol* 53:364, 1994.

Riethdorf S, Fritsche H, Müller V, et al.: Detection of circulating tumor cells in peripheral blood of patients with metastatic breast cancer: a validation study of the CellSearch system, *Clin Cancer Res* 13:920–928, 2007.

Roddam AW, Duffy MJ, Hamdy FC, et al.: Use of prostate-specific antigen (PSA) isoforms for the detection of prostate cancer in men with a PSA level of 2-10 ng/mL: systematic review and meta-analysis, *Eur Urol* 48:386–399, 2005.

Roupret M, Hupertan V, Yates DR, et al.: Molecular detection of localized prostate cancer using quantitative methylation-specific PCR on urinary cells obtained following prostate massage, *Clin Cancer Res* 13:1720–1725, 2007.

Rubinstein JC, Nicolcon NG, Ahuja N: Next-generation sequencing in the management of gastric and esophageal cancers, *Surg Clin North Am* 99(3):511–527, 2019.

Sabour L, Sabour M, Ghorbian S: Clinical applications of next-generation sequencing in cancer diagnosis, *Pathol Oncol Res* 23(2):225–234, 2017.

Salami SS, Schmidt F, Laxman B, et al.: Combining urinary detection of TMPRSS2:ERG and PCA3 with serum PSA to predict diagnosis of prostate cancer, *Urol Oncol* 31:566–571, 2013.

Sanger N, Effenberger KE, Riethdorf S, et al.: Disseminated tumor cells in the bone marrow of patients with ductal carcinoma in situ, *Int J Cancer* 129:2522–2526, 2011.

Sangrajrang S, Arpornwirat W, Cheirsilpa A, et al.: Serum p53 antibodies in correlation to other biological parameters of breast cancer, *Cancer Detect Prev* 27:182–186, 2003.

Saylor PJ, Karoly ED, Smith MR: Prospective study of changes in the metabolomics profiles of men during their first three months of androgen deprivation therapy for prostate cancer, *Clin Cancer Res* 18:3677–3685, 2012.

Scattoni V, Lazzeri M, Lughezzani G, et al.: Head to head comparison of prostate health index and urinary PCA3 for predicting cancer at initial or repeat biopsy, *J Urol* 190:496–501, 2013.

Schippinger W, Regitnig P, Bauernhofer T, et al.: The course of serum HER-2/neu levels as an independent prognostic factor for survival in metastatic breast cancer, *Oncol Rep* 11:1331–1336, 2004.

Schlichtholz B, Legros Y, Gillet D, et al.: The immune response to p53 in breast cancer patients is directed against immunodominant epitopes unrelated to the mutational hot spot, *Cancer Res* 52:6380–6384, 1992.

Schmidt B, Carstensen T, Engel E, et al.: Detection of cell-free nucleic acids in bronchial lavage fluid supernatants from patients with lung cancer, *Eur J Cancer* 40:452, 2004.

Schneider J, Philipp M, Velcovsky HG, et al.: Pro-gastrin-releasing peptide (ProGRP), neuron specific enolase (NSE), carcinoembryonic antigen (CEA), and cytokeratin 19-fragments (CYFRA 21-1) in patients with lung cancer in comparison to other lung diseases, *Anticancer Res* 23:885–893, 2003.

Schröder FH, Carter HB, Wolters T, et al.: Early detection of prostate cancer in 2007. Part 1: PSA and PSA kinetics, *Eur Urol* 53:468–477, 2008.

Schröder FH, Hugosson J, Roobol MJ, et al.: Screening and prostate-cancer mortality in a randomized European study, *N Engl J Med* 360:1320–1328, 2009.

Schröder FH, van der Cruijsen-Koeter I, de Koning HJ, et al.: Prostate cancer detection at low prostate specific antigen, *J Urol* 163:806–812, 2000.

Schummer M, Ng WV, Bumgarner RE, et al.: Comparative hybridization of an array of 21,500 ovarian cDNAs for the discovery of genes overexpressed in ovarian carcinomas, *Gene* 238:375–378, 1999.

Schwarz AK, Stanulla M, Cario G, et al.: Quantification of free total plasma DNA and minimal residual disease detection in the plasma of children with acute lymphoblastic leukemia, *Ann Hematol* 88:897–905, 2009.

Schwarzenbach H, Muller V, Stahmann N, et al.: Detection and characterization of circulating microsatellite DNA in blood of patients with breast cancer, *Ann NY Acad Sci* 1022:25, 2004.

Sciarra A, Monti S, Gentile V, et al.: Variation in chromogranin A serum levels during intermittent versus continuous androgen deprivation therapy for prostate adenocarcinoma, *Prostate* 55:168–179, 2003.

Sethi S, Ali S, Kong D, et al.: Clinical implication of microRNAs in molecular pathology, *Clin Lab Med* 33:773–786, 2013.

Sheen-Chen SM, Eng HL, Huang CC, et al.: Serum levels of soluble E-selectin in women with breast cancer, *Br J Surg* 91:1578–1581, 2004.

Shimada Y, Kameyama H, Nagahashi M, et al.: Comprehensive genomic sequencing detects important genetic differences between right-sided and left-sided colorectal cancer, *Oncotarget* 55:93567–93579, 2017.

Sidransky D, Von Eschenbach A, Tsai YC, et al.: Identification of p53 gene mutations in bladder cancers and urine samples, *Science* 252:706–709, 1991.

Silva JM, Gonzalez R, Dominguez G, et al.: TP53 gene mutations in plasma DNA of cancer patients, *Genes Chromosomes Cancer* 24:160, 1999.

Silva JM, Rodriguez R, Garcia JM, et al.: Detection of epithelial tumour RNA in the plasma of colon cancer patients is associated with advanced stages and circulating tumour cells, *Gut* 50:530, 2002.

Sita-Lumsden A, Fletcher CE, Dart DA, et al.: Circulating nucleic acids as biomarkers of prostate cancer, *Biomark Med* 7:867–877, 2013.

Smith TJ, Davidson NE, Schapira DV, et al.: American Society of Clinical Oncology 1998 update of recommended breast cancer surveillance guidelines, *J Clin Oncol* 17:1080–1082, 1999.

Sokoll LJ, Sanda MG, Feng Z, et al.: A prospective, multicenter, National Cancer Institute Early Detection Research Network study of [–2]proPSA: improving prostate cancer detection and correlating with cancer aggressiveness, *Cancer Epidemol Biomarkers Prev* 19:1193–1200, 2010.

Sorenson GD, Pribish DM, Valone FH, et al.: Soluble normal and mutated DNA sequences from single-copy genes in human blood, *Cancer Epidemiol Biomarkers Prev* 3:67, 1994.

Soussi T, Beroud C: Assessing TP53 status in human tumours to evaluate clinical outcome, *Nat Rev Cancer* 1:233–240, 2001.

Soussi T: p53 Antibodies in the sera of patients with various types of cancer: a review, *Cancer Res* 60:1777–1778, 2000.

Spindler KL, Pallisgaard N, Andersen RF, et al.: Changes in mutational status during third-line treatment for metastatic colorectal cancer—results of consecutive measurement of cell free DNA, KRAS and BRAF in the plasma, *Int J Cancer* 135:2215–2222, 2014.

Stenman UH, Leinonen J, Alfthan H, et al.: A complex between prostate-specific antigen and alpha 1-antichymotrypsin is the major form of prostate-specific antigen in serum of patients with prostatic cancer: assay of the complex improves clinical sensitivity for cancer, *Cancer Res* 51:222–226, 1991.

Stephan C, Rittenhouse H, Cammann H, et al.: New markers and multivariate models for prostate cancer detection, *Anticancer Res* 29:2589–2600, 2009.

Su WC, Shiesh SC, Liu HS, et al.: Expression of oncogene products HER2/Neu and Ras and fibrosis-related growth factors bFGF, TGF-beta, and PDGF in bile from biliary malignancies and inflammatory disorders, *Dig Dis Sci* 46:1387–1392, 2001.

Syrigos KN, Salgami E, Karayiannakis AJ, et al.: Prognostic significance of soluble adhesion molecules in Hodgkin's disease, *Anticancer Res* 24:1243–1247, 2004.

Tarle M, Ahel MZ, Kovacic K: Acquired neuroendocrine-positivity during maximal androgen blockade in prostate cancer patients, *Anticancer Res* 22:2525–2529, 2002.

Thierry AR, Mouliere F, El Messaoudi S, et al.: Clinical validation of the detection of KRAS and BRAF mutations from circulating tumor DNA, *Nat Med* 20:430–435, 2014.

Thompson IM, Ankerst DP, Chi C, et al.: Operating characteristics of prostate-specific antigen in men with an initial PSA level of 3.0 ng/mL or lower, *J Am Med Assoc* 294:66–70, 2005.

Thompson IM, Pauler DK, Goodman PJ, et al.: Prevalence of prostate cancer among men with a prostate-specific antigen level < or = 4.0 ng per milliliter, *N Engl J Med* 350:2239–2246, 2004.

Thurm H, Ebel S, Kentenich C, et al.: Rare expression of epithelial cell adhesion molecule on residual micrometastatic breast cancer cells after adjuvant chemotherapy, *Clin Cancer Res* 9:2598–2604, 2003.

Tondini C, Hayes DF, Gelman R, et al.: Comparison of CA15-3 and carcinoembryonic antigen in monitoring the clinical course of patients with metastatic breast cancer, *Cancer Res* 48:4107–4112, 1988.

Tonus C, Sellinger M, Koss K, et al.: Faecal pyruvate kinase isoenzyme type M2 for colorectal cancer screening: a meta-analysis, *World J Gastroenterol* 18:4004–4011, 2012.

Truong M, Yang B, Jarrad DF: Toward the detection of prostate cancer in urine: a critical analysis, *J Urol* 189:422–429, 2013.

Tsigris C, Karayiannakis AJ, Syrigos KN, et al.: Clinical significance of soluble c-erbB-2 levels in the serum and urine of patients with gastric cancer, *Anticancer Res* 22:3061–3065, 2002a.

Tsigris C, Karayiannakis AJ, Zbar A, et al.: Clinical significance of serum and urinary c-erbB-2 levels in colorectal cancer, *Cancer Lett* 184:215–222, 2002b.

Uhr JW: Cancer diagnostics: one-stop shop, *Nature* 450:1168–1169, 2007.

Ulivi P, Silvestrini R: Role of quantitative and qualitative characteristics of free circulating DNA in the management of patients with non–small cell lung cancer, *Cell Oncol* 36:439–448, 2013.

Utting M, Werner W, Dahse R, et al.: Microsatellite analysis of free tumor DNA in urine, serum, and plasma of patients: a minimally invasive method for the detection of bladder cancer, *Clin Cancer Res* 8:35, 2002.

Vaissière T, Cuenin C, Paliwal A, et al.: Quantitative analysis of DNA methylation after whole bisulfitome amplification of a minute amount of DNA from body fluids, *Epigenetics* 4:221–230, 2009.

van Ginkel JH, Huibers MMH, van Es RJJ, de Bree R, Willems SM: Droplet digital PCR for detection and quantification of circulating tumor DNA in plasma of head and neck cancer patients, *BMC Canc* 17(1):428, 2017, Published 2017 Jun 19, https://doi.org/10.1186/s12885-017-3424-0.

Vessella RL, Lange PH: Issues in the assessment of prostate-specific antigen immunoassays: an update, *Urol Clin North Am* 24:261–268, 1997.

Vlaeminck-Guillem V, Ruffion A, André J, et al.: Urinary prostate cancer 3 test: toward the age of reason? *Urology* 75:447–453, 2010.

Von Eyben FE: Laboratory markers and germ cell tumors, *Crit Rev Clin Lab Sci* 40:377–427, 2003.

Wang H, Tso V, Wong C, et al.: Development and validation of a highly sensitive urine-based test to identify patients with colonic adenomatous polyps, *Clin Transl Gastroenterol* 5(3), 2014. e54.

Whitman EJ, Groskopf J, Ali A, et al.: PCA3 score before radical prostatectomy predicts extracapsular extension and tumor volume, *J Urol* 180:1975–1978, 2008.

Wilmanns C, Grossmann J, Steinhauer S, et al.: Soluble serum E-cadherin as a marker of tumour progression in colorectal cancer patients, *Clin Exp Metastasis* 21:75–78, 2004.

Winter JM, Yeo CJ, Brody JR: Diagnostic, prognostic, and predictive biomarkers in pancreatic cancer, *J Surg Oncol* 107(1):15–22, 2013.

Woodrum D, French C, Shamel LB: Stability of free prostate-specific antigen in serum samples under a variety of sample collection and sample storage conditions, *Urology* 48(Suppl):33–39, 1996.

Woodson K, Hanson J, Tangrea J: A survey of gene-specific methylation in human prostate cancer among black and white men, *Cancer Lett* 205:181–188, 2004.

Woodson K, O'Reilly KJ, Hanson JC, et al.: The usefulness of the detection of GSTP1 methylation in urine as a biomarker in the diagnosis of prostate cancer, *J Urol* 179:508–511, 2008.

Wooster R, Neuhausen SL, Mangion J, et al.: Localization of a breast cancer susceptibility gene, BRCA2, to chromosome 13q12–13, *Science* 265:2088–2090, 1994.

Wu JT, Carlisle P: Low frequency and low level of elevation of serum CA 72-4 in human carcinomas in comparison with established tumor markers, *J Clin Lab Anal* 6:59–64, 1992.

Wu JT, Clayton F, Myers S, et al.: A simple radial immunodiffusion method for assay of β2-microglobulin in serum, *Clin Chem* 32:2070–2073, 1986.

Wu JT, Erickson AJ, Tsao KC, et al.: Elevated serum chromogranin A is detectable in patients with carcinomas at advanced disease stages, *Ann Clin Lab Sci* 30:175–178, 2000.

Wu JT, Liu GH: Advantages of replacing the total PSA assay with the assay for PSA-alpha 1-antichymotrypsin complex for the screening and management of prostate cancer, *J Clin Lab Anal* 12:32–40, 1998.

Wu JT: Assay for prostate specific antigen (PSA): problems and possible solutions, *J Clin Lab Anal* 8:51–62, 1994.

Wu JT: Expression of monoclonal antibody-defined tumor markers in four carcinomas, *Ann Clin Lab Sci* 19:17–26, 1989.

Wu JT: Serum alpha-fetoprotein and its lectin reactivity in liver diseases: a review, *Ann Clin Lab Sci* 20:98–105, 1990.

Xiao WB, Liu YL: Elevation of serum and ascites cancer antigen 125 levels in patients with liver cirrhosis, *J Gastroenterol Hepatol* 18:1315–1316, 2003.

Yamamoto H, Lambert-Messerlian GM, Silver HM, et al.: Maternal serum levels of type I and type III procollagen peptides in preeclamptic pregnancy, *J Matern Fetal Med* 10:40–43, 2001.

Yang M, Shen H, Qiu C, et al.: High expression of miR-21 and miR-155 predicts recurrence and unfavourable survival in non–small cell lung cancer, *Eur J Cancer* 49:604–615, 2013.

Yegnasubramanian S, Kowalski J, Gonzalgo ML, et al.: Hypermethylation of CpG islands in primary and metastatic human prostate cancer, *Cancer Res* 64:1975–1986, 2004.

Yoh K, Seto T, Satouchi M, et al.: Vandetanib in patients with previously treated RET-rearranged advanced non-small cell lung cancer (LURET): an open-label, multicenter phase 2 trial, *Lancet Respir Med* 5:42–50, 2017.

Yu J, Gu G, Ju S: Recent advances in clinical applications of circulating cell-free DNA integrity, *Lab Med* 45:6–12, 2014.

Yu YH, Schlossman DM, Harrison CL, et al.: Coexpression of different antigenic markers on moieties that bear CA 125 determinants, *Cancer Res* 51:468–475, 1991.

Zhang L, Riethdorf S, Wu G, et al.: Meta-analysis of the prognostic value of circulating tumor cells in breast cancer, *Clin Cancer Res* 18:5701–5710, 2012.

Zidan J, Husseiwwwn O, Basher W, et al.: Serum CA125: a tumor marker for monitoring response to treatment and follow-up in patients with non-Hodgkin's lymphoma, *Oncol* 9:417–421, 2004.

CHAPTER 77

ONCOPROTEINS AND EARLY TUMOR DETECTION

Matthew R. Pincus, Martin H. Bluth, Paul W. Brandt-Rauf, Wilbur B. Bowne, Charles LaDoulis

OVERVIEW, 1525
Cell Biology and Mitogenesis, 1525
Signal Transduction Pathways, 1525
Other Signal Transduction Pathways, 1526
ONCOPROTEINS IN TUMOR DETECTION, 1527
Growth Factors, 1528
Growth Factor Receptors, 1530
G-Proteins, 1532
Cytosolic Mitogenic Kinases, 1533
Nuclear Oncoproteins, 1533
USE OF MULTIPLE PROTEIN MARKERS IN THE DIAGNOSIS OF CANCER: PROTEOMICS, 1536
Protein Arrays Hold Promise In Detecting Both New Biomarker Proteins and Protein Expression Patterns and Antiprotein Antibodies and Their Patterns of Expression in Sera, 1536
Alternate Proteomic Approaches to Detection of Cancer in Serum and Other Body Fluids, 1538
Diagnostic Efficacy of Serum Oncoproteins, 1539
Origins of Malignancies, 1539
Tumor Size and Oncoprotein Levels, 1541
EVALUATION AND CONCLUSIONS, 1541
SELECTED REFERENCES, 1541

KEY POINTS

- As a result of the vast progress that has been made very recently in sequencing the entire human genome and in illuminating pathways that are involved in tumorigenesis, it has become clear that the malfunctioning of mutant proteins is the central cause of human cancers.
- These proteins—growth factors, growth factor receptors, G-proteins such as ras-p21, the mitogen-activated protein kinases, and nuclear proteins such as Myc, Fos, Jun, and p53—are critical in signal transduction pathways in which proliferation signals from growth factors at the cell membrane are transduced to the nucleus and stimulate cell division.
- The mutations in these proteins result in amino acid substitutions or deletions that cause them to be permanently activated. Mutations in regulatory domains of the genes encoding these proteins can result in protein overexpression, which can also result in continuous mitogenic signaling.
- These proteins and antibodies to them can be used to detect the presence of cancers in patients at early stages—and even to predict their future occurrence.
- Although mutated signal transduction proteins are involved in many different human cancers, it appears that there are patterns of expression of mutated proteins that typify specific cancers.

OVERVIEW

As a result of the vast progress that has been made recently in sequencing the entire human genome and in illuminating pathways that are involved in tumorigenesis, it has become clear that the malfunctioning of mutant proteins is the central cause of human cancers. This has given rise to a whole new field of proteomics—that is, detection of these aberrant proteins in the blood and other body fluids of patients. This chapter explains these new approaches and emphasizes that many of these aberrant proteins are actually involved in the transmission of proliferation signals on signal transduction pathways, prominent examples of which are discussed. This chapter explains signal transduction pathways in cell proliferation; illustrates how different mutant proteins on these pathways can cause abnormal, continuous proliferation signaling, leading to cell transformation; demonstrates how these proteins and antibodies to them can be used to detect the presence—and even to predict the future occurrence—of cancers in patients; and shows how new proteins that are strongly associated with different types of cancers have been discovered and can be used to detect these cancers at early stages.

CELL BIOLOGY AND MITOGENESIS

Control of the process of cell division in eukaryotic cells, especially in the higher forms of life, is vital to the processes of cell proliferation and differentiation. The fine balance between these two processes is regulated by numerous proteins that interact in the cell to ensure that this balance is maintained. Virtually all these proteins, many of which are critical in regulating the cell cycle, are encoded by oncogenes. Mutations in oncogenes can result in the production of proteins that become either permanently activated in stimulating cell growth and proliferation (e.g., the ras gene–encoded p21 protein). There can also be silencing or attenuation of genes and their products that inhibit cell proliferation (e.g., the p53 protein), otherwise known as tumor suppressor genes. Both events give rise to malignant tumor cells.

Knowledge not only of the existence of these oncogenes and their encoded oncoproteins but also of the mechanisms by which they exert their effects has resulted in a new series of highly sensitive assays for both mutated oncogenes and their encoded mutant proteins. Assays using amplification methods such as real-time polymerase chain reaction (RT-PCR) for mutated oncogenes are discussed extensively in Part 8 and are further discussed in this chapter. However, the main focus of this chapter is how the detection of oncogenic *proteins*, or *oncoproteins*, that occur in the serum of patients with malignant tumors enables the diagnosis of malignancy to be made, often at an early stage of tumor development. Because the finding of elevated levels of any of these oncoproteins or mutated forms of these proteins in human serum indicates the likely presence of a malignant tumor, these proteins are also referred to in this chapter as *tumor markers*. Additionally, in view of the enormous strides that have been made in PCR and other molecular technology, allowing the detection of very few copies of aberrant DNA, we also discuss in this chapter recently developed new detection methods for oncogenic DNA present in the sera and other body fluids of patients with cancer, further allowing early tumor detection.

Oncogenesis, the process by which normal cells become malignant, involves multiple steps that can be broadly classified into tumor initiation and tumor promotion. Mitogenesis itself is a multistep process that commences at the cell membrane as a result of the activation of a growth factor receptor, which then activates other membrane and cytosolic proteins and second-messenger molecules that transduce the mitogenic "signal" to the nucleus. The pathway in which this orderly progression of activation of successive proteins, mostly kinases, occurs from the cell membrane to the nucleus is referred to as a *signal transduction pathway*.

SIGNAL TRANSDUCTION PATHWAYS

A number of the steps on the signal transduction pathway that are involved in the transduction of the growth factor–initiated signal to the nucleus

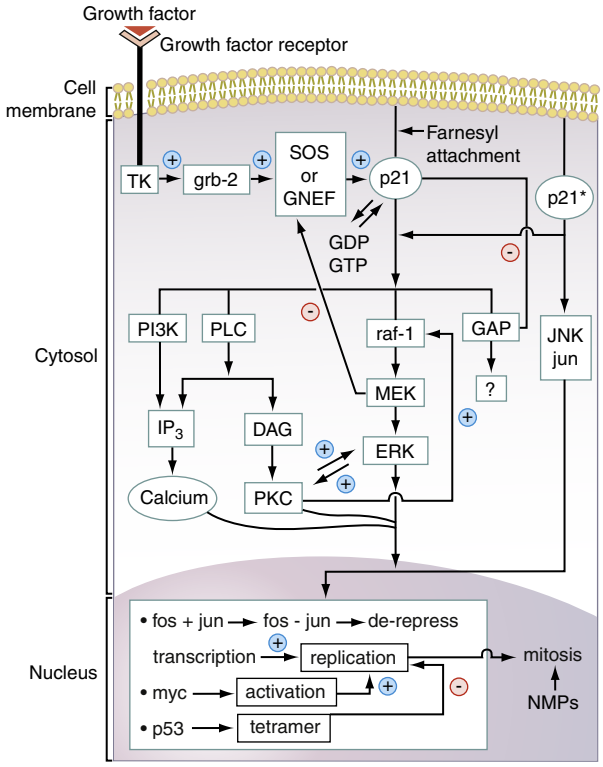

Figure 77.1 Schematic of some of the known components of the ras signal transduction pathway beginning *(top, left)* when a growth factor binds to its cell receptor. Note that binding of the growth factor to the growth factor receptor induces receptor dimerization, which is not explicitly shown in this figure but is shown in Fig. 77.2. The remainder of events is explained in the text. *DAG*, Diacylglycerol; *GAP*, GTPase-activating protein, which promotes hydrolysis of GTP to GDP bound to p21; *grb-2,* the adaptor protein that concurrently binds p21 and the guanine nucleotide exchange protein or factor (*GNEF*), SOS; *PI3K,* phosphoinositol-3-hydroxy kinase, an enzyme that induces synthesis of IP3 and is involved in many aspects of mitogenic signal transduction; *IP3,* inositol triphosphate; *MAP-2 kinase,* mitogen-activated protein kinase or microtubule-associated protein kinase-2 (ERK in the figure, also called MAP-2K); *myc, fos,* and *jun*, nuclear oncogenes that code for nuclear proteins; *NMP,* nuclear matrix protein; *PKC,* protein kinase C; *PLC,* phospholipase C; *raf-1,* the oncogene-encoded p74 protein, which functions as a kinase that phosphorylates another kinase of molecular mass 43 kDa, called MAP-2 kinase, MEK (as in the figure, or MAP-KK; ras-p21 protein, ras-p21, defined in the text); *TK,* tyrosine kinase.

have become elucidated, but many of the steps that are involved are still not fully understood. One well-established pathway, for the ras oncogene–induced mitogenic signaling pathway, is summarized in Figure 77.1. This figure shows that when a growth factor, such as epidermal growth factor (EGF), HER2/*neu*, or insulin, binds to its receptor on the cell surface, it induces receptor activation. Most commonly, receptor activation is a result of receptor dimerization as illustrated in Figure 77.2. The activated receptor in turn activates several intermediary proteins (Grb-2 and SOS, in Fig. 77.1) that activate the all-important G-protein (i.e., guanosine triphosphate [GTP]–binding protein), ras-p21. This membrane-bound 21-kDa protein, containing 189 amino acids, is activated when the SOS protein induces it to bind GTP in place of guanosine diphosphate (GDP). In its activated (GTP-bound) state, ras-p21 directly activates Raf (Moodie et al., 1993; Stokoe et al., 1994), which in turn induces a sequential protein kinase cascade beginning with the kinase MEK (formerly called MAP kinase kinase) and mitogen-activated protein (MAP) kinase encoded by the *ERK* gene, as shown in Figure 77.1.

MAP kinase directly activates nuclear transcription factors, one of these being Fos. This important protein forms a heterodimeric complex with another nuclear transcription factor, Jun, which is directly activated by Jun kinase (JNK). The Fos–Jun complex, also called AP1, binds to specific regions of genomic DNA, inducing the transcription of mitogenic proteins such as the cyclins. Transcription of these proteins is blocked by the antioncogene p53 protein (see Fig. 77.1), which further induces the transcription of antimitotic proteins such as Bax and caspases that are critical to the process of apoptosis in which the cell dies in a programmed manner.

Figure 77.1 shows that there are several other important nuclear oncogene–encoded proteins such as Myc, a 75-kDa protein that is overexpressed in Burkitt lymphoma. This oncogene protein is not directly on the ras signal transduction pathway. Interestingly, there are cell lines that when transfected with either the ras oncogene or with the myc oncogene do not undergo cell transformation but when transfected with both oncogenes simultaneously do undergo cell transformation. These results indicate that ras and myc may be interdependent and are an excellent prototypical example of the multistage nature of oncogenesis.

Figure 77.1 also illustrates that in normal mitogenic signal transduction, antiproliferative proteins, also called antioncogene proteins—that is, products of tumor suppressor genes, such as p53—become activated and downregulate mitogenic events. If these proteins become mutated at critical positions in their polypeptide chains, they become inactivated, allowing mitogenic events to occur with less inhibition and regulation. Numerous other antioncogene proteins occur, including p16, mutations that have been implicated as a major causative factor of bladder cancer; Rb (retinoblastoma antioncogene protein); and APC (adenomatosis polyposis coli) protein, mutations of which have been implicated in causing familial adenomatous polyposis and colon cancer.

A central feature of the signal transduction events summarized in Figure 77.1 is that the activation cascades are ordered and are under tight regulatory control. Thus, for example, whereas SOS activates ras-p21, GTPase-activating protein induces hydrolysis of GTP bound to Ras-p21, causing its inactivation (see Fig. 77.1). Activated MEK downregulates SOS, diminishing GDP–GTP exchange by Ras-p21 (Holt et al., 1996).

If one or more proteins on pathways such as the one shown in Figure 77.1 become mutated so they cannot be downregulated, continuous mitogenic signaling becomes possible, leading ultimately to neoplasia. The more such mutations occur, the more likely it is that the cell will undergo malignant transformation. Thus, progressive lesions in a mitogenic pathway or in more than one mitogenic pathway may correspond to the multiple steps in carcinogenesis. This model has been employed in the explanation for the pathogenesis of colorectal cancer (Vogelstein et al., 1988) and pancreatic cancer (Hruben et al., 2001).

These considerations have critically important practical consequences for both the diagnosis and treatment of patients with cancer. In colon cancer, overexpression of the epidermal growth factor receptor (EGFr) can occur, resulting in continuous mitogenic signaling. In addition, as a second occurrence, the ras gene encoding the ras-p21 protein can become mutated, resulting in expression of oncogenic ras-p21 and also resulting in continuous mitogenic signaling. Note in Figure 77.1 that ras occurs downstream of the growth factor receptor (EGFr in this case). If elevated levels of EGFr are found in the serum or tissue of a patient with colorectal cancer, an effective therapy is to treat the patient with anti-EGFr agents such as monoclonal antibodies (e.g., cetuximab and panitumumab). Unfortunately, treatment with EGFr inhibitors has no effect on oncogenic ras-p21 signaling. Therefore, it is necessary, prior to treatment, to ascertain whether oncogenic ras-p21 is present (Normanno et al., 2009). If it is not present, EGFr inhibitor administration is effective. If oncogenic ras-p21 is present, however, this treatment cannot be employed.

Table 77.1 summarizes the mechanisms by which each type of signal transduction element has been found to induce cell transformation, beginning with growth factors, progressing to growth factor receptors, then to G proteins and the kinase cascades, and finally to nuclear proteins. These mechanisms are discussed in more detail in each section of this chapter devoted to these different signal transduction proteins.

A number of these pathways seem to be activated in specific types of neoplasia. The ras-pathway itself has been found to be activated in so-called solid tissue (epithelial cell) tumors such as pancreatic cancers (>90%) and colon cancers (~70%).

OTHER SIGNAL TRANSDUCTION PATHWAYS

As discussed in Chapters 78 and 79, a number of other signal transduction pathways leading to mitogenesis have been discovered. Several of these interact with the ras pathway described above. Two prominent examples of these are the Akt-mTOR (target of rapamycin) pathway and the JAK-STAT (Janus kinase–signal transducer and activator of transcription) pathway.

The Akt-mTOR Pathway

Note that in Figure 77.1, activated ras-p21associates with several "downstream" proteins, one of which is phosphoinositol-3-hydroxykinase (PI3K). This enzyme catalyzes the synthesis of inositol triphosphate (IP3) that is a critical second messenger molecule that is vital in mobilization calcium ions that are required for kinase activation. In addition, PI3K itself activates a vital kinase called Akt or protein kinase B, which in turn activates mTOR, a critical kinase. This protein is discussed in Chapter 24 as being vital in promoting activation of cyclin kinases that activate cyclins that in turn induce progression of T cells (and other cell types) from G1 to S

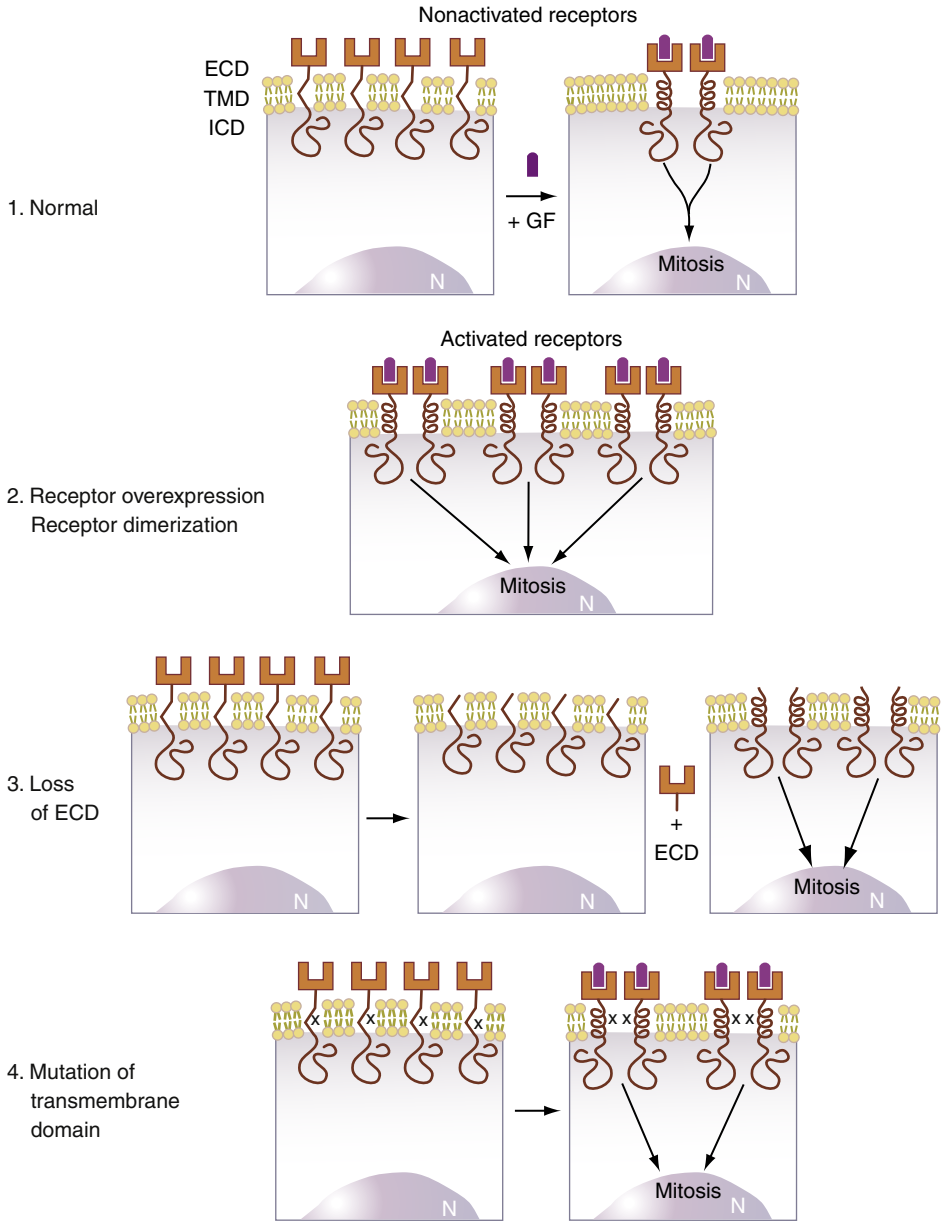

Figure 77.2 Mechanisms for continuous mitogenic signaling by growth factor receptors. *Scheme 1* shows that these receptors have three domains: an extracellular, growth factor-binding domain (ECD); a transmembrane domain (TMD); and an intracytoplasmic domain (ICD). A growth factor (GF) binds to the receptor, causing it to dimerize, setting in motion a cascade of intracellular events that are transduced to the nucleus (N) described in Fig. 77.1. There are three known ways in which continuous cell signaling by the growth factor receptor can occur, resulting in malignant transformation of cells. *Scheme 2* depicts the first of these: overexpression of the receptor that results in many activation processes and continuous signaling to the nucleus. *Scheme 3* shows the second mechanism wherein the ECD is either absent or cleaved off by intracellular proteases, leading to spontaneous dimerization. *Scheme 4* shows the third mechanism, in which a mutation in the growth factor receptor gene results in an amino acid substitution (X in the figure) in the transmembrane domain, leading to formation of α helices that associate (Brandt-Rauf et al., 1990), resulting in spontaneous dimerization that can occur in the absence or presence of the ligand.

phase in the cell cycle in blast transformation. Constitutive activation of Akt can therefore lead to uncontrolled cell proliferation and cancer. In the PI3K-Akt cascade, another protein becomes activated called phosphatase and tensin homologue protein (PTEN). This protein catalyzes the dephosphorylation of IP3 to inactivate this second messenger and inactivates phosphorylated Akt. Thus PTEN, like p53, is an anti-oncogene protein.

The JAK-STAT Pathway

Certain growth factors, cytokines being prominent among them, interact with transmembrane receptors to induce receptor dimerization. In the dimerized state, each receptor binds to one kinase protein called Janus kinase or JAK that, in turn, induces phosphorylation of each receptor. After being phosphorylated, each receptor binds to kinases called signal transducer and activator of transcription proteins (STATs). JAK then phosphorylates each STAT such that each STAT molecule is doubly phosphorylated; in the doubly phosphorylated states, the two STAT molecules dimerize, dissociate from JAK, and enter the nucleus, where they act as transcription activators. Receptors that have been phosphorylated by JAK also bind to PI3K, which in turn activates Akt, which activates mTOR and activation of cyclins as discussed in the preceding paragraph.

ONCOPROTEINS IN TUMOR DETECTION

Detection of mutated signal transduction proteins or high levels of the wild-type proteins in serum or body fluids is strongly suggestive of neoplasia. Therefore, many assays for different oncoproteins are now available commercially in kit form, including enzyme-linked immunosorbent assay (ELISA) assays for the growth factors, transforming growth factors (TGF)-α and -β and fibroblast growth factor (FGF); the growth factor receptor proteins EGFr and HER2/*neu*, Ras-p21; and the nuclear proteins p53, Myc, and NMP22 from such companies as Abcam, Lifespan Biosciences, and Fischer Thermo Scientific. A number of studies also employ the technique of western blotting or immunoblotting, as described elsewhere in this book.

Numerous studies have documented alterations in oncogene, oncoprotein, or growth factor expression in terms of messenger RNA (mRNA) or protein in tumor tissue compared with normal tissue (Pimentel, 1989; Brandt-Rauf & Pincus, 1998; Pincus & Friedman, 2003). Several studies have examined oncoprotein or growth factor expression in biologic fluids such as urine or effusions and demonstrated the feasibility of using these peptides and proteins as markers for the presence of neoplasia (Niman et al., 1985; Yeh & Yeh, 1989). Succeeding studies have confirmed these initial findings, resulting in the clinical use of these markers to detect the presence of neoplasia.

Recent studies have now revealed that oncogenes themselves can be detected in the body fluids of patients with different types of cancer. With the advent of microarray techniques for both gene expression and protein detection (see Chapter 70), it is now possible to assay for the presence of multiple oncogenes and oncoproteins in the body fluids, especially serum, of patients with cancer. A new, parallel approach for cancer screening has been developed, called *proteomics*, in which serum samples are subjected to mass spectroscopy and pattern analysis to detect the patterns of expression of proteins that are unique to the blood of patients with cancer. This type of analysis has recently resulted in the identification of not only oncoproteins

but also other proteins that are expressed at abnormally elevated or abnormally low levels in specific types of cancer. In fact, these techniques are being applied to other body-derived fluids to find similar oncoproteins. For example, research on urine biomarkers for breast cancer remains investigational but promising (Beretov et al., 2014).

This chapter focuses on the identification of different oncoproteins and growth factors, as well as their respective genes, in the serum, plasma, or urine in patients with cancer or who are at risk for the development of cancer. It also focuses on expression of other proteins that occur at abnormally elevated or low levels in specific types of cancer. Table 77.2 summarizes some of the many (>100) known oncogenes and their functions in the cell. ELISA or western blotting kits are commercially available for all of these oncogene-encoded proteins.

GROWTH FACTORS

Because various growth factors are believed to play a role in influencing cellular proliferation during tumorigenesis and because growth factors are actively secreted into the extracellular environment, they are attractive targets for detection in blood during cancer development. Several studies have demonstrated differences in blood levels of growth factors in patients with cancer and noncancer control participants.

TABLE 77.1
Mechanisms for Induction of Carcinogenesis by Mitogenic Pathway Elements

Pathway Element	Mechanism of Action
1. Growth factors	a. Overproduction by cell into surroundings b. Interaction of growth factors with high-affinity receptors
2. Growth factor receptors	a. Overexpression leading to high concentration of dimers b. Loss of extracellular domain, resulting in permanent dimerization of growth factor receptor and continuous signaling c. Amino acid substitutions in transmembrane domain, leading to permanent dimerization
3. Cytosolic proteins	a. Overexpression of normal G-proteins and protein kinases b. Amino acid substitutions that permanently change conformation to activated form c. Mutations that remove regulatory domains of kinases
4. Nuclear oncoproteins	a. Overexpression of transcription and replication proteins b. Mutations in antioncogene proteins that inactivate them c. Mutations that remove regulatory domains

Transforming Growth Factors α and β

TGF-α is a polypeptide with 50 amino acids that binds to the EGF receptor, which dimerizes upon binding to TGF-α or to EGF. TGF-β is a family of proteins labeled β_1 to β_5. TGF-β_1 is a homodimer of two 12-kDa subunits linked together by disulfide bonds. When bound to its receptor, it induces activation of Smads (small body size gene in *Caenorhabditis elegans* worms) that are involved in DNA binding and transcriptional activation. Even though TGF-β has been found to be elaborated by many different types of human malignant tumors, elevated serum levels of this growth factor have been found predominantly in cancers of the liver (Jeng et al., 2014) and bladder (see later). Interestingly, TGF-β has been found to inhibit mitosis in specific cell lines in culture, such as mink bronchial epithelial cells. It is not clear how TGF-β is triggered to act as a tumor suppressor versus tumor promotor. The pathway for tumor promotion has been somewhat elucidated. TGF-β binds to the inhibitor of DNA binding 1 (ID1), a transcriptional regulator resulting in decreased levels of E-cadherin (Pickup et al., 2013), thereby diminishing the number of tight junctions between cells and causing loss of contact inhibition. This growth factor also has been implicated in the interconversions of epithelial cells into mesenchymal cells and vice versa. These interconversions (called epithelial-to-mesenchymal transformation (EMT) and mesenchymal-to-epithelial transition [MET], the reverse process) are thought to be steps involved in tumorigenesis (Polyak & Weinberg, 2009).

TGF-β activity, which is determined using this technique, has been found to be markedly elevated in patients with hepatocellular carcinoma (HCC) but not in age-matched control participants (Shirai et al., 1992). More recently, TGF-β has been found to promote the formation of a tumor microenvironment together with other growth factors, such as platelet-derived growth factor (PDGF), vascular endothelial growth factor (VEGF) and FGF, in hepatocellular carcinogenesis (Salajegheh, 2016).

In the sera of patients who have undergone surgical resection of these tumors, the activity of TGF-β is barely detectable, suggesting that the tumor was the source of the elevated levels of growth factor in serum. Interestingly, in many patients with HCC, TGF-β has been found to be elevated in urine (Tsai et al., 1997). In this regard, in a study on the development of HCC in patients with hepatitis C (see Chapter 22), TGF-β_1 was found to be elevated in the sera of patients with hepatitis C and hepatitis C–induced fibrosis and cirrhosis but was not elevated in the sera of patients in whom HCC subsequently developed, resulting from the antecedent disease. Thus TGF-β_1 may be an early marker for HCC, but lower levels may be required for progression of disease (Ali et al., 2004). However, in

TABLE 77.2
Summary of Some Important Oncogenes and Their Protein Products[a]

Oncogene	Protein Product[b]	Function
1. erbB	EGF receptor	Binds to EGF; dimerizes; activates tyrosine kinases in signal transduction; works through ras
2. erbB-2	GF receptor	Very similar to EGF receptor; works through ras
3. sis	β-chain of PDGF	Growth factor receptor; may work through ras
4. src	Tyrosine kinase	Transduces signal through ras
5. ras	p21 proteins; H-, K-, and N-forms	G-proteins; bind to cell membrane and transduce signals through second messengers and Raf, GAP (?), JNK, PKC, and PLC
6. rap-1A	Anti-ras oncogene; in ras family	Blocks ras action in cells.
7. raf	74-kDa protein	Phosphorylates MEK, which then phosphorylates MAPK
8. erk-1 and erk-2	MAPK family 43-kDa proteins	Involved in cytoskeletal rearrangements and nuclear signaling
9. myc	62/64-kDa nuclear protein	Turns on transcription factors involved in replication
10. jun	Nuclear protein	Forms complex with fos
11. fos	Nuclear protein	Forms complex with jun; fos–jun complex activates transcription factors
12. p53	53-kDa nuclear antioncogene protein	Forms tetramers, then binds DNA segments to block transcription and replication
13. NMP22	236-kDa nuclear matrix protein	Involved in mitotic spindle formation

[a]Only a few of the many (>100) oncogenes are listed in this table. The ones that are listed here encode proteins for which assays have been developed or are closely related to these proteins. No growth factors except *platelet-derived growth factor (*PDGF) are included in this table.
[b]Assay kits for all of the oncogene-encoded proteins listed in this are commercially available.
EGF, Epidermal growth factor; *GAP,* GTPase-activating protein; *GF,* growth factor; *MAPK,* mitogen-activated protein kinase; *MEK,* mitogen-activated protein kinase; *NMP22,* nuclear matrix protein 22; *PKC,* protein kinase C; *PLC,* phospholipase C. The names of the oncogenes are commonly used and relate to the sources from which they were originally discovered. For example, *ras* is an abbreviation for rat sarcoma viral oncogene.

other studies, TGF-β_1 was found to be elevated in small (<3 cm) HCC far more frequently than α-fetoprotein (AFP), the classic marker for HCC (see Chapter 75; Song et al., 2002). Using a cutoff of 800 pg/mL for TGF-β_1 and 200 pg/mL for AFP, in which the specificities of both markers were 95% (i.e., few false-positive results), the sensitivity of TGF-β_1 was 68% versus only 24% for AFP. Thus TGF-β_1 may be a reliable marker for small HCC. The same conclusion has been reached in a study of HCC in which the sera of 23% of patients with this disease were positive for TGF-β_1 but not for AFP (Sacco et al., 2000). TGF-β_1 has also been found to be elevated in patients with metastatic prostate cancer (Adler et al., 1999). Levels of TGF-β have also been associated with extraprostatic extension of the tumor. Serum levels TGF-β together with levels of interleukin-6 (IL-6) soluble receptor can be used to predict progression of the disease after surgery (Kattan et al., 2003).

Use of an ELISA with a monoclonal antibody directed against TGF-β_2 has revealed that TGF-β_2 is elevated in a high proportion of patients with invasive bladder cancer but not in patients with noninvasive bladder cancers or in cancer-free patients (Klocker et al., 1994; Brandt-Rauf & Pincus, 1998; Pincus & Friedman, 2003). Recently, a new tumor marker for bladder cancer that appears to be more accurate in diagnosing both noninvasive and invasive bladder cancer is the nuclear matrix protein NMP22, detected in urine described later in this chapter.

Thus, serum assays for TGF-β are highly useful in diagnosing and following HCC. They are less useful in the diagnosis of carcinoma of the bladder, although for invasive bladder cancer, this growth factor has high sensitivity and specificity.

TGF-α has been found to be elevated in a large number of patients with epithelial cell tumors (Katoh et al., 1990; Chakrabarty et al., 1994), predominantly breast (almost 100%), lung, stomach (Moskal et al., 1995), colon, liver, and ovarian. It has been found to be elevated frequently in the sera of patients with gastric carcinoma (Choi et al., 1999). In contrast, normal individuals have very low serum levels. With respect to liver, TGF-α has been found to be elevated in the sera of patients with HCC but not in patients with cirrhosis. The elevated levels were reduced in patients who had been treated for HCC (Tomiya & Fujiwara, 1996).

Recent studies confirm that TGF-α is an effective predictor of the occurrence of malignancies at an early stage. For example, in 36 patients who had a history of asbestosis and subsequently developed a cancer, mainly adenocarcinoma or squamous cell carcinoma of the lung, more than one third were found to be seropositive for TGF-α. Blood samples from all of these patients were collected and then banked at the time of the diagnosis of asbestosis and before the diagnosis of malignancy. Significantly, all but one of these seropositive patients were found to have elevated TGF-α levels in their banked blood (Brandt-Rauf & Pincus, 1998).

TGF-α thus appears to be an excellent marker for the presence of malignancy. Unlike the case for TGF-β, these elevations are not tumor specific. Nonetheless, it is clear that TGF-α is extremely useful in screening patients for the presence of malignant solid tissue tumors.

Platelet-Derived Growth Factor

PDGF, a protein of molecular mass 28 kDa, exists as a dimer of A and B chains, as the A–A, A–B, or B–B dimer forms. Either chain can be glycosylated, increasing the molecular mass to 30 kDa. This growth factor, originally isolated from platelets, binds to a transmembrane growth factor receptor. The B chain is encoded by the sis oncogene. It has been found to be a potent mitogen in lymphoid, myeloid, and fibroblastic cell lines. Overexpression of PDGF has been found in both lung and pleural tumors. It has also been examined in the blood of patients with cancer. Overall, this growth factor has been found to be significantly elevated in more than 15% of patients with carcinomas, sarcomas, and lymphomas but not at all in normal individuals. In patients with breast cancer, there is an excellent correlation between the stage of the cancer and the serum level of the growth factor (Ariad et al., 1991). Higher levels predict shorter survivals. In addition, PDGF-B (Sis) in breast tissue appears to correlate with increased cellular proliferation because its expression increases with both nonmalignant and malignant states and decreases after menopause. Elevated serum levels of PDGF-B have also been found to occur in esophageal carcinoma that has infiltrated into lymph nodes (Krzystek-Korpacka et al., 2011). In malignancy, PDGF-B does not correlate with p53 expression, estrogen and progesterone status, or tumor grade (Coltrera et al., 1995). Levels of PDGF-A and PDGF-B were found to be elevated highest in patients with ovarian cancer compared with normal, benign, and borderline patients (Madsen et al., 2012). The role of PDGF-B as a marker in colorectal cancer is less clear (Lindmark et al., 1993). Serum PDGF-A levels in patients with cholangiocarcinoma were 1.4-fold higher than in normal control participants ($P = .014$) (Boonjaraspinyo et al., 2012).

PDGF-receptor A (PDGFRA) mutations have also been implicated in the pathogenesis of gastrointestinal stromal tumors. Most recent genetic analysis reveals that exon 18 is the commonest site of these mutations, although exon 12 can be involved as well (Ahmad et al., 2015). In addition, overexpression of PDGFRA has been found to occur in more than 20% of patients with triple-negative breast cancer, correlates with severity of disease (i.e., is a marker for disease progression), and correlates with prognosis, with higher levels indicating worse prognoses (Jansson et al., 2018).

As discussed later, both oncoproteins and antibodies to oncoproteins can be elevated in the sera of patients with cancer. Anti-PDGF antibody (PDGF-Ab) in serum has been found to be potentially diagnostic for pleural mesothelioma in patients with histories of exposure to asbestos. The serum levels of PDGF-Ab correlate positively with severity of the disease and show a significant negative correlation with survival—that is, higher levels correlate with shorter survival times (Filiberti et al., 2005).

Basic Fibroblast Growth Factor

Basic fibroblast growth factor (bFGF) is a protein containing 155 amino acids. It is a growth factor for mesenchymal cells but has also been found to have relatively high concentrations in the central nervous system (CNS). Interestingly, bFGF has been found to be present in high concentrations in the sera of patients with epithelial cell tumors. Prominent among these tumors is renal cell carcinoma. More than 50% of patients with this disease have markedly elevated serum levels of bFGF (Fujimoto et al., 1991; Ii et al., 1993), as determined either by ELISA or by enhanced chemiluminescent assays. This growth factor is also elevated in the sera of more than 50% of patients with CNS tumors, 90% of patients with lung cancers (Ii et al., 1993), and more than 60% of patients with lymphomas (Kurobe et al., 1993). It is not elevated, however, in the sera of large populations of normal (control) individuals.

In patients with colorectal cancer with tumors 30 mm or smaller, serum bFGF levels were 7.65 ± 1.11 pg/mL, whereas those with tumors greater than 30 mm had bFGF levels of 8.53 ± 3.22 pg/mL. Although these are small differences, it has been found that serum bFGF levels could be used to predict tumor size in colorectal cancer (Jibiki et al., 2014).

Elevated serum levels of bFGF have been found to be a good prognostic factor in patients with non–small cell carcinomas of the lung (NSCLCs; Brattstrom et al., 1998). More recently, the extent of overexpression of bFGF appears to correlate with prognosis for both small cell carcinoma of the lung and NSCLC, with higher levels indicating worse prognosis (Hu et al., 2016). Thus, TGF-α and TGF-β, PDGF, and bFGF all appear to be elevated in the sera of a significant number of patients with epithelial cell tumors but are not completely tumor specific. TGF-α has some specificity for breast cancer and TGF-β for HCC. bFGF is elevated in a variety of malignancies, including nonepithelial cell tumors, such as CNS tumors and lymphomas. PDGF shows little specificity for tumor type, but high levels in serum indicate the presence of malignancy.

Given the development of protein–antibody and gene arrays, it is possible to assay the sera and other body fluids of cohorts of patients who are at risk for developing cancer because of such factors as occupational exposure for multiple oncogene proteins concurrently. Discovery of the elevation of or the presence of oncogenic mutations in one or more of these proteins in a patient's serum or other body fluid identifies the patient as either having a cancer or developing one in the near future. Recently, serial levels of both TGF-β and PDGF were determined by ELISA (see Chapter 45) on a cohort of workers with long-term exposure to asbestos. PDGF, but not TGF-β, was found to predict both the development of NSCLC and (1) the radiographically determined severity of the disease and (2) the levels of PDGF correlating with severity of cancer and with fibrosis of the lung, which may be a predisposing factor (Li et al., 2009). These studies parallel the results of other studies, such as the study with TGF-α described earlier, in which the sera of patients with occupational or environmental risks have been found to be positive for one or more oncogene proteins prior to appearance of a cancer.

Epidermal Growth Factor

Earlier studies have suggested that EGF is elevated in the sera of some patients with stomach cancer (Pawlikowski et al., 1989) and cancer of the tongue (Bhatavdekar et al., 1993) but unchanged or decreased in other cancers (Nedvidkova et al., 1992). However, recently it has been found that EGF is significantly elevated in bronchial alveolar lavage fluid (BALF) in patients with lung cancer (Sun et al., 2017). Levels of EGF, Ca-125 (serum marker for ovarian cancer; see Chapter 76) and Ca 15-3 (breast cancer mucin; see Chapter 76) were studied in cohorts of patients with lung cancer and a control group with no lung cancer. Only EGF was found to be significantly elevated in the patients with lung cancer. The sensitivity was

found to be 63.6% and the specificity 65.7%, indicating that use of EGF in BALF may be a promising approach to aid in diagnosis of lung cancer.

Hepatocyte Growth Factor

Hepatocyte growth factor (HGF) is a growth factor that is cleaved post-translationally into α and β chains that are connected by a disulfide bond and binds to the c-MET receptor that is present on many different types of cells. Binding of HGF to c-MET results in activation of processes that result in cell proliferation, motility, migration, and invasion (Organ & Tsao, 2011). Elevated serum levels of HGF have been reported in HCC, but this growth factor appears to be unique in that elevated levels also occur in nonmalignant liver diseases (Hioki et al., 1993), diminishing its utility as a tumor marker for this disease. On the other hand, HGF has been found to be an important marker for evaluating prognosis and response to treatment of melanoma (Hügel et al., 2016).

Vascular Endothelial Growth Factor

This growth factor induces growth of endothelial cells and contributes to the growth of blood vessels in tumors. In addition, it has been found to have numerous functions outside of the vascular system including bone formation, hematopoiesis and cell migration of neurons in the central nervous system. This growth factor has been implicated in inducing tumor cell resistance to chemoradiation and is considered an anti-apoptotic factor enabling tumor cell growth. Significantly, VEGF has been found to be present in the bronchoalveolar lavage fluid of patients with NSCLC (Cao et al., 2013). Following up on this finding, a recent Asian study was performed in which sera from 180 patients with NSCLC, 136 patients with benign pulmonary nodules, and 119 healthy control participants were subjected to ELISA assays for VEGF (Lai et al., 2018). Patients with NSCLC had significantly higher serum concentrations of this growth factor than those from patients with benign pulmonary nodules from healthy control participants ($P < .0001$). The areas under the receiver operating characteristic (ROC) curves for VEGF as a diagnostic marker for NSCLC was 0.839 with a sensitivity of 0.75 for NSCLC and a specificity of 0.933 compared with benign pulmonary nodules and a ROC area of 0.824 with a sensitivity of 0.75 and specificity of 0.956 for NSCLC compared with healthy control participants. These values were significantly higher than for other markers for NSCLC such as CA125 (normally used for ovarian cancer; see Chapter 75), CEA (see Chapter 75) and cytokeratin 19 fragments (Cyfra 21-1) used in immunohistochemical (IHC) evaluation of lung tissue. On the other hand, use of the VEGF ELISA assay together with ELISA assays for these other three biomarkers raised the sensitivities to significantly higher values (0.84 and 0.85, respectively), although the specificities were slightly reduced to 0.9 and 0.92. Also of interest, VEGF was found to detect NSCLC at early stages with a significantly higher efficacy than any of the other markers and was found to be elevated before surgical removal of the tumors and was significantly reduced postoperatively, indicating its use for monitoring tumor status. Thus, VEGF appears to be a strong candidate for screening patients with this disease.

GROWTH FACTOR RECEPTORS

Growth factor receptors are often structured such that they contain three major domains: an extracellular domain that binds to the growth factor, a transmembrane domain often containing hydrophobic amino acid sequences that interact with lipid in the membrane lipid bilayer, and an intracytosolic domain that often contains a tyrosine kinase. Normally, growth factors bind to their growth factor receptors, generally inducing the receptors to dimerize. For receptors that contain intracytosolic tyrosine kinases, this dimerization activates these kinases, starting in motion a sequence of protein activations that occur on a signal transduction pathway. Figure 77.1 illustrates this phenomenon on the ras pathway. Activation of the receptor tyrosine kinase (TK in Fig. 77.1) results in phosphorylation of tyrosine residues of the adapter protein grb-2 that then binds both to the receptor tyrosine kinase and to the guanine nucleotide exchange protein, SOS, that in turn binds to ras-p21, causing it to exchange GDP for GTP, resulting in its activation.

At the growth factor receptor level, there are several mechanisms by which uncontrolled mitogenesis may be initiated. These are summarized in Figure 77.2. For both the EGF receptor and the *neu* (HER)–encoded p185 growth factor receptor protein, strongly associated with breast cancer (Brandt-Rauf & Pincus, 1998; Slamon et al., 1989; Pincus & Friedman, 2003), receptor dimerization results in activation of tyrosine kinases involved in the phosphorylation of proteins that initiate the transduction of the mitogenic signal to the nucleus. Three pathologic mechanisms can cause abnormally prolonged receptor dimerization that results in continuous mitogenic signaling. These are loss of the extracellular binding domain (ECD), mutations in the transmembrane domain that promote dimerization (Brandt-Rauf et al., 1990; Pincus & Friedman, 2003), and overexpression of the receptor.

Transmembrane growth factor receptors encoded by the erbB family of oncogenes (i.e., erbB, which encodes the EGF receptor, also called EGFr, and HER2/*neu* [erbB-2]) are particularly attractive targets for detection in blood during cancer development because it has been found that in human cancers induced by these receptors, the mechanism appears to be proteolysis of the extracellular receptor-binding domain (see Fig. 77.2, third illustration). The liberated extracellular domains, termed *ECD*, then enter the circulation and can be readily detected in serum using conventional immunoassay techniques (Brandt-Rauf et al., 1994a, 1994b; Brandt-Rauf & Pincus, 1998; Pincus & Friedman, 2003).

Epidermal Growth Factor Receptor

Overexpression of or oncogenic amino acid substitutions in the amino acid sequence of EGFr and in the closely related HER2/*neu* receptor are the primary causes of a large number of human epithelial cell tumors. These include colon, breast, lung, and ovarian cancers (Baron et al., 2009). This observation has been extended to CNS tumors, in particular, glioblastoma multiforme (Quaranta et al., 2007). As discussed earlier, serum EGFr is not only important for diagnostic purposes but also suggests a therapeutic strategy (Vincent et al., 2012)—that is, administration of EGFr inhibitors, the efficacy of which can be monitored by assaying for serum EGFr.

A particularly important use of serum EGFr is in following patients with known histories of exposure to environmental agents known to cause specific tumors. Elevations of circulating levels of the ECD of this growth factor receptor have been studied in patients with asbestosis (Brandt-Rauf et al., 1992), which is known to predispose to malignancies. It has been found that patients with ECD serum levels of 636 fmol/mL or higher either have an asbestos-associated malignancy (carcinoma of the lung or mesothelioma) or subsequently develop such a malignancy. Large numbers of normal individuals have been found to have much lower serum ECD levels. Thus, EGFr appears to be an excellent marker for asbestos-induced tumors. These results are also of interest because they suggest that the primary effect of asbestos as a carcinogen is to cause mutations in the *EGFr* gene (Brandt-Rauf & Pincus, 1998).

As discussed, many patients with colon cancers are treated with EGFr inhibitors. An important indication of efficacy of treatment is to measure circulating levels of EGFr. It was recently found that baseline levels of serum EGFr were strong predictors of outcome, higher values predicting better responses to treatment with EGFr inhibitors than lower values (Zampino et al., 2008).

Of considerable interest is the recent finding that serum levels of EGFr can detect the presence of prostate cancer (Milanese et al., 2009). Use of EGFr in detection of prostate cancer was motivated by the finding that overexpression of EGFr or critical amino acid substitutions in the amino acid sequence of prostate EGFr are strongly associated with prostate cancer. It was found that, using a cutoff value of 67.9 ng/mL for serum EGFr, the sensitivity and specificity of serum EGFr were 93.3% and 98%, respectively. In this study, it was further found that the best serodiagnostic marker for spread of prostate cancer beyond the prostate (e.g., into the seminal vesicle) was urokinase-type plasminogen activator receptor. These results suggest that both biomarkers may offer a new approach to diagnosis and monitoring of prostate cancer.

HER2/*neu* Receptor

This protein is discussed in Chapter 75 as a marker for breast cancer and a number of other cancers. Here we consider its potential as a marker for different stages of this cancer and for other human epithelial neoplasms. Current American Society of Clinical Oncology (ASCO) guidelines recommend evaluating the HER2/*neu* status of all primary tumors, primarily to guide therapy if trastuzumab is a suitable agent (Harris et al., 2007). Because of the documented strong association between breast cancer and mutations in the HER2/*neu* gene, many studies have examined the p185 erbB2 ECD in the blood of patients with cancer, particularly breast cancer. In prior studies on *neu* oncogene–induced overexpression of the p185 protein (Slamon et al., 1989), it was found that the level of expression of the *neu* oncogene in breast cancer biopsy tissue correlated with the extent of the tumor and was the best prognostic indicator of survival rates, exceeding even the extent of lymph node involvement as a prognostic indicator.

Results on quantitation of p185 ECD in the serum of patients with breast cancer parallel those of the prior genetic results. Between 25% and 50% of patients with stage III or IV breast cancer have been found to have markedly elevated levels of p185 ECD in their sera (40- to 190-fold higher

than in the sera of normal control individuals) (Mori et al., 1990; Carney et al., 1991; Kath et al., 1993). For patients from whom tumor biopsy material is available, there is an excellent correlation between serum ECD levels and tissue level of expression (Breuer et al., 1993, 1994; Ludovini et al., 2008). There is also an excellent correlation between levels of serum ECD and recurrent disease (Brandt-Rauf & Pincus, 1998).

ECD levels in serum have also been found to be an excellent prognostic indicator for breast cancer (Molina et al., 1996). In a study of patients with stage I to III breast cancer, it was found that presurgical serum ECD level was an independent prognosticator of disease-free survival in early breast cancer (Ludovini et al., 2008). This is an important finding because it identifies patients with early breast cancer with complete apparent surgical removal who are at significant risk for recurrence. In a large study, ECD levels were elevated in the sera of 44% of HER2-positive and, perhaps more important, in 15.8% of patients with HER2-negative breast cancer who developed recurrence, suggesting that HER2 status may change with disease progression (Kim et al., 2014).

Because serum levels of p185 ECD correlate with tumor load and stage, detection of incipient breast cancer using serum levels of p185 ECD is less effective for these patients. Overall, the rate of detection of stages I and II breast cancers using serum levels of ECD, based on conventional ELISA techniques, ranges from 10% to 15%. However, use of a sensitive ELISA assay for p185 ECD in patients with breast cancer resulted in discovery of carcinoma in situ in 43% of patients with this disease (Breuer et al., 1993, 1994). This latter result indicates that the use of more sensitive assays for p185 ECD identifies a significant increase in the number of patients with carcinoma in situ (i.e., at an early stage of development).

Treatment for patients with breast cancer that is positive for HER2/neu is with one or more agents that block the HER2/neu receptor or inhibit its tyrosine kinase activity (Duffy et al., 2017). The anti-HER2/neu receptor blockers are two monoclonal antibodies trastuzumab, also known as Herceptin, that blocks growth factor–induced activation of the receptor and pertuzumab that blocks HER2/neu receptor dimerization. The tyrosine kinase inhibitor lapatinib blocks autophosphorylation by ATP of the HER/neu receptor (and of EGFr). Depending on the stage of the tumor, one or more of these agents are used often in combination with more general anti–breast cancer agents such as Taxol. Although serum levels of ECD have not been found to predict responsiveness of HER2/neu–positive tumors to these chemotherapy regimens, newer assay techniques are being investigated that can accomplish this goal (Duffy et al., 2017).

*HER2/*neu *Detects Pulmonary Neoplasms*

p185 ECD is also elevated in a high percentage of patients with pulmonary cancers. HER2 expression has been detected in about a quarter of specimens of NSCLCs (Bellezza et al., 2013). More tellingly, a recent meta-analysis of 40 studies comprising more than 6000 patients revealed that HER2 overexpression was associated with a poor prognosis in patients with lung cancer (Liu et al., 2011). This trend has been observed in another large study of HER2 mutations in patients in the Lung Cancer Mutation Consortium with adenocarcinoma of the lung (Pillai et al., 2017). Of 920 patients in this study, 24 (3%) were found to have *HER2* mutations. Survival times for patients with HER2 mutations were lower than for patients with adenocarcinomas that were negative for mutations in HER2. Treatment with specific anti-HER2 agents as discussed earlier resulted in significantly prolonged median survival times.

Elevated serum levels of EGFr in early tumor detection have been employed to screen patients with known predisposition, such as pneumoconioses, for developing these cancers. In 70% of patients with pneumoconioses, elevated serum p185 ECD levels have been found prior to the onset of frank malignancy. In almost 100% of patients with this predisposing factor who have cancer of the lung, serum p185 ECD is markedly elevated (Brandt-Rauf et al., 1994a). Clearly, this protein is a highly sensitive marker for pulmonary cancers. In contrast, no elevations of p185 ECD have been found in the sera of large numbers of normal individuals (Brandt-Rauf & Pincus, 1998; Pincus & Friedman, 2003).

*HER2/*neu *in the Detection of Hepatocellular Carcinomas and Gastric Cancers*

Hepatocellular Carcinomas. It was noted previously that TGF-β is a good marker for HCC. There are now strong indications that p185 ECD is also a sensitive marker for this disease. Serum p185 ECD has been found to be elevated in almost 100% of East Asian people who have known risk factors for developing this disease (Luo et al., 1993; Yu et al., 1994a, 1994b). However, tissue expression of c-erbB-2 in biopsies derived from patients with HCC and adenoma showed neither overexpression nor amplification by fluorescence in situ hybridization or IHC (Vlasoff et al., 2002). Furthermore, no such elevations have been observed in normal individuals of similar age and race or in those with exposure to risk factors for this disease but who did not subsequently develop cancer.

By looking at a subset of HCC patients, however, HER2/*neu* IHC may be more instructive. It has been observed that HER2/*neu* upregulation in response to hepatitis B infection, specifically the hepatitis B x antigen (HBxAg), is an important mediator of hepatocyte proliferation and ultimately of malignant transformation to HCC. Patients with hepatitis B with liver specimens that stain strongly for HER2/*neu* develop HCC and have poorer survival. HER2/*neu* may be a sentinel of malignant transformation in this subset of patients (Liu et al., 2009).

Further studies indicate that there is amplification of HER2 mRNA in 14/17 HCC samples and in several human HCC cell lines. In these cells, HER2 appeared to induce upregulation of β catenin and inhibition of SMAD3 (Shi et al., 2019). Peculiarly, however, HER2 was found to be downregulated in high-grade HCCs.

Gastroesophageal Tumors. HER2 has been observed to be overexpressed in a significant number (4.4%–53.4%; mean, 17.9%) of gastroesophageal tumors (Abrahao-Machado & Scapulatempo-Neto, 2017). As found with other tumors in other tissues, survival times are lower for patients with HER2 overexpression compared with those found in patients with the same tumors without HER2 overexpression. Treatment of these patients with anti-HER2–directed agents appears to prolong life.

p185erbB-2 Extracellular Binding Domain in Other Tumors

Elevated serum erbB-2 ECD levels have now been found to occur in patients with colorectal, pancreatic, prostatic, hepatic, and ovarian cancers (Wu et al., 1993) at lower frequencies of detection (15%–20%) and were also found to be significantly higher in patients with nasopharyngeal carcinoma (Yazici et al., 2001). Excellent correlations between serum levels and tissue levels have been found in many of these cases. Serum p185erbB-2 ECD levels correlate well with the stage of oral cavity squamous cell carcinoma, as well as the response to therapy (Chen et al., 2004). These levels do not correlate with tumor size, nodal status, or metastases. There is a direct correlation between serum levels of p185 ECD and tumor size for premalignant adenomas of the colon (Brandt-Rauf et al., 1994b). Because colonic neoplasia usually progresses through well-defined steps from adenoma to carcinoma with the malignant potential of adenomas increasing with size, serum erbB-2 ECD levels may be useful in monitoring this progression. Gene amplification and protein overexpression of c-erbB-2 were also found in adenocarcinoma derived from Barrett esophagus (Geddert et al., 2002). In addition, pretreatment serum ECD has been found to be a reliable prognosticator of recurrence of metastatic prostate cancer and significantly more reliable than tissue p185 (Tambo et al., 2009).

E-Cadherin

E-cadherin, a cell-adhesion transmembrane protein, has been found to be responsible for METs and EMTs, activities that stabilize tumors in their local environment. One of the major proteins involved in this interconversion is β-catenin that is transported across the nuclear membrane and stabilizes transcription of mRNA that encodes EMT-promoting factors. However, E-cadherin binds to β-catenin, inhibiting its ability to enter the nucleus. Downregulation of E-cadherin results in decreased binding of β-catenin, allowing increased entry of β-catenin to the nucleus, where it activates EMT. Less certain is the mechanism of METs, likely caused by upregulation of E-cadherin and binding of β-catenin, reducing EMT (Polyak &Weinberg, 2009).Thus E-cadherin is a negative regulator of EMT and cell transformation.

However, E-cadherin is cleaved intracellularly to so-called soluble E-cadherin or sE-cad that is released from cells. This form of E-cadherin has been found to break cell–cell junctions in murine mammary tumor cells, suggesting that sE-cad reduces contact inhibition of cell growth that can lead to uncontrolled proliferation. sE-cad has been detected in the serum of patients with cancer.

Elevated levels of sE-cad have been detected in NSCCL and bladder, colorectal, ovarian, prostate, skin, esophageal, gastric, and hepatocellular cancers (Katayama et al., 1994; Grabowska & Day, 2012). The appearance of these cell adhesion molecules in blood circulation can indicate more than the mere presence of neoplasm and can be seen as a marker of metastases or poor prognosis. Indeed, elevated levels of sE-cad have been shown to be valid prognostic markers for gastric cancer and correlated well with late-stage colorectal cancer (Chan, 2006; Weiss et al., 2011). Most recently, it was found useful as a marker of preoperative chemotherapy response for breast cancer (Hofmann et al., 2013). In this study, levels of sE-cad were significantly reduced in patients with pathological complete response compared to those without pathological complete response, and the decreases

in the sE-cad levels were significantly different between these two groups. This may have great potential in identifying patients with breast cancer. The caveat to using this marker is that it is also found to be elevated in diseases causing inflammatory states, such as diabetes and HIV (Katayama et al., 1994; Grabowska & Day, 2012).

Metalloproteases in Pancreatic Cancer

Matrix metalloproteases (MMPs) constitute a class of many enzymes responsible for cleavage of the ECD of E-cadherin (Grabowska & Day, 2012). Their levels in serum have also been shown to be upregulated in the sera of patients with pancreatic ductal adenocarcinoma (PDAC), specifically MMP-1, -3, -7, -9, -10, and -12, compared with normal control patients' sera. MMP-7 and -12 had specificities and sensitivities greater than 90%. MMP-2, however, was significantly downregulated in the sera of patients with PDAC (Kahlert et al., 2014). Other useful tests are urinary MMP-2 (uMMP-2) and urinary tissue inhibitor of metalloprotease (TIMP-1). These markers were elevated to significantly higher levels in the urine of patients with pancreatic neuroendocrine tumors and PDACs than in the urine of normal control participants (Roy et al., 2014).

G-PROTEINS

ras-p21 Protein

As for growth factor receptors, signaling proteins that occur downstream of the growth factor receptors become oncogenic primarily from overexpression and amino acid substitutions at critical positions in their polypeptide chains. Less commonly, for some proteins, such as Raf (see Fig. 77.1 and Table 77.2), loss of regulatory domains may also lead to oncogenesis. Amino acid substitutions in signal transducing proteins cause these proteins to undergo conformational changes that result in their becoming permanently activated to stimulate cell division (Pincus et al., 1992, 2000, 2004, 2007, 2011).

This mechanism has been well documented for the ras oncogene–encoded p21 protein, for which substitutions of most amino acids for glycine 12 or glutamine 61 result in an oncogenic protein. Many p21 proteins with such substitutions have been cloned and directly microinjected into normal cells in culture such as NIH 3T3 cells (Barbacid, 1987). The cells undergo malignant transformation that lasts until the added mutant protein is metabolized and cleared from the cells. Oncogenic mutant forms of the ras gene and of its encoded p21 protein have been found in approximately one of three common human epithelial cell tumors, in more than 90% of human pancreatic tumors, and 75% of human colon cancers (Forester et al., 1987; Almoguera et al., 1988).

One of the consequences of amino acid substitutions in p21 and presumably in other signal transducing proteins is the abnormal activation of alternate, unregulated signal transduction pathways. Oncogenic ras-p21 protein (p21 in Fig. 77.1) has been found to interact directly with Jun, the nuclear transcription factor, and its activating kinase, JNK. This binding process results in the direct activation of these nuclear transcription–inducing proteins, thereby bypassing the normal cellular controls. This bypass or short-circuit pathway is shown on the right side of Figure 77.1 for p21 (Adler et al., 1995; Amar et al., 1997; Pincus et al., 2007; Pincus et al., 2011). In addition, oncogenic ras-p21 protein requires activation of protein kinase C as a downstream event on its signal transduction pathway (Pincus et al., 1992), as illustrated in Figure 77.1.

As noted previously, the ras oncogene–encoded p21 proteins are 21-kDa membrane-associated G-proteins that have been implicated in the growth signal transduction process from the cell membrane to cytoplasmic kinases. Qualitative (i.e., point mutations) and quantitative (i.e., overexpression) changes in p21 have been identified as contributing to human carcinogenesis (Barbacid, 1987). By undefined mechanisms, p21 proteins gain access to the extracellular environment. Thus increased amounts of p21 or point-mutated forms of p21 can be detected by immunoblotting with monoclonal antibodies in the supernatant of cells in culture known to overexpress p21 or to express mutant p21, respectively (Brandt-Rauf, 1991; Brandt-Rauf & Pincus, 1998; Pincus & Friedman, 2003).

Similarly, mice with tumors that overexpress p21 or express mutant p21 are found by immunoblotting to have increased amounts of p21 or mutant forms of p21 in their serum, respectively (Hamer et al., 1991). These results suggest that the detection of increased p21 or mutant p21 in blood is possible in humans.

Because of its central role in mitogenic signal transduction, overexpressed or mutated p21 protein might be expected to be present in a wide variety of human tumors. Indeed, elevated serum p21 has been identified in the serum of up to 68% of patients with many different cancers, including breast, prostate, colon, lung, and liver cancer. On the other hand, only a small percentage of normal individuals have been found to have detectable serum levels (Weissfeld et al., 1994). Newer assays based on RT-PCR have detected the ras oncogene in the stool of a high percentage of patients with colonic cancer (Pincus, 2004).

ras-p21 in Pancreatic Cancer

There has been a well-defined association of oncogenic k-ras-p21 with pancreatic cancer. K-ras mutations are present in 90% of all pancreatic adenocarcinomas, most of these resulting in the substitution of Val for Gly 12 (G12V) (Almoguera et al., 1988), and are also found frequently in early precursor lesions, even in low-grade pancreatic intraepithelial neoplasia (PanIN 1A) lesions (Morris et al., 2010; Kanda et al., 2012). Further studies in genetically modified adult mouse models indicate that the oncogenic protein is activated for prolonged time periods and, in the presence of inflammatory events, initiates the formation of intraductal pancreatic carcinoma (Logsdon & Lu, 2016). Thus, oncogenic ras-p21 is a major causative factor of pancreatic carcinoma.

Studies have focused on employing assays for the ras oncogene itself in the sera of patients with this disease. Patients with pancreatic cancer and a control group of patients with pancreatitis used RT-PCR to detect mutant ras DNA in the sera of these patients in combination with a serum assay for CA 19-9, a marker for pancreatic cancer, as discussed in Chapter 75 (Däbritz et al., 2009). Using DNA amplification techniques to detect oncogenes in serum is discussed later. In this study, no patients with pancreatitis were found to have oncogenic ras genes in their sera, whereas 36% of patients with pancreatic cancer were found to have detectable serum levels of this oncogene. Overall, using both markers, 91% of the patients with pancreatic cancer were found to have either elevated levels of CA 19-9 or oncogenic ras-p21 or both. Of these, 35% were found to have detectable oncogenic ras but nonelevated or only moderately elevated CA 19-9. Using restriction fragment length polymorphism (RFLP)-PCR on serum samples from patients with pancreatic cancer before and after chemoradiation therapy (CRT), it was found that in patients whose post-CRT sera were negative for oncogenic ras had significantly more favorable survivals (Olsen et al., 2009).

ras-p21 in Colon Cancer

PCR for K-ras mutant genes with base changes at codons 12 and 13 has been performed concurrently on tumor tissue and serum from patients with different stages of colorectal cancer (De Kok et al., 1997). Changes at codon 13, in particular, had a significant negative impact on Dukes classification, lymph node status, and high S-phase fraction (Bazan et al., 2002). In more than 90% of the patients with specific mutant ras genes found in tumor tissue, the same mutated ras gene was discovered in their sera, regardless of the stage of the tumor.

Mutant ras p21 oncogene DNA containing mutations at codon 12 was detected in the sera of 29 patients with advanced colon cancer using a two-stage PCR method, but this oncogene was not detected in 32 normal individuals (Kopreski et al., 1997). Other studies using similar techniques have found that expression of ras p21 protein in serum is associated with worse prognosis, especially if the same mutant protein is found in the tumors themselves (Su et al.+, 2008; Thomsen et al., 2016, 2017).

ras-p21 in Lung Cancer

Similarly encouraging results have been obtained using the sputum of patients with lung cancer. Parallel results have now been obtained using the ELISA for the p21 protein using the serum of patients with lung and colonic carcinoma. Elevated levels (five times more than control participants) of serum ras-p21 have been found in up to 83% of patients with cancer lung, whereas only low levels were found in the sera of normal individuals (Brandt-Rauf, 1991; Brandt-Rauf & Pincus, 1998). Meta-analysis of 41 trials comprising nearly 7000 patients found that K-RAS mutations were associated with poorer outcomes in patients with NSCLC (Meng et al., 2013).

In the previous discussion of the HER2/*neu*-oncogene–encoded p185 protein, it was noted that elevations of the serum levels of this protein were found in patients with pneumoconioses who then progressed to develop frank malignancies. A parallel study has been performed on patients with pneumoconioses in which assays were carried out for ras-p21 in their sera. For patients with this predisposing condition, 39% were found by western blotting to have elevated serum levels of the ras-p21 protein. Almost all of these patients developed a malignant lung tumor subsequent to the observed elevations of the p21 protein. Thus, like p185 ECD, elevated serum p21 is a biomarker of early malignant disease in patients with a known predisposition. An obvious study that is yet to be performed is to assay the sera of these patients for both HER2/*neu* and ras-p21 to increase the sensitivity of the assays.

The aforementioned studies are concerned with detecting elevated serum levels of p21 in serum as an indicator of malignancy. As noted previously, a major mechanism for oncogenesis induced by the ras-p21 protein is amino acid substitutions in its sequence that result in its permanent activation. Identification of mutant ras genes by PCR and direct sequencing of DNA isolated from the serum or plasma of three patients with pancreatic cancer has been described (Sorenson et al., 1994), but until recently, the direct detection of mutant p21 protein had not been reported in human blood (De Kok et al., 1997). Now, however, oncogenic amino acid substitutions in the p21 protein can be identified through the use of monoclonal antibodies that recognize specific oncogenic amino acid substitutions, including at positions 12, 13, 59, and 61. Use of these antibodies on the sera of patients with known risk factors for cancer appears to offer much promise for early tumor detection.

ras-p21 in Angiosarcoma

Mutated p21 has been found in the serum of patients with a known history of exposure to the carcinogen vinyl chloride. This chemical has been shown to predispose individuals to developing angiosarcomas (Brandt-Rauf & Pincus, 1998; Brandt-Rauf et al., 2012). Tissue studies of these angiosarcomas reveal that a mutant ras gene that codes for aspartic acid in place of the normally occurring glycine at position 13 in the polypeptide chain is present in the tumor cells. A monoclonal antibody that recognizes the Asp13 form of the p21 protein has been obtained (Oncogene Science/Siemens). This mutant p21 protein has been identified in the sera of 80% of patients with vinyl chloride–induced angiosarcoma of the liver but not in normal individuals (DeVivo et al., 1994). There is a direct correlation, moreover, between the degree of exposure of patients to vinyl chloride and the probability of discovering the oncogenic form of the protein in their sera.

Serum ras-p21 in Other Cancers

Breast Cancer. Although ras-p21 is not known to occur frequently in breast cancers, in a recent study of 259 patients with breast cancer, ras-p21 protein was elevated in the sera of 39 (12%) of the patients. Cox analysis of overall survival and prognosis showed that the group with elevated serum ras-p21 had significantly lower overall survival times and a worse prognosis than the patients with no serum elevations of this protein. This study suggests that in patients with breast cancer with elevated serum ras-p21, treatment with anti-ras agents would be beneficial (Banys-Paluchowsky et al., 2018).

Ras-p21 in Leukemias. Overexpression of ras-p21 has been found in acute myeloid (AML), lymphoblastic (ALL), and chronic myeloid (CML) but not in chronic lymphoid (CLL) leukemias (Nelli et al., 2006). In this study, the reference range for this protein was established in 48 normal participants as 5 to 422 ng/mL. Of 52 patients with leukemia, 16 (30%) were found to have elevated (>422 ng/mL) serum ras-p21 levels. The breakdown by category was almost half of patients with ALL or CML, 25% of patients with AML, and only about 12% of patients with CLL. This study suggests the possibility that ras-p21 as an important agent involved in three types of leukemia. Oncogenic ras-p21 has been further implicated in mixed-lineage leukemias with monocytoid features (Chandra et al., 2010).

CYTOSOLIC MITOGENIC KINASES

Raf

As shown in Figure 77.1 and Table 77.2, Raf is a 74-kDa protein that is a critical target of ras-p21. It directly activates MEK, which in turn activates mitogen-activated protein kinase (MAPK or ERK) (see Fig. 77.1 and Table 77.2). It is involved in cell growth, proliferation, apoptosis, and differentiation. There are several different isoforms of Raf, such as Raf A and Raf B, which may differ in their exact cellular functions. More than 30 mutations of the B-raf gene associated with human cancers have been identified (Wan et al., 2004). Western blot analysis showed that activated Raf was overexpressed in tissues obtained from patients with cirrhosis and HCC (91.2% and 100%, respectively) (Hwang et al., 2004). B-raf mutations have also been found in patients with colon cancer, although less frequently than K-ras (Monstein et al., 2004). The presence of mutant B-raf DNA in the serum of patients with colorectal cancer is an indication of less favorable prognosis if the tumors have proficient mismatch repair (Thompsen et al., 2017). However, Raf is found minimally to not at all in tissues from patients with bladder or endometrial carcinoma (Mutch et al., 2004; Stoehr et al., 2004). In contrast, mutant Raf (V600E) has been found to occur frequently in melanomas, although the same mutant Raf has also been found in a majority of benign nevi (Wellbrock et al., 2004). Ninety percent of the mutations result in substitution of glutamic acid for the normally occurring valine at position 600. Antibodies to B-raf V600E have been used in the diagnosis of some hematologic malignancies, particularly hairy cell leukemia. IHC with this mutation-specific antibody has a sensitivity and specificity of 88% and 97%, respectively (Uppal et al., 2015). These results suggest that this antibody may be useful in detecting the mutant Raf protein in serum. Because Raf is immediately downstream of ras-p21 on the ras signal transduction pathway (see Fig. 77.1), oncogenic mutations in Raf might also be expected to diminish the efficacy of anti-EGFr agents in cancers, especially colorectal cancers. This has been found to be the case for metastatic colon cancer (Di Nicolantonio et al., 2008).

NUCLEAR ONCOPROTEINS

As noted previously, two important nuclear proteins that appear to play critical roles in the regulation of cell growth and division are the tumor suppressor gene protein p53 and the p62/75 protein encoded by the c-myc oncogene for which serum assays have been developed. Furthermore, nuclear skeletal or matrix proteins are the targets of signal transducing kinases such as MAP kinase, as indicated in Figure 77.1.

p53 and c-myc Proteins

Human p53 protein contains 393 amino acid residues and is known to bind to specific sequences of DNA to suppress the mitotic process. In addition, activation of p53 in transformed cells results in apoptosis via activation of proapoptotic proteins such as Bax and caspases. Thus, p53 is an antioncogene protein. In its most effective form, p53 exerts its intracellular effects as a homotetramer.

There are four domains in p53: the transactivation domain, residues 1 to 93; the DNA binding domain, residues 93 to 312; the tetramerization domain, residues 307 to 355; and the negative regulatory domain (NRD), residues 356 to 393. The transactivation domain includes a subdomain, residues 12 to 29, that are involved in the binding of p53 to the HDM-2 protein (human double minute-binding protein) that is involved in promoting mitogenesis. This binding event induces ubiquitination of p53 that targets this protein for degradation in the proteosome, resulting in shortened lifetimes for this protein.

Many different point mutations in p53 have been identified in human tumors (Soussi et al., 1994). These mutations cause a loss of the normal vital growth-inhibitory function of p53, and at the same time, some of these mutations result in p53 proteins with considerably increased half-lives so that the mutant proteins accumulate in the transformed cells (Soussi et al., 1994). Some of these mutated p53 proteins are thought to be involved actively in cell transformation. Common point mutations resulting in inactivation or direct cell transformation are H179L, R249W, and I255F. The latter two mutations occur in a mutational "hot spot" region of the protein and appear to cause similar changes in the conformation of the protein, recognized by the P240 anti-p53 monoclonal antibody, which recognizes only p53 protein mutated in this domain (reviewed by Pincus et al., 2007; Brandt-Rauf et al., 1996). Other antibodies to p53 include PAb 1620, which recognizes only native p53, and the monoclonal antibody DO1, which binds to the transactivating domain including amino acid residues 12 to 29, which recognizes total p53.

Among the "inactivating" mutations of p53 are homozygous deletions of the whole gene, as has been found in a number of colon and bladder cancers. Absence of p53 in cells results in tumor formation.

These considerations present several diagnostic problems. First, because a significant number of cancers, especially colorectal and breast cancers, have the p53 gene homozygously deleted, p53 protein is absent in serum. Thus, the absence of serum p53 in types of cancers in which it may often be overexpressed may not signify a negative result. Unfortunately, at present, no serodiagnostic testing can detect p53 homozygous deletion. Second, as noted earlier, there are numerous antibodies to p53. Some of these antibodies recognize specific mutant p53 proteins but not all mutant proteins. Absence of mutant p53 in serum as detected by a specific antibody may be attributable to the nonreactivity of the antibody to the specific mutant p53 protein that is present in serum. Finally, antibodies to common determinants in both wild-type and mutant p53 can be used to detect elevated serum levels of this protein. However, these antibodies may miss circulating mutant forms of p53 that are present within the reference range but are actually oncogenic and are expressed by a cancer.

The c-myc oncoprotein is activated to cause cell transformation by overexpression, so it, too, accumulates in transformed cells (Field & Spandidos, 1990). Thus, for both p53 and p62/75 myc, increased levels of the proteins can be detected in transformed cells and human tumors (Field & Spandidos, 1990; Soussi et al., 1994). This overexpression apparently

results in leakage of the proteins into the extracellular environment. Not only can these proteins therefore be detected in serum and other body fluids, but these normally sequestered proteins are also recognized as foreign, so some patients with cancer develop antibodies to p53 or p62/75 myc. As a result, increased concentrations of p53 or p62/75 or of antibodies to these proteins in blood are excellent markers for tumor detection for following treatment efficacy and prognosis.

Detection of Malignancies by Assaying for p53 Protein

Hepatocellular Carcinoma. Increased levels of mutant p53 in serum by ELISA (>0.3 ng/mL, the upper limit of 100 normal participants) have been found in 20% of patients with HCC and 30% of patients with cirrhosis, a group known to be at increased risk for the development of HCC (Virji et al., 1992). In addition, mutant p53 protein has been implicated as a major causative factor in HCC (Meng et al., 2014). Because patients with cirrhosis have high levels of p53 in their sera and a known risk factor for developing HCC, the elevated p53 levels may be an early indicator of tumorigenesis.

From a meta-analysis in 2012 (Liu et al., 2012), elevated mutant p53 levels in serum from patients with HCC were associated with higher rates of recurrence and lower rates of overall survival than in patients whose sera were found not to have elevated mutant p53 levels. This indicates that mutant p53 levels can also be a prognostic indicator (Liu et al., 2012).

Breast and Lung Cancers. There have been few studies on p53 as a tumor marker in the sera of patients with breast and lung cancers. Elevated serum mutant p53 levels determined by ELISA have been reported in 8% of patients with breast cancer, with levels decreasing after surgical resection of the tumors (Rosanelli et al., 1993), indicating that the tumors were the source of the elevated p53. Elevations of p53 protein have not been observed in the sera of any normal individuals. Levels of p53 are elevated in lower stages of invasive ductal carcinoma compared with higher stages—that is, the sera of 63% of patients with stage I, 71% with stage II, and 53% with stage III cancers have elevated levels of p53. This finding suggests that serum levels of p53 can be used for early detection of breast cancer (Balogh et al., 2010).

For lung cancer, elevated serum mutant p53 levels determined by ELISA and immunoblotting have been found in up to 34% of patients with lung cancer but not in normal individuals (Fontanini et al., 1994). For these patients, IHC staining of subsequently obtained biopsy tissue showed elevated p53 levels, correlating with the serum findings. Elevated serum p53 protein (mutated and wild type) were found in 57% of patients with all types of lung cancer in a study with lung patients with 201 cancer and 54 control participants. None of the control sera were found to have elevated p53 (Mattioni et al., 2015).

Colon Cancer. An important mechanism believed to be operative in the development of colonic carcinoma is the deletion of the normal p53 gene or mutation of the gene leading to a nonfunctional antioncogenic protein. Elevated serum mutant p53 determined by ELISA has been found in about 1 in 5 patients with colon carcinomas and in approximately 1 in 10 patients with colonic adenomas. Normal individuals were found to be negative for serum p53 protein. These results show relatively low sensitivity of this marker for colon cancer (Meng et al., 2018), possibly because deletion of the p53 gene occurred in a high percentage of the tumors studied.

Bladder Cancer. Studies on the urine of patients with bladder cancer using PCR for p53 on shed cells in urine samples found that the p53 gene was mutated in a high proportion of these patients (Sidransky et al., 1991, Darabi et al., 2006), supporting the use of p53 in screening for this disease in a completely noninvasive manner. As discussed later, p53, together with several other promising markers, may result in a set of tests that have a high positive predictive value.

Leukemia. Elevations of serum p53 and EGFR have been found to occur both in ALL and AML (Abdel-Aziz, 2013). The sensitivities for diagnosing ALL were 52% and 73.9% for p53 and EGFR, respectively, and the specificities were 100% and 95.8%, respectively. In contrast, no elevations of either protein were observed in the control group of individuals with no disease.

Detection of soluble p53 in B-cell chronic lymphocytic leukemia (B-CLL) can predict stage and progression of disease. In a recent study, 197 patients with B-CLL had plasma p53 levels measured. Using the cutoff of 3.5 U/mL, significant differences were seen in levels of patients with Rai staging levels of low, intermediate, and high, with higher p53 levels correlating with higher stage. Likewise, this cutoff was significant for predicting progression of disease. Significantly, it was found that, using the above cutoff, progression-free survival at 9 years was 67% for patients with serum values less than this cutoff, but it was only 5% for patients whose serum values were greater than this cutoff. In addition, overall survival at 11 years of patients with B-CLL whose serum values for soluble p53 were less than the cutoff was 97%, but it was only 15% for patients whose serum values were greater than the cutoff ($P < .0001$) (Del Principe et al., 2004).

Circulating Anti-p53 Antibodies in Tumor Detection

Serum antibodies against p53 have been reported to be a frequent occurrence in patients with several types of cancer. Production of antibodies to p53 and other oncoproteins has been attributed to their accumulation in necrotic cells and their subsequent release into the circulation, where they are recognized as foreign (Pincus & Friedman, 2003). There is another cause for the development of antibodies to oncogenic p53. Like oncogenic ras-p21, mutant p53 proteins, containing single amino acid substitutions at critical positions in the polypeptide chain, themselves become oncogenic. These amino acid substitutions induce major changes in the conformation of the p53 protein (Brandt-Rauf et al., 1996; Adler et al., 1998). Among these changes is the exposure of specific antigenic determinants that are not normally exposed (Pincus & Friedman, 2003; Pincus et al., 2007). If the protein diffuses into the circulation, antibodies against these determinants often develop. In a systematic review, it was found that patients with circulating p53 antibodies were more likely to have cancer than patients with no circulating antibodies to p53 (odds ratio, 6:1) (Zhang et al., 2014).

Antibodies to p53 Are Present in the Sera of Many Patients with Epithelial Cell Tumors and Lymphomas. In several major studies (including a large study of 1392 patients with cancer), elevated serum levels of anti-p53 antibodies were found in patients with ovarian and colon cancers (15%); lung cancers, including small cell tumors (up to 25%); and breast cancers, including intraductal carcinoma (up to 15%). Normal individuals did not have elevated serum levels of these antibodies (Angelopoulou et al., 1994). In a significant number of patients who have been followed for the presence of anti-p53 antibodies in their sera, the appearance of these antibodies has been found to precede the occurrence of malignant tumors. Anti-p53 antibodies are also found to occur in more than 20% of patients with bladder cancer (mostly at more advanced stages), as well as a high proportion of patients with pancreatic cancer and HCC and in childhood lymphomas.

In a more recent study of 569 patients with cancer compared with 879 normal control participants, 15% of the patients with cancer tested positive for anti-p53 antibodies, whereas 1% of the normal patients tested positive. Four percent of patients with cancer tested positive for p53 protein in serum compared with 0.34% in the normal control participants. Whereas the sensitivity and specificity of anti-p53 antibodies in detecting cancer were 15% and 99%, respectively, they were 4% and 100%, respectively, for serum p53 (Wu et al., 2010). As noted earlier, certain specific cancers such as ductal breast carcinomas result in elevated levels of serum p53 at significantly higher rates.

Anti-p53 in Ovarian Cancer. Mutant p53 is known to occur with a high frequency in epithelial ovarian carcinomas. This finding suggests that mutant p53 can be detected in the serum of patients with this disease (Zhang et al., 2016). Studies on the expression of anti-p53 antibodies in the sera of patients with ovarian cancer have been performed (Tsai-Turton et al., 2009). Patients with type 2 ovarian cancer, a more aggressive form of this cancer, were found to have anti-p53 antibodies in their sera, whereas no patients with less aggressive type 1 cancers were found to have these antibodies in their sera. All of these patients with anti-p53 in their sera were found to have mutant forms of p53 in their cancers; those who did not have mutant p53 in their tumors were not found to have anti-p53 antibodies in their sera, suggesting that mutant p53 is required to provoke this immune response. In all of these seropositive patients, extensive assays for cytokines revealed that IL-4 and IL-12 were consistently elevated in serum, whereas IL-8 was consistently decreased. Further studies indicate that anti-mutant p53 antibodies are present in the sera of 42% of patients with serous ovarian carcinomas with a specificity of 92%. Importantly, meta-analysis in two databases suggest that there is a significant association of serum p53 antibodies with increased risk of epithelial ovarian carcinoma (reviewed in Zhang et al., 2016).

Anti-p53 in Hepatocellular Carcinoma. Continuing follow-up studies on anti-p53 antibodies in patients with different cancers reveal that up to half of the patients with HCC, regardless of their sizes, have markedly elevated serum levels of anti-p53 (Ryder et al., 1996). These elevated levels correlate with the known elevation of p53 in the sera of patients with this type of cancer.

Sensitivity and specificity of anti-p53 antibodies in detecting HCC are 91.5% and 84.6%, respectively. When correlated with AFP (an HCC tumor marker), r^2 (r is the correlation coefficient) values are 0.70 and 0.88 for nonviral and viral-associated HCC, respectively (El Azm et al., 2013).

Anti-p53 in Oral and Esophageal Cancers. Anti-p53 antibodies have likewise been found in the sera of patients with oral lesions, and many of these patients were found to have premalignant lesions (Kaur et al., 1997), indicating that anti-p53 antibodies are markers for early detection of oral cancer. Anti-p53 has also been found to be elevated in more than 50% of patients with esophageal squamous cell carcinoma (Shimada et al., 1998), indicating that anti-p53 may be a very useful one in the diagnosis of this disease (Li & Zhang, 2015). In a meta-analysis, the combined diagnostic odds ratio of serum anti-p53 antibodies in detecting esophageal cancer was 9.65 (95% CI: 7.04–13.22) (Zhang et al., 2012).

Anti-p53 in Lung Cancers. In a prospective study of patients with carcinoma of the lung, serum anti-p53 levels were found in 100% of patients with large cell carcinoma, 28% with adenocarcinomas, 55% with squamous cell carcinomas, and 71% with small cell carcinomas (Segawa et al., 1998). These results demonstrate that elevated serum anti-p53 levels are tumor type specific for carcinoma of the lung, showing high positivity rates for large and small cell lung carcinomas.

Anti-p53 Predicts Cancer Occurrence in Patients with Asbestos Exposure. A retrospective study (Li et al., 2004) of 103 patients with a known prolonged exposure to asbestos whose serum was banked between the years 1980 and 1988 has been performed. These patients were all followed until the end of 2001. Assays for anti-p53 antibodies were performed on the banked sera. It was found that of 49 patients who developed cancer, 13 (26.5%) had significantly elevated levels of anti-p53 antibodies in their sera, although 4 of the 54 (7.4%) individuals who did not develop cancer were found to also have these antibodies. In all four cases, the antibody levels were found initially to be marginally greater than the cutoff for positivity, but for all 4, subsequent banked serum samples were found to be antibody negative.

In contrast, in all 13 patients with cancer for whom multiple samples were available, all samples were positive for these antibodies. Statistical analysis of these results showed that the presence of anti-p53 antibodies is an independent predictor of cancer occurrence and that survival in anti-p53–antibody-free patients is significantly greater than in anti-p53–antibody-positive patients.

Anti-p53 in Colorectal Cancer. Serum anti-p53 antibodies have been found to be reliable indicators of postoperative recurrence of colorectal cancer (Tang et al., 2009). In patients whose preoperative anti-p53 titers were elevated, elevated postoperative serum anti-p53 antibody titers were found to be better indicators of tumor recurrence than serum elevation of carcinoembryonic antigen (CEA), the classic serum marker for colorectal cancer, as discussed in Chapter 76. In a recent systematic review, sensitivity of detecting colorectal cancer increases (to 51%) when using both as markers as opposed to anti-p53 (17%) or CEA (42%) alone (Suppiah & Greenman, 2013).

Negative Regulator of p53, S100, as a Tumor Marker for Malignant Melanoma. S100 is a low-molecular-weight calcium-binding protein expressed in a wide variety of cells from the neural crest lineage and is composed of two subunits, α and β. Calcium-bound S100 binds wild-type p53, disrupting its tumor suppressive role by breaking up the p53 tetramer (Baudier et al., 1992) and by binding to p53 in its NRD (see earlier), involving amino acid residues 374 to 388. This domain is autoregulatory and blocks the interaction of p53 with DNA sites, resulting in its inactivation. Contained in this domain is the phosphorylation site Ser 376-Thr 377-Ser 378. Phosphorylation of at least one of these residues results in the inability of S100 to bind to this domain of p53, allowing p53 to maintain its function. By binding to p53 in the NRD, S100 blocks phosphorylation and allows the NRD to block p53 functioning (Rustandi et al., 2000; Carty et al., 2018). The form that is found in melanoma is the αβ dimer. Serum levels of the β subunit are associated with a variety of brain and inflammatory processes; with brain diseases excluded, an elevated S100 β level is specific to malignant melanoma, especially metastases to skeletal muscle and liver. It is found to have low sensitivity but high prognostic value. S100 β correlates with disease severity, tumor mass, and progression and regression of the disease in response to therapy (Al-Shaer et al., 2010).

S100 is superseded among melanoma tumor markers only by lactate dehydrogenase (LDH). Although not strictly an oncoprotein, this biologic surrogate has great clinical utility. Elevated serum LDH levels have long been associated with poor prognosis in late-stage malignant melanoma and have been included in the AJCC staging guidelines (Gogas et al., 2009). Furthermore, LDH levels can stratify melanoma patients based on susceptibility to specific agents (Kelderman et al., 2014).

myc Oncogene–Encoded Protein in Tumor Detection

The myc gene codes for a protein of molecular mass of 75 kDa that functions as a transcription factor. When activated, it derepresses expression of other genes that encode proteins involved in replication. This oncogene is overexpressed in a number of tumors, including Burkitt lymphoma, in which the myc gene on chromosome 8 is translocated to a long terminal repeat–like region of an immunoglobulin (Ig)-coding region of chromosome 14. Long terminal repeat regions allow constitutive expression of genes that are adjacent to them.

c-myc–related proteins and antibodies to the c-myc protein, such as p53 and antibodies to it, have been identified in the serum of patients with cancer. Detection of this 62/75-kDa protein is hampered by its short half-life in serum. However, it is possible to detect a specific c-myc–related p40 protein in the serum of these patients, using immunoblotting. The highest frequencies of occurrence of myc protein in human serum have been found to occur in breast (~20%) and colon cancers. Treatment of both types of cancer results in marked diminution in the serum levels of this protein. Recurrences result in elevated levels; c-myc protein is therefore useful in following the course of malignant tumors. It has not been detected in the sera of normal individuals.

Serum Anti–c-myc Protein Antibodies in Tumor Detection in Breast Cancer, Ovarian Cancer, Leukemias, and Lymphomas

High serum levels of anti–c-myc antibodies have been found in the sera of patients with colorectal cancer (55%–65%) and in the sera of patients with both myeloid leukemias and Burkitt lymphoma. Anti-myc and anti-HDM-2 antibodies have been found in early stages of lung cancer (Lia et al., 2016) and may be excellent markers for the early diagnosis of this condition. Lower occurrences of elevated antibodies have been reported in patients with breast cancers (~10%) and ovarian cancers (10%). Anti–c-myc antibodies have not been found in the sera of normal individuals.

In a study of serum from 546 patients with cancer, elevated anti–c-myc antibodies were found in 12% of patients. In HCC, 25% displayed elevated anti–c-myc antibodies; in breast cancer, 19%; in esophageal cancer, 12%; and in gastric cancer, 15% (Megliorino et al., 2005).

Combined Oncogene Marker Proteins for Detection of Colorectal Cancer

As discussed later, since the development of gene, mRNA, and protein arrays, it is possible to screen for multiple oncogene proteins at the same time. Clinical guidelines, however, do not currently recommend routine testing of multiple oncogenes (Locker et al., 2006). The only tumor marker with ASCO endorsement is CEA, for staging and treatment purposes, as well as to monitor response to therapy. Recently, a study was performed in which the peripheral blood leukocytes of patients with colorectal cancer at all stages and of a control group were assayed for overexpression of ras-p21, myc, and p53 proteins. All of the patients with colorectal cancer were found to have marked overexpression of all three oncoproteins compared with the control group (Csontos et al., 2008). This study is significant both because three oncoproteins were overexpressed consistently in this disease and because it involves the novel use of leukocytes, rather than serum, to assay for oncoprotein expression, pointing to a new diagnostic approach.

Nuclear Matrix Proteins and Detection of Bladder Cancer

Important targets of oncogene-encoded proteins are nuclear matrix proteins (NMPs) (see Fig. 77.1), also referred to as *nuclear skeletal proteins*, and nuclear mitotic apparatus proteins. These 236-kDa proteins are vital for correct mitotic spindle formation. They contain a globular head and tail separated by a central rod-like α-helical core domain consisting of heptad repeat sequences. These proteins vary by cell type, stage of differentiation, and cell cycle. Crucially, a number of tumor-associated NMPs has been identified, each specific for one of five tumor types (bladder, prostate, breast, colon, and bone). The best studied is one strongly associated with transitional cell carcinoma of the bladder, NMP22, which functions as a nuclear mitotic apparatus protein, involved with chromosomal separation during mitosis (Hughes & Cohen, 1999). The amount of this protein in malignant transitional epithelial cells is 10 to 20 times that in normal cells.

NMP-22 Is an Excellent Biomarker for Bladder and Urothelial Cancers

Antibodies that are specific for this NMP have been developed and are now used in a commercial ELISA on urine (Matritech/Berlex). Because malignant urothelial cells in patients with bladder cancer are frequently exfoliated into the urine of these patients, this protein from the lysed cancer cells can be detected at elevated levels. Multiple studies of patients who have bladder cancers of a variety of different stages reveal that the sensitivity is close to 90% in malignant, invasive cancer and 75% in carcinoma in situ. The latter result is highly encouraging because this stage

is the earliest detectable one. For malignant papillary, noninvasive carcinoma, the sensitivity is 62%. The overall specificity for this marker ranges from around 73% to as high as 90%, depending on the specific study.

Comparison of the sensitivity of NMP22 ELISA with that of cytology reveals that the two methods are about 83% sensitive for invasive carcinoma, but for grade I transitional cell carcinoma, NMP22 is 61% sensitive, whereas cytology is only 17% sensitive (Landman et al., 1998). For grades II and III cancers, the NMP22 ELISA is more sensitive at 78% and 93% than cytology at 50% and 87%, respectively (Landman et al., 1998).

Although the results of a recent study of 31 patients with non–muscle-invasive bladder cancer suggest that NMP-22 has a low sensitivity (12%) and a high specificity (100%) (Pilcher et al., 2017) for diagnosing this specific condition, multiple other studies have compared overall sensitivity and specificity of NMP-22 with the sensitivity and specificity of urine cytology in screening for urothelial cancer of all types and stages. One prospective study of 103 patients found that NMP-22 and cytology gave approximately the same sensitivities and specificities—that is, 69% sensitivity and 76% specificity for NMP-2 and 75% sensitivity and 73% specificity for urine cytology (Hautmann et al., 2007). On the other hand, another large study of 93 patients with bladder cancer, 42 patients with benign urothelial conditions, and 50 normal volunteers found that NMP-22 had a sensitivity of 78% and a specificity of 73%, whereas cytology had a sensitivity of 24% and a specificity of 97% (Tsui et al., 2007). In a study of recurrent bladder cancer in a large cohort of patients, it was found that the sensitivity (85.7%), specificity (77.5%), positive predictive value (70.6%), and negative predictive value (89.6%) of NMP-22 alone were almost the same when combined with urine cytologic findings, presumably because the sensitivity of NMP-22 is higher than that for urine cytology (Gupta et al., 2009). These findings again suggest that NMP-22 is more effective overall in screening for bladder cancer than urine cytology.

NMP-22 testing has been approved by the U.S. Food and Drug Administration, both for screening for the presence of bladder cancer and for the follow-up of bladder cancer in patients who have been treated for this disease. With respect to the latter use of this method, clinical studies have been performed in which the NMP22 ELISA was performed on the urine of patients who have been treated for transitional cell carcinoma, 20 to 60 days after treatment, who were then subjected to cystoscopy 2 to 6 months after treatment. Using a cutoff of 10 U/mL, 86% of patients with negative (<10 U/mL) NMP22 values were found to have negative cystoscopic results, and 71% of patients with values greater than 10 U/mL were found to have positive cystoscopic findings. These results, combined with those of other studies, suggest that this methodology may obviate the necessity for performing cystoscopy on many patients who are being followed for tumor recurrence (Miyanaga et al., 1997).

NMP-22 can be used to monitor the recurrence of bladder cancer after resection. However, because recurrent tumors are smaller than initial tumors, cutoff values should be altered in these cases because the sensitivity of this test increases from 19% to 49% when the cutoff value is reduced to 5.0 U/mL (Miyanaga et al., 2003).

Bladder Tumor Antigen or Urinary Bladder Cancer Antigen

Several other biomarkers for bladder cancer are also being used to aid in the diagnosis and follow-up of this disease. Prominent among these is the so-called bladder tumor antigen (BTA), which measures a human complement H protein that is produced by malignant but not by normal transitional epithelial cells. This marker has a somewhat lower sensitivity than that for NMP-22 (Tsui et al., 2007) and has a lower specificity because of false-positive results from trauma to the urothelial tract. However, use of NMP-22 together with bladder tumor antigen and a number of other markers, including urokinase-type plasminogen activator, can improve the overall sensitivity of bladder cancer detection (Shariat et al., 2003). In the study on non–muscle-invasive bladder cancer referred to in the preceding section (Pilcher et al., 2017), it was found that the highest sensitivities (~61%–64%) of serum markers for this condition were obtained using BTA on either urine or barbotage fluid with specificities of 77% and 81%; cytologies on these fluids were found to have low sensitivities and specificities in the 30% range.

It should be further noted that other tests on urine, such as those for mutant or absent p53, discussed previously, and for homozygous deletion of the 9p21 chromosome (see Chapter 76) also have high diagnostic yields. Because these tests are relatively simple to perform, it is conceivable that they can be placed on a chip that will allow for simultaneous evaluations. A positive result on one or more test would suggest the occurrence of bladder cancer.

Minichromosome Maintenance Proteins

Minichromosome maintenance proteins (MCM2-7) are present in nuclei of cells during replication, and all six proteins are required for replication. They form a heterohexamer at the end of metaphase and are downregulated when cells are senescent. They have been found in serum and body fluids of patients with cancer. In bladder cancer, MCM5 in urine detected cancer with high sensitivity and specificity. The areas under the ROC curves for MCM5 and NMP22 were 0.75 and 0.72, respectively. When used in combination, they detected 100% of muscle-invading cancers, 46% of grade 1, 64% of grade 2, and 96% of grade 3 tumors (Kelly et al., 2012).

In patients with biliary strictures, biliary aspirates are routinely checked for pancreaticobiliary malignancy. Using an immunofluorometric assay for MCM5 in the aspirates yielded a sensitivity and specificity of 66% and 94%, respectively, compared with 20% and 100% for brush cytology (Ayaru et al., 2008).

In detection of HCC, MCM6 protein assay had a sensitivity of 67% and a specificity of 89.9%. In AFP-negative patients, MCM6 protein combined with assays for MCM6 mRNA could detect 76.9% of cases of HCC. When combined with AFP, MCM6 as a tumor marker increased detection of small HCCs from 71.4% to 85.7% (Zheng et al., 2014). In an extensive meta-analysis of data on 7653 patients with cancer in 31 criteria-satisfying publications in which MCMs were measured in body fluids, there was a strong correlation between levels of expression of these proteins, especially MCM2, MCM5, and MCM7 proteins, and overall survival, with higher levels being associated with lower survival times (Gou et al., 2018).

USE OF MULTIPLE PROTEIN MARKERS IN THE DIAGNOSIS OF CANCER: PROTEOMICS

Early detection of cancer using oncoproteins has been enhanced by the development of proteomics (i.e., identification of differential protein expression in the sera and body fluids of patients with specific cancers compared with expression in the sera and body fluids of control groups). This approach also includes analysis of patterns of protein expression wherein cancers of specific tissues show characteristic "signatures" that typify cancers that are occurring in them (Sallam, 2015; Huang & Zhu, 2017).

PROTEIN ARRAYS HOLD PROMISE IN DETECTING BOTH NEW BIOMARKER PROTEINS AND PROTEIN EXPRESSION PATTERNS AND ANTIPROTEIN ANTIBODIES AND THEIR PATTERNS OF EXPRESSION IN SERA

Since the revolution in the development of microchip technology, it is now possible to impregnate microchips, called arrays, either with multiple antibodies to different potential tumor marker proteins or multiple proteins from cancer and control cell lysates, especially those known to be expressed in specific types of cancers (Huang & Zhu 2017). These proteins are isolated either using micro separation techniques or are cloned from cDNA expression of multiple proteins often in baculovirus in insect sp9 cells to obtain proteins that are posttranslationally modified as in human cells. The multiple protein arrays are called reverse-phase protein arrays (RPPAs). The antibody arrays serve to identify proteins that are expressed in the sera or other body fluids of patients with specific types of cancers and are identified usually by labeled secondary antibodies to these proteins. The RPPAs are used usually to identify antibodies to specific proteins expressed in the sera of or other body fluids (e.g., anti-p53 or anti-myc as discussed earlier) of patients with cancer and are then identified by incubating the array with labeled antihuman antibodies. In both cases, the position of each antibody or protein on the array is set so as to enable identification.

The sera (or other body fluids) of patients with tumors in a specific tissue are then incubated on these arrays to determine if there is a pattern of increased expression of some proteins and perhaps a decreased expression of other proteins compared with the patterns from the sera of normal healthy individuals and of other individuals who are known to have benign conditions of the tissue.

Although the trend is to employ the arrays using many antibodies or cell proteins, the technology has also been applied to more focused studies using oncoproteins known to be involved in signal transduction in cancer cells. Here, the object is to identify the *presence* of a tumor and *not to identify its tissue of origin*. For example, elevations of p53 protein or anti-p53 protein

have high probabilities of identifying the occurrence of a tumor but do not reveal its source because different tumors in different tissues can result in expression of p53 or antibodies to it. We now discuss application of this microchip array technology to cancer detection using predominantly sera.

Mini-Arrays in the Detection of Cancer

Based on the findings that many patients with cancers are found to have antibodies to a variety of oncoproteins, such as anti-p53 and anti-Myc, as discussed earlier, studies have been performed to detect one or more such antibodies in patients' sera. In one such study, a mini-array of up to seven full-length recombinant oncoproteins was prepared and included such oncoproteins as Myc and p53.

This array was employed to detect antibodies in sera from 527 patients with six different types of cancer (Zhang et al., 2003). The antibody frequency to any one oncoprotein was on the order of 15% to 20%, but inclusion of all seven oncoproteins resulted in detection of up to 68%. Furthermore, distinct patterns of antibody expression were found for patients with breast, lung, and prostate cancer, whereas no discrete patterns were found for patients with gastric cancer, colorectal cancer, or HCC. These encouraging results can be enhanced by the inclusion of more oncoproteins. Given the results regarding detection of single oncoproteins, it would seem even more effective to construct arrays with the antibodies to the large number of known oncoproteins in patients with cancer to assay for the presence of increased levels of these or mutated forms.

In another, prospective study focused on 46 patients with a history of exposure to carcinogens with attendant pneumoconiosis, the sera of these patients were analyzed for elevated levels of five oncoproteins. Eighteen of these patients were found to have cancer, including 13 with lung cancer or mesothelioma, at the time the assays were performed. Of these 18 patients, 13 were found to have markedly elevated levels of at least one of the five oncoproteins for which the assays were performed. Eight of these patients were found to have elevations of at least two of these proteins. Another seven patients were found to have elevations of at least two of these oncoproteins but were not found to have cancer. Although some of these latter patients were lost to follow-up, long-term follow-up revealed the subsequent development of cancer in all of the remaining patients. More important, several of the patients with only one elevated marker were found to have elevations of different tumor markers in their serum, again emphasizing the importance of assaying for as many different oncoproteins as possible (Qin & Tang, 2002).

Use of Large Arrays with Multiple Cancer-Associated Proteins in Detection of Cancer

Here the objectives of the arrays are to diagnose the presence of a tumor and to identify its tissue source. There have been extensive studies of such arrays for identifying different types of cancers (Sallam, 2015; Huang & Zhu, 2017). Here, we illustrate how large protein arrays can be used to detect cancers serologically.

Pancreatic Cancer

Diagnosis and treatment of this disease is one of the biggest challenges in medicine. The 5-year survival for patients diagnosed with pancreatic cancer is around 5%. Because the pancreas is retroperitoneal, signs and symptoms of the disease occur late in the development of the tumor, and, thus far there are no reliable markers for this disease, including serum levels of the marker CA 19-9, as discussed in Chapter 76. Most pancreatic cancers, when they are diagnosed, are found to be inoperable. Obviously, there is a major need to find markers for the occurrence of this cancer at an early stage so that surgical removal is possible.

Combination of Serum Marker DNA and Serum Protein and Other Markers. Before reviewing some of the more recent protein array work in detecting pancreatic cancer, we note the results of a major recent multicenter study on 221 patients with relatively low-grade pancreatic cancer that has *combined* use of DNA probes for the presence in serum of circulating tumor (ct) DNA, such as k-ras-oncogene DNA containing oncogenic mutations at codons 12 and 61, or expression of at least one of four potential serum markers including CA 19-9 (see Chapter 76), HGF (discussed earlier), CEA (see Chapter 75), and the protein osteopontin (OPN) (Cohen et al., 2017). The three latter proteins were selected because serum elevations of these proteins out of a large group of candidate proteins best correlated with pancreatic cancer occurrence. This study focused on detecting these markers in the sera of patients with relatively *low-grade* pancreatic cancers (i.e., stages I, IIA, and IIB). Patients with higher stages were excluded. The purpose was to determine whether these markers could identify the presence of pancreatic cancer at relatively early stages. Importantly, to detect k-ras ctDNA, use was made of the safe sequencing system that utilizes molecular barcodes that specifically label each template enabling sensitive detection of mutant k-ras DNA down to 1 mutant template in 10,000 normal ones (Kinde et al., 2011).

A total of 66 of 221 patients in this study were found to harbor oncogenic mutations in the k-ras gene. Tumor DNA was available from 50 of these 66 patients; the mutations in the k-ras tumor DNA was identical to that found in serum on all 50 patients, confirming the validity of the assay. When combined with serum CA 19-9, the sensitivity of a positive test (either ct k-ras or elevated CA19-9 or both) was greater than 60%. Because expression of ctDNA alone was about 10% and of CA 19-9 alone was about 30%, combined use of these two markers clearly results in a major increase in sensitivity. There was only one false-positive result in a patient found to have ct k-ras with no apparent cancer. Overall, the sensitivity of the test including the three proteins (HGF, OPN, and CEA) was about 65%. These encouraging results suggest that further similar studies should be performed on an expanded number of patients diagnosed with low-grade pancreatic cancer to determine if this combination of markers can detect the presence of this cancer, enabling surgical removal.

Protein Array Studies. A major study was performed in which 92 antibodies to potential tumor markers were impregnated on these microchips and incubated with the sera of 61 patients with known pancreatic cancer and, as control participants, the sera of 31 patients with benign pancreatic disease and 50 normal healthy control participants. Use of a logistic regression algorithm in evaluating the results allowed for distinguishing the sera from patients with pancreatic cancer from those of the normal, healthy control participants with a sensitivity and specificity of over 90%. The same results were obtained in analysis comparing the sera of patients with pancreatic cancer to those of patients with benign disease of the pancreas (e.g., pancreatitis) (Orchekowski et al., 2005). This study has been followed up with expanded antibody arrays with similar results (Ingvarsson et al., 2008; Gerdtsson et al., 2015) with similar high values for sensitivity and specificity suggesting that this approach can be employed to screen for pancreatic cancer.

It should be noted that the proteins used in the arrays in each of these studies were different from one another so that the results cannot be compared. For example, in the Orchekowski study (2005), C-reactive protein, PIKVA II (de-carboxy [inactive] prothrombin), α-1 anti-trypsin, IgA, cathepsin, and alkaline phosphatase were found to be elevated in the sera of patients with pancreatic ductal carcinoma compared with sera from healthy, normal individuals, whereas PIKVA II and CA 15-3 (see Chapter 75) were elevated compared with the levels found in the sera of patients with benign pancreatic disease. In the Gerdtsson et al study (2015), proteins including VEGF proteins, complement components, several interleukins, monocyte chemotactic protein 1 (MCP-1), CA 19-9, and others, were found to be elevated in sera from patients with pancreatic cancer compared with those from normal, healthy individuals, whereas many of these or like proteins were also expressed at higher levels in the sera from patients with pancreatic cancer versus sera from patients with benign pancreatic disease. In addition, other proteins such as cystatin C, CD-40, Apo A4, and others were also expressed in the cancer sera at higher levels compared with the levels in the sera of patients with benign pancreatic disease. It would be of benefit to combine the protein arrays so as to obtain increased diagnostic accuracy.

Other Possible Array Approaches to Diagnose Pancreatic Cancer. As can be inferred from these studies, there has been an expansion in the number of serum proteins used to define patterns of expression that characterize pancreatic cancer. However, there have not as yet been studies that utilize knowledge of specific oncogene proteins that are already known to be expressed in a high percentage of these cancers. As discussed earlier in this chapter, 90% of pancreatic cancers have been found to contain the mutant k-ras oncogene (Almoguerra et al., 1987). Because k-ras-p21 protein is bound to the inner cell membrane, cancer cell death would probably result in its early extrusion from the necrosed tumor cell. By far the most common oncogenic mutation in the ras gene results in the substitution of a valine residue for the normally occurring glycine residue (G12V). It would seem desirable to make high-affinity monoclonal antibodies to this mutant G12V k-ras p21 protein and other known oncogenic mutations (e.g., G12D, G13D,Q61L) and assay the sera of patients with this disease and control groups (as discussed earlier) for the presence of one or more of these proteins. As illustrated in Figure 77.1, activated ras-p21 binds to and activates downstream target proteins such as raf, PI3K, GAP, and JNK (oncogenic ras-p21). These proteins, in turn, activate downstream targets such as MEK, which activates MAPK (or ERK) and PKC. These signal transduction proteins themselves are biomarkers for transformed cells, especially in their phosphorylated forms. because monoclonal antibodies to phosphorylated forms of these proteins are available, these antibodies

can be impregnated on the microchip arrays that can be used in detecting these proteins in addition to mutant ras-p21.

Breast Cancer

Other monoclonal antibody arrays show promise in detection of breast cancer in much the same manner as detection of pancreatic cancer. In these studies, a number of proteins have been identified that occur at elevated serum levels in this disease, including casein kinase-1-epsilon, p53, MAPK-7 (a form of MAPK discussed earlier), annexin 11, and eukaryotic translation initiation factor 4E (Hudelist et al., 2004; Huang & Zhu, 2017).

In another study using a similar approach for breast cancer detection, the sera from 4500 patients with different cancer types, including nonmetastatic breast cancer, were screened using 50 different protein markers, of which 35 were selected (Kim et al., 2009). When compared with results from control participants, EGF, soluble CD40-ligand, and proapolipoprotein A1 were all found to be increased in breast patients with cancer, whereas high-molecular-weight kininogen, apolipoprotein A1, soluble vascular cell adhesion molecule-1, plasminogen activator inhibitor-1, vitamin D–binding protein, and fibronectin were decreased in the cancer group. Diagnostic accuracy using these proteins was approximately 90%, indicating that the breast cancer array has promise in early detection of this disease.

Ovarian Cancer

Using a protein array consisting of 5005 purified human proteins, many of which have been observed to be expressed at high levels in ovarian cancers, the sera of 30 patients with diagnosed ovarian cancers and 30 normal healthy individuals were screened for antibodies to one or more of these proteins (Hudson et al., 2007). A total of 94 antibodies that recognized tumor antigens were identified as occurring preferentially in the sera of the patients with ovarian cancer. Among the antigens were lamins A and C, structure-specific recognition protein-1 (SSRP-1) and ral binding protein. These proteins appear to be promising in the diagnosis of this disease.

Prostate Cancer

Using a 123-protein array consisting of proteins found to be expressed in prostate cancer, autoantibodies to these proteins were assayed (Adeola et al., 2016). Compared with results on the sera of healthy normal individuals and patients with benign prostatic hyperplasia, the sera of patients with prostate cancer were found to have 24 different proteins upregulated and 11 proteins downregulated. Among the upregulated proteins in prostate cancer were G antigen-1 (GAGE) protein, an antigen that occurs on tumor but not on normal cells except for spermatozoa; rhophilin-associated tail protein (ROPN1), also present on sperm cells, SPANXA1 protein (sperm protein associated with the nucleus) encoded on the X chromosome and involved in sperm maturation; protein kinase zeta; and melanoma antigen family B1 MAGEB1). These results suggest that this pattern can distinguish prostate cancer from benign conditions and may prove effective in diagnosing prostate cancer in patients with prostate-specific antigen (PSA) serum levels that do not definitively diagnose prostate cancer, especially in the range of 4 to 10 ng/mL (see Chapter 76).

Gastric Cancer

Probably the largest protein array that has been employed thus far has been for diagnosis of gastric cancer for which there are no well-defined markers. Using an array onto which 17,000 proteins were impregnated, in a two-step procedure to focus on the most likely diagnostic proteins, Yang et al (2016) analyzed 1401 serum samples from patients with this disease and 550 normal healthy individuals. Four autoantigens were identified that included photomorphogenesis protein (COP9) signalosome complex subunit 2 (COPS2), cathepsin F, 5′-nucleotidase, and telomeric repeat binding factor (TERF1). In distinguishing patients with gastric cancer from normal individuals, the sensitivity was 95%, and specificity was 92%.

Lung Cancer

Proteomic methodology has been applied to the sera of a large cohort of patients with squamous cell carcinoma of the lung and a control group (Dowling et al., 2007). To increase the diagnostic sensitivity of the method, all sera were immunodepleted of all major common serum proteins, such as albumin, and were then subjected to high-resolution two-dimensional electrophoresis and mass spectroscopy. It has been found that a set of proteins—apolipoprotein A-IV precursor, chain F; human complement component C3c; haptoglobin; serum amyloid A protein precursor; and Ras-related protein Rab-7b—is reproducibly elevated. In addition, another set of proteins—α-2-HS glycoprotein, hemopexin precursor, proapolipoprotein, antithrombin III, and SP40—were reproducibly decreased. This resulting lung cancer array appears to be very useful in screening for this disease.

Squamous Cell Carcinomas of the Head and Neck

To identify proteins that, as a group, are expressed in oral squamous cell carcinomas (OSCCs), human OSCCs were xenotransplanted into mice. Protein expression in the sera of these mice was compared with that in control sera of nontransplanted mice (Bijian et al., 2009). It was possible to identify a number of proteins whose expressions exhibited major differences between the two groups. Large increases in expression in the sera of mice transplanted with the OSCCs included EGFr, cytokeratins, a G-protein–coupled receptor, Rab11 GTPase, and several other proteins. Arrays containing antibodies to these proteins are being used to screen for this disease.

In a modification of the proteomic method, a large expression array consisting of multiple oncoproteins, cytokines, chemokines, and tumor markers, such as those discussed in Chapter 73, was used to select the best diagnostic combination of these for head and neck cancers (Linkov et al., 2007). These cancers can be diagnosed with a sensitivity of 84.5% and a specificity of 98% if the following combination of biomarkers was used: EGF, EGFr, IL-8, tissue plasminogen activator inhibitor-1, AFP, matrix metalloproteinase-2, matrix metalloproteinase-3, interferon (IFN)-α, IFN-γ, IFN-inducible protein-10, regulated on activation, normal T cell expressed and secreted (RANTES) protein, macrophage inflammatory protein-1α, IL-7, IL-17, IL-1 receptor-α, IL-2 receptor, granulocyte colony-stimulating factor, mesothelin, insulinlike growth factor binding protein 1, E-selectin, cytokeratin-19, vascular cell adhesion molecule, and cancer antigen-125. Using this array on a group of patients with known cancers of the head and neck and a group without this disease, 92% of the patients were correctly diagnosed with this disease.

ALTERNATE PROTEOMIC APPROACHES TO DETECTION OF CANCER IN SERUM AND OTHER BODY FLUIDS

The aforementioned approaches to tumor detection are based on *immunologic* determination of patterns of expression of proteins in the sera and other body fluids of patients harboring specific tumors. Alternatively, other approaches have been developed to search for the expression of multiple proteins that occur uniquely in the body fluids of patients with cancers and not in in the body fluids of normal individuals or patients with benign conditions. These techniques involve two-dimensional polyacrylamide gel electrophoresis on protein extracts, from tissue and serum, which are first labeled with different fluorochromes (Wulfkuhle et al., 2003). The resulting gels from patients with cancer are compared with those from normal participants to detect differences in fluorescent labeling. Bands that differ are eluted and subjected to mass spectrometry (see Chapter 5) to determine molecular weight and fragmentation patterns and even the partial amino acid sequence.

An offshoot of this approach is the *phosphoproteomic* analysis of tumor samples. Given the new paradigm in oncologic therapeutic practice that relies on small kinase inhibitors and monoclonal antibodies, this phosphoproteomic approach aims to clarify the phosphorylation status of key biomarkers identified in the proteome. The main platforms are planar and bead array, reverse-phase protein microarray, phosphor-specific flow cytometry, and automated quantitative analysis (AQUA) (Pierobon et al., 2014). As an illustration of the great potential of this approach, a recent study of breast cancer investigated more than 8000 phosphorylation sites on nearly 3500 proteins, identifying 133 phosphopeptides that were differentially expressed between high- and low-risk recurrence groups. Fifteen of these were successfully quantified using advanced highly selective mass spectrometry techniques, such as selective reaction monitoring. Further investigation is necessary, but preliminary results suggest that the phosphoproteomic approach is well suited to identify and validate more biomarkers and oncoproteins based on their phosphorylation status (Shi et al., 2012).

Ultimately, mass spectroscopy, the principles of which are described in Chapter 5, can be used to obtain sequence information on these proteins. Using this technique, the RS/DI-1 protein that regulates protein–RNA interactions has been identified as a circulating protein in the sera of breast patients with cancer but not in normal individuals. Likewise, the protein PGP9.5, a ubiquitin hydrolase often elevated in tumor cells, has been found to occur in the sera of patients with lung cancer (Wulfkuhle et al., 2003).

Select humoral and cellular immune-related components have also been shown to differ in malignancy. Studies by Fu et al (2008) demonstrated the presence of a 50-kD protein that is recognized uniquely by IgE obtained from patients with pancreatic cancer. The characterization and function of this protein are unknown, and future studies will investigate the role of this

protein in pancreatic cancer. Interestingly, related studies by Nakasura et al (2002) have identified unique Ig responses to pancreatic cancer antigens by serologic analysis of recombinant cDNA expression libraries (SEREX). In these studies, antigens recognized by IgE were distinct from those of IgG and were not correlated with allergic status; the nature of the antigens was not identified. Furthermore, antigen-specific IgG and IgE antibodies are produced in patients with pancreatic cancer, and such antibodies can mediate antitumor effects through mechanisms such as antibody-dependent cell-mediated cytotoxicity (ADCC), which has been described as an effective anticancer modality for immunotherapeutics (Weiner, 2007). ADCC mediated by IgG has been described as an anticancer mechanism in HCC (Kuwata et al., 1998), colon and prostate cancer, melanoma, and pancreatic cancer. Meanwhile, IgE-mediated ADCC has been described in ovarian cancer (Karagiannis et al., 2007) and has been shown to inhibit the growth of colorectal carcinoma cells (Kershaw et al., 1998). Taken together, the presence of unique antigen-specific IgG and IgE in pancreatic as well as other patients with cancer, in addition to other immune-related mechanism, remains an important prospect for further investigation.

These approaches have therefore shown promise in identifying unique markers for different types of cancer. However, in certain cases, it requires high concentrations of proteins to enable detection on the two-dimensional gels and is quite time consuming. Nonetheless, it is a powerful method for the discovery of select proteins that are unique to specific types of tumor.

Mass Spectroscopy on Sera from Patients with and without Cancer

In this method, the sera of patients is directly applied to a chip, which allows for the partial separation of the proteins in the sample. The chip is then subjected to surface-enhanced laser desorption ionization time of flight (SELDI-TOF) mass spectrometry, as described in Chapters 5 and 78. This produces a complex pattern of protein and protein ion fragments with different mass-to-charge ratios (Wulfkuhle et al., 2003).

The patterns for the sera of patients with cancer are compared with those from normal individuals using computer pattern-recognition algorithms (some of them based on neural network theory) that can distinguish cancer patterns from normal ones. More important, the normal sera provide a "training set" of patterns that define the normal pattern, and a second set of sera from known patients with cancer define the cancer training set (Wulfkuhle et al., 2003).

This method was applied to 25 patients with ovarian cancers at all stages and a group of unaffected individuals. The sera were analyzed in a blind study. The method resulted in detecting 100% of the patients with ovarian cancer, including 18 who had stage I (early) disease. All the sera from the unaffected patients were identified as being negative for ovarian cancer (Wulfkuhle et al., 2003). On the other hand, the sera from patients with other types of cancer could not be classified by the algorithm, suggesting that ovarian cancer has a unique protein "profile."

Similar results were obtained with prostate and breast cancer sera. In the prostate study, the method could accurately predict the occurrence of cancer in 95% of patients with PSA values in the indeterminate zone of 4 to 10 ug/mL (see earlier) and could detect 70% (107 of 153) of patients with benign disease in the PSA range greater than 4 ng/mL (Wulfkuhle et al., 2003).

This approach has been criticized in that is that there were no tests for reproducibility of results using different patients and control participants, different equipment, and different reagents (Ransohoff, 2005). There is also the problem that there is no identity of the proteins involved in the fragmentograms obtained in the study.

Also, in the case of prostate cancer detection, different groups that have analyzed the sera of prostate patients with cancer and unaffected individuals have obtained different diagnostic protein patterns, none of which contained PSA (Diamandis, 2003). Yet PSA is known to be elevated in around 80% of patients with prostate cancer. Further questions have been raised as to whether important protein molecules such as PSA are present in sufficiently high concentration in a serum sample to be detected by the method and whether the actual patterns really characterize prostate tissue. With identification of the proteins in the training sets, these questions should be resolved. Although this approach has apparently been de-emphasized, the original results are intriguing, and further studies should be performed.

DIAGNOSTIC EFFICACY OF SERUM ONCOPROTEINS

The results of assays for the different oncoproteins discussed earlier in serum and urine (NMP-22), on several thousand patients, are summarized in Figure 77.3 for different tumor types. The figure shows three-dimensional graphs of tumor type (*y*-axis), tumor marker (*x*-axis), and percentage of cases of each tumor type successfully detected by each marker. The results for each marker are given as a specifically colored three-dimensional bar graph. From Figure 77.3, it is clear that of the proteins studied thus far, positivity rates (sensitivities) vary from less than 30% (myc oncoprotein sensitivity is 8% in breast cancer) to more than 80% (e.g., ras in angiosarcoma). However, all of the control groups (given adjacent to each tumor type, with an "N" in parentheses) show very low positivity rates and are, in most instances, 0. Therefore, whereas the sensitivities of oncoprotein markers vary, *their specificities are exceptionally high*, in the 95% to 100% range; in other words, there are very few false-positive results. If a mutated or overexpressed oncoprotein is detected in the serum or other body fluid of a patient, there is a high probability that the patient has some form of malignancy. Also, the sensitivities and specificities of oncoproteins in diagnosing cancer exceed those of the oncofetal antigens, such as CEA or AFP (see Chapter 75).

How Specific Is Oncoprotein Expression for Different Cancer Types?

Interestingly, although the oncoproteins studied are from signal transduction pathways that are involved in many different types of cells, there seems to be some specificity of expression of particular oncoproteins for certain types of cancer. For example, the growth factor TGF-α is elevated in a large proportion of colorectal, brain, and ovarian cancers, whereas TGF-β is elevated in hepatocellular, lung, and bladder cancers. The p185 ECD (neu) protein is elevated in the sera of many patients with breast carcinomas at more advanced stages (see Fig. 77.3B). Ras-p21 protein is elevated in colorectal cancer, HCC, angiosarcomas of the liver, and lung cancer. p53 is elevated in colorectal and lung cancers and is elevated uniquely in oropharyngeal cancers, although as discussed earlier, protein arrays designed for diagnosis of these cancers are now available. In addition, it is elevated in a high proportion of lymphomas. Anti-Myc antibody is elevated in many colon cancers and, interestingly, in a high proportion of prostate cancers. This last finding suggests the need for further investigation. For example, elevated serum anti-Myc may aid in the definitive diagnosis of prostate cancer in patients with elevated serum PSA. In view of the recent findings that the ECD of EGFr is elevated in 93% of patients with prostate cancer in one series (Milanese et al., 2009), this oncoprotein may likewise enable definitive diagnosis of prostate cancer.

Sensitivities of Oncoprotein Expression

As noted earlier, the sensitivities of oncoproteins in diagnosing specific cancers vary. Because of the multistep nature of carcinogenesis, many potential oncoproteins may become abnormal. In some types of cancers, pathways may be activated that are not activated in other types of cancers. This phenomenon occurs even within one type of cancer. For example, ras and neu are elevated in the sera of patients with lung cancer but not in patients with lymphomas because different signal transduction proteins are involved in these two different types of cancers. Also, ras and neu do not detect all lung cancers because these cancers differ with respect to affected signal transduction proteins among themselves, and some of them do not involve these two signal transduction proteins.

Therefore, the next step in using these oncoprotein markers in the early diagnosis of cancer is to assay for multiple markers in a given patient's serum because discovery of at least one aberrant component of the signal transduction pathway is much more likely. If at least one positive result is found, the patient can be followed for signs of the development of a tumor.

As discussed previously, progress has been made in this area. Protein and gene arrays for multiple oncoproteins and oncogenes have been constructed and have succeeded in increasing the rate of positive diagnoses for cancer in patients as discussed earlier. Furthermore, the advent of the proteomic–pattern recognition approach to cancer detection is proving to be successful in studies in which it has been thus far tested—that is, in the diagnosis of ovarian, prostate, and breast cancers. Combination of these two methods would result in high diagnostic yields; use of both would be feasible in that each can be performed rapidly.

ORIGINS OF MALIGNANCIES

Figure 77.3 indicates that discovery of an elevated level of an oncoprotein in the serum of a patient does not generally give conclusive information as to the source of the malignancy. For example, although ras-p21 has been found to be elevated with some specificity in colon, lung, and

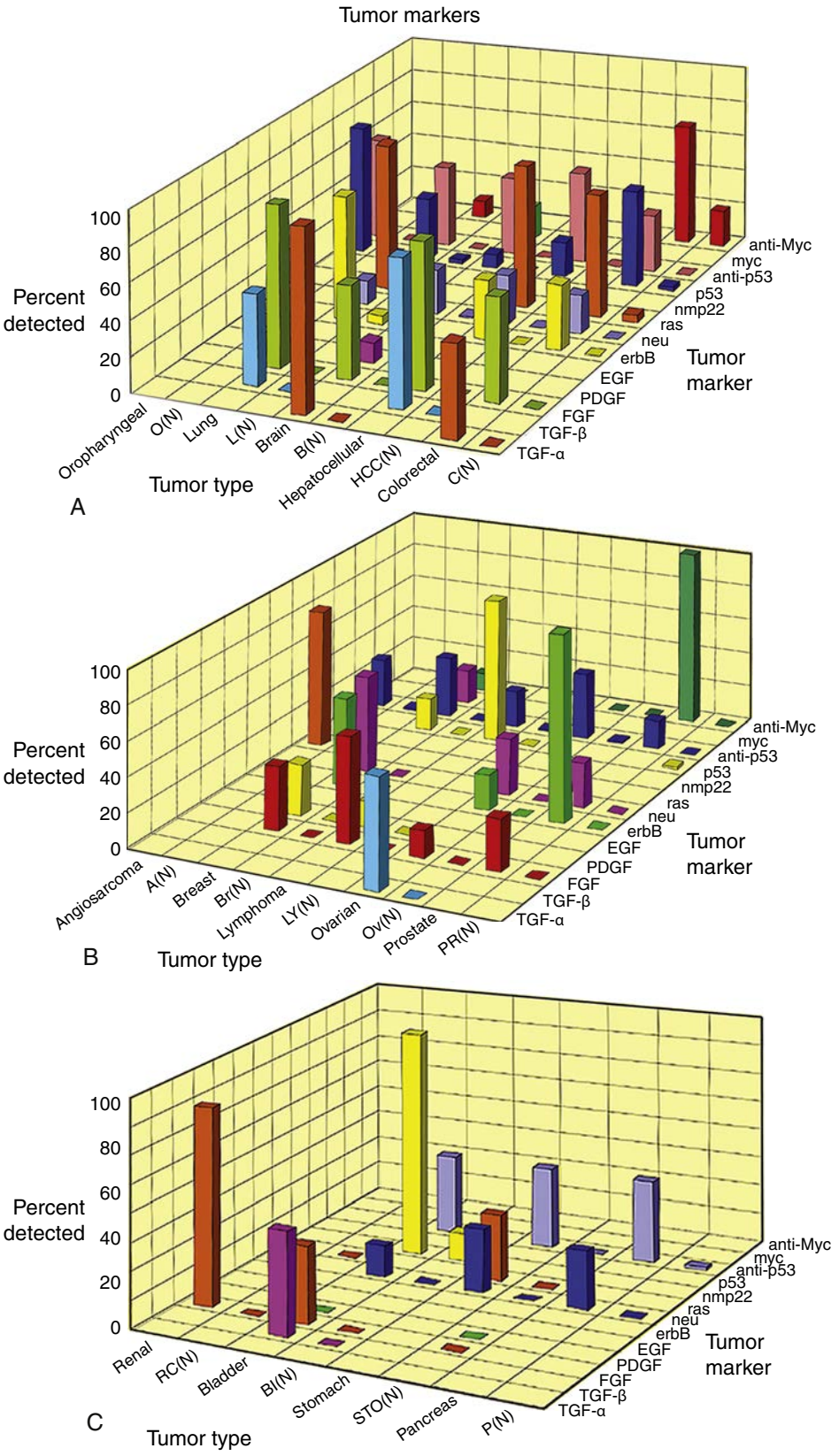

Figure 77.3 Summary of results of serum assays for different components of mitogenic signaling pathways. These are three-dimensional plots of tumor type on the *x*-axis, pathway component on the *y*-axis, and the percentage detected or the frequency of finding each of the pathway components elevated in the serum of patients with each tumor type on the perpendicular *z*-axis. Next to the results for each tumor type, the results for control groups are labeled as "N" for "normals"—that is, age- and sex-matched control participants who were tumor free. The control participants for patients with each tumor type are abbreviated with a single letter (with "N" in parentheses) for each tumor type, such as "B" for brain. *anti-Myc,* Antibody to the Myc protein; *anti-p53,* anti-p53 antibody; *EGF,* epidermal growth factor; *erbB,* epidermal growth factor (EGF) receptor; *FGF,* fibroblast growth factor; *myc,* a nuclear oncogene that encodes the Myc protein; *Neu,* p185 protein that is similar to the erbB protein and is also called erbB-2 and HER2; *NMP-22,* nuclear matrix protein number 22; *p53,* an antioncogene protein; *PDGF,* platelet-derived growth factor; *Ras,* p21 protein; *TGF-α,* transforming growth factor-α; *TGF-β,* transforming growth factor-β.

angiosarcomas of the liver and HER2/*neu* (c-erbB-2) p185 ECD has been found to be elevated in colon, lung, and breast cancers, elevation of one of these oncoproteins in a patient's serum would not allow identification of exactly the tissue of origin of a malignancy. Because the signal transduction pathways in most cells are remarkably similar to one another, an increase in any oncoprotein can signify malignancy in a number of different cell types. On the other hand, using the proteomic approach discussed earlier, serum protein patterns are uniquely characteristic of specific tumors so that this approach can identify the tissue of origin of the tumor.

Additionally, many studies on the correlations between the presence of tumors and serum levels of oncoproteins remain to be performed. For example, there are no published data on the occurrence of detectable forms of mutant ras-p21 protein in the serum of patients with pancreatic carcinoma with control groups consisting of age- and sex-matched control individuals and with groups containing patients with pancreatitis but no tumors. This is a vitally needed study because more than 90% of pancreatic cancers express oncogenic ras-p21 (Almoguera et al., 1988) as noted in our previous discussion of proteomic arrays for pancreatic cancer.

One manner of using serum oncoproteins could be to detect specific tumors at an early stage in tumor progression in populations known to be at risk for developing these cancers. These include patients with a history of occupational exposure to carcinogens or mutagens, as seen from the example of patients with a history of vinyl chloride exposure associated with angiosarcoma of the liver. In addition, patients can be followed who have been exposed chronically to asbestos and silica and who have consequent pneumoconioses associated with lung cancer and mesothelioma. Both conditions are associated with elevated serum levels of ras-p21 protein or mutant forms of this protein. Patients with pneumoconioses can also be followed with serum levels of p185neu.

TUMOR SIZE AND ONCOPROTEIN LEVELS

Currently, there is little information on the minimum size of a tumor that gives rise to serum elevations of oncoproteins. However, there are indications that small lesions may give rise to significant levels of certain oncoproteins.

First, in a significant number of patients with known cancer risks, oncoproteins were discovered in their sera before the development of detectable cancer. Thus, in patients with asbestosis, the ECD of the p185erbB protein became elevated *before* lung tumors were diagnosed. Overexpression of the p185 ECD occurred in a number of patients before the diagnosis of breast cancer. East Asian patients who had high serum levels of p185 ECD went on to develop HCC. Patients with pneumoconioses were found to have elevated levels of p185 ECD or ras-p21 protein and subsequently developed lung carcinomas. Mutant (Asp 13-) p21 protein was discovered in the serum of a very high percentage of patients with vinyl chloride exposure who subsequently developed angiosarcoma. Anti-p53 antibodies were found in the sera of individuals who subsequently developed angiosarcomas or lung cancers. For viral-associated HCC, anti-p53 antibodies were significantly correlated with tumor size and tumor number (El Azm et al., 2013). All these studies suggest that malignant lesions that are undetectable by conventional techniques may be detected by measuring the serum levels of oncoproteins or antibodies to oncoproteins, especially in patients with known exposures or risk factors for cancer.

Second, carcinomas in situ are known to cause elevated levels of oncoproteins in serum, as evidenced by elevated serum levels of p185neu protein in incipient breast cancer and NMP-22 in carcinoma in situ of the bladder. These findings suggest that serum oncoprotein levels are effective in detecting the presence of small tumors in individuals at an early stage.

It also seems clear that as the stage progresses, the tumors elaborate higher levels of oncoproteins so that there appears to be a good correlation, at least in some patients, between serum levels of marker oncoproteins and tumor size or level of expression of the marker in the tumor tissue itself. In this regard, some small adenomas (<1 cm) have been found to give rise to elevated levels of p185 ECD or ras-p21 in these patients' sera. For both ras-p21 protein and p185erbB ECD, there is an excellent correlation between serum level of these markers and the pretreatment and posttreatment clinical status of the patient. Nonetheless, substantially more correlation studies between tumor size and serum level of oncoproteins remain to be performed. One confounding factor may be that a small tumor may produce large amounts of the marker, whereas larger tumors may produce smaller amounts because of such factors as changes in the oncogenic lesions, affecting which oncoproteins are mutated or are overexpressed.

EVALUATION AND CONCLUSIONS

Well-defined pathways for mitogenic signal transduction exist between the membrane and the nucleus of cells. These pathways consist mainly of proteins, mutations in or overexpression of which can give rise to uncontrolled mitogenic signaling and cancer. More recently, based on proteomic approaches, other proteins are being discovered that characteristically are either overexpressed or expressed at much lower levels in the sera of patients with specific types of cancers compared with the levels found in the sera of control groups (Huang & Zhu, 2017).

Despite the foregoing caveats in interpretations of elevations of serum levels of oncoproteins or the detection of abnormal forms of these proteins in serum and the need for further correlation studies to be performed, assays for the presence of oncoproteins in serum show exceptional promise for detection of malignant tumors at an early stage and for monitoring their progression, response to therapy, remission, and recurrence.

SELECTED REFERENCES

Brandt-Rauf PW, Pincus MR: Molecular markers of carcinogenesis, *Pharmacol Ther* 77:135–148, 1998.

This is a review of the relevant oncoproteins that have proved to be markers for early tumor detection or that show great promise as biomarkers for early cancer detection.

Huang Y, Zhu H: Protein array-based approaches for biomarker discovery in cancer, *Dev Reprod Biol* 15:73–81, 2017.

This is a concise, excellent summary of the types of multiprotein arrays and their application to detecting specific types of tumors from serum protein expression.

Pincus MR, Friedman FK: Oncoproteins in the detection of human malignancies, *Mol Diagn* 1:23–38, 2003.

This is a review of oncoproteins as markers for early tumor detection, with an emphasis on oncoproteins as elements of signal transduction pathways.

Segawa Y, Kageyama M, Suzuki S, et al.: Measurement and evaluation of serum anti-p53 antibody levels in patients with lung cancer at its initial presentation: a prospective study, *Br J Cancer* 78:667–672, 1998.

This is a valuable study on the use of anti-p53 antibodies as a means for detecting lung cancers.

Slamon DJ, Godolphin W, Jones LA, et al.: Studies on the HER-2/neu proto-oncogene in human breast and ovarian cancer, *Science* 244:707–712, 1989.

This landmark paper established Her2/neu as an important factor in breast cancer causation and its use as a prognostic factor for disease progression.

Wulfkuhle JD, Liotta LA, Petricoin EF: Proteomic applications for the early detection of cancer, *Nat Rev Cancer* 3:267–275, 2003.

This clearly written review of different proteomic approaches in detecting cancer in blood samples explains the bases for these approaches that enable a good understanding of each method.

Zhang JY, Casiano CA, Peng XX, et al.: Enhancement of antibody detection in cancer using panel of recombinant tumor-associated antigens, *Cancer Epidemiol Biomarkers Prev* 12:136–143, 2003.

This important paper shows that using panels of oncoproteins on blood and body fluids is more effective than using single oncoproteins alone in detecting cancer.

Access the complete reference list online at Elsevier eBooks for Practicing Clinicians.

REFERENCES

Abdel-Aziz MM: Clinical significance of serum p53 and epidermal growth factor receptor in patients with acute leukemia, *Asian Pac J Cancer Prev* 14:4295–4299, 2013.

Abrahao-Machado LF, Scapulatempo-Neto C: HER2 testing in gastric cancer: an update, *World J Gastroenterol* 22:4619–4625, 2016.

Adeola HA, Smith M, Kaestner L, et al.: Novel potential serological prostate cancer biomarkers using CT100+ cancer antigen microarray platform in a multicultural South African Cohort, *Oncotarget* 7:13945–13964, 2016.

Adler HL, McCurdy MA, Kattan MW, et al.: Elevated levels of circulating interleukin-6 and transforming growth factor-beta1 in patients with metastatic prostatic carcinoma, *J Urol* 161:182–187, 1999.

Adler V, Pincus MR, Brandt-Rauf PW, et al.: Complexes of ras-p21 with jun-N-kinase and c-jun proteins, *Proc Natl Acad Sci U S A* 92:10585–10589, 1995.

Adler V, Pincus MR, Minamoto T, et al.: Conformation-dependent phosphorylation of p53, *Proc Natl Acad Sci U S A* 94:1686–1691, 1998.

Ahmad F, Lad P, Bhatia S, et al.: Molecular spectrum of c-KIT and PDGFRA gene mutations in gastrointestinal stromal tumor: determination of frequency, distribution pattern and identification of novel mutations in Indian patients, *Med Oncol* 32(1):424, 2015.

Ali MA, Koura BA, el Mashad N, et al.: The Bcl-2 and TGF-beta1 levels in patients with chronic hepatitis C, liver cirrhosis, and hepatocellular carcinoma, *Egypt J Immunol* 11:83–90, 2004.

Almoguera C, Shibata D, Forrester K, et al.: Most human carcinomas of the endocrine pancreas contain mutant c-K-ras genes, *Cell* 53:549–554, 1988.

Al-Shaer M, Gollapud D, Papgeorgio C: Melanoma biomarkers: Vox clamantis in deserto, *Oncol Lett* 1(3):399–405, 2010.

Amar S, Glozman A, Chung DL, et al.: Selective inhibition of oncogenic ras-p21 in vivo by agents that block its interaction with jun-N-kinase (JNK) and jun proteins: implications for the design of selective chemotherapeutic agents, *Cancer Chemother Pharmacol* 41:79–85, 1997.

Angelopoulou K, Diamandis EP, Sutherland DJ, et al.: Prevalence of serum antibodies against the p53 tumor suppressor gene protein in various cancers, *Int J Cancer* 58:480–487, 1994.

Ariad S, Seymour L, Bezwoda WR: Platelet-derived growth factor (PDGF) in plasma of breast cancer patients: correlation with stage and rate of progression, *Breast Cancer Res Treat* 20:11–17, 1991.

Ayaru L, Stoeber K, Webster GJ, et al.: Diagnosis of pancreaticobiliary malignancy by detection of minichromosome maintenance protein 5 in bile aspirates, *Br J Cancer* 98(9):1548–1554, 2008.

Balogh GA, Mailo D, Nardi H, et al.: Serological levels of mutated p53 protein are highly detected at early stages in breast cancer patients, *Exp Ther Med* 1(2):357–361, 2010.

Banys-Paluchowski M, Fehm T, Janni W, et al.: Elevated serum RAS p21 is an independent prognostic factor in metastatic breast cancer, *BMC Canc* 18:541–552, 2018.

Barbacid M: Ras genes, *Ann Rev Biochem* 56:779–827, 1987.

Baron AT, Wilken JA, Haggstrom DE, et al.: Clinical implementation of soluble EGFR (sEGFR) as a theragnostic serum biomarker of breast, lung and ovarian cancer, *Idrugs* 12:302–308, 2009.

Baudier J, Delphin C, Grunwald D, et al.: Characterization of the tumor suppressor protein p53 as a protein kinase C substrate and a S100b-binding protein, *Proc Natl Acad Sci U S A* 89:11627–11631, 1992.

Bazan V, Migliavacca M, Zanna I, et al.: Specific codon 13 K-ras mutations are predictive of clinical outcome in colorectal cancer patients, whereas codon 12 K-ras mutations are associated with mucinous histotype, *Ann Oncol* 13(9):1438–1446, 2002.

Bellezza G, Del Sordo R, Colella R, et al.: Co-expression of receptors of the HER family correlates with clinical outcome in nonsmall cell lung cancer (NSCLC), *Virchows Arch* 463(5):663–667, 2013.

Beretov J, Wasinger VJ, Graham PH, et al.: Proteomics for breast cancer urine biomarkers, *Adv Clin Chem* 63:123–167, 2014.

Bhatavdekar JM, Patel DD, Vora HH, et al.: Circulating markers and growth factors as prognosticators in men with advanced tongue cancer, *Tumour Biol* 14:55–58, 1993.

Bijian K, Mlynarek AM, Balys RL, et al.: Serum proteomic approach for the identification of serum biomarkers contributed by oral squamous cell carcinoma and host tissue microenvironment, *J Proteome Res* 8:2173–2185, 2009.

Boonjaraspinyo S, Boonmars T, Wu Z, et al.: Platelet-derived growth factor may be a potential diagnostic and prognostic marker for cholangiocarcinoma, *Tumour Biol* 33(5):1785–1802, 2012.

Brandt-Rauf PW: Oncogene proteins as biomarkers in the molecular epidemiology of occupational carcinogenesis: the example of the ras oncogene-encoded p21 protein, *Int Arch Occup Environ Health* 63:1–8, 1991.

Brandt-Rauf PW, Chen JM, Marion M-J, et al.: Conformational effects in the p53 protein of mutations induced during chemical carcinogenesis: molecular dynamic and immunologic analyses, *J Protein Chem* 15:367–375, 1996.

Brandt-Rauf PW, Li Y, Long C, et al.: Plastics and carcinogenesis: the example of vinyl chloride, *J Carcinog* 11(5), 2012.

Brandt-Rauf PW, Luo JC, Carney WP, et al.: The detection of increased amounts of the extracellular domain of the c-erbB-2 oncoprotein in serum during pulmonary carcinogenesis in humans, *Int J Cancer* 56:383–386, 1994a.

Brandt-Rauf PW, Pincus MR, Carney WP: The c-erbB-2 protein in oncogenesis: molecular structure to molecular epidemiology, *Crit Rev Oncog* 5:313–329, 1994b.

Brandt-Rauf PW, Rackovsky S, Pincus MR: Correlation of the conformation of the transmembrane domain of the neu oncogene-encoded p185 protein with its function, *Proc Natl Acad Sci U S A* 87:8660–8675, 1990.

Brandt-Rauf PW, Smith S, Hemminki K, et al.: Serum oncoproteins and growth factors in asbestosis and silicosis patients, *Int J Cancer* 50:881–885, 1992.

Brattstrom D, Bergvist M, Larsson A, et al.: Basic fibroblast growth factor and vascular endothelial growth factor in sera from non–small cell lung cancer patients, *Anticancer Res* 18:1123–1127, 1998.

Breuer B, DeVivo I, Luo JC, et al.: erbB-2 and myc oncoproteins in sera and tumors of breast cancer patients, *Cancer Epidemiol Biomarkers Prev* 3:63–66, 1994.

Breuer B, Luo JC, DeVivo I, et al.: Detection of elevated c-erbB-2 oncoprotein in the serum and tissue in breast cancer, *Med Sci Res* 21:383–384, 1993.

Cao C, Sun SF, Lv, et al.: Utility of VEGF and sVEGFR-1 in bronchoalveolar lavage fluid for differential diagnosis of primary lung cancer, *Asian Pac J Cancer Prev* 14:2443–2446, 2013.

Carney WP, Hamer PJ, Petit D, et al.: Detection and quantitation of the human neu oncoprotein, *Tumor Marker Oncol* 6:53, 1991.

Carty RP, Lin B, Fridman D, Pincus MR: Low energy conformations for S100 binding peptide from the negative regulatory domain of p53, *Prot J* 37:510–517, 2018.

Chakrabarty S, Huang S, Moskal TL, et al.: Elevated serum levels of transforming growth factor-alpha in breast cancer patients, *Cancer Lett* 79:157–160, 1994.

Chan AO: E cadherin in gastric cancer, *World J Gastroenterol* 12(2):199–203, 2006.

Chandra P, Luthra R, Zuo Z, et al.: Acute myeloid leukemia with t(9;11)(p21-22;q23) common properties of dysregulated ras pathway signaling and genomic progression characterize de novo and therapy-related cases, *Am J Clin Path* 133:686–693, 2010.

Chen CH, Lin YS, Lin CC, et al.: Elevated serum levels of a c-erbB-2 oncogene product in oral squamous cell carcinoma patients, *J Oral Pathol Med* 33(10):589–594, 2004.

Choi JH, Kim HC, Lim HY, et al.: Detection of transforming growth factor-alpha in the serum of gastric carcinoma patients, *Oncology* 57:236–241, 1999.

Cohen JD, Javed AA, Thoburne C, et al.: Combined circulating tumor DNA and protein biomarker-based liquid biopsy for the earlier detection of pancreatic cancers, *Proc Natl Acad Sci USA* 114:10202–10207, 2017.

Coltrera MD, Wang J, Porter PL, et al.: Expression of platelet-derived growth factor B-chain and the platelet-derived growth factor receptor beta subunit in human breast tissue and breast carcinoma, *Cancer Res* 55:2703–2708, 1995.

Csontos Z, Nádasi E, Csejtey A, et al.: Oncogene and tumor suppressor gene expression changes in the peripheral blood leukocytes of patients with colorectal cancer, *Tumori* 94:79–82, 2008.

Däbritz J, Preston R, Hänfler J, et al.: Follow-up study of K-ras mutations in the plasma of patients with pancreatic cancer: correlation with clinical features and carbohydrate antigen 19-9, *Pancreas* 38:534–541, 2009.

Darabi M, Meibodi NT, Mahdavi R, Arab D: p53 Protein in serum and urine samples of patients with bladder transitional cell carcinoma and its overexpression in tumoral tissue, *Urol Oncol* 4:216–219, 2006.

De Kok JB, van Solinge WW, Ruers TJ, et al.: Detection of tumor DNA in serum of colorectal cancer patients, *Scand J Clin Lab Invest* 57:601–604, 1997.

Del Principe MI, Del Poeta G, Venditti A, et al.: Clinical significance of soluble p53 protein in B-cell chronic lymphocytic leukemia, *Haematologica* 89(12):1468–1475, 2004.

DeVivo I, Marion MJ, Smith SJ, et al.: Mutant c-Ki-ras p21 protein in chemical carcinogenesis in humans exposed to vinyl chloride, *Cancer Causes Control* 5:273–278, 1994.

Diamandis EP: Point: proteomic patterns in biological fluids—do they represent the future of cancer diagnostics? *Clin Chem* 49:1272–1275, 2003.

Di Nicolantonio F, Martini M, Molinari F, et al.: Wild-type BRAF is required for response to panitumumab or cetuximab in metastatic colorectal cancer, *J Clin Oncol* 26:5705–5712, 2008.

Dowling P, O'Driscoll L, Meleady P, et al.: 2-D difference gel electrophoresis of the lung squamous cell carcinoma versus normal sera demonstrates consistent alterations in the levels of ten specific proteins, *Electrophoresis* 28:4302–4310, 2007.

Duffy MJ, Harbeck N, Nap M, et al.: Clinical use of biomarkers in breast cancer: updated guidelines from the European Group on Tumor Markers (EGTM), *Eur J Cancer* 75:284–298, 2017.

El Azm ARA, Yousef M, Salah R, et al.: Serum anti-P53 antibodies and alpha-fetoprotein in patients with non-B non-C hepatocellular carcinoma, *SpringerPlus* 2(1):69, 2013.

Field JK, Spandidos DA: The role of ras and myc oncogenes in human solid tumours and their relevance in diagnosis, *Anticancer Res* 10:1–22, 1990.

Filiberti R, Marroni P, Neri M, et al.: Serum PDGF-AB in pleural mesothelioma, *Tumor Biol* 25:221–226, 2005.

Fontanini G, Fiore L, Bigini D, et al.: Levels of p53 antigen in serum of non–small lung cancer patients correlate with positive p53 immunohistochemistry on tumor sections, tumor necrosis and nodal involvement, *Int J Oncol* 5:553, 1994.

Forester K, Almoguera C, Han K, et al.: Detection of high incidence of K-ras oncogenes during human colon tumorigenesis, *Nature* 327:298–303, 1987.

Fu S, Pierre J, Smith-Norowitz TA, Hagler M, et al.: IgE antibodies from pancreatic cancer patients mediate antibody-dependent cell meditate cytotoxicity (ADCC) against pancreatic cancer cells, *Clin Exp Immunol* 153:401–409, 2008.

Fujimoto K, Ichimori Y, Kakizoe T, et al.: Increased serum levels of basic fibroblast growth factor in patients with renal cell carcinoma, *Biochem Biophys Res Commun* 180:386–392, 1991.

Geddert H, Zeriouh M, Wolter M, et al.: Gene amplification and protein overexpression of c-erb-b2 in Barrett carcinoma and its precursor lesions, *Am J Clin Pathol* 118:60–66, 2002.

Gerdtsson AS, Malats N, Säll A, et al.: A multicenter trial defining a serum protein signature associated with pancreatic ductal adenocarcinoma, *Int J Proteomics* 2015:587250, 2015.

Gogas H, Eggermont AM, Hauschild A, et al.: Biomarkers in melanoma, *Ann Oncol* 20(Suppl 6):vi8–vi13, 2009.

Gou K, Liu J, Feng X, et al.: Expression of minichromosome maintenance proteins (MCM) and cancer prognosis: a meta-analysis, *J Cancer* 9:1518–1526, 2018.

Grabowska MM, Day ML: Soluble E-cadherin: more than a symptom of disease, *Frontiers in Bioscience (Landmark Edition)* 17:1948–1964, 2012.

Gupta NP, Sharma N, Kumar R: Nuclear matrix protein 22 as adjunct to urine cytology and cystoscopy in follow-up of superficial TCC of urinary bladder, *Urology* 73:592–596, 2009.

Hamer PJ, LaVecchio J, Ng S, et al.: Activated Val-12 ras p21 in cell culture fluids and mouse plasma, *Oncogene* 6:1609–1615, 1991.

Harris L, Fritsche H, Mennel R, et al.: American Society of Clinical Oncology 2007 update of recommendations for the use of tumor markers in breast cancer, *J Clin Oncol* 25(33):5287–5312, 2007.

Hautmann S, Eggers J, Meyhoff H, et al.: Tumor markers for bladder cancer: up-to-date study by the Kiel Tumor Bank, *Urologe* 46:1508–1513, 2007.

Hioki O, Watanabe A, Minemura M, et al.: Clinical significance of serum hepatocyte growth factor levels in liver diseases, *J Med* 24:35–46, 1993.

Hofmann G, Balic M, Dandachi N, et al.: The predictive value of serum soluble E-cadherin levels in breast cancer patients undergoing preoperative systemic chemotherapy, *Clin Biochem* 46(15):1585–1589, 2013. h.

Holt KH, Kasson BG, Pessin JE: Insulin stimulation of MEK-dependent but ERK-independent SOS protein kinase, *Mol Cell Biol* 16:577–583, 1996.

Hruben RH, Adsay NV, Albores-Saavedra J, et al.: Pancreatic intraepithelial neoplasia: a new nomenclature and classification system for pancreatic duct lesions, *Am J Surg Pathol* 25(5):579–586, 2001.

Hu M, Hu Y, He J, Li B: Prognostic value of basic fibroblast growth factor (bfgf) in lung cancer: a systematic review with meta-analysis, *PloS One* 11(1):e0147374, 2016.

Hudelist G, Pacher-Zavisin M, Singer CF, et al.: Use of high throughput protein array for profiling of differentially expressed proteins in normal and malignant breast tissue, *Breast Cancer Res Treat* 86:281–291, 2004.

Hudson ME, Pozdnyakova I, Haines K, et al.: Identification of differentially expressed proteins in ovarian cancer using high density protein microarrays, *Proc Natl Acad Sci USA* 104:7494–7499, 2007.

Hügel R, Muendlein A, Volbeding L, et al.: Serum levels of hepatocyte growth factor as a potential tumor marker in patients with malignant melanoma, *Melanoma Res* 26:354–360, 2016.

Hughes JH, Cohen MB: Nuclear matrix proteins and their potential applications to diagnostic pathology, *Am J Clin Pathol* 111:267–274, 1999.

Hwang YH, Choi JY, Kim S, et al.: Over-expression of c-raf-1 proto-oncogene in liver cirrhosis and hepatocellular carcinoma, *Hepatol Res* 29:113–121, 2004.

Ii M, Yoshida H, Aramaki Y, et al.: Improved enzyme immunoassay for human basic fibroblast growth factor using a new enhanced chemiluminescence system, *Biochem Biophys Res Commun* 193:540–545, 1993.

Ingvarsson J, Wingren C, Carlsson A, et al.: Detection of pancreatic cancer using antibody microarray-based serum protein profiling, *Proteomics* 8:221–2219, 2008.

Janson S, Aaltonen K, Bendahl P-O, et al.: The PDGF pathway in breast cancer is linked to tumour aggressiveness, triple-negative subtype and early recurrence, *Breast Cancer Res Treat* 169:231–241, 2018.

Jeng JE, Tsai MF, Tsai HR, et al.: Urinary transforming growth factor α and serum α-fetoprotein as tumor markers of hepatocellular carcinoma, *Tumour Biol* 3689–3698, 2014.

Jibiki N, Saito N, Kameoka S, et al.: Clinical significance of fibroblast growth factor (FGF) expression in colorectal cancer, *Int Surg* 99(5):493–499, 2014.

Kahlert C, Fiala M, Musso G, et al.: Prognostic impact of a compartment-specific angiogenic marker profile in patients with pancreatic cancer, *Oncotarget* 5(24):12978–12989, 2014.

Kanda M, Matthei H, Wu J, et al.: Presence of somatic mutations in most early-stage pancreatic intraepithelial neoplasia, *Gastroenterology* 142:730–733, e9, 2012.

Karagiannis SN, Bracher MG, Hunt J, et al.: E-antibody-dependent immunotherapy of solid tumors: cytotoxic and phagocytic mechanisms of eradication of ovarian cancer cells, *J Immunol* 179:2832–2843, 2007.

Katayama M, Hirai S, Kamihagi K, et al.: Soluble E-cadherin fragments increased in circulation of cancer patients, *Br J Cancer* 69(3):580–585, 1994.

Kath R, Hoffken K, Otte C, et al.: The neu-oncogene product in serum and tissue of patients with breast carcinoma, *Ann Oncol* 14:585–590, 1993.

Katoh M, Inagaki H, Kurosawa-Ohsawa K, et al.: Detection of transforming growth factor alpha in human urine and plasma, *Biochem Biophys Res Commun* 167:1065–1072, 1990.

Kattan MW, Shariat SF, Andrews B, et al.: The addition of interleukin-6 soluble receptor and transforming growth factor beta1 improves a preoperative nomogram for predicting biochemical progression in patients with clinically localized prostate cancer, *J Clin Oncol* 21(19):3573–3579, 2003.

Kaur J, Srivastava A, Ralhan R: Serum p53 antibodies in patients with oral lesions: correlation with p53/HSP70 complexes, *Int J Cancer* 74:609–613, 1997.

Kelderman S, Heemskerk B, van Tinteren H, et al.: Lactate dehydrogenase as a selection criterion for ipilimumab treatment in metastatic melanoma, *Cancer Immunol Immunother* 63(5):449–458, 2014.

Kelly JD, Dudderidge TJ, Wollenschlaeger A, et al.: Bladder cancer diagnosis and identification of clinically significant disease by combined urinary detection of Mcm5 and nuclear matrix protein 22, *PloS One* 7(7):e40305, 2012.

Kershaw MH, Darcy PK, Trapani JA, et al.: Tumor-specific IgE-mediated inhibition of human colorectal carcinoma xenograft growth, *Oncol Res* 10:133–142, 1998.

Kim H-A, Lee JK, Kim E-K, et al.: Serum human epidermal growth factor receptor 2 levels as a real-time marker for tumor burden in breast cancer patients, *J Surg Oncol* 109(5):421–425, 2014.

Kim BK, Lee JW, Park PJ, et al.: The multiplex bead array approach to identifying serum biomarkers associated with breast cancer, *Breast Cancer Res* 11:R22, 2009.

Kinde I, Wu J, Papadopoulos N, et al.: Detection and quantification of rare mutations with massively parallel sequencing, *Proc Natl Acad Sci USA* 108:9530–9535, 2011.

Klocker EI, Stenzl A, Cronauer MV, et al.: Quantitative determination of transforming growth factor-alpha in serum and urine in patients with bladder cancer and its expression in malignant and non-malignant primary epithelial cells, *Proc Am Assoc Cancer Res* 35:A261, 1994.

Kopreski MS, Benko FA, Kwee C, et al.: Detection of mutant K-ras DNA in plasma or serum of patients with colorectal cancer, *Br J Cancer* 76:1293–1299, 1997.

Krzystek-Korpacka M, Diakowska D, Gamian A, Matusiewicz M: Increase in serum platelet-derived growth factor (pdgf)-bb reflects lymph node involvement in esophageal cancer patients independently from platelet count, *Exp Oncol* 33:140–144, 2011.

Kurobe M, Takei Y, Ezawa H, et al.: Increased level of basic fibroblast growth factor (bFGF) in sera of patients with malignant tumors, *Horm Metab Res* 25:395–396, 1993.

Kuwata T, Haruta I, Hasegawa K, et al.: Antibody dependent cell-mediated cytotoxicity using hepatocellular carcinoma reactive monoclonal antibody, *J Gastroenterol Hepatol* 13:137–144, 1998.

Lai Y, Wang X, Zeng T, Xing S, et al.: Serum VEGF levels in the early diagnosis and severity assessment of non-small cell lung cancer, *J Cancer* 9:1538–1547, 2018.

Landman J, Chang Y, Kavaler E, et al.: Sensitivity and specificity of NMP-22, telomerase and BTA in the detection of human bladder cancer, *Urology* 52:398–402, 1998.

Li Y, Karjalainen A, Koskinen H, et al.: p53 autoantibodies predict subsequent development of cancer, *Int J Cancer* 114:157–160, 2004.

Li Y, Karjalainen A, Koskinen H, et al.: Serum growth factors in asbestosis patients, *Biomarkers* 14:61–66, 2009.

Li Y, Zhang J: Expression of mutant p53 in oral squamous cell carcinoma is correlated with the effectiveness of intra-arterial chemotherapy, *Oncol Lett* 10:2883–2887, 2015.

Lia P, Shia J-X, Daia L-P, et al.: Serum anti-MDM2 and anti-c-Myc autoantibodies as biomarkers in the early detection of lung cancer, *Oncoimmunol* 5:e1138200–e1138210, 2016.

Lindmark G, Sundberg C, Glimelius B, et al.: Stromal expression of platelet-derived growth factor beta-receptor and platelet-derived growth factor B-chain in colorectal cancer, *Lab Invest* 69:682–689, 1993.

Linkov F, Lisovich A, Yurkovetsky Z, et al.: Early detection of head and neck cancer: development of a novel screening tool using multiplexed immunobead-based biomarker profiling, *Cancer Epidemiol Biomarkers Prev* 16:102–107, 2007.

Liu L, Ahiekpor A, Li L, et al.: Increased expression of ErbB-2 in liver is associated with hepatitis B x antigen and shorter survival in patients with liver cancer, *Int J Cancer* 125(8):1894–1901, 2009.

Liu J, Ma Q, Zhang M, et al.: Alterations of TP53 are associated with a poor outcome for patients with hepatocellular carcinoma: evidence from a systematic review and meta-analysis, *Eur J Cancer* 48(15):2328–2338, 2012.

Liu L, Shao X, Gao W, et al.: The role of human epidermal growth factor receptor 2 as a prognostic factor in lung cancer, *J Thorac Oncol* 5:1922–1932, 2011.

Locker GY, Hamilton S, Harris J, et al.: ASCO 2006 update of recommendations for the use of tumor markers in gastrointestinal cancer, *J Clin Oncol* 24(33):5313–5327, 2006.

Logsdon CD, Lu W: The significance of Ras activity in pancreatic cancer initiation, *Int J Biol Sci* 113:338–346, 2016.

Ludovini V, Gori S, Colozza M, et al.: Evaluation of serum HER2 extracellular domain in early breast cancer patients: correlation with clinicopathological parameters and survival, *Ann Oncol* 19:883–890, 2008.

Luo JC, Yu MW, Chen CJ, et al.: Serum c-erbB-2 oncopeptide in hepatocellular carcinogenesis, *Med Sci Res* 21:305, 1993.

Madsen CV, Steffensen KD, Olsen DA, et al.: Serum platelet-derived growth factor and fibroblast growth factor in patients with benign and malignant ovarian tumors, *Anticancer Res* 32(9):3817–3825, 2012.

Mattioni M, Soddu S, Prodosmo A, et al.: Prognostic role of serum p53 antibodies in lung cancer, *BMC Canc* 15:148–159, 2015.

Megliorino R, Shi F-D, Peng X-X, et al.: Autoimmune response to anti-apoptotic protein survivin and its association with antibodies to p53 and c-myc in cancer detection, *Cancer Detect Prev* 29(3):241–248, 2005.

Meng D, Yuan M, Li X, et al.: Prognostic value of K-RAS mutations in patients with non–small cell lung cancer: a systematic review with meta-analysis, *Lung Canc* 81(1):1–10, 2013.

Meng R, Wang Y, He L, et al.: Potential diagnostic value of serum p53 antibody for detecting colorectal cancer: a meta-analysis, *Oncol Lett* 15:5489–5496, 2018.

Meng X, Franklin DA, Dong J, Zhang Y: MDM2-p53 pathway in hepatocellular carcinoma, *Cancer Res* 74:7161–7167, 2014.

Milanese G, Dellabella M, Fazioli F, et al.: Increased urokinase-type plasminogen activator receptor and epidermal growth factor receptor in serum of patients with prostate cancer, *J Urol* 181:1393–1400, 2009.

Miyanaga N, Akaza H, Ishikawa S, et al.: Clinical evaluation of nuclear matrix protein 22 (NMP22) in urine as a novel marker for urothelial cancer, *Eur Urol* 31:163–168, 1997.

Miyanaga N, Akaza H, Tsukamoto S, et al.: Usefulness of urinary NMP22 to detect tumor recurrence of superficial bladder cancer after transurethral resection, *Int J Clin Oncol* 8:369–373, 2003.

Molina R, Jo J, Filella X, et al.: C-erb-B oncoprotein in the sera and tissue of patients with breast cancer: utility in prognosis, *Anticancer Res* 16:2295–2300, 1996.

Monstein HJ, Fransen K, Dimberg J, et al.: K-ras and B-raf gene mutations are not associated with gastrin- and CCK2-receptor mRNA expression in human colorectal tumour tissues, *Eur J Clin Invest* 34:100–106, 2004.

Moodie SA, Willumsen BM, Weber MJ, et al.: Complexes of Ras-GTP with Raf-1 and mitogen-activated protein kinase kinase, *Science* 260:1658–1661, 1993.

Mori S, Mori Y, Mukaiyama T, et al.: In vitro and in vivo release of soluble erbB-2 protein from human carcinoma cells, *Jpn J Cancer Res* 81:489–494, 1990.

Morris JP, Wang SC, Hebrok M, et al.: KRAS, Hedgehog, Wnt and the twisted developmental biology of pancreatic ductal adenocarcinoma, *Nat Rev Cancer* 10:683–695, 2010.

Moskal T, Huang S, Ellis LM, et al.: Serum levels of transforming growth factor Alpha in gastrointestinal cancer patients, *Cancer Epidemiol Biomarkers Prev* 4:127–131, 1995.

Mutch DG, Powell MA, Mallon MA, et al.: RAS/RAF mutation and defective DNA mismatch repair in endometrial cancers, *Am J Obstet Gynecol* 190:935–942, 2004.

Nakatsura T, Senju S, Ito M, et al.: Cellular and humoral immune responses to a human pancreatic cancer antigen, coactosin-like protein, originally defined by the SEREX method, *Eur J Immunol* 32:826–836, 2002.

Nedvidkova J, Nemec J, Stolba P, et al.: Epidermal growth factor (EGF) in serum of patients with differentiated carcinoma of thyroids, *Neoplasma* 39:11–14, 1992.

Nelli EM, Leitzel K, Ali SM, et al.: Elevated serum ras levels in patients with hematologic malignancies, *Proc Am Assoc Cancer Res* 47:1144, 2006.

Niman HL, Thompson AM, Yu A, et al.: Anti-peptide antibodies detect oncogene-related proteins in urine, *Proc Natl Acad Sci U S A* 82:7924–7928, 1985.

Normanno N, Tejpar S, Morgillo F, et al.: Implications for KRAS status and EGFR-targeted therapies in metastatic CRC, *Nat Rev Clin Oncol* 6:519–527, 2009.

Olsen CC, Schefter TE, Chen H, et al.: Results of a phase I trial of 12 patients with locally advanced pancreatic carcinoma combining gefitinib, paclitaxel, and 3-dimensional conformal radiation: report of toxicity and evaluation of circulating K-ras as a potential biomarker of response to therapy, *Am J Clin Oncol* 32:115–121, 2009.

Orchekowski R, Hamelinck D, Li L, et al.: Antibody microarray profiling reveals individual and combined serum proteins associated with pancreatic cancer, *Cancer Res* 65:11194–11202, 2005.

Organ L, Tsao M-S: An overview of the c-MET signaling pathway, *Ther Adv Med Oncol* 3(1 Suppl):S7–S19, 2011.

Pawlikowski M, Cicslak D, Stepien H, et al.: Elevated blood serum levels of epidermal growth factor in some patients with gastric cancer, *Endokrynol Pol* 40:149–153, 1989.

Pichler R, Tulchiner G, Fritz J, et al.: Urinary UBC rapid and NMP-22 test for bladder cancer surveillance in comparison to urinary cytology: results from a prospective single-center study, *Int J Med Sci* 14:811–819, 2017.

Pickup M, Novitskiy S, Moses HL: The roles of TGFβ in the tumour Pickup microenvironment, *Nat Rev Cancer* 13(11):788–799, 2013.

Pierobon M, Wulfkuhle J, Liotta L, et al.: Application of molecular technologies for phosphoproteomic analysis of clinical samples, *Oncogene* 34:805–814, 2015.

Pillai R, Behera M, Berry LD, et al.: *HER2* mutations in lung adenocarcinomas: a report from the Lung Cancer Mutation Consortium, *Cancer* 123:4099–4105, 2017.

Pimentel E: *Oncogenes*, ed 2, Boca Raton, FL, 1989, CRC Press.

Pincus MR: Development of new anti-cancer peptides from conformational energy analysis of the oncogenic Ras-p21 protein and its complexes with target proteins, *Front Biosci* 9:3486–3509, 2004.

Pincus MR, Brandt-Rauf PW, Michl J, et al.: ras-p21-induced cell transformation: unique signal transduction pathways and implications for the design of new chemotherapeutic agents, *Cancer Invest* 18:39–50, 2000.

Pincus MR, Chung D, Dykes DC, et al.: Pathways for activation of the ras-oncogene-encoded p21 protein, *Ann Clin Lab Sci* 22:323–342, 1992.

Pincus MR, Fenelys M, Yazdi ES, et al.: Anti-cancer peptides from ras-p21 and p53 proteins, *Curr Pharm Des* 17:2677–2698, 2011.

Pincus MR, Michl J, Bowne W, et al.: Anti-cancer peptides from the ras-p21 and p53 proteins: research advances in cancer. In Mohan RM, editor: *Research advances in cancer*, Kerala, India, 2007, Global Research Network Publishers, pp 65–90.

Polyak K, Weinberg RA: Transitions between epithelial and mesenchymal states: acquisition of malignant and stem cell traits, *Nat Rev Cancer* 9(4):265–273, 2009.

Qin LX, Tang ZY: The prognostic molecular markers in hepatocellular carcinoma, *World J Gastroenterol* 8:385–392, 2002.

Quaranta M, Divella R, Daniele A, et al.: Epidermal growth factor receptor serum levels and prognostic value in malignant gliomas, *Tumori* 93:275–280, 2007.

Ransohoff DF: Lessons from controversy: ovarian cancer screening and serum proteomics, *J Nat Cancer Inst* 97:315–319, 2005.

Rosanelli GP, Wirnsberger GH, Purstner P, et al.: DNA flow cytometry and immunohistochemical demonstration of mutant p53 protein versus TPS and mutant p53 protein serum levels in human breast cancer, *Proc Am Assoc Cancer Res* 34:A1353, 1993.

Roy R, Zurakowski D, Wischhusen J, et al.: Urinary TIMP-1 and MMP-2 levels detect the presence of pancreatic malignancies, *Br J Cancer* 111(9):1772–1779, 2014.

Rustandi RR, Baldisseri DM, Weber DJ: Structure of the negative regulatory domain of p53 bound to S100B (ββ), *Nat Struct Biol* 7:570–574, 2000.

Ryder SD, Rizzi PM, Volkmann M, et al.: Use of a specific ELISA for the detection of antibodies directed against p53 protein in patients with hepatocellular carcinoma, *J Clin Pathol* 4:295–299, 1996.

Sacco R, Leuci D, Tortorella C, et al.: Transforming growth factor beta1 and soluble Fas serum levels in hepatocellular carcinoma, *Cytokine* 12:811–814, 2000.

Salajegheh A: Transforming growth factor α and β (TGF-α and TGF-β). In *Angiogenesis in health, disease and malignancy*, New York, 2016, Springer, pp 331–337.

Sallam RM: Proteomics in cancer biomarkers discovery: challenges and applications, *Dis Markers* 2015:1–12, 2015.

Shariat SF, Casella R, Monoski MA, et al.: The addition of urinary urokinase-type plasminogen activator to urinary nuclear matrix protein 22 and cytology improve the detection of bladder cancer, *J Urol* 170:2244–2247, 2003.

Shi T, Fillmore TL, Sun X, et al.: Antibody-free, targeted mass-spectrometric approach for quantification of proteins at low picogram per milliliter levels in human plasma/serum, *Proc Natl Acad Sci U S A* 109:15395–15400, 2012.

Shi J-H, Guo W-Z, Jim Y, et al.: Recognition of HER2 expression in hepatocellular carcinoma and its significance in postoperative tumor recurrence, *Cancer Med* 8:1269–1278, 2019.

Shimada H, Nakajima K, Ochiai T, et al.: Detection of serum p53 antibodies in patients with esophageal squamous cell carcinoma: correlation with clinicopathological features and tumor markers, *Oncol Rep* 5:871–874, 1998.

Shirai Y, Kawata S, Ito N, et al.: Elevated levels of plasma transforming growth factor-beta in patients with hepatocellular carcinoma, *Jpn J Cancer Res* 83:676–679, 1992.

Sidransky D, Von Eschenbach A, Tsai YC, et al.: Identification of p53 gene mutation in bladder cancers and urine samples, *Science* 252:706–709, 1991.

Song BC, Chung YH, Kim JA, et al.: Transforming growth factor-beta1 as a useful serologic marker of small hepatocellular carcinoma, *Cancer* 94:175–180, 2002.

Sorenson GD, Pribish DM, Valone FH, et al.: Soluble normal and mutated DNA sequences from single-copy genes in human blood, *Cancer Epidemiol Biomarkers Prev* 3:67–71, 1994.

Soussi T, Legros Y, Lubin R, et al.: Multifactorial analysis of p53 alteration in human cancer: a review, *Int J Cancer* 57:1–9, 1994.

Stoehr R, Brinkmann A, Filbeck T, et al.: No evidence for mutation of B-RAF in urothelial carcinomas of the bladder and upper urinary tract, *Oncol Rep* 11:137–141, 2004.

Stokoe D, MacDonald SG, Cadwallader K, et al.: Activation of Raf as a result of recruitment to the plasma membrane, *Science* 275:1463–1467, 1994.

Su Y-H, Wang M, Brenner DE, et al.: Detection of mutated K-ras DNA in urine, plasma, and serum of patients with colorectal carcinoma or adenomatous polyps, *Ann N Y Acad Sci* 1137:197–206, 2008.

Sun S, Chen Z, Cao C, et al.: Diagnostic value of epidermal growth factor,cancer antigen 125, and cancer antigen 15-3 in bronchoalveolar lavage fluid of lung cancer, *Curr Oncol* 24:e180–e184, 2017.

Suppiah A, Greenman J: Clinical utility of anti-p53 auto-antibody: systematic review and focus on colorectal cancer, *World J Gastroenterol* 19(29):4651–4670, 2013.

Tambo M, Higashihara E, Terado Y, et al.: Comparison of serum HER2/neu with immunohistochemical HER2/neu expression for the prediction of biochemical progression in metastatic prostate cancer, *Int J Urol* 16:369–374, 2009.

Tang R, Yeh CY, Wang JY, et al.: Serum p53 antibody as tumor marker for follow-up of colorectal cancer after curative resection, *Ann Surg Oncol* 16:2516–2523, 2009.

Thomsen CB, Appelt AL, Andersen RF, et al.: The prognostic impact of RAS and RAF serum mutations in localized colon cancer, *Ann Oncol* 27(Suppl 6):vi15–vi42, 2016.

Thomsen CEB, Appelt AL, Andersen RF, et al.: The prognostic value of simultaneous tumor and serum RAS/RAF mutations in localized colon cancer, *Cancer Med* 6:928–936, 2017.

Tomiya T, Fujiwara K: Serum transforming growth factor-alpha level as a marker of hepatocellular carcinoma complicating cirrhosis, *Cancer* 77:1056–1060, 1996.

Tsai JF, Jeng JE, Chuang LY, et al.: Urinary transforming growth factor-beta 1 in relation to serum alpha-fetoprotein in hepatocellular carcinoma, *Scand J Gastroenterol* 32:254–260, 1997.

Tsai-Turton M, Santillan A, Lu D, et al.: p53 autoantibodies, cytokine levels and ovarian carcinogenesis, *Gynecol Oncol* 114:12–17, 2009.

Tsui KH, Chen SM, Wang TM, et al.: Comparisons of voided urine cytology, nuclear matrix protein-22 and bladder tumor associated antigen tests for bladder cancer of geriatric male patients in Taiwan, China, *Asian J Androl* 9:711–715, 2007.

Uppal G, Ly V, Wang ZX, et al.: The utility of BRAF V600E mutation-specific antibody VE1 for the diagnosis of hairy cell leukemia, *Am J Clin Pathol* 143(1):120–125, 2015.

Vincent MD, Kuruvilla MS, Leighl NB, Kamel-Reid S: Biomarkers that currently affect clinical practice: EGFR, ALK, MET, KRAS, *Curr Oncol* 19:S33–S44, 2012.

Virji MA, Rosendale B, Piper M, et al.: Circulating levels of a mutant p53 protein in patients with hepatocellular carcinoma, *Proc Am Assoc Cancer Res* 33:A1508, 1992.

Vlasoff DM, Baschinsky DY, De Young BR, et al.: C-erb B2 (Her2/neu) is neither overexpressed nor amplified in hepatic neoplasms, *Appl Immunohistochem Mol Morphol* 10:237–241, 2002.

Vogelstein B, Fearon ER, Hamilton SR, et al.: Genetic alterations during colorectal-tumor development, *N Engl J Med* 319(9):525–532, 1988.

Wan PT, Garnett MJ, Roe SM, et al.: Mechanism of activation of the RAF-ERK signaling pathway by oncogenic mutations of B-RAF, *Cell* 116:855–867, 2004.

Weiner GJ: Monoclonal antibody mechanisms of action in cancer, *Immunol Res* 39:271–278, 2007.

Weiss JV, Klein-Scory S, Kübler S, et al.: Soluble E-cadherin as a serum biomarker candidate: elevated levels in patients with late-stage colorectal carcinoma and FAP, *Int J Cancer* 128(6):1384–1392, 2011.

Weissfeld JL, Larsen RD, Niman HL, et al.: Evaluation of oncogene-related proteins in serum, *Cancer Epidemiol Biomarkers Prev* 3:57–62, 1994.

Wellbrock C, Ogilvie L, Hedley D, et al.: V599EB-RAF is an oncogene in melanocytes, *Cancer Res* 75:2338–2342, 2004.

Wu JT, Astill ME, Zhang P: Detection of the extracellular domain of c-erbB-2 oncoprotein in sera from patients with various carcinomas: correlation with tumor markers, *J Clin Lab Anal* 7:31–40, 1993.

Wu M, Mao C, Chen Q, et al.: Serum p53 protein and anti-p53 antibodies are associated with increased cancer risk: a case-control study of 569 patients and 879 healthy controls, *Mol Biol Rep* 37(1):339–343, 2010.

Yang L, Wang J, Li J, et al.: Identification of serum biomarkers for gastric cancer diagnosis using a human proteome microarray, *Mol Cell Proteomics* 15:614–623, 2016.

Yazici H, Altun M, Hafiz G, et al.: Serum and tissue c-erb B2, bcl-2, and mutant p53 oncoprotein levels in nasopharyngeal cancer, *Cancer Invest* 19:773–778, 2001.

Yeh J, Yeh JC: Transforming growth factor-alpha and human cancer, *Biomed Pharmacother* 43:651–659, 1989.

Yu MW, Chen CJ, Luo JC, et al.: Correlations of chronic hepatitis B virus infection and cigarette smoking with elevated expression of neu oncoprotein in the development of hepatocellular carcinoma, *Cancer Res* 54:5106–5110, 1994a.

Yu MW, Luo JC, Brandt-Rauf PW, et al.: Correlations of chronic hepatitis B virus infection and cigarette smoking with elevated expression of the neu oncoprotein in the development of hepatocellular carcinoma, *Proc Am Assoc Cancer Res* 35:A1754, 1994b.

Zampino MG, Magni E, Santoro L, et al.: Epidermal growth factor receptor serum (sEGFR) level may predict response in patients with EGFR-positive advanced colorectal cancer treated with gefitinib? *Cancer Chemother Pharmacol* 63:139–148, 2008.

Zhang J, Xu Z, Yu L, et al.: Assessment of the potential diagnostic value of serum p53 antibody for cancer: a meta-analysis, *PloS One* 9(6):e99255, 2014.

Zhang J, Xv Z, Wu X, et al.: Potential diagnostic value of serum p53 antibody for detecting esophageal cancer: a meta-analysis, *PloS One* 7:e52896, 2012.

Zheng T, Chen M, Han S, et al.: Plasma minichromosome maintenance complex component 6 is a novel biomarker for hepatocellular carcinoma patients, *Hepatol Res* 44(13):1347–1356, 2014.

Zhang J-Y, Casiano CA, Peng X-X, et al.: Enhancement of antibody detection in cancer using panel of recombinant tumor-associated antigens, *Cancer Epidemiol Biomarkers Prev* 12:136–143, 2003.

Zhang Y, Cao L, Nguyen D, Lu H: TP53 mutations in epithelial ovarian cancer, *Transl Cancer Res* 5:650–663, 2016.

Zhang J-Y, Casiano CA, Peng X-X, et al.: Enhancement of antibody detection in cancer using panel of recombinant tumor-associated antigens, *Cancer Epidemiol Biomarkers Prev* 12:136–143, 2003.

CHAPTER 78

MOLECULAR DIAGNOSIS OF HEMATOPOIETIC NEOPLASMS

Rong He, David S. Viswanatha

MOLECULAR DIAGNOSIS OF LYMPHOID NEOPLASMS, 1543
Immunoglobulin and T-Cell Receptor Gene Rearrangements: Background and Methods, 1544
Lymphoblastic Leukemia/Lymphoma: Risk Stratification and Minimal Residual Disease, 1547
Low Grade B-Cell Lymphomas, 1551
Aggressive B-Cell Lymphomas, 1554
Plasma Cell Myeloma, 1555
Mature T-Cell Neoplasms, 1555
MOLECULAR DIAGNOSIS OF MYELOID NEOPLASMS, 1556
Acute Myeloid Leukemia, 1556
Chronic Myeloid Neoplasms, 1567
Myeloid Neoplasms with Germline Predisposition, 1575
Clonal Hematopoiesis of Indeterminate Potential, 1576
Myeloid/Lymphoid Neoplasms with Eosinophilia, 1577
SELECTED REFERENCES, 1578

KEY POINTS

- General considerations in the diagnosis, classification, prognosis, and monitoring of hematolymphoid disorders
- Summary of the major genetic abnormalities and molecular detection methods in chronic and acute myeloid neoplasms.
- Basis of lymphoid antigen receptor gene rearrangements and molecular techniques to assess lymphoid clonality
- Concept of risk-adapted therapy for optimized management of childhood acute lymphoblastic leukemias and significance of minimal residual disease assessment
- Summary of the major genetic abnormalities and molecular detection methods in the lymphoid neoplasms.
- Landscape of genetic abnormalities and clinical relevance in acute myeloid leukemias
- Molecular classification of chronic myeloid neoplasms
- Chronic myeloid leukemia: paradigm for targeted therapy and response monitoring
- Germline susceptibility and risk of developing myeloid neoplasms
- Clonal hematopoiesis and clinical significance

Our knowledge, classification, and management of hematolymphoid neoplasms continues to evolve as a result of the rapid pace of new discovery, made possible by new genetic sequencing technologies and the increasing development of rational ("targeted") therapeutic options. Whereas traditional morphologic (light microscopic) evaluation of glass slides still occupies the centerpiece of pathologic diagnosis, the judicious application of ancillary methods, such as special cytochemistry, immunohistochemistry (IHC), flow cytometry, cytogenetics, fluorescence in situ hybridization (FISH), and molecular genetics, has allowed for more precise, biologically driven characterization. The 2017 update of the World Health Organization (WHO) classification of hematopoietic and lymphoid neoplasms (Swerdlow et al., 2017) incorporates a greater proportion of disease-defining or associated genetic abnormalities encompassing both previously known entities and novel provisional categories. The relative ease of sampling sites such as the lymph nodes and bone marrow, as well as the procurement of easily disaggregated viable cell samples for analysis, has driven this paradigm of diagnostic evaluation. Furthermore, improvements in molecular methods have enabled ever more comprehensive utilization of formalin-fixed paraffin-embedded (FFPE) tissue sources. The nature of the hematolymphoid system is also highly conducive to repeated sampling following therapy to assess treatment response or recurrence, which represents another important facet in the management of many patients with these illnesses.

Given the wide array of diagnostic technical options available to hematopathologists, when is molecular testing of greatest necessity or practicality? There are perhaps four major scenarios in which molecular diagnostic analysis of an atypical hematolymphoid process is important. First, molecular investigation can *establish a diagnosis* in situations wherein morphologic details and results of other laboratory tests are inconclusive for malignancy. The presence of specific genetic abnormalities or the demonstration of tumor genetic clonality of a cell population can establish the presence of a pathologic process. Second, molecular methods are used to *subclassify* disease entities. To this end, the current WHO classification of hematologic neoplasms includes molecular characterization as a defining or strongly associated feature of most leukemias and lymphomas (Swerdlow et al., 2017). Next, specific genetic anomalies in hematolymphoid malignancies have important *prognostic or therapeutic value*, which in turn can influence the initial treatment of certain tumors to produce an optimal clinical outcome. Finally, being potentially of high analytical sensitivity, molecular techniques can be used to assess patients after the onset of therapy by monitoring for the presence and extent of minimal residual disease (MRD), which is becoming increasingly critical as therapeutic options improve and patients are surviving longer. As current and new molecular technologies accumulate, attention is appropriately shifting to the analysis and incorporation of different types of data ("multiomics") and leveraging powerful computational approaches to derive even more profound insights into tumor biology and patient-specific treatment (i.e., precision medicine). A major impetus in this regard has been the rapid development and deployment of massively parallel sequencing methods (next-generation sequencing [NGS]), which is simultaneously transforming discovery and diagnostics (Goodwin et al., 2016; Jennings et al., 2017; Johnsen et al., 2013; Kohlmann et al., 2013; Lindsley & Ebert, 2013; Mullighan, 2013).

This chapter focuses on the background, clinical rationale, and pertinent technical considerations underlying the molecular diagnostic evaluation and monitoring of hematopoietic and lymphoid tumors. The intent is to summarize the molecular diagnostic approaches typically employed in hematopathology practice, although it is evident that the rate of discovery and new knowledge in this field are rapidly expanding, requiring continuous attention to the most current literature. Of note, it is apparent that the detection of tumor-specific genetic abnormalities can be achieved by different analytic means—for example, cytogenetics, fluorescence in situ hybridization (FISH), polymerase chain reaction (PCR), Sanger sequencing, or NGS. Although at first glance these various methods may seem redundant or duplicative, these laboratory techniques are often complementary, and the choice of methodologies is determined by a number of factors, including the nature of the tumor genetic or genomic alterations, knowledge of assay analytic sensitivities, sample or source-specific limitations (e.g., FFPE tissues), required turn-around time for results, and diagnosis versus posttherapy monitoring, among others. Table 78.1 summarizes the major molecular methods in use in most clinical diagnostic laboratories. When applying and interpreting molecular diagnostic tests, one caveat that cannot be emphasized enough is that the results of these investigations must never be considered in isolation but rather in conjunction with the clinical presentation and morphologic and additional relevant laboratory data concerning the individual patient. Regardless of the remarkable specificity

TABLE 78.1
Relative Sensitivities of Common Techniques Used to Detect Leukemia or Lymphoma-Associated Genomic and Genetic Abnormalities

Method	Analytic Sensitivity (%)	Notes
Cytogenetics	5	• Requires fresh, sterile cells for culture and metaphase assessment • Global genomic assessment; detects numerical and structural chromosome aberrations • Requires several days to provide analyzed result • Limited resolution below 5–10 megabase (Mb) using standard banding techniques (e.g., Giemsa)
FISH	1–5	• Fluorescent-labeled DNA probe based targeted assessment of genomic abnormalities; detects numerical and structural changes in chromosome regions including translocation events • Enumeration probes (chromosome counting) and locus-specific probes can be used; latter category includes break-apart probes and dual-color or dual-fusion probes • Technically straightforward and rapid • Can be performed on cultured (metaphase) or fixed (interphase) nuclei, including FFPE tissues • Identifies genomic alterations to 50-100 kilobase (Kb) resolution, but not able to assess smaller CNAs
DNA microarray	15–30	• Hybridization of patient DNA (or cDNA) specimen to tiled DNA probe arrays on a solid substrate (glass, silicon, and so on) • Identifies structural variations (e.g., CNA) with nominally 50- to 100-Kb resolution (depends on density and type of array) • SNP arrays are most commonly used and can identify segmental gains or losses (i.e., gene region amplifications, copy gains and losses), including CN-LOH • Tiled oligoprobe microarrays can be used for GEP; requires reverse transcribed RNA (cDNA) as template
PCR	10^{-2}–10^{-4}	• Can be performed from DNA or RNA extracted from fresh or FFPE sources • RNA requires a RT step before PCR • Logarithmic amplification enables use of small amounts of input DNA or RNA (5–100 ng) • Efficiency and sensitivity varies by amplification product (amplicon) size: larger target regions flanked by PCR probes are amplified less efficiently • Targeted assessment of specific genetic regions to identify single base changes, small insertion/deletion events, some chromosomal translocation products • PCR products are often subjected to downstream analyses (e.g., sequencing) to resolve specific base-level alterations in the regions of interest • Use of fluorescent-labeled probes and optimized conditions permits highly sensitive and specific detection of desired targets (i.e., RQ-PCR) for MRD applications • PCR design variations are numerous and include AS-PCR and many others
Sanger sequencing	15–20	• Base-level assessment of SNVs or small insertion/deletion (indel) events • Requires PCR-amplified template; can interrogate only a single genetic region per Sanger assay • Automated methodologies (cycle sequencing) and software analysis have improved analytical performance, but interpretation can be challenging with more complex genetic changes • Cannot resolve biallelic versus same strand alterations (i.e., phasing) when more than one abnormality is present • Cannot accurately evaluate larger scale copy changes (exon deletions or loss of heterozygosity)
NGS	5-10	• Massively parallel sequencing with wide spectrum of applications, including targeted gene panels, WES, WGS, and transcriptome (RNA seq), as well as specialized methods (epigenetics, immunogenetics, and so on) • Short read methodologies (75–400 base segments) are most common (e.g., Illumina, Ion Torrent platforms), but long-read technologies (10s of kilobases) are increasingly common for structural variant detection (e.g., Pacific Biosystems, Oxford Nanopore) • NGS generates millions of sequence reads, requiring mapping to current human reference genome build and sophisticated bioinformatics secondary processing for determination of sequence variants; subsequent comprehensive tertiary analysis is required to interpret, categorize, and curate detected alterations for clinical reporting • NGS can resolve base-level changes, including SNV, small indel, CNA, and even genomic rearrangements (with specialized approaches) • Phasing of complex mutation patterns (e.g., biallelic, homozygous, compound heterozygote) and inference of subclonal populations (e.g., in cancer NGS testing) is possible • Analytic sensitivity for NGS standard methods is ~5%–10% VAF but can be improved with method alterations • Clinical data analysis requires a dedicated team of technical, medical, scientific, genetic counselor, and bioinformatics personnel

AS-PCR, Allele-specific amplification; *CNA,* copy number alteration; *CN-LOH,* copy-neutral loss of heterozygosity; *FFPE,* formalin-fixed paraffin-embedded; *FISH,* fluorescence in situ hybridization; *GEP,* gene expression profiling; *MRD,* minimal residual disease: *NGS,* next-generation sequencing; *PCR,* polymerase chain reaction; *RQ-PCR,* real-time quantitative polymerase chain reaction; *RT,* reverse transcription; *SNP,* single nucleotide polymorphism; *SNV,* single nucleotide variant; *VAF,* variant allele fraction; *WES,* whole-exome sequencing; *WGS,* whole-genome sequencing.

and sensitivity of molecular markers, the evident complexity of hematolymphoid neoplasia mandates such a fully integrated approach to diminish the possibility of serious diagnostic error.

MOLECULAR DIAGNOSIS OF LYMPHOID NEOPLASMS

The subclassification of non-Hodgkin lymphomas (NHL) and lymphoid leukemias is established by a combination of characteristic light microscopic tumor cell features, immunophenotypic cell marker profiling (e.g., by flow cytometry and IHC), and the presence of recurrent, nonrandom tumor genetic abnormalities (i.e., structural and numerical genomic variants, somatic gene mutations) (Swerdlow et al., 2017). Molecular diagnostic evaluation of abnormal lymphoid proliferations often involves FISH analysis, PCR, and DNA sequencing (including use of targeted NGS panels). A central paradigm in the diagnosis of lymphoid neoplasms is the demonstration of monoclonality, which is highly correlated with the malignant state. In many instances, a monoclonal lymphoid proliferation can be suggested or established with the aid of immunophenotypic studies—for example, by demonstrating light chain restriction in the case of B-cell neoplasms or aberrant antigen expression patterns in the setting of suspicious T-cell malignancies. However, there are often instances in which the foregoing analyses may be insufficient, and the determination of

TABLE 78.2

Summary of Polymerase Chain Reaction Analysis for Immunoglobulin and T-Cell Receptor Gene Rearrangements (Lymphoid Clonality Assessment)

Advantages	Pitfalls
• Rapid (24–96 hours), inexpensive, technically straightforward • Useful lower range of input DNA (e.g., 10–500 ng) and relatively short-amplicon products (e.g., 100–400 bp) enables evaluation of many tissue sources, including FFPE • Analytically relatively sensitive (~1%–5% detection of a clonal subpopulation) with FCE analysis • Evaluation of multiple loci (e.g., *IGH* + *IGK*, *TRB* + *TRG*) increases clinical sensitivity for detecting monoclonality • Adaptable to highly sensitive and specific NGS platforms for direct sequence analysis (e.g., CLL *IGH*-V somatic hypermutation status, MRD)	• False-positive risk from sample contamination or skewed T-cell repertoires (e.g., age related, viral infection, posttransplant), causing "pseudoclonal" results • False-negative risk with consensus primer methods (e.g., somatic *IGH* hypermutation in B cells) • Difficult interpretation in oligoclonal lymphoid proliferations and in samples with "limited DNA template" • Analytic sensitivity can be adversely affected by presence of abundant polyclonal lymphocyte background • Patient-related and technical factors can exacerbate subjective bias in interpretation

CLL, Chronic lymphocytic leukemia; *FCE,* fluorescent capillary electrophoresis; *MRD,* minimal residual disease; *NGS,* next-generation sequencing.

clonality in a lymphoid population by molecular methods remains key to establishing a definitive diagnosis. In these situations, which may include samples with uninformative phenotypic features, small tissue biopsies, or partially degraded specimens such as paraffin-embedded tissues, the molecular assessment of antigen receptor gene rearrangements is often very useful and commonly employed. Standard PCR-based clonality detection methods are often employed to resolve the definitive diagnosis of lymphoid neoplasms with features potentially mimicking benign hyperplasias (e.g., follicular lymphomas [FLs] or extranodal marginal zone B-cell lymphomas) and to aid in the diagnosis of neoplastic T-cell lymphoproliferations. Immunoglobulin and T-cell receptor (TCR) gene PCR evaluation has continued to further evolve with the application of NGS technology.

Chromosome translocation events or aneuploidies identified by FISH techniques also serve to establish the presence of a clonal neoplasm. Recurrent chromosomal translocations occur in many lymphomas and provide the basis for accurate diagnostic characterization and classification (Table 78.2) (Swerdlow et al., 2017). In general, chromosome translocations are more prevalent in B-cell NHL and result in the fusion of two genetic loci, commonly involving the *IGH* locus. As a result of this process, a normally highly regulated proto-oncogene becomes constitutively activated by juxtaposition to the immunoglobulin gene enhancer region, leading to overexpression of the translocated gene locus (e.g., t(8;14)/*MYC-IGH*). In some lymphomas, however, the gene fusion is expressed as a chimeric mRNA transcript and novel oncoprotein (e.g., t(2;5)/*NPM1-ALK*). In either case, interference with normal processes of lymphoid cell growth, homeostasis, or cell death (apoptosis) is central to lymphomagenesis. Lymphoma-associated translocation events are thought in many cases to be linked to aberrant behavior of the recombinase activating gene (RAG) and DNA breakage-repair enzyme systems that are active during the time of normal antigen receptor gene rearrangement or through germinal center processes such as somatic hypermutation (SHM) and class switch recombination (CSR), both of which require the enzyme activation-induced cytidine deaminase (AID) (Pasqualucci et al., 2008; Robbiani & Nussenzweig, 2013). The exact mechanisms underlying translocation events in leukemias and lymphomas are nevertheless incompletely understood but may involve nonrandom spatial proximity of genes during cell cycling, fragile sites such as single-stranded intermediates of DNA prone to breakage and recombination, or other factors (Raghavan & Lieber, 2004; Roix et al., 2003). A small proportion of lymphoma-associated translocations can be detected by PCR methods using genomic DNA (Table 78.3), but only if substantial breakpoint clustering exists in both partner genes to enable consensus primer strategies and the genomic target distance is amenable to efficient PCR amplification. In many cases, however, PCR detection is not possible or practical because of the substantial and inconsistent breakpoint locations over large genomic regions. Thus, FISH methods (break-apart probe [BAP-FISH], dual-probe FISH [D-FISH]) are most often employed to detect specific rearrangements.

Recurrent lymphoma-associated somatic gene mutations represent another class of abnormalities assessable by molecular diagnostic evaluation (see Table 78.2) (Blombery et al.,2015; Garces et al., 2017; Miles et al., 2016). Alterations characterized by single base changes in a "hot spot" codon (e.g., *MYD88*, *BRAF*) can be detected by sensitive allele-specific PCR methods; however, other mutation events can occur over multiple exon regions (e.g., *TP53*), requiring alternate and typically less analytically sensitive approaches, such as Sanger sequencing. NGS methodology has again begun to change the diagnostic landscape in lymphoma by evaluating multiple genes and regions in a single assay with a relatively uniform limit of detection (e.g., 5% variant frequency detection). Targeted NGS panels that can utilize DNA isolated from fixed paraffin-embedded tissues as well as fresh biopsy samples are therefore becoming more commonplace for lymphoma molecular diagnosis. The following sections first describe the molecular basis and methodology for assessing clonal status in lymphoid B-cell and T-cell neoplasms using antigen receptor gene rearrangements followed by descriptions of specific lymphoid malignancies and their associated tumor genetic alterations.

IMMUNOGLOBULIN AND T-CELL RECEPTOR GENE REARRANGEMENTS: BACKGROUND AND METHODS

Mechanism of Antigen Receptor Gene Rearrangements

The antigen receptor genes (*IGH*, *IGK*, *IGL*, *TRA*, *TRD*, *TRB*, *TRG*) are rearranged during the early development of immature B and T lymphocytes in the bone marrow and thymus, respectively, to produce a functional immune cell receptor repertoire. The process of DNA rearrangement in these genomic regions involves the splicing and recombination of *v*ariable (V), *d*iversity (D) and *j*oining (J) genes; the immunoglobulin kappa light chain (*IGK*) and T-cell receptor gamma loci (*TRG*) lack D genes but otherwise conform to the same process. These gene rearrangements occur across large segments of the specific genomic loci with looping out of intervening DNA between the rearranged junctions. The rearrangement process requires a complex of specialized proteins involved in site-specific DNA recognition, unwinding, splicing, nuclease activity, and addition of random junctional nucleobases and DNA repair (Bassing et al., 2002; Perlot & Alt, 2008). The recombinase activating gene enzymes (RAG1 and 2) are a major component of this process. Enormous diversity exists among the immunoglobulin (IG) and T-cell receptors (TCRs), resulting to a significant degree from the potential for genetic recombination between the numerous V, (D), and J genes at their respective loci. The activity of the enzyme terminal deoxynucleotidyl transferase (TdT) randomly adds a variable number of non-templated ("n") nucleic acid bases at the junctions of the rearranged V(D)J gene segments, further substantially increasing sequence diversity (Fig. 78.1A). An important aspect of the recombination process is that each IG or TCR rearrangement is highly unique at the DNA and peptide level, in large part conferred by the combinatorial nature of the process and associated TdT-mediated junctional nucleotide insertions. This is exemplified by the "CDR3" region of a rearranged immunoglobulin heavy chain (*IGH*) gene, in which the V(D)J junction sequence is highly specific for an individual B lymphocyte. The resulting rearranged V(D)J gene is subsequently joined with a downstream *c*onstant (C) region gene of the antigen receptor locus to produce a completed coding sequence capable of translation to a functional antigen receptor protein with both extracellular and intracellular domains (Bassing et al., 2002). Immune cells incapable of producing functional receptor proteins undergo deletion by apoptosis. For B cells in early development stages, the *IGH* on chromosome 14(q32) is the first to undergo this segmental locus rearrangement followed in turn by the *IGK* on 2(p12). If the latter attempt is unsuccessful (i.e., nonproductive) at both alleles, the lambda locus (*IGL*) on 22(q11) undergoes rearrangement in order to generate the final tetrameric immunoglobulin molecule, consisting of two identical heavy chains and two identical light chains. For T cells, the TCR delta (*TRD*) on 14(q11) and gamma (*TRG*) on 7(p15) loci initiate this process in thymic T lymphocytes; however, many of these gene rearrangements, particularly involving the *TRD* locus (which is embedded within the *TRA* region), fail to produce a functional heterodimeric gamma/delta TCR protein. Thus, rearrangement continues essentially simultaneously at the TCR alpha (*TRA*) and beta (*TRB*) loci, located on chromosomes 14(q11) and 7(q34), respectively,

TABLE 78.3

Risk Stratification or Outcome Prediction in Childhood B-Lineage Acute Lymphoblastic Leukemia[a]

Abnormality	Prognostic Significance	Notes
High hyperdiploidy (>52 chromosomes)	Favorable	• Relatively common • Hyperdiploid tumors with particular trisomic chromosomes (e.g., +4, +10, +17) associated with very favorable outcome
t(12;21)/*ETV6-RUNX1*	Favorable	• Relatively common • Very favorable outcome, but appreciable incidence of late relapses
t(1;19)/*TCF3-PBX1*	Intermediate	• Intensive therapy results in good outcome
Hypodiploidy (<44 chromosomes)	Unfavorable	• Rare incidence • Very high risk for relapse/refractory disease
iAMP21	Unfavorable	• Uncommon, results from complex chromosome 21 rearrangement pattern with variable genomic region amplifications (e.g., *RUNX1*) or losses
t(9;22)/*BCR-ABL1*	Unfavorable	• More common in adolescents and adults versus young children • High risk for relapse/refractory disease
BCR-ABL1-like genetics	Unfavorable	• Incidence increases with age, more prevalent in older children and adults • Complex spectrum of genetic abnormalities but shared gene expression signature with *BCR-ABL1*+ B-lymphoblastic leukemias • *CRLF2* gene alterations in ~50% of cases • Activation of kinase genes is common, including expressed chimeric gene fusions involving *ABL1* or *ABL2*, mutations or rearrangements in *JAK1* and *JAK2*, and translocations causing overexpression of *EPOR*, *PDGFRB* • Disruption of B-cell transcriptional program (alterations in *PAX5*, *IKZF1*) • Requires multimodal molecular diagnostic approach for evaluation
11q23/*KMT2A (MLL)* gene rearrangements	Unfavorable	• Highly prevalent in infant ALL; also considered high risk factor for older children • Many gene partners with *KMT2A*; FISH method is optimal for detection
MRD positivity at end-induction therapy	Unfavorable	• High risk of relapse in patients with MRD above 10^{-3} to 10^{-4}, detected by flow cytometric or molecular methods • NGS of immunoglobulin receptor gene rearrangements is highly sensitive for MRD detection

[a]Tumor genetic features and early MRD are considered in conjunction with clinical and laboratory findings, including age, presenting blast count, and evidence of extramedullary disease. These risk factors therefore modify and refine traditional parameters for predicting therapeutic response.

resulting in expression of a TCR alpha/beta protein in the large majority (>90%) of developing T cells. The basic structures of immunoglobulin and TCR proteins are illustrated in Fig. 78.1B. As an important point related to molecular diagnostic analysis, nearly all mature alpha/beta T-cells still retain residual gamma (*TRG*) locus gene rearrangement(s) at the DNA level, which can be utilized as a valuable marker for T-cell lymphoid clonality assessment.

Techniques to Detect Antigen Receptor Gene Rearrangements: Polymerase Chain Reaction/Fragment Analysis and Next-Generation Sequencing

As a result of the largely random nature of the immunoglobulin and TCR gene rearrangement process and variable junctional nucleotide diversity, individual B and T lymphocytes harbor a myriad of specific gene rearrangement sequences and express correspondingly unique antigen receptor immune proteins on their cell surfaces, enabling a tremendous range of potential antigen recognition and binding affinities. In a polyclonal lymphoid expansion, therefore, a highly diverse and variable distribution of individual antigen receptor gene rearrangements at the DNA level is generally found, whereas a monoclonal population is characterized by a single identical gene rearrangement in each progeny cell. This concept is exploited by several techniques, including DNA-based PCR and capillary or gel fragment sizing, NGS and Southern blot hybridization (SBH) analysis, to distinguish polyclonal ("benign") from monoclonal ("malignant") lymphocytic proliferations. The SBH method has largely been supplanted by comprehensive PCR-based approaches for routine lymphoid clonality determination and thus will not be discussed further.

Despite the large spectrum of antigen receptor gene rearrangements encoding this diverse immune repertoire, rearranged V(D)J genes can be reliably detected and analyzed by relatively simple PCR techniques made possible by the presence of relatively conserved DNA sequences within V and J genes that flank the rearrangements (Fig. 78.1C). For example, the *IGH* locus contains approximately 70 to 80 V-region genes that can be grouped into seven families based on partial sequence similarities. These more homologous sequence sites allow the use of "consensus" PCR primers that can bind and amplify the rearranged V(D)J genes in a DNA sample. Most commonly, PCR-based lymphoid clonality assays target the *IGH*, *IGK*, *TRG*, and *TRB* loci using the consensus primer design strategy. PCR amplification products can be displayed by agarose or polyacrylamide gel electrophoresis, in which polyclonal distributions are seen as broad smears and monoclonal populations are identified as discrete bands; however, current practice employs fluorescently labeled PCR primers and capillary gel electrophoresis (CGE) of the PCR products. CGE enables a high-resolution readout of amplitude (relative PCR product intensity) versus amplicon fragment size distribution (Fig. 78.1D). Substantial refinements have been made over time to optimize PCR approaches for lymphoid clonality evaluation, and many standard methods follow the guidelines proposed by the BIOMED-2 consortium (Bruggemann et al., 2007; Evans et al., 2007; Langerak et al., 2012; van Dongen et al., 2003; van Krieken et al., 2007), which provide recommendations on consensus primer design and primer multiplexing of reactions. In general, PCR techniques have gained wide popularity for clonality determination, principally because of their relative ease of performance and rapidity (see Table 78.3). PCR methods are advantageous in that they are fast (3–5 days), relatively inexpensive, and require relatively minimal starting DNA quantity. Moreover, PCR can be performed using DNA extracted from fresh samples and FFPE tissue sources, although certain fixatives (e.g., B5) or agents commonly used in lymph node or bone marrow biopsy processing may cause suboptimal results. Clonality assessment by PCR has a nominal analytical sensitivity of 1% to 5%, although a prominent coexisting polyclonal B or T-cell background can significantly reduce the ability of the technique to detect a coexistent monoclonal lymphocyte population.

Although immunoglobulin and TCR PCR is generally very informative, the technique is occasionally subject to false-negative assay results because it is not possible to design consensus-type primers to capture all possible antigen receptor gene rearrangements in lymphoid cells. For B-cell lymphomas, the issue of SHM of the *IGH* genes can also be problematic; SHM occurs during the germinal center reaction and is mediated by the enzyme AID (Di Noia & Neuberger, 2007). AID activity generates nucleotide base substitutions and corresponding amino acid changes in the V genes and is especially notable in the junctional region of the VDJ rearrangement. This biologic process enhances the binding of specific immunoglobulins for cognate epitope regions of target antigens (known as affinity maturation). In the setting of germinal center–associated or postgerminal center B-cell lymphomas (e.g., follicular and large B-cell lymphomas, myeloma), SHM can result in loss of consensus primer binding recognition, failure of PCR amplification, and inability to detect a monoclonal B-cell population. Nevertheless, the effect of SHM in B-cell lymphomas can be largely overcome by using multiple PCR primer strategies and by including analysis of the *IGK* locus. In contrast, the problem of analytic false positivity is sometimes encountered when interpreting T-cell (TCR) gene rearrangement results by PCR. This situation is most evident when evaluating the *TRG* locus. The *TRG* locus has limited overall V- and J-gene recombination potential, which can occasionally lead to a preferential amplification of certain rearrangements in non-neoplastic T cell proliferations, thus mimicking a

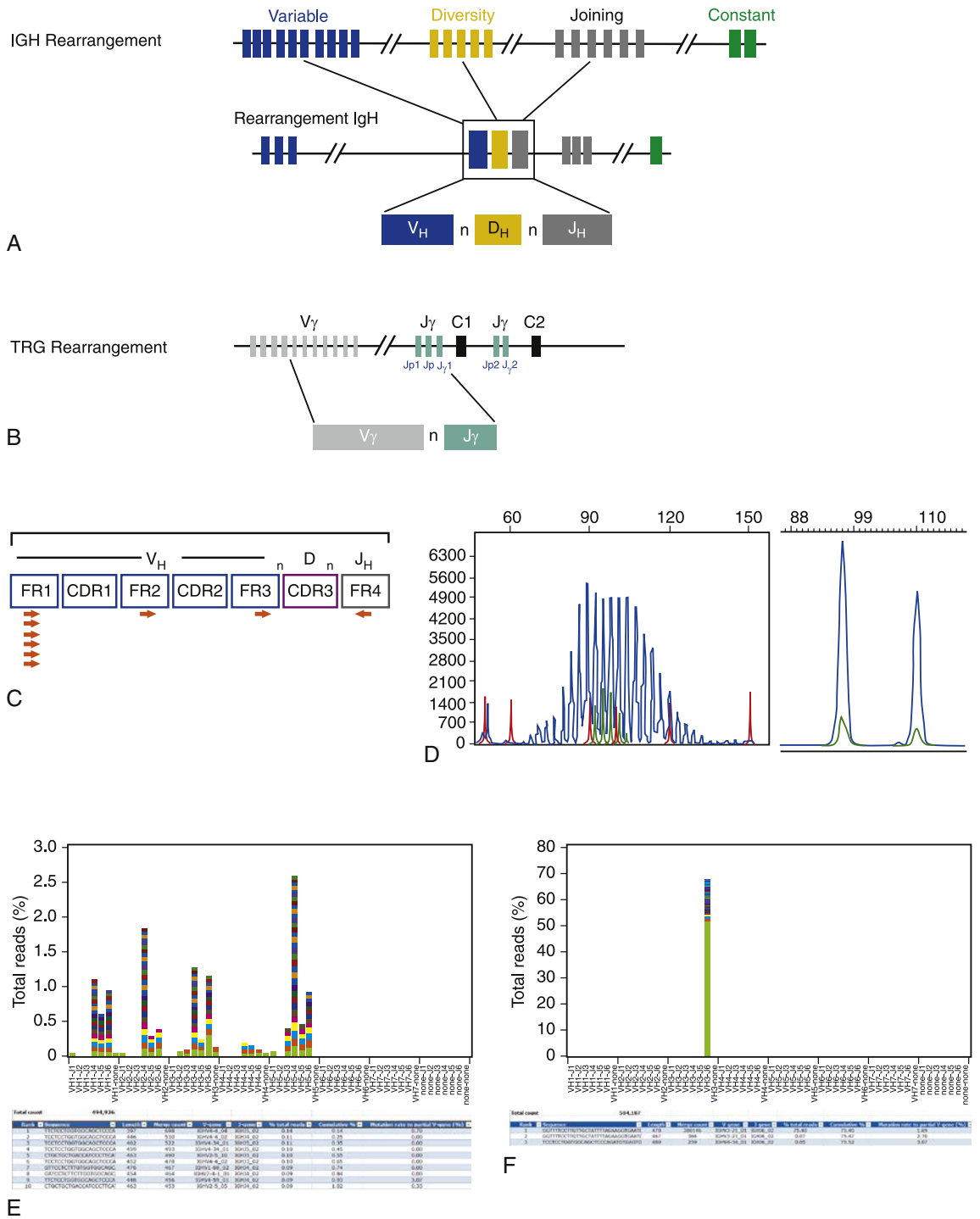

Figure 78.1 Immunoglobulin and T-cell receptor gene rearrangements and determination of clonality in lymphoid proliferations. **A,** Schematic representation of somatic rearrangements of the immunoglobulin heavy chain (*IGH*) locus (chromosome 14q32) occurring in B-cell development. Selection and rearrangement of *IGH* diversity (DH) and joining (JH) genes initiates over a large region of intervening DNA followed by the recruitment of a variable region (VH) gene to form a rearranged VDJ coding gene. VH genes can be grouped based on sequence similarities into seven "families." Substantial immunoglobulin diversity is generated at the nucleotide level because of the large combinatorial selection of the many possible individual V, D, and J genes, as well as by the activity of the enzyme terminal deoxynucleotidyl transferase (TdT), which inserts a random number of "nontemplated" (n) nucleotides at the rearranged junctions. **B,** The T-cell receptor gamma gene (*TRG*) located at chromosome 7p15 shares similar structural and rearrangement features, with the exception that D genes are not present. The *TRG* gene is also less complex, having only 11 functional Vγ genes capable of functional rearrangements, along with two sets of J-genes (Jp and Jγ) and two constant (C) regions. **C,** Detailed schematic of a rearranged *IGH* gene showing the joined VDJ coding region. The VH gene segment encodes much of the variable component of the immunoglobulin heavy chain peptide. Three relatively conserved framework regions (FR1–3) are identified in the V segment, as well as three more variable sequence "complementary determining regions" (CDR1–3). The CDR3 is composed of the junction between V, D, and J genes, along with inserted nontemplated (n) nucleotides (mediated by the enzyme terminal deoxynucleotidyl transferase [TdT]); this heterogeneous region thus represents a highly unique nucleotide sequence in each B cell. The presence of focal areas of shared sequence homology within the V-gene families (e.g., *IGH* FR segments) and in the J genes provides the basis for polymerase chain reaction (PCR)–based detection of the nearly all gene rearrangements occurring in a population of B- or T-cell lymphocytes; the placement of such flanking "consensus" oligonucleotide forward and reverse primers is depicted by the *arrows*. The same strategy is employed to cover gene rearrangements at other antigen receptor genomic loci (e.g., *IGK, TRB, TRG*). **D,** Results of *IGH* PCR using fluorescently labeled consensus primers and capillary gel electrophoresis (CGE) analysis. In this figure, the *y*-axis is fluorescence intensity, and the *x*-axis is fragment size. In a polyclonal B-cell population (*left side* of image), a finite range of VDJ rearrangement sizes exists, delimited both by the relative sizes of the recombined V, D, and J genes and the number of inserted junctional n-nucleotides. This fragment size range is normally distributed, and the area contained under each peak represents a "bin" of many similarly sized rearranged *IGH* fragment sizes. In contrast, a monoclonal B-cell population is characterized by reduction to a homogeneous single- or double-peak rearrangement pattern, as demonstrated in the *right side* of the image. **E** and **F,** *IGH* gene rearrangement analysis performed by next-generation sequencing (NGS). Polyclonal (**E**) and monoclonal (**F**) patterns are visually similar to those seen by PCR and CGE analysis; however, the NGS data represent a sequence-based distribution. In **E**, the proportion of distinct *IGH* VDJ rearrangements is indicated by the relative heights of the color bars. The V-gene family and J-gene rearrangement combinations are displayed across the *x*-axis representing a different type of distribution relative to CGE size-based data for a polyclonal B-cell population. **F** reveals a single dominant rearranged *IGH* population indicative of a monoclonal result. Direct determination of the DNA sequence of every rearranged VDJ sequence is possible by NGS and a sampling of tabular data (including VDJ sequences amplicon lengths, V and J genes used, proportion of total reads, and percent identity to nearest germline V gene) is shown below the graphical output. NGS is currently more expensive than CGE but is very powerful for immunoglobulin or T-cell receptor gene repertoire profiling at the DNA sequence level and allows for evaluation of several specimens in a single experiment (batch processing) with the use of specimen bar code indexing.

clonal population (i.e., "pseudoclonal" result) (Cushman-Vokoun et al., 2010). Such skewed T-cell populations can be encountered in several situations, including autoimmune disorders, after allogeneic organ transplantation, or as a consequence of immune repertoire contraction with normal aging. Therefore, diagnostic interpretation of T-cell clonality studies by PCR is somewhat more problematic, with the propensity for encountering "equivocal" results in a number of cases. Nonetheless, PCR-based methods provide a rapid and cost-effective approach for interrogating both immunoglobulin and TCR loci, keeping in mind the foregoing caveats that (1) the analytical specificity for identifying monoclonal populations is slightly less than 100%, (2) the potential for false-positive results (especially with T-cell receptor gene rearrangements) can occur, and (3) interpretation is inherently subjective (see Table 78.3). It is clear that PCR analysis of antigen receptor gene rearrangements must always be interpreted alongside all relevant clinical, pathologic, and other laboratory data. PCR analysis provides one additional capability: because the monoclonal antigen receptor gene rearrangements in individual lymphoid neoplasms are unique, these highly specific DNA sequences can also be used as tumor-specific markers for very sensitive (e.g., $<10^{-4}$) detection of MRD in blood or bone marrow after therapy (van der Velden et al., 2007; van der Velden & van Dongen, 2009).

The evolution of lymphoid clonality analysis is now entering a new phase characterized by combining comprehensive consensus PCR primer design with NGS. By altering the PCR primer design appropriately, lymphoid cell antigen receptor gene rearrangements can be directly analyzed by NGS, which correspondingly replaces the concept of a PCR product fragment size distribution with a DNA sequence distribution. Furthermore, individual sample barcoding (indexing) allows for simultaneous evaluation of multiple samples in the same run. The advent of NGS methodology has brought new opportunities and a profound increase in knowledge and diagnostic capability. Using a similar consensus PCR primer strategy, an amplicon library can be prepared with attached NGS adapters and sample-specific bar codes. Deep sequencing of these PCR products provides specific sequence identities of the many thousands of V(D)J rearrangements within a lymphoid population and enables quantitation of relative species abundance (Fig. 78.1E and F). NGS applications in this area are also providing an unprecedented opportunity to study epitope mapping, explore lymphocyte subsets, and better understand adaptive or cellular immune responses and repertoires. For *IGH* locus rearrangements, SHM status can be readily determined (McClure et al., 2015; Blachly et al., 2015). To a large extent, these analyses have been made possible by the establishment of high-quality antigen receptor gene specific reference sequence database resources, such as the IMGT Immunogenetics (http://www.imgt.org) and IGBLAST (https://www.ncbi.nlm.nih.gov/igblast) website repositories. In hematopathology practice, NGS is creating a deeper and richer data set to redefine and explore the concept of "clonality" and antigen receptor diversity in lymphoid proliferations (Arcila et al., 2019; Calis & Rosenberg, 2014; Georgiou et al., 2014; Langerak et al., 2017; Schumacher et al., 2014; Warren et al., 2013; Xu et al., 2017). The ability to generate hundreds of thousands to millions of sequence reads from a single sample also provides a powerful advantage for NGS in the direct evaluation of MRD; because each gene rearrangement is unique at the DNA sequence level, an individual lymphoid tumor cell population can be specifically identified and precisely quantified within a large background of other sequences. In step with therapeutic advancements for several lymphoid neoplasms, deep sequencing of immunoglobulin and TCR gene rearrangements is finding increasing utility for MRD detection in patients with B- and T-cell lymphoblastic leukemias, chronic lymphocytic leukemia (CLL), mantle cell lymphoma (MCL), and multiple myeloma (MM) (Bruggemann et al., 2019; Logan et al., 2011; Oberle et al., 2017; Rustad et al., 2019; Theunissen et al., 2019; Wood et al., 2018; Wu et al., 2014; Wu et al., 2012).

LYMPHOBLASTIC LEUKEMIA/LYMPHOMA: RISK STRATIFICATION AND MINIMAL RESIDUAL DISEASE

B-cell lymphoblastic leukemia (precursor B-cell acute lymphoblastic leukemia [B-LBL or B-ALL]) in the pediatric population represents a model linking tumor genetics with therapeutic stratification and clinical outcomes. In childhood B-LBL, a wide spectrum of genomic alterations has been identified, including numerical and structural chromosome alterations, activating chimeric kinase gene fusions, gene amplifications, and pathogenic gene alterations (single nucleotide mutations, insertions and deletions) (Armstrong & Look, 2005; Inaba et al., 2013; Roberts & Mullighan, 2015; Tasian & Hunger, 2017). These events have distinct prognostic value and help to classify patients according to relapse risk (e.g., standard, low, or high risk) and in turn provide the basis of current risk-adjusted therapy (Hunger & Mullighan, 2015; Pui et al., 2012). Several similar genetic changes are also found in a subset of adult patients with B-LBL, whereas others are more exclusive to childhood presentations. Recurrent tumor genetic associations in B-LBL are described in more detail later and summarized in Table 78.4. Genetic abnormalities in T-cell lymphoblastic leukemia/lymphoma (T-LBL) continue to become better defined and include translocations of *HOX* genes with the TCR gene loci; mutations of *NOTCH1*, *FBXW7*, *PHF6*, or *JAK* genes; *TAL1* oncogene activation; and gene fusions involving *ABL1* (Liu et al., 2017). Cases of early T-cell precursor (ETP) acute lymphoblastic leukemia have been characterized by gene mutations involving cell signaling (e.g., *RAS*, *FLT3*, *JAK1/3*), transcription factors (e.g., *RUNX1*, *ETV6*) and epigenetic modification (e.g., *EZH2*, *SUZ12*) that unusually overlap with abnormalities observed in myeloid malignancies (Zhang et al., 2012). Molecular diagnostic evaluation of T-LBL beyond FISH analysis for specific genomic rearrangements is not otherwise widespread in the clinical laboratory and is therefore not further detailed in this section.

Somatic numerical and recurrent structural genetic variations are identified in approximately half of pediatric patients with B-LBL (see Table 78.4) (Roberts & Mullighan, 2015; Tasian & Hunger, 2017). Hyperdiploid chromosome aneuploidy is present in nearly one-third of pediatric B-LBL at diagnosis, defined by the presence of more than 52 tumor cell chromosomes. Hyperdiploidy is typically associated with trisomies of chromosomes 4, 10, and 17, and these patients have a "good" risk profile with a favorable long-term outlook. Hyperdiploid leukemias can be identified by cytogenetics or by flow cytometric assessment of relative DNA content analysis of lymphoblast cell nuclei (DNA index >1.16) coupled with targeted FISH probe analysis (to detect +4, +10, and +17). Conversely, the presence of a hypodiploid chromosome number (<44) defines a rare group of individuals with aggressive disease and early treatment failure; these patients may be considered as early candidates for allogeneic stem cell transplantation. Intrachromosomal amplification of chromosome 21 ("iAMP21") has also recently been associated with poor outcome, arising from complex break-fusion events (chromothripsis) mainly involving the long (q) arm of the chromosome and leading to amplification of transcription factor genes such as *RUNX1* and *ERG* (Harrison, 2015). Cases of iAMP21 can be identified by FISH analysis of specific loci (e.g., *RUNX1*) or genomic microarray methods to detect the variable somatic copy number alterations.

In approximately 25% of pediatric B-LBL cases, common recurrent chromosome translocations are identified (see Table 78.4) (Armstrong & Look, 2005; Roberts & Mullighan, 2015; Tasian & Hunger, 2017), which include the t(12;21)(p13;q22)/*ETV6-RUNX1*, t(9;22)(p34;q11)/*BCR-ABL1*, and t(1;19)(q23;p13)/*TCF3-PBX1* and rearrangements of the *KMT2A* (*MLL*) gene. The t(12;21)/*ETV6-RUNX1* fusion is the most common recurrent gene fusion in pediatric B-LBL (20% of cases) but is very rarely identified in adult patients. *ETV6-RUNX1*–positive patients have an excellent clinical outcome after chemotherapy, similar to the group with chromosome hyperdiploidy and associated "good prognosis" trisomies, although late relapses in *ETV6-RUNX1* B-LBL can be a concern for a subset of these individuals (Forestier et al., 2008; Raimondi et al., 1997). The *ETV6* gene, which encodes an Ets family transcription factor, is joined with the *RUNX1* transcription factor to form a novel fusion gene on chromosome 12p. The resulting ETV6-RUNX1 oncoprotein disrupts the normal function of core binding factor (CBF) transcriptional activity (similar to the *RUNX1-RUNX1T1* in acute myeloid leukemia [AML]), leading to pathogenic effects on normal progenitor cell proliferation and differentiation (Zelent, et al., 2004). A large proportion of *ETV6-RUNX1* B-lymphoblastic leukemias also harbor deletions of the remaining *ETV6* allele on 12p, as well as additional clonal findings (Forestier et al., 2007; Wiemels et al., 2008). In the majority of t(12;21)/*ETV6-RUNX1*–positive B-LBL cases, the translocation is cytogenetically cryptic, requiring either reverse transcription polymerase chain reaction (RT-PCR) or FISH molecular methods for detection. Breakpoints in the *ETV6* gene are generally invariant within intron 5; however, the *RUNX1* gene can show heterogeneity both in genomic break-site location, as well as alternative RUNX1 splice variants in the chimeric mRNA transcripts (von Goessel et al., 2009; Zelent et al., 2004). As a result, potentially four ETV6-RUNX1 fusion forms can thus be detected by RT-PCR technique in any given patient; however, the most frequent types involve fusion of ETV6 exon 5 with exons 2 or 3 of RUNX1. FISH technique also readily detects the *ETV6-RUNX1* translocation in pediatric B-LBL, and this approach further enables the simultaneous identification of an accompanying deletion of the nontranslocated *ETV6* allele, if present.

The t(9;22)(q34;q11)/*BCR-ABL1* abnormality is identified in 3% of B-LBL cases in children and 20% to 25% of adult patients (Armstrong & Look, 2005)), and is associated with a poor prognosis characterized by

TABLE 78.4

Genetic Alterations and Detection in Non-Hodgkin Lymphomas and Chronic Leukemias

Disease Entity	Common Genetic Abnormalities	Molecular Pathogenesis Hallmarks	Molecular Diagnostic Detection	Key Notes
Follicular lymphoma (FL)	Structural variants: t(14;18)/*BCL2-IGH* Genetic variants: *EZH2*, *CREBBP*, *EP300*, *KMT2D* (*MLL2*)	Overexpression of BCL2 protein; protection from apoptosis	• D-FISH (or BAP FISH) • PCR (limited)	• ~10% of FL cases lack *BCL2-IGH* rearrangement • Alterations in chromatin modifier genes are involved in FL pathogenesis
Mantle cell lymphoma (MCL)	Structural variants: t(11;14)/*CCND1-IGH* Genetic variants: *TP53*, *ATM*, *NOTCH1*, *NOTCH2*	Overexpression of G1-phase cell cycle protein cyclin D1; cell proliferation	• D-FISH	• *TP53* gene mutation is an adverse progression-related factor • Rare cases of *CCND1*-negative MCL with identical phenotype and gene expression profile show rearrangements of *CCND2* or *CCND3* genes • *NOTCH1/2* alterations associated with poor outcome in MCL
Splenic and extranodal marginal zone lymphomas (SMZL, EN-MZL)	**SMZL:** Structural variants: del7q Genetic variants: *TNFAIP3, KLF2, NOTCH2, MYD88* L265P **EN-MZL:** Structural variants: +3, +18; del6(q23); t(11;18)/*BIRC3-MALT1* (gastric); t(14;18)/*MALT1-IGH* (lung) Genetic variants: *KMT2C, CREBBP, KMT2D, TET2, NOTCH1/2*	Common pathway in EN-MZL is aberrant NF-κB signal transduction; epigenetic modifier alterations and NOTCH pathway disruption also appear significant	• FISH for structural variants • RT-PCR for expressed *BIRC3-MALT1* mRNA • Targeted NGS panels for specific gene mutations	• *NOTCH2* mutations associated with poor outcome in SMZL • ~10% of SMZL cases associated with *MYD88* mutation
Chronic lymphocytic leukemia/small lymphocytic lymphoma (CLL/SLL)	Structural variants: 13/del13q, +12, del11q, del17p Genetic variants: *TP53*, *SF3B1*, *NOTCH1*, *ATM*, *BIRC3* gene Other: SHM status of clonal *IGH* V gene (i.e., unmutated >98% or mutated ≤98% relative to germline identity)	Multiple altered pathways, including loss of tumor suppressor activity (e.g., TP53), aberrant B-cell receptor signaling, apoptosis avoidance	• Locus-specific FISH for recurrent chromosome abnormalities • Targeted NGS for genetic alterations • *IGH* V-gene Sanger sequencing or NGS analysis for SHM status	• Favorable findings: isolated 13q-/del13q, mutated *IGH*-V gene status • Adverse prognostic findings: unmutated *IGH*-V gene status, del11q, del17p, *TP53*, *SF3B1*, *NOTCH1* mutations • *IGH* rearrangement sequence stereotypy may also have prognostic impact
Lymphoplasmacytic lymphoma (LPL)	Structural variants: N/A Genetic variants: *MYD88* L265P (>90%), *CXCR4* (30%)	Aberrant NF-κB and B-cell receptor signaling	• Allele-specific or quantitative PCR (for *MYD88* L265P) • Sanger sequencing • Targeted NGS panel	• *CXCR4* S338* or C-terminal frameshift alterations occur in setting of *MYD88* L265P and are associated with suboptimal therapeutic response
Hairy cell leukemia (HCL)	Structural variants: N/A Genetic variants: *BRAF* V600E (>95%), *MAP2K1* (rare)	MAPK pathway activation	• Allele-specific or quantitative PCR • Sanger sequencing • Targeted NGS panel	• *BRAF* mutation is potential target for vemurafenib in treatment-refractory HCL • Rare HCL cases with V4-34 *IGH* rearrangements have *MAP2K1* genetic alterations
Diffuse large B-cell lymphoma (DLBCL) and high-grade B-cell lymphoma (HGBCL)	**GCB type:** Structural variants: 18q21/*BCL2* (20%–30%), 8q24/*MYC* (5%–10%) Genetic variants: *KMT2D* (*MLL2*), *CREBBP*, *EP300*, *EZH2* **ABC type:** Structural variants: 3q27/*BCL6* (30%) Genetic variants: *CD79A*, *CD79B*, *MYD88*, *CARD11*, *PRDM1*, *TNFAIP3* **HGBCL (mostly GCB):** Structural variants: *MYC* + *BCL2* and/or *BCL6* "double hit"	Cellular proliferation, avoidance of apoptosis, B-cell maturation, aberrant B-cell receptor signaling, epigenetic alterations, immune surveillance escape	• BAP and D-FISH for *MYC*, *IGH*, *BCL2*, *BCL6* rearrangements (possibly include *IGK* and *IGL* in *MYC* rearranged DLBCL lacking *IGH* partner) • Targeted NGS panel for recurrent genetic alterations	• Specific subsets of acquired genetic or genomic abnormalities generally correlate with cell of origin phenotypes • GCB-type DLBCL associated with alterations in epigenetic modifying genes • ABC type DLBCL associated with alterations in B-cell receptor and signal transduction genes (e.g., NF-κB pathway) • Reflex FISH strategy is effective for rapid prognostic evaluation

Continued

TABLE 78.4—cont'd

Disease Entity	Common Genetic Abnormalities	Molecular Pathogenesis Hallmarks	Molecular Diagnostic Detection	Key Notes
Burkitt lymphoma (BL)	Structural variants: t(8;14)/*MYC-IGH* and variant *MYC* translocations Genetic variants: *TCF3*, *ID3*	Overexpression of potent early response mitogenic transcriptional factor MYC	• BAP and D-FISH for *MYC*, *IGH*, (possibly include *IGK* and *IGL*, and add *BCL2*, *BCL6* if HGBCL is in differential diagnosis) • Targeted NGS panel for genetic alterations	• True BL is more likely restricted to pediatric and young adult (<40 years) presentations
Multiple myeloma	Structural variants: Hyperdiploidy (typically odd chromosomes); t(11;14)/*CCND1-IGH* t(4;14)/*WHSC1-IGH* t(14;16)/*MAF-IGH* t(14;20)/*MAFB-IGH* del17p del1p gain1q Genetic variants: *TP53*, *FAM46C*, *DIS3*, *N/KRAS*, *ATM*, *BRAF*, *CCND1*, *IRF4*	Multiple pathways, including deregulated cell proliferation, apoptosis avoidance, abnormal B-cell programming, disrupted transcription or translation	• Locus-specific and D-FISH • Targeted NGS panel for gene mutations	• Primary prognostic classification is based on structural and numerical chromosomal abnormalities detected by FISH • Hyperdiploidy and *CCND1-IGH* associated with more favorable outcome • *MAF* and *WHSC1* translocations, del17p/*TP53*, del1p and 1q+ associated with poor outcome • Major altered pathways identified by somatic gene mutation abnormalities include RAS-MEK-ERK, NF-κB, epigenetic modification and cell cycle
Anaplastic large-cell lymphoma (ALCL)	Structural variants: ALK-positive t(2;5)/*NPM1-ALK* and variant *ALK* translocation partners (e.g., *TPM3*, *TFG*, *ATIC*) ALK-negative 6p25.3/*DUSP22*, 3q28/*TP63*	Constitutive activation and abnormal localization of ALK tyrosine kinase (ALK-positive cases); loss of tumor suppressor function of *DUSP22* or *TP63* (ALK-negative cases)	• BAP-FISH for *ALK* (all *ALK*-positive cases) • FISH for *DUSP22* and *TP63* gene loci (*ALK*-negative cases)	• Immunohistochemistry for ALK overexpression is commonly used at diagnosis; staining pattern (cellular localization) is correlated with gene fusion partner type in ALK positive tumors • Nodal *ALK* negative ALCL with *DUSP22* rearrangement is associated with more favorable outcome (similar to *ALK* positive cases) • *TP63* ALCL is associated with poor outcome
Peripheral T-cell lymphoma (PTCL)	Structural variants: t(5;9)/*ITK-SYK* *CTLA4-CD28* Genetic variants: *RHOA*, *IDH2*, *DNMT3A*, *TET2*, *CD28* (mainly seen in AITL and other TFH PTCLs)	Disordered follicular helper T-cell program, epigenetic modifications, immune dysregulation	• Targeted NGS panel for gene mutations	• PTCL is genetically heterogeneous and less is understood among non-ALCL lymphomas • *IDH2* inhibitor is a potential therapy target for TFH type PTCL (e.g., AITL)
T-cell prolymphocytic leukemia (T-PLL)	inv14 or t(14;14)/*TCL1A*	Overexpression of TCL1A transcription factor	• BAP FISH for *TCL1A* rearrangement	• TCL1A overexpression can be detected by immunohistochemistry in tissue biopsy samples
T-cell large granular lymphocytic leukemia (T-LGLL)	*STAT3*, *STAT5B* gene mutations	Aberrant signaling through JAK-STAT pathway	• Targeted NGS panel for gene mutations	• Patients may present clinically mimicking a myelodysplastic presentation

BAP-FISH, Break-apart probe fluorescence in situ hybridization; *D-FISH,* dual-probe fluorescence in situ hybridization; *FISH,* fluorescence in situ hybridization; *JAK,* Janus kinase; *N/A,* not applicable; *NF-κB,* nuclear factor kappa B; *NGS,* next-generation sequencing; *PCR,* polymerase chain reaction; *RT-PCR,* reverse transcriptase polymerase chain reaction; *SMH,* somatic hypermutation; *STAT,* signal transducer and activator of transcription; *THF,* T-follicular helper.

therapeutic resistance and high relapse risk (L.K. Jones & Saha, 2005; Yanada et al., 2009). Approximately 80% to 90% of pediatric and two-thirds of adult Ph-positive B-LBL produce an e1-a2 BCR-ABL1 fusion mRNA transcript, resulting in a 190-kD oncoprotein. The remaining cases are associated with e13-a2 or e14-a2 (formerly b2-a2 or b3-a2) BCR-ABL1 transcripts and a corresponding p210 chimeric protein. The BCR-ABL1 protein disrupts several normal cell functions and principally results in constitutive deregulation of the ABL1 tyrosine kinase, leading to increased cellular proliferation. BCR-ABL1 is readily transforming in in vivo transduction models of leukemia, but its phenotypic and clinical manifestations (e.g., B-LBL vs chronic myeloid leukemia [CML]) are dependent on the hematopoietic cell context in which the genetic abnormality is acquired (i.e., pluripotent stem cell vs committed lymphoid progenitor). Despite the generally poor prognostic significance for *BCR-ABL1* positive B-LBL, chemotherapy regimens now typically include tyrosine kinase inhibitors (TKIs; e.g., imatinib and related agents). Durable responses were initially difficult to achieve, but more patients are attaining longer hematologic remissions, providing a bridge to curative allogeneic hematopoietic stem cell transplantation (Gruber et al., 2009; L. K. Jones & Saha, 2005; Soverini et al., 2019; Yanada et al., 2009). Molecular details of the *BCR-ABL1* fusion gene are discussed in more detail in the section on CML and illustrated in Fig. 78.10. The *BCR-ABL1* abnormality can be readily identified at diagnosis by cytogenetics, FISH, or RT-PCR, although quantitative RT-PCR (QRT-PCR) is required for disease burden monitoring after therapy. As with CML, B-LBL patients treated with TKI therapy can develop acquired resistance mutations in the kinase domain of *BCR-ABL1*, necessitating ongoing molecular follow-up and vigilance. Deletions involving the *IKZF1* gene locus encoding the transcription factor Ikaros have also been identified in many cases of *BCR-ABL1* B-LBL, and these alterations represent an important cooperative lesion strongly influencing aggressive behavior in this subset of patients (Mullighan et al., 2008; Mullighan et al., 2009; Obhi et al., 2009).

A small proportion of pediatric B-lineage ALL, most commonly with a "pre-B" cell (cytoplasmic IgM positive) immunophenotype, harbors an unbalanced t(1;19)(q23;p13) with the resultant formation of a chimeric *TCF3-PBX1* oncogene (the *TCF3* gene is also known as *E2A*) and corresponding novel leukemogenic protein (Hunger et al., 1991; Paulsson et al., 2007). TCF3 is an important mediator of normal lymphoid cell and myocyte development, whereas PBX1 is a DNA binding protein that is not expressed in normal lymphocytes. Patients with leukemia who have this translocation fusion gene have been linked to more aggressive disease biology, although optimized therapeutic management has now improved the clinical outcome in most cases. A single chimeric TCF3-PBX1 mRNA is produced in nearly all cases, and this transcript can be readily detected

by RT-PCR analysis; FISH technique can also be employed to detect the genomic abnormality. Rare occurrences of a balanced t(1;19)(q23;p13) also occur in B-LBL and do not involve the *TCF3* and *PBX1* genes but rather create novel *DAZAP1-MEF2D* and reciprocal *MEF2D-DAZAP1* gene fusions, which are associated with poor outcome (Prima & Hunger, 2007).

The mixed-lineage leukemia gene (*MLL*, now designated *KMT2A*) is located on chromosome 11(q23) and is rearranged in approximately 5% of childhood leukemias, including the majority of B-LBL cases occurring in infants younger than 1 year of age (Armstrong & Look, 2005; Chowdhury & Brady, 2008; Silverman, 2007). Infantile acute leukemias with *KMT2A* gene rearrangements present in a clinically aggressive fashion and exhibit a dismal prognosis, particularly when associated with a poor therapeutic steroid response (Chowdhury & Brady, 2008; Forgione et al., 2020; Pui et al., 2003; Winters & Bernt, 2017). The *KMT2A* gene product encodes histone-lysine N-methyltransferase 2A (MLL1 protein), which differentially regulates a set of homeobox or *HOX* genes that are variably responsible for coordinated skeletal development during embryogenesis and significantly, normal postfetal hematopoietic progenitor cell development (Dorrance et al., 2006; Ernst et al., 2004; Hess, 2004; Krivtsov & Armstrong, 2007; Ono et al., 2005; Soshnikova & Duboule, 2008; Yu et al., 1995). In B-LBL, *KMT2A* becomes juxtaposed with a different genetic locus via chromosome translocation, resulting in the formation of a chimeric gene product. Abnormal MLL1 fusion proteins can promote leukemogenesis by aberrantly deregulating certain *HOX* gene subsets in hematopoietic stem cells (McGonigle et al., 2008). Numerous (>50) described reciprocal translocation partner genes have been described in *KMT2A* gene disruption (Broeker et al., 1996; Chowdhury & Brady, 2008; Harper & Aplan, 2008; Liu et al., 2009; Meyer et al., 2018). The t(4;11)(q21;q23) is most commonly encountered in infant B-LBL, resulting in the formation of the *KMT2A-AFF1* fusion (Sanjuan-Pla et al., 2015). In this event, the *KMT2A* gene exhibits substantial genomic breakpoint heterogeneity encompassing a large genomic region containing exons 5 to 11. Likewise, the *AFF1* gene (also known as *AF4*) also shows variability of breakpoint location among B-LBL cases. A second translocation, the t(11;19)/*MLLT1*(or *ENL*)-*KMT2A* abnormality, is also encountered in infant B-LBL, as well as lymphoblastic leukemia and AML in older children and adults. *KMT2A* translocation, in particular the t(9;11)/*MLLT3-KMT2A*, is also prevalent in the subgroup of therapy-related AML after prior exposure to DNA topoisomerase II inhibiting agents (e.g., etoposide, daunorubicin). Therapy-related AML is associated with a very poor prognosis (Godley & Larson, 2008). Although a single chimeric MLL fusion transcript type is associated with any given translocation event in an individual leukemic tumor, the presence of so many potential rearranging partner genes in *KMT2A* translocations with associated breakpoint junction heterogeneity poses significant challenges for molecular diagnostic detection. Multiplex RT-PCR approaches have been designed to identify many different *KMT2A* gene fusions; however, comprehensive molecular evaluation of this gene in childhood leukemias by PCR methods remains problematic because of both biologic and technical complexity, thus limiting clinical sensitivity. FISH technique based on a BAP strategy (with probes spanning either side of the breakpoint cluster region in the *KMT2A* gene) is very powerful for rapidly identifying genomic disruption at this locus, and this strategy is diagnostically very sensitive for *KMT2A* rearrangements regardless of the translocation partner; D-FISH can then be employed to define the specific translocation variants in many cases. FISH analysis also discriminates between true 11(q23)/*KMT2A* locus rearrangements and other genetic alterations (e.g., deletions) not involving the gene but clustering within the 11(q22-q25) region; this distinction may be difficult to discern by routine cytogenetic analysis. More recently, targeted next-generation RNA sequencing approaches have been employed to successfully detect *KMT2A* gene fusions (Afrin et al., 2018).

Interestingly, *KMT2A* gene rearrangements present in many B-LBL cases occurring in infancy have been traced back to their corresponding neonatal (preleukemic) blood spots, indicating in utero acquisition in the fetal bone marrow (Greaves, et al., 2003; Greaves & Wiemels, 2003). This finding has similarly been demonstrated in a subset of older children with *ETV6-RUNX1* B-LBL and some other types of acute leukemias in childhood. However, the latency period from initial acquisition of a genetic alteration to potential disease presentation differs between subtypes of genetically defined B-LBL, suggesting that the specific hematopoietic context, with unknown driver gene mutations, environmental influences, or both play important roles in determining whether leukemogenesis proceeds in a given individual. In infantile B-LBL, for example, *KMT2A* mutation acquired in utero appears necessary and sufficient for postnatal rapid development of B-LBL, whereas this is not similar for other leukemia subtypes. Furthermore, healthy newborn or umbilical cord blood population screening studies have shown an appreciable prevalence (~0.1%–1%) of leukemia-associated translocations events, albeit at very low quantitative levels ($<10^{-4}$); these data again point to the requirement for cooperating oncogenic mutations and a conducive background in the generation of overt leukemia. Nevertheless, the realization that at least some childhood leukemias have prenatal origins has sparked interest in identifying risk-modifying factors. For example, recent evidence shows that low penetrance population genetic variations in some genes (e.g., *IKZF1*, *PAX5*) or polymorphic loci may increase the risk of developing B-LBL (Churchman et al., 2018; Gocho & Yang, 2019; Perez-Andreu et al., 2015; Vijayakrishnan et al., 2019).

Data from comprehensive genomic analyses in the era of NGS have further advanced the characterization of childhood B-LBL. A wider array of genomic and genetic alterations that deregulate key cytokine receptor or kinase signaling pathways is now known in B-LBL (Roberts et al., 2012; Roberts et al., 2018; Tasian, Loh, & Hunger, 2017). For example, translocations of the *IGH* gene with the erythropoietin receptor (*EPOR*) or the type 1 cytokine receptor *CRLF2* result in overexpression of these proteins leading to autonomous receptor activity. Other genomic rearrangements result in pathogenic activation of tyrosine kinase genes (e.g., *ABL1*, *ABL2*, *PDGFRB*, *JAK2*) (Reshmi et al., 2017; Roberts et al., 2014). Single base mutations and small insertion/deletion (indel) type alterations are also evident in a number of genes, including members of the Janus kinase (*JAK*) family. Importantly, many of these alterations converge through the JAK-STAT (signal transducer and activator of transcription) signal transduction pathway. This diverse subset of B-LBL cases nonetheless shares a common gene expression signature similar to *BCR-ABL1*-positive (Ph+) B-LBL, leading to their designation as "*BCR-ABL1*–like" leukemias (see Table 78.4). Additional genetic deletion or mutation events in critical B-cell transcription factors, notably *IKZF1* and *PAX5*, are observed in both *BCR-ABL1*–positive and *BCR-ABL1*–like high-risk B-LBL. The proportion of B-LBL with *BCR-ABL1*–like genetic changes increases with age at presentation, with greater frequency seen among older children and young adults (Tasian et al., 2017); these patients are generally associated with poor outcome. Nevertheless, convergent disruption of known signal transduction pathways in these leukemias is providing new therapeutic opportunities for management using inhibitors of JAK and tyrosine kinases. Comprehensive detection of the complex genomic and genetic aberrations in *BCR-ABL1*–like B-LBL is difficult using standard molecular diagnostic methods and instead requires a multimodal strategy including targeted NGS (for gene mutations and small insertion/deletions), FISH (for specific translocations), RT-PCR (for selected expressed gene fusion mRNAs), chromosome arrays (for deletion/duplication analysis), and cytogenetics. *CRLF2* gene rearrangement is present in approximately half of *BCR-ABL1*–like tumors; genomic or immunophenotypic evaluation of CRLF2 overexpression can detect many of these patients at diagnosis. Targeted gene expression profiling approaches have also been developed to accurately and inexpensively identify the vast majority of *BCR-ABL1*–like B-LBL cases (Kang et al., 2012), although elucidation of the specific underlying genetic abnormalities with potential for targeted therapy requires more detailed downstream analyses as noted.

Risk Stratification in Childhood Acute Lymphoblastic Leukemia and Minimal Residual Disease Assessment

In childhood B-LBL, a comprehensive but directed molecular diagnostic testing approach can achieve a high rate of detection of most "favorable-risk" and "high-risk" tumor genetic factors, including the more heterogeneous group of *BCR-ABL1*–like cases. The identification of prognostic and predictive molecular markers in pediatric B-LBL has significantly driven the development of risk-adapted practices for managing lower risk and high-risk patients (see Table 78.4). This approach is based on the principles of achieving optimal clinical responses while minimizing toxic effects and other late sequelae, such as therapy-related neoplasms. For B-lineage LBL, in particular, initial clinical risk assessment (e.g., age, white blood cell and blast count, extramedullary involvement) is further modified by the presence and type of tumor genetic abnormalities, as outlined earlier. The *BCR-ABL1* gene fusion, hypodiploid karyotype, *KMT2A* rearrangement, *BCR-ABL1*–like genotype or phenotype, iAMP21, *IKZF1* deletion (often seen in *BCR-ABL1*–like disease), or therapeutic induction failure each constitute very high-risk patient subtypes. Conversely, B-LBL cases with hyperdiploidy and "favorable" trisomies or the *ETV6-RUNX1* gene fusion are considered good prognostic factors. Early genetic classification (i.e., before the end-induction treatment phase) thereby influences the chemotherapy protocol intensity and duration for a given patient. Most large children's cancer groups utilize this strategy of tumor genetic risk stratification in slightly different formats. Useful as these parameters have

been for more appropriately stratifying patients earlier to receive optimized therapy, a significant subset of children continues to experience treatment failure and leukemic relapse, indicating some enduring lack of precision in the risk assessment models. Better predictive surrogate markers of biologic response and disease clearance have therefore been sought, and MRD detection has emerged as a very powerful method of posttherapeutic prediction, contributing to a more "individualized" approach of risk evaluation. Many large clinical studies have now confirmed the utility of MRD in determining relapse potential in childhood B- and T-lineage B-LBL. Levels of MRD greater than 10^{-4} at the end of induction therapy have been shown to be highly correlated with significant risk of relapse compared to MRD negative status and this relationship has been shown to be strongly independent of most clinical and tumor genetic factors in multivariate analyses (Galimberti et al., 2018; Berry et al., 2017; Borowitz et al., 2008, 2015; Bruggemann et al., 2010; Conter et al., 2010). MRD can be assessed by flow cytometry techniques or molecular diagnostic methods. Targets for molecular MRD measurements include expressed chimeric fusion gene mRNA transcripts and tumor-specific clonal antigen receptor gene rearrangements.

Immunoglobulin or TCR gene rearrangements are unique and specific markers for MRD assessment in the large majority of individual lymphoid malignancies compared with leukemia-specific fusion gene transcripts, which are present in less than one-third of cases. Notably, in B-lineage LBL, "illegitimate" or cross-lineage gene rearrangements also occur frequently at the TCR genes, such that most B-lineage tumors have at least one and as many as two to three unique gene rearrangements available for MRD monitoring. The clonal V(D)J rearrangements in lymphoblastic leukemia cells can be amplified, then Sanger sequenced for the design of tumor-specific PCR primers, and probes that can be used in subsequent targeted QPCR analysis. However, this approach has relatively poor technical reproducibility and is highly labor intensive, significantly limiting routine adoption in many laboratories. Recent developments using NGS technology for deep sequencing of immunoglobulin and TCR genes (see Fig. 78.1E and F) have demonstrated an alternative and very powerful means of detecting tumor-specific clones at very high analytical sensitivity (~10^{-6}). Using an optimized consensus PCR primer strategy, a library pool of rearranged antigen receptor gene products can be prepared for high throughput NGS (Langerak et al., 2017; Wood et al., 2018; Wu et al., 2014; Wu et al., 2012; Theunissen et al., 2019). Relying on the highly specific nature of V(D)J segmental recombination and the unique CDR3 junctional region sequence in each lymphoid cell, the presence of tumor-specific DNA clonal disease can be directly and specifically queried in a single assay as long as the initial clonal immunoglobulin or TCR gene sequence of the tumor cells was determined at diagnosis. The development of commercial platforms (e.g., Lymphotrack, Invivoscribe; clonoSEQ, Adaptive Biotechnologies) has greatly facilitated clinical molecular laboratory access to this technology and the related bioinformatics software to effectively analyze the large amount of sequence data generated. Flow cytometric protocols can achieve comparable analytic sensitivity to molecular methods and have a potential advantage of being more easily standardized between laboratories, although at the extremes of analytical sensitivity (e.g., 10^{-5} to 10^{-6}), NGS methods appear to be more reliable. Incorporation of MRD data as a routine component of risk assessment enables higher risk MRD-positive patients to be rapidly stratified into more intensive therapy arms. Timing of MRD assessment is critical in this regard; in general, the end of induction therapy is considered a significant and highly informative time point in B-LBL, although ongoing serial measurements can further increase the predictive value.

LOW GRADE B-CELL LYMPHOMAS

Follicular Lymphoma

The t(14;18)(q21;q32) abnormality is a common translocation in B-lineage lymphomas, present in the majority of FLs (80%–90%) and in a subset of diffuse large B-cell lymphomas (DLBCLs; 20%–30%). At the molecular level, this translocation results in the juxtaposition of the *BCL2* gene located on chromosome 18q21 with the *IGH* locus at 14q32. As a consequence, *BCL2* gene expression becomes subject to the highly active *IGH* enhancer element on the derivative 14q32, leading to marked overexpression of BCL2 protein. The BCL2 gene product is a prototypic antiapoptotic protein that acts to protect cells from the process of programmed cell death (Cory & Adams, 2002; Rohde et al., 2008). Although regulation of apoptosis is important in normal cell physiologic contexts, aberrant BCL2 overexpression can inappropriately shield neoplastic cells from a variety of otherwise lethal cytotoxic events and promote a milieu favoring acquisition of additional tumor progression-related genetic abnormalities

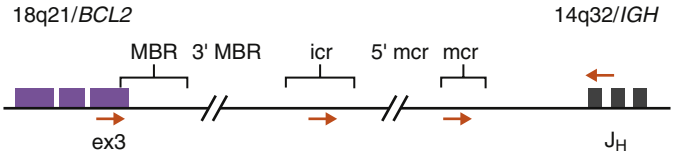

Figure 78.2 The t(14;18)/*BCL2-IGH* abnormality in non-Hodgkin lymphomas. The *BCL2* gene is rearranged by translocation to the *IGH* locus in most follicular lymphomas and a subset of large B-cell lymphomas. Most genomic breakpoints are relatively tightly clustered in the 3′ aspect of the noncoding third exon of the *BCL2* gene in a region termed the *major breakpoint region* (MBR). Up to four additional *BCL2* breakpoint clusters have been described: the minor cluster region (mcr), the intermediate cluster region (icr), and two areas near distal and proximal to the MBR and mcr, respectively (i.e., 3′ MBR and 5′ mcr). For the *IGH* gene, breakpoints occur within the JH region. Because of the clustered nature of a number of breakpoints and the relatively short intervening genomic distances between *BCL2* and *IGH*-JH in the rearranged configurations, *BCL2* and JH PCR region primers *(orange arrows)* can be used to detect a slight majority of *BCL2-IGH* gene fusions arising from the t(14;18)(q21;q32). Nevertheless, a significant minority (30%–40%) of *BCL2* rearrangements cannot be identified by polymerase chain reaction (PCR) methods because of breakpoint heterogeneity over the *BCL2* locus. This situation is common to most lymphoma-associated chromosomal translocations of a proto-oncogene with an antigen receptor gene (e.g., *IGH*); the wide and unpredictable distribution of genomic breaksites precludes identification by short-range PCR methods. In contrast, fluorescence in situ hybridization analysis is the method of choice for detection of these events.

(Green et al., 2013).The partial genomic structure of the *BCL2* gene locus is illustrated in Figure 78.2. The largest proportion (50%–65%) of break-fusion sites in the *BCL2* gene occurs in a tightly clustered area of approximately 150 bp in the 3′ noncoding segment of exon 3 known as the major breakpoint region (MBR). Additional breakpoint regions in *BCL2* have been described, including the minor cluster (mcr), intermediate cluster (icr), and areas 3′ of the MBR and 5′ of the mcr (Akasaka et al., 1998; Albinger-Hegyi et al., 2002). *BCL2* gene rearrangements in FL involving the MBR can be detected by PCR methods using genomic DNA and consensus primers situated near the MBR and in the *IGH*-JH region (see Fig. 78.2) (Aster & Longtine, 2002; Hsi, et al., 2002; Iqbal et al., 2004). Other *BCL2* break sites are more difficult to target by PCR because of heterogeneity in distribution. PCR approaches, however, achieve only 60% to 70% detection for *BCL2-IGH* rearrangement, particularly when compared with FISH analysis using dual-color *BCL2* and *IGH* locus-specific probes (Einerson et al., 2005). FISH is a versatile and relatively rapid approach that can be performed on nuclei extracted from fresh or paraffin-embedded tissues and remains the mainstay for identifying *BCL2* rearrangements in lymphomas.

The identification of *BCL2* gene rearrangements in neoplastic lymphoid proliferations is useful to establish a diagnosis and for disease subclassification. Cases of atypical or florid but benign follicular hyperplasia can be histologically and phenotypically difficult to differentiate from FL, and in this situation, the presence of the *BCL2-IGH* abnormality definitively establishes the latter diagnosis. Furthermore, identification of *BCL2* gene rearrangement can be used to specifically distinguish low-grade FL from other small B-cell lymphomas with potentially overlapping morphologic patterns, such as mantle cell or marginal zone types exhibiting follicle colonization. The presence of *BCL2* gene rearrangements in these contexts is relatively specific for FL and is almost always correlated with BCL2 protein overexpression. Conversely, it is important to note that many B-cell lymphomas and lymphoid leukemias are also associated with deregulated BCL2 protein expression in the absence of structural *BCL2* gene translocations (e.g., via gene amplification or possibly epigenetic mechanisms), indicating that the protein expression itself cannot be used for specific lymphoma subtyping (Green et al., 2013). As noted, a small proportion of FLs lacks the t(14;18)/*BCL2-IGH*. *BCL2*-rearrangement–negative FLs often demonstrate higher cytologic grade (e.g., grade 3) and may be associated with translocations involving the *BCL6* proto-oncogene (Green et al., 2013; Katzenberger et al., 2004). No significant survival differences have been observed between *BCL2*-positive and *BCL2*-negative FLs, but high-resolution genomics and gene expression profiling studies have suggested the presence of distinct molecular pathways (Leich et al., 2009, 2016). Recent genomic studies in FL have also found recurrent mutation events in several genes involved in chromatin modification, including *KMT2D* (*MLL2*), *CREBBP*, *EP300*, *TNFRSF14*, and *EZH2* (Bodor et al., 2013; Cheung et al., 2010; Green, 2018; Green et al., 2013; Lackraj et al., 2018; Okosun et al., 2014; Qu et al., 2019). These results suggest a central role for epigenetic deregulation in the pathogenesis of FL (see Table 78.4). Genomic data have also been evaluated alongside standard risk assessments in improving prognostic models for FL (Kridel, et al., 2017; Pastore et al., 2015).

Mantle Cell Lymphoma

The t(11;14)(q13;q32) is essentially pathognomonic for MCL in the differential diagnosis of small B-cell neoplasms. This translocation is also detected in a subset of MMs. The t(11;14) places a genomic region on 11q13 called *BCL1* in proximity to the JH region of the *IGH* gene. The gene encoding cyclin D1 (*CCND1*) is located telomeric to the majority of *BCL1* break sites but nonetheless is the consistent target of transcriptional deregulation by the *IGH* locus as a result of the translocation. Cyclin D1 is an early G1-phase cell cycle protein required for the normal activity of cyclin-dependent kinases 4 and 6 (cdk4, cdk6); these holoenzyme complexes promote progression through the G1/S transition of the cell cycle in proliferating cells through phosphorylation of the retinoblastoma (Rb) protein (Massague, 2004; Pestell, 2013). Cyclin D1 (in contrast to other related proteins cyclins D2 and D3) is not expressed by normal B cells. Aberrant overexpression of the D1-type cyclin is thus thought to play a key role in the pathogenesis of MCL and is supported by the overall "proliferative" transcriptional signature in MCL cells as identified by gene expression profiling studies (Hartmann et al., 2010; Rosenwald et al., 2003). The presence of a proliferative and antiapoptotic tumor phenotype underlies the relatively poor prognosis of MCL, relative to more indolent small B-lymphocyte neoplasms (Jares et al., 2012; Navarro et al., 2011; Perez-Galan, et al., 2011).

Successful detection of the t(11;14) or *CCND1* genetic rearrangements in MCL depends on the methodology employed. The *BCL1* breakpoint region encompasses a large area of 11q13. Approximately half of *BCL1* locus breakpoints occur over a small, well-defined site, referred to as the major translocation cluster region (MTC) (Chibbar et al., 1998; Williams et al., 1993). The MTC is located nearly 120 kb centromeric of the *CCND1* gene. Other breakpoints are found either more distal to the MTC or are located in the immediate 5′ region of *CCND1* (Williams, et al., 1991; Williams et al., 1992). SBH approaches using probes targeting the MTC and other genomic regions have previously mapped *BCL1* alterations in up to 70% of MCL cases; however, SBH is impractical for routine diagnostic purposes. DNA-based PCR technique has been successfully used to identify a subset of *BCL1-IGH* fusions involving the MTC region but only in approximately 30% to 40% of cases (Chibbar et al., 1998). It is thus evident that the large and widely distributed breakpoint region encompassed by the *BCL1* locus presents substantial difficulties for common molecular approaches. Break-apart and dual-fusion FISH assays are therefore ideal for resolving t(11;14)/*CCND1-IGH* genomic rearrangements in diagnostic specimens, including interphase nuclei obtained from fixed paraffin blocks (Belaud-Rotureau et al., 2002; Remstein et al., 2000). Cyclin D1 protein overexpression can be readily detected by immunohistochemical techniques in fixed, paraffin-embedded tissues, providing a rapid, widely applicable and complementary method in the diagnosis of MCL, although in situations in which cyclin D1 immunostaining is not successful, FISH for *CCND1* locus rearrangement remains of high utility for the identification of MCL. Cyclin D1 overexpression can also be observed in other B-cell neoplasms in the absence of *BCL1/CCND1* rearrangements, including hairy cell leukemia (HCL), the proliferation centers in occasional cases of CLL/small lymphocytic lymphoma (CLL/SLL), and a in subset of large B-cell lymphomas; however, these lymphoid neoplasms can usually be readily distinguished from MCL by morphology and cell marker studies.

Of note, rare cases of classical MCL are recognized that lack the t(11;14)/*CCND1* rearrangement and cyclin D1 overexpression yet exhibit the same morphology, immunophenotype, and gene expression signature (Rosenwald et al., 2003). These atypical MCL cases have been associated with translocations involving the *CCND2* or *CCND3* genes, which are detectable by specific FISH assays (Martin-Garcia et al., 2019; Salaverria et al., 2013). SOX11 protein expression is diagnostically helpful in these rare instances because it is present in both classical *CCND1*/cyclin D1-positive MCL and *CCND1*-negative MCL variant cases (Mozos et al., 2009). Finally, a subset of primarily leukemic presentations of MCL have been described characterized by the presence of *CCND1* rearrangement, somatic *IGH*-V gene hypermutation, absence of SOX11 expression, lack of bulky adenopathy, and a relatively nonaggressive clinical course (Clot et al., 2018; Fernandez et al., 2010; Navarro et al., 2012); these "indolent" MCL cases have a distinct gene expression profile relative to classical MCL.

Marginal Zone B-Cell Lymphomas

Marginal zone lymphomas (MZLs) include nodal and extranodal presentations, with the latter encompassing splenic and mucosa-associated lymphoid tissue (MALT) subtypes. Although they share similar morphologic and phenotypic features, MZL at certain sites harbor relatively distinct genetic findings, most notably seen among the extranodal MZL (EN-MZL) of MALT type (see Table 78.4). Common to MZL are certain recurrent numerical or structural chromosomal alterations, although these are not disease-specific associations. These alterations include +3, +18, and deletions of 6q23 with loss of the *TNFAIP3* gene locus (Cascione et al., 2019; Spina et al., 2016; Zucca & Bertoni, 2016). Splenic MZLs (SMZLs) are often associated with del7(q) (Salido et al., 2010), as well as acquired mutations in the *KLF2* and *NOTCH2* genes in 10% to 40% of cases (Jaramillo Oquendo et al., 2019; Kiel et al., 2012; Martinez et al., 2014). *NOTCH2* alterations are associated with an adverse prognosis in SMZL. A small number of SMZL (≤10%) may have the *MYD88* Leu265Pro somatic alteration, discussed in more detail with lymphoplasmacytic lymphoma (LPL). The EN-MZLs, also referred to as MALT lymphomas, are uncommon and biologically unusual lymphoid tumors. In addition to neoplastic growth in many diverse extranodal tissue sites (e.g., stomach, lung, salivary gland, thyroid), these tumors are often characterized by the presence of predisposing infectious or autoimmune conditions and a preceding or coexistent reactive lymphoid component. Gastric EN-MZL is a prototypic example: a significant subset of these lymphomas arises in the presence of *Helicobacter pylori* infection, which appears to play a key role in early disease pathogenesis (Isaacson & Du, 2004; Zucca & Bertoni, 2016). In addition to underlying infectious or inflammatory conditions, several recurrent genetic abnormalities have been more distinctly associated with EN-MZL in various tissue sites (Cascione et al., 2019; Du, 2007; Remstein et al., 2006; Streubel et al., 2004a; Zucca & Bertoni, 2016). The t(11;18)(q21;q21)/API2-MALT1 abnormality is characterized by fusion of an inhibitor-of-apoptosis gene (Ye et al., 2003). *BIRC3-MALT1*–positive tumors have a predilection for gastric and lung sites, with infrequent occurrences elsewhere. A second translocation event occurring in EN-MZL is characterized by the t(14;18)(q21;q32)-derived *MALT1-IGH* gene fusion (Ye et al., 2005). Notably, the *MALT1* gene is situated slightly centromeric to the *BCL2* locus on chromosome 18q, and as such, these two t(14;18)-associated gene fusions are indistinguishable by standard cytogenetics; however, FISH analysis can provide specific delineation. *MALT1-IGH*–positive lymphomas are distributed in orbital, parotid, lung, and cutaneous sites and are very uncommonly encountered in the stomach. Other rare translocations described sporadically in EN-MZL are the t(1;14)(p22;q32)/*BCL10-IGH* and t(3;14)(p14.1;q32)/*FOXP1-IGH* abnormalities (Streubel et al., , 2005). Despite the diversity of translocation-associated abnormalities and apparent variability in tissue distribution in EN-MZL, a common pathogenesis links these events. Overexpression of MALT1 or BCL10 proteins or expression of a chimeric MALT1 oncoprotein (e.g., from the *BIRC3-MALT1* gene fusion) each results in constitutive activation of the nuclear factor kappa B (NF-κB) signal transduction pathway, leading to altered effects on cell growth, immunity, and apoptosis regulation (Cascione et al., 2019; Du, 2007, 2011). NGS-based investigations are also beginning to shed additional perspective on genetic and epigenetic alterations in MALT lymphomas, revealing common defects in pathways involving chromatin modification and NOTCH signaling, as well as NF-κB regulation (Cascione et al., 2019).

Detection of specific translocation events or numerical chromosome alterations can be accomplished using FISH techniques (Remstein et al., 2006) and can be useful in some cases to establish the diagnosis of MZL; these situations might include morphologically challenging biopsies with prominent reactive or hyperplastic features, or when distinguishing MZL from a different subtype of low-grade B-cell lymphoma (e.g., *MALT1*+ MZL versus *BCL2*+ FL). RT-PCR analysis for the *BIRC3-MALT1* transcript has been described as an alternative method for detecting the t(11;18) (Zhang et al., 2006); however, owing to substantial breakpoint heterogeneity in both genes, comprehensive primer design can be problematic and obtaining sufficient high-quality RNA may be a limiting factor in small paraffin-embedded biopsies. Detection of the *BIRC3-MALT1* genetic lesion in gastric EN-MZL is potentially important for therapeutic management. Broad-spectrum antibiotic eradication of *H. pylori* can induce tumor regression in a significant subset of translocation-negative gastric EN-MZL, whereas the presence of the *BIRC3-MALT1* gene fusion implicates a distinct pathogenesis that is refractory to this non-cytotoxic option (Liu et al., 2001, 2002; Streubel et al., 2004b). PCR methods to identify a monoclonal immunoglobulin gene rearrangement in biopsied tissue are often used to support a diagnosis of gastric or other EN-MZL. Follow-up immunoglobulin PCR for assessing residual disease is also sometimes employed in patients with treated gastric EN-MZL; however, the significance of detecting clonal B cells by PCR technique in posttreatment gastric biopsies has been controversial, with some reports suggesting prolonged persistence of monoclonality after histologic eradication of lymphoma and others paradoxically showing the presence of clonotypic B-cell populations in benign gastric lymphoid proliferations (Bertoni et al., 2002; Noy et al.,

2005; Wundisch et al., 2003). These studies suggest that the reduction in PCR-detectable clonotypic B cells generally lags behind the histologic normalization of gastric tissue in successfully treated patients and follow-up PCR studies should be interpreted with caution.

Chronic Lymphocytic Leukemia/Small Lymphocytic Lymphoma

CLL and its nodal manifestation small lymphocytic lymphoma (CLL/SLL) are among the most common B-cell malignancies and typically are considered to be indolent entities. Yet, advances in the past 2 decades have revealed distinct prognostic subgroups in CLL/SLL, in turn identifying a proportion of patients at risk for early progressive disease and adverse outcome (Amin & Malek, 2016; Crassini et al., 2019; Fabbri & Dalla-Favera, 2016; Gaidano & Rossi, 2017; Nabhan et al., 2015). This area of malignant hematology is illustrative of the convergence of phenotypic, cytogenetic, and molecular genetic tumor features to produce a more refined approach for outcome prediction. Well-known phenotypic adverse factors in CLL include high expression of cell surface CD38 antigen and the overexpression of the signaling kinase ZAP-70. Several recurrent cytogenetic anomalies have been identified in CLL/SLL (see Table 78.4), none of which are disease specific. These abnormalities include deletions of chromosome 13 or 13q, deletions of 11q, deletions of 17p, and trisomy 12. The presence of isolated 13q- has been associated with relatively favorable outcome. In contrast, 11q- and 17p- alterations confer a more aggressive disease course with early requirement for chemotherapy (Dohner et al., 2000). In the latter two situations, minimally deleted regions of these chromosomal loci include the *ATM* and *TP53* genes, respectively. These CLL prognostic cytogenetic changes are most reliably identified with targeted DNA probes using FISH technique. In most cases of CLL with loss of 17p, the remaining allele shows mutation of *TP53*, indicating biallelic loss of tumor suppressor p53 activity (Dicker et al., 2009; Fabris et al., 2008; Del Giudice et al., 2012; Domenech et al., 2012). Although 17p- CLL cases account for 10% or less of all treatment-naive patients, the prevalence is higher in those with advanced disease or therapy resistance; these individuals exhibit an aggressive disease course requiring earlier therapeutic intervention. *TP53* mutated CLL patients are also poorly responsive to commonly used purine nucleoside analog chemotherapeutic agents and require alternative treatment regimens. *TP53* gene mutations can be evaluated by the clinical molecular laboratory using PCR and Sanger sequencing (typically of exons 4–9); recommended guidelines for *TP53* mutation analysis have also been described (Malcikova et al., 2018). The SHM status of the clonal *IGH* V-region is also an important prognostic marker in this disease. CLL/SLL cases with mutated *IGH* V genes (defined as >2% nucleotide deviation from the corresponding germline V-gene DNA sequence) are associated with significantly better outcome compared with cases with unmutated status (≤2% divergent from germline) (Damle et al., 1999; Hamblin et al., 1999; Oscier et al., 2002; Tobin & Rosenquist, 2005). Mutational analysis of *IGH* V genes involves PCR of the complete VDJ clonal rearrangement (i.e., encompassing the VH-FR1 though JH region, including the CDR3 sequence), with precise V-gene family delineation by Sanger sequencing, or increasingly now by NGS methods (see Figs. 78.1E and F) (Logan et al., 2011; McClure et al., 2015). The determination of VH gene identity and SHM status has been greatly facilitated by standardized recommendations and the establishment of comprehensive antigen receptor gene reference databases (e.g., ImmunoGenetics, http://imgt.cines.fr, IGBLAST, https://www.ncbi.nlm.nih.gov/igblast) (Alamyar et al.,2012; Ghia et al., 2007; Rosenquist et al., 2017).

NGS studies of CLL/SLL using targeted gene panels, whole-exome sequencing (WES), or whole-genome sequencing (WGS) have also identified several recurrent and prognostically relevant genetic alterations (see Table 78.4), including acquired mutations in *SF3B1*, *NOTCH1*, *BIRC3*, *POT1*, and *MYD88* genes, as well as known genetic changes in *TP53* and *ATM* (Foa et al., 2013; Landau et al., 2015; Martinez-Trillos et al., 2013; Nadeu et al., 2016; Puente et al., 2011). Utilizing the wide and complex array of genetic and phenotypic prognostic parameters in CLL/SLL for optimizing patient management is challenging, but it has become increasingly apparent that specific prognostic subgroups are strongly associated with outcome or specific therapy considerations (Baliakas et al., 2015b; Crassini et al., 2019; Fabbri & Dalla-Favera, 2016; Hallek et al., 2018; Hu et al., 2019; Nabhan et al., 2015; Rossi et al., 2013). *IGH* V-gene SHM status appears to be an initial dichotomization for general patient prognostic categories, with additional genetic alterations further refining disease biologic features and course. More complexity also continues to emerge, with the discovery of "stereotyped" (i.e., constrained receptor motif) classes of rearranged *IGH* V genes (e.g., VH3–21), some of which can exhibit prognostic features either independently or in concert with coexisting adverse or favorable factors (Baliakas et al., 2015a; Stamatopoulos, et al., 2017). The role and understanding of ancillary genetic testing in CLL is being further modified by the presence of newer classes of non-cytotoxic therapeutic agents, such as the Bruton tyrosine kinase (BTK) inhibitor ibrutinib, PI3 kinase delta inhibitors, BCL2 antagonists (e.g., venetoclax), and newer types of therapeutic monoclonal antibodies (Yosifov et al., 2019; Zalcberg et al., 2019). To summarize, current standard molecular and cytogenetic approaches to evaluate CLL/SLL tend to include a targeted FISH panel, *IGH* V-gene SHM analysis, and *TP53* mutation screening. The application of gene-specific NGS panels for evaluating additional genetic alterations is increasing, but the clinical relevance of these findings requires further validation. Finally, because more patients are being managed using non-chemotherapeutic agents, treatment-resistant mutations can arise in CLL subclones, as evidenced by acquired *BTK* and *PLCG2* gene alterations in patients receiving ibrutinib treatment (Ahn et al., 2017; Landau et al., 2017; Quinquenel et al., 2019; Woyach et al., 2014); these drug resistance variants can also be assessed using PCR and sequencing-based methods. With more patients achieving durable responses from improved risk stratification and newer treatment options, the need for MRD monitoring has emerged. Tracking of clonal CLL cells can be accomplished using flow cytometry, but NGS-based *IGH* V-region deep sequencing (see Figs. 78.1E and F) is also being increasingly utilized for this purpose (Del Giudice et al., 2019; Thompson et al., 2019).

Lymphoplasmacytic Lymphoma

LPL is characterized by a small lymphocytic and variably prominent plasmacytic component and by its association with the clinical syndrome of Waldenstrom macroglobulinemia (Swerdlow et al., 2017). Morphologic distinction from other small B-lymphocyte lymphomas with plasmacytic features (e.g., some MZLs) can be challenging and the typical elevation of IgM monoclonal serum protein may also occur in the setting of other B-cell neoplasms. LPL is strongly associated with the presence of a recurrent somatic mutation in the *MYD88* gene, which results in an amino acid substitution of leucine to proline at codon 265 (i.e., p.Leu265Pro or L265P) (Castillo et al., 2015; Rossi, 2014; Treon et al., 2014). This genetic alteration is identified in more than 90% of LPL cases but is also found in approximately 10% of splenic MZL cases, one-third of nodal DLBCL (mostly of ABC type) cases, and at high prevalence in DLBCL occurring in extranodal sites (Angelova et al., 2019; Hamadeh et al., Cook, 2015; Jimenez et al., 2013; Martinez-Lopez et al., 2015; Ondrejka et al., 2013; Shin et al., 2016; Swerdlow et al., 2016; Treon et al., 2012). *MYD88* L265P also occurs in approximately 50% of patients with IgM monoclonal gammopathy of uncertain significance (MGUS) but is absent in true cases of IgM-positive MM (Mori et al., 2013); this finding suggests a relationship between IgM MGUS patients with *MYD88* mutation and the development of LPL (Baldini et al., 2005). In the context of low-grade B-cell lymphomas, the presence of lymphoplasmacytic differentiation, characteristic histopathologic features in the bone marrow, IgM monoclonal paraproteinemia, and presence of *MYD88* L265P are together essentially diagnostic of LPL (Bassarova et al., 2015); however, the small proportion of patients with splenic MZL who also harbor *MYD88* L265P can pose a challenge in some diagnostic situations (Martinez-Lopez et al., 2015). Notably, IgG or IgA expressing lymphomas with lymphoplasmacytic features are less frequently associated with *MYD88* mutation (King et al., 2016; Manasanch et al., 2014).

Molecular detection of *MYD88* L265P mutation can be accomplished in several ways. PCR of exon 5 followed by Sanger sequencing can be performed to directly identify the single base change but has limited analytic sensitivity (15%–20%). Because of the patchy and often fibrotic nature of bone marrow infiltrates, more sensitive methods such as allele-specific or QPCR (Jimenez et al., 2014) and droplet digital PCR (Drandi et al., 2018) are more desirable for formalin-fixed paraffin-embedded tissues, as well as peripheral blood samples, which typically have a low number of circulating lymphoma cells (Fig. 78.3A). In approximately one-third of patients with LPL with *MYD88* L265P, a second somatic genetic alteration can be detected in the chemokine gene *CXCR4*. C-terminal truncation or frameshift alterations in *CXCR4* can be identified by PCR and Sanger sequencing (Ballester et al., 2016); Ser338* is a commonly observed *CXCR4* mutation (Fig. 78.3B). Co-occurrence of *CXCR4* mutations with *MYD88* L265P in LPL is associated with several adverse features, including decreased blood counts, higher lymphoma burden, and impaired response to targeted ibrutinib therapy (Schmidt et al., 2015; Treon et al., 2014; Castillo et al., 2019; Gustine et al., 2019; Hunter et al., 2014). *CXCR4* mutation does not appear to occur independently of *MYD88* L265P in LPL; furthermore, when present together, these genetic alterations are relatively specific for the diagnosis of LPL in the setting of low-grade B-cell lymphoma. Current evaluation of LPL thus now includes *MYD88* L265P and *CXCR4* mutation analyses by molecular techniques.

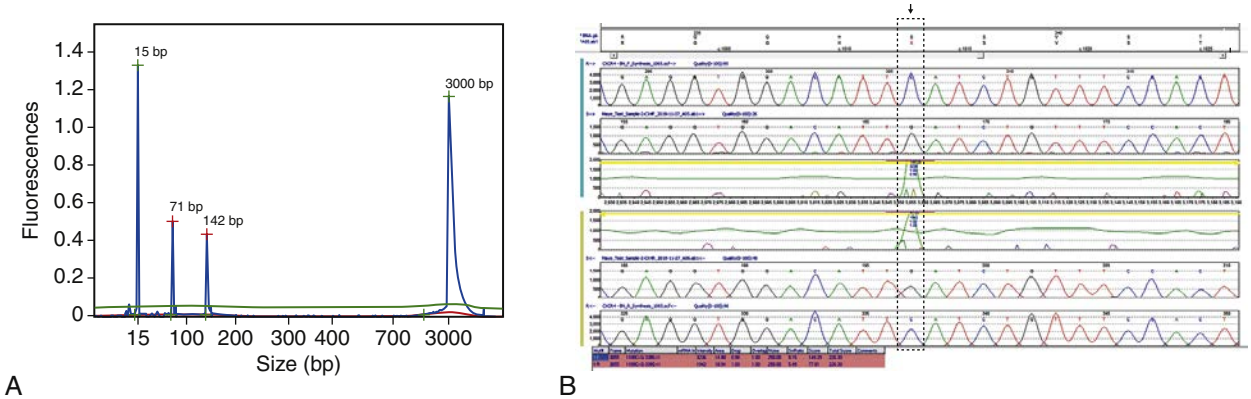

Figure 78.3 *MYD88* p. Leu265Pro and related *CXCR4* genetic alterations in lymphoplasmacytic lymphoma (LPL). **A,** A single reaction allele-specific polymerase chain reaction (AS-PCR) result detecting the presence of the *MYD88* p.Leu265Pro (L265P) mutation. Outside PCR primers produce a larger amplicon (142 bp) that covers the target gene region. A second mutant allele-discriminating primer reaction is nested within the target region and produces a smaller amplicon (71 bp) but only in the presence of the single base substitution event causing the L265P change. If the *MYD88* region is unaltered at this codon, then only the 142-bp product is observed. Electropherogram size standards are shown at either end of the display (15 and 3000 bp). The *MYD88* L265P is highly associated with LPL (>90% of cases), although it can be seen in rare cases of splenic marginal zone lymphoma and chronic lymphocytic leukemia, as well as diffuse large B-cell lymphoma. **B,** Sanger sequencing showing detection of Ser338* abnormality in the *CXCR4* gene (*arrow* and *hatched box*, C>G nucleotide substitution), occurring in the same patient with *MYD88* L265P shown in **A**. *CXCR4* acquired alterations occur in a subset (~30%) of *MYD88* mutated LPL patients and are associated with poorer responses to ibrutinib therapy.

Hairy Cell Leukemia

HCL is often readily diagnosed based on its cytologic features, pattern of bone marrow infiltration, and characteristic immunophenotype (Swerdlow et al., 2017). Occasionally however, HCL can be difficult to distinguish from other small B-cell neoplasms, particularly splenic MZL. In these difficult cases, molecular analysis for *BRAF* Val600Glu mutation (i.e., V600E) can be a useful and relatively specific diagnostic adjunct. As discussed in Chapter 77, BRAF is a member of the RAS/RAF/MEK/ERK mitogen-activated protein kinase (MAPK) pathway, and aberrant activation by acquired mutation results in deregulated signal transduction (Grever et al., 2014; Tiacci et al., 2013). *BRAF* V600E is identified in more than 95% of patients with HCL and is not significantly observed in those with other low-grade B-cell neoplasms (Tiacci et al., 2011). Of note, *BRAF* V600E mutation is also present in approximately 50% to 60% of patients with Langerhans cell histiocytosis (Badalian-Very et al., 2010) and in most patients with the rare Erdheim-Chester disease (Haroche et al., 2012). In addition to providing a molecular marker for diagnostic subclassification of HCL, the presence of *BRAF* mutation provides a potential targeted therapy option using the small-molecule inhibitor vemurafenib in patients who respond inadequately to standard cladribine or pentostatin treatment. The *BRAF* V600E alteration can be detected by PCR and Sanger sequencing; however, HCL is often associated with significant reticulin fibrosis in the bone marrow, and "dry tap" aspirate samples are not uncommon, thus necessitating more highly sensitive methods for mutation detection. Allele-specific or QPCR methods can be used for this purpose but require careful optimization to achieve specific mutant allele nucleotide discrimination relative to wild type (Schnittger et al., 2012c; Szankasi et al., 2013). In fixed paraffinized bone marrow core biopsies, the use of a BRAF V600E-specific antibody is a simple and often informative addition to a HCL diagnostic IHC panel (Brown et al., 2015; Uppal et al., 2015). In a small number of HCL cases associated with VH4-34 *IGH* clonal gene rearrangements, *BRAF* V600E mutation is not present, and it is similarly absent in cases of so-called of HCL variant (Waterfall et al., 2014; Xi et al., 2012); these rare cases may harbor acquired alterations in the *MAP2K1* gene, further highlighting the importance of MAPK pathway deregulation in HCL.

AGGRESSIVE B-CELL LYMPHOMAS

Diffuse Large B-Cell Lymphoma, High-Grade B-Cell Lymphoma, and Burkitt Lymphoma

Diffuse large B-cell lymphoma (DLBCL) is the most common type of aggressive lymphoma and is biologically and clinically heterogeneous (Swerdlow et al., 2017; Liu & Barta, 2019). DLBCL is broadly subclassified according to germinal center B-cell (GCB) or activated B-cell (ABC) "cell or origin" (COO) phenotypes, which were originally identified by unbiased gene expression profiling (GEP) studies (Alizadeh et al., 2000). IHC approaches such as the Hans algorithm are often used to define GCB or ABC types; more recently, targeted GEP techniques have been developed as an alternative to IHC in the clinical setting. COO status in DLBCL can generally identify subsets of patients with better or poorer outcomes on rituximab + CHOP (R-CHOP)–based immunochemotherapy; however, substantial variability in tumor aggressiveness and outcomes still exists both within and between COO subgroups. Recurrent genetic alterations are well known in DLBCL (see Table 78.4) and frequently include gene rearrangements involving *MYC*, *BCL2*, or *BCL6* loci, most often in conjunction with immunoglobulin gene (e.g., *IGH*) translocation events. *BCL2* (18q21) and *BCL6* (3q26) gene rearrangements each occur in approximately 20% to 30% of cases of DLBCL (Alizadeh et al., 2000; Iqbal et al., 2007). *BCL2* locus abnormalities in DLBCL further appear linked to cell of origin classification. The presence of the t(14;18)/*BCL2-IGH* is correlated with a GCB phenotype in DLBCL and poorer outcome with standard therapy (Ennishi et al., 2017). More comprehensive genetic analysis has indicated that genomic gains at the *BCL2* locus (e.g., gene amplification) without structural rearrangements are associated instead with ABC phenotype DLBCL, and these cases have an adverse prognosis (Ennishi et al., 2017; Obermann et al., 2009). *BCL6* rearrangements also occur more commonly in the ABC group of DLBCL. These associations suggest that specific genomic alterations may underlie distinct biologic and phenotypic subgroups of DLBCL, and this notion has been confirmed to some extent by a large body of research literature (Davis et al., 2010; Ennishi et al., 2017; Karube et al., 2018; Morin et al., 2010; Morin et al., 2011; Morin et al., 2013; Pasqualucci & Dalla-Favera, 2015, 2018; Pasqualucci et al., 2011; Reddy et al., 2017; Schmitz et al., 2018). For example, acquired genetic abnormalities in the B-cell receptor (BCR) signaling pathway (e.g., *CD79A*, *CD79B*), and the NF-κB signaling pathway (e.g., *CARD11*, *MYD88*) are associated with ABC type DLBCL, whereas alterations in other genes involved in epigenetic modulation (e.g., *EZH2*, *KMT2D*, *CREBBP*, *EP300*) characterize GCB tumors. These genetic alterations in turn define major pathways of oncogenesis in DLBCL, including aberrant signal transduction, apoptosis avoidance, immune surveillance evasion, and alterations in tumor-associated microenvironment. Some genetic alterations, such as *MYD88* L265P, show much greater prevalence in extranodal DLBCL presentations (Bonzheim et al., 2015; Kraan et al., 2013; Kraan et al., 2014; Pham-Ledard et al., 2014). *TP53* gene mutations are also present in a subset of DLBCL and are associated with adverse prognosis (Xu-Monette et al., 2012; Zenz et al., 2017).

MYC gene rearrangement occurs in 5% to 10% of de novo DLBCL cases and has been associated in most, but not all, studies with adverse prognostic outcome. *MYC* translocations typically occur with the *IGH* or less so *IGK* and *IGL* genes, although a small number of cases involve nonimmunoglobulin partners. The net pathogenic effect is constitutive activation of the *MYC* gene via the strong *IGH* enhancer element, leading to unchecked Myc expression and cellular proliferation. Aberrant Myc overexpression induces cellular apoptosis in normal cells, so tumor cells concurrently activate additional mechanisms to prolong cell survival (e.g., *BCL2* family upregulation, *TP53* inactivation) in the face of proliferative stress. The presence of *MYC* gene rearrangement with coexisting *BCL2* and/or *BCL6* gene rearrangements is of major clinical relevance in large B-cell lymphomas (Swerdlow et al., 2017; Ennishi et al., 2019; Kuhnl et al., 2017; Ok & Medeiros, 2019; Scott et al., 2018; Sesques & Johnson, 2017). This pattern of "double- (or triple-) hit" gene rearrangements is observed

in a subset (5%–15%) of mainly GCB lymphomas with "high-grade" or blastic nuclear features, although some cases can present as morphologically typical DLBCL. These B-cell lymphomas are highly aggressive and respond poorly to standard R-CHOP treatment, requiring instead dose-intensive alternative immunochemotherapy regimens. Some studies have suggested that the adverse association of *MYC* rearrangement is mainly confined to cases with immunoglobulin gene (IG) partners, suggesting that lymphomas with nonimmunoglobulin (non-IG) gene reciprocal translocations do not appear to behave as aggressively; however, this is controversial, with recent reports finding either no difference in outcomes or a worse prognosis only when *MYC* translocation is present along with additional rearrangements of *BCL2* and/or *BCL6* genes (Chong et al., 2018; McPhail et al., 2018; Rosenwald et al., 2019).

The complexity of DLBCL as defined in terms of GEP subtypes, recurrent genetic rearrangements, and gene-level somatic mutations creates a major challenge for molecular diagnostic assessment. Currently, the COO subtype is determined by IHC or less commonly targeted GEP (Scott et al., 2014, 2015). The mainstay of DLBCL evaluation involves FISH analysis to identify structural rearrangements of *MYC*, *BCL2*, *BCL6*, and *IGH* (or *IGK*, *IGL*) genes using break-apart and dual fusion probes. A reflex testing strategy is very effective in this regard, beginning, for example, with *MYC* BAP assessment followed by *IGH/MYC*, *BCL2*, and *BCL6* analysis only if *MYC* is rearranged. This approach establishes prognostic categories according to *MYC*-normal, *MYC*-rearranged, or double- or triple-hit (*MYC* with *BCL2* and/or *BCL6*) status, the latter defining high grade B-cell lymphoma. The role of recurrent tumor genetic sequence alterations in DLBCL continues to be better defined, but it is increasingly apparent that more precise classification and individualized management of these patients will require this information, provided by way of clinically validated targeted NGS gene panels. It is thus apparent that evaluating any single genetic abnormality in DLBCL is increasingly insufficient and more comprehensive diagnostic profiling will be required. A better understanding DLBCL pathogenesis is also more relevant in light of targeted or novel therapies including the BTK inhibitor ibrutinib, the BCL2 antagonist venetoclax, and others.

Burkitt lymphoma (BL) is a relatively rare yet distinct subtype of aggressive B-cell lymphoma that is diagnosed by its signature morphologic features, germinal center phenotype (with absence of BCL2 expression), and variable association with Epstein-Barr virus (EBV) (Dunleavy et al., 2016). In this lymphoma, the *MYC* gene on chromosome 8 translocates to *IGH* on chromosome 14 or immunoglobulin light chain genes, resulting in its overexpression; these translocations are also a hallmark, being present in 100% of cases. Endemic BL (i.e., sub-Saharan Africa) is highly associated with EBV. In this setting, the *MYC* gene is translocated to the JH region of the *IGH* locus, likely as a result of aberrant AID activity occurring during the SMH process (Casellas et al., 2016; Greisman et al., 2012). Sporadic BL is infrequently associated with EBV and the translocation event with *MYC* involves the *IGH* switch region. BL is far more commonly encountered in the pediatric age population; in contrast, significant morphologic overlap exists between BL and DLBCL or high grade B-cell lymphomas in older adults, suggesting caution when diagnosing BL in the latter cases (Bouska et al., 2017). In general, a diagnosis of true BL is less likely to be encountered in adults given the greater incidence of DLBCL and high-grade B-cell lymphomas with double-hit genetics. Therapy and prognosis are likewise critical considerations because BL requires intensive treatment on B-lymphoblastic leukemia type protocols, in contrast to R-CHOP chemotherapy in DLBCL, or alternative dose-adjusted intensive regimens for high-grade lymphoma. Recurrent tumor-associated mutations in *TCF3* and *ID3* genes have more recently emerged as relatively specific for BL based on results of research studies using NGS (Grande et al., 2019; Schmitz et al., 2012). TCF3 is a helix–loop–helix domain transcription factor that is negatively regulated by ID3. Alteration of these genes affects signaling by the BCR complex, creating a "tonic" state of cellular activation. In difficult differential diagnostic situations, identification of *TCF3* and/or *ID3* tumor genetic changes can therefore be helpful to establish the classification of BL, in conjunction with results from standard break-apart and dual fusion probe FISH evaluation for the presence of *MYC*, *BCL2*, *BCL6*, and immunoglobulin gene rearrangements.

PLASMA CELL MYELOMA

Plasma cell or MM is a relatively common hematologic malignancy with complexity in disease presentation and distribution (Swerdlow et al., 2017). Significant improvements in patient survival have been achieved with a combination of nonchemotherapeutic drugs and hematopoietic stem cell transplantation (most commonly autologous). Tumor-associated genetic abnormalities in MM form the basis of risk stratification for these patients and broadly are grouped by structural and numerical chromosomal lesions (see Table 78.4) (Fonseca et al., 2009; Kuehl & Bergsagel, 2012; Morgan et al., 2012). Cytogenetic hyperdiploidy is a common finding in MM and is unusually represented by trisomic gains in odd-numbered chromosomes. Structural variants are characterized by genomic translocations with the *IGH* locus, including the t(4;14), t(14;16), t(14;20), and t(11;14) events, which involve the *WHSC1* (aliases *NSD2*, *MMSET*), *MAF*, *MAFB* and *CCND1* (cyclin D1) genes, respectively. Recurrent gains or losses of chromosome segments are also identified in MM, including 1q amplification, del1p, del13q, and del17p, the last of these being associated with loss of the *TP53* tumor suppressor locus. The prognostic framework for MM is based largely on these abnormalities: hyperdiploid MM and cases with *CCND1* rearrangements are associated with relatively favorable outcomes, whereas genomic rearrangements or alterations involving *MAF/MAFB*, *WHSC1*, del17p, and 1p or 1q loci are associated with adverse outcome (Fonseca et al., 2009; Kuehl & Bergsagel, 2012). *MYC* gene rearrangements also occur in a subset of MM patients, associated with increased risk of progression (Misund et al., 2020; Walker et al., 2015b). The range of structural and numerical changes in MM is optimally evaluated in the diagnostic laboratory using a panel of FISH probes for enumeration and locus-specific interrogation of target genomic regions. NGS profiling of MM has also revealed recurrent mutations in a number of genes, including *NRAS*, *KRAS*, *TP53*, *BRAF*, *IRF4*, *FAM46C*, and *DIS3*, among others (Dutta et al., 2017; Walker et al., 2015a, 2018, 2019). Comprehensive genomic profiling has identified key affected pathways, including MEK-ERK, cell cycle, NF-κB, and epigenetic modification (Morgan et al., 2018). These studies have also revealed a more intricate relationship of certain acquired genetic mutations with subgroups of structural or numerical chromosome abnormalities in MM. Some genes (e.g., *FAM46C*) encode proteins whose functions are inadequately understood at the present time. Others, such as alterations in proteasome complex genes (e.g., *PSMB5*) or cereblon (*CRBN*), an E3 ubiquitin ligase cofactor, have been associated with acquired resistance to common myeloma therapeutics, such as bortezomib and lenalidomide (Barrio et al., 2019; Ushio et al., 2016). These genetic alterations may affect multiple aspects of MM pathogenesis, such as drug susceptibility or resistance and disease progression. Although the utility of clinical NGS testing to detect gene mutations remains to be determined in relation to the current well-established karyotypic stratification, an intriguing finding is that some recurrently altered genetic targets also reside in regions affected by structural variation (e.g., *FAM46C* on 1p, *DIS3* on 13q, *TP53* on 17p), suggesting a role for tumor suppressor loss in both initiation and progression of disease. Furthermore, insights from genomic analysis of MM have identified the relative tumor mutation burden and presence of neutral mutation evolution as important prognostic factors for outcome (Johnson et al., 2017; Walker et al., 2018).

MATURE T-CELL NEOPLASMS

Anaplastic Large-Cell Lymphoma

Anaplastic large-cell lymphoma (ALCL) is a unique subtype of peripheral T-cell NHL that may present as a primary cutaneous disease or, more commonly, as a systemic form involving lymph nodes, visceral organs, and skin (Ferreri et al.,2012; Irshaid & Xu, 2019; Montes-Mojarro et al., 2018; Shustov & Soma, 2019; Xing & Feldman, 2015). A rare presentation occurs in breast capsule tissue in patients with silicone prosthetic implants (Aladily et al., 2012; Quesada et al., 2019). A phenotypic hallmark in nearly all cases of ALCL is strong uniform expression of the CD30 (Ki-1) antigen, an activation marker and member of the tumor necrosis factor family. Many cases of ALCL either show minimal T-cell–associated markers, and some exhibit a "null" cell phenotype, but these cases can usually be confirmed as being of T-cell lineage based on T-cell receptor gene rearrangement studies. A significant subset of systemic ALCL is characterized by translocations involving the anaplastic lymphoma kinase (*ALK*) gene located on chromosome 2p23 (see Table 78.4). *ALK* encodes a tyrosine kinase that is not normally expressed in lymphoid cells. Approximately 90% of *ALK*-rearranged ALCL harbor the t(2;5)(p23;q35) abnormality, leading to a fusion of the *ALK* gene with the *NPM1* gene (Falini et al., 2007; Montes-Mojarro et al., 2018; Stein et al., 2000). Most genomic translocations in lymphomas aberrantly induce expression of a critically regulated gene (e.g., *BCL2*, *MYC*) under the promoter or enhancer element of the genetic partner. In ALCL, the *NPM1-ALK* chimeric fusion produces a novel oncoprotein that drives ALK overexpression in the neoplastic T cells. As a result of the *NPM1-ALK* gene fusion, the tyrosine kinase activity and intracellular location of ALK protein become deregulated, contributing to lymphomagenesis through increased target protein phosphorylation and signal

transduction (Chiarle et al., 2008; Montes-Mojarro et al., 2018; Pulford et al., 2004). Research data have shown that *ALK* activation is associated with downregulation of T cell–associated protein expression, NF-κB target gene activation, functional inactivation of normal p53 tumor suppression, and immunosuppressive effects mediated through STAT3 signaling (Morgan et al., 2018; Werner et al., 2017; Zamo et al., 2002). In addition to *NPM1-ALK*, several less common variant genetic rearrangements of *ALK* are also described in ALCL, including the t(1;2)(q25;p23)/*TPM3-ALK*, t(2;3)(p23;q35)/*TFG-ALK*, and inv(2)(p23q35)/*ATIC-ALK* abnormalities, all similarly resulting in *ALK* gene deregulation (reviewed in Montes-Mojarro et al., 2018). Notably, the abnormal cellular sublocalization of constitutive ALK kinase activity is mediated by the fusion partner protein moiety. Thus, NPM1-ALK oncoproteins are situated in both a nuclear and cytosolic pattern, whereas TPM3-ALK products show diffuse cytoplasmic distribution, in accordance with the usual site of the *TPM3* gene product tropomyosin-3. Several clinical studies have demonstrated a relatively favorable prognosis for *ALK*-positive ALCL, regardless of the underlying type of translocation (Hapgood & Savage, 2015). *ALK*-positive ALCL is more prevalently seen in younger patients (e.g., younger than 50 years) and in the pediatric population. Of note, the primary cutaneous form of ALCL is not commonly associated with *ALK* gene abnormalities or aberrant *ALK* expression and has a very favorable outcome. A second group of systemic ALCL is now recognized by absence of *ALK* gene disruption (*ALK*-negative ALCL) but instead with rearrangements of the *DUSP22/IRF4* gene locus (6q25.3) or the p53-related *TP63* gene (3q28) (see Table 78.4). *DUSP22* and *TP63* ALCL share similar morphologic features and expression of CD30 antigen as *ALK*-positive cases. Most significant, *ALK*-negative ALCL with *DUSP22* gene rearrangement has a relatively favorable prognosis similar to *ALK*-positive counterparts, whereas *TP63* gene rearrangement identifies a subset of ALCL with very poor outcome (Feldman et al., 2011; Hapgood & Savage, 2015; Parrilla Castellar et al., 2014; Pedersen et al., 2017; Vasmatzis et al., 2012; Zeng & Feldman, 2016). In part, the better outcomes for *DUSP22* rearranged ALCL may be related to the presence of an immunogenically primed state, establishing a more robust host response (Luchtel et al., 2018).

Genomic breakpoints in cases of t(2;5)-positive ALCL lie consistently within the same intron regions in both *NPM1* and *ALK* genes, resulting in the generation of a single, unique *NPM1-ALK* chimeric mRNA. As a result, RT-PCR technique can be used to detect the fusion transcript with high specificity and sensitivity (Beylot-Barry et al., 1996; Ladanyi, Cavalchire, Morris, Downing, & Filippa, 1994; Yee et al., 1996). In addition, long-distance DNA PCR has also been successfully employed to identify the genomic *NPM1-ALK* abnormality (Ladanyi & Cavalchire, 1996; Sarris et al., 1996). The latter approach requires high molecular weight DNA but obviates the need for RNA isolation and reverse transcription. FISH methodology is nevertheless the most widely employed diagnostic modality to detect *ALK* gene rearrangements (Cataldo et al., 1999; Mathew et al., 1997; Perkins et al., 2005). Essentially all translocation-associated alterations can be detected using a BAP method directed to the *ALK* locus; elucidation of the specific translocation gene partner is not required because of its limited clinical value. As with other gene overexpression phenomena in the NHLs, *ALK*-positive ALCL can also be readily diagnosed using monoclonal antibodies against the ALK portion of the oncoprotein. The immunohistochemical staining pattern of the abnormal ALK protein, as suggested previously, also correlates to some extent with the causative translocation event, reflecting the contribution of the fusion partner segment to cellular localization (Duyster et al., 2001; Falini et al., 1999; Stein et al., 2000). The subset of *ALK*-negative ALCL with *DUSP22* or *TP63* gene rearrangements can be reliably detected by specific FISH probe techniques. The presence of *ALK*, *DUSP22*, or *TP63* gene rearrangements provides important prognostic information in ALCL and can also be helpful in the differential diagnosis between ALCL and classical Hodgkin lymphoma.

As a footnote on *ALK*-positive lymphomas, rare presentations of an aggressive large B-cell lymphoma with t(2;17)(p23;q23)/*CLTC-ALK* or t(2;5)/*NPM1-ALK* gene fusions have been described, in association with IgA heavy chain expression and plasmablastic cytologic features (De Paepe et al., 2003; Gascoyne et al., 2003; Laurent et al., 2009). These tumors are also recognized by the presence of plasmacytic cell markers but lack of CD20 expression and are CD30 negative. The *CLTC* gene encodes clathrin, and the chimeric CLTC-ALK protein has a unique granular membranous cellular immunohistochemical pattern, corresponding to ALK localization in clathrin-coated pits.

Peripheral T-Cell Lymphomas

The genomic pathology of peripheral T-cell lymphoma (PTCL) is becoming better understood in the era of NGS and comprehensive tumor genetic profiling (Heavican et al., 2019; Lemonnier et al., 2018; Schatz et al., 2015; Vallois et al., 2016). One example is that of angioimmunoblastic T-cell lymphoma (AITL) and related entities under the subgroup of lymphomas of T-follicular helper (TFH) cell origin (Lunning & Vose, 2017). NGS studies have identified certain recurrent acquired genetic changes associated with TFH lymphomas, including mutations involving *IDH2* (particularly *IDH2* Arg172), *RHOA*, *CD28*, *DNMT3A*, and *TET2* genes (Dobay et al., 2017; Lemonnier et al., 2012; Odejide et al., 2014; Vallois et al., 2016; Wang et al., 2015a). Gene fusions such as the t(5;9)/*ITK-SYK* and *CTLA4-CD28* occur in small subsets of PTCL (including some cases of AITL). Molecular diagnostic evaluation of PTCL (excluding ALCL) currently does not require extensive studies beyond TCR gene rearrangement PCR analysis to establish monoclonality in some cases. However, the presence of recurrent gene mutations or chimeric gene fusion abnormalities suggests that a focused NGS approach may be of value for diagnosis and subclassification. Furthermore, the availability of selective inhibitors of mutated *IDH2* (e.g., enasidenib) may provide a potential therapeutic option for these patients in future. Despite significant gains in our understanding of PTCL molecular pathogenesis (most evidently for ALCL and TFH lymphoma), the wider category of PTCL-unspecified remains genetically complex, requiring ongoing research efforts to improve outcomes for these patients.

Chronic T-Cell Leukemias

T-cell large granular lymphocytic leukemia (T-LGLL) and T-cell prolymphocytic leukemia (T-PLL) are examples of chronic T-cell lymphoproliferative neoplasms with characteristic tumor genetic alterations. Acquired mutations of *STAT3* (present in approximately one-third of cases) and less frequently *STAT5B* (<5% of cases) occur in T-LGLL (Andersson et al., 2016; Coppe et al., 2017; Jerez et al., 2012a; Kerr et al., 2019; Koskela et al., 2012; Rajala et al., 2013, 2014). *STAT3* gene mutations are also observed in a subset of chronic lymphoproliferative disorders of natural killer (NK) cells. Mutations in these genes are considered to deregulate signaling through the JAK-STAT pathway. *STAT3* and *STAT5B* alterations can be identified by PCR and Sanger sequencing, allele-specific PCR, or as part of a targeted NGS panel. The latter testing approach may be of particular value given that many cases of T-LGLL are associated with unexplained peripheral blood cytopenias (mainly neutropenia), raising the differential diagnostic consideration of a myelodysplastic syndrome (MDS). NGS results can help to delineate a possible T-LGLL process from MDS provided that *STAT3* and *STAT5B* are included in the NGS panel design. The presence of *STAT* gene mutations may be useful to distinguish T-LGLL from reactive granular lymphocyte expansions in some patients, especially when TCR gene rearrangement analysis is equivocal.

T-PLL is a well-known lymphoid neoplasm with heterogeneous clinical presentation and course, and is associated with recurrent rearrangements of the *TCL1A* gene (Staber et al., 2019). T-PLL often demonstrates cutaneous involvement in addition to peripheral blood, bone marrow, and spleen (Hsi et al., 2014). *TCL1A* is deregulated in 80% of T-PLL cases as a result of an inv14(q11q32) or t(14;14)(q11;q32) event (Maljaei, et al., 1998). *TCL1A* is a proto-oncogene and after translocation to the TCR-α locus (*TRA*) on 14(q11) becomes activated, leading to overexpression of the TCL1A transcription factor, which is normally not present in mature T cells (but is expressed in a subset of B lymphocytes). *TCL1A* gene rearrangement is not identified in other T-cell neoplasms and is thus a relatively specific genetic marker for T-PLL (Sud & Dearden, 2017). FISH analysis is most often employed to detect 14q translocation or inversion abnormalities affecting the *TCL1A* locus, although IHC is a rapid alternative to demonstrate the overexpressed TCL1A protein (e.g., in paraffin-embedded bone marrow biopsy specimens). Rare patients with T-PLL lack *TCL1A* rearrangements but instead have alternate t(X;14)(q28;q11) or t(X;7)(q28;q35) events (Maljaei et al., 1998; Stern et al., 1993), resulting in translocation of the *TCL1A*-related gene *MTCP1* to the *TRA* or TCR-β (*TRB*) loci, respectively. These cases are more challenging to identify without specific FISH probes or karyotype studies. The finding of *TCL1A* rearrangement by FISH analysis or TCL1A overexpression by IHC is valuable in distinguishing T-PLL from other mature T-cell neoplasms with overlapping morphologic or immunophenotypic features.

MOLECULAR DIAGNOSIS OF MYELOID NEOPLASMS

ACUTE MYELOID LEUKEMIA

The importance of genetic markers is reflected in the present WHO classification, in which AMLs are increasingly defined by their characteristic

BOX 78.1

2017 World Health Organization Classification of Acute Myeloid Leukemia and Related Precursor Neoplasms

AML with Recurrent Genetic Abnormalities

- AML with t(8;21)(q22;q22.1); RUNX1-RUNX1T1
- AML with inv(16)(p13.1q22) or t(16;16)(p13.1;q22); *CBFB-MYH11*
- Acute promyelocytic leukemia with *PML-RARA*
- AML with t(9;11)(p21.3;q23.3); *KMT2A-MLLT3*
- AML with t(6;9)(p23;q34.1); *DEK-NUP214*
- AML with inv(3)(q21.3q26.2) or t(3;3)(q21.3;q26.2); *GATA2, MECOM*
- AML (megakaryoblastic) with t(1;22)(p13.3;q13.1); *RBM15-MKL1*
- AML with *BCR-ABL1*: provisional
- AML with gene mutations
  - AML with mutated *NPM1*
  - AML with biallelic mutation of CEBPA
  - AML with mutated *RUNX1*: provisional

AML with Myelodysplasia-Related Changes

Therapy-Related Myeloid Neoplasms

AML, Not Otherwise Specified

Myeloid Sarcoma

Myeloid Proliferation Associated with Down syndrome

AML, Acute myeloid leukemia.

genetic abnormalities in relation to morphologic and immunophenotypic features, prognosis, and therapeutic implications. The identification of specific genetic markers can thus establish the diagnosis of AML subclassification, provide important prognostic information, guide therapeutic intervention, and reveal insights into tumor biology (Swerdlow et al., 2017; Dohner et al., 2017; Tallman et al., 2019).

Cytogenetic studies of large cohorts of patients with AML have shown that balanced gene rearrangements underlie the disease pathogenesis in 30% to 50% of pediatric and younger AML patients and a minority of older AML patients (Grimwade, et al., 2016). These changes had been recognized in the WHO classification under the category of "AML with recurrent genetic abnormalities" (Box 78.1). Although the diagnosis of AML routinely requires at least 20% myeloblasts in the peripheral blood or bone marrow, detection of t(8;21)(q22;q22.1); *RUNX1-RUNX1T1*, inv(16)(p13.1q22)/t(16;16)(p13.1;q22); *CBFB-MYH11*, or t(15;17)(q24.1;q21.2); *PML-RARA* warrants a diagnosis of AML regardless of blast count. Therapy-related myeloid neoplasms may also harbor these balanced translocations or inversion and should be diagnosed as therapy-related myeloid neoplasms with the genetic abnormalities noted. At the time of AML diagnosis, cytogenetic analysis is a crucial component of the work-up not only because it defines AML subtypes in the context of patient's clinical and therapeutic history and molecular findings but also because it serves as the cornerstone for AML risk stratification.

The prognosis of patients with AML is determined by multiple factors, including patient demographics and clinical and treatment variables as well as a major impact from genetic abnormalities. AML had historically been assigned into "favorable," "intermediate," or "adverse" prognosis types based on cytogenetic findings. However, in the past decade, the molecular landscape of AML has been unveiled with the advent of high-throughput sequencing. Recurrent somatic mutations were observed in several common functional pathways: signaling and kinase pathways, NPM1, transcription factors, epigenetic modifiers, spliceosome complex, cohesin complex, and tumor suppressors (Table 78.5). Although a normal karyotype is seen in about 40% to 50% of patients with AML, somatic mutations are seen in 90% to 95% of patients with AML with a median of three or four mutations per case (Patel, et al., 2012; Cancer Genome Atlas Research et al., 2013; Metzeler et al., 2016; Papaemmanuil et al., 2016). These findings shed light on the genetic basis of AML, particularly in the cytogenetic intermediate-risk group with normal karyotype or chromosomal gains or losses. Because AML is clinically and genetically heterogeneous with co-occurrence of competing clones and genetic abnormalities impacting different yet interacting functional pathways, and naturally comes with dynamic clonal evolution, a major challenge for today's medical practitioners is to accurately decipher the clinical impact encrypted by the various combinations of genetic abnormalities and translate them into clinical gain for individual patients. Aided by numerous correlative clinical studies, progress has been made to this end, as reflected in the 2017 European LeukemiaNet (ELN) recommendation and 2020 National Comprehensive Cancer Network (NCCN) guideline in which mutational status further refined the cytogenetic-based risk stratification system, particularly

TABLE 78.5

Functional Pathways of Commonly Mutated Genes in Myeloid Neoplasms

Function or Pathway	Genes
Epigenetic modifier	*DNMT3A*
DNA methylation and hydroxymethylation	*TET2*
	IDH1
	IDH2
	WT1
Epigenetic modifier	*EZH2*
Chromatin histone acetylation and methylation	*ASXL1*
	MLL/KMT2A
	BCOR
Spliceosome complex	*SRSF2*
	U2AF1
	SF3B1
	ZRSR2
Signaling and kinase pathway	*FLT3*
	KRAS
	NRAS
	KIT
	PTPN11
	NF1
	CBL
Transcription factors	*CEBPA*
	RUNX1
	GATA2
	ETV6
	BCOR
Tumor suppressor	*TP53*
	PHF6
Cohesin complex	*RAD21*
	STAG1
	STAG2
	SMC1A
	SMC3
Nucleophosmin	*NPM1*
Poorly defined	*SETBP1*

in the intermediate cytogenetic risk group (Table 78.6) (Dohner et al., 2017; Tallman et al., 2019). Recent years have also witnessed meaningful advancement in targeted therapy in AML, and the U.S. Food and Drug Administration (FDA) has approved FLT3 inhibitors midostaurin and gilteritinib, IDH1 inhibitor ivosidenib, and IDH2 inhibitor enasidenib for adult AML patients harboring these respective mutations. The field of genomics for AML and other myeloid neoplasms is rapidly evolving, and at the time of AML diagnosis, multiple clinically relevant molecular markers such as *FLT3*, *NPM1*, *CEBPA*, *KIT*, *RUNX1*, *ASXL1*, *TP53*, *IDH1*, and *IDH2* should be evaluated (most efficiently by NGS) along with cytogenetics for comprehensive prognostic assessment and possible targeted therapy.

This section focuses on the common AML-related genetic abnormalities that are currently considered to be the most clinically relevant because of frequency of occurrence and impact on prognosis and therapeutic intervention.

Acute Myeloid Leukemia with Recurrent Cytogenetic Abnormalities

Acute Promyelocytic Leukemia with PML-RARA

Acute promyelocytic leukemia (APL), or AML-M3 (according to the previous French-American-British [FAB] classification of AML) accounts for 5% to 10% of de novo AML cases. Patients typically present with symptoms from peripheral blood cytopenias (e.g., anemia, absolute neutropenia, and thrombocytopenia) and have a high propensity for life-threatening coagulopathy. Morphologically, APL consists of a proliferation of hypergranular promyelocytes; however, a microgranular variant form is also frequently encountered (Mantadakis et al., 2008). Immunophenotypically, the

TABLE 78.6
Acute Myeloid Leukemia Risk Stratification by Genetics

Risk Category	Genetic Abnormality
Favorable	*PML-RARA*
	t(8;21)(q22;q22.1); *RUNX1-RUNX1T*
	inv(16)(p13.1q22) or t(16;16)(p13.1;q22); *CBFB-MYH11*
	Mutated *NPM1* without *FLT3*-ITD or with *FLT3*-ITD^{low}
	Biallelic mutated *CEBPA*
Intermediate	Mutated *NPM1* and *FLT3*-ITD^{high}
	Wild-type *NPM1* without *FLT3*-ITD or with *FLT3*-ITD^{low} (without adverse-risk genetic lesions)
	t(9;11)(p21.3;q23.3); *MLLT3-KMT2A*
	Cytogenetic abnormalities not classified as favorable or adverse
Adverse	t(6;9)(p23;q34.1); *DEK-NUP214*
	t(v;11q23.3); *KMT2A* rearranged
	t(9;22)(q34.1;q11.2); *BCR-ABL1*
	inv(3)(q21.3q26.2) or t(3;3)(q21.3;q26.2); *GATA2,MECOM(EVI1)*
	-5 or del(5q); -7; -17/abn(17p)
	Complex karyotype, monosomal karyotype
	Wild-type *NPM1* and *FLT3*-ITD^{high}
	Mutated *RUNX1* in the absence of favorable risk AML subtypes
	Mutated *ASXL1* in the absence of favorable risk AML subtypes
	Mutated *TP53*

AML, Acute myeloid leukemia.
Adapted from Dohner H, Estey E, Grimwade D, et al., Diagnosis and management of AML in adults: 2017 ELN recommendations from an international expert panel, *Blood* 129:424–447, 2017.

cells are characterized by a lack of CD34 and HLA-DR. APL is genetically defined by the presence of the t(15;17)(q24.1;q21.2) abnormality, resulting in the fusion of the retinoic acid receptor-α gene, *RARα* (also called *RARA*) [17(q21.2)] with the *PML* gene [15(q24.1)] to form a *PML-RARA* chimeric gene on the derivative chromosome 15q (Grignani et al., 1994; Jurcic et al., 2007).

The *RARA* gene product is a subunit of a heterodimeric nuclear receptor for the naturally occurring ligand retinoic acid, or vitamin A. The retinoid nuclear receptor pathway is functional in many aspects of normal cell proliferation and differentiation (Chambon, 1996; Collins, 2008; Mark et al., 2009). *PML* encodes a DNA-binding zinc finger protein and associates with several other proteins in a macromolecular complex, forming discrete nuclear bodies (Dyck et al., 1994; Weis et al., 1994; Reineke & Kao, 2009). This interesting protein appears to have multiple possible cellular functions, including transcriptional regulation, apoptosis, and possibly immune surveillance (Quignon et al., 1998; Wang et al., 1998; Grimwade, 1999; Zhong et al., 2000; Borden & Culjkovic, 2009; Reinecke & Kao, 2009; Gabali, 2013). The chimeric PML-RARA protein is clearly involved in disrupting numerous intracellular processes, primarily resulting in a lack of terminal differentiation of neoplastic myeloid precursors beyond the promyelocytic stage. Nonetheless, the significance of APL as a "therapeutic paradigm" for leukemia resides in the ability of pharmacologic doses of *all trans* retinoic acid (ATRA) to induce leukemic cell differentiation in vivo (Huang et al., 1988). When used in combination with cytotoxic chemotherapy, the synergistic effects with ATRA induce complete remission in 90% to 98% of patients and prolonged remission in more than 80% of patients (Tallman et al., 1997; 2002; Shen et al., 2004; Clavio et al., 2009; Sanz et al., 2009; Patel et al., 2012). This remarkable finding has intensified efforts to identify other avenues for "cytodifferentiative" therapy in AML. Even though the effect of ATRA would seem superficially related to the interaction with the RARA moiety in the abnormal PML-RARA protein, further investigations have revealed the basic molecular mechanisms underlying the success of this agent. The normal retinoic acid receptor, when not bound to its retinoic acid ligand, associates with histone deacetylase in a nuclear protein corepressor complex (Guidez et al., 1998; Lefebvre, 2001; Wei, 2004). This interaction reduces the accessibility of chromatin to transcription factors (and thus locus-specific transcriptional activity) yet is reversible in normal marrow cells upon exposure to physiologic concentrations of retinoic acid. The PML-RARA oncoprotein stabilizes and enhances the state of transcriptional repression by this multiprotein complex; however, therapeutic doses of ATRA appear to overcome this abnormal condition and relieve the cellular differentiation block (Melnick & Licht, 1999; Hormaeche & Licht, 2007; Collins, 2008; Licht, 2009). Whereas some evidence suggests that the PML-RARA oncoprotein may also disrupt the normal proapoptotic functions of PML, thus potentiating transformation via pathways involving both partners in the translocation (*PML-RARA* and *RARA-PML*), the direct contribution of altered PML to leukemogenesis remains controversial (Strudwick & Borden, 2002; Collins, 2008; Brown et al., 2009). Functional haploinsufficiency of one remaining normal *PML* gene may also be important in the pathobiology of APL.

The molecular anatomy of the *PML-RARA* fusion gene and mRNA products in APL is summarized diagrammatically in Figure 78.4. The *PML* gene exhibits breakpoint heterogeneity in that one of three possible break sites can be encountered in any given patient, involving either intron 3 or intron 6, or occurring within exon 6 (Grignani et al., 1994; Gallagher et al., 1995; Reiter et al., 2003). In contrast, the *RARA* breakpoints are uniformly distributed in intron 2 of the gene. Thus, one of three possible *PML-RARA* chimeric mRNAs can result from this genetic fusion after transcription and mRNA splicing: *PML* exon 6/*RARA* exon 3 [long (L)-form, or BCR 1], *PML* exon 3/*RARA* exon 3 [short (S)-form, or BCR 3], and *PML* exon 6Δ/*RARA* exon 3 [variable (V)-form, or BCR 2]. The V-form transcript is unique in that the *PML* break occurs within exon 6, and a variable proportion of this exon is retained, although additional nucleotides may be added or deleted. Notably, an in-frame fusion mRNA is produced in each case of APL, underscoring the critical requirement for the PML-RARA protein in leukemogenesis. The L-form (BCR 1) and S-form (BCR 3) *PML-RARA* fusions are most commonly found in APL (~45%–50% of cases each), whereas the V-form (BCR 2) is only rarely encountered (~5% of APL cases). The strategy for RT-PCR amplification of these *PML-RARA* transcripts is depicted in Figure 78.4B, as is a representative diagnostic PCR assay in a patient with APL (Fig. 78.4C).

The clinical relevance in detecting the *PML-RARA* fusion in cases of suspected APL is evident from the efficacy of administering specific therapy (ATRA plus arsenic trioxide [ATO] or anthracycline-based chemotherapy) with a high possibility of long-term remission and survival. RT-PCR analysis is a rapid and highly specific means of confirming the *PML-RARA* fusion in suspected patients with APL, for whom early treatment with ATRA can prevent the development of catastrophic APL-associated coagulopathy. The fusion can also be detected by FISH techniques using dual-color, dual-fusion probes. FISH methods are also very rapid and of high utility for initial diagnosis of APL; however, FISH and RT-PCR should be considered complementary in the diagnostic setting. FISH is also useful in identifying rare cases of "APL-variant" leukemias, which share morphologic and immunophenotypic similarities with classical APL, but have alternative translocations of *RARA* to genes other than *PML*. These variant AML types are characterized by t(11;17)/*ZBTB16(PLZF)-RARA*, t(11;17)/*NUMA1-RARA*, t(5;17)/*NPM1-RARA*, or t(17;17)/*STAT5B-RARA* abnormalities (Melnick & Licht, 1999; Grimwade et al., 2000; Sainty et al., 2000; Zelent et al., 2001; Balusu et al., 2011). Notably, *ZBTB16(PLZF)-RARA* and *STAT5B-RARA* APL variants are resistant to ATRA and are associated with less favorable outcomes (Jansen & Löwenberg, 2001; Redner, 2002). APL with t(5;17) with *NPM1-RARA* fusion appears to respond to ATRA (Melnick & Licht, 1999). Molecular assays with probes specific for the *PML-RARA* fusion will not detect these variant transcripts, and FISH results for *PML-RARA* would be negative; however, the presence of *RARA* region breakage by FISH is helpful for distinction from true APL and for further subclassification. Other morphologic AML subtypes characterized by increased promyelocytes are similarly ATRA unresponsive and also require distinction from true *PML-RARA* positive APL.

Although APL is potentially curable, relapses are not uncommon. Molecular reappearance of the *PML-RARA* mRNA usually precedes hematologic relapse by several weeks to months, thus enabling a window for early detection and secondary intervention. RQ-PCR–based molecular monitoring is a powerful tool for predicting relapse in patients with APL. Clinical testing should achieve a minimum analytic sensitivity of 10^{-4}, and the test should be performed in the same laboratory to ensure consistency of analytical sensitivity, given the current lack of an international standard for this assay (Schuurhuis et al., 2018; Tallman et al., 2019). The timing of molecular MRD evaluation (i.e., phase of disease therapy) is very important in this regard. MRD evaluation at the end of induction is not informative because of the delayed clearance of the differentiating *PML-RARA*–positive leukemic cells. At the end of consolidation therapy,

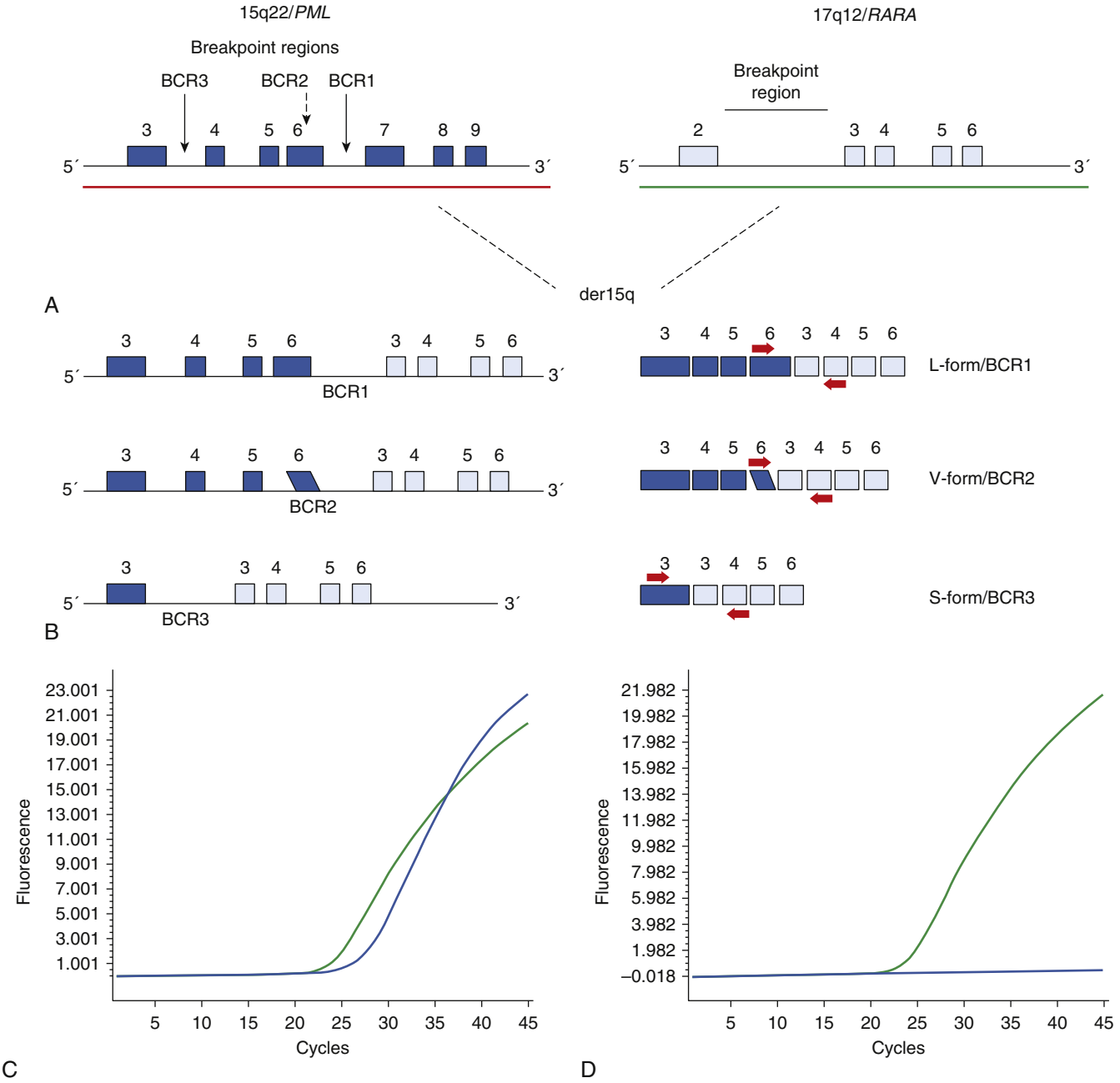

Figure 78.4 The t(15;17)/*PML-RARA* abnormality in acute promyelocytic leukemia (APL). **A,** Arrangement of *PML* and *RARA* genes on their respective chromosomes. Genomic breakpoints in the *RARA* locus occur invariantly in intron 2. This results in consistent fusion of *RARA* exon 3 to the *PML* gene. Break sites in *PML* are heterogeneous and can involve one of three breakpoint cluster regions (BCR) in any given patient with APL: in intron 6 (BCR1), within exon 6 (BCR2) or in intron 3 (BCR3). Of these, the BCR1 and BCR3 breakpoints are the most common, accounting for more than 90% of APL cases. Fluorescence in situ hybridization probes for the *PML* and *RARA* genes (*red* and *green bars,* respectively) typically span the entire genomic loci (including all breakpoint regions) and are designed to extend several hundred kilobases telomeric to each gene (not fully shown here). **B,** The three possible *PML-RARA* gene fusions *(left side)* and corresponding chimeric mRNA species *(right side)*. Because the BCR1 type *PML-RARA* fusion results in the longest transcript, it is also known as the long (L) form, in contrast to the BCR3 product, which conversely is designated as the short (S) form. The BCR2 event, owing to the inconstant intraexonic break-fusion location in each case, is also known as the Variable (V) form transcript. Reverse transcription polymerase chain reaction approaches to specifically amplify these various *PML-RARA* fusion mRNA species are schematically depicted by *small red arrows* representing PCR primer locations. **C,** Representative positive result of real-time quantitative polymerase chain reaction (RQ-PCR) analysis for the *PML-RARA* fusion mRNA in a patient with APL. *Blue curve, PML-RARA* fusion transcript amplified or detected; *green curve,* housekeeping gene *ABL1* transcript. **D,** Representative negative result of quantitative RQ-PCR analysis for the *PML-RARA* fusion mRNA in the same patient with APL in molecular remission. *Blue curve,* no *PML-RARA* transcript amplified or detected; *green curve,* housekeeping gene *ABL1* transcript.

however, conversion to or persistence of PCR positivity is a strong predictor for relapse in patients who may otherwise have apparently achieved clinical complete response. The positive predictive value for overt relapse is also highest in patients who repeatedly tested positive for *PML-RARA* by RQ-PCR on consecutive occasions. Thus, a major therapeutic goal in APL is the achievement and maintenance of "molecular remission" (i.e., a PCR-negative status). The results from several clinical studies have not only shown the benefit of using RQ-PCR to detect MRD and predict relapse risk but have also underscored the ability to successfully salvage patients with molecular disease and prevent recurrence of hematologic disease (Santamaria et al., 2007; Kohno et al., 2008; Lo Coco et al., 2008; Grimwade et al., 2010; Paschka et al., 2012; Patel et al., 2012; Schuurhuis et al., 2018). The 2020 NCCN guideline for AML recommends RQ-PCR on a peripheral blood specimen at the completion of consolidation to document molecular remission. In patients receiving an ATRA/ATO regimen, earlier testing at 3 to 4 months during consolidation is recommended. With confirmed molecular remission, subsequent monitoring in blood every 3 months for 2 years is recommended for high-risk patients (white blood cell count >10 × 10^9/L at diagnosis), those older than 60 years of age, and patients with long interruptions during consolidation or therapeutic intolerance during maintenance. The risk of relapse has been shown to be minimal for low-risk patients who achieve molecular remission at the completion of consolidation, and MRD monitoring may not be necessary except for clinical trial purposes. If RQ-PCR is positive at

any level, the result needs to be confirmed by a repeat testing on a blood sample in 2 to 4 weeks in a reliable laboratory. If repeated positive, the case should be treated as first relapse; if repeated negative, frequent monitoring (every 3 months for 2 years) is strongly recommended (Tallman et al., 2019). Because the sensitivity of transcript detection after treatment onset can be 1 to 2 logs lower in peripheral blood than in bone marrow, the ELN adopted a more conservative approach and recommended MRD assessment following consolidation every 3 months for 24 months in bone marrow and peripheral blood or alternatively in peripheral blood every 4 to 6 weeks. In patients on ATRA/ATO with low- or intermediate-risk Sanz score, MRD testing should be continued until patients have achieved MRD-negative complete remission. Beyond diagnosis, the role of FISH for MRD monitoring in APL is virtually nonexistent because the detection sensitivity required for prognostic and clinical decision-purposes cannot be reliably attained at sample time points beyond induction therapy.

Acute Myeloid Leukemia with Core Binding Factor Gene Rearrangement: t(8;21)(q22;q22.1); RUNX1-RUNX1T1 and Inv(16)(p13.1q22) or t(16;16)(p13.1;q22); CBFB-MYH11

AML with t(8;21)(q22;q22.1) and inv(16)(p13.1q22)/t(16;16)(p13.1;q22) cytogenetic abnormalities account for approximately 11% to 18% of de novo cases (Schnittger et al., 2007; Cheng et al., 2009). CBF-related AML cases are roughly evenly distributed between those with t(8;21) and inv(16)/t(16;16) (Dombret et al., 2009). Whereas t(8;21) is generally associated with AML showing maturation (FAB type AML-M2), inv(16)/t(16;16) are highly correlated with acute myelomonocytic leukemia with abnormal eosinophils (FAB type AML-M4Eo) (Le Beau et al., 1983). Clinically, these genetically defined AML subtypes are responsive to chemotherapy (especially high-dose cytarabine regimens) and are considered to be prognostically favorable compared with AML in general (Appelbaum et al., 2006; Dombret et al., 2009; Paschka et al., 2012; Patel et al., 2012).

Although different respective leukemia phenotypes derive from these translocations, a remarkable and common pathobiologic feature of both t(8;21) and inv(16)/t(16;16) AML is disruption of the CBF transcriptional regulatory pathway (Speck et al., 1999; Paschka, 2008). CBF is a heterodimeric transcription factor that consists of a DNA binding α-subunit (CBFα) and a peptide-interacting β-subunit (CBFβ), which acts to stabilize CBFα at sites of DNA interaction. In normal cells, CBF acts at "core" enhancer sequences in a number of genes required for proper myeloid and lymphoid cell differentiation, maturation, or both. The binding of CBF facilitates the access of other transcription factor complexes to these chromatin sites, in part through increased acetylation of DNA-bound histone proteins (Lorsbach & Downing, 2001; Yamagata et al., 2005). In AML with t(8;21), the *RUNX1* gene (formerly designated *AML1*, or *CBFA2*) encoding an isoform of CBFα is joined to a putative transcription factor, *RUNX1T1* (formerly *ETO*, or *MTG8*) to form the *RUNX1-RUNX1T1* fusion (Downing, 1999; Peterson et al., 2007; Patel et al., 2012). In the case of the inv(16)/t(16;16), the gene-producing CBFβ (*CBFB*) is juxtaposed to a smooth muscle myosin heavy chain gene *MYH11* to form the hybrid *CBFB-MYH11* (Liu et al., 1995; Mrózek et al., 2008; Pratcorona et al., 2012). In either case, profound disruption of the normal cellular differentiation program is thought to be central to the causation of acute leukemia. The prominence of CBF pathway alterations in leukemogenesis is additionally emphasized by the finding of *RUNX1* gene translocations in several other types of leukemia and myelodysplasia, including the t(12;21); *ETV6-RUNX1* abnormality, the most common single genetic abnormality in pediatric ALL.

From a mechanistic viewpoint, the RUNX1-RUNX1T1 leukemic fusion protein is thought to act in a dominant negative manner to normal RUNX1 (i.e., CBFα) by recruiting or stabilizing elements of transcriptional repression, including histone deacetylase complexes, at critical DNA sites (Lorsbach & Downing, 2001; Yamagata et al., 2005). Normal gene expression patterns are also disrupted by the altered affinity of the abnormal fusion protein for specific core enhancer sequences, including an increased propensity to bind sites with such sequences in duplicate (Okumura et al., 2008). The CBFβ-MYH11 chimeric protein sequesters the normal CBFα protein in the cytoplasm, thereby abrogating heterodimeric CBF assembly in the nucleus, but may also create an abnormally repressive transcriptional complex in a manner analogous to that of RUNX1-RUNX1T1 (Shigesada et al., 2004; Pratcorona et al., 2012). In either case, the resultant inhibition of transcription at key genes alters the genetic program for normal proliferation and differentiation in hematolymphoid stem or progenitor cells.

In keeping with the concept outlined previously that an individual genetic aberrancy is of itself not likely sufficient for carcinogenesis, transgenic mice engineered to conditionally express the *RUNX1-RUNX1T1* chimeric protein develop AML only on subsequent exposure to a promoting mutagen (Lorsbach & Downing, 2001; Peterson et al., 2007; Müller et al., 2008). In CBF leukemias, the pathognomonic translocations create a block in cellular differentiation (class II mutations), but affected cells often acquire secondary class I mutations that endow them with enhanced proliferative capacity. Indeed, there is a particularly strong association in CBF leukemias with secondary mutations to the gene encoding the c-KIT tyrosine kinase (stem cell factor [SCF] receptor), a potent regulator of cell growth. Approximately 25% to 35% of CBF leukemias carry *KIT* mutations; in contrast, approximately 5% of all AML cases show such mutations (Müller et al., 2008). Many of these *KIT* mutations involve the D816 "hotspot" amino acid in exon 17 (that is also present in systemic mastocytosis), but mutations have been described in other exons as well, such as exon 8. The presence of *KIT* mutations in CBF leukemias has been associated with increased relapse risk and, in some studies, poorer overall survival, particularly in AML with t(8;21), although the findings currently remain somewhat controversial (Cairoli et al., 2006; Paschka et al., 2006; Mrózek et al., 2008; Müller et al., 2008; Faderl et al., 2011). Recent comprehensive mutation profiling studies revealed association with signaling pathway mutations in both types of CBF-AML (*NRAS*, *KIT*, *KRAS*, *FLT3*-TKD) and differential enrichment of chromatin-modifying gene and cohesin complex gene mutations in AML with t(8;21);*RUNX1-RUNX1T1* (Duployez et al., 2016; Faber et al., 2016; Papaemmanuil et al., 2016). To date, although testing of *KIT* mutation is endorsed at the time of diagnosis for AML, both ELN and NCCN guidelines do not recommend its usage in AML risk stratification assignment. Rather, MRD monitoring is recommended as negative MRD status appears to abrogate the effect of mutant KIT (Dohner et al., 2017; Tallman et al., 2019).

The genetic locus rearrangements in both t(8;21) and inv(16) are also readily amenable to detection using standard FISH techniques at the time of AML diagnosis. FISH is especially helpful for diagnosing inv(16)/t(16;16) abnormalities, which can be more subtle and difficult to identify by standard karyotype banding. The molecular rearrangements underlying the *RUNX1-RUNX1T1* fusion are such that the breakpoint-fusion sites invariably involve the same limited set of intron regions in both genes, resulting in a consistent in-frame *RUNX1-RUNX1T1* mRNA molecule, although some degree of variant transcripts derived from alternative splicing and differential promoter usage can also be seen (Zhang et al., 2002; Lafiura et al., 2007; Pratcorona et al., 2012). In contrast, standard RT-PCR detection of the *CBFβ-MYH11* chimeric transcript is complicated by the marked breakpoint heterogeneity, mainly in the *MYH11* gene, as well as by rare alternate breakage sites described in *CBFB*. In all, more than 10 *CBFB-MYH11* fusion transcripts have been identified to date (Liu et al., 1995; Viswanatha et al., 1998; Kadkol et al., 2004; Schnittger et al., 2007). Despite this complexity, the *CBFB-MYH11* gene fusion can be readily detected by RT-PCR because approximately 90% of these neoplasms harbor the "type A" chimeric mRNA, characterized by fusion of *CBFB* nucleotide 495 to *MYH11* nucleotide 1921 to form a transcript of relatively short length (Schnittger et al., 2007). More comprehensive PCR strategies have also emerged to detect the majority of the other rare *CBFB-MYH11* fusion types (Kadkol et al., 2004). The value of posttherapeutic MRD monitoring by RQ-PCR in patients with CBF-associated AML has been examined in several studies and has shown strong relapse prediction. In *RUNX1-RUNX1T1* AML, measuring log reduction of leukemic mRNA transcripts after induction therapy or transcript copy number quantity after consolidation has been correlated with relapse risk. Nonetheless, some patients with the *RUNX1-RUNX1T1* abnormality can have persistent, very low levels of leukemic mRNA in the bone marrow, even after achieving stable long-term remission. The *CBFβ-MYH11* chimeric transcript also serves as a tumor-specific marker of MRD monitoring. In either case, serial time-point measurements using RQ-PCR technique are required for the most accurate prediction of relapse risk. Because multiple clinical studies have highlighted the significance of sensitive MRD testing to identify patients at high risk of disease recurrence, MRD assessment is endorsed by international guidelines (Dohner et al., 2017; Schuurhuis et al., 2018; Tallman et al., 2019). Similar to APL with *PML-RARA*, the role of FISH for MRD monitoring is virtually non-existent because the detection sensitivity required for prognostic and clinical decision purposes cannot be reliably attained at sample time-points beyond induction therapy.

Acute Myeloid Leukemia with t(9;11)(p21.3;q23.3); KMT2A-MLLT3

In AML, the presence of t(9;11)(p21.3;q23.3); *KMT2A-MLLT3* portends an intermediate prognosis, superior to AML with other 11q23.3 translocations (Mrozek et al., 1997; Rubnitz et al., 2002). It is seen in approximately 9% of pediatric and 2% of adult AML cases. The translocated *KMT2A* (previously known as *MLL*) gene is reported in de novo AML, around 3% to 4%, as well as in therapy-related AML (t-AML). Numerous

genes have been reported to partner with the *KMT2A* gene, but in around 80% of cases, the partner includes t(4;11)(q21;q23); *KMT2A-AFF1 (AF4)*, t(9;11)(q21;q23); *KMT2A-MLLT3*, or t(11;19)(q23;p13); *KMT2A-MLLT1* (*ENL*). *KMT2A-AFF1* and *KMT2A-MLLT3* are predominantly seen in lymphoblastic leukemia and de novo AML, respectively, and *KMT2A-MLLT3* and *KMT2A-MLLT1* are the most common balanced translocations in therapy-related AML, particularly in patients with a history of topoisomerase II inhibitor therapy. The most common breakpoints reported in the translocated *KMT2A* gene are present between exons 5 and 11. Some of the translocations/insertions can be too small and cryptic, thus limiting their detectability by conventional karyotyping. BAP FISH analysis is widely used to detect *KMT2A* abnormalities and can detect gene amplification or *KMT2A* rearrangements when the partner is unknown. RT-PCR is the most sensitive approach for detecting specific subtypes of *KMT2A* rearrangements when the partner gene is known (Ramchandren et al., 2013).

Acute Myeloid Leukemia with t(6;9)(p23;q34.1); DEK-NUP214

AML with t(6;9)(p23;q34.1); *DEK-NUP214* is identified in around 0.7% to 1.8% of AML cases. Characteristically, these cases are seen in children and younger adults and are associated with significant multilineage dysplasia, absolute basophilia in bone marrow and/or peripheral blood, and the myeloblasts may express TdT. The presence of this translocation in AML is considered a poor prognostic indicator and tends to be accompanied by *FLT3*-ITD mutation, which does not appear to negatively impact the prognosis in pediatric patients (Tarlock et al., 2014). Detection of such translocations can be achieved by conventional karyotyping, FISH, as well as RT-PCR, because the breakpoints in both genes are constant (Ramchandren et al., 2013).

Acute Myeloid Leukemia with inv(3)(q21.3q26.2) or t(3;3)(q21.3;q26.2); GATA2, MECOM

Recurring inv(3)(q21.3q26.2) or t(3;3)(q21;q26.2) with deregulated *MECOM* and *GATA2* expression is observed in about 1% to 2% of AML cases. It results from reposition of a distal *GATA2* enhancer leading to activation of *MECOM* expression and *GATA2* haploinsufficiency (Groschel et al., 2014; Yamazaki et al., 2014). It is associated with a poor prognosis with an aggressive disease course. Around 10% to 20% of patients with this genetic abnormality have peripheral thrombocytosis and dysplastic changes involving the granulocytic and megakaryocytic lineages. This type of leukemia may be preceded by a myelodysplastic picture with or without chromosomal abnormalities, which more commonly involve chromosome 7 than chromosome 5. Therefore, the presence of this abnormality is critical for diagnosing this condition. Genetic abnormalities of t(1;3)(p36.3;q21.1), t(3;21)(q26.2;q22.1), t(2;3)(p15;q26.2), and t(3;12)(q26.2;p13) are excluded from this diagnosis because they are more closely associated with myelodysplastic syndrome. The inv(3) or t(3;3) genetic anomaly can be detected by conventional karyotyping, FISH, and RT-PCR (Ramchandren et al., 2013).

Acute Myeloid Leukemia (Megakaryoblastic) with t(1;22)(p13.3;q13.1); RBM15-MKL1

This entity of AML is reported in fewer than 1% of cases of AML. It occurs most commonly in infants without trisomy 21 (Down syndrome) and is a de novo AML restricted to infants and young children (3 years or younger). The translocation results in the formation of *RBM15-MKL1* fusion transcript that causes defects in megakaryoblastic proliferation and differentiation. The bone marrow demonstrates increased megakaryoblasts with bone marrow fibrosis. This type of AML is associated with poor outcome, and most patients present with hepatosplenomegaly. The genetic abnormality can be detected by conventional karyotyping, FISH analysis, or RT-PCR (Ramchandren et al., 2013).

Acute Myeloid Leukemia with BCR-ABL1

This provisional entity from the 2017 WHO revision is defined as a de novo AML with exclusion of CML, mixed-phenotype acute leukemia, therapy-related myeloid neoplasms, and other AML types with recurrent genetic abnormalities. It accounts for fewer than 1% of AML cases and fewer than 1% of *BCR-ABL1*-positive acute or chronic leukemia cases. In comparison to CML, splenomegaly and basophilia are less frequent in these patients. They predominantly harbor the p210 fusion form (e13-a2 followed by e14-a2) and less frequently p190. *FLT3*-ITD, *NPM1* mutation, loss of *IKZF1* and *CDKN2A*, and cryptic deletion of the *IGH* and *TRG* genes have been reported to be preferentially associated with this entity in contrast to CML blastic transformation (Konoplev et al., 2013; Nacheva et al., 2013). AML with *BCR-ABL1* appears to behave aggressively with poor response to conventional AML therapy or TKI therapy alone. These patients may benefit from TKI therapy followed by allogeneic stem cell transplant (Bhatt et al., 2014; Fei et al., 2012). Detection and monitoring of *BCR-ABL1* would not be different from the analysis tools discussed in the section on CML.

Recurrent Gene Mutations in Acute Myeloid Leukemia

As mentioned earlier, AML is genetically heterogeneous, complex, and dynamic, characterized by multiple acquired genetic abnormalities, coexisting competing clones, and disease evolution. The advent of high-throughput NGS technology in recent years has greatly facilitated the investigation of the molecular landscape of AML, which provides important insight into the molecular abnormalities of AML, particularly in the previously poorly characterized intermediate-risk AML with normal karyotype or with chromosomal gains or losses, and further refines risk stratification. WGS, WES, RNA sequencing, and targeted sequencing in multiple studies have revealed recurrent genes mutated in AML, commonly involving signaling and kinase pathways, NPM1 biology, transcription factors, epigenetic modifiers, spliceosome complex, cohesin complex, and tumor suppressors (see Table 78.5). These genes are also recurrently mutated in other myeloid neoplasms, however, with disparate distribution patterns and frequencies, which provide genetic basis for the distinct biological behavior and clinical outcomes seen in these disease categories. The top 10 most commonly mutated genes in AML overall are *FLT3*, *NPM1*, *DNMT3A*, *NRAS*, *TET2*, *IDH2*, *RUNX1*, *PTPN11*, *CEBPA*, and *WT1*, in descending order of frequency (Fig. 78.5). Somatic mutations are seen in 90% to 95% of AML patients with a median of three or four mutations per case using NGS panels covering the commonly mutated genes.

It is worth noting that the competing clones of each individual AML commonly show distinct yet variably overlapping genetic compositions. Within each clone, the genetic abnormalities may also occur at multiple levels, from large chromosomal structural rearrangements as can be seen by conventional karyotyping, down to point mutations or small insertions or deletions only detectable at the nucleotide level by molecular techniques such as NGS. Similar to the possible coexistence of multiple chromosomal abnormalities within or among different clones, somatic mutations can co-occur. Multiple studies have demonstrated nonrandom patterns of co-occurrence and mutual exclusiveness of genetic abnormalities in AML. For example, *NPM1* and biallelic *CEBPA* mutations are characteristically associated with a normal karyotype; signal pathway mutations (*FLT3*, *KIT*) frequently accompany translocations involving hematopoietic transcription factors (*PML-RARA*, *RUNX1-RUNX1T1*, *CBFβ-MYH11*); *FLT3*-ITD frequently co-occur with *NPM1* mutations; and *IDH1/IDH2* and *TET2* mutations are mutually exclusive (Fig. 78.6). The genetic abnormalities impact on different yet relating functional pathways with intricate interplay and determine the unique biological trajectory of each clone and its fate in clonal competition and selection (Cancer Genome Atlas Research et al., 2013; Dohner et al., 2017; Grimwade et al., 2016; Papaemmanuil et al., 2016; Patel et al., 2012). Variant allele fraction (VAF) of mutations has been used to partially infer the development and clonal progression leading to AML. Studies following patients' clonal evolution and patient-derived xenografts have shown that mutations of epigenetic modifiers (most commonly *DNMT3A*, *TET2*, and *ASXL1*) occur early during leukemogenesis in the hematopoietic stem cells or progenitor cells, establishing the functionally immortalized preleukemic clone with maintenance of pluripotent differentiation capacity. Mutations in *NPM1* and kinase pathways (e.g., *FLT3*, *RAS*) emerge later in the disease course and confer a competitive advantage of the harboring clone over other clones with the initiating mutations, leading to the outgrowth and development of the dominant leukemia clone at the time of AML diagnosis (Fig. 78.7). The preleukemic ancestral cells capable of multilineage reconstitution may persist through chemotherapy and serve as a potential reservoir for recurrent disease (Corces-Zimmerman et al., 2014; Kronke et al., 2013; Shlush et al., 2014). Mutations of the spliceosome complex (*SF3B1*, *SRSF2*, *U2AF1*, *ZRSR2*) are highly specific for secondary AML and may also occur early in leukemogenesis events and persist in clonal remissions (Lindsley et al., 2015).

World Health Organization–Defined Acute Myeloid Leukemia with Gene Mutations

The 2008 WHO classification of AML has been broadened to include additional entities characterized by specific gene mutations. In the 2017 WHO classification revision, the provisional entities of AML with mutated *NPM1* and AML with biallelic *CEBPA* became distinct entities. A new provisional entity of AML with mutated *RUNX1* was added (Swerdlow et al., 2017).

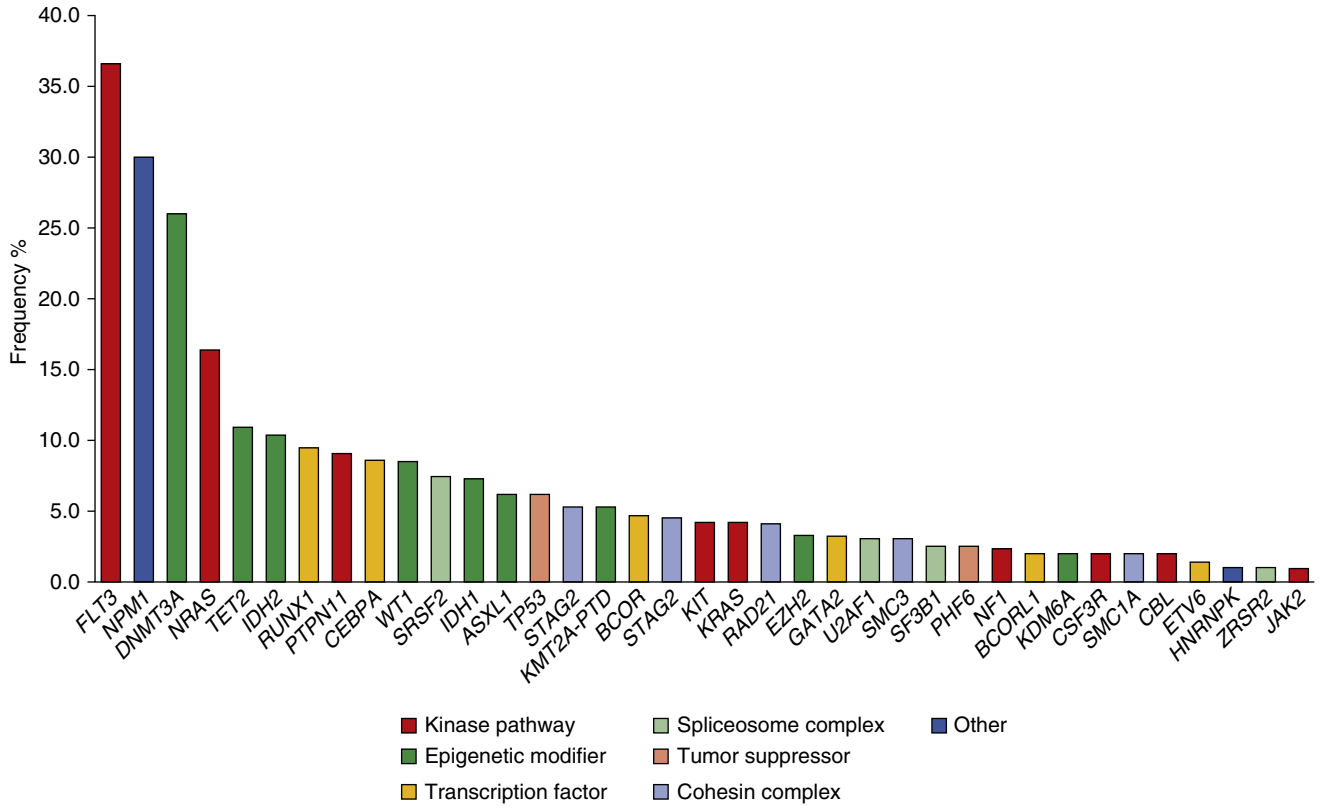

Figure 78.5 Molecular landscape of acute myeloid leukemia (AML). Frequency of common driver mutations identified in AML. *FLT3* and *NPM1* are the two most common mutations seen in AML. Mutations recurrently involve functional pathways of signaling and kinase pathways, NPM1, transcription factors, epigenetic modifiers, spliceosome complex, cohesin complex, and tumor suppressors (color coded). The median number of driver mutations is three or four per case in AML. Mutations impacting different yet interacting pathways commonly coexist, and the effect of one mutation may be modified by other concomitant genetic abnormalities.

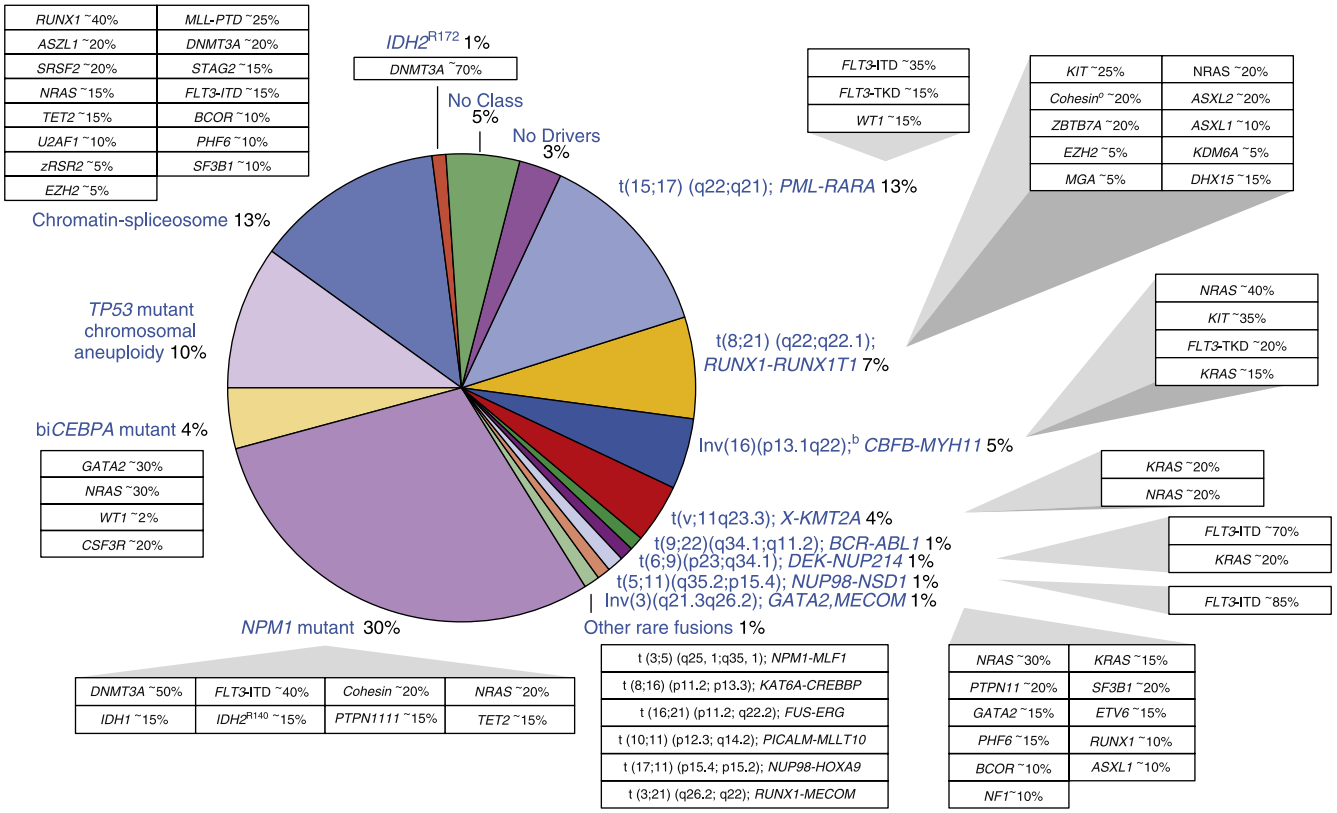

Figure 78.6 Genetic classes and concurrent mutations in adult patients with acute myeloid leukemia (AML) up to the age of 65 years. This figure highlights the complexity of genetic abnormalities in AML, which occur at both the cytogenetic level and molecular or nucleotide levels, with nonstochastic patterns of coexistence and mutual exclusiveness. AML class definitions were based on the study by Papaemmanuili et al (2016) in younger patients with AML. The frequent co-occurring mutations of each AML class are listed in their respective boxes. (Adapted from Dohner H, Estey E, Grimwade D, et al: Diagnosis and management of AML in adults: 2017 ELN recommendations from an international expert panel. *Blood* 129: 424–447, 2017.)

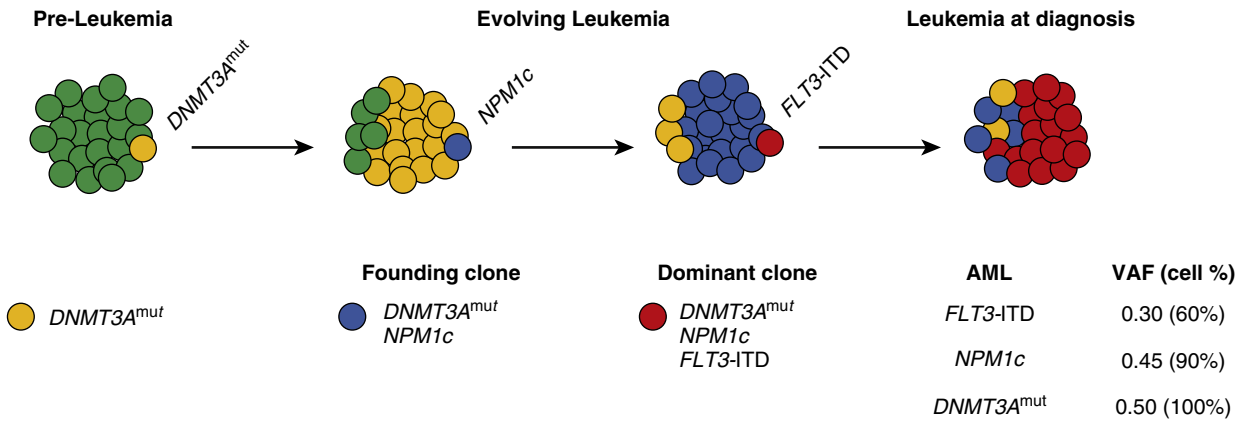

Figure 78.7 Acute myeloid leukemia (AML) clonal heterogeneity and evolution. Clonal evolution of AML in a hypothetical patient harboring cooperative driver mutations in *DNMT3A*, *NPM1*, and *FLT3*-ITD at the time of AML diagnosis. The earliest event is the *DNMT3A* mutation occurring in the preleukemia stage, which facilitates clonal expansion (preleukemic clone, *orange*) but is not sufficient to induce overt leukemogenesis. *NPM1* mutation then emerges within the preleukemic clone and defines the founding AML clone *(blue)* with leukemogenesis and evolution into AML. This leukemia expansion phase is further accelerated by acquisition of a *FLT3*-ITD, leading to the dominant clone *(red)* present at the time of diagnosis. For simplicity, only a linear evolution path is shown here, although branching evolution is frequently encountered. The evolutionary path of any given AML is also variable, although some common patterns are recognized. The relative variant allele fractions (VAFs) of the mutated genes indirectly reflect the temporal order of mutation acquisition and clonal hierarchy of the bulk disease analyzed. Mutations with higher VAFs are suggestive of earlier events in the disease process, and those with lower VAFs likely emerged later. Higher VAFs may also be encountered when there is concurrent acquired uniparental disomy (copy neutral loss of heterozygosity) at the genetic locus where the specific mutation occurs. (Adapted from Grimwade D, Ivey A, Huntly JP: Molecular landscape of acute myeloid leukemia in younger adults and its clinical relevance. *Blood* 12:27–41, 2016.)

Acute Myeloid Leukemia with Mutated NPM1

NPM1 is located on chromosome 5q35 and encodes nucleophosmin, a nuclear-cytoplasmic shuttle protein. *NPM1* mutation is one of the most common mutations in AML. It typically presents de novo in normal karyotype-AML and is seen in approximately 30% of adult AML cases (Falini et al., 2005; Balusu et al., 2011; Falini et al., 2013). Phenotypically, it commonly shows monocytic differentiation and lack of CD34 expression. The diagnosis of AML with mutated *NPM1* requires exclusion of therapy-related myeloid neoplasms, AML with recurrent cytogenetic abnormalities, and AML with myelodysplasia-related changes (AML-MRC) following the updated 2017 WHO diagnostic criteria. Multilineage dysplasia alone does not exclude this diagnosis. The prognostic effect of *NPM1* mutations is influenced by coexisting genetic abnormalities, particularly *FLT3*-ITD, which is seen in about 40% of *NPM1*-mutated cases: the presence of mutated *NPM1* is significantly associated with a good prognosis in normal karyotype AML but only in the absence of *FLT3*-ITD or *FLT3*-ITD with a low allelic ratio (AR) less than 0.5 (Schlenk et al., 2008; Baldus et al., 2006; Pratcorona et al., 2013; Schlenk et al., 2014). *NPM1* mutations in AML involve small insertions of variable length and sequence in the last exon of the gene, producing a frameshift that alters the amino acid sequence at the C-terminus of the protein. This portion of nucleophosmin carries a nuclear localization signal (NLS) important for its nuclear retention. The altered protein, lacking the NLS and incorporating instead a nuclear export signal, is aberrantly retained in the cytoplasm, which serves as a surrogate marker for *NPM1* mutation (Chen et al., 2006; Balusu et al., 2011). More than 40 distinct types of *NPM1* mutations have been identified in AML, and the majority (types A, B and D, ~90%) involve a 4-bp insertion at the hotspot codon W288 in exon 12 (Falini et al., 2007; Konoplev et al., 2009; Balusu et al., 2011). Because *NPM1* mutations change the length of the DNA sequence relative to the wild type, standard PCR amplification of the genomic region followed by fluorescent fragment size analysis by capillary electrophoresis suffices to detect the changes at diagnosis. In the current NGS era, many experienced laboratories have included *NPM1* in NGS panels, which offers the advantage of simultaneous evaluation of multiple clinically informative markers. Additionally, *NPM1* mutation is stable over the course of disease, and its persistence after therapy is a strong predictor of relapse. MRD monitoring is therefore recommended in patients with *NPM1*-positive AML at informative clinical time points. Besides multiparameter flow cytometry (MFC), *NPM1*-specific molecular assessment can be performed using the technique of real-time QPCR. Because *NPM1* mutant transcripts are commonly overexpressed compared with the housekeeping genes (e.g., *ABL1*), QPCR may offer improved sensitivity over MFC (Dohner et al., 2017; Schuurhuis et al., 2018). New technologies such as digital PCR and NGS are also emerging for MRD testing in AML.

Acute Myeloid Leukemia with Biallelic Mutation of CEBPA

CEBPA is located on chromosome 19q13.1 and encodes the CCAAT enhancer binding protein α, one of the basic region leucine zipper (bZIP) transcriptional factors that binds target genes and regulates their expression. In hematopoiesis, *CEBPA* expression is restricted to the myelomonocytic cell lineage and plays important roles in granulocytic differentiation (Koschmieder et al., 2009). About 10% to 15% of patients with AML harbor *CEBPA* mutations, and most are associated with a normal karyotype. AML with biallelic *CEBPA* mutations shows no distinct phenotypic features, and the diagnosis requires exclusion of therapy-related myeloid neoplasms, AML with recurrent cytogenetic abnormalities, and AML-MRC following the updated 2017 WHO diagnostic criteria. Multilineage dysplasia alone does not exclude this diagnosis. Biallelic (double) mutations typically composed of an N-terminal (p.1-120) frameshift/nonsense mutation and a C-terminal (p.278-358) in-frame/missense mutation have been associated with a more favorable prognosis than CEBPA-unmutated or CEBPA-single mutation cases. However, the favorable outcome of CEBPA double mutation may be lost with a concurrent FLT3-ITD mutation (Renneville et al., 2009a, 2009b; Wouters et al., 2009; Green et al., 2010; Dufour et al., 2012; Fasan et al., 2014). The N-terminal frameshift/nonsense mutations prevent translation of the full-length p42 isoform, but an alternative start site downstream permits continued production of a dominant-negative p30 isoform that inhibits the function of the wild-type p42 protein. In contrast, C-terminal mutations are in frame and are thought to impair CEBPA protein function of DNA binding, dimerization, or both. Although the N- and C-terminal mutations are most common, mutations have been described throughout the intervening region. Consequently, molecular detection strategies must be capable of detecting various types of mutations throughout the entire coding region of this single-exon gene, which is best achieved using a sequencing platform such as Sanger sequencing or NGS with the latter providing better analytical sensitivity. Of note, approximately 10% of patients with AML who have *CEBPA* mutations may harbor a germline *CEBPA* mutation, which predisposes them to the development of AML without a preexisting syndromic disorder or organ dysfunction. These patients should be diagnosed as AML with germline *CEBPA* mutations, and further evaluation of a familial predisposition syndrome is warranted. These AML cases usually present with younger age (younger than 50 years) with the germline mutations commonly clustering in the N-terminal region as heterozygous events, and accompanying somatic C-terminus mutation present at the time of AML diagnosis. These germline mutations show an autosomal dominant inheritance pattern with high penetrance. The favorable outcome of biallelic CEBPA mutations is maintained in familial cases (Tawana et al., 2015; Nickels et al., 2013; Pabst et al., 2008; Renneville et al., 2009b). In patients suspected to harbor germline *CEBPA* mutations, further evaluation to confirm/exclude a germline status is warranted.

Acute Myeloid Leukemia with Mutated RUNX1

RUNX1 is located on chromosome 21q22 and encodes RUNX1, the DNA-binding α subunit of the CBF. It interacts with the beta subunit of the core-binding factor (CBFβ), and together they function as a heterodimeric transcription factor targeting gene promoter regions through

TABLE 78.7
Molecular Markers in Myeloid Neoplasms

Diseases	Included in WHO Diagnostic Criteria	Prognostic Implications	Therapeutics Implications
AML	*NPM1*, CEBPA*, RUNX1**	*FLT3*-ITD, *NPM1, KIT, TP53, ASXL1, RAR RUNX1*	*FLT3, IDH1, IDH2, RAR TP53*
MPN	*JAK2, CALR, MPL, CSF3R*	*JAK2, CALR, MPL, ASXL1, IDH1/2, EZH2, SRSF2, TP53, U2AF1 Q157*	
MDS	*SF3B1*	*ASXL1, EZH2, SF3B1, SRSF2, U2AF1, ZRSR2, RUNX1, TP53, STAG2, NRAS, IDH2, BCOR, FLT3, NPM1, WT1*	*TP53*
MN with Germline disposition	*CEBPA, DDX41, RUNX1, ANKRD26, ETV6, GATA2*, BM failure syndrome and telomere biology disorders genes		

MDS, Myelodysplastic syndrome; *MN,* myeloid neoplasm; *MPN,* myeloproliferative neoplasms; *WHO,* World Health Organization.
*In the context of established acute myeloid leukemia (AML) diagnosis, for subclassification only.

the conserved Runt homology domain (RHD) and play important roles in hematopoietic differentiation. Loss-of-function through translocation or mutation has been described in the tumorigenesis of myeloid neoplasms (Rio-Machin et al., 2012; Silva et al., 2003). AML with mutated *RUNX1* is a new provisional category introduced in the 2017 WHO classification revision. This diagnosis requires exclusion of other AML with recurrent genetic abnormalities, therapy-related myeloid neoplasms, and AML with myelodysplasia-related changes (AML-MRC) following the 2017 WHO diagnostic criteria. Cases in this category demonstrate no specific phenotypic features and are by definition de novo AML. Somatic mutation in RUNX1 is seen in approximately 4% to 16% of AML cases and has been reported to be associated with worse overall survival in multivariate analysis. Concurrence with *ASXL1* mutations has also been reported to be associated with an adverse prognosis (Swerdlow et al., 2017; Gaidzik et al., 2011; Mendler et al., 2012; Paschka et al., 2015; Tang et al., 2009). Acquired *RUNX1* mutations are distributed across the gene and include missense, nonsense, frameshift, or splice-site mutations as well as exon or full gene deletions. Co-occurrence with *NPM1*, *CEBPA*, or balanced translocations is uncommon. The wide spectrum of mutations makes sequencing the best choice for a comprehensive assessment of the *RUNX1* gene. It can be done by Sanger sequencing or more conveniently by NGS, which offers the advantage of simultaneous evaluation of multiple clinically informative molecular markers and better analytical sensitivity. Whole-gene deletion associated with kb-range genetic material loss may not be reliably detected by Sanger sequencing or NGS (particularly amplicon based). Other technical platforms such as long-range PCR or genomic microarray analysis can aid in the detection of microdeletions and assessment of copy number variation. Myeloid neoplasms with germline *RUNX1* mutation are a recently recognized distinct entity in the 2017 WHO classification revision. It is an autosomal dominant syndrome with patients harboring a heterozygous germline *RUNX1* mutation with a familial platelet disorder and propensity for the development of MDS/AML. Most patients show a lifelong mild to moderate bleeding tendency caused by abnormalities in platelet number, or function, or both. Their risk of MDS/AML progression varies from 11% to 100% (median, 44%) with a median age of onset at 33 years (West, et al., 2014). Besides the most commonly encountered MDS/AML, development of chronic myelomonocytic leukemia (CMML), T-lymphoblastic leukemia/lymphoma, and B-cell neoplasms have also been reported (Godley, 2014). Progression into MDS/AML likely requires acquisition of additional mutations such as a mutation on the second allele of *RUNX1* or other genes. The "two-hit" theory also helps explain the observed variability in penetrance and neoplasm phenotypes (Preudhomme et al., 2009; West et al., 2014). The incidence of germline *RUNX1* mutation has not been well established, although a wide variety of mutations have been documented. In patients suspected to harbor germline *RUNX1* mutations with predisposition to myeloid neoplasms, further evaluation to confirm or exclude a germline status is warranted.

Other Genes Commonly Mutated in Acute Myeloid Leukemia and Related Myeloid Neoplasms

Genes with well-established diagnostic, prognostic, and therapeutic significance are summarized in Table 78.7.

Kinases and Signaling Pathways

FLT3. *FLT3* is located on chromosome 13(q12) and encodes a class III receptor tyrosine kinase FMS-like tyrosine kinase 3, which plays important roles in hematopoietic cell survival, proliferation, and differentiation. It binds its ligand and activates downstream signaling pathways, including RAS, AKT1, ERT, and mTOR (mammalian target of rapamycin) (Chen et al., 2010; Kiyoi & Naoe, 2002; Mizuki et al., 2000; Zhang et al., 1999). *FLT3* mutation is the most common mutation seen in AML and present in approximately 30% to 40% of AML cases, with most patients showing a normal karyotype. It most frequently takes the form of internal tandem duplication (*FLT3*-ITD) in the juxtamembrane domain with a net addition of nucleotides in multiples of 3, which maintains the reading frame of this tyrosine kinase and produces an abnormal, constitutively active mutant FLT3 protein through mitigation of the autoinhibitory effect of the juxtamembrane region on the tyrosine kinase domain (Gilliland & Griffin, 2002). Less often (~20% of *FLT3* mutations), a second type of activating lesion occurs in the downstream tyrosine kinase domain (*FLT3*-TKD) at the hotspot amino acid sites D835/I836 in the "activation loop" (Yamamoto et al., 2001; Bacher et al., 2008). The constitutively active mutant FLT3 tyrosine kinase initiates increased activity in its downstream signaling cascade, providing a pro-proliferative stimulus to the myeloid cells (Kontzias et al., 2012). Thus, *FLT3* belongs to the "class I" group of AML-related genetic abnormalities. The prognostic significance of *FLT3* mutations is most apparent in cytogenetically normal AML. *FLT3*-ITD is a well-established risk marker, and in AML with a normal karyotype, it is associated with inferior therapy response, higher risk of relapse, and decreased survival, particularly in those showing high *FLT3*-ITD ARs (Fröhling et al., 2002; Pratcorona et al., 2013; Schlenk et al., 2014). A high and low AR cutoff ratio of 0.5 has been endorsed by the ELN and NCCN guidelines to refine the risk stratification of *FLT3*-ITD–positive AML in the context of *NPM1* and cytogenetic findings (see Table 78.6). The prognostic impact of *FLT3*-TKD alteration is less well defined and remains somewhat controversial (Fröhling et al., 2002; Moreno et al., 2003; Yanada et al., 2005; Mead et al., 2007). However, acquired *FLT3*-TKD mutations involving D835 and F691 have been described as a mechanism of resistance to type II FLT3 inhibitors such as quizartinib (Levis, 2014). Significant advancement has been made in recent years in targeted therapy against FLT3. Beside cytogenetically normal AML, *FLT3*-ITD can be seen in other genetically defined subtypes of AML, including APL with *PML-RARA* (35%), t(6;9); *DEK-NUP214* (70%), and t(5;11); *NUP98-NSD1* (85%) (see Fig. 78.6). Its presence in these AML subtypes does not show significant impact on the clinical outcome (Dohner et al., 2017). *FLT3*- ITDs are innately heterogeneous with the ITD insertion sites spanning from exon 14, intron 14 to exon 15 (most commonly exon 14), sizes ranging from 3 bp up to ~400 bp, with the vast majority (>90%) falling between 20 and 100 bp and being simple tandem duplications or with insertion of extra nucleotides (Gale et al., 2008; Schnittger et al., 2012b; He et al., 2019). *FLT3*-ITDs have been detected by PCR using primers flanking exons 14 and 15 followed by fragment size analysis (e.g., by fluorescent capillary electrophoresis) in which the *FLT3*-ITD presents as a larger amplicon shifted away from the wild-type product. The *FLT3*-ITD AR is calculated from the fluorescent intensity of the ITD peak over the wild-type peak. Point mutations involving the D835 site can be identified by several methods, such as allele-specific PCR, digital PCR, Sanger sequencing, pyrosequencing, or restriction enzyme digestion of the PCR product. Both *FLT3*-ITD and *FLT3*-TKD mutations can also be assessed by NGS. Given the innate heterogeneity and the significant clinical and therapeutic impact of *FLT3*-ITD, thorough validation and refinement of NGS tests is required to meet the clinical need of reliable detection of *FLT3*-ITD. A capture-based NGS strategy aided by adequate probe tiling, optimized bioinformatic pipeline, and dedicated analysis is superior to an amplicon-based NGS approach in successfully detecting the larger size ITDs (He et al., 2019; Spencer et al., 2013). However, because the

FDA-approved FLT3 inhibitor midostaurin is indicated at day 8 during AML induction therapy, *FLT3* testing is time sensitive. If the NGS test cannot meet the clinical turn-around-time (TAT) requirement, a single gene *FLT3* test with a shorter TAT should be performed to ensure prompt initiation of FLT3 inhibitor therapy.

KIT. *KIT* is located on chromosome 4q12 and encodes a transmembrane receptor tyrosine kinase (KIT), which binds the ligand SCF. Ligand binding induces phosphorylation and dimerization of the KIT receptor and activation of downstream signaling pathways of PI3K (phosphoinositide 3 kinase)/AKT, RAS/MAPK/MEK, and/or JAK/STAT. Normal KIT has an important role in the growth and differentiation of hematopoietic stem cells, mast cell development and function, and development and function of other nonhematopoietic tissues such as melanogenesis and gastrointestinal cell function. It is therefore unsurprising that *KIT* mutations are also present in solid tumors such as melanoma, gastrointestinal stromal tumor (GIST), and germ cell tumors besides hematopoietic neoplasms (Orfao et al., 2007). *KIT* mutations are seen in approximately 25% to 35% of cases of CBF-AML of inv(16)/t(16;16); *CBFB-MYH11* or t(8;21); *RUNX1-RUNX1T1*. More specifically, they have been identified in the activation loop of the tyrosine kinase domain encoded by exon 17 (16%–20%), extracellular dimerization domain encoded by exon 8 (4%–12%), and other exons (~1%) (Orfao et al., 2007; Takahashi, 2011; Haferlach et al., 2010; Paschka et al., 2006). The presence of *KIT* mutation in CBF-AML appears to confer an adverse clinical outcome, particularly in patients with t(8;21); however, this finding was not observed in all studies, and the absence of MRD by real-time QPCR monitoring of the *CBFB-MYH11* or *RUNX1-RUNX1T1* transcripts appeared to abrogate the negative impact of *KIT* (Foran, 2010; Jourdan et al., 2013; Paschka & Dohner, 2013). Therefore, *KIT* mutational status does not change the genetic risk category of CBF-AML (Dohner et al., 2017; Tallman et al., 2019). Nevertheless, the NCCN guideline recommends *KIT* testing in CBF-AML, which is commonly performed through a sequencing approach (Sanger sequencing, pyrosequencing, or as part of NGS), given the multiple types of mutations and exons to be covered.

RAS Oncogenes. The RAS oncogene and its 21 kDa product, RAS-p21 protein, are also discussed in Chapter 77. Recurrent RAS signalling pathway mutations have been identified in *NRAS*, *KRAS*, *PTPN11*, *CBL*, and *NF1*. Activating mutations lead to the activation of the RAS/RAF/MEK and PI3K/AKT/mTOR pathways. Oncogenic ras-p21 protein has also been found to activate jun kinase (JNK) directly resulting in activation of the important transcription protein, jun (Pincus et al., 2000).

- ***NRAS* and *KRAS:*** *NRAS* is located on chromosome 1p13.2, and *KRAS* is located on chromosome 12p12.1; each encodes a member of the RAS family of small GTPases that mediate transduction of growth signals. Activation of RAS signaling leads to cellular proliferation, differentiation, and survival through activation of the downstream RAF/MEK/ERK and PI3K/AKT/mTOR pathways (Pylayeva-Gupta et al., 2011; Kahn et al., 1987) as discussed further in Chapter 77. Mutations often occur at hotspots G12, G13, or Q61 and result in constitutive activation of the pathway. *NRAS* and *KRAS* mutations show no clear impact on clinical outcome of AML, MDS, and CMML, although *NRAS* mutations may be associated with disease progression in CMML (Al-Kali et al., 2013; Bejar et al., 2011; Itzykson & Solary, 2013; McCullough & Patnaik, 2015; Metzeler et al., 2016; Patel et al., 2012). On the other hand, oncogenic mutations in k-RAS have been found in more than 90% of pancreatic cancers, and 70% of colon cancers and have been found to be expressed in relatively high frequencies in a number of other solid tissue tumors (see Chapter 77). Germline *NRAS* or *KRAS* mutations have rarely been described in Noonan syndrome (NS), a familial syndrome associated with an increased risk for a transient myeloproliferative disorder in early childhood that may resemble juvenile myelomonocytic leukemia (JMML), which usually resolves spontaneously with a small percentage (~10%) of cases progressing to JMML. The association with *NRAS* or *KRAS* is rare in this setting compared with the most frequently mutated *PTPN11* (Aoki & Matsubara, 2013; Niemeyer, 2014).
- ***PTPN11*:** *PTPN11* is located on chromosome 12q24 and encodes the cytoplasmic protein tyrosine phosphatase non-receptor type 11 (also known as SHP2), a signaling molecule with two tandem N-terminal SH2 (sarc homology-2) domains and a phosphatase domain (Tartaglia & Gelb, 2005). PTPN11 interacts with and regulates protein tyrosine kinases and is required for RAS-MAPK/ERK pathway signaling (see Chapter 77). It is critical in the regulation of diverse cellular activities, including proliferation, differentiation, and the cell cycle, and is essential for normal hematopoietic cell differentiation (Chan & Feng, 2007). *PTPN11* mutations do not show clear impact on AML clinical outcome (Metzeler et al., 2016; Patel et al., 2012). Germline *PTPN11* mutations are seen in approximately 50% of patients with NS, a familial syndrome associated with an increased risk for a transient myeloproliferative disorder in early childhood that may resemble JMML, which usually resolves spontaneously with a small percentage (~10%) of cases progressing to JMML (Aoki & Matsubara, 2013; Mohi & Neel, 2007; Niemeyer, 2014). Approximately 35% of patients with JMML harbor somatic *PTPN11* mutations, and they have demonstrated a gain-of function effect stronger than that observed with germline *PTPN11* mutations seen in patients with NS or transient myeloproliferative disorder. JMML associated with neurofibromatosis, NS, or NS-like disorders is recently recognized as a distinct entity in the 2017 WHO classification revision (Swerdlow et al., 2017).
- ***CBL*:** *CBL* is located on chromosome 11q23.3 and encodes the Casitas B-cell lymphoma (CBL) protein, a ring finger (RF) family ubiquitin ligase (E3s), targeting receptor and nonreceptor tyrosine kinases (including PDGFR and FLT3) and functions as a negative modulator of tyrosine kinase signaling. CBL also serves as an adaptive protein and a positive regulator of signaling transduction (i.e., the PI3K pathway) (Kales et al., 2010; Schnittger et al., 2012a). Point mutations and deletion involving the linker and RF regions of CBL are associated with loss of CBL ubiquitination of receptor tyrosine kinases such as FLT3 and result in the induction of cellular transformation. In myeloid neoplasms, most somatic *CBL* point mutations appear homozygous as associated with an acquired 11q uniparental disomy. The prognostic effect of *CBL* mutations in myeloid neoplasms has not been well established (Dunbar et al., 2008; Kales et al., 2010; Reindl et al., 2009; Schnittger et al., 2012a). Germline *CBL* mutations can occur in NS-like disorders. Approximately 15% of patients with JMML harbor germline *CBL* mutations, commonly as missense mutations in the linker and RF regions with a majority showing apparent homozygosity of the mutant *CBL* resulting from acquired uniparental disomy of 11q in the JMML cells (Caye et al., 2015; Loh et al., 2009; Muramatsu et al., 2010; Niemeyer et al., 2010; Perez et al., 2010). Most patients with JMML with germline *CBL* mutations show spontaneous regression with persistence of the uniparental disomy in the hematopoietic cells. JMML associated with neurofibromatosis, NS, or NS-like disorders is recently recognized as a distinct entity in the 2017 WHO classification revision.
- ***NF1*:** *NF1* is located on chromosome 17q11.2 and encodes neurofibromin-1, a GTPase activating protein (GAP) that enhances the hydrolysis of active GTP-RAS into inactive GDP-Ras. Loss of neurofibromin-1 has been shown to elevate the level of GTP-RAS and result in cellular proliferation. It is also considered a tumor suppressor gene (Abramowicz & Gos, 2015; Bollag et al., 1996). Direct inactivation of neurofibromin-1 is infrequent in de novo AML, and *NF1* deletion is associated with complex and monosomal karyotypes (Boudry-Labis et al., 2013). Germline *NF1* abnormalities are associated with neurofibromatosis type 1, which shows an increased risk of developing myeloid neoplasms, most commonly JMML. Approximately 10% of patients with JMML harbor germline NF1 mutations (Caye et al., 2015; Swerdlow et al., 2017). JMML associated with neurofibromatosis, NS, or NS-like disorders is recognized as a distinct entity in the 2017 WHO classification revision.

Epigenetic Modifiers

Epigenetic mechanisms are essential for normal development and differential gene expression in tissues in mammals. Epigenetics refer to heritable changes of gene expression that are irrelevant to the primary DNA sequences (Sharma et al., 2010; Wouters & Delwel, 2016). Major epigenetic regulations include DNA methylation, histone protein acetylation, and lysine methylation, and RNA-associated gene silencing (Fig. 78.8).

DNMT3A. *DNMT3A* is located on chromosome 2p23.3 and encodes the DNA (cytosine 5)-methyltransferase 3A, a member of a large family of enzymes involved in epigenetic regulation through DNA methylation (Chedin, 2011; Li et al., 2007). It adds a methyl group to cytosines in CpG dinucleotides at the 5-carbon position and converts it to a 5-methylcytosine (5mC) (Fig. 78.8A). *DNMT3A* is recurrently mutated in 20% to 30% of AML cases. It is commonly seen in patients with advanced age and coexists with *NPM1*, *FLT3*-ITD, or *IDH1* mutations. Approximately two-thirds of *DNMT3A* mutations occur at the hot-spot codon R882. The prognostic importance of *DNMT3A* mutations remains controversial in AML and other myeloid neoplasms, although in AML, the majority of literature reported association with poorer outcomes (Dohner et al., 2017; Roller et al., 2013; Tallman et al., 2019; Vannucchi et al., 2013). *DNMT3A*, *TET2*, and *ASXL1* are the most frequently mutated genes in clonal hematopoiesis of indeterminate potential (CHIP) described in aging individuals without apparent hematologic neoplasms (Genovese et al., 2014; Jaiswal et al., 2014).

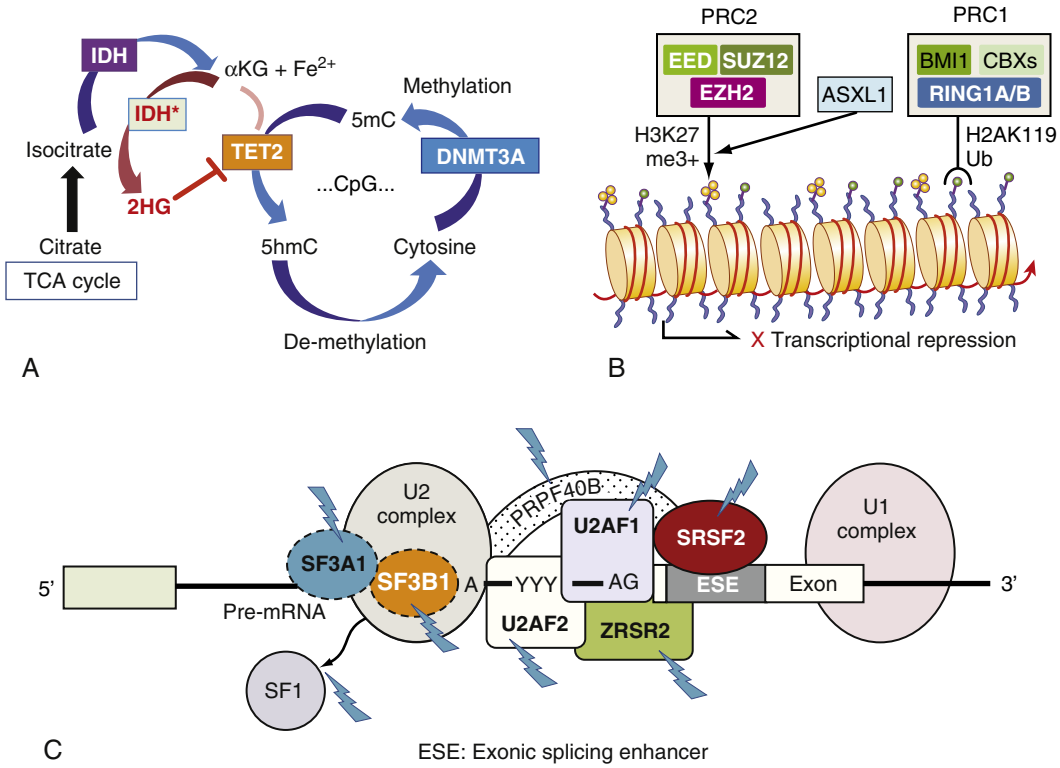

Figure 78.8 Epigenetic modifiers and spliceosome complex recurrently mutated in myeloid neoplasms. Genes encoding epigenetic modifiers involved in DNA methylation *DNMT3A, TET2, IDH1, IDH2* (**A**); chromatin histone modification *EZH2* and *ASXL1* (**B**); and spliceosome complex *SF3B1, SRSF2, U2AF1,* and *ZRSR2* (**C**) are recurrently somatically mutated in myeloid neoplasms. IDH*, mutated IDH protein. In **A,** 2HG is 2-hydroxyglutarate, the reduced form of α-ketoglutarate. The *symbol* to the upper right of 2HG between it and TET2 indicates that 2HG inhibits the activity of TET2 in oxidizing the 5-methylcytosine moiety to 5-hydroxymethyl cytosine. (Adapted from Ogawa S: Genetics of MDS, *Blood* 133(10):1049–1059, 2019.)

TET2. *TET2* is located on chromosome 4q24 and encodes methylcytosine dioxygenase, an important enzyme in the process of DNA demethylation, which converts methylcytosine (5mC) to 5-hydroxymethylcytosine (5hmC) (Guo et al., 2011; Ito et al., 2010) (see Fig. 78.8A). TET2 is widely expressed in hematopoietic cells. *TET2* mutations show no clear impact on the prognosis of myeloid neoplasms (Dohner et al., 2017; Itzykson et al., 2011; Patnaik et al., 2014; Tallman et al., 2019; Vannucchi et al., 2013). They are mutually exclusive of *IDH1* and *IDH2* mutations. *DNMT3A, TET2,* and *ASXL1* are the most frequently mutated genes in CHIP described in aging individuals without apparent hematologic neoplasms (Genovese et al., 2014; Jaiswal et al., 2014).

***IDH1* and *IDH2*.** *IDH1* and *IDH2* genes are located on chromosomes 2q33 and 15q26, respectively. They encode 2 isoforms of isocitrate dehydrogenase IDH1 and IDH2 that catalyze oxidative decarboxylation of isocitrate to α-ketoglutarate (α-KG) in cytoplasm/peroxisome and mitochondria, respectively (Rakheja et al., 2012). However, when mutated, their ability to catalyze the oxidative decarboxylation of isocitrate to α-KG was altered, coupled with a neomorphic gain-of-function to catalyze α-KG to 2-hydroxyglutarate (2-HG). The abnormal accumulation of 2-HG inhibits α-KG–dependent oxidative reactions, including TET2 and a number of histone demethylases, resulting in a hypermethylation state (Andersson et al., 2011; Tsukada et al., 2006; Yamane et al., 2006) (see Fig. 78.8A). The mutational hot spots involve R132 in *IDH1* and R140 and R172 in *IDH2*. IDH mutations in AML are predominantly associated with intermediate-risk karyotypes, and their impact on AML prognosis remains controversial (Chotirat et al., 2015; Dohner et al., 2017; Tallman et al., 2019). The FDA has approved IDH2 inhibitor enasidenib and IDH1 inhibitor ivosidenib in adult relapsed-refractory patients with AML harboring an *IDH2* or *IDH1* mutation, respectively. The FDA has also recently approved ivosidenib in newly diagnosed *IDH1*-positive patients with AML who are at least 75 years old or have comorbidities that preclude the use of intensive induction chemotherapy. The availability of targeted therapy for the mutation-positive patients imposes a turn-around-time (TAT) requirement for the *IDH1* and IDH2 tests. Although both are readily covered by NGS panels, a supplemental single gene test with quicker TAT using other less sophisticated techniques such as allele-specific PCR, digital PCR, pyrosequencing, or melting curve analysis (see Chapter 68) may be required to meet the clinical need.

WT1. *WT1* is located on chromosome 11p13 and encodes the Wilms tumor 1 protein, an important transcription factor for cell development and survival, which is normally expressed in hematopoietic progenitor cells and embryonic kidney cells (Gaidzik et al., 2009). WT1 has recently been shown to recruit TET2 to a specific genomic site to regulate WT-1-target gene expression, and WT1 and TET2 are functionally interdependent. *WT1* mutations demonstrate similar DNA methylation signatures as *TET2* and *IDH1/2* mutations, which explains their mutually exclusive nature in AML (Rampal et al., 2014; Wang et al., 2015b). *WT1* mutations appear to be more prevalent in patients with AML who have the *FLT3*-ITD abnormality. The presence of *WT1* mutations has been associated with poor clinical outcome, independent of *FLT3-ITD*. However, this finding was not consistently observed in all studies (Dohner et al., 2017; Tallman et al., 2019).

ASXL1. *ASXL1* is located at chromosome 20q11.21 and encodes a chromatin-binding protein required for normal embryonic segmentation and regulates epigenetic marks and transcription. It interacts with the polycomb repressive complex 2 (PRC2) and regulates trimethylation of histone H3 lysine 27 (H3K27me3), a chromatin modification process associated with gene silencing (see Fig. 78.8B). It also associates with the deubiquitinating enzyme BAP1 and may promote gene expression through removal of PRC1 complex-mediated H2A lysine 119 (H2AK119) ubiquitination (Abdel-Wahab et al., 2012; Inoue et al., 2013). Loss of ASXL1 functions result commonly from truncating or frameshift mutations that are associated with adverse prognosis in myeloid neoplasms including AML (Gelsi-Boyer et al., 2012) (Pratcorona et al., 2012; Thol et al., 2011; Vannucchi et al., 2013). *DNMT3A, TET2,* and *ASXL1* are the most frequently mutated genes in CHIP described in aging individuals without apparent hematologic neoplasms (Genovese et al., 2014; Jaiswal et al., 2014).

EZH2. *EZH2* is located on chromosome 7q36.1 and encodes enhancer of zeste 2 polycomb repressive complex (EZH2). It is expressed during normal cellular development and differentiation. EZH2 is the catalytic subunit of the polycomb repressive complex 2 (PRC2) and is involved in repressing gene expression through methylation of histone H3 on lysine 27 (H3K27) (McCabe et al., 2012) (see Fig. 78.8B). In AML, *EZH2* mutation is more commonly associated with secondary AML and worse clinical outcomes (Lindsley et al., 2015). The prognostic impact of *EZH2* mutations remains controversial in MDS and is insignificant in patients with CMML (Bejar et al., 2011; Papaemmanuil et al., 2013; Patnaik et al., 2014). Its co-occurrence with *IDH1/2, ASXL1,* or *SRSF2* mutations is reported to confer an unfavorable outcome in primary myelofibrosis (Guglielmelli et al., 2014).

RNA Splicing Machinery

***SF3B1, U2AF1, SRSF2,* and *ZRSR2*.** These genes encode protein components of the U2RNP complex of the splicing machinery see (Fig. 78.8C) and are located on chromosomes 2q33.1, 21q22.3, 17q25.1, and Xp22.2, respectively (Wahl, et al., 2009). Along with epigenetic modifiers,

RNA splicing factors are the most commonly mutated genes in MDS. *SF3B1*, *U2AF1*, and *SRSF2* commonly show hot-spot mutations without nonsense or frameshift variants, suggestive of neomorphic functions of the mutants. *ZRSR2*, however, shows predominance of frameshift and nonsense mutations with loss of protein functions. Mutations of the splicing factors are essentially mutually exclusive and result in widespread alterations in mRNA splicing such as usage of alternative 3′- or 5′- splice sites and enhanced or depressed intron retention (Boultwood et al., 2014; Yoshida et al., 2011; Ogawa, 2019; Shiozawa et al., 2018). *SF3B1* mutation is seen in 70% to 90% of cases of MDS with ring sideroblasts (MDS-RS) and myelodysplastic/myeloproliferative neoplasm (MDS/MPN) with ring sideroblasts and thrombocytosis (MDS/MPN-RS-T), and *SRSF2* mutation is seen in about half of CMML cases. They are present in approximately 10% of AML cases. In a recent study, mutations in *SRSF2*, *SF3B1*, *U2AF1*, or *ZRSR2* along with *ASXL1*, *EZH2*, *BCOR*, and *STAG2* are highly specific markers for secondary AML and portend worse clinical outcome in therapy-related AML and older adult de novo AML (Lindsley et al., 2015).

Tumor Suppressors

TP53. *TP53* is located at chromosome 17p13 and encodes a transcription factor that acts as a tumor suppressor through induction of apoptosis or growth arrest (see also Chapter 77). *TP53* is upregulated in response to a variety of cellular proliferative stress and DNA damage signals (Junttila & Evan, 2009; Kato et al., 2003; Willis, et al., 2004). P53 protein activity or its loss from mutation or other mechanisms has complex effects on normal hematopoiesis (Pant et al., 2012). Somatic *TP53* mutations are seen in approximately 5% to 10% of patients with MDS, with 25% showing high-grade diseases, 10% of de novo AML, and half of therapy-related myeloid neoplasms. *TP53* mutations often coexist with complex karyotypes with a high frequency of del(5q) and 17p loss of heterozygosity (LOH). These mutations confer chemoresistance and poor prognosis in myeloid neoplasms regardless of clinical or pathological diagnoses (Jerez et al., 2012b; Kulasekararaj et al., 2013; Wong et al., 2015; Yoshizato et al., 2017). *TP53* mutations in MDS patients with del(5q), either isolated or as part of a complex karyotype, are associated with inferior response and relapse after lenalidomide therapy (Mallo et al., 2013). In patients with AML and MDS harboring *TP53* mutations or unfavorable cytogenetic abnormalities, favorable clinical response and robust but incomplete mutation clearance have recently been described with decitabine therapy. In patients with AML, although the response was not durable, the overall survival rate was comparable to those with intermediate-risk cytogenetic abnormalities receiving decitabine (Welch et al., 2016). Germline mutations in *TP53* are associated with Li-Fraumeni syndrome with predisposition to development of multiple cancers, both solid and hematologic (Swaminathan et al., 2019).

Cohesin Complex

SMC1A, ***SMC3***, ***RAD21***, ***STAG1***, and ***STAG2*** are located on chromosomes Xp11.22, 10q25.2, 8q24.11, 3q22.3, and Xq25, respectively, and encode the multimeric protein components of the cohesin complex, which is a ring structure recruited onto chromatin to participate in the regulation of gene expression via formation of large-scale chromatin structures (Gruber et al., 2006; Hill et al., 2016). Cohesin complex gene mutations were seen in approximately 10% to 15% of patients with MDS, 6% of younger patients with non-APL AML, and 20% of patients with secondary AML. They are essentially mutually exclusive of each other and are commonly associated with mutations in *RUNX1*, *NPM1*, *BCOR*, and *ASXL1* with no clear impact on clinical outcome (Thol et al., 2014; Thota et al., 2014; Cancer Genome Atlas Research et al., 2013).

CHRONIC MYELOID NEOPLASMS

The chronic myeloid neoplasms broadly encompass MPNs, MDS, MDS/MPNs, and myeloid/lymphoid neoplasms with eosinophilia and gene rearrangement (Swerdlow et al., 2017). Within each subcategory there exist multiple pathologically or genetically distinct entities. In some neoplasms, specific molecular abnormalities are highly characteristic or disease defining; in other cases, recurrent genetic findings may be shared between different tumor types.

Myelodysplastic Syndromes

MDSs are clonal hematopoietic disorders characterized by cytopenia, morphologic dysplasia in one or more myeloid lineages, recurrent genetic abnormalities, ineffective hematopoiesis, and increased risk of progression to AML (Swerdlow et al., 2017). There are different subtypes of MDS as defined by the number of cytopenias, number of myeloid lineages showing dysplasia, peripheral blood and bone marrow blast count, presence of ring sideroblasts or Auer rods, and cytogenetic and molecular findings.

BOX 78.2

Presumptive Myelodysplastic Syndrome–Defining Cytogenetic Abnormalities

Chromosome Abnormalities

Unbalanced

- Loss of chromosome 7 or del(7q)
- del(5q)
- Isochromosome 17q or t(17p)
- Loss of chromosome 13 or del(13q)
- del(11q)
- del(12p) or t(12p)
- del(9q)
- idic(X)(q13)

Balanced

- t(11;16)(q23.3;p13.3)
- t(3;21)(q26.2;q22.1)
- t(1;3)(p36.3;q21.2)
- t(2;11)(p21;q23.3)
- inv(3)(q21.3q26.2)/t(3;3)(q21.3;q26.2)
- t(6;9)(p23;q34.1)

Recurring chromosomal abnormalities are seen in approximately 40% to 50% of patients with MDS and are characterized predominantly by loss of genetic material rather than translocation events. Cytogenetic findings aid in the diagnosis of MDS because the WHO has defined eight unbalanced and six balanced abnormalities as presumptive evidence of MDS in the setting of unexplained cytopenia, even in the absence of definitive morphologic dysplasia (Box 78.2). However, as a sole abnormality, the other three recurrent cytogenetic findings of gain of chromosome 8, del(20q), and loss of Y chromosome are not considered definitive evidence of MDS without diagnostic morphologic dysplasia (Swerdlow et al., 2017). The major risk stratification schemes of MDS include the international prognostic scoring system (IPSS), revised international prognostic scoring system (IPSS-R), and WHO-based prognostic scoring system (WIPSS). Although all included cytogenetic findings and variable indices of cytopenia in the scoring criteria, IPSS/IPSS-R and WIPSS also take into account BM blast percentage and the WHO-defined MDS subtype classifications, respectively (Greenberg et al., 2017). Karyotyping analysis of newly diagnosed MDS is therefore a required component of MDS evaluation. Meanwhile, multiple studies have consistently demonstrated limited additional diagnostic and prognostic value of FISH testing in MDS in the context of adequate karyotyping (He et al., 2016b; Jiang et al., 2012; Pitchford et al., 2010). A value and evidence-based cytogenetic testing approach in MDS has been endorsed by several national and international guidelines that reserve FISH analysis for patients with inadequate karyotyping (<20 metaphases) or those with karyotype ambiguity needing FISH clarification (Greenberg et al., 2017; Malcovati et al., 2013).

The advancement of NGS technology has greatly enhanced our understanding of the molecular landscape of MDS. Similar to AML, MDS is genetically heterogeneous, complex, and dynamic, characterized by coexisting competing clones and multiple genetic abnormalities affecting interacting functional pathways, with clonal shifts and evolution over the treatment and disease courses (Makishima et al., 2016; Ogawa, 2019). Recurrent somatic mutations have been reported in more than 40 genes, and 80% to 90% of patients with MDS harbor at least one somatic mutation, with a median of two or three mutations per case. The commonly affected pathways involve spliceosome machinery, epigenetic modifiers, transcription factors, cell signaling and kinase pathways, tumor suppressors, and the cohesin complex, similar to AML. However, the frequency and distribution of these mutations show patterns disparate from that of AML (Fig. 78.9) (Haferlach et al., 2014; Papaemmanuil et al., 2013; Yoshida et al., 2011). Spliceosome and epigenetic modifier mutations are most common and seen in more than half of patients with MDS, accentuating their importance in the early pathogenesis of MDS. During disease progression, clonal expansion occurs after emergence of additional genetic abnormalities in signaling pathway (*NRAS/KRAS*, *FLT3*, *PTPN11*), transcription factor (*RUNX1*, *ETV6*), and tumor suppressor (*TP53*, *PHF6*) genes, exhibiting complex interplay and cooperativity that bestow an ultimate competitive growth advantage to the dominant clone from a multiclone, cellular background characterized by the initial dysregulated pre-mRNA splicing and epigenetic modulation (Makishima et al., 2016; Ogawa, 2019).

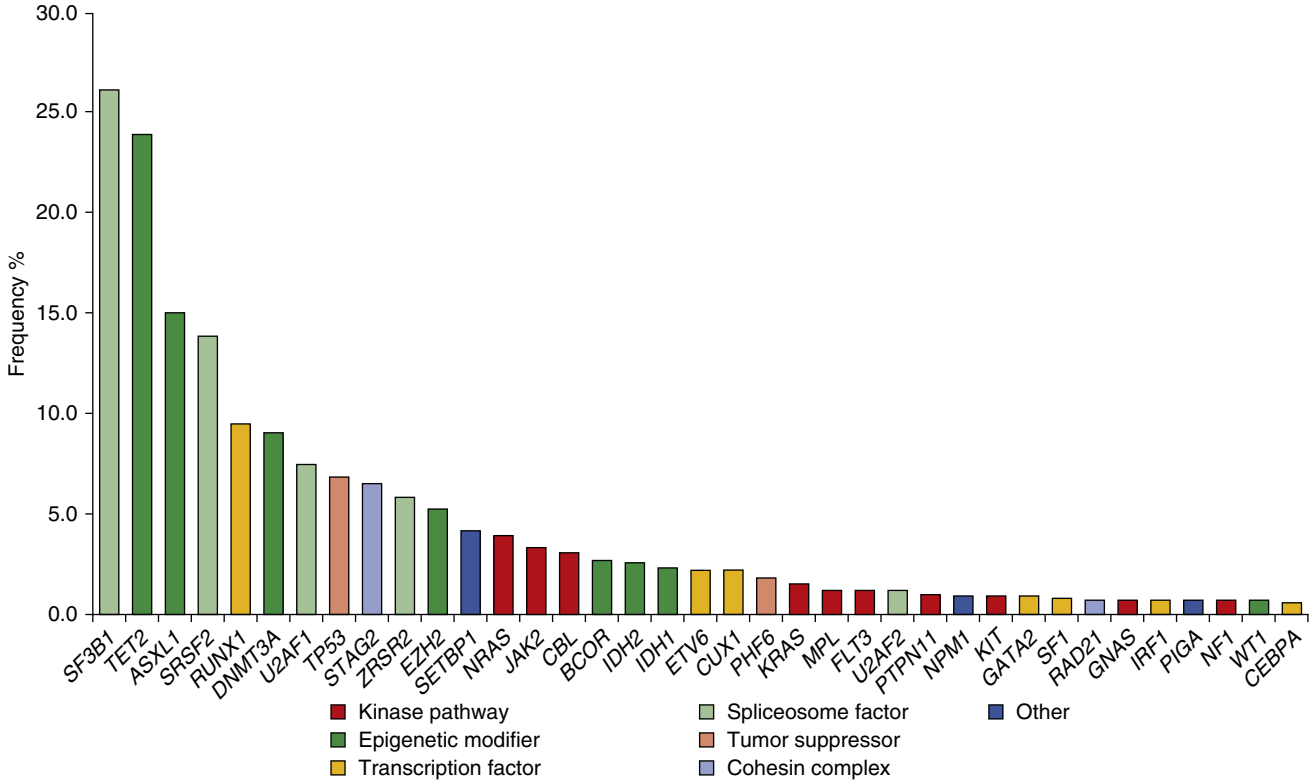

Figure 78.9 Molecular landscape of myelodysplastic syndrome (MDS). Frequency of common driver mutations identified in MDS. Note that mutations occur in similar functional pathways as acute myeloid leukemia (AML). However, the distribution pattern and frequency is different in MDS. Spliceosome and epigenetic modifier mutations in genes *SF3B1*, *TET2*, *AXSL1*, and *SRSF2* are the most common mutations in MDS, each present in more than 10% of patients. Disease progression of MDS is associated with acquisition of additional genetic abnormalities in the kinase signaling pathway, transcription factors, and tumor suppressor genes. Note: The presented frequency graph includes subsets of chronic myelomonocytic leukemia and MDS with ring sideroblasts and thrombocytosis cases.

Multiple studies have also demonstrated additional prognostic value provided by mutational data. Mutations in *TP53*, *EZH2*, *ETV6*, *RUNX1*, and *ASXL1* were found to be independent risk factors for adverse overall survival in multivariate analyses (Bejar et al., 2011). Higher number of mutations correlated with inferior leukemia-free survival and increased risk of leukemic transformation (Papaemmanuil et al., 2013). A clinical study using a novel prognostic model encompassing the mutational status of 14 genes, gender, age and IPSS-R showed better prognostic power than IPSS-R alone (Haferlach et al., 2014). With the poor lenalidomide response seen in *TP53*-mutated del5q-positive MDS patients, the 2017 WHO revision also recommended testing for *TP53* mutation in these cases. *TP53* gene mutation overall is a poor prognostic factor in myeloid neoplasms. Although currently mutational data have not been incorporated into the major MDS risk stratification scores such as IPSS, IPSS-R, and WIPSS, the widespread use and decreasing cost of NGS have greatly improved the accessibility of NGS testing and simultaneous availability of information on multiple clinical informative molecular markers. It seems inevitable that key gene mutations will become an integral component of MDS risk stratification scoring systems. The NCCN guideline recommends molecular profiling of recurrent mutations to augment diagnosis and prognostic risk assessment in MDS (Greenberg et al., 2019).

From the diagnostic perspective, the molecular marker *SF3B1* is the only one included in the 2017 WHO diagnostic criteria of MDS for the category of MDS-ring sideroblasts (MDS-RS): in the appropriate clinical setting, the presence of *SF3B1* mutation as a clonal marker qualifies a case for MDS-RS with 5% ring sideroblasts whereas in the absence of such a mutation, 15% ring sideroblasts are required. *SF3B1* mutations are usually missense alterations and can occur at codons E622, Y623, R625, N626, H662, T663, K666, K700, I704, G740, G742, and D781, spanning exons 14 to 16. The hot-spot mutation K700E accounts for more than half of somatic *SF3B1* mutations (Makishima et al., 2012; Yoshida et al., 2011). Overall, the presence of recurrent MDS-associated mutations provide evidence of a clonal process, particularly in cases with a normal karyotype, and further supports the diagnosis of MDS in cases fulfilling the WHO clinicomorphologic criteria. For cases that are suspicious or do not yet meet the diagnostic morphologic features of MDS, the presence of one or more mutations aids in the establishment of clonal hematopoiesis and may help to rule out benign causes of cytopenias in the appropriate clinical setting. Because MDS-associated mutations overlap with CHIP seen in approximately 10% of healthy individuals older than 70 years, the detection of similar alterations cannot be used as sufficient evidence for MDS if definitive morphologic features of dysplasia are lacking. However, in patients with unexplained cytopenia(s) with adequate clinical assessment who are not fulfilling the WHO diagnostic criteria for MDS but are showing the presence of a clonal marker (either mutations or cytogenetic abnormalities), the term clonal *cytopenia(s) with undetermined potential (CCUS)* applies. Patients with CCUS have shown similar mutational VAF and blood counts as MDS patients, and those harboring multiple mutations or spliceosome mutations exhibited a natural history similar to that of lower risk MDS patients (Kwok et al., 2015; Malcovati et al., 2017; Steensma et al., 2015), illustrating a blurred boundary between CCUS and MDS. Further clinical studies with adequate follow-up are required to elucidate the biology, natural history, and interrelationship between CHIP, CCUS, and MDS, which is of value for appropriate management of individuals with CHIP and patients with CCUS, and to improve risk prediction as well as refinement of MDS diagnosis. Conversely, because the vast majority of patients with MDS harbor at least one somatic mutation, the negative predictive value of finding no mutations is relatively high for excluding the possibility of MDS if a well-designed targeted NGS panel with adequate genetic coverage is used. In cases with negative NGS findings, non-neoplastic causes of cytopenias should be thoroughly evaluated and excluded before a diagnosis of MDS is rendered.

Myeloproliferative Neoplasms

MPNs are clonal hematopoietic disorders characterized by proliferation of one or more of the myeloid lineage cells (erythroid, granulocytic, megakaryocytic), effective hematopoiesis, with variable risk of progression to acute leukemia, myelofibrosis, or both. The basic pathogenesis is constitutive activation of tyrosine kinases involved in signal transduction pathways leading to excessive cellular proliferation and decreased apoptosis. The key driver genetic abnormalities of Philadelphia chromosome (Ph)-negative MPN are listed in Table 78.8.

*Chronic Myeloid Leukemia, **BCR-ABL1** Positive*

CML is a clonal marrow stem cell disease resulting from excessive proliferation of predominantly granulocytic lineage cells. The natural course

TABLE 78.8

Phenotypic Driver Mutations in Ph-Negative Myeloproliferative Neoplasms

Genetic Abnormality	Disease Associations (frequency)	Mutational Features and Pathogenesis	Diagnostic Detection	Notes
JAK2 V617F (exon 14)	PV (≥95%) ET (50%–60%) PMF (50%–60%)	*JAK2* V617F is a missense mutation in the autoinhibitory domain of JAK2, leading to constitutive activation of JAK-STAT pathway	Allele-specific qualitative/quantitative PCR; high-resolution melting curve analysis; Sanger sequencing; pyrosequencing; NGS	Also frequent in MDS/MPN-RS-T; rarely seen in AML, MDS, and CMML
JAK2 exon 12 mutation	PV (≤5%)	Small in-frame insertion and deletions in *JAK2* exon 12, leading to constitutive activation of JAK-STAT pathway	High-resolution melting curve analysis Sanger sequencing; pyrosequencing; NGS	Essentially exclusively seen in PV
CALR exon 9 mutation	PMF (20%–30%) ET (20%–30%)	1-bp frameshift insertion/deletion mutations in the last exon (fit the pattern of 3n + 1 for deletions and 3n + 2 for insertions), resulting in a C-terminus neoepitope that interacts with MPL and activates the JAK-STAT pathway	PCR and fragment analysis; Sanger sequencing; pyrosequencing; NGS	Not seen in PV; in-frame *CALR* mutations are of uncertain clinical significance and most are polymorphism; they do not create the pathogenic C-terminus neoepitope
MPL exon 10 mutation	PMF (5%–10%) ET (3%–5%)	Point mutation causes constitutive activation of thrombopoietin receptor (MPL) and JAK-STAT signaling; most common mutation site is W515	Allele-specific PCR (hot spot); Sanger sequencing; pyrosequencing; NGS	S505N germline mutation associated with familial ET

AML, Acute myeloid leukemia; *CMML,* chronic myelomonocytic leukemia; *ET,* essential thrombocythemia; *MDS,* myelodysplastic syndrome; *MDS/MPN-RS-T,* myelodysplastic/myeloproliferative neoplasm with ring sideroblasts and thrombocytosis; *JAK,* Janus kinase; *NGS,* next generation sequencing; *PCR,* polymerase chain reaction; *PMF,* primary myelofibrosis; *PV,* polycythemia vera; *STAT,* signal transducer and activator of transcription.

of CML is typified by a protracted chronic phase, often for several years, followed by a rapid transformation to an aggressive acute myeloid or lymphoid blast crisis with fatal outcome. The decades-long investigation of this disorder has led from the recognition of a disease-associated karyotypic abnormality to the unraveling of its molecular genetic pathogenesis and, currently, to the widespread use of highly effective targeted pharmacologic therapy in the form of imatinib mesylate (Gleevec, Novartis) or related second and third-generation agents (Zhou et al., 2018; Goldman & Melo, 2003). CML is characterized by the presence of the t(9;22)(q34;q11.2) chromosomal translocation, which was initially observed as an abnormal 22q- called the *Philadelphia chromosome* (Nowell & Hungerford, 1960; Rowley, 1973). This translocation leads to juxtaposition of the *ABL1* (Abelson murine leukemia viral oncogene homolog 1) tyrosine kinase gene (9q34) with the *BCR* gene (22q11.2) on the derivative chromosome 22q, resulting in formation of the *BCR-ABL1* fusion gene and mRNA, and production of a chimeric BCR-ABL1 protein (Melo, 1996; Deininger et al., 2000). The t(9;22)/*BCR-ABL1* is present in more than 99% of CML cases, but it is not pathognomonic of this entity because it also occurs in 20% to 25% of adult and approximately 3% of cases of pediatric B-lineage acute lymphoblastic leukemias (B-LBL). In patients with B-LBL, *BCR-ABL1* is associated with highly aggressive disease behavior.

The *ABL1* gene product is a highly regulated tyrosine kinase under normal physiologic conditions that participates in diverse cellular processes pertaining to actin organization, cellular differentiation, apoptosis, and TCR signaling. The function of the normal BCR protein is incompletely understood; it contains several functional domains, including a serine/threonine kinase and a Rho GTPase modulator (https://www.genecards.org). As a consequence of the abnormal genetic fusion, the localization and activity of the chimeric ABL1 tyrosine kinase is deregulated, producing complex effects on cellular signal transduction pathways, proliferation, apoptosis control, and cell adhesion (Deininger et al., 2000; Melo & Barnes, 2007; Quintas-Cardama & Cortes, 2009). In vivo topographic studies of the *BCR* and *ABL1* genes in cycling normal hematopoietic progenitor cells, as well as the surprising demonstration of very low levels of *BCR-ABL1* transcripts in the blood of some healthy participants, suggest that the t(9;22) occurs in normal human bone marrow cells (Brassesco, 2008; Kuan, et al., 2019); however, progression to overt CML (or Ph+ B-LBL) is dependent on the stem or progenitor cell type and fitness, host factors, and the acquisition of other initiating or permissive genetic or epigenetic changes, which are incompletely understood. Potentially curative treatment for patients with CML is achieved only by allogeneic bone marrow or stem cell transplantation (Craddock, 2018), although the frontline management of CML has now been significantly altered with the oral agent imatinib and related TKIs (e.g., dasatinib, nilotinib, bosutinib, ponatinib), such that the disease may now be controlled in most patients in a continuous clinical remission over long periods of time, although not entirely eliminated (Jain et al., 2016b; Rossari et al., 2018).

At the DNA level, the *BCR-ABL1* gene fusion exhibits breakpoint heterogeneity with three main recognized breakpoint loci in the *BCR* gene, as well as some alternative splice transcript variation (Fig. 78.10) (Melo,1996; Deininger et al., 2000; Foroni et al., 2009; Baccarani et al., 2019a). In virtually all cases of CML, the *BCR* gene breakpoints are situated in the so-called major breakpoint cluster region, or M-BCR. These break sites occur over a relatively small 5.8-kb genomic region spanning *BCR* exons e12 to e16, specifically in introns 13 or 14. In contrast, the breakpoints in the *ABL1* gene are distributed over a very large region of intronic DNA 5′ to exon a2. Therefore, two types of *BCR-ABL1* fusion mRNA transcripts can arise from M-BCR locus gene fusions in CML, designated e13-a2 or e14-a2. These two products encode a novel protein of 210 kD (p210). Most e14-a2–positive tumors also demonstrate alternative splicing to produce coexisting e13-a2 transcripts. Because both isoforms result in essentially the same protein product, they are sometimes collectively referred to as e13e14-a2 transcripts. In the pre-imatinib era, the types of major breakpoint locus *BCR-ABL1* fusion in CML were not considered clinically or prognostically distinct; however, recent data suggest the possibility of differential imatinib responses for the e14- versus e13-a2 transcript types, requiring further investigation (Baccarani, 2019b; Jain et al., 2016a; Lucas et al., 2009; Pfirrmann et al., 2017). The second common *BCR* breakpoint locus is termed the minor breakpoint cluster region, or m-BCR. Translocations involving this locus result in the formation of an e1-a2 *BCR-ABL1* fusion transcript, encoding a 190-kD *BCR-ABL1* protein (p190). The e1-a2 type *BCR-ABL1* is most typical of Ph+ B-LBL. Although a general correlation is apparent between *BCR-ABL1* breakpoint fusion location and disease phenotype (i.e., M-BCR with CML and m-BCR with B-LBL), these associations are not specific. Whereas the vast majority (~90%) of pediatric Ph+ B-LBL cases are of e1-a2 (m-BCR) type, approximately 30% to 40% of adult patients with Ph+ B-LBL demonstrate an e13e14-a2 (M-BCR) fusion. In the latter situation, the possibility of CML in lymphoid blast crisis requires consideration. In addition, at diagnosis, patients with CML who have the dominant e13e14-a2 *BCR-ABL1* transcript commonly demonstrate the concurrent presence of very low abundance e1-a2 mRNA caused by a minor degree of alternative splicing (Saglio et al., 1996; Van Rhee et al., 1996). Potentially more confounding is the occurrence of rare Ph+ CMLs with the e1-a2 fusion (p190) that are associated with atypical monocytic features rather than the usual left-shifted granulocytic myeloid cell predominance of classical

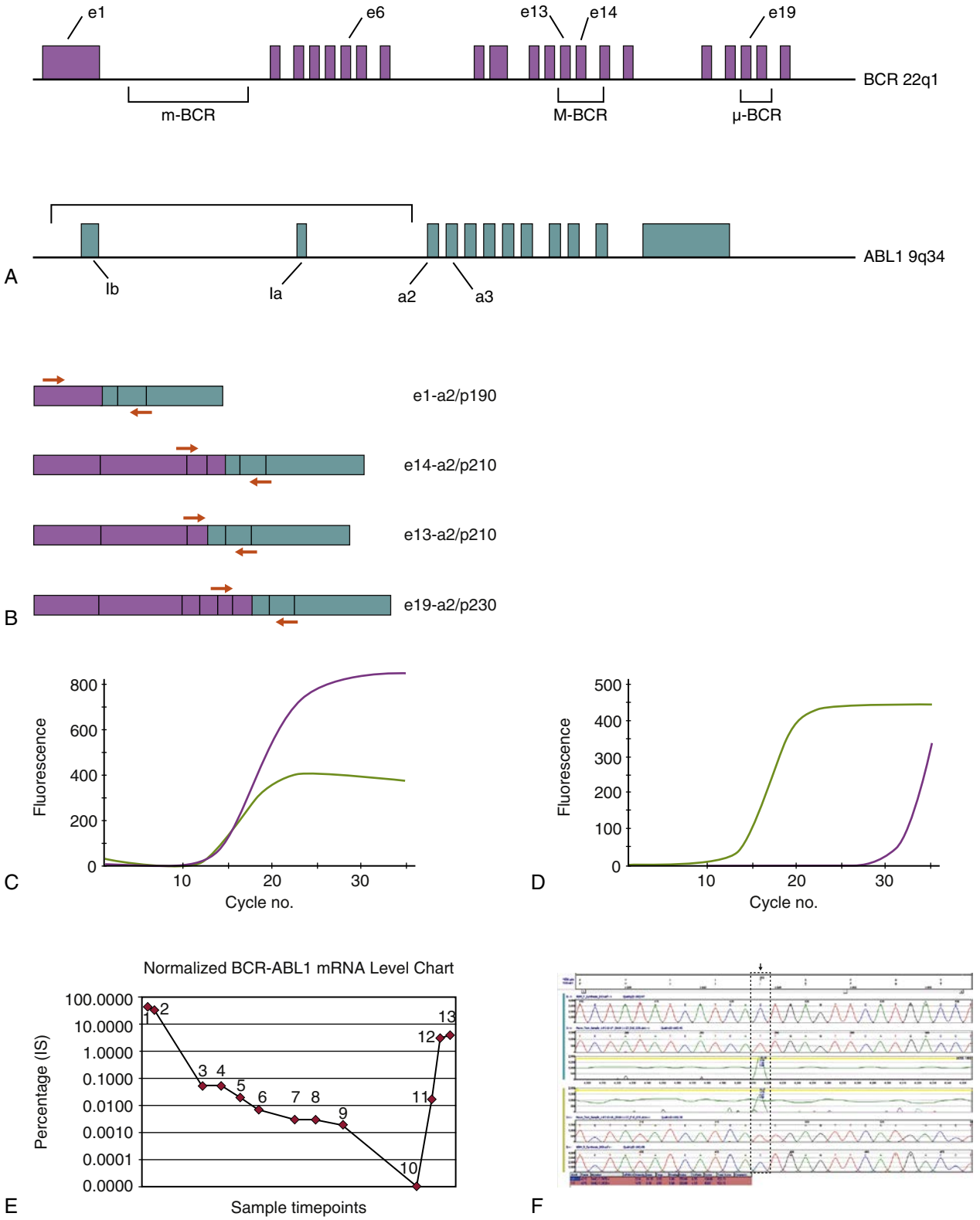

Figure 78.10 **t(9;22)**/*BCR-ABL1* abnormality in chronic myeloid leukemia (CML) and Ph+ B-lymphoblastic leukemia (B-LBL). **A,** Schematic of partial genomic organization of the *BCR* and *ABL1* genes. Three major recurrent breakpoint regions are recognized in the *BCR* gene: the minor breakpoint cluster region (m-BCR), the major breakpoint cluster region (M-BCR), and the μ-BCR. The M-BCR is involved in essentially all cases of CML but also in approximately one third of cases of de novo *BCR-ABL1*+ B-lineage adult acute lymphoblastic leukemias (B-LBL) and a small subset of childhood cases. Breakpoints within the m-BCR are observed in the majority of pediatric and adult *BCR-ABL1*+ B-LBL. Breakpoints at the μ-BCR have been associated with rare cases of CML. For the *ABL1* gene, genomic breakpoints are distributed throughout a large region 5′ of exon 2 (a2). **B,** Schematic representation of *BCR-ABL1* chimeric mRNA transcripts arising from these various translocation genomic breakpoints. The exon junctions are indicated for these fusion transcripts, with the corresponding BCR-ABl1 oncoprotein product sizes shown in kilodaltons (e.g., e1-a2 and p190; e13/e14-a2 and p210; e19-a2 and p230). The *orange arrows* indicate relative positions of polymerase chain reaction (PCR) primers to detect these various forms in qualitative or quantitative reverse transcriptase PCR assays. **C,** Example of real-time quantitative PCR (RQ-PCR) monitoring of *BCR-ABL1* mRNA in a patient with CML at diagnosis. The *green curve* represents *ABL1* control amplification, and the *purple curve* is the detected *BCR-ABL1* transcript. The percent *BCR-ABL1* normalized to *ABL1* is calculated and expressed on the International Scale (%IS); see text. **D,** RQ-PCR monitoring of a patient with CML on treatment with imatinib mesylate showing deep molecular response as evidenced by late occurrence of *BCR-ABL1* target amplification relative to *ABL1* control. **E,** Graphic of serial quantitative *BCR-ABL1* normalized transcript levels (IS%) in a patient treated with imatinib. The major molecular response threshold is defined as 0.1% (IS). The patient results indicate a favorable response profile over time with relatively rapid attainment of deep molecular response. Loss of response is shown after measurement time-point 10, with a rapid rise in normalized *BCR-ABL1* mRNA. **F.** *BCR-ABL1* kinase domain mutation (KDM) analysis performed between time-points 11 and 12 for monitored patient in **E**. Sanger sequencing reveals the presence of an acquired p.Thr315Ile (T315I) mutation (*arrow* and *hatched box*, C>T nucleotide substitution), which is relatively common and associated with resistance to most tyrosine kinase inhibitor agents used in CML therapy.

CML (Verma et al., 2009). A third breakpoint cluster region producing an uncommon *BCR-ABL1* gene fusion has been designated the μ-BCR and is associated with the formation of an e19-a2 mRNA; this event results in the translation of a 230-kD-size protein (p230) and is seen in rare patients with CML characterized by a greater relative proportion of mature neutrophils. Finally, very rare cases of CML or atypical MPNs and Ph+ B-LBL have been reported demonstrating alternate *BCR* or *ABL1* exon junctions, including e13-a3, e1-a3, e6-a2, and e8-a2 transcript forms (Baccarani et al., 2019b; Frederick et al., 2014; Melo, 1996; Deininger et al., 2000; Foroni et al., 2009).

Figure 78.10 schematically indicates the placement of oligonucleotide PCR primers to specifically amplify the M-BCR (e13e14-a2), m-BCR (e1-a2), and μ-BCR (e19-a2) fusion mRNA transcripts after reverse transcription; these RT-PCR molecular assays can be designed to be either qualitative or quantitative in nature. Qualitative RT-PCR assays for *BCR-ABL1* detection typically detect the most commonly encountered fusion forms at diagnosis (i.e., e13e14-a2, e1-a2), but more comprehensive multiple primer or probe approaches are capable of also identifying rarer transcript variants (such as the e19-a2) in a single assay as shown in Figure 78.10. FISH analysis for *BCR-ABL1* has very high clinical sensitivity and specificity and is often used at diagnosis to identify the translocation event, but it cannot determine precise mRNA transcript-level detail to enable disease monitoring after therapy; in contrast, given a sufficiently comprehensive multiplex RT-PCR approach, both the detection of *BCR-ABL1* and delineation of specific transcript type can be simultaneously obtained.

QRT-PCR specifically targeting the p210 fusion is subsequently used as the method of choice for ongoing evaluation of patients with CML after initiation of TKI therapy. Figure 78.10 shows a representative image of a standard QRT-PCR *BCR-ABL1* assay. The largest impact of QRT-PCR monitoring of *BCR-ABL1* in CML has come with the widespread use of targeted therapy with TKIs (e.g., imatinib and related drugs). Single-agent imatinib (previously called STI-571) was shown to be highly effective in inducing complete hematologic and cytogenetic responses in the majority of treated patients with CML within 12 months, as subsequently determined in the landmark International Randomized Study of Interferon and STI-571 (IRIS) clinical trial (Druker et al., 2001; Bechtold et al., 2009; Druker et al., 2006; O'Brien et al., 2003; Hughes et al., 2003; Hughes & Branford, 2009). Data derived from these and subsequent studies have demonstrated that the kinetics of *BCR-ABL1* reduction is strongly related to progression-free survival. Although criteria are continually being refined, several critical thresholds have been defined that indicate optimal response to imatinib and other TKIs. The vast majority of patients with CML receiving TKI therapy achieve complete hematologic remission within 3 months. Subsequently, overall survival and progression-free survival are strongly correlated with the attainment of a complete cytogenetic response by 12 months (or less) after therapy (complete cytogenetic response [CCyR], defined by the absence of Ph metaphases by cytogenetic analysis). Patients who continue to a deep level of *BCR-ABL1* suppression, termed a major molecular response (MMR), have favorable long-term outcome. The MMR level was originally defined by the IRIS group as 3-log reduction from a baseline pooled patient sample *BCR-ABL1* level, and this is now equivalent to a 0.1% normalized *BCR-ABL1* transcript ratio (i.e., *BCR-ABL1/ABL1*) using current highly standardized protocols as reported on the International Scale (IS: 100%–0.001%). The IS has also been alternatively expressed in terms of molecular log-fold response numbers (e.g., MR2 = 10%, MR3 = 0.1%, MR4.5 = 0.003%, and so on). A significant challenge for molecular hematopathology laboratories has been in establishing the reproducibility of QRT-PCR assays for *BCR-ABL1* that can meet the requirements of technical sensitivity and precision of IS reporting (Cross et al., 2016; Scott et al., 2017). The commercial-scale manufacture of high-quality reference materials calibrated to the original IS has greatly improved this situation for diagnostic testing laboratories, and at the present time, some reagents have received FDA approval for clinical use (e.g., Quantidex, Asuragen; GeneXpert Ultra, Cepheid). Newer methodology advances continue to emerge, capitalizing on the uniqueness of the *BCR-ABL1* fusion target to provide more sensitive or comprehensive assessment of CML cell populations during TKI therapy (Jennings et al., 2014; Radich et al., 2019).

Patients with CML who are taking TKI agents are now evaluated using a combination of clinical (i.e., hematologic), cytogenetic, and molecular response (QRT-PCR) criteria. FISH analysis for *BCR-ABL1* may have limited value at diagnosis but is not indicated after therapy in patients with CML. The combination of bone marrow cytogenetics and peripheral blood RQ-PCR for *BCR-ABL1* p210 levels is predictive of the risk of treatment failure and increased relapse and forms the basis of clinical management in CML. Patients who do not achieve less than 10% normalized IS *BCR-ABL1* transcript level at 3 months or 1% or less at 6 months generally do not obtain a timely complete cytogenetic response and thus are at risk for disease progression. Patients reaching an MMR relatively quickly (before or within a 12- to 18-month window after TKI therapy) have an excellent prognosis and a very low relapse risk (see Fig. 78.10). These benchmarks have been incorporated into guidelines issued by the ELN and NCCN for monitoring optimal and suboptimal responses to TKI therapy in patients with CML (Baccarani et al., 2013; Shanmuganathan & Hughes, 2018). Of note, a subset of individuals may also continue to deepen their molecular response and eventually become PCR negative (complete molecular response [CMR]), and drug withdrawal has been considered for some candidate patients meeting specific requirements (Fava et al., 2019; Hochhaus et al., 2017; Saussele et al., 2018; Shah et al., 2019). Attainment of CMR necessitates highly reproducible quantitative detection of *BCR-ABL1* e13e14-a2 mRNA at a very low level (currently 0.003%–0.002% IS by standardized platforms).

Although more than 80% of patients with CML taking imatinib are alive and without adverse events at 6 years (Hochhaus et al., 2009; Hughes & Branford, 2009; Hehlmann et al., 2017; Hoffmann et al., 2017), a significant subgroup develops resistance to imatinib or other TKI agents (Milojkovic & Apperley, 2009; Patel et al., 2017). TKI treatment failures are typically identified by loss of a previously attained CCyR, loss of MMR, or suboptimal responses as specified by consensus guidelines. Although resistance to TKI therapy is complex, more than half of patients with CML have acquired nucleotide single base substitutions (producing missense amino acid alterations) in the *ABL1* kinase domain of the chimeric *BCR-ABL1* gene that confer variable degrees of refractoriness to imatinib or second-generation agents (Ernst et al., 2011; Hughes et al., 2015; Jabbour et al., 2011a, 2011b). These mutations may occur at low level (i.e., in small subclones) and be selected for in the presence of these drugs, such that some neoplastic cells with *BCR-ABL1* kinase domain mutations (KDMs) gain a survival advantage and expand in the face of continued pharmacologic therapy. For patients being monitored by RQ-PCR, an increase in normalized *BCR-ABL1* transcript level of 0.5 to 1 log demonstrated in at least two consecutive samples is often correlated with the presence of an acquired *BCR-ABL1* KDM. These mutations can occur anywhere in the kinase domain, but they tend to preferentially involve critical amino acids in several regions corresponding to the phosphorylation loop (P-loop), activation loop (A-loop), and drug contact sites (Ernst et al., 2011; Hughes et al., 2015; Jabbour et al., 2011a, 2001b). Notably, P-loop and some direct contact site mutations are associated with high-level resistance to imatinib. Examples of common P-loop alterations include Q252H, Y253F/H, E255K/V, and G250E. Nonetheless, a significant number of imatinib resistance mutants can be overcome by either increasing the dosage of imatinib or by switching to a second-generation TKI, such as dasatinib, nilotinib, or bosutinib. Some therapy-associated alterations are also more typically associated with use of a particular TKI but not necessarily others (e.g., V299L and dasatinib resistance), suggesting a rational approach for drug modification in certain patients. Most problematic of all is the drug contact site mutation T315I, which is relatively frequently encountered and exhibits marked in vivo and clinical resistance to imatinib and all other currently approved second-generation TKI drugs, with the exception of ponatinib (Cortes et al., 2012; Cortes et al., 2018; Lipton et al., 2016; Nicolini et al., 2017). Furthermore, some cases of CML may harbor compound mutations (Khorashad et al., 2013). Molecular diagnostic evaluation for *BCR-ABL1* KDM is therefore an increasingly integral part of assessment for a subset of patients with CML (Jones et al., 2009; Soverini et al., 2011). Most commonly, a *BCR-ABL1* KDM is detected by sequencing of the *ABL1* segment derived from the amplified *BCR-ABL1* transcript. This approach is not highly analytically sensitive (~15%–20% by Sanger method), but it is successful in identifying a KDM when *BCR-ABL1/ABL1* mRNA levels are rising at or above the MMR and acquired drug resistance is most likely to be encountered. Finally, it should be noted that very low-level mutations can be identified using highly sensitive quantitative molecular techniques in patients with chronic phase CML, who are otherwise initially responsive to imatinib (Soverini et al., 2013; Willis et al., 2005). The significance of such small subclonal populations is not completely understood, and their detection by ultrasensitive methods may not necessarily be predictive of subsequent therapy resistance; however, recent data from NGS analysis of patients with CML receiving imatinib or other TKI agents has indicated that early occurrence of clinically relevant mutations can be detected more sensitively than by Sanger sequencing (Kizilors et al., 2019). Finally, it is notable that acquired *BCR-ABL1* KDM are more prevalent in patients with B-LBL receiving TKI therapy.

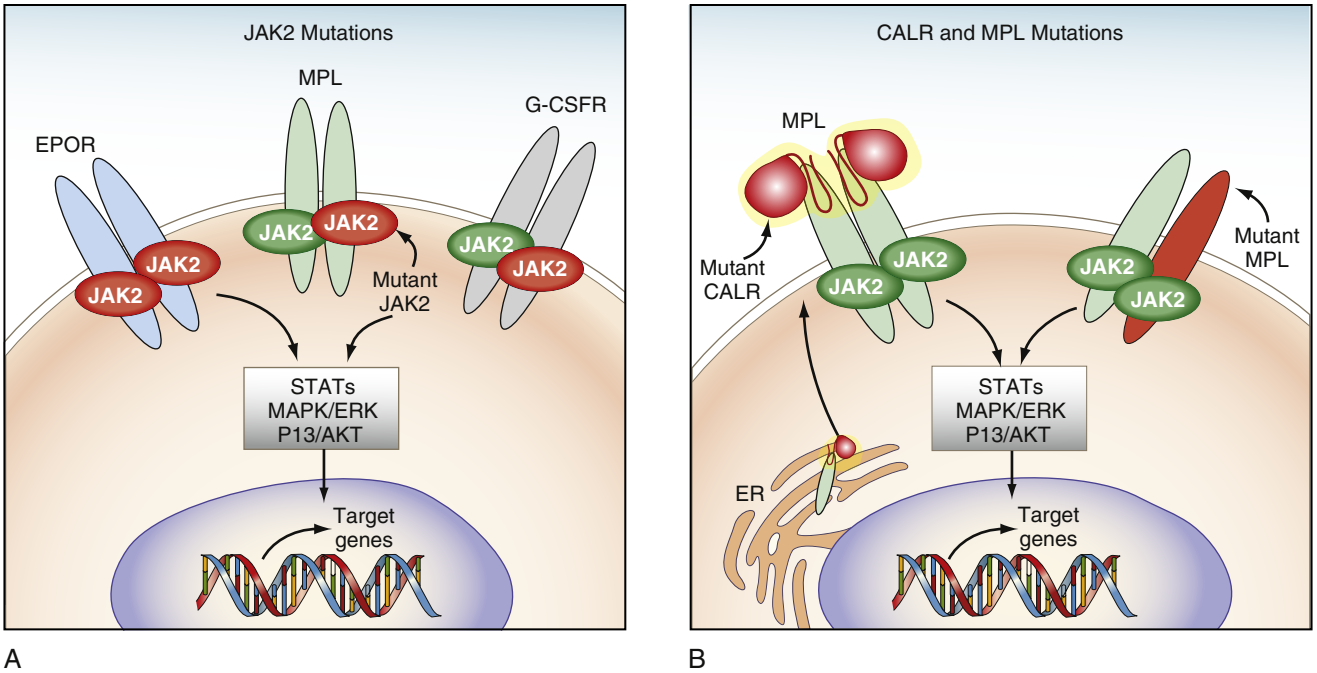

Figure 78.11 Molecular mechanism of *JAK2, CALR,* and *MPL* mutations in myeloproliferative neoplasm (MPN) pathogenesis. *JAK2, CALR,* and *MPL* mutations lead to constitutive activation of signaling pathways, resulting in myeloproliferation through various mechanisms. **A,** JAK2 is an intracellular tyrosine kinase closely associated with growth factor and cytokine receptors such as receptors for erythropoietin (EPOR), thrombopoietin (TPO) MPL, and granulocyte colony-stimulating factor (G-CSF). Binding of the ligand to its cognate receptor leads to activation of JAK2 *(green),* which then activates downstream signaling, including the Janus kinase–signal transducer and activator of transcription (JAK-STAT) and, to a lesser extent, mitogen-activated protein kinase/extracellular signal-regulated kinase (MAPK/ERK), and phosphoinositide 3 kinase (PI3K) pathways. Mutant JAK2 *(red)* is constitutively active in the absence of ligand-receptor binding. It is uncertain whether the mutant JAK2 dimerizes with mutant or wild-type JAK2. **B,** CALR and MPL mutants *(red)* lead to activation of downstream signaling through the MPL receptor. Mutant CALR binds the extracellular domain of MPL in the endoplasmic reticulum (ER) and then translocates to the cell surface. Both the C- and N-terminal of the mutant CALR and the extracellular domain of MPL are required for this interaction. (Adapted from Nangalia J, Green AR: Myeloproliferative neoplasms: from origins to outcomes, *Blood* 130:2475–2483, 2017.)

Philadelphia-Negative Classical Myeloproliferative Neoplasms: Polycythemia Vera, Essential Thrombocythemia, and Primary Myelofibrosis

The classical non-CML, or Ph-negative MPN include polycythemia vera (PV), essential thrombocythemia (ET), and primary myelofibrosis (PMF). These diseases are individually characterized by a defined set of clinical, laboratory, and morphologic features yet also exhibit overlap in all these aspects. Cytogenetic abnormalities are seen in 20% to 30% of patients with PV and PMF, most commonly +8, +9, del(20q) and del(13q). Cytogenetic abnormalities are rarer in ET (5%–10%) and commonly include +8, 9q abnormalities, and del(20q) (Swerdlow et al., 2017). In recent years, the expanded use of NGS technologies has greatly enhanced our understanding of the molecular genetic basis of MPN. In Ph-negative classical MPN, the molecular landscape has been well defined by phenotypic driver mutations (i.e., mutations that drive the development of an MPN phenotype) accounted for in more than 95% of cases by somatic mutations involving the *JAK2*, *CALR*, or *MPL* genes (Klampfl et al., 2013; Nangalia et al., 2013). Through various mechanisms, these mutations converge on the JAK-STAT signaling pathway, which helps to explain their essentially mutual exclusiveness in MPN (Fig. 78.11) (Ciboddo & Mullally, 2018). In PV, the missense mutation *JAK2* V617F in exon 14 is seen in at least 95% of cases with the vast majority of the reminder harboring a *JAK2* mutation in exon 12 (Scott et al., 2007). The mutational spectrums of ET and PMF are similar with the most frequent mutation being *JAK2* V617F (50%–60%) followed by *CALR* (20%–30%) and then *MPL* (5%–10% in PMF and 3%–5% in ET) (see Table 78.8). Because these molecular markers serve as one of the major diagnostic criteria for PV, ET and PMF by the 2017 WHO criteria, detection of such a mutation provides supporting evidence for the diagnosis of MPN in the appropriate clinicopathological setting and may be particularly helpful in cases morphologically equivocal for MPN and patients with unexplained cytosis or myelofibrosis suspicious for MPN.

JAK2 (also discussed in Chapter 77) is located on chromosome 9p24, and encodes Janus kinase 2 (JAK2), which intimately associates with the cytoplasmic portion of receptors of major hematopoietic growth factors and cytokines, such as erythropoietin, thrombopoietin (TPO), and granulocyte colony-stimulating factor (G-CSF). Under physiological conditions, binding of these ligands with their cognate heterodimeric transmembrane receptors leads to activation of the intracellular JAK2 through conformational changes and phosphorylation. The subsequent downstream activation is carried out through activation of the STAT (signal transducer and activator of transcription) signaling, and to a lesser extent, mitogen-activated protein kinase (MAPK) and phosphoinositide-3-kinase (PI3K) signaling pathways, resulting in eventual cellular proliferation (see Fig. 78.11A). The missense mutation (G1849T) in exon 14 replaces valine with phenylalanine at amino acid codon 617, resulting in the *JAK2* V617F missense mutation. This mutation is positioned in the pseudokinase (JH2) region of JAK2, which normally negatively regulates and inhibits autophosphorylation of the adjacent kinase domain in the absence of associated receptor-ligand activity. The V617F substitution abrogates this intrinsic negative regulatory control and results in autonomous cell signaling independent of receptor–cytokine engagement, with constitutive activation of the central JAK-STAT pathway as well as the MAPK and PI3K pathways (Ihle & Gilliland, 2007; Pfeifer et al., 2008).

The *JAK2* V617F mutation is most prevalent in patients with PV (>95%) and presents in the majority of patients with PMF and ET (50%–60%) (Baxter et al., 2005; James et al., 2005; Kralovics et al., 2005; Levine et al., 2005; Ramchandren et al., 2013). The V617F–wild-type allele ratio varies between individuals with the same diagnosis, reflecting tumor allele burden heterogeneity. Patients with PV and a subset of those with PMF are more likely to be homozygous for the V617F mutation and consequently have a higher mutated "allele burden" than do patients with ET. Interestingly, the homozygous mutation status is selected for by the process of uniparental disomy (copy-neutral LOH), usually through mitotic duplication of the mutated *JAK2* allele (Kralovics et al., 2002; Vannucchi et al., 2008). The wide spectrum of *JAK2* V617F allele burden seen in patients with MPN indicates that relatively sensitive assays are required for diagnostic work-up (Wang et al., 2008; Ramchandren et al., 2013). A variety of methods have been advocated for detecting *JAK2* V617F, including high-resolution melting curve analysis, Sanger sequencing or pyrosequencing, and allele-specific PCR (e.g., "amplification refractory mutation system," RQ-PCR). Of these, allele-specific PCR approaches using DNA as template offer the highest analytic sensitivity (see Table 78.8). Although quantitative reporting of mutation burden is not presently required for diagnostic or therapeutic purposes, the development of newer generation *JAK2* inhibitors may change this aspect as more data emerge. It should be noted that *JAK2* V617F has also been reported in rare cases (<5%) of other myeloid neoplasms, including MDS, CMML, atypical CML (aCML), and

de novo AML, as well as the majority of patients with MDS/MPN-RS-T (Malcovati et al., 2009; Steensma et al., 2005; Wang et al., 2014). Therefore, the presence of a *JAK2* V617F mutation does not specify the diagnosis of an MPN, and the result needs to be interpreted in the context of the overall clinical and pathological findings for a definitive diagnosis and classification. Conversely, a negative *JAK2* V617F analysis does not exclude the diagnosis of a classical MPN if definitive clinical and morphologic findings are present. The use of highly sensitive PCR methods can also identify very low-level (<0.1%) *JAK2* V617F mutation in individuals without apparent MPN (Xu et al., 2007). A recent Danish case-control study reported a prevalence of 3% for *JAK2* V617F in the general population with 83% showing a VAF below 1% by digital PCR and 2% carrying a MPN diagnosis at time of data collection (VAF range, 0.3%–96%). The mutation positive patients showed higher blood counts and increased odds for venous thromboembolism (Cordua et al., 2019). These findings caution that molecular diagnostic laboratories must be aware of the dynamic range of the *JAK2* V617F test they offer and understand the relative clinical validity of positive values, especially at low levels (<1%), when reporting the results. The importance of thorough clinical and pathologic correlation cannot be overemphasized in this setting. *JAK2* V617F was also included in the gene list of CHIP in several WES-based large population studies, with an overall lower incidence of about 0.2% (Genovese et al., 2014; Jaiswal et al., 2014; Xie et al., 2014). In these studies, the mutation was detected at significantly higher VAF than most other CHIP genes, and it is important to note that not all patients had a well-documented hematologic evaluation in these population studies. In one study of more than 12,000 participants with 2 to 7 years of longitudinal follow-up, approximately 29% (7 of 24) of individuals with *JAK2* V617F mutation either had an existing MPN or developed an MPN during the study. Although similarly lacking follow-up in the MPN-negative individuals for the 5% of participants showing greater than 10% VAF at the time of their case-control study, the Danish study did report an odds ratio of 1.14 per percent VAF for MPN diagnosis (Cordua et al., 2019). Further studies are thus warranted to explore whether the presence of *JAK2* V617F at relatively high VAF is truly a CHIP-associated age-related finding and better delineates its clinical significance.

A small group of PV patients (≤5%) lack the *JAK2* V617F mutation, and the vast majority of them have been found to harbor small in-frame insertion/deletion (indel) events or nucleotide substitutions involving codons 536-547 in exon 12 of *JAK2*, such as N542-E543del, H538-K539del, F537-K539delinsL (i.e., F537-K539 deleted and replaced with Leu), R541-E543delinsK, and K539L (Scott et al., 2007; Pietra et al., 2008). These alterations involve the region adjacent to the beginning of the JAK2 pseudo-kinase domain and disrupt its interaction with the kinase domain. They have been shown to induce cytokine-independent cell growth in vitro. Clinically, patients with PV who have *JAK2* exon 12 mutations do not show the same propensity to thrombocytosis as those with *JAK2* V617F mutations, but otherwise the disease appears clinically similar despite the alternate localization of the mutation (Kilpivaara & Levine, 2008). Morphologically, these cases may exhibit more subtle changes in bone marrow in comparison with the *JAK2* V617F-mutated PV. *JAK2* exon 12 presents a relatively large genomic area across which mutations may be scattered. Screening techniques, including high-resolution melting curve analysis, may be used to triage specimens and distinguish those that are apparently wild type from those deserving of additional scrutiny via direct sequencing (Jones et al., 2008; Rapado et al., 2009). Alternatively, they can be conveniently identified by NGS or other sequencing platforms (see Table 78.8).

CALR is located on chromosome 19p13.2 and encodes calreticulin, a multifunctional protein involved in endoplasmic reticulum (ER) protein folding, calcium homeostasis, and cellular proliferation and apoptosis. In 2013, two groups simultaneously reported highly prevalent somatic *CALR* mutations in *JAK2* and *MPL*-negative ET and PMF patients but not in those with PV patients (Klampfl et al., 2013; Nangalia et al., 2013). These mutations occur in the last exon (exon 9) of *CALR* and are always frameshift insertion/deletion (indels) with a net 1bp frameshift, resulting in the same alternative reading frame and generating a C-terminus neoepitope with loss of most of the acidic amino domain including a critical Lys-Asp-Glu-Leu (KDEL) signal sequence that allows retention of the protein in the endoplasmic reticulum, the so-called "ER-retention signal." More than 50 types of somatic indels have been documented thus far, all following the pattern of 3n+1 for deletions and 3n+2 for insertions. The two most common mutations are type 1 (52bp deletion, c.1092-1143del, p.Leu367fs*46) and type 2 (5 bp insertion, c.1154_1155insTTGTC, p.Lys385fs*47), accounting for about 53% and 32% of *CALR* mutations in MPN, respectively. *CALR* mutations have been identified in the neoplastic hematopoietic stem and progenitor cells. The mutant CALR protein has been shown to bind and constitutively activate MPL and the downstream JAK-STAT pathway (see Fig. 78.11B). The positive charge of the mutant CALR protein and its lectin-binding activity are required for the oncogenic activity (Elf et al., 2016, 2018). Defined by the deletion of stretches of negatively charged amino acids in the wild-type CALR C-terminus or statistically calculated helix propensity, non-type 1/2 *CALR* mutations can be classified into type 1–like or type 2–like mutations (Pietra et al., 2016; Tefferi et al., 2014). It has been shown that *CALR* type 1–like and type 2–like mutants were sufficient to induce an MPN phenotype in retroviral mouse models (Marty et al., 2016; Toppaldoddi et al., 2019). Type 1–like and type 2–like mutations are preferentially associated with PMF and ET phenotypes, respectively, with the former associated with a more favorable prognosis in PMF (Guglielmelli et al., 2015; Pietra et al., 2016; Tefferi et al., 2014). It is important to note that, occasionally, in-frame indels of *CALR* have been observed, and they are biologically distinct from the frameshift mutations and lack the pathogenic C-terminus neoepitope. In most cases, the in-frame indels are germline polymorphisms but they can rarely co-occur as a subclonal event along with a phenotypic driver mutation such as *JAK2* V617F or a frameshift *CALR* mutation in MPN (He et al., 2015). Because in-frame *CALR* variants can occasionally be encountered during routine screening tests, differentiation between frameshift and in-frame *CALR* mutation is important clinically to avoid errant interpretation. Given the size change associated with indel events in *CALR*, these alterations can be effectively identified by fragment sizing analysis following PCR of exon 9 or by sequencing techniques such as Sanger sequencing or NGS (see Table 78.8). One caveat is that the typical resolution of many fragment size analysis platforms is ± 1 to 3 bp depending on the size of the PCR product and platform used. Because differentiation between frameshift and in-frame indels is important for *CALR*, it is strongly recommended that the run controls of the fragment sizing analysis include at least the two most common *CALR* type 1 and type 2 mutations for variant size comparison and confirmation. For rare *CALR* mutations not matching sizes of the type 1 and type 2 run controls, supplemental sequencing should be pursued for confirmation of the indel size. One additional note about fragment sizing is that it cannot elucidate the nature of events that are of identical size change (e.g., different deletions can generate a 52-bp deletion size but may arise from a variety of different locations and sequence changes within *CALR* exon 9). Knowing the precise mutation sequence may be of clinical significance in light of the recent reports of favorable clinical outcome in type 1–like *CALR*-mutated PMF patients. Sequencing platforms provide information on the mutant sequences with higher analytical sensitivity seen with NGS in comparison to Sanger sequencing (see Table 78.8).

MPL is located on chromosome 1p34 and encodes the cell surface receptor for TPO serving as the major regulator of proliferation and differentiation of megakaryocytes and platelets (Ding et al., 2004). The receptor–ligand interaction initiates cell signaling through the JAK-STAT pathway, and activating mutations thus induce aberrant constitutive signaling effects, as observed similarly for mutated *JAK2* (see Fig. 78.11B). A minority of patients with PMF (5%–10%) and ET (3%–5%) lack *JAK2* and *CALR* mutations and instead harbor coding alterations in the *MPL* gene (Pikman et al., 2006; Tefferi, 2008; Beer et al., 2008). *MPL* mutations mostly occur in exon 10 at hot-spot codon W515 with amino acid substitutions of W515L (76%), W515K (11%), and W515R/S/A/G (<10% each). Somatic and germline S505N mutations have been reported, and the latter situation is associated with rare cases of familial ET (Ding et al., 2004). *MPL* mutational analysis may be performed using allele-specific PCR for hot-spot mutations or direct sequencing of PCR products (Pancrazzi et al., 2008; Daly et al., 2009).

In addition to the phenotypic driver mutations of *JAK2*, *CALR*, and *MPL*, patients with MPN frequently harbor other somatic mutations. These mutations commonly involve the epigenetic modifiers (*TET2*, *DNMT3A*, *IDH1/2*, *EZH2*, and *ASXL1*) and spliceosome machinery (*SF3B1*, *U2AF1*, *SRSF2*). In patients with PMF, mutations in *ASXL1*, *SRSF2*, *IDH1/2*, or *EZH2* were associated with shortened survival times and are considered high molecular risk (HMR) mutations. The number of HMR mutations also portends prognostic significance with multiple mutations correlated with a worse prognosis (Guglielmelli et al., 2014; Vannucchi et al., 2013). Among HMR only *ASXL1* mutations remain independently significant in the context of the IPSS/DIPSS+ (dynamic international scoring system) risk stratification scoring systems. These observations have led to proposals for new prognostic strategies incorporating molecular information, in addition to standard clinical and laboratory measures. Three recently proposed MF prognostic scoring models, Myelofibrosis Secondary to PV and ET-Prognostic model (MYSEC-PM), Mutation-Enhanced International Prognostic Score system (MIPSS) and

MIPSS-plus, and Genetically Inspired Prognostic Scoring System (GIPSS), incorporated the molecular markers of *CALR* unmutated genotype, presence of HMR/number of HMR/absence of a *CALR* type 1–like mutation, and *ASXL1/SRSF2/U2AF1* Q157/absence of a *CALR* type 1–like mutation in the scoring systems, respectively (Guglielmelli et al., 2018; Passamonti et al., 2017; Tefferi et al., 2018a, 2018b). In patients with ET and PV, the risk stratification has been primarily focused on estimation of thrombotic risk given the relative indolent clinical course. *JAK2* mutational status has been included into the thrombosis risk stratification scheme in patients with ET (Haider et al., 2016). NGS studies investigating molecular risk in ET and PV prognosis are emerging. One recent study reported unfavorable survival impact of *ASXL1*, *SRSF2*, and *IDH2* in patients with PV and *SH2B3*, *SF3B1*, *U2AF1*, *TP53*, *IDH2*, and *EZH2* in patients with ET (Tefferi et al., 2016). However, these findings need to be further validated in larger cohort studies to warrant expanded clinical molecular testing for these abnormalities in patients with ET or PV.

The current health care system emphasizes value-based, cost-effective laboratory testing for optimal and efficient patient care. For diagnosis purposes, the mutually exclusive nature of *JAK2*, *CALR*, and *MPL* mutations in ET and PMF, along with the distinct disease-associated frequencies makes these genes ideal candidates for reflexive testing based on a sequential analysis of *JAK2* V617F, *CALR*, and *MPL*, with the process halted when a positive result is encountered. This algorithmic approach has recently been incorporated into the NCCN guideline for the diagnostic work-up of patients with MPN (Mesa et al., 2017). Similarly, if the clinical suspicion is high for PV, a similar reflexive testing starting with *JAK2* V617F followed by *JAK2* exon 12 sequencing is recommended. Because other somatic mutations are of prognostic value in patients with myelofibrosis, a more comprehensive approach of NGS panel testing including *JAK2*, *CALR* and *MPL* and other genes can be performed in myelofibrosis patients for both diagnostic and prognostic purposes.

Chronic Neutrophilic Leukemia

Chronic neutrophilic leukemia (CNL) is a very rare, slowly progressive subtype of Ph-negative MPN characterized by persistent nonreactive peripheral neutrophilia with bone marrow–based myeloid hyperplasia and hepatosplenomegaly. Patients' survival is variable, and the disease may rarely progress to MDS or AML. Karyotyping studies are normal in nearly 90% of cases, and the rest demonstrate nonspecific cytogenetic findings. The *CSF3R* gene encoding the colony-stimulating factor 3 protein is essential for proliferation, differentiation, and survival of neutrophils and myeloid cells. Membrane-proximal activating *CSF3R* mutations in exon 14 have been reported in approximately 50% to 80% of cases of CNL, most commonly the T618I missense substitution. They constitutively activate the JAK-STAT pathway with resultant ligand-independent cell growth in vitro (Mehta et al., 2013; Maxson et al., 2013). Their association with aCML remains controversial (Maxson et al., 2013; Gotlib et al., 2013; Pardanani et al., 2013). Somatic cytoplasmic truncation mutations involving exon 17 were described in approximately 30% of patients with severe congenital neutropenia (SCN) and 80% of patients with SCN with leukemic transformation who are often on G-CSF therapy, although their role in leukemic transformation is uncertain (Bernard et al., 1998; Vandenberghe & Beel, 2011). They can also coexist with membrane-proximal mutations in CNL. Cytoplasmic truncation mutations of *CSF3R* result in loss of the negative regulatory domain on the C-terminus of the CSF3R protein and preferentially activate the downstream SRC family kinases (SFKs) and TNK2 signaling mediators with growth factor–independent cell line growth in vitro (Maxson et al., 2013; Germeshausen et al., 2007). Laboratory studies have shown JAK inhibitor sensitivity of membrane-proximal mutant T618I in vitro and in mouse model. It is promising that patients with CNL carrying the *CSF3R* mutation showed clinical improvement after the administration of the JAK2 inhibitor (Maxson et al., 2013). Because *CSF3R* mutations can occur at various sites in exons 14 and 17, they can be more conveniently detected by various sequencing platforms.

Myelodysplastic and Myeloproliferative Neoplasms

Chronic Myelomonocytic Leukemia

CMML is a clonal hematopoietic neoplasm exhibiting both myelodysplastic and myeloproliferative features with persistent peripheral blood monocytosis and 10% or more monocytes in white blood cell differentials. Cytogenetic abnormalities are seen in 20% to 40% of patients with CMML, and the most frequent findings are gain of chromosome 8 and loss of chromosome 7 or del(7q) (Swerdlow et al., 2017). However, these findings are not unique to CMML and overlap with other myeloid neoplasms and therefore are not disease defining. Recurrent somatic gene mutations have been identified in more than 90% of CMML cases, and the recurrently mutated genes are *TET2* (40%–60%); *SRSF2* (40%–50%); *ASXL1* (40%–50%); *RUNX1* (15%–20%); *NRAS* (10%–20%); and *SETBP1*, *CBL*, *EZH2*, *KRAS*, *SF3B1*, *ZRSF2*, *U2AF1*, *IDH2*, *JAK2*, *FLT3*, *NPM1*, *DNMT3A*, *IDH1*, and *TP53* (1%–10%), in descending order of frequency. Co-mutation of *TET2* and *SRSF2* is highly associated with a CMML phenotype, characterized by monocytosis and morphologic dysplasia (Itzykson et al., 2013; Jankowska et al., 2011; Mughal et al., 2015; Padron et al., 2015). Mutations of *TET2*, *SRSF2*, or *ASXL1* occur in 80% or more of patients with CMML and aid in the establishment of CMML diagnosis in the appropriate clinical setting in patients with persistent monocytosis yet lacking definitive dysplasia. It is worth noting that mutations in these genes can also occur as CHIP in aging individuals without evident hematologic neoplasms, most commonly as a solitary alteration. Therefore, their presence as a sole mutation, especially at low (<20%) VAF, needs to be interpreted with caution and considered in the context of the overall clinicopathologic picture. Patients with proliferative CMML show a higher frequency of mutations in the RAS pathway genes (*NRAS*, *KRAS*, *CBL*, and *PTPN11*) (Patnaik & Tefferi, 2018; Ricci et al., 2010). Among the recurrent somatic mutations, frameshift and truncating *ASXL1* mutations have been confirmed to be an independent poor prognostic marker in multiple studies. There are multiple risk stratification models for CMML with the more recent ones incorporating molecular markers of *ASXL1* in the Groupe Français des Myélodysplasies model and Mayo Molecular Model, and *ASXL1*, *RUNX1*, *NRAS* and *SETBP1* in the CMML-specific prognostic scoring system (CPSS-mol) model (Elena et al., 2016; Itzykson et al., 2013; Wassie et al., 2014). Of note, *NPM1* mutations can rarely be seen in CMML and are associated with high probability of progression toward AML, and they may require aggressive clinical intervention (Peng et al., 2016). Similar to other myeloid neoplasms, the spectrum of genetic mutations in CMML is most optimally detected using a targeted NGS strategy.

Juvenile Myelomonocytic Leukemia

JMML is a clonal hematopoietic neoplasm of childhood featured by granulocytic and monocytic proliferation. Cytogenetic abnormalities are seen in 35% of patients with JMML, with approximately 70% being monosomy 7 (Niemeyer et al., 1997). The JMML mutational landscape characteristically centers on the RAS signaling pathway with approximately 85% of cases showing recurrent mutations in RASopathy genes *PTPN11*, *KRAS/NRAS*, *NF1*, and *CBL*. Heterozygous somatic mutations in *PTPN11* and *KRAS/NRAS* account for approximately 35% and 20% to 25% cases, respectively, whereas germline mutations in *CBL* and *NF1* are present in approximately 15% and 10% of cases (Swerdlow et al., 2017; Caye et al., 2015; Niemeyer et al., 1997). CBL germline mutations are most commonly missense mutations involving the linker or RF domain, accompanied by an acquired uniparental disomy (UPD), resulting in a homozygous state of the mutant *CBL* in JMML cells. Germline *CBL* mutation-associated JMML spontaneously regress in most cases with the persistence of the UPD in hematopoietic cells (Loh et al., 2009; Muramatsu et al., 2010; Niemeyer et al., 2010; Perez et al., 2010). As reflected by the mutated genes, JMML is associated with the familial syndromes neurofibromatosis-1 (NF-1) and Noonan's syndrome (NS) or NS-like disorders. *PTPN11* is the most commonly mutated gene (50%) in NS followed by *SOS1*, *RAF1*, *KRAS*, *NRAS*, and others. Approximately 10% patients with NS develop a transient myeloproliferative disorder in early infancy, and the vast majority harbor germline *PTPN11* mutations, which were predicted to result in weaker gain-of-function effects than the somatic mutations seen in patients with JMML. Most of these cases spontaneously regress with about 10% progressing to JMML upon acquisition of additional genetic abnormalities (Aoki & Matsubara, 2013; Mohi & Neel, 2007; Niemeyer, 2014). Germline mutations in *PTPN11/KRAS/NRAS*, *CBL*, and *NF1* mutations are associated with NS, NS-like disorder, and neurofibromatosis, respectively. JMML in these clinical contexts is recognized under the new 2017 WHO entity of myeloid neoplasms with germline predisposition (Swerdlow et al., 2017). Similar to other myeloid neoplasms, the spectrum of genetic mutations in JMML can be conveniently detected using a targeted NGS strategy. Confirmation of the germline nature of suspicious mutations should be pursued and is further discussed in the section of Myeloid Neoplasms with Germline Disposition.

Myelodysplastic/Myeloproliferative Neoplasm with Ring Sideroblasts and Thrombocytosis

MDS/MPN-RS-T is characterized by thrombocytosis and increased ring sideroblasts (≥15%) (Swerdlow et al., 2017). It was previously designated as a provisional entity of refractory anemia with ring sideroblasts associated with marked thrombocytosis (RARS-T) and is now recognized as a distinct entity in the 2017 WHO revision given its established association

with spliceosome gene *SF3B1* mutations. *SF3B1* mutations are strongly associated with presence of ring sideroblasts as seen in 70% to 90% of cases of MDS/MPN-RS-T and MDS-RS (Malcovati et al., 2009; Schmitt-Graeff et al., 2008; Visconte et al., 2016; Yoshida et al., 2011). In MDS/MPN-RS-T, *SF3B1* mutations most frequently coexist with *JAK2* V617F (50%–65%) and less commonly (<10%) with *MPL* or *CALR* mutations. The coexistence of *SF3B1* and typical MPN driver mutations (*JAK2* V617F, *CALR*, or *MPL*) provides the genetic basis for the observed mixed MDS/MPN phenotype of thrombocytosis and ring sideroblasts in MDS/MPN-RS-T. These gene mutations can be examined simultaneously using targeted NGS panels or other platforms according to the specific mutation patterns and analytical sensitivity desired such as allelic-specific PCR for sensitive detection of the hot-spot *JAK2* V617F mutation, fragment analysis for *CALR* mutations, or Sanger sequencing.

Atypical Chronic Myeloid Leukemia, *BCR-ABL1*–Negative

aCML is characterized by dysgranulopoiesis and neutrophilia with left shift. It is distinct from CML by the absence of *BCR-ABL1* fusion and the presence of prominent dysgranulopoiesis. The latter is also a salient feature distinguishing aCML from chronic neutrophilic leukemia (CNL). Cytogenetic abnormalities are seen in up to 80% of cases of aCML, most commonly +8 and del(20q) (Breccia et al., 2006; Hernandez et al., 2000). Recurrent somatic mutations have been identified in *SETBP1*, *ETNK1* with a frequency of approximately 20% to 30% and 9%, respectively. Mutations of other genes such as *KRAS/NARS*, *ASXL1*, *SRSF2*, *TET2*, and *CBL* are also seen (Gotlib et al., 2013; Meggendorfer et al., 2013, 2014; Piazza et al., 2013). *CSF3R* is the most commonly mutated gene in CNL, and *CSF3R* mutations were initially reported in aCML; however, this finding was not confirmed in subsequent studies employing a strict pathologic definition of aCML (Gotlib et al., 2013; Maxson et al., 2013; Pardanani et al., 2013).

Mastocytosis

Clinical and pathologic manifestations of neoplastic mast cell proliferations are diverse, resulting in a relatively complex system of classification (Swerdlow et al., 2017). In the 2017 WHO revision, mastocytosis was separated out from MPN given its unique and wide spectrum of clinical and pathological presentations. Mastocytosis now encompasses three subcategories: cutaneous mastocytosis exhibiting predominantly localized involvement of the skin, systemic mastocytosis with involvement of at least one extracutaneous organ with or without skin lesions, and mast cell sarcoma. Mutations in the tyrosine kinase gene *KIT*, particularly the most common codon D816V abnormality, are strongly associated with mastocytosis. As discussed earlier, KIT is a transmembrane receptor tyrosine kinase that plays important roles in the proliferative activities essential to stem cell regeneration and the expansion of hematopoietic progeny. It is also expressed on melanocytes, germ cells, and gastrointestinal pacemaker cells (Metcalfe, 2008; Orfao et al., 2007). Activating *KIT* mutations obviate the normally regulated ligand-receptor mechanism and produce growth factor–independent cell proliferation. More important, *KIT* mutations are not specific for mastocytosis, in that they are detectable in a subset of CBF-AML (as discussed earlier), gastrointestinal stromal tumors, and a subset of melanomas (Orfao et al., 2007). The genomic distribution of *KIT* mutations is variable in these different tumors. Nevertheless, detection of an activating *KIT* D816 mutation fulfills one of the four minor diagnostic criteria for systemic mastocytosis and is thus often helpful in definitively supporting a diagnosis suspected on clinical, morphologic, or immunophenotypic grounds. The exon 17–situated D816V is the most common *KIT* mutation in mastocytosis, present in more than 90% of mastocytosis cases; this consistency presents an attractive target for molecular diagnostic methodologies amenable to the interrogation of specific sequence changes, including allele-specific PCR, restriction fragment length polymorphism-based analysis, and sequencing. The proportion of non-D816V cases is higher in cutaneous mastocytosis and mast cell leukemia, and atypical *KIT* mutations such as non-D816V codon 816 mutations or noncodon 816 mutations can be seen (Lanternier et al., 2008).

KIT-activating mutations may be amenable to targeted therapy with TKIs. However, the efficacy of TKI agents against KIT mutations is dependent on the tumor type, mutation location, and in some cases, specific amino acid changes (Ashman & Griffith, 2013; Yim et al., 2018). Whereas exon 11 mutations of *KIT* are sensitive to imatinib mesylate, the mutations in exon 9 are less sensitive and require a higher therapeutic dosage. Other mutations including *KIT* exon 13 and 17 (e.g., D816V) mutations are resistant to imatinib. The D816V mutant has alternatively shown responsiveness to the multitarget TKI midostaurin, which was approved by the FDA for the treatment of aggressive systemic mastocytosis (ASM) in adult patients, systemic mastocytosis with associated hematologic neoplasm (SM-AHN), and mast cell leukemia in 2017, thus complementing the approval of imatinib for non-D816V ASM patients in 2006 (Pardanani, 2013; Ustun et al., 2011; Vega-Ruiz et al., 2009). Molecular analysis of *KIT* mutations occurring at other locations in the gene besides D816V requires a more comprehensive approach involving sequencing of several exon regions and can be accomplished by various sequencing platforms, such as NGS, Sanger sequencing, and pyrosequencing with relatively lower analytic sensitivity seen in Sanger sequencing.

MYELOID NEOPLASMS WITH GERMLINE PREDISPOSITION

This new category was introduced in the 2017 WHO revision as it has become apparent that although most myeloid neoplasms arise sporadically, some MDS/AML cases are associated with germline mutations (inherited or de novo) and demonstrate characteristic genetic and clinical features. There are three major subtypes in this category: myeloid neoplasms with germline predisposition without a preexisting disorder or organ function, myeloid neoplasms with germline predisposition and preexisting platelet disorders, and myeloid neoplasms with germline predisposition and other organ dysfunction (Swerdlow et al., 2017). Clinically, it is important to recognize these cases, not only because a correct diagnosis is critical for the appropriate clinical management and long-term follow-up of the patient and timely evaluation of family members for counseling and planning, but also for careful donor selection in preparation of stem cell transplantation in patients with MDS/AML to avoid reintroduction of the same pathogenic mutation from a sibling donor (Furutani & Shimamura, 2017). These are a heterogeneous group of disorders with each familial syndrome showing unique genetic and clinical features (Table 78.9) (Gao et al., 2019; University of Chicago Hematopoietic Malignancies Cancer Risk, 2016). Some gene mutations such as *RUNX1*, *ETV6*, and *CEBPA* occur in both somatic and germline settings and are commonly picked up in targeted NGS panels. However, other subtypes, particularly the bone marrow failure syndromes, encompass a large number of genetic abnormalities of various types involving multiple genes, whose comprehensive detection would mandate a sufficiently large panel design (or WES). However, every technical platform has its advantages and limitations. Although WES covers much wider genetic regions than targeted NGS panels and is helpful in cases in which the latter is unrevealing, there will be poorly covered regions, and it does not cover noncoding regions. Given the sheer amount of data generated from WES, the bioinformatic analysis and annotation efforts also significantly increase with predictably increased numbers of variants of unknown significance (VUSs). Functional tests such as chromosomal breakage analysis and telomere length tests may help establish the pathogenicity of VUS variants in Fanconi anemia and telomeropathies, respectively (Furutani & Shimamura, 2017).

Although typically a heterozygous germline variant in an untreated patient would show a VAF near 50% in well-validated clinical tests, a word of caution is that VAF cannot be used as a reliable marker to differentiate between germline versus somatic variants. First, VAF around 50% can occur in somatic settings. Second, VAF values in a specific tumor sample are also influenced by other conditions such as copy number variation, LOH, allogenic stem cell transplant, and so on. For solid tumors, peripheral blood is commonly used for evaluation of germline variant. In hematologic malignancies, the gold standard sample for germline variant testing is often nonhematopoietic lineage skin fibroblasts. However, this testing process is cumbersome because it involves the invasive procedure of skin biopsy and culture of fibroblasts, which takes several weeks. Alternatively, the variant can be assessed in other sample types such as a complete remission blood sample in posttherapy AML patients, hair follicles, T lymphocytes, and buccal swabs. Testing in these samples may serve as a screening test for germline evaluation because the absence of the target variant in these samples in contrast to their presence in the diagnostic peripheral blood (PB) or bone marrow (BM) samples) is in keeping with a somatic nature of the target variant detected in the diagnostic sample and essentially excludes its germline nature. For patients showing persistence of the target variant irrespective of the VAF, the germline nature of the variant should be further evaluated and confirmed in a skin fibroblast test. One caveat is that there are rare reports of revertant somatic mosaicism in Fanconi anemia and dyskeratosis congenita, involving the *FANCA*, *FANCC*, or *TERC* genes in hematologic cells of myeloid and T- and B-cell lineages at variable degrees (Furutani & Shimamura, 2017; Gregory et al., 2001; Gross et al., 2002; Jongmans et al., 2012). Germline testing in the setting of these disorders would be best achieved with the gold standard skin fibroblast test. Germline genetic testing has profound psychosocial impacts, and the importance of multidisciplinary support and genetic counseling cannot be overstated.

TABLE 78.9

World Health Organization Classification of Myeloid Neoplasms with Germline Predisposition

Category	Genes	Pattern of Inheritance	Germline Genetic Alterations	Acquired Genetic Alterations During Leukemogenesis	Clinical Features
Myeloid Neoplasms with Germline Predisposition without a Preexisting Disorder or Organ Dysfunction					
AML with germline *CEBPA* mutation	*CEBPA*	AD	N-terminus frameshift or nonsense mutation	C-terminus missense or in-frame indel mutation on the other allele	AML with biallelic *CEBPA* mutations is associated with a more favorable prognosis
Myeloid neoplasms with germline *DDX41* mutation	*DDX41*	AD	p.D140Gfs*2 most common in whites; p.A500Cfs*9 most common in Asians	p.R525H most common	Long latency, with disease onset in older adults similar to sporadic MDS or AML
Myeloid Neoplasms with Germline Predisposition and Preexisting Platelet Disorders					
Myeloid neoplasms with germline *RUNX1* mutation	*RUNX1*	AD	Frameshift, nonsense mutations, or deletion cluster to *RUNX1* N-terminal region and less frequently C-terminal region	A second somatic *RUNX1* mutation, deletion or chromosome 21 aberration	History of thrombocytopenia of variable degree with or without bleeding tendency, development of myeloid neoplasms in the context of familial platelet disorder
Myeloid neoplasms with germline *ANKRD26* mutation	*ANKRD26*	AD	Single-nucleotide substitutions in 5′ untranslated region	Unknown	Moderate thrombocytopenia, no or mild spontaneous bleeding
Myeloid neoplasms with germline *ETV6* mutation	*ETV6*	AD	Frameshift, missense, and nonsense mutations in the DNA-binding and central domains	Unknown	Variable degree of thrombocytopenia, bleeding tendencies, some with erythroid macrocytosis but no anemia
Myeloid Neoplasms with Germline Predisposition and Other Organ Dysfunction					
Myeloid neoplasms with germline *GATA2* mutation	*GATA2*	AD	Truncating or missense mutations in the second zinc finger domain or mutations in the noncoding regulatory region	Somatic *ASXL1* mutation in 29% of patients with germline *GATA2* mutation	Monocytopenia, B/NK/dendritic cell deficiencies, atypical infections, lymphedema
Myeloid Neoplasms Associated with Inherited Bone Marrow Failure Syndromes and Telomere Biology Disorders					
Fanconi anemia	*FANCA, FANCC, FANCG, FANCD1/BRCA2*, etc	AR, XL	Null mutations, as results of frameshift, stop codon, and large deletions; missense, in-frame deletions, or C-terminus truncation mutations	Unknown; biallelic mutations may have increased risks	Progressive bone marrow failure during childhood, congenital abnormalities, increased risk of AML or MDS, solid tumors arise in adulthood
Dyskeratosis congenita	*DKC1, NOP10, NPH2, TCAB1, C16orf57, RTEL1, TERC, TERT, TINF2*	XL, AR, AD	Large and small deletions, insertions, and missense mutations throughout the coding regions	Unknown	Nail dystrophy, abnormal skin pigmentation, oral leukoplakia, pulmonary fibrosis, bone marrow failure
Telomere biology disorder	*TERT, TERC*	AD, AR (TERT)	Large and small deletions, insertions, and missense mutations throughout the coding regions	Unknown	Bone marrow failure, predisposition to AML and MDS, and a variety of solid tumors

AD, Autosomal dominant; *AML,* acute myeloid leukemia; *AR,* autosomal recessive; *indel,* insertion and/or deletion; *MDS,* myelodysplastic syndrome; XL, X-linked.
Adapted and modified from Gao J, Gong S, Chen, YH, et al: Myeloid neoplasm with germline predisposition: A 2016 update for pathologists, *Arch Pathol Lab Med* 143:3–22, 2019.

CLONAL HEMATOPOIESIS OF INDETERMINATE POTENTIAL

After the introduction of the sensitive PCR into clinical laboratories, low-level *BCL2* translocation and *BCR-ABL1* fusion were described in individuals without lymphoma or CML respectively (Biernaux et al.,1995; Limpens et al., 1995). In recent years, genome-wide association studies using single nucleotide polymorphism arrays have revealed acquired chromosomal abnormalities of aneuploidy and large segmental deletion in regions where genes involved in myeloid neoplasms are located. They were rare in persons younger than age 50 years but were observed in 2% to 3% of apparently healthy older individuals. These chromosomal mosaicisms conferred an approximately 10-fold increased risk of hematologic neoplasm development (Jacobs et al., 2012; Laurie et al., 2012). *TET2* mutations were also seen in approximately 5% of older women with age-related hematopoietic clonal skewing and normal blood counts (Busque et al., 1996). More recently, empowered by NGS technology, several large population-based studies have concordantly identified somatic mutations in genes commonly associated with myeloid neoplasms in individuals without apparent hematologic neoplasms. The most commonly involved genes are the epigenetic modifiers *DNMT3A*, *TET2*, and *ASXL1*. Similarly, the incidence of these mutations has been found to increase with age, approaching 10% to 20% between 65 to 90 years, and is rare in people younger than 40 years (Genovese et al., 2014; Jaiswal et al., 2014; Xie et al., 2014). In comparison with people without mutations, those harboring mutations showed an increased risk of subsequent development of hematologic neoplasms, at a rate of approximately 0.5% to 1% per year and a hazard ratio (HR) of approximately 11 to 13. This low progression rate is analogous to that seen

BOX 78.3

Common Features of Clonal Hematopoiesis of Indeterminate Potential

- Older age (older than 60 years)
- Only one myeloid-associated somatic mutation detected (rarely two)
- VAF ≥2%; most not exceeding 20%–30%
- Mutation seen in *DNMT3A, TET2, ASXL1, SF3B1, JAK2, TP53, SRSF2, U2AF1, CBL, BCOR, GNB1, CREBBP, CUX1, MLL2, SETD2, SETDB1, PPM1D, BCORL1*
- Does not meet diagnostic morphologic features of MDS
- Does not meet diagnostic criteria for PNH, MGUS, or MBL
- Progression rate to subsequent hematologic malignancy 0.5% to 1% per year

MDS, Myelodysplastic syndrome; *MGUS,* monoclonal gammopathy of undetermined significance; *PNH,* paroxysmal nocturnal hemoglobinuria; *VA* F Variant allele fraction.
Adapted from Steensma DP, Bejar R, Jaiswal S, et al: Clonal hematopoiesis of indeterminate potential and its distinction from myelodysplastic syndromes, *Blood* 126:9–16, 2015.

in MGUS and monoclonal B-cell lymphocytosis, with regards to progression to myeloma and CLL, respectively. The presence of mutations is also associated with increased rate of all-cause mortality (HR, 1.4) and coronary artery diseases (HR, 2.0). The latter has been shown to be related to accelerated atherosclerosis driven by endothelial inflammatory injury resulting from proinflammatory interactions between the macrophages derived from the clonal monocytes and endothelial cells (Fuster et al., 2017; Jaiswal et al., 2017). The presence of somatic mutations in individuals without significant cytopenias, morphologic dysplasia, hematologic neoplasia, or other clonal processes has been termed CHIP or age-related clonal hematopoiesis (ARCH), reflecting its premalignant nature and biological uncertainty (Shlush, 2018; Steensma et al., 2015). The presence of CHIP reflects the inability to eliminate or suppress the growth of mutated hematopoietic subclones that occur in individuals with more advanced age.

Typical CHIP mutations are characterized by the presence of a single somatic mutation, with a minimum threshold of 2% VAF (Box 78.3). The 2% cut-off was proposed to define the presence of CHIP based on the assay detection limits and clinical data from reported large population studies. The VAF of CHIP mutations commonly does not exceed 20% to 30%, but higher levels can be seen. Using more sensitive techniques, even lower levels of clonal hematopoiesis can be detected, although the clinical significance of such low-level somatic mutations is uncertain. In a study utilizing a highly sensitive NGS test with an analytical sensitivity of 0.03%, clonal hematopoiesis involving *DNMT3A* and *TET2* was seen in approximately 95% of healthy individuals in the age range of 50 to 60 years with a median VAF of 0.2%. Interestingly and importantly, these clonal mutations were present in multiple hematopoietic compartments and stable in longitudinal follow-up, highlighting the essentially ubiquitous nature of clinically silent, very low-level clonal hematopoiesis (Young et al., 2016). The emergence of more readily detectable levels of clonal hematopoiesis in the absence of overt disease results from the combined effects of cellular intrinsic and extrinsic factors, as modified by cooperative or mitigating co-mutations or genetic abnormalities and environmental stresses such as chemotherapy, inflammation, or infection. Additionally, the presence of CHIP mutations is associated with an increased risk of therapy-related myeloid neoplasms such as in patients with cancer receiving chemotherapy with expansion of a preexisting *TP53*-mutant clone (Gillis et al., 2017; Takahashi et al., 2017). In patients receiving autologous or allogeneic stem cell transplants, CHIP mutations present at the time of autologous stem cell transplant or engrafted from a donor are associated with posttransplant cytopenia (Gibson et al., 2017a, 2017b).

In patients with unexplained cytopenia(s) who do not meet the current WHO diagnostic criteria for a myeloid neoplasm, the presence of similar somatic mutations was associated with increased risk of myeloid neoplasm with an HR of 14. This condition is termed clonal cytopenia(s) of uncertain significance (CCUS) as previously discussed in the MDS section. Patients with CCUS showed similar mutational VAF and blood counts as patients with MDS, and those harboring multiple mutations or spliceosome mutations exhibited a natural history similar to lower risk MDS (Kwok et al., 2015; Malcovati et al., 2017; Steensma et al., 2015). These findings highlight the currently indistinct boundary between CCUS and MDS, and additional elucidation from further studies is needed to refine and improve the diagnostic criteria of MDS. Given the overlapping mutational landscape of CHIP, CCUS, and MDS, recognition of each entity is critical to avoid misdiagnosis of a myeloid neoplasm when not truly present or overinterpretation of persistent *DNMT3A*, *TET2*, or *ASXL1* (DTA) mutations during AML MRD monitoring (Jongen-Lavrencic et al., 2018). However, the relationships between CHIP, CCUS, and MDS warrant further investigation to more precisely define their relationships and delineate the relative risks of neoplastic progression.

MYELOID/LYMPHOID NEOPLASMS WITH EOSINOPHILIA

The trend to molecular classification of hematologic malignancies is further illustrated by the creation of a new subcategory of hematopoietic neoplasms in the 2008 WHO classification, defined almost exclusively on molecular grounds and including myeloid/lymphoid neoplasms with *PDGFRA*, *PDGFRB*, or *FGFR1* rearrangement. This category was further expanded in the 2017 WHO revision with the addition of the provisional entity myeloid/lymphoid neoplasms with *PCM1-JAK2* (Swerdlow et al., 2017). These neoplasms encompass a heterogeneous group of diseases of both myeloid and lymphoid lineages, previously existing as separate entities largely defined by morphologic, clinical, and certain cytogenetic features. A unifying feature is the formation of a fusion gene leading to deregulated activity of an aberrant tyrosine kinase and a tumor phenotype characterized by eosinophilia, although this is not invariable. In at least some cases within each group, the neoplastic cells originate from pluripotent stem cells with the potential of both myeloid and lymphoid differentiation. Therefore, these disorders can present as chronic MPNs, lymphoid neoplasms, or AML with variable frequency of occurrence. Although laboratory testing for these genetic abnormalities is accomplished mainly by FISH or conventional karyotyping, a short discussion of this entity is included here because it represents a good example of the reconfiguration of hematologic malignancies based on molecular characterization.

Rearrangement of the platelet-derived growth factor receptor α (*PDGFRA*) gene is diagnostic of a hematologic neoplasm typically characterized by chronic eosinophilic leukemia (CEL) but may in some cases present as AML or T-lymphoblastic leukemia/lymphoma (T-LBL) or both (Metzgeroth et al., 2007). Acute transformation can also occur in CEL. The presence of a *PDGFRA* rearrangement (rarely activating mutation of *PDGFRA*) thus defines this diagnostic entity at the genetic level regardless of the cellular component heterogeneity. The most common *PDGFRA* rearrangement is a karyotypically cryptic interstitial deletion at 4q12 that juxtaposes *PDGFRA* with an adjacent gene, *FIP1L1*. The resultant expression of a *FIP1L1-PDGFRA* fusion protein disrupts the autoinhibitory domain of *PDGFRA* and leads to its constitutive tyrosine kinase activity (Stover et al., 2006). An intervening gene called *CHIC2* is deleted in the 4q12 rearrangement; thus, assessment of the *CHIC2* locus by the FISH technique serves as an effective surrogate marker to identify the chromosomal microdeletion and establish the presence of a *PDGFRA* rearrangement (Pardanani et al., 2003; Fink et al., 2009; Ramchandren et al., 2013). Of note, a subset of CEL with *PDGFRA* rearrangements also exhibits abnormal mast cell expansions in the bone marrow, but the *KIT* D816V abnormality is not present in these cases. The overlapping nature of neoplastic myeloid cellular proliferations therefore underscores the comprehensive molecular approach to subclassification of these diseases. Most significantly, patients with *PDGFRA*-positive CEL are remarkably sensitive to treatment with even low doses of imatinib, highlighting the power of molecularly targeted therapy (Pardanani et al., 2003).

Myeloid/lymphoid neoplasms with platelet-derived growth factor receptor β (*PDGFRB*) gene rearrangement are conceptually similar. These neoplasms are typically characterized morphologically as CMMLs with eosinophilia, although less common variant presentations of aCML, CEL, MPN with eosinophilia, AML, and JMML are also recognized. Patients with *PDGFRB* rearranged neoplasms are also expected to benefit from treatment with imatinib (David et al., 2007; Apperley et al., 2002). A karyotypic abnormality of t(5;12)(q32;p1.23) is commonly associated with the deregulation of *PDGFRB* via creation of a chimeric *ETV6(TEL)-PDGFRB* fusion gene and protein; however, other translocation partners of *PDGFRB* have also been described. Alterations of the *PDGFRB* locus are usually detectable by conventional chromosome analysis, showing breakpoints at 5q31-33. Given the therapeutic implications of *PDGFRB* rearrangement, FISH or RT-PCR is indicated for fusion confirmation. Rare cases are FISH negative in the face of a submicroscopic *ETV6-PDGFRB* gene fusion, indicating that comprehensive detection may require a combination of molecular and cytogenetic approaches.

In contrast to myeloid/lymphoid neoplasms with rearrangements of *PDGFRA* or *PDGFRB*, patients with neoplasms overexpressing aberrant fibroblast growth factor receptor-1 (*FGFR1*) differ in certain key respects. First, the translocated gene encodes a tyrosine kinase receptor involved

in a similar but nonetheless distinct cell signaling pathway. Second, these cases are particularly associated with presentations of lymphoblastic (e.g., T-LBL) or mixed phenotype acute leukemias, MPN or AML, as well as often prominent neoplastic eosinophilia. Finally, an effective TKI therapy has yet to be established in the setting of *FGFR1* rearrangement. Cytogenetic and FISH analyses can be used to diagnose the presence of *FGFR1* gene rearrangements.

In the 2017 WHO revision, the new provisional entity of myeloid/lymphoid neoplasms with *PCM1-JAK2* was added (Swerdlow et al., 2017). This hematologic neoplasm is characterized by t(8;9)(p22;p24.1) with heterogeneous clinical presentations including CEL, PMF, and aCML, often with eosinophilia. AML, B-LBL, T-LBL have also been documented (Bain & Ahmad, 2014). *JAK2* rearrangement with other partners, specifically t(9;12)(p24.1;p13.2) resulting in *ETV6-JAK2* fusion and t(9;22)(p24.1;q11.2) resulting in *BCR-JAK2* fusion, are considered variants of this disorder. They show more heterogeneous presentations than cases with *PCM-JAK2*, with the *ETV6-JAK2* fusion more commonly presenting as B or T-LBL and less commonly as myeloid neoplasms with an uncommon association with eosinophilia, and the *BCR-JAK2* fusion more frequently presenting as myeloid neoplasms and occasionally as B-LBL. In B-LBL, cases have the features of *BCR-ABL1*-like B-LBL and are best classified as such. Studies and case reports have shown that these patients may benefit from the JAK2 inhibitor ruxolitinib (Bain & Ahmad, 2014; Roberts et al., 2014). It is worth noting that t(9;22) (p24.1;q11.2); *BCR-JAK2* should not be confused with t(9;22)(q34.1; q11.2); *BCR-ABL1* as seen in CML: although both are located on chromosome 9, the breakpoint of *JAK2* occurs at 9p24.1 whereas the *ABL1* breakpoint occurs at 9q34.1. Importantly, patients harboring *BCR-JAK2* do not respond to imatinib like patients with CML, but they are candidates for JAK2 inhibitors (He et al., 2016a).

SELECTED REFERENCES

Baccarani M, Deininger MW, Rosti G, et al.: European LeukemiaNet recommendations for the management of chronic myeloid leukemia, *Blood* 122:872–884, 2013.

Recent update of molecular monitoring and therapy guidelines in patients with chronic myeloid leukemia. Also, specific recommendations are made for patients in the accelerated and blastic phases and for allogeneic stem cell transplantation.

Baldus CD, Mrózek K, Marcucci G, et al.: Clinical outcome of de novo acute myeloid leukaemia patients with normal cytogenetics is affected by molecular genetic alterations: a concise review, *Br J Haematol* 137(5):387–400, 2007.

Good review of molecular genetics and clinical significance of normal karyotype acute myeloid leukemia.

Breen KA, Grimwade D, Hunt BJ: The pathogenesis and management of the coagulopathy of acute promyelocytic leukaemia, *Br J Haematol* 156:24–36, 2012.

Excellent review describing the underlying possible mechanisms of coagulopathy in patients with acute promyelocytic leukemia.

de Leval L, Hasserjian RP: Diffuse large B-cell lymphomas and Burkitt lymphoma, *Hematol Oncol Clin N Am* 23:791–827, 2009.

Excellent review of aggressive lymphomas.

Dohner H, Estey EH, Amadori S, et al.: Diagnosis and management of acute myeloid leukemia in adults: recommendations from an international expert panel, on behalf of the European LeukemiaNet, *Blood* 115:453–474, 2010.

Excellent review that emphasizes the new standardized reporting system for correlation of cytogenetic and molecular genetic data with clinical data in acute myeloid leukemia.

Downing JR, Wilson RK, Zhang J, et al.: The pediatric cancer genome Project, *Nat Genet* 44:619–622, 2012.

An overview of the international effort to identify somatic mutations that drive pediatric cancers through global cancer genome sequencing.

Grimwade D, Jovanovic JV, Hills RK, et al.: Prospective minimal residual disease monitoring to predict relapse of acute promyelocytic leukemia and to direct pre-emptive arsenic trioxide therapy, *J Clin Oncol* 27(22):3650–3658, 2009.

This study shows compelling data for PCR monitoring of minimal residual disease in acute promyelocytic leukemia and illustrates the successful use of therapeutic intervention for molecular relapse.

Hochhaus A, Druker B, Sawyers C, et al.: Favorable long-term follow-up results over 6 years for response, survival, and safety with imatinib mesylate therapy in chronic-phase chronic myeloid leukemia after failure of interferon-α treatment, *Blood* 111:1039–1043, 2008.

Results of a large study showing durable efficacy of imatinib in the treatment of chronic phase chronic myeloid leukemia.

Ishikawa Y, Kiyoi H, Tsujimura A, et al.: Comprehensive analysis of cooperative gene mutations between class I and class II in de novo acute myeloid leukemia, *Eur J Haematol* 83(2):90–98, 2009.

Overview of the cooperative nature of gene mutations in the pathogenesis of acute myeloid leukemia.

Jones D, Kamel-Reid S, Bahler D, et al.: Laboratory practice guidelines for detecting and reporting BCR-ABL drug resistance mutations in chronic myelogenous leukemia and acute lymphoblastic leukemia: a report of the Association for Molecular Pathology, *J Mol Diagn* 11(4–11), 2009.

Useful consensus document for the laboratory detection of BCR-ABL1 drug resistance mutations.

Kantarjian HM, Larson RA, Cortes JE, et al.: Current practices in the management of chronic myeloid leukemia, *Clin Lymphoma Myeloma Leuk* 13:48–54, 2013.

Update on the current theme of chronic myeloid leukemia therapy.

Langerak AW, Groenen PJTA, Bruggemann M, et al.: EuroClonality/BIOMED-2 guidelines for interpretation and reporting of Ig/TCR clonality testing in suspected lymphoproliferations, *Leukemia* 26:2159–2171, 2012.

Updated review of PCR-based approaches for determination of B and T cell clonality in lymphoid proliferations.

Loghavi S, Zuo Z, Ravandi F, et al.: Clinical features of de novo acute myeloid leukemia with concurrent DNMT3A, FLT3, and NPM1 mutations, *J Hematol Oncol* 7:74, 2014.

Excellent review of acute myeloid leukemia with the referred mutations.

Malcovati L, Hellström-Lindberg E, Bowen D, et al.: Diagnosis and treatment of primary myelodysplastic syndromes in adults: recommendations from the European LeukemiaNet, *Blood* 122:2943–2964, 2013.

Excellent review of myelodysplastic syndrome and therapy consideration.

Pui CH, Mullighan CG, Evans WE, et al.: Pediatric acute lymphoblastic leukemia: where are we going and how do we get there? *Blood* 120:1165–1174, 2012.

Excellent review and update on prognostic factors in the management of pediatric acute lymphoblastic leukemia.

Ramchandren R, Jazaerly T, Gabali AM: Molecular diagnosis of hematopoietic neoplasms, *Clin Lab Med* 33:817–833, 2013.

Reviews the role of molecular testing in hematologic malignancy management and discusses the utility, advantages, and disadvantages of molecular tests.

Solh M, Yohe S, Weisdorf D, et al.: Core-binding factor acute myeloid leukemia: heterogeneity, monitoring, and therapy, *Am J Hematol* 89:1121–1131, 2014.

Updated and comprehensive review of core binding factor acute myeloid leukemia, with emphasis on the histopathologic, genetic, molecular, and clinical heterogeneity.

Van Dongen JJM, Langerak AW, Bruggemann M, et al.: Design and standardization of PCR primers and protocols for detection of clonal immunoglobulin and T-cell receptor gene recombinations in suspect lymphoproliferations: report of the BIOMED-2 Concerted Action BMH4-CT98-3936, *Leukemia* 17:2257–2317, 2003.

Landmark publication detailing very comprehensive assessment of polymerase chain reaction–based techniques versus Southern blot methods to detect clonal B- and T-cell populations in lymphoid proliferations.

Access the complete reference list online at Elsevier eBooks for Practicing Clinicians.

REFERENCES

Abdel-Wahab O, Adli M, LaFave LM, et al.: ASXL1 mutations promote myeloid transformation through loss of PRC2-mediated gene repression, *Canc Cell* 22(2):180–193, 2012.

Abramowicz A, Gos M: [Neurofibromin - protein structure and cellular functions in the context of neurofibromatosis type I pathogenesis], *Postepy Hig Med Dosw* 69:1331–1348, 2015.

Afrin S, Zhang CRC, Meyer C, et al.: Targeted next-generation sequencing for detecting MLL gene fusions in leukemia, *Mol Cancer Res* 16(2):279–285, 2018.

Ahn IE, Underbayev C, Albitar A, et al.: Clonal evolution leading to ibrutinib resistance in chronic lymphocytic leukemia, *Blood* 129(11):1469–1479, 2017.

Akasaka T, Akasaka H, Yonetani N, et al.: Refinement of the BCL2/immunoglobulin heavy chain fusion gene in t(14;18) (q32;q21) by polymerase chain reaction amplification for long targets, *Genes Chromosomes Cancer* 21:17–29, 1998.

Akasaka T, Akasaka H, Yonetani N, et al.: Refinement of the BCL2/immunoglobulin heavy chain fusion gene in t(14;18)(q32;q21) by polymerase chain reaction amplification for long targets, *Genes Chromosomes Cancer* 21(1):17–29, 1998.

Aladily TN, Medeiros LJ, Amin MB, et al.: Anaplastic large cell lymphoma associated with breast implants: a report of 13 cases, *Am J Surg Pathol* 36(7):1000–1008, 2012.

Alamyar E, Duroux P, Lefranc MP, Giudicelli V: IMGT((R)) tools for the nucleotide analysis of immunoglobulin (IG) and T cell receptor (TR) V-(D)-J repertoires, polymorphisms, and IG mutations: IMGT/V-QUEST and IMGT/HighV-QUEST for NGS, *Methods Mol Biol* 882:569–604, 2012.

Albinger-Hegyi A, Hochreutener B, Abdou M-T, et al.: High frequency of t(14;18)-translocation breakpoints outside of major breakpoint and minor cluster regions in follicular lymphomas. Improved polymerase chain reaction protocols for their detection, *Am J Pathol* 160:823–832, 2002.

Albinger-Hegyi A, Hochreutener B, Abdou MT, et al.: High frequency of t(14;18)-translocation breakpoints outside of major breakpoint and minor cluster regions in follicular lymphomas: improved polymerase chain reaction protocols for their detection, *Am J Pathol* 160(3):823–832, 2002.

Alizadeh AA, Eisen MB, Davis RE, et al.: Distinct types of diffuse large B-cell lymphoma identified by gene expression profiling, *Nature* 403:503–511, 2000.

Al-Kali A, Quintas-Cardama A, Luthra R, et al.: Prognostic impact of RAS mutations in patients with myelodysplastic syndrome, *Am J Hematol* 88(5):365–369, 2013.

Amin NA, Malek SN: Gene mutations in chronic lymphocytic leukemia, *Semin Oncol* 43(2):215–221, 2016.

Andersson AK, Miller DW, Lynch JA, et al.: IDH1 and IDH2 mutations in pediatric acute leukemia, *Leukemia* 25(10):1570–1577, 2011.

Andersson EI, Tanahashi T, Sekiguchi N, et al.: High incidence of activating STAT5B mutations in CD4-positive T-cell large granular lymphocyte leukemia, *Blood* 128(20):2465–2468, 2016.

Angelova EA, Li S, Wang W, et al.: IgM plasma cell myeloma in the era of novel therapy: a clinicopathological study of 17 cases, *Hum Pathol* 84:321–334, 2019.

Aoki Y, Matsubara Y: Ras/MAPK syndromes and childhood hemato-oncological diseases, *Int J Hematol* 97(1):30–36, 2013.

Appelbaum FR, Kopecky KJ, Tallman MS, et al.: The clinical spectrum of adult acute myeloid leukaemia associated with core binding factor translocations, *Br J Haematol* 135(2):165–173, 2006.

Apperley JF, Gardembas M, Melo JV, et al.: Response to imatinib mesylate in patients with chronic myeloproliferative diseases with rearrangements of the platelet-derived growth factor receptor beta, *N Engl J Med* 347(7):481–487, 2002.

Arcila ME, Yu W, Syed M, et al.: Establishment of immunoglobulin heavy (IGH) chain clonality testing by next-generation sequencing for routine characterization of B-cell and plasma cell neoplasms, *J Mol Diagn* 21(2):330–342, 2019.

Armstrong SA: Look AT: molecular genetics of acute lymphoblastic leukemia, *J Clin Oncol* 23(26):6306–6315, 2005.

Ashman LK, Griffith R: Therapeutic targeting of c-KIT in cancer, *Expert Opin Investig Drugs* 22(1):103–115, 2013.

Aster JC, Longtine JA: Detection of BCL2 rearrangements in follicular lymphoma, *Am J Pathol* 160:759–763, 2002.

Baccarani M, Castagnetti F, Gugliotta G, et al.: The proportion of different BCR-ABL1 transcript types in chronic myeloid leukemia, *An international overview*, *Leukemia* 33(5):1173–1183, 2019a.

Baccarani M, Rosti G, Soverini S: Chronic myeloid leukemia: the concepts of resistance and persistence and the relationship with the BCR-ABL1 transcript type, *Leukemia* 33(10):2358–2364, 2019b.

Bacher U, Haferlach C, Kern W, et al.: Prognostic relevance of FLT3-TKD mutations in AML: the combination matters—an analysis of 3082 patients, *Blood* 111(5):2527–2537, 2008.

Badalian-Very G, Vergilio JA, Degar BA, et al.: Recurrent BRAF mutations in Langerhans cell histiocytosis, *Blood* 116(11):1919–1923, 2010.

Bain BJ, Ahmad S: Should myeloid and lymphoid neoplasms with PCM1-JAK2 and other rearrangements of JAK2 be recognized as specific entities? *Br J Haematol* 166(6):809–817, 2014.

Baldini L, Goldaniga M, Guffanti A, et al.: Immunoglobulin M monoclonal gammopathies of undetermined significance and indolent Waldenstrom's macroglobulinemia recognize the same determinants of evolution into symptomatic lymphoid disorders: proposal for a common prognostic scoring system, *J Clin Oncol* 23(21):4662–4668, 2005.

Baldus CD, Thiede C, Soucek S, et al.: BAALC expression and FLT3 internal tandem duplication mutations in acute myeloid leukemia patients with normal cytogenetics: prognostic implications, *J Clin Oncol* 24(5):790–797, 2006.

Baliakas P, Agathangelidis A, Hadzidimitriou A, et al.: Not all IGHV3-21 chronic lymphocytic leukemias are equal: prognostic considerations, *Blood* 125(5):856–859, 2015a.

Baliakas P, Hadzidimitriou A, Sutton LA, et al.: Recurrent mutations refine prognosis in chronic lymphocytic leukemia, *Leukemia* 29(2):329–336, 2015b.

Ballester LY, Loghavi S, Kanagal-Shamanna R, et al.: Clinical validation of a CXCR4 mutation screening assay for Waldenstrom macroglobulinemia, *Clin Lymphoma Myeloma Leuk* 16(7):395–403, 2016. e391.

Balusu R, Fiskus W, Rao R, et al.: Targeting levels or oligomerization of nucleophosmin 1 induces differentiation and loss of survival of human AML cells with mutant NPM1, *Blood* 118:3096–3106, 2011.

Barrio S, Munawar U, Zhu YX, et al.: IKZF1/3 and CRL4-CRBN E3 ubiquitin ligase mutations and IMiD resistance in multiple myeloma, *Haematologica* 105(5):e237–e241, 2019.

Bassarova A, Troen G, Spetalen S, et al.: Lymphoplasmacytic lymphoma and marginal zone lymphoma in the bone marrow: Paratrabecular involvement as an important distinguishing feature, *Am J Clin Pathol* 143(6):797–806, 2015.

Bassing CH, Swat W, Alt FW: The mechanism and regulation of chromosomal V(D)J recombination, *Cell* 109, 2002. S45–S55.

Baxter EJ, Scott LM, Campbell PJ, et al.: Acquired mutation of the tyrosine kinase JAK2 in human myeloproliferative disorders, *Lancet* 365:1054–1061, 2005.

Bechtold AG, Patel G, Hochhaus G, Scheuer DA: Chronic blockade of hindbrain glucocorticoid receptors reduces blood pressure responses to novel stress and attenuates adaptation to repeated stress, *Am J Physiol Regul Integr Comp Physiol* 296(5):R1445–1454, 2009.

Beer PA, Campbell PJ, Scott LM, et al.: MPL mutations in myeloproliferative disorders: analysis of the PT-1 cohort, *Blood* 112:141–149, 2008.

Bejar R, Stevenson K, Abdel-Wahab O, et al.: Clinical effect of point mutations in myelodysplastic syndromes, *N Engl J Med* 364(26):2496–2506, 2011.

Belaud-Rotureau MA, Parrens M, Dubus P, et al.: A comparative analysis of FISH, RT-PCR, PCR, and immunohistochemistry for the diagnosis of mantle cell lymphomas, *Mod Pathol* 15:517–525, 2002.

Bernard T, Gale RE, Evans JP, Linch DC: Mutations of the granulocyte-colony stimulating factor receptor in patients with severe congenital neutropenia are not required for transformation to acute myeloid leukaemia and may be a bystander phenomenon, *Br J Haematol* 101(1):141–149, 1998.

Berry DA, Zhou S, Higley H, et al.: Association of minimal residual disease with clinical outcome in pediatric and adult acute lymphoblastic leukemia: a meta-analysis, *JAMA Oncol* 3(7), 2017. e170580.

Bertoni F, Conconi A, Capella C, et al.: Molecular follow-up in gastric mucosa-associated lymphoid tissue lymphomas: early analysis of the LY03 cooperative trial, *Blood* 99:2541–2544, 2002.

Beylot-Barry M, Lamant L, Vergier B, et al.: Detection of t(2;5)(p23;q35) translocation by reverse transcriptase polymerase chain reaction and in situ hybridization in CD30-positive primary cutaneous lymphoma and lymphomatoid papulosis, *Am J Pathol* 149(2):483–492, 1996.

Bhatt VR, Akhtari M, Bociek RG, et al.: Allogeneic stem cell transplantation for Philadelphia chromosome-positive acute myeloid leukemia, *J Natl Compr Canc Netw* 12(7):963–968, 2014.

Biernaux C, Loos M, Sels A, et al.: Detection of major bcr-abl gene expression at a very low level in blood cells of some healthy individuals, *Blood* 86(8):3118–3122, 1995.

Blachly JS, Ruppert AS, Zhao W, et al.: Immunoglobulin transcript sequence and somatic hypermutation computation from unselected NA-seq reads in chronic lymphocytic leukemia, *Proc Natl Acad Sci U S A* 112(14):4322–4327, 2015.

Blombery PA, Wall M, Seymour JF: The molecular pathogenesis of B-cell non-Hodgkin lymphoma, *Eur J Haematol* 95(4):280–293, 2015.

Bodor C, Grossmann V, Popov N, et al.: EZH2 mutations are frequent and represent an early event in follicular lymphoma, *Blood* 122(18):3165–3168, 2013.

Bollag G, Clapp DW, Shih S, et al.: Loss of NF1 results in activation of the Ras signaling pathway and leads to aberrant growth in haematopoietic cells, *Nat Genet* 12(2):144–148, 1996.

Bonzheim I, Giese S, Deuter C, et al.: High frequency of MYD88 mutations in vitreoretinal B-cell lymphoma: a valuable tool to improve diagnostic yield of vitreous aspirates, *Blood* 126(1):76–79, 2015.

Borden KL, Culjkovic B: Perspectives in PML: a unifying framework for PML function, *Front Biosci* 14:497–509, 2009.

Borowitz MJ, Devidas M, Hunger SP, et al.: Clinical significance of minimal residual disease in childhood acute lymphoblastic leukemia and its relationship to other prognostic factors: a Children's Oncology Group study, *Blood* 111(12):5477–5485, 2008.

Borowitz MJ, Wood BL, Devidas M, et al.: Prognostic significance of minimal residual disease in high risk B-ALL: a report from Children's Oncology Group study AALL0232, *Blood* 126(8):964–971, 2015.

Boudry-Labis E, Roche-Lestienne C, Nibourel O, et al.: Neurofibromatosis-1 gene deletions and mutations in de novo adult acute myeloid leukemia, *Am J Hematol* 88(4):306–311, 2013.

Boultwood J, Dolatshad H, Varanasi SS, et al.: The role of splicing factor mutations in the pathogenesis of the myelodysplastic syndromes, *Adv Biol Regul* 54:153–161, 2014.

Bouska A, Bi C, Lone W, et al.: Adult high-grade B-cell lymphoma with Burkitt lymphoma signature: genomic features and potential therapeutic targets, *Blood* 130(16):1819–1831, 2017.

Brassesco MS: Leukemia/lymphoma-associated gene fusions in normal individuals, *Genet Mol Res* 7(3):782–790, 2008.

Breccia M, Biondo F, Latagliata R, et al.: Identification of risk factors in atypical chronic myeloid leukemia, *Haematologica* 91(11):1566–1568, 2006.

Broeker PL, Super HG, Thirman MJ, et al.: Distribution of 11q23 breakpoints within the MLL breakpoint cluster region in de novo acute leukemia and in treatment-related acute myeloid leukemia: correlation with scaffold attachment regions and topoisomerase II consensus binding sites, *Blood* 87(5):1912–1922, 1996.

Brown NJ, Ramalho M, Pedersen EW, et al.: PML nuclear bodies in the pathogenesis of acute promyelocytic leukemia: active players or innocent bystanders? *Front Biosci* 14:1684–1707, 2009.

Brown NA, Betz BL, Weigelin HC, et al.: Evaluation of allele-specific PCR and immunohistochemistry for the detection of BRAF V600E mutations in hairy cell leukemia, *Am J Clin Pathol* 143(1):89–99, 2015.

Bruggemann M, Kotrova M, Knecht H, et al.: Standardized next-generation sequencing of immunoglobulin and T-cell receptor gene recombinations for MRD marker identification in acute lymphoblastic leukaemia; a EuroClonality-NGS validation study, *Leukemia* 33(9):2241–2253, 2019.

Bruggemann M, Schrauder A, Raff T, et al.: Standardized MRD quantification in European ALL trials: proceedings of the second international Symposium on MRD assessment in Kiel, Germany, 18-20 September 2008, *Leukemia* 24(3):521–535, 2010.

Bruggemann M, White H, Gaulard P, et al.: Powerful strategy for polymerase chain reaction-based clonality assessment in T-cell malignancies Report of the BIOMED-2 Concerted Action BHM4 CT98-3936, *Leukemia* 21(2):215–221, 2007.

Busque L, Mio R, Mattioli J, et al.: Nonrandom X-inactivation patterns in normal females: lyonization ratios vary with age, *Blood* 88(1):59–65, 1996.

Cairoli R, Beghini A, Grillo G, et al.: Prognostic impact of c-KIT mutations in core binding factor leukemias: an Italian retrospective study, *Blood* 107(9):3463–3468, 2006.

Calis JJ, Rosenberg BR: Characterizing immune repertoires by high throughput sequencing: strategies and applications, *Trends Immunol* 35(12):581–590, 2014.

Cancer Genome Atlas Research Network, Ley TJ, Miller C, et al.: Genomic and epigenomic landscapes of adult de novo acute myeloid leukemia, *N Engl J Med* 368(22):2059–2074, 2013.

Cascione L, Rinaldi A, Bruscaggin A, et al.: Novel insights into the genetics and epigenetics of MALT lymphoma unveiled by next generation sequencing analyses, *Haematologica* 104(12), 2019. e558–e561.

Casellas R, Basu U, Yewdell WT, et al.: Mutations, kataegis and translocations in B cells: understanding AID promiscuous activity, *Nat Rev Immunol* 16(3):164–176, 2016.

Castillo JJ, Ghobrial IM, Treon SP: Biology, prognosis, and therapy of Waldenstrom macroglobulinemia, *Cancer Treat Res* 165:177–195, 2015.

Castillo JJ, Xu L, Gustine JN, et al.: CXCR4 mutation subtypes impact response and survival outcomes in patients with Waldenstrom macroglobulinaemia treated with ibrutinib, *Br J Haematol* 187(3):356–363, 2019.

Cataldo KA, Jalal SM, Law ME, et al.: Detection of t(2;5) in anaplastic large cell lymphoma: comparison of immunohistochemical studies, FISH, and RT-PCR in paraffin-embedded tissue, *Am J Surg Pathol* 23(11):1386–1392, 1999.

Caye A, Strullu M, Guidez F, et al.: Juvenile myelomonocytic leukemia displays mutations in components of the RAS pathway and the PRC2 network, *Nat Genet* 47(11):1334–1340, 2015.

Chambon P: A decade of molecular biology of retinoic acid receptors, *FASEB J* 10:940–954, 1996.

Chan RJ, Feng GS: PTPN11 is the first identified proto-oncogene that encodes a tyrosine phosphatase, *Blood* 109(3):862–867, 2007.

Chedin F: The DNMT3 family of mammalian de novo DNA methyltransferases, *Prog Mol Biol Transl Sci* 101:255–285, 2011.

Chen W, Rassidakis GZ, Medeiros LJ: Nucleophosmin gene mutations in acute myeloid leukemia, *Arch Pathol Lab Med* 130(11):1687–1692, 2006.

Chen W, Drakos E, Grammatikakis I, et al.: mTOR signaling is activated by FLT3 kinase and promotes survival of FLT3-mutated acute myeloid leukemia cells, *Mol Cancer* 9:292, 2010.

Cheung KJ, Johnson NA, Affleck JG, et al.: Acquired TNFRSF14 mutations in follicular lymphoma are associated with worse prognosis, *Cancer Res* 70(22):9166–9174, 2010.

Cheung KJ, Delaney A, Ben-Neriah S, et al.: High resolution analysis of follicular lymphoma genomes reveals somatic recurrent sites of copy-neutral loss of heterozygosity and copy number alterations that target single genes, *Genes Chromosomes Cancer* 49(8):669–681, 2010.

Chiarle R, Voena C, Ambrogio C, et al.: The anaplastic lymphoma kinase in the pathogenesis of cancer, *Nat Rev Cancer* 8:11–23, 2008.

Chibbar R, Leung K, McCormick S, et al.: bcl-1 gene rearrangements in mantle cell lymphoma: a comprehensive analysis of 118 cases, including B-5-fixed tissue, by polymerase chain reaction and Southern transfer analysis, *Mod Pathol* 11(11):1089–1097, 1998.

Chong LC, Ben-Neriah S, Slack GW, et al.: High-resolution architecture and partner genes of MYC rearrangements in lymphoma with DLBCL morphology, *Blood Adv* 2(20):2755–2765, 2018.

Chotirat S, Thongnoppakhun W, Wanachiwanawin W: Auewarakul CU: acquired somatic mutations of isocitrate dehydrogenases 1 and 2 (IDH1 and IDH2) in preleukemic disorders, *Blood Cells Mol Dis* 54(3):286–291, 2015.

Chowdhury T, Brady HJ: Insights from clinical studies into the role of the MLL gene in infant and childhood leukemia, *Blood Cells Mol Dis* 40(2):192–199, 2008.

Churchman ML, Qian M, Te Kronnie G, et al.: Germline genetic IKZF1 variation and predisposition to childhood acute lymphoblastic leukemia, *Canc Cell* 33(5):937–948, 2018. e938.

Ciboddo M, Mullally A: JAK2 (and other genes) be nimble with MPN diagnosis, prognosis, and therapy, *Hematology Am Soc Hematol Educ Program*(1)110–117, 2018.

Clavio M, Ghiso A, Ghiggi C, et al.: Seventeen years of experience with ATRAATRAATRA-based therapy for acute promyelocytic leukaemia: long-term follow-up of patients treated at S, *Martino Hospital*, *Genoa*, *Oncol Rep* 21(4):1045–1052, 2009.

Clot G, Jares P, Gine E, et al.: A gene signature that distinguishes conventional and leukemic nonnodal mantle cell lymphoma helps predict outcome, *Blood* 132(4):413–422, 2018.

Collins SJ: Retinoic acid receptors, hematopoiesis and leukemogenesis, *Curr Opin Hematol* 15(4):346–351, 2008.

Conter V, Bartram CR, Valsecchi MG, et al.: Molecular response to treatment redefines all prognostic factors in children and adolescents with B-cell precursor acute lymphoblastic leukemia: results in 3184 patients of the AIEOP-BFM ALL 2000 study, *Blood* 115(16):3206–3214, 2010.

Coppe A, Andersson EI, Binatti A, et al.: Genomic landscape characterization of large granular lymphocyte leukemia with a systems genetics approach, *Leukemia* 31(5):1243–1246, 2017.

Corces-Zimmerman MR, Hong WJ, Weissman IL, et al.: Preleukemic mutations in human acute myeloid leukemia affect epigenetic regulators and persist in remission, *Proc Natl Acad Sci U S A* 111(7):2548–2553, 2014.

Cordua S, Kjaer L, Skov V, et al.: Prevalence and phenotypes of JAK2 V617F and calreticulin mutations in a Danish general population, *Blood* 134(5):469–479, 2019.

Cortes JE, Kantarjian H, Shah NP, et al.: Ponatinib in refractory Philadelphia chromosome-positive leukemias, *N Engl J Med* 367(22):2075–2088, 2012.

Cortes JE, Kim DW, Pinilla-Ibarz J, et al.: Ponatinib efficacy and safety in Philadelphia chromosome-positive leukemia: final 5-year results of the phase 2 PACE trial, *Blood* 132(4):393–404, 2018.

Cory S, Adams JM: The Bcl2 family: regulators of the cellular life-or-death switch, *Nat Rev Cancer* 2(9):647–656, 2002.

Craddock CF: We do still transplant CML, don't we?, *Hematology Am Soc Hematol Educ Program* (1)177–184, 2018.

Crassini K, Stevenson WS, Mulligan SP, Best OG: Molecular pathogenesis of chronic lymphocytic leukaemia, *Br J Haematol* 186(5):668–684, 2019.

Cross NC, White HE, Ernst T, et al.: Development and evaluation of a secondary reference panel for BCR-ABL1 quantification on the International Scale, *Leukemia* 30(9):1844–1852, 2016.

Cushman-Vokoun AM, Connealy S, Greiner TC: Assay design affects the interpretation of T-cell receptor gamma gene rearrangements: comparison of the performance of a one-tube assay with the BIOMED-2-based TCRG gene clonality assay, *J Mol Diagn* 12(6):787–796, 2010.

Daly S, Conneally E, Langabeer SE: Identification of MPL W515L/K mutations in patients with primary myelofibrosis and essential thrombocythaemia by allele-specific polymerase chain reaction, *Acta Haematol* 121(4):221–222, 2009.

Damle RN, Wasil T, Fais F, et al.: Ig V gene mutation status and CD38 expression as novel prognostic indicators in chronic lymphocytic leukemia, *Blood* 94(6):1840–1847, 1999.

David M, Cross NCP, Burgstaller S, et al.: Durable responses to imatinib in patients with PDGFRB fusion gene-positive and BCR-ABL-negative chronic myeloproliferative disorders, *Blood* 109:61–64, 2007.

Davis RE, Ngo VN, Lenz G, et al.: Chronic active B-cell-receptor signalling in diffuse large B-cell lymphoma, *Nature* 463(7277):88–92, 2010.

De Paepe P, Baens M, Van Krieken H, et al.: ALK activation by the CLTC-ALK fusion is a recurrent event in large B-cell lymphoma, *Blood* 102:2638–2641, 2003.

Deininger MW, Goldman JM, Melo JV: The molecular biology of chronic myeloid leukemia, *Blood* 96(10):3343–3356, 2000.

Del Giudice I, Rossi D, Chiaretti S, et al.: NOTCH1 mutations in +12 chronic lymphocytic leukemia (CLL) confer an unfavorable prognosis, induce a distinctive transcriptional profiling and refine the intermediate prognosis of +12 CLL, *Haematologica* 97(3):437–441, 2012.

Del Giudice I, Raponi S, Della Starza I, et al.: Minimal residual disease in chronic lymphocytic leukemia: a new goal? *Front Oncol* 9:689, 2019.

Di Noia JM, Neuberger MS: Molecular mechanisms of antibody somatic hypermutation, *Annu Rev Biochem* 76:1–22, 2007.

Dicker F, Herholz H, Schnittger S, et al.: The detection of TP53 mutations in chronic lymphocytic leukemia independently predicts rapid disease progression and is highly correlated with a complex aberrant karyotype, *Leukemia* 23:117–124, 2009.

Ding J, Komatsu H, Wakita A, et al.: Familial essential thrombocythemia associated with a dominant-positive activating mutation of the c-MPL gene, which encodes for the receptor for thrombopoietin, *Blood* 103(11):4198–4200, 2004.

Dobay MP, Lemonnier F, Missiaglia E, et al.: Integrative clinicopathological and molecular analyses of angioimmunoblastic T-cell lymphoma and other nodal lymphomas of follicular helper T-cell origin, *Haematologica* 102(4), 2017. e148–e151.

Dohner H, Estey E, Grimwade D, et al.: Diagnosis and management of AML in adults: 2017 ELN recommendations from an international expert panel, *Blood* 129(4):424–447, 2017.

Dohner H, Stilgenbauer S, Benner A, et al.: Genomic aberrations and survival in chronic lymphocytic leukemia, *N Engl J Med* 343(26):1910–1916, 2000.

Dombret H, Preudhomme C, Boissel N: Core binding factor acute myeloid leukemia (CBF-AML): is high-dose Ara-C (HDAC) consolidation as effective as you think? *Curr Opin Hematol* 16(2):92–97, 2009.

Domenech E, Gomez-Lopez G, Gzlez-Pena D, et al.: New mutations in chronic lymphocytic leukemia identified by target enrichment and deep sequencing, *PloS One* 7(6), 2012. e38158.

Dorrance AM, Liu S, Yuan W, et al.: Mll partial tandem duplication induces aberrant Hox expression in vivo via specific epigenetic alterations, *J Clin Invest* 116(10):2707–2716, 2006.

Downing JR: The AML1-ETO chimaeric transcription factor in acute myeloid leukaemia: biology and clinical significance, *Br J Haematol* 106:296–308, 1999.

Drandi D, Genuardi E, Dogliotti I, et al.: Highly sensitive MYD88(L265P) mutation detection by droplet digital polymerase chain reaction in Waldenstrom macroglobulinemia, *Haematologica* 103(6):1029–1037, 2018.

Druker BJ, Talpaz M, Resta DJ, et al.: Efficacy and safety of a specific inhibitor of the BCR-ABL tyrosine kinase in chronic myeloid leukemia, *N Engl J Med* 344:1031–1037, 2001.

Druker BJ, Guilhot F, O'Brien SG, et al.: Five-year follow-up of patients receiving imatinib for chronic myeloid leukemia, *N Engl J Med* 355(23):2408–2417, 2006.

Du MQ: MALT lymphoma: recent advances in aetiology and molecular genetics, *J Clin Exp Hematop* 47(2):31–42, 2007.

Du MQ: MALT lymphoma: many roads lead to nuclear factor-kappab activation, *Histopathology* 58(1):26–38, 2011.

Dufour A, Schneider F, Hoster E, et al.: Monoallelic CEBPA mutations in normal karyotype acute myeloid leukemia: independent favorable prognostic factor within NPM1 mutated patients, *Ann Hematol* 91:1051–1063, 2012.

Dunbar AJ, Gondek LP, O'Keefe CL, et al.: 250K single nucleotide polymorphism array karyotyping identifies acquired uniparental disomy and homozygous mutations, including novel missense substitutions of c-Cbl, in myeloid malignancies, *Cancer Res* 68(24):10349–10357, 2008.

Dunleavy K, Little RF, Wilson WH: Update on Burkitt lymphoma, *Hematol Oncol Clin North Am* 30(6):1333–1343, 2016.

Duployez N, Marceau-Renaut A, Boissel N, et al.: Comprehensive mutational profiling of core binding factor acute myeloid leukemia, *Blood* 127(20):2451–2459, 2016.

Dutta AK, Hewett DR, Fink JL, et al.: Cutting edge genomics reveal new insights into tumour development, disease progression and therapeutic impacts in multiple myeloma, *Br J Haematol* 178(2):196–208, 2017.

Duyster J, Bai RY, Morris SW: Translocations involving anaplastic lymphoma kinase (ALK), *Oncogene* 20(40):5623–5637, 2001.

Dyck J, Maul GG, Miller WH, et al.: A novel macromolecular structure is a target of the promyelocytic-retinoic acid receptor oncoprotein, *Cell* 76:333–343, 1994.

Einerson RR, Kurtin PJ, Dayharsh GA, et al.: FISH is superior to PCR in detecting t(14;18)(q32;q21)-IgH/bcl-2 in follicular lymphoma using paraffin-embedded tissue samples, *Am J Clin Pathol* 124(3):421–429, 2005.

Elena C, Galli A, Such E, et al.: Integrating clinical features and genetic lesions in the risk assessment of patients with chronic myelomonocytic leukemia, *Blood* 128(10):1408–1417, 2016.

Elf S, Abdelfattah NS, Baral AJ, et al.: Defining the requirements for the pathogenic interaction between mutant calreticulin and MPL in MPN, *Blood* 131(7):782–786, 2018.

Elf S, Abdelfattah NS, Chen E, et al.: Mutant calreticulin requires both its mutant C-terminus and the thrombopoietin receptor for oncogenic transformation, *Cancer Discov* 6(4):368–381, 2016.

Ennishi D, Jiang A, Boyle M, et al.: Double-hit gene expression signature defines a distinct subgroup of germinal center B-cell-like diffuse large B-cell lymphoma, *J Clin Oncol* 37(3):190–201, 2019.

Ennishi D, Mottok A, Ben-Neriah S, et al.: Genetic profiling of MYC and BCL2 in diffuse large B-cell lymphoma determines cell-of-origin-specific clinical impact, *Blood* 129(20):2760–2770, 2017.

Ernst P, Fisher JK, Avery W, et al.: Definitive hematopoiesis requires the mixed-lineage leukemia gene, *Dev Cell* 6(3):437–443, 2004.

Ernst T, La Rosee P, Muller MC, Hochhaus A: BCR-ABL mutations in chronic myeloid leukemia, *Hematol Oncol Clin North Am* 25(5):997–1008, 2011. v–vi.

Evans PA, Pott C, Groenen PJ, et al.: Significantly improved PCR-based clonality testing in B-cell malignancies by use of multiple immunoglobulin gene targets, *Report of the BIOMED-2 Concerted Action BHM4-CT98-3936*, *Leukemia* 21(2):207–214, 2007.

Fabbri G, Dalla-Favera R: The molecular pathogenesis of chronic lymphocytic leukaemia, *Nat Rev Cancer* 16(3):145–162, 2016.

Faber ZJ, Chen X, Gedman AL, et al.: The genomic landscape of core-binding factor acute myeloid leukemias, *Nat Genet* 48(12):1551–1556, 2016.

Fabris S, Mosca L, Todoerti K, et al.: Molecular and transcriptional characterization of 17p loss in B-cell chronic lymphocytic leukemia, *Genes Chromosomes Cancer* 47:781–793, 2008.

Faderl S, Bueso-Ramos C, Liu Z, et al.: Kit inhibitor APcK110 extends survival in an AML xenograft mouse model, *Invest New Drugs* 29:1094–1097, 2011.

Falini B, Mecucci C, Tiacci E, et al.: Cytoplasmic nucleophosmin in acute myelogenous leukemia with a normal karyotype, *N Engl J Med* 352(3):254–266, 2005.

Falini B, Mecucci C, Tiacci E, et al.: Mutations and targeted therapies in AML 41, *Am J Blood Res* 3(1):29–51, 2013.

Falini B, Nicoletti I, Martelli MF, et al.: Acute myeloid leukemia carrying cytoplasmic/mutated nucleophosmin (NPMc+ AML): biologic and clinical features, *Blood* 109(3):874–885, 2007.

Falini B, Nicoletti I, Bolli N, et al.: Translocations and mutations involving the nucleophosmin (NPM1) gene in lymphomas and leukemias, *Haematologica* 92(4):519–532, 2007.

Falini B, Pulford K, Pucciarini A, et al.: Lymphomas expressing ALK fusion protein(s) other than NPM-ALK, *Blood* 94(10):3509–3515, 1999.

Fasan A, Haferlach C, Alpermann T, et al.: The role of different genetic subtypes of CEBPA mutated AML, *Leukemia* 28(4):794–803, 2014.

Fava C, Rege-Cambrin G, Dogliotti I, et al.: Observational study of chronic myeloid leukemia Italian patients who discontinued tyrosine kinase inhibitors in clinical practice, *Haematologica* 104(8):1589–1596, 2019.

Fei XH, Wu SL, Sun RJ, et al.: [Clinical analysis of 12 cases of acute myeloid leukemia with Ph chromosome and BCR-ABL positive], *Zhongguo Shi Yan Xue Ye Xue Za Zhi* 20(3):545–548, 2012.

Feldman AL, Dogan A, Smith DI, et al.: Discovery of recurrent t(6;7)(p25.3;q32.3) translocations in ALK-negative anaplastic large cell lymphomas by massively parallel genomic sequencing, *Blood* 117(3):915–919, 2011.

Fernandez V, Salamero O, Espinet B, et al.: Genomic and gene expression profiling defines indolent forms of mantle cell lymphoma, *Cancer Res* 70(4):1408–1418, 2010.

Ferreri AJ, Govi S, Pileri SA, Savage KJ: Anaplastic large cell lymphoma, ALK-positive, *Crit Rev Oncol Hematol* 83(2):293–302, 2012.

Fink SR, Belomgie KJ, Paternoster SF, et al.: Validation of a new three-color fluorescence in situ hybridization (FISH) method to detect CHIC2 deletion, FIP1L1/PDGFRA fusion and PDGFRA translocations, *Leuk Res* 33:843–846, 2009.

Foa R, Del Giudice I, Guarini A, et al.: Clinical implications of the molecular genetics of chronic lymphocytic leukemia, *Haematologica* 98(5):675–685, 2013.

Fonseca R, Bergsagel PL, Drach J, et al.: International Myeloma Working Group molecular classification of multiple myeloma: spotlight review, *Leukemia* 23(12):2210–2221, 2009.

Foran JM: New prognostic markers in acute myeloid leukemia: perspective from the clinic, *Hematology Am Soc Hematol Educ Program*47–55, 2010.

Forestier E, Andersen MK, Autio K, et al.: Cytogenetic patterns in ETV6/RUNX1-positive pediatric B-cell precursor acute lymphoblastic leukemia: a Nordic series of 245 cases and review of the literature, *Genes Chromosomes Cancer* 46(5):440–450, 2007.

Forestier E, Heyman M, Andersen MK, et al.: Outcome of ETV6/RUNX1-positive childhood acute lymphoblastic leukaemia in the NOPHO-ALL-1992 protocol: frequent late relapses but good overall survival, *Br J Haematol* 140(6):665–672, 2008.

Forgione MO, McClure BJ, Eadie LN, et al.: KMT2A rearranged acute lymphoblastic leukaemia: Unravelling the genomic complexity and heterogeneity of this high-risk disease, *Cancer Lett* 469:410–418, 2020.

Foroni L, Gerrard G, Nna E, et al.: Technical aspects and clinical applications of measuring BCR-ABL1 transcripts number in chronic myeloid leukemia, *Am J Hematol* 84:517–522, 2009.

Frederick L, Beardell F, Viswanatha DS: Novel BCR-ABL1 fusion identified by targeted next-generation sequencing in a patient with an atypical myeloproliferative neoplasm, *Hum Pathol* 45(8):1784–1789, 2014.

Fröhling S, Schlenk RF, Breitruck J, et al.: Prognostic significance of activating FLT3 mutations in younger adults (16 to 60 years) with acute myeloid leukemia and normal cytogenetics: a study of the AML Study Group Ulm, *Blood* 100:4372–4380, 2002.

Furutani E, Shimamura A: Germline genetic predisposition to hematologic malignancy, *J Clin Oncol* 35(9):1018–1028, 2017.

Fuster JJ, MacLauchlan S, Zuriaga MA, et al.: Clonal hematopoiesis associated with TET2 deficiency accelerates atherosclerosis development in mice, *Science* 355(6327):842–847, 2017.

Gaidano G, Rossi D: The mutational landscape of chronic lymphocytic leukemia and its impact on prognosis and treatment, *Hematology Am Soc Hematol Educ Program* (1)329–337, 2017. 2017.

Gaidzik VI, Bullinger L, Schlenk RF, et al.: RUNX1 mutations in acute myeloid leukemia: results from a comprehensive genetic and clinical analysis from the AML study group, *J Clin Oncol* 29(10):1364–1372, 2011.

Gaidzik VI, Schlenk RF, Moschny S, et al.: Prognostic impact of WT1 mutations in cytogenetically normal acute myeloid leukemia: a study of the German-Austrian AML Study Group, *Blood* 113(19):4505–4511, 2009.

Gale RE, Green C, Allen C, et al.: The impact of FLT3 internal tandem duplication mutant level, number, size, and interaction with NPM1 mutations in a large cohort of young adult patients with acute myeloid leukemia, *Blood* 111(5):2776–2784, 2008.

Galimberti S, Devidas M, Lucenti A, et al.: Validation of minimal residual disease as surrogate endpoint for event-free survival in childhood acute lymphoblastic leukemia, *JNCI Cancer Spectr* 2(4):pky069, 2018.

Gallagher RE, Li Y-P, Rao S, et al.: Characterization of acute promyelocytic leukemia cases with PML-RARα break/fusion sites in PML exon 6: identification of a subgroup with decreased in vitro responsiveness to all-trans retinoic acid, *Blood* 86:1540, 1995.

Gao J, Gong S, Chen YH: Myeloid neoplasm with germline predisposition: a 2016 update for pathologists, *Arch Pathol Lab Med* 143(1):13–22, 2019.

Garces S, Medeiros LJ, Patel KP, et al.: Mutually exclusive recurrent KRAS and MAP2K1 mutations in Rosai-Dorfman disease, *Mod Pathol* 30(10):1367–1377, 2017.

Gascoyne RD, Lamant L, Martin-Subero JI, et al.: ALK-positive diffuse large B-cell lymphoma is associated with clathrin-ALK rearrangements: report of 6 cases, *Blood* 102(7):2568–2573, 2003.

Gelsi-Boyer V, Brecqueville M, Devillier R, et al.: Mutations in ASXL1 are associated with poor prognosis across the spectrum of malignant myeloid diseases, *J Hematol Oncol* 5:12, 2012.

Genovese G, Kahler AK, Handsaker RE, et al.: Clonal hematopoiesis and blood-cancer risk inferred from blood DNA sequence, *N Engl J Med* 371(26):2477–2487, 2014.

Georgiou G, Ippolito GC, Beausang J, et al.: The promise and challenge of high-throughput sequencing of the antibody repertoire, *Nat Biotechnol* 32(2):158–168, 2014.

Germeshausen M, Ballmaier M, Welte K: Incidence of CSF3R mutations in severe congenital neutropenia and relevance for leukemogenesis: results of a long-term survey, *Blood* 109:93–99, 2007.

Ghia P, Stamatopoulos K, Belessi C, et al.: ERIC recommendations on IGHV gene mutational status analysis in chronic lymphocytic leukemia, *Leukemia* 21(1):1–3, 2007.

Gibson CJ, Kennedy JA, Nikiforow S, et al.: Donor-engrafted CHIP is common among stem cell transplant recipients with unexplained cytopenias, *Blood* 130(1):91–94, 2017a.

Gibson CJ, Lindsley RC, Tchekmedyian V, et al.: Clonal hematopoiesis associated with adverse outcomes after autologous stem-cell transplantation for lymphoma, *J Clin Oncol* 35(14):1598–1605, 2017b.

Gilliland DG, Griffin JD: The roles of FLT3 in hematopoiesis and leukemia, *Blood* 100(5):1532–1542, 2002.

Gillis NK, Ball M, Zhang Q, et al.: Clonal haemopoiesis and therapy-related myeloid malignancies in elderly patients: a proof-of-concept, case-control study, *Lancet Oncol* 18(1):112–121, 2017.

Gocho Y, Yang JJ: Genetic defects in hematopoietic transcription factors and predisposition to acute lymphoblastic leukemia, *Blood* 134(10):793–797, 2019.

Godley LA: Inherited predisposition to acute myeloid leukemia, *Semin Hematol* 51(4):306–321, 2014.

Godley LA, Larson RA: Therapy-related myeloid leukemia, *Semin Oncol* 35(4):418–429, 2008.

Goldman JM, Melo JV: Chronic myeloid leukemia--advances in biology and new approaches to treatment, *N Engl J Med* 349(15):1451–1464, 2003.

Goodwin S, McPherson JD, McCombie WR: Coming of age: ten years of next-generation sequencing technologies, *Nat Rev Genet* 17(6):333–351, 2016.

Gotlib J, Maxson JE, George TI, Tyner JW: The new genetics of chronic neutrophilic leukemia and atypical CML: implications for diagnosis and treatment, *Blood* 122(10):1707–1711, 2013.

Grande BM, Gerhard DS, Jiang A, et al.: Genome-wide discovery of somatic coding and noncoding mutations in pediatric endemic and sporadic Burkitt lymphoma, *Blood* 133(12):1313–1324, 2019.

Greaves MF, Wiemels J: Origins of chromosome translocations in childhood leukaemia, *Nat Rev Cancer* 3(9):639–649, 2003.

Greaves MF, Maia AT, Wiemels JL, Ford AM: Leukemia in twins: lessons in natural history, *Blood* 102(7):2321–2333, 2003.

Green CL, Koo KK, Hills RK, et al.: Prognostic significance of CEBPA mutations in a large cohort of younger adult patients with acute myeloid leukemia: impact of double CEBPA mutations and the interaction with FLT3 and NPM1 mutations, *J Clin Oncol* 28:2739–2747, 2010.

Green MR: Chromatin modifying gene mutations in follicular lymphoma, *Blood* 131(6):595–604, 2018.

Green MR, Gentles AJ, Nair RV, et al.: Hierarchy in somatic mutations arising during genomic evolution and progression of follicular lymphoma, *Blood* 121(9):1604–1611, 2013.

Greenberg PL, Stone RM, Al-Kali A, et al.: *Myelodysplastic syndromes, version 1.2020, NCCN clinical practice guidelines in Oncology*, National Comprehensive Cancer Network, 2019.

Gregory Jr JJ, Wagner JE, Verlander PC, et al.: Somatic mosaicism in Fanconi anemia: evidence of genotypic reversion in lymphohematopoietic stem cells, *Proc Natl Acad Sci U S A* 98(5):2532–2537, 2001.

Greisman HA, Lu Z, Tsai AG, et al.: IgH partner breakpoint sequences provide evidence that AID initiates t(11;14) and t(8;14) chromosomal breaks in mantle cell and Burkitt lymphomas, *Blood* 120(14):2864–2867, 2012.

Grever MR, Blachly JS, Andritsos LA: Hairy cell leukemia: update on molecular profiling and therapeutic advances, *Blood Rev* 28(5):197–203, 2014.

Grignani F, Fagioli M, Alcalay M, et al.: Acute promyelocytic leukemia: from genetics to treatment, *Blood* 83:10–25, 1994.

Grimwade D: The pathogenesis of acute promyelocytic leukaemia: evaluation of the role of molecular diagnosis and monitoring in the management of the disease, *Br J Haematol* 106:591–613, 1999.

Grimwade D, Biondi A, Mozziconacci M, et al.: Characterization of acute promyelocytic leukemia cases lacking the classic t(15;17): results of the European Working Party, *Blood* 96:1297–1308, 2000.

Grimwade D, Hills RK, Moorman AV, et al.: Refinement of cytogenetic classification in acute myeloid leukemia: determination of prognostic significance of rare recurring chromosomal abnormalities among 5876 younger adult patients treated in the United Kingdom Medical Research Council trials, *Blood* 116:354–365, 2010.

Grimwade D, Ivey A, Huntly BJ: Molecular landscape of acute myeloid leukemia in younger adults and its clinical relevance, *Blood* 127(1):29–41, 2016.

Groschel S, Sanders MA, Hoogenboezem R, et al.: A single oncogenic enhancer rearrangement causes concomitant EVI1 and GATA2 deregulation in leukemia, *Cell* 157(2):369–381, 2014.

Gross M, Hanenberg H, Lobitz S, et al.: Reverse mosaicism in Fanconi anemia: natural gene therapy via molecular self-correction, *Cytogenet Genome Res* 98(2–3):126–135, 2002.

Gruber F, Mustjoki S, Porkka K: Impact of tyrosine kinase inhibitors on patient outcomes in Philadelphia chromosome-positive acute lymphoblastic leukaemia, *Br J Haematol* 145(5):581–597, 2009.

Gruber S, Arumugam P, Katou Y, et al.: Evidence that loading of cohesin onto chromosomes involves opening of its SMC hinge, *Cell* 127(3):523–537, 2006.

Guglielmelli P, Lasho TL, Rotunno G, et al.: MIPSS70: mutation-enhanced international prognostic score system for transplantation-age patients with primary myelofibrosis, *J Clin Oncol* 36(4):310–318, 2018.

Guglielmelli P, Lasho TL, Rotunno G, et al.: The number of prognostically detrimental mutations and prognosis in primary myelofibrosis: an international study of 797 patients, *Leukemia* 28(9):1804–1810, 2014.

Guglielmelli P, Rotunno G, Fanelli T, et al.: Validation of the differential prognostic impact of type 1/type 1-like versus type 2/type 2-like CALR mutations in myelofibrosis, *Blood Cancer J* 5, 2015. e360.

Guidez F, Ivins S, Zhu J, et al.: Reduced retinoic acid-sensitivities of nuclear receptor corepressor binding to PML- and PLZF-RARα underlie molecular pathogenesis and treatment of acute promyelocytic leukemia, *Blood* 91:2634–2642, 1998.

Guo JU, Su Y, Zhong C, et al.: Hydroxylation of 5-methylcytosine by TET1 promotes active DNA demethylation in the adult brain, *Cell* 145(3):423–434, 2011.

Gustine JN, Xu L, Tsakmaklis N, et al.: CXCR4 (S338X) clonality is an important determinant of ibrutinib outcomes in patients with Waldenstrom macroglobulinemia, *Blood Adv* 3(19):2800–2803, 2019.

Haferlach C, Dicker F, Kohlmann A, et al.: AML with CBFB-MYH11 rearrangement demonstrate RAS pathway alterations in 92% of all cases including a high frequency of NF1 deletions, *Leukemia* 24(5):1065–1069, 2010.

Haferlach T, Nagata Y, Grossmann V, et al.: Landscape of genetic lesions in 944 patients with myelodysplastic syndromes, *Leukemia* 28(2):241–247, 2014.

Haider M, Gangat N, Lasho T, et al.: Validation of the revised international prognostic score of thrombosis for essential thrombocythemia (IPSET-thrombosis) in 585 Mayo clinic patients, *Am J Hematol* 91(4):390–394, 2016.

Hallek M, Cheson BD, Catovsky D, et al.: iwCLL guidelines for diagnosis, indications for treatment, response assessment, and supportive management of CLL, *Blood* 131(25):2745–2760, 2018.

Hamadeh F, MacNamara SP, Aguilera NS, et al.: MYD88 L265P mutation analysis helps define nodal lymphoplasmacytic lymphoma, *Mod Pathol* 28(4):564–574, 2015.

Hamblin TJ, Davis Z, Gardiner A, et al.: Unmutated Ig V(H) genes are associated with a more aggressive form of chronic lymphocytic leukemia, *Blood* 94:1848–1854, 1999.

Hapgood G, Savage KJ: The biology and management of systemic anaplastic large cell lymphoma, *Blood* 126(1):17–25, 2015.

Haroche J, Charlotte F, Arnaud L, et al.: High prevalence of BRAF V600E mutations in Erdheim-Chester disease but not in other non-Langerhans cell histiocytoses, *Blood* 120(13):2700–2703, 2012.

Harper DP: Aplan PD: chromosomal rearrangements leading to MLL gene fusions: clinical and biological aspects, *Cancer Res* 68(24):10024–10027, 2008.

Harrison CJ: Blood Spotlight on iAMP21 acute lymphoblastic leukemia (ALL), a high-risk pediatric disease, *Blood* 125(9):1383–1386, 2015.

Hartmann EM, Campo E, Wright G, et al.: Pathway discovery in mantle cell lymphoma by integrated analysis of high-resolution gene expression and copy number profiling, *Blood* 116(6):953–961, 2010.

He R, Devine DJ, Tu ZJ, et al.: Hybridization capture-based next generation sequencing reliably detects FLT3 mutations and classifies FLT3-internal tandem duplication allelic ratio in acute myeloid leukemia: a comparative study to standard fragment analysis, Mod Pathol, 2019.

He R, Greipp PT, Rangan A, et al.: BCR-JAK2 fusion in a myeloproliferative neoplasm with associated eosinophilia, *Cancer Genet* 209(5):223–228, 2016a.

He R, Wiktor AE, Durnick DK, et al.: Bone marrow conventional karyotyping and fluorescence in situ hybridization: defining an effective utilization strategy for evaluation of myelodysplastic syndromes, *Am J Clin Pathol* 146(1):86–94, 2016b.

Heavican TB, Bouska A, Yu J, et al.: Genetic drivers of oncogenic pathways in molecular subgroups of peripheral T-cell lymphoma, *Blood* 133(15):1664–1676, 2019.

Hehlmann R, Lauseker M, Saussele S, et al.: Assessment of imatinib as first-line treatment of chronic myeloid leukemia: 10-year survival results of the randomized CML study IV and impact of non-CML determinants, *Leukemia* 31(11):2398–2406, 2017.

Hernandez JM, del Canizo MC, Cuneo A, et al.: Clinical, hematological and cytogenetic characteristics of atypical chronic myeloid leukemia, *Ann Oncol* 11(4):441–444, 2000.

Hess JL: Mechanisms of transformation by MLL, *Crit Rev Eukaryot Gene Expr* 14(4):235–254, 2004.

Hill VK, Kim JS, Waldman T: Cohesin mutations in human cancer. *Biochim Biophys Acta* 1866(1), 1-11, 2016.

Hochhaus A, O'Brien SG, Guilhot F, et al.: Six-year follow-up of patients receiving imatinib for the first-line treatment of chronic myeloid leukemia, *Leukemia* 23:1054–1061, 2009.

Hochhaus A, Masszi T, Giles FJ, et al.: Treatment-free remission following frontline nilotinib in patients with chronic myeloid leukemia in chronic phase: results from the ENESTfreedom study, *Leukemia* 31(7):1525–1531, 2017.

Hoffmann VS, Baccarani M, Hasford J, et al.: Treatment and outcome of 2904 CML patients from the EUTOS population-based registry, *Leukemia* 31(3):593–601, 2017.

Hormaeche I, Licht JD: Chromatin modulation by oncogenic transcription factors: new complexity, new therapeutic targets, *Canc Cell* 11(6):475–478, 2007.

Hsi AC, Robirds DH, Luo J, et al.: T-cell prolymphocytic leukemia frequently shows cutaneous involvement and is associated with gains of MYC, loss of ATM, and TCL1A rearrangement, *Am J Surg Pathol* 38(11):1468–1483, 2014.

Hsi ED, Tubbs RR, Lovell MA, et al.: Detection of bcl-2/J(H) translocation by polymerase chain reaction: a summary of the experience of the Molecular Oncology Survey of the College of American Pathologist, *Arch Pathol Lab Med* 126(8):902–908, 2002.

Hu B, Patel KP, Chen HC, et al.: Association of gene mutations with time-to-first treatment in 384 treatment-naive chronic lymphocytic leukaemia patients, *Br J Haematol* 187(3):307–318, 2019.

Huang ME, Ye YC, Chen SR, et al.: Use of all-trans retinoic acid in the treatment of acute promyelocytic leukemia, *Blood* 72(2):567–572, 1988.

Hughes TP, Branford S: Monitoring disease response to tyrosine kinase inhibitor therapy in CML, *Hematology*477–487, 2009. 2009.

Hughes TP, Kaeda J, Branford S, et al.: Frequency of major molecular responses to imatinib or interferon alfa plus cytarabine in newly diagnosed chronic myeloid leukemia, *N Engl J Med* 349:1423–1432, 2003.

Hughes TP, Saglio G, Quintas-Cardama A, et al.: BCR-ABL1 mutation development during first-line treatment with dasatinib or imatinib for chronic myeloid leukemia in chronic phase, *Leukemia* 29(9):1832–1838, 2015.

Hunger SP, Mullighan CG: Acute lymphoblastic leukemia in children, *N Engl J Med* 373(16):1541–1552, 2015.

Hunger SP, Galili N, Carroll AJ, et al.: The t(1;19)(q23;p13) results in consistent fusion of E2A and PBX1 coding sequences in acute lymphoblastic leukemias, *Blood* 77(4):687–693, 1991.

Hunter ZR, Xu L, Yang G, et al.: The genomic landscape of Waldenstrom macroglobulinemia is characterized by highly recurring MYD88 and WHIM-like CXCR4 mutations, and small somatic deletions associated with B-cell lymphomagenesis, *Blood* 123(11):1637–1646, 2014.

Ihle JN, Gilliland DG: Jak2: normal function and role in hematopoietic disorders, *Curr Opin Genet Dev* 17(1):8–14, 2007.

Inaba H, Greaves M, Mullighan CG: Acute lymphoblastic leukaemia, *Lancet* 381(9881):1943–1955, 2013.

Inoue D, Kitaura J, Togami K, et al.: Myelodysplastic syndromes are induced by histone methylation-altering ASXL1 mutations, *J Clin Invest* 123(11):4627–4640, 2013.

Iqbal J, Greiner TC, Patel K, et al.: Distinctive patterns of BCL6 molecular alterations and their functional consequences in different subgroups of diffuse large B-cell lymphoma, *Leukemia* 21(11):2332–2343, 2007.

Iqbal S, Jenner MJ, Summers KE, et al.: Reliable detection of clonal IgH/Bcl2 MBR rearrangement in follicular lymphoma: methodology and clinical significance, *Br J Haematol* 124(3):325–328, 2004.

Irshaid L, Xu ML: ALCL by any other name: the many facets of anaplastic large cell lymphoma, *Pathology*, 2019.

Isaacson PG, Du MQ: MALT lymphoma: from morphology to molecules, *Nat Rev Cancer* 4(8):644–653, 2004.

Ito S, D'Alessio AC, Taranova OV, et al.: Role of Tet proteins in 5mC to 5hmC conversion, ES-cell self-renewal and inner cell mass specification, *Nature* 466(7310):1129–1133, 2010.

Itzykson R, Solary E: An evolutionary perspective on chronic myelomonocytic leukemia, *Leukemia* 27(7):1441–1450, 2013.

Itzykson R, Kosmider O, Cluzeau T, et al.: Impact of TET2 mutations on response rate to azacitidine in myelodysplastic syndromes and low blast count acute myeloid leukemias, *Leukemia* 25(7):1147–1152, 2011.

Itzykson R, Kosmider O, Renneville A, et al.: Prognostic score including gene mutations in chronic myelomonocytic leukemia, *J Clin Oncol* 31(19):2428–2436, 2013.

Jabbour E, Branford S, Saglio G, et al.: Practical advice for determining the role of BCR-ABL mutations in guiding tyrosine kinase inhibitor therapy in patients with chronic myeloid leukemia, *Cancer* 117(9):1800–1811, 2011a.

Jabbour E, Parikh SA, Kantarjian H, Cortes J: Chronic myeloid leukemia: mechanisms of resistance and treatment, *Hematol Oncol Clin North Am* 25(5):981–995, 2011b. v.

Jacobs KB, Yeager M, Zhou W, et al.: Detectable clonal mosaicism and its relationship to aging and cancer, *Nat Genet* 44(6):651–658, 2012.

Jain P, Kantarjian H, Patel KP, et al.: Impact of BCR-ABL transcript type on outcome in patients with chronic-phase CML treated with tyrosine kinase inhibitors, *Blood* 127(10):1269–1275, 2016a.

Jain P, Kantarjian H, Sasaki K, et al.: Analysis of 2013 European LeukaemiaNet (ELN) responses in chronic phase CML across four frontline TKI modalities and impact on clinical outcomes, *Br J Haematol* 173(1):114–126, 2016b.

Jaiswal S, Fontanillas P, Flannick J, et al.: Age-related clonal hematopoiesis associated with adverse outcomes, *N Engl J Med* 371(26):2488–2498, 2014.

Jaiswal S, Natarajan P, Silver AJ, et al.: Clonal hematopoiesis and risk of atherosclerotic cardiovascular disease, *N Engl J Med* 377(2):111–121, 2017.

James C, Ugo V, Le Couedic JP, et al.: A unique clonal JAK2 mutation leading to constitutive signalling causes polycythaemia vera, *Nature* 434:1144–1148, 2005.

Jankowska AM, Makishima H, Tiu RV, et al.: Mutational spectrum analysis of chronic myelomonocytic leukemia includes genes associated with epigenetic regulation: UTX, EZH2, and DNMT3A, *Blood* 118(14):3932–3941, 2011.

Jansen JH, Löwenberg B: Acute promyelocytic leukemia with a PLZF-RARalpha fusion protein, *Semin Hematol* 38(1):37–41, 2001.

Jaramillo Oquendo C, Parker H, et al.: Systematic review of somatic mutations in splenic marginal zone lymphoma, *Sci Rep* 9(1):10444, 2019.

Jares P, Colomer D, Campo E: Molecular pathogenesis of mantle cell lymphoma, *J Clin Invest* 122(10):3416–3423, 2012.

Jennings LJ, Arcila ME, Corless C, et al.: Guidelines for validation of next-generation sequencing-based oncology panels: a joint consensus recommendation of the Association for Molecular Pathology and College of American Pathologists, *J Mol Diagn* 19(3):341–365, 2017.

Jennings LJ, George D, Czech J, et al.: Detection and quantification of BCR-ABL1 fusion transcripts by droplet digital PCR, *J Mol Diagn* 16(2):174–179, 2014.

Jerez A, Clemente MJ, Makishima H, et al.: STAT3 mutations unify the pathogenesis of chronic lymphoproliferative disorders of NK cells and T-cell large granular lymphocyte leukemia, *Blood* 120(15):3048–3057, 2012a.

Jerez A, Gondek LP, Jankowska AM, et al.: Topography, clinical, and genomic correlates of 5q myeloid malignancies revisited, *J Clin Oncol* 30(12):1343–1349, 2012b.

Jiang H, Xue Y, Wang Q, et al.: The utility of fluorescence in situ hybridization analysis in diagnosing myelodysplastic syndromes is limited to cases with karyotype failure, *Leuk Res* 36(4):448–452, 2012.

Jimenez C, Chillon Mdel C, Balanzategui A, et al.: Detection of MYD88 L265P mutation by real-time allele-specific oligonucleotide polymerase chain reaction, *Appl Immunohistochem Mol Morphol* 22(10):768–773, 2014.

Jimenez C, Sebastian E, Chillon MC, et al.: MYD88 L265P is a marker highly characteristic of, but not restricted to, *Waldenstrom's macroglobulinemia*, *Leukemia* 27(8):1722–1728, 2013.

Johnsen JM, Nickerson DA, Reiner AP: Massively parallel sequencing: the new frontier of hematologic genomics, *Blood* 122(19):3268–3275, 2013.

Johnson DC, Lenive O, Mitchell J, et al.: Neutral tumor evolution in myeloma is associated with poor prognosis, *Blood* 130(14):1639–1643, 2017.

Jones AV, Cross NC, White HE, et al.: Rapid identification of JAK2 exon 12 mutations using high-resolution melting analysis, *Haematologica* 93(10):1560–1564, 2008.

Jones D, Kamel-Reid S, Bahler D, et al.: Laboratory practice guidelines for detecting and reporting BCR-ABL drug resistance mutations in chronic myelogenous leukemia and acute lymphoblastic leukemia: a report of the Association for Molecular Pathology, *J Mol Diagn* 11(1):4–11, 2009.

Jones LK, Saha V: Philadelphia positive acute lymphoblastic leukaemia of childhood, *Br J Haematol* 130(4):489–500, 2005.

Jongen-Lavrencic M, Grob T, Hanekamp D, et al.: Molecular minimal residual disease in acute myeloid leukemia, *N Engl J Med* 378(13):1189–1199, 2018.

Jongmans MC, Verwiel ET, Heijdra Y, et al.: Revertant somatic mosaicism by mitotic recombination in dyskeratosis congenita, *Am J Hum Genet* 90(3):426–433, 2012.

Jourdan E, Boissel N, Chevret S, et al.: Prospective evaluation of gene mutations and minimal residual disease in patients with core binding factor acute myeloid leukemia, *Blood* 121(12):2213–2223, 2013.

Junttila MR, Evan GI: p53—a Jack of all trades but master of none, *Nat Rev Cancer* 9(11):821–829, 2009.

Jurcic JG, Soignet SL, Maslak AP: Diagnosis and treatment of acute promyelocytic leukemia, *Curr Oncol Rep* 9(5):337–344, 2007.

Kadkol S, Bruno A, Dodge C, et al.: Comprehensive analysis of CBFβ-MYH11 fusion transcripts in acute myeloid leukemia by RT-PCR analysis, *J Mol Diag* 6:22–27, 2004.

Kahn S, Yamamoto F, Almoguera C, et al.: The c-K-ras gene and human cancer (review), *Anticancer Res* 7(4A):639–652, 1987.

Kales SC, Ryan PE, Nau MM, et al.: Cbl and human myeloid neoplasms: the Cbl oncogene comes of age, *Cancer Res* 70(12):4789–4794, 2010.

Kang H, Wilson CS, Harvey RC, et al.: Gene expression profiles predictive of outcome and age in infant acute lymphoblastic leukemia: a Children's Oncology Group study, *Blood* 119(8):1872–1881, 2012.

Karube K, Enjuanes A, Dlouhy I, et al.: Integrating genomic alterations in diffuse large B-cell lymphoma identifies new relevant pathways and potential therapeutic targets, *Leukemia* 32(3):675–684, 2018.

Kato S, Han SY, Liu W, et al.: Understanding the function-structure and function-mutation relationships of p53 tumor suppressor protein by high-resolution missense mutation analysis, *Proc Natl Acad Sci U S A* 100(14):8424–8429, 2003.

Katzenberger T, Ott G, Klein T, et al.: Cytogenetic alterations affecting BCL6 are predominantly found in follicular lymphomas grade 3B with a diffuse large B-cell component, *Am J Pathol* 165(2):481–490, 2004.

Kerr CM, Clemente MJ, Chomczynski PW, et al.: Subclonal STAT3 mutations solidify clonal dominance, *Blood Adv* 3(6):917–921, 2019.

Khorashad JS, Kelley TW, Szankasi P, et al.: BCR-ABL1 compound mutations in tyrosine kinase inhibitor-resistant CML: frequency and clonal relationships, *Blood* 121(3):489–498, 2013.

Kiel MJ, Velusamy T, Betz BL, et al.: Whole-genome sequencing identifies recurrent somatic NOTCH2 mutations in splenic marginal zone lymphoma, *J Exp Med* 209(9):1553–1565, 2012.

Kilpivaara O, Levine RL: JAK2 and MPL mutations in myeloproliferative neoplasms: discovery and science, *Leukemia* 22(10):1813–1817, 2008.

King RL, Gonsalves WI, Ansell SM, et al.: Lymphoplasmacytic lymphoma with a non-IgM paraprotein shows clinical and pathologic heterogeneity and may harbor MYD88 L265P mutations, *Am J Clin Pathol* 145(6):843–851, 2016.

Kiyoi H, Naoe T: FLT3 in human hematologic malignancies, *Leuk Lymphoma* 43(8):1541–1547, 2002.

Kizilors A, Crisa E, Lea N, et al.: Effect of low-level BCR-ABL1 kinase domain mutations identified by next-generation sequencing in patients with chronic myeloid leukaemia: a population-based study, *Lancet Haematol* 6(5):219, 2019. e276–e284.

Klampfl T, Gisslinger H, Harutyunyan AS, et al.: Somatic mutations of calreticulin in myeloproliferative neoplasms, *N Engl J Med* 369(25):2379–2390, 2013.

Kohlmann A, Grossmann V, Nadarajah N, et al.: Next-generation sequencing—Feasibility and practicality in haematology, *Br J Haematol* 160(6):736–753, 2013.

Kohno A, Morishita Y, Iida H, et al.: Hematopoietic stem cell transplantation for acute promyelocytic leukemia in second or third complete remission: a retrospective analysis in the Nagoya Blood and Marrow Transplantation Group, *Int J Hematol* 87(2):210–216, 2008.

Konoplev S, Huang X, Drabkin HA, et al.: Cytoplasmic localization of nucleophosmin in bone marrow blasts of acute myeloid leukemia patients is not completely concordant with NPM1 mutation and is not predictive of prognosis, *Cancer* 115(20):4737–4744, 2009.

Konoplev S, Yin CC, Kornblau SM, et al.: Molecular characterization of de novo Philadelphia chromosome-positive acute myeloid leukemia, *Leuk Lymphoma* 54(1):138–144, 2013.

Kontzias A, Kotlyar A, Laurence A, et al.: A new class of kinase inhibitors in cancer and autoimmune disease, *Curr Opin Pharmacol* 12:464–470, 2012.

Koschmieder S, Halmos B, Levantini E, et al.: Dysregulation of the C/EBPalpha differentiation pathway in human cancer, *J Clin Oncol* 27(4):619–628, 2009.

Koskela HL, Eldfors S, Ellonen P, et al.: Somatic STAT3 mutations in large granular lymphocytic leukemia, *N Engl J Med* 366(20):1905–1913, 2012.

Kraan W, Horlings HM, van Keimpema M, et al.: High prevalence of oncogenic MYD88 and CD79B mutations in diffuse large B-cell lymphomas presenting at immune-privileged sites, *Blood Cancer J* 3:e139, 2013.

Kraan W, van Keimpema M, Horlings HM, et al.: High prevalence of oncogenic MYD88 and CD79B mutations in primary testicular diffuse large B-cell lymphoma, *Leukemia* 28(3):719–720, 2014.

Kralovics R, Guan Y, Prchal JT: Acquired uniparental disomy of chromosome 9p is a frequent stem cell defect in polycythemia vera, *Exp Hematol* 30(3):229–236, 2002.

Kralovics R, Passamonti F, Buser AS, et al.: A gain-of-function mutation of JAK2 in myeloproliferative disorders, *N Engl J Med* 352:1779–1790, 2005.

Kridel R, Sehn LH, Gascoyne RD: Can histologic transformation of follicular lymphoma be predicted and prevented? *Blood* 130(3):258–266, 2017.

Krivtsov AV, Armstrong SA: MLL translocations, histone modifications and leukaemia stem-cell development, *Nat Rev Cancer* 7(11):823–833, 2007.

Kronke J, Bullinger L, Teleanu V, et al.: Clonal evolution in relapsed NPM1-mutated acute myeloid leukemia, *Blood* 122(1):100–108, 2013.

Kuan JW, Su AT, Leong CF, et al.: Systematic review of normal subjects harbouring BCR-ABL1 fusion gene, *Acta Haematol* 143(2):1–16, 2019.

Kuehl WM, Bergsagel PL: Molecular pathogenesis of multiple myeloma and its premalignant precursor, *J Clin Invest* 122(10):3456–3463, 2012.

Kuhnl A, Cunningham D, Counsell N, et al.: Outcome of elderly patients with diffuse large B-cell lymphoma treated with R-CHOP: results from the UK NCRI R-CHOP14v21 trial with combined analysis of molecular characteristics with the DSHNHL RICOVER-60 trial, *Ann Oncol* 28(7):1540–1546, 2017.

Kulasekararaj AG, Smith AE, Mian SA, et al.: TP53 mutations in myelodysplastic syndrome are strongly correlated with aberrations of chromosome 5, and correlate with adverse prognosis, *Br J Haematol* 160(5):660–672, 2013.

Kwok B, Hall JM, Witte JS, et al.: MDS-associated somatic mutations and clonal hematopoiesis are common in idiopathic cytopenias of undetermined significance, *Blood* 126(21):2355–2361, 2015.

Lackraj T, Goswami R, Kridel R: Pathogenesis of follicular lymphoma, *Best Pract Res Clin Haematol* 31(1):2–14, 2018.

Ladanyi M, Cavalchire G: Detection of the NPM-ALK genomic rearrangement of Ki-1 lymphoma and isolation of the involved NPM and ALK introns, *Diagn Mol Pathol* 5(3):154–158, 1996.

Ladanyi M, Cavalchire G, Morris SW, et al.: Reverse transcriptase polymerase chain reaction for the Ki-1 anaplastic large cell lymphoma-associated t(2;5) translocation in Hodgkin's disease, *Am J Pathol* 145(6):1296–1300, 1994.

Lafiura KM, Bielawski DM, Posecion Jr NC, et al.: Association between prenatal pesticide exposures and the generation of leukemia-associated T(8;21), *Pediatr Blood Cancer* 49(5):624–628, 2007.

Landau DA, Sun C, Rosebrock D, et al.: The evolutionary landscape of chronic lymphocytic leukemia treated with ibrutinib targeted therapy, *Nat Commun* 8(1):2185, 2017.

Landau DA, Tausch E, Taylor-Weiner AN, et al.: Mutations driving CLL and their evolution in progression and relapse, *Nature* 526(7574):525–530, 2015.

Langerak AW, Bruggemann M, Davi F, et al.: High-throughput immunogenetics for clinical and research applications in immunohematology: potential and challenges, *J Immunol* 198(10):3765–3774, 2017.

Langerak AW, Groenen PJ, Bruggemann M, et al.: EuroClonality/BIOMED-2 guidelines for interpretation and reporting of Ig/TCR clonality testing in suspected lymphoproliferations, *Leukemia* 26(10):2159–2171, 2012.

Lanternier F, Cohen-Akenine A, Palmerini F, et al.: Phenotypic and genotypic characteristics of mastocytosis according to the age of onset, *PloS One* 3(4), 2008:e1906.

Laurent C, Do C, Gascoyne RD, et al.: Anaplastic lymphoma kinase-positive diffuse large B-cell lymphoma: a rare clinicopathologic entity with poor prognosis, *J Clin Oncol* 27(25):4211–4216, 2009.

Laurie CC, Laurie CA, Rice K, et al.: Detectable clonal mosaicism from birth to old age and its relationship to cancer, *Nat Genet* 44(6):642–650, 2012.

Le Beau MM, Larson RA, Bitter MA, et al.: Association of an inversion of chromosome 16 with abnormal marrow eosinophils in acute myelomonocytic leukemia. A unique cytogenetic-clinicopathological association, *N Engl J Med* 309:630–636, 1983.

Lefebvre P: Molecular basis for designing selective modulators of retinoic acid receptor transcriptional activities, *Curr Drug Targets Immune Endocr Metabol Disord* 1(2):153–164, 2001.

Leich E, Hoster E, Wartenberg M, et al.: Similar clinical features in follicular lymphomas with and without breaks in the BCL2 locus, *Leukemia* 30(4):854–860, 2016.

Leich E, Salaverria I, Bea S, et al.: Follicular lymphomas with and without translocation t(14;18) differ in gene expression profiles and genetic alterations, *Blood* 114(4):826–834, 2009.

Lemonnier F, Couronne L, Parrens M, et al.: Recurrent TET2 mutations in peripheral T-cell lymphomas correlate with TFH-like features and adverse clinical parameters, *Blood* 120(7):1466–1469, 2012.

Lemonnier F, Gaulard P, de Leval L: New insights in the pathogenesis of T-cell lymphomas, *Curr Opin Oncol* 30(5):277–284, 2018.

Levine RL, Wadleigh M, Cools J, et al.: Activating mutation in the tyrosine kinase JAK2 in polycythemia vera, essential thrombocythemia, and myeloid metaplasia with myelofibrosis, *Canc Cell* 7:387–397, 2005.

Levis M: Quizartinib for the treatment of FLT3/ITD acute myeloid leukemia, *Future Oncol* 10:1571–1579, 2014.

Li JY, Pu MT, Hirasawa R, et al.: Synergistic function of DNA methyltransferases Dnmt3a and Dnmt3b in the methylation of Oct4 and Nanog, *Mol Cell Biol* 27(24):8748–8759, 2007.

Licht JD: Acute promyelocytic leukemia—Weapons of mass differentiation, *N Eng J Med* 360:928–930, 2009.

Limpens J, Stad R, Vos C, et al.: Lymphoma-associated translocation t(14;18) in blood B cells of normal individuals, *Blood* 85(9):2528–2536, 1995.

Lindsley RC, Ebert BL: The biology and clinical impact of genetic lesions in myeloid malignancies, *Blood* 122(23):3741–3748, 2013.

Lindsley RC, Mar BG, Mazzola E, et al.: Acute myeloid leukemia ontogeny is defined by distinct somatic mutations, *Blood* 125(9):1367–1376, 2015.

Lipton JH, Chuah C, Guerci-Bresler A, et al.: Ponatinib versus imatinib for newly diagnosed chronic myeloid leukaemia: an international, randomised, open-label, phase 3 trial, *Lancet Oncol* 17(5):612–621, 2016.

Liu PP, Hajra A, Wijmenga C, et al.: Molecular pathogenesis of the chromosome 16 inversion in the M4Eo subtype of acute myeloid leukemia, *Blood* 9:2289–2302, 1995.

Liu H, Cheng EH, Hsieh JJ: MLL fusions: pathways to leukemia, *Cancer Biol Ther* 8(13):1204–1211, 2009.

Liu H, Ruskon-Fourmestraux A, Lavergne-Slove A, et al.: Resistance of t(11;18) positive gastric mucosa-associated lymphoid tissue lymphoma to Helicobacter pylori eradication therapy, *Lancet* 357(9249):39–40, 2001.

Liu H, Ye H, Ruskone-Fourmestraux A, et al.: T(11;18) is a marker for all stage gastric MALT lymphomas that will not respond to H. pylori eradication, *Gastroenterology* 122(5):1286–1294, 2002.

Liu Y, Barta SK: Diffuse large B-cell lymphoma: 2019 update on diagnosis, risk stratification, and treatment, *Am J Hematol* 94(5):604–616, 2019.

Liu Y, Easton J, Shao Y, et al.: The genomic landscape of pediatric and young adult T-lineage acute lymphoblastic leukemia, *Nat Genet* 49(8):1211–1218, 2017.

Lo Coco F, Ammatuna E, Montesinos P, et al.: Acute promyelocytic leukemia: recent advances in diagnosis and management, *Semin Oncol* 35(4):401–409, 2008.

Logan AC, Gao H, Wang C, et al.: High-throughput VDJ sequencing for quantification of minimal residual disease in chronic lymphocytic leukemia and immune reconstitution assessment, *Proc Natl Acad Sci U S A* 108(52):21194–21199, 2011.

Loh ML, Sakai DS, Flotho C, et al.: Mutations in CBL occur frequently in juvenile myelomonocytic leukemia, *Blood* 114(9):1859–1863, 2009.

Lorsbach RB, Downing JR: The role of the AML1 transcription factor in leukemogenesis, *Int J Hematol* 74:258–265, 2001.

Lucas CM, Harris RJ, Giannoudis A, et al.: Chronic myeloid leukemia patients with the e13a2 BCR-ABL fusion transcript have inferior responses to imatinib compared to patients with the e14a2 transcript, *Haematologica* 94(10):1362–1367, 2009.

Luchtel RA, Dasari S, Oishi N, et al.: Molecular profiling reveals immunogenic cues in anaplastic large cell lymphomas with DUSP22 rearrangements, *Blood* 132(13):1386–1398, 2018.

Lunning MA, Vose JM: Angioimmunoblastic T-cell lymphoma: the many-faced lymphoma, *Blood* 129(9):1095–1102, 2017.

Makishima H, Visconte V, Sakaguchi H, et al.: Mutations in the spliceosome machinery, a novel and ubiquitous pathway in leukemogenesis, *Blood* 119(14):3203–3210, 2012.

Makishima H, Yoshizato T, Yoshida K, et al.: Dynamics of clonal evolution in myelodysplastic syndromes, *Nat Genet* 49(2):204–212, 2016.

Malcikova J, Tausch E, Rossi D, et al.: ERIC recommendations for TP53 mutation analysis in chronic lymphocytic leukemia-update on methodological approaches and results interpretation, *Leukemia* 32(5):1070–1080, 2018.

Malcovati L, Della Porta MG, Pietra D, et al.: Molecular and clinical features of refractory anemia with ringed sideroblasts associated with marked thrombocytosis, *Blood* 114(17):3538–3545, 2009.

Malcovati L, Galli A, Travaglino E, et al.: Clinical significance of somatic mutation in unexplained blood cytopenia, *Blood* 129(25):3371–3378, 2017.

Malcovati L, Hellstrom-Lindberg E, Bowen D, et al.: Diagnosis and treatment of primary myelodysplastic syndromes in adults: recommendations from the European LeukemiaNet, *Blood* 122(17):2943–2964, 2013.

Maljaei SH, Brito-Babapulle V, Hiorns LR, et al.: Abnormalities of chromosomes 8, 11, 14, and X in T-prolymphocytic leukemia studied by fluorescence in situ hybridization, *Cancer Genet Cytogenet* 103(2):110–116, 1998.

Mallo M, Del Rey M, Ibanez M, et al.: Response to lenalidomide in myelodysplastic syndromes with del(5q): influence of cytogenetics and mutations, *Br J Haematol* 162(1):74–86, 2013.

Manasanch EE, Braylan R, Stetler-Stevenson M, et al.: Lack of MYD88 L265P in non-immunoglobulin M lymphoplasmacytic lymphoma, *Leuk Lymphoma* 55(6):1402–1403, 2014.

Mantadakis E, Samonis G, Kalmanti M: A comprehensive review of acute promyelocytic leukemia in children, *Acta Haematol* 119(2):73–82, 2008.

Mark M, Ghyselinck NB, Chambon P: Function of retinoic acid receptors during embryonic development, *Nucl Recept Signal* 7, 2009:e002.

Martinez N, Almaraz C, Vaque JP, et al.: Whole-exome sequencing in splenic marginal zone lymphoma reveals mutations in genes involved in marginal zone differentiation, *Leukemia* 28(6):1334–1340, 2014.

Martinez-Lopez A, Curiel-Olmo S, Mollejo M, et al.: MYD88 (L265P) somatic mutation in marginal zone B-cell lymphoma, *Am J Surg Pathol* 39(5):644–651, 2015.

Martinez-Trillos A, Quesada V, Villamor N, et al.: Recurrent gene mutations in CLL, *Adv Exp Med Biol* 792:87–107, 2013.

Martin-Garcia D, Navarro A, Valdes-Mas R, et al.: CCND2 and CCND3 hijack immunoglobulin light-chain enhancers in cyclin D1(-) mantle cell lymphoma, *Blood* 133(9):940–951, 2019.

Marty C, Pecquet C, Nivarthi H, et al.: Calreticulin mutants in mice induce an MPL-dependent thrombocytosis with frequent progression to myelofibrosis, *Blood* 127(10):1317–1324, 2016.

Massague J: G1 cell-cycle control and cancer, *Nature* 432(7015):298–306, 2004.

Mathew P, Sanger WG, Weisenburger DD, et al.: Detection of the t(2;5)(p23;q35) and NPM-ALK fusion in non-Hodgkin's lymphoma by two-color fluorescence in situ hybridization, *Blood* 89(5):1678–1685, 1997.

Maxson JE, Gotlib J, Pollyea DA, et al.: Oncogenic CSF3R mutations in chronic neutrophilic leukemia and atypical CML, *N Engl J Med* 368(19):1781–1790, 2013.

McCabe MT, Ott HM, Ganji G, et al.: EZH2 inhibition as a therapeutic strategy for lymphoma with EZH2-activating mutations, *Nature* 492(7427):108–112, 2012.

McClure R, Mai M, McClure S: High-throughput sequencing using the Ion Torrent personal genome machine for clinical evaluation of somatic hypermutation status in chronic lymphocytic leukemia, *J Mol Diagn* 17(2):145–154, 2015.

McCullough KB, Patnaik MM: Chronic myelomonocytic leukemia: a genetic and clinical update, *Curr Hematol Malig Rep* 10(3):292–302, 2015.

McGonigle GJ, Lappin TR, Thompson A: Grappling with the HOX network in hematopoiesis and leukemia, *Front Biosci* 13:4297–4308, 2008.

McPhail ED, Maurer MJ, Macon WR, et al.: Inferior survival in high-grade B-cell lymphoma with MYC and BCL2 and/or BCL6 rearrangements is not associated with MYC/IG gene rearrangements, *Haematologica* 103(11):1899–1907, 2018.

Mead AJ, Linch DC, Hills RK, et al.: FLT3 tyrosine kinase domain mutations are biologically distinct from and have a significantly more favorable prognosis than FLT3 internal tandem duplications in patients with acute myeloid leukemia, *Blood* 110:1262–1270, 2007.

Meggendorfer M, Bacher U, Alpermann T, et al.: SETBP1 mutations occur in 9% of MDS/MPN and in 4% of MPN cases and are strongly associated with atypical CML, monosomy 7, isochromosome i(17)(q10), ASXL1 and CBL mutations, *Leukemia* 27(9):1852–1860, 2013.

Meggendorfer M, Haferlach T, Alpermann T, et al.: Specific molecular mutation patterns delineate chronic neutrophilic leukemia, atypical chronic myeloid leukemia, and chronic myelomonocytic leukemia, *Haematologica* 99(12):e244–246, 2014.

Mehta HM, Glaubach T, Long A, et al.: Granulocyte colony-stimulating factor receptor T595I (T618I) mutation confers ligand independence and enhanced signaling, *Leukemia* 27(12):2407–2410, 2013.

Melnick A, Licht JD: Deconstructing a disease: RARα, its fusion partners, and their roles in the pathogenesis of acute promyelocytic leukemia, *Blood* 93:3167–3215, 1999.

Melnick A, Licht JD: Deconstructing a disease: RARalpha, its fusion partners, and their roles in the pathogenesis of acute promyelocytic leukemia, *Blood* 93(10):3167–3215, 1999.

Melo JV: The diversity of BCR-ABL fusion proteins and their relationship to leukemia phenotype, *Blood* 88:2375–2384, 1996.

Melo JV, Barnes DJ: Chronic myeloid leukaemia as a model of disease evolution in human cancer, *Nat Rev Cancer* 7(6):441–453, 2007.

Mendler JH, Maharry K, Radmacher MD, et al.: RUNX1 mutations are associated with poor outcome in younger and older patients with cytogenetically normal acute myeloid leukemia and with distinct gene and MicroRNA expression signatures, *J Clin Oncol* 30(25):3109–3118, 2012.

Mesa RA, Jamieson C, Bhatia R, et al.: NCCN guidelines insights: myeloproliferative neoplasms, version 2.2018, *J Natl Compr Canc Netw* 15(10):1193–1207, 2017.

Metcalfe DD: Mast cells and mastocytosis, *Blood* 112(4):946–956, 2008.

Metzeler KH, Herold T, Rothenberg-Thurley M, et al.: Spectrum and prognostic relevance of driver gene mutations in acute myeloid leukemia, *Blood* 128(5):686–698, 2016.

Metzgeroth G, Walz C, Score J, et al.: Recurrent finding of the FIP1L1-PDGFRA fusion gene in eosinophilia-associated acute myeloid leukemia and lymphoblastic T-cell lymphoma, *Leukemia* 21(6):1183–1188, 2007.

Meyer C, Burmeister T, Groger D, et al.: The MLL recombinome of acute leukemias in 2017, *Leukemia* 32(2):273–284, 2018.

Miles RR, Shah RK, Frazer JK: Molecular genetics of childhood, adolescent and young adult non-Hodgkin lymphoma, *Br J Haematol* 173(4):582–596, 2016.

Milojkovic D, Apperley J: Mechanisms of resistance to imatinib and second-generation tyrosine inhibitors in chronic myeloid leukemia, *Clin Cancer Res* 15(24):7519–7527, 2009.

Misund K, Keane N, Stein CK, et al.: MYC dysregulation in the progression of multiple myeloma, *Leukemia* 34(1):322–326, 2020.

Mizuki M, Fenski R, Halfter H, et al.: Flt3 mutations from patients with acute myeloid leukemia induce transformation of 32D cells mediated by the Ras and STAT5 pathways, *Blood* 96(12):3907–3914, 2000.

Mohi MG, Neel BG: The role of Shp2 (PTPN11) in cancer, *Curr Opin Genet Dev* 17(1):23–30, 2007.

Montes-Mojarro IA, Steinhilber J, et al.: The pathological spectrum of systemic anaplastic large cell lymphoma (ALCL), *Cancers* 10(4):107, 2018.

Moreno I, Martin G, Bolufer P, et al.: Incidence and prognostic value of FLT3 internal tandem duplication and D835 mutations in acute myeloid leukemia, *Haematologica* 88:19–24, 2003.

Morgan GJ, He J, Tytarenko R, et al.: Kinase domain activation through gene rearrangement in multiple myeloma, *Leukemia* 32(11):2435–2444, 2018.

Morgan GJ, Walker BA, Davies FE: The genetic architecture of multiple myeloma, *Nat Rev Cancer* 12(5):335–348, 2012.

Mori N, Ohwashi M, Yoshinaga K, et al.: L265P mutation of the MYD88 gene is frequent in Waldenstrom's macroglobulinemia and its absence in myeloma, *PloS One* 8(11), 2013. e80088.

Morin RD, Johnson NA, Severson TM, et al.: Somatic mutations altering EZH2 (Tyr641) in follicular and diffuse large B-cell lymphomas of germinal-center origin, *Nat Genet* 42(2):181–185, 2010.

Morin RD, Mendez-Lago M, Mungall AJ, et al.: Frequent mutation of histone-modifying genes in non-Hodgkin lymphoma, *Nature* 476(7360):298–303, 2011.

Morin RD, Mungall K, Pleasance E, et al.: Mutational and structural analysis of diffuse large B-cell lymphoma using whole-genome sequencing, *Blood* 122(7):1256–1265, 2013.

Mozos A, Royo C, Hartmann E, et al.: SOX11 expression is highly specific for mantle cell lymphoma and identifies the cyclin D1-negative subtype, *Haematologica* 94(11):1555–1562, 2009.

Mrózek K, Marcucci G, Paschka P, et al.: Advances in molecular genetics and treatment of core-binding factor acute myeloid leukemia, *Curr Opin Oncol* 20(6):711–718, 2008.

Mrozek K, Heinonen K, Lawrence D, et al.: Adult patients with de novo acute myeloid leukemia and t(9; 11)(p22; q23) have a superior outcome to patients with other translocations involving band 11q23: a cancer and leukemia group B study, *Blood* 90(11):4532–4538, 1997.

Mughal TI, Cross NC, Padron E, et al.: An International MDS/MPN Working Group's perspective and recommendations on molecular pathogenesis, diagnosis and clinical characterization of myelodysplastic/myeloproliferative neoplasms, *Haematologica* 100(9):1117–1130, 2015.

Müller AM, Duque J, Shizuru JA, et al.: Complementing mutations in core binding factor leukemias: from mouse models to clinical applications, *Oncogene* 27(44):5759–5773, 2008.

Mullighan CG: Genome sequencing of lymphoid malignancies, *Blood* 122(24):3899–3907, 2013.

Mullighan CG, Miller CB, Radtke I, et al.: BCR-ABL1 lymphoblastic leukaemia is characterized by the deletion of Ikaros, *Nature* 453(7191):110–114, 2008.

Mullighan CG, Su X, Zhang J, et al.: Deletion of IKZF1 and prognosis in acute lymphoblastic leukemia, *N Engl J Med* 360(5):470–480, 2009.

Muramatsu H, Makishima H, Jankowska AM, et al.: Mutations of an E3 ubiquitin ligase c-Cbl but not TET2 mutations are pathogenic in juvenile myelomonocytic leukemia, *Blood* 115(10):1969–1975, 2010.

Nabhan C, Raca G, Wang YL: Predicting prognosis in chronic lymphocytic leukemia in the contemporary era, *JAMA Oncol* 1(7):965–974, 2015.

Nacheva EP, Grace CD, Brazma D, et al.: Does BCR/ABL1 positive acute myeloid leukaemia exist? *Br J Haematol* 161(4):541–550, 2013.

Nadeu F, Delgado J, Royo C, et al.: Clinical impact of clonal and subclonal TP53, SF3B1, BIRC3, NOTCH1, and ATM mutations in chronic lymphocytic leukemia, *Blood* 127(17):2122–2130, 2016.

Nangalia J, Massie CE, Baxter EJ, et al.: Somatic CALR mutations in myeloproliferative neoplasms with nonmutated JAK2, *N Engl J Med* 369(25):2391–2405, 2013.

Navarro A, Clot G, Royo C, et al.: Molecular subsets of mantle cell lymphoma defined by the IGHV mutational status and SOX11 expression have distinct biologic and clinical features *Cancer*, *Res* 72(20):5307–5316, 2012.

Navarro A, Royo C, Hernandez L, et al.: Molecular pathogenesis of mantle cell lymphoma: new perspectives and challenges with clinical implications, *Semin Hematol* 48(3):155–165, 2011.

Nickels EM, Soodalter J, Churpek JE, et al.: Recognizing familial myeloid leukemia in adults, *Ther Adv Hematol* 4(4):254–269, 2013.

Nicolini FE, Basak GW, Kim DW, et al.: Overall survival with ponatinib versus allogeneic stem cell transplantation in Philadelphia chromosome-positive leukemias with the T315I mutation, *Cancer* 123(15):2875–2880, 2017.

Niemeyer CM: RAS diseases in children, *Haematologica* 99(11):1653–1662, 2014.

Niemeyer CM, Arico M, Basso G, et al.: Chronic myelomonocytic leukemia in childhood: a retrospective analysis of 110 cases, *European Working Group on Myelodysplastic Syndromes in Childhood (EWOG-MDS)*, *Blood* 89(10):3534–3543, 1997.

Niemeyer CM, Kang MW, Shin DH, et al.: Germline CBL mutations cause developmental abnormalities and predispose to juvenile myelomonocytic leukemia, *Nat Genet* 42(9):794–800, 2010.

Nowell PC, Hungerford DA: A minute chromosome in human chronic granulocytic leukemia, *Science* 132:1497, 1960.

Noy A, Yahalom J, Zaretsky L, et al.: Gastric mucosa-associated lymphoid tissue lymphoma detected by clonotypic polymerase chain reaction despite continuous pathologic remission induced by involved-field radiotherapy, *J Clin Oncol* 23(16):3768–3772, 2005.

Oberle A, Brandt A, Voigtlaender M, et al.: Monitoring multiple myeloma by next-generation sequencing of V(D)J rearrangements from circulating myeloma cells and cell-free myeloma DNA, *Haematologica* 102(6):1105–1111, 2017.

Obermann EC, Csato M, Dirnhofer S, Tzankov A: BCL2 gene aberration as an IPI-independent marker for poor outcome in non-germinal-centre diffuse large B cell lymphoma, *J Clin Pathol* 62(10):903–907, 2009.

Obhi SS, Matkovich S, Chen R: Changing the "when" and "what" of intended actions, *J Neurophysiol* 102(5):2755–2762, 2009.

O'Brien SG, Guilhot F, Larson RA, et al.: Imatinib compared with interferon and low-dose cytarabine for newly diagnosed chronic-phase chronic myeloid leukemia, *N Eng J Med* 348:994–1004, 2003.

Odejide O, Weigert O, Lane AA, et al.: A targeted mutational landscape of angioimmunoblastic T-cell lymphoma, *Blood* 123(9):1293–1296, 2014.

Ogawa S: Genetics of MDS, *Blood* 133(10):1049–1059, 2019.

Ok CY, Medeiros LJ: *High-grade B-cell lymphoma: a term re-purposed in the revised WHO classification*, *Pathology*, 2019.

Okosun J, Bodor C, Wang J, et al.: Integrated genomic analysis identifies recurrent mutations and evolution patterns driving the initiation and progression of follicular lymphoma, *Nat Genet* 46(2):176–181, 2014.

Okumura AJ, Peterson LF, Okumura F, et al.: t(8;21)(q22;q22) fusion proteins preferentially bind to duplicated AML1/RUNX1 DNA-binding sequences to differentially regulate gene expression, *Blood* 112:1392–1401, 2008.

Ondrejka SL, Lin JJ, Warden DW, et al.: MYD88 L265P somatic mutation: its usefulness in the differential diagnosis of bone marrow involvement by B-cell lymphoproliferative disorders, *Am J Clin Pathol* 140(3):387–394, 2013.

Ono R, Nosaka T, Hayashi Y: Roles of a trithorax group gene, MLL, in hematopoiesis, *Int J Hematol* 81(4):288–293, 2005.

Orfao A, Garcia-Montero AC, Sanchez L, et al.: Recent advances in the understanding of mastocytosis: the role of KIT mutations, *Br J Haematol* 138:12–30, 2007.

Oscier DG, Gardiner AC, Mould SJ, et al.: Multivariate analysis of prognostic factors in CLL: clinical stage, IGVH gene mutational status, and loss or mutation of the p53 gene are independent prognostic factors, *Blood* 100(4):1177–1184, 2002.

Pabst T, Eyholzer M, Haefliger S, et al.: Somatic CEBPA mutations are a frequent second event in families with germline CEBPA mutations and familial acute myeloid leukemia, *J Clin Oncol* 26(31):5088–5093, 2008.

Padron E, Garcia-Manero G, Patnaik MM, et al.: An international data set for CMML validates prognostic scoring systems and demonstrates a need for novel prognostication strategies, *Blood Cancer J* 5:e333, 2015.

Pancrazzi A, Guglielmelli P, Ponziani V, et al.: A sensitive detection method for MPLW515L or MPLW515K mutation in chronic myeloproliferative disorders with locked nucleic acid-modified probes and real-time polymerase chain reaction, *J Mol Diagn* 10(5):435–441, 2008.

Pant V, Quintas-Cardama A, Lozano G: The p53 pathway in hematopoiesis: lessons from mouse models, implications for humans, *Blood* 120(26):5118–5127, 2012.

Papaemmanuil E, Gerstung M, Bullinger L, et al.: Genomic classification and prognosis in acute myeloid leukemia, *N Engl J Med* 374(23):2209–2221, 2016.

Papaemmanuil E, Gerstung M, Malcovati L, et al.: Clinical and biological implications of driver mutations in myelodysplastic syndromes, *Blood* 122(22):3616–3627, 2013. quiz 3699.

Pardanani A: Systemic mastocytosis in adults: 2013 update on diagnosis, risk stratification, and management, *Am J Hematol* 88(7):612–624, 2013.

Pardanani A, Ketterling RP, Brockman SR, et al.: CHIC2 deletion, a surrogate for FIP1L1-PDGFRA fusion, occurs in systemic mastocytosis associated with eosinophilia and predicts response to imatinib therapy, *Blood* 102:3093–3096, 2003.

Pardanani A, Lasho TL, Laborde RR, et al.: CSF3R T618I is a highly prevalent and specific mutation in chronic neutrophilic leukemia, *Leukemia* 27(9):1870–1873, 2013.

Parrilla Castellar ER, Jaffe ES, Said JW, et al.: ALK-negative anaplastic large cell lymphoma is a genetically heterogeneous disease with widely disparate clinical outcomes, *Blood* 124(9):1473–1480, 2014.

Paschka P, Du J, Schlenk RF, et al.: Secondary genetic lesions in acute myeloid leukemia with inv(16) or t(16; 16): a study of the German-Austrian AML Study Group (AMLSG), *Blood* 121:170–177, 2012.

Paschka P: Core binding factor acute myeloid leukemia, *Semin Oncol* 35(4):410–417, 2008.

Paschka P, Dohner K: Core-binding factor acute myeloid leukemia: can we improve on HiDAC consolidation?, *Hematology Am Soc Hematol Educ Program*209–219, 2013. 2013.

Paschka P, Marcucci G, Ruppert AS, et al.: Adverse prognostic significance of KIT mutations in adult acute myeloid leukemia with inv(16) and t(8;21): a Cancer and Leukemia Group B Study, *J Clin Oncol* 24(24):3904–3911, 2006.

Paschka P, Schlenk RF, Gaidzik VI, et al.: ASXL1 mutations in younger adult patients with acute myeloid leukemia: a study by the German-Austrian Acute Myeloid Leukemia Study Group, *Haematologica* 100(3):324–330, 2015.

Pasqualucci L, Dalla-Favera R: The genetic landscape of diffuse large B-cell lymphoma, *Semin Hematol* 52(2):67–76, 2015.

Pasqualucci L, Dalla-Favera R: Genetics of diffuse large B-cell lymphoma, *Blood* 131(21):2307–2319, 2018.

Pasqualucci L, Bhagat G, Jankovic M, et al.: AID is required for germinal center-derived lymphomagenesis, *Nat Genet* 40(1):108–112, 2008.

Pasqualucci L, Trifonov V, Fabbri G, et al.: Analysis of the coding genome of diffuse large B-cell lymphoma, *Nat Genet* 43(9):830–837, 2011.

Passamonti F, Giorgino T, Mora B, et al.: A clinical-molecular prognostic model to predict survival in patients with post polycythemia vera and post essential thrombocythemia myelofibrosis, *Leukemia* 31(12):2726–2731, 2017.

Pastore A, Jurinovic V, Kridel R, et al.: Integration of gene mutations in risk prognostication for patients receiving first-line immunochemotherapy for follicular lymphoma: a retrospective analysis of a prospective clinical trial and validation in a population-based registry, *Lancet Oncol* 16(9):1111–1122, 2015.

Patel AB, O'Hare T, Deininger MW: Mechanisms of resistance to ABL kinase inhibition in chronic myeloid leukemia and the development of next generation ABL kinase inhibitors, *Hematol Oncol Clin North Am* 31(4):589–612, 2017.

Patel JP, Gonen M, Figueroa ME, et al.: Prognostic relevance of integrated genetic profiling in acute myeloid leukemia, *N Engl J Med* 366(12):1079–1089, 2012.

Patnaik MM, Tefferi A: Chronic myelomonocytic leukemia: 2018 update on diagnosis, risk stratification and management, *Am J Hematol* 93(6):824–840, 2018.

Patnaik MM, Itzykson R, Lasho TL, et al.: ASXL1 and SETBP1 mutations and their prognostic contribution in chronic myelomonocytic leukemia: a two-center study of 466 patients, *Leukemia* 28(11):2206–2212, 2014.

Paulsson K, Jonson T, Ora I, et al.: Characterisation of genomic translocation breakpoints and identification of an alternative TCF3/PBX1 fusion transcript in t(1;19)(q23;p13)-positive acute lymphoblastic leukaemias, *Br J Haematol* 138(2):196–201, 2007.

Pedersen MB, Hamilton-Dutoit SJ, Bendix K, et al.: DUSP22 and TP63 rearrangements predict outcome of ALK-negative anaplastic large cell lymphoma: a Danish cohort study, *Blood* 130(4):554–557, 2017.

Peng J, Zuo Z, Fu B, et al.: Chronic myelomonocytic leukemia with nucleophosmin (NPM1) mutation, *Eur J Haematol* 96(1):65–71, 2016.

Perez B, Mechinaud F, Galambrun C, et al.: Germline mutations of the CBL gene define a new genetic syndrome with predisposition to juvenile myelomonocytic leukaemia, *J Med Genet* 47(10):686–691, 2010.

Perez-Andreu V, Roberts KG, Xu H, et al.: A genome-wide association study of susceptibility to acute lymphoblastic leukemia in adolescents and young adults, *Blood* 125(4):680–686, 2015.

Perez-Galan P, Dreyling M, Wiestner A: Mantle cell lymphoma: biology, pathogenesis, and the molecular basis of treatment in the genomic era, *Blood* 117(1):26–38, 2011.

Perkins SL, Pickering D, Lowe EJ, et al.: Childhood anaplastic large cell lymphoma has a high incidence of ALK gene rearrangement as determined by immunohistochemical staining and fluorescent in situ hybridisation: a genetic and pathological correlation, *Br J Haematol* 131(5):624–627, 2005.

Perlot T, Alt FW: Cis-regulatory elements and epigenetic changes control genomic rearrangements of the IgH locus, *Adv Immunol* 99:1–32, 2008.

Pestell RG: New roles of cyclin D1, *Am J Pathol* 183(1):3–9, 2013.

Peterson LF, Boyapati A, Ahn EY, et al.: Acute myeloid leukemia with the 8q22;21q22 translocation: secondary mutational events and alternative t(8;21) transcripts, *Blood* 110(3):799–805, 2007.

Pfeifer AC, Timmer J, Klingmüller U: Systems biology of JAK/STAT signalling, *Essays Biochem* 45:109–120, 2008.

Pfirrmann M, Evtimova D, Saussele S, et al.: No influence of BCR-ABL1 transcript types e13a2 and e14a2 on long-term survival: results in 1494 patients with chronic myeloid leukemia treated with imatinib, *J Cancer Res Clin Oncol* 143(5):843–850, 2017.

Pham-Ledard A, Beylot-Barry M, Barbe C, et al.: High frequency and clinical prognostic value of MYD88 L265P mutation in primary cutaneous diffuse large B-cell lymphoma, leg-type, *JAMA Dermatol* 150(11):1173–1179, 2014.

Piazza R, Valletta S, Winkelmann N, et al.: Recurrent SETBP1 mutations in atypical chronic myeloid leukemia, *Nat Genet* 45(1):18–24, 2013.

Pietra D, Li S, Brisci A, et al.: Somatic mutations of JAK2 exon 12 in patients with JAK2 (V617F)-negative myeloproliferative disorders, *Blood* 111(3):1686–1689, 2008.

Pietra D, Rumi E, Ferretti VV, et al.: Differential clinical effects of different mutation subtypes in CALR-mutant myeloproliferative neoplasms, *Leukemia* 30(2):431–438, 2016.

Pikman Y, Lee BH, Mercher T, et al.: MPLW515L is a novel somatic activating mutation in myelofibrosis with myeloid metaplasia, *PLoS Med* 3, 2006. e270.

Pincus MR, Brandt-Rauf PM, Michl J, et al: ras-p21-induced cell transformation: Unique signal transduction pathways and implications for the design of new chemotherapeutic agents, *Cancer Invest*, 18:39-50, 2000.

Pitchford CW, Hettinga AC, Reichard KK: Fluorescence in situ hybridization testing for -5/5q, -7/7q, +8, and del(20q) in primary myelodysplastic syndrome correlates with conventional cytogenetics in the setting of an adequate study, *Am J Clin Pathol* 133(2):260–264, 2010.

Pratcorona M, Abbas S, Sanders MA, et al.: Acquired mutations in ASXL1 in acute myeloid leukemia: prevalence and prognostic value, *Haematologica* 97(3):388–392, 2012.

Pratcorona M, Brunet S, Nomdedeu J, et al.: Favorable outcome of patients with acute myeloid leukemia harboring a low-allelic burden FLT3-ITD mutation and concomitant NPM1 mutation: relevance to post-remission therapy, *Blood* 121(14):2734–2738, 2013.

Preudhomme C, Renneville A, Bourdon V, et al.: High frequency of RUNX1 biallelic alteration in acute myeloid leukemia secondary to familial platelet disorder, *Blood* 113(22):5583–5587, 2009.

Prima V, Hunger SP: Cooperative transformation by MEF2D/DAZAP1 and DAZAP1/MEF2D fusion proteins generated by the variant t(1;19) in acute lymphoblastic leukemia, *Leukemia* 21(12):2470–2475, 2007.

Puente XS, Pinyol M, Quesada V, et al.: Whole-genome sequencing identifies recurrent mutations in chronic lymphocytic leukaemia, *Nature* 475(7354):101–105, 2011.

Pui CH, Chessells JM, Camitta B, et al.: Clinical heterogeneity in childhood acute lymphoblastic leukemia with 11q23 rearrangements, *Leukemia* 17(4):700–706, 2003.

Pui CH, Mullighan CG, Evans WE, et al.: Pediatric acute lymphoblastic leukemia: where are we going and how do we get there? *Blood* 120(6):1165–1174, 2012.

Pulford K, Lamant L, Espinos E, et al.: The emerging normal and disease-related roles of anaplastic lymphoma kinase, *Cell Mol Life Sci* 61(23):2939–2953, 2004.

Pylayeva-Gupta Y, Grabocka E, Bar-Sagi D: RAS oncogenes: weaving a tumorigenic web, *Nat Rev Cancer* 11(11):761–774, 2011.

Qu X, Li H, Braziel RM, et al.: Genomic alterations important for the prognosis in patients with follicular lymphoma treated in SWOG study S0016, *Blood* 133(1):81–93, 2019.

Quesada AE, Medeiros LJ, Clemens MW, et al.: Breast implant-associated anaplastic large cell lymphoma: a review, *Mod Pathol* 32(2):166–188, 2019.

Quignon F, De Bels F, Koken M, et al.: PML induces a novel caspase-independent death process, *Nat Genet* 20:259–265, 1998.

Quinquenel A, Fornecker LM, Letestu R, et al.: Prevalence of BTK and PLCG2 mutations in a real-life CLL cohort still on ibrutinib after 3 years: a FILO group study, *Blood* 134(7):641–644, 2019.

Quintas-Cardama A, Cortes J: Molecular biology of bcr-abl1-positive chronic myeloid leukemia, *Blood* 113(8):1619–1630, 2009.

Radich J, Yeung C, Wu D: New approaches to molecular monitoring in CML (and other diseases), *Blood* 134(19):1578–1584, 2019.

Raghavan SC, Lieber MR: Chromosomal translocations and non-B DNA structures in the human genome, *Cell Cycle* 3(6):762–768, 2004.

Raimondi SC, Shurtleff SA, Downing JR, et al.: 12p abnormalities and the TEL gene (ETV6) in childhood acute lymphoblastic leukemia, *Blood* 90(11):4559–4566, 1997.

Rajala HL, Eldfors S, Kuusanmaki H, et al.: Discovery of somatic STAT5b mutations in large granular lymphocytic leukemia, *Blood* 121(22):4541–4550, 2013.

Rajala HL, Porkka K, Maciejewski JP, et al.: Uncovering the pathogenesis of large granular lymphocytic leukemia-novel STAT3 and STAT5b mutations, *Ann Med* 46(3):114–122, 2014.

Rakheja D, Konoplev S, Medeiros LJ, et al.: IDH mutations in acute myeloid leukemia, *Hum Pathol* 43(10):1541–1551, 2012.

Rampal R, Alkalin A, Madzo J, et al.: DNA hydroxymethylation profiling reveals that WT1 mutations result in loss of TET2 function in acute myeloid leukemia, *Cell Rep* 9(5):1841–1855, 2014.

Rapado I, Grande S, Albizua E, et al.: High resolution melting analysis for JAK2 Exon 14 and Exon 12 mutations: a diagnostic tool for myeloproliferative neoplasms, *J Mol Diagn* 11(2):155–161, 2009.

Reddy A, Zhang J, Davis NS, et al.: Genetic and functional drivers of diffuse large B cell lymphoma, *Cell* 171(2):481–494 e415, 2017.

Redner RL: Variations on a theme: the alternate translocations in APL, *Leukemia* 16(10):1927–1932, 2002.

Reindl C, Quentmeier H, Petropoulos K, et al.: CBL exon 8/9 mutants activate the FLT3 pathway and cluster in core binding factor/11q deletion acute myeloid leukemia/myelodysplastic syndrome subtypes, *Clin Cancer Res* 15(7):2238–2247, 2009.

Reineke EL, Kao HY: Targeting promyelocytic leukemia protein: a means to regulating PML nuclear bodies, *Int J Biol Sci* 5(4):366–376, 2009.

Reiter A, Saussele S, Grimwade D, et al.: Genomic anatomy of the specific reciprocal translocation t(15;17) in acute promyelocytic leukemia, *Genes Chromosomes Cancer* 36(2):175–188, 2003.

Remstein ED, Dogan A, Einerson RR, et al.: The incidence and anatomic site specificity of chromosomal translocations in primary extranodal marginal zone B-cell lymphoma of mucosa-associated lymphoid tissue (MALT lymphoma) in North America, *Am J Surg Pathol* 30(12):1546–1553, 2006.

Remstein ED, Kurtin PJ, Buno I, et al.: Diagnostic utility of fluorescence in situ hybridization in mantle-cell lymphoma, *Br J Haematol* 110(4):856–862, 2000.

Renneville A, Boissel N, Gachard N, et al.: The favorable impact of CEBPA mutations in patients with acute myeloid leukemia is only observed in the absence of associated cytogenetic abnormalities and FLT3 internal duplication, *Blood* 113(21):5090–5093, 2009a.

Renneville A, Mialou V, Philippe N, et al.: Another pedigree with familial acute myeloid leukemia and germline CEBPA mutation, *Leukemia* 23(4):804–806, 2009b.

Reshmi SC, Harvey RC, Roberts KG, et al.: Targetable kinase gene fusions in high-risk B-ALL: a study from the Children's Oncology Group, *Blood* 129(25):3352–3361, 2017.

Ricci C, Fermo E, Corti S, et al.: RAS mutations contribute to evolution of chronic myelomonocytic leukemia to the proliferative variant, *Clin Cancer Res* 16(8):2246–2256, 2010.

Rio-Machin A, Menezes J, Maiques-Diaz A, et al.: Abrogation of RUNX1 gene expression in de novo myelodysplastic syndrome with t(4;21)(q21;q22), *Haematologica* 97(4):534–537, 2012.

Robbiani DF, Nussenzweig MC: Chromosome translocation, B cell lymphoma, and activation-induced cytidine deaminase, *Annu Rev Pathol* 8:79–103, 2013.

Roberts KG, Mullighan CG: Genomics in acute lymphoblastic leukaemia: insights and treatment implications, *Nat Rev Clin Oncol* 12(6):344–357, 2015.

Roberts KG, Li Y, Payne-Turner D, et al.: Targetable kinase-activating lesions in Ph-like acute lymphoblastic leukemia, *N Engl J Med* 371(11):1005–1015, 2014.

Roberts KG, Morin RD, Zhang J, et al.: Genetic alterations activating kinase and cytokine receptor signaling in high-risk acute lymphoblastic leukemia, *Canc Cell* 22(2):153–166, 2012.

Roberts KG, Reshmi SC, Harvey RC, et al.: Genomic and outcome analyses of Ph-like ALL in NCI standard-risk patients: a report from the Children's Oncology Group, *Blood* 132(8):815–824, 2018.

Rohde G, Kermer P, Reed JC, Bahr M, Weishaupt JH: Neuron-specific overexpression of the co-chaperone Bcl-2-associated athanogene-1 in superoxide dismutase 1(G93A)-transgenic mice, *Neuroscience* 157(4):844–849, 2008.

Roix JJ, McQueen PG, Munson PJ, et al.: Spatial proximity of translocation-prone gene loci in human lymphomas, *Nat Genet* 34(3):287–291, 2003.

Roller A, Grossmann V, Bacher U, et al.: Landmark analysis of DNMT3A mutations in hematological malignancies, *Leukemia* 27(7):1573–1578, 2013.

Rosenquist R, Ghia P, Hadzidimitriou A, et al.: Immunoglobulin gene sequence analysis in chronic lymphocytic leukemia: updated ERIC recommendations, *Leukemia* 31(7):1477–1481, 2017.

Rosenwald A, Bens S, Advani R, et al.: Prognostic significance of MYC rearrangement and translocation partner in diffuse large B-cell lymphoma: a study by the Lunenburg Lymphoma Biomarker Consortium, *J Clin Oncol* 37(35):3359–3368, 2019.

Rosenwald A, Wright G, Wiestner A, et al.: The proliferation gene expression signature is a quantitative integrator of oncogenic events that predicts survival in mantle cell lymphoma, *Canc Cell* 3(2):185–197, 2003.

Rossari F, Minutolo F, Orciuolo E: Past, present, and future of Bcr-Abl inhibitors: from chemical development to clinical efficacy, *J Hematol Oncol* 11(1):84, 2018.

Rossi D: Role of MYD88 in lymphoplasmacytic lymphoma diagnosis and pathogenesis, *Hematology Am Soc Hematol Educ Program*(1)113–118, 2014.

Rossi D, Rasi S, Spina V, et al.: Integrated mutational and cytogenetic analysis identifies new prognostic subgroups in chronic lymphocytic leukemia, *Blood* 121(8):1403–1412, 2013.

Rowley JD: A new consistent chromosomal abnormality in chronic myelogenous leukaemia identified by quinacrine fluorescence and Giemsa staining, *Nature* 243:290–293, 1973.

Rubnitz JE, Raimondi SC, Tong X, et al.: Favorable impact of the t(9;11) in childhood acute myeloid leukemia, *J Clin Oncol* 20(9):2302–2309, 2002.

Rustad EH, Misund K, Bernard E, et al.: Stability and uniqueness of clonal immunoglobulin CDR3 sequences for MRD tracking in multiple myeloma, *Am J Hematol* 94(12):1364–1373, 2019.

Saglio G, Pane F, Gottardi E, et al.: Consistent amounts of acute leukemia-associated P190BCR/ABL transcripts are expressed by chronic myelogenous leukemia patients at diagnosis, *Blood* 87:1075–1080, 1996.

Sainty D, Liso V, Cantu-Rajnoldi A, et al.: A new morphological classification system for acute promyelocytic leukemia distinguishes cases with underlying PLZF-RARA rearrangements, *Blood* 96:1287–1296, 2000.

Salaverria I, Royo C, Carvajal-Cuenca A, et al.: CCND2 rearrangements are the most frequent genetic events in cyclin D1(-) mantle cell lymphoma, *Blood* 121(8):1394–1402, 2013.

Salido M, Baro C, Oscier D, et al.: Cytogenetic aberrations and their prognostic value in a series of 330 splenic marginal zone B-cell lymphomas: a multicenter study of the Splenic B-Cell Lymphoma Group, *Blood* 116(9):1479–1488, 2010.

Sanjuan-Pla A, Bueno C, Prieto C, et al.: Revisiting the biology of infant t(4;11)/MLL-AF4+ B-cell acute lymphoblastic leukemia, *Blood* 126(25):2676–2685, 2015.

Santamaria C, Chillon MC, Fernandez C, et al.: Using quantification of the PML-RARα transcript to stratify the risk of relapse in patients with acute promyelocytic leukemia, *Haematologica* 92:315–322, 2007.

Sanz MA, Grimwade D, Tallman MS, et al.: Management of acute promyelocytic leukemia: recommendations from an expert panel on behalf of the European LeukemiaNet, *Blood* 113(9):1875–1891, 2009.

Sarris AH, Luthra R, Papadimitracopoulou V, et al.: Amplification of genomic DNA demonstrates the presence of the t(2;5) (p23;q35) in anaplastic large cell lymphoma, but not in other non-Hodgkin's lymphomas, Hodgkin's disease, or lymphomatoid papulosis, *Blood* 88(5):1771–1779, 1996.

Saussele S, Richter J, Guilhot J, et al: Discontinuation of tyrosine kinase inhibitor therapy in chronic myeloid leukaemia (EURO-SKI): a prespecified interim analysis of a prospective, multicentre, non-randomised, trial, Lancet Oncol 19(6):747–757.

Schatz JH, Horwitz SM, Teruya-Feldstein J, et al.: Targeted mutational profiling of peripheral T-cell lymphoma not otherwise specified highlights new mechanisms in a heterogeneous pathogenesis, *Leukemia* 29(1):237–241, 2015.

Schlenk RF, Döhner K, Krauter J, et al.: Mutations and treatment outcome in cytogenetically normal acute myeloid leukemia, *N Engl J Med* 358(18):1909–1918, 2008.

Schlenk RF, Kayser S, Bullinger L, et al.: Differential impact of allelic ratio and insertion site in FLT3-ITD-positive AML with respect to allogeneic transplantation, *Blood* 124(23):3441–3449, 2014.

Schmidt J, Federmann B, Schindler N, et al.: MYD88 L265P and CXCR4 mutations in lymphoplasmacytic lymphoma identify cases with high disease activity, *Br J Haematol* 169(6):795–803, 2015.

Schmitt-Graeff AH, Teo SS, Olschewski M, et al.: JAK2V617F mutation status identifies subtypes of refractory anemia with ringed sideroblasts associated with marked thrombocytosis, *Haematologica* 93(1):34–40, 2008.

Schmitz R, Wright GW, Huang DW, et al.: Genetics and pathogenesis of diffuse large B-cell lymphoma, *N Engl J Med* 378(15):1396–1407, 2018.

Schmitz R, Young RM, Ceribelli M, et al.: Burkitt lymphoma pathogenesis and therapeutic targets from structural and functional genomics, *Nature* 490(7418):116–120, 2012.

Schnittger S, Bacher U, Haferlach C, et al.: Rare CBFB-MYH11 fusion transcripts in AML with inv(16)/t(16;16) are associated with therapy-related AML M4eo, atypical cytomorphology, atypical immunophenotype, atypical additional chromosomal rearrangements and low white blood cell count: a study on 162 patients, *Leukemia* 21(4):725–731, 2007.

Schnittger S, Bacher U, Alpermann T, et al.: Use of CBL exon 8 and 9 mutations in diagnosis of myeloproliferative neoplasms and myelodysplastic/myeloproliferative disorders: an analysis of 636 cases, *Haematologica* 97(12):1890–1894, 2012a.

Schnittger S, Bacher U, Haferlach C, et al.: Diversity of the juxtamembrane and TKD1 mutations (exons 13-15) in the FLT3 gene with regards to mutant load, sequence, length, localization, and correlation with biological data, *Genes Chromosomes Cancer* 51(10):910–924, 2012b.

Schnittger S, Bacher U, Haferlach T, et al.: Development and validation of a real-time quantification assay to detect and monitor BRAFV600E mutations in hairy cell leukemia, *Blood* 119(13):3151–3154, 2012c.

Schumacher JA, Duncavage EJ, Mosbruger TL, et al.: A comparison of deep sequencing of TCRG rearrangements vs traditional capillary electrophoresis for assessment of clonality in T-Cell lymphoproliferative disorders, *Am J Clin Pathol* 141(3):348–359, 2014.

Schuurhuis GJ, Heuser M, Freeman S, et al.: Minimal/measurable residual disease in AML: a consensus document from the European LeukemiaNet MRD Working Party, *Blood* 131(12):1275–1291, 2018.

Scott LM, Tong W, Levine RL, et al.: JAK2 Exon 12 mutations in polycythemia vera and idiopathic erythrocytosis, *N Engl J Med* 356:459–468, 2007.

Scott LM, Beer PA, Bench AJ, et al.: Prevalance of JAK2 V617F and exon 12 mutations in polycythaemia vera, *Br Haematol* 139(3):511–512, 2008.

Scott DW, King RL, Staiger AM, et al.: High-grade B-cell lymphoma with MYC and BCL2 and/or BCL6 rearrangements with diffuse large B-cell lymphoma morphology, *Blood* 131(18):2060–2064, 2018.

Scott DW, Mottok A, Ennishi D, et al.: Prognostic significance of diffuse large B-Cell lymphoma cell of origin determined by digital gene expression in formalin-fixed paraffin-embedded tissue biopsies, *J Clin Oncol* 33(26):2848–2856, 2015.

Scott DW, Wright GW, Williams PM, et al.: Determining cell-of-origin subtypes of diffuse large B-cell lymphoma using gene expression in formalin-fixed paraffin-embedded tissue, *Blood* 123(8):1214–1217, 2014.

Scott S, Travis D, Whitby L, Bainbridge J, et al.: Measurement of BCR-ABL1 by RT-qPCR in chronic myeloid leukaemia: findings from an international EQA Programme, *Br J Haematol* 177(3):414–422, 2017.

Sesques P, Johnson NA: Approach to the diagnosis and treatment of high-grade B-cell lymphomas with MYC and BCL2 and/or BCL6 rearrangements, *Blood* 129(3):280–288, 2017.

Shah NP, Garcia-Gutierrez V, Jimenez-Velasco A, et al.: Dasatinib discontinuation in patients with chronic-phase chronic myeloid leukemia and stable deep molecular response: the DASFREE study, *Leuk Lymphoma*1–10, 2019.

Shanmuganathan N, Hughes TP: Molecular monitoring in CML: how deep? How often? How should it influence therapy? *Blood* 132(20):2125–2133, 2018.

Sharma S, Kelly TK, Jones PA: Epigenetics in cancer, *Carcinogenesis* 31(1):27–36, 2010.

Shen ZX, Shi ZZ, Fang J, et al.: All-trans retinoic acid/As2O3 combination yields a high quality remission and survival in newly diagnosed acute promyelocytic leukemia, *Proc Natl Acad Sci U S A* 101(15):5328–5335, 2004.

Shigesada K, Van de Sluis B, Liu PP: Mechanism of leukemogenesis by the inv(16) chimeric gene CBFB//PEBP2B-MHY11, *Oncogene* 23:4297–4307, 2004.

Shin SY, Lee ST, Kim HY, et al.: Detection of MYD88 L265P in patients with lymphoplasmacytic lymphoma/Waldenstrom macroglobulinemia and other B-cell non-Hodgkin lymphomas, *Blood Res* 51(3):181–186, 2016.

Shiozawa Y, Malcovati L, Galli A, et al.: Aberrant splicing and defective mRNA production induced by somatic spliceosome mutations in myelodysplasia, *Nat Commun* 9(1):3649, 2018.

Shlush LI: Age-related clonal hematopoiesis, *Blood* 131(5):496–504, 2018.

Shlush LI, Zandi S, Mitchell A, et al.: Identification of pre-leukaemic haematopoietic stem cells in acute leukaemia, *Nature* 506(7488):328–333, 2014.

Shustov A, Soma L: Anaplastic large cell lymphoma: contemporary concepts and optimal management, *Cancer Treat Res* 176:127–144, 2019.

Silva FP, Morolli B, Storlazzi CT, et al.: Identification of RUNX1/AML1 as a classical tumor suppressor gene, *Oncogene* 22(4):538–547, 2003.

Silverman LB: Acute lymphoblastic leukemia in infancy, *Pediatr Blood Cancer* 49(7 Suppl):1070–1073, 2007.

Soshnikova N, Duboule D: Epigenetic regulation of Hox gene activation: the waltz of methyls, *Bioessays* 30(3):199–202, 2008.

Soverini S, Bassan R, Lion T: Treatment and monitoring of Philadelphia chromosome-positive leukemia patients: recent advances and remaining challenges, *J Hematol Oncol* 12(1):39, 2019.

Soverini S, De Benedittis C, Machova Polakova K, et al.: Unraveling the complexity of tyrosine kinase inhibitor-resistant populations by ultra-deep sequencing of the BCR-ABL kinase domain, *Blood* 122(9):1634–1648, 2013.

Soverini S, Hochhaus A, Nicolini FE, et al.: BCR-ABL kinase domain mutation analysis in chronic myeloid leukemia patients treated with tyrosine kinase inhibitors: recommendations from an expert panel on behalf of European LeukemiaNet, *Blood* 118(5):1208–1215, 2011.

Speck NA, Stacy T, Wang Q, et al.: Core-binding factor: a central player in hematopoiesis and leukemia, *Cancer Res* 59(Suppl), 1999. 1789S–1793S.

Spencer DH, Abel HJ, Lockwood CM, et al.: Detection of FLT3 internal tandem duplication in targeted, short-read-length, next-generation sequencing data, *J Mol Diagn* 15(1):81–93, 2013.

Spina V, Khiabanian H, Messina M, et al.: The genetics of nodal marginal zone lymphoma, *Blood* 128(10):1362–1373, 2016.

Staber PB, Herling M, Bellido M, et al.: Consensus criteria for diagnosis, staging, and treatment response assessment of T-cell prolymphocytic leukemia, *Blood* 134(14):1132–1143, 2019.

Stamatopoulos K, Agathangelidis A, Rosenquist R, et al.: Antigen receptor stereotypy in chronic lymphocytic leukemia, *Leukemia* 31(2):282–291, 2017.

Steensma DP, Bejar R, Jaiswal S, et al.: Clonal hematopoiesis of indeterminate potential and its distinction from myelodysplastic syndromes, *Blood* 126(1):9–16, 2015.

Steensma DP, Dewald GW, Lasho TL, et al.: The JAK2 V617F activating tyrosine kinase mutation is an infrequent event in both "atypical" myeloproliferative disorders and myelodysplastic syndromes, *Blood* 106(4):1207–1209, 2005.

Stein H, Foss HD, Durkop H, et al.: CD30(+) anaplastic large cell lymphoma: a review of its histopathologic, genetic, and clinical features, *Blood* 96(12):3681–3695, 2000.

Stern MH, Soulier J, Rosenzwajg M, et al.: MTCP-1: a novel gene on the human chromosome Xq28 translocated to the T cell receptor alpha/delta locus in mature T cell proliferations, *Oncogene* 8(9):2475–2483, 1993.

Stover EH, Chen J, Folens C, et al.: Activation of FIP1L1-PDGFRalpha requires disruption of the juxtamembrane domain of PDGFRalpha and is FIP1L1-independent, *Proc Natl Acad Sci U S A* 103(21):8078–8083, 2006.

Streubel B, Simonitsch-Klupp I, Mullauer L, et al.: Variable frequencies of MALT lymphoma-associated genetic aberrations in MALT lymphomas of different sites, *Leukemia* 18(10):1722–1726, 2004a.

Streubel B, Ye H, Du MQ, et al.: Translocation t(11;18)(q21;q21) is not predictive of response to chemotherapy with 2CdA in patients with gastric MALT lymphoma, *Oncology* 66(6):476–480, 2004b.

Streubel B, Vinatzer U, Lamprecht A, et al.: T(3;14)(p14.1;q32) involving IGH and FOXP1 is a novel recurrent chromosomal aberration in MALT lymphoma, *Leukemia* 19(4):652–658, 2005.

Strudwick S, Borden KL: Finding a role for PML in APL pathogenesis: a critical assessment of potential PML activities, *Leukemia* 16(10):1906–1917, 2002.

Sud A, Dearden C: T-cell prolymphocytic leukemia, *Hematol Oncol Clin North Am* 31(2):273–283, 2017.

Swaminathan M, Bannon SA, Routbort M, et al.: Hematologic malignancies and Li-Fraumeni syndrome, *Cold Spring Harb Mol Case Stud* 5(1), 2019.

Swerdlow SH, Campo E, Harris NL, et al.: *WHO classification of tumours of hematopoietic and lymphoid tissues*, Lyon, France, 2017, IARC Press.

Swerdlow SH, Kuzu I, Dogan A, et al.: The many faces of small B cell lymphomas with plasmacytic differentiation and the contribution of MYD88 testing, *Virchows Arch* 468(3):259–275, 2016.

Szankasi P, Reading NS, Vaughn CP, et al.: A quantitative allele-specific PCR test for the BRAF V600E mutation using a single heterozygous control plasmid for quantitation: a model for qPCR testing without standard curves, *J Mol Diagn* 15(2):248–254, 2013.

Takahashi K, Wang F, Kantarjian H, et al.: Preleukaemic clonal haemopoiesis and risk of therapy-related myeloid neoplasms: a case-control study, *Lancet Oncol* 18(1):100–111, 2017.

Takahashi S: Current findings for recurring mutations in acute myeloid leukemia, *J Hematol Oncol* 4:36, 2011.

Tallman MS, Wang ES, Altman JK, et al.: Acute myeloid leukemia, version 3.2019, NCCN clinical practice guidelines in oncology, *J Natl Compr Canc Netw* 17(6):721–749, 2019.

Tang JL, Hou HA, Chen CY, et al.: AML1/RUNX1 mutations in 470 adult patients with de novo acute myeloid leukemia: prognostic implication and interaction with other gene alterations, *Blood* 114(26):5352–5361, 2009.

Tarlock K, Alonzo TA, Moraleda PP, et al.: Acute myeloid leukaemia (AML) with t(6;9)(p23;q34) is associated with poor outcome in childhood AML regardless of FLT3-ITD status: a report from the Children's Oncology Group, *Br J Haematol* 166(2):254–259, 2014.

Tartaglia M, Gelb BD: Germ-line and somatic PTPN11 mutations in human disease, *Eur J Med Genet* 48(2):81–96, 2005.

Tasian SK, Hunger SP: Genomic characterization of paediatric acute lymphoblastic leukaemia: an opportunity for precision medicine therapeutics, *Br J Haematol* 176(6):867–882, 2017.

Tasian SK, Hurtz C, Wertheim GB, et al.: High incidence of Philadelphia chromosome-like acute lymphoblastic leukemia in older adults with B-ALL, *Leukemia* 31(4):981–984, 2017.

Tasian SK, Loh ML, Hunger SP: Philadelphia chromosome-like acute lymphoblastic leukemia, *Blood* 130(19):2064–2072, 2017.

Tawana K, Wang J, Renneville A, et al.: Disease evolution and outcomes in familial AML with germline CEBPA mutations, *Blood* 126(10):1214–1223, 2015.

Tefferi A: JAK and MPL mutations in myeloid malignancies, *Leuk Lymphoma* 49(3):388–397, 2008.

Tefferi A, Guglielmelli P, Lasho TL, et al.: MIPSS70+ version 2.0: mutation and karyotype-enhanced international prognostic scoring system for primary myelofibrosis, *J Clin Oncol* 36(17):1769–1770, 2018a.

Tefferi A, Guglielmelli P, Nicolosi M, et al.: GIPSS: genetically inspired prognostic scoring system for primary myelofibrosis, *Leukemia* 32(7):1631–1642, 2018b.

Tefferi A, Lasho TL, Guglielmelli P, et al.: Targeted deep sequencing in polycythemia vera and essential thrombocythemia, *Blood Adv* 1(1):21–30, 2016.

Tefferi A, Lasho TL, Tischer A, et al.: The prognostic advantage of calreticulin mutations in myelofibrosis might be confined to type 1 or type 1-like CALR variants, *Blood* 124(15):2465–2466, 2014.

Theunissen PMJ, de Bie M, van Zessen D, et al.: Next-generation antigen receptor sequencing of paired diagnosis and relapse samples of B-cell acute lymphoblastic leukemia: clonal evolution and implications for minimal residual disease target selection, *Leuk Res* 76:98–104, 2019.

Thol F, Bollin R, Gehlhaar M, et al.: Mutations in the cohesin complex in acute myeloid leukemia: clinical and prognostic implications, *Blood* 123(6):914–920, 2014.

Thol F, Friesen I, Damm F, et al.: Prognostic significance of ASXL1 mutations in patients with myelodysplastic syndromes, *J Clin Oncol* 29(18):2499–2506, 2011.

Thompson PA, Srivastava J, Peterson C, et al.: Minimal residual disease undetectable by next-generation sequencing predicts improved outcome in CLL after chemoimmunotherapy, *Blood* 134(22):1951–1959, 2019.

Thota S, Viny AD, Makishima H, et al.: Genetic alterations of the cohesin complex genes in myeloid malignancies, *Blood* 124(11):1790–1798, 2014.

Tiacci E, Schiavoni G, Martelli MP, et al.: Constant activation of the RAF-MEK-ERK pathway as a diagnostic and therapeutic target in hairy cell leukemia, *Haematologica* 98(4):635–639, 2013.

Tiacci E, Trifonov V, Schiavoni G, et al.: BRAF mutations in hairy-cell leukemia, *N Engl J Med* 364(24):2305–2315, 2011.

Tobin G, Rosenquist R: Prognostic usage of V(H) gene mutation status and its surrogate markers and the role of antigen selection in chronic lymphocytic leukemia, *Med Oncol* 22(3):217–228, 2005.

Toppaldoddi KR, da Costa Cacemiro M, Bluteau O, et al.: Rare type 1-like and type 2-like calreticulin mutants induce similar myeloproliferative neoplasms as prevalent type 1 and 2 mutants in mice, *Oncogene* 38(10):1651–1660, 2019.

Treon SP, Cao Y, Xu L, et al.: Somatic mutations in MYD88 and CXCR4 are determinants of clinical presentation and overall survival in Waldenstrom macroglobulinemia, *Blood* 123(18):2791–2796, 2014.

Treon SP, Xu L, Yang G, et al.: MYD88 L265P somatic mutation in Waldenstrom's macroglobulinemia, *N Engl J Med* 367(9):826–833, 2012.

Tsukada Y, Fang J, Erdjument-Bromage H, et al.: Histone demethylation by a family of JmjC domain-containing proteins, *Nature* 439(7078):811–816, 2006.

University of Chicago Hematopoietic Malignancies Cancer Risk T: How I diagnose and manage individuals at risk for inherited myeloid malignancies, *Blood* 128(14):1800–1813, 2016.

Uppal G, Ly V, Wang ZX, et al.: The utility of BRAF V600E mutation-specific antibody VE1 for the diagnosis of hairy cell leukemia, *Am J Clin Pathol* 143(1):120–125, 2015.

Ushio R, Yamamoto M, Nakashima K, et al.: Digital PCR assay detection of circulating Mycobacterium tuberculosis DNA in pulmonary tuberculosis patient plasma, *Tuberculosis* 99:47–53, 2016.

Ustun C, DeRemer DL, Akin C: Tyrosine kinase inhibitors in the treatment of systemic mastocytosis, *Leuk Res* 35(9):1143–1152, 2011.

Vallois D, Dobay MP, Morin RD, et al.: Activating mutations in genes related to TCR signaling in angioimmunoblastic and other follicular helper T-cell-derived lymphomas, *Blood* 128(11):1490–1502, 2016.

van der Velden VH, van Dongen JJ: MRD detection in acute lymphoblastic leukemia patients using Ig/TCR gene rearrangements as targets for real-time quantitative PCR, *Methods Mol Biol* 538:115–150, 2009.

van der Velden VH, Panzer-Grumayer ER, Cazzaniga G, et al.: Optimization of PCR-based minimal residual disease diagnostics for childhood acute lymphoblastic leukemia in a multi-center setting, *Leukemia* 21(4):706–713, 2007.

van Dongen JJ, Langerak AW, Bruggemann M, et al.: Design and standardization of PCR primers and protocols for detection of clonal immunoglobulin and T-cell receptor gene recombinations in suspect lymphoproliferations: report of the BIOMED-2 Concerted Action BMH4-CT98-3936, *Leukemia* 17(12):2257–2317, 2003.

van Krieken JH, Langerak AW, Macintyre EA, et al.: Improved reliability of lymphoma diagnostics via PCR-based clonality testing: report of the BIOMED-2 Concerted Action BHM4-CT98-3936, *Leukemia* 21(2):201–206, 2007.

Van Rhee F, Hochhaus A, Lin F, et al.: p190 BCR-ABL mRNA is expressed at low levels in p210-positive chronic myeloid and acute lymphoblastic leukemias, *Blood* 87:5213–5217, 1996.

Vandenberghe P, Beel K: Severe congenital neutropenia, a genetically heterogeneous disease group with an increased risk of AML/MDS, *Pediatr Rep* 3(Suppl 2), 2011. e9.

Vannucchi AM, Antonioli E, Guglielmelli P, et al.: Clinical correlates of JAK2V617F presence or allele burden in myeloproliferative neoplasms: a critical reappraisal, *Leukemia* 22(7):1299–1307, 2008.

Vannucchi AM, Lasho TL, Guglielmelli P, et al.: Mutations and prognosis in primary myelofibrosis, *Leukemia* 27(9):1861–1869, 2013.

Vasmatzis G, Johnson SH, Knudson RA, et al.: Genome-wide analysis reveals recurrent structural abnormalities of TP63 and other p53-related genes in peripheral T-cell lymphomas, *Blood* 120(11):2280–2289, 2012.

Vega-Ruiz A, Cortes JE, Sever M, et al.: Phase II study of imatinib mesylate as therapy for patients with systemic mastocytosis, *Leuk Res* 33(11):1481–1484, 2009.

Verma D, Kantarjian HM, Jones D, et al.: Chronic myeloid leukemia (CML) with P190 BCR-ABL: analysis of characteristics, outcomes, and prognostic significance, *Blood* 114(11):2232–2235, 2009.

Vijayakrishnan J, Qian M, Studd JB, et al.: Identification of four novel associations for B-cell acute lymphoblastic leukaemia risk, *Nat Commun* 10(1):5348, 2019.

Visconte V, Tabarroki A, Hasrouni E, et al.: Molecular and phenotypic heterogeneity of refractory anemia with ring sideroblasts associated with marked thrombocytosis, *Leuk Lymphoma* 57(1):212–215, 2016.

Viswanatha DS, Chen IM, Liu PP, et al.: Characterization and use of an antibody detecting the CBFB/SMMHC fusion protein in inv 16/t(16;16)-associated acute myeloid leukemias, *Blood* 91:1882–1890, 1998.

von Goessel H, Jacobs U, Semper S, et al.: Cluster analysis of genomic ETV6-RUNX1 (TEL-AML1) fusion sites in childhood acute lymphoblastic leukemia, *Leuk Res* 33(8):1082–1088, 2009.

Wahl MC, Will CL, Luhrmann R: The spliceosome: design principles of a dynamic RNP machine, *Cell* 136(4):701–718, 2009.

Walker BA, Boyle EM, Wardell CP, et al.: Mutational spectrum, copy number changes, and outcome: results of a sequencing study of patients with newly diagnosed myeloma, *J Clin Oncol* 33(33):3911–3920, 2015a.

Walker BA, Mavrommatis K, Wardell CP, et al.: A high-risk, double-hit, group of newly diagnosed myeloma identified by genomic analysis, *Leukemia* 33(1):159–170, 2019.

Walker BA, Mavrommatis K, Wardell CP, et al.: Identification of novel mutational drivers reveals oncogene dependencies in multiple myeloma, *Blood* 132(6):587–597, 2018.

Walker BA, Wardell CP, Murison A, et al.: APOBEC family mutational signatures are associated with poor prognosis translocations in multiple myeloma, *Nat Commun* 6:6997, 2015b.

Wang ZG, Ruggero D, Ronchetti S, et al.: Pml is essential for multiple apoptotic pathways, *Nat Genet* 20:266–272, 1998.

Wang C, McKeithan TW, Gong Q, et al.: IDH2R172 mutations define a unique subgroup of patients with angioimmunoblastic T-cell lymphoma, *Blood* 126(15):1741–1752, 2015a.

Wang SA, Hasserjian RP, Fox PS, et al.: Atypical chronic myeloid leukemia is clinically distinct from unclassifiable myelodysplastic/myeloproliferative neoplasms, *Blood* 123(17):2645–2651, 2014.

Wang Y, Xiao M, Chen X, et al.: WT1 recruits TET2 to regulate its target gene expression and suppress leukemia cell proliferation, *Mol Cell* 57(4):662–673, 2015b.

Wassie EA, Itzykson R, Lasho TL, et al.: Molecular and prognostic correlates of cytogenetic abnormalities in chronic myelomonocytic leukemia: a Mayo Clinic-French Consortium Study, *Am J Hematol* 89(12):1111–1115, 2014.

Waterfall JJ, Arons E, Walker RL, et al.: High prevalence of MAP2K1 mutations in variant and IGHV4-34-expressing hairy-cell leukemias, *Nat Genet* 46(1):8–10, 2014.

Wei LN: Retinoids and receptor interacting protein 140 (RIP140) in gene regulation, *Curr Med Chem* 11(12):1527–1532, 2004.

Weis K, Rambaud S, Lavau C, et al.: Retinoic acid regulates aberrant nuclear localization of PML-RARα in acute promyelocytic leukaemia cells, *Cell* 76:345–356, 1994.

Welch JS, Petti AA, Miller CA, et al.: TP53 and decitabine in acute myeloid leukemia and myelodysplastic syndromes, *N Engl J Med* 375(21):2023–2036, 2016.

West AH, Godley LA, Churpek JE: Familial myelodysplastic syndrome/acute leukemia syndromes: a review and utility for translational investigations, *Ann N Y Acad Sci* 1310:111–118, 2014.

Wiemels JL, Hofmann J, Kang M, et al.: Chromosome 12p deletions in TEL-AML1 childhood acute lymphoblastic leukemia are associated with retrotransposon elements and occur postnatally, *Cancer Res* 68(23):9935–9944, 2008.

Williams ME, Meeker TC, Swerdlow SH: Rearrangement of the chromosome 11 bcl-1 locus in centrocytic lymphoma: analysis with multiple breakpoint probes, *Blood* 78(2):493–498, 1991.

Williams ME, Swerdlow SH, Meeker TC: Chromosome t(11;14)(q13;q32) breakpoints in centrocytic lymphoma are highly localized at the bcl-1 major translocation cluster, *Leukemia* 7(9):1437–1440, 1993.

Williams ME, Swerdlow SH, Rosenberg CL, Arnold A: Characterization of chromosome 11 translocation breakpoints at the bcl-1 and PRAD1 loci in centrocytic lymphoma, *Cancer Res* 52(19 Suppl), 1992. 5541s–5544s.

Willis A, Jung EJ, Wakefield T, Chen X: Mutant p53 exerts a dominant negative effect by preventing wild-type p53 from binding to the promoter of its target genes, *Oncogene* 23(13):2330–2338, 2004.

Willis SG, Lange T, Demehri S, et al.: High-sensitivity detection of BCR-ABL kinase domain mutations in imatinib-naive patients: correlation with clonal cytogenetic evolution but not response to therapy, *Blood* 106(6):2128–2137, 2005.

Winters AC, Bernt KM: MLL-rearranged leukemias—an update on science and clinical approaches, *Front Pediatr* 5(4), 2017.

Wong TN, Ramsingh G, Young AL, et al.: Role of TP53 mutations in the origin and evolution of therapy-related acute myeloid leukaemia, *Nature* 518(7540):552–555, 2015.

Wood B, Wu D, Crossley B, et al.: Measurable residual disease detection by high-throughput sequencing improves risk stratification for pediatric B-ALL, *Blood* 131(12):1350–1359, 2018.

Wouters BJ, Lowenberg B, Erpelinck-Verschueren CAJ, et al.: Double CEBPA mutations, but not single CEBPA mutations, define a subgroup of acute myeloid leukemia with a distinctive gene expression profile that is uniquely associated with a favorable outcome, *Blood* 113:3088–3091, 2009.

Wouters BJ, Delwel R: Epigenetics and approaches to targeted epigenetic therapy in acute myeloid leukemia, *Blood* 127(1):42–52, 2016.

Woyach JA, Furman RR, Liu TM, et al.: Resistance mechanisms for the Bruton's tyrosine kinase inhibitor ibrutinib, *N Engl J Med* 370(24):2286–2294, 2014.

Wu D, Emerson RO, Sherwood A, et al.: Detection of minimal residual disease in B lymphoblastic leukemia by high-throughput sequencing of IGH, *Clin Cancer Res* 20(17):4540–4548, 2014.

Wu D, Sherwood A, Fromm JR, et al.: High-throughput sequencing detects minimal residual disease in acute T lymphoblastic leukemia, *Sci Transl Med* 4(134):134ra163, 2012.

Wundisch T, Neubauer A, Stolte M, et al.: B-cell monoclonality is associated with lymphoid follicles in gastritis, *Am J Surg Pathol* 27(7):882–887, 2003.

Xi L, Arons E, Navarro W, et al.: Both variant and IGHV4-34-expressing hairy cell leukemia lack the BRAF V600E mutation, *Blood* 119(14):3330–3332, 2012.

Xie M, Lu C, Wang J, et al.: Age-related mutations associated with clonal hematopoietic expansion and malignancies, *Nat Med* 20(12):1472–1478, 2014.

Xing X, Feldman AL: Anaplastic large cell lymphomas: ALK positive, ALK negative, and primary cutaneous, *Adv Anat Pathol* 22(1):29–49, 2015.

Xu X, Zhang Q, Luo J, et al.: JAK2(V617F): prevalence in a large Chinese hospital population, *Blood* 109(1):339–342, 2007.

Xu L, You X, Zheng P, et al.: Methodologic considerations in the application of next-generation sequencing of human TRB repertoires for clinical use, *J Mol Diagn* 19(1):72–83, 2017.

Xu-Monette ZY, Wu L, Visco C, et al.: Mutational profile and prognostic significance of TP53 in diffuse large B-cell lymphoma patients treated with R-CHOP: report from an International DLBCL Rituximab-CHOP Consortium Program Study, *Blood* 120(19):3986–3996, 2012.

Yamagata T, Maki K, Mitani K: Runx1/AML1 in normal and abnormal hematopoiesis, *Int J Hematol* 82(1):1–8, 2005.

Yamamoto Y, Kiyoi H, Nakano Y, et al.: Activating mutation of D835 within the activation loop of FLT3 in human hematologic malignancies, *Blood* 97:2434–2439, 2001.

Yamane K, Toumazou C, Tsukada Y, et al.: JHDM2A, a JmjC-containing H3K9 demethylase, facilitates transcription activation by androgen receptor, *Cell* 125(3):483–495, 2006.

Yamazaki H, Suzuki M, Otsuki A, et al.: A remote GATA2 hematopoietic enhancer drives leukemogenesis in inv(3)(q21;q26) by activating EVI1 expression, *Canc Cell* 25:415–427, 2014.

Yanada M, Matsuo K, Suzuki T, et al.: Prognostic significance of FLT3 internal tandem duplication and tyrosine kinase domain mutations for acute myeloid leukemia: a meta-analysis, *Leukemia* 19:1345–1349, 2005.

Yanada M, Ohno R, Naoe T: Recent advances in the treatment of Philadelphia chromosome-positive acute lymphoblastic leukemia, *Int J Hematol* 89(1):3–13, 2009.

Ye H, Gong L, Liu H, et al.: MALT lymphoma with t(14;18)(q32;q21)/IGH-MALT1 is characterized by strong cytoplasmic MALT1 and BCL10 expression, *J Pathol* 205(3):293–301, 2005.

Ye H, Liu H, Raderer M, et al.: High incidence of t(11;18)(q21;q21) in Helicobacter pylori-negative gastric MALT lymphoma, *Blood* 101(7):2547–2550, 2003.

Yee HT, Ponzoni M, Merson A, et al.: Molecular characterization of the t(2;5) (p23; q35) translocation in anaplastic large cell lymphoma (Ki-1) and Hodgkin's disease, *Blood* 87(3):1081–1088, 1996.

Yim E, An HJ, Cho U, et al.: Two different KIT mutations may lead to different responses to imatinib in metastatic gastrointestinal stromal tumor, *Korean J Intern Med* 33(2):432–434, 2018.

Yoshida K, Sanada M, Shiraishi Y, et al.: Frequent pathway mutations of splicing machinery in myelodysplasia, *Nature* 478(7367):64–69, 2011.

Yoshizato T, Nannya Y, Atsuta Y, et al.: Genetic abnormalities in myelodysplasia and secondary acute myeloid leukemia: impact on outcome of stem cell transplantation, *Blood* 129(17):2347–2358, 2017.

Yosifov DY, Wolf C, Stilgenbauer S, et al.: From biology to therapy: the CLL success story, *Hemasphere* 3(2):e175, 2019.

Young AL, Challen GA, Birmann BM, et al.: Clonal haematopoiesis harbouring AML-associated mutations is ubiquitous in healthy adults, *Nat Commun* 7:12484, 2016.

Yu BD, Hess JL, Horning SE, et al.: Altered Hox expression and segmental identity in Mll-mutant mice, *Nature* 378(6556):505–508, 1995.

Zalcberg I, D'Andrea MG, Monteiro L, et al.: *Multidisciplinary diagnostics of chronic lymphocytic leukemia: European Research Initiative on CLL - ERIC recommendations*, Hematol Transfus Cell Ther, 2019.

Zamo A, Chiarle R, Piva R, et al.: Anaplastic lymphoma kinase (ALK) activates Stat3 and protects hematopoietic cells from cell death, *Oncogene* 21(7):1038–1047, 2002.

Zelent A, Guidez F, Melnick A, et al.: Translocations of the RARalpha gene in acute promyelocytic leukemia, *Oncogene* 20(49):7186–7203, 2001.

Zelent A, Greaves M, Enver T: Role of the TEL-AML1 fusion gene in the molecular pathogenesis of childhood acute lymphoblastic leukaemia, *Oncogene* 23(24):4275–4283, 2004.

Zeng Y, Feldman AL: Genetics of anaplastic large cell lymphoma, *Leuk Lymphoma* 57(1):21–27, 2016.

Zenz T, Kreuz M, Fuge M, et al.: TP53 mutation and survival in aggressive B cell lymphoma, *Int J Cancer* 141(7):1381–1388, 2017.

Zhang Y, Strissel P, Strick R, et al.: Genomic DNA breakpoints in AML1/RUNX1 and ETO cluster with topoisomerase II DNA cleavage and DNase I hypersensitive sites in t(8;21) leukemia, *Proc Natl Acad Sci USA* 99:3070–3075, 2002.

Zhang J, Ding L, Holmfeldt L, et al.: The genetic basis of early T-cell precursor acute lymphoblastic leukaemia, *Nature* 481(7380):157–163, 2012.

Zhang S, Mantel C, Broxmeyer HE: Flt3 signaling involves tyrosyl-phosphorylation of SHP-2 and SHIP and their association with Grb2 and Shc in Baf3/Flt3 cells, *J Leukoc Biol* 65(3):372–380, 1999.

Zhang W, Garces J, Dong HY: Detection of the t(11;18) API2/MALT1 translocation associated with gastric MALT lymphoma in routine formalin-fixed, paraffin-embedded small endoscopic biopsy specimens by robust real-time RT-PCR, *Am J Clin Pathol* 126(6):931–940, 2006.

Zhong S, Salomoni P, Pandofi PP: The transcriptional role of PML and the nuclear body, *Nature Cell Biol* 2, 2000. E85–E90.

Zhou T, Medeiros LJ, Hu S: Chronic myeloid leukemia: beyond BCR-ABL1, *Curr Hematol Malig Rep* 13(6):435–445, 2018.

Zucca E, Bertoni F: The spectrum of MALT lymphoma at different sites: biological and therapeutic relevance, *Blood* 127(17):2082–2092, 2016.

CHAPTER 79

MOLECULAR GENETIC PATHOLOGY OF SOLID TUMORS

Yu Bai, Shilpa Jain, Matthew R. Pincus, Peng Lee

MOLECULAR GENETIC PATHOLOGY OF SPECIFIC SOLID TUMORS BY MAJOR ORGAN, 1580
Brain Tumor, 1580
Breast Cancer, 1583
Thyroid Cancer, 1586
Lung Cancer, 1587
Hepatocellular Carcinoma, 1588
Gastric Cancer, 1589
Colorectal Cancer, 1590
Pancreatic Cancer (Nonneuroendocrine Tumor), 1593
Pancreatic Neuroendocrine Tumors, 1594
Kidney Tumor, 1595
Bladder Cancer, 1596
Prostate Cancer, 1596
Cervical Cancer, 1597
Endometrial Cancer, 1598
Ovarian Cancer, 1598
Melanoma, 1599
MOLECULAR GENETIC PATHOLOGY OF SARCOMA, 1599
Sarcomas with Fusion Genes, 1600
Sarcomas with Oncogenic Mutations, 1601
Sarcomas with Variable Other Specific Pattern, 1602
Sarcomas with Variable Complex Genetic Alterations with No Specific Pattern, 1602
MOLECULAR GENETIC PATHOLOGY OF MULTIPLE ENDOCRINE NEOPLASIA, 1602
CANCERS OF UNKNOWN ORIGIN, 1604
miRNA in Cancer, 1604
CLINICAL APPLICATION OF NEXT-GENERATION SEQUENCING, 1604
SELECTED REFERENCES, 1606

KEY POINTS

- Solid-tissue (predominantly epithelial cell) tumors are mainly caused by genetic lesions of three types: deletion or inactivation of tumor suppressor genes, mutation in or overexpression of oncogenes (i.e., genes encoding proteins that are vital in control of the cell cycle), and hypermethylation of the promoter regions.
- These genetic lesions can be detected using the techniques described in Part 8 of this textbook involving real-time polymerase chain reaction, fluorescence in situ hybridization, immunohistochemistry, enzyme-linked immunosorbent assay, and so on.
- Detection of genetic lesions in solid-tissue tumors is of great value for the diagnosis of specific types, for classification of the tumor, and for determining prognosis for a patient with a specific type of cancer. A common mutation in several of these cancers is overexpression of the epidermal growth factor receptor (EGFR). Discovery of this lesion allows for implementation of anti-EGFR therapy. However, because ras-p21 is a downstream target of EGFR and because it is commonly mutated in many human cancers, it is necessary to test for oncogenic mutations in the *ras* gene. If these are found, the efficacy of anti-EGFR agents is diminished.
- Less commonly, oncogenic mutations can be found in downstream targets of *ras-p21*, such as *BRAF*, which makes treatment with anti-EGFR agents less effective.
- Many solid-tissue tumors express the same oncogenes, such as *BRAF*, in melanoma and thyroid cancer, but other cancers have genetic lesions that appear to be specific for that type of cancer, such as *RET* in medullary thyroid carcinoma.
- Although not formally classified as solid-tissue tumors, sarcomas often behave in a manner identical to that of solid-tissue tumors. These cancers have been found to be caused by reciprocal translocations resulting in oncogenic fusion transcripts (accounting for 15%–20% of cases) and by specific oncogenic mutations (e.g., *KIT* and *PDGFRA* mutations in gastrointestinal stromal tumors). Both types of genetic alterations are often specific to certain types of sarcomas.
- Because the genetic alterations or changes that underlie many familial types of cancers are known, it is possible to screen for these in the children and close relatives of patients known to have a form of familial cancer to detect the presence of these cancers as rapidly as possible.
- Next-generation sequencing is currently widely used in the selection of pathway-based therapy and prediction of treatment resistance of many types of cancer.

Cancer is largely a genetically encoded disease. Recent research on cancer molecular genetics, epigenetics, and genomics, as well as their application, has vastly changed the practice of cancer diagnosis, classification, prognosis, and treatment. Application of molecular genetics to solid tumors is a major milestone in diagnostic pathology. Molecular diagnosis was initially introduced for accurate diagnosis of solid tumors based on the unique genetics. Now, the utility of molecular diagnosis is far beyond its original intention, and it is no longer just an adjunct method. It has become an indispensable tool that is widely used to predict clinical outcome, including disease prognosis, selection of optimal therapeutic regimens, and anticipation in response to treatment. It has not only revolutionized the concept and practice of diagnostic pathology for solid tumors, it has also become the basis for personalized medicine.

The principles and method in molecular diagnostics of solid tumors are similar to those used in other fields of molecular diagnosis. Techniques commonly used in cancer molecular pathology include detection or identification of specific sequences of genes (deoxyribonucleic acid [DNA] and/or its transcribed ribonucleic acid [RNA]) or gene product (protein) alterations. They include amplification-based techniques (i.e., polymerase chain reaction [PCR], reverse-transcriptase PCR [RT-PCR], branched DNA testing), hybridization methods (i.e., in situ hybridization, or fluorescence in situ hybridization [FISH]), microarray-based approaches (i.e., comparative genomic hybridization [CGH], DNA, RNA, microRNA [miRNA] microarray), and sequencing. PCR and FISH are among the most commonly used methods, whereas high-throughput techniques, such as array-based tests and next-generation sequencing (NGS) have a promising future but have not been fully established in clinical settings due to the lack of standards. Each method is described in Part 8 of this textbook.

Tissue sources of diagnostic materials of molecular pathology for solid tumor include paraffin-embedded tissue, fresh tissue, and cytologic specimens. Fresh tissue is a preferred choice for preservation of DNA, RNA, or protein. In most cases, only fresh tissue is usable in array-based methods; however, it is usually not readily available or accessible. Thus, paraffin-embedded tissue is used most commonly because of its availability and ease of access. It also allows use of the corresponding hematoxylin and eosin–stained slides for morphologic study. However, exposure of nucleic acid to formalin is associated with the major inherent problems of increased nucleic acid fragmentation and low integrity of DNA, RNA, and protein. Tissue fixation in formalin for longer than 24 hours will likely reduce the yield of high-molecular-weight nucleic acid. Thus, longer formalin fixation, paraffin embedding, and long storage at room temperatures can lead to false-negative results. A second problem is impurity of tumor cells, which usually are mixed with normal cells and stromal cells. Relatively pure tumor cells can be achieved by employing microdissection that isolates the

tumor cells, even a single tumor cell, by a manual or instrument-assisted method. Cytologic specimens, including cells from fine-needle aspiration (FNA), urine, and blood, and swabs for molecular pathology, are used most often to assist in accurate diagnosis of superficial solid tumors, such as human epidermal growth factor receptor (*Her*)-*2/neu* (*ERBB2*) for breast cancer, human papillomavirus (HPV) testing for cervical cancer, and UroVysion (Abbott Laboratories, Abbott Park, IL) for bladder cancer.

Molecular diagnoses of solid tumors rely on our understanding of the molecular mechanism involved in carcinogenesis of solid tumors. Genetic alterations can be inherited or can result from carcinogenesis, as described in Chapter 77. In several tumors, polygenic mutations occur. However, often in these cases, some unique or specific genetic alterations lead to carcinogenesis. Those genetic or epigenetic components mainly belong to the following:

1. Tumor suppressor genes (TSGs) (e.g., *Rb*, *SMAD*, adenomatous polyposis coli [*APC*]).
2. Oncogenes (e.g., *EWS*, *cKIT*, *Her2/neu*, *KRAS*, *BRAF*).
3. Promoter regions with methylation/inactivation activity.
4. Copy number alteration (CNA) has also been found to play an important role in tumor genesis.

Application of molecular diagnosis of solid tumors has been used clinically as follows:

1. **Assistance in disease diagnosis and classification:** For example, small "blue-cell" tumors encompassing Ewing sarcoma, lymphoma, rhabdomyosarcoma, and so forth, can be diagnosed by identification of specifically altered genes (e.g., Ewing sarcoma–specific gene translocations). In cervical cancer, detection of HPV assists in the diagnosis of neoplastic change on cervical biopsies or smears. Moreover, analysis of microarray data of the tumor detects gene signatures.
2. **Determination of prognosis:** With better understanding of the molecular genetics of solid tumors, a greater number of prognostic markers can be identified. Thus, detection of those markers in some cases has become a routine practice. For example, detection of overexpression/amplification of *Her2/neu* in breast cancer and 1p19q deletion in brain tumor has been used to predict prognosis or clinical outcome.
3. **Determination of therapeutic options:** Many drugs have been developed to target certain genes and gene products (i.e., proteins) and related pathways. Examples include tyrosine kinase inhibitors (TKIs) and monoclonal antibodies to EGFRs in lung and colon cancer. Moreover, only certain groups of patients with unique genetic profiles can respond to these treatments. Thus, providing the right management not only will increase the chances for cure but also will improve patient quality of life by avoiding unnecessary side effects.
4. **Combination of the above:** In most cases, detection of molecular markers may provide both diagnostic and prognostic information, such as c*KIT* mutations and chromosomal abnormalities detected by UroVysion, and amplification of *Her2/neu*.

This chapter focuses on the clinical application of molecular pathology in cancer diagnosis, prognosis, and predicting treatment response in common solid tumors. The major genetic findings in each tumor type are summarized in Table 79.1.

MOLECULAR GENETIC PATHOLOGY OF SPECIFIC SOLID TUMORS BY MAJOR ORGAN

BRAIN TUMOR

Primary central nervous system (CNS) gliomas, originating exclusively from brain cells such as astrocytes, oligodendrocytes, and ependymal cells, account for only about 1.35% of all cancers, but rank second among the causes of death from neurologic disease. Glioblastomas are the most common primary CNS tumor and are categorized as World Health Organization (WHO) grades I to IV based on histologic characteristics. With the advent of new treatment modalities, the use of microscopic examination alone is insufficient for the histologic classification and grading of gliomas. Under the 2016 WHO classification schema, molecular and genetic data as layer 4 information supports histologic classification (Louis, 2016).

Glioblastoma Multiforme

Glioblastoma multiforme (GBM) consists of anaplastic malignant astrocytic tumors characterized by predominant microvascular and endothelial proliferation. The current standard of care for GBM is surgical resection, followed by radiation therapy. However, the association of specific molecular genetics not only assists in diagnosis and prognosis but also leads to the development of new adjuvant chemotherapy (e.g., temozolomide) (Stupp et al., 2005). Glioblastomas (WHO grade IV) may develop de novo (primary glioblastomas) or through progression from low-grade astrocytomas (secondary glioblastomas). The two types show similar histologic features. However, they differ in terms of molecular alterations, with primary glioblastomas showing activation of the EGFR pathway, whereas secondary glioblastomas are more commonly associated with *TP53* mutations. Thus, the molecular genetics of these tumors demonstrates that they are distinct diseases and, therefore, may exhibit different prognoses and responsiveness to therapy (Ohgaki & Kleihues, 2007). Tyrosine kinase inhibitors, such as erlotinib and gefitinib, may offer a therapeutic option for primary tumors in which EGFR signaling is upregulated (Ohgaki & Kleihues, 2007).

Comprehensive genetic screens of GBM (Parsons et al., 2008) have confirmed that genetic loss is scattered across the entire genome, affecting numerous chromosomes. **Loss of heterozygosity (LOH) on chromosome 10 is the most frequent genetic loss in GBM,** occurring in 60% to 80% of cases. Allelic losses on 1p and 7q have also been seen in GBM, but at lower frequencies. Loss of 1p occurs in 6% to 20% of GBMs, and in combination with 19q loss may indicate a better prognosis and improved responsiveness to therapy. However, the combined loss of 1p/19q is a rare event in GBM (Kanu et al., 2009).

Gains in gene expression have also been demonstrated in GBM in the form of duplication of entire chromosomes, intrachromosomal amplification of specific alleles, or extrachromosomal amplification (often in the form of double minutes) and activating mutations. Many genes have been shown to be amplified in glioma; these include *EGFR*, *CDK4*, *SAS*, *MDM2*, *GLI*, *PDGFRA*, *MYC*, *N-MYC*, *MYCL1*, *MET*, *GADD153*, and *cKIT*. The most commonly amplified genes in glioblastoma are *EGFR* on chromosome 7 (in ≈40% of cases), *CDK4*, and *SAS* (in ≈15%).

Other molecular mechanisms of gliomagenesis include loss of the DNA repair enzyme, O(6)-methyl guanine DNA methyltransferase (MGMT), which specifically removes promutagenic alkyl groups from the O6-position of guanine in DNA (Kanu et al., 2009). Expression of MGMT protects normal cells from carcinogens; however, it can also protect cancer cells from chemotherapeutic alkylating agents. This has been implicated as an important mechanism of drug resistance because it reduces the cytotoxicity of alkylating chemotherapeutic agents. Loss of MGMT expression may be caused by methylation of promoter CpG islands, which have been detected in 75% of secondary GBMs—much more frequently than in primary GBMs (36%). Immunohistochemical staining for MGMT does not offer a reliable way to stratify GBM (Kanu et al., 2009); therefore, PCR assay is necessary. *TP53* is one of the more commonly studied TSGs in GBM. Loss of normal *TP53* function due to mutation occurs more frequently in secondary GBM. Thus, the major molecular targets of glioblastomas are EGFR, TP53, 10q LOH, and deletion of the *MGMT* gene. These can be detected using RT-PCR, methylation-specific PCR, and FISH. The main clinical applications are related to prognosis and treatment response. These findings are summarized in Table 79.1 and, in greater detail, in Table 79.2.

Oligodendroglioma

Oligodendroglioma is an infiltrating glioma of the cerebral cortex diagnostically characterized by a triad of uniformly round to ovoid nuclei, perinuclear halos, and an even distribution of cells, together with a delicate chicken wire type of vasculature. However, in a significant number of these lesions, the microscopic morphology is not so clear-cut, and distinction from other diffuse glial lesions may be difficult. Combined loss of 1p and 19q (Fig. 79.1A to 79.1C) is typical in oligodendroglioma (Aldape et al., 2007), and loss of 19q occurs in astrocytoma and mixed oligoastrocytoma (Aldape et al., 2007). The incidence of 1p/19q loss varies from 50% to 80% in oligodendroglioma in different studies and is 1% to 10% in other gliomas, which indicates its utility in differentiating the diagnosis. Recent studies suggest that the combined loss of 1p/19q may follow a (1;19)(q10;p10) translocation, with subsequent loss of the derivative chromosome der(1;19)(q10;p10) (Aldape et al., 2007). Identification of 1p/19q loss is associated with two unique features of tumor biology with clinical indications: first, they grow slowly, even those that are anaplastic in nature; second, they correlate with better prognosis and response to chemotherapy (Kuo et al., 2009). In terms of treatment response, initial studies suggested that 1p/19q loss is a marker of response to PCV (procarbazine, lomustine/CCNU, and vincristine) or temozolomide chemotherapy (Kuo et al., 2009). Thus, the 1p/19q status has become an important part of diagnosis, prognosis, and predicted therapeutic response of oligodendrogliomas. In addition to 1p/19q alteration, LOH mutations in *p53* and *p16* may be associated with poor survival or tumor progression (Kuo et al., 2009).

Nearly all 1p/19q codeleted oligodendrogliomas are also mutated on isocitrate dehydrogenases (IDHs), IDH1 or IDH2 (Labussiere et al., 2010).

TABLE 79.1

Most Common Genetic Alterations in Solid-Tissue Tumors

Tumor Type	Major Molecular Target(s)*	Main Method(s) of Detection	Clinical Application(s)
Solid-Tissue Tumors			
Glioblastoma	*EGFR, TP53,* 10q, MGMT, mutations in *TP53* and *PTEN, P16INK4a* deletions	RT-PCR, methylation-specific PCR, FISH	Prognosis, treatment response
Oligodendroglioma	1p and 19q deletions, *EGFR, TP53*	FISH, RT-PCR, LOH	Diagnosis, prognosis, treatment response
Sporadic, nonhereditary breast cancer	*Her2/neu*, multiplex genes	FISH, IHC, RT-PCR, Oncotype, MammaPrint	Molecular classification, prognosis, treatment response
Hereditary breast cancer	*BRCA1, BRCA2, EGFR*	High-throughput sequencing, multiplex PCR, genetic counseling	Diagnosis, genetic counseling
Papillary thyroid cancer	*BRAF, RAS, RET, PTC1, PTC3*	FISH, RT-PCR, direct sequencing	Diagnosis, prognosis, therapeutic option
Follicular thyroid cancer	*PAX8-PPARG*	IHC, FISH, RT-PCR	Diagnosis, prognosis
Medullary thyroid carcinoma	*RET*	Sequencing, PCR	Diagnosis, screening, surveillance
Non–small cell cancers of the lung	*EGFR, ALK, ROS1*	PCR, sequencing, FISH	Prognosis, treatment response
Liver (hepatocellular)	*EGFR, PIK3CA, p53*, β-catenin, microRNA (miR-122a), multiple genes	FISH, PCR, sequencing, microarray	Diagnosis, prognosis, targeted therapy
Gastric cancer, intestinal type	*p73* mutations, *MSI* (*MLH1* and *MSH2*), LOH/mutations of *APC* genes, and Her2/neu	FISH, PCR, IHC	Diagnosis, prognosis
Gastric cancer, diffuse type	*CDH1*	FISH, PCR, IHC	Diagnosis, prognosis
Colon cancer	Mutated oncogenes: mainly *EGFR, KRAS, BRAF,* and *PI3K.*	FISH, PCR, microarray, methylation-specific PCR, sequencing, array technology	Diagnosis, prognosis
	Mutated or deleted antioncogenes: *p53, APC, TGFBRI, SMAD2, SMAD4*		
	Microsatellite instability (MSI) genes and CpG island methylator (CIMP) genes		
Pancreatic cancer	Most pancreatic cancers: *KRAS* mutations	PCR, sequencing	Diagnosis
	Inactivating mutation or deletion or methylation of genes encoding *TP53, SMAD4, p16/CDKN2A*	PCR, methylation-specific PCR	Diagnosis (rarely), prognosis
	miRNAs (miR-196a, 217, 221, 376a, and 301)	RT-PCR	Diagnosis, prognosis
Renal cell carcinoma (RCC)	Chromosome 3p deletion, von Hippel–Lindau *(VHL)* gene deletion; *PI3K/AKT/MTOR*	Sequencing, FISH (for VHL)	Diagnosis
Translocation-associated RCC	t(X;17)(p11.2;q25); *ASPL-TFE3* and *PRCC-TFE3* fusion genes	RT-PCR, FISH, IHC for the C-terminal domain of nuclear TFE3	Diagnosis, classification
RCC, clear cell	Carbonic anhydrase IX	Gene expression arrays, IHC	
	Genes of immune response and proangiogenesis		
	Proximal nephron markers: megalin, cubilin, adipophilin		Diagnosis, prognosis, classification
RCC, papillary	Proximal nephron marker α-methylacyl-coA racemase	Gene expression arrays, IHC	Diagnosis, prognosis, classification
	CDKN2A, CIMP		
RCC, chromophobe	Abundant mitochondria	Gene expression arrays, IHC	
	TP53, PTEN, TERT		
	Distal nephron markers: β-defensin, parvalbumin, chloride channel Kb, claudin 7 and 8, and EGF		Diagnosis, prognosis, classification
RCC, oncocytoma	Abundant mitochondria	Gene expression arrays, IHC	
	Distal nephron markers: β-defensin, parvalbumin, chloride channel Kb, claudin 7 and 8, EGF		Diagnosis, prognosis, classification
Bladder cancer	Aneuploidy of chromosomes 3, 7, and 17 and/or deletion of the 9p21 (encoding p16); *NMP 22*	FISH	Diagnosis
Prostate cancer	*TMPRSS2* (*21q22.3*) to transcripts of the ETS family member genes: overexpression of ETS proteins (e.g., ERG, ETV1, ETV4, ETV5)	FISH, ELISA, RT-PCR, gene expression arrays	Diagnosis, classification
Cervical cancer	HPV-6 and -18	Hybrid capture DNA assay, RT-PCR, Southern blot, dot blot	Diagnosis, follow-up of abnormal PAP smears
Ovarian Cancer			
Low-grade serous	*KRAS, BRAF*	PCR, Southern blot	Diagnosis, classification
High-grade serous	*p53* deletion/mutation; Wnt/β-catenin or PI3K/PTEN signaling pathway defects	PCR, Southern blot	Diagnosis, classification
Mucinous	*KRAS, BRAF*	PCR, Southern blot	Diagnosis, classification
Clear cell	*PI3K/PTEN* mutations	PCR, Southern blot	Diagnosis, classification
Endometrioid	Mutations of *CTNNB1* (β-catenin)	PCR, Southern blot	Diagnosis, classification

Continued

TABLE 79.1 —cont'd

Tumor Type	Major Molecular Target(s)*	Main Method(s) of Detection	Clinical Application(s)
Melanoma	*CDKN2A, p14,* and *p16* inactivation; *NRAS* (G12V) and *BRAF* oncogenic mutations (V600E)	PCR, sequencing	Diagnosis, classification, therapy
Sarcoma			
Sarcoma with fusion genes involving the *TET* gene: Ewing's sarcoma	t(11;22)(q24;q12) translocation; fusion of *EWSR1* and an *ETS* family gene, mainly *FLI1*	RT-PCR, FISH, Southern blot	Diagnosis Prognosis
Sarcoma with fusion genes involving receptor tyrosine kinase: congenital fibrosarcoma	t(12;15)(p13;q25) translocation, resulting in fusion of *ETS* gene, *ETV6* with neurotropin receptor (that has tyrosine kinase activity), *NTRK3* gene	RT-PCR, FISH, Southern blot	Diagnosis
Sarcoma with fusion genes involving chromatin remodeling: synovial sarcoma (SS)	t(X;18)(p11.2;q11.2) translocation resulting in fusion of *SS18(SYT)* gene with one of the *SSX* genes on the X chromosome, creating *SS18-SSX1, SS18-SSX2,* or *SS18-SSX4* chimeric genes Downstream targets of above fusion proteins: *CCND1* (cyclin D1) and *TLE1* that encodes a transcriptional corepressor	FISH, RT-PCR IHC	Diagnosis, classification
Sarcoma with fusion genes involving growth factors: dermatofibrosarcoma protuberans (DFSP) and giant cell fibroblastoma (GCF)	t(17;22)(q11;q13.1) translocation resulting in fusion of the *COL1A1* gene on chromosome 17 with the *PDGFB* gene on chromosome 22, leading to *PDGFRB* overexpression	RT-PCR	Diagnosis, classification
Sarcoma with other types of fusion genes: alveolar rhabdomyosarcoma (ARMS)	t(2;13)(q35:q14) translocation that results in fusion of *PAX3* with *FOXO1A*	FISH	Diagnosis
Sarcoma with oncogenic mutations: gastrointestinal stromal tumor (GIST)	*cKIT/PDGFRA*	PCR, sequencing, Southern blot	Diagnosis
Sarcoma with no consistent genetic lesions: leiomyosarcoma (LMS)	Loss of 1p12-pter, 2p, 13q14-q21 (targeting the Rb pathway), 10q (targeting *PTEN*), 16q. Gains of 17p, 8q, and 5p14 pter. Activation of the PI3K-AKT pathway and mTOR	FISH	Diagnosis
Syndromatic Cancers			
Familial adenomatous polyposis syndrome	Adenomatous polyposis coli *(APC)* (long arm of chromosome 5) or MutY human homologue *(MYH)* gene involved in repair of oxidative damage to DNA	PCR, sequencing, Southern blot	Diagnosis
Hereditary nonpolyposis colorectal cancer (HNPCC): Lynch syndrome	Microsatellite instability (MSI) in mismatch repair *(MMR)* genes, including *MLH1, MSH2, MSH6, MLH3,* and *PMS2*	IHC, PCR, sequencing	Diagnosis, classification, genetic counseling
Familial juvenile polyposis syndrome	Germline mutations of *SMAD4, BMPR1A*, and *ENG*; also, mutations in kinase, *BMPR1A* (bone morphogenetic protein receptor type IA), on chromosome 10q22.3. Involvement of TGF-β signal transduction pathway	PCR, sequencing	Diagnosis, classification
Peutz-Jeghers syndrome (PJS): melanotic mucocutaneous hyperpigmentation and GI hamartomas, which occur anywhere from the stomach to the anus; multiple polyps in small bowel	*STK11/LKB1* gene	PCR, sequencing	Diagnosis, classification
Multiple endocrine neoplasia (MEN)			
MEN type 1: tumors in the parathyroid glands; the stomach, pancreas, and intestinal tract; anterior pituitary gland; endocrine pancreas; and duodenum, and by the presence of other nonendocrine tumors such as hemangioma, ependymoma, and leiomyoma, often at a young age	MEN 1 tumor suppressor gene, *MEN 1*	PCR	Diagnosis, classification
MEN type 2: medullary thyroid carcinoma (MTC) and associated pheochromocytoma and hyperparathyroidism	*RET* (chromosome 10q11.2) (encoding a tyrosine kinase) mutations	PCR, sequencing	Diagnosis, classification
von Hippel–Lindau syndrome (VHL): neoplasia syndrome characterized by hemangioblastomas in the central nervous system and retina, pheochromocytomas, renal cysts and clear cell renal cell carcinoma, pancreatic cysts and islet cell tumors, endolymphatic sac tumors, and papillary cystadenomas of the epididymis and broad ligament	*VHL* tumor suppressor gene (three exons) on chromosome 3p25. Encodes VHL protein, critical in regulating hypoxia-inducible factor (HIF-α and -β)	PCR, sequencing	Diagnosis, classification

TABLE 79.1 —cont'd

Tumor Type	Major Molecular Target(s)*	Main Method(s) of Detection	Clinical Application(s)
Familial paraganglioma syndromes	Mutation of three genes encoding subunits of mitochondrial succinate dehydrogenase (SDH complex): *SDHB* at 1p36.1 (PGL4), *SDHC* at 1q21 (PGL3), and *SDHD* at 11q23 (PGL1)	PCR	Diagnosis, classification
Cowden syndrome (CS); breast, thyroid, and endometrial cancers and other benign conditions, including multiple hamartomas in the colon, lipomas, fibromas	*PTEN* mutations	PCR	Diagnosis, classification
Li-Fraumeni syndrome; soft-tissue sarcomas, breast cancer, osteosarcoma, brain tumors, childhood leukemias, and adrenocortical carcinoma	*p53* gene mutations	PCR, IHC	Diagnosis, classification
Neurofibromatosis 1 (NF1); neurofibroma and, less commonly, gliomas and other abnormalities (learning disability, vasculopathy, and bony abnormalities)	*NF1*, located on chromosome 17q11.2; diminished GTPase activating (GAP) activity activating the ras signal transduction pathway	FISH, direct sequencing, long-range PCR with Southern blot analysis, and/or cytogenetic analysis	Diagnosis, classification
Neurofibromatosis (NF2) and schwannomatosis. NF2 involves schwannomas, meningiomas, and ependymomas	*NF2* gene (chromosome 22)	Sequencing, mutation scanning, duplication/deletion testing, PCR, quantitative PCR, microarray, comparative genomic hybridization, or combination	Diagnosis, classification

ELISA, Enzyme-linked immunosorbent assay; *FISH,* fluorescent in situ hybridization; *IHC,* immunohistochemistry; *LOH,* loss of heterozygosity; *PCR,* polymerase chain reaction; *RT-PCR,* real-time PCR.
*Full names and functions of molecular targets (i.e., oncogenes and oncoproteins) listed in the second column may be found in the corresponding sections of this chapter describing these targets and the corresponding references.

TABLE 79.2
Common Genetic Alterations in Glioblastoma Multiforme

	Primary GBM	Secondary GBM
LOH 10q	70%	63%
EGFR amplification	36%	8%
P16INK4a deletion	31%	19%
TP53 mutation	28%	65%
PTEN mutation	25%	4%

Data from Ohgaki H, Kleihues P: Genetic pathways to primary and secondary glioblastoma, *Am J Pathol* 170:1445–1453, 2007.
EGFR, Epidermal growth factor receptor; *GBM,* glioblastoma multiforme; *LOH,* loss of heterozygosity; *PTEN,* phosphate and tensin homologue deleted on chromosome 10.

IDH1 has been found to be mutated in a vast majority of astrocytic, oligodendroglial, and oligoastrocytic gliomas (WHO grades II to III) as well as in secondary glioblastomas (WHO grade IV). However, IDH1 mutation is very rare in primary glioblastoma and is not involved in pilocytic astrocytomas. IDH1 and IDH2 are homologous, $NADP^+$-dependent cytoplasmic and mitochondrial enzymes, respectively. The role of these enzymes is the conversion of isocitrate to α-ketoglutarate with the simultaneous reduction of $NADP^+$ to NADPH. The most common mutation is a heterozygous point mutation with substitution of arginine by histidine at residue 132 (R132H), located in the substrate-binding site. This IDH1-R132 mutation has a reported frequency of 50% to 93% (Parsons et al., 2008; Yan et al., 2009). IDH2 gene mutations affecting the amino acid R172 are much less common than the IDH1 isoform, 3% to 5%, yet have been identified in a small subset of gliomas that lack the typical IDH1 mutation with predominance in oligodendrogliomas (Yan et al., 2009). *IDH1* and *IDH2* genes appear to behave dominantly and are mutually exclusive. *IDH1* mutation has been shown to be a strong, independent positive prognostic biomarker in diffuse gliomas, glioblastomas, and oligodendroglioma (Sanson et al., 2009). *IDH* mutation was also identified as a marker for response to temozolomide in low-grade gliomas (Houillier et al., 2010).

Rhabdoid Tumor

Rhabdoid tumors are highly malignant (WHO grade IV) embryonal CNS tumors of infants and very young children showing rhabdoid features. Similar to renal and other extrarenal rhabdoid tumors, over 90% of atypical teratoid/**rhabdoid** tumors (AT/RT) demonstrate loss of all or part of chromosome 22, particularly involving 22q11.2. *INI1* (hSNF5/SMARCB1/BAF47), a putative suppressor gene, is mapped to the 22q11.2 region. *INI1* deletions and/or mutation have been detected in the majority of AT/RT cases. Nearly all AT/RTs demonstrate absence of the nuclear immunohistochemical expression of INII/BAF47 protein. FISH for monosomy 22, 22q and deletion or the *INI1* gene are commonly utilized as adjunct molecular studies in the diagnosis of AT/RTs and other pediatric embryonal tumors (Wei et al., 2014).

BREAST CANCER

Breast cancer is the most common cancer in women and the second most common cause of cancer death in women in the United States. Until recently, breast cancer was characterized according to tumor type (ductal vs. lobular carcinoma), histologic grade (I to III), steroid hormone receptors (estrogen receptor [ER] and progesterone receptor [PR]), and *Her2/neu* status (positive vs. negative), along with metastasis to lymph nodes and distant organs, for its prognosis and treatment. Gene expression profiling has also been utilized as an adjunct for the management of breast cancer. Gene panel study and germline testing using NGS have been introduced to search for actionable mutations and identify genetic predisposition for counseling and screening.

Sporadic, Nonhereditary Breast Cancer

Various genetic, epigenetic, and genomic changes have been associated with breast cancer. Traditionally, ER and PR status is used as a prognostic and predictive marker for breast cancer. *Her2/neu* (detailed in Chapter 77) status has been added in the past decade as a breast cancer prognostic and predictive marker. The FISH method has been used primarily to determine the copy number of the *Her2/neu* gene (see Fig. 79.1D and 79.1E) for the purpose of selecting Her2-targeted therapies such as trastuzumab and lapatinib in both adjuvant and neoadjuvant settings. Enumeration of 20 interphase nuclei from tumor cells on a given case is reported as the ratio of average *Her2/neu* copy number to that of chromosome enumeration probe 17 for centromere, CEP17. Specimens with amplification showed a *Her2/neu*:CEP17 signal ratio ≥2.0 as abnormal and a ratio <2.0 as normal. A three-color FISH assay has been commercialized for assessment of standalone prognosis in ER-positive and ER-negative stage I breast cancers (Ross, 2009). In addition, HercepTest (Dako Corp, Carpinteria, CA), an immunohistochemistry (IHC) test for *Her2/neu* using a polyclonal antibody, was the first approved by the U.S. Food and Drug

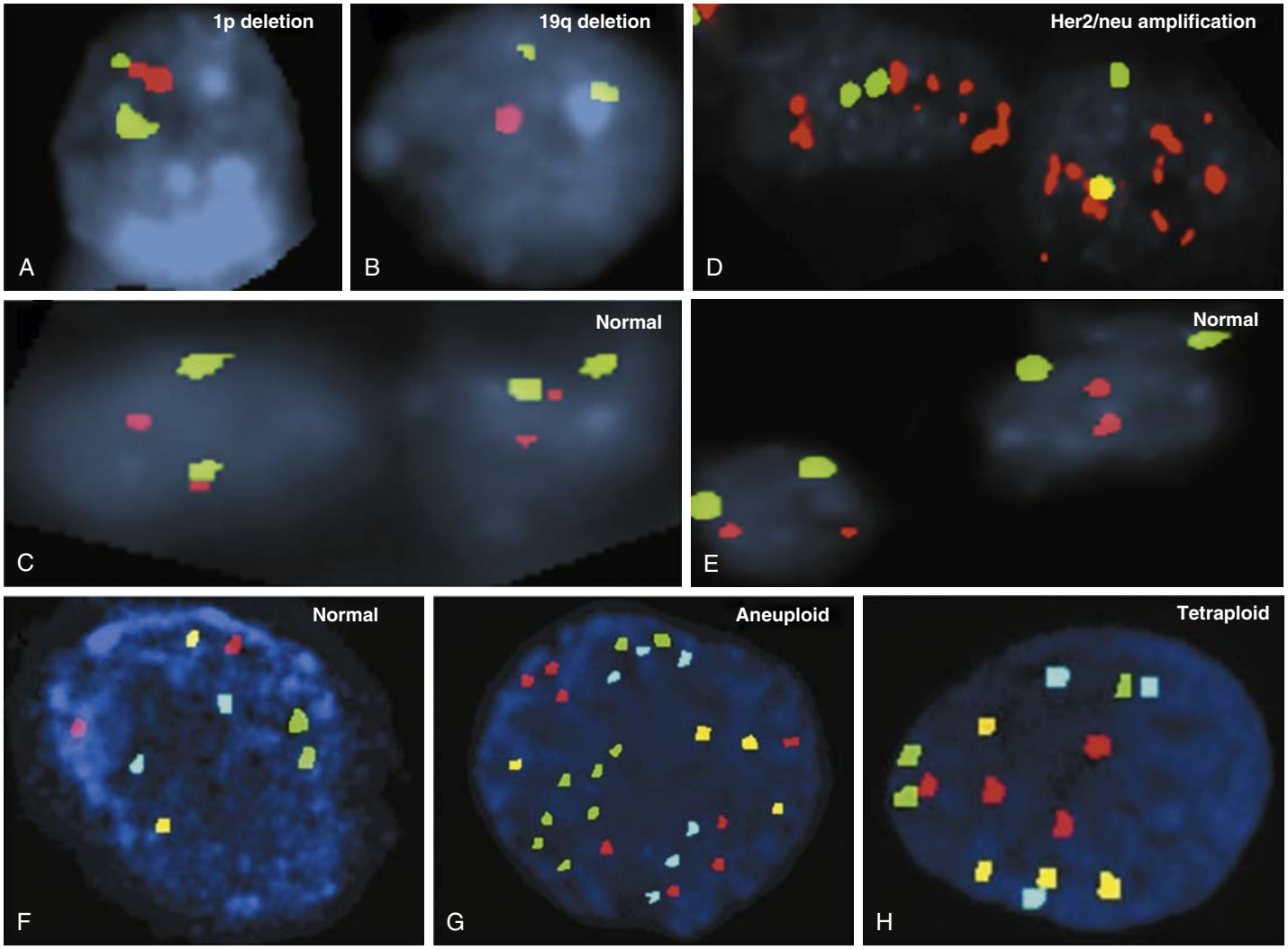

Figure 79.1 Examples of fluorescence in situ hybridization in cancer diagnosis. Oligodendroglioma with **A,** 1p and **B,** 19q deletions compared with **C,** normal cells. Green color in *A,* 1q probe; red color in *A,* 1p probe; green color in *B,* 19p probe; red color in *B,* 19q probe. **D,** Her2/neu amplification compared with **E,** normal cells. Green color: CEP17 probe. Red color: Her2/neu probe. UroVysion showing **F,** normal; **G,** aneuploid; and **H,** tetraploid cells. Aqua color: chromosome 17. Yellow (gold) color: 9p21 locus. Red color: chromosome 3. Green color: chromosome 7.

Administration (FDA). Subsequently, Pathway (Ventana Medical Systems, Tucson, AZ) produced a monoclonal antibody (CB11) for *Her2/neu* for the same response indication, which has also been FDA-approved and is used in combination with FISH (Fig. 79.2). IHC is widely used to measure prognostic factors, including ER, PR, *Her2/neu*, and the proliferation marker, Ki-67, and to predict response to hormonal and Her2-targeted therapies (Ross, 2009).

Concerns associated with IHC-based assays for multiple markers include the nonlinear nature of IHC staining, the different subcellular localizations of different markers, and the impact of different slide-scoring thresholds for different antibodies. The introduction of whole-genome profiling technologies has greatly expanded our knowledge of the genomic pathways associated with the development and progression of breast cancer (Bao & Davidson, 2008). These research results have led to the development of several commercialized tests with multigenes/proteins as prognostic and predictive tools for clinical application using IHC, FISH, RT-PCR, and genomic microarray technologies with integrated bioinformatic/statistical algorithms designed to calculate disease recurrence and patient survival (Ross et al., 2008).

Molecular classification of breast cancer has been proposed, based on gene expression profiling, to include luminal-like, normal-like, Her2-positive, and basal-like subtypes of invasive breast cancer (Ross et al., 2008). It is important to note that all of the luminal groups of breast cancers are ER positive, and nearly two-thirds are of low or intermediate histologic grade, whereas 95% of all (Ross, 2009) basal-like cancers are ER negative and 91% of these tumors are of high grade (Bao & Davidson, 2008). Studies of clinical outcomes based on molecular subtypes have shown that luminal A is more sensitive to antiestrogen than is luminal B. Her2-positive responds to trastuzumab, an anti–Her2 antibody, whereas basal is more aggressive (but is especially sensitive to anthracycline-based neoadjuvant chemotherapy) than are the luminal breast cancers (Ross, 2009). Basal-like and Her2-positive subgroups are associated with the highest rates of pathologic complete response to neoadjuvant multiagent chemotherapy (Ross, 2009).

Several commercially available assays have been developed to predict the risk for recurrence. Prosigna Breast Cancer Assay, developed by NanoString, is based on the prediction analysis of the microarray-50 (PAM50) gene expression signature. The PAM50 gene signature measures the expression levels of 50 genes in a surgically resected breast cancer sample to classify a tumor as one of four intrinsic subtypes (Luminal A, Luminal B, HER2-enriched, and Basal-like). This test outputs a risk of recurrence (ROR) score in these intrinsic subtypes. Prosigna uses multiplexed gene-specific fluorescently labeled probe pairs to measure gene expression in frozen or formalin-fixed paraffin-embedded (FFPE) tissues with equivalent ease and efficiency (Nielsen et al., 2014). Clinical trials demonstrated its utility in prognostic information of distant recurrence in hormone receptor–positive, postmenopausal breast cancer patients treated with endocrine therapy (Dowsett et al., 2013) and in node-positive patients (Gnant et al., 2014). The other two gene microarray-based clinical tests are the OncotypeDx and MammaPrint assays (Fig. 79.3) (Kato, 2009; Oakman et al., 2009). Oncotype Dx (Genomic Health, Inc., Redwood City, CA) is a 21-gene multiplex prognostic and predictive RT-PCR assay performed on primary FFPE breast cancer samples. The original 16 informative genes (Paik et al., 2004) that calculate the recurrence score (RS) were discovered on archived FFPE samples by transcriptional profiling and then were converted to the FFPE RT-PCR assay (Ross et al., 2008). OncotypeDx determines the 10-year risk for disease recurrence in patients with ER-positive, lymph node–negative tumors by using a continuous variable algorithm and

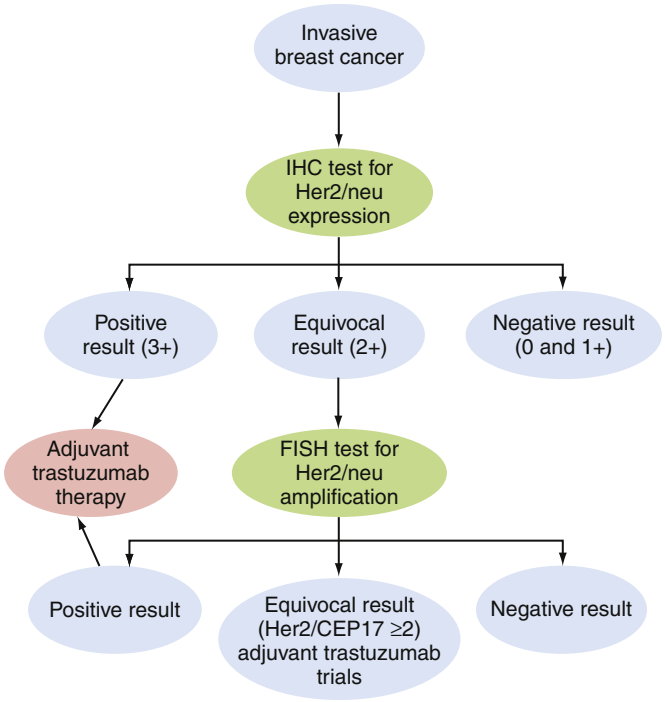

Figure 79.2 Algorithm using Her2/neu status in diagnosis and treatment of breast cancer.

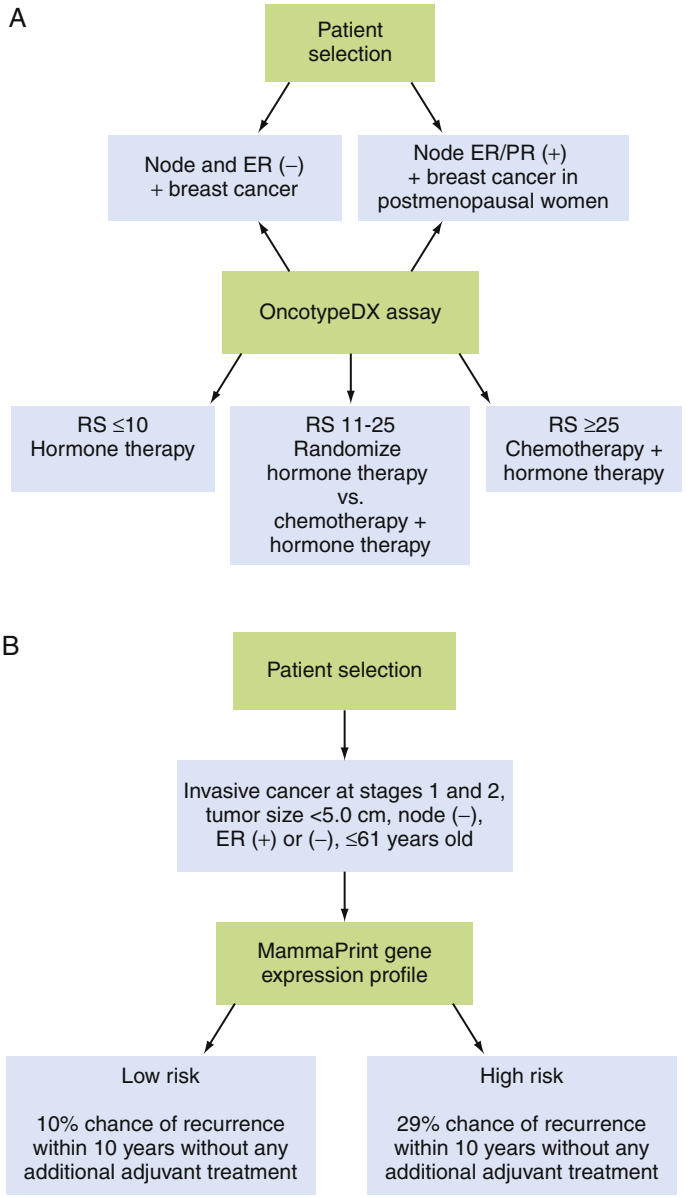

Figure 79.3 Algorithm of *A,* OncotypeDx and *B,* MammaPrint assays in breast cancer management.

assigning a tripartite RS (17, low risk; 18–30, intermediate risk; >30, high risk). Of the multiple pathways assessed by this assay, the proliferation and ER pathways are the most influential in RS calculation, followed by the Her2 pathway. High relative levels of ER messenger RNA (mRNA) and low levels of Ki-67 proliferation gene mRNA have a low RS. Low levels of ER mRNA and high levels of Ki-67 mRNA have a high RS. The other 14 informative mRNA levels play their greatest roles in determining the RS in tumors with intermediate ER and Ki-67 mRNA levels. It should also be noted that OncotypeDx is best suited for detecting breast cancers with a low potential for recurrence. The MammaPrint assay (Agendia BV, Amsterdam, The Netherlands) was the first fully commercialized microarray-based multigene assay for breast cancer. This test is offered as a prognostic test for lymph node–negative breast cancer in women younger than 61 years of age with an ER-positive or ER-negative tumor. The prospective RASTER trial showed that MammaPrint testing could spare from chemotherapy 94 of 295 patients (32%) for whom chemotherapy would have been recommended by a standard (non–gene-based) decision tool (Drukker et al., 2013). The clinical utility of the assay supported the test to be the first assay approved by the FDA's new in vitro diagnostic multivariate index assay classification. Like Prosigna and OncotypeDx, both fresh-frozen and FFPE tissues can be used for analysis. The 70 genes that make up the MammaPrint assay are focused primarily on proliferation. Additional genes are associated with invasion, metastasis, stromal integrity, and angiogenesis. Of note, the OncotypeDx and MammaPrint assays have only one gene in common—the *SCUBE2* gene, which is a member of the ER pathway. Unlike the OncotypeDx test, which features a continuous RS result, the MammaPrint test uses a dichotomous "high risk versus low risk" result format. The MammaPrint test does not include ER, PR, or Her2 in the 70-gene microarray.

Multigene testing procedures such as disease classifiers and prognostic and predictive markers have been introduced with the use of slide-based methods (e.g., IHC, FISH) or molecular platform–based methods such as quantitative multiplex PCR and genomic array profiling. Morphologically based mRNA extraction performed with the use of tissue macrodissection or microdissection is recommended for analysis as it is highly enriched for invasive carcinoma and is not diluted with cells from benign tissues and in situ carcinoma areas (Ross et al., 2008). The heterogeneous expression of important mRNAs—such as ER, Her2, and Ki-67, often reflected in the varying histologic grades seen in larger tumors—can influence the predictive accuracy of transcriptional profiling measurements. One caveat is that, although the number of genes that can be simultaneously assessed by multiplex qRT-PCR is significantly greater than that for IHC, multiplex qRT-PCR requires a more complex statistical evaluation of the gene expression profiles. Nevertheless, the RT-PCR technique has been used to predict overall prognosis and response to both hormonal and cytotoxic therapies.

High-throughput NGS has made it possible to sequence large numbers of genes to identify actionable mutations in the tumor. The diagnostic yield of breast NGS has been studied but is difficult to define and measure (Ian, 2016). Sequencing of 46 cancer-related genes in 415 breast cancer samples (including some primary-metastatic pairs) revealed somatic nonsynonymous mutations in 220 of 354 patients (62.1%) (Roy-Chowduri et al., 2015). A systematic multinational study of NGS profiling in breast cancer is underway (Zardavas et al., 2014).

Hereditary Breast Cancer

Hereditary breast cancer (HBC) accounts for approximately 10% of all breast cancers. Positive family history is the strongest risk factor, as it is present in about 20% of breast cancer cases. Population-based studies indicate that 15% of familial risk can be attributed to *BRCA* gene mutations and that a further 10% involve *TP53*, phosphate and tensin homologue (*PTEN*), serine/threonine kinase 11 (*STK11*), cadherin 1 (*CDH1*) and *ATM*. The rest may be explained by a polygenic model. A significant number of HBC-prone families are characterized by the more common hereditary breast-ovarian cancer syndrome. The *BRCA* genes operate as TSGs, and germline mutations affecting one allele of *BRCA1* or *BRCA2* confer susceptibility to breast and ovarian cancers. The cumulative risk for developing breast cancer by 70 years of age approaches 50% to 70% in *BRCA1*-mutation carriers; for ovarian cancer, the risk is 30% to 40% (Venkitaraman, 2009). For *BRCA2*-mutation carriers, the risk is 40% to 50% for breast cancer and 10% to 15% for ovarian cancer. However, individuals

who carry *BRCA2* mutations also have an increased risk for other cancers, including those of the male breast (≈75–fold relative risk), pancreas (fourfold to eightfold), and prostate (twofold to fourfold) (Venkitaraman, 2009). The spontaneous instability of chromosome structure and number is a hallmark of *BRCA*-deficient cells and arises from the distinct cellular functions performed by the BRCA1 and BRCA2 proteins in DNA repair and mitotic control. Since the discovery of *BRCA* genes and the development of methods for mutation screening, identification of *BRCA*-mutation carriers during the clinical management of familial cancer cases has become widespread. Gene expression profiling has revealed that tumors from patients who are *BRCA1*-mutated segregate within the basal subgroup of breast cancers (Venkitaraman, 2009) of the five different molecular groups, as discussed earlier. Tumors from *BRCA1*-mutation carriers are likely to stain positive for basal cytokeratins 5/6 and 14, and to exhibit negative estrogen receptor staining. These breast carcinomas also commonly stain for EGFR. *BRCA1*-associated tumors are commonly of high grade and are *p53*-mutated. They have a tendency to occur in younger women and carry a poor prognosis (Venkitaraman, 2009).

THYROID CANCER

Thyroid cancer is the most common endocrine neoplastic condition. The two most frequent types of thyroid malignancy derived from follicular cells are papillary and follicular carcinomas, which constitute approximately 80% and 15%, respectively, of all thyroid cancers. These follicular cell–derived tumors are well differentiated, in contrast to poorly differentiated and anaplastic carcinomas, which constitute about 2% of cases. Another malignancy of the thyroid is medullary carcinoma, which originates from parafollicular C cells and accounts for approximately 3% of cases. Several genetic alterations in various thyroid tumors have been well documented, including translocations and point mutations. The genetic alteration in thyroid cancer involves *BRAF*, *RAS*, *RET*, and *PAX8*.

Papillary Thyroid Carcinoma

Recent studies have characterized papillary thyroid carcinoma (PTC) into two classes: "BRAF-V600E-like" and "RAS-like." These mutations are mutually exclusive (Nikiforov, 2017).

RAF, as noted earlier (see Chapter 77), is a direct target of ras-p21. The *BRAF* gene mutation is the most commonly known genetic alteration in papillary carcinoma, found in approximately 45% of these tumors (Nikiforova & Nikiforov, 2008). A majority of mutations involve T1799A transversion mutation in exon 15 of the gene, which causes amino acid change from valine to glutamic acid at amino acid residue 600 (V600E), leading to constitutive activation of BRAF kinase, subsequent phosphorylation of MEK and ERK protein kinases (see Chapter 77), and downstream effectors of the mitogen-activated protein kinase (MAPK) pathway, as is summarized in Chapter 77 (see Fig. 77.1). It is believed that BRAF-V600E-like tumors carry profound downregulation of expression of thyroid differentiation markers (TCGA Network, 2014a). Other mechanisms of *BRAF* activation, although rare, include K601E point mutation, small in-frame insertions or deletions surrounding codon 600, and *AKAP9-BRAF* rearrangement, which is more commonly associated with radiation exposure papillary carcinoma. *BRAF V600E* mutation is highly prevalent in papillary carcinoma with classical histology and in the tall cell variant while tumors that harbor the K601E BRAF mutation typically have the follicular variant of papillary carcinoma histology (Nikiforov & Nikiforova, 2011) and are associated with a low recurrence risk (Yip et al., 2015). The *BRAF V600E* mutation has been correlated with aggressive features such as extrathyroid extension, advanced tumor stage at presentation, recurrence, and lymph node involvement and/or distant spread (Xing et al., 2005), conferring an intermediate risk of disease recurrence (Yip et al., 2015). This mutation also occurs in 20% to 40% of poorly differentiated thyroid carcinomas and 30% to 40% of anaplastic thyroid carcinomas. Many of these carcinomas also reveal areas of well-differentiated papillary cancer, and BRAF V600E is present in both tumor components, which suggests that this mutation is an early event that predisposes the tumor to dedifferentiation (Nikiforova, 2011). Cancers with these mutations have decreased ability to trap radioiodine, which leads to treatment failure and more aggressive tumor behavior (Nikiforova & Nikiforov, 2008).

Detection of the *BRAF* mutation can be achieved by direct sequencing, colorimetric mutation detection assay based on shifted terminal assay (Xing et al., 2004), real-time PCR, and allele-specific SYBR green PCR on an FNA sample, which is virtually diagnostic of papillary carcinoma. The *BRAF* mutation represents an attractive therapeutic target for papillary carcinoma with the advent of various BRAF inhibitors (e.g., BAY43-9006) (Wan et al., 2004; Wilhelm et al., 2004).

Human *HRAS*, *KRAS*, and *NRAS* genes encode the ras-p21 proteins, which are highly conserved in sequence from yeast to humans and are strongly homologous in amino acid sequence to one another. As described in Chapter 77, the ras-p21 protein is a G-protein, that is, a guanosine triphosphate (GTP)–binding protein that is activated when GTP binds in place of guanosine diphosphate (GDP). The exchange is promoted by the SOS or GNEF (guanine nucleotide exchange factor) that, in turn, is activated when a tyrosine kinase–containing receptor binds to its growth factor. The activated tyrosine kinase binds to the growth factor receptor–bound (grb) adapter protein that binds simultaneously to SOS-GNEF, activating it to bind to ras-p21 thereby promoting GTP-GDP exchange. To be active, ras-p21 must bind to the inner cell membrane in a covalent link between a farnesyl moiety in the membrane and the thio group of Cys 186. In its active form, ras-p21 binds directly to raf, thereby activating the raf-MEK-MAP kinase (or ERK) pathway as described in Chapter 77. Simultaneously, it activates phosphatidylinositol-3-hydroxy kinase (PI3K), which activates AKT. Unlike BRAF V600E-driven tumors, RAS-like tumors typically preserve the expression of thyroid differentiation genes (TCGA Network, 2014a). Point mutations involving several specific sites (codons 12, 13, and 61) in *NRAS* and *HRAS* are more common in thyroid cancer. They are found in 10% to 20% of cases of papillary carcinoma, 40% to 50% of follicular carcinomas, and 20% to 40% of poorly differentiated and anaplastic carcinomas. Among papillary carcinomas, virtually all tumors that harbor a RAS mutation grow, forming neoplastic follicles and no papillary structures. Therefore, they are diagnosed as the follicular variant of papillary carcinoma (Zhu et al., 2003).

RAS mutations are also found in 20% to 40% of benign follicular adenomas (Motoi et al., 2000). The finding of this mutation in benign adenomas as well as in follicular-patterned carcinomas suggests that RAS-positive follicular adenomas may serve as a precursor for RAS-positive follicular carcinomas and the follicular variant of papillary carcinomas. Furthermore, RAS mutations may predispose well-differentiated cancers to dedifferentiation, resulting in anaplastic tumors. With regard to the rare but important cribriform morular variant of papillary carcinoma, nuclear β-catenin accumulation is essentially a defining feature that is diagnostically invaluable.

The *RET/PTC* gene rearrangement is another prominent genetic alteration that plays a role in the pathogenesis of up to 20% of sporadic PTCs (Nikiforova & Nikiforov, 2008). The *RET* gene, located on chromosome 10q11.2, encodes the tyrosine kinase receptor consisting of an extracellular ligand-binding domain for the glial-derived neurotrophic factor family of growth factors, a cysteine-rich region, a transmembrane domain, and an intracellular tyrosine kinase domain. *RET* is highly expressed in parafollicular C cells and at very low levels in thyroid follicular cells (Nikiforov, 2008). *RET/PTC* rearrangements are a very early event in thyroid cancer development; this would explain their high prevalence in occult or microscopic PTC. Twelve forms of *RET/PTC* rearrangements have been reported to date, linking the 3′ portion of the *RET* gene with the 5′ portion of various different genes of the PTC family (Nikiforova & Nikiforov, 2008), the two most common of which are *PTC1* (*H4*) and *PTC3* (*ELE1*, *ARA70*, *NCOR4*), which account for up to 70% and 30% of rearrangements in sporadic PTC, respectively (Nikiforova & Nikiforov, 2008). In particular, *RET/PTC* rearrangements are more frequent in individuals exposed to ionizing radiation (50%–80%) (Nikiforova & Nikiforov, 2008), with the exception of *ELKS-RET* (ELKS is a polypeptide sequence that is rich in glutamic acid [E], leucine [L], lysine [K], and serine [S]) and *HOOK3RET* fusion (HOOK3 encodes the protein Hook homolog 3). *RET/PTC* rearrangements are also more frequent in children (40%–70%) (Nikiforova & Nikiforov, 2008) as compared with the general population (15%–30%). Papillary carcinomas with *RET/PTC* gene rearrangements typically present in younger individuals and exhibit a high rate of lymph node metastasis with classical papillary histology and lower stage at presentation, particularly in cases harboring *RET/PTC1* (Nikiforova & Nikiforov, 2008). In tumors arising after radiation exposure, *RET/PTC1* was found to be associated with classic papillary histology, whereas the *RET/PTC3* type was more common among solid variants (Nikiforova & Nikiforov, 2008).

Activated RET kinase has been explored as a target of therapy using TKIs such as ZD6474 (Nikiforova & Nikiforov, 2008). The distribution of *RET/PTC* rearrangements within each tumor may vary from involving almost all neoplastic cells (clonal *RET/PTC*) to being detected only in a small fraction of tumor cells (nonclonal *RET/PTC*) (Nikiforov, 2008). This heterogeneity is a potential problem in RET receptor–targeted therapy.

Follicular Carcinoma

Most of the frequent genetic alterations in follicular carcinoma are *RAS* point mutations and *PAX8-PPARG* rearrangements, altering the PI3K/

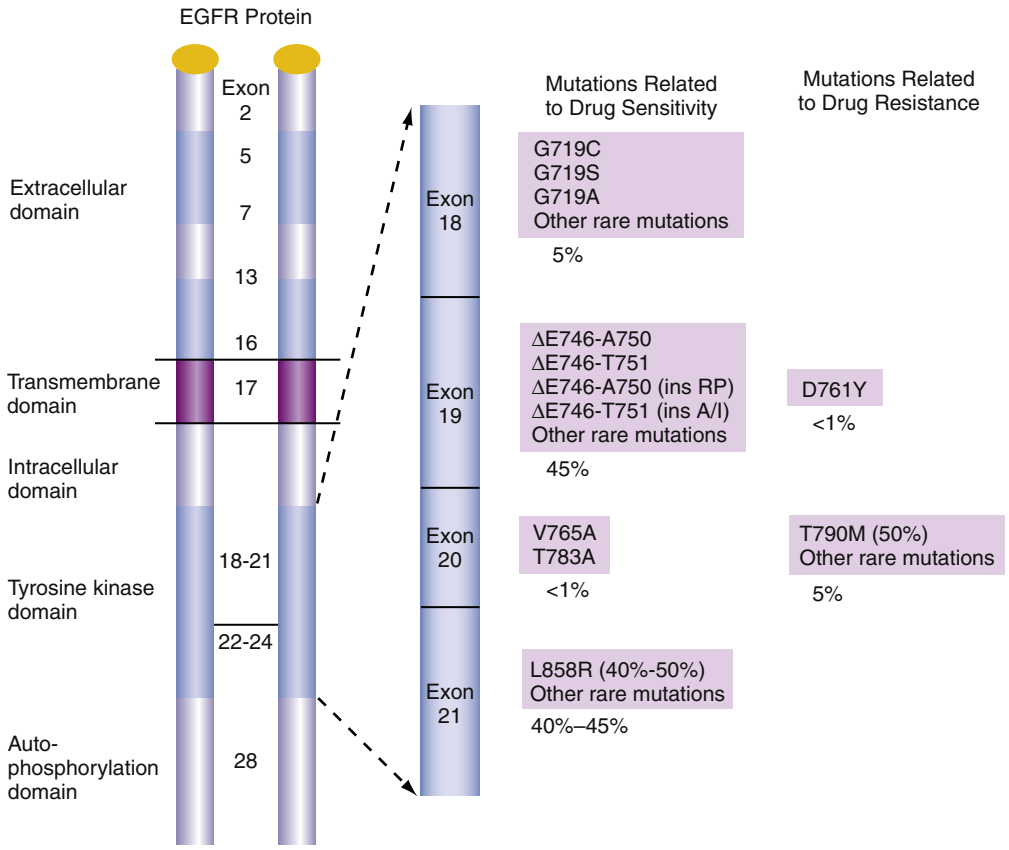

Figure 79.4 Clinically significant mutations of epidermal growth factor receptor mutation in cancer.

AKT signal pathway. Several studies have reported the utility of molecular testing in diagnosing this type of thyroid cancer preoperatively on FNA specimens.

A *RAS* mutation is found in 40% to 50% of conventional follicular carcinomas and in 20% to 40% of adenomas. It is interesting to note that the most common *ras* mutations, instead of occurring at codon 12, as in most other cancers, occur at codon 61 for *NRAS* and *HRAS* (Nikiforova & Nikiforov, 2008). These mutations are associated with tumor dedifferentiation, a less favorable prognosis, and metastasis to bone (Nikiforova & Nikiforov, 2008). Furthermore, RAS mutations are potentially transformative as indicated by a 20% to 40% prevalence in poorly differentiated and undifferentiated carcinoma.

The *PAX8-PPARG* gene rearrangement is a result of the translocation t(2;3)(q13;p25). It leads to a fusion between the *PAX8* gene, which encodes a thyroid-specific paired domain transcription factor, and the *PPARG* gene. It occurs in 35% of conventional follicular carcinomas and has a lower prevalence in oncocytic (Hürthle cell) carcinomas (Nikiforova & Nikiforov, 2008). This translocation may also be seen in up to 13% of follicular adenomas and approximately 5% of follicular variants of papillary carcinoma. Tumors harboring *PAX8-PPARG* rearrangements tend to present in a younger age group, are smaller, and exhibit solid or nested patterns and more frequent vascular invasion. This rearrangement results in overexpression of the PPARG protein that is detectable on IHC (Nikiforova et al., 2003). This molecular overlap between follicular adenoma, follicular carcinoma, and follicular variant of papillary thyroid carcinoma thus likely reflects a biological continuum.

Medullary Carcinoma

Medullary thyroid carcinoma (MTC) is a sporadic malignancy in a majority of cases (75%), with the remainder spanning three familial syndromes, including multiple endocrine neoplasia (MEN 2A and MEN 2B) and familial MTC (FMTC). In MTC, *RET* is activated by point mutations in contrast to its activation by chromosomal rearrangement in PTC. In sporadic medullary carcinomas, somatic mutations of *RET* are found in 20% to 80% of cases without a germline mutation. Germline mutations in *RET* are found in almost all patients with familial forms of medullary carcinoma; this correlates with the aggressiveness of MTC. However, it must be noted that sporadic tumors may also harbor RET mutations (30%–66%) as well as *HRAS* or *KRAS* mutations (up to 25%).

Thyroid-specific gene panels using microarray or NGS have also been developed (Nikiforov, 2017). The tumor profile data, including telomerase reverse transcriptase (TERT) gene promoter mutations may improve individualized patient management.

LUNG CANCER

Lung cancer remains the most common cause of cancer-related death among men and women worldwide. Epithelial tumors of the lung are of four principal types: squamous cell carcinoma, adenocarcinoma, large cell carcinoma, and small cell carcinoma. Clinically, the most important distinction is noted between small cell carcinoma and the others, which can be grouped together as non–small cell carcinoma. Small cell cancers respond to chemotherapy, whereas non–small cell lung cancers (NSCLCs) are removed surgically if possible. However, with the rapid advancements in the understanding of NSCLCs and the corresponding growth in available molecularly targeted therapy, recognition of specific molecular alterations is required for optimal patient care.

EGFR mutations have been identified in many human cancers, such as lung, breast, head and neck, colorectal, pancreatic, and bladder cancers; glioma; squamous cell carcinoma; Wilms tumor; and certain NSCLCs (adenocarcinoma). EGFR is a *membranous oncoprotein* that induces cell proliferation upon activation. Binding of a ligand to a receptor activates its tyrosine kinase activity, which phosphorylates several substrates on a number of signal transduction pathways, leading to increased signaling activity and activation of downstream effectors. This results in uncontrolled cell proliferation, tumor invasion, angiogenesis, and resistance to normal apoptotic signals (see Chapter 77). Increased EGFR signaling can be the result of *EGFR* gene amplification, protein overexpression, or specific activation mutations in the *EGFR* gene, as described in detail in Chapter 77.

It has been shown that a subset of patients with NSCLC (10%–40%) (Coate et al., 2009) have specific activating mutations in the *EGFR* gene (Fig. 79.4) that are associated with increased sensitivity to TKIs, such as gefitinib (Iressa) or erlotinib (Tarceva), targeting EGFR in lung cancer. Common activating *EGFR* mutations occur most often in exons 18 to 21 and cluster in two major hot spots. The prototype mutation *L858R* in exon 21 (40% of *EGFR* mutations) encoding the tyrosine kinase domain and small in-frame deletions in exon 19 (>50%) are reportedly most often constituting up to 90% and are associated with responses to EGFR TKI therapy. Mutations in exons 18 and 20 account for the remaining 10% of *EGFR* mutations in NSCLC (Sholl et al., 2009). Recent guidelines suggest that routine EGFR assays should include EGFR exon 19 for deletions and insertions, EGFR exon 18 for E709 and G719 mutations; exon

20 for S768I, T790M, and insertions; and exon 21 for L858R, T854, and L861Q mutations. Clinical EGFR mutation testing should be able to detect all individual mutations that have been reported with a frequency of at least 1% of EGFR-mutated lung adenocarcinomas (Lindeman et al., 2013). Studies have reported that *EGFR* gene mutations are more common among females, Asians, and nonsmokers with adenocarcinoma; these are the same groups that have the highest response rates to TKIs (Sequist & Lynch, 2008). However, recent guidelines (Lindeman et al., 2013) suggest that EGFR molecular testing should be done in all patients with lung adenocarcinoma component. T790M mutation detection is required by 2018 guidelines reversion for relapse cases (Kalemkerian et al., 2018).

Immunohistochemistry for total EGFR and EGFR copy number analysis (i.e., FISH or chromogenic in situ hybridization) are not recommended for selection of EGFR TKI therapy according to recent guidelines. Recent studies have demonstrated that in patients with *EGFR* mutations, the EGFR locus is often concurrently amplified.

ALK gene chromosomal rearrangement is found in another ~7% of lung adenocarcinomas, most commonly in the form of an intrachromosomal inversion leading to the EML4-ALK fusion product associated with ALK protein overexpression. This mutation is present more frequently in lung adenocarcinomas from younger patients with either no or only light smoking history (Kwak et al., 2010; Shaw et al., 2009). However, recent guidelines suggest that ALK molecular testing should be done in all patients with a lung adenocarcinoma component. Some studies have reported associations with solid, mucinous cribriform and/or signet ring histology (Yoshida et al., 2011; Shaw et al., 2009). The translocation is infrequent in pure squamous cell carcinoma but has been reported in adenosquamous carcinoma (Chaft et al., 2012). Patients with this tumor type are responsive to therapy with the multitargeted TKI crizotinib (Takeuchi et al., 2012). FISH using break-apart probes is currently considered the gold standard for detection of ALK rearrangements (Febbo et al., 2011). Polysomy (multiple copies) at the ALK locus is common in lung adenocarcinoma and, when present, confirms that FISH has been performed in a tumor cell population. ALK immunohistochemistry has been included as an alternative to FISH by 2018 updated guidelines (Kalemkerian et al., 2018). However, current evidence suggests that it does not predict response/resistance to targeted therapies. RT-PCR is not recommended as an alternative to FISH for selecting patients for ALK inhibitor therapy (Lindeman et al., 2013).

Recent recommendations for EGFR and ALK testings are as follows: EGFR and ALK testing is not recommended in lung cancers that lack any adenocarcinoma component, such as "pure" squamous cell carcinomas, "pure" small cell carcinomas, or large cell carcinomas lacking any IHC evidence of adenocarcinoma differentiation. EGFR and ALK testing are the most important uses of the diagnostic sample after a diagnosis of adenocarcinoma is established. If specimens are insufficient for molecular testing, patients may need to undergo another invasive diagnostic procedure before they can be treated. NGS enables the use of small specimens for multiple molecular marker detection, avoiding the risks associated with obtaining surgical biopsies. Cell-free circulating DNA can be used for T790M detection in relapse (Kalemkerian et al., 2018). EGFR and ALK results should be available within 2 weeks (10 working days) of receiving the specimen in the testing laboratory (Lindeman et al., 2013).

Mutations in *KRAS*, frequently in codons 12 and 13, have been reported in up to 30% of cases of lung adenocarcinoma (Coate et al., 2009). These mutations are usually found in cancers of smokers and are more common in adenocarcinoma (30%–50%) than in NSCLC (15%–20%). Conversely, oncogenic mutations in the *KRAS* gene were reportedly associated with resistance to EGFR-TKIs in metastatic colorectal cancer. Thus, testing for *KRAS* mutations as a negative predictor of response to EGFR TKI has become part of molecular diagnostic algorithms for lung adenocarcinoma in many centers. However, more recent data suggest that EGFR wild-type tumors have less favorable outcomes if they are treated with EGFR TKI than if they are treated with conventional platinum-based chemotherapy. Therefore, *KRAS* mutation testing is not recommended as a sole determinant of anti-EGFR TKI therapy (Lindeman et al., 2013).

Lung adenocarcinomas contain a number of other less common alterations that may lead to treatment with targeted inhibitors. These include *RET* (~2% of lung adenocarcinomas) (Takeuchi et al., 2012), increased copies of *MET* (Engelman et al., 2007), and sequence-altering mutations in *ERBB2* (*HER2*), *BRAF*, and *PIK3CA* (Cardarella et al., 2012) as well as chromosomal rearrangements involving *ROS1* (~2% of lung adenocarcinomas; may respond to treatment with crizotinib). In fact, *ROS1* mutation detection has been strongly recommended for all lung cancer patients regardless of clinical characteristics according to the updated guidelines. According to the updated guidelines from Association for Molecular Pathology (AMP), the College of American Pathologists (CAP) and the International Association for the Study of Lung Cancer (IASLC), multiplexed genetic sequencing panels (e.g., NGS testing with detection of *BRAF*, *ERBB2*, *MET*, *RET*, and *KRAS* gene alterations) are preferred over multiple single-gene tests to identify other treatment options beyond *EGFR*, *ALK*, and *ROS1* (Kalemkerian et al., 2018).

HEPATOCELLULAR CARCINOMA

Hepatocellular carcinoma (HCC) is the sixth most common malignancy and the third most common cause of cancer death worldwide. Major risk factors include chronic viral infection (hepatitis B virus [HBV] and hepatitis C virus [HCV]), alcoholic/nonalcoholic liver disease, environmental carcinogens (e.g., aflatoxin B1), and inherited genetic disorders (e.g., Wilson disease, hemochromatosis, α_1-antitrypsin deficiency, tyrosinemia) (McGlynn & London, 2005; Parkin et al., 2005; Clark, 2006; Motola-Kuba et al., 2006). The development of HCC is a multistep process, comprising hyperplastic change, dysplasia, early HCC, and well-developed HCC in the setting of chronic hepatitis or cirrhosis (Takayama et al., 1990; Theise et al., 2002). A small percentage of HCC develops in patients with nonalcoholic steatohepatitis (~14%), with 37% with no cirrhosis (Bengtsson et al., 2019).

The genomic abnormality of HCC is heterogeneous, largely as the result of various molecular mechanisms of carcinogenesis related to different causes and multifactorial processes (Jain et al., 2010a). Two major mutually exclusive subtypes of HCC are classified by CTNNB1 (the gene encoding β-catanine) and p53 mutations. Tumors with CTNNB1 mutations are featured with nuclear β-catenin staining and downregulation of the interleukin (IL)-6/JAK-STAT pathway. They are larger well-differentiated tumors with microtrabecular and pseudoglandular architecture. The tumors are cholestatic and are not associated with significant inflammatory infiltrate. Tumors with p53 mutations are related to activation of the PI3K/AKT pathway. They are poorly differentiated, highly proliferative, massive tumors with macrotrabecular architecture and pleomorphic histology, often with sarcomatous and multinucleated components. They have a high propensity for both macrovascular and microvascular invasion. In addition, somatic mutations with TERT are frequent genetic alterations in dysplastic nodules and HCC (Calderaro et al., 2017; Torbenson, 2017).

Detailed molecular findings in various subtypes of HCC include the following. (1) Scirrhous HCC has been found to express the tuberous sclerosis genes, *TSC1* and *TSC2*, that promote epithelial to mesenchymal transition (transforming growth factor-β, VIM) and PI3/AKT pathway activation. CTNNB1 is not activated. (2) Steatohepatitic HCC is associated with IL-6/JAK-STAT involvement. It is also featured with lack of Wnt/β-catenin pathway activation. (3) A macrotrabecular massive variant of HCC has been found to express Tp53 mutations, FGF19 amplifications, ATM mutations, angiogenesis activation consisting of upregulation of the ANGPT2 gene, and vascular endothelial growth factor (VEGF) A expression. (4) Carcinosarcomas have been found to have overexpressed or mutant Tp53 involvement, which is found in both the carcinoma and sarcoma parts, PI3K involvement in the carcinoma part and FGFR3 involvement in the sarcoma sections. Activation of protein kinase A resulting from deletion on Chr 19 is reported in (5) fibrolamellar HCC, which leads to fusion between the *DNAJB1* gene and the *PRKACA* gene (Rondell et al., 2015). Homologous recombination of telomeres has been involved in the pathogenesis of (6) chromophobe HCC. Wnt/β-catenin and transforming growth factor-β signaling are reported to be significantly activated in mixed (7) HCC–cholangiocarcinoma (CCA). (8) A stem cell subclass of HCC is associated with the MYC, mTOR, and NOTCH signaling pathways. Upregulation of the insulin-like growth factor 2 pathway and genes implicated in liver progenitor cells (*PROX1*, *HNF-1β*, *FOXA1*, *FOXA3*) may also be involved (Calderaro et al., 2017; Torbenson, 2017; Moeini et al., 2017).

In addition, differential expression of miRNA in HCC has been reported to have prognostic value and pathogenesis significance (Tang et al., 2016; Lee et al., 2014). The only curative therapy for HCC is surgical resection or liver transplantation. PD-L1 tumoral expression is observed in 16% of HCC from recent reports (Sia et al., 2017). However, the identification of accurate predictive markers and/or immune classifiers to select ideal candidates for immunotherapy is still under investigation (Sia et al., 2017).

Using genome-wide expression profiling analysis six, five, eight, and nine samples were analyzed for HBV, HCV, AC, and NAFLD HCC, respectively. The regulatory networks for HBV HCC revealed E2F1 as activated UR, regulating genes involved in cell cycle and DNA replication, and HNF4A and HNF1A as inhibited UR. In HCV HCC, interferon-γ, involved in cellular movement and signaling, was activated, while IL1RN,

mitogen-activated protein kinase 1 involved in IL-22 signaling and immune response, was inhibited. In alcohol consumption HCC, ERBB2 involved in inflammatory response and cellular movement was activated, whereas HNF4A and NUPR1 were inhibited. For HCC derived from nonalcoholic fatty liver disease, miR-1249-5p was activated, and NUPR1 involved in cell cycle and apoptosis was inhibited. The prognostic value of representative genes identified in the regulatory networks for HBV HCC can be further validated by an independent HBV HCC data set established in our laboratory with survival data (Seshachalam et al., 2018).

Fibrolamellar Carcinoma

A subtype of HCC usually occurs in children and young adults in the noncirrhotic liver. Histologically, it is identified by a proliferation of large hepatocytes with abundant granular eosinophilic cytoplasm and round nuclei with prominent, centrally placed nucleoli. Recent studies have identified activation of protein kinase A as the defining molecular feature of this tumor, the vast majority of which demonstrate fusion of the *DNAJB1* and *PRKACA* genes (Graham et al., 2015). A separate genetic defect in the regulatory subunit of the protein kinase A complex, PRKAR1A, was also recently identified as the underlying genetic defect in a small subset of cases, some of which are associated with the Carney complex.

Hepatic Adenomas

Hepatic adenoma (HA) is an uncommon, benign, hepatic neoplasm that typically occurs in women of childbearing age, often with a history of long-term use of oral contraceptive drugs. Molecular studies have revealed that HAs bear several recurrent mutations that involve unique molecular pathways that are distinct from hepatocellular carcinoma. In a recent review, hepatic adenoma has been reclassified from the four groups that were originally proposed by the French Bordeaux collaborative group into 6 groups, based on the molecular characteristics, as determined by IHC markers and their correlation with histologic features. These six subtypes are (1) HAs with inactivating mutations of hepatocyte nuclear factor 1a (HNF1A; HCA-H), either somatic or germline steatosis; (2) HAs with activating mutations of β-catenin gene (HCA-B) in exon 3; (3) HAs with activating mutations of β-catenin gene (HCA-B) in exons 7 and 8; (4) HAs with inflammatory features and associated with activation of JAK/STAT pathway—these neoplasms may also harbor β-catenin mutations (HCA-I); (5) HAs with activation of sonic hedgehog signaling (sh-HCA); and (6) unclassified HAs that have no specific gene mutations or unique morphologic features (HCA-U) (Zucman-Rossi et al., 2006; Zhang et al., 2018).

TCF1 (transcription factor 7, also known as *HNF1A*) is a tumor suppressor gene involved in liver tumorigenesis. It is located on the long arm of chromosome 12. It encodes transcription factor HNF1, which, in the liver, is implicated in hepatocyte differentiation and is required for expression of certain liver-specific genes, including albumin, b-fibrinogen, and α_1-antitrypsin (Rebouissou et al., 2007). The French Bordeaux group showed that HAs with biallelic inactivating mutations in the TCF1 (*HNF1A*) gene constituted a homogenous, morphologically distinct group that comprises 35% to 40% of all HAs, and classified the group as *HNF1A-mutated hepatic adenomas* (*HA-H*). In most of this subtype of HAs (about 85%), mutations are somatic in origin. However, in a few cases, one mutation is somatic and the other is germline in origin. Furthermore, heterozygous germline mutations in the *TCF1* gene have been associated with occurrence of a rare autosomal-dominant condition, maturity-onset diabetes mellitus of youth, type 3 (MODY3), which presents in early adulthood (usually younger than 25 years of age). *HNF1A* mutation increases lipogenesis by promotion of fatty acid synthesis and downregulation of liver-type fatty acid–binding protein 1 (L-FABP), leading to diffuse intralesional steatosis (Rebouissou et al., 2007).

The β-catenin gene (*CTNNB1*) is a component gene of the Wnt/β-catenin pathway, which is important in hepatocellular development and physiology. In normal hepatocytes, activation of the β-catenin gene is transient, followed by rapid degradation of the β-catenin protein, which is facilitated by a set of genes, including *axins*, glycogen S-kinase 3 (*GSK3*), and adenomatosis polyposis coli (*APC*). β-Catenin mutations in exon 3 are associated with strong nuclear expression of β-catenin; exons 7 and 8 mutations show weak activation of β-catenin. Decreased degradation, sustained activation, and nuclear accumulation of β-catenin protein could be due to either a mutation of the β-catenin gene or mutations in the *axin*, *APC*, or *GSK3* genes. Activating β-catenin mutation is reported in 15% to 19% of HA cases (Rebouissou et al., 2008). β-Catenin mutations have also been seen in 20% to 34% of well-differentiated HCCs (Bioulac-Sage et al., 2010). Mutations bearing high expression are more frequently associated with malignant transformation (Bioulac-Sage et al., 2010).

Some hepatic adenomas show sustained activation of IL-6 receptor signaling because of somatic gain-of-function mutations of the IL-6 signal transducer gene (*IL6ST*), which encodes glycoprotein-130 (gp130); gp130 is a component of the IL-6 receptor (Rebouissou et al., 2009). This activation of IL-6 promotes the signal transducer and activation of the JAK/STAT3 signaling pathway and induces an acute-phase inflammatory response within neoplastic hepatocytes. This is manifested as overexpression of acute-phase reactants, such as serum amyloid A and C-reactive protein (CRP), and inflammatory cell infiltration of the tumor. Such HAs are referred to as inflammatory HA (HA-I) and comprise 30% to 35% of all HAs (Bioulac-Sage et al., 2010). Somatic mutations of the *IL6ST* gene are seen in about 60% of the HA-I subtype. About 10% of HA-I cases show coexistent β-catenin mutations. Historically, the HA-I subtype was referred to as *telangiectatic focal nodular hyperplasia* and was thought to belong to the focal nodular hyperplasia (FNH) family. In certain studies, the telangiectatic focal nodular hyperplasias are monoclonal neoplasms that are morphologically and biologically closer to HAs and included within the subgroup HA-I in the new classification scheme (Paradis et al., 2004; Bioulac-Sage et al., 2005). This classification is clinically relevant because it identifies a subset of HAs, specifically HA-B, with increased potential for malignant transformation (Farges & Dokmak, 2010; Columbo, 2016).

Furthermore, it helps in identifying cases for which genetic counseling is recommended in the subset of patients with hepatic adenomatosis that shows a steatotic morphology resembling HNF1A-mutated adenomas. This familial form of hepatic adenomatosis involves germline mutations of *HNF1A* and is associated with maturity-onset diabetes mellitus of youth, type 3 (MODY3). Hence, the rationale for genetic counseling is to search for germline mutations of *HNF1A* in the family. Reclassification of telangiectatic FNH as HA-I, based on molecular genetics and proteomic profiling, has added to the morphologic and molecular heterogeneity of HAs (Bioulac-Sage et al., 2005).

Cholangiocarcinoma

Cholangiocarcinomas are tumors arising from the biliary tract that can be intrahepatic or extrahepatic. Based on histology, they are divided into large-duct and small-duct type (also referred to in the literature as *cholangiolar* and, occasionally, *cholangiocellular*). Small-duct type tumor is characterized by low-grade cytologic atypia, anastomosing cords, and glands resembling cholangioles or canals of Hering. Immunohistochemically, CD56 (also known as *neural cell adhesion molecule* [NCAM]), N-cadherin, and CRP expression have been thought of as combined hepatocellular-choriocarcinoma with stem cell features or distinct liver tumor. However, a recent study of identified cholangiolocellular carcinoma based on genomic profiling (IDH1/2 mutations, FGFR2 fusions, chromatin-remodeling gene mutations such as ARID1A, PBRM1, and copy number alterations) found that this condition is a subtype of cholangiocarcinoma (Balitzer et al., 2019). In fact, IHC and molecular features of cholangiolocellular carcinoma are similar to well-differentiated intrahepatic cholangiocarcinoma.

GASTRIC CANCER

Stomach cancer represents 1.6% of all new cancer cases in the U.S. (Surveillance, Epidemiology, and Ends Results). The average annual percent change (AAPC) from 2012 to 2016 is significantly decreased by 1.7%. A majority of gastric cancers (GCs) are adenocarcinomas, historically classified into two major groups by Lauren's classification: intestinal type with glandular pattern, and diffuse or poorly differentiated type with a signet ring cell morphology in some cases (Lauren, 1965). These two types of GCs have a distinct molecular basis of carcinogenesis, and clinical and genetic characteristics. The main causes of the intestinal type include dietary habits, environmental factors, and *Helicobacter pylori* infection (Kelley & Duggan, 2003). Gastric cancer risk is also associated with hereditary tumor syndromes, such as hereditary diffuse-type gastric cancer syndrome, hereditary nonpolyposis colorectal cancer (HNPCC), Li-Fraumeni syndrome, and Peutz-Jeghers syndrome (PJS; i.e., familial adenomatous polyposis [FAP] and juvenile polyposis) (Traverso et al., 2002; Napieralski et al., 2005).

The development of intestinal-type GC is a multistep process that proceeds from gastritis (chronic or atrophic) and related changes (e.g., pernicious anemia) to intestinal metaplasia, dysplasia, and, eventually, carcinoma (Oberhuber & Stolte, 2000; Kelley & Duggan, 2003). These processes are accompanied by a series of genetic alterations. The molecular alterations occur in the early stage of carcinogenesis, including molecules leading to genetic instability, inactivation of TSGs by methylation of CpG, telomerase activation, and *p53* gene loss and mutation. Elevated telomerase activity was observed in precancerous lesions (Yasui et al., 1999). The inactivation

mutation of the TSG *p53* (see Chapter 77) is also seen in 38% to 71% of GCs (Joypaul et al., 1993; Shiao et al., 1994; Xiangming et al., 2000). Mutation in *p73*, a member of the *p53* family, is indicated in the development of GC associated with *H. pylori* infection in mouse model. A high level of microsatellite instability (MSI-H) is frequently seen in intestinal-type GC, largely caused by hypermethylation of the promoter regions of mismatch repair genes (most commonly, *MLH1* and *MSH2*) or gene mutations (in a small percentage of GCs) (Lee et al., 2004a; Gu et al., 2009; Seo et al., 2009). The CpG island methylator phenotype, originally found in colorectal cancer, has been detected in 24% to 47% of GCs (Toyota et al., 1999; Oue et al., 2003; Lee et al., 2004b). The oncogene product *Her2/neu* is frequently amplified in intestinal-type GC (Wang et al., 2002).

The molecular pathogenesis of diffuse-type GC is less clear. *H. pylori* infection seems not to be related to the diffuse type of GC according to epidemiologic studies. It can be part of a hereditary gastric cancer predisposition syndrome (Guilford et al., 1998). The unique molecular abnormality of diffuse-type GC distinct from intestinal-type GC is deficiency in cell-cell adhesion caused by loss or downregulation of the *E-cadherin* gene (*CDH1*) as a result of genetic or epigenetic alterations. The abnormality in *CDH1* can be found in the early stages of diffuse GC development. Decreased *CDH1* expression is detected in 50% of diffuse-type GCs, and more than 70% of those somatic *CDH1* mutations consist of complete or partial deletion of exons (Berx et al., 1998; Napieralski et al., 2005). The unique molecular genetics of GC might be useful for diagnosis in that *CDH1* mutations can be detected by PCR on paraffin-embedded tissue. Detection of the germline mutation in *CDH1* may help in identification of carriers of asymptomatic mutations involved in the GC family syndrome and may offer an opportunity for prophylactic total gastrectomy in patients carrying the *CDH1* mutation (Fitzgerald & Caldas, 2002). Other frequently altered genes or gene products in diffuse-type GC include the met proto-oncogene, encoding the hepatocyte growth factor receptor, and the SC-1 antigen, an apoptosis receptor (Kuniyasu et al., 1992; Vollmers et al., 1998a, 1998b).

Currently, the most valuable predictive and prognostic factor for GC is clinical staging independent of cancer type, but it does not reflect the heterogeneity of tumor biology. Molecular biomarkers have been investigated as alternatives or supplements to the current system and have shown very promising results in predicting prognosis and therapeutic response. For example, microsatellite instability (MSI) results in an accumulation of genetic abnormalities during the early stages of gastric carcinogenesis (Yokozaki et al., 2001). MSI-H is shown in only 4% of stomach carcinomas, especially in well-differentiated types in elderly patients. It is usually associated with intestinal-type GC, commonly seen in the distal stomach or antrum, and is associated with less frequent local lymph node metastasis. However, whether patients with MSI-H GC have more favorable long-term survival than those with MSH-L GC (novel tumor bands with one marker)/microsatellite stable [MSS], no novel tumor bands) remains controversial (Hayden et al., 1997; Wirtz et al., 1998). Expression in tumor tissue of caudal-type homeobox transcription factor 2 (*CDX2*), in combination with normal *E-cadherin* and nonexpression of the transmembrane protein mucin 1 (*MUC1*), is a favorable prognostic factor for patients with GC (Tanaka et al., 2003; Fondevila et al., 2004).

Abnormal methylation is present in multiple TSGs, such as *p16*, *CDH1* (*E-cadherin*), *hMLH1*, *RAR-beta*, *RUNX3*, *MGMT* (O6-methylguanine methyltransferase), *TSP1* (thrombospondin-1), *HLTF* (helicase-like transcription factor), and *RIZ1* (retinoblastoma protein-interacting zinc finger gene-1). A 12-gene study has shown that methylation changes are more frequently observed in stages III/IV cancers compared with stages I/II cancers (Oue et al., 2006). Overexpression of growth factors, such as EGF/TGF-α and EGFR, is associated with cancer progression and often indicative of poor prognosis (Choi et al., 2019). VEGF overexpression enhances tumor angiogenesis; thus, it is associated with lymph node metastasis, hepatic metastasis, and shorter survival time.

In addition, mutation or abnormal expression of *p53* may predict a reduced cumulative survival and is associated with lymph node metastasis and lower chemosensitivity (Fondevila et al., 2004; Pinto-de-Sousa et al., 2004; Oh et al., 2008).

An alternative system, proposed by the WHO, divides GC into papillary, tubular, mucinous (colloid), and poorly cohesive carcinomas (Lauwers et al., 2010). These classification systems have little clinical utility, making the development of robust classifiers that can guide patient therapy an urgent priority. Recently, The Cancer Genome Atlas (TCGA, 2014b) project proposed a molecular classification dividing GC into four subtypes: (1) Epstein-Barr virus–associated tumors (~9%, which display recurrent PI3KCA mutations, extreme DNA hypermethylation, and amplification of JAK2, CD274 [also known as PD-L1] and PDCD1LG2 [also known as PD-L2], EBV-CIMP, CDKN2A silencing, and immune cell signaling); (2) microsatellite unstable tumors (~22%), which show elevated mutation rates, including mutations of genes encoding targetable oncogenic signaling proteins; (3) genomically stable tumors (~20%), which are enriched in the diffuse histologic variant and have mutations of *RHOA* or fusions involving RHO-family GTPase-activating proteins, CLDN18-ARHGAP fusion, or mutation in the cell adhesion gene CDH1; and (4) tumors with chromosomal instability (~50%), which show intestinal histology, TP53 mutation, RTK-RAS activation, marked aneuploidy, and focal amplification of receptor tyrosine kinases (Bass et al., 2014). Notably, the chromosomal instability tumors were predominant (65%) in the gastroesophageal junction and the gastric cardia, whereas the EBV-positive tumors (62%) were primarily noted in the fundus and body of the stomach (Bass et al., 2014).

Importantly, these molecular subtypes showed distinct salient genomic features, providing a guide to targeted agents that should be evaluated in clinical trials for distinct populations of GC patients. Through existing testing for MSI and EBV and the use of emerging genomic assays that query focused gene sets for mutations and amplifications, the classification system developed through this study can be applied to new GC cases.

The ToGA trial, an international multicenter phase III clinical study involving 24 countries globally, has shown that the anti-HER2/neu humanized monoclonal antibody trastuzumab (Herceptin) is effective in prolonging survival in patients with HER2/neu-positive adenocarcinoma of the stomach and the gastroesophageal junction (Bang et al., 2010; van Cutsem et al., 2015). Molecular therapy targeting HER2/neu is now approved for patients with inoperable locally advanced, recurrent, or metastatic adenocarcinoma of the stomach or esophagogastric junction if the tumor shows unequivocal HER2/neu overexpression by IHC (score 3+) or amplification by FISH or chromogenic in situ hybridization (CISH). Therefore, HER2 testing in gastric carcinoma is warranted for determination of treatment eligibility.

The prognosis of GC is relatively poor. Treatment of GC, especially late-stage tumor, usually requires a multidisciplinary approach that includes chemotherapy in combination with surgical resection. TCGA studies has developed a genetic profile of somatic gene alteration in GC using GNS (Network CGAR, 2014; TCGA, 2014b). With such high-throughput technology, potential novel biomarkers—that is, genes (genomics), mRNA (transcriptomics), proteins (proteomics), and metabolites (metabolomics)—are able to be discovered.

COLORECTAL CANCER

Colorectal cancer (CRC) is the third most common malignancy worldwide (Ferlay et al., 2004). Prognostication of newly diagnosed CRC predominantly relies on stage or anatomic extent of disease based on the International Union Against Cancer and the American Joint Committee on Cancer staging classifications. However, CRC should be regarded as a heterogeneous, multipathway disease—an observation substantiated by the fact that histologically identical tumors may have neither similar prognosis nor similar response to therapy (Umar et al., 2004). Mutations and/or epigenetic alterations in TSGs (e.g., *APC*, *DCC*, *SMAD-2*, *SMAD-4*, *p53*) and oncogenes (e.g., *KRAS*, *p53*) are molecular determinants during the development of sporadic CRC, which was first summarized in the adenoma-carcinoma sequence described by Fearon and Vogelstein (1990). Based on genetic background, sporadic CRCs can be subclassified into two major types: (1) chromosomal unstable and (2) microsatellite unstable, plus an additional group with CpG island methylator phenotypes. Various genetic syndromes are known to predispose to colorectal carcinoma and to have specific inherited gene defects. These molecular markers are currently being investigated as a means of improving the identification of patients likely to have poor clinical outcomes and, therefore, possibly benefiting from adjuvant treatment (Eschrich et al., 2005; Ghadimi et al., 2005; Liang et al., 2009).

EGFR (a receptor tyrosine kinase) overexpression is detected in up to 80% of CRCs (Messa et al., 1998). Tumors with a high level of EGFR expression usually have a poor prognosis (Ghadimi et al., 2005; Liang et al., 2009). These data have led to the clinical use of EGFR blockade in the treatment of CRCs with anti-EGFR monoclonal antibodies such as cetuximab or panitumumab (see Chapter 77). Cetuximab is a mouse-human hybrid monoclonal antibody approved by the FDA in 2004 as second-line treatment of CRC. Panitumumab is a fully human immunoglobulin G_2 monoclonal antibody approved by the FDA in 2007 as third-line monoclonal antibody therapy of refractory CRC. Both drugs are expensive and have significant side effects. Thus, it is imperative to use a biomarker to predicate the therapeutic response. However, use of EGFR as a biomarker to

predict response to EGFR monoclonal antibodies has had limited success. Only detection of increased EGFR copy number by FISH has predictive value (Liang et al., 2009), and it has been proven that EGFR expression levels detected by IHC are not as useful. In contrast to *EGFR* mutation in lung cancer, *EGFR* mutation in CRC is a rare event that occurs in fewer than 1% of cases (Plesec & Hunt, 2009). Current studies are focused on finding the downstream effectors of the EGFR pathway that may serve as biomarkers for predicting the effectiveness of anti-EGFR therapy.

As summarized earlier in this chapter and in Chapter 77 Ras-p21 proteins are guanosine triphosphate (GTP)-coupled proteins that are important in many receptor tyrosine kinases that utilize signaling on the Ras/Raf/Erk/Map kinase signal transduction pathway. Mutations that result in single amino acid substitutions at critical positions in the amino acid sequence of this protein, such as Gly 12, Gly 13, and Gln 61, occur in the Ras protein and cause its constitutive activation. This leads to a series of oncogenic events that activate downstream signaling pathways, promoting tumor initiation and tumor growth and progression, including local invasion, angiogenesis, metastasis, and even immune response (Rowinsky et al., 1999; Smakman et al., 2005).

The *KRAS* mutation occurs in at least 35% to 45% of cases of CRC and, in some series, in up to 75% of cases. Mutations of this gene occur almost exclusively in three hot spots (codons 12, 13, and 61) and rarely in others, including codon 146 (Ogino et al., 2005; Smakman et al., 2005). Because *KRAS* is the downstream effector of EGFR and is frequently mutated in CRC, the mutation status of *KRAS* has become an important predictive marker for the effectiveness of cetuximab or panitumumab on metastatic CRCs. The American Society of Clinical Oncology (ASCO) has recommended that patients with diagnosed metastatic colon cancer who are candidates for anti-EGFR therapy should be tested for *KRAS* mutations in a Clinical Laboratory Improvement Amendments (CLIA)-accredited laboratory. If negative for *KRAS* mutations, these patients are deemed suitable for treatment with anti-EGFR antibody (cetuximab or panitumumab) therapy. This recommendation is based on the results of phase II and phase III clinical trials. Retrospective subset analyses of these trial data suggest that patients who have *KRAS* mutations detected in codon 12 or 13 do not benefit from this therapy. This was further confirmed by five randomized, controlled trials of cetuximab or panitumumab response in relation to *KRAS* mutational status (no mutation [wild type] and mutated [abnormal]) and another five single-arm retrospective studies undertaken to evaluate tumor response according to *KRAS* mutational status.

According to the CAP Perspectives on Emerging Technology (POET) guideline published in 2009, acceptable samples for *KRAS* mutation include fresh, frozen, and FFPE tissues. Acceptable assay types are RT-PCR and direct sequencing analysis. However, other methods, such as pyrosequencing or microarray (chip)–based tests, have also been developed (Pajkos et al., 2000; Ogino et al., 2005). As of the time of this writing, no type of *KRAS* testing has been approved by the FDA. Although recommended testing is limited to codons 12 and 13 of exon 2, which make up the vast majority of cases with *KRAS* mutations, many laboratories and commercial kits also include testing for other mutations, such as for codons 61 and 146.

The 2016 National Comprehensive Cancer Network (NCCN) guidelines state that patients with any known *KRAS* or *NRAS* mutation should not receive an EGFR inhibitor. This opinion is shared by ASCO (De Roock et al., 2010).

BRAF is an immediate downstream effector of *RAS* in the Ras/Raf/Map kinase pathway (see Fig. 79.1). Mutation of *BRAF* has been identified in approximately 10% of CRCs (Di Nicolantonio et al., 2008). A vast majority of the point mutations are V600E, a mutational hot spot at nucleotide 1796 within exon 15, accounting for a T:A transversion mutation and a valine-to-glutamic acid substitution. All point mutations occur within the kinase domain of B-Raf protein, leading to constitutive activation of B-Raf kinase (Davies et al., 2002). The *BRAF* mutation is almost mutually exclusive with *KRAS* mutations. Unlike the *KRAS* mutation, *BRAF* mutations frequently occur in female patients older than 75 years of age with proximal lesions. These tumors exhibit MSI with higher frequency than those in other patients with colon cancer (Barault et al., 2008), which appears to be due to epigenetic effects involving hypermethylation of the promoter regions of mismatch repair genes. This finding helps in differentiating between sporadic MSI-H tumors with somatic mutations in the V600E hot spot in *BRAF* and Lynch-associated cancers with *MLH1* or *MSH2* mutations.

BRAF mutations in tumors have been characteristically associated with a worse survival than in those without mutations and with resistance to treatment with anti-EGFR monoclonal antibodies, cetuximab, or panitumumab for metastatic CRCs. Currently, molecular testing for *BRAF* mutation V600E has been performed in many clinical laboratories as a therapeutic indicator for anti-EGFR treatment in combination with *KRAS* mutation analysis (Siena et al., 2009).

PI3KCA is a membrane lipid kinase that phosphorylates the 3-hydroxyl group of phosphatidylinositol. This critical enzyme, which binds directly to ras-p21 protein, can be activated by EGFR-mediated signaling in parallel with the K-ras/B-raf/MAP kinase pathway. Activation of PI3KCA counteracts PTEN, an antioncogene protein, and promotes AKT1 phosphorylation, stimulating cell proliferation, survival, and angiogenesis in cooperation with other pathways. The *PIK3CA* (phosphatidylinositol-4,5-bisphosphate 3-kinase, catalytic subunit α) gene is mutated in about 20% of CRCs (Sartore-Bianchi et al., 2009a). The mutation of *PIK3CA* usually occurs in the hot spots in exon 9 (E542K, E545K) and exon 20 (H1047R), both of which are oncogenic in CRC cellular models. Unlike the *BRAF* mutation, *PIK3CA* and *KRAS* mutations may coexist. In addition to their association with poor prognosis (i.e., local recurrence and increased mortality of CRCs), *PIK3CA* mutations can independently predict resistance to anti-EGFR therapy with panitumumab or cetuximab for metastatic CRCs (Ogino et al., 2009a; Sartore-Bianchi et al., 2009b; Siena et al., 2009). Testing for combinations of the *PIK3CA/PTEN* and *KRAS* mutations can detect up to 70% of patients who are unlikely to respond to anti-EGFR therapy, although more validation is required for clinical practice (Siena et al., 2009).

Loss of PTEN has been found to co-occur with *KRAS*, *BRAF*, and *PIK3CA* mutations (Laurent-Puig et al., 2009; Frattini et al., 2007; Loupakis et al., 2009; Sartore-Bianchi et al., 2009a). The recorded frequency of loss of PTEN expression varies from 19% to 36%, with some studies reporting an effect on response rate and survival, whereas others found an effect only on progression-free or overall survival. Moreover, data on the loss of PTEN expression are not concordant in primary and metastatic tissues (Loupakis et al., 2009). It has been suggested that loss of PTEN expression, as determined by immunohistochemistry, is associated with lack of benefit from cetuximab in metastatic colorectal cancer (Laurent-Puig et al., 2009; Frattini et al., 2007; Loupakis et al., 2009; Sartore-Bianchi et al., 2009b). Two recent retrospective studies reported an association between *PIK3CA* mutations and better outcomes among patients taking aspirin after a diagnosis of colorectal carcinoma (Domingo et al., 2013 and Liao et al., 2012).

The *APC* gene, a tumor necrosis factor-stimulated gene (TSG), encodes a 2843-amino acid protein and is located on chromosome 5q21-22, regulating Wnt/β-catenin signaling (Phelps et al., 2009). Mutations of this gene can be point mutations or small deletions or insertions. The latter cause frameshifts that generate stop codons. Germline mutations of this gene are responsible for FAP, whereas somatic mutations occur in the majority of sporadic CRCs. Somatic mutations of this gene may initiate and promote carcinogenesis of sporadic CRCs, and can be found in early neoplastic stages, even in dysplastic cryptic foci (Varesco, 2004; Phelps et al., 2009; Sweeney et al., 2009). CRCs with *APC* mutation usually are those with chromosomal instability or MSS (Luceri et al., 2002). The *APC* gene can serve as a biomarker for early detection or as a risk factor for familial polyposis syndrome. Detection methods include various types of PCR, LOH, and others (Varesco, 2004). Screening for *APC* mutations may detect patients with relatively early CRC by purified DNA from routinely collected stool samples (Traverso et al., 2002).

p53 (or TP53) is a tumor suppressor that regulates the cell cycle and is involved in apoptosis and DNA repair. This protein is discussed at length in Chapters 76 and 77. It is located on the short arm of chromosome 17 (17p13.1) (Isobe et al., 1986). Mutation or homozygous deletion of TP53 is found in 40% to 50% of CRCs. Loss of wild-type p53 activity is thought to be a major predictor of failure to respond to radiotherapy and chemotherapy in various human cancers, including CRCs, and predicts lower survival (Weller et al., 1998; Zlobec & Lugli, 2008). Although *TP53* mutation analysis has shown promising prognostic value, the ASCO Tumor Markers Expert Panel does not currently recommend its use in routine practice.

TGFBR1, SMAD2, and SMAD4 are proteins involved in the transforming growth factor-β (TGF-β) signaling pathway (see Chapter 77). SMAD proteins are the principal components mediating the TGF-β signaling pathway, which negatively regulates the growth of epithelial cells (Kouvidou et al., 2006). It has been found that germline allele-specific expression (ASE) of the gene encoding the TGF-β type I receptor (TGFBR1) occurs in 10% to 20% of CRCs in both familial (dominantly inherited and segregated) and sporadic forms (Valle et al., 2008). The presence of multiple-mutated TGF-β has been linked with poor prognosis in a subset of CRC patients. Approximately 50% to 60% of CRCs have been found to harbor *SMAD4* mutations (Woodford-Richens et al., 2001); in contrast, only a few have been found to have *SMAD2* mutations. Both *SMAD2* and *SMAD4* are mapped to chromosome 18q21 (Woodford-Richens et al.,

2001; Miyaki & Kuroki, 2003). Most mutations of *SMAD2* and *SMAD4* occur in their so-called *MH2 domain*. Inactivation of the *SMAD4* gene through germline mutation and loss of the unaffected wild-type allele are responsible for familial juvenile polyposis, whereas inactivation of the *SMAD4* gene through homozygous deletion or intragenic mutation occurs frequently in CRC and pancreatic cancer. *SMAD4* mutation occurs at a later stage of colorectal carcinogenesis and is an indicator of advanced phenotypes. Loss or low levels of *SMAD4* expression in CRCs are found to be associated with poor prognosis following surgery and 5-fluorouracil (5-FU)-based adjuvant therapy. However, the predictive value of *SMAD4* mutation/inactivation is controversial (Miyaki & Kuroki, 2003; Alhopuro et al., 2005). Chromosomal loss at 18q encompassing both *SMAD2* and *SMAD4* has been reported in up to 70% of CRCs (Alhopuro et al., 2005). Patients with locally advanced stage II or stage III disease appear to demonstrate a significantly poorer prognosis with loss of 18q (Popat & Houlston, 2005).

MSI is involved in approximately 75% to 85% of CRCs, characterized by aneuploidy, allelic losses, amplifications, translocations, and mutations of *APC*, *KRAS*, and *TP53* (Jones et al., 2008). Although the prognosis of patients with MSI CRC is stage and grade dependent, tumors with identical morphologic features display considerable heterogeneity in terms of clinical outcome. The remaining 15% to 20% of CRCs have MSI-H characterized by inactivation of mismatch repair (*MMR*) genes (Umar et al., 2004), as discussed in Chapter 77. Sporadic *MSI-H* cases have been shown to arise predominantly through promoter hypermethylation and silencing of the *hMLH1* gene in contrast to a hereditary form of *MSI-H* CRC, HNPCC, which typically shows germline mutations in one of the DNA *MMR* genes (Weisenberger et al., 2006). Tumors with *MSI-H* tend to be more proximally located, poorly differentiated, and of mucinous histologic type, and to show considerable lymphocytic infiltration; they have been linked with *TGFBRII* and *BRAF* mutations (Zlobec & Lugli, 2008). Patients with colon cancers demonstrating MSI-H have a stage-independent improved survival compared with patients with MSS tumors in most, although not all, studies. However, they do not benefit from treatment with 5-FU in randomized adjuvant therapy trials (Ribic et al., 2003). In stage II patients, when the tumor is MSI-H, no additional treatment is necessary because, based on trial, further chemotherapy or radiation treatment will not be beneficial and can potentially be harmful for this group of patients. Recently *MSI* is also defined as a predictor for a positive response to immunotherapy. Pembrolizumab is an anti–PD-1 (programmed cell death protein 1) immune checkpoint inhibitor that induces an objective response in 40% of patients with treatment-refractory metastatic, microsatellite unstable colorectal cancers. On the other hand, immunoexpression of PD-1 ligands on tumor cells does not seem to be a predictive marker of response to PD-1 blockade (Le et al., 2015).

HER2

Approximately 3% of colorectal cancers show amplification of HER2 (Kavuri et al., 2015). Preclinical models of HER2-amplified colorectal tumors have shown that the combination of an antibody and TKI leads to sustained tumor shrinkage. Both HER2-amplified and HER2-mutated cancers can show de novo and acquired resistance to EGFR inhibitors, resulting in persistent signaling in the presence of an EGFR inhibitor (Bertotti et al., 2015).

The *CpG island methylator phenotype* (*CIMP*$^+$), or simultaneous hypermethylation of the promoter regions of a number of TSGs, is one of the principal mechanisms of colorectal carcinogenesis, independent of chromosomal instability or MSI. CIMP$^+$ is found in approximately 20% of patients with CRCs. These patients usually are female and of more advanced age, with a history of cigarette smoking. These cancers occur predominantly in the proximal colon and are associated with MSI, wild-type *TP53*, *BRAF* mutation, and β-catenin activation (Grady, 2007; Ogino et al., 2009b). The association between CIMP status and prognosis is controversial, however, and later studies suggest that the occurrence of CIMP appears to be an independent predictor of a low colon cancer–specific mortality and survival advantage and a high responsive rate to 5-FU–based treatment (Iacopetta et al., 2008; Ogino et al., 2009b). Additional studies, including randomized clinical trials, are required to confirm the value of CIMP$^+$ and associated molecular features for the prediction of clinical outcomes of CRCs.

Hereditary Colonic Cancer Syndrome

Approximately 5% to 10% of CRCs are hereditary, predominantly in a form of autosomal-dominant transmission. Genetic polyposis syndrome accounts for less than 0.5% of all CRCs, whereas nonpolyposis forms of hereditary CRC are seen in a much higher percentage in overall hereditary CRCs (Lynch & de la Chapelle, 2003; Kievit et al., 2004). The next section offers a brief introduction of the genetics of common hereditary colonic cancer syndromes.

Familial Adenomatous Polyposis Syndrome

FAP is a rare disease characterized by numerous colorectal polyps (usually more than 100) (Winawer et al., 2003). Diagnosis of FAP is based on clinical and endoscopic findings. Classic FAP is an autosomal-dominant inheritable disease, with nearly 100% penetrance. It is mainly attributable to the mutation/deletion of the *APC* gene, located at the long arm of chromosome 5. So far, more than 500 different germline *APC* mutations have been identified in FAP families (Varesco, 2004). About one-third of patients are found to harbor de novo mutations. However, 5% to 30% of FAP patients show no *APC* mutations on current genetic testing. Among those patients with *APC*-negative FAP, biallelic mutations in a different gene, the *MutY human homologue* (*MYH*) gene, may be found. The *MYH* gene encodes a member of the base excision repair pathway that is involved in repairing oxidative damage to DNA. Those *APC*-negative FAP patients may have a family history compatible with recessive inheritance (Sieber et al., 2003; Varesco, 2004), indicating that this may be a different disease. Genetic testing may be helpful in screening and diagnosis of atypical FAP cases and in the management of affected patients. PCR-based methods have been developed to detect *APC* germline mutations (Varesco, 2004).

Hereditary Nonpolyposis Colorectal Cancer (Lynch Syndrome)

HNPCC is an autosomal-dominant genetic condition characterized by high predisposition to CRC and other cancers outside of the colorectum, including the genitourinary and female reproduction systems, the upper gastrointestinal tract, hepatobiliary tract, brain, and skin. Approximately 3% of all diagnosed cases of CRC belong to HNPCC, which makes it the most common hereditary CRC-predisposing syndrome (Lynch & de la Chapelle, 2003; Lynch et al., 2009). It has been found to have lifetime risks of approximately 80% for CRC and 40% to 60% for endometrial disease. Colorectal cancer develops in younger patients (average 45 years of age); two-thirds of these cancers occur in the proximal colon. Histologically, HNPCC is not associated with a large number of colorectal polyps, as seen in FAP; rather, it forms a large nonpolypoid malignant lesion. Compared with sporadic CRC of equivalent staging, patients with HNPCC may have a better response to chemotherapy and better clinical outcomes (Lynch et al., 2009).

The molecular basis for the development of HNPCC is due to MSI, which is a consequence of inherited or germline mutations of DNA *MMR* genes. Among the nine *MMR* genes discovered, mutations in *MLH1*, *MSH2*, *MSH6*, *MLH3*, and *PMS2* are associated with the development of HNPCC (Peltomaki, 2005). The significance of mutations in two other *MMR* genes, *TGFBR2* and *PMS1*, is less clear (Table 79.3). Among those identifiable mutations associated with HNPCC, 90% occur in *MLH1* or *MSH2* (Chung & Rustgi, 2003), 7% to 10% in *MSH6*, and 1% to 2% in *PMS2* or *MLH3* (Lawes et al., 2005). Most germline mutations in *MSH2* lead to complete loss of gene expression and usually are accompanied by loss of expression of *MSH6*. CRC with *MLH1* mutation is frequently caused by missense mutations. Mutations of *MMR* genes cause abnormal mismatch repair function, failing to correct a larger number of insertions and deletions, eventually leading to frameshift within the microsatellites or MSI (Jacob & Praz, 2002; de Vos et al., 2005). However, approximately 50% of all HNPCCs have no identifiable mutations in *MMR* genes according to current methods of detection (Umar et al., 2004).

TABLE 79.3
Molecular Genetics of Hereditary Nonpolyposis Colorectal Cancer

MMR Gene	OMIM Name	Chromosomal Locus	% of HNPCC with Mutation
MLH1	HNPCC2	3p21	50
MSH2	HNPCC1	2p16	40
MSH6	HNPCC5	2p15	≈7–10
PMS2	HNPCC4	7p22	1–2
MLH3	HNPCC7	14q24.3	1
PMS1a	HNPCC3	7p22	Unclear
TGFBR2	HNPCC6	3p22	Case report

HNPCC, Hereditary nonpolyposis colorectal cancer; *MMR,* mismatch repair; *OMIM,* Online Mendelian Inheritance in Man (database).

Two rare but distinct variants of HNPCC are known: (1) Muir-Torre syndrome, resulting from mutations in the *MSH2* gene and showing coexisting sebaceous skin tumors with small and large intestinal, gastric, kidney, endometrial, and ovarian cancer (Lynch et al., 2009); and (2) Turcot syndrome, resulting from mutations in the *MLH1* and *PMS2* genes and showing coexistent glioblastoma with CRCs (Abdel-Rahman & Peltomaki, 2004).

The diagnosis of HNPCC is based mainly on clinical information and familial history. Genetic testing has been introduced for diagnostic purposes. A testing kit for germline mutations is commercially available for blood samples. *MMR* dysfunction can be analyzed by immunohistochemistry on paraffin-embedded tissues. PCR and sequencing are methods commonly used to detect MSI. According to the Bethesda Guidelines, five microsatellite markers are to be tested. Of these, three are dinucleotide repeats, and two mononucleotide repeats. MSI-H is defined as LOH in two or more of five markers in tumor tissue compared with a normal tissue control. However, although it is a sensitive test, MSI testing is not specific for HNPCC, as HNPCC can be MSI-low and MSI-stable in some cases, and sporadic CRCs may also show MSI-H. Thus, genetic testing may be useful only after patients at risk for HNPCC are identified by the Amsterdam or Bethesda clinical criteria (Abdel-Rahman & Peltomaki, 2004; Umar et al., 2004; Lynch et al., 2009).

Familial Juvenile Polyposis Syndrome

Familial juvenile polyposis syndrome (JPS) is a rare disorder inherited in an autosomal-dominant fashion in at least 30% of patients. The incidence of JPS is approximately 1 per 100,000 births, and it is the most common of the hamartomatous syndromes (Schreibman et al., 2005).

Germline mutations of *SMAD4*, *BMPR1A*, and *ENG* have all been described in patients with JPS. *SMAD4* is located on chromosome 18q21.1 and usually is found to be mutated in approximately 15% of cases of JPS (Mishra et al., 2006). *BMPR1A* (bone morphogenetic protein receptor type 1A), located on chromosome 10q22.3, is a serine threonine kinase that is a mediator of the bone morphogenetic protein intracellular signaling pathway (Zbuk & Eng, 2007). It has been identified as mutated in about 25% of affected patients with JPS. Both genes mentioned previously encode proteins that are involved in the TGF-β signaling pathway, which is an important modulator of many cellular processes (e.g., cell growth, apoptosis, growth arrest) (Zhou et al., 2003).

The lifetime risk for CRC is about 70%, and the risk for pancreatic, gastric, and duodenal carcinoma is increased in these patients (Gatalica & Torlakovic, 2008). Molecular screening of individuals at risk within a JPS family for a known genetic mutation would allow clinicians to make the diagnosis at an earlier age and would lead to closer endoscopic screening and follow-up. Individuals without the mutation would need less frequent endoscopic screening and perhaps endoscopy only after 50 years of age, as is provided in the normal population. Therefore, genetic testing can help to define the recommended interval for screening and surveillance; it is hoped that it will help to prevent malignancy by early polypectomy and heightened surveillance (Mishra et al., 2006).

Peutz-Jeghers Syndrome

PJS is an autosomal-dominant hamartomatous polyposis syndrome characterized by melanotic mucocutaneous hyperpigmentation and gastrointestinal hamartomas, which occur anywhere from the stomach to the anus, with a prevalence of approximately 1 in 200,000. Polyps usually are fewer than 20 in number and are most prevalent in the small intestine (Bourke et al., 2006). The only identifiable germline mutation causing PJS is seen in the *STK11* (also known as *LKB1*) gene. PJS patients have increased risk for esophageal, gastrointestinal, and pancreatic cancer, and the risk for these cancers markedly increases with age. By 65 years of age, the risk for CRC is about 39% (Gatalica & Torlakovic, 2008). In women with PJS, the risk for breast cancer is also reported to be substantially increased. PJS patients need to be educated as to the resources available for genetic testing, which can be very helpful, although the diagnosis can be made clinically in most cases when the family history is positive. A positive *LKB1* mutation test will confirm that individuals need careful screening and follow-up; a negative test will allow individuals to be spared of unnecessary screening procedures (Schreibman et al., 2005).

Serrated Polyposis Syndrome (Formerly Known as Hyperplastic Polyposis Syndrome)

Serrated polyposis syndrome usually presents in the 6th decade with approximately 100 hyperplastic or serrated polyps or sessile adenomas identified on colonoscopy. The presence of more than five large hyperplastic polyps proximal to the sigmoid colon is one indication that this syndrome might affect the patient. The inheritance pattern in a study was compatible with an autosomal-recessive mode of transmission (Young & Jass, 2006). Depending on the studies, the risk for developing colon cancer ranges from 37% to 69%. Up to 70% of colonic neoplasms in serrated polyposis syndrome have a *BRAF* mutation. By comparison, the *BRAF* mutation is extremely rare in Lynch syndrome and is found in only 15% of unselected colorectal carcinomas. Another molecular trait of patients with the serrated polyposis syndrome is the presence of numerous sites of DNA methylation, including methylation of MLH1, in the polyps and in carcinomas.

MYH Polyposis and Inherited Colon Cancer Due to MYH Inactivation

This syndrome was discovered when a family with multiple adenomas and colon cancer had no germline mutation of APC, but instead a germline mutation in a gene located on the short arm of chromosome 1, called *MUTYH glycosylase* (now referred to as *MYH*). The normal function of the gene is to repair DNA damage occurring as a result of oxidation—in particular, oxidative damage caused by an oxidized form of guanine, which acts as a mutagen. The repair performed by *MYH* consists of removing adenine when it inappropriately pairs with the oxidized form of guanine or guanine itself. If not repaired by *MYH*, oxidized guanine is recognized as thymine during DNA replication and, therefore, aberrantly pairs with adenine. The function of the wild-type *MYH*-encoded protein is to recognize this mispaired adenine and excise the mispair. When *MYH* is mutated, this repair function is lost and C:G to T:A transversion persists, which may involve several important genes, such as *KRAS*, which is often mutated in this condition. Most *MYH* mutations are located at Y165C and G382D, and are found in up to 2% of the general population. Unlike FAP, MYH polyposis has an autosomal-recessive mode of transmission. Patients with heterozygous *MYH* mutations in their germline DNA have a 1.3-fold increased risk for developing colorectal cancer compared with a 177-fold increase in subjects with biallelic mutations. Colorectal cancers associated with germline biallelic *MYH* mutations are more likely to be low grade as compared with sporadic carcinomas, or in cancers found in carriers of monoallelic MYH mutations (O'Shea et al., 2008). Hyperplastic and serrated polyps are present in MYH-associated polyposis; characteristically, they contain G:C to T:A transversions in the *KRAS* gene (Boparai et al., 2008). Although inconsistent, it was found that the presence of multiple hyperplastic polyps in the context of adenomatous polyposis is an indication that the polyposis could be due to an *MYH* genetic alteration (Jass, 2008).

MYH-associated polyposis is associated with extracolonic manifestations, with duodenal adenomas or carcinomas found in up to 17% of patients (Vogt et al., 2009). Also, ovarian, bladder, and skin cancers are found at higher frequency, compared with sporadic colorectal cancer cases. Molecular methods, such as PCR followed by denaturing high-pressure liquid chromatography (dHPLC), are required to test germline DNA (Croitoru et al., 2007).

PANCREATIC CANCER (NONNEUROENDOCRINE TUMOR)

Pancreatic cancer is one of the leading causes of cancer-related death worldwide (Parkin et al., 2001) and ranks as the fourth most common cause of cancer death in the United States (Jemal et al., 2008). Most pancreatic cancer is of exocrine origin, and most cases involve invasive pancreatic ductal adenocarcinoma (PDAC) and its variants (Hruban & Fukushima, 2007; Ranganathan et al., 2009). Other nonendocrine, nonductal carcinomas—such as acinic cell carcinoma, solid-pseudopapillary neoplasm, and pancreatoblastoma—are uncommon (Hruban & Adsay, 2009). It should be noted, however, that the actual cell of origin of certain pancreatic carcinomas is not known, and much debate continues regarding this issue.

PDAC is the result of accumulation of inherited (germline) and/or acquired (somatic or epigenetic) gene mutations, including oncogenes such as, most prominently, mutated (Val-for-Gly 12) *K-RAS*-p21; TSGs such as *p53*, *p16*, and *SMAD4*; and genome maintenance genes such as *BRCA2*, telomerase, and MSI (Su & Kern, 2000; Ranganathan et al., 2009). Genetic alterations seen in pancreatic intraepithelial neoplasia are *KRAS* at early stages, *p16/CDKN2A* inactivation during the middle stages, and *SMAD4/DPC4* and *p53* during later stages (Moskaluk et al., 1997; Jimenez et al., 1999; Wilentz et al., 2000). Oncogenic ras-p21 protein has been identified in more than 90% of human pancreatic cancers; therefore, it is considered a major causative factor in this disease (see Chapter 77). DNA mismatch repair genes are mutated in 2% to 3% of pancreatic cancers.

The genetic alterations that have been observed in pancreatic cancer may be reflected by chromosome gain, loss, or copy number changes. PDACs frequently have loss of chromosomes 18, 17, 6, 21, 22, Y, 10, 4, 15p, 14p 5, 13p, 9p, 21p, and 17p (Johansson et al., 1992; Ranganathan et al., 2009). Among them, allelic loss of chromosome 18 is the most common event, and about one-third of pancreatic carcinomas have a consensus region of homozygous deletion at 18q21 (Hahn et al., 1996a). More specific genetic alterations or mutations have been identified by many studies using different molecular approaches. One study by Jones and colleagues (2008) identified more than 1500 somatic mutations affecting 1007 genes in pancreatic cancers. Activation of *KRAS* (95%), inactivation of *p16/CDKN2A* (75%–80% mutation and 15% hypermethylation), *TP53* (80%), and inactivation of *SMAD4* (95%) are the most frequent and well-known gene mutations (Hruban et al., 1993; Caldas et al., 1994; Redston et al., 1994; Hahn et al., 1996b; Jones et al., 2008). Activating point mutation of *KRAS* occurs commonly in codon 12 and much less frequently in codons 13 and 61. Germline mutations in *BRCA2*, a predisposing factor to pancreatic cancer, are frequently detected in the Ashkenazi Jewish population (Ranganathan et al., 2009). Inactivation of genes by hypermethylation is also important in the development of pancreatic cancer. Aberrant methylation has been identified in the promoter regions of *p16/CDKN2A*, *APC*, *TSLC/IGSF4*, *SOCS-1*, *cyclin D2*, *RASSF1A*, *WWOX*, *RUNX3*, *CDH13*, *DUSP6*, *HHIP*, and *SLC5A8*, and in pancreatic cancer and precancerous lesions (Sato et al., 2002; Ranganathan et al., 2009). Those gene mutations or genetic alterations may affect one or more signaling pathways and MSI. As stated earlier, the most commonly affected signaling pathways include the EGFR/RAS/MAPK pathway as well as the PI3K/AKT pathway, VEGF, the WNT/β-catenin pathway, and TGF-β signaling (Buchholz & Gress, 2009; Hruban & Adsay, 2009). miRNAs are also associated with pancreatic carcinogenesis. miR-216, miR-196a, miR-217, and miR-210 were identified specifically for or were frequently associated with PDAC (Bloomston et al., 2007; Szafranska et al., 2007; Hoimes et al., 2009).

Precancerous lesions, including pancreatic intraductal neoplasia (PanIN) and intraductal papillary-mucinous neoplasms (IPMNs), may also have *KRAS*, *TP53*, *SMAD4*, and *p16/CDKN2A* mutations, as seen in PDACs (Hruban & Adsay, 2009; Ranganathan et al., 2009). Loss of *SMAD4/DPC4* within IPMNs was the best marker for the presence of invasive carcinoma. However, intestinal-type IPMNs, a precursor to invasive colloid carcinomas, always have intact *SMAD4/DPC4* and harbor *PI3KCA* mutations in 10% of cases; this usually does not occur in PDACs (Hruban & Adsay, 2009; Ranganathan et al., 2009).

Undifferentiated carcinoma may have loss of E-cadherin. Acinar carcinomas are, on the basis of some studies, thought not to have activation of *KRAS* and inactivation of *TP53*, *p16/CDKN2A*, or *SMAD4*, as seen in PDACs, but may have loss of chromosome 11p and *APC/β-catenin* gene mutations in some cases (Hoorens et al., 1993; Abraham et al., 2002; Hruban & Adsay, 2009). On the other hand, nontransformed pancreatic acinar cells in culture are readily and stably transformed into malignant pancreatic cancer cells by transfection of oncogenic *K-ras* or by exposure to carcinogens present in cigarette smoke, a known major risk factor for developing this disease. A common finding in these transformed acinar cells is oncogenic ras-p21.

Solid-pseudopapillary neoplasms commonly have abnormal expression of β-catenin (Hruban & Adsay, 2009). The most common genetic abnormality in pancreatoblastomas is loss of one copy of the short arm of chromosome 11 near the *WT-2* locus (11p15.5) (Abraham et al., 2001; Kerr et al., 2002). Those genetic differences may dictate their different morphology and clinical/biological behaviors in different types of pancreatic exocrine carcinomas.

A vast majority of pancreatic cancers are sporadic; however, familial forms have also been reported. Familial pancreatic cancers most often are associated with many genetic cancer syndromes, including hereditary breast and ovarian cancer syndrome, Peutz-Jeghers syndrome, HNPCC syndrome, FAP, familial pancreatic cancer, and hereditary pancreatitis (associated with mutations of *PRSS1* and *SPINK1*; see respective sections later in the chapter).

The molecular changes noted in pancreatic cancer, as described previously, may serve as diagnostic markers. Detection of mutations of *KRAS*, telomerase (*hTERT*), and others has been used or proposed for the diagnosis of pancreatic carcinoma, which can be potentially applied in surgically resected pancreatic specimens and pancreatic fluid samples (Seki et al., 2001; Mishra et al., 2006), although the usefulness of these techniques requires further evaluation (Fry et al., 2008). The levels of *hTERT* expression could differentiate PDACs from adenoma and pancreatitis (Nakashima et al., 2009). Although deletion/inactivation of *SMAD4* is also a relatively highly frequent event in pancreatic cancer, it is not specific. Thus, its utility in molecular diagnosis requires further evaluation (Hruban & Adsay, 2009; Ranganathan et al., 2009). Aberrant methylation of certain genes may also have diagnostic utility (Matsubayashi et al., 2006; Ranganathan et al., 2009). Yan and colleagues showed that a panel of molecular markers (methylated *p16*, *p53* mutations, and *KRAS* mutations) could stratify patients in high-risk groups from negligible risk to greater than 50% probability of an early cancer (Yan et al., 2005). In addition, the expression pattern of a group of 112 miRNAs could correctly distinguish pancreatic cancer tissue from adjacent normal and benign tissues, including pancreatitis. Three of the top differentially expressed miRNAs (miR-221, miR-376a, and miR-301) were specifically localized to pancreatic carcinoma, but not to the stroma or to normal acini or ducts (Lee et al., 2007; Liang et al., 2009). Other potentially useful diagnostic markers for pancreatic cancers include miR-217 and miR-196a (Szafranska et al., 2007).

Amplification of *KRAS2* and *CMYC* and loss of *TP53* genes are found to be correlated with tumor grade and survival (Ranganathan et al., 2009). Alterations of *p16* and *hTERT* may also be a prognostic indicator of pancreatic cancer, which conferred a worse outcome by univariate and multivariate analysis (Kumari et al., 2009). Giovannetti found that patients with high levels of human equilibrative nucleoside transporter-1 (hENT1) mRNA had significantly longer overall survival than patients with a low level of hENT1 expression, suggesting that hENT1 levels may be a predictor of survival (Giovannetti et al., 2006; Liang et al., 2009). Iacobuzio-Donahue found that *SMAD4/DPC4* loss is usually associated with death related to multiple metastases, whereas patients found to have intact *SMAD4* genes are more likely to have localized disease, although many of these cancers are also fatal (Hruban & Adsay, 2009; Iacobuzio-Donahue et al., 2009). The presence of miR-21 and miR-196a-2 has been found to be a significant predictor of poor survival (Bloomston et al., 2007; Dillhoff et al., 2008). *BRCA2* gene mutation, seen in 7% of PDACs and in more cases of familial disease, is a predicting marker for responsiveness to poly-(adenosine diphosphate [ADP]-ribose) polymerase-1 (PARP) inhibitors and to DNA cross-linking agents such as mitomycin C (Helleday et al., 2005; van der Heijden et al., 2005; McCabe et al., 2006). Sufficient pancreatic tissue sampling is a clinical challenge. The PathFinderTG pancreas molecular test developed by RedPath Integrated Pathology can be used adjunctively when a definitive pathologic diagnosis cannot be made because of inadequate specimen or equivocal histologic or cytologic findings. This test uses loss of heterozygosity markers, oncogene mutations, and DNA content abnormalities to stratify patients according to their risk for progression to cancer. The sample can be taken from pancreatobiliary fluid/ERCP, a brush, pancreatic masses, or pancreatic tissue. Similarly, the PathFinderTG Biliary on Biliary brush/supernatants uses oncogene mutations and loss of heterozygosity markers to identify whether patients with biliary strictures have a malignant neoplasm or benign reactive disease.

PANCREATIC NEUROENDOCRINE TUMORS

Pancreatic neuroendocrine neoplasms (PanNENs) are the second most common malignancy of the pancreas and account for 1.3% to 2.8% of new pancreatic malignancies each year (Franko et al., 2010). The genetic alterations between well-differentiated pancreatic neuroendocrine tumors (PanNETs grades 1 and 2) have been compared with those in pancreatic neuroendocrine carcinoma (PanNEC grade 3). In PanNECs, activating *KRAS* mutations (2 of 7) and inactivating mutations in *TP53* (4 of 7) and *RB1* (5 of 7) were seen. By contrast, none of these mutations were found in 11 well-differentiated PanNETs. Abnormal expression of the TP53 (95%) and RB1 (75%) proteins was also frequently seen in PanNEC, but not in well-differentiated PanNETs. Furthermore, all PanNECs retained expression of ATRX and DAXX, while, as noted earlier, PanNETs showed loss of expression of ATRX and DAXX in 45% of cases (Yachida et al., 2012).

This led to the 2017 revision of the WHO classification of Pan NENs, which addresses these findings by introducing a separate G3 well-differentiated NET category intermediate between G2 NET and G3 NEC.

Low-Grade Neuroendocrine Tumors (LGNETs). A recent study on LGNETs revealed that there is a strikingly high correlation of decreased PTEN expression and/or increased activated (phosphorylated) Akt (Akt-P) and tendency for tumor recurrence or metastasis (Jayakumar, 2018). In this study, a series of 18 patients diagnosed with this uncommon tumor were followed up for possible tumor recurrences after a 5-year period. The cell blocks from the original tumors were stained for both of these critical signal transduction proteins. Significantly, of 10 patients whose tumors showed loss of PTEN expression, 9 were found to have recurrence of disease and/or metastatic disease. Importantly, lung and appendiceal LGNETs were found to have high PTEN expression and a

markedly better prognosis than their gastrointestinal and pancreatic counterparts. Loss of PTEN correlated significantly with the positive expression of pAKT and aggressive behavior of LGNETs. Though the sample size was small due to the uncommon occurrence of LGNETs, the results strongly suggest that PTEN and Akt-P are important markers for predicting future tumor behavior.

KIDNEY TUMOR

In accordance with the increased understanding of the morphologic, immunohistochemical, molecular, and epidemiologic characteristics of renal cell tumors, the WHO classification of renal cell tumors has been modified (Inamura, 2017; Ricketts, 2018).

Clear-Cell Renal Cell Carcinoma (RCC)

Clear cell RCC, the most common subtype of renal cancer (65%–70%), is characterized by an encapsulated solid mass with alveolar or acinar arrangement of clear polygonal cells. Chromosome 3p deletion is seen in 70% to 90% of cases (Crossey et al., 1994; Lonser et al., 2003), and TSG von Hippel–Lindau (VHL) located on the 3p25 chromosome is consistently inactivated in 100% of familial renal cancer syndromes and 57% of sporadic cases (Gnarra et al., 1994). The VHL protein regulates expression of the transcription factor, hypoxia-inducible factor (HIF), implicated in tumor growth and angiogenesis. VHL syndrome–associated clear-cell carcinoma is caused by a germline mutation at birth in one copy of the *VHL* gene; a second hit can result from deletion, nonsense mutations, allelic loss, or hypermethylation of the VHL promoter region. Loss of both *VHL* genes leads to tumorigenesis. According to the TCGA (2013), clear-cell RCCs are characterized by recurrent mutations in the PI3K/AKT/MTOR pathway (a potential therapeutic target), mutations in *SETD2* (associated with widespread DNA hypomethylation), and mutations involving the SWI/SNF chromatin remodeling complex (*PBRM1*, *ARID1A*, and *SMARCA4*). Aggressive clear-cell RCCs demonstrate a metabolic shift (TCGA, 2013).

Papillary RCC

Papillary RCC is the second most common type of renal carcinoma, constituting 15% to 20% of renal cancers, and can be morphologically classified into 2 types (Kovacs et al., 1989). Type I is characterized architecturally by fibrovascular papillae lined by a single layer of cuboidal neoplastic cells with small, uniform, oval nuclei with inconspicuous nucleoli (Fuhrman nuclear grades I to II) and a pale basophilic cytoplasm. In contrast, type II papillary carcinomas are composed of fibrovascular papillae lined by a pseudostratified layer of larger neoplastic cells that have large pleomorphic nuclei with prominent nucleoli (Fuhrman nuclear grades II to III) and an abundant eosinophilic cytoplasm. Papillary carcinomas containing histologic features of both types are occasionally encountered. Because of the difficulty in classifying these tumors with mixed features, clinical studies examining the survival of patients with these carcinomas often do not distinguish between types I and II (Delahunt et al., 2013). It has been suggested that type II papillary RCC is associated with a more aggressive behavior, usually presenting at higher stage, and carries worse survival than type I papillary RCC (Mejean et al., 2003; Pignot et al., 2007). Conventionally, the most common chromosomal abnormality of papillary RCC involves trisomies of chromosomes 7 and 17 and loss of chromosome Y. Additionally, loss of 9q correlated with reduced survival in these tumors. By comparative genomic hybridization analyses, it was found that full-length gains of chromosomes 7 and 17 are more frequently detected in type I papillary RCC (PRCC) than in type II tumors (Jiang et al., 1998).

Inherited forms of type I and type II tumors are described for conditions known as *hereditary papillary renal cell* and *hereditary leiomyomatosis and RCC* (*HLRCC*), respectively. According to the comprehensive molecular profiling of PRCCs by TCGA (Linehan et al., 2016) type I PRCCs are characterized by *MET* alterations, whereas type II PRCCs are featured with *CDKN2A* silencing, *SETD2* mutations, and increased expression of the NRF2-antioxidant response element pathway. Using multiplatform analyses, type II PRCCs have been categorized into three clusters (C2a, C2b, and C2c). C2c PRCCs are CpG island methylator phenotype (CIMP)–associated tumors, characterized by poor survival and *FH* mutations. C2a PRCCs are associated with early stages of tumor development. C2b PRCCs are associated with later stages of tumor development and *SETD2* mutations (Linehan et al., 2016).

Chromophobe Tumors

Chromophobe tumors commonly have widespread copy number alterations seen at chromosomes 1, 2, 6, 10, 13, and 17 (Tan et al., 2010). Patients with the hereditary RCC syndrome (Birt-Hogg-Dubé [BHD] syndrome) exhibit chromophobe histology in 30% of tumors (Pavlovich et al., 2002). While mutations in the folliculin (FLCN) gene are associated with this hereditary syndrome (Nickerson et al., 2002), this genetic abnormality is rarely found in sporadic non-BHD cases of chromophobe RCC (Nagy et al., 2004). Mutations of *TP53* and *PTEN*, imbalanced chromosome duplication (ICD), and high *TERT* expression by DNA rearrangement within *TERT* promotor region (Davis et al., 2014) have been recognized in metastatic evolution for chromophobe RCC (Casuscelli et al., 2017).

Microphthalmia Transcription Factor (MiT) Family Translocation Renal Cell Carcinoma

A class of tumors called *translocation renal tumors* involves somatic translocations of transcription factors that are members of the MiT family. Transcription factors binding to IGHM enhancer 3 (TFE3) and transcription factor EB (TFEB) located on chromosomes Xp11 and 6p21, respectively, have diverse tissue-specific functions and are included in this category. At least five recurrent translocations of TFE3 are known to occur. TFEB translocations are less common, with only 30 confirmed cases reported in the literature (Green et al., 2013). Translocation leads to high levels of expression of TFE3 or TFEB fusion protein(s) with increased nuclear localization (Weterman et al., 2000; Tsuda et al., 2007), subsequently activating their target genes.

TFE3 and TFEB translocation renal tumors appear to be more common in women. Additionally, cytotoxic chemotherapy during childhood is a suspected risk factor for developing these lesions (Argani et al., 2006). In fact, translocation tumors are one of the most common renal malignancies in adolescents and young adults, accounting for approximately one-third of cases (Bruder et al., 2004). Similar to other rare subtypes of RCC, translocation tumors exhibit extremely aggressive clinical behavior and are associated with early nodal involvement (Geller et al., 2008).

Xp11 Translocation or TFE3-Associated RCC

Renal cell carcinoma with Xp11 translocation is a recently recognized entity with unique morphology and genetic characteristics. The most common translocations associated with these tumors are t(X;17)(p11.2;q25), the same cytogenetic abnormality (with identical breakpoints) observed in alveolar soft part sarcomas, which gives rise to the *ASPL-TFE3* fusion gene, and t(X;1)(p11.2;q21), which results in the *PRCC-TFE3* fusion gene.

In this entity, translocation fuses the *TFE3* transcription factor gene at Xp11.2 to *ASPL*, a novel gene at 17q25, or 1q21, which results in the fusion protein ASPL-TFE3 or PRCC-TFE3, respectively (Tomlinson et al., 1991; Meloni et al., 1992, 1993; Hernandez-Marti et al., 1995; Sidhar et al., 1996; Carcao et al., 1998; Heimann et al., 1998; Argani et al., 2001; Heimann et al., 2001; Ladanyi et al., 2001; Argani et al., 2002; Argani & Ladanyi, 2003a). Both the *ASPL-TFE3* and *PRCC-TFE3* fusion genes encode chimeric gene products that retain the ability of the TFE3 protein to migrate to the nucleus and participate in transcriptional activation of target genes (Weterman et al., 2000; Skalsky et al., 2001). Originally described as affecting the pediatric age group and now recognized in both pediatric and adult populations, the age at diagnosis for Xp11 renal tumor ranges from 17 months to 78 years of age (Argani et al., 2001, 2006, 2007). It is interesting to note that pediatric tumors show no particular sex preference, whereas adult tumors demonstrate a strong female predilection (Argani et al., 2002, 2007).

Grossly, the tumors resemble clear-cell RCCs (Argani et al., 2001). The histopathologic appearance is that of papillary carcinoma (Argani & Ladanyi, 2003b). ASPL-TFE3 renal carcinomas are characterized by voluminous, clear to eosinophilic cytoplasm of the cells, discrete cell borders, vesicular nuclear chromatin, and prominent nucleoli (Argani et al., 2001). Psammoma bodies are constant and sometimes extensive, often arising within characteristic hyaline nodules. In contrast, PRCC-TFE3 renal carcinomas generally feature less abundant cytoplasm, fewer psammoma bodies, fewer hyaline nodules, and a more nested, compact architecture (Argani et al., 2002). Renal carcinomas with Xp11.2-associated translocations characteristically underexpress cytokeratin, epithelial membrane, and vimentin antigen by IHC. The tumors, however, consistently label for the RCC marker antigen and CD10, similar to conventional renal carcinomas. The most distinctive immunohistochemical feature of these tumors is the nuclear pattern for the TFE3 protein using an antibody to the C-terminal portion of TFE3, which is retained in the gene fusions (Argani & Ladanyi, 2003a)—a common feature in all Xp11.2-associated carcinomas and ASPS, and not in other adult-type renal carcinomas (Argani & Ladanyi, 2003a).

(6;11) Translocation TFEB-Associated RCC

A lesser well-known member of the translocation RCC family is the tumor characterized by the t(6;11)(p21;q12), which results in an *α-TFEB* gene

fusion. This neoplasm typically demonstrates distinctive biphasic morphology, comprising larger and smaller epithelioid cells, with the latter often clustered around basement membrane material. However, the full spectrum of the morphologic appearances of the t(6;11) RCC is not known. Cases without the small cell component and instead dominated by sclerosis, clear cells, or papillary architecture have been reported. The t(6;11) RCC differs from most conventional RCCs in that they consistently express melanocytic IHC markers such as HMB-45 and Melan-A but are either negative or only focally positive for epithelial markers such as cytokeratins. Nuclear labeling for TFEB protein by IHC is a sensitive and specific assay for these neoplasms (Argani et al., 2005). However, IHC is highly fixation dependent and has proven to be particularly difficult for this protein. Recently, a break-apart FISH assay for *TFEB* gene fusions has been developed for archival material and has allowed expansion of the clinical and morphologic spectrum of the t(6;11) RCC (Argani et al., 2012).

Succinate Dehydrogenase B (SDHB) Mutation–Associated RCC

Renal carcinomas have been reported with germline SDHB mutations that are associated with pheochromocytoma/paraganglioma syndrome type 4 (PGL4) (Gill et al., 2011). This syndrome is characterized by a predilection to pheochromocytoma, paraganglioma, so-called type 2 gastrointestinal stromal tumors (similar to those frequently seen in children and in association with Carney syndrome), and an estimated approximate 14% lifetime risk for renal neoplasia. Fewer than 10 cases of RCC associated with germline *SDHB* mutations have been reported. Most have affected young adults, with most having an indolent course on limited follow-up. Morphologically, these neoplasms are usually unencapsulated and composed of compact nests of eosinophilic polygonal cells, with entrapped renal tubules at the periphery. The cells may have vacuolated cytoplasm or distinctive pale eosinophilic cytoplasmic inclusions, which correspond to giant mitochondria by ultrastructural examination. Loss of the SDHB protein by IHC is reported to be a sensitive and specific marker for these neoplasms.

ALK Translocation RCC

Two cases of RCC harboring a t(2;10)(p23;q22) translocation resulting in a fusion of the gene for the cytoskeletal protein vinculin (VCL) with the anaplastic lymphoma kinase (*ALK*) gene have been reported. Both cases occurred in young patients (6 and 16 years of age) with sickle cell trait (raising the differential diagnosis of renal medullary carcinoma [RMC]) and demonstrated distinctive morphology characterized by polygonal to spindle cells with abundant eosinophilic cytoplasm and frequent intracytoplasmic lumina. Although the case numbers are small, the findings suggest that VCL-ALK RCCs have distinctive clinical and pathologic features.

Gene Expression Profiling in RCC

Several RCC biomarkers identified in gene expression profiling by Affymetrix oligonucleotide microarrays have been verified as potential prognostic markers using IHC. For example, adipophilin, which was discovered as a clear-cell RCC biomarker using gene expression microarrays, was subsequently associated with favorable outcome by IHC (Yao et al., 2005). Many genes overexpressed in RCC are therapeutically significant. Angiogenesis genes are overexpressed in clear-cell RCC, likely related to VHL and HIF1A dysregulation, both of which result in activation of multiple angiogenic tyrosine kinase molecules (e.g., VEGF, platelet-derived growth factor [PDGF]). TKIs (e.g., sunitinib, sorafenib, and cabozantinib) proved to have a significant role in metastatic RCC. Targeted RNA NGS has recently been utilized in searching for druggable targets in RCC personalized therapy (van den Huevel et al., 2019).

BLADDER CANCER

Bladder cancer is the second most common malignancy affecting the urinary system. Urothelial carcinoma (i.e., transitional cell carcinoma) is the most common form of bladder cancer, accounting for about 90% of cases. Remaining forms include squamous cell carcinoma (about 5%), most commonly provoked by *Schistosoma hematobium*, adenocarcinoma, and small cell carcinoma. Serum and urine markers used for early detection of bladder cancer, including genetic tests for *p16* TSG deletion (UroVysion, Abbott Laboratories, Abbott Park, IL), NMP22, and others, are discussed in Chapter 77.

For diagnosis of bladder cancer, invasive urethrocystoscopy and urinary cytology with low sensitivity for low-grade cancer have generated interest in other noninvasive and more sensitive diagnostic tools. The diagnosis of urothelial carcinoma (UC) is further compounded by the need for accurate pathologic staging, with one of the most critical challenges arising in identification of muscularis propria (detrusor muscle) invasion, which ultimately drives patient management. About 25% of patients with bladder cancer have advanced disease (muscle-invasive or metastatic disease) at presentation and are candidates for systemic chemotherapy. On the basis of the pivotal importance of diagnosing and staging bladder cancer, numerous recent studies have examined novel markers to aid diagnosis, prognosis, and treatment. Molecular and genetic changes in UC of the bladder can be broadly classified into three interrelated processes: (1) chromosomal alteration, triggering the initial carcinogenic event; (2) cancer cell proliferation, caused by loss of cell cycle regulation and derangements in normal apoptotic turnover; and (3) metastasis, in which the initial tumor spreads and brings into play processes such as angiogenesis and loss of cell adhesions (Quek et al., 2003).

Research has focused on molecular changes that occur in noninvasive low-grade papillary UCs, which only rarely progress to muscle-invasive disease (Holmang et al., 1999; Holmang et al., 2001). Activating mutations in the *HRAS* oncogene, discussed previously in Chapter 77, are one of the best characterized alterations in this population and have been associated with progression from urothelial hyperplasia to low-grade noninvasive papillary carcinoma (Spruck et al., 1994; Fitzgerald et al., 1995). Activating mutations in fibroblast growth factor receptor-3 (FGFR3), a tyrosine kinase receptor, have been documented in 70% to 80% of noninvasive low-grade papillary UCs, in contrast to only approximately 20% of invasive carcinomas (Billerey et al., 2001; van Rhijn et al., 2001). High-grade tumors with FGFR3 mutation have unique histologic features characterized by a bulky, exophytic component with branching papillary architecture as well as irregular nuclei with a koilocytotic appearance, which can facilitate the identification of this subset of tumors (Al-Ahmadie et al., 2011). High-grade papillary UC and flat carcinoma in situ (CIS) share common molecular alterations with invasive UC, the most commonly studied of which include *TP53* and *RB* gene mutations. Invasive UCs commonly demonstrate immunoreactivity for cytokeratins 7 and 20, p63, and high-molecular-weight cytokeratins, such as CK903. Benign urothelial tissue, however, demonstrates at least focal reactivity for these immunomarkers, including CK7 expression within the urothelial mucosa, CK20 expression in the umbrella cell layer, and p63 nuclear expression in the basal and parabasal cell layers.

Genetic studies of flat (and papillary) urothelial hyperplasia in patients with papillary low-grade UC showed frequent genetic alterations in chromosome 9, whereas chromosomal changes more specifically associated with aggressive bladder cancer (loss of 17p, 2q, 4, 11p) were uncommon (Obermann et al., 2003). With the FISH technique, chromosomal anomalies can be detected in exfoliated bladder cells from the patient's voided urine. A currently commercially available test, the UroVysion Bladder Cancer Kit (UroVysion, Abbott Laboratories, Abbott Park, IL) (see Figs. 79.1F to 79.1H) is intended to detect aneuploidy for chromosomes 3, 7, and 17, and loss of the 9p21 locus, encoding the p16 tumor suppressor protein using FISH (discussed further in the cervical cancer section). The indication for UroVysion includes hematuria and monitoring for tumor recurrence in patients previously diagnosed with UC. A minimum of 25 morphologically abnormal cells should be analyzed. The abnormal profile for chromosomes 3, 7, and 17 and the 9p21 locus includes aneuploidy of chromosomes 3 (red color), 7 (green color), and 17 (aqua color) and/or deletion of the 9p21 (yellow/gold) locus. Criteria for abnormal results include 4 aneuploid cells, 12 cells with deletion of the 9p21 locus, or 10 cells with a tetraploid or near-tetraploid profile.

Genetic changes can precede appearance of the lesions. Positive results include UC of renal pelvis, ureter, urethra, and urinary bladder (Halling & Kipp, 2008). Negative UroVysion results could occur with a positive diagnosis of UC by cytopathology or biopsy because certain UCs do not have the cytogenetic change of UroVysion. However, many of these cancers can be detected using the marker NMP22 in voided urine specimens, as described in Chapter 77.

PROSTATE CANCER

Prostate cancer is the most common noncutaneous cancer among males. Almost all cancers of the prostate are adenocarcinomas that occur in more than one site (multifocal) in more than 85% of cases. Adenocarcinomas of the prostate are graded according to the Gleason grading system to predict their prognosis and overall aggressiveness. The most common biomarker in serum that is used in diagnosing prostate cancer is prostate-specific antigen (PSA), as discussed in detail in Chapter 76. This chapter focuses on new genetic markers in tissue that are diagnostic for this condition.

It has been shown that approximately 50% (Hermans et al., 2006; Perner et al., 2006; Soller et al., 2006; Nam et al., 2007; Rajput et al., 2007) of

prostate cancers harbor a recurrent chromosomal rearrangement, resulting in the fusion of androgen-regulated *TMPRSS2* (*21q22.3*) to the erythroblastosis virus E26 transforming sequence (ETS) family of transcription factors. The latter is a group of genes that encode transcription factors. *TMPRSS2* is regulated by androgen (Afar et al., 2001) and estrogen (Setlur et al., 2008). Fusion leads to overexpression of the ETS family of genes (Petrovics et al., 2005), including *ERG* (*21q22.2*), *ETV1* (*7q21.2*), or *ETV4* (*17q21*) (Tomlins et al., 2005; Cerveira et al., 2006; Perner et al., 2006; Wang et al., 2006; Yoshimoto et al., 2006; Clark et al., 2007). In about two-thirds of cases resulting in the fusion protein, fusion is the result of genomic deletion (Liu et al., 2006; Perner et al., 2006) of the intervening DNA sequence, but fusion may also occur by a more complex rearrangement, such as a translocation (Tomlins et al., 2005; Hermans et al., 2006). The most common variant is fusion between the 5′-untranslated region of *TMPRSS2* and the 3′ region of *ERG* (Perner et al., 2006; Mehra et al., 2007a; Tu et al., 2007). However, more than 20 other fusion variants have now been described (involving more than 10 different genes [e.g., *ETV1*, *ETV4*, *ETV5*]).

Histologic features are reportedly associated with the presence of gene fusion: the presence of blue-tinged mucin, a cribriform growth pattern, macronucleoli, intraductal tumor spread, and signet ring cell features. These features are also associated with an aggressive clinical course of prostate cancer, but neither Gleason grade nor stage was found to correlate with presence of the fusion gene (Perner et al., 2006; Nam et al., 2007; Rajput et al., 2007; Tu et al., 2007). Results to date have been inconsistent, but most studies suggest that presence of the fusion protein is not correlated with other markers of risk. Thus, the clinical significance of the presence of the *TMPRSS2:ERG* gene fusion product for prostate cancer presentation and progression is not fully understood, but studies to date suggest that this may be a biomarker of risk.

The *Myc* oncogene is located at 8q24 and is found amplified and highly expressed in primary and metastatic prostate cancer, with C-Myc levels increasing with tumor progression (Jenkins et al., 1997; Bubendorf et al., 1999; Sato et al., 2006). As shown in Figure 77.3B, antibodies to C-MYC have been detected in the sera of patients with prostate cancer but not in normal controls. C-Myc expression correlated strongly with higher histopathologic grade, Gleason score, earlier disease progression, aggressive disease, and earlier prostate cancer–related death (Cher et al., 1996). Several important Myc target genes have been identified that regulate numerous pathways involved in prostate cancer progression and metastasis. Myc overexpression has been correlated with downregulation of *FOXP3*, an X-linked tumor suppressor gene. *FOXP3* binds to the promoter region of Myc and represses its transcription and, hence, loss of *FOXP3*-increased Myc expression (Wang et al., 2009a). Higher C-Myc mRNA levels significantly correlated with positive surgical margins upon prostatectomy, higher Gleason score, and pathologic stage (Hawksworth et al., 2010). C-Myc amplification and overexpression was a predictor of biochemical recurrence (Fromont et al., 2013). c-Myc elevation confers resistance to PI3K inhibitors (Liu et al., 2011) and overrides the mTOR dependence of prostate lesions arising from constitutive AKT activation (Zafarana et al., 2012). C-Myc levels in prostate cancer have been quantified via FISH, RT-PCR, and microarray (Jenkins et al., 1997; Bubendorf et al., 1999; Sato et al., 2006; Hawksworth et al., 2010).

The PTEN genetic alterations, including mutation, deletion, and rearrangement, are present in prostate cancer. PTEN loss correlates with high Gleason score and advanced stage (McMenamin et al., 1999). Its loss results in a hyperactive PI3K/Akt pathway that further promotes cancer progression (Vivanco & Sawyers, 2002). These findings parallel those for low-grade neuroendocrine tumors discussed earlier. Heterozygous and homozygous deletions have been identified in a subset of primary prostate cancer, and their prognostic value is indicated in clinical studies (Yoshimoto et al., 2006). PTEN loss is also associated with resistance to PI3K pathway inhibitors and treatment failure (Ilic et al., 2011). Of note, allelic loss of PTEN and gain of c-Myc coexisted in 3% human PCa, suggesting innate resistance to PI3K inhibitors in this subtype.

Recently, a few laboratory-developed tests (LDTs) were introduced that have not been approved by the FDA but are offered under a laboratory's CLIA certificate. The LDT is required to demonstrate certain analytic performances. However, the validation is much more limited as compared with the requirements for regulatory approval. The major concern is the variability of such validation studies from laboratory to laboratory. Caution should be exercised in judging the acceptance of some of these tests.

Oncotype DX (Genomic Health Inc., Redwood City, CA) is an LDT that was developed to test small (1-mm) fixed paraffin–embedded tissue samples obtained by needle biopsy. The assay measures the expression of 12 cancer-related genes that represent four different biological pathways (the androgen pathway [AZGP1, KLK2, SRD5A2, and RAM13C]; cellular organization [FLNC, GSN, TPM2, and GSTM2]; proliferation pathway [TPX2]; and stromal response [BGN, COL1A1, and SFRP4]) and five reference genes (used to normalize and control preanalytic and analytic variability), which are algorithmically combined to calculate the Genomic Prostate Score (GPS) (Knezevic et al., 2013). Together with NCCN risk criteria, the GPS improves risk discrimination of prostate cancer with the categories of very low, low, and modified intermediate risk in order to help clinicians select appropriate candidates for active surveillance.

Prolaris (Myriad Genetics, Inc., Salt Lake City, UT) offers a molecular test that directly measures tumor cell growth characteristics to stratify disease risk of progression. By testing FFPE tissue obtained by biopsy or prostatectomy, Myriad tests 46 different gene expressions, which include 31 cell-cycle progression (CCP) genes and 15 housekeeper genes that were selected because of correlation with proliferation of prostate cancer (Cuzick et al., 2012; Freedland et al., 2013). It was found that low expression is associated with a low risk for disease progression, whereas high expression is more indicative of higher risk for disease progression, suggesting either close monitoring or additional therapy for the latter group of patients.

Decipher (GenomeDX, Vancouver, Canada) was initially designed to predict treatment response with a 22-gene panel spanning genes involved in cell proliferation, cell cycle, differentiation, adhesion, and androgen pathway (Nakagawa et al., 2008).

Regardless of their initial discovery purpose, they are used in the setting of localized prostate cancer managing active surveillance.

Studies have compared results using all three test systems and found agreement of 50% to 75% (Alam et al., 2019). Uniquely, Confirm MDX (MDxHealth, Irvine, CA) utilizes the cancer field effect on methylation of GSPT1, APC and RASSF1 to detect possible cancer on patients with biopsy-proven negative cases (Stewart et al., 2013). A recent survey suggests that there is approximately 50% to 75% concordance among the three different genetic screens (Alam, 2019).

CERVICAL CANCER

Cervical carcinoma is the second most prevalent cancer in women worldwide (Parkin et al., 2001). The primary cause of cervical cancer is HPV infection. HPV infection initiates and promotes the development of cervical neoplasia from the precancerous lesion, cervical intraepithelial neoplasia (CIN) I or low-grade squamous intraepithelial lesion (LSIL), to in situ cancer III or high-grade squamous intraepithelial lesion (HSIL) and invasive cancer (Kisseljov et al., 2008; Herrington et al., 2009). Other cellular or environmental factors, such as genetic and immune disorders, hormonal contraception, high parity, tobacco smoking, coinfection with other microorganisms (e.g., HIV), and dietary deficiencies, are also implicated in cervical carcinogenesis. These factors are important for the progression from cervical HPV infection to cervical intraepithelial lesions and cancer (Munoz et al., 2006).

HPVs are double-stranded, circular DNA viruses that contain seven early (*E1* to *E7*) and two late (*L1* to *L2*) genes necessary for viral replication. Among them, two genes (*E6* and *E7*) play a pivotal role in the initiation of cervical carcinogenesis and maintain the transformed phenotype (Mantovani & Banks, 2001; Munger et al., 2001). The E7 protein binds to the retinoblastoma TSG product pRB, preferably the underphosphorylated or "active" form of *pRB*. HPV E6 proteins can also associate with the p53 tumor suppressor protein. Inactivation of pRB and p53 by the HPV oncoproteins E7 and E6 likely represents major steps in cervical carcinogenesis. HPV may also be integrated with the human genome, which is important in the progression of HPV-associated neoplasia. This integration may cause upregulation of HPV E6 and E7 expression and other genetic abnormalities, including telomerase activation and chromosomal alterations leading to the development of high-grade intraepithelial and invasive squamous carcinoma. In addition, HPV infection can induce many epigenetic changes, including methylation of the promoter of TSGs involved in cell proliferation and differentiation (Kisseljov et al., 2008; Gupta et al., 2010; Herrington et al., 2009).

Although more than 100 HPV types have been identified, studies show that HPV-16 and, to a lesser extent, HPV-18 play a dominant role in cervical carcinogenesis and are jointly responsible for 70% of the world's cervical cancer cases. Based on their capability for tumorigenicity, HPVs are classified into high- and low-risk groups (Table 79.4), with high-risk HPV types causing high-grade cervical intraepithelial lesions (CIN2/3 or HSIL), and with low-risk HPV types leading to low-grade cervical intraepithelial lesions (CIN1 or LSIL) (Kisseljov et al., 2008; Herrington et al., 2009).

Because a strong causative association has been observed between HPV infection and cervical cancer, identification of HPVs in tissue or cytologic

TABLE 79.4
Oncogenicity of HPV

Oncogenicity	HPV Types
High-risk HPV types	16, 18, 31, 33, 35, 39, 45, 52, 56, 58, 59, 67, 68
Low-risk HPV types	6, 11, 40, 42, 43, 44, 54, 61, 70, 72, 74, 81, 83, 84
Probable high-risk types	26, 51, 53, 56, 66, 69, 82

HPV, Human papillomavirus.

specimens has become a routine practice not only for screening purposes but also for the diagnosis of cervical cancer and for follow-up of abnormal changes detected by a cervical Papanicolaou (Pap) smear. The combination of HPV testing and Pap smear evaluation has significantly improved the sensitivity and specificity of the diagnosis of precancerous lesions and cancer (Cuzick et al., 2008). Among various platforms for HPV infection detection, the Digene Hybrid Capture (Digene Corporation, Gaithersburg, MD) is an in vitro, solution hybridization, signal-amplified test used to detect HPV DNA targets. First introduced by Digene in 1995, it was designed to detect 14 HPV types, including the high-risk types HPV 16, 18, 31, 33, 35, 45, 51, 52, and 56; and the low-risk types HPV 6, 11, 42, 43, and 44. The Hybrid Capture test is performed on the residual liquid portion of the patient's Pap smear specimen, such as the thin preparation containing HPV DNA. This reacted viral DNA is combined with viral-specific RNA probes, creating hybrids. These RNA:DNA hybrids are then combined onto a solid phase coat, with subsequent capture by universal antibodies that are specific for that particular RNA:DNA nucleic acid hybrid. In turn, the RNA:DNA antibody is detected by a signaling antibody conjugated to alkaline phosphatase, resulting in chemiluminescence that, when amplified, can be measured in relative light units (RLUs). The second generation of the hybrid capture assay, Hybrid Capture 2, replaces the tubes with microtiter plates to improve performance and suitability for automation. It is the first FDA-approved form of HPV testing for high-risk groups for HPV.

The Cobas HPV test (Roche Molecular Diagnostics, Inc., Indianapolis, IN) was FDA approved in 2011. These tests can individually report on HPV-16 and HPV-18 subtypes within a pool of an additional 12 high-risk subtypes. For the first time, this test platform enabled stratification of women into those infected with HPV-16/18 versus those infected with high-risk groups other than HPV-16/18 without the need for a secondary test. The importance of identifying these subtypes is also evidenced in the 2012 revised guidelines for the prevention and early detection of cervical cancer (Saslow et al., 2012).

The Aptima HPV assay (Hologic Inc., Marlborough, MA), stands apart from the other tests in that it targets the detection of E6/E7 mRNA, which is associated with integration of the virus into the host cell genome and malignant transformation (Morris, 2005). It therefore probes the most clinically relevant infections. While Gen-Probe does offer two Aptima tests, the latter allowing detection of either pooled high-risk virions or HPV-16/18/45 versus HPV-18 and HPV-45, this assay is unable to distinguish between HPV-18 and HPV-45 subtypes, which does not meet the revised screening guidelines.

The FDA approved two other HPV tests in 2009, both of which utilize an isothermal enzymatic DNA amplification process with a fluorescent readout used with ThinPrep samples (Hologic Inc.). One of these tests, the Cervista HPV HR (Hologic Inc.), is designed to identify 14 high-risk types of HPV. These include the 13 types detected by the Hybrid Capture 2 HPV DNA assay (16, 18, 31, 33, 35, 39, 45, 51, 52, and 56, as well as 58, 59, and 68) and HPV 66. The other test, Cervista HPV 16/18, is designed to specifically detect HPV-16 and HPV-18. Other technologies are also used by some laboratories, including PCR, DNA microarray, dot blot, Southern blot, and genotyping, such as TaqMan PCR genotyping assay, GenProbe (GenProbe Inc., San Diego, CA), and APTIMA1 HPV assay (Aptima Inc., Woburn, MA).

p16 (*CDKN2A* or *MTS1*) is located at 9p21.3 and belongs to a group of tumor suppressor genes that includes *p15INK4b*, *p21waf1*, and *p27KIP1*, all of which negatively regulate the G1 phase of the cell cycle (Serrano et al., 1993). Specifically, p16 binds the cyclin-dependent protein kinases CDK4 and CDK6, inhibiting their interactions with cyclin D1. As a result, pRb phosphorylation is inhibited and the E2F transcription factors are sequestered, blocking G1 to S phase progression. p16 expression loss allows cells to escape G1 arrest (Cobrinik et al., 1992). The HPV E7 oncoprotein binds pRb, causing E2F release, resulting in G1 to S progression despite high p16 expression (Mantovani & Banks, 2001; Munger et al., 2001; Khleif et al., 1996). Thus, high p16 expression is a sensitive marker for HPV E7 protein expression. Cuschieri and Wentzensen (2008) reviewed 9 studies, including 2178 cases, and found that 7% of nondysplastic, 54% of CIN1 cases, 86% of CIN2 cases, and 96% of CIN3 and invasive cancers showed diffuse p16 expression, demonstrating high specificity and sensitivity of p16 staining as a measure of HPV infection. As with Ki-67, p16 staining is not entirely specific for a neoplastic process or HPV infection. For example, benign cervical tubal metaplasia shows p16 positivity (Horree et al., 2007).

ENDOMETRIAL CANCER

Endometrial cancer is a common gynecologic malignancy in Western countries, fourth in incidence after breast, lung, and colon cancer. Between 2008 and 2019, the incidence of endometrial cancer increased by 6% to 7% yearly, and the mortality rate remained at 3% to 4% with no significant improvement in the last decade (Cancer Statistics, 2008-2019). The molecular genetics of endometrial cancer vary with clinical characteristics (type I or II), tissue differentiation, and histologic type. Endometrioid adenocarcinoma, a type I endometrial cancer, exhibits rates of *K-Ras* and *p53* mutations of 26% and 17%, respectively. In serous adenocarcinoma, a type II endometrial cancer, these rates are 2% and 93%, respectively (Lax et al., 2000). Similarly, in clear-cell adenocarcinoma, a particular histologic type of endometrial cancer, the levels of estrogen receptor (ER), progesterone receptor (PR), and Ki-67 are similar to those in serous adenocarcinoma while p53 is significantly lower, whereas ER and PR are significantly lower, Ki-67 is significantly higher, and p53 tends to be higher compared with endometrioid adenocarcinoma (Lax et al., 1998). Thus, the patterns of genetic mutations and the developmental mechanisms may vary among histologic types.

Approximately 5% of endometrioid carcinomas are associated with Lynch syndrome, which can either be endometrium or extrauterine endometrial tissues, the latter usually associated with endometriosis. A large percentage of these tumors have mutations in the ARID1A protein, an ATPase-containing protein that is involved with destabilizing histone-DNA complexes and allowing transcription, especially at A-T–rich regions of DNA. Assays for this protein, which are associated with nonserous endometrial tumors (Wiegand et al., 2010), could provide the basis for another molecular test, allowing distinction between these tumors and the less aggressive endometrioid and clear-cell tumors.

OVARIAN CANCER

Ovarian cancer is one of the most common gynecologic malignancies and is the fifth leading cause of cancer mortality in women in the United States (Jemal et al., 2009). Ovarian epithelial cancers are classified on the basis of morphology depending on invasiveness (tumor grade) and type of differentiation (e.g., serous, mucinous, endometrioid, clear cell, and transitional type).

Studies on the molecular pathology of ovarian cancer show that each of the four major histopathologic types of ovarian carcinoma is characterized by rather distinctive, although not necessarily unique, genetic abnormalities. For example, *TP53* gene mutations are extremely common in high-grade serous carcinomas, while low-grade serous and mucinous adenocarcinomas have a high prevalence of *KRAS* and *B-RAF* mutations (75% in primary mucinous adenocarcinomas) (Cho & Shih, 2009). Mutations of *CTNNB1*, the gene encoding β-catenin and PTEN, are common in endometrioid adenocarcinoma but are rare in serous, mucinous, and clear-cell carcinomas. Mutations of *PIK3CA*, which encodes the catalytic subunit of PI3K (phosphoinositide 3-kinase), are observed most frequently in clear-cell carcinomas. In addition, genetic differences exist within a given type of ovarian cancer.

Molecular subgroups of endometrioid adenocarcinomas correlate with tumor grade, stage of disease, and clinical outcome. Serous carcinomas can be subdivided into low-grade serous carcinoma (LGSC) and high-grade serous carcinoma (HGSC).

Histologic Subtypes of Serous Carcinoma

LGSC, also called International Federation of Gynecology and Obstetrics (FIGO) stage I, is defined as malignancy of one (Ia) or both (Ib) ovaries. These carcinomas characteristically have *KRAS* or *BRAF* mutations, but lack *TP53* mutations (Gilks & Prat, 2009). *KRAS* or *BRAF* mutations lead to constitutive activation of the MAPK signaling pathway. Low-grade tumors have also been found to contain mutations that deregulate the canonical Wnt/β-catenin and PI3K/PTEN signaling pathways and typically lack *TP53* mutations (Cho & Shih, 2009).

On the other hand, HGSCs are characterized by high-grade nuclei, have short latent precursor lesions, and have rapid tumor progression into invasive carcinoma. HGSCs are often identified in the advanced stage and have a high prevalence (50%–70%) of *TP53* gene mutations (Wen et al., 1999). However, unlike in LGSC, *KRAS* and *BRAF* mutations are rare. Most HGSC cancers further lack Wnt/β-catenin or PI3K/PTEN signaling pathway defects (Kolasa et al., 2006), which are common in the LGSCs. Moreover, it is important to note that most HGSCs have genetic and somatic alterations of *BRCA1* and *BRCA2* (germline or somatic mutation or promoter methylation and loss of expression) (Kobel et al., 2008). These changes occur early during oncogenesis and result in loss of ability to repair DNA double-strand breaks, which, in turn, leads to chromosomal instability.

Molecular Classification of Ovarian Cancer

Molecular studies led to the proposal of a new model for classifying ovarian carcinomas in which surface epithelial tumors can be divided into two broad categories, designated type I and type II, based on their pattern of tumor progression and molecular genetic changes (Landen et al., 2008; Levanon et al., 2008). Type I tumors include low-grade endometrioid carcinoma, mucinous carcinoma, and a subset of clear-cell carcinomas that develop in a stepwise fashion from well-recognized precursors, in most cases, borderline tumors, which generally are large and often are confined to the ovary at diagnosis. In contrast, type II tumors are of high grade and almost always have spread beyond the ovaries at presentation. These include high-grade serous carcinoma, undifferentiated carcinoma, some clear-cell carcinomas, and malignant mixed Müllerian tumor. Type I and type II tumors also differ in their molecular profiles. Type I tumors often harbor somatic mutations of genes encoding protein kinases, including *KRAS*, *BRAF*, *PIK3CA*, and *ERB-2* (*Her2/neu*), and other signaling molecules, including CTNNB1 and PTEN. In contrast, type II tumors generally lack these mutations but are characterized by a high frequency of *TP53* mutations, which are rare in type I tumors. Chromosomal instability levels, as reflected by genome-wide changes in DNA copy number, are much higher in type II tumors than in type I tumors (Mayr et al., 2006).

Clear-Cell Ovarian Carcinoma

Mutations in *KRAS*, *BRAF*, and *TP53* are present in some clear-cell carcinomas, but their frequency is generally low. Mutations predicted to deregulate PI3K/PTEN signaling are more common in clear cell carcinomas, with *PIK3CA* mutations reported in 20% to 25%, and *PTEN* mutations in 8% of tumors (Cho & Shih, 2009).

BRCA1 and *BRCA2* in Ovarian Cancer

These genes encode proteins that are required for DNA double-strand break repair by homologous recombination. Cells lacking *BRCA1*- or *BRCA2*-dependent DNA repair tend to develop chromosomal rearrangements and genomic instability. Inheritance of DNA repair defects involving *BRCA1* and *BRCA2* contributes to as many as 10% to 15% of ovarian cancers (Lancaster et al., 1996). The lifetime risk for developing ovarian cancer in mutation carriers varies with the genetic defect (for *BRCA1*, 30%–60%, and for *BRCA2*, 15%–30%). *BRCA*-related familial ovarian cancers are more frequently multifocal and progress faster. Carcinomas arising in patients with germline *BRCA1* or *BRCA2* mutations are almost invariably of the high-grade serous type discussed previously. Fortunately, however, ovarian cancers that contain mutations affecting *BRCA1* and *BRCA2* are more sensitive to DNA damage induced by chemotherapeutic agents such as platinum drugs and PARP inhibitors because they are less able to repair the DNA damage caused by these agents. Thus, these drugs are particularly effective in the presence of defects in homologous recombination repair; clinical trials with these agents are underway in ovarian cancer patients with inherited *BRCA1* and *BRCA2* mutations (Yap et al., 2009).

Although *BRCA1* and *BRCA2* genes have been thought to be mutated only rarely in sporadic ovarian cancers, somatic mutations have recently been documented in approximately 10% of nonfamilial cases, particularly in high-grade serous epithelial ovarian cancers, and expression of *BRCA1* and *BRCA2* can be silenced by methylation in additional cancers. This contributes to their sensitivity to platinum-containing therapies in HGSC. PARP inhibitors might also find broader clinical application in these sporadic cancers, in which these pathways are also defective. Thus, in some regions, all patients presenting with an HGSC are referred for genetic counseling and screening for *BRCA* mutations (Risch et al., 2001).

MELANOMA

Malignant melanoma is an aggressive tumor that originates from pigment-producing melanocytes, mainly in skin. About 80% of melanomas are diagnosed early and can be cured by surgical excision (Gray-Schopfer et al., 2007). However, metastatic melanomas are refractory to current chemotherapy or radiotherapy and have a very poor prognosis, with a median survival of 6 months (Miller & Mihm, 2006). A majority (90%) of melanoma cases are sporadic, and 10% are familial melanomas, also known as *dysplastic nevus syndrome*. Four melanoma-predisposing genes have been identified in familial melanoma based on the discovery of germline mutations in multiple-case families; three are high penetrance, and one is low penetrance. The best characterized high-penetrance gene is cyclin-dependent kinase inhibitor 2A. It is located on chromosome 9p21 and encodes two distinct melanoma-predisposing genes: *p16* (discussed in the Bladder Cancer section earlier in the chapter) and *p14* (Mehra et al., 2007b). The protein product of *p16* is INK4a, and the protein product of *p14* is ARF. From 25% to 40% of familial melanoma cases harbor an inactivating mutation in *CDKN2A* (Miller & Mihm, 2006; Gray-Schopfer et al., 2007). Cyclin-dependent kinase 4 (*CDK4*), located on 12q14, is the third high-penetrance melanoma susceptibility gene (Zuo et al., 1996). Finally, melanocortin-1 receptor (*MC1R*) is a low-penetrance gene implicated in melanomagenesis.

The RAS/RAF/MEK/ERK signaling pathway has emerged as a major player in the induction and maintenance of sporadic melanoma. Among *RAS* family members, mutations in *NRAS* occur most frequently in melanocytes, with rates approaching 56% in congenital nevi (Demunter et al., 2001; Miller & Mihm, 2006), 33% in primary melanomas, and 26% in metastatic melanomas (Garnett et al., 2005).

However, as in papillary thyroid carcinoma and in some forms of colorectal cancer, the most important signaling molecule in melanoma downstream of RAS is BRAF. *BRAF* somatic missense mutations are found in 66% of malignant melanomas, of which 80% involve a single base substitution of valine by glutamic acid at position 600 (V600E). Most of these mutations activate BRAF kinase activity from 1.5- to 700-fold, although a small number actually are inactivating mutations. However, even these inactive mutants can stimulate cellular signaling through the MEK-ERK pathway because they activate the related family member *C-RAF* (Garnett et al., 2005).

It is interesting to note that genetic alterations in *NRAS* and *BRAF* rarely coexist in melanoma (Zuo et al., 1996; Tsao et al., 2004; Miller & Mihm, 2006), suggesting that mutant *BRAF* or *NRAS* alone is able to activate the pathway. Recent studies have revealed deregulation of PI3K signaling in a high proportion of melanomas. Indeed, in about 45% of melanomas, *PTEN* is deleted and the downstream *AKT* gene is amplified (Zhou et al., 2003; Stahl et al., 2004). Additionally, RAS binds and activates PI3K, thereby activating the AKT pathway and preventing apoptosis (Sekulic et al., 2008). These data suggest that loss of *PTEN* and oncogenic activation of RAS are equivalent (Zhou et al., 2003).

The high mutation rate of *BRAF* in melanoma makes it an attractive therapeutic target. Investigators have focused much attention on agents that specifically target *BRAF*, such as sorafenib, as well as on molecules that function both upstream and downstream of BRAF. A nonspecific inhibitor of BRAF, sorafenib is not effective as a single agent in advanced-stage melanoma patients (Sekulic et al., 2008). Of interest downstream of BRAF is the direct inhibition of ERK and MEK. Although no mutations have been documented in either molecule, inhibition of MEK has proved effective in the presence of a mutated *BRAF* (Sekulic et al., 2008). Several MEK inhibitors are currently in clinical trials. Several BRAF and MEK inhibitors are approved by the European Medicines Agency (EMA) and FDA to be used in metastatic or unresectable melanoma with BRAF V600 mutations (Robert et al., 2015; Larkin et al., 2014). AKT, PI3K, and ERK inhibitors are under development (Greco & Hainsworth, 2014; Siegel et al., 2012; Siegel et al., 2017). Upstream of BRAF, RAS is an attractive target for inhibition. Farnesyltransferase inhibitors (FTIs) interfere with posttranslational processing of RAS, disenabling its insertion into the inner cell membrane, thereby inhibiting the downstream effects of RAS. Immune checkpoint inhibitors targeting cytotoxic T-lymphocyte–associated antigen-4 (CTLA-4) and programmed death 1 (PD-1) have also been evaluated (Melis et al., 2017) (NCCN, 2018).

MOLECULAR GENETIC PATHOLOGY OF SARCOMA

Sarcomas are malignant neoplasms arising in connective tissue, fat, muscle, blood vessels, deep skin tissues, nerves, bones, and cartilage. These types of cancers often are not considered classical "solid-tissue tumors," although often their biological behavior is similar to that of the types of solid-tissue tumors discussed previously. However, because major advances have been made in the area of the molecular biology of sarcomas, and because these

advances have illuminated the nature of specific genetic lesions that cause cell transformation, we describe them in this section. This section is meant to show the principles that have been discovered in sarcomatous cell transformation and is not meant to be a detailed discussion of specific genetic lesions in each of the myriad different sarcomas that have been described. Rather, we present specific examples of each type of genetic lesion that has been discovered. The reader is referred to other texts that describe the genetic lesions in each sarcoma type.

Many sarcomas harbor specific translocations or other characteristic genetic defects that aid in the diagnosis of each tumor type and, in some cases, impart prognostic or predictive information influencing clinical management (Jain et al., 2010b). Recent molecular cytogenetic analysis has demonstrated that the sarcomas can be divided into two main categories:

1. Sarcomas with specific genetic alterations. These can be subclassified further into sarcomas that harbor reciprocal translocations resulting in oncogenic fusion transcripts (accounting for 15%–20% of cases [e.g., SS18-SSX in synovial sarcoma]) and sarcomas that harbor specific oncogenic mutations (e.g., *KIT* and *PDGFRA* mutations in gastrointestinal stromal tumors) (Hirota et al., 1998; Miettinen & Lasota, 2006).
2. Sarcomas displaying multiple complex karyotypic abnormalities with no specific pattern, including malignant fibrous histiocytoma (MFH) and leiomyosarcoma (LMS).

SARCOMAS WITH FUSION GENES

Fusion Genes Involving *TET* Genes

Nearly half of the fusion proteins believed to participate in initiation and development of sarcoma contain a portion of the so-called *TET* gene family products, including *EWSR1*, *TLS/FUS*, and *TAFII68*. TET family proteins contain a characteristic 87–amino acid RNA recognition motif that is thought to be implicated in protein-RNA binding and to participate in transcription and RNA metabolism.

Ewing Sarcoma/Primitive Peripheral Neuroectodermal Tumor

This is a prime example of a fusion gene–induced sarcoma. The tumor itself is a small blue cell tumor that primarily affects long bones or the vertebral area in young adults and children. Histologically, it is characterized by sheets of small round cells that may form Homer-Wright rosettes. Ewing sarcoma family tumors (ESFTs) can be subclassified into Ewing sarcomas or primitive peripheral neuroectodermal tumor (PNET), the latter showing evidence of neuroendocrine differentiation immunohistochemically (Olsen et al., 2006). However, the distinction between them is no longer considered critical for clinical management, as prognosis and therapy are similar.

ESFTs characteristically harbor a recurring t(11;22)(q24;q12) that juxtaposes the *FLI1* and *EWSR1* genes to encode a chimeric RNA and protein. About 10% of Ewing family tumors have an alternate translocation involving the *EWSR1* gene, implying that disruption of *EWSR1* is the critical molecular event underlying tumorigenesis. Except for *FUS-ERG*, all fusion transcripts identified so far in ESFTs consist of *EWSR1* and an ETS family transcription factor, including *FLI1*, *ERG*, *ETV1*, *ETV4*, and *FEV* genes (de Alava & Gerald, 2000). Approximately 85% to 90% of ESFTs are associated with the *EWSR1-FLI1* fusion gene, 9% to 14% with the *EWR1-ERG* gene, and the remaining 1% to 5% with other rare variants (de Alava & Gerald, 2000).

Karyotype is the analytic method used for the initial workup of a suspected Ewing family tumor because the characteristic t(11;22) is evident in approximately 90% of these tumors. However, in a case of strong suspicion of Ewing's sarcoma/PNET with normal karyotype, FISH should be considered as an additional test for the genetic defects. FISH, using a break-apart probe targeting the *EWSR1* gene, is an excellent method to identify or exclude a *EWSR1* gene rearrangement. FISH may be carried out on metaphase cells (requiring fresh tissue) or on interphase cells (feasible on a wide variety of sample types, including fine-needle aspirates, touch preparations, smears, or paraffin-embedded tissue) (Kilpatrick et al., 2006). An advantage unique to RT-PCR is its ability to define which of two prognostically relevant transcript structures is present: type 1 fusion transcripts *(EWSR1-FLI1)* are not transcribed as actively and carry a good prognosis compared with alternative fusions. Another advantage of RT-PCR is its ability to detect minimal residual disease after therapy (Vermeulen et al., 2006). Immunohistochemical analyses of *CD99* and *FLI1* reveal overexpression in most Ewing's/PNET tumors harboring a t(11;22) translocation (Hameed, 2007).

Clear Cell Sarcoma

Clear cell sarcoma is a malignant neoplasm with melanocytic differentiation. Tumors generally occur in young adults, without significant sex predilection, and are typically found in the deep tissues of the extremities. Tumors are characterized by reciprocal t(12;22)(q13;q13) translocations (Reeves et al., 1992). This leads to the formation of an EWSR1-ATF1 fusion product (Zucman et al., 1993; Speleman et al., 1997; Hiraga et al., 1997). Exons 7, 8, and 10 of EWSR1 have been reported to fuse with exon 4 or 5 of ATF1. More recently, EWSR1-CREB1 fusion products have been described in clear cell sarcomas arising in both the soft tissues and gastrointestinal locations (Hisaoka et al., 2008; Antonescu et al., 2006; Wang et al., 2009b). RT-PCR remains an excellent means of diagnosing this tumor (Wang et al., 2009b; Coindre et al., 2006). Given the presence of multiple fusion partners, FISH with a break-apart EWSR1 probe is convenient. The fusion type does not appear to be associated with outcome (Coindre et al., 2006).

Extraskeletal Myxoid Chondrosarcoma

Extraskeletal myxoid chondrosarcoma typically occurs in bone of adults without a consistent sex predisposition. Tumors are aggressive, with a high rate of metastasis on presentation and follow-up, in addition to frequent local recurrence. Histologically, small and round spindle shaped cells are arranged in chains, nests, or filigree-like, with a lobular pattern within a chondromyxoid stroma, but lack actual hyaline cartilage. Cytogenetic analysis has revealed a t(9;22)(q22;q12) in a majority of cases (Turc-Carel et al., 1988). This involves rearrangement of NR4A3 with EWSR1. As a result, FISH, using a commercially available EWSR1 break-apart probe, is a useful diagnostic marker (Wang et al., 2008), in addition to RT-PCR. There are, however, additional fusion products that do not involve EWSR1. For example, t(9;17)(q22;q11) (Bjerkehagen et al., 1999) and t(9;15)(q22;q21) (Sjogren et al., 2000) translocations were subsequently described. Secondary structural abnormalities are a common feature on cytogenetic analysis. The latter tumors respectively partner NR4A3 with TAF15 and TCF12 (Panagopoulos et al., 2002; Sjogren et al., 2000). There are commercially available NR4A3 break-apart probes that help broaden the sensitivity of FISH for this diagnosis.

Atypical Lipomatous Tumor, Well-Differentiated and Dedifferentiated Liposarcoma

Liposarcoma is the most common type of soft-tissue sarcoma. It typically occurs in middle-aged adults and affects males and females equally. Atypical lipomatous tumor (ALT) and well-differentiated liposarcoma (WD-LPS) are synonymous, with the former term employed for extremity-based lesions. Histologically, tumors are composed of sheets of adipocytes of variable size and shape with scattered lipoblasts. Dedifferentiated liposarcoma (DD-LPS) more frequently occurs in the retroperitoneum and mediastinum. Histologically they are characterized by spindle cells with a storiform pattern and a greater degree of pleomorphism, mitotic activity, and necrosis. This heralds a more aggressive tumor with the potential for metastatic spread. Some cytogenetic findings in WD-LPS and DD-LPS are similar. Fluorescence in situ hybridization (FISH) and comparative genomic hybridization (CGH) consistently show amplification in the q14 to q15 regions containing the *MDM2* gene, in both these lesions. Amplification of this region results in increased cell proliferation and decreased apoptosis (Coindre et al., 2010). Immunohistochemistry is available but it is less sensitive and specific than FISH. FISH for MDM2 amplification is now routinely used to facilitate the diagnosis of WD-LPS/DD-LPS, as over 90% of these tumors will show this alteration (Sirvent et al., 2007; Weaver et al., 2010). Polymerase chain reaction (PCR)-based techniques have also been shown to be diagnostically useful (Weaver et al., 2010; Shimada et al., 2006; Ma et al., 2006).

Myxoid/Round Cell Liposarcoma

Myxoid/round cell liposarcoma represents approximately 15% to 20% of liposarcomas, which more commonly occur in the deep soft tissues of the extremities in young males (Moreau et al., 2012). Over 90% of cases contain a recurrent t(12;16) (q13;p11) translocation involving DDIT3 (formerly CHOP) and TLS (formerly FUS) (Lopez-Gines et al., 1989). Less commonly, cytogenetics reveal a t(12;22) (q13;q12) translocation, whereby DDIT3 is partnered with EWSR1 (Mrozek et al., 1997). Diagnosis of myxoid/round cell is usually confirmed by FISH for TLS (and EWS when presented with a negative TLS result and classic histomorphology); alternatively, a DDIT3 break-apart probe can be used to cover both forms of rearrangements (Narendra et al., 2011). TLS has several common variable breakpoints fusing exons 5, 7, and 8, with exon 2 of DDIT3; this leads to three basic transcript types: type I (7-2), type 2 (5-2), and type 3 (8-2), which do not appear to have prognostic significance (Bridge et al., 2001).

Low-Grade Fibromyxoid Sarcoma

Low-grade fibromyxoid sarcoma (LGFMS) and hyalinizing spindle cell tumor with giant rosettes fall on a histologic continuum. These malignant

fibroblastic tumors are rare and frequently characterized by a long clinical history prior to presentation and late metastases. They predominate in young adults (from 2 to 70 years of age) (Billings et al., 2005) and are frequently located in the trunk and extremities (Evans, 2011). The majority of cases of LGFMS are characterized by a t(7;16)(q32–34;p11) translocation derived from fusion of FUS and CREB3L2, with a minority exhibiting a t(11;16)(p11;p11) translocation that results in the pairing of FUS and CREB3L1. Recently, two cases exhibiting fusion of EWSR1 and CREB3L1 were described (Lau et al., 2013). Both FISH and RT-PCR are useful diagnostic techniques for identifying this translocation. Given the possibility of multiple different fusion products, the use of commercially available EWSR1 and FUS break-apart probes represents a convenient means of diagnostic confirmation. The different fusion products do not appear to be associated with morphologic or immunohistochemical differences; at present there is insufficient information to know if the fusion product is associated with differences in clinical behavior (Lau et al., 2013).

Hemangioma of Bone

Benign vascular neoplasms usually occur throughout the body, in any age group, without any sex predilection. Despite their high prevalence, not much is known about their pathophysiology. Recently, a t(18;22)(q23;q12) translocation bridging the *EWSR1-NFATC1* genes was identified in a case of hemangioma of bone (Arbajian et al., 2013). The prevalence of this translocation in other vascular lesions remains to be determined. NFATC1 is a member of the NFAT transcription factor family, which has a pleiotropic effect on cells; EWSR1-NFATC1 chimeras have rarely been reported in Ewing Family of Tumors (Arbajian et al., 2013).

Fusion Genes Involving Receptor Tyrosine Kinase Genes

Congenital fibrosarcoma (CFS) is a low-grade pediatric soft-tissue sarcoma, principally arising in the extremities, generally in the first year of life. Recently, CFSs were shown to contain a novel t(12;15)(p13;q25) translocation, resulting in *ETV6-NTR*K3 gene fusion. *ETV6* is a member of the ETS family of transcription factors containing a basic helix-loop-helix (bHLH) dimerization domain, which was originally found at the breakpoint in translocations in leukemia and myeloproliferative syndromes. NTRK3 is the cell surface receptor for neurotropin 3 expressed primarily in the CNS. The ETV6-NTRK3 fusion protein forms a homodimer or heterodimer with wild-type NTRK3, which displays receptor tyrosine kinase (RTK) activity and undergoes autophosphorylation at tyrosine residues (Knezevich et al., 1998). Cytogenetic t(12;15) translocations may not be identified in several cases (CMN4, CFS1, and CFS5), but RT-PCR and FISH analyses revealed ETV6-region rearrangements in those same cases. Detection of *ETV6-NTRK3* fusion transcripts in most CFSs using RT-PCR methods with archival, formalin-fixed, paraffin-embedded tissues, therefore, is a useful diagnostic adjunct.

Sarcoma with Fusion Genes Involving Chromatin Remodeling Genes

Synovial sarcomas (SSs) often arise deep in the soft tissue near a joint in the extremity of a young adult patient. Most SSs are characterized by t(X;18)(p11.2;q11.2), resulting in a fusion between the *SS18(SYT)* gene on chromosome 18 and one of the *SSX* genes on the X chromosome, creating *SS18-SSX1*, *SS18-SSX2*, or *SS18-SSX4* chimeric genes (Skytting et al., 1999; Nishio et al., 2001, 2002a, 2002b, 2005; Kanemitsu et al., 2007). Two common histologic and genetic variants of synovial sarcoma are known: a monophasic variant comprising vimentin-expressing spindle cells usually carrying *SS18-SSX2* translocation, and a biphasic variant that consists of a mixture of vimentin-expressing spindle cells and keratin-expressing glandular epithelial cells harboring the *SS18-SSX1* or *SS18-SSX2* translocation (Ladanyi et al., 2002). The biphasic variant may resemble adenocarcinoma or more typically carcinosarcoma and carries a worse prognosis, at least in early-stage patients. Karyotype is helpful when it is positive, but negative results could reflect failure of the tumor cells to divide sufficiently in culture, or other mechanisms of false-negative results. FISH using an SS18 break-apart probe is helpful for demonstrating t(X;18), but it cannot distinguish which partner gene is involved for prognostic purposes. RNA from frozen or paraffin-embedded tissue is suitable for RT-PCR to detect and to distinguish the two common translocation variants (Sieber et al., 2003). From a mechanistic standpoint, the translocation creates a chimeric gene encoding a fusion protein that redirects the transcription factor function of SS18. Relevant downstream targets include *CCND1* (cyclin D1), which enhances cell cycle progression. *TLE1* encodes a transcriptional corepressor that is overexpressed in synovial sarcomas. Gene and tissue microarray studies have identified TLE1 as an excellent biomarker for distinguishing synovial sarcoma from other soft-tissue malignancies on immunohistochemistry (Jagdis et al., 2009).

Sarcoma with Fusion Genes Involving Growth Factors

Dermatofibrosarcoma protuberans (DFSP) is a rare skin tumor of low-grade malignancy that shows local recurrence. The reciprocal chromosomal translocation t(17;22)(q11;q13.1) or a supernumerary ring chromosome derived from t(17;22) is found in this type of tumor, which results in fusion of the *COL1A1* gene on chromosome 17 with the *PDGFB* gene on chromosome 22 (Simon et al., 1997). Because the point of fusion is highly specific for *PDGFB* but is spread over almost the entire locus for *COL1A1*, the role of the *COL1A1* gene may be simply to upregulate the expression of the platelet-derived growth factor receptor (PDGFR). Imatinib mesylate is an inhibitor of tyrosine kinases, including PDGFR, and has shown a dramatic response to treatment in adults. The use of other PDGFR inhibitors such as sunitinib and sorafenib has recently commenced in patients with metastatic DFSP (McArthur, 2006).

Giant cell fibroblastoma (GCF) represents the juvenile form of DFSP, which shows local recurrence. Although histologically different, these two diseases share several features, including CD34 positivity and, most important, the genetic alteration t(17;22)(q11;q13.1), involving the *COL1A1* gene as found in DFSP (Simon et al., 1997).

Sarcoma with Other Types of Fusion Genes

Rhabdomyosarcoma (RMS), a malignant tumor of skeletal muscle cells, is the most common soft-tissue sarcoma in children and young adults, often arising from extremities, paranasal sinus, or retroperitoneum. The main histologic subtypes are alveolar (ARMS) (20%), embryonal (ERMS) (60%), and pleomorphic (PRMS); survival rates for these subtypes vary from <25% to >95%, respectively (Breneman et al., 2003). Histologically, striated muscle differentiation is noted with concomitant expression of vimentin, muscle-specific actin, desmin, myogenin, and MyoD1.

In ARMS, 70% of cases harbor the translocation t(2;13)(q35:q14), which fuses the 5′ end of *PAX3* with the 3′ end of the *FOXO1A* gene. A further 10% of ARMS cases are associated with fusion of *PAX7* to the *FOXO1A* gene. The remaining 20% of ARMS cases do not have these fusion genes detectable by routine RT-PCR and constitute cases with very low expression of a fusion gene or a rare variant fusion gene, or with no detectable fusion gene. FISH using a break-apart probe identifies rearrangement of the *FOXO1A* gene (Matsumura et al., 2008; Mehra et al., 2008). The karyotype typically reveals t(2;13)(q35;q14) *PAX3-FOXO1A* or t(1;13)(p36;q14) *PAX7-FOXO1A*, with the latter being less common but imparting a better prognosis (Davicioni et al., 2006). It should be noted that ARMS tends to have a poor prognosis overall, especially when presenting with disseminated disease, so genetic testing may be moot in stage IV patients. Testing is most useful when the histologic features are not classic (e.g., mixed alveolar and embryonal patterns).

Epithelioid Hemangioendothelioma

Epithelioid hemangioendothelioma is a malignant vascular neoplasm that can occur at essentially any age, but that predominates in the second decade. Recurrent t(1;3)(p36.3;q25) translocation was identified in epithelioid hemangioendothelioma (Mendlick et al., 2001), which results in a *WWTR1-CAMTA1* gene fusion (Errani et al., 2011; Tanas et al., 2011). This involves fusion of exon 3 or 4 of *WWTR1* with exon 8 or 9 of *CAMTA1* (Errani et al., 2011, 2012; Tanas et al., 2011). Both break-apart FISH and RT-PCR are effective diagnostic tools for detecting the fusion. Interestingly, recently a subset of epithelioid hemangioma showing an atypical morphology was discovered to contain a YAP-TFE3 fusion partner (Antonescu et al., 2013). Parenthetically, these tumors are readily identified using immunohistochemistry for TFE3, which is diffusely and strongly positive.

SARCOMAS WITH ONCOGENIC MUTATIONS

KIT and *PDGFRA* in Gastrointestinal Stromal Tumor

Gastrointestinal stromal tumor (GIST) is the most common mesenchymal tumor in the gastrointestinal tract. Activating mutations of the *cKIT* gene were found in 75% to 80% of cases and of *PDGFRA* in 5% to 10%; cases with no mutation in either of these are extremely rare. The cKIT protein, which encodes a tyrosine kinase receptor (TKR) for stem cell/PDGFR, comprises a long extracellular domain, a transmembrane segment, and an intracellular domain. In all cases, mutated receptors transmit growth signals in a ligand-independent manner, inducing dysregulated cell proliferation, as described in Chapter 77. Mutations generally occur in exon 11, encoding the intracellular receptor domain, but can also occur in exons 9 and (rarely) 13, and 1 in GIST. Mutations in *cKIT* and *PDGFRA* are mutually exclusive.

Detection of overexpression or mutation of *cKIT/PDGFRA* has become a standard diagnostic tool for GIST. Drugs targeting the activating tyrosine kinase, such as imatinib mesylate (Glivec/Gleevec), have been used successfully to treat patients with metastatic GIST showing the previously described mutations. D816V point mutations in *cKIT* exon 17 are responsible for resistance to targeted therapy drugs such as imatinib mesylate (Miettinen & Lasota, 2006).

GISTs that are negative for both *KIT* and *PDGFRA* mutations have been referred to as *wild-type GISTs*. It is now becoming clear that many of these carry mutations in one of the succinate dehydrogenase *(SDH)* genes and are now known as *SDH-deficient GISTs* (Janeway et al., 2011). SDH mutations are relatively common, particularly in the stomach, accounting for 5% to 10% of all gastric GISTs (Miettinen et al., 2011). SDH-deficient GISTs are characterized by a distinct multinodular and plexiform growth pattern and are almost always epithelioid in morphology (Miettinen et al., 2011). This pattern was previously observed in children (known as *pediatric-type* GIST) and in patients with Carney triad. Unlike conventional GISTs, the behavior of SDH-deficient GISTs cannot be predicted based on size and mitotic activity. In addition, tumors are often multifocal, tend to metastasize to lymph nodes, and despite resistance to imatinib therapy, have an indolent clinical course (Janeway et al., 2009). These SDH-deficient GISTs may occur as part of Carney triad or Carney-Stratakis syndrome that are characterized by multifocal GISTs, paraganglioma, and pheochromocytoma, or they can occur sporadically as a result of germ-line mutation in one of the SDH subunits.

SARCOMAS WITH VARIABLE OTHER SPECIFIC PATTERN

Nodular Fasciitis

Nodular fasciitis is a common and benign soft-tissue tumor that can occur at any age, but is most common in young adults. It typically manifests in the subcutis of upper limbs and head and neck region. Historically, nodular fasciitis was thought to be a reactive lesion, perhaps instigated by trauma. Recently, it was found that most cases are characterized by rearrangement of USP6 (ubiquitin-specific peptidase 6). In approximately 90% of cases, there is fusion with MYH9 (myosin heavy chain 9, non-muscle) (Erickson-Johnson et al., 2011; Swanson et al., 2012; Amary et al., 2013). Both FISH-and PCR-based assays have proved useful as diagnostic markers for nodular fasciitis. The translocation leads to overexpression of USP6, a protein shown to be involved in proliferation, inflammation, and cell signaling (Erickson-Johnson et al., 2011).

Inflammatory Myofibroblastic Tumor

Inflammatory myofibroblastic tumor (IMT) is a neoplasm showing (myo) fibroblastic differentiation. This tumor spans a broad demographic, ranging from prenatal to older adults, and is not restricted by anatomic location. Roughly 10% to 30% of cases are associated with fever and weight loss along with a number of hematologic findings. Approximately half of inflammatory myofibroblastic tumors contain rearrangement of the 2p23 region corresponding to the *ALK* gene (Griffin et al., 1999). Molecular diagnostic confirmation is becoming imperative given the emergence of targeted therapies based on inhibition of ALK tyrosine kinase (Butrynski et al., 2010). Numerous fusion partners have been reported, including TPM3 and TPM4 (Lawrence et al., 2000), CLTC, RANBP2 (Ma et al., 2003), ATIC (Debiec-Rychter et al., 2003), CARS (Debelenko et al., 2003), SEC31L1 (Panagopoulos et al., 2006), and PPFIBP (Takeuchi et al., 2011), with new fusion partners continually being identified. The mechanism of tumorigenesis in cases without ALK rearrangement remains to be explained. Given the large percentage of ALK-negative cases, it should be emphasized that the diagnosis frequently rests on morphologic and immune-histochemical criteria. Some fusion products have been reported to be associated with a worse prognosis, such as RANBP2-ALK (Marino-Enriquez et al., 2011). Interestingly, at least some of these cases are associated with an epithelioid morphology; in addition, rather than showing the typical cytoplasmic pattern of ALK expression, they may be a perinuclear or nuclear membrane decoration (Marino-Enriquez et al., 2011). Other molecular changes have been described in inflammatory myofibroblastic tumor, including p53 mutations and MDM2 amplification (Yamamoto et al., 2003). The various fusion partners are reported to share an N-terminal oligomerization motif that leads to ALK kinase catalytic activation (Ma et al., 2003).

Aneurysmal Bone Cyst

Aneurysmal bone cyst may arise de novo, or secondary to another underlying lesion such as giant cell tumor of bone. It is most common in the first 2 decades and most frequently involves the metaphysis of long bones and the spine.

Recurrent clonal karyotypic abnormalities have been reported in primary aneurysmal bone cyst, including a t(16;17)(q22;p13) translocation (Panoutsakopoulos et al., 1999; Sciot et al., 2000), which involves production of a CDH11-USP6 fusion product (Oliveira et al., 2004); other reported translocations include t(1;17)(p34.1–34.3;p13), t(3;17) (q21;p13), t(5;17)(q33;p13), t(9;17)(q22;p11 to 12), t(11;16)(q13;q22 to 23), t(17;17) (q12;p13), and t(6;13)(q15;q34) translocations (Dal Cin et al., 2000; Nielsen et al., 2002; Oliveira et al., 2005; Mentzel et al., 2012). Based on the fact that most translocations involve USP6, and a varied number of fusion partners, break-apart FISH for USP6 would be the most diagnostically helpful.

SARCOMAS WITH VARIABLE COMPLEX GENETIC ALTERATIONS WITH NO SPECIFIC PATTERN

Tumors in this group are characterized by pleomorphic/spindle cell morphology, including MFH, LMS, and malignant peripheral nerve sheath tumor (MPNST). Chromosomal breakpoints in these tumors are widely scattered, with no predilection for any of the recurrent breakpoints and no losses to any of the morphologic subtypes. A prime example of this type of sarcoma is LMS, a malignant tumor of smooth muscle.

Leiomyosarcomas are adult soft-tissue sarcomas that show varying degrees of smooth muscle differentiation and can develop anywhere in the body. LMSs usually show complex karyotypic alterations in the form of gains, losses, and amplifications in chromosomes. Some gains and losses of chromosomal material tend to correlate with poor outcome, large tumor size, and metastatic dissemination, and include loss of 1p12-pter, loss of 2p, loss of 13q14-q21 (targeting the Rb pathway), loss of 10q (targeting PTEN), and loss of 16q, as well as gains of 17p, 8q, and 5p14 pter. Activation of the *PI3K-AKT* pathway through different mechanisms (e.g., activation of insulin-like growth factor receptor [IGFR]; inactivation of PTEN, a negative regulator of *PI3K-AKT*) also plays a crucial role in the development and maintenance of LMS. This activation leads to the concomitant activation of downstream effectors such as mTOR (target of rapamycin protein; discussed in Chapter 24, see Fig. 24.15) and its targets (e.g., β-catenin, pS6, p4E-BP), as well as to stabilization of a particularly important promitotic protein, HDM-2 (human double minute-binding protein). Clinical trials have shown that analogs of rapamycin such as everolimus (RAD001), an mTOR inhibitor, have some efficacy in patients with LMS. It is known that the more differentiated retroperitoneal LMSs tend to behave more aggressively as a result of amplification/overexpression of myocardin. This protein is a transcriptional cofactor for regulating smooth muscle differentiation, and its inactivation is associated with less differentiated histology. Myocardin might constitute a promising therapeutic target.

MOLECULAR GENETIC PATHOLOGY OF MULTIPLE ENDOCRINE NEOPLASIA

Multiple endocrine neoplasia (MEN) syndromes consist of a group of benign and malignant tumors in the pituitary gland, thyroid gland, parathyroid glands, adrenal glands, endocrine pancreas, paraganglia, or nonendocrine organs. Currently, the well-recognized MEN syndrome includes type 1 MEN and type 2 MEN. Some hereditary diseases are not classic for, but should be included in, the MEN syndromes, such as VHL syndrome, familial paraganglioma syndromes, Cowden syndrome, Carney complex, hyperparathyroidism jaw tumor syndrome, and other uncommon conditions (Callender et al., 2008).

Multiple endocrine neoplasia type 1, also known as *Wermer syndrome*, is characterized by tumors in the parathyroid glands, stomach, pancreas and intestinal tract, anterior pituitary gland, endocrine pancreas, and duodenum, and by the presence of other, nonendocrine tumors such as hemangioma, ependymoma, and leiomyoma, often at a young age (Callender et al., 2008; Dreijerink et al., 2009). The syndrome is caused by inactivating germ-line mutations of the MEN 1 TSG, *MEN1*, encoding a gene product that is involved in the regulation of gene transcription, DNA replication and repair, and chromatin modification (Dreijerink et al., 2009). Approximately 10% of patients are the first affected person in their family, or the index patient. By 50 years of age, approximately 80% of patients with mutations in the *MEN1* TSG will have the disease, and 90% to 95% of these patients will have abnormal biochemical screening results (Trump et al., 1996; Chandrasekharappa & Teh, 2001; Callender et al., 2008). Genetic testing is complicated, as it may detect hundreds of disease-causing mutations (e.g., *MEN1*), as well as polymorphisms. It may potentially identify those with early asymptomatic hyperparathyroidism, allowing for early nonsurgical intervention to avoid invasive surgery (Chew, 2009).

Multiple endocrine neoplasia type 2 is characterized by strong penetrance of the MTC and associated pheochromocytoma and hyperparathyroidism. It can be further categorized into MEN 2A, MEN 2B, and FMTC, based on the risk for pheochromocytoma or hyperparathyroidism, and the presence or absence of characteristic physical features (Callender et al., 2008; Raue et al., 2009). MEN 2 is caused by germ-line activating mutations of the *RET* proto-oncogene due to missense mutations, predominantly in exons 10, 11, or 13 to 16, and rarely in exons 5 and 8 (Da Silva et al., 2003; Dvorakova et al., 2005). *RET* is located on chromosome 10q11.2 and encodes a TKR that appears to transduce growth and differentiation signals in several developing tissues, including those derived from the neural crest. Constitutive activation of *RET* leads to uncontrolled cell growth and survival. Genetic testing for germ-line *RET* mutations is available for a definitive diagnosis of MEN 2 in patients who have an equivocal presentation or family history.

Close genotype-phenotype correlations have been noted in MEN 2. Certain specific *RET* mutations (genotype) are associated with age at onset, aggressiveness of MTC, and the presence or absence of other endocrine neoplasms (phenotype) (Eng et al., 1996; Yip et al., 2003). MEN 2A, the most common subtype, has a detectable *RET* mutation in at least 95% of patients (Mulligan et al., 1994; Schuffenecker et al., 1994). Among those mutations, codon 634 (exon 11) and codons 609, 611, 618, and 620 are found to be mutated in 85% of patients with MEN 2A and in 10% to 15% of patients with MEN 2B. MEN 2B, the rarest subtype of MEN 2, has *RET* mutations in codon 918 (exon 16) in more than 95% of patients, and rarely in codon 883 of exon 15 (A883F in the encoded protein) (Mulligan et al., 1995; Gimm et al., 1997). Patients with FMTC who develop only MTC with its germ-line mutations have these mutations from exons 13 to 15 of *RET* (Brauckhoff et al., 2002). Based on the mutation sites and numbers, MEN 2 can be stratified into three different levels of risk for MTC development (Brandi et al., 2001; Frank-Raue et al., 2006): high-risk group with mutations (codons 609, 768, 790, 791, 804, and 891), higher-risk group with mutations (codons 611, 618, 620, and 634), and highest-risk group with mutations (codons 883 and 918). Genetic testing may help to determine appropriate treatment options for individual patients, including prophylactic thyroidectomy, as well as the extent of surgery.

von Hippel–Lindau syndrome is an autosomal dominant inheritable neoplasia syndrome characterized by hemangioblastomas in the CNS and retina, pheochromocytomas, renal cysts and clear cell RCC, pancreatic cysts and islet cell tumors, endolymphatic sac tumors, and papillary cystadenomas of the epididymis and broad ligament (Maher et al., 1991). It has a strong penetrance, and more than 90% of affected individuals have the disease by 65 years of age. As discussed in the earlier section on renal tumors, VHL disease is caused by inactivating germ-line mutations of the VHL TSG, which contains three exons and is located on chromosome 3p25. VHL is critical in the process of regulating HIF-α and -β, which participate in the cell's response to hypoxia, as discussed earlier. Similar to MEN 2, a clear relationship has been noted between the type of genetic mutation of *VHL* (the genotype) and the pattern of tumors that developed in that particular family (the phenotype) (Crossey et al., 1994; Maher et al., 1996; Webster et al., 1998). The syndrome is associated with an increased risk for a variety of tumors in an allele-specific manner. Genetic testing is available for definite diagnosis of VHL syndrome in patients with equivocal disease and apparently sporadic *VHL*-related disease (Stolle et al., 1998).

Familial paraganglioma syndromes are inherited in an autosomal dominant manner and are characterized by multiple head and neck, thoracic, and abdominal paragangliomas and/or pheochromocytomas. Four familial paraganglioma syndromes have been described: PGL 1, PGL 2, PGL 3, and PGL 4 (Callender et al., 2008; Myssiorek et al., 2008). Most familial cases of paraganglioma have been found to be associated with the mutation of three genes encoding subunits of the mitochondrial II/succinate dehydrogenase (SDH) complex: *SDHB* at 1p36.1 (PGL4), *SDHC* at 1q21 (PGL3), and *SDHD* at 11q23 (PGL1) (most common) by linkage and candidate gene studies (Myssiorek et al., 2008). Individuals with *SDHB* mutation usually have paragangliomas in the abdomen and less frequently in the head and neck, the chest, and the adrenal gland, and are associated with an increased risk for malignancy. Individuals with *SDHD* mutation develop paragangliomas most often in the head and neck (Neumann et al., 2004; Benn et al., 2006). *SDHD* mutation is usually associated with low risk for malignancy of paragangliomas (Neumann et al., 2004; Dreijerink et al., 2009). Individuals with *SDHC* mutations are rare, and paragangliomas usually present in the head and neck, with a benign course (Schiavi et al., 2005).

The genetic screening method is very useful for predicting risk for malignancy, because so far the biologic behavior of all neuroendocrine tumors cannot be determined by conventional histologic examination alone. Genetic screening for the three genes previously discussed has been offered for familial paraganglioma (Oosterwijk et al., 1996). This test can identify individuals with mutations, allowing earlier detection and earlier intervention.

Cowden syndrome is a rare autosomal dominant, cancer-predisposing condition characterized by increased risk for breast, thyroid, and endometrial cancers and other benign conditions, including multiple hamartomas in the colon, lipomas, and fibromas (Callender et al., 2008; Hobert & Eng, 2009). It is caused by germ-line mutations in the *TSG phosphate and tensin homologue deleted on chromosome 10. PTEN* encodes a tumor suppressor promoting G1 cell-cycle arrest or apoptosis by downregulating *PI3K* and *AKT* and, concurrently, the raf-MEK-ERK pathway (Waite & Eng, 2002; Hobert & Eng, 2009).

Genetic testing for this condition is commercially available to identify mutations and/or deletions within *PTEN* (Marsh et al., 1998; Zhou et al., 2003). Approximately 85% of patients with Cowden syndrome have an identifiable *PTEN* mutation or deletion (Marsh et al., 1998; Eng, 2003; Zhou et al., 2003). This method includes multiplex ligation–dependent probe amplification (the preferred method), Southern blotting, monochromosomal hybrid analysis, real-time polymerase chain reaction, and semiquantitative multiplex PCR. Promoter analysis is also used for genetic testing in the research setting. Identification of *PTEN* mutations not only can confirm the clinical diagnosis, but also can help in prenatal diagnosis and prediction of mutations in affected families (Callender et al., 2008; Hobert & Eng, 2009).

Li-Fraumeni syndrome is a rare autosomal dominant disorder characterized by increased risk for soft-tissue sarcoma, breast cancer, and osteosarcoma, as well as brain tumor, childhood leukemia, and adrenocortical carcinoma (Moule et al., 2006; Callender et al., 2008).

Most individuals or families with Li-Fraumeni syndrome have the germ-line mutation in the TSG encoding the p53 protein on chromosome 17p13.1. Unlike other TSGs, such as *RB* and *p16*, germ-line mutations in only one copy of *p53* can result in cancer development (Yoon et al., 2002). Most *p53* germ-line mutations are missense mutations, and only 10% are due to deletions (Olivier et al., 2003). A few cases of Li-Fraumeni syndrome and Li-Fraumeni–like syndrome show mutations in another TSG, *CHEK2*, without *p53* mutation (Bell et al., 1999).

Certain genotypes of *p53* mutations have prognostic significance. Cancers harboring missense *p53* mutations are associated with more aggressive behavior; these mutations therefore suggest poorer prognoses. Missense mutations within the DNA binding region of the *p53* gene are more likely predisposed to early onset of breast cancer and brain tumor, whereas mutations outside the DNA binding region are more commonly seen in adrenocortical carcinoma. Mutations leading to a *p53* null phenotype are associated with earlier onset of brain tumor (Olivier et al., 2003).

Genetic testing for a mutation of *p53* in a patient with Li-Fraumeni or Li-Fraumeni–like syndrome can confirm the clinical diagnosis and screen family members at risk. However, it should also be noted that inactivating *p53* mutations and homozygous deletions of this gene are observed in a significant number of other types of cancer, including colon, breast, and bladder cancers.

Neurofibromatoses are a group of genetically distinct disorders with predisposition to induce nerve sheath tumor. They include neurofibromatosis 1 (NF1), neurofibromatosis 2 (NF2), and schwannomatosis.

Neurofibromatosis 1 (also referred to as *von Recklinghausen's disease*), the most common type, is an autosomal dominant multisystem disorder with 100% penetrance and variable expression. It predisposes to the development of benign and malignant tumors, typically neurofibroma, and less commonly glioma and other abnormalities (learning disability, vasculopathy, and bony abnormalities) (Arun & Gutmann, 2004; Boyd et al., 2009). Patients with this condition often are observed to have multiple tumors and café-au-lait spots on their body surfaces.

NF1 results from a mutation in the *NF1* gene, *NF1*, located on chromosome 17q11.2, and encodes for the large protein, neurofibromin. Of major importance, neurofibromin contains at least one domain that has GTPase-activating (GAP) activity with the ras-p21 protein. As discussed in Chapter 77, wild-type ras-p21 is activated by exchanging guanosine diphosphate for GTP. GAP inactivates wild-type ras-p21 by promoting the hydrolysis of ras-p21–bound GTP. Mutations in *NF1* result in loss of function of neurofibromin, leading to increased Ras activity, particularly in neurocutaneous tissues, as well as to increase proliferation and tumorigenesis (Boyd et al., 2009). The mutations are near evenly split between the sporadic and the inherited. Types of mutations of *NF1* include complete gene deletions, insertions, stop codons, splicing mutations, amino acid substitutions, and chromosomal rearrangements (Messiaen et al., 2000).

Molecular testing for *NF1* is clinically available. Because of the large gene size and lack of hot spots of *NF1* mutations, comprehensive screening approaches have been established to detect all or most mutations and may detect 95% of *NF1* mutations (Messiaen et al., 2000). These approaches include the optimized protein truncation test (an in vitro coupled transcription/translation synthesis assay designed as a tool to detect mutations that lead to premature translational termination), FISH, direct sequencing, RT-PCR with Southern blot analysis, and/or cytogenetic analysis (Messiaen et al., 2000; Boyd et al., 2009).

Molecular testing of *NF1* mutations is used mainly for definitive diagnosis in suspicious cases, and for prenatal or preimplantation genetic diagnosis. However, it is not indicated for the routine clinical care of patients with NF1. Because of the lack of genotype-phenotype correlations, genetic testing, although useful for confirming the diagnosis of NF1, does not predict disease severity or outcome.

Neurofibromatosis 2 is also a dominantly inherited tumor predisposition syndrome characterized by the development of multiple schwannomas, meningiomas, and ependymomas. Most patients present with hearing loss due to inevitable development of schwannomas affecting both vestibulocochlear (eighth) nerves (Evans, 2009a, 2009b).

NF2 is caused by mutations in the *NF2* gene on chromosome 22. More than 50% of patients have new mutations, and about one third are mosaic for the underlying disease. Germ-line mutations are most frequently truncating mutations (nonsense and frameshifts) that are associated with the most severe disease. However, single and multiple exon deletions may cause mild disease. Most mutations in *NF2* found on sequence analysis are pathogenic. Some missense mutations or in-frame deletions may be harmless (Evans, 2009b). Diagnosis of NF2 is based on clinical criteria; molecular genetic testing for *NF2* mutations can confirm the diagnosis because *NF2* is the only gene known to be associated with this disease. Methods of genetic testing for NF2 include sequence analysis, mutation scanning, duplication/deletion testing, RT-PCR, real-time PCR, array comparative genomic hybridization, and combinations of these. Large deletions encompassing *NF2*, ring chromosome 22, and translocation disrupting *NF2* can be detected by cytogenetic analysis, and smaller deletions can be identified by FISH. Molecular testing may also be used for appropriate surveillance, earlier detection, and early intervention of disease among relatives at risk (Evans, 2009a, 2009b).

Schwannomatosis is a recently recognized third major form of NF, characterized by multiple nonvestibular schwannomas in the absence of meningiomas, intraspinal ependymomas, and other clinical signs of NF2. Schwannomatosis and NF2 are clinically and molecularly distinct (MacCollin et al., 2003), but their phenotypes frequently overlap. In contrast to patients with NF2, multiple tumors from the same individual with schwannomatosis do not share a constitutional mutation (Jacoby et al., 1997; Kaufman et al., 2003). Schwannomatosis-derived schwannomas have been shown to have truncating mutations of the *NF2* gene (Jacoby et al., 1997). Commercially available *NF2* mutational analysis does not help differentiate between schwannomatosis and NF2 (MacCollin et al., 1994; Moyhuddin et al., 2003). Definitive diagnosis of schwannomatosis and its distinction from NF2 await identification of the schwannomatosis locus or gene.

CANCERS OF UNKNOWN ORIGIN

Cancer of unknown primary (CUP) is defined by the presence of cytologically or histologically proven metastases, for which no primary tumor can be identified despite standardized and extensive diagnostic workup. It constitutes approximately 2% of all malignancies, of which 90% are adenocarcinoma (60% well to moderately differentiated and 29% poorly differentiated), 5% are squamous cell carcinoma, 5% are undifferentiated neoplasm on light microscopy (Horlings et al., 2008) and 1% neuroendocrine tumors (Hainsworth et al., 1988; Moertel et al., 1991). Accordingly, failure to identify the primary tumor theoretically incurs the risk for failure to administer appropriate systemic combination chemotherapy, as well as targeted molecular therapy. Although the metastatic pattern in these patients is often atypical, no direct evidence indicates that molecular genetic abnormalities in these tumors differ from those seen in metastatic cancers of known primary site. With expansion of tissue-specific targeted therapy, it is believed that patient prognosis can be better predicted when the primary site of metastatic tumors is assigned.

This has increased the need for identification of the tissue of origin, which further makes the immunohistochemical analysis a crucial component of clinical workup. However, the current success rate of the diagnostic workup, including clinical, radiologic, and extensive pathologic methods, varies between 20% and 30% (Horlings et al., 2008). Therefore, new methods are required to increase diagnostic accuracy.

The development of molecular technology that allows gene expression profiling of tumors provides an opportunity for improved diagnosis of patients with CUP. Quantitative reverse transcriptase polymerase chain reaction (RT-PCR) is a technique that allows gene expression profiling of FFPE tissue specimens, and therefore is a potential diagnostic tool with broad applicability. These techniques have enabled researchers to develop expression profiles unique to a wide variety of well-characterized primary cancers. The accuracy of diagnosis of primary site obtained by comparing these known unique signatures with those from unknown primary cancers is approximately 75% (Kandalaft & Gown, 2016). This is based on the finding that metastatic cancers retain at least the basic genetic signature found in their respective primary cancers. Gene expression profiling has also shown important potential diagnostic and therapeutic implications in CUP. The CUP colon cancer profile can be identified, and patients appear to respond well to current regimens for metastatic CRC (Varadhachary et al., 2008). Expression profiling of certain genes (e.g., *EGFR*, *cKIT/PDGFR*, *RAS*, *BCL2*, *Her/2neu*, and *p53*) and chromosomal abnormalities for CUP will benefit patients by revealing therapies that can be used to target these molecules (Pentheroudakis et al., 2007).

To date, several gene expression–based tests have demonstrated an increase in overall accuracy for the primary site of origin to 78% to 88% (Horlings et al., 2008). A few gene panels such as OncotypeDx and Pathwork Tissue of Origin Test have achieved FDA approval. However, the National Comprehensive Cancer Network (NCCN) panel has determined that gene expression profiling along with ICH has focused more on establishing a tissue of origin than on determining whether such identification leads to better outcomes in patients. Thus, although there is a diagnostic benefit to gene expression profiling, it is not recommended for the identification of tissue of origin as standard management in the diagnostic workup of patients with CUP at this time (NCCN 2018).

miRNA IN CANCER

MicroRNA (miRNA) are small, noncoding endogenous single-stranded RNAs comprising only 19 to 25 nucleotides in length but on average about 22 nucleotides in length. First described in 1993, these molecules are actively involved in the regulation of multiple physiologic and pathologic procedures in humans, animals, and plants. Recent studies have also demonstrated their key roles in the pathogenetic evolution, progression, and metastasis of carcinomas. miRNA expression profiling has been recently evaluated as a reliable diagnostic biomarker for differentiating between normal and tumor specimens. In addition to distinguishing normal from cancerous tissues, molecular markers can also be used to determine the tissue of origin in tumors of unknown primary (Lu et al., 2005). The miRNA expression enhances (oncogenic miRNA) or reduces (tumor suppressor) tumor growth as the tumor progresses and was found to be associated with drug resistance (Ali et al., 2010). Although some miRNAs are tumor-specific (Liang et al., 2007), miR-21 has proved to be the global oncogenic miRNA in many solid tumors (Gall et al., 2013; Hermansen et al., 2013; Si et al., 2013; Sicard et al., 2013; Tang et al., 2013; Yang et al., 2013). The miRNAs with oncogenic potential include miR-155, miR-17-92, and miR-217, but it is not limited to these alone. The level of expression of miR-155 is upregulated in various carcinomas (Yang et al., 2013, Zhang et al., 2012). However, they are specifically significant in pancreatic cancers, where they have prognostic relevance (Zhang et al., 2012). They can be used for early diagnosis, treatment, and prognosis.

Similarly, the miRNA let-7 family and miR-200 family is frequently downregulated in many types of cancer, suggesting their role as a general tumor suppressor (Bhutia et al., 2013). Low levels of let-7 miRNA49 have been shown to indicate poorer prognosis with shorter postoperative survival in human lung cancer (Xia et al., 2010). The tumor suppressor miR-34 is directly transactivated and induced by p53 signaling in the inhibition of human pancreatic cancer tumor-initiating cells (Vogt et al., 2011). The miR409-3p, miR-7, and miR93 panel can be used for early detection of colorectal cancer (Wang et al., 2015). Low expression of miR-34b and miR-129-3p are associated with a poor clinical outcome of gastric cancer patients, and hypermethylation of miR-129-2 and miR-34b CpG islands had a tendency to show poor clinicopathologic features.

CLINICAL APPLICATION OF NEXT-GENERATION SEQUENCING

Next-generation sequencing (NGS) has been applied to whole-genome sequencing (WGS), whole-exome sequencing (WES), and RNA profiling (RNA-Seq). High-throughput sequencing (i.e., NGS) technologies

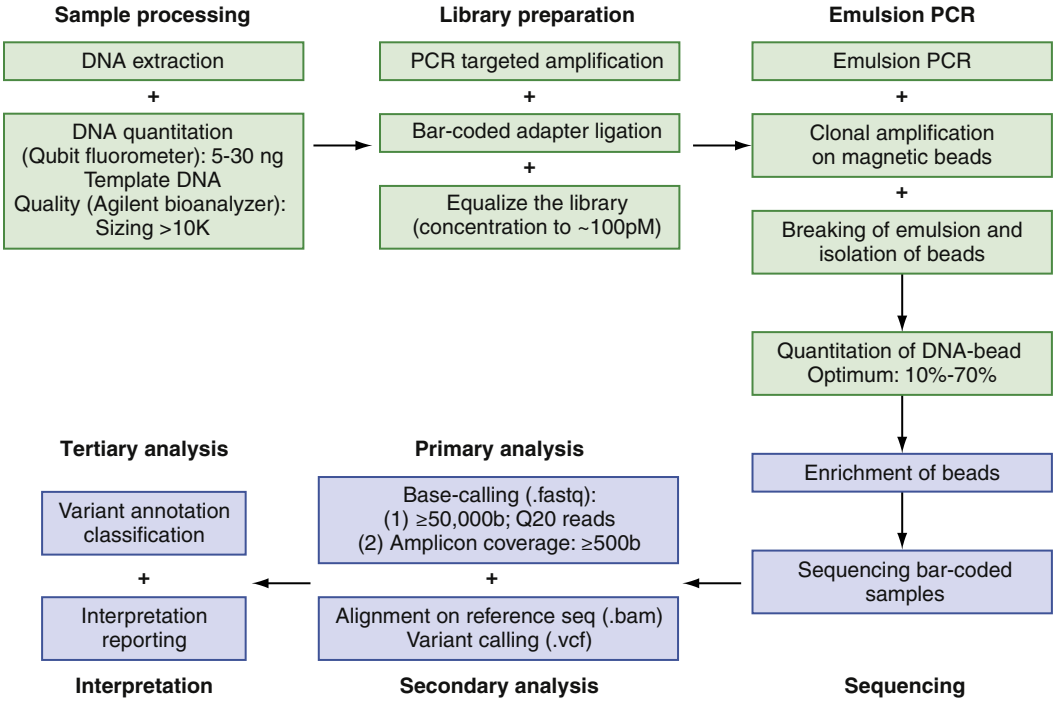

Figure 79.5 Workflow and data analysis of targeted sequencing by next-generation sequencing platforms for clinical applications.

parallelize the sequencing process of millions of reactions, producing thousands or millions of sequences concurrently (Metzker, 2010). A fundamental process of NGS is that clonally amplified DNA templates, or single DNA molecules, are sequenced in a massively parallel fashion in a flow cell (Fig. 79.5). As a result, the cost of DNA sequencing is significantly reduced to the point that it can routinely be applied in clinical settings.

Currently several platforms of NGS are available including Pacific Biosciences (single-molecular real-time sequencing), Ion Torrent (ion semiconductor), Illumina (sequencing by synthesis), 454 (pyrosequencing, see Chapter 68), SOLiD (sequencing by ligation). The two most commonly used NGS platforms in clinical laboratories are Ion Torrent PGM (Personal Genetic Machine) (Life Technology) and Illumina MiSeq, as both offer significant advantages such as read length (100 to 200 bp), accuracy (>98%), reads per run (up to 80 million), time per run (2 hours to 24 hours), cost per million bases (<$1), cost of equipment (<$100,000), and low concentration of DNA (especially FFPE).

Ion Torrent PGM sequencing is based on using standard sequencing chemistry with a semiconductor-based detection system (Mardis, 2013). This method of sequencing is based on the detection of hydrogen ions (H^+) that are released during DNA synthesis. By combining the speed and scalability of semiconductor technology with a system of measuring pH fluctuations produced during DNA synthesis in real-time, the Ion Torrent is able to directly turn genetic information into digital data. A variety of chips are available from 10 Mb to greater than 1 Gb, allowing highly accurate sequence data to be generated for 16 samples per run in less than 2 hours. With a raw accuracy rate of 99.5% and a detection sensitivity of around 5%, the Ion Torrent is a suitable platform for single-nucleotide variant (SNV) detection and mutational analysis. The Ion AmpliSeq Cancer Hotspot Panel v2 uses a single pool of primers to perform multiplex PCR for preparation of amplicon libraries from genomic "hot spot" regions that are frequently mutated in human cancer genes (Singh et al., 2013). It includes 207 amplicon and 2800 COSMIC point mutations and small indels in 50 oncogenes and tumor suppressor genes. It is compatible with FFPE samples and uses only 10 ng of DNA.

The Illumina MiSeq platform is a reversible terminator-based sequencing by synthesis chemistry (Mardis et al., 2013). MiSeq is a bench-top sequencer and delivers a high sequencing output and a fast data-generation rate. It is able to process larger numbers of samples and to decode larger and more complex genomes. The fluorescence generated during the DNA synthesis is captured digitally by image. The TruSeq Amplicon cancer panel developed by Illumina on the MiSeq platform is a single-tube multiplex PCR. It includes 212 amplicons from 48 cancer-related genes to detect point mutations and small indels. It is compatible with FFPE samples and runs 96 samples at one time. The disadvantage is that it takes a longer time (>48 hours) to generate sequencing data than Ion Torrent PGM.

Since NGS produces millions of reads, analysis of the data requires strong bioinformatics support (Meldrum et al., 2011). NGS data analysis can be divided into several processes: base calling, read alignment, variant calling, and variant annotation (see Fig. 79.5). Base calling is the identification of the specific nucleotide present at each position in a single sequencing read. Read alignment involves correctly positioning short DNA sequence reads (often 50 to 200 base pairs) along the genome in reference sequences. Variant calling is the detection of the DNA variants in the sequence analyzed as compared with a reference sequence. The accuracy of identifying variants greatly depends on the depth of sequence coverage, and increased coverage improves correct variant calling. Because some regions may have low sequence coverage or are difficult to sequence, it is important to visually examine the sequence alignment to resolve an ambiguous call or false call. Variant annotation adds information about each variant detected. For example, annotation pipelines will determine whether a variant is within or near a gene, where the variant is located within that gene (e.g., untranslated region, exon, intron), and whether the variant causes a change in an amino acid within the encoded protein. This process is facilitated by comparing with available databases (i.e., COMICS) and its potential impact on protein function. Finally the potential pathogenic variants have to be interpreted with correlation of clinical information (e.g., tumor types, pathology features) to determine their clinical significance.

NGS has been adopted in clinical diagnostic laboratories for genetic diagnosis and cancer stratification (Meldrum et al., 2011). Genetic changes in cancer genome serve as biomarkers for cancer diagnosis, prognosis, and treatment guidance (i.e., companion diagnosis) (Gonzalez de Castro et al., 2013). The utility of these markers has generally been demonstrated by randomized, controlled trials that select patients with the marker, and report significant improvements in outcomes compared among those with or without biomarkers or those with targeted therapy or with standard therapy. The National Comprehensive Cancer Network (NCCN) guidelines as well as many insurance companies have accepted testing genetic markers as the standard of care for cancer patients. It is expected that the diagnosis and treatment of many, if not all, cancers requires understanding the genomic landscape, with an increased understanding of the cancer genome and the development of new target-specific drugs.

Application of NGS in cancer genome testing faces several challenges. Cancer is considered a genetic disorder in which somatic mutations alter the critical signaling pathways leading to uncontrolled proliferation, invasion, and metastasis. These genetic changes range from a single nucleotide change, to structural chromosomal changes (insertions, deletions, rearrangements), to variations in copy number. However, only a portion of these changes are clinically significant in influencing the diagnosis, prognosis, and therapy. These critical changes are often confused with germ-line changes and high-frequency bystander variants (>90% frequency). Therefore, it is critical to filter out these noncritical variants. Clinical interpretation of these genetic changes requires understanding not only the function of these alterations but also documentation of the clinical importance, such as response to treatment, either clinically or experimentally. Another challenge is tumor

sample selection. Cancer cells are heterogeneous; therefore, small sampling of a large tumor may miss the critical but low-level mutations. Furthermore, background non-neoplastic cells may interfere with the detection of mutations harbored in a small number of tumor cells. This is especially true for small biopsy or fine-needle aspiration samples. The criteria of acceptable samples are based on the assay sensitivity (usually 5%) and coverage (usually >500×). In general, >10% tumor content or >1000 tumor cells for targeted sequencing are required. For all these reasons, molecular pathologists play a very important role in the entire process of NGS, including sample selection, quality control of NGS data, and final interpretation in the context of clinical relevance. It is anticipated that future molecular tumor boards will consist of a group of experts including pathologists, geneticists, experts in bioinformatics, oncologists, and so on, to jointly determine the result interpretation and patient management.

SELECTED REFERENCES

Aldape K, Burger PC, et al.: Clinicopathologic aspects of 1p/19q loss and the diagnosis of oligodendroglioma, *Arch Pathol Lab Med* 131:242–251, 2007.

Detection of 1p/19q loss greatly improved the ability to accurately diagnose oligodendrogliomas, in particular distinguishing it from other brain tumors, such as astrocytoma and mixed oligoastrocytoma as well as to predict prognosis.

El-Zammar OA, Zhang S, et al.: Comparison of FISH, PCR, and immunohistochemistry in assessing EGFR status in lung adenocarcinoma and correlation with clinicopathologic features, *Diagn Mol Pathol* 18:133–137, 2009.

Amplification and activation mutation of EGFR is associated with a number of cancers including lung cancer. This article compares various methods used in identifying the altered copy number, mutation, and protein expression levels in lung cancer.

Halling KC, Kipp BR: Bladder cancer detection using FISH (UroVysion assay), *Adv Anat Pathol* 15:279–286, 2008.

UroVysion is developed and FDA approved to assist in the detection of chromosomal abnormality for bladder cancer in urine specimens. This article discusses its utility in bladder cancer detection and treatment follow-up.

Kato K: Algorithm for in vitro diagnostic multivariate index assay, *Breast Cancer* 16:248–251, 2009.

This article reviews the current knowledge for the marker development and their application in breast cancer including precurrence prediction with Oncotype, a 21-gene panel, and Mammaprint, a 70-gene-microarray test, in women who have invasive breast cancer.

Oakman C, Bessi S, et al.: Recent advances in systemic therapy: new diagnostics and biological predictors of outcome in early breast cancer, *Breast Cancer Res* 11:205, 2009.

This article reviews the current knowledge for the marker development and their application in breast cancer including precurrence prediction with Oncotype, a 21-gene panel, and Mammaprint, a 70-gene-microarray test, in women who have invasive breast cancer.

Access the complete reference list online at Elsevier eBooks for Practicing Clinicians.

REFERENCES

Abdel-Rahman WM, Peltomaki P: Molecular basis and diagnostics of hereditary colorectal cancers, *Ann Med* 36:379–388, 2004.

Abraham SC, Wu TT, et al.: Distinctive molecular genetic alterations in sporadic and familial adenomatous polyposis-associated pancreatoblastomas: frequent alterations in the APC/beta-catenin pathway and chromosome 11p, *Am J Pathol* 159:1619–1627, 2001.

Abraham SC, Wu TT, et al.: Genetic and immunohistochemical analysis of pancreatic acinar cell carcinoma: frequent allelic loss on chromosome 11p and alterations in the APC/beta-catenin pathway, *Am J Pathol* 160:953–962, 2002.

Afar DE, Vivanco I, et al.: Catalytic cleavage of the androgen-regulated TMPRSS2 protease results in its secretion by prostate and prostate cancer epithelia, *Cancer Res* 61:1686–1692, 2001.

Al-Ahmadie HA, Iyer G, et al.: Somatic mutation of fibroblast growth factor receptor-3 (FGFR3) defines a distinct morphological subtype of high-grade urothelial carcinoma, *J Pathol* 224:270–279, 2011.

Alam S, Tortora J, et al.: Prostate cancer genomics: comparing results from three molecular assays, *Can J Urol* 26(3):9758–9762, 2019.

Alhopuro P, Alazzouzi H, et al.: SMAD4 levels and response to 5-fluorouracil in colorectal cancer, *Clin Cancer Res* 11:6311–6316, 2005.

Ali S, Ahmad A, et al.: Gemcitabine sensitivity can be induced in pancreatic cancer cells through modulation of miR-200 and miR-21 expression by curcumin or its analogue CDF, *Cancer Res* 70:3606–3617, 2010.

Amary MF, Ye H, et al.: Detection of USP6 gene rearrangement in nodular fasciitis: an important diagnostic tool, *Virchows Arch* 463:97–98, 2013.

Antonescu CR, Le Loarer F, et al.: Novel YAP1-TFE3 fusion defines a distinct subset of epithelioid hemangioendothelioma, *Genes Chromosomes Cancer* 52:775–784, 2013.

Antonescu CR, Nafa K, et al.: EWS-CREB1: a recurrent variant fusion in clear cell sarcoma—association with gastrointestinal location and absence of melanocytic differentiation, *Clin Cancer Res* 12:5356–5362, 2006.

Arbajian E, Magnusson L, et al.: A benign vascular tumor with a new fusion gene: EWSR1-NFATC1 in hemangioma of the bone, *Am J Surg Pathol* 37:613–616, 2013.

Argani P, Antonescu CR, et al.: Primary renal neoplasms with the ASPL-TFE3 gene fusion of alveolar soft part sarcoma: a distinctive tumor entity previously included among renal cell carcinomas of children and adolescents, *Am J Pathol* 159:179–192, 2001.

Argani P, Antonescu CR, et al.: PRCC-TFE3 renal carcinomas: morphologic, immunohistochemical, ultrastructural, and molecular analysis of an entity associated with the t(X;1)(p11.2;q21), *Am J Surg Pathol* 26:1553–1566, 2002.

Argani P, Ladanyi M: Recent advances in pediatric renal neoplasia, *Adv Anat Pathol* 10:243–260, 2003a.

Argani P, Ladanyi M: Distinctive neoplasms characterised by specific chromosomal translocations comprise a significant proportion of paediatric renal cell carcinomas, *Pathology* 35:492–498, 2003b.

Argani P, Lae M, et al.: Renal carcinomas with the t(6;11)(p21;q12). Clinicopathologic features and demonstration of the specific Alpha-TFEB gene fusion by immunohistochemistry, RT-PCR, and DNA-PCR, *Am J Surg Pathol* 29:230–240, 2005.

Argani P, Lae M, et al.: Translocation carcinomas of the kidney after chemotherapy in childhood, *J Clin Oncol* 24:1529–1534, 2006.

Argani P, Olgac S, et al.: Xp11 translocation renal cell carcinoma in adults: expanded clinical, pathologic, and genetic spectrum, *Am J Surg Pathol* 31:1149–1160, 2007.

Argani P, Yonescu R, et al.: Molecular confirmation of the t(6;11)(p21;q12) renal cell carcinomas in archival paraffin embedded material using a break-apart TFEB FISH assay expands its clinicopathologic spectrum, *Am J Surg Pathol* 36:1516–1526, 2012.

Arun D, Gutmann DH: Recent advances in neurofibromatosis type 1, *Curr Opin Neurol* 17:101–105, 2004.

Balitzer D, Joseph NM, et al.: Immunohistochemical and molecular features of cholangiolocellular carcinoma are similar to well-differentiated intrahepatic cholangiocarcinoma, *Mod Pathol*, 2019. [Epub ahead of print].

Bang YJ, Van Cutsem E, et al.: Trastuzumab in combination with chemotherapy versus chemotherapy alone for treatment of HER2-positive advanced gastric or gastro-oesophageal junction cancer (ToGA): a phase 3, open-label, randomised controlled trial, *Lancet* 376:687–697, 2010.

Bao T, Davidson NE: Gene expression profiling of breast cancer, *Adv Surg* 42:249–260, 2008.

Barault L, Veyrie N, et al.: Mutations in the RAS-MAPK, PIK (phosphatidylinositol-3-OH kinase) signaling network correlate with poor survival in a population-based series of colon cancers, *Int J Cancer* 122:2255–2259, 2008.

Bass AJ, Thorsson V, et al.: Comprehensive molecular characterization of gastric adenocarcinoma, *Nature* 513:202–209, 2014.

Bell DW, Varley JM, et al.: Heterozygous germ line hCHK2 mutations in Li-Fraumeni syndrome, *Science* 286:2528–2531, 1999.

Bengtsson B, Stål P1, et al.: Characteristics and outcome of hepatocellular carcinoma in patients with NAFLD without cirrhosis, *Liver Int* 39(6):1098–1108, 2019.

Benn DE, Gimenez-Roqueplo AP, et al.: Clinical presentation and penetrance of pheochromocytoma/paraganglioma syndromes, *J Clin Endocrinol Metab* 91:827–836, 2006.

Bertotti A, Papp E, et al.: The genomic landscape of response to EGFR blockade in colorectal cancer, *Nature* 526:263–267, 2015.

Berx G, Becker KF, et al.: Mutations of the human E-cadherin (CDH1) gene, *Hum Mutat* 12:226–237, 1998.

Bhutia YD, Hung SW, et al.: Differential processing of let-7a precursors influences RRM2 expression and chemosensitivity in pancreatic cancer: role of LIN-28 and SET oncoprotein, *PloS One* 8:e53436, 2013.

Billerey C, Chopin D, et al.: Frequent FGFR3 mutations in papillary non-invasive bladder (pTa) tumors, *Am J Pathol* 158:1955–1959, 2001.

Billings SD, Giblen G, et al.: Superficial low-grade fibromyxoid sarcoma (Evans tumor): a clinicopathologic analysis of 19 cases with a unique observation in the pediatric population, *Am J Surg Pathol* 29:204–210, 2005.

Bioulac-Sage P, Balabaud C, et al.: Subtype classification of hepatic adenoma, *Dig Surg* 27:39–45, 2010.

Bioulac-Sage P, Rebouissou S, et al.: Clinical, morphologic, and molecular features defining so called telangiectatic focal nodular hyperplasias of the liver, *Gastroenterology* 128:1211–1218, 2005.

Bjerkehagen B, Dietrich C, et al.: Extraskeletal myxoid chondrosarcoma: multimodal diagnosis and identification of a new cytogenetic subgroup characterized by t(9;17)(q22;q11), *Virchows Arch* 435:524–530, 1999.

Bloomston M, Frankel WL, et al.: MicroRNA expression patterns to differentiate pancreatic adenocarcinoma from normal pancreas and chronic pancreatitis, *J Am Med Assoc* 297:1901–1908, 2007.

Boparai KS, Dekker E, et al.: Hyperplastic polyps and sessile serrated adenomas as a phenotypic expression of MYH-associated polyposis, *Gastroenterology* 135:2014–2018, 2008.

Bourke B, Broderick A, et al.: Peutz-Jeghers syndrome and management recommendations, *Clin Gastroenterol Hepatol* 4:1550, 2006. author reply 1550.

Brandi ML, Gagel RF, et al.: Guidelines for diagnosis and therapy of MEN type 1 and type 2, *J Clin Endocrinol Metab* 86:5658–5671, 2001.

Brauckhoff M, Gimm O, et al.: Papillary thyroid carcinoma in patients with RET proto-oncogene germline mutation, *Thyroid* 12:557–561, 2002.

Breneman JC, Lyden E, et al.: Prognostic factors and clinical outcomes in children and adolescents with metastatic rhabdomyosarcoma—a report from the Intergroup Rhabdomyosarcoma Study IV, *J Clin Oncol* 21:78–84, 2003.

Bridge JA, Kanamori M, et al.: Fusion of the ALK gene to the clathrin heavy chain gene, CLTC, in inflammatory myofibroblastic tumor, *Am J Pathol* 159:411–415, 2001.

Bruder E, Passera O, et al.: Morphologic and molecular characterization of renal cell carcinoma in children and young adults, *Am J Surg Pathol* 28:1117–1132, 2004.

Bubendorf L, Kononen J, et al.: Survey of gene amplifications during prostate cancer progression by high-throughput fluorescence in situ hybridization on tissue microarrays, *Cancer Res* 59:803–806, 1999.

Buchholz M, Gress TM: Molecular changes in pancreatic cancer, *Expert Rev Anticancer Ther* 9:1487–1497, 2009.

Butrynski JE, D'Adamo DR, et al.: Crizotinib in ALK-rearranged inflammatory myofibroblastic tumor, *N Engl J Med* 363:1727–1733, 2010.

Calderaro J, Couchy G, et al.: Histological subtypes of hepatocellular carcinoma are related to gene mutations and molecular tumor classification, *J Hepatol* 67:727–738, 2017.

Caldas C, Hahn SA, et al.: Frequent somatic mutations and homozygous deletions of the p16 (MTS1) gene in pancreatic adenocarcinoma, *Nat Genet* 8:27–32, 1994.

Callender GG, Rich TA, et al.: Multiple endocrine neoplasia syndromes, *Surg Clin North Am* 88:863–895, 2008. viii.

Cancer Genome Atlas Research Network: Integrated genomic characterization of papillary thyroid carcinoma, *Cell* 159:676–690, 2014.

Carcao MD, Taylor GP, et al.: Renal-cell carcinoma in children: a different disorder from its adult counterpart? *Med Pediatr Oncol* 31:153–158, 1998.

Cardarella S, Ortiz TM, et al.: The introduction of systematic genomic testing for patients with non-small-cell lung cancer, *J Thorac Oncol* 7:1767–1774, 2012.

Casuscelli J, Weinhold N, et al.: Genomic landscape and evolution of metastatic chromophobe renal cell carcinoma, *JCI Insight* 2:92688, 2017.

Cerveira N, Ribeiro FR, et al.: TMPRSS2-ERG gene fusion causing ERG overexpression precedes chromosome copy number changes in prostate carcinomas and paired HGPIN lesions, *Neoplasia* 8:826–832, 2006.

Chaft JE, Rekhtman N, et al.: ALK- rearranged lung cancer: adenosquamous lung cancer masquerading as pure squamous carcinoma, *J Thorac Oncol* 7:768–769, 2012.

Chandrasekharappa SC, Teh BT: Clinical and molecular aspects of multiple endocrine neoplasia type 1, *Front Horm Res* 28:50–80, 2001.

Cher ML, Bova GS, et al.: Genetic alterations in untreated metastases and androgen-independent prostate cancer detected by comparative genomic hybridization and allelotyping, *Cancer Res* 56:3091–3102, 1996.

Chew SL: Use of mutation analysis in endocrine neoplasia syndromes, *Clin Med* 9:362–363, 2009.

Cho KR: Shih IeM: ovarian cancer, *Annu Rev Pathol* 4:287–313, 2009.

Choi R, et al.: Current and future molecular diagnostics of gastric cancer, *Expert Rev Mol Diagn* 19:1–12, 2019.

Chung DC, Rustgi AK: The hereditary nonpolyposis colorectal cancer syndrome: genetics and clinical implications, *Ann Intern Med* 138:560–570, 2003.

Clark JM: The epidemiology of nonalcoholic fatty liver disease in adults, *J Clin Gastroenterol* 40(Suppl 1):S5–S10, 2006.

Clark J, Merson S, et al.: Diversity of TMPRSS2-ERG fusion transcripts in the human prostate, *Oncogene* 26:2667–2673, 2007.

Coate LE, John T, et al.: Molecular predictive and prognostic markers in non-small-cell lung cancer, *Lancet Oncol* 10:1001–1010, 2009.

Cobrinik D, Dowdy SF, et al.: The retinoblastoma protein and the regulation of cell cycling, *Trends Biochem Sci* 17:312–315, 1992.

Coindre JM, Hostein I, et al.: Diagnosis of clear cell sarcoma by real-time reverse transcriptase-polymerase chain reaction analysis of paraffin embedded tissues: clinicopathologic and molecular analysis of 44 patients from the French sarcoma group, *Cancer* 107:1055–1064, 2006.

Coindre JM, Pedeutour F, et al.: Well-differentiated and dedifferentiated liposarcomas, *Virchows Arch* 456:167–179, 2010.

Columbo M1, Forner A1, et al.: EASL Clinical Practice Guidelines on the management of benign liver tumours, *J Hepatol* 65(2):386–398, 2016.

Croitoru ME, Cleary SP, et al.: Germline MYH mutations in a clinic-based series of Canadian multiple colorectal adenoma patients, *J Surg Oncol* 95:499–506, 2007.

Crossey PA, Richards FM, et al.: Identification of intragenic mutations in the von Hippel-Lindau disease tumor suppressor gene and correlation with disease phenotype, *Hum Mol Genet* 3:1303–1308, 1994.

Cuschieri K, Wentzensen N: Human papillomavirus mRNA and p16 detection as biomarkers for the improved diagnosis of cervical neoplasia, *Cancer Epidemiol Biomarkers Prev* 17:2536–2545, 2008.

Cuzick J, Arbyn M, et al.: Overview of human papillomavirus-based and other novel options for cervical cancer screening in developed and developing countries, *Vaccine* 26(Suppl 10):K29–K41, 2008.

Cuzick J, Berney DM, et al.: Prognostic value of cell cycle progression signature for a prostate cancer death in a conservatively managed needle biopsy cohort, *Br J Cancer* 106:1095–1099, 2012.

Da Silva AM, Maciel RM, et al.: A novel germ-line point mutation in RET exon 8 (Gly(533)Cys) in a large kindred with familial medullary thyroid carcinoma, *J Clin Endocrinol Metab* 88:5438–5443, 2003.

Dal Cin P, Kozakewich HP, et al.: Variant translocations involving 16q22 and 17p13 in solid variant and extraosseous forms of aneurysmal bone cyst, *Genes Chromosomes Cancer* 28:233–234, 2000.

Davicioni E, Finckenstein FG, et al.: Identification of a PAX-FKHR gene expression signature that defines molecular classes and determines the prognosis of alveolar rhabdomyosarcomas, *Cancer Res* 66:6936–6946, 2006.

Davies H, Bignell GR, et al.: Mutations of the BRAF gene in human cancer, *Nature* 417:949–954, 2002.

Davis CF, Ricketts CJ, et al.: The somatic genomic landscape of chromophobe renal cell carcinoma, *Canc Cell* 26:319–330, 2014.

De Alava E, Gerald WL: Molecular biology of the Ewing's sarcoma/primitive neuroectodermal tumor family, *J Clin Oncol* 18:204–213, 2000.

De Vos M, Hayward B, et al.: Phenotype associated with recessively inherited mutations in DNA mismatch repair (MMR) genes, *Biochem Soc Trans* 33(Pt 4):718–720, 2005.

Debelenko LV, Arthur DC, et al.: Identification of CARS-ALK fusion in primary and metastatic lesions of an inflammatory myofibroblastic tumor, *Lab Invest* 83:1255–1265, 2003.

Debelenko LV, Raimondi SC, et al.: Renal cell carcinoma with novel VCL-ALK fusion: new representative of ALK-associated tumor spectrum, *Mod Pathol* 24:430–442, 2011.

Debiec-Rychter M, Marynen P, et al.: ALK-ATIC fusion in urinary bladder inflammatory myofibroblastic tumor, *Genes Chromosomes Cancer* 38:187–190, 2003.

Delahunt B, Cheville JC, Martignoni G, et al.: The International Society of Urological Pathology (ISUP) grading system for renal cell carcinoma and other prognostic parameters, *Am J Surg Pathol* 37:e33–e47, 2013.

Demunter A, Stas M, et al.: Analysis of N- and K-ras mutations in the distinctive tumor progression phases of melanoma, *J Invest Dermatol* 117:1483–1489, 2001.

De Roock W, Claes B, et al.: Effects of KRAS, BRAF, NRAS, and PIK3CA mutations on the efficacy of cetuximab plus chemotherapy in chemotherapy-refractory metastatic colorectal cancer: a retrospective consortium analysis, *Lancet Oncol* 11(8):753–762, 2010.

Di Nicolantonio F, Martini M, et al.: Wild-type BRAF is required for response to panitumumab or cetuximab in metastatic colorectal cancer, *J Clin Oncol* 26:5705–5712, 2008.

Dillhoff M, Liu J, et al.: MicroRNA-21 is overexpressed in pancreatic cancer and a potential predictor of survival, *J Gastrointest Surg* 12:2171–2176, 2008.

Domingo E, Church DN, et al.: Evaluation of PIK3CA mutation as a predictor of benefit from nonsteroidal anti-inflammatory drug therapy in colorectal cancer, *J Clin Oncol* 31:4297–4305, 2013.

Dowsett M, Sestak I, et al.: Comparison of PAM50 Risk of Recurrence Score with Oncotype DX and IHC4 for predicting risk of distant recurrence after endocrine therapy, *J Clin Oncol* 31:2783–2790, 2013.

Dreijerink KM, Lips CJ, et al.: Multiple endocrine neoplasia type 1: a chromatin writer's block, *J Intern Med* 266:53–59, 2009.

Drukker CA, Bueno-de-Mesquita JM, et al.: A prospective evaluation of a breast cancer prognosis signature in the observational RASTER study, *Int J Cancer* 133:929–936, 2013.

Dvorakova S, Vaclavikova E, et al.: Exon 5 of the RET proto-oncogene: a newly detected risk exon for familial medullary thyroid carcinoma, a novel germ-line mutation Gly321Arg, *J Endocrinol Invest* 28:905–909, 2005.

Eng C: PTEN: one gene, many syndromes, *Hum Mutat* 22:183–198, 2003.

Eng C, Clayton D, et al.: The relationship between specific RET proto-oncogene mutations and disease phenotype in multiple endocrine neoplasia type 2. International RET mutation consortium analysis, *J Am Med Assoc* 276:1575–1579, 1996.

Engelman JA, Zejnullahu K, et al.: MET amplification leads to gefitinib resistance in lung cancer by activating ERBB3 signaling, *Science* 316:1039–1043, 2007.

Erickson-Johnson MR, Chou MM, et al.: Nodular fasciitis: a novel model of transient neoplasia induced by MYH9-USP6 gene fusion, *Lab Invest* 91:1427–1433, 2011.

Errani C, Sung YS, et al.: Monoclonality of multifocal epithelioid hemangioendothelioma of the liver by analysis of WWTR1-CAMTA1 breakpoints, *Cancer Genet* 205:12–17, 2012.

Errani C, Zhang L, et al.: A novel WWTR1-CAMTA1 gene fusion is a consistent abnormality in epithelioid hemangioendothelioma of different anatomic sites, *Genes Chromosomes Cancer* 50:644–653, 2011.

Eschrich S, Yang I, et al.: Molecular staging for survival prediction of colorectal cancer patients, *J Clin Oncol* 23:3526–3535, 2005.

Evans DG: Neurofibromatosis 2 [Bilateral acoustic neurofibromatosis, central neurofibromatosis, NF2, neurofibromatosis type II], *Genet Med* 11:599–610, 2009a.

Evans DG: Neurofibromatosis type 2 (NF2): a clinical and molecular review, *Orphanet J Rare Dis* 4(16), 2009b.

Evans HL: Low-grade fibromyxoid sarcoma: a clinicopathologic study of 33 cases with long-term follow-up, *Am J Surg Pathol* 35:1450–1462, 2011.

Farges O, Dokmak S: Malignant transformation of liver adenoma: an analysis of the literature, *Dig Surg* 27:32–38, 2010.

Fearon ER, Vogelstein B: A genetic model for colorectal tumorigenesis, *Cell* 61:759–767, 1990.

Febbo PG, Ladanyi M, et al.: NCCN Task Force report: evaluating the clinical utility of tumor markers in oncology, *J Natl Compr Canc Netw* 9(Suppl 5):S1–S32, 2011.

Ferlay JBF, Pisani P, Parkin DM: Globocan 2002: cancer incidence, mortality and prevalence worldwide, IARC CancerBase, no. 5, version 2.0, Lyon, France, 2004, IARC Press.

Fitzgerald RC, Caldas C: E-cadherin mutations and hereditary gastric cancer: prevention by resection? *Dig Dis* 20:23–31, 2002.

Fitzgerald JM, Ramchurren N, et al.: Identification of H-ras mutations in urine sediments complements cytology in the detection of bladder tumors, *J Natl Cancer Inst* 87:129–133, 1995.

Fondevila C, Metges JP, et al.: p53 and VEGF expression are independent predictors of tumor recurrence and survival following curative resection of gastric cancer, *Br J Cancer* 90:206–215, 2004.

Franko J, Feng W, et al.: Non-functional neuroendocrine carcinoma of the pancreas: incidence, tumor biology, and outcomes in 2158 patients, *J Gastrointest Surg* 14:541–548, 2010.

Frank-Raue K, Buhr H, et al.: Long-term outcome in 46 gene carriers of hereditary medullary thyroid carcinoma after prophylactic thyroidectomy: impact of individual RET genotype, *Eur J Endocrinol* 155:229–236, 2006.

Frattini M, Saletti P, et al.: PTEN loss of expression predicts cetuximab efficacy in metastatic colorectal cancer patients, *Br J Cancer* 97:1139–1145, 2007.

Freedland SJ, Gerber L, et al.: Prognostic utility of cell cycle progression score in men with prostate cancer after primary external beam radiation therapy, *Int J Radiat Oncol Biol Phys* 86:848–853, 2013.

Fromont G, Godet J, et al.: 8q24 amplification is associated with Myc expression and prostate cancer progression and is an independent predictor of recurrence after radical prostatectomy, *Hum Pathol* 44:1617–1623, 2013.

Fry LC, Monkemuller K, et al.: Molecular markers of pancreatic cancer: development and clinical relevance, *Langenbeck's Arch Surg* 393:883–890, 2008.

Garnett MJ, Rana S, et al.: Wild-type and mutant B-RAF activate C-RAF through distinct mechanisms involving heterodimerization, *Mol Cell* 20:963–969, 2005.

Gatalica Z, Torlakovic E: Pathology of the hereditary colorectal carcinoma, *Fam Cancer* 7:15–26, 2008.

Geller JI, Argani P, et al.: Translocation renal cell carcinoma: lack of negative impact due to lymph node spread, *Cancer* 112:1607–1616, 2008.

Ghadimi BM, Grade M, et al.: Effectiveness of gene expression profiling for response prediction of rectal adenocarcinomas to preoperative chemoradiotherapy, *J Clin Oncol* 23:1826–1838, 2005.

Gilks CB, Prat J: Ovarian carcinoma pathology and genetics: recent advances, *Hum Pathol* 40:1213–1223, 2009.

Gill AJ, Pachter NS, Chou A: Renal tumors associated with germline SDHB mutation show distinctive morphology, *Am J Surg Pathol* 35:1578–1585, 2011.

Gimm O, Marsh DJ, et al.: Germline dinucleotide mutation in codon 883 of the RET proto-oncogene in multiple endocrine neoplasia type 2B without codon 918 mutation, *J Clin Endocrinol Metab* 82:3902–3904, 1997.

Giovannetti E, Del Tacca M, et al.: Transcription analysis of human equilibrative nucleoside transporter-1 predicts survival in pancreas cancer patients treated with gemcitabine, *Cancer Res* 66:3928–3935, 2006.

Gnant M, Filipits M, et al.: Predicting distant recurrence in receptor-positive breast cancer patients with limited clinicopathological risk: using the PAM50 Risk of Recurrence score in 1478 postmenopausal patients of the ABCSG-8 trial treated with adjuvant endocrine therapy alone, *Ann Oncol* 25:339–345, 2014.

Gnarra JR, Tory K, et al.: Mutations of the VHL tumor suppressor gene in renal carcinoma, *Nat Genet* 7:85–90, 1994.

Gonzalez de Castro D, Clarke PA, et al.: Personalized cancer medicine: molecular diagnostics, predictive biomarkers, and drug resistance, *Clin Pharmacol Ther* 93:252–259, 2013.

Grady WM: CIMP and colon cancer gets more complicated, *Gut* 56:1498–1500, 2007.

Gray-Schopfer V, Wellbrock C, et al.: Melanoma biology and new targeted therapy, *Nature* 445:851–857, 2007.

Greco FA, Hainsworth JD: Cancer of Unkonwn primary site. In DeVita VT, et al.: *Principles & practice of Oncology*, ed 10th, Philadelphia, 2014, Lippincott Williams & Wilkins, pp 1720–1737.

Green WM, Yonescu R, et al.: Utilization of a TFE3 break-apart FISH assay in a renal tumor consultation service, *Am J Surg Pathol* 37:1150–1163, 2013.

Griffin CA, Hawkins AL, et al.: Recurrent involvement of 2p23 in inflammatory myofibroblastic tumors, *Cancer Res* 59:2776–2780, 1999.

Gu M, Kim D, et al.: Analysis of microsatellite instability, protein expression and methylation status of hMLH1 and hMSH2 genes in gastric carcinomas, *Hepato-Gastroenterology* 56:899–904, 2009.

Guilford P, Hopkins J, et al.: E-cadherin germline mutations in familial gastric cancer, *Nature* 392:402–405, 1998.

Gupta N, Srinivasan R, Rajwanshi A: Functional biomarkers in cervical precancer: an overview, *Diagn Cytopathol* 38:618–623, 2010.

Hahn SA, Hoque AT, et al.: Homozygous deletion map at 18q21.1 in pancreatic cancer, *Cancer Res* 56:490–494, 1996a.

Hahn SA, Schutte M, et al.: DPC4, a candidate tumor suppressor gene at human chromosome 18q21.1, *Science* 271:350–353, 1996b.

Hainsworth JD, Johnson DH, et al.: Poorly differentiated neuroendocrine carcinoma of unkown primary site: a newly recognized clinicopathologic entity, *Ann Intern Med* 109:364–371, 1988.

Hameed M: Small round cell tumors of bone, *Arch Pathol Lab Med* 131:192–204, 2007.

Hawksworth D, Ravindranath L, et al.: Overexpression of C-MYC oncogene in prostate cancer predicts biochemical recurrence, *Prostate Cancer Prostatic Dis* 13:311–315, 2010.

Hayden JD, Cawkwell L, et al.: Prognostic significance of microsatellite instability in patients with gastric carcinoma, *Eur J Cancer* 33:2342–2346, 1997.

Heimann P, Devalck C, et al.: Alveolar soft-part sarcoma: further evidence by FISH for the involvement of chromosome band 17q25, *Genes Chromosomes Cancer* 23:194–197, 1998.

Heimann P, Housni HE, et al.: Fusion of a novel gene, RCC17, to the TFE3 gene in t(X;17)(p11.2;q25.3)-bearing papillary renal cell carcinomas, *Cancer Res* 61:4130–4135, 2001.

Helleday T, Bryant HE, et al.: Poly(ADP-ribose) polymerase (PARP-1) in homologous recombination and as a target for cancer therapy, *Cell Cycle* 4:1176–1178, 2005.

Hermans KG, van Marion R, et al.: TMPRSS2:ERG fusion by translocation or interstitial deletion is highly relevant in androgen-dependent prostate cancer, but is bypassed in late-stage androgen receptor-negative prostate cancer, *Cancer Res* 66:10658–10663, 2006.

Hermansen SK, Dahlrot RH, et al.: MiR-21 expression in the tumor cell compartment holds unfavorable prognostic value in gliomas, *J Neuro Oncol* 111:71–81, 2013.

Hernandez-Marti MJ, Orellana-Alonso C, et al.: Renal adenocarcinoma in an 8-year-old child, with a t(X;17)(p11.2;q25), *Cancer Genet Cytogenet* 83:82–83, 1995.

Herrington CS: Recent advances in molecular gynaecological pathology, *Histopathology* 55:243–249, 2009.

Hiraga H, Nojima T, et al.: Establishment of a new continuous clear cell sarcoma cell line. Morphological and cytogenetic characterization and detection of chimaeric EWS/ATF-1 transcripts, *Virchows Arch* 431:45–51, 1997.

Hirota S, Isozaki K, et al.: Gain-of-function mutations of c-kit in human gastrointestinal stromal tumors, *Science* 279:577–580, 1998.

Hisaoka M, Ishida T, et al.: Clear cell sarcoma of soft tissue: a clinicopathologic, immunohistochemical, and molecular analysis of 33 cases, *Am J Surg Pathol* 32:452–460, 2008.

Hobert JA, Eng C: PTEN hamartoma tumor syndrome: an overview, *Genet Med* 11:687–694, 2009.

Hoimes CJ, Moyer MT, Saif MW: Biomarkers for early detection and screening in pancreatic cancer. Highlights from the 45th ASCO annual meeting. Orlando, FL, USA. May 29-June 2, 2009, *JOP* 10:352–356, 2009.

Holmang S, Andius P, et al.: Stage progression in Ta papillary urothelial tumors: relationship to grade, immunohistochemical expression of tumor markers, mitotic frequency and DNA ploidy, *J Urol* 165:1124–1128, 2001. discussion 1128–1130.

Holmang S, Hedelin H, et al.: Recurrence and progression in low grade papillary urothelial tumors, *J Urol* 162:702–707, 1999.

Hoorens A, Lemoine NR, et al.: Pancreatic acinar cell carcinoma. An analysis of cell lineage markers, p53 expression, and Ki-ras mutation, *Am J Pathol* 143:685–698, 1993.

Horlings HM, van Laar RK, et al.: Gene expression profiling to identify the histogenetic origin of metastatic adenocarcinomas of unknown primary, *J Clin Oncol* 26:4435–4441, 2008.

Horree N, Heintz AP, et al.: p16 is consistently expressed in endometrial tubal metaplasia, *Cell Oncol* 29:37–45, 2007.

Houillier C, Wang X, et al.: IDH1 or IDH2 mutations predict longer survival and response to temozolomide in low-grade gliomas, *Neurology* 75:1560–1566, 2010.

Hruban RH, Adsay NV: Molecular classification of neoplasms of the pancreas, *Hum Pathol* 40:612–623, 2009.

Hruban RH, Fukushima N: Pancreatic adenocarcinoma: update on the surgical pathology of carcinomas of ductal origin and PanINs, *Mod Pathol* 20:S61–S70, 2007.

Hruban RH, van Mansfeld AD, et al.: K-ras oncogene activation in adenocarcinoma of the human pancreas. A study of 82 carcinomas using a combination of mutant-enriched polymerase chain reaction analysis and allele-specific oligonucleotide hybridization, *Am J Pathol* 143:545–554, 1993.

Iacobuzio-Donahue CA, Fu B, et al.: DPC4 gene status of the primary carcinoma correlates with patterns of failure in patients with pancreatic cancer, *J Clin Oncol* 27:1806–1813, 2009.

Iacopetta B, Kawakami K, et al.: Predicting clinical outcome of 5-fluorouracil-based chemotherapy for colon cancer patients: is the CpG island methylator phenotype the 5-fluorouracil-responsive subgroup? *Int J Clin Oncol* 13:498–503, 2008.

Ian S: Hagemann: molecular testing in breast cancer: a guide to current practices, *Arch Path Lab Med* 40:815–824, 2016.

Ilic N, Utermark T, et al.: PI3K-targeted therapy can be evaded by gene amplification along the MYC-eukaryotic translation initiation factor 4E (eIF4E) axis, *Proc Natl Acad Sci U S A* 108:E699–E708, 2011.

Inamura K: Renal cell tumors: understanding their molecular pathological epidemiology and the 2016 WHO classification, *Int J Mol Sci* 18:2195–3009, 2017.

Isobe M, Emanuel BS, et al.: Localization of gene for human p53 tumor antigen to band 17p13, *Nature* 320:84–85, 1986.

Jacob S, Praz F: DNA mismatch repair defects: role in colorectal carcinogenesis, *Biochimie* 84:27–47, 2002.

Jacoby LB, Jones D, et al.: Molecular analysis of the NF2 tumor-suppressor gene in schwannomatosis, *Am J Hum Genet* 61:1293–1302, 1997.

Jagdis A, Rubin BP, et al.: Prospective evaluation of TLE1 as a diagnostic immunohistochemical marker in synovial sarcoma, *Am J Surg Pathol* 33:1743–1751, 2009.

Jain S, Lee P, et al.: Molecular genetics of hepatocellular neoplasia, *Am J Transl Res* 2:105–118, 2010a.

Jain S, Xu R, et al.: Molecular classification of soft tissue sarcomas and its clinical applications, *Int J Clin Exp Pathol* 3:416–428, 2010b.

Janeway KA, Albritton KH, et al.: Sunitinib treatment in pediatric patients with advanced GIST following failure of imatinib, *Pediatr Blood Cancer* 52:767–771, 2009.

Janeway KA, Kim SY, et al.: Defects in succinate dehydrogenase in gastrointestinal stromal tumors lacking KIT and PDGFRA mutations, *Proc Natl Acad Sci U S A* 108:314–318, 2011.

Jass JR: Colorectal polyposes: from phenotype to diagnosis, *Pathol Res Pract* 204:431–447, 2008.

Jayakumar R, Lanjewar S: Axiotis CA Loss of PTEN and increased pAkt expression distinguishes aggressive low-grade neuroendocrine tumors, *Ann Clin Lab Sci* 48:565–572, 2018.

Jemal A, Siegel R, et al.: Cancer statistics, 2008, *CA Cancer J Clin* 58:71–96, 2008.

Jemal A, Siegel R, et al.: Cancer statistics, 2009, *CA Cancer J Clin* 59:225–249, 2009.

Jenkins RB, Qian J, et al.: Detection of c-myc oncogene amplification and chromosomal anomalies in metastatic prostatic carcinoma by fluorescence in situ hybridization, *Cancer Res* 57:524–531, 1997.

Jiang F, Richter J, et al.: Chromosomal imbalances in papillary renal cell carcinoma: genetic differences between histological subtypes, *Am J Pathol* 153:1467–1473, 1998.

Jimenez RE, Warshaw AL, et al.: Sequential accumulation of K-ras mutations and p53 overexpression in the progression of pancreatic mucinous cyctic neoplasms to malignancy, *Ann Surg* 230:501–509, 1999.

Johansson B, Bardi G, et al.: Nonrandom chromosomal rearrangements in pancreatic carcinomas, *Cancer* 69:1674–1681, 1992.

Jones S, Zhang X, et al.: Core signaling pathways in human pancreatic cancers revealed by global genomic analyses, *Science* 321:1801–1806, 2008.

Joypaul BV, Newman EL, et al.: Expression of p53 protein in normal, dysplastic, and malignant gastric mucosa: an immunohistochemical study, *J Pathol* 170:279–283, 1993.

Kalemkerian GP, Narula N, et al.: Molecular testing guideline for the selection of lung cancer patients for treatment with targeted tyrosine kinase inhibitors: American Society of clinical oncology Endorsement summary of the College of American pathologists/international association for the study of lung cancer/association for molecular pathology clinical practice guideline update, *J Oncol Pract* 14:323–327, 2018.

Kandalaft PL, Gown AM: Practical applications in immunohistochemistry: carcinomas of unknown primary site, *Arch Pathol Lab Med* 140:508–523, 2016.

Kanemitsu S, Hisaoka M, et al.: Molecular detection of SS18-SSX fusion gene transcripts by cRNA in situ hybridization in synovial sarcoma using formalin-fixed, paraffin-embedded tumor tissue specimens, *Diagn Mol Pathol* 16:9–17, 2007.

Kanu OO, Mehta A, et al.: Glioblastoma multiforme: a review of therapeutic targets, *Expert Opin Ther Targets* 13:701–718, 2009.

Kaufman DL, Heinrich BS, et al.: Somatic instability of the NF2 gene in schwannomatosis, *Arch Neurol* 60:1317–1320, 2003.

Kavuri SM, Jain N, et al.: HER2 activating mutations are targets for colorectal cancer treatment, *Cancer Discov* 5:832–841, 2015.

Kelley JR, Duggan JM: Gastric cancer epidemiology and risk factors, *J Clin Epidemiol* 56:1–9, 2003.

Kerr NJ, Chun YH, et al.: Pancreatoblastoma is associated with chromosome 11p loss of heterozygosity and IGF2 overexpression, *Med Pediatr Oncol* 39:52–54, 2002.

Khleif SN, DeGregori J, et al.: Inhibition of cyclin D-CDK4/CDK6 activity is associated with an E2F-mediated induction of cyclin kinase inhibitor activity, *Proc Natl Acad Sci U S A* 93:4350–4354, 1996.

Kievit W, de Bruin JH, et al.: Current clinical selection strategies for identification of hereditary non-polyposis colorectal cancer families are inadequate: a meta-analysis, *Clin Genet* 65:308–316, 2004.

Kilpatrick SE, Bergman S, et al.: The usefulness of cytogenetic analysis in fine needle aspirates for the histologic subtyping of sarcomas, *Mod Pathol* 19:815–819, 2006.

Kisseljov F, Sakharova O, et al.: Cellular and molecular biological aspects of cervical intraepithelial neoplasia, *Int Rev Cell Mol Biol* 271:35–95, 2008.

Knezevic D, Goddard AD, et al.: Analytical validation of the Oncotype DX prostate cancer assay—a clinical RT-PCR assay optimized for prostate needle biopsies, *BMC Genom* 14:690–702, 2013.

Knezevich SR, McFadden DE, et al.: A novel ETV6-NTRK3 gene fusion in congenital fibrosarcoma, *Nat Genet* 18:184–187, 1998.

Kobel M, Huntsman D, Gilks CB: Critical molecular abnormalities in high-grade serous carcinoma of the ovary, *Expert Rev Mol Med* 10:e22, 2008.

Kolasa IK, Rembiszewska A, et al.: PTEN mutation, expression and LOH at its locus in ovarian carcinomas. Relation to TP53, K-RAS and BRCA1 mutations, *Gynecol Oncol* 103:692–697, 2006.

Kouvidou C, Latoufis C, et al.: Expression of Smad4 and TGF-beta2 in colorectal carcinoma, *Anticancer Res* 26:2901–2907, 2006.

Kovacs G, Wilkens L, Papp T: Differentiation between papillary and nonpapillary renal cell carcinomas by DNA analysis, *J Natl Cancer Inst* 81:527–530, 1989.

Kumari A, Srinivasan R, et al.: Positive regulation of human telomerase reverse transcriptase gene expression and telomerase activity by DNA methylation in pancreatic cancer, *Ann Surg Oncol* 16:1051–1059, 2009.

Kuniyasu H, Yasui W, et al.: Frequent amplification of the c-met gene in scirrhous type stomach cancer, *Biochem Biophys Res Commun* 189:227–232, 1992.

Kuo LT, Kuo KT, et al.: Correlation among pathology, genetic and epigenetic profiles, and clinical outcome in oligodendroglial tumors, *Int J Cancer* 124:2872–2879, 2009.

Kwak EL, Bang YJ, et al.: Anaplastic lymphoma kinase inhibition in non-small-cell lung cancer, *N Engl J Med* 363:1693–1703, 2010.

Labussiere M, Idbaih A, et al.: All the 1p19q codeleted gliomas are mutated on IDH1 or IDH2, *Neurology* 74:1886–1890, 2010.

Ladanyi M, Antonescu CR, et al.: Impact of SYT-SSX fusion type on the clinical behavior of synovial sarcoma: a multi-institutional retrospective study of 243 patients, *Cancer Res* 62:135–140, 2002.

Ladanyi M, Lui MY, et al.: The dert(X;17)(p11;q25) of human alveolar soft part sarcoma fuses the TFE3 transcription factor gene to ASPL, a novel gene at 17q25, *Oncogene* 20:48–57, 2001.

Lancaster JM, Wooster R, Mangion J, et al.: BRCA2 mutations in primary breast and ovarian cancers, *Nat Genet* 13:238–240, 1996.

Landen Jr CN, Birrer MJ, et al.: Early events in the pathogenesis of epithelial ovarian cancer, *J Clin Oncol* 26:995–1005, 2008.

Larkin J, Ascierto PA, et al.: Combined Vemurafenib and Cobimetinib in-mutated melanoma, *New Eng J Med* 371:1867–1876, 2014.

Lau PP, Lui PC, et al.: EWSR1-CREB3L1 gene fusion: a novel alternative molecular aberration of low-grade fibromyxoid sarcoma, *Am J Surg Pathol* 37:734–738, 2013.

Lauren P: The two histological main types of gastric carcinoma: diffuse and so-called intestinal-type carcinoma. an attempt at a histo-clinical classification, *Acta Pathol Microbiol Scand* 64:31–49, 1965.

Laurent-Puig P, Cayre A, et al.: Analysis of PTEN, BRAF, and EGFR status in determining benefit from cetuximab therapy in wild-type KRAS metastatic colon cancer, *J Clin Oncol* 27:5924–5930, 2009.

Lauwers YG, Franceschi S, Carneiro F, et al.: *WHO classification of tumors of the stomach. WHO classification of tumors of digestive system*, Lyon, 2010, IARC, pp 46–47.

Lawes DA, Pearson T, et al.: The role of MLH1, MSH2 and MSH6 in the development of multiple colorectal cancers, *Br J Cancer* 93:472–477, 2005.

Lawrence B, Perez-Atayde A, et al.: TPM3-ALK and TPM4-ALK oncogenes in inflammatory myofibroblastic tumors, *Am J Pathol* 157:377–384, 2000.

Lax SF, Kendall B, et al.: The frequency of p53, K-ras mutations, and microsatellite instability differs in uterine endometrioid and serous carcinoma: evidence of distinct molecular genetic pathways, *Cancer* 88:814–824, 2000.

Lax SF, Pizer ES, et al.: Clear cell carcinoma of the endometrium is characterized by a distinctive profile of p53, Ki-67, estrogen, and progesterone receptor expression, *Hum Pathol* 29:551–558, 1998.

Le DT, Uram JN, et al.: PD-1 blockade in tumors with mismatch-repair deficiency, *N Engl J Med* 372:2509–2520, 2015.

Lee EJ, Gusev Y, et al.: Expression profiling identifies microRNA signature in pancreatic cancer, *Int J Cancer* 120:1046–1054, 2007.

Lee JH, Park SJ, et al.: Frequent CpG island methylation in precursor lesions and early gastric adenocarcinomas, *Oncogene* 23:4646–4654, 2004b.

Lee JS, Chu IS, et al.: Classification and prediction of survival in hepatocellular carcinoma by gene expression profiling, *Hepatology* 40:667–676, 2004a.

Lee SC, Tan HT, et al.: Prognostic biomarkers for prediction of recurrence of hepatocellular carcinoma: current status and future prospects, *World J Gastroenterol* 20:3112–3124, 2014.

Levanon K, Crum C, Drapkin R: New insights into the pathogenesis of serous ovarian cancer and its clinical impact, *J Clin Oncol* 26:5284–5293, 2008.

Liang JJ, Kimchi ET, et al.: Diagnostic and prognostic biomarkers in pancreatic carcinoma, *Int J Clin Exp Pathol* 2:1–10, 2009.

Liang Y, Ridzon D, et al.: Characterization of microRNA expression profiles in normal human tissues, *BMC Genom* 8:166, 2007.

Liao X, Lochhead P, et al.: Aspirin use, tumor PIK3CA mutation, and colorectal-cancer survival, *N Engl J Med* 367:1596–1606, 2012.

Lindeman NI, Cagle PT, et al.: Molecular testing guideline for selection of lung cancer patients for EGFR and ALK tyrosine kinase inhibitors: guideline from the College of American pathologists, international association for the study of lung cancer, and association for molecular pathology, *J Thorac Oncol* 8:823–859, 2013.

Linehan WM, Spellman PT, et al.: Comprehensive molecular characterization of papillary renal-cell carcinoma, *N Engl J Med* 374:135–145, 2016.

Liu W, Chang B, et al.: Comprehensive assessment of DNA copy number alterations in human prostate cancers using Affymetrix 100K SNP mapping array, *Genes Chromosomes Cancer* 45:1018–1032, 2006.

Liu P, Cheng H, et al.: Oncogenic PIK3CA-driven mammary tumors frequently recur via PI3K pathway-dependent and PI3K pathway independent mechanisms, *Nat Med* 17:1116–1120, 2011.

Lonser RR, Glenn GM, et al.: von Hippel-Lindau disease, *Lancet* 361:2059–2067, 2003.

Lopez-Gines C, Navarro S, et al.: Malignant myxoid liposarcoma: an immunohistochemical, electron-microscopical and cytogenetical analysis, *Appl Pathol* 7:285–293, 1989.

Louis DN, Perry A, et al.: The 2016 World Health Organization classification of tumors of the central nervous system: a summary, *Acta Neuropathol* 131:803–820, 2016.

Loupakis F, Pollina L, et al.: PTEN expression and KRAS mutations on primary tumors and metastases in the prediction of benefit from cetuximab plus irinotecan for patients with metastatic colorectal cancer, *J Clin Oncol* 27:2622–2629, 2009.

Lu J, Getz G, et al.: MicroRNA expression profiles classify human cancers, *Nature* 435:834–838, 2005.

Luceri C, De Filippo C, et al.: Microsatellite instability in a population of sporadic colorectal cancers: correlation between genetic and pathological profiles, *Dig Liver Dis* 34:553–559, 2002.

Lynch HT, de la Chapelle A: Hereditary colorectal cancer, *N Engl J Med* 348:919–932, 2003.

Lynch HT, Lynch PM, et al.: Review of the Lynch syndrome: history, molecular genetics, screening, differential diagnosis, and medicolegal ramifications, *Clin Genet* 76:1–18, 2009.

Ma Z, Hill DA, et al.: Fusion of ALK to the Ran-binding protein 2 (RANBP2) gene in inflammatory myofibroblastic tumor, *Genes Chromosomes Cancer* 37:98–105, 2003.

Ma XJ, Patel R, et al.: Molecular classification of human cancers using a 92-gene real-time quantitative polymerase chain reaction assay, *Arch Pathol Lab Med* 130:465–473, 2006.

MacCollin M, Ramesh V, et al.: Mutational analysis of patients with neurofibromatosis 2, *Am J Hum Genet* 55:314–320, 1994.

MacCollin M, Willett C, et al.: Familial schwannomatosis: exclusion of the NF2 locus as the germline event, *Neurology* 60:1968–1974, 2003.

Maher ER, Iselius L, et al.: Von Hippel-Lindau disease: a genetic study, *J Med Genet* 28:443–447, 1991.

Maher ER, Webster AR, et al.: Phenotypic expression in von Hippel-Lindau disease: correlations with germline VHL gene mutations, *J Med Genet* 33:328–332, 1996.

Mantovani F, Banks L: The human papillomavirus E6 protein and its contribution to malignant progression, *Oncogene* 20:7874–7887, 2001.

Mardis ER: Next-generation sequencing platforms, *Annu Rev Anal Chem* 6:287–303, 2013.

Marino-Enriquez A, Wang WL, et al.: Epithelioid inflammatory myofibroblastic sarcoma: an aggressive intra-abdominal variant of inflammatory myofibroblastic tumor with nuclear membrane or perinuclear ALK, *Am J Surg Pathol* 35:135–144, 2011.

Marino-Enriquez A, Ou WB, et al.: ALK rearrangement in sickle cell trait-associated renal medullary carcinoma, *Genes Chromosomes Cancer* 50:146–153, 2011.

Marsh DJ, Coulon V, et al.: Mutation spectrum and genotype-phenotype analyses in Cowden disease and Bannayan-Zonana syndrome, two hamartoma syndromes with germline PTEN mutation, *Hum Mol Genet* 7:507–515, 1998.

Matsubayashi H, Canto M, et al.: DNA methylation alterations in the pancreatic juice of patients with suspected pancreatic disease, *Cancer Res* 66:1208–1217, 2006.

Matsumura T, Yamaguchi T, et al.: Advantage of FISH analysis using FKHR probes for an adjunct to diagnosis of rhabdomyosarcomas, *Virchows Arch* 452:251–258, 2008.

Mayr D, Kanitz V, et al.: Analysis of gene amplification and prognostic markers in ovarian cancer using comparative genomic hybridization for microarrays and immunohistochemical analysis for tissue microarrays, *Am J Clin Pathol* 126:101–109, 2006.

McArthur GA: Dermatofibrosarcoma protuberans: a surgical disease with a molecular savior, *Curr Opin Oncol* 18:341–346, 2006.

McCabe N, Turner NC, et al.: Deficiency in the repair of DNA damage by homologous recombination and sensitivity to poly(ADP-ribose) polymerase inhibition, *Cancer Res* 66:8109–8115, 2006.

McGlynn KA, London WT: Epidemiology and natural history of hepatocellular carcinoma, *Best Pract Res Clin Gastroenterol* 19:3–23, 2005.

McMenamin ME, Soung P, et al.: Loss of PTEN expression in paraffin embedded primary prostate cancer correlates with high Gleason score and advanced stage, *Cancer Res* 59:4291–4296, 1999.

Mehra R, Han B, et al.: Heterogeneity of TMPRSS2 gene rearrangements in multifocal prostate adenocarcinoma: molecular evidence for an independent group of diseases, *Cancer Res* 67:7991–7995, 2007a.

Mehra R, Tomlins SA, et al.: Comprehensive assessment of TMPRSS2 and ETS family gene aberrations in clinically localized prostate cancer, *Mod Pathol* 20:538–544, 2007b.

Mehra S, de la Roza G, et al.: Detection of FOXO1 (FKHR) gene break-apart by fluorescence in situ hybridization in formalin-fixed, paraffin-embedded alveolar rhabdomyosarcomas and its clinicopathologic correlation, *Diagn Mol Pathol* 17:14–20, 2008.

Mejean A, Hopirtean V, et al.: Prognostic factors for the survival of patients with papillary renal cell carcinoma: meaning of histological typing and multifocality, *J Urol* 170:764–767, 2003.

Meldrum C, Doyle MA, et al.: Next-generation sequencing for cancer diagnostics: a practical perspective, *Clin Biochem Rev* 32:177–195, 2011.

Meloni AM, Dobbs RM, et al.: Translocation (X;1) in papillary renal cell carcinoma. A new cytogenetic subtype, *Cancer Genet Cytogenet* 65:1–6, 1993.

Meloni AM, Sandberg AA, et al.: Translocation (X;1)(p11.2;q21). A subtype of renal adenocarcinomas, *Cancer Genet Cytogenet* 63:100–101, 1992.

Mendlick MR, Nelson M, et al.: Translocation t(1;3)(p36.3;q25) is a nonrandom aberration in epithelioid hemangioendothelioma, *Am J Surg Pathol* 25:684–687, 2001.

Mentzel T, Schildhaus HU, et al.: Postradiation cutaneous angiosarcoma after treatment of breast carcinoma is characterized by MYC amplification in contrast to atypical vascular lesions after radiotherapy and control cases: clinicopathological, immunohistochemical and molecular analysis of 66 cases, *Mod Pathol* 25:75–85, 2012.

Messa C, Russo F, et al.: EGF, TGF-alpha, and EGF-R in human colorectal adenocarcinoma, *Acta Oncol* 37:285–289, 1998.

Messiaen LM, Callens T, et al.: Exhaustive mutation analysis of the NF1 gene allows identification of 95% of mutations and reveals a high frequency of unusual splicing defects, *Hum Mutat* 15:541–555, 2000.

Metzker ML: Sequencing technologies—the next generation, *Nat Rev Genet* 11:31–46, 2010.

Miettinen M, Lasota J: Gastrointestinal stromal tumors: review on morphology, molecular pathology, prognosis, and differential diagnosis, *Arch Pathol Lab Med* 130:1466–1478, 2006.

Miettinen M, Wang ZF, et al.: Succinate dehydrogenase-deficient GISTs: a clinicopathologic, immunohistochemical, and molecular genetic study of 66 gastric GISTs with predilection to young age, *Am J Surg Pathol* 35:1712–1721, 2011.

Miller AJ, Mihm Jr MC: *Melanoma*, *N Engl J Med* 355:51–65, 2006.

Mishra G, Zhao Y, et al.: Determination of qualitative telomerase activity as an adjunct to the diagnosis of pancreatic adenocarcinoma by EUS-guided fine-needle aspiration, *Gastrointest Endosc* 63:648–654, 2006.

Miyaki M, Kuroki T: Role of Smad4 (DPC4) inactivation in human cancer, *Biochem Biophys Res Commun* 306:799–804, 2003.

Moeini A, Sia D, et al.: Mixed hepatocellular cholangiocarcinoma tumors: cholangiocellular carcinoma is a distinct molecular entity, *J Hepatol* 66:952–961, 2017.

Moskaluk CA, Hruban RH, et al.: p16 and K-ras mutations in the intraductal precursors of human pancreatic adenocarcinoma, *Can Res* 57:2140–2143, 1997.

Moertel CG, Kvols LK, et al.: Treatment of neuroendocrine carcinomas with combined etoposide and cisplatin: evidence of major therapeutic activity in the anaplastic variants of these neoplasma, *Cancer* 68:227–232, 1991.

Motoi N, Sakamoto A, Yamochi T, et al.: Role of ras mutation in the progression of thyroid carcinoma of follicular epithelial origin, *Pathol Res Pract* 196:1–7, 2000.

Moreau LC, Turcotte R, et al.: Myxoid\round cell liposarcoma (MRCLS) revisited: an analysis of 418 primarily managed cases, *Ann Surg Oncol* 19:1081–1088, 2012.

Morris BJ: Cervical human papillomavirus screening by PCR: advantages of targeting the E6/E7 region, *Clin Chem Lab Med* 43:1171–1177, 2005.

Motola-Kuba D, Zamora-Valdes D, et al.: Hepatocellular carcinoma. An overview, *Ann Hepatol* 5:16–24, 2006.

Moule RN, Jhavar SG, et al.: Genotype phenotype correlation in Li-Fraumeni syndrome kindreds and its implications for management, *Fam Cancer* 5:129–133, 2006.

Moyhuddin A, Baser ME, et al.: Somatic mosaicism in neurofibromatosis 2: prevalence and risk of disease transmission to offspring, *J Med Genet* 40:459–463, 2003.

Mrozek K, Szumigala J, et al.: Round cell liposarcoma with the insertion (12;16)(q13;p11.2p13), *Am J Clin Pathol* 108:35–39, 1997.

Mulligan LM, Eng C, et al.: Specific mutations of the RET proto-oncogene are related to disease phenotype in MEN 2A and FMTC, *Nat Genet* 6:70–74, 1994.

Mulligan LM, Marsh DJ, et al.: Genotype-phenotype correlation in multiple endocrine neoplasia type 2: report of the International RET Mutation Consortium, *J Intern Med* 238:343–346, 1995.

Munger K, et al.: Biological activities and molecular targets of the human papillomavirus E7 oncoprotein, *Oncogene* 20:7888–7898, 2001.

Munoz N, et al.: 1: HPV in the etiology of human cancer, *Vaccine* 24(Suppl 3):1–10, 2006.

Myssiorek D, Ferlito A, et al.: Screening for familial paragangliomas, *Oral Oncol* 44:532–537, 2008.

Nagy A, Zoubakov D, et al.: Lack of mutation of the folliculin gene in sporadic chromophobe renal cell carcinoma and renal oncocytoma, *Int J Cancer* 109:472–475, 2004.

Nakagawa T1, Kollmeyer TM, et al.: A tissue biomarker panel predicting systemic progression after PSA recurrence post-definitive prostate cancer therapy, *PloS One* 3(5):e2318, 2008.

Nakashima A, Murakami Y, et al.: Usefulness of human telomerase reverse transcriptase in pancreatic juice as a biomarker of pancreatic malignancy, *Pancreas* 38:527–533, 2009.

Nam RK, Sugar L, et al.: Expression of the TMPRSS2:ERG fusion gene predicts cancer recurrence after surgery for localised prostate cancer, *Br J Cancer* 97:1690–1695, 2007.

Napieralski R, Ott K, et al.: Combined GADD45A and thymidine phosphorylase expression levels predict response and survival of neoadjuvant-treated gastric cancer patients, *Clin Cancer Res* 11:3025–3031, 2005.

Narendra S, Valente A, et al.: DDIT3 gene break-apart as a molecular marker for diagnosis of myxoid liposarcoma—assay validation and clinical experience, *Diagn Mol Pathol* 20:218–224, 2011.

Network CGAR: Comprehensive molecular characterization of gastric adenocarcinoma, *Nature* 513:202, 2014.

NCCN: *National comprehensive cancer Newwork guidelines version 1*, 2018. Occult primary.

Neumann HP, Pawlu C, et al.: Distinct clinical features of paraganglioma syndromes associated with SDHB and SDHD gene mutations, *J Am Med Assoc* 292:943–951, 2004.

Nickerson ML, Warren MB, et al.: Mutations in a novel gene lead to kidney tumors, lung wall defects, and benign tumors of the hair follicle in patients with the Birt-Hogg-Dube syndrome, *Canc Cell* 2:157–164, 2002.

Nielsen GP, Fletcher CD, et al.: Soft tissue aneurysmal bone cyst: a clinicopathologic study of five cases, *Am J Surg Pathol* 26:64–69, 2002.

Nielsen T, Wallden B, et al.: Analytical validation of the PAM50-based Prosigna breast cancer prognostic gene signature assay and nCounter analysis system using formalin-fixed paraffin-embedded breast tumor specimens, *BMC Canc* 14:177, 2014.

Nikiforov YE: Thyroid carcinoma: molecular pathways and therapeutic targets, *Mod Pathol* 21(Suppl 2):S37–S43, 2008.

Nikiforov YE: Role of molecular markers in thyroid nodule management: then and now, *Endocri Pract* 23:979–988, 2017.

Nikiforova MN, Lynch RA, et al.: RAS point mutations and PAX8-PPAR gamma rearrangement in thyroid tumors: evidence for distinct molecular pathways in thyroid follicular carcinoma, *J Clin Endocrinol Metab* 88:2318–2326, 2003.

Nikiforov YE, Nikiforova MN: Molecular genetics and diagnosis of thyroid cancer, *Nat Rev Endocrinol* 7:569–580, 2011.

Nikiforova MN, Nikiforov YE: Molecular genetics of thyroid cancer: implications for diagnosis, treatment and prognosis, *Expert Rev Mol Diagn* 8:83–95, 2008.

Nishio J, Iwasaki H, et al.: Identification of syt-ssx fusion transcripts in both epithelial and spindle cell components of biphasic synovial sarcoma in small tissue samples isolated by membrane-based laser microdissection, *Virchows Arch* 439:152–157, 2001.

Nishio J, Iwasaki H, et al.: Establishment of a new human synovial sarcoma cell line, FU-SY-1, that expresses c-Met receptor and its ligand hepatocyte growth factor, *Int J Oncol* 21:17–23, 2002a.

Nishio J, Iwasaki H, et al.: Synovial sarcoma with a secondary chromosome change dert(17;22)(q12;q12), *Cancer Genet Cytogenet* 137:23–28, 2002b.

Nishio J, Iwasaki H, et al.: Identification of a ring chromosome with spectral karyotyping in a pleural synovial sarcoma, *Cancer Genet Cytogenet* 160:174–178, 2005.

Oberhuber G, Stolte M: Gastric polyps: an update of their pathology and biological significance, *Virchows Arch* 437:581–590, 2000.

Obermann EC, Junker K, et al.: Frequent genetic alterations in flat urothelial hyperplasias and concomitant papillary bladder cancer as detected by CGH, LOH, and FISH analyses, *J Pathol* 199:50–57, 2003.

Ogino S, Kawasaki T, et al.: Sensitive sequencing method for KRAS mutation detection by Pyrosequencing, *J Mol Diagn* 7:413–421, 2005.

Ogino S, Nosho K, et al.: CpG island methylator phenotype, microsatellite instability, BRAF mutation and clinical outcome in colon cancer, *Gut* 58:90–96, 2009a.

Ogino S, Nosho K, et al.: PIK3CA mutation is associated with poor prognosis among patients with curatively resected colon cancer, *J Clin Oncol* 27:1477–1484, 2009b.

Oh SY, Kwon HC, et al.: Clinicopathologic significance of HIF-1alpha, p53, and VEGF expression and preoperative serum VEGF level in gastric cancer, *BMC Canc* 8:123, 2008.

Ohgaki H, Kleihues P: Genetic pathways to primary and secondary glioblastoma, *Am J Pathol* 170:1445–1453, 2007.

Oliveira AM, Hsi BL, et al.: USP6 (Tre2) fusion oncogenes in aneurysmal bone cyst, *Cancer Res* 64:1920–1923, 2004.

Oliveira AM, Perez-Atayde AR, et al.: Aneurysmal bone cyst variant translocations upregulate USP6 transcription by promoter swapping with the ZNF9, COL1A1, TRAP150, and OMD genes, *Oncogene* 24:3419–3426, 2005.

Olivier M, Goldgar DE, et al.: Li-Fraumeni and related syndromes: correlation between tumor type, family structure, and TP53 genotype, *Cancer Res* 63:6643–6650, 2003.

Olsen SH, Thomas DG, et al.: Cluster analysis of immunohistochemical profiles in synovial sarcoma, malignant peripheral nerve sheath tumor, and Ewing sarcoma, *Mod Pathol* 19:659–668, 2006.

Oosterwijk JC, Jansen JC, et al.: First experiences with genetic counselling based on predictive DNA diagnosis in hereditary glomus tumors (paragangliomas), *J Med Genet* 33:379–383, 1996.

O'Shea AM, Cleary SP, et al.: Pathological features of colorectal carcinomas in MYH-associated polyposis, *Histopathology* 53:184–194, 2008.

Oue N, Mitani Y, et al.: Accumulation of DNA methylation is associated with tumor stage in gastric cancer, Cancer, *Interdiscip Int J Am Cancer Soc* 106:1250–1259, 2006.

Oue N, Oshimo Y, et al.: DNA methylation of multiple genes in gastric carcinoma: association with histological type and CpG island methylator phenotype, *Cancer Sci* 94:901–905, 2003.

Paik S, Shak S, et al.: A multigene assay to predict recurrence of tamoxifen-treated, node-negative breast cancer, *N Engl J Med* 351:2817–2826, 2004.

Pajkos G, Kiss I, et al.: The prognostic value of the presence of mutations at the codons 12, 13, 61 of K-ras oncogene in colorectal cancer, *Anticancer Res* 20:1695–1701, 2000.

Panagopoulos I, Mertens F, et al.: Molecular genetic characterization of the EWS/CHN and RBP56/CHN fusion genes in extraskeletal myxoid chondrosarcoma, *Genes Chromosomes Cancer* 35:340–352, 2002.

Panagopoulos I, Nilsson T, et al.: Fusion of the SEC31L1 and ALK genes in an inflammatory myofibroblastic tumor, *Int J Cancer* 118:1181–1186, 2006.

Panoutsakopoulos G, Pandis N, et al.: Recurrent t(16;17)(q22;p13) in aneurysmal bone cysts, *Genes Chromosomes Cancer* 26:265–266, 1999.

Paradis V, Benzekri A, et al.: Telangiectatic focal nodular hyperplasia: a variant of hepatic adenoma, *Gastroenterology* 126:1323–1329, 2004.

Parkin DM, Bray F, et al.: Estimating the world cancer burden: Globocan 2000, *Int J Cancer* 94:153–156, 2001.

Parkin DM, Bray F, et al.: Global cancer statistics, 2002, *CA Cancer J Clin* 55:74–108, 2005.

Parsons DW, Jones S, et al.: An integrated genomic analysis of human glioblastoma multiforme, *Science* 321:1807–1812, 2008.

Pavlovich CP, Walther MM, et al.: Renal tumors in the Birt-Hogg-Dube syndrome, *Am J Surg Pathol* 26:1542–1552, 2002.

Peltomaki P: Lynch syndrome genes, *Fam Cancer* 4:227–232, 2005.

Pentheroudakis G, Briasoulis E, et al.: Cancer of unknown primary site: missing primary or missing biology? *Oncol* 12:418–425, 2007.

Perner S, Demichelis F, et al.: TMPRSS2:ERG fusion-associated deletions provide insight into the heterogeneity of prostate cancer, *Cancer Res* 66:8337–8341, 2006.

Petrovics G, Liu A, et al.: Frequent overexpression of ETS-related gene-1 (ERG1) in prostate cancer transcriptome, *Oncogene* 24:3847–3852, 2005.

Phelps RA, Broadbent TJ, et al.: New perspectives on APC control of cell fate and proliferation in colorectal cancer, *Cell Cycle* 8:2549–2556, 2009.

Pignot G, Elie C, et al.: Survival analysis of 130 patients with papillary renal cell carcinoma: prognostic utility of type 1 and type 2 subclassification, *Urology* 69:230–235, 2007.

Pinto-de-Sousa J, Silva F, et al.: Clinicopathological significance and survival influence of p53 protein expression in gastric carcinoma, *Histopathology* 44:323–331, 2004.

Plesec TP, Hunt JL: KRAS mutation testing in colorectal cancer, *Adv Anat Pathol* 16:196–203, 2009.

Popat S, Houlston RS: A systematic review and meta-analysis of the relationship between chromosome 18q genotype, DCC status and colorectal cancer prognosis, *Eur J Cancer* 41:2060–2070, 2005.

Quek ML, Quinn DI, et al.: Molecular prognostication in bladder cancer—a current perspective, *Eur J Cancer* 39:1501–1510, 2003.

Rajput AB, Miller MA, et al.: Frequency of the TMPRSS2:ERG gene fusion is increased in moderate to poorly differentiated prostate cancers, *J Clin Pathol* 60:1238–1243, 2007.

Ranganathan P, Harsha HC, et al.: Molecular alterations in exocrine neoplasms of the pancreas, *Arch Pathol Lab Med* 133:405–412, 2009.

Raue F, Frank-Raue K: Genotype-phenotype relationship in multiple endocrine neoplasia type 2. Implications for clinical management, *Hormones (Basel)* 8:23–28, 2009.

Rebouissou S, Amessou M, et al.: Frequent in-frame somatic deletions activate gp130 in inflammatory hepatocellular tumors, *Nature* 457:200–204, 2009.

Rebouissou S, Bioulac-Sage P, et al.: Molecular pathogenesis of focal nodular hyperplasia and hepatocellular adenoma, *J Hepatol* 48:163–170, 2008.

Rebouissou S, Imbeaud S, et al.: HNF1 alpha inactivation promotes lipogenesis in human hepatic adenoma independently of SREBP-1 and carbohydrate-response element-binding protein (ChREBP) activation, *J Biol Chem* 282:14437–14446, 2007.

Redston MS, Caldas C, et al.: p53 mutations in pancreatic carcinoma and evidence of common involvement of homocopolymer tracts in DNA microdeletions, *Cancer Res* 54:3025–3033, 1994.

Reeves BR, Fletcher CD, et al.: Translocation t(12;22)(q13;q13) is a nonrandom rearrangement in clear cell sarcoma, *Cancer Genet Cytogenet* 64:101–103, 1992.

Ribic CM, Sargent DJ, Moore MJ, et al.: Tumor microsatellite-instability status as a predictor of benefit from fluorouracil-based adjuvant chemotherapy for colon cancer, *N Engl J Med* 349:247–257, 2003.

Ricketts CJ, De Cubas AA, et al.: The cancer genome Atlas comprehensive molecular characterization of renal cell carcinoma, *Cell Rep* 23(1):313–326, 2018.

Risch HA, McLaughlin JR, Cole DE, et al.: Prevalence and penetrance of germline BRCA1 and BRCA2 mutations in a population series of 649 women with ovarian cancer, *Am J Hum Genet* 68:700–710, 2001.

Robert C, Karaszewska B, et al.: Improved overall survival in melanoma with combined Dabrafenib and Trametinib, *New Eng J Med* 372:30–39, 2015.

Rondell P, Graham LJ, et al.: *DNAJB1-PRKACA* is specific for fibrolamellar carcinoma, *Mod Pathol* 28:822–829, 2015.

Ross JS: Multigene classifiers, prognostic factors, and predictors of breast cancer clinical outcome, *Adv Anat Pathol* 16:204–215, 2009.

Ross JS, Hatzis C, et al.: Commercialized multigene predictors of clinical outcome for breast cancer, *Oncol* 13:477–493, 2008.

Roy-Chowdhuri S, de Melo Gagliato D, et al.: Multigene clinical mutational profiling of breast carcinoma using next-generation sequencing, *Am J Clin Pathol* 144:713–721, 2015.

Rowinsky EK, Windle JJ, et al.: Ras protein farnesyltransferase: a strategic target for anticancer therapeutic development, *J Clin Oncol* 17:3631–3652, 1999.

Sanson M, Marie Y, et al.: Isocitrate dehydrogenase 1 codon 132 mutation is an important prognostic biomarker in gliomas, *J Clin Oncol* 27:4150–4154, 2009.

Sartore-Bianchi A, Di Nicolantonio F, et al.: Multi-determinants analysis of molecular alterations for predicting clinical benefit to EGFR-targeted monoclonal antibodies in colorectal cancer, *PloS One* 4:e7287, 2009b.

Sartore-Bianchi A, Martini M, et al.: PIK3CA mutations in colorectal cancer are associated with clinical resistance to EGFR-targeted monoclonal antibodies, *Cancer Res* 69:1851–1857, 2009a.

Saslow D, Solomon D, et al.: American cancer Society, American Society for Colposcopy and cervical pathology, and American Society for clinical pathology screening guidelines for the prevention and early detection of cervical cancer, *Am J Clin Pathol* 137:516–542, 2012.

Sato H, Minei S, et al.: Fluorescence in situ hybridization analysis of c-myc amplification in stage TNM prostate cancer in Japanese patients, *Int J Urol* 13:761–766, 2006.

Sato N, Ueki T, et al.: Aberrant methylation of CpG islands in intraductal papillary mucinous neoplasms of the pancreas, *Gastroenterology* 123:365–372, 2002.

Schiavi F, Boedeker CC, et al.: Predictors and prevalence of paraganglioma syndrome associated with mutations of the SDHC gene, *J Am Med Assoc* 294:2057–2063, 2005.

Schreibman IR, Baker M, et al.: The hamartomatous polyposis syndromes: a clinical and molecular review, *Am J Gastroenterol* 100:476–490, 2005.

Schuffenecker I, Billaud M, et al.: RET proto-oncogene mutations in French MEN 2A and FMTC families, *Hum Mol Genet* 3:1939–1943, 1994.

Sciot R, Dorfman H, et al.: Cytogenetic-morphologic correlations in aneurysmal bone cyst, giant cell tumor of bone and combined lesions. A report from the CHAMP study group, *Mod Pathol* 13:1206–1210, 2000.

Seki K, Suda T, et al.: Diagnosis of pancreatic adenocarcinoma by detection of human telomerase reverse transcriptase messenger RNA in pancreatic juice with sample qualification, *Clin Cancer Res* 7:1976–1981, 2001.

Sekulic A, Haluska Jr P, et al.: Malignant melanoma in the 21st century: the emerging molecular landscape, *Mayo Clin Proc* 83:825–846, 2008.

Seo HM, Chang YS, et al.: Clinicopathologic characteristics and outcomes of gastric cancers with the MSI-H phenotype, *J Surg Oncol* 99:143–147, 2009.

Sequist LV, Lynch TJ: EGFR tyrosine kinase inhibitors in lung cancer: an evolving story, *Annu Rev Med* 59:429–442, 2008.

Serrano M, Hannon GJ, et al.: A new regulatory motif in cell cycle control causing specific inhibition of cycling D/CDK4, *Nature* 366:704–707, 1993.

Seshachalam VP, Sekar K, et al.: Insights into the etiology-associated gene regulatory networks in hepatocellular carcinoma from the Cancer Genome Atlas, *J Gastroenterol Hepatol* 33(12):2037–2047, 2018.

Setlur SR, Mertz KD, et al.: Estrogen-dependent signaling in a molecularly distinct subclass of aggressive prostate cancer, *J Natl Cancer Inst* 100:815–825, 2008.

Shaw AT: Yeap BY, et al: clinical features and outcome of patients with non-small-cell lung cancer who harbor EML4-ALK, *J Clin Oncol* 27:4247–4253, 2009.

Shiao YH, Rugge M, et al.: p53 alteration in gastric precancerous lesions, *Am J Pathol* 144:511–517, 1994.

Shimada S, Ishizawa T, et al.: The value of MDM2 and CDK4 amplification levels using real-time polymerase chain reaction for the differential diagnosis of liposarcomas and their histologic mimickers, *Hum Pathol* 37:1123–1129, 2006.

Sholl LM: Yeap BY, et al: lung adenocarcinoma with EGFR amplification has distinct clinicopathologic and molecular features in never-smokers, *Cancer Res* 69:8341–8348, 2009.

Si H, Sun X, et al.: Circulating microRNA-92a and microRNA-21 as novel minimally invasive biomarkers for primary breast cancer, *J Cancer Res Clin Oncol* 139:223–229, 2013.

Sia D, Jiao Y, Martinez-Quetglas I, et al.: Identification of an immune specific class of hepatocellular carcinoma, based on molecular features, *Gastroenterology* 153:812–826, 2017.

Sicard F, Gayral M, et al.: Targeting miR-21 for the therapy of pancreatic cancer, *Mol Ther* 21:986–994, 2013.

Sidhar SK, Clark J, et al.: The t(X;1)(p11.2;q21.2) translocation in papillary renal cell carcinoma fuses a novel gene PRCC to the TFE3 transcription factor gene, *Hum Mol Genet* 5:1333–1338, 1996.

Sieber OM, Lipton L, et al.: Multiple colorectal adenomas, classic adenomatous polyposis, and germ-line mutations in MYH, *N Engl J Med* 348:791–799, 2003.

Siegel R, Naishadham D, et al.: Cancer statistics, *CA Cancer J Clin* 62:10–29, 2012.

Siegel RL, Miller KD, Jemal A: Cancer statistics, *CA Cancer J Clin* 67:7–30, 2017.

Siena S, Sartore-Bianchi A, et al.: Biomarkers predicting clinical outcome of epidermal growth factor receptor-targeted therapy in metastatic colorectal cancer, *J Natl Cancer Inst* 101:1308–1324, 2009.

Simon MP, Pedeutour F, et al.: Deregulation of the platelet-derived growth factor B-chain gene via fusion with collagen gene COL1A1 in dermatofibrosarcoma protuberans and giant-cell fibroblastoma, *Nat Genet* 15:95–98, 1997.

Singh RR, Patel KP, et al.: Clinical validation of a next-generation sequencing screen for mutational hotspots in 46 cancer-related genes, *J Mol Diagn* 15:607–622, 2013.

Sirvent N, Coindre JM, et al.: Detection of MDM2-CDK4 amplification by fluorescence in situ hybridization in 200 paraffin-embedded tumor samples: utility in diagnosing adipocytic lesions and comparison with immunohistochemistry and real-time PCR, *Am J Surg Pathol* 31:1476–1489, 2007.

Sjogren H, Wedell B, et al.: Fusion of the NH2-terminal domain of the basic helix-loop-helix protein TCF12 to TEC in extraskeletal myxoid chondrosarcoma with translocation t(9;15)(q22;q21), *Cancer Res* 60:6832–6835, 2000.

Skalsky YM, Ajuh PM, et al.: PRCC, the commonest TFE3 fusion partner in papillary renal carcinoma is associated with pre-mRNA splicing factors, *Oncogene* 20:178–187, 2001.

Skytting B, Nilsson G, et al.: A novel fusion gene, SYT-SSX4, in synovial sarcoma, *J Natl Cancer Inst* 91:974–975, 1999.

Smakman N, Borel Rinkes IH, et al.: Control of colorectal metastasis formation by K-Ras, *Biochim Biophys Acta* 1756:103–114, 2005.

Soller MJ, Isaksson M, et al.: Confirmation of the high frequency of the TMPRSS2/ERG fusion gene in prostate cancer, *Genes Chromosomes Cancer* 45:717–719, 2006.

Sorosky JI: Endometrial cancer, *Obstet Gynecol* 120:383–397, 2012.

Speleman F, Delattre O, et al.: Malignant melanoma of the soft parts (clear-cell sarcoma): confirmation of EWS and ATF-1 gene fusion caused by a t(12;22) translocation, *Mod Pathol* 10:496–499, 1997.

Spruck 3rd CH, Ohneseit PF, et al.: Two molecular pathways to transitional cell carcinoma of the bladder, *Cancer Res* 54:784–788, 1994.

Stahl JM, Sharma A, et al.: Deregulated Akt3 activity promotes development of malignant melanoma, *Cancer Res* 64:7002–7010, 2004.

Stewart GD, Van Neste L, et al.: Clinical utility of an epigenetic assay to detect occult prostate cancer in histopathologically negative biopsies: results of the MATLOC study, *J Urol* 189(3):1110–1116, 2013.

Stolle C, Glenn G, et al.: Improved detection of germline mutations in the von Hippel-Lindau disease tumor suppressor gene, *Hum Mutat* 12:417–423, 1998.

Stupp R, Mason WP, et al.: Radiotherapy plus concomitant and adjuvant temozolomide for glioblastoma, *N Engl J Med* 352:987–996, 2005.

Su GH, Kern SE: Molecular genetics of ductal pancreatic neoplasia, *Curr Opin Gastroenterol* 16:419–425, 2000.

Swanson DB, Cohen E, et al.: MYH9-USP6 fusion transcript in nodular fasciitis: an institutional review, *Mod Pathol* 25:20A, 2012.

Sweeney C, Boucher KM, et al.: Oncogenetic tree model of somatic mutations and DNA methylation in colon tumors, *Genes Chromosomes Cancer* 48:1–9, 2009.

Szafranska AE, Davison TS, et al.: MicroRNA expression alterations are linked to tumorigenesis and non-neoplastic processes in pancreatic ductal adenocarcinoma, *Oncogene* 26:4442–4452, 2007.

Takayama T, Makuuchi M, et al.: Malignant transformation of adenomatous hyperplasia to hepatocellular carcinoma, *Lancet* 336:1150–1153, 1990.

Takeuchi K, Soda M, et al.: Pulmonary inflammatory myofibroblastic tumor expressing a novel fusion, PPFIBP1-ALK: reappraisal of anti-ALK immunohistochemistry as a tool for novel ALK fusion identification, *Clin Cancer Res* 17:3341–3348, 2011.

Takeuchi K, Soda M, et al.: RET, ROS1 and ALK fusions in lung cancer, *Nat Med* 18:378–381, 2012.

Tan MH, Wong CF, et al.: Genomic expression and single-nucleotide polymorphism profiling discriminates chromophobe renal cell carcinoma and oncocytoma, *BMC Canc* 10:196, 2010.

Tanaka M, Kitajima Y, et al.: Combined evaluation of mucin antigen and E-cadherin expression may help select patients with gastric cancer suitable for minimally invasive therapy, *Br J Surg* 90:95–101, 2003.

Tanas MR, Sboner A, et al.: Identification of a disease-defining gene fusion in epithelioid hemangioendothelioma, *Sci Transl Med* 3, 2011. 98ra82.

Tang D, Shen Y, et al.: Identification of plasma microRNAs as novel noninvasive biomarkers for early detection of lung cancer, *Eur J Cancer Prev* 22:540–548, 2013.

Tang S, Wu WK, et al.: Stratification of digestive cancers with different pathological features and survival outcomes by microRNA expression, *Sci Rep* 6:2466, 2016.

TCGA: The Cancer Genome Atlas Research Network Comprehensive molecular characterization of clear cell renal cell carcinoma, *Nature* 499:43–49, 2013.

TCGA: The cancer genome Atlas research network integrated genomic characterization of papillary thyroid carcinoma, *Cell* 159(3):676–690, 2014a, https://doi.org/10.1016/j.cell.2014.09.050.

TCGA: The cancer genome Atlas research network comprehensive molecular characterization of gastric adenocarcinoma, *Nature* 513(7517):202–209, 2014b, https://doi.org/10.1038/nature13480.

Theise ND, Park YN, et al.: Dysplastic nodules and hepatocarcinogenesis, *Clin Liver Dis* 6:497–512, 2002.

Tomlins SA, Rhodes DR, et al.: Recurrent fusion of TMPRSS2 and ETS transcription factor genes in prostate cancer, *Science* 310:644–648, 2005.

Tomlinson GE, Nisen PD, et al.: Cytogenetics of a renal cell carcinoma in a 17-month-old child. Evidence for Xp11.2 as a recurring breakpoint, *Cancer Genet Cytogenet* 57:11–17, 1991.

Torbenson MS: Morphologic subtypes of hepatocellular carcinoma, *Gastrenterol Clin North Am* 46:365–391, 2017.

Toyota M, Ahuja N, et al.: Aberrant methylation in gastric cancer associated with the CpG island methylator phenotype, *Cancer Res* 59:5438–5442, 1999.

Traverso G, Shuber A, et al.: Detection of APC mutations in fecal DNA from patients with colorectal tumors, *N Engl J Med* 346:311–320, 2002.

Trump D, Farren B, et al.: Clinical studies of multiple endocrine neoplasia type 1 (MEN1), *QJM* 89:653–669, 1996.

Tsao H, Goel V, et al.: Genetic interaction between NRAS and BRAF mutations and PTEN/MMAC1 inactivation in melanoma, *J Invest Dermatol* 122:337–341, 2004.

Tsuda M, Davis IJ, et al.: TFE3 fusions activate MET signaling by transcriptional up-regulation, defining another class of tumors as candidates for therapeutic MET inhibition, *Cancer Res* 67:919–929, 2007.

Tu JJ, Rohan S, et al.: Gene fusions between TMPRSS2 and ETS family genes in prostate cancer: frequency and transcript variant analysis by RT-PCR and FISH on paraffin-embedded tissues, *Mod Pathol* 20:921–928, 2007.

Turc-Carel C, Dal Cin P, et al.: Recurrent breakpoints at 9q31 and 22q12.2 in extraskeletal myxoid chondrosarcoma, *Cancer Genet Cytogenet* 30:145–150, 1988.

Umar A, Boland CR, et al.: Revised Bethesda Guidelines for hereditary nonpolyposis colorectal cancer (Lynch syndrome) and microsatellite instability, *J Natl Cancer Inst* 96:261–268, 2004.

Valle L, Serena-Acedo T, et al.: Germline allele-specific expression of TGFBR1 confers an increased risk of colorectal cancer, *Science* 321:1361–1365, 2008.

van Cutsem E, et al.: HER2 screening data from ToGA: targeting HER2 in gastric and gastroesophageal junction cancer, *Gastric Cancer* 18:476–484, 2015.

van der Heijden MS, Brody JR, et al.: In vivo therapeutic responses contingent on Fanconi anemia/BRCA2 status of the tumor, *Clin Cancer Res* 11:7508–7515, 2005.

van den Heuvel C, van Ewijk A, et al.: Molecular profiling of druggable targets in clear cell renal cell carcinoma through targeted RNA sequencing, *Front Oncol* 9:117–130, 2019.

van Rhijn BW, Lurkin I, et al.: The fibroblast growth factor receptor 3 (FGFR3) mutation is a strong indicator of superficial bladder cancer with low recurrence rate, *Cancer Res* 61:1265–1268, 2001.

Varadhachary GR, Talantov D, et al.: Molecular profiling of carcinoma of unknown primary and correlation with clinical evaluation, *J Clin Oncol* 26:4442–4448, 2008.

Varesco L: Familial adenomatous polyposis: genetics and epidemiology, *Tech Coloproctol* 8(Suppl 2):S305–S308, 2004.

Venkitaraman AR: Linking the cellular functions of BRCA genes to cancer pathogenesis and treatment, *Annu Rev Pathol* 4:461–487, 2009.

Vermeulen J, Ballet S, et al.: Incidence and prognostic value of tumor cells detected by RT-PCR in peripheral blood stem cell collections from patients with Ewing tumor, *Br J Cancer* 95:1326–1333, 2006.

Vivanco I, Sawyers CL: The phosphatidylinositol 3-kinase AKT pathway in human cancer, *Nat Rev Cancer* 2:489–501, 2002.

Vogt S, Jones N, et al.: Expanded extracolonic tumor spectrum in MUTYH-associated polyposis, *Gastroenterology* 137:1976–1985, 2009. e1–e10.

Vogt M, Munding J, et al.: Frequent concomitant inactivation of miR-34a and miR-34b/c by CpG methylation in colorectal, pancreatic, mammary, ovarian, urothelial, and renal cell carcinomas and soft tissue sarcomas, *Virchows Arch* 458:313–322, 2011.

Vollmers HP, Hensel F, et al.: Tumor-specific apoptosis induced by the human monoclonal antibody SC-1: a new therapeutical approach for stomach cancer, *Oncol Rep* 5:35–40, 1998a.

Vollmers HP, Zimmermann U, et al.: Adjuvant therapy for gastric adenocarcinoma with the apoptosis-inducing human monoclonal antibody SC-1: first clinical and histopathological results, *Oncol Rep* 5:549–552, 1998b.

Waite KA, Eng C, Protean PTEN: Form and function, *Am J Hum Genet* 70:829–844, 2002.

Wan PT, Garnett MJ, et al.: Mechanism of activation of the RAF-ERK signaling pathway by oncogenic mutations of B-RAF, *Cell* 116:855–867, 2004.

Wang J, Cai Y, et al.: Expression of variant TMPRSS2/ERG fusion messenger RNAs is associated with aggressive prostate cancer, *Cancer Res* 66:8347–8351, 2006.

Wang L, Liu R, et al.: Somatic single hits inactivate the X-linked tumor suppressor FOXP3 in the prostate, *Canc Cell* 16:336–346, 2009a.

Wang WL, Mayordomo E, et al.: Fluorescence in situ hybridization is a useful ancillary diagnostic tool for extraskeletal myxoid chondrosarcoma, *Mod Pathol* 21:1303–1310, 2008.

Wang WL, Mayordomo E, et al.: Detection and characterization of EWSR1/ATF1 and EWSR1/CREB1 chimeric transcripts in clear cell sarcoma (melanoma of soft parts), *Mod Pathol* 22:1201–1209, 2009b.

Wang YL, Sheu BS, et al.: Overexpression of c-erb-B2 proteins in tumor and non-tumor parts of gastric adenocarcinoma—emphasis on its relation to *H. pylori* infection and clinicohistological characteristics, *Hepato-Gastroenterology* 49:1172–1176, 2002.

Wang S, Xiang J, et al.: A plasma microRNA panel for early detection of colorectal cancer, *Int J Cancer* 136:152–161, 2015.

Weaver J, Rao P, et al.: Can MDM2 analytical tests performed on core needle biopsy be relied upon to diagnose well-differentiated liposarcoma? *Mod Pathol* 23:1301–1306, 2010.

Webster AR, Richards FM, et al.: An analysis of phenotypic variation in the familial cancer syndrome von Hippel-Lindau disease: evidence for modifier effects, *Am J Hum Genet* 63:1025–1035, 1998.

Wei D, Goldfarb D, et al.: SNF5/INI1 deficiency redefines chromatin remodeling complex composition during tumor development, *Mol Cancer Res* 12:1574–1585, 2014.

Weisenberger DJ, Siegmund KD, et al.: CpG island methylator phenotype underlies sporadic microsatellite instability and is tightly associated with BRAF mutation in colorectal cancer, *Nat Genet* 38:787–793, 2006.

Weller M, Rieger J, et al.: Predicting chemoresistance in human malignant glioma cells: the role of molecular genetic analyses, *Int J Cancer* 79:640–644, 1998.

Wen WH, Reles A, et al.: p53 mutations and expression in ovarian cancers: correlation with overall survival, *Int J Gynecol Pathol* 18:29–41, 1999.

Weterman MJ, van Groningen JJ, et al.: Nuclear localization and transactivating capacities of the papillary renal cell carcinoma-associated TFE3 and PRCC (fusion) proteins, *Oncogene* 19:69–74, 2000.

Wiegand KC, Shah SP, et al.: ARID1A mutations in endometriosis-associated ovarian carcinomas, *N Engl J Med* 363:1532–1543, 2010.

Wilentz RE, Iacobuzio-Donahue CA, et al.: Loss of expression of Dpc4 in pancreatic intraepithelial neoplasia: evidence that DPC4 inactivation occurs late in neoplastic progression, *Cancer Res* 60:2002–2006, 2000.

Wilhelm SM, Carter C, et al.: BAY 43–9006 exhibits broad spectrum oral antitumor activity and targets the RAF/MEK/ERK pathway and receptor tyrosine kinases involved in tumor progression and angiogenesis, *Cancer Res* 64:7099–7109, 2004.

Winawer S, Fletcher R, et al.: Colorectal cancer screening and surveillance: clinical guidelines and rationale—update based on new evidence, *Gastroenterology* 124:544–560, 2003.

Wirtz HC, Muller W, et al.: Prognostic value and clinicopathological profile of microsatellite instability in gastric cancer, *Clin Cancer Res* 4:1749–1754, 1998.

Woodford-Richens KL, Rowan AJ, et al.: SMAD4 mutations in colorectal cancer probably occur before chromosomal instability, but after divergence of the microsatellite instability pathway, *Proc Natl Acad Sci U S A* 98:9719–9723, 2001.

Xiangming C, Hokita S, et al.: p21 expression is a prognostic factor in patients with p53-negative gastric cancer, *Cancer Lett* 148:181–188, 2000.

Xing M, Tufano RP, et al.: Detection of BRAF mutation on fine needle aspiration biopsy specimens: a new diagnostic tool for papillary thyroid cancer, *J Clin Endocrinol Metab* 89:2867–2872, 2004.

Xing M, Westra WH, et al.: BRAF mutation predicts a poorer clinical prognosis for papillary thyroid cancer, *J Clin Endocrinol Metab* 90:6373–6379, 2005.

Xia XM, Jin WY, et al.: Clinical significance and the correlation of expression between Let-7 and K-ras in non-small cell lung cancer, *Oncol Lett* 1:1045–1047, 2010.

Yachida S, Vakiani E, et al.: Small cell and large cell neuroendocrine carcinomas of the pancreas are genetically similar and distinct from well-differentiated pancreatic neuroendocrine tumors, *Am J Surg Pathol* 36:173–184, 2012.

Yamamoto H, Oda Y, et al.: p53 mutation and MDM2 amplification in inflammatory myofibroblastic tumors, *Histopathology* 42:431–439, 2003.

Yan L, McFaul C, et al.: Molecular analysis to detect pancreatic ductal adenocarcinoma in high-risk groups, *Gastroenterology* 128:2124–2130, 2005.

Yan H, Parsons DW, et al.: IDH1 and IDH2 mutations in gliomas, *N Engl J Med* 360:765–773, 2009.

Yang M, Shen H, et al.: High expression of miR-21 and miR-155 predicts recurrence and unfavourable survival in non-small cell lung cancer, *Eur J Cancer* 49:604–615, 2013.

Yao M, Tabuchi H, et al.: Gene expression analysis of renal carcinoma: adipose differentiation-related protein as a potential diagnostic and prognostic biomarker for clear-cell renal carcinoma, *J Pathol* 205:377–387, 2005.

Yasui W, Tahara E, et al.: Immunohistochemical detection of human telomerase reverse transcriptase in normal mucosa and precancerous lesions of the stomach, *Jpn J Cancer Res* 90:589–595, 1999.

Yap TA, Carden CP, et al.: Beyond chemotherapy: targeted therapies in ovarian cancer, *Nat Rev Cancer* 9:167–181, 2009.

Yip L, Cote GJ, et al.: Multiple endocrine neoplasia type 2: evaluation of the genotype-phenotype relationship, *Arch Surg* 138:409–416, discussion 416, 2003.

Yip L, Nikiforova MN, et al.: Tumor genotype determins phenoty and disease-related outcomes in thyroid cancer: a study of 1510 patients, *Ann Surg* 262:519–525, 2015. discussion 524-525.

Yokozaki H, Yasui W, et al.: Genetic and epigenetic changes in stomach cancer, *Int Rev Cytol* 204:49–95, 2001.

Yoon H, Liyanarachchi S, et al.: Gene expression profiling of isogenic cells with different TP53 gene dosage reveals numerous genes that are affected by TP53 dosage and identifies CSPG2 as a direct target of p53, *Proc Natl Acad Sci U S A* 99:15632–15637, 2002.

Yoshida A, Tsuta K, et al.: Comprehensive histologic analysis of ALK-rearranged lung carcinomas, *Am J Surg Pathol* 35:1226–1234, 2011.

Yoshimoto M, Joshua AM, et al.: Three-color FISH analysis of TMPRSS2/ERG fusions in prostate cancer indicates that genomic microdeletion of chromosome 21 is associated with rearrangement, *Neoplasia* 8:465–469, 2006.

Young J, Jass JR: The case for a genetic predisposition to serrated neoplasia in the colorectum: hypothesis and review of the literature, *Cancer Epidemiol Biomarkers Prev* 15:1778–1784, 2006.

Zafarana G, Ishkanian AS, et al.: Copy number alterations of c-MYC and PTEN are prognostic factors for relapse after prostate cancer radiotherapy, *Cancer* 118:4053–4062, 2012.

Zardavas D, Maetens M, et al.: The AURORA initiative for metastatic breast cancer, *Br J Cancer* 111:1881–1887, 2014.

Zbuk KM, Eng C: Hamartomatous polyposis syndromes, *Nat Clin Pract Gastroenterol Hepatol* 4:492–502, 2007.

Zhang L, Bluth MH, et al.: Molecular diagnostics in the neoplasms of the pancreas, liver, Gallbladder, and Extrahepatic biliary tract: 2018 update, *Clin Lab Med* 38:367–384, 2018.

Zhang Y, Roccaro AM, et al.: LNA-mediated anti-miR-155 silencing in low-grade B-cell lymphomas, *Blood* 120:1678–1686, 2012.

Zhou XP, Waite KA, et al.: Germline PTEN promoter mutations and deletions in Cowden/Bannayan-Riley-Ruvalcaba syndrome result in aberrant PTEN protein and dysregulation of the phosphoinositol-3-kinase/Akt pathway, *Am J Hum Genet* 73:404–411, 2003.

Zhu Z, Gandhi M, et al.: Molecular profile and clinical-pathologic features of the follicular variant of papillary thyroid carcinoma. An unusually high prevalence of ras mutations, *Am J Clin Pathol* 120:71–77, 2003.

Zlobec I, Lugli A: Prognostic and predictive factors in colorectal cancer, *J Clin Pathol* 61:561–569, 2008.

Zucman J, Delattre O, et al.: EWS and ATF-1 gene fusion induced by t(12;22) translocation in malignant melanoma of soft parts, *Nat Genet* 4:341–345, 1993.

Zucman-Rossi J, Jeannot E, et al.: Genotype-phenotype correlation in hepatocellular adenoma: new classification and relationship with HCC, *Hepatology* 43:515–524, 2006.

Zuo L, Weger J, et al.: Germline mutations in the p16INK4a binding domain of CDK4 in familial melanoma, *Nat Genet* 12:97–99, 1996.

CHAPTER 80

HIGH-THROUGHPUT GENOMIC AND PROTEOMIC TECHNOLOGIES IN THE POSTGENOMIC ERA

Martin H. Bluth

OVERVIEW, 1607

THE HUMAN GENOME PROJECT, 1608
Public Sequencing Effort (Hierarchical Shotgun Sequencing), 1608
Private Sequencing Effort (Whole-Genome Shotgun Sequencing), 1609
Finishing the Sequence of the Human Genome, 1609

HIGH-THROUGHPUT TECHNOLOGIES, 1609
Genomic, 1609
Proteomic, 1614

MOLECULAR MARKERS FOR THE DIAGNOSIS OF HUMAN NEOPLASIA, 1615
Genomic, 1615
Proteomic, 1615

DIAGNOSTIC CANCER APPLICATIONS, 1616
Small, Round Blue Cell Tumors, 1616
Barrett Esophagus, 1616
Thyroid Carcinoma, 1617
Adenocarcinoma, 1617
Pancreatic Cancer, 1617
Other Cancers, 1617

PROGNOSTIC MOLECULAR MARKERS OF DISEASE, 1618
Genomic, 1618
Integrating Genomics and Proteomics, 1619

PITFALLS OF MOLECULAR MARKERS FOR BOTH PROGNOSTICS AND DIAGNOSTICS, 1620
Microarray Data Sets, 1620
"Overfitting" The Predictor, 1620
The "Bystander" Effect, 1620
Limitations of Proteomic Techniques, 1620

EMERGING TECHNOLOGIES, 1620
CRISPR, 1620
Next-Generation Sequencing, 1621
Ion Torrent Sequencing, 1622

CONCLUSION AND FUTURE CHALLENGES, 1622

SELECTED REFERENCES, 1623

KEY POINTS

- Completion of the Human Genome Project has provided scientists with a detailed map of the human genome and predicted coding regions that have facilitated the emergence of high-throughput genomic and proteomic technologies.
- A number of mature platforms exist for high-throughput profiling of gene expression in human tissue, including serial analysis of gene expression (SAGE), deoxyribonucleic acid (DNA) microarrays, and real competitive polymerase chain reaction.
- Proteomic technologies, including mass spectrometry and protein arrays, have begun to explore the dynamic and complex protein composition of healthy and diseased human tissue.
- DNA microarray and SAGE technologies have identified diagnostic gene-expression signatures for a number of hematologic and solid malignancies that are often difficult to distinguish using traditional histologic analysis.
- Prognostic gene and protein expression profiles have been identified in a large number of cancer settings, including lymphoma, lung cancer, breast cancer, and acute myeloid leukemia, among others.
- Validation in large clinical trials, standardization of techniques and controls, and inclusion of analytic standards are needed before widespread clinical implementation of these technologies can be achieved.

OVERVIEW

With the complete sequence of human and other genomes recently elucidated, we have witnessed an explosion of information and high-throughput tools that are profoundly altering biomedical research and the culture of science. This revolution, which began in the mid-1980s, emerged from developments in three areas: (1) molecular biology, most notably, breakthroughs in rapid deoxyribonucleic acid (DNA) sequencing; (2) information technology, in particular, the ability to store and analyze unprecedented quantities of data; and, most important, (3) progress in human genetics, especially the identification of thousands of single-gene human disorders. The convergence of these technological and scientific advances raises promise for the rapid identification of disease-related genes, leading to improved diagnostic tests and more effective therapies.

Detailed maps of human and other genomes provide the information needed to chart a course toward understanding and treating many diseases. However, this course remains a long and difficult one. Although progress will come most readily for disorders following Mendelian patterns of inheritance, even these disorders will pose significant difficulties. For example, although the biology and genetics of sickle cell anemia have been reasonably well understood for more than half a century—a single valine replaces glutamic acid at position 6 in the β-hemoglobin chain—effective treatment has been slow to develop. The penetrance of genetic diseases thought to be due to single mutations often relies on more complex interactions between the mutation and a variety of concurrent gene polymorphisms, such as those seen in the genes encoding surface proteins on postcapillary venule endothelial cells, which, in part, account for sickle cell disease severity.

Many common diseases—in particular, cardiovascular disease, mental illness, and almost all cancers—stem from multigenic causes. In addition, these diseases invariably have strong environmental components, presenting a substantial challenge to the development of effective and economical diagnostic and prognostic tests. Even in the absence of a confounding environmental influence, linking the quantifiable phenotype of a disease to a set of distinct alleles is a complex undertaking. Further complicating matters, many disorders do not have sharply defined, quantifiable phenotypes.

In a chapter filled with information on promising technologies, we make these sobering remarks to emphasize that greater understanding never guarantees cures or therapies. However, greater understanding does aid the development of rational strategies to detect and control disease. The reference genome allows us to rapidly characterize polymorphisms across the human population; it also enables molecular fingerprinting technologies that permit identification of the precursors and consequences of normal and pathologic changes in gene and protein expression. We can feel confident that the power of genomic technologies is well beyond anything previously available, and that it will make possible during the next several decades a host of new diagnostics and therapeutics for cancer and other common diseases, profoundly altering the practice of medicine. As discussed in Chapter 75, genomic technologies have already made an impact in the area of pharmacogenomics, in which drug protocols are

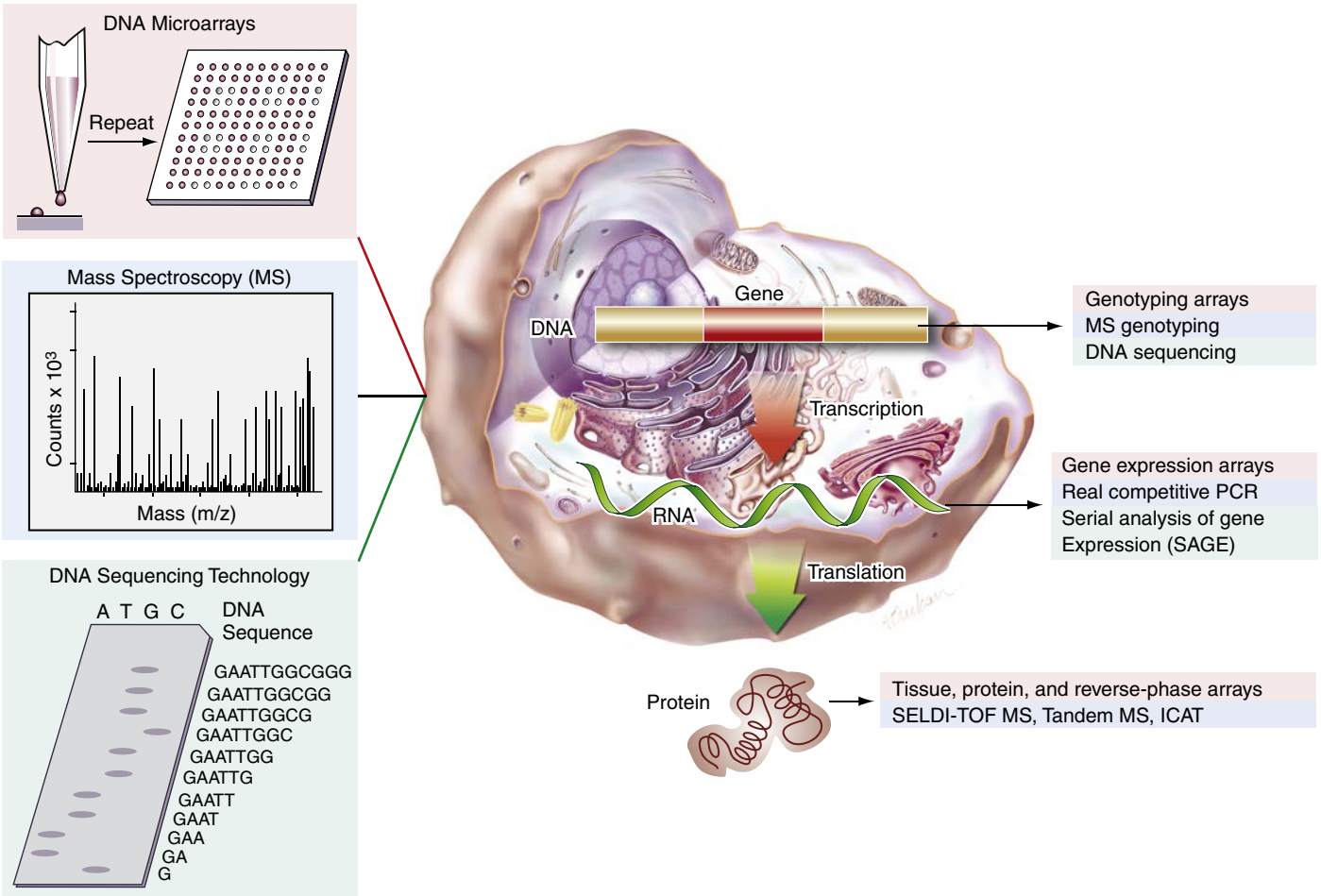

Figure 80.1 High-throughput platforms and the central dogma of biology. The three major technologies responsible for rapid analysis of biological systems include mass spectrometry, sequencing, and microarrays. Examples of each technology have been listed as applied to each broad stage of biological information, that is, DNA, RNA, and protein. *ICAT,* Isotope-coded affinity tags; *m/z,* mass-to-charge ratio; *MS,* mass spectroscopy; *SELDI-TOF-MS,* surface-enhanced laser desorption ionization, time-of-flight mass spectroscopy. (Modified with permission from Kufe DW, Holland JF: *Cancer Medicine,* ed 6, Hamilton, Ontario, 2003, BC Decker; Wilson J, Hunt T: *Molecular Biology of the Cell,* ed 4, New York, 2003, Garland Science; Brown TA: *Genomes*, ed 2, New York, 2002, John Wiley & Sons.)

being designed from the cytochrome P450 genetic profiles of patients, allowing for maximally effective therapeutic regimens for each patient.

This chapter focuses on several high-throughput genomic and proteomic technologies that have the potential to influence disease classification and prognostication (Fig. 80.1). These molecular tools have affected virtually all forms of human pathology. However, given the public health implications and the preponderance of recent publications in the field, we will concentrate on diagnostic and prognostic applications related to cancer, although we will mention other salient disease states where applicable. After presenting a brief overview of the Human Genome Project and resultant high-throughput technologies, we will discuss examples of applications in the setting of several hematologic and solid malignancies. The scope of the chapter has been constrained to focus on high-throughput technologies; therefore, this chapter does not represent a comprehensive overview of all technologies being used in clinical genomic and proteomic studies. In addition, among the technologies presented, some are highlighted in greater detail because of their widespread use. As more data are produced using these technologies, strategies combining data sets may become powerful approaches to developing accurate clinical tools. Along with measuring gene and protein expression levels, understanding human genetic variation in DNA will be important in elucidating disease markers and mechanisms. A discussion of high-throughput genotyping technologies to assay single-nucleotide polymorphisms is beyond the scope of this chapter, however (for reviews, see Syvanen, 2001; Ding & Jin, 2009).

THE HUMAN GENOME PROJECT

PUBLIC SEQUENCING EFFORT (HIERARCHICAL SHOTGUN SEQUENCING)

Sequencing of the human genome was a 15-year, $3 billion project, initiated in 1990 as a joint effort between the U.S. Department of Energy and the National Institutes of Health (Collins et al., 2003). From the time of the project's inception through 1995, genetic and physical maps of human and mouse genomes were constructed, and yeast and worm genomes were sequenced. These initial projects, coupled with advances in sequencing technology and sequence data analysis, outlined cost-effective strategies and techniques while demonstrating the feasibility of sequencing the human genome. In March 1999, the effort to sequence the human genome commenced in earnest. Sequencing was set to be completed in two phases: the first phase would include completion of a draft sequence and the second would be a finishing phase for resolution of misassembled regions and filling in of sequence gaps. By June 2000, centers involved in the project were producing raw sequence data at a rate of about 1000 nucleotides per second, 24 hours a day, 7 days a week (Lander et al., 2001).

The first phase of the Human Genome Project, a collaborative endeavor of 20 groups in six countries, was completed and published in February 2001 in the journal *Nature* (Genome International Sequencing Consortium, 2001; Lander et al., 2001). The draft sequence covered about 96% of the euchromatic part (gene-rich) of the human genome and 94% of the entire genome, with an average of fourfold coverage (i.e., each base sequenced an average of four times). The International Human Genome Sequencing Consortium employed a sequencing strategy referred to as *hierarchical shotgun sequencing* (also known as *map-based*, *bacterial artificial chromosome* (*BAC*)*–based*, or *clone-by-clone sequencing*) (Olson, 2001). Genomic DNA obtained from volunteers from a variety of racial and ethnic backgrounds was partially digested with restriction endonucleases. Fragments of 1 to 2 MB in length were cloned into BACs. Eight DNA libraries containing overlapping insert clones were created, representing 65-fold coverage of the genome (each base is represented on average 65 times, as seen on examination of all 8 libraries).

BACs containing fragments of the human genome are inserted into bacteria and are replicated as the bacteria grow and divide. Each BAC clone is completely digested with a restriction enzyme to produce a unique

pattern of DNA fragments, known as a *fingerprint*. The fingerprints from different BAC clones can be compared to allow selection of a set of overlapping BAC clones that cover a portion of the genome (a large region of the genome covered by overlapping clones is called a *contig*). Contigs can be positioned along the chromosome by using known markers from previously constructed genetic and physical maps of the human genome. Selected BAC clones are sheared into smaller overlapping fragments, subcloned, and sequenced. Subcloning is necessary because each sequencing reaction can reliably read only about 500 base pairs (bp). The sequence of the BAC clone can be reconstructed from the set of sequences obtained from the subclones, and BAC fingerprints guide the assembly of several BAC clones into contigs.

Draft sequences were required to obtain an average of fourfold coverage with 99% accuracy as determined by software (i.e., PHRED, PHRAP; CodonCode Corporation, Dedham, MA) that assigns base quality scores and assembles sequences according to the scores. Throughout the duration of the project, sequences longer than 2 KB were required to be deposited in public databases within 24 hours (data are available from the Genome Browser of the University of California at Santa Cruz, www.genome.ucsc.edu; the GenBank of the National Center for Biotechnology Information, http://www.ncbi.nlm.nih.gov/genbank/; and Ensembl of the European Bioinformatics Institute and the Sanger Centre, www.ensembl.org). Assembly of the draft sequence was a three-part process that involved filtering the sequence data to eliminate bacterial and mitochondrial sequences, constructing a layout of clones along the genome, and merging overlapping clones to produce a draft sequence.

The hierarchical shotgun sequencing approach was chosen by the public consortium for several reasons. Dividing the work among sequencing centers was straightforward with the use of clones. Also, the assembly of clones to produce a draft sequence probably would enhance accuracy because approximately 46% of the human genome comprises repeat sequences and exhibits widespread individual sequence variation. In addition, this approach could address cloning bias, and underrepresented sequences could be targeted for sequencing.

PRIVATE SEQUENCING EFFORT (WHOLE-GENOME SHOTGUN SEQUENCING)

In 1998, a private company, Celera Genomics (Alameda, CA), led by Craig Venter, announced its intention of sequencing the human genome in 3 years using a different approach, known as *whole-genome shotgun sequencing*. Celera's draft of the human genome sequence was reported in the February 2001 issue of *Science* (Venter et al., 2001). Celera generated 14.8 billion bp of DNA sequence in 9 months to produce a 2.91 billion–bp consensus sequence of the euchromatic part of the human genome with an average of fivefold coverage. The company used genomic DNA obtained from three females and two males of the following ethnogeographic groups: African American, Asian-Chinese, Hispanic-Mexican, and white. A total of 16 different DNA libraries were constructed with three different insert sizes: 2 KB, 10 KB, and 50 KB. Both ends of the insert from clones chosen at random were sequenced to produce "mate pair" sequencing reads. The average distance between mate pairs was known because the range of insert sizes for a clone taken from a particular library could be characterized by calculating the distance between mate pairs in previously sequenced stretches of the genome. Celera generated a set of 27.26 million reads with an average length of 543 bp.

Celera combined its sequence data with all data from the publicly funded efforts available up to September 2000 in GenBank and pursued two different assembly strategies. The whole-genome assembly strategy involved "shredding" the publicly funded sequences into small fragments, combining these fragments with Celera's reads, identifying overlapping sequences, and joining them to produce long, continuous consensus sequences. These contigs were ordered, and gaps between contigs were quantified using information obtained from the mate pair reads. A variant of the process described previously, known as *compartmentalized shotgun assembly*, yielded slightly better results because sequences were first clustered, based on mapping information, to a region of the chromosome before the process already described was performed.

Analyses of draft sequences performed by the two groups yielded similar results. Some genes were derived from bacteria or transposable elements, and large segmental duplications were apparent throughout the genome. The distribution of genes, CpG islands, recombination sites, and repeats was found to be highly variable across the genome. Widespread genetic variation was apparent, and about 2.1 million single-nucleotide polymorphisms—1 per 1250 bp—were discovered. One of the most surprising results revealed by completion of the draft sequence was the estimate that the genome contained about 30,000 protein-coding genes, considerably fewer than the 100,000 or more that had been postulated. The number is only one-third greater than that of the worm. However, probably a much larger number of different proteins were noted because of alternative splicing (Claverie, 2001). Scientists used many gene-prediction methods to arrive at the gene estimate of 30,000. Gene-prediction algorithms predict the location of unknown genes in the genome using sequence characteristics learned from known genes, including codon and nucleotide composition within coding regions and conserved sequences at exon/intron boundaries and within promoter regions. The human genome sequence has a low signal-to-noise ratio because the coding regions represent only about 3% of the genome; therefore, algorithms produce a large number of false-positives. Most algorithms, however, use two other important sources of information: (1) similarity to known human proteins and expressed transcripts and (2) homology to proteins and sequences characterized in other organisms. (For a review of gene prediction algorithms, see Mathe et al., 2002.)

FINISHING THE SEQUENCE OF THE HUMAN GENOME

In October 2004, in the journal *Nature*, the International Human Genome Sequencing Consortium published an article entitled, "Finishing the Euchromatic Sequence of the Human Genome" (International Human Genome Sequencing Consortium, 2004). This article reported that the draft sequence was missing about 10% of the euchromatic portion of the genome, contained about 150,000 gaps, and had many sequence segments that had not been assigned an order or orientation. The current sequence contains 2.35 billion nucleotides, covers about 99% of the genome, and has only 341 gaps (with an error rate of 1 mistake every 100,000 bases). The sequence revision predicts between 20,000 and 25,000 protein-coding genes; this discrepancy in number is due to differences in gene prediction algorithms. The newly published sequence reveals that segmental duplications cover about 5.3% of the euchromatic portion, providing insight into the evolution of the human genome and aiding the study of diseases caused by deletions and rearrangements of these regions (e.g., DiGeorge syndrome) (Stankiewicz & Lupski, 2002). This latest sequence also makes it possible to trace the birth and death of genes—genes recently born as a result of gene duplication and genes lost as a result of mutation.

Sequencing of the human genome is a monumental achievement that "holds an extraordinary trove of information about human development, physiology, medicine, and evolution" (Lander et al., 2001). It has provided the infrastructure for sequencing other genomes and for understanding the structure and complexity of human genetic variation. This detailed map of the human genome and predicted coding regions has facilitated the emergence of several high-throughput technologies through which scientists have begun to explore the complete set of gene and protein expressions in healthy and diseased human tissue. These technologies promise to revolutionize the classification of human disease and to usher in an era of individualized molecular medicine.

HIGH-THROUGHPUT TECHNOLOGIES

GENOMIC

An intimate understanding of cellular machinery represents the first step toward unraveling the complexity of human disease. Important insights into the function of a gene can be deduced by determining the cell type and conditions under which a gene is expressed, and by quantifying the level of message transcribed. A technique commonly used to assay the level of expression of a single gene (represented by messenger ribonucleic acid [mRNA]) across a few different conditions is a Northern blot. This "gene-by-gene" approach began to change in the early 1990s as a result of the success of the Human Genome Project and various technological advances that enabled the development of high-throughput gene-expression analyses whereby several genes could be assayed simultaneously. Three different genomic high-throughput technologies are discussed here. Serial analysis of gene expression (SAGE) (Velculescu et al., 1995) and DNA microarrays (Schena et al., 1995; Lockhart et al., 1996) were both developed in the 1990s and are currently in widespread use. Real competitive polymerase chain reaction (PCR) using matrix-assisted laser desorption ionization time-of-flight mass spectroscopy (MALDI-TOF-MS) was first published in 2003 (Ding & Cantor, 2003). The basic principles underlying DNA microarrays are discussed in Chapter 68; those underlying real competitive PCR are discussed in Chapter 69.

Depending on the experimental design, samples are obtained from cell cultures or surgical tissues, and total RNA is isolated. Techniques such as laser

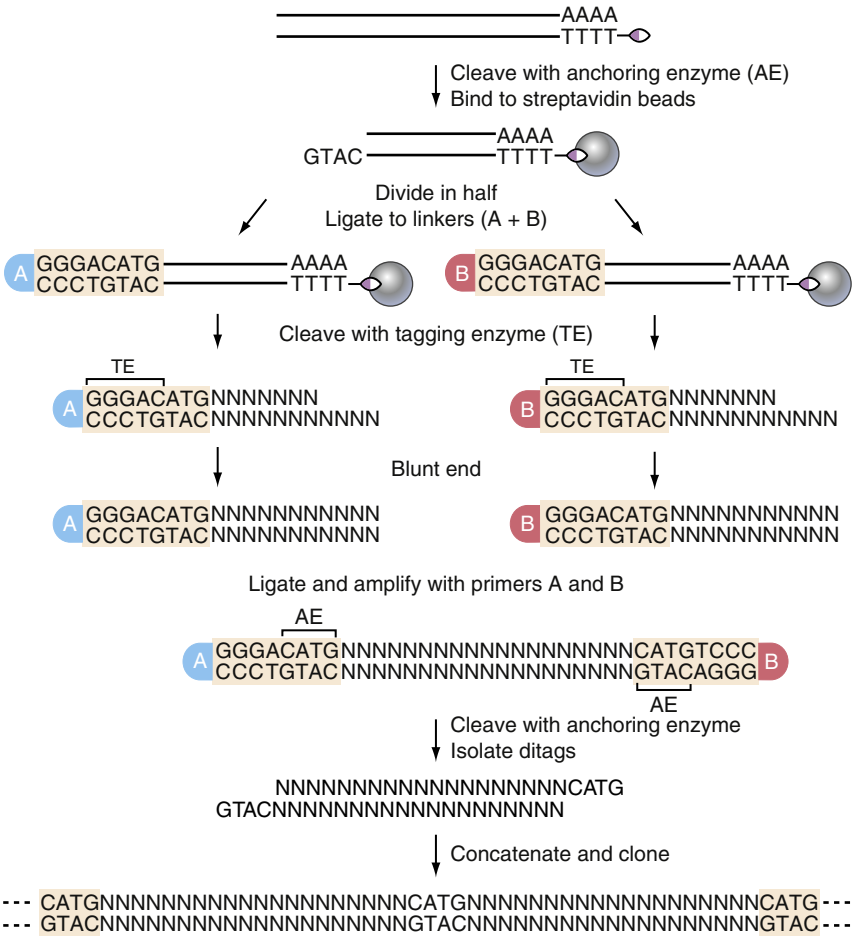

Figure 80.2 Serial analysis of gene expression (SAGE) is a technique that measures the expression levels of genes in a sample of interest. RNA is isolated from the sample, complementary DNA (cDNA) is synthesized, and several thousand short base pair (bp) tags are isolated. SAGE uses two types of restriction enzyme: one, called the *anchoring enzyme* (i.e., NlaIII), recognizes a specific 4-bp sequence and cleaves DNA every 256 bp, immediately 5′ of the sequence tag. The second enzyme, called the *tagging enzyme* (i.e., BsmFI), behaves differently and cleaves DNA 14 to 15 bp immediately 3′ of its recognition sequence. First, cDNA fragments are cut with the anchoring enzyme, captured using streptavidin-biotin affinity chromatography, purified, and split into two pools—A and B. Second, two different linkers (A and B) are ligated to the 5′ ends of the cDNA fragments in their respective pools. The cDNA fragments in each pool are then cut with the tagging enzyme *(TE)*, resulting in a new fragment that contains the linker plus a short 10-bp region of the cDNA, known as a *tag*. The two pools of cDNA fragments are ligated together, creating ditags, which are amplified by polymerase chain reaction (PCR) using primers designed on the basis of sequences in linkers A and B. After amplification, the anchoring enzyme is used to cleave the linkers off the ends of the ditags. Ditags from different reactions are ligated together to form strings of 10 to 50 tags. The concatenated strings of ditags are cloned into plasmids and sequenced. Sequences of the tags are used to identify the corresponding genes and represent a measure of transcript abundance. (Modified with permission from Yamamoto M, Wakatsuki T, Hada A, et al.: Use of serial analysis of gene expression [SAGE] technology, *J Immunol Methods* 250:45–66, 2001.)

capture microdissection (Emmert-Buck et al., 1996) are often used before RNA isolation to obtain a homogeneous population of cells from tissue specimens. After total RNA or mRNA is obtained and is reverse transcribed to make complementary DNA (cDNA) (see Chapter 69), each technology uses a different protocol to rapidly measure the transcript levels of the genes in each sample. The principles of each method, as well as corresponding advantages and disadvantages, are outlined in the following sections.

Serial Analysis of Gene Expression

SAGE measures the expression level of genes in a sample by isolating and sequencing several thousand short 10- to 14-bp tags isolated from cDNA. Two important pieces of information can be deduced from the output: (1) the sequences of the tags usually allow identification of their corresponding genes and (2) the number of times a particular tag is sequenced is a measure of transcript abundance. The ability to uniquely identify a transcript using as short a sequence as 9 bp resides in the probability of defining this sequence from others. Such a sequence can distinguish 262,144 transcripts (4^9)—a number greater than current estimates of the number of transcripts in the human genome (Velculescu et al., 1995; Pennisi, 2000).

The SAGE protocol involves isolating RNA from a sample of interest. RNA is converted to double-stranded cDNA using a biotinylated oligo primer for first-strand synthesis. SAGE then uses two types of restriction enzymes. The first, called an *anchoring enzyme*, recognizes a specific 4-bp sequence (e.g., NlaIII). Any 4-bp–recognizing enzyme may be used because, on average, enzymes cleave every 256 bp (4^4). The anchoring enzyme leaves a short, overhanging, single-stranded piece of DNA at the 5′ end of the site of cleavage. The biotinylated fragment, which represents the 3′ end of the gene, then is bound to streptavidin beads, capturing only digested cDNA fragments that contain a portion of the poly(A+) tail. Captured fragments are purified and are randomly split equally into two pools. The second enzyme, called the *tagging enzyme*, behaves differently and cleaves DNA 14 to 15 bp immediately 3′ of its recognition sequence (e.g., BsmFI). The recognition sequence for the tagging enzyme is engineered into the sequence of linkers described in the following section.

After the purified fragments are split into two pools, two different oligonucleotide linkers, each containing a different PCR primer sequence (for purposes of discussion, the linkers will be labeled A and B)—the tagging enzyme recognition sequence and a single-stranded DNA overhang that is part of the anchoring enzyme recognition sequence—are designed and synthesized. Linker A is ligated to the 5′ ends of cDNA fragments in one pool, and linker B is ligated to the 5′ ends of cDNA fragments in the other pool. Ligation proceeds by means of base pairing between complementary single-stranded overhanging DNA ends on both cDNA fragments and linkers, creating an intact anchoring enzyme recognition sequence. The cDNA fragments in each pool are then cut with the tagging enzyme, resulting in a new fragment that contains the linker plus a short, 10-bp region of cDNA, known as a *tag* (the remaining cDNA fragment and the poly[A+] portion of the tail are removed). The two pools of cDNA fragments are ligated together, creating ditags (the new sequences are as follows: linker A–tag–tag–linker B). Ditags are amplified by PCR using primers designed on the basis of sequences in linkers A and B.

Creation of the ditags is important for several reasons. First, ditags can be amplified by PCR for subsequent cloning steps. Second, each tag within a ditag is linked tail to tail and is flanked by anchoring enzyme–recognition sequences, providing important orientation information used to identify the genes corresponding to each tag. Finally, even if tags are highly abundant, the probability of creating identical ditags is extremely low. As a result, the occurrence of identical ditags indicates PCR bias; these ditags are excluded from the final analysis to ensure accurate quantification of transcript abundance (Velculescu et al., 1995; Yamamoto et al., 2001).

After amplification, the anchoring enzyme is used to cleave the linkers from the ditags. Ditags from different reactions are ligated together end to end to form strings of 10 to 50 tags. The concatenated strings of ditags are cloned into plasmids and are sequenced. Typically, about 50,000 tags are sequenced for each sample of interest using a high-throughput sequencer. (For additional details on the method, see the review by Madden et al., 2000.) The absolute expression levels of genes in the sample are quantified by counting the number of sequenced tags that correspond with each gene. Figure 80.2 provides a visual scheme of the procedure.

SAGE technology has continued to mature, and technologies have been used to refine this technology toward its application, including an increase in sequencing efficiency (deepSAGE), improved tag-to-transcript

mapping of SAGE tags (longSAGE), and reduction of the amount of required input RNA (microSAGE). The expansion of SAGE application from solely transcriptosome-based analysis to genomic analysis has given rise to Serial Analysis of Chromatin Occupancy, which identifies genomic signature tags that pinpoint transcription factor–binding sites. Because of the advent of microSAGE, small amounts of material obtained from needle biopsies and from specific cell types (obtained via fluorescence-activated cell sorting or laser microdissection) are sufficient to allow characterization of global gene expression (Datson, 2008).

The Cancer Genome Anatomy Project of the National Cancer Institute has chosen SAGE technology to sequence more than 5 million tags across more than 100 different human cell types. Data are stored in a public database known as SAGEmap (Lal et al., 1999; Lash et al., 2000). Several tools, such as SAGE Genie (Boon et al., 2002), are available for reliably assigning tags to genes and for performing data analysis and visualization. Additional information and details can be obtained at https://sagebionetworks.org/.

SAGE differs from microarray in that the former employs a sequence-based sampling technique that is not contingent on hybridization and does not require well-defined known genes or sequences. Through this approach, novel genes or gene variants can be elucidated. Furthermore, SAGE provides better gene quantification because it directly counts the number of gene transcripts and is less subject to background "noise" of the microarray; however, it is more expensive. Modifications of SAGE, such as longSAGE, utilize different restriction endonucleases as the tagging enzyme that cuts 17 bp 3′ from the anchoring site, generating a tag with a uniqueness probability of >99% and providing the ability to tag a greater proportion of the unannotated genome. Other modifications that require minimal quantities of mRNA for library construction (SAGE-Lite and Micro-SAGE) have also been described (Datson et al., 1999; Patino et al., 2002).

Microarray

DNA microarrays are orderly arrays of spots, each composed of DNA representing a single gene and immobilized onto a solid support such as a glass slide, as described in Chapter 70. DNA microarrays take advantage of Watson-Crick base pairing; therefore, only strands of DNA that are complementary will hybridize and produce a signal that can be used as a measure of gene expression. Production and use of microarrays requires several steps—including creation of probes, array fabrication, target hybridization, fluorescence scanning, and image processing—to produce a numeric readout of gene expression. Throughout this chapter, a *probe* will refer to a nucleic acid sequence that is attached to a solid support and the *target* will be a complementary free sequence of nucleic acids measured for its abundance with the use of microarrays. A detailed description regarding the fabrication of cDNA and oligonucleotide arrays, along with how the RNA is prepared and hybridized to these platforms, is found in Chapter 70.

DNA microarray experiments can produce millions of data points; this requires a suite of data-processing steps to select relevant genes. Although no standard protocol is available, the following steps usually are included in analysis of a DNA microarray experiment (Fig. 80.3). Image files are converted to numeric values that are normalized and summarized using a software program. Both free and commercially available programs, such as Affymetrix (Affymetrix Inc., Santa Clara, CA) and Agilent (Agilent Technologies, Wilmington, DE), among others, may be used (Li & Wong, 2001; Irizarry et al., 2003). Poor-quality arrays are removed from the analysis. Genes that are not accurately detected by the array and genes that show little variation across samples are filtered out. Then, a variety of computational and statistical analyses are performed. Exploratory data analyses, including classification and identification of differentially expressed genes, can be divided into two categories: *supervised* and *unsupervised* methods. Supervised methods, such as class-prediction algorithms, use predefined groups of samples (referred to as the *training set*) to identify genes that can distinguish between groups to accurately classify unknown samples (referred to as the *test set*). A large number of supervised class-prediction algorithms have been applied to microarray data, including linear or quadratic discriminant analysis (Dudoit, 2002), k-nearest neighbors (Simon & Lam, 2004), weighted voting (Golub et al., 1999), artificial neural networks (Khan et al., 2001), support vector machines (Brown et al., 2000), and shrunken centroids (Tibshirani et al., 2002). Supervised algorithms—such as significance analysis of microarrays (SAM) (Tusher et al., 2001), as well as parametric and nonparametric statistical tests between groups of samples—can be used to identify differentially expressed genes. Unsupervised methods, also known as *class-discovery methods*, can be used to find previously unknown classes, such as novel cancer subtypes, within a data set. Various clustering techniques, such as hierarchical clustering (Eisen et al., 1998) and self-organizing maps, are commonly used class-discovery algorithms (for a general review, see Kaminski & Friedman, 2002; for a cDNA array analysis review, see Leung & Cavalieri, 2003; and for an oligonucleotide array analysis review, see Tumor Analysis Best Practices Working Group, 2004).

The Gene Expression Omnibus database (GEO; available at http://www.ncbi.nlm.nih.gov/geo) is a central repository for high-throughput gene-expression data through which a wide range of microarray data from published experiments is publicly available. All microarray data deposited in GEO adhere to the Minimum Information About a Microarray Experiment guidelines established to provide basic information about experimental designs, samples, and types of technology used. In addition to GEO, a wide range of bioinformatics tools is available for microarray data analysis (Quackenbush, 2001; Zhang et al., 2009). No standards for analyzing microarray data have been established, and various methods can often produce different results (for a discussion, see Tumor Analysis Best Practices Working Group, 2004). Validation studies with larger sample sizes or using a different technology are usually necessary to confirm significant findings.

Real Competitive Polymerase Chain Reaction

Real competitive PCR combines conventional competitive PCR techniques with single base extension and MALDI-TOF-MS to measure gene-expression levels. The principles of mass spectroscopy are discussed in Chapter 5, and its applications to drug analysis, identification and speciation of microorganisms and proteomics of cancer-associated proteins are discussed in Chapters 5, 24, 57 and 77, respectively. The use of MALDI-TOF-MS in high-throughput genomic studies is a recent innovation that is capable of absolute gene quantification with extremely high sensitivity and produces results consistent with real-time PCR and DNA microarrays. The basic principles underlying real-time PCR are discussed in Chapter 69.

Analogous to real-time PCR, use of this technique requires previous knowledge of the sequences of the genes of interest. Through this approach (Figs. 80.4 and 80.5), total RNA from a sample is reverse transcribed using random hexamers or gene-specific primers. An 80- to 100-bp region is selected from the gene of interest, and primers are designed to amplify this region in a PCR. A known concentration of an 80- to 100-bp DNA oligonucleotide of the same length and sequence, except for a single-point mutation (known as the *competitor*), is added to the PCR for amplification with the gene of interest. The competitor and the gene of interest will be amplified with the same kinetics because their sequences are almost identical. As a result, the concentration of the gene of interest can be calculated on the basis of the amount of competitor present in the PCR. A series of PCRs are performed with different concentrations of the oligonucleotide competitor to accurately titrate the final concentration of the candidate gene. Next, each PCR is subjected to a base extension reaction. A short base extension primer (approximately 23 nucleotides long) is designed to anneal to both 80-bp amplified PCR products adjacent to the site of the single-point mutation. A base extension reaction is then carried out with three dideoxydinucleotide triphosphates and one deoxynucleotide triphosphate to produce two extension products that differ in their terminal nucleotide. As a result of this one-nucleotide difference, MALDI-TOF-MS is able to identify and quantify the two products on the basis of their different molecular weights. The throughput of the assay can be increased by a technique known as *multiplexing*, whereby several genes are quantified in a single PCR and primer extension reaction using unique primers, competitors, and extension oligonucleotides for each gene.

This system, initially developed for high-throughput genotyping, was adapted for gene-expression analysis in 2003 (Ding & Cantor, 2003) and was marketed by a California-based company (Sequenom, Inc., San Diego, CA). Thus, public data and analysis resources are in the process of development. Applications of the technique include measurement of expression levels for three genes in RNA isolated from buccal mucosal cells obtained from smokers versus nonsmokers (Spira et al., 2004), measurement of allele-specific expression of *ABCD1*, a gene involved in X-linked adrenoleukodystrophy (Ding et al., 2004), and detection of infectious diseases (Arbefeville et al., 2014; McIver et al., 2014). Variations of this methodology, such as phage display–mediated immunopolymerase chain reaction (PD-IPCR) and competitive quantitative real-time polymerase chain reaction (cqPCR) have also been applied to the food industry to detect toxins (Liu et al., 2014) and allergens (Holzhauser et al., 2014), respectively.

The three genomic high-throughput technologies highlighted previously use very different techniques to measure the abundance of gene transcripts; each technique has a unique set of advantages and disadvantages. A brief overview comparing the three different platforms can be found in Table 80.1. The major limitation of SAGE is that it requires many laborious PCR and sequencing reactions per sample and, thus, is

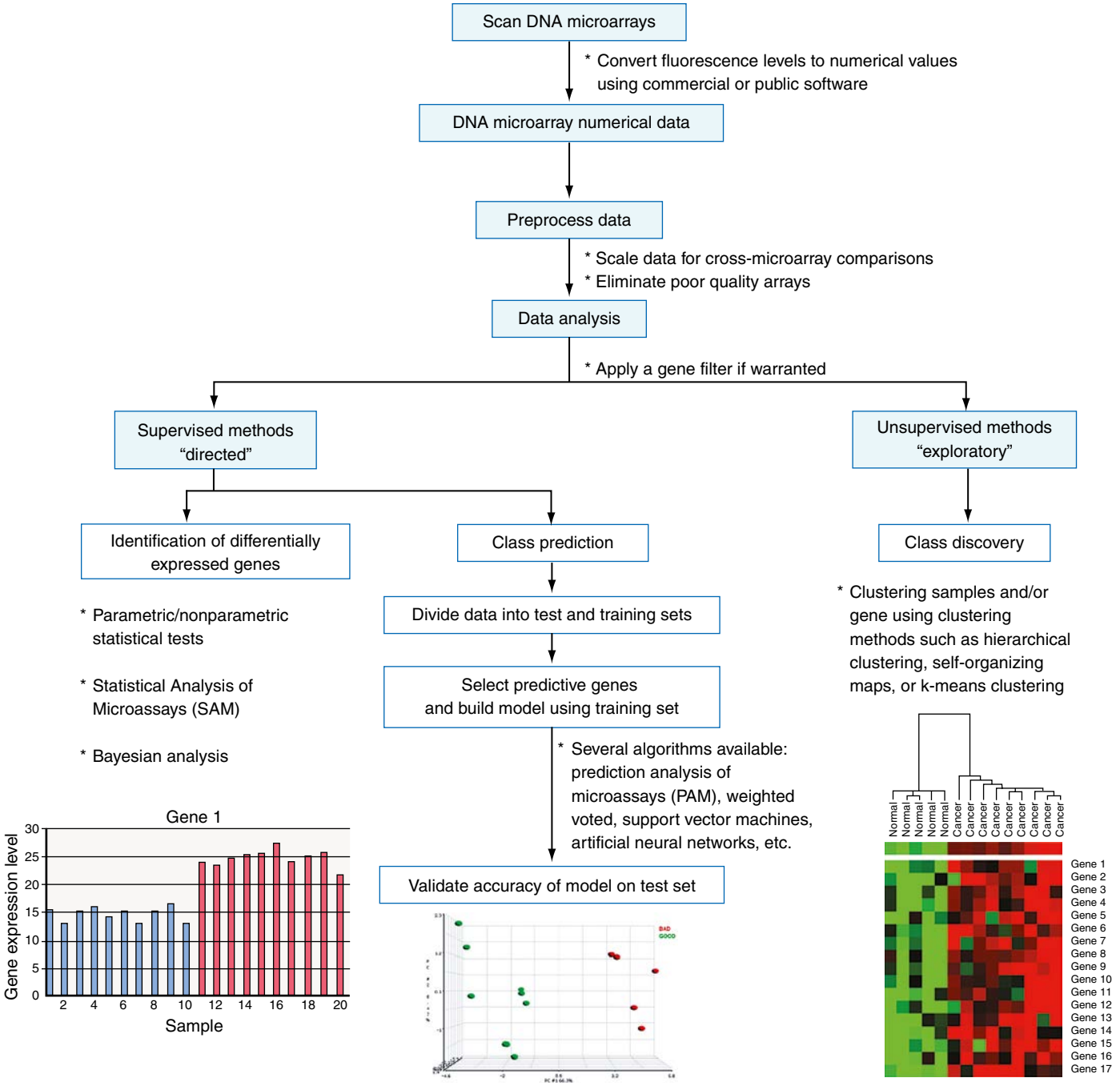

Figure 80.3 Analysis of DNA microarray data. The schematic diagram outlines the various steps required in the analysis of DNA microarray data. Image files are converted to numeric values; normalized, poor-quality arrays are removed from the analysis; and genes that are not accurately detected by the array and genes that show little variation across samples are filtered out. Downstream computational and statistical analysis of the data can be divided into two categories: supervised and unsupervised methods. Supervised methods, such as *class prediction algorithms*, use predefined groups of samples to identify genes that can distinguish between groups and can accurately classify unknown samples. Unsupervised methods, also known as *class discovery methods*, try to find previously unknown classes, such as novel cancer subtypes, within a data set.

high-throughput in terms of genes, not samples. Another drawback of SAGE is that it requires a large amount of starting RNA. However, as noted earlier, several modifications have been made to the protocol; a new technique known as microSAGE requires only 1 to 5 ng of poly(A+) RNA (Datson, 2008). Advantages of the technology include that it is not based on prior sequence information and that it is capable of discovering novel transcripts. The output from SAGE consists of sequence data that allow direct transcript identification with the use of public sequence databases.

DNA microarrays, on the other hand, are higher throughput than SAGE in terms of genes and samples. DNA microarrays are practical for studies assaying clinical samples for which high throughput of samples is required and only small amounts of starting RNA can be obtained. The gene-expression levels obtained from DNA microarrays are only relative transcript levels (in contrast to absolute levels with SAGE) that are dependent on probe selection, making cross-platform comparisons difficult.

Finally, with the use of real competitive PCR, it is difficult to assay several thousand genes, because each gene requires the design of specific primers for the PCR and base extension reactions. Once the assay has been designed, however, the technique can be high throughput in terms of samples. As a result, real competitive PCR probably will not be used as a discovery platform in the way that SAGE and DNA microarrays are used. Rather, it will serve as a validation tool and a potential clinical tool for assaying relatively small numbers of genes across large numbers of individual samples. Continuously evolving ultra high–throughput genomic technologies offered by various vendors (Illumina/Solexa, San Diego, CA; ABI/SOLiD, Foster City, CA; 454/Roche, Branford, CT; and Helicos, Cambridge, MA) will likely be able to provide even greater throughput at reduced cost.

Multiplex PCR

Multiplex PCR (mpPCR) consists of multiple primer sets within a single PCR mixture to produce amplicons of differing sizes that specifically identify different DNA sequences. Primer sets are designed so that their annealing temperatures are optimized to work correctly within a single reaction.

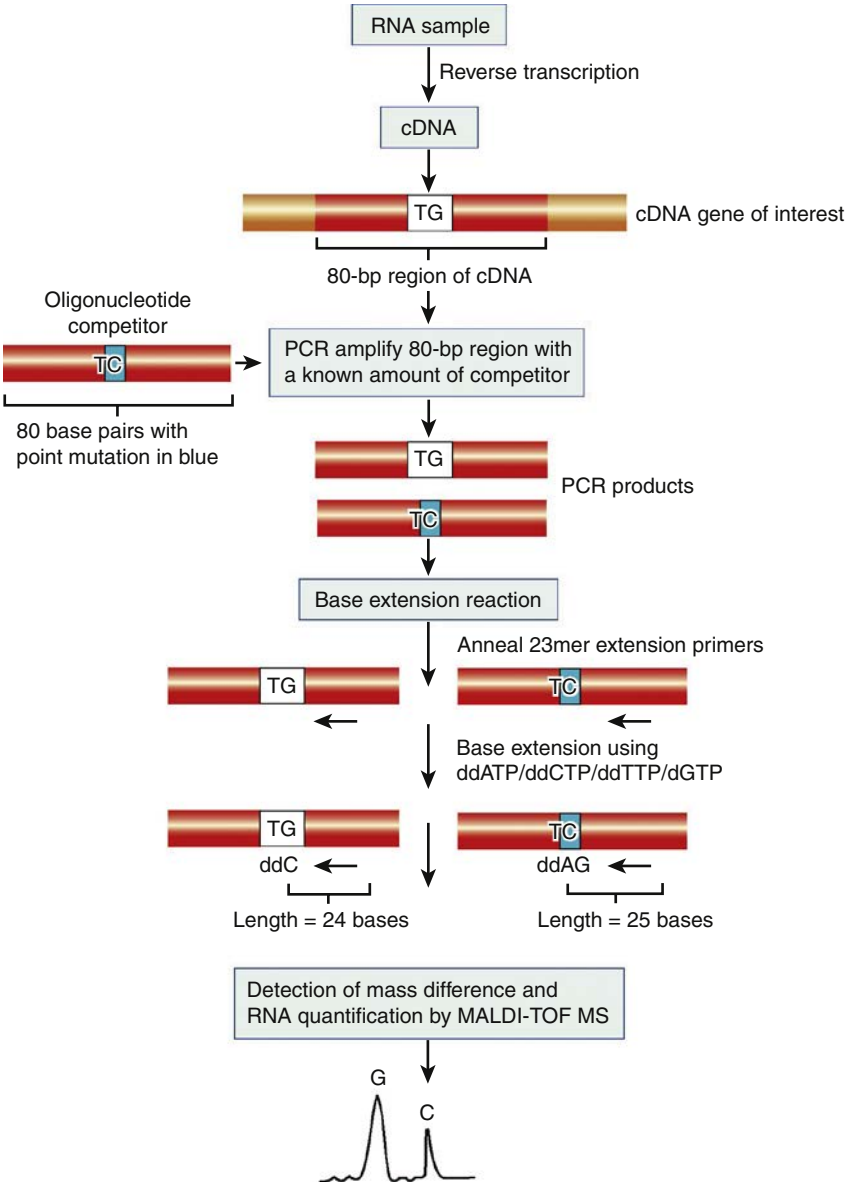

Figure 80.4 Real competitive polymerase chain reaction (PCR) coupled with matrix-assisted laser desorption ionization time-of-flight mass spectroscopy (MALDI-TOF-MS) is a technique used to measure the transcript abundance of a gene in a sample of interest. RNA is isolated, complementary DNA (cDNA) is synthesized from a sample, and a region (≈80 bp) of the gene of interest is selected for PCR amplification. A known concentration of an oligonucleotide competitor of the same length and sequence except for a single-point mutation is added to the PCR reaction for amplification. A short base extension primer (≈23 bp) is designed to anneal to both amplified products adjacent to the site of the single-point mutation. A base extension reaction is then carried out with three dideoxydinucleotide-triphosphates (ddNTPs) and one deoxynucleotide-triphosphate (dNTP) to produce two extension products that differ in their length by one base. As a result of this difference of one nucleotide, MALDI-TOF-MS is able to identify and quantify the two products on the basis of their different molecular weights. (Adapted with permission from Ding C, Cantor CR: A high-throughput gene expression analysis technique using competitive PCR and matrix-assisted laser desorption ionization time-of-flight MS, *Proc Natl Acad Sci U S A* 100:3059–3064, 2003.)

The resultant amplicons are different enough in size to form distinct bands when visualized by gel electrophoresis. By its original design, this assay is typically efficient for elucidating the presence and relative concentrations of from 2 to 20 distinct messages and is limited by the resolution capacity of electrophoretic gel separation (for a review, see Bluth & Bluth, 2013).

xTAG Technology

xTAG technology (Luminex Corp, Austin, TX) is a next-generation form of multiplexing that overcomes the resolution limits of mpPCR by combining the methods of multiplex amplification with particle-based flow cytometry. Like mpPCR, multiple reactions can be carried out in a single reaction. However, because of the added flow component, many more tests can be run and resolved at the same time.

Using a viral panel as an example, after obtaining a biological sample, the mRNA is reverse transcribed to cDNA. The cDNA is then amplified using a panel of primers that can specifically amplify many different pathologic/pathogenic nucleic acid sequences at the same time. Each pathogen-specific primer used is tagged with a unique oligonucleotide sequence (called the *tag*) as well as a fluorophore. After the multiplex amplification step is completed, the reaction is mixed with microscopic beads that are internally tagged with varying amounts of fluorescent molecules at the time of production. Each different type of bead is also labeled with a unique oligonucleotide sequence that is complementary to the unique tag on the pathogen-specific primer (called the *anti-tag*). If both the tag and the anti-tag are present, then hybridization occurs, binding the fluorophore-labeled amplicon to its appropriate fluorophore-labeled bead. The beads are then processed and placed in a special flow-enabled luminometer equipped with two lasers for reading. The first laser identifies the bead based on its internal dye content. The second laser detects how much, if any, tagged amplicon is bound to its surface.

This technology allows for the resolution of 100 or more tests from one sample at one time in one tube. It is adaptable to perform tests on nucleic acids, peptides, and proteins in a variety of sample matrixes (for a review, see Bluth & Bluth, 2013).

High-Resolution Melting Analysis

High-resolution melting (HRM) analysis is a technique for fast, high-throughput post-PCR analysis of genetic mutations or variance in nucleic acid sequences. It enables researchers to detect and categorize genetic mutations rapidly (e.g., single-nucleotide polymorphisms), identify new genetic variants without sequencing (gene scanning), or determine the genetic variation in a population (e.g., viral diversity) before sequencing.

The first step of the HRM protocol is the amplification of the region of interest, using standard PCR techniques, in the presence of a specialized double-stranded DNA (dsDNA) binding dye (e.g., SYBR Green). This specialized dye is highly fluorescent when bound to dsDNA and poorly fluorescent in the unbound state. This change allows the user to monitor the DNA amplification during PCR (as in real-time or quantitative PCR). After completion of the PCR step, a high-resolution melt curve is produced by increasing the temperature of the PCR product, typically in increments of 0.008°C to 0.2°C, thereby gradually denaturing an amplified DNA target. Because SYBR Green is fluorescent only when bound to dsDNA, fluorescence decreases as duplex DNA is denatured, which produces a characteristic melting profile; this is termed *melting analysis*.

The melting profile depends on the length, GC content, sequence, and heterozygosity of the amplified target. When set up correctly, HRM is sensitive enough to allow the detection of a single base change between otherwise identical nucleotide sequences (for a review, see Bluth & Bluth, 2013).

PROTEOMIC

Current proteomic technology offers a variety of promising high-throughput approaches to the investigation of cellular biology. As one moves from the slowly changing, relatively static genome to RNA transcription, and ultimately to protein translation and additional downstream modifications, the information becomes increasingly more dynamic. An estimated 30,000 genes (Lander et al., 2001) are present in the human genome and are translated into more than 1 million proteins (Anderson & Anderson, 2002); the complexity of this system belies simple global analysis (Oh et al., 2004). Inability to amplify proteins often necessitates working with small quantities of biological samples. In addition, the range of protein concentrations, spanning several log units, can obscure signals of clinical utility.

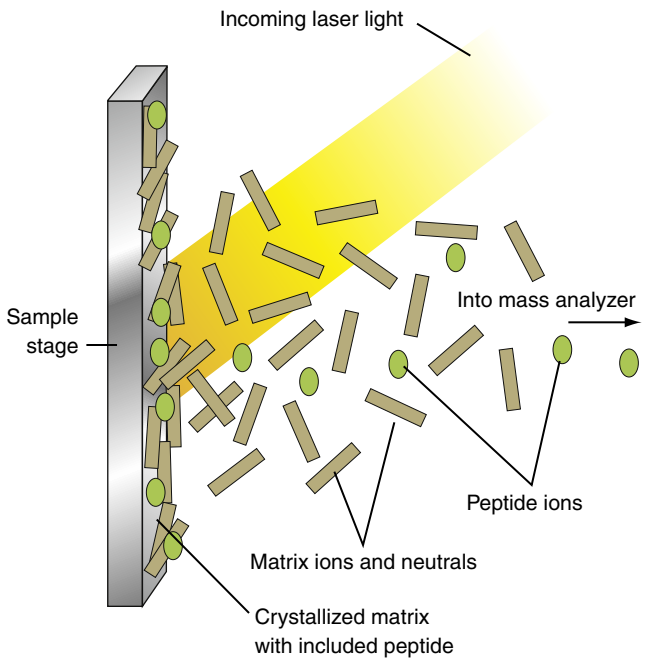

Figure 80.5 Matrix-assisted laser desorption ionization time-of-flight mass spectroscopy (MALDI-TOF-MS). A laser pulse provides energy for the matrix solution to ionize peptides and oligonucleotides, which travel downstream to the mass analyzer. (Redrawn from Kintner M, Sherman NE: *Protein sequencing and identification using tandem mass spectrometry*, New York, 2000, John Wiley & Sons.)

Mass Spectrometry

Mass spectrometry (MS) is the tool used most often to investigate the protein composition of complex biological samples. The principles of MS are discussed in Chapter 5, and its applications to drug analysis, identification and speciation of microorganisms and proteomics of cancer-associated proteins are discussed in Chapters 24, 57, and 77 respectively. Before the discoveries that made MS protein analysis feasible, protein identification depended on more labor-intensive techniques such as Edman sequencing or antibody-based assays. The major obstacle to high-throughput protein analysis using MS has been the technical difficulty of ionizing proteins. The innovations of John Fenn, working with electrospray ionization, and of Koichi Tanaka, who developed laser desorption ionization, opened the door to the field of proteomics. For their contributions to the field, both scientists shared half of the 2002 Nobel Prize in Chemistry. Electrospray ionization creates small, charged droplets of protein in solution. As the droplets move toward a vacuum chamber, the liquid evaporates, leaving behind a charged protein moiety. In laser desorption, a protein is placed in a chemical solution (called a *matrix*) in which high-energy electron beams are focused on the protein, resulting in its ionization. Once ionized, the mass-to-charge (m/z) ratio can be determined by migration of the protein in an electrical field.

Additional analytic problems arise from the elaborate structure of proteins and from the sheer abundance seen in most biological samples. With its secondary, tertiary, and quaternary structures, as well as its posttranslational modifications, protein structure is much more complex and is less predictable than that of DNA or RNA. Advances in protein analysis have allowed more rapid identification. However, many of these methods are subject to variation because of the context in which the protein is found, in particular, its shape and the protein environment in which it is analyzed. Separation remains an important step in reducing complex biological specimens into more manageable samples. Most of proteomic experiments rely on separation of constituent proteins over a two-dimensional gel, a time- and labor-intensive method that slows the discovery process and requires relatively large amounts of starting sample. Other techniques used to improve the resolution of data include proteomic analysis of whole-cell lysate, usually separated by high-pressure liquid chromatography, and multidimensional liquid chromatography.

Although the quantity of a peptide in a sample can increase the amplitude of the m/z spike seen on MS, other factors such as propensity of a peptide to ionize or surrounding ions at the time of measurement can also affect amplitude, making it difficult to comparatively quantify similar samples from different experimental conditions. The use of isotope-coded affinity tags allows quantitative comparison of samples. The tag consists of a biotin marker and a link, which contains eight hydrogens or eight deuteriums. To compare the amount of a single protein present in two different samples, one would label one sample with a light marker and the other with a heavy marker. This is done before MS analysis is performed, which would then show a series of paired peaks for individual peptide fragments, with heavy tag samples having an m/z 8 units greater than light tag samples. One can then compare the relative amplitude of the two samples.

Multidimensional protein identification technology allows identification of proteins in a digested sample. Protein fragments are introduced

TABLE 80.1
Comparison of High-Throughput Genomic Technologies

	SAGE	DNA Microarray	Real Competitive PCR
Equipment needed	Sequencer	Arrayer (cDNA only), array scanner	Nanodispenser, MALDI-TOF-MS
Throughput			
Genes	Medium, ≈2000–20,000 tags/day, depending on sequencer	Highest, ≈40,000/array	Medium, ≈100/day
Samples	Low, ≈1/week	Medium, ≈10–20/day	High, ≈100/day
Cost	$1500–$2500/sample if between 50,000 and 100,000 tags are sequenced	$500–$1000/chip	$1–$2/gene/sample
Amount of starting material required	500–1000 μg total RNA/sample	1–15 μg total RNA/sample, as little as 10–100 ng total RNA/sample can be used with a modified protocol	5 ng total RNA/gene/sample
Gene sequences need to be known a priori	No	Yes	Yes
Absolute gene quantification	Yes	No	Yes

cDNA, Complementary DNA; *MALDI-TOF-MS,* matrix-assisted laser desorption ionization time-of-flight mass spectroscopy; *PCR,* polymerase chain reaction; *SAGE,* serial analysis of gene expression.

through high-pressure liquid chromatography into a tandem mass spectrometer. The m/z ratio for each peptide is measured in the first MS chamber, after which the peptide is fragmented. By comparing the relative weights of these fragments, one can determine the amino acid responsible for the change—in effect, sequencing the peptide. Measured peptide sequences are then matched to predicted fragments of known proteins, generating the identity of a large number of proteins from a complex biological sample.

Protein Arrays

Tissue microarrays produce a compact arrangement of sections from frozen or paraffin-embedded tissue, combining samples onto a single platform. Before the sampling advances described by Kononen and colleagues in 1998, the number of sections that could be arranged in parallel limited the simultaneous investigation of multiple tissue sections. Currently, a tissue microarray can hold up to 1000 samples, which can be tagged and labeled via in situ hybridization or immunohistochemical assay (Kononen et al., 1998; Russo et al., 2003). Such large-scale parallel inquiry may provide a more rapid means of answering questions about the biological mechanisms involved in progression from normal tissue to neoplasia (Kononen et al., 1998) or the pathways related to variable prognoses among tumors of similar histology (Bubendorf et al., 1999), providing a ready means of validating results from other genomic or proteomic experiments (Chen et al., 2003), as well as tumor classification (Djidja et al., 2010).

Paweletz and colleagues pioneered the development of reverse-phase protein microarrays. Rather than spotting small sections of tissue, these slides hold arrays of whole-cell lysate from a specific cellular portion of tissue (Paweletz et al., 2001). Under the microscope, scientists can "hand pick" those cells of interest, capturing them with a small, focused laser that binds cells to an overlying transfer film.

In contrast to arrays containing tissue or cells of interest, other arrays can hold material designed to bind proteins from a sample applied to the surface of the array. Antibodies, DNA, RNA, and ribosomes—any substance with an affinity for a protein—can be used as a probe on the surface of the array. Manufacturing of these slides uses spotting technology similar to that described for oligonucleotide arrays (see earlier discussion).

Secretome

A subset of the proteome includes the secretome, characterized as proteins that are secreted externally by the cells (Mukherjee & Mani, 2013). Such secretory proteins are important for maintaining cell-cell communication and proliferation. Secretory proteins include growth factors, enzymes, and hormones, as well as stimulating and inhibiting growth factors, among others. They often operate in a transmembrane manner, where amino and carboxyl termini facilitate key signals and enzyme/cleavage instructions via the endoplasmic reticulum and Golgi apparatus. Various methods have been employed to assess the secretome, including, but not limited to, microarray, mass spectrometry, nucleic acid sequencing, SAGE, and antibody- and bead-based arrays (Mukherjee & Mani, 2013). Understanding of the human secretome has demonstrated promise toward the identification of novel biomarkers in malignancy, including lung, breast, and colorectal carcinoma (Schaaij-Visser et al., 2013), as well as facilitating a better understanding of stem cell regeneration for application to cardiovascular, neurodegenerative, and genitourinary diseases (Tran & Damaser, 2015).

MOLECULAR MARKERS FOR THE DIAGNOSIS OF HUMAN NEOPLASIA

GENOMIC

One clinically relevant application of genomic high-throughput technologies is the identification of diagnostic molecular markers for human diseases such as cancer. Histologic analysis complemented by immunohistochemistry, electron microscopy, and molecular analysis of chromosomal abnormalities is frequently used to classify cancers. Definitive diagnoses can be difficult to determine but are important because they often influence patient treatment, response, and prognosis. The first paper to use DNA microarrays in clinical samples to develop gene-expression profiles for cancer classification was published in 1999 by Golub and colleagues (Golub et al., 1999). Since that time, DNA microarrays have been used extensively across a wide range of malignant and normal tissue specimens in an attempt to develop diagnostic and prognostic tests.

As mentioned in Chapter 78, a pioneering study has been performed using DNA microarrays to distinguish acute myeloid leukemia (AML) from acute lymphoblastic leukemia (ALL). In this study, Affymetrix GeneChips containing approximately 6800 human genes were employed to measure gene expression of bone marrow mononuclear cells obtained from patients with either of these diseases (Golub et al., 1999). In this study, the choice of acute leukemia, a hematologic malignancy, was important for several reasons. Previous DNA microarray experiments had obtained reproducible results on cell lines; however, clinical specimens introduce additional noise that may obscure differences. Mononuclear cells reduce noise because they are a relatively homogeneous cancer cell population, in contrast to biopsies of solid tumors that exhibit varying quantities of surrounding stromal cells. In addition, distinction between acute leukemia subtypes is difficult with existing techniques, and the discovery of additional molecular markers would enhance the accuracy of diagnosis, ultimately influencing the choice of a therapeutic regimen.

To explore whether differences in gene expression could be detected between 27 ALL and 11 AML samples in this study, a method called *neighborhood analysis* was used. This method ranks genes whose expression patterns across patients are highly correlated with the class of the sample (ALL or AML). A gene that is expressed at high levels across all patients but at low levels in AML patients, for example, would be highly ranked. Significance, or how likely the correlation is by chance, was assessed by randomly assigning class labels to each of the samples and repeating the analysis. Approximately 1100 genes were significantly correlated with class labels. The top 50 genes were subsequently used in a weighted-vote class prediction algorithm that predicts the class of unknown samples. Each of these 50 genes casts a vote indicating the class of the new sample. Each gene's "vote"—AML or ALL—was determined by calculating whether the expression value for the gene in the unknown sample was closer to the mean expression value for the gene across all or all AML patients. Votes were then weighted according to the strength of the correlation between gene-expression levels and class vector. The votes for each class were summed, and the unknown sample was assigned to the class with the larger total vote. An additional metric, known as *prediction strength*, can be calculated to determine the margin of victory. (For additional details, see Reich et al., 2004.) The accuracy of this prediction method was evaluated by "leave-one-out" cross-validation, wherein one of the 38 samples is withheld, the analysis is repeated, and the class of the left-out sample is predicted. Using this approach, this study found that 36 of the 38 samples were classified correctly, and 2 were classified as uncertain on cross-validation. The predictor was tested on an independent set of 34 additional samples and was correctly classified in 29 of the 34 samples. The committee of 50 genes contained known markers of lymphoid versus myeloid cell lineage, as well as genes related to carcinogenesis.

In addition to identifying markers capable of distinguishing AML and ALL, Golub and colleagues used an unsupervised clustering method known as *self-organizing maps* (*SOMs*) to evaluate whether the two subtypes of leukemia could be found within the gene-expression data without prior knowledge of the two leukemia classes. SOM group samples were divided into a user-defined number of clusters based on gene-expression pattern similarities. Two-cluster SOMs produced one cluster containing 24 of the 25 ALL samples and another cluster with 10 of the 13 AML samples. A four-cluster SOM was capable of distinguishing among T-lineage ALL, B-lineage ALL, and AML. The success of this initial experiment and its exciting implications—as well as improvements in DNA microarray technology, analysis, and availability—have resulted in an exponential increase in the number of clinical studies using microarrays. Additional information can be found in Chapter 78.

PROTEOMIC

In Chapter 77, an intriguing approach to the early detection of several different types of cancer based on patterns of protein expression, called proteomics, is discussed. This approach does not search for specific known proteins but rather searches for differences in patterns of protein expression (the identity of many of these proteins is unknown) based on the use of MS as illustrated in Figure 80.6. Given the more favorable prognosis seen with malignancies diagnosed at earlier stages, a great deal of interest has been expressed in using proteomic tools to search for diagnostic markers in readily available biological samples such as blood, urine, or saliva. As discussed in Chapter 77, methods of detection of protein expression in human samples include high resolution two-dimensional electrophoresis and surface-enhanced laser desorption ionization (SELDI)-TOF-MS coupled with a mass spectrometer that measures the time of flight (TOF) of ionized proteins from laser to detector as described in Chapter 5.

In brief, serum samples are placed on a chip with embedded weak cations, which provide the "surface enhancement" of SELDI. Excess serum is washed off, and proteins bound to weak cations remain on the chip, where they are combined with a matrix solution and ionized when

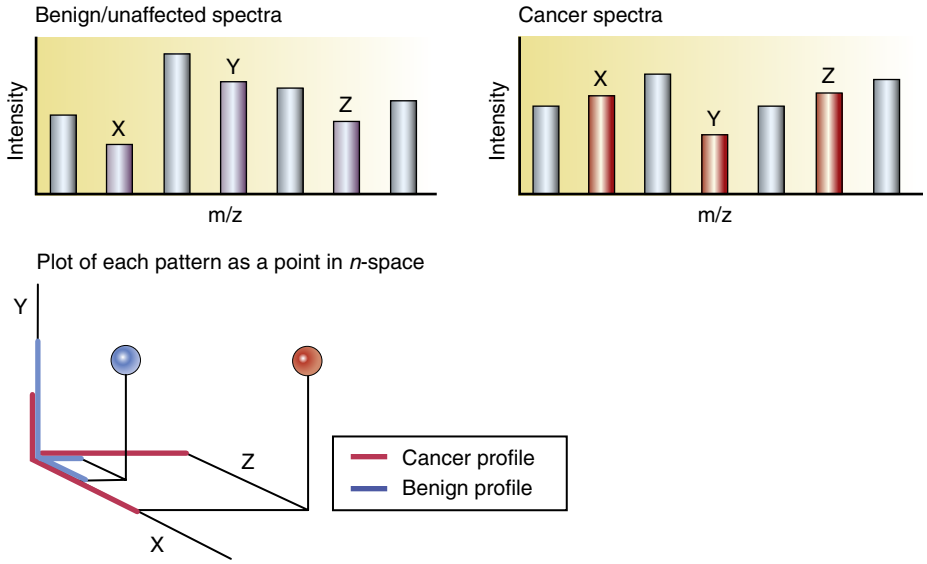

Figure 80.6 Proteomic pattern diagnostics. Pattern analysis identifies m/z ratios with the "most fit" combination of proteins for distinguishing between clinical states of interest. (Redrawn from Petricoin EF, Zoon KC, Kohn EC, et al.: Clinical proteomics: translating benchside promise into bedside reality, *Nat Rev Drug Discov* 1:683–695, 2002.)

exposed to a laser. Each serum sample results in approximately 15,000 mass-to-charge (m/z) values of varying amplitude. The bioinformatic tools used to parse through such a complicated data set rely on class prediction based on a genetic algorithm. Class prediction involves a "training" set of known cancer and noncancer samples. The genetic algorithm selects a panel of m/z values and tests its ability to differentiate between cancer and control. The "genetics" of a genetic algorithm represents a biological analogy describing repeated mixing and matching of the most successful m/z values, allowing "survival of the fittest" values in successive generations of testing, ultimately producing the most discriminatory panels, which are then tested on a "masked" group of patients and controls (i.e., the condition of each patient is withheld before the test result is obtained).

As described in Chapter 77, this methodology was employed on cohorts of women with ovarian cancer and non-cancer patients and was found to have 100% sensitivity and 95% specificity in diagnosing ovarian cancer specifically (Petricoin et al., 2002). As noted in Chapter 77, although the panel used in this study resulted in a test with high diagnostic accuracy, validation in a more realistic clinical setting remains to be done. The idea of studying a group of markers in parallel would seem appropriate, given the complexity of tumor biology and its interaction with the host. The absence of protein identification with this technique constrains the test. It is not clear whether the values included represent participants in tumor biology shed into the bloodstream or nonspecific markers of inflammation. With 15,000 data points to choose from in each serum sample, the risk of overfitting any model so that it would have little clinical utility in a practical setting is significant. In addition, array-based assessments may not correlate with classical diagnostic approaches (immunohistochemistry) or with survival (Dahl Steffensen et al., 2010) and may differ depending on the choice of specimen interrogated (Sanchez-Carbayo, 2010). However, the approach appears to be a promising one.

DIAGNOSTIC CANCER APPLICATIONS

SMALL, ROUND BLUE CELL TUMORS

Another cancer that is difficult to accurately diagnose using a variety of histologic and specialized molecular analyses is small, round blue cell tumor (SRBT) of childhood (see Chapter 79), which includes neuroblastoma, rhabdomyosarcoma, non-Hodgkin lymphoma, and the Ewing family of tumors (EWS). Ewing sarcomas are discussed in Chapter 79, where we noted that the most common characteristic finding is the t(11;22) translocation, which juxtaposes the *FLI1* and *EWSR1* genes, giving rise to chimeric (*EWSR1-FLI1*) mRNAs and protein.

Khan and colleagues were among the first to identify molecular markers predictive of SRBT subtypes (Khan et al., 2001). Predictive genes were chosen using artificial neural networks (ANNs), which are pattern-recognition computer programs modeled after the neural structure and behavior of the human brain. Similar to the human brain, ANNs are capable of learning from experience. A neuron can accept many inputs but has only one output. In an analogous manner, artificial neurons output a signal based on several inputs. ANNs consist of several connected artificial neurons that can recognize patterns in training data through optimization of several parameters (weights assigned to the links between neurons) to accurately predict the tumor type of unknown samples.

Khan and colleagues used a cDNA microarray containing 6567 genes to measure the gene expression of 63 samples, which included both tumor biopsies (13 EWS and 10 rhabdomyosarcoma) and cell lines (10 EWS, 10 rhabdomyosarcoma, 12 neuroblastoma, and 8 Burkitt lymphoma, a subset of non-Hodgkin lymphoma). Using a filtered set of 2308 genes, the 63 samples representing four SRBT diagnostic categories were used to train linear ANN models. A total of 96 probes corresponding to 93 genes were selected on the basis of ANN models because they minimized the misclassification error rate to 0%. The algorithm was validated on a test set of 25 samples that consisted of a mixture of cell lines, tumor biopsies, and five non-SRBTs. In all, 17 SRBT test samples were classified correctly; the remaining three SRBTs, along with the five non-SRBTs, could not be assigned a subtype. It is interesting to note that even though only data from neuroblastoma cell lines were used in the training set, the model accurately predicted neuroblastoma tumor biopsy specimens in the test set. Results suggest that the use of cell lines may be beneficial in reducing noise created by stromal contamination of tumor specimens.

Many of the 96 predictive genes reported in the study just discussed were expressed at high levels in 1, 2, or 3 of the 4 diagnostic categories. One marker, MIC2, is currently used to diagnose EWS, although this is not as specific as the (*EWSR1-FLI1*) fusion genes and their products. Also, MIC2 was highly expressed in EWS and in some rhabdomyosarcomas, suggesting that the marker may lack specificity when used alone. Another molecular marker, FGFR4, a tyrosine kinase receptor related to myogenesis and upregulated only in rhabdomyosarcoma samples, was investigated by immunostaining across a variety of tissues. FGFR4 was found to be upregulated in some other cancers and normal tissues, providing clues to its potential biological importance while reducing its potential as a specific molecular marker. This finding illustrates that a compendium of genes, instead of a single molecular marker, may increase diagnostic sensitivity and specificity. This complements the conclusions of Chapter 77 on oncoproteins in tumor diagnosis: arrays of oncoproteins are more effective than individual oncoproteins in early tumor detection.

BARRETT ESOPHAGUS

In addition to these studies, several other DNA microarray and SAGE experiments have been conducted to develop diagnostic tests for human cancers that are difficult to classify using conventional histologic methods. Barrett esophagus, in which the lining of the esophagus is replaced with a metaplastic columnar lining, is a condition associated with gastroesophageal reflux disease that can lead to the development of squamous cell carcinoma or adenocarcinoma. Esophageal cancer is usually difficult to detect

at an early stage and has a high mortality rate. Hierarchical clustering and ANNs were used to discover gene-expression profiles measured by cDNA microarrays that could distinguish between esophageal cancer and Barrett metaplasia specimens (Selaru et al., 2002; Xu et al., 2002). The expression levels of a small subset of predictor genes were quantified with Taqman quantitative reverse-transcriptase (RT)-PCR (Applied Biosystems, Inc., Carlsbad, CA) in 39 patients with Barrett metaplasia or esophageal cancer to assess their clinical usefulness (Brabender et al., 2004). Other studies have demonstrated the utility of microRNA (miRNA) expression in prognosticating patients with Barrett esophagitis (Mathe et al., 2009). In those studies, miR-21, miR-223, miR-192, and miR-194 expression was elevated, whereas miR-203 expression was reduced, in cancerous compared with noncancerous tissue obtained from the same patient (tissue pairs), and reduced levels of miR-375 were strongly correlated with worse prognosis in Barrett patients. Collectively, these studies illustrate the potential of array-based interrogation toward diagnostic and prognostic application.

THYROID CARCINOMA

In Chapter 79, we discuss the most common genetic lesions that have been found in thyroid carcinomas. About half of follicular thyroid carcinomas contain oncogenic *ras*, and many also express the *PAX8-PPARγ* fusion gene and its products. A high percentage of papillary thyroid carcinomas express mutant *BRAF* and *RET/PTC* gene rearrangements. Medullary thyroid carcinomas express mutant forms of *RET* (as opposed to fusion gene products).

Distinguishing Follicular Thyroid Carcinoma from Adenoma

New diagnostic molecular markers are needed to distinguish between follicular-patterned thyroid lesions as to whether they are benign or malignant. Papillary thyroid carcinoma is usually diagnosed with fine-needle aspiration (FNA) after detection of a thyroid nodule and can be further characterized by its expression of the markers noted previously and in Chapter 79. However, FNA cannot differentiate between follicular thyroid adenoma (FTA) and follicular thyroid carcinoma (FTC); a more invasive surgical biopsy is usually warranted. Cerutti and colleagues have attempted to develop a preoperative diagnostic test by constructing and analyzing three SAGE libraries using an FTA, an FTC, and a normal thyroid specimen (Cerutti et al., 2004). More than 360,000 tags were sequenced among the three libraries, and 305 genes were significantly differentially expressed between the three groups. A subset of these genes was chosen for validation with RT-PCR on independent samples that included 10 FTAs, 13 FTCs, and 8 patient-matched normal thyroid tissues. RT-PCR was performed on a subset of the 305 genes: 12 of the most highly expressed genes in FTC and 5 of the most highly expressed genes in FTA/normal thyroid were chosen for validation with RT-PCR. Four genes (*DDIT3*, *ARG2*, *ITM1*, and *C1orf24*) validated the SAGE results and were able to predict 19 of the 23 samples correctly on leave-one-out cross-validation. In addition, immunohistochemistry was performed on 32 FTA and 27 FTC paraffin-embedded tissues using antibodies against two of the four genes, *DDIT3* and *ARG2*. *DDIT3* and *ARG2* showed staining for FTCs and negative staining for ARG2 in most samples, suggesting that these markers might improve the preoperative diagnosis of thyroid nodules. Thus, these four genes, in addition to expression of oncogenic *ras*, are promising for use in the diagnosis of FTC.

ADENOCARCINOMA

Histologic identification of the primary tumor site in patients presenting with metastatic adenocarcinoma can also be difficult. SAGE data sets suggest that primary and metastatic adenocarcinomas cluster together according to their site of origin. A variety of RNA quantification methods, including DNA microarrays and SAGE, as well as the literature, were used to select tumor- and site-specific molecular markers (Dennis et al., 2002). Buckhaults and colleagues analyzed a set of 11 SAGE libraries of ovarian, breast, pancreatic, and colon adenocarcinomas to select five genes that could discriminate among these carcinomas of different tissue origins (Buckhaults et al., 2003). A class prediction algorithm, known as a *two-dimensional gene-expression–based classification map*, was able to correctly classify tissue origin in 81% of 62 independent samples of ovarian, breast, pancreatic, and colorectal carcinomas based on RT-PCR data from the five genes. A related study, aimed at identifying molecular markers of metastasis in primary tumors, compared gene-expression profiles of unpaired primary adenocarcinomas and metastatic nodules from different individuals across a broad spectrum of tumor types. A total of 128 genes were identified whose expression patterns could distinguish primary from metastatic adenocarcinoma (Ramaswamy et al., 2003). Ramaswamy and colleagues demonstrated that a subset of the 128 genes was associated with metastasis in independent data sets from primary lung, breast, and prostate adenocarcinomas, as well as from medulloblastomas and large B-cell lymphomas. These findings challenge the hypothesis that metastatic potential arises in a few cells in the primary tumor and suggest that the ability to metastasize is preexistent in the primary tumor. If this is correct, gene-expression patterns in primary tumors could potentially predict future risks for distant metastasis.

PANCREATIC CANCER

In Chapters 77 and 79, it was noted that more than 90% of pancreatic cancers express the oncogenic k-*ras* gene and its ras-p21 protein product. Other common genetic lesions include aberrant methylations of a series of genes, including *p16/CDKN2A*, *APC*, *TSLC/IGSF4*, *SOCS-1*, *cyclin D2*, *RASSF1A*, *WWOX*, *RUNX3*, *CDH13*, *DUSP6*, *HHIP*, and *SLC5A8*. In addition, mutations in *SMAD4*, *PI3K*, and *p53* genes have been found in these cancers.

Microarray, semiquantitative PCR, and SAGE methods have been further applied to identify differentially expressed genes in pancreatic cancer (Iacobuzio-Donahue et al., 2002; Hustinx et al., 2004; Watanabe et al., 2005). Such prostate stem cell antigens as mesothelin and osteopontin were identified as overexpressed in pancreatic carcinoma, the latter of which demonstrated a sensitivity of 80% and a specificity of 97% for pancreatic cancer (Koopmann et al., 2004). Nonogaki and colleagues developed a three-dimensional microarray technology to assess RNA from endoscopic ultrasound-guided FNA (EUS-FNA) samples obtained from patients with pancreatic cancer (Nonogaki et al., 2010). They found that CDK2A, CD44, S100A4, and MUC1 were differentially expressed between cancer and noncancer groups subsequent to two orders of hierarchical clustering analysis. Furthermore, cDNA microarray analysis identified that the secreted protein acidic and rich in cysteine (*SPARC*) gene (also known as *osteonectin* or *BM-40*) and its ligand (*SPARCL1*) are overexpressed in pancreatic cancer tissues but not in their noncancerous counterparts (Jinawath et al., 2004). Specific SPARC protein antigens are now being evaluated as candidates for immunotherapy for pancreatic and other cancers (Inoue et al., 2010). Therefore, these genes may be important in the diagnosis of pancreatic carcinoma.

OTHER CANCERS

High-throughput genomic technologies have been used to aid in disease diagnosis and identification of novel disease subtypes in a variety of other diseases, including bladder carcinoma (Dyrskjot et al., 2003) (see Chapter 77), central nervous system embryonal tumor (Pomeroy et al., 2002), ovarian cancer (Sawiris et al., 2002; Tinelli et al., 2009), breast cancer (Perou et al., 2000; Porter et al., 2001, 2003a; Vera-Ramirez et al., 2010), lung cancer (Bhattacharjee et al., 2001; Ocak et al., 2009), hepatocellular carcinoma (Zender et al., 2010), and colorectal cancer (Buckhaults et al., 2001). The use of high-throughput genomic technologies to develop disease diagnostics is an inherently difficult problem because predictive genes identified by a training set are based on histopathologic diagnoses. However, the histologic methods used for classification of certain cancers may be imperfect, making it difficult to assess the true accuracy of the molecular markers. In addition, it is difficult to verify the existence of novel disease subtypes found in DNA microarray experiments if no complementary histologic evidence is available. In the future, pathologists probably will use high-throughput genomic technology to facilitate accurate diagnosis in difficult cases. A majority of studies using genomic high-throughput methods have chosen to focus on identifying gene-expression profiles predictive of disease prognosis given the limited number of histologic or clinical indicators of disease outcome (see discussion later in the chapter).

Application of proteomics in the search for a clinically useful biomarker has been reported in patients with breast (Kuerer et al., 2002), prostate (Ornstein et al., 2004), colorectal (Zhou et al., 2010), and lung cancers (Chen et al., 2003), among others (Djidja et al., 2010). When these techniques of detection and analysis are applied to prostate cancer, preliminary data from men with an indeterminate elevation of prostate-specific antigen (PSA) suggest that an *ion signature* is present that distinguishes between men with prostate cancer and those with benign prostatic hyperplasia with 100% sensitivity and 67% specificity (Ornstein et al., 2004).

Because the serum represents a particularly complicated specimen for two-dimensional polyacrylamide gel electrophoresis (2D-PAGE)–based proteomic analysis, other specimens in proximity to the tissue in question

may be more readily available and simpler to work with. Nipple aspirate fluid is easily obtained and, in the case of unilateral disease, allows for a simple paired sample from the unaffected breast. Kuerer and colleagues used 2D-PAGE in an initial descriptive study comparing protein expression in the nipple aspirate from both breasts in patients with unilateral breast cancer and a healthy volunteer (Kuerer et al., 2002). Their results showed highly concordant protein electrophoresis patterns when nipple aspirate fluid was compared from each breast in the control subject as opposed to samples obtained from patients with breast cancer, which exhibited a larger number of proteins unique to the affected breast compared with the unaffected breast in the same patient. This finding suggests that localized breast malignancy significantly alters protein expression in nipple aspirate fluid, raising the possibility of a diagnostic marker pattern.

PROGNOSTIC MOLECULAR MARKERS OF DISEASE

GENOMIC

Patients diagnosed with the same type of cancer and treated using similar protocols often respond differently and have varying survival rates. Several clinical and histologic variables—such as age, serum protein levels, and stage or grade of tumor—can be used to assess a patient's prognosis with variable accuracy. Many studies have utilized genomic high-throughput technologies, especially DNA microarrays, as described at length in Chapter 70, to identify gene-expression signatures that predict patient survival or relapse rates. Instead of comparing two different disease states, as detailed earlier in the technologies section, the experimental design for the development of molecular prognostic indicators usually attempts to stratify a particular cancer into subtypes according to outcome, using unsupervised or supervised computational approaches (see Fig. 80.3). The marker associated with poor prognosis may provide clues about the biological mechanisms underlying resistance to chemotherapeutics and may aid in the identification of new drug targets.

Diffuse Large B-Cell Lymphoma (see also Chapter 78)

Identifying molecular markers that predict patient survival involves distinguishing subtle differences between specimens. As previously noted in the technologies section, many studies have been conducted on hematologic malignancies in which a homogeneous population of cells can be isolated easily. Diffuse large B-cell lymphoma (DLBCL), the most common adult lymphoid neoplasm, accounts for 30% to 40% of all non-Hodgkin lymphomas. DLBCLs commonly contain *BCL6* gene fusions, as discussed in Chapter 78. Response to chemotherapy is highly variable, and less than half of treated patients achieve long-term remission. Currently, the International Prognostic Index (IPI) is used to approximate the outcome of patients diagnosed with DLBCL based on several clinical factors, such as serum lactate dehydrogenase and stage.

As noted in Chapter 78, a paradigm shift has occurred in the classification of DLBCLs based on the use of gene arrays. Here, we discuss this approach further. Alizadeh and colleagues constructed a specialized cDNA microarray, known as the *lymphochip*, which included 17,856 probes chosen from germinal center B cells, DLBCLs, and other lymphoma cDNA libraries (Alizadeh et al., 2000). In all, 128 lymphochips were used to assay 96 normal and malignant samples from leukemia and lymphoma cell lines and from patients with DLBCL, follicular lymphoma, and chronic lymphocytic leukemia. Hierarchical clustering of the microarrays revealed three subgroups of DLBCL samples based on genes related to proliferation: T cells, lymph node biology, and germinal center B cells. DLBCLs are thought to arise at different stages of B-cell differentiation, and hierarchical clustering of just DLBCL samples across the genes related to germinal center B cells separated the sample into two distinct clusters: germinal center B cell–like DLBCLs and activated B cell–like DLBCLs, as discussed in Chapter 78. The two subtypes were shown to have statistically different overall survival (72% of germinal cell B cell–like DLBCL subjects were alive after 5 years in comparison with 16% of activated B cell–like DLBCL subjects); the two classes could be used to further stratify patients identified as low risk by the IPI. This study was one of the first to relate tumor subtypes identified by global gene-expression profiling to patient outcome. Use of the DNA microarray in diagnosing this condition and further subtyping it into the germinal center B cell–like group and the activated B cell–like group is discussed in Chapter 78.

A follow-up study by Shipp and colleagues tested whether a gene-expression profile could be identified, without prior discovery of subtypes, that predicted survival in DLBCL patients (Shipp et al., 2002). Affymetrix HuGeneFL microarrays containing approximately 6800 probes were used to measure global gene-expression profiles across 58 patients with DLBCL (32 patients with cured disease, 26 patients with refractory/fatal disease). The weighted vote class prediction algorithm with cross-validation was used to identify a gene-expression signature of 13 genes capable of distinguishing between patients with cured disease and those with fatal disease. The prediction model was also able to stratify patients into good and poor prognosis groups within categories defined by the IPI. As additional validation, results of the current study were compared with previous findings reported by Alizadeh's group. The studies used microarray platforms that interrogated two different but overlapping sets of genes. Genes used to distinguish the two subtypes of DLBCL in the Alizadeh study that were also present on the HuGeneFL microarray separated the 58 DLBCLs into two groups, but the groups did not correlate with overall survival rates. However, of 13 predictive genes identified by Shipp and colleagues, 3 were present on the lymphochip and correlated with survival across patients in the Alizadeh study.

In a related study, Rosenwald and colleagues used the lymphochip to study 240 patients with untreated DLBCL who subsequently received anthracycline-based chemotherapy (Rosenwald et al., 2002). Using a training set of 160 samples, gene-expression levels were correlated with survival times using the Cox proportional hazards model. A total of 670 genes had expression patterns that were significantly correlated with prognosis; these genes were clustered to identify sets of genes with similar expression patterns. Highly correlated genes were involved in similar biological processes. Four sets of correlated genes related to proliferation, major histocompatibility complex class II, lymph node biology, and germinal center B cells were used to develop a class prediction model. The gene-expression levels of genes within each set were averaged; these composite values were used to build a multivariate prediction model. The model was capable of assigning each sample in the test set a score related to the risk for succumbing to the disease. Scores assigned by the model to the entire set of samples were stratified into quartiles, with a 5-year survival of 73% in the first group compared with 15% in the fourth group.

Follicular Lymphoma

A similar survival prediction model was used to predict the prognosis of patients with follicular lymphoma, a cancer similarly arising from germinal-center B cells (Dave et al., 2004). Treatment may involve chemotherapy, immunologic therapy, or hematopoietic stem cell transplantation. However, no consensus has been reached as to which regimen is superior, and outcome is highly variable. Tumor biopsies from 191 patients with follicular lymphoma were divided into training and test sets. With use of the Cox proportional hazards model to correlate genes with survival, two highly correlated sets of genes were chosen to build a multivariate predictive model. The set associated with a favorable prognosis contained genes highly expressed in T cells and macrophages, whereas the set associated with poor prognosis contained genes expressed in macrophages and dendritic cells. In additional experiments on biopsy specimens separated into malignant and nonmalignant fractions, two sets of gene signatures culled from the initial 10-set gene signature patterns were highly predictive of survival. These findings support the notion that immune-related responses by way of gene signatures reflect biological characteristics that may predict length of survival.

The lymphoma studies already discussed demonstrate that microarrays may be successful in accurately predicting patient prognosis and may complement currently used methods, such as the IPI. Results imply that biopsies obtained at the time of diagnosis can be used to predict prognosis and could influence treatment decisions. As noted earlier, however, disagreement between studies has resulted from several factors, including the DNA microarray platform used, patient population, differences in treatment regimens, sample size, the variable quality of long-term follow-up data, and choice of prediction methods (see the Pitfalls of Molecular Markers for Both Prognostics and Diagnostics section later in the chapter). The follicular lymphoma study also shows the importance of the tumor microenvironment—something that is not typically explored in DNA microarray studies.

Acute Myeloid Leukemia

In Chapter 78, patterns of oncogene expression in different phenotypes of AML that are currently used for therapeutic and prognostic purposes are discussed. Certain patterns of expression of these oncogenes suggest not only possible effective therapeutic regimens but also prognosis. For example, oncogenes found frequently in promyelocytic leukemia include the retinoic acid receptor-α (PML-RARα) fusion genes, whose presence suggests a favorable prognosis and indicates that treatment with all-*trans* retinoic acid (aTR) will be of therapeutic benefit. However, the

presence of *RAR* fusion genes with other, non-PML genes—including *ZBTB16(PLZF)-RARA*, t(11;17)/*NUMA1-RARA*, t(5;17)/*NPM1-RARA*, and t(17;17)*STAT5B-RARA*—is a strong indicator that aTR will not be as effective and that the prognosis is not favorable. In addition, core-binding domain fusion genes such as *RUNX1-RUNX1T1* and *CBFβ-MYH11* are expressed in other AMLs (such as myelomonocytic leukemia) and correlate with specific chromosomal abnormalities. The presence of these fusion genes suggests susceptibility of the tumor to high-dose cytarabine regimens and often indicates a favorable prognosis. On the other hand, the presence of the *FLT3* oncogene alone or together with these other fusion genes suggests a less-favorable prognosis despite the suggested chemotherapeutic regimen. Additional aspects of gene mutations that affect therapeutic responses can be found in Chapter 78.

Overall, the presence of specific fusion genes in AML does not always reflect the molecular heterogeneity of the disease because the presence or absence of other fusion oncogenes or mutations in proto-oncogenes may not be detected, and other genes, not thus far identified, may also be involved in the cell transformation process. To attempt to identify which genes may be involved in cell transformation in AML and to detect patterns of gene expression in AML that correlate with prognosis and suggest effective therapies, several studies using gene-expression microarrays from patients with AML have been carried out. Despite potential problems with this type of approach, discussed in the preceding section, two studies published in the *New England Journal of Medicine* identified gene-expression profiles that can be used as prognostic indicators in AML (Bullinger et al., 2004; Valk et al., 2004).

Bullinger's group used cDNA microarrays (≈39,000 probes) to obtain global gene-expression profiles for 116 patients with AML, and Valk's group used Affymetrix human U133A microarrays (≈22,000 probes) to assay 285 patients with AML. Unsupervised hierarchical clustering in both studies revealed clusters that correlated with cytogenetic and molecular abnormalities present in the tumors. Using the Cox proportional hazards model implemented in SAM software (Tusher et al., 2001), Bullinger and colleagues identified gene-expression patterns that correlated with survival. K-means clustering was used to divide the training samples into two groups, representing good and bad outcomes, based on genes selected by SAM. The prediction analysis of microarrays (PAM) algorithm was used to develop an outcome predictor using 133 genes based on the two identified groups in the training set. PAM was applied to the test samples and was able to separate them into two groups that differed significantly in terms of survival times. In this study, it was found that expression of so-called "forkhead" genes such as the forkhead box *O1A* gene (*FOXO1A*, also known as *FKHR*) in AML is associated with a favorable prognosis. On the other hand, expression of such genes as *MAP7*, *GUCY1A3*, *TCF4*, and *MSI* prognosticates a less favorable prognosis. Overexpression of genes involved in homeobox regulation—such as *HOXB2*, *HOXB5*, *PBX3*, *HOXA*, and *HOXA10*—has occurred in multiple different phenotypic AMLs, suggesting their importance in leukemogenesis. Expression of mutant or overexpressed *FLT3* was associated with a poor outcome, as discussed in Chapter 78 (Bullinger et al., 2004).

Valk's group used similar methods to identify genes that could classify samples into disease subgroups previously identified by clustering analysis. These subgroups were associated with cytogenetic and molecular abnormalities as well as with patient prognosis (Valk et al., 2004). Both studies demonstrated the usefulness of global gene-expression analysis in dissecting the heterogeneity that exists within tumors of the same type. The high degree of overlapping results between these two studies shows the potential that microarray technology has to distinguish between subtle tumor subtypes and to add prognostic information to current clinical practice.

Breast Cancer

Although similar prognostic biomarker studies have been carried out in prostate cancer (Dhanasekaran et al., 2001), lung adenocarcinoma (Beer et al., 2002), and multiple myeloma (Tian et al., 2003), identification of prognostic biomarkers in breast cancer best demonstrates how successful high-throughput genomic studies can translate into important clinical tools. In Chapter 70, we discuss how the use of gene arrays has been successful in enabling prognosis and treatment of different breast cancers. The most important markers for these purposes are estrogen receptor (ER), progesterone receptor (PR), the proliferation marker protein, Ki67, and the *HER2/neu* oncogene.

Additional prognostic molecular markers were identified from gene-expression studies using primary breast cancer biopsies from patients younger than 55 years of age with sporadic node-negative disease that did and did not develop metastases within 5 years. The predictive power of these molecular markers was deemed to be greater than that of other clinical and histologic factors, such as tumor grade, size, angioinvasion, or ER status (van't Veer et al., 2002). Similar studies on breast cancer were subsequently conducted (van de Vijver et al., 2002; Huang et al., 2003; Sotiriou et al., 2003). A recent paper describes the development of a predictive model that uses gene-expression, clinical, and histologic data to more accurately estimate prognosis (Pittman et al., 2004).

One bottleneck to performing DNA microarray studies is the dearth of snap-frozen tissues obtained from patients with long-term follow-up. Snap-freezing tissue preserves the integrity of the RNA and is ideal for DNA microarray experiments. However, most tissue banks and clinical trials have collected paraffin-embedded tissue. Paraffin-embedded tissue contains partially degraded RNA that usually is insufficient to allow high-quality DNA microarray results (although advances in this area are ongoing; Drury et al., 2010). Technologies such as real competitive PCR and real-time PCR are being used to measure gene-expression levels in these tissues, but the amount of RNA obtained from tissue blocks often limits assays to a few hundred genes. Using RT-PCR, Paik and colleagues studied 21 genes (16 cancer-related and 5 reference genes for normalization) chosen from the breast cancer DNA microarray studies outlined previously. Samples included 675 paraffin-embedded tissue blocks obtained from patients enrolled in the National Surgical Adjuvant Breast and Bowel Project B-14 trials (Paik et al., 2004). All tissue blocks were obtained from tamoxifen-treated patients who had node-negative, ER-positive primary breast cancer. Expression levels of the 16 cancer-related genes were used to calculate a score representing the risk for cancer recurrence at a distant site. Patients were stratified into low-, intermediate-, and high-risk groups based on the recurrence score. The recurrence score provided significant predictive information beyond tumor grade, age, and tumor size. The simplified 21-gene assay can be translated easily into a clinical prognostic test designed to help physicians decide which tamoxifen-treated, node-negative, ER-positive breast cancer patients should receive additional chemotherapy.

Prognostic molecular markers for breast cancer have been identified using SAGE technology. SAGE, unlike DNA microarrays, cannot be used to assay hundreds of clinical samples. However, it is not restricted to known genes, nor is it limited by the selection of probes on a microarray. SAGE is capable of identifying novel transcripts that have not been described previously, possibly because of their tissue-specific expression (an advantage in developing therapeutics). Two studies using SAGE libraries obtained from normal tissue, as well as from ductal carcinoma in situ (DCIS), invasive, and metastatic breast tumors, were used to identify transcripts that changed between disease states (Porter et al., 2001, 2003a). Several DCIS or invasive/metastatic "specific" genes were assayed by mRNA in situ hybridization using 18 frozen DCIS and invasive breast cancer samples, and by immunohistochemistry using 769 DCIS, invasive, and metastatic breast tumor samples. S100A7, a member of the S100 family of calcium-binding proteins, was preferentially expressed in DCIS (with highest levels restricted to high-grade comedo DCIS) versus normal or invasive/metastatic tumors. Although S100A7 is expressed less strongly in invasive tumors, its levels are higher in ER-negative, poorly differentiated, lymph node–positive tumors, suggesting that its expression in DCIS may be a useful prognostic indicator. In a follow-up study, Porter and colleagues further characterized dermcidin, identified in previous studies as preferentially expressed in invasive and metastatic tumors. Dermcidin is a 110 amino acid–containing protein that is expressed mainly in sweat glands and the pons of the brain (Porter et al., 2003b) and is proteolyzed to a 47 amino acid–containing peptide. The marker was expressed in a subset of invasive tumors by immunohistochemistry, and its expression correlated with larger tumor size and the presence of metastatic lymph nodes. In a subset of cases, higher expression levels were attributable to gene amplification at the gene locus on chromosome 12. Dermcidin was shown to enhance cell growth and survival and may be a promising prognostic indicator of overall and distant metastatic-free survival.

INTEGRATING GENOMICS AND PROTEOMICS

The development of high-throughput technology allows one not only to look at how multiple genes or proteins might predict a clinical feature of interest but also to study overlap in transcriptional activity and protein translation. Chen and colleagues looked at the ability of genetic profiling and protein translation in lung adenocarcinoma to predict survival (Chen et al., 2003). After filtering low-abundance genes, they found approximately 5000 genes consistently expressed across a cohort of 86 adenocarcinoma samples and 10 normal tissue samples. Hierarchical clustering and leave-one-out cross-validation generated a list of the 50 genes that were most effective in dividing patients into high- and low-risk groups for mortality

over several years of follow-up. Of particular interest was the observation that stage I patients, those most likely to experience a surgical cure of their disease, could also be divided into high- and low-risk groups, potentially identifying a novel group that would benefit from adjuvant chemotherapy.

A total of 76 tumor samples underwent both microarray and proteomic analysis. In the examples of genes found along with their corresponding protein products, correlation peaked at 0.39. Although statistically significant, the low degree of correlation underlines the point that the oversimplified model of transcription and translation is in reality a much more elaborate system of translational regulation, glycosylation, phosphorylation, and additional downstream modifications. As the authors conclude, many of the transcripts probably do not correlate well with their protein counterparts as a result of this continued posttranslational development. Extension of their investigation to include genomics and proteomics uncovered a significant cohort of genes and proteins involved in the glycolytic pathway and upregulated among patients with a high risk for mortality, suggesting that this integration of genomics and proteomics has particular value in shedding light on the molecular pathogenesis of disease states.

PITFALLS OF MOLECULAR MARKERS FOR BOTH PROGNOSTICS AND DIAGNOSTICS

MICROARRAY DATA SETS

Diffuse large B-cell lymphoma studies conducted by Alizadeh and Shipp (2000) identified subsets of genes that specified two subtypes of DLBCL patients who differed in terms of survival. Shipp and colleagues (2002) also identified two subtypes of DLBCL patients; however, these types did not correlate with survival. The example presented earlier illustrates one of many DNA microarray studies in which little or no overlap of results is evident. Several potential causes seen in the experimental design and analysis of DNA microarray results may account for the widespread discrepancies (Simon et al., 2003). Two different studies performed using similar tissue samples may involve slightly different patient populations and sample sizes. Tissue heterogeneity is also a problem. Biopsies obtained from different locations have varying numbers of normal cells contaminating the tumor samples. Additionally, no standard is used for preprocessing and analyzing microarray data. New computational approaches are continually emerging, and two groups analyzing the same data set will often produce disparate gene lists. Finally, methods used to compare data sets generated using different DNA microarray platforms are currently being developed, and similar studies with nonoverlapping results may have employed inadequate methods of comparison.

"OVERFITTING" THE PREDICTOR

Traditionally, clinical studies aim to associate a handful of variables across several hundred patients, whereas DNA microarray studies contain thousands of variables (gene-expression levels) across relatively small numbers of patients (typically, 20–200 patients). Many class prediction algorithms yield accurate results for samples in the study from which they were derived, but when they are applied to an independent patient sample, performance drops significantly—a phenomenon known as *overfitting* (Ransohoff, 2004). Results of DNA microarray studies, therefore, are most robust when the data are divided into a training set and a test or validation set (Ntzani & Ioannidis, 2003). In addition to the need for independent sample validation, it is important for investigators to validate gene-expression levels using different technology. To realize the true promise of these technologies, it is critical to develop methods that combine several gene-expression studies to identify markers that are consistently correlated with disease class or outcome and then to validate these markers using different technology and a different cohort of patients.

THE "BYSTANDER" EFFECT

Miklos and Maleszka compared DNA microarray studies measuring prefrontal cortex gene expression in patients with and without schizophrenia versus nonmicroarray studies that included genetic, RNA, and protein measurements obtained through a variety of approaches (Miklos & Maleszka, 2004). Little overlap was noted between DNA microarray and nonmicroarray experiments. One reason for this may be that genes identified using DNA microarray studies are "bystanders," that is, not involved in the pathogenesis of the disease state. Genes identified by genetic linkage studies are usually causally related to a disease; however, expression levels of these genes may remain constant because the genetic alteration affects only mRNA splicing or posttranscriptional regulation. Also, DNA microarray technologies may not be sensitive enough to accurately measure gene-expression changes in genes expressed at low levels.

Despite the suggested cautions, DNA microarray studies in the recent literature have begun to explore the biological significance and therapeutic potential of promising genes in greater depth using in vitro and in vivo models. For example, using DNA microarrays, Tian and colleagues (2003) identified a gene, *DKK1*, that was differentially expressed in multiple myeloma patients with and without focal bone lesions. Patients with bone lesions expressed higher levels of *DKK1* RNA and protein. *DKK1* is involved in bone formation through the Wnt signaling pathway, and marrow plasma from patients with bone lesions was shown to block osteoblast differentiation in vitro, indicating a causal role in disease progression and a potential therapeutic target. Another study, using cDNA microarrays to study liver samples from patients with hepatitis B–positive hepatocellular carcinomas with and without intrahepatic metastases, found that paired primary and metastatic tumors had similar gene-expression patterns (Ye et al., 2003). Many differentially expressed genes, however, were identified between primary carcinomas that did and did not metastasize. Osteopontin, a glycosylated phosphoprotein that acts as a cytokine, was overexpressed in primary tumors with metastasis. Additional experimental studies showed that cellular invasiveness was reduced in hepatoma-derived cell lines treated with neutralizing osteopontin antibody. In addition, nude mice injected with hepatocellular carcinoma cells had a reduced incidence of metastasis when treated with osteopontin-specific antibody.

LIMITATIONS OF PROTEOMIC TECHNIQUES

Proteomic studies suffer from problems similar to those outlined previously for DNA microarrays, including tissue heterogeneity, overfitting of predictive models, and identification of causative disease proteins. Specific criticism of proteomic techniques for the diagnosis of cancer focuses largely on the SELDI-TOF-MS technique. Diamandis (2004a, 2004b), the most widely published critic of this approach, has outlined several shortcomings of the technology. Although several papers have published impressive diagnostic yields using a panel of mass spectra, or "ion signatures," few positive identifications of proteins responsible for those peaks have occurred. Some of the proteins identified have been studied previously as tumor markers but were dismissed as acute-phase reactants. The absence of more positive protein identification limits the interpretation of published results, which potentially record differences attributable to something other than the underlying cancer, such as generalized inflammation.

The narrow dynamic detection range of MS technology also limits proteomic studies. In the case of serum samples, minimal preprocessing generally occurs prior to MS analysis. This involves surface enhancement attained through incubation on a weakly cationic protein chip—a nonspecific process that would likely bind only to the most abundant proteins in the sample, failing to detect potentially informative low-abundance proteins. One would likely not expect the proteins shed from a malignancy such as prostate cancer to be the most abundant proteins in a serum sample. By some estimates, SELDI-TOF-MS could not detect proteins at less than 1 μg/dL—a concentration many times higher than that of most known tumor markers (Diamandis, 2003).

EMERGING TECHNOLOGIES

CRISPR

Clustered regularly interspaced short palindromic repeats (CRISPR) and CRISPR-associated (Cas) proteins is a system originally found to be involved in defense against viral (phage) infection to bacteria (*Escherichia coli*). The genetic components of CRISPR contain short segments of bacteriophage genomes separated by the palindromic repeats and bacteria are resistant to infection by phages harboring corresponding sequences. These affordable and easily programmable molecular modalities enable virtually unlimited genetic manipulations in most organisms and hold the promise of curing human genetic disorders. The methodology pertaining to CRISPR–Cas9 systems for genome editing introduces DNA double-strand breaks at specific genomic locations that, in turn, activate host DNA repair pathways to introduce specific DNA modifications. CRISPR–Cas9 systems are also modified to modulate gene expression, track genomic loci and mRNA transcripts, or modify epigenetic markings (Pelletier, 2017). It is posited that genome editing can prevent and cure any disease as long as the disease-specific target gene is identified and validated and that new therapeutic possibilities may mature toward clinical considerations, for example, gene therapy, genome editing, or nucleic acid therapeutics. Novel classes of medicines may also be generated from a series of consequences

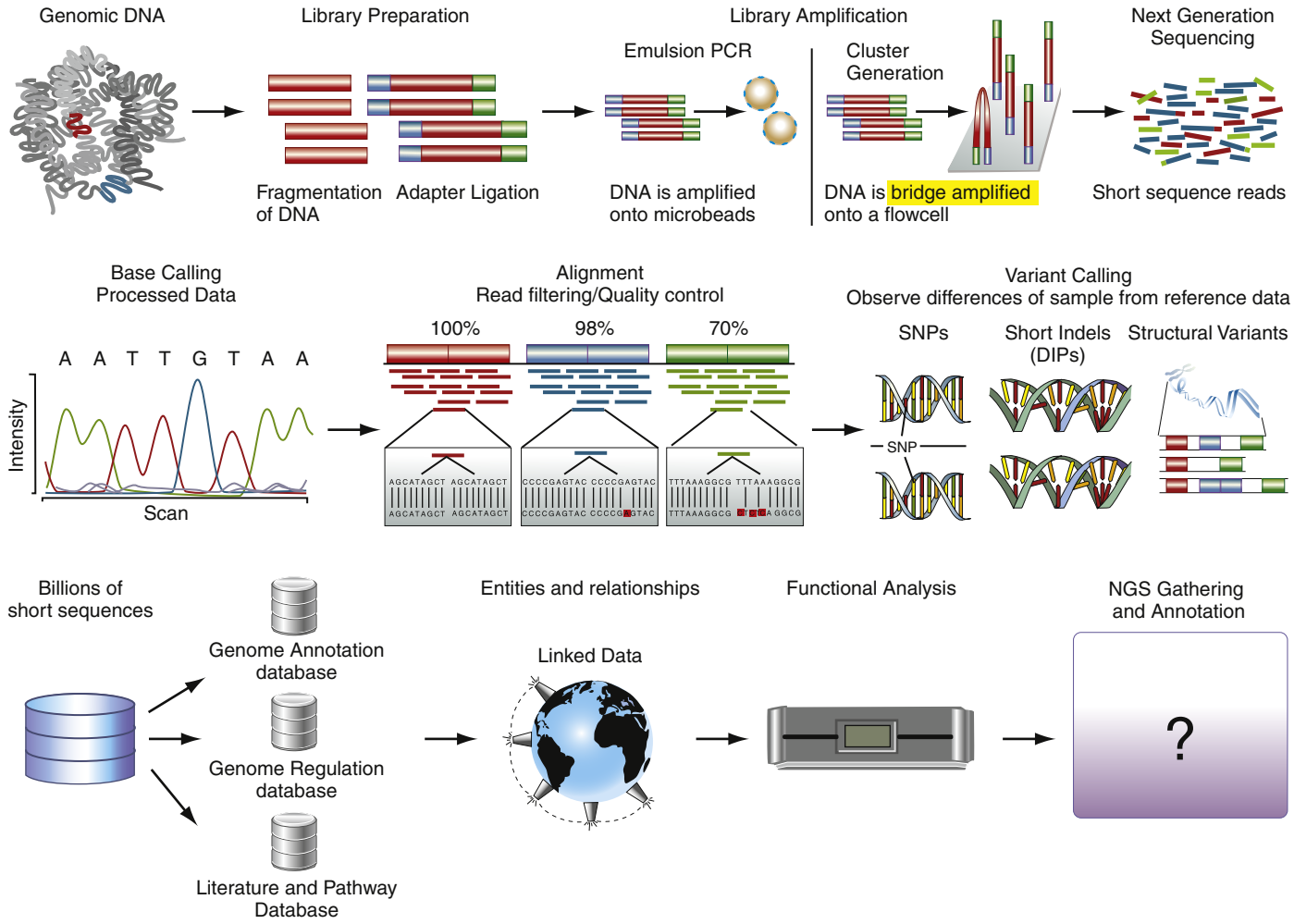

Figure 80.7 Next-generation sequencing methodology. (Reprinted with permission from Nayarisseri A, Yadav M, Bhatia M, et al.: Impact of next-generation whole-exome sequencing in molecular diagnostics, *Drug Invention Today* 5:327–334, 2013.)

after clinical application of genome editing (Porteus, 2019). With increasing precision editing, transplantation of genome-engineered cells and embryonic cells may be an alternative for the prevention and treatment of genetic and nongenetic diseases (Wang & Wang, 2019). Although this technology has been predominantly applied to genetic engineering pursuits in prokaryotes and lower vertebrates, recent studies by Bell et al. (2019) have utilized CRISPR to interrogate nongenetic drug resistance in acute myeloid leukemia. CRISPR-Cas9 screens were used to identify regulators of enhancer function that served as important modulators of the resistant cell state. They showed that inhibition of lysine-specific histone demethylase 1A (LSD1), also known as lysine (K)-specific demethylase 1A (KDM1A), was able to overcome stable epigenetic resistance by facilitating the binding of the pioneer factor Pu.1 and transcription cofactor Irf8 to nucleate new enhancers that regulate the expression of key survival genes. This enhancer switching resulted in the redistribution of transcriptional coactivators, including Brd4, and provided the opportunity to disable their activity and overcome epigenetic resistance. This approach suggests that disabling the process of enhancer remodeling, which is the cornerstone of nongenetic adaptation and resistance, may be preferable to inhibiting the final transcriptional state/pathway of resistant cells, which is likely to be a constantly moving target in an inherently plastic cell. In this way, CRISPR-based technology may dovetail with classic molecular pathology diagnostic techniques toward providing unique therapy options that result from such personalized medicine approaches.

NEXT-GENERATION SEQUENCING

Next-generation sequencing (NGS) is an established test method for germline (inherited) and somatic (acquired mutations) genetic mutations in many clinical laboratories. For inherited diseases, testing for germline mutations may include targeted panels, whole-exome, whole-genome, or mitochondrial DNA sequencing. In principle, NGS is similar to conventional (Sanger) sequencing methodology. However, while the Sanger method sequences only a single DNA fragment at a time, NGS is massively parallel, sequencing millions of fragments simultaneously per run. This high-throughput process translates into sequencing hundreds to thousands of genes at one time, as illustrated in Figure 80.7 (Nayarisseri, 2013). NGS also offers greater discovery power to detect novel or rare variants with deep sequencing. Targeted panel testing, which varies between laboratories, is possible for a wide variety of inherited disorders, such as immunodeficiencies, bone marrow failure syndromes, blindness, deafness, mitochondrial disorders, renal disorders, neurologic disorders, connective tissue disorders, cardiomyopathies, and cancer predisposition syndromes, among others (Yohe & Thyagarajan, 2017). While still a research tool in most cases, several new applications for NGS have more recently moved into the clinical arena or are being actively researched for clinical use, including circulating tumor DNA testing, human leukocyte antigen (HLA) typing, microbial analysis, RNA sequencing and expression, methylation, hematologic disorders, epilepsy, gastric and other cancers, among others (Yohe & Thyagarajan, 2017; Dunn et al., 2018; Zhang et al., 2019; Coccaro et al., 2019; Cai et al., 2019).

A more cost-effective model of NGS is referred to as whole-exome sequencing (WES), which interrogates the protein-coding regions of the genome. This approach is focused on the understanding that ~85% of disease-causing mutations reside in the exome and has proven successful in identifying new causal mutations for diseases of previously unknown etiology. The technique requires the extraction of high-quality genomic DNA (gDNA) from biological samples, most commonly extracted from peripheral blood leukocytes. Saliva or formalin-fixed paraffin-embedded samples are other biological samples, although their purity and/or yield may be an issue. The DNA is enriched following sample extraction, and exome capture kits are available from commercial vendors (Agilent, Illumina, and NimbleGen), which provide (1) DNA fragmentation, (2) adaptor ligation, and (3) target enrichment (see Fig. 80.8) (Seaby, 2016). The resultant captured library (following exon enrichment) is subject to high-throughput, massively parallel sequencing to produce millions of short

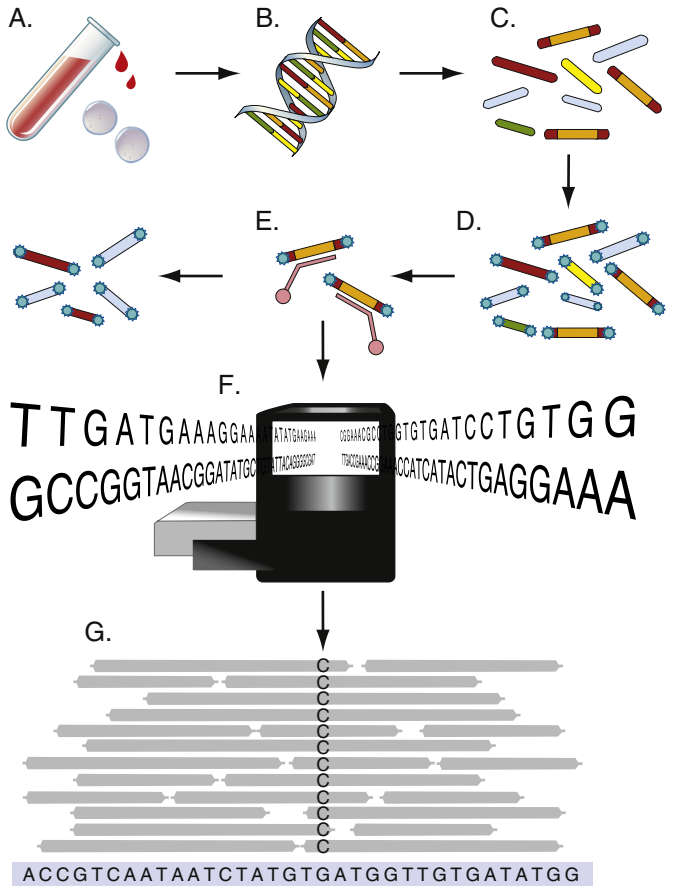

Figure 80.8 Workflow example of whole exome sequencing (WES). **A,** A blood sample is collected containing peripheral lymphocytes. **B,** gDNA is extracted from white blood cells using extraction kits or the salting-out method, and the quality and quantity is assessed. **C,** DNA is fragmented either by sonication or enzymatic methods, which vary between library preparations. **D,** Fragment ends are repaired by removing overhanging nucleotides, and the ends are ligated to adaptors *(stars)*. Rectangular regions within fragments represent exons present in DNA fragments. **E,** Aqueous-phase hybridization capture enriches exonic sequences *(rectangular regions)* by ligation of fragments to biotinylated baits (probes) as used by most enrichment platforms. Hybridized fragments are recovered by biotin-streptavidin–based magnetic bead pulldown. Uncaptured regions are washed away. The enriched library of exonic fragments are eluted and amplified. **F,** The resultant exome library is sequenced using massively parallel sequencing technologies, producing millions of sequenced reads (**G**). Raw data are aligned to the human genome reference sequence, and downstream in silico tools analyze output data. (A color version of this figure is available online at http://bfg.oxfordjournals.org) (From Seaby EG, Pengelly RJ, G, Ennis S: Exome sequencing explained: a practical guide to its clinical application, *Briefings in Functional Genomics*, 15(5):374-384, 2016.)

reads. Paired-end reads are created after the sequencing of both the forward and reverse strands, which provide longer-range information than single reads, yielding greater alignment accuracy when computationally mapped to the human genome reference sequence. This target-mapping process allows for the identification of coding nucleotide and splice site changes in the patient's DNA that vary from the reference sequence (variants). Although this technology is being applied to a number of clinical conditions with beneficial outcomes, there are various hurdles that have to be overcome to use WES in routine health care, including ethical, legal, social, and policy challenges, among others (Bertier, 2019). Nonetheless, WES remains a promising technology that will gain increased visibility and application over time.

ION TORRENT SEQUENCING

Another variation of NGS includes ion torrent sequencing, which measures the direct release of H+ (protons) from the incorporation of individual bases by DNA polymerase and, therefore, differs from other sequencing methods in that it does not measure light. In ion torrent sequencing, DNA is fragmented, attached to a bead, and amplified. The fragment is subsequently sequenced using a semiconductor chip. When each nucleic acid (ATCG) is successfully incorporated (referred to as a *base call*), it liberates a proton that is detected by a change in pH. Each individual well where this reaction occurs can be considered its own pH meter. For an excellent video on this technology, the reader is referred to https://www.thermofisher.com/us/en/home/life-science/sequencing/next-generation-sequencing/ion-torrent-next-generation-sequencing-technology.html.

CONCLUSION AND FUTURE CHALLENGES

The recent completion of the Human Genome Project and advances within the biotechnology sector offer unprecedented opportunities for identification of biomarkers associated with cancer and other pathologies. Genome sequence data combined with high-throughput biomarker discovery will facilitate the correlation of genetic variation with disease diagnosis and biological outcomes. The emerging fields of functional genomics and functional proteomics offer the opportunity to translate these advances into a full comprehension of the pathophysiology of cancer and other complex multigenic diseases.

High-throughput genomic and proteomic technologies have the potential to transform clinical practice and are likely to lead to the supplementation or replacement of traditional diagnostic and prognostic biomarkers. Many of the studies detailed in this chapter have demonstrated the utility of gene-expression profiles for the classification of tumors into distinct, clinically relevant subtypes and for the prediction of clinical outcomes. In addition, emerging proteomics platforms have just begun to add another layer of molecular information to the study of human disease. These technologies should lead to a new era of individualized molecular medicine, whereby all patients will be treated on the basis of genetic changes in their tumors and their own genetic makeup, resulting in more effective and less toxic therapy.

These high-throughput platforms offer the promise of influencing the practice of medicine. However, a number of obstacles to widespread clinical implementation of these technologies remain. Genomic and proteomic biomarkers are an emerging class of laboratory tests that present special implementation challenges for the clinical laboratory, including analytic, bioinformatics, and bioethical issues. Considerable efforts are required to provide the necessary clinical laboratory infrastructure for standard high-throughput analyzers capable of detecting genomic and proteomic alterations within a variety of biological samples and within various high-performance computing and advanced data-management capabilities. Significant improvements in analytic tools are needed, as are efforts to standardize techniques, controls, and reference standards. The application of such information to medical diagnosis and treatment will require considerable changes in the training of physicians. The most pressing need, however, is for extensive independent validation of the profiles described in the previous sections using large, statistically powered data sets. Inclusion of genomic- and proteomic-based molecular profiling techniques into clinical trial protocols will be needed to realize the potential of this technology to improve diagnosis and to tailor treatment of human disease.

SELECTED REFERENCES

Alizadeh AA, Eisen MB, Davis RE, et al.: Distinct types of diffuse large B-cell lymphoma identified by gene expression profiling, *Nature* 403:503–511, 2000.

This study analyzed diffuse large B-cell lymphoma patient samples using DNA microarrays and was one of the first to relate tumor subtypes identified by global gene-expression profiling to patient outcome.

Bluth MJ, Bluth MH: Molecular pathology techniques, *Clin Lab Med* 33:753–772, 2013.

This is a comprehensive review of commonly utilized molecular pathology techniques employed in the clinical laboratory for elucidating disease pathophysiology in addition to diagnosis, prognosis, and therapeutic monitoring for patient management.

Chen G, Gharib TG, Wang H, et al.: Protein profiles associated with survival in lung adenocarcinoma, *Proc Natl Acad Sci U S A* 100:13537–13542, 2003.

This study analyzed resected lung tumors that underwent both DNA microarray and proteomic analysis. It reported that gene and protein expression levels were mostly poorly correlated. However, integration of the two techniques revealed components of the glycolysis pathway associated with poor patient survival.

Golub TR, Slonim DK, Tamayo P, et al.: Molecular classification of cancer: class discovery and class prediction by gene expression monitoring, *Science* 286:531–537, 1999.

This article describes the first use of DNA microarrays to assay the gene expression of thousands of genes in clinical samples (human acute leukemias) to identify new cancer classes and to predict the class of unknown samples.

Lander ES, Linton LM, Birren B, et al.: Initial sequencing and analysis of the human genome, *Nature* 409:860–921, 2001.

A thorough presentation of the history of the Human Genome Project, the method used by the public consortium, the quality of the draft sequence, and the biological insights revealed by initial analyses.

Access the complete reference list online at Elsevier eBooks for Practicing Clinicians.

REFERENCES

Arbefeville S, Levi MH, Ferrieri P: Development of a multiplex real-time PCR assay for the detection of Bordetella pertussis and Bordetella parapertussis in a single tube reaction, *J Microbiol Methods* 97:15–19, 2014.

Anderson NL, Anderson NG: The human plasma proteome: history, character, and diagnostic prospects, *Mol Cell Proteomics* 1:845–867, 2002.

Beer DG, Kardia SL, Huang CC, et al.: Gene-expression profiles predict survival of patients with lung adenocarcinoma, *Nat Med* 8:816–824, 2002.

Bell CC, Fennell KA, Chan YC, et al.: Targeting enhancer switching overcomes non-genetic drug resistance in acute myeloid leukaemia, *Nat Commun* 10:2723, 2019.

Bertier G, Hétu M, Joly Y: Unsolved challenges of clinical whole-exome sequencing: a systematic literature review of end-users' views, *BMC Med Genomics* 9:52, 2016.

Bhattacharjee A, Richards WG, Staunton J, et al.: Classification of human lung carcinomas by mRNA expression profiling reveals distinct adenocarcinoma subclasses, *Proc Natl Acad Sci U S A* 98:13790–13795, 2001.

Boon K, Osorio EC, Greenhut SF, et al.: An anatomy of normal and malignant gene expression, *Proc Natl Acad Sci U S A* 99:11287–11292, 2002.

Brabender J, Marjoram P, Salonga D, et al.: A multigene expression panel for the molecular diagnosis of Barrett's esophagus and Barrett's adenocarcinoma of the esophagus, *Oncogene* 23:4780–4788, 2004.

Brown MP, Grundy WN, Lin D, et al.: Knowledge-based analysis of microarray gene expression data by using support vector machines, *Proc Natl Acad Sci U S A* 97:262–267, 2000.

Bubendorf L, Kolmer M, Kononen J, et al.: Hormone therapy failure in human prostate cancer: analysis by complementary DNA and tissue microarrays, *J Natl Cancer Inst* 91:1758–1764, 1999.

Buckhaults P, Rago C, St Croix B, et al.: Secreted and cell surface genes expressed in benign and malignant colorectal tumors, *Cancer Res* 61:6996–7001, 2001.

Buckhaults P, Zhang Z, Chen YC, et al.: Identifying tumor origin using a gene expression–based classification map, *Cancer Res* 63:4144–4149, 2003.

Bullinger L, Dohner K, Bair E, et al.: Use of gene-expression profiling to identify prognostic subclasses in adult acute myeloid leukemia, *N Engl J Med* 350:1605–1616, 2004.

Cai H, Jing C, Chang X, et al.: Mutational landscape of gastric cancer and clinical application of genomic profiling based on target next-generation sequencing, *J Transl Med* 17:189, 2019.

Cerutti JM, Delcelo R, Amadei MJ, et al.: A preoperative diagnostic test that distinguishes benign from malignant thyroid carcinoma based on gene expression, *J Clin Invest* 113:1234–1242, 2004.

Claverie JM: Gene number: what if there are only 30000 human genes? *Science* 291:1255–1257, 2001.

Coccaro N, Anelli L, Zagaria A, Specchia G, Albano F: Next-generation sequencing in acute lymphoblastic leukemia, *Int J Mol Sci* 20, 2019. E2929.

Collins FS, Morgan M, Patrinos A: The Human Genome Project: lessons from large-scale biology, *Science* 300:286–290, 2003.

Dahl Steffensen K, Waldstrom M, Kolby Christensen R, et al.: Lack of relationship between TIMP-1 tumour cell immunoreactivity, treatment efficacy and prognosis in patients with advanced epithelial ovarian cancer, *BMC Canc* 10:185, 2010.

Datson NA: Scaling down SAGE: from miniSAGE to microSAGE, *Curr Pharm Biotechnol* 9:351–361, 2008.

Datson NA, van der Perk-de Jong J, van den Berg MP, et al.: MicroSAGE: a modified procedure for serial analysis of gene expression in limited amounts of tissue, *Nucleic Acids Res* 27:1300–1307, 1999.

Dave SS, Wright G, Tan B, et al.: Prediction of survival in follicular lymphoma based on molecular features of tumor-infiltrating immune cells, *N Engl J Med* 351:2159–2169, 2004.

Dennis JL, Vass JK, Wit EC, et al.: Identification from public data of molecular markers of adenocarcinoma characteristic of the site of origin, *Cancer Res* 62:5999–6005, 2002.

Dhanasekaran SM, Barrette TR, Ghosh D, et al.: Delineation of prognostic biomarkers in prostate cancer, *Nature* 412:822–826, 2001.

Diamandis EP: Analysis of serum proteomic patterns for early cancer diagnosis: drawing attention to potential problems, *J Natl Cancer Inst* 96:353–356, 2004a.

Diamandis EP: Mass spectrometry as a diagnostic and a cancer biomarker discovery tool: opportunities and potential limitations, *Mol Cell Proteomics* 3:367–378, 2004b.

Diamandis EP: Point: proteomic patterns in biological fluids: do they represent the future of cancer diagnostics? *Clin Chem* 49:1272–1275, 2003.

Ding C, Cantor CR: A high-throughput gene expression analysis technique using competitive PCR and matrix-assisted laser desorption ionization time-of-flight MS, *Proc Natl Acad Sci U S A* 100:3059–3064, 2003.

Ding C, Jin S: High-throughput methods for SNP genotyping, *Methods Mol Biol* 578:245–254, 2009.

Ding C, Maier E, Roscher AA, et al.: Simultaneous quantitative and allele-specific expression analysis with real competitive PCR, *BMC Genet* 5:8, 2004.

Djidja MC, Claude E, Snel MF, et al.: Novel molecular tumour classification using MALDI-mass spectrometry imaging of tissue micro-array, *Anal Bioanal Chem* 397:587–601, 2010.

Drury S, Salter J, Baehner FL, et al.: Feasibility of using tissue microarray cores of paraffin-embedded breast cancer tissue for measurement of gene expression: a proof-of-concept study, *J Clin Pathol* 63:513–517, 2010.

Dudoit S: FJST: comparison of discrimination methods for the classification of tumors using gene expression data, *J Am Statistical Assoc* 97:77–87, 2002.

Dunn P, Albury CL, Maksemous N, et al.: Next generation sequencing methods for diagnosis of epilepsy syndromes, *Front Genet* 9:20, 2018.

Dyrskjot L, Thykjaer T, Kruhoffer M, et al.: Identifying distinct classes of bladder carcinoma using microarrays, *Nat Genet* 33:90–96, 2003.

Eisen MB, Spellman PT, Brown PO, et al.: Cluster analysis and display of genome-wide expression patterns, *Proc Natl Acad Sci U S A* 95:14863–14868, 1998.

Emmert-Buck MR, Bonner RF, Smith PD, et al.: Laser capture microdissection, *Science* 274:998–1001, 1996.

Genome International Sequencing Consortium: Initial sequencing and analysis of the human genome, *Nature* 409:860–921, 2001.

Holzhauser T, Kleiner K, Janise A, et al.: Matrix-normalised quantification of species by threshold-calibrated competitive real-time PCR: allergenic peanut in food as one example, *Food Chem* 163:68–76, 2014.

Huang E, Cheng SH, Dressman H, et al.: Gene expression predictors of breast cancer outcomes, *Lancet* 361:1590–1596, 2003.

Hustinx SR, Cao D, Maitra A, et al.: Differentially expressed genes in pancreatic ductal adenocarcinomas identified through serial analysis of gene expression, *Cancer Biol Ther* 3:1254–1261, 2004.

Iacobuzio-Donahue CA, Maitra A, Shen-Ong GL, et al.: Discovery of novel tumor markers of pancreatic cancer using global gene expression technology, *Am J Pathol* 160:1239–1249, 2002.

Inoue M, Senju S, Hirata S, et al.: Identification of SPARC as a candidate target antigen for immunotherapy of various cancers, *Int J Cancer* 127:1393–1403, 2010.

International Human Genome Sequencing Consortium: Finishing the euchromatic sequence of the human genome, *Nature* 431:931–945, 2004.

Irizarry RA, Bolstad BM, Collin F, et al.: Summaries of Affymetrix GeneChip probe level data, *Nucleic Acids Res* 31, 2003. e15.

Jinawath N, Furukawa Y, Hasegawa S, et al.: Comparison of gene expression profiles between diffuse- and intestinal-type gastric cancers using a genome-wide cDNA microarray, *Oncogene* 23:6830–6844, 2004.

Kaminski N, Friedman N: Practical approaches to analyzing results of microarray experiments, *Am J Respir Cell Mol Biol* 27:125–132, 2002.

Khan J, Wei JS, Ringner M, et al.: Classification and diagnostic prediction of cancers using gene expression profiling and artificial neural networks, *Nat Med* 7:673–679, 2001.

Kononen J, Bubendorf L, Kallioniemi A, et al.: Tissue microarrays for high-throughput molecular profiling of tumor specimens, *Nat Med* 4:844–847, 1998.

Koopmann J, Fedarko NS, Jain A, et al.: Evaluation of osteopontin as biomarker for pancreatic adenocarcinoma, *Cancer Epidemiol Biomarkers Prev* 13:487–491, 2004.

Kuerer HM, Goldknopf IL, Fritsche H, et al.: Identification of distinct protein expression patterns in bilateral matched pair breast ductal fluid specimens from women with unilateral invasive breast carcinoma: high-throughput biomarker discovery, *Cancer* 95:2276–2282, 2002.

Lal A, Lash AE, Altschul SF, et al.: A public database for gene expression in human cancers, *Cancer Res* 59:5403–5407, 1999.

Lash AE, Tolstoshev CM, Wagner L, et al.: SAGEmap: a public gene expression resource, *Genome Res* 10:1051–1060, 2000.

Leung YF, Cavalieri D: Fundamentals of cDNA microarray data analysis, *Trends Genet* 19:649–659, 2003.

Li C, Wong WH: Model-based analysis of oligonucleotide arrays: expression index computation and outlier detection, *Proc Natl Acad Sci U S A* 98:31–36, 2001.

Liu X, Xu Y, Xiong YH, et al.: VHH phage-based competitive real-time immunopolymerase chain reaction for ultrasensitive detection of ochratoxin A in cereal, *Anal Chem* 86:7471–7477, 2014.

Lockhart DJ, Dong H, Byrne MC, et al.: Expression monitoring by hybridization to high-density oligonucleotide arrays, *Nat Biotechnol* 14:1675–1680, 1996.

Madden SL, Wang CJ, Landes G: Serial analysis of gene expression: from gene discovery to target identification, *Drug Discov Today* 5:415–425, 2000.

Mathe C, Sagot MF, Schiex T, et al.: Current methods of gene prediction, their strengths and weaknesses, *Nucleic Acids Res* 30:4103–4117, 2002.

Mathe EA, Nguyen GH, Bowman ED, et al.: MicroRNA expression in squamous cell carcinoma and adenocarcinoma of the esophagus: associations with survival, *Clin Cancer Res* 15:6192–6200, 2009.

McIver CJ, Bell SM, Er N: Development of an internal amplification control system for a real-time PCR assay for detection of Neisseria meningitidis in CSF and EDTA blood, *Pathology* 46:344–347, 2014.

Miklos GL, Maleszka R: Microarray reality checks in the context of a complex disease, *Nat Biotechnol* 22:615–621, 2004.

Nayarisseri A, Yadav M, Bhatia M, Pandey A, Elkunchwar A, Paul N, Sharma D, Kumar G: Impact of Next-Generation Whole-Exome sequencing in molecular diagnostics, *Drug Invent Today* 5:327–334, 2013.

Mukherjee P, Mani S: Methodologies to decipher the cell secretome, *Biochim Biophys Acta* 1834:2226–2232, 2013.

Nonogaki K, Itoh A, Kawashima H, et al.: A preliminary result of three-dimensional microarray technology to gene analysis with endoscopic ultrasound-guided fine-needle aspiration specimens and pancreatic juices, *J Exp Clin Cancer Res* 29:36, 2010.

Ntzani EE, Ioannidis JP: Predictive ability of DNA microarrays for cancer outcomes and correlates: an empirical assessment, *Lancet* 362:1439–1444, 2003.

Ocak S, Sos ML, Thomas RK, et al.: High-throughput molecular analysis in lung cancer: insights into biology and potential clinical applications, *Eur Respir J* 34:489–506, 2009.

Oh P, Li Y, Yu J, et al.: Subtractive proteomic mapping of the endothelial surface in lung and solid tumours for tissue-specific therapy, *Nature* 429:629–635, 2004.

Olson MV: The maps: clone by clone by clone, *Nature* 409:816–818, 2001.

Ornstein DK, Rayford W, Fusaro VA, et al.: Serum proteomic profiling can discriminate prostate cancer from benign prostates in men with total prostate specific antigen levels between 2.5 and 15.0 ng/ml, *J Urol* 172:1302–1305, 2004.

Paik S, Shak S, Tang G, et al.: A multigene assay to predict recurrence of tamoxifen-treated, node-negative breast cancer, *N Engl J Med* 351:2817–2826, 2004.

Patino WD, Mian OY, Hwang PM: Serial analysis of gene expression: technical considerations and applications to cardiovascular biology, *Circ Res* 91:565–569, 2002.

Paweletz CP, Charboneau L, Bichsel VE, et al.: Reverse phase protein microarrays which capture disease progression show activation of pro-survival pathways at the cancer invasion front, *Oncogene* 20:1981–1989, 2001.

Pennisi E: And the gene number is …? *Science* 288:1146–1147, 2000.

Perou CM, Sorlie T, Eisen MB, et al.: Molecular portraits of human breast tumours, *Nature* 406:747–752, 2000.

Pittman J, Huang E, Dressman H, et al.: Integrated modeling of clinical and gene expression information for personalized prediction of disease outcomes, *Proc Natl Acad Sci U S A* 101:8431–8436, 2004.

Pomeroy SL, Tamayo P, Gaasenbeek M, et al.: Prediction of central nervous system embryonal tumour outcome based on gene expression, *Nature* 415:436–442, 2002.

Porter D, Lahti-Domenici J, Keshaviah A, et al.: Molecular markers in ductal carcinoma in situ of the breast, *Mol Cancer Res* 1:362–375, 2003a.

Porter D, Weremowicz S, Chin K, et al.: A neural survival factor is a candidate oncogene in breast cancer, *Proc Natl Acad Sci U S A* 100:10931–10936, 2003b.

Porter DA, Krop IE, Nasser S, et al.: A SAGE (serial analysis of gene expression) view of breast tumor progression, *Cancer Res* 61:5697–5702, 2001.

Porteus MH: A new class of medicines through DNA editing, *N Engl J Med* 380:947–959, 2019.

Quackenbush J: Computational analysis of microarray data, *Nat Rev Genet* 2:418–427, 2001.

Ramaswamy S, Ross KN, Lander ES, et al.: A molecular signature of metastasis in primary solid tumors, *Nat Genet* 33:49–54, 2003.

Ransohoff DF: Rules of evidence for cancer molecular-marker discovery and validation, *Nat Rev Cancer* 4:309–314, 2004.

Reich M, Ohm K, Angelo M, et al.: GeneCluster 2.0: an advanced toolset for bioarray analysis, *Bioinformatics* 20:1797–1798, 2004.

Rosenwald A, Wright G, Chan WC, et al.: The use of molecular profiling to predict survival after chemotherapy for diffuse large-B-cell lymphoma, *N Engl J Med* 346:1937–1947, 2002.

Russo G, Zegar C, Giordano A: Advantages and limitations of microarray technology in human cancer, *Oncogene* 22:6497–6507, 2003.

Sanchez-Carbayo M: Antibody array-based technologies for cancer protein profiling and functional proteomic analyses using serum and tissue specimens, *Tumour Biol* 31:103–112, 2010.

Sawiris GP, Sherman-Baust CA, Becker KG, et al.: Development of a highly specialized cDNA array for the study and diagnosis of epithelial ovarian cancer, *Cancer Res* 62:2923–2928, 2002.

Schena M, Shalon D, Davis RW, et al.: Quantitative monitoring of gene expression patterns with a complementary DNA microarray, *Science* 270:467–470, 1995.

Seaby EG, Pengelly RJ, Ennis S: Exome sequencing explained: a practical guide to its clinical application, *Briefings in Functional Genomics* 15, 2016. 374–38.

Selaru FM, Zou T, Xu Y, et al.: Global gene expression profiling in Barrett's esophagus and esophageal cancer: a comparative analysis using cDNA microarrays, *Oncogene* 21:475–478, 2002.

Schaaij-Visser TB, de Wit M, Lam SW, et al.: The cancer secretome, current status and opportunities in the lung, breast and colorectal cancer context, *Biochim Biophys Acta* 1834:2242–2258, 2013.

Shipp MA, Ross KN, Tamayo P, et al.: Diffuse large B-cell lymphoma outcome prediction by gene-expression profiling and supervised machine learning, *Nat Med* 8:68–74, 2002.

Simon R, Lam AP: *BRB ArrayTools*, *version 3.5*, *Bethesda*, *Md*, Biometrics Research Branch, 2004, National Cancer Institute.

Simon R, Radmacher MD, Dobbin K, et al.: Pitfalls in the use of DNA microarray data for diagnostic and prognostic classification, *J Natl Cancer Inst* 95:14–18, 2003.

Sotiriou C, Neo SY, McShane LM, et al.: Breast cancer classification and prognosis based on gene expression profiles from a population-based study, *Proc Natl Acad Sci U S A* 100:10393–10398, 2003.

Spira A, Beane J, Schembri F, et al.: Noninvasive method for obtaining RNA from buccal mucosa epithelial cells for gene expression profiling, *Biotechniques* 36:484–487, 2004.

Stankiewicz P, Lupski JR: Genome architecture, rearrangements and genomic disorders, *Trends Genet* 18:74–82, 2002.

Syvanen AC: Accessing genetic variation: genotyping single nucleotide polymorphisms, *Nat Rev Genet* 2:930–942, 2001.

Tian E, Zhan F, Walker R, et al.: The role of the Wnt-signaling antagonist DKK1 in the development of osteolytic lesions in multiple myeloma, *N Engl J Med* 349:2483–2494, 2003.

Tibshirani R, Hastie T, Narasimhan B, et al.: Diagnosis of multiple cancer types by shrunken centroids of gene expression, *Proc Natl Acad Sci U S A* 99:6567–6572, 2002.

Tinelli A, Vergara D, Martignago R, et al.: An outlook on ovarian cancer and borderline ovarian tumors: focus on genomic and proteomic findings, *Curr Genomics* 10:240–249, 2009.

Tumor Analysis Best Practices Working Group: Expression profiling—best practices for data generation and interpretation in clinical trials, *Nat Rev Genet* 5:229–237, 2004.

Tran C, Damaser MS: Stem cells as drug delivery methods: application of stem cell secretome for regeneration, *Adv Drug Deliv Rev* 82–83:1–11, 2015.

Tusher VG, Tibshirani R, Chu G: Significance analysis of microarrays applied to the ionizing radiation response, *Proc Natl Acad Sci U S A* 98:5116–5121, 2001.

Valk PJ, Verhaak RG, Beijen MA, et al.: Prognostically useful gene-expression profiles in acute myeloid leukemia, *N Engl J Med* 350:1617–1628, 2004.

Van de Vijver MJ, He YD, van't Veer LJ, et al.: A gene-expression signature as a predictor of survival in breast cancer, *N Engl J Med* 347:1999–2009, 2002.

van't Veer LJ, Dai H, van de Vijver MJ, et al.: Gene expression profiling predicts clinical outcome of breast cancer, *Nature* 415:530–536, 2002.

Velculescu VE, Zhang L, Vogelstein B, et al.: Serial analysis of gene expression, *Science* 270:484–487, 1995.

Venter JC, Adams MD, Myers EW, et al.: The sequence of the human genome, *Science* 291:1304–1351, 2001.

Vera-Ramirez L, Sanchez-Rovira P, Ramirez-Tortosa CL, et al.: Gene-expression profiles, tumor microenvironment, and cancer stem cells in breast cancer: latest advances towards an integrated approach, *Cancer Treat Rev* 36:477–484, 2010.

Wang DC, Wang X: Off-target genome editing: a new discipline of gene science and a new class of medicine Cell, *Biol Toxicol* 35:179–183, 2019.

Watanabe H, Okada G, Ohtsubo K, et al.: Expression of mesothelin mRNA in pure pancreatic juice from patients with pancreatic carcinoma, intraductal papillary mucinous neoplasm of the pancreas, and chronic pancreatitis, *Pancreas* 30:349–354, 2005.

Xu Y, Selaru FM, Yin J, et al.: Artificial neural networks and gene filtering distinguish between global gene expression profiles of Barrett's esophagus and esophageal cancer, *Cancer Res* 62:3493–3497, 2002.

Yamamoto M, Wakatsuki T, Hada A, et al.: Use of serial analysis of gene expression (SAGE) technology, *J Immunol Methods* 250:45–66, 2001.

Ye QH, Qin LX, Forgues M, et al.: Predicting hepatitis B virus–positive metastatic hepatocellular carcinomas using gene expression profiling and supervised machine learning, *Nat Med* 9:416–423, 2003.

Yohe S, Thyagarajan B: Review of clinical next-generation sequencing, *Arch Pathol Lab Med* 141:1544–1557, 2017.

Zender L, Villanueva A, Tovar V, et al.: Cancer gene discovery in hepatocellular carcinoma, *J Hepatol* 52:921–929, 2010.

Zhang X, Liang Z, Wang S, et al.: Tumor biomarker committee OBOCSOCOC application of next-generation sequencing technology to precision medicine in cancer: joint consensus of the tumor biomarker committee of the Chinese Society of clinical Oncology, *Cancer Biol Med* 16:189–204, 2019.

Zhang Y, Szustakowski J, Schinke M: Bioinformatics analysis of microarray data, *Methods Mol Biol* 573:259–284, 2009.

Zhou J, Belov L, Huang PY, et al.: Surface antigen profiling of colorectal cancer using antibody microarrays with fluorescence multiplexing, *J Immunol Methods* 355:40–51, 2010.

APPENDIX 1

PHYSIOLOGIC SOLUTIONS, BUFFERS, ACID-BASE INDICATORS, STANDARD REFERENCE MATERIALS, AND TEMPERATURE CONVERSIONS

PHYSIOLOGIC SOLUTIONS

A physiologic solution is one that contains various salts in concentrations that closely approximate the composition of fluids in the human body. The simplest of these is physiologic saline, which has the same osmotic pressure as the blood. There are more elaborate solutions, for example, to maintain tissues in a metabolically active state for longer periods of time. Table A1.1 lists formulas of some solutions that are isotonic with respect to blood.

BUFFERS*

Buffers have the ability to resist changes in pH. Buffers usually consist of a weak acid and its salt or a weak base and its salt. The Henderson-Hasselbalch equation is useful in calculating the ratio of acid (or base) to salt required to establish a desired pH from a buffer system:

$$pH = pK + \log [salt] / [acid] \qquad \text{(Eq. A1.1)}$$

EXAMPLE 1

If the pH of a 0.1-M acetate buffer is known to be 4.90, calculate the concentration of acetic acid and sodium acetate in the buffer (pK for acetic acid = 4.76).

Substituting values of pH and pK in Equation A1.1:

$$\log [acetate] / [acetic\ acid] = 4.90 - 4.76 = 0.14$$
$$[acetate] / [acetic\ acid] = 1.38$$
$$[acetate] = 1.38\,[acetic\ acid]$$

Because the total buffer/L concentrations is 0.1 M,

$$[acetate] + [acetic\ acid] = 0.1\ M \qquad \text{(Eq. A1.2)}$$

Substituting the value of acetate in Equation A1.2:

$$1.38\,[acetic\ acid] + [acetic\ acid] = 0.1\ M$$

Hence,

$$[acetic\ acid] = 0.042\ M$$
$$[acetic\ acid] = 2.52\ g/L$$
$$[acetate] = 0.058\ M = 4.76\ g/L$$

EXAMPLE 2

If 648 mL of 0.025 molar diethylbarbituric acid and 10 mL of 0.5 molar sodium diethylbarbiturate are mixed and diluted to 1 L, calculate the pH of the solution (pK for diethylbarbituric acid = 7.98 and molar concentration = mol/L).

The following relationship exists between molarity and volume of a solution:

$$M1V1 = M2V2 \qquad \text{(Eq. A1.3)}$$

where M1 = molarity of the initial solution, V1 = volume of the initial solution, M2 = molarity of the final solution, and V2 = volume of the final solution.

Use Equation A1.3 to calculate changes in salt and acid concentrations after dilution to 1 L:

$$[Sodium\ \ diethylbarbiturate] = 0.025 \times 0.648 = 0.0162\ mol/L$$

$$[Diethylbarbituric\ acid] = 0.5 \times 0.01 = 0.005\ mol/L$$

Calculate pH of the solution using Equation A1.1:

$$pH = 7.98 - \log (0.0162 / 0.005) = 7.98 - \log 3.24 = 7.98 - 0.51 = 7.47$$

The maximum buffering capacity is at the pK value of the weak acid or base. For instance, for acetic acid with a pH value of 4.76, more acid is required to change the pH of an acetate buffer from 4.76 to 4.66 than from 4.20 to 4.10. Efficient buffering capacity covers a pH range of about 1 unit on either side of the pK value of the weak acid or base. For acetic acid, this would be from about pH 3.8 to 5.8.

SORENSEN'S PHOSPHATE BUFFERS

These buffer solutions are generally useful because the range of the mixtures is from pH 5 to 8.

Prepare 0.1-molar solutions of monobasic potassium phosphate (13.6 g/L) and dibasic sodium phosphate (14.2 g/L). Mix solutions in the ratio indicated in Table A1.2 to obtain the buffer of desired pH.

TRIS(HYDROXYMETHYL)AMINOMETHANE BUFFER*

Tris(hydroxymethyl)aminomethane buffer can be used for a pH range between 7.0 and 9.0, but its best buffer capacity is between 7.5 and 8.5. It is practically ineffective below pH 7.0 and above pH 9.0. One advantage of the buffer is its excellent stability. The buffer can be prepared by weighing the desired amount of tris(hydroxymethyl)aminomethane, dissolving it in water, and adjusting the pH to the desired value with HCl. For example, if 100 mL of 0.05 M buffer is desired, place 0.6057 g of tris(hydroxymethyl)aminomethane into a 100-mL volumetric flask. This is dissolved in approximately 50 mL of distilled water. Add 0.1 N HCl, as indicated in Table A1.3, and fill up to the mark with distilled water. The table shows the pH values obtained when 0.6057 g of tris(hydroxymethyl)aminomethane dissolved in water is mixed with the indicated amounts of 0.1 N HCl and diluted to 100 mL.

ACID-BASE INDICATORS†

An acid-base indicator is a weak acid or a weak base, the undissociated form of which has a color and constitution other than the ionogenic form. Color change takes place over a certain narrow range of hydrogen ion concentrations. This range is called the *color change interval* and is expressed in terms of pH (the negative logarithm of the hydrogen ion concentration). A great number of substances show indicator properties, although relatively few

*For a comprehensive discussion, including preparation of buffer solutions of a definite ionic strength, consult Bates RG: *Determination of pH—theory and practice*, ed 2, New York, 1973, John Wiley and Sons.

*If buffers of a higher molarity are desired, the 0.1N HCl may have to be replaced by 1.0N HCl.

† Based on Dean JA, editor: *Handbook of chemistry*, revised ed 13, New York, 1985, McGraw-Hill.

TABLE A1.1
Physiologic Solutions

	Saline	Locke's Solution	Ringer's Solution	Tyrode's Solution
Sodium chloride	0.85 g	0.9 g	0.7 g	0.8 g
Calcium chloride		0.024 g	0.0026 g	0.02 g
Potassium chloride		0.042 g	0.035 g	0.02 g
Sodium bicarbonate		0.01–0.03 g		0.1 g
D-Glucose		0.01–0.25 g		0.1 g
Magnesium chloride				0.01 g
Monosodium phosphate				0.005 g
Distilled water	100 mL	100 mL	100 mL	100 mL

TABLE A1.2
Sorensen's Table of Buffer Mixtures

Na_2HPO_4 Solution (mL)	KH_2PO_4 Solution (mL)	pH
0.25	9.75	5.288
0.5	9.5	5.589
1.0	9.0	5.906
2.0	8.0	6.239
3.0	7.0	6.468
4.0	6.0	6.643
5.0	5.0	6.813
6.0	4.0	6.979
7.0	3.0	7.168
8.0	2.0	7.381
9.0	1.0	7.731
9.5	0.5	8.043

TABLE A1.3
Tris(hydroxymethyl)aminomethane Buffer

mL 0.1 N HCl Added	Resulting pH at 23°C	Resulting pH at 37°C
5.0	9.10	8.95
7.5	8.92	8.78
10.0	8.74	8.60
12.5	8.62	8.48
15.0	8.50	8.37
17.5	8.40	8.27
20.0	8.32	8.18
22.5	8.23	8.10
25.0	8.14	8.00
27.5	8.05	7.90
30.0	7.96	7.82
32.5	7.87	7.73
35.0	7.77	7.63
37.5	7.66	7.52
40.0	7.54	7.40
42.5	7.36	7.22
45.0	7.20	7.05

TABLE A1.4
Acid-Base Indicators

Indicator	pH Range	Quantity of Indicator per 10 mL	Color Acid	Alkaline
Thymol blue (A)*†	1.2–2.8	1–2 drops 0.1% solution in aqueous	Red	Yellow
Methyl orange (B)	3.1–4.4	1 drop 0.1% solution in aqueous	Red	Orange
Bromophenol blue (A)†	3.0–4.6	1 drop 0.1% solution in aqueous	Yellow	Blue-violet
Bromocresol green (A)†	4.0–5.6	1 drop 0.1% solution in aqueous	Yellow	Blue
Methyl red (A)†	4.4–6.2	1 drop 0.1% solution in aqueous	Red	Yellow
Bromocresol purple (A)†	5.2–6.8	1 drop 0.1% solution in aqueous	Yellow	Purple
Bromothymol blue (A)†	6.2–7.6	1 drop 0.1% solution in aqueous	Yellow	Blue
Phenol red (A)†	6.4–8.0	1 drop 0.1% solution in aqueous	Yellow	Red
Neutral red (B)	6.8–8.0	1 drop 0.1% solution in 70% alcohol	Red	Yellow
Thymol blue (A)†‡	8.0–9.6	1–5 drops 0.1% solution in aqueous	Yellow	Blue
Phenolphthalein (A)	8.0–10.0	1–5 drops 0.1% solution in 70% alcohol	Colorless	Red
Thymolphthalein (A)	9.4–10.6	1 drop 0.1% solution in 90% alcohol	Colorless	Blue

(A), acid; *(B)*, base.
*For the acid range.
†Sodium salt.
‡For the alkaline range.

are practically applied for neutralization reactions and pH determinations. Commonly used acid-base indicators are listed in Table A1.4. In general, weak acids should be titrated in the presence of indicators that change in slightly alkaline solutions. Weak bases should be titrated in the presence of indicators that change in slightly acid solutions. Commonly used acids and alkalis are listed in Table A1.5.

The availability of precision pH meters allows titration to a selected endpoint (pH) and may replace use of indicators for several applications.

STANDARD REFERENCE MATERIALS

Standard reference materials (SRMs) are available for many substances with defined identities and concentrations in solutions or as other materials, such as thermometers or optical filters with specified transmission wavelengths (Table A1.6). SRMs are used as standards or controls against which assays may be calibrated with high certainty of accuracy in both identity and concentration of the substance or other property.

TEMPERATURE CONVERSION

Temperature is expressed in either Fahrenheit (F) or centigrade (C) scale according to the convention of the country, editorial policy of journals, and local practices. The simple relationship between these two temperature scales is:

$$\text{Temperature in degrees Fahrenheit} = 1.8 \times \text{temperature in degrees centigrade} + 32$$

Often it is more convenient to look up corresponding values for these two temperature scales in a list of values (Table A1.7). A unique value occurs at −40°, where the two scales intersect and the values coincide (i.e., −40° F = −40° C).

TABLE A1.5

Commonly Used Acids and Alkalis*

Solution	Molecular Weight	Specific Gravity†	g/L†	Molarity†	Normality†	Approximate Number of mL Required to Make 1000 mL of 1 N Solution
Concentrated HCl	36.46	1.19	440	12	12	83
Concentrated H_2SO_4	98.08	1.84	1730	18	36	28
Concentrated HNO_3	63.02	1.42	990	16	16	64
Concentrated lactic acid	90.08	1.21	1030	11	11	87
Glacial acetic acid	60.08	1.06	1060	17.5	17.5	57
Concentrated NH_4OH	35.05	0.90	250	15	15	67

*Commercially available.
†Figures may vary slightly according to the lot or manufacturer.

TABLE A1.6

Standard Reference Materials for Clinical Measurements

SRM No.	SRM Type	Stoichiometric Purity Mass Fraction in %	Certified Use	Unit Size (g)
40h	Sodium oxalate	99.972	Reductometric standard	60
83d	Arsenic trioxide	99.9926	Reductometric standard	60
84k	Potassium hydrogen phthalate	99.9911	Acidimetric standard	60
136e	Potassium dichromate	99.984	Oximetric standard	60
350a	Benzoic acid	99.9958	Acidimetric standard	30
723c	Tris(hydroxymethyl) aminomethane	99.901	Acidimetric standard	50
911b	Cholesterol	99.8	Identity and purity	2.0
912a	Urea	99.9	Identity and purity	25
913	Uric acid	99.7	Identity and purity	10
914a	Creatinine	99.7	Identity and purity	10
915a	Calcium carbonate	99.9	Identity and purity	20
916a	Bilirubin	98.3	Identity and purity	0.1
917a	D-Glucose (dextrose)	99.7	Identity and purity	25
918a	Potassium chloride	99.9817	Identity and purity	30
919a	Sodium chloride	99.89	Identity and purity	30
930e	Glass filters, transmittance		Wavelength range (440–635 nm)	3 filters
931f	Liquid filters, absorbance		Wavelength range (302–678 nm)	Ampules
934	Clinical laboratory thermometers (0, 25, 30, 37)		Temperature	One each
937	Iron metal	99.90		50
955b	Lead in blood			Set of 4 ampules

SRM, Standard reference materials.

TABLE A1.7

Temperature Conversions

Centigrade (°)	Fahrenheit (°)	Centigrade (°)	Fahrenheit (°)
110	230	38	100.4
100	212	37.5	99.5
95	203	37	98.6
90	194	36.5	97.7
85	185	36	96.8
80	176	35.5	95.9
75	167	35	95
70	158	34	93.2
65	149	33	91.4
60	140	32	89.6
55	131	31	87.8
50	122	30	86
45	113	25	77
44	111.2	20	68
43	109.4	15	59
42	107.6	10	50
41	105.8	+5	41
40.5	104.9	0	32
40	104	–5	23
39.5	103.1	–10	14
39	102.2	–15	+5
38.5	101.3	–20	–4

1° F = –17.2° C.
1° C = 33.8° F.
To convert Fahrenheit into centigrade, subtract 32 and multiply by 0.555.
To convert centigrade to Fahrenheit, multiply by 1.8 and add 32.

SELECTED REFERENCES

Dean JA, editor: *Handbook of chemistry*, ed 13, New York, 1985, McGraw-Hill.

Fasman GD, editor: *Handbook of biochemistry and molecular biology*, ed 3, Cleveland, OH, 1976, CRC Press.

Meinke WW: Standard reference materials for clinical measurements, *Anal Chem* 43:28A, 1971.

The Merck index: In *an encyclopedia of chemicals and drugs*, ed 12, Whitehouse Station, NJ, 1996, Merck and Co.

APPENDIX 2

DESIRABLE WEIGHTS, BODY SURFACE AREA, AND BODY MASS INDEX

TABLE A2.1

Comparison of the Weight-for-Height Tables from Actuarial Data: Non–Age-Corrected Metropolitan Life Insurance Company and Age-Specific Gerontology Research Center Recommendations

HEIGHT		METROPOLITAN 1983 WEIGHTS* (25–59 YEARS)		GERONTOLOGY RESEARCH CENTER* (AGE-SPECIFIC WEIGHT RANGE FOR MEN AND WOMEN)				
ft	in	Men	Women	20–29 Years	30–39 Years	40–49 Years	50–59 Years	60–79 Years
4	10		100–131	84–111	92–119	99–127	107–135	115–142
4	11		101–134	87–115	95–123	103–131	111–139	119–147
5	0		103–137	90–119	98–127	106–135	114–143	123–152
5	1	123–145	105–140	93–123	101–131	110–140	118–148	127–157
5	2	125–148	108–144	96–127	105–136	113–144	122–153	131–163
5	3	127–151	111–148	99–131	108–140	117–149	126–158	135–168
5	4	129–155	114–152	102–135	112–145	121–154	130–163	140–173
5	5	131–159	117–156	106–140	115–149	125–159	134–168	144–179
5	6	133–163	120–160	109–144	119–154	129–164	138–174	148–184
5	7	135–167	123–164	112–148	122–159	133–169	143–179	153–190
5	8	137–171	126–167	116–153	126–163	137–174	147–184	158–196
5	9	139–175	129–170	119–157	130–168	141–179	151–190	162–201
5	10	141–179	132–173	122–162	134–173	145–184	156–195	167–207
5	11	144–183	135–176	126–167	137–178	149–190	160–201	172–213
6	0	147–187		129–171	141–183	153–195	165–207	177–219
6	1	150–192		133–176	145–188	157–200	169–213	182–225
6	2	153–197		137–181	149–194	162–206	174–219	187–232
6	3	157–202		141–186	153–199	166–212	179–225	192–238
6	4			144–191	157–205	171–218	184–231	197–244

From Andres R: Mortality and obesity: the rationale for age-specific height–weight tables. In Hazzard WR, Bierman EL, Blass JP, et al., editors: *Principles of geriatric medicine and gerontology,* ed 3, New York, 1994, McGraw-Hill, p 847, with permission.

*Values in this table are for height without shoes and weight without clothes. The Metropolitan Life Insurance Company (1983 Metropolitan height and weight tables, *Stat Bull Metropol Life Ins Co* 64[Jan–Jun]:2, 1983) presented a table for nude heights and weights (Table 4) as well as a table for heights and weights clothed (Table 1).

TABLE A2.2

Body Mass Index Table

To use the following table, find the appropriate height in the left-hand column. Move across to a given weight. The number at the top of the column is the body mass index at the height and weight. Pounds are rounded off.

BMI		19	20	21	22	23	24	25	26	27	28	29	30	31	32	33	34	35
		Body Weight (lb)																
Height (in)	58	91	96	100	105	110	115	119	124	129	134	138	143	148	153	158	162	167
	59	94	99	104	109	114	119	124	128	133	138	143	148	153	158	163	168	173
	60	97	102	107	112	118	123	128	133	138	143	148	153	158	163	168	174	179
	61	100	106	111	116	122	127	132	137	143	148	153	158	164	169	174	180	185
	62	104	109	115	120	126	131	136	142	147	153	158	164	169	175	180	186	191
	63	107	113	118	124	130	135	141	146	152	158	163	169	175	180	186	191	197
	64	110	116	122	128	134	140	145	151	157	163	169	174	180	186	192	197	204
	65	114	120	126	132	138	144	150	156	162	168	174	180	186	192	198	204	210
	66	118	124	130	136	142	148	155	161	167	173	179	186	192	198	204	210	216
	67	121	127	134	140	146	153	159	166	172	178	185	191	198	204	211	217	223
	68	125	131	138	144	151	158	164	171	177	184	190	197	203	210	216	223	230
	69	128	135	142	149	155	162	169	176	182	189	196	203	209	216	223	230	236
	70	132	139	146	153	160	167	174	181	188	195	202	209	216	222	229	236	243
	71	136	143	150	157	165	172	179	186	193	200	208	215	222	229	236	243	250
	72	140	147	154	162	169	177	184	191	199	206	213	221	228	235	242	250	258
	73	144	151	159	166	174	182	189	197	204	212	219	227	235	242	250	257	265
	74	148	155	163	171	179	186	194	202	210	218	225	233	241	249	256	264	272
	75	152	160	168	176	184	192	200	208	216	224	232	240	248	256	264	272	279
	76	156	164	172	180	189	197	205	213	221	230	238	246	254	263	271	279	287

BMI		36	37	38	39	40	41	42	43	44	45	46	47	48	49	50	51	52
		Body Weight (lb)																
Height (in)	58	172	177	181	186	191	196	201	205	210	215	220	224	229	234	239	244	248
	59	178	183	188	193	198	203	208	212	217	222	227	232	237	242	247	252	257
	60	184	189	194	199	204	209	215	220	225	230	235	240	245	250	255	261	266
	61	190	195	201	206	211	217	222	227	232	238	243	248	254	259	264	269	275
	62	196	202	207	213	218	224	229	235	240	246	251	256	262	267	273	278	284
	63	203	208	214	220	225	231	237	242	248	254	259	265	270	278	282	287	293
	64	209	215	221	227	232	238	244	250	256	262	267	273	279	285	291	296	302
	65	216	222	228	234	240	246	252	258	264	270	276	282	288	294	300	306	312
	66	223	229	235	241	247	253	260	266	272	278	284	291	297	303	309	315	322
	67	230	236	242	249	255	261	268	274	280	287	293	299	306	312	319	325	331
	68	236	243	249	256	262	269	276	282	289	295	302	308	315	322	328	335	341
	69	243	250	257	263	270	277	284	291	297	304	311	318	324	331	338	345	351
	70	250	257	264	271	278	285	292	299	306	313	320	327	334	341	348	355	362
	71	257	265	272	279	286	293	301	308	315	322	329	338	343	351	358	365	372
	72	265	272	279	287	294	302	309	316	324	331	338	346	353	361	368	375	383
	73	272	280	288	295	302	310	318	325	333	340	348	355	363	371	378	386	393
	74	280	287	295	303	311	319	326	334	342	350	358	365	373	381	389	396	404
	75	287	295	303	311	319	327	335	343	351	359	367	375	383	391	399	407	415
	76	295	304	312	320	328	336	344	353	361	369	377	385	394	402	410	418	426

Source: http://www.nhlbi.nih.gov/guidelines/obesity/bmi_tbl.htm.

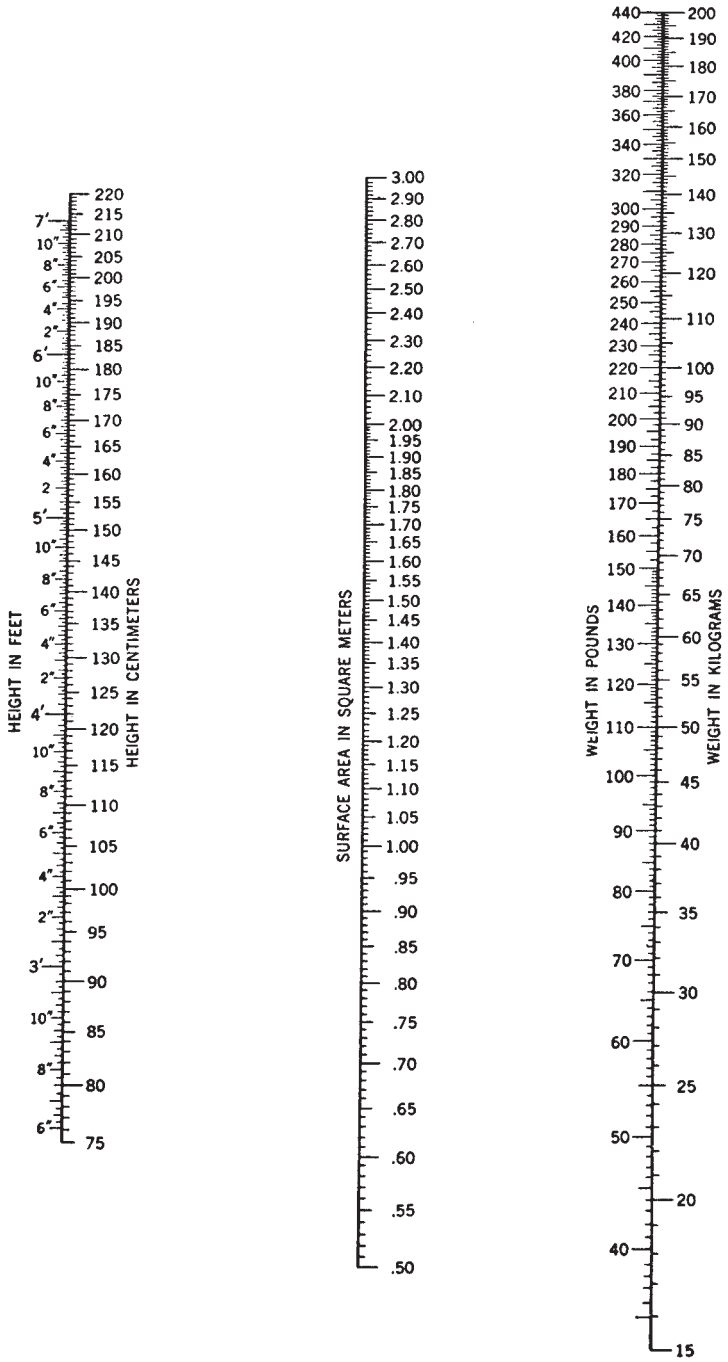

Figure A2.1 Nomogram for the determination of body surface area of children and adults. (From Boothby WM, Sandiford RB: Nomographic charts for the calculation of the metabolic rate by the gasometer method, *Boston Med Surg J* 185:337, 1921, with permission.)

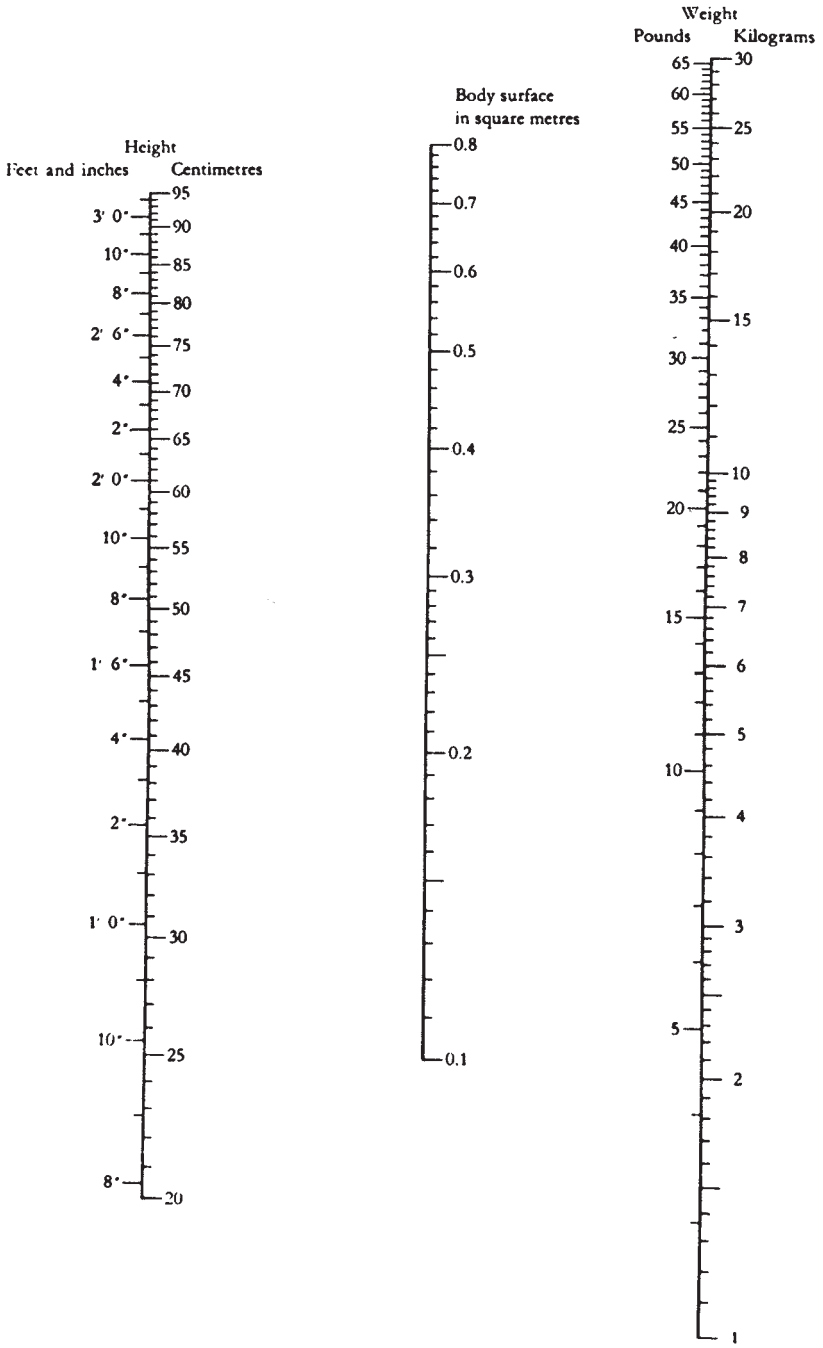

Figure A2.2 Nomogram for the determination of body surface area of children. (From DuBois EF: *Basal metabolism in health and disease*, Philadelphia, PA, 1936, Lea & Febiger.)

The formula for calculating body mass index (BMI) is:

$$\text{BMI} = \text{Weight (kg)} / \text{Height (m}^2)$$

or

$$\text{BMI} = 703 \times \text{Weight (lb)} / \text{Height (in}^2)$$

The interpretation of BMI (kg/m^2) with risk for type 2 diabetes in adults 20 years old and older varies according to populations as follows:

White European Populations	Asian Populations	Interpretation
<18.5	<18.5	Underweight
18.5–24.9	18.5–23	Normal; increasing but acceptable risk
25–29.9	23–27.5	Overweight; increased risk
30 or higher	27.5 or higher	Obese; high risk

From Centers for Disease Control and Prevention: *About BMI for adults*. http://www.cdc.gov/healthyweight/assessing/bmi/adult_bmi/index.html.

Assessing body mass index and waist circumference thresholds for intervening to prevent ill health and premature death among adults for black, Asian, and other minority ethnic groups in the UK, NICE (National Institute for Health and Care Excellence) guidelines [PH46], July 2013. www.nice.org.uk/guidance/ph46/chapter/recommendations.

APPENDIX 3

APPROXIMATIONS OF TOTAL BLOOD VOLUME

When estimating a patient's total blood volume (TBV), a commonly used approximation is 70 mL of TBV per kilogram body weight. While useful in many patients, in others, particularly children and overweight or thin adults, this figure offers only a poor approximation of actual TBV. In these patients, other methods of estimation of TBV are more appropriate.

ADULTS

The COBE Spectra uses the Nadler and Allen formula to calculate approximate TBV for patients (*COBE Spectra Apheresis System Operator's Manual*, 1997). This formula uses patient height, weight, and sex to calculate TBV. The formula is:

$$\text{Males}: \text{TBV (mL)} = 604 + [367 \times \text{height}^3 \text{ (m)}] + [32.2 \times \text{weight (kg)}]$$

$$\text{Females}: \text{TBV (mL)} = 183 + [356 \times \text{height}^3 \text{ (m)}] + [33.1 \times \text{weight (kg)}]$$

TBV can also be approximated using the patient's calculated body surface area (Shoemaker, 1989):

$$\text{Males}: \text{TBV} = 2740 \text{ mL/m}^2$$

$$\text{Females}: \text{TBV} = 2370 \text{ mL/m}^2$$

Another relatively simple approximation uses Gilcher's so-called "rule of fives," reproduced here, as an estimate of blood volume, which is more tailored to the individual patient than the 70 mL/kg rule (Gilcher, 1996).

	Obese	**Thin**	**Normal**	**Muscular**
Males	60	65	70	75
Females	55	60	65	70

CHILDREN

The Nadler and Allen calculation can be particularly inaccurate in children, especially prepubertal boys, in whom it has been recommended that the female gender be entered to improve the estimation (Kim, 2000). The following values for TBV per kilogram body weight can be used (Oski, 1993):

Premature infants	89–105 mL/kg
Term newborns	82–86 mL/kg
Infants and preschoolers	73–82 mL/kg

SELECTED REFERENCES

COBE Spectra Apheresis System operator's manual, Lakewood, CO, 1997, Gambro BCT, p 1.

Gilcher RO: Apheresis: principles and practices. In Rossi EC, Simon TL, Moss GS, et al.: *Principles of transfusion medicine*, ed 2, Baltimore, MD, 1996, Williams & Wilkins, p 542.

Kim HC: Therapeutic pediatric apheresis, *J Clin Apheresis* 15:129–157, 2000.

Oski FA: The erythrocyte and its disorders. In Nathan DG, Oski FA, editors: *Hematology of infancy and childhood*, ed 4, Philadelphia, PA, 1993, WB Saunders, p 28.

Shoemaker WC: Fluids and electrolytes in the acutely ill adult. In Shoemaker WC, Ayres S, Grenvik A, et al.: *Textbook of critical care*, ed 2, Philadelphia, PA, 1989, WB Saunders, p 1130.

APPENDIX 4

PERIODIC TABLE OF THE ELEMENTS

A short history of the development of the periodic table is presented in the article by Roberts (2019).

Newly discovered elements are added to the periodic table with names agreed upon by the IUPAC. Four new elements were added in 2016: Nihonium (Nh, 113), Moscovium (Mc, 115), Tennessine (Ts, 117), and Oganesson (Og, 118) (St. Fleur, 2016). Upon their initial discovery, these elements had been given the placeholder names ununtrium, ununpentium, ununseptium, and ununoctium, respectively, prior to their official designations. Flerovium (Fl, 114) and Livermorium (Lv, 116) had been added previously.

New notation → 1, 2, 13, 14, 15, 16, 17, 18
Previous IUPAC form → 1, 2, 13, 14, 15, 16, 17, 18
CAS version → 1, 2, 13, 14, 15, 16, 17, 18

KEY TO CHART

Atomic number → 50 ← Oxidation state (+2)
Symbol → Sn (+4)
1989 Atomic weight → 118.71
← Electron configuration (18 18 4)

Group	1 IA	2 IIA	3 IIIA IIIB	4 IVA IVB	5 VA VB	6 VIA VIB	7 VIA VIIB	8	9 VIIIA VIII	10	11 IB	12 IIB	13 IIIB IIIA	14 IVB IVA	15 VB VA	16 VIB VIA	17 VIIB VIIA	18 VIIIA	Shell
	1 +1 H −1 1.00794 1																	2 0 He 4.0020602 2	K
	3 +1 Li 6.941 2-1	4 +1 Be 9.012182 2-2											5 +3 B 10.811 2-3	6 +2 C +4 −4 12.011 2-4	7 +1 +2 +3 +4 +5 −1 −2 −3 N 14.00674 2-5	8 −2 O 15.9994 2-6	9 −1 F 18.998403 2	10 0 Ne 20.1797 2-8	K-L
	11 +1 Na 22.989768 2-8-1	12 +2 Mg 24.3050 2-8-2											13 +3 Al 26.981539 2-8-3	14 +2 Si +4 −4 28.0855 2-8-4	15 +3 P +5 −3 30.97362 2-8-5	16 +3 S +5 −2 32.066 2-8-6	17 +1 Cl +5 +7 −1 35.4527 2-8-7	18 0 Ar 39.948 2-8-8	K-L-M
	19 +1 K 39.0983 -8-8-1	20 +2 Ca 40.078 -8-8-2	21 +3 Sc 44.955910 -8-9-2	22 +2 Ti +3 +4 47.88 -8-10-2	23 +2 V +3 +4 +5 50.9415 -8-11-2	24 +2 Cr +3 +6 51.9961 -8-13-1	25 +2 Mn +3 +4 +7 54.93085 -8-13-2	26 +2 Fe +3 55.847 -8-14-2	27 +2 Co +3 58.93320 -8-15-2	28 +2 Ni +3 58.6934 -8-16-2	29 +1 Ni +2 63.546 -8-18-1	30 +2 Zn 65.39 -8-18-2	31 +3 Ga 69.723 -8-18-3	32 +2 Ge +4 72.61 -8-18-4	33 +2 As +5 −3 74.92159 -8-18-5	34 +4 Se +6 −2 78.96 -8-18-6	35 +1 Br +5 −1 79.904 -8-18-7	36 0 Kr 83.80 -8-18-8	-L-M-N
	37 +1 Rb 85.4678 -18-8-1	38 +2 Sr 87-62 -18-8-2	39 +3 Y 88-90585 -18-9-2	40 +4 Zr 91.224 -18-12-1	41 +3 Nb +5 92.90638 -18-10-2	42 +6 Mo 95.94 -18-13-1	43 +4 Tc +6 +7 (98) -18-13-2	44 +3 Ru 101.07 -18-15-1	45 +3 Rh 102.90550 -18-16-1	46 +2 Pd +4 106.42 -18-18-0	47 +1 Ag 107.8682 -18-18-1	48 +2 Cd 112.411 -18-18-2	49 +3 In 114.818 -18-18-3	50 +2 Sn +4 118.710 -18-18-4	51 +3 Sb +5 −3 121.757 -18-18-5	52 +4 Te +6 −2 127.60 -18-18-6	53 +1 I +5 +7 −1 126.90447 -18-18-7	54 0 Xe 131.29 -18-18-8	-M-N-O
	55 +1 Cs 132.90543 -18-8-1	56 +2 Ba 137.327 -18-8-2	57* +3 La 139.9055 -18-9-2	72 +4 Hf 178.49 -32-10-2	73 +5 Ta 180.9479 -32-11-2	74 +6 W 183.84 -32-12-2	75 +4 Re +6 +7 186.207 -32-13-2	76 +3 Os +4 190.23 -32-14-2	77 +3 Ir +4 192.22 -32-15-2	78 +2 Pt +4 195.08 -32-16-2	79 +1 Au +3 196.96654 -32-18-1	80 +1 Hg +2 200.59 -32-18-2	81 +1 Tl +3 204.3833 -32-18-3	82 +2 Pb +4 207.2 -32-18-4	83 +3 Bi +5 208.98037 -32-18-5	84 +2 Po +4 (209) -32-18-6	85 At (210) -32-18-7	86 0 Rn (222) -32-18-8	-N-O-P
	87 +1 Fr (223) -18-8-1	88 +2 Ra 226.025 -18-8-2	89** Ac +3 227.08 -18-9-2	104 Rf +4 (261) -32-10-2	105 Db (262) -32-11-2	106 Se (266) -32-12-2	107 Bh (264) -32-13-2	108 Hs (267) -32-14-2	109 Mt (268) -32-15-2	110 Ds (271) -32-17-2	111 Rg (272) -32-18-1	112 Cn (285) -32-18-2	113 Nh (284) -32-18-3	114 Fl (289) -32-18-4	115 Mc (288) -32-18-5	116 Lv (292) -32-18-6	117 Ts (295) -32-18-7	118 Og (294) -32-18-8	O P Q

*Lathanides	58 +3 Ce +4 140.115 -19-9-2	59 +3 Pr 140.90765 -21-8-2	60 +3 Nd 144.24 -22-8-2	61 +3 Pm (145) -23-8-2	62 +2 Sm +3 150.36 -24-8-2	63 +2 Eu +3 151.965 -25-8-2	64 +3 Gd 157.25 -25-9-2	65 +3 Tb 158.92534 -27-8-2	66 +3 Dy 162.50 -28-8-2	67 +3 Ho 164.93032 -29-8-2	68 +3 Er 167.26 -30-8-2	69 +3 Tm 168.93421 -32-8-2	70 +2 Yb +3 173.04 -32-8-2	71 +3 Lu 174.967 -32-9-2		N O P
**Actinides	90 +4 Th 232.0381 -18-10-2	91 +5 Pa +4 231.03588 -20-9-2	92 +3 +4 +5 +6 U 238.0289 -21-9-2	93 +3 +4 +5 +6 Np 237.048 -22-9-2	94 +3 +4 +5 +6 Pu (244) -24-8-2	95 +3 +4 +5 +6 Am (243) -25-8-2	96 +3 Cm (247) -25-9-2	97 +3 Bk +4 (247) -27-8-2	98 +3 Cf (251) -28-8-2	99 +3 Es (252) -29-8-2	100 +3 Fm (257) -30-8-2	101 +2 Md +3 (258) -31-8-2	102 +2 No +3 (259) -32-8-2	103 +3 Lr (260) -32-9-2		O P Q

Modified from Lide DR, Frederikse HPR: *CRC handbook of chemistry and physics 1993–1994,* ed 74, Boca Raton, FL, 1993, CRC Press. The new International Union of Pure and Applied Chemistry (IUPAC) format numbers the groups from 1 to 18. The previous IUPAC numbering system and the system used by Chemical Abstracts Service (CAS) are also shown. For radioactive elements that do not occur in nature, the mass number of the most stable isotope is given in parentheses.

REFERENCES

Chemical and Engineering News: It's elemental: the periodic table—introduction, National Chemistry Week. October:19–24, 2009. http://pubs.acs.org/cen/80th/elements.html.

Leigh GJ, editor: *Nomenclature of inorganic chemistry*, Oxford, 1990, Blackwell Scientific.

Los Alamos National Laboratory: *Periodic table of elements:*, LANL, 2015. periodic.lanl.gov/index.shtml.

Roberts S: Is it time to upend the periodic table?, *New York Times*, August 27, 2019. https://www.nytimes.com/2019/08/27/science/periodic-table-elements-chemistry.html.

St. Fleur N: Four elements on the periodic table get new names, *New York Times June* 8, 2016. https://www.nytimes.com/2016/06/09/science/four-elements-on-the-periodic-table-get-new-names.html?action=click&module=RelatedLinks&pgtype=Article.

The periodic table of videos, University of Nottingham. http://www.periodicvideos.com.

Professor Martyn Poliakoff and chemistry staff from the University of Nottingham have produced "The Periodic Table of Videos" as entertaining and educational discussions and laboratory demonstrations of chemical properties of each of the elements..

APPENDIX 5

SI UNITS

The International System of Units (French: *Système International d'Unités*, SI) consists of seven dimensionally independent base units, which are listed in Table A5.1, along with the symbols to be used to denote these units. Table A5.2 lists a number of derived units of the SI that are used in the clinical laboratory. There are two kinds of derived units: (1) coherent units, which are derived directly from the base units without the use of conversion factors, and (2) noncoherent units, which are constructed from the base units and contain a numerical factor to make the numbers more convenient to use. The prefixes to denote fractions or multiples of base and derived SI units are given in Table A5.3. A complete description of the SI and its application in medicine may be found in the World Health Organization publication *The SI for the Health Professions* (World Health Organization, 1977). See Tietz (1995) for a comprehensive list of quantities and their internationally recommended SI units.

The reference intervals used in this presentation should be considered typical values to illustrate principles of analysis; however, they are not intended to be used for interpretation of laboratory results for specific patients, which should be evaluated according to reference ranges established by the laboratory performing those measurements. In making the conversion to recommended SI units (Tables A5.4 through A5.13), the following guidelines were followed:

1. All reference intervals have been converted to SI units except in cases in which the measurements are not quantitative.
2. Chemical names have not been changed; for example, urea is retained instead of changing to carbamide.
3. Factors are those published by the American National Metric Council (Lundberg et al., 1986; Beeler, 1987; Young, 1987), based on the Metric Commission of Canada (1981) factors.
4. Factors are calculated to the base unit for volume of 1 L.
5. The order of magnitude of the factors is calculated to make the values in SI units convenient numbers, that is, with prefixes, a number not greater than 1000 or smaller than 0.001.
6. The number in recommended SI units is equal to the number in conventional units times the factor.
7. For compounds for which relative molecular masses are not definitely known (e.g., proteins), reference intervals are converted to mass amounts per liter.
8. For mixtures of indeterminate composition (e.g., phospholipids), reference intervals are converted to mass amounts per liter or are based on a given standard, for example, DHEA for 17-ketosteroids.
9. Quantities of a relative nature that are usually expressed as percentages—for example, fractions of LD isoenzymes—are given as fractions.
10. Enzyme units are given as the international unit per liter (U/L). Although the coherent SI unit for catalytic activity (including enzymes), the katal, has been defined as the number of moles of substrate converted per second under defined conditions, its adoption is limited.
11. The pH scale is retained for measurement of hydrogen ion concentrations.
12. It is recommended that the unit millimeters of mercury (mm Hg) be retained for pressure (P_{CO_2}, P_{O_2}) at the present time.
13. Percentages are expressed as fractions in the SI, where a fraction is a dimensionless quantity given by the number of defined particles constituting a specified component divided by the total number of defined particles in the system.

TABLE A5.1
SI Base Units

Quantity	Name	Symbol
Length	meter	m
Mass	kilogram	kg
Time	second	s
Electric current	ampere	A
Thermodynamic temperature	kelvin	K
Luminous intensity	candela	cd
Amount of substance	mole	mol

TABLE A5.2
SI Derived Units

Quantity	Unit Name	Unit Symbol
Area	square meter*	m^2
Volume	cubic meter*	m^3
	liter†	$L = dm^3$‡
Concentration		
Mass	kilogram/liter†	kg/L
Substance	mole/liter†	mol/L
Molality	mole/kilogram	mol/kg
Density	kilogram/liter†	kg/L
Mass fraction	kilogram/kilogram	kg/kg
Mole fraction	mole/mole	mol/mol
Number concentration	number/liter	L^{-1}
Temperature	degree celsius*	°C = °K – 273.15
Pressure	pascal*	$Pa = kg/m^2$
Frequency	hertz*	Hz = 1 cycle/s
Clearance	liter/second†	L/s
Electrical potential	volt*	$V = kgm^2/s^3$
Energy	joule*	$J = kgm^2/s^2$

*Derived coherent unit.
†Derived noncoherent unit.
‡Both "L" and "l" are symbols for the liter.

TABLE A5.3
Prefixes

Prefix	Prefix Symbol	Factor
exa	E	10^{18}
peta	P	10^{15}
tera	T	10^{12}
giga	G	10^{9}
mega	M	10^{6}
kilo	k	10^{3}
hecto	h	10^{2}
deca	da	10^{1}
deci	d	10^{-1}
centi	c	10^{-2}
milli	m	10^{-3}
micro	μ	10^{-6}
nano	n	10^{-9}
pico	p	10^{-12}
femto	f	10^{-15}
atto	a	10^{-18}
zepto	z	10^{-21}
yocto	y	10^{-24}

TABLE A5.4

Whole Blood, Serum, and Plasma Chemistry

Component	System	TYPICAL REFERENCE INTERVALS		
		Conventional Units	Factor*	Recommended SI Units†
Acetoacetic acid				
Qualitative	Serum	Negative	—	Negative
Quantitative	Serum	0.2–1 mg/dL	97.95	20–100 μmol/L
Acetone				
Qualitative	Serum	Negative	—	Negative
Quantitative	Serum	0.3–2 mg/dL	172.95	20–340 μmol/L
Albumin				
Qualitative	Serum	3.2–4.5 g/dL (salt fractionation)	10	32–45 g/L
		3.2–5.6 g/dL (electrophoresis)		32–56 g/L
		3.8–5 g/dL (eye binding)		38–50 g/L
Alcohol, ethyl	Serum or whole blood	Negative–but presented as mg/dL	0.2171	Negative–but presented as mmol/L
Aldolase	Serum			
	Adults	3–8 Sibley-Lehninger U/dL at 37°C	7.4	22–59 mU/L at 37°C
	Children	Approximately 2× adult levels	—	Approximately 2× adult levels
	Newborn	Approximately 4× adult levels	—	Approximately 4× adult levels
α-Amino acid nitrogen	Serum	3.6–7 mg/dL	0.7139	2.6–5 mmol/L
δ-Aminolevulinic acid	Serum	0.01–0.03 mg/dL	76.26	0.8–2.3 μmol/L
Ammonia	Plasma	20–120 μg/dL (diffusion)	0.5872	12–70 μmol/L
		40–80 μg/dL (enzymatic method)		23–47 μmol/L
		12–48 μg/dL (resin method)		7–28 μmol/L
Amylase	Serum	16–120 Somogyi units/dL	1.85	30–220 U/L
Argininosuccinate lyase	Serum	0–4 U/dL	10	0–40 U/L
Arsenic‡	Whole blood	<7 μg/dL	0.05055	<0.4 μmol/L
Ascorbic acid (vitamin C)	Plasma	0.6–1.6 mg/dL	56.78	34–91 μmol/L
	Whole blood	0.7–2 mg/dL		40–114 μmol/L
Barbiturates	Serum, plasma, or whole blood	Negative	—	Negative
Base excess	Whole blood			
	Male	−3.3 to +1.2 mEq/L	1	−3.3 to +1.2 mmol/L
	Female	−2.4 to +2.3 mEq/L		−2.4 to +2.3 mmol/L
Base, total	Serum	145–160 mEq/L	1	145–160 mmol/L
Bicarbonate	Plasma	21–28 mmol/L	1	21–28 mmol/L
Bile acids	Serum	0.3–3 mg/dL	10	3–30 mg/L
Bilirubin				
Direct (conjugated)	Serum	<0.3 mg/dL	17.10	<5 μmol/L
Indirect (unconjugated)	Serum	0.1–1 mg/dL		2–17 μmol/L
Total	Serum	0.1–1.2 mg/dL		2–21 μmol/L
Newborns total	Serum	1–12 mg/dL		17–205 μmol/L
Blood gases (see Chapters 9 and 15)				
pH	Whole blood	7.38–7.44 (arterial)	1	7.38–7.44
		7.36–7.41 (venous)		7.36–7.41
P_{CO_2}	Whole blood	35–40 mm Hg (arterial)	0.1333	4.7–5.3 kPa
		40–45 mm Hg (venous)		5.3–6 kPa
P_{O_2}	Whole blood	95–100 mm Hg (arterial)	0.1333	12.7–13.3 kPa
Bromide	Serum	<5 mg/dL	0.125	<0.63 mmol/L
Calcium				
Ionized	Serum	4–4.8 mg/dL	0.2500	1–1.2 mmol/L
		2–2.4 mEq/L	0.5000	
		30%–58% of total	0.01	0.30–1.58 of total
Total	Serum	9.2–11.0 mg/dL	0.2500	2.30–2.74 mmol/L
		4.6–5.5 mEq/L	0.5000	
Carbon dioxide (CO_2 content)	Whole blood (arterial)	19–24 mmol/L	1	19–24 mmol/L
	Plasma or serum (arterial)	21–28 mmol/L		21–28 mmol/L

Continued

TABLE A5.4

Whole Blood, Serum, and Plasma Chemistry—cont'd

Component	System	TYPICAL REFERENCE INTERVALS		
		Conventional Units	Factor*	Recommended SI Units†
Carbon dioxide	Whole blood (venous)	22–26 mmol/L	1	22–26 mmol/L
	Plasma or serum (venous)	24–30 mmol/L		24–30 mmol/L
CO_2 combining power	Plasma or serum (venous)	24–30 mmol/L	1	24–30 mmol/L
CO_2 partial pressure (P_{CO_2})	Whole blood (arterial)	35–40 mm Hg	0.1333	4.7–5.3 kPa
Whole blood (venous)	40–45 mm Hg			5.3–6 kPa
Carbonic acid (H_2CO_3)	Whole blood (arterial)	1.05–1.45 mmol/L	1	1.05–1.45 mmol/L
	Whole blood (venous)	1.15–1.50 mmol/L		1.15–1.50 mmol/L
	Plasma (venous)	1.02–1.38 mmol/L		1.02–1.38 mmol/L
Carboxyhemoglobin (carbon monoxide hemoglobin)	Whole blood			
	Suburban nonsmokers	<1.5% saturation of hemoglobin	0.01	Fraction hemoglobin saturated: <0.015
	Nonsmokers	2%–3% saturation		
	Smokers	1.5%–5% saturation		0.015–0.050
	Heavy smokers	5%–9% saturation		0.050–0.090
Carotene, β	Serum	40–200 μg/dL	0.01863	0.7–3.7 μmol/L
Ceruloplasmin	Serum	23–50 mg/dL	10	230–500 mg/L
Chloride	Serum	95–103 mEq/L	1	95–103 mmol/L
Cholesterol				
Total (see Chapters 18 and 28)	Serum	150–250 mg/dL (varies with diet, sex, and age)	0.02586	3.88–6.47 mmol/L
Esters	Serum	65%–75% of total cholesterol	0.01	Fraction of total cholesterol: 0.65–0.75
Cholinesterase (pseudocholinesterase)	Erythrocytes	0.65–1.3 pH units	1	0.65–1.3 units§
	Plasma	0.5–1.3 pH units	1	0.5–1.3 units
		8–18 U/L at 37° C		
Citrate	Serum or plasma	1.7–3 mg/dL	52.05	88–156 μmol/L
Copper	Serum, plasma			
	Male	70–140 μg/dL	0.1574	11–22 μmol/L
	Female	80–155 μg/dL		13–24 μmol/L
Cortisol	Plasma			
	8 AM–10 AM	5–23 μg/dL	27.59	138–635 nmol/L
	4 PM–6 PM	3–13 μg/dL		83–359 nmol/L
Creatine	Serum or plasma			
	Male	0.1–0.4 mg/dL	76.25	8–31 μmol/L
	Female	0.2–0.7 mg/dL		15–53 μmol/L
Creatine kinase (CK)	Serum			
	Male	55–170 U/L at 37° C	1	55–170 U/L at 37° C
	Female	30–135 U/L at 37°C	1	30–135 U/L at 37°C
Creatinine (see Chapters 9 and 15)	Serum or plasma	0.6–1.2 mg/dL (adult)	88.40	53–106 μmol/L
		0.3–0.6 mg/dL (children <2 yr)		27–53 μmol/L
Creatinine clearance (endogenous) (see Chapters 9 and 15)	Serum or plasma and urine			
	Male	107–139 mL/min	0.01667	1.78–2.32 mL/sec
	Female	87–107 mL/min		1.45–1.78 mL/sec
Cryoglobulins	Serum	Negative	—	Negative
Electrophoresis, protein	Serum			
Albumin		52%–65% of total protein	0.01	Fraction of total protein: 0.52–0.65
α-1		2.5%–5% of total protein	0.01	0.025–0.05
α-2		7%–13% of total protein	0.01	0.07–0.13
β		8%–14% of total protein	0.1	0.08–0.14
γ		12%–22% of total protein	0.01	0.12–0.22
	Serum	Concentration		
Albumin		3.2–5.6 g/dL	10	32–56 g/L
α-1		0.1–0.4 g/dL		1–4 g/L
α-2		0.4–1.2 g/dL		4–12 g/L
β		0.5–1.1 g/dL		5–11 g/L
γ		0.5–1.6 g/dL		5–16 g/L
Fats, neutral (see Triglycerides)				
Fatty acids				
Total (free and esterified)	Serum	9–15 mmol/L	1	9–15 mmol/L

TABLE A5.4

Whole Blood, Serum, and Plasma Chemistry—cont'd

Component	System	TYPICAL REFERENCE INTERVALS		
		Conventional Units	Factor*	Recommended SI Units†
Free (nonesterified)	Plasma	300–480 μEq/L	1	300–480 μmol/L
Ferritin	Serum			
	Male	15–200 ng/mL	1	15–200 μg/L
	Female	12–150 ng/mL	1	15–150 μg/L
Fibrinogen	Plasma	200–400 mg/dL	0.01	2–4 g/L
Fluoride	Whole blood	<0.05 mg/dL	0.5263	<0.027 mmol/L
Folate	Serum			11–57 nmol/L
		≥3.5 ng/mL (immunoassay)	2.266	>5 nmol/L
	Erythrocytes	166–640 ng/mL (bioassay)		376–1450 nmol/L
		>140 ng/mL (immunoassay)		>317 nmol/L
Galactose	Whole blood			
	Adults	None	—	None
	Children	<20 mg/dL	0.05551	<1.11 mmol/L
Gammaglobulin	Serum	0.5–1.6 g/dL	10	5–16 g/L
Globulins, total	Serum	2.3–3.5 g/dL	10	23–35 g/L
Glucose, fasting	Serum or plasma	70–110 mg/dL	0.05551	3.9–6.1 mmol/L
	Whole blood	60–100 mg/dL		3.3–5.6 mmol/L
Glucose tolerance	Serum or plasma			
Oral	Fasting	70–110 mg/dL	0.05551	3.9–6.1 mmol/L
	30 min	30–60 mg/dL above fasting		1.7–3.3 mmol/L above fasting
	60 min	20–50 mg/dL above fasting		1.1–2.8 mmol/L above fasting
	120 min	5–15 mg/dL above fasting		0.3–0.8 mmol/L above fasting
	180 min	Fasting level or below	—	Fasting level or below
Intravenous	Serum or plasma			
	Fasting	70–110 mg/dL	0.05551	3.9–6.1 mmol/L
	5 min	Maximum of 250 mg/dL		Maximum of 13.9 mmol/L
	60 min	Significant decrease	—	Significant decrease
	120 min	Below 120 mg/dL	0.05551	Below 6.7 mmol/L
	180 min	Fasting level	—	Fasting level
Glucose-6-phosphate dehydrogenase (G6PD)	Erythrocytes	250–5000 U/10^6 cells	1	250–5000 μU/cell
		1200–2000 mU/mL packed erythrocytes	1	1200–2000 U/L packed erythrocytes
γ-Glutamyltransferase	Serum	5–40 U/L	1	5–40 U/L at 37°C
Glutathione	Whole blood	24–37 mg/dL	0.03254	0.78–1.20 mmol/L
Growth hormone	Serum	<10 ng/mL	1	<10 μg/L
Guanase	Serum	<3 nmol/mL/min	1	<3 U/L at 37°C
Haptoglobin	Serum	60–270 mg/dL	0.01	0.6–2.7 g/L
Hemoglobin	Serum or plasma			
	Qualitative	Negative	—	Negative
	Quantitative	0.5–5 mg/dL	10	5–50 mg/L
	Whole blood			
	Female	12–16 g/dL	10	120–160 g/L
	Male	13.5–18 g/dL		135–180 g/L
α-Hydroxybutyrate dehydrogenase	Serum	140–350 U/mL	1	140–350 kU/L
17-Hydroxycorticosteroids	Plasma			
	Male	7–19 μg/dL	25.59¶	193–524 mmol/L
	Female	9–21 μg/dL		248–579 mmol/L
	After 24 USP units of ACTH intramuscularly	35–55 μg/dL		966–1517 nmol/L
Immunoglobulins	Serum			
IgG		800–1801 mg/dL	0.01	8–18 g/L
IgA		113–563 mg/dL		1.1–5.6 g/L
IgM		54–222 mg/dL		0.5–2.2 g/L
IgD		0.5–3 mg/dL	10	5–30 mg/L
IgE		0.01–0.04 mg/dL		0.1–0.4 mg/L
Insulin	Plasma bioassay	11–240 μU/mL	7.175‖	79–1722 pmol/L
	Immunoassay	4–24 μU/mL		29–172 pmol/L

Continued

TABLE A5.4

Whole Blood, Serum, and Plasma Chemistry—cont'd

Component	System	TYPICAL REFERENCE INTERVALS		
		Conventional Units	Factor*	Recommended SI Units†
Insulin tolerance (0.1 unit/kg)	Serum			
	Fasting	Glucose of 70–110 mg/dL	0.05551	Glucose of 3.9–6.1 mmol/L
	30 min	Fall to 50% of fasting level	0.01	Fall to 0.5 of fasting level
	90 min	Fasting level	—	Fasting level
Iron, total	Serum	60–150 μg/dL	0.1791	10.7–26.9 μmol/L
Iron-binding capacity	Serum	250–400 μg/dL	0.1791	44.8–71.6 μmol/L
Iron saturation	Serum	20%–55%	0.01	Fraction of total iron-binding capacity: 0.20–0.55
Isocitric dehydrogenase	Serum	50–240 U/mL at 25°C (Wolfson-Williams Ashman units)	0.0166	0.83–4.18 U/L at 25°C
Ketone bodies	Serum	Negative	—	Negative
17-Ketosteroids	Plasma	25–125 μg/dL	34.67**	866–4334 nmol/L
Lactic acid (as lactate)	Whole blood			
	Venous	5–20 mg/dL	0.1110	0.6–2.2 mmol/L
	Arterial	3–7 mg/dL		0.3–0.8 mmol/L
Lactate dehydrogenase (LD)	Serum	(lactate → pyruvate) 80–120 U at 30°C	0.48	38–62 U/L at 30°C
		(pyruvate → lactate) 185–640 U at 30°C	0.48	90–310 U/L at 30°C
		(lactate → pyruvate) 100–190 U/L at 37°C	1	100–190 U/L at 37°C
Lactate dehydrogenase isoenzymes	Serum			Fraction of total LD
LD_1 (anode)		17%–27%	0.01	0.17–0.27
LD_2		27%–37%		0.27–0.37
LD_3		18%–25%		0.18–0.25
LD_4		3%–8%		0.03–0.08
LD_5 (cathode)		0%–5%		0.00–0.05
Lactate dehydrogenase (heat stable)	Serum	30%–60% of total	0.01	Fraction of total LD: 0.30–0.6
Lactose tolerance	Serum	Serum glucose changes similar to glucose tolerance test	—	Serum glucose changes similar to glucose tolerance test
Lead	Whole blood	<50 μg/dL	0.04826	<2.41 μmol/L
Leucine aminopeptidase (LAP)	Serum			
	Male	80–200 U/mL (Goldbarg–Rutenberg)	0.24	19.2–48 U/L
	Female	75–185 U/mL (Goldbarg–Rutenberg)		18–44.4 U/L
Lipase	Serum	0–1.5 U/mL (Cherry–Crandall)	278	0–417 U/L
		14–280 mU/mL	1	14–280 U/L
Lipids, total	Serum	400–800 mg/dL	0.01	4–8 g/L
Cholesterol (see Chapters 18 and 28)		150–250 mg/dL	0.02586	3.88–6.47 mmol/L
Triglycerides (see Chapter 18 and 28)		10–90 mg/dL	0.01129††	0.11–2.15 mmol/L
Phospholipids		150–380 mg/dL	0.01	1.50–3.80 g/L
Fatty acids (free)		9–15 mmol/L	1	9–15 mmol/L
Phospholipid phosphorus		8–11 mg/dL	0.3229	2.58–3.55 mmol/L
Lithium	Serum	Negative	—	Negative
Therapeutic interval		0.5–1.4 mEq/L	1	0.5–1.4 mmol/L
Long-acting thyroid-stimulating hormone (LATS)	Serum	None detected	—	None detected
Luteinizing hormone (LH)	Serum			
	Male	6–30 mU/mL	1	6–30 U/L
	Female	Midcycle peak: 3× baseline value	—	Midcycle peak: 3× baseline value
		Premenopausal <30 mU/mL	1	Premenopausal <30 U/L
		Postmenopausal >35 mU/mL		Postmenopausal >35 U/L

TABLE A5.4

Whole Blood, Serum, and Plasma Chemistry—cont'd

Component	System	TYPICAL REFERENCE INTERVALS		
		Conventional Units	Factor*	Recommended SI Units†
Macroglobulins, total	Serum	70–430 mg/dL	0.01	0.7–4.3 g/L
Magnesium	Serum	1.3–2.1 mEq/L	0.5000	0.65–1.05 mmol/L
		1.8–3 mg/dL	0.4114	0.74–1.23 mmol/L
Methemoglobin	Whole blood	<0.24 g/dL	10	<2.4 g/L
		<1% of total hemoglobin	0.01	Fraction of total hemoglobin <0.01
Mucoprotein	Serum	80–200 mg/dL	0.01	0.8–2 g/L
Muramidase	Serum	4–13 mg/L	1	4–13 mg/L
Myoglobin	Serum	<90 μg/L	1	<90 μg/L
Nonprotein nitrogen (NPN)	Serum or plasma	20–35 mg/dL	0.7139	14.3–25 mmol/L
	Whole blood	25–50 mg/dL		17.8–35.7 mmol/L
5′-Nucleotidase	Serum	0–1.6 U at 37°C	1	0–1.6 U at 37°C
Ornithine carbamyl transferase	Serum	8–20 mU/mL at 37° C	1	8–20 U/L at 37°C
Osmolality	Serum	280–295 mOsm/kg	1	280–295 mmol/kg
Oxygen (see Chapters 9 and 15)				
Pressure (P_{O_2})	Whole blood (arterial)	95–100 mmHg	0.1333	2.7–13.3 kPa
Content	Whole blood (arterial)	15–23 volume	0.01	Volume fraction: 0.15–0.23
Saturation	Whole blood (arterial)	94%–100%	0.01	Fraction saturated: 0.94–1
pH	Whole blood (arterial)	7.38–7.44	1	7.38–7.44
	Whole blood (venous)	7.36–7.41		7.36–7.41
	Serum or plasma (venous)	7.35–7.45		7.35–7.45
Phenylalanine	Serum			
	Adults	<3 mg/dL	60.54	<182 μmol/L
	Newborns (term)	1.2–3.5 mg/dL		73–212 μmol/L
Phosphatase				
Acid phosphatase	Serum	0.13–0.63 U/L at 37°C (*p*-nitrophenylphosphate)	16.67	2.2–10.5 U/L at 37°C
Alkaline phosphatase	Serum	20–130 U/L at 37°C (*p*-nitrophenylphosphate in AMP buffer)	1	20–130 U/L at 37°C
Phospholipid phosphorus (see Lipids, total)				
Phospholipids (see Lipids, total)	Serum			
	Adults	2.3–4.7 mg/dL	0.3229	0.74–1.52 mmol/L
Phosphorus, inorganic	Children	4–7 mg/dL		1.29–2.26 mmol/L
Potassium	Plasma	3.8–5 mEq/L	1	3.8–5 mmol/L
Prolactin	Serum			
	Female	1–25 ng/mL	1	1–25 μg/L
	Male	1–20 ng/mL		1–20 μg/L
Proteins (see Chapter 20)	Serum			
Total		6–7.8 g/dL	10	60–78 g/L
Albumin		3.2–4.5 g/dL		32–45 g/L
Globulin		2.3–3.5 g/dL		23–35 g/L
Protein fractionation, see Electrophoresis				
Protoporphyrin	Erythrocytes	15–50 mg/dL	0.01777	0.27–0.89 μmol/L
Pyruvate	Whole blood	0.3–0.9 mg/dL	113.6	34–102 μmol/L
Salicylates	Serum	Negative	—	Negative
Therapeutic interval		15–30 mg/dL	0.07240	1.08–2.17 mmol/L
Sodium	Plasma	136–142 mEq/L	1	136–142 mmol/L
Sulfate, inorganic	Serum	0.2–1.3 mEq/L	0.5	0.10–0.65 mmol/L
		0.9–6 in mg/dL as SO_4^{-2}	0.1042	0.09–0.63 mmol/L as SO_4^{-2}
Sulfhemoglobin	Whole blood	Negative	—	Negative
Sulfonamides	Serum or whole blood	Negative	—	Negative
Testosterone	Serum or plasma			
	Male	300–1200 ng/dL	0.03467	10.4–41.6 nmol/L
	Female	30–95 ng/dL		1–3.3 mmol/L

Continued

TABLE A5.4

Whole Blood, Serum, and Plasma Chemistry—cont'd

Component	System	TYPICAL REFERENCE INTERVALS		
		Conventional Units	Factor*	Recommended SI Units†
Thiocyanate	Serum	Negative	—	Negative
Thyroid hormone tests (see Chapter 25)	Serum			
Thyroxine, total (T4)		5.5–12.5 μg/dL	12.87	71–161 nmol/L
Thyroxine, free (FT4)		0.9–2.3 ng/dL	12.87	12–30 pmol/L
T3 resin uptake		25–38 relative % uptake	0.01	Relative uptake fraction: 0.25–0.38
Thyroxine-binding globulin (TBG)	Serum	10–26 μg/dL	10	100–260 μg/L
Thyrotropin (TSH)	Serum	0.5–5 μU/mL	1	0.5–5 μU/L
Triiodothyronine (T3)		80–200 mg/dL	0.0154	1.23–3 of nmol/L
Transferases				
Aspartate aminotransferase (AST or SGOT)	Serum	8–33 U/L at 37°C	1	8–33 U/L at 37°C
Alanine aminotransferase (ALT or SGPT)	Serum	4–36 U/L at 37°C	1	4–36 U/L at 37°C
γ Glutamyl transferase (GGT)		5–40 U/L at 37°C	1	5–40 U/L at 37°C
Triglycerides (see Chapter 18 and 28)	Serum	10–190 mg/dL	0.01129††	0.11–2.15 mmol/L
Troponin I	Serum	<2 mg/mL		0–0.6 μg/L 0–0.1 μg/L
Urea nitrogen	Serum	8–23 mg/dL	0.357	2.9–8.2 mmol/L
Urea clearance	Serum and urine			
Maximum clearance		64–99 mL/min	0.01667	1.07–1.65 L/s
Standard clearance		41–65 mL/min, or more than 75% of normal clearance		0.68–1.08 L/s or more than 0.75 of normal clearance
Uric acid	Serum			
	Male	4–8.5 mg/dL	0.05948	0.24–0.51 mmol/L
	Female	2.7–7.3 mg/dL		0.16–0.43 mmol/L
Vitamin A	Serum	15–60 μg/dL	0.03491	0.52–2.09 μmol/L
Vitamin A tolerance	Serum	15–60 μg/dL	0.03491	0.52–2.09 μmol/L
	Fasting 3 hr or 6 hr after 5000 U vitamin A/kg	200–600 μg/dL	0.03491	6.98–20.95 μmol/L
	24 hr	Fasting values or slightly above	—	Fasting values or slightly above
Vitamin B_{12}	Serum	160–950 pg/mL	0.7378	118–701 pmol/L
Unsaturated vitamin B_{12}-binding capacity	Serum	1000–2000 pg/mL	0.7378	738–1475 pmol/L
Vitamin C	Plasma	0.6–1.6 mg/dL	56.78	34–91 μmol/L
Xylose absorption	Serum normal in malabsorption	25–40 mg/dL 1–2 hr Maximum ≈10 mg/dL Dose: Adult 25 g D-xylose/kg; children 0.5 g D-xylose/kg	0.06661	1.67–2.66 mmol/L 1–2 hr Maximum ≈0.67 mmol/L
Zinc	Serum	50–150 μg/dL	0.1530	7.7–23 μmol/L

*Factor = number factor (note that units are not presented).
†Value in SI units = value in conventional units × factor.
‡Usually not measured in blood (preferred specimen is urine, hair, or nails except in acute cases, when gastric contents are used).
§Unit based on hydrogen ion concentration.
¶As cortisol.
‖1 International unit of insulin corresponds to 0.04167 mg of the 4th International Standard (a mixture of 52% beef insulin and 48% pig insulin).
**As DHEA.
††As triolein.

TABLE A5.5

Urine

Component	Type of Urine System	TYPICAL REFERENCE INTERVALS		
		Conventional Units	Factor*	Recommended SI Units†
Acetoacetic acid	Random	Negative	—	Negative
Acetone	Random	Negative	—	Negative
Addis count	12-hr collection	WBC and epithelial cells: 1,800,000/12 hr	1	1.8×10^6/12 hr
		RBC 500,000/12 hr	1	0.5×10^6/12 hr
		Hyaline casts: <5000/12 hr	1	$<5 \times 10^3$/12 hr
Albumin				
Qualitative	Random	Negative	—	Negative
Quantitative	24 hr	15–150 mg/day	0.001	0.015–0.150 g/day
Aldosterone	24 hr	2–26 μg/day	2.774	6–72 nmol/day
Alkapton bodies	Random	Negative	—	Negative
α-Amino acid nitrogen	24 hr	100–290 mg/day	0.07139	7.1–20.7 mmol/day
δ-Aminolevulinic acid	Random			
	Adults	0.1–0.6 mg/dL	76.26	8–46 μmol/L
	Children	<0.5 mg/dL		<38 μmol/L
	24 hr	1.5–7.5 mg/day	7.626	11–57 μmol/day
Ammonia nitrogen	24 hr	20–70 mEq/day	1	20–70 mmol/day
		500–1200 mg/day	0.07139	35.6–85.7 mmol/day
Amylase	2 hr	35–260 Somogyi U/hr	0.1850	6.5–48.1 U/hr
Arsenic	24 hr	<50 μg/L	0.01335	<0.67 μmol/L
Ascorbic acid	Random	1–7 mg/dL	56.78	57–397 μmol/L
	24 hr	>50 mg/day	5.678	>284 μmol/day
Bence Jones protein	Negative	—	Negative	
Beryllium	24 hr	<0.05 μg/day	111	<5.55 nmol/day
Bilirubin, qualitative	Negative	—	Negative	
Blood, occult	Negative	—	Negative	
Borate	24 hr	<2 mg/L	16.44	<32 μmol/L
Calcium				
Qualitative (Sulkowitch)	Random	1 + turbidity	1	1 + turbidity
Quantitative	24 hr			
	Average diet	100–240 mg/day	0.02495	2.5–6 mmol/day
	Low-calcium diet	<150 mg/day		<3.7 mmol/day
	High-calcium diet	240–300 mg/day		6–7.5 mmol/day
Catecholamines	Random	<14 μg/dL	59.11*	<828 nmol/L
	24 hr	<100 μg/day (varies with activity)	5.911*	<591 nmol/day
Epinephrine		<10 ng/day	5.458	<55 nmol/day
Norepinephrine		<100 ng/day	5.911	<591 nmol/day
Total free catecholamines		4–126 μg/day	5.911*	24–745 nmol/day
Total metanephrines		0.1–1.6 mg/day	5.458†	0.5–8.7 μmol/day
Chloride	24 hr	140–250 mEq/day	1	140–250 nmol/day
Concentration test (Fishberg)	Random—after fluid restriction			
Specific gravity		>1.025	1	>1.025
Osmolality		>850 mOsm/kg	1	>850 mmol/kg
Copper	24 hr	<50 μg/day	0.01574	<0.8 μmol/day
Coproporphyrin	Random			
	Adult	3–20 μg/dL	15.27	46–305 nmol/L
	24 hr			
	Adult	50–160 μg/day	1.527	76–244 nmol/day
	Children	<80 μg/day		<122 nmol/day
Creatine	24 hr			
	Male	<40 mg/day	7.625	<305 μmol/day
	Female	<100 mg/day		<763 μmol/day
		Higher in children and during pregnancy	—	Higher in children and during pregnancy
Creatinine	24 hr			
	Male	20–26 mg/kg/day	8.840	177–230 μmol/kg/day
		1–2 g/day	8.840	8.8–17.7 mmol/day
	Female	14–22 mg/kg/day	8.840	124–195 μmol/kg/day
		0.8–1.8 g/day	8.840	7.1–15.9 mmol/day

Continued

TABLE A5.5

Urine—cont'd

Component	Type of Urine System	TYPICAL REFERENCE INTERVALS		
		Conventional Units	Factor*	Recommended SI Units†
Cystine, qualitative	Random	Negative	—	Negative
Cystine and cysteine	24 hr	10–100 mg/day	4.161‡	42–416 μmol/day
Dehydroepiandrosterone	24 hr			
	Male	0.2–2 mg/day	3.467	0.7–6.9 μmol/day
	Female	0.2–1.8 mg/day		0.7–6.2 μmol/day
Diacetic acid	Random	Negative	—	Negative
Epinephrine	24 hr	<20 μg/day	5.458	<109 nmol/day
Estrogens, total	24 hr			
	Male	5–18 μg/day	3.468§	17–62 nmol/day
	Female			
	Ovulation	28–100 μg/day	3.468	97–347 nmol/day
	Luteal peak	22–80 μg/day		76–364 nmol/day
	At menses	4–25 μg/day		14–87 nmol/day
	Pregnancy	Up to 45,000 μg/day	0.003468	Up to 156 μmol/day
	Postmenopausal	Up to 10 μg/day	3.468	Up to 35 nmol/day
Estrogens, fractionated	24 hr, nonpregnant, midcycle			
Estrone (E1)	—	2–25 μg/day	3.699	7–93 nmol/day
Estradiol (E2)	—	<10 μg/day	3.671	<37 nmol/day
Estriol (E3)	—	2–30 μg/day	3.468	7–104 nmol/day
Etiocholanolone	24 hr			
	Male	1.4–5 mg/day	3.443	4.8–17.2 μmol/day
	Female	0.8–4 mg/day		2.8–13.8 μmol/day
Fat, qualitative	Random	Negative	—	Negative
FIGLU (*N*-formiminoglutamic acid)	24 hr	<3 mg/day	5.740	<7.2 μmol/day
	After 15 g of l-histidine	4 mg/8 hr		23 μmol/8 hr
Fluoride	24 hr	<1 mg/day	52.63	<53 μmol/day
Follicle-stimulating hormone (FSH)	24 hr			
	Adult	4–25 U/L	1	4–25 U/L
	Prepubertal	4–30 U/L	1	4–30 U/L
	Postmenopausal	40–50 U/L	1	40–50 U/L
	Midcycle	2 × baseline	1	2 × baseline
Fructose	24 hr	30–65 mg/day	0.005551	0.17–0.36 mmol/day
Glucose, qualitative	Random	Negative	—	Negative
Glucose, quantitative	24 hr			
Copper-reducing substances		0.5–1.5 g/day	1	0.5–1.5 g/day
Total sugars		Average 250 mg/day	1	Average 250 mg/day
Glucose		Average 130 mg/day	0.005551	Average 0.72 mmol/day
Gonadotropins, pituitary (FSH and LH)	24 hr	10–50 U/L	1	10–50 U/day
11-Hydroxyandrosterone	24 hr			
	Male	0.1–0.8 mg/day	3.263	0.3–2.6 μmol/day
	Female	<0.5 mg/day		<1.6 μmol/day
11-Hydroxyetiocholanolone	24 hr			
	Male	0.2–0.6 mg/day	3.26	0.7–2 μmol/day
	Female	0.1–1.1 mg/day		0.3–3.63 μmol/day
11-Ketoandrosterone	24 hr			
	Male	0.2–1 mg/day	3.274	0.7–3.3 μmol/day
	Female	0.2–0.8 mg/day		0.7–2.6 μmol/day
11-Ketoetiocholanolone	24 hr			
	Male	0.2–1 mg/day	3.274	0.7–3.3 μmol/day
	Female	0.2–0.8 mg/day		0.7–2.6 μmol/day
Lactose	24 hr	14–40 mg/day	2.291	41–117 μmol/day
Lead	24 hr	<100 μg/day	0.004826	<0.48 μmol/day
Magnesium	24 hr	6–8.5 mEq/day	0.5000	3–4.3 mmol/day
Melanin, qualitative	Random	Negative	—	Negative
Mucin	24 hr	100–150 mg/day	1	100–150 mg/day
Muramidase (lysozyme)	24 hr	1.3–36 mg/day	1	1.3–36 mg/day

TABLE A5.5

Urine—cont'd

Component	Type of Urine System	TYPICAL REFERENCE INTERVALS		
		Conventional Units	Factor*	Recommended SI Units†
Myoglobin	24 hr	14–40 mg/day	2.291	41–117 μmol/day
Qualitative	Random	Negative	—	Negative
Quantitative	24 hr	<4 mg/L	1	<4 mg/L
Osmolality	Random	500–800 mOsm/kg water	1	500–800 mmol/kg
Pentoses	24 hr	2–5 mg/kg/day	1	2–5 mg/kg/day
pH	Random	4.6–8	1	4.6–8
Phenolsulfonphthalein (PSP)	Urine timed after 6 mg PSP IV			Fraction dye excreted:
	15 min	20%–50% dye excreted	0.01	0.20–0.50
	30 min	16%–24% dye excreted		0.16–0.24
	60 min	9%–17% dye excreted		0.09–0.17
	120 min	3%–10% dye excreted		0.03–0.10
Phenylpyruvic acid, qualitative	Random	Negative	—	Negative
Phosphorus	Random	0.9–1.3 g/day	32.29	29–42 mmol/day
Porphobilinogen				
Qualitative	Random	Negative	—	Negative
Quantitative	24 hr	<1 mg/day	4.420	<4.4 μmol/day
Potassium	24 hr	40–80 mEq/day	1	40–80 mmol/day
Pregnancy tests	Concentrated morning specimen	Positive in normal pregnancies or with tumors producing chorionic gonadotropin	—	Positive in normal pregnancies or with tumors producing chorionic gonadotropin
Pregnanediol	24 hr			
	Male	<1.5 mg/day	3.120	<4.7 μmol/day
	Female	1–8 mg/day	3.120	3–25 μmol/day
	Peak	1 week after ovulation	—	1 week after ovulation
	Pregnancy	<50 mg/day	3.120	<156 μmol/day
	Children	Negative	—	Negative
Pregnanetriol	24 hr			
	Male	0.4–2.4 mg/day	2.972	1.2–7 μmol/day
	Female	0.5–2 mg/day		1.5–5.9 μmol/day
	Children	Up to 1 mg/day		Up to 3 μmol/day
Protein, qualitative	Random	Negative	—	Negative
	24 hr	40–150 mg/day	1	40–150 mg/day
Reducing substances, total	24 hr	0.5–1.5 mg/day	1	0.5–1.5 mg/day
Sodium	24 hr	75–200 mEq/day	1	75–200 mmol/day
Solids, total	24 hr	55–70 g/day	1	55–70 g/day
		Decreases with age to 30 g/day	—	Decreases with age to 30 g/day
Specific gravity	Random			Relative density (U 20°C/water 20°C):
		1.016–1.022 (normal fluid intake)	1	1.016–1.022 (normal fluid intake)
		1.001–1.035 (range)		1.001–1.035 (range)
Sugars (excluding glucose)	Random	Negative	—	Negative
Titratable acidity	24 hr	20–50 mEq/day	1	20–50 mmol/day
Urea nitrogen	24 hr	6–17 g/day	35.70	214–607 mmol/day
Uric acid	24 hr	250–750 mg/day	0.005948	1.5–4.5 mmol/day
Urobilinogen	2 hr	0.3–1 Ehrlich units	1	0.3–1 U
	24 hr	0.05–2.5 mg/day or	1.693	0.1–4.2 μmol/day
		0.5–4 Ehrlich units/day	1	0.5–4 U/day
Uropepsin	Random	15–45 U/hr (Anson)	7.37	111–332 U/hr
	24 hr	1500–5000 units/day (Anson)		11–37 kU/hr
Uroporphyrins				
Qualitative	Random	Negative	—	Negative
Quantitative	24 hr	10–30 μg/day	1.204	12–36 nmol/day
Vanillylmandelic acid (VMA)	24 hr	1.5–7.5 mg/day	5.046	7.6–37.9 μmol/day
Volume, total	24 hr	600–1600 mL/day	0.001	0.6–1.6 L/day
Zinc	24 hr	0.15–1.2 mg/day	15.30	2.3–18.4 μmol/day

*As norepinephrine.
†As normetanephrine.
‡Based on cystine.
§Based on estriol.

TABLE A5.6

Synovial Fluid

Component	TYPICAL REFERENCE INTERVALS		
	Conventional Units	Factor	Recommended SI Units
Blood-serum-synovial fluid glucose difference	<10 mg/dL	0.05551	<0.56 mmol/L
Differential cell count	Granulocytes <25% of nucleated cells	0.01	Granulocyte number fraction: <0.25 of nucleated cells
Fibrin clot	Absent	—	Absent
Mucin clot	Abundant	—	Abundant
Nucleated cell count	<200 cells/μL	10^6	<200 × 10^6 cells/L
Viscosity	High	—	High
Volume	<3.5 mL	0.001	<0.0035 L

TABLE A5.7

Seminal Fluid

Component	TYPICAL REFERENCE INTERVALS		
	Conventional Units	Factor	Recommended SI Units
Liquefaction	Within 20 min		Within 20 min
Sperm morphology	>70% normal, mature spermatozoa	0.01	Number fraction: >0.70 normal, mature spermatozoa
Sperm motility	>60%	0.01	Number fraction: >0.60
pH	>7 (average 7.7)	1	>7 (average 7.7)
Sperm count	60–150 × 10^6/mL	10^3	60–150 × 10^9/L
Volume	1.5–5 mL	0.001	0.0015–0.005 L

TABLE A5.8

Gastric Fluid

Component	TYPICAL REFERENCE INTERVALS		
	Conventional Units	Factor	Recommended SI Units
Fasting residual volume	20–100 mL	0.001	0.02–0.10 L
pH	<2	1	<2
Basal acid output (BAO)*	0–6 mEq/hr	1	0–6 mmol/hr
Maximum acid output (MAO; after histamine stimulation)	5–40 mEq/hr	1	5–40 mmol/hr
BAO/MAO ratio	<0.4	1	<0.4

*Varies between male and female and ages.

TABLE A5.9

Hematology

Component	TYPICAL REFERENCE INTERVALS				
	Conventional Units		Factor	Recommended SI Units	
Red cell volume					
Male	20–36 mL/kg body weight		0.001	0.020–0.036 L/kg body weight	
Female	19–32 mL/kg body weight			0.019–0.032 L/kg body weight	
Plasma volume					
Male	25–43 mL/kg body weight		0.001	0.025–0.043 L/kg body weight	
Female	28–45 mL/kg body weight			0.028–0.045 L/kg body weight	
Coagulation and hemostatic tests					
Bleeding time	Depends on location and orientation of cut and on particular device, typically 2–8 min				
Activated partial thromboplastin time (APTT)	Depends on activator and phospholipid reagents used, typically 25–35 s				
Antithrombin IIII					
Immunologic	20–30 mg/dL		10	200–300 mg/L	
Functional	80–120 U/dL		10	800–1200 U/L	
Clot lysis time					
Euglobulin factor	1.5–4 hr at 37°C				
Whole blood	None by 24 hr at 37°C				
Clot retraction	Complete by 4 hr at 37°C				
Coagulation factors	0.50–1.50 μ/mL		1000	500–1500 U/L	
Factor XIII (screening test)	Clot insoluble in 5 mol/L urea at 24 hr				
Fibrinogen	200–400 mg/dL		0.01	2–4 g/L	
Fibrin(ogen) degradation products					
Serum FDP	<10 μg/mL		1	<10 mg/L	
Plasma D-dimers	<200 ng/mL		1	<200 μg/L	
Plasminogen					
Immunologic	10–20 mg/dL		10	100–200 mg/L	
Functional	80–120 U/dL		10	800–1200 U/L	
Protein C	0.7–1.4 μ/mL		10	700–1400 U/L	
Protein S (total)	0.7–1.4 μ/mL		10	700–1400 U/L	
Prothrombin time	Depends on thromboplastin reagent used, typically 10–13 s				
Thrombin time	Depends on concentration of thrombin reagent used, typically 17–25 s				
von Willebrand factor					
Immunologic	50–150 U/dL		10	500–1500 U/L	
Ristocetin cofactor activity	50–150 U/dL			500–1500 U/L	
Complete blood count (CBC)					
Hematocrit				Volume fraction:	
Male	41.5%–50.4%		0.01	0.415–0.504	
Female	35.9%–44.6%			0.359–0.446	
Hemoglobin					
Male	14–17.5 g/dL		10	140–175 g/L	
Female	12.3–15.3 g/dL			123–153 g/L	
Red cell count					
Male	$4.5–5.9 \times 10^6/\mu L$		10^6	$4.5–5.9 \times 10^{12}/L$	
Female	$4.5–5.1 \times 10^6/\mu L$			$4.1–5.1 \times 10^{12}/L$	
White cell count	$4.4–11 \times 10^3/\mu L$		10^6	$4.4–11.3 \times 10^9/L$	
Erythrocyte indices					
Mean corpuscular volume (MCV)	$80–96\ \mu m^3$		1	80–96 fL	
Mean corpuscular hemoglobin (MCH)	27.5–33.2 pg		1	27.5–33.2 pg	
Mean corpuscular hemoglobin concentration (MCHC)	33.4%–35.5%		0.01	Concentration fraction: 0.334–0.355	
White blood cell differential (adult)	Mean %	Range of absolute counts		Mean number fraction*	Range of absolute counts
Segmented neutrophils	56	1800–7800/μL	10^6	0.56	$1.8–7.8 \times 10^9/L$

Continued

TABLE A5.9

Hematology—cont'd

Component	TYPICAL REFERENCE INTERVALS						
	Conventional Units		Factor	Recommended SI Units			
Bands	3	0–700/μL		0.03	0–0.70 × 10^9/L		
Eosinophils	2.7	0–450/μL		0.027	0–0.45 × 10^9/L		
Basophils	0.3	0–200/μL		0.003	0–0.20 × 10^9/L		
Lymphocytes	34	1000–4800/μL		0.34	1.0–4.8 × 10^9/L		
Monocytes	4	0–800/μL		0.04	0–0.80 × 10^9/L		
Hemoglobin A2	1.5%–3.5% of total hemoglobin		0.01	Mass fraction: 0.015–0.035 of total hemoglobin			
Hemoglobin F	<2%		0.01	Mass fraction: <0.02			
Osmotic fragility		% Lysis				Lysed Fraction	
	% (w/v) NaCl	Fresh	24 hr at 37° C	% NaCl – 171 % Lysis – 0.01	NaCl mmol/L	Fresh	24 hr at 37°C
	0.2	—	95–100		34.2	—	0.95–1
	0.3	97–100	85–100		51.3	0.97–1.00	0.85–1
	0.35	90–99	75–100		59.8	0.90–0.99	0.75–1
	0.4	50–95	65–100		68.4	0.50–0.95	0.65–1
	0.45	5–45	55–95		77.0	0.05–0.45	0.55–0.95
	0.5	0.6	40–85		85.5	0–0.06	0.40–0.85
	0.55	—	15–70		94.1	0	0.15–0.70
	0.6	—	0–40		102.6	—	0–0.40
	0.65	—	0–10		111.2	—	0–0.10
	0.7	—	0–5		119.7	—	0–0.05
	0.75	—	95–100		128.3	—	0
Platelet count	150,000–450,000/μL	10^6	150–450 × 10^9/L				
Reticulocyte count	0.5%–1.5%	0.01	Number fraction: 0.005–0.015				
	25,000–75,000 cells/μL	10^6	25–75 × 10^9/L				
Sedimentation rate (ESR) (Westergren)							
Men younger than 50 yr	<15 mm/hr						
Men 50–85 yr	<20 mm/hr						
Men older than 85 yr	<30 mm/hr						
Women younger than 50 yr	<20 mm/hr						
Women 50–85 yr	<30 mm/hr						
Women older than 85 yr	<42 mm/hr						
Viscosity	1.4–1.8 times water	1	1.4–1.8 times water				
Zeta sedimentation ratio	41%–54%	0.01	Fraction: 0.41–0.54				

*All percentages are multiplied by 0.01 to give fraction.

TABLE A5.10

Amniotic Fluid

Component	TYPICAL REFERENCE INTERVALS		
	Conventional Units	Factor	Recommended SI Units
Appearance			
Early gestation	Clear	—	Clear
Term	Clear or slightly opalescent	—	Clear or slightly opalescent
Albumin			
Early gestation	0.39 g/dL	10	3.9 g/L
Term	0.19 g/dL		1.9 g/L
Bilirubin			
Early gestation	<0.075 mg/dL	17.10	<1.3 μmol/L
Term	<0.025 mg/dL		<0.41 μmol/L
Chloride			
Early gestation	Approximately equal to serum chloride	—	Approximately equal to serum chloride
Term	Generally 1–3 mEq/L lower than serum chloride	1	Generally 1–3 mmol/L lower than serum chloride

Continued

TABLE A5.10

Amniotic Fluid—cont'd

Component	TYPICAL REFERENCE INTERVALS		
	Conventional Units	Factor	Recommended SI Units
Creatinine			
Early gestation	0.8–1.1 mg/dL	88.40	71–97 μmol/L
Term	1.8–4 mg/dL (generally >2 mg/dL)		159–354 μmol/L (generally >177 μmol/L)
Estriol			
Early gestation	<10 μg/dL	3.468	<347 nmol/L
Term	<60 μg/dL		>2081 nmol/L
Lecithin: sphingomyelin			
Early (immature)	<1 : 1	1	<1 : 1
Term (mature)	>2 : 1		>2 : 1
Osmolality			
Early gestation	Approximately equal to serum osmolality	—	Approximately equal to serum osmolality
Term	230–270 mOsm/kg	1	230–270 mmol/kg
P_{CO_2}			
Early gestation	33–55 mm Hg	0.1333	4.4–7.3 kPa
Term	42–55 mm Hg (increases toward term)		5.6–7.3 kPa (increases toward term)
pH			
Early gestation	7.12–7.38	1	7.12–7.38
Term	6.91–7.43 (decreases toward term)		6.91–7.43
Protein, total			
Early gestation	0.60 ± 0.24 g/dL	10	60 ± 2.4 g/L
Term	0.26 ± 0.19 g/dL		2.6 ± 1.9 g/L
Sodium			
Early gestation	Approximately equal to serum sodium	—	Approximately equal to serum sodium
Term	7–10 mEq/L lower than serum sodium	1	7–10 mmol/L lower than serum sodium
Staining, cytologic			
Oil Red O			
Early gestation	Stained fraction: <10%	0.01	Stained fraction: <0.1
Term	Stained fraction: >50%		>0.5
Nile blue sulfate			
Early gestation	Stained fraction: 0	0.01	Stained fraction: <0.0
Term	Stained fraction: >20%		>0.2
Urea			
Early gestation	18 ± 5.9 mg/dL	0.1665	3.00 ± 0.98 mmol/L
Term	30.3 ± 11.4 mg/dL		5.04 ± 1.90 mmol/L
Uric acid			
Early gestation	3.72 ± 0.96 mg/dL	59.48	221 ± 57 μmol/L
Term	9.90 ± 2.23 mg/dL		589 ± 133 μmol/L
Volume			
Early gestation	450–1200 mL	0.001	0.45–1.2 L
Term	500–1400 mL (increases toward term)		0.5–1.4 L (increases toward term)

TABLE A5.11

Cerebrospinal Fluid

Component	TYPICAL REFERENCE INTERVALS		
	Conventional Units	Factor	Recommended SI Units
Albumin	<10–30 mg/dL	10	100–300 mg/L
Cell count	<5 cells/μL	10^6	$<5 \times 10^6$/L
Glucose	40–80 mg/dL	0.05551	2.8–4.4 mmol/L
Lactate dehydrogenase (LD)	Approximately 10% of serum level	—	Activity fraction: approximately 0.1 of serum level
Proteins	12–60 mg/dL	10	120–600 mg/L
Protein electrophoresis			Fraction:
Prealbumin	2%–7%	0.01	0.2–0.07
Albumin	56%–76%		0.56–0.76
α-1 Globulin	2%–7%		0.02–0.07
α-2 Globulin	4%–12%		0.04–0.12
β Globulin	8%–18%		0.08–0.18
γ Globulin	3%–12%		0.03–0.12
Xanthochromia	Negative	—	Negative

TABLE A5.12

Miscellaneous

Component	TYPICAL REFERENCE INTERVALS			
	Specimen	Conventional Units	Factor	Recommended SI Units
Bile, qualitative	Random stool	Negative in adults	—	Negative in adults
		Positive in children	—	Positive in children
Chloride	Sweat	4–60 mEq/L	1	4–60 mmol/L
Clearances	Serum and urine (timed)			
	Creatinine, endogenous	115 ± 20 mL/min	0.01667	1.92 ± 0.33 mL/s
	Diodrast	600–720 mL/min		10–12 mL/s
	Inulin	100–150 mL/min		1.67–2.50 mL/s
	PAH	600–750 mL/min		10–12.50 mL/s
Diagnex blue (tubeless gastric analysis)	Urine	Free acid present	—	Free acid present
Fat	Stool, 72 hr			
	Total fat	<5 g/24 hr	1	<5 g/day
		10%–25% of dry matter	0.01	Mass fraction: 0.1–0.25 of dry matter
	Neutral fat	1%–5% of dry matter		0.01–0.05 of dry matter
	Free fatty acids	5%–13% of dry matter		0.05–0.13 of dry matter
	Combined fatty acids	5%–15% of dry matter		0.05–0.15 of dry matter
Nitrogen, total	Stool, 24 hr	10% of intake		Mass fraction: 0.1 of intake
		1–2 g/24 hr	71.39	71–143 mmol/day
Sodium	Sweat	10–80 mEq/L	1	10–80 mmol/L
Trypsin activity	Random, fresh stool	Positive (2+ to 4+)	—	Positive (2+ to 4+)
Thyroid iodine-131 uptake		7.5%–25% in 6 hr	0.01	Fraction uptake: 0.075–0.25 in 6 hr
Urobilinogen				
Qualitative	Random stool	Positive	—	Positive
Quantitative	Stool, 24 hr	40–200 mg/24 hr	1.693	68–339 μmol/day
		80–280 Ehrlich units/24 hr		

TABLE A5.13

Selected Pediatric Reference Values

Parameter	Value	
S-Acid phosphatase		
Newborn	7.4–19.4 U/L	
2–13 yr	6.4–15.2 U/L	
S-Aldolase		
Newborn	to 4× adult value	
Child	to 2× adult value	
S-Alkaline phosphatase		
Newborn	40–300 U/L	
Child	60–270 U/L	
S-α-fetoprotein		
Newborn	Up to 150 mg/L or higher	
1–2 yr	Up to 87 mg/L	
S-Amylase		
Newborn	Little, if any, amylase activity	
1 yr	Adult values	
S-Aspartate aminotransferase		
Newborn	16–74 U/L	
1–3 yr	6–30 U/L	
S-Bilirubin, newborn	Preterm	Full-term
24 hr	17–103 μmol/L (10–60 mg/L)	34–103 μmol/L (20–60 mg/L)
48 hr	17–103 μmol/L (10–60 mg/L)	103–120 μmol/L (60–70 mg/L)
3–5 day	171–257 μmol/L (100–150 mg/L)	68–205 μmol/L (40–120 mg/L)
S-Calcium		
Preterm, first week	1.50–2.50 mmol/L (60–100 mg/L)	
Full-term, first week	1.75–3 mmol/L (70–120 mg/L)	
1–2 yr	2.50–3 mmol/L (100–120 mg/L)	
2–16 yr	2.25–2.87 mmol/L (90–115 mg/L)	
U-Catecholamines	Norepinephrine:	Epinephrine:
1 yr	30–90 nmol/day (5.4–15.9 μg/day)	1–23 nmol/day (0.1–4.3 μg/day)
1–5 yr	50–180 nmol/day (8.1–30.8 μg/day)	4–50 nmol/day (0.8–9.1 μg/day)
6–15 yr	110–420 nmol/day (19–71.1 μg/day)	7–339 nmol/day (1.3–10.5 μg/day)
>15 yr	200–510 nmol/day (34.4–87 μg/day)	19–72 nmol/day (3.5–13.2 μg/day)
U-Chloride (varies with chloride intake)		
Infant	1.7–8.5 mmol/day	
Child	17–34 mmol/day	
S-Cholesterol		
Cord blood	1.2–2.5 mmol/L (460–980 mg/L)	
1–2 yr	1.8–4.9 mmol/L (700–1900 mg/L)	
2–16 yr	3.5–6.5 mmol/L (1350–2500 mg/L)	
U-Cortisol (free)		
4 mo–10 yr	6–74 nmol/day (2–27 μg/day)	
11–20 yr	2–152 nmol/day (0.7–55 μg/day)	
S-Creatine kinase		
Newborn	3× adult values	
3 wk–3 mo	1.5× adult values	
>1 yr	Adult values	
S-Creatinine	Upper reference value:	
Up to 5 yr	44 μmol/L (5 mg/L)	
Up to 6 yr	53 μmol/L (6 mg/L)	
Up to 7 yr	62 μmol/L (7 mg/L)	
Up to 8 yr	71 μmol/L (8 mg/L)	
Up to 9 yr	80 μmol/L (9 mg/L)	
Up to 10 yr	88 μmol/L (10 mg/L)	
>10 yr	106 μmol/L (12 mg/L)	
S-Estradiol		
0–2 yr	0–26 pmol/L (0–7 pg/mL)	
2–4 yr	0–26 pmol/L (0–7 pg/mL)	
4–6 yr	0–51 pmol/L (0–14 pg/mL)	
6–8 yr	0–37 pmol/L (0–10 pg/mL)	
8–10 yr	0–367 pmol/L (0–100 pg/mL)	

Continued

TABLE A5.13

Selected Pediatric Reference Values—cont'd

Parameter	Value	
10–12 yr	0–367 pmol/L (0–100 pg/mL)	
12–14 yr	0–367 pmol/L (0–100 pg/mL)	
14–16 yr	26–385 pmol/L (7–105 pg/mL)	
16–26 yr	26–1175 pmol/L (7–320 pg/mL)	
Fecal fat		
Preterm newborn	Up to 0.40 excreted	
Full-term newborn	Up to 0.20 excreted	
3 mo–1 yr	Up to 0.15 excreted	
1 yr	Up to 0.085 excreted	
P-Nonesterified fatty acids		
Newborn	0–1845 mmol/L	
4 mo–10 yr	300–1100 mmol/L	
S-Glucose		
Preterm newborn	1.1–3.6 mmol/L (200–656 mg/L)	
Full–term newborn	1.1–6.1 mmol/L (200–1100 mg/L)	
Child	3.3–5.8 mmol/L (600–1050 mg/L)	
S-γ-Glutamyltransferase		
Premature newborn	56–233 U/L	
Newborn–3 wk	10–103 U/L	
3 wk–3 mo	4–111 U/L	
1–5 yr	2–23 U/L	
6–15 yr	2–23 U/L	
16 yr–adult	2–35 U/L	
S-Haptoglobin		
Newborn	Detectable haptoglobin in only 0.1–0.2	
≥1 yr	Adult values	
S-Immunoglobulin G		
0–5 wk	7500–15,000 mg/L	
6 mo	1500–7000 mg/L	
1 yr	1400–10,300 mg/L	
5 yr	3700–15,000 mg/L	
10 yr	4400–15,500 mg/L	
S-Immunoglobulin A		
0–5 wk	None	
6 mo	200–1300 mg/L	
1 yr	200–1300 mg/L	
5 yr	300–2000 mg/L	
10 yr	500–2300 mg/L	
0–5 wk	None	
S-Immunoglobulin M		
0–5 wk	<200 mg/L	
6 mo	300–600 mg/L	
1 yr	300–1600 mg/L	
5 yr	200–2200 mg/L	
10 yr	300–1700 mg/L	
Inulin clearance		
<1 mo	29–88 mL/min per 1.73 m^2 of body surface	
1–6 mo	40–112 mL/min per 1.73 m^2 of body surface	
6–12 mo	62–121 mL/min per 1.73 m^2 of body surface	
>1 yr	78–164 mL/min per 1.73 m^2 of body surface	
U-17-Ketosteroids*		
0–3 day	0–0.2 μmol/day (0–0.5 mg/day)	
1–3 yr	<7.0 μmol/day (<2.0 mg/day)	
3–6 yr	2–10 μmol/day (0.5–3.0 mg/day)	
6–9 yr	3–14 μmol/day (0.8–4.0 mg/day)	
	Male	Female
10–12 yr	2–21 μmol/day (0.7–6.0 mg/day)	2–17 μmol/day (0.7–5.0 mg/day)
Adolescent	10–52 μmol/day (3–15 mg/day)	10–42 μmol/day (3–12 mg/day)

TABLE A5.13

Selected Pediatric Reference Values—cont'd

Parameter	Value	
S-Lactate dehydrogenase		
1–3 day	Up to 2× → adult values	
S-Phosphorus (inorganic)		
Preterm newborn	1.81–2.58 mmol/L (56.0–80.0 mg/L)	
6–10 day	1.97–3.78 mmol/L (61–117 mg/L)	
4 mo	1.55–2.62 mmol/L (48–81 mg/L)	
1 yr	1.26–1.94 mmol/L (39–60 mg/L)	
2–16 yr	0.84–1.61 mmol/L (26–50 mg/L)	
S-Potassium		
Preterm newborn	4.5–7.2 mmol/L	
Full-term newborn	5.0–7.7 mmol/L	
2 day–2 wk	4.0–6.4 mmol/L	
2 wk–3 mo	4.0–6.2 mmol/L	
3 mo–1 yr	3.7–5.6 mmol/L	
1–16 yr	3.6–5.2 mmol/L	
S-Testosterone	Male	Female
0–2 yr	0.14–1.28 nmol/L (0–0.4 ng/mL)	0.24–0.62 nmol/L (0.1–0.2 ng/mL)
2–4 yr	0.17–5.55 nmol/L (0–1.6 ng/mL)	0.24–0.69 nmol/L (0.1–0.2 ng/mL)
4–6 yr	0.28–1.39 nmol/L (0.1–0.4 ng/mL)	0.35–0.69 nmol/L (0.1–0.2 ng/mL)
6–8 yr	0.21–9.72 nmol/L (0.1–2.8 ng/mL)	0.52–1.04 nmol/L (0.1–0.3 ng/mL)
8–10 yr	0.31–1.74 nmol/L (0.1–0.5 ng/mL)	0.69–1.39 nmol/L (0.2–0.4 ng/mL)
10–12 yr	0.29–10.06 nmol/L (0.1–2.9 ng/mL)	0.69–1.74 nmol/L (0.2–0.5 ng/mL)
12–14 yr	0.17–26.37 nmol/L (0–7.6 ng/mL)	1.04–2.43 nmol/L (0.3–0.7 ng/mL)
14–16 yr	3.12–19.43 nmol/L (0.9–5.6 ng/mL)	1.21–3.30 nmol/L (0.3–1.0 ng/mL)
16–18 yr	9.02–25.33 nmol/L (2.6–7.3 ng/mL)	1.39–3.30 nmol/L (0.4–1.0 ng/mL)
18–20 yr	13.88–24.98 nmol/L (4.0–7.2 ng/mL)	1.39–3.30 nmol/L (0.4–1.0 ng/mL)
20–25 yr	11.80–38.86 nmol/L (3.4–11.2 ng/mL)	1.39–3.30 nmol/L (0.4–1.0 ng/mL)
S-Thyroxine		
1–3 day	142–296 nmol/L (11.0–23.0 μg/dL)	
1 wk–1 mo	116–232 nmol/L (9.0–18.0 μg/dL)	
1–4 mo	97–212 nmol/L (7.5–16.5 μg/dL)	
4–12 mo	71–187 nmol/L (5.5–14.5 μg/dL)	
1–6 yr	71–174 nmol/L (5.5–13.5 μg/dL)	
6–10 yr	64–161 nmol/L (5.0–12.5 μg/dL)	

Information based on Meites S, editor: *Pediatric clinical chemistry*, Washington, DC, 1977, American Association for Clinical Chemistry.
P, Plasma; *S,* serum; *U,* urine.
*As DHEA

REFERENCES

Beeler MF: SI units and the AJCP, *Am J Clin Pathol* 87:140, 1987.

Lundberg GD, Iverson C, Radulescu G: Now read this: the SI units are here, *JAMA* 255:2329, 1986.

Metric Commission of Canada: *The SI manual in healthcare*, Ottawa, 1981, Sector 9.10 Health and Welfare, Metric Commission of Canada.

Tietz NW, editor: *Clinical guide to laboratory tests*, ed 3, Philadelphia, PA, 1995, WB Saunders.

World Health Organization: *The SI for the health professions*, Geneva, 1977, WHO.

Young DS: Implementation of SI units for clinical laboratory data: style specifications and conversion tables, *Ann Intern Med* 106:114, 1987.

APPENDIX 6

COMMON CHIMERIC GENES IDENTIFIED IN HUMAN MALIGNANCIES

Peng Lee, Naif Z. Abraham Jr., Matthew R. Pincus

Tables A6.1 and A6.2 give well-known examples of common recurrent translocations identified in a number of malignancies. Table A6.1 correlates the specific translocation and genes involved with the respective malignancy. For example, in chronic myelogenous leukemia (CML), the typical chromosomal translocation present is t(9; 22) (q34q11), where typically the long arms of chromosome 22 and nine are involved in a reciprocal translocation or genetic fusion. The bcr gene is located on chromosome 22q11, whereas the abl oncogene resides on chromosome 9q34. This translocation produces an abnormal bcr/abl fusion gene. This gene, in turn, is transcribed into an abnormal bcr/abl fusion mRNA, which, in turn, is translated into the leukemia-producing bcr/abl protein molecule. This fusion protein possesses an abnormally increased tyrosine kinase activity that is involved in malignant transformation of hematopoietic cells to produce CML.

Table A6.2 indicates the genes and their chromosomal locations, their apparent protein product, and the abbreviation or nomenclature used in the research and medical literature to identify them. For example, in transformation to CML, key genes involved are bcr and abl, where the nomenclature *bcr* stands for "breakpoint cluster region" and *abl* refers to the human homologue of the oncogene of the Abelson murine leukemia virus, or v-abl.

These tables and their "explanations" of the gene nomenclature are intended to help clarify to the student of molecular and clinical pathology the function and/or particular research history of these genes and protein products. All information in these tables is derived from references listed.

TABLE A6.1

Common Recurrent Chromosome Changes with Common Chimeric Genes and Protein Fusions Identified in Malignancies

Malignancy	Translocation, Genes/Proteins Involved
Hematopoietic malignancies	
Chronic myelogenous leukemia	t(9;22)(q34q11), BCR/ABL
Acute myeloid leukemia	t(8;21)(q22;q22), AML1/ETO
Acute promyelocytic leukemia	t(15;17)(q22;q12), PML/RAR α
AML with abnormal eosinophils	t(16;16)(p13;q22) or inv(16) (p13q22), CBFb/MYH11
Burkitt lymphoma	t(8;14)(q24;q32), c-MYC/Ig heavy-chain locus
Precursor B ALL/lymphoma	t(9;22)(q34;q11.2), BCR/ABL
	t(4;11)(q21;q23), AF4/MLL
	t(1;19)(q23;p13.3), PBX/E2A
	t(12;21)(p13;q22), TEL/AML1
Mantle cell lymphoma	t(11;14)(q13;q32), Ig heavy-chain locus/BCL1
Follicular lymphoma	t(14;18)(q32;q21), BCL2 rearranged
MALT lymphoma	t(11;18)(q21;q21), API2/MLT
Anaplastic large-cell lymphoma	t(2;5)(p23;q35), ALK/NPM
T-cell prolymphocytic leukemia	t(14;14)(q11;q32), TCR α/TCL1
	inv14q(q11;q32), TCR α/TCL1
Mesenchymal malignancies	
Alveolar soft part sarcoma	t(X;17)(p11;q25), ASPL/TFE3
Alveolar rhabdomyosarcoma	t(2;13)(q35;q14), PAX3/FKHR
	t(1;13)(q36;q14), *PAX7-FOXO1A*
Congenital fibrosarcoma	t(12;15)(p13;q25), ETV6/NTRK3
Clear-cell sarcoma	t(12;22)(q13;q12), *EWSR1-ATF1*
	t(2;22)(q33;q12), *EWSR1-CREB1*
Dermatofibrosarcoma protuberans	t(17;22)(q22;q13), COLIA1/PDGFB
Desmoplastic small round-cell tumor	t(11;22)(p13q;12), EWS/WT1
	t(21;22)(q22;q12), *EWSR1-ERG**
Ewing sarcoma/peripheral primitive neuroectodermal tumor	t(11;22)(q24;q12), EWS/FLI1
Extraskeletal myxoid chondrosarcoma	t(9;22)(q22;q12), EWS/TEC
Malignant melanoma of soft parts/clear-cell sarcoma	t(12;22)(q13;q12), EWS/ATF1
Myxoid/round-cell liposarcoma	t(12;16)(q13;p11), TLS/CHOP
Synovial sarcoma	t(X;18)(p11.23;q11), SYT/SSX1
	t(X;18)(p11;q11), *SS18-SSX2*

TABLE A6.1

Common Recurrent Chromosome Changes with Common Chimeric Genes and Protein Fusions Identified in Malignancies—cont'd

Malignancy	Translocation, Genes/Proteins Involved
Carcinomas	
Renal cell carcinoma, papillary type	t(X;1)(p11;q21), TFE3/PRCC
	t(X;1)(p11;p34), TFE3/PSF
Papillary carcinoma of thyroid	2 proto-oncogenes identified in some cancers: RET and NTRK1 fused to the amino-terminus of different gene products
Prostate cancer	Deletion of TMPRSS2 with fusion to ETS family proteins, including:
	TMPRSS2/ERG
	TMPRSS2/ETV1
	TMPRSS2/ETV4
Follicular carcinoma of thyroid	T(2;3)(q13;p25), PAX8-PPAR γ

Sources: Alberti et al., 2003; Barone et al., 1994; Beckmann et al., 1990; Bernard et al., 1996; Bongarzone & Pierotti, 2003; Bursen et al., 2004; Cooper, 2002; Deng et al., 1993; DiMartino & Cleary, 1999; Ernst et al., 2002; Hart & Foroni, 2002; Hisaoka et al., 2004; Jaffe et al., 2001; Kundu et al., 2002; Labelle et al., 1995; Lasota, 2003; Lerman et al., 1983; Mathur et al., 2003; Oikawa & Yamada, 2003; Patton et al., 1993; Pekarsky et al., 2001a, 2001b; Pierotti, 2001; Pierotti et al., 1995; Ponder, 2002; Pulford et al., 1997; Ro & Roncari, 1991; Rosenwald et al., 2004; Santoro et al., 1995, 2004; Schaefer et al., 2004; Sidhar et al., 1996; Soulez et al., 1999; Takahashi & Cooper, 1987; Takahashi et al., 1985; Thayer & Singer, 1983; Thompson, 2004; Tong et al., 1986; Whitman et al., 2001; Yonezumi et al., 2001.

TABLE A6.2

Genes and Proteins Involved in Malignancies

Hematopoietic Malignancies	
BCR	Breakpoint cluster region gene, codes for a putative serine/threonine kinase, maps to chromosome 22q11
ABL	Human homologue of the oncogene of the Abelson murine leukemia virus, or v-abl, codes for a nonreceptor tyrosine kinase, maps to chromosome 9q34
AML1	Acute myelogenous leukemia-1 gene, codes for a transcription factor, maps to chromosome 21q22; also known as core binding factor α 2 or CBF α 2, RUNX1, PEBP2 α B
ETO	Eight-twenty-one gene, codes for a transcription factor, maps to chromosome 21q22
PML	Promyelocytic leukemia gene, codes for a nuclear factor that may influence transcription, maps to chromosome 15q22
RAR α	Retinoic acid receptor α gene, codes for a ligand-dependent nuclear retinoic acid receptor with transcription factor activity, maps to chromosome 17q21
CBF β	Core binding factor β, codes for a transcription factor, maps to chromosome 16q22; also known as PEBP2B or polyoma enhancer binding protein
MYH11	Myosin heavy chain 11 gene, codes for smooth-muscle myosin heavy chain, maps to chromosome 16p13
c-MYC	Cellular homologue of the v-myc oncogene from the avian myelocytomatosis retrovirus, codes for a transcription factor, maps to chromosome 8q24
Ig heavy-chain locus	Codes for the principal constituent (i.e., the heavy or H chain) of the immunoglobulin molecule and determines the class (IgA, IgD, IgE, IgG, IgM) of the molecule, maps to chromosome 14q32
AF4	ALL-1 fused gene on chromosome 4, codes for a putative transcription factor, maps to chromosome 4q21; also known as FEL
MLL	Mixed-lineage leukemia or myeloid/lymphoid leukemia gene, codes for a transcriptional regulator, maps to chromosome 11q23; also known as HRX and ALL-1
PBX1	Pre-B-cell leukemic homeobox 1 gene, codes for a transcriptional activator, maps to chromosome 1q23
E2A	Enhancer binding A gene (encoding two proteins that bind to the κ E2 site in the enhancer region of the κ light-chain gene), codes for a transcription factor required in B-cell development, maps to chromosome 19p13.3
TEL	Translocated ETS (E26-transformation specific) leukemia gene, codes for a transcription factor, maps to chromosome 12p13; also known as ETV6
BCL1	B-cell leukemia/lymphoma 1 gene, codes for a growth factor sensor protein involved in regulation of cell cycle division, maps to chromosome 11q13; also known as PRAD1/CCND1 or cyclin D1
BCL2	B-cell leukemia/lymphoma 2 gene, codes for BCL-2 protein, which inhibits apoptosis (programmed cell death), maps to chromosome 18q21.3
API2	Apoptosis inhibitor 2 gene, codes for an inhibitor of apoptosis, maps to chromosome 11q21; also known as c-IAP2, HIAP1, MIHC
MLT	MALT (mucosa-associated lymphoid tissue) lymphoma-associated translocation, codes for protein of unknown function, maps to chromosome 18q21
ALK	Anaplastic lymphoma kinase gene, codes for a receptor tyrosine kinase (expressed in neural tissue), maps to chromosome 2p23
NPM	Nucleophosmin (a nonribosomal nucleolar phosphoprotein involved in transporting ribosomal components between the nucleus and the cytoplasm for ribosomal assembly), coded by the NPM gene, maps to chromosome 5q35
TCR	T-cell antigen receptor, a T-cell membrane/surface receptor for antigen, composed of polypeptide chains from the α/δ (chromosome 14q11), β (chromosome 7q34), and/or γ (chromosome 7p) gene sets
TCL1	T-cell leukemia/lymphoma 1 gene, codes for a protein of unknown function but may be involved in lymphoid cell proliferation and/or survival, maps to chromosome 14q32.1

Continued

TABLE A6.2

Genes and Proteins Involved in Malignancies—cont'd

Mesenchymal Malignancies	
ASPL	Alveolar soft part sarcoma locus, function unknown, maps to chromosome 17q25
c-Kit	Mast/stem cell growth factor receptor gene encodes a tyrosine-protein kinase, maps to chromosome 4q11-q12
TFE3	Gene codes for a transcription factor that binds to the IgH intronic enhancer muE3 DNA region, maps to chromosome Xp11.2
PAX3	Paired box transcription factor 3 gene, codes for a transcription factor, maps to chromosome 2q35
FKHR	Forkhead-related gene, codes for a transcription factor, maps to chromosome 13q14; also known as FOXO1A
ETV6	Ets variant 6 gene, codes for a transcription factor, maps to chromosome 12p13; also known as TEL
NTRK3	Neurotrophin transmembrane receptor tyrosine kinase 3 gene, codes for a receptor that induces the release of neurotrophins, maps to chromosome 15q25; also known as TRKC or transmembrane receptor tyrosine kinase C
COL1A1	Collagen type 1 α 1 chain gene, codes for an extracellular matrix protein, maps to chromosome 17q22
PDGFB	Platelet-derived growth factor β chain gene, codes for a growth factor or mitogen, maps to chromosome 22q13; a human homologue of v-sis (simian sarcoma virus) oncogene
EWS	Ewing sarcoma gene, a putative nuclear RNA binding protein, maps to chromosome 22q12
WT1	Wilms tumor protein 1 gene, codes for a transcription factor, maps to chromosome 11p13
FLI1	Freund leukemia integration site 1 gene and an ETS family gene, codes for a transcriptional regulator protein, maps to chromosome 11q
TEC	Translocated in extraskeletal chondrosarcoma, codes for a steroid nuclear receptor/transcription factor thought to be involved in control of cellular proliferation and apoptosis, maps to chromosome 9q22; also known as CHN (chondrosarcoma), NOR1 (neuron-derived orphan receptor 1)—a receptor is termed an orphan when its ligand has not been isolated
ATF1	Activating transcription factor 1 gene, codes for a transcription factor, maps to chromosome 12q13
TLS	Translocated in liposarcoma gene, a putative nuclear RNA binding protein, maps to chromosome 16p11; also known as FUS or fusion
CHOP	C/EBP homologous protein—where C/EBP refers to CCAAT/enhancer-binding protein—codes for a transcription factor, maps to chromosome 12q13; also known as GADD153, DDIT3
SYT	Synovial sarcoma translocation gene, a putative transcriptional activator, maps to chromosome 18q11
SSX1	Synovial sarcoma X chromosome breakpoint gene 1, a putative transcriptional repressor/DNA binding factor, maps to chromosome Xp11
Carcinomas	
BRCA1/BRCA2	Breast and ovarian cancer susceptibility proteins, BRCA1 maps to chromosome 17q21 and BRCA2 maps to chromosome 13q12.3
BRAF	B-Raf proto-oncogene encoding serine/threonine-protein kinase, maps to chromosome 7q34
EGFR	Epidermal growth factor receptor encodes transmembrane tyrosine-protein kinase, maps to chromosome 7p12
HER2/neu	Human epidermal growth factor receptor 2, maps to chromosome 17q11.2-q12
TFE3	Gene codes for a transcription factor that binds to the IgH intronic enhancer muE3 DNA region, maps to chromosome Xp11.2
PRCC	Papillary renal cell carcinoma gene, a ubiquitously expressed nuclear protein, maps to chromosome 1q21.2
PSF	PTB-associated splicing factor gene where PTB = polypyrimidine tract-binding protein, codes for a ubiquitously expressed, putative multifunctional, nuclear protein possibly involved in transcription, maps to chromosome 1p34
RAS	Rat sarcoma oncogene encodes ras p21 protein (protein of molecular mass 21 kD), a membrane-bound G-protein that is the target of different activated growth factor receptors. Mutations that cause amino acid substitutions at critical positions, such as Val-for-Gly 12, are oncogenic. There are three major ras types: Harvey (Ha), Kirsten (K), and N. K-ras with the Val-for Gly 12 substitution has been found in over 90% of pancreatic cancers and over 50% of colon cancers and occurs in about 1 in every three common solid-tissue tumors. K-ras maps to chromosome 12p12.1
RET	Rearranged during transfection, codes for a tyrosine kinase receptor, maps to chromosome 10q11
NTRK1	Neurotrophin transmembrane receptor tyrosine kinase 1 gene, codes for a tyrosine kinase receptor for nerve growth factor, maps to chromosome 1q21-22; also known as TRKA or transmembrane receptor tyrosine kinase A
SRC	Encodes a tyrosine kinase protein that activates other tyrosine kinases intracellularly. It has been implicated in tumor progression in colorectal cancer and other cancers.

Sources: Alberti et al., 2003; Barone et al., 1994; Beckmann et al., 1990; Bernard et al., 1996; Bongarzone & Pierotti 2003; Bursen et al., 2004; Cooper, 2002; Deng et al., 1993; DiMartino & Cleary, 1999; Ernst et al., 2002; Hart & Foroni, 2002; Hisaoka et al., 2004; Jaffe et al., 2001; Kundu et al., 2002; Labelle et al., 1995; Lasota, 2003; Lerman et al., 1983; Mathur et al., 2003; Oikawa & Yamada, 2003; Patton et al., 1993; Pekarsky et al., 2001a, 2001b; Pierotti, 2001; Pierotti et al., 1995; Ponder, 2002; Pulford et al., 1997; Ro & Roncari, 1991; Rosenwald et al., 2004; Santoro et al., 1995, 2004; Schaefer et al., 2004; Sidhar et al., 1996; Soulez et al., 1999; Takahashi & Cooper, 1987; Takahashi et al., 1985; Thayer & Singer, 1983; Thompson, 2004; Tong et al., 1986; Whitman et al., 2001; Yonezumi et al., 2001.

REFERENCES

Alberti L, Carniti C, Miranda C, et al.: RET and NTRK1 proto-oncogenes in human diseases, *J Cell Physiol* 195:168–186, 2003.

Barone MV, Crozat A, Tabaee A, et al.: CHOP (GADD153) and its oncogenic variant, TLS-CHOP, have opposing effects on the induction of G1/S arrest, *Genes Dev* 8:453–464, 1994.

Beckmann H, Su LK, Kadesch T: TFE3: a helix-loophelix protein that activates transcription through the immunoglobulin enhancer muE3 motif, *Genes Dev* 4:167–179, 1990.

Bernard OA, Romana SP, Poirel H, et al.: Molecular cytogenetics of t(12;21)(p13;q22), *Leuk Lymphoma* 23:459–465, 1996.

Bongarzone I, Pierotti MA: The molecular basis of thyroid epithelial tumorigenesis, *Tumori* 89:514–516, 2003.

Bursen A, Moritz S, Gaussmann A, et al.: Interaction of AF4 wild-type and AF4-MLL fusion protein with SIAH proteins: Indication for t(4;11) pathobiology? *Oncogene* 23:6237–6249, 2004.

Cooper CS, editor: *Translocations in solid tumors*, Georgetown, TX, 2002, Landes Bioscience.

Deng Z, Liu P, Marlton P, et al.: Smooth muscle myosin heavy chain locus (MYH11) maps to 16p13.13-p13.12 and establishes a new region of conserved synteny between human 16p and mouse 16, *Genomics* 18:156–159, 1993.

DiMartino JF, Cleary ML: MLL rearrangements in haematological malignancies: lessons from clinical and biological studies, *Br J Haematol* 106:614–626, 1999.

Ernst P, Wang J, Korsmeyer SJ: The role of MLL in hematopoiesis and leukemia, *Curr Opin Hematol* 9:282–287, 2002.

Hart SM, Foroni L: Core binding factor genes and human leukemia, *Haematologica* 87:1307–1323, 2002.

Hisaoka M, Ishida T, Imamura T, et al.: TFG is a novel fusion partner of NOR1 in extraskeletal myxoid chondrosarcoma, *Genes Chromosomes Cancer* 40:325–328, 2004.

Jaffe ES, Harris NL, Stein H, editors: *WHO classification of tumours: Pathology and genetics of tumours of haematopoietic and lymphoid tissues*, Lyon, France, 2001, IARC Press.

Kundu M, Chen A, Anderson S, et al.: Role of Cbfb in hematopoiesis and perturbations resulting from expression of the leukemogenic fusion gene Cbfb-MYH11, *Blood* 100:2449–2456, 2002.

Labelle Y, Zucman J, Stenman G, et al.: Oncogenic conversion of a novel orphan nuclear receptor by chromosome translocation, *Hum Mol Genet* 4:2219–2226, 1995.

Lasota J: Genetics of soft tissue tumors. In Miettinen M, editor: *Diagnostic soft tissue pathology*, New York, 2003, Churchill Livingstone, pp 99–142.

Lerman MI, Thayer RE, Singer MF: Kpn I family of long interspersed repeated DNA sequences in primates: polymorphism of family members and evidence for transcription, *Proc Natl Acad Sci U S A* 80:3966–3970, 1983.

Mathur M, Das S, Samuels HH: PSF-TFE3 oncoprotein in papillary renal cell carcinoma inactivates TFE3 and p53 through cytoplasmic sequestration, *Oncogene* 22:5031–5044, 2003.

Oikawa T, Yamada T: Molecular biology of the Ets family of transcription factors, *Gene* 303:11–34, 2003.

Patton JG, Porro EB, Galceran J, et al.: Cloning and characterization of PSF, a novel pre-mRNA splicing factor, *Genes Dev* 7:393–406, 1993.

Pekarsky Y, Hallas C, Croce CM: Molecular basis of mature T-cell leukemia, *JAMA* 286:2308–2314, 2001a.

Pekarsky Y, Hallas C, Croce CM: The role of TCL1 in human T-cell leukemia, *Oncogene* 20:5638–5643, 2001b.

Pierotti MA: Chromosomal rearrangements in thyroid carcinomas: a recombination or death dilemma, *Cancer Lett* 166:1–7, 2001.

Pierotti MA, Bongarzone I, Borrello MG, et al.: Rearrangements of TRK proto-oncogene in papillary thyroid carcinomas, *J Endocrinol Invest* 18:130–133, 1995.

Ponder BAJ: Multiple endocrine neoplasia type 2. In Vogelstein B, Kinzler KW, editors: *The genetic basis of human cancer*, ed 2, New York, 2002, McGraw-Hill, pp 501–513.

Pulford K, Lamant L, Morris SW, et al.: Detection of anaplastic lymphoma kinase (ALK) and nucleolar protein nucleophosmin (NPM)-ALK proteins in normal and neoplastic cells with the monoclonal antibody ALK1, *Blood* 89:1394–1404, 1997.

Ro HS, Roncari DAK: The C/EBP-binding region and adjacent sites regulate expression of the adipose P2 gene in human preadipocytes, *Mol Cell Biol* 11:2303–2306, 1991.

Rosenwald A, Staudt LM, Duyster JG, et al.: Molecular aspects of non-Hodgkin lymphomagenesis. In Greer JP, Foerster J, Lukens JN, editors: *Wintrobe's clinical hematology*, ed 11, Philadelphia, 2004, Lippincott Williams & Wilkins, pp 2325–2361.

Santoro M, Grieco M, Melillo RM, et al.: Molecular defects in thyroid carcinomas: role of the RET oncogene in thyroid neoplastic transformation, *Eur J Endocrinol* 133:513–522, 1995.

Santoro M, Melillo RM, Carlomagno F, et al.: RET: normal and abnormal functions, *Endocrinology* 145:5448–5451, 2004.

Schaefer KL, Brachwitz K, Wai DH, et al.: Expression profiling of t(12;22) positive clear cell sarcoma of soft tissue cell lines reveals characteristic up-regulation of potential new marker genes including ERBB3, *Cancer Res* 64:3395–3405, 2004.

Sidhar SK, Clark J, Gill S, et al.: The t(X;1)(p11.2;q21.2) translocation in papillary renal cell carcinoma fuses a novel gene PRCC to the TFE3 transcription factor gene, *Hum Mol Genet* 5:1333–1338, 1996.

Soulez M, Saurin AJ, Freemont PS, et al.: SSX and the synovial-sarcoma-specific chimaeric protein SYT-SSX co-localize with the human polycomb group complex, *Oncogene* 18:2739–2746, 1999.

Takahashi M, Cooper GM: Ret transforming gene encodes a fusion protein homologous to tyrosine kinases, *Mol Cell Biol* 7:1378–1385, 1987.

Takahashi M, Ritz J, Cooper GM: Activation of a novel human transforming gene, ret, by DNA rearrangement, *Cell* 42:581–588, 1985.

Thayer RE, Singer MF: Interruption of an α-satellite array by a short member of the KpnI family of interspersed, highly repeated monkey DNA sequences, *Mol Cell Biol* 3:967–973, 1983.

Thompson MA, et al.: Molecular genetics of acute leukemia. In Greer JP, Foerster J, Lukens JN, editors: *Wintrobe's clinical hematology*, ed 11, Philadelphia, 2004, Lippincott Williams & Wilkins, pp 2045–2062.

Tong BD, Levine SE, Jaye M, et al.: Isolation and sequencing of a cDNA clone homologous to the v-sis oncogene from human endothelial cells, *Mol Cell Biol* 6:3018–3022, 1986.

Whitman SP, Strout MP, Marcucci G, et al.: The partial nontandem duplication of the MLL (ALL1) gene is a novel rearrangement that generates three distinct fusion transcripts in B-cell acute lymphoblastic leukemia, *Cancer Res* 61:59–63, 2001.

Yonezumi M, Suzuki R, Suzuki H, et al.: Detection of API2-MALT1 chimaeric gene in extranodal and nodal marginal zone B-cell lymphoma by reverse transcription polymerase chain reaction (PCR) and genomic long and accurate PCR analyses, *Br J Haematol* 115:588–594, 2001.

APPENDIX 7

DISEASE/ORGAN PANELS

ANEMIA

CBC with indices, reticulocyte count, and microscopic examination
Microcytic: *Iron studies*,* ferritin, ESR
Normocytic: ESR, *hemolysis profile*
Macrocytic: B_{12}, folate, TSH

ARTERIAL BLOOD GAS

pH
P_aCO_2
O_2 saturation
P_aO_2
CO_2 content
$P_{A-a}O_2$

ARTHRITIS

ESR (sedimentation rate)
Uric acid
ANA (antinuclear antibody)
C-reactive protein
Rheumatoid factor
Cyclic citrullinated peptide antibody

BONE/JOINT

Albumin
Calcium
Phosphorus
Osteocalcin
Protein, total
Uric acid
Alkaline phosphatase
25-OH Vitamin D

CARDIAC INJURY

Creatine kinase (CK)
CK-MB
Cardiac troponin-I or troponin-T

COAGULATION SCREENING

Prothrombin time
Thrombin time
Partial thromboplastin time
Platelet count
Platelet function test
Fibrinogen

COLLAGEN DISEASE/SLE

ESR
C-reactive protein
C_3
C_4
ANCA (antibody neutrophil cytoplasmic antibody)
ANA
Anti-DNA

COMA

Basic Metabolic Panel
Toxicology screen
Salicylate
Ammonia
Anion gap
Arterial blood gas profile
Alcohol
Lactic acid
Calcium (total and ionized)
Serum osmolality

DISSEMINATED INTRAVASCULAR COAGULATION (DIC)

Platelet count
Thrombin time
Fibrinogen
D-dimers
Prothrombin time
Partial thromboplastin time
CBC with examination of blood film

DIABETES MELLITUS MANAGEMENT

Basic Metabolic Panel
Hemoglobin A1c
Anion gap
Lipid profile

ELECTROLYTE/FLUID MANAGEMENT

Basic Metabolic Panel
Plasma and urine osmolality
Creatinine clearance
Free water clearance
Anion gap

ENTERAL/PARENTERAL NUTRITION MANAGEMENT

Basic Metabolic Panel
Magnesium
Albumin
Total protein
Alkaline phosphatase
Phosphorus
Triglycerides
Prealbumin
CBC

GENERAL HEALTH

CBC
Comprehensive Metabolic Panel
Lipid Panel
Uric acid
TSH

HEMOLYSIS

CBC
Bilirubin
Haptoglobin
Free hemoglobin (plasma and urine)
Lactate dehydrogenase (LD)
Direct Antiglobulin Test
Reticulocyte count

HEPATITIS SEROLOGY, CHRONIC CARRIER

Hepatitis Be Ab
Hepatitis Be Ag
Hepatitis B surface Ag
Hepatitis C Ab

HUMAN IMMUNODEFICIENCY VIRUS

HIV 1 and 2 Ab (EIA) with Western blot confirmation
HIV p24 antigen
HIV viral load
HIV genotype
CBC with CD4 and CD8 lymphocyte subsets

HYPERTENSION

Basic Metabolic Panel
Urinary free cortisol
Renin
Thyroid Screening
Urinary metanephrines
Urinalysis

IRON/HEMOCHROMATOSIS

Serum iron
TIBC (total iron-binding capacity)
% Saturation
Ferritin
Alanine aminotransferase (ALT)

HEPATIC FUNCTION

Albumin
Prothrombin time
Bilirubin (total and direct)
GGT
Protein, total
Alanine aminotransferase (ALT)
Aspartate aminotransferase (AST)
Alkaline phosphatase
5′-Nucleotidase
Lactate dehydrogenase (LDH)

NEWBORN SCREENING

Adrenoleukodystrophy (ALD)
Argininemia (ARG)
Argininosuccinic acidemia (ASA)

*Test name in *italics* refers to panel of that name.

Beta-ketothiolase deficiency (βKT)
Biotinidase deficiency (BIOT)
Carnitine uptake defect (CUD)
Citrullinemia (CIT)
Congenital adrenal hyperplasia (CAH)
Congenital hypothyroidism (CH)
Cystic fibrosis (CF)
Galactosemia (GALT)
Glutaric acidemia type I (GA I)
Guanidinoacetate methyltransferase (GAMT) deficiency
Hemoglobin sickle/beta-thalassemia (Hb S/βTh)
Hemoglobin sickle/C disease (Hb S/C)
Homocystinuria (HCY)
Hypermethionemia (HMET)
Isobutyryl-CoA dehydrogenase (IBCD) deficiency
Isovaleric acidemia (IVA)
Krabbe disease
Long-chain hydroxyacyl-CoA dehydrogenase deficiency (LCHAD)
Malonic aciduria (MA)
Maple syrup urine disease (MSUD)
Medium-chain acyl-CoA dehydrogenase deficiency (MCAD)
Methylmalonic acidemia (mutase deficiency; MUT)
Methylmalonic acidemia (Cbl A,B)
Mucopolysaccharidosis type I (MPS-I)
Multiple acyl-CoA dehydrogenase deficiency (MADD)
Multiple carboxylase deficiency (MCD)
Phenylketonuria (PKU)
Pompe disease (GAA; glycogen storage disorder type II)
Propionic acidemia (PROP)
Severe combined immunodeficiency (SCID)
Short-chain acyl-CoA dehydrogenase (SCAD) deficiency
Spinal muscular atrophy (SMA)
Sickle cell disease (S/S and S/C) and sickle cell trait (carriers)
Trifunctional protein deficiency (TFP)
Tyrosinemia type I (TYR I)
Very long–chain acyl-CoA dehydrogenase deficiency (VLCAD)
3-Hydroxy 3-methyl glutaric aciduria (HMG)
3-Methylcrotonyl-CoA carboxylase deficiency (3MCC)
Newborn testing for secondary target conditions varies by state

PANCREATIC

Amylase
Calcium (total and ionized)
Triglycerides
Lipase
Glucose

PARATHYROID

Albumin
Alkaline phosphatase
Magnesium
Creatinine
PTH (whole molecule, amino terminal)
Protein, total
Calcium (total and ionized)
Phosphorus
Urinary calcium

PRENATAL SCREENING

CBC
BUN
Uric acid
ABO and Rh typing
Urinalysis
Toxoplasmosis Ab
CMV Ab
Hepatitis B surface Ag
HIV antibody
Cervical Pap smear
Cervical culture/amplification for GC, Chlamydia, group B Streptococci
Glucose
Creatinine
Free T4
Erythrocyte antibody screen
Urine culture
Rubella titer
Syphilis serology (RPR)
Herpes simplex I and II Ab
Selected genetic testing according to population

RENAL

Basic Metabolic Panel
Magnesium
Albumin
24-Hour urine protein
Creatinine clearance
Phosphorus
Protein, total
24-Hour creatinine
CBC

THYROID SCREENING

Thyroxine (free T4)
TSH (third or fourth generation)

TOXICOLOGY SCREENING (URINE)

Amphetamines
Benzodiazepines
Marijuana metabolites
Methaqualone
Phencyclidine
Barbiturates
Cocaine and cocaine metabolites
Methadone
Opiates and opiate metabolites
Propoxyphene

AMA DESIGNATED DISEASE/ORGAN PANELS

CPT 80048 BASIC METABOLIC PANEL

Calcium
Carbon Dioxide
Chloride
Creatinine
Glucose
Potassium
Sodium
Urea Nitrogen (BUN)

CPT 80076 HEPATIC FUNCTION PANEL

Albumin
Alkaline Phosphatase
Alanine Aminotransferase (ALT)
Aspartate Aminotransferase (AST)
Direct Bilirubin
Total Bilirubin
Total Protein

CPT 80069 RENAL FUNCTION PANEL

Albumin
Calcium
Carbon Dioxide
Chloride
Creatinine
Glucose
Phosphorus
Potassium
Sodium
Urea Nitrogen (BUN)

CPT 80053 COMPREHENSIVE METABOLIC PANEL

Albumin
Alkaline Phosphatase
Alanine Aminotransferase (ALT)
Aspartate Aminotransferase (AST)
Calcium
Carbon Dioxide
Chloride
Creatinine
Glucose
Potassium
Sodium
Total Bilirubin
Total Protein
Urea Nitrogen (BUN)

CPT 80074 ACUTE HEPATITIS PANEL

Hepatitis A Antibody, IgM
Hepatitis B Core Antibody, IgM
Hepatitis B Surface Antigen
Hepatitis C Antibody
Consider testing for hepatitis E based on travel history

CPT 80051 ELECTROLYTE PANEL

Carbon Dioxide
Chloride
Potassium
Sodium

CPT 80061 LIPID PANEL

Triglycerides
HDL-Cholesterol, Direct
Total Cholesterol
LDL-Cholesterol, Calculated

REFERENCES

Current procedural terminology, standard edition, Chicago, IL, 2015, American Medical Association.

Department of Practice Parameters: *Principles of practice parameters*, Chicago, IL, 1995, American Medical Association, pp 1–18.

Glenn GC, Altshuler CH, Gambino R, et al.: Practice parameter on laboratory panel testing for screening and case finding in asymptomatic adults, *Arch Pathol Lab Med* 120:929–941, 1996.

Henry JB, Howantiz PJ: Organ panels and the relationship of the laboratory to the physician. In *AMA Council on Scientific Affairs: Laboratory tests in medical practice*, Chicago, IL, 1980, American Medical Association.

National Newborn Screening and Genetics Resource Center (NNSGRC): National newborn screening status report through the University of Texas at Austin, updated online periodically at http://genes-r-us.uthscsa.edu/%3Cfront%3E.

INDEX

A

A antigen, 711
Abacavir, 1495
Abbreviated or immediate-spin cross match, 754
ABCB1 transporters, 1486t, 1487, 1488t, 1498–1499
ABCC1 and ABCC2 transporters, 1486t, 1487–1488, 1488t
ABCG2 transporter, 1488–1489, 1488t
Abetalipoproteinemia, 265, 340
ABL1 gene, 1569
Abnormal cells, agents hemolytic to, 624
Abnormal hemoglobin syndromes, 611
Abnormalities, of proteins, patterns of, 288–289, 288f–289f
Abnormal laboratory values, interpreting and correlating, 100–101
Abnormal localization of immature precursors (ALIP), 654
ABO and H blood group systems, 711–714, 712t
  biochemistry of, 711
  null and weak phenotypes of, 711
ABO antibodies, 713–714
ABO gene locus, 711
ABO grouping, in compatibility testing, 750–751
  discrepancies in, 750–751, 751t
  of donors, 750
  of recipients, 750
Aβ precursor protein *(APP)*, 1464
Abscesses, specimens from, 1365
Absorbance check, 42
Absorption spectroscopy, 35
Abuse
  drugs of, 354–364
  laxative, 341
Acanthamoeba keratitis, 1314
Accuracy, 42
  of analysis, 127
  in analytic bias, imprecision and, in quality control, 131
  predictive value and, 94, 94t
  testing for, weights for, 54–55
Accuracy-based proficiency testing programs, 147
AccuVein, blood collection and, 27
Acetaminophen, 373–374
Acetylcholine acylhydrolase, 310
Acetylcholinesterase (EC 3.1.1.7) and butyrylcholinesterase (EC 3.1.1.8), 310–311
  abnormal results of, causes of, 310–311
  biochemistry and physiology of, 310
  measurement of, 310
  reference ranges and preanalytic variation of, 310
N-Acetyltransferase, 1483, 1485–1486
Acid and base, definition of, 201
Acid-base balance
  evaluation of, 181–207.e2
  whole body, 201–202
Acid-base disorders, 201–207
  acid and base, definition of, 201
  bicarbonate and CO_2 buffer system, 201
  metabolic acidosis, 202–205, 202b
  metabolic alkalosis, 205, 205b
  mixed, 207, 207b
  respiratory acidosis, 206, 206b
  respiratory alkalosis, 206, 206b
  serum anion gap, 203–204, 203b, 204f
  whole-body acid-base balance, 201–202
Acid-base disturbances, and hemapheresis, 813–814
Acid elution slide test, for F cells, 608
α_1-Acid glycoprotein, 286
Acid phosphatase (EC 3.1.3.2), 305–306
  abnormal results of, causes of, 306
  biochemistry and physiology of, 305–306
  measurement of, 306
  reference ranges and preanalytic variation of, 306
ACID properties of databases, 152t
Acinetobacter, 1148
  antimicrobial susceptibility of, 1148
  clinical manifestations and pathogenesis of, 1148
  laboratory diagnosis of, 1148
Acquired coagulation disorders, 843–845
Acquired coagulation factor deficiencies, 844
Acquired coagulation protein inhibitors, lupus anticoagulant and, 845
Acquired combined hyperlipidemia, 264
Acquired extrinsic hemolysis, 623–628
  chemical agents, 623–624
  immune hemolytic anemias, 625–628, 625b
  infectious agents, 625
  physical agents, 624–625
Acquired immunity, complement and, 975
Acquired immunodeficiency syndrome, 645, 1273–1274, 1280–1282, 1281f
  blood transfusion products, 1282
  etiology of, 645
  hematologic features of, 645
  NAAT testing, 1282
  parvovirus, enterovirus, and hepatitis B virus, 1273–1274
  vertical transmission, 1282
Acquired pure red cell aplasia, 602
Acquired storage pool disease, 863
Acquired von Willebrand syndrome (AVWS), 867
Acridinium esters, used as labels, 919, 919f
Acrodermatitis enteropathica, 451
ACTH. *See* Adrenocorticotropic hormone (ACTH)
Activated complex, 293f
Activated partial thromboplastin time (APTT), 834, 880, 882, 885, 887
  mixing study, 834
  normal, and PT, 843
    fibrinolysis, hereditary hemorrhagic disorders of, 843
    FVII deficiency, 843
    FXIII deficiency, 843
  prolonged, and PT, 842–843
    combined deficiency of vitamin K-dependent clotting factors, 843
    disorders of fibrinogen, 842
    factor XI, 841
    FII deficiency, 842
    FV and FVIII, combined deficiency of, 842–843
    FV deficiency, 842
    FX deficiency, 842
    FXII, prekallikrein, and high molecular weight kininogen, 841–842
Activated protein C resistance and factor V_{Leiden}, 874, 874f
Activation energy barrier, 293f
Active site, 292
Acute basophilic leukemia, 660
Acute biliary obstruction, 113
Acute bleeds, treatment of, 839–840
Acute coronary syndrome (ACS), 267–268
  diagnosis of, 270–272, 271f, 271t
Acute fulminant hepatic failure, 113
Acute hemolytic reactions, 782
Acute infectious lymphocytosis (AIL), 642
Acute inflammatory demyelinating polyneuropathy, and therapeutic plasma exchange, 807–808
Acute kidney injury (AKI)
  biomarkers of, 192–193
  classification for, 192t
  fatty acid-binding protein, 193
  interleukin-18, 193
Acute kidney injury *(Continued)*
  kidney injury molecule-1, 193
  neutrophil gelatinase-associated lipocalin, 193
  RIFLE criteria for, 192t
Acute leukemia, 105, 693–697
  of ambiguous lineage, 662, 663b
    NOS, 659
  diagnosis and classification of, 693–695, 696f–699f, 696t
  mixed phenotype
    B/myeloid, NOS, 662
    NOS-other rare types, 662
    with t(9;22)(q34;q11.2); BCR-ABL1, 662
    with t(v;11q23); MLL rearranged, 662
    T/myeloid, NOS, 662
  and myelodysplastic syndromes, 862
  myelogenous, predisposition to, with familial platelet disorder, 861
  natural killer cell lymphoblastic leukemia/lymphoma, 662
  prognostic factors of, 695–696, 700t
  with recurrent genetic abnormalities, 655–658
    with balanced translocations/inversions, 655–658, 657f
    with gene mutations, 658
  residual disease monitoring in, 700
  therapeutic targets of, 695–696
  undifferentiated, 662
Acute lymphoblastic leukemia
  childhood B-Lineage, risk stratification/outcome prediction in, 1545t
  risk stratification in childhood, 1550–1551
Acute megakaryoblastic leukemia, 659–660, 661f
Acute monoblastic and acute monocytic leukemia, 659, 660f–661f
Acute monocytic leukemia, 659
Acute myeloblastic leukemia
  with maturation, 659, 660f
  minimally differentiated, 659, 660f
  without maturation, 659, 660f
Acute myeloid leukemia, 655–662, 656t–657t, 656b, 1556–1567, 1557t–1558t, 1557b, 1618–1619
  acute promyelocytic leukemia with PML-RARA, 1557–1560, 1559f
  with balanced translocations/inversions, 655–658
    acute promyelocytic leukemia with t(15;17) (q22l;q12), PML/RARA variants, 656, 658f
    AML with inv(16)(p13q22) or t(16:16) (p13.1;q22), CFβ/MYH11, 656, 658f
    AML with (t5;21)(q22;q22), RUNX1-RUNX1T1, 655–656
    AML with t(6;9)(p23;q34); DEK-NUP214, 657
    AML with t(9;11)(p22;q23); MLLT3-MLL, 657, 658f
    AML (megakaryoblastic) with t(1;22) (p13;q13); RMB15-MKL1, 657
  with BCR-ABL1, 1561
  with biallelic mutation of CEBPA, 1563
  clonal heterogeneity and evolution, 1563f
  with core binding factor gene rearrangement: t(8;21) (q22;q22.1); RUNX1-RUNX1T1 and Inv(16) (p13.1q22) or (16;16)(p13.1;q22); CBFB-MYH11, 1560
  with gene mutations, 658, 1561–1564
    AML with *CEBPA* mutation, 658
    AML with *NPM1* mutation, 658
  with inv(3)(q21.3q26.2) or t(3;3) (q21.3;q26.2); GATA2, MECOM, 1561
  with mutated NPM1, 1554
  with mutated RUNX1, 1563–1564
  with myelodysplasia-related changes, 658
  not otherwise specified, 657t, 659–661
  other genes mutated, and related myeloid neoplasms, 1564–1567
  prognosis of, 1557

Pages followed by *b*, *t*, or *f* refer to boxes, tables, or figures, respectively.

Acute myeloid leukemia *(Continued)*
with recurrent cytogenetic abnormalities, 1557–1561
recurrent gene mutations in, 1561, 1562f–1563f
with t(1;22) (p13.3;q13.1); RBM15-MKL1, 1561
with t(6;9)(p23;q34.1); DEK-NUP214, 1561
with t(9;11)(p21.3;q23.3); KMT2A-MLLT3, 1560–1561
Acute myelomonocytic leukemia, 659, 660f, 699f
Acute pancreatitis, 332–334, 333t
Acute panmyelosis, with myelofibrosis, 660, 662f
Acute phase reactants, 287–288
Acute posthemorrhagic anemia, 603
Acute poststreptococcal glomerulonephritis (APSGN), 1097–1098, 1097f–1098f
Acute promyelocytic leukemia, 698f
Acute pulmonary infection, *Histoplasma* in, 1212
Acute renal failure, causes of
postrenal, 471
prerenal, 471
ADAM10, 1465
ADAMTS13 testing, 864, 868
Adaptive immunity, 930
ADCY2, 1457
Addiction medicine, 1503
Addison disease, autoimmune, 1111
treatment of, 1111
Additives, blood collection and, 27–28
Adenocarcinoma, 1617
Adenoma, follicular thyroid carcinoma from, 1617
Adenomatous polyps, of colon, urine metabolic test for, 1524
Adenosine deaminase, 520
Adenovirus, 1269–1270, 1285
Adequate intake (AI), 441–442
Adhesion molecules, and metastasis, 1510
Adoptive cell transfer, 824–825
Adrenal cortex, hormones of, 407–419
adrenal cortical enzyme deficiencies, congenital disorders of, 408–413, 410f, 411t
cortisol and glucocorticoids, 413–419
mineralocorticoid axis, 407–408, 409t
Adrenal cortical enzyme deficiencies, congenital disorders of, 408–413, 410f, 411t
aldosterone synthetase deficiency, 413
11-β-hydroxylase deficiency, 410–412, 412f
3-β-hydroxysteroid dehydrogenase deficiency, 412, 413f
congenital lipoid adrenal hyperplasia, 412, 415f
17-hydroxylase deficiency, 412, 414f
21-hydroxylase deficiency, 409–410, 411f
Adrenal function, 115–116, 116t, 404–420
adrenal cortex, hormones of, 407–419
adrenal medulla, hormones of, 405–407, 405f
Adrenal glands, 404–405
Adrenal insufficiency, 419–420
tests for, 419–420
Adrenal medulla, hormones of, 405–407, 405f
neuroblastoma, 407
pheochromocytoma and paraganglioma, 405–407, 405b, 406t–407t, 408f
Adrenocortical autoimmunity, 1111
Adrenocorticotropic hormone (ACTH)
laboratory measurement of, 414–415
stimulation test, 419–420
Adsorption (liquid-solid) chromatography, 51
Adults, cytogenetics in, 1425
Adult T cell leukemia-lymphoma, 677–679, 679f
Advanced beneficiary notice (ABN), 167
Aerial mycelium, 1195
Aerobic actinomycetes, 1141
clinical manifestations and pathogenesis, 1141–1142
laboratory diagnosis, 1142
Aerococcus, Gemella and, 1137
Aeromonas
antimicrobial susceptibility of, 1150
characteristics, 1150
clinical manifestations and pathogenesis of, 1150
laboratory diagnosis of, 1150
Affinity
of antibody, 954
chromatography, 51, 279
maturation, 954
Affinity-labeled probe detection systems, 1381f
Affymetrix, gene expression profiling by, in RCC, 1596
African tick bite, 1256
African trypanosomiasis, 1310
Agammaglobulinemia, 340, 959
Agglutination, 430, 851
Aggregatibacter, 1153–1154
antimicrobial susceptibility of, 1154
characteristics, 1153
clinical manifestations and pathogenesis of, 1154
laboratory diagnosis of, 1154
Aggressive B-cell lymphomas, 1554–1555
Burkitt lymphoma, 1554–1555
diffuse large B-cell lymphoma, 1554–1555
high-grade B-cell lymphoma, 1554–1555
plasma cell myeloma, 1555
Aggressive NK cell leukemia, 677, 679f
Agranulocytosis, 637
Air embolus, 816
AKAP9, 1465
AKI. *See* Acute kidney injury (AKI)
Akt-mTOR pathway, 1526–1527
Alanine aminotransferase (ALT), aspartate aminotransferase (AST) and, 320, 462–463
Alarms, and flags, 89–90
Albright's hereditary osteodystrophy. *See* Pseudohypoparathyroidism (PHP)
Albumin, 281–282, 282f, 456
calcium and, 109–110
IgG measurements and, 516–518
ischemia modified, 270
as replacement fluid, 808–809
total protein and, 456
Alcohol dehydrogenase *(ADH)*, 1459
Alcoholic hepatitis, 327
Alcohols, glycols and, 381–382
Alcohol use, 1459–1460
Aldehyde dehydrogenase *(ALDH)*, 1459
Alder-Reilly anomaly, 639, 640f
Aldosterone. *See also* Renin-aldosterone axis.
concentration, and abnormalities in potassium metabolism, 194
deficit of, 106t, 107
measurements of, 423, 423t
Aldosterone synthetase deficiency, 413
Alimentary hypoglycemia, 236
Alkaline phosphatase (ALP), 220, 306–308, 321, 463
abnormal results of, causes of, 307–308
biochemistry and physiology of, 306
isoforms of, 307
measurement of, 307
reference ranges and preanalytic variation of, 307, 307t
Alkaptonuria, 508
methods for, 508
ALK gene, 1588
abnormalities, in anaplastic large cell lymphomas, 1555–1556
chromosomal rearrangement of, in lung cancer, 1588
in renal cell carcinoma, 1596
ALK inhibitors, 1501
Alkylating agents, mutagenic effects of, 658
Alleles
definition of, 1411
frequencies, and mass population screening, 1438
Allen test, modified, 30b
Allergen component families, 1121t
Allergen molecules, protein component families, molecular structures and cross-reactivity, 1120–1121, 1121t
Allergen-specific IgE antibodies, measurement of, 1123
Allergic, anaphylactoid, and anaphylactic reactions, to hemapheresis, 814–815
Allergic bronchopulmonary aspergillosis (ABPA), 1122
Allergic diseases, 1115–1128.e2
allergen molecules, protein component families, molecular structures and cross-reactivity, 1120–1121, 1121t
allergen *vs.* allergenic component, 1116
laboratory testing for, 1120–1128
component-resolved diagnostics and testing, by microarray methods, 1121t, 1127–1128
immediate hypersensitivity reactions, mediators of, 1128
measurement of allergen-specific immunoglobulin E antibodies
analytic methods, 1123
clinical applications, 1123–1127, 1124f–1125f, 1125t, 1127f
measurement of IgE, analytic methods and reference ranges, 1121–1122, 1122t
pathogenesis of, 1116–1120
atopy and allergic phenotype, genetic influences and candidate genes, 1116, 1117t
immediate hypersensitivity, mechanisms of, 1116
Allergic diseases *(Continued)*
immediate hypersensitivity reactions, cells and mediators of, 1118–1120, 1119f
immunoglobulin E, 1117–1118, 1118t, 1119f
molecular and cellular interactions, regulation of IgE synthesis, 1117, 1118f
prevalence of, 1115–1116
rationale for, 1120
signs and symptoms of, 1116
total serum IgE, measurement of, 1122
in vivo test techniques, skin tests and end-organ challenge tests, 1121
Allergic march, 1123–1124
Allergic phenotype, genetic influence and candidate genes, 1116, 1117t
Allergic reactions, to transfusion, 781
severe (anaphylactic), 781–782
Allergic rhinitis, 1124–1125
Allergies, 898–899
Alloantibodies and autoantibodies, blood group, 710
Allogeneic hematopoietic progenitor cell transplantation, 1012–1013
Allogenic versus autologous hematopoietic progenitor cell harvest, 795
Alloimmune hemolytic disease of the newborn (HDN), 627
Allopurinol, 1022, 1496
All trans retinoic acid (ATRA), 1558
Alpha-2-antiplasmin deficiency, acquired, 843
Altered repertoire model, 1495
Alternative hypothesis (Halt), 122
Alternative pathway, 979
Alzheimer disease, 1464–1465, 1466f
angiotensin-converting enzyme (ACE), 1465
Apolipoprotein E (APOE), 1464
Aβ precursor protein *(APP)*, 1464
genetic loci, 1464–1465
next-generation sequencing for, 1465
presenilins, 1464
Ambient mass spectrometry, 68–69
Amebae
Blastocystis hominis and, 1319
Entamoeba histolytica, 1315–1318
nonpathogenic amebae, 1315f–1317f, 1318–1319, 1319t–1320t
opportunistic free-living, 1313–1315, 1314f
Amebiasis, 1315–1318
Amenorrhea, 431, 432f
American Association of Tissue Banks (AATB), 817–820
American trypanosomiasis, 1311
Aminoacidurias, 507–509
Aminoacyl-tRNA synthetases (ARS), 1046–1047
Amino transferase, 462–463
Aminotransferases (transaminases), 320–321
Amiodarone, 368–369
Ammonia, 317, 458
amines, amino acids and, 520
Ammonium biurate, 496, 497f
Amorphous phosphates, 496, 496f
Amorphous urates, 493
AmpC cefoxitin-ethylenediaminetetraacetic acid test., 1175, 1176f
AmpC enzymes, 1175
Amperometry, 48
Amphetamines, 360–361
acute toxicity of, 361
chronic usage, 361
clinical symptoms of, 360–361
"designer", 361
detection of, 361
treatment of, 361
Ampicillin (high dosage), 497, 498f
Amplification
methods of, for nucleic acid analysis, 1383
preparation, for DNA, 1007
Amplitude, of sine wave, 36
Amylase, 333, 463–464, 464f, 530, 535
Amylin, 226–227
Amyloidosis, 345
primary, 670
β-Amyloid protein 42 and τ protein, 518–519
Anaerobic bacteria, 1160–1163
antimicrobial susceptibility of, 1163
definitions and characteristics of, 1160
laboratory diagnosis of, 1161–1162, 1161f–1164f, 1162t–1165t
pathogenesis and virulence factors of, 1160–1161
Analbuminemia, 281
Analgesic, and antiinflammatory drugs, 372–374, 373f

Analogs, codeine and, 359
Analysis
of accuracy, 127
of clinical laboratory automation, 74–80.e1
data, 120
discrete, 124–125, 124t
general analytic methods and issues for, 53–58
of aqueous solution, 57–58
of chemicals, 53
of heating blocks, dry-bath incubators, and ovens, 57
of laboratory glassware and plasticware, 55
of mass, measurement of, 54–55
of mixing, 57
of thermometry, 56–57
of volumetric laboratoryware, 55–56
of water, 53–54
of water baths, 57
instrumentation, principles of, 35–59.e1
capillary electrophoresis in, 52, 52f
conductance in, 48
electrochemistry in, 47–48
electrophoresis and densitometry in, 48
flow cytometry in, 45–46
impedance in, 48
isoelectric focusing in, 48–49, 49f
mass spectrometry in, 51–52
molecular luminescence spectroscopy (fluorometry) in, 43–44
nephelometry and turbidimetry in, 44–45
nuclear magnetic resonance spectroscopy in, 52–53, 53f
osmometry in, 46–47
reflectometry in, 43
refractometry in, 46
scintillation counter in, 52
spectrophotometry in, 35–42, 36f
involving multiple variables, 126–127
precision of, 127
of sensitivity, 127–128
of specificity, 128
of specimens, additional, 90
statistical, resources for, 128–129
Analysis of covariance (ANCOVA), 126–127
Analysis of variance (ANOVA), 119, 126, 127f
multiple, 126–127
two-way, 126
Analyte assays and common interferences, chemical basis for, 453–466.e1
analyte concentrations, enzymes as reagents for, 458–466
enzymes, assays for, 462–466
ion-selective electrodes, 453–454, 454f
spectrophotometric determinations, 454–458
Analyte concentrations
enzyme reactions determined by, 458–462
enzymes as reagents for, 458–466
NADH and NADPH as quantitative indicators, 458
rate versus end-point methods, 458
Analytes
quantitation of, 456–458
serum, 328–329
Analytic bias and imprecision, of quality control, 121f, 130–131
Analytic correctness, of results, assessment of, 89–90
Analytic immune studies, 942–943, 942b
Analytic sensitivity, 127–128
Analytic specificity, 128
Analytic system, flow of immunoassay in, 920, 920f
Analytic techniques
for calcitonin, 214
for calcium, 210
for intraoperative PTH, 213
for magnesium, 211–212
for parathyroid hormone, 212
for parathyroid hormone-related peptide, 213
for phosphatonins, 215
for phosphorus, 211
for vitamin D and metabolites, 214–215
Anaphylactic reaction, to hemapheresis, 814–815
Anaphylactoid reaction, to hemapheresis, 814–815
Anaphylatoxins, 972–973
Anaplasma, infections caused by organisms of, 1259–1261, 1259t
Anaplastic large cell lymphoma, 682, 1555–1556
ALK gene encodes, 1555–1556
ANCA, for primary sclerosing cholangitis, 322–323
ANCA-associated small vessel vasculitis, 1064–1068
clinical laboratory testing of, 1067–1068, 1067f
definition and epidemiology of, 1064–1065, 1064t
diagnosis, treatment, and prognosis of, 1068
etiology and pathogenesis of, 1066
pathology of, 1065–1066, 1065f–1066f
Anchoring enzyme, 1610
ANCOVA. *See* Analysis of covariance (ANCOVA)
Ancylostoma duodenale, 1329
Anderson's disease. *See* Chylomicron retention disease
Andexanet alfa, 887–888
Anemias, 101–104, 588–630. *See also* Aplastic anemia; Iron deficiency anemia.
associated with bone marrow infiltration, 598–599
blood loss, 603
in B lymphoblastic leukemia/lymphoma, 663–664
of chronic disease, 597–598
common types of, 101t
congenital dyserythropoietic, 602–603
in endocrine disease, 598
general manifestations of, 588, 589t
hemolysis, 623–628
hemolytic, 102–103
immune, 625–628, 625b
microangiopathic, 103
hypochromic, 629
impaired production
iron deficiency anemia, 588–592
megaloblastic anemia, 592–597
other, 597–603
laboratory investigations of, 628–630
in liver disease, 598
macrocytic, 104, 629
microcytic, 101–102
normocytic, 102
hyperproliferative, 102–103
hypoproliferative, 103–104
pernicious, 1084–1085, 1084f
posthemorrhagic
acute, 603
chronic, 603
of renal failure, 104
of renal insufficiency, 598
sickle cell, 805–806, 805b
sideroblastic, 602
thalassemias, 616–620
Anergy, 942, 942b
Aneuploidy, 1419–1420, 1419f
Aneurysmal bone cyst, 1602
Angelman syndrome, 1430, 1445, 1445f
Angina pectoris, 267–268
Angiogenesis, 1515
Angiogenic factors, 1515
Angioimmunoblastic T cell lymphoma, 681, 682f
Angiosarcoma, ras-p21 protein in, 1533
Angiostrongyliasis, 1341
Angiostrongylus cantonensis, 1341
Angiostrongylus costaricensis, 1341
Angiotensin-converting enzyme, 308–310
abnormal results of, causes of, 308–310
biochemistry and physiology of, 308, 308f
inhibitors, 815
design of, 308
measurement of, 308
reference ranges and preanalytic variation of, 308
Angiotensin-converting enzyme (ACE), 1465
Angiotensinogen, 308
Anion-exchange chromatography, 279
Anion gap, 108
Anisakis spp., 1342
Ankylosing spondylitis, 1020
Ankyrin 3 (ANK3), 1458
Annexin A5, 871
Annexins A2, 871
Anodic stripping voltammetry, 48
ANOVA. *See* Analysis of variance (ANOVA)
Anti-A,B, 713
Anti-α-Fodrin antibody, 1041
Antiapoptosis cell survival pathways, 1454
Anti–asialoglycoprotein receptor autoantibodies, 1086–1087
Antiasthmatics, 371–372, 372f
Antibiotics, and neutrophilia, 637
Antibiotic stewardship programs, 1180
Antibiotic susceptibility testing (AST)
definition, 1166
dilution testing, 1168, 1168f
direct β-lactamase tests, 1169–1170
disk diffusion, 1169, 1169f
gradient diffusion, 1168–1169, 1169f
Antibiotic susceptibility testing *(Continued)*
phenotypic methods in, 1169
technical considerations in
incubation conditions, 1167
inoculum, 1167
media, 1167
test interpretation, 1167–1168, 1168f
Antibodies
anti-α-Fodrin, 1041
anticarbamylated protein, 1046
anti-DFS70, 1040
to antieukaryotic initiation factor-2B, 1044
antigens and, 1037, 1037t
antikeratin, 1045
anti-Ku, 1038
antimitochondrial, 1086
for primary biliary cirrhosis, 322
antinucleosome, 1040
antiphospholipid antibodies, 1038
anti-SS-A/Ro60
and anti-SS-B/La, 1040, 1041t
elevated levels of, 1038
to bicaudal D2, 1042
catalytic, new, with predetermined enzyme activity, 304–305, 305f
characteristics of, 902
to citrullinated peptides, 1045–1046
clinically important, 1113t–1114t
detection techniques, 1012
diversity of, genetic basis of, 955, 955f, 956t
drug binding to, 348
glycosylated, 1046
identification, 1011
monoclonal, 902
to native DNA, 1037
to nuclear protein NA14, 1041
to nucleolar antigen fibrillarin (U3-snoRNP), 1044
peptidylarginine deiminase, 1046
to PM/SCL, 1044
polyclonal, 902
production of, 1028–1029
novel immunogens for assessment of, 1032
by recombinant technology, 902
proliferating cell nuclear antigen multiprotein complex, 1038
removal of, for antigen typing, 759
to ribosomal P proteins, 1038
to RNA polymerases, 1042–1043
to SCL-70, 1042
to Sm and nuclear ribonucleoprotein, 1037
to SS-A/Ro and SS-B/La, 1038
structural properties of, 952–955
targeting nucleolar organizing region, 1044
titering of, 691
to topoisomerase I, 1042
to U11/U12 RNA associated ribonucleoprotein C3 (RNPC3), 1044
Antibody adsorption, 757
Antibody-antigen interaction, 953–955, 954f
Antibody-based techniques, for measuring enzymes, 300
Antibody-dependent cell-mediated cytotoxicity (ADCC) assay, 945f
Antibody detection, 751–756, 1299–1300, 1300t
antibody identification, 752–754
crossmatching, 754–755
interpreting the results of, 753–754, 753t, 754f
protocols of, 752
for column agglutination technologies, 752
for solid-phase adherence tests, 752
for tube tests, 752
reagent red blood cells in, 751–752
Antibody elution, 758–759
Antibody identification, 752–754
crossmatching, 754–755
antiglobulin crossmatch, 755
compatibility testing in emergencies, 755
electronic crossmatch, 754–755, 755b
immediate spin serologic crossmatch, 754
preoperative crossmatch protocols, 755
interpreting the results of, 753–754, 753t, 754f
prenatal, postnatal, and infant testing in, 755–756
special techniques for, 756–760
serum antibody titration as, 757–758
serum procedures to eliminate antibody reactivity as, 756–757
special red cell procedures as, 758–760
Antibody molecule, 952–953, 953f, 954t
Anticarbamylated protein antibodies, 1046
α_1-Antichymotrypsin (AAC), 287

Anticipation, 1438
Anticitrullinated peptides, 1045–1046
Anticoagulants, blood collection and, 27–28, 1469b
Anticoagulation protein systems, 831–832
Anticodon, 1376
Anticonvulsants, 369–371, 370f
Antidepressants, 376–377
  therapeutic levels and metabolism of, 378
  tricyclic, 377–378, 377f
Antidiuretic hormone (ADH), 392–395
  metabolism, 197–200
Anti-EGFR monoclonal antibodies, 1501
Anti-eIF2B antibodies, 1044
Anti-factor Xa assays, 882
Antigen-antibody reaction
  general characteristics of, 901–902
  kinetics of, 902–903
Antigen capture assays, 769
Antigen expression
  abnormal patterns of
    acute leukemia, 693–697, 696f–699f, 696t, 700t
    in hematopoietic neoplasia, 693–705
    myelodysplastic syndromes and myeloproliferative disorders, 703–705, 707f
    paroxysmal nocturnal hemoglobinuria, 705, 707f
    plasma cell neoplasms, 703, 706f
  lymphoma, 697–700, 701f–704f
  normal patterns of, 693, 693f–695f
Antigenic assays, complement levels by, 982–983
Antigenic fragments, class I and II molecules relating to, 1005
Antigen-induced activation, of T lymphocytes, 931
Antigen-presenting cells, 895, 895f
Antigen receptor gene rearrangements
  mechanism of, 1544–1545
  techniques to detection, 1545–1547
Antigens
  and antibodies, erythrocyte, 711–744, 712t–713t
  carcinoembryonic, 520–521
  characteristics of, 902
  density of, 709, 939
  detection of, 1288, 1294t, 1297–1299
  histocompatibility, 896
  red cell, destruction of, 758
  typing, removal of antibody from red cells for, 759
Antigen-specific stimulation, signal transduction following, 931
Antiglobulin crossmatch, 755
Anti-glomerular basement membrane disease, 1068–1069
  clinical laboratory testing of, 1069
  definition and epidemiology of, 1068, 1068t
  diagnosis, treatment, and prognosis of, 1069
  etiology and pathogenesis of, 1069
  pathology of, 1068–1069, 1069f
Anti-glomerular basement membrane glomerulonephritis, 1098–1099, 1099f–1100f
Antigram, 751–752
Antihistone antibodies, drug-induced lupus erythematosus and, 1039–1040
Anti-human globulin cytotoxicity assay, 1012
Antihuman globulin test, 746–748
  quality control of, 748
  reagents and procedures for, 747–748
    choosing of, 747–748
    monospecific reagents, 747
    polyspecific reagents, 747
  sensitivity of, 748
Anti-I and anti-i antibodies, 742
Anti-idiotype antibody-based immunoassay, 923
Antiinflammatory and analgesic drugs, 372–374, 373f
Antikeratin antibody, 1045
Anti-Ku antibodies, 1038
Anti–liver cytosol type 1 autoantibodies, 1086
Anti–liver-kidney microsomal type 1 autoantibodies, 1086
Antimetatype antibody-based immunoassay, 923–925
Antimicrobial agents, in vitro testing of, 1166–1182.e3
  antibiotics selection for, 1179–1180
    reporting of, 1180
  antimicrobial susceptibility
    cumulative reports for, 1180–1181
    molecular-based testing for, 1171–1179
  bactericidal testing, 1170
  definitions of, 1166–1167
  dilution testing, 1168, 1168f
  disk diffusion, 1169, 1169f
  gradient diffusion, 1168–1169, 1169f
  guidance documents for, 1166–1167
  resistance phenotypes detection, 1172–1177
Antimicrobial agents, in vitro testing of *(Continued)*
  aminoglycosides, 1172
  AmpC cefoxitin-ethylenediaminetetraacetic acid test., 1175, 1176f
  chromogenic media, 1172
  D-zone approximation test, 1173, 1173f
  E-test, 1175, 1175f
  extended-spectrum β-lactamases, 1174–1175, 1174t
  glycopeptide resistance, 1172–1173
  inhibition test for classify carbapenemases, 1177, 1177f
  methicillin resistance, 1172
  modified Hodge test, 1176, 1176f
  MRSA and CoNS, 1172
  nitrocefin β-lactamase test, 1172
  oxacillin screen disk diffusion method, 1172
  penicillin-intermediate and -resistant isolates, 1172
  supplementary phenotypic tests, 1176
  vancomycin susceptibility testing, 1173
  VISA, 1173
  VRE screening, 1173
  susceptibility testing
    indications for, 1179
    inhibitory methods of, 1168–1170
    technical considerations in, 1167–1168
Antimicrobial stewardship program (ASP), 1179
Antimicrobial susceptibility
  of *Acinetobacter*, 1148
  of *Aeromonas*, 1150
  of *Aggregatibacter*, 1154
  of anaerobic bacteria, 1163
  of *Bacillus*, 1140–1141
  of *Bordetella*, 1156
  of *Brucella*, 1157
  of *Burkholderia*, 1149
  of *Calymmatobacterium granulomatis*, 1159
  of *Campylobacter*, 1151
  of *Capnocytophaga*, 1159
  of *Cardiobacterium hominis*, 1154
  of *Corynebacterium*, *Arcanobacterium*, 1138
  cumulative reports for, 1180–1181
  of *Eikenella*, 1154
  of *Enterobacterales*, 1146
  of *Erysipelothrix*, 1139
  of *Francisella tularensis*, 1158
  of *Gardnerella*, 1158
  of *Haemophilus*, 1153
  of *Helicobacter*, 1151
  of *Kingella*, 1154
  of *Legionella*, 1155
  of *Listeria*, 1139
  molecular-based testing for, 1171–1179
  of *Neisseria*, 1143–1144
  of *Nocardia*, 1141
  of *Pasteurella*, 1157
  of *Plesiomonas*, 1147
  of *Pseudomonas*, 1147–1148
  of *Staphylococcus*, 1133, 1133f
  of *Stenotrophomonas maltophilia*, 1149
  of *Streptobacillus*, 1160
  of *Streptococcus* and *Enterococcus*, 1136–1137
  of *Vibrio*, 1150
Antimitochondrial antibodies, 1086
  for primary biliary cirrhosis, 322
Anti-Mullerian Hormone (AMH), 433
Antimuscarinic type 3 receptor (M3R) autoantibodies, 1040–1041
Antineutrophil cytoplasmic autoantibodies (ANCA), 1086, 1099–1102, 1101f
Antinuclear autoantibodies, 1086
Antinucleosome antibodies, 1040
Antiperinuclear factor, 1044
Antiphospholipid antibodies, in systemic lupus erythematosus, 1038
Antiphospholipid syndrome, and lupus anticoagulant, 875–876, 875b
Antiplatelet therapy, 888–890
  aspirin, 888–889
  glycoprotein IIb/IIIa inhibitors, 890
  P2Y12 inhibitors, 889–890, 889f, 889t
Anti–smooth muscle autoantibodies, 1086
Antisoluble liver antigen/liver-pancreas autoantibodies, 1086
Anti-SS-A/Ro60 antibodies, 1040, 1041t
Anti-SS-B/La antibodies, 1040, 1041t
Antisynthetase syndrome (aSS), 1047
Anti-tag, 1613
Antithrombin, 832, 870–871
Antithrombin deficiency, 873
Antithrombin-dependent parenteral anticoagulants, 882–885
  fondaparinux, 883
  heparin
    low molecular weight, 883, 884t
    unfractionated, 882–883, 882f–883f
  heparin-induced thrombocytopenia, 883–885, 884f, 885t, 886f
  unfractionated heparin, 882–883, 882f–883f
Antithrombin III (AT_3), 287
Antithrombotic therapy, 879–892.e3
  antiplatelet therapy, 888–890
    aspirin, 888–889
    glycoprotein IIb/IIIa inhibitors, 890
    P2Y12 inhibitors, 889–890, 889f, 889t
  antithrombin-dependent parenteral anticoagulants, 882–885
    fondaparinux, 883
    heparin-induced thrombocytopenia, 883–885, 884f, 885t, 886f
    low molecular weight heparin, 883, 884t
    unfractionated heparin, 882–883, 882f–883f
  target-specific anticoagulants, 885–888
    oral agents, 885–887
    parenteral agents, 885
  vitamin K antagonists, 879–882, 880f, 881t, 881b
    brodifacoum, 882
    long-acting anticoagulant rodenticides, 882
α_1-Antitrypsin, 282–283, 319
Antiviral resistance testing, 1285–1286
Anti-Xa activity assay, for heparin monitoring, 835
Ants, 1347
Anxiety disorders, 1463–1464
Aortic valve replacement, 820
APC gene, 1591
Apheresis, 773
Apheresis platelets, benefits of, 790
Apixaban, 887
Aplastic anemia, 103, 599–601
  associated with other disease, 600–601
  chemical or physical agents associated with, 600
  clinical features of, 599
  etiology of, 599
  idiopathic acquired, 600
  inherited, 601
  management of, 599
  pathogenesis of, 599
  prognosis of, 599
ApoA-I deficiency, and ApoC-III deficiency, 266
ApoA-I variants, 266
ApoA-V, 264
ApoC-II deficiency, 264
ApoC-III deficiency, ApoA-I deficiency and, 266
ApoC-III excess, 264
Apoenzyme reactivation immunoassay (ARIS), 914, 916f
Apolipoprotein E (APOE), 1464
Apolipoproteins, 244, 248, 248t–249t
  analysis of, 257
Aptima HPV assay, 1598
Aqueous solution, 57–58
  acids, alkalis, and pH in, 58
  buffer solution in, 58
  dilutions in, 58, 58b
  millimoles in, 57
  molal in, 57–58, 58b
  molarity in, 57, 57b
  normality in, 57, 58b
Arachidonic acid, abnormalities in metabolism of, and platelet signaling pathway, 860
Arachnids, 1347–1349, 1348f
Arboviral infections, 1286–1287
Arboviruses, 1275
Arcanobacterium, *Corynebacterium* and, 1137–1138, 1137f
Argasid ticks, 1243, 1243f
Argatroban, 885
Arginine vasopressin/antidiuretic hormone, 392–395
Arsenic, 382
Arterial puncture, 29–30
  procedure, 30b
Arthritis, rheumatoid, 1022. *See also* Rheumatoid arthritis.
Arthropods, medically important, 1344, 1345t
  arachnids as, 1347–1349, 1348f
    mites, 1348f–1349f, 1349
    scorpions, 1348, 1348f
    spiders, 1348
    ticks, 1348–1349
  biological characteristics of, 1344
  centipedes as, 1350

Arthropods, medically important *(Continued)*
crustaceans as, 1350–1351
insects as, 1346–1347, 1346f
bedbugs and kissing bugs, 1346f, 1347
bees, wasps and ants, 1347
beetles, 1347
cockroaches, 1347
fleas, 1346f, 1347
flies, mosquitoes and midges, 1347
moths and butterflies, 1347
parasitic lice, 1346–1347
sucking lice, 1344
laboratory approaches to identification of, 1346
mechanisms of injury of, 1344–1346
blood loss as, 1344
direct tissue invasion as, 1344
envenomation as, 1344
hypersensitivity reactions as, 1345
infectious agents as, transmission of, 1344–1345
psychological manifestations as, 1345–1346
vesication as, 1344
millipedes as, 1349–1350
pentastomids as, 1344
Artificial intelligence, 157–159, 158f
Asbestos exposure, cancer occurrence in, anti-p53 in, 1535
Ascariasis, 1328–1329
Ascaris lumbricoides, 1328–1329
Ascites, 533
Ascorbate (vitamin C), 446
Ascorbate cyanide test, 622–623
Ascorbic acid, 484–485
methods for detecting, 484
reagent strip, 485
Aseptate, 1195
Aspartate aminotransferase (AST) and alanine aminotransferase (ALT), assays for, 321, 462–463
Aspergillosis, 1222
hyaline fungi as cause of, 1222–1225
pathology of, 1221t, 1223, 1223f
Aspirates, 1297
Aspirin, 373, 374f, 888–889
and platelet function, 863
Assay
for ammonia, 317
procedures for, 270
Assay systems, instrument automation and modulation of, 919–921
analytic system, flow of immunoassay in, 920, 920f
heterogeneous immunoassay systems, 919
high throughput fully automated, 920–921, 921t
instrumentation and key points for, 920
homogeneous assay systems, 919
remote maintenance of, 921
Assisted reproductive technology (ART), 433
Asthma, 898
ASXL1 gene, 1566
Asymptomatic (smoldering) myeloma, 670
Atherosclerosis, 267–268. *See also* Cardiac injury, atherosclerosis, thrombotic disease.
Atmospheric pressure chemical ionization, 62
Atmospheric pressure photoionization, 62
ATP2A1 (Sarcoplasmic/Endoplasmic Reticulum Calcium AT Pase 1), 1461
ATP-binding cassette transporters, 1487–1489
Attenuated familial adenomatous polyposis, 1447–1448
Atypical chemokine receptors, 990–992
Atypical chronic myeloid leukemia, 1575
BCR-ABL1 negative, 652
CSF3R gene mutation, 1575
Atypical chronic myeloid leukemia, *BCR-ABL1*-negative, 1575
Atypical lipomatous tumor, 1600
Auer rods, 655, 657f
AUG antibodies, 743
Augustine blood group systems, 743
biochemistry, 743
biological role, 743
molecular biology, 743
Authorship, 179
AUTION HYBRID System, 505
AUTION MAX AX-4030 urinalysis system, 502–503
Autism spectrum disorder (ASD), 1465–1466
Autoadsorption, 761
Autoantibodies, 1011
alloantibodies and, 710
anti-ARS, 1047
anti–liver cytosol type 1, 1086
anti–liver-kidney microsomal type 1, 1086
anti-Mi-2, 1048
antimuscarinic type 3 receptor, 1040–1041
Autoantibodies *(Continued)*
antinuclear, 1086
anti–smooth muscle, 1086
clinically important, 1113t–1114t
to complement proteins, 983
drug-dependent, 763
nonimmunologic adsorption of serum proteins in, 763
reactivity of, with drug-coated cells, 763
reactivity of, with uncoated cells, 763
drug-independent, 763
glutamic acid decarboxylase, 1108–1109
3-hydroxy-3-methylglutaryl-coenzyme A reductase, 1048
induction by drugs of, 628
insulin, 1108, 1109f
insulinoma-2-associated, 1109
insulinomimetic insulin receptor, 1110
islet cell cytoplasmic, 1108, 1108f
MDA5 (CADM-140), 1048
MJ/NXP2, 1048
myositis-associated, 1049
other, 1086–1087
as predictors of disease, 1078–1079
profile of, in systemic lupus erythematosus, 1037–1038, 1037t
rheumatoid arthritis, 1044, 1045t
signal recognition particle, 1048
small ubiquitin-like modifier activating enzyme (SAE), 1048
techniques used to detect
cell-based assays, 1057
computer-assisted ANA IFA technology, 1050
dot blots and line immunoassays, 1056
double immunodiffusion analysis, 1057
enzyme-linked immunosorbent assays, 1056
general considerations, 1049–1050
immunoblotting, 1056, 1056f
indirect immunofluorescence in HEp-2 cells, 1050, 1051f–1054f, 1055t
multiplex bead-based assays, 1056–1057
to nuclear and intracellular antigens, detection methods of, 1050, 1050t
thyroglobulin, 1110
thyroid gland relating to, 401
thyroperoxidase, 1110, 1110f
TIF1-γ/TIF1-α(P155/140), 1048
zinc transporter-8, 1109, 1109t
Autoantigens
centromere protein, 1042
Th/To, 1043–1044
Autoanti-P, 762
Autohemolysis test, 605
Autoimmune diseases, organ-specific, 1074–1114.e6, 1076b
application of testing to, 898
autoantibodies, as predictors of disease, 1078–1079
autoimmunity versus, definition of, 1074–1075, 1075f
classification of, 1075–1076
cutaneous, 1079–1084, 1079b, 1080t
dermatitis herpetiformis, 1082–1083, 1083f
epidermolysis bullosa acquisita, 1082, 1083f
linear IgA dermatosis, 1082
paraneoplastic pemphigus, 1081
systemic lupus erythematosus, 1102, 1105
vasculitis, 1083–1084
vitiligo, 1084
endocrinopathies, 1111–1112
gastrointestinal, 1084–1089
celiac disease, 1085
hepatic and hepatobiliary, 1086–1089
inflammatory bowel disease, 1085–1086
pancreatitis, 1089
pernicious anemia, 1084–1085, 1084f
glomerular, 1089–1107
glomerulonephritides, 1093–1107
glomerulopathies, 1090–1093
injury, mechanisms of, 1089–1090
renal biopsy, approach to, 1090
immunoendocrinopathies, 1108–1112
Addison disease, 1111
carbohydrate metabolism, 1108–1110
laboratory tests for evaluating, 1076–1077, 1077f
of muscle, 1112–1113
of nervous system, 1112–1113
Eaton-Lambert myasthenic syndrome, 1112
multiple sclerosis, 1112
myasthenia gravis, 1112
paraneoplastic neurologic syndromes, 1112
polymyositis, 1113
Stiff-Person syndrome, 1112–1113
Autoimmune diseases, organ-specific *(Continued)*
of neuromuscular junction, 1112–1113
of ovary, 1111
recent advances in diagnostic technologies, 1078
serum autoantibody levels in, interpretation of, 1077–1078
pemphigoid, 1081–1082
pemphigus, 1079–1081
therapeutics for, 899
thyroid gland, 1110–1111
Autoimmune hemolytic anemia (AIHA), 625–626, 626t
associated with warm and cold antibodies, 626
associated with warm antibody, 626
cold, 761–762, 762t
cold agglutinin disease and, 761–762
paroxysmal cold hemoglobinuria and, 762
etiology and pathophysiology of, 625
investigation of, 760–762
warm, 760–761
serologic characteristics of, 761
serologic testing beyond the DAT of, 761
Autoimmune hepatitis, 1087–1088, 1087f, 1087t
prognostic relevance of autoantibodies in, 1087–1088
Autoimmune hypoglycemia, 1110
Autoimmune lymphoproliferative syndrome, 645
Autoimmune markers, 322–323
ANCA, for primary sclerosing cholangitis, 322–323
antimitochondrial antibody, for primary biliary cirrhosis, 322
serum, for hepatitis, 323
Autoimmune myelofibrosis, 637
Autoimmune-related hypoglycemia, 236
Autoimmune thrombocytopenia, 769
Autoimmune thyroid disease (AITD), treatment of, 1111
Autoimmunity, 1075, 1075f
adrenocortical, 1111
autoimmune diseases versus, definition of, 1074–1075, 1075f
Autologous cells, separation of transfused red cells from, 759–760
Autologous donation, 773
Autologous versus allogenic hematopoietic progenitor cell harvest, 795
Automated chemistry analyzer, core components of, 76–77
Automated delivery, 75
Automated differential leukocyte counting, 550–551
Automated reticulocyte counting, 551
Automated specimen inspection, 75
Automated specimen processing, 75
Automated system, selection of, 1171
Autosomal aneuploidies, 1427–1428, 1428f
Autosomal dominant hypercholesterolemia, 263–264
Autosomal recessive hypercholesterolemia, 263–264
Autosome, definition of, 1411
Avidin, 446

B

Babesia species, 1304–1309, 1309f–1310f
Babesiosis, 786, 1304–1309, 1309f–1310f
Bacillary angiomatosis, 1263–1264, 1263t
Bacilli. *See* Medical bacteriology
Bacillus, 1139–1141, 1140f
antimicrobial susceptibility of, 1140–1141
characteristics, 1139
clinical manifestations and pathogenesis of, 1139–1140
laboratory diagnosis of, 1140, 1140f
prevention of, 1141
Bacteremia, blood specimen timing for, 1353–1354
Bacteria, 498, 498f. *See also* Medical bacteriology.
Bacterial contamination, of blood components, 782–783
Bacterial culture, from CSF, sample processing of, 1356
Bacterial meningitis, 521, 521f
Bacterial pathogens, in feces, 1363–1364
Bactericidal testing, of antimicrobial agents, 1170
Bacteriology. *See* Medical bacteriology
Bacteriuria, 483–484
Bairnsdale ulcer, 1186
Balances
specifications for, 55
types of, 54
Balance sheet, 170
Balantidium coli, 1322–1323
Banding pattern, 1414
Bandpass, 39
Bannwarth syndrome, 1239

B antigen, 711
Barbiturates, sedative-hypnotics, 362
Barcoding, 154–155, 155f
Bare lymphocyte syndrome, 1005
Barrett esophagus, 1616–1617
Barrier layer cell, 41
Bartonella, infections caused by organisms of, 1254, 1263–1264
Bartter's syndrome, 106t, 107
Basal hormone measurements, 419
Basic fibroblast growth factor, 1529
Basophilia, 641, 642f, 642b
Basophils
  mast cells and, 580–581, 896
    distribution and kinetics of, 581
    function of, 581, 581b
    morphology of, 580–581, 581f
Bassen-Kornzweig syndrome. *See* Abetalipoproteinemia
Bayes theorem, 94, 95t
B cell ALL, 1547
B cell development: bone marrow, 583–584, 584f
B cell lymphoblastic leukemia/lymphoma, 1547
B cell lymphoma, unclassifiable, 676
  with features intermediate between DLBCL and Burkitt lymphoma, 676
  with features intermediate between DLBCL and classical Hodgkin lymphoma, 676
B cell prolymphocytic leukemia, 665, 667f
B cell responses, in cellular immunity, 933, 933f
BCL1 gene, 1552
BCL2 gene, 1551
BCL10 proteins, 1552
BCR-ABL1 fusion gene, 1547–1549, 1568–1569
BCR-ALB fusion gene, 1501
BD Vacutainer, 31
Bead arrays, 1382–1383
Bead-based antibody capture assays, 766–767
Bedbugs, 1346f, 1347
Beer-Lambert law, 37–38, 37f, 38b
Beer's law, 454
Bees, 1347
Beetles, 1347
Belmont Report, 175–176, 175b
Bence Jones proteinuria, 475
Benchmarking and productivity measures, 171, 171t
Benign pediatric viral exanthems, 1278
Benzodiazepines, 361
Bernard-Soulier syndrome, 858
Bernard-Soulier syndrome (BSS), 852f, 853, 858
Beta-2 microglobulin, 191
Beta trace protein, 191
Bicarbonate and CO_2 buffer system, 201
Bicarbonate ions (HCO^{3-}), 459
Bile salts, tests for, 318
Biliary obstruction, 316
Bilineal acute leukemia, 662, 694–695
Bilirubin, 314–317, 456–457, 535
  casts, 493
  conjugated, elevated serum levels of, 316
    biliary obstruction, 316
    Dubin-Johnson syndrome, 316
  derangements of, 316
  laboratory tests for, 316–317
  metabolic functions of, 314–317
  methemoglobin and, 519
  normal bilirubin metabolism, 314–316, 315f
  unconjugated, elevated serum levels of, 316
    Gilbert's syndrome and Crigler-Najjar syndrome, 316
    hemolysis, 316
  in urine, 482–483, 482t
Bilirubinuria, 482
Binding specificity, 291–292
Biochemical and clinical correlations, of cirrhosis, 329
Biochemical identification, 1204, 1204t
Biochemical markers
  of bone metabolism, 208–224.e2
  of bone remodeling, 219–221
Biochemistry
  nucleic acid, 1373–1379
  and physiology
    of acetylcholinesterase (EC 3.1.1.7) and butyrylcholinesterase (EC 3.1.1.8), 310
    of acid phosphatase (EC 3.1.3.2), 305–306
    of alkaline phosphatase (EC 3.1.3.1), 306
    of angiotensin-converting enzyme (EC 3.4.15.1), 308
    of lactate dehydrogenase (EC 1.1.1.27), 311
Biocompatibility, complement relating to, 980
Bioinformatics, 1406–1407, 1407f
Bio-intact PTH, 212–213
Biological drugs, 899
Biological hazards, clinical laboratory and, 10–11
Biological variation, in blood sampling and storage, 252
Biology
  cell, mitogenesis and, 1525
  normal platelet, 847–849
  of von Willebrand factor, 864–865, 864f
Biomarkers, of acute kidney injury, 192–193, 192t
BIOMIC System, 1169
Biomolecule database building, 68
Biosimilar drugs, 899
Bioterrorism, rickettsiae, as agents of, 1257
Biotin, 445
Biphenotypic acute leukemia, 694–695
Bipolar disorder, 1456–1459, 1457t
  calcium channel protein, 1457
  copy number variants in, 1458
  neural development and nerve transmission, protein for, 1457–1458
  neuronal stability, protein involved in, 1458
  pharmacogenomic studies, 1458
  proteins with other functions, 1458
  and schizophrenia, 1459
  transcription and cell cycle regulation, protein for, 1458
Bisalbuminemia, 281, 282f
Biuret method, 280
Bivalirudin, 885
Black Death. *See* Plague
Black grains, 1219
Black-top tubes, anticoagulants and additives, 27–28, 27t
Bladder cancer, 1581t–1583t, 1596
  nuclear matrix proteins in, 1535–1536
  p53 protein in, 1534
Bladder tumor antigen, 1536
Blastic plasmacytoid dendritic cell neoplasm, 662
Blastocystis hominis, 1319
Blastocystis spp, 1318f, 1319
Blastomycosis, pathology of, 1213, 1214f
Blast phase, 646
Bleeding time, 849
Blood
  banking of, complement system and, 710–711
  and bone marrow, examination of
    blood film examination, 551–563
  collection of, tubes for, inhibitory compounds in, 300
  culture systems of, 1354
    automated, 1354
    manual, 1354
  enzymes in, lifetime of, 294–295
  fecal occult testing of, 343
  hematology principles and procedures, 540–551
  hemoglobin, hemosiderin, and myoglobin, in urine, 479–482
  lead in, 384
  loss, as mechanism of injury, 1344
  manual cell counts of, 544–549
  for medical parasitology, examination of, 1301–1326
    concentration techniques in, 1293–1294
    thick and thin blood films, 1293, 1293f
  megakaryocytes in, 583, 583f
  in newborn feces, 343
  sampling and storage of, 252–253
  specimen of, for diagnosis of infectious diseases, 1353–1355
    automated blood culture systems, 1354
    bacteremia and fungemia, timing for detection of, 1353–1354
    collection of, 1353
    microorganisms in, recovery of, 1354
    parasites in, detection of, 1355
    positive cultures in, detection and notification of, 1354–1355
    specimen draws, 1354
    timing, 1353–1354
    viruses in, detection of, 1355
    volume of, 1353–1354
  stains of, 551–552
  thick and thin blood films, for medical parasitology, examination of
    slides for, preparation of, 1293, 1293f
    smears, examination of, 1293
    staining of, 1293
  and tissue protozoa, for medical parasitology, 1301–1326
    babesiosis, 1304–1309
    hemoflagellates, 1309–1312
    malaria, 1301–1304
    opportunistic free-living amebae, 1313–1315, 1314f
    toxoplasmosis, 1312–1313
Blood banking, 771
Blood cell distribution width, red, 102
Blood collection
  devices, 29
  overview of, 27–29
  techniques, 29–31
  and transfusion medicine, 771–773
  tubes for, inhibitory compounds in, 300
Blood components
  bacterial contamination of, 782–783
  manufacture of, 773–775
    cryoprecipitated antihemophilic factor, 774
    leukocyte components, 774
    leukocyte-reduced blood components, 774
    pathogen reduction, 775
    plasma, 773–774
    platelet concentrates, 774
    red blood cells, 773
    special components, 774–775
  selection of, 775–776
    platelets, 776
    red blood cells, 775–776
Blood component therapy, 777–779
  cryoprecipitate transfusion, 779, 779b
  plasma transfusion, 779, 779b
  platelet transfusion, 778–779, 778b–779b
  red cell transfusion, 777–778
Blood film
  examination of, 551–563
    making and staining of, 551–552
  leukocytes on peripheral blood smear examination, 547t, 557–561
  Spinner method of, 551
Blood gas abnormalities, 110–111, 110t
Blood group alloantibodies and autoantibodies, 710
Blood group antibodies, blood group alloantibodies and autoantibodies, 710
Blood group antigens, 709
  antigen, density, 709, 709t
  chemical characteristics, 709
  immunogenicity, 709, 709t
Blood loss anemia, 603
Blood storage, and preservation, 29
Blood urea nitrogen (BUN), 108, 462
Bloody CSF, differential diagnosis of, 512
B lymphoblastic leukemia/lymphoma, 663–664, 664f
  BCR-ABL1- Like, 664
  clinical features of, 663
  cytogenetics of, 663
  with hyperdiploidy, 664
  with hypodiploidy, 664
  with iAMP21, 664
  marrow in, 663
  not otherwise specified, 664
    precursor T lymphoblastic leukemia/lymphoblastic lymphoma, 664
  with t(9;22)(q34;q11.2);BCR-ABL1, 663
  with t(1;19)(q23;p13.3); E2A-PBX1, 663
  with t(5;14)(q31;q32); IL3-IGH, 664
  with t(v;11q23); MLL rearranged, 663
  with t(12;21)(p12;q22); TEL-AML1 (ETV6-RUNX1), 663
B lymphocytes, 895
Body fluid(s)
  chemical measurements in, 537–538
  composition of, 184–185
    extracellular, 184, 184b
    intracellular, 184–185, 184b
  osmolality of, 182–186
    plasma, measurement of, 185–186
    specific gravity and, 186
  specimens of, 1355–1357
  urine and, 31–33
  volume of, 182–186, 184b
    measurement of, 183
Bone
  hemangioma of, 1601
  infection of, *Cryptococcus* in, 1209
Bone allografts, 819
Bone banking, 819
Bone formation markers, 220–221
Bone marrow, 822
  B cell development relating to, 583–584, 584f, 584t
  infiltration of, anemia associated with, 598–599
  natural killer cell relating to, 585–586
Bone metabolism, biochemical markers of, 208–224.e2
  bone remodeling, biochemical markers of, 219–221
  metabolic bone disease, 221–224
  mineral and bone metabolism, 208–215, 209f
Bone remodeling, biochemical markers of, 219–221

Bone resorption markers, 220
Bordetella, 1155–1156
  antimicrobial susceptibility of, 1156
  characteristics, 1155–1156
  clinical manifestations and pathogenesis of, 1156
  laboratory diagnosis of, 1156
Bordetella pertussis, 642
Borrelia, 1237–1244
Bottom-up proteomics, 67–68
Bound/fixed separation and washing systems, 920
Boutonneuse fever, 1256
Bradykinin, 983
BRAF, mutations, 1501
BRAF gene mutation, 1586
  in colorectal cancer, 1591
  in melanoma, 1599
BRAF inhibitors, 1501
BRAF V600E mutation, 1586
Brain tumor, 1580–1583
Branched DNA, 1399
BRCA1, in ovarian cancer, 1599
BRCA2, in ovarian cancer, 1599
Breakage syndromes, 1431, 1432t
Breakeven point, 171
Breakpoint cluster region (bcr), 1378–1379
Breakpoint heterogeneity, 1550, 1552–1553, 1558, 1569–1571
Breakpoints, 1166–1168
Breast cancer, 1583–1586, 1619
  anti-c-myc protein in, 1535
  hereditary, 1585–1586
  p53 protein in, 1534
  protein arrays for, 1538
  protein array to, 1538
  sporadic, nonhereditary, 1583–1585, 1584f–1585f
Breast implant–associated anaplastic large-cell lymphoma, 682–683
Breast-ovarian cancer, hereditary, 1447
Breathalyzer testing, 381
Breath testing, 537
Bright-field microscopy, 487
  supravital stain reagents for, 487
    procedure of, 487
Bring your own device (BYOD), 159
Broad casts, 493
Brodifacoum, 882
Bromocresol green (BCG), 280
Bronchiolitis, RSV, 1266, 1268
Bronchoscopy specimens, 1360, 1360f
Broth macrodilution method, 1168
Broth microdilution method, 1168
Brucella species, 1156–1157
  antimicrobial susceptibility of, 1157
  characteristics, 1156
  clinical manifestations and pathogenesis of, 1156–1157
  laboratory diagnosis of, 1157
Brugia malayi, 1339–1340, 1339f
Budding, 1195
Budgeting, 169, 170t
Buffer zone, 1168
Bullae, specimens of, 1365
Bullous lupus erythematosus, 1082
Bullous pemphigoid, 1081, 1082f
BUN. *See* Blood urea nitrogen (BUN)
Buprenorphine, 360
Burkholderia
  antimicrobial susceptibility of, 1149
  characteristics, 1148
  clinical significance and pathogenesis of, 1148
  laboratory diagnosis of, 1148–1149
Burkitt lymphoma, 675–676, 676f, 1554–1555
"Burning feet syndrome", 445
Buruli ulcer, 1186
Busulfan, 379
Butterflies, 1347
Butyrylcholinesterase (EC 3.1.1.8). *See* Acetylcholinesterase (EC 3.1.1.7) and butyrylcholinesterase (EC 3.1.1.8)
β-VLDL ("floating β" lipoprotein), 248
  detection of, 257
BYOD. *See* Bring your own device (BYOD)
Bystander effect, 1620

C

CA 72-4, 1517
CA 125, 1516–1517
CA 15-3 and CA 27.29, 1516
CA 19-9, CA 50 and CA 19-5, 1516
CACNA1A gene, 1454–1456
CACNA1I, 1456
CACNB2, 1456
CADM2 (Cell adhesion molecule 2), 1460
CADPS (calcium-dependent activator protein for secretion), 1466
Calcitonin, 213–214, 404, 404t, 1517
Calcium, 208–210, 457
  albumin and, 109–110
  analytic techniques for, 210
  determinations, ion-selective electrodes for, 457
  mobilization, defects in, and platelet signaling pathways, 860
  phosphate and, 109
  physiology of, 208–210
  reference interval for, 210
  total and ionized, 210
Calcium carbonate, 496
Calcium channel proteins, 1454–1457
Calcium homeostasis, 209–210, 209f
Calcium mobilization pathways, 1454, 1455f
Calcium oxalate dihydrate crystals, 525
Calcium oxalates, 495–496, 495f–496f
Calcium pyrophosphate dihydrate (CPPD) crystals, 525, 525f
Calcium stones, hypercalciuria and, 506
Calcofluor white stain, for examination, 1202–1203, 1202f, 1202b
Calculi, 505–507
Calibration
  issues in quality control, 131–132, 131f
  for measurement of mass, 54–55
  of pipet, 55–56
  of thermometer, 56–57
  verification of, 131–132
  of volumetric glassware, 56
Calibrator, new lot of, verifying method performance of, 143
Calmagite, 458, 458f
CALR gene, 1573
CALR mutations, 1572f, 1573–1574
Calymmatobacterium granulomatis
  antimicrobial susceptibility of, 1159
  characteristics, 1159
  clinical manifestations and pathogenesis of, 1159
  laboratory diagnosis of, 1159
CAMKMT gene, 1463
Campylobacter
  antimicrobial susceptibility of, 1151
  characteristics, 1150, 1150f
  clinical manifestations and pathogenesis of, 1150–1151
  laboratory diagnosis of, 1151
Canalicular injury, enzyme relating to, 321–322
Cancer
  cell-free nucleic acid testing, in, 1521
  chemotherapy for, pharmacogenomics in, 1496–1501
    5-fluorouracil, 1496–1497, 1497f
    irinotecan, 1497–1499, 1498f
    tamoxifen, 1499–1501, 1500f
    thiopurines, 1496
  colorectal, hereditary syndromes of, 1447
  detection of, molecular pathology's application to, 1370–1371
  diagnosis of, multiple oncoprotein markers for, 1536–1541
  familial, 1445–1448, 1446t, 1448f
  genetics, 1425–1427, 1426t, 1427f
  and immune response, 940
  immunotherapy, use of dendritic cells in, 824
  mini-arrays in detection of, 1537
  prostate
    serum markers for, 1518–1520
    urine markers for, 1523–1524
  of unknown primary, 1604
"Candidatus *Neoehrlichia mikurensis*", human infections caused by, 1260
Candidiasis, 1207–1211
Cannabis. *See* Marijuana (Cannabis)
Capecitabine, 1496–1497, 1497f
Capillaria hepatica, 1342
Capillaria philippinensis, 1328
Capillariasis, 1342
Capillary electrophoresis, 52, 52f, 279, 608, 609f
Capital acquisition methods, 172–173, 172t
Capital budget, 169
Capital project, evaluating of, 171–172, 172t
Capnocytophaga
  antimicrobial susceptibility, 1159
  characteristics, 1158
  clinical manifestations and pathogenesis of, 1158–1159, 1159f
  laboratory diagnosis, 1159
Captopril, 308
Carbamates, 384–385
Carbamazepine (Tegretol), 367t, 370–371, 1022, 1495
Carbamylation, 1046
Carbapenemase-producing carbapenem- resistant Entero-bacteriaceae (CP-CRE), 1176
Carbapenemase-producing organisms (CPO), 1176
Carbapenem-resistant *Enterobacteriaceae* (CRE), 1176
Carbohydrate antigen 19-9 (CA 19-9), 344
Carbohydrate metabolism
  autoimmune disorders of, 1108–1110
  inborn errors of, 238–243, 239t–241t
    disorders of gluconeogenesis, 238–242
    fructose metabolism in, defects in, 242–243
    galactose metabolism in, defects in, 242
    glycogen storage diseases, 238
    lactic acidosis, 242–243
Carbohydrates, 225–243.e3
  diabetes mellitus and, 229–234, 229t–230t
  endocrine pancreas and, functions of, 226–228
  glucose measurements and, 228–229
  hypoglycemia and, 234–238, 235b
Carbon monoxide (CO), 380–381
Carbon-13-urea breath test, 537
Carboxyhemoglobin, 541
Carcinoembryonic antigen (CEA), 344, 520–521, 536, 1516
Carcinogens, environmental, 380
Carcinoid syndrome, 345
Cardiac function tests, 113–114
Cardiac glycosides, 367–368
Cardiac injury, atherosclerosis, thrombotic disease, 267–275.e2
  background of, 267–269, 268t, 268b
  congestive heart failure, markers of, 273–275
  coronary risk, markers of, 272
  myocardial damage, markers of, 269–270
    assay procedures, 270
    cardiac troponin, 269–270
    clinical protocols, 270–273
    historical development, 269
    other markers—copeptin, 270
  other conditions associated with, 275
  overview in, 267, 268b
Cardiac natriuretic peptides, 273–275, 274f
Cardiac troponin, 269–270
Cardiac valves, 820
Cardiac valvular disease and prostheses, 624
Cardiobacterium hominis, 1154
  antimicrobial susceptibility of, 1154
  characteristics, 1154
  clinical manifestations and pathogenesis of, 1154
  laboratory diagnosis of, 1154
Cardiotropics, 366–369, 367f
Cardiovascular diseases, 980
Carrier, screening, 1436
Carryover, 920
Cartilage oligomeric matrix protein (COMP), 832
Cartwright antibodies, 733
Cascade reporting, 1180
Case reports, 176
Cash flows, statement of, 170–171
Casts, 490, 490b
  broad, 493
  cellular, 491–492
  inclusion, 492
  pigmented, 492–493
Catalysis, 291
  enzyme, molecular basis of, 292–293, 293f
Catalytic antibodies, new, with predetermined enzyme activity, 304–305, 305f
Catalytic efficiency, 302–305
  high rate enhancements in, 303
  high rates of reactions in, 302
  transition state theory in drug design for, 303–305, 303f
Cathinones (bath salts), 363
β-Catenin gene *(CTNNB1)*, 1589
Cation-exchange chromatography, 279
Cation-exchange high-performance liquid chromatography (HPLC), 608, 609f
C-banding, 1414
C3b/C4b inactivator, 973
CBFB-MYH11 gene fusion, 1560

CBF transcriptional regulatory pathway, 1560
C8-binding protein, 974
CBL gene, 1565
C2, C4, CFB genes
  disease associations with, 1017
  and typing, 1016–1017
CCHF. *See* Crimean Congo hemorrhagic fever (CCHF)
CCND1 gene, 1555
C3: complement activation pathways, central molecule of, 970, 971f
CD20, 700
CD59 antibodies, 743
CD147 antibodies, 740
CD34 antigen, 821
CD59 blood group systems, 743
  biochemistry and molecular biology, 743
CD36 deficiency, 769
CD4, expression of, 699–700
CD10, expression of, 699
cDNA microarrays, 1404
CEBPA mutations, in acute myeloid leukemia, 1561
Celiac disease, 341–342, 342t, 1020–1021, 1085
Cell adhesion molecule 2 (CADM2), 1460
Cell adhesion molecules, 992–993, 993t
Cell adhesion proteins, 1460
Cell-associated regulatory proteins, 973–974
Cell-based assays, 1057
Cell culture, 1250
Cell cycle, 938f
Cell DNA testing, for cancer, using fluorescence in situ hybridization, 1522–1523
Cell free DNA (cfDNA), 484
Cell-free nucleic acid testing, in cancer, 1521
Cell growth pathways, 1454
Cell lysis syndrome, 313
Cells
  abnormal, formed elements and, 497–499
  biology of, mitogenesis and, 1525
  culture of, of chromosomes, 1412–1413, 1413f
  and mediators, of immediate hypersensitivity reactions, 1119f
  proliferation of, oncoproteins for, 1509–1510
Cell surface markers, additional, 1032
Cell surface receptors, 1032
Cellular casts, 491–492
Cellular detection, of class II molecules, 1009
Cellular immune defects, infections associated with, 1026f
Cellular immune system, laboratory evaluation of, 929–951.e7
  cellular immunity, flow and image cytometry in evaluation of, 933–936
  cellular immunology, general principles of, 930–933
    B cell responses, in cellular immunity, 933, 933f
    lymphocyte activation and proliferation, 930–931
    signal transduction, following antigen-specific stimulation, 931
    T cell recognition, activation, and signal transduction, 931
    T cell responses, 932–933
  gating and data analysis, 936–939
    DNA analysis, 937–939
    immunophenotypic analysis, 936–937
    quantitative flow cytometry, 939
  granulocyte and monocyte function, 946–949
  lymphocyte function, 943–946
  methodologic approach, 940–943
  quality control and quality assurance, 949–950
Cellular immune system, testing of clinical interpretation of, 939–940
  methodologic approach to, 940–943
  significance of, 939–940, 939b
  stages of
    analytic immune studies, 942–943, 942b
    confirming, 941–942, 942b
    screening, 941, 941f, 942b
Cellular immunity, 897–899
  B cell responses in, 933, 933f
  flow and image cytometry, 933–936
Cellular immunology
  DNA studies relating to, 939
  general principles of, 930–933
Cellular maturation, abnormal, types of, 651, 652f
Center for International Blood and Marrow Transplant Research (CIBMTR), 821
Centipedes, 1350
Central molecule, of complement activation pathways, 970, 971f
Central nervous system, infection of, *Cryptococcus* in, 1209
Central or class III region, genes in, 1015–1017, 1015f
Central tendency, 120–121
Central venous access devices (CVADs), 30–31
Centrifugation phase, of specimen processing, 34
Centromere protein autoantigens, 1042
Cerebrospinal fluid (CSF), 32–33, 510–522
  bloody, differential diagnosis of, 512
  chemical analysis of, 515–521, 516t
    proteins, 515–519, 516t
  collection of, specimen, opening pressure and, 510–511
  examination for
    gross, 511–512
    microbiological, 521–522, 521t
    microscopic, 512
  indications and recommended tests for, 511, 511b
  oligoclonal immunoglobulin bands in, 963–964, 965f
  specimen, 1355–1356, 1355t
    bacterial and fungal culture from, sample processing for, 1356
    collection and transport of, 1355, 1356t
    diagnostic tests for, 1356, 1356f
    viral and parasite infections in, diagnosis of, 1356
Cerebrovascular accident, 275
Ceruloplasmin, 285–286, 319, 449–450
Cerumen, 537
Cervical cancer, 1581t–1583t, 1597–1598
Cervista HPV HR, 1598
C1 esterase inhibitor, 287
Cestodes, 1330–1335, 1342–1344
  coenurosis, 1344
  cysticercosis, 1342
  Diphyllobothrium spp., 1333–1334
  Dipylidium caninum, 1334–1335
  hydatidosis, 1342–1343
  Hymenolepis diminuta, 1332–1333
  Hymenolepis nana, 1332
  sparganosis, 1344
  Taenia saginata, 1331–1332
  Taenia solium, 1332, 1342, 1343f
Cetuximab, 1126, 1501
CF. *See* Cystic fibrosis (CF)
CFTR. *See* Cystic fibrosis transmembrane conductance regulator (CFTR)
CFU. *See* Colony-forming units (CFU)
C3 glomerulopathy, 1096–1097
Chain of custody, 354
α-Chain variants, 615
β-Chain variants, 614–615
Charge-transfer devices, 42
Check cells, 748
Check-Points assays, 1177
Chédiak-Higashi syndrome, 639, 1031
Chemical agents, acquired, extrinsic hemolysis relating to, 623–624
Chemical analysis
  of CSF, 515–521, 516t
  of pericardial fluid, 532–533
  of peritoneal fluid, 535–536
  of pleural fluid, 529–531
  of synovial fluid, 526, 526t
Chemical basis, for analyte assays and common interferences, 453–466.e1
Chemical hazard(s)
  clinical laboratory and, 11
Chemical ionization, 62
Chemical measurements, in body fluids, 537–538
Chemical precipitation, selective, 256
Chemical profiling, 65
Chemicals, 53
Chemical screening, of urinalysis, 472–486, 473b
  acid urine, 473
  alkaline urine, 473
  methods of, 473
    pH electrode, 473
    reagent strip, 473
    urine, titratable acidity of, 473
  normal pH, 473
  tests for, 484–486
  urine pH, 473
  urine, protein in, 473–476
Chemiluminescence, 44
Chemiluminescent enzyme immunoassay (CL-EIAs), 912–913, 913f
Chemiluminescent immunoassay, 919
  acridinium esters as labels used for, 919, 919f
  background of, 919
  electrochemiluminescent, 919
Chemistry
  conjugation, 903–904, 904f
  point-of-care testing in, 83–84
  serum, 507
Chemistry analyzer, automated, core components of, 76–77
Chemistry automation, continuum of, 77
Chemokine, 988–992, 989t
  atypical receptors, 990–992
  receptor homologues, 992
Chemokine-based therapeutics, clinically useful, 989–990, 990t
Chemotherapeutic agents, 379
Chemotherapy, cancer, pharmacogenomics in, 1496–1501
  5-fluorouracil, 1496–1497, 1497f
  irinotecan, 1497–1499, 1498f
  tamoxifen, 1499–1501, 1500f
  thiopurines, 1496
Chido/Rodgers antibodies, 736
Chido/Rodgers blood group system, 736
  biochemistry/molecular biology, 736
  biological role, 736
Chikungunya virus (CHIKV), 1286–1287
Childhood
  cytogenetics in, 1425
  EBV-positive T cell lymphoproliferative disorders of, 677
  hypoglycemia in, 236–238
  leukemias in, 1550
  myelodysplastic syndromes of, 654–655
Children, high cholesterol in, 260, 260t
Child-Turcotte-Pugh score, 329
Chilomastix mesnili, 1321
Chimeric antigen receptors, 824–825
Chimeric antigen receptor T-cell (CAR T-cell) therapy, 899
Chi-square test, 124–125, 125t
Chlamydial infections, 1246–1250, 1247t
  classification, 1246
  differentiating species of, 1246, 1247t
  laboratory diagnosis of, 1249–1250
  replication of, 1246–1247
  structure of, 1246
  treatment of, 1250
Chlamydia psittaci, 1248
Chlamydia trachomatis, 1247–1248
  clinical manifestations, 1247–1248
  detection of, 1249t
  epidemiology, 1247–1248
  LGV, 1247, 1250
  non-LGV, 1247, 1249–1250
  pathology, 1247–1248
Chlamydophila, 1247t, 1248–1249
Chlamydophila pneumoniae, 1248–1249
  clinical manifestations, 1249
  epidemiology, 1249
  laboratory diagnosis, 1250
  pathogenesis, 1249
Chlamydophila psittaci, 1248
  clinical manifestations, 1248
  epidemiology, 1248
  laboratory diagnosis, 1250
  pathogenesis and pathology, 1248
Cholangiocarcinoma, 1589
Cholangiocellular, 1589
Cholangiolar, 1589
Cholecalciferol. *See* Vitamin D
Cholesterol, 253, 459–460, 535
  HDL, 460
  high
    in children, 260, 260t
    with high LDL-C, 260
    with high triglycerides, 264–265
    triglyceride and low HDL, 265–266
  LDL, 460
  lipoprotein, estimation of, 254–255
  low total, and triglyceride, 265
  normal, high triglycerides with, 264
  quinoneimine strategy, 460
  testing and management of, guidelines for, 258–260, 258t, 258b–259b
  tests for, 317–318
Cholesterol 7-alpha-hydroxylase deficiency, 265
Cholesterol crystals, in synovial fluid, 526, 526f
Cholesteryl ester transfer protein gene defects, 266
Choline transporter-like protein 2 (CTL2/SLC44A2), 744
Chopper, in double-beam spectrophotometer, 42

Chromatin remodeling genes, fusion genes involving, 1601
Chromatographic techniques, for drug detection, in serum and urine, 348–353
  high-performance liquid chromatography, 350–352, 352f
  reliability of, 350
  specific drugs, identification of, 350, 351f
  thin-layer chromatography, 348, 350f
  toxi-lab procedures, 348–350
Chromatography, 49–51, 49f
  gas, 50, 50f, 352, 353f
  liquid, 50–51, 51f, 350–352, 352f
  thin-layer, 348, 350f
Chromium (Cr), 448–449
Chromoblastomycosis, 1220, 1220f
Chromogenic FVIII assay, 835
Chromogenic test, 1169–1170
Chromogranin A, 1517
Chromomycosis, 1219
Chromophobe tumors, 1595
Chromosomal aneuploidy syndromes, 1427–1429
Chromosomal microarray, 1435
Chromosomes, 1412–1418, 1412f. *See also* Cytogenetics, in modern pathology, applications of.
  abnormalities, 1418–1423
    nomenclature for, 1423, 1424t
    numerical, 1418–1420, 1419f
    structural, 1420–1423, 1421f–1422f
  cell culture of, 1412–1413, 1413f
  computer-assisted imaging of, 1415
  definition of, 1411
  fluorescence in situ hybridization of, 1415–1417, 1416f
  karyotype analysis of, 1414–1415
  microarray technology on, 1417–1418, 1418f
  staining of, 1414, 1414f
  structure of, 1412, 1413f
Chronic active EBV infection of T-and NK-cell type, 677
Chronic discoid lupus, and other cutaneous variants, 1038–1040, 1039f
Chronic eosinophilic leukemia, 649–650, 1577
Chronic familial neutropenia, 637
Chronic fatigue syndrome, 1271
Chronic granulomatous disease, 639
Chronic idiopathic myelofibrosis (CIM), 647
Chronic leukemias, genetic alterations and detection in, 1548t–1549t
Chronic lymphocytic leukemia, 105
Chronic lymphocytic leukemia/small lymphocytic lymphoma (CLL/SLL), 665, 667f, 1553
Chronic lymphocytosis/persistent polyclonal B cell lymphocytosis, 642
Chronic lymphoproliferative disorders, of NK cells, 677
Chronic myelogenous leukemia, 105
Chronic myeloid leukemia (CML), 646, 703–705, 1570f
Chronic myeloid neoplasms, 1567–1575
  chronic neutrophilic leukemia, 1574
  myelodysplastic and myeloproliferative neoplasms, 1574–1575
  myelodysplastic syndromes, 1567–1568, 1568f
  myeloproliferative neoplasms, 1568–1574
Chronic myelomonocytic leukemia, 651–652, 653f, 1574
Chronic myeloproliferative disease unclassifiable, 649
Chronic neutrophilic leukemia, 646–647, 1574
  with *CSF3R* gene mutation, 1574
Chronic passive congestion, 327
Chronic posthemorrhagic anemia, 603
Chronic pulmonary histoplasmosis, 1212
Chronic Q fever, 1261–1262
Chronic T-cell leukemias, 1556
Chylomicron retention disease, 265
Chylomicrons, 246
Chyluria, 471
CI. *See* Confidence interval (CI)
Ciliates, 1322–1326
  Balantidium coli, 1322–1323
Cimetidine-enhanced creatinine clearance, 189
C1-inhibitor and factor H, functional assay of, 982
Circulating anti-p53 antibodies, in tumor detection, 1534–1535
Circulating nucleic acids, in peripheral blood, 1521–1523
Circulating tumor cells, in peripheral blood, 1520–1521
Cirrhosis, 112–113, 327–329, 844
  biochemical and clinical correlations of, 329
  diagnosing and following cirrhosis, fibrosis, and necroinflammation of liver, using serum analytes, 328–329
  primary biliary, antimitochondrial antibody for, 322
Class-discovery methods, 1611
Class I and class II alleles, DNA-based typing of, 1007–1009
Class I and class II molecules
  MHC and, 1032
Classical Hodgkin lymphoma, 683
Classical pathway, 971
Classic trachoma, 1247
Classic treponemal disease, 1230–1233
Class I genes
  expression, regulation of, 1001–1002
  organization of, 1001
  other, 1003
    HLA-E, 1003
    HLA-F, 1003
    HLA-G, 1003
Class II genes
  expression, regulation of, 1005
  linkage disequilibrium, 1004–1005
  organization of, 1003f, 1004
  other, 1005
Class II molecules, 1003–1005
  cellular detection of, 1009
  HLA-DR, HLA-DQ, HLA-DP subregions, 1003–1005
    class II genes, other, 1005
    function of, 1005
    structure of, 1003–1004
Class I molecules—HLA-A, HLA-B, HLA-C subregions, 998–1003
Clearance, concept of, 187–188
Clear cell ovarian carcinoma, 1599
Clear cell renal cell carcinoma, 1595
Clear cell sarcoma, 1600
Cleavase/invader technology, 1397–1399, 1399f
CLIA. *See* Clinical Laboratory Improvement Acts of 1988 and 2003
Client-server model, 159
Clinical and Laboratory Standards Institute (CLSI), 1166–1167, 1179–1180
Clinical chemistry, abnormalities in, 106–116
  blood gas, 110–111, 110t
  cardiac function tests, 113–114
  combined acid- base conditions, 110
  diabetes mellitus, 112
  electrolyte, 106–108, 106f
  endocrine function testing, 114–115, 115t
  glucose, 111–112
  inflammatory conditions, markers for, 114
  liver function tests, 112–113, 112t
  pancreatic function tests, 114
  renal disease, 108–110
  skeletal muscle function, 114
Clinical disease, array technology in, 1408
Clinical enzymology, 291–313.e3
  catalytic efficiency and, 302–305
  enzymes in
    inhibition of, 300–302, 302f, 303t
    kinetics of, 295–300
    properties of, 291–295
    specific, 305–313
Clinical hemostasis, 833–836
  coagulation disorders, approach to patients with, 836
  laboratory evaluation of hemostasis, 833–836
  primary hemostasis, 833
  secondary hemostasis, 833
Clinical laboratories, 61
Clinical Laboratories Standards Institute (CLSI), 154–155
Clinical laboratory
  array technology in, 1408
  general concepts of, 1–12.e1
  hazard(s)
    biological, 10–11
    chemical, 11
    ergonomic, 11
    prevention strategies in, 10t
  human resource management, 5–6
  laboratory design and service models, 6, 7b
  leadership, 2
  quality systems management, 3–5
    Lean, 5
    Quality System Essentials, 5, 5b
    six sigma, 4–5, 5t
    traditional versus TQM thinking, 5t
Clinical laboratory *(Continued)*
  regulation, accreditation, and legislation, 6–10
    CLIA categories, 9b
    governmental agencies, laboratory-related, 8t
    laboratory regulations, 7t
    nongovernmental organizations, laboratory-related, 9t
    record and specimen retention, guidelines, 9t
    states, requiring laboratory personnel licensure, 9b
  safety, 10–11
  strategic planning, 3
    marketing program issues, 4t
    strengths, weaknesses, opportunities, and threats (SWOT) analysis, for new hospital outreach program, 4b
Clinical laboratory automation
  analysis of, 74–80.e1
  evolution of, 74–75, 75b
  in other sections of the lab, 77–79
  planning for, 79, 79t, 79b
  preanalytic and postanalytic, 75–76
    steps of, 75b
Clinical Laboratory Improvement Acts of 1988 and 2003, 81–82
  categories, 7t
  certificates, types of, 82b
Clinical laboratory informatics, 150–161.e1
  artificial intelligence, 157–159, 158f
  barcoding, 154–155, 155f
  database fundamentals, 151–154
    common database operations, 153, 153f
    database deletions, 154
    database insertions, 153
    database updates, 153–154
    data normalization, 153
    key database concepts, 151–152, 151t
    key database structures, 152–153
    single source of truth, 153
    transformational operations, 153
  design, implementation, and maintenance, 151–154
  fundamentals of, 150–151
  laboratory information systems. *See* Laboratory information systems (LIS)
  machine learning, 157–159, 158f
  positive patient identification, 154–155
  positive specimen identification, 154–155
Clinical laboratory testing, rheumatoid vasculitis and, 1072–1073
Clinical mass spectrometry, 60. *See also* Mass spectrometry (MS).
  future perspectives on, 73
  limitation, 73
  workflow of clinical diagnostics, 65f
Clinical practice guidelines, 98, 98b
Clinical protocols, 270–273
Clinical significance, of results, assessment of, 90–92
Clinical signs and symptoms, of immunodeficiency disorders, 1025–1026, 1026f
Clinical trial phases, 178
Clinical use, of calcitonin, 213–214
Clinical viral infectious syndromes, 1266–1289
Clinicopathological correlations, clinical cases with, 116–118
Clinitek Novus Automated Urine Chemistry Analyzer, 502
Clinitek Status+ Analyzer, 500
Clonal hematopoiesis of indeterminate potential, 1576–1577, 1577b
Clone-by-clone sequencing, 1608
Cloned enzyme donor immunoassay, 915–916, 917f
Clonorchis sinensis, 1336–1337, 1336f
Closed reagent systems, 76
Close out of research study, 177
Clostridium difficile-associated diarrhea, 339, 339t
Clot formation, and heparin, 883
Clot retraction, 852
Clotting factors, 319
CLSI. *See* Clinical Laboratories Standards Institute (CLSI)
Clustered regularly interspaced short palindromic repeats (CRISPR), 1620–1621
Clusterin (CLU), 1465
CMV reactivation, 1284
c-myc proteins, 1533–1535
CNVs. *See* Copy number variants (CNVs)

Coagulation disorders, 105–106
acquired coagulation disorders, 843–845
acquired coagulation protein inhibitors and lupus anticoagulant, 845
disseminated intravascular coagulation, 843–844, 844t
liver disease, 844
massive transfusion, 845
vitamin K deficiency, 844–845
approach to patients with, 836, 837t
hematologic disorders and, pregnancy with, 439
screening tests for, 835, 836f
differential diagnosis of, 837t
Coagulation factor assays, 835
Coagulation factors
deficiency of, 105
elevation of levels of, 875
Coagulation, fibrinolysis and, 827–846.e3
clinical hemostasis, 833–836
coagulation disorders, approach to patients with, 836, 837t
laboratory evaluation of hemostasis, 833–836
primary hemostasis, 833
secondary hemostasis, 833
coagulation disorders, screening tests for, 835, 836f
hereditary coagulation protein defects, 836–843
factor VIII or factor IX, deficiency of, 837–840, 837t
of other coagulation factors, 840–843
physiologic hemostasis, 828–833
anticoagulation protein systems, 831–832
coagulation protein system, 829–830
endothelium, platelets and, 828–829, 829f
fibrin and fibrinolytic system, formation of, 830–831, 831f
hemostatic system, hypothesis for initiation of, 832–833
Coagulation proteins
characterization of, 829–830, 829t, 830f
system of, 829–830
Coagulopathy, and hemapheresis, 816
Coated blade spray, 69f, 71
Cobalamin (vitamin B_{12}), 445
defective absorption of, 593
detecting cause of deficiency, 595
diagnosis of deficiency, 594
lack of availability of, 594
Cobalt (Co), 449
Cobas HPV test, 1598
Cobas u 411 urinalysis test system, 500
Cocaine, 358–359
benzoate ester moiety of, 304–305, 305f
metabolism of, 358–359
Cocci. *See* Medical bacteriology
Coccidia, 1323
Cryptosporidium spp., 1323–1325
Cyclospora cayetanensis, 1325
Cystoisospora belli, 1324f–1325f, 1325
Sarcocystis spp., 1325–1326
Cockroaches, 1347
Codeine, analogs and, 359
Codominant alleles, definition of, 1412
Codons, 1376
Coefficient of variation (CV), 119, 121
Coenurosis, 1344
Cofactors, of enzymes, 293–294, 294t, 296b
Cognitive disorders, pharmacogenomics in, 1502–1503
Cohesin complex, 1567
Coincidence, 690
Cold agglutinin disease, 626–627
Cold agglutinin disease (CAD), 761–762
Collectins, 972
Collection-associated variables, interference with, 24, 24f, 24t
Collection, of specimen, 1267, 1284t
Collision-induced dissociation (CID), 64
Colon, adenomatous polyps of, urine metabolic test for, 1524
Colon cancer
inherited, due to *MYH* inactivation, 1593
p53 protein in, 1534
ras-p21 protein in, 1532
Colonic cancer syndrome, hereditary, 1592–1593
Colony-forming assays, 821
Colorectal cancer, 1590–1593
anti-p53 in, 1535
combined oncogene marker proteins in, 1535
hereditary nonpolyposis, 1592–1593, 1592t
hereditary syndromes of, 1447
Colorimeter, 42
Colorimetric enzyme immunoassay, 912
Colton antibodies, 735
Colton blood group system, 735
biochemistry, 735, 735f
biological role, 735
molecular biology, 735
Column agglutination technologies, 752
Column separations, 279
Combined DNA Index System (CODIS), 1468–1469
Commercial automated instrument systems, 1170–1171
Comparative statistics, 122–124
Compatibility testing, 748–751, 750t
ABO grouping in, 750–751
discrepancies in, 750–751, 751t
of donors, 750
of recipients, 750
documentation and record keeping of, 749–750
check of previous records in, 750
general considerations in, 749–750
in emergencies, 755
specimen requirements of, 748–749
age of sample as, 749
appearance as, 749
recipient sample identification, 748–749
sample storage as, 749
type of sample as, 749
Compensation, 691, 692f
Competitor, 1611
Complement, 285, 896–897
acquired immunity and, 975
action regulation of, 973–974, 973t
activity of, in disease, 977–978, 977t–978t
assays of, 981–983
biosynthesis relating to, 974
clinically useful inhibitors, 981
in disease states, 978–981
evaluation of, 1030
genetics and, 974–975, 975t
levels of, by antigenic assays, 982–983
receptors, 974, 974t
role of, in erythrocyte destruction, 710–711
system of
blood banking and, 710–711
structure and function of, 969–975
Complementary base pairing, conditions for, 1381
Complement consumption, 899
Complement, cytokines, adhesion molecules, 969–983.e3
complement activity, in disease, assessment of, 977–978, 977t
complement, assays of, 981–983
alternative pathway, functional evaluation of, 982
C1-inhibitor and factor H, functional assay of, 982
classical pathway, functional evaluation of, 982
complement levels, by antigenic assays, 982–983
general principles of, 981–982
complement, in disease states, 978–981
biocompatibility, 980
cardiovascular diseases, 980
dermatologic diseases, 979
hematologic diseases, 979–980
hereditary angioedema, 979
infectious diseases, 979
neurologic diseases, 980
ophthalmologic diseases, 979
organ transplantation, 980–981, 981f
renal diseases, 979
rheumatologic disease, 978–979
complement inhibitors, clinically useful, 981
complement system, structure and function of, 969–975
alternative pathway, 971–972
anaphylatoxins, 972–973
C3: complement activation pathways, central molecule of, 970, 971f
classical pathway, 971
complement action, regulation of, 973–974, 973t
complement and acquired immunity, 975
complement biosynthesis, 974
complement genetics, 974–975, 975t
complement receptors, 974, 974t
mannan-binding lectin pathway, 972
nomenclature, 969–970, 970f
terminal complement components, 972
genetic complement deficiencies, 976–977, 976t
perspectives and, 983
Complement receptor 1 (CR1), 1465
Complex prostate-specific antigen (PSA), 1519
Compliance, for point-of-care testing and physician office laboratories, 83
Complotypes, 1017, 1017t
Component-resolved diagnostics and testing, by microarray methods, 1121t, 1127–1128
Compound heterozygosities, with Hb S, 614
Computer-assisted ANA IFA technology, 1050
Computer-assisted imaging, of chromosomes, 1415
Computer cross-match, 776
COMT gene, 1462
Concentration and activity, of enzymes, 292, 292f
Conductance, 48
Cone and plate analyzer, 849
Confidence interval (CI), 119
Confidentiality of genetic information, 178
Confirmatory bilirubin tests, 482
Conflict of interest, 175
Conflict of interest disclosures (COIDs), 175
Congenital adrenal hyperplasia, due to 21-hydroxylase deficiency, 1020
Congenital afibrinogenemia, 285
Congenital and perinatal viral infections, 1271–1273
Congenital defects, 597
Congenital dyserythropoietic anemias (CDAs), 602–603
Congenital fibrosarcoma (CFS), 1601
Congenital hyperinsulinism, 237–238
Congenital hypoplastic anemia, 601–602
Congenital lipoid adrenal hyperplasia (lipoid CAH), 412, 415f
Congenital red cell aplasia, 601–602
Congestive heart failure
diagnosis of, 114
markers of, 273–275
Conidia, 1196
Conidiogenous cells, 1197–1198
Conidiophores, 1197–1198
Conjugation chemistry, 903–904, 904f
Conjunctival specimens, 1357
Conjunctivitis, 1266, 1273
Connective tissue disease, mixed, 1049
Consolidation, optimizing performance and, 19–20
Constitutional cytogenetics, 1423–1425
Contact system, 829
Contaminants, and artifacts, 499, 499f
Contamination, bacterial, of blood components, 782–783
Contigs, 1608
Contiguous gene syndromes, 1430–1431, 1430t, 1431f
Continuous quality improvement (CQI), 4
Continuum source, 38
Contracaecum spp., 1342
Conversion of clearance in L/week to mL/min, 188
Cooley's anemia, 617
Cooley's trait, 617–618
Coomassie brilliant blue dye, 280, 517
Coombs control cells, 748
Coombs test, 746–747
Copeptin, 270
Copper, 449–450
biochemistry of, 449
dietary sources of, 449
genetic diseases and, 450
metabolism of, 449
testing of, 449–450
Copper reduction tests, 477–478, 478t
chemistry of, 478
five-drop method of, 478
precautions of, 478
procedure of, 478
two-drop method of, 478
Copy number variants, 1456
in bipolar disorder, 1458
Copy number variants (CNVs), 1435
Cordocentesis, 1413
Core binding factor leukemia, 656
Cornea, 820
Corneal graft, 820
Corneal specimens, 1357–1358
Coronary angiography, 268
Coronary heart disease (CHD), 267–268
risk factors for, 268, 268b
Coronary risk, markers of, 272
Coronavirus, 1269
Corpus luteum, 427
Corrected count increment, 779, 779b
Corticosteroid-binding globulin (CBG), 425–426
Corticotropin-releasing hormone test, 420
Cortisol, glucocorticoids and, 413–419
ACTH, laboratory measurement of, 414–415
hypercortisolism: Cushing's syndrome, 416
plasma corticotropin-releasing hormone, 415
salivary cortisol, 415–416
serum cortisol measurements, 415
urinary free cortisol measurements, 416

Corynebacterium, *Arcanobacterium* and, 1137–1138, 1137f
antimicrobial susceptibility of, 1138
characteristics, 1137
clinical manifestations and pathogenesis of, 1137
laboratory diagnosis of, 1137–1138
prevention of, 1138
Costs, defining and identifying of, 162–164, 163f, 163t, 165t
Coulomb, 47
Coulometry, 47
Coumadin, 105
Counting chamber, leukocyte counts and, 546
Coupled enzymatic reactions, 298
Cowden syndrome, 1603
Coxiella, 1254, 1261t
Coxiella burnetii, infections caused by, 1261–1263
laboratory diagnosis, 1262–1263
Q fever, 1261–1262
structure and function, 1261, 1261t
treatment, 1263
CpG island methylator phenotype (CIMP+), 1592
Crack, 358
CRE. *See* Carbapenem-resistant *Enterobacteriaceae* (CRE)
C-reactive protein (CRP), 272–273, 272b, 286–287, 518, 530–531
Creatine kinase (CK), 269, 464, 520
Creatine phosphokinase, 313
Creatinine, 108, 457
clearance of
as an estimate of GFR, formulas for, 189–190
cimetidine-enhanced, 189
measurement of, 189
as a measure of renal function, 188–190
ratio of, in serum, 191
urea and, 535
Cri-du-chat, 1430
Crigler-Najjar syndrome, 316
Crimean-Congo hemorrhagic fever orthonairovirus (CCHFV), 1288
CRISPR, 1620–1621
Criterion-based job description, human resource management and, 6
Critical values, 90
Crohn's disease (CD), 1085
Cromer blood group systems, 737–738, 738t
antibodies, 738
biochemistry, 738
biological role, 738
molecular biology, 738
null/weak phenotypes, 738
Crossing over, definition of, 1338, 1412
Cross-linked telopeptides, 220
Cross-match, 776
Crossmatching, 754–755
antiglobulin crossmatch, 755
compatibility testing in emergencies, 755
electronic crossmatch, 754–755, 755b
immediate spin serologic crossmatch, 754
preoperative crossmatch protocols, 755
Cross-reactivity, 1006, 1009
Croup, 1268
Crustaceans, 1350–1351
Cryoglobulinemic vasculitis, 1069–1070
clinical laboratory testing of, 1070
definition and epidemiology of, 1069–1070
diagnosis, treatment, and prognosis of, 1070
etiology and pathogenesis of, 1070
pathology of, 1070, 1070f
Cryoglobulins, 961
testing, 963, 964f
Cryohydrocytosis (CHC), 606
Cryoprecipitated antihemophilic factor, 774
Cryoprecipitate transfusion, 779, 779b
Cryopreservation, 818–819
of hematopoietic grafts, 823–824
Cryptic species, 1222
Cryptococcosis, yeast as cause of, 1207–1211
Cryptococcus, 1209–1210
Cryptosporidium spp., 1323–1325
Crystal casts, 492
Crystal examination, for synovial fluid, 524–526, 525f
Crystalline phosphates, 496, 496f
Crystalline urates, 493, 495f
Crystalline uric acid, 493–495, 495f
Crystals, 493, 494t
in abnormal urine, 496–497
in normal acid urine, 493–496
in normal alkaline urine, 496
Crystal scintillation, 52
CSF. *See* Cerebrospinal fluid (CSF)
CSF3R gene mutation, 1574
CSF/serum albumin index, 516
CSF/serum IgG index, 516–517
CTNNB1 gene, 1588–1589
Culture
cell, 1250, 1270, 1273
isolation of, for herpes simplex virus, 1272–1273, 1276t
viral growth in, 1282–1283
isolation in, 1203
blood cultures for, 1203
inoculation and incubation for, 1203
media selection for, 1203
methods, for mycobacteria diagnosis, 1189–1190, 1190t
mixed lymphocyte, 944, 945f
techniques, for specimen processing, 1131
Cumulative probability of exclusion (CPE), 1470–1471, 1475, 1475f
Cumulative sum (CUSUM), 137
CUSUM. *See* Cumulative sum (CUSUM)
Cutaneous autoimmune diseases, 1079–1084, 1079b, 1080t
Cutaneous disease, 1208
Cutaneous infection
Aspergillus in, 1223
Malassezia in, 1210
Cutaneous leishmaniasis, 1312
Cutaneous T cell lymphoma, as indication for extracorporeal photopheresis, 806, 806b
Cutaneous ulcers, specimens from, 1366
Cuvette-based particle analysis, 503–504
Cuvets. *See* Sample containers (cuvets)
CV. *See* Coefficient of variation (CV)
CVA collection technique, 31
Cyanide, 380
Cycle threshold (CT), 1390
Cyclic enzyme instability, 299
Cyclic neutropenia, 637
Cyclin D1, 1552
Cyclospora cayetanensis, 1325
Cyclosporine, 375–376
Cylindroids, 490
CYP2C9 gene, 1482t–1483t, 1483
CYP2C19 gene, 1483
CYP2D6 gene, 1483
CYP genes, 1483
Cystatin C, 190
Cysticercosis, 1342
Cystic fibrosis (CF), 331–332, 1438–1439, 1439t
Cystic fibrosis transmembrane conductance regulator (CFTR), 1438–1439
Cystine, 496, 497f
stones, 507
Cystinuria, 508
methods of, 508
procedure of, 508
Cystoisospora belli, 1324f–1325f, 1325
Cytocentrifuge method, 512–513
Cytochemistry, 549–550
Cytogenetic disorders, 1427–1431
Cytogenetic findings, of schizophrenia, 1456
Cytogenetic microarray, 1417–1418, 1418f
Cytogenetic phenomena, 1431
Cytogenetics, 157
Cytogenetics, in modern pathology, applications of, 1411–1433.e2
chromosome abnormalities, 1418–1423
nomenclature for, 1423, 1424t
numerical, 1418–1420, 1419f
structural, 1420–1423, 1421f–1422f
chromosomes, 1412–1418, 1412f
cell culture of, 1412–1413, 1413f
computer-assisted imaging of, 1415
fluorescence in situ hybridization of, 1415–1417, 1416f
karyotype analysis of, 1414–1415
microarray technology on, 1417–1418, 1418f
staining of, 1414, 1414f
structure of, 1412, 1413f
clinical, 1423–1431
cancer genetics, 1425–1427, 1426t, 1427f
in childhood and adult, 1425
constitutional, 1423–1425
cytogenetic disorders, 1427–1431
cytogenetic phenomena, 1431
postnatal, 1425
prenatal, 1423–1425, 1424t, 1425f
Cytokeratin 19 fragment, 1517
Cytokine-based therapeutics, clinically useful, 986–988
Cytokines, 984–995.e2, 896–899
assays, 986
cell adhesion molecules, 992–993, 993t
chemokine and chemokine receptor family, 988–992, 989t
in disease states, 986
family, 984
grouped by receptor class, 985t
leukocyte extravasation, 994, 994f
perspectives, 995
receptors, 984–986
by type and function, 985t
Cytokines receptors, 1031–1032
Cytomegalovirus, 644, 785, 1272, 1283f, 1286f
Cytopenia, refractory, with multilineage dysplasia, 654
Cytoskeletal linking proteins, defects in, 860
Cytosolic mitogenic kinases, 1533
Cytotoxicity assays, 944–946
cytotoxic T cell, 945–946
microlymphocytotoxicity, 946, 948f
natural killer cell-mediated cytotoxicity, 946
Cytotoxic T cell (CTL) assays, 945–946
Cytotoxic T cell lymphoma, aggressive, epidermotropic, primary cutaneous CD8-positive, 681

D

Dabigatran etexilate, 885, 887, 888f
D antigen, 721–723, 721f
C/c, E/e, and compound Rh antigens, 722
G antigen, 722
partial D, 721–722
Rh-negative phenotype, 722
weak D, 721
Darkfield microscopy, 1233, 1233f
Darvon. *See* Propoxyphene (Darvon)
Data
acquisition of, 692
analysis of, 120, 937–939
Database, 151
ACID properties of, 152t
deletions, 154
insertions, 153
operations, 153, 153f
master keys, 153
subordinate keys, 153
schema, 153
updates, 153–154
Data collection techniques, 13–16
instrument audit, 14–16
interviews, 16
processing mode and load balancing, 16
sample and test mapping, 13
task mapping, 16
test menu, 16
tube analysis, 14
workstation analysis, 14
Data denormalization, 153
Data normalization, 153
Data processing and real-time monitoring, in automated chemistry analyzer, 76–77
Data provenance, 151–152
Data security strategy, 159
Data type overload, 152–153
D-Dimers, 834
DDN, 1458
Decontamination agents, in clinical laboratory, 11b
Decoy cells, 498
Degenerate code, 1376
Degrees of freedom (df), 120
Dehydration, 107, 107t
DEK-NUP214, in acute myeloid leukemia, 1561
Delayed hemolytic transfusion reactions (DHTRs), 782
Deletion, 1414–1415, 1420
Deletional pancellular hereditary persistence of fetal hemoglobin, 619
Delivery, automated, 75
Delta check, 90, 143, 143t
Demargination, 636
Dematiaceous, 1195–1196
Dematiaceous fungi, mycoses caused by, 1219–1220
chromoblastomycosis, 1220, 1220f
clinical diseases of, 1219–1220
mycetoma, 1219, 1219f–1220f
phaeohyphomycosis, 1220
sick building syndrome, 1220
Dendritic cell neoplasms, 686, 686f

Dendritic cell sarcoma
follicular, 686
interdigitating, 686
Dendritic cells, use of, in cancer immunotherapy, 824
Dendroaspis angusticeps, 273
Dengue virus (DENV), 1286–1287
Densitometry, electrophoresis and, 48
Density, PSA, 1520
Dental fluorosis, 450
Dentatorubral-pallidoluysian atrophy, 1442
Deoxypyridinoline. *See* Pyridinium cross-links
Deoxyribonucleic acid (DNA), 1373
analysis of, 610–611, 937–939
cellular immunology, DNA studies relating to, 939
general aspects of, 937, 938f
sample preparation of, 937–939
branched, 1399
in crime laboratory, 1473–1474, 1473f
duplication process, 1375–1376
mutations, 1378–1379, 1378t
or double-stranded DNA, antibodies relating to, 1037
in pathology laboratory, 1474, 1474t
preparation and amplification of, 1007
repair mechanisms, 1377–1378
replication, 1375–1376
sequencing of, for nucleic acid analysis, 1384, 1384f
transcription of, to RNA, 1376
Deoxyuridine suppression test, 595
Depakene. *See* Valproic acid (Depakene)
Depression and mania, therapeutic drug monitoring for, 376–378
Derangements, of bilirubin metabolism, 316
Dermatitis herpetiformis, 1082–1083, 1083f
Dermatofibrosarcoma protuberance (DFSP), 1601
Dermatologic diseases, 979
Dermatomyositis (DM), 1046
Dermatophytoses, 1216–1218
clinical diseases of, 1217
laboratory diagnosis of, 1217–1218, 1217f–1218f
risk factors for, 1217
1-Desamino-8D-arginine vasopressin (DDAVP), 861–862
Descriptive statistics, 120–122
Des-γ-carboxy prothrombin (DCP), 319–320
"Designer" amphetamines, 361
Desorption electrospray ionization (DESI), 69f, 70–71
Detection
in automated chemistry analyzer, 76
hybridization, detection and image analysis, 1405–1406, 1406f
DHCP. *See* Dynamic host configuration protocol (DHCP)
DHCP reservation, 159
Diabetes
gestational, 437
diagnosis of, 229–230, 230t
glycemic control for, measures of, 232–234, 232t
insipidus, 107, 107t, 393–394, 393t, 394f, 395b
ketone testing for, 234
mellitus, 112, 229–234, 229t–230t
type 1, 1022–1023, 1108–1109, 1108t
pharmacogenomics in, 1501–1502
type 1, 230–232, 231t
type 2, 231t, 232
Diabetic hyperosmolar state, 106t, 107
Diabetic ketonuria, 479
Diagnostic accuracy, of laboratory results, 92–94
Diagnostic cancer applications, 1616–1618
adenocarcinoma, 1617
Barrett esophagus, 1616–1617
other cancers, 1617–1618
pancreatic cancer, 1617
small, round blue cell tumors, 1616
thyroid carcinoma, 1617
Diagnostic genetic testing, 1436–1437
Diagnostic molecular pathology, 1370–1371
Diagnostic peritoneal lavage, 533–534, 534b
Diagnostic techniques, for mycotic diseases, 1200–1207
Dialysis, peritoneal, 534
Diamond-Blackfan anemia (DBA), 601–602
Diarrhea, 336–340, 337t
causes of, 338
Clostridium difficile-associated, 339, 339t
disaccharidase deficiency, 338
drug-induced, 338
gut peptides in, 338
HIV-related, 340
lactose tolerance test, 338
vasoactive intestinal peptide, 339
Diazo tablet method, 482
procedure of, 482–483
DIC. *See* Disseminated intravascular coagulopathy (DIC)
Diego antibodies, 731
Diego blood group system, 731–732
biochemistry, 731
biological role, 731–732
molecular biology, 731
Dientamoeba fragilis, 1319–1320
Dietary Reference Intakes (DRI), 441–442
Diet, as physiologic factor, 22–23
Differential cell count, for CSF, 512–515, 513f–515f, 513t, 513b
Differential leukocyte count
and cytology, 528–529, 529f, 530b
for synovial fluid, 524, 524f
Diffuse large B cell lymphoma, 1554–1555, 1618
NOS, 673–674, 674f
Diffusion-controlled limit, 302
Digene Hybrid Capture, 1597–1598
Digital image processing, 550–551
Digital polymerase chain reaction, 1392–1393
Digitoxin, 368
Digoxin, 366t, 367–368
Dilantin. *See* Phenytoin (Dilantin)
Diluting fluid, leukocyte counts and, 546
Dilution testing, 1168, 1168f
Dimethyl sulfoxide (DMSO), 818–819
Dimorphic fungi, mycoses caused by, 1211–1216, 1212f
Dimorphism, 1199–1200
Diphyllobothrium spp., 1333–1334
Diploid, definition of, 1411
Dipylidium caninum, 1334–1335
Direct agglutinins, 745
Direct analysis in real time (DART), 71
Direct antiglobulin test (DAT), 748, 748t
in investigation of autoimmune hemolytic anemia, 760–762
positive, and hemolytic anemia induced by medication, 763
stimulation of red cell autoantibody production in, 763
Direct bilirubin, 456–457
Direct complement-dependent cytotoxicity, 1012
Direct costs, 162
Direct determination, 454
Direct examination, of mycotic diseases, 1200–1203
calcofluor white stain for, 1202–1203, 1202f, 1202b
Giemsa stain for, 1202
Gram stain for, 1202
histopathologic stains for, 1202
immunohistochemical stains for, 1203
India ink preparation for, 1202, 1202f
wet preparation for, 1202, 1202b
Wright stain for, 1202
Direct fluorescent antibody (DFA) tests, 1250
Direct immunofluorescence microscopy, 1080f
Direct LDL-C measurement, 256
Direct mutation tests, 1435
Direct sampling ionization
bioanalytic method validation criteria, 69
coated blade spray, 69f, 71
desorption electrospray ionization, 69f, 70–71
direct analysis in real time, 71
laser ablation electrospray ionization, 71
paper spray ionization, 69–70, 69f
Direct tissue invasion, 1344
Direct-to-consumer genetic testing, 1504
Direct wet mount, for medical parasitology, 1295
Disaccharidase deficiency, 338
Discontinuous atmospheric pressure interface (DAPI), 72–73
Discrete data, analyzing, 124–125, 124t
Disease
cytokines in, 986
diagnosis of, 961–966
cryoglobulin testing, 963
heavy-light chain immunoassay, 963
immunofixation, 961–962, 962f
immunoglobulin free light-chain analysis, 962–963
monoclonal bands detection, problems in, 964–966
oligoclonal immunoglobulin bands in cerebrospinal fluid, 963–964
oligoclonal immunoglobulin bands in serum, 966
laboratory evaluation of, 1385
pathogenesis of, 959–961
prevalence of, predictive value and, 93–94, 94t
prevention and therapy of, 966–967
redefining, 1371
Disease associations
of MHC, 1018–1023
monogenic, 1019–1020, 1020t
of polygenic diseases, 1020–1023, 1020t
Dishonest behavior, 179
Disk diffusion, 1169, 1169f
Dispersion, 121–122, 121f
Disseminated histoplasmosis, 1212
Disseminated infection, *Aspergillus* in, 1223
Disseminated intravascular coagulation, 843–844, 844t
Disseminated intravascular coagulopathy (DIC), 103
Disseminated viral infection, 1278, 1285
Distillation, 53–54
Disulfide knot, 285
Diuresis, 199, 199b
osmotic, 471
Diuretics, 107
Diurnal variation
as physiologic factor, 22
tests affected by, 23t
DNA analysis, for identity testing, 1468–1479.e1
advantages of, 1469
extraction and quantification in, 1470
genetic markers for, 1470–1473
historical background of, 1468–1469
parentage in
combined probability of exclusion of, 1475, 1475f
estimating of, with absent parent, 1477, 1477t
exclusion of, 1474–1475, 1475t
families in, reconstruction of, 1477, 1477f
inclusion of, 1475–1477, 1475f
likelihood of, 1476, 1476b
paternity index calculation in, 1476, 1476t
probability of exclusion of, 1474–1475
quality assurance standards for, 1478
samples and specimen collection for, 1469–1470
software systems for, 1473
test data in, 1473–1474
DNA in crime laboratory, 1473–1474, 1473f
DNA in pathology laboratory, 1474, 1474t
test methods and marker systems for, 1470–1473
mitochondrial DNA sequencing as, 1472
next-generation sequencing, 1472–1473, 1473b
short tandem repeats as, 1470–1471, 1471f, 1472t
single nucleotide polymorphisms, 1472–1473
X and Y chromosome markers as, 1471–1472, 1472f, 1473b
DNA-based allele designations, 1006–1007
DNA-based typing
of class I and class II alleles, 1007–1009
resolution of, 1008–1009
DNA chip technology, 1382–1383
DNA fingerprinting, 1468
DNA microarrays, 1611, 1612f
DNA ploidy analysis, 536
DNA repair genes, 1489–1491, 1491f, 1492t–1493t
DNA sequencing, genome-level, 1449–1451, 1449f–1450f, 1451b
DNMT3A gene, 1565, 1566f
DNS. *See* Domain name system (DNS)
Döhle inclusion bodies, 638
Domain name system (DNS), 159
Dombrock antibodies, 734–735
Dombrock blood group system, 734–735, 734t
biological role, 735
null/weak phenotypes, 734
Dominant allele, definition of, 1412
Donath-Landsteiner (DL) antibody, 762
Donor
concerns, of hematopoietic progenitor cell, 798
haploidentical, 821–822, 824
screening of, 818, 818b
Donor cytapheresis, 790–798
Donor erythrocytapheresis, 794–795
Donor leukocytapheresis, 791–794
Donor lymphocyte infusion, 774
Donor/patient complications, common to all hemapheresis procedures, 811–816
Donor plasmapheresis, 798–799
Donor plateletpheresis, 790–791
Donor-specific crossmatch, 1011–1012
physical crossmatch, 1011–1012
virtual crossmatch, 1012
Dot blots assay, 1056
Dot or linear array hybridization, 1382
Double reciprocal plot. *See* Lineweaver-Burk plot
Double-beam spectrophotometer, 42, 43f
Doubling time, PSA, 1520

Down syndrome, 436, 436f
  myeloid proliferations related to, 661–662
    blastic plasmacytoid dendritic cell neoplasm, 662
    myeloid leukemia associated with, 661
    transient abnormal myelopoiesis, 661
DP subregion, 1004
DQ subregion, 1003f, 1004
Dracunculiasis, 1341
Dracunculus medinensis, 1341
Dried blood spot testing, 353
DR subregion, 1003f, 1004
Drug(s). *See also* Therapeutic drug monitoring.
  of abuse, 354–364
  binding, to antibodies, 348
  design, transition state theory in, 303–305, 303f
  effects of, 25–26
  metabolism relating to, 318
  reaction, with eosinophilia and systemic symptoms, 1495–1496
Drug-independent autoantibodies, 763
Drug-induced diarrhea, 338
Drug-induced hypoglycemia, 234–235
Drug-induced immune hemolytic anemia (DIIHA), 627–628, 763
Drug-induced immune thrombocytopenia (DITP), 856
Drug-induced lupus erythematosus, antihistone antibodies, 1039–1040
Drug-induced thrombocytopenia, 769
Drug-metabolizing enzyme pharmacogenomics, 1481–1486, 1481f
Drug-transporter pharmacogenomics, 1486–1489, 1487f
Dubin-Johnson syndrome, 316
Duchenne muscular dystrophy, 1439–1440, 1440f
Duffy antibodies, 729–730
Duffy antigen, 990–992
Duffy blood group system, 728–730, 729t
  biochemistry, 729, 729f
  biological role, 730
  molecular biology, 729
Duplication, 1420
Dutcher bodies, 668
Dyes, 26
Dynamic host configuration protocol (DHCP), 159
Dysbetalipoproteinemia, 264–265
Dyserythropoiesis, 651, 652f
Dysfibrinogenemia, 285, 875
Dysgranulopoiesis, 651, 652f–653f
Dyslipidemia, 265
  study methods for, 256–258
Dyslipoproteinemia. *See* Lipids
Dysmegakaryocytopoiesis, 651, 653f
Dysmorphic erythrocytes, 487–488, 488f
Dysmyelopoietic syndrome, 651
Dysplasia, multilineage, with refractory cytopenia, 654
Dysplastic nevus syndrome, 1599
Dysproteinemias, 862
D-zone approximation test, 1173, 1173f

E

Early T-cell precursor lymphoblastic leukemia (ETP-ALL), 664
Eaton-Lambert myasthenic syndrome, 1112
Ebola viral disease (EVD), 1288
EBV infection, 1284–1285
EBV-positive DLBCL of the elderly, 674
EBV-positive mucocutaneous ulcer, 674
EBV-positive T cell lymphoproliferative disorders of childhood, 677
E-cadherin, 1531–1532
E-cadherin gene, 1590
Echinococcus spp., 1342–1343
Eclampsia, 625
Ecthyma gangrenosum, 1366
Ectopic tumor markers, 1512–1514, 1515t
E domain, 285
Edoxaban, 887
Effusion, 527
EGFR mutations
  colorectal cancer and, 1590–1591
  lung cancer and, 1587
Egg studies, for enteric parasites, 1296
EHR. *See* Electronic health record (EHR)
Ehrlichia canis Ehrlichiosis, human, 1260
Ehrlichia ewingii, human infection with, 1260
Ehrlichia, infections caused by organisms of, 1259–1261, 1259t
Ehrlichia muris eauclairensis, 1260
Ehrlichiosis
  human *Ehrlichia canis*, 1260
  human monocytotropic, 1259–1260
Eikenella, 1154
  antimicrobial susceptibility of, 1154
  characteristics, 1154
  clinical manifestations and pathogenesis of, 1154
  laboratory diagnosis of, 1153t, 1154
Electrical impedance, of instrument technology, 549
Electrochemiluminescent immunoassay, 919
Electrochemistry, 47–48
Electroimmunodiffusion, 517
Electrolyte(s)
  abnormalities of, 106–108, 106f
    hyperkalemia, 108
    hypernatremia, 107, 107t
    hypokalemia, 107–108
    hyponatremia, 106–107, 106t
    pseudohyponatremia, 107
  acid-base balance and, 520
  and acid-base disturbances, and hemapheresis, 813–814
  renal function, water, and acid-base balance, evaluation of, 181–207.e2
Electromagnetic radiation (EMR), 35–36, 37f
  energy of, 36, 36b
Electronic balances, 54
Electronic crossmatch, 754–755, 755b
Electronic health record (EHR), 150, 155
Electron- impact ionization, 62
Electron ionization, 62
Electro-osmosis, 278
Electrophoresis, 277–279, 278f
  capillary, 52, 52f
  and densitometry, 48
Electrophoretic methods, 255
Electrophoretic separation, 1379, 1379f
Electrophoretic techniques, of albumin and IgG measurements, 517–518
Electrospray ionization (ESI), 62
Elevated white blood cell (WBC)
  chronic lymphocytic leukemia relating to, 105
  chronic myelogenous leukemia relating, 105
  infection relating to, 104
  leukemoid reaction relating to, 104–105
Elevation of coagulation factor levels, 875
Elevation of prothrombin, 875
Elution, 761
  antibody, 758–759
Embolization, 275
Embryonic and fetal hematopoiesis, 572
Embryonic hemoglobins, 608
Emerging technologies, 1620–1622
  CRISPR, 1620–1621
  ion torrent sequencing, 1622
  next-generation sequencing, 1621–1622, 1621f
EML4-ALK fusion gene, 1501
EMR. *See* Electromagnetic radiation (EMR)
Encephalitis, 1274–1275, 1275t, 1278, 1284–1285
Endemic syphilis, 1232–1233
Endocarditis-associated glomerulonephritis, 1098, 1098f
Endocervical specimens, 1362
Endocrine disease, anemia in, 598
Endocrine function
  evaluation of, 387–424.e6
    adrenal, 404–420
    pituitary, 387–395, 388f, 388b
    renin-aldosterone axis, 420–424, 420f–421f
    thyroid, 395–404, 397f
  testing, 114–115, 115t
    adrenal function, 115–116, 116t
    thyroid function, 114–115, 115t
Endocrine pancreas, functions of, 226–228
Endocytosis, assays of, 947–948
Endogenous anticoagulant pathways, 870–871, 871f
  annexin A2, 871
  annexin A5, 871
  antithrombin, 870–871, 871f
  fibrinolytic system, 871
  protein C, 871
  protein S system, 871
  tissue factor pathway inhibitor, 870, 871f
Endogenous erythroid colonies (EECs), 647
Endogenous hyperinsulinism, 236
Endogenous substances, GFR with, 188
Endometrial cancer, 1598
Endophenotype, 1502–1503
Endosmosis, 278
Endothelium, platelets and, 828–829, 829f
End-point method, 454
Endpoint quantitative polymerase chain reaction, 1389
End-product inhibition, 300
Energy, of electromagnetic radiation, 36, 36b, 37f
Entamoeba histolytica, 1315–1318
  diagnosis of, 1316
  epidemiology of, 1317
Enteric parasites, 1296
  egg studies for, 1296
  nematode culture and recovery techniques for, 1296
  objects resembling, 1296–1297
  paddle techniques, 1296
  pinworms, cellulose tape technique, 1296
Enteritis, 1284
Enterobacterales, 1144–1146
  antimicrobial susceptibility of, 1146
  characteristics, 1144, 1144f
  clinical manifestations and pathogenesis of, 1144–1145
  laboratory diagnosis of, 1145–1146, 1145t–1146t
Enterobius vermicularis, 1327–1328, 1327f–1328f
Enterococcus, 1133–1137, 1134f, 1134t
Enteropathy-associated T cell lymphoma, 679, 680f
Enterovirus, 1273, 1278
Envenomation, 1344
Environmental carcinogens, 380
Environmental concerns, for best weighing accuracy, 55
Enzymatic activity and intracellular killing, assays of, 948–949, 948f
Enzymatic methods, 253
Enzyme activity, 297
  coupled enzymatic reactions and, 298
  factors affecting, 298–299
    inhibitors and interferences, 299
    pH, 299
    salt and protein concentrations, 299
    temperature, 298–299
  measuring, 297
  plasma, factors affecting, 294
  predetermined, new catalytic antibodies with, 304–305, 305f
  spectrophotometric assays and, 297–298
Enzyme assays
  caveats in, 299–300
    competing reactions, 300
    cyclic enzyme instability, 299
    enzyme inhibitors and, presence, 299
    inhibitory compounds, in blood collection tubes, 300
    K_M-type mutations, 299
    time-dependent inactivation, 300
    unstable enzymes, protease degradation of, 299
  under nonsaturating conditions, 298
Enzyme inhibitory homogeneous immunoassay, 914–915, 916f
Enzyme kinetics: total enzyme concentrations, in serum and other body fluids, 295–300
  enzyme activity, factors affecting, 298–299
  enzyme assays in, caveats in, 299–300
  measuring enzymes in, antibody-based techniques for, 300
  Michaelis-Menten equation in, 295–298
Enzyme-linked immunosorbent assay (ELISA), 1056
  for heparin-induced thrombocytopenia, 884–885, 886f
Enzyme-linked immunosorbent spot (ELISPOT) assay, 947f
Enzyme-multiplied immunoassay technique, 914, 915f
Enzymes, 520, 526, 530, 532, 535
  assays for, 462–466
  canalicular injury relating to, 321–322
    ALP, 321
  cellular locations of, 320, 320f
  drug-metabolizing, pharmacogenomics, 1481–1486, 1481f
  homogeneous, 914–916, 914t
  immunoassay, 911–917
    background and classification of, 911, 911t, 912b
    heterogeneous, 911–912, 912t, 913f
    homogeneous, 914–916, 914t
  inhibition of, 300–302, 301f, 303t
    competitive, 300
    noncompetitive, simple and mixed, 301–302
    uncompetitive, 301
  inhibitors of, presence of, 299
  lipolytic, and other proteins, 248, 250t
  measurement, for metabolic defects, 1030–1031
  measuring, antibody-based techniques for, 300
  nucleic acid-associated, 1375, 1375f, 1375t
  plasma levels relating to, 320–322

Enzymes *(Continued)*
properties of, 291–295
catalysis, 291–293, 293f
cofactors, 293–294, 294t, 296b
concentration and activity of, 292, 292f
isoenzymes, 293, 294t
lifetime of, in blood, factors affecting, 294–295
nomenclature of, 293, 293t
plasma enzyme activities in, factors affecting, 294
specificity of, 291–292
as reagents, for analyte concentrations, 458–466
release of, mechanisms of, 320–321
specific, 305–313, 305t
acetylcholinesterase (EC 3.1.1.7), and butyrylcholinesterase (EC 3.1.1.8), 310–311
acid phosphatase (EC 3.1.3.2), 305–306
alkaline phosphatase (EC 3.1.3.1), 306–308
angiotensin-converting enzyme (EC 3.4.15.1), 308–310
lactate dehydrogenase (EC 1.1.1.27), 311–312
5'-nucleotidase (EC 3.1.3.5), 312
Enzymology. *See* Clinical enzymology
Eosinophilia, 640–641, 642f, 642b
myeloid and lymphoid neoplasms with, 650–651
myeloid/lymphoid neoplasms with, 1577–1578
Eosinophilic leukemia, chronic, 649–650
Eosinophilic leukemoid reactions, 646
Eosinophil precursors, morphology of, 580, 580f, 580b
Eosinophils, 488, 488f, 579–580
distribution and kinetics of, 580
function of, 580
and neutrophils, 896
Epidermal growth factor, 1529–1530
Epidermal growth factor receptor, 1494–1495, 1494f, 1501, 1528t, 1530
Epidermal growth factor receptor inhibitors, 1501
Epidermolysis bullosa acquisita, 1082, 1083f
Epigenetic influences, and nonmendelian inheritance, 1438
Epigenetics, 1503–1504, 1565–1566
gene regulation and, 1377
Epigenomics, pharmacogenomics in, 1503–1504, 1504f
Epithelial cells, 488–490
renal tubular, 489, 489f
squamous, 488, 489f
transitional (urothelial), 489, 489f
tumors of, antibodies to p53 in, 1534
Epithelioid hemangioendothelioma, 1601
Epsilometer, 1168–1169, 1169f
Epstein-Barr virus (EBV), 1270–1271, 1271t, 1282t
EQC. *See* Equivalent Quality Control (EQC)
Equipment, in specimen processing, 34
ERB-B2, 1458
Ergonomic hazards, clinical laboratory and, 11
Errors
in preanalysis, 22, 23t
quality systems management and, 3–5
Erysipelothrix, 1139
antimicrobial susceptibility of, 1139
clinical manifestations and pathogenesis of, 1139
laboratory diagnosis of, 1139, 1139t
prevention of, 1139
Erythema migrans, 1239
Erythroblastosis fetalis, 436–437, 437f
Erythrocytapheresis
benefits of, 794, 794b
donor
concerns of, 795
selection of, 794–795
product requirements, 794
Erythrocyte(s), 487
in blood, effective survival measurement of, 577–578
destruction of, 576
role of complement in, 710–711
effective production measurement of, 577, 577t
indices of, 543–544
manual counts of, 544
semiautomated methods of, 544
or hemoglobin
total destruction measurement of, 577
total production measurement of, 576–577
physiologic variation in, 544–545, 545f, 545t
survival studies relating to, 603, 604f
Erythrocyte antigens and antibodies, 711–744, 712t–713t
Erythrocyte (red blood cell) casts, 491, 491f
Erythrocyte lysis, 692
Erythrocyte production, 572–576
hemoglobin
structure and function of, 574–576, 574f, 576f
synthesis of, 574
megaloblastic maturation, 574
normoblastic maturation, 572–574, 572f–573f
regulation of, 574
Erythrocytic disorders, 588–635.e2
anemias, 588–630
polycythemia, 581b
Erythrokinetics, 576–578
erythrocytes
in blood, effective survival measurement of, 577–578
effective production measurement of, 577, 577t
erythrocytes or hemoglobin
total destruction measurement of, 576–577
total production measurement of, 576–577
Erythroleukemia, 659, 661f
Erythropoiesis, transitory arrest of, 601
Esophageal cancer, anti-p53 in, 1535
Essential fructosuria, 242
Essential thrombocythemia, 649, 650f, 1572–1574, 1572f
clinical features of, 649
diagnosis of, 649
genetics of, 649
laboratory features of, 649
blood in, 649
marrow in, 649
Estimated average requirement (EAR), 441–442
Estimating risk factors, in cholesterol testing, 258–260
Estradiol, 427
Estrone, 425
E-test, for extended- spectrum β-lactamases detection, 1175, 1175f
E-test strip, 1168–1169, 1169f
Ethanol, 26, 381, 381t
Ethical behavior, in laboratory medicine, 174
authorship, 179
case reports, 176
clinical trial phases, 178
close out of research study, 177
confidentiality of genetic information, 178
dishonest behavior, 179
Hippocratic oath, 174
human subject research, 175–178
kickbacks/bribery, 179
method validation/newly developed assays, 177
ownership of specimens, 179–180
regulations, 174
conflict of interest, 175
privacy, 175
Ethical principle of equipoise, 178
Ethnic variation, of MHC, 998, 1001f
Ethosuximide (Zarontin), 370
Ethylenediaminetetraacetic acid (EDTA), 27–28
effect on blood tests, 28t
Ethylene glycol, 382
E26 transformation specific-related gene (ERG), 1523
ETV6-RUNX1 ALL, 1547
EUCAST. *See* European Committee on Antimicrobial Susceptibility Testing (EUCAST)
Eumycetoma, 1219
Euploidy, 1418–1419, 1419f
European Committee on Antimicrobial Susceptibility Testing (EUCAST), 1166–1167
Evans syndrome, 627
EVD. *See* Ebola viral disease (EVD)
Event, in flow cytometry, 45
Evidence-based medicine, 97, 97f
Ewing's sarcoma, primitive peripheral neuroectodermal tumor in, 1600
EWMA. *See* Exponentially weighted moving averages (EWMA)
Exempt From Informed Consent (EFIC) study, 175
Exempt review category, 176–177
Exercise, as physiologic factor, 22
Exertional angina, 267–268
Exhaled breath condensate (EBC), 537
Exhaled nitric oxide (NO), 537
Exogenous substances, GFR with, 188
Exosomes, 1408–1410
Expedited review, 177
Expert systems, 151, 1168
Exponentially weighted moving averages (EWMA), 137
Expressivity, variable penetrance and, 1437
Extended haplotypes, 1017–1018, 1018f, 1018t–1019t
Extended-spectrum β-lactamases (ESBLs), 1174
Extensive liver disease, 328
Extracellular volume, regulation of, 186–187
water and electrolyte balance, nonrenal control of, 187
Extracorporeal photopheresis, 806–807
indications for, 806–807
procedure for, 807
Extraction
in molecular diagnostics, 25
and quantification, of DNA, 1470
Extranodal marginal zone B cell lymphoma *MALT1*, *BCL10* and *FOXP1* gene
of mucosa-associated lymphoid tissue, 671, 671f
Extranodal NK/T cell lymphoma, nasal type, 679, 680f
Extraosseous plasmacytoma, 670
Extraskeletal myxoid chondrosarcoma, 1600
Extravascular hemolysis, 710–711
Extrinsic pathway, 833
Eye, specimens from, 1357–1358
conjunctival, 1357
corneal, 1357–1358
EZH2 gene, 1566

F

FACS. *See* Fluorescence-activated cell sorter
Factor VIII or factor IX, deficiency of, 837–840, 837t
disruptive therapies for hemophilias, 840
evaluation of carriers of, 838
gene therapy for hemophilias, 840
treatment of, 838–839
acute bleeds associated with neutralizing alloantibody inhibitors in hemophilia A and B, 839–840
complications of, 839, 840f
Factor V_{Leiden}, 874
Falling drop method, 472
Fallopian tubes, 428
False negatives, 61–62
False positives, 61–62
Familial adenomatous polyposis, 1447–1448
Familial adenomatous polyposis syndrome, 1592
Familial cancers, 1445–1448, 1446t, 1448f
Familial combined hyperlipidemia (type 2B), 264
Familial defective ApoB, 263
Familial hypercholesterolemia, 261–263, 263f
Familial hypertriglyceridemia, 264
Familial hypoalphalipoproteinemia, 265–266
Familial juvenile polyposis syndrome (JPS), 1581t–1583t, 1593
Familial paraganglioma syndromes, 1603
Familial platelet disorder, with disposition to acute myelogenous leukemia, 861
Familial pseudohyperkalemia (FP), 606
Familial testing, 1473–1474, 1477f
Fanconi's anemia (FA), 601, 637
Faraday, in coulometry, 47
Fasciola hepatica, 1335–1336, 1336f
Fascioliasis, 1335–1336
Fasciolopsis buski, 1335, 1336f
Fast atom bombardment, 62
Fasting, 252
Fat, 345–346
Fat-soluble vitamins, 442t, 446–447
Fatty acid-binding protein (FABP), 193
Fatty casts, 492, 493f
Febrile nonhemolytic reactions, to transfusion, 781
Fecal elastase, 341
Fecal occult blood testing (FOBT), 343
and mutant protein markers, in stool, 1524
Fecal specimens, for medical parasitology, examination of, 1294–1297
collection, handling, and preservation of, 1294–1295, 1294t
concentration techniques in, 1295
direct wet mount of, 1295
enteric parasites, 1296
iron hematoxylin stain for, 1296
macroscopic, 1295
microscopic, 1295–1296
microsporidia in, stains for
modified acid-fast stains for, 1296
permanent stains for, 1295–1296
Wheatley's trichrome stain for, 1295
Feces
newborn, blood in, 343
specimens from, 1363–1365
bacterial pathogens in, 1363–1364
parasites in, 1364–1365
viruses in, 1363

Feet, 1195
Felbamate, 371
Felty's syndrome (FS), 637
Female reproduction, regulation of, 427–428, 427f–428f, 431–433, 432f
Fentanyl, 360
Ferroportin, 450
Fetal hematopoiesis, 572
Fetal hemoglobin, hereditary persistence of, 619
Fetal lung maturity, 437–438
Fetal status, intrapartum assessment of, 439
α-fetoprotein (AFP), 322, 1515
Fever
  Boutonneuse, 1256
  Oroya, 1264
  Q, 1261–1262
  relapsing, 1243–1244, 1243f, 1244t
  spotted
    fleaborne, 1256
    Rocky Mountain, 1255–1256
  trench, 1263t, 1264
Fibrin and fibrinolytic system, formation of, 830–831, 831f
Fibrin clot formation, 830f
Fibrinogen, 285, 286f
  disorders of, 842
Fibrinogen assay, 834
Fibrinolysis, hereditary hemorrhagic disorders of, 843
Fibrinolytic system and fibrin, formation of, 830–831, 831f
Fibrinolytic system, rebalanced, 844
Fibronectin, 518, 535
Fibrosing mediastinitis, 1212
FII deficiency, 842
Filamin A, 860
Filarial, 1338–1341
Filters, 39–40, 39f
Financial calculations, interpretation of, 171–172
Financial lease, 173
Financial management, 162–173.e1
  capital acquisition methods, 172–173, 172t
  capital project, evaluating, 171–172, 172t
    breakeven point, 171
    financial calculations, interpretation of, 171–172
    internal rate of return, 171
    net present value, 171
    payback period, 171
    return on investment, 171
  costs, defining and identifying of, 162–164, 163f, 163t, 165t
  industry overview of, 162
  payers and reimbursement, 164–166
    government payers, 164–166
    private insurance, 164
  performance and monitoring of, 169–171
    benchmarking and productivity measures, 171, 171t
    budgeting, 169, 170t
    financial reporting and statements, 170–171, 170t
    variance analysis, 169–170
  reimbursement coding systems, 166–169
    accurate coding, 166–167, 168t–169t
    Medicare reimbursement, 167–169, 169t
  revenue, 164, 166t
Financial reporting and statements, 170–171, 170t
Finger or heel skin puncture, 30–31
Fingerprint, 537, 1608
Firewall, 159
Fisher's exact method, 753
F2-isoprostanes, 519
Fixed costs, 162
Flagellates, 1319–1322, 1323t
  Chilomastix mesnili, 1321
  Dientamoeba fragilis, 1319–1320
  Giardia duodenalis, 1320–1321
  Pentatrichomonas hominis, 1322
  Trichomonas vaginalis, 1322
Flags
  alarms and, 89–90
  for problematic results, 90
  for problem specimens, 89–90
  for specimens that require additional analysis, 90
Flame ionization detectors (FIDs), 50
Fleaborne spotted fever, 1256
Fleas, 1346f, 1347
Flies, 1346f, 1347
"Floating β" lipoprotein. *See* β-VLDL
FLI1 mutations, 861
Floret cells, 678
Flow cytometer, 934–936
  colors, applications and fluorochromes relating to, 935–936
  flow cell, 934–935
  fluidics, 934–935
  immunophenotypic lymphocyte subset analysis, 936f
  light source and signal processing of, 934, 934f
  structural components and function of, 934f
Flow cytometric analysis, 935t
  polymorphonuclear leukocyte, 949f
Flow cytometric evaluation, of hematopoietic neoplasia, 689–707.e3
Flow cytometric immunoassay, 926–927
Flow cytometric particle analysis, 504–505
Flow cytometry, 45–46, 46f, 156–157, 689, 766
  detection of F cells by, 608
  quantitative, 939
  use of, for platelet function evaluation, 852, 852f
Flow imaging particle analysis, 503
FLT3 mutations, in acute myeloid leukemia, 1564–1565
Fluid delivery type, and sampling, 920
Fluid-filled lesions, 1365
Fluid-phase regulators, 973
Fluorescence, 44
Fluorescence-activated cell sorter, 45–46, 46f
Fluorescence assays, time-resolved, 44
Fluorescence excitation transfer immunoassay, 918
Fluorescence in situ hybridization, 1415–1417, 1416f
  cell DNA testing for cancer using, 1522–1523
Fluorescence polarization assay, 918, 918f
Fluorescence polarization immunoassay (FPIA), 348
Fluorescence resonance energy transfer (FRET), 1391
Fluorescent dyes, 935
Fluorescent enzyme immunoassay, 912
Fluorescent immunoassay, 917–919
  background and classification, 917
  fluorescence excitation transfer, 918
  fluorescence polarization assay, 918, 918f
  fluorescent protection immunoassay, 918–919
  fluoroimmunometric method, 917
  heterogeneous, 917–918
  homogeneous, 918–919
  radial partition immunofluorometric, 917
  time-resolved fluoroimmunoassay, 917–918
Fluorescent protection immunoassay, 918–919
Fluorescent proteins, 936
Fluorescent spot test, 623
Fluoride (Fl), 450
Fluorochromes, 935–936, 935t
  emission spectra of, 690f
  tandem, 690–691, 691f
Fluoroimmunometric method, 917
Fluorometers, components of, 44, 44f
Fluorometry. *See* Molecular luminescence spectroscopy (fluorometry)
Fluoropyrimidines, 1496–1497
Fluoroquinolone, 1253
5-Fluorouracil, 1496–1497, 1497f
Folate, 445
  defective absorption of, 596
  evolution of laboratory abnormalities in, 596
  inadequate intake of, 596
  inadequate utilization of, 596
  increased requirement for, 596
Folate-cobalamin relationship, 595
Folate deficiency, diagnosis of, 596
Folic acid
  deficiency of, 596–597
  metabolism of, 595
  prevention of, 434–435
Folin-Ciocalteu reagent, 280
Follicular carcinoma, 1586–1587
Follicular dendritic cell sarcoma/tumor, 686
Follicular lymphoma, 671–672, 672f–673f, 672t, 1551, 1618
Follicular thyroid carcinoma from adenoma, 1617
Folliculogenesis, 427
Fondaparinux, 883
Food and Drug Administration (FDA)
  on CLIA waiver, 81–82
FORS blood group system, 716–718
FQDN. *See* Fully qualified domain name (FQDN)
Fractalkine, 988
Fractional excretion (FE), 192
Fractional reabsorption (FR), 192
Fragile X syndrome, 1431, 1431f
Francisella tularensis
  antimicrobial susceptibility of, 1158
  characteristics, 1157
  clinical manifestations and pathogenesis of, 1157–1158
  laboratory diagnosis of, 1158
Fraudulent activity, 179. *See also* Dishonest behavior.
Fredrickson Classification, 260, 261t
Free prostate-specific antigen (PSA), 1519, 1520f
Free thyroxine, 400
Freezing-point osmometer, 47
  principle of, 47
French-American-British Cooperative Group, 655
Frequency, of sine wave, 36
Fresh frozen plasma (FFP), 798–799
  as replacement fluid, 808–809
Friedewald calculation, 255
Friedreich ataxia, 1443
Frontal electrophoresis, 277–278
Fructosamine. *See* Glycosylated albumin
Fructose
  intolerance, hereditary, 241
  metabolism in, defects in, 242–243
  in urine, 478
Fructose-1,6-biphosphatase deficiency, 241
Full IRB panel review, 177
Full-width at half maximum (FWHM), 62
Fully automated urinalysis systems, 505
Fully qualified domain name (FQDN), 159
Fulminant hepatic failure, 330
Functional tests, for heparin-induced thrombocytopenia, 884–885
Fungal colony, 1195, 1197f
Fungal culture, from CSF, sample processing of, 1356
Fungal meningitis, 522
Fungal pigment, 1195–1196
Fungemia, blood specimen timing for, 1353–1354
Fungi, 498, 498f–499f
  imperfect, 1195
Fungus ball, 1219
Fusariosis, hyaline fungi as cause of, 1222–1225
Fusarium, 1224–1225, 1224f
Fusion genes
  chromatin remodeling genes in, 1601
  involving growth factors, 1601
  involving receptor tyrosine kinase genes, 1601
  involving *TET* genes, 1600
  other types of, sarcoma with, 1601
  sarcomas with, 1600–1601
FV deficiency, 842
  and FVII, combined, 842–843
FVIIa-TF complex, 833
FVII deficiency, 843
FVIII (antihemophilic factor), 829–830
  and FV, combined deficiency of, 842–843
FX deficiency, 842
FXIII deficiency, 843

G

Gabapentin, 371
Galactokinase deficiency, 242
Galactose, in urine, 478
Galactose metabolism, defects in, 242
Galactose-1-phosphate uridyl transferase (GALT), 242
Gamma-glutamyl transferase (GGT), 464–465
G antigen, 722
Gardnerella
  antimicrobial susceptibility of, 1158
  characteristics, 1158
  clinical manifestations and pathogenesis of, 1158
  laboratory diagnosis of, 1158
Gas chromatography, 50, 50f
  with infrared spectroscopy, 353
Gas chromatography (GC), 62
Gas chromatography-mass spectroscopy, 66, 352, 353f
Gastrectomy, megaloblastic anemia and, 594
Gastric cancer, 1589–1590
  protein array to, 1538
Gastrinoma, 345
Gastroenteritis, 1278–1279, 1279t
Gastrointestinal bleeding, 343
Gastrointestinal candidiasis, 1208
Gastrointestinal disorders, laboratory diagnosis of, 331–346.e3
  diarrhea and malabsorption, 336–342
  macroscopic examination for, 345
  microscopic examination for, 345–346
  peptic ulceration, 335
  stool collection for, 345–346
  Zollinger-Ellison syndrome, 335–336
Gastrointestinal stromal tumor (GIST), 1601–1602
GATA-1, mutations in, 861
Gatekeeper, 1180
Gatifloxacin, 234–235

Gating and data analysis, 936–939
Gaussian distribution, 121, 121f
  definition of, 120
G-banding, 1414
Gc-globulin, 286
GCKR (Glucokinase regulator protein) gene *(rs1260326)*, 1459
Gelatinous transformation, 638
Gelatin particle agglutination, 907, 909f
Gel filtration, 279
Gemella, *Aerococcus* and, 1137
Genealogy testing, 1473–1474
Gene arrays, detecting oncoprotein abnormalities, 1521–1522
"Gene-by-gene" approach, 1609
GeneChip array manufacture, 1403f
Gene-encoded dopamine receptors, 1453–1454
Gene expression profiling, 1554–1555
  in RCC, 1596
Gene mutations, 1522
Genes, 1376
  and allergic phenotype, 1117t
  in central or class III region, 1015–1017, 1015f
  definition of, 1411
  and phenotype frequencies, 1023
  regulation of
    epigenetics and, 1377
    small RNA and, 1377, 1377f
Gene therapy for hemophilias, 840
Genetic abnormalities, recurrent, acute leukemia with, 655–658
  balanced translocations/inversions, 655–658
    acute promyelocytic leukemia with t(15;17) (q22l;q12), PML/RARA variants, 656, 658f
    AML with inv(3)(q21q26.2)or t(3;3) (q21;q23.2) RPN1-EVI1, 656, 658f
    AML with (t5;21)(q22;q22), RUNX1-RUNX1T1, 655–656, 657f
    AML with t(6;9)(p23;q34); DEKNUP214, 657
    AML with t(9;11)(p22;q23); MLLT3-MLL, 657
    AML (megakaryoblastic) with t(1;22) (p13;q13); RMB15-MKL1, 657
  with gene mutations, 658
    AML with *CEBPA* mutation, 658
    AML with *NPM1* mutation, 658
    AML with RUNX1 mutation, 658
Genetic basis
  of antibody diversity, 955, 955f, 956t
  of transplantation, 1009–1010, 1010f
Genetic complement deficiencies, 976–977, 976t
Genetic diseases, molecular diagnosis of, 1434–1451.e2
  applications for, 1435–1437
  new frontier of, 1449–1451, 1449f–1450f, 1451b
  special concepts in, 1437–1438
    allele frequencies and mass population screening, 1438
    anticipation, 1438
    epigenetic influences and nonmendelian inheritance, 1438
    imprinting, 1437–1438
    molecular heterogeneity, 1437
    predictive genetic testing, 1438
    uniparental disomy, 1437
    variable penetrance and expressivity, 1437
  specific examples of, 1438–1449
    cystic fibrosis, 1438–1439, 1439t
    Duchenne muscular dystrophy, 1439–1440, 1440f
    familial cancers, 1445–1448, 1446t, 1448f
    hemochromatosis, 1441
    hereditary thrombophilias, 1440–1441, 1441f
    mitochondrial DNA disorders, 1448
    Prader-Willi and Angelman syndromes, 1445
    sickle cell anemia, hemoglobinopathies and, 1440
    spinal muscular atrophy, 1440
    trinucleotide repeat expansion disorders, 1441–1444, 1443t
  techniques for, 1435, 1436f
Genetic information, confidentiality of, 178
Genetic markers, 1023, 1470–1473
Genetic polymorphism, 1023
Genetics
  complement, 974–975, 975t
  of major histocompatibility complex (MHC), 997–998
    basic, 997–998
    ethnic variation, 998, 1001f
    inheritance, 998
    linkage disequilibrium, 998
    MHC, composition of, 998, 999t, 1000f
    MHC genes, localization of, 998
Genital mycoplasmas, 1252
  clinical manifestations, 1252
  epidemiology, 1252
  laboratory diagnosis, 1252–1253
Genital tract infections, 430
Genital tract, specimens from, 1362–1363
  endocervical and urethral specimens, 1362
  ulcers, 1295, 1363
  vaginal secretions, 1362, 1362f
  vesicles, 1362–1363, 1363f
Genome-wide association studies, 1452–1453
  copy number variants, 1456
  on major depression disorder, 1462
  in pharmacogenomics, 1456
  proteins from opioid addiction, 1461
  of PTSD, 1463
Genomics, 1609–1614
  human neoplasia, molecular markers for diagnosis of, 1615
  prognostic molecular markers of disease, 1618–1619
Genotype, definition of, 1411
Genus *Aspergillus*, 1222–1224
  aspergillosis, pathology of, 1221t, 1223, 1223f
  clinical diseases of, 1222–1223
    cutaneous infection, 1223
    disseminated infection, 1223
    ocular infections, 1223
    otic infections, 1223
    primary pulmonary infection, 1223
    sinus infection, 1223
  laboratory diagnosis, 1223–1224, 1224f
  risk factors for, 1222
Genus *Blastomyces*, 1213–1214
  blastomycosis, pathology of, 1213, 1214f
  clinical diseases of, 1213
  laboratory identification of, 1213–1214, 1214f
  risk factors for, 1213
Genus *Candida*, 1207–1209
  clinical diseases of, 1207–1208
    cutaneous disease as, 1208
    gastrointestinal candidiasis as, 1208
    invasive candidiasis as, 1208
    oral candidiasis as, 1208
    urinary tract infection as, 1208
    vaginal candidiasis as, 1208
  laboratory diagnosis for, 1204f, 1205t, 1208–1209, 1208f
  pathology of, 1208
  risk factors for, 1207
Genus *Coccidioides*, 1214–1215
  clinical diseases of, 1214–1215
  laboratory diagnosis of, 1215
  pathology of, 1215, 1215f
  risk factors for, 1214
Genus *Cryptococcus*, 1209–1210
  clinical disease of, 1209
    bone and joint infection, 1209
    central nervous system infection, 1209
    in respiratory tract, 1209
    in skin lesions, 1209
  laboratory diagnosis of, 1209f, 1210
  pathology of, 1209
  risk factors for, 1209
Genus *Fusarium*, 1224–1225, 1224f
Genus *Histoplasma*, 1211–1213
  clinical diseases of, 1212
    acute pulmonary infection, 1212
    chronic pulmonary histoplasmosis, 1212
    disseminated histoplasmosis, 1212
    granulomatous and fibrosing mediastinitis, 1212
  laboratory diagnosis of, 1212–1213, 1213f
  pathology of, 1212, 1213f
  risk factors for, 1211–1212
Genus *Malassezia*, 1210–1211
  clinical diseases of, 1210
    cutaneous infection, 1210
    systemic infection, 1210
  infection from, pathology of, 1210, 1210f
  laboratory diagnosis for, 1210–1211, 1211f
  risk factors for, 1210
Genus *Scedosporium*, 1225, 1225f
Genus *Sporothrix*, 1215–1216
  clinical diseases of, 1216
  laboratory diagnosis of, 1216, 1216f
  risk factors for, 1216
  sporotrichosis, pathology of, 1216
Geometric mean, 121
Gerbich antibodies, 737
Gerbich blood group system, 736–737
  biochemistry, 736, 737f
  biological role, 737
  molecular biology, 736–737, 737t
  null/weak phenotypes, 736
Germline predisposition, myeloid neoplasms with, 1575, 1576t
Gestational diabetes, 437
  diagnosis of, 229–230, 230t
GFI1B mutations, 861
Ghost cells, 487
Ghrelin, 228
Giant cell arteritis, 1061–1062
  clinical laboratory testing of, 1061–1062
  definition and epidemiology of, 1061
  diagnosis, treatment, and prognosis of, 1062
  etiology and pathogenesis of, 1061
  pathology of, 1061, 1061f
Giant cell fibroblastoma (GCF), 1601
Giardia duodenalis, 1320–1321
Giemsa stain, 1202
GIL antibodies, 742
Gilbert's syndrome, 316
GIL blood group systems, 742
  biochemistry, 742
  biological role, 742
  molecular biology, 742
GINA. *See* Genetic Information Nondiscrimination Act
Glanzmann thrombasthenia, 857–858
Glassware, and plasticware, for laboratory, 55
Glioblastoma multiforme, 1580, 1583t
Glioma tissue analysis, 72f
Global hemostasis assays, 835–836
GLOB blood group system, 716–718
Globin gene clusters, 608, 608f
Globin synthesis, 574
Glomerular autoimmune diseases, 1089–1107
Glomerular filtration rate (GFR)
  creatinine clearance as an estimate of, 189–190
  measurement of, 188–191
    beta-2 microglobulin, 191
    beta trace protein, 191
    cystatin C, 190
    with endogenous substances, 188
    with exogenous substances, 188
    tryptophan glycoconjugate, 191
  renal plasma flow, filtration fraction and, 191–192
Glomerulonephritides, 1093–1107
Glomerulonephritis
  acute poststreptococcal, 1097–1098, 1097f–1098f
  endocarditis-associated, 1098, 1098f
  infection-associated, 1097–1098
  membranoproliferative, 1095–1096, 1095f–1096f
  pauci-immune, 1099–1102, 1100f–1101f
  postinfectious, 1097
Glomerulopathies, 1090–1093
Glove powder, 526
Glucagon, 227
Glucagonoma, 345
Glucose, 460–461, 519, 526, 529, 532, 535
  abnormalities, 111–112
  interstitial, 229
  measurements for, 228–229
Glucose oxidase, 228–229
Glutamate and *N*-Methyl-D-Aspartate (NMDA) receptors, 1454
Glutamic acid decarboxylase autoantibodies, 1108–1109
γ-Glutamyl transferase, 321–322
Glutathione S-transferases, 1483, 1484t–1485t, 1485
Glycemic control, measures of, 232–234, 232t
Glycogenoses
  hepatic, 239t
  muscle, 240t–241t
Glycogen phosphorylase, 270
Glycols, 381–382
Glycolytic enzyme deficiencies, 623
Glycoprotein Ib α (CD42b,c), 858
Glycoprotein IIb/IIIa inhibitors, 890
Glycoproteins Ib (CD42b,c)/IX (CD42a)/V, 858
Glycoprotein VI *(GP6)*, 858
Glycosuria, 476
  causes of, 477
Glycosylated albumin, 281–282
Glycosylated hemoglobin (GHb), 232, 233f, 233t, 608
Gonadotropin-releasing hormone (GnRH), 427
Gout, 525
Gouty arthritis, 525
Government payers, 164–166
GP130 gene, 1589

G-proteins, 848–849, 1532–1533
  defects in, and platelet signaling pathways, 860
Gradient diffusion, 1168–1169, 1169f
Graft-versus-host disease, 783–784, 784f, 784b
  as indication for extracorporeal photopheresis, 806–807, 806b
Gram-negative bacilli, miscellaneous, 1154–1160
Gram-negative bacteria
  bacilli, 1144–1147
  cocci, 1142–1144
  HACEK, 1153–1154, 1153t
  nonfermentative bacilli, 1147–1153
Gram-positive cocci, 1131–1137
Gram-positive rods, 1137–1142
Gram stain, 1202
  specimen processing relating to, 1130–1131, 1131f
Granular casts, 492, 493f
Granules, of platelets, and secretion, disorders of, 847, 858–859
Granule stores, deficiency of, 858–859
  gray platelet syndrome, 859
  Quebec platelet syndrome (QPS), 859
  δ-storage pool, 858
Granulocyte agglutination test, 766
Granulocyte and monocyte function, 946–949
Granulocyte antibody testing, 766
  flow cytometry, 766
  granulocyte agglutination test, 766
  granulocyte immunofluorescence test, 766
Granulocyte collection procedure, 793
Granulocyte colony-stimulating factor (G-CSF), 823
Granulocyte donor
  concerns of, 793–794
  selection of, 792
  stimulation of, 792–793
Granulocyte immunofluorescence test, 766
Granulocyte product requirements, 793
Granulocytes, 774
Granulocyte serology, 763–767
  granulocyte antibody testing, 766
  human neutrophil antigens, 763–766, 764t
  monoclonal antibody-immobilized granulocyte antigen assay, 766–767
Granulocyte transfusions, 791–792
Granulocytic and monocytic disorders, 636–641
  leukocyte adhesion deficiency (LAD) diseases as, 640
  neutropenia, 637–638, 638b
  neutrophilia, 636–637, 638f, 638b
  neutrophils
    functional disorders of, 639–640
    morphologic alterations in, 638–639, 639b
Granulocytotropic anaplasmosis, human, 1260
Granulomatous amebic meningoencephalitis (GAE), 1313
Granulomatous mediastinitis, 1212
Gray platelet syndrome (GPS), 859
Gray-top tubes, anticoagulants and, 27t, 28
Gross/physical examination, of urine, 469–472
  appearance of, 469–471, 470t
  color, 469–470, 470t
    blue, green, or blue-green, 470
    dark brown or black, 469
    orange-red or orange-brown, 469
    red, 469
    yellow-brown or green-brown, 469
  odor, 471
  volume, 471
Ground state, 293f
Group O, 714
Growth
  factors of, 572
  rate of, 1203
  temperature, 1203
Growth factor receptors, 1526f, 1530–1532
Growth factors, 1528–1530
  fusion genes involving, 1601
Growth hormone (GH), 390–392, 390f
  deficiency of, 391
  excess of, 391–392
Guanidinosuccinic acid, 862–863
Guinea worms, 1341
Gut peptides, in diarrhea, 338
Gynecomastia, 431

H

HACEK bacteria, 1153–1154, 1153t
Haemophilus, 1152–1153
  antimicrobial susceptibility of, 1153
  characteristics, 1152, 1152f
Haemophilus (Continued)
  clinical manifestations and pathogenesis of, 1152, 1152f
  laboratory diagnosis of, 1152–1153, 1152t–1153t, 1153f
Hair and nails, 536–537
Hairy cell leukemia, 667, 668f, 699, 702f, 1554
  variant, 667–668, 669f
Hand, foot, and mouth disease (HFMD), 1278
Hansen disease, 1186
H antigen, 711
Haploid, definition of, 1411
Hapten model, 1495
Haptoglobin, 283–284, 284f
Hb A_2 quantitation, 608
Hb C/β⁺-thalassemia, 615
HbC/β0-thalassemia, 615
Hb C disease, 614
Hb concentration, measurement of, 541–542
Hb C trait (β6 glu→lys), 614
Hb D Los Angeles (Punjab) (β121 glu→gln), 615
Hb E (β26 glu→lys), 615
Hb E/ β–thalassemia, 615
Hb E trait (Hb AE), 615
Hb G Philadelphia (α 68asn→lys), 615
Hb Kenya, 619
Hb S/β-thalassemia, 614
Hb S/O Arab, 614
Hb SS/α-thalassemia, 614, 615t
hCG, early pregnancy and, 433–434
HDL-C values, determining, 255
Health Insurance Portability and Accountability Act (HIPAA), 8–9, 175
Heart failure (HF), 268–269
  biomarkers, 275
Heart fatty acid binding protein, 270
Heat, hemolysis and, 624
Heat instability test, 616
Heat of fusion, 818–819
Heat-shock protein 70 genes, 1016
α Heavy chain disease, 669
γ Heavy chain disease, 668–669
μ Heavy chain disease, 669
Heavy chain diseases, 668–669
Heavy-light chain immunoassay (HLC), 963
Heavy proteinuria, 474
Heinz bodies, 622, 622f
Helicase-dependent amplification (HDA), 1397, 1397f
Helicobacter
  antimicrobial susceptibility of, 1151
  characteristics, 1151
  clinical manifestations and pathogenesis of, 1151
  laboratory diagnosis of, 1151
Helicobacter pylori infection, 1589
Hemagglutination, 744–746, 745f, 745t, 905–907, 907f–908f
  inhibition of, 756, 757t
  reactions, grading of, 746
  specific, factors affecting, 745, 745t
Hemangioendothelioma, epithelioid, 1601
Hemangioma, of bone, 1601
Hemapheresis, 788–816.e4
  donor cytapheresis
    donor erythrocytapheresis, 794–795
    donor leukocytapheresis, 791–794
    donor platelet apheresis, 790–791
    hematopoietic progenitor cell collection, by apheresis, 795–798
    multicomponent apheresis donation, 795, 795b
  donor/patient complications common to procedures, 811–816, 813t
    air embolus, 816
    allergic, anaphylactoid and anaphylactic reactions, 814–815
    angiotensin-converting enzyme inhibitors, 815
    electrolyte and acid-base disturbances, 813–814
    hydroxyethyl starch and coagulopathy, 816
    hydroxyethyl starch and renal dysfunction, 816
    hydroxyethyl starch and side effects, 816
    hypovolemia and vasovagal reactions, 815–816
  donor plasmapheresis
    plasma donor concerns, 799
    plasma donor selection, 799
    plasma products, 798–799
  hematopoietic progenitor cell collection, by apheresis, 795–798
  introduction to, 788–790
    basic principles of, 789–790, 789f
    definitions of, 788
  therapeutic, indications for, 799–811, 799t–803t
  therapeutic plasma exchange, 807–811, 808f, 809b–810b
Hematocrit, 542–543
  gross examination of, 543
  micromethod measurement of, 543
    centrifugation, 543
    equipment, 543
    interpretation of results, 543
    other errors, 543
    procedure, 543
    sample, 543
Hematocrit effect, 455–456
Hematogones, 694
Hematologic and coagulation disorders, pregnancy with, 439
Hematologic cells, ex vivo manipulation of, 824
Hematologic diseases, 979–980
Hematology
  analyzers, 549–550
  laboratory automation for, 77–78, 78f
  point-of-care testing in, 83
  principles and procedures of, for blood and bone marrow examination, 539–569.e2
  profile of, abnormalities in, 101–106
    anemias, 101–104, 101t
    coagulation disorders, 105–106
    quantitative white blood cell (WBC) abnormalities, 104–105
Hematolymphoid neoplasia, diagnosis and prognosis of, 1542–1578.e11
Hematopoiesis, 570–587.e1
  basophils and mast cells, 580–581
  embryonic and fetal, 572
  eosinophils, 579–580
  erythrocyte
    destruction of, 576
    erythrokinetics, 576–578
    production of, 572–576
  hematopoietic tissues, 572
  lymphocytes, 583–586
  megakaryocytes, 582–583
  monocytes and macrophages, 581–582
  neutrophils, 578–579
  postnatal, 572
  stem cells, 570–572
Hematopoietic grafts
  cryopreservation of, 818–819
  sources of, 821–823, 822t
    bone marrow as, 822
    peripheral blood progenitor cells, 822–823
    umbilical cord blood as, 823
Hematopoietic growth factors, 572
Hematopoietic neoplasms
  flow cytometric evaluation of, 689–707.e3
    interpretive considerations of, 693–705
    technical considerations of, 689–692
  leukemias
    acute lymphoblastic leukemia, 1550–1551
    acute myeloid, 1556–1567, 1557t–1558t, 1557b
    acute promyelocytic, 1557–1560
    childhood, 1550
  molecular diagnosis of, 1542–1578.e11, 1543t
  myeloproliferative neoplasms, 1568–1574
  non-Hodgkin lymphomas, 1548t–1549t, 1551f
    overview of, 645
Hematopoietic progenitor cell banking, 821–825, 821b
  adoptive cell transfer/chimeric antigen receptors, 824–825
  dendritic cells in cancer immunotherapy, 824
  ex vivo manipulation of hematologic cells in, 824
  hematopoietic grafts
    cryopreservation of, 823–824, 824t
    sources of, 821–823, 822t
  quantification and potency evaluation, 821
  reinfusion of progenitor cell products in, 824
  T-cell depletion in, 823
Hematopoietic progenitor cells (HPCs), 570–571, 571f, 571b, 774
  autologous versus allogenic harvest of, 795
  collection of
    by apheresis, 795–798
    procedure of, 798, 798t
  donor concerns of, 799
  dose of, 795–796, 796t
  mobilization of, 796–798, 796t, 797f
Hematopoietic stem cells, 570–571, 571f, 571b
Hematopoietic tissues, 572
  embryonic and fetal hematopoiesis, 572
  postnatal hematopoiesis, 572
Hematopoietic transplantation, indications for, 821b
Hematuria, 479–480, 481t
Heme synthesis, 574, 575f

Hemiglobin, 540–541
Hemiglobincyanide method
  of measurement, 541–542
  principle of, 541, 542f, 542t
  reagent of, 541–542
Hemizygous, definition of, 1411
Hemochromatosis, 332, 1441
Hemoflagellates, 1309–1312, 1311f
  Leishmania, 1312
  Toxoplasma gondii, 1312–1313
  Trypanosoma, 1310–1311
Hemoglobin, 540–542
  abnormal syndromes of, 611
  degradation of, 576
  derivatives of, 540–541
  destruction of, 603–604
    blood film of, 604–605
    bone marrow in, 605
  disorders of
    hemolysis relating to, 607–616
    screening and prenatal diagnosis of, 620
  electrophoresis and isoelectric focusing relating to, 608, 609f–612f
  fetal, hereditary persistence of, 619
  function and stability of, disorders of, 615–616
  Hb concentration, measurement of, 541–542
  hemosiderin, myoglobin, blood, and, in urine, 479–482
  mean cell, 543
  normal, 607–608, 607f
  reticulocyte content of, 592
  spectrophotometric identification of, 542
  structural variants of, 611, 613t–614t
  structure and function of, 574–576, 574f, 576f
  synthesis of, 574
  total destruction measurement of, 576–577
  total production measurement of, 576–577
Hemoglobin A (α2β2), 607
Hemoglobin A2 (α2γ2), 608
Hemoglobin Bart's hydrops fetalis, 619
Hemoglobin (blood) casts, 492–493, 493f
Hemoglobin constant spring (αCSα/), 620
Hemoglobin E disease, 615
Hemoglobin F (α2γ2), 607–608
Hemoglobin H disease, 620, 620f
Hemoglobin H, preparation of, 620, 620f
Hemoglobinometry, errors in, 542
  in equipment, 542
  in method, 542
  in sample, 542
Hemoglobinopathies
  sickle cell anemia and, 1440
  thalassemias and, laboratory investigation of, 608–611
Hemoglobin S, 611–615
Hemoglobin SC disease, 613–614
Hemoglobin SD disease, 614
Hemoglobinuria, 479–480, 481t, 606–607
  paroxysmal nocturnal, 705, 707f
Hemolysis, 102, 316
  anemia relating to
    acquired, extrinsic, 623–628
    general, 603–605
    hemoglobin disorders, 607–616
    membrane disorders, 605–607
    metabolic disorders, 621–623
  collection-associated variables, interference with, 24
  extravascular, 710–711, 711t
  intravascular, 710
  nonimmune, 784–785
Hemolytic anemia, 102–103
  autoimmune
    cold, 761–762
    investigation of, 760–762
    warm, 760–761
  immune, drug-induced, 763
  induced by medication, and positive direct antiglobulin tests, 763
  stimulation of red cell autoantibody production in, 763
Hemolytic disease, Rh antibodies in, 723
Hemolytic-uremic syndrome (HUS), 624–625
Hemopexin, 286
Hemophagocytic syndromes, 686, 687f
Hemophilias
  disruptive therapies for, 840
  gene therapy for, 840
  treatment of, 838–839
    complications of, 839, 840f
Hemosiderin
  casts, 493
  detection of, in urine, 481, 482f
    dry procedure, 481
    procedure, 482
    reagents, 481–482
    wet procedure, 482
  myoglobin, blood, hemoglobin, in urine, 479–482, 481f
Hemostatic system, hypothesis for initiation of, 832–833
Henoch-Schönlein purpura, 1070–1071, 1071f
Heparin
  as anticoagulant, 27–28
  effect on blood tests, 28t
  low molecular weight, 883, 884t
  resistance to, 883
  unfractionated, 882–883, 882f–883f
Heparin-induced extracorporeal low-density lipoprotein precipitation (HELP), 811
Heparin-induced thrombocytopenia, 883–885, 884f, 885t, 886f
Heparin-induced thrombocytopenia and thrombosis (HITT), 883–884
Heparin monitoring, 834–835
  anti-Xa activity assay for, 835
Hepatic adenomas, 1589
Hepatic adenomas with inflammatory features (HA-I), 1589
Hepatic autoantibodies, 1086–1087
Hepatic autoimmunity, 1086–1089
Hepatic glycogenoses, 239t
Hepatic lipase deficiency, 265
Hepatitis, 327, 785. *See also* Viral-induced.
  A, 323, 323f
  acute injuries and, 112
  alcoholic, 327
  B, 323–325, 324f, 325t
  B virus, 1279–1280, 1285
  chronic, 327
  C virus, 1058, 1070, 1280, 1285
  D virus, 1280
  E virus, 1280
  serum for, 323
  A virus, 1279
Hepatitis C (HCV)-induced hepatocellular carcinoma (HCC), 326
Hepatobiliary autoimmunity, 1086–1089
Hepatocellular carcinomas, 1588–1589
  anti-p53 in, 1534
  HER2/*neu* receptor and, 1531
  p53 protein in, 1534
Hepatocyte growth factor, 1530
Hepatolenticular degeneration. *See* Wilson's disease
Hepatosplenic T cell lymphoma, 679–680, 680f
Hepcidin, 450
HER2, 1592
Hereditary angioedema, 287, 979
Hereditary breast-ovarian cancer, 1447
Hereditary coagulation protein defects, 836–843
  factor VIII or factor IX, deficiency of, 837–840, 837t
  of other coagulation factors, 840–843
Hereditary colonic cancer syndrome, 1592–1593
Hereditary colorectal cancer syndromes, 1447
Hereditary elliptocytosis (HE), 606
  common, 606
Hereditary fructose intolerance, 241
Hereditary hemochromatosis (HH), 332
  HFE gene and, 1019–1020
Hereditary leiomyomatosis and RCC (HLRCC), 1595
Hereditary nonpolyposis colorectal cancer, 1447, 1592–1593
Hereditary papillary renal cell carcinoma, 1595
Hereditary proteinuria, 474
Hereditary pyropoikilocytosis (HPP), 606
Hereditary renal cell carcinoma syndromes, 1595
Hereditary sideroblastic anemias, 603
Hereditary spherocytosis, 605–606
Hereditary stomatocytosis, 606
Hereditary thrombophilias, 1440–1441, 1441f
HER2/*neu* (c-*erb*B-2) oncoprotein, 1517–1518
HER2/*neu* receptor, 1530–1531
Heroin, 359
Herpes simplex virus (HSV), 1272–1274, 1276t, 1277f
  cell culture isolation of, 1272–1273, 1276t
  direct detection of, 1272
  HSV-1, 1277, 1285
  HSV-2, 1277, 1285
  nucleic acid-based detection of, 1268
  traditional tube and shell vial cultures, 1267, 1272
Heterocellular hereditary persistence of fetal hemoglobin, 619
Heterogeneity, of parathyroid hormone, 212
Heterogeneous enzyme immunoassays, 911–912, 912t, 913f
  chemiluminescent, 912–913, 913f
  colorimetric, 912
  fluorescent, 912
Heterogeneous fluorescent immunoassay, 917–918
Heterogeneous immunoassay systems, 919
  high throughput fully automated, 920–921, 921t
  instrumentation and key points for, 920
Heterologous interpolation, 1123
Heterophile-negative infectious mononucleosis, 1270–1271
Heterophilic antibody, 1515
Heterophyes, 1335
Heterozygous β-thalassemia, 617–618, 618f
Heterozygous, definition of, 1411
HFE gene, hereditary hemochromatosis and, 1019–1020
HHV-6 infection, 1285
HHV8-positive DLBCL, NOS, 675
Hierarchical shotgun sequencing, 1608–1609
High cholesterol
  in children, 260, 260t
  with high LDL-C, 260
  with high triglycerides, 264–265
High-density lipoproteins, 247
High-grade B-cell lymphoma (HGBL), 1554–1555
  with MYC and BCL2 and/ or BCL6 rearrangements, 676
  NOS, 676
High-grade serous carcinoma (HGSC), 1598–1599
Highly active antiretroviral therapy (HAART), 1501
High oxygen affinity
  hemoglobins associated with, 615
High-performance liquid chromatography (HPLC), 51, 51f
  for drug detection, in serum and urine, 350–352, 352f
High-resolution melting analysis, 1613–1614
High specificity, versus high sensitivity, need for, 93
High throughput fully automated heterogeneous immunoassay systems, 920–921, 921t
High-throughput genomic and proteomic technologies, in postgenomic era
  diagnostic cancer applications, 1616–1618
    adenocarcinoma, 1617
    Barrett esophagus, 1616–1617
    other cancers, 1617–1618
    pancreatic cancer, 1617
    small, round blue cell tumors, 1616
    thyroid carcinoma, 1617
  emerging technologies, 1620–1622
    CRISPR, 1620–1621
    ion torrent sequencing, 1622
    next-generation sequencing, 1621–1622, 1621f
  human genome project
    private sequencing effort, 1609
    public sequencing effort, 1608–1609
    sequence of, 1609
  human neoplasia, molecular markers for diagnosis of, 1615–1616
    genomic, 1615
    proteomics, 1615–1616, 1616f
High-throughput platforms and central dogma of biology, 1608f
High-throughput technologies, 1609–1615
  genomic, 1609–1614
  proteomic, 1614–1615
High triglycerides
  high cholesterol with, 264–265
  with normal cholesterol, 264
Hinge region, 953
Histamine, 1119
Histiocytic and dendritic cell neoplasms, 686, 686f
Histocompatibility, 156
Histocompatibility antigens, 896
Histopathologic stains, 1202
HITECH Act, 8–9
HIV. *See* Human immunodeficiency virus (HIV)
HIV NAAT testing, 1282
HLA-A subregion, 998–1003
HLA-B subregion, 998–1003
HLA-C subregion, 998–1003
HLA-DP subregion, 1003–1005
HLA-DQ subregion, 1003–1005
HLA-DR subregion, 1003–1005
HLA-E genes, 1003
HLA-F genes, 1003

HLA-G genes, 1003
HLA matching, 1010–1011
HLA nomenclature, 1006–1007
HLA polymorphisms, identification techniques of, 1007–1009
HLA-specific antibody detection in recipient serum, 1011
HLA testing, 898
HLA typing, 1013
  sera trays, 1009
HLC. *See* Heavy-light chain immunoassay (HLC)
HNA-1 system, 764, 764t
HNA-2 system, 764–765
HNA-3 system, 765–766
HNA-4 system, 766
HNA-5 system, 766
HNF1A gene, 1589
HNF1A-mutated hepatic adenomas (HA-H), 1589
Hodgkin lymphoma, 683–685, 683f
  classical, 683
    unclassifiable B cell lymphoma with features intermediate between DLBCL and, 676
Hoesch test, 485–486
Holoenzyme, 293–294
Homeostasis
  calcium, 209–210, 209f
  magnesium, 211
  phosphorus, 210–211
  volume, defective hormonal regulation of, 471
Homocysteine, 273, 273f
Homocysteine assays, 595
Homocystinuria, 443–445, 508–509
Homogeneous assay systems, 919
Homogeneous enzyme immunoassay, 914–916, 914t
  apoenzyme-reactivation immunoassay, 914, 916f
  background of, 914
  cloned enzyme donor, 915–916, 917f
  enzyme inhibitory homogenous, 914–915, 916f
  enzyme-multiplied immunoassay technique, 914, 915f
  substrate-labeled fluorescent, 914, 915f
Homogeneous fluorescent immunoassay, 918–919
Homogeneous immunoassay, 348
Homologous chromosomes, definition of, 1411
Homologues, definition of, 1411
Homozygous β-thalassemia, 617
Homozygous, definition of, 1411
Honeycombed exudates, 1227
Honor codes, 179
Hook effect, 954
Hookworm, 1329, 1330f–1331f
Hormones. *See also* Antidiuretic hormone (ADH); Pituitary gland; Thyroid gland.
  analysis of, male reproduction relating to, 430–431, 431f
  deficiencies, hypoglycemia and, 235
  plasma corticotropin-releasing, 415
  regulating mineral metabolism, 212–215
  synthesis and metabolism, of thyroid gland, 396–398, 398t
Hormone therapy, 26
Hospitals, in point-of-care testing program, 86–87
HOX genes, 1547
HRF-20, 974
hTERT, 1594
HTLA antibodies, 758
HTR2A, 1462
Human antimouse antibodies (HAMAs), immunoassays and, 25
Human chorionic gonadotropin, 1517
Human *Ehrlichia canis* ehrlichiosis, 1260
Human equilibrative nucleoside transporter-1 (hENT1), 1594
Human genome, 1374–1375
Human genome project
  private sequencing effort, 1609
  public sequencing effort, 1608–1609
  sequence of, 1609
Human granulocytotropic anaplasmosis, 1260
Human immunodeficiency virus (HIV), 522, 785, 1273–1274, 1280–1282, 1281f
  blood transfusion products, 1282
  diarrhea relating to, 340
  infection, syphilis and, 1231–1232
  lymphomas associated with, 685
  NAAT testing, 1282
  parvovirus, enterovirus, and hepatitis B virus, 1273–1274
  pharmacogenomics in, 1502
Human immunodeficiency virus *(Continued)*
  protease inhibitors, in treating HIV-AIDS, 303–304, 303f–304f
  type 1 (HIV-1), 642–643
  vertical transmission, 1282
Human immunoglobulins
  physical properties of, 957t
  properties of, 957t
Human infection with *Ehrlichia ewingii*, 1260
Humanization, 966
Human leukocyte antigen (HLA), 899
  complex, 896
  pharmacogenomics, 1495–1496
Human leukocyte antigens, 998–999
Human metapneumovirus, 1268
Human monocytotropic ehrlichiosis, 1259–1260
Human neoplasia, molecular markers for diagnosis of, 1615–1616
  genomic, 1615
  proteomics, 1615–1616, 1616f
Human neutrophil antigens (HNAs), 763–766, 764t
  HNA-1 system, 764, 764t–765t
  HNA-2 system, 764–765
  HNA-3 system, 765–766
  HNA-4 system, 766
  HNA-5 system, 766
Human papillomavirus (HPV), 1276–1277
  infection, in cervical cancer, 1597–1598, 1598t
Human placental lactogen (HPL), 428, 767–769
Human platelet alloantigens, 767–769, 768t
  autoimmune thrombocytopenia, 769
  CD36 deficiency, 769
  drug-induced thrombocytopenia, 769
  and neonatal alloimmune thrombocytopenia, 767
  platelet antibody testing, 769
  and posttransfusion purpura, 767–769
Human resource management, clinical laboratory and, 5–6
Human subject research
  categories of
    exempt review category, 176–177
    expedited review, 177
    full IRB panel review, 177
  in clinical laboratories, 177–178
  federal regulations, development of, 176
  principles of, 175, 175b
Human T-cell lymphotropic virus, 785
Human T lymphotropic virus type 1 (HTLV-1), 642–643
Humoral factors, of immune system, 896
Humoral hypercalcemia of malignancy (HHM), 216
Humoral immunity, 897, 899
Huntington disease, 1442
Hyaline, 1195–1196
Hyaline casts, 490
Hyaline fungi, aspergillosis, fusariosis and other mycoses caused by, 1222–1225
Hyaline molds, septate, 1225
Hyalohyphomycosis, 1222
Hybrid capture, 1404–1405
Hybrid capture assays, 1399
Hybridization array technologies, 1401–1410.e3
  applications of, 1408–1410
    in clinical disease, 1408
    in clinical laboratory, 1408
    exosomes, 1408–1410
    limitations of, 1410
  bioinformatics in, 1406–1407, 1407f
  cDNA microarrays in, 1404
  delivery technologies for, 1402–1403
  detection and image analysis in, 1405–1406, 1406f
  hybrid capture in, 1404–1405
  intellectual property issues in, 1407–1408
  macroarrays in, 1402
  microarray fabrication in, 1402–1403
  microarrays in, 1402
  microarray substrates in, 1402
  oligonucleotide microarrays in, 1403–1404
  reverse line-blot hybridization in, 1405
  sequencing arrays in, 1404
  in situ synthesis for, 1403, 1403f
Hybridization assays, 1380–1381
  complementary base pairing in, conditions for, 1381
  formats for, 1381–1383
    dot or linear array hybridization as, 1382
    liquid or solution phase hybridization as, 1382
    microarray hybridization as, 1382–1383
    in situ hybridization as, 1383
    solid-support hybridization as, 1382
    Southern and Northern hybridizations as, 1382
Hybridization assays *(Continued)*
  hybrids in, detection of, 1381, 1385f
  probe in, 1380–1381, 1380f
  sample of, 1381
Hybridization, nucleic acid, 1379–1380, 1380f
Hybrids, detection of, 1381, 1385f
Hydatidosis, 1342–1343
Hydrodynamic focusing, 45
Hydrophobic chromatography, 279
Hydroxyethyl starch (HES)
  and coagulopathy, and hemapheresis, 816
  and other side effects, in hemapheresis, 816
  and renal dysfunction, and hemapheresis, 816
  as replacement fluid, 809
5-Hydroxyindoleacetic acid, 485
  screening test of, 485
11-β-Hydroxylase deficiency, 410–412, 412f
17-Hydroxylase deficiency, 412, 414f
21-Hydroxylase deficiency, 409–410, 411f
  congenital adrenal hyperplasia relating to, 1020
  diagnosis of, 409–410
3-Hydroxy-3-methylglutaryl-coenzyme A reductase, 1048
3-β-Hydroxysteroid dehydrogenase deficiency, 412, 413f
Hymenolepiasis, 1332
Hymenolepis diminuta, 1332–1333
Hymenolepis nana, 1332
Hyperacute rejection, 980
Hyperaldosteronism, 107, 107t
Hypercalcemia, 215–217
  causes of, 109, 215b
Hypercalciuria, calcium stones and, 506
Hypercarbia, as a cause of hypoxia, 111
Hypercholesterolemia
  autosomal dominant, 263–264
  autosomal recessive, 263–264
  familial, 261–263, 263f
  polygenic (nonfamilial), 260–261
Hyperchylomicronemia. *See* Lipoprotein lipase deficiency
Hypercortisolism: Cushing's syndrome, 416
  pseudo-Cushing's syndrome, 419
  tests for, 416–419
    confirmatory tests for, 418
    for defining cause of, 418–419, 418t
    screening for, 416–418, 417f
    in special populations, 418
Hyperdiploidy, with B lymphoblastic leukemia/lymphoma, 664
Hyperglycemia, on serum Na+, effect of, 185–186
Hyperhomocysteinemia, 877
Hyper-IgE syndrome, 1030
Hyper-IgM syndrome, 1028
Hyperimmunoglobulinemia, 959
Hyperinsulinism
  congenital, 237–238
  endogenous, 236
Hyperkalemia, 108
  cause and pathogenesis of, 196–197, 196b
  differential diagnosis of, 197
Hyperleukocytosis, 804
Hyperlipidemia
  combined
    acquired, 264
    familial, 264
  phenotypes, classical, 247t
Hyperlipoproteinemia type 1. *See* Lipoprotein lipase deficiency
Hypermagnesemia, 219
Hypermethylation, promoter, 1522
Hypernatremia, 107, 107t
  causes and pathogenesis of, 200, 200b
Hyperoxaluria, 506
Hyperphosphatemia, 218–219, 219b
Hyperplastic polyposis syndrome, 1593
Hyperproliferative normocytic anemias, 101t, 102–103
Hypersensitive aplastic anemias, 600
Hypersensitivity reactions, 898–899, 1345
Hypertension, renin and, 421–423, 421b–422b
Hypertriglyceridemia, 264
Hypertrophic cardiomyopathy, 269
Hyperuricuria, 506
Hypervitaminosis D, 446
Hyperzincemia, 452
Hyphae, yeasts and, structure of, 1195, 1197f–1198f
Hypobetalipoproteinemia, 265
Hypocalcemia, 217–218
  causes of, 107–108, 217b

Hypocomplementemic urticarial vasculitis, 1071–1072
clinical laboratory testing of, 1072
definition and epidemiology of, 1071–1072
diagnosis, treatment, and prognosis of, 1072
etiology and pathogenesis of, 1072
pathology of, 1072
Hypodiploidy, B lymphoblastic leukemia/ lymphoma with, 664
Hypofibrinolysis, 874–875
Hypoglobulinemia, 959
Hypoglycemia, 112, 234–238, 235b
alimentary, 236
autoimmune, 236, 1110
congenital hyperinsulinism and, 237–238
drug-induced, 234–235
endogenous hyperinsulinism and, 236
hormone deficiencies and, 235
in infancy and childhood, 236–238
non-beta cell tumors and, 235–236
severe medical illnesses and, 235
Hypokalemia, 107–108
cause and pathogenesis of, 195–196, 195b
differential diagnosis of, 196
Hypomagnesemia, 219
causes of, 219b
Hyponatremia, 106–107, 106t
causes and pathogenesis of, 199–200, 199b
Hypoparathyroidism, 217
Hypophosphatemia, 219
Hypoproliferative normocytic anemias, 101t, 103–104
Hyposthenuric urine, 472
Hypotensive reactions, 784
Hypothalamic-pituitary-thyroid axis, 398–401
Hypotonic cell lysis, 760
Hypovolemia, 815–816
Hypoxia
hypercarbia as a cause of, 111

I

I blood group systems, 741–742, 741f
biochemistry, 741, 741f
biological role, 742
molecular biology, 741–742, 741f
null phenotype, 741
iChemVELOCITY, 502
Idarucizumab, 887
IDH1 gene, 1566
IDH2 gene, 1566
Idiopathic acquired aplastic anemia, 600
blood in, 600
bone marrow in, 600
erythrokinetics in, 600
Idiopathic hypereosinophilic syndrome (HES), 641, 641b, 642f, 649–650
Idiopathic inflammatory myopathies, 1046–1049
aminoacyl-tRNA synthetases, 1046–1047
autoantigens and autoantibodies in, 1046, 1047t
cytosolic 5'-nucleotidase 1A, 1048–1049
3-hydroxy-3-methylglutaryl-coenzyme A reductase, 1048
MDA5 (CADM-140), 1048
Mi-2/NuRD complex, 1048
MJ/NXP2, 1048
myositis-associated autoantibodies, 1049
signal recognition particle, 1048
small ubiquitin-like modifier activating enzyme, 1048
TIF1-I/TIF1-α (P155/140), 1048
IgA
nephropathy, 1093–1095, 1093f–1094f
pemphigus, 1081
IgA vasculitis (Henoch-Schönlein purpura), 1070–1071
clinical laboratory testing of, 1071
definition and epidemiology of, 1070–1071
diagnosis, treatment, and prognosis of, 1071
etiology and pathogenesis of, 1071
pathology of, 1071, 1071f
IgE. *See* Immunoglobulin E (IgE)
IgE antibodies
allergen-specific, measurement of, 1123
measurement of, 1123–1127, 1124f–1125f, 1125t, 1127f
clinical applications of, 1122, 1122t
IgG, 1271t
measurements of, albumin and, 516–518
subclasses of, 1029
IgG synthesis rate, 517
IgM, 1271t
iKnife, 72
IL17 receptor, 985–986
Image analysis, in array technologies, 1405–1406, 1406f
Imaging
of chromosomes, computer-assisted, 1415
radiologic, 1028
Imatinib, 1501
Imidazopyridine zolpidem, 363
Immediate hypersensitivity
mechanisms of, 1116
reactions to
cells and mediators of, 1118–1120, 1119f
tests for mediators of, 1128
Immune cell function, 932f
Immune glomerular diseases, pathologic features of, 1090t
Immune hemolytic anemias, 625–628, 625b
Immune response
age and, 940
cancer and, 940
malnutrition and, 940
Immune system and immunologic disorders, overview of, 893–900.e1
histocompatibility antigens, 896
humoral factors, 896
complement, 896
cytokines, 896
immunoglobulins, 896
immunologic assessment, laboratory applications of, 897–898, 897b
immunologic injury, mechanism of, 896–897
immunology, therapeutics in, 898–899, 898b
lymphoid cells, 894–896
antigen-presenting cells, 895, 895f
B lymphocytes, 895
natural killer cells, 895–896
T lymphocytes, 894–895
nonlymphoid cells, 896
basophils and mast cells, 896
neutrophils and eosinophils, 896
Immune system, evaluation of, 1026–1034, 1027f
adjunctive tests
pathology, 1028
pulmonary function, 1028
radiologic imaging, 1028
advanced evaluation, 1030–1034
antibody production, novel immunogens for assessment of, 1032
cell surface markers, additional, 1032
cytokines and cytokine receptors, 1031–1032
functional assays, 1032
metabolic defects, enzyme measurements for, 1030–1031
MHC class I and II molecules, 1032
molecular genetics, 1032–1034, 1033t–1034t
natural killer cell assays, 1031
newborn blood screening, 1033–1034, 1034f
phagocyte analyses, additional, 1031
prenatal diagnosis, 1033
targeting cell surface receptors, treatment by, 1032
Toll-like receptor (TLR) assays, 1031
basic evaluation, 1026–1028
clinical history and physical examination, 1026–1027
complete blood count, 1027
immunoglobulins, 1027–1028
intermediate evaluation, 1028–1030
complement evaluation, 1030
IgG subclasses, 1029
lymphocyte subsets, 1029
polymorphonuclear killing assays, 1030
specific antibody production, 1028–1029
T cell functional assessment, 1029–1030
Immune thrombocytopenias, 855–856, 855t
drug-induced, 856
Immunity, 929–930
Immunoassays, and immunochemistry, 901–928.e2
in analytic system, flow of, 920, 920f
antibodies, characteristics of, 902
antigen-antibody reaction
general characteristics of, 901–902
kinetics of, 902–903
antigens, characteristics of, 902
assay systems, instrument automation and modulation of, 920
chemiluminescent immunoassay, 919
classes of, 903, 903t
conjugation chemistry, 903–904, 904f
enzyme, 911–917
fluorescent, 917–919
interference with, 24–25
Immunoassays, and immunochemistry *(Continued)*
nephelometric, 904
noncompetitive immunoassay, for small molecules, 923–925
particle, 905–909
particle agglutination, principle of, 905–907, 905f–906f, 905t
particle-counting, 907
point-of-care testing, devices for, 921–923, 922f
precipitin and nephelometric immunoassays, 904
background and principles of, 904
principles of, overview of, 903–904
radioimmunoassay, 909–911, 910f
assay principles and methods, 909–911, 910f–911f
background, 909, 909f, 909t
sensitive immunoassay, using specimen pretreatment methods, 925–926
simultaneous multiple immunoassays, 926–927
single molecule detection, 927–928
solid phase of, 904, 905t
Immunoblot, 1235
Immunoblotting, 1056, 1056f
Immunochemical methods, of drug detection, 348, 349f
Immunochromatographic devices, 921–922, 922f
Immunocompromised host, parasitic infections and, 1350t, 1351
Immunodeficiency-associated lymphoproliferative disorders, 685, 685b
Immunodeficiency disorders, 1025–1034.e2, 1026f
clinical signs and symptoms, 1025–1026, 1026f
immune system, evaluation of. *See* Immune system, evaluation of
novel approaches for treatment of, 1034
patterns of, 1027f
primary/secondary, 1025
Immunodiagnostic methods, for medical parasitology, 1297–1300
Immunodominant structures, 709
Immunoendocrinopathies, 1108–1112
Immunofixation, 961–962, 962f
Immunofixation electrophoresis (IFE), 517
Immunoglobulin E (IgE)
measurement of, analytic methods and reference ranges, 1121–1122, 1122t
physicochemical properties of, 1118t
structural and functional characteristics, 1117–1118, 1118t, 1119f
synthesis of, regulation of, 1117, 1118f
total serum measurement, clinical applications, 1122
Immunoglobulin free light chain analysis, 962–963
Immunoglobulin function and humoral immunity, laboratory evaluation of, 952–968.e2
antibodies, structural properties of, 952–955
antibody-antigen interaction, 953–955, 954f
antibody molecule, 952–953, 953f, 954t
antibody diversity, genetic basis of, 955, 955f, 956t
immunoglobulins
clinical significance of, 959–967
general properties of, 955–959
Immunoglobulin G isoelectric focusing (IgG-IEF), 517, 518f
Immunoglobulin heavy chain locus *(IGH)*, 1544–1545
Immunoglobulins, 896, 1027–1028
A, 956–957, 957t, 958f
clinical significance of, 959–967
D, 957–959, 957t
E, 957t, 959
G, 956, 957t–958t
general properties of, 955–959
human, 957t–958t
M, 955–956, 957t
nonimmunologic adsorption of, to red cell membrane, 628
variants, 956t
Immunoglobulins with restricted heterogeneity, 960
Immunohematology, 708–770.e6
basic concepts of, 708–711
blood group alloantibodies and autoantibodies, 710
blood group antigens, 709
blood group systems
ABO and H, 711–714, 712t
Augustine, 743
CD59, 743
Chido/Rodgers, 736, 736t
Colton, 735, 735f
Cromer, 737–738, 738t
Diego, 731–732, 732f
Dombrock, 734–735
Duffy, 728–730, 729f–730f, 729t–730t
Gerbich, 736–737, 737f, 737t

Immunohematology *(Continued)*
GIL, 742
I, 741–742, 741f
Indian, 739–740
JMH, 740–741
JR, 742
KANNO, 744
Kidd, 730–731
Knops, 738–739, 739t
Lan, 742–743
Lewis blood group system, 727–728, 728f
Lutheran blood group system, 723–725, 724f, 724t–725t, 726f, 727t
LW, 735–736, 736t
MNSs, 714–716, 715f, 715t
OK, 740
P1PK, GLOB and FORS, 716–718, 717t
RAPH, 740
RH and RHAG blood group systems, 718–723, 719t–721t, 721f–722f
Scianna, 733–734, 733t–734t
SID, 744
Vel, 743
Xg, 733
YT, 732–733, 733f
complement system, blood banking and, 710–711
erythrocyte antigens and antibodies, 711–744, 712t–713t
granulocyte serology, 763–767
granulocyte antibody testing, 766
human neutrophil antigens, 763–766, 764t
monoclonal antibody-immobilized granulocyte antigen assay, 766–767
platelet serology, 767–769
positive direct antiglobulin tests and hemolytic anemia, induced by medication, 763
tests and procedures for, 744–762
antibody detection, 751–756, 753t, 754f
antibody identification, 752–754, 754f
antihuman globulin test, 746–748
autoimmune hemolytic anemia, investigation of, 760–762
compatibility testing, 748–751, 750t
hemagglutination, basic principles, 744–746, 745f, 745t
special antibody identification techniques in, 756–760
Immunohistochemical microscopy, 1233
Immunohistochemical stains, 1203
Immunologic assessment, laboratory applications of, 897–898, 897b
Immunologic diseases, 601
Immunologic injury, mechanism of, 896–897
Immunologic studies
of pericardial fluid, 533
of pleural fluid, 531
of synovial fluid, 527
Immunologic tests, for male reproduction, regulation of, 430
Immunologic thrombocytopenic purpura (ITP), 855t
Immunology testing, 897b
Immunology, therapeutics in, 898–899, 898b
Immunophenotypic analysis, 936–937
Immunophenotyping lymphocyte subpopulations, 942b
Immunophilins, 348–350
Immunosignature, 897
Immunosuppressives, 374–376, 375f
Impedance, 48
Imperfect fungi, 1195
Implementation, of quality control procedures, 133–141
Imprinting, 1437–1438
Inclusion casts, 492
Income statement, 170
Incretin, 228
Incubation
conditions, for susceptibility testing, 1167
mixing and, in automated chemistry analyzer, 76
Independent assortment, definition of, 1412
Indeterminate leprosy, 1187
India ink preparation, for examination, 1202, 1202f
Indian antibodies, 740
Indian blood group systems, 739–740
biochemistry, 739
biological role, 740
molecular biology, 739–740
null/weak phenotypes, 739
Indirect agglutinins, 745
Indirect antiglobulin test (IAT), 746–747, 749t
Indirect bilirubin, 456–457
Indirect crossmatch techniques, 1012
Indirect determination, 454
Indirect exclusion, 1474
Indirect immunofluorescence in HEp-2 cells, 1050, 1051f–1054f, 1055t
Indirect immunofluorescence microscopy, 1081f
Individualized Quality Control Plan (IQCP), 139
Induced fit, of substrate binding, 292, 292f
Industry overview, of financial management, 162
Infancy and childhood, hypoglycemia in, 236–238
Infection(s)
aplastic anemia and, 600
Bartonella, 1263–1264, 1263t
Coxiella, 1261t
elevated WBC due to, 104
pregnancy with, 439
Rickettsial, 1254–1264, 1255t
ureaplasmal, 1250–1253
Infectious agents
acquired, extrinsic hemolysis relating to, 625
transmission of, 1344–1345
Infectious diseases, 979, 1368
Infectious mononucleosis
diagnosis of, 1270–1271
Epstein-Barr virus infection and, 643–644, 644f
clinical features of, 643
complications of, 643
course of, 644
differential diagnosis for, 644
etiology and pathophysiology of, 643
hematologic features of, 643
serologic findings, in immunocompromised patients, 644
and related infections, 1270–1271
Inflammation, DLBCL associated with, 674
Inflammatory bowel disease, 342, 342t, 1085–1086
Inflammatory conditions, markers for, 114
Inflammatory myofibroblastic tumor, 1602
Influenza, 1267
clinical implications, 1267
clinical presentation, 1267
epidemiology, 1267
laboratory diagnosis, 1267
licensed antivirals, 1267
molecular tests, 1267
virology, 1267
Influenza pneumonia, 1266
Information technology (IT), 155
Informed consent document, 175
Infrared spectroscopy, gas chromatography with, 353
Inheritance, 998
Inherited aplastic anemia, 601
Inherited metabolic disease, urinary screening for, 507–509
Inhibitory methods, for susceptibility testing, 1168–1170
Ink-jet technologies, 1403
Inoculum, susceptibility testing, 1167
Insects, 1346–1347, 1346f
In situ hybridization, 1383
In situ synthesis, for microarray fabrication, 1403, 1403f
In-space mass analyzers, 64
Institutional review board (IRB), 176
human subjects research, oversight of, 176b
waived and expedited reviews, 176
Instrumentation, 689–690, 690f
principles of, 35–59.e1
Instrument technology, 549–551
cytochemistry, 549–550
electrical impedance of, 549
error, sources of, 548t, 550
light scattering, 549, 550f
radiofrequency conductivity, 549
reporting/flagging, 550, 550f, 550t
Insulin, 226–227
Insulin autoantibodies (IAA), 1108, 1109f
Insulinoma, 345
Insulinoma-2-associated autoantibodies, 1109
Insulinomimetic insulin receptor autoantibodies, 1110
Insulin resistance, type B, 1110
Insurance, private, 164
Integration, optimizing performance and, 20
Integrin $\alpha_2\beta_1$ (Glycoprotein Ia/IIa; VLA-2; CD49b/CD29) *(ITGA1/ITGA2)*, 858
Integrin $\alpha_{IIb}\beta_3$ (Glycoprotein IIb/IIIa; CD41/CD61), 857–858
Integrins, 992–993, 993t
Inter-α-trypsin inhibitor (IATI), 287
Intercept Blood System (IBS), 775
Interference filter, 40f
Interferences, 455–456. *See also* Analyte assays and common interferences, chemical basis for.
biotin, 24–25
common, of precollection variables, 23–24
in vitro, collection-associated variables, 24, 24f, 24t
in vivo, tobacco smoking, 23
drugs, effects of, 25–26
dyes, 26
ethanol, 26
hormone therapy, 26
immunoassays, 24–25
molecular diagnostics, 25
monoclonal antibodies, 25
specimen matrix effects, 25
transgender, 26
Interfering substances, 253
Interferon- γ, 530, 532
Interleukin-8, 535–536
Interleukin-18 (IL-18), 193
Intermediate-density lipoproteins, 248
Internal rate of return (IRR), 171
Internal Standard (IS), 61
International Chapel Hill Consensus Conference, 1059b, 1060t
International normalized ratio (INR), 879
and prothrombin time, 833–834
International units, 297
Internet/Intranet, 160
Interstitial deletion, 1420, 1421f–1422f
Interstitial glucose, 229
Interstitial keratitis, of cornea, 443
Interval scale, 119
Interviews, data collection techniques and, 16
Intestinal helminths, 1326–1338
Intestinal protozoa, in medical parasitology, 1315, 1315f–1317f
Intracellular antigens, methods for detection of autoantibodies to, 1050, 1050t
Intracellular killing, assays of, 948–949, 948f
Intracellular processes, proteins involved with, 1460–1461
Intracytoplasmic sperm injection (ICSI), 433
Intraductal papillary-mucinous neoplasms (IPMNs), 1594
Intraoperative PTH, 213
Intrapartum assessment, of fetal status, 439
Intravascular hemolysis, 710
Intravascular large B cell lymphoma, 675
Intrinsic tenase, 833
Introns, 1001
Invasive candidiasis, 1208
Inversion, 1420, 1421f–1423f
Inversion loop, 1420–1421
Investment, return on, 171
In vitro antibiotic susceptibility testing (AST), 1166
In vitro fertilization (IVF), 820
In vitro testing, of antimicrobial agents, 1166–1182.e3
Iodine (I), 450
Ion detector, 64
Ion-exchange chromatography, 51, 279
Ionization, 62
Ionized (free) calcium, reference interval for, 210
Ionized (free) magnesium, 211–212
Ionizing radiation, aplastic anemia and, 600
Ion-photon conversion detectors, 64
Ions, bicarbonate, 459
Ion-selective electrodes, 47, 453–454, 454f
for calcium determinations, 457
Ion signature, 1617
Ion Torrent PGM sequencing, 1605
Ion torrent sequencing, 1622
Ion trap mass analyzers, 62–64
IP address, 160
iQ200 analyzer, 503
iQ lamina, 503
IQCP. *See* Individualized Quality Control Plan (IQCP)
Irinotecan, 1497–1499, 1498f
Iron, 383, 450–451, 457–458. *See also* Serum iron.
intoxication relating to, 383
Iron-binding capacity, 102, 383, 457–458
Iron deficiency anemia (IDA), 590–592
clinical features of, 590
differential diagnosis of, 592
iron metabolism, 588–590, 589f
laboratory features of, 590–592
blood, 590, 591f
erythrocyte porphyrins, 591
hepcidin level, 592
marrow, 590, 591f
reticulocyte hemoglobin content, 592

Iron deficiency anemia *(Continued)*
serum ferritin, 591
serum iron, 590
serum (total) iron-binding capacity, 590
serum transferrin receptors, 591–592
serum transferrin receptor-to-serum ferritin ratio, 592
TIBC, percent saturation of, 591
management of, 592
Iron hematoxylin stain, 1296
Iron-refractory iron deficiency anemia (IRIDA), 592
IRR. *See* Internal rate of return (IRR)
Irradiation, of blood components, 775
Ischemia modified albumin, 270
Islet autoantibody testing, 1109t
Islet cell cytoplasmic autoantibodies (ICA), 1108f
testing, 1077f
Isochromosome, 1422
Isocitrate dehydrogenase (IDH) I and II, 72–73
Isoelectric focusing, 48–49, 49f
Isoenzymes, 293, 294t
Isoforms, 293
Isolated HDL-C
high, 266
low, 265–266
Isolated neutropenia, 638
Isolation
Isopropanol precipitation test, 616
Isosthenuria, 472

J

JAK2 mutations, 1572, 1572f
JAK-STAT pathway, 1527
JAK2 V617F mutation, 1572–1573
Japanese encephalitis virus (JEV), 1288
J (joining) chain, 956
JMH antibodies, 741
JMH blood group systems, 740–741
biochemistry, 741
biological role, 741
molecular biology, 741
variant and null phenotypes, 740–741
Joint, infection of, *Cryptococcus* in, 1209
Jr antibodies, 742
JR blood group systems, 742
biochemistry, 742
molecular biology, 742
Juvenile myelomonocytic leukemia, 652–653, 1574
Juvenile polyposis syndrome (JPS), familial, 1581t–1583t, 1593

K

k_2 and K_M, knowledge of, 296, 296f
KANNO antibodies, 744
KANNO blood group systems, 744
biochemistry, 744
biological role, 744
molecular biology, 744
Karyogram, definition of, 1411
Karyotype
analysis, of chromosomes, 1414–1415
definition of, 1411
Kawasaki disease, 1063–1064
clinical laboratory testing of, 1064
definition and epidemiology of, 1063
diagnosis, treatment, and prognosis of, 1064
etiology and pathogenesis of, 1064
pathology of, 1063–1064, 1063f
KCNC1, 1461
KCNG2, 1461
Kell and KX blood group systems, 725–727, 725t
biochemistry, 726, 726f
biological role, 727
molecular biology, 726
null and weak phenotypes, 725–726
Kell antibodies, 726–727
Ketoacidosis, 203
Ketones
tests for, 234, 479
in urine, 479
Ketonuria
diabetic, 479
nondiabetic, 479
Key database
concepts, 151–152, 151t
structures, 152–153
tables, 152–153, 152f
Kickbacks/bribery, 179
Kidd antibodies, 731
Kidd (JK) blood group system, 730–731, 730t
biochemistry, 730–731
biological role, 731
molecular biology, 731
null phenotypes, 730
Kidney injury molecule-1 (KIM-1), 193
Kidney tumor, 1595–1596
Kinases and signaling pathways, 1564–1565
Kindlin-3 deficiency, 860
Kinetics, of antigen-antibody reaction, 902–903
Kingella, 1154
antimicrobial susceptibility of, 1154
characteristics, 1154
clinical manifestations and pathogenesis of, 1154
laboratory diagnosis of, 1154
Kininogen, high molecular weight, 841–842
Kinins and kinin-generating system, 983
Kirby-Bauer test, 1169
Kissing bugs, 1346f, 1347
KIT-activating mutations, 1575
KIT D816V gene mutation, 1577
KIT mutations, 658, 1560, 1565
in gastrointestinal stromal tumor, 1601–1602
Kjeldahl technique, 279–280
KLB gene *(rs11940694)*, 1459
Klebsiella granulomatis, 1159
Klebsiella pneumoniae carbapenemases (KPCs), 1176
Kleihauer-Betke test, 756
Klinefelter syndrome, 1428–1429
KMT2A gene rearrangements, 1550
KMT2E, 1466
Knops antibodies, 739
Knops blood group systems, 738–739, 739t
biochemistry, 739
biological role, 739
molecular biology, 739
Kostmann's syndrome, 637
KRAS gene, 1565
mutations in, 1501
in colorectal cancer, 1591
in lung cancer, 1588

L

Laboratory. *See also* Clinical laboratory.
design and service models, 6, 7b
glassware and plasticware for, 55
hazard prevention strategies, 10t
medical parasitology methods of, 1292–1301
mercury-free, 56
performance, optimizing, 19–21, 21t
regulations and their significance, 7t
safety of, 1200
technology
breakthrough, 18b
role of, 18–19
understanding of, 18–19
testing process, 14f
workflow
analysis, 16–18
data collection techniques and, 13–16
and performance, 13–21.e1
understanding of, 13–18
Laboratory Compliance Program, clinical laboratory and, 8
Laboratory-developed tests (LDT), 73
for prostate cancer, 1597
Laboratory directorship, in point-of-care testing and physician office laboratories, 82–83
Laboratory information systems (LIS), 155–157
specialized modules, 156–157
cytogenetics, 157
flow cytometry, 156–157
histocompatibility, 156
molecular diagnostics, 157
system selection, 155–156
Laboratory-related governmental agencies, 8t
Laboratory-related nongovernmental organizations, 9t
Laboratory results
interpretation of, 92–97
interpreting, 100–118.e2
abnormal laboratory values, 100–101
clinical cases with clinicopathological correlations, 116–118
clinical chemistry, abnormalities in, 106–116
hematology profile, abnormalities in, 101–106
variability of, 91–92, 91t
Laboratory statistics, 119–129.e1
analyzing data
discrete, 124–125, 124t
preparation, 120
comparative, 122–124
definitions for, 119–120
descriptive, 120–122
method validation and process control for, 127–128
resources for, 128–129
trend evaluation and correlative, 125–127
variables, 120
LabUMat 2, 503
β-Lactam antibiotics, and platelet function, 864
β-Lactamase
classification, 1174t
direct tests for, 1169–1170
Lactate, 461, 519, 529–530, 535
Lactate dehydrogenase (LD), 269, 311–312, 321, 465, 520
abnormal results of, causes of, 312
biochemistry and physiology of, 311, 311t
measurement of, 311–312
reference ranges and preanalytic variation of, 311
Lactic acid dehydrogenase, 293
Lactic acidosis, 202, 203b, 242–243, 243b, 479
methods of, 479
nitroprusside tablet test for, 479
reagent strip for, 479
D-lactic acidosis, 203
Lactose, in urine, 477
Lactose tolerance test, 338
Lagging strand, 1375–1376
Lan antibodies, 743
Lan blood group systems, 742–743
biochemistry, 742
biological role, 743
molecular biology, 743
Langerhans histiocytosis, 686, 687f
Large B cell lymphoma, arising in HHV8-associated multicentric Castleman's disease, 675
Large B-cell lymphoma with IRF4 rearrangement, 672
Large granular lymphocyte leukemia, 677
Large granular lymphoproliferative disorder, 700
Large vessel vasculitis, 1059–1062, 1060f, 1060t
giant cell arteritis, 1061–1062
Takayasu arteritis, 1060–1061
Larval migrans, 1341–1342
Laser ablation electrospray ionization (LAESI), 71
Lasers, 45
Laser source, 39
Lassa mammarenavirus (LASV), 1288
Latex agglutination, 907
Latex turbidimetric assay, 907
Laxative abuse, 341
LBRF. *See* Louse-borne relapsing fever (LBRF)
LDL-C measurement, 255
Lead, 383–384
in blood, 384
Leadership, 2
Leading strand, 1375–1376
Lean
optimizing performance and, 20
quality systems management and, 3–5
Lecithin/cholesterol acyltransferase (LCAT) deficiency, 266
Lectin reagents, red blood cell typing with, 759
Leflunomide (LFM), 376
Left ventricular ejection fraction (LVEF), 269
Legionella, 1154–1155
antimicrobial susceptibility of, 1155
characteristics, 1154, 1155f
clinical manifestations and pathogenesis of, 1154–1155, 1155f
laboratory diagnosis of, 1155, 1155f
Leiomyosarcomas, 1602
Leishmania, 1312
cutaneous, 1312
diagnosis of, 1312
mucocutaneous, 1312
visceral, 1312
Leishmaniasis, 1312
Lepirudin, 885
Lepore hemoglobins, 619
Lepromas, 1187
Lepromatous leprosy, 1187
Leprosy, 1186–1187
Leptospira, 1236–1237
characteristics, 1236
clinical manifestations of, 1236
epidemiology of, 1236

Leptospira (Continued)
laboratory diagnosis of, 1237
pathology and pathogenesis of, 1236
species, 1236
treatment of, 1237
Lesion(s), 108
of skin, *Cryptococcus* in, 1209
space-occupying, 113, 329
Leucine, 497, 497f
Leukemias
acute lymphoblastic leukemia, 1550–1551
acute myeloid, 1556–1567, 1557t–1558t, 1557b
acute promyelocytic, 1557–1560
anti-c-myc protein in, 1535
childhood, 1550
p53 protein in, 1534
pure erythroid, 659
ras-p21 protein in, 1533
Leukemoid reactions, 645–646
and congenital neutrophilia, 646
elevated WBC due to, 104–105
eosinophilic, 646
leukoerythroblastosis and, 646
lymphocytic, 646
neutrophilic, 646
Leukocyte(s), 346, 488, 636
components, 774
manual count of, 545–546
due to equipment, 546
due to nature of sample, 546
hemocytometer method, 545
inherent or field errors, 546
nucleated red blood cells, 546
operator's errors, 546
procedure, 546, 546f
reference value, 546
sources of error, 546
specimen collection, 545–546
on peripheral blood smear examination, 547t
physiologic variation in, 546, 547t
Leukocyte adhesion deficiency (LAD), 860
diseases, 640
type 1, 1031
type 2, 1031
Leukocyte (WBC) casts, 491, 491f
Leukocyte esterase, 484
methods of detecting, 484
reagent strip, 484
Leukocyte extravasation, 994, 994f
Leukocyte-reduced blood components, 774
Leukocytic disorders, 636–688.e4
leukocytes, 636
neoplastic disorders, primarily involving leukocytes, 646–686
nonneoplastic, 636–646
granulocytic and monocytic, 636–641
lymphocytic and plasmacytic, 641–645
Leukocytosis, due to acute leukemias, 105
Leukoerythroblastosis, 646
Leukopenia, Gram-negative sepsis as a cause of, 105
Levetiracetam, 371
Lewis antibodies, 728
Lewis blood group system, 727–728, 727t
biochemistry, 727
biological role, 728
molecular biology, 727–728, 728f
LHPP, 1462
Lidocaine, 368
Lifetime, of enzymes, in blood, 294–295
Li-Fraumeni syndrome, 1603
Light blue-top tubes, anticoagulants and additives, 27–28, 27t
Light scattering, 549, 550f
Likelihood ratio, 94–95, 95t
Limit of detection, 62
Limits of quantitation, 62
Linear array hybridization, 1382
Linear IgA dermatosis, 1082
Linearity, 42
Linear regression, 125, 125f
definition of, 120
Line immunoassays, 1056
Line source, 38
Lineweaver-Burk plot, 296–297, 296f
Linkage
analysis, 1436
definition of, 1412
disequilibrium, 998
of class II genes, 1004–1005
Lipase, 334, 465–466
Lipid crystals, 526
Lipids, 244, 526–527, 530, 532
dyslipoproteinemia and, 244–266.e2
cholesterol testing and management in, guidelines for, 258–260, 258t, 258b–259b
lipoproteins, apolipoproteins, and related proteins in, 246–248
overview of, 244, 245f–246f, 245t
and lipoprotein measurement, 251–256
lipoproteins, and disease, 260–265, 261t, 262f–263f
obesity and metabolic syndrome, 265
in renal tubular epithelial cells, 489, 490f
tests for, 317–318
transport of, and lipoprotein metabolism, 248–251
Lipiduria, 471
Lipolytic enzymes, and other proteins, 248, 250t
β-Lipoprotein, 284
Lipoprotein lipase deficiency, 264
Lipoproteins, 244, 248
apolipoproteins, and related proteins in, 246–248
chemical composition of, 245t
classification of, 246f
detection of, 257
high-density, 247
intermediate-density, 248
lipids, and disease, 260–265, 261t, 262f–263f
and lipoprotein cholesterol, estimation of, 254–255
low-density, 247
LpX, 248
major, 246–247
metabolism of, 246f
important proteins in, 248
minor and abnormal, 248
modified, 257
particle number, measurement of, 256
physicochemical characteristics of, 245t
structure of, 245f
subclasses, measurement of, 256–257
very-low-density, 246–247
Liposarcoma, well-differentiated and dedifferentiated, 1600
Liquid chromatography, 51, 51f, 62
Liquid chromatography-mass spectroscopy, 66, 352–353
Liquid or solution phase hybridization, 1382
Liquid scintillation, 52
LIS. *See* Laboratory information systems (LIS)
LIS Functionality Assessment Toolkit (LIS-FAT), 156
LIS system selection, 155–156
Listeria, 1138–1139, 1138f
antimicrobial susceptibility of, 1139
characteristics, 1138
clinical manifestations and pathogenesis of, 1138–1139
laboratory diagnosis of, 1139, 1139t
List-mode data (Flow Cytometry), 159–160
Lithium, 376
Liver
fibrosis of, 328–329
metabolism in, 365–366
necroinflammation of, 328–329
synthetic functions of, 318–320
Liver disease, 596, 844
anemia in, 598
Liver function, evaluation of, 314–330.e4
diseases, diagnosis of, 327–330
chronic passive congestion, 327
cirrhosis, 327–329
fulminant hepatic failure, 330
hepatitis, 327
posthepatic biliary obstruction, 329
space-occupying lesions, 329
injury, tests of, 320–327
autoimmune markers, 322–323
plasma enzyme levels, 320–322
viral-induced hepatitis, testing for, 323–327
normal, 314–320
metabolic functions of, 314–318
synthetic functions of, 318–320
prothrombin and INR used in, 319
tests, 112–113, 112t
Load balancing, test menu and, 16
Loa loa, 1340, 1340f
"Lock-and-key" appearance, antigen antibody, 955
Lock-and-key fit, 292, 292f
Locus, definition of, 1411
Loeffler syndrome, 641
Logarithm of the odds (LOD) score method, 1023–1024
Lomentospora, 1225, 1225f
Long-acting anticoagulant rodenticides, 882
Long-QT syndrome, 269–270
Loop-mediated amplification (LAMP), 1395–1397, 1396f
Louse-borne relapsing fever (LBRF), 1243–1244
Louse-borne typhus, murine typhus and, 1256–1257
Low-density lipoproteins, 247
selective removal of, 810–811
Low grade B-cell lymphomas, 1551–1554
chronic lymphocytic leukemia/small lymphocytic lymphoma, 1553
follicular lymphoma, 1551
hairy cell leukemia, 1554
lymphoplasmacytic lymphoma, 1553, 1554f
mantle cell lymphoma, 1552
marginal zone B-cell lymphomas, 1552–1553
Low-grade fibromyxoid sarcoma, 1600–1601
Low-Grade Neuroendocrine Tumors (LGNETs), 1594–1595
Low-grade serous carcinoma (LGSC), 1598
Low molecular weight heparin, 883, 884t
Low oxygen affinity, hemoglobins associated with, 615–616
Lowry assay, 280
Low total cholesterol, and triglyceride, 265
Low white cell counts, 105
LpX lipoprotein, 248
L-Thyroxine, uses of, 403–404
Luciferase immunoprecipitation system (LIPS), 1078
Lumbar punctures (LPs), cerebrospinal fluid and, 32
Luminescence, 43–44
Lung, acute injury of, transfusion-related, 783
Lung cancer, 1587–1588, 1587f
anti-p53 in, 1535
p53 protein in, 1534
protein arrays for, 1538
protein array to, 1538
ras-p21 protein in, 1532–1533
Lupus anticoagulant, 845
and acquired coagulation protein inhibitors and, 845
and antiphospholipid syndrome, 875–876, 875b
Lupus erythematosus (LE) cells, 524
"Lupus-like" syndromes and diseases, 1036–1037
Lupus nephritis, 1102–1107, 1102f–1107f
Lutheran antibodies, 725
Lutheran blood group system, 723–725
biochemistry, 724, 724f
biological role, 725
molecular biology, 724–725
null/weak phenotypes, 723–724, 724t
LW antibodies, 736
LW blood group system, 735–736
biochemistry, 735
biological role, 736
molecular biology, 735
Lyme disease, 1237–1243
antigen-detection assays, 1242
clinical manifestations of, 1239–1240, 1239f
culture of, 1242
epidemiology and pathogenesis of, 1237–1239, 1238f
genomic amplification techniques, 1241–1242
laboratory diagnosis of, 1240–1242, 1241f
nucleic acid detection, 1242
PCR, 1242
serologic tests for, 1240–1241, 1242f
treatment and prevention of, 1242–1243
xenodiagnosis of, 1242
Lyme-like disease, 1237–1243
antigen-detection assays, 1242
clinical manifestations of, 1239–1240, 1239f
culture of, 1242
epidemiology and pathogenesis of, 1237–1239, 1238f
genomic amplification techniques, 1241–1242
laboratory diagnosis of, 1240–1242, 1241f
nucleic acid detection, 1242
PCR, 1242
serologic tests for, 1240–1241, 1241f–1242f
treatment and prevention of, 1242–1243
xenodiagnosis of, 1242
Lymphadenopathy, nonneoplastic causes of, 645
Lymphoblastic leukemia/lymphoma, 1547–1551
risk stratification and minimal residual disease, 1547–1551
Lymphochip, 1618
Lymphocyte(s), 488
activation and proliferation, 930–931
activation of, biochemical pathways of, 931
depletion of, 683, 685f
donor-specific crossmatch, 1011–1012

Lymphocyte(s) *(Continued)*
function of
laboratory evaluation of, 943–946
and physiology of, 586, 586f
hematopoiesis, 583–586
in normal individuals, 641
preparation of, 1009
primary lymphoid tissue, 583–586
secondary lymphoid tissue, 586
Lymphocyte microcytotoxicity assay, 1009
Lymphocyte stimulation assay, principle of, 943f
Lymphocyte subsets, 1029
Lymphocyte transformation
assays, 943–944
lymphocyte transformation, principles of, 943
mitogen-induced blastogenesis, 943–944, 943f
mixed lymphocyte culture, 944, 945f
principles of, 943
Lymphocytic and plasmacytic disorders, 641–645
lymphocytes, in normal individuals, 641
lymphocytopenia, 645, 646b
lymphocytosis, 642–645, 643b
Lymphocytic choriomeningitis virus (LCMV), 1274
Lymphocytic leukemoid reactions, 646
Lymphocytopenia, 645, 646b
Lymphocytosis, 642–645, 643b
associated with viral infection, 642
chronic/persistent polyclonal B cell, 642
monoclonal B cell, 665
Lymphoepithelial lesions, 671, 671f
Lymphogranuloma venereum, 1363
Lymphoid cells, 894–896
antigen-presenting cells, 895, 895f
B lymphocytes, 895
natural killer cells, 895–896
T lymphocytes, 894–895
Lymphoid clonality analysis, 1547
Lymphoid neoplasms
aggressive B-cell lymphomas, 1554–1555
with eosinophilia, 650–651
immunoglobulin and T-cell receptor gene rearrangements, 1544–1547, 1546f
low grade B-cell lymphomas, 1551–1554
lymphoblastic leukemia/lymphoma, 1547–1551
mature T-cell neoplasms, 1555–1556
molecular diagnosis of, 1543–1556
precursor, 663–664
Lymphoid tissue, 583–586
mucosa-associated, extranodal marginal zone B-cell lymphoma of, 671, 671f
Lymphoma(s), 697–700, 701f
anti-c-myc protein in, 1535
breast implant-associated anaplastic large-cell, 682–683
diagnosis and classification of, 697–700, 702f–704f
minimal residual disease detection in, 700
prognostic factors of, 695
therapeutic targets of, 695–696
tumors of, antibodies to p53 in, 1534
Lymphomatoid granulomatosis, 674–675, 675f
Lymphoplasmacytic lymphoma, 668, 669f, 1553, 1554f
Lymphoproliferative disorders
immunodeficiency-associated, 685, 685b
of NK cells, chronic, 677
posttransplant, 685, 686f
primary cutaneous CD30-positive T cell, 680–681
Lymphoproliferative syndrome, autoimmune, 645
Lymphotoxin A and B genes, tumor necrosis factor and, 1016
Lynch syndrome, 1592–1593
Lysergic acid diethylamide (lysergide), 363
Lysozyme, 520

M

Machine learning, 157–159, 158f
Macroamylasemia, 334, 334t
Macroangiopathic hemolytic anemia, 624
Macroarrays, 1402
Macrocytic anemia, 101t, 104
Macrocytosis, with normoblastic marrow, 592
Macroenzymes, 294
α_2-Macroglobulin, 283, 518
Macrolide, 1253
Macropapular cutaneous mastocytosis (MPCM), 650
Macrophages, monocytes and, 581–582
Macroscopic examination, for gastrointestinal and pancreatic disorders, 345–346
Maculopapular eruption, 1495
Magnesium, 211–212, 458
homeostasis, 211
Magnetic biosensor assay, 922–923
Magnetic force restoration balance, 54
Major depression disorder, 1461–1463
COMT gene, 1462
GWAS on, 1462
HTR2A, 1462
LHPP, 1462
pharmacogenomics of, 1462–1463
serotonin-related genes (SERT), 1462
sirtuin, 1461–1462
SLC6A4 (sodium-dependent serotonin transporter), 1462
SNPs in, 1463t
tryptophan metabolic pathways, 1462
Major histocompatibility complex, disease and, 1014–1024.e4
central or class III region, genes in, 1015–1017, 1015f
C2, *C4*, *CFB* genes and typing, 1016–1017
complotypes, 1017, 1017t
heat-shock protein 70 genes, 1016
tumor necrosis factor and lymphotoxin A and B genes, 1016
disease associations of, 1018–1023
of MHC monogenic, 1019–1020, 1020t
polygenic diseases, 1020–1023, 1020t
DNA sequence of, overview of, 1014–1015
extended haplotypes, 1017–1018, 1018f, 1018t–1019t
genetic markers and, 1023
association, strength of, 1023
gene and phenotype frequencies, 1023
genetic polymorphism, 1023
LOD score method, 1023–1024
mode of inheritance, 1023
Major histocompatibility complex (MHC) of man
class I and II molecules, antigenic fragments bound by, 1005
class II molecules—HLA-DR, HLA-DQ, HLA-DP subregions, 1003–1005
class II gene expression, regulation of, 1005
class II genes, linkage disequilibrium of, 1004–1005
class II genes, organization of, 1003f, 1004
class II genes, other, 1005
class II genes, structure of, 1003–1004
function of, 1005
class I molecules—HLA-A, HLA-B, HLA-C subregions, 998–1003
class I gene expression, regulation of, 1001–1002
class I genes, organization of, 1001
class I genes, other, 1003
function of, 1002–1003
structure of, 999–1000, 1002f
genetics of, 997–998
HLA nomenclature, 1006–1007
DNA-based allele designations, 1006–1007
serologic and cellular specificities, 1006
HLA polymorphisms, identification techniques of, 1007–1009
class I and class II molecules, serologic detection of, 1009
class II molecules, cellular detection of, 1009
DNA-based typing, of class I and class II alleles, 1007–1009
human leukocyte antigen (HLA) as, 996–1013.e3, 997f
minor histocompatibility molecules, 1006
molecules, foreign, recognition of, 1005–1006
tissue/organ transplantation, 1009–1013
allogeneic hematopoietic progenitor cell transplantation, 1012–1013
genetic basis of, 1009–1010, 1010f
histocompatibility matching, 1010–1012
nonrenal, 1012
renal, 1012
Malabsorption syndromes, 340–342, 594
abetalipoproteinemia, 340
agammaglobulinemia, 340
celiac disease, 341–342, 342t
inflammatory bowel disease, 342, 342t
laxative abuse, 341
steatorrhea, tests for, 340–341
tests for, 341
Whipple's disease, 342
Malaria, 786, 1301–1304
as clinical disease, 1303
diagnosis of, 1303–1304, 1304t, 1305f–1310f
epidemiology of, 1303
life cycle of, 1302–1303, 1302f, 1305f–1308f
Malassezia infection, pathology of, 1210, 1210f
MALDI-TOF mass spectrometry, 1206
Male reproduction, regulation of, 427, 427f, 429–431
hormone analysis of, 430–431, 431f
semen analysis of, 429–430
accessory glands and, 430
examination in, 429–430
image analysis of, 430
immunologic tests of, 430
sample collection in, 429
Malignancies, origins of, 1539–1541, 1540f
Malignancy-associated hypercalcemia, 216
MALT1 gene abnormalities in, 1552
MammaPrint assay, 1584–1585, 1585f
Management, 2–3
responsibilities, 3b
Managers, leadership and management, 2
Managing utilization, optimizing performance and, 20
Manganese (Mn), 451
Mania, depression and, therapeutic drug monitoring for, 376–378
Mannan-binding lectin pathway, 972
MANOVA. *See* Multiple analysis of variance (MANOVA)
Mansonella spp., 1340
Mantle cell lymphoma, 672–673, 673f, 1552
t(11;14)/*CCND1-IGH* in, 1552
Manual blood cell counts, 544–549
MAO inhibitors, 378
Maple syrup urine disease, 508
methods for, 508
procedure of, 508
Mapping
sample, 13, 14f
task, 16, 17f
test, 13, 14f
Marburgvirus (MARV), 1288
Marginal zone B-cell lymphomas, 1552–1553
Marijuana (Cannabis), 362–363
Marker chromosome, 1423
Markers
biochemical
of bone metabolism, 208–215, 209f
of bone remodeling, 219–221
in body fluids, 1523–1524
bone formation, 220–221
bone resorption, 220
cell surface, 1032
genetic, 1023, 1470–1473
monoclonal antibody–defined tumor, 1510–1511, 1512t
multiple oncoproteins, 1536–1541
mutant protein, 1524
tumor, 520–521, 536
urine, 1523–1524
X and Y chromosome, 1471–1472, 1472f, 1473b
Mass analyzer, 62–64
Massively parallel sequencing, 1542
Massive transfusion, 779–780, 845
Mass, measurement of, 54–55
MasSpec Pen, 72
Mass population screening, and allele frequencies, 1438
Mass spectrometry (MS), 51–52, 1614–1615
analytic methods
chemical profiling, 65
quantitative analysis, 65
tandem mass spectrometry, 64–65
analytic systems, 63f
clinical applications, 65–67
definitions and terminology, 60–62
imaging
matrix-assisted laser desorption ionization, 66–67
secondary ion mass spectrometry, 67
implementation challenges, 68–73
principles of, 62–64
ion detector, 64
ionization, 62
mass analyzer, 62–64
primary components, 62
separation and extraction, 62
on sera, 1539
technology development, timeline of, 61f
Mass- to- charge ratio, 60–61
Mast cell leukemia, 650
Mast cells
and basophils, 896
basophils and, 580–581
Master keys, 153
Mastocytosis, 650, 651f, 1575
Matrix-assisted laser desorption ionization, 62, 66–67

Matrix Assisted Laser Desorption Ionization Time-of-Flight Mass Spectrometry (MALDI-TOF MS), 1178
Matrix effect, 61
Matrix-free laser desorption ionization (LDI), 67
Maturation
acute myeloblastic leukemia with, 659, 660f
acute myeloblastic leukemia without, 659, 660f
arrest, 637–638
cellular, abnormal, 651, 652f
megaloblastic, 574
normoblastic, 572–574, 572f–573f
Mature B cell neoplasms, 664–676, 666t
Mature T cell and natural killer cell neoplasms, 676–683, 678t
Mature T-cell neoplasms, 1555–1556
anaplastic large-cell lymphoma, 1555–1556
chronic T-cell leukemias, 1556
peripheral T-cell lymphomas, 1556
Maximal velocity, 296
May-Hegglin anomaly, 638–639, 640f
MCB. *See* Monoclonal band (MCB)
MDA5 (CADM-140), autoantibodies, 1048
Mean, 120
Mean cell hemoglobin, 543
concentration of, 543–544
Mean cell volume, 543
Mean platelet volume (MPV), 849
Measles morbillivirus, 1278
Measurements, reliability of, in cholesterol testing, 257–258, 258t
Meat fiber, 346
Mechanical masks or barriers, 1403
Meconium, 536
Media access control address (MAC address), 160
Median, 120
Media, susceptibility testing, 1167
Medical bacteriology, 1129–1165.e4
medically important bacteria, 1131–1163
anaerobic bacteria, 1160–1163
Gram-negative bacteria-bacilli, 1144–1147
Gram-negative bacteria-cocci, 1142–1144
Gram-negative bacteria-HACEK, 1153–1154
Gram-negative bacteria–nonfermentative bacilli, 1147–1153
Gram-positive cocci of, 1131–1137
Gram-positive rods, 1137–1142
miscellaneous Gram-negative bacilli, 1154–1160
specimen processing, 1130–1131
culture techniques of, 1131
Gram stain of, 1130–1131, 1131f
Medical centers, in point-of-care testing program, 86–87
Medical decision making, 89–99.e1
analytic correctness, of results, assessment of, 89–90
clinical significance, of results, assessment of, 90–92
evidence-based medicine, 97, 97f
laboratory results, interpretation of, 92–97
Bayes theorem in, 94, 95t
diagnostic accuracy in, 92–94, 94t
likelihood ratio in, 94–95, 95t
positivity criterion in, 96–97, 97t
receiver operator characteristic curves in, 95–96, 96f
systematic reviews of clinical effectiveness research and clinical practice guidelines, 36b, 98, 98b
Medically important bacteria, 1131–1163
Medical mycology, 1194
Medical parasitology, 1290–1351.e3, 1291t–1292t
arthropods in, medically important, 1344, 1345t
blood and tissue protozoa in, 1301–1326
babesiosis, 1304–1309
hemoflagellates, 1309–1312
malaria, 1301–1304
opportunistic free-living amebae, 1313–1315, 1314f
toxoplasmosis, 1312–1313
immunodiagnostic methods for, 1297–1300
intestinal and urogenital protozoa in, 1315, 1315f
amebae, 1315–1319, 1316f–1317f
Blastocystis spp., 1319
ciliates, 1318f, 1322–1326
coccidia, 1318f, 1323
flagellates, 1318f, 1319–1322, 1321f–1322f
microsporidia, 1297
intestinal helminths in', 1326–1338
cestodes, 1330–1335
nematodes, 1326–1330
trematodes, 1335–1338
Medical parasitology *(Continued)*
laboratory methods for, 1292–1301
blood, examination of, 1292–1294
fecal specimens, examination of, 1294–1297
urogenital and other specimens, examination of, 1297
molecular diagnostic methods for, 1300, 1301t
parasite classification and taxonomy in, 1292
parasite culture techniques for, 1297
parasitic infections and immunocompromised host, 1350t, 1351
quality assurance, quality improvement and safety for, 1300–1301
tissue helminths in, 1338–1344
cestodes, 1342–1344
nematodes, 1338–1341
trematodes, 1344
Medicare, 164–166
inpatients in, 167
outpatients in, 167–169, 169t
reimbursement of, 167–169, 169t
Medicine
evidence-based, 97, 97f
pathology and, molecular diagnostics on practice of, 1371
data analysis in, 1371
molecular biology used in disease treatment in, 1371
in redefining disease, 1371
personalized, pharmacogenomics and, 1480–1506.e6
transfusion, 771
Medium vessel vasculitis, 1060f, 1062–1064, 1062t
Kawasaki disease, 1063–1064, 1063f
polyarteritis nodosa, 1062–1063
Medullary angiitis, 1099–1101, 1101f
Medullary carcinoma, 1587
Megakaryocytes, 582–583
distribution and kinetics of, 583
function of, 583
morphology of, 582–583, 583f
Megaloblastic anemia, 592–593
acute, 597
blood relating to, 592–593, 593f
folic acid deficiency, 596–597
folic acid metabolism, 595
macrocytosis, with normoblastic marrow, 592
marrow relating to, 592, 593f
therapy for, 597
Megaloblastic maturation, 574
Meiosis, definition of, 1412
Melanin, 485
Melanized dark, 1195–1196, 1219
Melanoma, 1599
malignant, p53 protein in, 1535
Melanosomes, 485
MELD score, 319, 328–329
Melting, 1373–1374
Melting point, 1373–1374
Membrane
disorders of, hemolysis relating to, 605–607
permeability of, assays of, 949
premature rupture of, 438–439
Membrane inhibitor of reactive lysis, 974
Membranoproliferative glomerulonephritis, 1095–1096, 1095f–1096f
Membranous nephropathy (MN), 1090–1093, 1091f–1092f
Meningitis, 1273–1275
Meningoencephalitis, granulomatous amebic, 1313
Menkes syndrome, 450
Menstrual cycle, 427
Meprobamate, 364
MER2 antibodies, 740
Mercury, 382–383
MERS-CoV. *See* Middle Eastern Respiratory Syndrome Coronavirus (MERS-CoV)
Mesobilifuscin, 483
Metabolic acidosis, 202–205, 202b
classification of, 202–203, 202b
D-lactic, 203
ketoacidosis, 203
lactic, 202, 203b
organic, 202–203
renal, 202
Metabolic alkalosis, 205, 205b
Metabolic bone disease, 221–224
Metabolic defects, enzyme measurements for, 1030–1031
Metabolic disorders, hemolysis relating to, 621–623
erythrocyte metabolism, 621–622, 621f
glucose-6-phosphate dehydrogenase deficiency, 622–623, 622b
Metabolic functions, of liver, 314–318
bilirubin, 314–317
drug metabolism, 318
lipids, 317–318
other metabolic tests, 317–318
Metabolic syndrome, 264–265
Metabolic tests, 317–318
ammonia, 317
Metabolism
antidiuretic hormone, 197–200
of calcitonin, 213
of folic acid, 595
iron, 588–590
of lipoproteins, 246f
important proteins in, 248
in liver, 365–366
mineral
disorders of, 215–219, 215b, 217b
hormones regulating, 212–215
therapeutic levels and, of antidepressants, 378
of thyroid gland, 396–398, 398t
of vitamin D and metabolites, 214
Metabolomics, 68
Metagonimus, 1335
Metallochaperones, 449
Metalloproteases, in pancreatic cancer, 1532
Metapneumovirus, 1268
Metastasis, adhesion molecules and, 1510
Metformin, 1489
Methadone, 360
Methanol, 382
Methaqualone (Quaalude), 362
Methemoglobin, bilirubin and, 519
Methicillin-resistant coagulase-negative staphylococci (CoNS), 1172
Methicillin-resistant *Staphylococcus aureus* (MRSA), 1172
Method validations, 87
Methotrexate, 379, 379t
Methylmalonic acid, 595
MHC monogenic disease association, 1019–1020, 1020t
congenital adrenal hyperplasia, due to 21-hydroxylase deficiency, 1020
hereditary hemochromatosis, HFE gene and, 1019–1020
MHC restriction, 1002
MH2 domain, 1591–1592
M hemoglobins, 616
MIC. *See* Minimum inhibitory concentration (MIC)
Michaelis constant, 295
Michaelis-Menten equation
derivation of, 295
for determination of total enzyme concentration, 296
enzyme activity in, 297
enzyme assays and, under nonsaturating conditions, 298
enzymes, inhibition of
competitive, 300–301
noncompetitive, simple and mixed, 302
uncompetitive, 301
k_2 and K_M in, 296, 296f
K_M in, a word about, 297
Lineweaver-Burk plot and, 296–297, 296f
measuring enzyme activity in, 297
saturation, initial rate at, 296
Microalbuminuria, 475
Microangiopathic hemolytic anemia, 103, 624
Microarray data sets, 1620
Microarray hybridization, 1382–1383
Microarrays, 1402, 1611, 1612f
of cDNA sequences, 1404
fabrication for, 1402–1403
methods of, component-resolved diagnostics and testing by, 1121t, 1127–1128
oligonucleotide, 1403–1404
substrates, 1402
Microarray technology, 1417–1418, 1418f
Microbial stains, 1188–1189, 1188f–1189f, 1190t
Microbiological examination
for CSF, 521–522, 521t
bacterial meningitis, 521, 521f
fungal meningitis, 522
human immunodeficiency virus, 522
primary amebic meningoencephalitis, 522
spirochetal meningitis, 521–522
tuberculous meningitis, 522
viral meningitis, 522
for synovial fluid, 527
Microbiology
laboratory automation for, 79
point-of-care testing in, 84–85

Microchannel assay, compact disk used for, 927
Microcytic anemia, 101–102, 101t
Microdeletion syndromes, and contiguous gene syndromes, 1430–1431, 1430t, 1431f
β_2-Microglobulin, 518, 1515
Microlymphocytotoxicity assay, 946, 948f
Micronutrients, 441
Microorganisms, recovery of, 1354
Microphthalmia transcription factor (MiT) family, translocation renal cell carcinoma, 1595
Micropipets, 55–56
MicroRNA (miRNA), 531
  circulating, 1522
Microsatellite alterations, 1522
Microsatellite instability, high (MSI-H), 1589–1590
  in colorectal cancer, 1592
Microsatellite stable (MSS), 1590
Microscan, 1171–1172
Microscopic components, of urine sediment, 487–499
Microscopic examination
  for CSF, 512
  for gastrointestinal and pancreatic disorders, 345
  for synovial fluid, 524–526
  of urine sediment, 503
Microscopy, 486, 1233, 1233f
Microsporidia, 1315
  stains for, 1297
Microsporidiosis, 1225–1226
  laboratory diagnosis, 1226, 1226f
  pathology, 1225–1226
  risk factors, 1225
Microspot assay, 926
Middle Eastern respiratory syndrome coronavirus (MERS-CoV), 1288
Middleware, 77
Midges, 1347
Milk-alkali syndrome, 217
Miller-Dieker syndrome, 1430
Millipedes, 1349–1350
Mineral metabolism
  and bone metabolism, 208–215, 209f
  disorders of, 215–219, 215b, 217b
  hormones regulating, 212–215
Mineralocorticoid axis, 407–408, 409t
Mini-arrays in detection of cancer, 1537
Miniature mass spectrometry systems for clinical use, 72–73
Minichromosome maintenance proteins, 1536
Minimal proteinuria, 475
Minimal residual disease, 1385
Minimal residual disease assessment, 1550–1551
Minimum bactericidal concentration (MBC), 1170
Minimum inhibitory concentration (MIC), 1167–1168
  by broth microdilution, 1168f
Minor groove binder, 1391
Mi-2/nucleosome remodeling and deacetylase (NuRD) complex, 1048
Mi-Prostate Score, 1523
miRNA, in cancer, 1604
Missense mutations, 1379
Mites, 1348f–1349f, 1349
Mitochondrial DNA
  disorders of, 1448
  sequencing of, 1472
Mitogenesis, cell biology and, 1525
Mitogen-induced blastogenesis, 943–944, 943f
Mitosis, definition of, 1412
Mixed acid-base disorders, 207, 207b
Mixed agglutination reaction (MAR) tests, 430
Mixed cellular casts, 492, 492f
Mixed cellularity, 683, 683f
Mixed connective tissue disease (MCTD), 1049
Mixed cryoglobulin, 961
Mixed leukocyte culture, 1009
Mixed lymphocyte culture, 944, 945f
Mixed lymphocyte reaction, 1009
Mixed-type AIHA, 762
Mixing, 57
  and incubation, in automated chemistry analyzer, 76
MLL gene, 1550
  in childhood leukemias, 1560–1561
MMR genes, in colorectal cancer, 1592
MNS blood group system, 714–716
  biochemistry of, 714–715, 715f
  biological role, 716
  molecular biology, 715–716
  null phenotypes, 714
MNSs antibodies
  anti-M and anti-N, 716
  anti-S, -s, and -U, 716
Mobile robots, for automated delivery, 75
Mode, 120
Mode of inheritance
  based on population studies, 1023
  based on sibling pairs, 1023
Moderate proteinuria, 474–475
Modified acid-fast stains, 1296
Modified Hodge test, 1176, 1176f
Molar absorptivity, 38
Mold, 1195
  morphology, 1204
Molecular allergy diagnosis, and testing by microarray methods, 1121t, 1127–1128
Molecular and cellular interactions, regulation of IgE synthesis, 1117, 1118f
Molecular-based testing, for antimicrobial susceptibility, 1171–1179
Molecular basis, for enzyme catalysis, 292–293, 293f
Molecular biology, in disease treatment, 1371
Molecular composition and structure, 1373–1375, 1374f, 1375t
Molecular defects, of thalassemias, 616–617
Molecular detection methods, 1267, 1275
Molecular diagnosis, 1385. *See also* Genetic diseases, molecular diagnosis of.
Molecular diagnostics, 25, 157
  basic principles and techniques of, 1373–1386.e1
    nucleic acid analyses in, 1379–1385
    nucleic acid biochemistry and biology in, 1373–1379
  disease in, laboratory evaluation of, 1385
    beyond diagnosis in, 1385
    molecular diagnosis in, 1385
  for medical parasitology, methods for, 1300, 1301t
Molecular genetics, for immunodeficiencies analysis, 1032–1034
  gene mutations
    affected proteins, and primary immunodeficiencies, 1032–1033, 1033t
    and susceptibility to pathogens, 1032–1033, 1034t
  mutation registries and databases, 1033
  newborn screening, 1033–1034, 1034f
  next generation sequencing, 1033
  polymerase chain reaction, 1032–1033
  prenatal diagnosis, 1033
Molecular heterogeneity, 1437
Molecular identification, 1205–1206, 1205t
Molecular luminescence spectroscopy (fluorometry), 43–44
Molecular major histocompatibility complex (MHC), 930
Molecular pathology, introduction to, 1367–1372.e1
  application of, to cancer detection, 1370–1371
  cancer, 1368–1369
  caveats to, 1372
  diagnostic, discussion of, 1370–1371
  financial management reimbursement, 1371–1372
  implications of, on practice of pathology and medicine, 1371
    data analysis relating to, 1371
    molecular biology used in disease treatment, 1371
    in redefining disease, 1371
  infectious disease, 1368
  inherited disorders, 1369
  molecular biology revolution's impact on, 1369–1370
  molecular diagnostic tests, 1368–1369
  quality assurance in, 1371
Molecular testing, for *Borrelia*, 1242
Molecular typing, 760
Molecular weight, 60
Molluscum contagiosum virus (MCV), 1275, 1276f
Molybdenum (Mo), 451
Monoclonal antibodies, 899, 902
Monoclonal antibody-defined tumor markers, 1510–1511, 1512t
Monoclonal antibody-immobilized granulocyte antigen (MAIGA) assay, 766–767
  bead-based antibody capture assays, 766–767
Monoclonal band (MCB), 961f
  detection of, 964–966
Monoclonal B cell lymphocytosis, 665, 697–698
Monoclonal gammopathy of undetermined significance (MGUS), 669, 670b, 960
Monoclonal immunoglobulin deposition diseases, 670
  monoclonal light and heavy chain deposition diseases, 670
  primary amyloidosis as, 670
Monoclonal immunoglobulins (Ig), 960–961, 960f, 960b
Monoclonal light and heavy chain deposition diseases, 670
Monocytes
  granulocytes and, function, 946–949
  and macrophages, 581–582
    distribution and kinetics of, 582
    function of, 582, 582b
    morphology of, 581–582, 582f, 582b
Monocytopenia, 641
Monocytosis, 641, 642b
Monomorphic epitheliotropic intestinal T-cell lymphoma, 679
Mononuclear leukocytes, 488
Monosodium urate (MSU) crystals, 525, 525f
Monospecific reagent, for antihuman globulin test, 747
Moraxella catarrhalis, 1143t, 1144, 1144f
Morphologic identification, 1199t, 1203–1204
Morphology
  of basophils and mast cells, 580–581
  of eosinophil precursors, 580, 580f, 580b
  of megakaryocytes, 582–583, 583f
  mold, 1204
  of monocytes and macrophages, 581–582, 582f, 582b
  of neutrophil precursors, 578–579, 578f
  of yeast, 1203–1204, 1204f, 1204b
Mosquitoes, 1347
Moths, 1347
MOdulator/DEModulator (MODEM), 160
Moving boundary, 277–278
MPL gene mutations, 1573
MRSA. *See* Methicillin-resistant *Staphylococcus aureus* (MRSA)
MS-based omics
  biomolecule database building, 68
  metabolomics, 68
  proteomics, 67–68
M. tuberculosis infection, latent, testing for, 1187
MTBC. *See* Mycobacterium tuberculosis complex (MTBC)
Mucin clot test, 526
Mucocutaneous leishmaniasis, 1312
Mucormycetes, 1220–1221
Mucosa-associated lymphoid tissue
  extranodal marginal zone B cell lymphoma of, 671
  lymphoma of, 671, 671f
Mucous membrane pemphigoid (MMP), 1082
Mucus, 345
Muir-Torre syndrome, 1593
Multianalyte microarray immunoassay, 926, 926f
Multicolor fluorescence in situ hybridization, 1417, 1417f
Multicomponent apheresis donation, 795
Multidrug resistance-related proteins, 1487
Multiparameter fluorescent immunoassay, 767
Multiple analysis of variance (MANOVA), 126–127
Multiple endocrine neoplasia type 1, 1602
Multiple endocrine neoplasia type 2, 1446, 1603
Multiple myeloma, 960, 964, 966
Multiple oncoprotein markers, for cancer diagnosis, 1536–1541
Multiple reaction monitoring (MRM), 65
Multiple sclerosis, 1112
Multiple-tube mixers, 57
Multiplex bead-based assays, 1056–1057
Multiplexing, 1611
Multiplex PCR (mpPCR), 1612–1613
Multiplex polymerase chain reaction, 1389
Multivalent, 953
Murine typhus, louse-borne typhus and, 1256–1257
Muscle glycogenoses, 240t–241t
Muscle relaxants, 364
Musculoskeletal tissues, 819–820
Mutation, definition of, 1411
Myasthenia gravis, 1112
Mycelium, 1195
Mycetoma, 1219, 1219f–1220f
MYC gene rearrangement, 1554–1555
Mycobacteria, 1183–1193.e3
  identification tests for, 1190–1191
  laboratory diagnosis for, 1187–1192
    culture methods in, 1189–1190, 1190t
    microbial stains in, 1188–1189, 1188f–1189f, 1190t
    specimens in, 1187–1188, 1188f
  M. tuberculosis infection, latent, testing for, 1187
  Mycobacterium tuberculosis complex, 1183–1184, 1192
  nontuberculous, 1184–1187
    classification of, 1184t
    Mycobacterium avium complex as, 1185, 1192
    Mycobacterium genavense as, 1185
    Mycobacterium gordonae as, 1185

Mycobacteria *(Continued)*
Mycobacterium haemophilum as, 1185
Mycobacterium kansasii as, 1185
mycobacterium leprae as, 1186–1187
Mycobacterium marinum as, 1185–1186
Mycobacterium ulcerans as, 1186
Mycobacterium xenopi as, 1186
prevention of, 1192
rapidly growing, 1186
susceptibility testing of, 1191–1192, 1191t
treatment of, 1192, 1192t
Mycobacterium avium complex, 1185, 1192
Mycobacterium genavense, 1185
Mycobacterium gordonae, 1185
Mycobacterium haemophilum, 1185
Mycobacterium kansasii, 1185
Mycobacterium leprae, 1186–1187
Mycobacterium marinum, 1185–1186
Mycobacterium tuberculosis complex (MTBC), 1171, 1183–1184, 1192
Mycobacterium ulcerans, 1186
Mycobacterium xenopi, 1186
myc oncogene-encoded protein, in tumor detection, 1535
Myc oncogene, in prostate cancer, 1597
Mycophenolate mofetil, 376
Mycoplasmal infections, 1250–1253
genital, 1252
laboratory diagnosis of, 1252–1253
treatment of, 1253
Mycoplasma pneumoniae, 1251–1252
clinical manifestations, 1251–1252
epidemiology, 1251
laboratory diagnosis, 1252
pathogenesis and pathology, 1251
Mycoplasmas, genital, 1252–1253
Mycoses
dematiaceous fungi as cause of, 1219–1220
dimorphic fungi as cause of, 1211–1216, 1212f
hyaline fungi as cause of, 1222–1225
Mycosis fungoides, Sézary syndrome and, 680, 681f, 699–700
Mycotic diseases, 1194–1228.e7
dematiaceous fungi, mycoses caused by, 1219–1220
dermatophytoses, 1216–1218
clinical diseases of, 1217
laboratory diagnosis of, 1217–1218, 1217f–1218f
risk factors for, 1217
diagnostic techniques for, 1200–1207
biochemical identification as, 1204, 1204t
culture as, isolation in, 1203
direct examination as, 1200–1203
growth rate in, 1203
growth temperature in, 1203
laboratory safety in, 1200
MALDI-TOF mass spectrometry as, 1206
molecular identification as, 1205–1206, 1205t
morphologic identification as, 1203–1204
serologic identification as, 1205
specimen collection and transport in, 1200, 1201t
susceptibility testing as, 1206–1207
dimorphic fungi as caused of, 1211–1216, 1212f
hyaline fungi, aspergillosis, fusariosis and other mycoses caused by, 1222–1225
nomenclature, taxonomy, fungal morphology of, 1195–1200, 1196t–1197t
dimorphism in, 1199–1200
fungal colony in, 1195, 1197f
fungal pigment in, 1195–1196
reproductive structures in, 1196–1199, 1198f–1200f, 1199t
yeasts and hyphae in, structure of, 1195, 1197f–1198f
Pneumocystis pneumonia, 1226–1227
clinical diseases of, 1226
laboratory diagnosis of, 1226–1227, 1226f–1227f
risk factors for, 1226
protothecosis, 1227, 1227f
yeast, candidiasis, cryptococcosis, other infections as cause of, 1207–1211
zygomycosis, 1220–1222
clinical diseases of, 1221
laboratory diagnosis of, 1221–1222, 1222f
pathology of, 1221, 1221t
risk factors for, 1221
Mycotoxins, 385
MYD88 mutation, 1553
Myelin basic protein (MBP), 518
Myelodysplasia-related changes, acute myeloid leukemia with, 658
Myelodysplastic and myelodysplastic/myeloproliferative neoplasms, 651–653
genetics and epigenetics of, 651
and types of abnormal cellular maturation, 651, 652f
Myelodysplastic and myeloproliferative neoplasms, 1574–1575
Myelodysplastic/myeloproliferative disease, unclassifiable, 653–654
refractory anemia with ring sideroblasts associated with marked thrombocytosis, 653–654
Myelodysplastic/myeloproliferative neoplasms, 651–653
Myelodysplastic syndromes, 103–104, 597, 602, 654–655, 655t, 1567–1568, 1568f
and acute leukemia, 862
childhood, 654–655
with isolated del (5q), 654
myeloproliferative disorders and, 703–705, 707f
refractory cytopenia
with multilineage dysplasia, 654
unclassified, 654
Myelofibrosis
with acute panmyelosis, 660, 662f
autoimmune, 637
primary, 647–649, 1572–1574, 1572f
biology of, 648
course of, 648–649
Myeloid and lymphoid neoplasms, with eosinophilia and abnormalities of PDGFRA, PDGFRB, or FGFR1, 650–651
Myeloid leukemia, associated with Down syndrome, 661
Myeloid/lymphoid neoplasms with eosinophilia, 1577–1578
Myeloid neoplasms
acute myeloid leukemia, 1556–1567
chronic myeloid neoplasms, 1567–1575
clonal hematopoiesis of indeterminate potential, 1576–1577, 1577b
with germline predisposition, 1575, 1576t
molecular diagnosis of, 1556–1578
myeloid/lymphoid neoplasms with eosinophilia, 1577–1578
therapy related, 658–659
Myeloid proliferations, Down syndrome related to, 661–662
blastic plasmacytoid dendritic cell neoplasm, 662
myeloid leukemia associated with, 661
transient abnormal myelopoiesis, 661
Myeloid sarcoma, 661, 662f
Myelokathexis, 639
Myeloma
asymptomatic (smoldering), 670
kidney, 475, 670
nonsecretory, 670
Myelophthisic anemia, 598–599
Myeloproliferative disease, chronic, unclassifiable, 649
Myeloproliferative disorders, myelodysplastic syndromes and, 703–705, 707f
Myeloproliferative neoplasm (MPN), 646–655, 862, 1568–1574, 1572f
chronic myeloid leukemia, *BCR-ABL1* positive, 1568–1571
Philadelphia-negative classical myeloproliferative neoplasms: polycythemia vera, essential thrombocythemia, and primary myelofibrosis, 1572–1574
unclassifiable, 649
MYH-associated polyposis, 1448
MYH gene, 1592
MYH polyposis, due to *MYH* inactivation, 1593
MYH9-related macrothrombocytopenia, 853
Myocardial damage, markers of, 269–270
Myocardial infarction (MI), 267–268
and acute coronary syndrome, diagnosis of, 113–114
Myofibroblastic tumor, inflammatory, 1602
Myoglobin, 270
blood, hemoglobin, hemosiderin, in urine, 479–482
casts, 493
qualitative test for, 481
Myoglobinuria, 480–481, 481t
Myositis-associated autoantibodies, 1049
Myotonic dystrophy, 1442–1443
Mysoline. *See* Primidone (Mysoline)
Myxoid/round cell liposarcoma, 1600

N

NAAT. *See* Nucleic acid amplification testing (NAAT)
NAC. *See* Network admission control (NAC)
N-acetyl-*p*-aminobenzoquinoneimime (NAPQI), 373–374
Nano-DESI, 71
Nanophyetus salmincola, 1335
NanoString's Prosigna Breast Cancer Prognostic Gene Signature Assay, 1584–1585
Narcolepsy, 1021
Nasopharyngeal specimens, 1358
National Glycohemoglobin Standardization Program (NGSP), 232–233
Natural killer cell lymphoblastic leukemia/ lymphoma, 662
Natural killer cell-mediated cytotoxicity, 946
Natural killer cells, 895–896
assays, 1031
bone marrow relating to, 585–586
and mature T cell neoplasms, 676–683, 678t
NCAM1 (neural cell adhesion molecule 1), 1460
NCAN (NeuroCAN), 1457–1458
Necator americanus, 1329, 1330f–1331f
Neighborhood analysis, 1615
Neisseria, 1142–1144
antimicrobial susceptibility of, 1143–1144
characteristics, 1142, 1142f
clinical manifestations and pathogenesis of, 1142
laboratory diagnosis of, 1142–1143, 1143t
prevention of, 1144
Nematodes, 1326–1330, 1338–1341
Ancylostoma duodenale, 1329
Angiostrongylus cantonensis and *Angiostrongylus costaricensis*, 1341
Anisakis, Pseudoterranova and *Contracaecum* spp., 1342
Brugia malayi, 1339–1340, 1339f
Capillaria hepatica, 1342
culture and recovery techniques for, 1296
Dracunculus medinensis, 1341
filarial, 1338–1341
hookworms, 1329, 1330f–1331f
Larval migrans, 1341–1342
Loa loa, 1340, 1340f
Mansonella spp., 1340
Necator americanus, 1329, 1330f–1331f
Onchocerca volvulus, 1340, 1340f
Strongyloides stercoralis, 1329–1330, 1330f–1331f
Trichinella species, 1341
Trichostrongylus spp., 1329
Wuchereria bancrofti, 1338–1339, 1339f
Zoonotic Filarial Nematodes, 1340–1341
Neoantigen formation, 628, 628b
Neoehrlichia, 1259t
Neonatal alloimmune thrombocytopenia, 767
Neonatal and pediatric transfusion, 780, 781b
Neonatal hypothyroidism, screening for, 402
gastrointestinal and pancreatic neuroendocrine, 343–345
Neoplastic disorders, primarily involving leukocytes, 646–686
acute myeloid leukemia, 655–662, 656t–657t, 656b
histiocytic and dendritic cell neoplasms, 686, 686f
Hodgkin lymphoma, 683–685, 683f
immunodeficiency-associated lymphoproliferative disorders, 685, 685b
mature B cell neoplasms, 664–676, 666t
mature T cell and natural killer cell neoplasms, 676–683, 678t
myeloproliferative neoplasms, overview of, 646–655
precursor lymphoid neoplasms, 663–664
Neorickettsia, 1259, 1259t
Nephelometer, 45
Nephelometric immunoassays, 904
Nephelometry, 280
and turbidimetry, 45, 45f
Nephrolithiasis, 505
Nephrotic versus nephritic disease, 108–109
Nervous system, autoimmune diseases of, 1112–1113
Nested polymerase chain reaction, 1388–1389
Net acid excretion, 202
Net acid production, 201–202
Net present value (NPV), 171
Network, 160
Network admission control (NAC), 160
Network interface controller (NIC), 160
Neu/HER2, 1458
Neural cell adhesion molecule (NCAM), 1589
Neural cell adhesion molecule 1 (NCAM1), 1460
Neural tube defects (NTDs), 434–436
folic acid prevention of, 434–435
screening for, 435–436, 436f
Neuroblastoma, 407
Neurodegenerative disorders, 1442

Neuroendocrine neoplasms, 344–345
Neurofibromatoses, 1603
Neurofibromatosis 1, 1603–1604
Neurofibromatosis 2, 1604
Neuroleptics, antipsychotic major tranquilizers, 378–379
Neurologic diseases, 980
Neuromyelitis optica spectrum disorder, 980
Neuronal exon, 1458
Neuronal stability, protein involved in, 1458
Neuropsychiatric diseases, 1453–1466
  Alzheimer disease, 1464–1465
  anxiety disorders, 1463–1464
  autism spectrum disorder (ASD), 1465–1466
  bipolar disorder, 1456–1459, 1457t
  major depression disorder, 1461–1463
  posttraumatic stress disorder, 1463–1464
  schizophrenia, 1453–1456
  substance use disorders, 1459–1461
Neuropsychiatric disorders, molecular genetics of, 1452–1467.e3, 1466
  genome-wide association studies, 1452–1453
    copy number variants, 1456
    in pharmacogenomics, 1456
    proteins from opioid addiction, 1461
  neuropsychiatric diseases, 1453–1466
    Alzheimer disease, 1464–1465
    anxiety disorders, 1463–1464
    autism spectrum disorder (ASD), 1465–1466
    bipolar disorder, 1456–1459, 1457t
    major depression disorder, 1461–1463
    posttraumatic stress disorder, 1463–1464
    schizophrenia, 1453–1456
    substance use disorders, 1459–1461
Neutropenia, 637–638, 638b
  chronic familial, 637
  cyclic, 637
  of hypersplenism, 638
  isolated, 638
  transient, 638
Neutrophil gelatinase-associated lipocalin (NGAL), 193
Neutrophilia, 636–637
  congenital, 646
  determinants of, 637
  mechanisms of, 636–637
Neutrophilic activation, assays of, 946–947
Neutrophilic leukemias, chronic, 1574
Neutrophilic leukemoid reactions, 646
Neutrophil precursors, morphology of, 578–579, 578f, 579b
Neutrophils, 488, 488f, 578–579
  distribution and kinetics of, 579
  and eosinophils, 896
  functional disorders of, 639–640
  function of, 579
  morphologic alterations in, 638–639, 639b
Neutrophil-specific granule deficiency, 1031
Nevirapine, 1496
Newborn blood screening (NBS), 1033–1034, 1034f
Newborn feces, blood in, 343
Newborn metabolite screening, 66
Newborn screening, 1436
New catalytic antibodies, with predetermined enzyme activity, 304–305, 305f
Next-generation sequencing, 1279, 1282, 1289, 1434, 1472–1473, 1473b, 1510, 1621–1622, 1621f
  for Alzheimer disease, 1465
  for antigen receptor gene rearrangements detection, 1545–1547
  clinical application of, 1604–1606, 1605f
Next-generation sequencing (NGS), 157, 1033
NF1 gene, 1565
NGS. *See* Next-generation sequencing (NGS)
Niacin (nicotinic acid), 443
NIC. *See* Network interface controller (NIC)
Nicking endonuclease amplification, 1397
Nicotiana tabacum, 385–386
Nicotinamide adenine dinucleotide (NADH), 458, 458f
Nicotinamide adenine dinucleotide phosphate (NADPH), 458, 458f
Nicotinic acid. *See* Niacin (nicotinic acid)
Nicotine, 385–386
  metabolic pathway, 385f
Ninhydrin, 280
Nipah henipavirus (NiV), 1288–1289
Nitric oxide, 832
Nitrite, 484
  methods of detecting, 484
    reagent strip, 484
Nitroblue tetrazolium (NBT) reduction assay, 948f
Nitroprusside tablet test for, 479
  procedure of, 479
Nocardia, 1141, 1141f
  antimicrobial susceptibility of, 1141
  characteristics, 1141
  clinical manifestations and pathogenesis of, 1141
  laboratory diagnosis of, 1141
Nodal marginal zone lymphoma, 671, 672f
Nodular fasciitis, 1602
Nodular lymphocyte predominant HL, 683–684
Nodular lymphocyte-rich classical HL, 684–685
Nodular sclerosis, 683, 684f
Nomenclature, 969–970, 970f
  of enzymes, 293, 293t
  taxonomy, fungal morphology and, of mycotic diseases, 1195–1200, 1196t–1197t
    dimorphism in, 1199–1200
    fungal colony in, 1195, 1197f
    fungal pigment in, 1195–1196
    reproductive structures in, 1196–1199, 1198f–1200f, 1199t
    yeasts and hyphae in, structure of, 1195, 1197f–1198f
Nominal scale, 119
Nominal wavelength, 39
Non-beta cell tumors, hypoglycemia and, 235–236
Nonbiological drugs, 899
Noncompetitive immunoassay, for small molecules, 923–925
  anti-idiotype antibody-based immunoassay, 923
  antimetatype antibody-based immunoassay, 923–925
  background of, 923, 924f
  open-sandwich, 923
Nondeletional pancellular hereditary persistence of fetal hemoglobin, 619
Nondiabetic ketonuria, 479
Nondisjunction, definition of, 1412
Non-Hodgkin lymphomas, 515, 1548t–1549t, 1551f
  genetic alterations and detection in, 1548t–1549t
Nonimmune hemolysis, 784–785
Non-islet cell tumor hypoglycemia (NICTH), 235–236
Nonlymphoid cells, 896
Nonmendelian inheritance, and epigenetic influences, 1438
Nonneoplastic disorders, 636–646
Nonneuroendocrine tumor, 1593–1594
Non-organ-specific autoimmune diseases, 1076b
Nonparallel curve, 835
Nonparametric measures, 122, 122f–123f
Nonparametric test, 124
Nonpathogenic amebae, 1315f–1317f, 1318–1319, 1319t–1320t
Nonrenal organ transplantation, 1012
Nonsaturating conditions, enzyme assays under, 298
Nonsecretory myeloma, 670
Nonseptate fungi, 1195
Non-small cell carcinomas (NSCLCs), of lung, 1587–1588
Nonstandard specimens, test billing for, 537
Nonsteroidal estrogen receptor modulator, 433
Nonsusceptible category, antibacterial, 1168
Nonthyroidal illness, 402
Nontreponemal serologic tests, 1233–1234, 1234f, 1234t
Nontuberculous mycobacteria, 1184–1187
  classification of, 1184t
  Mycobacterium avium complex as, 1185, 1192
  Mycobacterium genavense as, 1185
  mycobacterium gordonae as, 1185
  Mycobacterium haemophilum as, 1185
  Mycobacterium kansasii as, 1185
  mycobacterium leprae as, 1186–1187
  Mycobacterium marinum as, 1185–1186
  Mycobacterium ulcerans as, 1186
  Mycobacterium xenopi as, 1186
Normal cells, agents hemolytic to, 624
Normal hemoglobins, 607–608, 607f
Normal platelet biology, 847–849
Normoblastic marrow, macrocytosis with, 592
Normoblastic maturation, 572–574, 572f–573f
Normocytic anemia, 101t, 102
Northern hybridization, 1382
NPM1-ALK gene fusion, 1555–1556
NPM1 mutations, in acute myeloid leukemia, 1563
NRAS gene, 1565
NPV. *See* Net present value (NPV)
Nuclear magnetic resonance spectroscopy, 52–53, 53f
Nuclear matrix proteins, and detection of bladder cancer, 1535–1536
Nuclear methods, for detection of autoantibodies to, 1050, 1050t
Nuclear oncoproteins, 1528t, 1533–1536
Nuclear protein NA14, antibodies to, 1041
Nucleic acid amplification, 1249–1250
  technology, polymerase chain reaction and, 1387–1400.e1
Nucleic acid amplification testing (NAAT), 1271, 1273, 1282
Nucleic-acid amplification tests (NAATs), 1171–1172
Nucleic acid analyses, 1379–1385
  amplification methods for, 1383
  DNA sequencing for, 1384, 1384f
  electrophoretic separation in, 1379, 1379f
  hybridization assays in, 1380–1381
  nucleic acid hybridization in, 1379–1380, 1380f
  polymorphism detection assays for, 1383–1384, 1383f
  pyrosequencing, 1384–1385, 1385f
Nucleic acid-associated enzymes, 1375, 1375f, 1375t
Nucleic acid-based detection, of herpes simplex virus, 1268
Nucleic acid biochemistry and biology, 1373–1379
  DNA in
    mutations of, 1378–1379, 1378t
    repair of, mechanisms of, 1377–1378, 1378t
    replication of, 1375–1376
    to RNA, transcription of, 1376
  molecular composition and structure in, 1373–1375, 1374f, 1375t
  nucleic acid-associated enzymes in, 1375, 1375f, 1375t
  posttranscriptional modification in, 1376
  RNA to protein in, translation of, 1376
  transcriptional control in, 1376–1377, 1376f
Nucleic acid hybridization, 1379–1380, 1380f
Nucleic acid methods, urine, 483–484
Nucleic acid sequence-based amplification (NASBA), 1393–1394
Nucleic acid sequence data, 1404
Nucleic acid sequencing, 1007
Nucleolar antigen fibrillarin, antibodies to, 1044
Nucleolar organizing region (NOR)-90 antibodies, 1044
Nucleolar organizing region, antibodies targeting, 1044
Nucleoprotein synthesis, defects of, 597
5'-Nucleotidase (EC 3.1.3.5), 312
NucliSENS EasyQ KPC assay, 1177
Null cells, 895–896
Null hypothesis (Ho), 120
Numerical chromosome abnormalities, 1418–1420, 1419f
Nutritional folate deficiency, 596

O

Obesity, 265
Occupational Safety and Health Administration (OSHA), 27, 29, 286–287
Ocular infections, *Aspergillus* in, 1223
ODZ gene-encoded teneurins, 1457
OK blood group systems, 740
  biochemistry and molecular biology, 740
  biological role, 740
Oligoclonal bands (OCBs), 517
Oligoclonal immunoglobulin bands
  in cerebrospinal fluid, 963–964, 965f
  in serum, 966
Oligodendroglioma, 1580–1583, 1584f
Oligonucleotide microarrays, 1403–1404
Onchocerca volvulus, 1340, 1340f
Oncogenes, 1446
Oncogenic mutations, sarcomas with, 1601–1602
Oncoprotein abnormalities, gene arrays detecting, 1521–1522
Oncoprotein expression
  sensitivities of, 1539
  specificity of, 1539
Oncoproteins, 1525–1541.e3
  for cell proliferation, 1509–1510
  in detecting biomarker proteins and protein expression patterns in sera, 1536–1538
  detection of cancer in serum, proteomic approaches to, 1538–1539
    antiprotein antibodies and their patterns of expression in sera, 1536–1538
    biomarker proteins and protein expression patterns, 1536–1538
    efficacy of, 1539, 1540f
    origin of malignancies in, 1539–1541
    tumor size and oncoprotein levels in, 1541

Oncoproteins *(Continued)*
evaluation and conclusions of, 1541
multiple markers of, for cancer diagnosis, 1536–1541
overview of, 1525–1527
cell biology and mitogenesis in, 1525
signal transduction pathways in, 1525–1526, 1526f–1527f, 1528t
in tumor detection, 1527–1536
cytosolic mitogenic kinases, 1533
G-proteins, 1532–1533
growth factor receptors, 1526f, 1530–1532
growth factors, 1528–1530
nuclear oncoproteins, 1533–1536
Oncotype Dx
in breast cancer, 1584–1585, 1585f
in prostate cancer, 1597
"One-cell-one-immunoglobulin", 957–958
Oocyte, 428
Open reagent systems, 76
Open-sandwich immunoassay, 923
Operating costs, 163
Operating lease, 173
Ophthalmologic diseases, 979
Opiates, 359–360
Opioid use, 1461
Opisthorchis viverrini, 1336
Opportunistic free-living amebae, 1313–1315, 1314f
Opsonization, assays of, 949
Oral allergy syndrome (OAS), 1120–1121
Oral cancer, anti-p53 in, 1535
Oral candidiasis, 1208
Oral glucose tolerance tests, 229
Orbitrap mass analyzers, 62–64
Order of draw, catheter lines, 31b
Ordinal scale, 119
Organic acidosis, 202–203
Organic acids, 526
Organic anion transporter, 1486t, 1489, 1490t–1491t
Organic anion transporting peptides, 1486t, 1489, 1490t–1491t
Organic cation transporter, 1486t, 1489, 1490t–1491t
Organophosphates, and carbamates, 384–385
Organ transplantation, 980–981, 981f
Orientia tsutsugamushi, as cause of scrub typhus, 1258–1259, 1258t
Origin, in genome, 1375–1376
Orosomucoid. *See* α_1-Acid glycoprotein
Oroya fever, 1264
Osmolal gap, 382
Osmolality, 471–472. *See also* Plasma.
of body fluid, 182–186
methods of, 472
plasma, measurement of, 185–186
specific gravity and, 186
Osmometer, freezing-point, 47
Osmometry, 46–47
Osmotic diuresis, 199, 471
Osmotic fragility test, 605, 605f
Osteitis fibrosa cystica
hyperthyroidism and, 216
renal osteodystrophy and, 222–223
Osteocalcin, 221
Osteomalacia
in renal osteodystrophy, 222, 223f
and rickets, 222
Osteopenia, 221
Osteoporosis, 221–222
pharmacogenomics in, 1502
Otic infections, *Aspergillus* in, 1223
Ovarian cancer, 1598–1599
anti-c-myc protein in, 1535
anti-p53 in, 1534
BRCA1 and *BRCA2* in, 1599
molecular classification of, 1599
protein array to, 1538
Ovary, autoimmune diseases of, 1111
Overfitting predictor, 1620
Overflow proteinuria, 475
Overhydration, 106–107
Overlap syndromes, 1088–1089
concept of, 1049
computer-assisted ANA IFA technology, 1050
immunoblotting, 1056, 1056f
line immunoassays, 1056
multiplex bead-based assays, 1056–1057
mixed connective tissue disease, 1049
Overnight metyrapone test, 420
Oviduct, 428
Ownership of specimens, 179–180
Oxycodone, 360
Oxygenation, 110–111
Oxytocin, 392

P

Paget's disease, 223–224
PAM50 gene signature, 1584–1585
Pancreas
autoimmune diseases of, 1089
endocrine, functions of, 226–228
in systemic disease, 331–332
cystic fibrosis, 331–332
hemochromatosis, 332
Pancreatic adenocarcinoma, 343–344, 344t
CA 19-9, 344
carcinoembryonic antigen, 344
early detection markers, 344
Pancreatic cancer, 1593–1594, 1617
metalloproteases in, 1532
ras-p21 protein in, 1532
Pancreatic disorders, laboratory diagnosis of, 331–346.e3
inflammatory diseases, 332–335
acute pancreatitis, 332–334, 333t
macroamylasemia, 334, 334t
macroscopic examination for, 345
microscopic examination for, 345–346
stool collection for, 345–346
in systemic disease, 331–332
cystic fibrosis, 331–332
hemochromatosis, 332
Pancreatic ductal adenocarcinoma, 1593
Pancreatic function tests, 114
Pancreatic intraductal neoplasia (PanIN), 1594
Pancreatic neuroendocrine tumors, 1594–1595
Pancreatic polypeptide, 228
Pancreatitis, autoimmune, 1089
Panel design, 691, 693t
Panitumumab, 1501
Pantothenic acid, 445
Paper spray ionization (PSI) mass spectrometry, 69–70, 69f
illicit and therapeutic drugs analyzed by, 70t
Papillary renal cell carcinoma, 1595
Papillary thyroid carcinoma, 1586
Paracentesis, 533
Paraganglioma, 405–407, 405f
Paragonimiasis, 1337
Paragonimus spp., 1337
Parainfluenza, 1267–1268
Parametric statistics, 120
Paraneoplastic neurologic syndromes, 1112
Paraneoplastic pemphigus, 1081
Parasites, 498–499
classification and taxonomy of, 1292
culture techniques, for medical parasitology, 1297
detection of, in blood specimen, 1364–1365
from feces, 1364–1365
infections of, diagnosis of, 1364
Parasitic infections and immunocompromised host, 1350t, 1351
Parasitic lice, 1346–1347
Parasitologic examination, 1357
Parathyroid hormone (PTH), 212
vitamin D and, 115–116, 116t
Parathyroid hormone-related peptide, 213, 1518
Parechovirus, 1273
Parietal cell autoantibodies (PCA), 1084, 1084f
gastric, 1084f
Paroxysmal cold hemoglobinuria, 627
Paroxysmal nocturnal hemoglobinuria (PNH), 601, 606–607, 705, 707f
laboratory diagnosis of, 607
Particle agglutination, principle of, 905–907, 905f–906f, 905t
Particle-counting immunoassays, 907
Particle immunoassay, 905–909
Partition (liquid-liquid) chromatography, 51
Parturition, 428
Parvovirus B-19, 785, 1278
Passive congestion, 113
Pasteurella
antimicrobial susceptibility of, 1157
characteristics, 1157
clinical manifestations and pathogenesis of, 1157
laboratory diagnosis of, 1157
Paternity index calculation, 1476, 1476t
Pathogen
reduction, 775
yeast and yeastlike, 1211, 1211f
Pathology
laboratory of, DNA in, 1474, 1474t
molecular diagnostics on practice of
data analysis relating to, 1371
molecular biology used in disease treatment in, 1371
in redefining disease, 1371
Pathology informatics, 151
Pathway interactions, 1454
Patient(s)
data
delta check for, 143, 143t
in quality control procedures, 143–144
for statistical quality control, 144
verifying consistency of, in method, 143–144, 143f
inpatients, Medicare, 167
outpatients, Medicare, 167–169, 169t
risk of harm to, quality control samples and, 139
Patient/donor complications, common to all hemapheresis procedures, 811–816, 813t
Pauci-immune glomerulonephritis, 1099–1102, 1100f–1101f
Pautrier's abscesses, 680
PAX8-PPARG gene rearrangement, 1587
Payback period, 171
Payers, reimbursement and, 164–166
PBP. *See* Penicillin binding protein (PBP)
pCO_2 electrode, 47
PCR. *See* Polymerase chain reaction (PCR)
PDGFRA, in gastrointestinal stromal tumor, 1601–1602
Pediatric nodal marginal zone lymphoma, 671
Pediatric transfusion, 780, 781b
Peer group grading, 145, 145f
Pelger-Huët anomaly, 639, 640f
Pellagra, 443
Pemphigoid, 1081–1082
Pemphigoid gestationis (PG), 1081–1082
Pemphigus, 1079–1081
Pemphigus foliaceus, 1080–1081
Pemphigus vulgaris, 1079–1080, 1080f–1081f
Penicillin, allergens derived from, 1127f
Penicillin binding protein (PBP), 1169–1170
Pentastomids, 1344
Pentatrichomonas hominis, 1322
Pentose, in urine, 477
Pepsin, pepsinogen and, 336
Peptic ulceration, 335
Peptides
cardiac natriuretic, 273–275, 274f
parathyroid hormone-related, 213
procollagen type I N-terminal and C-terminal, 221
Peptidylarginine deiminase (PAD) antibodies, 1046
p185erbB-2 ECD, in other tumors, 1531
Percutaneous umbilical blood sampling (PUBS), 1413
Performance
and monitoring, of financial management, 170–171, 170t
optimizing, 19–21, 21t
Pericardial fluid, 33, 531–533, 532b
chemical analysis of, 532–533
collection of, 531–532
examination of
gross, 532
microbiological, 533
microscopic, 532
exudates and transudates, 532
immunologic studies of, 533
Perinatal viral infections, 1271–1273
Period, of sine wave, 36
Peripheral blood progenitor cells, 821–823
Peripheral blood smear examination, leukocytes on, 547t
Peripheral T-cell lymphomas, 1556
Peritoneal dialysis, 534
Peritoneal fluid, 33, 533–536
chemical analysis of, 535–536
collection of, 533–534
examination of
gross, 534
microbiological, 536
microscopic, 534–535, 534f
tests for, 534, 534b
transudates and exudates, 533, 533b
Peritoneal washings, 534
Permeability defects, 606–607
Pernicious anemia (PA), 1084–1085, 1084f
in children, 594
immune abnormalities of, 594
Pertussis, 642
Peutz-Jeghers syndrome (PJS), 1593

PFA-100/200, 849
p53 gene, 1518, 1591
proteins, 1533–1535
pH, 530, 535
Phaeohyphomycosis, 1220
Phaeoid, 1195–1196, 1219
Phagocyte analyses, 1031
Phagocytosis and endocytosis, assays of, 947–948
Pharmacogenetics, 1480
Pharmacogenomics, 1480
in bipolar disorder, 1458
in genome-wide association studies, 1456
of major depression disorder, 1462–1463
Pharmacogenomics, personalized medicine and
basic concepts of, 1480, 1481f
in cancer chemotherapy, 1496–1501
5-fluorouracil, 1496–1497, 1497f
irinotecan, 1497–1499, 1498f
tamoxifen, 1499–1501, 1500f
thiopurines, 1496
drug-metabolizing enzyme
pharmacogenomics, 1481–1486, 1481f
phase I enzymes, 1481–1483, 1481f, 1482t–1483t
phase II enzymes, 1481f, 1483–1486, 1484t–1485t
drug target pharmacogenomics, 1489–1495
DNA repair genes in, 1489–1491, 1491f, 1492t–1493t
epidermal growth factor receptor in, 1494–1495, 1494f
thymidylate synthase in, 1493–1494, 1493f, 1494t
drug-transporter pharmacogenomics, 1486–1489, 1487f
ABCB1 transporters, 1486t, 1487, 1488t, 1498–1499
ABCC1 and ABCC2 transporters, 1486t, 1487–1488, 1488t
ABCG2 transporters, 1488–1489, 1488t
OATPs, 1486t, 1489, 1490t–1491t
OATs, 1486t, 1489, 1490t–1491t
OCTs, 1486t, 1489, 1490t–1491t
human leukocyte antigen pharmacogenomics, 1495–1496
in other diseases, 1501–1504
diabetes, 1501–1502
epigenomics, 1503–1504, 1504f
human immunodeficiency virus, 1502
osteoporosis, 1502
psychiatric and cognitive disorders, 1502–1503
Pharmacokinetics, 364–366, 364f
liver, metabolism in, 365–366
volume of distribution, 365
Phase-contrast microscopy, 487, 487f
Phase I enzymes, 1481–1483, 1481f, 1482t–1483t
Phase II enzymes, 1481f, 1483–1486, 1484t–1485t
Phase III trials, 178
Phase II trials, 178
Phase I trials, 178
Phase IV trials, 178
Phase 0 trials, 178
pH electrode, 47
Phencyclidine, 362
Phenobarbital, 366t, 369, 370f
Phenotype
definition of, 1412
frequencies, genes and, 1023
Phenylketonuria, 507–508
methods for, 507–508
Phenytoin (Dilantin), 366t, 369
Pheochromocytoma, 405–407, 405b, 406t–407t, 408f
additional follow-up testing of, 407
testing procedures of, 407
Phe-Psi residue, 303–304
Phi bodies, 655
Philadelphia (Ph') chromosome, 651, 1568–1569
Ph-negative myeloproliferative neoplasms, 1569t
Phoenix system, 1171
Phosphate, 458
calcium and, 109
Phosphatonins, 215
Phospholipase C, defects in activation of, and platelet signaling pathways, 860
Phospholipase D3, 1465
Phospholipids, 254, 848, 849t
Phosphorescence, 43–44
Phosphorus, 210–211
Phosphorus homeostasis, 210–211
Photodetectors, 40–42
Photodiode arrays, 41–42, 41f
Photolithographic synthesis, 1403, 1403f
Photometers, 42
Photometric accuracy, 42
Photometric instruments, types of, 42
Photomultiplier tubes (PMTs), 40–41, 41f
Photovoltaic cell, 41
Physical agents
acquired, extrinsic hemolysis relating to, 624–625
aplastic anemia associated with, 600
Physician office laboratories. *See* Point-of care testing (POCT), and physician office laboratories
Physician offices, in point-of-care testing program, 85–86
Physiologic factors
of precollection variables, 22–23
tests affected by diurnal variation, posture, and stress, 23t
Physiologic hemostasis, 828–833
anticoagulation protein systems, 831–832
coagulation protein system, 829–830
endothelium, platelets and, 828–829, 829f
fibrin and fibrinolytic system, formation of, 830–831, 831f
hemostatic system, hypothesis for initiation of, 832–833
Physiologic protein assemblies, 830
Physiologic role
of calcitonin, 213–214
of vitamin D and metabolites, 214
Physiologic variables, of thyroid function, 402–403, 402f
Physiologic variation
in erythrocyte, 544–545, 545f, 545t
in leukocyte, 546, 547t
in platelet, 549
Physiology
of bio-intact PTH, 212–213
of calcitonin, 213–214
of calcium, 208–210
of magnesium, 211
of parathyroid hormone, 212
of parathyroid hormone-related peptide, 213
of phosphorus, 210–211
of vitamin D and metabolites, 214
Phytomenadione. *See* Vitamin K
Pigmented casts, 492–493
Pigment, in renal tubular epithelial cells, 490
PI3KCA, 1591
p16 (CDKN2A or MTS1), in cervical cancer, 1598
Pink-top tubes, anticoagulants and additives, 27, 27t
Pinta, 1233
Pinworms
cellulose tape technique for, 1296
infection, 1328
Piperazines, 361
Pipets, 55–56
Pituitary function, 387–395, 388f, 388b
growth hormone, 390–392, 390f
posterior pituitary hormones, 392–395
prolactin, 389–390, 389b
tumors, 388, 389t
Pituitary gland, 387
Placenta, 428
Planar configuration, 303
Plasma, 773–774
donor of, 799
enzyme activities of, factors affecting, 294
enzyme levels of, 320–322
flow of, glomerular filtration rate (GFR), and filtration fraction (FF), 191–192
osmolality, measurement of, 185–186
hyperglycemia, serum Na+ and, 185–186
specific gravity and, 186, 472
tonicity, 186
versus serum, 252–253
transfusion of, 779
Plasma aldosterone concentration, in potassium metabolism, 194
Plasmablastic lymphoma, 675
Plasma cell leukemia, 670, 671f
Plasma cell myeloma, 669–670, 670f, 670b, 1555
clinical variants of, 670
asymptomatic (smoldering) myeloma, 670
extraosseous plasmacytoma as, 670
plasma cell leukemia as, 670, 671f
solitary plasmacytoma of bone as, 670
Plasma cell neoplasms, 669–670, 670b, 703, 706f
Plasma corticotropin-releasing hormone, 415
Plasmacytoma, extraosseous, 670
Plasmacytosis, 645, 646b
Plasma homocysteine assay, 597
Plasma lipids, estimation of, 253–254
Plasma products, 798–799
Plasma proteins, 280–288, 281t
acute phase reactants and, 287–288
components of
major, 280–285
minor, 285–287
protease inhibitors in, 287
Plasma pyridoxal 5-phosphate (PLP), 445
Plasma renin activity, in potassium metabolism, 194
Plasma transfusion, 779, 779b
Plasmin-cleaved soluble fibrinogen or fibrin, 831f
Plasmodium species, 1301–1304
as clinical disease, 1303
diagnosis of, 1303–1304, 1304t, 1305f–1310f
epidemiology of, 1303
life cycle of, 1302–1303, 1302f, 1305f–1308f
Plasticware, for laboratory, 55
Platelet antibody testing, 769
Plateletpheresis donor
concerns of, 791
selection of, 790–791
Plateletpheresis, therapeutic, 803–807
Platelet-derived growth factor, 1529
Platelet-derived growth factor receptor α *(PDGFRA)* gene, 1577
Platelet disorders
acquired, 862–864
acquired storage pool disease, 863
acute leukemias and myelodysplastic syndromes, 862
in antiplatelet antibodies and platelet function, 863
from drugs that inhibit platelet function, 863–864, 863b
dysproteinemias, 862
myeloproliferative neoplasms, 862
uremia, 862–863
of adhesion, 848
of aggregation, 848
familial, with predisposition to acute myelogenous leukemia, 861
of granules, and secretion, 858–859
inherited, 857–862, 857b, 858f
cytoskeletal linking proteins, defects in, 860
cytoskeletal proteins, defects in, 860
evaluation of patients with suspected, 861
of glycoprotein adhesion, abnormalities of, 857–858
high-throughput DNA sequencing for diagnosis of, 852
platelet granules, abnormalities of, 858–859
platelet receptors, signaling pathways, and secretion, abnormalities of, 860
of procoagulant activities, 860–861
therapy of, 861–862
and transcription factor mutations, 861
laboratory evaluation of, 849–852
flow cytometry used in, 852
initial, 849
platelet aggregation and secretion studies, 849–852
studies of platelet function in, 849
platelet receptors, signaling pathways, and secretion, abnormalities of, 860
and arachidonic acid metabolism, abnormalities of, 860
defects in G-proteins and their activation in, 860
defects in phospholipase C activation, calcium mobilization, and protein phosphorylation in, 860
defects in receptors and, 860
and thromboxane synthesis, abnormalities of, 860
quantitative, 852–857
thrombocytopenia, 852–856
thrombocytosis, 856–857
and von Willebrand disease
inherited platelet defects, 857–862
laboratory evaluation of, 849–852
and normal platelet biology, 847–849
Platelet membrane glycoproteins, and phospholipids, 848
Platelet product requirements, 790
Platelets, 498, 776
activation and signaling events of, 848–849
activation mechanisms of, and platelets, in hemostasis, 848–849
aggregation of, and secretion studies, 849–852, 851f
apheresis, benefits of, 790
coagulant activity of, 849
concentrates of, 774
counts of, 546–548, 547f
calculation of, 548
diluent solution in, 547

Platelets *(Continued)*
falsely elevated counts, 548
falsely low counts, 548
hemocytometer method of, 547
procedure of, 547
sources of error, 548
specimen of, 547
dysfunction of, transcription factor mutations associated with, 861
endothelium and, 828–829, 829f
function of
and antiplatelet antibodies, 863
bleeding time measures of, 105
drugs and food supplements, 856b, 863–864
in hemostasis, platelet activation mechanisms and, 848–849, 850f
physiologic variation in, 549
refractoriness, 776
reticulated, 548
selection of, 776
structure of, 847, 848f
transfusion of, 778–779, 778b
Platelet serology, 767–769
human platelet alloantigens, 767–769, 768t
autoimmune thrombocytopenia, 769
CD36 deficiency, 769
drug-induced thrombocytopenia, 769
and neonatal alloimmune thrombocytopenia, 767
platelet antibody testing, 769
and posttransfusion purpura, 767–769
Platelet transfusions, 778–779, 778b–779b, 861–862
Platelet-type or pseudo- von Willebrand disease *(gp1ba)*, 858
Plerixafor, 989–990
Plesiomonas, 1146–1147
antimicrobial susceptibility, 1147
characteristics, 1146
clinical manifestations and pathogenesis, 1146–1147
laboratory diagnosis, 1147
Pleural fluid, 33, 527–531
chemical analysis of, 529–531
collection of, specimen, 527
examination of
gross, 528, 529t
microbiological, 531
immunologic studies of, 531
microscopic examination of, 528–529
cell counts, 528
differential leukocyte count and cytology, 528–529, 529f, 530b
tests for, 527–528, 528t, 528b
transudates and exudates, 527, 527b
PML-RARA gene, 1557–1560
PMTs. *See* Photomultiplier tubes (PMTs)
Pneumatic tube(s)
for automated delivery, 75
transport, of specimens, 18
Pneumocystis carinii pneumonia, 312
Pneumocystis pneumonia, 1226–1227
clinical diseases, 1226
laboratory diagnosis, 1226–1227, 1226f–1227f
risk factors, 1226
pO_2 gas-sensing electrode, 48
Point-of-care mass spectrometry devices
cartridge development, 71–72
miniature mass spectrometry systems, 72–73
in vivo clinical analysis, 72
Point- of- care settings, 61
Point-of-care testing (POCT), 81, 83t, 455–456
advantages and disadvantages of, 85, 85b
committee and management team, 86
selection of appropriate testing devices and method of, 86–87
selection of appropriate tests of, 86
definition of, 81
devices, 921–923, 922f
background of, 921
immunochromatographic devices, 921–922, 922f
magnetic biosensor assay, 922–923
interfaces in, 86f
laboratory design and service models, 6, 7b
and physician office laboratories, 81–88.e1
compliance for, 83
connectivity and data management in, 85, 86f
laboratory directorship in, 82–83
regulatory requirements for, 81–82
program
implementation of, 85–86
maintenance of, 85
types of, 83–85
Poisoning, acute, toxins and, 380–386
Polarized microscopy, 487
Policies, on point-of-care testing program, 87
Polyacrylamide gel electrophoresis (PAGE), 278
Polyanion precipitation methods, 255
Polyarteritis nodosa, 1062–1063
clinical laboratory testing of, 1063
definition and epidemiology of, 1062
diagnosis, treatment, and prognosis of, 1063
etiology and pathogenesis of, 1063
pathology of, 1062–1063, 1062f–1063f
Polyclonal antibodies, 902
Polyclonal hyperimmunoglobulinemias, 960t
Polyclonal immunoglobulins, 959, 961
Polycythemia, 581b
hemoglobins associated with, 615
Polycythemia vera, 647, 1572–1574
clinical features of, 647
laboratory features of, 647
blood in, 647
marrow in, 647, 649f
Polygenic diseases, with MHC association
ankylosing spondylitis, 1020
celiac disease, 1020–1021
narcolepsy, 1021
rheumatoid arthritis, 1022
Type 1 diabetes, 1022–1023
Polygenic diseases, with MHC associations, 1020–1023, 1020t
Polygenic (nonfamilial) hypercholesterolemia, 260–261
Polymerase chain reaction (PCR), 532–533, 1235, 1387–1393, 1388f
allele-specific, 1393
digital, 1392–1393
end-point quantitative, 1389
for antigen receptor gene rearrangements detection, 1545–1547
for lymphoid clonality analysis, 1547
multiplex, 1389
nested, 1388–1389
and nucleic acid amplification technology, 1387–1400.e1
probe amplification methods in, 1397–1399, 1399f
signal amplification methods in, 1397–1399, 1399f
target amplification methods in, 1387–1397, 1388f, 1390f, 1392f
rapid-cycle, 1392
real-time, 1390–1392, 1390f
reverse-transcriptase, 1387–1388
Polymorphism
class II, 1004
genetic, 1023
HLA, identification techniques of, 1007–1009
Polymorphism detection assays, for nucleic acid analysis, 1383–1384, 1383f
Polymorphonuclear killing assays, 1030
Polymyositis (PM), 1046, 1113
Polyomavirus infections, 1285
Polyspecific reagents, for antihuman globulin test, 747
Polyuria, 199, 471
Pooled human γ-globulin, 966
Porphobilinogen tests, 483
physiology of, 586f
Porphyrins, 485–486
fluorescence screening procedure for, 486
methods of, 485
Positive cultures, detection and notification of, in blood specimen, 1354–1355
Positive patient identification, 154–155
Positive specimen identification, 154–155
Positivity criterion, 96–97, 97t
Postanalytic processing, 75–76
Posterior pituitary hormones, 392–395
arginine vasopressin/antidiuretic hormone, 392–395
diabetes insipidus relating to, 393–394, 393t, 394f, 395b
oxytocin, 392
SIADH, 394–395, 395t, 396f, 396b
Posthepatic biliary obstruction, 329
Postinfectious glomerulonephritis, 1097
Postnatal cytogenetics, 1425
Postnatal hematopoiesis, 572
Postpericardiotomy syndrome, 531
Postsample filters, 40
Posttranscriptional modification, 1376
Posttransfusion purpura (PTA), 767–769
Posttransplant lymphoproliferative disorders, 685, 686f
Posttransplant viral load testing, 1284–1286, 1284t
Posttraumatic stress disorder, 1463–1464
GWAS of, 1463
SNPs in, 1464t
Postural proteinuria, 474
Posture
in blood sampling and storage, 252
as physiologic factor, 23
tests affected by, 23t
Potassium
collection-associated variables and, 24
disorders of, 193–197
hyperkalemia
cause and pathogenesis of, 196–197, 196b
differential diagnosis of, 197
hypokalemia
causes and pathogenesis of, 195–196, 195b
differential diagnosis of, 196
metabolism, abnormalities in, 194
plasma aldosterone concentration, 194
plasma renin activity, 194
renal excretion, control of, 194, 194f
transcellular flux, control of, 193–194, 194f
Potassium hydroxide (KOH), preparation of, 1202b
Potentiometry, 47
POU3F2, 1458
Power function graphs, in quality control, 137, 138f
Prader-Willi syndrome, 1430, 1445, 1445f
Prealbumin, 280–281
Preanalysis, 22–34.e1
blood collection
overview, 27–29
techniques, 29–31
errors, 23t
precollection variables, 22–26
specimen
collection, 26
processing, 33–34
transport, 33
urine and other body fluids, collection of, 31–33
Precentrifugation phase, of specimen processing, 33–34
Precipitation, 279
Precipitin and nephelometric immunoassays, 904
background and principles of, 904
Precision, of analysis, 127
Precollection variables, 22–26
common interferences, 23–24
physiologic factors, 22–23
Precursor lymphoid neoplasms, 663–664
Prediction of T1DM, 1109
Prediction strength, 1615
Predictive genetic testing, 1438
Predictive value
and accuracy, 94, 94t
and prevalence of disease, 93–94, 94t
Preeclampsia, 438, 625
Pregnancy. *See* Reproductive function, pregnancy and
Pregnancy-associated plasma protein A (PAPP-A), 436
Preimplantation genetic testing for aneuploidy (PGT-A), 433
Prekallikrein, 828–829, 841–842
Preleukemias, 651
Premature rupture of membranes, 438–439
Prenatal cytogenetics, 1423–1425, 1424t, 1425f
Prenatal/neonatal viral infection, 1272
Prenatal testing, 1437
Preoperative crossmatch protocols, 755
Prerenal disease, 108
Presample filters, 39
Presenilins, 1464
Presymptomatic DNA testing, 1437
Preterm labor, 439
Pretransfusion testing, 776
Prevalence of disease, predictive value and, 93–94, 94t
Primary amebic meningoencephalitis, 522
Primary amyloidosis, 670
Primary biliary cirrhosis, 1086, 1088, 1088f
antimitochondrial antibody for, 322
Primary components, of mass spectrometry systems, 62
Primary cutaneous CD8-positive aggressive epidermotropic cytotoxic T cell lymphoma, 681
Primary cutaneous CD4-positive small-medium T cell lymphoma, 681
Primary cutaneous CD30-positive T cell lymphoproliferative disorder, 680–681, 682f
Primary cutaneous DLBCL, leg type, 674
Primary cutaneous γδ T cell lymphoma, 681
Primary DLBCL, of the CNS, 674
Primary effusion lymphoma, 529, 675
Primary hemostasis, 833
rebalanced, 844
Primary hyperaldosteronism, 422
differentiating causes of, 422–423, 423t
Primary hyperparathyroidism (PHPT), 215–216

Primary immunodeficiencies (PIDDs), 1025–1026
Primary lymphoid tissue, 583–586
Primary mediastinal (thymic) large B cell lymphoma, 675
Primary myelofibrosis, 647–649
  biology of, 648
  course of, 648–649
Primary osteoporosis, 222
Primary pulmonary infection, *Aspergillus* in, 1223
Primary red cell hydration disorders, 606–607
Primary sclerosing cholangitis (PSC), 1088, 1089f
  ANCA, 322–323
Primidone (Mysoline), 369–370
Primitive peripheral neuroectodermal tumor, 1600
Prion, 786
Privacy regulations, 175
Private insurance, 164
Private sequencing effort, 1609
Probability of exclusion, 1474–1475
Probe amplification methods, 1397–1399, 1399f
Probe, hybridization assays and, 1380–1381, 1380f
Procainamide (Pronestyl), 366t, 368
Procedures, on point-of-care testing program, 87
Processing mode, test menu and, 16
Procollagen type I N-terminal and C-terminal peptides, 221
Productivity measures, 171, 171t
Proficiency testing (PT), 144–147
  materials, noncommutability of, 145, 145f
  programs for, accuracy-based, 147
  results of
    interpretation of, 145–147, 146f, 147b
    limitations in, 146–147
    reporting, 145, 145f
Progenitors, hematopoietic stem cells and, 570–571, 571f, 571b
Prognostic molecular markers of disease, 1618–1620
  genomics, 1618–1619
  integrating genomics and proteomics, 1619–1620
  pitfalls of, 1620
Programmed cell death protein 1 (PD-1), 899
Programmed cell death protein 1 and its ligand (PD-L1), 899
Proinsulin, 226–227, 226f
Prolactin, 389–390, 389b
Prolaris, in prostate cancer, 1597
Proliferating cell nuclear antigen multiprotein complex, 1038
Proliferating cell nuclear antigen (PCNA) proteins, 1038
Promonocyte, 651–652, 654f
Promoter hypermethylation, 1522
Promyelocytic hyperplasia, 637–638
Proofreading, 1375–1376
Pronestyl. *See* Procainamide (Pronestyl)
Propagation, velocity of, 36, 36b
Propoxyphene (Darvon), 362
Propranolol, 368
proPSA, 1519–1520
Prostacyclins, 832
Prostarix, 1523
Prostate cancer, 1596–1597
  protein array to, 1538
  serum markers for, 1518–1520
  urine markers for, 1523–1524
Prostate Health Index, 1519–1520
Prosthetic groups, 293–294
Protease degradation, of unstable enzymes, 299
Protease inhibitors, 287
Protected Health Information (PHI), 175
Protectin, 974
Protein 14-3-3, 519
Protein(s), 515–519, 526, 529, 532, 535
  β-amyloid protein 42 and τ protein, 518–519
  anticarbamylated antibodies, 1046
  beta trace, 191
  C, 871, 873
  c-myc, p53 and, 1533–1535
  C/protein S system, 832
  C-reactive, 272–273, 272b
  defects in phosphorylation of, and platelet signaling pathways, 860
  fatty acid-binding, 193
  markers of, 1524
  myelin basic, 518
  nuclear matrix, 1535–1536
  P ribosomal, antibodies to, 1038
  regulatory, cell-associated, 973–974
  S, 871, 873–874
Protein(s) *(Continued)*
  and salt concentrations, affecting enzyme activity, 299
  specific, 276–290.e2
    abnormalities of, patterns of, 288–289, 288f–289f
    detection and quantitation of, 279–280
    plasma, 280–288, 281t
    separation of, techniques for, 277–279
    structure of, 276–277
  synthesis of, 318–320
  total, albumin and, 456
  urine in, 473–476
Protein arrays, 1536–1538, 1615
Protein C deficiency, 873
Protein C pathway, 872f
Protein S deficiency, 873–874
Protein trafficking, 1460–1461
Proteinuria
  Bence Jones, 475
  heavy, 474
  methods for, 475–476
  minimal, 475
  moderate, 474–475
  in older adults, 474
  overflow, 475
  postural, 474
  qualitative categories of, 475
    glomerular pattern, 475
    tubular pattern, 475
  quantification, 474–475
  screening for, 475t
    Bence Jones determination methods, 476
    microalbuminuria determination methods, 476
    quantitative protein determinations and confirmatory methods, 476
    reagent strip, 476
    sulfosalicylic acid method, 476
Proteomics, 1527–1528, 1536–1541, 1614–1615
  human neoplasia, molecular markers for diagnosis of, 1615–1616, 1616f
  limitations of, 1620
Prothrombin (PT) and INR, liver function relating to, 319
Prothrombinase complex, 833
Prothrombin g20210a, 875
Prothrombin time, 833–834, 879
Protothecosis, 1227, 1227f
Provider-performed microscopy procedures (PPMP), 81–82, 82b
Prozone effect, 954
Pseudocholinesterase, 310
Pseudochylous/chyliform effusions, 528
Pseudo-Cushing's syndrome, 419
Pseudocyanosis, 616
Pseudogout, 525
Pseudohyphae, 1195
Pseudohyponatremia, 454
Pseudohypoparathyroidism (PHP), 217–218
Pseudomonas, 1147–1148
  antimicrobial susceptibility of, 1147–1148
  characteristics, 1147, 1147f
  clinical manifestations and pathogenesis of, 1147
  laboratory diagnosis of, 1147, 1147f, 1148t
Pseudo-neutropenia, 638
Pseudo-Pelger-Huët anomaly, 639
Pseudoterranova spp., 1342
Psychiatric and cognitive disorders, pharmacogenomics in, 1502–1503
Psychological manifestations, in mechanism of injury, 1345–1346
PTBP2 (polypyrimidine tract binding protein 2), 1466
PT. *See* Proficiency testing (PT)
PTEN, 1583t, 1591
  in prostate cancer, 1597
PTPN11 gene, 1565
Public sequencing effort, 1608–1609
Pulmonary function, 1028
Pulmonary histoplasmosis, chronic, 1212
Pulmonary infection
  acute, *Histoplasma* in, 1212
  primary, *Aspergillus* in, 1223
Pulmonary neoplasms, HER2/*neu* receptor and, 1531
Pure erythroid leukemia, 659
Pure red cell aplasia, 601–602
Purification, of water, 53–54
Pus, 345
Pustules, specimens of, 1365
P2Y12 inhibitors, 889–890, 889f, 889t
Pyogenic bacteria, and neutrophilia, 637
Pyridinium cross-links, 220
Pyridoxine (vitamin B_6), 443–445
Pyrimidine-5'-nucleotidase deficiency, 623
Pyrosequencing, 1384–1385, 1385f
Pyruvate kinase (PK) deficiency, 623
Pyuria, 488

Q

Q-banding, 1414
QC. *See* Quality control (QC)
Q fever, 1261–1262
Quaalude. *See* Methaqualone (Quaalude)
Quadrupole, 62–64
Quadrupole mass analyzers, 62–64
Quality assurance
  program, 87
  quality improvement and safety, for medical parasitology, 1300–1301
  in spectrophotometry, 42
  standards of, for DNA analysis, 1478
Quality control (QC), 130–149.e1
  analytic bias and imprecision, 121f, 130–131
  calibration issues in, 131–132, 131f
  calibrator, new lot of, verifying method performance following, 143
  data, reviewing, 140–141
  materials for
    limitations of, 134
    selection of, 133–134
  measurement problem with, corrective action for, 140, 140f, 140t
  in measurement procedure, for intended medical use, 136, 136t, 137f
  plan, individualized, 139
  procedures for, 132–133, 133f
    implementing, 133–141
    using patient data in, 143–144
  proficiency testing, 144–147
  and quality assurance, of cellular immune system, 949–950
  quality management and, 147–148, 148t–149t
  results of, rules to evaluate, 137–139, 138f, 139t
  samples of
    event-based, 139–140
    frequency to, 139–140
    harm to a patient, risk of, 139
    stability of, 139
  statistical, 144, 144f
  target value and standard deviation, establishing, 134–136, 135f, 135t
  verifying, evaluation parameters following a reagent lot change, 141–142, 141f–142f
Quality management (QM)
  quality control and, 147–148, 148t–149t
Quality System Essentials, quality systems management and, 5, 5b
Quality systems management, clinical laboratory and, 3–5
Quantification, of DNA, 1470
Quantile normalization, 1406
Quantitative assay
  of glucose-6-phosphate dehydrogenase deficiency, 623
  of pyruvate kinase deficiency, 623
Quantitative counts, 487
Quantitative flow cytometry, 939
Quantitative platelet disorders, 852–857
  thrombocytopenia, 852–856
  thrombocytosis, 856–857
Quantitative white blood cell abnormalities, 104–105
Quaternary structure, 277
Quebec platelet syndrome, 859
Quinidine, 368

R

RABEP2 (Rab GTPase-Binding Effector Protein 2 or Rabaptin), 1461
Radial partition immunofluorometric assay, 917
Radiant energy sources, 38–39
Radiation, scattering of, 37
Radioallergosorbent test (RAST), 1123
Radiofrequency conductivity, 549
Radiographic media (meglumine diatrizoate), 497, 498f
Radioimmunoassay, 909–911, 910f
  assay principles and methods, 909–911, 910f–911f
  background, 909, 909f, 909t
Radiologic examination, of urine, 507

Radiologic imaging, for immunodeficiency evaluation, 1028
Raf, 1533
Raman scattering, 37
Random access analyzer, 74
Randomized controlled trial (RCT) evidence, 1267
Rapamycin (Sirolimus), 376
RAPH blood group systems, 740
  biochemistry, 740
  biological role, 740
  molecular biology, 740
  null phenotypes, 740
Rapid-cycle polymerase chain reaction, 1392
Rapid evaporative ionization mass spectrometry (REIMS), 72
RARA gene, 1557–1558
Rare calculi, 507
Rare variant studies, 1456
RAS mutations, 1586
RAS oncogenes, 1565
ras-p21 protein, 1532–1533
Rayleigh scattering, 37
R-banding, 1414
RBC sensitization, 745
R-binder/transcobalamin I, 445
RBM15-MKL1 fusion transcript, 1561
RDW. *See* Red cell distribution width (RDW)
Reaction coordinate, 293f
Reaction cuvette, 920
Reaction specificity, 291–292
Reading frame, of protein, 1376
Read-only, 153
Reagent handling, in automated chemistry analyzer, 76
Reagent lot change, verifying quality control evaluation parameters following, 141–142, 141f–142f
Reagent red blood cells, 751–752
Reagents, 690–691, 690f–691f
  enzymes as, for analyte concentrations, 458–466
Reagent strip, 472–473, 476–477, 479, 482
Real competitive polymerase chain reaction, 1611–1612, 1613f–1614f, 1614t
Real-time clot, viscoelastic measurement of, 835–836
Real-time polymerase chain reaction, 1390–1392, 1390f
Receiver operator characteristic curves, 95–96, 96f
Receptor tyrosine kinase genes, 1601
Recessive allele, definition of, 1412
Recipient sample identification, 748–749
Recombinant technology, antibody production by, 902
Recombination, definition of, 1412
Recommended dietary allowance (RDA), 441–442
Record and specimen retention, guidelines for, 9t
Red blood cells, 773
  blood components, selection of, 775–776
  frozen, 775
  selection of, 775–776
  typing of, with lectin reagents, 759
Red cell antigens, destruction of, 758
Red cell autoantibody, stimulation of production of, 763
  drug-dependent autoantibodies, 763
  drug-independent autoantibodies, 763
  drug-induced immune hemolytic anemia, 763
Red cell distribution width (RDW), 102
Red cell exchange, 805–806
Red cell folate, serum and, 596, 597t
Red cell grouping, 750
Red cell hydration disorders, primary, 606–607
Red cell membrane, adsorption of drug to, 628
Red cell transfusion, 777–778
Red-top tube, anticoagulants and, 27t, 28
Reference electrodes, 47
Reference interval(s)
  for calcitonin, 214
  for calcium, 210
  definition of, 90
  for magnesium, 212
  for parathyroid hormone, 212
  for parathyroid hormone-related peptide, 213
  for phosphatonins, 215
  for phosphorus, 211
  for vitamin D and metabolites, 215
Reference laboratories, 61
Reference ranges, 90–92, 127
  determination of, 91
  factors that influence, 91
  laboratory results in, variability of, 91–92
Referential integrity failure, 153
Reflectometers, 43, 44f
Reflectometry, 43
Refractive index, 280
Refractometer, 472
  procedure of, 472
Refractometry, 46
Refractoriness, of platelets, 776
Refractory anemia(s), with ring sideroblasts, 602
Regulation, accreditation, and legislation, 6–10
Regulatory requirements, for point-of-care testing and physician office laboratories, 81–82
Reimbursement
  coding systems for, 166–169
    accurate coding, 166–167, 168t–169t
  Medicare, 167–169, 169t
  payers and, 164–166
Relapsing fever, 1243–1244, 1243f, 1244t
Relational database, 160
Relative quantity value, 1392
Relative standard deviation (RSD), 62
Renal acidosis, 202
Renal and postrenal disease, 108
Renal cell carcinoma, 1595
Renal diseases, 979
Renal excretion, of potassium, control of, 194, 194f
Renal failure
  anemia of, 104
  casts, 491
  index of, 192
Renal function, measurement of, 187–192
  clearance, concept of, 187–188
    conversion of clearance in L/week to mL/min, 188
    formulas for the calculation of, 188
  creatinine as, 188–190
  fractional excretion (FE), 192
  fractional reabsorption (FR), 192
  glomerular filtration rate (GFR), 188–191
    renal plasma flow (RPF), and filtration fraction (FF), 191–192
  renal failure index (RFI), 192
  urea as, 190
  urea clearance and urea/creatinine ratio in serum, 191
Renal function, water, electrolytes, and acid-base balance, evaluation of, 181–207.e2
  body fluid, volume and osmolality of, 182–186
    composition of, 184–185
    measurement of, 183
    plasma, measurement of, 185–186
  extracellular volume, regulation of, 186–187
    water and electrolyte balance, nonrenal control of, 187
Renal medullary angiitis, 1099–1101, 1101f
Renal osteodystrophy, 222, 223f
  osteomalacia in, 223f
  secondary hyperparathyroidism and, 216, 217f, 218t
Renal parenchymal disease, 471
Renal plasma flow, glomerular filtration rate, filtration fraction and, 191–192
Renal salt/water absorption, defective, 471
Renal transplantation, 1012
Renal tubular epithelial cells, 489, 489f
  casts, 491–492, 492f
  lipids in, 489, 490f
  pigment in, 490
Renin
  hypertension and, 421–423, 421b–422b
  measurements of, 423–424
Renin-aldosterone axis, 420–424, 420f–421f
  aldosterone measurements, 423, 423t
  renin, 421–423, 421b–422b
Renin-angiotensin system, 308f
Replication of DNA, 1375–1376
Reporting/flagging, of instrument technology, 550, 550f, 550t
Reproducibility, 62
Reproductive function, pregnancy and, 425–440.e2
  aplastic anemia and, 601
  laboratory evaluation of, 429–433, 429t, 434t
    assisted reproductive technology, 433
    Down syndrome, 436, 436f
    erythroblastosis fetalis, 436–437, 437f
    for female, 431–433, 432f
    fetal lung maturity, 437–438
    gestational diabetes, 437
    hCG and early pregnancy, 433–434
    with hematologic and coagulation disorders, 439
    with infection, 439
    intrapartum assessment, of fetal status, 439
    for male, 429–431
    neural tube defects, 434–436, 435f
    preeclampsia, 438
    premature rupture of membranes, 438–439
    preterm labor, 439
    testosterone replacement therapy, 439–440
Reproductive function, pregnancy and *(Continued)*
  normal physiology of, 425–429
    female reproduction, regulation of, 427–428, 427f–428f
    male reproduction, regulation of, 427, 427f
    pregnancy, 428–429, 428f
    sex steroids, 425–427, 426f
Reproductive structures, of mycotic diseases, 1196–1199, 1198f–1200f, 1199t
Reproductive tissue, 820–821
Request for proposal (RFP), 156
  for laboratory automation, 79, 79t
Resistance phenotypes detection, 1172–1177
  aminoglycosides, 1172
  AmpC cefoxitin-ethylenediaminetetraacetic acid test., 1175, 1176f
  chromogenic media, 1172
  D-zone approximation test, 1173, 1173f
  E-test, 1175, 1175f
  extended-spectrum β-lactamases, 1174–1175, 1174t
  glycopeptide resistance, 1172–1173
  inhibition test for classify carbapenemases, 1177, 1177f
  methicillin resistance, 1172
  modified Hodge test, 1176, 1176f
  MRSA and CoNS, 1172
  nitrocefin β-lactamase test, 1172
  oxacillin screen disk diffusion method, 1172
  penicillin-intermediate and -resistant isolates, 1172
  supplementary phenotypic tests, 1176
  vancomycin susceptibility testing, 1173
  VISA, 1173
  VRE screening, 1173
Resolution, 62
Resolving power, 62
Respiratory acidosis, 110, 110t, 206, 206b
Respiratory alkalosis, 206, 206b
Respiratory syncytial virus (RSV), 1268
  bronchiolitis and, 1266, 1268
Respiratory tract
  cryptococcal infection of, 1209
  specimens from, 1358–1360
Respiratory tract infections
  in adults, 1266–1270
  in children, 1266–1270
  diagnostic testing, 1267
Respiratory viruses, 1266–1270
  RNA viruses, 1285
Restriction fragment length polymorphism (RFLP), 1468
Resurfacing, 966
Reticulated platelets, 548
Reticulocyte count, 544–545, 577, 577t
  principle of, 544
    controls, 544
    interpretation, 544
    procedure, 544
    reagent, 544
    reference values, 544
    sources of variation, 544–545
Reticulocyte hemoglobin content, 592
Reticulocyte production index
Retinoblastoma, 1445–1446
Retinol, 446. *See also* Vitamin A.
RET/PTC gene rearrangement, 1586
Retrovirus-associated diseases and conditions, 642–643
Return on investment (ROI), 171
Revenue, 164, 166t
Reverse line-blot hybridization, 1405
Reverse-transcriptase polymerase chain reaction, 1387–1388
Reverse triiodothyronine, 400
RFP. *See* Request for proposal (RFP)
RGMA gene, 1461
RGMA-promoted signal transduction pathways block cell growth, 1461
Rhabdoid tumor, 1583
Rhabdomyolysis, 313
Rhabdomyosarcoma (RMS), 1601
RH and RHAG blood group systems, 718–723
  biochemistry, 719–721, 721f
  biological role, 723
  hemolytic disease, Rh antibodies in, 723
  molecular biology, 721
  Rh antibodies, 723
  Rh inheritance and classification system, theories of, 718–719, 719t

Rheumatoid arthritis, 1022, 1044–1046
anticarbamylated protein antibodies, 1046
anticitrullinated peptides (CCP), 1045–1046
antikeratin antibody, 1045
autoantibodies, 1044, 1045t
characteristics, 1044
diagnostic and prognostic markers, 1044, 1045f
glycosylated antibodies, 1046
PAD antibodies, 1046
rheumatoid factor (RF), 1044–1045
Rheumatoid factor (RF), 1044–1045
Rheumatoid vasculitis, 1072–1073
clinical laboratory testing, 1072–1073
definition and epidemiology of, 1072
diagnosis, treatment, and prognosis of, 1073
etiology and pathogenesis of, 1072
pathology of, 1072
Rheumatologic disease, 978–979
Rhinoviruses (HRV), 1268–1269
Rh typing, in compatibility testing, 751
discrepancies, 751
of donors, 751
of recipients, 751
Riboflavin (vitamin B_2), 443
Ribonuclease, 293
Ribonucleic acid (RNA), 1373
DNA to, transcription of, 1376
to protein in, translation of, 1376
to protein, translation of, 1376
small, gene regulation and, 1377
Rickets, 222
Rickettsia
as agents of bioterrorism, 1257
organisms of, 1254–1258
Rickettsial infections, 1254–1264, 1255t
Rickettsia, organisms of, 1254–1258, 1255t
Rickettsialpox, 1256
Ring chromosome, 1422–1423
Ring sideroblasts
associated with marked thrombocytosis (RARS-T), 1574–1575
with refractory anemia, marked thrombocytosis associated with, 653–654
Risk factors, estimating, in cholesterol testing, 258–260
Ristocetin cofactor assay, 865
Rivaroxaban, 885, 887
RNA polymerases, antibodies to, 1042–1043
RNA splicing machinery, in acute myeloid leukemia, 1566–1567
RNA to protein, translation of, 1376
Robertsonian translocations, 1422, 1424f
Rocky Mountain spotted fever, 1255–1256
"Rogue testing", 82–83
ROI. *See* Return on investment (ROI)
Rosette test, 756
Round cell liposarcoma, 1600
Router, 160
Rubella, 1271–1272
Rubella virus, 1278
RUNX1 gene, 1563–1564
RUNX1 *(RUNX1)* mutations, 861
RUNX1-RUNX1T1 fusion, 1560
RUNX1T1 gene, 1560

S

Safety, in clinical laboratory, 10–11
Salary costs, 163
Saline, as replacement fluid, 809
Saliva, 536
Salivary cortisol, 415–416
Salt, and protein concentrations, affecting enzyme activity, 299
Sample containers (cuvettes), 40
Sample mapping, data collection techniques and, 13, 14f
Sample matrix, 61
Samples and specimen collection, for DNA analysis, 1469–1470
Sample transfer, between tubes, 28
Sampling
in automated chemistry analyzer, 76
and storage, of blood, 252–253
Saponification, 461
Sarcocystis spp., 1325–1326
Sarcoma(s), 1581t–1583t, 1599–1602
dendritic cell
follicular, 686
interdigitating, 686
Sarcoma(s) *(Continued)*
Ewing's sarcoma, 1600
with fusion genes, 1600–1601
molecular genetic pathology of, 1599–1602
myeloid, 661, 662f
with oncogenic mutations, 1601–1602
with variable complex genetic alterations with no specific pattern, 1602
with variable other specific pattern, 1602
Saturation, initial rate at, 296
SC. *See* Secretory component (SC)
Scattering, of radiation, 37
Scedosporium, 1225, 1225f
Schema. *See* Database schema
Schistosoma haematobium, 1338, 1338f
Schistosoma intercalatum, 1338
Schistosoma japonicum, 1337, 1338f
Schistosoma mansoni, 1337, 1338f
Schistosoma mekongi, 1338
Schistosoma spp., 1337–1338
Schistosomiasis, 1337–1338
Schizophrenia, 1453–1456
and bipolar disorder, 1459
calcium channel proteins, 1454–1456
cytogenetic findings, 1456
gene-encoded dopamine receptors, 1453–1454
glutamate and *N*-Methyl-D-Aspartate (NMDA) receptors, 1454
rare variant studies, 1456
single nucleotide polymorphisms, 1453t
Schwannomatosis, 1604
Scianna antibodies, 734
Scianna (Sc) blood group system, 733–734
biochemistry, 733
biological role, 734
molecular biology, 733–734
Scintillation counter, 52
Scleroderma. *See* Systemic sclerosis (SSc)
Sclerotic bodies, 1195, 1220
Scorpion probes, 1390f, 1391
Scorpions, 1348, 1348f
Scott syndrome, 860–861
Scrub typhus, *Orientia tsutsugamushi* as cause of, 1258–1259, 1258t
Sd^a antibodies, 744
SD. *See* Standard deviation (SD)
SDD. *See* Susceptible dose dependent (SDD)
SDI. *See* Standard deviation index (SDI)
Secondary hemostasis, 833
rebalanced, 844
Secondary hyperparathyroidism, 216, 217f, 218t
Secondary ion mass spectrometry, 67
Secondary lymphoid tissue, 586
Secondary osteoporosis, 222
Secondary (drug- or toxin-induced) sideroblastic anemia, 602
Secondary structure, 276–277
Second-order rate process, 455
Secretion
of parathyroid hormone, 212
studies of, and platelet aggregation, 849–852, 851f
Secretome, 1615
Secretory component (SC), 956, 958f
Selected engineered therapeutic agents, 987t–988t
Selectins, 993
Selective chemical precipitation, 256
Selective serotonin reuptake inhibitors (SSRIs), 378
and platelet function, 864
Select statement, 153
Selenium (Se), 451
Self-organizing maps (SOMs), 1615
SEM. *See* Structural equation modeling (SEM)
Semen analysis, male reproduction relating to, 429–430
accessory glands and, 430
examination in, 429–430
image analysis of, 430
immunologic tests of, 430
sample collection in, 429
Semi-automated urine chemistry analyzers, 500
Semiconservative replication, 1375–1376
Seminiferous tubules, of testis, 427
Sensitive immunoassay, using specimen pretreatment methods, 925–926
background of, 925
highly sensitive, for viral antigen using, 925, 925f
for host antigen without influence of auto-antibody, 925–926
Sensitivity
high, versus high specificity, need for, 93
and specificity, of diagnostic accuracy, 92–93, 92t–93t
Septate, 1195
Sequence-specific oligonucleotide hybridization, 1008, 1008f
Sequence-specific priming, 1007–1008
Sequencing arrays, 1404
Sequential screening, 436
Serial analysis of gene expression (SAGE), 1610–1611, 1610f
Serologic and cellular specificities, 1006
Serologic detection, of class I and class II molecules, 1009
Serologic diagnosis, 1275, 1277
for medical parasitology, 1299
Serologic findings, in immunocompromised patients, 644
Serologic identification, 1205
Serologic markers, for cancer diagnosis and management, 1507–1524.e5
circulating nucleic acids, in peripheral blood, 1521–1523
cell DNA testing for cancer, using fluorescence in situ hybridization, 1522–1523
cell-free nucleic acid testing in cancer, 1521
circulating microRNA, 1522
gene arrays detecting oncoprotein abnormalities, 1521–1522
gene mutations, 1522
microsatellite alterations, 1522
promoter hypermethylation, 1522
circulating tumor cells, in peripheral blood, 1520–1521
clinical applications of, 1511
diagnosis, 1511
prognosis: recurrence, metastasis and survival, 1511
screening, 1511
treatment response, monitoring of, 1511
conclusions in, 1524
as effective tool, 1509, 1509f
fecal occult blood testing and mutant protein markers, in stool, 1524
functional classification of, 1509–1511
adhesion molecules and metastasis as, 1510
monoclonal-antibody-defined tumor markers, 1510–1511
next-generation sequencing, 1510
oncoproteins, for cell proliferation, 1509–1510
other, 1511
tumor suppressors/cell differentiation, 1510
individual, 1515–1520
angiogenic factors in, 1515
β_2-microglobulin in, 1515
CA 72-4, 1517
CA 125, 1516–1517
CA 15-3 and CA 27.29, 1516
CA 19-9, CA 50 and CA 19-5, 1516
calcitonin in, 1517
carcinoembryonic antigen in, 1516
chromogranin A in, 1517
cytokeratin 19 fragment in, 1517
α-fetoprotein in, 1515
HER2/*neu* (c-*erb*B-2) oncoprotein in, 1517–1518
human chorionic gonadotropin in, 1517
parathyroid hormone-related peptide in, 1518
p53 in, 1518
serum free light chain determinations in, 1515–1516
serum markers, for prostate cancer in, 1518–1520
recommendations for ordering of, 1512–1515, 1513t–1514t
Serologic tests, 1085, 1250
for *Borrelia*, 1240–1241, 1242f
for *Treponema*, 1233, 1234f, 1234t
Serotonin-related genes (SERT), 1462
Serotonin transporter, 1462
Serous carcinoma, histologic subtypes of, 1598–1599
Serous effusion, 527
Serous fat atrophy, 638
Serrated polyposis syndrome, 1593
Serum
body fluids and, total enzyme concentrations in, 295–300
elevated levels of, for bilirubin, 316
for hepatitis, 323
HLA-specific antibody detection in recipient, 1011
immunoglobulin E (IgE), 1122t
Na+, effect of hyperglycemia on, 185–186
oligoclonal immunoglobulin bands in, 966
plasma versus, 252–253
red cell folate and, 596, 597t

Serum *(Continued)*
screening of, 1011
total, measurement of, 1121–1122
urea clearance and urea/creatinine ratio in, 191
and urine, drug detection in, 347–354
Serum analytes, 328–329
Serum anion gap (AG), 203–204, 203b, 204f
Serum-ascites albumin gradient (SAAG), 533
Serum autoantibody levels in, interpretation of, 1077–1078
Serum bactericidal titer (SBT), 1170
Serum chemistry, 507
Serum cobalamin assay, 595
Serum cortisol measurements, 415
Serum ferritin levels, 102
Serum free light chain determinations, 1515–1516
Serum grouping, 750
Serum immunoglobulin levels, 959
Serum iron
assays for, 383
use of, 102
Serum lethal titer, 1170
Serum markers, for prostate cancer, 1518–1520
Serum prostate-specific antigen (PSA), 1518–1520
Serum protein
α1-Antitrypsin, 319
ceruloplasmin, 319
DCP, 319–320
determining levels of, 318
electrophoresis, 960f, 961
Serum transferrin receptors, 591–592
Serum transferrin receptor-to-serum ferritin ratio, 592
Severe acute respiratory syndrome coronavirus (SARS-CoV), 1269, 1288
Severe allergic (anaphylactic) reactions, to transfusion, 781–782
Severe combined immunodeficiency (SCID), 898
Severe medical illnesses, hypoglycemia and, 235
Sex, as physiologic factor, 23
Sex chromosome abnormalities, 1429, 1429f
Sex chromosome aneuploidies, 1428–1429, 1429t
Sex hormone-binding globulin (SHBG), 425–426
Sex steroids, 425–427, 426f
Sézary syndrome, mycosis fungoides and, 680, 681f
SF3B1 gene, 1566–1567
SHANK2, 1457
Shell vial cultures, 1267, 1272
Shewhart plot. *See* Levey-Jennings plot
Shiga toxin-related hemolytic uremic syndrome (HUS), 868
Short tandem repeats, 1470–1471, 1471f, 1472t
SIADH. *See* Syndrome of inappropriate ADH (SIADH) secretion
Shotgun proteomics, 67
Sialylated tumor-related antigen (sTRA), 344
Sick building syndrome, 1220
Sickle cell anemia, 805–806, 805b
hemoglobinopathies and, 1440
Sickle cell disease (Hb SS), 611–613
complications of, 612
diagnosis of, 613, 614f
Sickle cell trait (Hb AS), 611
Sickle solubility test, 610
Sickling test-metabisulfite slide test, 609–610, 613f
SID blood group systems, 744
biochemistry and molecular biology, 744
biological role, 744
choline transporter-like protein 2, 744
Sideroblastic anemia, 602
Siderophilin. *See* Transferrin
Sigma metric, in measurement procedure, 136
Signal amplification methods, 1397–1399, 1399f
Signal processors, and readout, in spectrophotometer, 42
Signal recognition particle, 1048
Signal transduction
following antigen-specific stimulation, 931
pathways, 1525–1526, 1526f–1527f, 1528t
recognition, activation, and, of T cell, 931, 932f
Signal transduction pathways, 1454
Significance level, 120
Silent carrier α-thalassemia, 620
Simultaneous multiple immunoassays, 926–927
background, 926
flow cytometric, 926–927
microchannel assay, using compact discs, 927
microspot assay, 926
multianalyte microarray immunoassay, 926, 926f
Single-chain urokinase plasminogen activator (ScuPA), 828
Single fluorescent dyes, 935
Single-fluorescent immunoassay, 927
Single molecule detection, 927–928
background of, 927
ELISA, 927
single-fluorescent immunoassay, 927
Single-molecule ELISA, 927
Single nucleotide polymorphisms (SNPs), 1452–1453, 1470, 1472–1473, 1485
arrays, 1576–1577
autism spectrum disorder (ASD), 1466t
in bipolar disorder, 1457t
in major depression disorder, 1463t
in schizophrenia, 1453t
in substance use disorders, 1460t
Single source of truth, 153
Single-tube mixers, 57
Sinus infection, *Aspergillus* in, 1223
Sirolimus. *See* Rapamycin (Sirolimus)
Sirtuin, 1461–1462
Sitosterolemia, 263
SIX homeobox 3 (SIX3) gene, 1460
Six Sigma
optimizing performance and, 20
quality systems management and, 4–5, 5t
Size-exclusion chromatography, 51
Sjögren syndrome (SjS), 1040–1041
anti-α-Fodrin antibody, 1041
antibodies to nuclear protein NA14, 1041
antimuscarinic type 3 receptor autoantibodies, 1040–1041
anti-SS-A/Ro60 and anti-SS-B/La antibodies, 1040
autoantibodies prevalence in primary, 1040, 1041t
classification, 1040
clinical and laboratory characteristics of, 1040, 1041f
clinical conditions associated with, 1040, 1040b
Skin
banking of, 819
lesions of, *Cryptococcus* in, 1209
puncture technique, 31b
subcutaneous lesions and, specimens of, 1365–1366
Skin testing, 942
anergy, 942b
confirming stage, 941–942
SLC6A4 (sodium-dependent serotonin transporter), 1462
SLC39A8 and 13, 1460
Sleep aids, 363
Slides, preparation of, 1293
Slug-flow microextraction direct sampling, 72–73
SMAD2 gene, 1591–1592
SMAD4 gene, 1591–1592
SMAD proteins, 1591–1592
Small RNA, gene regulation and, 1377
Small, round blue cell tumors, 1616
Small ubiquitin-like modifier activating enzyme (SAE), 1048
Small vessel vasculitis, 1060f, 1064–1073
ANCA-associated small vessel vasculitis, 1064–1068, 1064t, 1065f–1067f
anti-glomerular basement membrane disease, 1068–1069, 1068t, 1069f
cryoglobulinemic, 1069–1070, 1070f
hypocomplementemic urticarial, 1071–1072
IGA (Henoch-Schönlein purpura), 1070–1071, 1071f
rheumatoid, 1072–1073
Smell brain, 354
Snorting, 358
Software systems, for DNA analysis, 1473
Solid organ rejection, as indication for extracorporeal photopheresis, 806–807
Solid-phase adherence tests, 752, 753f
Solid phase, characteristics of, 904
Solid-pseudopapillary neoplasms, 1594
Solid-support hybridization, 1382
Solid tumors, molecular genetic pathology of, 1579–1606.e7, 1581t–1583t
cancers, of unknown origin, 1604
clinical application of next-generation sequencing, 1604–1606, 1605f
by major organ, 1580–1599
bladder cancer, 1581t–1583t, 1596
brain tumor, 1580–1583
breast cancer, 1583–1586
cervical cancer, 1581t–1583t, 1597–1598
colorectal cancer, 1590–1593
endometrial cancer, 1598
gastric cancer, 1589–1590
hepatocellular carcinoma, 1588–1589
kidney tumor, 1595–1596
Solid tumors, molecular genetic pathology of *(Continued)*
lung cancer, 1587–1588, 1587f
melanoma, 1599
ovarian cancer, 1598–1599
pancreatic cancer, 1593–1594
prostate cancer, 1596–1597
thyroid cancer, 1586–1587
miRNA in cancer, 1604
multiple endocrine neoplasia, 1602–1604
sarcoma, 1581t–1583t, 1599–1602
Ewing's sarcoma, 1600
with fusion genes, 1600–1601
with oncogenic mutations, 1601–1602
with variable complex genetic alterations with no specific pattern, 1602
with variable other specific pattern, 1602
Solitary plasmacytoma of bone, 670
Soluble fibrin monomers, 830
Solute carrier transporters, 1489
Solvent exclusion effect, 25
Somatostatin, 227–228
Somatostatinoma, 345
Southeast Asian ovalocytosis, 606
Southern blot hybridization, 1545
Southern hybridization, 1382
Space-occupying lesions, 113, 329
"Spacer oligonucleotide typing", 1405
Sparganosis, 1344
Specialized LAB information system modules, 156–157
cytogenetics, 157
flow cytometry, 156–157
histocompatibility, 156
molecular diagnostics, 157
Special urine collection techniques, 31
Species complex, 1195
Specific granule deficiency (SGD), 639
Specific gravity
osmolality and, 471–472
methods of, 472
plasma osmolality and, 186
Specificity, high, versus high sensitivity, need for, 93
Specimen(s)
additional analysis required of, 90
alternative, 536–537
chromosome, 1412–1413
collection of, 26, 1267, 1284t
for DNA analysis, 1469–1470
for pleural fluid, 527
for synovial fluid, 523
and transport of, for mycotic diseases, 1200, 1201t
considerations, for glucose measurements, 228
handling of, and sample preparation, 692
inspection of, automated, 75
matrix effects, 25
for mycobacterial infection diagnosis, 1187–1188, 1188f
nonstandard, test billing for, 537
problem, flags for, 90
processing, 33–34
processing of, 1130–1131
automated, 75
culture techniques of, 1131
Gram stain of, 1130–1131, 1131f
transport, 33
urine, evaluation of, 469
urogenital, for medical parasitology, 1297
Specimen, for diagnosis of infectious diseases, collection and handling of, 1352–1366.e2
from blood, 1353–1355
from body fluids, 1355–1357
from eye, 1357–1358
conjunctival, 1357
corneal, 1357–1358
from feces, 1363–1365
general principles of, 1352–1353
on collection, 1352
on referral testing, 1353
on standard precautions, 1353
on timing, 1352
on transport, 1352–1353
on unacceptable specimens, 1353
on volume, 1352
from genital tract, 1362–1363
from respiratory tract, 1358–1360
bronchoscopy, 1360, 1360f
nasopharyngeal, 1358
sputum and tracheal aspirates, 1359–1360, 1359f
throat, 1358

Specimen, for diagnosis of infectious diseases, collection and handling of *(Continued)*
from skin and subcutaneous lesions, 1365–1366
cutaneous ulcers, 1366
vesicles, bullae, pustules, 1365
from tissues, 1357
urinary tract, 1361–1362
collection and transport for, 1361
processing for, 1361–1362, 1361f
from wound infections and abscesses, 1365–1366
Specimen validity testing, 354
Spectral bandwidth, 39, 39f
Spectrometer, 42
Spectrophotofluorometers, components of, 44
Spectrophotometer, components of, 38–42, 38f
charge-transfer devices, 42
filters in, 39–40, 40f
photodetectors in, 40–42
radiant energy sources of, 38–39
sample containers (cuvettes) in, 40
signal processors and readout in, 42
wavelength selectors in, 39
Spectrophotometric assays, 297–298
Spectrophotometric determinations, 454–458
analytes, quantitation of, 456–458
Beer's law, 454
end-point versus rate method, 454–455
interferences, 455–456
Spectrophotometric identification, of hemoglobins, 542
Spectrophotometry, 35–42, 36f
Beer-Lambert law in, 37–38, 37f, 38b
energy of EMR, 36–37, 36b, 37f
quality assurance in, 42
radiation, scattering of, 37
velocity, of propagation, 36, 36b
Spectroscope, 42
Spherocytic hereditary elliptocytosis, 606
Spherule, 1195
Spiders, 1348
Spinal muscular atrophy, 1440
Spinocerebellar ataxias, 1442
Spirochetal meningitis, 521–522
Spirochete infections, 1229–1245.e4
Borrelia, 1237–1244
Leptospira, 1236–1237
spirochetosis, agents of, 1244
Treponema, 1229–1236
Spirochetosis, agents of, 1244
characteristics, 1244
epidemiology and clinical manifestations of, 1244
laboratory diagnosis of, 1244
pathology and pathogenesis of, 1244, 1245f
species, 1244
treatment of, 1244
Spirometra spp., 1343f, 1344
Splendore-Hoeppli phenomenon, 1216
Splenic B cell lymphoma/leukemia, unclassifiable, 667
splenic diffuse red pulp small B-cell lymphoma, 667, 669f
Splenic diffuse red pulp small B-cell lymphoma, 667, 669f
Splenic marginal zone lymphoma, 665–667, 667f–668f
Sporangiospores, 1196
Sporangium, 1196
Sporotrichosis, pathology of, 1216
SPSS. *See* Statistical Package for the Social Sciences (SPSS)
Sputa, 1297
Sputum aspirates, 1359–1360, 1359f
SQL. *See* Structured Query Language (SQL)
Squamous cell carcinomas, of head and neck, 1538
Squamous cell carcinomas of the head and neck protein array to, 1538
Squamous epithelial cells, 488, 489f
SRSF2 gene, 1566–1567
Stable isotope standards and capture by antipeptide antibodies (SISCAPA), 67–68
Staining, 1293
of chromosomes, 1414, 1414f
Stains
Gram, specimen processing relating to, 1130–1131, 1131f
microbial, 1188–1189, 1188f–1189f, 1190t
Standard deviation (SD), 120
in quality control, 130, 142
Standard deviation index (SDI), 120
Standard error
of the mean, 121
of regression, 125
Standardization, optimizing performance and, 20
Standing plasma test, 257
Staphylococcus, 1131–1133, 1132f
antimicrobial susceptibility of, 1133, 1133f
characteristics, 1131
clinical manifestations and pathogenesis of, 1131–1132
laboratory diagnosis of, 1133
States, requiring laboratory personnel licensure, 9b
StatisPro™, 126, 126f
Statistical analysis, resources for, 128–129
Statistical Package for the Social Sciences (SPSS), 128
Statistical power, 120
Statistical quality control, 132–133, 144, 144f
Status flag, 154
Steatorrhea, tests for, 340–341
Stem cells, 570–572
hematopoietic, and progenitors, 570–571, 571f, 571b
hematopoietic growth factors, 572
Stenotrophomonas maltophilia, 1149
Steroidal cell autoantibodies (SCA), 1111f
Stiff-Person syndrome, 1112–1113
Stone analysis, 507
Stone formers, laboratory tests for, 507
Stool, fecal occult blood testing and mutant protein markers in, 1524
Storage, of blood, 253
δ-Storage pool deficiency, 859
Strand-displacement amplification (SDA), 1394–1395, 1395f
Strategic planning, in clinical laboratory, 3
Stray light, 42
Strength, weaknesses, opportunities, and threats (SWOT) analysis, 3
for new hospital outreach program, 4b
Streptobacillus, 1159–1160
antimicrobial susceptibility of, 1160
characteristics, 1159, 1160f
clinical manifestations and pathogenesis of, 1159
laboratory diagnosis of, 1159
Streptococcus and *enterococcus*, 1133–1137
antimicrobial susceptibility of, 1136–1137
characteristics, 1133–1134
classification of, 1133–1134, 1134t
clinical manifestations of, 1134–1135
Gram stain of *S. pyogenes*, 1133–1134, 1134f
laboratory diagnosis of, 1135–1136, 1135f–1136f, 1136t
Stress
as physiologic factor, 23
tests affected by, 23t
Stroke, 275
Strongyloides stercoralis, 1329–1330, 1330f–1331f
Strongyloidiasis, 1329–1330
Structural chromosome abnormalities, 1420–1423, 1421f–1422f
Structural chromosome anomalies, 1429–1430
Structural equation modeling (SEM), 127
Structural hemoglobin variants, 611, 613t–614t
Structure
of chromosomes, 1412, 1413f
of proteins, 276–277
Structured Query Language (SQL), 152
Student t-test, 120, 122–124, 124f
sample size, 124
significance, 122–124
S100, tumor marker for malignant melanoma, 1535
Subcutaneous lesions, specimens of, 1365–1366
Subcutaneous panniculitis-like T cell lymphoma, 680, 681f
Subordinate keys, 153
Substance use disorders, 1459–1461
alcohol use, 1459–1460
cannabis use, 1460–1461
future studies, 1461
opioid use, 1461
SNPs in, 1460t
Substrate, 291
Substrate-labeled fluorescent immunoassay, 914, 915f
Succinate dehydrogenase B (SDHB) mutation-associated renal cell carcinoma, 1596
Sucking lice, 1344
Sucrose hemolysis tests, 607
Sucrose, in urine, 477
Sugars, tests for, 478
Sulfhemoglobin (SHb), 541, 541f
Sulfonamide (sulfadiazine) crystals, 497, 497f
Sulfotransferases, 1484t–1485t, 1485
Surface-bound proenzymes, 829
Surface-enhanced laser desorption ionization (SELDI), 1616
Surface-enhanced laser desorption ionization time of flight (SELDI-TOF) mass spectrometry, 1539
Surfactant, 437–438
Susceptibility testing
antibiotics selection for, 1179–1180
commercial automated instrument systems, 1170–1171
dilution testing, 1168, 1168f
direct β-lactamase tests, 1169–1170
disk diffusion, 1169, 1169f
gradient diffusion, 1168–1169, 1169f
indications for, 1179
inhibitory methods of, 1168–1170
for mycobacteria, 1191–1192, 1191t
for mycotic diseases, 1206–1207
phenotypic methods in, 1169
S. pneumoniae, 1172
technical considerations in
incubation conditions, 1167
inoculum, 1167
media, 1167
test interpretation, 1167–1168, 1168f
Susceptible dose dependent (SDD), 1168
Sweat chloride, 332
Swiss-type hereditary persistence of fetal hemoglobin, 619
Syndrome of inappropriate ADH (SIADH) secretion, 106t, 107, 394–395, 395t, 396f, 396b
SYNE1, 1458
Synovial fluid, 33, 522–527, 523t
chemical analysis of, 526, 526t
collection of, 523
differential leukocyte count for, 524, 524f
examination for
crystal, 524–526, 525f
gross, 523–524
microbiological, 527
microscopic, 524–526
immunologic studies of, 527
recommended tests for, 523, 523b
total cell count for, 524
Synovial sarcomas, 1601
Synthesis
globin, 574
heme, 574, 575f
of hemoglobin, 574
metabolism and
of calcitonin, 213
of vitamin D and metabolites, 214
nucleoprotein, defects of, 597
of parathyroid hormone, 212
protein, 318–320
of thyroid gland, 396–398, 398t
Synthetic functions, of liver, 318–320
protein synthesis, 318–320
Synthetic inhibitors, 597
Syphilis, 1230–1232
characteristics, 1230, 1230f
clinical manifestations of, 1231–1232, 1232f
endemic, 1232–1233
epidemiology, 1230, 1230f
nontreponemal serologic tests, 1234, 1234t
pathogenesis and pathology of, 1230–1231, 1231f
Sysmex UD-10, 504
Sysmex XN-9000™, for hematology automation, 77–78, 78f
Systematic reviews, 98, 98b
Systemic autoimmune rheumatic diseases (SARDs), 1035–1057.e8
autoantibodies. *See also* Autoantibodies.
to nuclear and intracellular antigens, detection methods of, 1050t
in systemic rheumatic diseases, profiles of, 1049
characteristics, 1035
classification, 1035, 1036b
concept of overlap syndromes, 1049
idiopathic inflammatory myopathies, 1046–1049, 1047t
aminoacyl-tRNA synthetases, 1046–1047
cytosolic 5'-nucleotidase 1A, 1048–1049
3-hydroxy-3-methylglutaryl-coenzyme reductase, 1048
MDA5 (CADM-140), 1048
Mi-2/NuRD complex, 1048
MJ/NXP2, 1048
myositis-associated autoantibodies, 1049
signal recognition particle, 1048
small ubiquitin-like modifier activating enzyme, 1048

Systemic autoimmune rheumatic diseases *(Continued)*
and related disorders, 1036b
rheumatoid arthritis. *See* Rheumatoid arthritis
Sjögren syndrome. *See* Sjögren syndrome (SjS)
systemic lupus erythematosus and related lupus-like disorders, 1036–1040
systemic sclerosis, 1041–1044, 1043f
Systemic disease, pancreas relating to, 331–332
Systemic infection, *Malassezia* in, 1210
Systemic lupus erythematosus (SLE), 1036–1040, 1102, 1105
autoantibodies, 1037–1038, 1055t
antigens and, 1037, 1037t
anti-Ku, 1038
antiphospholipid antibodies, 1038
anti-SS-A/Ro60 elevated levels, 1038
to native DNA, 1037
proliferating cell nuclear antigen multiprotein complex, 1038
to ribosomal P proteins, 1038
to Sm and nuclear ribonucleoprotein, 1037
to SS-A/Ro and SS-B/La, 1038
chronic discoid lupus and other cutaneous variants, 1038–1040, 1039f
anti-DFS70 Antibodies, 1040
antinucleosome antibodies, 1040
drug-induced, antihistone antibodies, 1039–1040
classification criteria for, 1036
"lupus-like" syndromes and diseases, 1036–1037
and neutropenia, 637
significant features, 1036
Systemic mastocytosis, 650
Systemic sclerosis (SSc), 1041–1044
antibodies to
antieukaryotic initiation factor-2B, 1044
bicaudal D2, 1042
NOR-90, 1044
nucleolar antigen fibrillarin (U3-snoRNP), 1044
PM/SCL, 1044
RNA polymerases, 1042–1043
topoisomerase I (SCL-70), 1042
U11/U12 RNA associated ribonucleoprotein C3 (RNPC3), 1044
autoantigens and autoantibodies in, 1041–1042, 1042t
centromere protein autoantigens, 1042
classification criteria of, 1042
clinical and laboratory characteristics of, 1042, 1043f
Th/To autoantigens, 1043–1044

T

Tacrolimus (FK-506), 376
Taenia multiceps, 1344
Taenia saginata, 1331–1332
Taenia serialis, 1344
Taeniasis, 1331–1332
Taenia solium, 641, 1332, 1342, 1343f
Tag, 1610, 1613
Tagging enzyme, 1610
Takayasu arteritis, 1060–1061
clinical laboratory testing of, 1060–1061
definition and epidemiology of, 1060
diagnosis, treatment, and prognosis of, 1061
etiology and pathogenesis of, 1060
pathology of, 1060
Tamoxifen, 1499–1501, 1500f
Tandem dye, 936
Tandem mass spectrometry (MS/MS or MS²)
neutral loss scan, 65
precursor ion scan, 64
product ion scan, 64
scan modes, 64f
selected reaction monitoring, 65
Tangier disease, 266
Target amplification methods, 1387–1397, 1388f, 1390f, 1392f
Targeted analytic mass spectrometry systems, 66
Target imbalance, 1242
Targeting cell surface receptors, treatment by, 1032
Target of rapamycin (TOR), 374
Target-specific anticoagulants, 885–888
oral agents, 885–887, 887t, 888f
parenteral agents, 885
Task mapping, data collection techniques and, 16, 17f
TBRF. *See* Tick-borne relapsing fever (TBRF)
T cell
depletion of, 823
development of, thymus relating to, 584–585
functional assessment of, 1029–1030
recognition, activation, and signal transduction of, 931, 932f
responses of, 932–933
T cell/histiocyte-rich large B cell lymphoma, 673–674, 674f
T cell lymphoblastic leukemia/lymphoma, 1547, 1577
T cell proliferations, 697
T cell prolymphocytic leukemia, *TCL1A* gene abnormalities in, 1556
T-cell receptor excision circle (TREC) screening, 1034f
TCF1 gene, 1589
TCF3-PBX1 gene fusion, 1549–1550
TCL1A gene abnormalities, 1556
TCO. *See* Total cost of ownership (TCO)
TCP/UDP packet type, 160–161
Technical considerations in susceptibility testing, 1167–1168
Technology
breakthrough, 18b
role of, 18–19
understanding of, 18–19
Tegretol. *See* Carbamazepine (Tegretol)
Telangiectatic focal nodular hyperplasia, 1589
Telescoped sediment, 493
Telopeptides, cross-linked, 220
TEMPI syndrome, 671
Teratozoospermic index, 430
Terminal complement components, 972
Terminal deletion, 1420, 1421f–1422f
Ternary complexes, formation of, 628, 628b
Tertiary hyperparathyroidism, 216, 218t
Tertiary structure, 277
Test
data from, use of, in DNA analysis, 1473–1474
familial and genealogy, 1473–1474
future of, DNA analysis, 1474
mapping, data collection techniques and, 13, 14f
menu, workstation analysis and, 16
methods of, and marker systems, for DNA analysis, 1470–1473
Test cutoff, altering of, 93
Testing process, laboratory, 13, 14f
Test methods, 1250
Test order(s), specimen collection and, 26
Testosterone replacement therapy (TRT), 439–440
TET2 gene, 1566
TET genes, fusion genes with, 1600
Tetracycline, 1253
Tetrahedral intermediate, of peptide bond, 303, 303f
TFE3-associated renal cell carcinoma, 1595
TFEB-associated renal cell carcinoma, 1595–1596
TGFBR1 gene, 1591–1592
δβ⁺-Thalassemia, 619
Thalassemia major, 617
Thalassemia minor, 617–618
α-Thalassemia trait, 620
β-Thalassemia trait, 617–618, 618f
with normal Hb A_2, 618
Thalassemias, 608–611, 616–620
β-thalassemias, 617–619, 618t
fetal hemoglobin, hereditary persistence of, 619
molecular defects of, 616–617
α-thalassemias, 619–620
α-Thalassemias, 619–620
β-Thalassemias, 617–619, 618t
α-Thalassemias syndromes, 619–620, 619t
β1-Tubulin (TUBB1), 860
The Cancer Genome Atlas (TCGA), 1590
Theophylline, 372
Therapeutic cytapheresis, 803–807
Therapeutic drug monitoring, 347–386.e3. *See also* Toxicology, therapeutic drug monitoring and.
antiasthmatics, 371–372, 372f
anticonvulsants, 369–371, 370f
antiinflammatory and analgesic, 372–374, 373f
cardiotropics, 366–369, 367f
chemotherapeutic agents, 379
immunosuppressives, 374–376, 375f
for mania and depression, 376–378
neuroleptics, antipsychotic major tranquilizers, 378–379
pharmacokinetics, 364–366, 364f
Therapeutic hemapheresis, indications for, 799–811, 799t–803t
Therapeutic leukocytapheresis, 804
indications for, 804
Therapeutic levels and metabolism, of antidepressants, 378
Therapeutic plasma exchange, 807–811, 808f, 809b–810b
efficacy of removal in, 808, 808f
indications for, 811
mechanisms of action of, 807–808
patient concerns in, 809–810, 809b
procedures for selective removal of plasma components in, 810–811
low-density lipoproteins, 810–811, 810b
replacement fluids in, 808–809
Therapeutic plateletpheresis, 803–804
Therapeutic thrombocytapheresis, indications, 804
Therapeutic trial, of cobalamin deficiency, 594
Thermistors, 56
Thermocouple, 56
Thermometers, types of, 56
Thermometry, 56–57
Thick client, 161
Thin client, 161
Thin-layer chromatography, 348, 350f
Thiol reagents, 757
Thiopurines, 1496
Thiopurine S-methyltransferase, 1486
Thirst, regulation of, ADH release and, 197–198
Throat specimens, 1358
Thrombin-activated fibrinolytic inhibitor (TAFI), 871
Thrombin generation, 833, 840–841
Thrombin time, 834, 879
Thrombocythemia, essential, 1572–1574
Thrombocytopenia, 852–856, 853t
in chronic lymphocytic leukemia/small lymphocytic lymphoma, 663
congenital
autosomal dominant, 853
autosomal recessive, 853–854
heparin-induced, 883–885, 884f, 885t, 886f
immune, 855–856
drug-induced, 856
inherited, 852–855, 854t
sex-linked, 854–855
Thrombocytosis, 803–804, 804t, 804b, 856–857, 856t
marked, refractory anemia with ring sideroblasts associated with, 653–654
Thrombomodulin, 871
Thrombophilic factors, 872t
Thrombospondin-5, 832
Thrombotic disease. *See* Cardiac injury, atherosclerosis, thrombotic disease
Thrombotic microangiopathy, 624
Thrombotic risk, laboratory approach to, 870–878.e2
appropriate laboratory utilization, 877–878
endogenous anticoagulant pathways, 870–871, 871f
annexin A2, 871
annexin A5, 871
antithrombin, 870–871, 871f
fibrinolytic system, 871
protein C, 871
protein S system, 871
tissue factor pathway inhibitor, 870, 871f
hyperhomocysteinemia, 877
prothrombotic states, 872–877, 872t–873t
activated protein C resistance and factor V_{Leiden}, 874, 874f
antiphospholipid syndrome and lupus anticoagulants, 875–876, 876f
antithrombin deficiency, 873
dysfibrinogenemia, 875
elevation of coagulation factor levels, 875
hypofibrinolysis, 874–875
other and novel genetic variants, 876–877
protein C deficiency, 873
protein S deficiency, 873–874
tissue factor pathway inhibitor deficiency, 872
Thrombotic thrombocytopenic purpura (TTP), 625, 864–868
Thromboxane synthesis, abnormalities in, and platelet signaling pathway, 860
Th/To autoantigens, 1043–1044
Thymic presence, 942
Thymidylate synthase, 1493–1494, 1493f, 1494t
Thymoma, 601
Thyroglobulin, 400–401
Thyroglobulin autoantibodies, 1110
Thyroid
autoantibodies relating to, 401
cancer, 1586–1587
diseases of, 403, 1110–1111
function, 114–115, 115t, 395–404, 397f

Thyroid *(Continued)*
calcitonin and, 404, 404t
hormone synthesis and metabolism, 396–398, 398t
hypothalamic-pituitary-thyroid axis, 398–401
L-thyroxine, uses of, 403–404
neonatal hypothyroidism, screening for, 402
nonthyroidal illness, 402
physiologic variables of, 402–403, 402f
tests, medications and, 403
thyroid disease, screening for, 403
thyroid illness and, 403
urinary iodine measurement, 401, 401t
function of, tests of, medications and, 403
illness of, 403
Thyroid carcinoma, 1617
Thyroid gland, 395
autoimmune, 1110–1111
Thyroid-stimulating hormone (TSH), 398–399, 399t
Thyroid-stimulating immunoglobulins (TSIs), 1077, 1077f, 1110
Thyroperoxidase autoantibodies, 1110, 1110f
Thyrotropin-binding inhibitor immunoglobulins, 1110–1111
Thyrotropin-releasing hormone (TRH), 398
Thyroxine, 399–400, 399t, 400f
free, 400
Thyroxine-binding globulin (TBG), 401, 401t
Thyroxine-binding prealbumin (TBPA), 280
Tick bite, African, 1256
Tick-borne relapsing fever (TBRF), 1243–1244, 1244t
Ticks, 1348–1349
Time-of-flight (TOF) analyzers, 62–64
Time, of specimen collection, 26
Time-resolved fluoroimmunoassay, 917–918
Tissue bank activities, 817–819, 818b
Tissue banking, and progenitor cells, 817–826.e2, 818b
and adoptive cell transfer/chimeric antigen receptors, 824–825
and cardiac valves, 820
and cornea, 820
ex vivo manipulation of hematologic cells in, 824
hematopoietic progenitor cell banking, 821–825, 821b
and musculoskeletal tissues, 819–820
reinfusion of progenitor cell products and, 824
and reproductive tissue, 820–821
and skin banking, 819
and tissue bank activities, 817–819, 818b
cryopreservation, 818–819
donor screening in, 818, 818b
and tissue, sources of, 817
and use of dendritic cells, in cancer immunotherapy, 824
Tissue factor pathway inhibitor, 832, 838, 870, 871f
Tissue factor pathway inhibitor deficiency, 872
Tissue helminths, 1338–1344
Tissue/organ transplantation, 1009–1013
Tissue plasminogen activator (tPA), 830–831, 831f
Tissues
aspirates of, 537
lymphoid, 583–586
musculoskeletal, 819–820
sources of, 817
specimens from, 1357
T lymphoblastic leukemia/lymphoblastic lymphoma, precursor, 664
genetics of, 664
morphology of, 664
T lymphocytes, 894–895
antigen-induced activation of, 931
Tobacco smoking, interference with, 23
Tocopherol. *See* Vitamin E (tocopherol)
ToGA trial, 1590
Tolerable upper intake level (UL), 441–442
Toll-like receptor (TLR) assays, 1031
Tonicity, 186
Top-down proteomics, 67
Topiramate, 371
Top-loading balances, 54
Total activity unit, 296–297
Total and ionized calcium, 210
Total bilirubin, 456–457
Total cell count
for CSF, 512
for synovial fluid, 524
Total cost of ownership (TCO), 164
Total iron-binding capacity, 457–458
Total laboratory automation, 75, 77, 78f
Total magnesium, 211
Total protein, 456, 515–516, 516t
methods of, 516
reference values of, 515–516, 516b
Total quality management (TQM), 4, 5t
Tourniquet, posture and, 23
Toxic aplastic anemias, 600
Toxic granulation, 638, 638f–639f
Toxicity, vitamins and, 443
Toxicology, therapeutic drug monitoring and, 347–386.e3
drugs of abuse, 354–364
amphetamines, 360–361
barbiturates, sedative-hypnotics, 362
benzodiazepines, 361
cathinones, 363
cocaine, 358–359
codeine and analogs, 359
extent of use of, 354–358
fentanyl, 360
lysergic acid diethylamide (lysergide), 363
marijuana, 362–363
mechanisms of action, 354, 355f–358f
methadone, 360
methaqualone, 362
muscle relaxants, 364
opiates, 359–360
phencyclidine, 362
piperazines, 361
propoxyphene, 362
sleep aids, 363
tryptamines, 361
serum and urine, drug detection in, 347–354
chromatographic techniques for, 348–353
drug binding, to antibodies, 348
drugs of abuse, screening for, 354
gas chromatography-mass spectroscopy, 352, 353f
gas chromatography, with infrared spectroscopy, 353
immunochemical methods of, 348, 349f
liquid chromatography-mass spectroscopy, 352–353
toxins and acute poisoning, 380–386
Toxi-lab procedures, 348–350
Toxins, and acute poisoning, 380–386
Toxogenomics, 1480
Toxoplasma gondii, 644, 1312–1313
Toxoplasmosis, 644–645, 645f, 1312–1313
TP53 gene, 1567, 1580
T-prolymphocytic leukemia, 677
TQM. *See* Total quality management (TQM)
Trace elements, vitamins and, 447–452, 447t–448t
Tracheal aspirates, 1359–1360, 1359f
Trachoma, classic, 1247
Training and competency, oversight of, 87
Training set, 1611
Transcellular flux, of potassium, control of, 193–194, 194f
Transcriptional control, 1376–1377, 1376f
Transcription and cell cycle regulation, protein for, 1458
Transcription-based amplification, 1393–1394
Transcription factor mutations, platelet dysfunction associated with, 861
Transcription-mediated amplification (TMA), 1393–1394, 1394f
Transcriptomics, 897
Transducers
multichannel photon, 41
silicon diode, 41, 41f
Transferrin, 284–285, 285f
and CSF leakage, 519
Transfer RNAs (tRNAs), 1376
Transformational operations, 153
Transforming growth factors α and β, 1528–1529
Transfused red cells, separation of autologous cells from, 759–760
Transfusion
administration of, 777–780
blood component therapy, 777–779
granulocyte, 791–792
massive, 779–780, 845
medicine, 771
background of, 771
and blood collection, 771–773, 772t, 773b
blood component manufacture and, 773–775
blood components, selection of, 775–776
pretransfusion testing, 776
neonatal and pediatric transfusion, 780
of plasma, 779
of platelets, 778–779, 779b
reactions to, 781–786
acute hemolytic, 782
allergic, 781
Transfusion *(Continued)*
bacterial contamination, of blood components, 782–783
delayed hemolytic, 782
febrile nonhemolytic, 781
graft-versus-host disease, 783–784, 784f, 784b
hypotensive reactions, 784
nonimmune hemolysis, 784–785
severe allergic, 781–782
transfusion-associated circulatory overload, 783
transfusion-related acute lung injury, 783
transfusion-transmitted disease, 785–786
Transfusion-associated circulatory overload, 783
Transfusion-related acute lung injury, 783
Transfusion-transmitted disease, 785–786
babesiosis, 786
cytomegalovirus, 785
hepatitis, 785
human immunodeficiency virus, 785
human T-cell lymphotropic virus, 785
malaria, 786
parvovirus B-19, 785
transmissible spongiform encephalopathies, 786
Trypanosoma cruzi, 786
West Nile virus, 785–786
Zika virus, 786
Transgender, 26
Transient abnormal myelopoiesis, 661
Transient aplastic crises, 601
Transient erythroblastopenia of childhood (TEC), 601
Transient neutropenia, 638
Transient proteinuria, 474
Transitional (urothelial) epithelial cells, 489, 489f
Transition state, 292–293
theory, in drug design, 303–305, 303f
catalytic antibodies, new, with predetermined enzyme activity, 304–305, 305f
HIV protease inhibitors, in treating HIV-AIDS, 303–304, 303f–304f
Translocation renal cell carcinoma, 1595
Translocations, 1378–1379, 1383, 1421, 1421f–1422f
Transmissible spongiform encephalopathies, 786
Transmission lines, 161
Transplant-associated viral infections, 1284–1286, 1284t
Transplantation
and ABO antibodies, 714
nonrenal organ, 1012
organ, 980–981, 981f
renal, 1012
tissue/organ, 1009–1013
Transplant donor and recipient screening, 1283, 1284t
Transthyretin (TTR), 280
Transudates and exudates, 527, 527b, 533, 533b
Traumatic hemolysis, 624
T regulatory (Treg) cells, 895
TREM2, 1465
Trematodes, 1335–1338, 1344
Clonorchis sinensis and *Opisthorchis spp.*, 1336–1337
Fasciola hepatica, 1335–1336, 1336f
Fasciolopsis buski, 1335, 1336f
Heterophyes and *Metagonimus*, 1335
Nanophyetus salmincola, 1335
Paragonimus spp., 1337
Schistosoma spp., 1337–1338
Trench fever, 1263t, 1264
Treponema, 1229–1236
classic treponemal disease, 1230–1233
other diseases of, 1236
treponematoses
laboratory diagnosis of, 1233–1235
treatment of, 1235–1236
Treponemal serologic test, 1234–1235, 1234t
Treponematoses
laboratory diagnosis of, 1233–1235
treatment of, 1235–1236
Trichinella species, 1341
Trichinella spiralis, 641
Trichinellosis, 1341
Trichinosis, 1341
Trichomonas vaginalis, 1322
Trichostrongylus spp., 1329
Trichuris trichiura, 1328
Tricyclic antidepressants, 377–378, 377f
toxicity of, 378
treatment of, 378
Triglyceride blanks, 254
Triglycerides, 254, 461–462. *See also* High triglycerides.
Triiodothyronine, 400
reverse, 400

Trinder reagents, 460
Trinucleotide repeat expansion disorders, 1441–1444, 1443t
Troponin, cardiac, 269–270
Trueness, in analytic bias, imprecision and, in quality control, 147
Truth table, 92, 92f–93f, 92t
Trypanosoma cruzi, 786
Trypanosoma spp., 1310–1311
Trypsinogen, 334
Tryptamines, 361
Tryptase, 1119–1120, 1128
Tryptase-positive round cell infiltrates (TROCI), 650
Tryptophan glycoconjugate, 191
Tryptophan metabolic pathways, 1462
Tryptophan-rich prealbumin, 280–281
4T system, 884, 885t
Tube analysis, 14
  chemistry, 15t
Tube labor, 14
Tuberculostearic acid (TSA), 531, 536
Tuberculous meningitis, 522
Tube reactions, 746, 746f, 746t
Tumor cells, 497–498
Tumor marker tests, recommendations for ordering, 1512–1515, 1513t–1514t
Tumor necrosis factor, lymphotoxin A and B genes and, 1016
Tumors
  detection of
    circulating anti-p53 antibodies in, 1534–1535
    myc oncogene-encoded protein in, 1535
    oncoproteins in, 1527–1536
    serum anti-c-myc protein antibodies in, 1535
  markers for, 520–521, 531, 536
  non-beta cell, 235–236
  of pituitary gland, 388, 389t
  primitive peripheral neuroectodermal, 1600
Tumor suppressor genes, 1445–1446
Tumor suppressors/cell differentiation, 1510, 1567
Turbidimetric methods, 280
Turbidimetry, 45, 45f
Turcot's syndrome, 1593
Turner syndrome, 1428f, 1429, 1429t
Tuskegee Health Survey, 176
Two-dimensional electrophoresis (2-DE), 278
Two-dimensional gene-expression-based classification map, 1617
Two-factor authentication, 159
Two-way analysis of variance (two-way ANOVA), 126
Tyndall effect, 37
Type B insulin resistance, 1110
Type 1 diabetes, 230–232, 231t, 1022–1023
Type 2 diabetes, 231t, 232
Type I error, 120
Type II error, 120
Tyrosine, 496–497, 497f
Tyrosine kinase inhibitor (TKI), for chronic myeloid leukemia, 646
Tyrosinuria, 508
  methods for, 508

U

U2AF1 gene, 1566–1567
UF-100 analyzer, 504
Ulcerative colitis (UC), 1085
Ulcers, 1363, 1366
ULI. *See* Unique laboratory identifier (ULI)
Ultracentrifugation methods, 255
Umbilical cord blood, 823
UNC5C, 1465
Undifferentiated acute leukemia, 662
Unequal-arm substitution balances, 54
Unfractionated heparin, 882–883, 882f–883f
Uniparental disomy, 1437
Unique laboratory identifier (ULI), 154–155
Unstable angina (UA), 267–268
Unstable enzymes, protease degradation of, 299
Unstable hemoglobins, 616
Urea, 462
  clearance and urea/creatinine ratio in serum, 191
  as measure of renal function, 190
Ureaplasmal infections, 1250–1253
Uremia, 862–863
Urethral specimens, 1362
Uric acid, 462, 526
Uridine diphosphate GALE deficiency, 242
Uridine diphosphate glucuronosyltransferases, 1484t–1485t, 1485
Urinalysis
  components of, 468–499
    chemical screening, 472–486, 473b
    gross/physical examination of, 469–472
    specimen evaluation of, 469
  methods for, 499–505
    automated, 500–503, 504f–505f
    automated microscopy analyzers, 503–505
    basic (routine), 499–500, 501t
    integrated/fully automated, 505
Urinary bladder cancer antigen, 1536
Urinary calcium, reference interval for, 210
Urinary calculi, 505–507
Urinary formiminoglutamic acid (FIGLU), 597
Urinary free cortisol measurements, 416
  method of, 416
Urinary iodine measurement, 401, 401t
Urinary screening, for inherited metabolic diseases, 507–509
Urinary tract infection, 483–484, 1208
Urinary tract, specimens, 1361–1362
  collection and transport for, 1361
  processing for, 1361–1362, 1361f
Urine, 31–33
  basic examination of, 467–509.e6, 469t
  bilirubin in, 482–483, 482t
  blood, hemoglobin, hemosiderin, and myoglobin in, 479–482
  changes in, with delayed testing, 32t
  concentration and dilution of, 198–199, 198f
  cuvette-based particle analysis, 503–504
  examinations of, 507
  flow cytometric particle analysis, 504–505
  flow imaging particle analysis, 503
  formation of, 468
  fructose in, 478
  galactose in, 478
  glucose and other sugars in, 476–479
  ketones in, 479
  lactose in, 477
  pentose in, 477
  protein in, 473–476
  sediment in
    examination of, 486–499
    microscopic components of, 487–499
  serum and, drug detection in, 347–354
  special testing and monitoring techniques for, 505–509
  storage and preservation of, 32
  sucrose in, 477
  testing modalities of, 509
  urobilinogen in, 483
Urine hypermethylated glutathione S-transferase pi 1 gene, 1523–1524
Urine markers, for prostate cancer, 1523–1524
Urine metabolic test, for adenomatous polyps of colon, 1524
Urine prostate cancer antigen 3, 1523
Urine TMPRSS2, 1523
Urine volume
  decreases in, 471
  increases in, 471
Urinometer, 472
  procedure of, 472
Urinothorax, 530
UriSed, 503–504
Urisys 1100 urine analyzer, 500
Urobilinogen, in urine, 483
Urogenital protozoa, in medical parasitology, 1315, 1315f
Urogenital specimens, examination of, for medical parasitology, 1297
Urothelial cancer, NMP-22, 1535–1536
Urticaria pigmentosa (UP), 650
U.S. Clinical Laboratory Improvement Act (CLIA), 139
U.S. Food and Drug Administration submission trials for, 177
U variants, 714

V

Vacuum phototubes, 41
Vaginal candidiasis, 1208
Vaginal secretions, 1362, 1362f
Valproic acid (Depakene), 371
Variable complex genetic alterations, with no specific pattern, sarcomas with, 1602
Variable costs, 162
Variable number of tandem repeat (VNTR) loci, 1470
Variable penetrance, and expressivity, 1437
Variables, 119
Variance analysis, 126, 127f, 169–170
Varicella zoster virus (VZV), 1271, 1274, 1276t, 1277–1278, 1285
Vascular endothelial growth factor, 1530
Vasculitis, 1058–1073.e2, 1083–1084. *See also* Rheumatoid vasculitis.
  diagnostic classification of, 1058–1059
  large vessel, 1059–1062, 1060f, 1060t
  medium vessel, 1060f, 1062–1064, 1062t
  putative pathogenic mechanisms for, 1059b
  small vessel, 1064–1073, 1064t
Vasoactive intestinal peptide (VIP), in diarrhea, 339
Vasovagal reactions, 815–816
Vegetative mycelium, 1195
Vel antibodies, 743
Vel blood group systems, 743
  biochemistry, 743
  molecular biology, 743
Velocardiofacial syndrome, 1417f, 1425, 1431
Velocity
  of propagation, 36, 36b
  PSA, 1520
Venereal syphilis
  clinical manifestations of, 1232f
  etiologic agents of, 1229–1230
  incidence, 1230
  in vitro diagnostic modalities for, 1233, 1233f
Venous puncture technique, 30b
Venous versus capillary samples, 252
Verapamil, 369
Verigene Gram-Positive Blood Culture Nucleic Acid Test, 1178
Verruga peruana, 1264
VersaTREK system, 1354
Very late activation antigens (VLAs), 992
Very-low-density lipoproteins, 246–247
Vesication, 1344
Vesicles
  from genital tract, 1362–1363, 1363f
  from skin, 1365
Vesicular rash, 1277–1278
Vibrio
  antimicrobial susceptibility of, 1150
  characteristics, 1149, 1149t
  clinical manifestations and pathogenesis of, 1149
  laboratory diagnosis of, 1149–1150, 1149t
VIPoma, 345
Viral exanthems and common cutaneous infections, 1278
Viral gastroenteritis, 1278–1279, 1279t
Viral growth, 1282–1283
Viral hemorrhagic fever, 1287–1288
Viral hepatitis, 1279–1280
Viral inclusion cells, 498
Viral-induced hepatitis, testing for, 323–327
  hepatitis A, 323, 323f
  hepatitis B, 323–325, 324f, 325t
  hepatitis C, 325–326, 325t
  hepatitis D, 326
  hepatitis E, 326–327
  hepatitis G, 327
Viral infections, 1266–1289.e5, 1276f
  clinical viral infectious syndromes, 1266–1289
    acquired immunodeficiency syndrome, 1273–1274, 1280–1282, 1281f
    congenital and perinatal viral infections, 1271–1273
    viral exanthems and common cutaneous infections, 1278
    viral gastroenteritis, 1278–1279, 1279t
    viral hepatitis, 1279–1280
  in immunocompromised hosts, 1283–1286
  introduction to, 1266, 1271t, 1283f
    antigen detection, 1288
    cell culture, 1270, 1273
    nucleic acid amplification testing, 1271, 1273, 1282
    specimen collection, 1267, 1284t
    viral serology, 1269, 1275, 1278–1279
    virus antigen assays, 1268
  laboratory methods for diagnosis of, 1276t
  pediatric and adult viral respiratory syndromes, 1266–1270
  in returning travelers, 1286–1289, 1287t
  with skin and mucosal manifestations, 1275–1278, 1276t
  syndromes, clinical, 1266–1289

Viral infections *(Continued)*
transplant donor and recipient screening, 1283, 1284t
viral meningitis and encephalitis, 1273–1275
virus-associated neoplasia, 1282–1283
Viral meningitis, 522, 1273–1274
encephalitis and, 1273–1275
Viral respiratory syndromes, pediatric and adult, 1266–1270
Viral serology, 1269, 1275, 1278–1279
Virus antigen assays, 1268
Virus-associated neoplasia, 1282–1283
Viruses
detection of, in blood specimen, 1355
in feces, 1363
infections of, diagnosis of, 1356
Virus isolation, 1272–1273, 1276t
Visceral leishmaniasis, 1312
Vitamin A, 446
prealbumin and, 280–281
Vitamin B1. *See* Thiamine pyrophosphate (TPP) (vitamin B1)
Vitamin B2. *See* Riboflavin (vitamin B2)
Vitamin B6. *See* Pyridoxine (vitamin B6)
Vitamin B12. *See* Cobalamin (vitamin B12)
Vitamin C. *See* Ascorbate (vitamin C)
Vitamin D, 115–116, 116t, 446
deficiency, 222
intoxication, 217
and metabolites, 214–215
synthesis, pathways of, 214f
Vitamin E (tocopherol), 446
Vitamin K, 446–447
deficiency of, 844–845
Vitamin K antagonists, 879–882, 880f, 881t, 881b
brodifacoum, 882
long-acting anticoagulant rodenticides, 882
Vitamin K-dependent clotting factors, combined deficiency of, 843
Vitamins, 442–447, 442t, 444t–445t
fat-soluble, 446–447
trace elements and, 447–452, 447t–448t
water-soluble, 443–446
Vitek System, 1171
Vitiligo, 1084
Vitronectin, 973
VLDL-C/plasma triglyceride ratio, 257
Voltammetry, 48
Volume
of blood specimen, 1352–1354
homeostasis, defective hormonal regulation of, 471
Volumetric flasks, 56
Volumetric laboratoryware, 55–56
von Hippel-Lindau syndrome, 1603
von Recklinghausen's disease, 1603
von Willebrand disease, 838
laboratory evaluation of, 849–852
and normal platelet biology, 847–849
and platelet disorders, 847–869.e5
qualitative abnormalities of, 866–867
platelet type, 867
type 2A, 866
type 2B, 866
type 2M, 866
type 2N (Normandy), 866–867
type 1: partial quantitative abnormality, 865–866, 866f
type 3: severe quantitative abnormality, 866
and von Willebrand factor, 864–868
biology of, 864–865, 864f
laboratory tests for, 865
von Willebrand factor
biology of, 864–865, 864f
laboratory tests for, 865
and von Willebrand disease, 865–867
von Willebrand syndrome, acquired, 867
VPN tunnel, 161
VRE. *See* Vancomycin-resistant enterococci (VRE)
VTM. *See* Viral transport medium (VTM)

W

Waived testing, 81–82, 82t
Waldenström's macroglobulinemia (WM), 668
Warfarin, 879
control of, 881–882
drug and supplement interactions with, 881b
half-life of, 880
therapeutic index of, 881
true genetic resistance to, 880–881
Warm autoimmune hemolytic anemia, 760–761
serologic characteristics of, 761
serologic testing beyond the DAT of, 761
Washing, of RBCs and PCs, 775
Wash-through tablet method, 483
procedure of, 483
Wasps, 1347
Water, 53–54
baths of, 57
diuresis, 199, 199b
purification of, 53–54
purity of
monitoring, 54
types of, 53
renal function, electrolytes, and acid-base balance, evaluation of, 181–207.e2
sodium, and diuretic hormone metabolism, disorders of, 197–200
hypernatremia, causes and pathogenesis of, 200, 200b
hyponatremia, causes and pathogenesis of, 199–200, 199b
polyuria, 199, 199b
thirst, regulation of, ADH release and, 197–198
urine concentration and dilution, 198–199, 198f
Water load test, 394, 395t
Water-soluble vitamins, 442t, 443–446
Watson-Schwartz test, 485, 486f
Wavelength, 36
accuracy, 42
selectors, 39
units for, 36b
Waxy casts, 490–491, 491f
Weak ABO subtype, 714
Weights, handling, for testing accuracy, 54–55
Wermer syndrome, 1602
West Nile virus (WNV), 785–786, 1275
Wet preparation, for examination, 1202, 1202b
Wheatley's trichrome stain, 1295
WHIM (warts, hypogammaglobulinemia, infection, and myelokathexis) syndrome, 639
Whipple's disease, 342
"Whipple's triad," for hypoglycemic disorders, 234
Whipworm, 1328
Whistleblowers, 179
White blood cell (WBC), abnormalities in, 104–105
Whole blood glucose, 228–229
Whole-body acid-base balance, 201–202
Whole-cell granulocyte antibody assays, 766
Whole-exome sequencing (WES), 1621–1622, 1622f
Whole-genome shotgun sequencing, 1609
Whole platelet assays, 769
WHONET software, 1181
Wilcoxon signed-ranks test, 124
Williams syndrome, 1430–1431
Wilms' tumor 1 gene *(WT1)* mutations, in acute myeloid leukemias, 1566
Wilson's disease, 286, 450
Wiskott-Aldrich syndrome (WAS), 854–855, 854t, 860
Wolf-Hirschhorn syndrome, 1430
Workcell, 77
Workflow
analysis, 16–18
metric examples, 20t
modeling, 17–18
software models, interrelated variables simulated by, 18b
understanding of, 13–18
Workstation, 77
Workstation analysis, 14
instrument audit and, 14–16
test menu and, 16
Wound infections, specimens from, 1365–1366
Wright's stain, 1202
WT1 mutations, in acute myeloid leukemias, 1566
Wuchereria bancrofti, 1338–1339, 1339f

X

X and Y chromosome markers, 1471–1472, 1472f, 1473b
Xanthochromia, 512, 512t
Xg^a antibodies, 733
Xg blood group system, 733
biochemistry and molecular biology, 733
X-linked agammaglobulinemia (XLA), and neutropenia, 637
X-linked spinal and bulbar muscular atrophy, 1442
Xp11 translocation, renal cell carcinoma with, 1595
xTAG technology, 1613
Xylose absorption test, 341

Y

Yaws, 1232
Y chromosome markers, 1471–1472, 1472f, 1473b
Yeast
candidiasis, cryptococcosis and other infections caused by, 1207–1211
and hyphae, structure of, 1195, 1197f–1198f
morphology of, 1203–1204, 1204f, 1204b
and yeastlike pathogens, 1211, 1211f
YT blood group system, 732–733
biochemistry, 732–733, 733f
biological role, 733
molecular biology, 732–733

Z

Zarontin. *See* Ethosuximide (Zarontin)
Zero-based budget, 169
Zika virus (ZIKV), 786, 1286–1287
Zinc (Zn), 451–452
deficiency of, 451
dietary sources of, 451
metabolism of, 451
testing of, 452
Zinc transporter-8 autoantibodies, 1109, 1109t
ZNF704 (zinc finger protein 704), 1460–1461
ZNF804A gene, 1457
Zollinger-Ellison (ZE) syndrome, 216, 335–336
Zonal electrophoresis, 277–278
Zoonotic Filarial Nematodes, 1340–1341
ZRSR2 gene, 1566–1567
Zygomycetes, 1195
Zygomycosis, 1220–1222
Zymogen, 969–970

GUIDELINES FOR ORDERING BLOOD FOR ELECTIVE SURGERY

ALSO REFERRED TO AS MAXIMUM SURGICAL BLOOD ORDER SCHEDULE (MSBOS)

These guidelines present a range in numbers of units of blood to be ordered as practiced at three different institutions: University Hospital State University of New York Upstate Medical Center at Syracuse, New York; Virginia Commonwealth University Medical Center, Richmond, Virginia; and University of Michigan Hospitals, Ann Arbor, Michigan. Each institution should set its own guidelines for ordering blood products to take into account varying medical needs and practices in collaboration with the hospital medical and surgical staff.

KEY:
0 = no testing required
T&S = type and screen
1-6 = number of units crossmatched
AO = as ordered
* = varies with purpose

CARDIOPULMONARY/ CARDIOTHORACIC

A-V canal repair 3
Angioplasty ..... T&S
Aortic or ventricular aneurysm repair 4
Aortic dissection/repair 6
Aortic valve replacement ..... 2 to 3
Atrial septal defect repair 2
Atrial septectomy 2
Blalock-Taussig shunt 1
Bidirectional Glenn's shunt 2
CABG (coronary vein graft)
Off pump ..... T&S
On pump 2
Coarctation repair 2
Esophagogastrectomy 3
Esophageal hernia/hiatal ..... T&S
Esophagoscopy ..... T&S
Fontan's procedure ..... 3 to 4
Great vessel switch 3
Lobectomy ..... T&S
Mediastinoscopy ..... T&S
Mitral commissurotomy 2
Mitral valvuloplasty 2
Mitral valve annuloplasty 2
Mitral valve replacement 2
Mustard procedure 2
Open lung biopsy ..... T&S
Pacemaker insertion ..... T&S
Patent ductus arteriosus ligation ..... T&S
Pericardectomy 2
Pericardial window ..... T&S
Pneumonectomy ..... T&S
Pulmonary valve replacement 2
Pulmonary valvulotomy 2
Redo and repair 6
Septectomy 2
Sternal wire removal 0
Tetralogy of Fallot 2
Thoracotomy/lobectomy ..... T&S
Thoracoscopy ..... T&S
Transposition repair 2
Ventricular septal defect repair 2
Wedge resection ..... T&S

GENERAL SURGERY

Abdominoperineal resection ..... T&S
Amputations ..... T&S
Appendectomy 0
Bronchoscopy ..... T&S
Catheter insertion/removal 0
Cholecystojejunostomy ..... T&S
Cholecystectomy 0
Colon resection ..... T&S
Colostomy closure/takedown ..... T&S
Debridement (wound, burn) ..... AO
Denver peritoneal shunt insertion ..... T&S
Denver shunt revision ..... T&S
Dressing change 0
Exploratory laparotomy ..... T&S to 2
Gastric bypass ..... T&S
Gastrostomy tube insertion ..... 0 or T&S
Hemicolectomy ..... T&S
Hemorrhoidectomy 0
Hepatic lobectomy 4
Hernia repair, inguinal 0
Ileostomy ..... T&S
Iliac profunda bypass 2
Jejunostomy tube placement 0
Lumpectomy, breast mass 0
Mastectomy, simple 0
Mastectomy, modified radical 0
Mastectomy, radical ..... T&S
Mediastinoscopy 0
Myotomy (pyloric) 0
Parotidectomy 0
Pilonidal cyst 0
Portocaval shunt ..... 4 to 6
Pseudoaneurysm repair ..... 4 to 6
Rib resection 0
Sigmoidectomy ..... T&S
Sigmoidoscopy 0
Small bowel resection ..... T&S
Splenectomy ..... T&S to 2
Sympathectomy ..... T&S
Thyroidectomy 0
Total colon resection ..... T&S
Transjugular intrahepatic portosystemic shunt (TIPS) ..... T&S
Vagotomy 0
Vein stripping ..... T&S
Whipple's procedure ..... 2 to 4

GYNECOLOGY

Anterior-posterior repair 0
Cone biopsy (CO_2 laser) 0
Dilation and curettage (D&C) ..... 0 to 2
Ectopic pregnancy ..... T&S
Endometrium ablation 0
Examine under anesthesia (EUA) 0
Exploratory laparotomy ..... T&S to 2
Exenteration procedure 4
Hysterectomy, total abdominal ..... T&S
Hysteroscopy 0
Laparoscopy 0
Laser vaporization 0
Neosalpingostomy 0
Oophorectomy 0
Ovarian wedge resection 0
Salpingo-oophorectomy 0
Uterine suspension 0
Tubal ligation 0
Tuboplasty 0
Vaginectomy ..... T&S to 2
Vulvectomy ..... T&S to 2

NEUROSURGERY

Aneurysm clipping 2
Biopsy (cervical/brain) ..... T&S
Burr hole ..... T&S
Carpal tunnel release ..... 0 or T&S
Cervical decompression
1-2 level 0
>2 level ..... T&S
Cervical discectomy ..... T&S
Cordotomy ..... T&S
Cordectomy 1
Craniectomy 2
Cranioplasty ..... T&S
Craniotomy 2
Endarterectomy, carotid ..... T&S
Hypophysectomy ..... T&S to 1
Laminectomy
1-2 level 0
>2 level ..... T&S
Lobectomy 2
Neuroma removal ..... T&S
Nerve repair ..... T&S
Pituitary tumor resection 1
Spinal fusion ..... T&S
Stereotactic brain biopsy ..... T&S
Stereotactic hematoma ..... T&S
Ulnar nerve transplant 0
Ventricular-peritoneal shunt insertion ..... 0 or T&S

ORTHOPEDICS

Acromioplasty 0
Amputation ..... T&S
Arthroscopy 0
Arthroplasty 0
Arthrotomy 0
Biopsy, excisional 0
Bipolar transfer ..... T&S
Carpal tunnel release 0
Closed reduction 0
Debridement ..... AO
Decompression laminectomy
1-2 level 0
>2 level ..... T&S
Diskectomy ..... T&S
Fractures 0
*Fusions, other ..... T&S to 2
Hardware removal 0
Hip revision ..... T&S to 2
Hip screw and nailing ..... T&S to 2
Lumbar laminectomy
1-2 level 0
>2 level ..... T&S
Meniscectomy 0
Nerve transposition 0
Neuroma excision 0

Open reduction
- Femur, pelvis, acetabulum ..... T&S to 2
- Hand, foot 0
- Radius, humerus, elbow ..... 0 or T&S

Osteotomy 0
Posterior rod fusion 2
Prosthesis removal 0
Releases 0
Revascularization and exploration ..... T&S
Rodding (Grosse and Kempf) ..... T&S
Rotator cuff repair ..... T&S
Shoulder replacement ..... T&S
Shoulder repair 0
Spinal fusions ..... 2 to 4
Tendon repair 0
Total elbow 0
Total hip ..... T&S
Total knee ..... T&S

OTORHINOLARYNGOLOGY/ HEAD AND NECK SURGERY

Antrotomy 0
Atticoantrotomy 0
Bronchoscopy 0
Caldwell-Luc ..... 0 or T&S
Cochlear implant 0
Composite resection 4
Craniofacial resection ..... T&S
Dissecting laryngoscopy 0
Endoscopy 0
Esophageal reconstruction ..... T&S
Esophagoscopy 0
Ethmoid artery ligation 4
Ethmoidectomy ..... T&S
Excisional biopsy 0
Frontal sinus exploration ..... T&S
Glossectomy ..... T&S
Labyrinthectomy 0
Laryngectomy ..... T&S
Laryngoscopy 0
Mandibulectomy ..... T&S
Mastoidectomy 0
Maxillary fixation ..... T&S
Maxillectomy ..... T&S
Myringotomy 0
Nasopharyngoscopy 0
Neck dissection ..... T&S
Neurectomy ..... 0 or T&S
Panendoscopy 0
Parotidectomy 0
Plate removal 0
Septoplasty ..... 0 or T&S
Septorhinoplasty ..... 0 or T&S
Sphenoethmoidectomy ..... T&S
Sphenoidectomy ..... T&S
Stapedectomy 0
Thyroidectomy 0
Tonsillectomy 0
Tracheoscopy 0
Tracheostomy tube insertion 0
Tracheotomy ..... T&S
Tympanomastoidectomy ..... 0 or T&S
Tympanoplasty 0

PLASTIC SURGERY

Millard's repair ..... T&S
Orbitotomy ..... T&S
Reduction mammoplasty 0
Septorhinoplasty 0

RENAL TRANSPLANTATION

Arteriovenous fistula 0
Donor nephrectomy ..... T&S
Pancreas transplant 4
Renal artery-vein patch 3
Renal transplant ..... T&S to 2
Vascular catheter insertion/removal (Tenckhoff) ..... T&S

UROLOGY

Adrenalectomy 2
Bladder resection ..... T&S
Circumcision 0
Cystectomy
- Simple 0
- Radical 2

Cystoscopy 0
Cystotomy 0
Fulguration, bleeding bladder ..... T&S
Hydrocelectomy 0
Ileal conduit 1
Lithotomy, ureteral ..... T&S
Lithotripsy, shock wave 0
Meatotomy ..... T&S
Needle biopsy of prostate 0
Nephrectomy, donor ..... T&S
Nephrectomy, radical ..... T&S
Nephrolithotripsy 1
Nephrostomy ..... T&S
Orchiopexy 0
Orchiectomy 0
Penectomy 2
Penile prosthesis insertion 0
Prostatectomy ..... T&S
Pyelolithotomy ..... T&S
Reimplantation of ureter ..... T&S
Stamey's procedure ..... 0 or T&S
Transurethral resection of the prostate 0
Ureterectomy 0
Ureterolithotomy ..... T&S
Ureteroscopy 0
Urethral fistula excision ..... T&S
Vasectomy 0
Vasovasostomy 0

VASCULAR SURGERY

Abdominal aortic surgery 4
Aneurysm repair 2
Aortoiliac bypass 2
Arteriofemoral bypass 2
Arteriovenous fistula 0
Carotid endarterectomy ..... T&S
Catheter insertion/removal 0
Femoral bypass ..... T&S
Iliac profunda bypass 2
Renal artery repair 3
Splenorenal artery bypass ..... T&S